A publication of the
American Pharmaceutical Association—
the National Professional Society
of Pharmacists

JOURNAL OF PHARMACEUTICAL SCIENCES

Volume 73, 1984

JPMSAE 73(1-12) 1-1910 (1984)
ISSN 0022-3549

Sharon G. Boots
Editor

Sue A. Kruger
Production Editor

Margaret M. Madeleine
Assistant Production Editor

Karen A. Blakney
Copy Editor

Edward G. Feldmann
Contributing Editor

Samuel W. Goldstein
Contributing Editor

Patricia A. Evich
Editorial Secretary

Editorial Advisory Board

Jordan L. Cohen
Kenneth A. Connors
Louis Diamond
Ho-Leung Fung
Milo Gibaldi
Everett N. Hiestand
W. Homer Lawrence
Ian W. Mathison
Carl M. Metzler
Robert E. Notari
Paul L. Schiff, Jr.
Jane E. Shaw

Published monthly under the supervision of the Board of Trustees

FDA Commissioners—Their Function and Operation

Over the past eighteen years, we have witnessed a virtual procession of people serve as FDA Commissioners. In addition, there have been many other periods—some quite lengthy—during which various Acting Commissioners have bridged the gap between the departure of one Commissioner and the arrival of the next.

George P. Larrick was the last FDA Commissioner to "rise through the ranks" and follow the traditional promotion and selection process that had been used for the agency since its predecessor department was initially established at the turn of the century. In breaking with the past, a Public Health Service physician-administrator, James L. Goddard, was selected to head the FDA. Supposedly, this would transform the agency's enforcement and regulatory philosophy—which was attributed to the inspector background of Larrick and his immediate predecessors—into one with a more scientific and medical orientation associated with Goddard and his background.

Although Goddard and every subsequent occupant of the Commissioner's office have been medical or health care scientists, the overall orientation has changed relatively little—at least until the recent government-wide deregulation emphasis espoused by the Reagan Administration. And given the fact that FDA's primary mission is to protect and safeguard the public relative to foods, drugs, and cosmetics, it hardly could be otherwise. Simply put, FDA's major mission is neither research nor education—although both of these elements are highly important to it and to the public in FDA's ability to fulfill its regulatory role in the most efficient and effective manner possible.

However, in departing from the promotion from within practice, something did happen. The office became "political" rather than "career." In practical terms, this made the revolving-door syndrome one natural result; it also led to the instability and insecurity that has characterized the position for almost the past two decades; and it has contributed to certain rivalries between the FDA Commissioner and his or her boss, the Secretary of the U.S. Department of Health and Human Services (formerly, U.S. Department of Health, Education, and Welfare).

Without exception, each of the FDA Commissioners since Larrick has been competent, qualified, and has discharged his duties with skill and dedication. However, their individual personalities and operating styles have differed as greatly as night and day. This diversity began immediately with Goddard, whose authoritative rule, high management profile, and dominating personality earned him the nickname of "Dr. God."

But at the same time, these various FDA heads were obliged to mold their individual operating styles and their public images to "fit" with their respective bosses—namely, the person who happened to be HHS or HEW Secretary at that particular point in time.

And again, the personality and operating style of the respective HHS/HEW Secretaries has been every bit as broad and different as the FDA Commissioners. To this, add the fact that their relative interest in FDA and in FDA matters has been equally varied, and we have had situations ranging from one extreme to the other.

At no time was that phenomenon more evident than during the tenure of Arthur Hull Hayes. During the first portion of Hayes' term in office, Richard S. Schweiker was his boss—and Schweiker took such a strong personal interest in FDA matters that he virtually appeared to emasculate the Commissioner's office. Indeed, it was widely mentioned in Washington political circles that Schweiker served "as his own FDA Commissioner." This was the case despite the fact that both Hayes and Schweiker repeatedly claimed that they enjoyed a close, harmonious working relationship.

Then, when Schweiker resigned and Margaret M. Heckler was named Secretary, Hayes found himself in a profoundly different situation. No longer was the Secretary trying to run the FDA. Indeed, Heckler adopted and followed such an extreme "hands off" policy that when Hayes himself resigned many months later, it was reported that he had never once had a meeting with her during his entire term in office.

All of this makes interesting recounting for us and, we hope, interesting reading for our subscribers. But that is not our real purpose in reviewing this past history.

Rather, we wish to suggest that it may be appropriate to review the relationship that exists between the two offices involved; namely, HHS Secretary and FDA Commissioner. If so, such an examination and review would appear to be especially timely now with the FDA Commissionership currently vacant.

Former FDA Commissioner Alexander M. Schmidt wrote a guest commentary that appeared in the January 1983 issue of *Pharmaceutical Technology*. His editorial, written when Hayes and Schweiker were both still in office, was extremely tactful and diplomatic. But, in spite of his careful choice of words and phraseology, Schmidt clearly delineated what he saw as the respective roles of the two positions, as well as the hazard inherent in having the Secretary intrude too far into the realm of the Commissioner.

"It was my strongly held view as Commissioner," wrote Schmidt, "that the Secretary's job was to establish policy to govern the functioning of the agency. It was the Commissioner's job to be certain that the agency responded to the policy and was well run.

"The Commissioner, for his part, had to subscribe to the mandated policy or leave. The Secretary had to be fully satisfied with the Commissioner and his performance or replace him, but should never become involved with the operation of the agency or assume the Commissioner's function. I always insisted," continued Schmidt, "that one Commissioner of Food and Drugs was enough!"

Schmidt then went on to detail various managerial and pragmatic reasons why he felt such a clean division of responsibility should be established and followed. He summed up by saying, "There is a much more important reason for the Commissioner to run the agency, however, and that is simply that the higher FDA's decisions go in the administrative hierarchy, the more political and less scientific the decisions are likely to be . . . Good science certainly protects the public interest and in the long run, also protects the interests of industry and FDA."

Well said, Dr. Schmidt! We earnestly hope that your words of advice will have a positive influence in shaping the future roles and interrelationships between these two highly important government offices.

—EDWARD G. FELDMANN
American Pharmaceutical Association
Washinton, DC 20037

0022-3549/84/0100-0001$01.00/0
© 1984, American Pharmaceutical Association

JOURNAL OF PHARMACEUTICAL SCIENCES

JANUARY 1984
VOLUME 73 NUMBER 1

RESEARCH ARTICLES

Mechanism of Freeze–Thaw Instability of Aluminum Hydroxycarbonate and Magnesium Hydroxide Gels

MARY I. ZAPATA *, JOSEPH R. FELDKAMP ‡, GARNET E. PECK *, JOE L. WHITE ‡, and STANLEY L. HEM *x

Received August 2, 1982, from the *Department of Industrial and Physical Pharmacy and the ‡Department of Agronomy, Purdue University, West Lafayette, IN 47907. Accepted for publication November 24, 1982.

Abstract □ The effect of freeze–thaw cycles on the physical stability of aluminum hydroxycarbonate and magnesium hydroxide gels was studied. Coagulation following a freeze–thaw cycle, leading to the formation of visible aggregates, affected the content uniformity of both gels. The freeze–thaw cycles did not affect the crystal form or surface characteristics of the gels as determined by X-ray powder diffraction and point of zero charge, but caused a slight reduction in the rate of acid neutralization and a large increase in the rate of sedimentation. The greatest effect was observed after the first freeze–thaw cycle. While the duration of freezing was not a factor, the rate of freezing was important and was inversely related to the aggregate size. The aggregates which formed following a freeze–thaw cycle were not redispersed by shaking, but were reversed by ultrasonic treatment or homogenization. The adsorption of polymers or surface-active agents prior to freezing reduced and, in some cases, prevented the formation of aggregates. The physical instability produced by a freeze–thaw cycle was explained by the modified DLVO theory. The force exerted on the particles by the growing ice crystals forced the particles into the primary minimum, producing strong interparticle attraction. On thawing, simple agitation did not provide enough force to overcome the attractive force of the primary minimum. Adsorption of polymers or surface-active agents increased the steric repulsive force and prevented the particles from reaching the primary minimum.

Keyphrases □ Aluminum hydroxycarbonate gel—freeze–thaw instability, mechanism, effect of added polymers and surface-active agents □ Magnesium hydroxide gel—freeze–thaw instability, mechanism, effect of added polymers and surface-active agents □ Freeze–thaw cycles—stability of aluminum hydroxycarbonate and magnesium hydroxide gels, effects of added polymers and surface-active agents, mechanisms

A pharmaceutical suspension must be composed of small, uniformly sized particles which do not settle rapidly and which can be easily redispersed to provide the patient with an accurate dose. Unfortunately, the physical characteristics of many suspensions are adversely affected by freeze–thaw cycles, causing the formation of visible lumps which settle rapidly and do not redisperse even after vigorous shaking (1). Aluminum hydroxycarbonate and magnesium hydroxide gels are widely recognized examples of suspensions whose physical stability is adversely affected by freeze–thaw cycles. Products containing these gels frequently bear a warning on the label to protect from freezing.

The homogeneity of parenteral chloramphenical suspensions is affected so adversely by freeze–thaw cycles that they can not be administered due to needle blockage (2). The rate of sedimentation of insulin suspensions was at least three times faster after undergoing a freeze–thaw cycle (3). The rate of thawing of the frozen insulin suspensions did not affect the sedimentation rate. The biological activity of the insulin suspensions was not affected by the freeze–thaw cycle, but it was difficult to obtain a reproducible dose. A change in particle size distribution following a freeze–thaw cycle has also been observed for suspensions of titanium dioxide, zinc oxide, glass beads, prednisolone acetate, and sulfadimethoxine (2).

Physical stability problems, such as oil separation, have been associated with freeze–thaw cycles of oil-in-water emulsions (1, 4–8). The mechanism responsible for the freeze–thaw instability of emulsions is not fully understood, but a common mechanism may be operating in both suspensions and emulsions.

The present study was undertaken to investigate the mechanism responsible for the freeze–thaw instability of suspensions in the belief that this basic information will lead to methods of stabilizing suspensions which are exposed to freezing. Gels of aluminum hydroxycarbonate and magnesium hydroxide were chosen as model suspensions because of their history of freeze–thaw stability problems. In addition, these gels provide a valuable comparison as

0022-3549/84/0100-0003$01.00/0
© 1984, American Pharmaceutical Association

Table I—Percent of Theoretical Dose Obtained Under Simulated Administration of Aluminum Hydroxycarbonate and Magnesium Hydroxide Gels

Aluminum Hydroxycarbonate Gel		Magnesium Hydroxide Gel	
Never Frozen	After One Freeze–Thaw Cycle	Never Frozen	After One Freeze–Thaw Cycle
99.6	118.2	99.1	136.9
99.6	109.8	99.1	121.8
99.6	112.0	99.1	109.3
99.6	108.4	99.1	83.6
99.1	110.9	99.1	100.0
99.6	113.8	98.7	132.4
98.7	117.8	99.1	101.3
99.6	112.0	99.1	92.4
99.6	107.8	99.1	91.6
99.6	109.3	99.1	92.4
Mean 99.5	112.0	99.1	106.2
SD 0.3	3.6	0.1	18.4

aluminum hydroxycarbonate gel is amorphous, but can undergo transformation to crystalline polymorphs, while magnesium hydroxide gel possesses the stable crystalline structure of the mineral brucite (9).

EXPERIMENTAL

The aluminum hydroxycarbonate and magnesium hydroxide gels studied were prepared by diluting a commercial aluminum hydroxycarbonate gel to 4% equivalent aluminum oxide or a commercial magnesium hydroxide gel to 6.8% magnesium hydroxide with doubly distilled water and homogenizing[1]. A standard procedure was followed for the freeze–thaw cycle. The gel (350 mL) in a 500-mL linear polyethylene bottle was placed in a freezer at −24°C. After 24 h, the sample was returned to room temperature. The effect of a rapid freezing rate was determined by immersing a 350-mL sample contained in a 500-mL linear polyethylene bottle in an acetone–dry ice bath (−86°C) for 24 h.

The aluminum or magnesium content was determined by chelatometric titration (10) and was expressed as equivalent aluminum oxide or magnesium oxide. The content uniformity was determined by inverting the 350-mL sample 20 times and immediately withdrawing a sample which would theoretically neutralize 3.75×10^{-4} M equivalent Al_2O_3. The sample was withdrawn by syringe and accurately weighed. The moles of acid actually neutralized by the sample at pH 3.0, 25°C was determined by an automated[2] pH-stat titration (11).

Samples were prepared for X-ray diffraction by air drying the gel and preparing a power by trituration with an agate mortar and pestle. Randomly oriented powder samples were prepared in McCreery mounts. Diffractograms were recorded[3] from 4° to 65° 2θ under the following conditions: CuK_α radiation, 30 kV, 28 mA, 1000 cps, and 2°/min.

A titration technique (12, 13) was used to determine the point of zero charge. The rate of acid neutralization was determined by an automated pH-stat titration at pH 3.0, 25°C and expressed as t_{50}, the time required for 50% of the theoretical amount of acid to be neutralized (11). The rate of sedimentation was determined by monitoring the density[4] of the upper region of the sample (14). Entrapped air was removed from the sample by placing 350 mL in a 1-L sidearm flask and applying vacuum for 15 min.

Samples were examined microscopically at a magnification of 400× using the following dilutions: aluminum hydroxycarbonate gel, 1 drop of gel with 4 drops of supernatant; aluminum hydroxycarbonate gel after one freeze–thaw cycle, 1 drop of gel with 2 drops of supernatant; magnesium hydroxide gel, 1 drop of gel with 6 drops of supernatant; and magnesium hydroxide gel after one freeze–thaw cycle, no dilution.

Samples were processed using the following equipment: ultrasonic dispersor[5] for 12 min at an output control of 4, one pass through a colloid mill[6] at a clearance of 7.62×10^{-3} cm, one pass through a hand homogenizer set at the smallest opening, and a magnetic stirrer for 12 min. Samples containing hydroxypropyl methylcellulose[7], sodium lauryl sulfate, cetyltrimethylammonium bromide, or polysorbate 80 were prepared by appropriate dilution of stock solutions.

The surface tension of the supernatant of surface-active agent–aluminum hydroxycarbonate gel mixtures was measured with a DuNouy tensiometer[8]. The average of three readings was reported. The following procedure was necessary to obtain a clear supernatant:

1. The equilibrated surface-active agent–aluminum hydroxycarbonate gel mixture was centrifuged at 6000 rpm for 20 min and the supernatant (cloudy) was collected.
2. The pH of the supernatant was adjusted to the point of zero charge of the aluminum hydroxycarbonate gel (pH 6.7) with 0.5 M NaOH (the number of drops was recorded).
3. The mixture was centrifuged at 5000 rpm for 10 min, and the supernatant (clear) was collected. The surface tension of solutions containing the same concentration of surface-active agent and 0.5 M NaOH served as controls.

Table II—X-ray Diffractogram of Magnesium Hydroxide Gel Before and After Freeze–Thaw Cycles

	dhkl (I/I_0)		
	Magnesium Hydroxide Gel		
Brucite[a]	Never Frozen	After 1 Freeze–Thaw Cycle	After 10 Freeze–Thaw Cycles
4.77(90)	4.7663(40)	4.7663(41)	4.7663(38)
2.72(6)	2.7281(4)	2.7281(4)	2.7281(5)
2.365(100)	2.3659(100)	2.3659(100)	2.3659(100)
1.7941(55)	1.7957(38)	1.7957(38)	1.7957(38)
1.573(35)	1.5739(35)	1.5739(35)	1.5739(34)
1.494(19)	1.4955(14)	1.4955(14)	1.4955(14)

[a] *Selected Powder Diffraction Data for Minerals*, Joint Committee on Powder Diffraction Standards, Swathmore, Pa. 1947, File 7-239.

RESULTS AND DISCUSSION

Aluminum hydroxycarbonate and magnesium hydroxide gels exhibit excellent content uniformity, as the mean dose was within 99% of the theoretical following the simulated administration of 10 doses (Table I). However, the ability to obtain an accurate dose of either gel was lost following one freeze–thaw cycle. Lumps were observed in both gels following the freeze–thaw cycle; however, the lumps in the magnesium hydroxide gel appeared to be larger. This difference may be responsible for the greater standard deviation for magnesium hydroxide (±18.4%) than for aluminum hydroxycarbonate gel (±3.6%) following a freeze–thaw cycle.

Freeze–thaw cycles did not affect the polymorphic form of the solid phase, as aluminum hydroxycarbonate gel remained amorphous by X-ray diffraction after 10 freeze–thaw cycles. The X-ray diffractogram of magnesium hydroxide gel was identical to brucite and did not change after 10 freeze–thaw cycles (Table II). Freeze–thaw cycles also do not

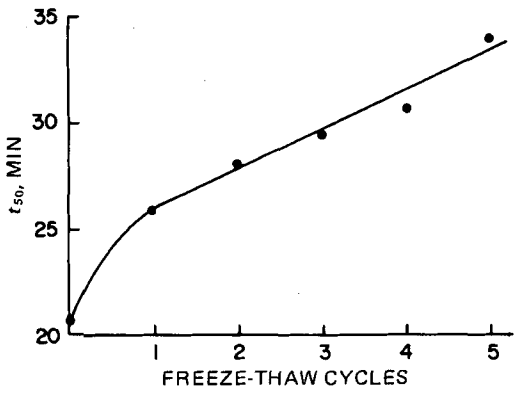

Figure 1—*Effect of repeated freeze–thaw cycles on the rate of acid neutralization of aluminum hydroxycarbonate gel.* t_{50} *represents the time required for 50% of the theoretical amount of acid to be neutralized at pH 3.*

[1] Eppenbach Homo Mixer; Gifford-Wood Co., Hudson, N.Y.
[2] PHM 26, TTT II, ABU 12 (2.5 mL), TTA 3, SBR 2, Radiometer, Copenhagen, Denmark.
[3] Siemens AG Kristalloflex 4 generator, type F diffractometer; Karlsruhe, West Germany.
[4] Hydrometer, model H8705-8 and cylinder model C-9010-340; American Scientific Products, McGaw Park, Ill.
[5] Sonicator, model W-370; Heat Systems Ultrasonics, Plainview, N.Y.
[6] Tri-Homo Dispersor, Tri-Homo Corp., Salem, Miss.
[7] Methocel E50 Premium; Dow Chemical Co., Midland, Mich.
[8] Autotensiomat, Model 215; Fisher Scientific Co., Chicago, Ill.

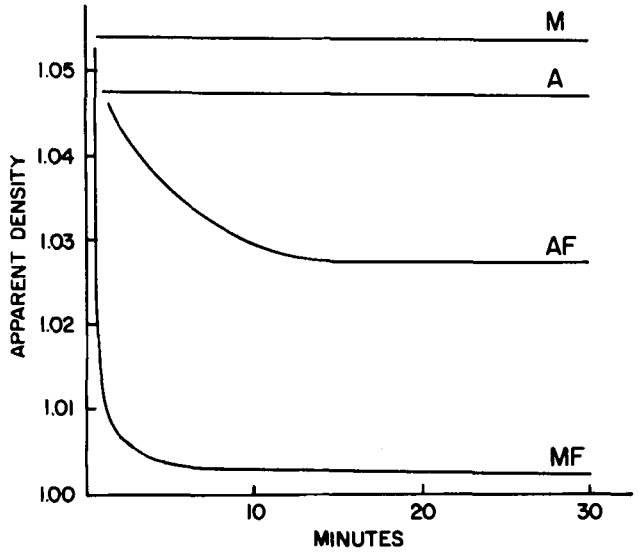

Figure 2—*Apparent density of the upper region of aluminum hydroxycarbonate or magnesium hydroxide gels. Key: (M) magnesium hydroxide gel, never frozen; (MF) magnesium hydroxide gel after one freeze–thaw cycle; (A) aluminum hydroxycarbonate gel, never frozen; (AF) aluminum hydroxycarbonate gel after one freeze–thaw cycle.*

appear to affect the surface groups of either gel as the point of zero charge (ZPC) was unaltered by 10 freeze–thaw cycles (ZPC of aluminum hydroxycarbonate, 6.7; ZPC of magnesium hydroxide, 10.8).

The rate of acid neutralization decreased slightly following freeze–thaw cycles. This effect was seen most clearly for aluminum hydroxycarbonate gel (Fig. 1). The initial freeze–thaw cycle caused the greatest decrease in the rate of acid neutralization, although a consistent decrease in the rate of acid neutralization occurred following each freeze–thaw cycle. The rate of acid neutralization of magnesium hydroxide is so rapid (t_{50}, 1.3 min) that the small effect of a freeze–thaw cycle was difficult to detect.

The decrease in the rate of acid neutralization was too small to attribute to the formation of a crystalline phase in aluminum hydroxycarbonate gel, as the crystalline forms of aluminum hydroxide are virtually unreactive at pH 3 (10). Thus both the X-ray diffraction and rate of acid neutralization data conflict with Gamame and Yoshida's (15) conclusion that freeze–thaw cycles promote the crystallization of aluminum hydroxide. An explanation for this apparent discrepancy is that Gamame and Yoshida used chloride-, nitrate-, and sulfate-containing aluminum hydroxide gels, which convert to crystalline forms very rapidly under normal aging (16, 17).

The duration of freezing is not significant, as samples of aluminum hydroxycarbonate or magnesium hydroxide gel which were frozen for 1, 3, 5, or 7 d all exhibited the same rate of acid neutralization (t_{50}, 26.0 min.). The freeze–thaw process seems to be the key element rather than the duration of freezing.

The rate of sedimentation as measured by the decrease in the density of the upper region of the sample proved to be a good indicator of the effects of a freeze–thaw cycle on the particle size distribution (14). The density of the upper region of aluminum hydroxycarbonate or magnesium hydroxide gel which had never been frozen remained essentially constant for at least 30 min, indicating a very low rate of sedimentation (Fig. 2). However, the density of the upper region of each gel decreased sharply following a freeze–thaw cycle. The sedimentation method is not as sensitive to the effect of repeated freeze–thaw cycles as the rate of acid neutralization, because a similar density curve was obtained regardless of the number of freeze–thaw cycles while the rate of acid neutralization steadily decreased with repeated freeze–thaw cycles (Fig. 1).

The greater particle size of magnesium hydroxide gel following a freeze–thaw cycle, which was suggested by the content uniformity data in Table I, was confirmed by the density data in Fig. 2. The density of the upper region of the aluminum hydroxycarbonate gel dropped rapidly to 1.0275 following a freeze–thaw cycle while the density of the upper region of the magnesium hydroxide gel rapidly approached the density of water. This indicates that the rate of sedimentation in magnesium hydroxide gel following a freeze–thaw cycle was very rapid and produced a particle-free upper region within several minutes. Photomicrographs of aluminum hydroxycarbonate and magnesium hydroxide gels confirm that

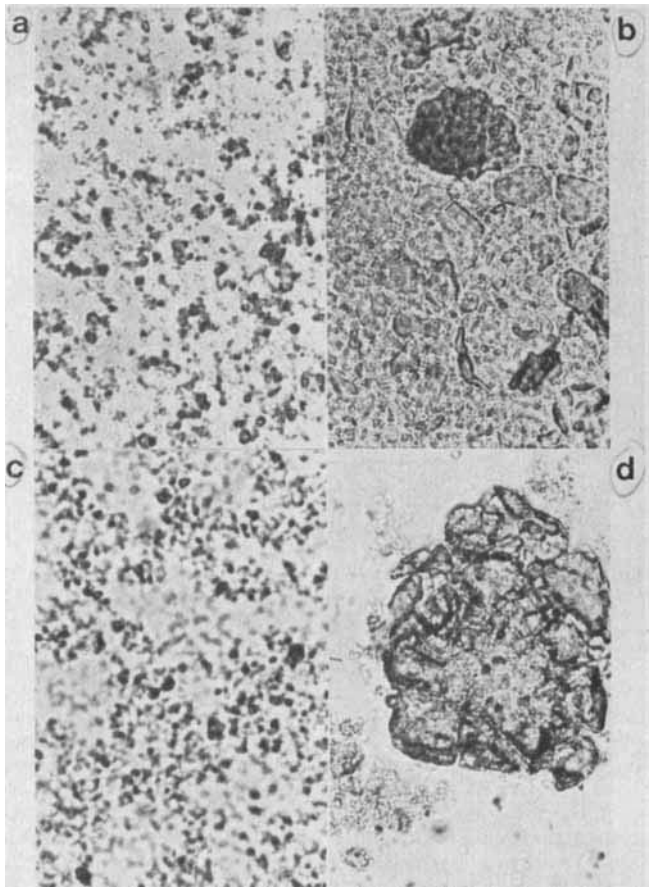

Figure 3—*Photomicrographs of gels at an original magnification of 400×. Key: (a) aluminum hydroxycarbonate gel; (b) aluminum hydroxycarbonate gel after one freeze–thaw cycle; (c) magnesium hydroxide gel; (d) magnesium hydroxide gel after one freeze–thaw cycle.*

aggregates ranging from ~65 to 160 μm form following a freeze–thaw cycle (Fig. 3).

The effects of a freeze–thaw cycle were reversed if adequate energy was applied to the suspension. As observed in Fig. 4, magnesium hydroxide gel which had undergone a freeze–thaw cycle was restored to its original settling characteristics by treatment with an ultrasonic dispersor. The effectiveness of various processing methods in restoring the original particle size distribution of the magnesium hydroxide gel appears (Fig. 4) to be directly related to the energy input as the order of effectiveness was ultrasonic dispersor > hand homogenizer > colloid mill > magnetic stirrer. The settling characteristics of aluminum hydroxycarbonate gel were similarily restored by the processing equipment.

The rate of freezing was found to be an important factor in the formation of aggregates during a freeze–thaw cycle. The rate of sedimentation of aluminum hydroxycarbonate gel was unaffected (identical to curve A in Fig. 2) if the gel was exposed to an acetone–dry ice bath (−86°C) to produce a rapid rate of freezing, while a slower rate of freezing (freezer at −24°C) resulted in an increased particle size (identical to curve AF in Fig. 2).

The importance of the freezing process and the rate of freezing, the absence of crystallization following freeze–thaw cycles, and the ability of high shear to reverse the effects of the freeze–thaw cycle all led to the

Table III—Effect of Hydroxypropyl Methylcellulose on Rate of Acid Neutralization of Aluminum Hydroxycarbonate Gel at pH 3.0

Hydroxypropyl Methylcellulose, %	t_{50}, min
0	38
1	39.5
3	40.5
5	42
7	44.5

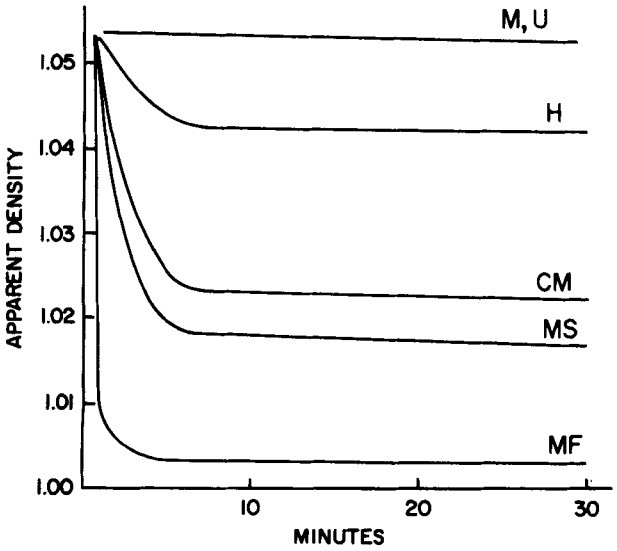

Figure 4—*Apparent density of the upper region of magnesium hydroxide gel. Key: (M) never frozen; (MF) after one freeze–thaw cycle; (U) ultrasonic dispersor after one freeze–thaw cycle; (H) hand homogenizer after one freeze–thaw cycle; (CM) colloid mill after one freeze–thaw cycle; (MS) magnetic stirrer after one freeze–thaw cycle.*

hypothesis that the freezing process forces the particles to form aggregates as described by the modified DLVO theory (Fig. 5) (18–22). The strong force exerted on the particles by ice formation was sufficient to overcome the repulsive barrier known as the primary maximum, and the particles were forced close enough together to experience the strong attractive force present in the primary minimum, thus forming aggregates. When the ice thawed, the aggregates remained intact unless enough energy was applied to overcome the energy barrier imposed by the primary maximum. The appearance of aggregates, the increased rate of sedimentation, the slight decrease in rate of acid neutralization, and the reversibility under high shear are all consistent with this mechanism.

The effect of the rate of freezing was also consistent with the modified DLVO theory. The more rapid rate of freezing caused a greater rate of nucleation and, therefore, a lower rate of crystal growth (23). The smaller ice crystals which were formed during the more rapid rate of freezing did not force as many suspension particles into an aggregate as occurred when large ice crystals formed during a slow rate of freezing. Therefore, aggregate size is inversely related to the rate of freezing. Furthermore, both theoretical and experimental studies showed that the maximum force exerted on a fixed spherical particle by a freezing interface was inversely related to the freezing rate (24, 25). Thus, the suspension particles experience a smaller force during a rapid freezing process.

The modified DLVO theory includes steric repulsive forces which are dependent on the size, geometry, and conformation of adsorbed molecules. Lecithin monolayers have been reported to exhibit strong repulsion at separation distances <20 Å (26). Steric repulsive forces have been observed on the close approach of mica sheets in an aqueous medium containing polyethylene oxide (27). A sharp increase in the repulsive force, which was attributed to forcing the polymer from between the mica surfaces, was observed when the distance of separation of the mica sheets was <5 Å.

It was hypothesized that adsorption of appropriate solutes will minimize aggregate formation during a freeze–thaw cycle by enhancing the primary maximum through the introduction of steric repulsive forces.

Table IV—Difference in Density of the Upper Region of Aluminum Hydroxycarbonate Gel Containing Various Concentrations of Hydroxypropyl Methylcellulose Following a Freeze–Thaw Cycle

Hydroxypropyl Methylcellulose, %	Initial Density	Equilibrium Density[a]	Δ Density
0	1.050	1.027 (10 min)	0.023
1	1.055	1.035 (10 min)	0.020
3	1.060	1.040 (10 min)	0.020
5	1.070	1.055 (15 min)	0.015
7	1.075	1.065 (20 min)	0.010

[a] Time to reach equilibrium density in parentheses.

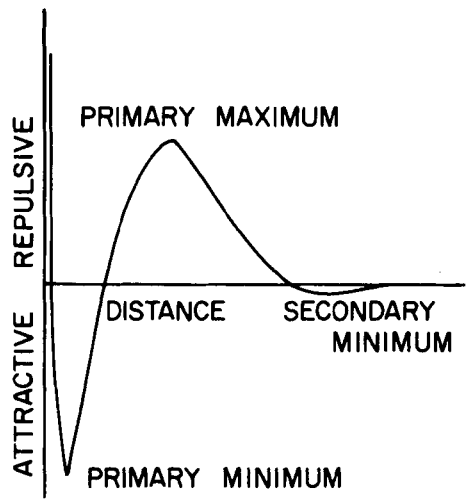

Figure 5—*Interparticle forces described by the modified DLVO theory.*

This hypothesis was tested by determining the effect of a polymer and several surface-active agents on the freeze–thaw stability.

Hydroxypropyl methylcellulose was adsorbed by aluminum hydroxycarbonate gel as evidenced by the decreased rate of acid neutralization in the presence of increased quantities of hydroxypropyl methylcellulose (Table III). The adsorbed hydroxypropyl methylcellulose was believed to reduce the rate of acid neutralization by occluding the surface and interfering with the approach of protons (28). The reduced rate of acid neutralization was not believed to be due to changes in viscosity as the hydroxypropyl methylcellulose–aluminum hydroxycarbonate gel sample was diluted 20 times prior to the pH-stat titration.

The addition of hydroxypropyl methylcellulose increased both the density and viscosity of the aluminum hydroxycarbonate gel. Therefore, to monitor the effect of a freeze–thaw cycle on the particle size distribution of the hydroxypropyl methylcellulose-containing aluminum hydroxycarbonate gel, it was necessary to modify the sedimentation procedure by comparing the difference in apparent density between the initial value (which increased with increasing hydroxypropyl methylcellulose concentration) and the relatively constant density which was ultimately reached. As seen in Table IV, aggregate formation due to a freeze–thaw cycle was reduced in direct relation to the concentration of hydroxypropyl methylcellulose.

The ability of polymers to minimize the effects of a freeze–thaw cycle was previously observed for polyvinylpyrrolidone, polyvinyl alcohol, methylcellulose, sodium carboxymethylcellulose, pectin, tragacanth, and sodium alginate (29). The protective effect was attributed to the formation by the polymer of a three-dimensional network in the aqueous phase which reduced the growth of ice crystals and immobilized the suspended particles, thereby reducing the formation of aggregates. While the structuring effect of polymers on the aqueous phase may be important and may have occurred in the hydroxypropyl methylcellulose–aluminum hydroxycarbonate system, it does not explain the protective effect which was also observed when surface-active agents were adsorbed by aluminum hydroxycarbonate or magnesium hydroxide gel.

The effect of sodium lauryl sulfate (an anionic surface-active agent), cetyltrimethylammonium bromide (a cationic surface-active agent), and polysorbate 80 (a neutral surface-active agent) on the freeze–thaw stabilities of aluminum hydroxycarbonate and magnesium hydroxide gels was studied. The rate of acid neutralization was reduced by the presence of the surface-active agents, with sodium lauryl sulfate causing the greatest effect (Table V). The reduction in the rate of acid neutralization was believed to be due to adsorption of the surface-active agents. Greater adsorption of sodium lauryl sulfate was expected, as both gels are positively charged under the conditions of the test (ZPC of aluminum hy-

Table V—Effect of Surface-Active Agents on the Rate of Acid Neutralization of Aluminum Hydroxycarbonate Gel at pH 3.0

Adsorbate	t_{50}, Min
Control	20.8
2.4×10^{-2} M Sodium lauryl sulfate	27.2
2.0×10^{-2} M Cetyltrimethylammonium bromide	22.2
2.6×10^{-2} M Polysorbate 80	22.5

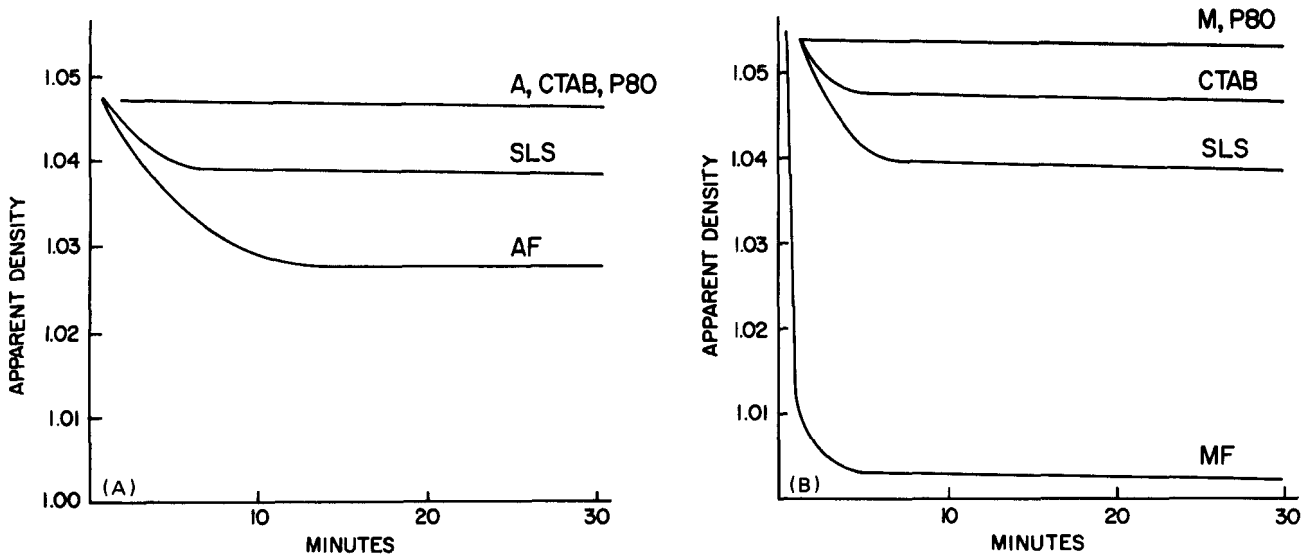

Figure 6—*Apparent density of the upper region of (A) aluminum hydroxycarbonate and (B) magnesium hydroxide gels. Key: (A, M) never frozen; (AF, MF) after one freeze–thaw cycle; (CTAB) containing 2.0 × 10^{-2} M cetyltrimethylammonium bromide after one freeze–thaw cycle; (SLS) containing 2.4 × 10^{-2} M sodium lauryl sulfate after one freeze–thaw cycle; (P80) containing 2.6 × 10^{-2} M polysorbate 80 after one freeze–thaw cycle.*

droxycarbonate gel 7.6, pH 5.4; ZPC of magnesium hydroxide gel 10.8, pH 9.9). Therefore, the greater reduction in the rate of acid neutralization which occurred when sodium lauryl sulfate was present confirms the adsorption hypothesis.

Adsorption of the surface-active agents was confirmed by a comparison of the surface tension of a solution of the surface-active agent with the surface tension of the supernatant after equilibration of the gel with the same solution of surface-active agent (Table VI) (30). Sodium lauryl sulfate was the most readily adsorbed agent, as the surface tension of the supernatant was 10–15 dynes/cm higher than the surface tension of the control solution. Adsorption of cetyltrimethylammonium bromide and polysorbate 80 also occurred, as the surface tension of each supernatant was greater than the control solution. In addition, it is likely that the freezing process favors adsorption since the solute will be concentrated in a solution of unfrozen water at the solid–liquid interface as freezing proceeds.

Each of the surface-active agents reduced aggregate formation following a freeze–thaw cycle (Fig. 6). Polysorbate 80 was the most effective surface-active agent in preventing an increase in the particle size distribution of either gel, while sodium lauryl sulfate was the least effective. The relative effectiveness of the surface-active agents can be rationalized based on the adsorption mechanism and the dimensions of the surface-active agent. The expected orientation of the adsorbed agents is shown in Fig. 7. The negative hydrophilic region of sodium lauryl sulfate will be adsorbed by the positive surface. However, the hydrophobic region will also be adsorbed (31), thereby reducing the thickness of the adsorbed layer. The hydrophobic region of cetyltrimethylammonium bromide will be adsorbed, while the positive hydrophilic region will experience electrostatic repulsion with the positive surface. The hydrophobic region of polysorbate 80 will be adsorbed, while the hydrophilic region will undergo little or no adsorption due to its compatibility with water.

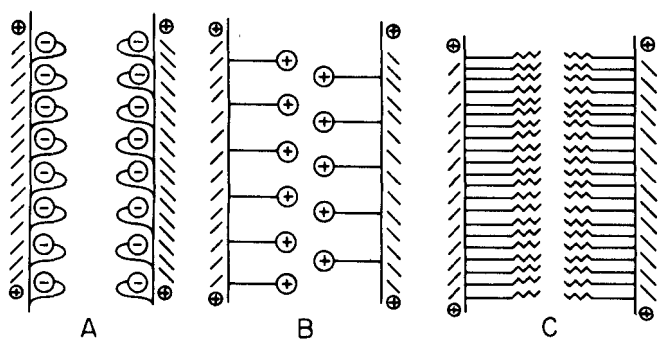

Figure 7—*Hypothetical steric repulsive region on adsorption of various surface-active agents. Key: (A) sodium lauryl sulfate; (B) cetyltrimethylammonium bromide; (C) polysorbate 80.*

The estimated molecular length of the surface-active agents is: sodium lauryl sulfate, 53 Å; cetyltrimethylammonium bromide, 76 Å; and polysorbate 80, 786 Å. Thus, the expected orientation of the adsorbed sodium lauryl sulfate suggests a steric repulsive region substantially <53 Å. The expected orientation of adsorbed cetyltrimethylammonium bromide suggests a steric repulsive region of ~76 Å. Polysorbate 80 will produce the largest steric repulsive region due to its large size and expected orientation. Examination of Fig. 6 reveals that the effectiveness of the surface-active agents in minimizing aggregate formation following a freeze–thaw cycle was directly related to the predicted size of the steric repulsive region produced by adsorption of the surface-active agent.

To determine if surface-active agents can produce disaggregation when added to a suspension following a freeze–thaw cycle, a sample of aluminum hydroxycarbonate gel was frozen for 24 h and then thawed. Polysorbate 80 was added with gentle stirring after thawing. Figure 8 shows that addition of a surface-active agent following a freeze–thaw cycle was partially effective in restoring the original particle size distribution. It has been reported (32) that irregular particles, when coagulating, will only come in contact at a limited number of points. Therefore, it is believed that polysorbate 80 added after a freeze–thaw cycle was adsorbed on the accessible interparticle space of the aggregates. The adsorption of polysorbate 80 produced a steric repulsive force between the particles, which led to partial disaggregation. However, the most effective steric repulsion

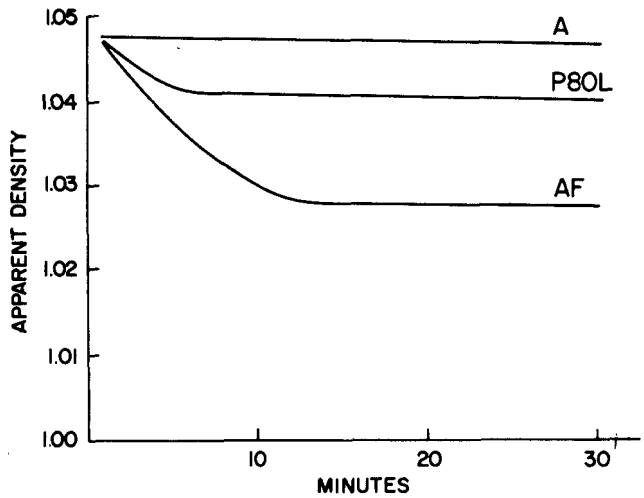

Figure 8—*Apparent density of the upper region of aluminum hydroxycarbonate gel. Key: (A) never frozen; (AF) after one freeze–thaw cycle; (P80L) 2.4 × 10^{-2} M polysorbate 80 added after one freeze–thaw cycle.*

Table VI—Comparison of Surface Tension of Solutions of Surface-Active Agents to the Surface Tension of the Supernatant After Equilibration with Aluminum Hydroxycarbonate Gel

Surface-Active Agent	Concentration, M	Surface Tension of Solution, dynes/cm	Surface Tension of Supernatant, dynes/cm
Sodium lauryl sulfate	5×10^{-5}	62	72
	1×10^{-4}	57	72
	2×10^{-4}	48	70
	3×10^{-4}	44	60
	4×10^{-4}	43	59
	5×10^{-4}	42	57
Cetyltrimethylammonium bromide	5×10^{-5}	52	55
	1×10^{-4}	49	52
	2×10^{-4}	47	50
	3×10^{-4}	44	47
	4×10^{-4}	40	41
	5×10^{-4}	40	41
Polysorbate 80	5×10^{-6}	44	45
	1×10^{-5}	41	42
	5×10^{-5}	39	40
	1×10^{-4}	38	39
	2×10^{-4}	38	38
	3×10^{-4}	38	38

was produced when the surface-active agent was adsorbed before the suspension was exposed to a freeze–thaw cycle.

Although only gels of aluminum hydroxycarbonate and magnesium hydroxide were examined, it is believed that the results of this study can be applied to any suspension and that the aggregation produced by freeze–thaw cycles will be more pronounced as the particle size of the suspension is smaller.

REFERENCES

(1) M. R. Cutie, *Drug Cosmet. Ind.*, **40**(January) (1980).

(2) A. Nakamura and R. Okada, *Colloid Polym. Sci.*, **254**, 718 (1976).

(3) D. T. Graham and A. R. Pomeroy, *Int. J. Pharm.*, **1**, 315 (1978).

(4) T. G. Rochow and C. W. Mason, *Ind. Eng. Chem.*, **28**, 1296 (1936).

(5) H. W. Walker, *J. Phys. Colloid Chem.*, **51**, 351 (1947).

(6) W. G. Barb and W. Mikuki, *J. Polym. Sci.*, **37**, 499 (1959).

(7) A. Buzagh and S. Rohrsetzer, *Kolloid Z. Z. Polym.*, **176**, 9 (1961).

(8) K. L. Blaze, E. Dvorak, and S. Mysik, *Kolloid Zh.*, **26**, 565 (1964).

(9) C. J. Serna, J. L. White, and S. L. Hem, *J. Pharm. Sci.*, **67**, 324 (1978).

(10) "The United States Pharmacopeia," 20th rev., United States Pharmacopeial Convention, Rockville, Md., 1980, p. 23.

(11) N. J. Kerkhof, R. K. Vanderlaan, J. L. White, and S. L. Hem, *J. Pharm. Sci.*, **66**, 1528 (1977).

(12) T. F. Tadros and J. Lyklema, *J. Electroanal. Chem.*, **17**, 267 (1968).

(13) J. R. Feldkamp, D. N. Shah, S. L. Meyer, J. L. White, and S. L. Hem, *J. Pharm. Sci.*, **70**, 638 (1981).

(14) B. H. Kaye, "Direct Characterization of Fine Particles," Wiley, New York, N.Y., 1981, pp. 159–168.

(15) S. Gamame and H. Yoshida, *J. Chem. Soc. Jpn.*, **82**, 1128 (1961).

(16) S. L. Hem, E. J. Russo, S. M. Bahal, and R. S. Levi, *J. Pharm. Sci.*, **59**, 317 (1970).

(17) C. J. Serna, J. L. White, and S. L. Hem, *Soil Sci. Soc. Am. J.*, **41**, 1009 (1977).

(18) J. N. Israelachvili, *Faraday Discuss. Chem. Soc.*, **65**, 20 (1976).

(19) J. N. Israelachvili and G. E. Adams, *J. Chem. Soc., Faraday Trans. 1*, **74**, 975 (1978).

(20) G. E. Adams and J. N. Israelachvili, in "Modification of Soil Structure," W. W. Emerson, R. D. Bond, and A. R. Dexter, Eds., Wiley, New York, N.Y., 1978, pp. 27–33.

(21) J. N. Israelachvili and B. W. Ninham, in "Colloid and Interface Science," M. Kerker, A. C. Zettlemoyer, and R. I. Rowell, Eds., Academic, New York, N.Y., 1978, p. 15.

(22) J. Th. G. Overbeek, in "Colloid and Interface Science," M. Kerker, A. C. Zettlemoyer, and R. I. Rowell, Eds., Academic, New York, N.Y., 1978, p. 431.

(23) A. W. Adamson, "Physical Chemistry of Surfaces," 3rd ed., Wiley, New York, N.Y., 1976, pp. 372–384.

(24) W. R. Wilcox, *J. Colloid Interface Sci.*, **77**, 213 (1980).

(25) G. Gupta, R. F. Rice, and W. R. Wilcox, *J. Colloid Interface Sci.*, **82**, 458 (1981).

(26) D. M. LeNevey, R. P. Rand, and V. A. Parsegian, *Nature (London)*, **259**, 601 (1976).

(27) J. N. Israelachvili, R. K. Tandon, and L. R. White, *J. Colloid Interface Sci.*, **78**, 430 (1980).

(28) D. N. Shah, J. L. White, and S. L. Hem, *J. Pharm. Sci.*, **70**, 1101 (1981).

(29) A. Nakamura and R. Okada, *Colloid Polym. Sci.*, **255**, 362 (1977).

(30) W. J. Knox, Jr. and T. O. Parshall, *J. Colloid Interface Sci.*, **40**, 290 (1972).

(31) D. N. Shah, J. R. Feldkamp, J. L. White, and S. L. Hem, *J. Pharm. Sci.*, **71**, 266 (1982).

(32) R. S. B. Greene, A. M. Posner, and J. P. Quirk, in "Modification of Soil Structure," W. W. Emerson, R. D. Bond, and A. R. Dexter, Eds., Wiley, New York, N.Y., 1978, pp. 35–40.

ACKNOWLEDGMENTS

Supported in part by a Graduate and Professional Opportunities Fellowship (M.I.Z.) and William H. Rorer, Inc. This report is Journal Paper 9135, Purdue University Agricultural Experiment Station, West Lafayette, IN 47907.

Excess Free Energy Approach to the Estimation of Solubility in Mixed Solvent Systems I: Theory

N. A. WILLIAMS * and G. L. AMIDON *x

Received July 22, 1982, from the *School of Pharmacy, University of Wisconsin, Madison, WI 53706.* Accepted for publication October 22, 1982. *Present address: College of Pharmacy, The University of Michigan, Ann Arbor, MI 48104-1065.

Abstract □ An approach is developed by which the solubility of an organic compound in mixed solvents may be estimated. In this approach, an expression for the excess Gibbs free energy of mixing for multicomponent solvent systems was used to obtain parameters characteristic of the interaction between the solvents. A fairly simple equation which predicts the solubility of a solute in a binary solvent system over the entire solvent composition range was then derived. The equation may be partitioned into terms that contain (*a*) pure solvent solubilities, (*b*) solvent–solvent interaction contributions, and (*c*) contributions from the solute–mixed solvent interactions. The required data are the molar volume of the solute, the pure solvent solubilities, and, theoretically, one experimentally determined solubility in a solvent mixture. The equation can be easily extended for systems with three or more solvents.

Keyphrases ■ Solubility—mixed solvent systems, estimation by an excess free energy approach, theory □ Excess free energy—use in estimating solubility in mixed solvent systems, theory □ Mixed solvent systems—estimation of solubility, excess free energy approach, theory

For pharmaceutical purposes, it is often necessary to dissolve a nonpolar or slightly polar drug in a mixture of water and one or more cosolvents such as ethanol, glycerol, propylene glycol, and low-molecular weight polyethylene glycols to increase its solubility. It is also often desirable to know if and where a maximum exists in the solubility profile of the drug in the mixture of solvents. Apart from determining such a profile experimentally over the whole solvent composition range, no general method exists at present which can, with a minimum of experiments, completely describe the solubility in the solvent mixture. Typical approaches to the estimation of solubility in mixed solvents merely express solubility in terms of a power series in mole or volume fraction multiplied by arbitrary numbers that have little physical meaning (1). Although useful such equations are by their nature restricted to and only useful for the particular solute–solvent systems for which they were formulated.

Recently Martin and coworkers (2–5) have attempted to use an extended form of the regular solution equation for the solubility of solids to estimate solubility in pure and mixed solvents. This is accomplished, in effect, by adding a term, W, to the expression for the regular solution activity coefficient to account for non-dispersion-type solute–solvent interactions. W is then estimated from differences between experimental and calculated solubilities using the regular solution equation. While their method is an improvement over the purely empirical approach, it does have a few disadvantages. For instance, it requires obtaining the heat of fusion, melting point, molar volume, and solubility parameter of the solute and the solubility parameter of the solvent or solvent mixture. When these data are not readily available, the experimental labor involved in determining them may be such as to frustrate the ultimate aim of the approach, *i.e.*, to estimate solubility with a minimal number of experiments. As the authors have also pointed out (2), the correction term (W) is difficult to determine independently, and the solubility parameter of the solute may assume a different value in a different solvent system (although this does not seriously affect the results) (4).

This paper presents the theoretical aspects of a method based on an excess free energy model which can be used to characterize the solubility of compounds in binary and ternary solvent systems. The method is general and applicable, in principle, to virtually any solute–mixed solvent system as long as the solubility is not high. The data required are the molar volume of the solute, the pure solvent solubilities, and, theoretically, one experimentally determined solubility in a solvent mixture. The last item is required for estimating C_2, a ternary interaction term. Although estimated empirically, C_2, unlike W, results logically from the development of the excess free energy model for the system. Subsequent papers in this series (6, 7) discuss the usefulness of this approach in describing experimental data from the literature.

THEORETICAL

For a solute in solution in equilibrium with its solid phase:

$$f_2^{soln} = f_2^{pure} \qquad \text{(Eq. 1)}$$

where f_2^{soln} is the fugacity of the solute in solution and f_2^{pure} is the fugacity of the pure solid. The fugacity of the solute in solution may be expressed as (8):

$$f_2^{soln} = x_2\gamma_2 f_2^0 \qquad \text{(Eq. 2)}$$

where x_2 is the mole fraction concentration of the solute, γ_2 is the symmetric convention activity coefficient, and f_2^0 is the fugacity of the hypothetical pure liquid at the same temperature and pressure as the solution (as is shown later, f_2^0 drops out of the equation and, therefore, its evaluation does not present a problem).

The symmetric convention activity coefficient (γ_2) has the property that $\gamma_2 \to 1$ as $x_2 \to 1$, while the unsymmetric convention activity coefficient (γ_2^*) has the property that $\gamma_2^* \to 1$ as $x_2 \to 0$. The relationship between the two activity coefficients has been derived by Prigogine and Defay (9):

$$\frac{\gamma_2}{\gamma_2^*} = \lim_{x_2 \to 0} \gamma_2 \qquad \text{(Eq. 3)}$$

If x_2 approaches zero, γ_2^* is equal to ~1 and Eq. 3 becomes:

$$\gamma_2 \approx \lim_{x_2 \to 0} \gamma_2 \qquad \text{(Eq. 4)}$$

This situation is described by Henry's Law which may be written as:

$$\lim_{x_2 \to 0} \frac{f_2^{soln}}{x_2} = H_2 \qquad \text{(Eq. 5)}$$

where H_2 is the Henry's Law constant.

If we assume that the mole fraction solubility is sufficiently small such that Henry's Law holds up to the solubility limit, we can write:

$$f_2^{soln} = f_2^{pure} = H_2 x_2^s \qquad \text{(Eq. 6)}$$

where x_2^s is the mole fraction solubility. In many cases of interest, the mole fraction solubility of the drug or chemical in question is low enough even in the pure cosolvent to justify such an assumption.

0022-3549/84/0100-0009$01.00/0
© 1984, American Pharmaceutical Association

Comparison of Eqs. 2 and 5 shows that:

$$\lim_{x_2 \to 0} \gamma_2 = \frac{H_2}{f_2^0} \qquad \text{(Eq. 7)}$$

If we take the logarithm of Eq. 7 and then write the expression for the solute in solvents 1 and 3 separately, we obtain for solvent 1:

$$\lim_{x_2 \to 0} \ln \gamma_{2,1} = \ln \frac{H_{2,1}}{f_2^0} \qquad \text{(Eq. 8a)}$$

and for solvent 3:

$$\lim_{x_2 \to 0} \ln \gamma_{2,3} = \ln \frac{H_{2,3}}{f_2^0} \qquad \text{(Eq. 8b)}$$

We note here that subscript 2 is used for the solute while subscripts 1, 3, 4, *etc.* are used for the pure solvents. For a binary mixture (denoted by subscript m) of solvents 1 and 3, Eq. 7 becomes:

$$\lim_{x_2 \to 0} \ln \gamma_{2,m} = \ln \frac{H_{2,m}}{f_2^0} \qquad \text{(Eq. 8c)}$$

If we take the logarithms of Eqs. 1, 2, and 4 and combine them, we obtain, at the solubility limit:

$$\ln x_2^s = \ln \left(\frac{f_2^{pure}}{f_2^0} \right) - \lim_{x_2 \to 0} \ln \gamma_2 \qquad \text{(Eq. 9)}$$

Substituting the expressions for $\ln \gamma_2$ in Eqs. 8a–c we obtain, for solvent 1:

$$\ln x_{2,1}^s = \ln \frac{f_2^{pure}}{H_{2,1}} \qquad \text{(Eq. 10a)}$$

for solvent 2:

$$\ln x_{2,3}^s = \ln \frac{f_2^{pure}}{H_{2,3}} \qquad \text{(Eq. 10b)}$$

and for a mixture of solvents 1 and 3:

$$\ln x_{2,m}^s = \ln \frac{f_2^{pure}}{H_{2,m}} \qquad \text{(Eq. 10c)}$$

We now define the volume fraction z_i of any component i in the mixture as:

$$z_i = \frac{x_i q_i}{\sum_i x_i q_i} \qquad \text{(Eq. 11)}$$

where q_i is the molar volume of component i. If we let x_2 approach zero, z_2 also approaches zero, and z_1 and z_3 become solute-free volume fractions, *i.e.*:

$$\hat{z}_1 + \hat{z}_3 = 1 \qquad \text{(Eq. 12)}$$

where the circumflex denotes solute-free terms. From Eq. 6 we can write:

$$\ln f_2^{pure} = \ln x_{2,1}^s + \ln H_{2,1} \qquad \text{(Eq. 13a)}$$

and

$$\ln f_2^{pure} = \ln x_{2,3}^s + \ln H_{2,3} \qquad \text{(Eq. 13b)}$$

If we multiply Eq. 13a by $\hat{z}_1$, Eq. 13b by $\hat{z}_3$, and add them, we obtain:

$$\ln f_2^{pure} = \hat{z}_1(\ln x_{2,1}^s + \ln H_{2,1}) + \hat{z}_3(\ln x_{2,3}^s + \ln H_{2,3}) \qquad \text{(Eq. 14)}$$

Eq. 14 substituted into Eq. 10c gives:

$$\ln x_{2,m}^s = \hat{z}_1 \ln x_{2,1}^s + \hat{z}_3 \ln x_{2,3}^s - (\ln H_{2,m} - \hat{z}_1 \ln H_{2,1} - \hat{z}_3 \ln H_{2,3}) \qquad \text{(Eq. 15)}$$

Equation 15 shows that the solubility of a compound in a binary solvent mixture is a volume fraction-weighted sum of the two pure solvent solubilities plus what can be termed an excess Henry's Law constant H_2^{Ex}. In general, we may write:

$$\ln x_{2,m}^s = \sum_{\text{solv } i} \hat{z}_1 \ln x_{2,i}^s - \ln H_2^{Ex} \qquad \text{(Eq. 16)}$$

$$\ln H_2^{Ex} = \ln H_{2,m} - \sum_{\text{solv } i} \hat{z}_1 \ln H_{2,i} \qquad \text{(Eq. 17)}$$

For Eqs. 15–17 to be useful, an expression for H_2^{Ex} must be developed. To obtain such an expression, we have employed an excess free energy model as proposed by Wohl (10).

Excess Free Energy Model—The total free energy (G) of a homogeneous system consisting of r components may be written as:

$$G = \sum_{i=1}^{r} n_i g_i^0 + RT \sum_{i=1}^{r} n_i \ln x_i + \left(\sum_{i=1}^{r} n_i \right) g^E \qquad \text{(Eq. 18)}$$

where n_i represents the number of moles of the ith component, x_i is the mole fraction of the ith component, and g^E is the excess free energy per mole. The first term represents the free energies of each of the pure components (g_i^0 being the free energy per mole of pure component i). The second term is the free energy of ideal mixing, and the third term represents the excess free energy arising from nonidealities in the mixing. The partial molar free energy of component j at constant temperature, pressure, and composition is given by:

$$\left(\frac{\partial G}{\partial n_j} \right)_{T,P,n_{i \neq j}} = g_j = g_j^0 + RT \ln x_j + RT \ln \gamma_j \qquad \text{(Eq. 19)}$$

where

$$\ln \gamma_j = \left[\frac{\partial \left[\sum_{i=1}^{r} n_i \frac{g^E}{RT} \right]}{\partial n_j} \right]_{T,P,n_{i \neq j}} \qquad \text{(Eq. 20)}$$

In 1946, Wohl (10) proposed a general method for expressing the excess free energies of mixtures in terms of increasing powers of the volume fractions (z) of the components. Thus, the excess free energy of a ternary system may be expressed as:

$$\begin{aligned} \frac{g^E}{RT(x_1q_1 + x_2q_2 + x_3q_3)} &= 2a_{12}z_1z_2 + 2a_{13}z_1z_3 + 2a_{23}z_2z_3 \\ &+ 3a_{112}z_1^2z_2 + 3a_{122}z_1z_2^2 + 3a_{113}z_1^2z_3 + 3a_{133}z_1z_3^2 \\ &+ 3a_{223}z_2^2z_3 + 3a_{233}z_2z_3^2 + 6a_{123}z_1z_2z_3 + 4a_{1112}z_1^3z_2 \\ &+ 6a_{1122}z_1^2z_2^2 + 4a_{1222}z_1z_2^3 + 4a_{1113}z_1^3z_3 + 6a_{1133}z_1^2z_3^2 \\ &+ 4a_{1333}z_1z_3^3 + 4a_{2223}z_2^3z_3 + 6a_{2233}z_2^2z_3^2 + 4a_{2333}z_2z_3^3 \\ &+ 12a_{1123}z_1^2z_2z_3 + 12a_{1223}z_1z_2^2z_3 + 12a_{1233}z_1z_3^2 \end{aligned} \qquad \text{(Eq. 21)}$$

where $z_1 = x_1q_1/(x_1q_1 + x_2q_2 + x_3q_3 \ldots)$ (see Eq. 11). The q values are usually considered a measure of the sizes of the molecules. In this report we have used molar volumes for the q-values; Wohl used the term "four-suffix q equation" in describing Eq. 21 to distinguish it from Margules-type equations which assume that all the molecules are of equal size. The "four" refers to the largest number of subscripts on an a term in the equation. As an example, a_{12} is a constant which represents the interaction between one molecule of component 1 and another of component 2. Also, as Prausnitz (8) has pointed out, the probability that any pair of two molecules consists of one molecule each of components 1 and 2 is given by $2z_1z_2$. Similarly a_{1133} is the interaction parameter for four interacting molecules two of which are components 1 and 3, respectively, and $6z_1^2z_3^2$ is the probability that any four neighboring molecules consist of two molecules each of components 1 and 3. Although the a values may be regarded, in a rough sense, as similar to virial coefficients, they do not have a rigorous theoretical basis (8). Their importance lies in the fact that they are physically meaningful parameters.

Higher- or lower-suffix q equations may also be written for the excess free energy depending on the degree of complexity required. A three-suffix equation contains only the first 10 terms on the right-hand side of Eq. 21, and a two-suffix equation contains only the first three terms.

Wohl (10) defined:

$$A_{2\text{-}1} = q_2(2a_{12} + 3a_{112} + 4a_{1112}) \qquad \text{(Eq. 22a)}$$

$$A_{1\text{-}2} = q_1(2a_{12} + 3a_{122} + 4a_{1222}) \qquad \text{(Eq. 22b)}$$

$$A_{3\text{-}1} = q_3(2a_{13} + 3a_{113} + 4a_{1113}) \qquad \text{(Eq. 22c)}$$

$$A_{1\text{-}3} = q_1(2a_{13} + 3a_{133} + 4a_{1333}) \qquad \text{(Eq. 22d)}$$

$$A_{3\text{-}2} = q_3(2a_{23} + 3a_{223} + 4a_{2223}) \qquad \text{(Eq. 22e)}$$

$$A_{2\text{-}3} = q_2(2a_{23} + 3a_{233} + 4a_{2333}) \qquad \text{(Eq. 22f)}$$

$$C_1 = q_1[(3a_{112} + 3a_{133} + 3a_{223} - 6a_{123}) + 4a_{1112} + 6a_{1122} - 4a_{1222} + 6a_{1133} + 4a_{2223} - 12a_{1123}] \qquad \text{(Eq. 22g)}$$

$$C_2 = q_2[(3a_{112} + 3a_{133} + 3a_{223} - 6a_{123}) + 4a_{2223} + 6a_{2233} - 4a_{2333} + 6a_{1122} + 4a_{1333} - 12a_{1223}] \qquad \text{(Eq. 22h)}$$

$$C_3 = q_3[(3a_{112} + 3a_{133} + 3a_{223} - 6a_{123}) + 4a_{1333} + 6a_{1133}$$

$$- 4a_{1113} + 6a_{2233} + 4a_{1112} - 12a_{1233}] \quad \text{(Eq. 22i)}$$

$$D_{12} = q_1[4a_{1112} + 4a_{1222} - 6a_{1122}] \quad \text{(Eq. 22j)}$$

$$D_{13} = q_3[4a_{1333} + 4a_{1113} - 6a_{1133}] \quad \text{(Eq. 22k)}$$

$$D_{23} = q_2[4a_{2223} + 4a_{2333} - 6a_{2233}] \quad \text{(Eq. 22l)}$$

If we introduce Eqs. 22a–l into Eq. 21 and differentiate the total excess free energy with respect to n_2, Eq. 23 is obtained:

$$\left[\frac{\partial n_T \dfrac{g^E}{RT}}{\partial n_2}\right]_{T,P,n_1,n_3} = \ln \gamma_{2,m}$$

$$= z_3^2\left[A_{2\text{-}3} + 2z_2\left(A_{3\text{-}2}\frac{q_2}{q_3} - A_{2\text{-}3} - D_{23}\right) + 3z_2^2 D_{23}\right]$$
$$+ z_1^2\left[A_{2\text{-}1} + 2z_2\left(A_{1\text{-}2}\frac{q_2}{q_1} - A_{2\text{-}1} - D_{12}\frac{q_2}{q_1}\right) + 3z_2^2 D_{12}\frac{q_2}{q_1}\right]$$
$$+ z_1 z_3\left[A_{3\text{-}2}\frac{q_2}{q_3} + A_{2\text{-}1} - A_{1\text{-}3}\frac{q_2}{q_1} + 2z_2\left(A_{1\text{-}2}\frac{q_2}{q_1} - A_{2\text{-}1}\right)\right.$$
$$\left. + 2z_1\left(A_{1\text{-}3}\frac{q_2}{q_1} - A_{3\text{-}1}\frac{q_2}{q_3}\right) - 3z_1 z_3 D_{13}\frac{q_2}{q_3} - C_2 z_2(2 - 3z_2)\right.$$
$$\left. - C_3\frac{q_2}{q_3}z_3(1 - 3z_2) - C_1\frac{q_2}{q_1}z_1(1 - 3z_2)\right] \quad \text{(Eq. 23)}$$

where n_T is the total number of moles. Since, in our convention, subscripts 1, 2, and 3 represent one solvent, the solute, and the other solvent, respectively, in the mixture m, $\gamma_{2,m}$ is the activity coefficient of a solute in a mixture of two solvents in which the solute is dissolved. If desired, the activity coefficients of each of the solvents may be obtained by appropriately interchanging the subscripts (10), but they are not needed in this analysis.

For the purpose of our analysis Eq. 23 may be simplified by making the following approximations:

$$3a_{122} \approx 3a_{112}, \quad 4a_{1222} \approx 4a_{1112} \quad \text{(Eq. 24a)}$$

$$3a_{233} \approx 3a_{223}, \quad 4a_{2333} \approx 4a_{2223} \quad \text{(Eq. 24b)}$$

With these approximations:

$$\frac{A_{1\text{-}2}}{A_{2\text{-}1}} = \frac{q_1}{q_2}, \quad \frac{A_{2\text{-}3}}{A_{3\text{-}2}} = \frac{q_2}{q_3} \quad \text{(Eq. 25)}$$

Equations 24a and b imply that we are neglecting three (or more)-body interactions between the solute and each of the solvents. This approximation seems reasonable in view of the fact that we are dealing in most cases with low concentrations of solute. If we apply the same approximation to solvent–solvent interactions, Eq. 23 reduces to the van Laar equations which have been used to fit activity coefficient data with some success.

Substituting Eq. 25 into Eq. 23 and letting x_2 (and hence z_2) approach zero, we obtain:

$$\lim_{x_2 \to 0} \ln \gamma_{2,m} = A_{2\text{-}3}\hat{z}_3 + A_{2\text{-}1}\hat{z}_1 + A_{1\text{-}3}\hat{z}_1\hat{z}_3(2\hat{z}_1 - 1)\frac{q_2}{q_1}$$
$$- A_{3\text{-}1}2\hat{z}_1^2\hat{z}_3\frac{q_2}{q_3} - D_{13}3\hat{z}_1^2\hat{z}_3^2\frac{q_2}{q_3} - C_3\hat{z}_1\hat{z}_3^2\frac{q_2}{q_3} - C_1\hat{z}_1^2\hat{z}_3\frac{q_2}{q_1} \quad \text{(Eq. 26)}$$

where $A_{2\text{-}3}$ is the constant arising from the interaction of the solute with pure solvent 3, and $A_{2\text{-}1}$ is the corresponding constant for the solute and pure solvent 1.

Comparison of Eqs. 8a and b with the first two terms in Eq. 26 shows that:

$$\lim_{x_2 \to 0} \ln \gamma_{2,1} = \ln \frac{H_{2,1}}{f_2^0} = A_{2\text{-}1} \quad \text{(Eq. 27a)}$$

and

$$\lim_{x_2 \to 0} \ln \gamma_{2,3} = \ln \frac{H_{2,3}}{f_2^0} = A_{2\text{-}3} \quad \text{(Eq. 27b)}$$

Substituting Eqs. 8c, 27a, and 27b into Eq. 26, we obtain:

$$\ln H_{2,m} = \hat{z}_1 \ln H_{2,1} + \hat{z}_3 \ln H_{2,3} + A_{1\text{-}3}\frac{q_2}{q_1}\hat{z}_1\hat{z}_3(2\hat{z}_1 - 1)$$
$$- A_{3\text{-}1}\frac{q_2}{q_3}2\hat{z}_1^2\hat{z}_3 - D_{13}\frac{q_2}{q_3}3\hat{z}_1^2\hat{z}_3^2 - C_3\frac{q_2}{q_3}\hat{z}_1\hat{z}_3^2 - C_1\frac{q_2}{q_1}\hat{z}_1^2\hat{z}_3 \quad \text{(Eq. 28)}$$

Note that f_2^0 does not appear in Eq. 28; it drops out since $\hat{z}_1 + \hat{z}_3 = 1$. If we substitute Eq. 28 into Eq. 15, we obtain the final equation:

$$\ln x_{2,m}^s = \hat{z}_1 \ln x_{2,1}^s + \hat{z}_3 \ln x_{2,3}^s - A_{1\text{-}3}\hat{z}_1\hat{z}_3(2\hat{z}_1 - 1)\frac{q_2}{q_1}$$
$$+ A_{3\text{-}1}2\hat{z}_1^2\hat{z}_3\frac{q_2}{q_3} + D_{13}3\hat{z}_1^2\hat{z}_3^2\frac{q_2}{q_3} + C_3\hat{z}_1\hat{z}_3^2\frac{q_2}{q_3} + C_1\hat{z}_1^2\hat{z}_3\frac{q_2}{q_1} \quad \text{(Eq. 29)}$$

The above equation will be referred to as the reduced four-suffix solubility equation since it was derived from the four-suffix excess free energy expression. Other solubility equations to be derived later will be referred to in a similar manner.

Equation 29 expresses the mole fraction solubility $x_{2,m}^s$ of the solute in the mixed solvent in terms of (*a*) the pure solvent solubilities given by the first two terms, (*b*) contributions from solvent–solvent interactions given by the next three terms, and (*c*) contributions from the interaction between the solute and the solvent mixture described by the last two terms. The data needed for the estimation of the solubility in Eq. 29 are:

1. The pure solvent solubilities $x_{2,1}^s$ and $x_{2,3}^s$.
2. The binary solvent data (usually vapor pressure as a function of composition) from which solvent–solvent interaction constants $A_{1\text{-}3}$, $A_{3\text{-}1}$, and D_{13} may be obtained,
3. The molar volumes of the pure compounds.
4. Two ternary experimental points (obtained from the solubility of the solute in the solvent mixture at two different compositions) from which C_1 and C_3 are calculated. It is important to note that the solvent–solvent interaction constants, once obtained at a particular temperature are fixed for the solvent system at that temperature.

Corresponding two- and three-suffix equations may also be written for the system described by Eq. 23. The three-suffix equation is obtained by setting the D values equal to zero or, in other words, by neglecting four-body interactions. If this is done, then:

$$C_2 = C_1\frac{q_2}{q_1}, \quad C_3 = C_1\frac{q_3}{q_1} \quad \text{(Eq. 30)}$$

and Eq. 23 becomes:

$$\ln \gamma_{2,m} = z_3^2\left[A_{2\text{-}3} + 2z_2\left(A_{3\text{-}2}\frac{q_2}{q_3} - A_{2\text{-}3}\right)\right]$$
$$+ z_1^2\left[A_{2\text{-}1} + 2z_2\left(A_{1\text{-}2}\frac{q_2}{q_1} - A_{2\text{-}1}\right)\right]$$
$$+ z_1 z_3\left[A_{3\text{-}2}\frac{q_2}{q_3} + A_{2\text{-}1} - A_{1\text{-}3}\frac{q_2}{q_1} + 2z_2\left(A_{1\text{-}2}\frac{q_2}{q_1} - A_{2\text{-}1}\right)\right.$$
$$\left. + 2z_1\left(A_{1\text{-}3}\frac{q_2}{q_1} - A_{3\text{-}1}\frac{q_2}{q_3}\right) - C_2(1 - 2z_2)\right] \quad \text{(Eq. 31)}$$

where $C_2 = q_2[3a_{112} + 3a_{133} + 3a_{223} - 6a_{123}]$ and the A values are as defined in Eqs. 22a–f without four-body interaction terms. Following the same treatment given in Eqs. 23–29, we arrive at the reduced three-suffix solubility equation:

$$\ln x_{2,m}^s = \hat{z}_1 \ln x_{2,1}^s + \hat{z}_3 \ln x_{2,3}^s - A_{1\text{-}3}\hat{z}_1\hat{z}_3(2\hat{z}_1 - 1)\frac{q_2}{q_1}$$
$$+ A_{3\text{-}1}2\hat{z}_1^2\hat{z}_3\frac{q_2}{q_3} + C_2\hat{z}_1\hat{z}_3 \quad \text{(Eq. 32)}$$

Equation 32 shows that only one constant, C_2, needs to be obtained from ternary data and, theoretically, only one point in the ternary system is needed.

The two-suffix equation is obtained by neglecting three- and four-body interactions. Then, Eq. 23 becomes:

$$\ln \gamma_{2,m} = z_3^2 A_{2\text{-}3} + z_1^2 A_{2\text{-}1} + z_1 z_3\left(A_{2\text{-}3} + A_{2\text{-}1} - A_{1\text{-}3}\frac{A_{2\text{-}1}}{A_{1\text{-}2}}\right) \quad \text{(Eq. 33)}$$

where

$$A_{1\text{-}2} = 2a_{12}q_1, \quad A_{2\text{-}1} = 2a_{12}q_2 \quad \text{(Eq. 34a)}$$

$$A_{1\text{-}3} = 2a_{13}q_1, \quad A_{3\text{-}1} = 2a_{13}q_3 \quad \text{(Eq. 34b)}$$

$$A_{2\text{-}3} = 2a_{23}q_2, \quad A_{3\text{-}2} = 2a_{23}q_3 \quad \text{(Eq. 34c)}$$

Again, following the same treatment given in Eqs. 23–29 (excepting that it is not necessary to make the van Laar-type approximation mentioned earlier because it is already implied in Eq. 34), Eq. 33 leads to the reduced two-suffix solubility equation:

Table I—Summary of Equations [a]

Starting Equation	Differential	Simplifications	Final Equation
Four-Suffix Excess Free Energy Model			
$[g^E/(RT)(x_1q_1 + x_2q_2 + x_3q_3)] = 2a_{12}z_1z_2 + 2a_{13}z_1z_3 + 2a_{23}z_2z_3 + 3a_{112}z_1^2z_2 + 3a_{122}z_1z_2^2 + 3a_{113}z_1^2z_3 + 3a_{133}z_1z_3^2 + 3a_{223}z_2^2z_3 + 3a_{233}z_2z_3^2 + 6a_{123}z_1z_2z_3 + 4a_{1112}z_1^3z_2 + 6a_{1122}z_1^2z_2^2 + 4a_{1222}z_1z_2^3 + 4a_{1113}z_1^3z_3 + 6a_{1133}z_1^2z_3^2 + 4a_{1333}z_1z_3^3 + 4a_{2223}z_2^3z_3 + 6a_{2233}z_2^2z_3^2 + 4a_{2333}z_2z_3^3 + 12a_{1123}z_1^2z_2z_3 + 12a_{1223}z_1z_2^2z_3 + 12a_{1233}z_1z_2z_3^2$	$\ln \gamma_{2,m} = [\delta n_T g^E/RT/\delta n_2]_{T,P,n_1,n_3} = z_3^2[A_{2\text{-}3} + 2z_2(A_{3\text{-}2}q_2/q_3 - A_{2\text{-}3} - D_{23}) + 3z_2^2D_{23}] + z_1^2[A_{2\text{-}1} + 2z_2(A_{1\text{-}2}q_2/q_1 - A_{2\text{-}1} - D_{12}q_2/q_1) + 3z_2^2D_{12}q_2/q_1] + z_1z_3[A_{3\text{-}2}q_2/q_3 + A_{2\text{-}1} - A_{1\text{-}3}q_2/q_1 + 2z_2(A_{1\text{-}2}q_2/q_1 - A_{2\text{-}1}) + 2z_1(A_{1\text{-}3}q_2/q_1 - A_{3\text{-}1}q_2/q_3) - 3z_1z_3D_{13}q_2/q_3 - C_2z_2(2 - 3z_2) - C_3q_2/q_3z_3(1 - 3z_2) - C_1q_2/q_1z_1(1 - 3z_2)]$	1. $3a_{112} = 3a_{122}$, $3a_{233} = 3a_{223}$, $4a_{1112} = 4a_{1222}$, $4a_{2333} = 4a_{2223}$. Then, $A_{1\text{-}2}/A_{2\text{-}1} = q_1/q_2$ and $A_{2\text{-}3}/A_{3\text{-}2} = q_2/q_3$. 2. Let $x_2 \to 0$. 3. $\text{limit}_{x_2\to 0} \ln \gamma_{2,1} = \ln (H_{2,1}/f_2^0) = A_{2\text{-}1}$ and $\text{limit}_{x_2\to 0} \ln \gamma_{2,3} = \ln (H_{2,3}/f_2^0) = A_{2\text{-}3}$	$\ln x_{2,m}^s = \hat{z}_1 \ln x_{2,1}^2 + \hat{z}_3 \ln x_{2,3}^s - A_{1\text{-}3}\hat{z}_1\hat{z}_3(2\hat{z}_1 - 1)q_2/q_1 + A_{3\text{-}1}2\hat{z}_1^2\hat{z}_3q_2/q_3 + D_{13}3\hat{z}_1^2\hat{z}_3^2q_2/q_3 + C_3\hat{z}_1\hat{z}_3^2q_2/q_3 + C_1\hat{z}_1^2\hat{z}_3q_2/q_1$
Three-Suffix Excess Free Energy Model			
Four-suffix equation with: $a_{1112} = a_{1122} = a_{1222} = a_{1113} = a_{1133} = a_{1333} = a_{2223} = a_{2233} = a_{2333} = a_{1123} = a_{1223} = a_{1233} = 0$	$\ln \gamma_{2,m} = z_3[A_{2\text{-}3} + 2z_2(A_{3\text{-}2}q_2/q_3 - A_{2\text{-}3})] + z_1^2[A_{2\text{-}1} + 2z_2(A_{1\text{-}2}q_2/q_1 - A_{2\text{-}1})] + z_1z_3[A_{3\text{-}2}q_2/q_3 + A_{2\text{-}1} - A_{1\text{-}3}q_2/q_1 + 2z_2(A_{1\text{-}2}q_2/q_1 - A_{2\text{-}1}) + 2z_1(A_{1\text{-}3}q_2/q_1 - A_{3\text{-}1}q_2/q_3) - C_2(1 - 2z_2)]$	1. $3a_{112} = 3a_{122}$, $3a_{233} = 3a_{223}$. Then, $A_{1\text{-}2}/A_{2\text{-}1} = q_1/q_2$ and $A_{2\text{-}3}/A_{3\text{-}2} = q_2/q_3$. 2. Simplifications 2 and 3 from the four-suffix model	$\ln x_{2,m}^s = \hat{z}_1 \ln x_{2,1}^s + \hat{z}_3 \ln x_{2,3}^s - A_{1\text{-}3}\hat{z}_1\hat{z}_3(2\hat{z}_1 - 1)q_2/q_1 + A_{3\text{-}1}2\hat{z}_1^2\hat{z}_3q_2/q_3 + C_2\hat{z}_1\hat{z}_3$
Two-Suffix Excess Free Energy Model			
Four-suffix equation with: $a_{112} = a_{122} = a_{113} = a_{133} = a_{223} = a_{233} = a_{123} = \ldots = 0$	$z_3^2A_{2\text{-}3} + z_1^2A_{2\text{-}1} + z_1z_3(A_{2\text{-}3} + A_{2\text{-}1} - A_{1\text{-}3}A_{2\text{-}1}/A_{1\text{-}2})]$	1. Simplifications 2 and 3 from the four-suffix model	$\ln x_{2,m}^s = \hat{z}_1 \ln x_{2,1}^s + \hat{z}_3 \ln x_{2,3}^s + A_{1\text{-}3}\hat{z}_1\hat{z}_3 q_2/q_1$

[a] The symbols are defined in the text. Note that the A values for the two-suffix equation are defined differently than those for the three- and four-suffix equations.

$$\ln x_{2,m}^s = \hat{z}_1 \ln x_{2,1}^s + \hat{z}_3 \ln x_{2,3}^s + A_{1\text{-}3}\hat{z}_1\hat{z}_3\frac{q_2}{q_1} \qquad \text{(Eq. 35)}$$

Examination of Eq. 35 shows that unlike the reduced three- and four-suffix solubility equations, it contains no constant to be estimated from ternary data. This, combined with the fact that the reduced three-suffix solubility equation with its fewer parameters (compared with the corresponding four-suffix equation) satisfactorily describes the data used (6), leads us to choose Eq. 32 as our working equation for a three-component system.

Four-Component Systems—For a four-component system, the three-suffix excess free energy expression is given by:

$$\frac{g^E}{RT\left(x_1 + x_2\frac{q_2}{q_1} + x_3\frac{q_3}{q_1} + x_4\frac{q_4}{q_1}\right)} = q_1(2a_{12}z_1z_2 + 2a_{13}z_1z_3 + 2a_{14}z_1z_4 + 2a_{23}z_2z_3 + 2a_{34}z_3z_4 + 2a_{24}z_2z_4 + 3a_{112}z_1^2z_2 + 3a_{122}z_1z_2^2 + 3a_{113}z_1^2z_3 + 3a_{133}z_1z_3^2 + 3a_{114}z_1^2z_4 + 3a_{144}z_1z_4^2 + 3a_{223}z_2^2z_3 + 3a_{233}z_2z_3^2 + 3a_{224}z_2^2z_4 + 3a_{244}z_2z_4^2 + 3a_{334}z_3^2z_4 + 3a_{344}z_3z_4^2 + 6a_{123}z_1z_2z_3 + 6a_{124}z_1z_2z_4 + 6a_{234}z_2z_3z_4 + 6a_{134}z_1z_3z_4 + 24a_{1234}z_1z_2z_3z_4) \qquad \text{(Eq. 36)}$$

With the following definitions:

$$A_{1\text{-}4} = q_1(2a_{14} + 3a_{144}) \qquad \text{(Eq. 37a)}$$

$$A_{4\text{-}1} = q_4(2a_{14} + 3a_{114}) \qquad \text{(Eq. 37b)}$$

$$A_{3\text{-}4} = q_3(2a_{34} + 3a_{344}) \qquad \text{(Eq. 37c)}$$

$$A_{4\text{-}3} = q_4(2a_{34} + 3a_{334}) \qquad \text{(Eq. 37d)}$$

$$A_{2\text{-}4} = q_2(2a_{24} + 3a_{244}) \qquad \text{(Eq. 37e)}$$

$$A_{4\text{-}2} = q_4(2a_{24} + 3a_{224}) \qquad \text{(Eq. 37f)}$$

$$G_{123} = 3a_{112} + 3a_{133} + 3a_{223} - 6a_{123} \qquad \text{(Eq. 37g)}$$

$$G_{234} = 3a_{223} + 3a_{334} + 3a_{244} - 6a_{234} \qquad \text{(Eq. 37h)}$$

$$G_{134} = 3a_{144} + 3a_{113} + 3a_{334} - 6a_{134} \qquad \text{(Eq. 37i)}$$

$$G_{124} = 3a_{112} + 3a_{224} + 3a_{144} - 6a_{124} \qquad \text{(Eq. 37j)}$$

$$K = 24a_{1234} \qquad \text{(Eq. 37k)}$$

Eq. 36 becomes:

$$\frac{g^E}{RT\left(x_1 + x_2\frac{q_2}{q_1} + x_3\frac{q_3}{q_1} + x_4\frac{q_4}{q_1}\right)} = z_1z_2\left(A_{2\text{-}1}z_1\frac{q_1}{q_2} + A_{1\text{-}2}z_2\right) + z_1z_3\left(A_{3\text{-}1}z_1\frac{q_1}{q_3} + A_{1\text{-}3}z_3\right) + z_1z_4\left(A_{4\text{-}1}z_1\frac{q_1}{q_4} + A_{1\text{-}4}z_4\right) + z_2z_3\left(A_{3\text{-}2}z_2\frac{q_1}{q_3} + A_{2\text{-}3}z_3\frac{q_1}{q_2}\right) + z_2z_4\left(A_{4\text{-}2}\frac{q_1}{q_4} + A_{2\text{-}4}z_4\frac{q_1}{q_2}\right) + z_3z_4\left(A_{4\text{-}3}z_3\frac{q_1}{q_4} + A_{3\text{-}4}z_4\frac{q_1}{q_3}\right) + z_1z_2z_3\left(A_{2\text{-}1}\frac{q_1}{q_2} + A_{3\text{-}2}\frac{q_1}{q_3} + A_{1\text{-}3} - G_{123}q_1\right) + z_1z_2z_4\left(A_{2\text{-}1}\frac{q_1}{q_2} + A_{4\text{-}2}\frac{q_1}{q_4} + A_{1\text{-}4} - G_{124}q_1\right) + z_2z_3z_4\left(A_{3\text{-}2}\frac{q_1}{q_3} + A_{4\text{-}3}\frac{q_1}{q_4} + A_{2\text{-}4}\frac{q_1}{q_2} - G_{234}q_1\right) + z_1z_3z_4\left(A_{1\text{-}4} + A_{3\text{-}1}\frac{q_1}{q_3} + A_{4\text{-}3}\frac{q_1}{q_4} - G_{134}q_1\right) + Kz_1z_2z_3z_4q_1 \qquad \text{(Eq. 38)}$$

where $A_{1\text{-}2}$, $A_{2\text{-}1}$, $A_{1\text{-}3}$, $A_{3\text{-}1}$, $A_{2\text{-}3}$, and $A_{3\text{-}2}$ are as defined in Eqs. 22a–f without the four-body interaction terms. If we consider this system as a solute (denoted by subscript 2) in a mixture of three solvents (denoted by subscripts 1, 3, and 4), then an approach similar to that given in Eqs. 23 to 29 yields the reduced three-suffix solubility equation for a four-component system:

$$\ln x_{2,m}^s = \hat{z}_1 \ln x_{2,1}^s + \hat{z}_3 \ln x_{2,3}^s + \hat{z}_4 \ln x_{2,4}^s - A_{1\text{-}3}\hat{z}_1z_3(2\hat{z}_1 + 2\hat{z}_4 - 1)\frac{q_2}{q_1} + A_{3\text{-}1}2\hat{z}_1\hat{z}_3(\hat{z}_1 + \hat{z}_4)\frac{q_2}{q_3} - A_{1\text{-}4}\hat{z}_1\hat{z}_4(2\hat{z}_1 - 1)\frac{q_2}{q_1} + A_{4\text{-}1}2\hat{z}_1^2\hat{z}_4\frac{q_2}{q_4} - A_{4\text{-}3}\hat{z}_3\hat{z}_4(2\hat{z}_4 - 1)\frac{q_2}{q_4} + A_{3\text{-}4}2\hat{z}_3\hat{z}_4^2\frac{q_2}{q_3} + G_{123}q_2\hat{z}_1\hat{z}_3$$

$$+ G_{124}q_2\hat{z}_1\hat{z}_4 + G_{234}q_2\hat{z}_3\hat{z}_4 - G_{134}q_2\hat{z}_1\hat{z}_3\hat{z}_4 - Kq_2\hat{z}_1\hat{z}_3\hat{z}_4 \quad \text{(Eq. 39)}$$

Equation 39 shows that only one constant, K, need be obtained from a quaternary system. The A values and G_{134} are obtained from solvent vapor pressure composition data. If we let $\hat{z}_4$ equal zero, Eq. 39 reduces to Eq. 32 with $C_2 = G_{123}q_2$. Thus G_{123}, G_{124}, and G_{234} are estimated from solubility data at points where solvent 4, solvent 3, and solvent 1, respectively, are absent. They are, therefore, not new parameters in the same sense as K. It is important to note that even with the more complex four-component system, we need to estimate only one quaternary constant to describe the system. It is clear that if Eq. 39 is used for predictive purposes (for systems in which it is valid) the experimental labor saved is substantial. The same consideration holds to a lesser degree for Eq. 32.

DISCUSSION

The reduced three-suffix solubility equation for a solute in a mixture of two solvents (Eq. 32) describes solubility in terms of pure solvent solubilities and contributions from solvent–solvent and solute–binary solvent interactions. The advantages of this approach over others are its generality and flexibility. Once the solvent–solvent interaction constants are obtained, they are fixed for that solvent system (provided one operates at or close to the temperature at which they were determined, usually 25°C). Thus, the only constant that needs to be determined to completely describe the solubility (assuming that the solubility of the solute in each solvent is known) is the ternary constant C_2. For a solute in a mixture of three solvents (four-component system), only one quaternary constant (K in Eq. 39) is needed to describe the solubility. The ternary constants G_{124}, G_{234}, and G_{123} are obtained in practice in the absence of solvents 3, 1, and 4, respectively. The essential aspects of this treatment are presented in Table I, including the n-suffix excess free energy model for the number of components involved and assumptions which simplify the solute–solvent interactions while keeping the solvent–solvent interaction terms as detailed as necessary.

REFERENCES

(1) M. A. Moustafa, A. M. Molokhia, and M. W. Gouda, *J. Pharm. Sci.*, **70,** 1172 (1981).

(2) A. Martin, J. Newburger, and A. Adjei, *J. Pharm. Sci.*, **69,** 487 (1980).

(3) A. Adjei, J. Newburger, and A. Martin, *J. Pharm. Sci.*, **69,** 659 (1980).

(4) A. Martin, A. N. Paruta, and A. Adjei, *J. Pharm. Sci.*, **70,** 1115 (1981).

(5) A. Martin, P. L. Wu, A. Adjei, A. Beerbower, and J. M. Prausnitz, *J. Pharm. Sci.*, **70,** 1260 (1981).

(6) N. A. Williams and G. L. Amidon, **73,** 14 (1984).

(7) N. A. Williams and G. L. Amidon, **73,** 18 (1984).

(8) J. M. Prausnitz, "Molecular Thermodynamics of Fluid-Phase Equilibria," Prentice-Hall, Englewood Cliffs, N.J., 1969, chap. 6.

(9) I. Prigogine and R. Defay, "Chemical Thermodynamics," Longmans, London, 1954, chap. 21.

(10) K. Wohl, *Trans. Am. Inst. Chem. Eng.*, **42,** 215 (1946).

ACKNOWLEDGMENTS

The authors thank Dr. J. C. Telotte of the Department of Chemical Engineering for many helpful suggestions.

Excess Free Energy Approach to the Estimation of Solubility in Mixed Solvent Systems II: Ethanol–Water Mixtures

N. A. WILLIAMS * and G. L. AMIDON *x

Received July 22, 1982, from the *School of Pharmacy, University of Wisconsin, Madison, WI 53706.* Accepted for publication October 22, 1982. *Present address: College of Pharmacy, The University of Michigan, Ann Arbor, MI 48109-1065.

Abstract □ The use of the reduced three-suffix solubility equation in characterizing solubility in ethanol–water mixtures is discussed. The equation states that $\ln x^s_{2,m} = \hat{z}_1 \ln x^s_{2,1} + \hat{z}_3 \ln x^s_{2,3} - A_{1\text{-}3}\hat{z}_1\hat{z}_3(2\hat{z}_1 - 1)(q_2/q_1) + A_{3\text{-}1}2\hat{z}_1^2\hat{z}_3(q_2/q_3) + C_2\hat{z}_1\hat{z}_3$, where $x^s_{2,1}$, $x^s_{2,3}$, and $x^s_{2,m}$ are the mole fraction solubilities of the solute in ethanol (subscript 1), water (subscript 3), and in the mixture (m); $A_{1\text{-}3}$ and $A_{3\text{-}1}$ are solvent–solvent interaction terms; C_2 is a solute–solvent interaction term; and the q- and z-values are molar volumes and solute-free volume fractions, respectively. The contributions of the various terms in the equation to solubility are examined, and the possible use of its derivative in indicating whether a maximum may exist in the solubility profile is discussed. Methods of obtaining the solvent–solvent interaction constant and the ternary constant C_2 are described, and the general effectiveness of the equation in describing solubility is examined. The equation is shown to be applicable to 10 compounds with widely different physical properties and, thus, appears to combine both ease of use and general utility.

Keyphrases □ Solubility—mixed solvent systems, estimation by an excess free energy approach, application to ethanol–water □ Excess free energy—use in estimating solubility in mixed solvent systems, application to ethanol–water □ Mixed solvent systems—estimation of solubility, excess free energy approach, application to ethanol–water

The previous paper (1) described the theoretical aspects of an excess free energy approach to the estimation of solubility in mixed solvent systems. In this report we discuss methods of obtaining the constants in the working equation and their use in characterizing solubility in the ethanol–water system.

THEORETICAL

For a solute (subscript 2) in a mixture of ethanol (subscript 1) and water (subscript 3), the reduced four-suffix solubility equation is:

$$\ln x^s_{2,m} = \hat{z}_1 \ln x^s_{2,1} + \hat{z}_3 \ln x^s_{2,3} - A_{1\text{-}3}\hat{z}_1\hat{z}_3(2\hat{z}_1 - 1)\frac{q_2}{q_1} + A_{3\text{-}1}2\hat{z}_1^2\hat{z}_3\frac{q_2}{q_3} + D_{13}3\hat{z}_1^2\hat{z}_3^2\frac{q_2}{q_3} + C_3\hat{z}_1\hat{z}_3^2\frac{q_2}{q_3} + C_1\hat{z}_1^2\hat{z}_3\frac{q_2}{q_1} \quad \text{(Eq. 1)}$$

The corresponding three-suffix and two-suffix equations are given by Eqs. 2 and 3, respectively:

$$\ln x^s_{2,m} = \hat{z}_1 \ln x^s_{2,1} + \hat{z}_3 \ln x^s_{2,3} - A_{1\text{-}3}\hat{z}_1\hat{z}_3(2\hat{z}_1 - 1)\frac{q_2}{q_1} + A_{3\text{-}1}2\hat{z}_1^2\hat{z}_3\frac{q_2}{q_3} + C_2\hat{z}_1\hat{z}_3 \quad \text{(Eq. 2)}$$

$$\ln x^s_{2,m} = \hat{z}_1 \ln x^s_{2,1} + \hat{z}_3 \ln x^s_{2,3} + A_{1\text{-}3}\hat{z}_1\hat{z}_3\frac{q_2}{q_1} \quad \text{(Eq. 3)}$$

Note that the numerical values of $A_{1\text{-}3}$ and $A_{3\text{-}1}$ differ in Eqs. 1–3 because they are defined differently in the three equations (1). We also note here that Eq. 2 may be rearranged to give:

$$\ln\left(\frac{x^s_{2,m}}{x^s_{2,3}}\right) = \hat{z}_1 \ln\left(\frac{x^s_{2,1}}{x^s_{2,3}}\right) - A_{1\text{-}3}\hat{z}_1\hat{z}_3(2z_1 - 1)\frac{q_2}{q_1} + A_{3\text{-}1}2\hat{z}_1^2\hat{z}_3\frac{q_2}{q_3} + C_2\hat{z}_1\hat{z}_3 \quad \text{(Eq. 4)}$$

In this report we evaluate the parameters in Eqs. 1–3 and discuss their ability to describe solubility in ethanol–water mixtures.

Evaluation of Interaction Constants—The solvent–solvent interaction constants (the A terms) are easily obtained from vapor–liquid equilibrium data. If partial pressure–composition data are available, the constants may be obtained by fitting the excess free energy calculated from such data to whichever n-suffix equation is chosen. As an example consider the three-suffix equation for a binary solvent mixture. The molar excess free energy is given by (2):

$$\frac{g^E}{RT} = \frac{A_{1\text{-}3}}{q_1}[z_1z_3^2(x_1q_1 + x_3q_3)] + \frac{A_{3\text{-}1}}{q_3}[z_1^2z_3(x_1q_1 + x_3q_3)] \quad \text{(Eq. 5)}$$

where

$$A_{1\text{-}3} = q_1(2a_{13} + 3a_{133}), \quad A_{3\text{-}1} = q_3(2a_{13} + 3a_{113}) \quad \text{(Eq. 6)}$$

But

$$\frac{g^E}{RT} = \sum_{\text{solv } i} x_i \ln \gamma_i = x_1 \ln \gamma_1 + x_3 \ln \gamma_3 \quad \text{(Eq. 7)}$$

and

$$\gamma_1 = \frac{p_1}{p_1^0}, \quad \gamma_3 = \frac{p_3}{p_3^0} \quad \text{(Eq. 8)}$$

where p_1 is the partial pressure of component 1 in the mixture of 1 and 3 and p_1^0 is the vapor pressure of pure component 1; p_3 and p_3^0 are defined similarly.

Combining Eqs. 5 and 7 we find:

$$x_1 \ln \gamma_1 + x_3 \ln \gamma_3 = A_{1\text{-}3}\left[\frac{z_1z_3^2(x_1q_1 + x_3q_3)}{q_1}\right] + A_{3\text{-}1}\left[\frac{z_1^2z_3(x_1q_1 + x_3q_3)}{q_3}\right] \quad \text{(Eq. 9)}$$

Equation 9 may be represented as:

$$y = \theta_1\chi_1 + \theta_2\chi_2 \quad \text{(Eq. 10)}$$

where $y = x_1 \ln \gamma_1 + x_3 \ln \gamma_3$, $\theta_1 = A_{1\text{-}3}$, χ_1 is the first term in parentheses,

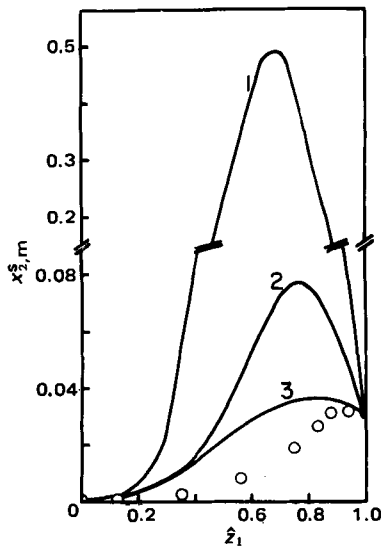

Figure 1—*Solubility profiles of barbital in ethanol calculated from Eqs. 1–3 without any solute–solvent interaction term (i.e., with $C_1 = C_2 = C_3 = 0$). Key: (1) reduced four-suffix solubility equation (Eq. 1); (2) reduced three-suffix solubility equation (Eq. 2); (3) reduced two-suffix solubility equation (Eq. 3); (○) experimental points.*

0022-3549/84/0100-0014$01.00/0
© 1984, American Pharmaceutical Association

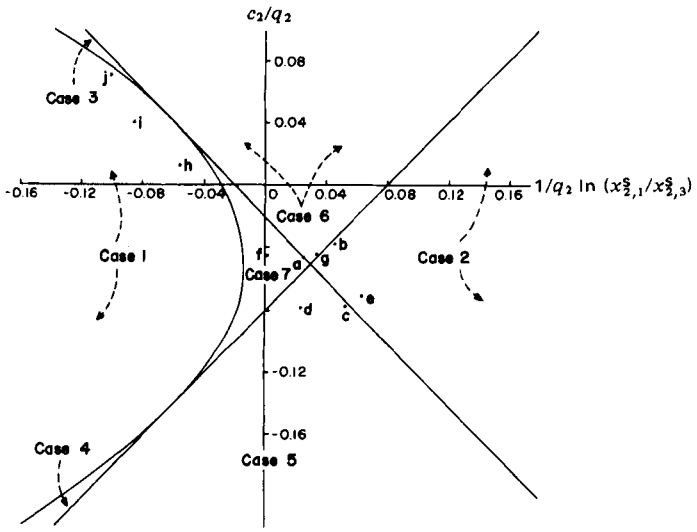

Figure 2—*Projection of* $\langle \hat{z}_1 \rangle$ *on to the* (C_2/q_2), $(1/q_2)$ *ln* $(x^s_{2,1}/x^s_{2,3})$ *plane. Key: (a) barbital; (b) acetanilide; (c) phenyl salicylate; (d) stearic acid; (e) o-nitrophenol; (f) antipyrine; (g) phenobarbital; (h) DL-valine; (i) glycine; (j) DL-alanine.*

$\theta_2 = A_{1\text{-}3}$, and χ_2 is the second term in parentheses. As shown by Eq. 10, y is a linear function of the parameters θ_1 and θ_2 and, so, $A_{1\text{-}3}$ and $A_{3\text{-}1}$ can be obtained by linear regression.

The constants for ethanol–water were obtained at 25°C from data in Ref. 5. If only the partial vapor pressure of one component is available, the Gibbs–Duhem relation may be used to calculate the other in the case of a binary system (3). It is usually easier to measure the total vapor pressure over a solvent mixture rather than partial pressures. From the total pressure, the interaction constants may be obtained as follows.

The total pressure P_T over a binary solvent mixture is given by:

$$P_T = p_1 + p_3 = x_1\gamma_1 p_1^0 + x_3\gamma_3 p_3^0 \qquad \text{(Eq. 11)}$$

If we differentiate Eq. 5 with respect to n_1, we obtain the expression for ln γ_1 in the solvent mixture:

$$\ln \gamma_1 = A_{1\text{-}3}[z_3^2(1 - 2z_1)] + A_{3\text{-}1}\left[2z_1 z_3^2 \frac{q_1}{q_3}\right] \qquad \text{(Eq. 12)}$$

Similarly:

$$\ln \gamma_3 = A_{1\text{-}3}\left[2z_1^2 z_3 \frac{q_3}{q_1}\right] + A_{3\text{-}1}[z_1^2(1 - 2z_3)] \qquad \text{(Eq. 13)}$$

Substituting Eqs. 12 and 13 into Eq. 11, we obtain:

$$P_T = p_1^0 x_1 e^{[A_{1\text{-}3}x_1 + A_{3\text{-}1}x_2]} + p_3^0 x_3 e^{[A_{1\text{-}3}x_3 + A_{3\text{-}1}x_4]} \qquad \text{(Eq. 14)}$$

Table I—Solvent–Solvent Interaction Terms

Excess Free Energy Model	Constants: Linear Regression	Constants: Total Pressure Fit[a]
Four-suffix	$A_{1\text{-}3} = 0.9385$ $A_{3\text{-}1} = 1.387$ $D_{13} = 0.6106$	
Three-suffix	$A_{1\text{-}3} = 1.216$ $A_{3\text{-}1} = 0.9093$	1.138 0.9047
Two-suffix	$A_{1\text{-}3} = 2.215$	

[a] Nonlinear.

where $\chi_1 = z_3^2(1 - 2z_1)$, $\chi_2 = 2z_1z_3^2(q_1/q_3)$, $\chi_3 = 2z_1^2z_3(q_3/q_1)$, and $\chi_4 = z_1^2(1 - 2z_3)$.

The parameters may be obtained from Eq. 14 by a total pressure fit using nonlinear regression. This method is more complicated, but it gives similar results to the excess free energy fit (Table I). Where partial pressure data are available, as in the case of ethanol–water, the linear regression fit is the method of choice because of its simplicity and much lower tendency to give non-unique constants than the nonlinear method, whose results sometimes depend on the choice of initial estimates.

Choice of a Working Equation—Figure 1 shows calculated solubility profiles for barbital in ethanol–water mixtures using Eqs. 1, 2, and 3 with the solvent–solvent interaction constants in Table I, but without any ternary solute–solvent interaction terms (*i.e.*, with $C_1 = C_2 = C_3 = 0$). When compared with experimental data (4), it is clearly seen that the reduced four-suffix solubility equation is the worst for predicting solubility. The three-suffix equation does better, but not as well as the two-suffix equation. A comparison of Eqs. 2 and 3, however, shows that while the reduced three-suffix solubility equation has one more constant that is related to, and can be evaluated from, ternary solute–solvent data, the two-suffix equation has none and this severely limits its use. The four-suffix equation has two constants, which may be estimated from ternary solute–solvent data. For the ethanol–water system, the three-suffix equation, with its one constant C_2 estimated from ternary data, satisfactorily predicts the solubilities of compounds in ethanol–water mixtures. This and the fact that it has less parameters than the four-suffix equation has led us to choose the three-suffix equation (Eq. 2) to characterize the solubilities in ethanol–water systems.

Estimation of C_2—The constant C_2, which accounts for the interaction between the solute and the two solvents, was estimated by linear regression from the difference between the reported experimental solubility at 25°C and the calculated solubility (without the C_2 term) at each point in the solvent composition range. The C_2 thus obtained was then used to estimate the solubility over the solvent composition range.

Analysis of Solubility in the Ethanol–Water System—Certain compounds are known to exhibit a maximum in their solubility in some solvent mixtures (4). In this work, we were interested in whether our reduced three-suffix solubility equation for a three-component system predicted a maximum and/or minimum and under what conditions. We used the ethanol–water system as a specific example; the results will therefore be applicable only to a solute in ethanol–water.

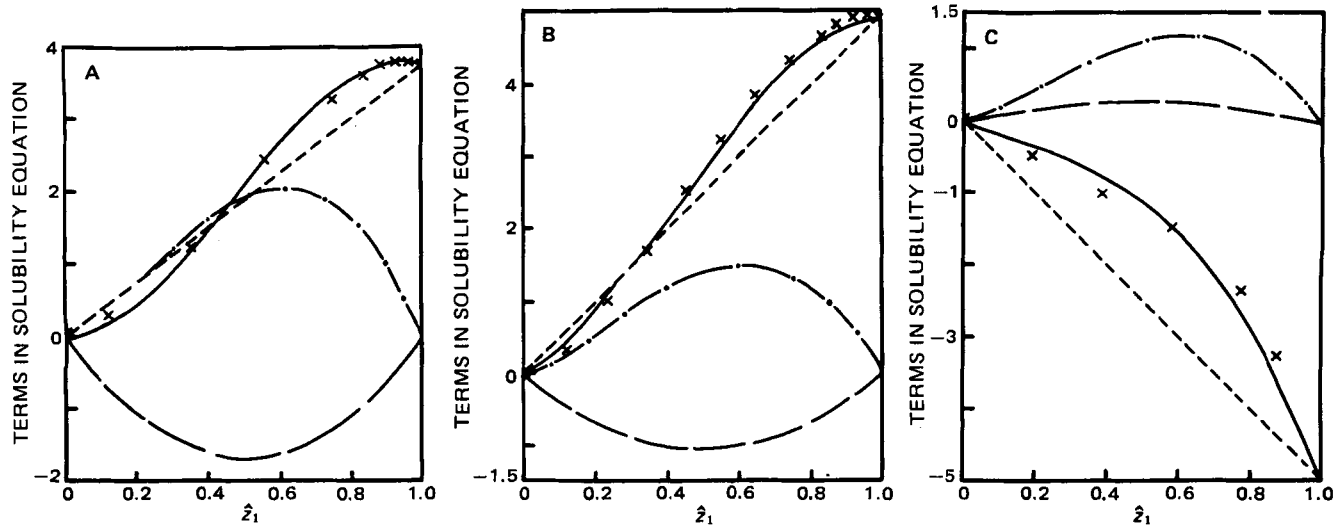

Figure 3—*Solubility profile of barbital (A), acetanilide (B), and DL-valine (C) in ethanol showing contributions from terms in Eq. 4. Key: (---)* $\hat{z}_1 \ln (x^s_{2,1}/x^s_{2,3})$; *(-·-)* $-A_{1\text{-}3}\hat{z}_1\hat{z}_3(2\hat{z}_1 - 1)(q_2/q_1) + A_{3\text{-}1}2\hat{z}_1^2\hat{z}_3(q_2/q_3)$; *(- -)* $C_2\hat{z}_1\hat{z}_3$; *(—) calculated ln* $(x^s_{2,m}/x^s_{2,3})$; *(X) experimental ln* $(x^s_{2,m}/x^s_{2,3})$.

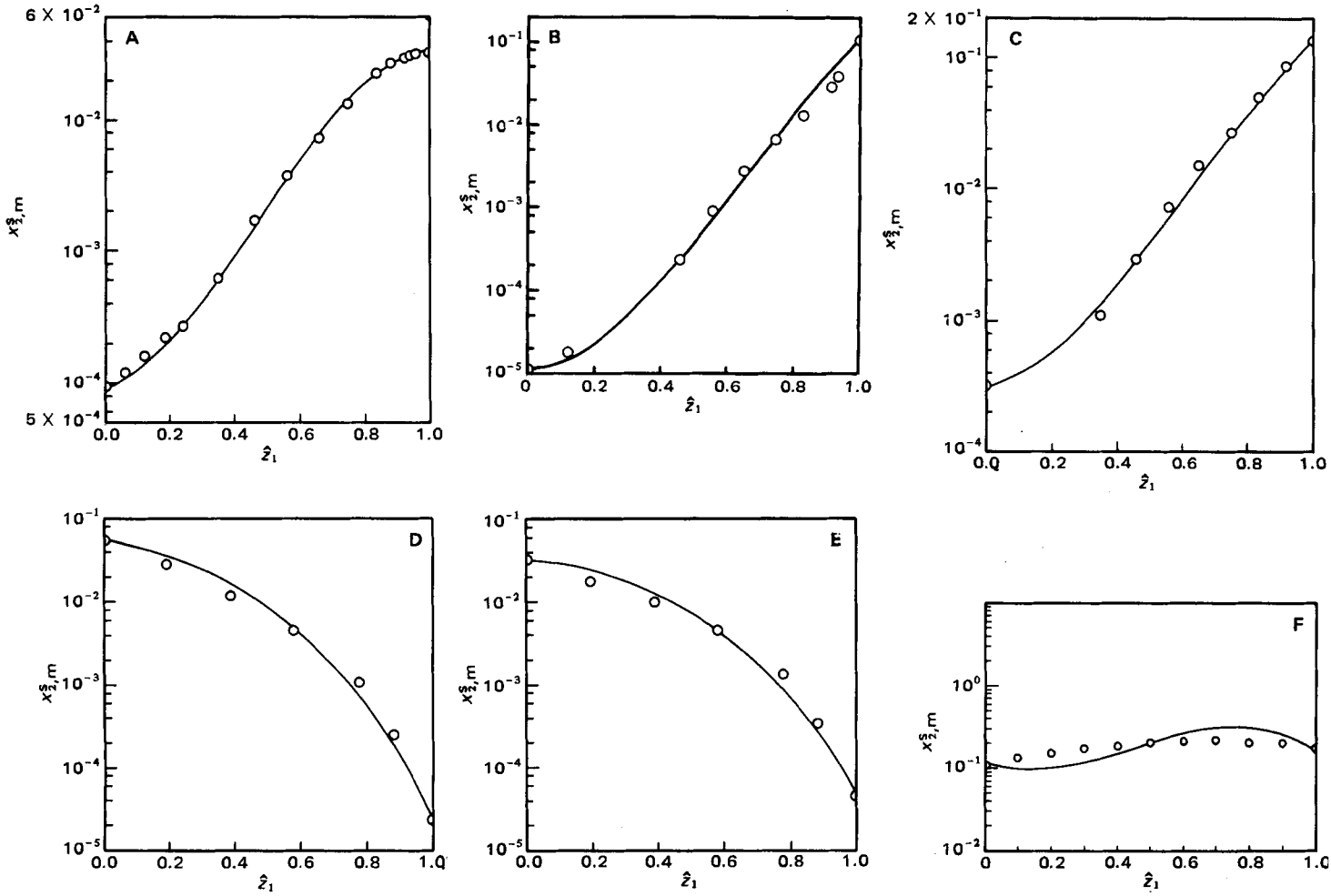

Figure 4—*Solubility profile of phenobarbital (A), pheny salicylate (B), o-nitrophenol (C), glycine (D), DL-alanine (E), and antipyrine (F) in ethanol. Key: (—) estimated solubility; (○) experimental solubility.*

Differentiating Eq. 2 with respect to $\hat{z}_1$ and equating it to zero yields:

$$\left(\frac{\partial \ln x^s_{2,m}}{\partial \hat{z}_1}\right)_{\hat{z}_3} = 0.1788\langle\hat{z}_1\rangle^2 + \left(\frac{2C_2}{q_2} - 0.0778\right)\langle\hat{z}_1\rangle - \left[0.0207 + \frac{1}{q_2}\ln\left(\frac{x^s_{2,1}}{x^s_{2,3}}\right) + \frac{C_2}{q_2}\right] = 0 \quad \text{(Eq. 15)}$$

where the values $A_{1\text{-}3} = 1.216$ and $A_{3\text{-}1} = 0.9093$ obtained from ethanol–water vapor–liquid equilibrium data (5) have been used and the maximum or minimum $\hat{z}_1$ is indicated by $\langle\hat{z}_1\rangle$. Equation 15 can be solved quadratically for $\langle\hat{z}_1\rangle$. Depending on the values of C_2/q_2 and $(1/q_2)\cdot\ln(x^s_{2,1}/x^s_{2,3})$, the range of possible values for the two roots of $\hat{z}_1$ are given in Table II. Cases 1–4 have no extrema in the 0–1 volume fraction range. Cases 5–6 have one extremum each in the 0–1 range, but without knowing C_2, q_2, and $\ln(x^s_{2,1}/x^s_{2,3})$, it is impossible to say if it is a maximum or minimum. No solubility profiles exhibiting a minimum have been found in the literature. Case 7 has two extrema which clearly must be a minimum and a maximum; to our knowledge, no such profiles have been found in the literature. The relationship between $\langle\hat{z}_1\rangle$ and the solute-dependent terms mentioned above is illustrated in Fig. 2, where the $\langle\hat{z}_1\rangle$ surface is projected onto the C_2/q_2 *versus* $(1/q_2)\cdot\ln(x^s_{2,1}/x^s_{2,3})$ plane. Theoretically, the question of whether a solute exhibits an extremum in ethanol–water mixtures may be answered by obtaining the above solute-characteristic terms and then locating the area in which they fall in Fig. 2. This will not always be successful since Fig. 2 arises from a purely mathematical treatment; however, it may be useful as a general guide.

Table II—Possible Solutions of Eq. 15

Cases	Roots	Remarks
1	Imaginary, Imaginary	No extremum
2	<0, >1	No extremum
3	<0, <0	No extremum
4	>1, >1	No extremum
5	0-1, >1	1 extremum
6	0-1, <0	1 extremum
7	0-1, 0-1	2 extrema

RESULTS AND DISCUSSION

Contributions of Various Terms to Solubility—Figure 3 shows a plot of the left-hand side of Eq. 4 against the volume fraction of ethanol for three compounds. Without ethanol, the left-hand side of Eq. 4 is zero because $x^s_{2,m}/x^s_{2,3} = 1$; hence, the curves all start from zero. With water absent, *i.e.*, with $\hat{z}_3 = 0$, only the first term on the right-hand side of Eq. 4 remains, all other terms going to zero as indicated in Fig. 3. If, in a mixture of ethanol and water, we set all the interaction constants equal to zero, then the solubility is given by the dashed straight line. This may be called the ideal mixture solubility since there are no contributing interaction terms. The solvent–solvent interactions contribute to solubility in the manner shown in Fig. 3. They go to zero at each end, as they must. The contribution from these terms usually (but not always) results in a maximum solubility being predicted for the compound without the C_2 term. The C_2 term not only corrects this tendency, but also adjusts the solubility to such an extent as to be able to reproduce the maximum solubility with respect to the value and the volume fraction of ethanol at which it occurs (Fig. 3A). Since C_2 accounts for interactions between solute and solvents, it must necessarily go to zero at both ends of the solvent composition.

Prediction Capabilities of the Reduced Three-Suffix Solubility Equation—Figures 3–5 show the results of using Eq. 2 and the parameters given in Table III to estimate reported solubilities in ethanol–water at 25°C. In the ethanol–barbital–water system in Fig. 3A, the solvent–solvent terms and C_2 make significant contributions to the solubility, but tend to compensate for each other. Since they are unsymmetrical with respect to $\hat{z}_1$, they combine to produce a lower than ideal mixture solubility at low volume fractions of ethanol and a higher than ideal mixture

Table III—Parameters Used to Estimate Solubilities[a] and Partition Coefficients

Compound	Formula	$\ln x^s_{2,1}$	$\ln x^s_{2,3}$	q_2^b	C_2	n	r	s^c	Log (PC) in Octanol–Water[d]	Solubility Data References
Barbital	$C_8H_{12}N_2O_3$	−3.479	−7.240	151.0	−6.76	10	0.999	0.069	0.71	(4)
Acetanilide	C_8H_9NO	−2.294	−7.233	110.9	−4.26	10	1.000	0.095	1.21	(6)
Phenyl salicylate	$C_{13}H_{10}O_3$	−2.266	−11.28	169.8	−13.3	7	0.997	0.315	3	(6)
Stearic acid	$C_{18}H_{36}O_2$	−4.237	−10.75	302.4	−23.8	7	0.993	0.438	6.8[e]	(6)
o-Nitrophenol	$C_6H_5NO_3$	−2.023	−8.037	93.68	−6.67	7	0.997	0.131	1.76	(7)
Antipyrine	$C_{11}H_{12}N_2O$	−1.716	−2.096	175.1	−7.94	9	0.952	0.365	0.26	(8)
Phenobarbital	$C_{12}H_{12}N_2O_3$	−3.450	−9.282	172.0	−7.63	15	1.000	0.062	1.41	(4)
DL-Valine	$C_5H_{11}NO_2$	−9.498	−4.529	89.02	1.15	5	0.996	0.282	−1.14[f]	(9)
Glycine	$C_2H_5NO_2$	−10.68	−2.871	90.66	3.67	5	0.998	0.359	−3.0	(9)
DL-Alanine	$C_3H_7NO_2$	−10.01	−3.433	62.57	4.43	5	0.997	0.367	−2.8	(9)

[a] The solvent–solvent term is $-1.216\hat{z}_1\hat{z}_3(2\hat{z}_1 - 1)(q_2/q_1) + 0.9093\,2\hat{z}_1^2\hat{z}_3(q_2/q_3)$. [b] $q_1 = 58.68$ (Ref. 11) and $q_3 = 18.07$ (Ref. 12) were used as molar volumes of ethanol and water, respectively; q_2 values were calculated from density data in Ref. 12. [c] s is the standard deviation of the error between $\ln (x^s_{2,m})_{obs}$ and $\ln (x^s_{2,m})_{est}$. [d] From Ref. 10; some values are averages of reported data. [e] *n*-Heptane–water; not used in the regression of C_2. [f] 1-Butanol–water; not used in the regression of C_2.

solubility at higher ethanol volume fractions. The maximum in the solubility at $\hat{z}_1 = 0.93$ is also due to the nonsymmetrical contributions of these two terms and the particular values they assume at this point. Figure 3B for acetanilide shows similar contributions from the various terms although there is no maximum; this is due to the lower contribution of the solvent–solvent terms because of a lower q_2. In Fig. 3C, which shows a case where the solubility of the solute (DL-valine) is higher in water than in ethanol, the deviation from the ideal mixture solubility is accounted for largely by the solvent–solvent terms.

Figure 4 shows semilogarithmic plots of solubility profiles for additional compounds. The results for phenobarbital, phenyl salicylate, and *o*-nitrophenol in Fig. 4A–C are similar to the barbital and acetanilide systems (Fig. 3A and B) previously discussed. Figure 4D and E shows the results for glycine and DL-alanine, which are similar to Fig. 3 for DL-valine.

Figure 5 shows a plot of the terms in Eq. 4 for stearic acid to indicate why a minimum is predicted (although the experimental data from Ref. 6 do not show it). It is seen that the minimum is caused by the large negative value (−3) of the C_2 term compared with the value (+1) of the sum of the solvent–solvent terms.

Figure 4F shows the solubility profile of antipyrine. The solubilities of antipyrine are reported as 620 mg/mL in water and 425 mg/mL in ethanol (8) which, converted to mole fraction solubilities, are 0.123 and 0.180, respectively. These high figures invalidate the assumption (made in the derivation of Eq. 2) that the mole fraction solubility is very small. In addition, the solubility of antipyrine changes very little between the end points. The shallow maximum and minimum in the predicted solubility profile result from the unsymmetric dependence of C_2 and the solvent–solvent terms on volume fraction (see Fig. 3). In summary, Figs. 3–5 show clearly that the reduced three-suffix solubility equation estimates solubilities in ethanol–water systems very well.

In practice, one would have little or no data from which to estimate C_2 as we have done here. In such a case it is still possible to estimate this term by other means requiring the determination of solubility at one or two points in the solvent composition. The significant point, in any case, is that it is possible to obtain the single ternary constant C_2 which, along with the other constants, adequately describes the solubility profile.

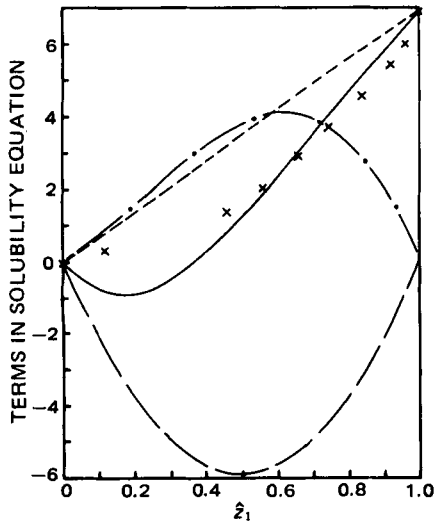

Figure 5—*Solubility profile of stearic acid in ethanol showing contributions from terms in Eq. 4. Key: (- - -) $\hat{z}_1$ ln $(x^s_{2,1}/x^s_{2,3})$; (- · -) $-A_{1\text{-}3}\hat{z}_1\hat{z}_3(2\hat{z}_1 - 1)(q_2/q_1) + A_{3\text{-}1}2\hat{z}_1^2\hat{z}_3\,(q_2/q_3)$; (– –) $C_2\hat{z}_1\hat{z}_3$; (——) calculated ln $(x^s_{2,m}/x^s_{2,3})$; (X) experimental ln $(x^s_{2,m}/x^s_{2,3})$.*

Significance of C_2—The solvent–solvent terms, when combined only with ideal mixture solubilities, usually (but not necessarily always) overpredict (as in Fig. 1 and with nonpolar compounds) or underpredict (as with the more polar amino acids in the solubility profiles shown) solubility. Therefore, the C_2 term usually has an opposite sign (but not always; see Fig. 3C) to the sum of the solvent–solvent terms. To determine what influence, if any, the polar or nonpolar nature of the solute has on C_2, we have obtained octanol–water partition coefficients (PC), when available (10), for the solutes whose solubility profiles we examined. There is an excellent trend in which C_2 becomes more negative as the solutes become more nonpolar and more positive as the solutes become more polar (Table III, Fig. 6). The regression equation is:

$$C_2 = -3.96 - 2.66\log (PC) \qquad n = 8,\quad r = 0.946,\quad s = 1.96 \qquad \text{(Eq. 16)}$$

where s is the standard deviation of the error between observed and predicted values of C_2. Equation 16 suggests that it may be possible to estimate C_2 from octanol–water partition coefficients and use the estimated term with the solvent–solvent terms and pure solvent solubilities to estimate the entire solubility profile.

A qualitative interpretation of C_2 is as follows. If the solvents interact in such a manner as to eliminate (*i.e.*, interact "negatively" with) the solute more effectively than would be expected from their interactions with each other (as indicated by the solvent–solvent constants), the predicted solubility without C_2 will tend to be higher than the observed solubility. This may be expected to happen with nonpolar solutes in ethanol–water. To correct this overprediction, C_2 has to be negative to decrease the predicted solubility. Conversely, if the solvents interact in such a manner as to incorporate the solute more effectively than would be expected from their interactions with each other, the predicted solubility will tend to be lower than the observed solubility. This could happen with more polar solutes. C_2 will therefore tend to be more positive in order to increase the solubility.

Prediction of Extrema in Solubility—As was mentioned earlier, it is possible to obtain some idea of whether a solute may exhibit a maxi-

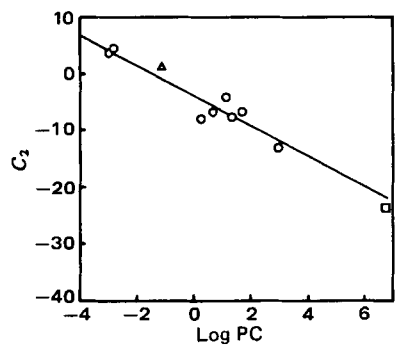

Figure 6—*Correlation of C_2 with the logarithm of the partition coefficient (octanol–water) where $C_2 = -3.96 - 2.66$ log (PC), n = 8, r = 0.946. Key: (△) 1-butanol–water; (□) n-heptane–water.*

mum (or a minimum, although we have not seen this) by computing its C_2/q_2 and $(1/q_2)\cdot\ln(x^s_{2,1}/x^s_{2,3})$ and locating them on Fig. 2. This was done for the solutes listed in Table III, and the values obtained for the above terms were plotted in Fig. 2. It is seen that the amino acids DL-valine, glycine, and DL-alanine fall in the case 1 area where no extrema are predicted (see Table II). They are, therefore, not expected to show any extrema in solubility, and they do not (Figs. 3C and 4D, E). Acetanilide and *o*-nitrophenol fall in the case 2 area and also show no extrema (Figs. 3B and 4C). Phenyl salicylate and stearic acid fall into case 5 where one extremum is predicted. The literature data we obtained do not show this, although, as expected, the estimated solubility curves in Figs. 4B and 5 indicate a minimum (the minimum in the case of phenyl salicylate is too shallow to be evident on the graph). If indeed these compounds do not show any minimum, the failure of Eq. 15 should not be surprising for reasons indicated earlier. Antipyrine falls into the case 7 area, but the solubility data show only one maximum in Fig. 4F instead of a minimum and maximum as predicted by Eq. 15. Even though the equation predicts a minimum not seen, the fact that it predicts a maximum which is seen makes it useful. Barbital falls in the borderline area between cases 6 and 7, while phenobarbital falls more into case 6 than case 2. The interesting point is that both show well-defined maxima in their solubility profiles in ethanol–water (4). Because the shapes of solubility curves change slightly when solubility is plotted as mole fraction rather than mg/L or mol/L and the fact that the log of the mole fraction solubility is used for most of the plots, the maximum is not pronounced in the case of barbital in Fig. 3A and it is not even evident with phenobarbital in Fig. 4B.

In summary it does seem that Fig. 2 may be of considerable help in indicating when a solute may be expected to show an extremum, usually a maximum, in its solubility in ethanol–water mixtures. Since we have seen no case in which a solute showed an experimental maximum without falling into one of cases 5–7, it may be possible to use a method such as this to *a priori* rule out possible maxima for solutes in ethanol–water (or other mixed solvent) systems.

CONCLUSIONS

The reduced three-suffix solubility equation (Eq. 2):

$$\ln x^s_{2,m} = \hat{z}_1 \ln x^s_{2,1} + \hat{z}_3 \ln x^s_{2,3} - A_{1\text{-}3}\hat{z}_1\hat{z}_3(2\hat{z}_1 - 1)\frac{q_2}{q_1} + A_{3\text{-}1}2\hat{z}_1^2\hat{z}_3\frac{q_2}{q_3} + C_2\hat{z}_1\hat{z}_3$$

provides a general method for characterizing and estimating solubility in mixed solvent systems. The equation may be partitioned into (*a*) the ideal mixture solubility described by the first two terms on the right-hand side, (*b*) solvent–solvent interaction contributions described by the next two terms, and (*c*) a solute–solvent interaction contribution described by the C_2 term. $A_{1\text{-}3}$ and $A_{3\text{-}1}$ are solvent–solvent interaction constants which, once obtained, are fixed for that particular mixed solvent system. Thus, apart from pure solvent solubilities, the only term needed to estimate the solubility of any solute in ethanol–water is C_2.

All systems investigated in this report were adequately described by Eq. 2, except antipyrine, which was not as well characterized because its high solubility in both solvents invalidates the assumptions made in deriving Eq. 2. The approach is also flexible enough to be appropriately altered. For example, it is possible to use the reduced four-suffix solubility equation (Eq. 1) for a system where the three-suffix equation does not satisfactorily describe the solubility. The method is readily applicable to pharmaceutically important cosolvents such as ethanol, propylene glycol, glycerol, and low-molecular weight polyethylene glycols.

REFERENCES

(1) N. A. Williams and G. L. Amidon, *J. Pharm. Sci.*, **73,** 9 (1984).

(2) K. Wohl, *Trans. Am. Inst. Chem. Eng.*, **42,** 215 (1946).

(3) J. M. Prausnitz, "Molecular Thermodynamics of Fluid-Phase Equilibria," Prentice-Hall, Englewood Cliffs, N.J., 1969, chap. 6.

(4) T. L. Breon and A. N. Paruta, *J. Pharm. Sci.*, **59,** 1306 (1970).

(5) H. J. E. Dobson, *J. Chem. Soc.*, **1925,** 2866.

(6) H. Stephen and T. Stephen, "Solubilities of Inorganic and Organic Compounds," vol. 2, Part 2, MacMillan, New York, N.Y., 1964.

(7) J. C. Duff and E. J. Bills, *J. Chem. Soc.*, **1930,** 1331.

(8) A. N. Paruta, *J. Pharm. Sci.*, **56,** 1565 (1967).

(9) J. P. Greenstein and M. Winitz, "Chemistry of the Amino Acids," vol. 1, Wiley, New York, N.Y., 1961, p. 547.

(10) C. Hansch and A. J. Leo, "Substituent Constants for Correlation Analysis in Chemistry and Biology," Wiley, New York, N.Y., 1979.

(11) R. C. Wilhoit and B. J. Zwolinski, *J. Phys. Chem.*, (Ref. Data), **2,** 1973.

(12) "Handbook of Physics and Chemistry," 60th ed., C. R. C. Press, Boca Raton, Fla., 1979.

Excess Free Energy Approach to the Estimation of Solubility in Mixed Solvent Systems III: Ethanol–Propylene Glycol–Water Mixtures

N. A. WILLIAMS * and G. L. AMIDON *x

Received July 22, 1982, from the *School of Pharmacy, University of Wisconsin, Madison, WI 53706.* Accepted for publication October 22, 1982.

*Present Address: College of Pharmacy, The University of Michigan, Ann Arbor, MI 48109-1065.

Abstract □ The reduced three-suffix solubility equation derived from the Wohl excess free energy expression is used to describe the solubility of phenobarbital in propylene glycol–water, ethanol–propylene glycol, and ethanol–water–propylene glycol mixtures and the solubility of hydrocortisone in propylene glycol–water mixtures. Solvent–solvent interaction constants were obtained by fitting total vapor pressure *versus* composition data, obtained at 25 ± 0.1°C, to the Wohl excess free energy model for the solvents. The equation describes solubility in these systems satisfactorily except for phenobarbital in ethanol–propylene glycol, where the solubility is fairly high and the assumptions involved in the derivation of the equation do not hold.

Keyphrases □ Solubility—mixed solvent systems, estimation by an excess free energy approach, application to binary and ternary mixtures of ethanol, propylene glycol, and water □ Excess free energy—use in estimating solubility in mixed solvent systems, application to binary and ternary mixtures of ethanol, propylene glycol, and water □ Mixed solvent systems—estimation of solubility, excess free energy approach, application to binary and ternary mixtures of ethanol, propylene glycol, and water

In previous reports, a general equation for describing and estimating solubility in mixed solvent systems was developed (1) and applied to ethanol–water systems (2). The equation, referred to as the reduced three-suffix solubility equation, was developed from an excess free energy model proposed by Wohl (3).

0022-3549/84/0100-0018$01.00/0

© 1984, American Pharmaceutical Association

mum (or a minimum, although we have not seen this) by computing its C_2/q_2 and $(1/q_2)\cdot\ln(x^s_{2,1}/x^s_{2,3})$ and locating them on Fig. 2. This was done for the solutes listed in Table III, and the values obtained for the above terms were plotted in Fig. 2. It is seen that the amino acids DL-valine, glycine, and DL-alanine fall in the case 1 area where no extrema are predicted (see Table II). They are, therefore, not expected to show any extrema in solubility, and they do not (Figs. 3C and 4D, E). Acetanilide and *o*-nitrophenol fall in the case 2 area and also show no extrema (Figs. 3B and 4C). Phenyl salicylate and stearic acid fall into case 5 where one extremum is predicted. The literature data we obtained do not show this, although, as expected, the estimated solubility curves in Figs. 4B and 5 indicate a minimum (the minimum in the case of phenyl salicylate is too shallow to be evident on the graph). If indeed these compounds do not show any minimum, the failure of Eq. 15 should not be surprising for reasons indicated earlier. Antipyrine falls into the case 7 area, but the solubility data show only one maximum in Fig. 4F instead of a minimum and maximum as predicted by Eq. 15. Even though the equation predicts a minimum not seen, the fact that it predicts a maximum which is seen makes it useful. Barbital falls in the borderline area between cases 6 and 7, while phenobarbital falls more into case 6 than case 2. The interesting point is that both show well-defined maxima in their solubility profiles in ethanol–water (4). Because the shapes of solubility curves change slightly when solubility is plotted as mole fraction rather than mg/L or mol/L and the fact that the log of the mole fraction solubility is used for most of the plots, the maximum is not pronounced in the case of barbital in Fig. 3A and it is not even evident with phenobarbital in Fig. 4B.

In summary it does seem that Fig. 2 may be of considerable help in indicating when a solute may be expected to show an extremum, usually a maximum, in its solubility in ethanol–water mixtures. Since we have seen no case in which a solute showed an experimental maximum without falling into one of cases 5–7, it may be possible to use a method such as this to *a priori* rule out possible maxima for solutes in ethanol–water (or other mixed solvent) systems.

CONCLUSIONS

The reduced three-suffix solubility equation (Eq. 2):

$$\ln x^s_{2,m} = \hat{z}_1 \ln x^s_{2,1} + \hat{z}_3 \ln x^s_{2,3} - A_{1\text{-}3}\hat{z}_1\hat{z}_3(2\hat{z}_1 - 1)\frac{q_2}{q_1} + A_{3\text{-}1}2\hat{z}_1^2\hat{z}_3\frac{q_2}{q_3} + C_2\hat{z}_1\hat{z}_3$$

provides a general method for characterizing and estimating solubility in mixed solvent systems. The equation may be partitioned into (*a*) the ideal mixture solubility described by the first two terms on the right-hand side, (*b*) solvent–solvent interaction contributions described by the next two terms, and (*c*) a solute–solvent interaction contribution described by the C_2 term. $A_{1\text{-}3}$ and $A_{3\text{-}1}$ are solvent–solvent interaction constants which, once obtained, are fixed for that particular mixed solvent system. Thus, apart from pure solvent solubilities, the only term needed to estimate the solubility of any solute in ethanol–water is C_2.

All systems investigated in this report were adequately described by Eq. 2, except antipyrine, which was not as well characterized because its high solubility in both solvents invalidates the assumptions made in deriving Eq. 2. The approach is also flexible enough to be appropriately altered. For example, it is possible to use the reduced four-suffix solubility equation (Eq. 1) for a system where the three-suffix equation does not satisfactorily describe the solubility. The method is readily applicable to pharmaceutically important cosolvents such as ethanol, propylene glycol, glycerol, and low-molecular weight polyethylene glycols.

REFERENCES

(1) N. A. Williams and G. L. Amidon, *J. Pharm. Sci.*, **73,** 9 (1984).

(2) K. Wohl, *Trans. Am. Inst. Chem. Eng.*, **42,** 215 (1946).

(3) J. M. Prausnitz, "Molecular Thermodynamics of Fluid-Phase Equilibria," Prentice-Hall, Englewood Cliffs, N.J., 1969, chap. 6.

(4) T. L. Breon and A. N. Paruta, *J. Pharm. Sci.*, **59,** 1306 (1970).

(5) H. J. E. Dobson, *J. Chem. Soc.*, **1925,** 2866.

(6) H. Stephen and T. Stephen, "Solubilities of Inorganic and Organic Compounds," vol. 2, Part 2, MacMillan, New York, N.Y., 1964.

(7) J. C. Duff and E. J. Bills, *J. Chem. Soc.*, **1930,** 1331.

(8) A. N. Paruta, *J. Pharm. Sci.*, **56,** 1565 (1967).

(9) J. P. Greenstein and M. Winitz, "Chemistry of the Amino Acids," vol. 1, Wiley, New York, N.Y., 1961, p. 547.

(10) C. Hansch and A. J. Leo, "Substituent Constants for Correlation Analysis in Chemistry and Biology," Wiley, New York, N.Y., 1979.

(11) R. C. Wilhoit and B. J. Zwolinski, *J. Phys. Chem.*, (Ref. Data), **2,** 1973.

(12) "Handbook of Physics and Chemistry," 60th ed., C. R. C. Press, Boca Raton, Fla., 1979.

Excess Free Energy Approach to the Estimation of Solubility in Mixed Solvent Systems III: Ethanol–Propylene Glycol–Water Mixtures

N. A. WILLIAMS * and G. L. AMIDON *x

Received July 22, 1982, from the *School of Pharmacy, University of Wisconsin, Madison, WI 53706.* Accepted for publication October 22, 1982.

*Present Address: College of Pharmacy, The University of Michigan, Ann Arbor, MI 48109-1065.

Abstract □ The reduced three-suffix solubility equation derived from the Wohl excess free energy expression is used to describe the solubility of phenobarbital in propylene glycol–water, ethanol–propylene glycol, and ethanol–water–propylene glycol mixtures and the solubility of hydrocortisone in propylene glycol–water mixtures. Solvent–solvent interaction constants were obtained by fitting total vapor pressure *versus* composition data, obtained at 25 ± 0.1°C, to the Wohl excess free energy model for the solvents. The equation describes solubility in these systems satisfactorily except for phenobarbital in ethanol–propylene glycol, where the solubility is fairly high and the assumptions involved in the derivation of the equation do not hold.

Keyphrases □ Solubility—mixed solvent systems, estimation by an excess free energy approach, application to binary and ternary mixtures of ethanol, propylene glycol, and water □ Excess free energy—use in estimating solubility in mixed solvent systems, application to binary and ternary mixtures of ethanol, propylene glycol, and water □ Mixed solvent systems—estimation of solubility, excess free energy approach, application to binary and ternary mixtures of ethanol, propylene glycol, and water

In previous reports, a general equation for describing and estimating solubility in mixed solvent systems was developed (1) and applied to ethanol–water systems (2). The equation, referred to as the reduced three-suffix solubility equation, was developed from an excess free energy model proposed by Wohl (3).

0022-3549/84/0100-0018$01.00/0

© 1984, American Pharmaceutical Association

Table I—Binary (A Terms) and Ternary (G_{134}) Solvent Constants [a]

System	A_{1-3}	A_{3-1}	A_{1-4}	A_{4-1}	A_{3-4}	A_{4-3}	G_{134}
Ethanol–Water	1.138	0.9047					
Ethanol–Propylene Glycol			0.1633	0.5688			
Water–Propylene Glycol					−0.0308	−0.0828	
Ethanol–Water–Propylene Glycol	1.138	0.9047	0.1633	0.5688	−0.0308	−0.0828	−0.1068 mol/cm^3

[a] Subscript 1 denotes ethanol, subscript 3 denotes water, and subcript 4 denotes propylene glycol.

THEORETICAL

For a solute (denoted by subscript 2) in a mixture (subscript m) of two solvents (denoted by subscripts 1 and 3):

$$\ln x^s_{2,1} = \hat{z}_1 \ln x^s_{2,1} + \hat{z}_3 \ln x^s_{2,3} - A_{1\text{-}3}\hat{z}_1\hat{z}_3(2\hat{z}_1 - 1)\frac{q_2}{q_1} + A_{3\text{-}1}2\hat{z}_1^2\hat{z}_3\frac{q_2}{q_3 + C_2\hat{z}_1\hat{z}_3} \quad \text{(Eq. 1)}$$

where $x^s_{2,m}$ is the mole fraction solubility of the solute in the solvent mixture; $x^s_{2,1}$ and $x^s_{2,3}$ are the solute mole fraction solubilities in solvents 1 and 3, respectively; $A_{1\text{-}3}$ and $A_{3\text{-}1}$ are solvent–solvent interaction constants; C_2 is a ternary solute–solvent interaction constant; q_1, q_2, and q_3 are the molar volumes of the first solvent, the solute, and the second solvent, respectively; and $\hat{z}_1$ and $\hat{z}_3$ are the solute-free volume fractions of solvents 1 and 3, respectively. Equation 1 may be rearranged to give:

$$\ln\left(\frac{x^s_{2,m}}{x^s_{2,3}}\right) = \hat{z}_1 \ln\left(\frac{x^s_{2,1}}{x^s_{2,3}}\right) - A_{1\text{-}3}\hat{z}_1\hat{z}_3(2\hat{z}_1 - 1)\frac{q_2}{q_1} + A_{3\text{-}1}2\hat{z}_1^2\hat{z}_3\frac{q_2}{q_1} + C_2\hat{z}_1\hat{z}_3 \quad \text{(Eq. 2)}$$

For a solute in a ternary solvent mixture (denoted by subscripts 1, 3, and 4), the reduced three-suffix solubility equation is:

$$\begin{aligned}\ln x^s_{2,m} = {} & \hat{z}_1 \ln x^s_{2,1} + \hat{z}_3 \ln x^s_{2,3} + \hat{z}_4 \ln x^s_{2,4} - A_{1\text{-}3}\hat{z}_1\hat{z}_3(2\hat{z}_1 + 2\hat{z}_4 - 1)\frac{q_2}{q_1} \\ & + A_{3\text{-}1}2\hat{z}_1\hat{z}_3(\hat{z}_1 + \hat{z}_4)\frac{q_2}{q_3} - A_{1\text{-}4}\hat{z}_1\hat{z}_4(2\hat{z}_1 - 1)\frac{q_2}{q_1} + A_{4\text{-}1}2\hat{z}_1^2\hat{z}_4\frac{q_2}{q_4} \\ & - A_{4\text{-}3}\hat{z}_3\hat{z}_4(2\hat{z}_4 - 1)\frac{q_2}{q_4} + A_{3\text{-}4}2\hat{z}_3\hat{z}_4^2\frac{q_2}{q_3} - G_{134}q_2\hat{z}_1\hat{z}_3\hat{z}_4 \\ & + G_{123}q_2\hat{z}_1\hat{z}_3 + G_{124}q_2\hat{z}_1\hat{z}_4 + G_{234}q_2\hat{z}_3\hat{z}_4 - Kq_2\hat{z}_1\hat{z}_3\hat{z}_4 \quad \text{(Eq. 3)}\end{aligned}$$

where $x^s_{2,4}$ is the solute mole fraction solubility in solvent 4; $\hat{z}_4$ is the volume fraction of solvent 4; $A_{1\text{-}4}$, $A_{4\text{-}1}$, $A_{4\text{-}3}$, $A_{3\text{-}4}$, and G_{134} are solvent–solvent interaction constants; G_{123} and G_{234} are ternary solute–solvent interaction constants accounting for the interaction of the solute with solvents 1 and 3, 1 and 4, and 3 and 4, respectively; and K is a quaternary solute–solvent interaction constant, which accounts for the interaction of the solute with a mixture of all three solvents. The other terms are as defined in Eq. 1. Examination of Eqs. 1 and 3 shows that Eq. 1 is identical to Eq. 3 with $\hat{z}_4 = 0$ and $G_{123}q_2 = C_2$. The q_2 in $G_{123}q_2$ arises from the slightly different definitions of C_2 and G_{123} (1).

Equation 3 shows that the logarithm of the mole fraction solubility of a solute in a ternary solvent mixture $\ln x^s_{2,m}$ may be described in the following terms:

1. The ideal mixture solubility, described by the first three terms which are a volume fraction weighted sum of the logarithm of the pure solvent solubilities.
2. Contributions from binary solvent–solvent interactions between solvents 1 and 3, 1 and 4, 3 and 4, described by the next six terms. Contributions from ternary solvent interactions are described by the G_{134} term. All the solvent interaction constants ($A_{1\text{-}3}$, $A_{3\text{-}1}$, $A_{1\text{-}4}$, $A_{4\text{-}1}$, $A_{3\text{-}4}$, $A_{4\text{-}3}$, and G_{134}), once obtained for a ternary solvent system at a particular temperature, are fixed for that solvent system and do not need to be determined again for any solute.
3. Contributions from ternary solute–solvent interactions described by the next three terms. These terms account for the interaction of the solute with two solvents in the absence of the third. For example, $G_{123}q_2\hat{z}_1\hat{z}_3$ (equivalent to $C_2\hat{z}_1\hat{z}_3$ in Eq. 1; see Ref. 1) is the contribution to solubility from the interaction of the solute with a mixture of solvents 1 and 3 only; the constant G_{123} is determined from solubility data in the absence of solvent 4.
4. Contributions from a quaternary solute–solvent interaction given by the last term. The constant K describes the interaction of the solute with all three solvents in the mixture. Since G_{123} and G_{124} are obtained for the special cases where solvents 4, 3, and 1, respectively, are absent, they, unlike K, are not new constants to be determined. K, theoretically, may be obtained from one solubility measurement somewhere in the ternary solvent composition range.

In this report, we measured total vapor pressures over ethanol–propylene glycol (denoted by subscripts 1 and 4, respectively, in Eq. 3) and ethanol–water–propylene glycol (denoted by subscripts 1, 3, and 4, respectively, in Eq. 3) mixtures at 25°C. With these data and reliable vapor pressure data for ethanol–water (4) and propylene glycol–water (5), the binary solvent interaction constants (the A terms) and the ternary solvent interaction constant (G_{134}) were obtained. These constants were then used to characterize the solubilities of (*a*) phenobarbital in propylene glycol–water, ethanol–propylene glycol, and ethanol–water–propylene

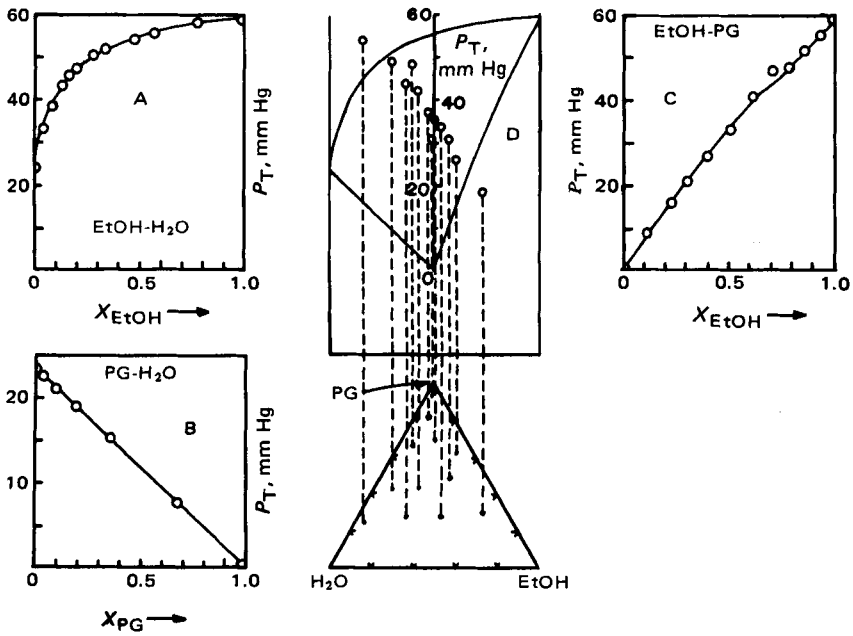

Figure 1—*Total vapor pressure* P_T *versus mole fraction composition* x. *Key: (A) ethanol–water; (B) propylene glycol–water; (C) ethanol–propylene glycol; (D) ethanol–water–propylene glycol; (—) calculated curves; (O) experimental points; (EtOH) ethanol; (*H_2O*) water; (PG) propylene glycol.*

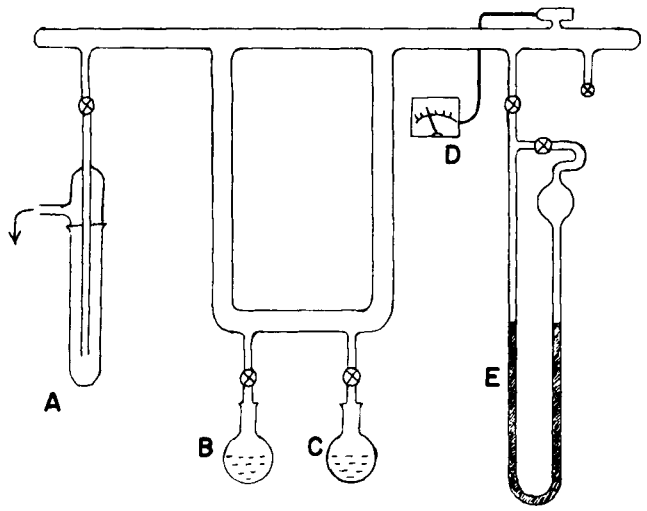

Figure 2—*Diagram of vapor pressure-measuring apparatus. Key: (A) cold trap; (B, C) flasks containing solvent mixtures; (D) pressure gauge; (E) mercury manometer.*

glycol mixtures and (*b*) hydrocortisone in propylene glycol–water mixtures at 25°C. The solubility of phenobarbital in ethanol–water mixtures has already been described (2).

Estimation of Binary Solvent Interaction Constants—Following the method described in the previous paper for the estimation of solvent interaction parameters from total pressure data, the data reported here for ethanol–propylene glycol and those for ethanol–water (4) and propylene glycol–water (5) were reduced to obtain the binary constants. The binary constants, including the ternary constant G_{134} to be discussed next, are shown in Table I. The experimental vapor pressure–composition data and the calculated curves using the binary solvent interaction constants in Table I are shown in Fig. 1 for three binary systems, ethanol–water, ethanol–propylene glycol, and propylene glycol–water.

Estimation of Ternary Solvent Interaction Constant G_{134}—For a ternary solvent mixture such as ethanol–water–propylene glycol, the excess free energy model is given by Eq. 36 of Ref. 1 except that all terms with subscript 2 are omitted. If we rewrite the equation in terms of the A values, multiply by the total number of moles, and differentiate with respect to the number of moles of each of the components, we obtain

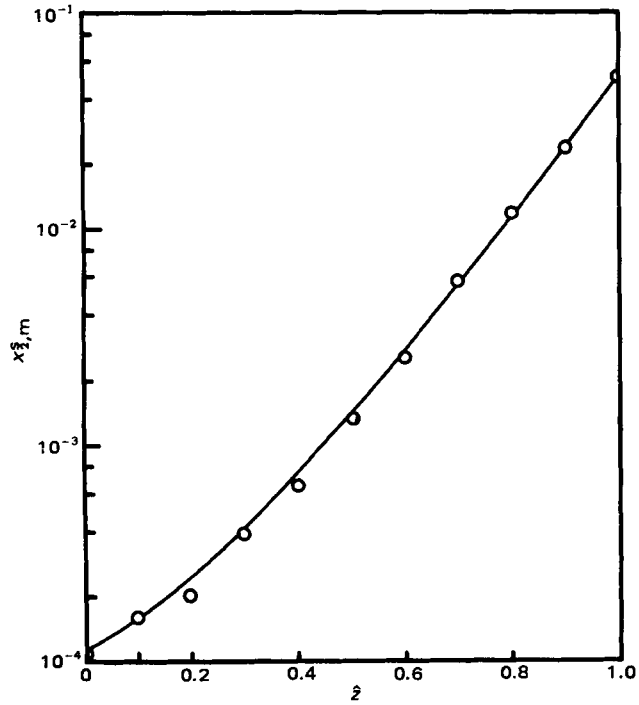

Figure 3—*Solubility profile of phenobarbital in propylene glycol–water mixtures.*

Table II—Total Vapor Pressure Results for Ethanol–Propylene Glycol

Mole Fraction		Vapor Pressure, mm Hg
Ethanol	Propylene Glycol	
0.0	1.0	0.32
0.1254	0.8746	9.00
0.2258	0.7742	16.43
0.2996	0.7004	21.27
0.3974	0.6026	26.71
0.5135	0.4865	33.12
0.6181	0.3819	40.77
0.7066	0.2934	46.87
0.7864	0.2136	47.28
0.8648	0.1352	51.23
0.9386	0.0614	55.31
1.0	0.0	58.57

expressions for the logarithm of the activity coefficients as already described (2). Thus, for a ternary solvent system:

$$\ln \gamma_1 = z_3^2\left[A_{1\text{-}3} + 2z_1\left(A_{3\text{-}1}\frac{q_1}{q_3} - A_{1\text{-}3}\right)\right] + z_4^2\left[A_{1\text{-}4} + 2z_1\left(A_{4\text{-}1}\frac{q_1}{q_4} - A_{1\text{-}4}\right)\right] + z_3z_4\left[A_{4\text{-}1}\frac{q_1}{q_4} + A_{1\text{-}3} - A_{3\text{-}4}\frac{q_1}{q_3} + 2z_1\left(A_{3\text{-}1}\frac{q_1}{q_3} - A_{1\text{-}3}\right) + 2z_3\left(A_{3\text{-}4}\frac{q_1}{q_3} - A_{4\text{-}3}\frac{q_1}{q_4}\right) - G_{134}q_1(1 - 2z_1)\right] \quad \text{(Eq. 4)}$$

$$\ln \gamma_3 = z_1^2\left[A_{3\text{-}1} + 2z_3\left(A_{1\text{-}3}\frac{q_3}{q_1} - A_{3\text{-}1}\right)\right] + z_4^2\left[A_{3\text{-}4} + 2z_3\left(A_{4\text{-}3}\frac{q_3}{q_4} - A_{3\text{-}4}\right)\right] + z_4z_1\left[A_{1\text{-}3}\frac{q_3}{q_1} + A_{3\text{-}4} - A_{4\text{-}1}\frac{q_3}{q_4} + 2z_3\left(A_{4\text{-}3}\frac{q_3}{q_4} - A_{3\text{-}4}\right) + 2z_4\left(A_{4\text{-}1}\frac{q_3}{q_4} - A_{1\text{-}4}\frac{q_3}{q_1}\right) - G_{134}q_3(1 - 2z_3)\right] \quad \text{(Eq. 5)}$$

$$\ln \gamma_4 = z_3^2\left[A_{4\text{-}3} + 2z_4\left(A_{3\text{-}4}\frac{q_4}{q_3} - A_{4\text{-}3}\right)\right] + z_1^2\left[A_{4\text{-}1} + 2z_4\left(A_{1\text{-}4}\frac{q_4}{q_1} - A_{4\text{-}1}\right)\right] + z_1z_3\left[A_{3\text{-}4}\frac{q_4}{q_3} + A_{4\text{-}1} - A_{1\text{-}3}\frac{q_4}{q_1} + 2z_4\left(A_{1\text{-}4}\frac{q_4}{q_1} - A_{4\text{-}1}\right) + 2z_1\left(A_{1\text{-}3}\frac{q_4}{q_1} - A_{3\text{-}1}\frac{q_4}{q_3}\right) - G_{134}q_4(1 - 2z_4)\right] \quad \text{(Eq. 6)}$$

The total vapor pressure, P_T, of a ternary solvent system is given by:

$$P_T = x_1p_1^0\gamma_1 + x_3p_3^0\gamma_3 + x_4p_4^0\gamma_4 \quad \text{(Eq. 7)}$$

$$P_T = x_1p_1^0e^{\ln \gamma_1} + x_3p_3^0e^{\ln \gamma_3} + x_4p_4^0e^{\ln \gamma_4} \quad \text{(Eq. 8)}$$

where x_1, x_3, and x_4 are the mole fraction compositions of solvents 1, 3, and 4 (in this case ethanol, water, and propylene glycol, respectively); p_1^0, p_3^0, and p_4^0 are the pure solvent vapor pressures; and γ_1, γ_3, and γ_4 are the activity coefficients.

Table III—Total Vapor Pressure Results for Ethanol–Water–Propylene Glycol

Mole Fraction			Vapor Pressure, mm Hg
Ethanol	Water	Propylene Glycol	
0.1191	0.3033	0.5776	18.44
0.0817	0.6219	0.2964	25.81
0.1857	0.4764	0.3379	30.71
0.0463	0.9265	0.0272	30.73
0.3246	0.2804	0.3950	33.27
0.1359	0.6994	0.1647	35.03
0.1096	0.8259	0.0645	37.03
0.3475	0.4415	0.2110	42.00
0.5003	0.2555	0.2442	43.70
0.2588	0.6638	0.0774	48.42
0.4874	0.4143	0.0983	48.79
0.7188	0.2272	0.0540	53.70

Table IV—Solute-Solvent Interaction Parameters

Compound	q_2[a]	Mixed Solvent System[b]	Solute-Solvent Interaction Constants	n[c]	γ[c]	s[c,d]
Phenobarbital	172.0	Ethanol–Propylene Glycol	$G_{124}q_2 = -0.092$	9	0.885	0.291
Phenobarbital	172.0	Propylene Glycol–Water	$G_{234}q_2 = -1.80$	9	0.999	0.129
Phenobarbital	172.0	Ethanol–Water	$G_{123}q_2 = -6.74$	9	0.995	0.21
Phenobarbital	172.0	Ethanol–Water–Propylene Glycol	$Kq_2 = 15.3$	20	0.996	0.135
Hydrocortisone	293	Propylene Glycol–Water	$C_2 = 1.44$	4	1.000	0.200

[a] $q_1 = 58.68$ (Ref. 11), $q_3 = 18.07$ (Ref. 15), and $q_4 = 73.69$ (Ref. 14), q_2 was calculated by group contribution from the molar volume of barbital (Ref. 15). [b] Subscript key: 1, ethanol; 2, solute; 3, water; 4, propylene glycol. [c] Linear regression parameters for the estimation of the constants in column 4. [d] s is the standard deviation of the error between $\ln (x^s_{2,m})_{obs}$ and $\ln (x^s_{2,m})_{est}$.

By substituting Eqs. 4–6 into Eq. 8, all seven interaction constants may be obtained by nonlinear regression since P_T, the mole fractions, and pure solvent–vapor pressures are known. To obtain G_{134}, the other six constants $A_{1\text{-}3}$, $A_{3\text{-}1}$, $A_{1\text{-}4}$, $A_{4\text{-}1}$, $A_{3\text{-}4}$, and $A_{4\text{-}3}$ were fixed so that only G_{134} was altered to obtain the best fit. If the six binary constants were allowed to vary, the estimates would become meaningless because of the complexity of the sum of squares surface for seven parameters. With this method, $G_{134} = -0.1069$ mol/cm^3 was obtained with the A terms as shown in Table I. It should be noted that, while the A terms are dimensionless, G_{134} has units of reciprocal molar volume because of the way it was defined in Eq. 37i of Ref. 1.

EXPERIMENTAL

Materials—Absolute ethanol and propylene glycol were used as received. Double-distilled water was used for all aqueous mixtures.

Method—All solvent mixtures were made by weighing the appropriate amounts of solvents. To prevent condensation of the solvent vapor on the mercury and in the manifold of the apparatus (Fig. 2), the manometer (E) and the manifold were wrapped with a heating tape kept at 3 ± 0.5°C above the temperature of the flask contents (B and C).

The method described here is similar to that used by Verlinde *et al.* (5). The solvent (or solvent mixture) was frozen using liquid nitrogen. The stopcock to the solvent was opened, and the air in the manifold and above the solvent was evacuated by means of a compound-stage vacuum pump until the pressure gauge (D) indicated a pressure of ≤2 μm. The stopcock was then closed, and the solvent was brought to room temperature and stirred by means of a glass-coated magnetic bar in the flask. The solvent was again frozen, the stopcock opened, and the air evacuated. By means of several such freeze–thaw cycles, the dissolved air in the solvent was removed. The process was stopped after the pressure gauge showed no significant increase in pressure on opening the stopcock to the frozen solvent.

After deaerating the solvent, it was brought to, and kept at, 25 ± 0.1°C. The solvent stopcock was opened, the vapor pressure was read by a cathetometer (graduated to 0.05 mm) after the mercury column had stopped moving, and the average was computed.

Two flasks containing two different concentrations of the solvent mixture were used so that deaerating the contents simultaneously saved considerable time. After deaerating, flask B was shut off while the vapor pressure of the contents of flask C was measured. Then flask C was shut off, the system evacuated, and the vapor pressure of the contents of flask B measured. Each averaged vapor pressure reading was corrected for the change in acceleration due to gravity, the change in the density of mercury at 28°C (temperature of the manometer), and capillary depression (6) using: corrected pressure = (uncorrected pressure) (g/g_0) $(d_t/d_0) + C_u - C_l$, where g is the acceleration due to gravity in Madison (980.368 cm/s^2) (7); g_0 = 980.665 cm/s^2 (6); d_t is the density of mercury at manometer temperature (28°C); d_0 is the density of mercury at 0°C; C_u and C_l are the capillary depression correction for the upper and lower columns of the manometer, respectively; and $d_t/d_0 = 0.994939$ (6). The results of four separate measurements with ethanol indicated a relative standard error of <1%.

Calculations (using the ideal gas equation $PV = nRT$), with the highest possible partial pressure values showed that with a void volume of 1324 ± 7 cm^3 occupied by the solvent or solvent mixture vapor, there was <0.6% change between initial and equilibrium weight fractions of the components. There was, therefore, no need to use equilibrium weight/mole fraction values.

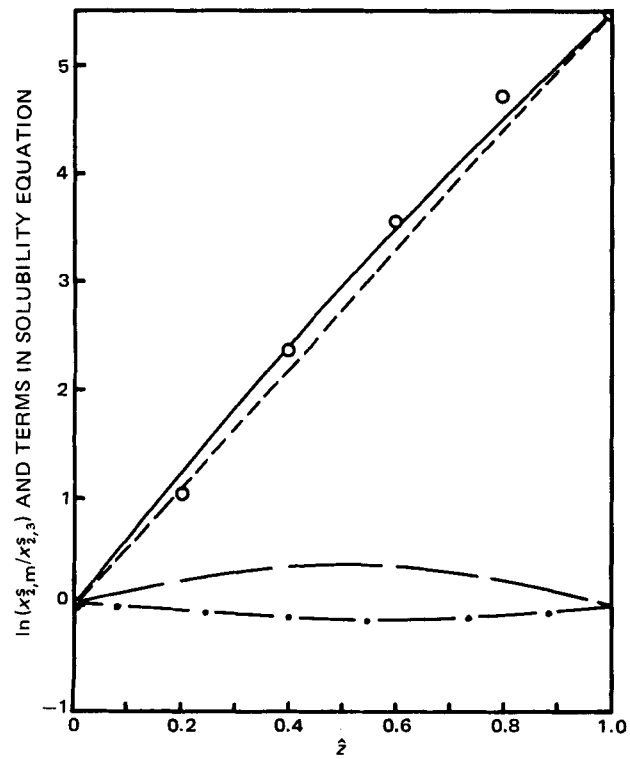

Figure 4—*Solubility profile of hydrocortisone in water–propylene glycol mixtures (showing contributions from terms in Eq. 4). Key: (- - - -) $\hat{z}_1$ ln $(x^s_{2,1}/x^s_{2,3})$; (— · — · —) $-A_{1\text{-}3}\hat{z}_1\hat{z}_3(2\hat{z}_1 - 1)$ q_2/q_1 + $A_{3\text{-}1}2\hat{z}_1^2\hat{z}_3q_2/q_3$; (— — —) $C_2\hat{z}_1\hat{z}_3$; (—) estimated ln $(x^s_{2,m}/x^s_{2,3})$; (O) experimental ln $(x^s_{2,m}/x^s_{2,3})$.*

RESULTS

Vapor Pressure Results—Corrected total vapor pressure readings at different solvent compositions are given in Tables II and III for ethanol–propylene glycol and ethanol–water–propylene glycol mixtures. For ethanol–water mixtures, partial vapor pressure readings that had been

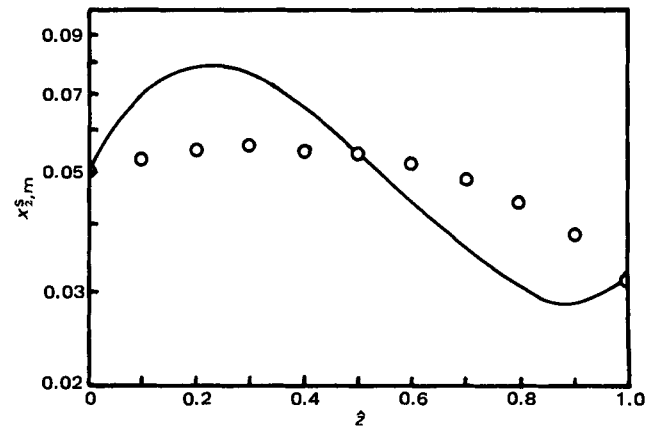

Figure 5—*Solubility profile of phenobarbital in ethanol–propylene glycol mixtures. Key: (—) estimated solubility; (O) experimental solubility.*

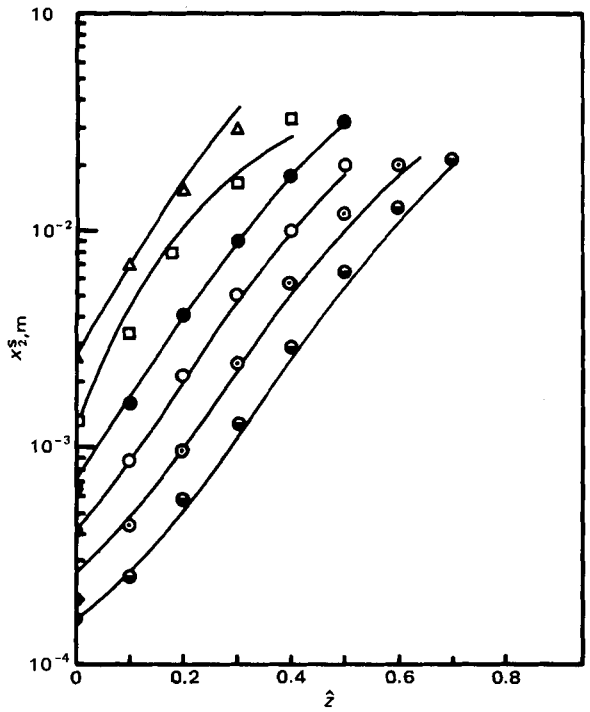

Figure 6—*Solubility profiles of phenobarbital in ethanol-water at designated volume fractions of propylene glycol. Lines represent estimated solubilities and points are the experimental solubilities. Volume fractions of propylene glycol: (◒) 0.1; (⊙) 0.2; (○) 0.3; (●) 0.4; (□) 0.5; (△) 0.6.*

tested for thermodynamic consistency (8) were taken from Ref. 4. For propylene glycol–water mixtures, total vapor pressure results from Ref. 5 were used after being checked with the apparatus described above.

Figure 1A–C shows the experimental points for the three binary systems. Figure 1D combines all three cases and the ternary mixture vapor pressures. The resulting vapor pressure surface is plotted above a triangular plane each of whose apices represent a pure solvent.

Solubility in Ethanol–Water–Propylene Glycol Mixtures—Figures 3 and 4 show the estimated and experimental solubility profiles of phenobarbital (9) and hydrocortisone (10) in propylene glycol–water mixtures obtained by methods described in the previous paper (2). In summary, the ternary solute–solvent interaction constant for this system, G_{234}, is estimated from differences between experimental solubilities and solubilities calculated with $G_{234} = 0$. The binary solvent–solvent interaction constants needed in this case are $A_{3\text{-}4}$ and $A_{4\text{-}3}$, whose values are given in Table I. With regard to Eq. 4, it means that one sets $\hat{z}_1 = 0$.

Figure 5 shows the estimated and experimental solubility profile of phenobarbital in ethanol–propylene glycol mixtures (9), and Fig. 6 shows the same compound in a mixture of all three solvents (9). In this case, K, the quaternary solute–solvent constant, was estimated from differences between experimental solubilities in mixtures of the three solvents and solubilities calculated from all the terms in Eq. 4 without the K term. G_{123}, G_{234}, and G_{124} were already known from the solubilities of phenobarbital in mixtures of ethanol–water, water–propylene glycol, and ethanol–propylene glycol, respectively. All ternary and quaternary solute–solvent interaction constants estimated are shown in Table IV.

DISCUSSION

Vapor Pressure Fit by Excess Free Energy Model—As shown in Fig. 1A–C, the three-suffix excess free energy model accurately predicts total vapor pressures for the three binary systems described here. This indicates that it is very reliable for obtaining binary solvent interaction constants which adequately represent interactions between the solvents. It is interesting to note that in Fig. 1B, the total vapor pressure over propylene glycol–water mixtures can be described by a straight line, which implies that the solvent mixture follows Raoult's Law for ideal mixtures. Raoult's Law states that the total vapor pressure, P_T, over an ideal mixture of solvents may be expressed as:

$$P_T = \sum_i x_i p_i^0 \qquad \text{(Eq. 9)}$$

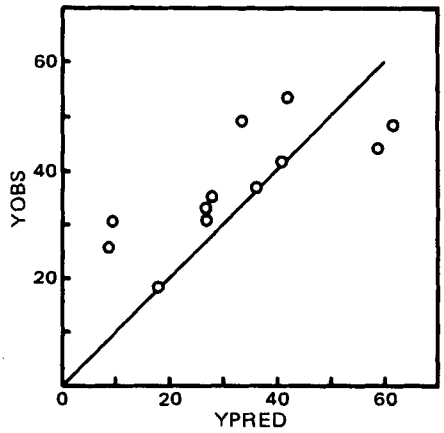

Figure 7—*Observed (YOBS)* versus *predicted (YPRED) vapor pressures for ethanol–water–propylene glycol mixtures;* n = *12,* r = *0.765,* s = *11.1.*

where x_i represents the mole fraction of each component i and p_i^0 is the pure vapor pressure of component i. In systems where Raoult's Law holds, the excess free energy of mixing is zero. The implications of this observation as it concerns solubility in propylene glycol–water mixtures will be discussed in the next section. The vapor pressure curve for ethanol–propylene glycol (Fig. 1C) follows that of a typical solute (with a relatively low vapor pressure) in a solvent. At high concentrations of ethanol, the total vapor pressure is practically equal to the partial pressure of ethanol, which, as expected, converges to the Raoult's Law line as the mole fraction of ethanol in the mixture approaches 1.

For the mixture of all three solvents, predicted vapor pressures (Fig. 7) were not as good as for the binary systems (Fig. 1), but if one considers the complexity of the ternary system, the fit is satisfactory. A better fit may be obtained by using the four-suffix excess free energy model (3), but the number of solvent constants to be estimated (12, see Ref. 3) becomes inconveniently high. Another excess free energy model which has been shown to better describe ternary vapor–liquid equilibrium data is the nonrandom two liquid (NRTL) model (12). However, we have not examined this model at this time for possible application to solid–solvent systems.

Estimation of Solubility in Ethanol–Water–Propylene Glycol Mixtures—As was mentioned above, the propylene glycol–water system is close to ideal in the Raoult's Law sense. This is also indicated by the binary solvent interaction constants (A terms) which are quite small in magnitude (Table I). Consequently, the solubility of a compound in their mixture should be approximately equal to the ideal mixture solubility discussed earlier if there is little interaction between the solute and mixed solvent. This is borne out by Figs. 3 and 4, in which the experimental solubility is close to a straight line between the two end points. This provides a rationale for the observation that the logarithm of the solubility of some compounds, *e.g.*, alkyl *p*-aminobenzoates (13), in propylene glycol–water mixtures increases linearly with the volume fraction of propylene glycol in the mixture.

Figure 4 shows the contributions of the various terms in Eq. 2 to the solubility of hydrocortisone in propylene glycol–water mixtures. Equation 2 is written for solvents 1 and 3. It may be applied to propylene glycol–water mixtures by temporarily designating propylene glycol as solvent 1. If we temporarily make this change, then we can refer to the ternary solute–solvent constant C_2 in Eq. 2 instead of $G_{234}q_2$ in Eq. 3. As seen in Fig. 4, the solvent interaction contribution (the sum of the A terms) is always close to zero and has no significant effect on the solubility. The C_2 term is responsible for the positive deviation from the ideal mixture solubility. The magnitude of the sum of the A terms in Eq. 2 is influenced by the ratio of the solute to solvent molar volumes q_2/q_1 and q_2/q_3. If we temporarily label propylene glycol "1" (water is still "3"), then since the molar volumes of hydrocortisone, propylene glycol, and water are 293 (10), 73.69 (14), and 18.07 cm^3/mol (15), respectively, $q_2/q_1 = 3.98$ and $q_2/q_3 = 16.2$. These ratios are about as high as they can get for many solutes. Therefore, the fact that the solvent interaction contribution is very small for hydrocortisone indicates that it is likely to be even smaller for many other solutes in this binary solvent mixture. One can conclude from these results that for propylene glycol–water systems, only the interaction between the solute and solvent mixture (estimated by C_2) contributes significantly to the deviation of the solubility profile from that estimated by using only the ideal mixture solubility terms.

The solubility of phenobarbital in ethanol–propylene glycol mixtures is not well described by Eq. 1, as seen in Fig. 5. However, if one takes into account that Fig. 5 is drawn on an expanded scale compared with, for example, Fig. 3, then the estimation is not overwhelmingly poor. The equation predicts a maximum and a minimum, whereas only the maximum is seen experimentally. The comparatively poor characterization of solubility in this case [as in the case of antipyrine in ethanol–water discussed previously (2)] is most likely due to the fairly high solubility of the drug in each of the solvents (149.5 mg/mL in propylene glycol and 117.9 mg/mL in ethanol) (9). These values are 0.051 and 0.032, respectively, in mole fraction units.

Figure 6 shows the estimated and experimental (9) solubility profiles of phenobarbital in ethanol–water–propylene glycol mixtures. The fit is remarkably good. One could argue that the curves could be well approximated by straight lines so that the effectiveness of Eq. 3 is not really demonstrated by Fig. 6. If the points are fitted to straight lines, two parameters would be required for each line. In this approach, however, only one parameter (K) is required to generate all the curves in Fig. 6, since the solvent–solvent constants (the A terms and G_{134} in Eq. 3) and the ternary solute–solvent constants (G_{123}, G_{124}, and G_{234} in Eq. 3) are known (Tables I and IV). Thus, this aproach is more flexible and requires fewer empirically adjusted parameters (compared with the straight line fit just discussed, for example) to describe solubility in a ternary solvent system.

As was pointed out earlier, the binary solvent interaction contributions from propylene glycol–water are quite small. It is, therefore, possible to drop these terms (*i.e.*, set $A_{3\text{-}4} = A_{4\text{-}3} = 0$) from Eq. 3 for mixtures of ethanol–water–propylene glycol without any significant loss in estimation capabilities.

CONCLUSION

The reduced three-suffix solubility equation for decreasing solubility in binary and ternary solvent mixtures has previously been shown to be quite successful for ethanol–water systems 2. In this report, its applicability to other binary systems and a ternary system is further demonstrated. Our results indicate that the solubility of compounds in propylene glycol–water systems may be described in terms of the volume fraction weighted sum of the pure solvent solubilities and a ternary solute–solvent interaction term, *i.e.*, solvent–solvent interaction terms make negligible contributions to the total solubility. This finding provides a rational explanation for the observation that the logarithms of the solubilities of a number of compounds in propylene glycol–water mixtures are a linear function of the volume fraction of the former.

Estimation of solubility in a ternary solvent system requires more terms than in a binary solvent system, which is not unexpected considering that the former is complicated. However, in both systems only one unknown parameter needs to be estimated from mixed solvent solubility data. For instance, to describe the solubility of phenobarbital in ethanol–water, ethanol–propylene glycol, and propylene glycol–water, we may use Eq. 1 or 3. To use Eq. 3 for ethanol–water, we set $\hat{z}_4 = 0$ and estimate G_{123} as already described; for ethanol–propylene glycol we set $\hat{z}_3 = 0$ and estimate G_{124}; and for propylene glycol–water, we set $\hat{z}_1 = 0$ and estimate G_{234}. To describe the solubility of phenobarbital in ternary mixtures of these solvents, the only known term to estimate in Eq. 3 is the quaternary solute–solvent constant K since the A terms and G_{134} are fixed for the solvent system and G_{123}, G_{124}, and G_{234} are fixed for the solute in this solvent system. With the estimated K, the entire solubility profile of phenobarbital in a mixture of these three solvents was described very well. It appears, then, that this approach is reasonably flexible and general while requiring relatively few empirically adjusted solute–solvent parameters.

The only apparent limitation of the reduced three-suffix solubility equation thus far is in describing relatively high solubilities. Bearing in mind that the equation was developed with the assumption that the solubility of the solute is very small, it is not surprising that the equation does not do well for compounds that are fairly to highly soluble in both (or all) of the pure solvents used. From a pharmaceutical point of view, a compound with appreciably high solubility in water does not need a cosolvent. Therefore, it seems that the equation is well suited for the systems for which it was derived: compounds whose very low solubility in water (or another solvent) necessitate the addition of a second solvent or solvents to increase their solubility.

REFERENCES

(1) N. A. Williams and G. L. Amidon, *J. Pharm. Sci.*, **73**, 9, (1984).

(2) N. A. Williams and G. L. Amidon, *J. Pharm. Sci.*, **73**, 14 (1984).

(3) K. Wohl, *Trans. Am. Inst. Chem. Eng.*, **42**, 215 (1946).

(4) H. J. E. Dobson, *J. Chem. Soc.*, **1925**, 2866.

(5) J. R. Verlinde, R. M. H. Verbeeck, and H. P. Thun, *Bull. Soc. Chim. Belg.*, **84**, 1119 (1975).

(6) D. F. Shriver, "The Manipulation of Air-Sensitive Compounds," McGraw Hill, New York, N.Y., 1969, p. 39.

(7) "International Critical Tables, Vol. 1," McGraw Hill, New York, N.Y., 1926.

(8) J. M. Prausnitz, "Molecular Thermodynamics of Fluid-Phase Equilibria," Prentice-Hall, Englewood Cliffs, N.J., 1969, chap. 6.

(9) C. F. Peterson and R. E. Hopponen, *J. Am. Pharm. Assoc., Sci. Ed.*, **42**, 540 (1953).

(10) T. A. Hagen, Ph.D. Thesis, University of Michigan, Ann Arbor, Mich., 1979.

(11) R. C. Wilhoit and B. J. Zwolinski, *J. Phys. Chem.* (Ref. Data) *Suppl.* 1, **2**, 1973.

(12) H. Renon and J. M. Prausnitz, *Am. Inst. Chem. Eng. J.*, **14**, 135 (1968).

(13) S. H. Yalkowsky, S. C. Valvani, and G. L. Amidon, *J. Pharm. Sci.*, **65**, 1488 (1976).

(14) G. O. Curme and F. Johnston, Eds., "Glycols," Reinhold, New York, N.Y. 1952.

(15) "Handbook of Physics and Chemistry," 60th ed., C. R. C. Press, Boca Raton, Fla., 1979.

Quantitative Determination of Dextromethorphan and Three Metabolites in Urine by Reverse-Phase High-Performance Liquid Chromatography

YOUNG HAN PARK, M. PETER KULLBERG, and ORVILLE N. HINSVARK ×

Received May 18, 1982, from the *Department of Analytical Chemistry, Pharmaceutical Division, Pennwalt Corporation, Rochester, NY 14623.* Accepted for publication November 10, 1982.

Abstract □ A high-performance liquid chromatographic (HPLC) method for the quantitation of dextromethorphan (I) and its three metabolites, dextrorphan (II), 3-hydroxy-9α,13α,14α-morphinan (III), and 3-methoxy-9α,13α,14α-morphinan (IV), in urine was developed. For the analysis of nonconjugated compounds, urine samples at pH 11–11.5, containing 3-methoxy-17-methyl-10-oxo-9α,13α,14α-morphinan as an internal standard, were applied to an extraction column, and the compounds were eluted with 10% *n*-butyl alcohol–hexane. The organic eluant was extracted with 0.1 M HCl, and an aliquot of the acidic extract was analyzed by HPLC utilizing a 5-μm phenyl column (25 × 0.46-cm i.d.) with a mobile phase of 10 mM potassium phosphate–acetonitrile (45:55, pH 4.0); the column effluent was monitored by UV detection at 280 nm. Free and conjugated metabolites in the enzyme-treated urine were analyzed by selective extraction of I and IV with hexane from urine samples at pH > 12 and extraction of II and III with 10% *n*-butyl alcohol–hexane from urine samples at pH 11–11.5. The minimum quantifiable levels of I–IV ranged from 0.017 to 0.09 μg of base/mL and from 0.11 to 0.21 μg of base/mL in nonhydrolyzed and hydrolyzed urine, respectively.

Keyphrases □ Dextromethorphan—quantitation with metabolites by high-performance liquid chromatography, human urine □ Dextrorphan—quantitation in human urine after administration of dextromethorphan, high-performance liquid chromatography □ Cough suppressants—dextromethorphan, dextrorphan, and metabolites, quantitation in human urine by high-performance liquid chromatography

Dextromethorphan (3-methoxy-17-methyl-9α,13α,-14α-morphinan, I), a widely used nonnarcotic antitussive agent, has been judged to be safe and effective, with a reported activity of about one-half the potency of codeine (1) against citric acid-induced cough. Considerable intersubject variations in plasma levels of I have been reported by Barnhart and Massad (2). O'Brien *et al.* described the measurement of I by GC with nitrogen detection and also reported variable human plasma levels of I following single and multiple doses (3). Hinsvark *et al.* suggested that these differences are attributable to genetic polymorphism (4). Therefore, a study to determine if differences in the elimination rates of I were related to different biotransformation routes was initiated in our laboratories. The initial phase required the development of a procedure capable of measuring I and its known metabolites in urine.

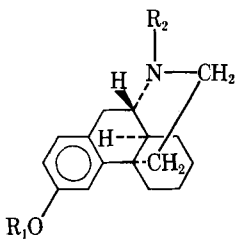

I: $R_1 = R_2 = CH_3$
II: $R_1 = H$, $R_2 = CH_3$
III: $R_1 = R_2 = H$
IV: $R_1 = CH_3$, $R_2 = H$

Recently, Barnhart described a GC procedure to measure the amount of I and three of its metabolites [dextrorphan (II), 3-hydroxy-9α,13α,14α-morphinan (III) and 3-methoxy-9α,13α,14α-morphinan (IV)] in urine (5). It suffers the usual problems associated with derivatization. The approach utilized in this paper uses high-performance liquid chromatography (HPLC) to simultaneously measure I and its metabolites in urine. The procedure is presented and data are provided which describe the accuracy and precision of the method. Examples of chromatograms from assay of 24-h urine samples of subjects who had received 60 mg of dextromethorphan hydrobromide orally are also presented.

EXPERIMENTAL

Materials—Dextromethorphan hydrobromide[1], dextrorphan tartrate[2], 3-hydroxy-9α,13α,14α-morphinan[2], and thebaine[3] were available commercially. The 3-methoxy-9α,13α,14α-morphinan hydrochloride was synthesized by *N*-demethylation of dextromethorphan (6). The internal standard, 3-methoxy-17-methyl-10-oxo-9α,13α,14α-morphinan[4] was prepared by a previously described method (7).

All reagents were analytical grade. The chromatographic solvents used in the chromatographic separation were HPLC grade. Membrane filters[5] were used for filtration of the mobile phase. Disposable extraction columns[6] were utilized for extraction. β-Glucuronidase–sulfatase[7] was used for hydrolysis of conjugated metabolites for the assay of total metabolites.

Instrumentation—A modular chromatograph consisting of a pump[8], an autosample injector[9], a fixed-wavelength absorbance detector[10], and a recorder[11] was used. A reverse-phase phenyl column[12] (25 × 0.46-cm i.d.) packed at 8000 psi was used for all analyses. A laboratory data system[13] was used for quantitation and identification of chromatographic peaks.

Chromatographic Conditions—The mobile phase was 10 mM potassium phosphate (monobasic)–acetonitrile (45:55, v/v) adjusted to pH 4.0 with 8.5% phosphoric acid. The flow rate was 1.2 mL/min. Following preparation, the mobile phase was filtered through a membrane filter and deaerated under vacuum. The detector was set at 280 nm with a sensitivity of 0.05 AUFS.

Preparation of Validation Samples and Standards—Validation samples, analyzed under single-blind conditions, were prepared in control human urine by spiking with combinations of I, II, III, and IV at various concentrations. One set of samples was analyzed on preparation; the other set was frozen for 2 weeks, thawed, and analyzed. Duplicate standards were prepared on each day of analysis of the validation samples by adding

[1] USP reference standard.
[2] Hoffmann-La Roche, Inc., Nutley, N.J.
[3] Mallinckrodt Chemical Co., St. Louis, Mo.
[4] Synthesized by Dr. Metro Fedorchuk in the Department of Organic Chemistry.
[5] 0.45-μm; Rainin Instrument Co., Woburn, Mass.
[6] Clin-Elut; Analytichem Internation, Inc., Lawndale, Calif.
[7] Glusulase; Endo Laboratories, Garden City, N.Y.
[8] Model M-45; Waters Associates, Milford, Mass.
[9] Model WISP-710B; Waters Associates, Milford, Mass.
[10] Model 440; Waters Associates, Milford, Mass.
[11] Omni-Scribe B-5000 Strip Chart Recorder; Houston Instrument, Austin, Texas.
[12] Spherisorb phenyl, 5-μm; Deeside Ind. Est., Clwyd. UK, Hauppauge, NY 11787.
[13] Model 3353E; Hewlett-Packard, Avondale, Pa.

0022-3549/84/0100-0024$01.00/0
© 1984, American Pharmaceutical Association

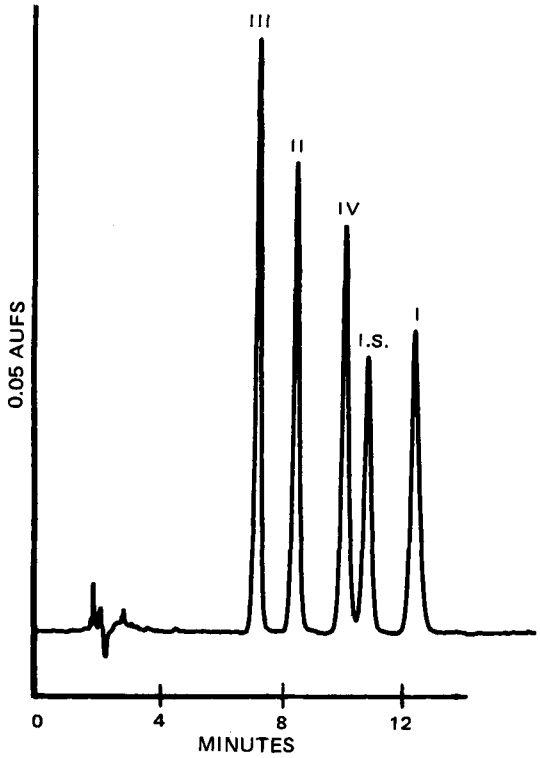

Figure 1—*Chromatogram at 280 nm of dextromethorphan and three metabolites with an internal standard (3 methoxy-17-methyl-10-oxo-9α,13α,14α-morphinan) using a 5-μm phenyl 25 × 0.46-cm column with 10 mM potassium phosphate–acetonitrile (45:55, pH 4.0) at 1.2 mL/min. Key: (I) dextromethorphan; (II) dextrorphan; (III) 3-hydroxy-9α,13α,14α-morphinan; (IV) 3-methoxy-9α,13α,14α-morphinan.*

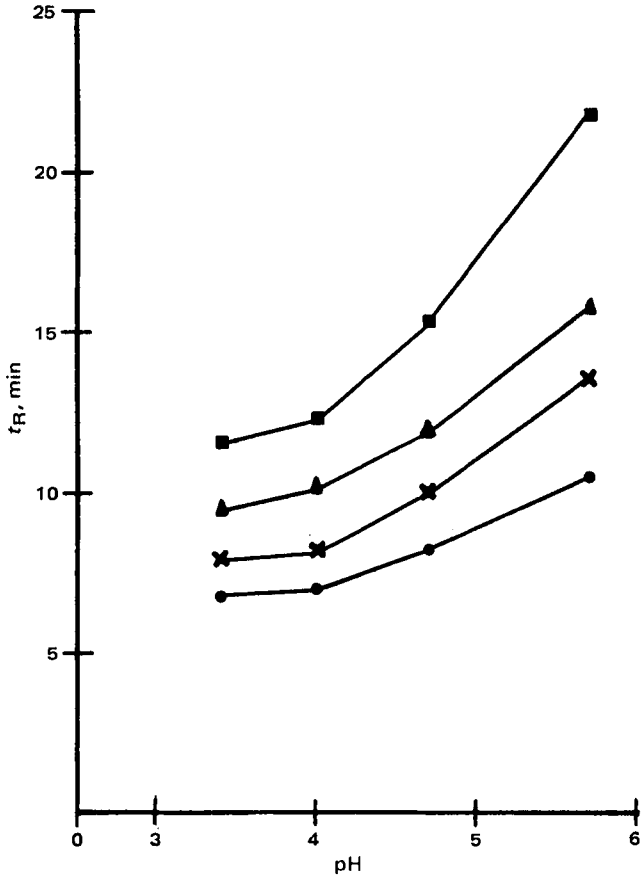

Figure 2—*Effect of pH of the mobile phase (10 mM potassium phosphate–acetonitrile, 45:55, pH 4.0) on the retention times (t_R) of dextromethorphan (■), dextrorphan (x), 3-hydroxy-9α,13α,14α-morphinan (●), and 3-methoxy-9α,13α,14α-morphinan (▲).*

100 μL of stock solutions to control human urine (2 mL) to give final concentrations of 0.00, 0.05, 0.10, 0.25, 1.25, 2.50, 5.00, and 10.00 μg of base/mL for all four compounds.

Extraction Procedures—*Dextromethorphan and Unconjugated Metabolites*—The urine sample (2 mL) was adjusted to pH 11–11.5 with concentrated ammonium hydroxide, and 50 μL of a solution of 3-methoxy-17-methyl-10-oxo-9α,13α,14α-morphinan (1 μg of base/50 μL in 0.01 M HCl) was added as the internal standard. The mixture was gently vortexed and transferred to an extraction column with a pipet. After 5 min, the column was eluted with 10% *n*-butyl alcohol–hexane (10 mL). The collected eluant (~7 mL) was extracted with 0.1 M HCl (0.4 mL) by roto-mixing for 40 min and centrifuged. The organic layer was aspirated and discarded. The acid extract (40 μL) was analyzed by HPLC.

Dextromethorphan and Total (Free and Conjugated) Metabolites—The urine sample (2 mL) was adjusted to pH 5–5.5 with 50 mM sodium acetate buffer (pH 3.5), and the β-glucuronidase–sulfatase mixture (0.2 mL) was added. After incubation at 37°C for 18 h, the mixture was adjusted to pH 12–12.5 with 1 M NaOH, and 50 μL of a solution of 3-methoxy-17-methyl-10-oxo-9α,13α,14α-morphinan (1 μg of base/50 μL in 0.01 M HCl) was added as the internal standard. The mixture was extracted with hexane (6 mL) by roto-mixing for 40 min and centrifuged. The aqueous layer was frozen in a dry ice–acetone bath. The hexane extract was decanted into a centrifuge tube and back-extracted with 0.1 M HCl (0.2 mL) by roto-mixing for 30 min. The acid extract (25 μL) was analyzed by HPLC for I and IV. The thawed aqueous layer was adjusted to pH 11–11.5 with 1 M HCl. After addition of 50 μL of a solution of thebaine, the internal standard (1 μg of base/50 μL in 0.01 M HCl), the mixture was extracted by the aforementioned method for the determination of free metabolites. The acid extract (25 μL) was analyzed for total II and III.

Extraction Efficiency—The extraction efficiency of each compound from urine was investigated at pH ranging from 2 to 13. The pH-adjusted urine samples (2 mL) were spiked with 100 μL of a mixture of I, II, III, and IV in solution and processed through the entire extraction procedure and chromatographic analysis for the determination of both free and total metabolites. The recovery of each compound was determined by comparing the peak heights of extracted standards with those of unextracted standards. The unextracted standards were prepared by the addition of stock solutions of I, II, III, and IV to 0.1 M HCl to give concentrations equivalent to that of extracted standards.

Quantitation—The duplicate fresh standards at seven different concentrations ranging from 0.05 to 10.0 μg of base/mL of I–IV were analyzed together with validation samples. From the standards, the peak height ratios of each compound to the internal standard were obtained with the aid of a laboratory data system. From linear regression of the peak height ratios of each compound with respect to its concentration in the standards, the concentrations of each compound in the validation samples were determined by inverse prediction.

RESULTS AND DISCUSSION

HPLC of Dextromethorphan and Metabolites—Figure 1 is a representative chromatogram of I, II, III, IV, and the internal standard on a phenyl column. The phenyl column was chosen after evaluation of octadecylsilanyl and cyano columns. Unlike the others, the phenyl column gave both symmetric peaks and baseline separations of compounds of diverse polarity.

The effect of pH and acetonitrile composition on retention times of the four compounds was investigated. The retention times of all four compounds increased as the pH of the mobile phase increased (Fig. 2). Similarly, the retention times of the compounds increased with decreasing concentrations of acetonitrile in the 10 mM potassium phosphate buffer at pH 4.0 (Fig. 3). These studies suggest that the chromatographic characteristics of dextromethorphan and its related alkaloids are dependent on both the pH and composition of the mobile phase. A mobile phase of 10 mM potassium phosphate buffer–acetonitrile (45:55) at pH 4.0 was chosen because it permitted the baseline separation of dextromethorphan and its three metabolites with reasonable analysis time and sensitivity.

Extraction and Recovery—In the development of this assay, several problems were encountered. The first was attaining an efficient simultaneous extraction of all four compounds from urine. The second was concentrating the compounds to give sufficient sensitivity for the analysis

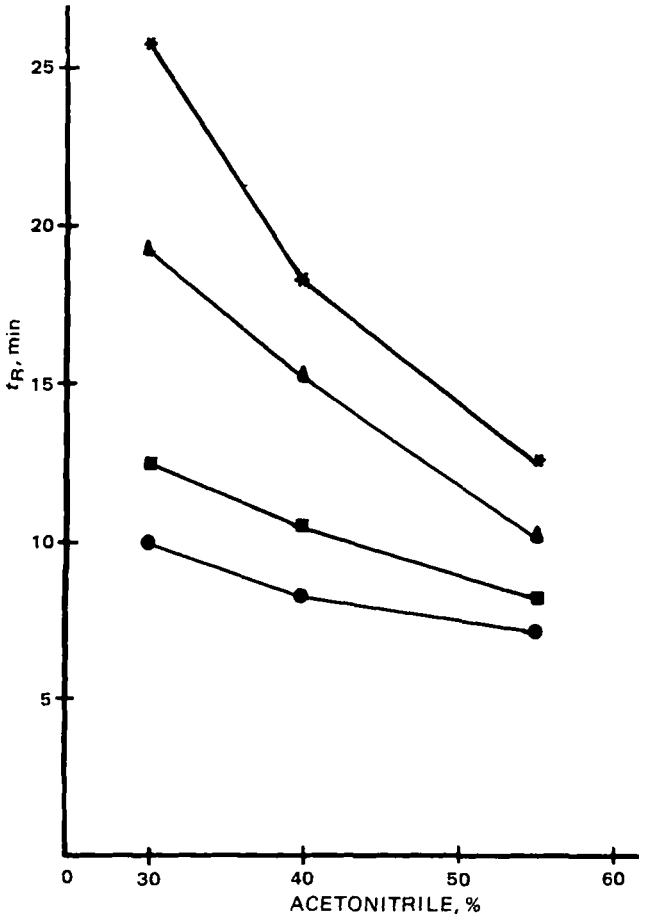

Figure 3—*Effect of acetonitrile percentage in 10 mM potassium phosphate buffer at pH 4.0 on the retention time (t_R) of dextromethorphan (*), dextrorphan (■), 3-hydroxy-9α,13α,14α-morphinan (●), and 3-methoxy-9α,13α,14α-morphinan (▲).*

of the free compounds in nonhydrolyzed urine, while using a solvent that gave little background interference from hydrolyzed and nonhydrolyzed urine samples. Thirdly, an unexpected problem arose in that the hydrochloride salts of I and IV were found to be fairly soluble in relatively polar organic solvents, resulting in a poor extraction efficiency of the amines from the organic phase into the acidic phase in the back-extraction procedure. A fourth problem was the concentration difference of I

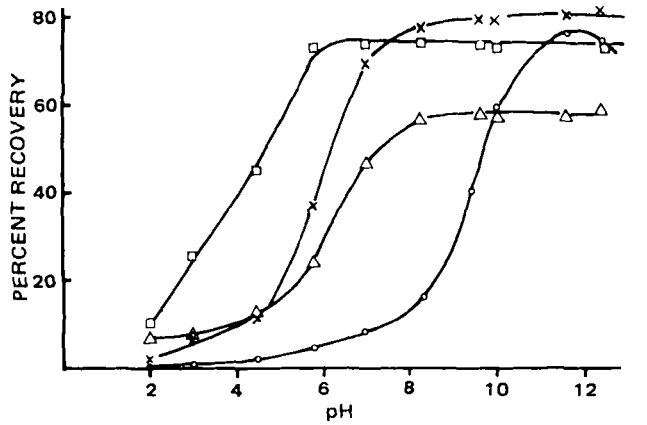

Figure 4—*Extraction efficiency* versus *pH value of urine samples. Two milliliters of urine containing a mixture of I–IV was extracted with 10% n-butyl alcohol–hexane at pH 11–11.5 by an extraction column. About 7 mL of the eluant was extracted with 0.4 mL of 0.1 M HCl. Each point represents the average of three determinations at four different concentrations. Key: (□) dextromethorphan (I); (x) dextrorphan (II); (○) 3-hydroxy-9α,13α,14α-morphinan (III); (△) 3-methoxy-9α,13α,-14α-morphinan (IV).*

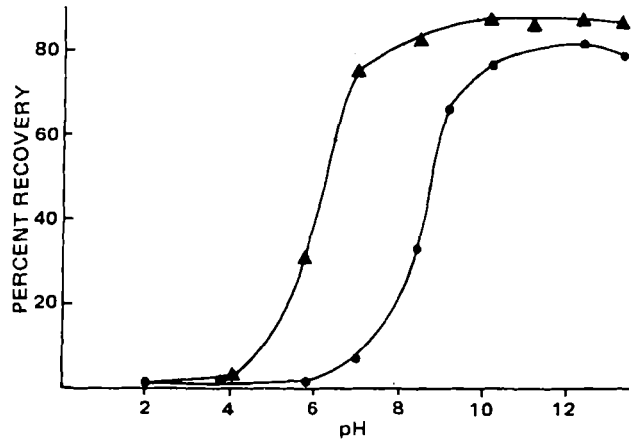

Figure 5—*Extraction efficiency* versus *pH value of urine samples. Two milliliters of enzyme-treated urine containing a mixture of I–IV was extracted with 6 mL of hexane at pH 12–12.5 by liquid–liquid extraction. The separated hexane extract was extracted with 0.2 mL of 0.1 M HCl. Each point represents the average of three determinations at three different concentrations. Key: (▲) dextromethorphan (I); (●) 3-methoxy-9α,13α,14α-morphinan (IV).*

and IV compared with II and III observed in hydrolyzed urine samples of humans who had received doses of dextromethorphan.

To carry out a simultaneous extraction of a mixture of compounds that have both acidic and basic functions, a pH profile is important. Using 10% *n*-butyl alcohol–hexane as the extracting solvent, the recoveries of I, II, and IV were constant over the pH range of 9–13. However, the recovery of III was markedly dependent on the pH, with the maximum occurring at pH 11–11.5 (Fig. 4).

Having optimized the pH, the next problem was efficient and clean extraction of dextromethorphan and its metabolites from urine, followed by back-extraction into a small volume of acid to effect removal of neutral materials and concentration of the compounds. A variety of solvents and solvent mixtures were investigated. Solvents such as hexane and toluene effectively extracted I and IV, but gave poor recovery of the more polar II and III. Relatively polar solvents such as 10 to 20% *n*-butyl alcohol in

Table I—Analysis of Dextromethorphan (I) in Nonhydrolyzed Validation Urine Samples

Nominal Value, μg/mL	Analyzed Value in Fresh Samples, μg/mL	Analyzed Value in Frozen Samples, μg/mL
0	<0.05	<0.09
	<0.05	<0.09
	<0.05	<0.09
0.5	0.50	0.52
	0.51	0.51
	0.49	0.50
Mean	0.50	0.51
SD (%)[a]	0.01 (2.0)	0.01 (1.9)
Mean % difference[b]	0.0	2.0
1.0	0.97	1.10
	1.03	1.05
	0.98	1.12
Mean	0.99	1.09
SD (%)[a]	0.03 (3.2)	0.03 (3.3)
Mean % difference[b]	−0.7	9.0
3.0	2.65	2.69
	2.64	2.70
	2.62	2.67
Mean	2.64	2.69
SD (%)[a]	0.01 (0.6)	0.01 (0.6)
Mean % difference[b]	−12.1	−10.4
5.0	4.57	4.71
	4.68	4.74
	4.44	4.57
Mean	4.56	4.67
SD (%)	0.12 (2.6)	0.09 (1.9)
Mean % difference[b]	−8.7	−6.5

[a] (%) = relative standard deviation = *SD*/mean × 100. [b] Mean % difference = (Mean − Nominal/Nominal) × 100.

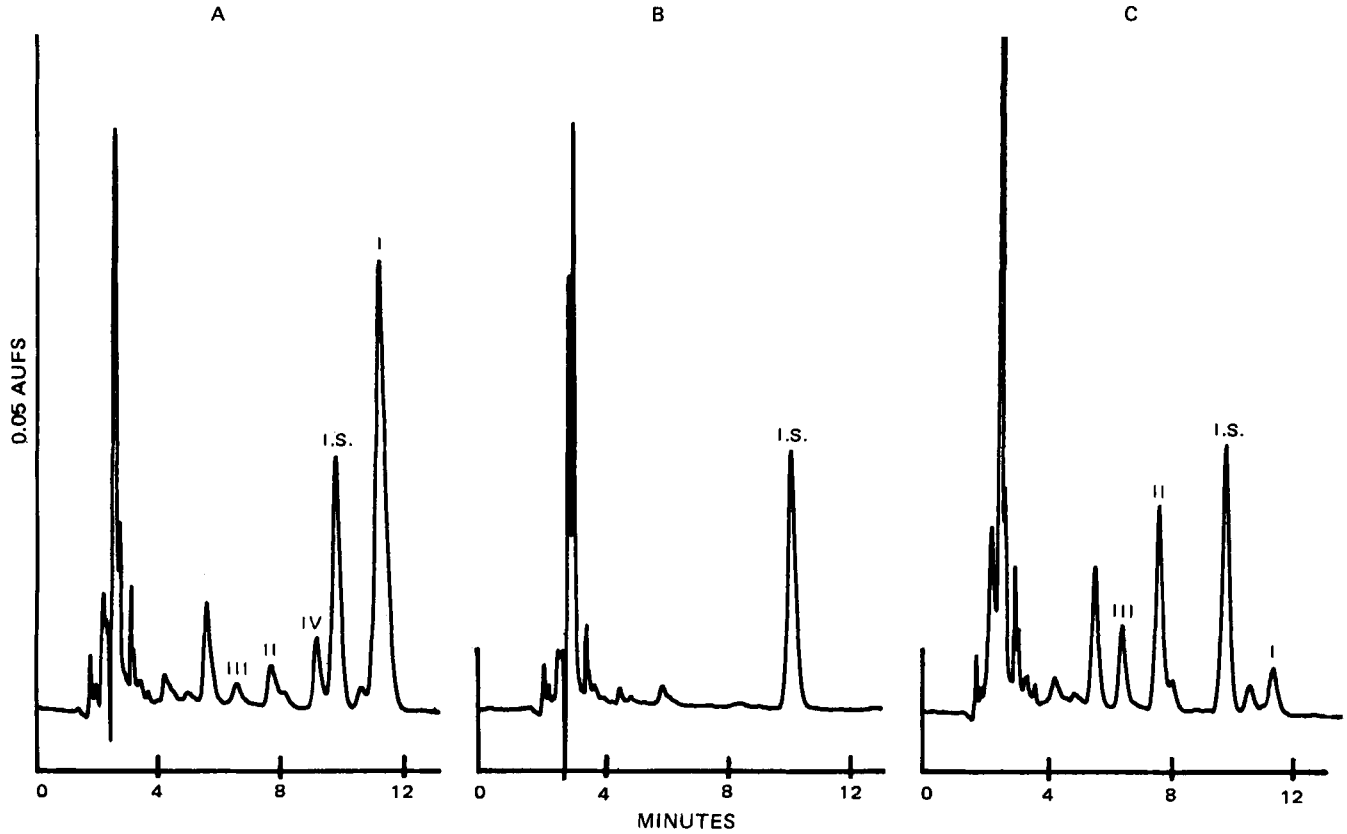

Figure 6—*Chromatograms of extracts of 2 mL of nonhydrolyzed 24-h urine samples from humans who were given 60 mg of dextromethorphan hydrobromide orally. Key: (A) sample determined to contain 0.04 μg of III, 0.26 μg of II, 0.66 μg of IV, and 4.83 μg of I/mL; (B) extracted control human urine samples containing only internal standard, 3-methoxy-17-methyl-10-oxo-9α,13α,14α-morphinan (0.5 μg/mL); (C) sample determined to contain 0.42 μg of III, 1.28 μg of II, and 0.49 μg of I/mL.*

either toluene or ethyl acetate gave high recoveries of I–IV, but the high solubility of their hydrochloride salts in the organic solvents gave poor extraction into the small volume of acidic phase needed for concentration and cleanup. The solvent chosen to satisfy all the criteria for the efficient simultaneous transfer of I–IV from the urine sample to a small volume of acid with low background was 10% *n*-butyl alcohol–hexane at pH 11–11.5. The recovery was ~80% for I, II, and III and 60% for IV.

A further problem that developed on analysis of hydrolyzed human

Table II—Analysis of Dextrorphan (II) in Nonhydrolyzed Validation Urine Samples

Nominal Value, μg/mL	Analyzed Value in Fresh Samples, μg/mL	Analyzed Value in Frozen Samples, μg/mL
0	<0.05	<0.033
	<0.05	<0.033
	<0.05	<0.033
0.2	0.20	0.19
	0.19	0.20
	0.20	0.21
Mean	0.20	0.20
SD (%)[a]	0.01 (2.9)	0.01 (5.0)
Mean % difference[a]	−1.7	0.0
1.0	1.03	0.96
	1.00	0.98
	1.02	0.96
Mean	1.02	0.97
SD (%)[a]	0.01 (1.5)	0.01 (1.2)
Mean % difference[a]	1.7	−3.3
3.0	2.90	3.04
	3.01	2.82
	2.88	3.05
Mean	2.93	2.97
SD (%)[a]	0.07 (2.4)	0.13 (4.4)
Mean % difference[a]	−2.3	−1.0
5.0	4.87	4.64
	4.83	4.82
	4.76	4.72
Mean	4.82	4.73
SD (%)[a]	0.06 (1.5)	0.09 (1.9)
Mean % difference[a]	−3.6	−5.5

[a] Defined in Table I.

Table III—Analysis of 3-Hydroxy-9α,13α,14α-morphinan (III) in Nonhydrolyzed Validation Samples

Nominal Value, μg/mL	Analyzed Value in Fresh Samples, μg/mL	Analyzed Value in Frozen Samples, μg/mL
0	<0.03	<0.017
	<0.03	<0.017
	<0.03	<0.017
0.2	0.21	0.21
	0.21	0.19
	0.21	0.22
Mean	0.21	0.21
SD (%)[a]	0.00 (0.0)	0.02 (7.4)
Mean % difference[a]	+5.0	+3.3
0.5	0.52	0.46
	0.52	0.47
	0.49	0.47
Mean	0.51	0.47
SD (%)[a]	0.02 (3.4)	0.01 (1.2)
Mean % difference[a]	+2.0	−6.7
2.0	2.06	1.81
	2.07	1.92
	1.93	1.95
Mean	2.02	1.89
SD (%)[a]	0.08 (3.8)	0.07 (3.9)
Mean % difference[a]	+1.0	−5.3
4.0	4.09	3.78
	4.03	4.21
	4.06	4.02
Mean	4.06	4.00
SD (%)[a]	0.03 (0.7)	0.21 (5.4)
Mean % difference[a]	+1.5	+0.08

[a] Defined in Table I.

Table IV—Analysis of 3-Methoxy-9α,13α,14α-morphinan (IV) in Nonhydrolyzed Validation Samples

Nominal Value, μg/mL	Analyzed Value in Fresh Samples, μg/mL	Analyzed Value in Frozen Samples, μg/mL
0	<0.05	<0.09
	<0.05	<0.09
	<0.05	<0.09
0.1	0.11	0.11
	0.10	0.11
	0.11	0.08
Mean	0.11	0.10
SD (%)[a]	0.01 (5.4)	0.02 (17.3)
Mean % difference[a]	6.7	0.0
0.5	0.51	0.52
	0.51	0.51
	0.50	0.52
Mean	0.51	0.52
SD (%)[a]	0.01 (1.1)	0.01 (1.1)
Mean % difference[a]	1.3	3.3
1.0	0.98	1.05
	1.01	1.03
	1.00	1.01
Mean	1.00	1.03
SD (%)[a]	0.01 (1.5)	0.02 (1.9)
Mean % difference[a]	−0.3	3.0
2.5	2.40	2.43
	2.40	2.54
	2.41	2.42
Mean	2.40	2.46
SD (%)[a]	0.01 (0.2)	0.07 (2.7)
Mean % difference[a]	−3.9	−1.5

[a] Defined in Table I.

urine samples from subjects given dextromethorphan was that the concentrations of I and IV were much lower than those of II and III. To increase sensitivity and decrease background interference for the analysis of I and IV, a sequential extraction procedure was designed. Compounds I and IV, which do not have a phenolic hydroxyl group, were selectively extracted from the enzyme-treated urine at pH 12–12.5 with hexane and back-extracted into 0.1 M HCl from the separated hexane extract. Compounds II and III, which remained in the aqueous layer, were extracted with 10% *n*-butyl alcohol–hexane at pH 11–11.5 as previously described for the simultaneous extraction of I–IV.

Two internal standards were required in this procedure: 3-methoxy-17-methyl-10-oxo-9α,13α,14α-morphinan was found to behave chemically and physically like I and IV, while thebaine was used for II and III. By this specific extraction procedure, the recoveries of I and IV were increased to 90–95% and 80–85%, respectively (Fig. 5), and the sensitivity for each compound was doubled, since the acid volume was reduced to one-half in the acid back-extraction. The recoveries of II and III were ~80%.

Table V—Analysis of Dextromethorphan (I) and 3-Methoxy-9α,13α,14α-morphinan (IV) in Enzyme-Treated Validation Samples

Dextromethorphan		3-Methoxy-9α,13α,14α-morphinan	
Nominal Value, μg/mL	Analyzed[a] Value, μg/mL	Nominal Value, μg/mL	Analyzed[a] Value, μg/mL
0.1	<0.15	0.1	<0.15
	<0.15		<0.15
	<0.15		<0.15
0.5	0.51	0.5	0.43
	0.49		0.40
	0.50		0.40
Mean	0.50		0.41
SD (%)[b]	0.01 (2.0)		0.02 (4.2)
Mean % difference[b]	0.0		−18.0
1.0	1.02	1.0	0.86
	1.03		0.85
	1.02		0.89
Mean	1.02		0.87
SD (%)[b]	0.01 (0.5)		0.02 (2.4)
Mean % difference[b]	2.3		−13.3
4.0	4.35	3.0	3.00
	3.85		2.91
	3.79		3.00
Mean	4.00		2.97
SD (%)[b]	0.30 (7.7)		0.05 (1.7)
Mean % difference[b]	−0.08		−1.0

[a] Analyzed immediately after preparation. [b] Defined in Table I.

Table VI—Analysis of Dextrorphan (II) and 3-Hydroxy-9α,13α,14α-morphinan (III) in Enzyme-Treated Validation Samples

Dextrorphan		3-Hydroxy-9α,13α,14α-morphinan	
Nominal Value, μg/mL	Analyzed[a] Value, μg/mL	Nominal Value, μg/mL	Analyzed[a] Value, μg/mL
0	<0.11	0.05	<0.21
	<0.11		<0.21
	<0.11		<0.21
0.5	0.53	0.2	0.31
	0.53		0.22
	0.53		0.23
Mean	0.53		0.25
SD (%)[b]	0.00 (0.0)		0.05 (19.5)
Mean % difference[b]	6.0		26.5
1.0	1.03	0.5	0.60
	1.00		0.47
	0.97		0.50
Mean	1.00		0.52
SD (%)[b]	0.03 (3.0)		0.07 (13.0)
Mean % difference[b]	0.0		4.7
3.0	2.99	2.0	2.21
	2.97		1.84
	2.97		2.05
Mean	2.98		2.03
SD (%)[b]	0.01 (0.4)		0.18 (9.1)
Mean % difference[b]	−0.8		1.7
5.0	4.88	4.0	4.37
	4.92		3.52
	5.13		3.85
Mean	4.98		3.91
SD (%)[b]	0.13 (2.7)		0.43 (10.9)
Mean % difference[b]	−0.47		−2.2

[a] Analyzed immediately after preparation. [b] Defined in Table I.

Assay Sensitivity and Precision—The standard curves for I–IV in nonhydrolyzed urine samples fit a linear model ($r > 0.997$) over the range of 0.05–5.0 μg of base/mL. Similarly, the standard curves for I–IV in hydrolyzed urine samples were linear ($r > 0.995$) over the range of 0.10–10.0 μg of base/mL. The range of minimum quantifiable levels, determined as that concentration whose lower 80% confidence limit just encompasses zero (8), was 0.017–0.09 μg of base/mL and 0.11–0.21 μg of base/mL for I–IV in nonhydrolyzed and hydrolyzed urine samples, respectively.

The accuracy of the assays, expressed as the mean percent difference, ranged from −12.1% to 9.0% over all concentrations of I–IV in nonhydrolyzed urine (Tables I–IV) and −18.0% to 26.5% in hydrolyzed urine (Tables V and VI). The precision of the assay, expressed as the mean % *SD*, was 2.93 ± 3.1% ($n = 32$) for all concentrations of I–IV in nonhydrolyzed urine samples and 5.51 ± 5.77% ($n = 14$) for all concentrations in hydrolyzed urine. Quantitation of each compound assayed immediately after preparation and after freezing (Tables I–IV) showed that there was no loss of drugs due to freezing the urine samples.

Chromatograms of I and free (unconjugated) II–IV in 24-h urine samples of humans who were dosed with 60 mg of dextromethorphan hydrobromide orally are presented in Fig. 6. Compared with Fig. 6C, Fig. 6A shows relatively high concentrations of I (4.83 μg of base/mL) and IV (0.66 μg of base/mL) and low concentrations of the polar metabolites, III (0.04 μg of base/mL) and II (0.26 μg of base/mL). In Fig. 6C, the concentrations of I, II, and III were 0.49, 1.28, and 0.42 μg of base/mL, respectively; IV was not detected. Figure 6B is a chromatogram of the extract of a control human urine sample containing the internal standard. Results of the assay of urine samples from clinical studies will be reported separately.

The simultaneous quantitation of dextromethorphan and its urinary metabolites provided several challenges in the development of both extraction and chromatographic methods. The methods presented are

precise, accurate, specific, and sensitive for the assay of dextromethorphan and its urinary metabolites and have been used to quantitate these compounds in urine from humans who received a therapeutic dose of dextromethorphan hydrobromide.

REFERENCES

(1) B. Calesnick and J. A. Christensen, *Clin. Pharmacol. Ther.*, **8**, 374 (1967).

(2) J. W. Barnhart and E. N. Massad, *J. Chromatogr.*, **163**, 390 (1979).

(3) J. E. O'Brien, O. N. Hinsvark, W. R. Newman, L. P. Amsel, J. E. Giering, and F. E. Leaders, Jr., *National Bureau of Standards Special Publication 519, Trace Organic Analysis:* A New Frontier in Analytical Chemistry, Proceedings of the 9th Materials Research Symposium, April 1978, NBS, Gaithersburg, Md.

(4) O. N. Hinsvark, J. O'Brien, W. Zazulak, L. Amsel, and J. E. Giering, Presented at Pittsburgh Conference on Analytical Chemistry and Applied Spectroscopy, Atlantic City, N.J., March 1981. *Abstracts*, p. 333.

(5) J. W. Barnhart, *Toxicol. Appl. Pharmacol.*, **35**, 43 (1980).

(6) M. M. Abdel-Monem and P. S. Portoghese, *J. Med. Chem.*, **15**, 208 (1972).

(7) O. Härlinger, A. Brossi, L. H. Chopard-dit-Jean, M. Walter, and O. Schnider, *Helv. Chim. Acta*, **39**, 2053 (1956).

(8) R. W. Ross and H. Stander, "Some Statistical Problems in Drug Metabolism," paper presented at the Princeton Conference on Applied Statistics, December 1975.

ACKNOWLEDGMENTS

Presented at the Chromatography Section, Northeast Regional Meeting of the American Chemical Society, Rochester, N.Y., October 1981.

Effect of Renal Failure and Bis(2-ethylhexyl) Phthalate Pretreatment on the Disposition and Metabolism of Antipyrine in the Rat

GARY M. POLLACK and DANNY D. SHEN ˣ

Received June 16, 1982, from the *Department of Pharmaceutics, School of Pharmacy, State University of New York at Buffalo, Amherst, NY 14260.* Accepted for publication October 15, 1982.

Abstract □ Renal failure patients undergoing hemodialysis are regularly exposed to phthalate plasticizers leached from dialysis tubings. Previous studies have shown that antipyrine is eliminated more rapidly in chronic renal failure patients compared with normal individuals. Therefore, the effect of bis(2-ethylhexyl) phthalate on the metabolism of antipyrine was investigated in normal and renal failure rats. In normal animals, the elimination kinetics of an intravenous dose of antipyrine (20 mg/kg) was determined before and after 14 days of peroral treatment with 2 mL/kg/d of bis(2-ethylhexyl) phthalate. The plasma clearance of antipyrine increased markedly after bis(2-ethylhexyl) phthalate treatment. There was a corresponding decrease in the elimination half-life of antipyrine, whereas the apparent volume of distribution was not affected. Both liver weight and hepatic cytochrome P_{450} content increased following exposure to bis(2-ethylhexyl) phthalate, indicating the induction of hepatic microsomal enzymes. The fractional urinary recovery of the *N*-demethyl, 4-hydroxy, and 3-hydroxymethyl metabolites of antipyrine was not altered, suggesting that all three oxidative pathways were induced to the same extent. Renal failure alone did not affect the elimination kinetics of antipyrine. However, antipyrine clearance was induced to a greater extent by bis(2-ethylhexyl) phthalate treatment in the renal failure rats as compared with the control animals. The potential for phthalate plasticizers to alter hepatic drug metabolism in hemodialysis patients should be considered.

Keyphrases □ Antipyrine—disposition, pharmacokinetics, effect of bis(2-ethylhexyl) phthalate pretreatment and renal failure, rats □ Bis(2-ethylhexyl) phthalate—pretreatment, effect on antipyrine disposition and pharmacokinetics, renal failure, rats □ Renal failure—effect on antipyrine disposition and pharmacokinetics, rats, bis(2-ethylhexyl) phthalate pretreatment

There is increasing evidence suggesting that the metabolism of some drugs may be altered in renal failure (1). In general, an inhibition of drug metabolism is observed; *e.g.*, the oxidative metabolism of propranolol (2) and propoxyphene (3) and the acetylation of drugs such as sulfisoxazole (4) and aminosalicylic acid (5) are apparently inhibited in uremia. Phenytoin (6, 7) and antipyrine (8–10) are apparent exceptions to this rule, as the metabolic clearance of these compounds has been reported to be increased in patients with renal insufficiency.

The increased metabolic clearance of phenytoin in patients with renal failure is attributed to reduced protein binding of this drug in uremic serum (11). Antipyrine, however, is only slightly bound to serum and tissue proteins (12), and a decrease in serum protein binding would not be expected to significantly alter the metabolic clearance of this drug. Alternative explanations for this phenomenon, therefore, should be considered.

It is known that plasticizers can be leached from plastic medical devices such as blood transfusion bags and hemodialysis tubing into blood and certain intravenous fluids. The most common plasticizer used in the production of medical-grade plastics, bis(2-ethylhexyl) phthalate (I), has been identified as a contaminant in blood that was stored in transfusion bags (13, 14) or passed through plastic tubing (15). Clinical studies have shown that patients undergoing maintenance hemodialysis are regularly exposed to I (16, 17). Serum concentrations of I in the microgram/milliliter range were observed in renal failure patients during hemodialysis. It is possible that impaired renal function and repeated dialysis may lead to significant accumulation of I and its metabolites in hemodialysis patients (18).

Animal studies have shown that chronic exposure to I can induce changes in the *in vitro* activities of a number of hepatic drug-metabolizing enzymes (19–23). Both inhibition and induction of hepatic enzymatic activities have been observed. The reason for these conflicting results between studies may be due to variations in the selection of drug substrate, treatment schedule, and route of ad-

0022-3549/84/0100-0029$01.99/0

© 1984, American Pharmaceutical Association

precise, accurate, specific, and sensitive for the assay of dextromethorphan and its urinary metabolites and have been used to quantitate these compounds in urine from humans who received a therapeutic dose of dextromethorphan hydrobromide.

REFERENCES

(1) B. Calesnick and J. A. Christensen, *Clin. Pharmacol. Ther.*, **8**, 374 (1967).

(2) J. W. Barnhart and E. N. Massad, *J. Chromatogr.*, **163**, 390 (1979).

(3) J. E. O'Brien, O. N. Hinsvark, W. R. Newman, L. P. Amsel, J. E. Giering, and F. E. Leaders, Jr., *National Bureau of Standards Special Publication 519, Trace Organic Analysis:* A New Frontier in Analytical Chemistry, Proceedings of the 9th Materials Research Symposium, April 1978, NBS, Gaithersburg, Md.

(4) O. N. Hinsvark, J. O'Brien, W. Zazulak, L. Amsel, and J. E. Giering, Presented at Pittsburgh Conference on Analytical Chemistry and Applied Spectroscopy, Atlantic City, N.J., March 1981. *Abstracts*, p. 333.

(5) J. W. Barnhart, *Toxicol. Appl. Pharmacol.*, **35**, 43 (1980).

(6) M. M. Abdel-Monem and P. S. Portoghese, *J. Med. Chem.*, **15**, 208 (1972).

(7) O. Härlinger, A. Brossi, L. H. Chopard-dit-Jean, M. Walter, and O. Schnider, *Helv. Chim. Acta*, **39**, 2053 (1956).

(8) R. W. Ross and H. Stander, "Some Statistical Problems in Drug Metabolism," paper presented at the Princeton Conference on Applied Statistics, December 1975.

ACKNOWLEDGMENTS

Presented at the Chromatography Section, Northeast Regional Meeting of the American Chemical Society, Rochester, N.Y., October 1981.

Effect of Renal Failure and Bis(2-ethylhexyl) Phthalate Pretreatment on the Disposition and Metabolism of Antipyrine in the Rat

GARY M. POLLACK and DANNY D. SHEN ˣ

Received June 16, 1982, from the *Department of Pharmaceutics, School of Pharmacy, State University of New York at Buffalo, Amherst, NY 14260.* Accepted for publication October 15, 1982.

Abstract □ Renal failure patients undergoing hemodialysis are regularly exposed to phthalate plasticizers leached from dialysis tubings. Previous studies have shown that antipyrine is eliminated more rapidly in chronic renal failure patients compared with normal individuals. Therefore, the effect of bis(2-ethylhexyl) phthalate on the metabolism of antipyrine was investigated in normal and renal failure rats. In normal animals, the elimination kinetics of an intravenous dose of antipyrine (20 mg/kg) was determined before and after 14 days of peroral treatment with 2 mL/kg/d of bis(2-ethylhexyl) phthalate. The plasma clearance of antipyrine increased markedly after bis(2-ethylhexyl) phthalate treatment. There was a corresponding decrease in the elimination half-life of antipyrine, whereas the apparent volume of distribution was not affected. Both liver weight and hepatic cytochrome P_{450} content increased following exposure to bis(2-ethylhexyl) phthalate, indicating the induction of hepatic microsomal enzymes. The fractional urinary recovery of the *N*-demethyl, 4-hydroxy, and 3-hydroxymethyl metabolites of antipyrine was not altered, suggesting that all three oxidative pathways were induced to the same extent. Renal failure alone did not affect the elimination kinetics of antipyrine. However, antipyrine clearance was induced to a greater extent by bis(2-ethylhexyl) phthalate treatment in the renal failure rats as compared with the control animals. The potential for phthalate plasticizers to alter hepatic drug metabolism in hemodialysis patients should be considered.

Keyphrases □ Antipyrine—disposition, pharmacokinetics, effect of bis(2-ethylhexyl) phthalate pretreatment and renal failure, rats □ Bis(2-ethylhexyl) phthalate—pretreatment, effect on antipyrine disposition and pharmacokinetics, renal failure, rats □ Renal failure—effect on antipyrine disposition and pharmacokinetics, rats, bis(2-ethylhexyl) phthalate pretreatment

There is increasing evidence suggesting that the metabolism of some drugs may be altered in renal failure (1). In general, an inhibition of drug metabolism is observed; *e.g.*, the oxidative metabolism of propranolol (2) and propoxyphene (3) and the acetylation of drugs such as sulfisoxazole (4) and aminosalicylic acid (5) are apparently inhibited in uremia. Phenytoin (6, 7) and antipyrine (8–10) are apparent exceptions to this rule, as the metabolic clearance of these compounds has been reported to be increased in patients with renal insufficiency.

The increased metabolic clearance of phenytoin in patients with renal failure is attributed to reduced protein binding of this drug in uremic serum (11). Antipyrine, however, is only slightly bound to serum and tissue proteins (12), and a decrease in serum protein binding would not be expected to significantly alter the metabolic clearance of this drug. Alternative explanations for this phenomenon, therefore, should be considered.

It is known that plasticizers can be leached from plastic medical devices such as blood transfusion bags and hemodialysis tubing into blood and certain intravenous fluids. The most common plasticizer used in the production of medical-grade plastics, bis(2-ethylhexyl) phthalate (I), has been identified as a contaminant in blood that was stored in transfusion bags (13, 14) or passed through plastic tubing (15). Clinical studies have shown that patients undergoing maintenance hemodialysis are regularly exposed to I (16, 17). Serum concentrations of I in the microgram/milliliter range were observed in renal failure patients during hemodialysis. It is possible that impaired renal function and repeated dialysis may lead to significant accumulation of I and its metabolites in hemodialysis patients (18).

Animal studies have shown that chronic exposure to I can induce changes in the *in vitro* activities of a number of hepatic drug-metabolizing enzymes (19–23). Both inhibition and induction of hepatic enzymatic activities have been observed. The reason for these conflicting results between studies may be due to variations in the selection of drug substrate, treatment schedule, and route of ad-

0022-3549/84/0100-0029$01.99/0

© 1984, American Pharmaceutical Association

Table I—Pharmacokinetic Parameters for Antipyrine Disposition in Normal Rats Receiving Corn Oil or Phthalate Treatment [a]

Parameter	Corn Oil		Phthalate	
	Pretreatment	Posttreatment	Pretreatment	Posttreatment
CL_p, mL/min/kg	3.30 (0.44)	4.18 (0.49)	3.86 (0.51)	7.81 (0.53)[b]
Vd_β (area), mL/kg	726 (98)	755 (79)	859 (58)	755 (56)
$t_{1/2\beta}$, min	153 (13)	128 (9)	165 (22)	67.2 (3.1)[b]

[a] Results are expressed as mean (±*SE*) of *n* determinations; $n = 9$ for corn oil and $n = 7$ for phthalate. [b] Significantly different from pretreatment, $p < 0.005$.

ministration of the phthalate. Moreover, appropriate *in vivo* metabolic studies are seldom available for *in vitro–in vivo* correlations.

The primary purpose of the present study was to determine whether chronic treatment with I can induce the *in vivo* metabolism of antipyrine in rats, which may provide a plausible explanation for the apparent increase in the metabolic clearance of this drug in chronic renal failure patients. Secondly, studies were performed in rats with experimentally induced renal failure to assess the effect of uremia on antipyrine metabolism. In addition, possible modulation of the metabolic effect of I in the presence of renal failure was investigated.

EXPERIMENTAL

Chemicals—Antipyrine, *N*-demethylantipyrine, 4-hydroxyantipyrine, and 3-hydroxymethylantipyrine were supplied[1]. Bis(2-ethylhexyl) phthalate[2], and β-glucuronidase–aryl sulfatase[3], in the form of limpet acetone powder (type I) were purchased and used without further purification.

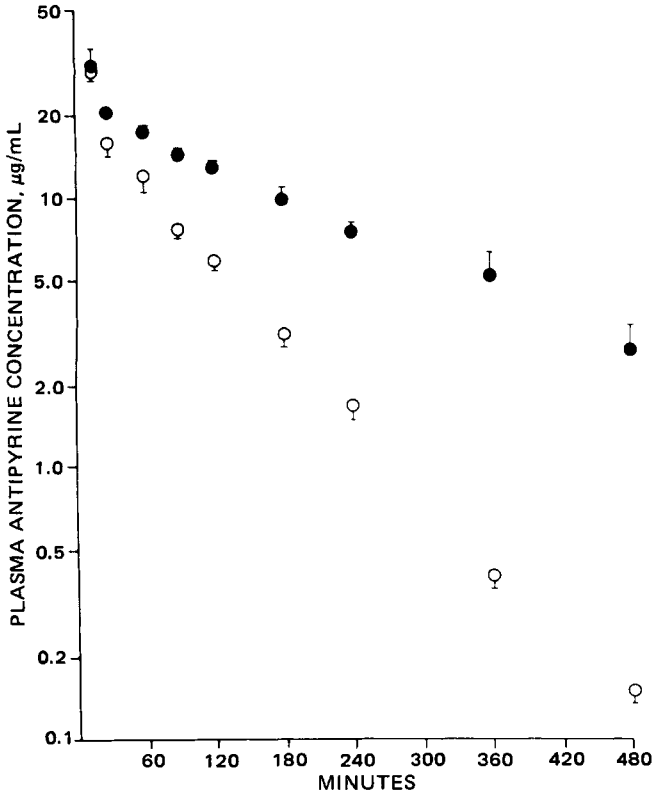

Figure 1—*Mean antipyrine plasma concentration–time profile in rats before (●) and after (○) a 14-d treatment with I. Bars represent* SE.

[1] Supplied by Dr. Charles Hignite, Veterans Administration Medical Center, Kansas City, Mo. and Professor Gerhard Levy, State University of New York at Buffalo.

[2] Aldrich Chemical Co., Milwaukee, Wis.

[3] Sigma Chemical Co., St. Louis, Mo.

Table II—Liver Weights and Antipyrine Clearance Normalized for Liver Weight in Corn Oil- and Phthalate-Treated Rats [a]

	Corn Oil	Phthalate
Wet liver weight, g/kg	30.7 (1.6)	48.2 (0.9)[b]
CL_p, mL/min/g of liver	0.139 (0.017)	0.162 (0.012)

[a] Results are expressed as mean (±*SE*) of *n* determinations; $n = 9$ for corn oil and $n = 7$ for phthalate. [b] Significantly different from corn oil, $p < 0.005$.

Table III—Comparison of Cumulative Urinary Recovery of Antipyrine and Metabolites Between Corn Oil and Phthalate Treatments [a]

Compound	Corn Oil	Phthalate
Antipyrine	2.11 (0.38)	3.26 (0.65)
N-Demethylantipyrine	2.97 (0.61)	2.08 (0.32)
4-Hydroxyantipyrine	17.8 (4.7)	13.0 (2.8)
3-Hydroxymethylantipyrine	26.1 (2.3)	24.9 (2.8)
Total	48.9 (5.5)	43.2 (3.4)

[a] Results are expressed as mean percent of dose (±*SE*) of six determinations.

Studies in Normal Rats—*Antipyrine Clearance Kinetics*—Male Sprague–Dawley rats[4] weighing 300–350 g were used. A silicone rubber cannula was implanted in the right jugular vein under ether anesthesia 48 h before the first experiment. Antipyrine (20 mg/kg) dissolved in physiological saline (10 mg/mL) was administered through the cannula. Serial venous blood samples (0.2–0.3 mL) were drawn through the cannula over an 8-h period and collected in heparinized tubes. The plasma was separated and stored at −20°C until assayed. Food was restricted only during the blood collection period, and water was available *ad libitum* throughout the entire experiment. The plasma concentration of antipyrine was determined by the high-performance liquid chromatographic (HPLC) procedure of Danhof *et al.* (24).

Following the blood sampling, I dissolved in corn oil (2:3 v/v) or corn oil alone was administered once daily for 14 days *via* gastric intubation. The total volume administered was 5 mL/kg/d, yielding a dosage of I of 2 mL/kg/d or 1.96 g/kg/d, which is comparable to dosages employed in previous studies of the effect of I on *in vitro* hepatic drug-metabolizing enzyme activities.

On the final treatment day, a silicone rubber cannula was implanted in the left jugular vein under ether anesthesia, and the posttreatment time course of antipyrine was determined 48 h later. The 48-h washout period was included to avoid the possibility of direct effects of the plasticizer on the disposition of antipyrine. It has been shown that a single dose of radiolabeled I is completely eliminated in the rat within this time period (25). Following blood sampling the animals were sacrificed and the livers were excised and weighed.

The pretreatment and posttreatment antipyrine plasma concentration time course data were fit to a biexponential equation using a nonlinear least-squares regression computer program (26). The apparent volume of distribution (Vd_β), plasma clearance (CL_p), and terminal disposition half-life ($t_{1/2\beta}$) were calculated.

Urinary Recovery of Antipyrine Metabolites—Rats weighing 300–350 g were treated with I or corn oil for 14 d as in the previous experiment. Antipyrine (20 mg/kg) was administered intravenously *via* the dorsal tail vein under light ether anesthesia 48 h following the final day of treatment. The rats were placed in plastic metabolism cages, and urine was collected for 24 h. Urinary excretion of antipyrine and its metabolites has been reported to be essentially complete within 8 h (27). Food and water were available *ad libitum* during the urine collection period. The urine samples were incubated with β-glucuronidase–aryl sulfatase (limpet acetone powder) at 37°C for 3 h, and the total (free plus conjugated) amounts of 4-hydroxyantipyrine, 3-hydroxymethylantipyrine, *N*-demethylantipyrine, and the parent drug were then assayed by the HPLC method of Danhof *et al.* (24).

Hepatic Hemoprotein Content—Rats weighing 265–315 g were treated for 14 d with I or corn oil as in the previous experiment. Twenty-four hours following the final treatment, the animals were anesthetized lightly with ether and exsanguinated by cutting the renal blood vessels. The livers were quickly excised, washed in ice-cold 0.25 M sucrose, blotted dry, and weighed. Following homogenization in ice-cold 0.25 M sucrose (1:4 w/v) the hepatic microsomes were isolated by the calcium precipi-

[4] Blue Spruce Farms, Altamont, N.Y.

Table IV—Hepatic Microsomal Protein and Hemoprotein Content in Rats Treated with Corn Oil or Phthalate [a]

	Corn Oil	Phthalate
Wet liver weight, g/kg	24.9 (2.1)	44.6 (3.1)[c]
Total microsomal protein, mg/g of liver	23.8 (4.0)	24.7 (9.4)
Cytochrome p_{450}, nmol/mg of protein	0.544 (0.004)	0.860 (0.112)[b]
nmol/g of liver	13.0 (1.1)	19.5 (1.6)[c]
Cytochrome b_5 nmol/mg of protein	0.310 (0.037)	0.338 (0.051)
nmol/g of liver	7.53 (1.24)	8.96 (2.57)

[a] Values are mean (±*SE*) of five determinations. [b] Significantly different from corn oil, $p < 0.05$. [c] Significantly different from corn oil, $p < 0.001$.

tation method of Kamath and Rubin (28). The microsomal content of cytochrome P_{450} and cytochrome b_5 was determined spectrophotometrically as described by Omura and Sato (29). Microsomal protein content was determined by the method of Lowry *et al.* (30).

Studies in Renal Failure Animals—Renal failure was induced by a two-step subtotal nephrectomy (31). Two-thirds of the right kidney was removed in the first step, followed by removal of the entire left kidney 1 week later. The sham procedure consisted of removal of the connective tissue surrounding the appropriate kidney on each of the 2 surgical days. Care was taken at all times to avoid damaging the adrenal glands. Penicillin-G (20,000 U/kg) and streptomycin (10 mg/kg) were administered intramuscularly following each surgical procedure to prevent infection and reduce mortality (31). Preliminary studies with this renal failure model showed that the procedure significantly elevated the serum creatinine level without affecting the serum glutamic pyruvic transaminase activity, indicating that subtotal nephrectomy does not produce hepatic damage.

Renal failure and sham-operated animals received the following treatments: (1) sham-operated rat dosed with corn oil; (2) renal failure rat dosed with corn oil; (3) sham-operated rat dosed with 0.5 mL/kg/d of I; (4) renal failure rat dosed with 0.5 mL/kg/d of I; (5) sham-operated rat dosed with 2 mL/kg/d of I; and (6) renal failure rat dosed with 2 mL/kg/d of I. The treatment scheme was designed to ascertain the effect of renal failure on antipyrine elimination. In addition, the combined effect of renal failure and phthalate pretreatment was assessed at low (0.5 mL/kg/d) and high (2 mL/kg/d) dosages of I.

Phthalate treatment began 48 h after the completion of the nephrectomy procedure (*i.e.*, after the second surgical day). The renal function of nephrectomized rats remains depressed for 10 d after surgery. Thereafter, a gradual recovery in renal function is observed in some animals. Therefore, the length of phthalate treatment was reduced to 7 d as compared with the 2-week period in the studies with normal animals. At 48 h after the final dose of I, the elimination kinetics of antipyrine was determined as previously described.

Statistical Analysis—The paired Student's t test was used to test the significance of differences between means of the pretreatment and posttreatment antipyrine pharmacokinetic parameters. Differences between the phthalate and corn oil treatment in normal animals were analyzed using the unpaired Student's t test. The Wilcoxon summed ranks test was used to test the significance of differences between the uremic and sham-operated animals receiving I or corn oil. A probability level of $p < 0.05$ was considered statistically significant.

RESULTS

Studies in Normal Rats—*Antipyrine Disposition*—The mean antipyrine pharmacokinetic parameters for the corn oil- and phthalate-treated animals are presented in Table I. The disposition of antipyrine was not significantly affected by corn oil administration, although there was a trend towards an increased CL_p and decreased $t_{1/2}$. In contrast, treatment with I resulted in a significant increase in plasma clearance and a decrease in the terminal disposition half-life of antipyrine. No alteration in the volume of distribution was observed. The mean pre- and posttreatment antipyrine concentration–time profiles for the phthalate-treated animals are presented in Fig. 1.

Liver weight data are presented in Table II. A significant increase in wet liver weight was observed following treatment with I. When the posttreatment plasma clearance of antipyrine was normalized for wet liver weight, the difference between the two groups was no longer statistically significant.

Urinary Excretion of Antipyrine Metabolites—A comparison of the mean cumulative urinary recovery of antipyrine and three of its oxidative metabolites in the corn oil and phthalate groups is presented in Table III. None of the differences between the two groups were statistically significant, indicating that the three major metabolic pathways of antipyrine, *i.e.*, *N*-demethylation, hydroxylation at the 4 position of the pyrazole ring, and hydroxylation at the 3-methyl side chain, were uniformly induced by I.

Hepatic Hemoproteins—The hepatic hemoprotein data are presented in Table IV. In comparison with control animals, treatment with I significantly increased the hepatic content of cytochrome P_{450} and the weight of the liver. The recovery of microsomal protein per gram of wet liver and the hepatic content of cytochrome b_5 were not significantly altered.

Table V—Mean Serum Creatinine Concentrations (mg/dL) in the Six Treatment Groups

Treatments[a]	Mean ± *SE*
1	0.356 ± 0.046
2	0.490 ± 0.041
3	0.452 ± 0.031
4	2.21 ± 0.51[b]
5	1.37 ± 0.06[b]
6	1.71 ± 0.35[b]

[a] See text for explanation of treatment codes. [b] Significantly different from their respective sham-operated controls ($p < 0.005$).

Studies in Renal Failure Rats—Serum creatinine concentrations at the time of antipyrine studies in the various treatment groups are given in Table V. Subtotal nephrectomy increased serum creatinine three- to fivefold, while phthalate treatment apparently had no effect on creatinine concentrations.

The mean antipyrine plasma clearances and half-lives for the nephrectomized animals and sham-operated controls are given in Tables VI and VII, respectively. Nephrectomy alone did not significantly affect the disposition of antipyrine in the corn oil-treated animals. As in the earlier study in normal rats, administration of I to the sham-operated animals resulted in a significant increase in CL_p and a corresponding decrease in $t_{1/2}$. Treatment with I at a dose of 2 mL/kg/d produced significantly greater changes in the elimination kinetics of antipyrine than a lower dose of 0.5 mL/kg/d, suggesting that the magnitude of the increase in antipyrine clearance is related to the dose of plasticizer administered. The apparent volume of distribution was not affected by nephrectomy, pretreatment with I, or combinations thereof. Equivalent doses of I tended to produce a greater increase in antipyrine clearance in the nephrectomized animals as compared with the sham-operated controls. The differences between the two groups are statistically significant at the low dose of I, but not at the high dose. The lack of a difference at the high dose of I may be due to the large variability in the clearance estimates in the renal failure group. Alternatively, near maximal induction may have been reached with the phthalate dosage of 2 mL/kg/d such that any enhancement in response in the presence of renal failure was not readily discernible.

The effects of nephrectomy and phthalate treatment on wet liver weight per kilogram of body weight are presented in Table VIII. Nephrectomy alone tended to decrease liver weight slightly, although the difference was statistically significant. It is likely that this difference is the result of a decreased food intake in these animals. Phthalate treatment led to a marked increase in liver weight in both renal failure and sham-operated control animals. There was no significant difference in liver weight between the nephrectomized and sham-operated control animals at either phthalate dosage level, possibly because the decrease in liver weight due to uremia was partly offset by an increase response to the plasticizer in the renal failure rats.

DISCUSSION

Chronic exposure to I can induce hepatic drug metabolism in the rat. The magnitude of increase in the plasma clearance and the decrease in terminal disposition half-life of antipyrine following chronic treatment with I is comparable to the reported changes in antipyrine disposition produced by phenobarbital (27), 3-methylcholanthrene (27), and polychlorinated biphenyls (32). Also, the increase in antipyrine clearance was dependent on the pretreatment dosage of I.

The urinary recovery of the *N*-demethyl and hydroxyl metabolites of antipyrine remained unchanged after treatment with I. Danhof *et al.* (27) showed that 3-methylcholanthrene preferentially induced the 4-hydroxylation pathway in the metabolism of antipyrine in rats, while phe-

Table VI—Antipyrine Clearance (mL/min/kg) in Renal Failure and Sham-Control Rats after Treatment with Corn Oil or Phthalate

Statistical Comparisons[a]	Treatments[b] 1	2	3	4	5	6
Mean (n)	3.71 (7)	3.83 (7)	5.14 (6)	6.56 (5)	7.54 (7)	9.53 (7)
SE	0.11	0.24	0.38	0.13	0.58	1.20
Between renal failure and sham-operated rats treated with corn oil	NS[c]	$p < 0.05$				
Between low- and high-dose phthalate in sham-operated rats			$p < 0.001$	$p < 0.05$		
Between low- and high-dose phthalate in renal failure rats			$p < 0.005$	$p < 0.001$	$p < 0.005$	
Between renal failure and sham-operated rats treated with phthalate				$p < 0.05$		NS

[a] Wilcoxon's summed rank test. [b] See text for explanation of treatment codes. [c] No statistically significant difference.

nobarbital treatment resulted in an almost uniform stimulation of all known metabolic pathways. The present urinary metabolite data suggest that induction of antipyrine metabolism by I resembles induction produced by phenobarbital more closely than that produced by 3-methylcholanthrene. However, it should be noted that in our study as well as in others, only ~50% of the antipyrine dose could be accounted for as either intact antipyrine or its known metabolites in urine. A previous study of Aarbakke (33) in rats with radiolabeled antipyrine showed that ~74% of the radioactive dose is recovered in urine while <3% appeared in the feces and expired air. Recently, 4,4′-dihydroxyantipyrine was identified as a metabolite in rat urine (34). Therefore, the effect of I on other metabolic pathways of antipyrine is presently unknown.

The increase in hepatic cytochrome P_{450} content following treatment with I is similar in magnitude to that reported by other investigators (19, 20, 22, 23). It is well recognized that treatment with 3-methylcholanthrene results in a shift in the wavelength maximum of the carbon monoxide difference spectrum of reduced hepatic microsomes from 450 nm to 448 nm, whereas no such shift is observed with liver microsomes from phenobarbital-induced animals. The carbon monoxide difference spectrum of reduced microsomes from both control and phthalate-treated rats in the present study displayed a maximum at 450 nm. This finding would also suggest that the inductive properties of I more closely resemble phenobarbital than 3-methylcholanthrene.

Treatment with I had no apparent effect on the hepatic content of cytochrome b_5. Little data concerning the induction of this cytochrome is available; however, phenobarbital (35) has been reported to increase hepatic cytochrome b_5. This may indicate a subtle difference between the inductive properties of I and phenobarbital. The importance of this difference, however, is not known.

It should be noted that normalizing the plasma clearance of antipyrine by liver weight rather than body weight, eliminates any significant difference between the phthalate and corn oil groups. This would suggest that the clearance of antipyrine is governed primarily by the amount of normally functioning hepatic tissue present in the organism. The lack of a significant difference in mean plasma clearance per gram of liver weight between the phthalate and corn oil groups also suggests that, while I increases the amount of hepatic tissue, it does not change the intrinsic metabolic activity of the newly generated tissue towards antipyrine.

The elimination of antipyrine was not altered by the impairment of renal function. Furthermore, the effect of I on antipyrine clearance was enhanced in the presence of renal failure. The *in vivo* data are consistent with the study by Leber *et al.* (20), who observed that pretreatment with I at a dosage of 0.2 mL/kg/d led to an increase in the *in vitro* drug-metabolizing enzyme activities in subtotally nephrectomized rats, but not in sham-operated controls. The enhanced response to phthalate treatment in uremic rats may be explained by a greater exposure to the inducing agent(s), as a result of accumulation of I and/or its metabolites during renal failure. Alternatively, uremia may promote the intrinsic response of the liver to treatment with the plasticizer.

The present animal data with I suggest that the increased metabolic clearance of antipyrine in renal failure patients could be a result of chronic exposure to phthalate ester plasticizers through repeated hemodialysis. However, it is important to note that in this study the antipyrine clearance measurements were all performed at 48 h after the last dose of I, by which time much of the administered dose of phthalate should have been eliminated. Hence, the possibility of a direct inhibitory effect on antipyrine metabolism cannot be ruled out. Metabolic inducers such as phenobarbital are known to also exhibit inhibitory activity (36). The potential for induction and inhibition of drug metabolism to occur simultaneously during continuous treatment with I should be recognized. In fact, a recent study by Agarwal *et al.* (23) showed that either induction or inhibition of *in vitro* hepatic microsomal oxidative enzyme activities

Table VII—Antipyrine Elimination Half-life (min) in Renal Failure and Sham-Operated Rats after Treatment with Corn Oil or Phthalate

Statistical Comparisons[a]	Treatments[b] 1	2	3	4	5	6
Mean (n)	157 (7)	152 (7)	108 (6)	70.9 (5)	76.9 (6)	70.2 (7)
SE	5	14	6	7.4	4.8	4.0
Between renal failure and sham-operated rats treated with corn oil	NS[c]					
Between low- and high-dose phthalate in sham-operated rats		$p < 0.005$	$p < 0.001$	$p < 0.005$		
Between low- and high-dose phthalate in renal failure rats			$p < 0.005$	$p < 0.001$	NS	
Between renal failure and sham-operated rats treated with phthalate				$p < 0.005$		NS

[a] Wilcoxon's summed rank test. [b] See text for explanation of treatment codes. [c] No statistically significant difference.

Table VIII—Liver Weights in Renal Failure and Sham-Operated Rats after Treatment with Corn Oil or Phthalate

Statistical Comparisons[a]	Treatments[b] 1	2	3	4	5	6
Mean (n)	35.7 (7)	31.2 (7)	43.6 (6)	46.6 (5)	54.3 (7)	52.7 (7)
SE	1.4	1.2	1.4	0.7	1.4	2.6
Between renal failure and sham-operated rats treated with corn oil		$p < 0.05$				
Between low- and high-dose phthalate in sham-operated rats		$p < 0.001$		$p < 0.001$		
			$p < 0.001$			
Between low- and high-dose phthalate in renal failure rats			$p < 0.005$		NS[c]	
				$p < 0.001$		
Between renal failure and sham-operated rats treated with phthalate				NS		NS

[a] Wilcoxon's summed rank test. [b] See text for explanation of treatment codes. [c] No statistically significant difference.

can result depending on the route of administration of I. Induction of metabolism was observed after oral administration of I, whereas inhibition was evident after intraperitoneal administration. Unfortunately, these investigators used very high doses of I (>2 mL/kg/d). Since the degree of metabolic inhibition is usually dependent on the dose or concentration of the inhibitor, the likelihood for metabolic inhibition to occur at phthalate levels that have been observed in human subjects is not known. Studies are currently underway to investigate the effects of phthalate plasticizers on hepatic drug metabolism under more clinically relevant experimental conditions.

In conclusion, the presence of circulating plasticizers in patients undergoing regular hemodialysis should be considered as a complicating factor in the interpretation of clinical data concerning the effect of renal failure on drug metabolism.

REFERENCES

(1) M. Reidenberg, *Am. J. Med.*, **62,** 482 (1977).

(2) D. Lowenthal, W. Briggs, T. Gibson, H. Nelson, and W. Cirksena, *Clin. Pharmacol. Ther.*, **16,** 761 (1974).

(3) T. Gibson, K. Giacomini, W. Briggs, W. Whitman, and G. Levy, *Clin. Pharmacol. Ther.*, **27,** 665 (1980).

(4) M. Reidenberg, H. Kostenbauder, and W. Adams, *Metabolism*, **18,** 209 (1969).

(5) C. Ogg, P. Toseland, and J. Cameron, *Br. Med. J.*, **2,** 283 (1968).

(6) H. Mellk, J. Lettieri, and P. Durante, *Ann. Int. Med.*, **72,** 801 (1970).

(7) M. Reidenberg, I. Odar-Cederlof, C. von Bahr, O. Borga, and F. Sjoqvist, *N. Engl. J. Med.*, **285,** 264 (1971).

(8) M. Lichter, M. Black, and I. Arias, *J. Pharmacol. Exp. Ther.*, **187,** 612 (1973).

(9) J. Maddocks, C. Wake, and M. Harber, *Br. J. Clin. Pharmacol.*, **2,** 339 (1975).

(10) I. Nemeth and T. Szeleczki, *Br. J. Clin. Pharmacol.*, **11,** 92 (1981).

(11) I. Odar-Cederlof and O. Borga, *Clin. Pharmacol. Ther.*, **20,** 36 (1976).

(12) B. Brodie and J. Axelrod, *J. Pharmacol. Exp. Ther.*, **98,** 97 (1950).

(13) W. Guess, J. Jacob, and J. Autian, *Drug Intell.*, **1,** 120 (1967).

(14) R. Jaeger and R. Rubin, *Science*, **170,** 460 (1970).

(15) R. Easterling, E. Johnson, and E. Napier, *Proc. Soc. Exp. Biol. Med.*, **147,** 572 (1974).

(16) T. Gibson, W. Briggs, and B. Boone, *J. Lab. Clin. Med.*, **87,** 519 (1976).

(17) L. Lewis, T. Flechtner, J. Kerkay, K. Pearson, W. Chen, K. Popowniak, and S. Nakamoto, *Trans. Am. Soc. Artif. Intern. Organs*, **23,** 566 (1977).

(18) W. Chen, J. Kerkay, and K. Pearson, *Anal. Lett.*, **12,** 517 (1979).

(19) B. G. Lake, S. D. Gangolli, P. Grasso, and A. G. Lloyd, *Toxicol. Appl. Pharmacol.*, **32,** 355 (1975).

(20) H. W. Leber, L. Gleumes, and G. Schutterle, *Kidney Int.*, **13,** S43 (1978).

(21) S. P. Srivastava, D. K. Agarwal, M. Mushtaq, and P. K. Seth, *Toxicology*, **11,** 271 (1978).

(22) A. Aitio and M. Parkki, *Arch. Int. Pharmacodyn. Ther.*, **235,** 187 (1978).

(23) D. K. Agarwal, S. Agarwal, and P. K. Seth, *Drug Metab. Dispos.*, **10,** 77 (1982).

(24) M. Danhof, E. de Groot-van der Vis, and D. Breimer, *Pharmacology*, **18,** 210 (1979).

(25) D. Williams and B. Blanchfield, *Bull. Environm. Contam. Toxicol.*, **10,** 371 (1971).

(26) C. Metzler, G. Elfring, and A. McEwen, *Biometrics*, **30,** 562 (1974).

(27) M. Danhof, D. Krom, and D. Breimer, *Xenobiotica*, **9,** 695 (1979).

(28) S. Kamath and E. Rubin, *Biochem. Biophys. Res. Commun.*, **49,** 52 (1972).

(29) T. Omura and R. Sato, *J. Biol. Chem.*, **239,** 2370 (1964).

(30) O. Lowry, N. Rosebrough, A. Farr, and R. Randall, *J. Biol. Chem.*, **193,** 265 (1951).

(31) R. Platt, M. Roscoe, and F. Smith, *Clin. Sci.*, **11,** 217 (1952).

(32) V. Krampl and M. Kontsekova, *Bull. Environm. Contam. Toxicol.*, **20,** 191 (1978).

(33) J. Aarbakke, *Acta Pharmacol. Toxicol.*, **43,** 64 (1978).

(34) H. Bässman, J. Böttcher, and R. Schuppel, *N.-S. Arch. Pharmacol.*, **309,** 203 (1979).

(35) Y. Kuriyama, T. Omura, P. Siekevitz, and G. Palade, *J. Biol. Chem.*, **244,** 2017 (1969).

(36) H. Kutt, *Epilepsia*, **16,** 393 (1975).

ACKNOWLEDGMENTS

This work was supported in part by United States Public Health Services Grants Nos. RR05454-19 and HL-25797 and by the Woodburn Fellowship (G.M.P.) from the State University of New York at Buffalo.

Protection of Murine L1210 Leukemia and Bone Marrow Progenitor Cells Against Mechlorethamine and Inhibition of Choline Uptake as a Structure–Activity Relationship of 2-Dimethylaminoethanol and Its Analogues

SAULIUS A. NAUJOKAITIS, JOYCE M. FISHER, and MARCO RABINOVITZ ×

Received September 2, 1981, from the *Laboratory of Medicinal Chemistry and Pharmacology, Developmental Therapeutics Program, Division of Cancer Treatment, National Cancer Institute, National Institutes of Health, Bethesda, Md. 20850.* Accepted for publication November 5, 1982.

Abstract □ The structure–activity relationships of 2-dimethylaminoethanol and its analogues as protectors against mechlorethamine cytotoxicity and as inhibitors of choline uptake were evaluated. Of a series of inhibitors and protectors, 2-dimethylaminoethanol was the most potent inhibitor of choline uptake and the most potent protector of both hematopoietic progenitor cells and murine L1210 leukemia cells. Two analogues that exhibited both potent protection and inhibition were 1-dimethylamino-2-propanol and 2-ethylmethylaminoethanol. 2-Di-*n*-butylaminoethanol, while protecting against mechlorethamine cytotoxicity, was not an inhibitor of choline uptake. 2-*n*-Butylmethylaminoethanol, while an inhibitor of choline uptake, was not a protector against mechlorethamine cytotoxicity. Addition of 2-dimethylaminoethanol to mechlorethamine in a mole ratio of 1000:1 did not improve survival of tumor-bearing mice beyond that of mice treated with mechlorethamine alone.

Keyphrases □ Structure–activity relationships—2-dimethylaminoethanol and its analogues, protection against mechlorethamine cytotoxicity, inhibition of choline uptake □ Antitumor activity—combination chemotherapy, 2-dimethylaminoethanol and mechlorethamine, differential antitumor activity □ 2-Dimethylaminoethanol—analogues, protection against mechlorethamine cytotoxicity, inhibition of choline uptake, combination chemotherapy with mechlorethamine

The limited capacity of membrane transport carriers allows use of nutritional and appropriate pharmacological substrates to protect cells from cytotoxicity by competing with cytotoxic agents dependent, at least in part, for uptake into the cell by transport carriers (1). 2-Dimethylaminoethanol, the tertiary amine corresponding to choline, is fully protonated at physiological pH and is a substrate for the choline transport system (2, 3). Mechlorethamine(2,2′-dichloro-*N*-methyldiethylamine), a nitrogen mustard, is a cytotoxic agent transported by the choline transport carrier (4). With the view of obtaining differential protection of sensitive host tissue against mechlorethamine cytotoxicity, a systematic evaluation of the structure–activity relationships of 2-dimethylaminoethanol and its analogues as protectors of hematopoietic precursor cells and murine L1210 leukemia cells against mechlorethamine cytotoxicity and as inhibitors of choline uptake into murine L1210 leukemia cells was undertaken. Mechlorethamine cytotoxicity was used as an indicator for its transport by the choline transport system (4), and protection against mechlorethamine cytotoxicity was employed as an indicator for inhibition of mechlorethamine uptake by competitors for the choline transport system (5). Since mechlorethamine is a highly reactive alkylating agent and the transport of its hydrolyzed product, diethanolmethylamine, is only partially inhibited by choline (6), the inhibition of choline transport by 2-dimethylaminoethanol and its analogues was used to identify potential inhibitors of mechlorethamine transport. The study concluded with the *in vivo* chemotherapy of L1210 tumor-bearing mice using 2-dimethylaminoethanol and mechlorethamine in a mole ratio of 1000:1.

EXPERIMENTAL

Material—Mechlorethamine hydrochloride[1], 2-dimethylaminoethanol[1], 2-dimethylamino-1-propanol[1], 2-dimethylamino-2-methyl-1-propanol[1], 1-dimethylamino-2-propanol[1], and the higher homologues[2] were purchased from commercial sources and were used as received.

L1210 Cloning Assay—The methods for the growth and maintenance of L1210 cells have been previously described (7). The L1210 cells were maintained in RPMI medium 1630[3] plus 16% heat-inactivated fetal bovine serum[4]. They were harvested in log phase (8–12 × 10^5/mL by centrifugation at 300×*g* for 5 min, washed twice in medium composed of Dulbecco's phosphate saline[5] plus 0.1 mM bovine serum albumin (pH 7.4) supplemented with 16 mM glucose (medium I), and resuspended to an appropriate cell density as determined with a cell counter[6]. The L1210 cells at a final density of 1 × 10^5/mL were added to the incubation medium containing the compounds to be tested and incubated for 15 min at 37°C. Mechlorethamine hydrochloride was then added to a final concentration of 1.0 μM (an LD_{99} dose), and the incubation was continued for 20 min. The incubation was terminated by placing the tubes containing the mixture into an ice-water bath for 5–10 min. The cells were washed three times in growth medium composed of medium 1630, 20% fetal bovine serum, and 40 μg/mL of gentamicin. The cell density was adjusted to 1 × 10^5/mL, and cytotoxicity was assayed by clonal growth in 0.13% soft nutrient agar according to the procedure of Chu and Fischer (8) with minor modifications. The surviving fractions were estimated in triplicate after 2 weeks of incubation. They were similar whether the protector and the mechlorethamine hydrochloride were added simultaneously to the L1210 cell suspension or the L1210 cell suspension was incubated 15 min with the protector prior to the addition of mechlorethamine hydrochloride.

Bone Marrow Colony-Forming Units in Culture—The method of obtaining colony-forming units in culture from bone marrow was adapted from a previously reported work (7). The central core of the femurs from male CDF_1 mice were flushed with medium I. The bone marrow cells were washed three times with this medium and resuspended to a nucleated cell concentration of 1 × 10^5/mL. The incubation of the cells with the test compounds was performed in the same manner as described for the murine L1210 leukemia clonal growth assay. The cells were then incubated with the LD_{95} dose of 0.5 μM mechlorethamine hydrochloride and for 20 min. They were then washed three times in McCoy's 5A medium[7] supplemented with 16% fetal bovine serum (non-heat in-

[1] Aldrich Chemical Co., Milwaukee, Wis.
[2] Sapon Laboratories, Division of Overlook Industries, Bloomsbury, N.J.
[3] Prepared by the NIH media unit.
[4] Flow Laboratories, McLean, Va.
[5] Miles Laboratories, Elkhart, Ind.
[6] Model ZBI; Coulter Electronics, Hialeah, Fla.
[7] Grand Island Biological Co., Grand Island, N.Y.

0022-3549/84/0100-0034$01.00/0
© 1984, American Pharmaceutical Association

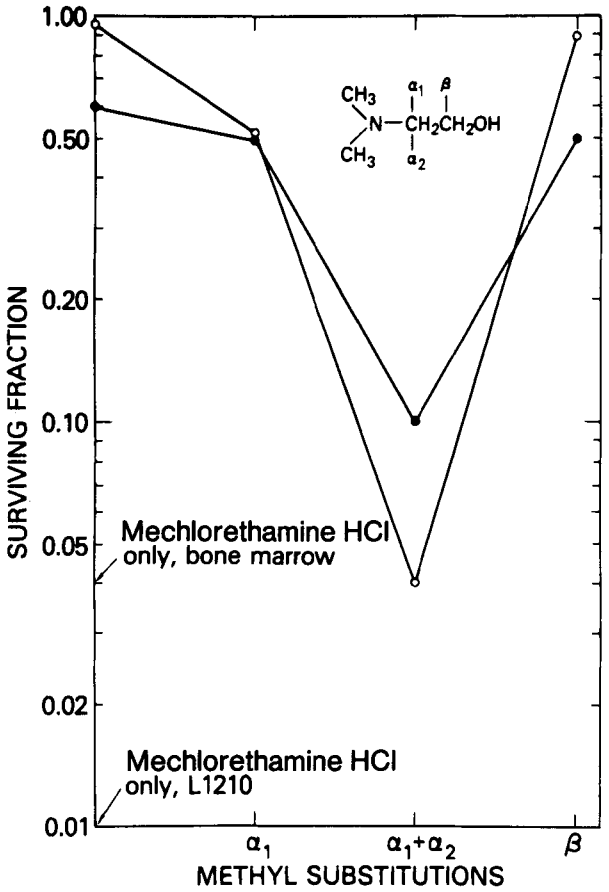

Figure 1—*Protection of murine L1210 leukemia cells and bone marrow colony-forming units by 2-dimethylaminoethanol and its α- and β-methyl derivatives against mechlorethamine cytotoxicity. The L1210 cells (○) and the bone marrow cells (●) at a density of 1 × 10⁵/mL were exposed to 200 μM 2-dimethylaminoethanol, 2-dimethylamino-1-propanol (α_1), 2-dimethylamino-2-methyl-1-propanol ($\alpha_1 + \alpha_2$), and 1-dimethylamino-2-propanol (β_1) plus 1.0 or 0.5 μM mechlorethamine hydrochloride, respectively, at 37°C. After 20 min the L1210 cells and bone marrow cells were washed and resuspended in their respective growth medium-containing agar; colonies were counted after 2 weeks and 1 week, respectively.*

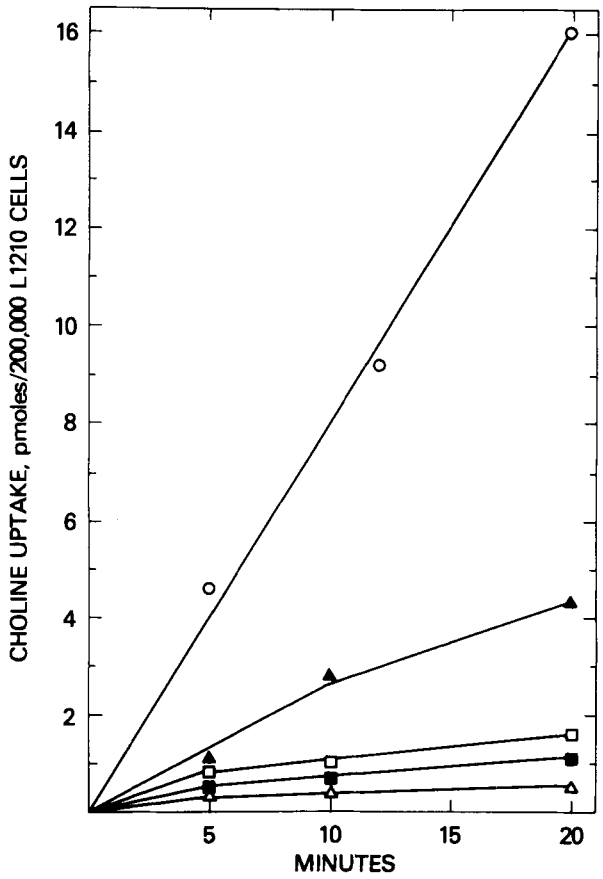

Figure 2—*Inhibition of choline uptake by 2-dimethylaminoethanol, 2-dimethylamino-1-propanol, 2-dimethylamino-2-methyl-1-propanol, and 1-dimethylamino-2-propanol. A volume of a L1210 cell suspension at a density of 2 × 10⁶/mL was added to an equal volume of transport medium at 37°C containing 1.0 μM [³H]choline (○) plus 200 μM 2-dimethylaminoethanol (△), 2-dimethylamino-1-propanol (□), 2-dimethylamino-2-methyl-1-propanol (▲), or 1-dimethylamino-2-propanol (■). At indicated time intervals triplicate 200-μL samples of the cell suspension were layered over silicone oil and centrifuged at 12,000×g. The centrifuge tips were placed in scintillation fluid and the incorporated [³H]choline was counted.*

activated), 20 U/mL of penicillin, and 20 μg/mL of streptomycin and plated in soft nutrient agar (0.3%) with colony-stimulating factor[8] such that 1 × 10⁵ nucleated cells gave 100 colonies after 7 d of growth at 37°C in a humidified, 10% carbon dioxide atmosphere. Colonies having 50 or more cells were counted in triplicate.

Choline Uptake Studies—Murine L1210 leukemia cells were washed three times in transport medium composed of Dulbecco's phosphate-balanced saline, 0.1 mM bovine serum albumin, and 6.4 mM glucose at 37°C, and the final cell density was adjusted to 1 × 10⁶/mL. Incubations were initiated by the addition of a volume of an L1210 cell suspension to an equal volume of medium containing [³H]choline[9] and the compounds to be tested. The incubation was terminated by layering 200 μL of medium over silicone oil[10] in microcentrifuge tubes and pelleting the cells through the silicone oil for 1 min at 12,000×*g* in a microcentrifuge[11]. The centrifuge tube tips containing the pellet were cut off, mixed with liquid scintillation fluor, and the incorporated radioactivity estimated in a liquid scintillation counter[12]. Each experimental point was determined in duplicate or triplicate.

Chemotherapy—L1210 cells (NCI stock) were maintained in female DBA/2 mice and grown intraperitoneally for experimental work in male CDF_1 mice[13], 8–12 weeks old and weighing 22–31 g. The mice were grouped by weight, 5 or 6 per plastic cage with wood chip bedding, and were given laboratory diet *ad libitum*. The L1210 cells were harvested 7 d after the passage inoculum, 1 × 10⁵ cells were injected intraperitoneally on day 0, and intraperitoneal chemotherapy was begun on day 1.

[8] Gift of Dr. T. R. Bradley of the Cancer Institute, Melbourne, Australia and Dr. R. Knazek, NCI, Bethesda, Md.

[9] New England Nuclear, Boston, Mass.

[10] Versilube F-50, specific gravity 1.045, viscosity 70 centistokes at 25°C; Harwick Chemical Corp., Cambridge, Mass.

[11] Model 235; Fisher Scientific Co., Rockville, Md.

[12] Model LS8100; Beckman Instruments Inc., Silver Spring, Md.

[13] Charles River Laboratories, Wilmington, Mass.

RESULTS

2-Dimethylaminoethanol and Its α- or β-Methyl Analogues—The structure–activity pattern of protection by 2-dimethylaminoethanol, 2-dimethylamino-1-propanol (α_1-methyl), 2-dimethylamino-2-methyl-1-propanol (α_1- plus α_2-methyl), and 1-dimethylamino-2-propanol (β-methyl) for L1210 cells quantitatively parallels that of the protection pattern for bone marrow progenitor cells (Fig. 1). Quantitatively, there are differences. The protector–mechlorethamine ratio was 400:1 during the incubation of precursor bone marrow cells and 200:1 during the incubation of L1210 cells. Yet, the surviving fraction of L1210 cells is uniformly greater except when the protector analogue has two α-methyl groups as in 2-dimethylamino-2-methyl-1-propanol, which results in an equally poor protector. Though this poor protector results in a greater survival of bone marrow colony-forming units compared with L1210 cells, the surviving fraction differs by a factor of ~2, consistent with the difference in their protector–mechlorethamine ratio.

The potent protectors 2-dimethylaminoethanol and 1-dimethylamino-2-propanol achieve an L1210 surviving fraction of 0.95 and 0.90, while the comparable surviving fractions of bone marrow colony-forming units are 0.6 and 0.5. 2-Dimethylaminoethanol and its α- and β-methyl analogues acting as inhibitors of choline uptake reflect their qualitative pattern of protection. 2-Dimethylamino-2-methyl-1-propanol is a rela-

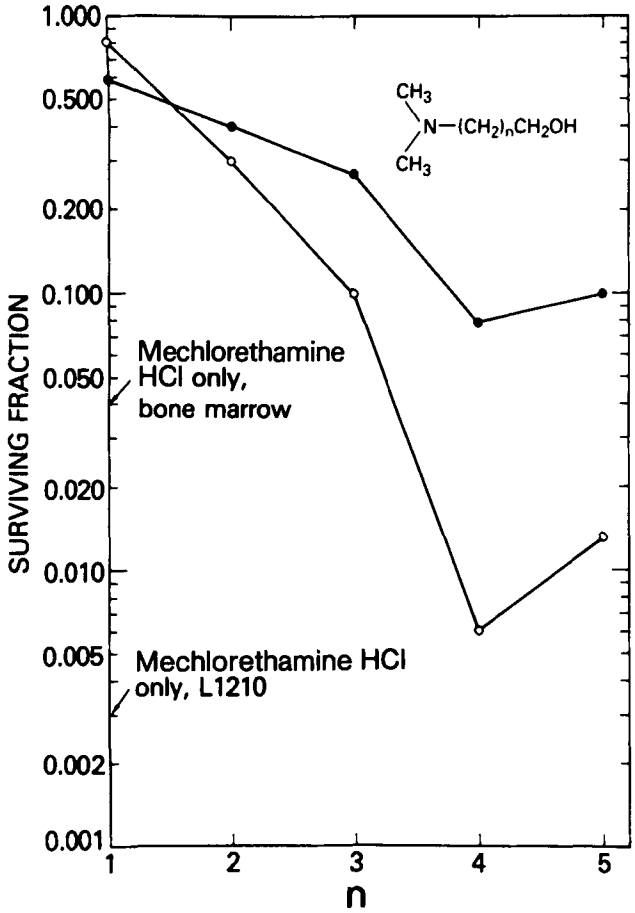

Figure 3—*Protection of murine L1210 leukemia cells and bone marrow colony-forming units by 2-dimethylaminoethanol and its higher homologues of the ethanol moiety against mechlorethamine cytotoxicity. The L1210 cells (○) and the bone marrow progenitor cells (●) at a density of 1 × 10^5/mL were exposed to 200 μM 2-dimethylaminoethanol (n = 1), 3-dimethylaminopropanol (n = 2), 4-dimethylaminobutanol (n = 3), 5-dimethylaminopentanol (n = 4), and 6-dimethylaminohexanol (n = 5) plus 1.0 or 0.5 μM mechlorethamine hydrochloride, respectively, at 37°C. The cells were processed in the same manner as described in the legend under Fig. 1.*

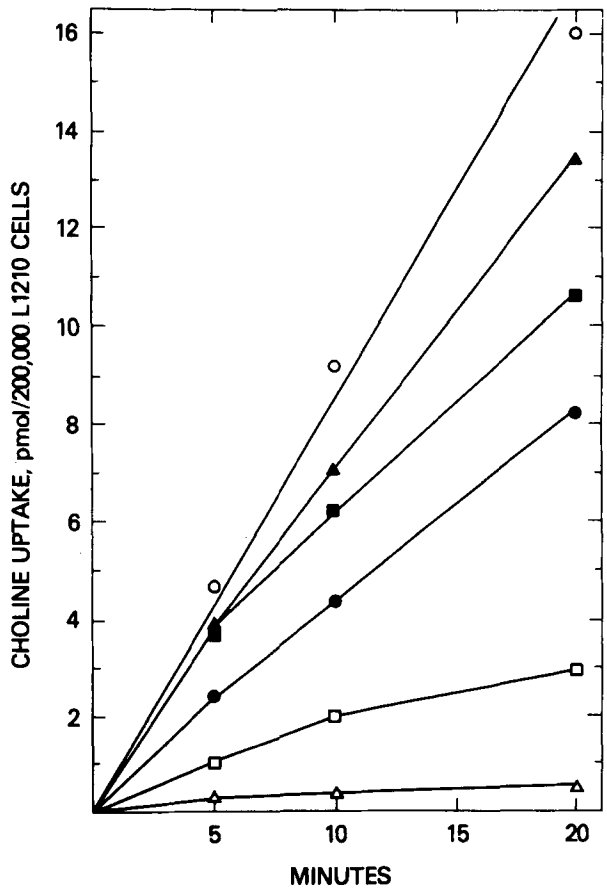

Figure 4—*Inhibition of choline uptake by 2-dimethylaminoethanol and its higher homologues of the ethanol moiety. A volume of a L1210 cell suspension at a density of 2 × 10^6/mL was added to an equal volume of transport medium at 37°C containing 1.0 μM [^{3}H]choline (○) plus 200 μM 2-dimethylaminoethanol (△), 3-dimethylaminopropanol (□), 4-dimethylaminobutanol (●), 5-dimethylaminopentanol (▲), or 6-dimethylaminohexanol (■). The cell suspension was sampled and the incorporated [^{3}H]choline was counted as described in the legend under Fig. 2.*

tively poor inhibitor compared with the other three in this series (Fig. 2). To compare choline with 2-dimethylaminoethanol, a β-methyl addition onto the choline molecule results in a compound with decreased inhibition of choline uptake, whereas a single α-methyl substitution slightly decreases the K_m of the compound for the choline transport carrier (2, 9, 10). However, a single methyl addition onto the β-position of 2-dimethylaminoethanol does not result in diminished protection against mechlorethamine cytotoxicity nor in decreased inhibition of choline uptake (Figs. 1 and 2).

2-Dimethylaminoethanol and Its Higher Methylene Homologues—With each successive increase in the number of methylene groups between the nitrogen and the hydroxyl group of 2-dimethylaminoethanol, generated higher homologues show decreased protection of both bone marrow and L1210 cells against mechlorethamine cytotoxicity (Fig. 3). Comparison of the surviving fractions of bone marrow with that of L1210 cells shows preferential protection of the bone marrow colony-forming units. A greater decrease in the surviving fraction of the L1210 cells occurs with each protector of the higher homologue than in that of the bone marrow cells. Protection by 5-dimethylaminopentanol results in a differential surviving fraction of the bone marrow cells, with the difference between these and L1210 surviving fractions being greater than an order of magnitude. This finding may describe differential protection of bone marrow progenitor cells or may be accounted for by the particular sensitivity of the L1210 cells, resulting in a survival fraction of 0.003 for mechlorethamine alone (Fig. 3). The pattern of choline uptake into L1210 cells produced by 2-dimethylaminoethanol and its higher homologues as competitors of choline is decreased inhibition of choline uptake by each higher homologue (Fig. 4). This structure–activity pattern of tertiary alkylamino alcohols is unlike that seen with the quaternary ammonium ions with the structure of alkyltrimethylammonium, which shows increased inhibition of choline uptake into erythrocytes with each methylene addition to the alkyl branch (11).

Methylene Additions onto a Single Alkyl Branch of 2-Dimethylaminoethanol—The analogues in the series from 2-dimethylaminoethanol to 2-methyl-*n*-propylaminoethanol show minimal differences in their protection of bone marrow and L1210 cells against mechlorethamine (Fig. 5). 2-*n*-Butylmethylaminoethanol is different from the rest of the series, showing a marked decrease in the ability to protect both bone marrow progenitor and L1210 cells. The entire series protected L1210 cells better than bone marrow cells. As inhibitors of choline uptake into L1210 cells, they are equally potent (Fig. 6). Compared with the pattern of inhibition of choline uptake by this series, the affinity for the choline transport carrier by quaternary ammonium analogues of choline, which were generated by increasing the number of methylene groups in a single alkyl branch, shows a biphasic pattern with maximum decrease occurring with the *n*-propyl and *n*-butyl derivatives and a progressive increase in affinity with *n*-pentyl and higher homologues (12). The alkyltrimethylammonium ions, containing no alcohol group, show a similar transition in affinity for the choline transport carrier occurring with the *n*-propyl to *n*-pentyl derivatives (11).

Methylene Additions into Both Alkyl Branches of 2-Dimethylaminoethanol—Protection of bone marrow progenitor and L1210 cells by 2-dimethylaminoethanol and its analogues, which are generated by methylene additions to both alkyl branches, shows a biphasic pattern (Fig. 7). Within the series the most potent protector is 2-dimethylaminoethanol and the least potent protector is 2-di-*n*-propylaminoethanol; at the transition to a potent protector is 2-di-*n*-butylaminoethanol.

2-Di-*n*-butylaminoethanol may detoxify mechlorethamine by func-

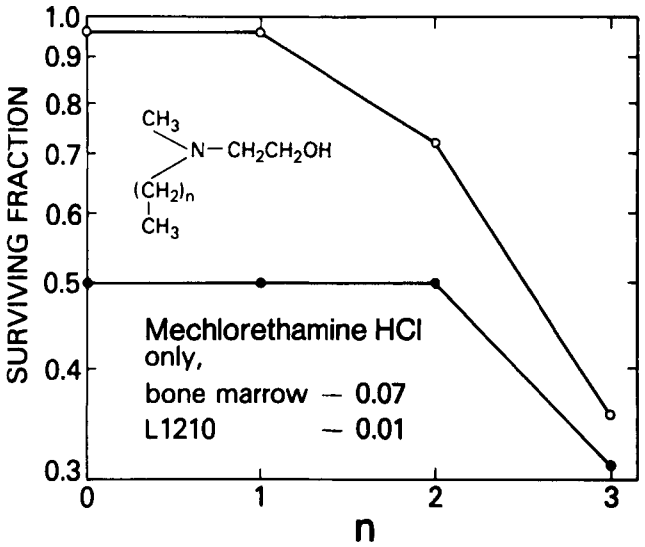

Figure 5—*Protection of murine L1210 leukemia cells and bone marrow colony-forming units by 2-dimethylaminoethanol and its analogues generated by methylene additions into a single alkyl branch. The L1210 cells (○) and the bone marrow progenitor cells (●) at a density of 1 × 10^5/mL were exposed to 200 μM 2-dimethylaminoethanol (n = 0), 2-ethylmethylaminoethanol (n = 1), 2-methyl-n-propylaminoethanol (n = 2), and 2-n-butylmethylaminoethanol (n = 3) plus 1.0 or 0.5 μM hydrochloride, respectively, at 37°C. The cells were processed in the same manner as described in the legend under Fig. 1.*

tioning as a potent nucleophile in the manner of 2-dimethylaminoethanol (13). In solution, mechlorethamine exists in various molecular forms (14) and is transported by a two-component transport system (6). Since it is a poor inhibitor of choline uptake (Fig. 8), 2-di-*n*-butylaminoethanol may protect against a larger number of mechlorethamine moieties which are not transported by the transport carrier inhibited by choline or its analogues. The small differential protection of bone marrow cells by 2-diethylaminoethanol and 2-di-*n*-propylaminoethanol may be due to the higher ratio of protector to mechlorethamine in its culture system (400:1 compared with 200:1 in the L1210 culture system).

2-Dimethylaminoethanol and 2-diethylaminoethanol are approximately equipotent inhibitors of choline uptake (Fig. 8). Their quaternary ammonium congeners, choline and diethylcholine, were found to show the same affinity for the high-affinity choline uptake system, but to differ in their affinity for the low-affinity system (15).

Treatment of L1210 Tumor-Bearing Mice with a Combination of 2-Dimethylaminoethanol and Mechlorethamine Hydrochloride—The *in vivo* treatment combination of 2-dimethylaminoethanol plus mechlorethamine hydrochloride in a mole ratio of 1000:1 decreased survival of the combination treatment group compared with the mechlorethamine hydrochloride only treatment group (Table I). This finding may be secondary to the detoxification of mechlorethamine by its ability to react with 2-dimethylaminoethanol (13). This point is possibly illustrated by the survival data, which show that the mean survival time of the group of animals which received mechlorethamine hydrochloride prior to the protector was longer (11.2 d) than the group which received the protector prior to mechlorethamine hydrochloride (9.8–10.5 d). The large doses of 2-dimethylaminoethanol produced minimal toxicity, such as salivation and shivering. The use of choline in high doses has been limited by its neurotoxicity, with a mole ratio of 30:1 of choline to mechlorethamine hydrochloride not protecting rats from a lethal dose of mechlorethamine hydrochloride (16).

Table I—Survival of Murine L1210 Leukemia-Bearing Mice Following Treatment with Mechlorethamine Hydrochloride or 2-Dimethylaminoethanol and Mechlorethane Hydrochloride

Treatment[a]	Mean Survival Time, d ± *SEM*	T/C, %
None or 5000 μmol/kg of 2-dimethylaminoethanol	7.7 ± 0.7	100
5 μmol/kg of mechlorethamine hydrochloride (days 1–5)	12.0 ± 0.9	156
5 μmol/kg of mechlorethamine hydrochloride and 5000 μmol/kg of 2-dimethylaminoethanol (0.25 hr, days 1–5)	11.2 ± 1.2[b]	146
5000 μmol/kg of 2-dimethylaminoethanol and 5 μmol/kg of mechlorethamine hydrochloride	9.8 ± 1.8[c]	114
0.25 h, days 1–5		
0.5 h, days 1–5	9.5 ± 1.1[d]	123
1 h, days 1–5	10.5 ± 0.8[e]	121

[a] L1210 cells, 1 × 10^5, were injected on day 0, and intraperitoneal chemotherapy was begun on day 1 and continued through day 5. In the combination treatment groups, the time indicates the interval between the two treatments. There were six mice per group. [b] No significant difference from mechlorethamine hydrochloride treatment only group at $p > 0.05$, as determined by the one-sided Student's *t* test. [c] Significantly different from the mechlorethamine hydrochloride treatment only group, $p < 0.02$. [d] Significantly different from the mechlorethamine hydrochloride treatment only group, $p < 0.01$. [e] Significantly different from the mechlorethamine hydrochloride treatment only group, $p < 0.05$.

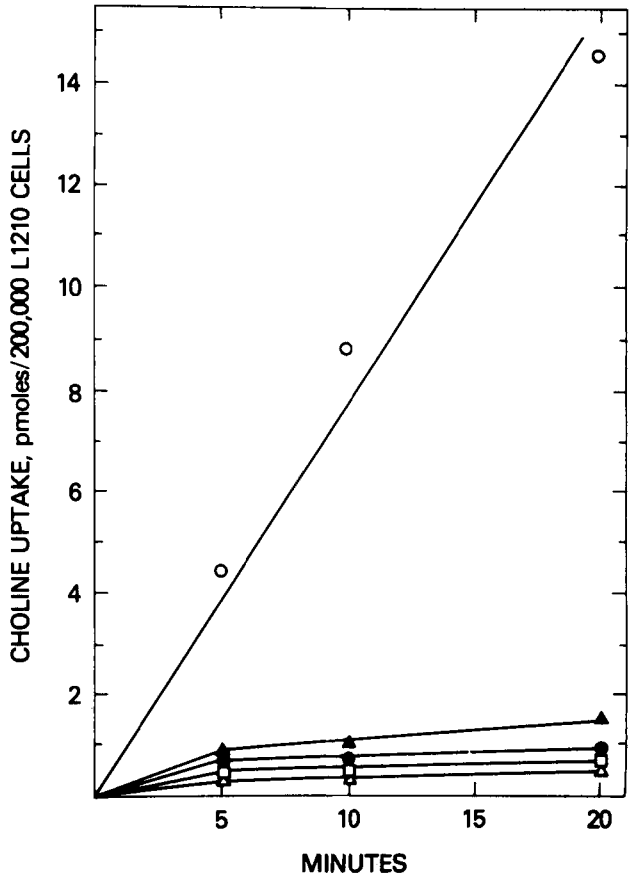

Figure 6—*Inhibition of choline uptake by 2-dimethylaminoethanol and its analogues generated by methylene additions into a single alkyl branch. A volume of a L1210 cell suspension at a density of 2 × 10^6/mL was added to an equal volume of transport medium at 37°C containing 1.0 μM [^{3}H]choline (○) plus 200 μM 2-dimethylaminoethanol (△), 2-ethylmethylaminoethanol (□), 2-methyl-n-propylaminoethanol (●), or 2-n-butylmethylaminoethanol (▲). The cell suspension was sampled and the incorporated [^{3}H]choline was counted as described in the legend under Fig. 2.*

DISCUSSION

With the possible exception of 5-dimethylaminopentanol (Fig. 3), the structure–activity relationships of 2-dimethylaminoethanol and its analogues to protection of bone marrow colony-forming units and L1210 cells did not identify a differential protector of bone marrow progenitor cells. During treatment with the protectors, the maximum achieved surviving fraction was observed with L1210 cells, unlike the plasmacytoma cell–bone marrow precursor cell culture system which showed preferential survival of bone marrow cells because of the differential sensitivity of the plasmacytoma cells to mechlorethamine (17). The maximum surviving fraction of bone marrow cells appears consistently fixed between 0.5 and 0.6 when they were exposed to 2-dimethylaminoethanol and mechlorethamine hydrochloride. The protector alone at

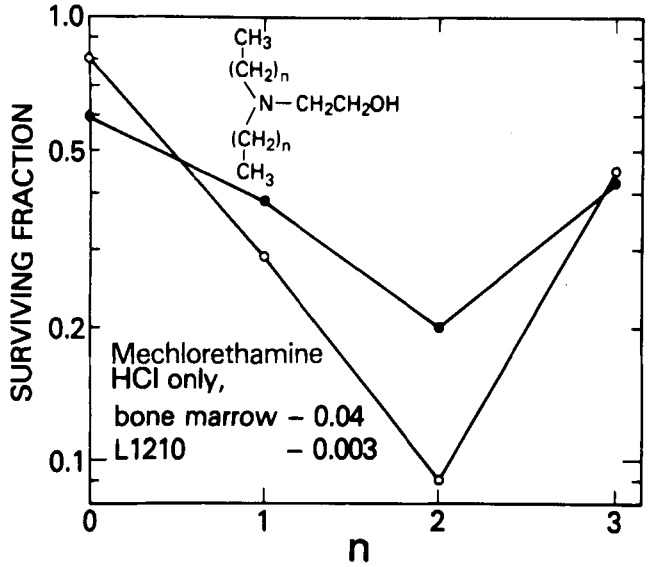

Figure 7—*Protection of murine L1210 leukemia cells and bone marrow colony-forming units by 2-dimethylaminoethanol and its analogues generated by methylene additions into the dialkyl branches. The L1210 cells (○) and the bone marrow progenitor cells (●) at a density of 1 × 10^5/mL were exposed to 200 μM 2-dimethylaminoethanol (n = 0), 2-diethylaminoethanol (n = 1), 2-di-n-propylaminoethanol (n = 2), and 2-di-n-butylaminoethanol (n = 3) plus 1.0 or 0.5 μM mechlorethamine hydrochloride, respectively, at 37°C. The cells were processed in the same manner as described in the legend under Fig. 1.*

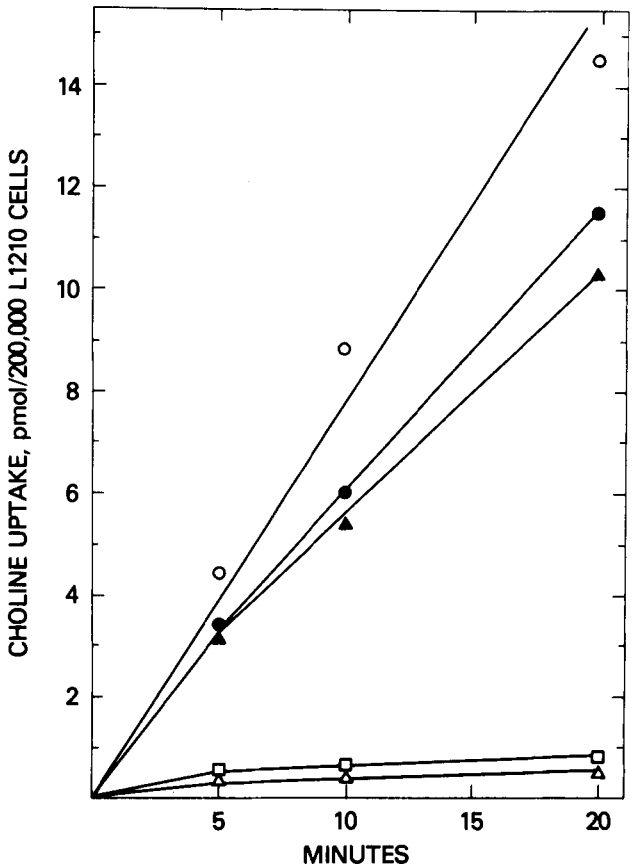

Figure 8—*Inhibition of choline uptake by 2-dimethylaminoethanol and its analogues generated by methylene additions into the dialkyl branches. A volume of a L1210 cell suspension at a density of 2 × 10^6/mL was added to an equal volume of transport medium at 37°C containing 1.0 μM [^{3}H]choline (○) plus 200 μM 2-dimethylaminoethanol (△), 2-diethylaminoethanol (□), 2-di-n-propylaminoethanol (●), or 2-di-n-butylaminoethanol (▲). The cell suspension was sampled and the incorporated [^{3}H]choline was counted as described in the legend under Fig. 2.*

the concentration used was not toxic to the bone marrow cells. Though an explanation for this persistent feature is not known, bone marrow precursor cells may have an increased number of choline transport sites or these sites may have a greater affinity for the various transformation products of mechlorethamine. In the milieu of the incubating bone marrow progenitor cells, the molar ratio of protector to mechlorethamine is 400:1, compared with 200:1 in that of the L1210 cells. Therefore, a counterflow phenomenon may exist (18). The increased intracellular concentration of protector may result in a preferential influx of mechlorethamine into the bone marrow progenitor cells.

The molecular transformations of mechlorethamine vary according to pH, and these products have different activities (13, 14). 2-Methyl-*n*-propylaminoethanol is an isostere of a hydrolysis product of mechlorethamine, 2-chloroethyl-2-hydroxyethylmethylamine. The isostere and its higher homologue, 2-*n*-butylmethylaminoethanol, are poor protectors against mechlorethamine cytotoxicity (Fig. 5); yet, both are potent inhibitors of choline uptake into the L1210 cells (Fig. 6). Another nonparallel finding between protection and inhibition is the potent protection against mechlorethamine cytotoxicity and the poor inhibition of choline uptake by 2-di-*n*-butylaminoethanol (Figs. 7 and 8). Using protection as an indicator of transport would have failed to identify an inhibitor of choline uptake in the former case (Figs. 5 and 6), while using inhibition of choline uptake as an indicator of protection would have failed to identify a protector in the latter case (Figs. 7 and 8). There may not be a direct correlation between protection against mechlorethamine cytotoxicity and inhibition of choline uptake by a choline analogue. Preincubation of the L1210 cell suspension with the compound to be tested rather than simultaneous addition of the compound and mechlorethamine hydrochloride to the cell suspension was selected because this approach would most closely represent the *in vivo* situation of maximizing protection of the sensitive host tissues.

In vivo experiments of interest would be the use of 2-di-*n*-butylaminoethanol as a protector against mechlorethamine host toxicity, with the possibility of avoiding the dose-limiting complications of neurotoxicity imposed by a substrate of the choline transport carrier, and use of 5-dimethylaminopentanol as a possible differential protector of the bone marrow progenitor cells. In the series of protectors that were tested, 2-dimethylaminoethanol consistently showed maximum protection of bone marrow and L1210 cells and was used in large doses as a protector against mechlorethamine toxicity *in vivo* with no benefit in survival to the tumor-bearing animal. There may be a role for 2-dimethylaminoethanol as a potent detoxifying agent, as with thiosulfate (19).

The correlation of the structure–activity relationship of choline and its congeners that are used in other disciplines (2, 9–12) to that of the murine L1210 leukemia cell is striking. Though exceptions have been found (15), such substrates can be used to predict similar structure–activity relationships in tumor systems.

REFERENCES

(1) M. Rabinovitz, Y. Uehara, and D. T. Vistica, *Science*, **206**, 1085 (1979).

(2) M. J. Dowdall, in "Cholinergic Mechanisms and Psychopharmacology," D. J. Jenden, Ed., Plenum, New York, N.Y., 1978 pp. 359–375.

(3) E. M. Cornford, L. D. Braun, and W. H. Oldendorf, *J. Neurochem.*, **30**, 299 (1978).

(4) G. J. Goldenberg, C. L. Vanstone, and I. Bihler, *Science*, **172**, 1148 (1971).

(5) D. T. Vistica, *Biochim. Biophys. Acta*, **550**, 309 (1979).

(6) R. M. Lyons and G. J. Goldenberg, *Cancer Res.*, **32**, 1679 (1972).

(7) D. T. Vistica, J. N. Toal, and M. Rabinovitz, *Biochem. Pharmacol.*, **27**, 2865 (1978).

(8) M. Chu and G. A. Fischer, *Biochem. Pharmacol.*, **17**, 753 (1968).

(9) J. R. Simon, T. W. Mittag, and M. J. Kuhar, *Biochem. Pharmacol.*, **24**, 1139 (1975).

(10) L. A. Baker and T. W. Mittag, *J. Pharmacol. Exp. Ther.*, **192**, 86 (1975).

(11) K. Martin, *Br. J. Pharmacol.*, **36**, 458 (1969).

(12) R. Deves and R. M. Krupka, *Biochim. Biophys. Acta*, **557**, 469 (1979).

(13) J. S. Fruton, W. J. Stein, M. A. Stahmann, and C. Golumbic, *J. Org. Chem.*, 11, 571 (1946).

(14) G. S. Tarnowski, F. A. Schmid, H. G. Satterwhite, E. M. Solney, and R. K. Barclay, *Biochem. Pharmacol.*, **17**, 989 (1968).
(15) R. T. Matthews and C. Y. Chion, *Biochem. Pharmacol.*, **28**, 405 (1979).
(16) G. J. Goldenberg and B. K. Sinha, *Cancer Res.*, **33**, 1253 (1973).
(17) M. Ogawa, D. E. Bergsagel, and E. A. McCulloch, *Cancer Res.*, **33**, 3172 (1973).
(18) P. G. W. Plagemann and D. P. Richey, *Biochim. Biophys. Acta*, **344**, 263 (1974).
(19) G. Owens and I. Hatiboglu, *Ann. Surg.*, **154**, 895 (1961).

ACKNOWLEDGMENTS

A preliminary report of this work has been presented [S. A. Naujokaitis, *Proc. Am. Assoc. Cancer Res.*, **20**, 1012 (1979)].

Simple Rapid Method for the Preparation of Enteric-Coated Microspheres

I. MAHARAJ *, J. G. NAIRN ‡, and J. B. CAMPBELL *x

Received August 31, 1982, from the **Department of Microbiology, Faculty of Medicine*, and ‡*Faculty of Pharmacy, University of Toronto, Toronto, Ontario, Canada. M5S 1A1.* Accepted for publication November 15, 1982.

Abstract □ A method is presented for encapsulating high molecular weight biological materials such as viral antigen, concanavalin A, and other proteins with cellulose acetate phthalate. The method is simple, inexpensive, and rapid; the process takes ~15 min. Capsules generated by this method are produced as microspheres 1–3 mm in diameter. They are stable for at least 6 h in simulated gastric conditions, but disintegrate rapidly under simulated intestinal conditions. Encapsulation had no effect on the activity of the biological materials. The method has potentially wide application for encapsulation of drugs and other substances.

Keyphrases □ Microspheres—enteric-coated, method for rapid preparation, encapsulation, cellulose acetate phthalate □ Encapsulation—method for the rapid preparation of enteric-coated microspheres, cellulose acetate phthalate □ Cellulose acetate phthalate—method for the preparation of enteric-coated microspheres, encapsulation □ Delivery systems—enteric-coated microspheres, cellulose acetate phthalate, method for rapid preparation

Cellulose acetate phthalate (I) has been used extensively as an enteric coating. Due to the presence of ionizable phthalate groups, the polymer is insoluble in acid media ≤pH 5, but is soluble when the pH is ≥6 (1). Since it is also remarkably inert *in vivo* (2), it is used to coat material for the release of drugs and other substances in the intestine. In recent years, I-coating technologies have been applied to the encapsulation of many biologically active materials, ranging from low molecular weight drugs [*e.g.*, sodium salicylate and phenacetin (3, 4)] to microorganisms [*e.g.*, viruses and bacteria (5–7)].

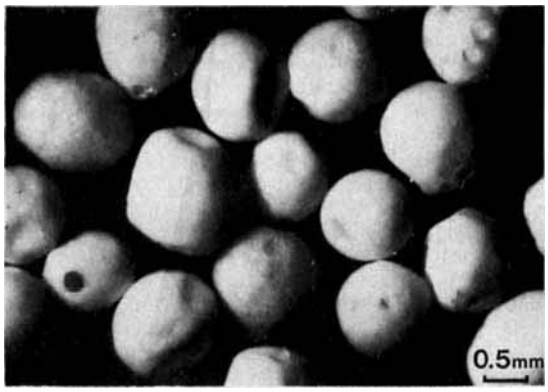

Figure 1—*Sucrose microspheres prepared as detailed in the text (formation time: 5 min).*

This report describes the development of an enteric coating for an oral vaccine used to protect wildlife against rabies. Studies on the vaccine itself will be reported elsewhere. The present report describes the principles of a method for encapsulation of the vaccine in the form of quasi-spherical particles ~1–3 mm in diameter (microspheres). The method is simple, rapid, and can be used to encapsulate a wide variety of materials. Therefore it has potential applications other than vaccine encapsulation.

EXPERIMENTAL

Materials—Core materials (*i.e.*, high molecular weight materials) that were encapsulated included rabies antigen (ERA-H strain of virus grown in BHK-21 cells and inactivated with β-propiolactone[1]), concanavalin A[1], and bovine serum albumin[1]. Radiolabeling of these materials with iodine-125 was carried out essentially as described by Thorell and Larson (8). Before use, the labeled preparations were passed through columns of Sephadex G-25[2] and extensively dialyzed against phosphate-buffered

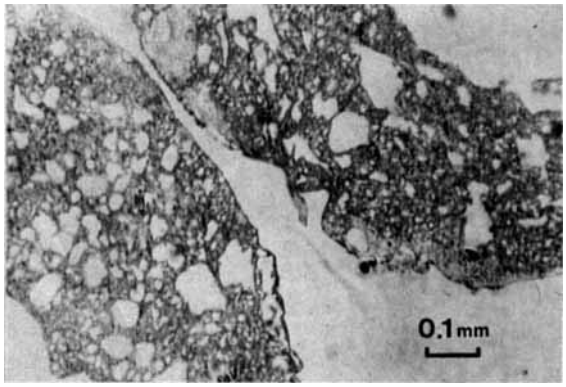

Figure 2—*Paraffin section (hematoxylin–eosin stain) of part of two sucrose microspheres showing the I matrix and the randomly distributed pockets that contained microparticles of the sucrose/core material. Hollow interiors of the microspheres are at the top right and bottom left of the photomicrograph.*

[1] Sigma Chemical Co., St. Louis, Mo.
[2] Pharmacia, Uppsala, Sweden.

0022-3549/84/0100-0039$01.00/0
© 1984, American Pharmaceutical Association

(14) G. S. Tarnowski, F. A. Schmid, H. G. Satterwhite, E. M. Solney, and R. K. Barclay, *Biochem. Pharmacol.*, **17**, 989 (1968).
(15) R. T. Matthews and C. Y. Chion, *Biochem. Pharmacol.*, **28**, 405 (1979).
(16) G. J. Goldenberg and B. K. Sinha, *Cancer Res.*, **33**, 1253 (1973).
(17) M. Ogawa, D. E. Bergsagel, and E. A. McCulloch, *Cancer Res.*, **33**, 3172 (1973).
(18) P. G. W. Plagemann and D. P. Richey, *Biochim. Biophys. Acta*, **344**, 263 (1974).
(19) G. Owens and I. Hatiboglu, *Ann. Surg.*, **154**, 895 (1961).

ACKNOWLEDGMENTS

A preliminary report of this work has been presented [S. A. Naujokaitis, *Proc. Am. Assoc. Cancer Res.*, **20**, 1012 (1979)].

Simple Rapid Method for the Preparation of Enteric-Coated Microspheres

I. MAHARAJ *, J. G. NAIRN ‡, and J. B. CAMPBELL *x

Received August 31, 1982, from the **Department of Microbiology, Faculty of Medicine*, and ‡*Faculty of Pharmacy, University of Toronto, Toronto, Ontario, Canada. M5S 1A1.* Accepted for publication November 15, 1982.

Abstract □ A method is presented for encapsulating high molecular weight biological materials such as viral antigen, concanavalin A, and other proteins with cellulose acetate phthalate. The method is simple, inexpensive, and rapid; the process takes ~15 min. Capsules generated by this method are produced as microspheres 1–3 mm in diameter. They are stable for at least 6 h in simulated gastric conditions, but disintegrate rapidly under simulated intestinal conditions. Encapsulation had no effect on the activity of the biological materials. The method has potentially wide application for encapsulation of drugs and other substances.

Keyphrases □ Microspheres—enteric-coated, method for rapid preparation, encapsulation, cellulose acetate phthalate □ Encapsulation—method for the rapid preparation of enteric-coated microspheres, cellulose acetate phthalate □ Cellulose acetate phthalate—method for the preparation of enteric-coated microspheres, encapsulation □ Delivery systems—enteric-coated microspheres, cellulose acetate phthalate, method for rapid preparation

Cellulose acetate phthalate (I) has been used extensively as an enteric coating. Due to the presence of ionizable phthalate groups, the polymer is insoluble in acid media ≤pH 5, but is soluble when the pH is ≥6 (1). Since it is also remarkably inert *in vivo* (2), it is used to coat material for the release of drugs and other substances in the intestine. In recent years, I-coating technologies have been applied to the encapsulation of many biologically active materials, ranging from low molecular weight drugs [*e.g.*, sodium salicylate and phenacetin (3, 4)] to microorganisms [*e.g.*, viruses and bacteria (5–7)].

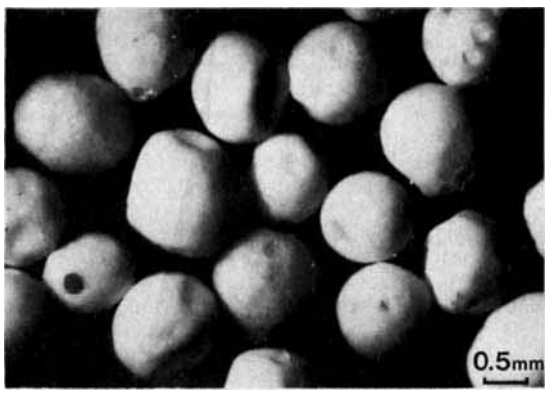

Figure 1—*Sucrose microspheres prepared as detailed in the text (formation time: 5 min).*

This report describes the development of an enteric coating for an oral vaccine used to protect wildlife against rabies. Studies on the vaccine itself will be reported elsewhere. The present report describes the principles of a method for encapsulation of the vaccine in the form of quasi-spherical particles ~1–3 mm in diameter (microspheres). The method is simple, rapid, and can be used to encapsulate a wide variety of materials. Therefore it has potential applications other than vaccine encapsulation.

EXPERIMENTAL

Materials—Core materials (*i.e.*, high molecular weight materials) that were encapsulated included rabies antigen (ERA-H strain of virus grown in BHK-21 cells and inactivated with β-propiolactone[1]), concanavalin A[1], and bovine serum albumin[1]. Radiolabeling of these materials with iodine-125 was carried out essentially as described by Thorell and Larson (8). Before use, the labeled preparations were passed through columns of Sephadex G-25[2] and extensively dialyzed against phosphate-buffered

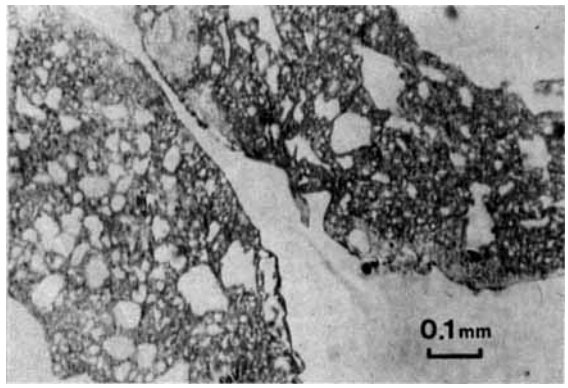

Figure 2—*Paraffin section (hematoxylin–eosin stain) of part of two sucrose microspheres showing the I matrix and the randomly distributed pockets that contained microparticles of the sucrose/core material. Hollow interiors of the microspheres are at the top right and bottom left of the photomicrograph.*

[1] Sigma Chemical Co., St. Louis, Mo.
[2] Pharmacia, Uppsala, Sweden.

0022-3549/84/0100-0039$01.00/0
© 1984, American Pharmaceutical Association

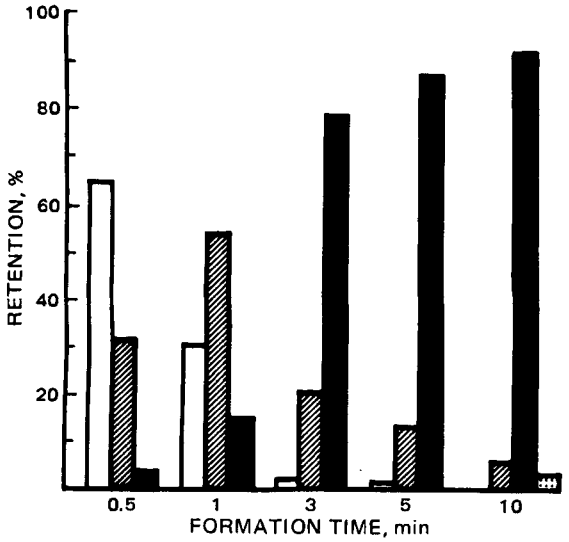

Figure 3—*Influence of formation time on the size of the microspheres. Formation was terminated by the addition of chloroform. Formed microspheres were collected, dried in air, and graded by passage through a series of U.S. standard stainless steel sieves mounted on a portable sieve shaker*[9]*, before being weighed. Key: (□) No. 50 sieve; (▨) No. 20 sieve; (■) No. 16 sieve; (▦) No. 12 sieve.*

saline to remove any free iodine. In the final preparations, >99% of the radioactivity was associated with trichloroacetic acid-precipitable (*i.e.*, high molecular weight) material.

Two lots of cellulose acetate phthalate[3] (A and B) were employed as the encapsulation material. Lot A had been stored for several years and had a pungent smell of acetic acid. Lot B was newly purchased and was practically odorless. Although both preparations were acceptable, they required slightly different conditions for optimal formation of microspheres.

Formation of Microspheres—The core material (maximum 50 mg) was suspended in 200 mL of 5% sucrose (w/v), shell-frozen, and then freeze-dried. The resulting powder was then triturated in a 1:4 ratio with finely divided sucrose containing up to 5% cornstarch and pressed through a No. 50 U.S. stainless steel sieve. This powder was then suspended in 200 mL of white paraffin oil[4] contained in a 400-mL beaker. The mixture

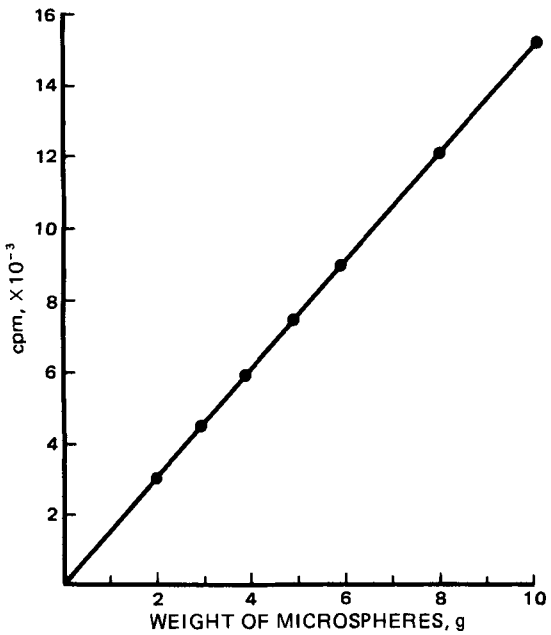

Figure 4—*Relationship between weight and core material content of the microspheres. Core material was [*^{125}*I]viral antigen, measured by radioactivity.*

[3] Lots #193(A) and #A9E(B); Eastman Kodak, Rochester, N.Y.
[4] Anachemia Chemicals Ltd., Mississauga, Ont.

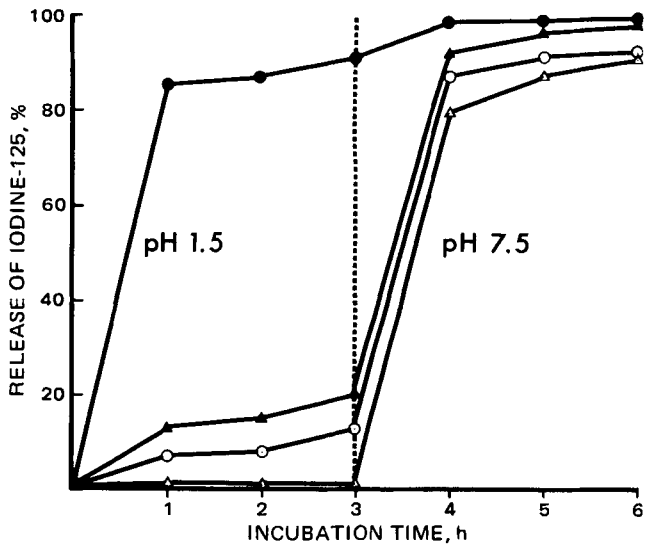

Figure 5—*Influence of pH of the incubation medium on the release of encapsulated viral radiolabel at 37°C. Key: (●) uncoated; (▲) I coated; (○) I–diethyl phthalate coated; (△) I–diethyl phthalate–wax coated.*

was dispersed by stirring at ~260 rpm with a 44-mm polyethylene three-blade paddle fitted to a high-torque stirrer[5]. To the suspension was added 20 mL of 10% (w/v) I in acetone–95% ethanol (9:1). Stirring was continued for 5 min to allow the microspheres to form, and then 75 mL of chloroform was added. The suspending medium was then decanted, and the microspheres were briefly resuspended in 75 mL of chloroform and air-dried at ambient temperature.

With one lot of I (B), some clumping of the microspheres was observed when they were removed from the chloroform. This was circumvented by stirring the suspension for 10–15 min after addition of the first volume of chloroform, prior to decanting.

In some preparations, the plasticizer diethyl phthalate[6] was included since it has been shown to increase the pliability and reduce the amount of moisture absorbed by I-coated capsules (9). The plasticizer (3% w/v) was dissolved in the I solution before addition to the encapsulation medium.

To further reduce the permeability of the microspheres, a wax coating was applied. Carnauba wax (1 g) was dissolved in 200 mL of white paraffin oil at 70°C and cooled to <45°C. The formed microspheres were then suspended in this for 15 min, with constant stirring. The wax solution was then decanted, and the microspheres were collected on filter paper to absorb the excess wax solution.

Release of Core Material—Stability of the microspheres was studied under conditions simulating those of the stomach and intestine. Breakdown or dissolution of the particles was monitored by measuring the release of iodine-125 and sucrose into the supernatant medium.

In most experiments, 2.5-g aliquots of the microsphere preparations were suspended in 20 mL of simulated gastric juice USP, without pepsin (*i.e.*, 0.08 M HCl containing 0.2% NaCl, pH 1.2). The suspension was incubated for 3 h at 37°C, with constant shaking at 160 rpm, on a clinical rotator[7]. At the end of each 1-h period, 1.0 mL of supernatant was removed, clarified by low-speed centrifugation (~7000×*g* for 10 min), and assayed for the presence of released encapsulated materials. Immediately following the 3-h incubation period, the simulated gastric medium was aspirated off, and the remaining microspheres were rinsed briefly with 5 mL of warm distilled water which was then discarded. The particles were incubated for a further 3 h at 37°C with 20 mL of simulated intestinal juice USP, without pancreatin (*i.e.*, 0.05 M KH_2PO_4 adjusted to pH 7.5 with 0.04 M NaOH). The hourly sampling process was repeated as before. The pH of the suspension was monitored by the addition of a few drops of 0.001% phenol red and adjusted when necessary with small volumes of alkali (usually 75 μL of 10 M NaOH after 1 and 2 h).

Assays—Levels of iodine-125 in the supernatant were measured by direct counting in a gamma-radiation counter[8]. Sucrose was measured by the anthrone reaction (10). There was no significant interference in this colorimetric reaction by dissolved I at the dilutions used.

[5] Type RZR1, "Caframo", Wiarton, Ont.
[6] BDH Chemicals, Toronto, Ont.
[7] Fisher Scientific Co., Fair Lawn, N.J.
[8] Gammacord; Ames Co., Elkhart, Ind.

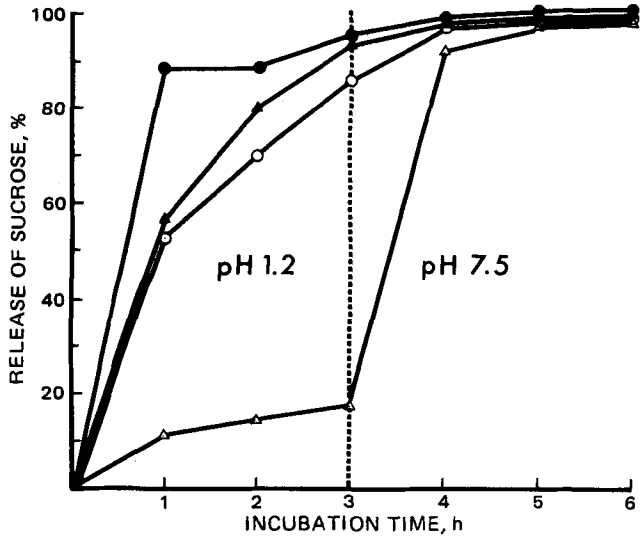

Figure 6—*Influence of pH of the incubation medium on the release of encapsulated sucrose at 37°C. Symbols are the same as in Fig. 5.*

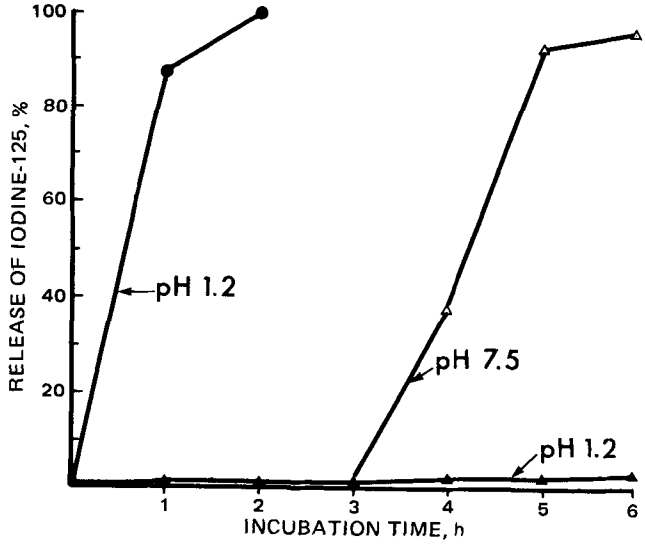

Figure 7—*Influence of pH of the incubation medium on the release of encapsulated concanavalin A at 37°C. Key: (●) uncoated; (▲, △) I–diethyl phthalate–wax coated.*

Before encapsulation, >99% of the iodine-125 activity was associated with trichloroacetic acid-precipitable material. To determine if any degradation or dissociation had occurred during the encapsulation and/or release studies, the hourly samples were adjusted to 10% with respect to trichloroacetic acid and incubated for 30 min at 4°C. Bovine serum albumin (1 mg) was added as a carrier. The resulting precipitates were separated from the supernatant by centrifugation, and both fractions were assayed for radioactivity.

Viral antigen and concanavalin A (a protein with lectin and immunostimulatory activity) were also assayed for biological activity before and after encapsulation. The virus was assayed by its ability to induce circulating antibody formation after intraperitoneal injection into mice, and the concanavalin A was assayed by its ability to agglutinate rabbit erythrocytes.

RESULTS AND DISCUSSION

Figure 1 illustrates the physical appearance of the microspheres. Preparations made with I lot A were dull white in color, whereas those produced with lot B were shiny white. Other characteristics of both preparations were similar. Most experiments presented in this report, however, were carried out with lot A.

Almost all of the microspheres were hollow, and in the large majority of particles the interior was completely sealed. A cross section of the particles revealed that the encapsulated material was dispersed throughout the I matrix in small pockets (Fig. 2). Fully formed quasi-spherical particles were apparent as early as 1 min after addition of the I solution. As seen from the data in Fig. 3, the size of the particles increased with time, reaching a maximum by 5–10 min after initiation. Coacervation of I, sucrose, and core material appeared to be complete since no I and only trace amounts of radioactivity (probably due to free iodine-125) were detected in the paraffin phase after separation of the microspheres.

It appears that formation of the microspheres occurs by stages. Initially, the finely divided suspension of sucrose/core material in the paraffin oil nonsolvent comes in contact with the I solution. Since the paraffin is also a nonsolvent for I, phase separation of the latter occurs with its deposition around the sucrose microparticles. Coated microparticles then aggregate, rapidly forming small hollow spheres. Further deposition of coated material around the aggregate results in the formation of larger spheres until all the suspended material has been utilized.

The data in Fig. 4 show a linear relationship between the weight of the microspheres and the amount of incorporated ^{125}I-labeled antigen. This indicates that the core material is dispersed uniformly among the particles.

Figures 5–7 summarize the disintegration characteristics of the microspheres under simulated gastric and intestinal conditions. From Fig. 5 it can be seen that, with a I–diethyl phthalate–wax coating, <1% of the encapsulated viral radiolabel was released into the gastric medium in 3 h. By comparison, the I–diethyl phthalate and I coatings were not as effective, releasing ~10 and 17%, respectively. Regardless of the coatings applied, however, most of the encapsulated protein was released within the first hour of incubation in the intestinal environment. Only 85–90% of the uncoated viral radiolabel (*i.e.*, lyophilized sucrose–viral antigen alone) was released in the first 3 h. The reason for this is not clear, but it may be due to an artifact in the assay system. There are a number of different proteins in the viral antigen preparation with radiolabel attached. Some of these proteins may have been denatured at the low pH of the simulated gastric juice and may have precipitated, in which case they would not have been measured in the supernatants, after centrifugation, as "released" material. Released under intestinal conditions, the same proteins would have remained soluble.

Although the I and I–diethyl phthalate coatings were effective in retaining the high molecular weight material, they had little effect on the retardation of the sucrose efflux, with almost all sucrose being released into the suspending medium within the 3-h test period. In contrast, when a I–diethyl phthalate-wax coating was applied, <20% was released under the same conditions (Fig. 6).

Figure 7 depicts the release of [^{125}I]concanavalin A from I–diethyl phthalate–wax-coated microspheres. Even after 6 h at low pH, there was <5% release, but there was almost complete breakdown at the intestinal pH of 7.5.

The size of the microspheres to some extent determined their release characteristics. In the experiment summarized in Fig. 8, I-coated microspheres prepared with [^{125}I]bovine albumin as the core material were graded through a series of Tyler sieves mounted on a portable sieve shaker[9]. It can be seen that the smaller the diameter, the more rapid the release. Since the size of the microspheres can be controlled to some extent by the time of addition of the chloroform (Fig. 3), the rate of release of their contents can also be controlled.

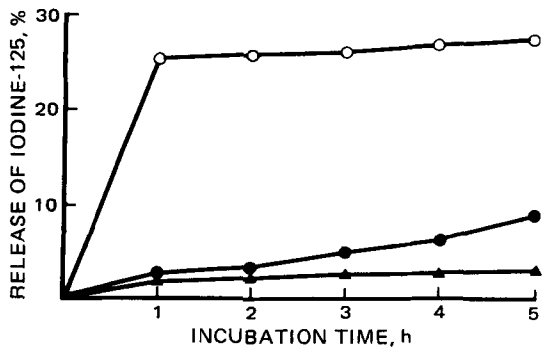

Figure 8—*Influence of size of the microspheres on the release of bovine albumin from simulated gastric juice (without enzymes), pH 1.2, at 37°C. Key: (○) particles retained by a No. 50 sieve; (●) particles retained by a No. 20 sieve; (▲) particles retained by a No. 12 sieve.*

[9] Model RX-24; W. S. Tyler Co. of Canada, Ltd., St. Catherines, Ont.

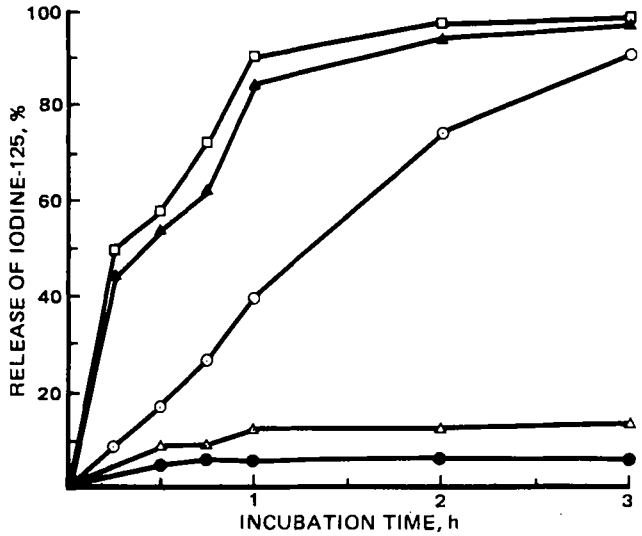

Figure 9—*Effect of pH on the release of viral radiolabel from citrate–phosphate buffer at 37°C. Key: (●) pH 2.5; (△) pH 5.0; (○) pH 6.0; (▲) pH 7.0; (□) pH 8.0.*

The above data indicate that the core materials were effectively released under simulated intestinal conditions. However, the data give no information about the physical state of the labeled material—specifically, whether or not it has been degraded during encapsulation and/or incubation. Studies on trichloroacetic acid-induced precipitation showed that >80% of the viral antigen- and concanavalin A-associated radiolabel was still acid insoluble after 3 h in each of the simulated gastric and intestinal conditions. Additionally, and more importantly, mice injected with the decapsulated viral antigen still produced protective neutralizing antibody titers against rabies virus (indicating that the antigenicity was largely intact), and the decapsulated lectin showed no significant loss of hemagglutinating activity with rabbit erythrocytes.

Figure 9 illustrates the pH dependency of the release of radiolabel from I-diethyl phthalate–wax-coated microspheres with a viral antigen core material. Conditions were the same as in previous experiments except that the buffer system was 0.1 M citrate–phosphate, ranging from pH 2.5 to 8.0. It is clear that the wax coating does not interfere with the release, which is minimal at pH ≤5. Between pH 5 and 7 there is increasingly rapid release, with no significant further increase above pH 7.

CONCLUSIONS

The encapsulation method described here is simple, inexpensive, and rapid; starting with the core material in the form of a finely divided powder, the whole procedure can take <15 min. Furthermore, no specialized equipment is required. The system has similarities to that described by Kitajima and coworkers (11); in their method, however, the core material is suspended in the I solution and the process required 5 h. In the system described here, it was found that if the stirring process was continued for > ~15 min prior to addition of the chloroform, clumping of the microspheres occurred. Since the microspheres were formed considerably before this time, this was no drawback.

In this report, the encapsulation of complex biologicals has been described, but the method can be applied to the encapsulation of many other substances. For example, microspheres have been prepared with such varied materials as cornstarch, tetracycline, saponin, and barium sulfate individually replacing the sucrose. Sucrose microspheres have been prepared containing the following active ingredients (2–60 mg/g of sucrose): scopolamine butylbromide[10], loperamide[11], trifluoperazine–isopropamide[12], and metoclopramide hydrochloride[13]. Encapsulation of cimetidine[14], however, was unsuccessful. The prime requirements appear to be that the materials to be encapsulated are in a finely divided state and that they are insoluble in both the acetone–ethanol and the paraffin phases. The microspheres can also be color-coded by addition of a dye such as malachite green to the I solution, the requirement here being that the dye is insoluble in the paraffin phase.

REFERENCES

(1) C. J. Malm, J. Emerson, and G. D. Hiatt, *J. Am. Pharm. Assoc., Sci. Ed.*, **40**, 520 (1951).

(2) H. C. Hodge, *J. Pharmacol. Exp. Ther.*, **80**, 250 (1944).

(3) H. P. Merkle and P. Speiser, *J. Pharm. Sci.*, **62**, 1444 (1973).

(4) P. L. Madan and S. R. Shanbhag, *J. Pharm. Pharmacol.*, **30**, 65 (1978).

(5) A. Gumma and A. Mirimanoff, *Pharm. Acta Helv.*, **46**, 278 (1971).

(6) D. H. Ferris and A. S. Arambulo, Ger. Offen. 2,343,570 (1974); *Chem. Abstr.*, **81**, 96437u (1974).

(7) R. M. Chanock, R. J. Huebner, and R. B. Couch, U.S. Pat. 3,317,393 (1967); *Chem. Abstr.*, **67**, 31018z (1967).

(8) J. I. Thorell and S. M. Larson, "Radioimmunoassay and Related Techniques. Methodology and Clinical Applications," C. V. Mosby, St. Louis, Mo., 1978.

(9) R. R. Crawford and O. K. Esmerian, *J. Pharm. Sci.*, **60**, 312 (1971).

(10) D. L. Morris, *Science*, **107**, 254 (1948).

(11) M. Kitajima, A. Kondo, S. Asaka, M. Moroshita, and J. Abe, Ger. Offen. 2,105,039 (1971); *Chem. Abstr.*, **75**, 152682k (1971).

ACKNOWLEDGMENTS

This work was supported by Provincial Lottery funds through a contract with the Ontario Ministry of Natural Resources.

[10] Buscopan; Boehringer Ingelheim (Canada) Ltd., Burlington, Ont.
[11] Imodium; Ortho Pharmaceutical (Canada) Ltd., Don Mills, Ont.
[12] Stelabid Forte; Smith, Kline and French (Canada) Ltd., Mississauga, Ont.
[13] Reglan; A. H. Robins Canada Ltd., Montreal, Que.
[14] Tagamet; Smith, Kline and French (Canada) Ltd., Mississauga, Ont.

Dynamics of Clomethiazole Edisylate Interaction with Plastic Infusion Systems

ELIZABETH A. KOWALUK ˣ, MICHAEL S. ROBERTS and ALAN E. POLACK

Received March 29, 1982, from the *School of Pharmacy, University of Tasmania, G.P.O. Box 252C, Hobart, Tasmania, 7001 Australia.* Accepted for publication November 22, 1982.

Abstract □ The dynamics of the interaction of clomethiazole edisylate (I) with polyvinyl chloride and cellulose propionate, the main plastics used in the manufacture of infusion bags and sets, was examined. An experimental system in which the plastic was either open or closed to the environment was used to determine the relative contribution of the sorption and permeation processes to loss from solutions of clomethiazole edisylate (I) in contact with the plastic infusion systems. Sorption by the plastic infusion materials accounted for most of the drug loss, while permeation into the external environment accounted for the remainder. The sorption and permeation into and through polyvinyl chloride was temperature dependent. The diffusion coefficient and permeation rate constant both increased with temperature, while the polyvinyl chloride–water partition coefficients were independent of temperature. The activation energy for the diffusion in polyvinyl chloride was 13.5 kcal/mol. The permeability of the infusion bag plastic and the evaporation across an unstirred air boundary layer adjacent to the external surface of the plastic both appeared to contribute to the overall diffusional resistance encountered in the permeation process. The plastic–water partition coefficients are independent of initial concentration, suggesting that the concentration-dependent loss of the drug from solutions stored in plastic infusion bags and burets is a result of the greater diffusivity of the drug in the plastic at the higher initial concentrations. Plasticization of the polymers by the drug is indicated by the increase in the diffusivity of the drug in polyvinyl chloride and cellulose propionate, the increase in the rate and extent of sorption of a radiolabeled marker (diazepam) by the plastic, and the decreased stiffness of polyvinyl chloride exposed to higher concentrations of the drug.

Keyphrases □ Clomethiazole edisylate—dynamics of interaction with plastic infusion systems, polyvinyl chloride, cellulose propionate □ Infusion systems, plastic—dynamics of clomethiazole edisylate interaction, polyvinyl chloride, cellulose propionate □ Polyvinyl chloride—dynamics of clomethiazole edisylate interaction with plastic infusion systems, cellulose propionate □ Cellulose propionate—dynamics of clomethiazole edisylate interaction with plastic infusion systems, polyvinyl chloride

Clomethiazole edisylate (I), a sedative and hypnotic with anticonvulsant properties (1), has been administered by intravenous infusion in the treatment of delirium tremors (1), pre-eclampsia, and eclampsia (2, 3) and to control status epilepticus (4, 5). Infusions of I have also been used for sedation of patients having surgery under epidural anesthesia (6) or receiving artificial ventilation of the lungs during intensive care (7).

During the course of recent investigations it was observed that the drug was lost from solutions stored in plastic infusion bags and during infusion through plastic administration sets. The loss was attributed to sorption and possibly permeation of the drug through the plastic components of the intravenous delivery systems (8, 9). Tsuei and coworkers (10) have also reported sorption of I by plastic infusion sets and have suggested that I is lost from the infusion set to the atmosphere. The present work reports on the relative contribution of sorption and permeation to the loss of I from solutions stored in polyvinyl chloride infusion bags and cellulose propionate buret chambers. The kinetics and thermodynamics of the sorption process are also examined, as are the kinetics of the permeation process.

Lingham *et al.* (11) have noted that "intravenous clomethiazole reacts with the plastic giving sets and may soften the burette." Softening of polyvinyl chloride infusion bags after contact with solutions has also been observed (8). It was suggested that this may be due to the ability of the drug to plasticize or swell the polyvinyl chloride resin. This hypothesis was investigated in the present work by monitoring the rate and extent of sorption of a radiolabeled marker substance (diazepam) by infusion bags and burets in the presence of varying concentrations of I. In addition, the softening of polyvinyl chloride on exposure to solutions of clomethiazole edisylate (I) was measured using tensile creep tests.

EXPERIMENTAL

Materials—Solutions of clomethiazole edisylate (I) were prepared by diluting I infusion solution[1] (0.8%) with 4% dextrose solution. The pH of each solution was measured[2] and found to be the same as that of the undiluted infusion solution (pH 5.8 ± 0.1). The storage studies were conducted using polyvinyl chloride infusion bags[3] and the cellulose

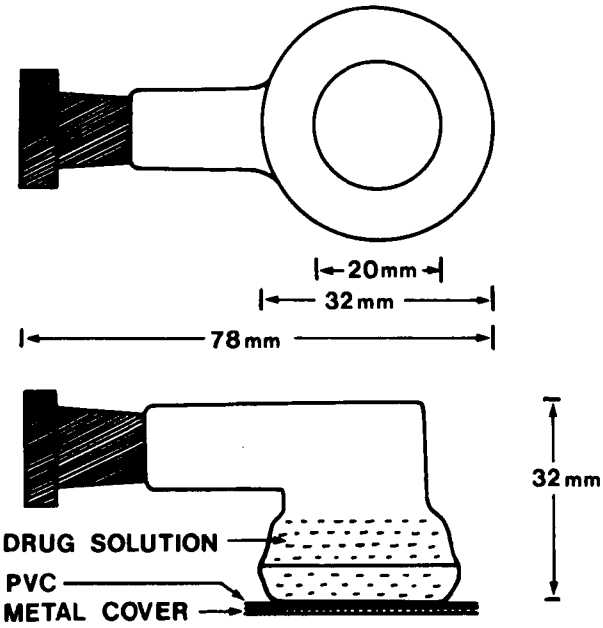

Figure 1—*Diagrammatic representation of the diffusion cell used in permeation studies. The plastic sheet (PVC) is held between the drug solution and the annular (open diffusion cell) or solid square (closed diffusion cell) metal cover by a metal clamp. The cells were stored resting on a wire gauze in the position shown in the lower diagram.*

[1] Heminevrin, batch FL1911 lot D106; Astra Pharmaceuticals, Sodertalje, Sweden.
[2] Metrohm Hensau E520 pH meter.
[3] Viaflex (polyvinyl chloride), code AHB8098 empty container, 500 mL, batch R39NO; Travenol Laboratories, Old Toongabbie, NSW, Australia, 2146.

0022-3549/84/0100-0043$01.00/0
© 1984, American Pharmaceutical Association

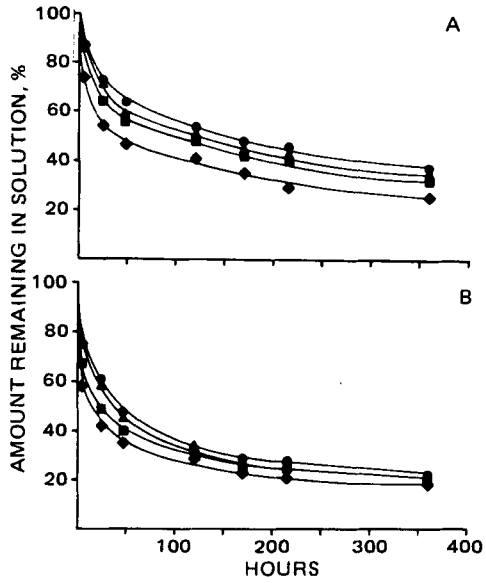

Figure 2—*Percentage of I remaining in solutions stored in polyvinyl chloride infusion bags (A) and cellulose propionate buret chambers (B). Initial I concentration: (●) 0.2%; (▲) 0.4%; (■) 0.6%; (◆) 0.8%.*

propionate buret chambers of the infusion sets[4]. The buret chambers were separated from the infusion tubing, and the outlet of each chamber was closed using a metal screw clamp. Where strips or sheets of polyvinyl chloride or cellulose propionate were required, these were cut from the unprinted areas of the infusion bags and buret chambers. The polyvinyl chloride tubing used for permeation studies was cut from an infusion set[4]. All experiments in the present study were performed in duplicate.

Storage Studies—Loss of clomethiazole edisylate (I) and the effect of this drug on the loss of the radiolabeled marker (diazepam) from solution during storage in plastic infusion bags and buret chambers were examined in the following manner. Each infusion bag and isolated buret chamber was filled with 500, and 150 mL, respectively, of I solution prepared at concentrations of 0.2, 0.4, 0.6, or 0.8%, or with diluent. In addition, each solution contained [methyl-^{3}H]diazepam[5] at a concentration of 1.8×10^{-8} mg/mL, 8.2×10^3 dpm/mL; 100 mL of each solution was stored in a glass container to act as a control. The infusion bags, buret chambers, and glass controls were stored in a controlled-temperature room at 20 ± 1°C. Aliquots of drug solution were removed from each container immediately after introduction of the solution and at regular intervals during storage, and assayed for I and diazepam content.

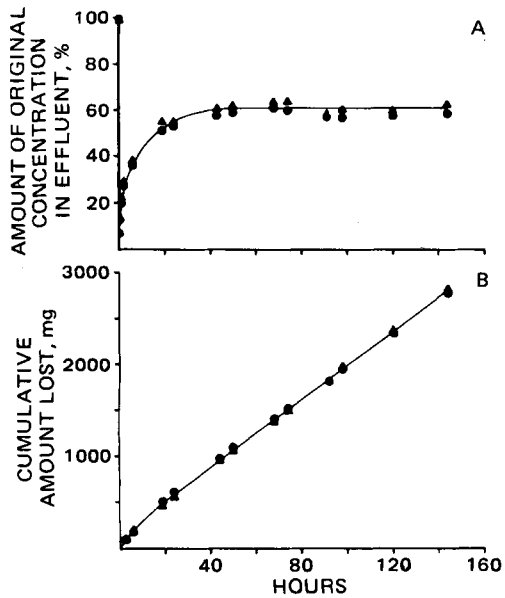

Figure 3—*Percentage of original I concentration in the effluent (A) and cumulative amount of I lost from solution (B) at various times during infusion through polyvinyl chloride tubing at a flow rate of 0.095 mL/min. Key: (●) infusion tubing only (open); (▲) infusion tubing encased by glass tubing (closed).*

[4] Code ACH0317 solution administration set, batch no. R39F8; Travenol Laboratories, Old Toongabbie, NSW, Australia.

[5] New England Nuclear, Boston, MA 02118.

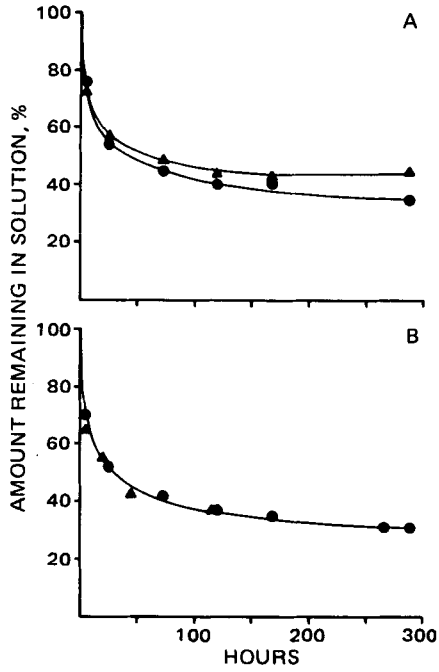

Figure 4—*Percentage of I remaining in solutions stored in open (●) and closed (▲) diffusion cells in contact with polyvinyl chloride (A) or cellulose propionate (B) sheets at 20°C.*

Permeation Studies—The permeation of clomethiazole edisylate (I) through polyvinyl chloride and cellulose propionate sheets was examined using the diffusion cell shown in Fig. 1. A sheet of polyvinyl chloride or cellulose propionate was held firmly in place across the cell opening by either an annular or solid square stainless steel sheet. In this way the plastic sheet was either open to the ambient environment, permitting transfer of molecules of I to the atmosphere, or closed, preventing such transfer. A volume of I infusion solution (4.4 mL) sufficient to result in the same surface area of plastic–volume ratio as in the infusion bags was stored in each diffusion cell at 4 ± 1°C, 10 ± 1°C, 20 ± 1°C, and 36 ± 1°C. Aliquots of solution were removed from the cells periodically during storage and assayed for clomethiazole edisylate content. Solutions were also stored in glass containers to act as controls.

Plastic–water partition coefficients were calculated as the ratio of the equilibrium concentration of the drug in the plastic and aqueous phases in the closed system. The concentrations were calculated as weight of drug per weight of water or plastic in contact with the solution.

Permeation of clomethiazole edisylate (I) through polyvinyl chloride tubing was examined using two 150-cm lengths of tubing—one encased tightly by glass tubing (closed), the other left exposed to the atmosphere (open). Infusion solution (0.8% of I) was infused[6] through the tubings at an average flow rate of 0.095 mL min for a period of 144 h. The effluent was collected over 10-min intervals at specified times for analysis.

Evaporation—The evaporation of I was examined at various temperatures by storing 9.8 mL of the 0.8% infusion solution in an open 25-mL glass beaker to give the same surface area of solution–volume ratio as in the infusion bags. The percentage of I remaining at various times was calculated by determining the drug concentration of the solution and correcting for water loss. Evaporation of water was monitored by weighing each beaker of solution at the time of assay. Evaporation rate constants were evaluated from the slopes of log percentage remaining *versus* time plots.

Tensile Properties—An experiment was designed to examine the stiffness of polyvinyl chloride strips exposed to solutions of clomethiazole edisylate (I). The stiffness of a plastic film can be assessed by examining its stress–strain curve. Because of the viscoelastic nature of plastics, stress–strain relationships are measured indirectly by tensile creep tests,

[6] Waters Associates M45 solvent delivery system.

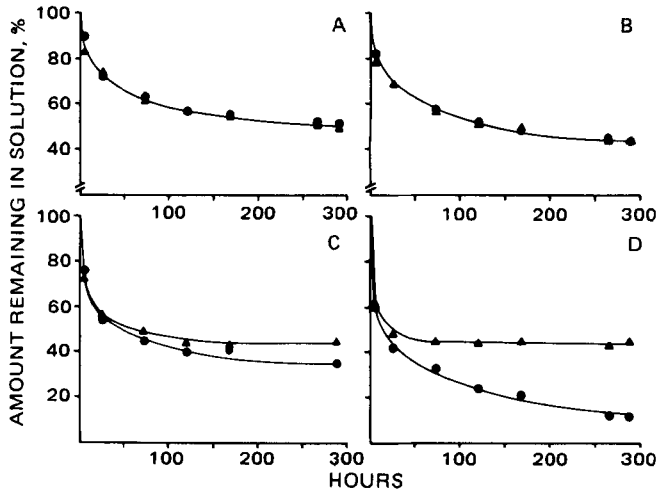

Figure 5—*Percentage of I remaining in solutions stored in open (●) and closed (▲) diffusion cells in contact with polyvinyl chloride sheets at 4°C (A), 10°C (B), 20°C (C), and 36°C (D).*

the results of which may be expressed in the form of strain–time curves at constant stress. Isochronous stress–strain curves can be plotted from the strain–time curves (12, 13). Strips of polyvinyl chloride (12.5 cm × 1 cm) were stored in I solution (0.2, 0.4, 0.6, and 0.8%) or in diluent in glass containers; after 9 d they were removed, rinsed lightly with distilled water, and allowed to dry. Each strip was suspended from a fixed clamp and loads of 517, 770, or 1020 g were applied to the end of the strip. The length of the strip was measured before and at regular intervals for at least 48 h after application of the load. Experiments were performed at room temperature (15–20°C).

Equilibrium Sorption Studies—Strips of polyvinyl chloride and cellulose propionate (1 × 1 cm) were stored in 5 mL of the drug solution (0.2, 0.4, 0.6, or 0.8%) in a glass container until equilibrium was reached (≤168 h). Plastic–water partition coefficients were calculated as the ratio of equilibrium concentrations of clomethiazole edisylate (I) in the plastic and the aqueous phases. The concentrations were calculated as weight of drug per weight of plastic or water.

Assay of Drug Solutions—Solutions of clomethiazole edisylate (I) were assayed spectrophotometrically[7]. Solutions were diluted 1:200 with distilled water, and the absorbance was measured at 257 nm. The absorbance of the infusion solutions was proportional to concentration of I over the concentration range studied. Solutions were analyzed for diazepam content by placing a 200-μL aqueous sample in a counting vial[8] together with 5 mL of scintillation cocktail[9] and determining the radioactivity by liquid scintillation counting[10].

RESULTS AND DISCUSSION

The loss of clomethiazole edisylate from aqueous solutions stored in polyvinyl chloride infusion bags and cellulose propionate buret chambers at 20°C is shown in Fig. 2. Extensive concentration-dependent losses are observed in both cases, confirming and extending previous reports (8, 9). It can be concluded, by comparing the losses found in this study with those previously observed (8, 9), that the loss of I was unaffected by the presence of trace amounts of radiolabeled diazepam. Significant I losses were also observed from solutions infused through polyvinyl chloride tubing (Fig. 3). Since the loss of I from solutions stored in glass for 400 h was negligible, it is reasonable to suggest that the loss of this drug during storage in plastic infusion bags and burets and during infusion through plastic tubing is the result of sorption of the drug by the plastic (and possibly its subsequent permeation into the atmosphere) (8–10). Sorption appears to be the predominant mechanism of the loss in all three cases (Figs. 3 and 4). Figure 4A shows that the loss is decreased, and eventually reaches equilibrium, when the polyvinyl chloride sheet is covered by metal. However, loss from solution in the open diffusion cell continued, suggesting that permeation also contributes to the loss from polyvinyl chloride infusion bags. No difference was observed in losses from solution

[7] Beckman DB-G grating spectrophotometer.
[8] Packard Minivial.
[9] Packard Insta-Gel Liquid scintillation cocktail.
[10] LKB Wallac RackBeta II Liquid scintillation counter.

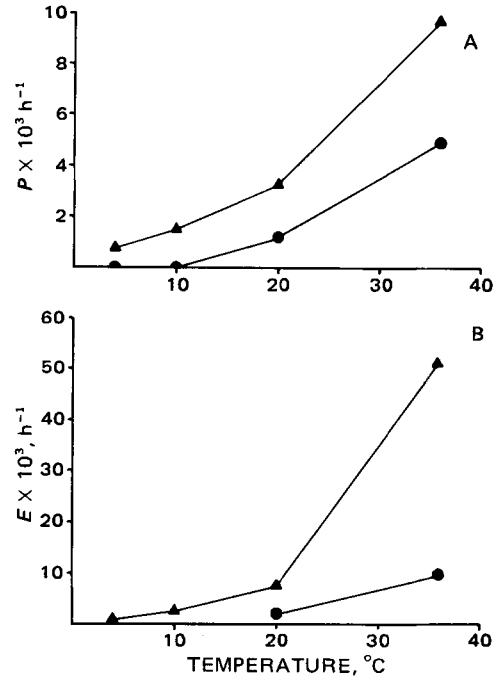

Figure 6—*(A) Rate constants for the permeation of I through polyvinyl chloride (P_{exp}) determined from open cell data (●) and membrane permeability rate constants (P_m) calculated by substituting D and K from closed cell data into Eq. 2 (▲). (B) Rate constants for the evaporation of I across the unstirred air boundary layer adjacent to the external surface of the polyvinyl chloride sheet in the open diffusion cell (●) and for the evaporation of I from aqueous solution (▲).*

in the open and closed infusion tubing (Fig. 3). However, the odor of I could be detected in the vicinity of the open tubing after the third day of infusion, suggesting that some permeation of I to the environment occurs. Permeation of I through cellulose propionate was not detected (Fig. 4B).

Kinetics of Sorption and Permeation—The sorption of clomethiazole edisylate (I) by polyvinyl chloride and cellulose propionate has been described previously as a diffusion-controlled process (8, 9). According to the diffusion model, the rate and extent of sorption is determined by the plastic–water partition coefficient of the solute and its diffusion

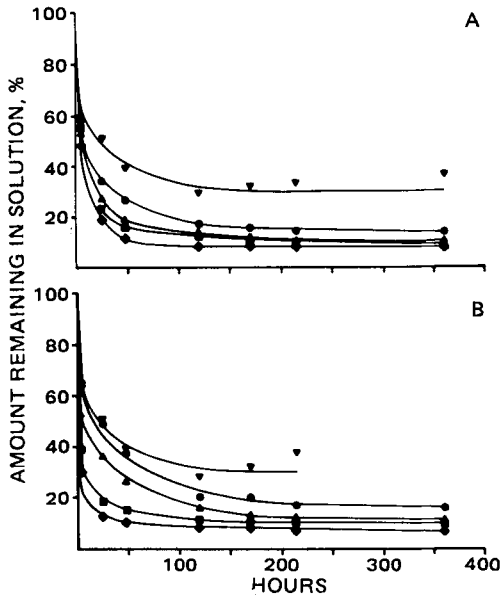

Figure 7—*Percentage of diazepam remaining in solutions containing different initial concentrations of I at various times during storage in polyvinyl chloride infusion bags (A) and cellulose propionate buret chambers (B). Key: (▼) diluent only; (●) 0.2%; (▲) 0.4%; (■) 0.6%; (◆) 0.8%.*

Table I—Diffusion Coefficients, Half-Times for Sorption, and Plastic–Water Partition Coefficients of I [a]

Temperature, °C	Apparent Diffusion Coefficient × 10^5, cm^2/h	$t_{1/2}$, h	Plastic–Water Partition Coefficient [b]
	Polyvinyl Chloride		
4	0.241	28	41
10	0.491	19	41
20	1.1	6.5	41
36	3.1	2	41
	Cellulose Propionate		
20	1.4	6.5	42

[a] Initial I concentration: 0.8%. [b] Determined from closed diffusion cell studies.

coefficient in the plastic. The fraction of the drug remaining in solution (F_t) at various times (t) is (14, 15):

$$\frac{F_t - F_\infty}{1 - F_\infty} = \sum_{n=1}^{\infty} \frac{2\alpha(1+\alpha)}{1 + \alpha + \alpha^2 q_n^2} \exp\left(-q_n^2 \frac{D_t}{l^2}\right) \qquad \text{(Eq. 1)}$$

where F_∞ is the fraction of I remaining in solution at equilibrium, $\alpha = F_\infty/(1 - F_\infty)$, q_n values are the nonzero positive roots of $\tan q = -\alpha q$, and D is the diffusion coefficient of solute in the plastic of thickness l. In the present work the diffusion coefficients of I in polyvinyl chloride and cellulose propionate were determined from plots of log $(F_t - F_\infty)$ *versus* time for the closed diffusion cell, using Eq. 1. In addition half-times for sorption were determined by inspection of disappearance profiles for the closed diffusion cell. These values and the plastic–water partition coefficients are shown in Table I.

The rate of sorption is temperature dependent, appearing to progress more rapidly at higher temperatures (Fig. 5). The half-time for sorption decreases and its diffusion coefficient increases with increasing temperature. In contrast, the plastic–water partition coefficients appear to be independent of temperature over the temperature range examined (Table I). The temperature dependence of the sorption process is, therefore, a result of the increased diffusivity in the polymer matrix, the equilibrium fractional uptake being unaffected by changes in temperature.

The permeation is also a temperature-dependent process. Figure 5 shows that while at the lower temperature permeation through polyvinyl chloride appears to be negligible, at 36°C a large percentage of the initial amount of the drug contained in the solution is lost by permeation to the atmosphere. Rate constants for the permeation process (P_{exp}) were determined from the slope of the terminal phase of log percentage I remaining in solution *versus* time plots for the open diffusion cell (Fig. 6A). It is apparent that the permeation process is more rapid at higher temperatures.

The membrane permeability rate constant (P_m) for I in polyvinyl chloride may be evaluated by substituting the values of the apparent diffusion coefficient (D) and the polyvinyl chloride–water partition coefficient (K) determined for the closed system (Table I) into the following (16):

$$P_m = \frac{DKA}{2.303Vl} \qquad \text{(Eq. 2)}$$

Table II—Plastic–Water Partition Coefficients of I at Different Initial Concentrations [a]

Concentration of I, %	Plastic–Water Partition Coefficient
Polyvinyl Chloride	
0.2	55
0.4	58
0.6	55
0.8	53
Cellulose Propionate	
0.2	80
0.4	71
0.6	77
0.8	77

[a] Determined using equilibrium sorption studies.

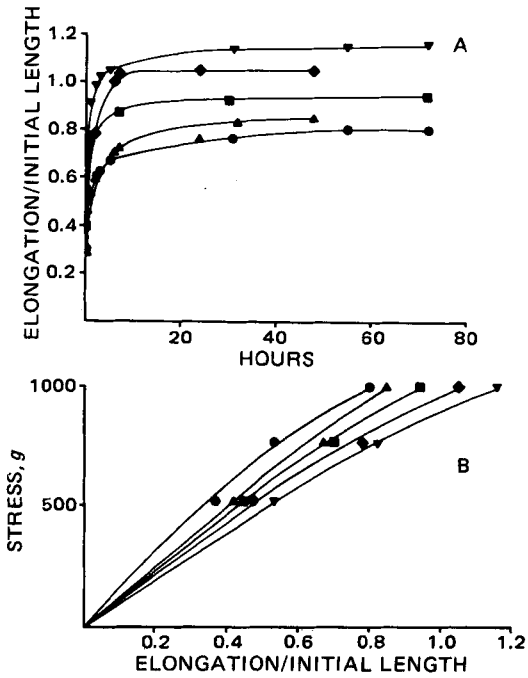

Figure 8—*Strain–time curves at a constant stress of 1020 g (A) and 48-h isochronous stress–strain curves (B) for polyvinyl chloride strips treated with I solutions of various initial concentrations. Key: (▲) 0.2%; (■) 0.4%; (◆) 0.6%; (▼) 0.8%; (●) diluent only.*

where V is the volume of I solution in contact with an area (A) of polyvinyl chloride of thickness l. The use of Eq. 2 in the present context assumes that the extent of plasticization in the open and closed systems is identical. P_m is related to the final observed permeation rate constant (P_{exp}) by (17, 18):

$$\frac{1}{P_{exp}} = \frac{1}{P_m} + \frac{1}{E} \qquad \text{(Eq. 3)}$$

where E represents the rate of evaporation of I across an unstirred air boundary layer adjacent to the external surface of the plastic in the open diffusion cell.

Figure 6A and B shows the individual rate constants at different temperatures. Values of E, calculated using Eq. 3, are of similar magnitude to the values of P_m, suggesting that the permeability of the infusion bag plastic and the evaporation of I across an unstirred air boundary layer contribute to a similar extent to the overall diffusional resistance encountered in the permeation process. Rate constants for the evaporation of I from aqueous solution at different temperatures are shown in Figure 6B. It is apparent that the evaporation of the drug from solution is faster than its evaporation from polyvinyl chloride, suggesting that I has a lower vapor pressure in the plastic than in water.

At a storage temperature of 20°C permeation is evident after 24 h (Fig. 5C). This lag time probably reflects the time required for the drug molecules to travel through the polyvinyl chloride film to its external surface. It can be seen from Fig. 5D that the lag time is much shorter at 36°C. This is consistent with increased diffusivity of I in the polyvinyl chloride at the higher temperature. The lag time for I in polyvinyl chloride tubing is apparently longer than in the infusion bag plastic, since no difference was observed in loss from the open and closed tubing during the 6 d of infusion (Fig. 3). The longer lag time is consistent with the greater thickness and density of the infusion tubing plastic compared with infusion bag plastic.

The results of this study suggest that the constant rate of I loss from solutions infused through a plastic administration set does not reflect loss of the drug to the atmosphere as suggested by Tsuei *et al.* (10), but that it results mainly from sorption. The constant rate of I sorption into the infusion tubing over 1–6 d (Fig. 3) is consistent with the plastic acting as a semi-infinite sink over this time. Kowaluk *et al.* (9) have reported that the sorption of a number of other drugs by plastic infusion tubing also shows a constant rate over a limited period and have described an equation relating the steady-state effluent concentrations of those drugs sorbed by tubing (in the period in which the plastic acts as a semi-infinite sink) to the infusion conditions.

Thermodynamics of Sorption—The plastic–water partition coeffi-

cient (K) can be related to the thermodynamic parameters in the partition process by (19, 20):

$$\log K = \frac{-\Delta H^0}{2.303RT} + \frac{\Delta S^0}{2.303R} \qquad \text{(Eq. 4)}$$

where ΔH^0 and ΔS^0 are the standard enthalpy and entropy changes of partition, respectively, R is the gas constant, and T is the temperature. Since the polyvinyl chloride–water partition coefficient is independent of temperature (Table I), the standard enthalpy of transfer is zero, implying an entropy-controlled partition process (20). The positive entropy change associated with this process probably reflects movement of I molecules from the relatively ordered aqueous environment to the more random environment of the polymer matrix.

The diffusion of solute molecules through a polymeric field has been described as a series of jumps from one hole to another, the holes being formed by movements of the polymer chains (21, 22). The energy required to move the polymer chains apart sufficiently to create a hole and to move the diffusing molecule into this hole corresponds to the activation energy of diffusion. This energy is supplied by the kinetic energy of the polymer chains and of the diffusing molecule (22). The activation energy of diffusion for I in polyvinyl chloride, determined from the Arrhenius equation, has a value of 13.5 kcal/mol. This value is of the same order as that for the organic nitrates (23) and would be consistent with the hypothesis (22) that the energy required for diffusion of solute molecules in polyvinyl chloride is supplied mainly by the kinetic energy of the polymer chains and to a lesser degree by the kinetic energy of the diffusing molecule. The increase in diffusivity of I in the polyvinyl chloride with temperature probably reflects an increase in the kinetic energy of the polymer chains at higher temperatures (22).

Plasticization—It has previously been suggested that the concentration-dependent loss of I from solutions stored in plastic infusion bags and burets (Fig. 2) is the result of the plasticization process (8, 9). Plasticizer molecules insert themselves between the polymer chains, reducing the intermolecular forces between the polymer chains and generating additional free volume (22–26). Consequently, plasticizers accelerate the diffusive process (21) and produce greater flexibility and softness of the material (22).

It is apparent that the increased drug loss at higher concentrations cannot be attributed to a greater affinity of I for the drug-impregnated plastic, since the I–plastic–water partition coefficients are independent of initial drug concentration (Table II). Increased loss is probably due to greater diffusivity of I in the polymer matrix at higher drug concentrations, consistent with plasticization. The rate and extent of sorption of the marker substance (diazepam) by plastic infusion bags and buret chambers [a diffusion-controlled process (8, 9)] is enhanced by the presence of I in the infusion solutions (Fig. 7), further suggesting plasticization of the plastic matrix of bags and burets by the drug (17). Bray and Meakin (27) have shown that the sorption and permeation of benzocaine through polyvinyl chloride increased with increasing concentration of the plasticizers di-2-ethylhexylphthalate and tri-*n*-butyl citrate.

Figure 8 shows strain–time curves at constant stress and isochronous stress–strain curves (12, 13) for I-treated polyvinyl chloride strips. These curves are concentration dependent; the stiffness of the polyvinyl chloride decreases with increasing drug concentrations. These data confirm the previously reported softening and greater pliability of plastic infusion bags in the presence of the solutions (8) and provides further evidence for plasticization of polyvinyl chloride by clomethiazole edisylate (I).

The present study has shown that the loss of I from solutions stored in plastic infusion bags and buret chambers or infused through plastic tubing depends on (*a*) the partitioning of the drug between the plastic and aqueous phases, (*b*) the diffusion of I in the plastic matrix, (*c*) the evaporation of the drug across an unstirred air boundary layer, (*d*) the type of plastic, and (*e*) changes in the permeability characteristics of the plastic with drug concentration. Each of these processes must be taken into account in arriving at a predictive method for determining the extent of drug interactions with intravenous delivery systems.

As we know of no other drug which plasticizes polyvinyl chloride, it is not possible to define, using structure–activity relationships, the factors determining the ability of I to act as a plasticizer. However, the possibility that other drugs may plasticize polyvinyl chloride cannot be overlooked.

REFERENCES

(1) Astra Pharmaceuticals Pty. Ltd., Heminevrin package insert, Sodertalje, Sweden.

(2) J. Varma, *J. Obstet. Gynaecol. Br. Emp.*, **79,** 513 (1972).

(3) E. Tischler, *Aust. N.Z. J. Obstet. Gynaecol.*, **13,** 137 (1973).

(4) P. K. P. Harvey, T. W. Higenbottam, and L. Loh, *Br. Med. J.*, **2,** 603 (1975).

(5) G. Bentley and R. Mellick, *Med. J. Aust.*, **1,** 537 (1975).

(6) S. A. Schweitzer, *Anesth. Intens. Care (Berlin)*, **6,** 248 (1978).

(7) D. B. Scott, D. Beamish, I. N. Hudson, and G. G. Jostell, *Br. J. Anaesth.*, **52,** 541 (1980).

(8) E. A. Kowaluk, M. S. Roberts, H. D. Blackburn, and A. E. Polack, *Am. J. Hosp. Pharm.*, **38,** 1308 (1981).

(9) E. A. Kowaluk, M. S. Roberts, and A. E. Polack, *Am. J. Hosp. Pharm.*, **39,** 460 (1982).

(10) S. E. Tsuei, R. L. Nation, and J. Thomas, *Eur. J. Clin. Pharmacol.*, **18,** 333 (1980).

(11) S. Lingham, H. Bertwhistle, H. M. Elliston, and J. Wilson, *Br. Med. J.*, **280,** 155 (1980).

(12) S. Levy and J. H. DuBois, "Plastics Product Design Engineering Handbook," Van Nostrand Reinhold, New York, N.Y., 1977.

(13) R. H. Ogorkiewicz, "The Engineering Properties of Plastics," Oxford University Press, Oxford, England, 1977.

(14) J. Crank, "The Mathematics of Diffusion," 2nd ed., Clarendon Press, Oxford, England, 1975.

(15) M. S. Roberts, P. A. Cossum, A. J. Galbraith, and G. W. Boyd, *J. Pharm. Pharmacol.*, **32,** 237 (1980).

(16) H. Davson, "A Textbook of General Physiology," 4th ed. Vol. 1, Churchill, London, 1970, p. 395.

(17) G. L. Flynn and S. M. Yalkowsky, *J. Pharm. Sci.*, **61,** 838 (1972).

(18) E. M. Wright and R. J. Pietras, *J. Membr. Biol.*, **17,** 293 (1974).

(19) J. M. Diamond and E. M. Wright, *Annu. Rev. Phys.*, **31,** 581 (1969).

(20) M. S. Roberts, R. A. Anderson, D. E. Moore, and J. A. Swarbrick, *Aust. J. Pharm. Sci.*, **6,** 77 (1977).

(21) G. L. Flynn in "Advances in Experimental Medicine and Biology," Vol. 47, A. C. Tanquary and R. E. Lacey, Eds., Plenum, New York, N.Y., 1974, p. 73.

(22) J. Autian in "Dispensing of Medication," E. W. Martin, Ed., Mack Publishing Co., Easton, Pa., 1971, p. 652.

(23) P. A. Cossum, M.Pharm. thesis, University of Tasmania, 1981.

(24) J. Autian, *J. Pharm. Sci.*, **52,** 1 (1963).

(25) J. A. Brydson, "Plastics Materials," 3rd ed., Newnes-Butterworths, London, 1975.

(26) P. D. Ritchie, "A Chemistry of Plastics and High Polymers," Cleaver-Hume Press, London, England, 1979.

(27) C. S. Bray and B. J. Meakin, *J. Pharm. Pharmacol.*, **29,** 49P (1975).

ACKNOWLEDGMENTS

This research was supported in part by a grant from the National Health and Medical Research Council, Australia.

The donations of infusion bags and sets by Travenol Laboratories and Heminevrin infusion solution by Astra Pharmaceuticals, Australia are acknowledged.

Effect of Systemic Anaphylaxis on the Absorption of Salicylic Acid from the Rat Small Intestine

AKIRA YAMAMOTO, JUNZO NAKAMURA, SHIGEYUKI TAKADA, TOSHIKIRO KIMURA, and HITOSHI SEZAKI ×

Received August 10, 1982, from the *Department of Pharmaceutics, Faculty of Pharmaceutical Sciences, Kyoto University, Kyoto 606, Japan.* Accepted for publication November 2, 1982.

Abstract □ Rats were immunized by intraperitoneal injection of ovalbumin (egg albumin) emulsified in Freund's incomplete adjuvant, and then the effect of an intravenous challenge with ovalbumin on salicylic acid absorption from the small intestine was examined by means of an *in situ* recirculation technique. The disappearance of salicylic acid from the luminal solution was significantly decreased in rats treated with ovalbumin compared with control groups treated with saline. The decreased absorption of salicylic acid in ovalbumin-immunized rats was related to the anti-ovalbumin antibody responses examined by passive cutaneous anaphylactic reactions. On the other hand, the decreased absorption of salicylic acid was not found in ovalbumin-immunized rats challenged intravenously with bovine γ-globulin. Similar results were also noted in rats immunized *via* the footpads with ovalbumin. However, no significant change was observed in the intestinal absorption of salicylic acid in normal (nonimmunized) rats challenged intravenously with ovalbumin. Furthermore, intestinal absorption of sulfadimethoxine and sulfanilamide was significantly decreased during systemic anaphylaxis, whereas no change was observed in the absorption of sulfisoxazole, quinine, sulfanilic acid, and phenolsulfonphthalein. This suggests that the intestinal absorption of rapidly absorbed drugs, including salicylic acid, is more sensitive to systemic anaphylaxis than that of poorly absorbed drugs.

Keyphrases □ Salicylic acid—intestinal absorption, effect of anaphylaxis, rats □ Absorption, intestinal—salicylic acid, effect of anaphylaxis, rats □ Anaphylaxis—effect on intestinal absorption of salicylic acid, rats

In a previous paper, it was reported that the intestinal absorption of salicylic acid was decreased by the intravenous challenge with bovine γ-globulin in rats immunized intraperitoneally with the same antigen, and it was suggested that systemic anaphylaxis influenced the intestinal absorption of drugs (1). The present report concerns the effect of intravenous challenge with ovalbumin on the intestinal absorption of salicylic acid in rats immunized parenterally with ovalbumin. Ovalbumin was chosen on the grounds that (*a*) ovalbumin induces a good humoral and cellular response in the guinea pig, as demonstrated by Audibert *et al.* (2), (*b*) ovalbumin is widely used for IgE antibodies (3, 4), and (*c*) ovalbumin is one of the most potent immunogens in rats (5–8). To prove the immunogenicity, the anti-ovalbumin antibody was examined by the passive cutaneous anaphylaxis technique (9–14), and the intestinal absorption of various drugs was investigated to clarify the mechanisms by which the absorption of salicylic acid was decreased during systemic anaphylaxis.

EXPERIMENTAL

Materials—Ovalbumin[1] (crystallized and lyophylized) and bovine γ-globulin[1] (Cohn fraction II) were used without further purification. Salicylic acid[2], sulfadimethoxine[2], sulfanilamide[2], sulfisoxazole[2], quinine[2], sulfanilic acid[2], phenolsulfonphthalein[2], and all reagents[2] used in these experiments were reagent grade.

The isotonic buffer solution (pH 6.5) was prepared from 0.123 M Na_2HPO_4 and 0.163 M NaH_2PO_4. Salicylic acid was dissolved in this buffer solution at a concentration of 1 mM for absorption experiments. All other drugs were dissolved in the same buffer solution at a concentration of 0.1 mM.

Immunization—Male Wistar albino rats, 150–200 g, were used in these studies and were maintained on a diet free of ovalbumin and bovine γ-globulin. For intraperitoneal immunization, 1 mg of ovalbumin dissolved in 0.25 mL of saline (0.9% w/v) was emulsified with an equal volume of Freund's incomplete adjuvant[3] and was injected into the peritoneal cavity under light ether anesthesia. For footpad immunization, 0.5 mL of ovalbumin dissolved in 0.05 mL of saline was emulsified with an equal volume of Freund's incomplete adjuvant and was injected into both the right and left footpads under light ether anesthesia. The same dose of antigen with adjuvant was administered at 10-d intervals thereafter. Animals were immunized 1–3 times, and absorption studies were carried out 1 week after the last immunization.

Antiserum and Passive Cutaneous Anaphylaxis—Blood obtained by heart puncture 10 days after the last immunization was allowed to clot at room temperature, stored overnight at 4°C, and centrifuged for 10 min at 3000 rpm. The passive cutaneous anaphylaxis method used was similar to that described by Goose and Blair (9). The titer of the antisera was estimated by serial dilution from 1:1 to 1:32. After light intraperitoneal pentobarbital anesthesia, the hair was removed from the back of the rat with an electric clipper. Diluted anti-ovalbumin sera (0.1 mL) was injected intracutaneously at six skin sites. Seventy-two hours after the intracutaneous injection, 10 mg of antigen dissolved in 1 mL of saline containing 0.5% (w/v) Evans blue dye was administered intravenously. The animals were killed 30 min after the challenge, and the skin was excised. The diameters of the blue discolorations were measured, and the wheals were scored as 0 for <5 mm, 1 for 5–10 mm, 2 for 10–15 mm, 3 for 15–20 mm, and 4 for >20 mm.

Absorption studies—The procedure of the *in situ* absorption study in the rat small intestine was the same as that reported previously (15). Briefly, animals were anesthetized with intraperitoneal pentobarbital, and the small intestine was cannulated for *in situ* recirculation. The entire length of the small intestine, from the pylorus to the ileocecal junction, was used for the absorption studies. The bile duct was ligated in all experiments. Ovalbumin dissolved in 0.25 mL of saline was administered into a right femoral vein for 5 min. Immediately thereafter, 40 mL of a drug solution kept at 37°C was recirculated through the intestine at a rate of 5 mL/min using a peristaltic pump. At the end of an experimental period, the perfused solution in the small intestine was withdrawn as completely as possible, and the intestinal lumen was washed with pH 6.5 buffer solution. The washings were combined with the perfused solution and made up to 100 mL with pH 6.5 buffer solution. The amount absorbed by the lumen was calculated as the difference between the amount of the drug in the initial and the final solutions. Results were expressed as the mean ± *SD*. Statistical analyses were performed using the Student's *t* test.

Analytical Methods—*Salicylic Acid*—Three milliliters of sample solution was acidified with 0.1 mL of concentrated HCl and extracted with 7 mL of chloroform. An aliquot of the organic phase was then shaken with 0.1 M NaOH, and the optical density of the aqueous phase was determined spectrophotometrically at 295 nm.

Aromatic Amines—All the aromatic amines were diazotized, coupled with 2-diethylaminoethyl-1-naphthylamine, and then were extracted with isoamyl alcohol after the addition of sodium chloride. The optical density of the organic layer was determined at each absorption maximum, 552–560 nm (16).

Quinine—Three milliliters of a sample solution was alkalinized with 1 ml of 3 M NaOH and extracted with 6 ml of ethylene dichloride. An

[1] Sigma Chemical Co., St. Louis, Mo.
[2] Nakarai Chemical Co., Japan.
[3] Difco Laboratories, Detroit, Mich.

0022-3549/84/0100-0048$01.00/0
© 1984, American Pharmaceutical Association

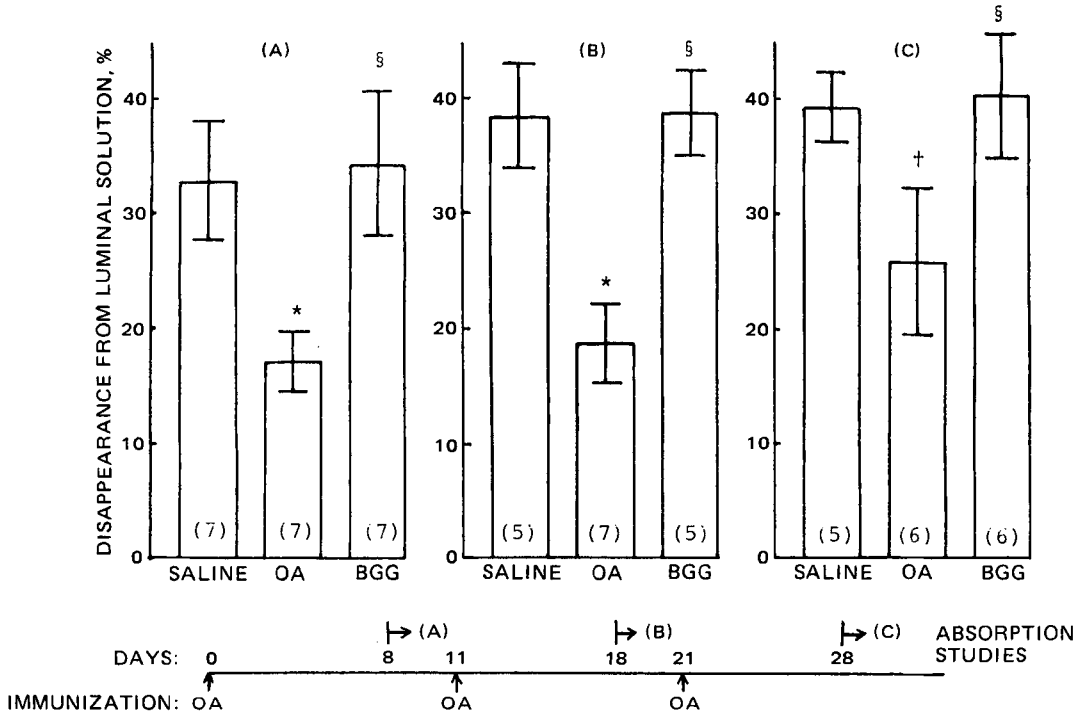

Figure 1—*Effect of intravenous challenge with ovalbumin(OA) or bovine γ-globulin (BGG) on the intestinal absorption of salicylic acid in 15 min in rats immunized intraperitoneally once (A), twice (B), or three times (C) with ovalbumin. Ovalbumin or bovine γ-globulin (0.5 mg) dissolved in 0.25 mL of saline was administered immediately before the start of intestinal recirculation. Numbers in parentheses represent the number of experiments; vertical bars indicate ±SD. Key: (*) p < 0.001; (†) p < 0.005; (§) not significantly different, compared with the appropriate control.*

aliquot of the organic phase was shaken with acidic media, and the optical density of the latter phase was determined spectrophotometrically at 251 nm (17).

Phenolsulfonphthalein—One milliliter of sample solution was alkalinized with 4 ml of 1 M NaOH and determined spectrophotometrically at 560 nm.

RESULTS

The absorption of salicylic acid from the small intestine was examined at pH 6.5 in ovalbumin-immunized rats using an *in situ* recirculation technique. The protocol of the immunization with ovalbumin and the absorption studies are shown in each figure and table.

The results of absorption studies in rats immunized once, twice, or three times with ovalbumin are summarized in Fig. 1. The disappearance of salicylic acid from the luminal solution in 15 min was significantly decreased in rats challenged intravenously with ovalbumin compared with control rats treated with saline. On the other hand, decreased absorption of the drug by the intravenous challenge with bovine γ-globulin was not observed in ovalbumin-immunized rats. These results indicate the remarkable specificity of antigen-antibody reactions.

In this study, the passive cutaneous anaphylaxis method was employed for the identification of the anti-ovalbumin antibodies. The results of the anaphylaxis experiment are shown in Table I. There is a good relationship between the decrease of salicylic acid absorption and passive cutaneous anaphylactic reactions. To examine the duration of the action, absorption studies and anaphylactic reactions were carried out 1, 5, 10, and 16 weeks after the third immunization. The results are shown in Fig. 2 and Table II, respectively. The reduction of salicylic acid absorption by the intravenous challenge with ovalbumin was observed for 10 weeks, but did not last for 16 weeks after the last immunization. Similarly, the sera withdrawn from rats 1, 5, and 10 weeks after the last immunization were able to sensitize rat skin for passive cutaneous anaphylaxis, but anaphylactic reactions were negative for the serum withdrawn from rats at 16 weeks, with one exception. Thus, the decreased salicylic acid absorption agrees with the passive cutaneous anaphylactic reactions.

Figure 3 shows the effect of intravenous administration of ovalbumin on salicylic acid absorption from the small intestine in nonimmunized rats. The decreased absorption of the drug by the intravenous challenge

Table I—Passive Cutaneous Anaphylactic Reactions in Rats Immunized Intraperitoneally Once, Twice, or Three Times with Ovalbumin [a]

No. of Immunizations	Antiserum Dilution 1:1	1:2	1:4	1:8	1:16	1:32
1	2.4	0.9	0.5	0.1	0	0
2	2.0	1.1	0.5	0.1	0	0
3	2.2	1.1	0.5	0.3	0	0

[a] The diameter of the blue discoloration was scored 0–4 as described in *Experimental*. Data represent the mean of 8–10 experiments.

Table II—Passive Cutaneous Anaphylactic Reactions in Rats Immunized Intraperitoneally Three Times with Ovalbumin [a]

Group [b]	Antiserum Dilution 1:1	1:2	1:4	1:8	1:16	1:32
A	2.8	1.7	0.9	0.6	0.4	0.4
B	1.2	0.3	0	0	0	0
C	0.4	0.1	0	0	0	0
D	0.25	0	0	0	0	0

[a] The diameter of the blue discoloration was scored 0–4 as described in *Experimental*. Data represent the mean of 8–10 experiments. [b] Passive cutaneous anaphylaxis experiments were carried out 1 week (A), 5 weeks (B), 10 weeks (C), and 16 weeks (D) after the last immunization.

Table III—Effect of Intravenous Challenge with Ovalbumin on the Intestinal Absorption of Various Drugs in 15 min in Rats Immunized Intraperitoneally with Ovalbumin [a]

Drug	Challenge: Saline, % absorbed	Challenge: Ovalbumin, % absorbed
Salicylic acid	38.5 ± 4.6 (5)	18.7 ± 3.4 (7) [b]
Sulfadimethoxine	28.7 ± 2.6 (6)	20.6 ± 2.5 (6) [b]
Sulfanilamide	17.8 ± 2.4 (5)	11.6 ± 1.2 (6) [b]
Sulfisoxazole	12.9 ± 1.5 (5)	11.3 ± 0.9 (5)
Quinine	11.3 ± 0.9 (6)	9.9 ± 1.3 (6)
Sulfanilic acid	4.3 ± 0.6 (5)	3.6 ± 0.8 (5)
Phenolsulfonphthalein	1.7 ± 0.6 (6)	1.7 ± 0.2 (6)

[a] 0.5 mg of ovalbumin dissolved in 0.25 mL of saline was administered immediately before the start of intestinal recirculation. Results are expressed as the mean ± *SD* followed by the number of experiments in parentheses. [b] $p < 0.001$, compared with the appropriate control.

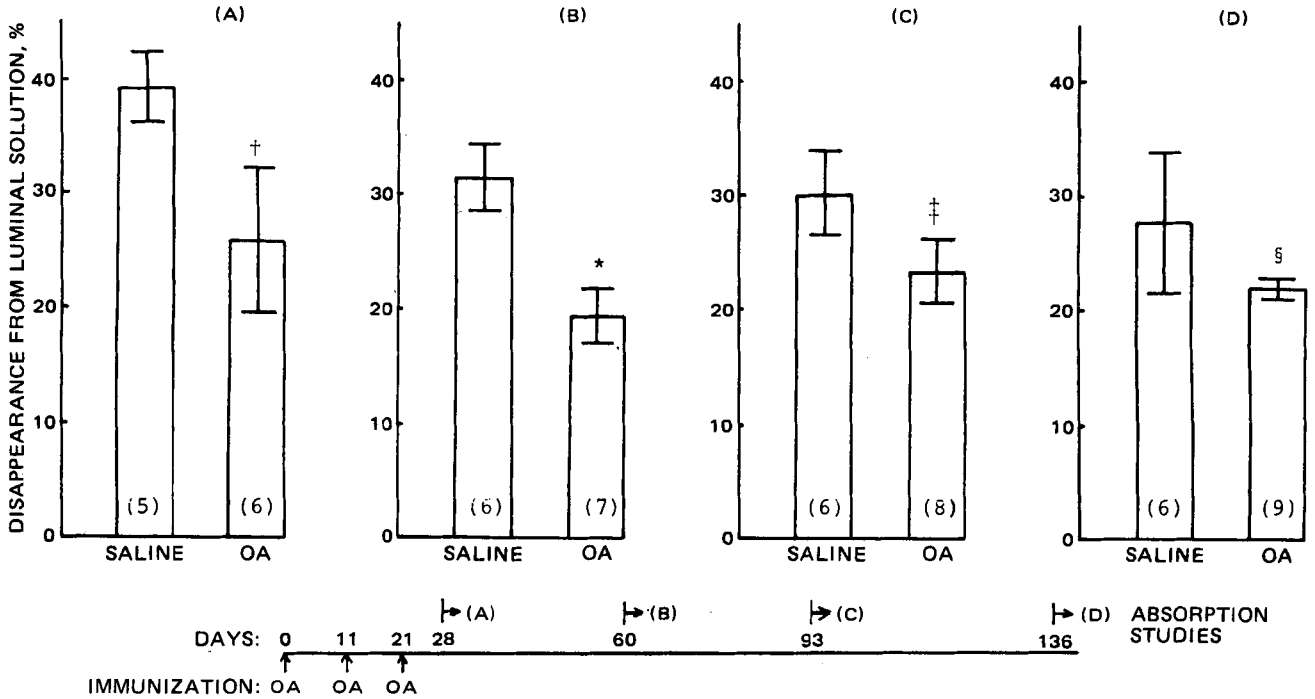

Figure 2—*Effect of intravenous challenge with ovalbumin(OA) on the intestinal absorption of salicylic acid in 15 min in rats immunized intraperitoneally three times with ovalbumin. Absorption studies were carried out 1 week (A), 5 weeks (B), 10 weeks (C), and 16 weeks (D) after the last immunization. Ovalbumin (0.5 mg) dissolved in 0.25 mL of saline was administered immediately before the start of intestinal recirculation. Numbers in parentheses represent the number of experiments, vertical bars indicate* ± SD. *Key: (*)* $p < 0.001$; *(†)* $p < 0.005$; *(‡)* $p < 0.01$; *(§) not significantly different, compared with the appropriate control.*

failed to be found in normal rats. From the results described above, it is reasonable to consider that systemic anaphylaxis results in the decrease of salicylic acid absorption. This result is consistent with previous data that salicylic acid absorption was decreased by the intravenous challenge with bovine γ-globulin in rats immunized with the same antigen. To elucidate the mechanism by which systemic anaphylaxis decreased salicylic acid absorption, the intestinal absorption of drugs with various absorbability was examined (Table III). Sulfadimethoxine is a rapidly absorbed drug like salicylic acid. Sulfanilamide, sulfisoxazole, and quinine are moderately absorbable drugs. Sulfanilic acid and phenolsulfonphthalein are poorly absorbed. As is evident from the table, the absorption of sulfadimethoxine and sulfanilamide was decreased by the intravenous challenge with ovalbumin; no significant change was observed in the intestinal absorption of sulfisoxazole, quinine, sulfanilic acid, and phenolsulfonphthalein.

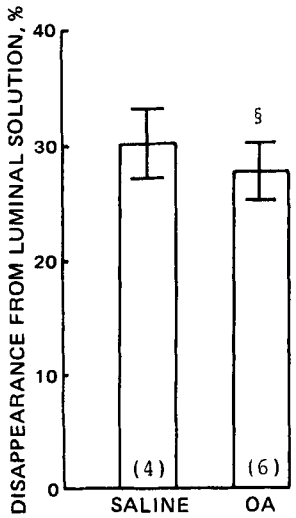

Figure 3—*Effect of intravenous challenge with ovalbumin (OA) on the intestinal absorption of salicylic acid in 15 min in normal (nonimmunized) rats. Ovalbumin (0.5 mg) dissolved in 0.25 mL of saline was administered immediately before the start of intestinal recirculation. Numbers in parentheses represent the number of experiments; vertical bars indicate* ± SD. *Key: (§) not significantly different compared with the control.*

To examine the effect of the route of immunization with the antigen, ovalbumin was injected into the footpads of rats twice and three times. As shown in Fig. 4, the intestinal absorption of salicylic acid was significantly decreased in rats challenged intravenously with ovalbumin compared with the control (challenged with saline). However, there was no effect of the intravenous challenge with the different antigen, bovine γ-globulin on salicylic acid absorption. These results agree well with the data shown in Fig. 1. In this case, the passive cutaneous anaphylaxis experiment can again be used to prove the existence of the anti-ovalbumin antibody in rats immunized *via* the footpads (Table IV). The data in the table provide definitive evidence for the existence of anti-ovalbumin antibodies in rats immunized *via* the footpads, as in rats immunized intraperitoneally.

DISCUSSION

There has been considerable interest recently in the immunological consideration of the GI tract. A previous paper reported the decreased absorption of salicylic acid following intravenous challenge with bovine γ-globulin in rats immunized intraperitoneally with this antigen (1). In the case of bovine γ-globulin, however, the decreased absorption of the drug by the antigen challenge was observed in rats immunized twice and three times, but not in rats immunized only once. Furthermore, the effect was maintained for at least 5 weeks after the third immunization, but disappeared within 10 weeks.

In the present study, the effect of intravenous challenge with ovalbumin on the intestinal absorption of salicylic acid was investigated in rats parenterally immunized with the same antigen. As shown in Figs. 1 and

Table IV—Passive Cutaneous Anaphylactic Reactions in Rats Immunized in the Footpads Once, Twice, or Three Times with Ovalbumin [a]

No. of Immunizations	Antiserum Dilution					
	1:1	1:2	1:4	1:8	1:16	1:32
1	2.3	0.9	0.5	0.1	0	0
2	4.0	4.0	4.0	4.0	2.6	1.2
3	3.7	3.2	2.9	2.1	2.0	2.0

[a] The diameter of the blue discoloration was scored 0–4 as described in *Experimental*. Data represent the mean of 10 experiments.

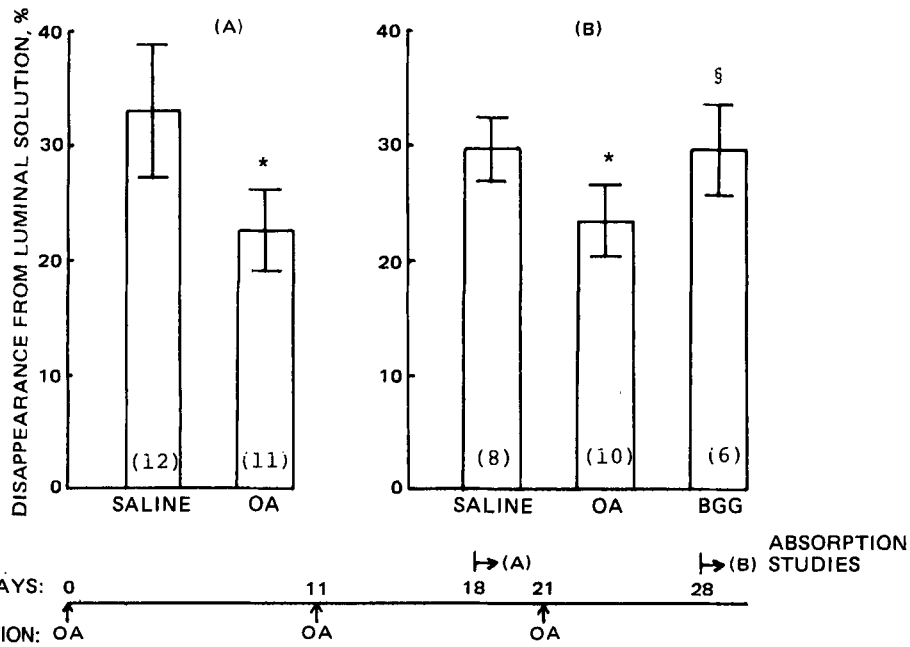

Figure 4—*Effect of intravenous challenge with ovalbumin (OA) on the intestinal absorption of salicylic acid in 15 min in rats immunized in the footpads twice (A) or three times (B) with ovalbumin. Ovalbumin or bovine γ-globulin (BGG) (0.5 mg) dissolved in 0.25 mL of saline was administered immediately before the start of intestinal recirculation. Numbers in parentheses represent the number of experiments; vertical bars indicate* ± SD. *Key: (§) not significantly different compared with the control.*

4, the intestinal absorption of salicylic acid was significantly decreased by the intravenous challenge with ovalbumin in ovalbumin-immunized rats. It seems likely that these results are not dependent on the route of immunization (intraperitoneal or intrafootpad). Figure 4 also shows that intravenous challenge with bovine γ-globulin failed to decrease salicylic acid absorption in ovalbumin-immunized rats. This indicates the specificity of the antigen–antibody reactions.

A significant decrease in the intestinal absorption of salicylic acid was noted by an ovalbumin challenge in rats immunized only once with ovalbumin (Fig. 1). This result is consistent with the passive cutaneous anaphylaxis data shown in Table I, but differs from our previous experiments where there was no significant change in the intestinal absorption of the drug in rats immunized only once with bovine γ-globulin. Furthermore, as shown in Fig. 2, intestinal absorption of salicylic acid was significantly decreased more than 10 weeks after the last immunization by the challenge with ovalbumin. In the case of bovine γ-globulin, the decreased absorption of salicylic acid was observed within 5 weeks and had disappeared within 10 weeks after the last immunization. From the results described above, it is reasonable to consider that ovalbumin is a more potent antigen than bovine γ-globulin in rats under these conditions.

The mammalian GI system contributes to the total immune response of the body. In both qualitative and quantitative terms, this contribution is no better defined than that of other organs. In addition, systemic anaphylaxis has been accompanied by changes in vascular and mucosal permeability in the rat. These changes are reflected in an enhanced retention of labeled serum albumin in intestinal tissues and by the increased concentration of such proteins in intestinal fluids. Bloch *et al.* suggested that during intestinal anaphylaxis, there is an increased movement of protein from the lumen into the systemic circulation (18, 19). Similarly, Thomas and Parrot could show that the systemic immune response, as well as the local immune answer, can change the normal protein absorption (20).

In contrast to the well-studied change of macromolecule transport during intestinal or systemic anaphylaxis (21–25), few studies have investigated the immunological consideration on the intestinal transport of low molecular weight organic compounds. Since, from the standpoint of biopharmaceutics, it might be worthy to examine the absorption of such compounds during intestinal or systemic anaphylaxis, the intestinal absorption of several low molecular weight drugs was examined in immunized rats by means of an *in situ* recirculation technique. As is evident from Table III, intestinal absorption of sulfadimethoxine and sulfanilamide was significantly decreased by the intravenous challenge with ovalbumin. There was, however, no significant change in the intestinal absorption of sulfisoxazole, quinine, sulfanilic acid, and phenolsulfonphthalein in rats challenged with ovalbumin. These findings indicate that poorly absorbed drugs are less sensitive to systemic anaphylaxis than well-absorbed drugs. As the absorption of poorly absorbed drugs was not increased by systemic anaphylaxis, it is suggested that progressive loss of structural integrity of the epithelium did not occur during systemic anaphylaxis.

The mechanism by which the intestinal absorption of salicylic acid was decreased during systemic anaphylaxis is not completely defined at present. In this case, various mechanisms may be considered. One of the most important mechanisms is the alteration of the mesenteric blood flow during anaphylaxis. It is well known that the absorption rates of rapidly absorbed drugs are controlled by the mesenteric blood flow. Beubler and Lêmbech showed that the absorption rate of salicylic acid was affected by the intestinal blood flow (26). Therefore, changes in the vascular system during systemic anaphylaxis might influence the absorption rate of the drug. Another possibility is that the release of histamine, serotonin, and other vasoactive substances induced by systemic anaphylaxis may contribute to the decreased absorption of salicylic acid. These chemical mediators play an important role in increased capillary permeability, vasodilation, and smooth muscle contraction. Moreover, Lake *et al.* have shown the enhanced release of goblet cell mucus during intestinal anaphylaxis (27, 28). This discharge of goblet cell mucus may also represent a barrier against the intestinal absorption of salicylic acid. Additional studies are needed to further clarify this observation.

REFERENCES

(1) J. Nakamura, A. Yamamoto, S. Takada, T. Kimura, and H. Sezaki, *J. Pharm. Dyn.*, **5**, 278 (1982).

(2) F. Audibert, I. Chedid, P. Lefrancier, J. Choay, and E. Lederer, *Ann. Immunol. (Inst. Pasteur)*, **128c**, 653 (1977).

(3) M. T. Lubet and J. R. Kettman, *Immunogenetics*, **6**, 69 (1978).

(4) E. M. Vaz, N. M. Vaz, and B. B. Levine, *Immunology*, **21**, 11 (1971).

(5) E. E. E. Jarret and D. C. Stewart, *Immunology*, **27**, 365 (1974).

(6) E. E. E. Jarret, D. M. Haig, W. McDougall, and E. McNulty, *Immunology*, **30**, 671 (1976).

(7) J. G. Vos, J. Boerkamp, J. Buys, and P. A. Steerenberg, *Scand. J. Immunol.*, **12**, 289 (1980).

(8) H. Brazin and B. Platteau, *Immunology*, **30**, 679 (1976).

(9) J. Goose and A. M. J. N. Blair, *Immunology*, **16**, 749 (1969).

(10) D. J. Stechschulte, R. P. Orange, and K. F. Austen, *J. Immunol.*, **105**, 1082 (1970).

(11) E. S. K. Assem and A. W. Richter, *Immunology*, **21**, 729 (1971).

(12) T. C. Kravis and N. J. Zvaifler, *J. Immunol.*, **113**, 244 (1974).
(13) T. Tada and K. Okumura, *J. Immunol.*, **106**, 1002 (1971).
(14) F. Fraga and I. Mota, *Immunology*, **30**, 655 (1976).
(15) J. Nakamura, Y. Yoshizaki, M. Yasuhara, T. Kimura, S. Muranishi, and H. Sezaki, *Chem. Pharm. Bull.*, **24**, 683 (1976).
(16) M. Yasuhara, H. Kobayashi, S. Muranishi, H. Sezaki, and T. Kimura, *J. Pharm. Dyn.*, **1**, 114 (1978).
(17) J. Nakamura, N. Muranushi, T. Kimura, S. Muranishi, and H. Sezaki, *Chem. Pharm. Bull.*, **26**, 857 (1978).
(18) K. J. Bloch, D. B. Bloch, M. Stearns, and W. A. Walker, *Gastroenterology*, **77**, 1039 (1979).
(19) K. J. Bloch and W. A. Walker, *J. Allergy Clin. Immunol.*, **67**, 312 (1981).
(20) H. C. Thomas and D. M. V. Parrot, *Immunology* **27**, 631 (1974).
(21) W. A. Walker, K. J. Isselbacher, and K. J. Bloch, *Science*, **177**, 608 (1972).
(22) W. A. Walker, K. J. Isselbacher, and K. J. Bloch, *J. Immunol.*, **111**, 221 (1973).
(23) W. A. Walker, M. Wu, K. J. Isselbacher, and K. J. Bloch, *J. Immunol.*, **115**, 854 (1975).
(24) W. A. Walker, M. Wu, K. J. Isselbacher, and K. J. Bloch, *Gastroenterology*, **69**, 1223 (1975).
(25) W. A. Walker, S. N. Abel, M. Wu, and K. J. Bloch, *J. Immunol.*, **117**, 1028 (1976).
(26) E. Beubler and F. Lembeck, *Naunyn-Schmiedeberg's Arch. Pharmacol.*, **292**, 73 (1976).
(27) A. M. Lake, K. J. Bloch, K. J. Sinclair, and W. A. Walker, *Immunology*, **39**, 173 (1980).
(28) A. M. Lake, K. J. Bloch, M. R. Neutra, and W. A. Walker, *J. Immunol.*, **122**, 834 (1979).

Effect of Microcapsule Core–Wall Ratio and Aggregate Size on the Properties of Tableted Microcapsules

JOSEPH R. NIXON and GEORGE A. AGYILIRAH *x

Received February 23, 1982, from the *Department of Pharmacy, Chelsea College. London University, London SW3 6LX, England.* Accepted for publication October 21, 1982. *Present address: Department of Industrial and Physical Pharmacy, School of Pharmacy and Pharmacal Sciences, Purdue University, West Lafayette, IN 47907.

Abstract □ Microcapsules containing sodium phenobarbital cores and ethylcellulose walls have been tableted. The thickness of the tablets, the breaking strength, and the dissolution characteristics were studied and found to be affected by the microcapsule core–wall ratio and the size of the microcapsule aggregates.

Keyphrases □ Microcapsules—sodium phenobarbital and ethylcellulose, tablets, effect of core–wall ratio and aggregate size on dissolution □ Dissolution—tablets composed of microcapsules, sodium phenobarbital and ethylcellulose, effect of core–wall ratio and aggregate size □ Sustained-release formulations—tableted microcapsules, sodium phenobarbital and ethylcellulose, effect of core–wall ratio and aggregate size on dissolution

Microcapsules consist of a thin wall which can enclose a solid or liquid core material. One of the many important reasons for microencapsulating medicaments is to achieve sustained release. Good sustained release has been achieved by microencapsulating poorly water-soluble medicaments such as aspirin and phenobarbital (1). With very water-soluble substances such as sodium phenobarbital, the rate of release is slowed by microencapsulation, being controlled partly by the wall thickness. However, no satisfactory sustained release has been achieved with water-soluble substances (1–3). Tableting of microcapsules has been shown to slow the release significantly and provide a sustained- or prolonged-action release (4–6). The microcapsules which have been tableted appear to be mainly those with ethylcellulose walls prepared using a modification of the method described by Fanger *et al.* (7); in most cases, this technique has produced aggregates (2, 5, 7). This work studies the effect of the aggregate size and the core–wall ratio on the properties of the prepared tablets.

EXPERIMENTAL

Materials—Phenobarbital sodium[1] (99.4% pure), ethylcellulose[1] (viscosity 5% w/w solution in 80:20 toluene–ethanol mixture: 14.13 cP; degree of substitution: 2.50; ethoxy content: 47.5%), and cyclohexane[2] (99.5% pure, bp 80–81°C, fp 5.95°C; wt/mL at 20°C: 0.776) were purchased commercially.

Preparation of Microcapsules—The method used was a modification of an original technique by Fanger *et al.* (7) as further modified by Agyilirah and Nixon (5). This method involves deposition of polymeric wall-forming material onto dispersed particles of core by cooling below a critical liquid–liquid phase separation temperature. A typical example of microcapsule preparation was as follows. Ten grams of sodium phenobarbital and 5 g of ethylcellulose were dispersed in 500 mL of cyclohexane. The stainless steel stirrer was adjusted to the middle of the dispersion to obtain uniform stirring and a speed of 500 rpm was used. The temperature was raised slowly to 80°C over a period of 1 h after which it was allowed to reflux for 30 min. While continuing the stirring, the temperature was allowed to decline at a controlled rate. The ethylcellulose separated, first as a liquid, which was deposited round the core particles, and when the temperature had reached 25°C the stirring was stopped so that the microcapsules could be filtered and dried.

Preparation of Tablets—The tablets were made by compressing 250-mg quantities of the dried microcapsules. The die was fitted onto a 9.5-mm flat lower punch, and 250 mg of microcapsules was placed in it. The upper punch was carefully placed in position, making sure no microcapsules were lost. The punch and die arrangement was placed under the compression head, which was lowered onto the upper punch until the required compression pressure was attained. A compression pressure of 315 kg/cm^2 was maintained for 1 min and then quickly removed. Tablets were prepared from microcapsules of core–wall ratios 4:1, 1:1, 1:2, and 1:4 as well as from 2:1 core–wall ratio microcapsules sieved into sizes of 215, 302.5, 427.5, 605, and 855 μm using British Standard sieves.

Determination of Tablet Thickness and Breaking Strength—The thickness of the tablets was determined by means of a micrometer screw gauge. For each tablet five different measurements were taken at five

[1] B.D.H. Chemicals Ltd., Poole, England.
[2] Fisons Scientific Apparatus, Loughborough, Leicestershire, England.

0022-3549/84/0100-0052$01.00/0
© 1984, American Pharmaceutical Association

(12) T. C. Kravis and N. J. Zvaifler, *J. Immunol.*, **113**, 244 (1974).
(13) T. Tada and K. Okumura, *J. Immunol.*, **106**, 1002 (1971).
(14) F. Fraga and I. Mota, *Immunology*, **30**, 655 (1976).
(15) J. Nakamura, Y. Yoshizaki, M. Yasuhara, T. Kimura, S. Muranishi, and H. Sezaki, *Chem. Pharm. Bull.*, **24**, 683 (1976).
(16) M. Yasuhara, H. Kobayashi, S. Muranishi, H. Sezaki, and T. Kimura, *J. Pharm. Dyn.*, **1**, 114 (1978).
(17) J. Nakamura, N. Muranushi, T. Kimura, S. Muranishi, and H. Sezaki, *Chem. Pharm. Bull.*, **26**, 857 (1978).
(18) K. J. Bloch, D. B. Bloch, M. Stearns, and W. A. Walker, *Gastroenterology*, **77**, 1039 (1979).
(19) K. J. Bloch and W. A. Walker, *J. Allergy Clin. Immunol.*, **67**, 312 (1981).
(20) H. C. Thomas and D. M. V. Parrot, *Immunology* **27**, 631 (1974).
(21) W. A. Walker, K. J. Isselbacher, and K. J. Bloch, *Science*, **177**, 608 (1972).
(22) W. A. Walker, K. J. Isselbacher, and K. J. Bloch, *J. Immunol.*, **111**, 221 (1973).
(23) W. A. Walker, M. Wu, K. J. Isselbacher, and K. J. Bloch, *J. Immunol.*, **115**, 854 (1975).
(24) W. A. Walker, M. Wu, K. J. Isselbacher, and K. J. Bloch, *Gastroenterology*, **69**, 1223 (1975).
(25) W. A. Walker, S. N. Abel, M. Wu, and K. J. Bloch, *J. Immunol.*, **117**, 1028 (1976).
(26) E. Beubler and F. Lembeck, *Naunyn-Schmiedeberg's Arch. Pharmacol.*, **292**, 73 (1976).
(27) A. M. Lake, K. J. Bloch, K. J. Sinclair, and W. A. Walker, *Immunology*, **39**, 173 (1980).
(28) A. M. Lake, K. J. Bloch, M. R. Neutra, and W. A. Walker, *J. Immunol.*, **122**, 834 (1979).

Effect of Microcapsule Core–Wall Ratio and Aggregate Size on the Properties of Tableted Microcapsules

JOSEPH R. NIXON and GEORGE A. AGYILIRAH *x

Received February 23, 1982, from the *Department of Pharmacy, Chelsea College. London University, London SW3 6LX, England.* Accepted for publication October 21, 1982. *Present address: Department of Industrial and Physical Pharmacy, School of Pharmacy and Pharmacal Sciences, Purdue University, West Lafayette, IN 47907.

Abstract □ Microcapsules containing sodium phenobarbital cores and ethylcellulose walls have been tableted. The thickness of the tablets, the breaking strength, and the dissolution characteristics were studied and found to be affected by the microcapsule core–wall ratio and the size of the microcapsule aggregates.

Keyphrases □ Microcapsules—sodium phenobarbital and ethylcellulose, tablets, effect of core–wall ratio and aggregate size on dissolution □ Dissolution—tablets composed of microcapsules, sodium phenobarbital and ethylcellulose, effect of core–wall ratio and aggregate size □ Sustained-release formulations—tableted microcapsules, sodium phenobarbital and ethylcellulose, effect of core–wall ratio and aggregate size on dissolution

Microcapsules consist of a thin wall which can enclose a solid or liquid core material. One of the many important reasons for microencapsulating medicaments is to achieve sustained release. Good sustained release has been achieved by microencapsulating poorly water-soluble medicaments such as aspirin and phenobarbital (1). With very water-soluble substances such as sodium phenobarbital, the rate of release is slowed by microencapsulation, being controlled partly by the wall thickness. However, no satisfactory sustained release has been achieved with water-soluble substances (1–3). Tableting of microcapsules has been shown to slow the release significantly and provide a sustained- or prolonged-action release (4–6). The microcapsules which have been tableted appear to be mainly those with ethylcellulose walls prepared using a modification of the method described by Fanger *et al.* (7); in most cases, this technique has produced aggregates (2, 5, 7). This work studies the effect of the aggregate size and the core–wall ratio on the properties of the prepared tablets.

EXPERIMENTAL

Materials—Phenobarbital sodium[1] (99.4% pure), ethylcellulose[1] (viscosity 5% w/w solution in 80:20 toluene–ethanol mixture: 14.13 cP; degree of substitution: 2.50; ethoxy content: 47.5%), and cyclohexane[2] (99.5% pure, bp 80–81°C, fp 5.95°C; wt/mL at 20°C: 0.776) were purchased commercially.

Preparation of Microcapsules—The method used was a modification of an original technique by Fanger *et al.* (7) as further modified by Agyilirah and Nixon (5). This method involves deposition of polymeric wall-forming material onto dispersed particles of core by cooling below a critical liquid–liquid phase separation temperature. A typical example of microcapsule preparation was as follows. Ten grams of sodium phenobarbital and 5 g of ethylcellulose were dispersed in 500 mL of cyclohexane. The stainless steel stirrer was adjusted to the middle of the dispersion to obtain uniform stirring and a speed of 500 rpm was used. The temperature was raised slowly to 80°C over a period of 1 h after which it was allowed to reflux for 30 min. While continuing the stirring, the temperature was allowed to decline at a controlled rate. The ethylcellulose separated, first as a liquid, which was deposited round the core particles, and when the temperature had reached 25°C the stirring was stopped so that the microcapsules could be filtered and dried.

Preparation of Tablets—The tablets were made by compressing 250-mg quantities of the dried microcapsules. The die was fitted onto a 9.5-mm flat lower punch, and 250 mg of microcapsules was placed in it. The upper punch was carefully placed in position, making sure no microcapsules were lost. The punch and die arrangement was placed under the compression head, which was lowered onto the upper punch until the required compression pressure was attained. A compression pressure of 315 kg/cm^2 was maintained for 1 min and then quickly removed. Tablets were prepared from microcapsules of core–wall ratios 4:1, 1:1, 1:2, and 1:4 as well as from 2:1 core–wall ratio microcapsules sieved into sizes of 215, 302.5, 427.5, 605, and 855 μm using British Standard sieves.

Determination of Tablet Thickness and Breaking Strength—The thickness of the tablets was determined by means of a micrometer screw gauge. For each tablet five different measurements were taken at five

[1] B.D.H. Chemicals Ltd., Poole, England.
[2] Fisons Scientific Apparatus, Loughborough, Leicestershire, England.

0022-3549/84/0100-0052$01.00/0
© 1984, American Pharmaceutical Association

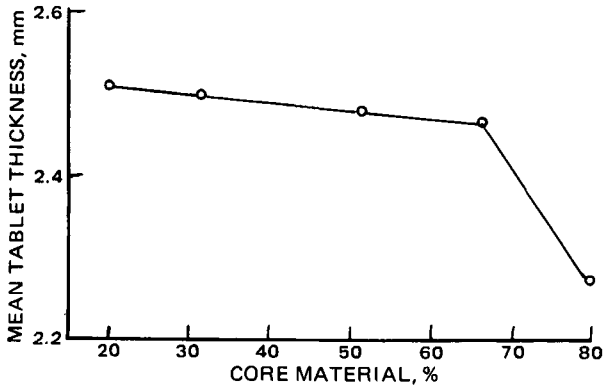

Figure 1—*Influence of microcapsule core–wall ratio on tablet thickness. Compression pressure: 315 kg/cm²; tablet weight: 250 mg; tablet diameter: 9.5 mm.*

different positions and the mean value recorded. Tablet breaking strength was determined by means of a hardness tester[3]. The tablet was pressed between platens across its diameter and the force increased until the tablet fractured. The force required to break the tablet was recorded as its breaking strength.

Dissolution Studies—The dissolution medium consisted of 2 L of distilled water in a 2500-mL flask at a temperature of 37°C. A stirring rate of 100 rpm was standardized using a 7-cm paddle. The dissolution flask was connected to the cells of a digital spectrophotometer[4] by an inlet tubing through which solution from the flask was continuously pumped through the 1-cm UV cells for assay. The solution once assayed returned to the flask *via* the outlet tubing. A wavelength of 240 nm was used and the instrument calibrated to give a direct reading of percent dissolved. One tablet was used for each dissolution.

RESULTS AND DISCUSSION

The effects of the microcapsule core–wall ratio and aggregate size on the thickness of the tablets are shown in Figs. 1 and 2, respectively. From Fig. 1 it can be seen that the thickness of the tablet decreased as the proportion of the core material increased. During the compression both the sodium phenobarbital and the ethylcellulose became compressed, with a greater elastic compression of the ethylcellulose wall due to its fibrous nature. On removal of the compression pressure there is a reexpansion of the ethylcellulose wall. The larger the amount of ethylcellulose present, the greater the expansion. This explains the reduction in the tablet thickness as the core–wall ratio increases, since the amount of ethylcellulose present becomes proportionately less under these conditions. The much smaller value for the 4:1 core–wall ratio (*i.e.*, 80% core) occurs because at this ratio the ethylcellulose wall is so thin that breakdown of the wall occurs during the compression. When wall destruction occurs, some sodium phenobarbital crystals penetrate the wall, making it impossible for any appreciable expansion on removal of the pressure.

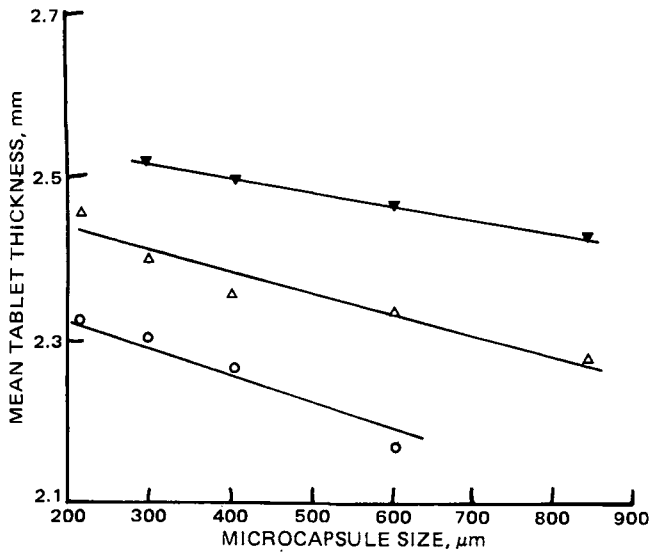

Figure 2—*Effect of microcapsule size on tablet thickness. Microcapsule core–wall ratios: (○) 4:1, (△) 2:1, (▼) 1:1. Compression pressure: 315 kg/cm²; tablet weight: 250 mg; tablet diameter: 9.5 mm.*

[3] Nottingham Engineering, Nottingham University, Notts, England.
[4] Cecil Instrument Co., Milton, Cambridgeshire, England.

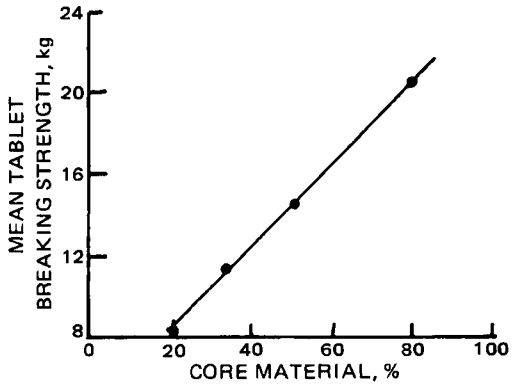

Figure 3—*Effect of the percent core material on the mean breaking strength of tablets prepared from 4:1, 1:1, 1:2, and 1:4 core–wall ratio microcapsules. Compression pressure: 315 kg/cm²; weight of tablet: 250 mg; tablet diameter: 9.5 mm.*

The decrease in the thickness with increasing microcapsule aggregate size is due to the breakdown of microcapsule aggregates during the compression. The smaller particles resulting from the breakdown would fill gaps between larger particles, thus producing a more compact mass.

The amount of sodium phenobarbital that resulted from assaying 100 mg of 1:1 core–wall ratio microcapsules of aggregate sizes 215, 302.5, 427.5, and 605 μm were 49.5, 51.0, 50.3, and 49.2 mg, respectively, showing that the amount of drug contained in a given amount of the same batch of microcapsules did not depend on the aggregate size. This finding is not surprising since the different aggregates are made up of microcapsules that existed as individual entities at one stage of their preparation and the different aggregate size only reflects the numbers of individual microcapsules in the aggregate.

Figures 3 and 4 show the relationship between the strength of the tablets, the core–wall ratio, and the microcapsule size. Figure 3 appears to complement the results shown in Fig. 1 in that when ethylcellulose expands after the removal of the compression pressure, the bonds formed during the compression are relaxed producing a less rigid tablet. This relaxation could explain the decrease found in the strength of the tablets as the core–wall ratio was reduced. The walls of the microcapsules also

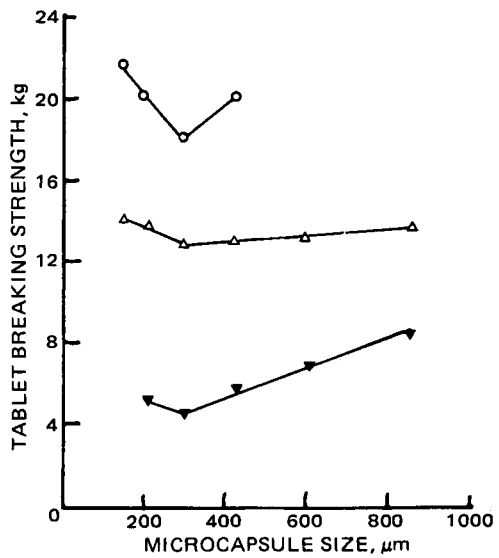

Figure 4—*Effect of microcapsule size on tablet breaking strength. Microcapsule core–wall ratio: (○) 4:1, (△) 2:1, (▼) 1:1. Compression pressure 315 kg/cm²; tablet diameter: 9.5 mm; tablet weight: 250 mg.*

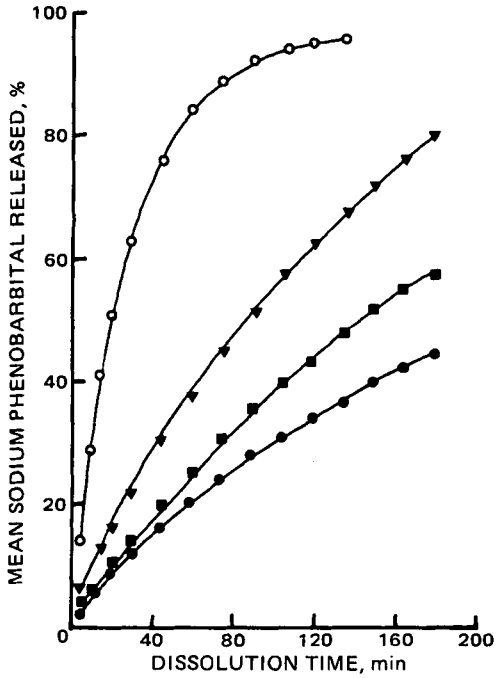

Figure 5—*Effect of microcapsule core–wall ratio on tablet dissolution. Core–wall ratio: (○) 4:1, (▼) 1:1, (■) 1:2, (●) 1:4. Dissolution medium: 2 L of distilled water (pH 5.4); dissolution temperature: 37°C; dissolution stirring rate: 100 rpm; compression pressure: 315 kg/cm²; tablet weight: 250 mg; tablet diameter: 9.5 mm.*

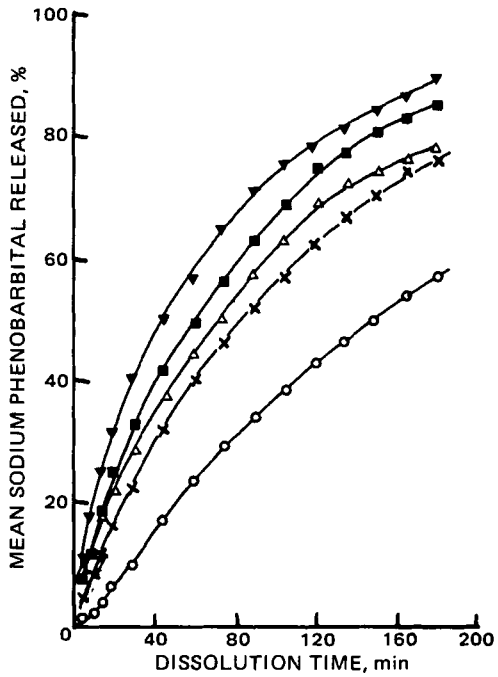

Figure 6—*Effect of microcapsule size on the dissolution from 2:1 core–wall ratio microcapsule tablets. Microcapsule size: (○) 215 μm, (×) 302.5 μm, (△) 427.5 μm, (■) 605 μm, (▼) 855 μm. Dissolution medium: 2 L of distilled water (pH 5.4); dissolution temperature: 37°C; dissolution stirring rate: 100 rpm; compression pressure: 315 kg/cm²; tablet weight: 250 mg; tablet diameter: 9.5 mm.*

became thinner with a decrease in the proportion of wall material. At higher core–wall ratios there is the possibility of wall breakage during the compression. When walls rupture, particles of core material are exposed and will interlock strongly, thus leading to stronger tablets.

An explanation of the effect of the microcapsule aggregate size on the tablet strength, as shown in Fig. 4, is that with the very small aggregates the large surface areas result in greater bonding. The strength of the tablet decreased as the aggregate size increased, and the surface area available for bonding decreased. A further rise in the size of the microcapsule aggregate brought about the breakdown of the aggregates and exposed fresh surfaces for bonding. The greater the aggregate size, the greater the extent of breakdown as found by Armstrong and Haines-Nutt (8) in the case of tablet granules. This would result in a larger fresh bonding surface being exposed and explain the second rise in the tablet strength curve at larger aggregate size.

Figures 5 and 6 show the release of sodium phenobarbital from these tablets. Dissolution was faster from the higher core–wall ratio microcapsules with greater strengths, although one would normally expect dissolution to be faster from a weaker tablet. When dissolution studies were conducted on untableted microcapsules, a faster release occurred from the higher core–wall microcapsules because these had thinner walls, making penetration of both the dissolution medium and the core solution through the walls easier. Also, because of the higher core–wall ratios, there were more core particles per microcapsule, resulting in a higher concentration gradient to boost dissolution.

These same considerations are controlling factors for dissolution from the tableted microcapsules since the microcapsule wall still has to be penetrated to release the core. The only difference is the compact nature of the tablet as compared with the corresponding microcapsules. Compacting the microcapsules results in a greatly reduced surface area being available for release. Even after release of core material from the individual microcapsules composing the tablet, the core solution has to permeate narrow channels prior to release between the compressed aggregates into the outside dissolution medium. The effect of reduced surface area and channel permeation results in a considerable slowing of the release from the tableted microcapsules compared with the untableted microcapsules.

The effects of microcapsule size on the dissolution from tablets are shown in Fig. 6. This illustration indicates that release was faster from tablets made from larger microcapsules. The increase in the release from tablets prepared using 215-μm microcapsules to those from 302.5-μm microcapsules followed the same pattern as the corresponding strength graph, which also showed a decrease. Beyond 302.5-μm microcapsule size, the tablet strength increased again; the corresponding increase in the release characteristic of the core material is in line with the explanation given for the increase in strength found in this region. The increase in strength found with microcapsules >302.5 μm was due to a breakdown of aggregates, possibly even to the breakdown of individual microcapsule walls, either of which conditions would expose fresh surfaces for dissolution. The breakdown would be greater the larger the initial microcapsule size, as confirmed by the dissolution results. We can conclude, therefore, that the aggregate size significantly affects the properties of the tablets and should be taken into consideration whenever one is designing a dosage form as it will affect the availability of the drug. Tablets made from different sized aggregates of the same preparation could give markedly different absorption rates because of the differences in drug release.

REFERENCES

(1) S. A. H. Khalil and A. S. El-Gamal, *Pharmazie*, **28,** 46 (1973).

(2) I. Jalsenjak, C. F. Nicolaidou, and J. R. Nixon, *J. Pharm. Pharmacol.*, **28,** 912 (1976).

(3) P. B. Deasy, M. R. Brophy, B. Ecanow, and M. M. Joy, *J. Pharm. Pharmacol.*, **32,** 15 (1980).

(4) I. Jalsenjak, C. F. Nicolaidou, and J. R. Nixon, *J. Pharm. Pharmacol.*, **29,** 169 (1977).

(5) G. A. Agyilirah and J. R. Nixon, *Acta Pharm. Technol.*, **26(4),** 251 (1980).

(6) I. Jalsenjak, J. R. Nixon, R. Senjkovic, and I. Stivic, *J. Pharm. Pharmacol.*, **32,** 678 (1980).

(7) G. O. Fanger, R. E. Miller, and R. G.McNiff, *U.S. Pat.*, 3,531,418, (1970).

(8) N. A. Armstrong and R. F. Haines-Nutt, *J. Pharm. Pharmacol.*, **25,** 147P (1970).

Assay of Chlordiazepoxide and Demoxepam in Chlordiazepoxide Formulations by Difference Spectrophotometry

A. G. DAVIDSON

Received July 6, 1982, from the *Department of Pharmacy, School of Pharmaceutical Sciences, University of Strathclyde, Glasgow G1 1XW, U.K.* Accepted for publication October 21, 1982.

Abstract □ Rapid difference spectrophotometric methods for chlordiazepoxide and demoxepam in chlordiazepoxide formulations are described which overcome the nonspecificity of the official spectrophotometric assays. The procedures are based on the measurement of the difference absorbance at 269 nm of equimolar solutions of chlordiazepoxide at pH 8 and pH 3 and the difference absorbance at 263 nm of equimolar solutions of demoxepam at pH 13 and pH 8. The methods are specific for chlordiazepoxide and demoxepam in the presence of both compounds, 2-amino-5-chlorobenzophenone, certain coformulated drugs, and formulation excipients. Analyses of commercial dosage forms of chlordiazepoxide have shown the presence of demoxepam at concentrations in excess of the pharmacopoeial specifications in some aged samples.

Keyphrases □ Chlordiazepoxide—assay with demoxepam in formulations, difference spectrophotometry □ Demoxepam—assay with chlordiazepoxide in chlordiazepoxide formulations, difference spectrophotometry □ Difference spectrophotometry—assay of chlordiazepoxide and demoxepam in chlordiazepoxide formulations

Methods of analysis of benzodiazepine drugs and their respective hydrolysis products in pharmaceutical formulations based on the direct measurement of absorbance in the UV region lack selectivity. For example, chlordiazepoxide (I) and its major hydrolysis product demoxepam (7-chloro-1,3-dihydro-5-phenyl-2*H*-1,4-benzodiazepin-2-one 4-oxide, II) have very similar UV spectra resulting in their mutual interference in direct spectrophotometric procedures. The presence of a minor hydrolysis product 2-amino-5-chlorobenzophenone (III) and absorbing coformulated drugs in certain chlordiazepoxide–drug combinations may further reduce the accuracy of direct spectrophotometric methods for I and II.

Current pharmacopoeial specifications in the United States (1) limit the content of II to 0.1% in chlordiazepoxide drug substance, 3% in capsules of the hydrochloride salt, and 4% in tablets of the free base. The British Pharmacopoeia 1980 (2) also specifies limits for II and other related substances in chlordiazepoxide and its formulations based on a comparison of the intensities of impurity spots on a thin-layer chromatogram of the sample with that of a specified quantity of I obtained by a dilution of the sample. The maximum permissible content of III is 0.01% (1) or 0.05% (2) in chlordiazepoxide drug substance and 0.1% in solid dosage forms (1, 2).

A variety of techniques have been used to assay chlordiazepoxide formulations including HPLC (3–5) and GLC (6) which quantitatively determine I and its hydrolysis products, spectrofluorometry (7, 8), polarography (9, 10), colorimetry (11, 12), and UV spectrophotometry (1, 2, 13). A column chromatographic–UV spectrophotometric assay has also been described for II (14).

Difference spectrophotometry has proved particularly useful in the assay of medicinal substances by eliminating specific interference from degradation products and coformulated drugs (15, 16) and also nonspecific irrelevant absorption from the formulation matrix. The technique may be applied to substances that exhibit a difference in absorbance between two equimolar solutions which has been induced by the addition of reagents to one or both of the solutions. The difference spectrophotometric assay of these substances in samples that also contain other absorbing components may be carried out provided the absorbances of the interfering substances remain unaltered by the reagents. This paper describes pH-induced simultaneous difference spectrophotometric procedures that are specific for I and II in the presence of III, certain coformulated drugs, and formulation excipients.

EXPERIMENTAL

Apparatus—Absorption and difference absorption spectra were recorded in 1-cm silica quartz cells using a recording double-beam spectrophotometer[1]. To measure the small difference absorbance of demoxepam accurately, the cells were carefully matched for transmission and path length so that the absorbance difference at 269 nm of neither a solution of I (10 μg/mL) at pH 8 nor of water in the two cells exceeded 0.001 AU.

Reagents—Chlordiazepoxide BP[2], demoxepam[2], and 2-amino-5-chlorobenzophenone[2] were dried as described in the USP XX (1). All other reagents and solvents were of analytical reagent quality. Stock pH 3 buffer was prepared by diluting 37.53 g of glycine and 114 mL of 1.00 M HCl to 1 L with water. Stock pH 8 buffer was prepared by diluting 60.57 g of Tris and 292 mL of 1.00 M HCl to 1 L with water.

Chlordiazepoxide Standard Solutions—Approximately 25 mg of chlordiazepoxide was accurately weighed into a 250-mL volumetric flask and dissolved in 20 mL of ethanol. The solution was slightly acidified by the addition of 0.4 mL of 1 M HCl and diluted to volume with water. A 5.0-mL aliquot was transferred to each of two 50-mL volumetric flasks containing stock pH 3 buffer (5 mL) and stock pH 8 buffer (5 mL), respectively, and diluted to volume with water. The difference absorbance at 269 nm (ΔA_{269}^{Std}) of the pH 8 solution in the sample cell was measured relative to the pH 3 solution in the reference cell after the zero absorbance had been set with the pH 8 buffer (stock buffer diluted 1:9 with water) in the sample cell and the pH 3 buffer (stock buffer diluted 1:9 with water) in the reference cell.

Demoxepam Standard Solutions—Approximately 25 mg of demoxepam, accurately weighed into a 250-mL volumetric flask, was dissolved in 20 mL of ethanol and diluted to volume with water. A 5.0-mL aliquot was transferred to two 50-mL volumetric flasks containing stock pH 8 buffer (5 mL) and 1 M NaOH (5 mL), respectively, and diluted to volume with water. The difference absorbance at 263 nm (ΔA_{263}^{Std}) of the pH 13 solution (in 0.1 M NaOH) in the sample cell was measured relative to the pH 8 solution in the reference cell after the zero absorbance had been set with 0.1 M NaOH and the pH 8 buffer in the sample and reference cells, respectively.

Sample Solutions—Twenty tablets or the contents of twenty capsules were thoroughly triturated. A quantity of powder containing ~10 mg of chlordiazepoxide or 11.2 mg of chlordiazepoxide hydrochloride was ac-

[1] Model 552 Spectrophotometer; Perkin-Elmer Ltd., Beaconsfield, Bucks, HP9 1QA, U.K.
[2] Roche Products Ltd., Welwyn Garden City, Herts AL7 3AY, U.K.

0022-3549/84/0100-0055$01.00/0
© 1984, American Pharmaceutical Association

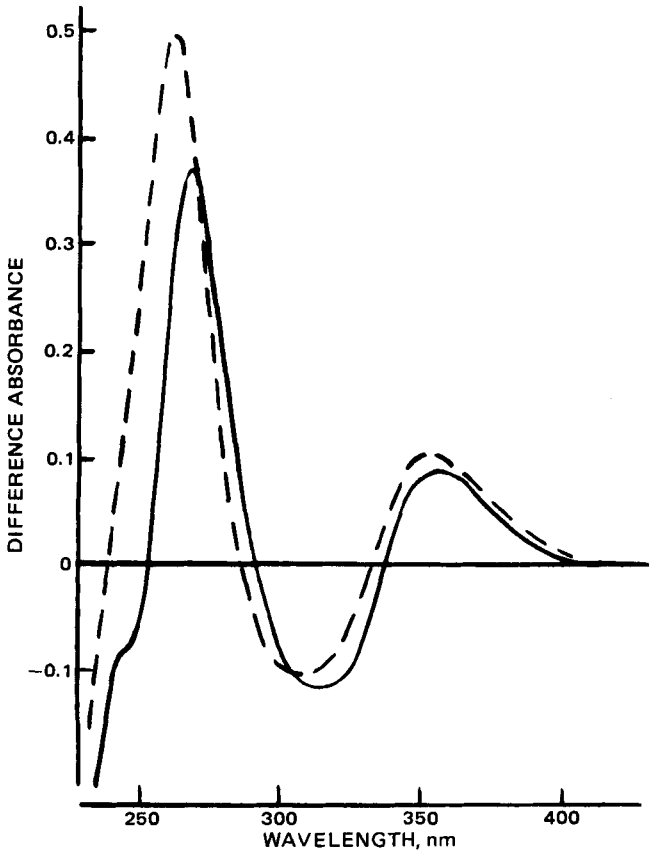

Figure 1—*Difference absorption spectra of chlordiazepoxide (10μg/mL) in pH 8* versus *pH 3 solutions (—) and demoxepam (10 μg/mL) in pH 13* versus *pH 8 solutions (- - -).*

curately weighed into a 100-mL volumetric flask and shaken for 10 min with 10 mL of ethanol. Water (60 mL) and 0.1 M HCl (10 mL) were added and the flask was shaken for an additional 20 min. The extract was diluted to volume with water and clarified by passing it through a filter paper[3] or membrane filter[4], with the first 10 mL of filtrate being discarded. Aliquots (5.0 mL) of the filtrate were transferred to three 50-ml volumetric flasks containing stock pH 3 buffer (5 mL), stock pH 8 buffer (5 mL), and 1 M NaOH (5 mL), respectively, and diluted to volume with water. The $\Delta A_{269}^{\text{sample}}$ of the pH 8 and pH 3 solutions were measured as described above for the standard chlordiazepoxide solutions, and the $\Delta A_{263}^{\text{sample}}$ of the solutions in 0.1 M NaOH and pH 8 buffer were measured as described above for the standard demoxepam solutions.

The concentrations of chlordiazepoxide (C_C) and demoxepam (C_D) in a tablet or capsule contents of average weight (AW) as a percentage of the stated quantity of chlordiazepoxide (C_t) were calculated using:

$$C_C = \frac{\Delta A_{269}^{\text{sample}} \times C_C^{\text{std}} \times \text{AW} \times 100}{\Delta A_{269}^{\text{std}} \times \text{weight of sample} \times C_t} \quad \text{(Eq. 1)}$$

$$C_D = \frac{\Delta A_{263}^{\text{sample}} \times C_D^{\text{std}} \times \text{AW} \times 100}{\Delta A_{263}^{\text{std}} \times \text{weight of sample} \times C_t} \quad \text{(Eq. 2)}$$

where C_C^{std} and C_D^{std} are the concentrations of the buffered standard solutions of I and II, respectively, in μg/mL and weights are in mg.

RESULTS AND DISCUSSION

Choice of Assay Conditions—The specificity of the difference spectrophotometric assays of I and II is due to the different spectral changes exhibited by these substances in aqueous solution on alteration of the pH. Chlordiazepoxide displays a bathochromic shift of its λ_{max} at 245 nm in acidic solution to 260 nm in alkaline solution (17). The difference absorption spectrum (Fig. 1) of a solution of I buffered at pH 8 relative to an identical solution buffered at pH 3 in the reference cell shows that the maximum difference occurs at 269 nm. The spectra of II are identical at pH 3 and pH 8, but basification to pH 13 results in a bathochromic shift of the maximum at 237 nm to 242 nm with a shoulder at 255 nm (17). The maximum difference absorbance of equimolar solutions of II at pH 13 (in 0.1 M NaOH) and at pH 8 occurs at 263 nm (Fig. 1).

[3] Whatman No. 1.
[4] Millipore Filter, 0.45 μm, 25 mm diameter.

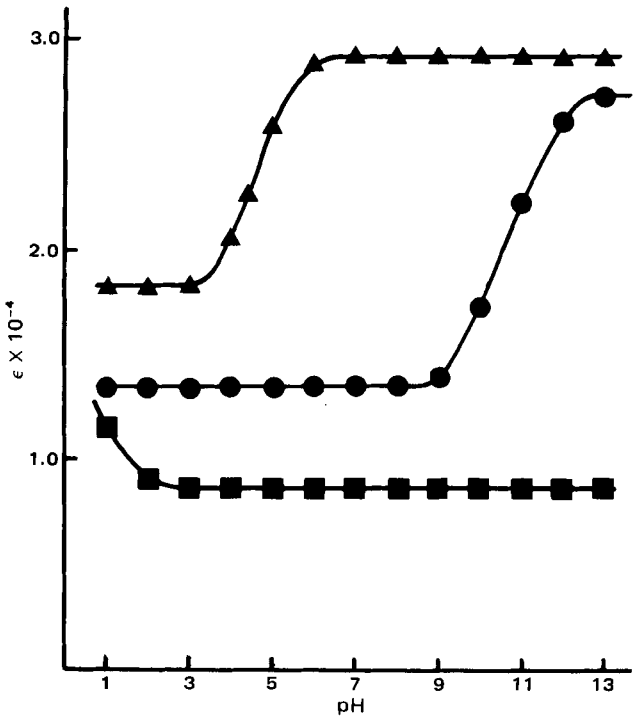

Figure 2—*Variation of molar absorptivity (ε) of chlordiazepoxide (▲) at 269 nm, demoxepam (●) at 263 nm, and 2-amino-5-chlorobenzophenone (■) at 269 nm with pH.*

Absorptivity—pH plots of equimolar solutions (3.34×10^{-5} M) of I, II, and III over the pH range of 1–13 (Fig. 2) show that each exhibits only one inflexion and that the pH regions over which these occur (pH ~4.6, ~10.5, and ~1.0, respectively) are sufficiently well separated to permit the selective determination of I and II in the presence of each other and in the presence of III. Buffers of pH 8 and pH 3 have been selected for the determination of I at 269 nm and buffers at pH 13 and pH 8 for the assay of II at 263 nm. The assay of III utilizing the spectral changes of pH ~1 has not been attempted in this work owing to the very low levels found in formulations, typically <0.03% (3, 6).

The sites of ionization which affect the absorption spectra of I and II are, respectively, the *N*-oxide oxygen atom where protonation in acidic solution occurs (18) and the C-3 position where deprotonation occurs in alkaline solution with stabilizing enolization in the direction of C-2 (19). An ionization of II (pK_a 4–5) associated with protonation of the *N*-oxide oxygen atom has been found in this work and previously (19) to have no effect on its absorption spectrum.

The midpoint of the sigmoidal curve (Fig. 2) for I occurred at pH 4.6, in agreement with the pK_a measured spectrophotometrically at 265 nm (18). However the midpoint of the inflexion given by II occurred at pH 10.5, considerably lower than 11.5, the pK_{a2} which has been determined spectrophotometrically at an unspecified wavelength (19). To resolve this difference, the pK_a of II (concentration, 10 μg/mL) was determined

Table 1—Recovery of Chlordiazepoxide and Demoxepam in Standard Mixtures

Composition of Mixture, μg/mL			Concentration Found			
			I		II	
I	II	III	μg/mL	Percent Added	μg/mL	Percent Added
99.2	0.0	0.0	99.2	100.0	0.0	—
98.2	1.05	0.0	98.0	99.8	0.92	87.6
96.2	2.10	0.0	96.6	100.4	2.23	106.2
94.2	4.20	1.02	93.6	99.4	4.30	102.4
89.3	8.40	2.04	89.9	100.7	8.16	97.1
79.4	16.80	4.07	79.9	100.6	16.83	100.2
59.5	31.49	10.18	60.2	101.2	31.40	99.7
19.8	62.99	20.36	20.1	101.5	63.40	100.7

Table II—Means, Standard Deviations (*SD*), and Coefficients of Variation (*CV*) for Standard Solutions of Chlordiazepoxide and Demoxepam

Composition of Mixture, μg/mL		ΔA_{269}			ΔA_{263}		
I	II	Mean[a]	$SD \times 10^3$	CV, %	Mean[a]	$SD \times 10^3$	CV, %
100.0	0.0	0.3704	1.30	0.35	0.0001	0.70	—
0.0	100.0	0.0008	0.92	—	0.4903	0.91	0.19
96.0	4.0	0.3551	1.13	0.32	0.0194	0.69	3.57
80.0	20.0	0.2960	1.05	0.36	0.0982	0.62	0.63

[a] Ten replicate measurements.

Table III—Assay of Chlordiazepoxide Formulations by the Difference (ΔA) and Official Spectrophotometric Procedures

Sample	Formulation	Coformulated Drug	Age, years	ΔA I[a]	ΔA II[a]	USP (1)[a]	BP (2)[a]
A	5-mg Capsule of I·HCl	—	New	102.7	<L.D.[b]	101.7	101.9
B	10-mg Capsule of I·HCl	—	New	98.9	<L.D.[b]	101.0	100.4
C	5-mg Capsule of I·HCl	—	6	98.1	2.47	100.0	100.9
D	10-mg Capsule of I·HCl	—	6	86.8	6.80	95.0	94.4
E	25-mg Tablet I (base)	—	1	99.0	<L.D.[b]	102.2	102.0
F	5-mg Tablet I (base)	—	5	98.2	1.91	100.2	99.7
G	5-mg Tablet I (base)	Clidinium bromide, 2.5 mg	4	92.1	8.31	—	—
H	5-mg Capsule I·HCl	Amitriptyline HCl, 12.5 mg	New	98.3	—	—	—
I	10-mg Capsule I·HCl	Amitriptyline HCl, 25.0 mg	4	96.8	—	—	—

[a] Expressed as percent of stated content. [b] Less than the limit of detection.

at 263 nm in seven buffers of 0.3 pH increments from pH 9.6 to 11.4 (20). The average pK_a was 10.55 ± 0.05.

Beer's Law and Specificity—Beer's law graphs for I showed that a proportional relationship exists between the ΔA_{269} of solutions at pH 8 and pH 3 and the concentration of I in the range 0–12.5 μg/mL. The regression equation obtained with six pairs of solutions was $y = 0.0370x - 0.0023$ and the correlation coefficient (r) was 0.99997, where y is the ΔA_{269} in 1-cm cells and x μg/mL is the concentration. An almost identical line ($y = 0.0369x - 0.0010$; $r = 0.99994$) was obtained for a similar series of solutions of I (0–12.5 μg/mL) containing II (2 μg/mL) confirming that the presence of II does not affect the absorptivity of I. Similarly, a proportional relationship exists between the ΔA_{263} of pH 13 and pH 8 solutions of II and their concentration in the range 0–12.5 μg/mL ($y = 0.0490x + 0.0020$; $r = 0.99994$) which is almost identical to that of a series of six mixtures containing a varying concentration of II (0–2.5 μg/mL) and a constant concentration (10 μg/mL) of I ($y = 0.0492x + 0.0020$; $r = 0.9994$). The chosen analytical concentration of I (10 μg/mL) gives absorbance values for the standard solution of I and sample solutions at pH 8 of ~1.0 at 269 nm and 1.2 at 263 nm, which are within the optimum range of absorbance providing minimum relative error.

To assess further the specificity of the method in samples containing I and II, two series each of six solutions were assayed using the procedures. The solutions in the first series contained a constant concentration of I (100 μg/mL) and a varying concentration (0–25 μg/mL) of II. The solutions in the second series contained a constant concentration of II (20 μg/mL) and a varying concentration of I (0–125 μg/mL). The ΔA_{269} of the pH 8 and pH 3 solutions of the first series all fell within 99.4–100.6% of that of the solutions of I containing no added II; in the second series, the ΔA_{263} of the pH 13 and pH 8 solutions fell within 97.6–101.3% of the solutions of II only. These results confirm that the concentrations of I and II may be selectively determined in mixtures by measurement of the ΔA_{269} of equal dilutions at pH 8 and pH 3 and of the ΔA_{263} of equal dilutions at pH 13 and pH 8, respectively.

Amitriptyline hydrochloride and clidinium bromide, coformulated with I in two commercial preparations, give zero ΔA_{269} and do not interfere in the assay of I in these formulations. Amitriptyline, however, precipitates in pH 13 solution, and the assay of II in amitriptyline–chlordiazepoxide combinations cannot, therefore, be carried out by the procedure. Clidinium bromide gives zero ΔA_{263} and does not affect the assay of II in clidinium–chlordiazepoxide combinations.

Isosbestic points (*i.e.*, wavelengths of zero difference absorbance owing to the equal absorptivity of the protonated and nonprotonated species) in the difference absorption spectra (Fig. 1) of I at 291 nm and 252 nm and of II at 287 nm and 240 nm were found to be identical in standard and sample solutions, which indicates that there was no interference from the formulation excipients of the samples (15).

Accuracy, Precision, and Limit of Detection of II—The accuracy of the procedures was assessed by analyzing in duplicate standard mixtures containing I, II, and III, prepared to simulate solutions of I which had undergone varying degrees of hydrolytic decomposition. The results in Table I show that the accuracy of the assay of I is excellent even in the presence of high concentrations of hydrolysis products. The recoveries of II, at and above the USP limit of 4% in chlordiazepoxide capsules, were also satisfactory. At lower concentrations of II, near the limit of detection, the recoveries of 87.6 and 106.2%, at approximate concentrations of II of 1 and 2%, respectively, reflect the difficulty of accurately measuring very small values of ΔA_{263}. At the specified analytical concentration of I, each 1% of II gives a ΔA_{263} value of ~0.005 AU. A high-performance spectrophotometer is therefore essential for the accurate and precise measurement of these small values.

Satisfactory precision was achieved in 10 replicate measurements of ΔA_{269} and ΔA_{263} of solutions of I and II separately and mixtures containing 4 and 20% of II (Table II). The limit of detection of II in I, calculated as twice the standard deviation of the ΔA_{263} of the solution containing no II (21), corresponded to a concentration of 0.286%.

Assay Results—To test the application of the methods, the levels of I and II were determined in a number of chlordiazepoxide tablets and capsules both newly purchased and stored for several years at room temperature. Tablets containing I and clidinium bromide were assayed for I and II and tablets containing I and amitriptyline hydrochloride were assayed for I only. For comparison, the chlordiazepoxide tablets and capsules were also assayed by the official procedures of the USP XX (1) and BP 1980 (2). The results (Table III) show that the new formulations contained undetectable levels of II, and that the levels of I were in good agreement with the declared content and, where appropriate, with those found by the official procedures. In the samples which had been stored, the levels of I were lower than label strength and significant amounts of II were found. In most of these samples the total content of I and II were in reasonable agreement with the declared strength and, where appropriate, with the concentration found by the official procedures. These results confirm the findings of other investigations using chromatographic techniques (3, 6) which showed that levels of II in excess of pharmacopoeial limits may be found in aged chlordiazepoxide samples and that the official nonspecific spectrophotometric procedures do not measure the concomitant loss of chlordiazepoxide.

REFERENCES

(1) "The United States Pharmacopeia," 20th rev., U.S. Pharmacopeial Convention, Rockville, Md., 1980, pp. 132–134.

(2) "British Pharmacopoeia 1980," Her Majesty's Stationery Office, London, United Kingdom, pp. 98, 99, 526, 745, 746.

(3) A. G. Butterfield, F. F. Matsui, S. J. Smith, and R. W. Sears, *J. Pharm. Sci.*, **66**, 684 (1977).

(4) J. B. Zagar, F. J. van Lenten, and G. P. Chrekian, *J. Assoc. Off. Anal. Chem.*, **61**, 678 (1978).

(5) S. L. Ali, *Int. J. Pharm.*, **5**, 85 (1980).
(6) D. B. Black, R. C. Lawrence, E. G. Lovering, and J. R. Watson, *J. Pharm. Sci.*, **70**, 208 (1981).
(7) J. T. Stewart and J. L. Williamson, *Anal. Chem.*, **48**, 1182 (1976).
(8) J. Troschuetz, *Arch. Pharm.*, **314**, 204 (1981).
(9) E. Jacobsen and T. V. Jacobsen, *Anal. Chim. Acta*, **55**, 293 (1971).
(10) W. Lund and L. Opheim, *Anal. Chim. Acta*, **88**, 275 (1977).
(11) H. Raber and J. Gruber, *Scientia Pharm.*, **40**, 35 (1972).
(12) Y. A. Beltagy, A. S. Issa, and M. S. Mahrous, *Egypt. J. Pharm. Sci.* **19**, 115 (1978).
(13) R. W. T. Seitzinger, *Pharm. Weekbl.*, **110**, 1073 (1975).
(14) W. N. French, F. F. Matsui, and S. J. Smith, *J. Pharm. Sci.*, **64**, 1545 (1975).
(15) T. D. Doyle and F. R. Fazzari, *J. Pharm. Sci.*, **63**, 1921 (1974).
(16) A. G. Davidson, *J. Pharm. Pharmacol.*, **28**, 795 (1976).
(17) I. Sunshine "CRC Handbook of Spectrophotometric Data of Drugs," CRC Press, Boca Raton, Fla., 1981 p. 143.
(18) J. Barrett, W. Franklyn Smyth, and I. E. Davidson, *J. Pharm. Pharmacol.*, **25**, 387 (1973).
(19) J. Barrett, W. Franklyn Smyth, and J. P. Hart, *J. Pharm. Pharmacol.*, **26**, 9 (1974).
(20) A. Albert and E. P. Serjeant "The Determination of Ionisation Constants," 2nd ed., Chapman and Hall, London, 1971, p. 44.
(21) A. L. Wilson, *Analyst*, **86**, 72 (1961).

Initial Slope Technique for Estimation of the Apparent Volume of Distribution During Constant-Rate Intravenous Infusion

JOSEPH F. COCCHETTO *, DAVID M. COCCHETTO ‡ ¶, THORIR D. BJORNSSON ‡ ×, and TOM BERGAN §

Received August 19, 1982, from the **School of Chemical Engineering, Cornell University, Ithaca, NY 14853-0294*, the ‡*Division of Clinical Pharmacology, Departments of Pharmacology and Medicine, Box 3813, Duke University Medical Center, Durham, NC 27710*, and the §*Department of Microbiology, Institute of Pharmacy, University of Oslo, Blindern, Oslo 3, Norway.* Accepted for publication October 21, 1982. ¶Present address: Merck Sharp and Dohme Research Laboratories, West Point, PA 19486.

Abstract □ A new technique is presented for estimating the apparent volume of distribution of drugs during constant-rate intravenous infusion. It is based on the initial slope of the plasma drug concentration *versus* time profile during the infusion. Equations are derived to provide estimates of the apparent volume of distribution for a one-compartment drug and for the central compartment of a two-compartment drug. The utility of the technique is illustrated by data obtained during constant-rate infusion of metronidazole in 11 healthy subjects. The average estimated value of the volume of the central compartment of metronidazole was 12% higher than the average value obtained by conventional pharmacokinetic analysis. The systematic error associated with this volume estimation procedure was assessed through the use of dimensionless concentration *versus* dimensionless time plots. The initial slope technique should prove useful in providing initial estimates of volume terms.

Keyphrases □ Pharmacokinetics—apparent volume of distribution, constant-rate infusion, estimation by an initial slope technique, application to metronidazole □ Initial slope technique—estimation of apparent volume of distribution, constant-rate infusion, application to metronidazole pharmacokinetics □ Infusion, constant-rate—estimation of apparent volume of distribution, initial slope technique, application to metronidazole pharmacokinetics

During the past few years, three research groups have described approaches for determining the apparent volume of distribution after administration of single and multiple intermittent, constant-rate, intravenous infusions. Sawchuk *et al.* (1, 2) derived an equation from which the apparent volume of distribution for a drug that follows a one-compartment open model can be calculated, based on knowledge of (*a*) the elimination rate constant, (*b*) the preinfusion residual plasma drug concentration, and (*c*) the plasma drug concentration at the end of infusion. Chiou *et al.* (3, 4) extended the technique by using post-infusion data and the midpoint back-extrapolation method to calculate the apparent volume of distribution for drugs that exhibit linear one-compartmental or multicompartmental characteristics. In addition, application of the Chiou–Hsu equation (5–7) to accurately estimate total body clearance during a constant-rate intravenous infusion requires an accurate estimate of the apparent volume of distribution. Barzegar-Jalali (8) used equally spaced sampling times during a zero-order intravenous infusion and the first derivative of the plasma drug concentration *versus* time profile to directly estimate both the elimination rate constant and steady-state plasma drug concentration for a drug with linear one-compartmental characteristics. The apparent volume of distribution could then be estimated from the latter two quantities.

Unfortunately, none of these approaches can be used to estimate directly the apparent volume of distribution or total body clearance from individual patient plasma drug concentration data gathered during the ongoing infusion. The purpose of this paper is to detail a method for estimating the apparent volume of distribution of a drug from the initial slope of the plasma drug concentration *versus* time profile during a constant-rate intravenous infusion.

THEORETICAL

If instantaneous drug distribution and first-order drug elimination are assumed, the plasma concentration of a drug given as a constant-rate intravenous infusion can be described by the following equation (9):

$$C = \frac{k_0}{KV}(1 - e^{-Kt}) \qquad \text{(Eq. 1)}$$

where C is concentration, k_0 is the zero-order infusion rate, K is the first-order elimination rate constant, V is the apparent volume of distribution, and t is time. Taking the first derivative of Eq. 1 with respect to time yields:

$$\frac{dC}{dt} = \frac{k_0 e^{-Kt}}{V} \qquad \text{(Eq. 2)}$$

0022-3549/84/0100-0058$01.00/0
© 1984, American Pharmaceutical Association

(5) S. L. Ali, *Int. J. Pharm.*, **5**, 85 (1980).
(6) D. B. Black, R. C. Lawrence, E. G. Lovering, and J. R. Watson, *J. Pharm. Sci.*, **70**, 208 (1981).
(7) J. T. Stewart and J. L. Williamson, *Anal. Chem.*, **48**, 1182 (1976).
(8) J. Troschuetz, *Arch. Pharm.*, **314**, 204 (1981).
(9) E. Jacobsen and T. V. Jacobsen, *Anal. Chim. Acta*, **55**, 293 (1971).
(10) W. Lund and L. Opheim, *Anal. Chim. Acta*, **88**, 275 (1977).
(11) H. Raber and J. Gruber, *Scientia Pharm.*, **40**, 35 (1972).
(12) Y. A. Beltagy, A. S. Issa, and M. S. Mahrous, *Egypt. J. Pharm. Sci.* **19**, 115 (1978).
(13) R. W. T. Seitzinger, *Pharm. Weekbl.*, **110**, 1073 (1975).
(14) W. N. French, F. F. Matsui, and S. J. Smith, *J. Pharm. Sci.*, **64**, 1545 (1975).
(15) T. D. Doyle and F. R. Fazzari, *J. Pharm. Sci.*, **63**, 1921 (1974).
(16) A. G. Davidson, *J. Pharm. Pharmacol.*, **28**, 795 (1976).
(17) I. Sunshine "CRC Handbook of Spectrophotometric Data of Drugs," CRC Press, Boca Raton, Fla., 1981 p. 143.
(18) J. Barrett, W. Franklyn Smyth, and I. E. Davidson, *J. Pharm. Pharmacol.*, **25**, 387 (1973).
(19) J. Barrett, W. Franklyn Smyth, and J. P. Hart, *J. Pharm. Pharmacol.*, **26**, 9 (1974).
(20) A. Albert and E. P. Serjeant "The Determination of Ionisation Constants," 2nd ed., Chapman and Hall, London, 1971, p. 44.
(21) A. L. Wilson, *Analyst*, **86**, 72 (1961).

Initial Slope Technique for Estimation of the Apparent Volume of Distribution During Constant-Rate Intravenous Infusion

JOSEPH F. COCCHETTO *, DAVID M. COCCHETTO ‡ ¶, THORIR D. BJORNSSON ‡ ×, and TOM BERGAN §

Received August 19, 1982, from the **School of Chemical Engineering, Cornell University, Ithaca, NY 14853-0294*, the ‡*Division of Clinical Pharmacology, Departments of Pharmacology and Medicine, Box 3813, Duke University Medical Center, Durham, NC 27710*, and the §*Department of Microbiology, Institute of Pharmacy, University of Oslo, Blindern, Oslo 3, Norway.* Accepted for publication October 21, 1982. ¶Present address: Merck Sharp and Dohme Research Laboratories, West Point, PA 19486.

Abstract □ A new technique is presented for estimating the apparent volume of distribution of drugs during constant-rate intravenous infusion. It is based on the initial slope of the plasma drug concentration *versus* time profile during the infusion. Equations are derived to provide estimates of the apparent volume of distribution for a one-compartment drug and for the central compartment of a two-compartment drug. The utility of the technique is illustrated by data obtained during constant-rate infusion of metronidazole in 11 healthy subjects. The average estimated value of the volume of the central compartment of metronidazole was 12% higher than the average value obtained by conventional pharmacokinetic analysis. The systematic error associated with this volume estimation procedure was assessed through the use of dimensionless concentration *versus* dimensionless time plots. The initial slope technique should prove useful in providing initial estimates of volume terms.

Keyphrases □ Pharmacokinetics—apparent volume of distribution, constant-rate infusion, estimation by an initial slope technique, application to metronidazole □ Initial slope technique—estimation of apparent volume of distribution, constant-rate infusion, application to metronidazole pharmacokinetics □ Infusion, constant-rate—estimation of apparent volume of distribution, initial slope technique, application to metronidazole pharmacokinetics

During the past few years, three research groups have described approaches for determining the apparent volume of distribution after administration of single and multiple intermittent, constant-rate, intravenous infusions. Sawchuk *et al.* (1, 2) derived an equation from which the apparent volume of distribution for a drug that follows a one-compartment open model can be calculated, based on knowledge of (*a*) the elimination rate constant, (*b*) the preinfusion residual plasma drug concentration, and (*c*) the plasma drug concentration at the end of infusion. Chiou *et al.* (3, 4) extended the technique by using post-infusion data and the midpoint back-extrapolation method to calculate the apparent volume of distribution for drugs that exhibit linear one-compartmental or multicompartmental characteristics. In addition, application of the Chiou–Hsu equation (5–7) to accurately estimate total body clearance during a constant-rate intravenous infusion requires an accurate estimate of the apparent volume of distribution. Barzegar-Jalali (8) used equally spaced sampling times during a zero-order intravenous infusion and the first derivative of the plasma drug concentration *versus* time profile to directly estimate both the elimination rate constant and steady-state plasma drug concentration for a drug with linear one-compartmental characteristics. The apparent volume of distribution could then be estimated from the latter two quantities.

Unfortunately, none of these approaches can be used to estimate directly the apparent volume of distribution or total body clearance from individual patient plasma drug concentration data gathered during the ongoing infusion. The purpose of this paper is to detail a method for estimating the apparent volume of distribution of a drug from the initial slope of the plasma drug concentration *versus* time profile during a constant-rate intravenous infusion.

THEORETICAL

If instantaneous drug distribution and first-order drug elimination are assumed, the plasma concentration of a drug given as a constant-rate intravenous infusion can be described by the following equation (9):

$$C = \frac{k_0}{KV}(1 - e^{-Kt}) \qquad \text{(Eq. 1)}$$

where C is concentration, k_0 is the zero-order infusion rate, K is the first-order elimination rate constant, V is the apparent volume of distribution, and t is time. Taking the first derivative of Eq. 1 with respect to time yields:

$$\frac{dC}{dt} = \frac{k_0 e^{-Kt}}{V} \qquad \text{(Eq. 2)}$$

0022-3549/84/0100-0058$01.00/0
© 1984, American Pharmaceutical Association

which can be evaluated at time zero to give:

$$\frac{dC}{dt}(t=0) = \frac{k_0}{V} \qquad \text{(Eq. 3)}$$

Rearrangement of Eq. 3 yields:

$$V = \frac{k_0}{\frac{dC}{dt}(t=0)} \qquad \text{(Eq. 4)}$$

Equation 4 indicates that the apparent volume of distribution can be calculated from the zero-order infusion rate and the initial slope of the plasma drug concentration *versus* time curve.

The above mathematical manipulations are readily extended to a drug undergoing biexponential disposition following drug administration by constant-rate intravenous infusion. Plasma drug concentration during infusion is given by (10):

$$C = \frac{k_0}{k_{10}V_c}\left[1 - \left(\frac{k_{10}-\beta}{\alpha-\beta}\right)e^{-\alpha t} - \left(\frac{\alpha-k_{10}}{\alpha-\beta}\right)e^{-\beta t}\right] \qquad \text{(Eq. 5)}$$

where α is the rapid disposition rate constant, β is the slow disposition rate constant, k_{10} is the first-order elimination rate constant from the central compartment, and V_c is the apparent volume of distribution of the central compartment. Taking the first derivative with respect to time yields:

$$\frac{dC}{dt} = \frac{\alpha k_0(k_{10}-\beta)}{k_{10}V_c(\alpha-\beta)}e^{-\alpha t} + \frac{\beta k_0(\alpha-k_{10})}{k_{10}V_c(\alpha-\beta)}e^{-\beta t} \qquad \text{(Eq. 6)}$$

which can be evaluated at time zero to give:

$$\frac{dC}{dt}(t=0) = \frac{k_0}{V_c} \qquad \text{(Eq. 7)}$$

Rearrangement of Eq. 7 yields:

$$V_c = \frac{k_0}{\frac{dC}{dt}(t=0)} \qquad \text{(Eq. 8)}$$

Equation 8 shows that, for a drug exhibiting two-compartmental characteristics, the apparent volume of distribution of the central compartment is equal to the quotient of the zero-order infusion rate and the initial slope of the plasma drug concentration *versus* time curve. Equations 4 and 8 indicate that the apparent volume of distribution can be estimated if the initial slope of the concentration *versus* time profile can be estimated. This initial slope can be estimated by:

$$\frac{dC}{dt}(t=0) \cong \frac{\Delta C}{\Delta t}(t \to 0) \qquad \text{(Eq. 9)}$$

which is equivalent to:

$$\frac{dC}{dt}(t=0) \cong \frac{C}{t} \qquad \text{(Eq. 10)}$$

when there is no residual drug concentration at time zero. Using this simple estimate of the initial slope, Eqs. 4 and 8 become:

$$V^{est} = \frac{k_0}{C/t} \qquad \text{(Eq. 4a)}$$

and

$$V_c^{est} = \frac{k_0}{C/t} \qquad \text{(Eq. 8a)}$$

where the superscript est indicates an estimated value of the volume term.

A detailed examination of the concentration *versus* time profiles for both the monoexponential and biexponential disposition cases is necessary to determine the systematic error associated with this volume estimation procedure. To make this error analysis generally applicable to drugs with a wide range of parameter values, it is advantageous to work with the concentration *versus* time equations in their dimensionless forms. The dimensionless equivalent of Eq. 1 is:

$$\frac{C}{C_{ss}} = 1 - e^{-\phi} \qquad \text{(Eq. 11)}$$

where $\phi \equiv Kt$ and $C_{ss} = (k_0/KV)$, *i.e.*, C at steady state. Equation 11 shows that the dimensionless concentration C/C_{ss} is a function only of the dimensionless time ϕ and therefore Eq. 11 is applicable to any drug undergoing monoexponential disposition. The dimensionless equivalent of Eq. 5 is:

$$\frac{C}{C_{ss}} = 1 - \left(\frac{1-\rho_2}{\rho_1-\rho_2}\right)e^{-\rho_1\phi} - \left(\frac{\rho_1-1}{\rho_1-\rho_2}\right)e^{-\rho_2\phi} \qquad \text{(Eq. 12)}$$

where $\phi \equiv k_{10}t$, $\rho_1 = \alpha/k_{10}$, $\rho_2 = \beta/k_{10}$, and $C_{ss} = (k_0/k_{10}V_c)$, *i.e.*, C at steady state. In concert with the classical definition for a conventional biexponential disposition model where $\alpha > k_{10} > \beta$, it follows that $\rho_1 > 1 > \rho_2$. In contrast to Eq. 11, Eq. 12 indicates that the dimensionless concentration of a two-compartmental drug is a function not only of the dimensionless time, but also of the dimensionless hybrid rate constants ρ_1 and ρ_2.

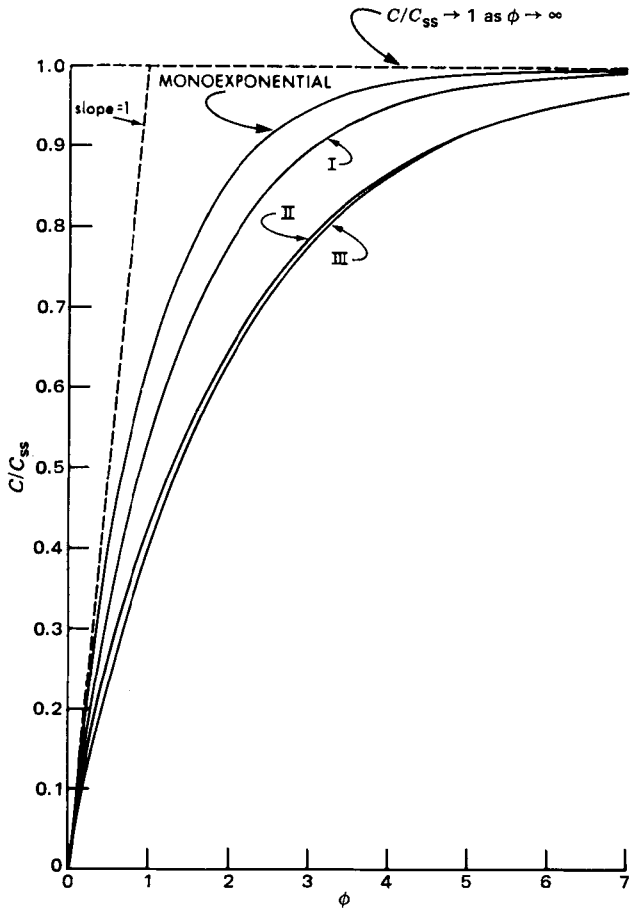

Figure 1—*Relationship between dimensionless concentration* C/C_{ss} *and dimensionless time* ϕ *for the universal monoexponential disposition model (Eq. 11) and three examples (I, II, and III) of the biexponential disposition model (Eq. 12). Parameter values were chosen to reflect the range of values observed for the metronidazole examples. Key: I:* $\rho_1 = 10$, $\rho_2 = 0.75$; *II:* $\rho_1 = 10$, $\rho_2 = 0.50$; *III:* $\rho_1 = 30$, $\rho_2 = 0.50$.

The utility of the dimensionless Eqs. 11 and 12 is illustrated in Fig. 1. The most striking feature of these curves is that they share common asymptotes at both $\phi = 0$ and $\phi = \infty$. In each case, the initial slope is unity (as indicated by the dashed line in Fig. 1). This is readily verified by differentiation of Eqs. 11 and 12 and evaluation of the respective derivatives at $\phi = 0$. Note that the unit initial slope feature for the biexponential disposition model is preserved only when the dimensionless parameters ϕ, ρ_1, and ρ_2 are defined as above. The family of exemplary curves for the biexponential model in Fig. 1 indicates that ρ_1 and ρ_2 are useful indices of the degree of biexponential character, *i.e.*, the extent of deviation from the monoexponential model. For a given value of ρ_2, the degree of biexponential character increases with increasing values of ρ_1, thereby reflecting the divergence of α and β. As ρ_2 increases (for a given value of ρ_1), the biexponential model exhibits less pronounced biexponential character and collapses to the monoexponential model as ρ_2 approaches 1, *i.e.*, as β becomes experimentally indistinguishable from k_{10}. Thus, the dimensionless plot (Fig. 1) affords inspection of both monoexponential and biexponential disposition cases under limiting conditions ($\phi \to 0$, $\phi \to \infty$) that supply equal asymptotes and elucidates the conditions under which collapse to the monoexponential case occurs.

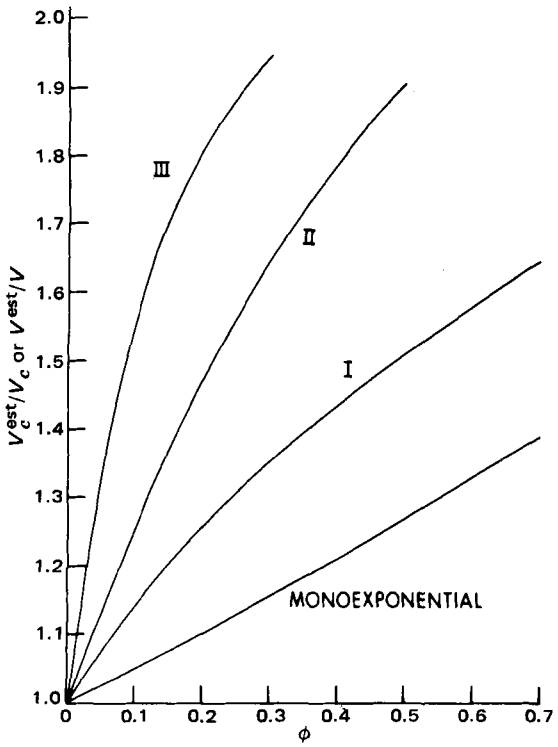

Figure 2—*Relationship between the ratio of estimated volume to true volume* versus *dimensionless time ϕ for the universal monoexponential disposition model (Eq. 16) and three examples (I, II, and III) of the biexponential disposition model (Eq. 19). The biexponential model cases are defined in Fig. 1.*

These features are useful in evaluation of the errors associated with volume estimation.

A convenient way to quantify the accuracy of the initial slope technique for volume estimation is to examine the ratio of the estimated volume to the true volume. Combination of Eqs. 4 and 4a yields:

$$\frac{V^{est}}{V} = \frac{\frac{dC}{dt}(t=0)}{C/t} \qquad \text{(Eq. 13)}$$

or

$$\frac{V^{est}}{V} = \frac{\frac{d(C/C_{ss})}{d\phi}[\phi = 0]}{\frac{(C/C_{ss})}{\phi}} \qquad \text{(Eq. 14)}$$

Recognize that the numerator in Eq. 14 is simply the unit initial slope of the previously developed dimensionless plot (Fig. 1). Therefore, Eq. 14 reduces to:

$$\frac{V^{est}}{V} = \frac{\phi}{C/C_{ss}} \qquad \text{(Eq. 15)}$$

which on substitution of Eq. 11 yields:

$$\frac{V^{est}}{V} = \frac{\phi}{1 - e^{-\phi}} \qquad \text{(Eq. 16)}$$

Equation 16 shows that the accuracy of the volume estimate is a function only of the dimensionless sampling time ϕ. In an analogous fashion for the biexponential model, Eqs. 8 and 8a yield:

$$\frac{V_c^{est}}{V_c} = \frac{\frac{dC}{dt}(t=0)}{C/t} \qquad \text{(Eq. 17)}$$

or

$$\frac{V_c^{est}}{V_c} = \frac{\frac{d(C/C_{ss})}{d\phi}[\phi = 0]}{\frac{(C/C_{ss})}{\phi}} \qquad \text{(Eq. 18)}$$

Table I—Calculated Sampling Time to Achieve an Acceptable Accuracy of Volume Estimation for Drugs Undergoing Monoexponential Disposition with Various Half-lives

Acceptable Accuracy, V^{est}/V	Maximum Allowable Value of ϕ[a]	$t_{1/2}$, h	Corresponding Maximum Allowable Intrainfusion Sampling Time (t), min[b]
1.01	0.020	2	3.5
		4	6.9
		8	13.9
		12	20.8
		24	41.6
1.02	0.040	1	3.5
		2	6.9
		4	13.9
		8	27.7
		12	41.6
		24	83.1
1.05	0.098	0.5	4.2
		1	8.5
		2	17.0
		4	33.9
		8	67.9
		12	101.8
		24	203.6
1.10	0.194	0.25	4.2
		0.50	8.4
		1	16.8
		2	33.6
		4	67.2
		8	134.4
		12	201.6
		24	403.1

[a] Calculated *via* Eq. 16. [b] Calculated *via* Eq. 21.

Substitution of the unit initial slope and Eq. 12 leads to an expression analogous to Eq. 16:

$$\frac{V_c^{est}}{V_c} = \frac{\phi}{1 - \left(\frac{1-\rho_2}{\rho_1-\rho_2}\right)e^{-\rho_1\phi} - \left(\frac{\rho_1-1}{\rho_1-\rho_2}\right)e^{-\rho_2\phi}} \qquad \text{(Eq. 19)}$$

Equation 19 shows that the accuracy of the volume estimate is a function of ρ_1 and ρ_2, as well as the dimensionless sampling time ϕ. The ratios of estimated volume to true volume calculated from Eqs. 16 and 19 are illustrated in Fig. 2. In Fig. 2, as in Fig. 1, the monoexponential disposition case applies to all drugs with such dispositional properties. Consistent with Fig. 1, Fig. 2 shows that the estimation error associated with the biexponential case approaches that of the monoexponential case as ρ_2 approaches 1. Note the tendency of the initial slope technique to overestimate the apparent volume of distribution. This is consistent with the fact that the true initial slope, $dC/dt(t = 0)$, is underestimated by C/t, which is the slope of a line from the origin to the point t,C (see Eq. 10 and Fig. 1). This tendency to overestimate the volume term can also be readily verified by estimation of the quotient C/t using Maclaurin series expansion (11) for limited term approximation of the exponential terms for concentration in Eqs. 1 and 5[1]. Clearly, accurate estimation of the apparent volume of distribution for both the monoexponential and biexponential model cases is best accomplished using a short intrainfusion dimensionless sampling time. Since this dimensionless sampling time is a function of both sampling time and the appropriate rate constant, it is useful to consider the accuracy of volume estimation in terms of sampling time (t) for drugs having a particular half-life ($t_{1/2}$). For the case of monoexponential disposition, $\phi \equiv Kt$ and therefore:

$$t = \frac{\phi}{K} \qquad \text{(Eq. 20)}$$

or

$$t = \frac{\phi t_{1/2}}{\ln 2} \qquad \text{(Eq. 21)}$$

Similarly, for the biexponential disposition case, $\phi \equiv k_{10}t$ and therefore:

$$t = \frac{\phi}{k_{10}} \qquad \text{(Eq. 22)}$$

[1] D. M. Cocchetto, unpublished calculations.

Table II—Comparison of the Estimates of V_c by the Initial Slope Technique and by Nonlinear Regression Analysis for 11 Subjects Receiving Metronidazole

Subject	Plasma Metronidazole Concentration At 15 min[a], μg/mL	C/t, μg/mL·min[b]	V_c^{est} (1) By Initial Slope Technique[c]	V_c (1) By Nonlinear Regression	$\frac{V_c^{est}}{V_c}$[d]	$\left(\frac{V_c^{est}}{V_c}\right)_{calc}$[e]
1	12.68	0.845	31.6	33.3	0.95	1.07
2	10.88	0.725	36.8	32.7	1.13	1.11
3	14.16	0.944	28.3	23.2	1.22	1.22
4	11.16	0.744	35.8	26.2	1.37	1.06
5	12.61	0.841	31.7	31.1	1.02	1.10
6	15.52	1.035	25.8	18.9	1.37	1.37
7	14.36	0.957	27.9	27.4	1.02	1.15
8	19.57	1.305	20.4	21.6	0.94	1.17
9	13.13	0.875	30.5	27.5	1.11	1.04
10	13.75	0.917	29.1	26.8	1.09	1.08
11	10.35	0.690	38.7	33.8	1.14	1.02

[a] Each subject received a constant-rate intravenous infusion of 800 mg of metronidazole over 30 min (k_0 = 26.67 mg/min). [b] An estimate of $dC/dt(t = 0)$ calculated as the slope of the line joining the origin to the point (15 min, C). [c] Calculated *via* Eq. 8a. [d] For each subject, this quantity is the quotient of the quantities in columns 4 and 5. [e] Calculated *via* Eq. 19 using the values of ϕ, ρ_1, and ρ_2 obtained for each subject (see footnote 2).

or

$$t = \frac{\phi t_{1/2}^{10}}{\ln 2} \qquad \text{(Eq. 23)}$$

where the superscript 10 signifies the half-life with respect to k_{10}. Table I summarizes the intrainfusion sampling time t, calculated *via* Eq. 21, required to achieve an acceptable accuracy of volume estimation for drugs undergoing monoexponential disposition with various half-lives. These results suggest that an accurate initial estimate of V (error ≤ 10%) can be obtained from a single intrainfusion concentration determined at a clinically realistic sampling time for drugs with a half-life as short as 15 min. Clearly, the accuracy of volume estimation increases as half-life increases for a series of drugs studied at the same intrainfusion sampling time.

Of special interest with respect to the monoexponential disposition case is the utility of multiple intrainfusion sampling times. Each of two or more sequential intrainfusion sampling times can be used to obtain increasingly errant overestimates of V. In view of the approximately linear character of the monoexponential curve in Fig. 2, a plot of these V^{est} values *versus* intrainfusion sampling time should be nearly linear. The time zero ordinate intercept of the V^{est} *versus* intrainfusion sampling time plot then provides a more accurate value of V^{est}. This intercept volume estimation procedure should prove particularly useful for drugs with short half-lives (<30 min) and monoexponential disposition characteristics, since an accurate value of V^{est} can be calculated from multiple values of V^{est} determined at intrainfusion sampling times that are long relative to the half-life.

An analysis similar to that summarized in Table I for the monoexponential case can be done for the biexponential disposition case, but numerical values of ρ_1 and ρ_2 must first be chosen. For example, for each of the biexponential cases illustrated in Fig. 2, the accuracy of volume estimation could be assessed and tabulated as a function of the half-life ($t_{1/2}^{10}$) by applying Eq. 19 to calculate the ϕ value yielding an acceptable accuracy and then using Eq. 23 to calculate the necessary sampling time t. Since this exercise requires estimates of ρ_1 and ρ_2 for an individual patient, it is best left to the reader having specific parameters for a drug of interest. Note that estimation of V_c as the time zero ordinate intercept of a plot of V_c^{est} *versus* intrainfusion sampling time is not recommended, since this approach would be accurate only if this relationship were approximately linear. The biexponential curves in Fig. 2 clearly show that reasonable linearity can not be ensured over the range of possible values of ρ_1 and ρ_2 for every drug.

RESULTS AND DISCUSSION

The utility of the initial slope technique in estimating the apparent volume of distribution of the central compartment will now be illustrated using data collected in a recent study on metronidazole administered as a constant-rate intravenous infusion. A total of 800 mg of metronidazole in solution was administered over 30 min to 11 healthy human volunteers[2]. The individual subject plasma metronidazole concentration *versus* time data were analyzed using the nonlinear least-squares regression program NONLIN (12, 13) in conjunction with a subroutine for the two-compartment open model with zero-order intravenous infusion input. For purposes of this example, the NONLIN parameter estimate of V_c for each patient will be compared to V_c^{est} calculated by Eq. 8a. The denominator in Eq. 8a is calculated from the plasma metronidazole concentration observed at 15 min after start of the infusion (the earliest sampling time in the study). Table II indicates the simplicity of this V_c^{est} calculation. Figure 3 illustrates the correlation between values of V_c^{est} and the nonlinear regression values of V_c.

This example demonstrates use of the initial slope technique in estimating V_c. Clearly, this estimate should be subsequently refined *via* more thorough characterization of the plasma drug concentration *versus* time profile. The predicted tendency of the initial slope technique of volume estimation to overestimate the true value of the volume term is confirmed by the example for metronidazole (Fig. 3, Table II) since 9 of the 11 subjects had higher initial slope estimates of V_c compared with the nonlinear regression values of V_c; on the average, the former estimates were 12% higher. The magnitudes of the observed V_c^{est}/V_c ratios (column 6 in Table II) are in reasonable agreement with the theoretical ratios of V_c^{est}/V_c (column 7 in Table II) calculated *via* Eq. 19 using the individual subject values of ϕ, ρ_1, and ρ_2. Deviation of the observed ratios from the theoretical ratios is probably due to measurement errors in blood sampling time and plasma metronidazole concentrations. Care must always be taken to minimize such measurement errors prior to using analytical results for pharmacokinetic parameter estimation.

A new technique has been presented for estimating the apparent vol-

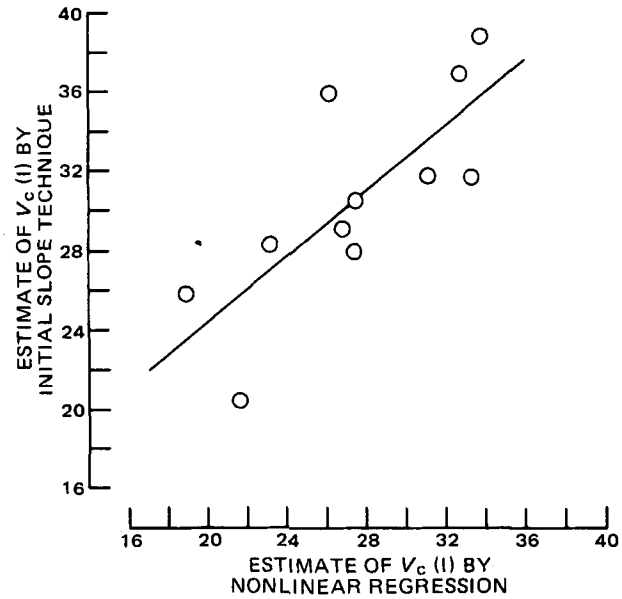

Figure 3—*Correlation between* V_c *estimated by the initial slope technique and the nonlinear regression estimate of* V_c *in 11 subjects receiving a constant-rate intravenous infusion of metronidazole. The linear regression line is shown (slope = 0.819, y-intercept = 8.09,* r = *0.768).*

[2] T. Bergan and D. M. Cocchetto, "Pharmacokinetics of Metronidazole After Intravenous, Oral, and Rectal Administration," manuscript in preparation.

ume of distribution of drugs during constant-rate intravenous infusion. This technique is based on the initial slope of the plasma drug concentration *versus* time profile during infusion. The resulting estimate of the apparent volume of distribution should prove useful as an initial estimate of this pharmacokinetic parameter, especially for investigational drugs for which no pharmacokinetic parameter estimates are available, until additional data permit estimation of the appropriate volume term by conventional methods (14). In addition, this estimate of the apparent volume of distribution can be used with two intrainfusion concentration *versus* time points as input to the Chiou–Hsu equation (5–7), from which total body clearance for individual patients can be calculated. In illustrating the theoretical principles and potential errors involved in the initial slope technique, equations were derived and plots presented of dimensionless concentration *versus* dimensionless time. To our knowledge such an approach, although widely used in engineering, has not been used previously in pharmacokinetics.

REFERENCES

(1) R. J. Sawchuk and D. E. Zaske, *J. Pharmacokinet. Biopharm.*, **4**, 183 (1976).

(2) R. J. Sawchuk, D. E. Zaske, R. J. Cipolle, W. A. Wargin, and R. G. Strate, *Clin. Pharmacol. Ther.*, **21**, 362 (1977).

(3) W. L. Chiou, G. W. Peng, and R. L. Nation, *J. Clin. Pharmacol.*, **18**, 266 (1978).

(4) W. L. Chiou, S. M. Huang, and Y. C. Huang, *Int. J. Clin. Pharmacol.*, **18**, 1 (1980).

(5) W. L. Chiou and F. H. Hsu, *Res. Commun. Chem. Pathol. Pharmacol.*, **10**, 315 (1975).

(6) W. L. Chiou, M. A. F. Gadalla, and G. W. Peng, *J. Pharmacokinet. Biopharm.*, **6**, 135 (1978).

(7) W. L. Chiou, *J. Pharm. Sci.*, **67**, 1776 (1978).

(8) M. Barzegar-Jalali, *Int. J. Pharm.*, **9**, 349 (1981).

(9) M. Gibaldi and D. Perrier, "Pharmacokinetics," Dekker, New York, N.Y., 1975, p. 28.

(10) M. Gibaldi and D. Perrier, "Pharmacokinetics," Dekker, New York, N.Y., 1975, p. 71.

(11) R. V. Churchill, "Operational Mathematics," 2nd ed., McGraw-Hill, New York, N.Y., 1958, p. 157.

(12) C. M. Metzler, G. L. Elfring, and A. J. McEwen, *Biometrics*, **30**, 562 (1974).

(13) C. M. Metzler, G. L. Elfring, and A. J. McEwen, "A Users Manual for NONLIN and Associated Programs," The Upjohn Co., Kalamazoo, Mich., 1974.

(14) M. Gibaldi and D. Perrier, "Pharmacokinetics," Dekker, New York, N.Y., 1975, Chap. 5.

Structure Determination of Polysaccharides in *Aloe saponaria* (Hill.) Haw. (Liliaceae)

AKIRA YAGI *x, KOZO HAMADA *, KUNIHIDE MIHASHI ‡, NOBUO HARADA §, and ITSUO NISHIOKA *

Received March 16, 1982, from the **Faculty of Pharmaceutical Sciences, Kyushu University, Maidashi, Higaski-ku, Fukuok,* ‡*Faculty of Pharmaceutical Sciences, Fukuoka University, Nanakuma, Minami-ku, Fukuoka,* and §*Banyu Pharmaceutical Co., Ltd., Nihonbashi, Honcho, Chuo-ku, Tokyo, Japan.* Accepted for publication September 15, 1982.

Abstract □ Neutral polysaccharides that inhibit carrageenin-induced edema in rats were isolated from the nondialysate of the pulp of *Aloe saponaria* by gel filtration. These were shown to be a linear polymer of a 1,4-linked β-D-mannopyranose (mol. wt. 15,000) containing 18% acetyl groups (As mannan 1), and a 1,4-linked α-D-mannopyranose polymer containing a single branch on the principal chain consisting of D-glucose residues linked at C-2 and C-4 (mol. wt. 66,000), with 10% acetyl groups (As mannan 2). As mannan 1 inhibited carrageenin-induced hind paw edema at 50 mg/kg ip in rats; As mannan 2 was not tested for pharmacological activity. A crude preparation of both As mannans was effective when given intraperitoneally, but was ineffective when given orally.

Keyphrases □ *Aloe saponaria*—isolation of neutral polysaccharides, As mannan 1, As mannan 2, structural determinations □ As mannans—isolation from *Aloe saponaria*, structural determinations, inhibition of carrageenin-induced edema in rats □ Edema, carrageenin-induced—inhibition in rats by neutral polysaccharides isolated from *Aloe saponica*, As mannan 1, As mannan 2

Pharmacological evidence for an anti-inflammatory effect was provided by the isolation from a nondialysate fraction of *Aloe saponaria*[1] of a glycoprotein with kininase activity (1). Further studies on the nondialysate led to the isolation of neutral polysaccharides that inhibit carrageenin-induced edema in rats. This paper describes the structural studies of the polysaccharides, As mannans 1 and 2, and the pharmacological evaluation of As mannan 1.

[1] This plant is also called spotted aloe or soap aloe.

EXPERIMENTAL[2]

Materials—The following materials were obtained commercially: agarose gel[3], diethylaminoethyl cellulose[4], dialysis membrane[5], bromelain[6], protease[7], anti-inflammatory drug[8], and a series of dextrans[9].

Methods of Analysis—The carbohydrate content of the sample was determined colorimetrically by the phenol–sulfuric acid method (2). Elution of material through gel[3] and diethylaminoethyl cellulose[4] filtration was monitored by absorbance of the effluent at 490 nm. Acid hydrolysis was carried out with 1M H_2SO_4 at 90°C for 2 h. Excess sulfuric acid was removed by precipitation as barium sulfate. The filtrate was passed through an ion-exchange column[10] to remove the remaining salts, and then the filtrate was evaporated to dryness. Partial hydrolysis was performed with 0.5M H_2SO_4 at 70°C for 4 h. Analysis of the carbohydrates by methylation was performed according to the method of Hakomori (3). This procedure was performed twice, to give permethylate showing no hydroxyl absorption in the IR spectrum. Paper partition chromatography[11] of the sugar moiety was performed using butanol–pyridine–water (6:4:3) and aniline hydrogen phthalate detection. Ultracentrifugation[12] was performed on an analytical ultracentrifuge with

[2] The IR spectra were obtained with a KOKEN DS-301 spectrometer. The ^1H- and ^{13}C-NMR spectra were recorded with a JEOL PS-100 (100 MHz) and a JEOL FX-100 (25 MHz) spectrometer, respectively. Chemical shifts were recorded in δ units relative to the internal standards 3-(trimethylsilyl)-1-propanesulfonic acid sodium salt or tetramethylsilane. Optical rotations were obtained on a JASCO DIP-4.

[3] Sepharose 6B; Pharmacia Fine Chemicals, Uppsala, Sweden.

[4] DE 32; Whatman Ltd., England.

[5] Visking tube; Union Carbide, Co.

[6] Nakarai Chemical Co., Ltd., Kyoto, Japan.

[7] Type III from papaya; Sigma Chemical Co.

[8] Indomethacin.

[9] Pharmacia Fine Chemicals, Uppsala, Sweden.

[10] Amberlite MR-3; Rohm and Hass Co., Ltd.

[11] Toyo Filter Paper No 50; Toyo Roshi, Co., Tokyo.

[12] Spinco Model E; Beckman Instrument Inc.

0022-3549/84/0100-0062$01.00/0

© 1984, American Pharmaceutical Association

ume of distribution of drugs during constant-rate intravenous infusion. This technique is based on the initial slope of the plasma drug concentration *versus* time profile during infusion. The resulting estimate of the apparent volume of distribution should prove useful as an initial estimate of this pharmacokinetic parameter, especially for investigational drugs for which no pharmacokinetic parameter estimates are available, until additional data permit estimation of the appropriate volume term by conventional methods (14). In addition, this estimate of the apparent volume of distribution can be used with two intrainfusion concentration *versus* time points as input to the Chiou–Hsu equation (5–7), from which total body clearance for individual patients can be calculated. In illustrating the theoretical principles and potential errors involved in the initial slope technique, equations were derived and plots presented of dimensionless concentration *versus* dimensionless time. To our knowledge such an approach, although widely used in engineering, has not been used previously in pharmacokinetics.

REFERENCES

(1) R. J. Sawchuk and D. E. Zaske, *J. Pharmacokinet. Biopharm.*, **4**, 183 (1976).

(2) R. J. Sawchuk, D. E. Zaske, R. J. Cipolle, W. A. Wargin, and R. G. Strate, *Clin. Pharmacol. Ther.*, **21**, 362 (1977).

(3) W. L. Chiou, G. W. Peng, and R. L. Nation, *J. Clin. Pharmacol.*, **18**, 266 (1978).

(4) W. L. Chiou, S. M. Huang, and Y. C. Huang, *Int. J. Clin. Pharmacol.*, **18**, 1 (1980).

(5) W. L. Chiou and F. H. Hsu, *Res. Commun. Chem. Pathol. Pharmacol.*, **10**, 315 (1975).

(6) W. L. Chiou, M. A. F. Gadalla, and G. W. Peng, *J. Pharmacokinet. Biopharm.*, **6**, 135 (1978).

(7) W. L. Chiou, *J. Pharm. Sci.*, **67**, 1776 (1978).

(8) M. Barzegar-Jalali, *Int. J. Pharm.*, **9**, 349 (1981).

(9) M. Gibaldi and D. Perrier, "Pharmacokinetics," Dekker, New York, N.Y., 1975, p. 28.

(10) M. Gibaldi and D. Perrier, "Pharmacokinetics," Dekker, New York, N.Y., 1975, p. 71.

(11) R. V. Churchill, "Operational Mathematics," 2nd ed., McGraw-Hill, New York, N.Y., 1958, p. 157.

(12) C. M. Metzler, G. L. Elfring, and A. J. McEwen, *Biometrics*, **30**, 562 (1974).

(13) C. M. Metzler, G. L. Elfring, and A. J. McEwen, "A Users Manual for NONLIN and Associated Programs," The Upjohn Co., Kalamazoo, Mich., 1974.

(14) M. Gibaldi and D. Perrier, "Pharmacokinetics," Dekker, New York, N.Y., 1975, Chap. 5.

Structure Determination of Polysaccharides in *Aloe saponaria* (Hill.) Haw. (Liliaceae)

AKIRA YAGI *x, KOZO HAMADA *, KUNIHIDE MIHASHI ‡, NOBUO HARADA §, and ITSUO NISHIOKA *

Received March 16, 1982, from the **Faculty of Pharmaceutical Sciences, Kyushu University, Maidashi, Higaski-ku, Fukuok,* ‡*Faculty of Pharmaceutical Sciences, Fukuoka University, Nanakuma, Minami-ku, Fukuoka,* and §*Banyu Pharmaceutical Co., Ltd., Nihonbashi, Honcho, Chuo-ku, Tokyo, Japan.* Accepted for publication September 15, 1982.

Abstract □ Neutral polysaccharides that inhibit carrageenin-induced edema in rats were isolated from the nondialysate of the pulp of *Aloe saponaria* by gel filtration. These were shown to be a linear polymer of a 1,4-linked β-D-mannopyranose (mol. wt. 15,000) containing 18% acetyl groups (As mannan 1), and a 1,4-linked α-D-mannopyranose polymer containing a single branch on the principal chain consisting of D-glucose residues linked at C-2 and C-4 (mol. wt. 66,000), with 10% acetyl groups (As mannan 2). As mannan 1 inhibited carrageenin-induced hind paw edema at 50 mg/kg ip in rats; As mannan 2 was not tested for pharmacological activity. A crude preparation of both As mannans was effective when given intraperitoneally, but was ineffective when given orally.

Keyphrases □ *Aloe saponaria*—isolation of neutral polysaccharides, As mannan 1, As mannan 2, structural determinations □ As mannans—isolation from *Aloe saponaria*, structural determinations, inhibition of carrageenin-induced edema in rats □ Edema, carrageenin-induced—inhibition in rats by neutral polysaccharides isolated from *Aloe saponica*, As mannan 1, As mannan 2

Pharmacological evidence for an anti-inflammatory effect was provided by the isolation from a nondialysate fraction of *Aloe saponaria*[1] of a glycoprotein with kininase activity (1). Further studies on the nondialysate led to the isolation of neutral polysaccharides that inhibit carrageenin-induced edema in rats. This paper describes the structural studies of the polysaccharides, As mannans 1 and 2, and the pharmacological evaluation of As mannan 1.

[1] This plant is also called spotted aloe or soap aloe.

EXPERIMENTAL[2]

Materials—The following materials were obtained commercially: agarose gel[3], diethylaminoethyl cellulose[4], dialysis membrane[5], bromelain[6], protease[7], anti-inflammatory drug[8], and a series of dextrans[9].

Methods of Analysis—The carbohydrate content of the sample was determined colorimetrically by the phenol–sulfuric acid method (2). Elution of material through gel[3] and diethylaminoethyl cellulose[4] filtration was monitored by absorbance of the effluent at 490 nm. Acid hydrolysis was carried out with 1M H_2SO_4 at 90°C for 2 h. Excess sulfuric acid was removed by precipitation as barium sulfate. The filtrate was passed through an ion-exchange column[10] to remove the remaining salts, and then the filtrate was evaporated to dryness. Partial hydrolysis was performed with 0.5M H_2SO_4 at 70°C for 4 h. Analysis of the carbohydrates by methylation was performed according to the method of Hakomori (3). This procedure was performed twice, to give permethylate showing no hydroxyl absorption in the IR spectrum. Paper partition chromatography[11] of the sugar moiety was performed using butanol–pyridine–water (6:4:3) and aniline hydrogen phthalate detection. Ultracentrifugation[12] was performed on an analytical ultracentrifuge with

[2] The IR spectra were obtained with a KOKEN DS-301 spectrometer. The ^1H- and ^{13}C-NMR spectra were recorded with a JEOL PS-100 (100 MHz) and a JEOL FX-100 (25 MHz) spectrometer, respectively. Chemical shifts were recorded in δ units relative to the internal standards 3-(trimethylsilyl)-1-propanesulfonic acid sodium salt or tetramethylsilane. Optical rotations were obtained on a JASCO DIP-4.

[3] Sepharose 6B; Pharmacia Fine Chemicals, Uppsala, Sweden.

[4] DE 32; Whatman Ltd., England.

[5] Visking tube; Union Carbide, Co.

[6] Nakarai Chemical Co., Ltd., Kyoto, Japan.

[7] Type III from papaya; Sigma Chemical Co.

[8] Indomethacin.

[9] Pharmacia Fine Chemicals, Uppsala, Sweden.

[10] Amberlite MR-3; Rohm and Hass Co., Ltd.

[11] Toyo Filter Paper No 50; Toyo Roshi, Co., Tokyo.

[12] Spinco Model E; Beckman Instrument Inc.

0022-3549/84/0100-0062$01.00/0

© 1984, American Pharmaceutical Association

a schlieren optical system in a single sector at 20°C and 56,000 rpm.

Gas chromatography (GC)[13] of the trimethylsilylated sugar from the hydrolysate was performed on a column of silicone SE 52 (3 mm × 2 m) on Chromosorb W AWDMCS (60–80 mesh) at 160°C with a nitrogen flow rate of 45 mL/min. Quantitative analysis of the acetyl content was determined by GC using a column of styrene divinylbenzene polymer (3 mm × 2 m)[14] at 158°C with a nitrogen flow rate of 55 mL/min, using propionic acid as an internal standard (4). GC analysis of the methanolysate was performed on a column of 1% neopentyl glycol succinate polyester (3 mm × 2 m) on Chromosorb W AWDMCS (60–80 mesh) at 147°C, with a nitrogen flow rate of 40 mL/min, and on a column of 5% 1,4-butanediol succinate (3 mm × 2 m) on Chromosorb W[15] (60–80 mesh) at 180°C, with a nitrogen flow rate of 60 mL/min.

The molecular weight estimation was determined on an agarose gel column (1.5 × 51.5 cm) using 0.1 M NaCl at a flow rate of 26 mL/h. A series of dextrans (10, 20, 40, 70, and T-500[9]) were used as a standard. The molecular weight was estimated from a linear correlation between the logarithm of the molecular weight of the polysaccharides and the ratio of their elution volume to the void volume from the column. The viscosities of As mannans 1 and 2 in an aqueous solution were determined by a capillary viscometer[16] at 26°C. The intrinsic viscosity (η) was obtained by the extrapolation to zero concentration of the straight line obtained by plotting η_{sp}/C *versus* concentration of each sample, where C is the concentration. η_{sp} is calculated by $\eta_{sp} = (t_1\rho_1/t_0\rho_0) - 1$, where t_1 is the time of efflux of the solution, ρ_1 is its density, t_0 is the time of efflux of the solvent, and ρ_0 is its density.

Assay Method for Carrageenin-Induced Edema—Male Wistar albino rats weighing 120–150 g were used. Edema was induced by the injection of 0.1 mL of 1% (w/v) carrageenin dissolved in saline beneath the plantar aponeuroses of the hind paws. One to twelve hours before the injection of carrageenin, drugs were administered intraperitoneally or per os. The swelling (in percent) of the rat hind paws was measured by a volume differential meter[17].

Preparation of Crude Material—The fresh leaves of *A. saponaria*[18] were harvested in September 1980 from the greenhouse of the herbal garden of Kyushu University. Fresh leaves were cut in half in a parallel manner, and colorless gelatinous pulp was separated carefully by scraping from the green cortical layer containing yellow phenolics. The homogenized pulp (3 kg) was centrifuged at 10,000 rpm for 30 min. The supernatant was membrane[5] dialyzed against distilled water for 48 h, and nondialysate was lyophilized to afford a colorless soft material (6 g).

Isolation and Purification of As Mannans 1 and 2—Crude material (yield, 0.012% from the fresh leaves) isolated from the pulp harvested in September 1980 was dissolved in 0.3 M NaCl and was subjected to column fractionation (4.8 × 20.5 cm, agarose gel) using the same solution as a solvent at a flow rate of 28 mL/h. The fraction (elution volume, 110–250 mL) containing carbohydrate was pooled, dialyzed, and lyophilized to give a colorless soft material (yield, 50.0%). This material (0.1 g) dissolved in 0.02 M NH_4HCO_3 (5 mL) was subjected to column fractionation (1.5 × 44 cm, DEAE-cellulose[4]) using the same solution as a solvent at a flow rate of 25 mL/h, and the fraction (elution volume, 40–75 mL) was pooled, dialyzed, and lyophilized to give As mannan 1 (yield, 35% from the crude material). In a similar manner, the crude material (yield, 0.05% from the fresh leaves) isolated from the pulp harvested in December 1980 was treated to give As mannan 2 (yield, 16% from the crude material).

Chemical and Physical Properties of As Mannans 1 and 2—Since As mannan 1 in 1% solution and As mannan 2 in 0.5% solution in 0.1 M NaCl gave single peaks having $S_{20,w} = 1.25\ S$ and $1.17\ S$, respectively, each appears to be homogeneous.

As Mannan 1—$[\alpha]_D^{20}$ −40.5° (c = 0.7, H_2O); ^{1}H-NMR [3-(trimethylsilyl)-1-propanesulfonic acid sodium salt, D_2O]: δ 2.13 (m, CH_3COO), 4.76 (br s, anomeric proton of the nonreducing carbon atom), 4.17, and 5.50 ppm (CH_3COOCH—); ^{13}C-NMR [3-(trimethylsilyl)-1-propanesulfonic acid sodium salt, 0.1 M NaCl]: δ 176.4 (CH_3COO) and 22.9 ppm (CH_3COO), with other signals listed in Table I. IR (KBr)ν_{max}: 1730 and 1250 cm^{-1}. This compound is very slightly soluble in water.

Hydrolysis of As Mannan 1—A sample of As mannan 1 (10 mg) was hydrolyzed to give D-mannose as the only sugar moiety by paper and gas (as a trimethylsilyl ether) chromatographic analyses. R_f values: glucose 0.31; galactose 0.25; mannose 0.34; and hydrolysate 0.34. GC retention times (in minutes): mannose 10.1 and 15.1; glucose 14.4 and 22.1; galactose 10.7, 12.6, and 15.7; the hydrolysate 10.1 and 15.1.

As Mannan 2—$[\alpha]_D^{20}$ +70.0° (c = 0.8, H_2O); ^{1}H-NMR [3-(trimethylsilyl)-1-propanesulfonic acid sodium salt, D_2O]: δ 2.13 (m, CH_3COO) and 5.00 ppm (br s, anomeric proton of the nonreducing carbon atom). ^{13}C-NMR [3-(trimethylsilyl)-1-propanesulfonic acid sodium salt, 0.1 M NaCl): δ 176.1 (CH_3COO) and 22.8 ppm (CH_3COO), with other signals listed in Table I. IR (KBr) ν_{max}: 1730 and 1245 cm^{-1}. This compound is soluble in water.

Hydrolysis of As Mannan 2—A sample of As mannan 2 (15 mg) was hydrolyzed to give D-mannose as the major sugar component and a minor amount of D-glucose by paper and gas (as a trimethylsilyl ether) chromatographic analyses. R_f values: mannose 0.37; glucose 0.31; galactose 0.26; the hydrolysate 0.31 and 0.36. GC retention times (in minutes): mannose 10.1 and 15.1; glucose 14.4 and 22.1; galactose 10.7, 12.6, and 15.7; the hydrolysate 10.1, 14.8, and 22.4. Mannose and glucose were detected using GC in a ratio of 95:5.

Analysis of As Mannan 1 by Methylation—A sample of As mannan 1 (20 mg) was methylated according to Hakomori's method (3). The product was chromatographed on a silica gel column using chloroform–methanol (20:1) to give material which showed no hydroxyl absorption in the IR spectrum; proton signals due to a methoxyl group (δ 3.3–3.8 ppm) and anomeric proton signals (δ 4.61 ppm) were observed in the ^{1}H-NMR spectrum. The permethylate (5 mg) was subjected to methanolysis with 4% hydrogen chloride in methanol (1 mL) in a sealed tube at 90°C for 2 h. After the removal of the solvent, the methanolysate (dissolved in ethyl acetate) was chromatographed on a silica gel column using ethyl acetate and ethyl acetate–methanol as solvents to give material which showed one spot on TLC [ethyl acetate–methanol (25:1)]. The methanolysate was subjected to GC analysis on columns of 1% neopentyl glycol succinate (*a*) and 5% 1,4-butanediol succinate (*b*). The following retention times were obtained: (*a*) methyl mannopyranosides of 2,3,4,6-tetramethyl-*O*-, 3,4,6-trimethyl-*O*-, 2,4,6-trimethyl-*O*-, 2,3,6-trimethyl-*O*-, and 2,3,4-trimethyl-*O*- derivatives: 1.8, 2.8, 3.3, 4.3, and 2.7 min and the methanolysate: 1.8 and 4.3 min. (*b*) methyl mannopyranosides of 2,3,4,6-tetramethyl-*O*-, 3,4,6-trimethyl-*O*-, 2,4,6-trimethyl-*O*-, 2,3,6-trimethyl-*O*-, and 2,3,4-trimethyl-*O*- derivatives: 4.1, 8.6, 10.1, 12.3, and 8.5 min and the methanolysate: 4.1 and 12.3 min.

Analysis of As Mannan 2 by Methylation—A sample of As mannan 2 (8 mg) was methylated according to Hakomori's method (3). In the same manner as for As mannan 1, the product was treated to give the methanolysate which showed a single spot on TLC [ethyl acetate–methanol (25:1)]. The methanolysate was subjected to GC analysis to give the following retention times on columns of 1% neopentyl glycol succinate (*a*) and 5% 1,4-butanediol succinate (*b*): (*a*) methyl mannopyranosides of 3,4,6-trimethyl-*O*-, 2,4,6-trimethyl-*O*-, 2,3,6-trimethyl-*O*-, and 2,3,4-trimethyl-*O*- derivatives: 3.4, 4.3, 5.6, and 3.4 min, methyl glucopyranosides of 3,4,6-trimethyl-*O*-, 2,4,6-trimethyl-*O*-, 2,3,6-trimethyl-*O*-, and 2,3,4-trimethyl-*O*- derivatives: 3.4, 5.4, 5.2, and 4.1 min, and the methanolysate 5.6 min. (*b*) methyl mannopyranosides of 2,3,4,6-tetramethyl-*O*-, 3,4,6-trimethyl-*O*-, 2,4,6-trimethyl-*O*-, 2,3,6-trimethyl-*O*-, 2,3,4-trimethyl-*O*-, 4,6-dimethyl-*O*-, 3,6-dimethyl-*O*-, and 3,4-dimethyl-*O*- derivatives: 4.9, 10.3, 12.0, 15.3, 12.0, 22.4, 20.5, and 20.2 min, methyl glycopyranosides of 4,6-dimethyl-*O*-, 3,6-dimethyl-*O*-, and 3,4-dimethyl-*O*-derivatives: 28.5, 29.3, and 25.7 min, and the methanolysate: 15.3 and 29.1 min.

Determination of the Molecular Weights of As Mannans 1 and 2—The molecular weights were estimated on a column of agarose gel using a series of dextrans as a standard. The molecular weights of As mannans 1 and 2 were determined to be 15,000 and 66,000, respectively.

Determination of the Viscosities of As Mannans 1 and 2—The viscosities were obtained with a capillary viscometer[16]. The intrinsic viscosities of As mannans 1 and 2 was determined to be 15.6 and 2.5 dL/g, respectively.

Alkaline Hydrolysis of As Mannans 1 and 2—Each sample of As mannan 1 (5 mg) or 2 (5 mg) was hydrolyzed with 4% NaOH for 30 min, and the mixture was dialyzed against distilled water followed by lyophilization to give material which showed no absorption in the IR spectrum due to acetyl groups. Deacetyl As mannan 1: ^{1}H-NMR [3-(trimethylsilyl)-1-propanesulfonic acid sodium salt, 1 M NaOD]: δ 4.55 ppm (br s); deacetyl As mannan 2: ^{1}H-NMR [3-(trimethylsilyl)-1-propanesulfonic acid sodium salt, 1 M NaOD]: δ 4.81 ppm (br s).

Partial Hydrolysis of As Mannan 1—On acid hydrolysis with 0.5M H_2SO_4 at 70°C for 4 h, As mannan 1 (38 mg) yielded the oligosaccharides. The products were fractionated on a cellulose column using acetone–water. On elution with acetone–water (10:1), (6:1), and (3:1), mannose

[13] Gas chromatograph GC-4BM; Shimadzu Seisakusho Ltd., Japan.
[14] Chromosorb 102; Johns-Manville.
[15] Shimalite W; Shimadzu Seisakusho Ltd., Japan.
[16] Ubbelohde instrument.
[17] Ugo Basile Co., Ltd., Italy.
[18] A voucher specimen is available for inspection at the Herbal Garden of Kyushu University, Fukuoka, Japan.

Table I—^{13}C-NMR Spectral Assignments

	As Mannan 1		As Mannan 2		Ivory Nut	
	1,4-β-Man[a]	Deacetyl[b]	1,4-α-Man[c]	Deacetyl[d]	Mannan[e]	Native D$_1$[f]
C-1	102.7[g]	103.0	100.1	101.3	101.7	102.1; 101.9
C-2	72.6	73.5	72.1	73.0	72.7	70.9; 71.1
C-3	74.1	74.7	72.7	73.4	73.5	70.2
C-4	79.1	78.6	76.1	77.5	78.8	74.8; 74.5
C-5	77.6	78.6	74.0	74.9	78.8	71.8; 69.3
C-6	63.3	63.4	63.2 67.3[h]	63.6 68.6[h]	62.1	64.1; 61.3

[a] Concentration: 30 mg/mL of 0.1 M NaCl at 28°C. [b] Concentration: 30 mg/mL of 0.1 M NaOD at 28°C. [c] Concentration: 50 mg/mL of 0.1 M NaCl at 28°C. [d] Concentration: 10 mg/mL of 0.1 M NaOD at 28°C. [e] From Ref. 5. [f] From Ref. 7; see text for chemical name. [g] Chemical shift (δ) was recorded at 25.5 MHz using tetramethylsilane as the internal standard. [h] Not assigned.

(4.3 mg), mannobiose (4.5 mg), and mannotriose (2.5 mg) were obtained. Mannobiose: $[\alpha]_D^{20}$ −6.4° (c = 0.66, H_2O); ^{1}H-NMR(tetramethylsilane, D_2O): δ 3.4–4.2 (m, 8, C*H*OH), 4.70 (s, 1, C_1 α-H), 4.88 (d, J = 0.7 Hz, C_1 α-H), and 5.15 ppm (d, J = 1.0 Hz, C_1 β-H); ^{13}C-NMR(tetramethylsilane, D_2O): δ 63.7, 63.1 (C_6, $C_{6'}$), 69.3 ($C_{4'}$), 71.6, 72.8, 73.2, 73.6, 77.4, 79.0 (C_2, C_3, C_5, $C_{2'}$, $C_{3'}$, $C_{5'}$), 79.5 (C_4), 96.4 (C_1), and 102.8 ppm ($C_{1'}$). The C—H coupling constants of the nonreducing anomeric carbon ($J_{C(1')-H}$) and of the reducing anomeric carbon ($J_{C(1)-H}$) were 163 and 172 Hz, respectively (nuclear Overhauser effect).

RESULTS AND DISCUSSION

To characterize the active component(s) in the crude material, 25 mg/kg ip of the crude material, treated by the following procedures, was administered to rats prior to the induction of edema by carrageenin. On heating at 100°C for 10 min or 1 h, crude material (150 mg) dissolved in distilled water (50 mL) did not show any change in the inhibitory activity, and on treatment of crude material (100 mg) with artificial gastric juice (40 mL, pH 1.2) at 37°C for 13 h, the same result was obtained. By allowing crude material (100 mg) to stand in 1% NH_4OH (20 mL) at room temperature for 13 h, followed by dialysis and lyophilization, the inhibitory activity of the material recovered (11 mg) appeared to be markedly elevated. On enzymatic hydrolysis of the crude material (160 mg) with protease[7] (5 mg) in 10 mM phosphate buffer (40 mL, pH 6.2) at 37°C for 57 h, followed by the precipitation of protease with trichloroacetic acid, filtration, dialysis, and lyophilization, the inhibitory activity of the material recovered (51 mg) appeared to be enhanced. From the above experiments it is concluded that the active substance(s) in the crude material is not an enzyme or protein. Furthermore, these results suggest that the inhibitory activity in the crude material may be due to a neutral polymer stable to heat, acid, and alkali. Neutral polysaccharides, As mannans 1 and 2, were isolated from the leaves harvested in September and December 1980, respectively, by gel filtration on agarose and DEAE-cellulose columns.

As Mannan 1—On acid hydrolysis D-mannose was the only sugar moiety detected by paper and gas chromatographic analyses. However, the IR spectrum gave a peak indicative of an *O*-acetyl substituent, and the ^{1}H- and ^{13}C-NMR spectral signals supported the presence of *O*-acetyl groups. The acetyl content was determined to be 18% by GC, and a molar ratio (1.2:1) of D-mannose to *O*-acetyl groups was confirmed by ^{1}H-NMR spectroscopy. On analysis by methylation the permethylate provided only 1,4-linked D-mannose residues on the GC spectrum. This indicated a linear structure made up of 1,4-linked D-mannopyranose. Table I indicated the downfield shifted signal due to 1,4-linkages at 102.7 and 79.1 ppm assigned to C-1 and C-4, respectively. On comparison of the ^{13}C-NMR spectral data with those of ivory nut mannan [1,4-linked β-D-mannan (5)], the assignment of the carbon resonances of As mannan 1 was reasonably accomplished. Accordingly, a linear chain structure having a repeating unit of 1,4-linked D-mannopyranose was proposed as As mannan 1. This conclusion was further confirmed by the partial hydrolysis. On treatment with 0.5M H_2SO_4 for 4 h at 70°C, As mannan 1 provided a mannobiose whose configuration was determined to be 4-*O*-β-D-mannopyranosyl-D-mannose based on the optical rotation value and the $J_{C(1)-H}$ coupling constants of the nonreducing anomeric carbon (163 Hz) and the reducing anomeric carbon (172 Hz) (6). As mannan 1 gave a $[\alpha]_D$ −40.5°, suggesting that all mannopyranose residues were β,D-linked. The direct bonded C—H coupling constant of the anomeric carbon ($J_{C(1)-H}$) may be useful for determining the configuration of the anomeric carbons in mannose-containing polysaccharides. However, it is evident that the wide diversity of ^{13}C-NMR spectra from mannose-containing polysaccharides is caused by differences in chain structure of the polysaccharides, and each peak width in the coupling between C-1 and H in the anomeric carbons in As mannan 1 are too broad. ^{1}H-NMR spectra have been used extensively for the characterization of anomeric protons of nonreducing carbon atoms in polysaccharides. It has been found that chemical shifts due to anomeric protons with an equatorial configuration appear further downfield (δ 5.02–5.92 ppm) than those with an axial configuration (δ 4.55–4.93 ppm) although deviation was observed depending on substituents, the aglycone, or the measurement condition. The anomeric proton signal at δ 4.76 was assigned as an axial proton, and the configuration of As mannan 1 was determined to be β-linked. Further evidence about the configuration of the glycosidation bonds was obtained from ^{1}H-NMR spectral data of the permethylate, indicating that the anomeric proton of the nonreducing carbon atom appeared at δ 4.61 ppm, and from the $J_{C(1)-H}$ coupling constant (163 Hz) of the nonreducing carbon atom in the mannobiose, indicating a repeating unit. The location of the *O*-acetyl substituents was suggested to be at C-6, by the ^{13}C-NMR spectral data, when comparing the chemical shift of C-6 with those of deacetyl As mannan 1 or ivory nut mannan. The signals at δ 4.17 ppm are assigned to the C-6 proton attached to the acetyl group, using comparison with signals of deacetyl As mannan 1 or D-mannopyranose pentaacetate on the ^{1}H-NMR spectra.

As Mannan 2—On acid hydrolysis, As mannan 2 gave D-mannose (major) and D-glucose (minor) components by paper and gas chromatographic analyses. The IR spectrum showed absorption indicative of an *O*-acetyl substituent, and the ^{1}H- and ^{13}C-NMR spectral signals supported the presence of *O*-acetyl groups. The acetyl content was determined to be 10% by GC, and a molar ratio of (2.4:1) of D-mannose to acetyl groups was confirmed by ^{1}H-NMR spectroscopy. On analysis by methylation the permethylate provided a 1,4-linked D-mannose residue (major) and a 1,4 and 1,2-linked glucose residue (minor) on GC. Further evidence for a 1,4-linkage of D-mannopyranose was shown by ^{13}C-NMR. Table I shows that the downfield shifted signal due to the 1,4-linkage was found at δ 100.1 and 76.1 ppm, assignable to C-1 and C-4, respectively.

Table II—Effect of Intraperitoneally Administered Crude Material, As mannan 1, and Indomethacin on Carrageenin-Induced Edema

Drug (Dose)	Postadministration Swelling, %[a]				
	1 h	2 h	3 h	4 h	5 h
Crude material (50 mg/kg)	16.2 ± 4.6	23.0 ± 5.3	17.6 ± 5.3	30.0 ± 13.1	43.4 ± 8.2
Indomethacin (2.5 mg/kg)	18.3 ± 6.8	20.8 ± 1.0	32.6 ± 5.5	37.7 ± 2.2	53.4 ± 6.6
As mannan 1 (50 mg/kg)	22.3 ± 6.7	19.1 ± 6.7	20.3 ± 9.4	37.1 ± 6.8	48.9 ± 12.8
Control (Saline)	24.8 ± 7.0	43.5 ± 10.1	63.1 ± 14.0	62.9 ± 16.6	72.4 ± 11.6

[a] The values are means ± *SD* from five rats.

Table III—Effect of Orally Administered Crude Material and Indomethacin on Carrageenin-Induced Edema

Drug (Dose)	Postadministration Swelling, %[a]				
	1 h	2 h	3 h	4 h	5 h
Crude material (400 mg/kg)	10.3 ± 3.8	32.3 ± 12.4	51.9 ± 19.1	53.7 ± 18.1	42.6 ± 19.3
Indomethacin (20 mg/kg)	1.7 ± 2.4[b]	5.2 ± 5.0[b]	9.5 ± 12.8[c]	17.3 ± 16.3	7.9 ± 9.3[c]
Control (saline)	14.1 ± 10.0	34.1 ± 7.1	41.4 ± 9.8	46.9 ± 4.8	33.4 ± 9.5

[a] The values are means ± *SD* from five rats; the drugs were administered per os. [b] Statistically significantly different from the control at $p < 0.05$. [c] Statistically significantly different from the control at $p < 0.01$.

Table IV—Effect of Crude Material and Bromelain Administered Orally 2, 4, 6, and 12 h Before Induction of Edema by Carrageenin Injection

Drug (Dose)	Time of Administration	Postinjection Swelling, %[a]				
		1 h	2 h	3 h	4 h	5 h
Crude material (100 mg/kg)	2 h	11.5 ± 1.9	39.3 ± 12.0	40.5 ± 15.1	55.7 ± 16.5	51.5 ± 8.0
Bromelain (100 mg/kg)		13.3 ± 1.3	29.9 ± 10.7	33.2 ± 14.1	46.5 ± 15.5	41.8 ± 13.5
Control (saline)		18.8 ± 8.3	40.4 ± 10.7	37.6 ± 6.7	47.0 ± 3.9	49.7 ± 5.6
Crude material (100 mg/kg)	4 h	14.1 ± 5.4	56.8 ± 6.8	61.7 ± 7.0	62.6 ± 6.7	60.4 ± 5.4
Bromelain (100 mg/kg)		13.1 ± 6.1	45.8 ± 14.7	51.9 ± 11.4	57.3 ± 7.1	56.9 ± 6.7
Control (saline)		12.8 ± 6.1	54.6 ± 13.4	58.6 ± 12.7	60.6 ± 11.7	61.7 ± 8.1
Crude material (100 mg/kg)	6 h	25.5 ± 3.7	42.4 ± 8.8	43.6 ± 9.6	58.4 ± 8.9	59.1 ± 7.3
Bromelain (100 mg/kg)		17.9 ± 9.9	34.1 ± 15.7	37.4 ± 14.5	63.9 ± 4.6	61.5 ± 5.3
Control (saline)		25.8 ± 9.0	48.5 ± 11.7	49.8 ± 12.3	64.7 ± 12.5	64.6 ± 8.9
Crude material (100 mg/kg)	12 h	17.9 ± 9.1	23.4 ± 7.3	35.8 ± 15.6	48.4 ± 17.1	49.9 ± 17.3
Bromelain (100 mg/kg)		22.7 ± 6.4	29.7 ± 9.1	38.6 ± 12.1	47.2 ± 9.6	41.0 ± 7.5
Control (saline)		16.9 ± 5.5	28.0 ± 5.6	36.3 ± 7.8	48.1 ± 6.7	48.2 ± 5.9

[a] The values are means ± *SD* from five rats.

On comparison of the ^{13}C-NMR spectral data with those of 1,4- and 1,2-linked α-D-mannan having an acetyl group at C-6 [native D_1 (7)], carbon resonances of As mannan 2 were assigned. As mannan 2 gave a $[\alpha]_D$ + 70°, suggesting mannopyranose residues were α,D-linked. On comparison of the ^{1}H-NMR spectra with those of As mannan 1, the anomeric proton signal of the nonreducing carbon atom at δ 5.00 ppm was assigned to be an equatorial proton, and the configuration of As mannan 2 was determined to be α-linked. The location of the acetyl group was ambiguous, because of a low content of acetyl groups in As mannan 2. Thus, a branched structure (I) was proposed for As mannan 2.

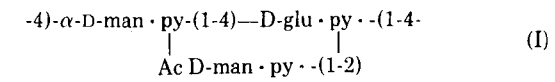

(I)

Inhibition of Carrageenin-Induced Edema—A potent inhibitory effect of the neutral polysaccharide, As mannan 1, for carrageenin-induced edema by the intraperitoneal route was found (Table II). With oral administration, however, both crude material and bromelain failed to induce any response in test animals at the dose used, while indomethacin gave apparent inhibition (Table III). No inhibitory activity of crude material or bromelain was found, even at a dose of 100 mg/kg, when given per os 2, 4, 6, or 12 h before induction of edema (Table IV). This may be due to poor absorption of As mannan when given orally.

REFERENCES

(1) A. Yagi, N. Harada, H. Yamada, S. Iwadare, and I. Nishioka, *J. Pharm. Sci.*, **71**, 1172 (1982).

(2) M. Dubois, K. A. Gilles, J. K. Hamilton, P. A. Rebers, and F. Smith, *Anal. Chem.*, **28**, 350 (1956).

(3) S. Hakomori, *J. Biochem.*, **55**, 205 (1964).

(4) B. Radhakrishnamurthy, E. R. Dalferes, Jr., and G. S. Bereson, *Anal. Biochem.*, **26**, 61 (1968).

(5) P. A. Gorin, *Can. J. Chem.*, **51**, 2375 (1973).

(6) R. Kasai, M. Okihara, J. Asakawa, K. Mizutani, and O. Tanaka, *Tetrahedron*, **35**, 1427 (1979).

(7) S. G. Wilkinson, *Carbohydr. Res.*, **93**, 269 (1981).

ACKNOWLEDGMENTS

The authors thank Prof. A. Koda (Department of Pharmacology and Immunology, Gifu College of Pharmacy), Dr. S. Yahara (Faculty of Pharmaceutical Sciences, Kyushu University), and Dr. S. Iwadare (Banyu Pharmaceutical Co. Ltd.) for valuable discussions. We acknowledge Mr. Y. Tanaka, Miss Y. Soeda, and Dr. T. Fukamizo for measurements of ^{1}H- and ^{13}C-NMR spectra and ultracentrifugation, and Miss Y. Ikeda for her technical assistance.

Prednisolone Levels in Plasma and Leukemia Cells During Therapy of Chronic Lymphocytic Leukemia

N. S. PANESAR *, C. C. BIRD *x, B. E. ROBERTS ‡, and J. A. CHILD ‡

Received March 26, 1982, from the **Pathology Department, University of Leeds, Leeds LS2 9JT, England*, and the ‡*Hematology Department, The General Infirmary, Leeds LS1 3EX, England.* Accepted for publication November 12, 1982.

Abstract □ The capacity of chronic lymphocytic leukemia cells to concentrate prednisolone has been evaluated *in vivo* and *in vitro* employing a radioimmunoassay for prednisolone. No evidence to suggest that leukemia cells are capable of selectively concentrating glucocorticoid was found. The relative uptake of glucocorticoid by leukemia cells was found to be greater *in vitro* than *in vivo*. This may be attributable to differences in steroid bioavailability to cells. Substantially lower levels than previously reported of free prednisolone were found in plasma of patients receiving oral treatment with prednisolone. This may result from the failure in previous studies to remove derivatives of prednisolone and other steroids prior to assay for hormones.

Keyphrases □ Prednisolone—levels in plasma and leukemia cells during therapy of chronic lymphocytic leukemia, glucocorticoid □ Lymphocytic leukemia—prednisolone levels in plasma and leukemia cells during therapy, chronic, glucocorticoid □ Glucocorticoids—prednisolone levels in plasma and leukemia cells during therapy of chronic lymphocytic leukemia

Glucocorticoid hormones, usually in combination with other chemotherapeutic agents, are used extensively for treatment of human leukemias and lymphomas. Clinical trials have clearly shown the efficacy of including glucocorticoid in treatment schedules, although the therapeutic mode of action of these steroids is still poorly understood (1). In the main, therapeutic effects have been attributed to the direct cytolethal and/or cytostatic action of the steroid on malignant cells, although glucocorticoids also have a wide variety of other effects on cells and tissues throughout the body (1).

In previous studies with a large series of human lymphoid cell lines (2–6) and freshly isolated leukemia cells from patients with chronic lymphocytic and hairy-cell leukemia (7), it was found that human lymphoid cells are remarkably resistant to the cytolethal and cytostatic effects of glucocorticoids *in vitro* despite the presence of substantial levels of cytoplasmic glucocorticoid receptors and evidence of uptake and binding of glucocorticoid by target cells. In nearly every case lymphoid cells required exposure to suprapharmacological concentration ($>10^{-6}$ M) of steroid for prolonged periods (>48–72 h) before significant cytolethal or cytostatic responses resulted. Since in therapeutic practice glucocorticoids are administered as repeated daily doses of low concentrations of steroid ($<10^{-6}$ M), it seems unlikely that leukemia cells *in vivo* are ever exposed to the glucocorticoid concentrations required to induce cytolethal responses *in vitro*. However, virtually nothing is known about target cell concentrations of glucocorticoids in leukemia patients during therapy and whether or not leukemia cells are capable of concentrating glucocorticoid to an extent that *in vitro* conditions may be simulated.

The results of such an investigation in which the concentrations of free prednisolone in plasma and leukemia cells of a small series of patients with chronic lymphocytic leukemia was measured at various time intervals after administration of a single oral therapeutic dose of prednisolone are reported herein. The results are compared with the *in vitro* uptake of prednisolone by freshly isolated leukemia cells. A radioimmunoassay (RIA) developed specifically to measure prednisolone levels also indicates that previous estimates of free prednisolone in plasma during therapy may be grossly inaccurate.

EXPERIMENTAL

Materials—[^{3}H]Prednisolone (25–50 Ci/mmol)[1] was purified by TLC before use. The xylene-based scintillation fluid contained *p*-bis-2-(5-phenyloxazole)[2] (0.02% w/v), 2,5-diphenyloxazole[3] (0.3% w/v), and isooctylphenoxypolyethoxyethanol[3] (25% v/v). Organic solvents[4] of analytical grade were used as supplied. Pharmaceutical [^{3}H]prednisolone (5 μCi/80 mg)[5] was prepared commercially and used as supplied.

Patients—Ethical restrictions required the complete study to be undertaken with 11 patients with hematologically confirmed chronic lymphocytic leukemia. Six patients (subjects 1–6) were used for the *in vivo* study and five patients (subjects 7–11) were used for the *in vitro* study.

In Vivo *Study*—Subjects 1–4 were given a single oral dose (45 mg/m^2) of prednisolone. In two other patients (subjects 5 and 6) the oral dose of steroid also included 5 μCi of [^{3}H]prednisolone. Blood samples (20–25 mL) were removed from the cubital vein at intervals up to 24 h. Leukemic lymphocytes were separated from other peripheral blood cells in a density gradient[6] (8). Plasma was drawn off without agitating the cell layer and stored at −20°C until assayed. Leukemia cells were washed twice in tissue culture medium[7] containing 10% heat-inactivated fetal calf serum[8], then counted before being stored as a pellet at −20°C. Normally cells were frozen within 1 hr of sample collection.

In Vitro *Study*—Leukemic lymphocytes were separated from the peripheral blood of five previously untreated patients (subjects 7–11) on the density gradient and washed twice with sterile tissue culture medium containing 10% heat-inactivated fetal calf serum. Approximately 25×10^6 viable eells were incubated at 37°C with a saturating concentration of [^{3}H]prednisolone ($7.22 \pm 0.062 \times 10^{-8}$ M) in 2 mL of growth medium. Cells were incubated for 1, 30, 60, and 120 min after which they were immediately centrifuged at 300×*g* for 1 min at 4°C. The pellet was washed with 3 × 2-ml aliquots of ice-cold medium and recovered by centrifugation (300×*g* for 1 min). The whole washing procedure took ~15 min to complete. After the third wash the pellet was resuspended in 2 mL of fresh medium, and 2 × 0.5-mL aliquots, each containing 6.25×10^6 viable cells, were added to 8 mL of scintillation fluid and assayed for radioactivity in a liquid scintillation counter[9] (efficiency ~50%). The remaining fraction was centrifuged, and a 0.5-mL aliquot was removed to determine the radioactivity of the supernatant. The latter was subtracted from the former to determine the activity in 6.25×10^6 viable cells. The intracellular concentration was calculated by assuming an average cell volume of 4.22×10^{-13} L (cell diameter 7.5 nm).

Radioimmunoassay for Prednisolone—Antiserum to prednisolone 21-hemisuccinate conjugated to bovine serum albumin (9) was raised in

[1] Amersham International, Amersham, Bucks, England.
[2] Nuclear Enterprises Ltd., Edinburgh, Scotland.
[3] Sigma London Chemical Co., Poole, Dorset, England.
[4] B.D.H. Ltd.; Poole, Dorset, England.
[5] Upjohn Ltd., Crawley, Sussex, England.
[6] Ficoll, Pharmacia Fine Chemicals AB, Uppsala, Sweden; Triosil, Nyegaard & Co., Oslo, Norway.
[7] RPMI 1640, Flow Laboratories, Irvine, Ayrshire, Scotland.
[8] Gibco Co., Paisley, Scotland.
[9] Nuclear Chicago Isocap 300—G.D. Searle, High Wycombe, Bucks, England.

0022-3549/84/0100-0066$01.00/0
© 1984, American Pharmaceutical Association

Table I—Plasma and Intracellular Concentrations of Prednisolone in Chronic Lymphocytic Leukemia Patients Following a Single Oral Dose of Prednisolone

Subject		Prednisolone Concentration, M					
		1 h	3 h	6 h	9 h	12 h	24 h
1	Plasma	7.94×10^{-9}	3.33×10^{-7}	1.53×10^{-7}	1.11×10^{-7}	ND[b]	ND
	Intracellular[a]	0.66×10^{-9}	0.90×10^{-9}	0.81×10^{-8}	0.53×10^{-8}	ND	ND
2	Plasma	4.83×10^{-7}	5.05×10^{-7}	2.69×10^{-7}	1.75×10^{-7}	9.16×10^{-8}	1.42×10^{-8}
	Intracellular[a]	1.05×10^{-8}	2.26×10^{-8}	1.18×10^{-8}	ND	2.50×10^{-9}	ND
3	Plasma	7.67×10^{-7}	5.04×10^{-7}	2.21×10^{-7}	1.65×10^{-7}	ND	ND
	Intracellular[a]	1.83×10^{-8}	1.08×10^{-8}	5.46×10^{-9}	3.88×10^{-9}	ND	ND
4	Plasma	7.53×10^{-7}	3.83×10^{-7}	2.06×10^{-7}	1.34×10^{-7}	ND	ND
	Intracellular[a]	1.06×10^{-8}	1.15×10^{-8}	7.30×10^{-9}	3.90×10^{-9}	ND	ND

[a] Determined assuming average cell volume 4.22×10^{-13} L (cell diameter 7 nm). [b] ND = not determined.

Table II—Total and Free Prednisolone Concentrations in Plasma of Chronic Lymphocytic Leukemia Patients Receiving a Single Oral Dose of Radioactive Prednisolone, 5 μCi

Subject		Prednisolone Concentration, M					
		1 h	3 h	6 h	9 h	12 h	24 h
5	Total Steroid[a]	3.90×10^{-6}	3.30×10^{-6}	2.30×10^{-6}	1.8×10^{-6}	1.40×10^{-6}	6.40×10^{-7}
	Free Steroid[b]	8.40×10^{-7}	ND[c]	1.87×10^{-7}	1.09×10^{-7}	3.67×10^{-8}	1.14×10^{-8}
6	Total Steroid[a]	3.90×10^{-6}	2.50×10^{-6}	1.80×10^{-6}	1.40×10^{-6}	1.00×10^{-6}	2.50×10^{-7}
	Free Steroid[b]	7.73×10^{-7}	5.1×10^{-7}	2.18×10^{-7}	1.03×10^{-7}	6.89×10^{-7}	8.30×10^{-9}

[a] Free prednisolone plus metabolites as determined by measuring total radioactivity. [b] Unmetabolized prednisolone assayed by column chromatography. [c] ND = not determined.

New Zealand White rabbits according to the method of Exley *et al.* (10). To plasma or cellular extracts (each cell pellet was resuspended, made up to 5 mL with water, and homogenized) was added ~26,000 dpm of [^{3}H]prednisolone to monitor recovery. These were extracted with dichloromethane, and the extracts were evaporated under a steady stream of nitrogen. The residue was reconstituted in 1 mL of benzene–ethanol (95:5) and loaded on a hydroxypropylated cross-linked dextran chromatography column[10] (10 × 0.8 cm) equilibrated in the above solvent system. The column was flushed with 55 mL of the eluant (benzene–ethanol, 95:5). The fraction that contained hydrocortisone was discarded. The column was further eluted with 30 mL of eluant, and the fraction was collected. This fraction contained virtually all (>99%) of the labeled prednisolone loaded to monitor recovery; there were no breakdown products. Aliquots (0.1 or 0.25 mL) of eluate were evaporated in triplicate for radioimmunoassay. The reference standard tubes containing 0, 17.3, 34.7, 69.4, 138.3, and 277.7 fmol of prednisolone were balanced with 0.1 or 0.25 ml of blank column eluate, and the organic phase was evaporated in a vacuum oven at 30°C. Phosphate buffer (0.1 mL, 0.01 M, pH 7.4) containing ~10,000 dpm of [^{3}H]prednisolone was added to each tube, and the tubes were thoroughly mixed. Antiserum solution (0.1 ml, diluted to 1:4000 with 0.1% gelatin and 0.01% menthiolate in phosphate buffer) was added to each tube, the contents mixed and incubated at 4°C for a minimum of 3 h. Dextran-coated charcoal solution (0.5 mL, 0.025% dextran and 0.25% charcoal in phosphate buffer) was added to each tube, and the solution was agitated and allowed to incubate for a further 10 min at 4°C. The tubes were centrifuged at 1000×*g* for 10 min at 4°C, the supernatant was decanted into a scintillation vial containing 8 mL of scintillation fluid, and the radioactivity was determined. A standard curve was constructed from reference standards and the results for test samples were read directly. The results were corrected for losses and expressed finally as molar concentrations. The intra- and interassay coefficients of variation were <4 and 8%, respectively.

RESULTS

***In Vivo* Study**—Figure 1 shows the mean plasma concentration of free (unmetabolized) prednisolone during the 24-h following a single oral dose of the glucocorticoid. A rapid rise in plasma concentration of free steroid occurred during the first 1–3 h followed by a rapid but progressively declining rate of fall in steroid level until barely detectable levels were reached by 24 h. Table I shows concurrent plasma and intracellular leukemia cell concentrations of free prednisolone during the 24-h period after an oral dose of nonradioactive steroid. As apparent from the results, there is nothing to suggest that leukemia cells are capable of selectively concentrating prednisolone. In Table II, total (unmetabolized and metabolized) and free (unmetabolized) concentrations of prednisolone in plasma of leukemia patients receiving radioactive steroid are shown. It is evident that prednisolone is rapidly metabolized *in vivo*, and 1 h after administration <25% of the total prednisolone remaining in plasma constitutes unmetabolized steroid.

***In Vitro* Study**—The intracellular concentration of prednisolone in leukemia cells as a function of time in the presence of constant extracellular steroid levels is shown in Table III. During the first hour progressive uptake of steroid occurred, but by 2 h the level had declined. In other experiments with cultured human lymphoid cell lines it was found that a similar rise and fall in intracellular steroid levels occurred over the same time interval (2). In no instance did intracellular concentrations of prednisolone reach or exceed extracellular levels.

DISCUSSION

These studies represent the first attempt to measure plasma and target cell concentrations of steroid concurrently in leukemia patients receiving therapeutic doses of glucocorticoid. The comparative *in vivo* and *in vitro* capacity of leukemia cells to concentrate glucocorticoid in the presence of known extracellular steroid levels has also been studied. It is evident that chronic lymphocytic leukemia cells do not possess the capacity for selectively concentrating glucocorticoids *in vivo* or *in vitro*, and steroid levels previously shown *in vitro* (5, 7) to be necessary for inducing cytolethal or cytostatic responses were not achieved in the plasma of leukemia patients receiving therapeutic doses of prednisolone.

The possible reasons for the apparent discrepancy between *in vitro* and *in vivo* glucocorticoid sensitivity of human lymphoid cells have been

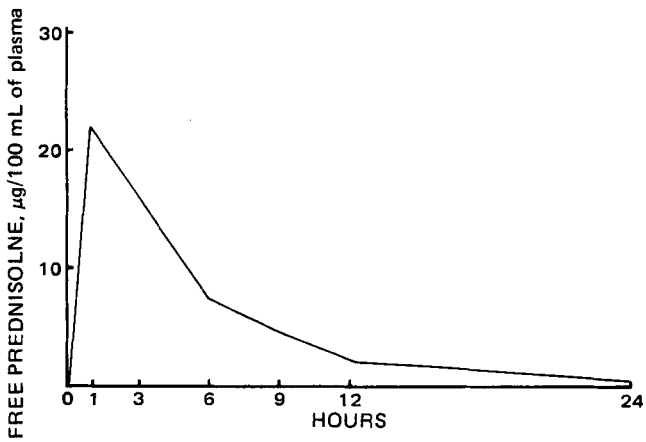

Figure 1—*Mean concentration of free prednisolone in plasma of chronic lymphocytic leukemia patients at various time intervals after a single oral dose of prednisolone.*

[10] Sephadex LH-20—Pharmacia Fine Chemicals AB, Uppsala, Sweden.

Table III—Intracellular and Extracellular Concentrations of Prednisolone in Cultured Chronic Lymphocytic Leukemia Cells

Subject	Extracellular Concentration, M	Intracellular Concentration, M[a]			
		1 min	30 min	60 min	90 min
7	8.1×10^{-8}	1.42×10^{-8}	2.72×10^{-8}	3.02×10^{-8}	2.72×10^{-8}
8	7.0×10^{-8}	1.27×10^{-8}	1.54×10^{-8}	1.53×10^{-8}	1.46×10^{-8}
9	6.8×10^{-8}	1.92×10^{-8}	3.44×10^{-8}	3.42×10^{-8}	3.10×10^{-8}
10	7.2×10^{-8}	1.52×10^{-8}	4.06×10^{-8}	3.83×10^{-8}	3.83×10^{-8}
11	7.0×10^{-8}	1.82×10^{-8}	3.37×10^{-8}	4.36×10^{-8}	4.06×10^{-8}
Mean ± *SD*	$7.22 \pm 0.26 \times 10^{-8}$	$1.59 \pm 0.08 \times 10^{-8}$	$3.03 \pm 0.92 \times 10^{-8}$	$3.23 \pm 1.52 \times 10^{-8}$	$3.03 \pm 1.07 \times 10^{-8}$

[a] Determined assuming average cell volume 4.22×10^{-13} L (cell diameter = 7.5 nm).

Table IV—Comparative Mean Plasma Concentration (μg/100 mL) [a] of Prednisolone Following Oral Steroid Administration

Sampling Time, h	*Colburn* and Buller (11)[b]	*DiSanto* and DeSante (12)[b]	Sullivan *et al.* (13)[b]	Present Study[c]
0	0	0	0	0
1.0	76.1	70.0	115.0	87.5
3.0	56.2	80.7	84.0	65.6
6.0	31.8	49.4	43.5	45.6
12.0	7.1	15.3	10.0	27.5
24.0	0	2.1	1.8	9.3

[a] Calculated as equivalent to a 50-mg oral dose of glucocorticoid. [b] Free (unmetabolized) steroid. [c] Total (unmetabolized and metabolized) steroid.

discussed in detail elsewhere (1). They cannot be attributed simply to differences in cytoplasmic receptor expression or the failure of target cells to take up and bind steroid (2–4, 7). If the therapeutic responses to glucocorticoids are mediated through direct cytolethal and/or cytostatic actions, it is evident the mechanisms involved *in vitro* and *in vivo* differ fundamentally since glucocorticoid concentrations required to induce these effects are of different orders of magnitude. Alternatively, *in vivo* responses to glucocorticoids may be mediated at least in part by indirect means by virtue of some synergistic action when used in combination with other chemotherapeutic agents or through some more generalized tissue or cellular response. Further studies to explore these possibilities are urgently required.

It is also evident from the findings reported here that the intracellular concentration of prednisolone in circulating leukemic lymphocytes was always <4% of that in concurrently removed (extracellular) plasma samples. By contrast, the relative intracellular concentration of steroid achieved *in vitro* was 4–15 times greater than that *in vivo* although in no instance did this reach or exceed extracellular concentrations. The relatively lower uptake of steroid *in vivo* may be accounted for by differences in availability of the glucocorticoid to target cells for a variety of reasons. First, although corticosteroid-binding globulin (transcortin) in plasma has a much lower affinity for prednisolone than hydrocortisone, free prednisolone will be sequestered to some extent *in vivo* by this steroid-binding protein. Since *in vitro* incubations were performed in medium containing heat-inactivated serum no transcortin was present to impede the uptake of steroid. In other experiments it has been found that cells incubated in medium containing non-heat-inactivated serum (thereby containing intact transcortin) show comparatively lower levels of steroid uptake. Second, prednisolone would be sequestered to some extent *in vivo* by adipose tissue with the production of a depot effect and reduced levels of circulating steroid. Third, in contrast to *in vitro* conditions, these results show that glucocorticoids are rapidly metabolized *in vivo* to produce water-soluble derivatives (sulfates and glucuronides), thus reducing the level of free steroid available for uptake by target cells. Finally, leukemic lymphocytes *in vivo* normally compete with other cells and tissues for unbound steroid in contrast to *in vitro* situations where leukemia cells have unrestricted access to the steroid.

In contrast to other workers (11–13), substantially lower concentrations of free prednisolone have been found in plasma following oral administration of the steroid. However, it is apparent from examination of results that the total (unmetabolized and metabolized) prednisolone levels in this study are roughly equivalent to what others have regarded as free (unmetabolized) glucocorticoid (Table IV). This study has shown that prednisolone is rapidly metabolized *in vivo*, and 1 h after oral administration <25% of prednisolone in plasma remains as free (unmetabolized) steroid. It must be assumed, therefore, that any discrepancies in findings between this and other studies are the result of differences in methods employed for assaying steroid levels. In the radioimmunoassay described here samples are purified by chromatography prior to assay to eliminate other cross-reacting steroids. Other workers have failed to remove such metabolites, and it would appear that most previous estimates of plasma concentrations of prednisolone during therapy are grossly inaccurate. Further studies are required to establish the true pharmacokinetics of prednisolone during steroid therapy.

REFERENCES

(1) C. C. Bird, in "7th Tenovus Workshop: Glucocorticoid Action and Leukemia," Alpha Omega, Cardiff, 1979, pp 123–139.

(2) I. D. Barrett, N. S. Panesar, C. C. Bird, A. C. Abbott, H. M. Burrow, and C. M. Steel, *Diagn. Histopathol.*, **4**, 189 (1981).

(3) C. C. Bird, A. W. Waddell, A. M. G. Robertson, A. R. Currie, C. M. Steel, and J. Evans, *Br. J. Cancer*, **32**, 700 (1975).

(4) C. C. Bird, A. M. G. Robertson, J. Read, and A. R. Currie, *J. Pathol.*, **123**, 145 (1977).

(5) H. M. Burrow, C. C. Bird, J. V. Warren, C. M. Steel, I. D. Barrett, and N. S. Panesar, *Diagn. Histopathol.*, **4**, 175 (1981).

(6) A. M. G. Robertson, C. C. Bird, A. W. Waddell, and A. R. Currie, *J. Pathol.*, **126**, 181 (1978).

(7) I. D. Barrett, N. S. Panesar, H. M. Burrow, C. C. Bird, J. C. Cawley, J. A. Child, and B. E. Roberts, *Clin. Lab. Haematol.*, **4**, 285 (1982).

(8) A. Boyum, *Scand. J. Clin. Lab. Invest., Suppl. 97*, **21**, 77 (1968).

(9) B. F. Erlander, F. Borek, S. M. Beiser, and S. Lieberman, *J. Biol. Chem.*, **228**, 713 (1957).

(10) D. Exley, M. W. Johnson, and P. D. G. Dean, *Steroids*, **18**, 605 (1971).

(11) W. A. Colburn and R. H. Buller, *Steroids*, **21**, 833 (1973).

(12) A. R. DiSanto and K. A. DeSante, *J. Pharm. Sci.*, **64**, 109 (1975).

(13) T. J. Sullivan, R. G. Stoll, E. Sakmar, D. C. Blair, and J. G. Wagner, *J. Pharmacokinet. Biopharm.*, **2**, 29 (1974).

ACKNOWLEDGMENTS

Supported by a grant to C. C. Bird from Yorkshire Cancer Research Campaign.

High-Performance Liquid Chromatographic Analysis of Neomycin in Petrolatum-Based Ointments and in Veterinary Formulations

R. BRUCE BINNS and KIYOSHI TSUJI ×

Received July 26, 1982, from the *Control Analytical Research and Development, The Upjohn Company, Kalamazoo, MI 49001.* Accepted for publication November 24, 1982.

Abstract □ A high-performance liquid chromatographic (HPLC) method has been developed for the assay of neomycin in petrolatum-based ophthalmic and topical ointments and in veterinary formulations. Neomycin assay interferences from drugs, such as bacitracin and polymyxin B and inactive components, *e.g.* wax, were eliminated by a methanol wash and/or a partitioning method. The extracted neomycin was derivatized with 2,4-dinitrofluorobenzene followed by normal-phase HPLC with detection at 254 nm. The average recovery of neomycin from spiked samples was ~100% with a relative standard deviation of <1%.

Keyphrases □ Neomycin—high-performance liquid chromatography petrolatum-based ointments, veterinary formulations □ Ointments—petrolatum-based, high-performance liquid chromatographic assay for neomycin, veterinary formulations □ Formulations, veterinary—high-performance liquid chromatographic assay for neomycin, petrolatum-based ointments

Neomycin has been formulated into many topical and ophthalmic ointments and veterinary products because of its broad spectrum of antimicrobial activity. The ointments are generally petrolatum based; some contain other antibiotics, such as bacitracin and polymyxin B, or steroidal anti-inflammatory agents, such as hydrocortisone acetate or methylprednisolone acetate.

The antimicrobial potency ratio of neomycins B and C varies with the species of microorganism, presence of divalent cations in the diffusion media, and culture conditions used in the microbiological assay (1). Thus, acceptable precision of the microbiological assay can only be realized if the composition of the unknown preparation is similar to that of the standard preparation. The agar diffusion cylinder cup assay method for neomycin in ointments (2) is often troublesome, giving low recovery with a relative standard deviation larger than desired.

The GC assay method for neomycin in ointments requires prior silylation of the samples, uses a column temperature of ~300°C (3), and is plagued with low recoveries, short column life, instability of derivatized samples, and tedious sample preparation. The high-performance liquid chromatographic (HPLC) method presented here is accurate, precise, and reliable.

EXPERIMENTAL

Apparatus—A modular liquid chromatograph equipped with a 254-nm UV monitor[1], a high-pressure pump[2], and a 40-μL automatic sample injector[3] was used. A normal-phase LiChrosorb column[4], 4.6-mm i.d. × 25 cm, was used to separate neomycins B and C. Peak area was determined using an electronic integrator[5].

Reagents—All the solvents used were distilled-in-glass and UV grade[6]. The 2,4-dinitrofluorobenzene[7] and anhydrous sodium borate[8] used were analytical reagent grade.

For the mobile phase, tetrahydrofuran–chloroform–water–glacial acetic acid (392:598:8:2) was used. The derivatization reagent was freshly prepared by diluting 4 mL of 2,4-dinitrofluorobenzene with 200 mL of methanol to give an ~0.15 M solution. The 0.02 M borate buffer solution (pH 9.0) was prepared from anhydrous sodium borate and water. The mobile phase was pumped through the column at a flow rate of ~1.0 mL/min.

Reference Standard Solution—Neomycin sulfate reference standard USP (Issue K) was dried (3 h, 60°C, <5 mm Hg) and then allowed to cool in a desiccator. A 2.0-g sample was rapidly and accurately weighed, placed in a 1000-mL volumetric flask, dissolved, and diluted to volume with the borate buffer. Aliquots of the neomycin sulfate reference standard solution were placed in tightly capped serum bottles and kept at −20°C until used.

For the determination of neomycin in ointments, 25.0 mL of thawed neomycin stock reference solution was transferred into a 100-mL volumetric flask, 60 mL of 20% methanol was added, and the solution was diluted to volume with the borate buffer. For the determination of neomycin in veterinary products, the 100-mL volumetric flask containing 25 mL of the thawed reference standard solution was diluted to volume with the borate buffer only. A 10-mL quantity of the diluted neomycin reference standard solution thus prepared was transferred into a 250-mL volumetric flask for derivatization.

Sample Preparation—*Ointments Containing Bacitracin and Polymyxin B*—Approximately 5 g of pooled and well-mixed ointment was accurately weighed into a 50-mL round-bottom centrifuge tube followed by 3 mL of methanol. The sample was heated in a 55°C water bath for 5 min with vortexing twice for 20 s, followed by centrifugation at 2000 × *g* for 2 min. The supernatant was removed by aspiration. The methanol wash was repeated twice.

Thirty milliliters of chloroform was then added, and the sample was placed in a 55°C water bath to melt the ointment, vortexing for 15 s. Ten milliliters of 20% methanol was added, vigorously shaken for 20 min on a reciprocating platform shaker, and the sample was centrifuged at 1000 × *g* for ~3 min. The upper aqueous layer was transferred to a 50-mL volumetric flask using a Pasteur pipet with care taken not to withdraw the emulsion interface layer. The methanol–water extraction step was repeated twice using 10 mL of 20% methanol, shaking the centrifuge tube for 10 min each time. The aqueous layer was pooled in a 50-mL volumetric flask, and the sample was diluted to volume with the borate buffer. A 10-mL portion of the diluted sample was accurately transferred into a 250-mL volumetric flask for derivatization.

Ointments Containing Steroids—Approximately 5 g of the ointment was accurately weighted into a 50-mL round-bottom centrifuge tube. The procedure described above for ointments containing bacitracin and polymyxin B was followed, omitting the initial methanolic wash.

Veterinary Formulations—Two types of veterinary formulations, a soluble dry powder containing sucrose and a solution containing salts, preservatives, and a stabilizer (reducing agent), were examined. A sample containing ~50 mg of neomycin sulfate was accurately transferred into a 100-mL volumetric flask and diluted to volume with the borate buffer. The sample was mixed and centrifuged if required. A 10-mL quantity of the sample was quantitatively transferred into a 200-mL volumetric flask for derivatization.

[1] Model 1203 UV monitor III; Laboratory Data Control, Riviera Beach, Fla.
[2] Model M19-60066-022 high-pressure mini-pump; Laboratory Data Control.
[3] Model 710B WISP; Waters Associates, Milford, Mass.
[4] SI-100, LiChrosorb Silica 5-μm particle size, Brownlee Labs, Santa Clara, Calif.
[5] Chromatopac-E1A; Shimadzu Seisakusha, Ltd., Kyoto, Japan.
[6] Burdick and Jackson Labs, Muskegon, Mich.
[7] Aldrich Chemical, Milwaukee, Mis.
[8] Mallinckrodt, St. Louis, Mo.

0022-3549/84/0100-0069$01.00/0
© 1984, American Pharmaceutical Association

Table I—Recovery of Neomycin From a Topical Ointment Containing Hydrocortisone Acetate

Drug Level, %	Neomycin Sulfate, mg/g Added	Recovered	Recovery, %
75	20.62	20.50	99.4
90	24.85	24.64	99.2
100	27.63	27.53	99.6
110	30.19	30.08	99.6
125	34.33	34.04	99.2
Mean			99.4
RSD			0.2
r			0.9999

Derivatization—A 15-mL quantity of the derivatization reagent was added to the 250-mL volumetric flask containing standard solution or sample, and the opening of the flask was covered with aluminum foil. The flask was then placed in a 100°C silicone oil bath for 45 min to form dinitrobenzene-neomycin. The amount of 2,4-dinitrofluorobenzene present was more than a 30-fold excess (4). The flask was then cooled, and mobile phase was added until the lower, yellow, organic phase reached the 250-mL mark. The top (aqueous) layer was removed by aspiration, and the yellow organic phase was chromatographed using the conditions described above. The derivatized neomycin is stable for over 1 week at room temperature when stored in the dark.

Calculations—The concentrations of neomycins B and C and the bioequivalent potency (5) were calculated by using the following equations:

$$\text{Neomycin B } (\mu g/g) = B_{smp}/B_{std} \times W_{std}/W_{smp} \times F1 \times F2 \quad \text{(Eq. 1)}$$

$$\text{Neomycin C } (\mu g/g) = C_{smp}/B_{std} \times W_{std}/W_{smp} \times F1 \times F2 \quad \text{(Eq. 2)}$$

$$\text{Bioequivalent Potency } (\mu g/g) = (\text{Neomycin B}) \times 1/2(\text{Neomycin C}) \quad \text{(Eq. 3)}$$

where B_{std} and B_{smp} are the peak areas of neomycin B in the reference standard and sample, respectively; C_{smp} is the peak area of neomycin C in samples; W_{std} and W_{smp} are the weight of the reference standard powder and samples, respectively; F1 is the dilution factor; and F2 is the assigned potency of the neomycin sulfate reference standard USP (765 μg/mg for Issue K).

RESULTS AND DISCUSSION

Derivatization—Recently, Helboe and Kryger noted formation of insoluble lumps on derivatization (6) which were eliminated when neomycin was derivatized at a lower temperature [60°C instead of 100°C as used by Tsuji *et al.* (4)]. To examine the problem, two lots each of the 2,4-dinitrofluorobenzene reagent obtained from two suppliers[7,9] were employed using the method of Tsuji *et al.* (4). Only one of the four lots of the reagent examined formed yellowish deposits which adhered to the wall of the flask. When derivatized at 60°C the peak areas of neomycins B and C were 94% and 45% of those derivatized at 100°C, respectively. Incomplete derivatization of neomycin in 60°C samples was evident from numerous peaks which eluted near the solvent front. Thus, the formation of insoluble lumps on derivatization may be due to impurities occasionally present in some lots of the derivatization reagent. The use of lower derivatization temperature may result in a serious underderivatization of neomycin.

The use of methanol in the partitioning extraction of neomycin occasionally increased the efficiency of derivatization, resulting in increased peak area. This potential difficulty was eliminated by inclusion of methanol in the reference standard solution prior to derivatization.

Extraction—Differential centrifugation with chloroform to dissolve excipients and to precipitate neomycin, as developed for the GC assay (3), was examined. Precipitated neomycin was dissolved in the borate buffer prior to derivatization. Centrifugation over an extended time (2000 × *g* for 30 min) failed to increase recovery of neomycin from spiked placebo above 98% and 93–95% for ophthalmic and topical ointments, respectively. Various solvents were added to chloroform to lower its specific gravity in an effort to facilitate precipitation of neomycin; no improvement in the recovery was noted.

[9] Eastman Organic Chemicals, Rochester, N.Y.

Table II—Analysis of Neomycin in Ophthalmic and Topical Ointments Containing Hydrocortisone Acetate[a]

Lot	Neomycin Base, mg/g HPLC	GC	Microbiological Assay
	Ophthalmic Ointment		
A	3.86	3.79	3.73
B	3.86	3.74	3.69
C	4.14	3.81	4.04
D	3.87	3.70	3.57
E	3.97	3.70	3.80
	Topical Ointment		
F	3.95	3.60	3.79
G	3.87	3.80	3.54
H	3.77	3.60	3.59
I	3.89	3.52	3.92
J	3.88	3.52	4.04

[a] All lots from The Upjohn Co.

It was noted that the recovery of neomycin from ophthalmic ointments was always higher than that from topical ointments. Topical ointments differ from ophthalmic ointments by inclusion of microcrystalline wax. It is possible that neomycin sulfate is encapsulated by the microcrystalline wax during the manufacturing process. This wax dissolves poorly in chloroform; heat and extended sonication are needed, and the resulting suspension is still turbid. A sample of neomycin was spiked in melted wax and dispersed by vortexing. The sample was then assayed by use of the differential centrifugation method. The recovery was 92%, suggesting the wax encapsulation or adsorption hypothesis. Efforts to remove the wax interference by extended heating and sonication failed to improve the recovery of neomycin.

Aqueous Extraction—Partitioning neomycin for extraction in a methanolic water–chloroform system was then examined. A 20% methanolic water solution was necessary to reduce emulsion formation at the water–chloroform interface.

Ointments Containing Steroids—Recovery of neomycin from both ophthalmic and topical ointments by the partitioning extraction method was examined. Neomycin was spiked in a steroid-containing ointment

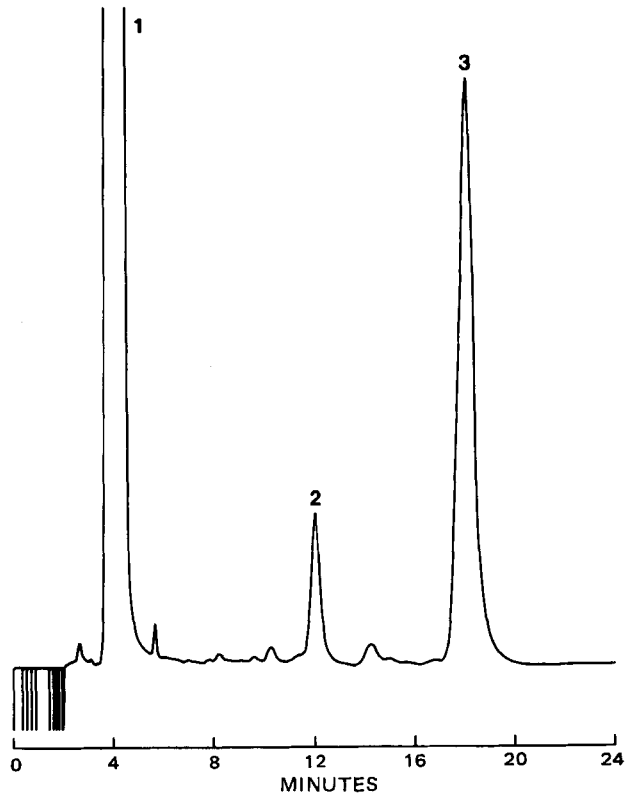

Figure 1—*Typical chromatogram of neomycin in a topical ointment containing hydrocortisone acetate. Key: (1) neomycin C; (2) neomycin B; (3) hydrocortisone acetate.*

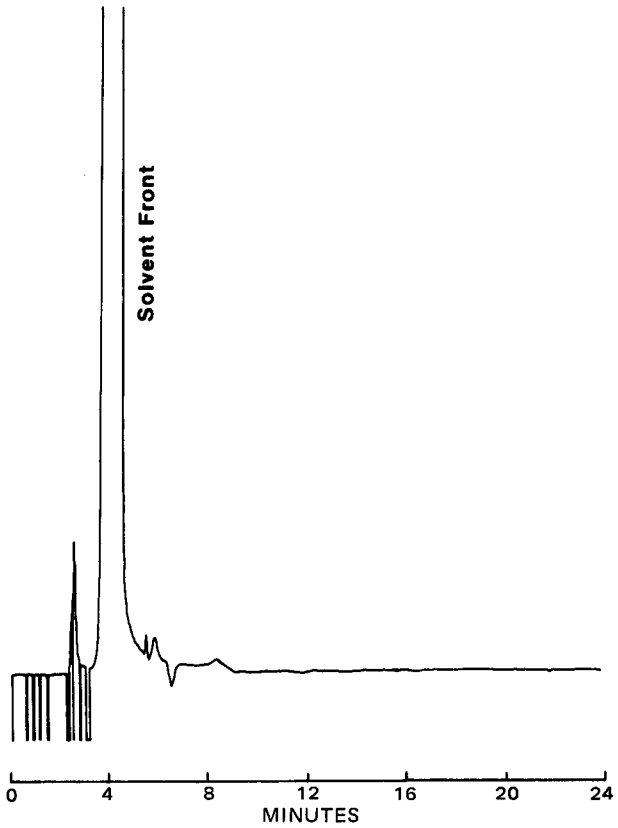

Figure 2—*Chromatogram of placebo of topical ointment containing hydrocortisone acetate, indicating no interfering peaks.*

base at 75–125% of the target. An example of the neomycin recovery study using a topical ointment containing hydrocortisone acetate is shown in Table I. The recovery of neomycin averaged 99.4%, with a relative standard deviation of 0.2%. The correlation coefficient (r) for the recovery study was 0.9999. Similar recoveries and precision were obtained for ophthalmic and topical ointments containing various steroids. Thus, the partitioning method for extraction of neomycin from ointment completely eliminated the interference of microcrystalline wax. Steroids, *e.g.*, hydrocortisone acetate, cortisone acetate, fluorometholone, methylprednisolone, and prednisolone acetate, showed no interference in the HPLC analysis of neomycin in ointments.

Precision of the HPLC method was also examined. Seven individually weighed and extracted samples were examined using the partitioning method. The relative standard deviation of the assay was 0.5%; similar precision was obtained for ophthalmic and topical ointments containing steroids. The HPLC method was then used to assay the ointments, and the values were compared with those of the GC and the microbiological assays. Table II shows an example of such comparison made using both ophthalmic and topical ointments containing hydrocortisone acetate. In general, the values obtained by the HPLC method were the closest to the target and higher than those of the GC or the microbiological methods. However, the difference between HPLC, GC, and microbiological

Table III—Recovery of Neomycin from Topical Ointments Containing Bacitracin and Polymyxin B

Drug Level, %	Day 1 Neomycin Sulfate, mg/g Added	Day 1 Neomycin Sulfate, mg/g Recovered	Day 1 Recovery, %	Day 2 Neomycin Sulfate, mg/g Added	Day 2 Neomycin Sulfate, mg/g Recovered	Day 2 Recovery, %
75	22.45	22.67	101.0	22.47	22.26	99.0
90	27.19	27.24	100.2	26.98	27.12	100.5
100	29.91	29.59	99.0	30.10	29.64	98.5
110	32.77	32.28	98.5	33.04	32.64	98.8
125	37.57	37.22	99.1	37.46	37.46	100.0
Mean			99.6%			99.4%
RSD			1.0%			0.9%
r			0.9996			0.9990

Table IV—Assay of Neomycin in Topical Ointments Containing Bacitracin and Polymyxin B[a]

Lot	Neomycin, mg/g[b] HPLC	Neomycin, mg/g[b] GC
A	4.03	3.75
B	4.25	3.88
C	4.26	3.80
D	4.29	3.88
E	4.33	3.76
F	4.26	3.82
G	4.25	3.84
H	4.24	3.80
I	4.27	3.74
J	4.34	3.90
K	4.25	3.91
L	4.34	3.81
Mean	4.26	3.82

[a] All lots from The Upjohn Co. [b] Manufacturing target: 4.2 mg/g.

Table V—Assay for Neomycin in a Veterinary Formulation[a]

Lot	Neomycin, mg/mL[b] HPLC	Neomycin, mg/mL[b] Microbiological Assay
A	142.7	149
B	142.8	152
C	142.3	148
D	146.5	155
E	136.5	137
F	136.0	136

[a] All lots from The Upjohn Co. [b] Manufacturing target: 142.8 mg/mL.

methods was not statistically significant. Typical chromatograms of the HPLC assay for neomycin in a topical ointment containing hydrocortisone acetate and its placebo are shown in Figs. 1 and 2.

Ointments Containing Bacitracin and Polymyxin B—Bacitracin and polymyxin B are polypeptide antibiotics, and primary amines present in the molecules compete effectively with neomycin for 2,4-dinitrofluorobenzene. Efforts to compensate for the competition by increasing the amounts of the derivatization reagent were unsuccessful. The recovery of neomycin in the presence of bacitracin and polymyxin B was ~92%.

Since bacitracin is readily soluble in methanol, and polymyxin B to a lesser extent, methanol was added to the ointment to remove the interference. (Neomycin sulfate is practically insoluble in methanol.) Samples of topical ointment placebo containing bacitracin and polymyxin B were spiked with neomycin at 75–125% of the manufacturing target. The results of the spiked recovery study are presented in Table III; the recovery of neomycin averaged 99.5% with a relative standard deviation of 1.0%, demonstrating complete removal of the interference.

Precision of the HPLC method for neomycin was examined by analyzing seven individually weighed and extracted ointment samples; the relative standard deviation of the assay was 0.86%. Twelve lots of topical ointments containing bacitracin and polymyxin B were then assayed (Table IV). Although there was significant difference in the assay values between the HPLC and GC methods, the HPLC data were extremely close to the manufacturing target for the product. The HPLC results averaged 101.4% of the target while the GC results averaged only 91%. Thus, the HPLC method was judged to give accurate results.

Veterinary Formulations—The veterinary formulations examined were all soluble in the borate buffer. Therefore, neomycin in the formulation was quantitated by simply derivatizing a dilute borate buffer mixture. The recovery of neomycin was ~100% with a relative standard deviation of <1%. Six lots of a liquid veterinary formulation were assayed for neomycin by HPLC, and the results were compared with those obtained by the microbiological assay method. As shown in Table V, no statistically significant difference existed between the HPLC and the microbiological assay results.

A petition to amend an antibiotic application for the use of the HPLC method as an alternative assay of neomycin in ointment products has been submitted to Food and Drug Administration for approval.

REFERENCES

(1) W. T. Sokolski, C. G. Chidester, and D. G. Kaiser, *J. Pharm. Sci.*, **53**, 726 (1964).

(2) Code of Federal Regulation, Title 21, U.S. Government Printing Office, Washington, D.C., 1981, pp. 471–477.
(3) B. van Giessen and K. Tsuji, *J. Pharm. Sci.*, **60**, 1068 (1971).
(4) K. Tsuji, J. F. Goetz, W. VanMeter, and K. A. Gusciora, *J. Chromatogr.*, **175**, 141 (1979).
(5) J. H. Robertson, R. Baas, R. L. Yeager, and K. Tsuji, *Appl. Microbiol.*, **22**, 1164 (1971).
(6) P. Helboe and S. Kryger, *J. Chromatogr.*, **235**, 215 (1982).

Pharmacokinetics of Heparin VII: Effect of Pregnancy on the Relationship Between Concentration and Anticoagulant Action of Heparin in Rats

LLOYD R. WHITFIELD, CRAIG WILKENFELD, and G. LEVY ˣ

Received September 13, 1982, from the *Department of Pharmaceutics, School of Pharmacy, State University of New York at Buffalo, Amherst, NY 14260.* Accepted for publication December 2, 1982.

Abstract □ The effect of pregnancy on the anticoagulant action of heparin was determined by comparing the slope of the relationship between the natural logarithm of the activated partial thromboplastin time (APTT) and heparin concentration (the heparin slope) in the plasma of pregnant and nonpregnant female inbred Lewis rats. Also determined were the prothrombin time, hematocrit, and the activities of coagulation factors II, VII, VIII, X, XI, and XII. The heparin slope was significantly decreased in pregnant rats at the 20th day of gestation but not in rats at the 10th day of gestation, indicative of a decreased anticoagulant action of heparin in late pregnancy. The hematocrit and prothrombin time were decreased, and the baseline APTT (*i.e.*, the APTT without added heparin) as well as the activities of factors II, VII, and X were increased in pregnant rats at the 20th day of gestation. Both pregnant and nonpregnant animals showed a significant negative correlation between prothrombin time and factor II activity and a significant positive correlation between the activities of factors II and X. The effects of pregnancy in rats on heparin slope, prothrombin time, hematocrit, and factors VII, VIII, X, and XII are qualitatively the same as those in pregnant women in the third trimester. The increases in factor II activity and baseline APTT found in the rats were not observed in humans. Pregnant rats, like pregnant women, are relatively resistant to the anticoagulant action of heparin.

Keyphrases □ Heparin—anticoagulant action, effect of pregnancy, rats □ Anticoagulants—heparin, effect of pregnancy on the anticoagulant action, rats □ Pregnancy—effect on the anticoagulant action of heparin in rats

Rats and humans exhibit grossly similar characteristics with respect to the pharmacokinetics and pharmacodynamics of heparin: both species eliminate heparin by dose-dependent kinetics that are not of the Michaelis–Menten type and both show an essentially linear relationship between an index of the anticoagulant response, the logarithm of the activated partial thromboplastin time of plasma (APTT), and the concentration of heparin added to plasma (1). Human pregnancy is associated with a state of progressive blood hypercoagulability due, in part, to increased concentrations or activities of certain components of the coagulation system (2). The heparin dose requirements for treatment or prevention of thromboembolic disorders are increased in human pregnancy (3–6). Recent studies in this laboratory have shown this to be due, at least in part, to a decreased anticoagulant effect of heparin (7). Changes in the distribution (7) and clearance (3) of heparin may also occur, but this is presently uncertain.

A previous investigation of blood coagulation characteristics and response to heparin in rats (8) has revealed a number of important differences relative to humans, despite the gross similarity in the pharmacokinetics and pharmacodynamics of heparin in the two species (1). To further explore the relative characteristics of the two species with respect to heparin, we have determined the effect of pregnancy on the anticoagulant action of heparin and on a number of related physiological variables in rats.

EXPERIMENTAL

Groups of two female inbred Lewis rats[1], 200–250 g, were placed in plastic cages with sawdust bedding taken from cages previously occupied by adult male rats. They had free access to food[2] and water at all times. After 2 d an adult male Sprague–Dawley rat was placed in each cage with the two females for an overnight period. The male rat was removed in the morning, and that day was designated as the first day of gestation. The female rats were then housed in groups of four per cage for the duration of the study; nonimpregnated females from the same colony were kept similarly. This procedure was repeated on three occasions. For the first study, groups of eight pregnant and eight control rats each were tested on the 10th and 20th days of gestation; for the second study, nine pregnant and nine control rats were tested on the 20th day of gestation; for the third study, seven pregnant and seven control rats were tested on the 20th day of gestation.

Blood samples were obtained from the abdominal aorta while the animals were under light ether anesthesia. The hematocrit was first determined from a small sample of blood (<0.1 mL) taken from the tail vein. Sufficient acid citrate anticoagulant (9) was then added to a 5-mL plastic syringe such as to yield a 6:1 plasma–citrate solution volume ratio when 4.5 mL of blood was drawn from the abdominal aorta into the syringe. The citrated blood was transferred to plastic tubes which were centrifuged to separate the plasma as previously described (8). The plasma samples were stored at −80°C for no longer than 3 d. Plasma from two of the control rats (10th day) in the first study contained small clots on thawing. To prevent this in subsequent experiments, the plasma–citrate solution volume ratio was changed from 6:1 to 5:1 in the second and third studies. All animals in the pregnant groups were dissected after blood sampling to confirm pregnancy.

The APTT was determined with a coagulation timer[3] after a 15-min plasma incubation time (unless stated otherwise), using automated APTT[4] as the principal reagent. Heparin of beef lung origin[5] was added to the plasma to yield concentrations of 0.1–0.7 U/mL in six steps; an equivalent volume of heparin-free solvent was added for baseline APTT determination. Details of these procedures have been described previ-

[1] Charles River Farms, Wilmington, Mass.
[2] Charles River Formula RMH 1000, Syracuse, N.Y.
[3] Fibrometer, Baltimore Biological Laboratories, Cockeysville, Md.
[4] General Diagnostics, Morris Plains, N.J.
[5] The Upjohn Co., Kalamazoo, Mich., (lot no. 955FW).

0022-3549/84/0100-0072$01.00/0
© 1984, American Pharmaceutical Association

(2) Code of Federal Regulation, Title 21, U.S. Government Printing Office, Washington, D.C., 1981, pp. 471–477.
(3) B. van Giessen and K. Tsuji, *J. Pharm. Sci.*, **60**, 1068 (1971).
(4) K. Tsuji, J. F. Goetz, W. VanMeter, and K. A. Gusciora, *J. Chromatogr.*, **175**, 141 (1979).
(5) J. H. Robertson, R. Baas, R. L. Yeager, and K. Tsuji, *Appl. Microbiol.*, **22**, 1164 (1971).
(6) P. Helboe and S. Kryger, *J. Chromatogr.*, **235**, 215 (1982).

Pharmacokinetics of Heparin VII: Effect of Pregnancy on the Relationship Between Concentration and Anticoagulant Action of Heparin in Rats

LLOYD R. WHITFIELD, CRAIG WILKENFELD, and G. LEVY ˣ

Received September 13, 1982, from the *Department of Pharmaceutics, School of Pharmacy, State University of New York at Buffalo, Amherst, NY 14260.* Accepted for publication December 2, 1982.

Abstract □ The effect of pregnancy on the anticoagulant action of heparin was determined by comparing the slope of the relationship between the natural logarithm of the activated partial thromboplastin time (APTT) and heparin concentration (the heparin slope) in the plasma of pregnant and nonpregnant female inbred Lewis rats. Also determined were the prothrombin time, hematocrit, and the activities of coagulation factors II, VII, VIII, X, XI, and XII. The heparin slope was significantly decreased in pregnant rats at the 20th day of gestation but not in rats at the 10th day of gestation, indicative of a decreased anticoagulant action of heparin in late pregnancy. The hematocrit and prothrombin time were decreased, and the baseline APTT (*i.e.*, the APTT without added heparin) as well as the activities of factors II, VII, and X were increased in pregnant rats at the 20th day of gestation. Both pregnant and nonpregnant animals showed a significant negative correlation between prothrombin time and factor II activity and a significant positive correlation between the activities of factors II and X. The effects of pregnancy in rats on heparin slope, prothrombin time, hematocrit, and factors VII, VIII, X, and XII are qualitatively the same as those in pregnant women in the third trimester. The increases in factor II activity and baseline APTT found in the rats were not observed in humans. Pregnant rats, like pregnant women, are relatively resistant to the anticoagulant action of heparin.

Keyphrases □ Heparin—anticoagulant action, effect of pregnancy, rats □ Anticoagulants—heparin, effect of pregnancy on the anticoagulant action, rats □ Pregnancy—effect on the anticoagulant action of heparin in rats

Rats and humans exhibit grossly similar characteristics with respect to the pharmacokinetics and pharmacodynamics of heparin: both species eliminate heparin by dose-dependent kinetics that are not of the Michaelis–Menten type and both show an essentially linear relationship between an index of the anticoagulant response, the logarithm of the activated partial thromboplastin time of plasma (APTT), and the concentration of heparin added to plasma (1). Human pregnancy is associated with a state of progressive blood hypercoagulability due, in part, to increased concentrations or activities of certain components of the coagulation system (2). The heparin dose requirements for treatment or prevention of thromboembolic disorders are increased in human pregnancy (3–6). Recent studies in this laboratory have shown this to be due, at least in part, to a decreased anticoagulant effect of heparin (7). Changes in the distribution (7) and clearance (3) of heparin may also occur, but this is presently uncertain.

A previous investigation of blood coagulation characteristics and response to heparin in rats (8) has revealed a number of important differences relative to humans, despite the gross similarity in the pharmacokinetics and pharmacodynamics of heparin in the two species (1). To further explore the relative characteristics of the two species with respect to heparin, we have determined the effect of pregnancy on the anticoagulant action of heparin and on a number of related physiological variables in rats.

EXPERIMENTAL

Groups of two female inbred Lewis rats[1], 200–250 g, were placed in plastic cages with sawdust bedding taken from cages previously occupied by adult male rats. They had free access to food[2] and water at all times. After 2 d an adult male Sprague–Dawley rat was placed in each cage with the two females for an overnight period. The male rat was removed in the morning, and that day was designated as the first day of gestation. The female rats were then housed in groups of four per cage for the duration of the study; nonimpregnated females from the same colony were kept similarly. This procedure was repeated on three occasions. For the first study, groups of eight pregnant and eight control rats each were tested on the 10th and 20th days of gestation; for the second study, nine pregnant and nine control rats were tested on the 20th day of gestation; for the third study, seven pregnant and seven control rats were tested on the 20th day of gestation.

Blood samples were obtained from the abdominal aorta while the animals were under light ether anesthesia. The hematocrit was first determined from a small sample of blood (<0.1 mL) taken from the tail vein. Sufficient acid citrate anticoagulant (9) was then added to a 5-mL plastic syringe such as to yield a 6:1 plasma–citrate solution volume ratio when 4.5 mL of blood was drawn from the abdominal aorta into the syringe. The citrated blood was transferred to plastic tubes which were centrifuged to separate the plasma as previously described (8). The plasma samples were stored at −80°C for no longer than 3 d. Plasma from two of the control rats (10th day) in the first study contained small clots on thawing. To prevent this in subsequent experiments, the plasma–citrate solution volume ratio was changed from 6:1 to 5:1 in the second and third studies. All animals in the pregnant groups were dissected after blood sampling to confirm pregnancy.

The APTT was determined with a coagulation timer[3] after a 15-min plasma incubation time (unless stated otherwise), using automated APTT[4] as the principal reagent. Heparin of beef lung origin[5] was added to the plasma to yield concentrations of 0.1–0.7 U/mL in six steps; an equivalent volume of heparin-free solvent was added for baseline APTT determination. Details of these procedures have been described previ-

[1] Charles River Farms, Wilmington, Mass.
[2] Charles River Formula RMH 1000, Syracuse, N.Y.
[3] Fibrometer, Baltimore Biological Laboratories, Cockeysville, Md.
[4] General Diagnostics, Morris Plains, N.J.
[5] The Upjohn Co., Kalamazoo, Mich., (lot no. 955FW).

0022-3549/84/0100-0072$01.00/0
© 1984, American Pharmaceutical Association

Table I—Effect of Pregnancy on Baseline APTT, *In Vitro* Anticoagulant Action of Heparin, Prothrombin Time, Hematocrit, and Body Weight of Rats (First Study)

Study Group[a]	Baseline APTT, s	Slope[b], mL/U	Intercept[b], s	Prothrombin Time, s	Hematocrit, %	Body Weight, g
10th Day of gestation						
Control	15.1 ± 1.0	2.72 ± 0.50	12.9 ± 1.3	21.0 ± 1.2	43.5 ± 2.2	254 ± 16
Pregnant	17.4 ± 2.0	2.06 ± 0.53	15.9 ± 1.8[c]	20.9 ± 0.8	41.5 ± 0.9[c]	275 ± 12[c]
20th Day of gestation						
Control	16.7 ± 1.2	2.29 ± 0.25	15.1 ± 0.7	18.5 ± 1.4	45.0 ± 1.1	243 ± 9
Pregnant	25.6 ± 2.8[c]	1.32 ± 0.32[c]	24.6 ± 2.1[c]	16.0 ± 0.8[c]	36.1 ± 2.8[c]	366 ± 26[c]

[a] Lewis inbred rats, eight per group. Results are expressed as mean ± *SD*. [b] Slope and intercept of the least squares regression line of ln APTT *versus* concentration of heparin added to plasma. APTT was measured after a 15-min incubation of the plasma–APTT reagent mixture. [c] Significantly different from the appropriate control group, $p < 0.01$.

Table II—Effect of Pregnancy on Baseline APTT, *In Vitro* Anticoagulant Action of Heparin, Prothrombin Time, Coagulation Factors Activity, Hematocrit, and Body Weight of Rats (Second Study)[a]

Variable	Control Rats	Pregnant Rats[b]
Baseline APTT, s	20.1 ± 4.5	26.2 ± 3.5[e]
Slope, mL/U[c]	2.45 ± 0.36	1.70 ± 0.08[e]
Intercept, s[c]	17.9 ± 6.3	23.6 ± 3.3[f]
Prothrombin time, s	19.0 ± 0.6	16.3 ± 0.3[e]
Factor II, %[d]	100 ± 8	133 ± 8[e]
Factor VII, %[d]	100 ± 19	203 ± 13[e]
Factor VIII, %[d]	100 ± 59	140 ± 69
Factor X, %[d]	100 ± 9	135 ± 13[e]
Factor XI, %[d]	100 ± 36	121 ± 34
Factor XII, %[d]	100 ± 33	85 ± 21
Hematocrit, %	45.7 ± 0.9	38.8 ± 1.4[e]
Body weight, g	254 ± 19	337 ± 12[e]

[a] Lewis inbred rats, nine per group. Results are expressed as mean ± *SD*. [b] At the 20th day of gestation. [c] See footnote b in Table I. [d] Determined by assay procedure for human coagulation factors; mean of control group taken as 100%. [e] Significantly different from the control group, $p < 0.01$. [f] Significantly different from the control group, $p < 0.05$.

ously (1, 8). Prothrombin time was determined as described previously (10). The activity of coagulation factors was determined by one-stage clotting assays using commercially available plasma deficient in the appropriate coagulation factor[6] as substrate, either actin-activated cephaloplastin reagent[6] or activated thromboplastin reagent[6], and the coagulation timer. The assay procedures were essentially as specified by the manufacturer.

The slope of the essentially linear portion of the relationship between ln APTT and heparin concentration (Fig. 1) and the intercept at zero heparin concentration were determined by linear regression analysis after transforming the APTT values to their natural logarithmic values. APTT values for the plasma samples without added heparin were not used in the regression analysis because these values were consistently higher than the extrapolated values based on the regression line for the other data (8). Results of the first study were analyzed statistically by two-way analysis of variance. If significant ($p < 0.05$) differences were found, the Student–Newman–Keuls test was used to determine, by multiple comparisons, which groups were different from one another. Differences between groups in the second and third studies were determined by unpaired t tests. Associations among variables were assessed by correlation analysis.

RESULTS

There was an essentially linear relationship between ln APTT and heparin concentration up to 0.7 U/mL ($r^2 > 0.96$) in plasma of both pregnant and nonpregnant rats, except that the APTT at zero heparin concentration was consistently higher than the extrapolated value (Fig. 1). Consequently, the intercept at zero heparin concentration of the least-squares regression line was always less than the actual baseline APTT.

The results of the first study are summarized in Table I. Pregnant rats at the 10th day of gestation had a lower hematocrit than the nonpregnant controls, but did not differ significantly from the controls with respect to baseline APTT and heparin slope. At the 20th day of gestation, the baseline APTT was significantly greater than and the slope was significantly lower than the corresponding control values. The prothrombin time and the hematocrit were decreased in late pregnancy.

The changes in baseline APTT, heparin slope, prothrombin time, and hematocrit in late pregnancy observed in the first study were confirmed in the second study which was performed ~6 months later. In addition, the activity of a number of coagulation factors was determined in the second study. This revealed a significant increase in the activities of factors II, VII, and X in late pregnancy (Table II).

A number of statistically significant correlations were found between pairs of some of the variables measured in this investigation (Table III). Of these, only the negative correlation between prothrombin time and factor II activity and between the activities of factors II and X are common to both the control and pregnant rats at the 20th day of gestation.

The APTT of rat plasma undergoes considerable change during incubation for activation of the intrinsic coagulation pathway (8). The APTT decreases rapidly in the first few minutes and then, unlike the APTT of human plasma under our experimental conditions (11), slowly increases (8). To minimize the effect of potential differences between pregnant and control rats with respect to the rate of this apparent *in vitro* degradation of some component(s) of the clotting process, a third study was performed in which the plasma incubation time was reduced from 15 to 3 min. The results of that study, summarized in Table IV, also show an increase in the baseline APTT and a decrease in heparin slope at the 20th gestational day, in agreement with the results of the first and second studies.

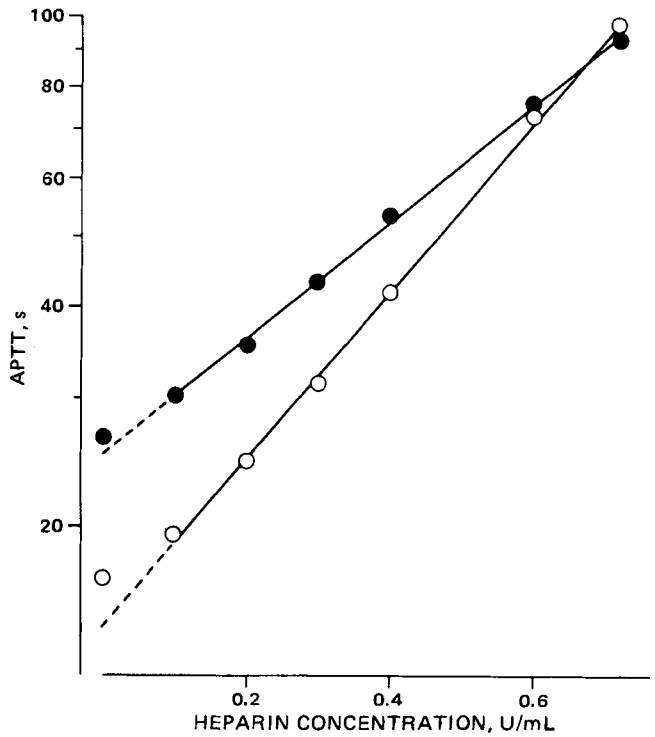

Figure 1—*Relationship between activated partial thromboplastin time (APTT) and heparin concentration in plasma of a pregnant rat (●) at the 20th day of gestation and a nonpregnant female control rat (○).*

[6] American Dade, Miami, Fla.

Table III—Correlations Among Variables in Control and Pregnant Rats of the Second Study [a]

Correlates	Control Rats		Pregnant Rats[b]	
	Correlation Coefficient	Statistical Significance (p)	Correlation Coefficient	Statistical Significance (p)
Prothrombin time–baseline APTT	0.76	<0.05	0.63	<0.1
Prothrombin time–hematocrit	0.85	<0.01	0.05	N.S.[c]
Prothrombin time–factor II	−0.68	<0.05	−0.76	<0.05
Prothrombin time–factor VII	−0.87	<0.01	−0.14	N.S.
Prothrombin time–factor X	−0.80	<0.05	−0.62	<0.1
Hematocrit–factor X	−0.73	<0.05	0.21	N.S.
Hematocrit–factor VII	−0.87	<0.01	−0.37	N.S.
Factor II–factor VII	0.69	<0.05	0.35	N.S.
Factor II–factor X	0.70	<0.05	0.76	<0.05
Factor VII–factor X	0.71	<0.05	0.15	N.S.
Factor XII–factor X	0.26	N.S.	−0.69	<0.05
Baseline APTT–factor II	−0.38	N.S.	−0.85	<0.01
Baseline APTT–factor X	−0.53	N.S.	−0.79	<0.05
Body weight–factor XI	0.06	N.S.	−0.72	<0.05

[a] Based on data summarized in Table II. [b] At the 20th day of gestation. [c] N.S. = not significant.

Table IV—Effect of Pregnancy on Baseline APTT and *In Vitro* Anticoagulant Action of Heparin Determined After a 3-min Incubation of the Plasma–APTT Reagent Mixture (Third Study) [a]

	Control Rats		Pregnant Rats[b]
Baseline APTT, s	12.9 ± 2.6	$p < 0.05$	16.0 ± 0.8
Slope, mL/U	1.24 ± 0.12	$p < 0.001$	0.95 ± 0.09
Intercept, s	12.8 ± 2.2	$p < 0.01$	15.4 ± 0.7

[a] Results are mean ± SD, $n = 7$. [b] At the 20th day of gestation.

DISCUSSION

This investigation has shown that rats, like humans, become relatively resistant to the anticoagulant effect of heparin in late pregnancy. The decrease of prothrombin time and hematocrit and the increase in the activities of clotting factors II, VII, and X in pregnant rats at the 20th day of gestation also occur in human pregnancy (7). One notable difference between rats and humans is that the baseline APTT increases in pregnant rats, but remains in the normal range during the third trimester of human pregnancy. The coagulation factor determinations in the second study were made to explore the possible reasons for this species difference.

The prothrombin time test is affected by alterations in the activity of clotting factors in the extrinsic coagulation pathway (factor VII) and in the common coagulation pathway (factors II, V, X, XIII, and fibrinogen). A deficiency in any of these components of the coagulation system or the presence of endogenous inhibitor(s) would be reflected by an increase in prothrombin time. In fact, the pregnant rats had a decreased prothrombin time and, consistent with this alteration, an increase in the activity of factors II, VII, and X. The decreased prothrombin time suggests that pregnancy is not associated with a deficiency of the components of the common coagulation pathway.

The APTT is affected by alterations in the activity of coagulation factors in the intrinsic coagulation pathway (factors VIII, IX, XI, XII, high molecular weight kininogen, and prekallikrein) and, like the prothrombin time, by factors in the common coagulation pathway. In view of the decreased prothrombin time, the increased baseline APTT in pregnancy is not likely to be due to a deficiency in any of the factors in the common coagulation pathway. Prolongation of the baseline APTT in pregnancy by an endogenous inhibitor was ruled out (12) because this prolongation was reversed on mixing equal volumes of plasma from pregnant and nonpregnant rats. This reversal, together with the other evidence, points to a deficiency of one or more components of the intrinsic coagulation pathway. Of these, factors VIII, XI, and XII were determined directly and were found not to be deficient. Factor IX activity was not measured, but since the other vitamin K-dependent factors (II, VII, and X) were actually above normal, it is probable that factor IX activity is not deficient. Thus, it appears that the increased baseline APTT in pregnant rats may be due to a deficiency of high molecular weight kininogen and/or prekallikrein, or to a deficiency of as yet unidentified factor(s) (13).

One more possibility was considered, namely that the prolonged baseline APTT in pregnant rats may have been due to more rapid *in vitro* degradation of one or several components of the coagulation system. That possibility is virtually excluded by the results of the third study, in which APTT was determined after 3 min rather than 15 min of plasma incubation for contact activation. The difference between pregnant and nonpregnant rats with respect to baseline APTT remained when the samples were incubated for only 3 min, although the absolute APTT values were different, as observed previously (8).

In summary, rats demonstrate many of the effects of pregnancy observed in humans with respect to blood coagulation: resistance to the anticoagulant effect of heparin relative to the response in nonpregnant individuals, increased activity of certain clotting factors, and decreased prothrombin time. However, there are also subtle differences, as reflected by the increased baseline APTT in pregnant rats which apparently does not occur in humans (7). The gestational age of the pregnant women (7) ranged from 33 to 41 weeks (mean, 36.8 weeks), and the correlation between their baseline APTT and gestational age was not statistically significant ($r = 0.63$, $n = 7$, $p > 0.1$). The rats were in their 20th day of gestation, *i.e.*, 1 d before parturition. Thus, their relative duration of gestation was similar.

REFERENCES

(1) T. D. Bjornsson and G. Levy, *J. Pharmacol. Exp. Ther.*, **210,** 237 (1979).

(2) D. G. McKay, *Contr. Nephrol.*, **25,** 108 (1981).

(3) J. Bonnar, in "Heparin: Chemistry and Clinical Uses," V. V. Kakkar and D. P. Thomas, Eds., Academic, London, U.K., 1976, p. 247.

(4) M. Hellgren and E.-B. Nygårds, *Gynecol. Obstet. Invest.*, **13,** 76 (1982).

(5) V. V. Kakkar and F. G. Bentley, *Brit. Med. J.*, **1,** 124 (1978) (Letter to Ed.).

(6) G. Spearing, I. Fraser, G. Turner, and G. Dixon, *Br. Med. J.*, **2,** 1457 (1978).

(7) L. R. Whitfield, A. S. Lele, and G. Levy, *Clin. Pharmacol. Ther.*, **34,** 23 (1983).

(8) L. R. Whitfield and G. Levy, *J. Pharm. Sci.*, **72,** 1141 (1983).

(9) R. R. Proctor and S. I. Rapaport, *Am. J. Clin. Pathol.*, **36,** 212 (1961).

(10) L. B. Wingard and G. Levy, *J. Pharmacol. Exp. Ther.*, **184,** 258 (1973).

(11) L. R. Whitfield, J. J. Schentag, and G. Levy, *Clin. Pharmacol. Ther.*, **32,** 503 (1982).

(12) E. J. W. Bowie and C. A. Owen, in "Progress in Hemostasis and Thrombosis," Vol. 5, T. H. Spaet, Ed., Grune and Stratton, New York, N.Y., 1980, p. 179.

(13) A. P. Kaplan, in "Progress in Hemostasis and Thrombosis," Vol. 4, T. H. Spaet, Ed., Grune and Stratton, New York, N.Y., 1978, p. 127.

ACKNOWLEDGMENTS

The previous (sixth) part of this series was L. R. Whitfield, A. S. Lele, and G. Levy, *Clin. Pharmacol. Ther.*, **34,** 23 (1983).

High-Performance Liquid Chromatographic Assay for Sodium Levothyroxine in Tablet Formulations: Content Uniformity Applications

R. L. GARNICK ˣ, G. F. BURT, D. A. LONG, J. W. BASTIAN, and J. P. ALDRED

Received August 12, 1982, from the *Armour Pharmaceutical Company, Kankakee, IL 60901.* Accepted for publication November 12, 1982.

Abstract □ Sodium levothyroxine was quantitated in 25–300 μg/tablet formulations. The procedure consisted of pulverization of a suitable sample, extraction into acetonitrile–water (40:60, v/v) containing 0.05% *o*-phosphoric acid, and injection onto a bonded-phase cyanopropyl column; the effluent was monitored by UV detection at 225 nm. Spiked placebo recovery studies demonstrated the linearity of the method over the range of 80–120% of the label claim. Stability studies indicated that no degradation products or excipients interfered with the quantitation of the intact drug. Data demonstrating the accuracy and precision of this assay are presented, and the method was applied to the measurement of single-tablet content uniformity.

Keyphrases □ Sodium levothyroxine—assay in tablet formulations, content uniformity, high-performance liquid chromatography □ Content uniformity—single-tablet, sodium levothyroxine, high-performance liquid chromatography □ Thyroid hormones—single-tablet content uniformity, high-performance liquid chromatography, sodium levothyroxine

High-performance liquid chromatography (HPLC), an increasingly popular procedure for the quantitation of a variety of medicinally important compounds, is particularly useful for the quantitation of drugs whose active components are present in extremely low concentrations, labile, and/or possess great biological activity. The synthetic thyroid hormones levothyroxine and liothyronine are good examples, typically present at levels of 3–300 μg/tablet. Historically, analyses of these hormones have been complex, often nonspecific (based on iodine content), required tedious sample preparation, and frequently required large samples (1).

Recently, a number of GC methods have been described for the quantitation of thyroid hormones in serum and tablet dosage forms (2–9). However, none of these procedures are capable of determining the stability of the active drug in the presence of its degradation products. In this report, an HPLC assay is described for sodium levothyroxine, which possesses sufficient sensitivity for single-tablet content uniformity studies. The sample preparation procedure is simple, and the method is capable of accurately determining the amount of active drug in the presence of degradation products.

BACKGROUND

The USP XX monograph for the analysis of sodium levothyroxine is based on the estimation of iodine content (1). This method is neither specific nor stability indicating, because it is unable to distinguish between active drug and iodine-containing decomposition products. Moreover, this method is quite insensitive, requiring 3 mg of sodium levothyroxine per assay. This assay requires 120 tablets of the 25-μg dosage form and, therefore, is not applicable to the determination of single-tablet content uniformity.

A survey of the literature indicated a number of analytical methodologies for the analysis of sodium levothyroxine (1–9); however, most were either nonspecific or insufficiently sensitive. Recently, two HPLC procedures for the determination of synthetic thyroid hormones in tablets were published, both using reverse-phase C-18 columns (8, 9). These procedures, while suitably accurate and precise, were not demonstrated to be stability indicating. We found that the quantitation of sodium levothyroxine by these methods was complicated by interferences observed in aged samples.

EXPERIMENTAL

Materials—Levothyroxine and liothyronine reference standards were obtained from the U.S. Pharmacopeial Convention. 3,5-Diiodo-L-thyronine was obtained commercially[1]. All chemicals were reagent or spectrophotometric grade.

Instrumentation—A modular chromatograph was used consisting of a constant-flow pump[2], a fixed-loop injector[3], a variable-wavelength UV detector operating at 225 nm[4], and a strip-chart recorder[5]. A suitable data system, equipped with a data interface printer/plotter was also used[6]. A bonded-phase cyanopropyl column[7] was used with a mobile phase of acetonitrile–water–phosphoric acid (40:60:0.05, v/v/v) at a flow rate of 1–2 mL/min. The mobile phase was deaerated prior to use.

Procedure—The average weight of 20 tablets was determined. The tablets were then ground to a fine powder, and a sample weight equivalent to ~100 μg of sodium levothyroxine was transferred to a 16 × 125-mm culture tube (equipped with a polytef-lined cap). Two glass beads were added to serve as an internal ball mill. Mobile solvent (10.0 mL) was then added to the tube, and the solution was vigorously mixed for 5 min using a vortex mixer. The solution was then centrifuged; the clear supernatant was used for the assay.

Content uniformity was established using single tablets with the addition of 10.0 mL of mobile solvent, as stated above, for the 25–150-μg dosage forms and 20.0 mL of mobile solvent for the 175–300-μg dosage forms. Sodium levothyroxine concentrations were determined by direct comparison with a standard solution. The standard solution was prepared using levothyroxine sodium reference standard USP, the concentration of which was corrected for the sodium content.

Spiked Placebo Recovery Procedure—Placebo material was prepared containing all of the excipients found in the 25–300-μg tablet formulations. Aliquots from solutions of mobile solvent containing 80, 100, and 120% of the theoretical formulated amount of sodium levothyroxine were added to the placebo material, and the resultant solutions were carried through the sample preparation procedure. The recoveries for sodium levothyroxine were 99–100% (Table I).

The precision of the assay was determined during the spiked placebo recovery study. Relative standard deviations of ±0.5 and ±0.12% were determined for the 25- and 300-μg formulations, respectively. Replicate analyses (n = 6) of the 25- and 300-μg tablets, each from a single composite, demonstrated sample-to-sample relative standard deviations of ±0.96 and ±0.35%, respectively.

Stability-Indicating Properties—The stability-indicating properties of the method were established by subjecting sodium levothyroxine bulk material, as well as the finished tablets, to extreme stress conditions designed to produce degradation products similar, or identical to, those which might be expected to occur under various storage conditions.

Single-Tablet Content Uniformity—The HPLC method was also applied to a single-tablet content uniformity assay. The only modification necessary for this purpose was an increase in the sample volume required for the larger dosages.

[1] Sigma Chemical Co., St. Louis, Mo.
[2] Model 110A, Beckman Instruments, Inc.
[3] Model 7125, Rheodyne.
[4] L.D.C. Spectromonitor III.
[5] Omniscribe Recorder.
[6] Sigma 10, Perkin-Elmer Co.
[7] Zorbax-CN, DuPont Co., Wilmington, Del.

0022-3549/84/0100-0075$01.00/0
© 1984, American Pharmaceutical Association

Table I—Spiked Placebo Recovery Studies for Sodium Levothyroxine Tablets

Dosage, μg	Formulated Amount Added (Nominal), %	Formulated Amount Recovered, %	Recovery, %
25	80	79.5	99.3
	80	79.9	99.9
	80	79.4	99.3
	100	99.7	99.7
	100	99.8	99.8
	100	99.6	99.6
	120	121.3	101.1
	120	119.8	99.9
	120	120.0	100.0
Mean ± *RSD*			99.8 ± 0.50
300	80	80.2	100.2
	80	79.8	99.8
	80	80.6	100.7
	100	100.1	100.1
	100	99.3	99.3
	100	99.9	99.9
	120	120.0	100.0
	120	119.9	99.9
	120	120.3	100.2
Mean ± *RSD*			100.0 ± 0.12

RESULTS AND DISCUSSION

A literature method was chosen as a starting point for the development of a stability-indicating assay for sodium levothyroxine in tablets (8). This method used a C-18 column with a mobile phase of methanol–water (50:50, v/v) containing 0.1% phosphoric acid. The method demonstrated excellent resolution between the diiodothyronine, triiodothyroxine, isotriiodothyronine, and levothyroxine peaks. However, under oxidative-degradation conditions, the method failed to resolve an unidentified impurity from the levothyroxine peak. Using several other reverse-phase columns, it was not possible to obtain results satisfactory for a stability-indicating method. A bonded phase cyanopropyl column was then investigated, as the nitrile group is of medium polarity and would be expected to afford a highly selective mode of separation. A mobile phase of acetonitrile–water (40:60, v/v) containing 0.05% phosphoric acid demonstrated excellent resolution between diiodothyronine, triiodothyroxine, isotriiodothyronine, levothyroxine, and other related compounds (Fig. 1). Significantly, the previously noted oxidative-degradation product, which was only partially resolved from the levothyroxine peak, did not interfere in this system.

It was observed that altering the acetonitrile concentration of the mobile solvent had little effect on the retention time of levothyroxine, whereas varying the phosphate ion concentration of the mobile solvent changed the retention time dramatically. This indicated that the separation mechanism was a form of ion suppression. In agreement with this was the observation that the retention time of levothyroxine decreased with increasing phosphate ion concentration.

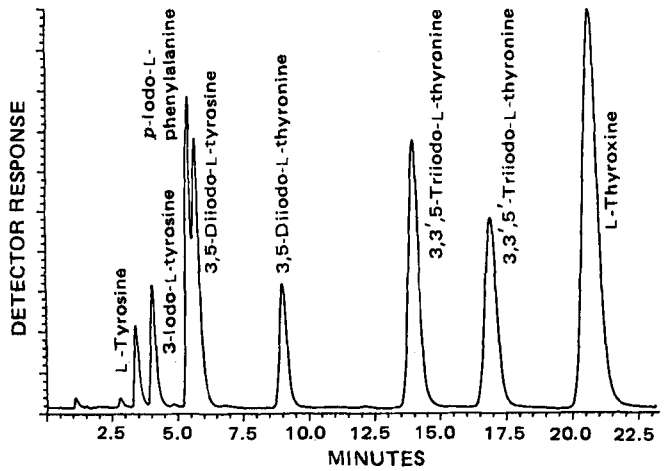

Figure 1—*Chromatogram of sodium levothyroxine and related compounds obtained on a bonded-phase cyanopropyl column using a mobile solvent of acetonitrile–water–phosphoric acid (40:60:0.05, v/v/v).*

Table II—Assay of Sodium Levothyroxine Tablets by the HPLC Method [a]

Sample	Dosage, μg	Age	Composite Tablet Assay	Percent of Labeled Strength
1	25	20 months	23.3	93.2
2	25	4 months	24.2	96.9
3	50	Initial	50.3	101
4	50	Initial	50.3	101
5	100	Initial	105.0	105
6	100	Initial	102.0	102
7	125	Initial	135	108
8	150	Initial	152.0	101
9	150	Initial	156.0	104
10	200	Initial	206	103
11	200	Initial	206	103
12	200	Initial	213	107
13	300	Initial	316	105
14	300	Initial	316	105

[a] All values were obtained for separate lots of sodium levothyroxine tablets.

Samples for assay were prepared by taking the tablet weight equivalent of 100 μg of sodium levothyroxine and extracting it into 10 mL of mobile solvent (Table II). The extract was then injected into the HPLC system, along with levothyroxine reference standard USP, at a concentration of ~10 μg/mL using a 100-μL injection loop (Fig. 2). The standard curve was constructed from eight concentration levels of standard solution. The plot of peak area *versus* the concentration of levothyroxine was linear over the range of 1–13 μg/mL (100–1300 ng/injection) as confirmed by a correlation coefficient of 0.999.

A spiked placebo recovery study was performed for sodium levothyroxine tablets at 80, 100, and 120% of the theoretical formulated amounts for both the 25- and 300-μg tablets. The results (Table I) demonstrate a mean recovery for sodium levothyroxine of 99.8% and 100% for the 25- and 300-μg tablets, respectively. Their respective relative standard deviations were ±0.50 and ±0.12%.

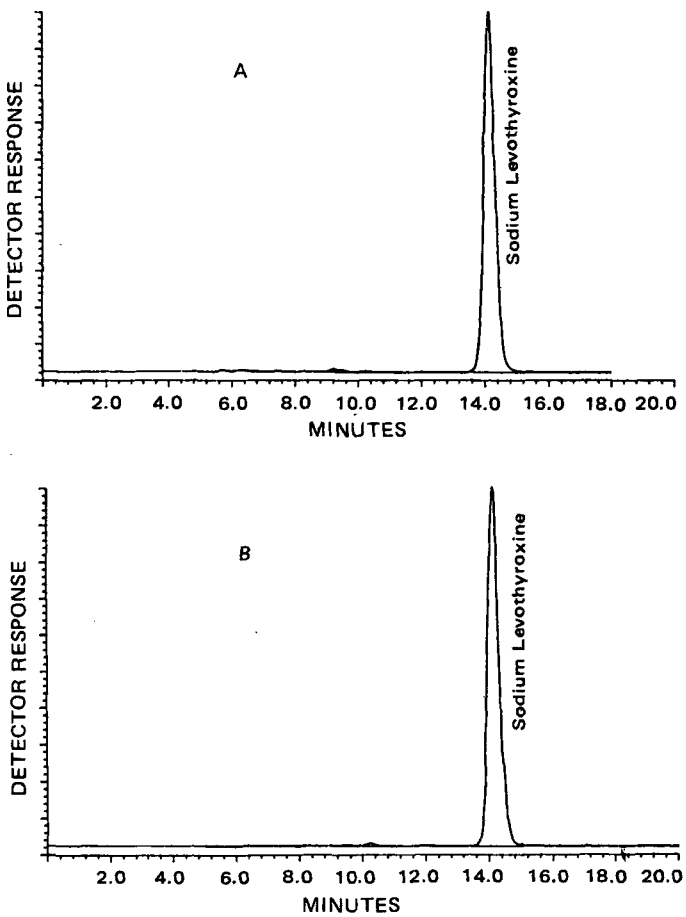

Figure 2—*Typical chromatograms of sample (A) and standard (B) preparations of sodium levothyroxine. See text for details.*

Table III—Degradation of Sodium Levothyroxine Raw Material and Finished Tablets Under Various Conditions [a]

Degradation Conditions	Reagents	Time, h	Amount Recovered, %
	Raw Material		
Thermal	80°C	168	100.8
Hydrolytic	0.1 M NaOH	87.5	90.6
	0.1 M HCl	44	92.8
Oxidative	*tert*-butyl hydroperoxide	1	37.5
Photochemical	UV light (shortwave)	144	98.9
	UV light (longwave)	48	101.4
	Intact Tablets		
Photochemical	UV light (longwave)	168	91.9
Thermal	80°C in air	168	50.0

[a] There were no HPLC interferences for any assay.

Table IV—25-μg Sodium Levothyroxine Tablet Content Uniformity *versus* Composite Assay Results

	Content Uniformity Assay	
Tablet	Tablet Wt., mg	Amount Found, μg/Tablet
1	86.09	23.20
2	86.75	24.43
3	87.63	24.25
4	88.43	25.27
5	86.80	24.26
6	87.30	24.22
7	87.12	23.52
8	87.29	23.81
9	88.35	24.15
10	85.46	23.63
Mean ± *RSD*		24.07 ± 2.41
	Composite Assay[a]	
Sample	Dosage Strength, μg	Amount Found, μg/Tablet
1	25	23.88
2	25	23.90
3	25	23.97
Mean ± *RSD*		23.92 ± 0.20

[a] All composite samples were unaged.

The degradation studies performed for sodium levothyroxine using the proposed method indicated that under oxidative, photochemical, hydrolytic, and thermal conditions, no degradation products were produced which interfered with the sodium levothyroxine peak. In these studies, there was little degradation of sodium levothyroxine *via* UV light (both short- and longwave) or *via* the thermal conditions utilized (Table III). However, oxidative degradation studies indicated that sodium levothyroxine may be subject to oxidative degradation by this means. Sodium levothyroxine was also moderately degraded under hydrolytic conditions (Table III).

Tablet recovery *versus* extraction time (1–10 min) indicated a rapid leaching of sodium levothyroxine from the tablet matrix. From these data a mean leaching time of 5 min was established for routine use.

Table V—300-μg Sodium Levothyroxine Tablet Content Uniformity *versus* Composite Assay Results

	Content Uniformity Assay	
Tablet	Tablet Wt., mg	Amount Found, μg/Tablet
1	87.68	303.27
2	88.44	299.55
3	89.21	302.25
4	89.07	305.48
5	87.49	306.48
6	87.42	303.00
7	89.27	305.08
8	90.55	311.51
9	86.60	292.96
10	88.96	301.37
Mean ± *RSD*		303.10 ± 1.60
	Composite Assay[a]	
Sample	Dosage Strength, μg	Amount Found, μg/Tablet
1	300	299.57
2	300	302.35
3	300	302.54
Mean ± *RSD*		301.49 ± 0.55

[a] All composite samples were unaged.

The assay was also used for a study of single-tablet content uniformity. The results of this study are presented in Tables IV and V for 25- and 300-μg tablets, respectively. These data demonstrate a good correlation with the tablet composite assay results also presented in the Tables. The only modification made to the assay was the use of a 20.0-mL aliquot of the mobile solvent for the 175–300-μg tablets to adjust the concentration to a suitable level.

The HPLC assay method for the determination of sodium levothyroxine in tablets has been demonstrated to be accurate, precise, and stability indicating. The method is simple, specific, and rugged, and is applicable to single-tablet content uniformity determination.

REFERENCES

(1) "The United States Pharmacopeia," 20th rev., U.S. Pharmacopeial Convention, Rockville, Md., 1975, pp. 282, 286.

(2) E. P. Lankmayr, B. Maichin, G. Knapp, and F. Nachtmann, *J. Chromatogr.*, **224**, 239 (1981).

(3) F. Nachtmann, G. Knapp, and H. Spitzy, *J. Chromatogr.*, **149**, 693 (1978).

(4) B. Petersen, R. Hanson, R. Giese, and B. L. Karger, *J. Chromatogr.*, **126**, 503 (1976).

(5) G. Skellern, M. Mahmoudian, and B. Knight, *J. Chromatogr.*, **179**, 213 (1979).

(6) M. Hearn, W. Hancock, and C. Bishop, *J. Chromatogr.*, **157**, 337 (1978).

(7) D. Smith and J. Graham, *J. Assoc. Off. Anal. Chem.*, **62**, 818 (1979).

(8) R. S. Rapaka, P. W. Knight, and V. K. Prasad, *J. Pharm. Sci.*, **70**, 131 (1981).

(9) D. J. Smith, M. Biesemeyer, and C. Yacin, *J. Chromatogr. Sci.*, **19**, 17 (1981).

Precipitation of Calcium Gluceptate from Aqueous Solutions

R. SURYANARAYANAN and A. G. MITCHELL ˣ

Received July 1, 1982, from the *Faculty of Pharmaceutical Sciences, University of British Columbia, Vancouver, BC V6T 1W5, Canada.* Accepted for publication November 5, 1982.

Abstract □ A precipitate encountered in solutions of calcium gluceptate was identified as hydrated calcium gluceptate. Precipitation was associated with a change from a very soluble amorphous anhydrous form to a sparingly soluble crystalline hydrate, the presence of seed crystals inducing crystallization, and unsuitable proportions of the α- and β-epimers of calcium gluceptate. Various commercial samples and the corresponding precipitates were examined by elemental analysis, thermal analysis, X-ray diffraction, IR spectroscopy, and GC–MS. The proportion of the α- and β-epimers in commercial samples was quantitated by GC. In this method, an aqueous solution of calcium gluceptate was converted into a mixture of glucoheptonic acids and their corresponding lactones by passage through a cation-exchange resin. The solution was freeze-dried, the acid–lactone mixture converted to the γ-lactones using concentrated hydrochloric acid, and the resulting material trimethylsilylated with trimethylsilylimidazole. Stability studies of solutions prepared from calcium gluceptate obtained from various commercial sources indicate that above ~50% α-epimer, stability decreased with an increase in the relative proportion of the α-epimer. Material complying with USP specifications (pure α-epimer) is the least stable in solution. It is suggested that calcium gluceptate containing approximately equal proportions of the α- and β-epimers be introduced in the USP monograph together with a method for estimating the proportions of the epimers.

Keyphrases □ Calcium gluceptate—precipitation in aqueous solutions, identification of α- and β-epimers, quantitation by GC □ Epimers—calcium gluceptate, quantitation by GC, role in precipitation in aqueous solutions □ Precipitation—calcium gluceptate in aqueous solutions, role of epimers, quantitation by GC

Calcium gluceptate used in the treatment of calcium deficiency (1), is described (2) as the calcium salt of D-*glycero*-D-*gulo*-heptonic acid (I), which is the α-epimer of glucoheptonic acid. However, the commercially available calcium gluceptate is often a mixture of the α- and β-[calcium D-*glycero*-D-*ido*-heptonate, (II)] epimers. These two forms differ only in their configuration at the second carbon atom (C-2).

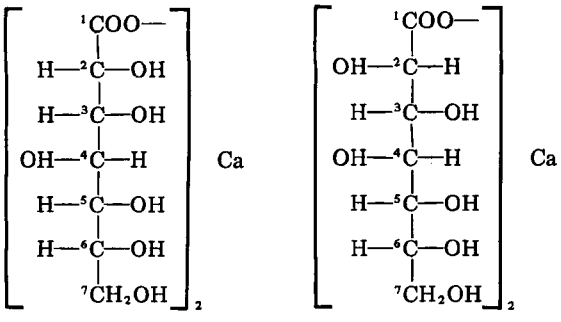

I II

Calcium gluceptate is highly soluble in water, and solutions containing 85% solids have been prepared which have not crystallized on prolonged standing[1]. However, since 1976 solutions of calcium gluceptate have shown a tendency to precipitate on storage[2] (3). According to Muller *et al.* (3), the precipitate can exist in two forms (A and B). They believed that the presence of seed crystals of form A was responsible for the precipitation, and that heating calcium gluceptate powder to 115–120°C destroyed the form A seed crystals, thus preventing nucleation and growth. However, this method offered no absolute guarantee of stability, whereas heating solutions of calcium gluceptate to a minimum temperature of 80°C for 30 min destroyed the form A seed crystals and offered complete protection against later crystallization. Holstein[2] indicates that the preparation of calcium gluceptate in the amorphous form has been impossible in recent years. He attributes precipitation to the presence of seed crystals or some other factor which initiates crystallization and suggests that the product is stable if prepared hot or autoclaved after packaging.

Preliminary stability studies indicated that the time for precipitation to commence depended on the commercial source of calcium gluceptate (4). Various commercial samples and the precipitate from solutions of these samples are examined in greater detail in this paper.

EXPERIMENTAL

Materials—Four samples of calcium gluceptate (source A[3], B[4], C[5], and D[6]) were obtained. Potassium chloride[7] was ground and dried at 105°C for 2 h. α-D-Glucoheptonic acid γ-lactone (III)[8], sulfonic cation-exchange resin[9], hydrochloric acid[10], methanol[11], sucrose[12], trimethylsilylimidazole in pyridine[13], and Tris[14] were used as received.

Characterization of Calcium Gluceptate and the Precipitate—Calcium gluceptate samples from commercial sources A, B, C, and D were dried under vacuum at 60°C for 16 h. For differential scanning calorimetric studies, calcium gluceptate was used as received. The precipitate obtained from solutions prepared with calcium gluceptate from sources A, B, and C was dried under vacuum at room temperature to constant weight unless otherwise stated.

Elemental Analysis—The percentage of carbon and hydrogen in calcium gluceptate (source C) and the precipitate [from the solution of calcium gluceptate (source C)] was determined by a commercial testing laboratory[15]. Calcium was estimated complexometrically with EDTA (ethylenediaminetetraacetic acid) using a modification of the USP method (5). Theoretically, calcium gluceptate consists of 34.3% carbon, 5.34% hydrogen, and 8.17% calcium. The commercial sample from source C gave 33.4% carbon, 5.48% hydrogen, and 8.12% calcium; the precipitate gave values of 32.6, 5.67, and 7.88%, respectively.

Thermal Analysis—Thermal analyses were performed using a dif-

[1] Product information of calcium gluceptate, Pfanstiehl Laboratories, Waukegan, Ill.

[2] Dr. A. G. Holstein, Pfanstiehl Laboratories, Waukegan, Ill., personal communication.

[3] Lot R 3679 BA, Givaudan; supplied by Stanley Drug Products, North Vancouver, British Columbia, Canada.

[4] Lot R 1432 TJ, Italsintex; supplied by Stanley Drug Products, North Vancouver, British Columbia, Canada.

[5] Lot 12953-D, USP grade (pure α-epimer); Pfanstiehl Laboratories, Waukegan, Ill.

[6] Lot 7311, α- and β-mixture; Pfanstiehl Laboratories, Waukegan, Ill.

[7] Analytical reagent; BDH Chemicals, Vancouver, British Columbia, Canada.

[8] Aldrich Chemical Co., Milwaukee, Wis.

[9] Amberlite IR-120 H; Mallinckrodt, Paris, Ky.

[10] ACS grade; Allied Chemical, Pointe Claire, Quebec, Canada.

[11] ACS grade; Caledon Laboratories, Georgetown, Ontario, Canada.

[12] Analytical reagent; BDH Chemicals, Vancouver, British Columbia, Canada.

[13] TRI-SIL Z; Pierce Chemical Co., Rockford, Ill.

[14] Parr Instrument Co., Moline, Ill.

[15] Canadian Microanalytical Service, Vancouver, British Columbia, Canada.

0022-3549/84/0100-0078$01.00/0
© 1984, American Pharmaceutical Association

ferential scanning calorimeter[16] (DSC) equipped for effluent gas analysis. After grinding with a glass pestle and mortar, 1- to 5-mg samples were weighed on an electrobalance[17] directly into aluminum volatile sample pans. Scans were made at various rates using closed pans and pans with a 0.1- to 0.2-mm pinhole.

Heat of Solution—About 500 mg of the sample was accurately weighed into the sample cell of a solution calorimeter[18]. After equilibration, the cell was lowered into 100 g of water contained in a fully silvered double-walled glass vessel and rotated at a constant speed of ~450 rpm. The dissolution of calcium gluceptate samples was almost instantaneous. Throughout the reaction, the temperature was monitored with a thermistor bridge system and recorded on a strip-chart recorder.

The change in enthalpy ΔH, at the mean reaction temperature (expressed in J/g) is[19]:

$$\Delta H = -\frac{(T_f - T_i)e}{m}$$

where T_f is the final temperature, T_i is the initial temperature, m is the weight of the sample, and e is the energy equivalent of the calorimeter and its contents[19] determined using Tris (505.89 J per degree). The calorimeter was standardized using potassium chloride–water (1:400) which gave a mean value for the heat of solution at 25°C of 231.9 ± 0.8 J/g, compared with reported values (6, 7) of 234.8 and 231.0 J/g, respectively. The heat of solution of the precipitate could not be determined because of its low aqueous solubility.

Surface Area—About 200 mg of each sample was accurately weighed into the sample cell of a surface area analyzer[20]. Krypton was used as the adsorbate, and helium was the carrier gas. The specific surface area was determined by the multipoint BET method (Brunauer, Emmett, and Teller) (8) using three different concentrations of adsorbate (0.030, 0.072, and 0.104 mol % krypton in helium). The desorption signals were calibrated with pure nitrogen injected into the flow stream.

X-ray Diffraction—Approximately 300 mg of the ground sample was exposed to Ni-filtered CuKα radiation (40 kV, 15 mA) in a wide-angle X-ray diffractometer[21] over a range of 2θ from 10° to 60°.

Infrared Spectra—One milligram of the sample was dissolved in 40 mL of chloroform, and the solution was scanned[22] in the 3800- to 625-cm^{-1} range. IR spectra were also obtained using compressed disks containing 200 mg of potassium bromide and 5 mg of sample.

Equilibrium Solubility of the Precipitate—An excess of the sample was added to 50 mL of water, and the mixture was agitated in a water-bath[23] maintained at 30°C. Aliquots were taken periodically, filtered, and analyzed for calcium gluceptate by a modification of the USP assay method (5).

Stability of Calcium Gluceptate Solutions—Solutions of calcium gluceptate in water (26.7% w/v)[24] were prepared from each commercial sample. Aliquots of each solution were treated as follows: (*a*) heated in a water-bath[23] at 85°C for 30 min, (*b*) autoclaved[25] at 121°C for 20 min, (*c*) filtered through a 0.22-μm membrane filter[26], and (*d*) left untreated (control). Solutions were also prepared using calcium gluceptate which had been heated at 120°C for 12 h and cooled in a desiccator.

Estimation of the Proportions of α- and β-Epimers in Calcium Gluceptate and the Precipitate—A gas chromatograph[27] (GC) equipped with a flame-ionization detector and data terminal[28] was used. A 1.8-m × 4-mm glass column packed with 3% phenyl–cyanopropyl methyl silicone[29] on a diatomaceous earth support (OV-225 on Chromosorb W) was employed with a carrier gas (helium) flow rate of 30 mL/min. The injector and the detector temperatures were 250°C. The column was maintained at 200°C for 10 min and then was temperature programmed from 200°C to 215°C at 5°C/min. It was maintained at the upper temperature until elution of the last peak.

[16] DSC-1B; Perkin-Elmer, Norwalk, Conn.
[17] Gram; Cahn Instrument Co., Paramount, Calif.
[18] Model 1451; Parr Instrument Co., Moline, Ill.
[19] Instrument manual for solution calorimeter, Model 1451; Parr Instrument Co., Moline, Ill.
[20] Quantasorb; Quantachrome Corp., Syosset, N.Y.
[21] Philips Electronic Instruments, Mount Vernon, N.Y.
[22] Unicam SP 1000; Philips Electronics Instruments, Mount Vernon, N.Y.
[23] Magni Whirl; Blue M Electric Co., Blue Island, Ill.
[24] This corresponds to the concentration of calcium gluceptate in a commercial formulation marketed by Stanley Drug Products, North Vancouver, British Columbia, Canada.
[25] General Purpose; American Sterilizer Co., Erie, Pa.
[26] Type GS; Millipore Corp., Bedford, Mass.
[27] Model 5830 A; Hewlett-Packard, Avondale, Pa.
[28] Model 18850 A; Hewlett-Packard, Avondale, Pa.
[29] Western Chromatography Supplies, New Westminster, British Columbia, Canada.

Table I—Heats of Solution and Surface Energy of Calcium Gluceptate

Calcium Gluceptate Source	Heat of Solution[a], J/g	Specific Surface Area, m^2/g	Surface Energy, J/m^2
B	16.9	0.619	27.3
A	20.4	0.421	48.5
D	33.0	0.145	228
C	45.3	0.156	290

[a] At 22°C; average of two determinations.

Sample Preparation—About 1 g of calcium gluceptate (preliminary studies with source D material) was weighed and dissolved in 20 mL of water. This solution was passed through a column of formic acid-washed cation-exchange resin. The eluate was analyzed for calcium in an atomic absorption spectrophotometer[30]. The calcium levels were found to be <5 ppm, confirming the efficiency of the ion-exchange process. This solution was freeze-dried[31] to a constant weight. About 70 mg of this dried material was accurately weighed, dissolved in sufficient methanol to give 100 mL, and 150, 200, and 250 μL of the solution were transferred to 1-mL vials[32]. The methanol was evaporated under reduced pressure[33], 50 μL of concentrated hydrochloric acid was added to each vial, and the vials were vortex mixed[34]. The hydrochloric acid was evaporated under reduced pressure; the addition and evaporation of hydrochloric acid was repeated 3 additional times.

About 60 mg of sucrose (internal standard) was accurately weighed and dissolved in pyridine, and the volume made up to 100 mL. To each vial 100 μL of the sucrose solution and 200 μL of trimethylsilylimidazole (to form the trimethylsilyl derivative) was added, the solution was vortex mixed, and 5 μL was injected into the GC. The precipitate was subjected to the same treatment.

Gas Chromatography–Mass Spectrometry—A mass spectrometer[35] interfaced to a GC was used to characterize source A drug and the precipitate from a solution from source A. The method of sample preparation and the GC conditions were the same as above. A beam energy of 70 eV was employed, and the separator temperature was 250°C. The injection volume was 5 μL.

RESULTS AND DISCUSSION

DSC thermograms of the different samples of calcium gluceptate showed no exothermic or endothermic peaks between 25 and 180°C, indicating that the samples were anhydrous as received and did not undergo any phase transitions in this temperature range. However, the precipitate (from solutions of calcium gluceptate from sources A, B, and C) gave a single endothermic peak at ~110°C in a closed sample pan with a pinhole, which allows water to evaporate. A weight loss was found on weighing the closed pan with a pinhole before and after the endothermic peak, and a peak was obtained on the effluent gas analyzer following the endothermic peak. When the precipitate was dried under vacuum at 76°C for 2 h and then subjected to DSC, the endothermic peak was not present. This indicates that the precipitate is a hydrate, but the weight loss was found to be highly variable.

The heats of solution and the surface energies (Table I) differ for each sample, but the values do not correlate with the stabilities of the corresponding solutions (Table II).

X-ray diffraction patterns of the calcium gluceptate samples were typical of amorphous materials. There were no characteristic diffraction peaks, contrary to the information received from Holstein[2] that production of the amorphous form has been impossible in recent years. The dried precipitate diffracted X-rays, showing its crystalline nature, and the diffraction patterns of the precipitates from different sources were very similar. When the precipitate was dried under vacuum at 80°C for 46 h, there were minor changes in the diffraction pattern (Table III). The results indicate that the crystal lattice of the hydrate does not collapse to an amorphous form when the water of hydration is removed.

The IR spectra of chloroform solutions of the four samples of calcium gluceptate and the three samples of the dried precipitates were identical.

[30] Model AA-5; Varian Techtron, Melbourne, Victoria, Australia.
[31] Freeze-Drying Unit; Vitris Co., Gardiner, N.Y.
[32] Reacti-Vial; Pierce Chemical Co., Rockford, Ill.
[33] Vac Torr S 35; Precision Scientific Company, Chicago, Ill.
[34] Vortex-Genie; Scientific Industries, Springfield, Mass.
[35] MAT 111; Varian Mat GmBH, West Germany. The mass spectrometer was coupled to a computer, Model 620/L, Varian Data Machines, Palo Alto, Calif.

Table II—Relationship Between the Proportions of the α- and β-Epimers and the Stability of Calcium Gluceptate in Solution

Calcium Gluceptate Source	Epimers in Calcium Gluceptate, % α	% β	Precipitation Begins, d	Epimers in Precipitate, % α	% β
C	100	0	<1	100	0
B	72.4	27.6	2	84.6	15.4
A	71.8	28.2	8	79.9	20.1
D	51.8	48.2	——Stable——		

The spectra of the potassium bromide disks of the samples were much less well defined than those of the chloroform solutions. The precipitate dried under vacuum at room temperature had a more clearly defined spectral pattern than the original sample, with an increase in the number of bands in the 1125- to 1000-cm^{-1} region, but after drying under vacuum at 80°C for 46 h the spectrum of the precipitate lost its sharpness and appeared like that of the original calcium gluceptate. This is in contrast with the X-ray results, where the more rigorous drying conditions caused only minor changes in the diffraction pattern rather than a return to the diffuse pattern of the original amorphous form.

Table III—X-ray Powder Diffraction Patterns of the Precipitate Obtained from the Solution of Calcium Gluceptate (Source C)

Dried Precipitate: Vacuum at Room Temperature[a] Interplanar Spacing, Å	Relative Intensity, %	Vacuum at 80°C[b] Interplanar Spacing, Å	Relative Intensity, %
		7.76	9
7.49	10	7.49	23
6.60	9	6.65	21
6.19	10	6.19	13
		5.86	12
5.50	13	5.50	22
5.34	27	5.37	36
5.27	6	5.24	14
4.87	7	4.87	34
4.74	22	4.72	18
		4.57	35
4.50	13	4.48	18
4.33	100	4.31	100
		4.23	22
		4.19	22
4.13	38	4.11	47
		4.02	7
3.90	31	3.88	23
3.85	44	3.83	56
		3.72	7
3.66	5	3.68	9
3.53	13	3.55	20
3.35	40	3.34	34
		3.29	18
3.25	14	3.25	22
3.23	7	3.22	10
3.16	5	3.17	8
3.10	22	3.09	22
3.05	8	3.05	16
2.98	27	2.96	23
2.92	6	2.92	8
		2.87	7
2.83	14	2.82	14
2.80	11		
2.70	19	2.70	22
2.64	5	2.64	8
2.49	11	2.49	14
2.43	31	2.43	28
2.38	14	2.38	12
2.33	15	2.32	16
2.26	8	2.25	12
		2.20	9
2.18	5		
		2.14	12
2.12	5		
2.07	8	2.07	9
2.03	10	2.03	7
1.97	6		
1.95	7		

[a] To constant weight. [b] For 46 h.

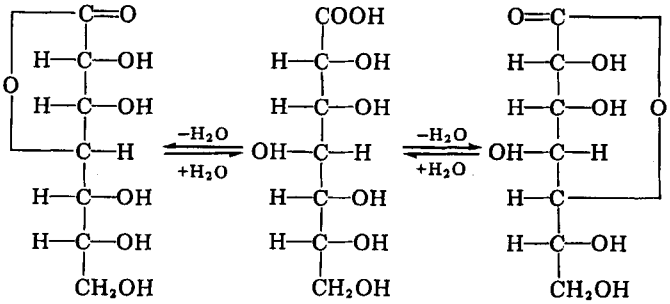

1,4-lactone of α-D-glucoheptonic acid (γ-lactone of α-D-glucoheptonic acid) | α-D-glucoheptonic acid | 1,5-lactone of α-D-glucoheptonic acid (δ-lactone of α-D-glucoheptonic acid)

Scheme I—Lactonization of α-D-glucoheptonic acid.

Attempts to determine the equilibrium solubility of each sample of calcium gluceptate were unsuccessful. Sources A, B, and D appeared to be infinitely soluble in water with >200% w/v going into solution. The accompanying increase in viscosity hindered dispersion and dissolution of additional solid. Concentrated solutions of source C were extremely unstable, becoming turbid and precipitating within minutes of dissolution. The precipitate (from the solution of source A) was found to have a solubility of 2.5% w/v in water.

Development of GC Method—Preliminary attempts to perform the GC analysis of calcium gluceptate were unsuccessful presumably due to the nonvolatile nature of this material. Hence, an aqueous solution of calcium gluceptate was first passed through a cation-exchange resin, freeze-dried, trimethylsilylated, and subjected to GC. This resulted in four peaks, presumably due to α-D-glucoheptonic acid, β-D-glucoheptonic acid, and the corresponding lactones, which result from lactonization of aldonic acids in solution (9). The formation of both the 1,4-lactone and 1,5-lactone is possible. The lactonization reactions of α-D-glucoheptonic acid are presented in Scheme I; β-D-glucoheptonic acid can undergo similar reactions.

In the presence of hydrochloric acid, aldonic acids are converted into their corresponding γ-lactones (1,4-lactones) (10). The number of substances eluted in the GC analysis was, therefore, reduced by treating the freeze-dried eluate from the ion-exchange column with hydrochloric acid. Treatment with hydrochloric acid also avoided possible complications due to the formation of 1,5-lactones (9, 10).

Identification of Calcium Gluceptate and the Precipitate—GC analysis of the treated calcium gluceptate (sources A, B, and D) indicated it to be a mixture of two compounds with retention times of 7.7 and 9.2 min (Fig. 1). GC–MS revealed that the compounds eluting as peaks 1 and 2 had similar mass spectral patterns as follows:

1. A molecular ion peak (M^+) recorded at m/z 568 in agreement with that calculated for the fully trimethylsilylated derivative of the lactone of glucoheptonic acid (11).
2. The ion M-15 (loss of one methyl group) was at m/z 553.
3. The ion M-43 was at m/z 525.
4. The ion M-105 was at m/z 463 due to the loss of methyl and trimethylsilanol groups.

The reference material III, when subjected to GC–MS analysis under the same conditions, had the same retention time and fragmentation pattern as the compound appearing as peak 2 in Fig. 1. Hence the identity of this compound as the trimethylsilyl derivative of III was confirmed.

The compounds eluting as peaks 1 and 2 (Fig. 1) have different retention times, but show mass spectral patterns with identical m/z values at the upper region of the spectrum. Hence, the chemical structures of the two compounds which gave rise to these peaks must be very similar. Since the identity of one of these compounds (peak 2) was established, peak 1 was ascribed to the trimethylsilyl derivative of β-D-glucoheptonic acid γ-lactone.

The precipitate, when subjected to the same treatment, was also found to be a mixture of two compounds with retention times of 7.7 and 9.2 min. Analysis by GC–MS showed that the mass fragmentation pattern of the compound eluting at 7.7 min was the same for both the treated calcium gluceptate and the treated precipitate. Similarly, the compounds appearing at 9.2 min also exhibited identical mass fragmentation patterns.

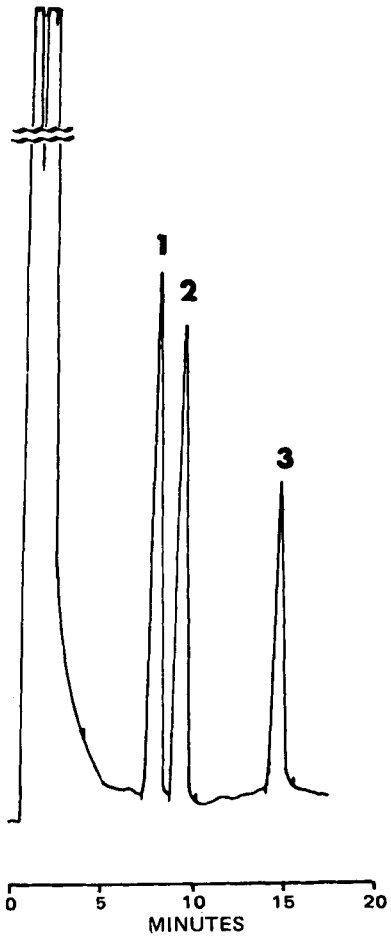

Figure 1—*Chromatogram of calcium gluceptate (source D) prepared for GC analysis. Key: (1) β-D-glucoheptonic acid γ-lactone; (2) α-D-glucoheptonic acid γ-lactone; (3) sucrose (internal standard).*

A linear relationship was established between the area ratio of peak 2 (trimethylsilyl derivative of III)–peak 3 (trimethylsilyl derivative of sucrose) and the weight ratio of III–sucrose (correlation coefficient 0.9989, slope 0.5174, intercept −0.0437). It was not possible to establish a similar relationship for β-D-glucoheptonic acid γ-lactone since this is not commercially available. Since β-D-glucoheptonic acid γ-lactone and III are epimers, the response factors were taken as being identical.

Elemental analysis, IR spectral (chloroform solutions), and GC–MS studies showed that calcium gluceptate and the precipitate were chemically similar. Since the DSC studies indicated that the precipitate was a hydrate, it was concluded that the precipitate was hydrated calcium gluceptate.

Stability of Solutions of Calcium Gluceptate—Calcium gluceptate consisting of the pure α-epimer (source C) has the lowest stability in solution, whereas the α–β mixture (source D) has the highest stability in solution (Table IV). Filtration increases the time before precipitation occurs, and autoclaved solutions showed no precipitation during 24 months of storage (Table IV). It is thought that precipitation could be due to one or more of the following factors:

1. A change from a very soluble amorphous anhydrous form to a sparingly soluble crystalline hydrate.
2. Unsuitable proportions of the α- and β-epimers. The problem of precipitation started only in 1976; prior to this time, solutions were apparently stable (3). It seems probable that in that year, a change occurred in the manufacturing procedure for calcium gluceptate which led to a change in the relative proportions of the α- and β-epimers.
3. The presence of seed crystals in the solution. Impurities or crystals of the required solute can act as nucleating agents or seed crystals (heterogeneous nucleation), inducing crystal growth at much lower degrees of supersaturation than for spontaneous (homogenous) nucleation.

Recrystallization of a Stable Form—X-ray studies showed that all the samples of calcium gluceptate were amorphous, whereas the precipitates were crystalline. Thermal analyses indicated that the initial materials were anhydrous, but the precipitates were hydrated. Hence, precipitation is due to the recrystallization of a stable hydrate from a solution made using an amorphous anhydrous form. This change produces a dramatic decrease in solubility from an infinitely soluble material to a precipitate with a water solubility of ~2.5% w/v.

Table IV—Stability of Calcium Gluceptate (26.7% w/v) in Aqueous Solution Stored at Room Temperature

Treatment	Time for Precipitation, d			
	Source A	Source B	Source C	Source D
Control[a]	2	8	<1	—[c]
Solution heated at 85°C × 30 min	13	7	<1	—
Solution autoclaved at 121°C × 20 min	—	—	—	—
Filtered	210	240	2	—
Solid heated[b] at 120°C × 12 h	3	3	<1	—

[a] Solution prepared by dissolving solid in water at room temperature; frequently contaminated with microbial growth. [b] Causes caramelization. [c] — no precipitation (during 24 months of storage).

Proportions of the α- and β-Epimers in Calcium Gluceptate and the Precipitate—There is a marked variation in the proportions of the α- and β-epimers in the different samples of calcium gluceptate, and there is a relationship between the stability in solution and the proportion of α- and β-epimers (Table II). Solutions prepared with source C (100% α-epimer) precipitated from solution within a day, whereas solutions prepared with source D (51.8% α-epimer) showed no precipitation during 24 months of storage.

The proportions of the α- and β-epimers in the precipitates obtained from solutions of calcium gluceptate were determined (Table II). There was an increase in the proportion of the α-epimer when compared with the original material. Since the precipitate is hydrated calcium gluceptate, it would appear that the hydrate of the β-epimer has a higher solubility in water than the hydrate of the α-epimer. Thus, the relative proportion of the α-epimer in the precipitate would increase.

Heating solutions of calcium gluceptate does not produce any change in the proportions of the α- and β-epimers. This became evident by determining the proportions of the α- and β-epimers before and after autoclaving solutions of calcium gluceptate.

Presence of Seed Crystals Inducing Crystallization—It has been shown that membrane filtration increases the time before precipitation occurs (Table IV), possibly by excluding the majority of seed crystals. The stability of the autoclaved solutions suggests that seed crystals are destroyed by heating at 121°C. This is above the DSC temperature of 110°C, at which the crystalline precipitate dehydrates, which suggests that the seed crystals are hydrated calcium gluceptate. Our results indicate that all three causes of instability postulated earlier are involved in precipitation, but the most important factor affecting the stability of nonautoclaved solutions is the relative proportion of the α- and β-epimers in the commercial material.

Some Comments About the USP Specifications of Calcium Gluceptate—Only the α-epimer of calcium gluceptate is official in the USP (2), but the stability results in Table IV indicate that the pure α-epimer (source C) is the least stable in aqueous solution, with precipitation occurring within a day. Moreover, the pharmacopeia offers no method of identification of the α-epimer. The USP identification test states that the IR spectrum of the sample under investigation must exhibit maxima only at the same wavelength as a similar preparation of USP Reference Standard (2). It has been found that the IR spectra of calcium gluceptate obtained from different sources (*i.e.*, containing different proportions of the α- and β-epimers) are superimposable. Thus, IR spectroscopy is incapable of distinguishing between the α- and β-epimers of calcium gluceptate.

The USP assay method consists of the complexometric estimation of calcium with EDTA and cannot distinguish between the α- and β-epimers. The rationale behind the choice of the pure α-epimer form of calcium gluceptate in the USP monograph is not known. It is apparent that in order to be stable in aqueous solution, calcium gluceptate must contain approximately equal proportions of the α- and β-epimers (as in the source D material). Hence, it is suggested that the USP should consider an α–β mixture, and the monograph should include a method for estimating the proportion of epimers in the mixture.

In our studies, based on the close structural similarity of the α- and β-epimers, the response factors of the two epimers were taken as being identical. For an absolute calculation of the proportions of the α- and β-epimers, it would be necessary to have pure reference standards for both

III and β-D-glucoheptonic acid γ-lactone. At present only III is commercially available.

REFERENCES

(1) "Martindale: The Extra Pharmacopoeia," 27th ed., Pharmaceutical Press, London, England, 1977, p. 286.

(2) "The United States Pharmacopeia," 20th rev., United States Pharmacopeial Convention, Rockville, Md., 1980, p. 107.

(3) R. Muller, J. Bardon, Y. Arnaud, J. Champy, and P. Roland, *Ann. Pharm. Fr.*, **37**, 301 (1979).

(4) R. Suryanarayanan and A. G. Mitchell, *J. Pharm. Pharmacol.*, **33**, 12P (1981).

(5) R. Suryanarayanan and A. G. Mitchell, *J. Pharm. Sci.*, **70**, 968 (1981).

(6) S. Sunner and I. Wadso, *Acta Chem. Scand.*, **13**, 97 (1959).

(7) "CRC Handbook of Chemistry and Physics," 62nd ed., R. C. Weast, Ed., CRC Press, Boca Raton, Fla., 1981, p. D-96.

(8) S. Lowell, *Anal. Chem.*, **45**, 1576 (1973).

(9) H. S. Isbell and H. L. Frush, in "Methods in Carbohydrate Chemistry," Vol. II, R. L. Whistler and M. L. Wolfrom, Eds., Academic, New York, N.Y., 1963, pp. 16, 17.

(10) M. B. Perry and R. K. Hulyalkar, *Can. J. Biochem.*, **43**, 573 (1965).

(11) G. Petersson, O. Samuelson, K. Anjou, and E. von Sydow, *Acta. Chem. Scand.*, **21**, 1251 (1967).

ACKNOWLEDGMENTS

Abstracted in part from a dissertation submitted by R. Suryanarayanan to the University of British Columbia, in partial fulfillment of the Master of Science degree requirements.

This investigation was supported by a research grant from the Medical Research Council of Canada, and R. Suryanarayanan acknowledges the receipt of a G.R.E.A.T. award from the Science Council of British Columbia. Appreciation is expressed to Stanley Drug Products Ltd., North Vancouver, British Columbia for suggesting this problem and also for financial support and chemical supplies.

The authors thank Mr. R. Butters, Dr. K. M. McErlane, and Dr. F. S. Abbott for their help.

Quantitative Determination of the Stabilizers Octanoic Acid and *N*-Acetyl-DL-tryptophan in Human Albumin Products

M. W. YU ˣ and J. S. FINLAYSON

Received July 7, 1982, from the *Division of Blood and Blood Products, National Center for Drugs and Biologics, Food and Drug Administration, Bethesda, MD 20205.* Accepted for publication November 29, 1982.

Abstract □ Methods were developed for the determination of octanoic acid and *N*-acetyl-DL-tryptophan, which are used as stabilizers in the human blood-derived therapeutic products normal serum albumin and plasma protein fraction. The method for octanoic acid uses GC; quantitation is achieved using heptanoic acid as the internal standard. The method for *N*-acetyl-DL-tryptophan is based on UV spectrophotometry of the acid-soluble fraction remaining after precipitation of the protein (ϵ_{280} for *N*-acetyl-DL-tryptophan, 5250). The coefficient of variation for replicate determinations of octanoic acid averaged 3.9% (range 2.1–5.5%); that of *N*-acetyl-DL-tryptophan averaged 1.9% (range 0.5–4.0%). Use of these methods for the analysis of 138 lots of commercial products for octanoic acid and 159 lots for *N*-acetyl-DL-tryptophan showed that the stabilizer contents of 132 and 158 of these lots, respectively, were within 20% of the value indicated on the product label.

Keyphrases □ *N*-Acetyl-DL-tryptophan—quantitative determination of stabilizers, octanoic acid, human albumin products □ Octanoic acid—quantitative determination of stabilizers, *N*-acetyl-DL-tryptophan, human albumin products □ Human albumin products—quantitation of stabilizers, octanoic acid and *N*-acetyl-DL-tryptophan

The major therapeutic human albumin products manufactured for intravenous use in the United States are normal serum albumin (prepared as a 5% or 25% protein solution) and plasma protein fraction (prepared as a 5% protein solution). These products are heated at 60°C for 10 h (1) to inactivate hepatitis viruses (2); to minimize changes in the protein during the heating procedure, stabilizers are added (3–5). The stabilizers permitted by federal regulations are the sodium salt of *N*-acetyl-DL-tryptophan (0.16 mmol) or a combination of sodium salts of *N*-acetyl-DL-tryptophan and octanoic acid (0.08 mmol of each) per gram of protein (1); in practice, only the combination is used. Both octanoic acid and *N*-acetyl-DL-tryptophan bind to human albumin (6). The strength of binding varies with the length of the carbon chain of the fatty acids (7, 8) and the steric configuration of tryptophan (9). Depending on the experimental conditions, lowering the concentration of either stabilizer can affect the thermal stability of albumin (5, 10, 11).

Numerous biological effects of octanoic acid have been reported, including inhibition of platelet aggregation (12, 13), hypoglycemia (14, 15), narcotic action in several animal species (16, 17), and suppression of liver clearance of long-chain fatty acids (18). The ability of the sera of certain individuals to agglutinate all human erythrocytes when octanoic acid is present has been described by several investigators (19). Although no untoward responses were elicited by administering octanoic acid-stabilized albumin to a recipient with such fatty acid-dependent ("caprylate-dependent") antibodies (20), some patients who had undergone anaphylactoid reactions to albumin products exhibited positive skin reactions to octanoic acid-treated albumin (21). In contrast, no adverse reactions have been reported for *N*-acetyl-DL-tryptophan. When given intravenously to human recipients, both the D- and the L-form are poorly utilized and rapidly excreted (22).

The present study was undertaken to develop precise and accurate methods for the quantitative determination of these stabilizers in concentrated protein solutions. The methods developed were then used to assess the stabilizer content of commercially manufactured normal serum albumin and plasma protein fraction[1].

[1] All lots of these products were submitted to the Bureau of Biologics before release for marketing; therefore, a sufficient number of samples could be analyzed to assure that the values obtained were representative of products in commercial distribution.

0022-3549/84/0100-0082$01.00/0

© 1984, American Pharmaceutical Association

III and β-D-glucoheptonic acid γ-lactone. At present only III is commercially available.

REFERENCES

(1) "Martindale: The Extra Pharmacopoeia," 27th ed., Pharmaceutical Press, London, England, 1977, p. 286.

(2) "The United States Pharmacopeia," 20th rev., United States Pharmacopeial Convention, Rockville, Md., 1980, p. 107.

(3) R. Muller, J. Bardon, Y. Arnaud, J. Champy, and P. Roland, *Ann. Pharm. Fr.*, **37**, 301 (1979).

(4) R. Suryanarayanan and A. G. Mitchell, *J. Pharm. Pharmacol.*, **33**, 12P (1981).

(5) R. Suryanarayanan and A. G. Mitchell, *J. Pharm. Sci.*, **70**, 968 (1981).

(6) S. Sunner and I. Wadso, *Acta Chem. Scand.*, **13**, 97 (1959).

(7) "CRC Handbook of Chemistry and Physics," 62nd ed., R. C. Weast, Ed., CRC Press, Boca Raton, Fla., 1981, p. D-96.

(8) S. Lowell, *Anal. Chem.*, **45**, 1576 (1973).

(9) H. S. Isbell and H. L. Frush, in "Methods in Carbohydrate Chemistry," Vol. II, R. L. Whistler and M. L. Wolfrom, Eds., Academic, New York, N.Y., 1963, pp. 16, 17.

(10) M. B. Perry and R. K. Hulyalkar, *Can. J. Biochem.*, **43**, 573 (1965).

(11) G. Petersson, O. Samuelson, K. Anjou, and E. von Sydow, *Acta. Chem. Scand.*, **21**, 1251 (1967).

ACKNOWLEDGMENTS

Abstracted in part from a dissertation submitted by R. Suryanarayanan to the University of British Columbia, in partial fulfillment of the Master of Science degree requirements.

This investigation was supported by a research grant from the Medical Research Council of Canada, and R. Suryanarayanan acknowledges the receipt of a G.R.E.A.T. award from the Science Council of British Columbia. Appreciation is expressed to Stanley Drug Products Ltd., North Vancouver, British Columbia for suggesting this problem and also for financial support and chemical supplies.

The authors thank Mr. R. Butters, Dr. K. M. McErlane, and Dr. F. S. Abbott for their help.

Quantitative Determination of the Stabilizers Octanoic Acid and *N*-Acetyl-DL-tryptophan in Human Albumin Products

M. W. YU ˣ and J. S. FINLAYSON

Received July 7, 1982, from the *Division of Blood and Blood Products, National Center for Drugs and Biologics, Food and Drug Administration, Bethesda, MD 20205.* Accepted for publication November 29, 1982.

Abstract □ Methods were developed for the determination of octanoic acid and *N*-acetyl-DL-tryptophan, which are used as stabilizers in the human blood-derived therapeutic products normal serum albumin and plasma protein fraction. The method for octanoic acid uses GC; quantitation is achieved using heptanoic acid as the internal standard. The method for *N*-acetyl-DL-tryptophan is based on UV spectrophotometry of the acid-soluble fraction remaining after precipitation of the protein (ϵ_{280} for *N*-acetyl-DL-tryptophan, 5250). The coefficient of variation for replicate determinations of octanoic acid averaged 3.9% (range 2.1–5.5%); that of *N*-acetyl-DL-tryptophan averaged 1.9% (range 0.5–4.0%). Use of these methods for the analysis of 138 lots of commercial products for octanoic acid and 159 lots for *N*-acetyl-DL-tryptophan showed that the stabilizer contents of 132 and 158 of these lots, respectively, were within 20% of the value indicated on the product label.

Keyphrases □ *N*-Acetyl-DL-tryptophan—quantitative determination of stabilizers, octanoic acid, human albumin products □ Octanoic acid—quantitative determination of stabilizers, *N*-acetyl-DL-tryptophan, human albumin products □ Human albumin products—quantitation of stabilizers, octanoic acid and *N*-acetyl-DL-tryptophan

The major therapeutic human albumin products manufactured for intravenous use in the United States are normal serum albumin (prepared as a 5% or 25% protein solution) and plasma protein fraction (prepared as a 5% protein solution). These products are heated at 60°C for 10 h (1) to inactivate hepatitis viruses (2); to minimize changes in the protein during the heating procedure, stabilizers are added (3–5). The stabilizers permitted by federal regulations are the sodium salt of *N*-acetyl-DL-tryptophan (0.16 mmol) or a combination of sodium salts of *N*-acetyl-DL-tryptophan and octanoic acid (0.08 mmol of each) per gram of protein (1); in practice, only the combination is used. Both octanoic acid and *N*-acetyl-DL-tryptophan bind to human albumin (6). The strength of binding varies with the length of the carbon chain of the fatty acids (7, 8) and the steric configuration of tryptophan (9). Depending on the experimental conditions, lowering the concentration of either stabilizer can affect the thermal stability of albumin (5, 10, 11).

Numerous biological effects of octanoic acid have been reported, including inhibition of platelet aggregation (12, 13), hypoglycemia (14, 15), narcotic action in several animal species (16, 17), and suppression of liver clearance of long-chain fatty acids (18). The ability of the sera of certain individuals to agglutinate all human erythrocytes when octanoic acid is present has been described by several investigators (19). Although no untoward responses were elicited by administering octanoic acid-stabilized albumin to a recipient with such fatty acid-dependent ("caprylate-dependent") antibodies (20), some patients who had undergone anaphylactoid reactions to albumin products exhibited positive skin reactions to octanoic acid-treated albumin (21). In contrast, no adverse reactions have been reported for *N*-acetyl-DL-tryptophan. When given intravenously to human recipients, both the D- and the L-form are poorly utilized and rapidly excreted (22).

The present study was undertaken to develop precise and accurate methods for the quantitative determination of these stabilizers in concentrated protein solutions. The methods developed were then used to assess the stabilizer content of commercially manufactured normal serum albumin and plasma protein fraction[1].

[1] All lots of these products were submitted to the Bureau of Biologics before release for marketing; therefore, a sufficient number of samples could be analyzed to assure that the values obtained were representative of products in commercial distribution.

0022-3549/84/0100-0082$01.00/0

© 1984, American Pharmaceutical Association

EXPERIMENTAL

Materials—The column packing used for gas chromatography (GC) was 80/100 Chromosorb W AW coated with 10% SP-1000[2]. Octanoic acid (>99.5% pure)[3], heptanoic acid (96% pure)[3], isoamyl acetate[3], perchloric acid (60%)[4], chloroform[4], *N*-acetyl-DL-tryptophan[5], and [1-^{14}C]octanoic acid (sodium salt, 1.628×10^{11} Bq/mol)[6] were obtained commercially and used without further purification. The human albumin solutions analyzed were normal serum albumin and plasma protein fraction prepared by 14 different manufacturers (designated A–N)[7]. The primary stabilizer-free albumin used was human fraction V powder prepared by manufacturer K. Other stabilizer-free albumin powders employed are described in the pertinent table. All albumin powders were held at −20°C until use.

Gas Chromatographic Conditions—A chromatograph[8] equipped with a flame-ionization detector, an integrator[9], and an automatic sampler[10] was used. A 1.22- or 1.83-m coiled-glass column (2-mm i.d.) was packed as indicated above and initially conditioned at 225°C by carrier gas (nitrogen) flow for 24 h. The operating conditions for the 1.22-m column were as follows: injection port temperature, 225°C; column, 160°C; detector, 300°C; nitrogen carrier gas flow rate 22 mL/min; detector pressures were hydrogen, 193 kPa (28 psig) and compressed air, 207 kPa (30 psig); automatic sampler pressure was compressed air, 552 kPa (80 psig); the volume of sample injected was ~0.5 μL. For the 1.83-m column, the conditions were the same except that the column temperature was 190°C and the nitrogen carrier gas flow rate was 35 mL/min. The retention times for heptanoic acid (the internal standard) and octanoic acid were, respectively, ~3.0 and ~4.6 min for the 1.22-m column and ~3.5 and ~5.0 min for the 1.83-m column.

Assay Procedure for Octanoic Acid—The method described by Kupferberg (23) for the determination of valproic acid in plasma was used. Protein solution (0.5 mL, 5%), 30 μL of internal standard solution (heptanoic acid, 11.52 mg/mL in chloroform), and 0.1 mL of 1.5 M perchloric acid were stirred vigorously with a vortex mixer for 1 min in a glass-stoppered 13-mL centrifuge tube. Chloroform (4 mL) was added, and the mixture was again stirred with a vortex mixer for a few minutes. The tubes were then centrifuged at 2800 rpm, and the aqueous layer was removed by aspiration. The chloroform layer was removed with a pipet (carefully so as not to remove any of the interphase, which contained mostly albumin) and transferred to a new centrifuge tube which contained 100 μL of isoamyl acetate. The chloroform was then removed at 30°C under reduced pressure[11]. The remaining isoamyl acetate solution was analyzed directly (GC). When 20 or 25% albumin[12] preparations were analyzed, 0.125- and 0.1-mL portions, respectively, were used and 0.9% NaCl was added to bring the volume to 0.5 mL.

A five-point standard curve for octanoic acid was prepared for each analysis by placing 10, 20, 30, 40, or 50 μL of octanoic acid standard solution (11.56 mg/mL in chloroform) plus 30 μL of the heptanoic acid internal standard solution, 4 mL of chloroform, and 100 μL of isoamyl acetate in glass-stoppered centrifuge tubes and evaporating as described above. This simplified procedure for preparing the standard curve was found to yield results identical to those obtained when stabilizer-free albumin was added and the entire extraction procedure (including acidification with perchloric acid) was performed or when perchloric acid was added in the absence of albumin. The octanoic acid standard solution could be kept at room temperature for as long as 2 months.

A typical GC profile of heptanoic and octanoic acids is shown in Fig. 1. With the equipment used in the present study[8,9], the area of each peak was integrated and printed automatically. Therefore, the ratio between the areas of the octanoic acid and heptanoic acid peaks was calculated for each sample and each point on the standard curve. The latter was obtained by plotting the area ratio against the amount of standard octanoic acid added (Fig. 2A, upper line), and the octanoic acid contents of the albumin samples were determined from their peak area ratios. However, a reliable standard curve can be constructed from the peak height ratios (Fig. 2A, lower line) and the octanoic acid contents of the samples determined accordingly.

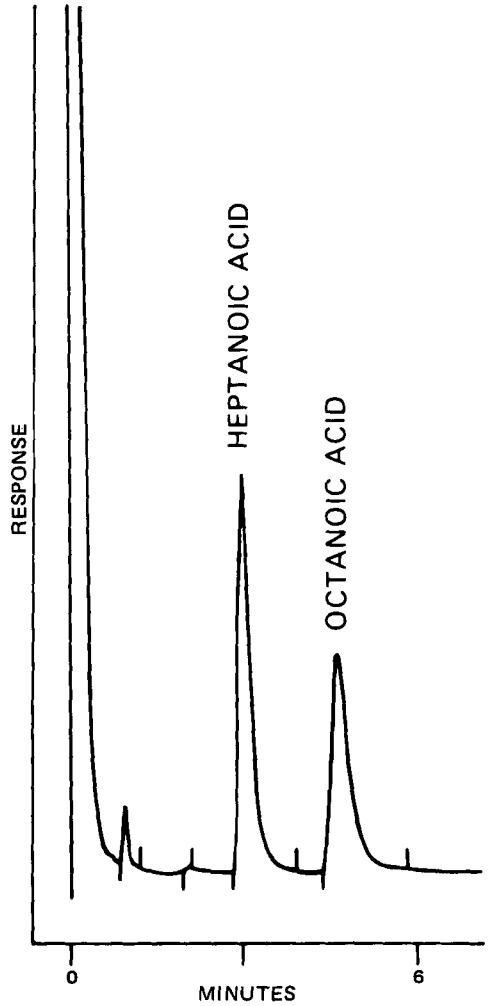

Figure 1—*Typical chromatogram obtained by GC analysis of a commercial human albumin. A 1.22-m column was used. In this experiment the retention times of the heptanoic acid internal standard and the octanoic acid from the albumin sample were 3.05 and 4.61 min, respectively.*

Assay Procedure for *N*-Acetyl-DL-tryptophan—*N*-Acetyl-DL-tryptophan was quantitated spectrophotometrically by precipitating the protein with perchloric acid and subsequently measuring the UV absorbance of the acid-soluble fraction. Virtually all of this absorbance was shown to be due to the *N*-acetyl-DL-tryptophan in the products analyzed (see below). In this procedure 0.1 mL of 5% protein solution, 0.1 mL of 0.9% NaCl, and 1.8 mL of 0.3 M perchloric acid were mixed and held for 10 min at room temperature before centrifuging at 2800 rpm for 10 min. The supernatant was decanted, and the absorbance was measured at 280 nm with a spectrophotometer[13]. When 20 or 25% albumin[12] solutions were analyzed, they were diluted to 5% protein before beginning the assay.

The molar absorption coefficient of *N*-acetyl-DL-tryptophan at 280 nm was determined by spectrophotometric analysis of solutions prepared from the compound dried to constant weight in a vacuum oven (maximum temperature 60°C). The dried compound was also analyzed for nitrogen by a semimicro-Kjeldahl procedure (expected 11.375%, found 11.33%). An 8-mM *N*-acetyl-DL-tryptophan stock solution was then prepared by dissolving the dried compound in 1 M NaOH and diluting with water (final concentration 0.01 M NaOH). The absorbance of this solution after further 100-fold dilution with water corresponded to a molar absorption coefficient of 5250. This figure was not altered by making the final dilution with 0.27 M perchloric acid. It agreed closely with the ϵ_{279} value of 5300 reported by McMenamy and Oncley (9).

As initially performed, the analysis involved a standard curve which was prepared by mixing 20, 40, 60, 80, or 100 μL of the 8-mM *N*-acetyl-DL-tryptophan stock solution (stable for at least 6 months when refrigerated and protected from light), 0.1 mL of 5% stabilizer-free albumin,

[2] Supelco, Bellefonte, Pa.
[3] Aldrich Chemical Co., Milwaukee, Wis.
[4] J. T. Baker Chemical Co., Phillipsburg, N.J.
[5] California Foundation for Biochemical Research, Los Angeles, Calif.
[6] New England Nuclear, Boston, Mass.
[7] Received by the Bureau of Biologics, FDA, before June, 1980.
[8] Model 5830A; Hewlett-Packard, Avondale, Pa.
[9] Model 18850A; Hewlett-Packard, Avondale, Pa.
[10] Model 7671A; Hewlett-Packard, Avondale, Pa.
[11] Evapomix; Buchler Instruments, Fort Lee, N.J.
[12] Normal serum albumin may also be prepared as a 20% protein solution (1). At present, this product is manufactured only for export.
[13] Model 250; Gilford Instrument Laboratories, Oberlin, Ohio.

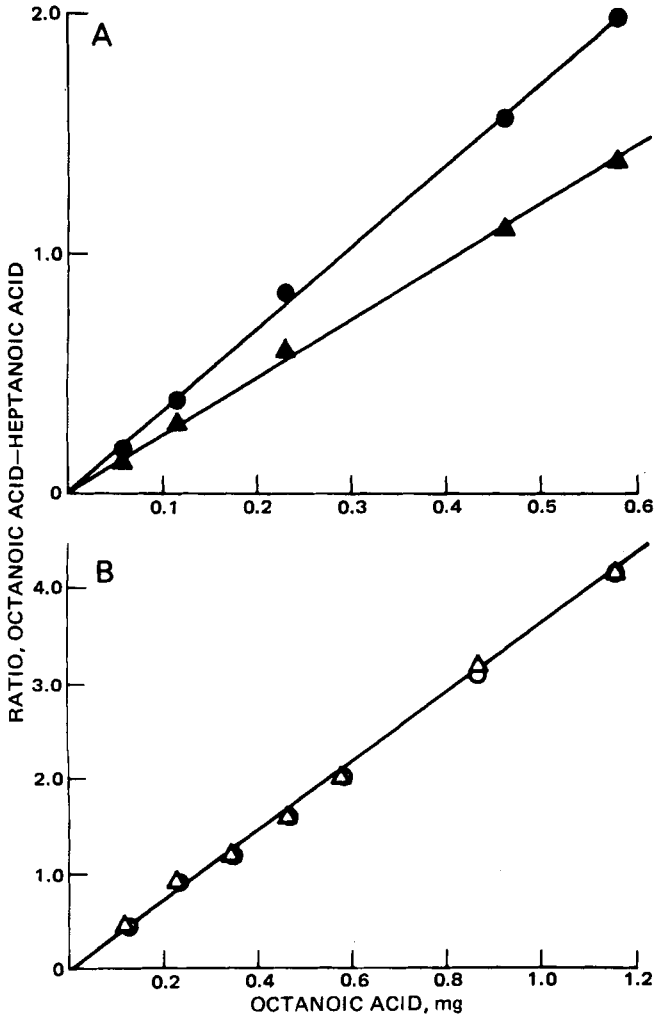

Figure 2—*Effect of experimental variants on the determination of octanoic acid. (A) Ordinate shows peak area (●) or peak height (▲) ratios; abscissa, milligrams of octanoic acid in the sample. A 1.22-m column was used. (B) Ordinate shows peak area ratios; abscissa, milligrams of octanoic acid in the sample. Portions of the same isoamyl acetate layers were chromatographed on 1.22-m (○) and 1.83-m (△) columns.*

sufficient 0.9% NaCl to bring the volume to 0.2 mL, and 1.8 mL of 0.3 M perchloric acid, and measuring the absorbance of the supernatant (after centrifugation) at 280 nm. It was found subsequently that an identical linear standard curve was obtained when 0.9% NaCl was used in place of the stabilizer-free albumin solution and, later, that the standard curve was so reproducible that the determination could be based on the molar absorption coefficient alone (see *Appendix* for calculations). Therefore, for routine analyses, no standard curve is used. When the same samples were analyzed with and without the use of a standard curve, the values for *N*-acetyl-DL-tryptophan content agreed within 2%.

RESULTS AND DISCUSSION

Octanoic Acid Analysis—*Development and Validation of the Method*—Before analysis, a 0.5-mL sample of 5% normal serum albumin was mixed with sodium [1-^{14}C]octanoate (3700 Bq). Counts obtained after acidification and extraction showed that >97% of the radioactivity was extracted into the chloroform layer. Because radiolabeled heptanoic acid was not available, recovery experiments were performed by mixing measured quantities of unlabeled heptanoic acid with stabilizer-free albumin or saline solutions and then adding a fixed amount of octanoic acid either before or after the acidification and extraction. The mean recovery of heptanoic acid was >97%. Subsequently, a series of samples were subjected to replicate analyses in which 2, 4, 6, or 8 mL of chloroform was used for the extraction step. The volume of chloroform used had no discernible effect on the value obtained for octanoic acid, indicating that any of these volumes can be used. For routine analyses, however, 4 mL of chloroform was always employed. Similarly, the 1.22- and the 1.83-m columns gave identical results over a wide range of octanoic acid concentrations (Fig. 2B). Because of the greater ease in packing, the shorter column was routinely used.

Table I—Assessment of Precision of Octanoic Acid Determination by GC [a]

Lot No.[b]	Mean ± *SD*, mM[c]	*CV*[d]
1	3.57 ± 0.15	4.2
2	3.57 ± 0.078	2.2
3	7.64 ± 0.31	4.1
4	3.50 ± 0.089	2.5
5	3.55 ± 0.073	2.1
6	20.4 ± 1.12	5.5
7	20.4 ± 0.75	3.7
8	20.0 ± 0.55	2.8
9	20.7 ± 0.98	4.7
10	20.5 ± 0.83	4.0
11	20.9 ± 0.76	3.6

[a] A 1.22-m column was used. [b] Lots 1–5 were 5% normal serum albumin from manufacturer G; lots 6–11 were 25% normal serum albumin from manufacturer N. [c] Standard deviation for five separate determinations; 0.08 mmol/g protein corresponds to concentrations of 4 mM and 20 mM in 5% and 25% protein solutions, respectively. [d] Coefficient of variation = *SD* × 100/mean.

To verify the accuracy of the analysis, the octanoic acid standard and the heptanoic acid internal standard were chromatographed individually. At the loads used in the present study, each showed only a single peak in addition to those produced by the solvent system. The octanoic acid standard solution was then titrated by the method of Marvel and Rands (24)[14]: nominal concentration 80 mM, by titration 78.7 mM. A solution of nominal concentration 80 mM was then prepared by dissolving sodium octanoate[15] in water. It was analyzed for sodium by flame photometry and for octanoic acid by the GC method described above: concentration by flame photometry 78.5 mM, by GC 79.3 mM, mean deviation 1.0%.

To assess the precision of the method, five lots of 5% normal serum albumin and six lots of 25% normal serum albumin were each subjected to five replicate analyses for octanoic acid. The coefficient of variation for replicate determinations ranged from 2.1 to 5.5% and averaged 3.9% (Table I).

Recovery was estimated by adding a series of incremental quantities of octanoic acid to replicate samples of normal serum albumin such that the largest amount approximately doubled the octanoic acid concentration. Analysis of these samples indicated that the recovery of added octanoic acid was 95.5 ± 4.2% (*SD*).

Analysis of Commercial Products—The octanoic acid concentrations of 138 lots of product were determined; of these, only six deviated >20% from the concentration given on the product label (Table II). Three of these lots were produced by manufacturer M, who used both venous plasma and placentas as source material. Preparation of albumin from placentas utilized octanoic acid in the purification procedure (25) as well as for stabilization and may account for the higher levels found in these samples. (Placentas are no longer used for the manufacture of albumin and globulin products in the United States.) One of the lots from manufacturer G had an octanoic acid concentration almost twice that of the others (Tables I and II), suggesting inadvertent repetition of stabilizer addition during manufacture. There is no obvious explanation for the low octanoic acid concentration in two lots from manufacturer K.

Comparison with Other Methods—Several methods for the determination of fatty acids involve extraction and subsequent titration in a two-phase (aqueous/nonpolar) system (24, 26, 27). Although these do not require preliminary evaporation of the solvent, the titration step does not readily lend itself to automation. Several other methods involve GC analysis after preparation of the methyl ester derivatives of the extracted fatty acids (28–30). One of these methods was specifically designed for the determination of octanoic acid and utilized sodium [1-^{14}C]octanoate as an internal standard to correct for losses during the procedure (29). The GC step in this analysis, like that described by Burnett *et al.* (30), was performed on a 1.83-m column; the packings employed were 80/100 mesh Gas-Chrom P coated with 15% diethylene glycol succinate (29) and 100/120 mesh Chromosorb W AW coated with 10% SP-2330 (30), respectively.

The method described in the present study requires neither derivatization of the octanoic acid nor the use of a radiolabeled tracer and utilizes

[14] The titration was performed as described except that 2% Triton X-100 (Rohm and Haas, Philadelphia, Pa.) was used in place of 2% Dreft.

[15] Nutritional Biochemical Corp., Cleveland, Ohio.

Table II—Octanoic Acid Concentration in Commercial Albumin Products

Manufacturer	Product[a]	No. of Lots Analyzed	Mean ± *SD*[b]	Lots >20% Beyond Labeled Value[c]
A	PPF	5	3.93 ± 0.08	0
	25%	5	19.68 ± 1.90	0
B	5%	8	3.48 ± 0.22	0
	25%	6	18.33 ± 0.72	0
C	25%	3	19.40 ± 1.04	0
D	5%	6	3.54 ± 0.12	0
	PPF	10	4.00 ± 0.24	0
	25%	5	19.44 ± 1.72	0
E	5%	6	3.98 ± 0.18	0
	PPF	6	4.09 ± 0.12	0
	25%	6	19.86 ± 2.18	0
F	25%	6	19.85 ± 1.65	0
G	5%	5	4.68 ± 2.32	1[d]
	25%	5	17.78 ± 1.19	0
H	25%	5	20.15 ± 1.92	0
I	25%	5	18.48 ± 0.73	0
J	25%	5	18.57 ± 1.04	0
K	5%	4	3.27 ± 0.35	2
	25%	5	18.56 ± 1.43	0
L	5%	5	3.74 ± 0.19	0
	25%	6	18.59 ± 1.35	0
M	5%	6	4.62 ± 0.43	2
	25%	6	22.75 ± 1.53	1
N	25%	9	20.93 ± 1.23	0

[a] PPF = plasma protein fraction (human); numbers refer to normal serum albumin (human) with the nominal protein concentration indicated. [b] Mean ± *SD* expressed as mM. [c] The labeled values for the octanoic acid concentrations of plasma protein fraction and of 5% and 25% normal serum albumin are 4, 4, and 20 mM, respectively. [d] This lot contained approximately twice the labeled value of octanoic acid; omission of this lot gave a value of 3.90 ± 0.19 (mean ± *SD*).

Table III—UV Absorbance of Acid-Soluble Fraction from Stabilizer-Free Albumin

Albumin[a]	Manufacturer	Absorbance at 280 nm
Human fraction V	K	0.048
Human fraction V	D	0.024
Human placental	I	0.025
Human fraction V	in-house	0.017
Bovine crystalline	O[b]	0.014
Human purified (from in-house)	in-house	0.014
Human purified (from normal serum albumin)	in-house	0.010

[a] Human albumin fraction V manufactured in-house was prepared from the plasma of two donors by cold ethanol fractionation (31). Purified albumins were prepared by ion exchange chromatography (32) of in-house human albumin fraction V and commercial normal serum albumin, respectively. [b] Distributed by Sigma Chemical Co., St. Louis, Mo.

a shorter (and thus more easily handled) 1.22-m column. Identical results were obtained when the 1.22- and 1.83-m columns (both packed with 80/100 mesh Chromosorb W AW coated with 10% SP-1000) were used to analyze human albumin products for octanoic acid. Moreover, a previous survey of such products involved GC on a 1.83-m column (100/120 mesh Supelcoport[2] coated with 5% diethylene glycol succinate) and yielded results similar to those presented above[16].

***N*-Acetyl-DL-tryptophan Analysis**—*Development and Validation of Method*—Several different protein precipitants, including isopropyl alcohol, trichloroacetic acid, and perchloric acid, were examined. The latter was ultimately chosen because it afforded essentially complete precipitation, consistent analytical results, and good recovery of *N*-acetyl-DL-tryptophan. No further improvement was achieved by carrying out the precipitation at 4°C; therefore, all operations in the analysis were performed at room temperature. Unlike the GC procedure, in which the retention time provides an internal identity criterion for octanoic acid, the spectrophotometric method for *N*-acetyl-DL-tryptophan includes no qualitative test. The underlying assumption is that virtually all the

[16] M. A. Gross and J. S. Finlayson, unpublished results. A preliminary sampling of 230 lots of NSA produced by 11 manufacturers and released before April 1979 indicated that 212 had octanoic acid concentrations within 20% of the labeled value.

Table IV—Assessment of Precision of *N*-Acetyl-DL-tryptophan Determination by UV Spectrophotometry[a]

Manufacturer	Product[b]	Mean ± *SD*, mM[c]	*CV*[d]
A	PPF	4.65 ± 0.046	1.0
	25%	22.8 ± 0.47	2.1
B	5%	3.65 ± 0.11	3.0
	25%	20.1 ± 0.32	1.6
C	PPF	4.06 ± 0.11	2.7
	5%	4.08 ± 0.11	2.7
	25%	19.9 ± 0.34	1.7
D	25%	20.7 ± 0.41	2.0
E	PPF	4.36 ± 0.058	1.3
	5%	4.30 ± 0.079	1.8
	25%	21.3 ± 0.40	1.9
G	5%	3.99 ± 0.076	1.9
	25%	22.9 ± 0.19	0.8
F	25%	20.7 ± 0.29	1.4
H	25%	19.0 ± 0.19	1.0
I	25%	21.0 ± 0.84	4.0
J	25%	20.0 ± 0.60	3.0
K	25%	18.1 ± 0.33	1.8
L	5%	4.12 ± 0.069	1.7
	25%	19.0 ± 0.53	2.8
M	5%	3.99 ± 0.067	1.7
J	25%	20.1 ± 0.11	0.5
N	25%	20.1 ± 0.47	2.3

[a] The standard curve procedure was used (see text). [b] PPF = plasma protein fraction; numbers refer to normal serum albumin with the nominal protein concentration indicated. [c] Mean ± *SD* for five separate determinations. [d] Coefficient of variation = *SD* × 100/mean.

Table V—*N*-Acetyl-DL-tryptophan Concentration in Commercial Albumin Products

Manufacturer	Product[a]	No. of Lots Analyzed	Mean ± *SD*[b]	Lots >20% Beyond Labeled Value[c]
A	PPF	6	4.59 ± 0.05	0
	25%	6	22.18 ± 1.13	1
B	5%	7	3.50 ± 0.10	0
	25%	5	19.00 ± 1.06	0
C	25%	3	20.37 ± 0.06	0
D	5%	6	4.05 ± 0.16	0
	PPF	7	4.06 ± 0.32	0
	25%	5	20.06 ± 1.02	0
E	5%	10	4.35 ± 0.25	0
	PPF	10	4.39 ± 0.12	0
	25%	6	20.27 ± 1.31	0
F	25%	8	19.90 ± 0.75	0
G	5%	5	4.09 ± 0.07	0
	25%	5	21.53 ± 1.25	0
H	25%	6	19.56 ± 1.44	0
I	25%	8	20.59 ± 0.77	0
J	25%	5	20.38 ± 0.70	0
K	5%	5	4.00 ± 0.20	0
	25%	5	20.18 ± 1.51	0
L	5%	5	4.21 ± 0.09	0
	25%	6	19.43 ± 0.63	0
M	5%	6	3.76 ± 0.32	0
	25%	7	17.60 ± 1.70	0
N	25%	17	19.20 ± 0.76	0

[a] PPF = plasma protein fraction (human); numbers refer to normal serum albumin (human) with the nominal protein concentration indicated. [b] Mean ± *SD* expressed mM. [c] The labeled values for *N*-acetyl-DL-tryptophan content of plasma protein fraction and of 5% and 25% normal serum albumin are 4, 4, and 20 mM, respectively.

UV absorbance of the acid-soluble fraction is due to *N*-acetyl-DL-tryptophan. To demonstrate the validity of this assumption a series of stabilizer-free albumin powders were used to prepare 5% protein solutions, which were then analyzed as described above. The absorbances found (Table III) corresponded to 0.95–4.6% of that obtained when 4 mM *N*-acetyl-DL-tryptophan[17] was treated in a similar manner, implying that at least 95–99% of the absorbance measured under the conditions of the method can be ascribed to the compound.

[17] A stabilizer/protein ratio of 0.08 mmol/g corresponds to stabilizer concentrations of 4, 16, and 20 mM in 5, 20, and 25% protein solutions, respectively.

The method precision was evaluated by performing five replicate analyses on each of 23 lots of product, including at least one lot from every manufacturer. The coefficient of variation for replicate determinations averaged 1.9% (range 0.5–4.0%) and did not differ among 5% normal serum albumin, 25% normal serum albumin, and plasma protein fraction (Table IV). Recovery was assessed by adding increments of *N*-acetyl-DL-tryptophan to replicate samples of normal serum albumin such that the largest increment more than doubled the concentration of this stabilizer. Analyses of these samples showed that the recovery of added *N*-acetyl-DL-tryptophan was 95.7 ± 2.0% (*SD*).

Analysis of Commercial Products—The *N*-acetyl-DL-tryptophan concentrations of 159 lots of product were determined. Only one of these deviated more than 20% from the value indicated on the label, and the mean concentration of most manufacturers' products was within 10% of the label value (Table V).

Applications of Octanoic Acid and *N*-Acetyl-DL-tryptophan Analyses—The procedures developed in the present study should be useful in the quality control of commercial albumin products. In addition, they may have other applications. For example, in a preliminary study, use of these methods showed that when solutions containing 4 mM *N*-acetyl-DL-tryptophan and 4 mM octanoic acid were heated for 10 h at 60°C, the concentrations of both stabilizers remained constant. This result was not altered by the presence or absence of albumin or by varying the pH between 4.9 and 8.6, indicating that within this range of conditions the stabilizers themselves are stable. In a separate investigation it was found that, as assessed by the present methods, stabilizer-free albumin monomer could be prepared by chromatography on agarose[18] columns at pH 8.0, whereas dialysis proved incapable of rendering normal serum albumin free of stabilizer[19]. Finally, because at least 96% of the protein in normal serum albumin is albumin (1), measurement of the total absorbance (280 nm) of a sample of normal serum albumin and concomitant determination of its *N*-acetyl-DL-tryptophan content may offer a rapid method for estimating the protein concentration[20].

APPENDIX: CALCULATION OF CONCENTRATIONS AND RATIOS

Octanoic Acid Concentration (mM)[17]:

(a) In 5% normal serum albumin or plasma protein fraction
= octanoic acid (mg) in 0.5-mL assay sample × 2 × 1000/mol. wt. of octanoic acid
= octanoic acid (mg) in 0.5-mL assay sample × 13.87

(b) In 20% normal serum albumin
= octanoic acid (mg) in 0.125-mL assay sample × 13.87 × 4
= octanoic acid (mg) in 0.125-mL assay sample × 55.48

(c) In 25% normal serum albumin
= octanoic acid (mg) in 0.1-mL assay sample × 13.87 × 5
= octanoic acid (mg) in 0.1-mL assay sample × 69.35

Octanoic Acid/Protein Ratio (mmol/g of protein):

In all products = octanoic acid (mg) in assay sample × 0.2774

***N*-Acetyl-DL-tryptophan Concentration (mM):**

(a) In 5% normal serum albumin or plasma protein fraction
= A_{280} of acid-soluble fraction × 2/0.1 × 5.25
= A_{280} of acid-soluble fraction × 3.81

(b) In 20% normal serum albumin
= A_{280} of acid-soluble fraction × 15.24

(c) In 25% normal serum albumin
= A_{280} of acid-soluble fraction × 19.05

***N*-Acetyl-DL-tryptophan/Protein Ratio (mmol/g of protein):**

= A_{280} of acid-soluble fraction × 0.0762

REFERENCES

(1) "Code of Federal Regulations," Title 21, Parts 640.80-640.86 and 640.90-640.96 (1982).

(2) S. S. Gellis, J. R. Neefe, J. Stokes, Jr., L. E. Strong, C. A. Janeway, and G. Scatchard, *J. Clin. Invest.*, **27**, 239 (1948).

(3) G. A. Ballou, P. D. Boyer, J. M. Luck, and F. G. Lum, *J. Biol. Chem.*, **153**, 589 (1944).

(4) G. Scatchard, L. E. Strong, W. L. Hughes, Jr., J. N. Ashworth, and A. H. Sparrow, *J. Clin. Invest.*, **24**, 671 (1945).

(5) P. D. Boyer, F. G. Lum, G. A. Ballou, J. M. Luck, and R. G. Rice, *J. Biol. Chem.*, **162**, 181 (1946).

(6) I. Y. Lee and R. H. McMenamy, *J. Biol. Chem.*, **255**, 6121 (1980).

(7) G. A. Ballou, P. D. Boyer, and J. M. Luck, *J. Biol. Chem.*, **159**, 111 (1945).

(8) J. D. Ashbrook, A. A. Spector, and J. E. Fletcher, *J. Biol. Chem.*, **247**, 7038 (1972).

(9) R. H. McMenamy and J. L. Oncley, *J. Biol. Chem.*, **233**, 1436 (1958).

(10) J. H. Hink, Jr. and F. F. Johnson, *J. Am. Pharm. Assoc. Sci. Ed.*, **40**, 517 (1951).

(11) M. E. Mackay and N. H. Martin, *Biochem. J.*, **65**, 284 (1957).

(12) O. Tangen, I. A. M. Wallenbeck, and D. Bergqvist, *Thromb. Res.*, **4**, 479 (1974).

(13) O. Tangen, I. A. M. Wallenbeck, and D. Bergqvist, *Scand. J. Clin. Lab. Invest.*, **35**, 19 (1975).

(14) S. S. Sanbar, G. Hetenyi, Jr., N. Forbath, and J. R. Evans, *Metabolism*, **14**, 1311 (1965).

(15) S. S. Sanbar, J. R. Evans, B. Lin, and G. Hetenyi, Jr., *Can. J. Physiol. Pharmacol.*, **45**, 29 (1967).

(16) F. E. Samson, Jr., N. Dahl, and D. R. Dahl, *J. Clin. Invest.*, **35**, 1291 (1956).

(17) F. J. Zieve, L. Zieve, W. M. Doizaki, and R. B. Gilsdorf, *J. Pharmacol. Exp. Ther.*, **191**, 10 (1974).

(18) J. L. Glenn and W. B. Hinshaw, *Proc. Soc. Exp. Biol. Med.*, **167**, 36 (1981).

(19) M. L. Beck, R. L. Edwards, S. R. Pierce, B. L. Hicklin, and W. L. Bayer, *Transfusion*, **16**, 434 (1976).

(20) A. A. Hossaini, A. J. Wasserman, and G. P. Vennart, *Am. J. Clin. Pathol.*, **65**, 513 (1976).

(21) J. Ring, W. Stephan, and W. Brendal, *Clin. Allergy*, **9**, 89 (1979).

(22) J. M. Luck, P. D. Boyer, and V. E. Hall, *Proc. Soc. Exp. Biol. Med.*, **62**, 177 (1946).

(23) H. J. Kupferberg, "Antiepileptic Drugs: Quantitative Analysis and Interpretation," C. E. Pippenger and J. K. Penry, Eds., Raven, New York, N.Y., 1978, pp. 147, 151.

(24) C. S. Marvel and R. D. Rands, Jr., *J. Am. Chem. Soc.*, **72**, 2642 (1950).

(25) H. L. Taylor, F. C. Bloom, K. B. McCall, and L. A. Hyndman, *J. Am. Chem. Soc.*, **78**, 1353 (1956).

(26) V. P. Dole, *J. Clin. Invest.*, **35**, 150 (1956).

(27) V. P. Dole and H. Meinertz, *J. Biol. Chem.*, **235**, 2595 (1960).

(28) L. Hagenfeldt, *Clin. Chim. Acta*, **13**, 266 (1966).

(29) J. D. McGarry and D. W. Foster, *J. Biol. Chem.*, **246**, 1149 (1971).

(30) D. A. Burnett, N. Lysenko, J. A. Manning, and R. K. Ockner, *Gastroenterology*, **77**, 241 (1979).

(31) E. J. Cohn, L. E. Strong, W. L. Hughes, Jr., D. L. Mulford, J. N. Ashworth, M. Melin, and H. L. Taylor, *J. Am. Chem. Soc.*, **68**, 459 (1946).

(32) J. S. Finlayson, R. T. Suchinsky, and A. L. Dayton, *J. Clin. Invest.*, **39**, 1837 (1960).

[18] Bio-Gel A-0.5m or A-1.5m, Bio-Rad Laboratories, Richmond, Calif.

[19] M. W. Yu, A. F. Shrake, and J. S. Finlayson, unpublished results.

[20] If the A_{280} of human albumin is 0.53, 44% of the absorbance of a solution of pure albumin containing 0.08 mmol of *N*-acetyl-DL-tryptophan/g of protein will be due to the *N*-acetyl-DL-tryptophan and 56% to the protein.

ACKNOWLEDGMENTS

The authors are grateful to Dr. H. J. Kupferberg for his generous aid and advice regarding analyses by GC, to Mr. A. V. Del Grosso for his assistance with the Hewlett-Packard instrument, to Ms. L. A. Reamer for her assistance in seeking conditions for the spectrophotometric analysis, and to Dr. M. A. Gross, who initiated this study.

Synthesis of Deuterium-Labeled Fluphenazine

H. UMESHA SHETTY, EDWARD M. HAWES ˣ, and KAMAL K. MIDHA

Received July 26, 1982, from the *College of Pharmacy, University of Saskatchewan, Saskatoon, Saskatchewan, Canada S7N OWO.* Accepted for publication December 3, 1982.

Abstract □ The propylpiperazine side chain of fluphenazine has been labeled with two, four, and six deuterium atoms by lithium aluminum deuteride reduction of the appropriate ester or imide. The γ-carbon of the propyl group was labeled with two deuterium atoms by reduction of 10- (2-methoxycarbonylethyl) -2-trifluoromethyl-10*H*-phenothiazine, while four deuterium atoms were incorporated into the piperazine ring by reduction of 10-[3-(3,5-dioxo-1-piperazinyl)propyl]-2-trifluoromethyl-10*H*-phenothiazine. The latter reduction gave the d_4-labeled *N*-deshydroxyethyl metabolite of fluphenazine.

Keyphrases □ Fluphenazine—synthesis of deuterium-labeled analogues, propylpiperazine side chain □ Synthesis—deuterium-labeled fluphenazine, propylpiperazine side chain

The quantitation of phenothiazine drugs in the plasma of patients under treatment is difficult due to low plasma concentrations, drug instability, and adsorptive losses. In the case of the piperazine-type phenothiazines, such as fluphenazine (I), the low doses used compound these

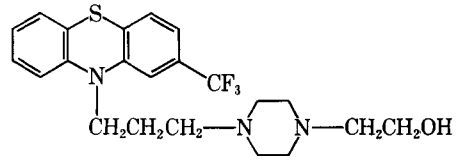

I

problems. In patients receiving normal therapeutic doses of the fatty acid ester depot formulations (fluphenazine decanoate or enanthate) intramuscularly, the plasma steady-state levels have been found to be in the low nanogram/milliliter range (1, 2) by radioimmunoassay (RIA). However, such biological methods of analysis have doubtful specificity and need to be certified by sensitive chemical methods. Thus, to verify the RIA method developed in these laboratories (3), which is capable of quantitating 0.25 ng of fluphenazine/mL of plasma using 200-μL plasma aliquots, we wanted to develop a GC–MS procedure. Such methods potentially have sensitivity comparable to RIA and, in general, can be performed using small plasma samples.

A stable isotope analogue of fluphenazine was needed as a reliable internal standard to obtain the required sensitivity of the GC–MS spectrometric procedure. Also, further stable isotopes of fluphenazine were required for administration to animals or humans by one or two routes so as to allow reliable pharmacokinetics, including absolute and relative bioavailability data, to be obtained, with the analysis of plasma concentrations by GC–MS using a selected ion monitoring technique. This would enable the definitive pharmacokinetics of fluphenazine to be determined using fewer administrations and far fewer individuals than would otherwise be possible.

This paper describes the synthesis of fluphenazine with two, four, and six deuterium atoms in the propylpiperazine side chain. This labeling site was chosen since it is generally not metabolically lost and allows variation in the number of deuterium atoms added.

RESULTS AND DISCUSSION

The syntheses of the piperazine-type phenothiazines, prochlorperazine (4) and trifluoperazine (5), labeled in the propylpiperazine side chain with two, four, and six deuterium atoms have been previously reported from these laboratories. Two deuterium atoms were incorporated in the propyl chain by reduction of a carbonyl group α to the piperazine ring. In a similar fashion we initially attempted to synthesize fluphenazine-d_2 by lithium aluminum deuteride reduction of the side-chain amide (III), obtained from the previously reported 2-trifluoromethyl-10*H*-phenothiazine-10-propionyl chloride (II) (5). Since only starting material was isolated from this reaction, and as lithium aluminum hydride is known to react with alcohol groups, it was decided to protect the alcohol group with 2-methoxyethoxymethyl (MEM) chloride. However, the protected alcohol (IV) on lithium aluminum hydride reduction gave none of the desired material, but instead 2-trifluoromethyl-10*H*-phenothiazine (V) and 10-(3-hydroxypropyl)-2-trifluoromethyl-10*H*-phenothiazine (VII*a*) (Scheme I). Similar reverse Michael reactions have been observed on attempted lithium aluminum hydride reduction of substituents in the N-10 side chain of phenothiazines: 2-chloro-10(2-cyanoethyl)-10*H*-phenothiazine yielded 2-chlorophenothiazine (6), while trace amounts of V and VII*a* were also obtained in the reduction of the intermediate 10-[3-(4-methyl-1-piperazinyl)-3-oxopropyl]-2-trifluoromethyl-10*H*-phenothiazine used in the synthesis of trifluoperazine-d_2[1].

The synthesis of fluphenazine-d_2 was successfully carried out as outlined in Scheme II (VI→VII*b*→VIII*b*→I*a*). The key reduction step used to incorporate deuterium, involving the conversion of 10-(2-methoxy-

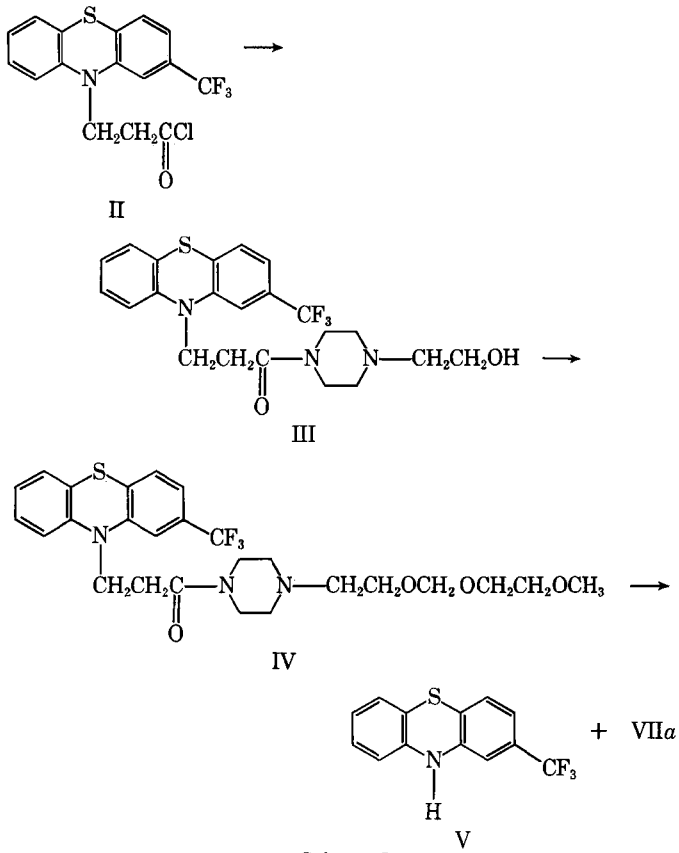

Scheme I

[1] H. U. Shetty, E. M. Hawes, and K. K. Midha, unpublished observations, subsequent to the publication of Ref. 5.

0022-3549/84/0100-0087$01.00/0
© 1984, American Pharmaceutical Association

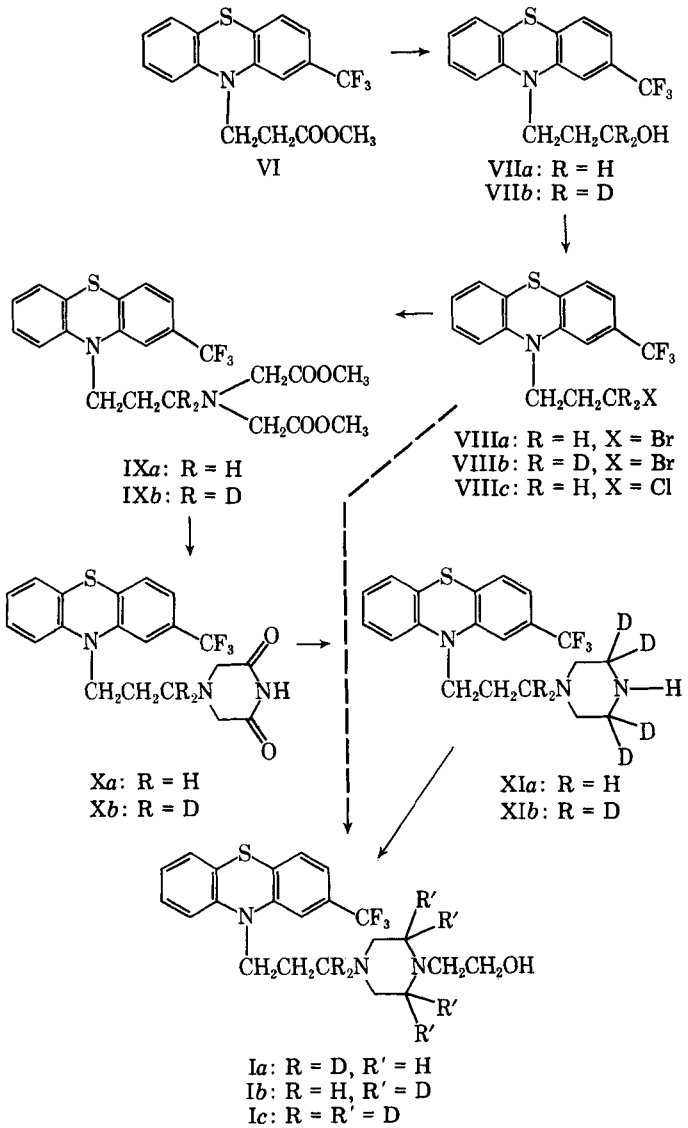

Scheme II—Synthesis of fluphenazine-d_2, -d_4, *and* -d_6.

carbonylethyl)-2-trifluoromethyl-10*H*-phenothiazine (VI) (7) to 2-trifluoromethyl-10*H*-phenothiazine-10-propanol (VII*a*) with lithium aluminum hydride has not been previously reported, although another route to this alcohol product is referred to in the patent literature (8). The final two steps, subsequent to the incorporation of deuterium, proceeded smoothly with the involvement of the newly reported bromopropyl compound (VIII*a*), synthesized by bromination of the alcohol with triphenylphosphine and *N*-bromosuccinimide (9), rather than the chloropropyl analogue (VIII*c*) invariably used in phenothiazine syntheses of this type.

For the previously reported syntheses of the d_4-labeled methylpiperazine-type phenothiazines, prochlorperazine (4) and trifluoperazine (5), the key intermediate involved was 1-methyl[3,3,5,5-$^2H_4$]piperazine, synthesized by lithium aluminum deuteride reduction of 1-methyl-3,5-piperazinedione. To synthesize labeled 2-hydroxyethylpiperazine-substituted phenothiazines in a similar fashion, suitable previously reported diketopiperazines appeared to be 1-(2-hydroxyethyl)-3,5-piperazinedione (XII) (10) and 1-(2-hydroxyethyl)-2,3-piperazinedione (XIII) (11). The former was obtained as a crude oil, which failed to distill under high vacuum, despite the report to the contrary (10); all subsequent attempts at purification failed to yield a sample of XII in a state suitable

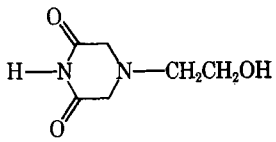

XII

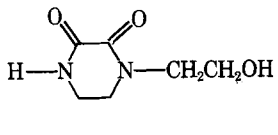

XIII

for the eventual synthesis of deuterium-labeled material for use as an internal standard and/or human administration. The 2,3-dione (XIII) was obtained in a pure form, but subsequent lithium aluminum hydride reduction gave none of the desired 1-(2-hydroxyethyl)piperazine even though none of the starting material (XIII) was recovered on GC of the reaction residue. This is hardly surprising in view of the report that under similar reaction conditions, the parent compound (piperazine-2,3-dione) was reduced quantitatively with ring opening to 1,2-diaminoethane (12).

The route utilized to synthesize fluphenazine-d_4 (Scheme II: VIII*c*→IX*a*→X*a*→XI*a*→I*b*) involves a novel route to piperazine-type phenothiazines. The piperazine ring was built stepwise onto the propyl side chain by amination of 10-(3-chloropropyl)-2-trifluoromethyl-10*H*-phenothiazine (VIII*c*) (13) with methyl iminodiacetate, followed by alkaline hydrolysis and subsequent urea fusion. The imide (X*a*) so formed was subsequently reduced with lithium aluminum deuteride to afford the labeled *N*-desalkyl metabolite of fluphenazine and trifluoperazine (XI*a*). Finally, alkylation gave greater yields with 2-bromoethanol than using ethylene oxide as reagent, to afford the desired fluphenazine-d_4 (I*b*). For each of the six steps involved in this synthesis, including the initial alkylation of 2-trifluoromethylphenothiazine with 1-bromo-3-chloropropane, yields were at least 70%. The synthesis of fluphenazine-d_6 was carried out in a similar fashion (VIII*b*→IX*b*→X*b*→XI*b*→I*c*) starting with the 10-(3-bromopropyl)-2-trifluoromethyl-10*H*-phenothiazine-d_2 (VIII*b*) discussed above.

The isotopic purity of the labeled purified products was determined by electron-impact mass spectrometry. The ratio for the molecular ions $^2H_0/^2H_n$ was determined to be 8.11, 3.49, and 0.01%, for the di-(n = 2) (I*a*), tetra-(n = 4) (I*b*), and hexa-(n = 6) (I*c*) deuterated fluphenazine, respectively. This purity of fluphenazine-d_6 is sufficient for its use as a reliable internal standard in GC–MS analyses and pharmacokinetic studies. However, in the case of fluphenazine-d_2 and -d_4 appropriate contribution from isotopes will be required, which can be easily carried out by the use of computerized data systems. These studies will be reported elsewhere.

EXPERIMENTAL[2]

10- [3-(4-Hydroxyethyl-1-piperazinyl)-3-oxopropyl] -2-trifluoromethyl-10*H*-phenothiazine (III)—To a solution of 2-hydroxyethylpiperazine (0.325 g, 2.5 mmol) in 10 mL of dry acetone, cooled to −50°C in a dry-ice bath, was added dropwise over 30 min a solution of 2-trifluoromethyl-10*H*-phenothiazine-10-propionyl chloride (II) (5) (0.715 g, 2.0 mmol) in 10 mL of dry acetone. The reaction mixture was stirred for 1 h, during which time the mixture was allowed to attain room temperature. The residue left after evaporation of the solvent was dissolved in methanol (10 mL), triturated with 1 M NaOH (10 mL), and the resulting suspension was heated on a water bath. The methanol was evaporated off and the resultant mixture was extracted with chloroform (3 × 20 mL). The chloroform extracts were combined, dried over magnesium sulfate, and evaporated under reduced pressure to afford a pale yellow liquid, which solidified on standing. Recrystallization from benzene–hexane resulted in 0.76 g (84%) of fine white needles, mp 111–112°C; ^{1}H-NMR ($CDCl_3$): δ 2.02–2.88 (m, 10, piperazine methylene and CH_2-piperazine), 3.00–3.85 (m, 5, CH_2CO and CH_2OH), 4.22 (t, 2, J = 7 Hz, CH_2-phenothiazine), and 6.6–7.4 ppm (m, 7, aromatic); MS: m/z 451 ($M^{+\cdot}$, 100%), 420(48), 320(24), 280(52), 266(30), 248(20), and 127(10).

Anal.—Calc. for $C_{22}H_{24}F_3N_3O_2S$: C, 58.52; H, 5.36; N, 9.31. Found: C, 58.75; H, 5.31; N, 9.27.

10-[3-(4-Methoxyethoxymethoxyethyl-1-piperazinyl)-3-oxopropyl]-2-trifluoromethyl-10*H*-phenothiazine (IV)—A mixture of III (0.451 g, 1 mmol), β-methoxyethoxymethyl chloride (0.249 g, 2 mmol), and triethylamine (0.202 g, 2 mmol) in dry acetonitrile (5 mL) was heated at reflux for 12 h. The solvent was removed, and the residue was partitioned between ether and water. The ether layer was washed with saturated brine solution and dried over anhydrous magnesium sulfate. Re-

[2] Melting points were determined with a Gallenkamp melting point apparatus and are uncorrected. All TLC were performed using Eastman Chromatogram Sheets, type 13254 (silica gel with fluorescent indicator); spots were observed under shortwave UV light. NMR spectra were determined on a Varian T-60 instrument with tetramethylsilane as internal reference. Low-resolution electron-impact mass spectra were routinely recorded on a VG Micromass MM16F instrument at 70 eV equipped with a VG 2025 data system. Microanalyses for samples dried over phosphorus pentoxide at 60°C under reduced pressure were performed by Mr. R. E. Teed, Department of Chemistry and Chemical Engineering, University of Saskatchewan. Lithium aluminum deuteride (>99% deuterium) was obtained from Merck Sharp and Dohme, Dorval, Quebec, and all other chemicals from Aldrich Chemical Co., Montreal, Quebec.

moval of the ether afforded an oil, which was passed through an alumina column (ether). Evaporation of the ether gave 0.51 g (95%) of the desired product as a colorless oil; ^{1}H-NMR ($CDCl_3$): δ 2.22–3.00 (m, 10, piperazine methylene and CH_2-piperazine), 3.20–3.87 (m, 13, CH_2CO and CH_2O-$CH_2OCH_2CH_2OCH_3$), 4.31 (t, 2, J = 7 Hz, CH_2-phenothiazine), and 6.7–7.4 ppm (m, 7, aromatic); MS: m/z 539 ($M^{+\cdot}$, 66%), 464(12), 420(100), 407(15), 320(37), 280(62), 266(38), 246(28), 127(35), and 99(24).

Anal.—Calc. for $C_{26}H_{32}F_3N_3O_4S$: C, 57.86; H, 5.97; N, 7.78. Found: C, 57.57; H, 5.97; N, 7.66.

Reduction of IV with Lithium Aluminum Hydride—To a suspension of lithium aluminum hydride (0.019 g, 0.5 mmol) in dry tetrahydrofuran (2 mL) was added dropwise a solution of IV (0.270 g, 0.5 mmol) in dry tetrahydrofuran (2 mL). After heating at reflux for 3 h with stirring, moist ether (10 mL) and water (0.5 mL) were successively added dropwise with stirring to the cooled reaction mixture. The precipitated inorganic material was filtered off, washed with ether, and the combined ether extracts were dried over anhydrous magnesium sulfate. Evaporation of the ether afforded a residue which on TLC (benzene–ethyl acetate 9:1) showed two spots corresponding to authentic samples of 2-trifluoromethyl-10*H*-phenothiazine (V) (R_f 0.81) and 10-(3-hydroxypropyl)-2-trifluoromethyl-10*H*-phenothiazine (VII*a*) (R_f 0.46). These authentic samples (V and VII*a*) gave identical GC retention times and electron-impact MS as the only two significant peaks resulting from GC–MS of the crude reaction mixture.

10-(3-Hydroxypropyl)-2-trifluoromethyl-10*H*-phenothiazine (VII*a*)—A solution of 1.765 g (5 mmol) of 10-(2-methoxycarbonylethyl)-2-trifluoromethyl-10*H*-phenothiazine (VI), bp 162–164°C/0.04 mm Hg [lit. (7) bp 172–175°C/55 μ] prepared as previously reported (7), in 10 mL of dry ether was added dropwise over 30 min to a magnetically stirred suspension under dry nitrogen of lithium aluminum hydride (0.190 g, 5 mmol) in 10 mL of dry ether at 0°C. After stirring for an additional hour at room temperature, the reaction mixture was heated at reflux for 30 min. Moist ether (10 mL) and 10% HCl (10 mL) were then successively added dropwise with stirring to the reaction mixture maintained at 0°C. The ether layer was separated, and the aqueous layer was washed with 10 mL of ether. The combined ether layers were dried (magnesium sulfate), evaporated, and the oily residue was passed through a neutral alumina column (ether). Evaporation of the solvent gave 1.531 g (94%) of a pale yellow oil which solidified on standing. An analytical sample was obtained by recrystallization from benzene–hexane, as pale yellow scales, mp 61–62°C; ^{1}H-NMR ($CDCl_3$): δ 1.62–2.30 (m, 3, propyl central methylene and OH), 3.76 (t, 2, J = 6 Hz, CH_2O), 4.06 (t, 2, J = 7 Hz, CH_2-phenothiazine), and 6.78–7.48 ppm (m, 7, aromatic); MS: m/z 325 ($M^{+\cdot}$, 82%), 280(61), 266(100), and 248(24).

Anal.—Calc. for $C_{16}H_{14}F_3NOS$: C, 59.06; H, 4.34; N, 4.31. Found: C, 58.88; H, 4.34; N, 4.32.

10-(3-Hydroxy[3,3-$^2H_2$]propyl)-2-trifluoromethyl-10*H*-phenothiazine (VII*b*)—This compound was prepared (95% yield) by the lithium aluminum deuteride reduction of VI using the method described for VII*a*, mp 60–61°C and not depressed when mixed with VII*a*; ^{1}H-NMR ($CDCl_3$): δ 1.72 (s, 1, OH), 2.02 (t, 2, J = 7 Hz, CH_2CD_2), 4.04 (t, 2, J = 7 Hz, CH_2-phenothiazine), and 6.65–7.42 ppm (m, 7, aromatic); MS: m/z 327 ($M^{+\cdot}$, 85%), 280(68), 266(100), and 248(25).

10-(3-Bromopropyl)-2-trifluoromethyl-10*H*-phenothiazine (VIII*a*)—To a stirred solution of 0.651 g (2 mmol) of VII*a* and 0.787 g (3 mmol) of triphenylphosphine in 5 mL of dry acetonitrile was added dropwise over 15 min a solution of 0.534 g (3 mmol) of *N*-bromosuccinimide in 5 mL of dry acetonitrile. The mixture was then stirred at room temperature for 1 h, the solvent was removed under reduced pressure, and the residue was partitioned between benzene and water. The organic phase was washed several times with water and dried over anhydrous magnesium sulfate. The residue left after removal of the solvent was digested with hexane (20 mL), cooled, and the precipitated triphenylphosphine oxide was removed by filtration and washed with *n*-hexane. The filtrate was passed through an alumina column, and on removal of solvent, the product was obtained as a white amorphous solid. Recrystallization from methanol afforded 0.670 g (86%) of white needles, mp 70–71°C; ^{1}H-NMR ($CDCl_3$): δ 2.32 (q, 2, J = 6 Hz, propyl central methylene), 3.56 (t, 2, J = 6 Hz, CH_2Br), 4.17 (t, 2, J = 7 Hz, CH_2-phenothiazine), and 6.78–7.47 ppm (m, 7, aromatic); MS: m/z 389 ($M^{+\cdot}$, 38%), 387(38), 280(83), 266(100), and 248(45).

Anal.—Calc. for $C_{16}H_{13}BrF_3N_3S$: C, 49.49; H, 3.37; N, 3.61. Found: C, 49.72; H, 3.34; N, 3.61.

10-(3-Bromo[3,3-$^2H_2$]propyl)-2-trifluoromethyl-10*H*-phenothiazine (VIII*b*)—This compound was prepared (90% yield) from VII*b* by the method described for VIII*a*, mp as for VIII*a*; ^{1}H-NMR ($CDCl_3$): δ 2.27 (t, 2, J = 7 Hz, CH_2CD_2), 4.10 (t, 2, J = 7 Hz, CH_2-phenothiazine), and 6.70–7.38 ppm (m, 7, aromatic); MS: m/z 391 ($M^{+\cdot}$, 73%), 389(73), 280(94), 266(100), and 248(32).

10-[[3-[4-(2-Hydroxyethyl)-1-piperazinyl]-[3,3-$^2H_2$]propyl]]-2-trifluoromethyl-10*H*-phenothiazine Dihydrochloride (I*a*)—A mixture of VIII*b* (0.781 g, 2 mmol) and 2-hydroxyethylpiperazine (0.521 g, 4 mmol) in methyl ethyl ketone was heated at reflux for 4 h. The solvent was removed under reduced pressure, and the residue was stirred with 10% HCl (20 mL). The acidic solution was washed with ether (3 × 10 mL), and the combined ether wash was extracted with 10% HCl (5 mL). The combined acid fractions were basified with sodium carbonate and extracted with ether (4 × 10 mL). The ether extracts were combined, washed with water, dried over anhydrous sodium sulfate, filtered, and evaporated to dryness *in vacuo*. The resulting pale yellow oil was dissolved in dry ether (10 mL), treated with ethereal HCl, and the solid which separated was recrystallized from absolute ethanol to afford 0.975 g (95%) of fluphenazine-d_2 dihydrochloride (I*a*), mp 235–237°C [lit. (8) unlabeled mp 235–237°C]. Mixed melting points with authentic nondeuterated samples (I), obtained commercially[3] or synthetically by amination of VIII*a*, were not depressed; TLC: R_f (acetone–ammonia, 100:1) 0.63; ^{1}H-NMR (free base, $CDCl_3$): δ 1.91 (t, 2, J = 7 Hz, CH_2CD_2), 2.28–2.87 (m, 10, piperazine methylene and CH_2-piperazine), 3.36 (s, 1, OH), 3.60 (t, 2, J = 5 Hz, CH_2O), 3.95 (t, 2, J = 7 Hz, CH_2-phenothiazine), and 6.69–7.46 ppm (m, 7, aromatic); MS: m/z 439 ($M^{+\cdot}$, 24%), 408(27), 280(100), 266(21), 248(20), 173(10), 145(39), 115(28), 100(21), 98(14), and 72(34).

10-[3-(*N*,*N*-Dimethoxycarbonylmethyl)aminopropyl]-2-trifluoromethyl-10*H*-phenothiazine (IX*a*)—A mixture of 6.87 g (20 mmol) of 10-(3-chloropropyl)-2-trifluoromethyl-10*H*-phenothiazine (VIII*c*), mp 69–70°C [lit. (14) mp 70–71°C] prepared in 70% yield by adaptation of the procedure used for the 2-chlorophenothiazine analogue (13), 8.058 g (50 mmol) of iminodiacetic acid dimethyl ester (15), and 3.0 g (20 mmol) of sodium iodide was heated at reflux in 50 mL of methyl ethyl ketone for 24 h. The solvent was evaporated to leave an oily residue, which was dissolved in 15% HCl. The acid was washed with ether (2 × 20 mL) and then neutralized with sodium carbonate. The oil that separated was extracted into ether (3 × 30 mL), and the combined ether extracts were washed with water (2 × 10 mL), dried over anhydrous magnesium sulfate, and evaporated to leave an oily residue. Vacuum distillation gave 6.8 g (73%) of the desired product as a viscous yellow oil, bp 208–210°/0.5 mmHg; ^{1}H-NMR ($CDCl_3$): δ 1.88 (q, 2, J = 6 Hz, propyl central methylene), 2.82 (t, 2, J = 6 Hz, CH_2-side chain N), 3.45 (s, 4, CH_2CO), 3.6 (s, 6, OCH_3), 3.99 (t, 2, J = 7 Hz, CH_2-phenothiazine), and 6.6–7.38 ppm (m, 7, aromatic); MS: m/z 468 ($M^{+\cdot}$, 12%), 307(13), 266(18), 248(23), 174(30), and 116(100).

Anal.—Calc. for $C_{22}H_{23}F_3N_2O_4S$: C, 56.39; H, 4.94; N, 5.98. Found: C, 56.29; H, 5.06; N, 5.98.

10-[3-(*N*,*N*-Dimethoxycarbonylmethyl)amino[3,3-$^2H_2$]propyl]-2-trifluoromethyl-10*H*-phenothiazine (IX*b*)—This was prepared (93% yield) from VIII*b* by the method decribed for IX*a*. The product was purified by silica gel chromatography (ether); ^{1}H-NMR ($CDCl_3$): δ 1.84 (t, 2, J = 7 Hz, CH_2CD_2), 3.46 (s, 4, CH_2CO), 3.61 (s, 6, OCH_3), 4.0 (t, 2, J = 7 Hz, CH_2-phenothiazine), and 6.61–7.34 ppm (m, 7, aromatic); MS: m/z 470 ($M^{+\cdot}$, 20%), 307(13), 266(18), 248(14), 176(14), and 118(100).

10-[3-(3,5-Dioxo-1-piperazinyl)propyl]-2-trifluoromethyl-10*H*-phenothiazine (X*a*)—Ester IX*a* (4.685 g, 10 mmol) was hydrolyzed by treatment with aqueous methanol (50 mL of methanol and 50 mL of water) containing sodium hydroxide (1.60 g, 40 mmol), heated under reflux on a steam bath for 1 h. The cooled solution was diluted with water (50 mL), and the pH was adjusted to 3.0. The precipitated product was filtered, washed with water, and dried to afford 4.14 g (94%) of the acid intermediate, mp 128–129°C. The finely powdered acid (4.4 g, 10 mmol) and urea (0.66 g, 11 mmol) were mixed, heated to 175°C on an oil bath, and held at this temperature for 2 h with stirring. The mixture was cooled, and the solidified product was dissolved in boiling ethanol, treated with activated charcoal, and filtered. On cooling 3.0 g (71%) of the desired product (X*a*) crystallized as pale yellow needles, mp 151–152°C; ^{1}H-NMR (DMSO-d_6): δ 1.84 (q, 2, J = 7 Hz, propyl central methylene), 3.28 (s, 6, piperazinedione methylene and CH_2-piperazinedione), 3.98 (t, 2, J = 7 Hz, CH_2-phenothiazine), 6.65–7.40 (m, 7, aromatic), and 10.9 ppm (s, 1, NH); MS: m/z 421 ($M^{+\cdot}$, 100%), 306(23), 280(39), 266(78), 248(42), 155(46), 127(63), 99(18), 83(25), and 71(42).

Anal.—Calc. for $C_{20}H_{18}F_3N_3O_2S$: C, 57.00; H, 4.30; N, 9.97. Found: C, 57.16; H, 4.37; N. 9.88.

10-[3-(3,5-Dioxo-1-piperazinyl)[3,3-$^2H_2$]propyl]-2-trifluoromethyl-10*H*-phenothiazine (X*b*)—This was prepared (68% yield) from

[3] A gift from Squibb Canada Inc., Montreal, Quebec.

ester IX*b* by the method described for X*a*, mp as for X*a*; ^{1}H-NMR (DMSO-d_6): δ 1.80 (t, 2, J = 7 Hz, CH_2CD_2), 3.24 (s, 4, piperazinedione methylene), 3.98 (t, 2, J = 7 Hz, CH_2-phenothiazine), 6.78–7.48 (m, 7, aromatic), and 10.9 ppm (s, 1, NH); MS: *m/z* 423 ($M^{+\cdot}$, 100%), 308(24), 280(46), 266(82), 248(46), 157(80), 129(69), 101(22), 85(25), and 73(26).

10-[[3-(1-[3,3,5,5-$^2H_4$]Piperazinyl)propyl]]-2-trifluoromethyl-10*H*-phenothiazine Dimaleate (XI*a*)—A solution of 1.264 g (3 mmol) of X*a* in 10 mL of dry tetrahydrofuran was added dropwise over 30 min to a stirred suspension of 0.504 g (12 mmol) of lithium aluminum deuteride in 10 mL of dry tetrahydrofuran at 0°C under nitrogen. After 2 h under reflux, 10 mL of moist ether and 2 mL of water were successively slowly added dropwise with stirring at 0°C. The precipitated inorganic material was filtered off and extracted with ether in a Soxhlet apparatus. The combined ether solution was dried over anhydrous sodium sulfate, filtered, and evaporated to dryness. The yellow oily residue was dissolved in acetone (10 mL) and treated with maleic acid (0.812 g, 7 mmol) in acetone (5 mL). The dimaleate salt was filtered and recrystallized from ethanol to afford 1.4 g (74%) of XI*a*, mp 152–154°C. Mixed melting points with the authentic nondeuterated samples, obtained by the same route with lithium aluminum hydride or from a commercial source[4], were not depressed; TLC: R_f (benzene–methanol, 8:2) 0.5; ^{1}H-NMR (free base, $CDCl_3$): δ 1.40 (s, 1, NH), 1.91 (q, 2, J = 7 Hz, propyl central methylene), 2.35 (m, 6, CH_2-piperazine and piperazine-2,6-methylene), 3.95 (t, 2, J = 7 Hz, CH_2-phenothiazine), and 6.62–7.4 ppm (m, 7, aromatic); MS: *m/z* 397 ($M^{+\cdot}$, 25%), 266(10), 248(10), 131(22), 103(84), 72(14), and 58(100).

10-[[3-(1-[3,3,5,5-$^2H_4$]Piperazinyl)[3,3-$^2H_2$]propyl]]-2-trifluoromethyl-10*H*-phenothiazine Dimaleate (XI*b*)—*N*-Deshydroxyethylfluphenazine-d_6 (XI*b*) was prepared (73% yield) by the lithium aluminum deuteride reduction of X*b* using the method described above for XI*a*, mp and TLC as for XI*a*; ^{1}H-NMR (free base, $CDCl_3$): δ 1.48 (s, 1, NH), 1.92 (t, 2, J = 7 Hz, propyl CH_2CD_2), 2.35 (s, 4, piperazine-2,6-methylene), 3.95 (t, 2, J = 7 Hz, CH_2-phenothiazine), and 6.67–7.34 ppm (m, 7, aromatic); MS: *m/z* 399 ($M^{+\cdot}$, 23%), 266(10), 248(11), 133(25), 105(75), 74(16), and 60(100).

10-[[3-[4-(2-Hydroxyethyl)-1-[3,3,5,5-$^2H_4$]piperazinyl]propyl]]-2-trifluoromethyl-10*H*-phenothiazine Dihydrochloride (I*b*)—A mixture of XI*a* (0.397 g of free base, 1 mmol), 2-bromoethanol (0.125 g, 1 mmol) and potassium carbonate (0.138 g, 1 mmol) in dry methyl ethyl ketone (10 mL) was refluxed under dry nitrogen for 10 h. The solvent was removed under reduced pressure, and the residue was stirred with ether (10 mL). The ether layer was washed with water (2 × 5 mL) and dried over anhydrous sodium sulfate. The dried extract was then added to a short column of alumina, which was eluted with ether. The oily residue left after removal of the ether was dissolved in 2 mL of dry ether and treated with ethereal HCl. The precipitated dihydrochloride salt was recrystallized from absolute ethanol–ether to afford 0.365 g (71%) of fluphenazine-d_4 dihydrochloride (I*b*) as fine white needles, mp 232–234°C. A mixed melting point with an authentic[3] nondeuterated sample was not depressed; TLC: as for I*a*; ^{1}H-NMR (free base, $CDCl_3$): δ 1.88 (q, 2, J = 7 Hz, propyl central methylene), 2.20–2.83 (m, 9, propyl CH_2-piperazine, piperazine-2,6-methylene, ethyl CH_2-piperazine, and OH), 3.53 (t, 2, J = 5 Hz, CH_2O), 3.90 (t, 2, J = 7 Hz, CH_2-phenothiazine), and 6.68–7.35 ppm (m, 7, aromatic); MS: *m/z* 441 ($M^{+\cdot}$, 17%), 410(18), 280(100), 266(14), 248(18), 161(13), 147(31), 117(22), 103(11), 102(10), and 72(25).

10-[[3-[4-(2-Hydroxyethyl)-1-[3,3,5,5-$^2H_4$]piperazinyl]-[3,3-$^2H_2$]propyl]]-2-trifluoromethyl-10*H*-phenothiazine Dihydrochloride (I*c*)—Fluphenazine-d_6 (I*c*) was prepared (74% yield) from XI*b* by the method described above for I*b*; mp and TLC as for I*b*; ^{1}H-NMR (free base, $CDCl_3$): δ 1.86 (t, 2, J = 7 Hz, propyl CH_2CD_2), 2.11–2.70 (m 6, piperazine-2,6-methylene and CH_2-piperazine), 3.53 (t, 2, J = 5 Hz, CH_2O), 3.90 (t, 2, J = 7 Hz, CH_2-phenothiazine), and 6.64–7.28 ppm (m, 7, aromatic); MS: *m/z* 443 ($M^{+\cdot}$, 27%), 412(28), 280(100), 266(25), 248(21), 163(16), 149(43), 119(30), 104(13), 103(13), 102(17), and 74(37).

[4] A gift from Smith, Kline and French Laboratories, Philadelphia, Pa.

REFERENCES

(1) D. H. Wiles and M. G. Gelder, *Br. J. Clin Pharmacol.*, **8**, 565 (1979).

(2) D. H. Wiles, M. Franklin, S. J. Dencker, R. Johansson, L. Lundin, and U. Malm, *Psychopharmacology (Berlin)*, **71**, 131 (1980).

(3) K. K. Midha, J. K. Cooper, and J. W. Hubbard, *Commun. Psychopharmacol.*, **4**, 107 (1980).

(4) E. M. Hawes, T. S. Gurnsey, H. U. Shetty, and K. K. Midha, *J. Pharm. Sci.*, **72**, 702 (1983).

(5) H. U. Shetty, E. M. Hawes, and K. K. Midha, *J. Labelled Comp. Radiopharm.*, **18**, 1633 (1981).

(6) J. C. Craig, L. D. Gruenke, and S.-Y.C. Lee, *J. Labelled Comp. Radiopharm.*, **15**, 31 (1978).

(7) P. N. Craig and J. J. Lafferty, U.S. pat. 2,919,271 (1959); through *Chem. Abstr.*, **54**, 6764 (1960).

(8) H. L. Yale, F. A. Sowinski, and J. Bernstein, U.S. pat. 3,227,708 (1966); through *Chem. Abstr.*, **64**, 9744f (1966).

(9) A. K. Bose and B. Lal, *Tetrahedron Lett.*, **1973**, 3937.

(10) *Belgian pat.* 624,686 (1962); through *Chem. Abstr.*, **59**, 10082 (1963).

(11) E. F. Cluff and H. F. McShane, Jr., *J. Org. Chem.*, **25**, 2059 (1960).

(12) A. T. Nielsen, *J. Heterocycl. Chem.*, **13**, 101 (1976).

(13) S. V. Zhuravlev, A. N. Gritsenko, and Z. I. Ermakova, *J. Gen. Chem. USSR*, **32**, 1889 (1962).

(14) H. L. Yale and F. Sowinski, *J. Am. Chem. Soc.*, **82**, 2039 (1960).

(15) L. L. Wood and R. A. Hamilton, U.S. pat. 3,607,910 (1971); through *Chem. Abstr.*, **75**, 129358a (1971).

ACKNOWLEDGMENTS

The authors gratefully acknowledge the Medical Research Council of Canada (grant MA-6767) for financial support for this research, Mr. K. Hall for the mass spectra, Mr. T. S. Gurnsey for technical assistance, and Mr. G. Grant for drafting.

Study of Intravenous Hyperalimentation: Effect of Selected Amino Acids on the Stability of *Intravenous* Fat Emulsions

AKIRA TAKAMURA *x, **FUMIYOSHI ISHII** *, **SHUN'ICHI NORO** *, **MASAAKI TANIFUJI** ‡, and **SHINOBU NAKAJIMA** ‡

Received August 2, 1982, from the *Meiji College of Pharmacy, 1-22-1, Yato-cho, Tanashi-shi, Tokyo, Japan and ‡Daigo Nutritive Chemicals, Ltd., 12-44, Nonakakita, 2-chome, Yodogawa-ku, Osaka, Japan. Accepted for publication November 22, 1982.

Abstract □ In an attempt to resolve the conflicts relevant to intravenous fat emulsion compatibility two amino acids, L-valine and L-histidine monohydrochloride monohydrate, were chosen as intravenous additives, and these substances were investigated as to whether they could induce significant changes in the physicochemical properties of an intravenous soybean oil emulsion. The stability of the fat emulsion was evaluated in terms of gross visual observation, particle size distribution, surface tension, pH, and the zeta potential. It was found that (*a*) no significant difference was produced on the particle size distribution up to 7 d after admixing, (*b*) the mean diameter of oil globules was ~0.21–0.24 μm, and (*c*) the fat emulsion was sufficiently stable, with a zeta potential ranging between −30 and −60 mV. The relationship of the isoelectric point (pI) of the amino acids and the pH of the buffer solutions was determined to be one of the most important factors in the stability of the fat emulsion.

Keyphrases □ Fat emulsions—stability, effect of L-valine and L-histidine monohydrochloride monohydrate additions, buffers □ Stability—long-term, fat emulsions admixed with L-valine and L-histidine monohydrochloride monohydrate and buffers □ Amino acids—L-valine, L-histidine monohydrochloride monohydrate, effect on fat emulsions, long-term stability of admixtures

Intravenous hyperalimentation has been developed for patients who cannot take food orally following surgery (1). Total parenteral nutrition regimens (2) by the intravenous route are important clinically for many renally impaired and/or burn patients.

Admixtures of fat emulsions with dextrose (3), amino acids (4), and electrolytes (5) are prepared and used for patients as needed. However, it is difficult and complex (6) to mix the fat emulsion with other additives at the time of use. Furthermore, it is necessary to use a large volume of the fat emulsion, (7) as it is continuously administered to the patients intravenously over a long period. If the long-term stability and safety of fat emulsion–parenteral additive mixtures can be corroborated, a more suitable product would result.

The evaluation of emulsion stability using a stepwise progression of procedures was reported by Ho and Higuchi (8). Frank (9) studied the stability of intravenous soybean oil emulsions by gross visual and microscopic examinations. Black and Popovich (10) investigated the effects of such common intravenous additives as physiological electrolytes, amino acid solutions, and/or dextrose on the particle size distribution of the emulsion. These studies, however, failed to characterize the long-term emulsion stability in the presence of the various additives.

In this study, two amino acids were chosen as intravenous additives and were investigated to determine whether or not additives could induce significant changes in the physicochemical properties of an intravenous soybean oil emulsion. The stability of the fat emulsion was evaluated in terms of gross visual observation (11), particle size and distribution of oil droplets measured with a scanning electron microscope (12) and an electronic counter (13), surface tension (14), pH (15), and the zeta potential at the oil–water interface (16). In addition, the effect of the isoelectric point (pI) (17) of the two amino acids and the pH of the buffer solution on emulsion stability were investigated. The study was instituted in an attempt to resolve the conflicts relevant to intravenous fat emulsion compatibility.

EXPERIMENTAL

Preparation of Intravenous Fat Emulsions—The fat emulsion was composed of 100 g of soybean oil (oil phase), 12 g of egg phospholipid (18) (emulsifier), and 25 g of glycerol (to adjust the pH to isotonic) in sufficient distilled water to make 1000 mL. The fatty acid composition of the egg phosphotidyl choline was palmitic acid (28.6%), palmitoleic acid (3.5%), stearic acid (10.6%), oleic acid (37.2%), linoleic acid (11.6%), polyvalent unsaturated fatty acids (6.8%), and other acids (1.7%).

The emulsifier was dissolved in the oil phase, kept at 80°C in a tank, and water preheated to 80°C was added to the solution. The emulsions prepared always contained 10% (w/v) of the oil phase. The agitator used was a mixer[1]; the temperature of the mixture was maintained at 80°C for 30 min after starting agitation in the tank. The impeller speed was kept at 11,200 rpm. The resulting coarse emulsion was quickly introduced into the homogenizer[2] (19) from the mixer and was vigorously stirred again at 4500 psi. Figure 1 illustrates the change of the mean diameter of the oil droplets with shear applications for the emulsions prepared, as measured with an electronic counter[3] (13). The number of shear applications had a large influence on the mean diameter of oil droplets in the emulsion: after eight shear applications, the mean diameter was reduced to ~0.20 μm. The homogenized emulsion was introduced into a glass vessel and was sterilized by heating in a free flame at 121°C for 30 min.

Admixture of the Amino Acids with the Fat Emulsion—In a previous experiment (20), 11 amino acids were selected as intravenous fat emulsion additives. The fat emulsion was admixed with equal parts of a 1% (w/v) amino acid solution. Each of the emulsion combinations was stored at 70°C for 24 h. The height of the separated oil phase appearing in the upper part of emulsion was observed visually at a constant time interval. Table I gives the height of the separated oil phase after admixing with 1% (w/v) amino acid solution. Significant changes in the separated oil phase were found for both the 12- and 24-h readings when L-histidine monohydrochloride monohydrate was admixed with the fat emulsion.

In the present experiments, L-histidine monohydrochloride monohydrate and L-valine were selected as the amino acid additives, because L-histidine monohydrochloride monohydrate has a high isoelectric point (7.64) and L-valine has a low value (5.96). Each amino acid was diluted with each of three solutions, acetate buffer (pH 4.0), phosphate buffer (pH 7.0), and borate buffer (pH 9.0). The amino acid concentration was kept at a constant value of 1% (w/v). The intravenous soybean oil emulsion was admixed with an equal volume of 1% (w/v) amino acid solution, and the mixture was stored at 20°C for 14 d. Fat emulsion admixed with an equal volume of distilled water was used as the control.

Evaluation of Emulsion Stability—The emulsion stability was

[1] Type IM; Tokushukika Co., Ltd., Osaka, Japan.
[2] Type 15M-8TA; Gaulin Co., Ltd., Mass.
[3] Coulter nanosizer; Coulter Electronics Inc., Hialeah, Fla.

0022-3549/84/0100-0091$01.00/0
© 1984, American Pharmaceutical Association

Table I—Height of the Separated Oil Phase of the Fat Emulsion after Adding the Amino Acid Solution[a]

Amino Acid	Height of Oil Phase, %[b] 10 h	12 h	24 h
L-Arginine monohydrochloride	—	—	+
Glycine	—	—	—
L-Histidine monohydrochloride monohydrate	0.67	2.00	2.67
L-Isoleucine	—	—	—
L-Leucine	—	—	—
L-Lysine monohydrochloride	—	—	—
L-Methionine	—	—	—
L-Phenylalanine	—	—	—
L-Threonine	—	—	—
L-Tryptophan	—	—	—
L-Valine	—	—	—

[a] Concentration of amino acid, 1% (w/v); temperature, 70°C; amino acid solution–fat emulsion, 1:1 (v/v). [b] – stable; + unstable.

evaluated by gross visual observation of creaming, particle size distribution, surface tension, pH, and/or zeta potential measurement. These methods have already proven useful in previous work (21). All bottles of the intravenous soybean oil emulsion were refrigerated at 4°C until used.

Gross visual analysis was used to observe separation and creaming of the emulsion after admixing. This analysis utilized five 50-mL glass tubes to display each of the emulsion combinations over the 14-d period. Assessment at predetermined times was qualitative.

The particle size distribution of the emulsions was determined with a scanning electron microscope. A specific fixation technique of the emulsions with malachite green was developed by modifying a previous method (22). Briefly, pieces of filter paper[4] were immersed in the emulsion and rapidly removed. The oil droplets adsorbed on the filter paper were fixed by immersion for 24 h at 4°C in 1% (w/v) glutaraldehyde–malachite green in a buffer solution (NaH_2PO_4–$NaHPO_4$, pH 7.4). After fixation the oil droplets were briefly washed with the buffer solution and allowed to react for 8 h with cold 1% (w/v) osmium tetroxide buffered with phosphate. All samples were subsequently dehydrated in a graded series of ethyl alcohol–water solutions. After critical point drying with liquid carbon dioxide, the fixed oil droplets were mounted on a sample stage with double-sided adhesive tape, vacuum coated with gold, and viewed in the scanning electron microscope[5]. An electronic counter was also used for the determination of the mean diameter of the soybean oil emulsion. The sizing data obtained with the electronic counter were confirmed to be in agreement with those obtained by electron microscopic techniques within an error of 5%.

The surface tensions of the fat emulsions were measured with a Dü-Nouy tensiometer[6]. The hydrogen ion concentration of the sample emulsions was determined using a pH meter[7]. The mean electrophoretic mobility of the oil droplets was obtained with a laser system[8] which measures the average particle mobility in an emulsion; the zeta potential was calculated with these data. All measurements were performed at a thermostatically controlled temperature of 20 ± 0.1°C.

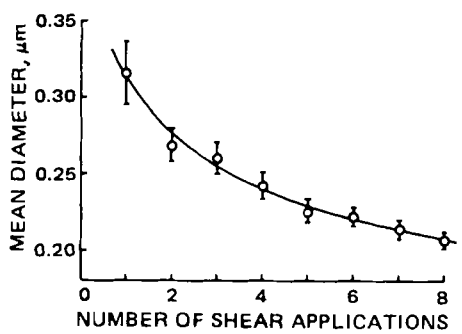

Figure 1—*Changes in the mean diameter of oil droplets in the fat emulsion by application of shear via an homogenizer, as measured by an electronic counter.*

[4] Type 2: Whatman Ltd., England.
[5] Model JSM-T200; JEOL Ltd., Tokyo, Japan.
[6] Shimadzu Seisakusyo Co., Kyoto, Japan.
[7] Model PT-5D; Toyo Kagaku Sangyo Co., Tokyo, Japan.
[8] Laser Zee, model 500; Pen Kem Inc., New York.

Table II—Flocculation Depth of the Fat Emulsion Stored at 20°C After Adding Various Solutions[a]

Solution	Acetate Buffer[b] pH 4.0	Phosphate Buffer[b] pH 7.0	Borate Buffer[b] pH 9.0
1% (v/v) L-Valine	+	+	—
1% (v/v) L-Histidine monohydrochloride monohydrate	1.9	1.5	—
Reference	—	2.9	0.5

[a] Stored temperature, 20°C; data taken 14 days after admixing; adding solution–fat emulsion, 1:1 (v/v). [b] – stable; + large oil droplets appeared on the fat emulsion.

RESULTS

Evaluation of Emulsion Stability in Terms of Separation and Creaming—Table II gives the heights of the separated fat emulsions stored at 20 ± 0.1°C after adding various solutions. In the case where the fat emulsion was admixed with equal parts of phosphate (pH 7.0) or borate (pH 9.0) buffer, separated oil phase was generated in the upper part of fat emulsion. When the fat emulsion was admixed with the borate buffer solution containing 1% (w/v) L-valine, no significant change was detected in the emulsion up to 14 d. However, some large oil droplets appeared on the surface of the fat emulsion when diluted with either acetate or phosphate buffer containing 1% (w/v) L-valine. On the other hand, the emulsion stability remained unchanged when the fat emulsion was diluted with the borate solution containing 1% (w/v) L-histidine monohydrochloride monohydrate. Accordingly, the fat emulsion would be comparatively stable if the admixed solution containing 1% (w/v) amino acid is diluted beforehand with basic buffer solution.

Evaluation of Emulsion Stability by the Particle Size Distribution—Figure 2 shows electron micrographs of oil droplets immediately and 7 d after adding the 1% (w/v) amino acid solutions to the fat emulsions. The amino acid was dissolved in distilled water, and the volume fraction of the fat emulsion to the amino acid solution was 1:1. The electron microscope characterized the fat emulsion as a dispersion of oil globules whose sizes were mostly distributed in a narrow range <1.0 μm.

Particle size distribution curves calculated using the micrographs in Fig. 2 are shown in Fig. 3. For the three samples, the distribution curves and peak heights were similar. A sharp size distribution with a peak at ~0.13 μm was observed. The mean diameter and standard deviation of oil globules were 0.23 μm and 0.11, respectively. The mean diameters as measured by the electronic counter are listed in Table III. No significant difference in the size distribution curves were found between those obtained by the electron microscope and the electronic counter.

Although particle size distributions were not significantly different from each other immediately and 7 d after admixing, a slight change reflected a diminished number of smaller globules (<0.1 μm) relative to the number of large globules (>0.3 μm). This pattern of net globule growth was due to coalescence and is indicative of emulsion instability.

Evaluation of Emulsion Stability in Terms of Surface Tension—Figure 4 shows the changes of surface tension of the fat emulsions with storage time after admixing with 1% (w/v) amino acid solutions. In the case of L-valine, the surface tensions of the fat emulsions diluted with acetate and phosphate buffer solutions decreased markedly at the early

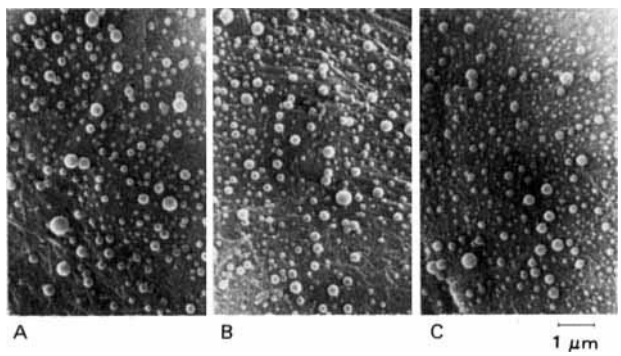

Figure 2—*Scanning electron micrographs of particles in the fat emulsion. The mixture was diluted with distilled water; the amino acid solution–fat emulsion ratio was 1:1 (v/v). Key: (A) L-valine; (B) reference solution; (C) L-histidine monohydrochloride monohydrate.*

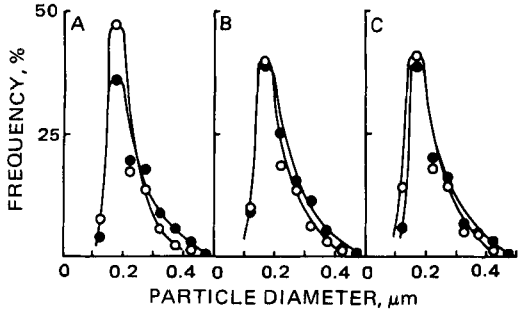

Figure 3—*Particle size distribution in the fat emulsion immediately (○) and 7 d (●) after adding a 1% (w/v) solution of amino acid in distilled water. The amino acid–fat emulsion ratio was 1:1 (v/v); the prepared final fat emulsion was stored at 20°C. Key: (A) L-valine; (B) reference solution; (C) L-histidine monohydrochloride monohydrate.*

stage of storage, and then leveled off after 4 d. However, the surface tension of the fat emulsion in borate buffer solution decreased slowly with increase in storage time.

In the case of L-histidine monohydrochloride monohydrate, the surface tension of the fat emulsion diluted with acetate buffer solution lowered suddenly to 33 dyn/cm after admixing. However, the surface tension of the fat emulsion containing L-histidine monohydrochloride monohydrate had the same tendency to decrease in both phosphate and borate buffer solutions.

A decrease of surface tension of an emulsion may be interpreted as showing that a certain number of large oil globules appear and move to the surface layer of the emulsion. Accordingly, the fat emulsions would be comparatively stable if the admixed solution containing 1% (w/v) amino acid is previously diluted with the basic buffer solution.

Evaluation of Emulsion Stability in Terms of pH—The effects of adding 1% (w/v) amino acid solutions on the pH of the fat emulsions are shown in Fig. 5. Addition of a 1% (w/v) solution of L-valine or L-histidine monohydrochloride monohydrate did not appreciably alter the pH of the fat emulsion in any of the buffer solutions. However, amino acid solutions immediately altered the pH of the fat emulsion when distilled water was used instead of the buffer solution. Thus, one should avoid the use of distilled water alone as a diluent when a fat emulsion is admixed with solutions of L-valine or L-histidine monohydrochloride monohydrate.

Evaluation of Emulsion Stability in Terms of Zeta Potential—Zeta potential is a controlling parameter in determining the stability of an emulsion. Figure 6 shows the change with time of the zeta potential of oil droplets in the fat emulsion containing 1% (w/v) amino acid. At the initial stage of admixing, the zeta potential ranged between −30 and −60 mV. Thus, the fat emulsion is likely to be sufficiently stable even though the amino acid is admixed because the strong electrostatic repulsion prevents two oil droplets from coalescing.

The zeta potential readings revealed that the addition of the amino acid solution altered the zeta potential of oil droplets within 1 d. However, after this initial change, the zeta potential remained constant throughout the 14-d observation period. This indicates that the amino acids changed the electrical properties of the oil–water interface very quickly at the early stage of admixing, and the zeta potential of the interface later shifted slightly as the storage time was increased.

DISCUSSION

When the fat emulsion admixed with 1% (w/v) L-histidine monohydrochloride monohydrate was stored at 70°C over a 24-h period, there was a significant change in the height of the separated oil phase. However,

Table III—Mean Diameter of Droplets in the Fat Emulsion [a]

Solution	Mean Diameter, μm: Scanning Electron Microscope, Day 0	Scanning Electron Microscope, Day 7	Electronic Counter, Day 0	Electronic Counter, Day 7
L-Valine	0.213	0.242	0.215	0.238
L-Histidine monohydrochloride monohydrate	0.211	0.230	0.213	0.235
Reference	0.214	0.227	0.212	0.224

[a] Mixture was diluted with distilled water; amino acid solution–fat emulsion, 1:1 (v/v); fat emulsion was stored at 20°C.

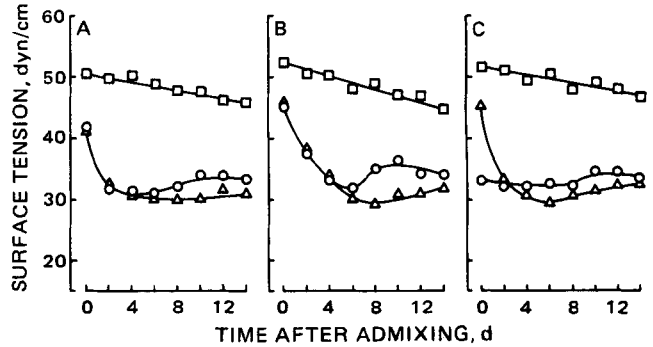

Figure 4—*Effect of adding 1% (w/v) solutions of L-valine (A), the reference (B), and L-histidine monohydrochloride monohydrate (C) on the surface tension of the fat emulsion. The amino acid solution–fat emulsion ratio was 1:1 (v/v); the prepared final fat emulsion was stored at 20°C. Key: (□) borate buffer, pH 9.0; (△) phosphate buffer, pH 7.0; (○) acetate buffer, pH 4.0.*

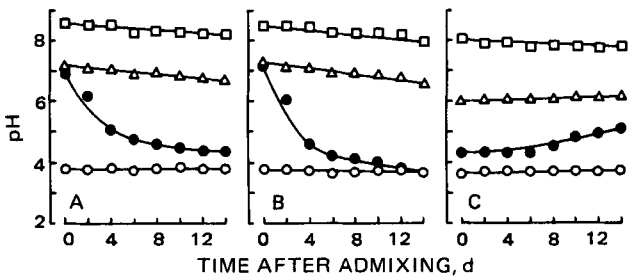

Figure 5—*Effect of adding 1% (w/v) solutions of L-valine (A), the reference (B), and L-histidine monohydrochloride monohydrate (C) on the pH of the fat emulsion. The amino acid solution–fat emulsion ratio was 1:1 (v/v); the prepared final fat emulsion was stored at 20°C. Key: (□) borate buffer, pH 9.0; (△) phosphate buffer, pH 7.0; (○) acetate buffer, pH 4.0; (●) distilled water.*

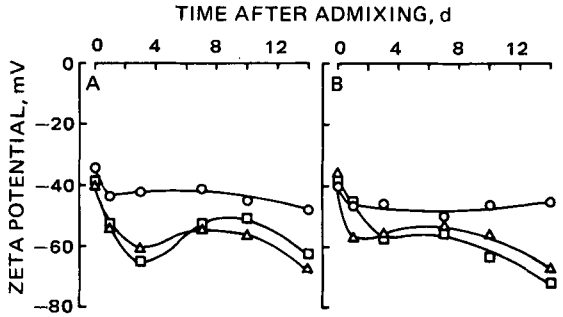

Figure 6—*Change with time of the zeta potential of oil droplets in the fat emulsion containing 1% (w/v) L-valine (A) or L-histidine monohydrochloride monohydrate (B). The amino acid solution–fat emulsion ratio was 1:1 (v/v); the prepared final fat emulsion was stored at 20°C. Key: (□) borate buffer, pH 9.0; (△) phosphate buffer, pH 7.0; (○) acetate buffer, pH 4.0.*

if the fat emulsion was stored at 20°C, the separated oil phase appeared gradually ~10 d after admixing. Hence, the rate of separation of the oil phase in the fat emulsion was considered to be very slow if the fat emulsion was stored at room temperature after being mixed with the 1% (w/v) amino acid solution.

The particle size distribution of the fat emulsion containing 1% (w/v) amino acid shifted only slightly to a larger size after a 7-d period. Accordingly, one may assume that coalescence or creaming of oil droplets rarely occurs in the fat emulsion.

The surface tension of the fat emulsion admixed with 1% (w/v) amino acid solution decreased markedly at the early stage of storage. Hence, it was considered that a certain number of large oil globules appeared and were concentrated in the surface layer of the fat emulsion.

No significant pH change was found when the fat emulsion was diluted with buffer solution instead of distilled water. Thus, buffered amino acid solutions only slightly affected the pH of the fat emulsion.

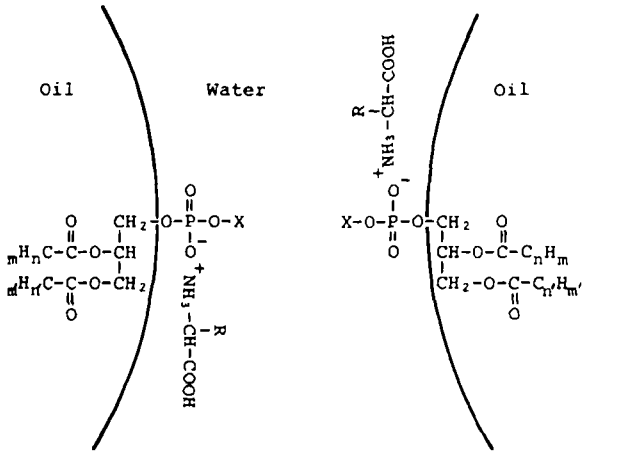

Figure 7—*Schematic representation of electrolytic dissociation of phospholipid and amino acid molecules adsorbed at the oil–water interface in acidic solution.*

At the initial stage of storage after admixing with 1% (w/v) amino acid solution, the absolute value of the zeta potential of the fat emulsion increased, and this increase was more frequently observed with the basic buffer solution than with the acidic buffer solutions. Therefore, it may be considered that amino acid in a basic buffer solution produced a strong electrostatic repulsion force at the surface of the oil droplets. These evaluations of emulsion stability concluded that the fat emulsion may be sufficiently stable even 14 d after adding 1% (w/v) amino acid if stored at 4°C.

Amino acids in aqueous solution exist generally as dipolar ions:

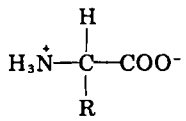

As the isoelectric point of L-valine is 5.96, it exists in acetate buffer solution (CH_3COOH–CH_3COONa, pH 4.0) as a positively charged ion. That is, L-valine as a positively charged ion in pH 4.0 buffer solution is adsorbed on the negatively charged oil droplet surface. As shown in Fig. 7, the charge will be neutralized. On the other hand, when hydroxyl ions are added to the amino acid solution, dissociation of the carboxyl group of the amino acid will take place.

L-Valine exists in pH 7.0 and pH 9.0 buffered solutions as a negatively charged ion. Accordingly, negatively charged oil droplets and amino acid molecules (L-valine molecules) will repel each other in the above buffer solutions. Figure 8 shows a schematic representation of electrolytic dissociation of phospholipid and amino acid molecules adsorbed at the oil–water interface in basic solution. In this state, oil droplets in the fat emulsion are electrically stabilized.

The dissociation of L-histidine monohydrochloride monohydrate in acidic or basic solution is illustrated in Scheme I.

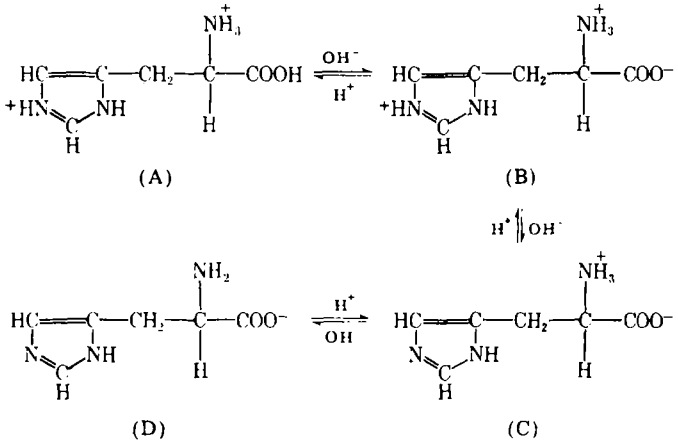

Scheme I

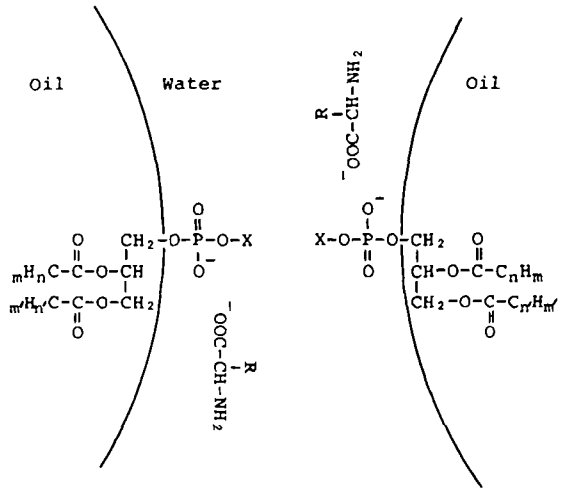

Figure 8—*Schematic representation of electrolytic dissociation of phospholipid and amino acid molecules adsorbed at the oil–water interface in basic solution.*

Since the pK_a value of the imidazole nitrogen is lower than that of the ammonium group, a proton on the imidazole nitrogen in weakly basic solution is removed; when hydroxyl ions are added, a proton on the ammonium group is removed. L-Histidine monohydrochloride monohydrate in pH 9.0 buffer solution is in the form of anion since the isoelectric point (pI) of L-histidine monohydrochloride monohydrate is 7.59. That is, negatively charged oil droplets and L-histidine monohydrochloride monohydrate molecules repel each other in this buffer solution. Thus, the fat emulsion is considered to be stable in basic solution. Accordingly, it will be necessary to take into account the effects of the isoelectric point of the amino acid and the hydrogen ion concentration of buffer solutions on the emulsion stability of intravenous fat emulsions.

REFERENCES

(1) S. J. Dudric, D. W. Wilmore, H. M. Vars, and J. E. Rhoads, *Surgery*, **64**, 134 (1968).

(2) J. Askanazi, Y. A. Carpentier, and D. H. Elwyn, *Ann. Surg.*, **191**, 40 (1980).

(3) B. S. R. Murty, J. N. Kappoor, and F. X. Smith, *Am. J. Hosp. Pharm.*, **34**, 205 (1977).

(4) G. P. Ellis, *Adv. Carbohydr. Chem.*, **14**, 63 (1959).

(5) D. H. Schuets and J. C. King, *Am. J. Hosp. Pharm.*, **35**, 33 (1978).

(6) H. H. LeVeen and G. P. Johnson, *Am. J. Clin. Nutr.*, **18**, 129 (1965).

(7) H. H. LeVeen and G. P. Johnson, *Arch. Surg.*, **83**, 311 (1961).

(8) N. F. H. Ho and W. I. Higuchi, *J. Pharm. Sci.*, **56**, 248 (1967).

(9) J. T. Frank, *Drug Intell. Clin. Pharm.*, **7**, 351 (1973).

(10) C. D. Black and N. G. Popovich, *Drug Intell. Clin. Pharm.*, **15**, 184 (1981).

(11) M. Temple, *Rec. Trav. Chim.*, **72**, 442 (1953).

(12) T. F. Anderson, *Trans. N.Y. Acad. Sci., Ser. II*, **13**, 130 (1951).

(13) S. Noro, A. Takamura, M. Miwa, S. Nakajima, and M. Kitauchi, *Bull. Meiji Coll. Pharm.*, **11**, 5 (1981).

(14) H. Toida, T. Ishizaka, and M. Koishi, *Cosmet. Toiletries*, **93**, 32 (1978).

(15) W. H. Dawes and M. J. Groves, *Int. J. Pharm.*, **1**, 141 (1978).

(16) M. Temple, *Rec. Trav. Chim.*, **72**, 419 (1953).

(17) Y. Kumano, S. Nakamura, S. Tahara, and S. Ohta, *J. Soc. Cosmet. Chem.*, **28**, 285 (1977).

(18) H. J. Zeringue, M. L. Brown, and W. S. Singleton, *J. Am. Oil Chem.*, **41**, 688 (1964).

(19) S. Noro, A. Takamura, and T. Minowa, *Chem. Pharm. Bull.*, **28**, 696 (1980).

(20) S. Noro, A. Takamura, F. Ishii, K. Fujioka, S. Nakajima, and M. Kitauchi, *Yakuzaigaku*, **42**, 17 (1982).

(21) S. Noro, A. Takamura, and M. Koishi, *Chem. Pharm. Bull.*, **27**, 309 (1979).

(22) G. Zografi and S. S. Tam, *J. Pharm. Sci.*, **65**, 1145 (1976).

Lumen Perfusion of the Human Rectum *In Situ*: A Method to Study Mechanisms for Rectal Drug Transport in Humans

W. M. BOTTGER ˣ, A. J. M. SCHOONEN, J. VISSER, and D. K. F. MEIJER

Received September 25, 1981, from the *Department of Pharmacology and Pharmacotherapeutics, Subfaculty of Pharmacy, State University of Groningen, 9713 AW Groningen, The Netherlands.* Accepted for publication November 12, 1982.

Abstract □ A lumen perfusion system was developed to study rectal transport mechanisms in humans. With this technique it is possible to perfuse a well-defined area of the rectum wall under single-pass and recirculation conditions. Sodium benzoate was used as a test drug. After absorption, sodium benzoate is conjugated with glycine to give hippuric acid which is rapidly eliminated ($t_{1/2}$ = 0.5 h). Due to the short half-life it is possible to reach a steady-state concentration within 2.5 h of perfusion. Plasma concentrations of hippuric acid were determined by HPLC. The absorption influx of sodium benzoate per unit area (Φ_{in}) could be calculated using the steady-state concentration of hippuric acid during rectal perfusion, the separately measured total body clearance after intravenous injection, and a designated absorption surface of the rectum. It was shown that with this technique reproducible Φ_{in} values within one subject could be obtained. Four volunteers were perfused with four different solutions of sodium benzoate, and it was found that Φ_{in} was proportional to the four concentrations used. In the case of recirculation perfusion (two volunteers), it was found that the amount of the perfusate lost equalled the amount absorbed into the general circulation. Therefore, the possibility of major drug accumulation in the rectal lumen or mucosa could be excluded. The perfusion technique elaborated in the present study can be used to investigate the mechanism of rectal absorption in humans as well as the factors that may influence this process.

Keyphrases □ Perfusion—lumen of the rectum, *in situ* technique in humans, sodium benzoate □ Drug transport, rectal—lumen perfusion, *in situ* technique in humans, sodium benzoate □ Sodium benzoate—*in situ* lumen perfusion of the rectum, humans

Drug absorption from the rectum is assumed to occur by mechanisms similar to those operating in other parts of the GI tract (1). Numerous studies have been done on drug absorption mechanisms *in vitro* as well as *in vivo*. Probably the most important mechanism of absorption is passive diffusion (2–5), but other mechanisms like convective, active, and ion-paired transport cannot be excluded (6, 7). Results from *in vitro* or *in vivo* rectal absorption studies in rats or rabbits are not always in agreement with the results from rectal absorption studies in humans (1, 8). Apart from anatomical species differences, an important factor in this respect may be the rectal formulations used, *e.g.*, suppositories and enemas.

Moolenaar and Schoonen (9) have investigated the rectal administration of various drugs with attention to the influence of physicochemical properties of drugs on the release from dosage forms *in vitro* and the absorption process *in vivo*. From these studies it was concluded that factors which markedly influence the delivery *in vitro* (*e.g.*, composition of suppository bases) have relatively little influence on the absorption *in vivo*. It was also shown that in case of poorly water-soluble drugs, the rectal absorption rate is determined by the release surface of the dosage form rather than the concentration of the drug. Finally, employing liquefied dosage forms they found a varying influence of pH of the administered solution on absorption rate.

When introducing a suppository or a rectal enema, however, neither the covered surface in the rectum nor changing conditions at the absorption site (*i.e.*, the rectal lumen) can be defined. Therefore, it was necessary to develop a technique that enabled these kinds of measurements. Devroede and Phillips (10) studied rectal absorption rates by perfusing a limited part of the rectal lumen, which involved separating the rectal lumen from the lumen of the colon by means of a distendable balloon fixed to the end of the perfusion apparatus. Bechaard (11) used an open perfusion technique with inner and outer tubes at a fixed distance from each other, and then instilled the perfusion solution until an equilibrium in the rate of inflow and outflow was reached and at this time measured the absorption. The rate and extent of absorption was determined either by the disappearance of the substance from the perfusion medium (10) or the appearance of the substance in the systemic circulation (11). A major problem encountered in these experiments was that a significant loss of perfusate through the colon could not be excluded, and therefore, the rectal absorption *per se* could not be accurately measured.

Other studies on rectal absorption in the human have been done with a dialyzing tube attached to a solid catheter, which was installed for 1 h in the rectum (12, 13). The initial and final drug concentrations of the rectally applied solution were measured to ascertain the amount absorbed. Although with these methods it was, in principle, possible to study rectal absorption as a function of the concentration in the perfusate, the technique did not allow quantitative measurement of the absorption process in a well-defined part of the rectum.

Therefore, a human rectal perfusion apparatus was developed enabling perfusion of a well-defined area of the rectal mucosa under single-pass and recirculation conditions. In the case of single-pass experiments, the apparatus delivers a solution with a constant rate creating a constant concentration of the substance under study within the lumen of the rectum. The absorption process can be measured as an influx per unit area of the rectal wall. In the case of the recirculation experiments, concentration in the perfusion fluid decreases. Since the total circulating volume can be estimated, the amount eliminated from the perfusate can be determined and compared with the total amount absorbed by the rectal wall.

Sodium benozate was used as the test drug because of its low toxicity, good water solubility (1:1.8), and convenient pharmacokinetic properties. It has been shown that after rectal administration, absorption of sodium benzoate is fast and complete (14). Benzoic acid is very rapidly conjugated with glycine in the liver to give hippuric acid.

0022-3549/84/0100-0095$01.00/0
© 1984, American Pharmaceutical Association

Table I—Recovery of Hippuric Acid from Human Plasma

Concentration Added, μg/mL	Concentration Determined[a], μg/mL	CV, %	Recovery, %
0.75	0.74 ± 0.10	13.5	98.7
1.50	1.39 ± 0.17	12.2	92.6
3.00	2.99 ± 0.33	11.0	99.6
6.00	6.01 ± 0.30	5.0	100.2
12.00	11.76 ± 0.46	3.9	98.0
18.00	17.68 ± 0.77	4.4	98.2
24.00	23.62 ± 0.85	3.6	98.4

[a] Mean ± *SD*, $n = 7$.

Hippuric acid is excreted in urine almost quantitatively with a biological half-life of ~30 min. It was also shown that benzoic acid absorption can be estimated by measuring plasma concentrations of hippuric acid, provided that the benzoic acid level does not exceed ~0.4 mg/mL (15). When this concentration is exceeded, the hepatic glycine pool may become exhausted and, in addition to hippuric acid, unchanged benzoic acid will accumulate in the plasma. In the present study benzoic acid levels in plasma remained below detectable amounts.

EXPERIMENTAL

Solution Preparation—The perfusion solutions employed contained 116, 155, 232, and 310 mmol of sodium benzoate[1], respectively. A sodium benzoate solution of 155 mmol is isotonic with blood plasma. The other solutions were not corrected for osmolarity to exclude possible effects of additives.

A 0.02 M buffer solution (pH 7.2) was prepared by dissolving 5.024 g of disodium hydrogen phosphate 12-hydrate[2] and 0.824 g of sodium dihydrogen phosphate 1-hydrate[3] in 1000 mL of distilled water. An internal standard solution was prepared by dissolving 0.50 g of 4-methoxyphenylacetic acid[4] in 1000 mL of methanol[5]. A standard solution of benzoic acid was prepared by dissolving 0.177 g of sodium benzoate in 100 mL of distilled water. A standard solution of hippuric acid was prepared by dissolving 0.168 g of sodium hippurate[6] in 100 mL of distilled water.

Chromatographic Conditions—A high-performance liquid chromatograph[7] was equipped with an automated sampling injector[8] and a spectrophotometric variable-wavelength detector set at 254 nm. Samples were analyzed on a 4.6-mm × 25-cm reverse-phase column[9] fitted with a 2.1-mm × 10-cm precolumn[10]. The mobile phase was a solvent system of methanol in 0.02 M Na_2HPO_4/NaH_2PO_4 buffer (15:18, pH 7.2), and the flow rate was 2 mL/min at a pressure of 1700 psi.

Assay of Plasma Samples—To 1.0 mL of plasma in a 10-mL glass-stoppered tube, 3.0 mL of the internal standard solution was added. After shaking for some minutes, the tube was centrifuged for 5 min at 4000 rpm, and 25 μL of the supernatant liquid was injected into the HPLC. The retention times were 3.0, 3.8, and 5.5 min for benzoic, hippuric, and 4-methoxyphenylacetic acids, respectively.

The ratio of the peak height of the sample component to that of the internal standard was used to calculate concentrations of benzoic acid and hippuric acid, based on calibration curves prepared from spiked plasma samples (Table I). With 1.0-mL plasma samples this method is accurate to concentrations as low as 1.5 μg/mL for benzoic acid and 0.75 μg/mL for hippuric acid. The recovery from plasma was determined for seven different concentrations of hippuric acid and was found to be essentially complete.

Kinetic Studies—Because of the short half-life of benzoic acid it was possible to reach a steady-state blood concentration within the perfusion period of 2.5 h. At steady-state concentration (C_{ss}) the amount of hippuric acid eliminated per unit of time should be equal to the amount absorbed. Since the perfused surface of the rectum can be estimated with the method described, it was possible to calculate the absorption rate per unit area (Φ_{in}) as follows:

$$\Phi_{in} = \frac{C_{ss} \times CL}{\text{Area}} \times 0.68\ \mu\text{g of benzoic acid/min} \cdot \text{cm}^2 \quad \text{(Eq. 1)}$$

in which the factor 0.68 accounts for the molar ratio of benzoic acid to hippuric acid, C_{ss} is the mean steady-state plasma concentration calculated from the last four data points of the plasma curve (μg/mL), *CL* is the total body plasma clearance (mL/min), and the perfused rectal area is calculated from the length and the volume of the filled dialysis membrane (cm^2).

The total body clearance of hippuric acid was determined for each volunteer participating in the perfusion experiments. Sodium hippurate (660 mg in 10 mL of distilled water) was injected in the cubiti medialis vein. Blood samples (8.0 mL) were taken from the other arm 1, 2, 3, 4, 5, 6, 8, 10, 12, 15, 20, 25, 30, 40, 50, 60, 75, 90, 105, 120, and 150 min postinjection. The blood samples were heparinized and centrifuged. The plasma thus obtained was immediately frozen until analyzed.

From the hippuric acid plasma disappearance curve, the pharmacokinetic parameters were calculated by a nonlinear curve-fitting program (16). Control experiments, in which hippuric acid clearance was determined several times within a few months, showed a good reproducibility with variations not deviating more than 5% from the mean value. To investigate whether the total body clearance of hippuric acid was dose dependent, a lower dose (250 mg of sodium hippurate in 10 mL of distilled water) was administered in addition to the high dose to three volunteers.

Perfusion Technique and Procedure—The apparatus consisted of an outer tube with a funnel-shaped end and an inner tube ending in a sphere with holes. Both tubes could be adjusted with respect to each other, so that the distance between sphere and funnel could be changed from 1 to 12 cm. A dialysis bag[11] (diameter 2.9 cm) was tightened over the funnel and sphere (Fig. 1).

The perfusion solution, warmed in a water bath to 37°C, was pumped by a peristaltic pump[12] through the outer tube into the dialysis bag and drained away through the holes of the inner tube (Fig. 2). In the case of single-pass studies, the perfusate was collected *via* an overflow vessel and a calibrated tube with a tap. By closing the tap, the flow rate of the effluent fluid can be estimated and compared with the infusion rate (10 mL/min). The difference in height between the outlet of the perfusion apparatus and the outlet of the overflow vessel was maintained at 110

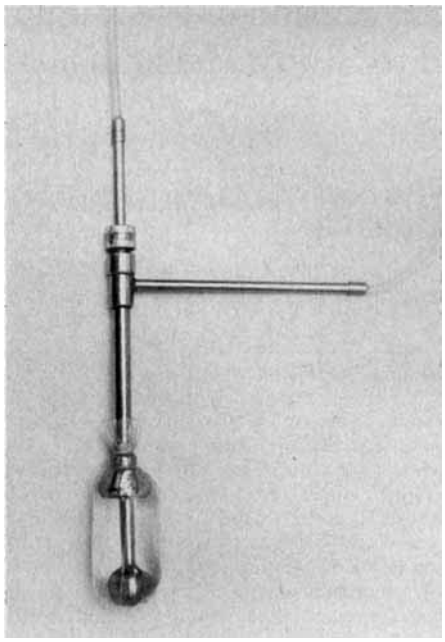

Figure 1—*Perfusion apparatus with filled dialysis bag.*

[1] Brocacef E 211, Maarsen, Netherlands.
[2] Merck 6579, Darmstadt, West Germany.
[3] Merck 6346, Darmstadt, West Germany.
[4] Aldrich M 1920-1, Beerse, Belgium.
[5] Merck 6009, Darmstadt, West Germany.
[6] Sigma, Chemical Co., St. Louis, Mo.
[7] Waters Associates model 440, Milford, Mass.
[8] Wisp; Waters Associates, Milford, Mass.
[9] Lichrosorb 10 RP 18; Chrompack, Middelburg, Netherlands.
[10] Vydac 201 SC; Chrompack, Middelburg, Netherlands.
[11] Thomas technological service, 3787 D50, Mw, Cutoff 12,000; Philadelphia, Pa.
[12] Gilson minipuls 2; Meyvis and Co., Bergen op Zoom, Netherlands.

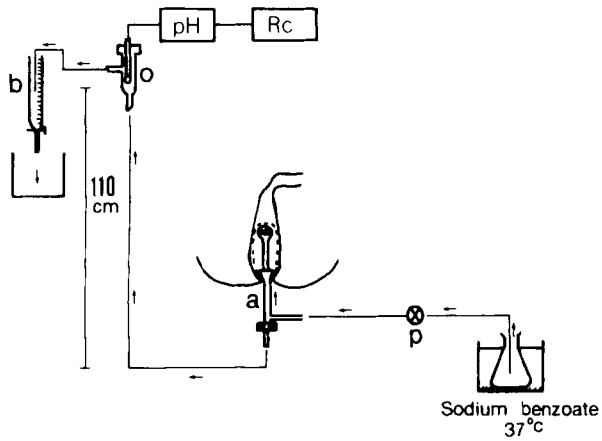

Figure 2—*Experimental setup for rectal absorption measurement* in vivo. *Key: (a) perfusion apparatus, (p) peristaltic pump, (o) overflow vessel, (b) buret, (pH) pH-electrode, (Rc) recorder. Arrows indicate the direction of flow.*

cm such that the inner pressure of the dialysis bag was constant. Due to the positive pressure in the system, the dialysis bag regained its maximal volume. A pH electrode was placed in the overflow vessel to record the pH of the perfusate during perfusion.

In the case of recirculation, a constant volume of perfusate was circulated by connecting the tube of the overflow vessel with the inlet tube of the perfusion apparatus. Before starting an experiment all the air was expelled by filling the whole system with perfusion solution. After emptying the dialysis bag, the apparatus was introduced into the rectum by placing the funnel on the inner side of the anus (Fig. 2). The perfused area of the rectum wall was in close contact with the surface of the dialysis bag.

The volunteers fasted overnight and throughout the perfusion experiment. Consequently, the endogenous hippuric acid level was almost zero before starting the infusion of sodium benzoate, confirming the results of Moolenaar *et al.* (14). One hour before the actual start of a perfusion, the rectum was cleaned by a phosphate buffer enema. The results of the experiment were rejected if the dialysis bag appeared to be contaminated with feces at the end of the perfusion.

The subject was seated on a specially designed chair so that the perfusion tube with connections did not cause inconvenience. After introducing the apparatus and filling it with the warm solution of sodium benzoate, the rectum was constantly perfused for 2.0–2.5 h under recirculation or single-pass conditions. Blood samples of 8.0 mL were taken every 15 min from a forearm vein and the plasma analyzed for hippuric acid and benzoic acid. Four volunteers were perfused for 2.5 h under single-pass conditions with four different concentrations of sodium benzoate on four different days. The time between the experiments was at least 14 d. From the established steady-state concentration, the Φ_{in} was calculated as described.

Two volunteers were perfused under recirculation conditions with a

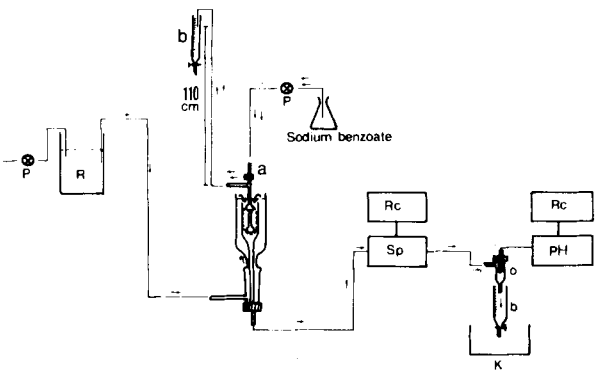

Figure 3—*Experimental setup for membrane-release measurement* in vitro. *Key: (a) perfusion apparatus; (R) reservoir; (p) peristaltic pump; (b) buret; (o) overflow vessel; (Sp) spectrophotometer; (Rc) recorder; (pH) pH-electrode; (k) collection vessel. Arrows indicate the direction of flow along the dialysis membrane (→) and through the dialysis membrane (⇉).*

Table II—Pharmacokinetic Parameters of Hippuric Acid after Intravenous Administration of Two Different Doses of Sodium Hippurate to Three Healthy Volunteers [a]

Parameter	Subject A	A	B	B	C	C
Dose (free acid), mg	588	222	588	222	588	222
AUC, μg·min/mL	1701	734	1828	657	1700	626
CL, mL/min	346	302	322	338	346	355

[a] Pharmacokinetic analysis was performed according to a two-compartment system with elimination from the central compartment.

155-mmol sodium benzoate solution. After 2 h the apparatus was taken out of the rectum, but blood sampling was continued for at least 1 h to determine the postperfusion elimination of hippuric acid. From the plasma concentration–time curve the area under the curve (AUC) was calculated using the trapezoidal rule. Using the AUC and clearance value, the total amount of absorbed sodium benzoate could be determined and compared with the amount that disappeared from the perfusate.

Determination of the Release from the Dialysis Bag *In Vitro*—To exclude the possibility that passage of sodium benzoate through the dialysis membrane would be rate limiting, the release of sodium benzoate from the dialysis bag was studied *in vitro* with the apparatus shown in Fig. 3. From a reservoir, nonbuffered water (pH 7.2) warmed to 37°C flowed into the outer tube and, *via* the inner tube, along the membrane, through a flow cell in the spectrophotometer, and was finally collected *via* overflow vessel and buret into a collection vessel. A pH-electrode was placed in the overflow vessel to detect any change in the pH of the solution coming out of the inner tube. The difference in height between the reservoir and the overflow vessel determined the water flow rate, which was measured by the buret.

The perfusion apparatus, with dialysis bag was hung inversely in the inner tube. The distance between the membrane and tube wall was such that a laminar water flow along the dialysis membrane occurred. The flow rate along the membrane (150–175 mL/min) ensured that measurements were performed under sink conditions, *i.e.*, that the concentration (C) in the water layer was almost zero compared with the concentration inside the membrane, C_0. The pressure inside the dialysis membrane was similar to that in the *in vivo* studies, since the distance between the inlet and outlet tubes of the perfusion apparatus was also maintained at 110 cm. In the case of *in vitro* recirculation experiments a pH electrode was also placed into the circulation system to detect any change of pH in the perfusate analogous to the *in vivo* situation.

The dialysis bag was filled with a solution of sodium benzoate and perfused until there was a steady-state release. Release per unit area was calculated as follows:

$$\Phi_{out} = \frac{C_{out} \times F}{\text{Area}} \ \mu\text{g/min} \cdot \text{cm}^2 \qquad \text{(Eq. 2)}$$

where C_{out} is the measured concentration of the solution coming out of the inner tube at steady state (μg/mL), F is the flow rate (mL/min), and Area = the membrane surface (cm^2).

Four different concentrations of sodium benzoate (72.5, 145, 218, and 290 mmol) were perfused as a single pass, and the release rate per unit of surface area was determined. To establish whether the membrane release characteristics change during perfusion *in situ*, control experiments were performed in which release from the dialysis bag was determined before and after use in a human rectal perfusion experiment. The presence of the bag in the human rectum for 2.5 h appeared not to change the *in vitro* release characteristics.

RESULTS AND DISCUSSION

Perfusion Under Single-Pass Conditions—Before starting the perfusion experiments it was determined whether dose-dependent kinetics in the elimination of hippuric acid could occur in the concentration range used for the perfusion studies. The clearance value can either be calculated according to the model-independent technique (CL = Dose/AUC, where AUC is the area under the plasma concentration *versus* time curve and dose is the amount of drug in the body) or by $CL = V_d \cdot \beta$, where V_d is the volume of distribution and β is the overall elimination rate constant. In the case of dose-dependent kinetics, a lower clearance value should be detected at the higher concentrations. The clearance will also change with any changes in V_d, when β remains constant. Table II shows the results of two different intravenous doses of sodium hippurate to three volunteers. No difference in CL was found, indicating that dose-dependent kinetics does not occur.

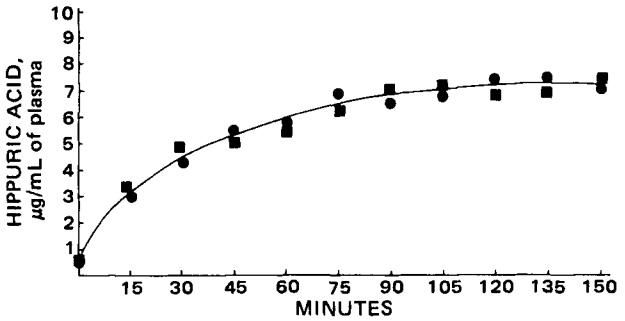

Figure 4—*Plasma concentration–time curves of perfusions with a 155-mmol sodium benzoate solution performed on two different occasions in one human subject.*

Figure 4 shows plasma concentration *versus* time curves following perfusions with 155 mmol on two different occasions in one subject. The calculated Φ_{in} values ($\mu g/min \cdot cm^2$) of the perfusion experiments, performed on two different occasions with four different concentrations of sodium benzoate, were, respectively, 19 and 16 for 116 mmol, 24 and 31 for 155 mmol, 58 and 59 for 232 mmol, 93 and 110 for 310 mmol of sodium benzoate. The identical curves and the established Φ_{in} values indicate a good reproducibility of the perfusion method.

Figure 5 shows the plots of the established Φ_{in} values of single-pass perfusion experiments with four different concentrations of sodium benzoate in four volunteers. The perfused length of the rectum was 7.0 cm. The plots show a linear relationship between Φ_{in} and sodium benzoate concentration. This pattern indicates a passive transport process, probably in the form of benzoic acid. However, paracellular or carrier transport in the form of sodium benzoate, operating under saturating conditions, can not be excluded at this stage. Further studies have been initiated to study the influence of pH on the absorption rate of this compound.

It is important that the perfused length of the rectum remains constant in these studies. Although Φ_{in} is determined per square centimeter, it is still unknown whether there is any difference in absorption between different parts of the rectum. Furthermore, there has to be a severe restriction in food intake the day before the experiment; otherwise, endogenous hippuric acid levels will be too high (2.0–8.0 μg/mL) and will influence steady-state concentration verifiability.

Figure 6 shows the *in vitro* transport across the membrane under sink conditions. For the sodium benzoate concentrations used in the present study, the transport across the membrane (per square centimeter) *in vitro* was found to be at least two times higher than the absorption rate (per square centimeter) observed *in vivo*. The amount transported was found to be proportional to the surface area of the membrane. Therefore, it is concluded that under the chosen conditions transport through the dialysis membrane is not rate limiting, so that the measured influx reflects the absorption capacity per unit area of the rectal membrane. This conclusion is supported by the high variation in Φ_{in} values between individuals, the good reproducibility of values within one individual, and the fact that membrane release does not change during the time of perfusion.

Perfusion Under Recirculation Conditions—Figure 7 shows a typical example of a perfusion curve following a recirculation experiment.

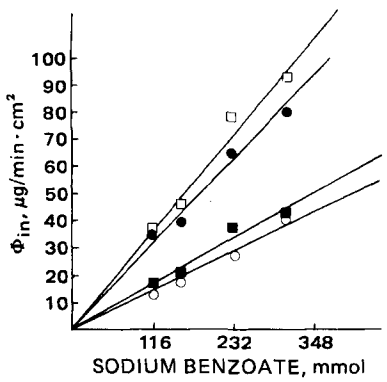

Figure 5—*Absorption rate (Φ_{in})* versus *sodium benzoate concentration after rectal perfusion with four different doses of sodium benzoate in four volunteers. Each symbol represents a single volunteer.*

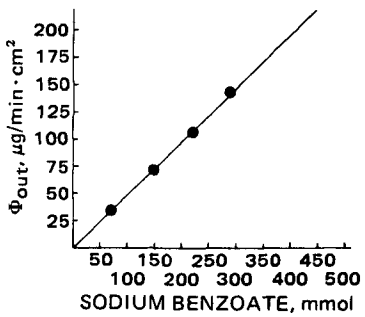

Figure 6—*Membrane release (Φ_{out})* versus *sodium benzoate concentration determined* in vitro.

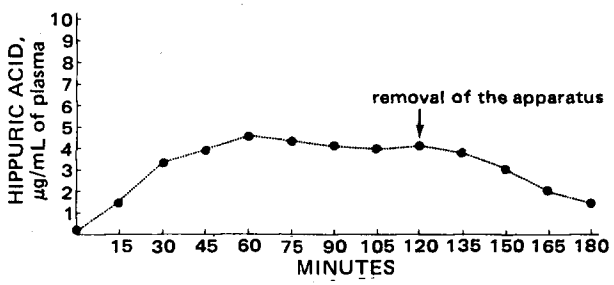

Figure 7—*Typical plasma concentration–time curve following a recirculation perfusion in one human subject.*

After the apparatus was taken out of the rectum, the plasma concentration of hippuric acid decreased very quickly. The slope of the terminal log concentration–time points (β-phase) was calculated and used to establish the $AUC_{t\to\infty}$. In the case of recirculation experiments, it is essential that the endogenous hippuric acid level is very low, because otherwise the calculated AUC is not in accordance with the amount really absorbed.

Table III represents the results of three recirculation experiments in two subjects (D and E). The total amount of absorbed benzoic acid equalled the measured amount of sodium benzoate eliminated from the perfusate. Thus, the loss of sodium benzoate within the lumen of the rectum or accumulation of sodium benzoate in the mucosa can be excluded.

In addition, it is interesting to note that in each experiment the pH of the perfusion solution rose during the time of perfusion at least one pH-unit, from 7.1 to 8.1. Assuming that sodium benzoate is absorbed in the uncharged form as benzoic acid, hydrogen ions have to be provided in the rectal wall or rectal lumen, because more benzoic acid disappeared from the perfusion solution than could be present at pH 7.1. With loss of benzoic acid, the sodium ion concentration increases, which combined with the hydroxyl ions from water cause the increase in pH. However, in our studies no relationship between the amount of sodium benzoate eliminated from the perfusion solution and the enhancement of the pH during perfusion was found. Therefore, it is concluded that the human rectum wall probably is able to secrete a fluid that adjusts the pH of the perfusion solution to a physiological pH. Crommelin *et al.* (17) found a similar phenomenon with perfusion experiments in rats. Future investigations should give a more quantitative picture of this process.

The rectal lumen perfusion technique described provides a reproducible method for quantitative absorption studies in humans. With sodium benzoate as the test drug, absorption could be measured as an influx per unit area of the rectal wall (Φ_{in} = $\mu g/min \cdot cm^2$). *In vitro* release studies indicate that the passage across the dialysis membrane of the perfusion apparatus is not rate limiting in the absorption process *in vivo*. With recirculation perfusion experiments it could be shown that the

Table III—Results of Recirculation Perfusion Experiments using 155-mmol Sodium Benzoate Solution in Two Subjects

Subject	Amount of Sodium Benzoate, mg Eliminated from the Perfusate	Absorbed	pH of the Perfusate Start	End
D	422	420	7.0	8.0
E	218	226	7.2	8.3
E	260	259	7.1	8.1

amount of sodium benzoate which disappeared from the perfusion solution equaled the amount of benzoic acid absorbed. With the single-pass perfusion experiments, a linear relationship between concentration of sodium benzoate and the rectal absorption was found, which may indicate passive diffusion possibly as benzoic acid.

REFERENCES

(1) N. Senior, "Advances in Pharmaceutical Sciences," vol. 4, Academic, London, 1974, p. 363.

(2) L. S. Schanker, D. J. Tocco, B. B. Brodie, and C. A. Hogben, *J. Pharmacol. Exp. Ther.*, **123**, 81 (1958).

(3) K. Kakemi, T. Arita, and S. Muranishi, *Chem. Pharm. Bull.*, **13**, 861 (1965).

(4) N. F. H. Ho and W. I. Higuchi, *J. Pharm. Sci.*, **60**, 537 (1971).

(5) S. Riegelman and W. J. Crowell, *J. Am. Pharm. Assoc., Sci. Ed.*, **47**, 115, 123, 127 (1958).

(6) R. E. Beck and S. Schultz, *Science*, **170**, 1302 (1970).

(7) K. Kakemi, T. Arita, R. Hori, R. Komishi, and K. Nishimura, *Chem. Pharm. Bull.*, **17**, 248 (1969).

(8) K. Thoma, "Arzneiformen zur Rectalen und Vaginalen Applikation," Werbe- und Vertriebsgesellschaft Deutscher Apotheker mbH, Frankfurt, West Germany, 1980, p. 17.

(9) F. Moolenaar and A. J. M. Schoonen, *Pharm. Int.*, **1**, 144 (1980).

(10) C. J. Devroede and S. F. Phillips, *Gut*, **11**, 438 (1970).

(11) E. Bechaard, *Acta Pharmacol. Toxicol.*, **33**, 123 (1973).

(12) N. I. McNeil, *Gut*, **20**, 400 (1979).

(13) C. J. Edmonds, *Gut*, **12**, 356 (1971).

(14) F. Moolenaar, A. G. G. Stuurman-Bieze, J. Visser, and T. Huizinga *Int. J. Pharm.*, **1**, 323 (1978).

(15) A. J. Quick, *Am. J. Med. Sci.*, **185**, 630 (1933).

(16) N. H. Nie and C. H. Hull *et al.*, "SPSS-6000," 2nd ed., McGraw-Hill, New York, N.Y., 1975, p. 4.

(17) D. J. A. Crommelin, J. Modderkolk, and C. J. De Blaey, *Int. J. Pharm.*, **3**, 299 (1979).

Quantitation of Norfloxacin, a New Antibacterial Agent in Human Plasma and Urine by Ion-Pair Reverse-Phase Chromatography

L. T. PAULIUKONIS, D. G. MUSSON ˣ, and W. F. BAYNE

Received August 12, 1982, from *Merck Sharp & Dohme Research Laboratories, West Point, PA 19486.* Accepted for publication November 22, 1982.

Abstract □ A specific and sensitive high-performance liquid chromatographic method for the analysis of norfloxacin in human plasma and urine is described. Norfloxacin was extracted from the sample matrix using dichloromethane under neutral conditions, followed by back extraction into dilute phosphoric acid for chromatographic analysis on a reverse-phase column with a mobile phase consisting of methanol, phosphate buffer, and ion-pairing reagent (pH 3.0) at a flow rate of 2.0 mL/min. The ability of this method to distinguish intact norfloxacin from its metabolites was demonstrated. The method is linear, quantitative, and reproducible for both plasma analysis (0.05–2.5 μg/mL) and urinalysis (1.0–500 μg/mL) using peak area ratios (norfloxacin–internal standard) for quantitation. The stability of norfloxacin and its metabolites in dilute phosphoric acid was studied. To assess the presence of norfloxacin conjugates in the urine of dosed individuals, the effects of urine hydrolysis on drug quantitation were examined. Urine and plasma levels of norfloxacin at selected time points following the administration of single drug doses are presented.

Keyphrases □ Norfloxacin—quantitation, antibacterial agent, human plasma and urine, ion-pair reverse-phase, high-performance liquid chromatography □ High-performance liquid chromatography—norfloxacin, human plasma and urine, ion pairing □ Antibacterial agents—quantitation of norfloxacin, human plasma and urine, ion-pair reverse-phase high-performance liquid chromatography

Norfloxacin (1-ethyl-6-fluoro-1,4-dihydro-4-oxo-7-(1-piperazinyl)-3-quinolinecarboxylic acid) (I) is a new quinolinecarboxylic acid antibiotic which exhibits a broad spectrum of antibacterial activity. *In vitro* studies have demonstrated its efficacy towards most Gram-positive and Gram-negative bacteria, including nalidixic acid-resistant pathogens (1, 2).

The development of a rapid, sensitive, and specific assay for norfloxacin quantitation was critical for the measurement of drug levels in clinical specimens. Although a high-performance liquid chromatographic (HPLC) method specific for norfloxacin has been described (3), this method proved unsuitable for use in clinical studies since it offers inadequate sensitivity and requires extensive sample preparation. The use of nonspecific microbiological methods[1] (4) in pharmacokinetic and bioavailability studies is also precluded due to the antibacterial nature of several norfloxacin metabolites (III–VIII) (3).

This report describes a reverse-phase ion-pair HPLC method developed for the quantitation of norfloxacin in plasma and urine, using pipemidic acid (II) as the internal standard. The assay was applied to the measurement of norfloxacin in the plasma and urine of human volunteers given increasing bolus doses of the drug.

EXPERIMENTAL

Reagents and Materials—All solvents[2] were distilled-in-glass and liquid chromatography grade, and purified water[3] was used throughout. All chemicals were ACS grade and used without further purification. Norfloxacin and its metabolites were used as received[4]. Pipemidic acid was extracted from 250-mg tablets[5].

Apparatus—The isocratic HPLC system consisted of a constant-flow pump[6], an autosampler[7], and variable-wavelength detectors; the assay for norfloxacin in plasma utilized a fluorescence detector[8] (excitation, λ = 280 nm; emission, λ = 445 nm; slits, 8 nm), while the urine assay used a UV absorbance detector[9] set at 280 nm. Data were recorded and reduced

[1] Dr. J. A. Bland, Merck Sharp & Dohme Research Laboratories, Rahway, N.J., personal communication.

[2] Burdick & Jackson Laboratories, Muskegon, Mich.

[3] Milli-Q System; Millipore Corp., Bedford, Mass.

[4] Kyorin Pharmaceutical Co., Ltd., Japan.

[5] Dolcol tabs from Dainippon Pharmaceutical Co., Japan.

[6] Model 6000A solvent delivery system; Waters Associates, Milford, Mass.

[7] WISP 710A autosampler; Waters Associates, Milford, Mass.

[8] 650S fluorescence detector equipped with 150B Xenon power supply; Perkin-Elmer, Norwalk, Conn.

[9] Schoeffel SF770 UV-spectroflow monitor; Kratos Analytical Instruments, Westwood, N.J.

0022-3549/84/0100-0099$01.00/0

© 1984, American Pharmaceutical Association

amount of sodium benzoate which disappeared from the perfusion solution equaled the amount of benzoic acid absorbed. With the single-pass perfusion experiments, a linear relationship between concentration of sodium benzoate and the rectal absorption was found, which may indicate passive diffusion possibly as benzoic acid.

REFERENCES

(1) N. Senior, "Advances in Pharmaceutical Sciences," vol. 4, Academic, London, 1974, p. 363.

(2) L. S. Schanker, D. J. Tocco, B. B. Brodie, and C. A. Hogben, *J. Pharmacol. Exp. Ther.*, **123**, 81 (1958).

(3) K. Kakemi, T. Arita, and S. Muranishi, *Chem. Pharm. Bull.*, **13**, 861 (1965).

(4) N. F. H. Ho and W. I. Higuchi, *J. Pharm. Sci.*, **60**, 537 (1971).

(5) S. Riegelman and W. J. Crowell, *J. Am. Pharm. Assoc., Sci. Ed.*, **47**, 115, 123, 127 (1958).

(6) R. E. Beck and S. Schultz, *Science*, **170**, 1302 (1970).

(7) K. Kakemi, T. Arita, R. Hori, R. Komishi, and K. Nishimura, *Chem. Pharm. Bull.*, **17**, 248 (1969).

(8) K. Thoma, "Arzneiformen zur Rectalen und Vaginalen Applikation," Werbe- und Vertriebsgesellschaft Deutscher Apotheker mbH, Frankfurt, West Germany, 1980, p. 17.

(9) F. Moolenaar and A. J. M. Schoonen, *Pharm. Int.*, **1**, 144 (1980).

(10) C. J. Devroede and S. F. Phillips, *Gut*, **11**, 438 (1970).

(11) E. Bechaard, *Acta Pharmacol. Toxicol.*, **33**, 123 (1973).

(12) N. I. McNeil, *Gut*, **20**, 400 (1979).

(13) C. J. Edmonds, *Gut*, **12**, 356 (1971).

(14) F. Moolenaar, A. G. G. Stuurman-Bieze, J. Visser, and T. Huizinga *Int. J. Pharm.*, **1**, 323 (1978).

(15) A. J. Quick, *Am. J. Med. Sci.*, **185**, 630 (1933).

(16) N. H. Nie and C. H. Hull *et al.*, "SPSS-6000," 2nd ed., McGraw-Hill, New York, N.Y., 1975, p. 4.

(17) D. J. A. Crommelin, J. Modderkolk, and C. J. De Blaey, *Int. J. Pharm.*, **3**, 299 (1979).

Quantitation of Norfloxacin, a New Antibacterial Agent in Human Plasma and Urine by Ion-Pair Reverse-Phase Chromatography

L. T. PAULIUKONIS, D. G. MUSSON ˣ, and W. F. BAYNE

Received August 12, 1982, from *Merck Sharp & Dohme Research Laboratories, West Point, PA 19486.* Accepted for publication November 22, 1982.

Abstract □ A specific and sensitive high-performance liquid chromatographic method for the analysis of norfloxacin in human plasma and urine is described. Norfloxacin was extracted from the sample matrix using dichloromethane under neutral conditions, followed by back extraction into dilute phosphoric acid for chromatographic analysis on a reverse-phase column with a mobile phase consisting of methanol, phosphate buffer, and ion-pairing reagent (pH 3.0) at a flow rate of 2.0 mL/min. The ability of this method to distinguish intact norfloxacin from its metabolites was demonstrated. The method is linear, quantitative, and reproducible for both plasma analysis (0.05–2.5 μg/mL) and urinalysis (1.0–500 μg/mL) using peak area ratios (norfloxacin–internal standard) for quantitation. The stability of norfloxacin and its metabolites in dilute phosphoric acid was studied. To assess the presence of norfloxacin conjugates in the urine of dosed individuals, the effects of urine hydrolysis on drug quantitation were examined. Urine and plasma levels of norfloxacin at selected time points following the administration of single drug doses are presented.

Keyphrases □ Norfloxacin—quantitation, antibacterial agent, human plasma and urine, ion-pair reverse-phase, high-performance liquid chromatography □ High-performance liquid chromatography—norfloxacin, human plasma and urine, ion pairing □ Antibacterial agents—quantitation of norfloxacin, human plasma and urine, ion-pair reverse-phase high-performance liquid chromatography

Norfloxacin (1-ethyl-6-fluoro-1,4-dihydro-4-oxo-7-(1-piperazinyl)-3-quinolinecarboxylic acid) (I) is a new quinolinecarboxylic acid antibiotic which exhibits a broad spectrum of antibacterial activity. *In vitro* studies have demonstrated its efficacy towards most Gram-positive and Gram-negative bacteria, including nalidixic acid-resistant pathogens (1, 2).

The development of a rapid, sensitive, and specific assay for norfloxacin quantitation was critical for the measurement of drug levels in clinical specimens. Although a high-performance liquid chromatographic (HPLC) method specific for norfloxacin has been described (3), this method proved unsuitable for use in clinical studies since it offers inadequate sensitivity and requires extensive sample preparation. The use of nonspecific microbiological methods[1] (4) in pharmacokinetic and bioavailability studies is also precluded due to the antibacterial nature of several norfloxacin metabolites (III–VIII) (3).

This report describes a reverse-phase ion-pair HPLC method developed for the quantitation of norfloxacin in plasma and urine, using pipemidic acid (II) as the internal standard. The assay was applied to the measurement of norfloxacin in the plasma and urine of human volunteers given increasing bolus doses of the drug.

EXPERIMENTAL

Reagents and Materials—All solvents[2] were distilled-in-glass and liquid chromatography grade, and purified water[3] was used throughout. All chemicals were ACS grade and used without further purification. Norfloxacin and its metabolites were used as received[4]. Pipemidic acid was extracted from 250-mg tablets[5].

Apparatus—The isocratic HPLC system consisted of a constant-flow pump[6], an autosampler[7], and variable-wavelength detectors; the assay for norfloxacin in plasma utilized a fluorescence detector[8] (excitation, λ = 280 nm; emission, λ = 445 nm; slits, 8 nm), while the urine assay used a UV absorbance detector[9] set at 280 nm. Data were recorded and reduced

[1] Dr. J. A. Bland, Merck Sharp & Dohme Research Laboratories, Rahway, N.J., personal communication.

[2] Burdick & Jackson Laboratories, Muskegon, Mich.

[3] Milli-Q System; Millipore Corp., Bedford, Mass.

[4] Kyorin Pharmaceutical Co., Ltd., Japan.

[5] Dolcol tabs from Dainippon Pharmaceutical Co., Japan.

[6] Model 6000A solvent delivery system; Waters Associates, Milford, Mass.

[7] WISP 710A autosampler; Waters Associates, Milford, Mass.

[8] 650S fluorescence detector equipped with 150B Xenon power supply; Perkin-Elmer, Norwalk, Conn.

[9] Schoeffel SF770 UV-spectroflow monitor; Kratos Analytical Instruments, Westwood, N.J.

0022-3549/84/0100-0099$01.00/0

© 1984, American Pharmaceutical Association

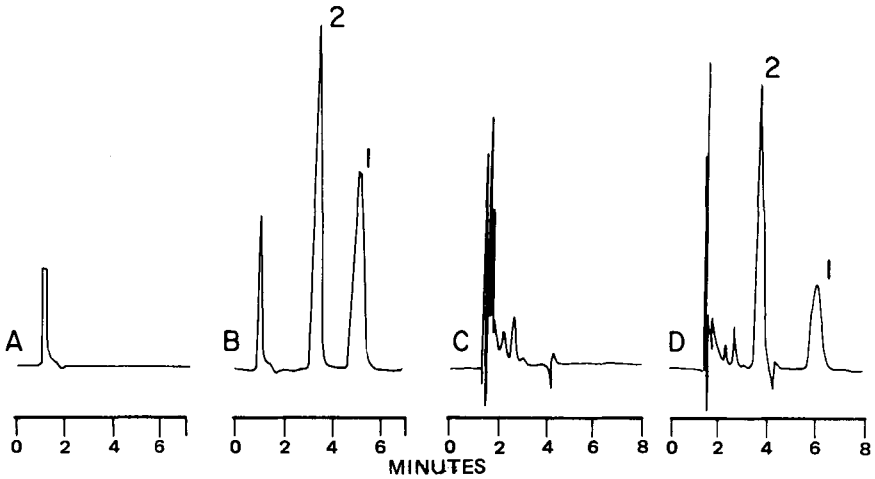

Figure 1—*Representative chromatograms; flow rate = 2.0 mL/min, chart speed = 0.5 cm/min. Key: (A) control plasma; (B) plasma spiked with 0.50 μg/mL of norfloxacin (1) and internal standard (2); (C) control urine; (D) urine spiked with 5.0 μg/mL of norfloxacin (1) and internal standard (2).*

by a computing integrator[10] set for peak area calculations at a chart speed of 0.5 cm/min and attenuation of 16 mV full scale.

Chromatographic Conditions—A 30-cm × 4-mm i.d. reverse-phase stainless steel column[11] was used for all assays. The mobile phase consisted of 300 mL of methanol and 700 mL of water, to which was added 1.74 g of monobasic potassium phosphate and 20 mg of ion-pairing reagent[12]. Prior to filtration through a 0.45-μm filter, the pH of the mobile phase was adjusted to a final value of pH 3.0 with ~1 mL of 85% phosphoric acid. All HPLC analyses were carried out at ambient temperature, using a 2-mL/min flow rate and a 30-μL sample injection volume.

Solution Preparation—Norfloxacin spiking solutions for use in the plasma assay were prepared by diluting a 100-μg/mL aqueous stock solution with water at 25.0, 10.0, 5.0, 2.5, 1.0, and 0.5 μg/mL. Similarly, for the urine assay a 5.0-mg/mL stock solution of norfloxacin in 0.05 M NaOH was diluted as necessary with water to obtain 5.0-, 2.5-, 1.0-mg/mL, 500-, 250-, 100-, 50-, and 10-μg/mL spiking solutions. All norfloxacin solutions were stored at 4°C.

The internal standard stock solution was prepared by dissolving pipemidic acid in 0.1 M NaOH and diluting with water to 100 μg/mL for the urine assay and to 25 μg/mL for the plasma assay. The acid was obtained by crushing a 250-mg tablet to a fine powder, dissolving the powder in 75 mL of 0.1 M NaOH, filtering through a 0.45-μm filter, and diluting the filtrate with water. Alternatively, the acid could also be continuously extracted from a crushed tablet with dichloromethane using a soxhlet apparatus. The solvent was removed from the extract *in vacuo* leaving a residue of pure pipemidic acid. The internal standard solutions were stored at 4°C.

Stock solutions (500 μg/mL) of norfloxacin metabolites M1, M2, M3, $M4_1$, $M4_2$, and M5 were prepared in dichloromethane using sonication and vortexed as needed to effect dissolution. These solutions were stored at −15°C. Aliquots of the stock solutions were diluted to 50 μg/mL with methanol for HPLC analysis.

Assay Procedure—Immediately following vigorous vortexing (or sonication), 100–1000 μL of plasma or urine was added to 100 μL of internal standard solution in a 40-mL centrifuge tube. This solution was then neutralized by adding 1.0 mL of 0.5 M phosphate buffer, pH 7.5. The resulting urine mixtures were extracted once, while the plasma mixtures were extracted twice with dichloromethane as follows. After addition of 10 mL of dichloromethane, each sample was vortexed 10 s, centrifuged[13] at 1000 rpm for 5 min, and the heavier organic layer was transferred to a second 40-mL centrifuge tube. Plasma samples were reextracted with 10 mL of dichloromethane, and this second extract was pooled with the first. The dichloromethane extracts were back-extracted into 0.085% phosphoric acid by adding 1.0 mL of the dilute acid to the organic extract and vortexing this mixture 10 s, followed by centrifugation at 1000 rpm for 5 min. Approximately 400 μL of the resulting acidic extracts were transferred into autosampler vials equipped with microvolume inserts.

[10] Model SP4100; Spectra Physics, Santa Clara, Calif.
[11] μBondapak C18; Waters Associates, Milford, Mass.
[12] Plasma assay: 1-hexanesulfonic acid, sodium salt; urine assay: 1-octanesulfonic acid, sodium salt.
[13] Model Centra 7; International Equipment Co., Needham Heights, Mass.

Preparation of the Standard Curve—Calibration standards were prepared by adding 100 μL of an appropriate spiking solution to 900 μL of urine or plasma and assaying as described above. The plasma assay used six calibration levels of norfloxacin for its standard curve (2.5, 1.0, 0.50, 0.25, and 0.10 μg/mL and 50 ng/mL), while the urine assay used eight calibrations (500, 250, 100, 50, 25, 10, 5.0, and 1.0 μg/mL). Concentrations of norfloxacin were calculated from calibration curves constructed by plotting the peak area ratio of norfloxacin to the internal standard *versus* the spiked concentration of norfloxacin. A freshly prepared set of calibration spikes was run daily, along with control blank extracts prepared both with and without the internal standard.

Urine Hydrolysis—To a 2.5-mL urine sample was added an equal volume of 2 M NaOH (hydrolysis pH 11.9) or 1 M HCl (hydrolysis pH 0.6–0.7). The mixture was vortexed briefly, and a 1.0-mL aliquot was removed immediately (t = 0 min), neutralized, and extracted according to the normal assay procedure. The remainder of the mixture was stoppered and placed in a constant temperature bath at 60°C. Additional 1.0-mL aliquots were removed, immediately neutralized, and assayed at t = 10, 20, and 30 min. Acid-hydrolyzed aliquots were neutralized by adding 0.5 mL of 2 M NaOH, while base-hydrolyzed aliquots were treated with 0.5 mL of 1 M HCl. The final pH of these mixtures after the addition of phosphate buffer (according to assay procedure) was in the range of pH 6.8–7.0.

Clinical Samples—The assay method was applied to both plasma and urine samples obtained from a clinical study in which five single doses of norfloxacin were orally administered to healthy male volunteers. All samples were stored at −20°C until the day of assay.

RESULTS AND DISCUSSION

A sensitive and specific HPLC method was developed utilizing the natural UV absorbing and fluorescing properties of norfloxacin. Using the chromatographic conditions described for this assay, norfloxacin (I) was completely resolved from each of its metabolites (III–VIII) and the internal standard (II), as is evident from the retention time data sum-

Table I—Chromatographic Properties of Norfloxacin, Pipemidic Acid, and Metabolites Under Urine and Plasma HPLC Assay Conditions

Compound	Retention Time, min	
	Plasma HPLC Conditions	Urine HPLC Conditions
Pipemidic acid (internal standard)	3.3	3.6
M2	4.0	4.4
Norfloxacin	5.1	5.6
M5	12.9	11.9
M3	19.0	17.8
M1	—[a]	21.3
$M4_2$	—[a]	30.9
$M4_1$	—[a]	42.6

[a] No fluorescence at 50 μg/mL.

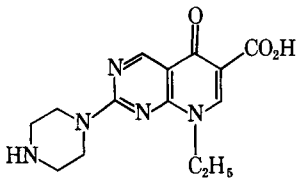

II

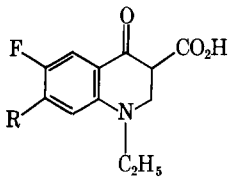

I [Norfloxacin]: R = —N NH

III [M1]: R = —N NH (O)

IV [M2]: R = —$NH(CH_2)_2NH_2$

V [M3]: R = —$NH(CH_2)_2NHCCH_3$ (O)

VI [$M4_1$]: R = —N N—CCH_3 (O)

VII [$M4_2$]: R = —N N—CHO

VIII [M5]: R = —NH_2

marized in Table I. Representative chromatograms of control urine and plasma and urine and plasma spiked with norfloxacin and internal standard shown in Fig. 1. The chromatograms obtained by injection of drug-free urine or plasma show no interfering peaks at the retention times of norfloxacin and the internal standard. Sample preparation for HPLC analysis involved initial extraction of the drug from an aliquot of urine or plasma into dichloromethane, followed by back-extraction into 0.085% phosphoric acid.

Norfloxacin and metabolites M2, M3, and M5 were found to be stable for at least 24 h at ambient temperature in the final acidic extraction medium. However, M1 slowly reacted under these conditions to form a new product which was detected only after 15 h as a fluorescing species

Table II—Representative Standard Curve Data

x: Standards, μg/mL	*y*: Area Ratio (norfloxacin/internal std.)
	Plasma Assay[a]
0.00	0.00
0.05	0.086
0.10	0.203
0.25	0.538
0.50	1.17
1.00	2.60
2.50	6.21
	Urine Assay[b]
0.00	0.00
1.0	0.091
5.0	0.467
10.0	1.19
25.0	2.90
50.0	6.16
100	12.45
250	32.83
500	63.65

[a] Least-mean-squares analysis: slope = 2.51, *y*-intercept = 0.03; correlation coefficient = 0.9996. [b] Least-mean-squares analysis: slope = 0.128; *y*-intercept = −0.103; correlation coefficient = 0.99986.

Table III—Norfloxacin Calibration Curve Replicate Analysis for the Plasma Assay

Plasma Concentration, μg/mL	*CV* (*n* = 6)
0.050	2.6%
0.10	6.5%
0.25	1.3%
0.50	4.3%
1.00	4.6%
2.50	2.2%

eluting ~2 min before norfloxacin. Similarly, $M4_1$ decomposed ($t_{1/2}$ = 23 h) in the dilute acid. In this case, however, no fluorescing products were observed for up to 27 h at ambient temperature. When dissolved in 0.085% phosphoric acid, $M4_2$ formed two fluorescing products. Both species were detected within 30 min of sample preparation. Their concentrations increased with time and reached maximum levels at 24–27 h. While one of these products (A) coeluted with $M4_2$, the retention time of the second degradation product (B) was coincident with that of norfloxacin. Since the amount of norfloxacin excreted in urine was 50 times that of $M4_2$ (3) and ~20% of $M4_2$ was converted to product B after 24 h in dilute acid at room temperature, the maximum norfloxacin quantitation error resulting from the appearance of this degradation product was only 0.4%. The $M4_2$ metabolite, as with the other metabolites and norfloxacin, attained a maximum excretion rate within 2.5–5 h. Later urinary excretion rates of the metabolites showed similar time-dependent variations to norfloxacin (3). Finally, when $M4_2$ was dissolved in 0.3 M NaOH, product B was again formed, along with two new products (C and D). No peak coeluting with $M4_2$ was detected at any time. As in acid, the concentration of product B increased with time, while the concentrations of C and D decreased during the same period. The identities of these degradation products were not pursued.

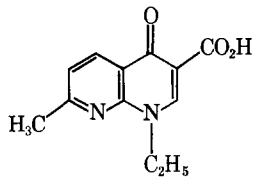

IX

The urine of subjects receiving nalidixic acid (IX) has been shown to contain conjugate derivatives of IX which were readily cleaved by hydrolysis (5). Because of the structural similarities between norfloxacin and nalidixic acid, the presence of analogous conjugates in the urine of norfloxacin-dosed individuals was assessed using conditions comparable with those described for the hydrolysis of nalidixic acid conjugates. It was found that even after 30 min of acid or base hydrolysis at 60°C, the apparent concentration of norfloxacin was unchanged. This suggests that norfloxacin conjugates are not formed in clinical urine specimens.

A structurally similar compound, pipemidic acid (II), was used as the internal standard, since it was found to exhibit favorable UV-absorbing, fluorescence extraction, and chromatographic properties. Using peak area ratios (norfloxacin–internal standard), the detector response was found to be linear in the 0.05–2.50-μg/mL range for plasma (fluorescence detection) and in the 1.0–500-μg/mL range of urine (UV absorbance). The mean recoveries of norfloxacin were 85.6 ± 16.7% in the plasma assay (double extraction), and 42.4 ± 6.0% in the urine assay (single extraction). The mean recoveries of the internal standard were 42.4 ± 6.0% for plasma and 21.7 ± 1.8% for urine. The recovery values are based on unextracted

Table IV—Norfloxacin Calibration Curve Replicate Analysis for the Urine Assay

Urine Concentration, μg/mL	*CV* (*n* = 6)
1.0	11.8
5.0	9.7
10.0	2.0
25.0	2.0
50.0	2.0
100.0	1.5
250.0	2.7
500.0	3.9

Table V—Norfloxacin in Plasma and Urine Following Single Oral Doses to an Individual

Dose, mg	Plasma Concentration, μg/mL Collection Time, h 0	0.5	1.0	1.5	2.0	3.0	4.0	6.0	8.0	12.0
200	0	0.63	1.22	0.81	0.60	0.28	0.47	0.33	0.21	0.14
400	0	0.51	1.42	1.21	0.91	0.74	0.52	0.42	0.28	0.22
800	0	2.91	3.22	2.43	2.20	1.88	1.31	0.83	0.73	0.41
1200	0	3.48	5.69	4.77	5.10	1.60	2.20	1.49	1.19	0.85
1600	0	0.73	2.73	4.61	5.15	4.61	3.54	2.26	1.63	1.13

Dose, mg	Urine Concentration[a] μg/mL Collection Interval, h 0–1	1–2	2–3	3–4	4–6	6–8	8–12	12–24	24–48
200	245	155	44	34	37	42	13	3	16
	(17.9)	(16.1)	(11.0)	(2.1)	(7.4)	(8.8)	(5.7)	(2.0)	(12.4)
400	271	69	41	129	102	109	32	6	4
	(14.4)	(35.9)	(16.8)	(9.8)	(11.6)	(10.0)	(14.4)	(1.1)	(3.0)
800	339	95	111	120	208	243	150	40	5
	(35.6)	(58.9)	(24.0)	(30.6)	(37.0)	(21.6)	(21.5)	(31.6)	(5.5)
1200	1125	1902	653	697	474	76	163	41	18
	(37.1)	(144.6)	(13.7)	(82.9)	(56.4)	(44.8)	(32.8)	(20.1)	(22.5)
1600	432	1414	505	161	524	583	134	70	10
	(34.6)	(60.8)	(72.2)	(67.6)	(74.4)	(43.1)	(56.3)	(39.9)	(30.4)

[a] Values in parentheses indicate total milligrams excreted.

standards. Representative standard curve data are shown in Table II. Reproducibility of this method was validated by the construction of calibration curves over the appropriate concentration ranges for plasma and urine analysis. The coefficients of variation so obtained are summarized in Tables III and IV. The day-to-day reproducibility of this method was demonstrated by assaying replicate aliquots of a spiked plasma sample. Thus, the interassay coefficient of variation was 8.7% (n = 8) for a 0.50-μg/mL plasma standard.

The assay method described in this report was used to quantitate norfloxacin levels in plasma and urine specimens from human subjects participating in an increasing-dose study of the drug. Representative data obtained for one of the volunteers is presented in Table V.

REFERENCES

(1) Y. Kumasaka, H. Nakahata, K. Imamura, and K. Takebe, *Chemotherapy*, **29(S-4)**, 56 (1981).

(2) K. Hirai, A. Ito, Y. Abe, S. Suzue, T. Irikura, M. Inoue, and S. Mitsuhashi, *Antimicrob. Agents Chemother.*, **19**, 188 (1981).

(3) T. Ozaki, H. Uchida, and T. Irikura, *Chemotherapy*, **29(S-4)**, 128 (1981).

(4) Y. Oomori, S. Murayama, Y. Abe, and T. Irikura, *Chemotherapy*, **29(S-4)**, 91 (1981).

(5) E. W. McChesney, E. J. Froelich, G. Y. Lesher, A. V. R. Crain, and D. Rosi, *Toxicol. Appl. Pharmacol.*, **6**, 292 (1964).

Application of Diffusion Theory to the Relationship Between Partition Coefficient and Biological Response

BRET BERNER ˣ and EUGENE R. COOPER

Received July 1, 1982, from *The Procter & Gamble Company, Miami Valley Laboratories, Cincinnati, OH 45247.* Accepted for publication December 14, 1982.

Abstract □ A diffusion model for transport through multilaminates is studied as a possible way to predict the optimal biological response of a set of congeners with respect to the oil–water partition coefficient, P. The model predicts the bilinear form typical of biological response data and, unlike the earlier kinetic model, also relates the results to physical processes, predicts the structure with the optimal response in terms of diffusion constants, and shows such an optimum prior to steady state for an infinite dose. Diffusion through an oil–water multilaminate causes extraordinary separation of permeating species based on partition coefficient and diffusion constant for times shorter than the lag time.

Keyphrases □ Multilaminates—oil–water, diffusion model, optimal biological response with respect to partition coefficient □ Partition coefficient—oil–water multilaminates, diffusion model, optimal biological response □ Optimal biological response—diffusion model, oil–water multilaminates, partition coefficient

In an earlier paper (1), we reviewed the kinetic (2) and equilibrium (3) models for predicting the optimal biological response of a set of congeners with respect to the partition coefficient, P. The kinetic models (1, 2) which treat this problem in terms of rate constants, can be a useful approximation for steady-state transport across a series of unstirred layers of the lipid–water interfaces. However, this kinetic model predicted a large degree of asymmetry (1) in the biological response curve with respect to P, and this asymmetry in transport is not satisfying from a fundamental physical viewpoint. Furthermore, the kinetic treatment neglects differences in diffusion between the lipid and aqueous phases. To understand the role of diffusion in transport across biological tissue of alternating physical properties, it is useful to apply classical diffusion theory to oil–water multilaminates.

Like the kinetic and equilibrium models, the diffusion model developed in this paper predicts a peak in the transport with respect to the partition coefficient for a multilaminated membrane. For a plot of the logarithm of

0022-3549/84/0100-0102$01.00/0

© 1984, American Pharmaceutical Association

Table V—Norfloxacin in Plasma and Urine Following Single Oral Doses to an Individual

Dose, mg	Plasma Concentration, μg/mL Collection Time, h 0	0.5	1.0	1.5	2.0	3.0	4.0	6.0	8.0	12.0
200	0	0.63	1.22	0.81	0.60	0.28	0.47	0.33	0.21	0.14
400	0	0.51	1.42	1.21	0.91	0.74	0.52	0.42	0.28	0.22
800	0	2.91	3.22	2.43	2.20	1.88	1.31	0.83	0.73	0.41
1200	0	3.48	5.69	4.77	5.10	1.60	2.20	1.49	1.19	0.85
1600	0	0.73	2.73	4.61	5.15	4.61	3.54	2.26	1.63	1.13

Dose, mg	Urine Concentration[a] μg/mL Collection Interval, h 0–1	1–2	2–3	3–4	4–6	6–8	8–12	12–24	24–48
200	245	155	44	34	37	42	13	3	16
	(17.9)	(16.1)	(11.0)	(2.1)	(7.4)	(8.8)	(5.7)	(2.0)	(12.4)
400	271	69	41	129	102	109	32	6	4
	(14.4)	(35.9)	(16.8)	(9.8)	(11.6)	(10.0)	(14.4)	(1.1)	(3.0)
800	339	95	111	120	208	243	150	40	5
	(35.6)	(58.9)	(24.0)	(30.6)	(37.0)	(21.6)	(21.5)	(31.6)	(5.5)
1200	1125	1902	653	697	474	76	163	41	18
	(37.1)	(144.6)	(13.7)	(82.9)	(56.4)	(44.8)	(32.8)	(20.1)	(22.5)
1600	432	1414	505	161	524	583	134	70	10
	(34.6)	(60.8)	(72.2)	(67.6)	(74.4)	(43.1)	(56.3)	(39.9)	(30.4)

[a] Values in parentheses indicate total milligrams excreted.

standards. Representative standard curve data are shown in Table II. Reproducibility of this method was validated by the construction of calibration curves over the appropriate concentration ranges for plasma and urine analysis. The coefficients of variation so obtained are summarized in Tables III and IV. The day-to-day reproducibility of this method was demonstrated by assaying replicate aliquots of a spiked plasma sample. Thus, the interassay coefficient of variation was 8.7% (n = 8) for a 0.50-μg/mL plasma standard.

The assay method described in this report was used to quantitate norfloxacin levels in plasma and urine specimens from human subjects participating in an increasing-dose study of the drug. Representative data obtained for one of the volunteers is presented in Table V.

REFERENCES

(1) Y. Kumasaka, H. Nakahata, K. Imamura, and K. Takebe, *Chemotherapy*, **29(S-4)**, 56 (1981).

(2) K. Hirai, A. Ito, Y. Abe, S. Suzue, T. Irikura, M. Inoue, and S. Mitsuhashi, *Antimicrob. Agents Chemother.*, **19**, 188 (1981).

(3) T. Ozaki, H. Uchida, and T. Irikura, *Chemotherapy*, **29(S-4)**, 128 (1981).

(4) Y. Oomori, S. Murayama, Y. Abe, and T. Irikura, *Chemotherapy*, **29(S-4)**, 91 (1981).

(5) E. W. McChesney, E. J. Froelich, G. Y. Lesher, A. V. R. Crain, and D. Rosi, *Toxicol. Appl. Pharmacol.*, **6**, 292 (1964).

Application of Diffusion Theory to the Relationship Between Partition Coefficient and Biological Response

BRET BERNER ˣ and EUGENE R. COOPER

Received July 1, 1982, from *The Procter & Gamble Company, Miami Valley Laboratories, Cincinnati, OH 45247.* Accepted for publication December 14, 1982.

Abstract □ A diffusion model for transport through multilaminates is studied as a possible way to predict the optimal biological response of a set of congeners with respect to the oil–water partition coefficient, P. The model predicts the bilinear form typical of biological response data and, unlike the earlier kinetic model, also relates the results to physical processes, predicts the structure with the optimal response in terms of diffusion constants, and shows such an optimum prior to steady state for an infinite dose. Diffusion through an oil–water multilaminate causes extraordinary separation of permeating species based on partition coefficient and diffusion constant for times shorter than the lag time.

Keyphrases □ Multilaminates—oil–water, diffusion model, optimal biological response with respect to partition coefficient □ Partition coefficient—oil–water multilaminates, diffusion model, optimal biological response □ Optimal biological response—diffusion model, oil–water multilaminates, partition coefficient

In an earlier paper (1), we reviewed the kinetic (2) and equilibrium (3) models for predicting the optimal biological response of a set of congeners with respect to the partition coefficient, P. The kinetic models (1, 2) which treat this problem in terms of rate constants, can be a useful approximation for steady-state transport across a series of unstirred layers of the lipid–water interfaces. However, this kinetic model predicted a large degree of asymmetry (1) in the biological response curve with respect to P, and this asymmetry in transport is not satisfying from a fundamental physical viewpoint. Furthermore, the kinetic treatment neglects differences in diffusion between the lipid and aqueous phases. To understand the role of diffusion in transport across biological tissue of alternating physical properties, it is useful to apply classical diffusion theory to oil–water multilaminates.

Like the kinetic and equilibrium models, the diffusion model developed in this paper predicts a peak in the transport with respect to the partition coefficient for a multilaminated membrane. For a plot of the logarithm of

0022-3549/84/0100-0102$01.00/0

© 1984, American Pharmaceutical Association

the concentration in the receptor compartment [log $C_R(t)$] *versus* log P, the diffusion model permits one to relate P_{max} (the partition coefficient which yields an optimal biological response) to the square root of the ratio of the diffusion constants in the water and oil phases. The initial and final slopes of such plots are equal to the number of oil laminates and water laminates, respectively. That is, non-steady-state permeation through multilaminates can produce an extraordinary separation of solutes with differing partition coefficients or diffusion constants. While this large separation factor is fascinating, it is atypical of biological response curves. To make the model more realistic, shunt pathways need to be introduced into the diffusion model.

Unlike the kinetic and equilibrium models, the diffusion model predicts a peak in the biological response with respect to P for both infinite and finite reservoirs (doses); the kinetic and equilibrium models predict an optimal biological response as a result of the depletion of the finite source (2). Provided water solubility is not the limiting factor, an infinite source reservoir may be used for biological response studies to determine whether equilibrium or nonequilibrium conditions prevail.

This paper presents the model for diffusion through multilaminates and relevant details of the finite difference method used to solve the equations. The theoretical transport curves obtained from this solution are also discussed. These results are then compared with the asymptotic solutions for times shorter than the lag time. [The details of the derivation of these asymptotic solutions and application to membrane separations are discussed elsewhere (4)]. The finite dose case is presented, and the time scale for diffusion is discussed.

THEORETICAL

An alternating series of n oil and $(n-1)$ water slabs (Fig. 1) separates a well-stirred water source compartment of initial solute concentration C_0 and a well-stirred water receptor compartment; the first oil membrane borders the source compartment. The variable to be solved for is $C_R(t)$, the concentration in the receptor compartment at time t, which is less than the characteristic time to reach equilibrium. This characteristic time is chosen to be the lag time for an identical membrane system with an infinite receptor compartment. The diffusing solute has an oil–water partition coefficient (P) and diffusion coefficients D_o and D_w in the oil and water phases, respectively. It is assumed that each barrier is uniform, and that solute equilibration at the interfaces is rapid compared with diffusion.

Within the ith membrane phase, the solute concentration, C_i, obeys Fick's law:

$$\frac{\partial C_i}{\partial t} = D_i \frac{\partial^2 C_i}{\partial x_i^2}, \qquad \text{(Eq. 1)}$$

where D_i equals D_o or D_w depending on the composition of that phase. At the interface, the following boundary conditions are satisfied:

$$D_i \left.\frac{\partial C_i}{\partial x_i}\right|_{\text{interface}} = D_i + 1 \left.\frac{\partial C_{i+1}}{\partial x_{i+1}}\right|_{\text{interface}} \qquad \text{(Eq. 2)}$$

and $C_{i+1} = \sigma C_i$ at the interface, where σ equals P or P^{-1} when the composition of the ith phase is water or oil, respectively. The initial conditions are:

$$C_1(x = 0, t = 0) = PC_o \text{ (water)} \qquad \text{(Eq. 3)}$$

and

$$C_i(x > 0, t = 0) = 0 \; (i = 1, 2, \ldots 2n-1),$$

where $x = 0$ denotes the interface of the source compartment and the first oil barrier. For these calculations the receptor compartment volume, V_R, was chosen to be 1 mL, the interfacial area to be 1 cm^2, and the source compartment volume, V_o, to be infinite or 1 mL. At the membrane–receptor interface, the boundary conditions are:

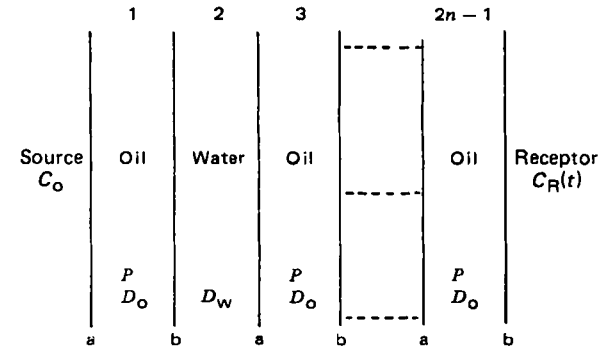

Figure 1—*The model for permeation through an oil–water multilaminate of* 2n − 1 *membranes.*

$$V_R \frac{\partial C_R}{\partial t} = -AD_o \frac{\partial C^b_{2n-1}}{\partial x_{2n-1}} \qquad \text{(Eq. 4)}$$

and $PC_R = C^b_{2n-1}$. The superscript b denotes the bth side of the $2n-1$ membrane. Analogous boundary conditions exist at the source–membrane interface for the finite source compartment case.

The method of finite differences (5) was used to solve Eq. 1 for $C_R(t)$. To obtain a stable numerical solution, the spatial and time increments, δx and δt, respectively, are selected subject to the condition (5):

$$\frac{D_i \delta t}{\delta x_i^2} = 0.5 \qquad \text{(Eq. 5)}$$

The important parameter to relate $C_R(t)$ to the biological response is C_0^{50}, the initial source concentration necessary to give 50% binding, A^{50}, at the receptor site at time t and partition coefficient P. Let there be a fixed, small volume fraction of lipophilic receptor binding sites in the receptor compartment; receptor binding is assumed to be rapid and, therefore, may be treated as an equilibrium process. C_0^{50} may be expressed as (1):

$$C_0^{50} = \frac{A^{50}}{aP^{\alpha}Q(t)} \qquad \text{(Eq. 6)}$$

where $Q(t) = C_R(t)/C_0$ and aP^{α} is the equilibrium constant for binding at the receptor sites. Since the details of the binding process are not known, it is appropriate to solve for $Q(t)$, which gives the main dependence of C_0^{50} on P for a given time. Note that throughout this paper $Q(t) = C_R(t)$.

Some of the parameters used in this model deserve comment. Although the volume ratio (oil–water) of 2:1 used in these calculations is not realistic for biological systems, calculations using a volume ratio of 1:10 showed no difference in any of the features discussed. It is not clear whether a constant total multilaminate thickness or a constant single membrane layer thickness as n varies is more appropriate for the modeling of biological response. There is no qualitative difference in the results of the two approaches, but t_L, the characteristic time for equilibration, for the latter is n^2 times t_l, for the former.

DISCUSSION

Diffusion Model Solution and Biological Response—To correlate the solution to the diffusion equation with biological response data, one needs to examine log $C_R(t)$ *versus* log P plots (Figs. 2 and 3). The bilinear function typical of biological response data (6) is in evidence for $n \geq 2$.

Even in the infinite source case shown (Figs. 2 and 3), the diffusion model predicts bilinear curves prior to establishing steady state. This is in contrast with the kinetic and equilibrium models, where this peaked function is due to the depletion of a finite dose reservoir. Since in the infinite source case the equilibrium model does not predict an optimal biological response, and the diffusion model does, an infinite dose biological experiment can be used to determine whether equilibrium or nonequilibrium processes prevail.

The shape of these bilinear curves is simply related to physical parameters in the diffusion model. The value of log P at which the peak in log $C_R(t)$ occurs (P_{max}) varies with the relative diffusion rate through each type of barrier (Fig. 2). In particular, it can be shown (4) that P_{max}

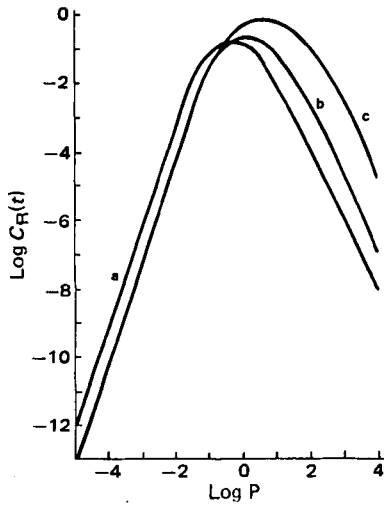

Figure 2—*Log* $C_R(t)$ versus *log P for* $D_o = 7 \times 10^{-5}$ *(a),* 7×10^{-6} *(b), and* 7×10^{-7} *(c)* cm^2/s, *where* D_w *is* 7×10^{-6} cm^2/s. *Note that the shift of the peak is proportional to* $(D_w/D_o)^{1/2}$, t = *1786, 7142, and 76,000 s, respectively, and* n = *3.*

is proportional to $(D_w/D_o)^{1/2}$. Provided the source is infinite, a knowledge of the solute diffusion constants in the two phases is sufficient to predict that structure of a homologous series which will give the optimal biological response. Since in biological systems $D_o < D_w$, the position of the peak must always be at log P >0.

While the position of the peak depends on the diffusion constants in the two phases, the initial and final slopes (Fig. 3) of a log $C_R(t)$ *versus* log P plot are n (the number of oil laminates) and $1 - n$ (the negative of the number of water laminates), respectively. For $0.1 < P < 10$, $C_R(t)$ is relatively insensitive to n. With increasing time, the peak becomes broader as does the range which is insensitive to n. Outside this range, however, there is exponential separation by the number of barriers based on partition coefficient; that is, $C_R(t)$ is proportional to P^n and $P^{(1-n)}$ for highly water- and oil-soluble solutes, respectively.

To relate these bilinear curves to a biological response, one recalls that biological response phenomena involve binding to lipophilic receptors, and therefore, the initial source concentration to give 50% binding is inversely proportional to $C_R(t)P^\alpha$ and not simply to $C_R(t)$ (Eq. 6). For a plot of log $C_R(t)P^\alpha$ *versus* P, a peak exists only when $n \geq 3$. The initial and final slopes of such plots are $(n + \alpha)$ and $(\alpha + 1 - n)$, respectively. P_{max} for a biological response is then approximately $[(D_w/D_o)^{1/2} + \alpha]$.

The slopes of these log $C_R(t)P^\alpha$ *versus* log P curves may be used to devise criteria for distinguishing which model best fits the data. To develop this criterion, α, which represents a difference in lipophilicity between the binding sites on the protein and the lipid phase, is approximated by one. Since $D_w/D_o > 100$, the optimal biological response occurs at a value of P > 10. At short times the initial slope predicted by both the diffusion and kinetic models is ≥2, whereas the initial slope predicted by the equilibrium model is 1 (1) (Table I). In marked contrast to the kinetic model, the final slope derived from diffusion theory need not be close to zero and, in fact, only equals 0 when $n = 2$ (Table I). Although measurement of the final slope is experimentally difficult, it is another method of distinguishing between the applicability of the diffusion model and other models. Note that for α exactly equal to one, only the diffusion model predicts an optimal biological response.

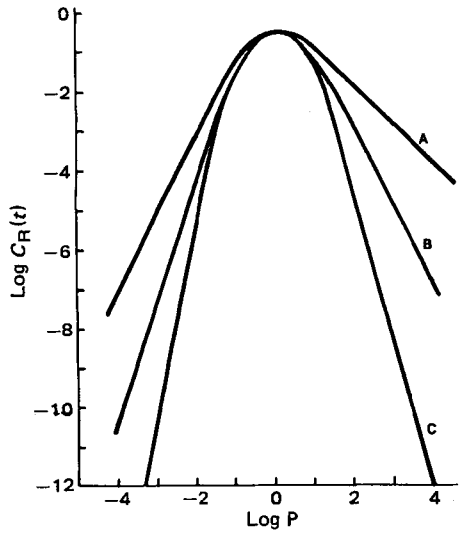

Figure 3—*Log* $C_R(t)$ versus *log P for* n = *2 (A), 3 (B), and 4 (C). The initial and final slopes are* n *and* −(n − *1), respectively;* t = *7142 s and* $D_w = 7 \times 10^{-6}$ cm^2/s.

Table I—Initial and Final Slopes for Models of Biological Response

Model	Initial Slope $P \ll 1$	Final Slope $P \gg 1$
Diffusion	$n + \alpha$	$\alpha + 1 - n$
Kinetic	$n + \alpha$	$\alpha - 1$
Equilibrium	α	$\alpha - 1$

While limited water solubility causes the final slopes of a biological response curve to be difficult to measure experimentally, the initial slope may be reasonably well determined. In an earlier paper, Kubinyi (6) fit a variety of biological data to the bilinear form:

$$\frac{bP^x}{(1 + \beta P)^y} \qquad \text{(Eq. 7)}$$

where x and y are adjustable parameters. Most of these data have initial slopes, $x \leq 1$. This result suggests that the equilibrium model is the best choice of operative process even though these data cannot be fit by the single adjustable parameter required in the equilibrium model. However, the initial slopes for the nonequilibrium model are time dependent and, at long times, may be closer to one.

Certain biological response data are probably governed by nonequilibrium transport phenomena, yet the data show $x \leq 1$. The proposed diffusion model may be inadequate due to neglect of certain physical processes. In particular, the inclusion of polar shunts through lipid membranes would shorten the equilibrium time for highly water-soluble permeating species. Consequently, the $P \ll 1$ regime might be best described by equilibrium or steady state, while the $P \gg 1$ region would be governed by non-steady-state phenomena. In this case, the initial slope of a log $P^\alpha C_R(t)$ *versus* P plot would be near unity. Inclusion of these shunts in the model creates a problem which is not easily solved and involves many adjustable parameters.

In summary, the advantages of the multilaminate diffusion model of biological response as compared to the kinetic model are (*a*) relating the results to physical processes, (*b*) the observation of a peak for an infinite dose in contrast to the other models, (*c*) the presence of a peak in log $P^\alpha C_R(t)$ *versus* log P, and (*d*) the existence of a simple asymptotic solution. However, as Hwang *et al.* (7) and Yalkowsky and Flynn (8) have shown for intestinal and vaginal absorption, a multilaminate model may not be appropriate for tissues in general, since aqueous pores may be present in the tissue.

Comparison with the Asymptotic Solutions for Short Times—Using a simple approximation, one can derive the asymptotic solutions for short times and P very different from unity (4). To understand the extreme separation predicted by this theory, it is useful to compare the finite-difference results with the asymptotic solutions.

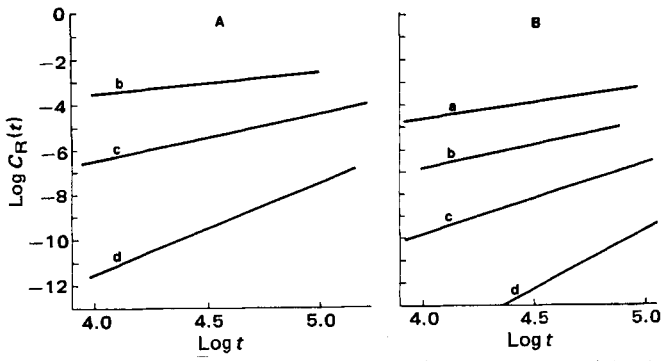

Figure 4—*Log* $C_R(t)$ versus *log* t *for* $P = 10^4$ *(A) and* $P = 10^{-4}$ *(B) for* n = *1 (a), 2 (b), 3 (c), and 4 (d). Note that the plots are linear with slopes of* n − *1 and* n *for* $P = 10^4$ *and* 10^{-4}, *respectively.*

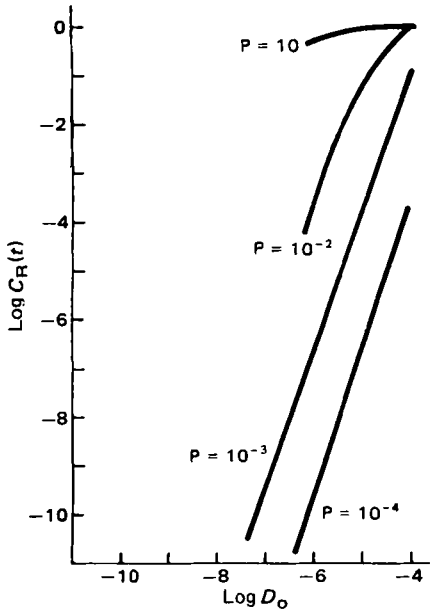

Figure 5—*Log* $C_R(t)$ versus *log* D_o *for several P. For* $P \ll 1$, *the plots are linear with a slope of 3 since* n = 3. *For larger P, log* $C_R(t)$ *is increasingly independent of* D_o; t = 71,390 *s.*

At short times ($t < t_L$) it may be shown that $P \ll P_{max}$:

$$C_R(t) \approx \frac{Al_w}{V_R n!}\left(\frac{D_o P t}{l_o l_w}\right)^n C_0 \qquad \text{(Eq. 8)}$$

and for $P \gg P_{max}$:

$$C_R(t) \approx \left(\frac{D_w t}{P l_o l_w}\right)^{n-1} \frac{C_0}{(n-1)!} \qquad \text{(Eq. 9)}$$

where t_L is the lag time (9) and l_o and l_w are the thickness of a single oil and water membrane, respectively. To demonstrate the validity of these equations, one examines the values of $C_R(t)$ obtained by the finite-difference method. If $t < t_L$ and $P \ll 1$, log $C_R(t)$ should be a linear function of log P, $-\log D_w$, $-\log t$, $\log l_o$, and l_w with a slope equal to the number of water barriers. Figure 4 is a plot of log $C_R(t)$ *versus* log t for several n. In Figs. 5 and 6 we plotted log $C_R(t)$ *versus* log D_o and log D_w, respec- of water barriers. Figure 4 is a plot of log $C_R(t)$ versus log t for several n. In Figs. 5 and 6 we plotted log $C_R(t)$ *versus* log D_o and log D_w, respectively, for various P; the separation of solutes at different diffusion constants is enormous. The predicted linear dependence and slopes stated in Eqs. 8 and 9 are all verified in these three figures. More important for the understanding of optimal biological response, log $C_R(t)$ should be a linear function of log P in the small and large P limits.

Permeation from a Finite Source—The effect of a finite source as a function of time is shown in Fig. 7. At short times, the curve is identical to the infinite source case. As t becomes longer the curve broadens and

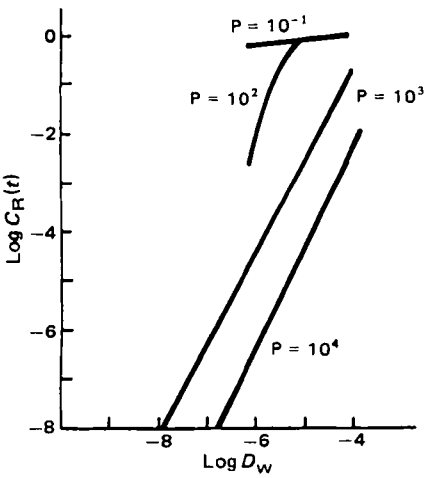

Figure 6—*Log* $C_R(t)$ versus *log* D_w *for several P. For* $P \gg 1$, *the plots are linear with a slope of 2 since* n = 3. *For smaller P, log* $C_R(t)$ *is increasingly independent of* D_w; t = 71,390 *s.*

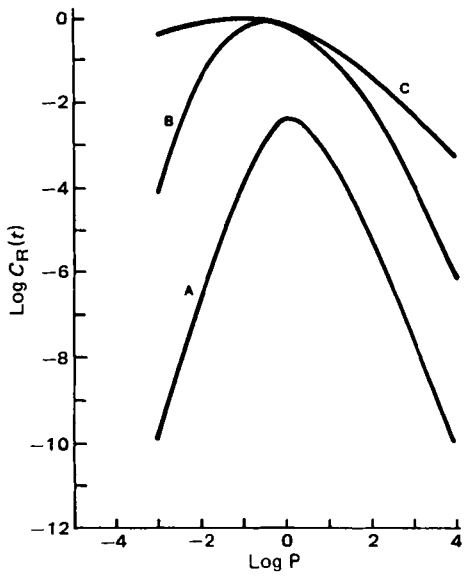

Figure 7- *Log* $C_R(t)$ versus *log P for* t = 1.786×10^3 *(A),* 7.829×10^4 *(B), and* 4.0×10^6 *s, with a finite source reservoir,* V_o = 1 *mL,* n = 3. *Note the shift of the peak and the flattening of the curve with increasing time.*

the peak shifts in the negative log P direction; at infinite time (the equilibrium case) the initial slope of a log $C_R(t)$ *versus* log P plot is zero, and the final slope is −1. According to the oil–water diffusion model, the peak in log $C_R(t)$ with respect to log P can occur at values of $P < 1$ only if there is a finite dose. Thus, with an infinite source, $P_{max} < 1$ should not occur unless water solubility is limiting. With a finite reservoir, such a peak position may result from either equilibrium or nonequilibrium processes.

Time Scale for Diffusion—It is useful to study the solution to Eq. 1 for the given initial and boundary condition in two limits: the long-time or equilibrium limit and the short-time nonequilibrium limit. A characteristic time which serves as an upper bound to the validity of the solution for short times needs to be defined; the diffusional lag time, t_L, is a lower limit to this characteristic time. For a large number of membrane pairs, $n^2 \gg 1$, t_L is given by (9):

$$t_L = \frac{V_o D_w + P V_w D_o}{6 D_o D_w}\left(V_o + \frac{V_w}{P}\right) l^2 \qquad \text{(Eq. 10)}$$

where l is the total thickness of the composite of slabs, and V_o and V_w are the volume fractions of oil and water, respectively. For *in vitro* experiments involving individual cells, t_L for distances equal to cell diameters is of the order of seconds, and the equilibrium model should be utilized in the interpretation of such biological response data. On the other hand, for *in vitro* or *in vivo* experiments involving diffusion through tissue, t_L for $l > 10$ μm can range from the order of hours to months for P very different from unity; consequently, the nonequilibrium model might be applicable for many experiments.

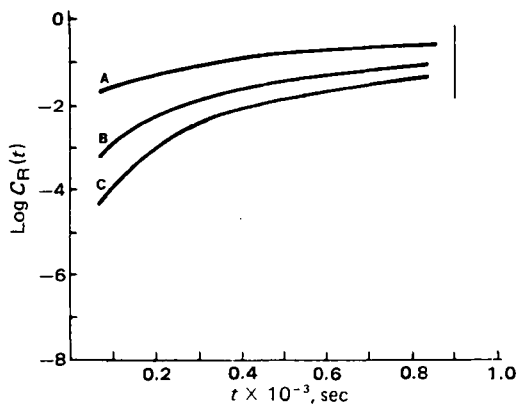

Figure 8—*Log* $C_R(t)$ versus t *for* $P = 10^{-2}$ *for* n = 1 *(A), 2 (B), and 3 (C) membranes. The lag time (perpendicular line) is shown as an estimate of the time of convergence of the curves for different* n.

The existence of aqueous shunts in the oil phase may shorten t_L drastically. To examine the validity of t_L as a characteristic time, one plots $C_R(t)$ against t for several values of n for an infinite source (Fig. 8). At long times, $C_R(t)$ asymptotically approaches the equilibrium solution, which for an infinite source is:

$$\lim_{t \to \infty} C_R(t) = C_0 \qquad \text{(Eq. 11)}$$

As shown in Fig. 8, the lag time, t_L, is a reasonable estimate of the time of convergence of the curves for different n.

REFERENCES

(1) E. R. Cooper, B. Berner, and R. Bruce, *J. Pharm. Sci.*, **70**, 57 (1981).

(2) J. T. Penniston, L. Beckett, D. L. Bentley, and C. Hansch, *Mol. Pharmacol.*, **5**, 333 (1969).

(3) T. Higuchi and S. S. Davis, *J. Pharm. Sci.*, **59**, 1376 (1970).

(4) B. Berner and E. R. Cooper, *J. Memb. Sci.*, **14**, 139 (1983).

(5) J. Crank, "The Mathematics of Diffusion," Oxford University Press, London, 1975.

(6) H. Kubinyi, *J. Med. Chem.*, **20**, 625 (1977).

(7) S. Hwang, E. Owada, T. Yotsuyanagi, L. Suhardja, N. F. H. Ho, G. L. Flynn, and W. I. Higuchi, *J. Pharm. Sci.*, **65**, 1576 (1976).

(8) S. H. Yalkowsky and G. L. Flynn, *J. Pharm. Sci.*, **62**, 210 (1973).

(9) R. M. Barrer, in "Diffusion in Polymers," J. Crank and G. S. Park, Eds., Academic, New York, N.Y., 1968.

Synthesis and Anticonvulsant Properties of Some 2-Aminoethanesulfonic Acid (Taurine) Derivatives

LARS ANDERSEN *, LARS-OLAV SUNDMAN *x, INGE-BRITT LINDÉN *, PIRJO KONTRO ‡, and SIMO S. OJA ‡

Received March 1, 1982, from the **Research Laboratories of Medica Pharmaceutical Company, Ltd., Box 325, SF-00101 Helsinki 10*, and ‡*Department of Biomedical Sciences, University of Tampere, Box 607, SF-33101 Tampere 10, Finland.* Accepted for publication September 2, 1982.

Abstract □ A series of 2-acylaminoethanesulfonamides were synthesized by treating the corresponding sulfonyl chlorides with ammonia, a primary, or a secondary amine. A few compounds displayed marked anticonvulsant activity in mice when tested for their potency in the maximal electroshock seizure test. The piperidino, benzamido, phthalimido, and phenylsuccinylimido derivatives were active, whereas the succinylimido, saccharinylimido, and norbornendicarboxylimido compounds showed no activity. The interference with the sodium-independent taurine binding to mouse brain synaptic membranes was assessed to elucidate the possible mode of anticonvulsant action.

Keyphrases □ Anticonvulsant agents—potential, 2-aminoethanesulfonic acid (taurine) derivatives, synthesis □ Synthesis—2-aminoethanesulfonic acid (taurine) derivatives, anticonvulsant activity in mice □ Taurine—synthesis of derivatives, anticonvulsant activity in mice

Taurine, 2-aminoethanesulfonic acid, is abundant in excitable mammalian tissues such as the brain, sensory organs, heart, and other muscles (1). In these tissues taurine has recently been considered an essential effector in the regulation of neuronal communication, possibly as an inhibitory synaptic transmitter, neuromodulator, or stabilizer of excitable membranes (2, 3). Taurine effectively prevents seizures when administered intracerebroventricularly to an animal model, but clinical trials with epileptic patients using oral or intravenous administration have been only partially successful (4).

Taurine is quite polar, and its penetration from plasma into brain tissue is apparently hampered by its hydrophilic properties (5). We have attempted to prepare more lipophilic derivatives of taurine which would still possess an inhibitory action at central synapses. Lipophilization of taurine was effected by both acylation and conversion of the sulfonic acid group to various amides. In this way the shape of the molecule and the intramolecular electron distribution, both of which may be essential for the taurine-like inhibitory action (6), were expected to be unchanged. It is also significant that sulfonamides are generally atoxic.

RESULTS AND DISCUSSION

The compounds studied are of the general structures A and B (see Table I for R_1 and R_2 designations).

$R_1CH_2CH_2SO_2NH_2$ (A) $\qquad$ $R_1CH_2CH_2SO_2R_2$ (B)

Although several earlier reports (7–10) have described similar compounds, these studies evaluated the compounds for antibacterial and antimalarial activity. They were either inactive or only slightly active in this respect.

Compounds II, IVa–g, V, and VIIIa–b inhibited maximal electroshock (MES)-induced convulsions in mice (Table II). The most potent compounds were II, IVc, IVd, IVe, IVg, and V, which had ED_{50} values ≤100 mg/kg. It was found that the sodium-independent binding of [^{3}H]taurine to isolated synaptic membranes was inhibited by III, IVa, V, and VIc. In general, no parallelism was observed between anticonvulsant action and inhibition of taurine binding. Only V may act by interfering with the attachment of taurine to its membrane binding sites.

The acyltaurinamides and *N*-substituted acyltaurinamides were synthesized from the corresponding sulfonyl chlorides and ammonia, a primary, or a secondary amine as described previously (7–9, 11). These compounds are colorless, crystalline substances with a somewhat bitter taste. They are insoluble or slightly soluble in water, but soluble in polar organic solvents.

EXPERIMENTAL[1]

***N*-[2-[(Methylamino)sulfonyl]ethyl]benzamide (IVb), *N*-[2-[(Ethylamino)sulfonyl]ethyl]benzamide (IVc), *N*-[2-[(Dimethylamino)sulfonyl]ethyl]benzamide (IVd), *N*-[2-[[(1-Methylethyl)amino]sulfonyl]ethyl]benzamide (IVe), *N*-[2-[(Butylamino)sulfonyl]ethyl]benzamide (IVf), and *N*-[2-[[(1,1-Dimethylethyl)amino]sulfonyl]ethyl]benzamide (IVg)**—These compounds were prepared as described below for IVg. To *tert*-butylamine (10.92 g, 0.150 mol) was added with cooling and stirring (ice-bath) the substituted sulfonyl chloride (7.66 g, 0.031 mol) over a 25-min period. After 20 min stirring additional *tert*-butylamine (3.64 g, 0.05 mol) was added, and the stirring was continued at room temperature. Water (75 mL) was added, and the excess amine was removed with a stream of air. The precipitate was re-

[1] Melting points were determined in open capillary tubes and are uncorrected. Elemental analyses were performed by Janssen Pharmaceutica NV, Analytical Department, Beerse, Belgium. NMR data were recorded on a JEOL FX-60 spectrophotometer.

0022-3549/84/0100-0106$01.00/0

© 1984, American Pharmaceutical Association

The existence of aqueous shunts in the oil phase may shorten t_L drastically. To examine the validity of t_L as a characteristic time, one plots $C_R(t)$ against t for several values of n for an infinite source (Fig. 8). At long times, $C_R(t)$ asymptotically approaches the equilibrium solution, which for an infinite source is:

$$\lim_{t \to \infty} C_R(t) = C_0 \qquad \text{(Eq. 11)}$$

As shown in Fig. 8, the lag time, t_L, is a reasonable estimate of the time of convergence of the curves for different n.

REFERENCES

(1) E. R. Cooper, B. Berner, and R. Bruce, *J. Pharm. Sci.*, **70**, 57 (1981).

(2) J. T. Penniston, L. Beckett, D. L. Bentley, and C. Hansch, *Mol. Pharmacol.*, **5**, 333 (1969).

(3) T. Higuchi and S. S. Davis, *J. Pharm. Sci.*, **59**, 1376 (1970).

(4) B. Berner and E. R. Cooper, *J. Memb. Sci.*, **14**, 139 (1983).

(5) J. Crank, "The Mathematics of Diffusion," Oxford University Press, London, 1975.

(6) H. Kubinyi, *J. Med. Chem.*, **20**, 625 (1977).

(7) S. Hwang, E. Owada, T. Yotsuyanagi, L. Suhardja, N. F. H. Ho, G. L. Flynn, and W. I. Higuchi, *J. Pharm. Sci.*, **65**, 1576 (1976).

(8) S. H. Yalkowsky and G. L. Flynn, *J. Pharm. Sci.*, **62**, 210 (1973).

(9) R. M. Barrer, in "Diffusion in Polymers," J. Crank and G. S. Park, Eds., Academic, New York, N.Y., 1968.

Synthesis and Anticonvulsant Properties of Some 2-Aminoethanesulfonic Acid (Taurine) Derivatives

LARS ANDERSEN *, LARS-OLAV SUNDMAN *x, INGE-BRITT LINDÉN *, PIRJO KONTRO ‡, and SIMO S. OJA ‡

Received March 1, 1982, from the **Research Laboratories of Medica Pharmaceutical Company, Ltd., Box 325, SF-00101 Helsinki 10*, and ‡*Department of Biomedical Sciences, University of Tampere, Box 607, SF-33101 Tampere 10, Finland.* Accepted for publication September 2, 1982.

Abstract □ A series of 2-acylaminoethanesulfonamides were synthesized by treating the corresponding sulfonyl chlorides with ammonia, a primary, or a secondary amine. A few compounds displayed marked anticonvulsant activity in mice when tested for their potency in the maximal electroshock seizure test. The piperidino, benzamido, phthalimido, and phenylsuccinylimido derivatives were active, whereas the succinylimido, saccharinylimido, and norbornendicarboxylimido compounds showed no activity. The interference with the sodium-independent taurine binding to mouse brain synaptic membranes was assessed to elucidate the possible mode of anticonvulsant action.

Keyphrases □ Anticonvulsant agents—potential, 2-aminoethanesulfonic acid (taurine) derivatives, synthesis □ Synthesis—2-aminoethanesulfonic acid (taurine) derivatives, anticonvulsant activity in mice □ Taurine—synthesis of derivatives, anticonvulsant activity in mice

Taurine, 2-aminoethanesulfonic acid, is abundant in excitable mammalian tissues such as the brain, sensory organs, heart, and other muscles (1). In these tissues taurine has recently been considered an essential effector in the regulation of neuronal communication, possibly as an inhibitory synaptic transmitter, neuromodulator, or stabilizer of excitable membranes (2, 3). Taurine effectively prevents seizures when administered intracerebroventricularly to an animal model, but clinical trials with epileptic patients using oral or intravenous administration have been only partially successful (4).

Taurine is quite polar, and its penetration from plasma into brain tissue is apparently hampered by its hydrophilic properties (5). We have attempted to prepare more lipophilic derivatives of taurine which would still possess an inhibitory action at central synapses. Lipophilization of taurine was effected by both acylation and conversion of the sulfonic acid group to various amides. In this way the shape of the molecule and the intramolecular electron distribution, both of which may be essential for the taurine-like inhibitory action (6), were expected to be unchanged. It is also significant that sulfonamides are generally atoxic.

RESULTS AND DISCUSSION

The compounds studied are of the general structures A and B (see Table I for R_1 and R_2 designations).

$R_1CH_2CH_2SO_2NH_2$ (A) $\qquad$ $R_1CH_2CH_2SO_2R_2$ (B)

Although several earlier reports (7–10) have described similar compounds, these studies evaluated the compounds for antibacterial and antimalarial activity. They were either inactive or only slightly active in this respect.

Compounds II, IVa–g, V, and VIIIa–b inhibited maximal electroshock (MES)-induced convulsions in mice (Table II). The most potent compounds were II, IVc, IVd, IVe, IVg, and V, which had ED_{50} values ≤100 mg/kg. It was found that the sodium-independent binding of [^{3}H]taurine to isolated synaptic membranes was inhibited by III, IVa, V, and VIc. In general, no parallelism was observed between anticonvulsant action and inhibition of taurine binding. Only V may act by interfering with the attachment of taurine to its membrane binding sites.

The acyltaurinamides and *N*-substituted acyltaurinamides were synthesized from the corresponding sulfonyl chlorides and ammonia, a primary, or a secondary amine as described previously (7–9, 11). These compounds are colorless, crystalline substances with a somewhat bitter taste. They are insoluble or slightly soluble in water, but soluble in polar organic solvents.

EXPERIMENTAL[1]

***N*-[2-[(Methylamino)sulfonyl]ethyl]benzamide (IVb), *N*-[2-[(Ethylamino)sulfonyl]ethyl]benzamide (IVc), *N*-[2-[(Dimethylamino)sulfonyl]ethyl]benzamide (IVd), *N*-[2-[[(1-Methylethyl)amino]sulfonyl]ethyl]benzamide (IVe), *N*-[2-[(Butylamino)sulfonyl]ethyl]benzamide (IVf), and *N*-[2-[[(1,1-Dimethylethyl)amino]sulfonyl]ethyl]benzamide (IVg)**—These compounds were prepared as described below for IVg. To *tert*-butylamine (10.92 g, 0.150 mol) was added with cooling and stirring (ice-bath) the substituted sulfonyl chloride (7.66 g, 0.031 mol) over a 25-min period. After 20 min stirring additional *tert*-butylamine (3.64 g, 0.05 mol) was added, and the stirring was continued at room temperature. Water (75 mL) was added, and the excess amine was removed with a stream of air. The precipitate was re-

[1] Melting points were determined in open capillary tubes and are uncorrected. Elemental analyses were performed by Janssen Pharmaceutica NV, Analytical Department, Beerse, Belgium. NMR data were recorded on a JEOL FX-60 spectrophotometer.

0022-3549/84/0100-0106$01.00/0

© 1984, American Pharmaceutical Association

Table I—Taurinesulfonamide Derivatives of $R_1CH_2CH_2SO_2R_2$

Compound	R_1	R_2	Recrystallization Solvent	Melting Point, °C	Formula	Analysis % Calc.	Found
I	H_2N-	$-NH_2$ HCl	90% ethanol	133–136[a]			
II		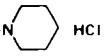	Ethanol-HCl	222–224[b]			
III			Ethanol-HCl	254–256[c]			
IVa		$-NH_2$	95% ethanol	168–171[d]			
IVb		$-NHCH_3$	Water	116–117	$C_{10}H_{14}N_2O_3S$	C 49.57 H 5.82 N 11.56	49.28 5.74 10.96
IVc		$-NHCH_2CH_3$	33% ethanol	112–114	$C_{11}H_{16}N_2O_3S$	C 51.54 H 6.29 N 10.93	51.45 6.32 11.00
IVd		$-N(CH_3)_2$	33% ethanol	113–115	$C_{11}H_{16}N_2O_3S$	C 51.54 H 6.29 N 10.93	51.72 6.35 11.11
IVe		$-NHCH(CH_3)_2$	33% ethanol	111–113	$C_{12}H_{18}N_2O_3S$	C 53.31 H 6.71 N 10.36	53.15 6.69 10.43
IVf		$-NH(CH_2)_3CH_3$	50% methanol	93–95	$C_{13}H_{20}N_2O_3S$	C 54.91 H 7.09 N 9.85	54.98 7.10 9.97
IVg		$-NHC(CH_3)_3$	75% methanol	91–94	$C_{13}H_{20}N_2O_3S$	C 54.91 H 7.09 N 9.85	54.77 7.03 9.93
V		$-NHCH_3$	95% ethanol	142–144	$C_{11}H_{12}N_2O_4S$	C 49.25 H 4.51 N 10.44	49.32 4.40 10.44
VIa		$-NH_2$	Acetone	195–197	$C_9H_{10}N_2O_5S_2$	C 37.24 H 3.47 N 9.65	37.12 3.48 9.68
VIb		$-NHCH_3$	Acetonitrile	179–182	$C_{10}H_{12}N_2O_5S_2$	C 39.47 H 3.97 N 9.20	39.43 4.01 9.22
VIc		$-NH(CH_2)_3CH_3$	Cyclohexane–ethylacetate (1:1)	72–77	$C_{13}H_{18}N_2O_5S_2$	C 45.07 H 5.24 N 8.09	44.86 5.07 7.92
VIIa		$-NH_2$	Water	189–191	$C_6H_{10}N_2O_4S$	C 34.95 H 4.89 N 13.58	34.75 4.88 13.60
VIIb		$-NHCH(CH_3)_2$	95% ethanol	101–102	$C_9H_{16}N_2O_4S$	C 43.54 H 6.50 N 11.28	43.46 6.54 11.28
VIIc		$-NH_2CH_2$	95% ethanol	110–112	$C_{13}H_{16}N_2O_4S$	C 52.69 H 5.44 N 9.45	52.78 5.48 9.48
VIIIa	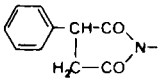	$-NH_2$	95% ethanol	157–159	$C_{12}H_{14}N_2O_4S$	C 51.05 H 5.00 N 9.52	50.50 4.91 9.66
VIIIb	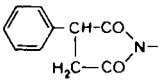	$-NHCH(CH_3)_2$	50% methanol	68–73	$C_{15}H_{20}N_2O_4S$	C 55.54 H 6.21 N 8.64	54.95 6.09 8.55
VIIIc	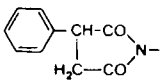	$-NHC(CH_3)_3$	95% ethanol	113–116	$C_{16}H_{22}N_2O_4S$	C 56.79 H 6.55 N 8.28	56.62 6.57 8.46
IX		$-NH_2$	Ethanol–dimethylformamide	242–245	$C_{14}H_{12}N_2O_4S$	C 55.26 H 3.97 N 9.21	55.06 3.90 9.21
Xa		$-NH_2$	Acetonitrile	206–209	$C_{11}H_{14}N_2O_4S$	C 48.88 H 5.22 N 10.36	48.89 5.21 10.21
Xb		$-NHCH(CH_3)_2$	Acetonitrile	131–134	$C_{14}H_{20}N_2O_4S$	C 53.83 H 6.45 N 8.97	53.93 6.52 8.88

[a] Lit. (8) mp 130–134°C. [b] Lit. (12) mp 202–206°C. [c] Lit. (12) mp 250–252°C. [d] Lit. (8) mp 169.5–170.5°C.

moved by filtration, washed with water, and recrystallized from the appropriate solvent (Table I).

1,3-Dihydro-*N*-methyl-1,3-dioxo-2*H*-isoindoleethanesulfonamide (V)—To methylene chloride (30 mL) were added the previously described sulfonyl chloride (2.74 g, 0.01 mol) (8) and methylamine hydrochloride (1.36 g, 0.02 mol). Then, 7 mL of 6 M K_2CO_3 was added with continuous stirring and cooling (~10°C) over a 10-min period. Water (25 mL) was added, and the organic phase was washed with water and dried over magnesium sulfate. The solvent was evaporated, and the product was recrystallized from the appropriate solvent (Table I).

3-Oxo-1,2-benzisothiazole-2(3*H*)-ethanesulfonamide 1,1-Dioxide (VIa), *N*-Methyl-3-oxo-1,2-benzisothiazole-2(3*H*)-ethanesulfon-

Table II—Anticonvulsant Activities (ED_{50}) of Taurinesulfonamide Derivatives in the Maximal Electroshock Test in Mice and the Effects on Sodium-Independent Taurine Binding in Mouse Brain Membrane Fractions

Compound	ED_{50}, mg/kg ip	Taurine Binding[a]
I	>300	102 ± 7 (5)
II	69	113 ± 6 (4)
III	>300	74 ± 10 (4)
IVa	209	80 ± 10 (5)
IVb	150	126 ± 10 (5)
IVc	84	140 ± 12 (4)
IVd	75	109 ± 10 (5)
IVe	77	121 ± 11 (5)
IVf	150	115 ± 11 (4)
IVg	82	136 ± 10 (5)
V	105	67 ± 4 (10)
VIa	>300	98 ± 9 (5)
VIb	>300	102 ± 9 (5)
VIc	>300	75 ± 10 (4)
VIIa	>300	
VIIb	>300	
VIIc	>300	
VIIIa	209	101 ± 13 (4)
VIIIb	244	84 ± 5 (3)
VIIIc	>300	
IX	>300	
Xa	>300	
Xb	>300	

[a] The binding of 0.1 μM [^{3}H]taurine to membrane fractions isolated from mouse whole brain in the presence of the compounds tested (concentration in the incubation medium: 1.0 mM except III and VIc, 0.5 mM, and IVg, 0.1 mM) is given as percentage of that in the control incubations without effectors (2.22 ± 0.32 nmol/kg fresh weight of synaptic membranes, n = 40, mean ± SEM). The number of experiments is in parentheses.

amide 1,1-Dioxide (VIb), and *N*-Butyl-3-oxo-1,2-benzisothiazole-2(3*H*)-ethanesulfonamide 1,1-Dioxide (VIc)—Sodium 1,2-benzisothiazol-3(2*H*)-one 1,1-dioxide (the sodium salt of saccharin) (205.2 g, 1 mol) and 1,2-dichloroethane (792 g, 8 mol) in dimethyl sulfoxide (1 L) were heated at 105°C for 6 h. The mixture was poured into water, and from the organic phase was isolated 153 g of the corresponding *N*-2-chloroethyl derivative, mp 63–66°C. This material was heated at 120°C for 2 h with thiourea (30.4 g, 0.4 mol). Dimethylformamide (20 mL) was added to the melt, and the mixture was allowed to cool. The material was slurried with acetone, filtered, and the resulting product washed with ethanol to give 38.9 g of the thiuronium hydrochloride, mp 210°C (dec.). This salt (83.2 g, 0.259 mol) was dissolved in warm water (1.9 L), and the mixture was filtered to remove the undissolved material (5.2 g). The solution was cooled to 5°C, and a stream of chlorine gas was bubbled through the solution over a 6-h period with cooling and stirring. The precipitate was isolated and recrystallized from toluene to give 56.2 g of 3-oxo-1,2-benzisothiazole-2(3*H*)-ethanesulfonyl chloride 1,1-dioxide.

Preparation of VIa—The aforementioned substituted sulfonyl chloride (9.66 g, 0.031 mol) was dissolved in methylene chloride (120 mL). With cooling and stirring, gaseous ammonia was introduced over a 15-min period. The solvent was removed by distillation, and the residue was slurried with water and then filtered. Recrystallization from acetone gave 2.09 g of VIa.

Preparation of VIb—The aforementioned substituted sulfonyl chloride (9.0 g, 0.029 mol) was dissolved in methylene chloride (100 mL), and methylamine (3.2 g, 0.19 mol) in isopropyl alcohol (16 mL) was added. After 3 min the mixture was poured into 200 mL of 0.3 M HCl, and after thorough mixing the organic layer was separated, dried, and the solvent evaporated. Several recrystallizations from acetonitrile gave 2.64 g of VIb.

Preparation of VIc—The aforementioned substituted sulfonyl chloride (9.3 g, 0.033 mol) was dissolved in methylene chloride (120 mL). *n*-Butylamine (2.44 g, 0.033 mol) in Na_2CO_3 solution (30 mL, 1.4 M) was added, the mixture was stirred for 6 min, and then water (50 mL) was added. The organic layer was separated and washed twice with water, dried over magnesium sulfate, and the solvent evaporated. The material was slurried with petroleum ether, filtered, and then recrystallized several times from a cyclohexane–ethyl acetate mixture (1:1) to give 0.95 g of VIc.

2,5-Dioxo-1-pyrrolidineethanesulfonamide (VIIa), *N*-(1-Methylethyl)-2,5-dioxo-1-pyrrolidineethanesulfonamide (VIIb), and 2,5-Dioxo -*N*- (phenylmethyl) -1- pyrrolidineethanesulfonamide (VIIc)—A mixture of 2-aminoethanesulfonic acid (taurine) 46.5 g, 0.37 mol), potassium acetate (49.0 g, 0.5 mol), succinic anhydride (50 g, 0.5 mol), and glacial acetic acid (300 mL) were heated at reflux for 2 h, with stirring. Acetic anhydride (25 mL) was added, and the heating was continued. The mixture was cooled overnight, and then the product was removed by filtration and washed with ethanol to give 54 g of the potassium salt of the succinylamide, which was used without purification.

A mixture of the aforementioned potassium salt (80 g, 0.41 mol), phosphorus pentachloride (115.8 g, 0.56 mol), and methylene chloride (689 mL) was stirred at 15–20°C for 5 h, and was then allowed to stand at room temperature for 48 h. The mixture was poured into ice-water (500 mL), and the organic layer was separated, washed with water, and dried over magnesium sulfate. The solvent was removed under reduced pressure, the residue was slurried with ether (150 mL), and the product was removed by filtration. Recrystallization from toluene gave 40 g of the sulfonyl chloride, mp 133–134°C.

Preparation of VIIa—The aforementioned sulfonyl chloride (11.25 g, 0.05 mol) was added with stirring and cooling (5–10°C) to a mixture of 15 mL of 6 M K_2CO_3, 15 mL of concentrated ammonium hydroxide, and methylene chloride (100 mL). The crystalline material was removed by filtration and washed with two 10-mL portions of cold water. Recrystallization gave 6 g of VIIa, mp 189–191°C. *N*-(1-Methylethyl)-2,5-dioxo-1-pyrrolidineethanesulfonamide (VIIb) and 2,5-dioxo-*N*-(phenylmethyl)-1-pyrrolidineethanesulfonamide (VIIc) were prepared in an analogous manner using isopropyl- and benzylamines, respectively.

2,5-Dioxo-3-phenyl-1-pyrrolidineethanesulfonamide (VIIIa), *N*-(1-Methylethyl)-2,5-dioxo-3-phenyl-1-pyrrolidineethanesulfonamide (VIIIb), and *N*-(1,1-Dimethylethyl)-2,5-dioxo-3-phenyl-1-pyrrolidineethanesulfonamide (VIIIc)—2-Phenylsuccinylimidoethanesulfonyl chloride was synthesized using the method described for phthalimidoethanesulfonyl chloride (7). Chloroethylphenylsuccinimide (87.3 g, 0.367 mol) gave the corresponding phenylsuccinylimidoethanethiuronium chloride in a yield of 56 g, mp 205–216°C. This material (49.4 g, 0.157 mol) afforded 39.4 g, of phenylsuccinylimidoethanesulfonyl chloride, mp 146–148°C, after recrystallization from toluene. Treatment of the aforementioned sulfonyl chloride with concentrated ammonium hydroxide gave VIIIa, while treatment with isopropylamine or *tert*-butylamine gave VIIIb or VIIIc, respectively.

In a similar fashion 1,3-dioxo-1*H*-benz[*de*]isoquinoline-2(3*H*)-ethanesulfonamide (IX) was prepared from the corresponding sulfonyl chloride (mp 164–165°C), and also 1,3,3a,4,7,7a-hexahydro-1,3-dioxo-4,7-methano-2*H*-isoindole-2-ethanesulfonamide (Xa) and 1,3,3a,4,7,7a-hexahydro-*N*-(1-methylethyl)-1,3-dioxo-4,7-methano-2*H*-isoindole-2-ethanesulfonamide (Xb) were prepared from the sulfonyl chloride, mp 158–160°C.

Anticonvulsant activity—All compounds were tested for anticonvulsant activity using the maximal electroshock seizure (MES) test which was carried out on mice subjected for 0.2 s to a current of 50 mA (60 Hz) delivered through corneal electrodes (13). The effect of the compounds on the sodium-independent binding of [^{3}H]taurine (0.1 mol/L, specific activity 0.33 PBq/mol) was measured in 0.05 M Tris buffer, pH 7.1, at 5°C (incubation time: 1 min) (14).

REFERENCES

(1) J. G. Jacobsen and L. H. Smith, Jr., *Physiol. Rev.*, **48,** 424 (1968).

(2) S. S. Oja, P. Kontro, and P. Lähdesmäki, *Prog. Pharmacol.*, **1,** 1 (1977).

(3) S. S. Oja and P. Kontro, in "Taurine and Neurological Disorders," A. Barbeau and R. J. Huxtable, Eds., Raven, New York, N.Y., 1978, pp. 181–200.

(4) S. S. Oja and P. Kontro, *Acta Neurol. Scand.*, Suppl. (in press).

(5) S. S. Oja, I. Lehtinen, and P. Lähdesmäki, *Q. J. Exp. Physiol.*, **61,** 133 (1976).

(6) P. Lähdesmäki and S. S. Oja, *J. Neurochem.*, **20,** 1411 (1973).

(7) E. Miller, J. M. Sprague, L. W. Kissinger, and L. F. McBurney, *J. Am. Chem. Soc.*, **62,** 2099 (1940).

(8) R. Winterbottom, I. W. Clapp, W. H. Miller, J. P. English, and R. O. Roblin, *J. Am. Chem. Soc.*, **69,** 1393 (1947).

(9) J. F. Mead and J. B. Koepfli, *J. Org. Chem.*, **12,** 295 (1947).

(10) J. W. Griffin and D. H. Hey, *J. Chem. Soc., London*, **1952,** 3334.

(11) M. Quaedvlieg, "Methoden der Organischen Chemie," Vol. 9, G. Thieme, Stuttgart, West Germany, 1955, pp. 398–400.

(12) A. A. Goldberg, *J. Chem. Soc., London*, **1945,** 464.

(13) J. E. P. Toman, E. A. Swinyard, and L. S. Goodman, *J. Neurophysiol.*, **9,** 231 (1946).

(14) S. J. Enna and S. H. Snyder, *Brain Res.*, **100,** 81 (1975).

Enhanced Rectal Absorption of Cefmetazole and Cefoxitin in the Presence of Epinephrine Metabolites in Rats and a High-Performance Liquid Chromatographic Assay for Cephamycin Antibiotics

TOSHIAKI NISHIHATA, HIDEKUNI TAKAHAGI, MIDORI YAMAMOTO, HISAO TOMIDA, J. HOWARD RYTTING ˣ, and TAKERU HIGUCHI

Received June 25, 1982, from the *Department of Pharmaceutical Chemistry, The University of Kansas, Lawrence, KS 66045.* Accepted for publication November 5, 1982.

Abstract □ 4-Hydroxy-3-methoxymandelic acid and 3,4-dihydroxymandelic acid were found to be potent adjuvants for the rectal absorption of water-soluble compounds in rats. Both adjuvants enhanced the absorption of two cephamycin antibiotics, cefmetazole and cefoxitin. Maximum plasma levels of the antibiotics were obtained within 30 min after rectal administration. The bioavailability of both antibiotics appeared to depend on the concentration of the adjuvant in the microenema, the dosage form used in these experiments. Instead of a microbial assay, a new chemical method involving high-performance liquid chromatography with an ion-pairing technique was developed for analyzing the cephamycin antibiotic plasma levels.

Keyphrases □ Epinephrine metabolites—4-hydroxy-3-methoxymandelic acid, 3,4-dihydroxymandelic acid, adjuvants, rectal absorption of cefmetazole and cefoxitin, rats □ Cefmetazole—rectal absorption in rats, use of epinephrine metabolites as adjuvants, high-performance liquid chromatographic assay in plasma □ Cefoxitin—rectal absorption in rats, use of epinephrine metabolites as adjuvants, high-performance liquid chromatographic assay in plasma

Cefmetazole and cefoxitin, cephamycin antibiotics which are effective against Gram-positive and Gram-negative bacteria, are differentiated from cephalosporins by a methoxy group at the 7-position of the isoxazole ring. Both antibiotic agents are currently administered by intravenous or intramuscular injection.

In a number of situations, rectal administration of these drugs would be advantageous, especially to reduce the muscle damage caused by repeated injections. Previous work (1–5) demonstrated that salicylates and several structurally related compounds (*e.g.*, sodium 5-methoxysalicylate) markedly enhanced the rectal absorption of many types of drugs, particularly those that are soluble in water, including cefmetazole. Also, a relatively high concentration (50 mg/mL) of salicylate did not appear to cause damage to the rectal mucosal membrane (3).

This paper describes the effect of two metabolites of epinephrine, 4-hydroxy-3-methoxymandelic acid (I) and 3,4-dihydroxymandelic acid (II), on the rectal absorption of sodium cefoxitin and sodium cefmetazole in rats. The rectal absorption of phenolsulfonphthalein, used as a model water-soluble compound, was also studied.

Often, microbial assays such as that reported by Simon and Yin (6) have been used to measure plasma concentrations of antibiotics such as cefmetazole and cefoxitin. Buhs *et al.* (7) have reported a high-performance liquid chromatographic (HPLC) assay of cefoxitin using a strong anion-exchange resin. In this paper, we describe HPLC assays (using reverse-phase columns) for cefmetazole and cefoxitin that were developed to avoid the interference of additives administered with the antibiotics.

EXPERIMENTAL

Materials—A pump[1] equipped with an injector[2], a reverse-phase column[3], and a UV detector[4] (254 nm), all operated at room temperature, was used for analysis of cefoxitin and cefmetazole. The compounds used included sodium cefoxitin[5], sodium cefmetazole[6], 4-hydroxy-3-methoxymandelic acid[7], 3,4-dihydroxymandelic acid[7], acetonitrile[8], citric acid[9], sodium citrate[9], tetrabutylammonium bromide[9], and phenolsulfonphthalein[9].

Sample Preparation—Plasma aliquots of 1.0 mL were mixed with 0.1 mL of 0.01 M phosphoric acid and 0.6 mL of acetonitrile in 15-mL test tubes for 20–30 s and then centrifuged at ~2000 rpm for 5 min. The supernatants were poured into 4-mL glass vials and evaporated to dryness under a nitrogen stream using evaporating manifolds[10]. The residues were dissolved in 0.1 mL of water just before analysis and stirred vigorously using a vortex mixer. Sample aliquots of 20 μL were then chromatographed. Blank plasma samples spiked with drug concentrations of up to 3.0 μg/mL were also analyzed to establish a calibration curve.

Chromatographic Conditions—Two different reverse-phase columns were used, and appropriate conditions were developed for each. A mobile phase consisting of 8 volumes of 0.005 M citrate buffer, pH 5.0, containing 0.002 M tetrabutylammonium bromide (ion-pairing agent) and 2 volumes of acetonitrile was used for the Ultrasphere ODS column[3]. A mixture consisting of 77.5% (v/v) 0.025 M citrate buffer, pH 5.0, containing 0.005 M tetrabutylammonium bromide and 22.5% (v/v) acetonitrile was used as the mobile phase for the OD-MP, RP-18 column[3]. The flow rate of the mobile phase was 1.0 mL/min. The column effluent was monitored by UV absorption at 254 nm, and peak height measurements were used for quantitation. The column was maintained at room temperature.

Animals—Sprague–Dawley male rats, 225–250 g, were fasted for 16 h prior to the experiment to avoid residual feces in the rectum which could reduce drug absorption. The rats were anesthetized with pentobarbital (60 mg/kg), and the rats' body temperatures were maintained at 38°C using a temperature-controlled platform.

***In Vivo* Absorption Study**—The drugs and adjuvants were administered rectally as a 0.3- or 0.6-mL microenema using 0.01 M phosphate buffer at pH 4.5 as the vehicle. Following administration of the drug solution to the rat, the anus was ligated with a thread to avoid leakage of the solution. Blood samples were withdrawn from the jugular vein at regular intervals into syringes pretreated with 3% sodium citrate (as anticoagulant) and centrifuged at 3000 rpm for 10 min.

Assay for Phenolsulfonphthalein in Plasma—Plasma samples of 0.3 mL were diluted with 0.3 mL of 0.1 M NaOH solution and measured with a spectrophotometer at 540 nm. As a blank, 0.3 mL of plasma was collected before administration of the phenolsulfonphthalein microenema.

RESULTS AND DISCUSSION

Drug Analysis—Due to the high polarity of cefoxitin and cefmetazole,

[1] Model 110A, Altex.
[2] Model 7010, Rheodyne.
[3] Ultrasphere ODS, 5 μm, 4.6 i.d. × 15-cm length; OD-MP, RP-18, 5 μm, 4.6 i.d. × 15-cm length; Altex.
[4] Model 153, Altex.
[5] Merck, Rahway, N.J.
[6] Sankyo Co., Tokyo, Japan.
[7] Sigma Chemical Co., St. Louis, Mo.
[8] Fisher Chemical Co., St. Louis, Mo.
[9] Aldrich Chemical Co., Milwaukee, Wis.
[10] Silli-Vap Evaporator; Pierce Chemical Co., Rockford, Ill.

0022-3549/84/0100-0109$01.00/0
© 1984, American Pharmaceutical Association

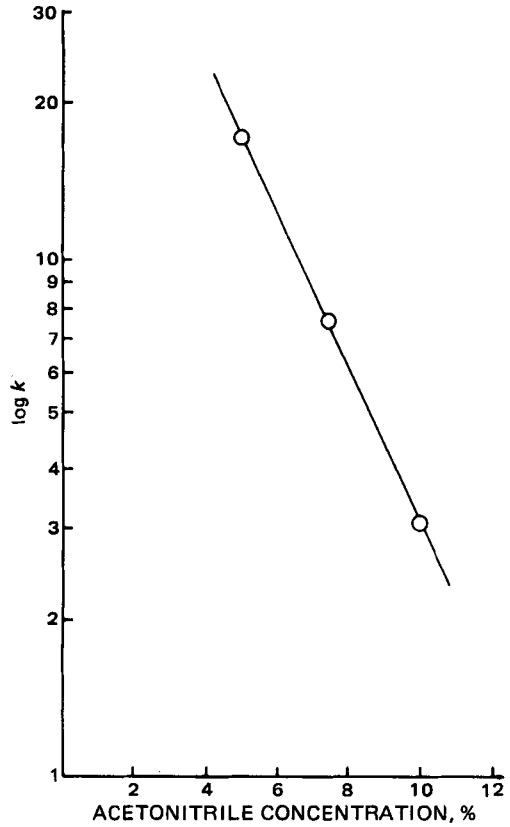

Figure 1—*Relationship between the capacity factor (k′) of cefmetazole and concentration of acetonitrile in the mobile phase. Chromatographic conditions: Ultrasphere ODS (4.6-mm × 15-cm) column with a mobile phase of 0.005 M citrate buffer (pH 5.0)–acetonitrile at a flow rate of 1 mL/min and detection at 254 nm.*

an aqueous or highly polar mobile phase with a high resolution reverse-phase column was used for the analysis. Reverse-phase chromatography using a mixture of buffer and acetonitrile as the mobile phase was the first analytical method attempted for the determination of cefmetazole and cefoxitin. With this method, the relationship between the percent concentration of acetonitrile in the mobile phase *versus* the capacity factor (log k') proved to be linear (Fig. 1). Optimum conditions for this method

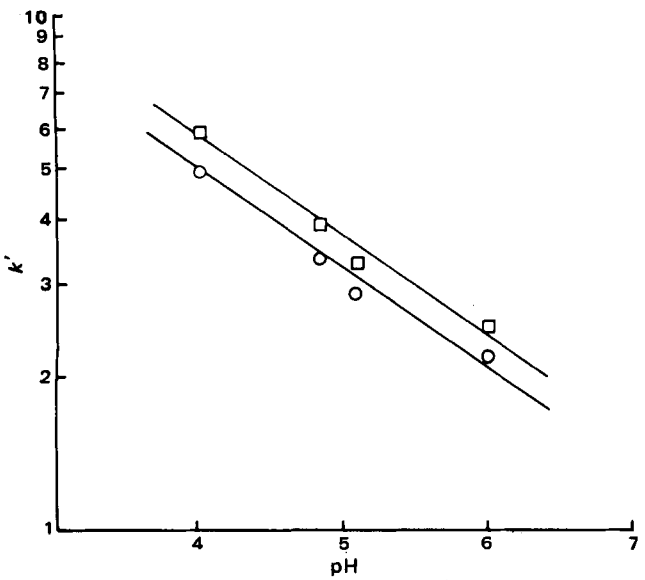

Figure 2—*Ion-pair reverse-phase chromatographic separation of cefmetazole (○) and cefoxitin (□) as a function of pH. Chromatographic conditions: Ultrasphere ODS (4.6-mm × 15-cm) column with a mobile phase of 0.002 M tetrabutylammonium bromide in 0.005 M citrate buffer–acetonitrile (8:2).*

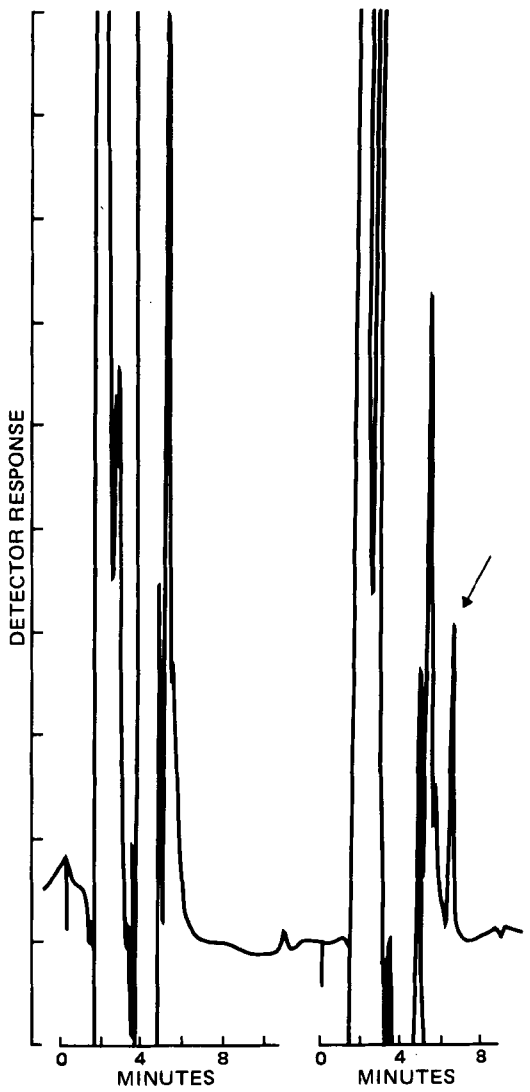

Figure 3—*Chromatogram of cefmetazole in plasma using an Ultrasphere ODS (4.6-mm × 15-cm) column with a mobile phase of 0.002 M tetrabutylammonium bromide in 0.005 M nitrate buffer (pH 5.0)–acetonitrile (8:2). The arrow indicates the cefmetazole peak, and the number of AUFS is 0.01.*

were obtained when the acetonitrile concentration was between 8 and 10% and the capacity factor was the only factor under consideration. It was critical that the retention time in each mobile phase be the same; however, using this method, some of the other plasma components interfered with the cefmetazole peak. Therefore, an ion-pairing agent (tetrabutylammonium bromide) was added to the mobile phase to enhance the retention of the drug.

Theoretically in reverse-phase ion-pairing chromatography, maximum k' values are obtained at intermediate pH levels, where the sample compounds are completely ionized and ion-pair formation is at a maximum. Since the pK_a values of cefoxitin and cefmetazole are 2.50 and 2.34, respectively, as the pH of the mobile phase increases, the k' values of these drugs should also increase if they are retained as ion-pair complexes. However, in our experiments, cefmetazole and cefoxitin appeared to be retained to a greater extent as the pH of the mobile phase decreased. The effect of pH on the separation of the components using tetrabutylammonium bromide as the source of the counter ion is shown in Fig. 2. One possible explanation for the results obtained may be that ion pairs were formed between the drugs and tetrabutylammonium bromide which increased the retention time possibly by modifying the properties of the stationary phase.

Figure 3 shows a typical chromatogram for the assay of cefmetazole in plasma using an Ultrasphere ODS column. Cefoxitin has a slightly longer retention time, as shown in Fig. 2. Adjuvants such as 4-hydroxy-3-methoxymandelic acid or 3,4-dihydroxymandelic acid present in the plasma samples did not interfere with the drug assay procedure.

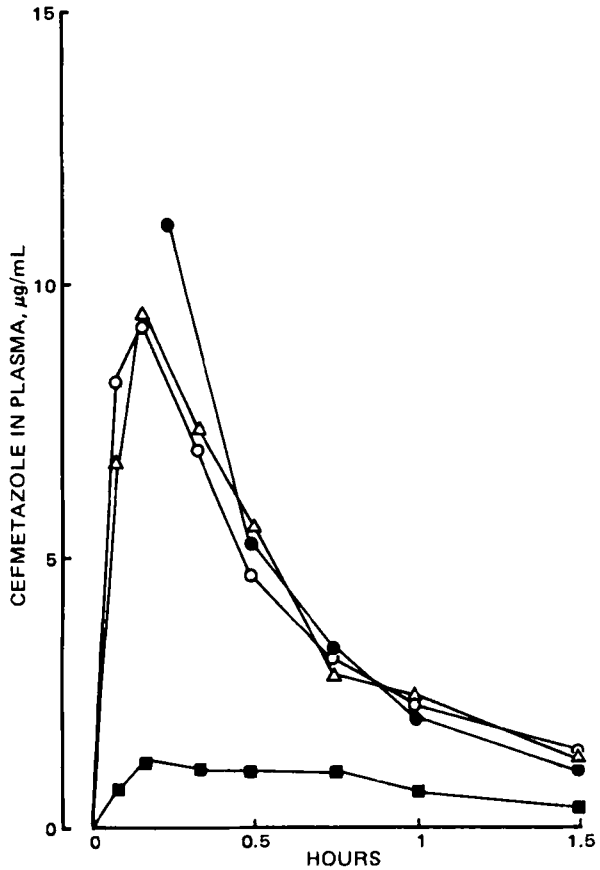

Figure 4—*Plasma cefmetazole levels in rats after intravenous injection of 6 mg/kg (●) and after rectal administration of a microenema containing 30 mg/mL/kg and 10 mg of sodium chloride (■); 30 mg/mL/kg, 10 mg of sodium chloride/mL, and 30 mg of I/mL/kg (○); or 30 mg/mL/kg, 10 mg of sodium chloride/mL, and 30 mg of II/mL/kg (△).*

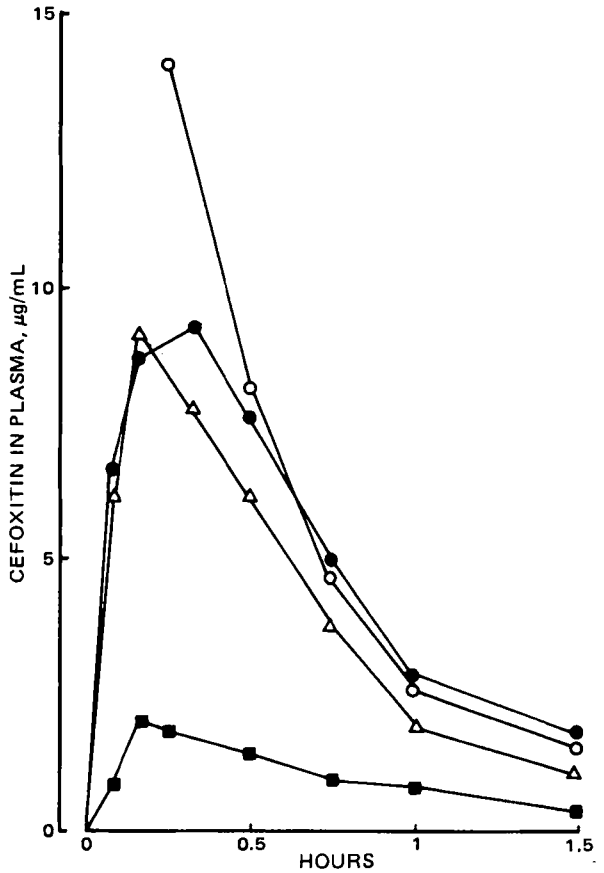

Figure 5—*Plasma cefoxitin levels in rats after intravenous injection of 6 mg/mL/kg (○) and after rectal administration of a microenema containing 30 mg/mL/kg and 10 mg of sodium chloride (■); 30 mg/mL/kg, 10 mg of sodium chloride, and 30 mg of I/mL/kg (●); or 30 mg/mL/kg, 10 mg of sodium chloride, and 30 mg of II/mL/kg (△).*

Linear calibration curves for cefoxitin and cefmetazole in water and plasma were obtained with concentrations ranging from 0.1 to 3.0 μg/mL. The reproducibility was indicated by coefficients of variation of 3.2% for cefmetazole and 1.5% for cefoxitin or five replicate analyses of 1.0-μg/mL samples. The recoveries of cefoxitin and cefmetazole, which were tested using plasma blanks containing the standard solution, were 91 and 90%, respectively. The limit for accurate quantitation appeared to be as low as 0.1 μg/mL for both compounds. When using columns from different manufacturers, minor modifications were necessary for good separation. Using OD-MP, RP-18, for example, the mobile phase described in the *Experimental* section was developed in order to get a separation comparable to the one shown in Fig. 3 with an Ultrasphere ODS column.

Table I—Relative Bioavailability of Cefmetazole (30 mg/kg) or Cefoxitin (30 mg/kg) after Rectal Administration in the Presence or Absence of Adjuvant

Adjuvant, mg/kg	Relative Bioavailability[a]	
	Cefmetazole	Cefoxitin
4-Hydroxy-3-methoxymandelic acid		
0	1.0	1.0
15	3.8 ± 1.3	2.6 ± 0.9
30	6.8 ± 2.5	5.7 ± 1.4
50	10.4 ± 2.8	9.3 ± 2.7
75	13.7 ± 3.4	15.6 ± 4.3
100	15.8 ± 3.1	17.5 ± 3.8
3,4-Dihydroxymandelic acid		
0	1.0	1.0
15	3.7 ± 0.8	2.9 ± 1.1
30	7.1 ± 2.1	4.8 ± 0.8
50	11.1 ± 2.3	7.4 ± 2.1
75	16.4 ± 4.2	14.2 ± 3.9
100	18.2 ± 4.8	19.3 ± 4.4

[a] Relative bioavailability = $([AUC]_{R \text{ in presence of adjuvant}}) \times (Dose_{\text{without adjuvant}}) / ([AUC]_{R \text{ without adjuvant}}) \times (Dose_{\text{in presence of adjuvant}})$.

Effects of Adjuvants—In a recent paper (5) describing the effects of several adjuvants on the rectal absorption of theophylline, lidocaine, cefmetazole, and levodopa, it was suggested that compounds which were effective in enhancing rectal absorption contained both hydroxy and carboxy functional groups. In these cases the groups were attached to a phenyl ring. To further elucidate the structural requirements for effective adjuvants, the present study involves two metabolites of epinephrine, 4-hydroxy-3-methoxymandelic acid (I) and 3,4-dihydroxymandelic acid (II), in which the carboxyl groups are not attached to a phenyl ring.

As seen in Figs. 4 and 5, respectively, these adjuvants improved the rectal absorption of cefmetazole and cefoxitin. Their action appeared to parallel that of 5-methoxysalicylate and other adjuvants described previously (5), in which relatively rapid absorption with high plasma levels was attained. Maximum plasma levels of cefmetazole appeared within 30 min after rectal administration with I or II. Higher plasma cefoxitin or cefmetazole levels were obtained after rectal administration of a microenema containing an adjuvant compared with the rectal administration of cefoxitin or cefmetazole alone (Figs. 4 and 5). As summarized in Table I, the relative bioavailabilities of cefmetazole and cefoxitin in the presence of adjuvants were significantly improved as determined from the typical relationship: $([AUC]_{R \text{ in presence of adjuvant}}) \times (Dose_{\text{without adjuvant}}) / ([AUC]_{R \text{ without adjuvant}}) \times (Dose_{\text{with adjuvant}})$.

The influence of adjuvant concentration is also illustrated in Table I. When the concentration of the adjuvant and drug in the microenema were cut in half by administering the same total amounts in double the solution volume, the cefmetazole plasma level decreased (Fig. 6). Therefore, the concentration of adjuvant and drug in the microenema appear to be important with regard to the efficacy of adjuvant-enhanced absorption.

Phenolsulfonphthalein has been used as an indicator to measure the change of perfusate volume in an *in situ* perfusion method since it is not readily absorbed (8). In this study, phenolsulfonphthalein was used as a typical water-soluble compound, *i.e.*, poorly absorbed from the rectum. In the absence of an adjuvant in the microenema, no phenolsulfonphthalein appeared in the plasma after rectal administration. However,

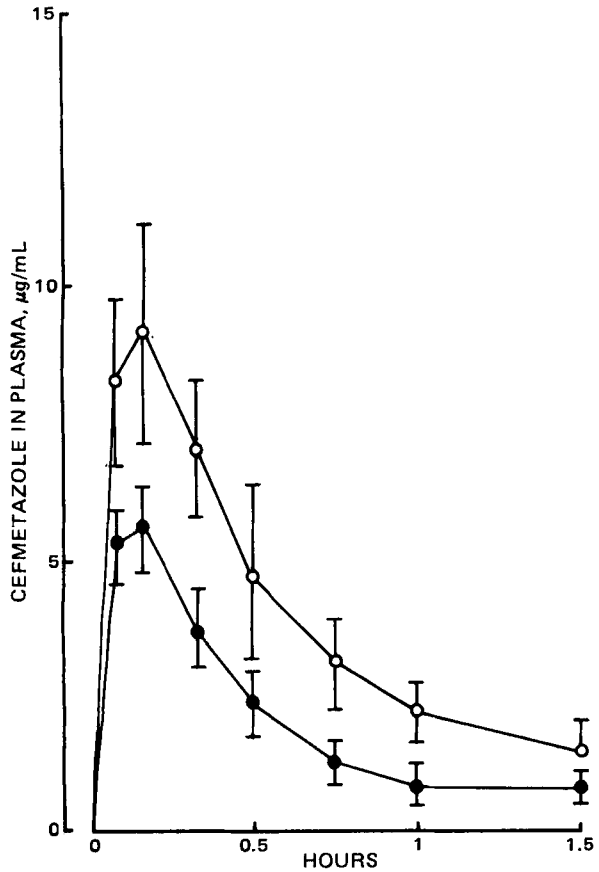

Figure 6—*Plasma cefmetazole levels in rats after rectal administration of a microenema containing 30 mg/mL/kg, 10 mg of sodium chloride, and 30 mg of I/mL/kg (○) or 30 mg/2 mL/kg, 10 mg of sodium chloride, and 30 mg of I/2 mL/kg (●). Statistical significance:* $p < 0.001$ ○ versus ● *except for 1.5 h.*

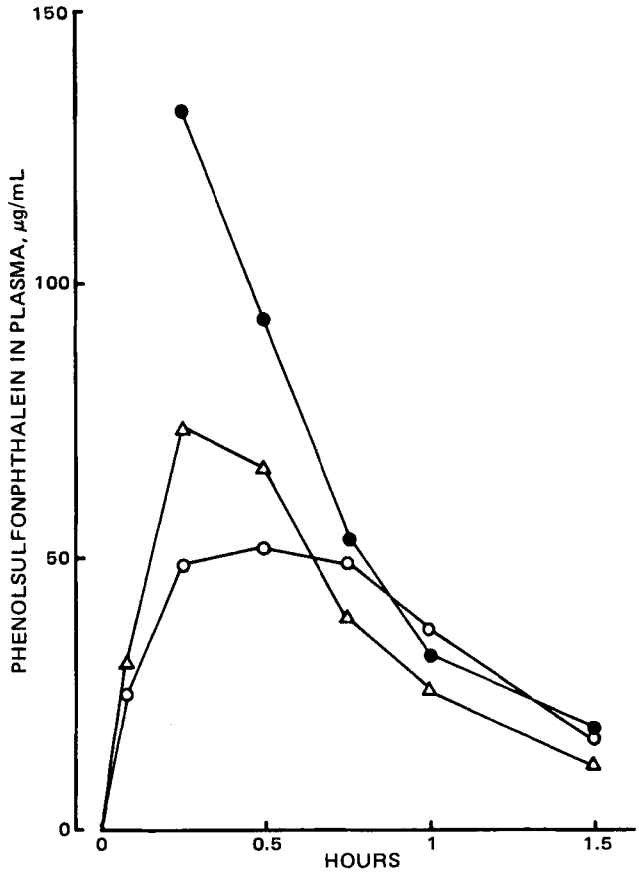

Figure 7—*Plasma phenolsulfonphthalein levels in rats after intravenous injection of 10 mg/kg and after rectal administration of a microenema containing 20 mg/mL/kg, 10 mg of sodium chloride, and 30 mg of I/mL/kg (○) or 20 mg/mL/kg, 10 mg of sodium chloride, and 30 mg of II/mL/kg (△).*

as shown in Fig. 7, absorption of phenolsulfonphthalein from the rectum was significantly enhanced in the presence of I or II. Bioavailability of phenolsulfonphthalein after rectal administration compared with intravenous injection was 32.4 ± 9.5% in the presence of 30 mg of I and 26.8 ± 5.7% in the presence of 30 mg of II.

The complete mechanism for the enhancement of rectal drug absorption in the presence of I and II has not been elucidated. It was reported earlier (1) that the enhancing action of salicylate was suppressed by the presence of the divalent ions of calcium and magnesium. Salicylate is known to complex with divalent metal ions, and it has been suggested that such interactions are responsible for at least some of the pharmacological and biochemical effects of salicylate (9). The presence of 10 mg/mL of calcium chloride in microenemas containing 30 mg/kg of cefoxitin or cefmetazole and 30 mg/kg of either I or II, reduced the peak plasma drug levels by ~50% compared with the absence of calcium chloride; *i.e.*, the presence of calcium chloride reduced the peak plasma levels of cefmetazole and cefoxitin from 9 μg/mL to 4 μg/mL in the presence of I and from 9 μg/mL to 5 μg/mL in the presence of II. Thus, it appears that the effects of I and II are similar to that of salicylate and that the adjuvants may require some complexation with divalent metal ions.

REFERENCES

(1) T. Nishihata, J. H. Rytting, and T. Higuchi, *J. Pharm. Sci.*, **70**, 71 (1981).

(2) T. Nishihata, J. H. Rytting, T. Higuchi, and L. Caldwell, *J. Pharm. Pharmacol.*, **33**, 334 (1981).

(3) T. Nishihata, J. H. Rytting, L. Caldwell, S. Yoshioka, and T. Higuchi, in "Optimization of Drug Delivery," Alfred Benzon Symposium 17, H. Bundgaard, A. B. Hansen, and H. Kofod, Eds., Munksgaard, Copenhagen, 1982, pp. 17–34.

(4) T. Nishihata, J. H. Rytting, and T. Higuchi, *J. Pharm. Sci.*, **71**, 869 (1982).

(5) T. Nishihata, J. H. Rytting, and T. Higuchi, *J. Pharm. Sci.*, **71**, 865 (1982).

(6) H. J. Simon and E. J. Yin, *Appl. Microbiol.*, **19**, 573 (1970).

(7) R. P. Buhs, T. E. Maxim, N. Allen, T. A. Jacob, and F. J. Wolf, *J. Chromatogr.*, **99**, 609 (1974).

(8) S. Kitazawa, H. Ito, and H. Sezaki, *Chem. Pharm. Bull.*, **23**, 1856 (1975).

(9) S. Grisolia, J. Mendelson, and D. Diederich, *FEBS Lett.*, **11**, 140 (1970).

ACKNOWLEDGMENTS

This work was supported in part by a grant from INTERx Research Corporation, a subsidiary of Merck & Co., Inc. The authors would also like to acknowledge the support provided by the Center for Biomedical Research, The University of Kansas.

Determination of Pantothenic Acid in Multivitamin Pharmaceutical Preparations by Reverse-Phase High-Performance Liquid Chromatography

THOMAS J. HUDSON ˣ and REBECCA J. ALLEN

Received April 19, 1982, from the *Forrest C. Shaklee Research Laboratories, Hayward, CA 94545.* Accepted for publication December 1, 1982.

Abstract □ A high-performance liquid chromatographic procedure was developed for the analysis of calcium pantothenate in nutritional supplements. The method involves a simple extraction using phosphate buffer and sonication. Chromatographic separation is obtained using an aminopropyl-loaded silica gel column in the reverse-phase mode. A UV detector set at 210 nm was used to monitor the effluent. Quantitative recoveries were obtained, and precision of the method is discussed. The method is applicable to multivitamin tablets, calcium pantothenate raw material, and yeast grown in the presence of high levels of calcium pantothenate. The results of the method are compared with results obtained from the USP microbiological method of analysis. It was concluded that the procedure is rapid, accurate, easily automated, and practical for routine quality control use.

Keyphrases □ Pantothenic acid—multivitamin preparations, HPLC □ Vitamins—pantothenic acid determination by HPLC □ High-performance liquid chromatography—pantothenic acid determination in multivitamins

Pantothenic acid is an important nutrient in the human diet and is a constituent of CoA, which is essential to the metabolism of both protein and fats. Since pantothenic acid can easily be destroyed by the prolonged heating often encountered in food and tablet processing, the more stable calcium salt is usually used in various fortified products.

Most chemical methods of analysis (1–4) require cleavage of the pantothenic acid molecule, reaction with a suitable derivatizing agent, and subsequent spectrophotometric measurement. The disadvantages associated with this approach include interferences from sugars and common pharmaceutical vehicles (4) as well as ascorbic acid and riboflavin. Considerable sample manipulation is required to remove these interferences, thus making the procedure very time consuming.

The traditional quality control procedure is the official microbiological assay (MBA) method (5). This method requires sample solution inoculation with *Lactobacillus plantarum*, incubation for 16–24 h, photometric measurement of the resulting turbidity, and interpolation of results using a standard growth response curve. This method suffers several disadvantages: it requires 24 h before data can be obtained and extensive manipulation by well experienced analysts to achieve reliable results. In addition, trace pantothenic acid contamination can easily cause erratic results since very small (<ppm) amounts are typically analyzed.

This report describes a high-performance liquid chromatographic (HPLC) procedure for the quantitative determination of pantothenic acid in multivitamin and multimineral tablets and raw materials.

EXPERIMENTAL

Apparatus—The HPLC system consisted of two solvent pumps[1], an autoinjector[2], an integrating recorder[3], and a UV absorbance detector[4] set at 210 nm. An aminopropyl-bonded silica gel column[5] was used and regulated at 25°C by a constant-temperature bath[6]. A high-output sonication device[7] was used to aid sample dissolution. The mobile phase was deaerated using a sonication water bath[8] and a vacuum pump[9]. All samples were filtered using a 0.45-μm filter unit[10].

Chemicals and Reagents—The solvents used were distilled in glass[11]. Potassium phosphate was HPLC grade[12] and calcium pantothenate was obtained as a USP reference standard[13]. Commercial vitamin preparations were obtained from local pharmacies and distributors.

Mobile Phase—A mixture of 0.005 M monobasic potassium phosphate (pH 4.5)–acetonitrile (13:87 v/v) was deaerated by sonication with vacuum and run at a flow rate of 2.0 mL/min using pump A. Pump B contained a mixture of water–acetonitrile (90:10) used as a final column washing step initiated after completion of an automated set of analyses.

Standard Preparation—An appropriate amount of calcium pantothenate reference standard was weighed and dissolved in 0.005 M potassium phosphate (pH 4.5) to obtain a concentration of 0.25 mg/mL.

Sample Preparation—A suitable number of weighed tablets were placed in a 200-mL volumetric flask. The final calcium pantothenate concentration was ~250 μg/mL. Approximately 100 mL of 0.005 M potassium phosphate solution (pH 4.5) was added, and the contents were sonicated at 75 W for 2 min. Thickly coated tablets required pulverization prior to sonication. The sample flask was diluted to volume with phosphate buffer after cooling to room temperature; a portion of the sample solution was filtered through a 0.45-μm filter unit, and 10 μL of the filtrate was injected into the liquid chromatograph.

Fortified yeasts, vitamin premixes, and raw material were treated in the same manner after appropriate sample amounts were selected.

RESULTS AND DISCUSSION

Pantothenic acid exhibits UV absorption between 200 and 225 nm, but no absorption in the 254–280-nm range, which is typically used for most HPLC analyses. Proper derivatization could provide a strong chromophore; however, this time-consuming step is impractical for the routine analyses of large numbers of samples. Analyses using UV detection <220 nm introduce problems caused by background UV absorption of mobile phase solvents and dissolved oxygen interference with a stable baseline (6). Solvents used for the mobile phase deaerated by sonication under vacuum were successful in this type of analysis. A problem associated with

[1] Model 6000A, Waters Associates, Milford, Mass.
[2] Model 710B, Waters Associates, Milford, Mass.
[3] Model 730, Waters Associates, Milford, Mass.
[4] Model LCL75, Perkin-Elmer Corp., Norwalk, Conn.
[5] Hibar II LiChrosorb NH_2 (10 μm), 250 mm × 4.6-mm i.d., Alltech Associates, Los Altos, Calif.
[6] Model FK, Haake, Saddlebrook, N.J.
[7] Model 184, Bronson Sonic Power Co., Danbury, Conn.
[8] Model 52H, Bronson Sonic Power Co., Danbury, Conn.
[9] Model 290, Thomas Co., Sheboygan, Wis.
[10] Type Ha, Millipore Corp., Bedford, Mass.
[11] Burdick & Jackson, Muskegon, Mich.
[12] Fisher Scientific Co., Fair Lawn, N.J.
[13] U.S. Pharmacopeial Convention, Rockville, Md.

0022-3549/84/0100-0113$01.00/0
© 1984, American Pharmaceutical Association

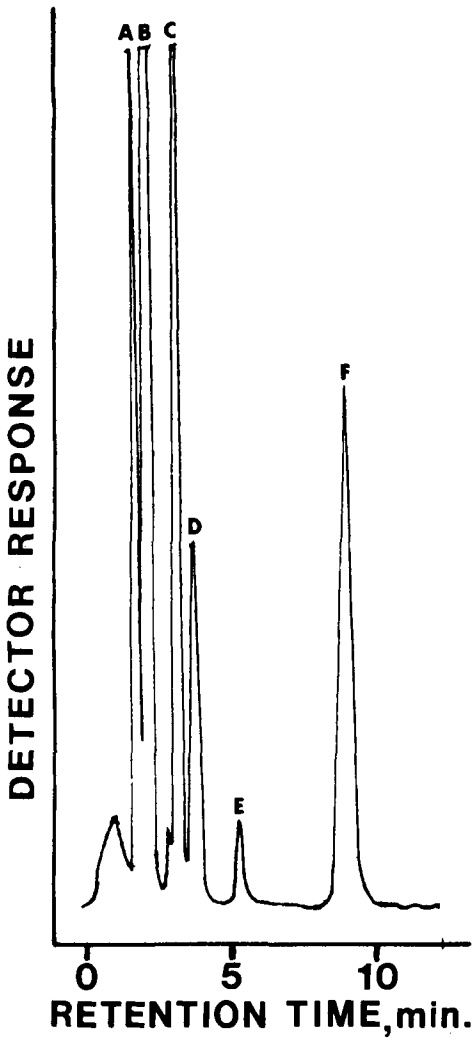

Figure 1—*Chromatogram of a multivitamin–multimineral tablet extract. Key: (A) niacinamide, (B) vitamin B_6, (C) vitamin B_2, (D) vitamin B_1, (E) unknown, (F) unknown, (G) pantothenic acid, (H) unknown.*

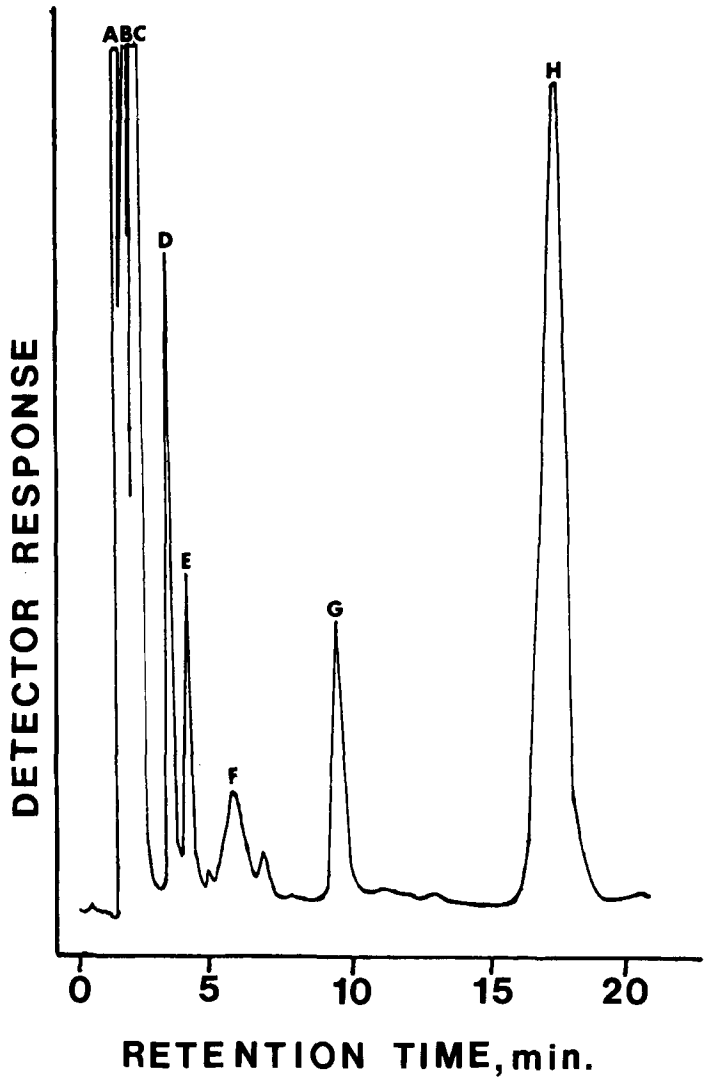

Figure 2—*Chromatogram of a high potency B complex tablet extract. Key: (A) niacinamide, (B) vitamin B_6, (C) vitamin B_2, (D) vitamin B_1, (E) unknown, (F) pantothenic acid.*

using the phosphate–acetonitrile solvent system is the potential for phosphate precipitation in the HPLC column. Considerable precipitation was encountered when the phosphate level was >0.15 M or the amount of acetonitrile was >95% in the mobile phase. A water–acetonitrile (90:10 v/v) column wash was very effective for maintaining column life. Over 500 routine samples were injected in duplicate using an automated system within a 3-month period with no appreciable loss in column performance. This is probably the result of using a small injection volume and performing the column washing step after every set of automated analyses.

Typical chromatographic separations of pantothenic acid in a multivitamin–multimineral tablet and in a B-complex tablet are shown in Figs. 1 and 2, respectively. The sample peak corresponding to the retention time of the pantothenic acid reference standard was recycled through the column four times with no further separation taking place. This technique is useful to determine the presence of any coeluting substances. The identity of the peak as pantothenic acid was confirmed by collecting the peak fractions from several sample injections, removing the acetonitrile portion of the mobile phase, and analyzing the peak material using the microbiological assay method.

A linearity study (ratio of concentration to peak area) showed complete linearity within the concentration range selected, 0.050–0.50 mg/mL, and a correlation coefficient of 0.998. Accuracy of the procedure was determined by spiking a placebo formulation and various samples with known concentrations of standard, while precision was determined by analyzing eight identical samples on different days. Recoveries of 96.4, 96.9, 96.8, and 100.1% and relative standard deviations (*RSD*) of 1.5, 2.2, 1.6, and 0.79% were obtained for multivitamin tablets, fortified yeast, vitamin premix, and raw material, respectively. A comparison of results from the HPLC method described and the USP microbiological method using the same sample is shown in Table I. Low levels of calcium pantothenate (<3 mg/tablet) were more precisely analyzed by the HPLC procedure (1.42% *RSD*) than the USP microbiological method (4.59% *RSD*). This may be related to the increase in sample size in the HPLC preparation and less sample manipulation than required in the microbiological assay method.

The HPLC method described can accurately and precisely determine calcium pantothenate or pantothenic acid in nutritional products. The procedure is rapid (~30 min for sample extraction and chromatography), easily automated with the use of an autoinjector, practical for routine

Table I—Comparison of Pantothenic Acid Results From the USP Microbiological Assay and the High-Performance Liquid Chromatographic Assay

Product[a]	Label Amount, mg/tablet	Amount Found[b], mg/tablet, ±*SD*	
		High-Performance Liquid Chromatographic Assay	Microbiological Assay
A	3.0	3.65 ± 0.075	3.73 ± 0.176
B	3.4	3.81 ± 0.099	3.88 ± 0.178
C	2.0	2.87 ± 0.041	2.66 ± 0.188
D	40.0	46.78 ± 0.823	47.0 ± 2.85
E	64.0	68.77 ± 2.077	67.84 ± 2.76
F	70.0	67.96 ± 1.990	66.47 ± 3.66
G	80.0	86.69 ± 1.830	87.41 ± 4.01

[a] Multivitamin-multimineral tablets: A, Vita Lea Chewable; B, Neo-Jr.; C, Vita Lea B-Complex tablets; D, Shaklee B-Complex; E, B-Guard; F, Generic B; G, stress formula B-Complex tablet, Hi Bee. [b] Average of five determinations.

quality control use, and the results compare favorably with the current official procedure.

REFERENCES

(1) W. Pregnolatto and I. Irelegi, *Rev. Inst. Adolfo Lutz*, **115**, 25 (1965/67).

(2) W. D. Hubbard and A. J. Sheppard, *J. Assoc. Off. Anal. Chem.*, **52**, 448 (1969).

(3) J. Vichek, *Pharmazie*, **21**, 222 (1966).

(4) M. Schmall and E. Wollish, *Anal. Chem.*, **29**, 1509 (1957).

(5) "The United States Pharmacopeia," 20th rev., U.S. Pharmacopeal Convention, Rockville, Md., 1979, pp. 889.

(6) J. Brown, M. Hewins, J. Van Der Linden, and R. Lynch, *J. Chromatogr.*, **204**, 115 (1981).

ACKNOWLEDGMENTS

A preliminary report of this work was presented at the 23rd Rocky Mountain Conference, Denver, Colo., August 1981.

The authors thank research microbiologists Nicolas Mattio and Eva Basa for performing the microbiological assay analyses.

Detection Limits for a GC Determination of Methanol and Methylene Chloride Residues on Film-Coated Tablets

DEBORAH R. WINKEL ˣ **and SHEILA A. HENDRICK**

Received June 15, 1982, from *Syntex Research, Palo Alto, CA 94304.* Accepted for publication November 22, 1982.

Abstract □ A GC assay was developed that quantitates methanol and methylene chloride at the lowest detectable levels for this mode of analysis. A statistical limit of detection was determined for both methanol and methylene chloride. This method is sensitive and reliable for detecting possible residues of these solvents on film-coated tablets.

Keyphrases □ Methanol—determination of detection limits for a GC method, methylene chloride, residues on film-coated tablets □ Methylene chloride—determination of detection limits for a GC method, methanol, residues on film-coated tablets □ Detection limits—determination, GC method for methanol and methylene chloride residues on film-coated tablets □ Film-coated tablets—determination of detection limits for a GC method, methanol and methylene chloride residues

Organic solvents are frequently used to dissolve film-coating materials such as methylcellulose and ethylcellulose to facilitate application onto compressed tablets. These tablets are subsequently air dried for varying periods of time until constant tablet weight is achieved. The assumption was made that drying removes all the organic solvents from the finished product. However, there are a scarcity of data documenting the actual organic solvent levels that may be found in the coated tablet.

Patt and Hartmann (1) studied the effect of tablet core porosity, spraying techniques, drying condition, and evaporation qualities of the solvents used during the film-coating process. The residual levels of organic solvents in the tablet cores and film coats were determined by a GC method. In the present study, a similar GC system was used to determine the levels of methanol and methylene chloride in tablets at various times during the film-coating process. These levels were monitored during a 24-h period of air drying after the film coating was complete. The analytical data were then evaluated by a method similar to Hubaux and Vos (2) to determine a statistically based limit of detection for this method. This technique is similar to the statistical methods defined by Parsons (3) and Currie (4).

EXPERIMENTAL

Materials—A GC[1] equipped with a flame-ionization detector was used with a 1.8-m × 3-mm coiled-glass column containing 80–100 mesh porous polymer packing[2]. Reagents included isopropyl alcohol (AR), chloroform, methanol, and methylene chloride; all reagents were glass distilled[3].

Tablet Coating—A solution of ethylcellulose and methylcellulose in methanol and methylene chloride was sprayed[4] onto the compressed tablets in a heated, rotating coating pan[5]. Uniform coating was achieved when a coating of ~3% of the tablet weight was deposited.

Analytical Procedure—Standard stock solutions of methanol and methylene chloride at concentrations of 24 and 40 ppm were prepared in chloroform, and dilutions were injected onto the GC at the lowest attenuation (where the baseline noise did not exceed 2 mm). The volume of injection of these dilutions was 2.5 μL. Quantitation of the peaks was done with isopropyl alcohol as the internal standard. At an oven temperature of 160°C and a gas flow rate of 60 mL/min, the methanol eluted at ~1–2 min, the methylene chloride at 3–4.5 min, and the isopropyl alcohol at 4–5 min. The limit of detectability, as determined by the instrument at a slope sensitivity of 1 and an attenuation of 8, was ~6 ppm for methanol and 10 ppm for methylene chloride. A calibration curve was prepared by injecting a series of six dilutions which varied fourfold in concentration. The range for methanol was 6–24 ppm, and for methylene chloride the range was 10–40 ppm.

A series of six spiked placebos at concentrations of 0–24 ppm for methanol and 0–40 ppm for methylene chloride were prepared to determine the linearity and recovery over the range of interest. A placebo was defined as a tablet manufactured with no organic solvents in the film-coating formulation.

Coating Studies—Once the lower limit was approximated and a range of linearity established, an experiment was designed to detect methanol and methylene chloride on tablets during the film-coating process. The film-coating formulation consisted of the following ingredients: hy-

Table I—Residual Methanol and Methylene Chloride During and After Film Coating

Sample	Concentration, ppm per tablet[a] Methanol	Methylene Chloride
Uncoated tablet (control)	0	0
5-min coating process	173	52
10-min coating process	312	74
15-min coating process	252	66
Immediately after coating	242	55
5-min heat drying	143	37
15-min air drying	118	31
30-min air drying	115	30
24-h air drying	—[b]	—[b]

[a] Average tablet weight is 760 mg. [b] — No detectable levels.

[1] Hewlett-Packard Model 5830A.

[2] Poropak R packing; Waters Associates, Milford, Mass.

[3] Glass-distilled solvents; Burdick and Jackson, Muskegon, Mich.

[4] Spray gun apparatus; Devilbiss, Toledo, Ohio.

[5] Erweka AR 400 coating pan.

0022-3549/84/0100-0115$01.00/0
© 1984, American Pharmaceutical Association

quality control use, and the results compare favorably with the current official procedure.

REFERENCES

(1) W. Pregnolatto and I. Irelegi, *Rev. Inst. Adolfo Lutz*, **115**, 25 (1965/67).

(2) W. D. Hubbard and A. J. Sheppard, *J. Assoc. Off. Anal. Chem.*, **52**, 448 (1969).

(3) J. Vichek, *Pharmazie*, **21**, 222 (1966).

(4) M. Schmall and E. Wollish, *Anal. Chem.*, **29**, 1509 (1957).

(5) "The United States Pharmacopeia," 20th rev., U.S. Pharmacopeal Convention, Rockville, Md., 1979, pp. 889.

(6) J. Brown, M. Hewins, J. Van Der Linden, and R. Lynch, *J. Chromatogr.*, **204**, 115 (1981).

ACKNOWLEDGMENTS

A preliminary report of this work was presented at the 23rd Rocky Mountain Conference, Denver, Colo., August 1981.

The authors thank research microbiologists Nicolas Mattio and Eva Basa for performing the microbiological assay analyses.

Detection Limits for a GC Determination of Methanol and Methylene Chloride Residues on Film-Coated Tablets

DEBORAH R. WINKEL ˣ **and SHEILA A. HENDRICK**

Received June 15, 1982, from *Syntex Research, Palo Alto, CA 94304.* Accepted for publication November 22, 1982.

Abstract □ A GC assay was developed that quantitates methanol and methylene chloride at the lowest detectable levels for this mode of analysis. A statistical limit of detection was determined for both methanol and methylene chloride. This method is sensitive and reliable for detecting possible residues of these solvents on film-coated tablets.

Keyphrases □ Methanol—determination of detection limits for a GC method, methylene chloride, residues on film-coated tablets □ Methylene chloride—determination of detection limits for a GC method, methanol, residues on film-coated tablets □ Detection limits—determination, GC method for methanol and methylene chloride residues on film-coated tablets □ Film-coated tablets—determination of detection limits for a GC method, methanol and methylene chloride residues

Organic solvents are frequently used to dissolve film-coating materials such as methylcellulose and ethylcellulose to facilitate application onto compressed tablets. These tablets are subsequently air dried for varying periods of time until constant tablet weight is achieved. The assumption was made that drying removes all the organic solvents from the finished product. However, there are a scarcity of data documenting the actual organic solvent levels that may be found in the coated tablet.

Patt and Hartmann (1) studied the effect of tablet core porosity, spraying techniques, drying condition, and evaporation qualities of the solvents used during the film-coating process. The residual levels of organic solvents in the tablet cores and film coats were determined by a GC method. In the present study, a similar GC system was used to determine the levels of methanol and methylene chloride in tablets at various times during the film-coating process. These levels were monitored during a 24-h period of air drying after the film coating was complete. The analytical data were then evaluated by a method similar to Hubaux and Vos (2) to determine a statistically based limit of detection for this method. This technique is similar to the statistical methods defined by Parsons (3) and Currie (4).

EXPERIMENTAL

Materials—A GC[1] equipped with a flame-ionization detector was used with a 1.8-m × 3-mm coiled-glass column containing 80–100 mesh porous polymer packing[2]. Reagents included isopropyl alcohol (AR), chloroform, methanol, and methylene chloride; all reagents were glass distilled[3].

Tablet Coating—A solution of ethylcellulose and methylcellulose in methanol and methylene chloride was sprayed[4] onto the compressed tablets in a heated, rotating coating pan[5]. Uniform coating was achieved when a coating of ~3% of the tablet weight was deposited.

Analytical Procedure—Standard stock solutions of methanol and methylene chloride at concentrations of 24 and 40 ppm were prepared in chloroform, and dilutions were injected onto the GC at the lowest attenuation (where the baseline noise did not exceed 2 mm). The volume of injection of these dilutions was 2.5 μL. Quantitation of the peaks was done with isopropyl alcohol as the internal standard. At an oven temperature of 160°C and a gas flow rate of 60 mL/min, the methanol eluted at ~1–2 min, the methylene chloride at 3–4.5 min, and the isopropyl alcohol at 4–5 min. The limit of detectability, as determined by the instrument at a slope sensitivity of 1 and an attenuation of 8, was ~6 ppm for methanol and 10 ppm for methylene chloride. A calibration curve was prepared by injecting a series of six dilutions which varied fourfold in concentration. The range for methanol was 6–24 ppm, and for methylene chloride the range was 10–40 ppm.

A series of six spiked placebos at concentrations of 0–24 ppm for methanol and 0–40 ppm for methylene chloride were prepared to determine the linearity and recovery over the range of interest. A placebo was defined as a tablet manufactured with no organic solvents in the film-coating formulation.

Coating Studies—Once the lower limit was approximated and a range of linearity established, an experiment was designed to detect methanol and methylene chloride on tablets during the film-coating process. The film-coating formulation consisted of the following ingredients: hy-

Table I—Residual Methanol and Methylene Chloride During and After Film Coating

Sample	Concentration, ppm per tablet[a] Methanol	Methylene Chloride
Uncoated tablet (control)	0	0
5-min coating process	173	52
10-min coating process	312	74
15-min coating process	252	66
Immediately after coating	242	55
5-min heat drying	143	37
15-min air drying	118	31
30-min air drying	115	30
24-h air drying	—[b]	—[b]

[a] Average tablet weight is 760 mg. [b] — No detectable levels.

[1] Hewlett-Packard Model 5830A.

[2] Poropak R packing; Waters Associates, Milford, Mass.

[3] Glass-distilled solvents; Burdick and Jackson, Muskegon, Mich.

[4] Spray gun apparatus; Devilbiss, Toledo, Ohio.

[5] Erweka AR 400 coating pan.

0022-3549/84/0100-0115$01.00/0
© 1984, American Pharmaceutical Association

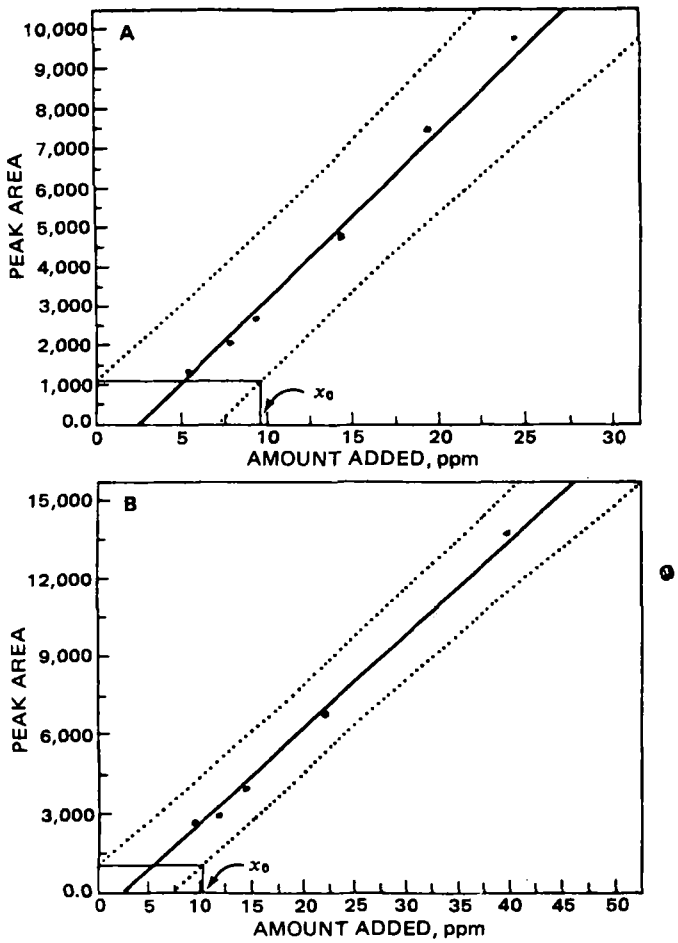

Figure 1—*Limit of detection curves for methanol (A) and methylene chloride (B) showing the statistical lower limit of detection as defined by Strobel (5). The lower limits of detection (x_0) were 9.552 ppm for methanol and 10.16 ppm for methylene chloride. Key: (—) regression line; (. . .) upper and lower 95% confidence lines.*

droxypropyl methylcellulose, ethylcellulose[6], diethyl phthalate, methanol, and methylene chloride. The film-coating process was performed using a coating pan and spray gun apparatus on a currently marketed tablet. Sampling consisted of pulling five tablets at each time interval of the coating process. Immediately after sampling, the tablets were submerged in 50 mL of chloroform to ensure complete recovery of the solvent residues. Tablets were collected from the coating pan after 5, 10, and 15 min of coating and immediately after the pan stopped. Additional collections were made after 5 min of heat drying and after 15 and 30 min of air drying; a sample was also taken after 24 h of air drying. The tablets were stored in plastic bags until packaging. Coated tablets from previous batches which had been packaged and maintained at room temperature were also assayed. Uncoated tablets were assayed as a control.

RESULTS AND DISCUSSION

Figure 1 represents the calibration curves used to statistically determine the lowest detectable limit with 95% confidence (2, 5). Concentration was plotted against peak area ratio, and a regression line was fitted through these points with confidence intervals[7]. The point of interception of the upper confidence line at the y-axis was extended horizontally to the lower confidence line, and where the two lines intersected a perpendicular was dropped to the x-axis. Parsons defines this point as the detection limit (3). For methanol, the value of this point was ~9 ppm per average tablet weight (Fig. 1). For methylene chloride, the value was approximated at 10 ppm per tablet (Fig. 1). Figure 2 shows the detector response for these values.

The results of the spiked placebo evaluation curve, evaluating solvent

[6] Methocel E-15 Premium, Ethocel 10 cps; Dow Chemical Co., Midland, Mich.
[7] Hewlett-Packard HP 85 Desk Top Computer equipped with an in-house program written for limits of detection determinations.

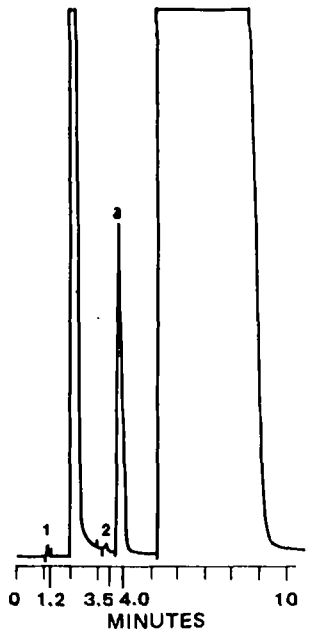

Figure 2—*Chromatogram showing detector response at the detection limit of methanol (1) and methylene chloride (2), with internal standard (3).*

added against the amount of solvent found, proved to be linear over the range studied. The precision of the method was determined by evaluating the results of six replicate injections of each standard solution. The standard deviations of the peak area measurements were 3.68% for methanol and 4.22% for methylene chloride. All samples and spiked placebos were evaluated against a standard containing 24 ppm of methanol and 40 ppm of methylene chloride (Fig. 3). Isopropyl alcohol was chosen as an internal standard because it was well resolved from the other peaks.

The results of the film-coating procedure are seen in Table I. Figure 4 depicts the methanol and methylene chloride peaks after 15 min of coating, where the residues are at a maximum. Table I shows that 24 h after the coating process, before packaging, no solvent residues were detected. No residues of methanol or methylene chloride were detected from the control or the older coated tablets.

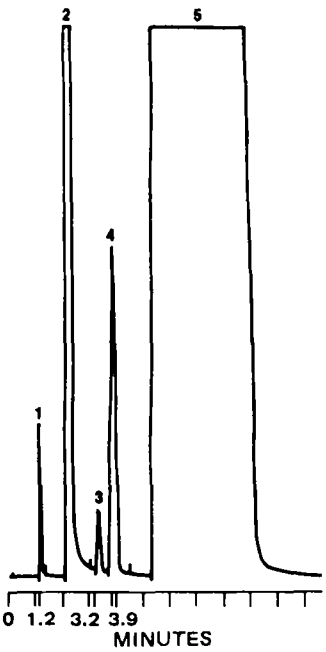

Figure 3—*Standard chromatogram for methanol and methylene chloride. Key: (1) methanol; (2) ethanol from solvent; (3) methylene chloride; (4) isopropyl alcohol (internal standard); (5) chloroform-solvent peak.*

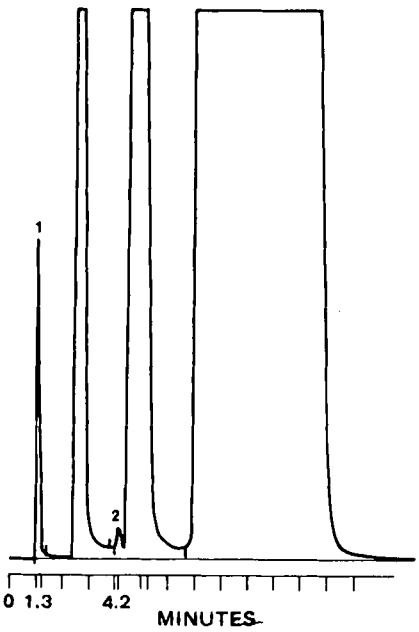

Figure 4—*Chromatogram of freshly coated tablets before drying, showing both methanol and methylene chloride after 15 min of coating. Key: (1) methanol; (2) methylene chloride.*

Statistical limits of detection were established for methanol at 9.5 ± 1.5 ppm per average tablet weight and for methylene chloride at 10.1 ± 2.3 ppm per tablet. Below these limits, sensitivity of the instrument was unreliable. All absolute values were approximate due to two factors. First, precision of measurement is decreased as concentrations used in the calibration curve approach the detection limit. As an alternative, a calibration curve could have been drawn at higher concentrations and extrapolated to the limit of detection (3). Second, this detection limit is also dependent on where the confidence lines are drawn about the regression line and is, at best, an estimate for a limit of guaranteed purity (2). Therefore, the values reported here represented a range within a specified precision for the standards, where the analytical method and the instrumentation were reliable for low-level determinations (6). The levels of solvent residues, ranging from 30 to 300 ppm, obtained during the film-coating process were statistically significant. However, after 24 h of drying, no peaks for either solvent were observed in the chromatograms.

This procedure is easy and reliable for monitoring organic residues on film-coated tablets. Determining lower limits of detection should be an integral part of any statistical package developed for a new analytical method.

REFERENCES

(1) L. Patt and V. Hartmann, *Pharm. Ind.*, **38**, 902 (1976).
(2) A. Hubaux and G. Vos, *Anal. Chem.*, **42**, 849 (1970).
(3) M. L. Parsons, *J. Chem. Educ.*, **46**, 290 (1969).
(4) L. A. Currie, *Anal. Chem.*, **40**, 586 (1968).
(5) H. A. Strobel, "Chemical Instrumentation," 2nd ed., Addison & Wesley, Menlo Park, Calif., 1973.
(6) W. J. Carpenter, *Proc. Anal. Div. Chem. Soc.*, **16**, 130 (1979).

ACKNOWLEDGMENTS

The authors thank Patricia Short for providing the computer program for the analyses and Dr. S. H. Wan for advice and assistance in the manuscript preparation. The authors also thank R. P. Hedge for the preparation of the tablets.

High-Performance Liquid Chromatographic Method for the Determination of Trace Amounts of Acetaminophen in Plasma

CHRYZANTA A. KORDUBA ˣ **and RALPH F. PETRUZZI**

Received July 15, 1982, from the *Department of Drug Metabolism and Pharmacokinetics, Schering-Plough Corporation, Bloomfield, NJ 07003.* Accepted for publication November 5, 1982.

Abstract □ A method is described for the rapid, sensitive, and precise quantitation of acetaminophen in human plasma. The assay involved a single acetonitrile extraction and high-performance liquid chromatographic analysis using a reverse-phase column, with a mobile phase of methanol and water. The limit of quantitation of acetaminophen by this method was 8 ng/mL; only 0.1 mL of the plasma sample was required for the determination. *N*-Propionyl-*p*-aminophenol was used as the internal standard.

Keyphrases □ Acetaminophen—high-performance liquid chromatography determination of trace amounts in plasma □ High-performance liquid chromatography—method for the determination of trace amounts of acetaminophen in plasma

Although acetaminophen is currently one of the most commonly used analgesics and antipyretics, hepatotoxicity has occurred in cases of acetaminophen overdose. Thus, a simple and rapid method for determining acetaminophen concentrations in plasma would be useful.

At present the most sensitive methods for plasma acetaminophen determination are liquid chromatography with electrochemical detection (1) or UV detection (2–6) and GC (7, 8). The quantitation limit for each of these methods is ~100 ng/mL with a 1-mL sample of plasma or serum. These methods, therefore, may be inadequate for microliter samples such as those obtained from newborn infants. Because of time requirements they may not be rapid enough for the determination of acetaminophen in overdose cases. A rapid, specific, high-performance liquid chromatographic (HPLC) method for the determination of acetaminophen in plasma using a 100-μL sample is described in this paper.

EXPERIMENTAL

Reagents and Materials—Acetaminophen[1] standard solutions were prepared in ethanol (1.0 mg/mL, stored at 4°C) and subsequent dilutions

[1] U.S. Pharmacopeial Convention, Inc., Rockville, Md.

0022-3549/84/0100-0117$01.00/0
© 1984, American Pharmaceutical Association

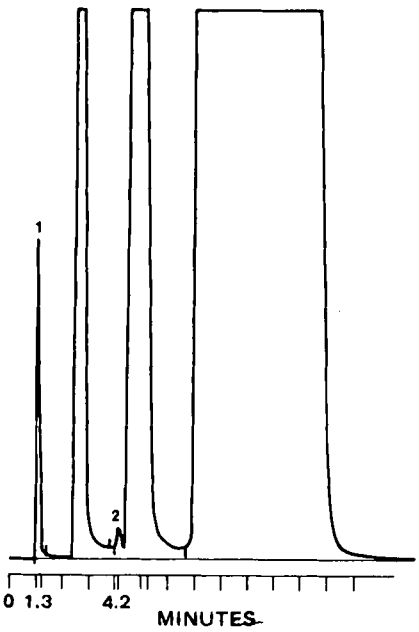

Figure 4—*Chromatogram of freshly coated tablets before drying, showing both methanol and methylene chloride after 15 min of coating. Key: (1) methanol; (2) methylene chloride.*

Statistical limits of detection were established for methanol at 9.5 ± 1.5 ppm per average tablet weight and for methylene chloride at 10.1 ± 2.3 ppm per tablet. Below these limits, sensitivity of the instrument was unreliable. All absolute values were approximate due to two factors. First, precision of measurement is decreased as concentrations used in the calibration curve approach the detection limit. As an alternative, a calibration curve could have been drawn at higher concentrations and extrapolated to the limit of detection (3). Second, this detection limit is also dependent on where the confidence lines are drawn about the regression line and is, at best, an estimate for a limit of guaranteed purity (2). Therefore, the values reported here represented a range within a specified precision for the standards, where the analytical method and the instrumentation were reliable for low-level determinations (6). The levels of solvent residues, ranging from 30 to 300 ppm, obtained during the film-coating process were statistically significant. However, after 24 h of drying, no peaks for either solvent were observed in the chromatograms.

This procedure is easy and reliable for monitoring organic residues on film-coated tablets. Determining lower limits of detection should be an integral part of any statistical package developed for a new analytical method.

REFERENCES

(1) L. Patt and V. Hartmann, *Pharm. Ind.*, **38**, 902 (1976).
(2) A. Hubaux and G. Vos, *Anal. Chem.*, **42**, 849 (1970).
(3) M. L. Parsons, *J. Chem. Educ.*, **46**, 290 (1969).
(4) L. A. Currie, *Anal. Chem.*, **40**, 586 (1968).
(5) H. A. Strobel, "Chemical Instrumentation," 2nd ed., Addison & Wesley, Menlo Park, Calif., 1973.
(6) W. J. Carpenter, *Proc. Anal. Div. Chem. Soc.*, **16**, 130 (1979).

ACKNOWLEDGMENTS

The authors thank Patricia Short for providing the computer program for the analyses and Dr. S. H. Wan for advice and assistance in the manuscript preparation. The authors also thank R. P. Hedge for the preparation of the tablets.

High-Performance Liquid Chromatographic Method for the Determination of Trace Amounts of Acetaminophen in Plasma

CHRYZANTA A. KORDUBA ˣ **and RALPH F. PETRUZZI**

Received July 15, 1982, from the *Department of Drug Metabolism and Pharmacokinetics, Schering-Plough Corporation, Bloomfield, NJ 07003.* Accepted for publication November 5, 1982.

Abstract □ A method is described for the rapid, sensitive, and precise quantitation of acetaminophen in human plasma. The assay involved a single acetonitrile extraction and high-performance liquid chromatographic analysis using a reverse-phase column, with a mobile phase of methanol and water. The limit of quantitation of acetaminophen by this method was 8 ng/mL; only 0.1 mL of the plasma sample was required for the determination. *N*-Propionyl-*p*-aminophenol was used as the internal standard.

Keyphrases □ Acetaminophen—high-performance liquid chromatography determination of trace amounts in plasma □ High-performance liquid chromatography—method for the determination of trace amounts of acetaminophen in plasma

Although acetaminophen is currently one of the most commonly used analgesics and antipyretics, hepatotoxicity has occurred in cases of acetaminophen overdose. Thus, a simple and rapid method for determining acetaminophen concentrations in plasma would be useful.

At present the most sensitive methods for plasma acetaminophen determination are liquid chromatography with electrochemical detection (1) or UV detection (2–6) and GC (7, 8). The quantitation limit for each of these methods is ~100 ng/mL with a 1-mL sample of plasma or serum. These methods, therefore, may be inadequate for microliter samples such as those obtained from newborn infants. Because of time requirements they may not be rapid enough for the determination of acetaminophen in overdose cases. A rapid, specific, high-performance liquid chromatographic (HPLC) method for the determination of acetaminophen in plasma using a 100-μL sample is described in this paper.

EXPERIMENTAL

Reagents and Materials—Acetaminophen[1] standard solutions were prepared in ethanol (1.0 mg/mL, stored at 4°C) and subsequent dilutions

[1] U.S. Pharmacopeial Convention, Inc., Rockville, Md.

0022-3549/84/0100-0117$01.00/0
© 1984, American Pharmaceutical Association

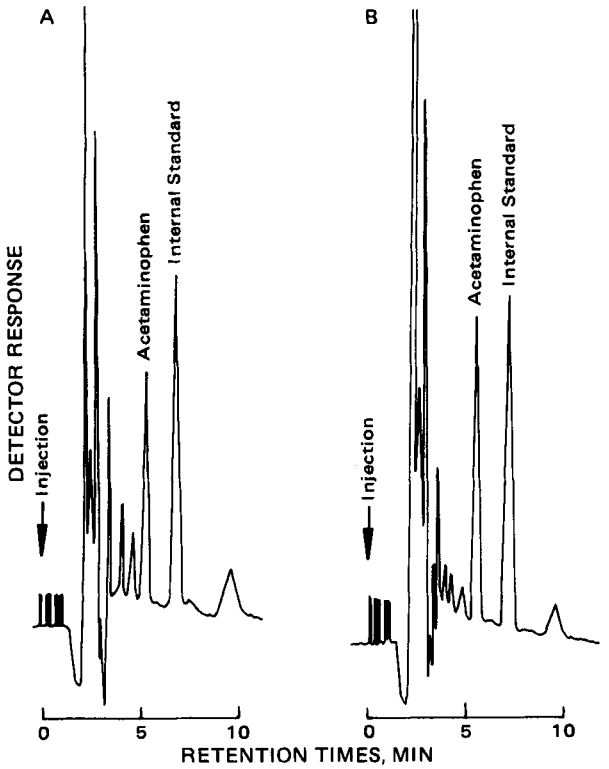

Figure 1—*High-performance liquid chromatogram of human plasma extract from: (A) drug-free plasma to which acetaminophen (1 μg/mL) was added and (B) plasma obtained from a human subject 9 h after 325.0 mg of acetaminophen was given at 0 and 6 hr. The column conditions are given in the text.*

were made with water. The internal standard (*N*-propionyl-*p*-aminophenol)[2] was also prepared in ethanol (1.0 mg/mL, stored at 4°C), with subsequent dilutions with water. Ethanol[3] and acetonitrile[4] (glass distilled) were used in the assay procedure.

Instrumentation—The chromatograph consisted of an automatic injector[5], a high-pressure pump[6], and a UV-absorbance detector[7] with a fixed wavelength of 254 nm. Separation was accomplished on a Spherisorb ODS (5-μm) reverse-phase column (0.46 cm × 25 cm)[8].

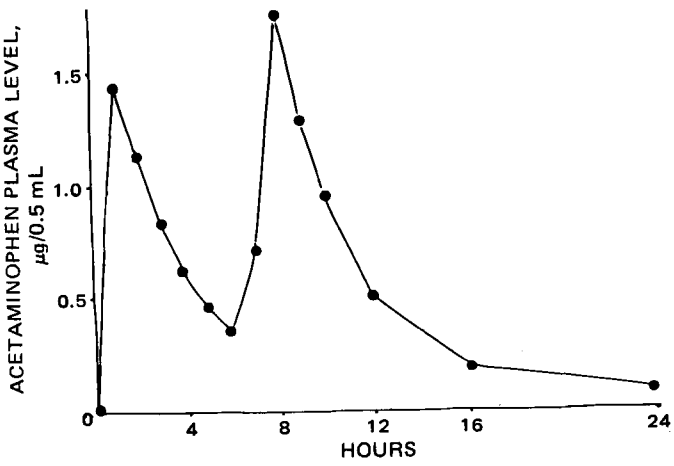

Figure 2—*Mean plasma levels of acetaminophen from nine human volunteers following oral 325.0-mg dose of acetaminophen at 0 and 6 h.*

[2] Schering Corp. (Batch βF504731), Bloomfield, N.J.
[3] Publicker Industries Inc., Philadelphia, Pa.
[4] MCB Manufacturing Chemist Inc., Cincinnati, Ohio.
[5] WISP 710A, Waters Associates Inc., Milford, Mass.
[6] Model 6000A, Waters Associates Inc., Milford, Mass.
[7] Model 440, Waters Associates Inc., Millford, Mass.
[8] Supelco Inc., Bellefonte, Pa.

Table I—Standard Curve of Acetaminophen [a]

Concentration, ng/mL	Peak Height Acetaminophen/ Peak Height Internal Standard Ratio			
	Mean	*SD*	*CV*, %	*n*
1.0	0.008	0.001	1.68	2
2.5	0.021	0.001	3.28	2
5.0	0.048	0.004	9.49	3
10.0	0.083	0.007	8.27	6
25.0	0.242	0.020	8.50	4
50.0	0.495	0.019	3.95	10
100.0	0.982	0.049	5.08	4
200.0	2.163	0.042	1.95	6
250.0	2.512	0.115	4.60	4
500.0	4.947	0.041	0.83	4
1000.0	10.185	0.021	0.20	2

[a] Various concentrations of acetaminophen were added to drug-free plasma samples prior to extraction as described in the text.

Analyses were performed using a deaerated mobile phase of methanol–water (25:75, v/v) at a flow rate of 1.0 mL/min (2200 psi). The UV detector was set at 0.02–2.0 AUFS. The absorbance detector output was monitored with a 1.0-mV recorder[9]. An automation system[10] was used for the measurements of peak height and retention time. All operations were done at ambient temperature.

Extraction and Analysis Procedure—To 0.1 mL of plasma in a 15-mL glass-stoppered centrifuge tube, 0.2 mL of *N*-propionyl-*p*-aminophenol (internal standard, 2.0 μg/mL) was added, mixed, and extracted with 5 ml of acetonitrile by shaking for 10 min on a shaker[11]. The tubes were then centrifuged for 10 min (1500 × *g*) after which 4.5 mL of the organic layer was transferred to another glass tube and evaporated to dryness under a nitrogen stream at 40°C. The residue was reconstituted with 2.0 mL of distilled water, and aliquots of 0.05 mL were injected into the HPLC using an automatic injector[5]. For calibration of detector response, various concentrations (0.10–20.0 μg/ml) of acetaminophen were added to several drug-free plasma samples, which were subsequently processed with each set of study samples. Calculation of acetaminophen concentration was based on the peak height ratio of acetaminophen relative to that of the internal standard. The linearity of the HPLC response was confirmed daily.

RESULTS AND DISCUSSION

The chromatogram yielded retention times (t_R) of 5.44 min, for acetaminophen and 6.86 min for the internal standard (Fig. 1). The extraction procedure using acetonitrile produced a clean extract. The absolute recoveries of acetaminophen from plasma were virtually complete (0.5 μg/mL gave 101.5% recovery, n = 7, and 1.0 μg/mL gave 99.8% recovery, n = 11); the recovery of the internal standard was 100.0%, n = 6. The linearity of the assay was evaluated by adding the acetaminophen to the drug-free plasma samples (Table I). The limit of acetaminophen quantitation in plasma by this method was 8.0 ng/mL (CV = 3.8%, n = 8). A straight line relationship was obtained between acetaminophen concentration and chromatographic response with a correlation coefficient of 1.000. The reproducibility of the assay was determined in six drug-free samples to which acetaminophen was added (CV of 2.7% at 0.5 μg/mL and CV of 1.8% at 2.0 μg/mL). The stability of acetaminophen was checked by reassaying the frozen and thawed plasma samples containing acetaminophen (over several weeks of storage). The coefficient of variation for the mean of three samples on each occasion and five determinations was 1.89%. None of the other drugs tested (theophylline, β-hydroxytheophylline, methylxanthine, theobromine, and caffeine) interfered with acetominophen detection; only the methylxanthine retention time (5.46 min) was close to that of acetaminophen. Table II shows individual plasma levels, and Fig. 2 illustrates the mean plasma levels of acetaminophen obtained from the nine human volunteers who received oral doses of 325.0 mg of acetaminophen[12] at 0 and 6 h. This simple, rapid, specific, and reproducible HPLC assay procedure developed for determination of acetaminophen in plasma could be used to monitor plasma acetaminophen levels in newborn infants, cases of overdose, and bioavailability studies.

[9] Model 9176, Varian, Palo Alto, Ca.
[10] Lab Automation System, Model 3353, Hewlett-Packard, Paramus, N.J.
[11] Model 6010, Eberbach Corp., Ann Arbor, Mich.
[12] McNEILAB, Inc., Spring House, Pa.

Table II—Plasma Levels of Acetaminophen (μg/0.5 mL) Following Administration of 325.0 mg of Acetaminophen at 0 and 6 h

Subject	Hours After Treatment													
	0	1	2	3	4	5	6	7	8	9	10	12	16	24
1	N.D.[a]	1.421	0.905	0.936	0.671	0.496	0.449	0.711	1.196	1.368	0.911	0.626	0.237	0.078
2	N.D.	1.058	0.923	0.615	0.464	0.294	0.238	0.343	1.688	1.178	0.814	0.454	0.187	0.065
3	N.D.	1.512	0.989	0.702	0.517	0.436	0.333	1.074	1.506	1.010	0.701	0.381	0.119	N.D.
4	N.D.	1.357	1.049	0.744	0.530	0.406	0.292	1.169	1.494	0.982	0.777	0.384	0.109	N.D.
5	N.D.	1.110	0.758	0.584	0.399	0.271	0.210	0.189	0.671	0.711	0.811	0.376	0.143	0.073
6	N.D.	1.239	1.542	0.798	0.617	0.361	0.249	0.651	1.954	1.233	0.861	0.400	0.165	0.078
7	N.D.	2.249	1.557	1.181	0.939	0.801	0.523	0.696	2.703	2.055	1.609	0.752	0.278	0.094
8	N.D.	1.265	1.360	1.110	0.702	0.554	0.441	0.885	2.212	1.354	0.878	0.494	0.172	0.056
9	N.D.	1.696	1.200	0.811	0.551	0.439	0.378	0.279	2.199	1.488	1.117	0.551	0.230	0.089

[a] N.D.—not detectable.

REFERENCES

(1) R. M. Riggin, A. L. Schmidt, and P. T. Kissinger, *J. Pharm. Sci.*, **64**, 680 (1975).

(2) G. R. Gothelli, P. M. Kabra, and L. J. Marton, *Clin. Chem.*, **23**, 957 (1977).

(3) L. T. Wong, G. Solomonraj, and B. H. Thomas, *J. Pharm. Sci.*, **65**, 1064 (1976).

(4) R. A. Horvitz and P. I. Jatlow, *Clin. Chem.*, **23**, 1596 (1977).

(5) D. Howie, P. I. Adriaenssens, and L. F. Prescott, *J. Pharm. Pharmacol.*, **29**, 235 (1977).

(6) B. Ameer, D. J. Greenblatt, M. Divoll, D. R. Abernethy, and L. Shargel, *J. Chromatogr.*, **226**, 224 (1981).

(7) W. A. Garland, K. C. Ksiao, E. J. Pantuck, and A. H. Conney, *J. Pharm. Sci.*, **66**, 340 (1977).

(8) M. A. Evans and R. D. Harbison, *J. Pharm. Sci.*, **66**, 1628 (1977).

Determination of a New Antihypertensive Agent (2*R*,4*R*)-2-(2-Hydroxyphenyl)-3-(3-mercaptopropionyl)-4-thiazolidinecarboxylic Acid in Blood by High-Performance Liquid Chromatography with Electrochemical Detection

KAZUTAKE SHIMADA *, MAKOTO TANAKA *, TOSHIO NAMBARA *x, and YUTAKA IMAI ‡

Received August 23, 1982, from the **Pharmaceutical Institute, Tohoku University, and* ‡*The Second Department of Internal Medicine, Tohoku University School of Medicine, Sendai 980, Japan.* Accepted for publication November 22, 1982.

Abstract □ A sensitive method has been developed for the determination of a new antihypertensive agent, (2*R*,4*R*)-2-(2-hydroxyphenyl)-3-(3-mercaptopropionyl)-4-thiazolidinecarboxylic acid (I), in human blood. Because the drug is unstable in biological fluids, it was immediately derivatized by treating the freshly drawn blood specimens with *N*-(4-anilinophenyl)maleimide. The adduct was separated and determined by high-performance liquid chromatography with electrochemical detection on a reverse-phase column. The assay method was satisfactory with respect to the sensitivity and precision, providing a quantitation limit of 2 ng/ml and coefficient of variation of 3%. Preliminary pharmacokinetic data were obtained by orally administering I to two patients with essential hypertension.

Keyphrases □ Antihypertensive agents—(2*R*,4*R*)-2-(2-hydroxyphenyl)-3-(3-mercaptopropionyl)-4-thiazolidinecarboxylic acid, determination in human blood, high-performance liquid chromatography with electrochemical detection □ High-performance liquid chromatography—determination of (2*R*,4*R*)-2-(2-hydroxyphenyl)-3-(3-mercaptopropionyl)-4-thiazolidinecarboxylic acid in human blood, electrochemical detection □ (2*R*,4*R*)-2-(2-Hydroxyphenyl)-3-(3-mercaptopropionyl)-4-thiazolidinecarboxylic acid—determination in human blood, high-performance liquid chromatography with electrochemical detection

(2*R*,4*R*) - 2 - (2-Hydroxyphenyl) - 3 - (3-mercaptopropionyl)-4-thiazolidinecarboxylic acid (SA 446, I), a newly developed potent and specific inhibitor of angiotensin-converting enzyme, appears to be a promising antihypertensive agent (1, 2). This drug is several times more potent *in vitro* than captopril, a specific and orally active inhibitor of angiotensin-converting enzyme proven useful in patients with hypertension and congestive heart failure (3, 4). The lower therapeutic dose of I requires a more sensitive method for the determination of the drug in biological fluids for pharmacokinetic studies. A sensitive GC method using an electron capture detector has been reported, but this procedure requires a two-step derivatization (5). High-performance liquid chromatography (HPLC) with

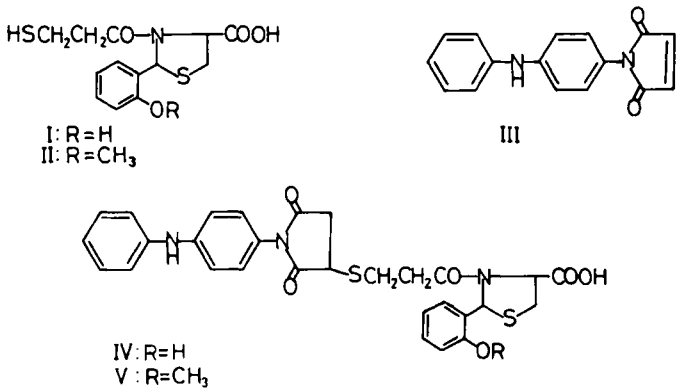

0022-3549/84/0100-0119$01.00/0

© 1984, American Pharmaceutical Association

Table II—Plasma Levels of Acetaminophen (μg/0.5 mL) Following Administration of 325.0 mg of Acetaminophen at 0 and 6 h

Subject	Hours After Treatment													
	0	1	2	3	4	5	6	7	8	9	10	12	16	24
1	N.D.[a]	1.421	0.905	0.936	0.671	0.496	0.449	0.711	1.196	1.368	0.911	0.626	0.237	0.078
2	N.D.	1.058	0.923	0.615	0.464	0.294	0.238	0.343	1.688	1.178	0.814	0.454	0.187	0.065
3	N.D.	1.512	0.989	0.702	0.517	0.436	0.333	1.074	1.506	1.010	0.701	0.381	0.119	N.D.
4	N.D.	1.357	1.049	0.744	0.530	0.406	0.292	1.169	1.494	0.982	0.777	0.384	0.109	N.D.
5	N.D.	1.110	0.758	0.584	0.399	0.271	0.210	0.189	0.671	0.711	0.811	0.376	0.143	0.073
6	N.D.	1.239	1.542	0.798	0.617	0.361	0.249	0.651	1.954	1.233	0.861	0.400	0.165	0.078
7	N.D.	2.249	1.557	1.181	0.939	0.801	0.523	0.696	2.703	2.055	1.609	0.752	0.278	0.094
8	N.D.	1.265	1.360	1.110	0.702	0.554	0.441	0.885	2.212	1.354	0.878	0.494	0.172	0.056
9	N.D.	1.696	1.200	0.811	0.551	0.439	0.378	0.279	2.199	1.488	1.117	0.551	0.230	0.089

[a] N.D.—not detectable.

REFERENCES

(1) R. M. Riggin, A. L. Schmidt, and P. T. Kissinger, *J. Pharm. Sci.*, **64**, 680 (1975).

(2) G. R. Gothelli, P. M. Kabra, and L. J. Marton, *Clin. Chem.*, **23**, 957 (1977).

(3) L. T. Wong, G. Solomonraj, and B. H. Thomas, *J. Pharm. Sci.*, **65**, 1064 (1976).

(4) R. A. Horvitz and P. I. Jatlow, *Clin. Chem.*, **23**, 1596 (1977).

(5) D. Howie, P. I. Adriaenssens, and L. F. Prescott, *J. Pharm. Pharmacol.*, **29**, 235 (1977).

(6) B. Ameer, D. J. Greenblatt, M. Divoll, D. R. Abernethy, and L. Shargel, *J. Chromatogr.*, **226**, 224 (1981).

(7) W. A. Garland, K. C. Ksiao, E. J. Pantuck, and A. H. Conney, *J. Pharm. Sci.*, **66**, 340 (1977).

(8) M. A. Evans and R. D. Harbison, *J. Pharm. Sci.*, **66**, 1628 (1977).

Determination of a New Antihypertensive Agent (2*R*,4*R*)-2-(2-Hydroxyphenyl)-3-(3-mercaptopropionyl)-4-thiazolidinecarboxylic Acid in Blood by High-Performance Liquid Chromatography with Electrochemical Detection

KAZUTAKE SHIMADA *, MAKOTO TANAKA *, TOSHIO NAMBARA *x, and YUTAKA IMAI ‡

Received August 23, 1982, from the **Pharmaceutical Institute, Tohoku University, and* ‡*The Second Department of Internal Medicine, Tohoku University School of Medicine, Sendai 980, Japan.* Accepted for publication November 22, 1982.

Abstract □ A sensitive method has been developed for the determination of a new antihypertensive agent, (2*R*,4*R*)-2-(2-hydroxyphenyl)-3-(3-mercaptopropionyl)-4-thiazolidinecarboxylic acid (I), in human blood. Because the drug is unstable in biological fluids, it was immediately derivatized by treating the freshly drawn blood specimens with *N*-(4-anilinophenyl)maleimide. The adduct was separated and determined by high-performance liquid chromatography with electrochemical detection on a reverse-phase column. The assay method was satisfactory with respect to the sensitivity and precision, providing a quantitation limit of 2 ng/ml and coefficient of variation of 3%. Preliminary pharmacokinetic data were obtained by orally administering I to two patients with essential hypertension.

Keyphrases □ Antihypertensive agents—(2*R*,4*R*)-2-(2-hydroxyphenyl)-3-(3-mercaptopropionyl)-4-thiazolidinecarboxylic acid, determination in human blood, high-performance liquid chromatography with electrochemical detection □ High-performance liquid chromatography—determination of (2*R*,4*R*)-2-(2-hydroxyphenyl)-3-(3-mercaptopropionyl)-4-thiazolidinecarboxylic acid in human blood, electrochemical detection □ (2*R*,4*R*)-2-(2-Hydroxyphenyl)-3-(3-mercaptopropionyl)-4-thiazolidinecarboxylic acid—determination in human blood, high-performance liquid chromatography with electrochemical detection

(2*R*,4*R*) - 2 - (2-Hydroxyphenyl) - 3 - (3-mercaptopropionyl)-4-thiazolidinecarboxylic acid (SA 446, I), a newly developed potent and specific inhibitor of angiotensin-converting enzyme, appears to be a promising antihypertensive agent (1, 2). This drug is several times more potent *in vitro* than captopril, a specific and orally active inhibitor of angiotensin-converting enzyme proven useful in patients with hypertension and congestive heart failure (3, 4). The lower therapeutic dose of I requires a more sensitive method for the determination of the drug in biological fluids for pharmacokinetic studies. A sensitive GC method using an electron capture detector has been reported, but this procedure requires a two-step derivatization (5). High-performance liquid chromatography (HPLC) with

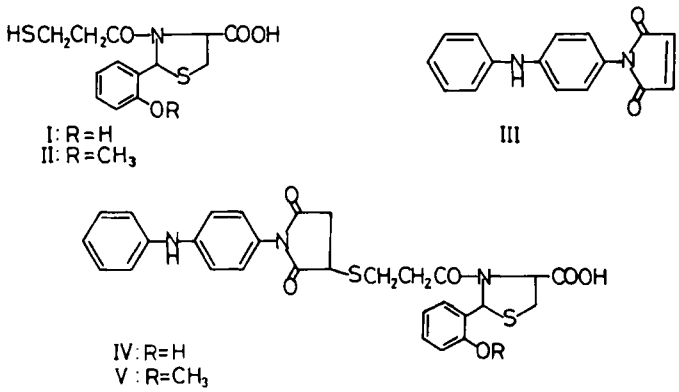

0022-3549/84/0100-0119$01.00/0

© 1984, American Pharmaceutical Association

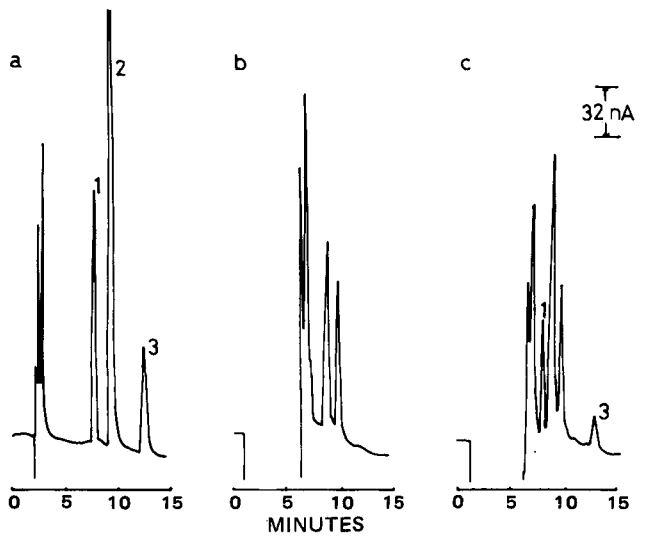

Figure 1—*Chromatograms obtained with (a) a standard 5-ng sample, (b) a blank sample, and (c) a blood sample of a patient orally administered 50 mg of I (325 ng/mL). Key: (1) I–*N*-(4-anilinophenyl)maleimide adduct; (2) N-(4-anilinophenyl)maleimide, (3) internal standard–N-(4-anilinophenyl)maleimide adduct.*

electrochemical detection (ED) continues to gain popularity for the sensitive and selective determination of trace components in complex biological samples (6, 7).

In our previous work we developed a sensitive method for the quantitation of captopril at therapeutic doses in human blood. Captopril was derivatized with *N*-(4-dimethylaminophenyl)maleimide into the electrochemically active adduct, which was then separated and determined by HPLC–ED (8). It was also found that *N*-(4-anilinophenyl)maleimide (III) was a better derivatization reagent for thiol compounds than *N*-(4-dimethylaminophenyl)-maleimide because of its higher sensitivity to ED (9). This paper describes a new method for the determination of I in whole blood, which involves derivatization with *N*-(4-anilinophenyl)maleimide into the electrochemically active form followed by HPLC–ED.

EXPERIMENTAL

Instruments—The apparatus used for this work was a high-performance liquid chromatograph[1] equipped with an electrochemical detector[2]. The applied potential was set at +1.0 V *versus* a silver–silver chloride reference electrode. A sample was introduced by a universal injector[3] with an effective volume of 2 mL. A reverse-phase column[4] (30.5 × 0.4-cm i.d.) was used under ambient conditions. A 1:1 mixture of acetonitrile and 0.8% $NH_4H_2PO_4$ (pH 3.0, adjusted with phosphoric acid) was used as a mobile phase at a flow rate of 1 mL/min.

Materials—(2*R*,4*R*)-2- (Hydroxyphenyl) -3-(3-mercaptopropionyl)-4-thiazolidinecarboxylic acid[5] and the internal standard[5], (2*R*,4*R*)-2-(2-methoxyphenyl)-3- (3-mercaptopropionyl) -4-thiazolidinecarboxylic acid (SA 427, II) were used as received. *N*-(4-Anilinophenyl)maleimide was prepared in-house as described in a previous paper (9). All other chemicals were of analytical reagent grade.

Standard Solutions—Standard solutions of I and the internal standard were each prepared by dissolving 2.0 mg of pure sample in 5.0 mL of methanol. These solutions were stable at least for 1 week when stored at −20°. A solution of 10 mg of *N*-(4-anilinophenyl)maleimide dissolved in 1.0 mL of acetone could be stored unchanged in a refrigerator for several months.

[1] Model ALC/GPC 202; Waters Associates, Milford, Mass.
[2] Model VMD 101; Yanagimoto Co., Kyoto, Japan.
[3] Model U6K; Waters Associates, Milford, Mass.
[4] μBondapak C_{18}; Waters Associates, Milford, Mass.
[5] Santen Pharmaceutical Co., Osaka, Japan.

Table I—Recovery of I Added to Human Blood

I Added, ng/mL	I Found, ng/mL	Recovery, %[a]
40	29.5	73.7±1.94
100	75.1	75.1±1.59
200	151	75.6±1.74
600	449	74.9±1.93
1000	740	74.0±1.77

[a] Mean ± *SD*; $n = 6$.

Subjects and Medication—Two female patients with essential hypertension were orally given 50 or 30 mg of I in capsule form after an overnight fast. The subjects were kept supine during the study period. Blood samples were withdrawn prior to administration of the drug and at intervals up to 2 h thereafter.

Assay Procedure—Duplicate 0.5-mL aliquots of each whole blood sample were poured immediately into tubes containing 20 μL of a 1% *N*-(4-anilinophenyl)maleimide solution and 0.3 mL of 0.033 M sodium-potassium phosphate buffer (pH 6.85). After addition of 100 ng of the internal standard, the tube was vortexed and then allowed to stand at 0°C for 30 min. The samples were frozen in a dry ice–acetone bath until analyzed.

The thawed sample was extracted twice with 2 mL of ether–hexane (1:1). After addition of ~500 μg of glutathione to consume the excess reagent, the aqueous layer was kept at 0°C for 20 min and then deproteinized with 3 mL of acetone. After centrifuging at 1500×*g* for 5 min, the precipitate was washed with 3 mL of acetone. The supernatant and washings were combined and evaporated to ~1 mL *in vacuo* at room temperature. The concentrate was diluted with 6 mL of water and applied to a reverse-phase cartridge[6]. After washing with 2 mL of water, the adducts of I and the internal standard with *N*-(4-anilinophenyl)maleimide were eluted with 8 mL of acetonitrile. The effluent was evaporated to dryness *in vacuo* below 40°C. The residue was dissolved in 0.2 mL of methanol, an aliquot of which was applied to the HPLC.

A calibration curve was constructed by assaying blood samples spiked with known amounts of I in the manner described above. The peak height ratio of I to the internal standard (II) was plotted against the blood concentration of I.

Derivatization of I—To a solution of 10 μg of *N*-(4-anilinophenyl)-maleimide in 1 ml of 0.033 M sodium-potassium phosphate buffer (pH 6.85) kept at 0°C in an ice-bath was added 4.0 μg of I. The reaction was terminated by extracting with 2 mL of ether–hexane (1:1) to eliminate the excess reagent. A 10-μL aliquot of the remaining aqueous layer was applied to the HPLC.

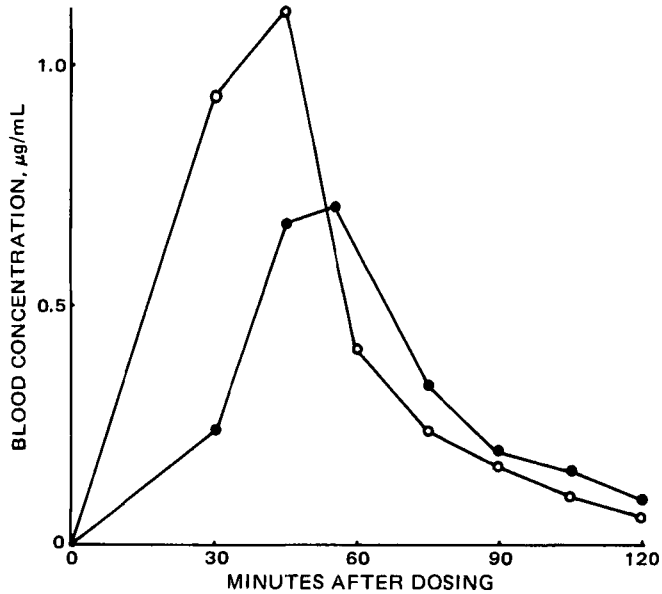

Figure 2—*Change in blood level after oral administration of I in two patients with essential hypertension. Key: (○) subject A, dose 50 mg; (●) subject B, dose 30 mg.*

[6] Sep-pak C_{18}; Waters Associates, Milford, Mass.

Table II—Accuracy and Precision of the Present Method for Determination of I in Human Blood

I Added, ng/mL	I Found, ng/mL[a]	CV, %
40	41± 1.2	3.0
200	200± 4.2	2.1
1000	1007±21	2.1

[a] Mean ± *SD*; $n = 6$.

RESULTS AND DISCUSSION

It is well known that thiol compounds are unstable, especially in biological fluids because of their high reactivity. In addition, the thiol compound I exhibits no prominent UV absorption responsive to UV detection. Therefore, appropriate precolumn labeling is needed for sensitive detection of I. The use of a derivatization reagent both reactive towards the thiol group and responsive to ED seemed to be promising. Accordingly, *N*-(4-anilinophenyl)maleimide, readily obtainable by a known method (9, 10), was chosen for investigation as a derivatization reagent.

First, the effect of reaction time on the formation of the adduct was investigated. After treatment with *N*-(4-anilinophenyl)maleimide in phosphate buffer at 0°C, I was quantitatively derivatized into the adduct (IV) in 10 min. The internal standard–*N*-(4-anilinophenyl)maleimide adduct (V) was similarly formed from II which was used as the internal standard. Among the columns tested, an octadecylsilane reverse-phase column[4] was the most favorable for efficient separation of the compounds. A hydrodynamic voltammogram of the I–*N*-(4-anilinophenyl)maleimide adduct indicated that the maximum sensitivity was obtainable at the potential of ~ +1.0 V, which was therefore used for the electrochemical detection. The electrochemical behavior of the internal standard–*N*-(4-anilinophenyl)maleimide adduct was similar to that of the I–*N*-(4-anilinophenyl)maleimide adduct. Typical chromatograms of the adducts formed from I and the internal standard (II) are illustrated in Fig. 1a. The detection limit (S/N = 2 at 4 nA full scale) was estimated to be 40 pg for I.

The next effort was focused on establishing a clean-up procedure for I in biological fluids. Compound I in human blood was immediately derivatized with *N*-(4-anilinophenyl)maleimide to prevent oxidative decomposition. Excess reagent was eliminated by extraction with ether–hexane and treatment with glutathione; the glutathione–*N*-(4-anilinophenyl)maleimide adduct was eluted at the solvent front on the chromatogram. More polar solvents such as ether or ethyl acetate were effective for removal of excess reagent, but reduced the recovery rate because the adducts of I and internal standard were also partially lost. The deproteinized sample was applied to a reverse-phase cartridge[6], and the adducts of I and the internal standard were eluted with acetonitrile. No interfering peaks were present with the blank specimen, as shown in Fig. 1b and c. Interferences of endogenous polar substances due to saturation of the output of the detector were overcome by disconnecting the detector for ~5 min after injection (11).

A known amount of I was added to the blood, and the overall recovery was estimated. Compound I spiked at five levels was recovered at the rate of >70% (Table I). In addition, the mean recovery rate for 100 ng of the internal standard (II) was 73.9±1.1%. When the peak height ratio of I/internal standard was plotted against the concentration of I (20–1000 ng/mL) spiked in a human blood specimen, a linear correlation was observed with the regression line defined by a slope of 11.96, a *y*-intercept of 0.018, and a correlation coefficient of 0.9998. The proposed method was also satisfactory with respect to both accuracy and precision (Table II).

Table III—Pharmacokinetic Parameters of I in Patients with Essential Hypertension

Subject	Age, yr	Body wt., kg	Dose, mg	t_{max}, min	C_{max}, μg/mL	$AUC_{0\to\infty}$, μg·min/mL	$t_{1/2}$, min
A	45	65.6	50	45	1.12	54.6	22
B	29	49.8	30	60	0.712	40.7	24

The present method was then applied to the determination of I in blood samples taken from two patients (subjects A and B) orally administered 50 and 30 mg of I, respectively. The blood concentration–time profiles observed are illustrated in Fig. 2; the individual pharmacokinetic data of the two patients are listed in Table III. The I levels reached maximum values, 1.12 and 0.721 μg/mL, at 45 and 60 min after administration, respectively. The blood concentrations decreased to 0.063 and 0.095 μg/ml at 120 min, with half-lives of 22 and 24 min, respectively.

The proposed method for the determination of I in human blood is satisfactory with respect to sensitivity and reliability and, hence, would be useful for clinical pharmacokinetic studies. The newly developed method may be widely applicable to the determination of biologically and pharmacologically important thiol compounds.

REFERENCES

(1) T. Iso, H. Yamauchi, H. Suda, K. Nakata, K. Nishimura, and J. Iwao, *Jpn. J. Pharmacol.*, **31,** 875 (1981).

(2) T. Unger, T. Yukimura, M. Marin-Grez, R. E. Lang, W. Rascher, and D. Ganten, *Eur. J. Pharmacol.*, **78,** 411 (1982).

(3) M. A. Ondetti, B. Rubin, and D. W. Cushman, *Science*, **196,** 441 (1977).

(4) D. G. Vidt, E. L. Bravo, and F. M. Fouad, *N. Engl. J. Med.*, **306,** 214 (1982).

(5) T. Iwatani, M. Naitoh, H. Takashina, S. Nagamori, Y. Itoh, and J. Iwao, *Chem. Pharm. Bull.*, **30,** 2087 (1982).

(6) P. T. Kissinger, *Anal. Chem.*, **49,** 447A (1977).

(7) W. R. Heineman and P. T. Kissinger, *Anal. Chem.*, **52,** 138R (1980).

(8) K. Shimada, M. Tanaka, T. Nambara, Y. Imai, K. Abe, and K. Yoshinaga, *J. Chromatogr.*, **227,** 445 (1982).

(9) K. Shimada, M. Tanaka, and T. Nambara, *Anal. Chim. Acta*, **147,** 375 (1983).

(10) M. Machida, M. I. Machida, and Y. Kanaoka, *Chem. Pharm. Bull.*, **25,** 2739 (1977).

(11) K. Shimada, M. Tanaka, and T. Nambara, *Anal. Lett.*, **13,** 1129 (1980).

ACKNOWLEDGMENTS

This work was supported in part by a grant from the Ministry of Education, Science and Culture of Japan.

The authors are grateful to Dr. Hiroshi Sekino, Kidney Center of Sendai Insurance Hospital, for his interest and support. Thanks are also due to Santen Pharmaceutical Co. for its generous gift of samples.

Structural Characteristics of Phospholipid Multilamellar Liposomes

D. LICHTENBERG ‡x and T. MARKELLO *

Received August 16, 1982, from the *Department of Biochemistry, University of Virginia School of Medicine, Charlottesville, VA 22908 and ‡Department of Physiology and Pharmacology, Tel Aviv University Sackler School of Medicine, Ramat Aviv 69978, Israel. Accepted for publication November 11, 1982.

Abstract □ The relative proportion of lipid on the external surface of spherical multilamellar vesicles and the aqueous volume trapped within them, can be computed as a function of a liposome's outer radius, interlamellar aqueous spacing, and the number of bilayers. When known experimental data is put into these calculations, the results lead to the conclusion that spontaneously formed liposomes are on the average composed of up to 10 lamellae, whose total thickness is ~0.1 μm, and traps an aqueous sphere whose average radius is ~0.5 μm. Most of the aqueous medium entrapped within the multi-bilayers is contained in the internal core of the liposome. When assuming spherical liposomes and using percent exposure data, this calculation overestimates the experimentally detected trapped volumes.

Keyphrases □ Liposomes—phospholipid, multilamellar, structural characteristics, determination of external lipid layer and aqueous volume □ Vesicles—multilamellar phospholipid liposomes, structural characteristics, determination of external lipid layers and aqueous volume □ Delivery systems—phospholipid liposomes, structural characteristics, determination of external lipid layers and aqueous volume

A wide variety of phospholipids spontaneously form multilamellar vesicles (liposomes) on hydration which are constructed of stacked concentric bimolecular lamellae interspersed with an aqueous medium (1, 2). These aggregates, often referred to as "onion-like" structures, are relatively impermeable to entrapped ions (3) and other solutes, which has generated interest in their use as an experimental tool for drug delivery (4). Despite extensive studies, the structural characteristics of these liposomes are not well defined. The properties of the liposomes depend on the composition and concentration of constituent phospholipids and the ionic strength of the aqueous medium (5, 6), as well as the method of phospholipid suspension and the time of hydration (5, 7).

A common feature of all dispersions made by shaking phospholipids in aqueous medium is the size heterogeneity of the resultant multilamellar liposomes. In egg phosphatidyl choline dispersions, electron microscopy reveals the existence of liposomes with diameters <0.2 μm as well as some with diameters >3 μm (5). Although average radius and average number of bilayers have limited significance as physical characteristics, attempts have been made to measure these parameters. Electron microscopic data are helpful for such studies; however, for these purposes the usefulness of electron microscopy is limited both by the need for vesicle fixation and by difficulties in the analysis of heterogeneous dispersions. Alternatively, two experimentally available parameters are the average trapped aqueous volume (V_T) and percent of lipid exposed on the external surface (E). Both these parameters have been examined for various liposome preparations, and the results have been interpreted in terms of the average liposome radius (R), number of bilayers (n), and/or the thickness of the intervening aqueous layers (d). For this kind of analysis, a relationship between the observed parameters and the intrinsic features of the liposomes must either be assumed or calculated on the basis of certain assumptions.

Assuming that the outer radius of the multi-bilayers is large when compared with the bilayer thickness, and that successive lamellae, therefore, have very similar surface areas, Schwartz and McConnell (7) calculated the average number of lamellae from the percent exposure of an ESR spin label to an externally added reducing agent. They concluded that this number varies between 6 and 10, depending on the exact method of liposome preparation. For large multilamellar vesicles (MLV) with an average radius of ~0.7 μm (5), successive lamellae of <50 Å thickness, and interlammelar spacing of <100 Å, the assumptions made by Schwartz and McConnell seem to be justified by their experimental results. However, in a recent review, Szoka and Papahadjopoulos (8) commented that accounting for the decreasing surface areas of successive lamellae and for the interlamellar spacing "would tend to considerably increase the calculated number of lamellae."

Formulas for calculating the number and surface areas of liposomes in any suspension from the trapped aqueous volume and the partial specific volume of the constituent lipids have recently been published by Pidgeon and Hunt (9). They have used these formulas to simulate electron microscopic results for number of lamellae and average radius in various lipid dispersions. In these calculations, Pidgeon and Hunt used combinations of liposomes with different interlamellar distances. This assumes *a priori* that significantly different interlamellar distances can occur within a liposome preparation. In fact, lipid dispersions made from a wide variety of lipids and lipid mixtures, both artificial and natural, show distinct X-ray diffraction bands. The presence of these bands strongly

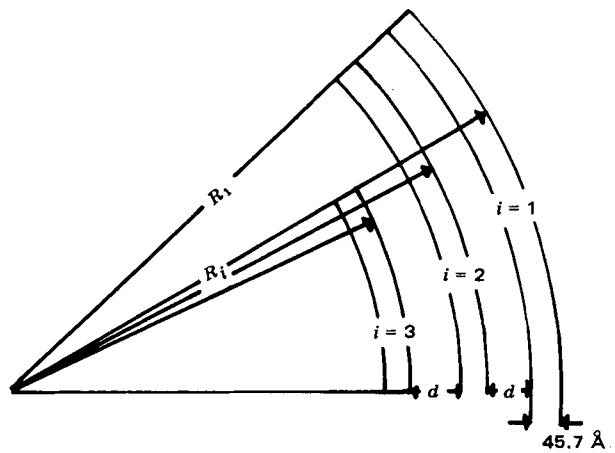

Figure 1—*Multilamellar structure of bilayers. Key: (R_1) outermost radius of the liposome; (i) serial number of the bilayer; (d) constant thickness of intervening aqueous shells.*

0022-3549/84/0100-0122$01.00/0
© 1984, American Pharmaceutical Association

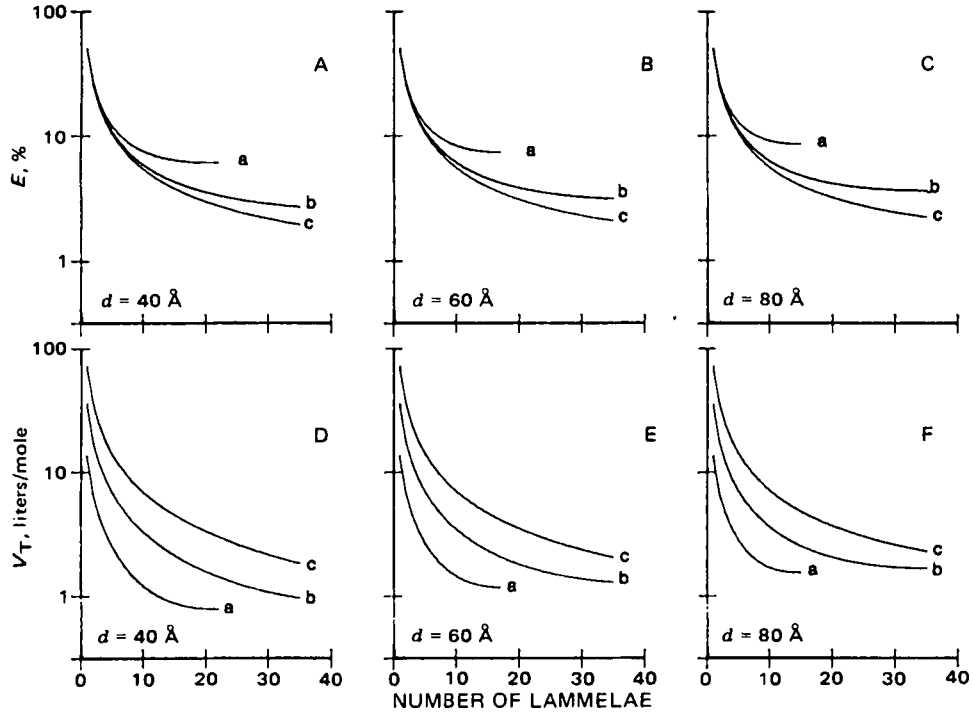

Figure 2—*Calculated dependence of percent exposure (E, Eq. 2) (A–C) and the total aqueous trapped volume (V_T, Eq. 3) (D–F) as a function of the number of lamellae, for various fixed interlamellar spacings (d). Key: (a) R_1 = 0.2 μm, (b) R_1 = 0.5 μm, (c) R_1 = 1.0 μm).*

argues that the majority of vesicles have a fixed repeat distance in a given preparation of liposomes (10).

In our view, there are several problems with the Pidgeon and Hunt model. Because they chose the innermost lamellae to begin their calculations, they were forced to assume that all of the vesicles had a fixed minimum radius common to all liposomes. In all cases they chose the radius determined for homogeneous sonicated vesicles, the smallest and most accurately known radius for any lipid vesicle (10), but one with no apparent constitutive relationship to multilamellar dispersions. The Pidgeon and Hunt formulas also are highly sensitive to deviations from the assumption of vesicle sphericity. This is because of the third-power relationship of entrapped volume (or encapsulation efficiency) to vesicle radius.

Percent exposure calculated from surface area measurements ($\propto r^2$) should be less sensitive to deviations from sphericity than trapped-volume measurements ($\propto r^3$).

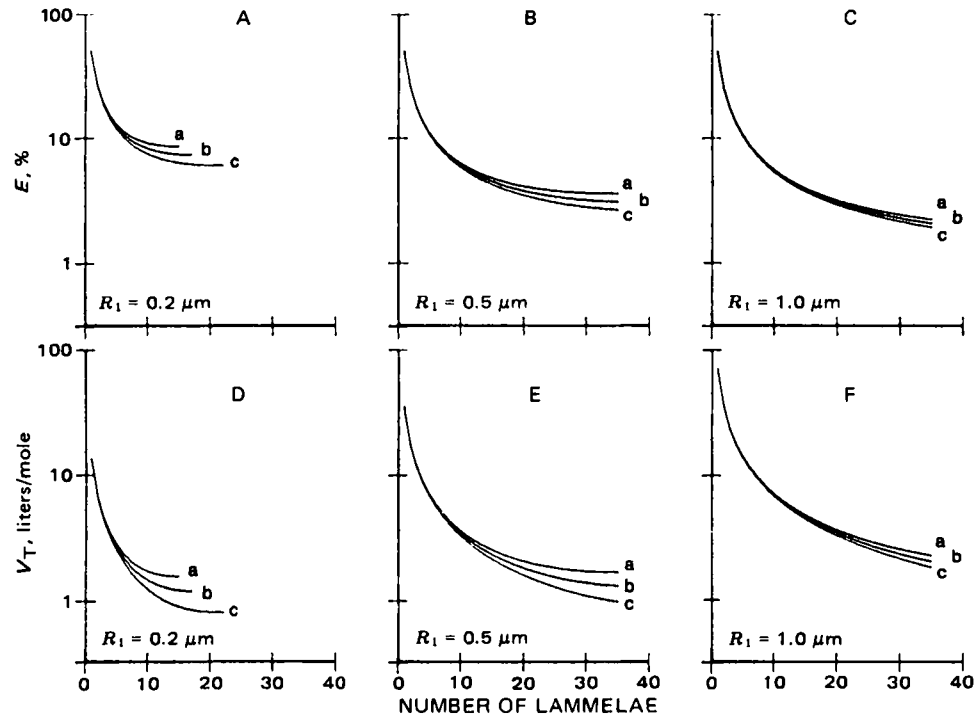

Figure 3—*Data in Fig. 2 plotted with various fixed* R_1 *radii. Key: (a)* d = 40 Å, *(b)* d = 60 Å, *(c)* d = 80 Å. *Calculations were terminated when* $R_n \leq 100$ Å *or* $n \geq 35$ *lamellae.*

Calculations based on percent exposure therefore, can be regarded as a more reliable basis for evaluating the number of lamellae in the multilamellar liposomes because this evaluation depends on the calculated radius. This is the approach which Schwartz and McConnell used. To avoid the criticism by Szoka and Papahadjopoulos, the differences in surface areas of successive lamellae and the existence of interlamellar spacing have been taken into consideration in the following treatment.

THEORETICAL

We adopted the assumption of vesicle sphericity as a first-order approximation. We also assumed that the thickness of the hydrated phospholipid bilayer is constant at 45.7 Å, and that the surface area per phospholipid molecule is constant at 72.5 Å^2 (11). In addition, we assumed that the bilayers are separated by intervening aqueous shells of constant thickness, d.

For a multilamellar structure of n bilayers, the radius of the outer surface of any given bilayer is:

$$R_i = R_1 - [(i - 1)(45.7 + d)] \qquad \text{(Eq. 1)}$$

where R_1 is the outermost radius of the liposome and i is the serial number of that bilayer, counted inward from the outermost bilayer (Fig. 1). The surface areas of both faces of the ith bilayer are closely approximated by $4\pi R_i^2$. The number of molecules for this bilayer is then twice this value divided by the surface area per molecule. The percent exposure is taken as equal to the external surface area of the outer bilayer ($4\pi R_1^2$) divided by the total surface area of all the bilayers and multiplied by 100:

$$E = \frac{100R_1^2}{\sum_{i=1}^{n} 2[R_1 - (i - 1)(45.7 + d)]^2}\% \qquad \text{(Eq. 2)}$$

Aqueous medium is trapped within the innermost bilayer shell (bilayer n) forming the aqueous core and between the concentric bilayers. The aqueous core has a radius of $R_n = R_1 - [45.7n + d(n - 1)]$ and a volume of $V_n = 4/3(\pi R_n^3)$. The volume of each of the inter-bilayer compartments can be calculated from the difference between the volumes of the two spheres defined by the inner radius of any given bilayer (i) and the outer radius of the next bilayer ($i + 1$). The moles of phospholipid per multibilayer are calculated as the sum of the surface areas of all bilayers divided by the assumed area per molecule and Avogadro's number. If the sum of all the trapped volume elements is divided by the moles of phospholipid, the following expression is obtained for the trapped volume as a function of R, d, and n:

$$V_T = 0.007274 \frac{\{R_1 - [45.7n + d(n - 1)]\}^3 + \sum_{i=1}^{n-1} \{[R_1 + d - i(45.7 + d)]^3 - [R_1 - i(45.7 + d)]^3\}}{\sum_{i=1}^{n} [R_1 - (i - 1)(45.7 + d)]^2} \frac{\text{L}}{\text{mol}} \qquad \text{(Eq. 3)}$$

RESULTS AND DISCUSSION

The dependence of the trapped volume (V_T) and the percent exposure (E) on the number of lamellae (n) is presented in Figs. 2 and 3. These curves are computed for various outermost radii (R_1) and interlamellar spacing (d) using Eqs. 2 and 3. These calculations suggest that both the trapped volume and percent exposure depend on R, d, and n. As previously proposed by Szoka and Papahadjopoulos (8), both the computed trapped volume and percent exposure decrease sharply as the number of lamellae increase. However, the dependence of the calculated trapped volume on the various parameters is quite different from the dependence of the calculated percent exposure.

Consider liposomes with ≤10 bilayers and radii >0.2 μm. The calculated percent exposure primarily depends on the number of lamellae and is insensitive to both the liposome outer radius (Fig. 2A) and the interlamellar distance (Fig. 3A). Furthermore, in liposomes with >10 bilayers, but radii of 0.5–1.0 μm and interlamellar distances of 40–80 Å, the major determinant of the calculated percent exposure is the number of lamellae and not the outer radius (R_1) (Fig. 2A–C) or interlamellar distance (Fig. 3A–C). On the other hand, the calculated trapped volume is very sensitive to R and d (Figs. 2D–F and 3D–F). For liposomes of ≤10 bilayers, the calculated trapped volume primarily depends on the number of lamellae and the outer radius of the liposome (Fig. 2D–F). In liposomes with more bilayers, the trapped volume becomes less sensitive to the number of lamellae (Figs. 2D–F and 3D–F), and the major factor is the outer radius of the liposome (Fig. 2D–F). The interlamellar spacing (d) in vesicles with an outer radius of 0.5 μm is significant only in multi-bilayers with >20 lamellae (Fig. 3E).

Average Number of Bilayers in Multilamellar Liposomes—The number of lamellae (not the radius nor interlamellar distance) is the major factor in determining the percent exposure. The radius, and to a lesser extent the interlamellar distance, markedly affect the trapped volume in spherical multi-bilayers. Thus, for multilamellar liposomes any approximation of the average number of lamellae would best be based on the fraction of exposed lipid and not on the encapsulated volume.

Schwartz and McConnell found in their ESR spin label experiments that liposomes made under specific conditions from dimyristoyl phosphatidyl choline, dipalmitoyl phosphatidyl choline, and binary mixtures of dipalmitoyl phosphatidyl choline and cholesterol "all have the same portion of external lipids" (7). The variation of the percent exposure in these uncharged liposomes was within the range of 5–9%, depending on the conditions of liposome preparation. This is similar to the value of 8.5% obtained previously for the percent of lipid exposed to UO_2^{2+} in liposomes composed of egg phosphatidyl choline (6). For liposomes of an average radius which is >0.4 μm (5, 6) and in this range of exposure (5–9%), the fraction of exposed lipid primarily reflects the average number of lamellae (Figs. 2 and 3). Therefore, we conclude that these liposomes are constructed of 5–10 bilayers on the average.

It should be pointed out that liposomes made of various phospholipids differ in their gel–liquid crystalline phase transition temperature. Thus, at room temperature egg phosphatidyl choline is in a liquid crystalline state, whereas dipalmitoyl phosphatidyl choline is in a gel state. The close similarity of the percent exposure, therefore, suggests that the average number of lamellae in the liposomes can only be slightly affected by the physical state of the phospholipid.

For negatively charged liposomes composed of 10% dicetyl phosphate and 90% dipalmitoyl phosphatidyl choline, 11% of the lipid is exposed to an externally added reagent (7). This may indicate that in the charged liposomes the average number of lamellae is smaller than in the uncharged liposome average.

The number of lamellae found by Schwartz and McConnell closely agrees with our calculations. Contrary to the suggestion of Szoka and Papahadjopoulos (8), accounting for the decreasing surface areas of successive bilayers and for the presence of interlamellar space does not increase the number of lamellae by more than one over the simple approximation of Schwartz and McConnell, which represents the minimal number of lamellae for any given percent exposure, since it models a liposome in which the radius of the inner aqueous core is very close to the external radius. Our computations support the suggestion of Schwartz and McConnell that for realistic values of the membrane thickness and aqueous interlamellar spacing, the multilamellar liposome can be described as having a large aqueous cavity entrapped within compact multilamella.

Trapped Volume and Shape of Multilamellar Liposomes—Consider egg phosphatidyl choline multilamellar liposomes with six bilayers [$E \simeq 8.5\%$ (6)] with an average radius in the range of 0.4–1.0 μm. The calculated trapped volume range of 4–12 L/mol is higher than that observed previously [1.5 L/mol (6)]. Moreover liposomes made of charged lipids, which are probably composed of fewer bilayers (7), have an average trapped volume that varies from 3 to 8 L/mol (5, 6). The upper limit of this range is obtained only in low ionic strength suspensions, where the liposomes are postulated to have fewer lamellae (12). In all other cases, the experimental values for the entrapped volumes are 1.5–4 times lower than predicted by our calculations.

Two factors may contribute to this large discrepancy. One possibility is a lower internal concentration of the trapped volume indicator within the liposome relative to the indicator concentration in the bulk medium. This could be due to the permanent exclusion of small solute molecules,

such as sucrose or other volume indicators, from a layer of water of hydration of the phospholipid. For dimyristoyl phosphatidyl choline liposomes, this "nonsolvent water" has been shown to be 11.5 mol of water/mol of phosphatidyl choline, or approximately one-third of the enclosed liposomal water (13). The second factor is the difference between the true liposomal structure and the geometric approximations made in our model. For example, any change in the shape of the model to a nonspherical geometry will decrease the trapped volume relative to the percent exposure (r^2 *versus* r^3). This does not imply that multi-bilayers are nonspherical, but deviations from sphericity can account for this discrepancy.

In conclusion, our calculations clearly show that the estimation by Schwartz and McConnell for the number of lamellae in multilamellar vesicles is essentially correct. This, in fact, implies that the wall of the average liposome spontaneously formed by hydration of phospholipids, consists of 5–10 bilayers and has a total thickness $< \sim 0.2$ μm. Thus, "fully swollen" (spherical) liposomes of a diameter of 1.4 μm, on the average, contain an inner aqueous cavity >1.0 μm. When viewed obliquely, a nonspherical multi-bilayer could result in the observed space-filling "onion-like" structures seen in some electron micrographs and give a somewhat misleading impression of the large central cavity which we calculate to be present in multilamellar liposomal structures. Finally, we conclude that therapeutic strategies using encapsulation of aqueous components into simple multilamellar lipid dispersions must take into account the fact that the vast majority of encapsulated material will reside in the central cavity of these liposomes.

REFERENCES

(1) V. Luzzati, in "Biological Membranes," D. Chapman, Ed., Academic, New York, N.Y., 1968, pp. 71–123.

(2) A. D. Bangham, M. W. Hill, and N. G. Miller, "Methods in Membrane Biology," E. D. Korn, Ed., Plenum, New York, N.Y., 1974, pp. 1–68.

(3) A. D. Bangham, M. M. Standish, and J. C. Watkins, *J. Mol. Biol.*, **13**, 238 (1965).

(4) G. Poste and D. Papahadjopoulos, in "Uses of Liposomes in Biology and Medicine," G. Gregoriadis and A. Allison, Eds., Wiley, London, 1979, pp. 101–151.

(5) F. Olson, C. A. Hunt, F. C. Szoka, W. J. Vail, and D. Papahadjopoulos, *Biochim. Biophys. Acta*, **557**, 9 (1979).

(6) A. D. Bangham, J. De Gier, and G. D. Greville, *Chem. Phys. Lipids*, **1**, 225 (1967).

(7) M. A. Schwartz and H. M. McConnell, *Biochemistry*, **17**, 837 (1978).

(8) F. Szoka, Jr. and D. Papahadjopoulos, *Annu. Rev. Biophys. Bioeng.*, **9**, 467 (1980),

(9) C. Pidgeon and C. A. Hunt, *J. Pharm. Sci.*, **70**, 173 (1981).

(10) C. Huang, *Biochemistry*, **8**, 344 (1969).

(11) B. A. Cornell, J. Middlehurst, and F. Separovic, *Biochim. Biophys. Acta*, **598**, 405 (1980).

(12) J. P. Reeves and R. M. Dowben, *J. Cell. Physiol.*, **73**, 49 (1979).

(13) Y. Katz and J. M. Diamond, *J. Membr. Biol.*, **17**, 87 (1974).

Epimerization of Benzylpenicilloic Acid in Alkaline Media

ISAAC GHEBRE-SELLASSIE *, STANLEY L. HEM ‡, and ADELBERT M. KNEVEL *x

Received November 2, 1981, from the **Department of Medicinal Chemistry and Pharmacognosy* and the ‡*Department of Industrial and Physical Pharmacy, School of Pharmacy and Pharmacal Sciences, Purdue University, West Lafayette, IN 47907.* Accepted for publication November 4, 1982.

Abstract □ 5*R*,6*R*-Benzylpenicilloic acid was found to epimerize slowly in alkaline media to 5*S*,6*R*-benzylpenicilloic acid until equilibrium was established. Epimerization proceeded *via* the imine tautomer of penamaldic acid rather than the enamine form and was found to favor the 5*S*,6*R*-epimer at equilibrium. The conversion process was monitored using both reverse-phase high-performance liquid chromatography and NMR spectroscopy.

Keyphrases □ Benzylpenicilloic acid—epimerization, alkaline media, imine tautomer of penamaldic acid as intermediate □ Epimerization—benzylpenicilloic acid in alkaline media, imine tautomer of penamaldic acid as intermediate □ Penamaldic acid—imine tautomer, intermediate in the epimerization of benzylpenicilloic acid

Penicilloic acid has been reported to be the principal hydrolysis and excretion product of penicillin (1, 2). It has also been cited as a minor antigenic determinant, although it is structurally incapable of reacting directly with proteins to form the highly reactive penicilloyl conjugate (3). This compound is believed to exert its antigenic activity by reacting with disulfide linkages of proteins (4). Despite the important role which penicilloic acid may play as an antigenic determinant and its reported existence as a mixture of isomers in alkaline media (5, 6), virtually no attempt has been made either to separate the isomers or to investigate the isomerization process.

In this paper, a combination of high-performance liquid chromatography (HPLC), NMR, polarography, and UV spectroscopy was used to separate the 5*R*,6*R*- and 5*S*,6*R*-epimers of benzylpenicilloic acid, monitor the conversion process, and examine the epimerization mechanism.

EXPERIMENTAL

Chemicals and Reagents—Penicillin G potassium[1] was obtained commercially and used without further treatment. Acetonitrile[2] was HPLC grade, while all other chemicals were either USP or reagent grade. Double-distilled water was used to prepare buffer solutions.

Preparation of Disodium Penicilloate—The disodium salts of 5*R*,6*R*- and 5*S*,6*R*-benzylpenicilloic acids were prepared by procedures similar to those used in the preparation of penicic and epipenicic acids (7).

Disodium 5R,6R-Benzylpenicilloate—An 8.64-g sample of penicillin G potassium was dissolved in 15 mL of double-distilled water and allowed to cool in an ice-salt bath. After the solution temperature reached ~0°C, 4.64 mL of cold 10 M NaOH was added in one increment. Fifteen minutes later, the pH was adjusted to 8.7 [the equivalence point of the disodium salt of benzylpenicilloic acid (7)] using 1 M HCl, and the reaction mixture was immediately lyophilized. ^{13}C-NMR: δ 26.4 and 26.7 (C-2$^{\alpha}$ and C-2$^{\beta}$), 42.5 (C-9), 58.6 (C-2), 59.9 (C-6), 66.1 (C-5), 75.4 (C-3), 127.4 (C-4′), 129.0 (C-3′), 129.4 (C-2′), 135.0 (C-1′), and 173.9, 175.4, and 175.9 (C-3$^{\alpha}$, C-6$^{\alpha}$, and C-8). ^{1}H-NMR (D_2O): δ 1.07 (s, CH_3), 1.34 (s, CH_3), 3.26 (s, H-3), 3.53

[1] Sigma Chemical Co., St. Louis, Mo.
[2] Waters Associates, Milford, Mass.

0022-3549/84/0100-0125$01.00/0

© 1984, American Pharmaceutical Association

such as sucrose or other volume indicators, from a layer of water of hydration of the phospholipid. For dimyristoyl phosphatidyl choline liposomes, this "nonsolvent water" has been shown to be 11.5 mol of water/mol of phosphatidyl choline, or approximately one-third of the enclosed liposomal water (13). The second factor is the difference between the true liposomal structure and the geometric approximations made in our model. For example, any change in the shape of the model to a nonspherical geometry will decrease the trapped volume relative to the percent exposure (r^2 *versus* r^3). This does not imply that multi-bilayers are nonspherical, but deviations from sphericity can account for this discrepancy.

In conclusion, our calculations clearly show that the estimation by Schwartz and McConnell for the number of lamellae in multilamellar vesicles is essentially correct. This, in fact, implies that the wall of the average liposome spontaneously formed by hydration of phospholipids, consists of 5–10 bilayers and has a total thickness $< \sim 0.2$ μm. Thus, "fully swollen" (spherical) liposomes of a diameter of 1.4 μm, on the average, contain an inner aqueous cavity >1.0 μm. When viewed obliquely, a nonspherical multi-bilayer could result in the observed space-filling "onion-like" structures seen in some electron micrographs and give a somewhat misleading impression of the large central cavity which we calculate to be present in multilamellar liposomal structures. Finally, we conclude that therapeutic strategies using encapsulation of aqueous components into simple multilamellar lipid dispersions must take into account the fact that the vast majority of encapsulated material will reside in the central cavity of these liposomes.

REFERENCES

(1) V. Luzzati, in "Biological Membranes," D. Chapman, Ed., Academic, New York, N.Y., 1968, pp. 71–123.

(2) A. D. Bangham, M. W. Hill, and N. G. Miller, "Methods in Membrane Biology," E. D. Korn, Ed., Plenum, New York, N.Y., 1974, pp. 1–68.

(3) A. D. Bangham, M. M. Standish, and J. C. Watkins, *J. Mol. Biol.*, **13**, 238 (1965).

(4) G. Poste and D. Papahadjopoulos, in "Uses of Liposomes in Biology and Medicine," G. Gregoriadis and A. Allison, Eds., Wiley, London, 1979, pp. 101–151.

(5) F. Olson, C. A. Hunt, F. C. Szoka, W. J. Vail, and D. Papahadjopoulos, *Biochim. Biophys. Acta*, **557**, 9 (1979).

(6) A. D. Bangham, J. De Gier, and G. D. Greville, *Chem. Phys. Lipids*, **1**, 225 (1967).

(7) M. A. Schwartz and H. M. McConnell, *Biochemistry*, **17**, 837 (1978).

(8) F. Szoka, Jr. and D. Papahadjopoulos, *Annu. Rev. Biophys. Bioeng.*, **9**, 467 (1980),

(9) C. Pidgeon and C. A. Hunt, *J. Pharm. Sci.*, **70**, 173 (1981).

(10) C. Huang, *Biochemistry*, **8**, 344 (1969).

(11) B. A. Cornell, J. Middlehurst, and F. Separovic, *Biochim. Biophys. Acta*, **598**, 405 (1980).

(12) J. P. Reeves and R. M. Dowben, *J. Cell. Physiol.*, **73**, 49 (1979).

(13) Y. Katz and J. M. Diamond, *J. Membr. Biol.*, **17**, 87 (1974).

Epimerization of Benzylpenicilloic Acid in Alkaline Media

ISAAC GHEBRE-SELLASSIE *, STANLEY L. HEM ‡, and ADELBERT M. KNEVEL *x

Received November 2, 1981, from the **Department of Medicinal Chemistry and Pharmacognosy* and the ‡*Department of Industrial and Physical Pharmacy, School of Pharmacy and Pharmacal Sciences, Purdue University, West Lafayette, IN 47907.* Accepted for publication November 4, 1982.

Abstract □ 5*R*,6*R*-Benzylpenicilloic acid was found to epimerize slowly in alkaline media to 5*S*,6*R*-benzylpenicilloic acid until equilibrium was established. Epimerization proceeded *via* the imine tautomer of penamaldic acid rather than the enamine form and was found to favor the 5*S*,6*R*-epimer at equilibrium. The conversion process was monitored using both reverse-phase high-performance liquid chromatography and NMR spectroscopy.

Keyphrases □ Benzylpenicilloic acid—epimerization, alkaline media, imine tautomer of penamaldic acid as intermediate □ Epimerization—benzylpenicilloic acid in alkaline media, imine tautomer of penamaldic acid as intermediate □ Penamaldic acid—imine tautomer, intermediate in the epimerization of benzylpenicilloic acid

Penicilloic acid has been reported to be the principal hydrolysis and excretion product of penicillin (1, 2). It has also been cited as a minor antigenic determinant, although it is structurally incapable of reacting directly with proteins to form the highly reactive penicilloyl conjugate (3). This compound is believed to exert its antigenic activity by reacting with disulfide linkages of proteins (4). Despite the important role which penicilloic acid may play as an antigenic determinant and its reported existence as a mixture of isomers in alkaline media (5, 6), virtually no attempt has been made either to separate the isomers or to investigate the isomerization process.

In this paper, a combination of high-performance liquid chromatography (HPLC), NMR, polarography, and UV spectroscopy was used to separate the 5*R*,6*R*- and 5*S*,6*R*-epimers of benzylpenicilloic acid, monitor the conversion process, and examine the epimerization mechanism.

EXPERIMENTAL

Chemicals and Reagents—Penicillin G potassium[1] was obtained commercially and used without further treatment. Acetonitrile[2] was HPLC grade, while all other chemicals were either USP or reagent grade. Double-distilled water was used to prepare buffer solutions.

Preparation of Disodium Penicilloate—The disodium salts of 5*R*,6*R*- and 5*S*,6*R*-benzylpenicilloic acids were prepared by procedures similar to those used in the preparation of penicic and epipenicic acids (7).

Disodium 5R,6R-Benzylpenicilloate—An 8.64-g sample of penicillin G potassium was dissolved in 15 mL of double-distilled water and allowed to cool in an ice-salt bath. After the solution temperature reached ~0°C, 4.64 mL of cold 10 M NaOH was added in one increment. Fifteen minutes later, the pH was adjusted to 8.7 [the equivalence point of the disodium salt of benzylpenicilloic acid (7)] using 1 M HCl, and the reaction mixture was immediately lyophilized. ^{13}C-NMR: δ 26.4 and 26.7 (C-2$^{\alpha}$ and C-2$^{\beta}$), 42.5 (C-9), 58.6 (C-2), 59.9 (C-6), 66.1 (C-5), 75.4 (C-3), 127.4 (C-4′), 129.0 (C-3′), 129.4 (C-2′), 135.0 (C-1′), and 173.9, 175.4, and 175.9 (C-3$^{\alpha}$, C-6$^{\alpha}$, and C-8). ^{1}H-NMR (D_2O): δ 1.07 (s, CH_3), 1.34 (s, CH_3), 3.26 (s, H-3), 3.53

[1] Sigma Chemical Co., St. Louis, Mo.
[2] Waters Associates, Milford, Mass.

0022-3549/84/0100-0125$01.00/0

© 1984, American Pharmaceutical Association

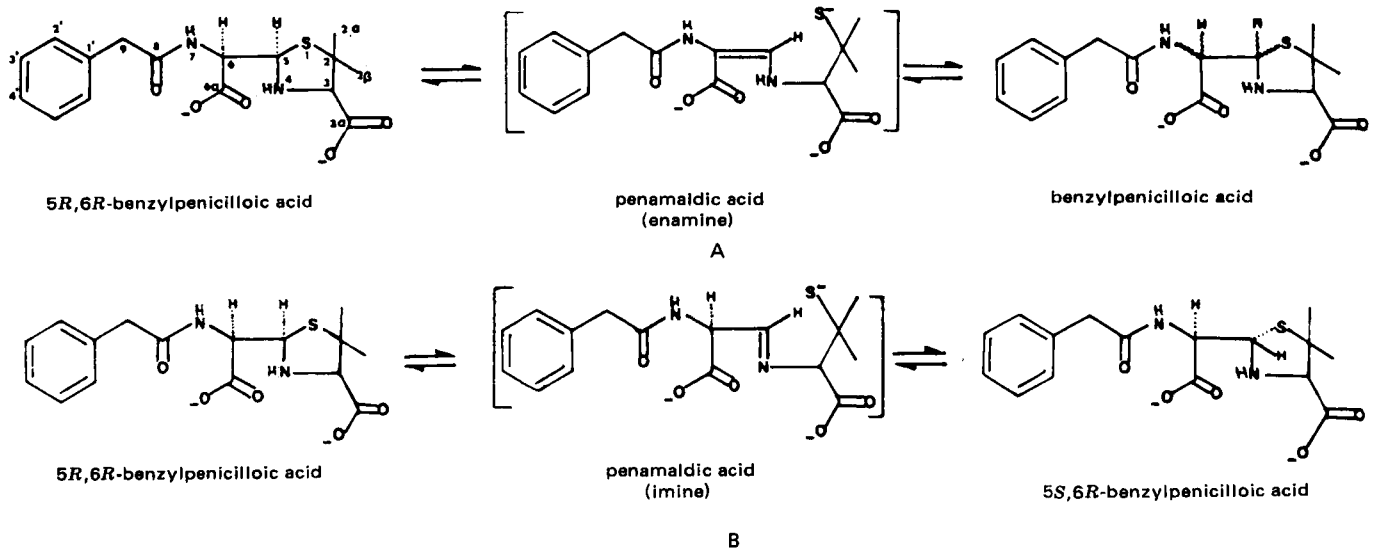

Scheme I—Proposed epimerization pathways for benzylpenicilloic acid.

(s, CH_2), 4.09 (d, J = 5.7 Hz, H-6), 4.92 (d, J = 5.7 Hz, H-5), and 7.23 (s, C_6H_5).

Disodium 5S,6R-Benzylpenicilloate—A 3.73-g sample of penicillin G potassium was dissolved in 100 mL of 0.2 M NaOH at 25°C. The mixture was stirred continuously using a magnetic stirrer, and the pH remained greater than 12 throughout the reaction time. After 30 min, the pH was adjusted to 8.7 by the addition of 1 M HCl, and the mixture was allowed to stand at 30°C for 48 h, and then was lyophilized. ^{13}C-NMR: δ 28.0 (C-2$^{\alpha}$ and C-2$^{\beta}$), 42.6 (C-9), 55.3 (C-6), 58.4 (C-2), 67.2 (C-5), 75.8 (C-3), 127.5 (C-4′), 129.2 (C-3′), 129.6 (C-2′), 134.4 (C-1′), and 174.6 and 174.8 (C-3$^{\alpha}$, C-6$^{\alpha}$, and C-8). ^{1}H-NMR (D_2O): δ 0.87 (s, CH_3), 1.41 (s, CH_3), 3.25 (s, H-3), 3.61 (s, CH_2), 4.61 (d, J = 3.1 Hz, H-6), 4.90 (d, J = 3.1 Hz, H-5), and 7.24 (s, C_6H_5).

Assignments of the structures of the 5*R*,6*R*- and 5*S*,6*R*-benzylpenicilloic acids were made after the ^{1}H- and ^{13}C-NMR spectra of the two isomers were examined. The proton-decoupled ^{13}C-NMR spectra showed clearly that these two epimers were distinctly different species. The structural difference of the two compounds was unequivocally established partly by focusing on the chemical shifts of C-5 and C-6, which are significantly different. Since one or both of these carbons are likely to participate in the isomerization of benzylpenicilloic acid, this distinction has also an additional importance in the present work. The peaks were assigned to the various carbons primarily on the basis of the proton-coupled ^{13}C-NMR spectra of the two isomers. In addition, comparison has been made with the reported assignments for penicillin G potassium (8). The ^{1}H-NMR spectra also revealed that the compounds have different coupling constants for the protons at C-5 and C-6. 5*R*,6*R*-benzylpenicilloic acid displayed a coupling constant of 5.7 Hz, while the 5*S*,6*R*-epimer exhibited a coupling constant of 3.1 Hz. This significant difference in coupling constants is in close agreement with that reported for the dimethyl esters of the two epimers (9). Moreover, examination of the signals of the protons on the methyl groups of C-2 and the chemical shifts of the proton on C-6 clearly demonstrate that the two compounds are indeed structurally different.

Table I—HPLC Data Demonstrating the Relative Peak Height Ratios of 5*R*,6*R*-Benzylpenicilloic Acid to 5*S*,6*R*-Benzylpenicilloic Acid as a Function of Time

Time, h	Peak Height Ratio (5*R*,6*R*/5*S*,6*R*)
0.50	11.4
1.00	7.8
1.50	5.9
2.00	4.9
3.00	3.6
6.00	2.1
12.00	1.0
24.00	0.5
48.00	0.3
72.00	0.2
96.00	0.2
120.00	0.2

Instrumentation—*HPLC*—A liquid chromatograph consisting of a solvent delivery system[3] and an UV absorbance detector[4] that operates at 254 nm was used. A commercially produced stainless steel column[5] (250 × 4.6-mm i.d.) prepacked with 5-μm particles that are chemically bonded to a monomolecular layer of octadecyl groups was employed. The mobile phase was composed of acetonitrile–0.05 M KH_2PO_4 (17:83) adjusted to pH 4.0 using 1 M H_3PO_4. The mixture was filtered through a 0.2-μm pore filter[6] and deaerated prior to use. Samples were introduced *via* an injection port[7] fitted with a 2.0-mL loop. The flow rate and chart speed were 1.2 mL/min and 0.25 cm/min, respectively.

^{13}C-NMR—The natural-abundance ^{13}C-NMR spectra were obtained on a spectrometer[8] operating at 25.1 MHz. The free-induction decays were recorded using a 5-KHz spectral width and 16K computer memory. This allowed a digital resolution of 0.61 Hz/data point in the transforms. The sample was irradiated with a 10-μs pulse (40° flip angle) at 4-s intervals. A noise-modulated 100-MHz frequency source was used to

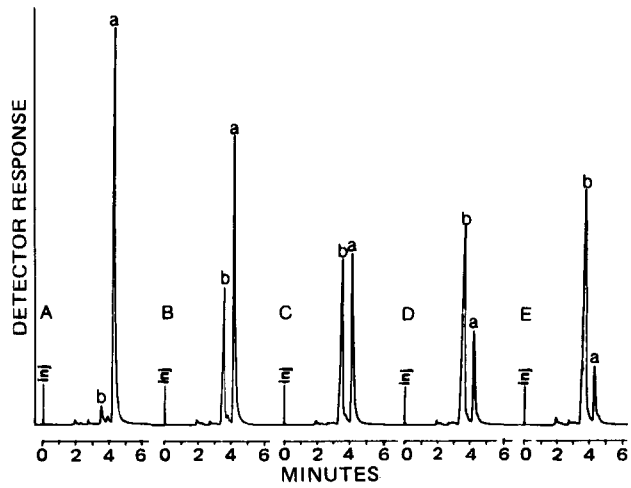

Figure 1—*Reverse-phase chromatograms of* 5R,6R-*penicilloic acid (a) and the* 5S,6R-*epimer (b) at specific time intervals during the epimerization process obtained using an ultrasphere-ODS column with a mobile phase of CH_3CN–0.05 M KH_2PO_4 (17:83) at pH 4.0 and detection at 254 nm. Key: (A) 0.03 h; (B) 6 h; (C) 12 h; (D) 24 h; (E) 48 h.*

[3] Model 6000A; Waters Associates.
[4] Model 440 Absorbance Detector; Waters Associates.
[5] Ultrasphere-ODS; Beckman Instruments, Irvine, Calif.
[6] Millipore Corp., Bedford, Mass.
[7] U6K; Waters Associates.
[8] Joel PFT-100; Joel Co., Cranford, N.J.

Table II—NMR Data Obtained During the Epimerization of 5*R*,6*R*-Benzylpenicilloic Acid to 5*S*,6*R*-Benzylpenicilloic Acid

Time, h	5*R*,6*R*/IS[a]	5*S*,6*R*/IS[a]	5*R*,6*R*/5*S*,6*R*
0.25	0.71	0.04	20
1.0	0.66	0.07	9.1
3.0	0.61	0.11	5.6
12.0	0.51	0.26	2.0
24.0	0.38	0.40	0.95
48.0	0.25	0.54	0.46
72.0	0.20	0.57	0.35
96.0	0.15	0.61	0.25
120.0	0.15	0.61	0.25

[a] IS = internal standard.

achieve broad-band decoupling of the protons. Proton-coupled ^{13}C-NMR spectra were obtained by gated decoupling (*i.e.*, decoupler off during acquisition) in order to maintain the nuclear Overhauser enhancement for the carbon signals. The carbon signals were referenced to an external standard of dioxane at 66.6 ppm.

^{1}H-NMR—The ^{1}H-NMR spectra of disodium penicilloate in deuterium oxide or sodium deuteroxide in deuterium oxide were obtained on a spectrometer[9] operating at 79.59 MHz. The free-induction decays were recorded using a 1000-Hz spectral width and 8K computer memory. This permitted a digital resolution of 0.24 Hz/data point in the transforms. The sample was irradiated with 15-μs pulse (30° flip angle) at 9-s intervals. All chemical shifts were referenced to acetone at 2.04 ppm.

Polarography—Polarographic data were obtained with a polarographic analyzer[10] which was used in conjunction with a drop timer[11]. Dropping mercury was used as the working electrode while the reference electrode was a saturated calomel electrode (SCE). A platinum wire was employed as an auxilliary electrode.

UV Spectroscopy—UV scans were made using a double-beam spectrophotometer[12] equipped with a single-pen recorder[13].

RESULTS AND DISCUSSION

Levine (1) investigated the decomposition of benzylpenicillin at pH 7.5 and 37°C and suggested that benzylpenicilloic acid appears to exist as a mixture of isomers. Furthermore, studies[14] on benzylpenicillin degradation indicated that benzylpenicilloic acid is extremely stable in mildly alkaline solutions and, hence, remains unchanged for extended periods of time. The epimerization of benzylpenicilloic acid was, therefore, studied in alkaline media where it is the most stable.

A reverse-phase HPLC technique was developed to separate the 5*R*,6*R*- and 5*S*,6*R*-epimers of benzylpenicilloic acid. The method was specific for the two epimers and, consequently, was utilized to monitor the epimerization process. The chromatograms in Fig. 1 demonstrate that in aqueous alkaline solutions, 5*R*,6*R*-benzylpenicilloic acid gradually epimerizes at room temperature to 5*S*,6*R*-benzylpenicilloic acid until equilibrium is established. At equilibrium, 5*S*,6*R*-benzylpenicilloic acid was found to be the favored product. Table I shows the ratios of the relative concentrations of the two epimers at specific time intervals.

^{1}H-NMR was also employed to examine the epimerization process. Once again, the spectra of benzylpenicilloic acid in alkaline media revealed the progressive conversion of 5*R*,6*R*-benzylpenicilloic acid to 5*S*,6*R*-benzylpenicilloic acid with a preponderance of the latter epimer forming at equilibrium (Table II). The conversion of 5*R*,6*R*-benzylpenicilloic acid to the 5*S*,6*R*-epimer was monitored by utilizing, respectively, the methyl signals at δ 1.07 and 6.87 ppm (Fig. 2). Acetone was used both as a reference for chemical shifts and as an internal standard. Integrations are not shown for the sake of clarity.

Based on mechanistic considerations, two pathways can be proposed for the epimerization process. The first (Scheme I, pathway A) involves the enamine tautomer of penamaldic acid, a compound which exhibits strong UV absorption at 280 nm, as an intermediate, while the second (Scheme I, pathway B) involves the imine tautomer, a compound which possesses a unique polarographically active group (C=N). These analytically significant differences in the proposed intermediates were, therefore, utilized not only to distinguish between the intermediates themselves, but also to elucidate the actual epimerization pathway.

[9] FT-80; Varian Instruments, Palo Alto, Calif.
[10] Model 174A; Princeton Applied Research Corp., Princeton, N.J.
[11] Model 174/70; Princeton Applied Research Corp., Princeton, N.J.
[12] Perkin-Elmer, Norwalk, Conn.
[13] Beckman Instruments, Irvine, Calif.
[14] Unpublished observations.

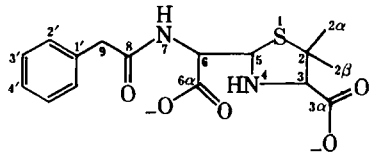

It has been suggested that the enamine form of penamaldic acid exists in equilibrium with benzylpenicilloic acid in alkaline solutions (10, 11). If this were the case, alkaline solutions of benzylpenicilloic acid would be expected to exhibit a strong absorption in the 280-nm region of the UV spectrum. In addition, deuterium exchange would occur at C-6 if C-6 were, indeed, involved in any way in the isomerization process (Scheme I, pathway A). However, solutions of the disodium salt of benzylpenicilloic acid in water, phosphate buffer (pH 7.4), or borate buffer (pH 10.0) did not show strong absorption at 280 nm during the lifetime of the experiment. This phenomenon was also observed by Busson and coworkers (9). Moreover, to determine whether C-6 participates in the epimerization process as would be the case if the enamine tautomer of penamaldic acid were an intermediate, a sample of disodium 5*R*,6*R*-benzylpenicilloate was dissolved in dilute aqueous solution of sodium deuteroxide and allowed to stand at room temperature. ^{1}H-NMR spectra revealed that conversion of the 5*R*,6*R*- to the 5*S*,6*R*-epimer proceeded without deu-

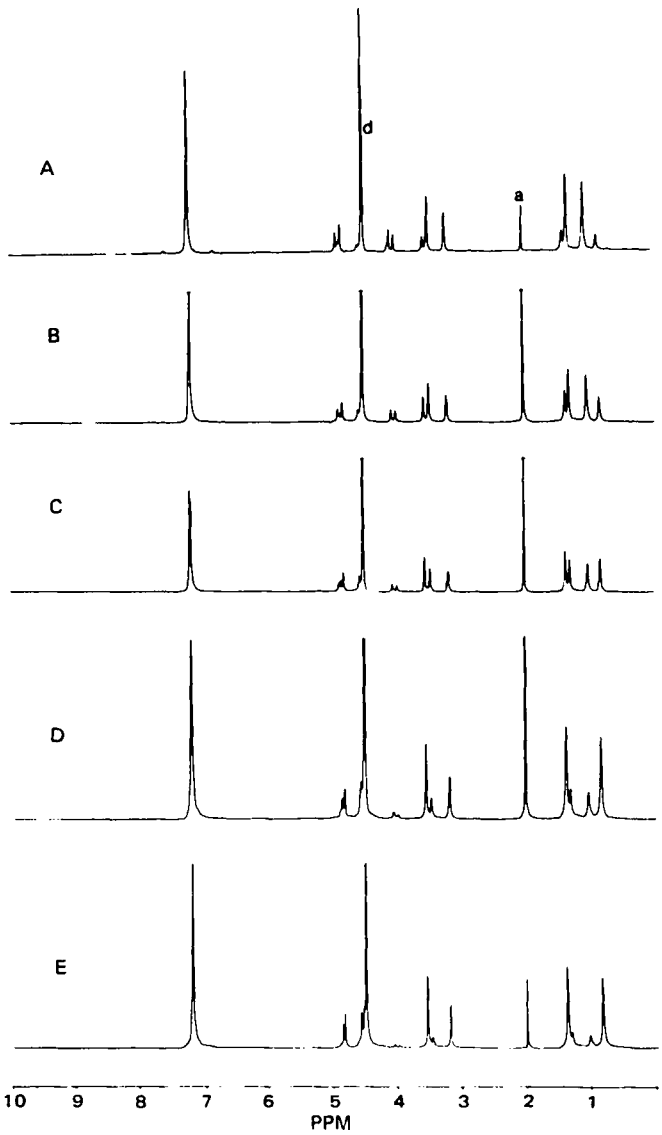

Figure 2—*^{1}H-NMR spectra showing the epimerization of* 5R,6R-*benzylpenicilloic acid (A) to* 5S,6R-*benzylpenicilloic acid (E) at specific time intervals. Key: (A) 6 h; (B) 12 h; (C) 24 h; (D) 48 h; (E) 120 h; (a) acetone; (d) water.*

terium incorporation. Though the chemical shifts of the protons at C-6 and C-5 and their coupling constants changed due to the conversion of one isomer to the other, the protons themselves remained coupled to each other, and the intensities of the peaks remained unchanged relative to the peaks of the other protons in the spectrum. These observations appear to contradict the suggestion that the enamine form of penamaldic acid exists in equilibrium with penicilloic acid in alkaline media and, consequently, exclude the enamine as an intermediate in the conversion of 5*R*,6*R*-benzylpenicilloic acid to the 5*S*,6*R*-epimer. Hence, the imine tautomer of penamaldic acid remains as the only probable intermediate involved in the epimerization process (Scheme I, pathway B).

An analytical technique employed to determine the imine in the presence of other degradation products including the enamine at very low concentrations was differential pulse polarography. Unlike the other compounds that may be present in solution, the imine tautomer contains a C=N group which is reducible at an electrode surface. Consequently, a solution of disodium 5*R*,6*R*-benzylpenicilloate was prepared and polarographed in the differential-pulse mode of operation. A reduction wave with a peak potential at −1.1 V *versus* SCE was observed. When aliquots were withdrawn from the reaction vessel after 12, 24, and 36 h and polarographed, the wave remained constant in height. An oxidation wave was also observed in the sulfhydryl region of the polarogram (~ −0.6 V *versus* SCE). However, it was not utilized for unequivocal identification since it is subject to interference from other sulfhydryl-containing compounds. Based on these results, it is concluded that in alkaline aqueous solutions 5*R*,6*R*-benzylpenicilloic acid epimerizes to 5*S*,6*R*-benzylpenicilloic acid and involves the imine tautomer rather than the enamine form of penamaldic acid as an intermediate.

The kinetic transformation of 5*R*,6*R*-benzylpenicilloic acid to its 5*S*,6*R*-epimer was determined quantitatively using the ^{1}H-NMR data presented in Table II. Assuming that the intermediate attains a steady-state concentration during the epimerization process and that the reaction rates are first order, the rate constants for both the forward and reverse reactions were computed using the following equations:

$$R \underset{k_r}{\overset{k_f}{\rightleftharpoons}} S \qquad \text{(Eq. 1)}$$

$$\log \frac{R_0 - R_{eq}}{R - R_{eq}} = \frac{(k_f + k_r)}{2.303} t \qquad \text{(Eq. 2)}$$

and

$$K = \frac{k_f}{k_r} = \frac{S_{eq}}{R_{eq}} \qquad \text{(Eq. 3)}$$

where R_0 is the initial concentration of 5*R*,6*R*-benzylpenicilloic acid, R_{eq} is the equilibrium concentration of 5*R*,6*R*-benzylpenicilloic acid, R is the concentration of 5*R*,6*R*-benzylpenicilloic acid at time t, k_f is the forward rate constant, k_r is the reverse rate constant, K is the equilibrium constant of the reaction, S is the concentration of 5*S*,6*R*-benzylpenicilloic acid at time t, and S_{eq} is the equilibrium concentration of 5*S*,6*R*-benzylpenicilloic acid; k_f was found to be 7.4×10^{-2} h^{-1}, while k_r was 1.8×10^{-2} h^{-1}. These values indicate that, at equilibrium, the ratio of the concentration of 5*R*,6*R*-benzylpenicilloic acid was ~0.2 × that of the 5*S*,6*R*-epimer, a value that is in agreement with the HPLC analysis (Table I).

REFERENCES

(1) B. B. Levine, *Nature (London)*, **187**, 939 (1960).

(2) T. L. Perry, *Nature (London)*, **206**, 895 (1965).

(3) B. B. Levine, *Arch. Biochem.*, **93**, 50 (1961).

(4) B. B. Levine, *Nature (London)*, **187**, 940 (1960).

(5) J. P. Hou and J. W. Poole, *J. Pharm. Sci.*, **60**, 503 (1971).

(6) R. Mozingo and K. Folkers, in "The Chemistry of Penicillin," M. T. Clark, J. R. Johnson, and B. Robinson, Eds., Princeton University Press, Princeton, N.J., 1949, p. 542.

(7) R. D. Carrol, S. Jung, and C. G. Sklavounos, *J. Heterocycl. Chem.*, **14**, 503 (1977).

(8) L. F. Johnson and W. C. Jankowski, "Carbon-13 NMR Spectra," Wiley-Interscience, New York, N.Y., 1972, p. 471.

(9) R. Busson, P. J. Claes, and H. Vanderhaeghe, *J. Org. Chem.*, **41**, 2556 (1976).

(10) M. A. Schwartz, *J. Pharm. Sci.*, **58**, 643 (1969).

(11) H. D. C. Rapson and A. E. Bird, *J. Pharm. Pharmacol.*, **15**, 222T (1963).

ACKNOWLEDGMENTS

Supported in part by Purdue Research Foundation and Biomedical Research Support Grant S07 RR 05586-11.

The authors wish to acknowledge John Kozlowski for his help in the presentation and interpretation of the NMR data.

Simultaneous Determination of Methyl, Ethyl, Propyl, and Butyl 4-Hydroxybenzoates and 4-Hydroxybenzoic Acid in Liquid Antacid Formulations by Gas Chromatography

GARY W. SCHIEFFER ˣ, PHILIP J. PALERMO *, and SUSAN POLLARD-WALKER ‡

Received October 20, 1982, from the *Analytical Chemistry Division, Norwich Eaton Pharmaceuticals, Inc., Norwich, NY 13815.* Accepted for publication December 13, 1982. Present address: *Proctor and Gamble Co., Sharon Woods Technical Center, Cincinnati, OH. ‡Savin Engineering and Manufacturing Division, Binghamton, NY 13902.

Abstract □ An isothermal chromatographic (GC) method employing an SE-30 column and flame-ionization detection has been developed for the simultaneous assay of methyl, ethyl, propyl, and butyl 4-hydroxybenzoates and 4-hydroxybenzoic acid in liquid antacid formulations. The method, which uses a silica column chromatographic cleanup step prior to GC, is specific for the compounds with respect to possible degradation products, impurities, and excipients.

Keyphrases □ 4-Hydroxybenzoic acid—simultaneous determination with its methyl, ethyl, propyl, and butyl esters, liquid antacid formulations, gas chromatography □ Antacid formulations—liquid, simultaneous determination of 4-hydroxybenzoic acid and its methyl, ethyl, propyl, and butyl esters, gas chromatography

The methyl (I), ethyl (II), propyl (III), and butyl (IV) esters of 4-hydroxybenzoic acid (V) in various combinations are commonly used as preservatives in liquid pharmaceutical preparations. Since the antimicrobial activity of various combinations of esters are generally more than additive (1), a method for simultaneously determining the

0022-3549/84/0100-0128$01.00/0

© 1984, American Pharmaceutical Association

terium incorporation. Though the chemical shifts of the protons at C-6 and C-5 and their coupling constants changed due to the conversion of one isomer to the other, the protons themselves remained coupled to each other, and the intensities of the peaks remained unchanged relative to the peaks of the other protons in the spectrum. These observations appear to contradict the suggestion that the enamine form of penamaldic acid exists in equilibrium with penicilloic acid in alkaline media and, consequently, exclude the enamine as an intermediate in the conversion of 5*R*,6*R*-benzylpenicilloic acid to the 5*S*,6*R*-epimer. Hence, the imine tautomer of penamaldic acid remains as the only probable intermediate involved in the epimerization process (Scheme I, pathway B).

An analytical technique employed to determine the imine in the presence of other degradation products including the enamine at very low concentrations was differential pulse polarography. Unlike the other compounds that may be present in solution, the imine tautomer contains a C=N group which is reducible at an electrode surface. Consequently, a solution of disodium 5*R*,6*R*-benzylpenicilloate was prepared and polarographed in the differential-pulse mode of operation. A reduction wave with a peak potential at −1.1 V *versus* SCE was observed. When aliquots were withdrawn from the reaction vessel after 12, 24, and 36 h and polarographed, the wave remained constant in height. An oxidation wave was also observed in the sulfhydryl region of the polarogram (~ −0.6 V *versus* SCE). However, it was not utilized for unequivocal identification since it is subject to interference from other sulfhydryl-containing compounds. Based on these results, it is concluded that in alkaline aqueous solutions 5*R*,6*R*-benzylpenicilloic acid epimerizes to 5*S*,6*R*-benzylpenicilloic acid and involves the imine tautomer rather than the enamine form of penamaldic acid as an intermediate.

The kinetic transformation of 5*R*,6*R*-benzylpenicilloic acid to its 5*S*,6*R*-epimer was determined quantitatively using the ^{1}H-NMR data presented in Table II. Assuming that the intermediate attains a steady-state concentration during the epimerization process and that the reaction rates are first order, the rate constants for both the forward and reverse reactions were computed using the following equations:

$$R \underset{k_r}{\overset{k_f}{\rightleftharpoons}} S \qquad \text{(Eq. 1)}$$

$$\log \frac{R_0 - R_{eq}}{R - R_{eq}} = \frac{(k_f + k_r)}{2.303} t \qquad \text{(Eq. 2)}$$

and

$$K = \frac{k_f}{k_r} = \frac{S_{eq}}{R_{eq}} \qquad \text{(Eq. 3)}$$

where R_0 is the initial concentration of 5*R*,6*R*-benzylpenicilloic acid, R_{eq} is the equilibrium concentration of 5*R*,6*R*-benzylpenicilloic acid, R is the concentration of 5*R*,6*R*-benzylpenicilloic acid at time t, k_f is the forward rate constant, k_r is the reverse rate constant, K is the equilibrium constant of the reaction, S is the concentration of 5*S*,6*R*-benzylpenicilloic acid at time t, and S_{eq} is the equilibrium concentration of 5*S*,6*R*-benzylpenicilloic acid; k_f was found to be 7.4×10^{-2} h^{-1}, while k_r was 1.8×10^{-2} h^{-1}. These values indicate that, at equilibrium, the ratio of the concentration of 5*R*,6*R*-benzylpenicilloic acid was ~0.2 × that of the 5*S*,6*R*-epimer, a value that is in agreement with the HPLC analysis (Table I).

REFERENCES

(1) B. B. Levine, *Nature (London)*, **187**, 939 (1960).

(2) T. L. Perry, *Nature (London)*, **206**, 895 (1965).

(3) B. B. Levine, *Arch. Biochem.*, **93**, 50 (1961).

(4) B. B. Levine, *Nature (London)*, **187**, 940 (1960).

(5) J. P. Hou and J. W. Poole, *J. Pharm. Sci.*, **60**, 503 (1971).

(6) R. Mozingo and K. Folkers, in "The Chemistry of Penicillin," M. T. Clark, J. R. Johnson, and B. Robinson, Eds., Princeton University Press, Princeton, N.J., 1949, p. 542.

(7) R. D. Carrol, S. Jung, and C. G. Sklavounos, *J. Heterocycl. Chem.*, **14**, 503 (1977).

(8) L. F. Johnson and W. C. Jankowski, "Carbon-13 NMR Spectra," Wiley-Interscience, New York, N.Y., 1972, p. 471.

(9) R. Busson, P. J. Claes, and H. Vanderhaeghe, *J. Org. Chem.*, **41**, 2556 (1976).

(10) M. A. Schwartz, *J. Pharm. Sci.*, **58**, 643 (1969).

(11) H. D. C. Rapson and A. E. Bird, *J. Pharm. Pharmacol.*, **15**, 222T (1963).

ACKNOWLEDGMENTS

Supported in part by Purdue Research Foundation and Biomedical Research Support Grant S07 RR 05586-11.

The authors wish to acknowledge John Kozlowski for his help in the presentation and interpretation of the NMR data.

Simultaneous Determination of Methyl, Ethyl, Propyl, and Butyl 4-Hydroxybenzoates and 4-Hydroxybenzoic Acid in Liquid Antacid Formulations by Gas Chromatography

GARY W. SCHIEFFER ˣ, PHILIP J. PALERMO *, and SUSAN POLLARD-WALKER ‡

Received October 20, 1982, from the *Analytical Chemistry Division, Norwich Eaton Pharmaceuticals, Inc., Norwich, NY 13815.* Accepted for publication December 13, 1982. Present address: *Proctor and Gamble Co., Sharon Woods Technical Center, Cincinnati, OH. ‡Savin Engineering and Manufacturing Division, Binghamton, NY 13902.

Abstract □ An isothermal chromatographic (GC) method employing an SE-30 column and flame-ionization detection has been developed for the simultaneous assay of methyl, ethyl, propyl, and butyl 4-hydroxybenzoates and 4-hydroxybenzoic acid in liquid antacid formulations. The method, which uses a silica column chromatographic cleanup step prior to GC, is specific for the compounds with respect to possible degradation products, impurities, and excipients.

Keyphrases □ 4-Hydroxybenzoic acid—simultaneous determination with its methyl, ethyl, propyl, and butyl esters, liquid antacid formulations, gas chromatography □ Antacid formulations—liquid, simultaneous determination of 4-hydroxybenzoic acid and its methyl, ethyl, propyl, and butyl esters, gas chromatography

The methyl (I), ethyl (II), propyl (III), and butyl (IV) esters of 4-hydroxybenzoic acid (V) in various combinations are commonly used as preservatives in liquid pharmaceutical preparations. Since the antimicrobial activity of various combinations of esters are generally more than additive (1), a method for simultaneously determining the

0022-3549/84/0100-0128$01.00/0

© 1984, American Pharmaceutical Association

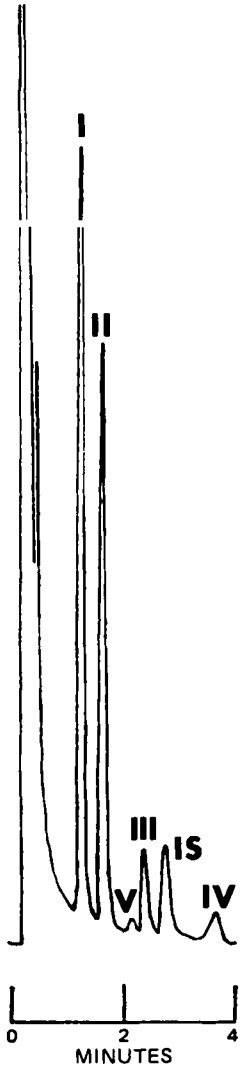

Figure 1—*Chromatogram of the trimethylsilyl derivatives of 1.5 μg of methyl 4-hydroxybenzoate (I), 1 μg of ethyl 4-hydroxybenzoate (II), 0.2 μg of propyl 4-hydroxybenzoate (III), 0.11 μg of butyl 4-hydroxybenzoate (IV), 0.03 μg of 4-hydroxybenzoic acid (V), and 0.75 μg of 3,4-dimethoxybenzoic acid internal standard (IS) using a 3% SE-30 column at 150°C.*

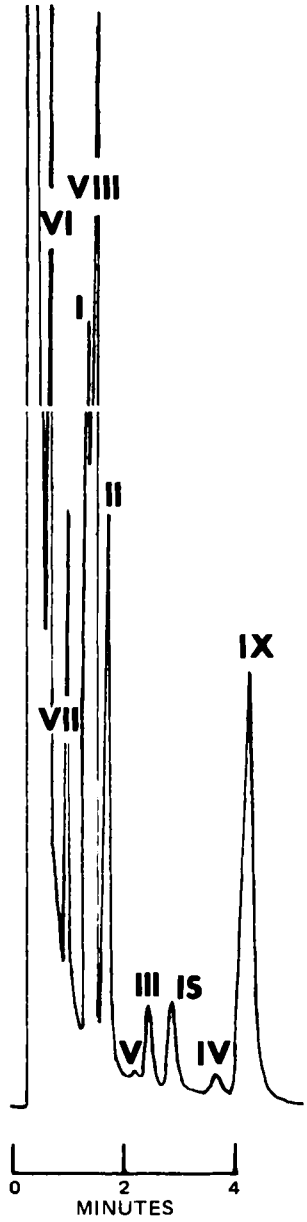

Figure 2—*Chromatogram of the trimethylsilyl derivatives of methyl (I), ethyl (II), propyl (III), and butyl (IV) 4-hydroxybenzoates, 4-hydroxybenzoic acid (V), 3,4-dimethoxybenzoic acid (IS), and possible impurities and degradation products: benzoic acid (VI), methyl salicylate (VII), salicylic acid (VIII), and 2,5-dihydroxybenzoic acid (IX) using a 3% SE-30 column at 150°C. A peak for phenol was not observed.*

concentrations of the four esters along with that of the hydrolytic degradation product (V) would be desirable. This would both aid the development of the optimum combination and concentration of the esters for maximum antibacterial effectiveness and assist in a study of the preservative stability in finished dosage forms.

Among the available assays, the HPLC assays of I–IV do not allow sufficient retention of V to separate it from the excipients. The weak eluant required for any significant retention on μ-phenyl or μ-C_{18} columns (2) makes elution of I–IV lengthy. The addition of a tetrabutylammonium ion pair does not significantly increase the retention of V on reverse-phase columns (3); however, this is not surprising since Doyle and Proctor have found that V yields low ion-pair extraction efficiency with tetrabutylammonium as the counter ion (4).

GC appears more promising for a simultaneous assay of I–V mainly because the large difference in the polarity of V from that of I–IV can be negated by the formation of derivatives of both the phenolic and carboxylic functions. SE-30 and OV-17 columns have been used to analyze plant extracts for trimethylsilyl derivatives of V and other phenolic acids (5). Similarly, OV-11 and OV-1 columns have been used to assay derivatized V and other aromatic acids in urine (6). A cyclohexane–dimethanol succinate column was used to assay trimethylsilyl derivatives of I–IV in an injection preservative (7), and a sucrose acetate isobutyrate column was used in the separation of the four esters in cosmetics (8). The present work involves similar approaches and the development of a column chromatographic cleanup step to yield a GC assay for simultaneously determining I–V in liquid antacid formulations.

EXPERIMENTAL

Reagents and Chemicals—All reagents and chemicals were ACS, USP, or NF quality and were used without further purification. Silyla-

Table I—Linearity of the Peak Height Ratios

Parameter	4-Hydroxybenzoate Esters				4-Hydroxybenzoic Acid
	Methyl	Ethyl	Propyl	Butyl	
Correlation coefficient	0.9997	0.9998	0.9998	0.9997	0.9996
Standard error of estimate ($SE_{y/x}$)	0.2	0.09	0.016	0.007	0.02
Intercept[a], %	3.7	−0.6	−3.6	−8.0	2.1
Variation[b], %	1.9	1.5	1.6	1.8	2.9

[a] (y-intercept/$\bar{y}$) × 100, where $\bar{y}$ is the average of y values (9). [b] ($SE_{y/x}/\bar{y}$) × 100.

tion-grade pyridine[1] and *N,O*-bis(trimethylsilyl)trifluoroacetamide[1] were used as received.

Apparatus—A chromatograph[2] equipped with a flame-ionization detector was used with a 1.8-m × 2-mm i.d. glass column[3] containing 3% SE-30 on 100–200 mesh support[4]. The gas flow rates were adjusted as follows: helium carrier gas, 30 mL/min; hydrogen, 50 mL/min; air, 400 mL/min. The detector and injector temperatures were both set at 250°C. The column temperature was set at 150°C for isothermal runs. Additional work was done with a 5% OV-1 column with temperature programming, as described below. Peak heights were determined either manually or with a computerized data acquisition system[5].

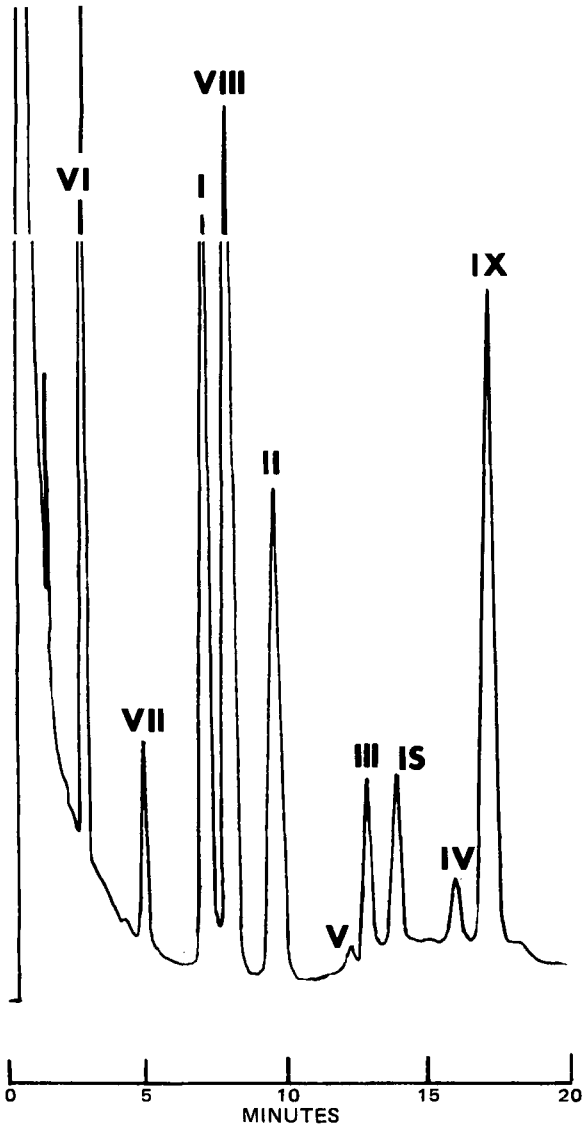

Figure 3—*Chromatogram of the trimethylsilyl 4-hydroxybenzoates, 4-hydroxybenzoic acid, impurities, and degradation products using a 5% OV-1 column, 150°C for 10 min, 32°C/min to 175°C. See Fig. 2 for peak identification.*

Table II—GC Assay of Commercial Liquid Antacids

Sample	Sample Weight, g	Amount Recovered, mg/mL I	II	III	IV	V
1[a]	0.7053	1.52	0.97	0.179	0.121	0.062
	0.7148	1.51	0.94	—	—	—
	0.6740	1.43	0.93	0.172	0.116	0.060
	0.9192	1.53	0.98	0.172	0.122	0.056
	0.9285	1.48	0.95	0.171	0.116	0.058
	0.8125	1.44	0.94	0.174	0.117	0.058
	1.038	1.45	0.95	0.178	0.120	0.060
	0.9910	1.48	0.93	0.168	0.117	0.057
	0.9424	1.45	0.93	0.173	0.118	0.061
	1.2885	1.50	0.96	0.170	0.116	0.060
	1.3027	1.52	0.98	—	—	—
	1.2816	1.48	0.96	0.174	0.121	0.061
Mean		1.48	0.95	0.173	0.118	0.059
RSD (1σ)		2.3%	1.8%	2.0%	1.9%	3.5%
2[b]	1.191	—	—	0.05	0.05	0.20
3[b]	1.001	0.12	—	0.21	—	0.81

[a] Sample 1, Experimental liquid antacid from Norwich Eaton; sample 2, Mylanta II; sample 3, Maalox. Label is 1.75 mg/mL for I, 1.02 mg/mL for II, 0.20 mg/mL for III, and 0.12 mg/mL for IV. [b] Label values not known.

Sample and Standard Preparation—One gram of liquid antacid, 0.4 mL of 1 M HCl, and 2.5 g of silica gel were mixed in a beaker until a fine, free-flowing powder formed. The powder was transferred to a 1-cm i.d. glass tube containing a glass wool pledget and eluted with 25–30 mL of ether at ~2 mL/min. Exactly 2.0 mL of a 0.2-mg/mL ether solution of 3,4-dimethoxybenzoic acid (internal standard) was added to the eluate, and the solution was evaporated to dryness under a nitrogen stream at room temperature. (Insufficient aqueous solubility precluded adding the internal standard prior to this step.) Similarly, 2.0–4.0 mL of an ether standard solution (depending on the expected 4-hydroxybenzoate content of the sample) containing 440 μg/mL of I, 225 μg/mL of II, 60 μg/mL of III, 60 μg/mL of IV, and 7.5 μg/mL of V was added to a test tube. Exactly 2.0 mL of the internal standard solution was added, and the solution was evaporated to dryness as for the sample. (Since studies have shown that no sample losses occur if an aqueous standard solution was eluted with ether through a silica column, a "method standard" was not necessary.) Trimethylsilyl derivatives of the compounds were formed by adding 0.4 ml of pyridine and 0.4 mL of *N,O*-bis(trimethylsilyl)trifluoroacetamide to the sample and standard residues. After briefly mixing, 1 μL of the solution was injected into the chromatograph.

Forced Degradation Sample—A fresh liquid antacid sample containing I and III (with no V initially present) was raised to a pH of ~10 by the addition of 2 M NaOH and heated in a stoppered container at 65°C for 48 h. The sample was extracted, derivatized, and chromatographed as described above.

RESULTS AND DISCUSSION

Initial attempts at solvent extraction of I–V from synthetic liquid antacid samples (placebo spiked with standard) yielded 100% recovery for I–IV but only ~50% recovery for V. Ion-pair extraction with tetraethylammonium ion also proved fruitless since V does not readily pair with other ions (4). A silica column chromatographic cleanup step, as described above, was found to be successful, yielding (after derivatization) the chromatogram shown in Fig. 1.

The compounds are resolved from possible degradation products (phenol, benzoic acid), impurities (methyl salicylate, 2,5-dihydroxybenzoic acid), and excipients. Salicylic acid is only partially resolved from

[1] Pierce Chemical Co., Rockford, Ill.
[2] Perkin-Elmer Model 900.
[3] Supelco, Bellefonte, Pa.
[4] Supelcort, Supelco.
[5] Hewlett-Packard Model 3356.

I; however, it was not present in the antacid formulations studied (Fig. 2). It was found that salicyclic acid could be better resolved, if necessary, by utilizing a 5% OV-1 column and temperature programming (150°C for 10 min, then 32°C/min to 175°C) (Fig. 3). However, chromatography time increased from ~5 min (SE-30 column) to >16 min (OV-1 column) per injection.

Assay of the forced degradation antacid sample revealed that ~10% of I had been converted to V. Compound III had not appreciably hydrolyzed during this short interval. No additional degradation peaks were observed.

The linearity data for I–V, determined by plotting peak height ratios (sample/internal standard) *versus* weight ratios injected, are presented in Table I. The correlation coefficients and percent variations (9) all indicate good linearity over the range studied: 0.75–6 μg for I, 0.5–3.8 μg for II, 0.1–0.9 μg for III, 0.06–0.5 μg for IV, and 0.014–0.7 μg for V. The percent intercepts indicate no serious problem with single-point standard calculations, except for IV. The significant negative intercept for IV demands that standard and sample concentrations be matched within 10%. Alternatively, a standard curve analysis could be run.

Assays of eight synthetic liquid antacid samples made by spiking placebo with solutions containing known amounts of standard I–V at levels of 60–125% of the theoretical yielded average recoveries and relative standard deviations of 99.0 ± 2.0% for I, 99.3 ± 1.9% for II, 98.7 ± 1.8% for III, 100.3 ± 1.6% for IV, and 100.0 ± 1.4% for V.

Twelve replicate assays of an actual liquid antacid sample containing all four preservatives and their common hydrolysis product V yielded good precision, as shown in Table II. The assay results of two other commercial liquid antacids are also shown in Table II. Since these samples had been stored for ~2 years prior to assay, relatively high concentrations of V were encountered. Although only antacids were examined in the present work, the technique should be readily applicable to other pharmaceutical preparations, such as liquids, elixirs, parenterals, creams, and gels.

REFERENCES

(1) G. Clarke and I. A. Rashid, *JAOAC*, **59**, 1175 (1976).

(2) F. M. Scriven, W. R. Day, and R. B. H. Wills, *J. Liq. Chromatogr.*, **2**, 125 (1979).

(3) P. Jandera and H. Engelhardt, *Chromatographia*, **13**, 18 (1980).

(4) T. D. Doyle and J. B. Proctor, *JAOAC*, **50**, 1175 (1976).

(5) R. J. Horvat and S. D. Senter, *J. Agric. Food Chem.*, **28**, 1292 (1980).

(6) R. F. Coward and P. Smith, *J. Chromatogr.*, **45**, 230 (1969).

(7) E. Hopp, *Medd. Nor. Farm. Selsk.*, **40**, 153 (1978).

(8) C. H. Wilson, *Am. Cosmet. Perfum.*, **87**, 43 (1972).

(9) M. J. Cardone, P. J. Palermo, and L. B. Sybrandt, *Anal. Chem.*, **52**, 1187 (1980).

Analysis of Ritodrine in Serum by High-Performance Liquid Chromatography with Electrochemical Detection

LI SHEI LIN *, STEVE N. CARITIS ‡, and LAN K. WONG *x

Received July 16, 1982, from the **Department of Pharmacology, School of Pharmacy* and the ‡*Department of Obstetrics and Gynecology, Magee-Womens Hospital, University of Pittsburgh, Pittsburgh, PA 15261.* Accepted for publication December 12, 1982.

Abstract □ A sensitive and specific assay for ritodrine in serum was developed using high-performance liquid chromatography (HPLC) with electrochemical detection. Serum samples were alkalinized to pH 9.4 by the addition of a sodium carbonate buffer and extracted with ethyl acetate. The extracts were evaporated to dryness and the residues were reconstituted in the HPLC mobile phase and chromatographed on a octadecylsilane reverse-phase column. The detection of ritodrine was achieved by an electrochemical detector with a glassy carbon electrode. The sensitivity was 0.2 ng for on-column injection. The extraction efficiency was 80%.

Keyphrases □ Ritodrine—analysis in serum, high-performance liquid chromatography with electrochemical detection □ High-performance liquid chromatography—analysis of ritodrine in serum, electrochemical detection

Ritodrine hydrochloride, *erythro*-*p*-hydroxy-α-[1-[(*p*-hydroxyphenethyl)amino]ethyl]benzyl alcohol hydrochloride (I), is a β-adrenergic receptor stimulant developed specifically for obstetrical use in the management of premature labor. Pharmacological studies have shown that ritodrine is a potent inhibitor of myometrial contractility with only minor cardiovascular effects (1–4). Studies on experimental animals have demonstrated the uterine relaxant properties of ritodrine. Depending on the animal species and the route of administration, the effective dose ranges from 5 μg/kg to 15 mg/kg (5). In humans, the therapeutic dose varies from 50 to 200 μg/min. The infusion rate is maintained 24–48 h according to the response of the patient and side effects (6). Treatment is usually followed with an oral 10-mg dose four to eight times daily for several days or until term. Human disposition studies have been carried out on healthy nonpregnant volunteers using tritiated ritodrine. It was found that the majority of the drug was excreted in the urine with a maximal excretion rate attained within 1 h after drug administration. The data suggested a two-compartment open model with half-lives of 2 and 13 h (5).

Analytical assay of ritodrine had been limited to the use of radioactively labeled drug (5) until recently when a sensitive RIA (7) was reported. The RIA has a sensitivity of <1 ng and has been used to measure serum levels of ritodrine in humans after oral or parenteral administration. Whereas good sensitivity was achieved by this procedure, some unexplained variability was observed in the data, possibly due to cross-reactivity with some endogenous interferences in the samples. The RIA antiserum is cur-

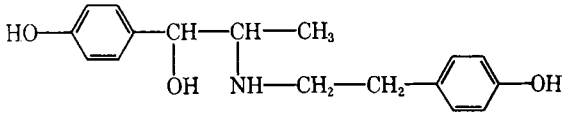

I

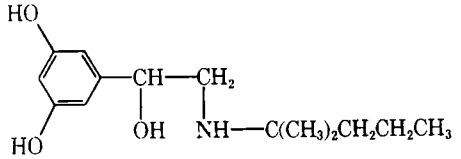

II

0022-3549/84/0100-0131$01.00/0

© 1984, American Pharmaceutical Association

I; however, it was not present in the antacid formulations studied (Fig. 2). It was found that salicyclic acid could be better resolved, if necessary, by utilizing a 5% OV-1 column and temperature programming (150°C for 10 min, then 32°C/min to 175°C) (Fig. 3). However, chromatography time increased from ~5 min (SE-30 column) to >16 min (OV-1 column) per injection.

Assay of the forced degradation antacid sample revealed that ~10% of I had been converted to V. Compound III had not appreciably hydrolyzed during this short interval. No additional degradation peaks were observed.

The linearity data for I–V, determined by plotting peak height ratios (sample/internal standard) *versus* weight ratios injected, are presented in Table I. The correlation coefficients and percent variations (9) all indicate good linearity over the range studied: 0.75–6 μg for I, 0.5–3.8 μg for II, 0.1–0.9 μg for III, 0.06–0.5 μg for IV, and 0.014–0.7 μg for V. The percent intercepts indicate no serious problem with single-point standard calculations, except for IV. The significant negative intercept for IV demands that standard and sample concentrations be matched within 10%. Alternatively, a standard curve analysis could be run.

Assays of eight synthetic liquid antacid samples made by spiking placebo with solutions containing known amounts of standard I–V at levels of 60–125% of the theoretical yielded average recoveries and relative standard deviations of 99.0 ± 2.0% for I, 99.3 ± 1.9% for II, 98.7 ± 1.8% for III, 100.3 ± 1.6% for IV, and 100.0 ± 1.4% for V.

Twelve replicate assays of an actual liquid antacid sample containing all four preservatives and their common hydrolysis product V yielded good precision, as shown in Table II. The assay results of two other commercial liquid antacids are also shown in Table II. Since these samples had been stored for ~2 years prior to assay, relatively high concentrations of V were encountered. Although only antacids were examined in the present work, the technique should be readily applicable to other pharmaceutical preparations, such as liquids, elixirs, parenterals, creams, and gels.

REFERENCES

(1) G. Clarke and I. A. Rashid, *JAOAC*, **59**, 1175 (1976).

(2) F. M. Scriven, W. R. Day, and R. B. H. Wills, *J. Liq. Chromatogr.*, **2**, 125 (1979).

(3) P. Jandera and H. Engelhardt, *Chromatographia*, **13**, 18 (1980).

(4) T. D. Doyle and J. B. Proctor, *JAOAC*, **50**, 1175 (1976).

(5) R. J. Horvat and S. D. Senter, *J. Agric. Food Chem.*, **28**, 1292 (1980).

(6) R. F. Coward and P. Smith, *J. Chromatogr.*, **45**, 230 (1969).

(7) E. Hopp, *Medd. Nor. Farm. Selsk.*, **40**, 153 (1978).

(8) C. H. Wilson, *Am. Cosmet. Perfum.*, **87**, 43 (1972).

(9) M. J. Cardone, P. J. Palermo, and L. B. Sybrandt, *Anal. Chem.*, **52**, 1187 (1980).

Analysis of Ritodrine in Serum by High-Performance Liquid Chromatography with Electrochemical Detection

LI SHEI LIN *, STEVE N. CARITIS ‡, and LAN K. WONG *x

Received July 16, 1982, from the **Department of Pharmacology, School of Pharmacy* and the ‡*Department of Obstetrics and Gynecology, Magee-Womens Hospital, University of Pittsburgh, Pittsburgh, PA 15261.* Accepted for publication December 12, 1982.

Abstract □ A sensitive and specific assay for ritodrine in serum was developed using high-performance liquid chromatography (HPLC) with electrochemical detection. Serum samples were alkalinized to pH 9.4 by the addition of a sodium carbonate buffer and extracted with ethyl acetate. The extracts were evaporated to dryness and the residues were reconstituted in the HPLC mobile phase and chromatographed on a octadecylsilane reverse-phase column. The detection of ritodrine was achieved by an electrochemical detector with a glassy carbon electrode. The sensitivity was 0.2 ng for on-column injection. The extraction efficiency was 80%.

Keyphrases □ Ritodrine—analysis in serum, high-performance liquid chromatography with electrochemical detection □ High-performance liquid chromatography—analysis of ritodrine in serum, electrochemical detection

Ritodrine hydrochloride, *erythro*-*p*-hydroxy-α-[1-[(*p*-hydroxyphenethyl)amino]ethyl]benzyl alcohol hydrochloride (I), is a β-adrenergic receptor stimulant developed specifically for obstetrical use in the management of premature labor. Pharmacological studies have shown that ritodrine is a potent inhibitor of myometrial contractility with only minor cardiovascular effects (1–4). Studies on experimental animals have demonstrated the uterine relaxant properties of ritodrine. Depending on the animal species and the route of administration, the effective dose ranges from 5 μg/kg to 15 mg/kg (5). In humans, the therapeutic dose varies from 50 to 200 μg/min. The infusion rate is maintained 24–48 h according to the response of the patient and side effects (6). Treatment is usually followed with an oral 10-mg dose four to eight times daily for several days or until term. Human disposition studies have been carried out on healthy nonpregnant volunteers using tritiated ritodrine. It was found that the majority of the drug was excreted in the urine with a maximal excretion rate attained within 1 h after drug administration. The data suggested a two-compartment open model with half-lives of 2 and 13 h (5).

Analytical assay of ritodrine had been limited to the use of radioactively labeled drug (5) until recently when a sensitive RIA (7) was reported. The RIA has a sensitivity of <1 ng and has been used to measure serum levels of ritodrine in humans after oral or parenteral administration. Whereas good sensitivity was achieved by this procedure, some unexplained variability was observed in the data, possibly due to cross-reactivity with some endogenous interferences in the samples. The RIA antiserum is cur-

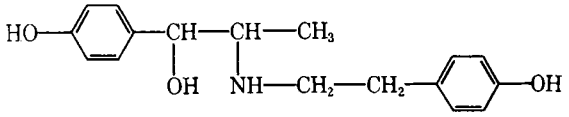

I

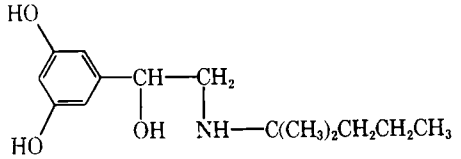

II

0022-3549/84/0100-0131$01.00/0

© 1984, American Pharmaceutical Association

rently unavailable precluding the routine clinical monitoring of ritodrine. Thus, it was deemed desirable to develop an alternative method for the assay of this drug in biological fluids. This report describes a simple, sensitive, and specific high-performance liquid chromatographic (HPLC) assay using electrochemical detection for the measurement of nanogram quantities of ritodrine in serum or plasma.

EXPERIMENTAL

Reagents and Materials—Ritodrine hydrochloride[1] and the internal standard[2], 1-(3,5-dihydroxyphenyl)-2-(1,1-dimethylbutylamino)ethanol (II), were used as received. Distilled-in-glass ethyl acetate[3] and methanol[4] were used in the extraction and chromatographic procedures, respectively. All other chemicals were reagent grade.

Apparatus—Chromatographic analyses were performed at ambient temperature on a liquid chromatograph[5] equipped with an electrochemical detector[6] fitted with a thin-layer cell containing a glassy carbon electrode. The electrochemical potential of the glassy carbon working electrode was set at +0.90 V relative to a silver–silver chloride reference electrode. A 4.6-mm × 26-cm prepacked octadecylsilane reverse-phase column[7] with a precolumn[8] (1.2 mm × 7.1 cm) was used. Samples were introduced onto the column through a septumless injector[9] with a 100-μL syringe. Chromatograms were recorded on a strip-chart recorder[10].

Chromatographic Condition—The chromatography was performed at an isocratic mode. The mobile phase was a methanol–phosphate buffer (25:75, v/v) with a flow rate of 1.5 mL/min. The phosphate buffer was composed of 0.01 M KH_2PO_4, 0.3 mM sodium octanesulfonate, and 0.1 mM EDTA (disodium ethylenediaminetetraacetate) and had a final pH of 4.5. The solvent mixture was deaerated by stirring under vacuum before use.

Extraction—A serum sample (1 mL) was adjusted to pH 9.4 by the use of 2 M sodium carbonate buffer. The internal standard (200 ng) was added to each sample, and the mixture was then vortexed and extracted with 6 mL of ethyl acetate by reciprocal shaking for 15 min. After centrifugation, the organic layer was transferred to another tube and evaporated to dryness under a nitrogen stream at 35°C. The dry residue was then redissolved in 400 μL of the HPLC mobile phase by vigorous vortexing. A 40-μL aliquot of the mixture was injected into the chromatograph for quantitation.

A set of standard samples prepared from blank serum spiked with known amounts of ritodrine and 200 ng of the internal standard were processed as above. The peak height ratios of ritodrine to the internal standard in these samples were determined, and a calibration curve was constructed from the resulting data. The concentrations of unknown samples were derived from this calibration curve. The recovery of ritodrine by the extraction procedure was 80%.

Mass Spectrometry—The identity of the ritodrine peak on the HPLC chromatogram was verified by MS. The eluate corresponding to the ritodrine fraction was collected from the HPLC, and the pH was adjusted to 9.4 with sodium carbonate. Ritodrine was extracted with ethyl acetate and evaporated to dryness under a nitrogen stream. The residue was applied to a sample vial of the spectrometer[11]. MS analysis was performed *via* a direct probe inlet in the electron-impact ionization mode at 70 eV. The mass spectrum of authentic ritodrine[1] showed the following characteristic fragment ions: *m/z* 121 (100%), 164 (65%), 107 (23%), 77 (21%), and 91 (10%). No molecular ion was observed for ritodrine. The HPLC peak of interest exhibited ions at *m/z* 121 (100%), 164 (65%), 107 (23%), 77 (21%), and 91 (10%). MS data were identical to those of the authentic sample.

RESULTS AND DISCUSSION

The sensitivity of detection for ritodrine during on-column injection was found to be 0.2 ng. This was established by observing that the peak height of 0.2 ng of ritodrine *versus* the internal standard was significantly different from zero when it was compared with the 95% confidence interval of the *y*-intercept. Under the described chromatographic conditions, the retention times of ritodrine and the internal standard were 7.8 and 12.0 min, respectively. Comparing the chromatogram (Fig. 1A) of an extracted blank serum sample pooled from pregnant women with that of a similar serum sample spiked with 40 ng of ritodrine hydrochloride and 200 ng of the internal standard (Fig. 1B), it can be concluded that little or no interferences from endogenous substances are present. A typical chromatogram from a patient receiving ritodrine for premature

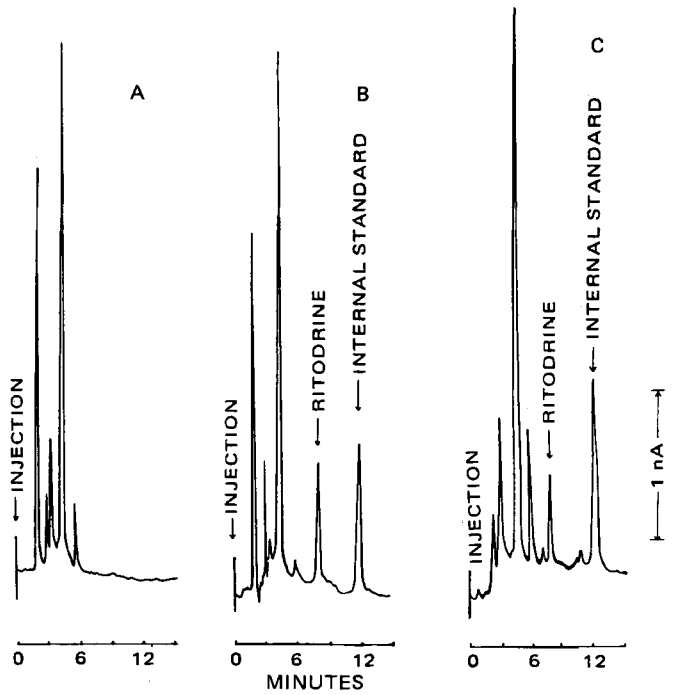

Figure 1—*Chromatograms of samples prepared from blank serum pooled from pregnant women (A), blank serum spiked with 40 ng of ritodrine hydrochloride and 200 ng of the internal standard (B), and serum of a patient receiving ritodrine therapy (C).*

Table 1—Analysis of Ritodrine Level in Serum

Ritodrine Spiked, ng/mL	Peak Height Ratio[a]	Mean Value Assayed, ng/mL	Ratio of Assayed to Spiked
2	0.095 0.091 0.119 0.098	2.08	1.04
5	0.131 0.165 0.144 0.130	5.31	1.06
10	0.207 0.210 0.237 0.186	9.20	0.920
20	0.400 0.345 0.366 0.460	19.6	0.978
40	0.731 0.760 0.708 0.752	39.9	0.998
80	1.35 1.57 1.50 1.43	82.3	1.03

[a] Ritodrine/internal standard.

[1] Philip-Duphar Research Laboratories, Weesp, The Netherlands.
[2] Research Laboratories of A B Draco, Lund, Sweden.
[3] Mallinckrodt, Paris, Ky.
[4] Burdick & Jackson Laboratories, Muskegon, Mich.
[5] Model M-45; Waters Associates, Milford, Mass.
[6] Model LC-4B; Bioanalytical Systems, West Lafayette, Ind.
[7] μBondapak C18; Waters Associates, Milford, Mass.
[8] HC Pellosil; Whatman, Clifton, N.J.
[9] Model U6K; Waters Associates, Milford, Mass.
[10] Linear Instruments, Irvine, Calif.
[11] Model 3200; Finnigan Corp., Sunnyvale, Calif.

labor is shown in Fig. 1C. The specificity of this method was also confirmed by mass spectral studies. The HPLC eluate corresponding to ritodrine was found to exhibit MS characteristics identical to those of pure ritodrine. The spectrum shows a base peak at m/z 121 and a strong fragment ion at m/z 164. No molecular ion is detectable for ritodrine in the electron-ionization spectrum.

The calibration curve for ritodrine using the internal standard bears a linear relationship ($r^2 = 0.9910$) over the range (2–80 ng/mL) studied. Table I illustrates the reproducibility of the method. To demonstrate the applicability of this method for the therapeutic monitoring of ritodrine, a serum sample from a pregnant woman receiving ritodrine for premature labor was analyzed. The patient received an intravenous infusion of ritodrine at 100 μg/min for 3.5 h. The serum level of ritodrine 20 min after the end of the infusion was 12.8 ng/mL. The concentration compares favorably with the results obtained by the RIA method (7). The degree of sensitivity achieved by the HPLC–EC method is suitable for drug monitoring and pharmacokinetic studies of ritodrine, since serum concentrations of the drug during clinical use usually range from several to ~100 ng/mL. The linearity of the calibration curve indicates that the assay methodology is appropriate for these measurements.

The usefulness of electrochemical detection has been demonstrated in the HPLC analysis of catecholamines (8–10), uric acid (11), ascorbic acid (11), and acetaminophen (12) in biological fluids and pharmaceutical preparations. Ritodrine, a compound structurally related to catecholamines, evokes a strong electrochemical response due to the two phenolic moieties in the molecule. The method described herein permits a rapid analysis of ritodrine at the nanogram level.

The sensitivity of the electrochemical detector is quite comparable with that of the RIA technique, and the assay speed of the two methods is also very comparable. The RIA method appears to be more convenient because no extraction is required. However, it takes ~40 min to incubate and equilibrate a sample with the antiserum plus additional time for scintillation counting, not to mention the time for preparing the antiserum. On the other hand, the analysis time by HPLC requires ~15 min according to the protocol. Most importantly the HPLC–EC method may be superior to the RIA in terms of specificity. Previous work in the assay of ritodrine by RIA showed negligible cross-reactivity with the drug conjugates (7). However, the possibility of cross-reactivity with endogenous catecholamines has not been evaluated. The fact that abnormal variability was observed in the data during the RIA quantitation of ritodrine (7) points to the potential problem of cross-reactivity. It is known that serum catecholamine levels are elevated during labor (13). This may cause erroneous determination of ritodrine by RIA under such conditions. On the other hand, the accuracy of the HPLC–EC method is not affected by these endogenous substances.

REFERENCES

(1) O. Jamissans, J. Esteban-Altirriba, and V. Maiques, *Br. J. Obstet. Gynecol.*, **76**, 656 (1969).

(2) T. P. Barden, *Am. J. Obstet, Gynecol.*, **112**, 645 (1972).

(3) D. J. Nochimson, H. D. Riffel, S.-Y. Yeh, M. S. Kreitzer, R. H. Paul, and E. H. Hon, *Am. J. Obstet. Gynecol.*, **118**, 523 (1974).

(4) A. S. I. Siimes and R. K. Creasy, *Am. J. Obstet. Gynecol.*, **126**, 1003 (1976).

(5) New Drug Application for ritodrine hydrochloride, no. 18280, submitted to the FDA on March 8, 1979, by Mid-West Medical Research, Inc., Columbus, Ohio, on behalf of Philip-Duphar B.V., Weesp, The Netherlands.

(6) A. Wesselins-deCasparis, M. Thiery, A. Y. L. Sian, K. Baungarten, I. Brosens, O. Gamisans, J. G. Stolk, and W. Vivier, *Br. Med. J.*, **3**, 144 (1971).

(7) R. Gander, L. W. de Zoeten, and J. B. van der Schoot, *Eur. J. Pharmacol.*, **17**, 117 (1980).

(8) C. Refshauge, P. T. Kissinger, R. Dreiling, L. Brank, R. Freeman, and R. N. Adams, *Life Sci.*, **14**, 311 (1974).

(9) R. M. Riggin, L.-D. Rau, R. L. Alcorn, and P. T. Kissinger, *Anal. Lett.*, **7**, 791 (1974).

(10) P. T. Kissinger, R. M. Riggin, R. L. Alcord, and L.-D. Rau, *Biochem. Med.*, **13**, 299 (1975).

(11) P. T. Kissinger, L. J. Felice, R. M. Riggin, L. A. Pachla, and D. C. Wenke, *Clin. Chem.*, **20**, 992 (1972).

(12) R. M. Riggin, A. L. Schmidt, and P. T. Kissinger, *J. Pharm. Sci.*, **64**, 680 (1975).

13) F. P. Zuspan, R. O'Shaughnessy, and J. D. Iams, *J. Reprod. Med.*, **26**, 483 (1981).

Remarks on the Structure–Activity Relationship of Silver Sulfanilamides

A. BULT *x, B. L. BAJEMA ‡, G. J. BOELEMA ‡, J. J. M. V. SAENE §, and D. A. DOORNBOS ‡

Received February 1, 1982, from the **Department of Pharmaceutical Analysis and Analytical Chemistry, State University of Leiden, 2300 RA Leiden, The Netherlands* and the ‡*Laboratory for Pharmaceutical and Analytical Chemistry* and the §*Laboratory for Pharmaceutical Technology and Dispensing, State University of Groningen, Groningen, The Netherlands.* Accepted for publication December 8, 1982.

Abstract □ The biological activity of a series of 10 silver sulfanilamides is studied in relation to the physical parameters pK_a, log K, and the aqueous solubility. None of the parameters demonstrate a simple relationship with the activity. A discussion of the significance of log K and the solubility in relation to the activity is given.

Keyphrases □ Silver sulfanilamides—structure-activity relationships, correlation between activity and pK_a, log K, and solubility □ Structure–activity relationships—silver sulfanilamides, correlation between activity and pK_a, log K, and solubility

An increasing interest in the silver sulfanilamide complexes was stimulated by the successful use of silver sulfadiazine (I) as an efficacious topical antibacterial agent in burn treatment (1). A number of efforts were made to account for the good *in vivo* activity of I as compared with other silver sulfanilamides (2–4). In this study the relevance of some physical parameters in relation to the *in vivo* antimicrobial activity are discussed.

BACKGROUND

The antimicrobial activity of I is thought to result from alteration of the mesosomal function of the microbial cell by the silver moiety of the molecule (5). The sulfadiazine moiety does not enter the cell and does not contribute appreciably to the antimicrobial action; therefore, I is not antagonized by *p*-aminobenzoic acid (3). A possible role of sulfadiazine is to localize the action of silver to the cell. The undissociated molecule I seems to interact with the microbial cell and is dissociated next at the cell surface into silver and sulfadiazine (6, 7).

The role of the sulfadiazine anion and other anions is rather unclear. Wysor assumed as a prerequisite for an active silver sulfanilamide that, like I, these compounds need to be stable in a chloride-containing solution

0022-3549/84/0100-0133$01.00/0

© 1984, American Pharmaceutical Association

labor is shown in Fig. 1C. The specificity of this method was also confirmed by mass spectral studies. The HPLC eluate corresponding to ritodrine was found to exhibit MS characteristics identical to those of pure ritodrine. The spectrum shows a base peak at m/z 121 and a strong fragment ion at m/z 164. No molecular ion is detectable for ritodrine in the electron-ionization spectrum.

The calibration curve for ritodrine using the internal standard bears a linear relationship ($r^2 = 0.9910$) over the range (2–80 ng/mL) studied. Table I illustrates the reproducibility of the method. To demonstrate the applicability of this method for the therapeutic monitoring of ritodrine, a serum sample from a pregnant woman receiving ritodrine for premature labor was analyzed. The patient received an intravenous infusion of ritodrine at 100 μg/min for 3.5 h. The serum level of ritodrine 20 min after the end of the infusion was 12.8 ng/mL. The concentration compares favorably with the results obtained by the RIA method (7). The degree of sensitivity achieved by the HPLC–EC method is suitable for drug monitoring and pharmacokinetic studies of ritodrine, since serum concentrations of the drug during clinical use usually range from several to ~100 ng/mL. The linearity of the calibration curve indicates that the assay methodology is appropriate for these measurements.

The usefulness of electrochemical detection has been demonstrated in the HPLC analysis of catecholamines (8–10), uric acid (11), ascorbic acid (11), and acetaminophen (12) in biological fluids and pharmaceutical preparations. Ritodrine, a compound structurally related to catecholamines, evokes a strong electrochemical response due to the two phenolic moieties in the molecule. The method described herein permits a rapid analysis of ritodrine at the nanogram level.

The sensitivity of the electrochemical detector is quite comparable with that of the RIA technique, and the assay speed of the two methods is also very comparable. The RIA method appears to be more convenient because no extraction is required. However, it takes ~40 min to incubate and equilibrate a sample with the antiserum plus additional time for scintillation counting, not to mention the time for preparing the antiserum. On the other hand, the analysis time by HPLC requires ~15 min according to the protocol. Most importantly the HPLC–EC method may be superior to the RIA in terms of specificity. Previous work in the assay of ritodrine by RIA showed negligible cross-reactivity with the drug conjugates (7). However, the possibility of cross-reactivity with endogenous catecholamines has not been evaluated. The fact that abnormal variability was observed in the data during the RIA quantitation of ritodrine (7) points to the potential problem of cross-reactivity. It is known that serum catecholamine levels are elevated during labor (13). This may cause erroneous determination of ritodrine by RIA under such conditions. On the other hand, the accuracy of the HPLC–EC method is not affected by these endogenous substances.

REFERENCES

(1) O. Jamissans, J. Esteban-Altirriba, and V. Maiques, *Br. J. Obstet. Gynecol.*, **76**, 656 (1969).

(2) T. P. Barden, *Am. J. Obstet, Gynecol.*, **112**, 645 (1972).

(3) D. J. Nochimson, H. D. Riffel, S.-Y. Yeh, M. S. Kreitzer, R. H. Paul, and E. H. Hon, *Am. J. Obstet. Gynecol.*, **118**, 523 (1974).

(4) A. S. I. Siimes and R. K. Creasy, *Am. J. Obstet. Gynecol.*, **126**, 1003 (1976).

(5) New Drug Application for ritodrine hydrochloride, no. 18280, submitted to the FDA on March 8, 1979, by Mid-West Medical Research, Inc., Columbus, Ohio, on behalf of Philip-Duphar B.V., Weesp, The Netherlands.

(6) A. Wesselins-deCasparis, M. Thiery, A. Y. L. Sian, K. Baungarten, I. Brosens, O. Gamisans, J. G. Stolk, and W. Vivier, *Br. Med. J.*, **3**, 144 (1971).

(7) R. Gander, L. W. de Zoeten, and J. B. van der Schoot, *Eur. J. Pharmacol.*, **17**, 117 (1980).

(8) C. Refshauge, P. T. Kissinger, R. Dreiling, L. Brank, R. Freeman, and R. N. Adams, *Life Sci.*, **14**, 311 (1974).

(9) R. M. Riggin, L.-D. Rau, R. L. Alcorn, and P. T. Kissinger, *Anal. Lett.*, **7**, 791 (1974).

(10) P. T. Kissinger, R. M. Riggin, R. L. Alcord, and L.-D. Rau, *Biochem. Med.*, **13**, 299 (1975).

(11) P. T. Kissinger, L. J. Felice, R. M. Riggin, L. A. Pachla, and D. C. Wenke, *Clin. Chem.*, **20**, 992 (1972).

(12) R. M. Riggin, A. L. Schmidt, and P. T. Kissinger, *J. Pharm. Sci.*, **64**, 680 (1975).

13) F. P. Zuspan, R. O'Shaughnessy, and J. D. Iams, *J. Reprod. Med.*, **26**, 483 (1981).

Remarks on the Structure–Activity Relationship of Silver Sulfanilamides

A. BULT *x, B. L. BAJEMA ‡, G. J. BOELEMA ‡, J. J. M. V. SAENE §, and D. A. DOORNBOS ‡

Received February 1, 1982, from the **Department of Pharmaceutical Analysis and Analytical Chemistry, State University of Leiden, 2300 RA Leiden, The Netherlands* and the ‡*Laboratory for Pharmaceutical and Analytical Chemistry* and the §*Laboratory for Pharmaceutical Technology and Dispensing, State University of Groningen, Groningen, The Netherlands.* Accepted for publication December 8, 1982.

Abstract □ The biological activity of a series of 10 silver sulfanilamides is studied in relation to the physical parameters pK_a, log K, and the aqueous solubility. None of the parameters demonstrate a simple relationship with the activity. A discussion of the significance of log K and the solubility in relation to the activity is given.

Keyphrases □ Silver sulfanilamides—structure-activity relationships, correlation between activity and pK_a, log K, and solubility □ Structure–activity relationships—silver sulfanilamides, correlation between activity and pK_a, log K, and solubility

An increasing interest in the silver sulfanilamide complexes was stimulated by the successful use of silver sulfadiazine (I) as an efficacious topical antibacterial agent in burn treatment (1). A number of efforts were made to account for the good *in vivo* activity of I as compared with other silver sulfanilamides (2–4). In this study the relevance of some physical parameters in relation to the *in vivo* antimicrobial activity are discussed.

BACKGROUND

The antimicrobial activity of I is thought to result from alteration of the mesosomal function of the microbial cell by the silver moiety of the molecule (5). The sulfadiazine moiety does not enter the cell and does not contribute appreciably to the antimicrobial action; therefore, I is not antagonized by *p*-aminobenzoic acid (3). A possible role of sulfadiazine is to localize the action of silver to the cell. The undissociated molecule I seems to interact with the microbial cell and is dissociated next at the cell surface into silver and sulfadiazine (6, 7).

The role of the sulfadiazine anion and other anions is rather unclear. Wysor assumed as a prerequisite for an active silver sulfanilamide that, like I, these compounds need to be stable in a chloride-containing solution

0022-3549/84/0100-0133$01.00/0

© 1984, American Pharmaceutical Association

Table I—Biological and Physical Data of the Silver Sulfanilamides

	Compound	mortality, %[a]	pK_a[b]	log K[c]	log K'[d]	Silver Ion Concentration, mg/100 mL[e]
I	Silver sulfadiazine	25.6	6.46 ± 0.02	3.62 ± 0.05	3.57	0.05 ± 0.001
II	Silver sulfathiazole	40	7.19 ± 0.01	4.18 ± 0.22	3.97	0.01 ± 0.003
III	Silver sulfisomidine	60	7.47 ± 0.01	3.69 ± 0.13	3.35	0.11 ± 0.003
IV	Silver sulfamethizole	65	5.63 ± 0.01	3.55 ± 0.18	3.54	0.10 ± 0.004
V	Silver sulfanilamide	77	10.57 ± 0.10	4.13 ± 0.11	0.96	0.70 ± 0.003
VI	Silver sulfamerazine	90	6.88 ± 0.11	3.91 ± 0.04	3.80	0.06 ± 0.003
VII	Silver sulfapyridine	75	8.57 ± 0.01	4.02 ± 0.04	2.82	0.11 ± 0.003
VIII	Silver 5-methylsulfadiazine	80	6.68 ± 0.05	3.66 ± 0.08	3.58	0.19 ± 0.002
IX	Silver 5-methoxysulfadiazine	80	6.67 ± 0.04	3.48 ± 0.08	3.41	0.06 ± 0.002
X	Silver benzenesulfonamidopyrimidine	100	6.12 ± 0.08	3.42 ± 0.04	3.40	0.05 ± 0.005

[a] Mortality for untreated mice: 88%; mortality for mice treated with ointment base: 65% (8). [b] Mean ± *SD*; n = 4–8. [c] Mean ± *SD*; n = 9–14. [d] Conditional stability constant (log K') = log K − log $\alpha_{L(H)}$ at pH 7.4. [e] Mean concentration of silver ion in a saturated aqueous solution ± *SD*; n = 5.

(no formation of silver chloride) (2). Only sulfanilamides with 2-pyrimidino as the N-1 substituent meet this criterion. Use of this information did not lead to the successful design of active compounds. Fox and Modak partly explained the large differences in *in vivo* antimicrobial activity of the silver sulfanilamides by differences in dissociation constants (pK_a) of the acidic N(1)—H of the parent sulfanilamides (3). Nesbitt and Sandmann reported a nonlinear relationship between the *in vivo* activity and pK_a + log K_s (solubility product) (4).

EXPERIMENTAL

A series of 10 silver sulfanilamides was selected for this study (Table I). The *in vivo* activity data (percentage of mortality of mice with burns over 30% of their bodies which were infected with *Pseudomonas aeruginosa*) were derived from the literature (8) or obtained from C. L. Fox, Jr., Columbia University, New York, N.Y. The acid dissociation constants (pK_a) of the sulfanilamides and the stability constants (log K) of their silver complexes were measured according to the method of Boelema *et al.* (9), using a microcomputer-controlled titration method in which the silver ion[1] and hydrogen ion[2] concentrations were determined in a combined measurement. The conditional stability constants (log K') were calculated from the pK_a and log K values using log K' = log K − log $\alpha_{L(H)}$, where $\alpha_{L(H)} = 1 + [H_3O^+]\cdot K_a^{-1}$ is the side reaction coefficient of the sulfanilamide with the hydrogen ion. The sulfanilamides (I–IX) used in this study were obtained commercially and recrystallized from acetone–water; X was synthesized as described previously (10).

The solubility measurements of the silver sulfanilamides were performed by equilibration in double-distilled water at 25 ± 0.1°C for 1 week in 100-mL vials wrapped with aluminum foil with covered[3] rubber closures. The vials were rotated during equilibration. The saturated solutions were filtered through a 25-mm diameter (1.2-μm average pore size) filter[4]; the first 25 mL of filtrate was discarded. The pH[5] of the filtrate was measured, and the filtrates were analyzed for sulfanilamide content by UV[6] and silver by atomic absorption spectroscopy[7]. The silver compounds used in this study are described elsewhere and were micronized[8] (10, 11).

RESULTS AND DISCUSSION

In Table I the biological and physical data of the 10 silver sulfanilamides are summarized. Efforts to measure the distribution coefficient (log P) for octanol–water failed; the silver compounds decomposed with the formation of metallic silver. Calculation of the correlation coefficients between percent mortality and pK_a, log K, log K', and the silver ion concentration reveals that a simple linear relationship between these sets of data does not exist; the coefficients are r = 0.07, 0.21, 0.21, and 0.19, respectively. Nesbitt and Sandmann (4) previously reported a nonlinear relationship between pK_a + log K_s and percent mortality. From Fig. 1 it is clear that this relationship is confirmed by our extended series; the points are spread randomly.

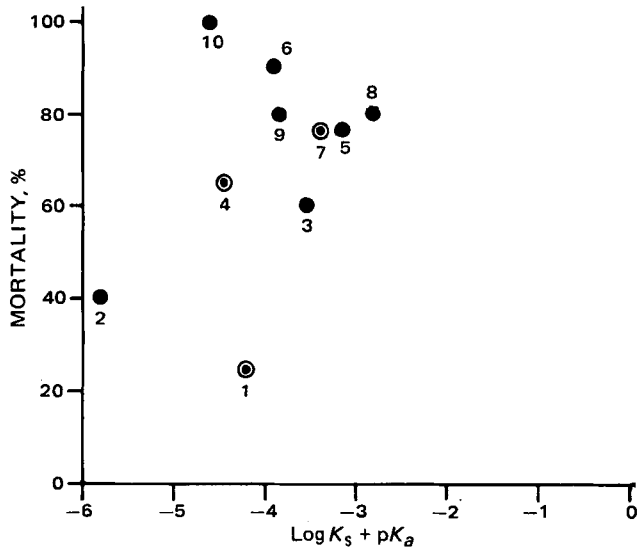

Figure 1—*Relationship between percent mortality and log* K_s + pK_a. *The points of Nesbitt and Sandmann (4) are marked by encircled dots. The solubility product* K_s *is calculated from* $[Ag]^2 = ([H_3O^+]\cdot K_s/K_a) + K_s$ *(4).*

The data for log K' (pH 7.4), the conditional stability constant, can explain in a qualitative way some of the observations made in earlier studies. Wysor (2) found that the silver sulfanilamides with 2-pyrimidino as the N-1 substituent (I, VI, VIII, IX, and X) were stable in a chloride-containing solution; V and VII, with lower log K' values, were unstable. Another example is the reaction of the silver compounds with human serum (3). Silver nitrate and V reacted completely within 2 h with the components of the serum, I reacted at a moderate rate (80% in 40 h), and II and VI reacted very slowly (~30% in 40 h). The log K' values of these compounds increase in the same order.

One unexpected result is that treatments with ointment bases containing the silver sulfanilamides V–X give rise to higher mortality rates than the ointment base alone. This is especially hard to understand for VI and VIII, which are structurally very similar to I. Also hard to understand in relation to the mortality data are the *in vitro* activities of the silver compounds. The minimum inhibitory concentration (MIC) of all the silver compounds in Table I are approximately the same for one type of microorganism. The MIC values for 10 different organisms vary between 6.3 and 200 μg·mL^{-1} (12). Thus, the differences in *in vivo* activity between the silver compounds are in no way reflected by their MIC values.

[1] Ion-selective silver sulfide electrode, Orion research 941600.
[2] Glass electrode, Radiometer G 2040.
[3] Using parafilm *M*.
[4] Selectron-filter, type ST 69; Schleicher-Schüll, Dassel, West Germany.
[5] pH-Meter, type PHM 22 r; Radiometer, Copenhagen, Denmark.
[6] Perkin-Elmer 124.
[7] Perkin-Elmer, type 303, acetylene-air flame, lamp: 3 UAX/Ag-Cathodeon Ltd, 328.1 nm.
[8] Trost Gem T Mill; Helme Chemicals, Inc., Helmetta, N.J.

REFERENCES

(1) C. L. Fox, *Arch. Surg.*, **96**, 184 (1968).
(2) M. S. Wysor, *Chemotherapy*, **21**, 284 (1975).
(3) C. L. Fox and S. M. Modak, *Antimicrob. Agents Chemother.*, **5**, 582 (1974).
(4) R. U. Nesbitt and B. J. Sandmann, *J. Pharm. Sci.*, **67**, 1012 (1978).

(5) H. S. Rosenkranz and H. S. Carr, *Antimicrob. Agents Chemother.*, **2**, 367 (1972).

(6) S. M. Modak and C. L. Fox, *Biochem. Pharmacol.*, **22**, 2391 (1973).

(7) J. E. Coward, H. S. Carr, and H. S. Rosenkranz, *Antimicrob. Agents Chemother.*, **3**, 621 (1973).

(8) J. W. Stanford, B. W. Rappole, and C. L. Fox, *J. Trauma*, **9**, 377 (1969).

(9) G. J. Boelema, A. Bult, H. J. Metting, B. L. Bajema, and D. A. Doornbos, *Pharm. Weekblad Sci. Ed.*, **4**, 38 (1982).

(10) A. Bult and H. B. Klasen, *J. Pharm. Sci.*, **67**, 284 (1978).

(11) A. Bult and H. B. Klasen, *Arch. Pharm. (Weinheim)*, **311**, 855 (1978).

(12) J. J. M. van Saene, A. Bult, and C. F. Lerk, *Pharm. Weekblad, Sci. Ed.*, **5**, 67 (1983).

COMMUNICATIONS

Enhancement of Fluoride Concentration in Saliva after Topical Application of Fluoride Sustained-Release Dosage Form on Orthodontic Plates

Keyphrases □ Fluoride, sustained release—topical application, concentration in whole saliva

To the Editor: The beneficial role of fluoride topical applications for caries prevention is now well established. The effectiveness of a topical treatment resides in the amount of fluoride incorporated in apatitic form (1) and in the continuous supply and renewal of the fluoride content of tooth enamel (2–3). None of the topical dosage forms of fluoride marketed today (dentifrices, mouth rinses, and gels) are able to supply fluoride for a long period of time. A sustained-release dosage form of fluoride for topical application should provide conditions that will result in the major product being a stable fluoroapatite. The research effort expended to date on the development of a sustained-release delivery system for fluoride is minor compared with efforts expended in the areas of other drugs; however, significant progress has been made.

Three general approaches are being taken now to develop a sustained-release delivery system of fluoride: (*a*) matrix tables (4), (*b*) aerosol containing microcapsules for direct application on the tooth surface (5), and (*c*) intraoral system (6).

In our previous *in vitro* work (7, 8) it was shown that fluoride release could be sustained by embedding NaF or CaF_2 in ethylcellulose polymers. The aim of this work was to establish the fluoride level of saliva in children using orthodontic plates coated with a long-acting fluoride application.

A group of nine children aged 7–12 undergoing orthodontic treatment participated in the study. The subjects resided in the Jerusalem area, which had ~0.4 ppm fluoride in the water supply. None of the children had brushed their teeth with a fluoride dentifrice or received a fluoride supplement (including tea) 2 d before or during the experiment. The palatinale part of the upper orthodontic plates was coated by immersing the plates in a 10% NaF suspension in ethanol solution of ethylcellulose and allowing them to dry at room temperature (8).

The amount of the coating layer on the orthodontic plates was determined by weighing the difference between the uncoated and coated materials. The fluoride (F) concentration was calculated from the weight ratio of fluoride and polymer used and was in the range of 4.8–5.1 mg/plate. Whole saliva samples were collected by chewing paraffin wax, and the F concentration was determined in the centrifuged sample with a fluoride ion electrode (9). Statistical significance was determined by the paired t test.

F release resulted in a significant ($p < 0.005$) increase in the amount of fluoride in the saliva during the first 4 days of the study but returned to its initial level on the 5th day (Table I). By the use of fluoride dentifrices or ingestion of 1-mg fluoride tablets, similar increases in the F content in the saliva were reported (10). However, the increase was for a short period only, with the F concentration returning to the initial levels after 90 min.

A relationship between the natural fluoride content in water and the prevalence of dental caries is well established today.

In communities with a fluoride content of ≥1 ppm, the prevalence of dental caries was less than in those communities whose water supplies contained fluoride at a concentration ≤0.6 ppm.

It has been shown by Yao and Grøn (9) that the fluoride content in the saliva of children who consumed drinking water containing 1 ppm of fluoride was 0.01–0.05 ppm.

These values are similar to the fluoride concentration obtained in the saliva of the children using sustained release application of fluoride in this study.

In our previous work (7) it was shown that thickness of the coating applied on the orthodontic plate did not affect

Table I—F Content in Mixed Saliva of Nine Children after Fluoride Sustained Release Application [a]

	Day after Application				
	1	2	3	4	5
F, mean ± *SD*	0.015 ± 0.003	0.02 ± 0.003	0.016 ± 0.003	0.01 ± 0.002	0.007 ± 0.0002
P	<0.005	<0.005	<0.005	<0.005	NS[b]

[a] Control (F concentration in saliva before the experiment) 0.008 ± 0.002 ppm. [b] NS = not significant.

0022-3549/84/0100-0135$01.00/0
© 1984, American Pharmaceutical Association

(5) H. S. Rosenkranz and H. S. Carr, *Antimicrob. Agents Chemother.*, **2**, 367 (1972).

(6) S. M. Modak and C. L. Fox, *Biochem. Pharmacol.*, **22**, 2391 (1973).

(7) J. E. Coward, H. S. Carr, and H. S. Rosenkranz, *Antimicrob. Agents Chemother.*, **3**, 621 (1973).

(8) J. W. Stanford, B. W. Rappole, and C. L. Fox, *J. Trauma*, **9**, 377 (1969).

(9) G. J. Boelema, A. Bult, H. J. Metting, B. L. Bajema, and D. A. Doornbos, *Pharm. Weekblad Sci. Ed.*, **4**, 38 (1982).

(10) A. Bult and H. B. Klasen, *J. Pharm. Sci.*, **67**, 284 (1978).

(11) A. Bult and H. B. Klasen, *Arch. Pharm. (Weinheim)*, **311**, 855 (1978).

(12) J. J. M. van Saene, A. Bult, and C. F. Lerk, *Pharm. Weekblad, Sci. Ed.*, **5**, 67 (1983).

COMMUNICATIONS

Enhancement of Fluoride Concentration in Saliva after Topical Application of Fluoride Sustained-Release Dosage Form on Orthodontic Plates

Keyphrases □ Fluoride, sustained release—topical application, concentration in whole saliva

To the Editor: The beneficial role of fluoride topical applications for caries prevention is now well established. The effectiveness of a topical treatment resides in the amount of fluoride incorporated in apatitic form (1) and in the continuous supply and renewal of the fluoride content of tooth enamel (2–3). None of the topical dosage forms of fluoride marketed today (dentifrices, mouth rinses, and gels) are able to supply fluoride for a long period of time. A sustained-release dosage form of fluoride for topical application should provide conditions that will result in the major product being a stable fluoroapatite. The research effort expended to date on the development of a sustained-release delivery system for fluoride is minor compared with efforts expended in the areas of other drugs; however, significant progress has been made.

Three general approaches are being taken now to develop a sustained-release delivery system of fluoride: (*a*) matrix tables (4), (*b*) aerosol containing microcapsules for direct application on the tooth surface (5), and (*c*) intraoral system (6).

In our previous *in vitro* work (7, 8) it was shown that fluoride release could be sustained by embedding NaF or CaF_2 in ethylcellulose polymers. The aim of this work was to establish the fluoride level of saliva in children using orthodontic plates coated with a long-acting fluoride application.

A group of nine children aged 7–12 undergoing orthodontic treatment participated in the study. The subjects resided in the Jerusalem area, which had ~0.4 ppm fluoride in the water supply. None of the children had brushed their teeth with a fluoride dentifrice or received a fluoride supplement (including tea) 2 d before or during the experiment. The palatinale part of the upper orthodontic plates was coated by immersing the plates in a 10% NaF suspension in ethanol solution of ethylcellulose and allowing them to dry at room temperature (8).

The amount of the coating layer on the orthodontic plates was determined by weighing the difference between the uncoated and coated materials. The fluoride (F) concentration was calculated from the weight ratio of fluoride and polymer used and was in the range of 4.8–5.1 mg/plate. Whole saliva samples were collected by chewing paraffin wax, and the F concentration was determined in the centrifuged sample with a fluoride ion electrode (9). Statistical significance was determined by the paired t test.

F release resulted in a significant ($p < 0.005$) increase in the amount of fluoride in the saliva during the first 4 days of the study but returned to its initial level on the 5th day (Table I). By the use of fluoride dentifrices or ingestion of 1-mg fluoride tablets, similar increases in the F content in the saliva were reported (10). However, the increase was for a short period only, with the F concentration returning to the initial levels after 90 min.

A relationship between the natural fluoride content in water and the prevalence of dental caries is well established today.

In communities with a fluoride content of ≥1 ppm, the prevalence of dental caries was less than in those communities whose water supplies contained fluoride at a concentration ≤0.6 ppm.

It has been shown by Yao and Grøn (9) that the fluoride content in the saliva of children who consumed drinking water containing 1 ppm of fluoride was 0.01–0.05 ppm.

These values are similar to the fluoride concentration obtained in the saliva of the children using sustained release application of fluoride in this study.

In our previous work (7) it was shown that thickness of the coating applied on the orthodontic plate did not affect

Table I—F Content in Mixed Saliva of Nine Children after Fluoride Sustained Release Application [a]

	Day after Application				
	1	2	3	4	5
F, mean ± *SD*	0.015 ± 0.003	0.02 ± 0.003	0.016 ± 0.003	0.01 ± 0.002	0.007 ± 0.0002
P	<0.005	<0.005	<0.005	<0.005	NS[b]

[a] Control (F concentration in saliva before the experiment) 0.008 ± 0.002 ppm. [b] NS = not significant.

0022-3549/84/0100-0135$01.00/0
© 1984, American Pharmaceutical Association

the release constant but determined the duration of fluoride release.

According to this it may be assumed that by an increase in the thickness of the coating applied to the plates, a prolonged continuous increase of F in saliva will be possible. The increase in the thickness of the coating may be easily achieved by adding additional layers of the coating solution.

The continuous presence of fluoride in saliva, achieved in this study, may favor the remineralization phase occurring between periods of enamel dissolution (2) and significantly increase the value of fluoride in caries prevention.

(1) V. Caslavska, E. C. Moreno, and F. Brudeveld, *Arch. Oral Biol.*, **20**, 333 (1975).

(2) B. Houwink, D. O. Backer, and G. W. Kwant, *Caries Res.*, **8**, 27 (1974).

(3) C. W. Lemke, J. H. Doherty, and M. C. Arra, *J. Am. Dent. Assoc.*, **80**, 782 (1970).

(4) P. M. Meier, J. Dilou, and D. D. Marco, Final report on Contract NO_1-DE-52448 to National Institutes of Health, Bethesda, 1976.

(5) D. L. Williams, P. M. Meier, T. J. Mullines, and K. R. St. John, 6th Report on Contract N01-DE-52448 to National Institutes of Health, Bethesda, 1977.

(6) D. M. Lewis, D. R. Cowsar, D. R. Miller, and L. Menaker, *J. Dent. Res.*, *56* 266 (1977) (Special issue).

(7) M. Friedman, *J. Dent. Res.*, **59**, 1392 (1980).

(8) M. Friedman, *Arch. Oral Biol.*, **26**, 131 (1981).

(9) K. Yao, and P. Grøn, *Caries Res.*, **4**, 321 (1970).

(10) P. Grøn, H. G. McCann, and F. Brudevold, *Arch. Oral Biol.*, **13**, 203 (1968).

*D. Harary**
M. Friedman ‡

* Departments of Orthodontic and ‡Pharmacy Schools of Dental Medicine and Pharmacy
The Hebrew University of Jerusalem
Jerusalem 91120, Israel

Received January 6, 1983.
Accepted for publication September 21, 1983.

Precursor–Metabolite Interaction in the Metabolism of Lidocaine

Keyphrases □ Lidocaine—precursor–metabolite interaction, metabolism □ metabolites—interaction with precursor in metabolism of lidocaine □ metabolism—lidocaine in the liver

To the Editor:

Lidocaine is a local anesthetic and antiarrhythmic drug that has been known to be extracted exclusively by the liver with a high extraction ratio after oral administration (1–4). As shown in Scheme I (5), lidocaine is extensively metabolized in rats to monoethylglycinexylidide (I) and 3-hydroxylidocaine (II) by P_{450}-dependent *N*-deethylase and 3-hydroxylase activities. These primary metabolites are further 3-hydroxylated and *N*-deethylated, respectively, to form a common secondary metabolite, 3-hydroxymonoethylglycinexylidide (III). In common with other drugs highly cleared by the liver, the areas under the blood concentration *versus* time curve (AUC) obtained after portal vein infusion of lidocaine at a dose range of

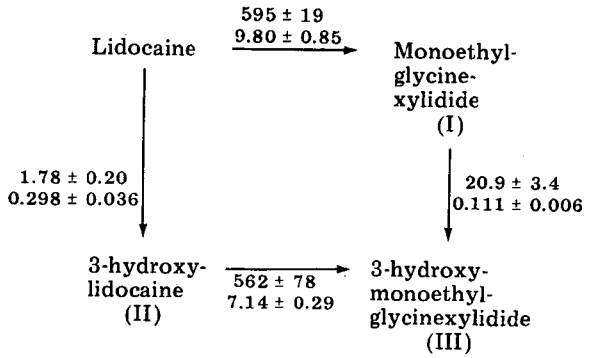

Scheme I—Parallel metabolic pathways of lidocaine and the kinetic parameters. The figures are expressed as means ±SE (n = 3) μM for apparent Michaelis constants (top numbers) and nmol/min·mg microsomal protein for maximum velocities (lower numbers). Substrate concentration range: 200–2000 μM for N-deethylation of lidocaine and 3-hydroxylidocaine (II); 1–100 μM for 3-hydroxylation of lidocaine and monoethylglycinexylidide (I).

1–10 mg/kg were smaller (approximately one half) than those after peripheral vein infusion of equal doses in rats (6). However, of special interest is our preliminary finding that the AUC of I, a pharmacologically active lidocaine metabolite, obtained after portal vein infusion of lidocaine was ~10 times as large as that obtained after peripheral vein infusion (6). The AUC of metabolite II, on the other hand, did not differ significantly depending on the route of administration of lidocaine. If a drug and its metabolites are eliminated linearly and exclusively by hepatic metabolism, the AUC of the metabolites, or the ratios of AUC of any two metabolites, are independent of the route of administration (4). The unusually high AUC of I and also the difference in the AUC ratios of the two metabolites of lidocaine depending on the route of administration can be explained by the following possibilities: (*a*) the elimination of I itself is nonlinear; (*b*) 3-hydroxylation of lidocaine is saturable at lidocaine concentrations attained by portal vein infusion but *N*-deethylation is not, resulting in the formation of I in higher concentrations; (*c*) lidocaine inhibits the metabolism of I in the liver and the elimination of I decreases in the presence of high concentrations of liodcaine. The AUC of I (1.5–7.5 mg/kg) was found to increase in an apparently linear fashion with increasing intraportal dosage (6). Therefore, either the second or the third possibility or both of them may be operative in these phenomena.

Studies by von Bahr *et al.* (7) and from our laboratory (8) have indicated that the 3-hydroxylation and *N*-deethylation pathways of lidocaine are catalyzed by different P_{450} species. It is then of interest to test if the parallel hydroxylation pathways (3-hydroxylations of lidocaine and I) are catalyzed by the same P_{450} species or different. If they are catalyzed by the same P_{450} species, lidocaine and I would be mutually competitive inhibitors of their metabolism. Then this would partly explain the unusually high AUC of I obtained after portal vein infusion of lidocaine as described above. By the same token, it is also of interest to examine if the *N*-deethylation pathways of lidocaine and II share the same species of P_{450}. In this communication, we report *in vitro* metabolic kinetics of lidocaine and its metabolites in order to characterize the nature of lidocaine metabolism and to investigate the

0022-3549/84/0100-0136$01.00/0
© 1984, American Pharmaceutical Association

the release constant but determined the duration of fluoride release.

According to this it may be assumed that by an increase in the thickness of the coating applied to the plates, a prolonged continuous increase of F in saliva will be possible. The increase in the thickness of the coating may be easily achieved by adding additional layers of the coating solution.

The continuous presence of fluoride in saliva, achieved in this study, may favor the remineralization phase occurring between periods of enamel dissolution (2) and significantly increase the value of fluoride in caries prevention.

(1) V. Caslavska, E. C. Moreno, and F. Brudeveld, *Arch. Oral Biol.*, **20**, 333 (1975).

(2) B. Houwink, D. O. Backer, and G. W. Kwant, *Caries Res.*, **8**, 27 (1974).

(3) C. W. Lemke, J. H. Doherty, and M. C. Arra, *J. Am. Dent. Assoc.*, **80**, 782 (1970).

(4) P. M. Meier, J. Dilou, and D. D. Marco, Final report on Contract NO_1-DE-52448 to National Institutes of Health, Bethesda, 1976.

(5) D. L. Williams, P. M. Meier, T. J. Mullines, and K. R. St. John, 6th Report on Contract N01-DE-52448 to National Institutes of Health, Bethesda, 1977.

(6) D. M. Lewis, D. R. Cowsar, D. R. Miller, and L. Menaker, *J. Dent. Res.*, *56* 266 (1977) (Special issue).

(7) M. Friedman, *J. Dent. Res.*, **59**, 1392 (1980).

(8) M. Friedman, *Arch. Oral Biol.*, **26**, 131 (1981).

(9) K. Yao, and P. Grøn, *Caries Res.*, **4**, 321 (1970).

(10) P. Grøn, H. G. McCann, and F. Brudevold, *Arch. Oral Biol.*, **13**, 203 (1968).

*D. Harary**
M. Friedman ‡

* Departments of Orthodontic and ‡Pharmacy Schools of Dental Medicine and Pharmacy
The Hebrew University of Jerusalem
Jerusalem 91120, Israel

Received January 6, 1983.
Accepted for publication September 21, 1983.

Precursor–Metabolite Interaction in the Metabolism of Lidocaine

Keyphrases □ Lidocaine—precursor–metabolite interaction, metabolism □ metabolites—interaction with precursor in metabolism of lidocaine □ metabolism—lidocaine in the liver

To the Editor:

Lidocaine is a local anesthetic and antiarrhythmic drug that has been known to be extracted exclusively by the liver with a high extraction ratio after oral administration (1–4). As shown in Scheme I (5), lidocaine is extensively metabolized in rats to monoethylglycinexylidide (I) and 3-hydroxylidocaine (II) by P_{450}-dependent *N*-deethylase and 3-hydroxylase activities. These primary metabolites are further 3-hydroxylated and *N*-deethylated, respectively, to form a common secondary metabolite, 3-hydroxymonoethylglycinexylidide (III). In common with other drugs highly cleared by the liver, the areas under the blood concentration *versus* time curve (AUC) obtained after portal vein infusion of lidocaine at a dose range of

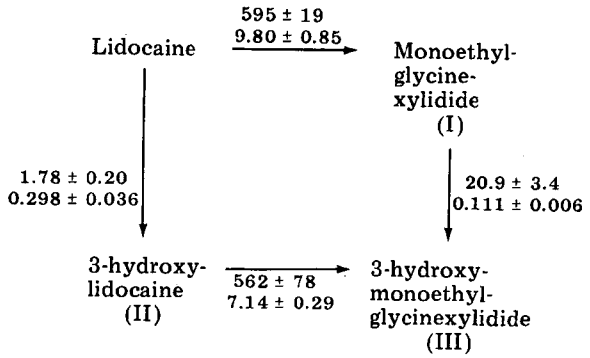

Scheme I—Parallel metabolic pathways of lidocaine and the kinetic parameters. The figures are expressed as means ±SE (n = 3) μM for apparent Michaelis constants (top numbers) and nmol/min·mg microsomal protein for maximum velocities (lower numbers). Substrate concentration range: 200–2000 μM for N-deethylation of lidocaine and 3-hydroxylidocaine (II); 1–100 μM for 3-hydroxylation of lidocaine and monoethylglycinexylidide (I).

1–10 mg/kg were smaller (approximately one half) than those after peripheral vein infusion of equal doses in rats (6). However, of special interest is our preliminary finding that the AUC of I, a pharmacologically active lidocaine metabolite, obtained after portal vein infusion of lidocaine was ~10 times as large as that obtained after peripheral vein infusion (6). The AUC of metabolite II, on the other hand, did not differ significantly depending on the route of administration of lidocaine. If a drug and its metabolites are eliminated linearly and exclusively by hepatic metabolism, the AUC of the metabolites, or the ratios of AUC of any two metabolites, are independent of the route of administration (4). The unusually high AUC of I and also the difference in the AUC ratios of the two metabolites of lidocaine depending on the route of administration can be explained by the following possibilities: (*a*) the elimination of I itself is nonlinear; (*b*) 3-hydroxylation of lidocaine is saturable at lidocaine concentrations attained by portal vein infusion but *N*-deethylation is not, resulting in the formation of I in higher concentrations; (*c*) lidocaine inhibits the metabolism of I in the liver and the elimination of I decreases in the presence of high concentrations of liodcaine. The AUC of I (1.5–7.5 mg/kg) was found to increase in an apparently linear fashion with increasing intraportal dosage (6). Therefore, either the second or the third possibility or both of them may be operative in these phenomena.

Studies by von Bahr *et al.* (7) and from our laboratory (8) have indicated that the 3-hydroxylation and *N*-deethylation pathways of lidocaine are catalyzed by different P_{450} species. It is then of interest to test if the parallel hydroxylation pathways (3-hydroxylations of lidocaine and I) are catalyzed by the same P_{450} species or different. If they are catalyzed by the same P_{450} species, lidocaine and I would be mutually competitive inhibitors of their metabolism. Then this would partly explain the unusually high AUC of I obtained after portal vein infusion of lidocaine as described above. By the same token, it is also of interest to examine if the *N*-deethylation pathways of lidocaine and II share the same species of P_{450}. In this communication, we report *in vitro* metabolic kinetics of lidocaine and its metabolites in order to characterize the nature of lidocaine metabolism and to investigate the

0022-3549/84/0100-0136$01.00/0
© 1984, American Pharmaceutical Association

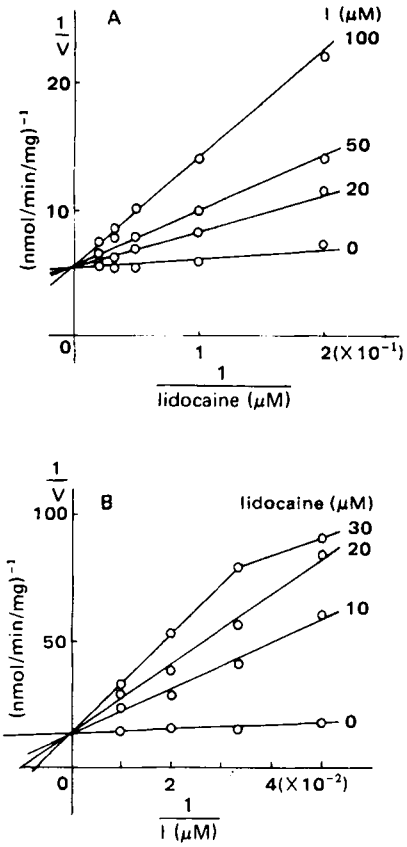

Figure 1—*Lineweaver–Burk plots of lidocaine and monoethylglycinexylidide (I) 3-hydroxylations in the presence of inhibitors, monoethylglycinexylidide(I) and lidocaine, respectively.*

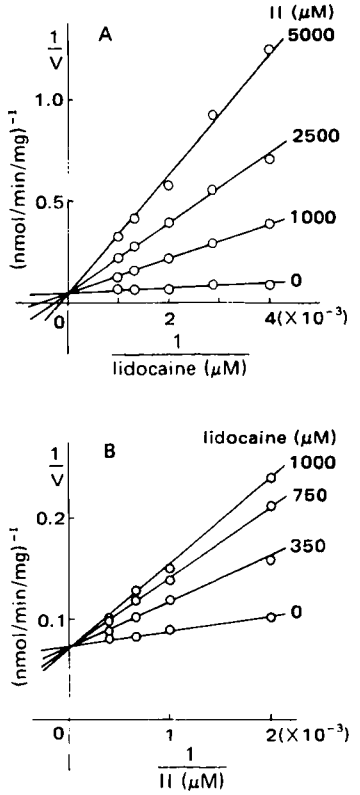

Figure 2—*Lineweaver–Burk plots of lidocaine and 3-hydroxylidocaine (II) (N)-deethylations in the presence of inhibitors, 3-hydroxylidocaine (II), and lidocaine, respectively.*

possible precursor–metabolite interactions between the parallel metabolic pathways.

N-deethylations and 3-hydroxylations of lidocaine and its metabolites were studied at 37°C using a hepatic microsomal suspension obtained from male Wistar rats weighing from 280 to 310 g. The incubation mixture contained the substrate, glucose-6-phosphate, glucose-6-phosphate dehydrogenase, and NADP in 50 mM Tris-HCl buffer, pH 7.4. The concentrations of I, II, and III after incubation for 2.5 min were determined using a reverse-phase[1] high-performance liquid chromatographic assay[2]. The rate of formation of I and II from lidocaine was linear up to 3 min at the substrate concentration range used in this study. Formation of III was not detected within this incubation period. The linearities of these reactions were lost, thereafter, due to the conversion of I and II into III. The formation rate of III from I or II was also linear, at least during the first 3 min.

Scheme I shows kinetic parameters for the metabolism of lidocaine and its metabolites. The metabolism of lidocaine consisted of *N*-deethylation with a large apparent Michaelis constant (K_m) and a high maximum velocity (V_{max}) and 3-hydroxylation with a small K_m and a low V_{max}. These data reflect the effects of substrate concentration on these reactions; that is, at low concentrations (<5 μM) larger fractions of lidocaine were 3-hydroxylated than *N*-deethylated, but at high concentrations larger fractions were *N*-deethylated than 3-hydroxylated. These results indicate that the second possibility stated above seems to be at least one of the reasons for the unusually high AUC of I after portal vein infusion of lidocaine. This also seems to be one of the reasons for the large difference in the AUC of I and II. The K_m of 3-hydroxylation of I was ~10-fold that of lidocaine 3-hydroxylation and V_{max}, about a third of that of lidocaine 3-hydroxylation. The *N*-deethylation of II possessed similar K_m and V_{max} values to those of lidocaine *N*-deethylation.

The results of the studies on the effects of lidocaine metabolites on lidocaine metabolism or *vice versa* are shown in Figs. 1 and 2.

Figure 1A shows the Lineweaver–Burk plots of the rate of formation of II from lidocaine (lidocaine 3-hydroxylase activities) in the presence of various concentrations of I. A clear competitive inhibition was observed. Figure 1B shows the Lineweaver–Burk plots of the rate of formation of III from I in the presence of various concentrations of lidocaine. Since III is formed from lidocaine added as an inhibitor *via* its metabolites (I and II) as well as from the substrate (I), the apparent rate of formation of III in this assay system is not the accurate rate of 3-hydroxylation of I, but is the sum of the rates of formation of III from I and lidocaine *via* its two metabolites. Therefore, the linearity of the plots in Fig. 1B obtained with this assay system, especially in the presence of a high lidocaine concentration, was not as good as the plots in Fig. 1A. However, the general pattern of these plots indicates the competitive nature, and since the inhibition of lidocaine 3-hydroxylation by I is competitive, it is naturally assumed

[1] μBondapak C-18; Waters, Associates, Milford, Mass.
[2] Unpublished data.

that the 3-hydroxylation of I is also competitively inhibited by lidocaine.

Figure 2A shows the Lineweaver–Burk plots of the rate of formation of I from lidocaine (lidocaine *N*-deethylase activities) in the presence of various concentrations of II. As in the case of the inhibition of lidocaine 3-hydroxylase activity by I, lidocaine *N*-deethylase activity was competitively inhibited by II. Figure 2B shows the Lineweaver–Burk plots of the rate of formation of III from II in the presence of various concentrations of lidocaine. Since III is formed from lidocaine as well as I, as stated above, the rate of formation of III does not accurately measure the rate of *N*-deethylation of II as in the case of the assay for 3-hydroxylation of I. However, these plots clearly show that the inhibition is of a competitive nature, as in the case of the inhibition of 3-hydroxylation of I by lidocaine.

The 3-hydroxylations of lidocaine and I and the *N*-deethylations of lidocaine and II are each mutually competitive, indicating that those two 3-hydroxylation pathways and *N*-deethylation pathways are each sharing the same species of P_{450}. The inhibition of 3-hydroxylation of I by lidocaine was more effective than that of lidocaine 3-hydroxylation by I. The inhibitions of *N*-deethylations of II and lidocaine by lidocaine and II, respectively, were of the same magnitude as expected from the K_m values of the corresponding inhibitors. The observed precursor inhibition, the inhibition of the further metabolism of a primary metabolite (I) by the precursor (lidocaine) may be operative in an *in vivo* system (the third possibility). The findings that 3-hydroxylation of lidocaine is saturable at a low concentration but *N*-deethylation is not, even at a high concentration, and that the precursor inhibition for II is much less effective than that for I may explain the difference in the ratios of the AUC of the two primary metabolites. Therefore, it appears that both the second and third possibilities stated above may cause the unusually high AUC of I only after portal vein infusion of lidocaine.

These types of precursor–metabolite interactions (precursor inhibition and product inhibition) between the metabolic pathways that are parallel to each other, as shown in Scheme I, is not an isolated phenomenon for lidocaine metabolism alone, but was observed in the metabolism of imipramine[3] and amitriptyline (9). These "parallel pathway interactions" may be observed in drugs possessing similar metabolic pathways, such as methamphetamine and diazepam.

(1) R. N. Boyes, D. B. Scott, P. J. Jebson, M. J. Godman, and D. G. Julian, *Clin. Pharmacol. Ther.*, **12**, 105 (1971).

(2) R. E. Stonson, R. T. Constantino, and D. C. Harrison, *Circulation*, **43**, 205 (1971).

(3) A. G. de Boer, D. D. Breimer, H. Mattie, J. Pronk, and J. M. Gubbens-Stibbe, *Clin. Pharmacol. Ther.*, **26**, 701 (1979).

(4) P. N. Bennett, L. J. Aarons, M. R. Bending, J. A. Steiner, and M. Rowland, *J. Pharmacokinet. Biopharm.*, **10**, 265 (1982).

(5) J. B. Keenaghan and R. N. Boyes, *J. Pharmacol. Exp. Ther.*, **180**, 454 (1972).

(6) Y. Saeki, MS Thesis Faculty of Pharmaceutical Sciences, Chiba University, 1980.

(7) C. von Bahr, I. Hedlund, B. Karlen, D. Backstrom, and H. Gransdalen, *Acta Pharmacol. Toxicol.*, **41**, 39 (1977).

(8) R. Kawai, J. Tatsuno, S. Fujita, and T. Suzuki, *J. Pharm. Dyn.*, **6**, s-79 (1983).

(9) B. Mellstrom and C. von Bahr, *Drug Metab. Dispos.*, **9**, 565 (1981).

Tokuji Suzuki[x]
Shoichi Fujita
Ryosei Kawai
Department of Biopharmaceutics
Faculty of Pharmaceutical Sciences
Chiba University
1-33, Yayoicho, Chiba, Japan

Received August 1, 1983.
Accepted for publication October 17, 1983.

[3] Unpublished data.

A publication of the
American Pharmaceutical Association—
the National Professional Society
of Pharmacists

JOURNAL OF PHARMACEUTICAL SCIENCES

Volume 73, 1984

JPMSAE 73(1-12) 1-1910 (1984)
ISSN 0022-3549

Sharon G. Boots
Editor

Sue A. Kruger
Production Editor

Margaret M. Madeleine
Assistant Production Editor

Karen A. Blakney
Copy Editor

Edward G. Feldmann
Contributing Editor

Samuel W. Goldstein
Contributing Editor

Patricia A. Evich
Editorial Secretary

Editorial Advisory Board

Jordan L. Cohen
Kenneth A. Connors
Louis Diamond
Ho-Leung Fung
Milo Gibaldi
Everett N. Hiestand
W. Homer Lawrence
Ian W. Mathison
Carl M. Metzler
Robert E. Notari
Paul L. Schiff, Jr.
Jane E. Shaw

Published monthly under the supervision of the Board of Trustees

JOURNAL OF PHARMACEUTICAL SCIENCES

FEBRUARY 1984
VOLUME 73 NUMBER 2

RESEARCH ARTICLES

Correlation Between the Bioavailability of Microencapsulated Bacampicillin Hydrochloride in Suspension and *In Vitro* Microcapsule Dissolution

JAN SJÖVALL *x, ROLF SJÖQVIST ‡, BERNHARD HUITFELDT §, and HÅKAN NYQVIST ‡

Received July 12, 1982, from the *Medical Department, the ‡Research and Development Laboratory, Pharmaceutics, and the §Medical Statistics Department, ASTRA LÄKEMEDEL AB, S-15185 Södertälje, Sweden. Accepted for publication December 2, 1982.

Abstract □ The relative bioavailability of microencapsulated bacampicillin hydrochloride in suspension was correlated with the *in vitro* dissolution half-lives of the microcapsules. Simultaneously, a sensory evaluation was performed to evaluate the taste acceptability of the suspension. The *in vitro* dissolution half-life is directly related to the coating thickness of the microcapsules. The four suspensions of bacampicillin hydrochloride, containing microcapsules with different coating thickness, were given as single 400-mg oral doses to 12 healthy volunteers after overnight fasting using a crossover design with balanced sequences. Bacampicillin is a prodrug of ampicillin, the concentration of which was determined in plasma and urine by bioassay. There were significant inverse linear relationships between the dissolution half-life and plasma peak concentration, area under the curve, and urinary recovery. The terminal exponential disposition phases of the curves were similar for all four suspensions. There was a significant direct linear relationship between the dissolution half-life and overall taste and bitterness. The results show that the mean bioavailability of bacampicillin hydrochloride from a microcapsule suspension can be predicted from an *in vitro* dissolution half-life. The results also suggest that bacampicillin hydrochloride can be given in a suspension with sufficient microcapsule film thickness to reduce the bitter taste of the drug and still retain adequate bioavailability.

Keyphrases □ Bioavailability—bacampicillin hydrochloride, microencapsulated oral suspensions, correlation with *in vitro* dissolution □ Bacampicillin hydrochloride—encapsulated oral suspensions, *in vivo* bioavailability correlations with *in vitro* dissolution, taste evaluation □ Dissolution—*in vitro*, microencapsulated bacampicillin hydrochloride in oral suspensions, correlation with *in vivo* bioavailability, taste evaluation

Bacampicillin hydrochloride, an oral prodrug of ampicillin, is absorbed more rapidly and to a greater extent than ampicillin (1, 2). The drug cannot be formulated as a simple solution due to its bitter taste. However, using an aqueous suspension of small particles of bacampicillin hydrochloride coated with a thin polymeric film of ethylcellulose (microencapsulated) and, for instance, adjusting the pH of the aqueous phase, the release of bacampicillin can be counteracted and the bitter taste masked[1]. Increased thickness of the microcapsule coating decreases the *in vitro* dissolution rate of bacampicillin in water. This might influence both the rate and extent of absorption of the drug. On the other hand, with too thin a coating it is possible that the microcapsules in the aqueous suspension may release bacampicillin in the mouth prematurely, thereby causing a bitter taste.

The purpose of this investigation was to compare the relative bioavailability of microencapsulated bacampicillin hydrochloride in four aqueous suspensions. The only difference between the suspensions was the coating thickness of the microcapsules. These were characterized by different *in vitro* dissolution half-lives of the bacampicillin. A sensory evaluation of the four suspensions was made simultaneously.

EXPERIMENTAL

Subjects—The study was conducted on three female and nine male nonobese volunteers, aged 23 to 37 years (mean 31 years) with body weights ranging from 56 to 86 kg (mean 74 kg). All were determined to be healthy by routine clinical and laboratory examinations within a 14-d period preceding the study and had no known allergy to penicillins or cephalosporins. The subjects had taken no other drugs for at least 1 week prior to the start of the study.

Pharmaceutical Preparations—Microcapsules of bacampicillin hydrochloride were prepared by fluid bed coating with ethylcellulose. Four different coating thicknesses were used for the microcapsules, with total polymer contents of 17, 23, 29, and 37%, respectively.

[1] R. Sjöqvist, J. Sjövall, H. Nyqvist, and D. Westerlund; unpublished data.

0022-3549/84/0200-0141$01.00/0
© 1984, American Pharmaceutical Association

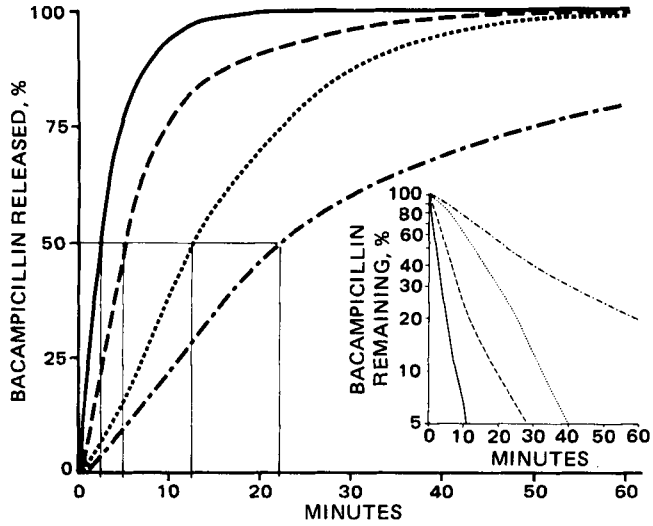

Figure 1—In vitro *dissolution, as a function of time, of four microcapsules of bacampicillin hydrochloride with different coating thicknesses expressed as the total content of polymer in the granules. Vertical lines indicate dissolution half-lives. Key: (—) 17%; (– – –) 23%; (- - -) 29%; (- · - ·) 37%.*

The microcapsules were characterized by different *in vitro* dissolution rates. The *in vitro* release rate of bacampicillin hydrochloride from the microcapsules was determined in the USP XX paddle apparatus with 500 mL of water (37°C) as the dissolution medium. The rotating speed of the shafts was 100 rpm. Six samples of 500 mg of microcapsules were run in each test. The amount of bacampicillin dissolved was monitored continuously in a spectrophotometer at 255 nm.

The microcapsules were administered as a flavored, aqueous suspension[2], of identical composition for the four different microcapsules. The suspension (40 mg/mL) was prepared 0.5 h before administration by adding a standardized volume (4.8 mL) of water to single dose cups containing an exact dose of microcapsules and excipients.

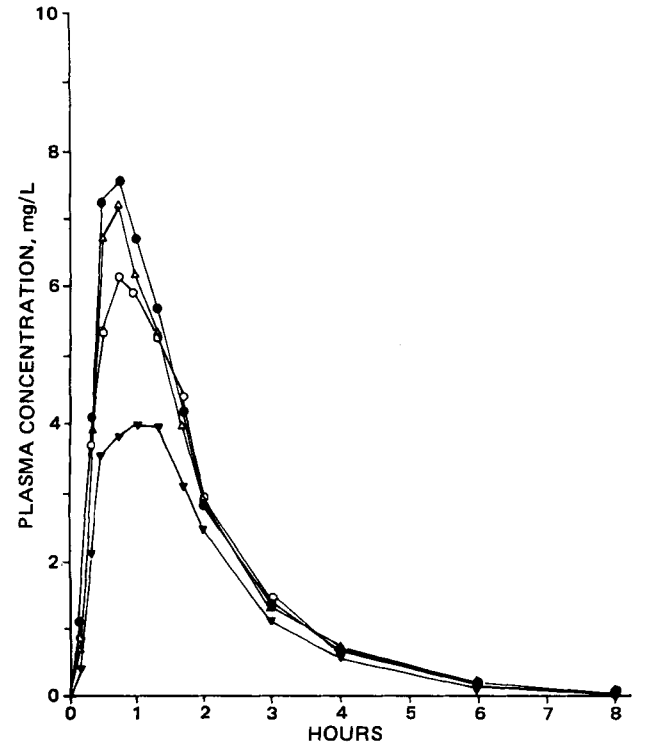

Figure 2—*Mean plasma concentrations after four single 400-mg doses of microencapsulated bacampicillin hydrochloride in suspension with different* in vitro *dissolution half-lives. Crossover study in 12 subjects. Key: (●) 2.5 min; (△) 5 min; (○) 12.5 min; (▼) 22 min.*

[2] PENGLOBE granules for reconstitution; Astra Läkemedel AB, Sweden.

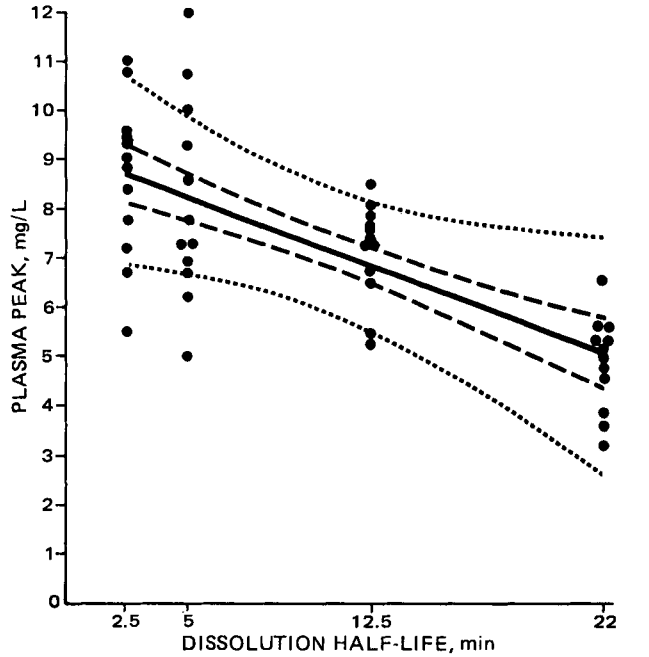

Figure 3—*Relationship between* in vitro *dissolution half-life and individual peak concentration after single 400-mg doses of microencapsulated bacampicillin hydrochloride in suspension. Crossover study in 12 subjects. The 95% confidence limits for the mean regression line (- - -) and for the prediction of a new observation in a random subject (. . .) after dosing with bacampicillin hydrochloride suspension with a given dissolution half-life are indicated.*

Experimental Design—The subjects were given the four suspensions according to a randomized, crossover design with balanced sequences and an interval of 1 week between doses. All subjects fasted for a minimum of 8 h (from midnight to drug administration) with the exception of 250 mL of water taken on rising, at least 1 h before dosing. The suspension was given in single oral doses containing 400 mg of bacampicillin hydrochloride. After swallowing the dose 150 mL of water was immediately ingested, part of which was used to rinse the cup twice. The subjects continued fasting for 3 h after drug ingestion, except for 150 mL of water given after 1 and 2 h and permitted *ad libitum* thereafter. A standardized meal was served 3 h after drug administration. The subjects were instructed not to engage in any strenuous or athletic activities during the days of drug administration. Smoking was permitted, but not snuff. The study protocol was reviewed and approved by a peer committee and written informed consent was obtained.

Sampling and Assay—Blood samples (5 mL) were drawn from the antecubital vein just prior to dosing and at 10, 20, 30, 45, 60, 80, and 100 min and 2, 3, 4, 6, and 8 h after drug administration. All samples were collected by direct puncture using evacuated heparinized blood collecting tubes[3]. Plasma was quickly separated by centrifugation and filtration[4]. The samples were frozen within 20 min of collection and were kept at −70°C in labeled vials until assayed. The total urine output was collected over 2-h intervals during the 8-h study period. The weight of the total volume collected during each interval was recorded and a 5 to 10-mL portion was frozen (−70°C) until assay. The plasma and urine samples were assayed for ampicillin by a microbiological technique using the cylinder plate method with *Micrococcus luteus* ATCC 9341 as the test organism (2).

Pharmacokinetic Calculations—The kinetics of ampicillin after intravenous injection can be adequately characterized by the two-compartment open model (3, 4). The individual plasma concentration *versus* time curves in the present study showed a biexponential decline, which also indicated that the two-compartment open model was valid. To determine the kinetics of absorption, the exponential parameters in the following equation were obtained using the nonlinear regression analysis program NONLIN (5):

$$C_p^t = Ae^{-\alpha t} + Be^{-\beta t} - Ce^{-k_a t} \text{ (mg/L)} \qquad \text{(Eq. 1)}$$

[3] Venoject; Terumo Europe NV, 3030 Leuven, Belgium.
[4] Sera-Clear; Technicon AB, Stockholm, Sweden.

Table I—Pharmacokinetic Variables After Single 400-mg Doses of Microencapsulated Bacampicillin Hydrochloride in Suspension [a]

Dissolution Rate						Urinary
$t_{50\%}$, min	k, h^{-1}	$C_{p,max}$, mg/L	k_a, h^{-1}	β, h^{-1}	AUC, mg·h/L	Recovery, %
2.5(0.13)	16.7(0.87)	8.7(1.6)	4.3(2.1)	0.60(0.24)	14.4(2.1)	76.7(11.3)[b]
5.0(0.23)	8.3(0.38)	8.2(2.0)	3.8(1.2)	0.57(0.13)	13.9(1.6)	74.0(12.3)
12.5(0.56)	3.3(0.15)	7.1(1.0)	3.6(1.9)	0.53(0.11)	13.3(2.2)	73.2(13.4)
22.0(0.72)	1.9(0.06)	4.9(0.94)	3.4(1.8)	0.52(0.14)	10.1(2.1)	53.7(14.2)

[a] Expressed as mean ± *SD* for a crossover study, $n = 12$. [b] $n = 11$.

where A, B, and C are the intercepts at the y-axis (at $t = 0$) obtained from the semilogarithmic plot of C_p^t *versus* t, α and β are first-order disposition rate constants of the biexponential decline of the curve, and k_a is the apparent first-order absorption rate constant. Initial parameter estimates used in NONLIN were calculated using a computer adaptation of the classical residual, peeling-off technique (CSTRIP) (6).

The areas under the plasma concentration–time curves (AUC) were calculated by use of the trapezoidal rule. The estimated area from the last sampling time t_x to infinity was calculated from

$$AUC_{t_x-\infty} = \frac{C_p^{t_x}}{\beta}(\text{mg} \cdot \text{h/L}) \qquad \text{(Eq. 2)}$$

where $C_p^{t_x}$ is the plasma concentration at the last sampling time. An estimation of the relative bioavailability of the four microcapsule suspensions was made by comparing the AUC values as well as the amount of ampicillin excreted in the urine during 8 h. The suspension with the shortest dissolution half-life was used as the standard.

Sensory Evaluation—Within 5–10 min after administration of each dose, the subjects recorded their sensory evaluation on two visual analogue scales. The first scale was related to the overall palatability, with the endpoints "extremely bad" and "excellent." The second was a rating of the bitter aftertaste with the endpoints "strong" and "none."

Statistical Analysis—The relationship between dissolution half-life and each of the response variables [plasma peak (C_{max}), area under the plasma concentration–time curve (AUC), and urinary recovery] was evaluated in a regression analysis. Since a crossover design was used, the observations within a subject are dependent in a manner requiring a modification of the standard regression technique. This modification is described in the *Appendix*.

For the sensory evaluation variables, for which a visual analogue scale was used, a nonparametric approach was taken in the analysis. The direct observations expressed as millimeters on the analogue scale were transformed to rank numbers after an overall ranking of the data. The rank numbers were then used in the regression analysis, a procedure which has been shown to give useful results for data on an ordinal scale (7).

A linear relationship between dissolution half-life and different variables was tested against the hypothesis of no relationship (slope of regression line = 0) using the Student's t test. The criterion for the choice between dissolution half-life ($t_{50\%}$) and dissolution constant [$k = (\ln 2)/t_{50\%}\ h^{-1}$] as the independent variable was the correlation between this variable and the response variable. The highest correlation coefficient was observed consistently for $t_{50\%}$; this measure was chosen, therefore, as the independent variable.

Since β was not expected to respond to differences in the dissolution rate, β was analyzed by using a two-way analysis of variance. The variable time-to-peak is a crude measurement of the absorption rate. Therefore, only descriptive methods were used in the evaluation of this variable. As such, these data give only supplementary information to the results of the nonlinear regression analysis.

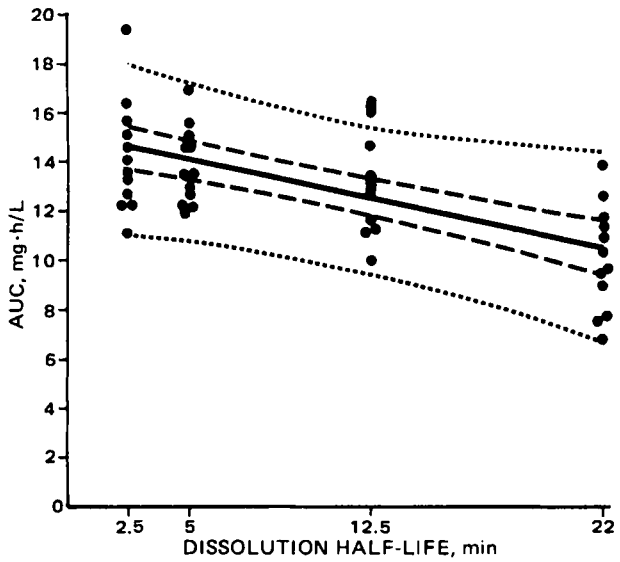

Figure 4—*Relationship between* in vitro *dissolution half-life and area under the plasma concentration–time curve (AUC) after single 400-mg doses of microencapsulated bacampicillin hydrochloride in suspension. Crossover study in 12 subjects. The lines are as defined for Fig. 3.*

RESULTS

***In Vitro* Dissolution**—The amount of polymer in the film coating applied had a strong influence on the *in vitro* dissolution rate of bacampicillin (Fig. 1), which followed first-order kinetics as shown by the linear curves in the inset diagram in Fig. 1. The mean calculated times for 50% of the drug to dissolve (dissolution half-life) were 2.5, 5.0, 12.5, and 22.0 min for the microcapsules with 17, 23, 29, and 37% film coating, respectively. A doubling of the thickness of the film coating thus increased the dissolution half-life by a factor of ~10. A variation in the stirring rate between 50 and 200 rpm did not affect the dissolution rate.

Dissolution Rate *versus* Plasma Levels—The highest mean plasma concentration–time curve was seen after the subjects received the suspension with the shortest dissolution half-life, and the lowest mean curve after receiving the suspension with the slowest dissolution rate (Fig. 2). The suspension with the slowest dissolution rate produced a lower and flatter maximum drug concentration. However, the slopes of the curves for the terminal disposition phase (β) of ampicillin did not differ significantly following administration of the four suspensions (Table I).

After receiving the three suspensions with the more rapid dissolution rates, no subject had a plasma peak below 5 mg/L, as compared with five subjects after receiving the suspension with a dissolution half-life of 22 min. An inverse linear relationship was noted between the plasma peak and dissolution half-life (Fig. 3). The regression lines had a mean (*SD*) slope of −0.19 (0.08), which is significantly different from zero at $p < 0.001$, and a mean correlation coefficient of 0.77 (0.18). There was a major deviation from the expected ranking order of the suspensions in only three subjects, all of whom had the highest peak after receiving the suspension with a dissolution half-life of 5 min. Proceeding from the lower limit of the 95% confidence interval for the regression line, a mean plasma peak of >5 mg/L can be predicted with a microcapsule suspension having a dissolution half-life of ≤19 min.

Dissolution Rate *versus* Absorption Rate—The absorption rate, as estimated from the time of the plasma peak concentrations, tended to increase with a decrease in the dissolution half-life (Table II). There tended to be less variation between individuals after receiving the suspension with the highest dissolution rate. The results of the nonlinear regression analysis show a slight tendency toward an increase in the apparent absorption rate with an increase in the dissolution rate (Table I). The regression lines had a mean (*SD*) slope of −0.04 (0.11), which is not

Table II—Frequency Distribution and Median Time of Plasma Peak Concentrations After Single 400-mg Doses of Microencapsulated Bacampicillin Hydrochloride in Suspension [a]

Dissolution Half-Life,	Time of Plasma Peak, h							
min	0.33	0.5	0.75	1.0	1.33	1.67	2.0	Median
2.5		6	5	1				0.63
5		4	3	1	4			0.75
12.5	1	2	4	2	2	1		0.75
22		4		3	4		1	1.0

[a] Crossover study, $n = 12$.

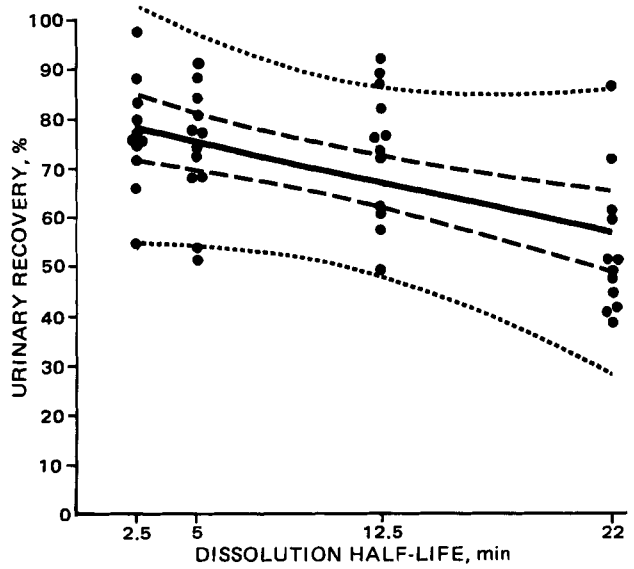

Figure 5—*Relationship between* in vitro *dissolution half-life and urinary recovery of ampicillin during 0–8 h after single 400-mg doses of microencapsulated bacampicillin hydrochloride in suspension. Crossover study in 12 subjects. The lines are as defined for Fig. 3.*

significantly different from zero, and a mean correlation coefficient of 0.61 (0.28).

Dissolution Rate *versus* Bioavailability—The extent of bioavailability was estimated from the AUC and the urinary recovery of ampicillin (Table I). Both of these variables correlated well with the dissolution half-life. The regression lines for the inverse relationship between AUC and dissolution half-life had a mean (*SD*) slope of −0.21 (0.10), which is significantly different from zero at $p < 0.001$, and a mean correlation coefficient of 0.77 (0.19) (Fig. 4). The linear regression lines between dissolution half-life and urinary recovery (Fig. 5) had a mean (*SD*) slope of −1.12 (0.82), significantly different from zero at $p < 0.001$, and a mean correlation coefficient of 0.67 (0.27). There were major deviations from the expected ranking order of the suspensions in only two subjects with regard to AUC and four with respect to urinary recovery. A mean urinary recovery of at least 60% can be predicted with 95% confidence for a suspension having a dissolution half-life of ≤14 min.

There was good agreement between the mean relative bioavailability when calculations were based on total AUC values and the amount of ampicillin recovered in urine (Table III) and a notable reduction in the bioavailability of the suspension with the longest dissolution half-life. The results with the two suspensions with the slowest dissolution rates were more variable when based on urinary excretion than on AUC.

Dissolution Rate *versus* Sensory Evaluation—There was a direct linear relationship between the dissolution half-life and the bitter aftertaste (Fig. 6) as well as the overall taste. The regression lines had mean (*SD*) slopes of 0.68 (0.71) and 0.53 (0.69), respectively, both significantly different from zero at $p < 0.01$ and $p < 0.05$. Their mean coefficients of correlation were 0.65 (0.29) and 0.56 (0.33), respectively. No adverse reactions were reported in any of the subjects.

DISCUSSION

The extent of bioavailability of bacampicillin hydrochloride from the three microcapsule suspensions with an *in vitro* dissolution rate of ≤12.5 min was similar to that previously reported with bacampicillin hydrochloride tablets. After 400-mg doses in tablet form, mean peak serum concentrations of 7.7–8.9 mg/L, a mean AUC of ~15 mg·h/L, and a mean urinary recovery of 71–75% have been reported (1, 2, 8). When given as tablets, 86–87% of the bacampicillin hydrochloride dose is absorbed (3, 4).

The significant correlation between the *in vitro* dissolution half-life of bacampicillin hydrochloride from the microcapsules and pharmacokinetic variables such as plasma peak, AUC, and urinary recovery can be used to predict the *in vivo* behavior of bacampicillin hydrochloride from *in vitro* tests of the microcapsule suspension. The 95% confidence limits for the mean regression lines in our study indicate that we can be fairly confident in predicting the mean of pharmacokinetic variables from *in vitro* data. The prediction of a new observation in a random subject is less accurate, however, due to the variation between individuals and the relatively small sample size in the present study.

Table III—Relative Bioavailability [a] After Single 400-mg Doses of Microencapsulated Bacampicillin Hydrochloride in Suspension

Dissolution Half-Life, min	Bioavailability, % AUC Method Mean	AUC Method *SD*	Urinary Recovery Method Mean [b]	Urinary Recovery Method *SD*
2.5	100.0		100.0	
5	97.9	17.6	97.1	17.1
12.5	93.4	14.9	99.1	24.8
22	70.1	11.9	72.3	22.7

[a] Based on the total AUC or amount of ampicillin recovered in the urine 0–8 h postdose in a crossover study, $n = 12$. [b] $n = 11$.

The bacampicillin hydrochloride microcapsules are coated with ethylcellulose, which is practically insoluble in aqueous solution. Thus, the rate-limiting step with respect to drug dissolution *in vitro* is diffusion through the film. That this process is also a rate limiting factor *in vivo* is supported by the good *in vitro–in vivo* correlation observed. Also, the lack of influence of stirring rate on the *in vitro* dissolution of the microcapsules favors a strong correlation and is similar to the findings of Levy *et al.* (9). The diffusion through the film is highly dependent on wall thickness, which has also been reported with regard to microcapsules containing phenethicillin potassium (10).

The weak correlation between the apparent absorption rate constant (k_a) and the dissolution rate constant (k) indicates that the diffusion through the microcapsule coating is not the rate-limiting step in the absorption process. The results of parameter estimation of a polyexponential model should be interpreted with great caution. This applies also to results obtained from computer programs based on nonlinear regression analysis. Especially when the exponents are close together, as is frequently the case with drugs with a short half-life like the penicillins, this approach may lead to inaccurate estimates of the parameters (11). Furthermore, in such cases the estimates are highly dependent on the choice of starting values in the iterative procedure. This was also obvious from some simulation in the present material, in which the nonlinear regression analysis gave very different estimates after even small changes in the initial values for some subjects.

The suspension with the slowest dissolution rate did not yield more sustained plasma concentrations than the others. A possible reason for this is that the microcapsules had passed the upper duodenum before bacampicillin was released. According to Swahn (12), the upper duodenum is where bacampicillin is most efficiently absorbed. Another possibility is that bacampicillin was released too far in the intestine and then decomposed to ampicillin which was destroyed by the β-lactamases which are abundant in the intestinal flora. The results clearly show that little benefit is to be expected from a slow-release formulation of microencapsulated bacampicillin hydrochloride.

A review of two previous bioavailability studies on volunteers verifies the correlation in the present study and indicates reproducible results. Thus, a similar microcapsule suspension with a dissolution half-life of ~20 min has been used and produced, after a 400-mg dose, a mean plasma peak, AUC, and urinary recovery of 5.2 mg/L, 10.8 mg·h/L, and 55.7%, respectively[5]. The same microcapsule batch (dissolution half-life 22 min) and dose as used in this study, but suspended in water without such excipients as sweeteners, flavoring, and thickening agents, generated a mean plasma peak, AUC, and urinary recovery of 4.3 mg/L, 7.8 mg·h/L, and 45%, respectively, in another group of volunteers[1]. Thus, the excipients do not seem to influence the bioavailability from the microcapsule suspension. A microcapsule formulation essentially similar to that used in the present study has also been found to be well absorbed in infants (13, 14).

Quantitative correlations have been reported between *in vitro* dissolution and *in vivo* bioavailability from other preparations of the present type, *e.g.*, estradiol suspensions with different rates of drug dissolution owing to differences in particle sizes (15). Sjögren and Bogentoft (16) were able to control aspirin absorption from enteric-coated granules with different *in vitro* dissolution profiles. The microcapsules were given in hard gelatin capsules. Wagner (17) and Smolen (18) have noted that *in vitro–in vivo* correlations have often been of little use in predicting the bioavailability of formulations not included in a study. However, the *in vitro–in vivo* correlation may apply to specific products manufactured

[5] J. Sjövall and R. Sjöqvist; unpublished data.

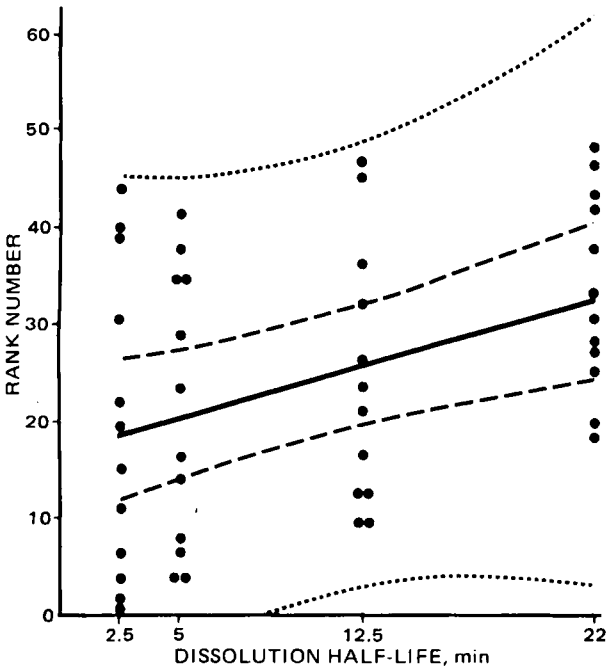

Figure 6—*Relationship between* in vitro *dissolution half-life and bitter aftertaste expressed as the rank number after an overall ranking of sensory recordings on a visual analogue scale. Crossover study in 12 subjects using single 400-mg doses of microencapsulated bacampicillin hydrochloride in suspension. High rank numbers indicate less bitterness. The lines are as defined for Fig. 3.*

by similar methods, *e.g.*, different amounts of coating agents, as shown in the present study. Substances with good solubility in water and lipids, and which show linear pharmacokinetics, offer more favorable conditions for a good *in vitro–in vivo* correlation. These factors are applicable to bacampicillin hydrochloride, which is soluble in both water and lipids. The total amount of bacampicillin hydrochloride absorbed is a linear function of the dose (19).

Although the present study was not optimally designed for a sensory evaluation of the taste of the suspension, a significant correlation between taste and dissolution rate was found. This verifies the results from prediction tests on volunteers in which the microencapsulation of bacampicillin hydrochloride was found to reduce the bitter taste in suspensions to a level similar to that of other aminopenicillins[6].

There is an inverse linear relationship between the bioavailability of bacampicillin hydrochloride from a microcapsule suspension and the microcapsule *in vitro* dissolution half-life. On the other hand, there is a direct linear relationship between masked bitterness and dissolution half-life. The present results suggest that bacampicillin hydrochloride can be administered in a microcapsule suspension with sufficient microcapsule film thickness to reduce the bitter taste and still retain good bioavailability.

APPENDIX

One important objective of this study was to evaluate the relationship between dissolution half-life (x) and each of the response variables (y) plasma peak concentration (C_{max}), area under the plasma concentration–time curve (AUC), urinary recovery, and the results of the sensory recordings. In this evaluation the standard linear regression analysis has been adapted to the crossover design. In principle, this means that individual regression equations have been estimated and then combined in an overall estimate. Formally, the following procedure was used. For each individual ($i = 1, \ldots, n$) the following linear regression model was assumed:

$$y = \alpha_i + \beta_i x + \epsilon, \qquad \text{(Eq. 3)}$$

where α is the intercept and β the slope of the regression line. The random error ϵ is assumed to be normally and independently distributed with mean = 0 and variance = σ_ϵ^2. Each of these models has been estimated separately by using the method of least squares, giving:

[6] R. Sjöqvist; unpublished data.

$$y = a_i + b_i x \qquad \text{(Eq. 4)}$$

An overall linear relationship has been estimated by averaging the individual regression model estimates, which yields:

$$y = a + bx, \qquad \text{(Eq. 5)}$$

where $a = (1/n)\,\Sigma a_i$ and $b = (1/n)\,\Sigma b_i$.

The standard error for $a + bx$ has been calculated according to:

$$SE(a + bx) = \left[\frac{1}{n}\left(SD^2(\bar{y}_i) + (x - \bar{x})^2 \cdot SD^2(b_i)\right)\right]^{1/2} \qquad \text{(Eq. 6)}$$

where $SD^2(\bar{y}_i)$ and $SD^2(b_i)$ is the variance of the mean value of y and the regression coefficients, respectively, calculated from the individual regression lines. $\bar{x}$ is the overall mean value of dissolution half-lives. A 95% confidence interval for the overall regression line has been calculated as follows:

$$(a + bx) \pm t^{0.95}_{n(k-2)} \cdot \mathrm{SE}(a + bx) \qquad \text{(Eq. 7)}$$

where $t^{0.95}_{n(k-2)}$ is the value of the Student's t distribution with $n(k - 2)$ degrees of freedom appropriate for a 95% interval.

The standard error of a new observation of y in a random subject with $x = x_0$ has been calculated as:

$$SE(a + bx_0) = \left[\left(1 + \frac{1}{n}\right)\left(SD^2(\bar{y}_i) + (x_0 - \bar{x})^2 \cdot SD^2(b_i)\right)\right]^{1/2} \qquad \text{(Eq. 8)}$$

The corresponding 95% prediction interval is:

$$(a + bx_0) \pm t^{0.95}_{n(k-2)} \cdot SE(a + bx_0) \qquad \text{(Eq. 9)}$$

This procedure is developed in analogy to that described in Brownlee (20).

REFERENCES

(1) J. Sjövall, L. Magni, and T. Bergan, *Antimicrob. Agents Chemother.*, **13,** 90 (1978).

(2) L. Magni, J. Sjövall, and E. Syvälahti, *Infection*, **6,** 283 (1978).

(3) T. Bergan, *Antimicrob. Agents Chemother.*, **13,** 971 (1978).

(4) M. Ehrnebo, S.-O. Nilsson, and L. O. Boréus, *J. Pharmacokinet. Biopharm.*, **7,** 429 (1979).

(5) C. M. Metzler, G. L. Elfring, and A. J. McEwen, *Biometrics*, **30,** 562 (1974).

(6) A. J. Sedman and J. G. Wagner, *J. Pharm. Sci.*, **65,** 1006 (1976).

(7) R. L. Iman and W. J. Conover, *Technometrics*, **21,** 499 (1979).

(8) L. Magni, B. Sjöberg, J. Sjövall, and J. Wessman, "Chemotherapy," vol. 5, Plenum, New York, N.Y., 1976, pp. 109–114.

(9) G. Levy, J. R. Leonards, and J. A. Procknal, *J. Pharm. Sci.*, **54,** 1719 (1965).

(10) H. O. Alpar and V. Walters, *J. Pharm. Pharmacol.*, **33,** 419 (1981).

(11) P. J. Fell and M. T. Stevens, *Eur. J. Clin. Pharmacol.*, **8,** 241 (1975).

(12) Å. Swahn, *Eur. J. Clin. Pharmacol.*, **9,** 299 (1976).

(13) T. Bergan, D. Bratlid, and A. Brøndbo, *J. Antimicrob. Chemother.*, **4,** 79 (1978).

(14) C. M. Ginsburg, G. H. McCracken, J. Clahsen, and T. Zweighaft, *Rev. Infect. Dis.*, **3,** 117 (1981).

(15) I. Kvorning and M. S. Christensen, *Drug. Dev. Ind. Pharm.*, **7,** 289 (1981).

(16) J. Sjögren and C. Bogentoft, in "Optimization of Drug Delivery," H. Bundgaard, A. Bagger Hansen, H. Kofod, Eds., Munksgaard, Copenhagen, 1982, pp. 53–66.

(17) J. G. Wagner, "Biopharmaceutics and Relevant Pharmacokinetics," Drug Intelligence Publications, Hamilton, Ill., 1971, pp. 58–88.

(18) V. F. Smolen, *J. Pharm. Sci.*, **60,** 878 (1971).

(19) J. Sjövall, *Infection*, **7,** Suppl. 5, 458 (1979).

(20) K. A. Brownlee, "Statistical Theory and Methodology in Science and Engineering," Wiley, New York, N.Y., 1965, pp. 376–388.

ACKNOWLEDGMENTS

The authors sincerely thank Lennart Magni for skillful technical assistance in the assay of ampicillin, Erik Vinnars for medical supervision, and Gunnar Alván and Rune Elofsson for valuable discussion.

Powder Suspension Method for Critically Re-Examining the Two-Site Model for Hydroxyapatite Dissolution Kinetics

W. I. HIGUCHI ˣ, E. Y. CESAR *, P. W. CHO, and J. L. FOX

Received October 18, 1982, from the *College of Pharmacy, Department of Pharmaceutics, University of Utah, Salt Lake City, UT 84112.* Accepted for publication December 15, 1982. *Present address: Lederele Laboratories, Pearl River, NY 10965.

Abstract □ A powder dissolution method has been developed, and experiments with the hydroxyapatite suspensions confirm earlier conclusions based on dissolution from hydroxyapatite disks. Although a quantitative assessment of the properties of site 1 was not possible from the data obtained in the present study, a rather accurate and independent evaluation of the properties and the behavior of site 2 of the two-site model for hydroxyapatite dissolution was possible, and the results clearly validate the original two-site model. The present work together with the earlier disk studies show that dissolution from site 2 is well described by a first-order expression, rate = k_{c2} ($C_{s2} - C$), where k_{c2} is a first-order rate constant, C_{s2} is the apparent solubility for site 2 (defined by an ion activity product, K_{HAP}, of the form $a^{10}_{Ca^{2+}} a^{6}_{PO_4^{3-}} a^{2}_{OH^-}$, and the solution conditions), and C is the microenvironmental solution concentration of hydroxyapatite. For four different precipitated hydroxyapatite preparations, a single K_{HAP} value of $1 \times 10^{-128} \pm 1$ was found to be consistent with experiments using solutions covering wide ranges of partial saturation and calcium–phosphate ratios. The hydroxyapatite powder and pellet methods (including the data evaluation procedures) now offer a powerful combination for investigating the complex kinetics associated with dental enamel dissolution in particular and enamel chemistry in general.

Keyphrases □ Hydroxyapatite—dissolution kinetics, powder suspension method for critically re-examining the two-site model □ Dissolution—powder suspension method for critically re-examining the two-site model for hydroxyapatite kinetics □ Kinetics—powder suspension method for critically re-examining the two-site model for hydroxyapatite dissolution □ Powder suspension method—re-examination of two-site model for hydroxyapatite dissolution kinetics

Because of the clinical importance (1, 2) there has been considerable interest in developing an understanding of the acid dissolution rate behavior of dental enamel and of hydroxyapatite, the principal mineral component of enamel. Research during the past 20 years has revealed, however, that the problem is extremely complicated both from the theoretical standpoint and from the experimental. Only recently, has progress been made toward achieving a degree of understanding at a generalizable level.

Recently, a model was presented for describing the acid dissolution rate of hydroxyapatite based on experiments with compressed hydroxyapatite disks (3). The model featured dissolution from two sites on the hydroxyapatite crystal and diffusion of species in the pores of the matrix as well as diffusion across the aqueous boundary layer. The purpose of the present study was to directly assess the crystal dissolution process by determining the dissolution rate of fine suspensions of hydroxyapatite crystals dispersed by ultrasonication so that the surface solution microenvironmental conditions were essentially the same as the bulk solution conditions.

BACKGROUND

Gray (4), following the postulate of Stralfors (5) that acid dissolution of dental enamel may be solution diffusion controlled, reported some carefully conducted experiments with block enamel using several acids under a variety of conditions. These experiments suggested an approach to the mechanistic study of the kinetics of dental enamel dissolution based on the use of mathematical modeling. In the earliest attempts, the dissolution of enamel in an acid buffer under sink conditions (*i.e.*, not partially saturated with hydroxyapatite) was described by a mathematical relationship (6–8):

$$J = AkC_s \qquad \text{(Eq. 1)}$$

where A is the exterior exposed enamel surface area, k is a rate constant which is a function of the hydrodynamics (solution agitation conditions), and C_s is the solubility of hydroxyapatite in the acid buffer. For the situation in which all species have about the same intrinsic diffusivity value (D_{aq}) and when diffusion potentials may be neglected, one may write $k = D_{aq}/h$ where h is the aqueous boundary layer thickness in the Nernst approximation.

In this diffusion-controlled model, it was assumed that the hydroxyapatite phase would determine C_s (which is a function of the solubility product for hydroxyapatite, the solution equilibrium constants, the acid buffer dissociation constant (K_a), the buffer concentration, buffer pH, and the activity coefficients for all the species in the system). An alternative model (6) was also considered at that time which assumed that the C_s-determining phase was dicalcium phosphate dihydrate. Analysis of the data of Gray on initial dissolution rates yielded results (6) that were remarkably consistent with the hydroxyapatite phase model, but not the dicalcium phosphate dihydrate model. Over a wide range of pH, acid buffers, buffer concentration, and common ion (*i.e.*, calcium and phosphate) concentrations, a single solubility product value for hydroxyapatite of $\sim 10^{-124}$ (based on $a^{10}_{Ca^{2+}} a^{6}_{PO_4^{3-}} a^{2}_{OH}$) was found to be consistent with all of the data of Gray. It was noted then (6), however, that this best-fit kinetic solubility product (hereafter designated as K_{HAP} value was somewhat low; it was much later that this low K_{HAP} value was understood to be not the actual thermodynamic solubility product of hydroxyapatite, but an apparent solubility product (and an ion activity product) governing the kinetics of dissolution (3, 8).

The hydroxyapatite model was extended to powdered dental enamel dissolution studies (9) under conditions similar to those utilized by Gray in his block enamel experiments. Essentially the same favorable results were obtained; *i.e.*, over a wide range of acetate and lactate buffer concentrations, pH, and common ion concentrations, the hydroxyapatite model with a single K_{HAP} value ($\sim 10^{-124}$) agreed well with all of the dissolution rate data. The best fitting K_{HAP} value, however, was again noted to be low compared with the currently published thermodynamic value ($\sim 10^{-116}$) (10) for the solubility product of hydroxyapatite.

A synthetic hydroxyapatite sample prepared by aqueous precipitation and digestion at 100°C was obtained[1]. This prototype sample was designated NBS hydroxyapatite and, subsequently, similar samples were prepared in these laboratories. The first studies with NBS hydroxyapatite were conducted using compacted pellets (to simulate block enamel) of this material in the rotating disk assembly with its well-developed hydrodynamics (11). All of the initial studies (8) were again under sink conditions paralleling the conditions of the experiments of Gray (4) and those studies (9) with the powdered enamel. Interestingly, all of the sink data, again obtained over a wide range of conditions, could be rather accurately fitted to the simple hydroxyapatite phase model with a single K_{HAP} value of 10^{-125} (very close to that obtained in the dental enamel experiments and, therefore, suggesting that NBS hydroxyapatite may be a good baseline model for enamel in kinetic studies).

It was learned from this study in which the hydrodynamics was quantitatively defined, however, that both aqueous diffusion and surface kinetics contributed significantly to the rate constant k (at low rotation speeds, k was predominantly diffusion controlled; at the higher speeds k was only 30–50% diffusion controlled). When these experiments with NBS hydroxyapatite were extended to acid buffers that were partially

[1] Supplied by Dr. P. R. Patel, American Dental Association, National Bureau of Standards.

0022-3549/84/0200-0146$01.00/0
© 1984, American Pharmaceutical Association

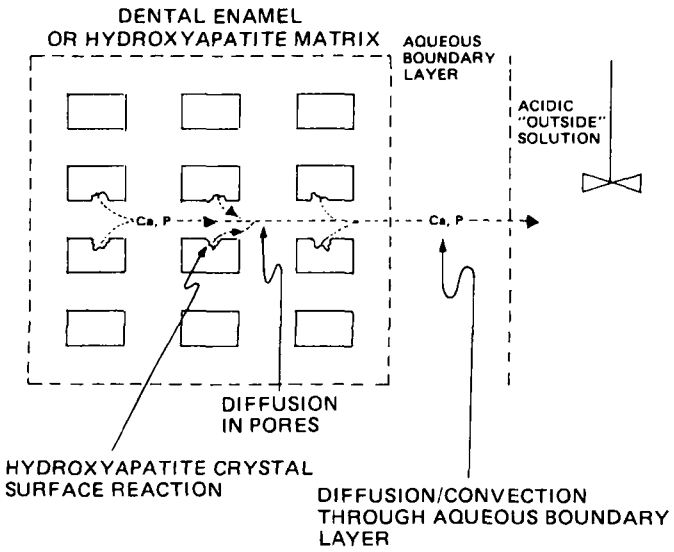

Figure 1—*General problem of hydroxyapatite crystal surface kinetics, pore diffusion, and bulk phase diffusion/convection.*

saturated with respect to hydroxyapatite, one of the most important results of this research followed. The large body of data obtained with NBS hydroxyapatite pellets under partially saturated conditions deviated significantly from the predictions of the one-site (or the one-phase) hydroxyapatite model (12). Subsequent theoretical work culminated in the deduction of a new NBS hydroxyapatite pellet dissolution model, the two-site model (3), and accompanying mathematics in which it is assumed that the NBS hydroxyapatite crystal dissolution may occur at two sites each characterized by an apparent solubility, C_s, and a first-order crystal surface–solution reaction rate constant, k_c. These conclusions based on kinetic studies were subsequently supported by electron microscopic experiments (13), which showed that dissolution into partially saturated buffers proceeded *via* formation of holes in the crystals while dissolution of comparable amounts of mineral into completely unsaturated buffers showed no such holes.

The development of the two-site model has been considered a breakthrough, as the model has been found to be capable of explaining a wide range of previously unexplained observations regarding hydroxyapatite behavior. Of particular interest is the ability of the model to predict all of the various sets of conditions leading to zonal (as opposed to surface) dissolution from NBS hydroxyapatite pellets. Zonal dissolution is believed to be a prerequisite for the formation of the pre-carious lesions known as "white spots" in clinical dentistry. The purpose of the present report is to describe the results of hydroxyapatite crystallite suspension dissolution rate studies aimed at critically evaluating the baseline two-site model, which had been developed entirely using experimental data involving compacted pellets of hydroxyapatite crystals.

THEORETICAL

The theory (3) as developed for the pellet dissolution system is relatively complex as, in addition to the events at the crystal–solution interface, diffusion of species in the pellet pores and in the aqueous boundary layer had to be taken into account. As discussed below, when appropriate crystallite or crystallite aggregate sizes and suitable hydrodynamics are employed as defined by the two-site model parameter values in crystallite suspension dissolution experiments, the crystal surface microenvironmental conditions are well approximated by the bulk solution conditions. Therefore solution diffusion, both in the aqueous boundary layer and in the aqueous pores in the case of crystal aggregates, may be neglected, and the dissolution rates may be related directly to the bulk solution conditions. The theory for dissolution from the pellet is insensitive, in certain situations, to some of the parameter values associated with defining the events at the crystal–solution interface; this is directly related to the above in that the contributions from diffusional processes in the aqueous pores of the pellet and in the aqueous boundary layer must be considered and accounted for in the calculations.

Table I—Best-Fit Parameter Values for the Two-Site Model

D	$pK_{HAP,1}$	$pK_{HAP,2}$	k'_{c1}, s/cm	k'_{c2}, s/cm
1.0×10^{-5} [a]	120	128	1252	111
1.5×10^{-5} [b]	122	130	844	65

[a] See Fig. 6 of Ref. 3. [b] See Fig. 7 of Ref. 3.

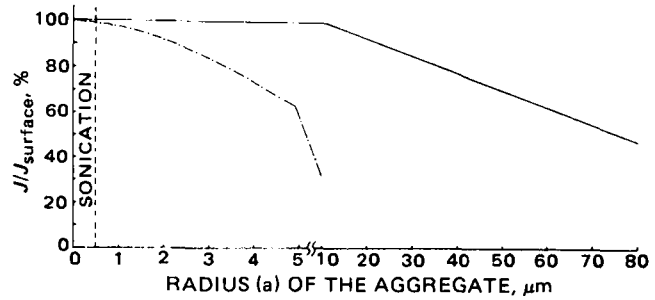

Figure 2—*Influence of the aggregate size on the extent to which the dissolution rate is controlled by crystal surface kinetics. Key: (—) $k = 0.30\ s^{-1}$; (- - - -) $k = 40\ s^{-1}$.*

A third problem associated with analyzing pellet dissolution data only with the theory has been how to deal with the question of quasi-steady-state *versus* non-steady-state conditions. The theory, as developed (3), is for steady-state conditions, and there are instances where transient effects resulting from slow diffusion in the pores may be long compared with experimental times, *e.g.*, when foreign agents are present in the bulk solution that may adsorb and influence the dissolution rates. Combined analysis of the pellet dissolution data with the crystal suspension data should help greatly in these situations. Finally, there are cases where phase changes may occur regionally in the pellet during dissolution; such situations would be extremely difficult to interpret using pellet data alone.

Parameter Values Deduced from the Two-Site Model and Hydroxyapatite Pellet Experiments—Figure 1 illustrates schematically the general problem of hydroxyapatite pellet dissolution into a stirred medium. The basic steady-state differential equation for describing the simultaneous diffusion (in the aqueous pores) and hydroxyapatite dissolution reaction within the pellet matrix is:

$$D'\frac{d^2C}{dx^2} + R = 0 \qquad \text{(Eq. 2)}$$

where C is the concentration of hydroxyapatite at point x, D' is the diffusivity (considered to be equal for all species in the matrix), and R is the rate of dissolution of crystalline hydroxyapatite at x. Equation 2 is for

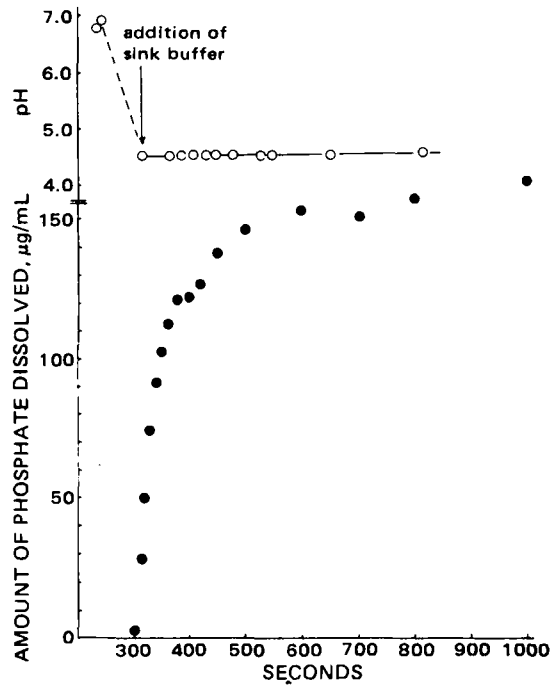

Figure 3—*pH profile of the dissolution medium during dissolution of hydroxyapatite powder (NBS–P). Initially, Ca = P = 0.*

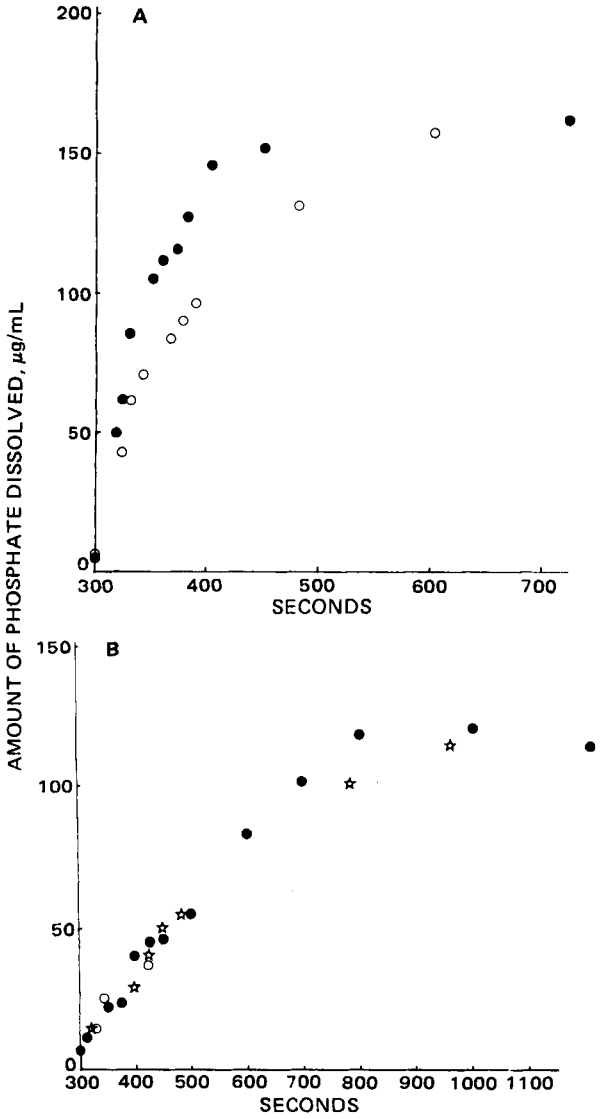

Figure 4—*Influence of ultrasonic radiation on the dissolution rate of hydroxyapatite powders UM-T (A) and NBS-P (B) suspension; Ca = P = 1.76 mM at t = 0 for UM-T; Ca = P = 3.5 mM at t = 0 for NBS-P. Key: (●), sonicated; (○, ☆), not sonicated.*

the one-dimensional problem, which is appropriate for the case of the pellet geometry employed in the previous investigation (3). The key assumption for the two-site model enters this equation *via* R by the function:

$$R = k_{c1}(C_{s1} - C) + k_{c2}(C_{s2} - C) \qquad \text{(Eq. 3)}$$

where C_{s1} and C_{s2} are the apparent solubilities associated with the two crystalline sites, and k_{c1} and k_{c2} are the respective first-order kinetic rate constants. C_{s1} and C_{s2} are functions of the bulk solution and the ion activity products, $K_{HAP,1}$ and $K_{HAP,2}$, which are the more basic parameters characterizing the driving forces for the dissolution reactions at the two sites. As discussed previously (3), C_{s1} and C_{s2} are defined as the moles of $Ca_{10}(PO_4)_6(OH)_2$ per liter that would have to be added to the bulk solution to saturate sites 1 and 2, respectively (see *Appendix* for how C_{s1} and C_{s2} values may be calculated for different solution conditions). C is defined as the number of moles of hydroxyapatite that would have to be added to the bulk solution to give a solution identical to that at point x. In the limit where diffusion is very rapid compared with the surface reactions, $C \rightarrow O$ in the pellet matrix.

It should be emphasized that C_{s1} and C_{s2} are not true solubilities in the thermodynamic sense. Rather they are apparent solubilities that one could deduce assuming solubility-controlled dissolution and extrapolating the dissolution rate *versus* concentration dependence to zero dissolution rate. Thus, apparent solubilities really represent a threshold concentration below which dissolution proceeds at a perceptible rate. That is,

Table II—Compositions of Dissolution Media Used in the Present Study

Nominal Percent Partial Saturation[a]	Solution pK_{HAP}	Ca–P Ratio	Calcium, mM	Phosphate, mM	pH	Ionic Strength
0	—	0:0	0	0	4.5	0.5
2	143.3	1:1	0.4405	0.4405	4.5	0.5
4	138.2	1:1	0.881	0.881	4.5	0.5
6	135.9	1:1	1.3215	1.3215	4.5	0.5
8	132.9	1:1	1.762	1.762	4.5	0.5
12	130.9	1:1	2.643	2.643	4.5	0.5
16	128.4	1:1	3.524	3.524	4.5	0.5
20	127.4	1:1	4.405	4.405	4.5	0.5
24	126.1	1:1	5.286	5.286	4.5	0.5
0	∞	1:0	1	0	4.5	0.5
0	∞	3:0	3	0	4.5	0.5
0	∞	5:0	5	0	4.5	0.5
0	∞	6:0	6	0	4.5	0.5
0	∞	10:0	10	0	4.5	0.5
0	∞	0:1	0	1	4.5	0.5
0	∞	0:3	0	3	4.5	0.5
0	∞	0.5	0	5	4.5	0.5
0	∞	0:6	0	6	4.5	0.5
0	∞	0:10	0	10	4.5	0.5
	135.2	2.14:1	1.881	0.881	4.5	0.5
	132.1	4.40:1	3.881	0.881	4.5	0.5
	130.3	6.68:1	5.881	0.881	4.5	0.5
	136.5	1:2.14	0.881	1.881	4.5	0.5
	134.7	1:4.41	0.881	3.881	4.5	0.5
	133.6	1:6.68	0.881	5.881	4.5	0.5

[a] Based on $K_{HAP} = 1 \times 10^{-116}$ as 100% saturation.

solution concentrations at or above these apparent solubilities do not result in precipitation or crystal growth, but merely a lack of dissolution. This situation must be distinguished from that for completely diffusion-controlled dissolution. In this latter case, the crystal surfaces are in rapid equilibrium with the adjacent solution, and the apparent solubility deduced from dissolution studies coincides with the thermodynamic solubility.

Table I presents the two-site model parameter values taken from the earlier study (3). These were determined by a best-fitting procedure employing a large amount of dissolution rate data obtained with NBS hydroxyapatite pellets in acetate buffers of varying degrees of partial saturation and calcium–phosphate ratios. A D value of 1×10^{-5} cm^2/s is believed to be a reasonable estimate (8) of the average aqueous solution diffusivity. The D value of 1.5×10^{-5} cm^2/s should represent an upper limit. The k'_c values, which were directly deduced from the best-fit procedures, are related to the k'_c values in Eq. 3 by:

$$k'_c\,(k_c D')^{-1/2} \qquad \text{(Eq. 4)}$$

As D' is the diffusivity in the pellet matrix, it can only be estimated *via* an expression such as:

$$D' = \frac{\epsilon}{\tau} D_{aq} \qquad \text{(Eq. 5)}$$

where ϵ is the porosity and τ is the tortuosity in the matrix. Both ϵ and τ are expected to be dependent on x.

Accordingly, estimates of k_{c1} and k_{c2} from the k'_{c1} and k'_{c2} values may be made using Eqs. 4 and 5. Using $D_{aq} = 1 \times 10^{-5}$ cm^2/s, $k'_{c1} = 1252$ s/cm, and k'_{c2} 111 s/cm from Table I, we have:

$$k_{c1} = \frac{1}{16\left(\frac{\epsilon_1}{\tau_1}\right)} \qquad \text{(Eq. 6)}$$

and

$$k_{c2} = \frac{1}{0.12\left(\frac{\epsilon_2}{\tau_2}\right)} \qquad \text{(Eq. 7)}$$

The average ϵ value may be 0.2–0.5 during pellet dissolution. The values would depend to some extent on whether initial rates are involved or whether quasi-steady-state conditions are approximated. In general, the average ϵ for site 2 kinetics would be expected to be larger than that for site 1 kinetics because of the greater "region-averaged" extent of dissolution for hydroxyapatite crystals involved in site 2 dissolution in the

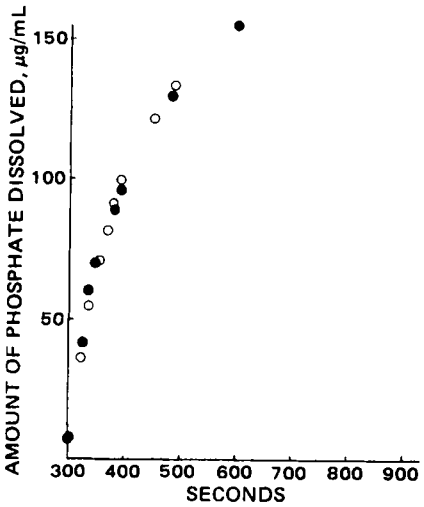

Figure 5—*Data showing little or no effect of rotation speed on the dissolution of hydroxyapatite powder (UM-T) in sink buffer (Ca = P = 0), pH 4.5. Key: (●), not sonicated, 600 rpm; (○), not sonicated, 400 rpm.*

pellet (*cf.* Fig. A1 in Ref. 3). The τ values are estimated to be 1.0–2.0 based on random spheres. It is found, therefore, that $\epsilon/\tau \simeq 0.2$, $k_{c1} \simeq 0.3\ s^{-1}$, and $k_{c2} \simeq 40\ s^{-1}$ from these numbers.

Conditions for Surface Controlled Kinetics in the Hydroxyapatite Crystal Suspension Dissolution Rate Experiments—The hydroxyapatite crystals in most of the preparations used in the present study, including the NBS hydroxyapatite (3, 13), are on the order of 10^2–10^3 Å in size. Light microscope examination of aqueous dispersions of these preparations show, however, the presence of large aggregates in the 20- to 100-μm range. As discussed later in this paper, ultrasonic irradiation of the aqueous dispersions effectively reduces the aggregate size to ≤1 μm. The following analysis shows that this aggregate size reduction is necessary if aqueous diffusion is to be eliminated as an important contributing step in the dissolution kinetics of these preparations.

If the dispersed aggregates of hydroxyapatite crystals are, as a first approximation, assumed to be spherical, we may write:

$$\frac{\partial C}{\partial t} = D\frac{1}{r^2}\frac{\partial}{\partial r}r^2\frac{\partial C}{\partial r} + k_c(C_s - C) \qquad \text{(Eq. 8)}$$

which is analogous to Eq. 2 but for the spherically symmetric one-dimensional case involving single-site dissolution. D is the diffusivity, r is the radial coordinate, and the other symbols have already been defined. The first term on the right-hand side represents diffusion, and the second term a first-order dissolution process as before. For the quasi-steady-state case, $\partial C/\partial t = 0$, and the differential equation is easily solved to yield the following equation for the dissolution rate:

$$J = \frac{4\pi aD'D_{aq}(\alpha a\cdot\cosh \alpha a - \sinh \alpha a)}{(D_{aq} - D')\cdot\sinh \alpha a + D'\alpha a\cdot\cosh \alpha a}C_s \qquad \text{(Eq. 9)}$$

where a is the radius of the spherical aggregate and $\alpha = (k_c/D')^{1/2}$. As previously, D' is the effective diffusivity in the matrix of the aggregate, D_{aq} is the diffusivity in the bulk aqueous solution, and C_s is the apparent hydroxyapatite solubility in the bulk solution.

Equation 9 describes the dissolution process for the one-site problem and takes into account a first-order surface process, diffusion in the matrix of the aggregate, and bulk diffusion from $r = a$ to $r = \infty$ (and therefore the worst case from the standpoint of bulk phase diffusion). It is instructive to use Eq. 9 for the purpose of determining how small the aggregate radius (a) must be so that diffusion processes are negligible compared with the surface kinetics. Calculations carried out for $k_c = 0.3\ s^{-1}$ (site 1) and $k_c = 40\ s^{-1}$ (site 2) are presented in Fig. 2 for different a values. Reasonable values for D' and D_{aq} have been employed based on the discussion in the previous section. First, it is seen that for $k_c = 0.3\ s^{-1}$ surface kinetics dominates even when a is rather large (*i.e.*, $r \simeq 25$ μm). For $k_c = 40\ s^{-1}$, however, it is necessary to have $a \lesssim 1$ μm (or a diameter of 2 μm) for the dissolution kinetics to be ≳98% surface controlled.

It is fortunate that, as discussed later in this paper, ultrasonic irradiation easily reduces hydroxyapatite aggregate sizes to ≤1 μm in diameter, and under these conditions, neither diffusion in the intercrystal

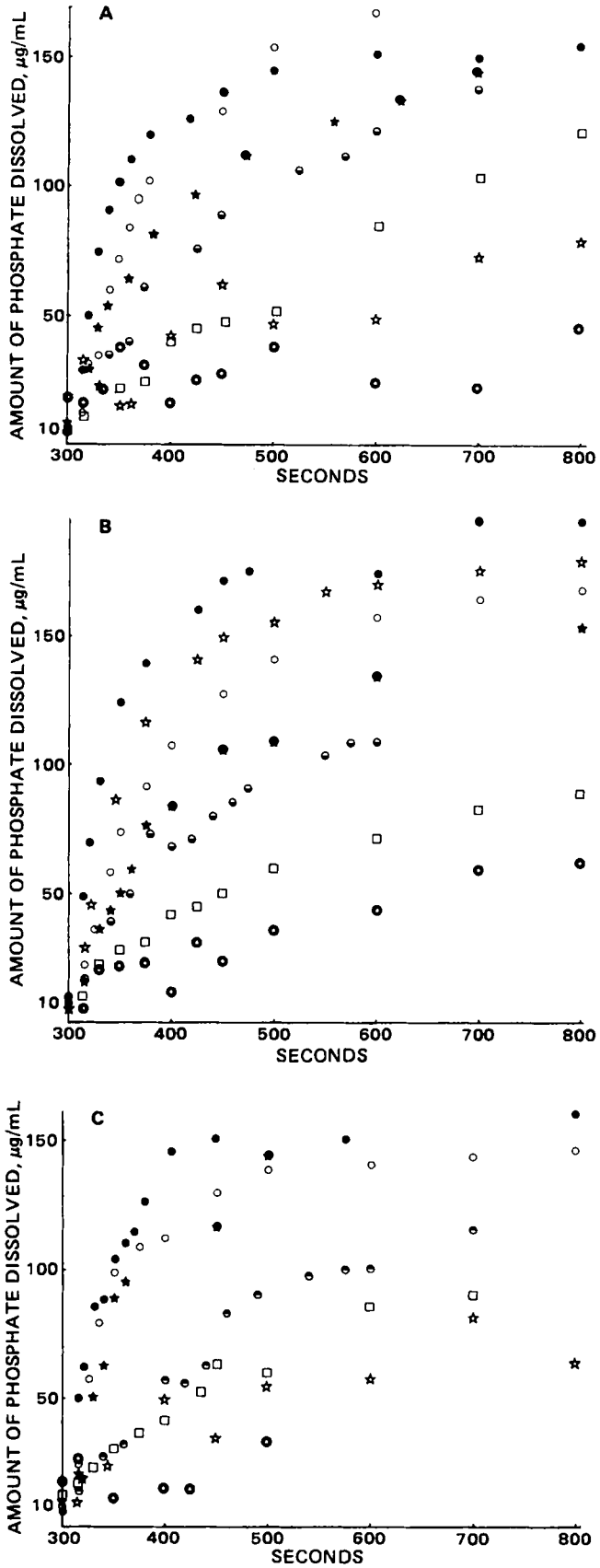

Figure 6—*Dissolution of sonicated hydroxyapatite powders NBS-P (A), NBS-B (B), and UM-T (C) in partially saturated solutions, pH 4.5, 0.1 M acetate buffer, 0.5 μ at 600 rpm. Key: (●) Ca = P = 0; (○) Ca = P = 0.881 mM; (★) Ca = P = 1.762 mM; (◓, ◒) Ca = P = 2.643 mM; (□) Ca = P = 3.524 mM; (☆) Ca = P = 4.405 mM for A and C, Ca = P = 0.4405 mM for B; (◐) Ca = P = 5.286 mM.*

Table III—Comparison of the Site 2 Parameters from the Present Powder Studies with Those Determined Previously from the Disk Experiments

Parameter Values	Powder Experiments	Disk Experiments
pK_{HAP} for Site 2	128 ± 1	128[a]
First-Order Rate Constant (k) for Site 2	40–60 s^{-1}	40 s^{-1} [b]

[a] Based on $D = 1 \times 10^{-5}$ cm^2/s. [b] Based on $\epsilon/\tau = 0.2$.

spaces nor bulk diffusion away from the aggregate should contribute significantly to the dissolution rates. Equation 9 reduces to the following equation under these conditions:

$$J = \frac{4}{3}\pi a^3 k_c C_s \qquad \text{(Eq. 10)}$$

and, by inspection, the appropriate limiting equation for the two-site model becomes:

$$J = \frac{4}{3}\pi a^3 (k_{c1} C_{s1} + k_{c2} C_{s2}) \qquad \text{(Eq. 11)}$$

For an experiment in which M is the total mass of hydroxyapatite crystals in suspension, since:

$$M = \frac{4}{3}\pi \rho \Sigma n_i a_i^3 \qquad \text{(Eq. 12)}$$

where n_i is the number of the crystal aggregates of radius a_i, and ρ_i is the average density of the aggregates, we have:

$$G = \frac{M}{\rho}(k_{c1} C_{s1} + k_{c2} C_{s2}) \qquad \text{(Eq. 13)}$$

where G is the total dissolution rate. Actually, Eq. 11 applies when the bulk solution conditions are unsaturated with respect to both sites and:

$$G = \frac{M}{\rho} k_1 C_{s1} \qquad \text{(Eq. 14)}$$

when the bulk solution conditions are unsaturated only with respect to site 1.

EXPERIMENTAL

Materials—*Hydroxyapatite*—Four different preparations of synthetic hydroxyapatite were used in this study; two were supplied by the National Bureau of Standards. NBS-P was made according to a method described by Avnimelech *et al.* (14)[1]. Pure phosphoric acid was slowly added to a carbon dioxide-free calcium oxide solution at 100°C or heated at reflux. The resulting precipitate was digested for 1 week at 100°C. The residue was washed with double-distilled water at 100°C, the precipitate was removed by filtration, rinsed with acetone, and then dried at 105°C. This was the original sample used in the pellet studies (3) from which the two-site model was developed. The calcium–phosphate ratio was 1.714; the surface area was 22.5 m^2/g.

The other NBS sample (NBS-B) was prepared[2] using the method developed by Mattamal[3]. In this preparation, dicalcium phosphate dihydrate was treated with calcium acetate in a pH 5.0 acetic acid solution. The mixture was heated at reflux for ~3 weeks with stirring in a nitrogen atmosphere. The solid was removed by filtration, washed with double-distilled water, and dried at ~150°C overnight. The calcium–phosphate ratio was 1.644.

The third hydroxyapatite sample (UM-T) was prepared in-house based on a method which is a slight modification of the one described by Avnimelech *et al.* (14). The digestion time was extended to 6 weeks. The calcium–phosphate ratio was 1.644.

Sample RZL was also supplied to us[4]. The detailed method is not known, but it was prepared by a precipitation procedure at 100°C.

All the preparations were of relatively high purity with good stoichiometric calcium–phosphate ratios. The NBS-P, NBS-B, and UM-T samples were studied extensively, while limited studies were conducted with the RZL sample.

Solutions—Calculated amounts of acetic acid and sodium acetate stock solutions were used to make buffer solutions of pH 4.50. Partially saturated buffer solutions were made by adding predetermined amounts of calcium chloride or sodium dihydrogen phosphate to the buffer. The pK_{HAP} values of these solutions were calculated with the computer program developed by Fox *et al.* (15). Sodium chloride was added to all buffer solutions to maintain an ionic strength of 0.5. The pH values of the solutions were measured to an accuracy of ±0.01 using a digital pH meter[5]. All chemicals were of reagent grade. The compositions of all dissolution media are listed in Table II.

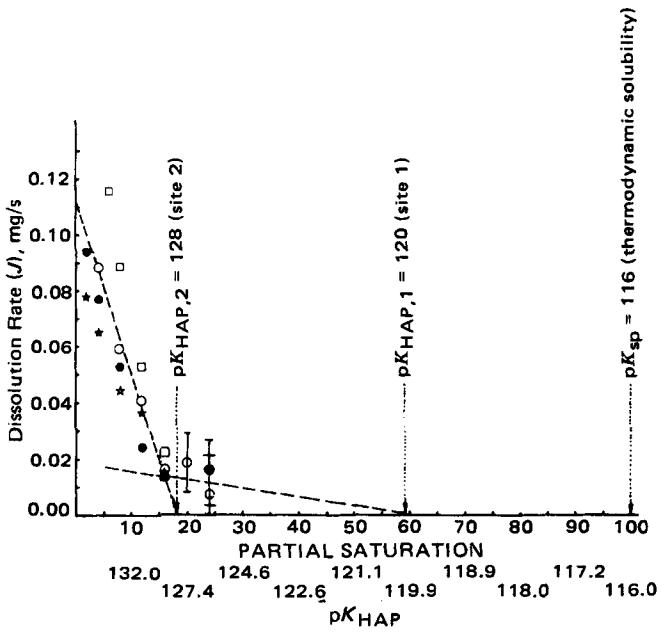

Figure 7—*Initial dissolution rate of hydroxyapatite as a function of the solution ion activity product, K_{HAP}. Key: (●) NBS-P; (☆) NBS-B; (○) UM-T; (□) RZL.*

Preparation of Suspensions—Clumps of hydroxyapatite were broken down by light grinding until no visible lumps were present. Exactly 10 mg of this powder was suspended in 12.5 mL of double-distilled water in a 50-mL water-jacketed (30°C) reaction vessel. This suspension was magnetically stirred for ~20 s at 600 or 400 rpm before being sonicated[6] for 30 s to produce a milky suspension. In cases where the powder was not preground, sonication was carried out for longer periods, usually ~60 s. After sonication, stirring was resumed, and 12.5 mL of dissolution medium (double concentration) was added to the suspension. Addition and mixing was completed in 1–2 s, and the pH at that point was recorded to be 4.50 ± 0.01 (Fig. 3). Samples of 0.5 mL were withdrawn at predetermined times during the dissolution experiment and immediately passed through filter paper[7] (GSU) with a pore size of 0.22 μm. Sampling and filtering was completed within 4–6 s. The filtrate was analyzed for phosphate and/or calcium, and whenever both were analyzed, the dissolution was always congruent with respect to hydroxyapatite under the conditions of these experiments. For cases in which the suspension was not sonicated, the above procedure was followed except for the sonication step.

Analytical Methods—*Phosphate Concentration*—Phosphate concentrations were determined according to the method of Gee *et al.* (16). The phospho–ammonium molybdate complex formed was reduced by stannous chloride. The absorbance of the resulting color was determined at the end of 15 min at λ = 720 nm in a spectrophotometer[8].

Calcium Concentration—Calcium concentrations were determined according to an unpublished method[9]. A purified arsenazo III[10] solution was mixed with small amounts of glacial acetic acid, and the pH was adjusted to 3.8 with tetrabutylammonium hydroxide[10]. It was then diluted with distilled water to the desired concentration. When a solution containing calcium was mixed with this reagent, a pink color was obtained, and the solution absorbance was determined at λ = 650 nm in a spectrophotometer[6].

[1] Provided by A. P. Brunetti, National Bureau of Standards.
[2] G. J. Mattamal, National Bureau of Standards, personal communication.
[3] Provided by R. Z. Legeros, New York University Dental Center.
[5] Altex Model 4500.
[6] Ultrasonic General Model AK500, Acoustica, Los Angeles, Calif.
[7] Millipore Corp.
[8] Beckman Model 25.
[9] Chow *et al.*, personal communication.
[10] Aldrich Chemical Co., Milwaukee, Wis.

RESULTS AND DISCUSSION

Preliminary Results and Assessment of the Method—Simple visual comparison of the dispersed hydroxyapatite aggregate particles, with 1.17-mm diameter polystyrene latex particles using an ordinary light microscope, showed that most of the hydroxyapatite crystals or the crystal aggregates in aqueous suspension after sonication were ≤ 1 μm in diameter. The unsonicated hydroxyapatite aggregates were found to be in the range of $< \sim 1$–100 μm with ~50% in the 15- to 50-μm range.

Figure 4A shows typical results demonstrating the effect of ultrasonic irradiation on the dissolution rate behavior of sample UM-T under sink conditions and under a moderately low partial saturation condition (Ca = P = 1.76 mM). The effect of sonication on the initial dissolution rate under these considerations is to increase the dissolution rate by a factor of $\leq \sim 2$. This is consistent with the predictions of the results in Fig. 2 with $k_c \simeq 40\ s^{-1}$, *i.e.*, a mass-mean diameter of 10–20 μm for the aggregate would be expected to show about a twofold reduction in rate over the 1-μm particles according to the theoretical calculations. Figure 4B shows that the sonication effect is absent or at least much smaller when the level of partial saturation is higher (Ca = P = 3.5 mM). From the results to be discussed later it may be interpreted that site 2 contributes little to the dissolution rate when Ca = P = 3.5 mM (which corresponds to a solution pK_{HAP} value of ~128) and only site 1 is primarily active under these conditions. According to the theoretical calculations (Fig. 2), sonication would be expected to have much less effect for this situation (*i.e.*, when k_c is $\sim 0.3\ s^{-1}$).

Figure 5 shows that changing the rotation speed from 400 to 600 rpm has a small or negligible effect even without sonication under sink conditions. These results suggest that even when moderately large aggregates are present, boundary layer diffusional resistance is small compared with both diffusional resistance in the intercrystal spaces (pores) of large aggregates and surface kinetic factors. This is as predicted by calculations with Eq. 7 using parameter values discussed earlier.

Initial Dissolution Rates at a Calcium–Phosphate Ratio of 1.0—The procedure implemented for most of the experiments involved 10 mg of hydroxyapatite in 25 mL of solution agitated at a stirring rate of 600 rpm. Figure 6A–C shows all of the raw rate data for hydroxyapatite samples NBS-P, NBS-B, and UM-T, respectively, with Ca/P = 1.0.

Initial slopes were estimated from the data in Fig. 6. With all three sets of data, reasonably linear initial regions could be determined up to partial saturations of Ca = P = 3.5 mM. When duplicate experiments were conducted, the reproducibility of the initial slopes were on the order of 10% except near sink conditions (Ca = P = 0), where the uncertainties were greater because of the extremely rapid rates. At the higher partial saturations, the data points scattered greatly and meaningful initial slopes could not be found. This was true with all of the hydroxyapatite preparations. This scatter in the data is believed to be not altogether related to the poorer precision of the phosphate and calcium analyses arising from high backgrounds. Some of the scatter is believed to be associated with the unusual dissolution rate behavior previously noted (17) for hydroxyapatite at moderate-to-high partial saturations and characterized by cyclical or oscillatory dissolution patterns.

The initial dissolution rates calculated from the data in Fig. 6 are presented in Fig. 7; results obtained with the fourth hydroxyapatite sample (RZL) are also presented. This figure shows the relationship of the rapid dissolution kinetics (predominantly site 2) region to the thermodynamic K_{sp} (14). Also indicated in Fig. 7 is the region where site 1 dissolution only was expected. Unfortunately, the larger variability in dissolution behavior in this region ($120 < pK_{HAP} < 128$) precludes making any quantitative judgments for the behavior in this region with this data.

The present focus is on how good the agreement is between the dissolution rate behavior in the site 2 region ($\infty > pK_{HAP} > 128$) and the findings and predictions of the earlier pellet studies (3). Table III summarizes both the best $K_{HAP,2}$ and the k_{c2} values estimated from the present work and the previous dissolution studies, and it is seen that the agreement is remarkably good. It should also be noted that except for the values obtained under sink conditions (*i.e.*, Ca = P = 0) the first-order assumption is obeyed rather well in the partial saturation region up to 16%, *i.e.*, the plots for all experiments are well approximated by straight lines going through the abscissa at 16–18% partial saturation (or $pK_{HAP} = 128 \pm 1$). It may be said, therefore, that not only are the parameter values for site 2 in good agreement, but the first-order approximation also seems to represent the facts rather satisfactorily.

Initial Dissolution Rates with a Calcium–Phosphate Ratio ≠ 1.0—The results of additional experiments conducted for Ca/P < 1.0 and Ca/P > 1.0 are presented for the UM-T sample in Fig. 8. Initial slopes

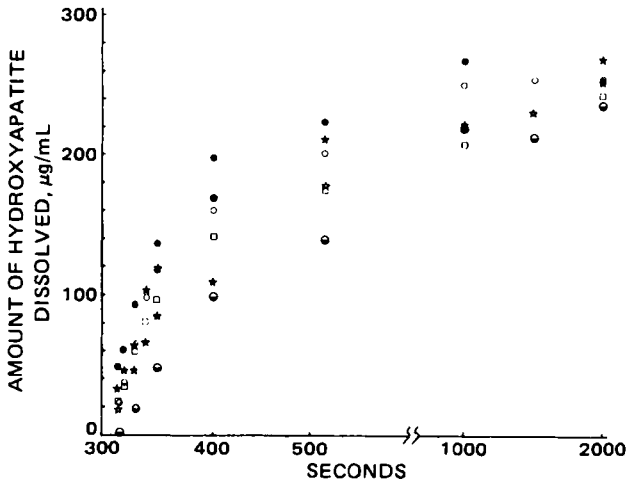

Figure 8—*Dissolution of sonicated hydroxyapatite powder (UM-T) in dissolution media with a Ca/P ratio <1 or a Ca/P ratio >1. Key: (●) Ca = 0.881 mM, P = 1.881 mM; (★) Ca = 0.881 mM, P = 3.881 mM; (□) Ca = 0.881 mM, P = 5.881 mM; (○) Ca = 1.881 mM, P = 0.881 mM; (☆) Ca = 3.881 mM, P = 0.881 mM; (◒) Ca = 5.881 mM, P = 0.881 mM.*

estimated from these data are plotted in Fig. 9 and compared with the theoretical line ($pK_{HAP} = 127.3$ and $k_2 = 36\ s^{-1}$).

The reasonably good agreement between the experimental results and theory further substantiates the conclusions presented in the previous section. These results at Ca/P ≠ 1.0, however, add an important new dimension. Because these experiments are over a 40-fold range in the Ca/P ratio, the good agreement between the experimental results and the theory strongly suggests that the form of the C_{s2} expression is essentially correct, *i.e.*, the apparent solubility (C_{s2}) in Eq. 3 indeed seems to be definable by the ion activity product expression, $K_{HAP} = a^{10}_{Ca^{2+}}\ a^{6}_{PO_4^{3-}}\ a^{2}_{OH^-}$ ($\simeq 1 \times 10^{-128}$), which is not a true solubility product, but defines a threshold below which dissolution occurs at an appreciable rate.

Relationship of the Present Powder Hydroxyapatite Studies to the Work of Others—Smith *et al.* (18) reported studies on the kinetics of the acid dissolution of hydroxyapatite powder using a pH-stat technique. The dissolution rates were determined by following the amount of acid added with time. Various mathematical expressions were compared with the data. These included first-, second-, third-order, and simultaneous (two parallel reactions) first-order equations. These investigators found that, while all of the equations fit the experimental data over varying periods of time, none would fit all the data in every case under all conditions. An expression which did fit the data more comprehensively was:

$$-\frac{dw}{dt} = k(w_\infty - w_n)\exp(-bw) \qquad \text{(Eq. 15)}$$

where w is the acid added at time t, w_∞ is the amount of acid necessary to dissolve the calcium and phosphate at saturation, and k and b are constants. Equation 15, which is referred to as the restriction model, is able to account for the fact that the decline in the dissolution rate for hydroxyapatite is much faster than that based on a single exponential (*i.e.*, a simple first-order law). These investigators, furthermore, ruled out the possibility that this rapid decline is due to an initial dissolution of small particles with a large specific surface because repeat experiments with the same sample yielded titration curves with similar shapes.

These findings by Smith *et al.* (18) are totally consistent with the results of our present investigations, and the data in Figs. 6 and 8. Our analysis (Figs. 7 and 9) was limited to initial ($t = 0$) conditions only in order that the dissolution rates under different solution conditions could be compared for the same state of the crystalline powder. It may be noted, however, that the shapes of most of our raw data curves are biphasic, *i.e.*, they are characterized by an initial fast-dissolving phase followed by a more slowly dissolving region. We have associated the fast-dissolving phase with that dominated by dissolution from site 2, for which the phenomenology is completely describable by the second term on the right-hand side of Eq. 3.

Another study on the dissolution rate behavior of hydroxyapatite crystals in suspension was reported recently by Christoffersen (19). All of the experiments in this study were conducted near pH 7.0 and, as in the experiments of Smith *et al.* (18), a pH-stat technique was used.

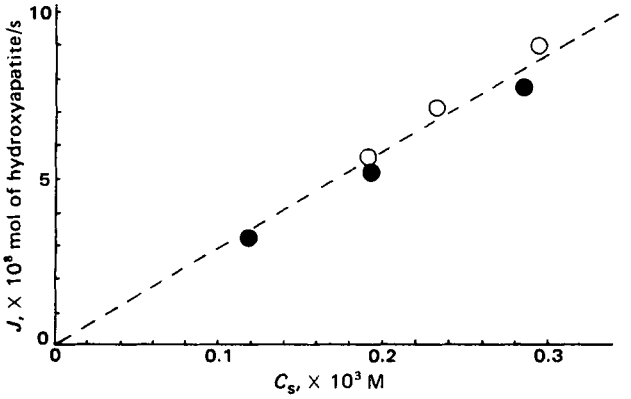

Figure 9—*A further test of the two-site model (Ca/P ≠ 1.0). Key: (○) Ca = 0.881 mM, P = 1.881, 3.881, and 5.881 mM; (●) P = 0.881 mM, Ca = 1.881, 3.881, and 5.881 mM; (---) theoretical* C_s *based on* pK_{HAP} = *127.3,* k = *36* s^{-1}.

Christoffersen analyzed the dissolution rate data entirely on the basis of a simple two-dimensional nucleation theory in two regimes, the mononuclear and the polynuclear regions.

Although the nucleation theory leads to explicit expressions for the rate as a function of solution conditions and although reasonably good consistency of the data with the model was obtained, it is difficult for a number of reasons to assess the applicability of the two-dimensional nucleation theory in hydroxyapatite dissolution kinetics. There is the usual objection (20) to treating the energetics of small particles as the sum of the bulk phase energetics and the surface energetics or the edge energetics (as in the present case). For hydroxyapatite, this problem requires special examination because one is dealing with the question of the meaning of a nucleus whose edge length (a) is less than one-half the dimension of the smallest of the three unit cell axes (*viz.*, 9.42, 9.42, and 6.88 Å). The theoretical treatment assumes the nuclei energetics to be the sum of bulk energetics and edge energetics when there is less than a representative unit cell present in the nucleus (at least, in one direction). Although it might be argued that the "averaging" law may apply, it would be a poor approximation in the case of hydroxyapatite as the calcium, phosphate, and hydroxide ion densities (both individually and collectively) are not uniform as one proceeds through the unit cell of hydroxyapatite (21, 22). This also begs the question of hydration at the surface, which may vary with the varying surface. Consequently, where smooth surfaces are stable (23), different lamellae in a unit cell could have different nucleation requirements. This may, however, be a basis for alternatively arguing that the relevant critical nucleus applies to that lamella in the unit cell associated with the highest free energy of activation which may not necessarily be the average for the unit cell.

Another difficulty in attempting to evaluate the applicability of the nucleation theory to hydroxyapatite dissolution kinetics is the lack of an independent experimental check. In the case of the three-dimensional nucleation of vapor-to-liquid, a direct independent test is possible (24, 25) because surface tensions may be measured directly and accurately. Unfortunately, in two-dimensional crystal growth or dissolution, the edge free energy (σ) cannot be determined experimentally. Consequently, σ becomes functionally an adjustable parameter in the examination of the theory with experimental dissolution rate data. It would be of interest, however, to test the hypothesis that, even though σ is ill defined, it may be relatively constant over a wide range of experimental conditions. More data than what is reported in the study of Christoffersen, however, would be needed to examine this possibility.

Finally, a third problem in comparing experimental data with the simple two-dimensional nucleation theory is that the theory, as presented by Christoffersen, assumes that the "averaging" law applies to all sites of dissolution and, therefore, that the parameters defining the dimensions and the energetics for the nuclei are the same for all sites. A recent study (13) in our laboratory has shown that different morphologies for hydroxyapatite crystals are found depending on the degree of solution unsaturation during dissolution. When the solution was partially saturated (acetate buffer, pH 4.5), a large number of holes were found within the hydroxyapatite crystals; for sink conditions (*i.e.*, highly unsaturated solutions), no such holes were found for the same extent of hydroxyapatite dissolution. These data suggest that prism plane and/or basal plane dissolution (*i.e.*, the thinning of crystals or the shortening of crystals) require higher levels of unsaturation than dissolution, leading to the formation of holes. Clearly, more studies on this point are needed, but the evidence to date suggests that a single-site model would be inadequate to describe hydroxyapatite dissolution kinetics.

APPENDIX: Calculation of C_{s1} and C_{s2} from $K_{HAP,1}$ and $K_{HAP,2}$

For i = 1 or 2, C_{si} is defined as the number of moles of hydroxyapatite that will be dissolved in the bulk solution, if the K_{sp} for hydroxyapatite were given by $K_{HAP,i}$. Thus, the calculation of C_s from K_{HAP} is done in exactly the same manner that hydroxyapatite solubility in a given solution is calculated.

The heart of the method is a technique for the merical solution of the calcium phosphate solution equilibrium problem; that is, the calculation of concentrations of all species when given total quantities of each element in a liter of solution (*e.g.*, total calcium, total phosphate, total buffer, total proton, total hydroxyl, *etc.*). This equilibrium problem can be stated mathematically as a nonlinear system of algebraic equations (two equations with two unknowns for the hydroxyapatite system). Our experience over the years with a number of numerical techniques indicates none more suitable than the Levenberg–Marquardt technique as implemented by Powell (26), and such problems are typically solved in 2–3 ms on a large mainframe computer.

Given an efficient technique for solving the equilibrium problem, the calculation of C_s can be done as follows. A trial guess, say x, is made for C_s. The total quantities per liter of each element are calculated for a bulk solution to which x mol of hydroxyapatite has been added. The solution equilibrium problem is solved for such a solution, and the ion activity product (IAP = $a^{10}_{Ca^{+2}}\, a^{6}_{PO_4^{-3}}\, a^{2}_{OH}$) is calculated and compared with the K_{HAP}. This procedure is repeated for different values of x until the calculated IAP is equal to K_{HAP}. Mathematically, we are trying to find the zero of a function of a single variable, and we use the so-called Pegasus algorithum as described by Jarratt (27), a technique which is guaranteed to converge and does so rapidly in practice.

REFERENCES

(1) W. E. Brown, *J. Dent. Res., Suppl.*, **53,** 204 (1974).

(2) W. I. Higuchi, *J. Dent. Res.*, **53,** 236 (1974).

(3) J. L. Fox, W. I. Higuchi, M. B. Fawzi, and M. S. Wu, *J. Colloid Interface Sci.*, **67,** 312 (1978).

(4) J. A. Gray, *J. Dent. Res.*, **41,** 633 (1962).

(5) A. Stralfors, *R. Roy. Schools Stockholm and Umei*, **Series 2:1,** 52 (1958).

(6) W. I. Higuchi, J. A. Gray, J. J. Hefferren, and P. R. Patel, *J. Dent. Res.*, **44,** 330 (1965).

(7) W. I. Higuchi, P. R. Patel, and J. J. Hefferren, *J. Pharm. Sci.*, **54,** 587 (1965).

(8) M. S. Wu, W. I. Higuchi, J. L. Fox, and M. Friedman, *J. Dent. Res.*, **55,** 496 (1976).

(9) W. I. Higuchi, N. A. Mir, P. R. Patel, J. W. Becker, and J. J. Hefferren, *J. Dent. Res.*, **48,** 396 (1969).

(10) E. C. Moreno, T. M. Gregory, and W. E. Brown, *J. Res. Nat. Bur. Stand. Sec. A*, **72A,** 773 (1965).

(11) V. G. Levich, "Physicochemical Hydrodynamics," Prentice Hall, Englewood Cliffs, N.J., 1962, p. 71.

(12) M. B. Fawzi, J. L. Fox, M. G. Dedhiya, W. I. Higuchi, and J. J. Hefferren, *J. Colloid Interface Sci.*, **67,** 304 (1978).

(13) E. N. Griffith, A. Katdare, J. L. Fox, and W. I. Higuchi, *J. Colloid Interface Sci.*, **67,** 331 (1978).

(14) Y. Avnimelech, E. C. Moreno, and W. E. Brown, *J. Res. Nat. Bur. Stand. Sec. A*, **77A,** 149 (1973).

(15) J. L. Fox, Ph.D. Thesis, The University of Michigan (1977).

(16) A. Gee, L. P. Domingues, and V. R. Deitz, *Anal. Chem.*, **26,** 1487 (1954).

(17) M. B. Fawzi, T. Sonobe, W. I. Higuchi, and J. J. Hefferren, *J. Dent. Res.*, **56,** 394 (1977).

(18) A. N. Smith, A. M. Posner, and J. P. Quirk, *J. Colloid Interface Sci.*, **62,** 475 (1977).

(19) J. Christoffersen, *J. Cryst. Growth*, **49,** 29 (1980).

(20) H. Reiss, *Ind. Eng. Chem.*, **44,** 1284 (1952).

(21) M. I. Kay, R. A. Young, and A. S. Posner, *Nature (London)*, **204,** 1050 (1964).

(22) D. McConnell, "Apatite," Springer-Verlag, New York, N.Y., 1962, chap. 4.

(23) P. Bennema and G. H. Gilmer, in "Crystal Growth: An Introduction," P. Hartman, Ed., North-Holland, Amsterdam, 1973, p. 272.

(24) W. I. Higuchi and C. T. O'Konski, *J. Colloid Interface Sci.*, **15**, 14 (1960).

(25) G. M. Pound, L. A. Madonna, and C. M. Sciulli, "Proceedings of the Conference on Interfacial Phenomena and Nucleation," Vol. 1, p. 85 (1955). Office of Technical Services, U.S. Dept. of Commerce, U.S. Research and Development Command, Cambridge, Mass.

(26) M. J. D. Powell, in "Numerical Methods for Nonlinear Algebraic Equations," P. Rabinowitz, Ed., Gordon & Breach Science Publishers, London, 1970.

(27) P. Jarratt, in "Numerical Methods for Nonlinear Algebraic Equations," P. Rabinowitz, Ed., Gordon & Breach Science Publishers, London, 1970.

ACKNOWLEDGMENTS

This investigation was supported by NIDR Grant DE01830.

Ultrastructural Alterations in Macrophages after Phagocytosis of Acrylic Microspheres

PETER EDMAN *§, INGVAR SJÖHOLM *§x, and ULF BRUNK‡

Received June 15, 1982, from the * *Department of Pharmaceutical Biochemistry, Biomedicum, S-751 23 Uppsala, Sweden* and ‡ *Linköping University, Department of Pathology, University Hospital, S-581 85 Linköping, Sweden.* Accepted for publication December 8, 1982. § Present address: National Board of Health and Welfare, Department of Drugs, Division of Pharmacy, S-751 25 Uppsala, Sweden.

Abstract □ The effect of microparticles on the survival of cultured mouse peritoneal macrophages was investigated using doses of 0.01–0.1 mg of lyophilized particles/ml of medium and 5×10^5 cells, corresponding to ~4000–40,000 particles per cell. The lowest dose did not significantly change the survival time as compared with the controls, while ~75% of the cells were lost during the first 48 h on exposure to the highest dose. High doses of particles induce cellular damage. The morphology and stability of the lysosomal apparatus was followed with electron microscopy, acid phosphatase cytochemistry, and acridine orange uptake. Alteration of the lysosomal vacuome was characterized by a greatly enhanced rate of autophagocytosis, the formation of huge secondary lysosomes containing microparticles, and labilization of the vacuome with loss of acidity and a tendency to leak acid phosphatase into the cell sap.

Keyphrases □ Microspheres—polyacrylamide, phagocytosis by cultured mouse peritoneal macrophages, ultrastructural cellular alterations □ Macrophages, peritoneal—cultured from mice, effect of phagocytosis of microparticles, ultrastructural cellular alterations □ Phagocytosis—microparticles, by cultured mouse peritoneal macrophages, ultrastructural cellular alterations

Acrylic polymer microparticles have been introduced recently as carriers for enzymes and other macromolecules (1). When such particles are injected intravenously into mice and rats they are eliminated rapidly from the circulatory system, mainly by the fixed macrophages of the reticuloendothelial system (RES) (2), and accumulate intracellularly within the lysosomal vacuome of these cells (3). This lysosomotropic character of the particles has been utilized in an experimental animal model to effect an artificial storage disease (4).

When massive doses of particles (160 mg/kg of body weight) were injected intravenously into mice, some adverse reactions occurred (3). The first general reaction was a megaly of the liver and spleen. This phenomenon, detected by light and electron microscopy, was due to initial cell damage with mitochondrial swelling, rupture of the cristae, and cellular edema. This was later followed by cellular necrosis and invasion of inflammatory cells (3). The megaly was thus due to both cellular swelling and accumulation of inflammatory cells in the affected organs. The microscopic study also showed that the megaly was reversible and that the normal anatomical structure of the tissues was restored in ~4 weeks. The effects detected are dose dependent and are not seen in mice after injection of moderate doses (40 mg/kg) (3).

The ultrastructural changes detected in the liver, spleen, and bone marrow after injection of large amounts of acrylic microspheres are of general interest, as they can be expected to occur on injection of any small-sized particles. Even injection of relatively rapidly degradable liposomes give rise to ultrastructural changes in the liver and spleen (5).

The relationship between the dose of particles and the cellular effect is not conveniently studied in animal models, where the relationship between particles and affected cells cannot be quantitatively controlled. It is therefore, necessary to develop a method in which the number of parti-

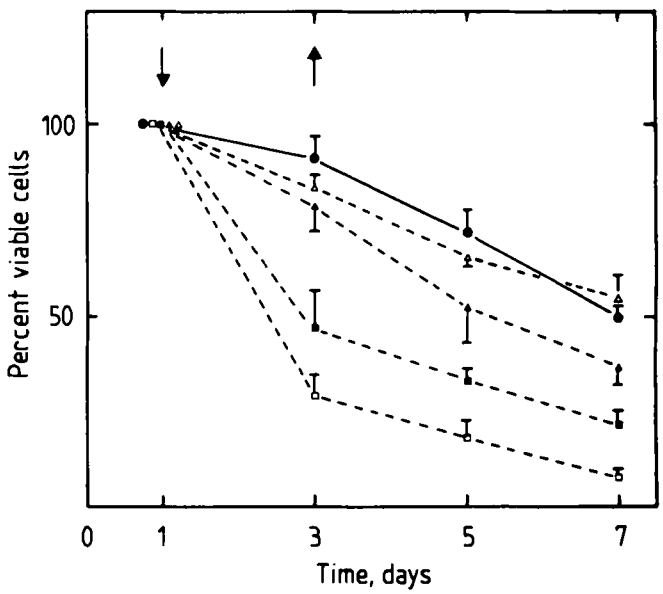

Figure 1—*Survival rates of cultured mouse peritoneal macrophages after exposure to microparticles at dose levels of 0.01 (△), 0.02 (▲), 0.05 (■), and 0.1 mg/mL (□). The normal survival rate (●) was followed during a period of 7 d. The arrows indicate the time of exposure to microparticles. Each point represents the mean ±SD from four experiments.*

0022-3549/84/0200-0153$01.00/0
© 1984, American Pharmaceutical Association

(24) W. I. Higuchi and C. T. O'Konski, *J. Colloid Interface Sci.*, **15**, 14 (1960).

(25) G. M. Pound, L. A. Madonna, and C. M. Sciulli, "Proceedings of the Conference on Interfacial Phenomena and Nucleation," Vol. 1, p. 85 (1955). Office of Technical Services, U.S. Dept. of Commerce, U.S. Research and Development Command, Cambridge, Mass.

(26) M. J. D. Powell, in "Numerical Methods for Nonlinear Algebraic Equations," P. Rabinowitz, Ed., Gordon & Breach Science Publishers, London, 1970.

(27) P. Jarratt, in "Numerical Methods for Nonlinear Algebraic Equations," P. Rabinowitz, Ed., Gordon & Breach Science Publishers, London, 1970.

ACKNOWLEDGMENTS

This investigation was supported by NIDR Grant DE01830.

Ultrastructural Alterations in Macrophages after Phagocytosis of Acrylic Microspheres

PETER EDMAN *§, INGVAR SJÖHOLM *§x, and ULF BRUNK‡

Received June 15, 1982, from the * *Department of Pharmaceutical Biochemistry, Biomedicum, S-751 23 Uppsala, Sweden* and ‡ *Linköping University, Department of Pathology, University Hospital, S-581 85 Linköping, Sweden.* Accepted for publication December 8, 1982. § Present address: National Board of Health and Welfare, Department of Drugs, Division of Pharmacy, S-751 25 Uppsala, Sweden.

Abstract □ The effect of microparticles on the survival of cultured mouse peritoneal macrophages was investigated using doses of 0.01–0.1 mg of lyophilized particles/ml of medium and 5×10^5 cells, corresponding to ~4000–40,000 particles per cell. The lowest dose did not significantly change the survival time as compared with the controls, while ~75% of the cells were lost during the first 48 h on exposure to the highest dose. High doses of particles induce cellular damage. The morphology and stability of the lysosomal apparatus was followed with electron microscopy, acid phosphatase cytochemistry, and acridine orange uptake. Alteration of the lysosomal vacuome was characterized by a greatly enhanced rate of autophagocytosis, the formation of huge secondary lysosomes containing microparticles, and labilization of the vacuome with loss of acidity and a tendency to leak acid phosphatase into the cell sap.

Keyphrases □ Microspheres—polyacrylamide, phagocytosis by cultured mouse peritoneal macrophages, ultrastructural cellular alterations □ Macrophages, peritoneal—cultured from mice, effect of phagocytosis of microparticles, ultrastructural cellular alterations □ Phagocytosis—microparticles, by cultured mouse peritoneal macrophages, ultrastructural cellular alterations

Acrylic polymer microparticles have been introduced recently as carriers for enzymes and other macromolecules (1). When such particles are injected intravenously into mice and rats they are eliminated rapidly from the circulatory system, mainly by the fixed macrophages of the reticuloendothelial system (RES) (2), and accumulate intracellularly within the lysosomal vacuome of these cells (3). This lysosomotropic character of the particles has been utilized in an experimental animal model to effect an artificial storage disease (4).

When massive doses of particles (160 mg/kg of body weight) were injected intravenously into mice, some adverse reactions occurred (3). The first general reaction was a megaly of the liver and spleen. This phenomenon, detected by light and electron microscopy, was due to initial cell damage with mitochondrial swelling, rupture of the cristae, and cellular edema. This was later followed by cellular necrosis and invasion of inflammatory cells (3). The megaly was thus due to both cellular swelling and accumulation of inflammatory cells in the affected organs. The microscopic study also showed that the megaly was reversible and that the normal anatomical structure of the tissues was restored in ~4 weeks. The effects detected are dose dependent and are not seen in mice after injection of moderate doses (40 mg/kg) (3).

The ultrastructural changes detected in the liver, spleen, and bone marrow after injection of large amounts of acrylic microspheres are of general interest, as they can be expected to occur on injection of any small-sized particles. Even injection of relatively rapidly degradable liposomes give rise to ultrastructural changes in the liver and spleen (5).

The relationship between the dose of particles and the cellular effect is not conveniently studied in animal models, where the relationship between particles and affected cells cannot be quantitatively controlled. It is therefore, necessary to develop a method in which the number of parti-

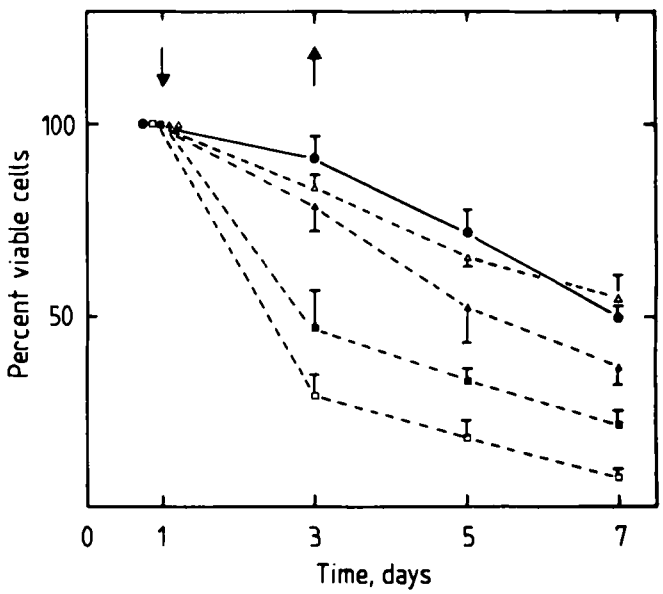

Figure 1—*Survival rates of cultured mouse peritoneal macrophages after exposure to microparticles at dose levels of 0.01 (△), 0.02 (▲), 0.05 (■), and 0.1 mg/mL (□). The normal survival rate (●) was followed during a period of 7 d. The arrows indicate the time of exposure to microparticles. Each point represents the mean ±SD from four experiments.*

0022-3549/84/0200-0153$01.00/0
© 1984, American Pharmaceutical Association

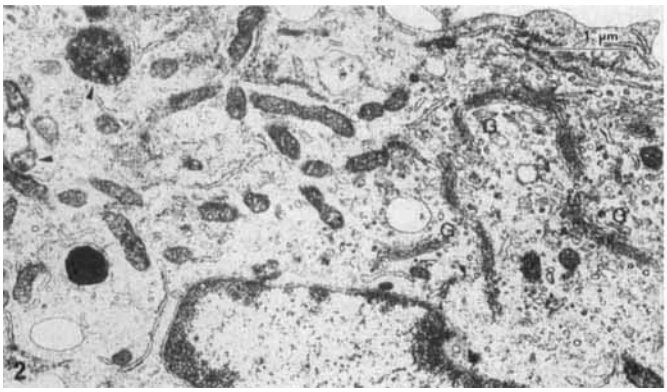

Figure 2—*Normal mouse macrophage cultured* in vitro, *showing elongated mitochrondria and secondary lysosomes (arrowheads). G denotes the Golgi apparatus.*

cles and phagocytic cells can be easily determined. The present paper describes a system in which mouse peritoneal macrophages in culture have been used to semiquantitatively study the effects of particles on cellular ultrastructure. The cellular alterations in the macrophages after exposure to particles were further correlated with biochemical and cytochemical changes in the cells.

EXPERIMENTAL

Acrylamide[1], *N,N'*-methylenebisacrylamide[1], cationized ferritin[2], *N,N,N',N'*-tetramethylethylenediamine[2], and other chemicals were of analytical grade. Pathogen-free male mice[3], weighing 20 g, were used throughout.

Preparation of Microparticles—Microparticles with immobilized cationized ferritin were prepared using a reported method (1, 3). The cationized ferritin (104 mg), acrylamide (0.3 g), and *N,N'*-methylenebisacrylamide (0.1 g) were dissolved in 5 mL of 0.005 M sodium phosphate buffer, pH 7.4, while maintaining a nitrogen atmosphere. The catalyst, ammonium peroxodisulfate (100 µL of a 0.5-g/mL solution in water) was added, the solution was poured into 200 mL of toluene–chloroform (4:1) containing 0.5 g of a detergent[4], and the resulting mixture homogenized to produce an oil-in-water emulsion. The accelerator *N,N,N',N'*-tetramethylethylenediamine (1.0 mL) was added to the emulsion, and after a few minutes polymerization started. The suspension was magnetically stirred for 20 min, and the microparticles were isolated by centrifugation and washed several times with buffer. After the last washing the particles were suspended in sterile physiological saline supplemented with antibiotics. Using this method, the microparticles had diameters ranging from 0.3–0.5 µm.

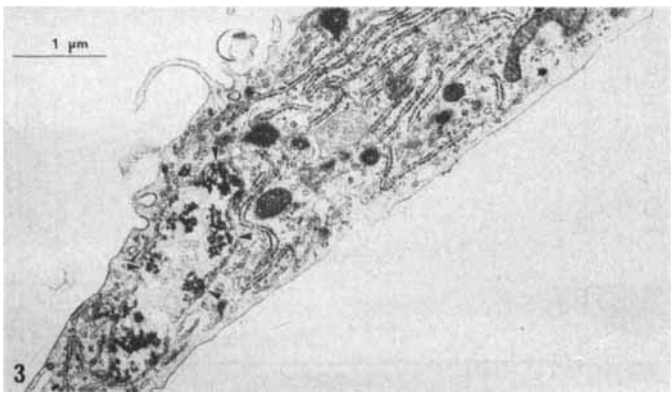

Figure 3—*Macrophage 72 h after exposure to ferritin-labeled microparticles (0.1 mg/mL of medium) showing a large vacuole containing ferritin-labeled particles (arrowheads).*

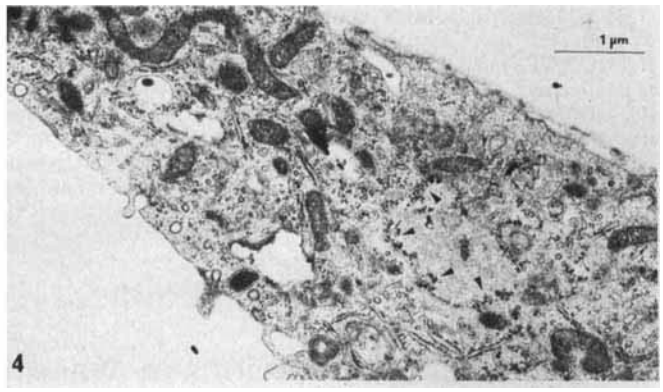

Figure 4—*Macrophage 72 h after exposure to ferritin-labeled microparticles (0.1 mg/mL). Note the localization of ferritin particles to the periphery of a large secondary lysosome (arrowheads).*

Preparation of Peritoneal Macrophage Cultures—Mouse peritoneal macrophages were collected by washing the unstimulated peritoneum of adult male mice with 3–4 mL of warm (37°C) phosphate-buffered saline, as described previously (3). The peritoneal exudate cells were suspended in 10 mL of cold (4°C) phosphate-buffered saline and centrifuged at 180× *g* for 10 min. The pellet was resuspended in a nutrient medium[5] (6) containing 15 mM 4-(2-hydroxyethyl)-1-piperazineethane sulfonic acid, pH 7.4. The medium was supplemented with penicillin G (100 U/mL), streptomycin (10 µg/mL), and 20% fetal calf serum. The cells were plated into 35-mm plastic dishes[6] at a concentration of 5×10^5 cells per dish and cultured at 37°C in air (85% relative humidity) containing 5% CO_2. After incubation for 2 h at 37°C, nonadherent cells were removed by washing with complete culture medium and fresh medium was added. The cultures were then incubated for 24 h. After that time, the medium was again changed and microparticles were added. During the ensuing cultivation period the medium was changed every 48 h.

Macrophage cultures were exposed to 0.01–0.1 mg/mL of microparticles containing ferritin as a marker. The cells were exposed to these particles for 24 or 48 h. To follow the number of viable and stretched macrophages in the dishes during the cultivation period, the mean number of cells counted in 10 different parts of the dishes was estimated every second day (before the medium was changed). With the aid of a stencil, 10 circles (diameter 3 mm) were drawn on the bottom of each dish in such a way as to ensure even distribution, but avoiding the exact center and the extreme periphery. In the center of each of these circles the cells were counted on a circular area of 0.24 mm^2 using an inverted phase-contrast microscope[7] and a 32× objective lens.

Preparation of Macrophages for Transmission Electron Microscopy—For morphological studies, the cells were fixed in 2% glutaraldehyde in 0.1 M cacodylate buffer with 0.1 M sucrose, pH 7.2 (total osmotic pressure 510 mOsm, effective osmotic pressure 300 mOsm) (7, 8) for 15 min at 37°C and for 45 min at 4°C. They were then rapidly rinsed in 0.15 M cacodylate buffer and postfixed in 1% OsO_4 in 0.15 M cacodylate buffer (pH 7.2) for 90 min at room temperature. The cells were then dehydrated *in situ* in an ethanol series, counter-stained *en block* for 12 h in 1% uranyl acetate in 50% ethanol, and embedded in plastic as described earlier (9). After polymerization, thin sections for transmission electron microscopy were cut with diamond knives, stained with lead citrate according to Reynolds (10), and examined at 60 kV in an electron microscope[8].

Demonstration of Acid Phosphatase—Coverslips with attached macrophages were fixed for 1 h at 0°C in 2% glutaraldehyde in 0.1 M sodium cacodylate–HCl buffer with 0.1 M sucrose (pH 7.2; total osmolality 510 mOsm, vehicle osmolality 300 mOsm), rinsed for 2 h in several changes of 0.1 M cacodylate buffer with 0.1 M sucrose (pH 7.2; 300 mOsm, 0°C), and incubated in a Gomori-type medium for acid phosphatase without the addition of sucrose or dimethyl sulfoxide to the incubating medium (7, 11, 12). The cells were incubated for 30, 45, and 60 min, and the secondary reaction product (lead phosphate) was converted to lead sulfide with a 1% solution of ammonium sulfide. After a light counterstaining with hematoxylin, the cells were dehydrated, cleared, and mounted in a synthetic resin.

[1] Eastman Kodak Co.
[2] Sigma Chemical Co.
[3] NMRI-mice; Anticimex, Stockholm, Sweden.
[4] Pluronics F-68 (polyoxyethylene-derived polyoxypropylene).
[5] F-10 medium; GIBCO BIO-CULT.
[6] Nunc. petri dishes.
[7] Leitz microscope.
[8] Philips 201.

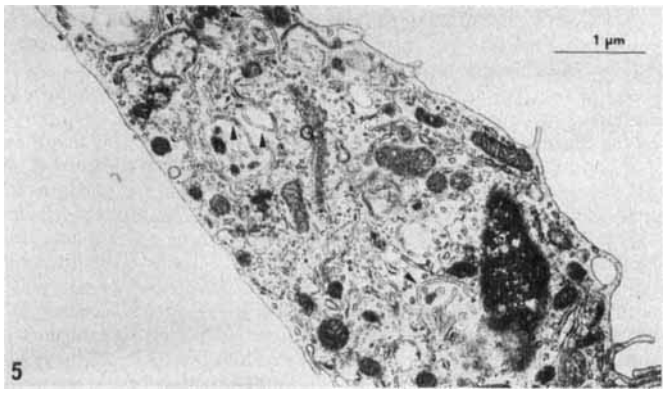

Figure 5—*Macrophage 72 h after exposure to microparticles. Note (arrowheads) the excessive formation of multilayer membranes wrapping around cytoplasmic areas (formation of autophagic vacuoles). G denotes a Golgi area.*

Visualization of the Lysosomal Vacuome with Acridine Orange—Coverslips with attached macrophages were cultured in plastic dishes[6]. Acridine orange was added to the medium to give a final concentration of 10 μg/mL. The cells were exposed to the dye for 10 min, whereupon the medium was changed twice. The cells were kept in fresh medium for 30 min in the dark in the incubation cabinet; the coverslips were then inverted on a drop of medium on an objective glass and rapidly examined under a fluorescent microscope[7] equipped with a high-pressure mercury lamp, a 5-mm BG-12 emission filter, and a 510-nm barrier filter. Acridine orange in lysosomes gives a bright red granular fluorescence, but in cells with a damaged lysosomal vacuome the nuclei and the cytoplasm show a diffuse green fluorescence with few remaining red granules. Micrographs were taken using black and white film[9].

RESULTS

Effect of Polyacrylamide Microspheres on the Survival of Cultured Mouse Peritoneal Macrophages—The effect of various doses (0.01, 0.02, 0.05, and 0.1 mg/mL of medium, total culture medium 2 mL) of polyacrylamide particles on the survival of macrophages is shown in Fig. 1. The cells were exposed to the particles over a 48-h period. As seen in the figure, the difference in survival between controls and macrophages treated with 0.01–0.02 mg/mL of microspheres is not significant, while concentrations of >0.02 mg/mL cause a rapid decline in survival rate. The significance of the difference was verified by variance analysis, $p < 0.01$. The highest dose (0.1 mg/mL) initiates a rapid decline in the number of viable and stretched macrophages. After an exposure time of 48 h, only ~30% of the initial cells remained, while the controls showed 90–100% viability.

Transmission Electron Microscopy—The control macrophages showed a normal ultrastructural appearance with extensive surface projections, many of which folded back on the plasma membrane under formation of macropinocytotic vacuoles. The nuclei were bean shaped with a euchromatic pattern and closely localized to them were several well-developed Golgi areas. The mitochondria were elonged, the endoplasmic net was regular, and the cells contained an abundance of secondary lysosomes with a moderate electron-dense, irregular matrix without any ferritin-like structures. Many of the lysosomes were large, and liquid droplets were observed (Fig. 2).

Following ingestion of ferritin-labeled microparticles, most secondary lysosomes were moderately enlarged and showed accumulations of ferritin particles in clusters (Fig. 3). The ferritin particles were usually localized near the periphery of the secondary lysosomes and sometimes formed a rim along the whole circumference (Fig. 4). In the cells exposed to acrylic microspheres there was a greatly enhanced rate of autophagocytosis with many flattened saccules wrapping around cellular structures during formation of autophagosomes (Fig. 5.)

Acid Phosphatase (Gomori Staining)—Control cells showed a distinct granular reaction product pattern with almost no diffuse staining and no nuclear impregnation. The cells had the same appearance 48 and 72 h after initiating the cultures.

Cells exposed to spheres in various concentrations (0.01, 0.05, and 0.1 mg/mL of cell medium) deviated from the control cells by a reduction

[9] Agfa, black and white 27 Din 400 ASA film.

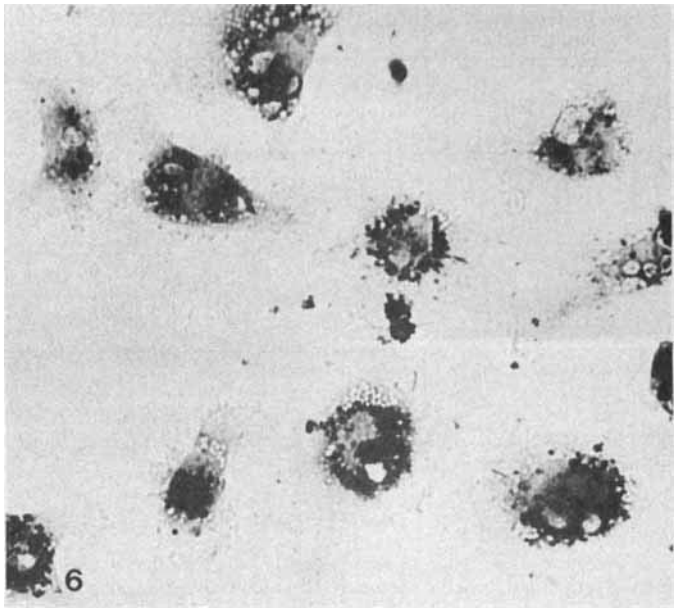

Figure 6—*Macrophages 48 h after exposure to microparticles (0.01 mg/mL). Reaction product, indicating acid phosphatase activity, is localized in granular sites in a way similar to control cells. Original magnification 640×.*

of granularity and an increase of diffuse cytoplasmic staining. The effect was dose dependent, with little or no effect at the 0.01-mg/mL dose (Fig. 6) and pronounced effect at the 0.1-mg/mL dose (Fig. 7). After 48 h many cells exposed to the high dose showed few remaining granular reaction sites and intense diffuse cytoplasmic staining. Many of these cells were becoming round and were obviously degenerating and dying. A number of cells in the 0.05- and 0.1-mg/mL groups contained no reaction product at all, neither granular nor diffuse.

Acridine Orange Uptake—Control cells showed distinct, red cytoplasmic granular fluorescence and weak nuclear green fluorescence. The red granular fluorescence corresponded well with the Gomori lysosomal pattern.

After treatment with high doses (0.05 and 0.1 mg/mL) of microparticles for 24 h, several cells, still being well stretched as detected by phase-contrast microscopy, had lost their granulated red fluorescence. As seen in Table I, this effect was dose dependent. Thus, 17% of the remaining

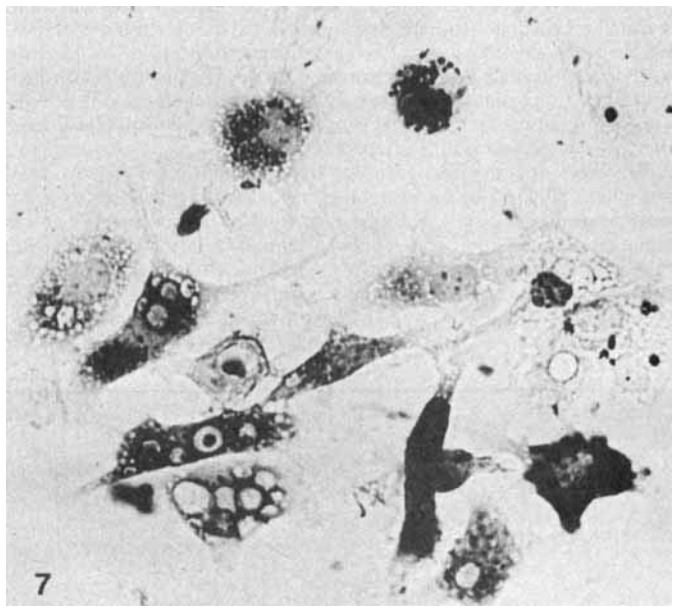

Figure 7—*Macrophages 24 h after exposure to microparticles (0.1 mg/mL). Compare with Fig. 6 and note cells with nongranular, diffuse reaction product as well as several almost unreactive cells. Original magnification 640×.*

Table I—Uptake of Acridine Orange by Macrophages Exposed to Microparticles

Exposure Time, h	Dose of Microparticles, mg/mL	Well-Stretched Cells with Granular Red Fluorescence, %[a]
24	Control	98.6 ± 0.0
	0.01	94.3 ± 3.6
	0.05	78.2 ± 5.5
	0.1	83.6 ± 4.2
48	Control	100 ± 0.0
	0.01	98.3 ± 1.1
	0.05	93.0 ± 2.1
	0.1	84.2 ± 2.3

[a] Mean ± *SE*; $n = 10$.

stretched cells exposed to a 0.1-mg/mL dose for 24 h contained no red granules at all and almost no green cytoplasmic or nulcear fluorescence.

DISCUSSION

The results presented in this study clearly show that the adverse effects on the reticuloendothelial system (RES) of massive doses of acrylic microspheres, previously demonstrated in mice (3), can be studied in greater detail in cultures of mouse peritoneal macrophages *in vitro*. The toxic reactions detected in these culture cells are strictly dose related and detectable only when the cells (5×10^5 cells/dish) are exposed to >0.01 mg of lyophilized particles/mL of medium (total culture medium per dish is 2 mL). From a particle density of 1.14 mg/mL (13) and a mean diameter of 0.25–0.3 μm, it can be estimated that 0.01 mg contains $\sim 1 \times 10^9$ particles. This means, that the ratio between the number of particles and cells is ~4000 when the cellular alterations can first be detected. In a previous study (3), it was shown that an intravenous injection of 1 mg of particles to mice (weighing ~20 g) produced only insignificant changes in the liver, spleen, and bone marrow. It was also shown that 50% of the injected dose was localized to the liver. This means that $\sim 50 \times 10^9$ particles were distributed to and taken up by the macrophages of the liver. It is reported by Knook and Sleyster (14) that the liver from a young rat contains 10×10^7 Kupffer cells per gram of tissue, and if we assume that the mouse liver is commensurable, it means that ~5000–6000 particles were taken up per phagocytosing cell before any reaction was detected in the tissue. The results of the present study thus indicate that cultured peritoneal macrophages are more sensitive to exposure of particles than fixed macrophages of the RES and that they may serve as a sensitive tool for studying the toxicity of microparticles.

The microspheres were phagocytosed by the macrophages and accumulated within large secondary lysosomes. Since the acrylic polymer itself has very little electron density, the particles had to be labeled with ferritin to allow visualization in the electron microscope. The uneven distribution of the ferritin particles within the secondary lysosomes (mostly peripheral) is probably due to partial resolution of the microspheres during dehydration and embedding in plastic[10].

The most drastic effect seen was the enormously enhanced rate of autophagocytosis seen in macrophages exposed to the largest concentration of microspheres. Autophagocytosis is a normal process and is enhanced as an unspecific response to a broad variety of cell-damaging processes (15). As judged from the cytochemical demonstration of the lysosomal enzyme acid phosphatase, there are indications of enhanced fragility of secondary lysosomes. Many exposed cells exhibited diffuse activity and few granular reaction sites. This may reflect alterations that occurred in a more pronounced way in the exposed cells than in control cells during fixation and the cytochemical procedure. It may, however, also indicate leakage of lysosomal enzymes from dilated secondary lysosomes already in culture as a response to the heavy loading of the lysosomal vacuome with microparticles. Such a conclusion is supported by the congruent result obtained with acridine orange showing that many exposed cells have few or no secondary lysosomes with the normal low pH. If so, such a leakage of hydrolytic lysosomal enzymes may contribute to the cell damage and stimulate the demonstrated autophagocytosis.

After exposure to high doses of microparticles some cells did not reveal any acid phosphatase at all with the Gomori method. About the same number of cells failed to accumulate the weak base acridine orange, which normally accumulates in the acidic milieu of the lysosomal vacuome (16). These findings suggest that some cells have completely lost the normal content of their lysosomal vacuome as a result of particle phagocytosis. Macrophages exposed to a variety of stimuli are subject to escape of the lysosomal enzymes during phagocytosis. This is referred to as regurgitation during feeding (17–19). Such regurgitation may possibly become extreme and lead to complete disappearance of lysosomal control, resulting in cells without the positive reaction for acid phosphatase and without uptake of acridine orange. Whether such cells will regain normal lysosomal content or will die and detach from their substratum is unknown.

[10] Epon.

REFERENCES

(1) P. Edman and I. Sjöholm, *J. Pharmacol. Exp. Ther.*, **211**, 663 (1979).

(2) I. Sjöholm and P. Edman, *J. Pharmacol. Exp. Ther.*, **211**, 656 (1979).

(3) P. Edman, I. Sjöholm, and U. Brunk, *J. Pharm. Sci.*, **72**, 658 (1983).

(4) P. Edman and I. Sjöholm, *Life Sci.*, **30**, 327 (1982).

(5) T. de Barsy, P. Devos, and F. van Hoof, *Lab. Invest.*, **34**, 273 (1976).

(6) R. G. Ham, *Exp. Cell Res.*, **29**, 515 (1963).

(7) B. Arborgh, P. Bell, U. Brunk, and V. P. Collins, *J. Ultrastruct. Res.*, **56**, 339 (1976).

(8) V. P. Collins, B. Arborgh, and U. Brunk, *Acta Path. Microbiol. Scan. A*, **85**, 157 (1977).

(9) U. Brunk, J. L. E. Ericsson, J. Pontén, and B. Westermark, *Exp. Cell Res.*, **67**, 407 (1971).

(10) E. S. Reynolds, *J. Cell Biol.*, **17**, 208 (1963).

(11) U. Brunk and J. L. E. Ericsson, *Histochem. J.*, **4**, 349 (1972).

(12) T. Barka and P. J. Anderson, *J. Histochem. Cytochem.*, **10**, 741 (1962).

(13) B. Ekman and I. Sjöholm, *J. Pharm. Sci.*, **67**, 693 (1978).

(14) D. L. Knook and E. C. Sleyster, *Biochem. Biophys. Res. Commun.*, **96**, 250 (1980).

(15) J. L. E. Ericsson, in "Lysosomes in Biology and Pathology," Vol II, J. T. Dingle and H. B. Fell, Eds., 1969, p. 345.

(16) D. de Duve, B. Poole, A. Trouet, P. Tulkens, and F. van Hoop, *Biochem. Pharmacol.*, **23**, 2495 (1974).

(17) B. C. Page, P. Davies, and A. C. Allison, *Arch. Oral. Biol.*, **18**, 1481 (1973).

(18) N. R. Acherman and J. R. Beebe, *Nature (London)*, **247**, 475 (1974).

(19) H. U. Schlorlemner, B. Burger, W. Hylton, and A. C. Allison, *Br. J. Exp. Pathol.*, **58**, 313 (1977).

ACKNOWLEDGMENTS

Supported by the Swedish Board for Technical Development, the Swedish Medical Research Council, and the I. F. Foundation for Pharmaceutical Research.

Colorimetric Prednisolone Assay and Its Application to Dissolution Studies

LILIAN CHONG KWAN *x and HANS SCHOTT

Received April 2, 1982, from the *School of Pharmacy, Temple University, Philadelphia, PA 19140.* Accepted for publication December 7, 1982. **Present address: Applebrook Research Center, SmithKline Animal Health Products, West Chester, PA 19380.*

Abstract □ The colorimetric method of Porter and Silber, originally developed for assaying cortisone and related corticosteroids, was adapted to the assay of prednisolone in the presence and absence of a surfactant, octoxynol 9. Optimal conditions for the colorimetric reaction between prednisolone and acidified phenylhydrazine solution were 30 min at 50°C. The slight interference of octoxynol 9 with the absorbance of the yellow prednisolone–phenylhydrazine complex at 410 nm was corrected by adding an equal surfactant concentration to the blank. When freshly prepared acidified phenylhydrazine solutions were used, the colorimetric method had a sensitivity of 0.2 μg/mL and a precision of 0.1 μg/mL. Its averaged relative standard deviation was 3.7% in the prednisolone concentration range of 10–300 μg/mL.

Keyphrases □ Prednisolone—colorimetric assay, application to dissolution, effect of octoxynol 9 □ Colorimetry—assay of prednisolone, application to dissolution, effect of octoxynol 9 □ Dissolution—prednisolone, colorimetric assay, effect of octoxynol 9

Surfactants such as octoxynol 9 NF enhance the dissolution rate of prednisolone from tablets. To study the effects of surfactants on the *in vitro* dissolution of prednisolone from different tablet formulations, a sensitive analytical method was required to determine the amount of dissolved prednisolone in the dissolution medium as a function of time. In the present application, a tablet containing 25 mg of prednisolone was dissolved in 900 mL of a 0.1 M HCl dissolution medium. At 4 and 100% dissolution, the concentrations of dissolved prednisolone in the dissolution medium correspond to 1 and 28 μg/mL, respectively. The analytical method should have a minimum sensitivity of 1 μg/mL to afford an accurate assay of the amount of dissolved prednisolone in the dissolution medium even at the beginning of a dissolution run.

The colorimetric assay of Porter and Silber (1) for the determination of cortisone and related 17,21-dihydroxy-20-ketosteroids in adrenal extracts has a sensitivity of 1 μg/mL, suitable for the present study. It is based on the development of a yellow color by the reaction between the steroid and an acidified phenylhydrazine reagent in a methanolic medium. Peterson *et al.* (2) developed a procedure for assaying hydrocortisone based on the Porter–Silber method. Since prednisolone and hydrocortisone have similar chemical structures, D'Arcy *et al.* (3) and Isbister *et al.* (4) used the Peterson procedure for the bioassay of prednisolone in plasma. These investigators made no attempt to develop specific reaction conditions appropriate for prednisolone. The present investigation shows that, at least for prednisolone, the age of the acidified phenylhydrazine solution as well as reaction time and temperature are crucial to the rate and extent of color development. Improper conditions resulted in poor reproducibility and led to considerable errors.

Direct spectrophotometric determination of prednisolone by UV absorption (5, 6) is not sensitive enough for *in vitro* dissolution testing. Radioimmunoassay (5) is complicated and requires special handling. Because a fast and accurate assay was required for studying the release characteristics of prednisolone from tablets in the presence and absence of octoxynol 9, the Porter–Silber method was specifically adapted to prednisolone. Optimum conditions for the rate of color development, stability and intensity of color, and sensitivity and accuracy of the assay were investigated.

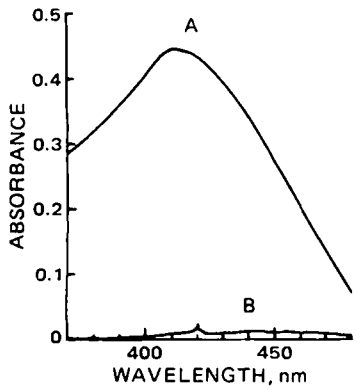

Figure 1—*Absorption spectra of the yellow prednisolone–phenylhydrazine complex (A) and of an octoxynol 9–phenylhydrazine solution (B).*

EXPERIMENTAL

Materials—The following tableting ingredients were employed. Two grades of prednisolone were used as received: anhydrous coarse powders[1] A and B, and anhydrous and micronized[2]. Most of the work, especially the tableting, dissolution, and deflocculation studies, was done with the anhydrous and micronized sample, and the other two coarser samples were merely included as additional sources of prednisolone to verify that the analytical method was independent of the origin of the steroid.

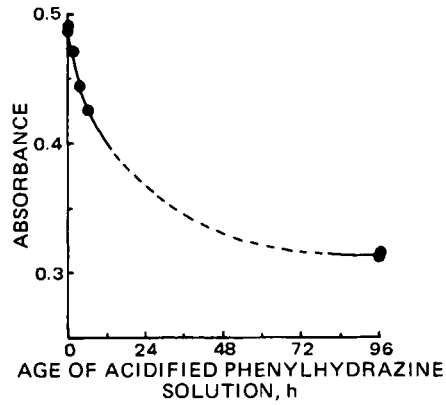

Figure 2—*Decrease in absorbance of the yellow prednisolone–phenylhydrazine complex at 410 nm with the age of the acidified phenylhydrazine solution. Prednisolone concentration = 150 μg/mL.*

[1] Coarse powder A supplied by Sigma Chemical Co., St. Louis, Mo., and coarse powder B supplied by The Upjohn Co., Kalamazoo, Mich.

[2] Schering Corp., Bloomfield, N.J.

0022-3549/84/0200-0157$01.00/0
© 1984, American Pharmaceutical Association

Table I—Formulations of Prednisolone Tablets

Ingredients[a]	Weight of Ingredients, mg Formulation I	Formulation II
Microcrystalline cellulose	75	75
Octoxynol 9	—	35
Spray-dried lactose	100	100
Prednisolone	25	25
Magnesium stearate	5	5
Spray-dried lactose	295	260

[a] Listed in the order of mixing.

Magnesium stearate[3] and spray-dried lactose[4] were USP grade. Octoxynol 9[5] and microcrystalline cellulose[6] were NF grade. The ACS-grade reagents used for the colorimetric assay were phenylhydrazine hydrochloride, anhydrous methanol, hydrochloric acid, and sulfuric acid. Double-distilled water was used throughout the experiments.

Equipment—Absorbances were measured with a double-beam grating spectrophotometer[7] equipped with a synchronized chart recorder[8] and 1-cm quartz cells. At an input voltage span of 1 mV, an absorbance value of 0.001 ± 0.0005 can be read directly from the chart. The temperatures for the colorimetric reaction were maintained within ±0.5°C.

Prednisolone tablets were prepared with a single-punch tablet press[9]. Membrane filters[10] were used to remove the undissolved tableting ingredients from the dissolution medium. The filters consisted of a mixture of cellulose nitrate and cellulose acetate and had two different porosities, 0.1 and 0.22 μm[11].

Reagents—Sulfuric acid at 68.7% w/w was prepared by diluting 1.63 parts by volume of concentrated sulfuric acid (93% w/w) with 1 part by volume of water. Porter and Silber investigated the effect of the sulfuric acid concentration on the cortisone acetate assay over a wide range and found that the concentration used for this study, 68.7% w/w, gave the best results. Acidified phenylhydrazine solution was prepared by dissolving 65 mg of phenylhydrazine hydrochloride in 100 mL of the 68.7% w/w sulfuric acid. Stock solutions of prednisolone were prepared in methanol at 10, 13.5, 15, 20, 28, 30, 60, 90, 150, 210, and 300 μg/mL. A stock solution of 0.4% w/v octoxynol 9 was prepared in 0.1 M HCl and diluted to 0.004, 0.01, and 0.05% w/v as required.

Prednisolone Tablets—Tablets containing 25 mg of prednisolone were prepared according to formulations I and II, as shown in Table I. Octoxynol 9 was excluded from the first formulation; 35 mg of octoxynol 9 was absorbed into the microcrystalline cellulose and incorporated into the second formulation. Several batches of 10 tablets each were prepared for each formulation using the following procedure. The tableting ingredients were triturated in a mortar and pestle. Compression at 10,000 psi on a single-punch tablet press yielded flat-faced cylindrical tablets with an average diameter of 12.8 mm, an average thickness of 2.8 mm, and an average tablet weight of 500 mg.

Dissolution—Individual prednisolone tablets were dissolved in 900 mL of 0.1 M HCl at 37°C using the USP XIX dissolution apparatus (7) and a 40-mesh metal basket rotated at 100 rpm. Five-milliliter aliquots of the dissolution medium containing dissolved prednisolone were withdrawn at appropriate time intervals and filtered through a 0.1-μm filter membrane that had been prewashed with 0.1 M HCl.

Prednisolone Assay—The accuracy of the Porter–Silber method applied to the assay of prednisolone was investigated as follows. The test solution consisted of 1 mL of a methanol solution containing a known amount of dissolved prednisolone and 8 mL of acidified phenylhydrazine solution placed in a stoppered test tube. The blank solution consisted of 1 mL of the dissolution medium and 8 mL of the acidified phenylhydrazine solution. Both solutions were heated for 20 min at 60°C (1), at which time the former developed a yellow color. After cooling to room temperature, the absorbance of the test solution was measured against the blank solution at 410 nm using 1-cm cells. Figure 1 shows a typical

[3] Impalpable powder; Mallinckrodt Inc., St. Louis, Mo.
[4] Manufactured by Foremost Dairies Inc. and supplied by SmithKline Beckman Corp., Philadelphia, Pa.
[5] Triton X-100; Rohm and Haas Co., Philadelphia, Pa.
[6] Avicel type PH-101; FMC Corp., Philadelphia, Pa.
[7] Coleman Model 124; Perkin-Elmer Corp., Norwalk, Conn.
[8] Coleman Model 165; Perkin-Elmer Corp., Norwalk, Conn.
[9] Carver Laboratory Press, Model C; Fred S. Carver Inc., Menomonee Falls, Wis.
[10] Fitted with Swinnex adaptors and Millipore membranes; Millipore Corp., Bedford, Mass.
[11] Type GSWP of 0.22-μm pore size and type VCWP of 0.1-μm pore size; Millipore Corp., Bedford, Mass.

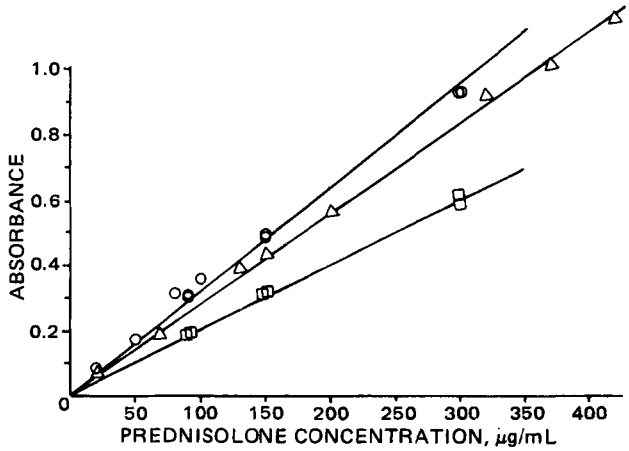

Figure 3—*Effect of aging the acidified phenylhydrazine solution on the relation between absorbance and prednisolone concentration. Key: (○) 0.5 h; (△) 6 h; (□) 96 h aging.*

absorption spectrum for the yellow prednisolone–phenylhydrazine complex, in which the maximum absorbance (A_1) occurred at 410 nm. This wavelength agrees well with the one reported by Porter and Silber for the phenylhydrazine complexes of cortisone and related compounds (1).

To correct for the absorbance due to the interaction between sulfuric acid and prednisolone in the absence of phenylhydrazine, a similar measurement was made omitting the phenylhydrazine solution from the reaction mixture. In this case, the absorbance (A_2) of a mixture of 1 mL of the methanol solution containing dissolved prednisolone and 8 mL of 68.7% w/w sulfuric acid was measured at 410 nm against a blank of 1 mL of the dissolution medium and 8 mL of the sulfuric acid solution. Both solutions were heated for 20 min at 60°C prior to the measurement. Subtracting the second absorbance (A_2) from the uncorrected absorbance (A_1) gave the correct absorbance for prednisolone solutions free from the interaction between sulfuric acid and prednisolone. Absorbance A_2 varied with each test sample and generally amounted to 5–15% of the uncorrected value.

RESULTS AND DISCUSSION

The adaptation of the Porter–Silber method to prednisolone and the optimization of the reaction conditions for maximum reproducibility and accuracy are discussed below.

Stability of the Acidified Phenylhydrazine Solution—Inconsistent results in preliminary experiments suggested that the acidified phenylhydrazine solution was unstable. The effect of aging of this solution on the absorbance of the colored complex with prednisolone was investigated.

A master batch of acidified phenylhydrazine solution was stored at

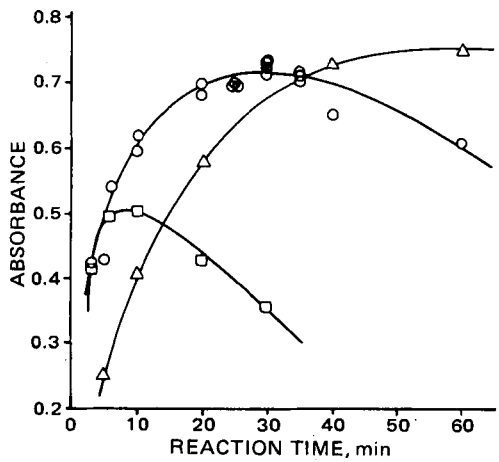

Figure 4—*Variation in absorbance of the prednisolone–phenylhydrazine complex at 410 nm with reaction time at different temperatures. Prednisolone concentration = 150 μg/mL. Key: (△) 40°C; (○) 50°C; (□) 60°C.*

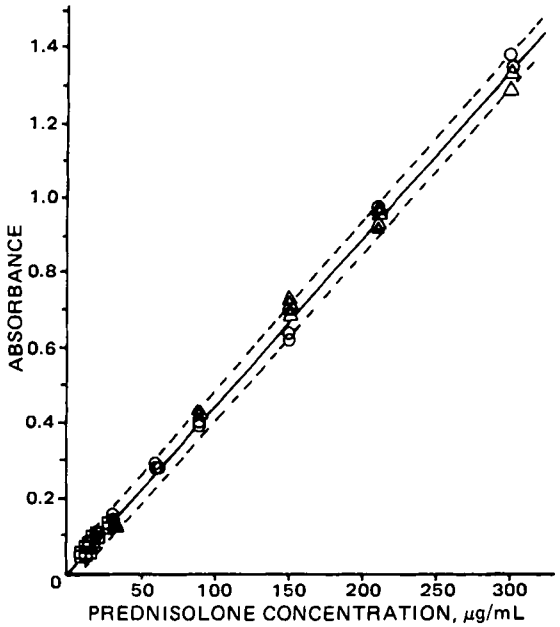

Figure 5—*Variation in absorbance of the prednisolone–phenylhydrazine complex with prednisolone concentration obtained with the standard procedure. Key: (○) anhydrous prednisolone coarse powder A; (△) anhydrous prednisolone coarse powder B; (□) micronized prednisolone. The broken lines represent the 95% confidence limits for the calculated absorbance.*

room temperature in the dark. Eight-milliliter aliquots were withdrawn immediately after the solution was prepared and after intervals of 0.5, 2, 4, 6, and 96 h. They were reacted with 1-mL volumes of prednisolone solution containing 150 μg/mL of dissolved prednisolone as described above. Corrected absorbance values at 410 nm are plotted against the age of the acidified phenylhydrazine solution in Fig. 2. A rapid initial decrease in absorbance is followed by a gradual leveling off.

Aging of the acidified phenylhydrazine solution for 96 h or more stabilized the absorbance of the yellow complex. However, it also reduced the molar absorptivity, or the slope of the Beer's-law plot, by ~40% (Fig. 3). The data of Fig. 3 were obtained by treating 1-mL aliquots of prednisolone solutions containing the indicated concentrations with 8-mL aliquots of acidified phenylhydrazine solutions aged 0, 6, and 24 h, respectively. Because of the high sensitivity required, subsequent prednisolone assays were performed within 1 h after the phenylhydrazine solution was prepared.

Dependence of Absorbance of the Yellow Complex on Reaction Time and Temperature—Porter and Silber reported that the absorbance values for the yellow complex of cortisone at 410 nm were reproducible when the colorimetric reaction was carried out at 60°C for 20 min. However, preliminary experiments suggested that the absorbance values for the prednisolone–phenylhydrazine complex were poorly reproducible under these reaction conditions. The influence of reaction time and temperature on the absorbance of the yellow complex was investigated.

One-milliliter aliquots of a 150-μg/mL prednisolone solution were reacted with 8-mL portions of freshly prepared acidified phenylhydrazine solutions at 40°C, 50°C, and 60°C. Absorbance values of the yellow complex were measured at 410 nm after 5, 10, 15, 20, 40, and 60 min for each temperature. The solutions were cooled to ambient temperature in a water bath before absorbance measurements. Figure 4 shows that the absorbance peaked at different reaction times for the three reaction temperatures. Lowering the reaction temperature reduced the reaction rate so that the peak value occurred after a longer reaction time. For example, as the reaction temperature was lowered from 60°C to 40°C, the time required to reach maximum absorbance increased from 10 to 40 min. The peak was broader at the lower temperatures, indicating that these absorbance values are more reproducible than those obtained at higher temperatures. While the maximum absorption occurred at 410 nm for the three temperatures, the absorbance at 410 nm was considerably stronger at the two lower temperatures.

Selection of Standard Reaction Conditions—Of the three experimental conditions required to attain maximum absorbance (50 min at 40°C, 30 min at 50°C, and 10 min at 60°C), the intermediate conditions were selected as the best compromise between reproducibility and reaction time. Subsequent colorimetric reactions were conducted at 50°C for 30 min.

Table II—Reproducibility of the Prednisolone Assay

Prednisolone Concentration, μg/mL	Average Absorbance	N^a	*SD*	*SE*	*RSD*, %
10.0	0.045	2	0.001	0.001	2.2
13.5	0.057	4	0.002	0.001	3.5
15.0	0.063	4	0.003	0.002	4.8
20.0	0.096	2	0.006	0.004	6.3
28.0	0.128	2	0.003	0.002	2.3
30.0	0.142	4	0.006	0.003	4.2
60.0	0.283	3	0.006	0.004	2.1
90.0	0.406	4	0.019	0.010	4.7
150.0	0.683	6	0.044	0.018	6.4
210.0	0.957	5	0.015	0.007	1.6
300.0	1.344	4	0.038	0.019	2.8

[a] Number of determinations.

Beer's Law Plot—The prednisolone assay for dissolution studies requires the use of a Beer's-law plot that correlates the absorbance of the prednisolone–phenylhydrazine complex with the prednisolone concentration. This plot was obtained by measuring the absorbance values of the yellow complex at 410 nm using prednisolone solutions of 11 different concentration levels in the range of 10–300 μg/mL. A total of 40 measurements were made, 14 with micronized prednisolone, 12 with the anhydrous prednisolone coarse powder A, and 14 with coarse powder B. Prednisolone samples from three suppliers were used to ensure that the results were independent of the source of the steroid.

The Beer's-law plot in Fig. 5 shows that the absorbance of the yellow complex is directly proportional to the prednisolone concentration up to at least 300 μg/mL. The absorbance values are independent of the source of prednisolone. The plot may be represented by the linear regression equation:

$$A = 0.0045C \qquad \text{(Eq. 1)}$$

where A is the absorbance at 410 nm, C is the prednisolone concentration in μg/mL, and 0.0045 is the slope. The absorptivity of prednisolone calculated from the slope is 0.0045 mL/μg·cm. It is equivalent to a molar absorptivity of 1622 L/mol·cm. The standard error for the slope of the regression line, SE_m, and the standard error of regression, SE_{AC}, were 0.00002 and 0.21, respectively (8, 9). The broken lines in Fig. 5 represent the 95% confidence limits for the calculated absorbance (9). The equations used for the linear regression analysis are given in the *Appendix*.

Reproducibility of the Prednisolone Assay—The standard deviation (*SD*), standard error (*SE*), and relative standard deviation (*RSD*) were calculated for each prednisolone concentration. Table II shows that the relative standard deviation varied randomly with the prednisolone concentration, ranging from 1.6 to 6.4% in the concentration range of 10–300 μg/mL. An average relative standard deviation ($\overline{RSD}$) was calculated for the entire concentration range using Eq. 2:

$$\overline{RSD} = \frac{\sum_{i=1}^{i=n} RSD}{n} \qquad \text{(Eq. 2)}$$

where RSD_i is the relative standard deviation at concentration C_i and n is the number of concentration levels used in the study. A value of 3.7% was obtained for $\overline{RSD}$ for concentrations ranging from 10 to 300 μg/mL. These statistics indicate that the measured absorbance is reproducible within ±4% for an entire dissolution run.

Sensitivity of the Prednisolone Assay—With an input voltage span of 1 mV for the recorder, an absorbance value of 0.001 ± 0.0005 can be determined directly from the chart. This is equivalent to a prednisolone concentration of 0.2 ± 0.1 μg/mL according to Eq. 1. The sensitivity of the assay is, therefore, at least 0.2 μg/mL, which is equivalent to 0.7% dissolution for a 25-mg tablet dissolving in 900 mL of dissolution medium. It far exceeds the required sensitivity of 1 μg/mL.

Dissolution Studies in the Absence of Octoxynol 9—When the dissolution experiment did not involve octoxynol 9, the test solution consisted of a 1-mL aliquot of the filtered dissolution sample and 8 mL of the freshly prepared acidified phenylhydrazine solution. The blank solution consisted of 1 mL of the dissolution medium and 8 mL of the phenylhydrazine solution. The absorbance of the prednisolone–phenylhydrazine complex was measured at 410 nm against the blank solution

Table III—Accuracy of the Prednisolone Assay in the Absence of Octoxynol 9

Tablet	Observed Prednisolone Content, mg/tablet[a]	
A	25.2	24.9
B	25.1	25.2
C	24.8	25.1
Mean	25.05	
N	6	
SE	0.07	
RSD	0.7%	

[a] Two determinations for each tablet.

using the standard reaction conditions and corrected for interference due to the interaction between prednisolone and sulfuric acid. The amount of dissolved prednisolone in the dissolution sample was calculated using Eq. 1. Results of the dissolution studies are reported in a separate publication (10).

Dissolution Studies in the Presence of Octoxynol 9—Preliminary experiments showed that 1 mL of a 0.0039% w/v octoxynol 9 solution and 8 mL of the acidified phenylhydrazine solution reacted at the standard conditions to develop a pale yellow color. The absorption spectrum for the reaction mixture is shown in Fig. 1. Three samples of the octoxynol 9–phenylhydrazine solution gave absorbance values at 410 nm ranging from 0.002 to 0.004.

Therefore, in dissolution studies where the surfactant was present in the dissolution medium the following procedure was employed to compensate for the slight interference of octoxynol 9 on the absorbance of the prednisolone–phenylhydrazine complex. The test solution consisted of a 1-mL aliquot of the filtered dissolution sample containing octoxynol 9 and the dissolved prednisolone plus an 8-mL portion of the acidified phenylhydrazine solution. The blank solution consisted of 1 mL of the 0.1 M HCl dissolution medium containing a quantity of the surfactant equal to the amount present in the test solution plus 8 mL of the acidified phenylhydrazine solution. The absorbance of the test solution was measured against this blank using the standard conditions and corrected for interference due to the prednisolone–sulfuric acid interaction.

In tablets containing octoxynol 9 (formulation II), the surfactant dissolved rapidly during prednisolone dissolution (10). Its concentration in the dissolution medium increased from 0 initially to a maximum of 0.0039% w/v at the complete release of the 35 mg of octoxynol 9 in the dissolution medium (900 mL). The faint yellow color produced by the interaction between octoxynol 9 in the filtered dissolution medium and phenylhydrazine remained essentially constant during an entire dissolution run: its absorbance was 0.003 at the time corresponding to the first prednisolone assay and 0.004 when all the prednisolone was dissolved.

In another experiment, conducted in the absence of prednisolone, an equal amount of the surfactant was added to the dissolution medium rather than incorporated into the tablets. Thus, the surfactant concentration remained constant at 0.0039% w/v throughout the entire dissolution run. The absorbance of this filtered dissolution medium when treated with the phenylhydrazine solution was 0.003 ± 0.001, comparable with the values obtained in the experiment where 35 mg of octoxynol 9 was incorporated into the tablets. Therefore, the absorbance due to the interference of octoxynol 9 with phenylhydrazine was essentially constant throughout a dissolution run regardless of whether the 35 mg of octoxynol 9 was originally incorporated into the tablet or added to the dissolution medium. A constant absorbance correction of 0.003 was made for both situations.

Accuracy of the Prednisolone Assay in Dissolution Studies—The accuracy of the prednisolone assay in the absence of octoxynol 9 was investigated by the following procedure. Three prednisolone tablets of formulation I were triturated individually with 10 mL of methanol to ensure the complete dissolution of the 25 mg of prednisolone incorporated into the tablet. Each mixture was diluted to 1 L with 0.1 M HCl, resulting in a final prednisolone concentration of 25 μg/mL. Each suspension was filtered individually through a 0.22-μm membrane that had been prewashed with a 5-mL portion of the 0.1 M HCl dissolution medium. Prednisolone assays were performed in duplicate for each filtrate as described above. The amount of dissolved prednisolone in the filtrate was calculated by means of Eq. 1.

The results of the prednisolone assays, summarized in Table III, shows that the experimental values of the drug content of the three tablets are in good agreement. The relative standard deviation was a mere 0.7%. The observed prednisolone contents are identical with the actual value of 25 mg per tablet. Therefore, the colorimetric assay has high accuracy and precision.

Nature of the Colored Complex—It is of interest to consider the chemical nature of the yellow color obtained by the reaction of prednisolone with phenylhydrazine. The reaction probably involves the following three steps:

1. The carbonyl group on C-3 reacts with one molecule of phenylhydrazine to form the phenylhydrazone.
2. The Mattox rearrangement involving the hydroxyl groups at C-17 and C-21 and the carbonyl group at C-20 produces the 17 β-glyoxal (C-20 and C-21 contain carbonyl groups, while the C-17 hydroxyl group is lost).
3. The carbonyl group at C-21 reacts with one molecule of phenylhydrazine to form a second phenylhydrazone.

The yellow pigment is thus the 20-keto-3,21-diphenylhydrazone (11).

APPENDIX

Slope m of the regression line is given by:

$$m = \frac{\sum_{i=1}^{i=n} C_i A_i}{\sum_{i=1}^{i=n} C_i^2} \qquad \text{(Eq. 3)}$$

where C_i is the prednisolone concentration in μg/mL, A_i is the absorbance of the yellow prednisolone–phenylhydrazine complex obtained at this concentration, and n is the number of concentration levels of prednisolone solution used for the regression analysis (8, 9).

The standard error of regression SE_{AC} is calculated by means of:

$$SE_{AC} = \left\{ \frac{\sum_{i=1}^{i=n} A_i^2 - \left[\left(\sum_{i=1}^{i=n} C_i A_i \right)^2 \Big/ \sum_{i=1}^{i=n} C_i^2 \right]}{n-1} \right\}^{1/2} \qquad \text{(Eq. 4)}$$

The standard error, SE_m, of the slope of the regression line is calculated by means of the equation:

$$SE_m = \frac{SE_{AC}}{\left(\sum_{i=1}^{i=n} C_i^2 \right)^{1/2}} \qquad \text{(Eq. 5)}$$

The linear regression equation (Eq. 1) is used to calculate the absorbance A_k for a known prednisolone concentration C_k. The 95% confidence limits for the calculated absorbance, A_k, at a specific value of prednisolone concentration, C_k, are calculated using:

$$\text{Absorbance} = A_k \pm t_{0.05}^{n-1} SE_{A,k} \qquad \text{(Eq. 6)}$$

where $t_{0.05}^{n-1}$ is the 5% point of a two-tailed t distribution with $n-1$ degrees of freedom, and $SE_{A,k}$ is a modified form of Eq. 6.12.1 in Ref. 9:

$$SE_{A,k} = SE_{AC} \left[1 + \frac{(\bar{C} - C_k)^2}{\sum_{i=1}^{i=n} (\bar{C} - C_i)^2} \right]^{1/2} \qquad \text{(Eq. 7)}$$

where $\bar{C}$ is the mean of all C_i values.

REFERENCES

(1) C. C. Porter and R. H. Silber, *J. Biol. Chem.*, **185**, 201 (1950).

(2) R. E. Peterson, A. Karrer, and S. L. Guerra, *Anal. Chem.*, **29**, 144 (1957).

(3) P. F. D'Arcy, J. P. Griffin, J. S. Jenkins, W. F. Kirk, and A. W. C. Peacock, *J. Pharm. Sci.*, **60**, 1028 (1971).

(4) J. P. Isbister, J. Speros, and A. W. Steinbeck, *Med. J. Aust.*, **1**, 1135 (1969).

(5) T. J. Sullivan, R. C. Stoll, E. Sakmar, D. C. Blair, and J. B. Wagner, *J. Pharmacokinet. Biopharm.*, **2**, 29 (1974).

(6) P. Hagemann, *Pharm. Acta Helv.*, **53**, 133 (1978).

(7) "United States Pharmacopeia XIX," U.S. Pharmacopeial Convention Inc., Rockville, Md., 1975, p. 650.

(8) W. J. Youden, "Statistical Methods for Chemists," Wiley, New York, N.Y., 1951, pp. 40–49.

(9) G. W. Snedecor and W. G. Cochran, "Statistical Methods," 6th

ed., The Iowa State University Press, Ames, Iowa, 1967, pp. 135–171.
(10) H. Schott, L. C. Kwan, and S. Feldman, *J. Pharm. Sci.*, 71, 1038 (1982).
(11) L. F. Fieser and M. Fieser, "Reagents for Organic Synthesis," Wiley, New York, N.Y., 1967, pp. 838–839.

ACKNOWLEDGMENTS

Adapted in part from a thesis submitted by L. Chong Kwan to Temple University in partial fulfillment of the Master of Science degree requirements.

Relationship Between Azo Dye Structure and Rat Hepatic Azoreductase Activity

LEON SHARGEL *x, ALI R. BANIJAMALI *, and SIMON H. KUTTAB ‡

Received March 9, 1982, from the *College of Pharmacy and Allied Health Professions, Northeastern University, Boston, MA 02115.* Accepted for publication December 2, 1982. Present addresses: *Massachusetts College of Pharmacy and Allied Health Sciences, Boston, MA 02115 and ‡Birzeit University, P.O. Box 14, Birzeit, West Bank, Israel.

Abstract □ The rate of reduction was determined for a variety of azo dyes using the rat hepatic azoreductase enzyme system. In decreasing order, the rates of reduction for the azo dyes expressed as nmol of arylamine product formed/min/0.25 g of liver were amaranth (33.2), azosulfamide (32.5), orange G (12.4), 1,2-dimethyl-4-*p*-(carboxyphenylazo)-5-hydroxybenzene (CPA) (9.27), brilliant crystal scarlet (8.00), sulfachrysoidine (7.27), and Sudan I (1.03). A comparison of the partition coefficient with its rate of reduction indicated that the water-soluble azo dyes were reduced more rapidly than the lipid-soluble ones. Furthermore, higher rates of reduction were observed for those dyes containing electron-withdrawing groups on the aromatic rings.

Keyphrases □ Azoreductase—rat hepatic activity, relationship to azo dye structure, amaranth, azosulfamide, orange G, 1,2-dimethyl-4-*p*-(carboxyphenylazo)-5-hydroxybenzene, brilliant crystal scarlet, sulfachrysoidine, Sudan I □ Azo dyes—relationship between structure and rat hepatic azoreductase activity, amaranth, azosulfamide, orange G, 1,2-dimethyl-4-*p*-(carboxyphenylazo)-5-hydroxybenzene, brilliant crystal scarlet, sulfachrysoidine, Sudan I

The azo dyes and pigments form a large group of synthetic colorants used in many dye applications including foods, cosmetics, and pharmaceuticals. The chromophoric system consists of the azo group (N=N—) in association with one or more aromatic system. Monoazo, diazo, triazo, and polyazo dyes contain one, two, three, or more azo groups, respectively, yielding a large range of colors including reds, oranges, and purples (1).

In mammals, several enzyme systems are capable of reducing the azo bond including the liver (2–7) and the GI flora (4, 8–10). These azoreductase enzyme systems reduce a variety of azo dye substrates and do not appear to have a strict structural requirement other than the azo bond (2, 4, 10). A number of azo dyes, such as dimethylaminoazobenzene (butter yellow), amaranth, and others have carcinogenic or suspected carcinogenic activity (4). This toxic activity may be due to the parent compound, which contains the intact azo bond, or to the resulting arylamine. Although the mechanism of the reduction of the azo bond has been studied (2, 3, 5, 11, 12) only a few papers have compared chemical structure with the rates of reduction of the azo bond (2, 13). The objective of this study was to investigate the relationship of the structure of selected azo dyes to the rate of reduction to the corresponding amine by the rat hepatic azoreductase enzyme system. The rat hepatic azoreductase enzyme system obtained from the 10,000 × *g* supernatant fraction of liver homogenates was chosen since the mechanism of azo bond reduction by this enzyme preparation has been characterized by a number of investigators (2, 3, 5–7, 11, 12).

EXPERIMENTAL

Reagents and Chemicals—Azo dyes including brilliant crystal scarlet[1], orange G[1], Sudan I[1], amaranth[1], sulfachrysoidine[2], azosulfamide[2], and 1,2-dimethyl-4-(carboxyphenylazo)-5-hydroxybenzene[3] (CPA) were checked for chemical purity by either TLC on silica gel plates (*n*-butyl alcohol–acetic acid–water, 6:1:3) or ascending paper chromatography (*n*-butyl alcohol–acetic acid–water 12:3:5). Cation-exchange[4] and anion-exchange[4] resins were washed with several volumes of distilled water prior to use. NADP[5], glucose-6-phosphate[5], and nicotinamide[5], as well as other reagents and solvents, were used without further purification.

Partition Coefficient—A partition coefficient, K, in *n*-octanol–0.05 M phosphate buffer (pH 7.4) was determined for each azo dye in duplicate at room temperature. For water-soluble dyes, 1 mL of an aqueous dye solution (~10 μmol) was placed in an extraction tube containing 4 mL of 0.05 M phosphate buffer (pH 7.4). To this sample was added 5 mL of *n*-octanol previously saturated with distilled water. Lipid-soluble dyes were initially dissolved in the water-saturated 1-octanol and added to 5 mL of 0.05 M phosphate buffer (pH 7.4). Each sample was shaken, allowed to stand for a few minutes, and centrifuged. The distribution of the dye in each phase at equilibrium was obtained from absorbance of the dye in a spectrophotometer[6] at an appropriate wavelength. The partition coefficient for each dye was calculated with respect to a standard curve or from the absorbance of the aqueous or lipid phase before and after equilibration.

Preparation of Liver Homogenates—Male albino Charles River CD rats (180–220 g) were used for all studies. Rats were weighed and then sacrificed by decapitation. Each liver was excised and immediately rinsed with ice-cold 1.15% KCl (isotonic). The livers were trimmed, weighed, and homogenized in three volumes of 1.15% KCl using a polytef pestle and glass mortar. All subsequent procedures were performed at 4°C. The tissue homogenates were centrifuged at 10,000×*g* for 15 min in a refrigerated centrifuge. The 10,000×*g* liver supernatant containing the microsomal enzymes and soluble fraction was filtered through gauze. Approximately 15 mL of the 10,000×*g* liver supernatant was placed in 50-mL glass ampules and shell-frozen in dry ice–acetone. This enzyme preparation is stable at dry ice temperature for a week or more. Previous studies have shown that lyophilization of this preparation stabilized the enzymes for as long as 6 months with no apparent loss of activity (14).

[1] Aldrich Chemical Co., Milwaukee, Wis.
[2] Sterling-Winthrop Research Institute, Rensselaer, N.Y.
[3] ICN Nutritional Biochemics, Cleveland, Ohio.
[4] Cation exchange resin (AG50W-X8, 200-400 mesh) and anion exchange resin (AGL-X2, 200-400 mesh); Bio-Rad Labs, Richmond, Calif.
[5] Sigma Chemical Co., St. Louis, Mo.
[6] UV/Vis; Beckman Instruments, Inc., Irvine, Calif.

0022-3549/84/0200-0161$01.00/0
© 1984, American Pharmaceutical Association

ed., The Iowa State University Press, Ames, Iowa, 1967, pp. 135–171.
(10) H. Schott, L. C. Kwan, and S. Feldman, *J. Pharm. Sci.*, 71, 1038 (1982).
(11) L. F. Fieser and M. Fieser, "Reagents for Organic Synthesis," Wiley, New York, N.Y., 1967, pp. 838–839.

ACKNOWLEDGMENTS

Adapted in part from a thesis submitted by L. Chong Kwan to Temple University in partial fulfillment of the Master of Science degree requirements.

Relationship Between Azo Dye Structure and Rat Hepatic Azoreductase Activity

LEON SHARGEL *x, ALI R. BANIJAMALI *, and SIMON H. KUTTAB ‡

Received March 9, 1982, from the *College of Pharmacy and Allied Health Professions, Northeastern University, Boston, MA 02115.* Accepted for publication December 2, 1982. Present addresses: *Massachusetts College of Pharmacy and Allied Health Sciences, Boston, MA 02115 and ‡Birzeit University, P.O. Box 14, Birzeit, West Bank, Israel.

Abstract □ The rate of reduction was determined for a variety of azo dyes using the rat hepatic azoreductase enzyme system. In decreasing order, the rates of reduction for the azo dyes expressed as nmol of arylamine product formed/min/0.25 g of liver were amaranth (33.2), azosulfamide (32.5), orange G (12.4), 1,2-dimethyl-4-*p*-(carboxyphenylazo)-5-hydroxybenzene (CPA) (9.27), brilliant crystal scarlet (8.00), sulfachrysoidine (7.27), and Sudan I (1.03). A comparison of the partition coefficient with its rate of reduction indicated that the water-soluble azo dyes were reduced more rapidly than the lipid-soluble ones. Furthermore, higher rates of reduction were observed for those dyes containing electron-withdrawing groups on the aromatic rings.

Keyphrases □ Azoreductase—rat hepatic activity, relationship to azo dye structure, amaranth, azosulfamide, orange G, 1,2-dimethyl-4-*p*-(carboxyphenylazo)-5-hydroxybenzene, brilliant crystal scarlet, sulfachrysoidine, Sudan I □ Azo dyes—relationship between structure and rat hepatic azoreductase activity, amaranth, azosulfamide, orange G, 1,2-dimethyl-4-*p*-(carboxyphenylazo)-5-hydroxybenzene, brilliant crystal scarlet, sulfachrysoidine, Sudan I

The azo dyes and pigments form a large group of synthetic colorants used in many dye applications including foods, cosmetics, and pharmaceuticals. The chromophoric system consists of the azo group (N=N—) in association with one or more aromatic system. Monoazo, diazo, triazo, and polyazo dyes contain one, two, three, or more azo groups, respectively, yielding a large range of colors including reds, oranges, and purples (1).

In mammals, several enzyme systems are capable of reducing the azo bond including the liver (2–7) and the GI flora (4, 8–10). These azoreductase enzyme systems reduce a variety of azo dye substrates and do not appear to have a strict structural requirement other than the azo bond (2, 4, 10). A number of azo dyes, such as dimethylaminoazobenzene (butter yellow), amaranth, and others have carcinogenic or suspected carcinogenic activity (4). This toxic activity may be due to the parent compound, which contains the intact azo bond, or to the resulting arylamine. Although the mechanism of the reduction of the azo bond has been studied (2, 3, 5, 11, 12) only a few papers have compared chemical structure with the rates of reduction of the azo bond (2, 13). The objective of this study was to investigate the relationship of the structure of selected azo dyes to the rate of reduction to the corresponding amine by the rat hepatic azoreductase enzyme system. The rat hepatic azoreductase enzyme system obtained from the 10,000 × *g* supernatant fraction of liver homogenates was chosen since the mechanism of azo bond reduction by this enzyme preparation has been characterized by a number of investigators (2, 3, 5–7, 11, 12).

EXPERIMENTAL

Reagents and Chemicals—Azo dyes including brilliant crystal scarlet[1], orange G[1], Sudan I[1], amaranth[1], sulfachrysoidine[2], azosulfamide[2], and 1,2-dimethyl-4-(carboxyphenylazo)-5-hydroxybenzene[3] (CPA) were checked for chemical purity by either TLC on silica gel plates (*n*-butyl alcohol–acetic acid–water, 6:1:3) or ascending paper chromatography (*n*-butyl alcohol–acetic acid–water 12:3:5). Cation-exchange[4] and anion-exchange[4] resins were washed with several volumes of distilled water prior to use. NADP[5], glucose-6-phosphate[5], and nicotinamide[5], as well as other reagents and solvents, were used without further purification.

Partition Coefficient—A partition coefficient, K, in *n*-octanol–0.05 M phosphate buffer (pH 7.4) was determined for each azo dye in duplicate at room temperature. For water-soluble dyes, 1 mL of an aqueous dye solution (~10 μmol) was placed in an extraction tube containing 4 mL of 0.05 M phosphate buffer (pH 7.4). To this sample was added 5 mL of *n*-octanol previously saturated with distilled water. Lipid-soluble dyes were initially dissolved in the water-saturated 1-octanol and added to 5 mL of 0.05 M phosphate buffer (pH 7.4). Each sample was shaken, allowed to stand for a few minutes, and centrifuged. The distribution of the dye in each phase at equilibrium was obtained from absorbance of the dye in a spectrophotometer[6] at an appropriate wavelength. The partition coefficient for each dye was calculated with respect to a standard curve or from the absorbance of the aqueous or lipid phase before and after equilibration.

Preparation of Liver Homogenates—Male albino Charles River CD rats (180–220 g) were used for all studies. Rats were weighed and then sacrificed by decapitation. Each liver was excised and immediately rinsed with ice-cold 1.15% KCl (isotonic). The livers were trimmed, weighed, and homogenized in three volumes of 1.15% KCl using a polytef pestle and glass mortar. All subsequent procedures were performed at 4°C. The tissue homogenates were centrifuged at 10,000×*g* for 15 min in a refrigerated centrifuge. The 10,000×*g* liver supernatant containing the microsomal enzymes and soluble fraction was filtered through gauze. Approximately 15 mL of the 10,000×*g* liver supernatant was placed in 50-mL glass ampules and shell-frozen in dry ice–acetone. This enzyme preparation is stable at dry ice temperature for a week or more. Previous studies have shown that lyophilization of this preparation stabilized the enzymes for as long as 6 months with no apparent loss of activity (14).

[1] Aldrich Chemical Co., Milwaukee, Wis.
[2] Sterling-Winthrop Research Institute, Rensselaer, N.Y.
[3] ICN Nutritional Biochemics, Cleveland, Ohio.
[4] Cation exchange resin (AG50W-X8, 200-400 mesh) and anion exchange resin (AGL-X2, 200-400 mesh); Bio-Rad Labs, Richmond, Calif.
[5] Sigma Chemical Co., St. Louis, Mo.
[6] UV/Vis; Beckman Instruments, Inc., Irvine, Calif.

0022-3549/84/0200-0161$01.00/0
© 1984, American Pharmaceutical Association

Table I—Structure and Partition Coefficients of Various Azo Dyes

Dye	Structure	Partition Coefficient[a]
Azosulfamide	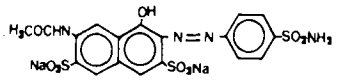	0.149
Orange G	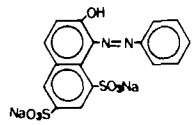	0.163
Amaranth	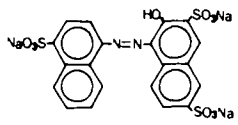	0.176
Brilliant crystal scarlet	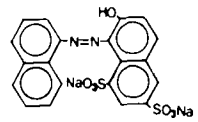	0.212
CPA[b]	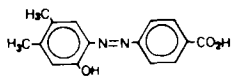	0.950
Sudan I	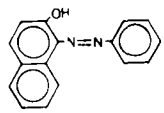	4.33
Sulfachrysoidine	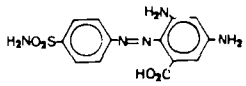	5.67

[a] Partition coefficient for *n*-octanol–0.05 M phosphate buffer. [b] 2-Dimethyl-4-*p*-(carboxyphenylazo)-5-hydroxybenzene

Enzyme Assays—The shell-frozen 10,000×*g* liver supernatant was used within 24–48 h and was slowly thawed on ice just prior to the azoreductase assay. Each azo dye (10 μmol) was incubated anaerobically in 5 mL of a reaction mixture containing 0.5 μmol of NADP, 40 μmol of glucose-6-phosphate, 20 μmol of nicotinamide, 22 μmol of magnesium chloride, 50 μmol of phosphate buffer, pH 7.4, and enzyme (10,000 × *g* liver supernatant, equivalent to 250 mg of liver). The reaction mixtures were incubated for 0, 5, 15, 30, 45, and 60 min at 37°C using a continuous nitrogen flush to obtain anaerobic conditions, with gentle shaking. The reaction was stopped by the addition of 5 mL of 10% trichloroacetic acid solution. The mixture was centrifuged, and the supernatant was assayed for the arylamine. The *in vitro* azoreductase activity of each azo dye was measured in parallel with the azoreductase activity of CPA, which acted as a positive control.

The azoreductase activity of CPA was measured by the rate of formation of *p*-aminobenzoic acid (13, 15), using the Bratton and Marshall procedure (16). Sulfanilamide was separated from azosulfamide or sulfachrysoidine using a cation-exchange resin. The resin was prepared according to the method of Hernandez *et al.* (3), and the amount of sulfanilamide was quantitated by the Bratton and Marshall procedure (16). Aniline and naphthylamine were separated similarly from their corresponding amines by column chromatography using an anion-exchange resin. For these assays, a 5-mL aliquot of the trichoroacetic acid supernatant was placed on the column along with an additional 5 mL of distilled water. The combined eluates were collected, mixed, and a 5-mL aliquot was used for the determination of either aniline or naphthylamine by the method of Bratton and Marshall (16). For each azo dye the quantitation of the arylamine product (either *p*-aminobenzoic acid, sulfanilamide, aniline, or naphthylamine) from each incubation flask was calculated by a suitable processed standard curve.

The enzymatic azoreduction of amaranth was measured by following the rate of formation of its metabolite, 4-amino-1-naphthalenesulfonic acid. Samples (15 μL) of the trichloroacetic acid supernatant collected after incubation with amaranth were subjected to HPLC[7] at room temperature on a microparticulate reverse-phase column[8] (4 mm × 30 cm). Amaranth and its metabolites were eluted with a mobile phase containing 2.5% acetonitrile in 0.01 M acetate buffer, pH 4 at a flow rate of 4 mL/min chart speed 1.27 cm/min. The compounds were detected by UV absorbance at 254 nm. The metabolite, 4-amino-1-naphthalenesulfonic acid, was quantitated from a processed standard curve.

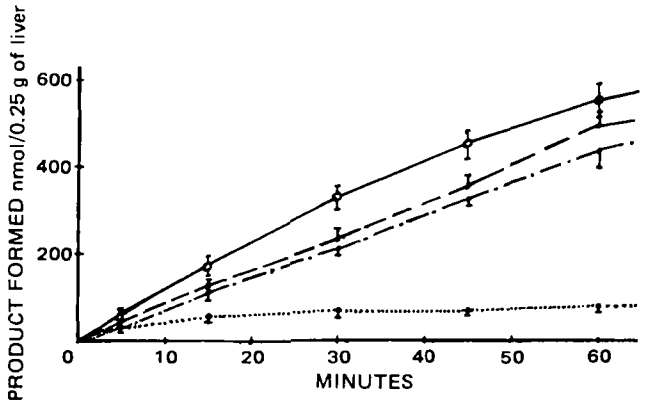

Figure 1—*Average hepatic azoreductase activity. Each azo dye (10 μmol) was incubated anaerobically with the 10,000×g rat liver supernatant and a NADPH-generating system (see text). The amount of arylamine product formed by the reduction of each dye was measured at the indicated time intervals. Key: (—) CPA, results include the* SEM; *(- - -) sulfachrysoidine; (- - -) brilliant crystal scarlet (·····) Sudan I. See Table I for individual values.*

RESULTS

The structures of various azo dyes and their partition coefficients (1-octanol–0.05 M phosphate buffer, pH 7.4) are shown in Table I. Dyes were chosen for their availability and chemical purity. The very lipid-soluble dyes sulfachrysoidine and Sudan I have partition coefficients of 5.67 and 4.33, respectively; the highly water-soluble dyes azosulfamide and amaranth have partition coefficients of 0.149 and 0.187, respectively.

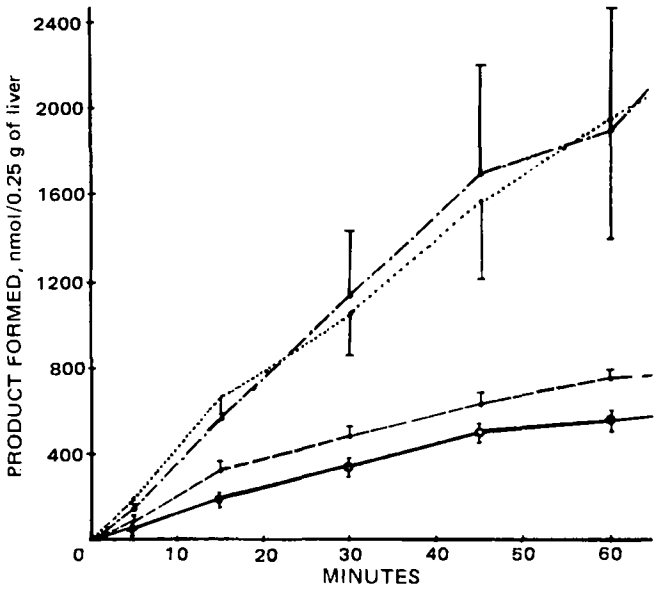

Figure 2—*Average hepatic azoreductase activity. Each azo dye (10 μmol) was incubated with the 10,000×g rat liver supernatant and a NADPH-generating system (see text). The amount of arylamine product formed by the reduction of each dye was measured at the indicated time intervals. Key: (—) CPA, results include the* SEM; *(- - -) amaranth; (·····) azasulfamide (- - -) orange G. See Table I for individual values.*

[7] Model ALC/GPC 204; Water Associates, Milford, Mass.
[8] μBondapak C_{18}; Water Associates, Milford, Mass.

Table II—Hepatic Azoreductase Activity [a]

Dye	n	Amount of Product Formed, nmol/0.25 g of liver					Azoreductase Activity[b]	r
		5 min	15 min	30 min	45 min	60 min		
CPA[c]	15	49.6	187	331	450	548	9.27	0.993
		(10.9)	(15.3)	(29.7)	(36.5)	(43.5)	(0.74)	
Amaranth	2	163	579	1130	1700	1890	33.2	0.990
		(50.1)	(19.1)	(304)	(577)	(577)	(11.9)	
Azosulfamide	3	198	669	1050	1576	1958	32.5	0.996
		(36.4)	(191)	(209)	(350)	(534)	(8.58)	
BCS	3	53	127	230	357	493	8.00	0.968
		(3.34)	(6.67)	(25.2)	(23.4)	(63.7)	(0.93)	
Sulfachrysoidine	3	36	124	226	329	438	7.27	0.996
		(6.94)	(18.3)	(10.9)	(6.67)	(36.3)	(0.40)	
Orange G	3	85	327	485	632	745	12.4	0.976
		(45.1)	(37.2)	(32.9)	(36.1)	(32.6)	(0.59)	
Sudan I	2	38	58	64	70	78	1.03	0.849
		(7.5)	(7.5)	(6.0)	(5.0)	(2.5)	(0.07)	

[a] Standard error in parentheses. [b] Azoreductase activity is equal to the slope of the linear regression line calculated from the nmoles of azo dye formed with respect to time (0–60 min). The azoreductase activity is expressed as nmoles of product formed/min/0.25 g liver. Each azoreductase activity was measured concurrently with CPA activity. [c] 1,2-Dimethyl-4-*p*-(carboxyphenylazo)-5-hydroxybenzene.

The rate of reduction of each azo dye by the 10,000×*g* supernatant fraction obtained from rat liver homogenates was measured by observing the formation of the arylamine with respect to time. The rate of reduction of CPA was measured concurrently with the azoreductase activity of each of the other azo dyes. Therefore, the integrity and consistency of the azoreductase enzyme preparation was verified. The rates of formation of the arylamine from each substrate are shown on Figs. 1 and 2. Azoreductase activity appeared to be linear for the reduction of each azo dye from 0 to 60 min. A regression line was calculated by the least-squares method comparing the product formed with respect to time (0 to 60 min). The slope of this computed regression line is equivalent to the azoreductase activity for each dye and is expressed as nmol of product formed/min/0.25 g of liver (Table II). With the exception of Sudan I, the coefficients of correlation for each azoreductase activity were excellent, implying that the azoreductase activities were linear for 60 min. The correlation coefficient for the azoreductase activity of Sudan I was 0.85.

The partition coefficient in 1-octanol–0.05 M phosphate buffer (pH 7.4) was determined for each dye and compared with its azoreductase activity. A direct correlation between partition coefficient and azoreductase activity was not observed. However, if the azoreductase activity is compared with the reciprocal of the partition coefficient, a regression line with a slope of 3.24 and correlation coefficient of 0.74 can be calculated (Fig. 3). However, if the azoreductase activity for orange G is excluded from the regression line calculation, a slope of 4.00 and correlation coefficient of 0.84 are obtained. Moreover, using the same data and comparing the rate of azoreductase activity with the logarithm of the partition coefficient (log K), a regression line calculated with a slope of −0.20 and a correlation coefficient of −0.75. Thus, there appears to be a trend in which azoreductase activity increases with aqueous solubility, but the correlation is not very strong.

DISCUSSION

From observation of each azo dye structure, factors other than lipid solubility may also affect the rate of azoreductase activity. Enzymatic reduction of azo dyes may either be a one- or two-electron transfer (17, 18). Therefore, the rate of reduction should be influenced by the electron density at the azo bond. Structural variations which can modify this electron density include the nature of the substituents around the ring systems and the potential for intramolecular hydrogen bonding of the substituents with the azo bond (19). For example, electron-withdrawing groups will decrease the electron density, thereby enhancing azo bond reduction. Moreover, hydroxyl or amino groups in close proximity to the azo bond can enhance reduction by hydrogen bonding with the azo bond. Furthermore, the nature of the aromatic systems around the azo bond should effect the rate of azo reduction. Thus, naphthalene provides greater steric hindrance, which should decrease the azoreductase activity in comparison with a phenyl ring.

Several different pathways for the reduction of azo dyes exist in the rat hepatic microsomal fraction, including NADPH cytochrome *c* reductase and cytochrome P_{450} (2–4, 10, 12). Apparently azo dyes with low reduction potentials are reduced more rapidly by cytochrome P_{450}, whereas azo dyes with higher reduction potentials are reduced more rapidly by NADPH cytochrome *c* reductase (5). In addition, amaranth azo reduction occurs primarily *via* cytochrome P_{450} and does not stimulate NADPH oxidation nor superoxide formation (5, 17). Furthermore, the cytosol fraction contains an azoreductase enzyme which is more selective in reducing azo dyes compared with the microsomal fraction (6, 7, 20). Many investigators have also noted that the azo dyes may be reduced nonenzymatically using reduced $NADPH_2$ (2, 3, 12) or reduced flavins (2, 12, 21). The nonenzymatic azo dye reduction is related to the reduction potential between $NADP^+$/NADPH and the substrate which acts as a final electron acceptor (20). Therefore, important factors for comparing the rates of reduction of azo dyes by hepatic enzymes include the reduction potential of the substrate and its affinity for the enzyme system.

The results of this investigation demonstrated that Sudan I had the slowest rate of azo dye reduction probably due to both the lack of electron-withdrawing groups on the aromatic ring system and its high lipid solubility. Higher rates of azo reduction are observed for those dyes containing electron-withdrawing substituents such as a sulfonamido group in sulfachrysoidine, a sulfonate group in both brilliant crystal scarlet and orange G, and carboxylic group in CPA. The higher rate of

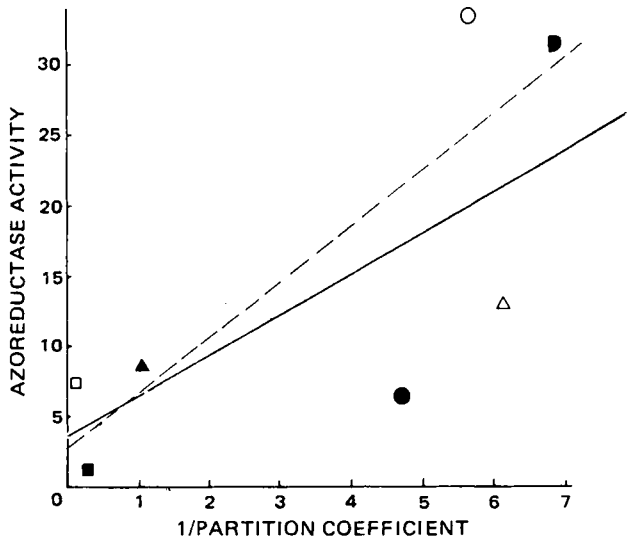

Figure 3—*Correlation of azoreductase activity and partion coefficient for each dye. The azoreductase activity (nmol of product formed/min 0.25 g of liver) for each dye is compared with the reciprocal of the corresponding partition coefficient (n-octanol–0.05 M phosphate buffer, pH 7.4). The calculated regression line (——) including the orange G azoreductase activity gives a slope of 3.24 and correlation coefficient of 0.74. The calculated regression excluding the orange G azoreductase activity (- - -) gives a slope of 4.00 and a correlation coefficient of 0.84. Key: (■) Sudan I; (□) sulfachrysoidine; (▲) CPA; (●) brilliant crystal scarlet; (△) orange G; (◑) azosulfamide; (○) amaranth.*

azo bond reduction observed with orange G compared with brilliant crystal scarlet may be due to steric hindrance in the latter. Amaranth and azosulfamide had the highest rates of azoreductase activity due to the presence of more electron-withdrawing groups (sulfonates) in the ring system. Sulfachrysoidine, a lipid-soluble azo dye, as indicated by its large partition coefficient has a greater than anticipated rate of azo reduction due to the presence of the sulfonamido group. The potential for the formation of an intramolecular hydrogen bond between the hydroxyl or amino group at the *ortho* position of the aromatic rings and the azo nitrogen is common to all the dyes investigated in this study and, therefore, should not be a major contributing factor in the observed differences in the rates of azo bond reduction.

Because of the wide variety of structures of azo dyes, it is difficult to determine which physicochemical factor influences the rate of azo reduction by the hepatic azoreductase enzymes the most. This investigation used the 10,000×*g* supernatant fraction from liver homogenates as the enzyme source to determine if an overall generalization could be determined for the rates of reduction of azo dyes. The results of this investigation show that both the partition coefficient and the presence of electron-withdrawing substituents will influence the rate of reduction of the azo bond. Apparently, the larger the number of electron-withdrawing groups, the more rapid the rate of reduction by the hepatic azoreductase system.

REFERENCES

(1) E. N. Abrhart "Dyes and Their Intermediates," 2nd ed., Edward Arnold, Ltd. London, 1977.

(2) J. R. Fouts, J. J. Kamm, and B. B. Brodie, *J. Pharmacol. Exp. Ther.*, **120,** 291 (1957).

(3) P. H. Hernandez, P. Mazel, and J. R. Gillette, *Biochem. Pharmacol.*, **16,** 1859 (1967).

(4) R. Walker, *Food Cosmet. Toxicol.*, **8,** 659 (1970).

(5) F. J. Peterson, R. P. Mason, and J. L. Holtzman, *Pharmacologist*, **19,** 210 (1977).

(6) S. Fujita and J. Peisach, *Biochem. Biophys. Res. Commun.*, **78,** 328 (1977).

(7) M. Huang, G. T. Miwa, and A. Y. H. Lu, *J. Biol. Chem.*, **254,** 3930 (1979).

(8) J. W. Daniel, *Toxicol Appl. Pharmacol.*, **4,** 572 (1962).

(9) J. J. Roxon, A. J. Ryan, and S. E. Wright, *Food Cosmet. Toxicol.*, **5,** 349 (1967).

(10) T. Watabe, N. Ozawa, and F. Kobayashi, *Food Cosmet. Toxicol.*, **18,** 349 (1980).

(11) R. P. Mason, F. J. Peterson, and J. L. Holtzman, *Biochem. Biophys. Res. Commun.*, **75,** 532 (1977).

(12) L. Shargel and P. Mazel, *Biochem. Pharmacol.*, **22,** 2365 (1973).

(13) L. Shargel, S. Akov, and P. Mazel, *J. Agr. Food Chem.*, **20,** 27 (1972).

(14) P. Hernandez, K. A. Pittman, and L. Shargel, *Pharmacologist*, **11,** 260 (1969).

(15) E. J. Smith and E. J. van Loon, *Anal. Biochem.*, **31,** 315 (1969).

(16) A. C. Bratton and E. K. Marshall, Jr., *J. Biol. Chem.*, **128,** 537 (1939).

(17) F. J. Peterson and J. L. Holtzman, in "Extrahepatic Metabolism of Drugs and Other Foreign Compounds," T. E. Gram, Ed., SP Medical and Scientific Books, New York, N.Y., 1981, pp. 27–28.

(18) F. G. Thomas and K. G. Boto, in "The Chemistry of the Hydrazo, Azo and Azoxy Groups, Pt 1," S. Patai, Ed., Wiley New York, N.Y., 1975, pp. 489–490.

(19) R. Walker and A. J. Ryan, *Xenobiotica*, **1,** 453 (1971).

(20) M. T. Huang, G. T. Miwa, and A. Y. H. Lu, *Biochem. Biophys. Res. Commun.*, **83,** 1253 (1978).

(21) L. D. Shargel, Ph.D. Dissertation, The George Washington University, Washington, D.C. (1969).

ACKNOWLEDGMENTS

Presented in part at the Spring Meeting of the Federation of American Societies for Experimental Biology [*Fed. Proc. Am. Soc. Exp. Biol.* **40,** 735 (1981)].

We would like to express our appreciation to Mr. Bijan Almassian for his excellent technical assistance.

High-Performance Liquid Chromatographic Analysis of the Semisynthetic Epipodophyllotoxins Teniposide and Etoposide Using Electrochemical Detection

JOSEPH A. SINKULE and WILLIAM E. EVANS ˣ

Received June 28, 1982, from the *Pharmacokinetics and Pharmacodynamics Section, St. Jude Children's Research Hospital, Memphis, TN 38101.* Accepted for publication December 13, 1982.

Abstract □ A high-performance liquid chromatographic (HPLC) assay was developed for the quantitation of two structurally similar and highly active anticancer drugs, etoposide (I) and teniposide (II), and their potential metabolites (hydroxy acid, picrolactone, and aglycone). The assay utilizes electrochemical detection, which imparts specificity and sensitivity sufficient to detect ≥20 ng/mL in plasma, urine, and CSF. The mean assay coefficients of variation were 5.1 and 8.1% for teniposide (10 μg/mL) and etoposide (5 μg/mL), respectively. The extraction efficiencies were 86% for etoposide, 70% for its hydroxy acid metabolite, 66% for teniposide, and 54% for the hydroxy acid of teniposide. The correlation coefficient of the multilevel standard curve was ≥0.995 over the concentration range of 0.05–50 μg/mL for the parent drugs and metabolites extracted from plasma. This method has been used to determine the concentrations of the parent drugs and their metabolites in the plasma, urine, and CSF of patients with cancer.

Keyphrases □ Etoposide—analysis with metabolites, high-performance liquid chromatography with electrochemical detection, human urine, plasma, and CSF □ Teniposide—analysis with metabolites, high-performance liquid chromatography with electrochemical detection, human urine, plasma, and CSF

Two relatively new and highly active antineoplastic drugs, etoposide {4′-demethylepipodophyllotoxin 9-[4,6-*O*-(*R*)-ethylidene-β-D-glucopyranoside], (I)} and teniposide {4′-demethylepipodophyllotoxin 9-[4,6-*O*-(*R*)-2-thenylidene-β-D-glucopyranoside], (II)} have clinical activity in childhood leukemias, lymphomas, neuroblastomas, brain tumors, and germ cell tumors and adult lung, brain, bladder, and testicular cancers as well as adult leukemias and lymphomas (1–5). The proposed metabolic scheme was derived from the known molecular transfor-

0022-3549/84/0200-0164$01.00/0

© 1984, American Pharmaceutical Association

azo bond reduction observed with orange G compared with brilliant crystal scarlet may be due to steric hindrance in the latter. Amaranth and azosulfamide had the highest rates of azoreductase activity due to the presence of more electron-withdrawing groups (sulfonates) in the ring system. Sulfachrysoidine, a lipid-soluble azo dye, as indicated by its large partition coefficient has a greater than anticipated rate of azo reduction due to the presence of the sulfonamido group. The potential for the formation of an intramolecular hydrogen bond between the hydroxyl or amino group at the *ortho* position of the aromatic rings and the azo nitrogen is common to all the dyes investigated in this study and, therefore, should not be a major contributing factor in the observed differences in the rates of azo bond reduction.

Because of the wide variety of structures of azo dyes, it is difficult to determine which physicochemical factor influences the rate of azo reduction by the hepatic azoreductase enzymes the most. This investigation used the 10,000×*g* supernatant fraction from liver homogenates as the enzyme source to determine if an overall generalization could be determined for the rates of reduction of azo dyes. The results of this investigation show that both the partition coefficient and the presence of electron-withdrawing substituents will influence the rate of reduction of the azo bond. Apparently, the larger the number of electron-withdrawing groups, the more rapid the rate of reduction by the hepatic azoreductase system.

REFERENCES

(1) E. N. Abrhart "Dyes and Their Intermediates," 2nd ed., Edward Arnold, Ltd. London, 1977.

(2) J. R. Fouts, J. J. Kamm, and B. B. Brodie, *J. Pharmacol. Exp. Ther.*, **120,** 291 (1957).

(3) P. H. Hernandez, P. Mazel, and J. R. Gillette, *Biochem. Pharmacol.*, **16,** 1859 (1967).

(4) R. Walker, *Food Cosmet. Toxicol.*, **8,** 659 (1970).

(5) F. J. Peterson, R. P. Mason, and J. L. Holtzman, *Pharmacologist*, **19,** 210 (1977).

(6) S. Fujita and J. Peisach, *Biochem. Biophys. Res. Commun.*, **78,** 328 (1977).

(7) M. Huang, G. T. Miwa, and A. Y. H. Lu, *J. Biol. Chem.*, **254,** 3930 (1979).

(8) J. W. Daniel, *Toxicol Appl. Pharmacol.*, **4,** 572 (1962).

(9) J. J. Roxon, A. J. Ryan, and S. E. Wright, *Food Cosmet. Toxicol.*, **5,** 349 (1967).

(10) T. Watabe, N. Ozawa, and F. Kobayashi, *Food Cosmet. Toxicol.*, **18,** 349 (1980).

(11) R. P. Mason, F. J. Peterson, and J. L. Holtzman, *Biochem. Biophys. Res. Commun.*, **75,** 532 (1977).

(12) L. Shargel and P. Mazel, *Biochem. Pharmacol.*, **22,** 2365 (1973).

(13) L. Shargel, S. Akov, and P. Mazel, *J. Agr. Food Chem.*, **20,** 27 (1972).

(14) P. Hernandez, K. A. Pittman, and L. Shargel, *Pharmacologist*, **11,** 260 (1969).

(15) E. J. Smith and E. J. van Loon, *Anal. Biochem.*, **31,** 315 (1969).

(16) A. C. Bratton and E. K. Marshall, Jr., *J. Biol. Chem.*, **128,** 537 (1939).

(17) F. J. Peterson and J. L. Holtzman, in "Extrahepatic Metabolism of Drugs and Other Foreign Compounds," T. E. Gram, Ed., SP Medical and Scientific Books, New York, N.Y., 1981, pp. 27–28.

(18) F. G. Thomas and K. G. Boto, in "The Chemistry of the Hydrazo, Azo and Azoxy Groups, Pt 1," S. Patai, Ed., Wiley New York, N.Y., 1975, pp. 489–490.

(19) R. Walker and A. J. Ryan, *Xenobiotica*, **1,** 453 (1971).

(20) M. T. Huang, G. T. Miwa, and A. Y. H. Lu, *Biochem. Biophys. Res. Commun.*, **83,** 1253 (1978).

(21) L. D. Shargel, Ph.D. Dissertation, The George Washington University, Washington, D.C. (1969).

ACKNOWLEDGMENTS

Presented in part at the Spring Meeting of the Federation of American Societies for Experimental Biology [*Fed. Proc. Am. Soc. Exp. Biol.* **40,** 735 (1981)].

We would like to express our appreciation to Mr. Bijan Almassian for his excellent technical assistance.

High-Performance Liquid Chromatographic Analysis of the Semisynthetic Epipodophyllotoxins Teniposide and Etoposide Using Electrochemical Detection

JOSEPH A. SINKULE and WILLIAM E. EVANS ˣ

Received June 28, 1982, from the *Pharmacokinetics and Pharmacodynamics Section, St. Jude Children's Research Hospital, Memphis, TN 38101.* Accepted for publication December 13, 1982.

Abstract □ A high-performance liquid chromatographic (HPLC) assay was developed for the quantitation of two structurally similar and highly active anticancer drugs, etoposide (I) and teniposide (II), and their potential metabolites (hydroxy acid, picrolactone, and aglycone). The assay utilizes electrochemical detection, which imparts specificity and sensitivity sufficient to detect ≥20 ng/mL in plasma, urine, and CSF. The mean assay coefficients of variation were 5.1 and 8.1% for teniposide (10 μg/mL) and etoposide (5 μg/mL), respectively. The extraction efficiencies were 86% for etoposide, 70% for its hydroxy acid metabolite, 66% for teniposide, and 54% for the hydroxy acid of teniposide. The correlation coefficient of the multilevel standard curve was ≥0.995 over the concentration range of 0.05–50 μg/mL for the parent drugs and metabolites extracted from plasma. This method has been used to determine the concentrations of the parent drugs and their metabolites in the plasma, urine, and CSF of patients with cancer.

Keyphrases □ Etoposide—analysis with metabolites, high-performance liquid chromatography with electrochemical detection, human urine, plasma, and CSF □ Teniposide—analysis with metabolites, high-performance liquid chromatography with electrochemical detection, human urine, plasma, and CSF

Two relatively new and highly active antineoplastic drugs, etoposide {4′-demethylepipodophyllotoxin 9-[4,6-*O*-(*R*)-ethylidene-β-D-glucopyranoside], (I)} and teniposide {4′-demethylepipodophyllotoxin 9-[4,6-*O*-(*R*)-2-thenylidene-β-D-glucopyranoside], (II)} have clinical activity in childhood leukemias, lymphomas, neuroblastomas, brain tumors, and germ cell tumors and adult lung, brain, bladder, and testicular cancers as well as adult leukemias and lymphomas (1–5). The proposed metabolic scheme was derived from the known molecular transfor-

0022-3549/84/0200-0164$01.00/0

© 1984, American Pharmaceutical Association

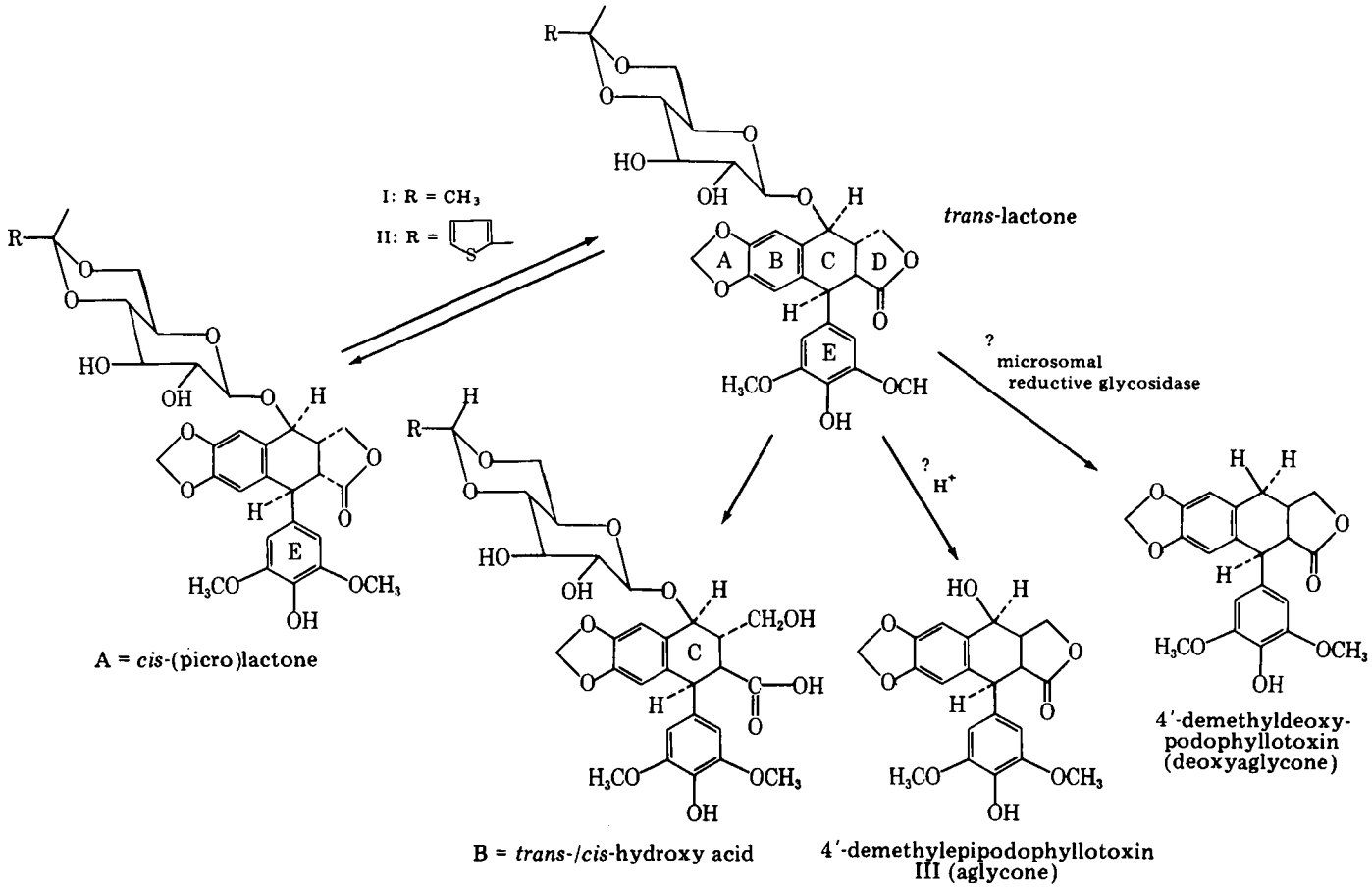

Scheme I—*Proposed metabolic transformations of the epipodophyllotoxin derivatives etoposide and teniposide.*

mations of podophyllotoxin, the compound from which these two drugs are synthesized (Scheme I). The biologically active molecules exist in a highly strained 2:3 *trans*-lactone ring that undergoes isomerization to a less active, more flexible, and less strained 2:3 *cis*-lactone or picro conformation hereafter referred to as picrolactones (IA, IIA) (6, 7). There are reports suggesting this isomerization takes place *in vivo* (8, 9). Initial Phase I pharmacokinetic studies using radiolabeled drug (10) measured total radioactivity in the chloroform-extractable layer and could not differentiate metabolites in human urine (11) and serum (12) that were later identified as chloroform-insoluble hydroxy acids (IB, IIB). Potential aglycones (III) formed by reductive or oxidative hydrolysis of the sugar moiety and glucuronide and/or sulfate conjugates are included as potential metabolites, although they have not yet been detected in biological fluids.

A new isocratic reverse-phase high-performance liquid chromatographic (HPLC) method utilizing the sensitivity and specificity of electrochemical detection was developed to quantitate these two drugs and their potential metabolites in the biological fluids of patients with cancer.

EXPERIMENTAL

Drugs, Reagents, and Equipment—Etoposide (NSC 141540) and teniposide (NCS 122819) were gifts from the manufacturer[1]. The potential metabolites of etoposide and teniposide were synthesized as described elsewhere (12) or provided by other sources[2]. Drug standards were dissolved in methanol (1 mg/mL) and stored at −70°C. The standards were routinely checked for purity by TLC and HPLC. HPLC-grade methanol, acetonitrile, ethyl acetate, and chloroform were used throughout. Water was deionized, distilled, and filtered for HPLC use. Other chemicals and glassware were of standard laboratory quality. TLC plates included commercially available analytical silica gel (0.25 mm), preparative silica gel (2 mm), and reverse-phase $KC_{18}F$ (0.2 mm). The HPLC apparatus consisted of an isocratic pump[3], an injector[4], a 10-μm reverse-phase phenyl precolumn and analytical column[5], and a UV ab-

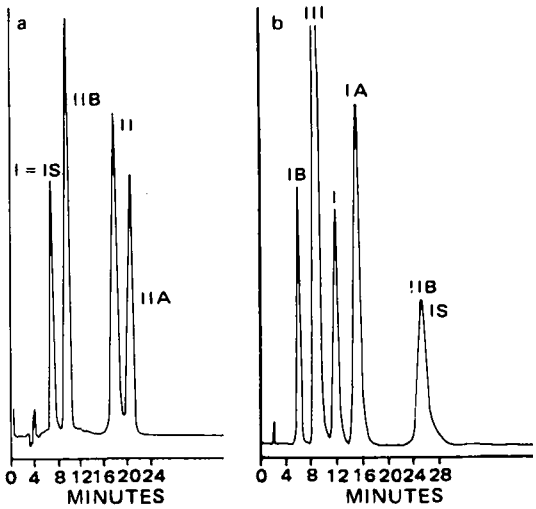

Figure 1—*Chromatographic separation of (a) teniposide (II) and its potential metabolites and (b) etoposide (I) and its potential metabolites. The HPLC conditions are described in the text.*

[1] Bristol Laboratories, Syracuse, N.Y.
[2] Dr. H. Stähelin, Sandoz LTD., Basel, Switzerland.
[3] Laboratory Data Control, Riviera Beach, Fla.
[4] Model 7125 with a 50-μL loop; Rheodyne, Berkeley, Calif.
[5] 4.6 mm × 250 mm, 10-μm, μBondapak phenyl; Water Associates, Milford, Mass.

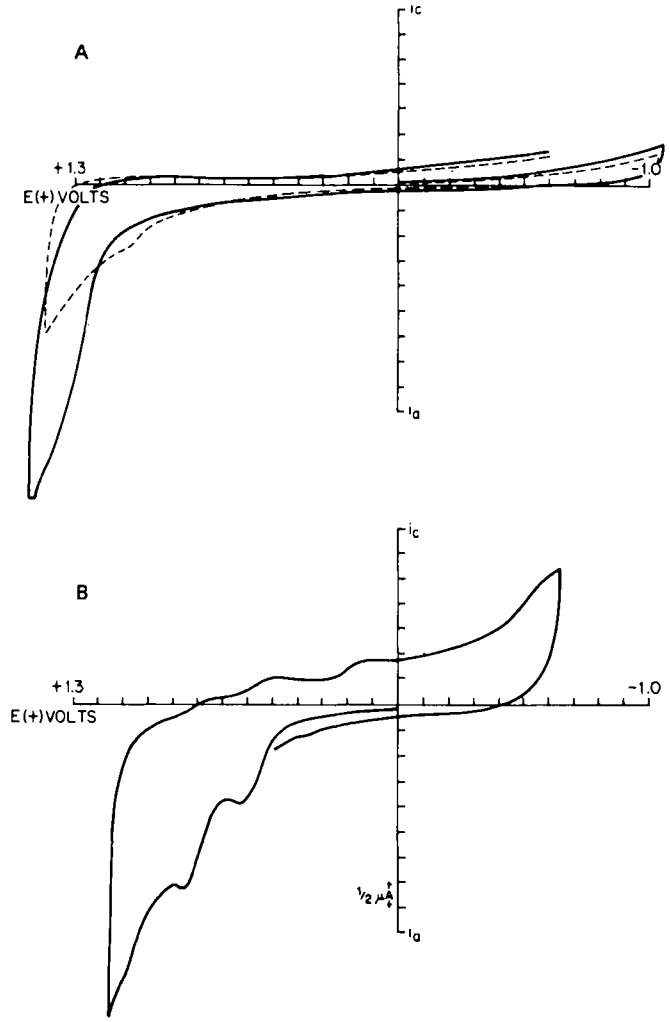

Figure 2—*Cyclic voltammograms of podophyllotoxin (A) and etoposide (B). Forward scan (anodic) from 0.0 applied potential; the broken line in A is the solvent scan.*

sorbance detector[6] connected in series to an amperometric (electrochemical) detector[7]. A dual-pen strip chart recorder was used for graphic display of the two detector outputs. Spectral identification of the metabolites was achieved by IR[8], ^{1}H-NMR[9], and MS[10]. Cyclic voltammograms were performed in 70% sodium acetate (pH 5) and 30% 2-propanol. The scans initiated at 0.0 applied potential with the oxidative (anodic) preceding the reductive (cathodic) scan and returning to 0.0 potential[11].

Liquid Chromatographic Conditions—A prefiltered mobile phase of water–acetonitrile–acetic acid 68:30:2 at a flow rate of ~1 mL/min (1500 psi) through a 10-μm reverse-phase HPLC column[5] was used to resolve teniposide and its metabolites (Fig. 1A). Assay conditions for etoposide and its metabolites were similar, with a mobile phase consisting of water–acetonitrile–acetic acid (74:25:1) (Fig. 1B).

Extraction of Biological Fluids—*Teniposide*—To 0.5 mL of plasma, urine, or CSF was added 0.5 mL of saturated ammonium sulfate followed by 4 mL of ethyl acetate and 10 μL of a 100-μg/mL stock solution of etoposide (used as an internal standard). The sample was vortexed for 5 min and then centrifuged at 3000 rpm for 15 min. The upper (organic) layer was collected and set aside. The aqueous layer was reextracted with 4 mL of ethyl acetate by vigorously vortexing, then centrifuged at 3000 rpm for 15 min. The organic layer was combined with the previously collected ethyl acetate layer. This organic extract was dried under a gentle nitrogen stream, and the residue was reconstituted with 200 μL of methanol before HPLC analysis.

Etoposide—To 0.5 mL of plasma, urine, or CSF was added 5 μL of a 2.5-μg/mL stock solution of IIB (internal standard for I analysis) followed by saturated ammonium sulfate and double ethyl acetate extraction, as described above. The organic layer was decanted, dried under a nitrogen stream, and reconstituted with 200 μL of methanol just prior to injection.

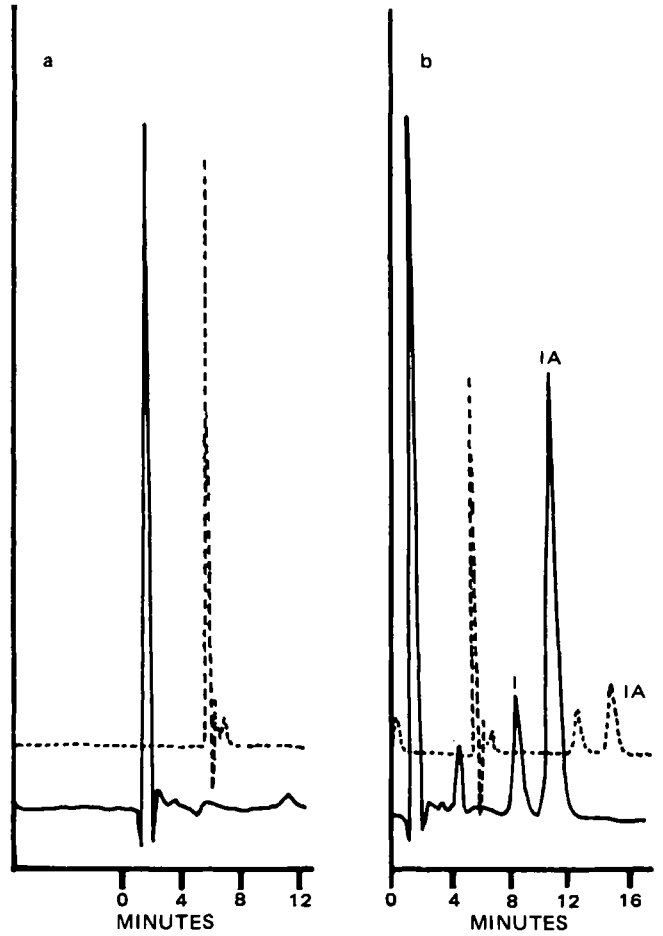

Figure 3—*Blank serum (a) and serum with etoposide and IA (b) showing relative UV (---) and electrochemical (—) response to the parent* trans*-lactone (I) and the picrolactone isomer (IA).*

Extraction Efficiency—To calculate the extraction efficiency, 10 aliquots of plasma containing either 10 μg/mL or 1 μg/mL of teniposide or etoposide and their respective metabolites were extracted, and the residues were reconstituted in 200 μL of methanol. Equivalent amounts (10 μg and 1 μg) of pure compounds in mobile phase were added to the residue of 1-mL blank plasma extracts. Extraction efficiency was calculated by the integrated area (or peak height) of the compound extracted, divided by the area (or height) of the same concentration of the compound added after extraction.

Precision and Accuracy—Teniposide or etoposide was added to 5 mL of pooled plasma (10 μg/mL) and thoroughly mixed. The sample was divided into 10 aliquots (0.5 mL each) and frozen at −70°C. All 10 samples were extracted and quantitated over a 3-d period. Daily (n = 4) and day-to-day (n = 3/d) coefficients of variation were calculated (expressed as percentage). Accuracy was determined by preparing samples containing unknown (blind) quantities of the compounds of interest. Percent recoveries were determined by two different operators on the same chromatographic system.

Multilevel Calibration Curves—Spiked samples in the concentration range of 0.05–50 μg/mL were extracted and each calibrator was analyzed in triplicate. Peak areas of the compounds were quantitated with the computing integrator, and peak heights were recorded by the strip-chart recorder attenuated to 100 mV. After chromatographic analysis, the peak areas, peak heights, peak area ratios (compound/internal standard), and peak height ratios were analyzed by linear regression against the known concentrations of the spiked samples.

[6] Model UV III, 284 nm; Laboratory Data Control, Riviera Beach, Fla.
[7] LC-4A Amperometric Detector; Bioanalytical Systems, Inc., West Lafayette, Ind.
[8] IR-20AX; Beckman, Berkeley, Calif.
[9] EM-930; Varian, Sunnyvale, Calif.
[10] Varian MAT; Varian, Sunnyvale, Calif.
[11] CV-1B Cyclic Voltameter; Bioanalytical Systems, Inc., West Lafayette, Ind.

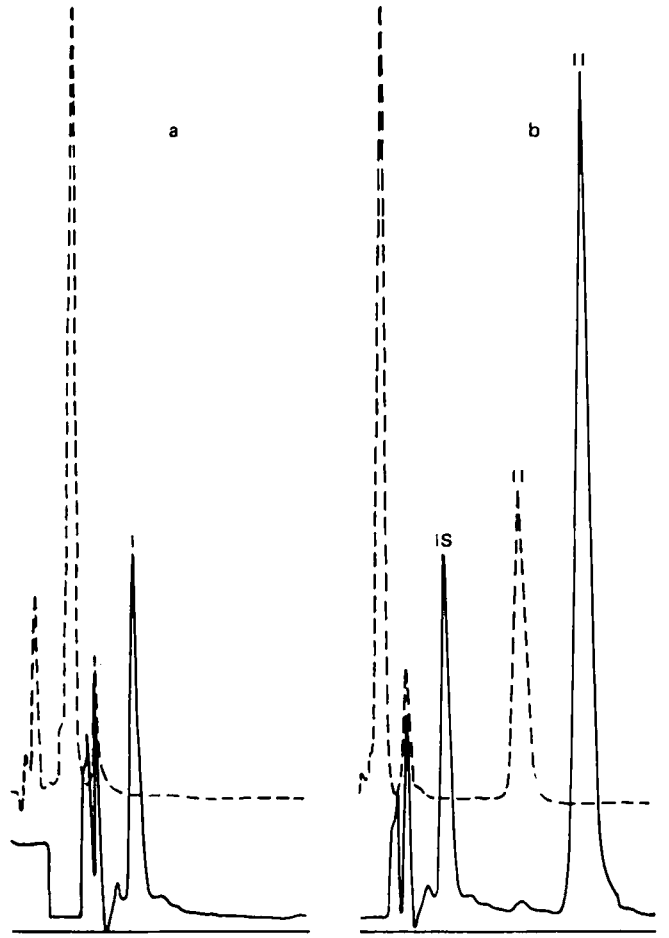

Figure 4—*Chromatograms of plasma obtained from a patient before (a) and 15 min after (b) a teniposide infusion. Key: (- - -) UV absorbance; (—) electrochemical response.*

Application to Biological Fluids—Blood (1–2 mL) was obtained in heparinized tubes prior to infusion and at 0.5, 1, 2, 4, 6, 8, 12, 24, and 48 h after the end of infusion and immediately placed on ice. Urine was collected for eight 6-h intervals in sterile containers and refrigerated.

RESULTS

Cyclic voltammograms of etoposide and podophyllotoxin are reproduced in Fig. 2. Optimal potentials for electrochemical detection of teniposide and etoposide were 0.75 and 0.85 V, respectively. Podophyllotoxin was not oxidized and its cyclic voltammogram was not substantially different from the solvent scan. Since the 4′-demethylepidophyllotoxin (aglycone III) of teniposide and etoposide possesses electrochemical activity, the moiety responsible for the electroactivity of teniposide and etoposide may be the phenolic hydroxyl group on the E-ring of these molecules, which is not present on podophyllotoxin. However, the exact redox mechanism remains to be elucidated.

Typical HPLC profiles of teniposide, etoposide, and their potential metabolites are shown in Fig. 1A and B, respectively. The relative response of the parent drug and the picrolactone with UV and electrochemical detectors can be seen in Fig. 3. The UV monitor was at maximal detector sensitivity, and the electrochemical detector could have been adjusted 50-fold more sensitive. The enhanced electroactivity of the picrolactone over that of the *trans*-lactone is as yet unexplained. Table I shows the retention volumes (V_R) and capacity factors (K') using the HPLC conditions noted above. Although separation of the *trans*-lactone from the picrolactone was not achieved using a nonpolar reverse-phase octadecylsilane (C_{18} or ODS) bonded phase, separation was accomplished using a more polar bonded phase such as phenyl or cyanonitrile.

The extraction efficiency of teniposide and its potential metabolites were: IIB, 70%; II, 66%; and IIA, 55%. The extraction efficiency of etoposide and its potential metabolites were: IB, 90%; I, 88%; and IA, 80%. The retention volumes (or retention times) for components of either assay were reproducible with a day-to-day CV of <2%. Quantitative precision (CV) for II (10 μg/mL, n = 10) was 5.1%, while the CV for I (5 μg/mL, n = 10) was 8.1%. Day-to-day variations (n = 3) for II, IIB, and IIA were 3.8, 7.6, and 4.2%.

Table I—Retention Volumes (V_R) and Capacity Factors (K') of I, II, and Their Potential Metabolites

Compound	V_R, mL	K'
I[a]	8	1.67
II[a]	26	7.67
IIB[a]	12	3.00
IIA[a]	30	9.00
III[a]	7.2	1.40
III[b]	14	3.67
I[b]	18	5.00
IB[b]	9	2.00
IA[b]	23	6.67
IIB[b]	30	9.00

[a] Retention data from a μBondapak phenyl column, 25 cm × 4.6 mm, with a mobile phase of water–acetonitrile–acetic acid (68:30:2) at a flow rate of 1 mL/min. [b] Retention data from a μBondapak phenyl column, 25 cm × 4.6 mm, with a mobile phase of water–acetonitrile–acetic acid (74:25:1) at 1 mL/min.

Least-squares regression analyses of teniposide and metabolite peak areas, peak area ratios, and peak height ratios to internal standard *versus* known concentration were linear from 0.05–50.0 μg/mL. The linear correlation coefficients of the best-fit line were >0.995 for the three methods of quantitation. Accuracy of the assay, determined by analysis of three prespiked unknown quantities of teniposide and metabolites was within ±5% of the true values.

A typical chromatogram of a preinfusion blank and 15-min postinfusion sample from one patient receiving teniposide (165 mg/m^2 over 40 min) is shown in Fig. 4. The concentration of teniposide in the sample chromatogram is 43.5 μg/mL. Figure 5 is a reproduction of a 15-min postinfusion chromatogram for a patient who received etoposide (250 mg/m^2 over 35 min); the plasma concentration shown was 72.2 μg/mL.

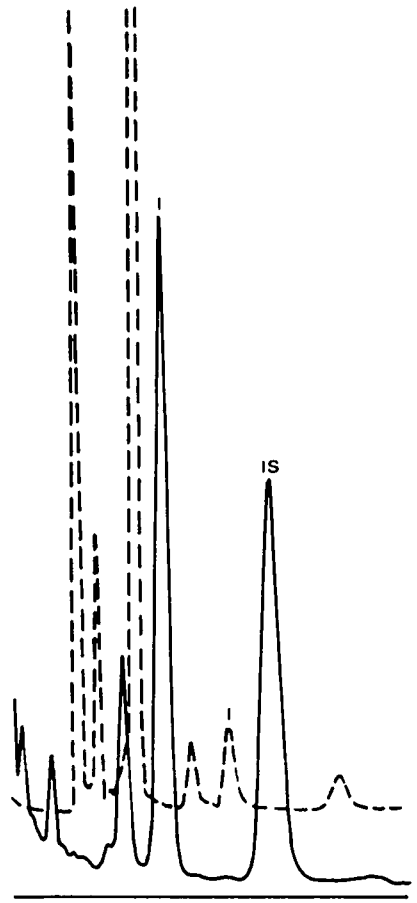

Figure 5—*Chromatogram of plasma obtained from a patient 15 min after an etoposide infusion. Key: (- - -) UV absorbance; (—) electrochemical response.*

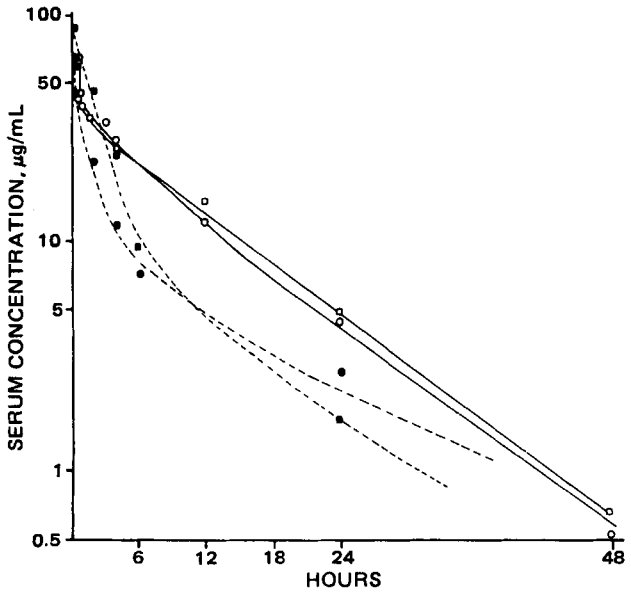

Figure 6—*Comparative plasma concentration* versus *time profiles of two patients who received etoposide at 250 mg/m² (■) and 200 mg/m² (●) and two patients who received teniposide at 165 mg/m² (□,○).*

Comparative plasma concentration *versus* time profiles of two patients are shown in Fig. 6.

DISCUSSION

Both etoposide and teniposide are undergoing extensive clinical investigation for the treatment of various pediatric and adult malignancies. For this reason, a sensitive, specific, and simple analytical method for the determination of both etoposide, teniposide, and potential metabolic products of these drugs is necessary.

With a slight variation in the mobile phase, I, II, and all potential metabolites are well resolved from any coeluting endogenous substances. A relatively inexpensive electrochemical detector provides an almost 10-fold greater sensitivity over previously described HPLC–UV methods. The multilevel calibration curve (0.05–50.0 μg/mL) gave a linear correlation coefficient of $r \geq 0.995$, and the *CV* of each calibration point was ≤8%. The single step extraction of both parent drugs and metabolites is not optimal, and we are currently pursuing more efficient methods of extraction.

The hydroxy acids of teniposide and etoposide (IIB and IB) appear to be the metabolites detectable in plasma and urine, based on chromatographic peaks eluting in the region of the *cis*-hydroxy acids. The picrolactones of I and II (IA and IIA) were detected in the plasma and urine of some patients, but the concentrations never exceeded 5.0 μg/mL. The aglycone (III) has not been detected in any biological fluid to date.

Clinical investigations are currently underway utilizing this sensitive and specific HPLC assay for etoposide, teniposide, and their metabolites. These data should describe the pharmacokinetics of the drugs, further define components of systemic clearance (*i.e.*, metabolic and renal clearance), and evaluate any differences in the extent of metabolism of etoposide and teniposide in pediatric and adult patients.

REFERENCES

(1) M. Rozencweig, D. D. Von Hoff, J. E. Henney, and F. M. Muggia, *Cancer*, **40**, 334 (1977).

(2) P. Dombernowsky, N. I. Nissen, and V. Larsen, *Cancer Chemother. Rep*, **56**, 71 (1972).

(3) M. Goldsmith and S. K. Carter, *Eur. J. Cancer*, **9**, 477 (1973).

(4) N. J. Vogelzang, D. Raghavan, and B. J. Kennedy, *Am. J. Med.*, **72**, 136 (1982).

(5) G. Rivera, W. P. Bowman, A. T. Look, W. E. Evans, D. Kalwinsky, and G. V. Dahl, *Cancer Treat. Rev.*, **9(S)**, 110 (1982).

(6) M. G. Kelly, and J. L. Hartwell, *J. Natl. Cancer Inst.*, **14**, 967 (1954).

(7) W. J. Gensler and C. D. Gatsonis, *J. Org. Chem.*, **29**, 3224 (1966).

(8) W. J. Gensler, C. D. Murthy, and M. H. Trammell, *J. Med. Chem.*, **20**, 635 (1977).

(9) C. F. Brewer, J. D. Loike, S. B. Horwitz, H. Sternlicht, and W. J. Gensler, *J. Med. Chem.*, **22**, 215 (1979).

(10) L. M. Allen and P. J. Creaven, *Eur. J. Cancer*, **11**, 697 (1975).

(11) L. M. Allen, C. Marks, and P. J. Creaven, *Proc. Am. Assoc. Cancer Res.*, **17**, 6 (1976).

(12) R. J. Strife, I. Jardine, and M. Colvin, *J. Chromatogr.*, **182**, 211 (1980).

ACKNOWLEDGMENTS

Supported in part by NIH Cancer Center CORE Grant CA 21765, Leukemia Program Project Grant CA 20180, and ALSAC.

Evaluation of the Bioavailability of Sarpicillin, the Methoxymethyl Ester of Hetacillin, in Humans

S. STAVCHANSKY *x, R. S. PEARLMAN *, D. R. VAN HARKEN ‡, R. D. SMYTH ‡, G. H. HOTTENDORF ‡, A. MARTIN *, J. NEWBURGER *, and L. W. SCHNEIDER *

Received March 15, 1982, from *The University of Texas at Austin, College of Pharmacy, Drug Dynamics Institute, Austin, TX 78712, and ‡Bristol Laboratories, Syracuse, NY 13201. Accepted for publication December 21, 1982.

Abstract □ The relative bioavailability of sarpicillin (the methoxymethyl ester of hetacillin) from three different oral dosage forms was compared in humans employing a three-way crossover study design. Each unit dose contained 250 mg of sarpicillin in terms of anhydrous ampicillin activity. The comparative bioavailability of a tablet containing added buffer, a liquid-filled capsule, and a standard powder-filled capsule was determined. The bioavailability parameters were C_{max}, t_{max}, and AUC of intact plasma sarpicillin levels and saliva ampicillin levels. Significant correlation was found between plasma sarpicillin levels and saliva ampicillin levels following the administration of sarpicillin. All three formulations yielded statistically similar C_{max} and AUC values with respect to plasma sarpicillin and saliva ampicillin levels. However, a more rapid absorption of intact sarpicillin was observed with the buffered tablet formulation, as reflected by significantly smaller t_{max} for both plasma sarpicillin and saliva ampicillin levels. The faster absorption from the tablet formulation gave more precise absorption among subjects.

Keyphrases □ Sarpicillin—evaluation of bioavailability, humans, methoxymethyl ester of hetacillin □ Bioavailability—sarpicillin, methoxymethyl ester of hetacillin, humans □ Hetacillin—methoxymethyl ester, evaluation of bioavailability of sarpicillin in humans

Ampicillin (II) is an acid-resistant form of penicillin, whose oral absorption is incomplete and erratic in humans. Factors which have been shown to account for differences in ampicillin bioavailability are intersubject variability (1), age of subjects (2), liver disease (3), and variation in forms [hydrate (4) and salt (5)] of ampicillin. Esters of penicillin, such as pivampicillin hydrochloride and hetacillin have been introduced in an effort to improve the properties of ampicillin. Hetacillin is susceptible to rapid hydrolysis both *in vivo* and *in vitro* (6, 7). However, this drug improves ampicillin bioavailability (8), and its activity depends on the formation of ampicillin.

Sarpicillin free base [methoxymethyl (2*S*,5*R*,6*R*)-6-(2,2-dimethyl-5-oxo-4-phenyl-1-imidazolidinyl)-3,3-dimethyl-7-oxo-4-thia-1-azabicyclo[3.2.0]heptane-2-carboxylate] (I) a new semisynthetic penicillin derivative, the methoxymethyl ester of hetacillin is a basic, nonionizable, highly lipophilic antibiotic possessing the same antimicrobial spectrum and activity as ampicillin. It is effective against Gram-negative pathogens such as *Hemophilus influenzae* and the coliform group. The chemical relationship of sarpicillin to ampicillin is apparent.

Distribution of antibiotics to tissues is of increasing clinical concern (9, 10). Sarpicillin is of particular importance because it results in high tissue concentrations of ampicillin, particularly in lipid-rich regions such as the brain and prostatic tissue, as well as in the CSF and lungs.

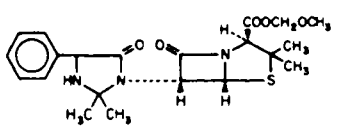

I

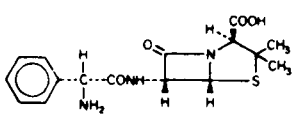

II

High concentrations of ampicillin are also observed in red blood cells following the administration of sarpicillin (11–14). Sarpicillin administered orally in a single dose appears to have advantages such as more rapid absorption, higher and earlier plasma levels, and a larger volume of distribution when compared with ampicillin (15). The objective of the present investigation was to prepare a formulation of sarpicillin base which would provide better systemic ampicillin levels compared with an equivalent dose of pure ampicillin and would protect sarpicillin from possible hydrolysis in the GI tract. Human plasma, saliva, and urine levels of sarpicillin in terms of ampicillin activity of three different formulations are presented.

EXPERIMENTAL

Study Design—Six normal healthy male volunteers, 20–35 years old, were selected for participation in the study. The range in subject weight did not exceed 30 kg.

Within 1 week preceding the study, subjects were given a thorough physical examination, and the following clinical laboratory tests were performed: (*a*) hematology: hemoglobin, hematocrit, sedimentation rate, white blood cell count, platelet estimate, and differential, (*b*) blood chemistry: SMA 12/60 analysis or equivalent, and (*c*) urinalysis: physical characteristics, albumin, sugar, and microscopic examination. Subjects whose values for any of the laboratory tests were outside of the normal range were excluded from the study.

Subjects were excluded from the study who: (*a*) had received any drugs, with the exception of moderate use of alcohol and tobacco, for a period of at least 2 weeks prior to the study; (*b*) showed significant physical or organ abnormality or disease; (*c*) required maintenance therapy with any drug or history of drug dependency; (*d*) had any recognizable surgical disease; (*e*) had a history of hypersensitivity to any antimicrobial agents

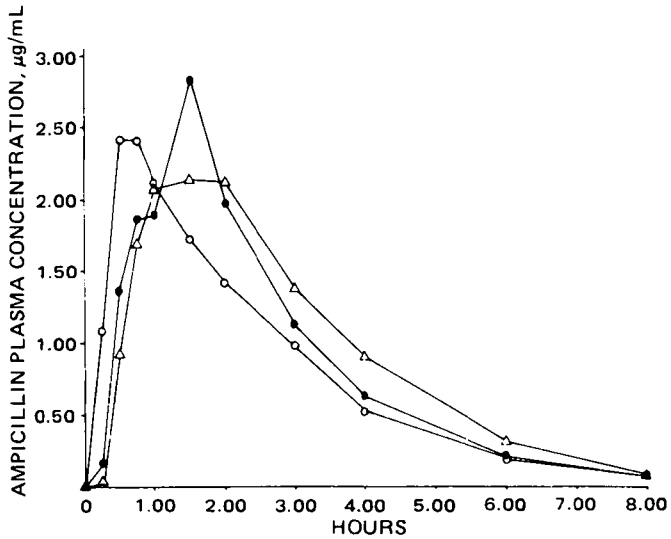

Figure 1—*Ampicillin plasma concentration obtained after single oral administration of treatments A, buffered tablet (○), B, soft gelatin capsule (●), and C, standard gelatin capsule (△).*

0022-3549/84/0200-0169$01.00/0
© 1984, American Pharmaceutical Association

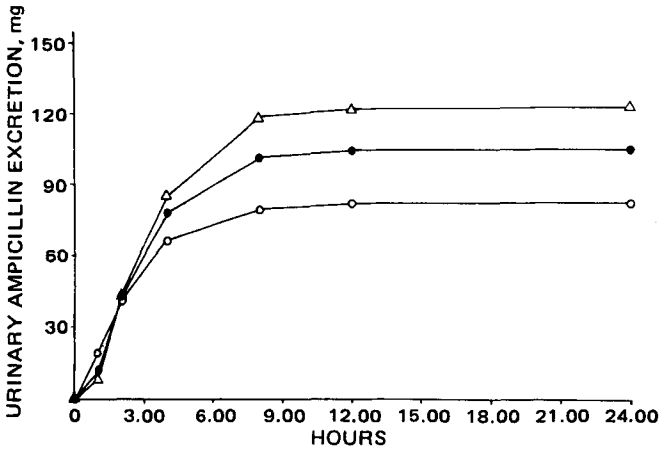

Figure 2—*Urinary ampicillin excretion after single oral administration of treatments A, buffered tablet (○), B, soft gelatin capsule (●), and C, standard gelatin capsule (△).*

or other allergens (pollens, *etc.*), previous use of any cardiac glycoside, any type of anemia, cardiac or respiratory diseases, renal or liver impairment, thyroid disease, recent GI or glucose-6-phosphate dehydrogenase deficiency. Informed consent was obtained from the subjects.

During the study day a physician was present, and all subjects were confined in the clinical facilities at the University of Texas Health Science Center at San Antonio. Subjects were fasted from midnight prior to the drug administration, and each subject drank at least 500 mL of fluids during the evening preceding the study day. No alcoholic beverages were allowed between supper and midnight. On the day of the study, no beverages were permitted during the fasting period. Following 4-h postdose fasting, the subjects were allowed to eat and drink a specific diet.

All subjects were given 200 mL of water at the start of the treatment, regardless of dosage administered. An additional 200 mL of water was given every 2 h after treatment while the fasting was still being maintained. After drug administration, the subjects were ambulatory throughout the test day, and proceeded with normal daily routine while being available for blood, saliva, and urine sampling.

The experimental design in the present study is an exact balance of formulations over weeks, and each subject received every formulation. The design was repeated twice for a total of two Latin squares. Each subject received single 250-mg oral doses of sarpicillin base on each of 3 study days.

Study days were separated by 1-week washout periods to allow for drug elimination as well as to allow for stabilization for the blood volumes of the subjects. Treatments A, B, and C consisted of a buffered tablet, a soft gelatin capsule, and a standard gelatin capsule, respectively. Each formulation contained 250 mg of sarpicillin base in terms of ampicillin activity[1].

Blood samples were drawn by serial venipuncture at time zero (prior to drug administration) and at 15, 30, 45 min, 1, 1.5, 2, 3, 4, 6, and 8 h after drug administration. All blood specimens were collected in heparinized tubes[2]. The heparinized tubes were gently inverted a few times to allow for complete mixing, cooled in ice for 3–5 min, and then centrifuged at 4500 rpm for 5 min in a refrigerated centrifuge. The plasma was transferred into polypropylene tubes, immediately flash frozen by immersion in an ethanol–dry ice bath, and was then kept frozen until assayed.

Urine specimens were collected at time zero (prior to drug administration). Saliva samples (~3–5 mL) were collected at time zero and at 15, 30, 45 min, 1, 1.5, 2, 3, 4, 6, and 8 h after drug administration. Saliva production was induced by instructing the subject to roll a glass marble in his mouth for 3–5 min prior to the collection period and then to expectorate into a plastic container. Each saliva sample was immediately frozen by immersion in an ethanol–dry ice bath and was kept frozen until assayed.

Analytical Methodology—Bioassays for antibiotic activity were performed by standard microbiological agar-diffusion assay methodology (16). Sarpicillin was determined by extracting the biological sample with chloroform after the addition of an equal volume of 0.1 M phosphate buffer, pH 7.4. The ampicillin remained in the aqueous phase. Antibiotic activity in each phase was quantitated by the disk-plate assay using

[1] Supplied by Bristol Laboratories, Syracuse, NY 13201.
[2] Becton, Dickinson, Rutherford, NJ 07070.

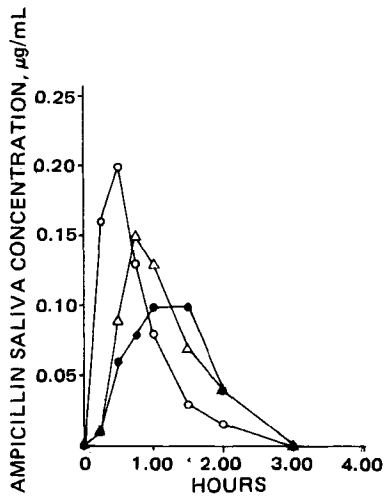

Figure 3—*Ampicillin saliva concentration obtained after single oral administration of treatments A, buffered tablet (○), B, soft gelatin capsule (●), and C, standard gelatin capsule (△).*

Sarcinea lutea ATCC 9341 as the assay organism. Ampicillin trihydrate and sarpicillin hydrochloride were used as the reference standards. Chloroform did not interfere with the assay.

Ampicillin trihydrate standards were prepared in distilled water, and sarpicillin base standards were prepared in chloroform. Standard solutions (1 mg/mL) were prepared for both compounds based on ampicillin potency. Two milliliters of each stock solution was diluted to 100 ml using the appropriate diluents. From this diluted standard, 1.0, 2.0, 3.0, 4.0, 5.0, 6.0, 7.0, 8.0, and 9.0 mL were placed in 100-mL volumetric flasks and diluted to volume. These dilutions yielded 1–9 ng of ampicillin activity when 5 μL of each standard solution was spotted on opposite site disks in duplicate. When completed, each dish was covered with cardboard, marked, and stored at 4°C until all samples were spotted.

Plasma, saliva, and urine samples were made for each dilution so that an average diameter value could be obtained. When the spotting of all samples was completed, the samples and standard dishes were placed in an incubator at 28°C overnight. Zone diameters for the various diluted samples were averaged and the concentrations determined from the appropriate standard curve.

RESULTS

Ampicillin—Average ampicillin plasma, saliva, and urine data obtained after oral administration of a buffered tablet, a liquid formulation in a soft gelatin capsule, and a standard gelatin capsule (treatments A, B, and C) containing 250 mg of sarpicillin base in terms of ampicillin activity are illustrated in Figs. 1–3, respectively. The data obtained represent unchanged ampicillin.

The average ampicillin level *versus* time curves (Fig. 1) for treatments A, B, and C were fitted to Eq. 1 (17) using the digital computer program NONLIN (18):

$$C_p = \frac{k_a \cdot D}{(k_a - K)Vd}\{e^{-K(t-L)} - e^{-k_a(t-L)}\} \qquad \text{(Eq. 1)}$$

where k_a is the first-order absorption rate constant, K is the overall first-order elimination rate constant, D represents the absorbed dose, Vd is the volume of distribution, C_p represents ampicillin plasma concentration, and L is the lag time for absorption. The parameters of the computer fit are K, k_a, D/Vd, and L. Based on R-squared values, slightly better fits were obtained when weights of $1/y_{obs}$ were used rather than weights of one. The results for the three treatments are summarized in Table I.

Based on the computer-generated parameters K, k_a, L, and D/Vd for ampicillin plasma data, estimates of the time to peak (t_{max}) peak concentration (C_{max}), and area under the curve (AUC) were calculated:

$$t_{max} = L + \frac{\ln (K/k_a)}{K - k_a} \qquad \text{(Eq. 2)}$$

$$C_{max} = \frac{k_a D}{(k_a - k)Vd}\{e^{-K(t_{max}-L)} - e^{-k_a(t_{max}-L)}\} \qquad \text{(Eq. 3)}$$

$$AUC = D/K \cdot Vd \qquad \text{(Eq. 4)}$$

Table I—Pharmacokinetic Parameters of Ampicillin After Administration of Sarpicillin

Parameter[a]	Treatment[b] A	B	C
K, h^{-1}	0.464 (0.016)	0.590 (0.068)	0.555 (0.061)
K^c, h^{-1}	0.453	0.441	0.507
k_a, h^{-1} [d]	6.958 (1.337)	1.528 (0.267)	1.320 (0.259)
L, h	0.184 (0.013)	0.221 (0.008)	0.295 (0.036)
D/V μg/mL	2.998 (0.081)	4.006 (0.438)	4.224 (0.454)
CL_R, L/h[e]	10.76	12.43	16.02

[a] See text for parameter definitions. Calculated from the NONLIN digital computer fit of average plasma ampicillin levels. Weights = $1/y_{obs}$ for treatment A (buffered tablet), treatment B (soft gelatin capsule), and treatment C (standard gelatin capsule). [b] *SD* in parentheses. [c] Values obtained from sigma-minus plots of urine data. [d] Paired t test at $p < 0.05$ indicates a significant difference between treatments A–B and A–C. [e] Values obtained from overall renal clearance plots.

The average of the observed values of t_{max}, C_{max}, and AUC for the individual ampicillin level *versus* time curves are listed in Table II along with the results of analysis of variance (ANOVA) and paired t tests.

The amount of ampicillin remaining to be excreted in the urine ($U_\infty - U_t$) was calculated and plotted *versus* time on a semilogarithmic scale (19). For these sigma-minus plots, the value of U_∞ was taken as the amount of ampicillin excreted in the urine after 24 h. Least-squares linear regression was used to determine the slope, intercept, and correlation coefficient for the straight line which best fit the data. The results for treatments A, B, and C are listed in Table I. Renal clearance plots were prepared by plotting the ampicillin urinary excretion rate for each collection interval *versus* the corresponding plasma ampicillin level at the midpoint of the collection interval. The data for each treatment (all six subjects) was fit to an equation for a straight line passing through the origin:

$$\frac{dU}{dt} = CL_R \cdot C_p \qquad \text{(Eq. 5)}$$

where dU/dt is the ampicillin urinary excretion rate and CL_R represents the ampicillin renal clearance. The slopes of these plots represent ampicillin renal clearance CL_R in liters per hour for treatments A, B, and C and are listed in Table I. The amount of unchanged ampicillin in the urine at time infinity (U_∞) for treatments A, B, and C are 82.04, 104.65, and 122.12 mg, respectively. The values for $\int_0^\infty C_p dt$, the plasma ampicillin AUC from time zero to infinity, were approximated by the values obtained after 24 h. From Table II, AUC values for treatments A, B, and C are 6.43, 7.07, and 7.58 h·mg/L, respectively. The calculated renal clearances are listed in Table I.

Saliva Ampicillin—The values of t_{max}, C_{max}, and AUC for saliva ampicillin are presented in Table III along with the results of paired t tests. In every subject, saliva ampicillin levels were <0.2 μg/mL.

Sarpicillin—Typical sarpicillin plasma levels obtained after oral administration of treatments A, B, and C are illustrated in Fig. 4. The average of the observed values of t_{max}, C_{max}, and AUC of the individual sarpicillin plasma level *versus* time curves are compared in Table IV with the observed t_{max}, C_{max}, and AUC of the average sarpicillin plasma level

Table II—Bioavailability Parameters and Statistics for Plasma Ampicillin After Administration of Sarpicillin

Parameter[a]	Treatment[b] A	B	C
t_{max}[c], h I	0.5	1.5	1.5
II	0.60	1.24	1.43
III	1.08(0.96)	1.25(0.50)	1.46(0.51)
C_{max},[c] (μg/mL) I	2.42	2.85	2.15
II	2.47	2.20	2.25
III	2.65(0.83)	3.38(1.06)	2.65(0.66)
AUC[c], μh · g/mL I	6.44	7.07	7.58
II	6.46	6.79	7.61
III	6.43(0.56)	7.07	7.58(0.86)

[a] I = Values observed from average data. II = Values from predicted points after NONLIN digital computer fit. t_1 max, C_{max}, and AUC were calculated from Eqs. 2, 3, and 4, respectively. III = Average of values observed for individual subject data. [b] Treatment A (buffered tablet), treatment B (soft gelatin capsule), and treatment C (standard gelatin capsule). *SD* in parentheses. [c] Paired t test at $p < 0.05$ indicates no significant difference between treatments.

Table III—Bioavailability Parameters and Statistics for Saliva Ampicillin After Administration of Sarpicillin

Parameter[a]	Treatment[b] A	B	C
t_{max}[c], h I	0.50	1.25	0.75
II	0.46(0.10)	1.04(0.39)	0.81(0.19)
C_{max}[c], μg/mL I	0.20	0.10	0.15
II	0.20(0.09)	0.15(0.05)	0.18(0.12)
AUC[c], h · μg/mL I	0.18	0.16	0.17
II	0.18(0.10)	0.16(0.05)	0.17(0.90)

[a] I = Values observed from average data. II = Average of values observed for individual subject data. [b] Treatment A (buffered tablet), treatment B (soft gelatin capsule), and treatment C (standard gelatin capsule). *SD* in parentheses. [c] Paired t test at $p < 0.05$ indicates a significant difference between treatments A–B and A–C.

data. Paired t tests between treatments for t_{max} are also included in Table IV. In every subject, traces of sarpicillin were found in the urine.

Saliva–Plasma Drug Ratios—Ratios of saliva ampicillin to plasma ampicillin and to plasma sarpicillin for each treatment are presented in Table V. AUC ratios are also listed, and all values are calculated from average data for the six subjects.

DISCUSSION

Kinetic Analysis—*Ampicillin*—Jusko and Lewis (8) used a two-compartment open-body model to describe the disposition kinetics of ampicillin after intravenous administration in humans. After oral administration of ampicillin, absorption and distribution occur simultaneously and could not be distinguished kinetically; a one-compartment open model was sufficient to fit the data (8). Pharmacokinetic analysis of the plasma ampicillin data after oral administration of sarpicillin also fit a one-compartment open model. A first-order input was used to represent intestinal absorption. Since the initial rise of ampicillin plasma levels were slightly delayed, a lag time, L, was incorporated into the mathematical model as seen in Eq. 1. This lag time may be the result of delayed absorption, conversion of sarpicillin to ampicillin, or a combination of both, since some conversion may occur prior to absorption. It would seem that this model is an oversimplification of the true situation considering the lipophilic nature of the prodrug. This is probably the case, but the data were fit very nicely by this model, as seen in Table I. The best fits of the data, as judged by the R-squared values and visual inspection, were obtained using weights of $1/y_{obs}$.

The sigma-minus plots of urine data also show first-order elimination of ampicillin. The slopes of these plots represent the overall elimination rate constants and are in reasonable agreement with those from the plasma data (Table I). Jusko and Lewis found β-phase elimination rate constants for ampicillin of 0.54 and 0.50 h^{-1} after intravenous ampicillin and hetacillin administration, respectively (8). These values are similar to the ampicillin elimination rate constants after sarpicillin administration (Table I). The much larger rate constant for absorption and shorter lag time, clearly indicate that ampicillin appears in the plasma more rapidly from the buffered tablet (treatment A) than from either of the capsules (treatments B and C). The larger D/Vd values for treatments B and C reflect the larger elimination rate constants and longer times to peak levels for these treatments.

Renal clearance, estimated from the slopes of clearance plots, are listed in Table I for the three treatments. The smaller clearance for treatment

Table IV—Bioavailability Parameters and Statistics for Plasma Sarpicillin

Parameter[a]	Treatment[b] A	B	C
t_{max}[c], h I	0.50	0.63	0.75
II	0.38(0.14)	0.92(0.47)	0.71(0.19)
C_{max}, μg/mL I	0.83	0.40	0.70
II	0.85(0.37)	0.72(0.23)	0.80(0.61)
AUC, h · μg/mL I	0.65	0.55	0.75
II	0.68(0.33)	0.57(0.22)	0.78(0.62)

[a] I = Observed values from average data. II = Average of values observed for individual subject data. [b] Treatment A (buffered tablet), treatment B (soft gelatin capsule), and treatment C (standard gelatin capsule). *SD* in parentheses. [c] ANOVA indicates a significant difference among treatments regarding t_{max} at $p < 0.01$. Paired t test at $p < 0.05$ indicates a significant difference for t_{max} between treatments A–B and A–C.

Table V—Saliva–Plasma Drug Ratios of Mean Data for Six Subjects [a]

	Treatment	Ratio						
		0.25 h	0.5 h	0.75 h	1.0 h	1.5 h	2.0 h	AUC
I/II	A	0.229	0.241	0.228	0.286	0.375	—	0.265
I/III	A	0.148	0.083	0.054	0.038	0.017	0.016	0.028
I/II	B	0.067	0.150	0.200	0.303	0.270	1.333	0.281
I/III	B	0.059	0.044	0.043	0.053	0.035	0.020	0.023
I/II	C	0.059	0.155	0.214	0.217	0.233	0.800	0.218
I/III	C	0.333	0.097	0.088	0.063	0.033	0.019	0.022

[a] I = Saliva ampicillin concentration; II = plasma sarpicillin concentration; III = plasma ampicillin concentration.

A appears to be due to the smaller amount of ampicillin eliminated in the urine compared with treatments B and C. Essentially no sarpicillin was detected in the urine, but if it is eliminated by this pathway, the residence time in the bladder would be sufficient for hydrolysis to occur. This would result in artificially high values of dU/dt and renal clearance for ampicillin.

Sarpicillin—As previously indicated, plasma sarpicillin data did not fit the one-compartment model (Eq. 1) to a statistically acceptable degree. As a result, only the simplest pharmacokinetic analysis of this data can be made, which is comparison of the t_{max}, C_{max}, and AUC values. No significant differences were observed for the AUC and C_{max} of sarpicillin plasma levels between treatments, but t_{max} for treatment A is significantly smaller than for treatments B or C, as seen in the paired t test in Table IV. The rate of sarpicillin delivery to plasma is faster for treatment A than B or C, whereas the extent of sarpicillin delivery to plasma is statistically the same for all three treatments.

Saliva–Plasma Drug Analysis—Although in this study sarpicillin saliva levels were found to be <0.2 μg/mL ($CV \leq 10\%$), it is likely that the ampicillin present in saliva originated from plasma sarpicillin which was converted to ampicillin after it reached the saliva. This becomes evident when saliva ampicillin levels are compared with plasma sarpicillin and ampicillin levels. Plasma sarpicillin and saliva ampicillin levels fall to undetectable levels at 3 h, while plasma ampicillin levels are relatively high at that time and become undetectable only after 8 h. For each treatment, the shape of the saliva ampicillin curve more closely resembles that of plasma sarpicillin. The ratios of saliva ampicillin to plasma sarpicillin in Table V are more constant for each treatment than the saliva ampicillin to plasma ampicillin ratios. This is in agreement with the findings of Kjaer and Madsen (13) who suggested that prostatic fluid ampicillin levels in dogs were dependent on the plasma sarpicillin levels. Due to its low pK_a, ampicillin is almost completely ionized in plasma at pH 7.4 while sarpicillin is not. Therefore, ampicillin would be less likely to cross the lipoidal parotid epithelium and enter saliva. In addition, the slight acidity of human saliva (20) creates an unfavorable driving force for pH partitioning of ampicillin from plasma to saliva. Melon and Reginster (21) found that passage of ampicillin into saliva of humans is irregular and very slight, as would be expected. Due to the highly enzymatic nature of saliva, one would expect sarpicillin there to be rapidly converted to ampicillin.

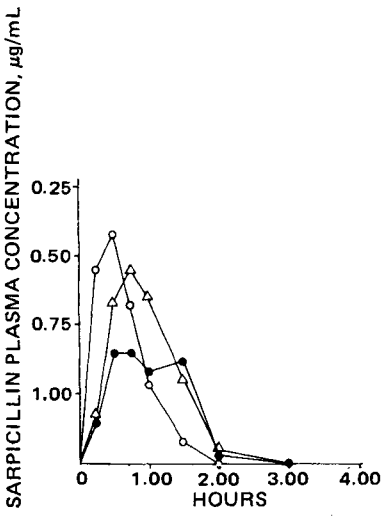

Figure 4—*Sarpicillin plasma concentration obtained after single oral administration of treatments A, buffered tablet (○), B, soft gelatin capsule (●), and C, standard gelatin capsule (△).*

Since saliva ampicillin levels, like plasma sarpicillin, fit the one compartment model poorly, the data were compared by t_{max}, C_{max}, and AUC. As shown by the t_{max} for saliva ampicillin levels in Table III, treatment A delivers ampicillin to saliva more rapidly than treatments B or C, which correlates with the more rapid delivery of sarpicillin to plasma by treatment A. The C_{max} and AUC values for saliva ampicillin levels are not significantly different for the three treatments.

CONCLUSIONS

Based on the time to peak, t_{max}, the rates of delivery of sarpicillin to plasma, ampicillin to plasma, and ampicillin to saliva were greater for the buffered tablet than either the soft gelatin capsule or the standard gelatin capsule. The absorption rate constant obtained from the computer fit of the average plasma ampicillin data (Table I) is statistically greater for the buffered tablet. The t_{max} calculated using k_a and Eq. 2 is also statistically smaller (Table II). However, statistical analysis of t_{max} obtained from the average of values observed graphically for individual subject data indicates no significant differences among or between treatments. The reason for this result is the large t_{max} obtained for subject 4 (3 h) in comparison with the range of values for t_{max} obtained in the rest of the subjects (0.5–1 h). If this subject is eliminated from the statistical analysis as an outlier, the data supports the contention that the plasma ampicillin time to peak is smaller for the buffered tablet than for the two capsule formulations.

Based on AUC values, the extent of delivery of sarpicillin to plasma, ampicillin to plasma, and ampicillin to saliva were statistically the same among treatments. The results of the present investigation suggest that the buffered tablet is a faster and more precise delivery system for sarpicillin than either the liquid formulation in the soft gelatin capsule or the standard gelatin capsule. Reduced excretion of ampicillin following the administration of the sarpicillin buffered tablet may be an indirect indicator of more extensive tissue distribution of sarpicillin and tissue metabolism to inactive metabolites.

Since ampicillin levels were observed in saliva after sarpicillin administration, it is likely that ampicillin levels in lipoidal tissues will be higher than after ampicillin administration. Clinical testing is necessary to determine whether this difference will result in a therapeutic advantage for sarpicillin over ampicillin.

This study is the first human bioavailability comparison of three formulations containing the same amount of sarpicillin base. Further investigation is needed to improve the oral absorption of antibiotics. The rationale for designing new drug delivery systems for sarpicillin and other antibiotics is partially for enhancement of GI absorption, which may potentially increase the tissue concentrations of sarpicillin and consequently maximize therapeutic activity.

REFERENCES

(1) E. L. Flotz, J. W. West, J. H. Breslow, and H. Wallick, *Antimicrob. Agents Chemother.*, **10**, 442 (1970).

(2) L. O. Boreus and B. Jalling, *Pediatr. Clin. North Am.*, **19**, 141 (1972).

(3) J. A. Davis, APhA Symposium on Pharmacokinetics in Disease, Houston, Texas, April 1972.

(4) J. W. Poole, G. Owen, J. Silverio, J. M. Freyhof, and S. B. Rosenman, *Curr. Ther. Res.*, **10**(June), 292 (1968).

(5) B. E. Cabana, L. F. Wilhite, and M. E. Bierwagen, *Antimicrob. Agents Chemother.*, 35 (1969).

(6) L. Magni, G. Ortengren, and S. Wahlqvist, *Scand. J. Lab. Invest.*, **20**, 195 (1967).

(7) C. M. Brown, D. P. Hannan, P. F. Langley, *Toxicol. Appl. Pharmacol.*, **15**(July), 136 (1969).

(8) W. J. Jusko and G. P. Lewis, *J. Pharm. Sci.*, **62**, 69 (1973).
(9) A. Whelton, D. G. Sapir, G. G. Carter, J. Kramer, and W. G. Walker, *J. Pharmacol. Exp. Ther.*, **179**, 419 (1971).
(10) A. T. K. Crockett, R. S. Moore, and A. P. Roberts, *Invest. Urol.*, **5**, 250 (1967).
(11) Disposition and Safety Evaluation Studies of BL-P1761, Bristol Laboratories, Syracuse, N.Y., Jan. 1974.
(12) T. B. Kjaer, P. G. Welling, and P. O. Madsen, *J. Pharm. Sci.*, **66**, 345 (1977).
(13) T. B. Kjaer and P. O. Madsen, *Invest. Urol.*, **14**(July), 57 (1976).
(14) J. A. Bodine, L. J. Strausbaught, and M. A. Sande, *Clin. Pharmacol. Ther.*, **20**, 727 (1976).
(15) M. Pfeffer, Human Study 107, Bristol Laboratories, Syracuse, N.Y., April 1975.
(16) D. C. Grove and W. A. Randall, "Assay Methods of Antibiotics: A Laboratory Manual," Medical Encyclopedia, New York, N.Y., 1955.
(17) M. Gibaldi and D. Perrier, "Pharmacokinetics," Dekker, New York, N.Y., 1975.
(18) C. M. Metzler, NONLIN, Technical Report 7292/60/7292/005, The Upjohn Company, Kalamazoo, Mich., 1969.
(19) B. K. Martin, *J. Pharmacol. Chemother.*, **29**, 181 (1967).
(20) F. Rasmussen, *Acta Pharmacol. Toxicol.*, **21**, 11 (1964).
(21) J. Melon and M. Reginster, *Acta Oto-Rhino-Laryngologica Belgica*, **30**, 643 (1976).

ACKNOWLEDGMENTS

This study was supported by a research grant from Bristol Laboratories.

Physicochemical Characterization of Spray-Dried Phenylbutazone Polymorphs

YOSHIHISA MATSUDA ˣ, SACHIYO KAWAGUCHI, HITOMI KOBAYASHI, and JUJIRO NISHIJO

Received September 28, 1982, from the *Kobe Women's College of Pharmacy, Higashinada, Kobe 658, Japan.* Accepted for publication December 17, 1982.

Abstract □ A spray-drying method was applied to the recrystallization of phenylbutazone, and the resulting samples were examined by X-ray powder diffractometry, differential thermal analysis, IR spectrophotometry, scanning electron microscopy, and hot-stage photomicroscopy. Three different crystalline forms (δ, β, and ϵ) could be prepared from methylene chloride solution by varying the drying temperature of sprayed droplets from 120°C to 30°C. Form ϵ, the fifth polymorph of phenylbutazone, was confirmed as a novel crystalline form which could not be prepared by recrystallization techniques. In this spray-drying system the composition of spray-dried samples was shown to be a function of the drying temperature. While the stable form δ was obtained at higher drying temperatures, form ϵ was obtained only under conditions affording a slower evaporation rate of the solvent. The dissolution properties of the pure modifications prepared by recrystallization techniques and the spray-dried samples were evaluated in simulated intestinal fluid. Form ϵ showed excellent *in vitro* availability and much higher solubility than any other of the forms.

Keyphrases □ Phenylbutazone—recrystallized polymorphs, spray-drying technique, physicochemical characterization □ Spray-drying—recrystallized polymorphs of phenylbutazone, physicochemical characterization □ Recrystallization—polymorphs of phenylbutazone, spray-drying technique, physicochemical characterization

The physicochemical properties of solid drug substances are of considerable importance in preformulation studies, because they are related to both the production of dosage forms and bioavailability. The nature of the crystalline forms affects bioavailability through the effect of crystal properties on dissolution rate. In a particular polymorphic form, many solids may be prepared *via* appropriate modification of the conditions of crystallization. Some important factors relating to the resulting crystalline forms when obtaining polymorphs by recrystallization techniques are the nature of solvent (its polarity and solvent power), temperature, and rate of cooling. The latter two factors can take part in the crystallization velocity. Although precise control of the recrystallization velocity is difficult for ordinary recrystallization techniques, a spray-drying method may enable one to produce different crystallization velocities by varying the drying conditions of the sprayed droplets.

While several papers dealing with the polymorphism of spray-dried drug substances have been published (1–5), little information is available on the relationship between the operating factors and the resulting crystalline forms. An interesting polymorphism of phenylbutazone was found using a spray-drying method (6). This paper describes a further investigation to provide basic physicochemical information on the polymorphic forms.

BACKGROUND

There have been several reports describing the polymorphism of phenylbutazone, including our previous communication (Table I). Matsunaga *et al.* (7) found that phenylbutazone gave three polymorphs, *i.e.*, forms I, II, and III, among which the former two polymorphs (available commercially) were considered to be a stable form and one of the metastable forms, respectively. The mutual transformation among them by heating or through grinding and compression has been investigated. Ibrahim *et al.* (8) independently reporting on the polymorphism and feasibility of crystalline structural changes under tableting conditions, found the presence of four forms (I, II, III, and IV). Müller (9) showed later that forms I and II were pseudopolymorphs resulting from solvation. This was also confirmed by our differential thermal analysis–thermogravimetry analysis (DTA–TG). While Müller suggested the existence of a fourth polymorph (form γ) other than forms α, β, and δ (which had been already identified), he could not isolate it, despite describing its thermogram. In the same year Chauvet *et al.* (10) reported the thermal behavior of three polymorphs, *i.e.*, forms I, II, and III, obtained by different methods, all of which were identical to those already found. They considered that form II was identical to that reported by Matsunaga; however, based on the results of thermomicroscopy and thermal analysis, we estimated that the form II should actually be identical to the form γ designated by Müller (9). In a previous publication, it was shown that a fifth crystalline form (form ϵ) is formed together with forms β and δ in a spray-drying system. In this system forms α and γ

0022-3549/84/0200-0173$01.00/0
© 1984, American Pharmaceutical Association

(8) W. J. Jusko and G. P. Lewis, *J. Pharm. Sci.*, **62**, 69 (1973).
(9) A. Whelton, D. G. Sapir, G. G. Carter, J. Kramer, and W. G. Walker, *J. Pharmacol. Exp. Ther.*, **179**, 419 (1971).
(10) A. T. K. Crockett, R. S. Moore, and A. P. Roberts, *Invest. Urol.*, **5**, 250 (1967).
(11) Disposition and Safety Evaluation Studies of BL-P1761, Bristol Laboratories, Syracuse, N.Y., Jan. 1974.
(12) T. B. Kjaer, P. G. Welling, and P. O. Madsen, *J. Pharm. Sci.*, **66**, 345 (1977).
(13) T. B. Kjaer and P. O. Madsen, *Invest. Urol.*, **14**(July), 57 (1976).
(14) J. A. Bodine, L. J. Strausbaught, and M. A. Sande, *Clin. Pharmacol. Ther.*, **20**, 727 (1976).
(15) M. Pfeffer, Human Study 107, Bristol Laboratories, Syracuse, N.Y., April 1975.
(16) D. C. Grove and W. A. Randall, "Assay Methods of Antibiotics: A Laboratory Manual," Medical Encyclopedia, New York, N.Y., 1955.
(17) M. Gibaldi and D. Perrier, "Pharmacokinetics," Dekker, New York, N.Y., 1975.
(18) C. M. Metzler, NONLIN, Technical Report 7292/60/7292/005, The Upjohn Company, Kalamazoo, Mich., 1969.
(19) B. K. Martin, *J. Pharmacol. Chemother.*, **29**, 181 (1967).
(20) F. Rasmussen, *Acta Pharmacol. Toxicol.*, **21**, 11 (1964).
(21) J. Melon and M. Reginster, *Acta Oto-Rhino-Laryngologica Belgica*, **30**, 643 (1976).

ACKNOWLEDGMENTS

This study was supported by a research grant from Bristol Laboratories.

Physicochemical Characterization of Spray-Dried Phenylbutazone Polymorphs

YOSHIHISA MATSUDA ˣ, SACHIYO KAWAGUCHI, HITOMI KOBAYASHI, and JUJIRO NISHIJO

Received September 28, 1982, from the *Kobe Women's College of Pharmacy, Higashinada, Kobe 658, Japan.* Accepted for publication December 17, 1982.

Abstract □ A spray-drying method was applied to the recrystallization of phenylbutazone, and the resulting samples were examined by X-ray powder diffractometry, differential thermal analysis, IR spectrophotometry, scanning electron microscopy, and hot-stage photomicroscopy. Three different crystalline forms (δ, β, and ϵ) could be prepared from methylene chloride solution by varying the drying temperature of sprayed droplets from 120°C to 30°C. Form ϵ, the fifth polymorph of phenylbutazone, was confirmed as a novel crystalline form which could not be prepared by recrystallization techniques. In this spray-drying system the composition of spray-dried samples was shown to be a function of the drying temperature. While the stable form δ was obtained at higher drying temperatures, form ϵ was obtained only under conditions affording a slower evaporation rate of the solvent. The dissolution properties of the pure modifications prepared by recrystallization techniques and the spray-dried samples were evaluated in simulated intestinal fluid. Form ϵ showed excellent *in vitro* availability and much higher solubility than any other of the forms.

Keyphrases □ Phenylbutazone—recrystallized polymorphs, spray-drying technique, physicochemical characterization □ Spray-drying—recrystallized polymorphs of phenylbutazone, physicochemical characterization □ Recrystallization—polymorphs of phenylbutazone, spray-drying technique, physicochemical characterization

The physicochemical properties of solid drug substances are of considerable importance in preformulation studies, because they are related to both the production of dosage forms and bioavailability. The nature of the crystalline forms affects bioavailability through the effect of crystal properties on dissolution rate. In a particular polymorphic form, many solids may be prepared *via* appropriate modification of the conditions of crystallization. Some important factors relating to the resulting crystalline forms when obtaining polymorphs by recrystallization techniques are the nature of solvent (its polarity and solvent power), temperature, and rate of cooling. The latter two factors can take part in the crystallization velocity. Although precise control of the recrystallization velocity is difficult for ordinary recrystallization techniques, a spray-drying method may enable one to produce different crystallization velocities by varying the drying conditions of the sprayed droplets.

While several papers dealing with the polymorphism of spray-dried drug substances have been published (1–5), little information is available on the relationship between the operating factors and the resulting crystalline forms. An interesting polymorphism of phenylbutazone was found using a spray-drying method (6). This paper describes a further investigation to provide basic physicochemical information on the polymorphic forms.

BACKGROUND

There have been several reports describing the polymorphism of phenylbutazone, including our previous communication (Table I). Matsunaga *et al.* (7) found that phenylbutazone gave three polymorphs, *i.e.*, forms I, II, and III, among which the former two polymorphs (available commercially) were considered to be a stable form and one of the metastable forms, respectively. The mutual transformation among them by heating or through grinding and compression has been investigated. Ibrahim *et al.* (8) independently reporting on the polymorphism and feasibility of crystalline structural changes under tableting conditions, found the presence of four forms (I, II, III, and IV). Müller (9) showed later that forms I and II were pseudopolymorphs resulting from solvation. This was also confirmed by our differential thermal analysis–thermogravimetry analysis (DTA–TG). While Müller suggested the existence of a fourth polymorph (form γ) other than forms α, β, and δ (which had been already identified), he could not isolate it, despite describing its thermogram. In the same year Chauvet *et al.* (10) reported the thermal behavior of three polymorphs, *i.e.*, forms I, II, and III, obtained by different methods, all of which were identical to those already found. They considered that form II was identical to that reported by Matsunaga; however, based on the results of thermomicroscopy and thermal analysis, we estimated that the form II should actually be identical to the form γ designated by Müller (9). In a previous publication, it was shown that a fifth crystalline form (form ϵ) is formed together with forms β and δ in a spray-drying system. In this system forms α and γ

0022-3549/84/0200-0173$01.00/0
© 1984, American Pharmaceutical Association

Table I—Crystalline Modifications of Phenylbutazone and Their Melting Points by Differential Scanning Calorimetry

Investigator	Modifications (Melting Points, °C)						
Matsunaga *et al.* (7)	I (103)	II (93, 103)	III (93)				
Ibrahim *et al.* (8)	IV (105)	III (93)				II (90)[a]	I (80)[a]
Müller (9)	δ (107.5)	α (93.5)	β (95.1)	γ (106.0)			
Chauvet *et al.* (10)	I (106)		III (96)	II (104)			
Matsuda *et al.* (6)	δ (103)[b]		β (91)[b]		ε (95)[b]		

[a] Solvates. [b] DTA data.

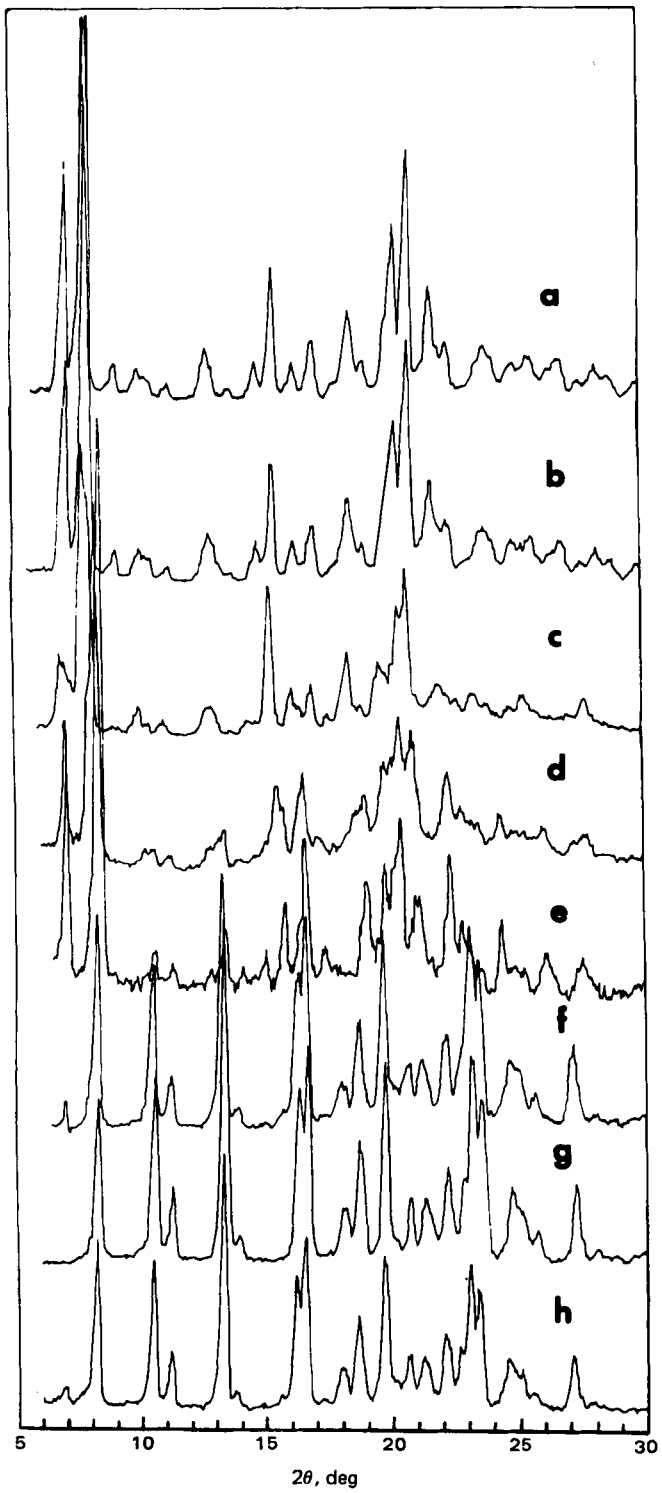

Figure 1—*X-ray powder diffraction patterns of form δ (a) and spray-dried samples prepared at drying temperatures of 120°C (b), 100°C (c), 80°C (d), 70°C (e), 60°C (f), 40°C (g), and 30°C (h).*

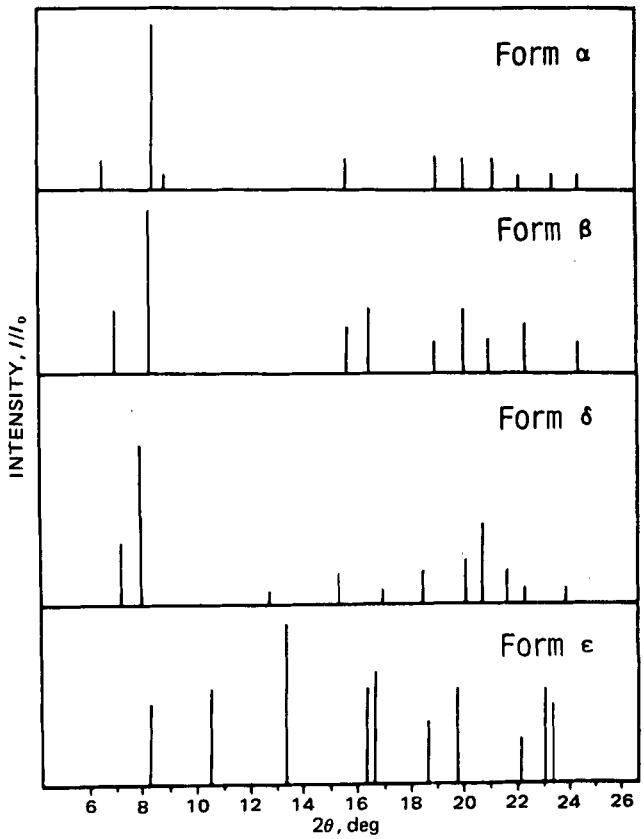

Figure 2—*Relative X-ray diffraction intensity patterns of forms α, β, and δ and the new form, ε.*

could not be obtained. The nomenclature of polymorphs in the present paper follows Müller's designations.

EXPERIMENTAL

Materials—A single batch of commercial phenylbutazone was used as received[1]. The drug was confirmed to be form δ (stable form) by X-ray powder diffraction analysis, differential thermal analysis (DTA), and IR spectroscopy. Form α was prepared by the method of Ibrahim (8); *i.e.*, water was added to a 2-propanol solution of form δ until it reached the cloud point, and Form β was prepared by pouring an ethanol solution of the same sample into cold water and stirring vigorously (9). These crystals were removed by filtration using a sintered-glass funnel and then dried under vacuum at room temperature. Methylene chloride was used as a solvent for spray drying. All the solvents were reagent grade and were used without further purification.

Spray Drying—Ten grams of phenylbutazone was dissolved in 200 mL of methylene chloride, and the solution was fed into a mini-spray drier[2] through a peristaltic pump at a flow rate of 20 mL/min. The temperature at the inlet of the drying chamber of the apparatus was varied in seven steps (120°C, 100°C, 80°C, 70°C, 60°C, 40°C, and 30°C) in seven runs; the temperature at the outlet varied from 64°C to 27°C, depending on the inlet temperature. Thus, seven samples (sample-120, -100, -80, -70, -60, -40, and -30, respectively) were prepared. The other operating

[1] Supplied by Ciba-Geigy (Japan) Ltd., lot no. 000978.
[2] Mini-Spray h_0; Yamato Kagaku Co., Tokyo, Japan.

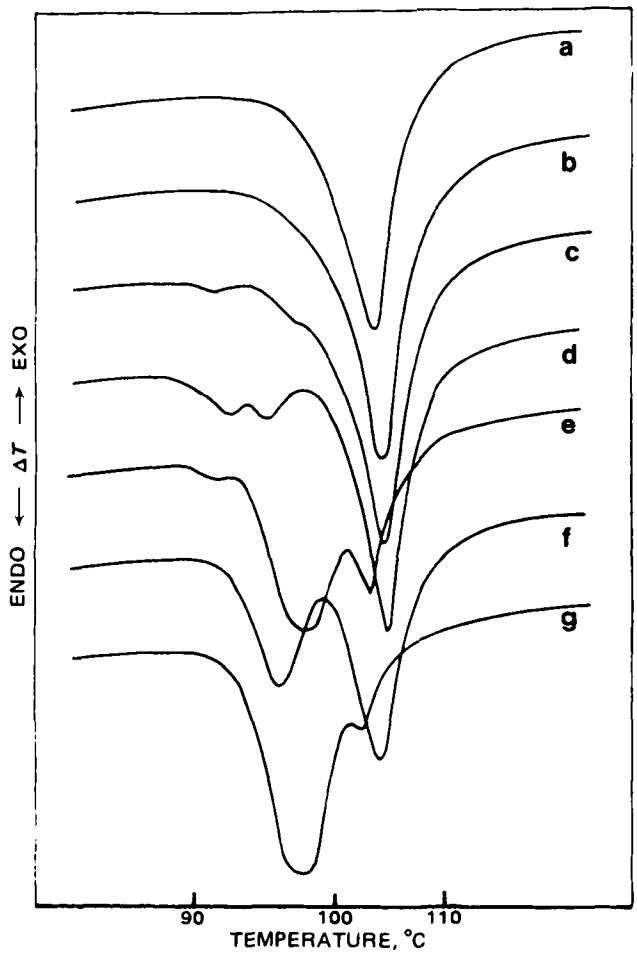

Figure 3—*DTA thermograms of spray-dried samples prepared at drying temperatures of 120°C (a), 100°C (b), 80°C (c), 70°C (d), 60°C (e), 40°C (f), and 30°C (g).*

conditions were: air pressure for atomizing, 2 kg/cm^2; flow rate of compressed air, 20 L/min; degree of reduced pressure in the drying chamber, 60–80 mm H_2O.

Characterization of Polymorphs—*X-ray Powder Diffraction Analysis*—X-ray diffraction patterns were recorded on a X-ray diffractometer[3] with Ni-filtered Cu-K_α radiation. The diffractometer was set at 35 kV–7 mA, 1° beam slit, and 0.2° detector slit with a count range of 2000 cps, a scanning speed of 1°/min, and a chart speed of 10 mm/min.

Differential Thermal Analysis—The thermograms of spray-dried samples and crystalline modifications prepared by the recrystallization method were recorded on a thermal analyzer[4] in an open-pan system; dry nitrogen at a constant flow rate was used as the carrier gas. α-Alumina served as a standard material. The rate of heating was 10°C/min unless otherwise stated. Thermogravimetry (TG) was also carried out for spray-dried samples to investigate the feasibility of the formation of solvates.

Infrared Spectroscopy—The IR spectra of forms δ and ϵ were recorded on a double-beam spectrophotometer[5] using the potassium bromide disk technique. No polymorphic changes in form ϵ were induced by grinding or compressing for sample preparation.

Scanning Electron Microscopy—The scanning electron photomicrographs of samples-120, -80, -60, and -30 were taken using a microscope[6] at magnifications ranging from 1000 to 3000×.

Photomicroscopy by the Hot-Stage Method—A photomicroscope equipped with a hot-stage was employed, and appearance changes during polymorphic transformation were observed for forms α and β and sample-30. The heating rate was 2°C/min.

Measurements of Solubility and Dissolution Rate—The solubilities

[3] Geigerflex 2011; Rigaku Denki Co., Tokyo, Japan.
[4] Model DTA-30; Shimadzu Co., Kyoto, Japan.
[5] Model 295; Hitachi Co., Tokyo, Japan.
[6] Model JSM-U3; Jeol Ltd., Tokyo, Japan.

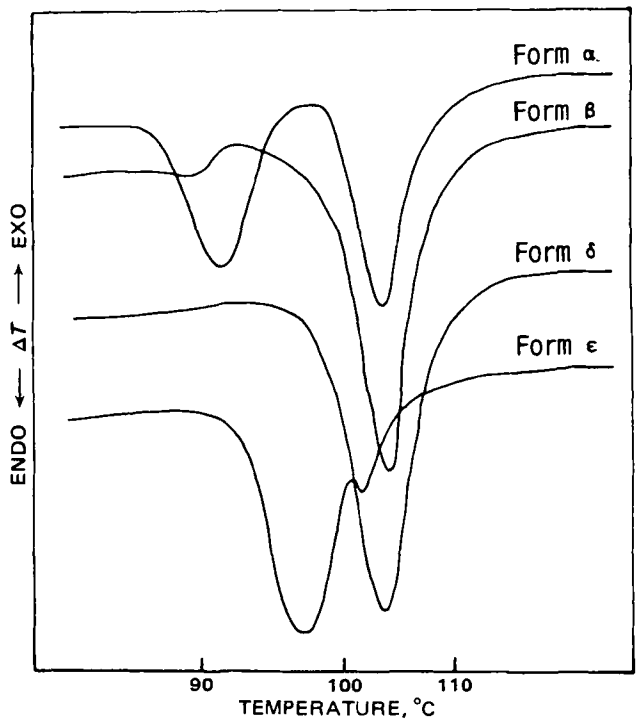

Figure 4—*DTA thermograms of forms α, β, δ, and ϵ.*

of different spray-dried samples were determined in simulated intestinal fluid (USP XIX), pH 7.5. An excess amount of powdered sample and 100 mL of the dissolution medium were placed in a 200-mL Erlenmeyer flask with a glass stopper. The flasks were fixed on the sample holder in a thermostatic water bath maintained at 37°C and mechanically shaken at a fixed rate of 60 strokes/min. Aliquots (2 mL) of the solution were withdrawn at designated intervals with a pipet fitted with a sintered-glass filter and suitably diluted with the dissolution medium. The concentrations of drugs were determined by measurement of the absorbance at 264 nm using a UV spectrophotometer. The resultant loss in volume was compensated for by adding dissolution medium maintained at the same temperature.

Using 500 mL of the dissolution medium, the dissolution rate was determined by a stationary disk method similar to that described by Wood

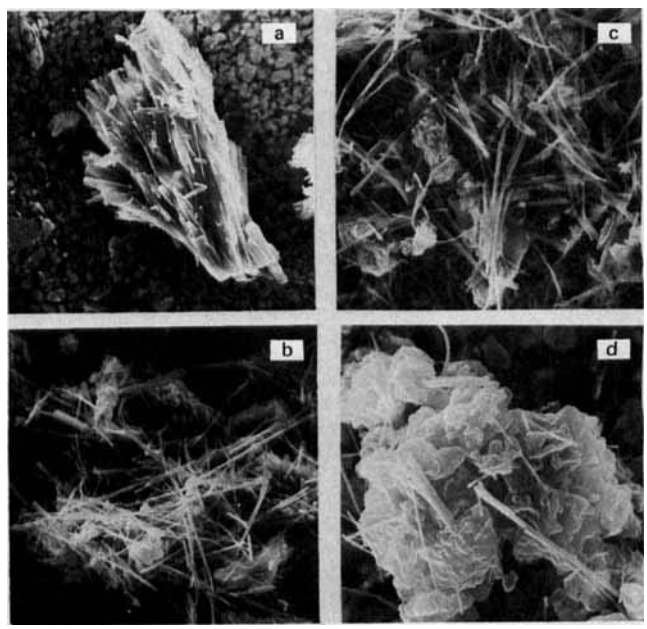

Figure 5—*Scanning electron microphotographs of spray-dried samples prepared at drying temperatures of 120°C (a), 80°C (b), 60°C (c), and 30°C (d). Original magnification for a, b, and c was 1000×; for d it was 3000×.*

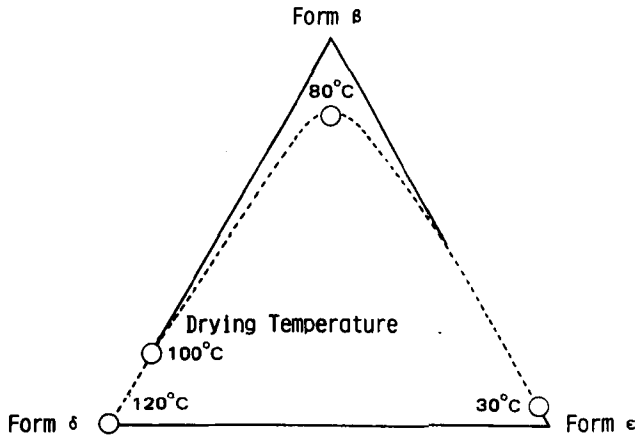

Figure 6—*Schematic phase diagram of spray-drying system of phenylbutazone.*

et al. (11) and Matsunaga *et al.* (7). A 100-mg portion of each sample was compressed in an 8-mm i.d. stainless steel die under the compression force of 1000 kg, using an accurate compression/tension-testing machine[7]. No polymorphic changes occurred during the compression for any of the samples. The rotation velocity of the stirring blade was maintained at 150 rpm during the experiment. The sampling procedures were the same as those described above; the rate was determined four times for each sample.

RESULTS AND DISCUSSION

Polymorphic Behavior—A wide range of drying temperature was applicable in this study; the spray drying could be performed successfully even at 120°C, which was much higher than the melting point of the stable form δ (103.0°C), because the surface temperature of recrystallizing crystals dropped below the melting point due to the evaporation heat of the solvent. Another extreme temperature (30°C) was applied to the present operating condition, although the boiling point of solvent was 40.1°C under atmospheric pressure.

Figure 1 shows the X-ray powder diffraction patterns of spray-dried phenylbutazone samples prepared at different drying temperatures together with a pure modification, form δ. The diffraction pattern of the sample-120 was quite similar to that of form δ. Within the range of 120–100°C the diffraction intensities decreased with a lowering in drying temperature, and the diffraction peak at 14.9° disappeared and new peaks appeared at 19.0° and 27.4°. This suggests that the sample-100 is not composed of only a single crystalline form. At the drying temperature of 80°C, although some of diffraction peaks attributable to the sample-120 still existed, the position of the maximum intensity peak at 8.0° (which was characteristic to form δ, sample-120, and sample-100) shifted to slightly higher diffraction angles, and the diffraction pattern was converted to one differing from that of the sample-120. At the temperature of 70°C new diffraction peaks appeared at 13.2°, 16.6°, 19.6°, and 23.1°, suggesting the presence of a third crystalline form in sample-70. Below 60°C the diffractograms showed quite different patterns from any of those obtained at temperatures above 70°C; they were no longer affected by drying temperature.

Figure 2 shows the relative X-ray diffraction intensity patterns of forms α, β, and δ [prepared by the recrystallization methods (8, 9)] and a new crystal form ε, obtained at 30°C. Distinct differences in the profiles were evident especially for form ε. Based on the collation of the diffraction patterns in Fig. 1 with those of pure crystal modifications, sample-120 was identified as form δ. However, sample-100 most likely consisted of a mixture of forms δ and β. Samples-80 and -70 seemed to be composed of mixtures of forms δ, β, and ε.

The X-ray diffraction analysis is not always able to distinguish a mixture of crystalline forms in a sample. The thermal behavior of a sample can be utilized as a supporting method for the identification and analysis of various forms in a mixture. The DTA curves of the samples in Fig. 1 and those of pure crystal modifications, together with sample-30, are illustrated in Figs. 3 and 4, respectively. The DTA curves for samples-120 and -100 showed a single endotherm at about 103°C corresponding to that of form δ despite of the differences in the X-ray diffraction patterns as seen in Fig. 1. The DTA curve for sample-80 showed an endothermic peak at 91°C, followed by a small exotherm characterizing transformation to form δ at ~93°C, a slight hollow at 95°C, and then a melting endotherm at 103°C. At the drying temperature of 70°C another small endothermic peak was observed at 95°C in addition to the peak at 92°C. Below 60°C such an endothermic change became more remarkable, showing another phase with thermodynamic instability. Conversely the endothermic peak at 91–92°C began to disappear as the drying temperature dropped. The possibility of the formation of solvate in the lower ranges of drying temperature was denied by the TG results and elemental analyses of these samples.

[7] Model IS-5000; Shimadzu Co., Kyoto, Japan.

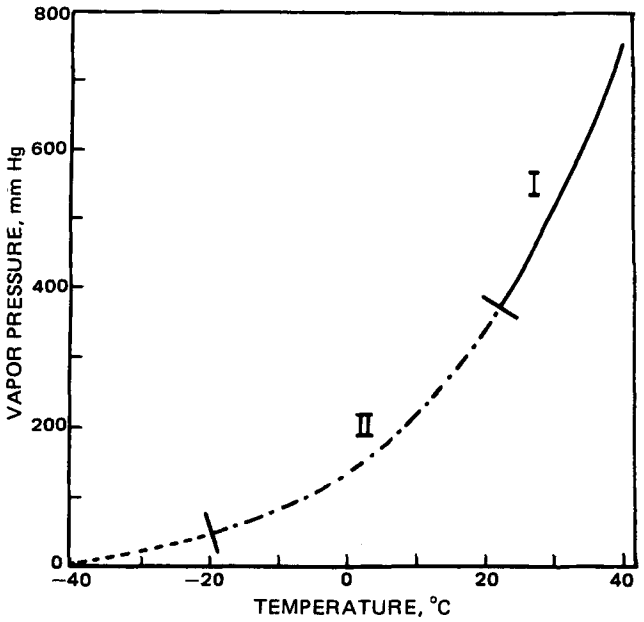

Figure 7—*Vapor pressure curve of methylene chloride and the resultant crystalline forms by the evaporation method. Key: (—) form δ; (·-·) mixture of forms δ and β; (- - -) not determined.*

Figure 5 shows the scanning electron photomicrographs of samples-120, -80, -60, and -30. As already pointed out by Müller (9), form δ did not differ essentially from form β in shape. Nevertheless, the shape of form δ in sample-120 was obviously a needle with round ends at higher magnifications, the individual single "crystal" being cluster of polycrystals. In the case of the sample-80 each crystal was entangled at random, but the crystals of forms δ and β were distinguishable from one another at higher magnifications. Simultaneously, the formation of form ε having a stony coral shape which was quite different from that of the other crystal modifications was detected. Although the amount of form ε obtained increased with a lowering in drying temperatures <60°C, form ε was not composed of a pure modification; a trace amount of form β existed even in sample-30.

The interpretation of X-ray diffractograms, thermograms, and scanning electron photomicrographs proved that sample-100 was composed of forms δ and β, and that sample-80 consisted of a mixture of forms δ, β, and ε, among which form β was the most abundant. The spray-drying system used in this investigation may qualitatively be summarized by a schematic phase diagram shown in Fig. 6. Very rapid evaporation of the solvent at higher temperatures in this system seemed to allow the maximum freedom for molecular orientation, resulting in the formation of the most stable form (δ) in the subsequent crystallization.

The evaporation rate of a single solvent is controlled by various factors including the vapor pressure of the solvent at a given temperature, the rate at which the heat is supplied, thermal conductivity and specific heat of the solvent, latent heat of evaporation, and the rate at which the vapor in contact with the solvent is removed. The transportation phenomena of vapor from a solution system, as in the case of this study, involve more complicated dynamic aspects. However, the major contributing factor in each case is the vapor pressure of the solvent. To simulate the evaporation of solvent from the sprayed droplets, the same solution was evaporated in a rotary evaporator at different temperatures under reduced pressure (15 mm Hg). The vapor pressure curve of methylene chloride and the forms of the resultant crystals are illustrated in Fig. 7. In this graph, while region I at higher temperatures gave only form δ, region II gave a mixture of forms δ and β. Though form ε could not be

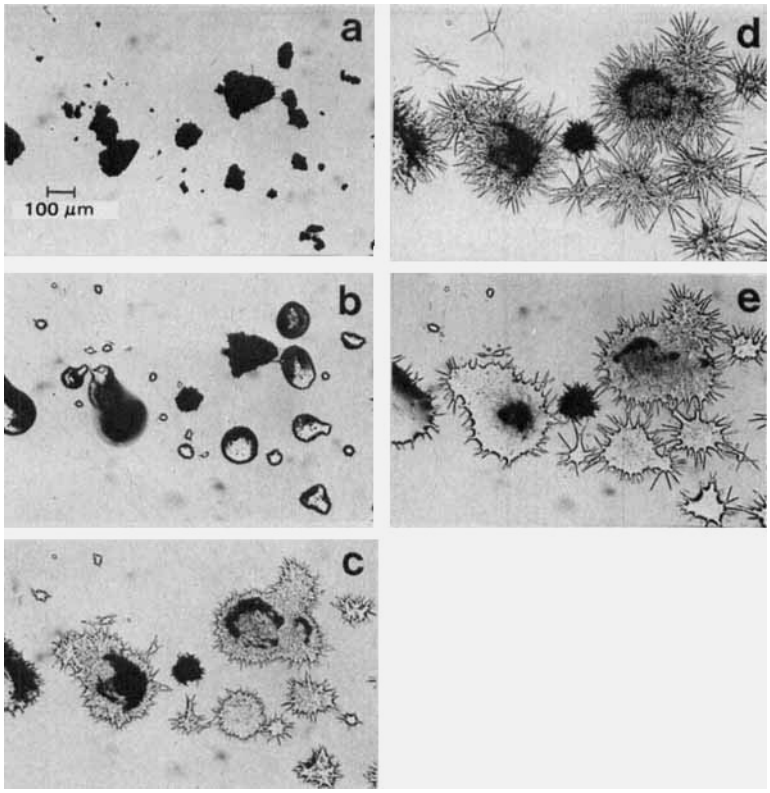

Figure 8—*Photomicrographs of form ϵ taken during the hot-stage microscopy study. Key: (a) 30°C; (b) 95°C; (c) 97°C; (d) 100°C; (e) 105°C.*

obtained within the range of the experimental condition, the result obtained in Fig. 7 may explain the present spray-drying system. From Figs. 6 and 7 form ϵ appears to be formed only at an extremely slow evaporation rate of the solvent.

Although form ϵ fused at its melting point and the liquid then recrystallized into form δ without generating a recrystallization exotherm under the ordinary analytical condition, the thermogram showed an exothermic peak at heating rates of <5°C/min. Such thermal behavior could also be

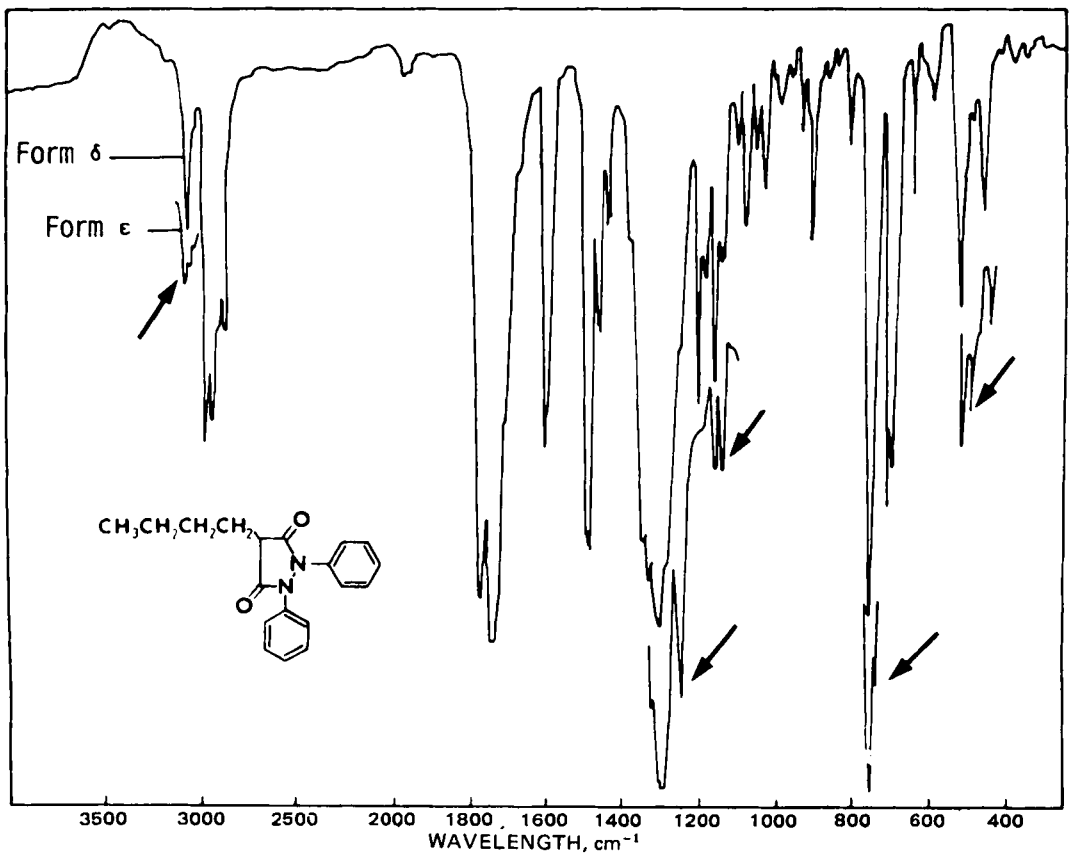

Figure 9—*IR spectra of forms δ and ϵ.*

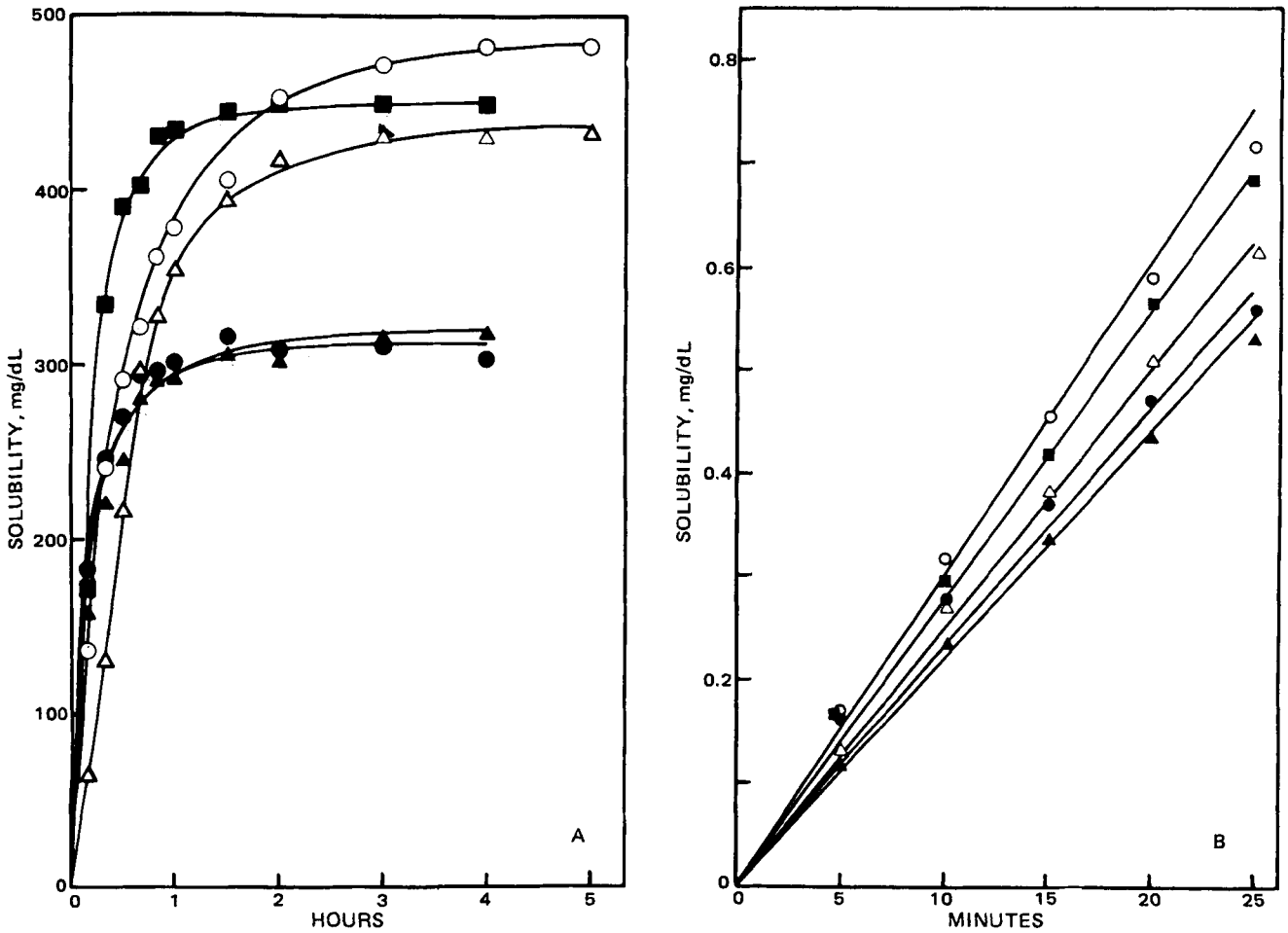

Figure 10—*Solubility profiles (A) and dissolution rates (B) of pure modifications and spray-dried samples prepared at different drying temperatures in simulated intestinal fluid at 37°C. Key: (●) form δ; (■) form β; (▲) sample at 120°C; (△) sample at 80°C; (○) sample at 30°C.*

evidenced by the hot-stage photomicroscopy. The result is shown in Fig. 8, visualizing the fusion of form ε at ~95°C and the polymorphic transformation to form δ in the range of 97–100°C.

Differing from the cases of forms α and β, grinding or compression did not induce the polymorphic transformation of form ε. Therefore, the IR spectrum of form ε was compared with that of form δ (Fig. 9). As indicated with arrows in Fig. 9, form ε was significantly different from form δ in five absorption bands (3050, 1293, 1130, 752, and 580 cm^{-1}). The differences for the C—N bonds between two nitrogen atoms and benzene rings and for the C—H bonds among individual benzene rings are attributable to the differences in crystalline structure.

Dissolution Properties—The dissolution behaviors of forms δ and β and of samples-120, -80, and -30 are depicted in Fig. 10A. Since the dissolution behavior of a mixture containing more than two polymorphs was hard to interpret even if the sample was of sufficient purity, only the three spray-dried samples in which one crystalline form was dominant were used in the dissolution study.

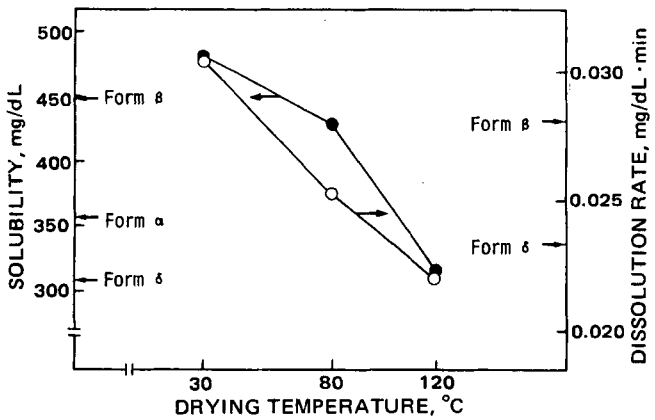

Figure 11—*Effect of drying temperature on the solubility (●) and dissolution rate (○) of spray-dried samples.*

The apparent equilibrium solubilities of forms β and ε were not affected by dissolution time, suggesting that they were not converted to form δ during the dissolution process. The dissolution rates of the samples in Fig. 10A are shown in Fig. 10B. Based on Müller's method (9), both the die and the punches were cooled with liquid nitrogen so as to prevent the polymorphic change during the disk preparation of sample-80. Good linear relationships were established for all the samples except for form δ, indicating that polymorphic transformation was also not induced during the dissolution measurement. The apparent dissolution rates calculated from the slopes of the regression lines, together with the solubilities in Fig. 10A, are given in Fig. 11 as functions of drying temperature. Both parameters increased with the increase in amount of form β in the sample, since the dissolution properties of form β were superior to those of form δ. As expected from the purity, the solubility of sample-80 reached nearly the same value as that of the pure modification β. However, the apparent dissolution rate was far smaller than that of form β. Below 80°C form ε contributed to both parameters more predominantly as the drying temperature dropped, and sample-30 gave a solubility ~1.56 times higher than that of form δ. Both the solubility and apparent dissolution rate of sample-30 were, of course, significantly higher than those of any of the other known crystalline forms including form α. The dependencies of these dissolution properties on the drying temperature were in good agreement, and the excellent *in vitro* availability of form ε was confirmed.

In the present investigation the spray-drying technique could be applied to prepare different crystalline forms by varying the operating condition. More extensive research is necessary to examine the possibility of controlling the purity of the crystalline form.

REFERENCES

(1) H. Junginger, *Acta Pharm. Technol.*, 22, 169 (1976).

(2) H. Junginger, *Pharm. Ztg.*, **121**, 1107 (1976).
(3) H. Junginger, *Pharm. Ind.*, **39**, 822 (1977).
(4) H. Takenaka, Y. Kawashima, and S. Y. Lin, *J. Pharm. Sci.*, **69**, 1388 (1980).
(5) H. Takenaka, Y. Kawashima, and S. Y. Lin, *J. Pharm. Sci.*, **70**, 1256 (1981).
(6) Y. Matsuda, S. Kawaguchi, H. Kobayashi, and J. Nishijo, *J. Pharm. Pharmacol.*, **32**, 579 (1980).
(7) J. Matsunaga, N. Nambu, and T. Nagai, *Chem. Pharm. Bull.*, **24**, 1169 (1976).
(8) H. G. Ibrahim, F. Pisano, and A. Bruno, *J. Pharm. Sci.*, **66**, 669 (1977).
(9) B. W. Müller, *Pharm. Acta Helv.*, **53**, 333 (1978).
(10) A. Chauvet and J. Masse, *Trav. Soc. Pharm. Montpellier*, **38**, 31 (1978).
(11) J. H. Wood, J. E. Syrato, and H. Letterman, *J. Pharm. Sci.*, **54**, 1068 (1965).

ACKNOWLEDGMENTS

The authors thank Ciba-Geigy (Japan) Ltd. for providing the bulk sample of phenylbutazone and are indebted to Dr. R. Higuchi of that corporation for his valuable suggestions. Thanks are also given to Dr. T. Nishino, Kyoto College of Pharmacy, for preparing the scanning electron photomicrographs.

Expanded Solubility Parameter Approach I: Naphthalene and Benzoic Acid in Individual Solvents

A. BEERBOWER ‡, P. L. WU *§, and A. MARTIN *x

Received September 13, 1982, from the *Drug Dynamics Institute, College of Pharmacy, University of Texas, Austin, TX 78712 and the ‡Energy Center, University of California at San Diego, La Jolla, CA 92093. Accepted for publication November 17, 1982. §Present address: China Chemical and Pharmaceutical Co., Taipei, Taiwan.

Abstract □ An expanded solubility parameter system was tested in conjunction with the extended Hansen solubility approach and the UNIFAC method to calculate the solubilities of naphthalene and benzoic acid in polar and nonpolar solvents. The expanded parameter system is characterized by δ_d for the dispersion force, δ_p for dipolar forces, a basic or electron-donor parameter, δ_b, and an acidic or electron-acceptor parameter δ_a. The correlation between the calculated and observed solubilities of benzoic acid was increased by use of the four-parameter system. An indicator variable was required to bring the solubilities into line in strongly dipolar solvents such as *N*,*N*-dimethylformamide. For naphthalene, use of the four-parameter approach proved not to be an improvement over the three-parameter extended Hansen solubility approach. The UNIFAC method was not successful in calculating solubilities of benzoic acid in the 40 polar and nonpolar solvents. A triangular plot of the three Hansen parameters for benzoic acid, *p*-hydroxybenzoic acid, and methyl *p*-hydroxybenzoate illustrated the contributions of dispersion, dipolar, and Lewis acid–base (hydrogen bonding) interaction forces among the three benzoic acid compounds and the various classes of solvents. A multiple regression procedure for calculating the four partial solubility parameters of drug solutes was developed.

Keyphrases □ Solubility parameters, expanded—individual solvents, four-parameter extended Hansen approach, UNIFAC, naphthalene, benzoic acid □ Extended Hansen approach—solubility of naphthalene and benzoic acid in individual solvents, four-parameter system, UNIFAC □ Benzoic acid—model drug, solubility in individual solvents, four-parameter extended Hansen approach, UNIFAC

Recently (1) the solubility of naphthalene was investigated in individual solvents. A new technique, the extended Hansen solubility approach, was compared with the universal functional group activity coefficient (UNIFAC) method (2) and the extended Hildebrand solubility approach (3). The present study was undertaken to investigate the extended Hansen method in more detail and to expand the number of partial solubility parameters from three in the original Hansen approach to four to account for Lewis acid–base (electron acceptor and donor) properties.

Naphthalene was studied in 26 solvents at 40°C and benzoic acid in 40 solvents at 25°C. Naphthalene data were obtained from the literature (1), and benzoic acid data were generated in this laboratory. Both three- and four-parameter solubility systems were used to correlate the solubilities for naphthalene and benzoic acid.

THEORETICAL

Extended Hansen Solubility Approach—The extended Hansen method (1) was successful in predicting the solubilities of naphthalene in individual solvents. Naphthalene is a good model to begin the study of nonpolar compounds in single solvents; however, it is a poor prototype of a drug molecule. Although naphthalene provides π-electrons for solute–solvent interaction, its lack of functional groups and side chains makes it considerably less irregular than molecules typically encountered in the pharmaceutical sciences. Benzoic acid, with its behavior in water and other polar solvents, provides a considerably better model of a drug.

The extended Hansen solubility equation is written:

$$\log \frac{X_2^i}{X_2} = \log \alpha_2 = C_0A + C_1A(\delta_{1d} - \delta_{2d})^2 + C_2A(\delta_{1p} - \delta_{2p})^2 + C_3A(\delta_{1h} - \delta_{2h})^2 \quad \text{(Eq. 1)}$$

where X_2^i is the solute ideal mole fraction solubility, X_2 is the observed solute mole fraction solubility, α_2 is the activity coefficient of the solute, and C_i (where i = 0,1,2,3) are regression coefficients obtained from regression analysis. δ_{jd} is the partial solubility parameter representing London dispersion forces, δ_{jp} is the Keesom dipolar solubility parameter, and δ_{jh} is a term for generalized electron-transfer bonding which includes hydrogen bonding and other Lewis acid–base interactions; j is 1 for solvent and 2 for solute. These parameters are always taken at 25°C, regardless of use. A is a term from regular solution theory (4):

$$A = \frac{V_2\phi_1^2}{2.303RT} \quad \text{(Eq. 2)}$$

where V_2 is the molar volume of the solid solute taken as a hypothetical supercooled liquid at 25°C, ϕ_1 is the volume fraction of the solvent, R is the molar gas constant, and T is the absolute temperature. The volume fraction of the solvent is defined as:

$$\phi_1 = \frac{(1 - X_2)V_1}{(1 - X_2)V_1 + X_2V_2} \quad \text{(Eq. 3)}$$

where V_1 is the molar volume of the solvent.

The partial solubility parameters, δ_{1d}, δ_{1p} and δ_{1h} for the solvents are found in the literature (5). Solubility parameters for solid solutes are seldom reported because organic compounds may decompose near their melting points and because of the low vapor pressures of these compounds. The properties of the solid phase cannot be used since the state

0022-3549/84/0200-0179$01.00/0
© 1984, American Pharmaceutical Association

(2) H. Junginger, *Pharm. Ztg.*, **121**, 1107 (1976).
(3) H. Junginger, *Pharm. Ind.*, **39**, 822 (1977).
(4) H. Takenaka, Y. Kawashima, and S. Y. Lin, *J. Pharm. Sci.*, **69**, 1388 (1980).
(5) H. Takenaka, Y. Kawashima, and S. Y. Lin, *J. Pharm. Sci.*, **70**, 1256 (1981).
(6) Y. Matsuda, S. Kawaguchi, H. Kobayashi, and J. Nishijo, *J. Pharm. Pharmacol.*, **32**, 579 (1980).
(7) J. Matsunaga, N. Nambu, and T. Nagai, *Chem. Pharm. Bull.*, **24**, 1169 (1976).
(8) H. G. Ibrahim, F. Pisano, and A. Bruno, *J. Pharm. Sci.*, **66**, 669 (1977).
(9) B. W. Müller, *Pharm. Acta Helv.*, **53**, 333 (1978).
(10) A. Chauvet and J. Masse, *Trav. Soc. Pharm. Montpellier*, **38**, 31 (1978).
(11) J. H. Wood, J. E. Syrato, and H. Letterman, *J. Pharm. Sci.*, **54**, 1068 (1965).

ACKNOWLEDGMENTS

The authors thank Ciba-Geigy (Japan) Ltd. for providing the bulk sample of phenylbutazone and are indebted to Dr. R. Higuchi of that corporation for his valuable suggestions. Thanks are also given to Dr. T. Nishino, Kyoto College of Pharmacy, for preparing the scanning electron photomicrographs.

Expanded Solubility Parameter Approach I: Naphthalene and Benzoic Acid in Individual Solvents

A. BEERBOWER ‡, P. L. WU *§, and A. MARTIN *x

Received September 13, 1982, from the *Drug Dynamics Institute, College of Pharmacy, University of Texas, Austin, TX 78712 and the ‡Energy Center, University of California at San Diego, La Jolla, CA 92093. Accepted for publication November 17, 1982. §Present address: China Chemical and Pharmaceutical Co., Taipei, Taiwan.

Abstract □ An expanded solubility parameter system was tested in conjunction with the extended Hansen solubility approach and the UNIFAC method to calculate the solubilities of naphthalene and benzoic acid in polar and nonpolar solvents. The expanded parameter system is characterized by δ_d for the dispersion force, δ_p for dipolar forces, a basic or electron-donor parameter, δ_b, and an acidic or electron-acceptor parameter δ_a. The correlation between the calculated and observed solubilities of benzoic acid was increased by use of the four-parameter system. An indicator variable was required to bring the solubilities into line in strongly dipolar solvents such as *N*,*N*-dimethylformamide. For naphthalene, use of the four-parameter approach proved not to be an improvement over the three-parameter extended Hansen solubility approach. The UNIFAC method was not successful in calculating solubilities of benzoic acid in the 40 polar and nonpolar solvents. A triangular plot of the three Hansen parameters for benzoic acid, *p*-hydroxybenzoic acid, and methyl *p*-hydroxybenzoate illustrated the contributions of dispersion, dipolar, and Lewis acid–base (hydrogen bonding) interaction forces among the three benzoic acid compounds and the various classes of solvents. A multiple regression procedure for calculating the four partial solubility parameters of drug solutes was developed.

Keyphrases □ Solubility parameters, expanded—individual solvents, four-parameter extended Hansen approach, UNIFAC, naphthalene, benzoic acid □ Extended Hansen approach—solubility of naphthalene and benzoic acid in individual solvents, four-parameter system, UNIFAC □ Benzoic acid—model drug, solubility in individual solvents, four-parameter extended Hansen approach, UNIFAC

Recently (1) the solubility of naphthalene was investigated in individual solvents. A new technique, the extended Hansen solubility approach, was compared with the universal functional group activity coefficient (UNIFAC) method (2) and the extended Hildebrand solubility approach (3). The present study was undertaken to investigate the extended Hansen method in more detail and to expand the number of partial solubility parameters from three in the original Hansen approach to four to account for Lewis acid–base (electron acceptor and donor) properties.

Naphthalene was studied in 26 solvents at 40°C and benzoic acid in 40 solvents at 25°C. Naphthalene data were obtained from the literature (1), and benzoic acid data were generated in this laboratory. Both three- and four-parameter solubility systems were used to correlate the solubilities for naphthalene and benzoic acid.

THEORETICAL

Extended Hansen Solubility Approach—The extended Hansen method (1) was successful in predicting the solubilities of naphthalene in individual solvents. Naphthalene is a good model to begin the study of nonpolar compounds in single solvents; however, it is a poor prototype of a drug molecule. Although naphthalene provides π-electrons for solute–solvent interaction, its lack of functional groups and side chains makes it considerably less irregular than molecules typically encountered in the pharmaceutical sciences. Benzoic acid, with its behavior in water and other polar solvents, provides a considerably better model of a drug.

The extended Hansen solubility equation is written:

$$\log \frac{X_2^i}{X_2} = \log \alpha_2 = C_0A + C_1A(\delta_{1d} - \delta_{2d})^2 + C_2A(\delta_{1p} - \delta_{2p})^2 + C_3A(\delta_{1h} - \delta_{2h})^2 \quad \text{(Eq. 1)}$$

where X_2^i is the solute ideal mole fraction solubility, X_2 is the observed solute mole fraction solubility, α_2 is the activity coefficient of the solute, and C_i (where i = 0,1,2,3) are regression coefficients obtained from regression analysis. δ_{jd} is the partial solubility parameter representing London dispersion forces, δ_{jp} is the Keesom dipolar solubility parameter, and δ_{jh} is a term for generalized electron-transfer bonding which includes hydrogen bonding and other Lewis acid–base interactions; j is 1 for solvent and 2 for solute. These parameters are always taken at 25°C, regardless of use. A is a term from regular solution theory (4):

$$A = \frac{V_2\phi_1^2}{2.303RT} \quad \text{(Eq. 2)}$$

where V_2 is the molar volume of the solid solute taken as a hypothetical supercooled liquid at 25°C, ϕ_1 is the volume fraction of the solvent, R is the molar gas constant, and T is the absolute temperature. The volume fraction of the solvent is defined as:

$$\phi_1 = \frac{(1 - X_2)V_1}{(1 - X_2)V_1 + X_2V_2} \quad \text{(Eq. 3)}$$

where V_1 is the molar volume of the solvent.

The partial solubility parameters, δ_{1d}, δ_{1p} and δ_{1h} for the solvents are found in the literature (5). Solubility parameters for solid solutes are seldom reported because organic compounds may decompose near their melting points and because of the low vapor pressures of these compounds. The properties of the solid phase cannot be used since the state

0022-3549/84/0200-0179$01.00/0
© 1984, American Pharmaceutical Association

of a solute is essentially that of the liquid phase, even if highly supercooled. Hansen and Beerbower (5) provide a group contribution method by which the partial solubility parameters can be estimated. A recent method based on multiple regression has been suggested to obtain partial solubility parameters for crystalline solid compounds (6).

For a given solute, δ_{2d}, δ_{2p}, and δ_{2h} are constants; therefore, $(\log \alpha_2)/A$ values are regressed only on δ_{1d}, δ_{1d}^2, δ_{1p}, δ_{1p}^2, δ_{1h}, and δ_{1h}^2, according to an expression obtained by expanding Eq. 1:

$$\frac{\log \alpha_2}{A} = C_1\delta_{1d}^2 + (-2C_1\delta_{2d})\delta_{1d} + C_2\delta_{1p}^2 + (-2C_2\delta_{2p})\delta_{1p} + C_3\delta_{1h}^2 + (-2C_3\delta_{2h})\delta_{1h} + (C_0 + C_1\delta_{2d}^2 + C_2\delta_{2p}^2 + C_3\delta_{2h}^2) \quad \text{(Eq. 4)}$$

According to the model:

$$\frac{\log \alpha_2}{A} = D_1\delta_{1d}^2 + D_2\delta_{1d} + D_3\delta_{1p}^2 + D_4\delta_{1p} + D_5\delta_{1h}^2 + D_6\delta_{1h} + D_0 \quad \text{(Eq. 5)}$$

where D_0 represents the last term of Eq. 4, made up exclusively of constants. This procedure eliminates the need for solubility parameters of the solute in the regression equation.

Expanded Parameter Approach—Karger *et al.* (7, 8) proposed five specific solubility parameters for solvents and adsorbents: dispersion, δ_d; induction, δ_{in}; orientation, δ_o; and δ_a and δ_b for acid and base effects, respectively. The authors used this expanded set of parameters to estimate selectivity in chromatography. According to their method, the dispersion solubility parameter is determined (9) from the refractive index fraction, $X = (n^2 - 1)/(n^2 - 2)$ and the expression:

$$\delta_d = -2.24 + 53X - 58X^2 + 22X^3 \quad \text{(Eq. 6)}$$

The orientation parameter (δ_o) is obtainable, in principle, from the dipole moment and molar volume of the substance. It can be calculated using the equation:

$$\delta_o^2 = (\delta_T^2 - \delta_d^2)/(1 + 0.0014\delta_d V) \quad \text{(Eq. 7)}$$

where δ_T is the total solubility parameter obtained from the energy of vaporization (4). The induction solubility parameter is obtained from the orientation parameter and molar volume:

$$\delta_{in} = 0.0007\delta_o^2 V \quad \text{(Eq. 8)}$$

For hydrogen bonding or acid–base effects, the $\delta_a\delta_b$ parameters of alcohols are obtained from:

$$\Delta H_{hb} = C^* V \delta_a \delta_b \quad \text{(Eq. 9)}$$

where ΔH_{hb} is the heat of hydrogen bonding, taken as 5200 cal/mol, and C^* is a proportionality constant. For alcohols C^* has a value of 1.8. With the assumption of equal values of δ_a and δ_b for all alcohols, it is possible to determine the acid and base parameters for other compounds *via* heats of hydrogen bonding. The expansion of Hansen solubility parameters as proposed here divides the electron transfer solubility parameter, δ_h, to yield acidic, δ_a, and basic, δ_b, solubility parameters in order to quantify electron-donor and -acceptor properties.

The detailed procedures employed in the current study for obtaining the partial solubility parameters of the solvents are as follows.

Dispersion Solubility Parameter, δ_d—The δ_d values proposed by Karger *et al.* (7, 8) are almost the same as Hansen's δ_d values (5). Since Hansen's δ_d has been refined over a long period of time, based on solubility data, the δ_d values of the solvents used in the current study are those provided by Hansen and Beerbower (5) with a few corrections.

Polar Solubility Parameter, δ_p—The polar parameter, δ_p, was calculated using the modified Boettcher equation (5, 10–12):

$$\delta_p^2 = \frac{12{,}108}{V^2} \cdot \frac{\epsilon - 1}{2\epsilon + n_D^2}(n_D^2 + 2)\mu^2 \quad \text{(Eq. 10)}$$

where V is the molar volume of the compound, ϵ is the dielectric constant, n_D is the refractive index for the D line of sodium, and μ is the dipole moment expressed in units of 10^{-18} esu-cm (Debye units). The δ_p values of the solvents in this study were obtained from Hansen and Beerbower (5).

Basic Solubility Parameter, δ_b—Recently Kamlet *et al.* (13) used spectrometric methods to obtain three solvatochromic parameters, π^*, α, and β. The α-scale of the solvent provided a measure of proton-donor capacity, and the β-scale quantified the ability of the solvent to accept a proton. Kamlet *et al.* have prepared an extensive table of β-values for solvents, and Karger *et al.* (7, 8) provided a limited number of δ_a and δ_b values for solvents. It was found in the current work that a linear relationship exists between the δ_b-value of Karger *et al.* and the β-value of Kamlet *et al.*:

$$V^{1/2}\delta_b = 60.1\beta + 2.45 \quad n = 22,\ r^2 = 0.918 \quad \text{(Eq. 11)}$$

The β-value provided by Kamlet *et al.* (13) in Eq. 11 yields δ_b of the solvent. For example, the β-value of dimethyl sulfoxide is 0.76 (13) and V = 71.3 (Table I): $V^{1/2}\delta_b = (60.1)(0.76) + 2.45$; $(71.3)^{1/2}\delta_b = 48.13$. Therefore, $\delta_b = (48.13)/(8.44) = 5.7$. Table I lists δ_b-values for the solvents. Solvents for which Kamlet *et al.* did not list β-values were evaluated by comparison with the extensive compilation of basicity and acidity parameters by Griffiths and Pugh (14). Some partial parameters were adjusted based on solubility data.

Acidic Solubility Parameter, δ_a—The α-values given by Kamlet *et al.* are less accurate than β-values, as noted by the authors (13). However, since δ_T, δ_d, δ_p, and δ_b are known, δ_a can be obtained using the following equation:

$$2\delta_a\delta_b = \delta_T^2 - \delta_d^2 - \delta_p^2 = \delta_h^2 \quad \text{(Eq. 12)}$$

For dimethyl sulfoxide, $\delta_b = 5.7$ as given above; $\delta_T = 13.04$, $\delta_d = 9.0$, and $\delta_p = 8.0$ are obtained from Table I. One gets δ_a for dimethyl sulfoxide by substituting these values into Eq. 12: $2\delta_a\delta_b = (13.04)^2 - (9.0)^2 - (8.0)^2 = 25.04$; $\delta_a = (25.04)/(2 \times 5.7) = 2.2$. The δ_a-values for the solvents are found in Table I.

Regression Approach Using Expanded Solubility Parameters—The solubility of a compound in a liquid solvent can be expressed as (7, 8):

$$\frac{\log \alpha_2}{A} = (\delta_{1d} - \delta_{2d})^2 + (\delta_{1o} - \delta_{2o})^2 + 2(\delta_{1d} - \delta_{2d})(\delta_{1in} - \delta_{2in}) + 2(\delta_{1a} - \delta_{2a})(\delta_{1b} - \delta_{2b}) \quad \text{(Eq. 13)}$$

where δ_{1d}, δ_{2d}, δ_{1o}, δ_{2o}, δ_{1a}, δ_{2a}, δ_{1b}, and δ_{2b} have already been defined. Since δ_p and δ_o are both contributed from the dipolar property of the compound, δ_p-values were used instead of δ_o in the present study. The induction solubility parameter, δ_{in}, a product term of δ_o and V, was found to be insignificant in improving the predicted solubilities[1] and was deleted. Equation 13 can then be transformed to:

$$\frac{\log \alpha_2}{A} = (\delta_{1d} - \delta_{2d})^2 + (\delta_{1p} - \delta_{2p})^2 + 2(\delta_{1a} - \delta_{2a})(\delta_{1b} - \delta_{2b}) \quad \text{(Eq. 14)}$$

The solubility of one compound in various single solvents can be predicted by expanding Eq. 14:

$$\frac{\log \alpha_2}{A} = \delta_{1d}^2 - 2\delta_{1d}\delta_{2d} + \delta_{2d}^2 + \delta_{1p}^2 - 2\delta_{1p}\delta_{2p} + \delta_{2p}^2 + 2\delta_{1a}\delta_{1b} - 2\delta_{1a}\delta_{2b} - 2\delta_{2a}\delta_{1b} + 2\delta_{2a}\delta_{2b} \quad \text{(Eq. 15)}$$

where δ_{2d}, δ_{2p}, δ_{2a}, and δ_{2b} are now the solubility parameters of the solute, which obviously are constant for a particular solute dissolved in a series of different solvents. Therefore, the solubilities are simply estimated by regressing $(\log \alpha_2)/A$ against δ_{1d}^2, δ_{1d}, δ_{1p}^2, δ_{1p}, $\delta_{1a}\delta_{1b}$, δ_{1a}, and δ_{1b} using the model suggested by Eq. 15:

$$\frac{\log \alpha_2}{A} = C_0 + C_1\delta_{1d}^2 + C_2\delta_{1d} + C_3\delta_{1p}^2 + C_4\delta_{1p} + C_5\delta_{1a}\delta_{1b} + C_6\delta_{1a} + C_7\delta_{1b} \quad \text{(Eq. 16)}$$

where C_0, C_1, . . . are the coefficients of the regression equation.

EXPERIMENTAL

Materials—The solubility of benzoic acid[2] in a number of solvents was compared with literature values, and the UV spectra of the various solutions were measured. The solvents were spectrophotometric or ACS grade or redistilled before used and are listed in Table I. The solubility data for naphthalene was obtained from the literature (1).

Heat of Fusion and Molar Volume—The heat of fusion of benzoic acid, determined by differential scanning calorimetry[3], was found to be

[1] P. L. Wu and A. Martin, unpublished data.
[2] Matheson Coleman Bell, Norwood, OH 45212.
[3] Perkin-Elmer DSC Model 1B, Norwalk, Conn.

Table I—Solubility Parameters and Molar Volumes of Commonly Used Solvents

No.	Solvent	Molar Volume (V_1)	Solubility Parameter: Dispersion (δ_d)	Dipolar (δ_p)	Hydrogen Bonding (δ_h)	Acidic (δ_a)	Basic (δ_b)	Total (δ_T)
1	Pentane	116.1	7.1	0.0	0.0	0.0	0.0	7.10
2	Hexane	131.6	7.3	0.0	0.0	0.0	0.0	7.30
3	Heptane	147.5	7.5	0.0	0.0	0.0	0.0	7.50
4	Nonane	179.7	7.7	0.0	0.0	0.0	0.0	7.70
5	Decane	195.9	7.7	0.0	0.0	0.0	0.0	7.70
6	Cyclohexane	108.8	8.2	0.0	0.0	0.0	0.0	8.20
7	Benzene	89.4	9.0	0.5	1.0	0.7	0.7	9.07
8	Toluene	106.9	8.8	0.7	1.0	0.8	0.6	8.88
9	Chlorobenzene	102.2	9.3	2.1	1.0	1.0	0.5	9.59
10	Ethylene dichloride	79.4	9.3	3.6	2.0	2.0	1.0	10.17
11	Ethylidene chloride	84.8	8.1	4.0	0.2	0.2	0.1	9.04
12	Chloroform	80.8	8.7	1.5	2.8	3.0	1.3	9.26
13	Carbon tetrachloride	97.1	8.7	0.0	0.3	0.05	0.9	8.71
14	Ethylene dibromide	87.0	9.3[a]	1.7	4.2	11.2	0.8	10.36
15	Ethylidene bromide	92.9	9.0[a]	2.5[a]	3.2[a]	10.0	0.5	9.86
16	Diethyl ether	104.8	7.1	1.4	2.5	0.5	6.3	7.66
17	Dipropyl ether	139.4	7.3	1.1	2.0	0.4	5.0	7.65
18	Dibutyl ether	170.4	7.6	0.8	1.5	0.3	3.9	7.79
19	Ethyl acetate	98.5	7.4	2.6	4.5	5.3	1.9	9.04
20	Propyl acetate	115.7	7.7	2.1	3.3	3.6	1.5	8.63
21	Butyl acetate	132.6	7.7	1.8	3.1	2.8	1.7	8.49
22	Hexyl acetate	164.5	7.8	1.5	2.9	1.9	2.2	8.45
23	Carbon disulfide	60.0	10.0	0.0	0.3	0.2	0.2	10.00
24	Acetone	74.0	7.6	5.1	3.4	2.4	2.4	9.76
25	Dioxane	85.7	9.3	0.9	3.6	1.0	6.5	10.01
26	Aniline	91.5	9.5	2.5	5.0	1.9	6.5	11.01
27	Nitrobenzene	102.7	9.8	4.2	2.0	2.0	1.0	10.85
28	Acetophenone	117.4	9.6	4.2	1.8	1.1	1.5	10.63
29	Benzyl alcohol	103.9	9.0	3.1	6.7	5.9	3.8	11.64
30	Cyclohexanol	106.0	8.5	2.0	6.6	7.3	3.0	10.96
31	Methyl alcohol	40.7	7.4	6.0	10.9	8.4	7.1	14.49
32	Ethyl alcohol	58.7	7.7	4.3	9.5	8.3	5.5	12.96
33	Propyl alcohol	75.1	7.8	3.3	8.5	7.5	4.8	11.99
34	Isopropyl alcohol	76.9	7.7	3.0	8.0	7.1	4.5	11.50
35	Butyl alcohol	92.0	7.8	2.8	7.7	6.4	4.6	11.29
36	Isobutyl alcohol	92.4	7.4	2.8	7.8	6.0	5.1	11.13
37	*sec*-Butyl alcohol	92.5	7.7	2.8	7.1	6.6	3.8	10.83
38	*tert*-Butyl alcohol	94.3	7.3	2.5	6.8	9.6	2.4	10.28
39	1-Pentanol	108.6	7.8	2.2	6.8	5.4	4.3	10.59
40	1-Hexanol	125.2	8.0	2.1	6.3	5.7	3.5	10.41
41	1-Heptanol	141.9	8.1	2.0	6.0	5.3	3.4	10.28
42	1-Octanol	158.4	8.3	1.6	5.8	5.2	3.2	10.23
43	Ethylene Glycol	55.9	8.3	5.4	12.6	17.9	4.4	15.99
44	1,2-Propanediol	73.7	8.2	4.6	11.4	14.1	4.6	14.77
45	1,3-Propanediol	72.5	8.1	5.3	12.7	10.9	7.4	15.97
46	Glycerol	73.2	8.5	5.9	14.3	20.0	5.1	17.64
47	1,4-Butanediol	88.6	8.2	8.1	11.6	18.2	3.7	16.36
48	Acetic acid	57.6	7.1	3.9	6.6	7.0	3.1	10.44
49	Propionic acid	75.0	7.2	3.8	6.0	6.0	3.0	10.11
50	Butyric acid	91.9	7.3	2.0	5.2	6.4	2.1	9.17
51	Dimethyl sulfoxide	71.3	9.0	8.0	5.0	2.2	5.7	13.04
52	Pyridine	80.9	9.3	4.3	3.0	1.4	3.2	10.67
53	Formamide	39.9	8.4	12.8	9.3	5.7	7.6	17.92
54	*N*-Methylformamide	59.1	8.4	10.1	6.1	4.8	3.9	14.49
55	*N,N*-Dimethylformamide	77.4	8.5	6.7	5.5	3.4	4.4	12.13
56	*N,N*-Diethylformamide	112.0	8.2	5.6	4.3	2.7	3.4	10.81
57	*N,N*-Dimethylacetamide	93.0	8.2	5.6	5.0	2.9	4.3	11.11
58	*N,N*-Diethylacetamide	126.6	8.2	4.1	3.7	2.1	3.2	9.87
59	Water	18.1	7.6	7.8	20.7	6.7	32.0	23.40

[a] Values recalculated.

4326 cal/mol (average of six measurements). The molar volume of supercooled benzoic acid at 25°C was taken as 104.3 cm^3/mol (15). The molar volumes of the solvents were obtained from the literature (16).

Ideal Solubility and Activity Coefficient—The ideal solubility of benzoic acid can be calculated from the heat of fusion of the solute and heat capacities of the solid and its supercooled liquid (17):

$$\log X_2^i = -\frac{\Delta H_m^f}{4.575}\left(\frac{T_m - T}{T_m T}\right) + \frac{\Delta C_p}{4.575}\left(\frac{T_m - T}{T}\right) - \frac{\Delta C_p}{1.987}\log\frac{T_m}{T} \quad \text{(Eq. 17)}$$

The ideal solubility of benzoic acid was calculated using the following data: ΔH_m^f = 4326 cal/mol, T_m = 395.45 K, T = 298.15 K, and $\Delta C_p = C_p^l - C_p^s$ = 13.83 cal/mol-deg (18). These quantities result in the following ideal solubility values at 25°C: $\log X_2^i = -0.6475$ or $X_2^i = 0.2251$. The activity coefficient is calculated from:

$$\log \alpha_2 = \log X_2^i - \log X_2 = \log\frac{X_2^i}{X_2} \quad \text{(Eq. 18)}$$

Solubility Determination—The solubility of benzoic acid was determined in individual solvents at 25°C. A suitable amount of an individual solvent was introduced into screw-capped vials containing an excess amount of the solute. After being sealed with several turns of plastic tape, the vials were submerged in water at 25 ± 0.2°C and were shaken at 100 cycles/min for 24 h in a constant-temperature bath[4]. Preliminary studies showed that this time period was sufficient to assure saturation at 25°C.

[4] Blue-M Electric Co., Blue Island, Ill.

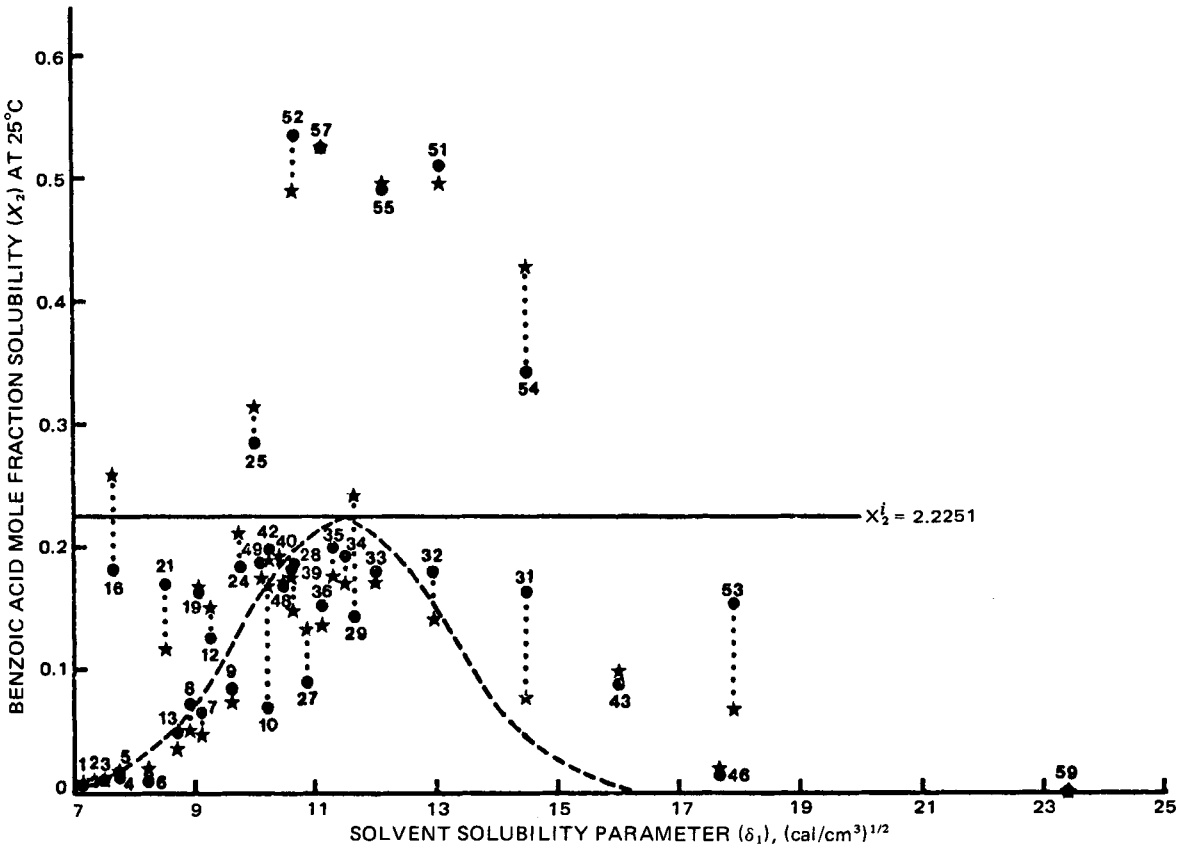

Figure 1—*Solubility profile of benzoic acid in individual solvents at 25°C. See Table I for solvent numbers. Key: (- - -) regular solution curve; (—) ideal solubility line, $X_2 = 0.2251$; (●) experimental solubilities; (★) solubilities calculated using Eq. 28.*

After equilibrium had been attained, each vial was removed, wiped dry, and analyzed. The solutions were transferred to a syringe and filtered using a filter[5] of pore size <1 μm. After suitable dilution, the solutions were assayed using a spectrophotometer[6] set at the λ_{max} of the solute. The solubility was determined at least six times for each solvent, and the average value was taken. The experimental variation in solubility was <3% in replicate samples and was consistent with an acid–base titration method (19). The densities of the saturated solutions were determined with a calibrated pycnometer at 25°C.

RESULTS AND DISCUSSION

Three-Parameter Solubility System—$(\text{Log } \alpha_2)/A$ for naphthalene solubility in 26 solvents at 40°C was regressed against the Hansen solvent parameters (Table I, Eq. 5) to yield:

$$\frac{\log \alpha_2}{A} = 0.6214\delta_{1d}^2 - 12.70\delta_{1d} - 0.1240\delta_{1p}^2 + 0.5383\delta_{1p} + 0.1292\delta_{1h}^2 - 0.2242\delta_{1h} + 64.62$$

$$n = 26, s = 1.37, r^2 = 0.986, F = 231, F(6,19,0.01) = 3.94 \quad \text{(Eq. 19)}$$

This regression equation is slightly different from the one reported earlier (6) due to recalculation of the solubility parameters of ethylene dibromide and ethylidene bromide.

To predict the solubility of naphthalene at 40°C in acetone, the calculation is made as follows. The partial solubility parameters for acetone are $\delta_{1d} = 7.6$, $\delta_{1p} = 5.1$, and $\delta_{1h} = 3.4$. Substituting these values in Eq. 19 yields $(\log \alpha_2)/A = 4.24$. The A-value is then calculated using Eq. 2 with $V_2 = 123$, $V_1 = 74.0$, $R = 1.987$, $T = 313.15$ K, and $X_2^i = 0.466$. The volume fraction of the solvent, ϕ_1, is unknown since it depends on the value of X_2 (Eq. 3). Hence, A is found by an iteration procedure (20), beginning with a value of 1 for ϕ_1 and iterating until X_2 or ϕ_1 no longer changes by more than some small desired value, *e.g.*, 0.0001. In the present example, the steps of the iteration are shown in Table II. The iteration yielded X_2 (calc.) = 0.379, a result that compares favorably with X_2 (obs.) = 0.378, and provides a predicted value within a 1% error relative to the observed mole fraction solubility. The back-calculated solubilities of naphthalene, using Eq. 19, are listed in Table III. They are within 30% error of the observed values, except for those in aniline (31%), isopropyl alcohol (38%), and acetic acid (68%). The residuals and percentage errors are also given in Table III. Thirty percent error is taken in this work as a criterion of acceptability. A maximum value of 15% would be highly desirable, but is unrealistic at this stage of development of the methods.

The mole fraction solubilities of benzoic acid in 40 solvents at 25°C are listed in Table IV. A mole fraction solubility profile of benzoic acid is plotted on the total solubility parameter scale in Fig. 1. The data points for observed solubilities are shown as filled circles, joined to the calculated values (stars) by dotted lines.

When benzoic acid is dissolved in a nonpolar solvent, it tends to self-associate, even at high dilution, through intermolecular hydrogen bonds and other attraction forces. In benzene at 25°C, benzoic acid forms dimers and trimers (21), in carbon tetrachloride it exists as dimers, and in alcohols it remains as the monomer (22). The degree of self-association of dissolved benzoic acid and the percentages of monomeric, dimeric, trimeric, and polymeric forms are not currently known for most solvents. Benzoic acid is therefore treated in this study as if it behaved as a monomer in all solvents, and the mole fraction solubility is calculated based on the monomeric form.

$(\text{Log } \alpha_2)/A$ of benzoic acid in 40 solvents at 25°C was regressed against

Table II—Iteration Procedure for Calculating the Solubility of Naphthalene in Acetone at 40°C Using Eq. 19

Step	ϕ_1	A	log α_2	X_2
1	1	0.08583	0.36394	0.20158
2	0.70440	0.04259	0.18058	0.30747
3	0.57538	0.02842	0.12049	0.35310
4	0.52431	0.02360	0.10005	0.37012
5	0.50590	0.02197	0.09314	0.37605
6	0.49956	0.02142	0.09082	0.37806
7	0.49742	0.02124	0.09005	0.37874
8	0.49670	0.02118	0.08979	0.37897
9	0.49646	0.02116	0.08970	0.37904
10	0.49637	0.02115	0.08967	0.37907
11	0.49635	0.02115	0.08966	0.37908

[5] Filter paper, Glass Fiber, Whatman Grade GF/F.
[6] Beckman, Model 25.

Table III—Back-Calculated Solubilities of Naphthalene in Solvents at 40°C Using Three- and Four-Parameter Systems

No.	Solvent	Mole Fraction Solubility (X_2)	Equation 29 X_2 (Calc.)	Equation 29 Residual	Equation 29 Error, %	Equation 19 X_2 (Calc.)	Equation 19 Residual	Equation 19 Error, %
2	Hexane	0.222	0.266	−0.044	−19.8	0.269	−0.047	−21.2
7	Benzene	0.428	0.446	−0.018	− 4.2	0.450	−0.022	− 5.1
8	Toluene	0.422	0.432	−0.010	− 2.4	0.436	−0.014	− 3.3
9	Chlorobenzene	0.444	0.453	−0.009	− 2.0	0.449	−0.005	− 1.1
10	Ethylene dichloride	0.452	0.455	−0.003	− 0.7	0.455	−0.003	− 0.7
11	Ethylidene chloride	0.437	0.416	0.021	4.8	0.409	0.028	6.4
12	Chloroform	0.467	0.419	0.048	10.3	0.426	0.041	8.8
13	Carbon tetrachloride	0.395	0.431	−0.036	− 9.1	0.441	−0.046	−11.6
14	Ethylene dibromide	0.439	0.442	−0.003	− 0.7	0.419	0.020	4.6
15	Ethylidene bromide	0.456	0.447	0.009	2.0	0.425	0.031	6.8
23	Carbon disulfide	0.494	0.473	0.021	4.3	0.469	0.025	5.1
24	Acetone	0.378	0.351	0.027	7.1	0.379	−0.001	− 0.3
26	Aniline	0.306	0.321	−0.015	− 4.9	0.402	−0.096	−31.4
27	Nitrobenzene	0.432	0.469	−0.037	− 8.6	0.466	−0.034	− 7.9
30	Cyclohexanol	0.232	0.241	−0.009	− 3.9	0.237	−0.005	− 2.2
31	Methyl alcohol	0.0412	0.0372	0.0040	9.7	0.0320	0.0092	22.3
32	Ethyl alcohol	0.0726	0.0686	0.0040	5.5	0.0599	0.0127	17.5
33	Propyl alcohol	0.0944	0.0930	0.0014	1.5	0.0910	0.0034	3.6
34	Isopropyl alcohol	0.0764	0.1023	−0.0259	−33.9	0.1051	−0.0287	−37.6
35	Butyl alcohol	0.116	0.104	0.012	10.3	0.114	0.002	1.7
36	Isobutyl alcohol	0.0925	0.0640	0.0285	30.8	0.0746	0.0179	19.4
37	*sec*-Butyl alcohol	0.1122	0.1284	−0.0162	−14.4	0.1364	−0.0242	−21.6
38	*tert*-Butyl alcohol	0.1009	0.1220	−0.0211	−20.9	0.1049	−0.0040	− 4.0
48	Acetic acid	0.117	0.192	−0.075	−64.1	0.197	−0.080	−68.4
50	Butyric acid	0.251	0.180	0.071	28.3	0.186	0.065	25.9
59	Water	1.76×10^{-5}	1.75×10^{-5}	1.0×10^{-7}	0.5	1.81×10^{-5}	5.0×10^{-5}	2.8

the Hansen parameters (Table I) to produce the regression equation:

$$\frac{\log \alpha_2}{A} = 5.498\delta_{1d}^2 - 92.79\delta_{1d} + 0.4686\delta_{1p}^2 - 7.397\delta_{1p} + 0.1597\delta_{1h}^2 - 0.6623\delta_{1h} + 403.17$$

$$n = 40, s = 7.47, r^2 = 0.71, F = 13.7, F(6,33,0.01) = 3.40 \quad \text{(Eq. 20)}$$

It has subsequently been found that a root-finder method (23) is more satisfactory than simple iteration, and this technique is now used in place of iteration *in the extended* Hansen solubility approach. Since the right-hand side of Eq. 20 is a function of the three partial parameters, which together constitute δ_1, it can be designated as $f(\delta_1)$. Combining this with Eqs. 2, 3, and 18, one obtains:

$$f(X_2) = (\log X_2^i - \log X_2)(2.303RT)[V_1(1 - X_2) + V_2X_2]^2 - V_2[V_1(1 - X_2)]^2 f(\delta_1) = 0 \quad \text{(Eq. 21)}$$

X_2 can be found by a trial and error method. For ethyl acetate ($\delta_{1d} = 7.4$, $\delta_{1p} = 2.6$, and $\delta_{1h} = 4.5$), one may substitute these partial solubility parameters into Eq. 20 and obtain $f(\delta_1) = 1.7836$. The mole fraction solubility of benzoic acid in ethyl acetate can then be estimated from Eq. 21 using $V_1 = 98.5$, $V_2 = 104.3$, $T = 298.15$ K, and $\log X_2^i = -0.6475$. Table V lists the values of X_2 found during the trial and error procedure, which can easily be accomplished by use of a programmable calculator. The root-finder subroutine ZBRENT found in The International Mathematics and Statistics Library (IMSL) (23) can be run on an electronic computer[7] to obtain the calculated solubilities. It was observed that 24 of the 40 solubilities were within 30% error of the experimental result. The calculated solubilities (Eq. 20) for benzoic acid at 25°C are found in Table IV.

Estimating the Partial Solubility Parameters of Benzoic Acid—Using the extended Hansen three-parameter system as previously reported for naphthalene (6), the regression equation obtained for benzoic acid can be transformed to a form that yields the partial solubility parameters of the solute. The steps are as follows:

$$\frac{\log \alpha_2}{A} = 5.489(\delta_{1d}^2 - 16.877\delta_{1d}) + 0.4686(\delta_{1p}^2 - 15.785\delta_{1p}) + 0.1597(\delta_{1h}^2 - 4.147\delta_{1h}) + 403.17 \quad \text{(Eq. 22)}$$

$$\frac{\log \alpha_2}{A} = 5.489(\delta_{1d}^2 - 16.877\delta_{1d} + 71.208) + 0.4686(\delta_{1p}^2 - 15.785\delta_{1p} + 62.292) + 0.1597(\delta_{1h}^2 - 4.147\delta_{1h} + 4.299) - (5.489)(71.208) - (0.4686)(62.292) - (0.1597)(4.299) + 403.17 \quad \text{(Eq. 23)}$$

Therefore, $71.208 = \delta_{2d}^2$ and $(71.208)^{1/2} = 8.44 = \delta_{2d}$; likewise for δ_{2p} and δ_{2h}:

$$\frac{\log \alpha_2}{A} = 5.498(\delta_{1d} - 8.44)^2 + 0.4686(\delta_{1d} - 7.89)^2 + 0.1597(\delta_{1h} - 2.07)^2 - 18.27 \quad \text{(Eq. 24)}$$

The partial solubility parameters, $\delta_{2d} = 8.44$, $\delta_{2p} = 7.89$, and $\delta_{2h} = 2.07$, have thus been obtained by a regression method involving only solvent partial solubility parameters, together with experimental data from which $(\log \alpha_2)/A$ is calculated. The total solubility parameter, δ_T, for benzoic acid by this method is:

$$\delta_T^2 = \delta_{2d}^2 + \delta_{2p}^2 + \delta_{2h}^2 = (8.44)^2 + (7.89)^2 + (2.07)^2 = 137.77$$

$$\delta_T = (137.77)^{1/2} = 11.74 \quad \text{(Eq. 25)}$$

This value compares favorably with $\delta_2 = 11.5$ given in the literature (15). An earlier publication (5) gave $\delta_{2d} = 8.9$, $\delta_{2p} = 3.4$, and $\delta_{2h} = 4.8$, from which $\delta_2 = 10.7$. These values appeared to be quite low, so they were recalculated in 1974[8] to be $\delta_{2d} = 10.5$, $\delta_{2p} = 2.8$, and $\delta_{2h} = 4.8$, from which $\delta_2 = 11.9$, in good agreement with δ_2 calculated by Eq. 25.

Agreement with the partial parameters of Eq. 25 is less satisfactory, partly because C_1 was allowed to have any value that the computer found gave the best fit to the solubilities in Table IV. That resulted in $C_1 = 5.489$, which is contrary to both theory and experience with London (dispersion) forces. Though they are omnidirectional and universal, they can interact only once with each nearest neighbor, so that any value of C_1 other than 1.000 must be an artifact. Trial runs with the computer constrained in that way show that the loss of accuracy in predicting solubility is not serious. It will be necessary to continue with this approach at a later time.

Graphical Solubility Relationships: Triangular Diagrams—To demonstrate graphically the effects of solvents, Teas (24) expressed the three solubility parameters of Hansen as functions:

$$f_d = \frac{\delta_d}{\delta_d + \delta_p + \delta_h}; \quad f_p = \frac{\delta_p}{\delta_d + \delta_p + \delta_h}; \quad f_h = \frac{\delta_h}{\delta_d + \delta_p + \delta_h} \quad \text{(Eq. 26)}$$

These functional values are plotted along the three axes of the triangular graphs in Fig. 2. The points for the solvents, numbered according to the listing in Table I, are then entered on each triangular graph. Solvents with high solvencies (mole fraction solubilities >0.150) for benzoic acid are plotted as filled circles, and those with low solvencies are plotted as open squares. A boundary line has been drawn around the solvents in Fig. 2A with solvencies for benzoic acid greater than $X_2 = 0.150$. Triangular solubility plots for *p*-hydroxybenzoic acid and for methyl *p*-hydroxy-

[7] University of Texas Cyber Computer System.

[8] Unpublished data.

Table IV—Calculated Solubilities of Benzoic Acid in Individual Solvents at 25°C

No.	Solvent	Mole Fraction Solubility (X_2)	UNIFAC			Equation 20			Equation 27			Equation 28		
			X_2 (Calc.)	Residual	Error, %	X_2 (Calc.)	Residual	Error, %	X_2 (Calc.)	Residual	Error, %	X_2 (Calc.)	Residual	Error, %
1	Pentane	0.0059	0.0100	−0.0041	−64.5	0.0053	0.0006	10.2	0.0024	0.0035	59.3	0.0078	−0.0019	−32.2
2	Hexane	0.0095	0.0101	−0.0006	−6.3	0.0086	0.0009	9.5	0.0045	0.0050	52.6	0.0097	−0.0002	−2.1
3	Heptane	0.0117	0.0103	0.0014	12.0	0.0130	−0.0013	−11.1	0.0075	0.0042	35.9	0.0118	−0.0001	−0.9
4	Nonane	0.0141	0.0109	0.0032	22.7	0.0180	−0.0039	−27.7	0.0115	0.0026	18.4	0.0138	0.0003	2.1
5	Decane	0.0154	0.0114	0.0040	26.0	0.0179	−0.0025	−16.2	0.0114	0.0040	26.0	0.0138	0.0016	10.4
6	Cyclohexane	0.0102	0.0112	−0.0010	−9.8	0.0310	−0.0208	−203.9	0.0220	−0.0118	−115.7	0.0191	−0.0089	−87.3
7	Benzene	0.0689	0.0623	0.0066	9.6	0.0532	0.0157	22.8	0.0459	0.0230	33.4	0.0476	0.0213	30.9
8	Toluene	0.0734	0.0407	0.0327	44.6	0.0798	−0.0064	−8.7	0.0707	0.0027	3.7	0.0512	0.0222	30.2
9	Chlorobenzene	0.0862	0.0747	0.0115	13.3	0.1832	−0.0970	−112.5	0.1265	−0.0403	−46.8	0.0762	0.0100	11.6
10	Ethylene dichloride	0.0695	0.1334	−0.0639	−91.9	0.3242	−0.2547	−366.5	0.2932	−0.2237	−321.9	0.1676	−0.0981	−141.2
12	Chloroform	0.1283	0.0038	0.1245	97.0	0.1954	−0.0671	−52.3	0.2185	−0.0902	−70.3	0.1537	−0.0254	−19.8
13	Carbon tetrachloride	0.0494	0.0178	0.0316	64.0	0.0322	0.0172	34.8	0.0352	0.0142	28.7	0.0356	0.0138	27.9
16	Diethyl ether	0.1837	0.0832	0.1005	54.7	0.0346	0.1491	81.6	0.2123	−0.0286	−15.6	0.2602	−0.0765	−41.6
19	Ethyl acetate	0.1649	0.1251	0.0398	24.1	0.1835	−0.0186	−11.3	0.1879	−0.0230	−13.9	0.1688	−0.0039	−2.4
21	Butyl acetate	0.1699	0.0937	0.0762	44.8	0.1655	0.0044	2.6	0.1874	−0.0175	−10.3	0.1171	0.0528	31.1
24	Acetone	0.1857	0.1671	0.0186	10.0	0.3810	−0.1953	−105.2	0.3830	−0.1973	−106.2	0.2111	−0.0254	−13.7
25	Dioxane	0.2853	0.2063	0.0790	27.7	0.0554	0.2299	80.6	0.2738	0.0115	4.0	0.3122	−0.0269	−9.4
27	Nitrobenzene	0.0897	—[a]	—	—	0.2630	−0.1733	−193.2	0.1643	−0.0746	−83.2	0.1332	−0.0435	−48.5
28	Acetophenone	0.1878	0.1232	0.0646	34.4	0.3282	−0.1404	−74.8	0.2704	−0.0826	−44.0	0.1475	0.0403	21.5
29	Benzyl alcohol	0.1441	0.1666	−0.0225	−15.6	0.2782	−0.1341	−93.1	0.3061	−0.1620	−112.4	0.2429	−0.0988	−68.6
31	Methyl alcohol	0.1632	0.1489	0.0143	8.8	0.1988	−0.0356	−21.8	0.1325	0.0307	18.8	0.0777	0.0855	52.4
32	Ethyl alcohol	0.1789	0.1231	0.0558	31.2	0.2292	−0.0503	−28.1	0.2030	−0.0241	−13.5	0.1413	0.0376	21.0
33	Propyl alcohol	0.1791	0.1099	0.0692	38.6	0.2156	−0.0365	−20.4	0.2208	−0.0417	−23.3	0.1690	0.0101	5.6
34	Isopropyl alcohol	0.1937	0.1102	0.0835	43.1	0.1918	0.0019	1.0	0.2041	−0.0104	−5.4	0.1694	0.0243	12.5
35	Butyl alcohol	0.2016	0.1013	0.1003	49.8	0.1983	0.0033	1.6	0.2318	−0.0302	−15.0	0.1787	0.0229	11.4
36	Isobutyl alcohol	0.1524	0.0956	0.0568	37.3	0.1127	0.0397	26.0	0.1325	0.0199	13.1	0.1375	0.0149	9.8
39	1-Pentanol	0.1839	0.0958	0.0881	47.9	0.1582	0.0257	14.0	0.2176	−0.0337	−18.3	0.1772	0.0067	3.6
40	1-Hexanol	0.1905	0.0920	0.0985	51.7	0.1886	0.0019	1.0	0.2463	−0.0558	−29.3	0.1932	−0.0027	−1.4
42	1-Octanol	0.1987	0.0873	0.1114	56.1	0.1561	0.0426	21.4	0.2294	−0.0307	−15.5	0.1895	0.0092	4.6
43	Ethylene glycol	0.0884	0.0476	0.0408	46.2	0.1838	−0.0954	−107.9	0.0556	0.0328	37.1	0.0977	−0.0093	−10.5
46	Glycerol	0.0164	0.0441	−0.0277	−168.9	0.0794	−0.0630	−384.1	0.0073	0.0091	55.5	0.0198	−0.0034	−20.7
48	Acetic acid	0.1675	0.1560	0.0115	6.9	0.1825	−0.0150	−9.0	0.1517	0.0158	9.4	0.1708	−0.0033	−2.0
49	Propionic acid	0.1887	0.1446	0.0441	23.4	0.2145	−0.0258	−13.7	0.1972	−0.0085	−4.5	0.1752	0.0135	7.2
51	Dimethyl sulfoxide	0.5102	—	—	—	0.4207	0.0895	17.5	0.4575	0.0527	10.3	0.4938	0.0164	3.2
52	Pyridine	0.5348	0.4255	0.1093	20.4	0.3602	0.1746	32.6	0.3847	0.1501	28.1	0.4890	0.0458	8.6
53	Formamide	0.1525	—	—	—	0.2059	−0.0534	−35.0	0.1942	−0.0417	−27.3	0.0674	0.0851	55.8
54	*N*-Methylformamide	0.3428	—	—	—	0.3835	−0.0407	−11.9	0.3781	−0.0353	−10.3	0.4269	−0.0841	−24.5
55	*N,N*-Dimethylformamide	0.4909	—	—	—	0.4364	0.0545	11.1	0.4576	0.0333	6.8	0.4959	−0.0050	−1.0
57	*N,N*-Dimethylacetamide	0.5245	—	—	—	0.4462	0.0783	14.9	0.4786	0.0459	8.8	0.5253	−0.0008	−0.2
59	Water (pH 2.0)	0.0005	0.0005	0.0	0.0	0.0002	0.0003	60.0	0.0007	−0.0002	−40.0	0.0007	−0.0002	−40.0

[a] Dashed lines indicate that X_2 (calc.) could not be obtained with UNIFAC because of lack of UNIFAC parameters for these solvents.

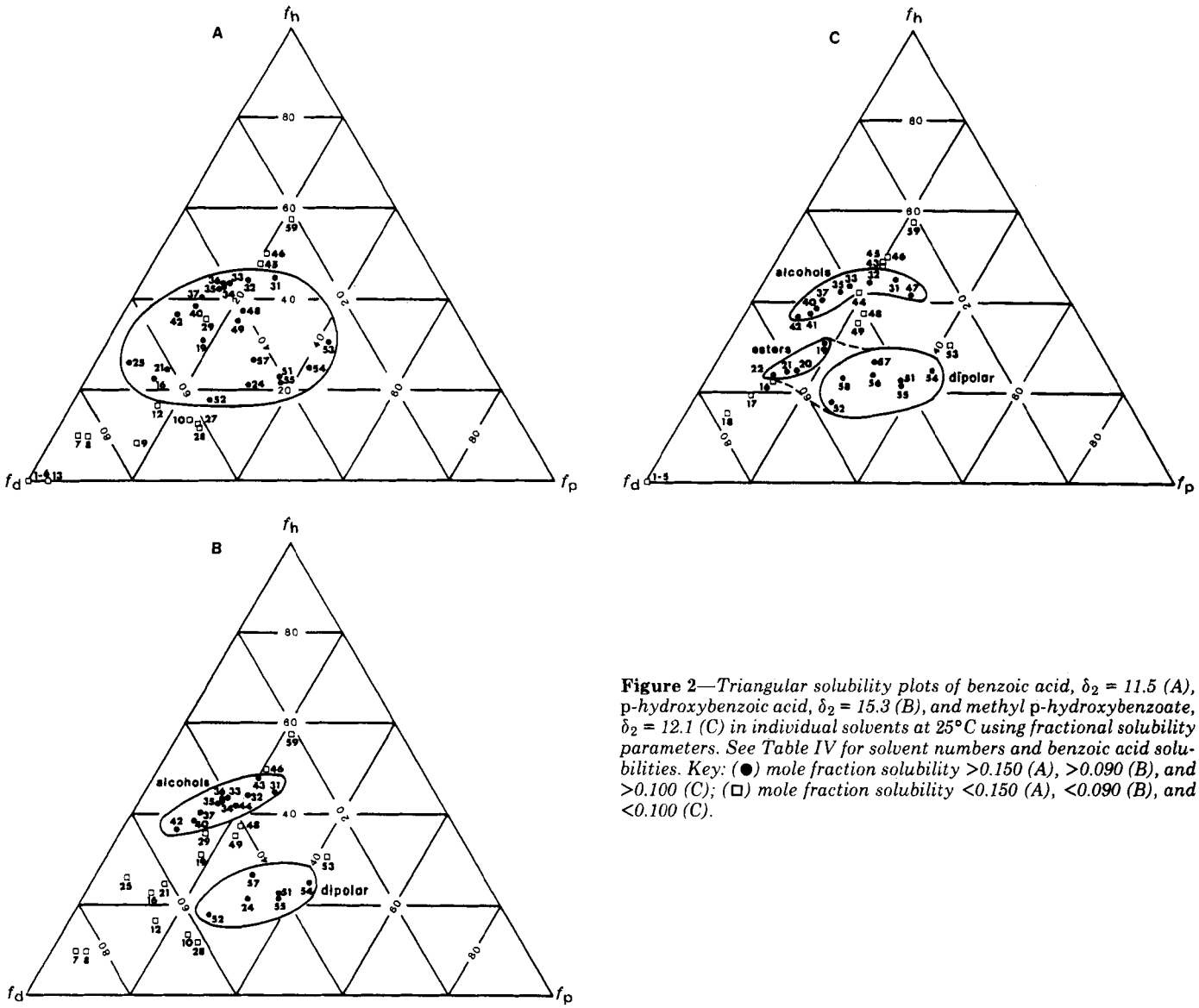

Figure 2—*Triangular solubility plots of benzoic acid, δ_2 = 11.5 (A), p-hydroxybenzoic acid, δ_2 = 15.3 (B), and methyl p-hydroxybenzoate, δ_2 = 12.1 (C) in individual solvents at 25°C using fractional solubility parameters. See Table IV for solvent numbers and benzoic acid solubilities. Key: (●) mole fraction solubility >0.150 (A), >0.090 (B), and >0.100 (C); (□) mole fraction solubility <0.150 (A), <0.090 (B), and <0.100 (C).*

benzoate are shown in Fig. 2B and C, respectively. The data for these compounds are given in the following paper (25).

As observed in Fig. 2A high solubility of benzoic acid occurs in solvents having f_d = 0.25–0.70, f_p = 0.05–0.45, and f_h = 0.17–0.45, which fall in the center region of the diagram. Solvents with high f_d values, such as numbers 1–9, result in low solubility of benzoic acid. Glycols and water with high f_h values (numbers 43, 46, and 59) also yield poor solubility of benzoic acid. Benzyl alcohol (number 29) produces intermediate solubility, X_2 = 0.144, and because of its δ_d-, δ_p-, and δ_h-values, falls within the boundary of good solvents in Fig. 2A.

The partial parameters of benzoic acid can be estimated from Fig. 2A, noting that the center of the high solubility region is at $f_d \simeq 0.47$, $f_p \simeq 0.23$, and $f_h \simeq 0.30$. Assuming that δ_2 = 11.45 as the average of the data above, we may calculate that δ_{2d} = 8.9, δ_{2p} = 4.4, and δ_{2h} = 5.7. These were much more definite than could be obtained by Hansen's (5) plotting method and quite possibly better than either Eq. 25 or the calculations done during 1974.

In Fig. 2B, it is observed that two distinct classes of solvents provide reasonable solubility for *p*-hydroxybenzoic acid, δ_2 = 15; the alcohols and glycols (excluding glycerol, number 46) on the one hand and the strongly dipolar solvents such as *N,N*-dimethylformamide (number 55) and dimethyl sulfoxide (number 51). The fact that the moderately dipolar pyridine (number 52) is a good solvent, but the strongly dipolar formamide (number 53) is not, shows the difficulty of classifying solvents in a general sense. It is the detailed matching of the partial parameters of solvent and solute that controls the specific solubilities. The two peak regions probably correspond to the two functional groups on the solute, as is found in elastomer swelling (5). Hydrocarbons, esters, and acids are not good solvents for *p*-hydroxybenzoic acid, presumably because one or more partial parameters do not match.

Methyl *p*-hydroxybenzoate, [δ_2 = 12.1 (26)] like benzoic acid [δ_2 = 11.5 (15)] is semipolar and is best dissolved by solvents located in the central region of Fig. 2C. The good solvents could be considered to constitute one large central region of the diagram, but they are better separated into three distinct regions representing esters, alcohols, and strongly dipolar

Table V—Demonstration of Trial and Error Process for Calculating Benzoic Acid Solubility in Ethyl Acetate at 25°C Using Eqs. 20 and 21

Step	X_2	$f(X_2)$
1	0.3	−2591063
2	0.1	3262236
3	0.2	−455342
4	0.15	1075195
5	0.19	−183640
6	0.185	−42185
7	0.183	15509
8	0.184	−13419
9	0.1835	1024
10	0.1836	−1868
11	0.18354	−133
12	0.18353	157
13	0.183535	12
14	0.1835352	6
15	0.1835354	0

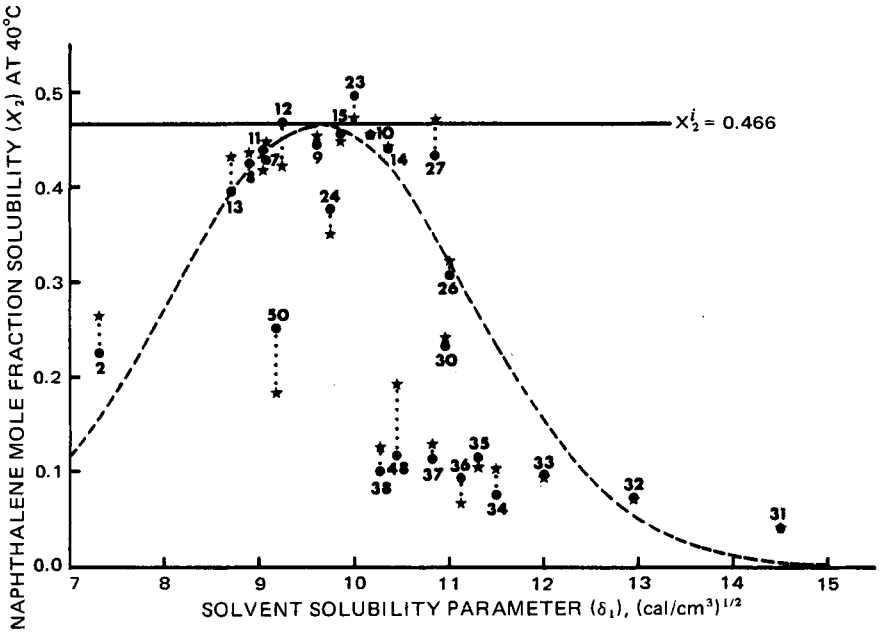

Figure 3—*Solubility profile of naphthalene in individual solvents at 40°C. See Table I for solvent numbers. Key: (– –) regular solution curve; (—) ideal solubility line,* $X_2^i = 0.466$*; (●) experimental solubilities; (★) solubilities calculated using Eq. 29.*

solvents, respectively. The two acidic solvents, acetic acid (number 48) and propionic acid (number 49) lie in the center of this general solubility region yet were poor solvents for methyl *p*-hydroxybenzoate. If the two lower peaks are combined with dashed lines as shown in Fig. 2C, they can be explained as an interaction of the solvent with the hydroxyl group of the solute, whereas the upper peak may be a response of the solvent hydroxyl group to the ester group of methyl *p*-hydroxybenzoate.

The triangular diagram of Teas (24) appears to characterize these three solutes and the solvents which dissolve them in an illuminating manner. It is observed that all nonpolar solvents are congregated in the lower left corner.

Universal Function Group Activity Coefficient (UNIFAC) Method for Benzoic Acid Solubility—The UNIFAC (2) program was used to calculate the solubilities of benzoic acid in most of the solvents at 25°C. For 34 predictions, 16 calculated solubilities are within 30% error. Six solvent results could not be calculated due to unavailability of the interaction energies needed for functional groups in the UNIFAC tables. The results are listed in Table IV.

A Four-Parameter Solubility System—$(\log \alpha_2)/A$ of benzoic acid was regressed with the four new partial solubility parameters listed in Table I, as suggested by Eq. 16. The regression equation obtained was:

$$\frac{\log \alpha_2}{A} = 7.186\delta_{1d}^2 - 121.0\delta_{1d} + 0.4734\delta_{1p}^2 - 6.969\delta_{1p} + 0.6503\delta_{1a}\delta_{1b} - 1.033\delta_{1a} - 2.874\delta_{1b} + 522.79$$

$$n = 40,\ s = 5.89,\ r^2 = 0.83,\ F = 21.9,\ F(7,32,0.01) = 3.25 \quad \text{(Eq. 27)}$$

The estimated mole fraction solubilities of benzoic acid from Eq. 27 are shown in Table IV using the root-finding method (Eq. 21, Table V). Of the 40 estimates, 25 predicted solubilities are within 30% error of the experimental values.

To account for facile electron donation by the strongly dipolar solvents (numbers 51, 52, and 54–57), an indicator variable, I, was incorporated in the regression yielding:

$$\frac{\log \alpha_2}{A} = 2.125\delta_{1d}^2 - 36.90\delta_{1d} + 0.2188\delta_{1p}^2 - 2.603\delta_{1p} + 0.6139\delta_{1a}\delta_{1b} - 1.966\delta_{1a} - 2.955\delta_{1b} + 174.25 - 20.27I$$

$$n = 40,\ s = 3.38,\ r^2 = 0.94,\ F = 66.5,\ F(8,31,0.01) = 3.15 \quad \text{(Eq. 28)}$$

In calculating the solubilities, I was assigned a value of one for strongly dipolar solvents and zero for all other solvents in the series. The improvement of Eq. 28 over Eq. 27 by the use of the indicator variable, I, suggests that the highly polar solvents (numbers 51, 52, and 54–57, which in most cases strongly accept a proton from the solute and do not self-associate through intermolecular hydrogen bonding) be treated as solvents uniquely superior in solubilizing effect on benzoic acid. Investigations should be made concentrating specifically on this class of unusual solvents for the dissolution of drugs, particularly of the proton-donor type.

As is evident to those familiar with the application of I, Eq. 28 in fact represents two equations. For solvents, exclusive of the dipolar ones, the equation contains terms in d-, p-, a-, and b-parameters plus the constant, 174.25. Here I equals zero. For solutions containing the dipolar solvents, I becomes unity and Eq. 28, in addition to identical terms in d, p, a, and b, now includes a constant, 174.25 − 20.27 = 153.98. This smaller value for the constant decreases $(\log \alpha_2)/A$ and accordingly increases X_2 for the solute in these solvents, as may be observed in Fig. 1. The inclusion of I therefore raises the parabolic-like curve of Eq. 28 sufficiently to pass through the experimental points for benzoic acid solubility in the strongly dipolar solvents. For methyl *p*-hydroxybenzoate and *p*-hydroxybenzoic acid, the very polar solvents form a separate subclass of solvents in Fig. 2B and C, and a simple addition of an indicator variable cannot provide a good fit of calculated values to experimental points (see Ref. 25).

The solubilities calculated from Eq. 28 using the root-finding method are listed in Table IV; 29 of 40 or almost three-quarters of the predictions are within 30% error. The mole fraction solubility of benzoic acid in the 40 solvents is plotted in Fig. 1. Calculated solubilities, using the four-parameter solubility system, are shown as stars on the figure and are connected by dotted lines to the experimental points, indicated by filled circles.

For naphthalene in single solvents at 40°C, the regression equation using the four-parameter solubility approach is:

$$\frac{\log \alpha_2}{A} = 0.5713\delta_{1d}^2 - 12.01\delta_{1d} - 0.09517\delta_{1p}^2 + 0.3381\delta_{1p} + 0.1673\delta_{1a}\delta_{1b} - 0.09187\delta_{1a} + 0.4824\delta_{1b} + 62.31$$

$$n = 26,\ s = 1.20,\ r^2 = 0.990,\ F = 257,\ F(7,18,0.01) = 3.85 \quad \text{(Eq. 29)}$$

The calculated solubilities are listed in Table III and plotted in Fig. 3. Of the 26 predictions, isopropyl alcohol (34%), isobutyl alcohol (31%), and acetic acid (68%) show >30% error. The four-parameter approach (Eq. 29) offers no significant advantage over three parameters (Eq. 19) for naphthalene, as observed in Table III.

Estimating Solubility Parameters of the Solute Using a Four-Parameter System—The regression equation obtained from the four-parameter system, as suggested by Eq. 16, can be transformed into an expression similar to Eq. 14 to predict the partial solubility parameters of the solute. For benzoic acid, Eq. 27 was rearranged to:

$$\frac{\log \alpha_2}{A} = 7.186(\delta_{1d} - 8.42)^2 + 0.4734(\delta_{1p} - 7.36) + 0.6503(\delta_{1a} - 4.42)(\delta_{1b} - 1.59) - 16.76 \quad \text{(Eq. 30)}$$

Comparing Eqs. 30 and 14, the solubility parameters of benzoic acid can be taken as $\delta_{2d} = 8.42$, $\delta_{2p} = 7.36$, $\delta_{2a} = 4.42$, and $\delta_{2b} = 1.59$. The total solubility parameter is:

$$\delta_T = (\delta_d^2 + \delta_p^2 + 2\delta_a\delta_b)^{1/2} = [(8.42)^2 + (7.36)^2 + 2(4.42)(1.59)]^{1/2}$$

$$\delta_T = 11.79 \quad \text{(Eq. 31)}$$

The regression equation containing an indicator, *i.e.*, Eq. 28, can be transformed to:

$$\frac{\log \alpha_2}{A} = 2.125(\delta_{1d} - 8.68)^2 + 0.2188(\delta_{1p} - 5.95)^2 + 0.6139(\delta_{1a} - 4.81)(\delta_{1b} - 3.20) - 3.13 - 20.27I \quad \text{(Eq. 32)}$$

Equation 32 suggests that $\delta_{2d} = 8.68$, $\delta_{2p} = 5.95$, $\delta_{2a} = 4.81$, $\delta_{2b} = 3.20$, and $\delta_T = 11.90$ for benzoic acid. The total solubility parameter, δ_T, for benzoic acid obtained from Eqs. 30 and 32 compares satisfactorily with the value (11.5) given in the literature (15).

For naphthalene, Eq. 29 can also be changed to:

$$\frac{\log \alpha_2}{A} = 0.5713(\delta_{1d} - 10.51)^2 - 0.09517(\delta_{1p} - 1.78)^2 + 0.1673(\delta_{1a} + 2.88)(\delta_{1b} - 0.55) - 0.24 \quad \text{(Eq. 33)}$$

Although Eq. 29 yields satisfactory solubilities for naphthalene, it is observed that δ_{2a} has been given the wrong sign in Eq. 33. If the sign is disregarded, $\delta_{2d} = 10.51$, $\delta_{2p} = 1.78$, $\delta_{2a} = 2.88$, and $\delta_{2b} = 0.55$, and the total solubility parameter is equal to 10.81. This value may be compared with $\delta_2 = 9.64$ for naphthalene as found in the literature (1). Since δ_{2a} has the wrong sign, however, the values must be rejected. Additional study is needed to determine why on occassion the regression procedure assigns the wrong sign to a parameter. The fault is not necessarily in the procedure, since Hansen's original plotting method has also been known to assign a negative value to a solute parameter—presumably because the center of maximum interaction lies closer to an axis than the radius of the circle of uncertainty (10–12).

Partial Solubility Parameters and Molecular Interactions—The magnitude of the solubility parameters of Table I should be noted as they relate to each class of solvents. The alcohols (numbers 29–42) like the carboxylic acids (numbers 48–50) show strong proton-donor, or acid, and moderately strong proton-acceptor, or basic, character. The glycols (numbers 43–47) have very high proton-donor qualities (δ_a). Dimethyl sulfoxide and pyridine (numbers 51 and 52, respectively) and the dialkylamides (numbers 55–58) are predominantly proton acceptors as reflected in their δ_b-values. Dimethyl sulfoxide has a large δ_p-value, as do formamide and methylformamide. Dioxane and aniline (numbers 25 and 26, respectively) are moderately strong Lewis bases (δ_b); aniline is also dipolar (δ_p). Ethylene dichloride and ethylidene chloride (numbers 10 and 11, respectively) show significant dipolarity by way of their δ_p-values, almost equal to that of acetone (number 24) and acetophenone (number 28). Methyl alcohol, (number 31), often considered to have solvent properties unlike the other alcohols, exhibits a relatively large δ_p-value. The ethers (numbers 16–18) are not dipolar, are weak Lewis acids (low δ_a-values), and show good proton-acceptor or basic (δ_b) character. The esters (numbers 19–22) show moderate dipolarity (δ_p). The moderate Lewis acid character of the esters, as reflected in their δ_a-values, is somewhat surprising. It is interesting to note the large Lewis acid (δ_a)-characteristics of ethylene bromide and ethylidene bromide (numbers 14 and 15).

A comparison of the partial solubility parameters of solvents and solutes provides an estimate of the molecular interactions between these species, particularly where high solubility results are found in Fig. 2. The partial solubility parameters for benzoic acid (Eq. 32) are $\delta_d = 8.68$, $\delta_p = 5.95$, $\delta_a = 4.81$, and $\delta_b = 3.20$. The solvents that dissolve benzoic acid to the greatest extent are dimethyl sulfoxide, pyridine, *N,N*-dimethylformamide, and *N,N*-dimethylacetamide. They have relatively large basic parameters, δ_b, favoring interaction with benzoic acid, which has an acidic parameter, $\delta_a = 4.8$. Formamide has a large basic parameter, $\delta_b = 7.6$, and should interact strongly with benzoic acid to produce significant solubility. The solubility is low (Table IV, Fig. 1) because formamide also has a large acidic parameter, $\delta_a = 5.7$ and tends to self-associate.

The partial solubility parameters of the solvents in Table I must be taken as tentative at this time; some will no doubt change as the work on solubility theory progresses. For now, these parameters lend a rough quantitative measure and a quasi-theoretical basis to the molecular forces involved in solvent–solvent and solvent–solute interactions.

CONCLUSIONS

This paper represents the second test of the extended Hansen solubility approach and the UNIFAC method. In an earlier study (1) the solubility of naphthalene in 24 solvents at 40°C was predicted satisfactorily by these two methods, UNIFAC being favored because it required no initial solubility data for regression as needed for the extended Hansen approach. It was recognized, however, that naphthalene was a poor model of a drug molecule.

In the present work, benzoic acid as well as naphthalene solubilities were studied in a wide range of solvents using UNIFAC and the extended Hansen solubility parameter approach. UNIFAC was less satisfactory for benzoic acid than the extended Hansen procedure, only 47% of the solubility results showing <30% error. (From solubility studies conducted in these laboratories, 30% was taken as a criterion of maximum allowable deviation from observed solubility.) Sixty percent of the solubilities were predicted by the Hansen approach (within 30% error of observed results). Apparently UNIFAC cannot satisfactorily reproduce the solubility results for more polar solutes like benzoic acid and its analogues; however, the interaction energy parameters for groups such as NH_2 and COOR are not currently found in the UNIFAC tables, and the application of UNIFAC to polar systems must await development of new parameters. The Hansen approach is also deficient, probably because its third solubility parameter, δ_h, cannot be expected to reflect both the electron-donor and electron-acceptor characteristics of complex organic drug molecules. An expanded four-parameter system was developed in this study, involving δ_d, δ_p, and both an electron-donor (δ_b) and electron-acceptor (δ_a) parameter. These new parameters were obtained as described and are listed in Table I for 59 solvents commonly used in pharmaceutical and industrial technology. Representative solvents were included from a number of classes: aliphatic and aromatic hydrocarbons, halogenated derivatives, ethers, esters, ketones, alcohols, glycols, acids, amides, and water. The four partial parameters of Table I are seen to describe the nonpolar, dipolar, and proton- or electron-transfer characteristics of each solvent.

Solubilities of naphthalene and benzoic acid were estimated using an expanded version of the Hansen equation with four, rather than three, solubility parameters. The success of the benzoic acid solubility correlations was increased by use of the new four-parameter system, 63% of the solubilities being predicted using four parameters as contrasted to 60% with three parameters. The strongly dipolar solvents (numbers 51, 52, and 54–58) were still not well represented with the four-parameter system. They were satisfactorily handled, however, when an indicator variable, I, was added to account for their irregular behavior.

The final equation involved separate parameters for weak dispersion forces, dipolar character, electron-donor and -acceptor effects, and a fifth "dummy" parameter or indicator variable for the strongly solvating amides and dimethyl sulfoxide. This expression, Eq. 28, successfully predicted benzoic acid solubilities for nearly three-fourths of the solvent systems. Cyclohexane (−87.3% error), ethylene chloride (−141.2% error), diethyl ether (−41.6% error), butyl acetate (31.1% error), nitrobenzene (−48.5% error), benzyl alcohol (−68.6% error), methyl alcohol (52.4% error), formamide (55.8% error), and *N,N*-dimethylacetamide (−40.0% error) produced errors larger than the accepted 30%. Only three were far above the 50% error range, and this is quite encouraging. For naphthalene, use of the four-parameter equation did not improve the accuracy over the three-parameter system. Only 3 of 26 solvents showed errors of >30% of the observed solubility whether the three- or the four-parameter approach was used.

Using the three-parameter system and triangular plots, the action of solvents on benzoic acid ($\delta_2 = 11.5$), *p*-hydroxybenzoic acid ($\delta_2 = 15$), and methyl *p*-hydroxybenzoate ($\delta_2 = 12$) was graphically demonstrated. Solvents of intermediate polarity (as measured by the three partial solubility parameters δ_d, δ_p, and δ_h), and belonging to various classes, successfully dissolved benzoic acid (Fig. 2A). *p*-Hydroxybenzoic acid was predominantly soluble in the alcohols and the dipolar amides (Fig. 2B); methyl *p*-hydroxybenzoate (Fig. 2C) was soluble in alcohols, esters, and the dipolar amide solvents. These triangular figures provide a particularly illuminating picture of the solubility of a drug in various groups of solvents, based on a three-parameter solubility classification. They also provide a means to calculate partial solubility parameters of drugs and other solid solutes. In a similar scheme, Snyder (27) has classified solvents into nine types on a triangular grid. The solubilities of *p*-hydroxybenzoic acid and methyl *p*-hydroxybenzoate are studied in some detail in the following report (25).

Benzoic acid, *p*-hydroxybenzoic acid, and methyl *p*-hydroxybenzoate appear to serve well as drug prototypes. The current study indicates the measure of success that can be expected with semiempirical approaches

to solubility theory at this stage of development. The four partial solubility parameters for solvents, particularly the new acid (δ_a) and base (δ_b) terms, should find use in the pharmaceutical sciences as well as in industrial technology. The multiple regression and triangular plot methods of estimating partial solubility parameters for solutes are promising steps toward characterizing the polar and nonpolar properties of drugs and related biochemicals. The partial solubility parameters of Table I are tentative and no doubt will be changed somewhat as dictated by additional findings.

REFERENCES

(1) A. Martin, P. L. Wu, A. Adjei, A. Beerbower, and J. M. Prausnitz, *J. Pharm. Sci.*, **70,** 1260 (1981).

(2) A. Fredenslund, J. Gmehling, and P. Rasmussen, "Vapor–Liquid Equilibrium Using UNIFAC," Elsevier, New York, N.Y., 1977.

(3) A. Martin, J. Newburger, and A. Adjei, *J. Pharm. Sci.*, **69,** 487 (1980).

(4) J. H. Hildebrand and R. L. Scott, "The Solubility of Nonelectrolytes," 3rd ed., Dover, New York, N.Y., 1964.

(5) C. M. Hansen and A. Beerbower, in "Encyclopedia of Chemical Technology," Suppl. Vol., 2nd ed., Wiley, New York, N.Y., 1971, pp. 889–910.

(6) P. L. Wu, A. Beerbower, and A. Martin, *J. Pharm. Sci.*, **71,** 1285 (1982).

(7) B. L. Karger, L. R. Snyder, and C. Eon, *J. Chromatogr.*, **125,** 71 (1962).

(8) B. L. Karger, L. R. Snyder, and C. Eon, *Anal. Chem.*, **50,** 2126 (1978).

(9) R. A. Keller, B. L. Karger, and L. R. Snyder, in "Gas Chromatography 1970," R. Stock, Ed., Institute of Petroleum, London, 1971, p. 125.

(10) C. M. Hansen, *J. Paint Technol.*, **39,** 104 (1967).

(11) C. M. Hansen, *J. Paint Technol.*, **39,** 505 (1967).

(12) C. M. Hansen and K. Skaarup, *J. Paint Technol.*, **39,** 511 (1967).

(13) M. J. Kamlet, J. L. M. Abboud, and R. W. Taft, "Progress in Physical Organic Chemistry," Wiley, New York, N.Y., 1981, pp. 485–630.

(14) T. R. Griffiths and D. C. Pugh, *Coord. Chem. Rev.*, **29,** 129–211 (1979).

(15) M. J. Chertkoff and A. Martin, *J. Am. Pharm. Assoc., Sci. Ed.*, **49,** 444 (1960).

(16) J. A. Riddick and W. B. Bunger, "Organic Solvents," Techniques of Chemistry, Vol. II, 3rd ed., Wiley, New York, N.Y., 1970.

(17) J. H. Hildebrand, J. M. Prausnitz, and R. L. Scott, "Regular and Related Solutions," Van Nostrand Reinhold, New York, N.Y., 1970, p. 22.

(18) D. C. Ginnings and G. T. Furukawa, *J. Am. Chem. Soc.*, **75,** 522 (1953).

(19) "United States Pharmacopeia," 20th rev., U.S. Pharmacopeial Convention, Rockville, Md., 1980, p. 929.

(20) A. Martin, J. Swarbrick, and A. Cammarata, "Physical Pharmacy," 3rd ed., Lea and Febiger, Philadelphia, Pa., 1983, p. 285.

(21) T. Krishnan, W. C. Duer, S. Goldman, and J. L. Fortier, *Can. J. Chem.*, **57,** 530 (1979).

(22) G. Allen, J. G. Watkinson, and K. H. Webb, *Spectrochim. Acta*, **22,** 807 (1966).

(23) IMSL Reference Manual, International Mathematical and Statistical Library, Houston, Texas, 1979.

(24) J. P. Teas, *J. Paint Technol.*, **40,** 19 (1968).

(25) A. Martin, P. L. Wu, and A. Beerbower, *J. Pharm. Sci.*, **73,** 188 (1984).

(26) A. Martin and J. Carstensen, *J. Pharm. Sci.*, **70,** 170 (1981).

(27) L. R. Snyder, *Chemtech*, **March,** 188 (1980).

ACKNOWLEDGMENTS

Supported in part by a grant from the University of Texas Research Institute. A. Martin is grateful to C. R. Sublett for the endowed professorship which also supported this work.

Expanded Solubility Parameter Approach II: *p*-Hydroxybenzoic Acid and Methyl *p*-Hydroxybenzoate in Individual Solvents

A. MARTIN *x, P. L. WU *§, and A. BEERBOWER ‡

Received September 13, 1982, from the **Drug Dynamics Institute, College of Pharmacy, University of Texas, Austin, TX 78712* and the ‡*Energy Center, University of California at San Diego, La Jolla, CA 92093.* Accepted for publication November 17, 1982. §Present address: China Chemical & Pharmaceutical Co., Ltd., Taipei, Taiwan.

Abstract □ The recently introduced four-parameter extended Hansen approach was used to study the solubility of *p*-hydroxybenzoic acid and methyl *p*-hydroxybenzoate in 32 and 35 individual solvents, respectively. The results are compared with those for benzoic acid in 40 solvents. Seventeen of the thirty-two or 53% of the calculated solubilities of *p*-hydroxybenzoic acid were within the established solubility criterion (*i.e.*, <30% error from the experimental value). Twenty-two of thirty-six or 61% of the calculated solubility values for methyl *p*-hydroxybenzoate met the solubility criterion. Experimental excess free energies of solution for *p*-hydroxybenzoic acid and methyl *p*-hydroxybenzoate were plotted against theoretical values using the expanded four-parameter solubility regression equations. From such results, adjustments may be made in the partial solubility parameters to bring the calculated solubilities in line with experimental results. Multiple regression analyses were used to estimate the total solubility parameter and the four partial solubility parameters of the two benzoic acid derivatives. Satisfactory results were obtained for methyl *p*-hydroxybenzoate, but poor agreement was found for *p*-hydroxybenzoic acid for the total parameter when compared with the Fedors group contribution method. Both the multiple regression and group contribution methods may yield inaccurate solubility parameters for relatively polar solid solutes. Factor analysis was used to test the adequacy of three- and four-parameter approaches in the evaluation of drug solubility. A principal factor method without iteration and orthogonal factor rotation were used to compare the two expanded solubility parameter approaches. Factor analysis showed that four solubility parameters were significantly more independent and presumably more satisfactory than three parameters.

Keyphrases □ Solubility parameters, expanded—individual solvents, four-parameter extended Hansen approach, *p*-hydroxybenzoic acid, methyl *p*-hydroxybenzoate □ Extended Hansen approach—solubility of *p*-hydroxybenzoic acid and methyl *p*-hydroxybenzoate in individual solvents, four-parameter system □ Benzoic acid derivatives—*p*-hydroxybenzoic acid, methyl *p*-hydroxybenzoate, use as model drugs, solubility in individual solvents, four-parameter extended Hansen approach

The solubility of a number of drugs in mixtures of two solvents has been analyzed with the extended Hildebrand solubility approach (1, 2). Subsequently, the solubility of naphthalene and benzoic acid in individual solvents was studied using the Hansen three-parameter solubility approach (3, 4) and a new four-parameter solubility system

0022-3549/84/0200-0188$01.00/0

© 1984, American Pharmaceutical Association

to solubility theory at this stage of development. The four partial solubility parameters for solvents, particularly the new acid (δ_a) and base (δ_b) terms, should find use in the pharmaceutical sciences as well as in industrial technology. The multiple regression and triangular plot methods of estimating partial solubility parameters for solutes are promising steps toward characterizing the polar and nonpolar properties of drugs and related biochemicals. The partial solubility parameters of Table I are tentative and no doubt will be changed somewhat as dictated by additional findings.

REFERENCES

(1) A. Martin, P. L. Wu, A. Adjei, A. Beerbower, and J. M. Prausnitz, *J. Pharm. Sci.*, **70,** 1260 (1981).

(2) A. Fredenslund, J. Gmehling, and P. Rasmussen, "Vapor–Liquid Equilibrium Using UNIFAC," Elsevier, New York, N.Y., 1977.

(3) A. Martin, J. Newburger, and A. Adjei, *J. Pharm. Sci.*, **69,** 487 (1980).

(4) J. H. Hildebrand and R. L. Scott, "The Solubility of Nonelectrolytes," 3rd ed., Dover, New York, N.Y., 1964.

(5) C. M. Hansen and A. Beerbower, in "Encyclopedia of Chemical Technology," Suppl. Vol., 2nd ed., Wiley, New York, N.Y., 1971, pp. 889–910.

(6) P. L. Wu, A. Beerbower, and A. Martin, *J. Pharm. Sci.*, **71,** 1285 (1982).

(7) B. L. Karger, L. R. Snyder, and C. Eon, *J. Chromatogr.*, **125,** 71 (1962).

(8) B. L. Karger, L. R. Snyder, and C. Eon, *Anal. Chem.*, **50,** 2126 (1978).

(9) R. A. Keller, B. L. Karger, and L. R. Snyder, in "Gas Chromatography 1970," R. Stock, Ed., Institute of Petroleum, London, 1971, p. 125.

(10) C. M. Hansen, *J. Paint Technol.*, **39,** 104 (1967).

(11) C. M. Hansen, *J. Paint Technol.*, **39,** 505 (1967).

(12) C. M. Hansen and K. Skaarup, *J. Paint Technol.*, **39,** 511 (1967).

(13) M. J. Kamlet, J. L. M. Abboud, and R. W. Taft, "Progress in Physical Organic Chemistry," Wiley, New York, N.Y., 1981, pp. 485–630.

(14) T. R. Griffiths and D. C. Pugh, *Coord. Chem. Rev.*, **29,** 129–211 (1979).

(15) M. J. Chertkoff and A. Martin, *J. Am. Pharm. Assoc., Sci. Ed.*, **49,** 444 (1960).

(16) J. A. Riddick and W. B. Bunger, "Organic Solvents," Techniques of Chemistry, Vol. II, 3rd ed., Wiley, New York, N.Y., 1970.

(17) J. H. Hildebrand, J. M. Prausnitz, and R. L. Scott, "Regular and Related Solutions," Van Nostrand Reinhold, New York, N.Y., 1970, p. 22.

(18) D. C. Ginnings and G. T. Furukawa, *J. Am. Chem. Soc.*, **75,** 522 (1953).

(19) "United States Pharmacopeia," 20th rev., U.S. Pharmacopeial Convention, Rockville, Md., 1980, p. 929.

(20) A. Martin, J. Swarbrick, and A. Cammarata, "Physical Pharmacy," 3rd ed., Lea and Febiger, Philadelphia, Pa., 1983, p. 285.

(21) T. Krishnan, W. C. Duer, S. Goldman, and J. L. Fortier, *Can. J. Chem.*, **57,** 530 (1979).

(22) G. Allen, J. G. Watkinson, and K. H. Webb, *Spectrochim. Acta*, **22,** 807 (1966).

(23) IMSL Reference Manual, International Mathematical and Statistical Library, Houston, Texas, 1979.

(24) J. P. Teas, *J. Paint Technol.*, **40,** 19 (1968).

(25) A. Martin, P. L. Wu, and A. Beerbower, *J. Pharm. Sci.*, **73,** 188 (1984).

(26) A. Martin and J. Carstensen, *J. Pharm. Sci.*, **70,** 170 (1981).

(27) L. R. Snyder, *Chemtech*, **March,** 188 (1980).

ACKNOWLEDGMENTS

Supported in part by a grant from the University of Texas Research Institute. A. Martin is grateful to C. R. Sublett for the endowed professorship which also supported this work.

Expanded Solubility Parameter Approach II: *p*-Hydroxybenzoic Acid and Methyl *p*-Hydroxybenzoate in Individual Solvents

A. MARTIN *x, P. L. WU *§, and A. BEERBOWER ‡

Received September 13, 1982, from the **Drug Dynamics Institute, College of Pharmacy, University of Texas, Austin, TX 78712* and the ‡*Energy Center, University of California at San Diego, La Jolla, CA 92093.* Accepted for publication November 17, 1982. §Present address: China Chemical & Pharmaceutical Co., Ltd., Taipei, Taiwan.

Abstract □ The recently introduced four-parameter extended Hansen approach was used to study the solubility of *p*-hydroxybenzoic acid and methyl *p*-hydroxybenzoate in 32 and 35 individual solvents, respectively. The results are compared with those for benzoic acid in 40 solvents. Seventeen of the thirty-two or 53% of the calculated solubilities of *p*-hydroxybenzoic acid were within the established solubility criterion (*i.e.*, <30% error from the experimental value). Twenty-two of thirty-six or 61% of the calculated solubility values for methyl *p*-hydroxybenzoate met the solubility criterion. Experimental excess free energies of solution for *p*-hydroxybenzoic acid and methyl *p*-hydroxybenzoate were plotted against theoretical values using the expanded four-parameter solubility regression equations. From such results, adjustments may be made in the partial solubility parameters to bring the calculated solubilities in line with experimental results. Multiple regression analyses were used to estimate the total solubility parameter and the four partial solubility parameters of the two benzoic acid derivatives. Satisfactory results were obtained for methyl *p*-hydroxybenzoate, but poor agreement was found for *p*-hydroxybenzoic acid for the total parameter when compared with the Fedors group contribution method. Both the multiple regression and group contribution methods may yield inaccurate solubility parameters for relatively polar solid solutes. Factor analysis was used to test the adequacy of three- and four-parameter approaches in the evaluation of drug solubility. A principal factor method without iteration and orthogonal factor rotation were used to compare the two expanded solubility parameter approaches. Factor analysis showed that four solubility parameters were significantly more independent and presumably more satisfactory than three parameters.

Keyphrases □ Solubility parameters, expanded—individual solvents, four-parameter extended Hansen approach, *p*-hydroxybenzoic acid, methyl *p*-hydroxybenzoate □ Extended Hansen approach—solubility of *p*-hydroxybenzoic acid and methyl *p*-hydroxybenzoate in individual solvents, four-parameter system □ Benzoic acid derivatives—*p*-hydroxybenzoic acid, methyl *p*-hydroxybenzoate, use as model drugs, solubility in individual solvents, four-parameter extended Hansen approach

The solubility of a number of drugs in mixtures of two solvents has been analyzed with the extended Hildebrand solubility approach (1, 2). Subsequently, the solubility of naphthalene and benzoic acid in individual solvents was studied using the Hansen three-parameter solubility approach (3, 4) and a new four-parameter solubility system

0022-3549/84/0200-0188$01.00/0

© 1984, American Pharmaceutical Association

Table I—Calculated Solubilities of Methyl *p*-Hydroxybenzoate[a] in Individual Solvents at 25°C

No.	Solvent	V_1	δ_d	δ_p	δ_a	δ_b	X_2 (Obs.)	Equation 7 X_2 (Calc.)	Residual	Error, %
1	Pentane	116.1	7.1	0.0	0.0	0.0	0.000063	0.000009	0.000054	85.7
2	Hexane	131.6	7.3	0.0	0.0	0.0	0.000077	0.000028	0.000049	63.6
3	Heptane	147.5	7.5	0.0	0.0	0.0	0.000083	0.000074	0.000009	10.8
4	Nonane	179.7	7.7	0.0	0.0	0.0	0.000106	0.000176	−0.000070	−66.0
5	Decane	195.9	7.7	0.0	0.0	0.0	0.000121	0.000176	−0.000055	−45.5
16	Diethyl ether	104.8	7.1	1.4	0.5	6.3	0.0840	0.0749	0.0091	10.8
17	Dipropyl ether	139.4	7.3	1.1	0.4	5.0	0.0314	0.0409	−0.0095	−30.3
18	Dibutyl ether	170.4	7.6	0.8	0.3	3.9	0.0268	0.0326	−0.0058	−21.6
19	Ethyl acetate	98.5	7.4	2.6	5.3	1.9	0.1270	0.0862	0.0408	32.1
20	Propyl acetate	115.7	7.7	2.1	3.6	1.5	0.1366	0.1639	−0.0273	−20.0
21	Butyl acetate	132.6	7.7	1.8	2.8	1.7	0.1326	0.0828	0.0538	39.4
22	Hexyl acetate	164.5	7.8	1.5	1.9	2.2	0.1164	0.0848	0.0316	27.1
31	Methyl alcohol	40.7	7.4	6.0	8.4	7.1	0.1254	0.1155	0.0099	7.9
32	Ethyl alcohol	58.7	7.7	4.3	8.3	5.5	0.1495	0.1745	−0.0250	−16.7
33	Propyl alcohol	75.1	7.8	3.3	7.5	4.8	0.1486	0.1745	−0.0259	−17.4
35	Butyl alcohol	92.0	7.8	2.8	6.4	4.6	0.1484	0.1743	−0.0259	−17.5
39	1-Pentanol	108.6	7.8	2.2	5.4	4.3	0.1528	0.1284	0.0244	20.0
40	1-Hexanol	125.2	8.0	2.1	5.7	3.5	0.1477	0.1694	−0.0217	−14.7
41	1-Heptanol	141.9	8.1	2.0	5.3	3.4	0.1483	0.2013	−0.0530	−35.7
42	1-Octanol	158.4	8.3	1.6	5.2	3.2	0.1381	0.1605	−0.0224	−16.2
43	Ethylene Glycol	55.9	8.3	5.4	17.9	4.4	0.0480	0.0304	0.0176	36.7
44	1,2-Propanediol	73.7	8.2	4.6	14.1	4.6	0.0941	0.0818	0.0123	13.1
45	1,3-Propanediol	72.5	8.1	5.3	10.9	7.4	0.0766	0.0560	0.0206	26.9
46	Glycerol	73.2	8.5	5.9	20.0	5.1	0.0064	0.0021	0.0043	67.2
47	1,4-Butanediol	88.6	8.2	8.1	18.2	3.7	0.1202	0.1438	−0.0236	−19.6
48	Acetic acid	57.6	7.1	3.9	7.0	3.1	0.0532	0.0820	−0.0288	−54.1
49	Propionic acid	75.0	7.2	3.8	6.0	3.0	0.0386	0.1436	−0.1050	−272.0
51	Dimethyl sulfoxide	71.3	9.0	8.0	2.2	5.7	0.5839	0.4965	0.0874	15.0
52	Pyridine	80.9	9.3	4.3	1.4	3.2	0.3243	0.4752	−0.1509	−46.5
53	Formamide	39.9	8.4	12.8	5.7	7.6	0.0765	0.1118	−0.0353	−46.1
54	*N*-Methylformamide	59.1	8.4	10.1	4.8	3.9	0.2981	0.3770	−0.0789	−26.5
55	*N,N*-Dimethylformamide	77.4	8.5	6.7	3.4	4.4	0.4605	0.4836	−0.0231	−5.0
56	*N,N*-Diethylformamide	112.0	8.2	5.6	2.7	3.4	0.4907	0.5346	−0.0439	−8.9
57	*N,N*-Dimethylacetamide	93.0	8.2	5.6	2.9	4.3	0.5418	0.5020	0.0398	7.3
58	*N,N*-Diethylacetamide	126.6	8.2	4.1	2.1	3.2	0.5299	0.5223	0.0076	1.4
59	Water	18.1	7.6	7.8	6.7	32.0	0.00027	0.00041	−0.00014	−51.9

[a] Solute properties: $\delta_2 = 12.1$, mp 399.65 K, $V_2 = 117.5$ cm³/mol, $X_2^i = 0.0988$, $\log X_2^i = -1.005$.

(4). The present study is an attempt to use the four-parameter method to reproduce the solubilities of two solid organic compounds, *p*-hydroxybenzoic acid and methyl *p*-hydroxybenzoate, which serve as models of drug molecules.

The substituted aromatic groups and flexible chains of drug molecules, exhibiting dipolar forces, hydrogen bonding, steric interferences, and ionic charges, make the prediction of solubility in drug research and development a formidable task. The results obtained with benzoic acid in the preceding paper (4) demonstrate the most satisfactory results that have been obtained in this laboratory for drug-like molecules by regression analysis and by the universal functional group activity coefficient (UNIFAC) procedure (5). The correlation found here between experimental data and a four-parameter equation can serve as a benchmark—a goal to be superseded in predicting the solubility of drugs in general. As in the previous paper (4) all solvents are "neat" or individual. The methods used here and the conclusions reached are not generally applicable to the binary solvent systems discussed earlier (1, 2).

EXPERIMENTAL

Methyl *p*-hydroxybenzoate USP[1] was used as obtained. *p*-Hydroxybenzoic acid[2] was recrystallized from aqueous alcohol (6) and dried at 105°C. Melting points measured by a hot-stage method[3] are 485.85°K and 399.65°K for *p*-hydroxybenzoic acid and methyl *p*-hydroxybenzoate, respectively. Heats of fusions of *p*-hydroxybenzoic acid and methyl *p*-hydroxybenzoate obtained by differential scanning calorimetry[4] are 7510 and 5400 cal/mol (7), respectively. The solvents were spectrophotometric grade, ACS grade or redistilled before use. The mole fraction solubilities X_2 of *p*-hydroxybenzoic acid and methyl *p*-hydroxybenzoate at 25°C were determined as described in the preceding paper (4).

RESULTS AND DISCUSSION

The solubilities of methyl *p*-hydroxybenzoate and *p*-hydroxybenzoic acid at 25°C are found in Tables I and II and in Fig. 1. The properties of the solutes are included in the footnotes of Tables I and II; solvent molar volumes and partial solubility parameters are also listed. Sources and methods of obtaining partial solubility parameters, δ_d, δ_p, δ_a, and δ_b, were described in the preceding paper (4). Briefly, δ_d and δ_p are the dispersion and dipolar solubility parameters of Hansen and Beerbower (8); δ_b, a basic parameter, was obtained using the expression:

$$V_1^{1/2}\delta_b = 60.1\beta + 2.45 \qquad \text{(Eq. 1)}$$

where V_1 is the molar volume of the solvent and β is a basicity parameter provided by Kamlet *et al.* (9). Since $\delta_h^2 = 2\delta_a\delta_b$, it is possible to obtain δ_a, an acid parameter, once δ_b is calculated from Eq. 1. The term, δ_h, is called a hydrogen bonding parameter (4) though it includes all transfer energies.

As in earlier papers of this series, the mole fraction solubilities (X_2) of the two drug prototypes, methyl *p*-hydroxybenzoate and *p*-hydroxybenzoic acid, are plotted (Fig. 1) as a function of the total solvent solubility parameter, δ_1. Shown in the graphs are the ideal mole fraction solubility line (X_2^i) for the solute and the regular solution curve, calculated using the Hildebrand equation (1). The observed solubilities are

[1] Tenneco Chemical Inc., Piscataway, NJ 08854.
[2] Matheson, Coleman and Bell, Norwood, OH 45212.
[3] Digital Melting Point Analyzer, Model 335, Fisher Scientific Co.
[4] Perkin-Elmer DSC Model 1B, Norwalk, CT.

Table II—Calculated Solubilities of *p*-Hydroxybenzoic Acid[a] in Individual Solvents at 25°C

No.	Solvents	V_1	δ_d	δ_p	δ_a	δ_b	X_2 (Obs.)	Equation 8 X_2 (Calc.)	Residual	Error, %
7	Benzene	89.4	9.0	0.5	0.7	0.7	0.000033	0.000012	0.000021	63.6
8	Toluene	106.9	8.8	0.7	0.8	0.6	0.000029	0.000027	0.000002	6.9
10	Ethylene dichloride	79.4	9.3	3.6	2.0	1.0	0.00011	0.00534	−0.00523	−4755.
12	Chloroform	80.8	8.7	1.5	3.0	1.3	0.00015	0.00322	−0.00307	−2047.
16	Diethyl ether	104.8	7.1	1.4	0.5	6.3	0.0521	0.1132	−0.0611	−117.
19	Ethyl acetate	98.5	7.4	2.6	5.3	1.9	0.0737	0.0438	0.0299	40.6
21	Butyl acetate	132.6	7.7	1.8	2.8	1.7	0.0574	0.0048	0.0526	91.6
24	Acetone	74.0	7.6	5.1	2.4	2.4	0.1185	0.1186	−0.0001	−0.1
25	Dioxane	85.7	9.3	0.9	1.0	6.5	0.0844	0.0939	−0.0095	−11.3
28	Acetophenone	117.4	9.6	4.2	1.1	1.5	0.0223	0.0029	0.0194	87.0
29	Benzyl alcohol	103.9	9.0	3.1	5.9	3.8	0.0784	0.1241	−0.0457	−58.3
31	Methyl alcohol	40.7	7.4	6.0	8.4	7.1	0.1142	0.0590	0.0552	48.3
32	Ethyl alcohol	58.7	7.7	4.3	8.3	5.5	0.1213	0.1077	0.0136	11.2
33	Propyl alcohol	75.1	7.8	3.3	7.5	4.8	0.1084	0.1156	−0.0072	−0.6
34	Isopropyl alcohol	76.9	7.7	3.0	7.1	4.5	0.1297	0.1011	0.0286	22.1
35	Butyl alcohol	92.0	7.8	2.8	6.4	4.6	0.1154	0.1094	0.0060	5.2
36	Isobutyl alcohol	92.4	7.4	2.8	6.0	5.1	0.0901	0.0660	0.0241	26.7
39	1-Pentanol	108.6	7.8	2.2	5.4	4.3	0.1145	0.0767	0.0378	33.0
40	1-Hexanol	125.2	8.0	2.1	5.7	3.5	0.1121	0.0815	0.0306	27.3
42	1-Octanol	158.4	8.3	1.6	5.2	3.2	0.1032	0.0445	0.0587	56.9
43	Ethylene glycol	55.9	8.3	5.4	17.9	4.4	0.1132	0.1343	−0.0211	−18.6
44	1,2-Propanediol	73.7	8.2	4.6	14.1	4.6	0.1308	0.1318	−0.0010	−0.8
46	Glycerol	73.2	8.5	5.9	20.0	5.1	0.0301	0.0225	0.0076	25.2
48	Acetic acid	57.6	7.1	3.9	7.0	3.1	0.0444	0.0826	−0.0382	−86.0
49	Propionic acid	75.0	7.2	3.8	6.0	3.0	0.0347	0.0919	−0.0572	−164.8
51	Dimethyl sulfoxide	71.3	9.0	8.0	2.2	5.7	0.3674	0.2769	0.0905	24.6
52	Pyridine	80.9	9.3	4.3	1.4	3.2	0.1044	0.0867	0.0177	17.0
53	Formamide	39.9	8.4	12.8	5.7	7.6	0.0341	0.0331	0.0010	2.9
54	*N*-Methylformamide	59.1	8.4	10.1	4.8	3.9	0.1025	0.1647	−0.0622	−60.7
55	*N,N*-Dimethylformamide	77.4	8.5	6.7	3.4	4.4	0.2137	0.2625	−0.0488	−22.8
57	*N,N*-Dimethylacetamide	93.0	8.2	5.6	2.9	4.3	0.2354	0.2782	−0.0428	−18.2
59	Water, pH 2.0	18.1	7.6	7.8	6.7	32.0	0.00060	0.00104	−0.00044	−73.3

[a] Solute properties: $\delta_2 = 15.3$, mp 485.85 K, $V_2 = 94.3$ cm³/mol, $X_2^i = 0.00747$, $\log X_2^i = -2.1267$.

plotted as filled circles and the predicted solubilities, obtained using Eq. 2 (below), are plotted as stars.

In the prior study (4), the solubilities of naphthalene and benzoic acid were found to lie on or near the regular solution line. In Fig. 1A most of the experimental points for methyl *p*-hydroxybenzoate fall near X_2^i and the regular solution line, but points 51, 52, and 54–58 (for the solute in strongly dipolar solvents) lie far above X_2^i and the regular solution line. In Fig. 1B, no relationship exists between *p*-hydroxybenzoic acid solubility points and the dashed regular solution line. *p*-Hydroxybenzoic acid is a relatively polar compound ($\delta_2 = 15.3$), and its solubility profile cannot be approximated by regular solution theory. However, it is possible with a four-parameter system to predict the solubilities of such a polar solute in polar (and nonpolar) solvents within a reasonable degree of accuracy (4). The results obtained here are not highly satisfactory, but adjustment of parameters and consideration of average molecular orientations in specific solute–solvent interactions may lead to improvements.

Estimation of Solubilities Using Four Partial Solubility Parameters—The solubility of a crystalline solid in a number of solvents can be expressed as (4):

$$\frac{\log \alpha_2}{A} = C_1(\delta_{1d} - \delta_{2d})^2 + C_2(\delta_{1p} - \delta_{2p})^2 + 2C_3(\delta_{1a} - \delta_{2a})(\delta_{1b} - \delta_{2b}) + C_0 \quad \text{(Eq. 2)}$$

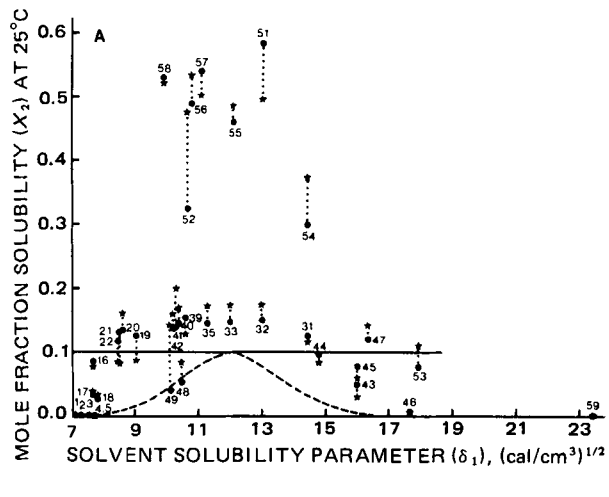

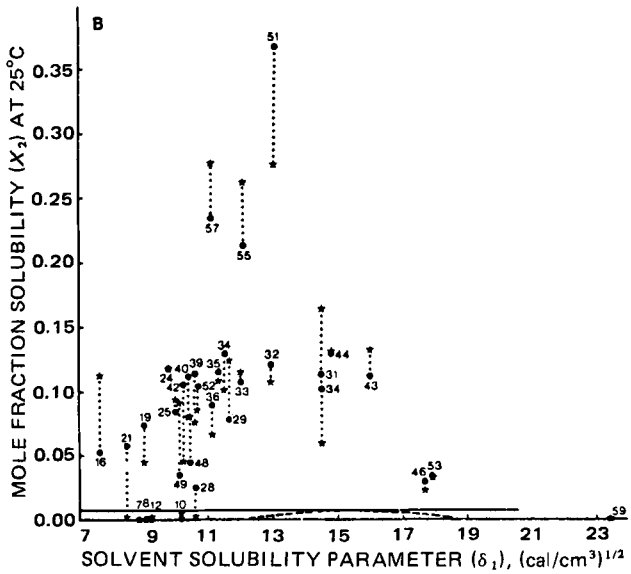

Figure 1—*Solubility profile of methyl* p*-hydroxybenzoate (A) and* p*-hydroxybenzoic acid (B) in individual solvents at 25°C. See Tables I–III for solvent numbers. Key: (- -) regular solution curve; (—) ideal solubility line, $X_2^i = 0.0988$ (A) and 0.00747 (B) (●) experimental solubilities; (★) solubilities calculated using Eq. 7(A) or Eq. 8(B).*

Table III—Excess Free Energies of Benzoic Acid and Its Derivatives In Individual Solvents at 25°C

No.	Solvent	Benzoic Acid			Methyl *p*-Hydroxybenzoate			*p*-Hydroxybenzoic Acid		
		$\overline{\Delta G}^E_{exp}$, cal/mol	ΔG^E_{calc}, cal/mol	Residual, cal/mol	$\overline{\Delta G}^E_{exp}$, cal/mol	$\overline{\Delta G}^E_{calc}$, cal/mol	Residual, cal/mol	$\overline{\Delta G}^E_{exp}$, cal/mol	ΔG^E_{calc}, cal/mol	Residual, cal/mol
1	Pentane	2157	1992	165	4359	5512	−1153	—	—	—
2	Hexane	1875	1863	12	4240	4839	−599	—	—	—
3	Heptane	1752	1747	5	4196	4264	−68	—	—	—
4	Nonane	1641	1654	−13	4051	3750	301	—	—	—
5	Decane	1589	1654	−65	3972	3750	222	—	—	—
6	Cyclohexane	1833	1461	372	—	—	—	—	—	—
7	Benzene	701	1397	−696	—	—	—	3212	3812	−600
8	Toluene	664	877	−213	—	—	—	3289	3331	−42
9	Chlorobenzene	569	642	−73	—	—	—	—	—	—
10	Ethylene dichloride	696	175	521	—	—	—	2499	199	2300
12	Chloroform	330	226	104	—	—	—	2335	499	1836
13	Carbon tetrachloride	898	1093	−195	—	—	—	—	—	—
16	Diethyl ether	120	−86	206	96	164	−68	−1150	−1610	460
17	Dipropyl ether	—	—	—	679	522	157	—	—	—
18	Dibutyl ether	—	—	—	773	657	116	—	—	—
19	Ethyl acetate	184	171	13	−149	81	−230	−1356	−1048	−308
20	Propyl acetate	—	—	—	−192	−300	108	—	—	—
21	Butyl acetate	167	387	−220	−174	105	−279	−1208	262	−1470
22	Hexyl acetate	—	—	—	−97	91	−188	—	—	—
24	Acetone	114	38	76	—	—	—	−1637	−1638	1
25	Dioxane	−140	−194	54	—	—	—	−1436	−1500	64
27	Nitrobenzene	545	311	234	—	—	—	—	—	—
28	Acetophenone	107	250	−143	—	—	—	−648	561	−1209
29	Benzyl alcohol	264	−45	309	—	—	—	−1393	−1665	272
31	Methyl alcohol	191	630	−439	−141	−93	−48	−1616	−1224	−392
32	Ethyl alcohol	136	276	−140	−245	−337	92	−1651	−1581	−70
33	Propyl alcohol	135	170	−35	−242	−337	95	−1585	−1623	38
34	Isopropyl alcohol	89	168	−79	—	—	—	−1691	−1543	−148
35	Butyl alcohol	65	137	−72	−241	−336	95	−1622	−1590	−32
36	Isobutyl alcohol	231	292	−61	—	—	—	−1475	−1291	−184
39	1-Pentanol	210	142	68	−258	−155	−103	−1617	−1380	−237
40	1-Hexanol	99	91	8	−238	−319	81	−1605	−1416	−189
41	1-Heptanol	—	—	—	−241	−422	181	—	—	—
42	1-Octanol	74	102	−28	−198	−287	89	−1556	−1057	−499
43	Ethylene glycol	554	494	60	428	698	−270	−1610	−1712	102
44	1,2-Propanediol	—	—	—	29	112	−83	−1696	−1700	4
45	1,3-Propanediol	—	—	—	151	336	−185	—	—	—
46	Glycerol	1552	1440	112	1621	2282	−661	−826	−653	−173
47	1,4-Butanediol	—	—	—	−116	−222	106	—	—	—
48	Acetic acid	175	164	11	367	110	257	−1056	−1424	368
49	Propionic acid	104	148	44	557	−222	779	−910	−1487	577
51	Dimethyl sulfoxide	−485	−465	−20	−1053	−956	−97	−2308	−2140	−168
52	Pyridine	−513	−460	−53	−704	−930	226	−1562	−1452	−110
53	Formamide	231	714	−483	152	−73	225	−900	−882	−18
54	*N*-Methylformamide	−249	−379	130	−162	−793	631	−1552	−1833	281
55	*N,N*-Dimethylformamide	−462	−468	6	−912	−941	29	−1987	−2109	122
56	*N,N*-Diethylformamide	—	—	—	−949	−1000	51	—	—	—
57	*N,N*-Dimethylacetamide	−501	−502	1	−1008	−963	−45	−2044	−2143	99
58	*N,N*-Diethylacetamide	—	—	—	−995	−986	−9	—	—	—
59	Water	3656	3420	236	3497	3249	248	1494	1168	326

where δ_d, δ_p, δ_a, and δ_b have previously been defined and C_0, C_1, C_2, and C_3 are the coefficients obtained as a result of multiple regression analysis. Log α_2 is the logarithm of the solute activity coefficient, where:

$$\alpha_2 = X_2^i/X_2 \qquad \text{(Eq. 3)}$$

and

$$A = \frac{V_2\phi_1^2}{2.303RT} \qquad \text{(Eq. 4)}$$

where V_2 is the molar volume of the solute, considered as a hypothetical supercooled liquid at the temperature of the solution. The molar volume of methyl *p*-hydroxybenzoate and *p*-hydroxybenzoic acid are 117.5 and 94.3 cm^3/mol, respectively, which are obtained as the average of apparent molar volume in the solutions (10) and by the group contribution method of Fedors (11). The solvent volume fraction, ϕ_1, and R and T have their usual meanings.

The ideal solubility, X_2^i, of the solute can be approximated by:

$$\log X_2^i = \frac{\Delta H_m^f}{2.303R}\left(\frac{1}{T_m} - \frac{1}{T}\right) \qquad \text{(Eq. 5)}$$

where ΔH_m^f is the heat of fusion of the solute, R is the gas constant, T_m and T are melting points of the solute and solution temperatures, respectively, in degrees Kelvin.

Once A is calculated, one can use the regression equation (Eq. 2) to calculate α_2, and knowing X_2^i for the solute, X_2 is obtained from Eq. 3. To obtain the A value, however, requires a value of the volume fraction of the solvent, ϕ_1; but, ϕ_1 depends on the value of X_2, the quantity sought. This difficulty can be overcome by simple iteration (3), or in a more satisfactory way by use of a root-finding method, as provided in the International Mathematical and Statistical Library (IMSL) (12) and described in the preceding paper (4).

The solubility of a solute, such as methyl *p*-hydroxybenzoate, in a solvent with known parameters can be calculated by expanding Eq. 2, recognizing that the partial solubility parameters for a particular solute are constants. Then:

$$\frac{\log \alpha_2}{A} = D_0 + D_1\delta_{1d}^2 + D_2\delta_{1d} + D_3\delta_{1p}^2 + D_4\delta_{1p} + D_5\delta_{1a}\delta_{1b} + D_6\delta_{1a} + D_7\delta_{1b} \qquad \text{(Eq. 6)}$$

where D_0 is a constant of regression and D_1–D_7 are regression coefficients associated with the partial solubility parameters. The regression equation was obtained by use of a multiple regression program (13) for methyl *p*-hydroxybenzoate in 36 solvents at 25°C and was found to be:

$$\frac{\log \alpha_2}{A} = 7.341\delta_{1d}^2 - 133.4\delta_{1d} + 1.138\delta_{1p}^2 - 16.57\delta_{1p} + 0.9032\delta_{1a}\delta_{1b} - 0.6605\delta_{1a} - 4.231\delta_{1b} + 623.85$$

$$n = 36,\ s = 10.61,\ r^2 = 0.87,\ F = 27.3,\ F(7,28,0.01) = 3.36 \qquad \text{(Eq. 7)}$$

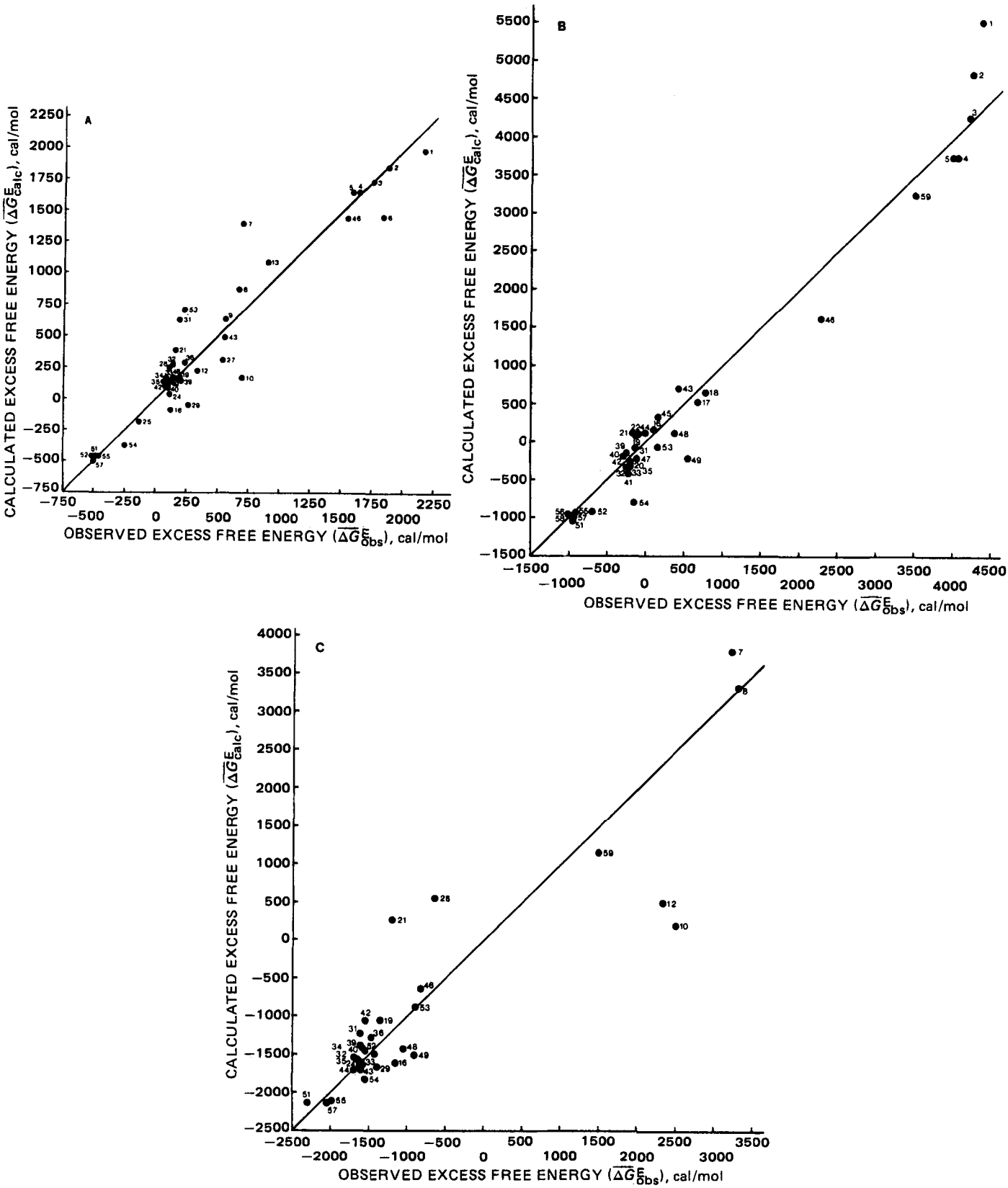

Figure 2—*Relationship between excess free energies of mixing of benzoic acid (A), methyl* p*-hydroxybenzoate (B), and* p*-hydroxybenzoic acid (C) derived from measured (Eq. 9) and calculated (Eq. 10 for benzoic acid) solubilities at 25°C. The line is drawn with unit slope and zero intercept. See Tables I–III for solvent numbers.*

The estimated solubilities of methyl *p*-hydroxybenzoate obtained from Eq. 7 are listed in Table I. The $(\log \alpha_2)/A$ values fall within a standard deviation of ±10.61. The coefficient of determination, r^2, which gives the fraction of the variance in the dependent variable that is explained by the regression equation, is 0.87. Therefore 87% of the solubility results (variances) are predicted by Eq. 7. As observed, the calculated F ratio (27.3) is significantly larger than the table value (3.36).

All statistical parameters, therefore, indicate that the relationship is

Table IV—Correlation Coefficients of Solubility Parameters[a]

	Three-Parameter System			
	δ_d	δ_p	δ_h	
δ_d	1.000			
δ_p	0.076	1.000		
δ_h	−0.183	0.623	1.000	
	Four-Parameter System			
	δ_d	δ_p	δ_a	δ_b
δ_d	1.000			
δ_p	0.076	1.000		
δ_a	−0.083	0.439	1.000	
δ_b	−0.143	0.468	0.252	1.000

[a] $n = 59$ for each system.

significant. Yet the most meaningful test is how close the calculated solubilities approach observed values. In previous work (3) an error of ≤30% from observed solubility was accepted as reasonable. A study of Table I shows that 22 of 36 or 61% of the predicted solubility values meet this criterion. The results are plotted in Fig. 1A where the calculated solubilities for methyl *p*-hydroxybenzoate (stars) are attached by dotted lines to the experimental points (filled circles).

Using the four-parameter system, the regression equation obtained for *p*-hydroxybenzoic acid at 25°C in 32 solvents was:

$$\frac{\log \alpha_2}{A} = 10.65\delta_{1d}^2 - 177.0\delta_{1d} + 1.040\delta_{1p}^2 - 14.73\delta_{1p} + 2.072\delta_{1a}\delta_{1b} - 8.107\delta_{1a} - 12.08\delta_{1b} + 790.82$$

$$n = 32, s = 10.93, r^2 = 0.81, F = 14.6, F(7,24,0.01) = 3.50 \quad \text{(Eq. 8)}$$

The calculated solubilities for *p*-hydroxybenzoic acid are shown in Table II and plotted in Fig. 1B. It is observed that 17 of the 32 results or 53% are within 30% of the observed solubility values. These are the best results that can be expected at this stage of the research for these highly irregular solutions. As shown in the preceding paper, both of these solutes show bimodal interactions (*cf.* Figs. 3 and 4 of Ref. 4), and that may be a major cause for perturbation of the single-peak models implied by Eqs. 6–8.

Thermodynamics of Irregular Solutions—Scatchard (14) suggested that nonideal behavior of a solute in solution could be expressed as an "excess free energy" of mixing:

$$\overline{\Delta G}^E = RT \ln (X_2'/X_2) \quad \text{(Eq. 9)}$$

The excess free energies of methyl *p*-hydroxybenzoate and *p*-hydroxybenzoic acid in solution at 25°C were obtained from Eq. 9 and are listed in Table III as experimental values. The $\overline{\Delta G}^E_{exp}$ values for benzoic acid, the solubility of which was reported earlier (4), were also included. The calculated results, $\overline{\Delta G}^E_{calc}$, are obtained from a rearrangement of the four-parameter regression equation, which for benzoic acid (4) is:

$$\overline{\Delta G}^E_{calc} = V_2\phi^2_{1,calc}(2.125\delta_{1d}^2 - 36.90\delta_{1d} + 0.2188\delta_{1p}^2 - 2.603\delta_{1p} + 0.6139\delta_{1a}\delta_{1b} - 1.966\delta_{1a} - 2.955\delta_{1b} + 174.25 - 20.27I) \quad \text{(Eq. 10)}$$

The $\overline{\Delta G}^E_{calc}$ along with $\overline{\Delta G}^E_{exp}$ and the residuals for methyl *p*-hydroxybenzoate and *p*-hydroxybenzoic acid at 25°C are listed in Table III. The previously reported (4) values for benzoic acid are included for comparison. The results for benzoic acid demonstrate that most of the calculated excess free energies, $\overline{\Delta G}^E_{calc}$, are within 500 cal/mol of the experimental values, except for two solvents, benzene (−696 cal/mol) and ethylene dichloride (521 cal/mol).

Table V—Factor Matrix Obtained from Principal Factor Without Iteration

	Three-Parameter System			
	Factor 1	Factor 2	Factor 3	
δ_d	−0.158	0.976	0.151	
δ_p	0.880	0.280	−0.383	
δ_h	0.913	−0.101	0.396	
	Four-Parameter System			
	Factor 1	Factor 2	Factor 3	Factor 4
δ_d	−0.132	0.972	0.080	0.180
δ_p	0.833	0.273	0.072	−0.476
δ_a	0.718	0.020	−0.650	0.248
δ_b	0.749	−0.152	0.558	0.324

Table VI—Varimax Rotated Factor Matrix for Three and Four Solubility Parameters

	Three-Parameter System			
	Factor 1	Factor 2	Factor 3	
δ_d	0.995	0.048	−0.092	
δ_p	0.062	0.941	0.333	
δ_h	−0.114	0.340	0.934	
	Four-Parameter System			
	Factor 1	Factor 2	Factor 3	Factor 4
δ_d	0.995	0.048	−0.042	0.072
δ_p	0.058	0.941	0.227	0.243
δ_a	0.046	0.208	0.972	0.103
δ_b	0.080	0.227	0.105	0.965

The estimated excess free energies are less satisfactory for the two benzoic acid derivatives. For methyl *p*-hydroxybenzoate, 5 of 36 calculated excess free energies have errors >500 cal/mol relative to the observed values. For *p*-hydroxybenzoic acid, 6 of 32 calculated excess free energies are >500 cal/mol in error.

The observed free energies $\overline{\Delta G}^E_{exp}$ are plotted (horizontal axis) *versus* $\overline{\Delta G}^E_{calc}$ (vertical axis) for benzoic acid, methyl *p*-hydroxybenzoate, and *p*-hydroxybenzoic acid in Fig. 2A–C. The straight lines plotted on these three graphs are drawn with slopes of unity and pass through the origin. The vertical distance of each point from the line is a measure of the residuals of Table III and gives an indication of the adjustment that must be made in the four parameters of the predicting equations. From the difference of excess free energies between the observed and estimated values, one can calculate the error in calories per mole caused by one unit difference in a solvent solubility parameter. With methyl *p*-hydroxybenzoate in glycerol, for example, δ_h was changed from 5.1 to 6.1 and δ_a was correspondingly adjusted from 20.0 to 16.8 (to keep δ_h the same) while holding the other values constant. The $\overline{\Delta G}^E_{calc}$ value obtained by this adjustment became 2070 cal/mol. Comparing this value with the original $\overline{\Delta G}^E_{calc}$ value (2282 cal/mol) demonstrates that an increase of one unit in δ_b decreased the predicted excess free energy by 212 cal/mol. This example suggests the changes in partial solubility parameters that are required to obtain more exact solubilities.

Estimating the Partial Solubility Parameters of the Solute—As reported earlier (4), the regression equation for a specific solute in a number of solvents can be used to estimate the partial solubility parameters of the solute. For methyl *p*-hydroxybenzoate, Eq. 7 can be rearranged to:

$$\frac{\log \alpha_2}{A} = 7.341(\delta_{1d} - 9.09)^2 + 1.138(\delta_{1p} - 7.28)^2 + 0.9032(\delta_{1a} - 4.68)(\delta_{1b} - 0.73) - 45.59 \quad \text{(Eq. 11)}$$

Comparing Eq. 11 with Eq. 2 shows that $\delta_{2d} = 9.09$, $\delta_{2p} = 7.28$, $\delta_{2a} = 4.68$, and $\delta_{2h} = 0.73$ for methyl *p*-hydroxybenzoate. The total solubility parameter δ_{2T} can be calculated by summing the squares of these partial values and taking the square root of the sum:

$$\delta_{2T}^2 = \delta_{2d}^2 + \delta_{2p}^2 + 2\delta_{2a}\delta_{2b} = (9.09)^2 + (7.28)^2 + 2(4.68)(0.73)\ \delta_{2T} = 11.94 \quad \text{(Eq. 12)}$$

This value compares satisfactorily with the value, 12.1, reported elsewhere (7).

The partial solubility parameters of *p*-hydroxybenzoic acid can be obtained by transforming Eq. 8 to the following:

$$\frac{\log \alpha_2}{A} = 10.65(\delta_{1d} - 8.31)^2 + 1.04(\delta_{1p} - 7.08)^2 + 2.072(\delta_{1a} - 5.83)(\delta_{1b} - 3.91) - 44.06 \quad \text{(Eq. 13)}$$

It is seen from Eq. 13 that $\delta_{2d} = 8.31$, $\delta_{2p} = 7.08$, $\delta_{2a} = 5.83$, $\delta_{2b} = 3.91$, and $\delta_{2T} = 12.84$ for *p*-hydroxybenzoic acid. The total solubility parameter for *p*-hydroxybenzoic acid calculated by Fedors (11) group contribution (15.3) and the value ($\delta_{2T} = 12.84$) obtained by regression show poor agreement. Undoubtedly, there are faults in both methods. Fedors' procedure, while generally accurate, tends to overestimate δ_T for aromatics.

Factor Analysis for Three- and Four-Parameter Solubility Systems—Factor analysis (15) offers the possibility of analyzing the

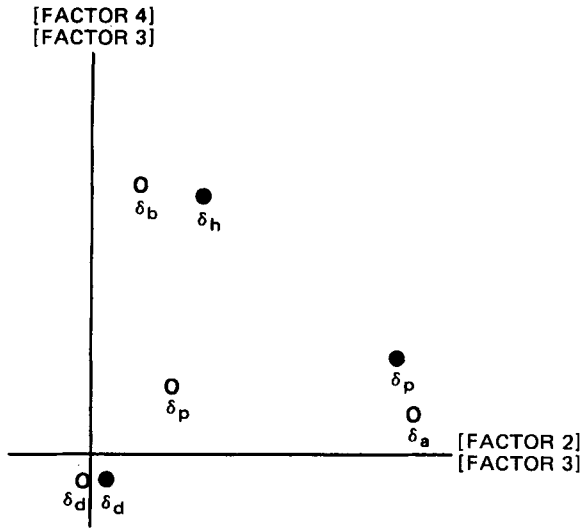

Figure 3—*Relative positions of δ_a and δ_b (four-parameter system, O) to that of [Factors 3 and 4] in comparison with the relative positions of δ_p and δ_h (three-parameter system, ●) to that of [Factors 2 and 3]. Note that the open point δ_a is closer to the [Factor 3] axis than closed point δ_p is to its [Factor 2] axis. Also, the open point δ_b is closer to its axis [Factor 4] than is the closed point δ_h to its [Factor 3] axis.*

independencies (noncorrelations) between the independent variables in regression equations. It can be used to test whether the three- or the four-parameter solubility approach forms a better set of variables. In multiple linear regression it is assumed that all the independent variables are mutually independent. In this study, the factor analysis program was obtained from SPSS (13) and was run on the University of Texas Cyber System. The three- and four-parameter systems are listed in Table I of the preceding paper (4); most of the data can also be found in Tables I and II. Table IV lists the correlation coefficients of these solubility parameter systems. As can be seen in Table IV, δ_d is almost uncorrelated with the other partial solubility parameters in both systems. For these solubility parameters, δ_p and δ_h are moderately correlated, with the correlation coefficient equal to 0.623 ($r^2 = 0.388$). This condition is undesirable, for it indicates that the variables are not independent of one another. For the expanded four-parameter solubility system, the correlation coefficient of δ_p and δ_a is 0.439 and that of δ_p and δ_b is 0.468 which are a little high, but are satisfactory in the present study ($r^2 < 0.22$ in both cases). The correlation coefficient between δ_a and δ_b is 0.252, which represents only slight correlation ($r^2 = 0.06$); therefore, these variables are independent of each other, a most desirable characteristic for multiple regression.

Table V lists the factor matrix obtained using the principal factor method without iteration (13). It can be seen from Table V that δ_p and δ_h are heavily loaded on Factor 1 and δ_d is loaded on Factor 2. Factor 3 does not contribute much in the three-parameter system. For the expanded four-parameter solubility system, δ_d is loaded on Factor 2, δ_p is loaded on Factor 1, but also slightly loaded on Factor 4; δ_a and δ_b are loaded on Factor 1 and Factor 3. The unrotated factors in Table V shows that four solubility parameters form a better system of independent variables than three solubility parameters.

Orthogonal factor rotation (13) was also used to compare these two systems of variables. Varimax-type rotation (13) was carried out by assuming the partial solubility parameters to be mutually independent. The procedure attempts to force independent variables to be loaded on different Factors and heavily on one Factor only. The results are found in Table VI. For the three-parameter system, δ_d is completely loaded on Factor 1, but δ_p and δ_h are less successful in loading on Factors 2 and 3, respectively.

For the four-parameter system, δ_d, δ_a, and δ_b are heavily loaded on Factors 1, 3, and 4, respectively; δ_p is less satisfactory in loading on Factor 2. The relative position of δ_a and δ_b to that of Factor 3 and Factor 4 for the four-parameter system was plotted in Fig. 3 in comparison with the relative position of δ_p and δ_h to that of Factor 2 and Factor 3 for the three-parameter system. It can be concluded that four solubility parameters are more independent than the quantities in the three-parameter solubility system. This is a desirable feature of the four-parameter system.

CONCLUSIONS

The UNIFAC (5) program which had been used earlier in computing solubilities of naphthalene (3) and benzoic acid (4) in individual solvents was not used in this study due to lack of parameters for interaction energies of phenolic —OH/—COOH groups in the data bank of the UNIFAC program.

The regression equation for predicting the solubility of a solute can be cast into the proposed model (Eq. 2) to get partial and total solubility parameters of the solute. The total solubility parameters obtained by this method are close to the values reported elsewhere for benzoic acid and methyl *p*-hydroxybenzoate. For *p*-hydroxybenzoic acid the total solubility parameter, 12.84, obtained from Eq. 13 is different from the value, 15.3, calculated by Fedors' (11) method.

The magnitude of the constant terms in Eqs. 11 and 13, namely −45.59 and −44.06, suggest that four solubility parameters are still not sufficient to explain all interactions between solute and solvent for the two solutes, methyl *p*-hydroxybenzoate and *p*-hydroxybenzoic acid, as compared with naphthalene and benzoic acid, whose simpler structures result in constant terms closer to zero (−0.24 and 3.13, respectively) in the transformed regression equations (4). On the other hand, this constant is not merely a catch-all for errors as in most regressions, but contains the entropies of mixing due to disparities in volume and shape between solvent and solute. Therefore, reducing the constant value to zero is not a realistic goal.

REFERENCES

(1) A. Martin, J. Newburger, and A. Adjei, *J. Pharm. Sci.*, **69,** 487 (1980).

(2) A. Martin, A. N. Paruta, and A. Adjei, *J. Pharm. Sci.*, **70,** 1115 (1981).

(3) A. Martin, P. L. Wu, A. Adjei, A. Beerbower, and J. M. Prausnitz, *J. Pharm. Sci.*, **70,** 1260 (1981).

(4) A. Beerbower, A. Martin, and P. L. Wu, *J. Pharm. Sci.*, **73,** 179 (1984).

(5) A. Fredenslund, J. Gmehling, and P. Rasmussen, "Vapor–Liquid Equilibrium Using UNIFAC," Elsevier, New York, N.Y., 1977.

(6) C. K. Hancock, J. N. Pawloski, and J. P. Indoux, *J. Org. Chem.*, **31,** 3801 (1966).

(7) A. Martin and J. Carstensen, *J. Pharm. Sci.*, **70,** 170 (1981).

(8) C. M. Hansen and A. Beerbower, "Encyclopedia of Chemical Technology," Suppl. Vol., 2nd ed., Wiley, New York, N.Y., 1971.

(9) M. J. Kamlet, J. L. M. Abboud, and R. W. Taft, *Prog. Phys. Org. Chem.*, **13,** 485 (1980).

(10) F. T. Gucker, Jr., W. I. Ford, and C. E. Moser, *J. Phys. Chem.*, **43,** 153 (1939).

(11) R. F. Fedors, *Polym. Eng. Sci.*, **14,** 147 (1974).

(12) IMSL Reference Manual, International Mathematical and Statistical Library, Houston, Texas, 1979.

(13) N. H. Nie, C. H. Hull, J. G. Jenkins, K. Steinbrenner, and D. H. Bent, "SPSS, Statistical Package for the Social Sciences," 2nd ed., McGraw-Hill, New York, N.Y., 1975, chap. 20.

(14) G. Scatchard, *Chem. Rev.*, **8,** 321 (1931).

(15) R. L. Rummel, "Applied Factor Analysis," Northwestern University Press, Evanston, Ill., 1970.

ACKNOWLEDGMENTS

Supported in part by a grant from the University of Texas Research Institute. A. Martin is grateful to Coulter R. Sublett for the endowed professorship which also supported this work.

The authors acknowledge review of the section on factor analysis by Drs. Mary Whiteside and Francis May, Statistics Division, University of Texas at Austin.

Stabilized Normal-Phase High-Performance Liquid Chromatographic Analysis of Aspirin and Salicylic Acid in Solid Pharmaceutical Dosage Forms

ROBERT N. GALANTE ˣ, ANTHONY J. VISALLI, and WAYNE M. GRIM

Received August 26, 1982, from the *Analytical and Physical Chemistry Department, Research and Development, William H. Rorer, Inc., Fort Washington, PA 19034.* Accepted for publication January 10, 1983.

Abstract □ A simultaneous analysis of aspirin and nonaspirin salicylates in solid pharmaceutical dosage forms is described. Two separate extraction procedures are employed, one for plain aspirin tablets and one for tablets containing aspirin plus buffers or antacids. The analyses of the extracted samples are accomplished by a stabilized normal-phase high-performance liquid chromatographic (HPLC) procedure. Prepared samples and standards are stable for up to 24 h, and the methodology is suitable for an automated HPLC system.

Keyphrases □ Aspirin—stabilized normal-phase high-performance liquid chromatographic analysis, solid pharmaceutical dosage forms, salicylic acid □ Salicylic acid—stabilized normal-phase high-performance liquid chromatographic analysis, solid pharmaceutical dosage forms, aspirin □ Solid dosage forms—stabilized normal-phase high-performance liquid chromatographic analysis of aspirin and salicylic acid

Successful analyses of aspirin and free salicylic acid by reverse-phase high-performance liquid chromatography (HPLC) have been reported (1–13). Effective adsorption HPLC procedures have also been described (14–16). All of these methods require immediate injections of prepared samples and standards into the HPLC. We described a stable assay preparation for aspirin and salicylic acid in tablets containing buffers or antacids *via* a chromatographic siliceous earth column with subsequent GC (17). The methodology described here combines some of these effective techniques into a stabilized normal-phase HPLC analysis. None of the previously published HPLC procedures allow the determination of salicylic acid as nonaspirin salicylates in tablets containing buffers or antacids.

EXPERIMENTAL

Materials and Equipment—HPLC-grade chloroform, methylene chloride, and acetonitrile and reagent-grade chloroform, formic acid (88%), methanol, hydrochloric acid, citric acid monohydrate, and chromatographic siliceous earth (acid washed by the USP procedure) were used. A modular high-pressure liquid chromatograph equipped with a variable-flow pump[1], an automatic injector[2] with a 20-μL loop, a variable-wavelength detector[3], and an electronic integrator[4] was used. The HPLC adsorption column was 4.6 mm × 25 cm packed with a porous 5-μm silica[5]. Reagent-grade chloroform saturated with citric acid was used as diluent for all sample and standard preparations.

Standards Preparation—*Aspirin*—About 125 mg of aspirin USP reference standard was accurately weighed, transferred to a 50-mL volumetric flask, and dissolved in ~10 mL of diluent. After adding 0.25 mL of formic acid, the mixture was diluted to volume with diluent. About 200 mg of citric acid crystals was added to the flask and mixed.

Salicylic Acid—A 1-mg/mL stock solution of salicylic acid USP reference standard was prepared in the diluent containing 0.5% formic acid. This solution was diluted to make standards containing 7.5, 25.0, 50.0, and 75.0 μg/mL, corresponding to 0.3, 1.0, 2.0, and 3.0% salicylic acid in the assay preparation.

Sample Preparation—*Plain Aspirin Tablets*—The average tablet weight of 20 tablets was determined, and the tablets were ground to a fine powder. A portion of the ground tablets equivalent to 250 mg of aspirin was transferred to a volumetric flask, and 100 mL of diluent containing 0.5 mL of formic acid was added to the flask. About 500 mg of citric acid crystals was added to the flask, and the assay preparation was placed in an ultrasonic bath for 2 min, then centrifuged or filtered for subsequent injection into the liquid chromatograph.

Aspirin Tablets Containing Buffers or Antacids—A portion of 20 ground tablets equivalent to 500 mg of aspirin was transferred to a small beaker containing 3.0 g of acid-washed chromatographic siliceous earth. The powders were mixed with a glass rod, 2.0 mL of 6 M HCl was added, and the powders were mixed again with the glass rod. The mixture was transferred to a 20 × 2.5-cm chromatographic column, and the beaker was dry washed with 1.0 g of siliceous earth (glass wool was used at both ends of the column). The column was packed uniformly and eluted with successive portions of diluent *via* the sample beaker, at the rate of ~10 mL/min. About 150 mL of the eluate was collected in a 200-mL volumetric flask. The tip of the column was rinsed with diluent, and 1.0 mL of formic acid was added. The flask was made to volume with the diluent. Approximately 500 mg of citric acid crystals were added to the flask and mixed.

Assay Procedure—The mobile phase, chloroform–methylene chloride–acetonitrile–formic acid (700:300:30:4), was placed in an ultrasonic bath to expel dissolved gases, and ~100 mL was allowed to pass through the column prior to the start of the analysis. At the completion of a 1-d run the column was washed with ~200 mL of methanol.

The variable-wavelength detector was set at 300 nm to maximize sal-

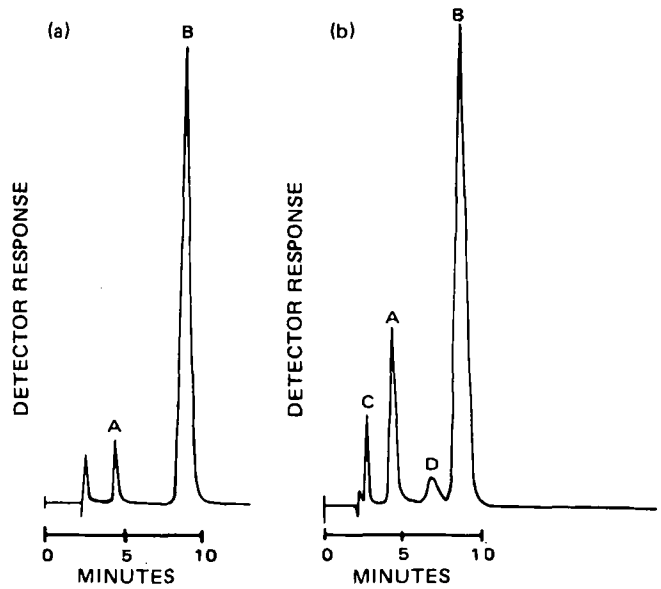

Figure 1—*Chromatograms of aspirin and salicylic acid (a) and a spiked aspirin sample (b) using a Zorbax-Sil column with chloroform–methylene chloride–acetonitrile–formic acid (700:300:30:4) at a flow rate of 2.0 mL/min. Detection was at 300 nm, 0.01 AUFS, with a recorder presentation of 128. Key: (A) salicylic acid; (B) aspirin; (D) acetylsalicylsalicylic acid; (C) acetylsalicylic acid anhydride.*

[1] Beckman Instruments, Model 110A.
[2] Micromeritics, Model 725.
[3] Laboratory Data Control, Spectromonitor III.
[4] Hewlett Packard, 3380A.
[5] Dupont Col, Zorbax-Sil.

0022-3549/84/0200-0195$01.00/0
© 1984, American Pharmaceutical Association

Table I—Assay Results on Commercial Aspirin Tablets

Product[a]	Aspirin, % of Claim		Salicylic Acid, %	
	HPLC	GC	HPLC	GC[b]
A	101.8	100.0	0.03	<0.30
B	98.9	97.8	0.05	<0.30
C	105.0	105.2	0.13	<0.30
D	99.7	100.3	0.06	<0.30
E	100.6	100.3	0.04	<0.30

[a] Products: A, Bayer; B, Empirin; C, Eckerd; D, Rite Aid; E, Treasury. [b] GC method determined by a 0.3% limit standard.

icylic acid detection. The detector sensitivity and the recorder presentation were adjusted so that the salicylic acid standard, containing 75 μg/mL, and the 2.5-mg/mL aspirin standard were both ~70% full scale. The pump flow rate was 2.0 mL/min. The relative standard deviation (n = 5) for the aspirin standard was <2.0%, and <2.0% for the salicylic acid standard at a concentration of 50 μg/mL. The retention times for salicylic acid, and aspirin were ~4 and 8 min, respectively (Fig. 1a).

Calculations—Integrated area counts were used to determine the amount of aspirin and salicylic acid in the assay preparation by external standard techniques. The aspirin was calculated as percent of label claim. The salicylic acid was calculated as a percentage of the theoretical aspirin content in the dosage form analyzed.

RESULTS AND DISCUSSION

The response linearity was suitable for the entire assay range, *i.e.*, aspirin 70–130% and salicylic acid 0.1–5.0%. The average relative standard deviation (n = 10) for the standard preparations was 0.48% for aspirin and 0.65% for salicylic acid. In most analyses a single point standard can be used for both aspirin and salicylic acid. Recoveries of salicylic acid and aspirin in spiked samples, standards, and placebos ranged from 97 to 102%. Recoveries of salicylic acid and aspirin from the chromatographic siliceous earth column have been previously reported (17). The rate of hydrolysis of aspirin to salicylic acid in the prepared samples and standards was 0.002%/h, which allows the preparation and storage of a large number of samples up to 24 h prior to injection without assay-induced hydrolysis. Since the aspirin and salicylic acid standards are injected separately into the liquid chromatograph, the rate of hydrolysis of the aspirin standard can be continuously monitored.

Tables I and II show the results of the analysis for plain and buffered tablets, respectively, by HPLC and GC. Results for the salicylic acid determination are reported as free salicylic acid in plain aspirin tablets and nonaspirin salicylates, in buffered tablets. Comparative analysis of the USP method to the GC method have been reported (17). Placebo tablet preparations of commonly used tablet excipients and binders showed no HPLC interferences.

The related compounds, acetylsalicylsalicylic acid and acetylsalicylic acid anhydride (Fig. 1b), are seldom seen in routine analysis. Salsalate has the same retention time as salicylic acid and, as in the current USP, is included as salicylic acid in the tablet analysis. Since the detector response for salicylic acid is ~20 times greater than aspirin at 300 nm, salicylic acid can be determined to the 0.02% level by use of integrated area counts.

The stability of aspirin in citric acid–chloroform has been previously described (15). One of the mechanisms for aspirin hydrolysis involves an intramolecular general base catalysis by the carboxylate anion. Citric acid, with a solubility in chloroform of 0.007 g/100 g, forms a more active carboxylate anion than aspirin, thereby competing more vigorously for trace amounts of water in the chloroform. In addition, a trace amount of hydronium ion from the citric acid has a stabilizing effect on the aspirin molecule. The results of 10 consecutive injections of the same assay preparations into the liquid chromatograph are shown in Table III. Recoveries of aspirin and salicylic acid from spiked placebos, samples, and standards are shown in Table IV.

Table II—Assay Results on Commercial Buffered Aspirin Tablets

Product[a]	Aspirin, % of Claim		Nonaspirin Salicylates, %	
	HPLC	GC	HPLC	GC
F	101.8	98.6	1.26	1.01
G	100.8	101.0	1.11	1.12
H	95.4	98.4	0.27	0.40
I	98.9	96.6	0.35	0.35
J	103.0	102.6	0.70	0.65

[a] Products: F, Treasury; G, Rite Aid; H, Bufferin; I, Bufferin Extra Strength; J. Eckerd.

Table III—Results of 10 Consecutive HPLC Analyses of the Same Assay Preparations, Spaced 20 Min Apart, for Plain and Buffered Aspirin Tablets

Run No.	Plain Tablets		Buffered Tablets	
	Aspirin, %	Salicylic Acid, %	Aspirin, %	Nonaspirin Salicylates, %
1	102.2	0.12	97.8	0.80
2	102.6	0.16	97.6	0.81
3	102.1	0.12	97.8	0.81
4	102.1	0.13	96.9	0.81
5	102.0	0.12	97.7	0.81
6	103.0	0.13	98.2	0.81
7	101.6	0.12	97.5	0.81
8	102.5	0.12	97.1	0.81
9	101.4	0.12	97.1	0.82
10	101.4	0.13	97.4	0.81
SD	0.53	0.013	0.43	0.007

Adsorption-Partition HPLC—Unlike bonded phases, silica columns are not subject to rapid deterioration. Silica columns used exclusively for a specific analysis can last for months, even years, as long as the column is kept clean. Washing the column with ~200 mL of methanol rids the active silanol sites of bound solutes. The composition of the mobile phase in the procedure described here requires no prior activation of the silica.

Chloroform and methylene chloride, the nonpolar solvents, are weakly held to the hydrogen-bonded water on the silica gel surface by disperson forces as a monolayer isotherm. Acetonitrile, a more polar solvent, forms a bilayer isotherm. The first layer is hydrogen bonded to water on the silica gel, and the second layer is formed by interacting with the first layer of the polar solvent (18–20). Under these circumstances the acetonitrile acts as the stationary phase proper. Therefore, the partitioning of the

Table IV—Aspirin and Salicylic Acid Recoveries from Spiked Placebos, Standards, and Assay Preparations

	Aspirin		
	Initial Amount, mg/mL	Amount Added, mg/mL	Total Recovery, %
Placebo			
1	0	.7640	101.0
2	0	1.9628	101.8
3	0	.2340	98.9
4	0	.4318	99.7
Standard preparation			
1	2.856	0.2946	99.8
2	2.5404	0.3975	101.0
3	2.183	0.5239	98.7
4	2.5204	0.5159	98.7
Assay preparation			
1	2.5027	0.2419	98.3
2	2.6511	0.6517	96.9
3	2.5052	0.5203	97.7
4	2.4180	0.3819	97.8
	Salicylic Acid		
	Initial Amount, μg/mL	Amount Added, μg/mL	Total Recovery, %
Placebo			
1	0	1.506	101.0
2	0	3.012	101.0
3	0	4.518	99.8
4	0	7.530	99.8
Standard preparation			
1	7.80	10.40	98.1
2	26.00	10.40	99.4
3	52.00	10.40	100.0
4	78.00	10.40	100.2
Assay preparation			
1	34.06	9.92	99.3
2	41.27	9.92	98.6
3	27.04	9.92	98.2
4	16.80	9.92	99.2

solutes passing through the column is dependent on the interaction or displacement of the acetonitrile, rather than displacement of hydrogen-bonded water on the silica gel surface. The mass of the three solvents produces a stable and self-activating chromatographic system in equilibrium. The presence of 1% ethanol or methanol, commonly used preservatives in chloroform and methylene chloride, does not adversely affect retention times or resolution of the solutes.

REFERENCES

(1) W. E. Juhl and R. D. Kirchhoefer, *J. Pharm. Sci.*, **69**, 544 (1980).

(2) R. D. Kirchhoefer and W. E. Juhl, *J. Pharm. Sci.*, **69**, 548 (1980).

(3) R. D. Kirchhoefer, J. C. Reepmeyer, and W. E. Juhl, *J. Pharm. Sci.*, **69**, 550 (1980).

(4) R. D. Kirchhoefer, *J. Pharm. Sci.*, **69**, 1188 (1980).

(5) *Pharmacopeal Forum*, **6**(5), 414 (1980).

(6) P. P. Ascione and C. P. Chrekian, *J. Pharm. Sci.*, **64**, 1029 (1975).

(7) R. G. Baum and F. F. Cantwell, *J. Pharm. Sci.*, **67**, 1066 (1978).

(8) P. J. Twitchett, A. E. P. Gorvin, and A. C. Moffat, *J. Chromatogr.*, **120**, 359 (1976).

(9) D. Blair, B. H. Rumack, and R. G. Peterson, *Clin. Chem.*, **24**, 1543 (1978).

(10) R. L. Stevenson and C. A. Burtis, *J. Chromatogr.*, **61**, 253 (1971).

(11) V. D. Gupta, *J. Pharm. Sci.*, **69**, 110 (1980).

(12) V. D. Gupta, *J. Pharm. Sci.*, **69**, 113 (1980).

(13) G. W. Peng, M. A. F. Gadalla, V. Smith, A. Peng, and W. L. Chiou, *J. Pharm. Sci.*, **67**, 710 (1978).

(14) S. L. Ali, *J. Chromatogr.*, **126**, 651 (1976).

(15) H. Bundgaard, *Arch. Pharm. Chem., Sci. Ed.*, **4**, 103 (1976).

(16) C. D. Pfeiffer and J. W. Pankey, *J. Pharm. Sci.*, **71**, 511 (1982).

(17) R. N. Galante, J. C. Egoville, A. J. Visalli, and D. M. Patel, *J. Pharm. Sci.*, **70**, 167 (1981).

(18) R. P. W. Scott, *J. Chromatogr. Sci.*, **18**, 297 (1980).

(19) R. P. W. Scott and P. Kucera, *J. Chromatogr.*, **149**, 93 (1978).

(20) R. P. W. Scott and P. Kucera, *J. Chromatogr.*, **171**, 37 (1979).

Particle Size and Surface Area Distributions of Pharmaceutical Powders by Microcomputerized Mercury Porosimetry

F. CARLI ˣ **and A. MOTTA**

Received June 1, 1982, from the *Physical Pharmacy Laboratory, Pharmaceutical Research and Development, Farmitalia Carlo Erba, Milan, Italy.* Accepted for publication December 16, 1982.

Abstract □ The Mayer–Stowe theory was applied to derive the particle size distribution of powders of pharmaceutical interest using mercury porosimetry. Particle size data obtained by this approach are fairly comparable with data derived by other, more popular, techniques such as the electrical sensing zone or the air jet sieving methods provided that the experimental value of the mercury–powder contact angle and the state of aggregation of the powder are carefully studied. Furthermore, by applying the Rootare–Prenzlow method a surface area distribution can also be derived from the same porosimetry data used to obtain the particle size distribution. All experiments were carried out with a microcomputerized mercury porosimeter, which allows storage of data during the analysis and a subsequent fast elaboration at the end of the run, with fully printed data on pore size, pore volume, surface area, and particle size of the powder sample.

Keyphrases □ Mercury porosimetry—application to particle size and surface area distributions, pharmaceutical powders □ Particle size—distribution in pharmaceutical powders, determination by mercury porosimetry □ Surface area—particles in pharmaceutical powders, distribution, determination by mercury porosimetry

The particle size of pharmaceutical powders plays a major role both in drug processing and bioavailability. Poorly soluble drugs are often rendered more available for absorption by reducing the particle size, *i.e.*, increasing the surface area (1–3). On the other hand, very important technological processes such as the compression (4) or mixing of powders (5) are strongly influenced by the particle size of the materials used. Not only the powdered drugs, but also the excipients, exhibit many particle size- or surface area-related properties. For example, (a) the lubricating efficacy of materials such as magnesium stearate is strongly influenced by the surface area of the powder (6), and (b) the disintegrating properties of povidone derivatives are dependent on particle size (7).

The growing need for particle size and surface area analyses has led to the introduction of such methods for particle size analysis as microscopic counting (8), the electrical sensing zone method (8, 9), the air jet sieving technique (8, 10), and simple sieving (8). The surface area analysis methods used range from gas adsorption techniques (11, 12) to gas diffusion or permeability (6).

Although mercury porosimetry is used mostly to characterize the porous structure of materials (13, 14), it has been used to determine the surface area (15) and the particle size of powders, both in the coarse region (16, 17) and in the submicron range (18). In pharmaceutics mercury porosimetry has been used almost exclusively to study the porous structure of tablets (19–21), granules (22, 23), or polymeric matrices (24, 25); no attempt has been made to characterize the micromeritics of pharmaceutical powders (26). In this paper, we use mercury porosimetry to measure the particle size and the surface area distributions of powdered drugs and excipients.

THEORETICAL

Particle Size Determination—The mercury porosimetry principle, based on the Washburn model, consists of registering the volume of pores penetrated at each intrusion pressure, which can be easily transformed into pore size *via* the Washburn equation (27) to give a complete pore size distribution. An alternative model describing the penetration of mercury was proposed by Frevel and Kressley (28) and subsequently developed by Mayer and Stowe (29). This treatment defines the solid being pene-

0022-3549/84/0200-0197$01.00/0

© 1984, American Pharmaceutical Association

solutes passing through the column is dependent on the interaction or displacement of the acetonitrile, rather than displacement of hydrogen-bonded water on the silica gel surface. The mass of the three solvents produces a stable and self-activating chromatographic system in equilibrium. The presence of 1% ethanol or methanol, commonly used preservatives in chloroform and methylene chloride, does not adversely affect retention times or resolution of the solutes.

REFERENCES

(1) W. E. Juhl and R. D. Kirchhoefer, *J. Pharm. Sci.*, **69**, 544 (1980).

(2) R. D. Kirchhoefer and W. E. Juhl, *J. Pharm. Sci.*, **69**, 548 (1980).

(3) R. D. Kirchhoefer, J. C. Reepmeyer, and W. E. Juhl, *J. Pharm. Sci.*, **69**, 550 (1980).

(4) R. D. Kirchhoefer, *J. Pharm. Sci.*, **69**, 1188 (1980).

(5) *Pharmacopeal Forum*, **6**(5), 414 (1980).

(6) P. P. Ascione and C. P. Chrekian, *J. Pharm. Sci.*, **64**, 1029 (1975).

(7) R. G. Baum and F. F. Cantwell, *J. Pharm. Sci.*, **67**, 1066 (1978).

(8) P. J. Twitchett, A. E. P. Gorvin, and A. C. Moffat, *J. Chromatogr.*, **120**, 359 (1976).

(9) D. Blair, B. H. Rumack, and R. G. Peterson, *Clin. Chem.*, **24**, 1543 (1978).

(10) R. L. Stevenson and C. A. Burtis, *J. Chromatogr.*, **61**, 253 (1971).

(11) V. D. Gupta, *J. Pharm. Sci.*, **69**, 110 (1980).

(12) V. D. Gupta, *J. Pharm. Sci.*, **69**, 113 (1980).

(13) G. W. Peng, M. A. F. Gadalla, V. Smith, A. Peng, and W. L. Chiou, *J. Pharm. Sci.*, **67**, 710 (1978).

(14) S. L. Ali, *J. Chromatogr.*, **126**, 651 (1976).

(15) H. Bundgaard, *Arch. Pharm. Chem., Sci. Ed.*, **4**, 103 (1976).

(16) C. D. Pfeiffer and J. W. Pankey, *J. Pharm. Sci.*, **71**, 511 (1982).

(17) R. N. Galante, J. C. Egoville, A. J. Visalli, and D. M. Patel, *J. Pharm. Sci.*, **70**, 167 (1981).

(18) R. P. W. Scott, *J. Chromatogr. Sci.*, **18**, 297 (1980).

(19) R. P. W. Scott and P. Kucera, *J. Chromatogr.*, **149**, 93 (1978).

(20) R. P. W. Scott and P. Kucera, *J. Chromatogr.*, **171**, 37 (1979).

Particle Size and Surface Area Distributions of Pharmaceutical Powders by Microcomputerized Mercury Porosimetry

F. CARLI ˣ **and A. MOTTA**

Received June 1, 1982, from the *Physical Pharmacy Laboratory, Pharmaceutical Research and Development, Farmitalia Carlo Erba, Milan, Italy.* Accepted for publication December 16, 1982.

Abstract □ The Mayer–Stowe theory was applied to derive the particle size distribution of powders of pharmaceutical interest using mercury porosimetry. Particle size data obtained by this approach are fairly comparable with data derived by other, more popular, techniques such as the electrical sensing zone or the air jet sieving methods provided that the experimental value of the mercury–powder contact angle and the state of aggregation of the powder are carefully studied. Furthermore, by applying the Rootare–Prenzlow method a surface area distribution can also be derived from the same porosimetry data used to obtain the particle size distribution. All experiments were carried out with a microcomputerized mercury porosimeter, which allows storage of data during the analysis and a subsequent fast elaboration at the end of the run, with fully printed data on pore size, pore volume, surface area, and particle size of the powder sample.

Keyphrases □ Mercury porosimetry—application to particle size and surface area distributions, pharmaceutical powders □ Particle size—distribution in pharmaceutical powders, determination by mercury porosimetry □ Surface area—particles in pharmaceutical powders, distribution, determination by mercury porosimetry

The particle size of pharmaceutical powders plays a major role both in drug processing and bioavailability. Poorly soluble drugs are often rendered more available for absorption by reducing the particle size, *i.e.*, increasing the surface area (1–3). On the other hand, very important technological processes such as the compression (4) or mixing of powders (5) are strongly influenced by the particle size of the materials used. Not only the powdered drugs, but also the excipients, exhibit many particle size- or surface area-related properties. For example, (a) the lubricating efficacy of materials such as magnesium stearate is strongly influenced by the surface area of the powder (6), and (b) the disintegrating properties of povidone derivatives are dependent on particle size (7).

The growing need for particle size and surface area analyses has led to the introduction of such methods for particle size analysis as microscopic counting (8), the electrical sensing zone method (8, 9), the air jet sieving technique (8, 10), and simple sieving (8). The surface area analysis methods used range from gas adsorption techniques (11, 12) to gas diffusion or permeability (6).

Although mercury porosimetry is used mostly to characterize the porous structure of materials (13, 14), it has been used to determine the surface area (15) and the particle size of powders, both in the coarse region (16, 17) and in the submicron range (18). In pharmaceutics mercury porosimetry has been used almost exclusively to study the porous structure of tablets (19–21), granules (22, 23), or polymeric matrices (24, 25); no attempt has been made to characterize the micromeritics of pharmaceutical powders (26). In this paper, we use mercury porosimetry to measure the particle size and the surface area distributions of powdered drugs and excipients.

THEORETICAL

Particle Size Determination—The mercury porosimetry principle, based on the Washburn model, consists of registering the volume of pores penetrated at each intrusion pressure, which can be easily transformed into pore size *via* the Washburn equation (27) to give a complete pore size distribution. An alternative model describing the penetration of mercury was proposed by Frevel and Kressley (28) and subsequently developed by Mayer and Stowe (29). This treatment defines the solid being pene-

0022-3549/84/0200-0197$01.00/0

© 1984, American Pharmaceutical Association

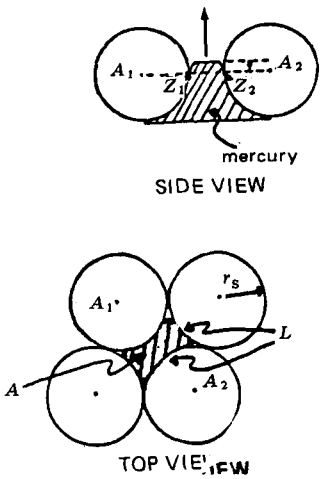

Figure 1—*Mayer–Stowe model for mercury intrusion between spherical particles. Breakthrough pressure (P) = $\gamma(L'/A)/r_s$, where γ is the surface tension of mercury, L′ is a parameter related to the cross-sectional perimeter (L) of mercury, A is the cross-sectional area of mercury at Z_1, Z_2, and r_s is the particle radius.*

trated by mercury as an assembly of spherical particles, packed together, and relates the size of the access opening to the radius of the spherical particles, rather than that of the cylindrical pore as in the case of the Washburn model.

The basic equation of the Mayer–Stowe model is given by:

$$P = \gamma \frac{(L')}{A} \Big/ r_s \qquad \text{(Eq. 1)}$$

where P is the intrusion or "breakthrough" pressure, r_s is the particle radius, L' is a parameter related to the perimeter L of the cross section of mercury intruding the touching spheres, A is the area of the cross section of intruding mercury, and γ is the surface tension of mercury (Fig. 1). The term L'/A is a function of the packing angle of the powder bed and the mercury contact angle. Mayer and Stowe calculated this ratio for all the possible packing angles originated by powder bed porosities in the range of 0.25–0.48 and contact angles from 180° to 100°; L'/A values calculated at 0.48 porosity can be extended to higher porosities, as stressed also by Stanley-Wood (18). Thus, once the correct L'/A value is chosen from the Mayer–Stowe table (29), one is able to directly derive from the experimental intrusion pressure the radius of the spherical particles originating the voids which are penetrated by mercury. At each intrusion pressure the mercury penetration volume is also registered; by expressing the volume as a percentage of the overall penetration volume measured at the end of the run, it is possible to derive a complete particle size distribution on a volume basis (16).

Surface Area Determination—Surface area values are usually derived by mercury porosimetry data assuming that pores are cylindrical (30, 31); at each intrusion pressure the mercury volume registered can be used to obtain a rough evaluation of the surface area of the pore walls by a simple geometrical calculation. An alternative model, based on no geometrical assumption and thus very much more reliable, has been developed by Rootare and Prenzlow (15). Their approach considers the process of mercury penetration from an energy point of view and leads to the following equation describing the work necessary to cover an infinitesimal area dA of a powder surface with mercury:

$$\gamma \cos \vartheta \cdot dA = -P \cdot dV_i \qquad \text{(Eq. 2)}$$

Where γ is the surface tension of mercury, ϑ is the mercury contact angle, dA is an infinitesimal area of powder surface, P is the intrusion pressure, and dV_i is the infinitesimal intrusion volume. The left-hand term of Eq. 2 is the work of immersion of the infinitesimal area dA into mercury and the right-hand term is the work effectively exerted by the mercury porosimeter in the course of the intrusion run.

Integration of Eq. 2 leads to:

$$A = \int dA = -\frac{1}{\gamma \cos \vartheta} \int_{V_0}^{V_{max}} P \cdot dV_i = -\frac{1}{\gamma \cos \vartheta} \int_{0}^{V_{max}} P \cdot dV_i \qquad \text{(Eq. 3)}$$

where A is the powder surface area, V_0 is the intrusion volume registered at $P = 0$ (*i.e.*, is equal to 0), and V_{max} is the final overall volume of mercury intrusion. Equation 3 may be used as a basis not only for calculating a total surface area from mercury porosimetry data, but also a surface area distribution on a particle size basis. In fact, at each intrusion pressure it is possible, on one side, to calculate the partial contribution to the overall value of the integral in Eq. 3 and, on the other side, to calculate from the P value the corresponding particle size value *via* Eq. 1.

EXPERIMENTAL

Materials—The powdered drugs used were indoprofen[1] (an organic weak acid) a morpholine derivative (drug A)[1], and an ergoline derivative (drug B)[1]. The other powders used were barium sulfate[1], cross-linked povidone[2], crystalline lactose[3], microcrystalline cellulose[4], magnesium stearate[1], and fumed silica[5]. All powders were used as received.

Mercury Porosimetry—Particle size and surface area analyses were carried out using a high-pressure mercury porosimeter[6], with intrusion pressures ranging from 1 to 2000 kg/cm^2, and with a low-pressure porosimeter[7], with pressure ranging from 0 to 3.5 kg/cm^2. The porosimeter was connected *via* an interface data logger[8] to a microcomputer[9] and a printer–plotter unit[8].

The powder samples (typical weights ranged from 100 to 300 mg) were introduced as received, in the dry state, into the sample container and then into the low-pressure porosimeter, where they were deaerated. The mercury penetration volume was subsequently registered while the intrusion pressure was increased to atmospheric pressure. The sample container was removed from the low-pressure unit and placed inside the high-pressure porosimeter; mercury penetration volume was registered while intrusion pressure was increased to 2000 kg/cm^2.

Mercury–Powder Contact Angle—Mercury–powder contact angles were measured by means of a wettability tester[10] using the method of Mack (32). Dimensions of the mercury droplets on the surface of a compact prepared with the sample powder were taken after increasing the droplet volume; thus, the derived contact angle can be considered as an advancing one (33). This seems to be the most correct value to be used in intrusion mercury runs (34), especially in loose powder beds, although some uncertainty remains (35). At least 10 replicates were carried out.

Electrical Sensing Zone Method—Particle size analyses were also carried out with an electrical sensing zone apparatus[11]. The suspension liquid used was 0.85% NaCl aqueous solution containing 0.1% surfactant. If necessary, this solution was saturated with the powder under examination. Disaggregation of the sample was further induced by sonicating the suspension. Orifice tubes of different size were used, allowing the determination of particles ≥ 0.6 μm.

Air Jet Sieving Technique—Particle size analyses by the air jet sieving technique were carried out with an air jet sieve[12]. The smallest detectable particle size was 32 μm.

Surface Area Determination by Gas Diffusion—Surface area analyses were carried out using a gas diffusion apparatus[13]. Powder samples were packed into the diffusion cell, and then helium was allowed to flow through the sample. From the rate of gas pressure decay, a surface area value was derived *via* a modified Knudsen equation (36).

Powder Density—The densities of the powders were measured with an air-comparison pycnometer[14].

RESULTS AND DISCUSSION

Mercury intrusion curves for crystalline lactose, microcrystalline cellulose, indoprofen, and magnesium stearate powders are shown in Fig. 2A–D, respectively. The particle size distribution for these powders are given in Figs. 3A–D.

Particle Size Determination—*Lactose*—In Fig. 2A, the mercury intrusion curves into a powdered sample of the widely used diluent crystalline lactose is shown. Curve A (the first mercury intrusion registered) presents a sharp increase in a very low range (0.1–1 kg/cm^2) of

[1] Farmitalia Carlo Erba, Italy.
[2] GAF.
[3] DMV, The Netherlands.
[4] Avicel PH 105, FMC Corp.
[5] Degussa, Germany.
[6] Model 200; Carlo Erba Strumentazione, Italy.
[7] Macropore Unit; Carlo Erba Strumentazione, Italy.
[8] Adcomp, Germany.
[9] Model CBM 4032; Commodore.
[10] Lorentzen-Wettre, Sweden.
[11] Coulter Counter Model TA II, Coulter Electronics, UK.
[12] Alpine, Germany.
[13] Alstan Diffusion Surface Area Meter, Powder Characterization Systems, U.K.
[14] Beckman.

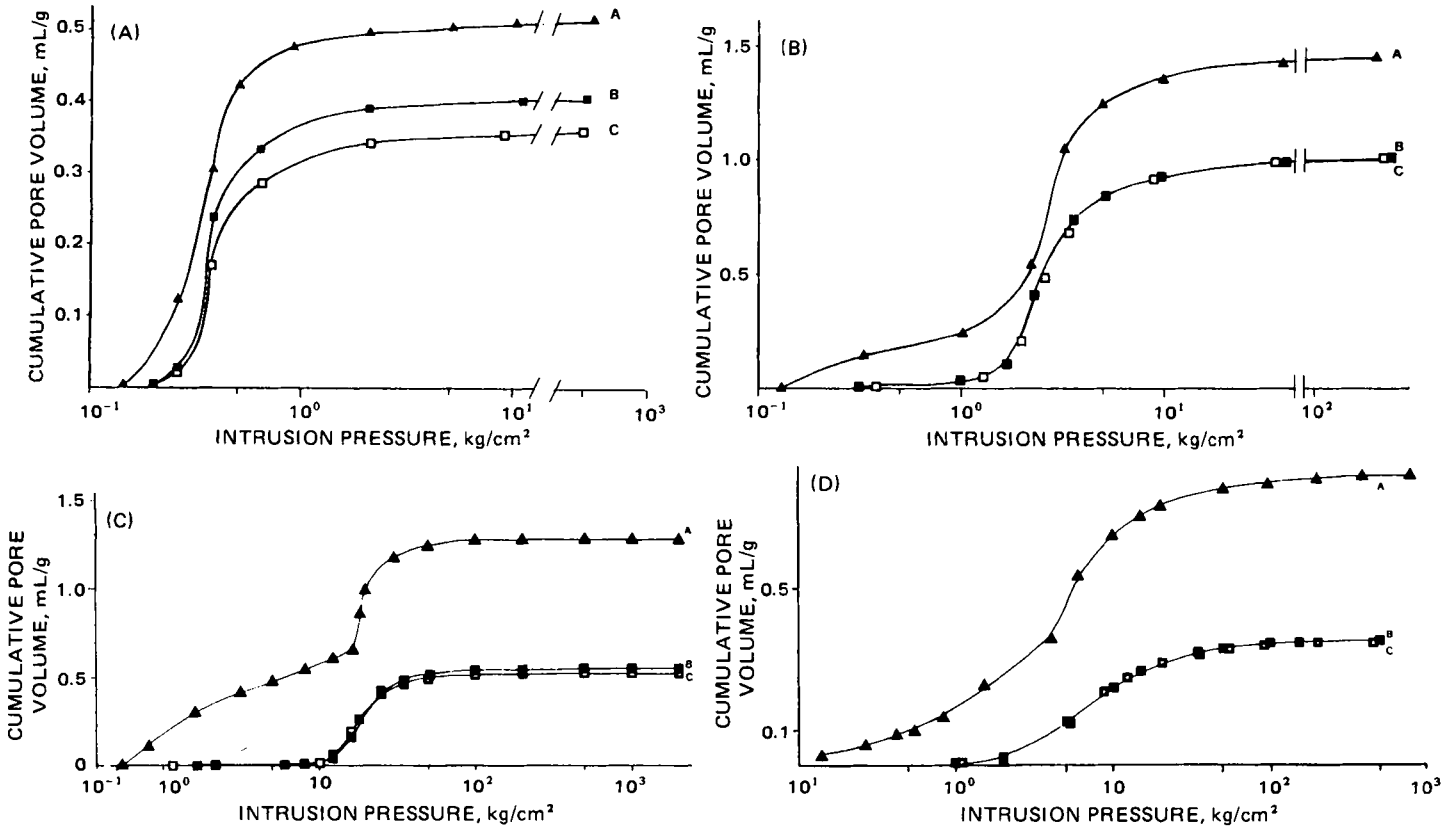

Figure 2—*Mercury intrusion of crystalline lactose (A), microcrystalline cellulose (B), indoprofen (C), and magnesium stearate (D) powders. Key: (▲) first run; (■) second run; (□) third run.*

pressures followed by a constant plateau value, suggesting the presence only of large interparticle voids. From the final overall volume of mercury penetration, the powder bed porosity is calculated by (18):

$$\epsilon = \frac{V_{max}}{V_{max} + 1/d} \qquad \text{(Eq. 4)}$$

where ϵ is the powder bed porosity, V_{max} is the final overall mercury intrusion volume, and d is the density of the powder sample. Once the ϵ value is calculated (in the case of the first run ϵ was 0.44), one can derive the powder bed packing angle σ from the Mayer and Stowe paper (Table 2 of Ref. 29) and subsequently obtain the L'/A value using the σ value and the experimental contact angle (Table 3 of Ref. 29). For lactose, the mercury contact angle was 144°.

The mercury intrusion pressures of Fig. 2A can be transformed into particle size *via* Eq. 1, and the mercury intrusion volumes expressed as percentages of the total intrusion volume. The particle size distribution of the crystalline lactose determined from the first intrusion run is shown in Fig. 3A, curve A. A satisfactory agreement is found with the particle size distribution measured by the air jet sieving technique (curve D, Fig. 3A).

If a second and a third mercury intrusion run are carried out on the same lactose sample after evacuation to extrude the already filled mercury, curves B and C (Fig. 2A) are obtained. Although the shape of these curves is very similar to that of the first run, the final intrusion volume is smaller, probably due to a different packing of the lactose powder particles caused by the first intrusion of mercury or to a partial entrapment of mercury. At any rate, by using the L'/A values derived from the porosities calculated by the second and third intrusion runs (ϵ = 0.38 and ϵ = 0.35, respectively), particle size distributions (curves B and C, Fig. 3A) are obtained which are practically superimposable with the curve derived from the first intrusion run.

Microcrystalline Cellulose—Microcrystalline cellulose is a powder well known for its intraparticle microporosity (37). Thus, it is interesting to study the applicability of the mercury porosimetry technique for particle size determination (based on the interparticle porosity) on this type of powder. Figure 2B shows the mercury intrusion curves into the microcrystalline cellulose powder. For all the intrusion runs, there is only one sharp penetration in a very low and restricted range of pressures (1–10 kg/cm²), which can be reasonably attributed to interparticle void intrusion. In fact, this low pressure range corresponds (*via* the Washburn equation) to a void size range of 8–0.8 μm, whereas the intraparticle pore sizes are <0.003 μm (37), the lowest pore size detectable by the porosimeter.

Thus, it is possible also in this case to apply the Mayer and Stowe approach to derive the particle size distribution of microcrystalline cellulose. The porosity values (0.68 for the first run, 0.60 for the second and third runs) derived from the intrusion curves and the mercury contact angle (145°) were used to obtain the particle size distributions shown in Fig. 3B. There is a good agreement between the mercury porosimetry (curves A, B, and C) and the electrical sensing zone technique (curve D), but this agreement is particularly good for the second and third runs (curves B and C). A tentative explanation may be the presence of a few aggregates in the microcrystalline cellulose powder, which could be eliminated by the first mercury intrusion. This interpretation can be further substantiated by carrying out porosimetry determinations on highly aggregated powders.

Aggregated Powders—In the case of lactose, no particular care was taken for the first or subsequent mercury intrusion runs in order to obtain porosimetry-derived particle size distributions comparable with the air jet sieving. But, particular attention must be paid when powder samples with aggregates are examined and when other reference techniques are used (*e.g.*, the electrical sensing zone method, which requires the dispersion of the sample into a suspension liquid prior to the test). In fact, mercury porosimetry tests are carried out directly on the powder samples in the dry state; consequently, mercury is forced not only between single

Table I—Mercury–Powder Contact Angles

Powder	Mercury Contact Angle
Povidone, cross-linked	154°
Magnesium stearate	152°
Barium sulfate	149°
Indoprofen	147°
Microcrystalline cellulose	145°
Lactose	144°
Morpholine derivative (drug A)	140°
Ergoline derivative (drug B)	140°
Fumed silica	136°

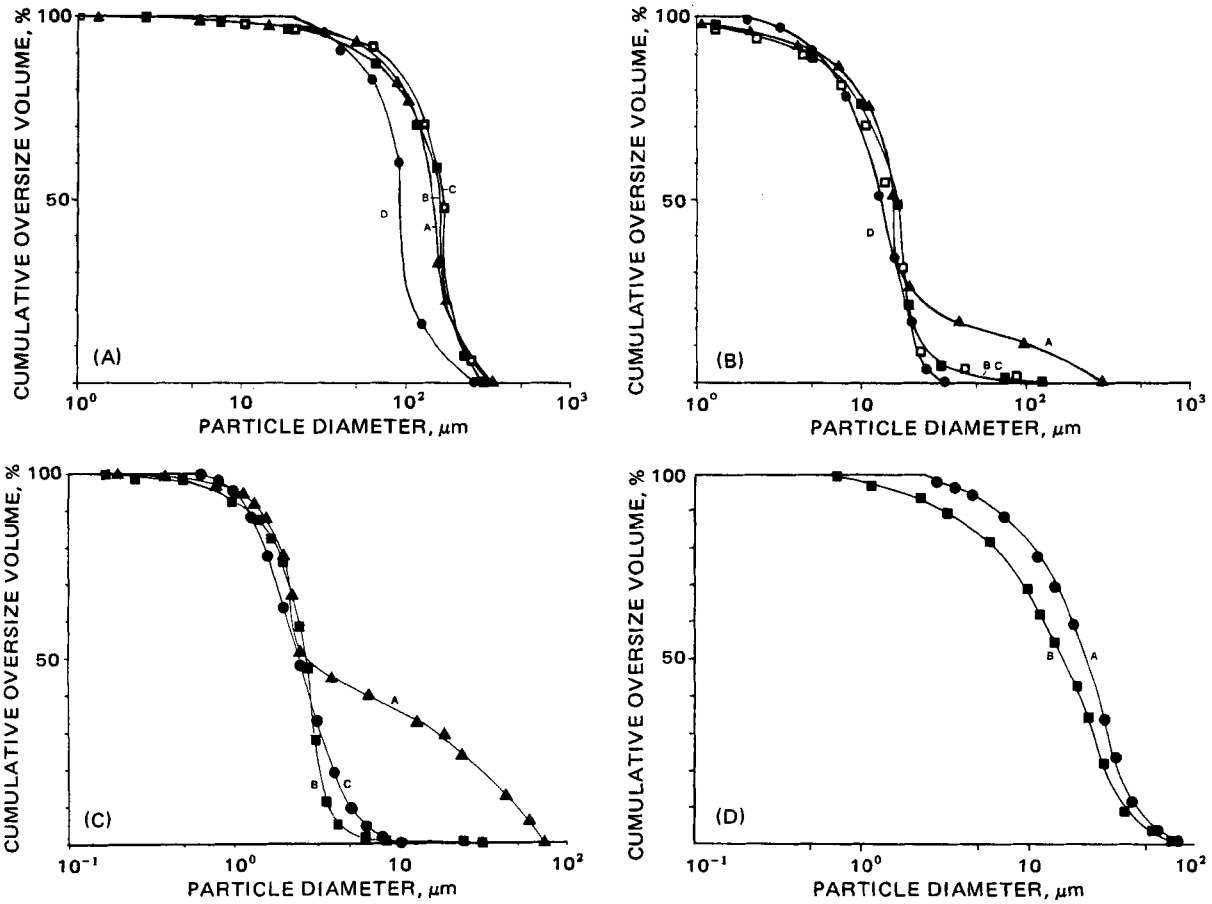

Figure 3—*Particle size distribution of crystalline lactose (A), microcrystalline cellulose (B), indoprofen (C), and magnesium stearate (D) powders. Key: (▲) derived from the first mercury intrusion run; (■) derived from the second intrusion run; (□) derived from the third intrusion run; (●) derived by air jet sieving (A) or electrical sensing zone method (B–D).*

particles, but (if present) also between aggregates and bundles of particles. If this is the case, particle size distributions derived by mercury porosimetry will differ from those derived by the electrical sensing zone technique after dispersion and sonication of the sample.

This point is illustrated by curves A and B in Fig. 2C (mercury intrusion curves) and Fig. 3C (particle size distributions) for the powdered drug indoprofen. The particle size distribution for indoprofen derived by mercury porosimetry (curve A, Fig. 3C) shows the presence of a high percentage of particles >10 μm, which are not detected by the particle counter method (curve C, Fig. 3C). This can be attributed to the presence of large aggregates in the dry indoprofen powder sample, which are eliminated by the dispersion and sonication techniques used prior to the electrical counting. If this interpretation is correct, disaggregation of the powder sample in the case of mercury porosimetry should eliminate the presence of larger particles. This is indeed the case, as shown by curve B in Fig. 3C, which was derived by a second mercury intrusion run (curve B, Fig. 2C) on the same indoprofen sample after evacuation to extrude the already filled mercury. In the first run (curve A, Fig. 2C), at low intrusion pressures (0.1–10-kg/cm^2 range) interaggregate voids are penetrated, whereas at higher pressures (20–50-kg/cm^2 range) both interparticle and intraaggregate penetration takes place, the latter leading to disaggregation of the powder, so that particle size distribution derived by a second mercury intrusion run is practically superimposable with that derived by the electrical sensing zone method. A third mercury intrusion run (curve C, Fig. 2C) showed no further change in the particle size distribution, suggesting that complete disaggregation of the powder samples is achieved after the first run and that no irreversible deformation of particles is caused by mercury intrusion.

Another example of this aggregation effect is given in Fig. 2D, showing porosimetry data for a magnesium stearate powder. In this case also, the second mercury intrusion run (curve B, Fig. 2D) greatly differs from the first run (curve A, Fig. 2D), indicating the presence of aggregates; in fact, if particle size data are derived only from the second mercury intrusion

Table II—Influence of Mercury–Powder Contact Angle on Particle Size Measurement

Powder	Particle Size at 50% Level, μm: Porosimetry, Calc. by Standard Contact Angle[a]	Porosimetry, Calc. by Experimental Contact Angle	Reference Technique[b]
Indoprofen	2.1	2.7 (147°)	2.5
Magnesium stearate	12.0	17.0 (152°)	21.0
Barium sulfate	1.7	2.1 (149°)	2.1

[a] 130°. [b] Electrical sensing zone.

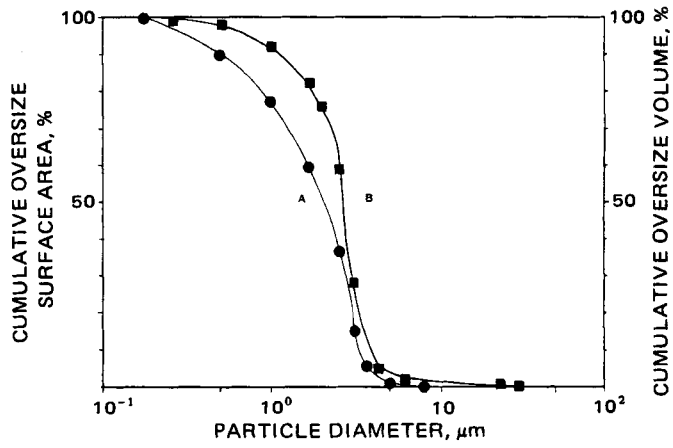

Figure 4—*Surface area distribution of indoprofen powder. Key: (●) surface area distribution derived from mercury intrusion, second run; (▲) particle size distribution derived from mercury intrusion, second run.*

Table III—Precision of Particle Size Analysis by Mercury Porosimetry: Reproducibility of Cumulative Oversize Volume Percentage Distribution Data of Morpholinic Derivative Drug A

Mercury Intrusion Pressure, kg/cm²	Particle Size, μm	Sample I, %	Sample II, %	Sample III, %	Sample IV, %	Sample V, %	Sample VI, %	Mean	*CV*, %
5	7.3	9.6	11.0	11.3	10.9	10.5	9.7	10.5	6.7
8	4.6	35.5	38.9	36.8	38.3	36.6	35.7	37.0	3.7
10	3.7	59.3	63.6	61.1	62.8	60.7	60.1	61.3	2.7
15	2.5	82.7	84.4	85.3	86.4	84.9	84.5	84.7	1.4
25	1.5	95.2	95.9	95.4	95.6	94.9	94.2	95.2	0.6

run (curve B, Fig. 3D) one can obtain a particle size distribution very similar to that derived by the electrical sensing zone method (curve A, Fig. 3D).

Influence of the Mercury–Powder Contact Angle—In previous papers showing particle size distributions derived by mercury porosimetry, standard contact angles of 130° (16, 18) or 140° (17) were used. The need for an experimentally measured value for each powder tested is illustrated in Table I, showing the large range of contact angle values found for a miscellaneous series of powders of pharmaceutical interest: from 154° for cross-linked povidone to 126° for fumed silica. Mercury contact angles influence the derived particle size data, as the value of the term L'/A in Eq. 2 is a function also of the contact angle itself (29). Table II stresses this point, showing that agreement between particle sizes at the 50% level measured by different techniques is improved by employing the experimentally measured contact angle instead of a standard value.

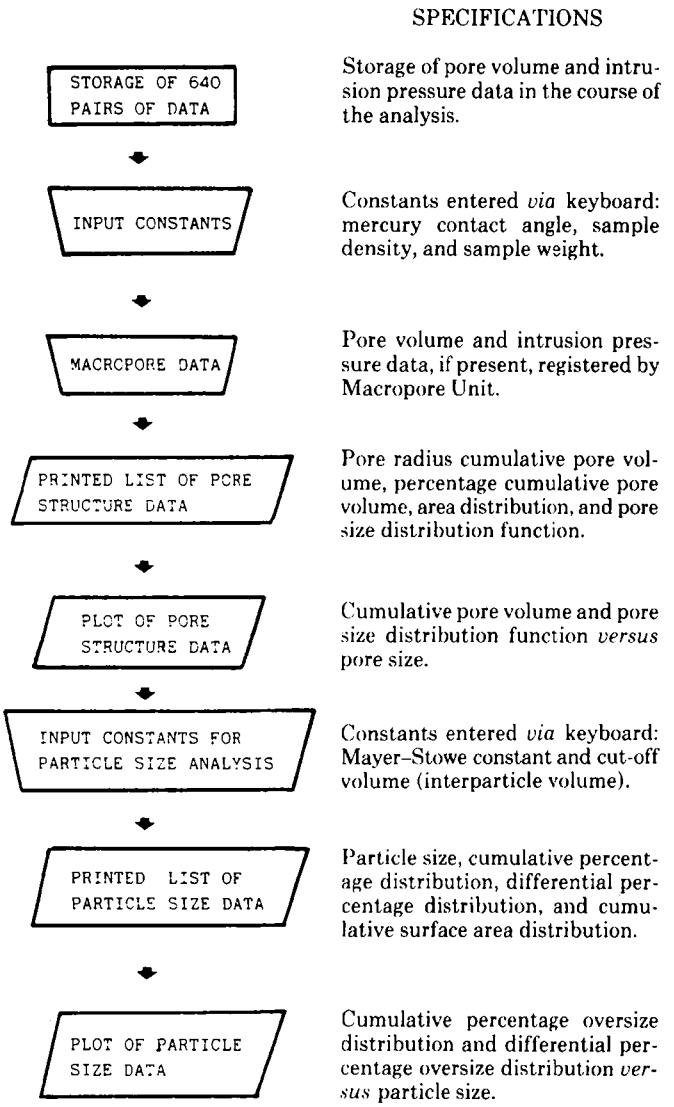

Scheme I—Flow diagram of microcomputer program for pore structure, surface area, and particle size analysis by mercury porosimetry.

Precision of the Method—Once the accuracy of the particle size distribution data derived by mercury porosimetry is optimized by taking into account the aggregation and contact angle effects, the precision of the method can be checked by carrying out many analyses on the same powder sample. Table III shows cumulative oversize volume percentage data of porosimetry analyses on samples of the morpholinic derivative (drug A). The data showed a very good reproducibility over the whole intrusion pressure range examined. The *CV* at any intrusion pressure is ≤3–6%, quite comparable with that usually found for a very reproducible method such as the electrical counting technique (typical *CV* of electrical counting data are usually <5–7%).

Surface Area Distribution Analysis—As shown in the theoretical considerations, at each intrusion pressure it is possible to derive a surface area value *via* Eq. 3. If this calculation is carried out over the whole intrusion pressure range and the surface area data are plotted against the particle sizes derived from the intrusion pressures, a surface area distribution on a particle size basis is obtained.

Figure 4 shows surface area distribution data (curve A) for the indoprofen powder, derived from curve B of Fig. 2C; the total surface area value is 3.38 m²/g. It is interesting to compare the surface area distribution (curve A) with the particle size distribution also reported in the same plot (curve B): the shape of the two curves differs quite notably in the small size range, indicating that smaller particles contribute much more to the overall surface area than to the volume distribution. For example, 24% (on a volume basis) of particles <2.0 μm originate 50% of the surface area, or 7% (by volume) of particles <1.0 μm originate 21% of the surface area.

As already outlined in the theoretical considerations, no geometrical assumption has to be made on the shape of the particles. In the electrical sensing zone method, surface area values are not experimentally measured, but simply calculated from the particle sizes assuming particle sphericity. From data in Table IV it appears quite evident that the geometrical approach can give only a rough estimate of the actual surface area. This observation is reinforced by comparing the total surface area values derived by porosimetry and electrical counting with the values found with another independent method such as the gas diffusion technique. As shown in Table IV, there is a fairly satisfactory agreement between porosimetry and gas diffusion, whereas electrical sensing zone data are lower. The particularly low surface area value derived by electrical counting for drug B is due to the presence of a large number of particles smaller than the minimum size detectable by this technique.

Microcomputer Program—The porosimeter is connected *via* an interface unit to a microcomputer and a printer–plotter. In the course of the analysis the microcomputer can store up to 640 pairs of data of intrusion pressures and mercury penetration volumes. At the end of the run, calculations are carried out as shown in the flow-chart presented in Scheme I. The main outputs of the program are: (*a*) printed lists of pore

Table IV—Comparison Between Mercury Porosimetry and Other Techniques of Surface Area Analysis

Powder	Specific Surface Area, m²/g: Porosimetry	Electrical Sensing Zone Method	Gas Diffusion
Indoprofen	3.38	2.13	2.93
Ergolinic derivative (drug B)	5.10	0.72	5.49
Magnesium stearate	1.48	0.40	1.80
Povidone, cross-linked	0.55	—[a]	0.84

[a] Not measured due to the swelling characteristics of the material.

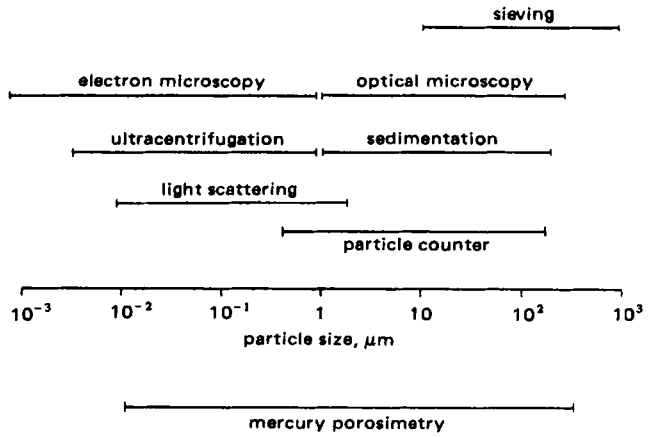

Figure 5—*Range of particle size measurement by different techniques.*

structure data, (*b*) plots of cumulative pore volume and pore size distribution functions, (*c*) printed lists of particle size and surface area analyses, and (*d*) plots of percentage cumulative and differential particle size distributions.

The program can be applied not only to powders with no intraparticle pores (as usually is the case with pharmaceutical powders), but also to porous powders. In fact the operator, after the pore structure data are fully printed and plotted, may decide to proceed to the particle size calculation. To do this, the operator must introduce, *via* the keyboard, the values of the Mayer–Stowe parameter and the "cut off" volume, *i.e.*, the found total interparticle void volume, which has to be distinguished from the intraparticle pore volume (18).

CONCLUSIONS

Mercury porosimetry can be a valuable method for deriving particle size distributions of pharmaceutical powders. Once the possible aggregation of the sample has been eliminated and the mercury contact angle has been measured, very good correlation is found between particle size data derived by mercury porosimetry and by other standard techniques. The basic advantages of the mercury porosimetry technique can be summarized as follows:

1. No particular treatment of the powdered samples is required. Powders are examined as received, in the dry state; this leads to a reduction in operator fatigue and time. Furthermore, possible damage or modification of the physical state of the sample caused by any treatment prior to the test, such as sonication, is ruled out.

2. As the powders are examined in the dry state, no limitation or trouble is posed by the solubility or swelling characteristics of the material. Highly soluble or swellable excipients (lactose, starch, powdered surfactants, *etc.*) can be analyzed easily.

3. A very wide range of particle sizes can be measured (Fig. 5). The upper particle size limit is given by the minimum intrusion pressure that can be exerted on the sample, usually given by the hydrostatic pressure of the mercury column. For example, for a mercury contact angle of 140° and a powder bed porosity of 0.36, the largest measurable particle size is 485 μm. The lower particle size limit is given by the maximum intrusion pressure which can be exerted by the porosimeter. For a maximum pressure of 2000 kg/cm^2, a mercury contact angle of 140°, and a powder bed porosity of 0.36, the smallest measurable particle size is 0.032 μm. This means that submicron powders can be analyzed with the same technique used for coarse powders, a major advantage over all other existing methods.

4. A surface area distribution on a particle size basis can be derived by the same mercury porosimetry analysis, requiring no additional experiment or apparatus. Furthermore, the surface area measurement is based on no geometrical assumption about the shape of the particles, allowing the derivation of an effective surface area comparable with data obtained by other experimental methods.

On the other hand, among the minor disadvantages of the technique, we should mention: (*a*) the possible difficulty in completely disaggregating some powder samples (although in the 30 powder samples we have examined thus far, this was never the case), (*b*) the assumption, only for the particle size derivation, that particles are spherical, as considered by the Mayer–Stowe model, and (*c*) the fact that particle size distribution data can be expressed only on a volume basis and not on a number basis. These minor limitations are furthermore reduced if we consider that practically all the existing particle size analysis methods, including the electrical sensing zone method or light scattering (8), make some assumptions on the particle geometry and that the volume or mass distribution is considered the most informative data for particle sizes of pharmaceutical powders. It must be stressed that particle sizes measured by mercury porosimetry are only indirectly derived from the data of interparticle void penetration, by assuming well-defined particle packing systems. This may pose severe problems with powder samples whose packing behavior (*e.g.*, needle-shaped particles or anomalous flow properties) cannot be interpreted by the classical theory.

On the whole, the advantages of the technique clearly outnumber the disadvantages, offering to workers in the physical pharmacy and pharmaceutical technology areas a new method of analyzing the particle size and the surface area distributions of powders. Furthermore, extension and application of the method to the qualitative or quantitative assessment of the degree of aggregation of powders caused by any process, such as micronization, is possible.

REFERENCES

(1) N. Watari, M. Hanano, and N. Kameniwa, *Chem. Pharm. Bull.*, **28,** 2221 (1980).

(2) N. Kameniwa, N. Watari, and H. Iijima, *Chem. Pharm. Bull.*, **26,** 2603 (1978).

(3) B. F. Johnson and J. O'Grady, *Br. J. Clin. Pharmacol.*, **5,** 465 (1978).

(4) J. T. Fell and J. M. Newton, *J. Pharm. Sci.*, **60,** 1866 (1971).

(5) N. A. Orr, Particle Size Analysis Conference, Loughborough, England, 1981.

(6) A. W. Hölzer and J. Syögren, *Int. J. Pharm.*, **2,** 145 (1979).

(7) Proceedings of the Symposium "Influenza Degli Eccipienti Sulla Cessione del Farmaco," BASF, Milan, 1979.

(8) T. Allen, "Particle Size Measurement," 2nd ed., Chapman and Hall, London, 1970.

(9) L. J. Beaubien and A. J. Vanderwielen, *J. Pharm. Sci.*, **69,** 651 (1980).

(10) A. E. Butcher and T. M. Jones, *J. Pharm. Pharmacol.*, 245, 1P (1972).

(11) P. V. Allen, P. D. Rahn, A. C. Sarapu, and A. J. Vanderwielen, *J. Pharm. Sci.*, **67,** 1087 (1978).

(12) C. F. Lerk, G. K. Bolhuis, and S. S. Smedema, *Pharm. Acta Helv.*, **52,** 33 (1977).

(13) S. M. Brown and E. W. Lard, *Powder Technol.*, **9,** 187 (1974).

(14) A. A. Liabastre and C. Orr, *J. Colloid Interface Sci.*, **64,** 1 (1978).

(15) H. M. Rootare and C. F. Prenzlow, *J. Phys. Chem.*, **71,** 2733 (1967).

(16) C. Orr, *Powder Technol.*, **3,** 117 (1969/70).

(17) M. Svata and Z. Zabranky, *Powder Technol.*, **3,** 296 (1969/70).

(18) N. G. Stanley-Wood, *Analyst*, **104,** 97 (1979).

(19) D. Sixsmith, *J. Pharm. Pharmacol.*, **29,** 82 (1977).

(20) H. Gucluyildiz, G. S. Banker, and G. E. Peck, *J. Pharm. Sci.*, **66,** 407 (1977).

(21) F. Carli, I. Colombo, L. Simioni, and R. Bianchini, *J. Pharm. Pharmacol.*, **33,** 129 (1981).

(22) W. D. Opankule and M. S. Spring, *J. Pharm. Pharmacol.*, **28,** 508 (1976).

(23) W. D. Opankule and M. S. Spring, *J. Pharm. Pharmacol.*, **28,** 806 (1976).

(24) R. C. Rowe, P. H. Elworthy, and D. Ganderton, *J. Pharm. Pharmacol.*, **25S,** 12 P (1973).

(25) F. Carli and L. Simioni, *Int. J. Pharm. Tech. Prod. Mfg.*, **2,** 23 (1981).

(26) P. J. Dees and J. P. Polderman, *Powder Technol.*, **29,** 187 (1981).

(27) E. W. Washburn, *Proc. Natl. Acad. Sci. USA*, **7,** 115 (1921).

(28) L. K. Frevel and L. J. Kressley, *Anal. Chem.*, **35,** 1492 (1963).

(29) R. P. Mayer and R. A. Stowe, *J. Colloid Sci.*, **20,** 893 (1965).

(30) L. G. Joiner, E. P. Barrett, and R. Skold, *J. Am. Chem. Soc.*, **73,** 3155 (1951).

(31) A. J. Goodsel, *Powder Technol.*, **9,** 191 (1974).

(32) G. L. Mack, *J. Phys. Chem.*, **40,** 159 (1936).

(33) R. E. Johnson and R. H. Dettre, "Surface Colloid Science," vol. 2, Wiley, New York, N.Y., 1969.

(34) S. Lowell and J. E. Shields, *J. Colloid. Interface Sci.*, **83**, 273 (1981).
(35) R. J. Good and R. S. Mikhail, *Powder Technol.*, **29**, 53 (1981).
(36) T. Allen and N. G. Stanley-Wood, *Powder Technol.*, **3**, 227 (1970).
(37) K. Marshall and D. Sixsmith, *Drug Dev. Commun.*, **1**, 51 (1974).

ACKNOWLEDGMENTS

Presented in part at the Particle Size Analysis Conference in Loughborough, UK (1981) and at the British Technology Conference in London, England (1982).

The authors thank M. Ulivieri for the electrical sensing zone measurements.

Liposome Disposition *In Vivo* VI: Delivery to the Lung

R. M. ABRA *, C. ANTHONY HUNT *[x], and D. T. LAU ‡

Received October 20, 1982 from the **School of Pharmacy* and ‡*Animal Care Facility, University of California, San Francisco, CA 94143.* Accepted for publication January 20, 1983.

Abstract □ The effect of negatively charged liposome components and vesicle size on the time course and dose dependency of liposome disposition in mice was studied with a view to optimizing liposome delivery to the lung. The disposition of large multilamellar liposomes was followed using ^{125}I-labeled *p*-hydroxybenzamidine phosphatidyl ethanolamine. Of the three negatively charged liposome compositions studied (phosphatidyl choline–X–cholesterol–α-tocopherol, molar ratio: 4:1:5:0.1; X = phosphatidyl serine, dipalmitoyl phosphatidic acid, or phosphatidyl glycerol), phosphatidyl serine liposomes resulted in the greatest accumulation in lungs. Lung levels decreased up to 95 h postdose, at which time 6% of the liposome dose present at 2 h still remained. The disposition of phosphatidyl serine-containing liposomes was independent of dose for the range 0.04–21 μmol/animal. When liposomes containing phosphatidyl choline were prepared using a variety of extrusion and dialysis conditions, a strong link between liposome size and lung accumulation was revealed. A maximum lung accumulation of 30.9% of the administered dose was achieved with no detectable gross pathological lung lesions up to 24 h postdose.

Keyphrases □ Liposomes—multilamellar, phosphatidyl serine, disposition *in vivo*, delivery to the lung, mice □ Disposition—multilamellar liposomes, *in vivo*, delivery to the lung, mice, phosphatidyl serine □ Phosphatidyl serine—multilamellar liposome disposition *in vivo*, delivery to the lung, mice

Liposomes may act as drug carriers (1, 2) but some degree of target specificity is necessary to maximize the therapeutic index of the drug. Intravenously administered liposomes generally become associated with organs of the reticuloendothelial system, mainly the liver and spleen (3, 4).

The lungs, because of their susceptibility to disease, *e.g.*, metastatic cancer (5), are a suitable target organ for attempts to localize drugs. Liposome preparations in common use generally do not accumulate in the lung to any significant extent after intravenous administration (6, 7). It is known, however, that liposome doses containing vesicles of ≥1-μm diameter exhibit improved localization in the lungs compared with smaller diameter preparations (8–10). This effect has been attributed to simple mechanical trapping in the capillary bed of the lungs (9). Liposomes bearing either positive (11) or negative (6, 10) surface charge accumulate in the lungs to a greater extent than neutral liposomes of similar size. However, there is some evidence that positively charged liposomes containing stearylamine may be toxic *in vivo* (12). Attempts have been made to deliver liposomes to the lungs *via* routes other than a distant intravenous site, *e.g.*, the ear vein of rabbits (13) and intratracheal instillation (14). Such approaches can have only specialized applications.

We have examined the effects of negatively charged liposome components and vesicle size on the time course and dose dependency of liposome disposition with a view to optimizing liposome delivery to the lungs. These results will be utilized for directing antitumor drugs to the lungs.

EXPERIMENTAL

Chemicals—Purified egg yolk phosphatidyl choline and phosphatidyl glycerol were prepared as previously described (15). Phosphatidyl serine[1], sodium dipalmitoyl phosphatidate[2], cholesterol[2], and α-tocopherol[2] were chromatographic grade. The method of Szoka and Mayhew (16) was used to synthesize the ^{125}I-labeled *p*-hydroxybenzamidine phosphatidyl ethanolamine (45 mCi/mg), subsequently referred to as the ^{125}I-marker. All other chemicals were at least reagent grade. The phosphate-buffered saline (pH 7.4) contained 92 mM sodium chloride, 43 mM anhydrous dibasic sodium phosphate, 11 mM monobasic sodium phosphate monohydrate, 100 USP U of penicillin, and 100 μg of streptomycin/mL. All buffer-containing solutions were routinely filtered through 0.22-μm pore size filters[3]. Dipalmitoyl phosphatidic acid was prepared by chloroform extraction of the sodium phosphatidate in 0.4 M HCl in 20% (v/v) methanolic aqueous solution.

Preparation of Liposomes—Liposomes were prepared as described previously (4). Three lipid compositions were used: (A) phosphatidyl choline, dipalmitoyl phosphatidic acid, cholesterol, and α-tocopherol; (B) phosphatidyl choline, phosphatidyl serine, cholesterol, and α-tocopherol; and (C) phosphatidyl choline, phosphatidyl glycerol, cholesterol, and α-tocopherol. In each case the molar ratio was 4:1:5:0.1. Sufficient lipid together with ~0.05 μCi of ^{125}I-marker per experimental animal was dried and suspended in buffer by mechanical agitation, yielding large multilamellar liposomes. In most cases these liposomes were subsequently extruded through polycarbonate membranes[4] having 8-, 5-, 3-, 2-, and 1-μm diameter pore sizes to generate populations having different mean diameters (17).

Liposomes were dialyzed at 4°C in the dark against frequent changes of buffer, for ~2 d. Dialysis was carried out in 1-mL dialysis cells fitted with 25-mm polycarbonate membranes[5] with a variety of pore sizes (specified below) to remove traces of dialyzable iodine-125 and some liposomes of smaller diameter than the membrane pores (17).

The final total lipid concentration was estimated by phosphorus assay (18) of extracted samples (19) and then corrected for the presence of non-phosphorus-containing lipids. Vesicle diameters were examed by electron microscopy following negative staining (4).

[1] Avanti Biochemicals Inc., Birmingham, Ala.
[2] Sigma Chemical Co., St. Louis, Mo.
[3] Millipore Corp., Bedford, Mass.
[4] Bio-Rad Labs, Richmond, Calif.
[5] Nucleopore, Bio-Rad Labs, Richmond, Calif.

0022-3549/84/0200-0203$01.00/0
© 1984, American Pharmaceutical Association

(34) S. Lowell and J. E. Shields, *J. Colloid. Interface Sci.*, **83**, 273 (1981).
(35) R. J. Good and R. S. Mikhail, *Powder Technol.*, **29**, 53 (1981).
(36) T. Allen and N. G. Stanley-Wood, *Powder Technol.*, **3**, 227 (1970).
(37) K. Marshall and D. Sixsmith, *Drug Dev. Commun.*, **1**, 51 (1974).

ACKNOWLEDGMENTS

Presented in part at the Particle Size Analysis Conference in Loughborough, UK (1981) and at the British Technology Conference in London, England (1982).

The authors thank M. Ulivieri for the electrical sensing zone measurements.

Liposome Disposition *In Vivo* VI: Delivery to the Lung

R. M. ABRA *, C. ANTHONY HUNT *[x], and D. T. LAU [‡]

Received October 20, 1982 from the **School of Pharmacy* and [‡]*Animal Care Facility, University of California, San Francisco, CA 94143.* Accepted for publication January 20, 1983.

Abstract □ The effect of negatively charged liposome components and vesicle size on the time course and dose dependency of liposome disposition in mice was studied with a view to optimizing liposome delivery to the lung. The disposition of large multilamellar liposomes was followed using ^{125}I-labeled *p*-hydroxybenzamidine phosphatidyl ethanolamine. Of the three negatively charged liposome compositions studied (phosphatidyl choline–X–cholesterol–α-tocopherol, molar ratio: 4:1:5:0.1; X = phosphatidyl serine, dipalmitoyl phosphatidic acid, or phosphatidyl glycerol), phosphatidyl serine liposomes resulted in the greatest accumulation in lungs. Lung levels decreased up to 95 h postdose, at which time 6% of the liposome dose present at 2 h still remained. The disposition of phosphatidyl serine-containing liposomes was independent of dose for the range 0.04–21 μmol/animal. When liposomes containing phosphatidyl choline were prepared using a variety of extrusion and dialysis conditions, a strong link between liposome size and lung accumulation was revealed. A maximum lung accumulation of 30.9% of the administered dose was achieved with no detectable gross pathological lung lesions up to 24 h postdose.

Keyphrases □ Liposomes—multilamellar, phosphatidyl serine, disposition *in vivo*, delivery to the lung, mice □ Disposition—multilamellar liposomes, *in vivo*, delivery to the lung, mice, phosphatidyl serine □ Phosphatidyl serine—multilamellar liposome disposition *in vivo*, delivery to the lung, mice

Liposomes may act as drug carriers (1, 2) but some degree of target specificity is necessary to maximize the therapeutic index of the drug. Intravenously administered liposomes generally become associated with organs of the reticuloendothelial system, mainly the liver and spleen (3, 4).

The lungs, because of their susceptibility to disease, *e.g.*, metastatic cancer (5), are a suitable target organ for attempts to localize drugs. Liposome preparations in common use generally do not accumulate in the lung to any significant extent after intravenous administration (6, 7). It is known, however, that liposome doses containing vesicles of ≥1-μm diameter exhibit improved localization in the lungs compared with smaller diameter preparations (8–10). This effect has been attributed to simple mechanical trapping in the capillary bed of the lungs (9). Liposomes bearing either positive (11) or negative (6, 10) surface charge accumulate in the lungs to a greater extent than neutral liposomes of similar size. However, there is some evidence that positively charged liposomes containing stearylamine may be toxic *in vivo* (12). Attempts have been made to deliver liposomes to the lungs *via* routes other than a distant intravenous site, *e.g.*, the ear vein of rabbits (13) and intratracheal instillation (14). Such approaches can have only specialized applications.

We have examined the effects of negatively charged liposome components and vesicle size on the time course and dose dependency of liposome disposition with a view to optimizing liposome delivery to the lungs. These results will be utilized for directing antitumor drugs to the lungs.

EXPERIMENTAL

Chemicals—Purified egg yolk phosphatidyl choline and phosphatidyl glycerol were prepared as previously described (15). Phosphatidyl serine[1], sodium dipalmitoyl phosphatidate[2], cholesterol[2], and α-tocopherol[2] were chromatographic grade. The method of Szoka and Mayhew (16) was used to synthesize the ^{125}I-labeled *p*-hydroxybenzamidine phosphatidyl ethanolamine (45 mCi/mg), subsequently referred to as the ^{125}I-marker. All other chemicals were at least reagent grade. The phosphate-buffered saline (pH 7.4) contained 92 mM sodium chloride, 43 mM anhydrous dibasic sodium phosphate, 11 mM monobasic sodium phosphate monohydrate, 100 USP U of penicillin, and 100 μg of streptomycin/mL. All buffer-containing solutions were routinely filtered through 0.22-μm pore size filters[3]. Dipalmitoyl phosphatidic acid was prepared by chloroform extraction of the sodium phosphatidate in 0.4 M HCl in 20% (v/v) methanolic aqueous solution.

Preparation of Liposomes—Liposomes were prepared as described previously (4). Three lipid compositions were used: (A) phosphatidyl choline, dipalmitoyl phosphatidic acid, cholesterol, and α-tocopherol; (B) phosphatidyl choline, phosphatidyl serine, cholesterol, and α-tocopherol; and (C) phosphatidyl choline, phosphatidyl glycerol, cholesterol, and α-tocopherol. In each case the molar ratio was 4:1:5:0.1. Sufficient lipid together with ~0.05 μCi of ^{125}I-marker per experimental animal was dried and suspended in buffer by mechanical agitation, yielding large multilamellar liposomes. In most cases these liposomes were subsequently extruded through polycarbonate membranes[4] having 8-, 5-, 3-, 2-, and 1-μm diameter pore sizes to generate populations having different mean diameters (17).

Liposomes were dialyzed at 4°C in the dark against frequent changes of buffer, for ~2 d. Dialysis was carried out in 1-mL dialysis cells fitted with 25-mm polycarbonate membranes[5] with a variety of pore sizes (specified below) to remove traces of dialyzable iodine-125 and some liposomes of smaller diameter than the membrane pores (17).

The final total lipid concentration was estimated by phosphorus assay (18) of extracted samples (19) and then corrected for the presence of non-phosphorus-containing lipids. Vesicle diameters were examed by electron microscopy following negative staining (4).

[1] Avanti Biochemicals Inc., Birmingham, Ala.
[2] Sigma Chemical Co., St. Louis, Mo.
[3] Millipore Corp., Bedford, Mass.
[4] Bio-Rad Labs, Richmond, Calif.
[5] Nucleopore, Bio-Rad Labs, Richmond, Calif.

0022-3549/84/0200-0203$01.00/0
© 1984, American Pharmaceutical Association

Table I—Effect of Extrusion Pore Size and Dialysis Treatment on the Various Liposome Batches

Batch	Extrusion Pore Size, μm	Dialysis Pore Size, μm	Total Lipid, μmol/mL	Loss of Liposome Material on Dialysis, %[a]
1	8	5.0	18.8	54
2	8	0.8	27.1	—
3	5	3.0	19.8	42
4	5	0.8	31.0	—
5	3	2.0	22.0	12
6	3	0.8	25.5	—
7	2	1.0	28.6	0
8	2	0.8	27.3	—
9	1	0.8	18.4	26
10	1	0.2	25.0	—

[a] Expressed as total radioactivity remaining after dialysis *versus* larger pore size membrane divided by total radioactivity remaining after dialysis *versus* smaller pore size membrane.

***In Vivo* Disposition Studies**—All experiments used male ICR mice[6] weighing 19–23 g. At the end of an experimental period, mice were lightly anesthetized with ether, and a 1-mL blood sample was rapidly removed from the jugular vein into an heparinized syringe. Livers, spleens, and lungs were subsequently removed, weighed, and stored at −20°C together with the remaining carcass. The bladder and contents were discarded prior to storage. Four experiments were performed. The mean weight of lungs sampled during these experiments was 0.16 ± 0.03 g (n = 83).

Experiment 1—To assess the effect of liposomal lipid composition on disposition, three batches of liposomes (A, B, and C) containing the ^{125}I-marker were prepared. Each batch was divided, and one-half extruded through an 8.0-μm pore size polycarbonate membrane. All six doses thus prepared were dialyzed *versus* 0.8-μm pore size polycarbonate membranes. Final total lipid concentrations were: (A) 32.5 μmol/mL, extruded 28 μmol/mL; (B) 45 μmol/mL, extruded 45.5 μmol/mL; and (C) 43.5 μmol/mL, extruded 36 μmol/mL. Groups of three mice each received 0.2-mL iv injections of liposome suspension *via* a tail vein and were sacrificed 4 h later.

Experiment 2—To establish the time course for the disposition of composition B liposomes, liposomes were prepared at 115 μmol of total lipid/mL and dialyzed *versus* 0.8-μm pore size polycarbonate membranes. Mice each received 0.2-mL iv injections, and groups of three mice were killed after 2, 5, 9.2, 24, and 94.8 h.

Experiment 3—To study the dose dependency of composition B liposomes, liposomes were prepared as described above at 105 μmol of total lipid/mL. Doses of 105, 33.5, 17, 13, and 0.2 μmol/mL were generated by serial dilution with buffer. Groups of three mice each received 0.2-mL iv injections and were sacrificed 4 h later.

Experiment 4—The effects of extrusion pore size and dialysis treatment on disposition were investigated for composition B liposomes. A batch of the liposomes was prepared as described above at a concentration of ~25 μmol/mL. The liposomes were then extruded twice at each pore size through a sequential series of 8.0-, 5.0-, 3.0-, 2.0-, and 1.0-μm pore size polycarbonate membranes. After each extrusion a sample was retained and, in this way, five batches of liposomes of different size were created. Each batch was then divided in half and dialyzed as follows: 8.0-μm pore size extruded, dialyzed *versus* either 5.0- or 0.8-μm pore size membranes; 5.0-μm pore size extruded, dialyzed *versus* either 3.0- or 0.8-μm membranes; 3.0-μm pore size extruded, dialyzed *versus* either 2.0- or 0.8-μm membranes; 2.0-μm pore size extruded, dialyzed *versus* either 1.0- or 0.8-μm membranes; and 1.0-μm pore size extruded, dialyzed *versus* either 0.8- or 0.2-μm membranes. Final dose concentrations are given in Table I. Each of 10 groups of three mice received intravenous doses of one of these preparations and were sacrificed 3 h later.

Analysis of Total Organ Radioactivity—Whole liver, spleen, lungs, 0.05-mL ^{125}I-labeled doses, and ~0.8 mL of blood were assayed for radioactivity by placing them in vials and counting in a γ-radiation counter[7]. Carcasses were cut into conveniently sized pieces and then assayed as above. Values for sample (cpm) were converted to percent of administered dose and a mean was calculated for the three animals in each group. Carcass values were corrected for blood volume remaining after sampling (4). Total radioactivity remaining *in vivo* was estimated by summation of the liver, spleen, total blood volume, lungs, and carcass values.

[6] Simonsen Laboratories Inc., Gilroy, Calif.

[7] Gamma 300; Beckman Instruments Inc., Mountain View, Calif.

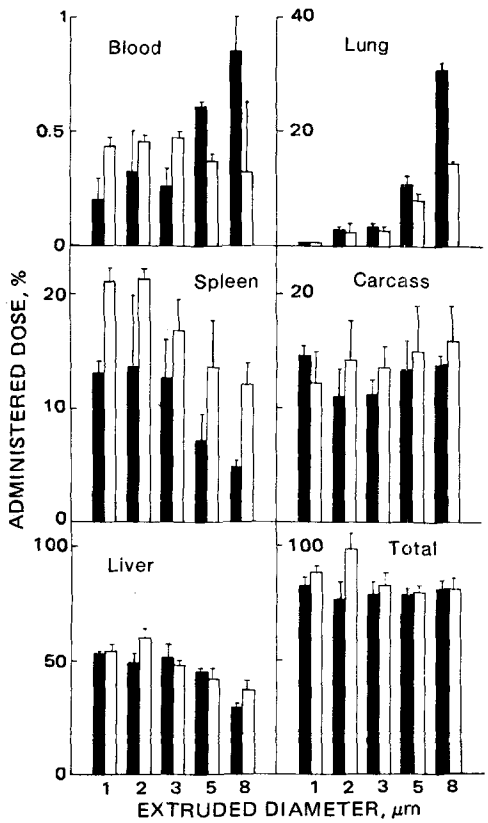

Figure 1—*Percentages of the administered dose (iodine-125) in blood (per milliliter), liver, lungs, spleen, carcass, and total remaining* in vivo *3 h after administration of composition B liposomes containing the ^{125}I-marker and prepared according to Table I. The histograms represent the mean of three mice for each extrusion pore diameter. Shaded bars represent liposomes dialyzed* versus *a membrane of pore size close to their extrusion pore size; clear bars represent liposomes dialyzed* versus *a membrane of pore size much smaller than their extrusion size. The vertical lines show one* SD.

Pathology—To examine the effect of liposomes on lung structure, groups of three 24-g mice[8] were injected intravenously with doses of 20.4 μmol of total lipid/animal (846 μmol/kg) of composition B liposomes. Three untreated mice served as controls. Two doses were prepared: one (lung-accumulating) was extruded through 8.0-μm pore size membranes and dialyzed against a 5.0-μm pore size membrane and the other (non-lung-accumulating) was extruded at 1.0-μm pore size and dialyzed against a 0.8-μm pore size membrane. Groups of mice were killed 1, 5, and 24 h postdose; their lungs were removed, washed in saline, and fixed overnight in 10% formalin. The lung samples were then dehydrated, embedded in paraffin wax, sectioned, and stained with hematoxylin and eosin (20). Sections from coded animals were examined under the light microscope for signs of damage; the nature of the treatment group was unknown at the time of examination.

RESULTS

Effects of Liposomal Lipid Composition on Disposition—The results of this experiment are given in Table II. All three compositions gave similar overall patterns of disposition, with the majority of the radiolabel residing in liver and carcass. Liposomes containing phosphatidyl serine accumulated in the lungs to a level four times that of phosphatidic acid-containing liposomes. Phosphatidyl glycerol-containing liposomes gave an intermediate level. This shift in disposition towards the lungs was at the expense of spleen and blood levels. All three doses were equally stable as judged by total radioactivity remaining *in vivo*. The extrusion treatment had no effect on radiolabel disposition. Electron micrographs taken of negatively stained liposomes failed to detect any differences in size distribution between the doses, but highlighted their extremely heterogeneous nature. Liposomes containing phosphatidyl serine (composition B) were chosen for all further experiments.

[8] CD-1; Charles River Breeding Laboratories, Wilmington, Mass.

Table II—Liposome Disposition *In Vivo* 4 h Postdose

Composition (mole ratio)[a]	Dose[b], μmol/animal	Disposition, % of Administered Dose[c]				
		Blood[d]	Liver	Spleen	Lungs	Total *In Vivo*[e]
PC/PA/CH/α-T	6.5 (U)	4.0 ± 2.1	23.2 ± 3.6	12.2 ± 4.4	4.8 ± 0.5	73.8 ± 5.3
(4:1:5:0.1)	5.6 (E)	4.0 ± 2.0	25.0 ± 6.6	12.9 ± 3.2	4.6 ± 0.9	83.4 ± 4.4
PC/PS/CH/α-T	9.0 (U)	1.0 ± 0.2	25.6 ± 1.4	9.3 ± 1.9	18.1 ± 2.1	81.0 ± 3.4
(4:1:5:0.1)	9.1 (E)	1.2 ± 0.3	30.3 ± 3.6	9.7 ± 1.2	16.9 ± 1.0	86.6 ± 1.1
PC/PG/CH/α-T	8.7 (U)	5.7 ± 2.9	31.7 ± 4.0	11.1 ± 0.7	9.5 ± 2.9	89.3 ± 5.4
(4:1:5:0.1)	7.2 (E)	3.6 ± 1.9	34.7 ± 4.4	16.5 ± 4.1	7.8 ± 1.5	94.0 ± 4.5

[a] Key: (PC) phosphatidyl choline; (CH) cholesterol; (α-T) α-tocopherol; (PA) dipalmitoyl phosphatidic acid; (PS) phosphatidyl serine; (PG) phosphatidyl glycerol. [b] Liposomes were prepared and dialyzed without extrusion (U) or were extruded through an 8-μm pore size membrane prior to dialysis. Quantitation was *via* the ^{125}I-marker. [c] Mean ± *SD*. [d] Per milliliter. [e] Calculated by summation of values for total blood volume, whole liver, spleen, lungs, and carcass.

Time Course for Disposition of Composition B Liposomes—Results are displayed in Table III. All organ levels of radioactivity were maximal at 2 h postdose and declined continuously up to 94.8 h postdose. The values for total radioactivity remaining *in vivo* reflected a net loss of radioactive label during this period.

Dose Dependency—Table IV gives the results for composition B liposomes. In the dose range of 0.04 to 21 μmol of total lipid/animal (1.7–871 μmol/kg) there was no apparent dose effect for blood, liver, or lung 4 h after dosing. However, there was a consistent increase in the percent associated with spleen for increasing dose. The *in vivo* stability of the dose (as estimated by total radioactivity remaining *in vivo*) was unaffected by dose.

Effect of Extrusion Pore Size and Dialysis Treatment on Disposition of Composition B Liposomes—Increasing the extrusion pore size led to an increase in accumulation of the radiolabel in the lungs and a decrease in the spleen (Fig. 1). Putative liposome size had little effect on levels in the blood, liver, carcass, or on total radioactivity remaining *in vivo*. The disposition of doses dialyzed *versus* membranes of a pore size close to that through which they were extruded (doses 1, 3, 5, 7, and 9; Table I) was markedly higher in the lungs than those doses dialyzed *versus* small pore size membranes (doses 2, 4, 6, 8, and 10; Table I). The reverse effect was noted in the spleen. A maximum lung accumulation of 30.9% of the administered dose (193.1 %/g wet weight) was achieved with 8.0-μm pore size extruded liposomes subsequently dialyzed *versus* a 5.0-μm pore size membrane. This contrasted with 0.5% of the dose (3.1%/g wet weight) for 1.0-μm pore size extruded liposomes dialyzed *versus* a 0.2-μm membrane.

Electron microscopic examination of these doses revealed, once again, a great heterogeneity of the vesicle size. In the fields examined, the largest diameter of a liposome noted for dose 1 (Table I) was 9.5 μm; for dose 3, 1.3 μm; for dose 5, 5.7 μm; and for dose 10, 2.0 μm.

Pathology—Light microscopy of stained lung sections from mice receiving one of the two liposome doses (20.4 μmol of total lipid either lung-accumulating or non-lung-accumulating) and the control group revealed no significant pathological features either within or between groups.

DISCUSSION

We have utilized a liposomal lipid label (the ^{125}I-marker) in order to follow the disposition of liposome doses *in vivo*. Abra *et al.* (7) have demonstrated that the use of such a label gives results equivalent to those obtained when inulin is used as an aqeuous space marker at times <5 h postdose. An important caveat is that blood levels are elevated for the lipid marker due to lipid exchange. We may therefore reasonably assume that radioactivity detected in organs other than blood, at least at 3–5 h postdose, for the protocols used here are indicative of the presence of liposomal lipid in the form of liposomes. We further assume, based on prior results (7), that we are observing a delivery of both liposomes and their contents at these early times. The question of subsequent liposome stability *in vivo*, which may be vital in the tailoring of liposomal properties to the pharmacokinetics of the encapsulated drug, cannot be answered with this kind of label. The degree to which tissue levels of the ^{125}I-marker reflect intact liposomes, free ^{125}I-marker, or its metabolites after ~5 h postdose is unknown.

It is immediately apparent that, of the negatively charged liposome compositions tested, composition B (phosphatidyl choline, phosphatidyl serine, cholesterol, α-tocopherol in the molar ratio of 4:1:5:0.1) gave the highest liposome levels in the lungs for a given preparation protocol. Fidler *et al.* (10) also found that phosphatidyl serine-containing liposomes accumulated in the lungs to a greater extent than phosphatidic acid-, ganglioside-, or dicetylphosphate-containing vesicles. The available data do not allow us to specify a mechanism accounting for this lung accumulation. Liposomes prepared identically but of different composition may in fact have different mean effective diameters. Phosphatidyl serine-containing liposomes may thus, on average, be larger than other negatively charged liposomes even though we were unable to detect such differences owing to the heterogeneity of the preparations. There may also be a specific, but unknown, interaction between phosphatidyl serine and the lung vasculature.

In the absence of any lung pathology, it seems unlikely that the larger liposomes actually form classical microemboli that block capillaries. It is more likely that liposomes bind to the capillary walls without completely blocking blood flow through that capillary. This binding may be dependent on two related variables, the transit time of liposomes through lung capillaries and the binding affinity between liposomes and lung capillary endothelial cells. As diameter increases, transit time (in the absence of binding) decreases. As diameter increases, the area available for endothelial cell contact increases and so the apparent binding constant (between liposomes and endothelial cells) increases per liposome. Thus, for some, but not all compositions, a critical diameter may be reached where prolonged attachment to endothelial cells will occur without capillary blockage. If this description is reasonable, then it follows that this critical diameter is smallest when the negative phospholipid is phosphatidyl serine, all other variables being constant.

There is no evidence that phosphatidyl serine-containing liposomes are toxic at doses of up to 20.4 μmol/mouse (864 μmol/kg). The LD_{50} of intravenously administered liposomes composed solely of phospholipids and cholesterol has been estimated to be ~18 mmol/kg (21, 22).

The time course of accumulation and retention of the ^{125}I-marker in the lungs is such that only 6% of the dose present in the lungs at 2 h remains by 95 h postdose. This remnant represents some 6% of the total liposome dose remaining *in vivo* at 95 h. We can not say if the ^{125}I-marker remains associated with intact liposomes at that time. Our assumption is that by 95 h considerable loss to the tissues has occurred. The fate of liposomes and their contents delivered to the lung can include binding and prolonged erosion, lysis and release of contents extracellularly, uptake by the local tissues *via* endocytosis, and uptake of leaked liposomal contents by local diffusion or pinocytosis.

The only evidence for dose dependency is that spleen levels of the ^{125}I-marker increase with increasing dose, consistent with previous studies of dose dependency using a similar dose range of smaller lipo-

Table III—*In Vivo* Disposition of Composition B Liposomes[a]

Time Postdose, h	Disposition, % of Administered Dose[c]				
	Blood[b]	Liver	Spleen	Lungs	Total *In Vivo*[d]
2	1.3 ± 0.2	24.2 ± 1.8	10.3 ± 1.7	16.5 ± 6.3	70.7 ± 7.4
5	0.9 ± 0.2	23.2 ± 2.8	8.4 ± 1.8	15.3 ± 1.7	65.6 ± 4.4
9.2	0.3 ± 0.01	22.4 ± 2.3	7.7 ± 2.3	12.1 ± 0.5	52.5 ± 1.0
24	0.4 ± 0.01	19.7 ± 1.2	6.1 ± 1.3	7.5 ± 0.8	44.0 ± 0.4
94.8	0.1 ± 0.02	9.6 ± 0.5	2.5 ± 0.4	1.0 ± 0.02	17.4 ± 0.4

[a] Mice received 23.0 μmol of total lipid each. Liposomes were unextruded, but were dialyzed against a 0.8-μm pore size membrane. Quantitation was *via* the ^{125}I-marker. [b] Per milliliter. [c] Mean ± *SD*. [d] Calculated by summation of values for total blood volume, whole liver, spleen, lungs, and carcass.

Table IV—Effect of Dose on *In Vivo* Levels of Composition B Liposomes 4 h Postdose [a]

Liposome Dose μmol of total lipid/animal	Disposition, % of Administered Dose [c]				
	Blood [b]	Liver	Spleen	Lungs	Total *In Vivo* [d]
21	1.3 ± 0.5	24.2 ± 2.8	8.2 ± 1.6	23.5 ± 7.3	80.7 ± 15.5
6.7	1.2 ± 0,2	24.5 ± 1.3	7.1 ± 0.6	18.7 ± 1.1	69.8 ± 3.0
3.4	1.1 ± 0.4	25.8 ± 3.9	5.6 ± 1.6	15.0 ± 1.5	68.8 ± 2.3
2.6	1.3 ± 0.2	25.6 ± 1.8	4.4 ± 1.0	16.4 ± 1.9	67.4 ± 3.0
0.04	1.7 ± 2.0	31.7 ± 7.4	2.6 ± 0.9	15.8 ± 3.2	77.5 ± 4.5

[a] Mice received intravenous doses of liposomes that were unextruded, but dialyzed against a 0.8-μm pore size membrane. Quantitation was *via* the ^{125}I-marker. [b] Per milliliter. [c] Mean ± *SD*. [d] Calculated by summation of values for total blood volume, whole liver, spleen, lungs, and carcass.

somes of composition A (4). The absence of a significant dose effect in other organs may be due, in part, to the presence in our doses of a whole range of liposome sizes which are able to interact with different organ binding sites (23).

The delivery of liposomes to the lungs clearly depends on liposome size, and in the absence of more definitive data, this may be due in some part to a requirement for microembolism formation to arrest liposomes in the lung capillaries (9, 10, 24). The composition data discussed above offer an alternative mechanism. Those liposome doses having a size distribution weighted toward the larger vesicles by dialysis against large pore size membranes (indicated by substantial losses of lipid during dialysis, see Table I) accumulate in the lung particularly well. Yet there is no evidence that such trapping in lung at doses of 846 μmol/kg results in any gross pathological damage. Our maximum delivery to lung, 30.9% of the administered dose or 193.1%/g wet weight, which was achieved with liposomes prepared by protocol 1 (Table I) represents the highest published figure for lung disposition that we are aware of.

We intend to utilize these techniques in the future to deliver antitumor drugs to a lung tumor model.

REFERENCES

(1) D. Papahadjopoulos, *Ann. Rep. Med. Chem.*, **14**, 250 (1979).

(2) G. Gregoriadis, *Nature (London)*, **283**, 814 (1980).

(3) H. K. Kimelberg, T. F. Tracy, S. M. Biddlecome, and R. S. Bourke, *Cancer Res.*, **36**, 2949 (1976).

(4) R. M. Abra and C. A. Hunt, *Biochim. Biophys. Acta*, **666**, 493 (1981).

(5) I. J. Fidler, D. M. Gersten, and I. R. Hart, *Adv. Cancer Res.*, **28**, 149 (1978).

(6) H. K. Kimelberg, *Biochim. Biophys. Acta*, **448**, 531 (1976).

(7) R. M. Abra, H. Schreier, and F. C. Szoka, *Res. Commun. Chem. Pathol. Pharmacol.*, **37**, 199 (1982).

(8) P. Sharma, D. A. Tyrrell, and B. E. Ryman, *Biochem. Soc. Trans.*, **5**, 1146 (1977).

(9) C. A. Hunt, Y. M. Rustum, E. Mayhew, and D. Papahadjopoulos, *Drug Metab. Dispos.*, **7**, 124 (1979).

(10) I. J. Fidler, A. Raz, W. E. Fogler, R. Kirsh, P. Bugelski, and G. Poste, *Cancer Res.*, **40**, 4460 (1980).

(11) M. M. Jonah, E. A. Cerruy, and Y. E. Rahman, *Biochim. Biophys. Acta*, **401**, 336 (1975).

(12) D. H. Adams, G. Joyce, V. J. Richardson, B. E. Ryman, and H. M. Wisniewski, *J. Neuro. Sci.*, **31**, 173 (1977).

(13) R. D. Zachman and F. H. C. Tsao, *Pediatr. Res.*, **14**, 24 (1980).

(14) R. L. Juliano and H. N. McCullough, *J. Pharmacol. Exp. Ther.*, **214**, 381 (1980).

(15) E. Mayhew, Y. M. Rustum, F. Szoka, and D. Papahadjopoulos, *Cancer Treat. Rep.*, **63**, 1923 (1979).

(16) F. Szoka and E. M. Mayhew, *Chem. Phys. Lipids*, in press.

(17) M. E. Bosworth, C. A. Hunt, and D. Pratt, *J. Pharm. Sci.*, **71**, 806 (1982).

(18) G. R. Bartlett, *J. Biol. Chem.*, **234**, 466 (1959).

(19) J. Folch, M. Lees, and G. H. Sloane-Stanley, *J. Biol. Chem.*, **226**, 497 (1957).

(20) C. F. A. Culling and W. L. Dunn, "Handbook of Histopathological and Histochemical Techniques," Butterworths, London, 1979.

(21) R. L. Juliano, *Trends Pharmacol. Sci.*, **2**, 39 (1981).

(22) F. Olson, E. Mayhew, D. Maslow, Y. Rustum, and F. Szoka, *Eur. J. Cancer*, **18**, 167 (1982).

(23) R. M. Abra and C. A. Hunt, *Res. Commun. Chem. Pathol. Pharmacol.*, **36**, 17 (1982).

(24) M. Kanke, G. H. Simmons, D. L. Weiss, B. A. Bivins, and P. P. DeLuca, *J. Pharm. Sci.*, **69**, 755 (1980).

ACKNOWLEDGMENTS

This work was supported by NIH grants GM-24612, GM-26691 and an Individual Investigator Research Award from the University of California Academic Senate Committee on Research to R.M.A.

We thank Dr. F. Szoka for kindly donating lipid samples; the members of the Drug Delivery Research Group for helpful discussions; and L. Carlson, E. Williams, and C. Abes for help in preparing this manuscript.

Improved Gas Chromatographic Determination of Diltiazem and Deacetyldiltiazem in Human Plasma

J. P. CLOZEL, G. CAILLÉ ˣ, Y. TAEYMANS, P. THÉROUX, P. BIRON, and J. G. BESNER

Received May 7, 1982, from the *Department of Pharmacology, School of Medicine, University of Montreal, Montreal, Quebec H3C 3J7, Canada.* Accepted for publication December 16, 1982.

Abstract □ This study describes an improved, simple, and specific gas chromatographic method for the determination of diltiazem (I) and deacetyldiltiazem (II) in human plasma using loxapine (III) as an internal standard. After extraction at pH 7.5 with anhydrous ether–ethyl acetate (1:1), II was silylated with *N*-methyl-*N*-(trimethylsilyl)trifluoroacetamide. The gas chromatograph, equipped with an electron-capture detector, allowed measurements as low as 2 ng/mL for I and 3 ng/mL for II. Recoveries of III, I, and II were 95, 85, and 79%, respectively. There were no interferences with endogenous substances in plasma or with common cardiovascular drugs. This method was used to measure plasma concentrations of two patients who received 20 mg iv of I. The areas under the curve for these two patients were 275 and 273 ng·h/mL, respectively. The apparent volumes of distribution were 493.6 and 288.6 L, and the elimination half-lives were 4.70 and 2.73 h. No deacetyldiltiazem could be detected in the blood after the single-dose diltiazem administration.

Keyphrases □ Diltiazem—human plasma, GC with electron-capture detection, concurrent assay with deacetyldiltiazem □ Deacetyldiltiazem—human plasma, GC with electron-capture detection, concurrent assay with diltiazem

Diltiazem hydrochloride, *cis*-(+)-3-acetoxy-5-(2-dimethylaminoethyl) -2,3-dihydro-2- (4-methoxyphenyl)-1,5-benzothiazepin-4(5*H*)-one hydrochloride (I), is a new calcium antagonist used in the treatment of clinical manifestations of variant angina (1–5). Several methods have been used to determine I and its metabolites in biological media including spectrophotometry (8), gas chromatography (GC) (7), and more recently HPLC (6). The latter technique (6) enables the determination of I and six of its metabolites in urine, but UV detection is not sensitive enough for pharmacokinetic studies involving the determination of I and its principal metabolite, deacetyldiltiazem (II), in human plasma. On the other hand, a GC method involving the use of a nitrogen-sensitive detector has been described (7). To achieve adequate sensitivity while maintaining high reproducibility and specificity, a GC technique using electron-capture detection with ^{63}Ni was chosen. The present study describes an assay for I and II in plasma, and some pharmacokinetic parameters obtained after intravenous administrations of 20 mg of I in two patients are given.

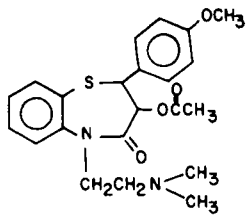

DILTIAZEM
I

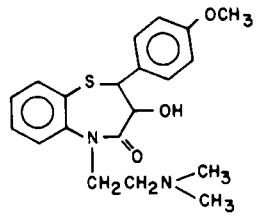

DEACETYLDILTIAZEM
II

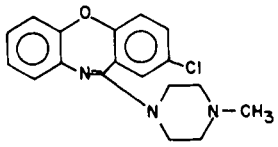

LOXAPINE
III

EXPERIMENTAL

Equipment—A gas chromatograph[1], equipped with an ^{63}Ni electron-capture detector and a computer for peak area integration[2], was used. The chromatographic column was a coiled glass tube, 2 m × 2-mm i.d., packed with 3% OV 7 on GasChrom Q, 80–100 mesh. The following conditions were used: oven temperature, 245°C; injection port temperature, 300°C; detector temperature, 300°C; argon–methane carrier gas at 60 mL/min.

Reagents and Chemicals—All solvents were certified grade. The hydrochloride salts of diltiazem (I), deacetyldiltiazem (II), and loxapine (III) were used. Standard solutions of I, II, and III were prepared in distilled water at concentrations of 0.5 mg%.

Assay Procedure—To 1 mL of plasma, contained in a culture tube, were added 100 μL of internal standard solution (500 ng) and 3 mL of phosphate buffer, pH 7.5. This mixture was vortexed for 30 s. Following the addition of 6 mL of 50% ether in ethyl acetate, the mixture was agitated for 10 min on a reciprocating shaker and then centrifuged at 800×*g*. The aqueous phase was discarded, and the organic phase was transferred to a second culture tube and dried under a nitrogen stream. *N*-Methyl-*N*-(trimethylsilyl)trifluoroacetamide (25 μL) and benzene (100 μL) were

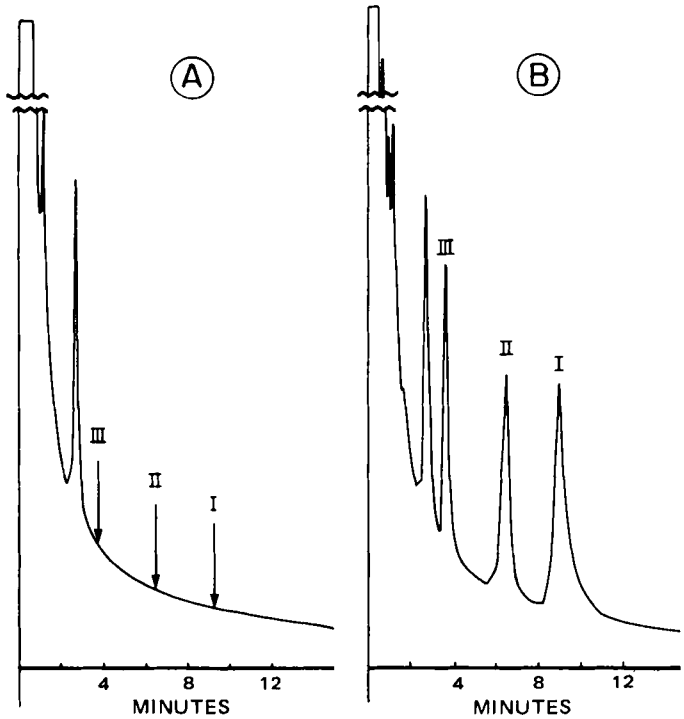

Figure 1—*Typical chromatograms of plasma extracts. Key: (A) blank; (B) containing I, II, and III.*

[1] Hewlett Packard model 5700.
[2] Hewlett Packard model 3300.

0022-3549/84/0200-0207$01.00/0
© 1984, American Pharmaceutical Association

Table I—Peak Height Ratios of Diltiazem (I) and Deacetyldiltiazem (II) in Plasma

Diltiazem			Deacetyldiltiazem		
Amount in Plasma, ng/mL	Peak Height Ratio	*CV*, %	Amount in Plasma, ng/mL	Peak Height Ratio	*CV*, %
10	0.049	3.9	7.5	0.031	8.5
20	0.100	4.9	15	0.065	5.4
50	0.245	4.1	30	0.126	2.6
100	0.490	4.5	60	0.242	5.3
200	1.000	2.0	120	0.497	3.0
400	2.020	3.1	240	0.985	3.5

added, and the tube was sealed and heated at 70°C for 1 h for the silylation of II. The solution was dried again under a nitrogen stream, 50 μL of methanol was added, and 5 μL of the resulting solution was injected into the chromatograph.

Standard samples were prepared by spiking human plasma with increasing concentrations of I (10, 25, 50, 100, 200, and 400 ng/mL) and of II (7.5, 15, 30, 60, 120, and 240 ng/mL). Four spiked samples were measured for each concentration, and calibration curves were obtained by plotting the ratios of the peak areas of I and II to the area of the internal standard *versus* the concentrations of I and II. Plasma recoveries of I and II were determined by comparing peak areas obtained by direct injection of I or silylated II with those obtained after the extraction procedure.

Clinical Study—Two fully informed patients with unstable angina received a bolus 20-mg iv dose of I. Blood samples were withdrawn into heparinized tubes at 0, 5, 10, 15, 20, 30, 45, 60, 90, 160, 180, 240, 360, and 480 min after administration. The blood samples were immediately centrifuged at 800×*g* and the plasma was removed and kept at −14°C until analysis (within 2 weeks).

Pharmacokinetic Data—Areas under the curve (AUC) were calculated by the trapezoidal rule:

$$AUC_{0\to t} = \sum_{i=1}^{n} 0.5(C_1 + C_2)\Delta t \qquad \text{(Eq. 1)}$$

The total area under the curve (AUC_∞) has been obtained by adding C_p/β:

$$AUC_\infty = \sum_{i=1}^{n} 0.5(C_1 + C_2)\Delta t + C_{p,n}/\beta \qquad \text{(Eq. 2)}$$

where C_p is the plasma concentration at 8 h and β the elimination constant calculated by logarithmic linear regression. The elimination half-life ($t_{1/2}$) and the apparent volume of distribution (Vd) were calculated by the following:

$$t_{1/2} = \frac{0.693}{\beta} \qquad \text{(Eq. 3)}$$

and

$$Vd = \frac{D_{iv}}{AUC \cdot \beta} \qquad \text{(Eq. 4)}$$

where D_{iv} is the intravenous dose.

RESULTS AND DISCUSSION

Assay Method—Before silylation, I and II had the same retention time in the assay. After silylation of II, the retention times for III, II, and I were 3.70, 6.55, and 9.15 min, respectively. Typical chromatograms of a plasma blank and a plasma extract spiked with the three standards are presented in Fig. 1. The extent of II silylation was 95%.

The calibration curves were linear throughout the range of the concentrations measured in this study ($r^2 = 0.9998$ for I and $r^2 = 0.9999$ for II). The equations of the calibration curves for I and II were, respectively, $y = 0.005x - 0.013$ and $y = 0.0041x + 0.00137$, where y is the peak height ratio and x is the plasma concentration of the drug.

The analytical recoveries of I, II, and III were 95, 79, and 85%, respectively. The sensitivity of the method was 2 ng/mL for I and 3 ng/mL for II; amounts as low as 0.5 ng/mL of I or II could be detected. Table I shows the peak area ratios and their coefficients of variation (*CV*) for the spiked samples.

Digoxin, propranolol, procainamide, nitroglycerin, isosorbide dinitrate, furosemide, flurazepam, and diazepam did not interfere with the plasma assay. Even if the frozen plasma was analyzed after 4–8 weeks, there were no interference peaks. The present study shows that the use of an electron-capture technique permitted a large increase in the sensitivity of the assay. Rovei *et al.*, with a nitrogen–phosphorus detector, could measure 10 ng/mL with 2 mL of plasma (5); in the present method, 2 ng/mL of I could be measured with 1 mL of plasma. Moreover, the plasma extraction with anhydrous ether–ethyl acetate permitted recoveries of 85 and 79%, respectively, for I and II, compared with 70 and 55% with the hexane-extraction method of Rovei *et al.* This improvement in recovery permits determination of lower concentrations of these compounds.

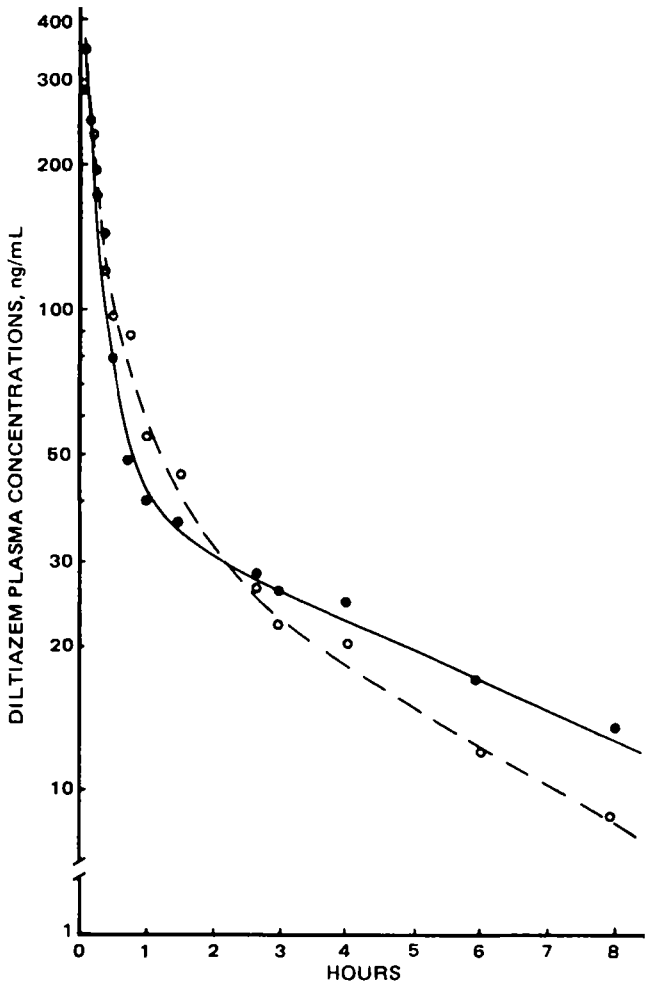

Figure 2—*Diltiazem plasma concentrations in two patients after a 20-mg iv dose. Key: (●) patient 1; (○) patient 2.*

Clinical Study—Figure 2 shows the plasma concentrations of I in two patients who were injected intravenously with 20 mg. Five minutes after the administration, the plasma concentrations were 289 and 344 ng/mL in the two patients. The distribution phase in both patients was rapid, and after 1 h the plasma concentrations were 40 and 59 ng/mL. The elimination half-lives were 4.70 and 2.73 h ($\beta = 0.1873$ and 0.2535, respectively). The areas under the curve were 275 and 273 ng·h/mL, and the apparent volumes of distribution were 493.6 and 288.6 L. The clearance values were 72.71 and 73.24 L/h, respectively.

The results are difficult to compare with those of previous investigations using oral administration. Rovei *et al.* found a half-life of 6 h after oral administration of 120 mg of the drug (7), and Kinney observed half-lives of 4.1, 5.1, and 5.6 h, with oral doses of 60, 90, and 120 mg of I, respectively (8). In the latter study, the AUC obtained after an oral dose of 40 mg was 514 ng·h/mL; in the present study a mean AUC of 274 ng·h/mL was found after a 20-mg iv dose. According to these results, the absolute bioavailability of I can be estimated by the following:

$$\text{Absolute bioavailability (\%)} = \frac{AUC_{po}/D_{po}}{AUC_{iv}/D_{iv}} \times 100 \qquad \text{(Eq. 5)}$$

By substituting into the equation the experimental values obtained for each term in the aforementioned studies, the absolute bioavailability of diltiazem is (514/50)/(274/20) = 62.5%.

No deacetyldiltiazem was detected in the plasma of the two patients after a 20-mg iv administration of I. More detailed studies are required for a better understanding of pharmacokinetics of diltiazem.

In summary, the present study has shown that the use of GC with electron-capture detection improves, to a large extent, the sensitivity of the previous HPLC and GC methods. This procedure is appropriate for monitoring plasma levels during single-dose pharmacokinetic studies.

REFERENCES

(1) S. J. Rosenthal, R. Ginsburg, I. H. Lamb, D. S. Baim, and J. S. Schroeder, *Am. J. Cardiol.*, **46**, 1027 (1980).

(2) P. Theroux, D. D. Waters, G. S. Affaki, J. Crittin, R. Bonan, and H. F. Mizgala, *Circulation*, **60**, 504 (1980).

(3) D. D. Waters, J. Szlachic, P. Théroux, F. Dauwe, and H. F. Mizgala, *Am. J. Cardiol.*, **47**, 179 (1981).

(4) K. Kohno, Y. Takeuchi, A. Etoh, and K. Noda, *Arzneim-Forsch.*, **27**, 1424 (1977).

(5) R. Rovei, M. Mitchard, and P. Morselli, *J. Chromatogr.*, **138**, 391 (1977).

(6) E. L. Kinney, R. M. Moskowitz and R. Zelis, *J. Clin Pharmacol.*, **21**, 337 (1981).

(7) V. Rovei, R. Gomeni, M. Mitchard, J. Larriband, C. Blatrix, J. J. Thebault, and P. L. Morselli, *Acta. Cardiol.*, **35**, 35 (1980).

(8) J. P. Clozel, G. Caillé, Y. Taemans, P. Thèroux, P. Biron, and F. Trudel, *J. Pharm. Sci.*, in press.

ACKNOWLEDGMENTS

The authors thank Mr. Leo Gosselin and Dr. David Bensemana of Laboratoires Nordic Inc. and Tanabe Seigaku Ltd. Japan for providing the diltiazem and deacetyldiltiazem.

Desorption of Carbonate from Aluminum Hydroxycarbonate Gel by Nitrogen Purging

EDWARD C. SCHOLTZ *, JOSEPH R. FELDKAMP ‡, JOE L. WHITE ‡, and STANLEY L. HEM*x

Received August 25, 1982, from the **Department of Industrial and Physical Pharmacy* and the ‡*Department of Agronomy, Purdue University, West Lafayette, IN 47907.* Accepted for publication January 13, 1983.

Abstract □ Carbonate was completely desorbed from amorphous aluminum hydroxycarbonate gel by purging with nitrogen. The reversibility of carbonate adsorption suggests that aluminum hydroxycarbonate particles are composed of planes of aluminum hydroxide with carbonate adsorbed at edge aluminum sites. A slow-reacting phase which was identified as a precursor of gibbsite, formed when the carbonate/aluminum molar ratio was <0.20.

Keyphrases □ Desorption—carbonate from aluminum hydroxycarbonate gel, nitrogen purging □ Carbonate—desorption from aluminum hydrocarbonate gel, nitrogen purging □ Nitrogen purging—desorption of carbonate from aluminum hydroxycarbonate gel □ Aluminum hydroxycarbonate gel—desorption of carbonate, nitrogen purging

The coordination of carbonate by aluminum in aluminum hydroxide has been demonstrated by Raman and IR analyses (1–3) as well as by the effect of carbonate adsorption on the point of zero charge of aluminum hydroxide (4). The term specific adsorption describes the adsorption of carbonate by aluminum hydroxide as it refers to the adsorption of anions by the formation of a partial covalent bond with structural metal atoms and the concomitant displacement of hydroxyl or water groups from the surface (5, 6).

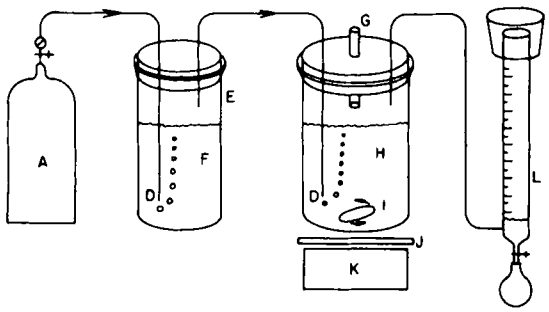

Figure 1—*Apparatus for purging aluminum hydroxycarbonate gel with nitrogen gas. Key: (A) nitrogen gas cylinder; (E) glass cylinder; (D) fritted glass gas disperser; (F) water; (G) sealable sampling port; (H) aluminum hydroxycarbonate gel; (I) magnetic stirring bar; (J) heat shield; (K) magnetic stirrer; (L) soap bubble flow meter.*

The importance of specifically adsorbed carbonate in maintaining the structure and antacid properties of aluminum hydroxide gel has been demonstrated by numerous kinetic studies (3, 7–11). Insight into adsorption mechanisms may be gained by studying desorption reactions. Hingston *et al.* (12) found that specific adsorption of phosphate, selenite, and fluoride by gibbsite or goethite varied between complete reversibility and almost complete irreversibility. The reversibility of the specifically adsorbed anion was related to the nature of the adsorption complex. Adsorption was reversible when only unidentate ligands formed between the anion and metal, *i.e.*, fluoride anion. However, multidentate ligands, bridging, or the formation of ring structures at the surface led to irreversibility. McBride (13) concluded from spin probe studies that easily desorbed anions were adsorbed on aluminum hydroxide by ligand exchange of a single surface hydroxyl while anions that could not be easily desorbed were adsorbed by bidentate bonds. Gast (6) also suggested that readily desorbed anions have one coordinated bond to the surface while those more strongly retained have two coordinated bonds. Therefore, the desorption of specifically adsorbed carbonate from aluminum hydroxycarbonate gel was studied as part of efforts to improve the antacid properties and stability of antacid products.

EXPERIMENTAL

The two aluminum hydroxycarbonate gels (CG1 and CG2) studied were obtained commercially[1] as 9.5% equivalent Al_2O_3 pourable gels and were diluted with distilled water to 5% equivalent Al_2O_3. IR analysis[2] was

[1] Reheis Chemical Co., Berkeley Heights, N.J. and Chattem Chemical, Chattanooga, Tenn.

[2] Model 180; Perkin-Elmer Co., Norwalk, Conn.

0022-3549/84/0200-0209$01.00/0

© 1984, American Pharmaceutical Association

In summary, the present study has shown that the use of GC with electron-capture detection improves, to a large extent, the sensitivity of the previous HPLC and GC methods. This procedure is appropriate for monitoring plasma levels during single-dose pharmacokinetic studies.

REFERENCES

(1) S. J. Rosenthal, R. Ginsburg, I. H. Lamb, D. S. Baim, and J. S. Schroeder, *Am. J. Cardiol.*, **46**, 1027 (1980).

(2) P. Theroux, D. D. Waters, G. S. Affaki, J. Crittin, R. Bonan, and H. F. Mizgala, *Circulation*, **60**, 504 (1980).

(3) D. D. Waters, J. Szlachic, P. Théroux, F. Dauwe, and H. F. Mizgala, *Am. J. Cardiol.*, **47**, 179 (1981).

(4) K. Kohno, Y. Takeuchi, A. Etoh, and K. Noda, *Arzneim-Forsch.*, **27**, 1424 (1977).

(5) R. Rovei, M. Mitchard, and P. Morselli, *J. Chromatogr.*, **138**, 391 (1977).

(6) E. L. Kinney, R. M. Moskowitz and R. Zelis, *J. Clin Pharmacol.*, **21**, 337 (1981).

(7) V. Rovei, R. Gomeni, M. Mitchard, J. Larriband, C. Blatrix, J. J. Thebault, and P. L. Morselli, *Acta. Cardiol.*, **35**, 35 (1980).

(8) J. P. Clozel, G. Caillé, Y. Taemans, P. Thèroux, P. Biron, and F. Trudel, *J. Pharm. Sci.*, in press.

ACKNOWLEDGMENTS

The authors thank Mr. Leo Gosselin and Dr. David Bensemana of Laboratoires Nordic Inc. and Tanabe Seigaku Ltd. Japan for providing the diltiazem and deacetyldiltiazem.

Desorption of Carbonate from Aluminum Hydroxycarbonate Gel by Nitrogen Purging

EDWARD C. SCHOLTZ *, JOSEPH R. FELDKAMP ‡, JOE L. WHITE ‡, and STANLEY L. HEM*x

Received August 25, 1982, from the **Department of Industrial and Physical Pharmacy* and the ‡*Department of Agronomy, Purdue University, West Lafayette, IN 47907.* Accepted for publication January 13, 1983.

Abstract □ Carbonate was completely desorbed from amorphous aluminum hydroxycarbonate gel by purging with nitrogen. The reversibility of carbonate adsorption suggests that aluminum hydroxycarbonate particles are composed of planes of aluminum hydroxide with carbonate adsorbed at edge aluminum sites. A slow-reacting phase which was identified as a precursor of gibbsite, formed when the carbonate/aluminum molar ratio was <0.20.

Keyphrases □ Desorption—carbonate from aluminum hydroxycarbonate gel, nitrogen purging □ Carbonate—desorption from aluminum hydrocarbonate gel, nitrogen purging □ Nitrogen purging—desorption of carbonate from aluminum hydroxycarbonate gel □ Aluminum hydroxycarbonate gel—desorption of carbonate, nitrogen purging

The coordination of carbonate by aluminum in aluminum hydroxide has been demonstrated by Raman and IR analyses (1–3) as well as by the effect of carbonate adsorption on the point of zero charge of aluminum hydroxide (4). The term specific adsorption describes the adsorption of carbonate by aluminum hydroxide as it refers to the adsorption of anions by the formation of a partial covalent bond with structural metal atoms and the concomitant displacement of hydroxyl or water groups from the surface (5, 6).

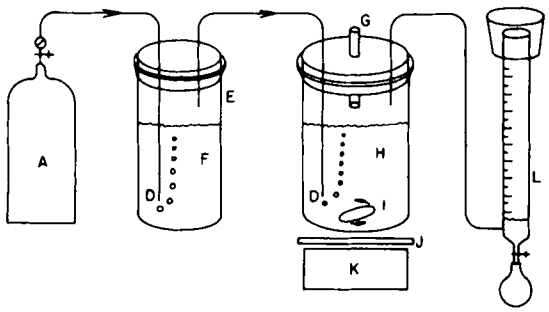

Figure 1—*Apparatus for purging aluminum hydroxycarbonate gel with nitrogen gas. Key: (A) nitrogen gas cylinder; (E) glass cylinder; (D) fritted glass gas disperser; (F) water; (G) sealable sampling port; (H) aluminum hydroxycarbonate gel; (I) magnetic stirring bar; (J) heat shield; (K) magnetic stirrer; (L) soap bubble flow meter.*

The importance of specifically adsorbed carbonate in maintaining the structure and antacid properties of aluminum hydroxide gel has been demonstrated by numerous kinetic studies (3, 7–11). Insight into adsorption mechanisms may be gained by studying desorption reactions. Hingston *et al.* (12) found that specific adsorption of phosphate, selenite, and fluoride by gibbsite or goethite varied between complete reversibility and almost complete irreversibility. The reversibility of the specifically adsorbed anion was related to the nature of the adsorption complex. Adsorption was reversible when only unidentate ligands formed between the anion and metal, *i.e.*, fluoride anion. However, multidentate ligands, bridging, or the formation of ring structures at the surface led to irreversibility. McBride (13) concluded from spin probe studies that easily desorbed anions were adsorbed on aluminum hydroxide by ligand exchange of a single surface hydroxyl while anions that could not be easily desorbed were adsorbed by bidentate bonds. Gast (6) also suggested that readily desorbed anions have one coordinated bond to the surface while those more strongly retained have two coordinated bonds. Therefore, the desorption of specifically adsorbed carbonate from aluminum hydroxycarbonate gel was studied as part of efforts to improve the antacid properties and stability of antacid products.

EXPERIMENTAL

The two aluminum hydroxycarbonate gels (CG1 and CG2) studied were obtained commercially[1] as 9.5% equivalent Al_2O_3 pourable gels and were diluted with distilled water to 5% equivalent Al_2O_3. IR analysis[2] was

[1] Reheis Chemical Co., Berkeley Heights, N.J. and Chattem Chemical, Chattanooga, Tenn.

[2] Model 180; Perkin-Elmer Co., Norwalk, Conn.

0022-3549/84/0200-0209$01.00/0

© 1984, American Pharmaceutical Association

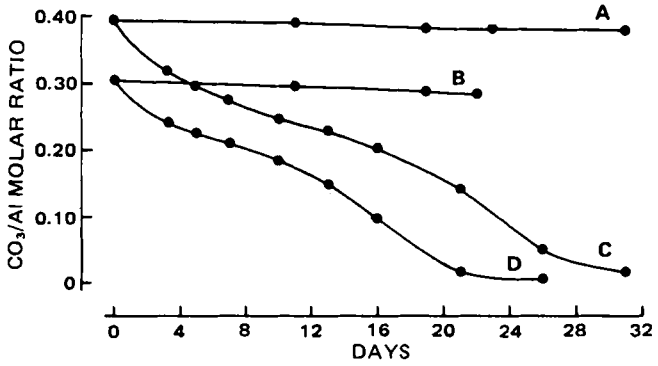

Figure 2—*Change in the carbonate content of two commercial aluminum hydroxycarbonate gels during the nitrogen purge. Key: (A) CG1, control; (B) CG2, control; (C) CG1, nitrogen purge; (D) CG2, nitrogen purge.*

performed on air-dried samples as potassium bromide pellets. Equivalent aluminum oxide content was determined by chelatometric titration (14).

Carbonate content was determined by a gasometric displacement technique (15) using the Chittick apparatus[3]. Because the addition of strong acid to aluminum hydroxycarbonate gel is an exothermic process, temperature control was required for accurate gas volume measurements. The Chittick reaction flask was immersed in a water bath maintained at room temperature, and the evolved carbon dioxide was passed through a copper coil (0.318 i.d. × 0.476 o.d. × 243 cm) inserted between the reaction flask and the measuring cylinder which was submerged in a water bath maintained at room temperature. The carbonate content was expressed as the carbonate–aluminum molar ratio.

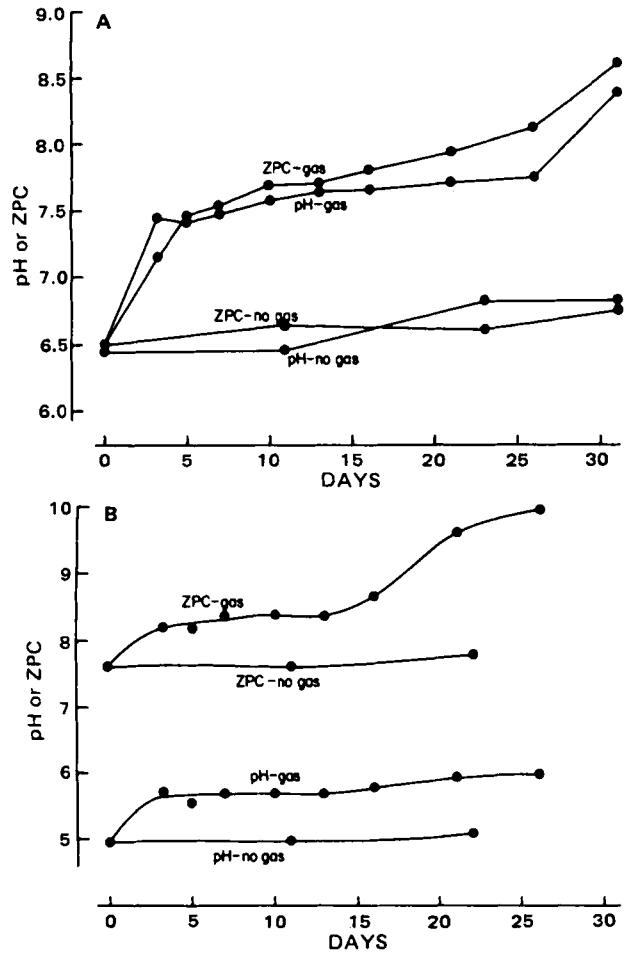

Figure 3—*Change in the pH and point of zero charge (ZPC) of CG1 (A) and CG2 (B) during the nitrogen purge. Key: (gas) nitrogen purge; (no gas) control.*

[3] Sargent-Welch Scientific Co., Skokie, Ill.

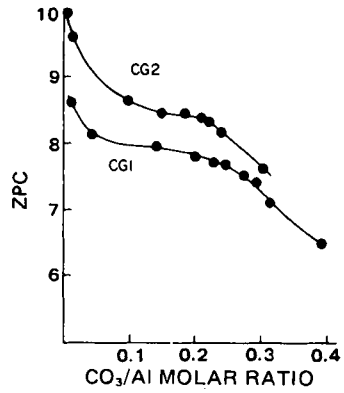

Figure 4—*Change in the point of zero charge (ZPC) during carbonate desorption from two commercial aluminum hydroxycarbonate gels.*

The point of zero charge (ZPC) was determined by a continuous potentiometric titration procedure (4). The acid reactivity was determined by the pH-stat technique at pH 3, 25°C employing an automatic titration apparatus[4] (16). X-ray powder diffractograms[5] were obtained on air-dried samples under the following operating conditions: CuK_α radiation, 30 kV, 28 mA, 3 s time constant, 6–30° 2θ.

A diagram of the apparatus used to purge the aluminum hydroxycarbonate gels with nitrogen is shown in Fig. 1. The nitrogen was saturated with water by bubbling through water prior to contact with the sample, thus minimizing the drying of the gel. The nitrogen flow was maintained at 153 mL/min; the initial sample was 1100 mL. As a consequence of

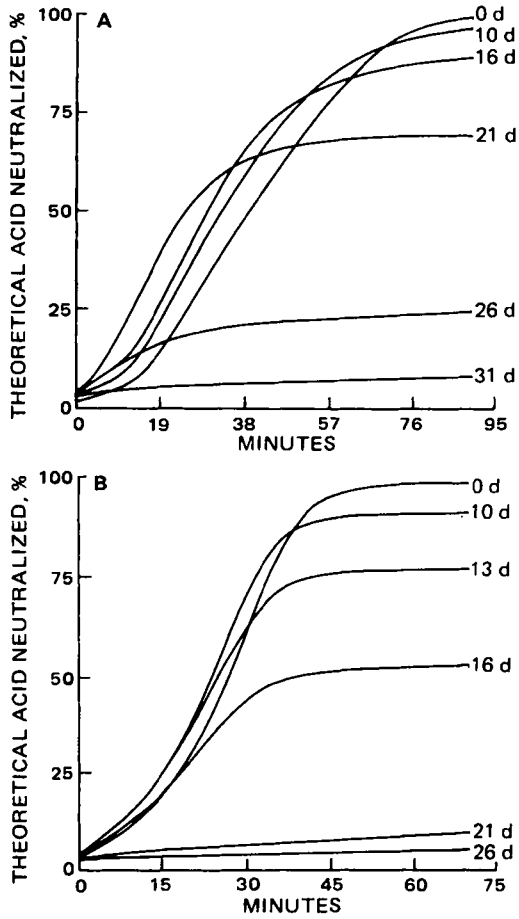

Figure 5—*pH-stat titrigram at pH 3, 25°C of CG1 (A) and CG2 (B) during nitrogen purging.*

[4] PHM 62, TTT 60, ABU 12 (2.5 mL), TTA 60, REA 160; Radiometer, Copenhagen, Denmark.

[5] Siemens Type F diffractometer; Siemens Corp., Iselin, NJ.

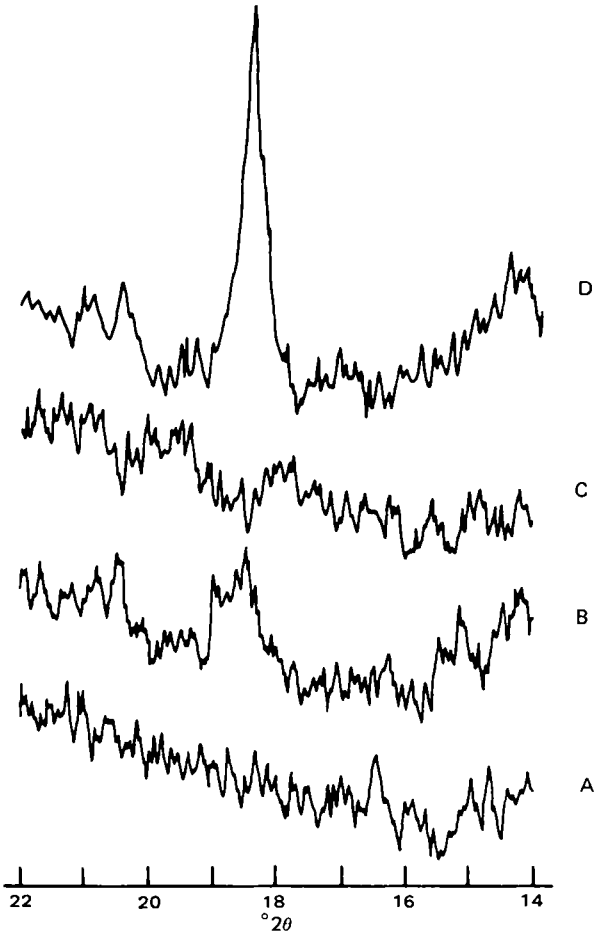

Figure 6—*X-ray powder diffractograms of CG1 and CG2 following nitrogen purging. Key: (A) CG1 control and after 31 d of nitrogen purging; (B) CG1 after 31 d of nitrogen purging followed by 16 d of aging at room temperature; (C) CG2 control and after 26 d of nitrogen purging; (D) CG2 after 26 d of nitrogen purging followed by 7 d of aging at room temperature.*

periodic sampling, ~350 mL remained at the end of the study. The control samples were not exposed to nitrogen and were stored in tightly sealed high-density polyethylene bottles at room temperature.

RESULTS AND DISCUSSION

The initial carbonate/aluminum molar ratios of CG1 and CG2 were 0.40 and 0.31, respectively. The IR spectrum of CG1 had absorption bands at 1510 and 1440 cm^{-1} and CG2 had absorption bands at 1505 and 1435 cm^{-1}, indicating that the carbonate was coordinated to aluminum (1–3). Further evidence of the specific adsorption of carbonate was provided by the point of zero charge (6.5 for CG1 and 7.6 for CG2) which was substantially lower than the 9–10 range reported for aluminum hydroxide (4).

Carbonate was readily removed from both aluminum hydroxycarbonate gels by purging with nitrogen (Fig. 2). Essentially complete carbonate removal was accomplished in 31 and 21 d for CG1 and CG2, respectively. The rate of desorption was similar. The only significant difference was the higher initial carbonate/aluminum molar ratio of CG1, which is a function of precipitation conditions and aging. The small loss of carbonate from the control samples indicates the inherent instability of aluminum hydroxycarbonate gels.

The complete removal of carbonate from the two aluminum hydroxycarbonate gels by nitrogen purging suggests that the carbonate sites are readily accessible, *i.e.*, edge sites. The complete removal of carbonate also suggests that adsorption is by unidentate rather than multidentate coordination (6, 12, 13). The same conclusion regarding unidentate coordination was reached based on the magnitude of the splitting of the degenerate ν_3 vibration of the carbonate anion in the IR spectrum of aluminum hydroxycarbonate gel (17). Thus, aluminum hydroxycarbonate particles are believed to be composed of sheets of aluminum hydroxide (18) with carbonate specifically adsorbed at the edges by unidentate coordination.

The point of zero charge of both aluminum hydroxycarbonate gels increased during the nitrogen purge (Fig. 3). The increase in the point of zero charge with the desorption of carbonate was expected because gibbsite, the stable polymorph of aluminum hydroxide, has a point of zero charge of 9–10 (4). As seen in Fig. 4, the point of zero charge changes rapidly at very low carbonate/aluminum molar ratios. Therefore, it is not accurate to extrapolate the data in Fig. 4 to zero carbonate content.

The desorption of specifically adsorbed carbonate had a substantial effect on the antacid properties of the aluminum hydroxycarbonate gels as seen in Fig. 5. The presence of a slow-reacting phase was observed within 10–16 d. When virtually all of the carbonate was desorbed, the slow-reacting phase represented nearly all of the sample. Aluminum hydroxycarbonate gels having such a slow rate of acid neutralization will be ineffective as antacids as the rate of acid neutralization is too slow to neutralize any significant quantity of gastric acid during the gastric residence time (19, 20).

The slow-reacting phase was first detected in CG1 on day 16, when the carbonate/aluminum molar ratio was 0.20, and on day 10 in CG2, when the carbonate/aluminum molar ratio was 0.18. This observation suggests that specifically adsorbed carbonate at a minimum carbonate/aluminum molar ratio of 0.20 is necessary to preserve the antacid properties of aluminum hydroxycarbonate gel.

X-ray diffractograms obtained immediately on termination of the nitrogen purging (Fig. 6A and C) were identical to the controls and indicated that CG1 and CG2 were amorphous following carbonate desorption. Thus, X-ray diffraction was insensitive to the structural changes responsible for the loss of acid reactivity as measured by pH-stat titration. This observation emphasizes the value of the pH-stat titration for studying structural changes in antacids. However, X-ray diffraction peaks were observed when the nitrogen-purged samples were allowed to age at room temperature (Fig. 6B and D), indicating that structural changes occur much more readily after specifically adsorbed carbonate has been removed. The position of the X-ray diffraction peak in the aged samples (4.84–4.67 Å in CG1 and 4.82 Å in CG2) suggests that gibbsite, a polymorph of aluminum hydroxide whose most intense X-ray diffraction peak is at 4.82 Å, is the final form of the slow-reacting phase.

The ability of nitrogen gas to remove specifically adsorbed carbonate is believed to be due to a transport mechanism involving a series of interrelated equilibria such as shown below:

$$[Al(OH)_x(H_2O)_y(OCO_2)_z]^q + zH_2O \rightleftharpoons [Al(OH)_x(H_2O)_y(OCO_2H)_z]^{q+z} + zOH^{-1} \quad \text{(Eq. 1)}$$

$$[Al(OH)_x(H_2O)_y(OCO_2H)_z]^{q+z} + zH_2O \rightleftharpoons [Al(OH)_{(x+z)}(H_2O)_y]^{q+z} + zH_2CO_3 \quad \text{(Eq. 2)}$$

$$H_2CO_3 \rightleftharpoons H_2O + CO_2\ (\text{solution}) \quad \text{(Eq. 3)}$$

$$CO_2\ (\text{solution}) \xrightarrow{N_2} CO_2\ (\text{gas}) \quad \text{(Eq. 4)}$$

Transporting carbon dioxide out of the system with nitrogen caused all of the equilibria to shift to the right, and carbonate was completely desorbed. An increase in pH was observed during carbonate desorption (Fig. 3) which is predicted by Eq. 1. The increase in pH supports a mechanism based on a series of equilibria such as hypothesized above, although any disaggregation which may be caused by the shear force of stirring or nitrogen bubbling may produce a change in pH as the newly exposed surface equilibrates by adsorbing protons in response to the pH-point of zero charge relationship (Fig. 3). The desorption of carbonate by a mechanism based on a series of equilibria as shown above was also proposed as the mechanism responsible for the reduced rate of acid neutralization that was observed following dilution of aluminum hydroxycarbonate gel with water (10). The reversible nature of carbonate adsorption requires that care be taken in the manufacture and packaging of aluminum hydroxycarbonate gel-containing antacids to minimize the desorption of specifically adsorbed carbonate.

REFERENCES

(1) J. L. White and S. L. Hem, *J. Pharm Sci.*, **64**, 468 (1975).

(2) C. J. Serna, J. L. White, and S. L. Hem, *Soil Sci. Soc. Am. Proc.*, **41**, 1009 (1977).

(3) C. J. Serna, J. L. White, and S. L. Hem, *J. Pharm. Sci.*, **67**, 1144 (1978).

(4) J. R. Feldkamp, D. N. Shah, S. L. Meyer, J. L. White, and S. L. Hem, *J. Pharm. Sci.*, **70**, 638 (1981).
(5) F. J. Hingston, A. M. Posner, and J. P. Quirk, *J. Soil Sci.*, **25**, 177 (1972).
(6) R. G. Gast, in "Minerals in Soil Environments," J. B. Dixon and S. B. Weed, Eds., Soil Science Society of America, Madison, Wis., 1977, p. 60.
(7) S. L. Hem, E. J. Russo, S. M. Bahal, and R. S. Levi, *J. Pharm. Sci.*, **59**, 317 (1970).
(8) C. J. Serna, J. C. Lyons, J. L. White, and S. L. Hem, *J. Pharm. Sci.*, **72**, 769 (1983).
(9) N. J. Kerkhof, J. L. White, and S. L. Hem, *J. Pharm. Sci.*, **66**, 1533 (1977).
(10) N. J. Kerkhof, J. L. White, and S. L. Hem, *J. Pharm. Sci.*, **64**, 940 (1975).
(11) M. K. Wang, J. L. White, and S. L. Hem, *J. Pharm. Sci.*, **69**, 668 (1980).
(12) F. J. Hingston, A. M. Posner, and J. P. Quirk, *J. Soil Sci.*, **25**, 16 (1974).
(13) M. B. McBride, *Clays Clay Miner.*, **30**, 438 (1982).
(14) "United States Pharmacopeia," 20th rev., U.S. Pharmacopeial Convention, Inc., Rockville, Md., 1980, p. 25.
(15) "Official Methods of Analysis of the Association of Official Analytical Chemists," 12th ed., W. Horwitz, Ed., Association of Official Analytical Chemists, Washington, D.C., 1975, p. 147.
(16) N. J. Kerkhof, R. K. Vanderlaan, J. L. White, and S. L. Hem, *J. Pharm. Sci.*, **66**, 1528 (1977).
(17) C. J. Serna, J. L. White, and S. L. Hem, *J. Pharm. Sci.*, **67**, 324 (1978).
(18) S. L. Nail, J. L. White, and S. L. Hem, *J. Pharm. Sci.*, **65**, 1188 (1976).
(19) *Fed. Regist.*, **39** (108) (June 4, 1974), 19,875.
(20) S. L. Hem, J. L. White, J. D. Buehler, J. R. Luber, W. M. Grim, and E. A. Lipka, *Am. J. Hosp. Pharm.*, **39**, 1925 (1982).

ACKNOWLEDGMENTS

Supported in part by William H. Rorer, Inc. This report is Journal Paper 9171, Purdue University Agricultural Experiment Station, West Lafayette, IN 47907.

Effect of Coadministration of Uracil on the Toxicity of Tegafur

JYUNJI YAMAMOTO *x, AKIHIRO HARUNO *, YUJI YOSHIMURA *, NORIO UNEMI *, YOSHIO KUNIMUNE ‡, KAZUMASA YAMASHITA ‡, and KEN'ICHI MORITA ‡

Received September 9, 1982, from the **Department of Pharmacology* and ‡*Drug Safety Research Laboratory, Taiho Pharmaceutical Co., Ltd., 224-2 Ebisuno, Hiraishi, Kawauchi-cho, Tokushima 771-01, Japan.* Accepted for publication January 10, 1983.

Abstract □ The cardiotoxic and neurotoxic effects of tegafur, an anticancer agent, were compared with those of uracil plus tegafur (4:1 mol/mol) in mice, rats, rabbits, cats and dogs. Uracil plus tegafur was shown to be less toxic than the drug alone in all the species, and uracil was found to decrease the toxicity of tegafur. α-Fluoro-β-alanine, a catabolic metabolite of the drug, had toxic effects similar to tegafur. The results suggest that administration of uracil with tegafur prevents the side effects of the drug on the heart and CNS by inhibiting the degradation of 5-fluorouracil.

Keyphrases □ Tegafur—coadministration with uracil, effect on toxicity, species comparison □ Uracil—coadministration with tegafur, effect on toxicity, species comparison □ Chemotherapeutic agents—coadministration of tegafur and uracil, effect on toxicity, species comparison

Tegafur [5-fluoro-1-(tetrahydro-2-furyl)uracil], synthesized by Hiller *et al.* (1), has been widely used clinically as an anticancer agent because it is a masked form of the pyrimidine antimetabolite, 5-fluorouracil. Jato and coworkers (2, 3) and Mukherjee and Heidelberger (4) reported that the antitumor activity and toxicity of fluorinated pyrimidines are increased by coadministration of pyrimidine. Fujii *et al.* (5–7) found that coadministration of uracil with tegafur increased the 5-fluorouracil level in tumors and the antitumor activity of tegafur, possibly because it inhibits the degradation in the liver of 5-fluorouracil formed from the drug. Moreover, it has been found that uracil plus tegafur (4:1 mol/mol) has stronger antitumor activity than the drug alone, both clinically and in animals (8–12).

Side effects of fluorinated pyrimidines on the heart and CNS have been observed clinically (13–15). But from the above findings, we suggested previously that uracil might prevent the cardiotoxic and neurotoxic effects of tegafur (16). To test this possibility, we compared the cardiotoxic and neurotoxic effects of the drug alone with those of uracil plus tegafur in mice, rats, rabbits, cats, and dogs.

EXPERIMENTAL

Drugs—The following drugs were used: tegafur[1], 5-fluorouracil[2], uracil[3], and α-fluoro-β-alanine hydrochloride[4]. Tegafur, uracil plus tegafur, and 5-fluorouracil were administered intravenously as their sodium salts and orally as suspensions in 5% gum arabic.

Animals—The following animals were used: male ddY mice (18–23 g)[5], male Wistar rats (160–200 g)[5], male Japanese White rabbits (2.5–3.5 kg)[6], mongrel cats of both sexes (2.3–3.4 kg)[6], and male Beagle dogs (9.5–10.0 kg)[7]. The animals were used for experiments after a period of acclimatization of at least 7 d in the laboratory at a controlled temperature of 23 ± 1°C and relative humidity of 55 ± 10% with a 12-h light/dark cycle. They were fasted for 18 h before oral administration of drugs.

Methods—Previously, we demonstrated that tegafur at high doses produces clonic convulsions in mice and rats, cardiac fibrillations in rabbits, and vomiting in dogs (16). 5-Fluorouracil has been reported to have a neurotoxic effect in cats (17). These cardiotoxic and neurotoxic effects of tegafur were compared with those of uracil plus the drug in the five species. The acute toxicity of tegafur in these animals was also compared with those of uracil plus tegafur and α-fluoro-β-alanine, a catabolic metabolite of the drug.

Convulsant Effects in Mice and Rats—Groups of 10 mice and rats

[1] Taiho Pharmaceutical Co., Ltd.
[2] Sigma Chemical Co.
[3] Wako Pure Chemical Industries.
[4] Tokyo Kasei Chemicals.
[5] Tokushima Laboratory Animals Co.
[6] Kearly Co.
[7] Laboratory Research Enterprise, Kalamazoo, Mich.

0022-3549/84/0200-0212$01.00/0
© 1984, American Pharmaceutical Association

(4) J. R. Feldkamp, D. N. Shah, S. L. Meyer, J. L. White, and S. L. Hem, *J. Pharm. Sci.*, **70**, 638 (1981).
(5) F. J. Hingston, A. M. Posner, and J. P. Quirk, *J. Soil Sci.*, **25**, 177 (1972).
(6) R. G. Gast, in "Minerals in Soil Environments," J. B. Dixon and S. B. Weed, Eds., Soil Science Society of America, Madison, Wis., 1977, p. 60.
(7) S. L. Hem, E. J. Russo, S. M. Bahal, and R. S. Levi, *J. Pharm. Sci.*, **59**, 317 (1970).
(8) C. J. Serna, J. C. Lyons, J. L. White, and S. L. Hem, *J. Pharm. Sci.*, **72**, 769 (1983).
(9) N. J. Kerkhof, J. L. White, and S. L. Hem, *J. Pharm. Sci.*, **66**, 1533 (1977).
(10) N. J. Kerkhof, J. L. White, and S. L. Hem, *J. Pharm. Sci.*, **64**, 940 (1975).
(11) M. K. Wang, J. L. White, and S. L. Hem, *J. Pharm. Sci.*, **69**, 668 (1980).
(12) F. J. Hingston, A. M. Posner, and J. P. Quirk, *J. Soil Sci.*, **25**, 16 (1974).
(13) M. B. McBride, *Clays Clay Miner.*, **30**, 438 (1982).
(14) "United States Pharmacopeia," 20th rev., U.S. Pharmacopeial Convention, Inc., Rockville, Md., 1980, p. 25.
(15) "Official Methods of Analysis of the Association of Official Analytical Chemists," 12th ed., W. Horwitz, Ed., Association of Official Analytical Chemists, Washington, D.C., 1975, p. 147.
(16) N. J. Kerkhof, R. K. Vanderlaan, J. L. White, and S. L. Hem, *J. Pharm. Sci.*, **66**, 1528 (1977).
(17) C. J. Serna, J. L. White, and S. L. Hem, *J. Pharm. Sci.*, **67**, 324 (1978).
(18) S. L. Nail, J. L. White, and S. L. Hem, *J. Pharm. Sci.*, **65**, 1188 (1976).
(19) *Fed. Regist.*, **39** (108) (June 4, 1974), 19,875.
(20) S. L. Hem, J. L. White, J. D. Buehler, J. R. Luber, W. M. Grim, and E. A. Lipka, *Am. J. Hosp. Pharm.*, **39**, 1925 (1982).

ACKNOWLEDGMENTS

Supported in part by William H. Rorer, Inc. This report is Journal Paper 9171, Purdue University Agricultural Experiment Station, West Lafayette, IN 47907.

Effect of Coadministration of Uracil on the Toxicity of Tegafur

JYUNJI YAMAMOTO *x, AKIHIRO HARUNO *, YUJI YOSHIMURA *, NORIO UNEMI *, YOSHIO KUNIMUNE ‡, KAZUMASA YAMASHITA ‡, and KEN'ICHI MORITA ‡

Received September 9, 1982, from the **Department of Pharmacology* and ‡*Drug Safety Research Laboratory, Taiho Pharmaceutical Co., Ltd., 224-2 Ebisuno, Hiraishi, Kawauchi-cho, Tokushima 771-01, Japan.* Accepted for publication January 10, 1983.

Abstract □ The cardiotoxic and neurotoxic effects of tegafur, an anticancer agent, were compared with those of uracil plus tegafur (4:1 mol/mol) in mice, rats, rabbits, cats and dogs. Uracil plus tegafur was shown to be less toxic than the drug alone in all the species, and uracil was found to decrease the toxicity of tegafur. α-Fluoro-β-alanine, a catabolic metabolite of the drug, had toxic effects similar to tegafur. The results suggest that administration of uracil with tegafur prevents the side effects of the drug on the heart and CNS by inhibiting the degradation of 5-fluorouracil.

Keyphrases □ Tegafur—coadministration with uracil, effect on toxicity, species comparison □ Uracil—coadministration with tegafur, effect on toxicity, species comparison □ Chemotherapeutic agents—coadministration of tegafur and uracil, effect on toxicity, species comparison

Tegafur [5-fluoro-1-(tetrahydro-2-furyl)uracil], synthesized by Hiller *et al.* (1), has been widely used clinically as an anticancer agent because it is a masked form of the pyrimidine antimetabolite, 5-fluorouracil. Jato and coworkers (2, 3) and Mukherjee and Heidelberger (4) reported that the antitumor activity and toxicity of fluorinated pyrimidines are increased by coadministration of pyrimidine. Fujii *et al.* (5–7) found that coadministration of uracil with tegafur increased the 5-fluorouracil level in tumors and the antitumor activity of tegafur, possibly because it inhibits the degradation in the liver of 5-fluorouracil formed from the drug. Moreover, it has been found that uracil plus tegafur (4:1 mol/mol) has stronger antitumor activity than the drug alone, both clinically and in animals (8–12).

Side effects of fluorinated pyrimidines on the heart and CNS have been observed clinically (13–15). But from the above findings, we suggested previously that uracil might prevent the cardiotoxic and neurotoxic effects of tegafur (16). To test this possibility, we compared the cardiotoxic and neurotoxic effects of the drug alone with those of uracil plus tegafur in mice, rats, rabbits, cats, and dogs.

EXPERIMENTAL

Drugs—The following drugs were used: tegafur[1], 5-fluorouracil[2], uracil[3], and α-fluoro-β-alanine hydrochloride[4]. Tegafur, uracil plus tegafur, and 5-fluorouracil were administered intravenously as their sodium salts and orally as suspensions in 5% gum arabic.

Animals—The following animals were used: male ddY mice (18–23 g)[5], male Wistar rats (160–200 g)[5], male Japanese White rabbits (2.5–3.5 kg)[6], mongrel cats of both sexes (2.3–3.4 kg)[6], and male Beagle dogs (9.5–10.0 kg)[7]. The animals were used for experiments after a period of acclimatization of at least 7 d in the laboratory at a controlled temperature of 23 ± 1°C and relative humidity of 55 ± 10% with a 12-h light/dark cycle. They were fasted for 18 h before oral administration of drugs.

Methods—Previously, we demonstrated that tegafur at high doses produces clonic convulsions in mice and rats, cardiac fibrillations in rabbits, and vomiting in dogs (16). 5-Fluorouracil has been reported to have a neurotoxic effect in cats (17). These cardiotoxic and neurotoxic effects of tegafur were compared with those of uracil plus the drug in the five species. The acute toxicity of tegafur in these animals was also compared with those of uracil plus tegafur and α-fluoro-β-alanine, a catabolic metabolite of the drug.

Convulsant Effects in Mice and Rats—Groups of 10 mice and rats

[1] Taiho Pharmaceutical Co., Ltd.
[2] Sigma Chemical Co.
[3] Wako Pure Chemical Industries.
[4] Tokyo Kasei Chemicals.
[5] Tokushima Laboratory Animals Co.
[6] Kearly Co.
[7] Laboratory Research Enterprise, Kalamazoo, Mich.

0022-3549/84/0200-0212$01.00/0
© 1984, American Pharmaceutical Association

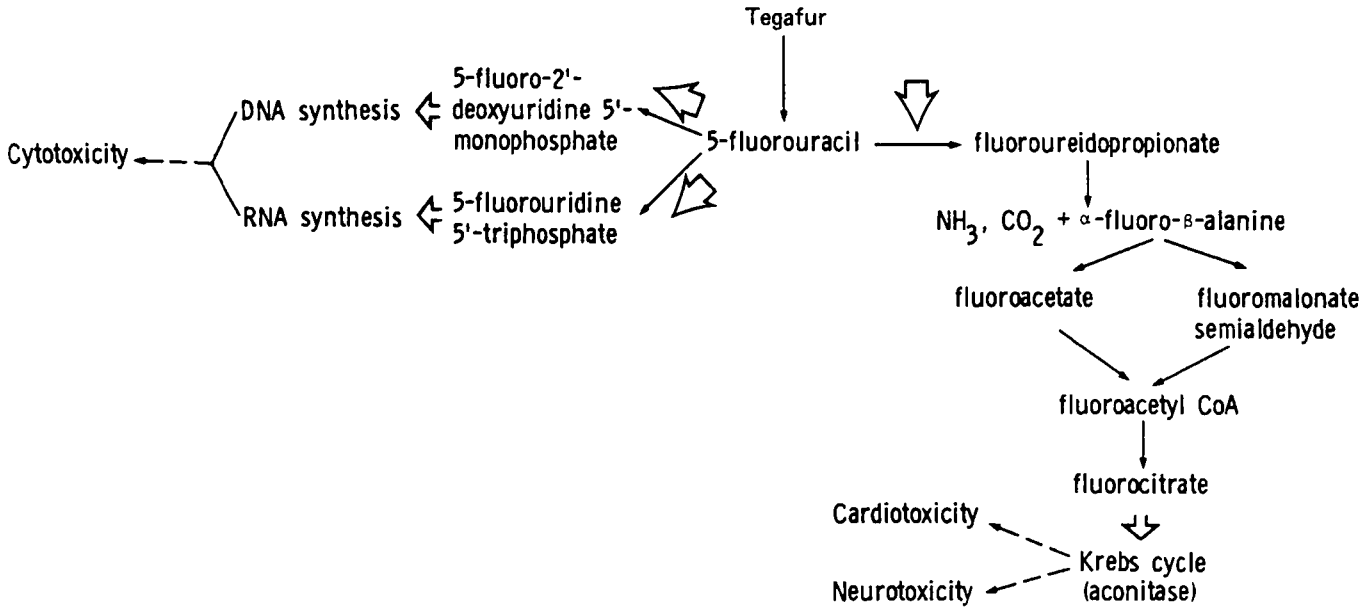

Figure 1—*Proposed mechanism of cyto-, cardio-, and neurotoxicity of tegafur and effect of uracil. Key: (⇦) coadministration of uracil.*

were observed for clonic convulsions after oral administration of the drugs. The CD_{50} values (doses producing clonic convulsions in 50% of the animals) were calculated by the method of Litchfield and Wilcoxon (18).

Cardiotoxic Effect in Rabbits—Groups of 8 rabbits were used. Cardiac fibrillations were determined from the ECG (A-B leads) using a polygraph[8] after intravenous administration of the drugs. The FD_{50} values (doses producing cardiac fibrillations in 50% of the animals) were calculated by the method of Litchfield and Wilcoxon (18).

Neurotoxic Effect in Cats—Cats were examined for gross behavioral changes after oral administration of drugs; tremors or abnormal gait was taken as an index of a neurotoxic effect. The ND_{50} values (doses producing neurotoxic effects in 50% of the animals) were calculated by the up and down method (19).

Neurotoxic Effect in Dogs—Vomiting was observed in dogs after administration of drugs. The VD_{50} values (doses producing vomiting in 50% of the animals) were calculated by the up and down method (19).

Acute Toxicities in Mice, Rats, Rabbits, Cats, and Dogs—Tegafur and uracil plus tegafur were administered orally to mice, rats, rabbits, cats, and dogs. The animals were then kept in cages with food and water, and all deaths within 21 d were recorded. The LD_{50} values in mice and rats were calculated by the method of Litchfield and Wilcoxon (18) and those in rabbits, cats, and dogs by the up and down method (19). In addition, α-fluoro-β-alanine was administered intraperitoneally to mice, rats, rabbits, cats, and dogs, and the LD_{50} values were calculated by the up and down method (19).

RESULTS

CD_{50} and LD_{50} in Mice and Rats—Tegafur at high doses caused two types of death in mice and rats: one following clonic convulsions ~4 h after treatment and the other by cytotoxicity, such as damage of the hematopoietic system, ~2 weeks after treatment. The CD_{50} values for uracil plus tegafur in mice and rats were 1.33 and 1.56 times those for the drug alone, respectively. On the other hand, the LD_{50} values for uracil plus tegafur in mice and rats were 0.28 and 0.34 times those for the drug alone, respectively (Table I). These results clearly demonstrated that coadministration of uracil decreased the convulsant effect of tegafur, but increased its acute toxicity.

FD_{50} and LD_{50} in Rabbits—Tegafur at high doses increased the voltage of the T-wave and decreased that of the ST-wave in the ECG after ~8 h, and caused cardiac fibrillation after ~15 h. Uracil plus tegafur induced cardiac fibrillation ~10 h later than the drug alone and had a weaker effect. 5-Fluorouracil induced more marked cardiac fibrillation than tegafur. The FD_{50} and LD_{50} values for uracil plus tegafur were 1.43 and 1.51 times those for the drug alone, respectively (Table I). Thus, coadministration of uracil decreased the cardiotoxic effect and acute toxicity of tegafur in rabbits.

ND_{50} and LD_{50} in Cats—Tegafur at high doses caused vomiting, tremors, and abnormal gait within 24 h. Uracil plus tegafur had similar, but weaker, effects which developed later after treatment. The effect of 5-fluorouracil was greater than that of tegafur. The ND_{50} and LD_{50} values for uracil plus tegafur were 1.18 and 1.20 times those for the drug alone, respectively (Table I). Therefore, coadministration of uracil decreased the neurotoxic effect and acute toxicity of tegafur in cats.

VD_{50} and LD_{50} in Dogs—Tegafur at high doses induced vomiting in dogs. Uracil plus tegafur had a weaker effect than the drug alone, which developed later, while 5-fluorouracil had a stronger effect than tegafur. The VD_{50} and LD_{50} values for uracil plus tegafur were 1.52 and 1.85 times those for the drug alone, respectively (Table I). Therefore, coadministration of uracil decreased the vomiting and acute toxicity induced by tegafur in dogs. In rabbits, cats, and dogs, no deaths were observed within 2 weeks after treatment, unlike mice and rats.

Toxic Effects of α-Fluoro-β-alanine in Mice, Rats, Rabbits, Cats,

Table I—Cardio- and Neurotoxic Effects and Acute Toxicities of Tegafur and Uracil plus Tegafur in Various Species

Species	Tegafur, mg/kg po	Uracil + Tegafur, mg/kg po[a]	Ratio[b]
Mice			
CD_{50}[c]	1850 (1480–2294)[h]	2470 (2266–2692)	1.33
LD_{50}[d]	1420 (1302–1547)	401 (371–474)	0.28
Rats			
CD_{50}	1340 (971–1849)	2100 (1826–2415)	1.56
LD_{50}	1410 (1308–1520)	487 (447–531)	0.34
Rabbits			
FD_{50}[e]	54.0[i] (40.9–71.3)	77.7[i] (65.8–91.7)	1.43
LD_{50}	71.0	107.7	1.51
Cats			
ND_{50}[f]	29.7	35.3	1.18
LD_{50}	35.5	42.7	1.20
Dogs			
VD_{50}[g]	30.9	47.2	1.52
LD_{50}	34.2	63.5	1.85

[a] In 4:1 mole ratio; dose is in terms of tegafur. [b] Uracil plus tegafur/tegafur. [c] Dose producing clonic convulsions in 50% of the animals, measured 3 d after drug treatment. [d] Lethal dose in 50% of the animals, measured for 21 d after drug treatment. [e] Dose producing cardiac fibrillation in 50% of the animals, measured 3 d after drug treatment. [f] Dose producing neurotoxic effects in 50% of the animals, measured 3 d after drug treatment. [g] Dose producing vomiting in 50% of the animals, measured 3 d after drug treatment. [h] Values in parentheses are 95% confidence limits. [i] Administered intravenously.

[8] San'ei-Sokki, 142-8.

Table II—LD_{50} Values for α-Fluoro-β-alanine in Various Species

Species	LD_{50}[a] mg/kg ip
Mice	167
Rats	218
Rabbits	27.4
Cats	9.4
Dogs	<24.5

[a] Measured for 21 d after drug treatment.

and Dogs—α-Fluoro-β-alanine, like tegafur, induced clonic convulsions in mice and rats, cardiac fibrillations in rabbits, and neurotoxic effects in cats and dogs. However, unlike tegafur, it did cause any deaths within 2 weeks after its administration. The LD_{50} values for α-fluoro-β-alanine in the five species are listed in Table II; rabbits, cats, and dogs were more sensitive than mice and rats to α-fluoro-β-alanine, as in the case of tegafur.

DISCUSSION

Previously, we suggested that uracil plus tegafur might have less cardio- and neurotoxicity than the drug alone (16). To test this possibility, in the present study we compared the pharmacological effects of tegafur alone and with uracil in mice, rats, rabbits, cats, and dogs, because tegafur has different effects in different species (16).

From our results on the effects of tegafur, 5-fluorouracil, and α-fluoro-β-alanine, we concluded that tegafur has two reactions, as illustrated in Fig. 1. One is due to the conversion of 5-fluorouracil to the phosphorylated anabolic metabolites, 5-fluoro-2′-deoxyuridine 5′-monophosphate and 5-fluorouridine 5′-triphosphate, which inhibit DNA and RNA syntheses. This is the mechanism of its antitumor activity (20). This action also results in damage of the hematopoietic system of mice and rats ~2 weeks after administration of tegafur. The other action is to induce clonic convulsions in mice and rats, cardiotoxicity in rabbits, and neurotoxicity in cats and dogs. These effects, which appear within 24 h after administration, were also observed after administration of α-fluoro-β-alanine.

The different effects in different species are very similar to those of methyl fluoroacetate or sodium fluoroacetate, which induce fluorocitrate intoxication (21). Thus, it has been suggested that the cardiotoxic and neurotoxic effects of 5-fluorouracil are due to fluorocitrate poisoning, probably as a result of catabolism of 5-fluorouracil (17, 22). Therefore, the second action of tegafur is caused by catabolic metabolites of 5-fluorouracil. Some metabolites may be converted to fluorocitrate, which inhibits the Krebs cycle, although no fluorocitrate has yet been detected in animals after treatment either with tegafur or 5-fluorouracil.

Rabbits, cats, and dogs are more sensitive to tegafur than mice and rats. This species difference in sensitivity might be due to species differences in the effects of fluorocitrate, because on clinical evaluation of tegafur (14), humans were found to be less sensitive than rabbits, cats, and dogs. Moreover, Meldrum and Bignell (23) reported that the sensitivity of humans to fluorocitrate is weaker than that of these animals. We think that the cardiotoxic and neurotoxic effects of fluorinated pyrimidines in clinical use (13–15) might also be caused by fluorocitrate.

On coadministration of uracil, Ikenaka *et al.* (24) found that uracil inhibited the degradation of 5-fluorouracil much more than its phosphorylation. Moreover, Unemi *et al.* (12) found that the antitumor activity of uracil plus tegafur is 5 times that of the drug alone, because uracil inhibits the degradation of 5-fluorouracil. Furthermore, Jato and coworkers (2, 3) and Mukherjee and Heidelberger (4) reported that coadministration of pyrimidine increased both the antitumor activity and the toxicity of fluorinated pyrimidines in mice.

In the present study, coadministration of uracil decreased the lethal dose of tegafur in mice and rats, but also increased the convulsant dose in these animals and the cardiotoxic, neurotoxic, and lethal doses in rabbits, cats, and dogs. These results can be explained by the fact that uracil inhibits the degradation of 5-fluorouracil, and so the effects of 5-fluoro-2′-deoxyuridine 5′-monophosphate and 5-fluorouridine 5′-triphosphate, anabolic metabolites of 5-fluorouracil, were increased while the effect of α-fluoro-β-alanine, a catabolic metabolite of 5-fluorouracil, was decreased. The extent of these effects probably depended on the relative inhibitions in degradation and phosphorylation of 5-fluorouracil caused by uracil (24). That the LD_{50} for tegafur in mice and rats was decreased and the LD_{50} in rabbits, cats, and dogs were increased by uracil can be explained by supposing that the acute toxicity in the former animals depends on anabolic rather than catabolic metabolites of 5-fluorouracil, whereas the acute toxicity in the latter animals depends on catabolic rather than anabolic metabolites.

The coadministrations of (aminooxy)acetate and acetamide were reported to reduce the toxicities of α-fluoro-β-alanine and fluoroacetate, respectively (25, 26). Furthermore, coadministration of malonate reduced citrate accumulation caused by fluoromalonate, which showed similar toxocity to fluorocitrate (27). Therefore, the inhibitory effect of uracil on the cardiotoxic and neurotoxic effects of tegafur may be explained not only by competitive inhibition of uracil with 5-fluorouracil, but also by competitive inhibition of the degradation of fluoroureidopropionate by ureidopropionate and of α-fluoro-β-alanine by β-alanine. Consequently, the actual concentration of fluorocitrate may be very low or the rate of formation of fluorocitrate may be very slow.

The present findings show that the side effects of tegafur on the heart and CNS are reduced by coadministration of uracil. Therefore, combination therapy with uracil and tegafur should be better than treatment with the drug alone.

REFERENCES

(1) S. A. Hiller, R. A. Zhuk, M. J. Lidak, and A. A. Zidermane, *British Patent* No. 1., 168 (1968).

(2) J. Jato and J. J. Windheuser, *J. Pharm. Sci.*, **62**, 1975 (1973).

(3) J. Jato, L. M. Lake, E. E. Grunden, and B. M. Johnson, *J. Pharm. Sci.*, **64**, 943 (1975).

(4) K. L. Mukherjee and C. Heidelberger, *J. Biol. Chem.*, **235**, 433 (1960).

(5) S. Fujii, K. Ikenaka, M. Fukushima, and T. Shirasaka, *Gann*, **69**, 763 (1978).

(6) S. Fujii, S. Kitano, K. Ikenaka, and T. Shirasaka, *Gann*, **70**, 209 (1979).

(7) S. Fujii, S. Kitano, K. Ikenaka, and T. Shirasaka, *Gann Kagakuryoho*, **6**, 377 (1979).

(8) K. Kimura, Y. Isobe, S. Suga, Y. Suzuoki, C. Konda, M. Shinoyama, T. Sakano, and K. Inoue, *Gann Kagakuryoho*, **6**, 237 (1979).

(9) T. Taguchi, Y. Nakano, K. Jikuya, S. Fujii, K. Ikenaka, M. Fukushima, and T. Shirasaka, *Gann Kagakuryoho*, **5**, 1161 (1978).

(10) T. Taguchi, Y. Nakano, S. Fujii, and T. Shirasaka, *Gann Kagakuryoho*, **5**, 1167 (1978).

(11) T. Taguchi and Y. Nakano, *Gann Kagakuryoho*, **6**, 257 (1979).

(12) N. Unemi, S. Takeda, K. Tajima, Y. Kawaguchi, and Y. Yasuda, *Chemotherapy*, **29**, 164 (1981).

(13) A. Pattage, S. Holt, S. Ludgate, and A. V. Langlands, *Br. Med. J.* **4** (March), 547 (1978).

(14) M. Valdivieso, G. P. Bodey, J. A. Gottlieb, and E. J. Freireich, *Cancer Res.*, **36**, 1821 (1976).

(15) H. D. Weiss, M. D. Walker, and P. H. Wiernih, *N. Engl. J. Med.*, **291**, 75 (1974).

(16) J. Yamamoto, K. Toide, A. Haruno, Y. Yoshimura, and N. Unemi, *Arzneim.-Forsch/Drug Res.*, **31**, 1268 (1981).

(17) H. Koenig and A. Patel, *Arch. Neural.*, **23**, 155 (1970).

(18) J. T. Litchfield and F. Wilcoxon, *J. Pharmacol. Exp. Ther.*, **96**, 99 (1949).

(19) K. A. Brownlee, J. L. Hodges J. R. Rosenblatt and M. Rosenblatt, *J.A.S.A.*, **48**, 262 (1953).

(20) W. Sadee and C. G. Wong, *Clin. Pharmacokinet.*, **2**, 437 (1977).

(21) F. L. M. Pattison and R. A. Peters, "Handbook of Experimental Pharmacology," vol XX, Springer-Verlag, Berlin-Heidelberg-New York, 1966, p. 409.

(22) I. Matsubara, J. Kamiya, and S. Imai, *Jpn. J. Pharmacol.*, **30**, 871 (1980).

(23) G. K. Meldrum and J. J. Bignell, *Aust. Vet. J.*, **33**, 186 (1957).

(24) K. Ikenaka, T. Shirasaka, S. Kitano, and S. Fujii, *Gann*, **70**, 353 (1979).

(25) Y. Hashimoto, *J. Hyg. Chem.*, **17**, 363 (1971).

(26) T. Winnick, R. E. Winnick and E. D. Bergman, *Biochim. Biophys. Acta.*, **69**, 48 (1963).

(27) A. C. Bilton, *Biochem. Pharmacol.*, **6**, 169 (1961).

ACKNOWLEDGMENTS

We thank Prof. S. Ueki, Department of Pharmacology, Faculty of Pharmaceutical Science, Kyushu University, for his helpful discussion.

Nonlinear Bioavailability of Metoclopramide in the Rat: Evidence for Saturable First-Pass Metabolism

R. P. KAPIL, J. E. AXELSON ˣ, R. ONGLEY, and J. D. E. PRICE

Received October 12, 1982, from the *Faculty of Pharmaceutical Sciences and Medicine, University of British Columbia, Vancouver, BC V6T 1W5, Canada.* Accepted for publication January 11, 1983.

Abstract □ *In vivo* and *in vitro* experiments were conducted in rats to examine the possibility of either extrahepatic metabolism or saturable first-pass effect as an explanation for the unusual presystemic clearance of metoclopramide (I) previously reported. *In vivo* studies involved two-thirds hepatectomized rats and animals pretreated with carbon tetrachloride to induce hepatic necrosis, whereas *in vitro* studies involved incubation of equal amounts of I (5.0 μmol/mL) with various tissue homogenates (*viz.*, liver, kidney, and lung) or their 9000×*g* supernatant fractions. Results suggest that the metabolism of I principally occurs in the rat liver, and there was no evidence suggesting the involvement of kidney or lung tissue in the metabolism of I. Forty-eight-hour cumulative urinary excretion studies following oral and intravenous administration of ≤5.0 mg/kg of metoclopramide hydrochloride were conducted. The bioavailability (F) values of I at dosage levels 0.1, 0.5, 1.0, and 5.0 mg/kg were 0.49, 0.75, 0.77, and 0.83, respectively. It is concluded that the liver is the primary organ for the metabolism of I in the rat and that the drug exhibits dose-dependent hepatic first-pass metabolism.

Keyphrases □ Bioavailability—nonlinear, metoclopramide in the rat, saturable first-pass metabolism □ Metoclopramide—nonlinear bioavailability, saturable first-pass metabolism, rat □ Metabolism—saturable, first-pass, nonlinear bioavailability, metoclopramide in the rat

Metoclopramide (I), a procainamide analogue, is a potent antiemetic and gastric motility modifier. Recent development of a sensitive and specific analysis for the quantitation of I in biological fluids has considerably facilitated the ability to study the pharmacokinetics of this drug in small animals (1, 2).

Tam *et al.* (1) have shown that after a dose of <15 mg/kg iv, the normal nonrenal clearance of I in the rat (CL_{NR} = 40 mL/min/kg) approaches the liver plasma flow, suggesting that the elimination of the drug may be perfusion limited and that the drug should be expected to undergo extensive hepatic first-pass metabolism in this species. However, after oral and intraperitoneal administration, I does not appear to undergo significant hepatic first-pass metabolism in the rat (1) over the dosage range studied (1–35 mg/kg). Hypotheses of extrahepatic metabolism of I and/or temporary saturation of the binding and metabolic sites in the liver during the absorption phase have been proposed. Recent work on the pharmacokinetics of I in rats with experimental hepatic dysfunction (2) has indicated that the liver is one of the major metabolic organs for I, but the monodeethylated metabolite of I may be formed extrahepatically.

Bateman and his coworkers (3, 4) have reported a fourfold increase in the terminal biological half-life ($t_{1/2}$) of I and a corresponding reduction in the total body clearance (CL_{TB}) of I in patients with chronic renal failure. A similar observation was made by Tam *et al.* (2) in rats with experimentally induced renal dysfunction. Both observations were somewhat unexpected since only ~20–25% of the dose is excreted as intact drug in both rat (2) and human urine (5–7), suggesting that the renal elimination pathway is relatively unimportant. In rats, Tam *et al.* (2) have also shown that a positive correlation (r^2 = 0.997) exists between the total body clearance of I and creatinine clearance, implying that the elimination of I is related to renal function. Based on the renal dysfunction studies in rats (2) and humans (3, 4), it has been proposed that a reduction of hepatic function secondary to renal injury takes place and/or there is loss of extrahepatic (*i.e.*, kidney) metabolic capabilities due to kidney malfunction.

We report the results of various *in vivo* and *in vitro* studies used to test the hypotheses proposed by previous workers in an attempt to explain the underlying mechanism(s) of the elimination of I. Results of bioavailability experiments using 48-h cumulative urinary excretion data are also reported following low-dose (≤5 mg/kg) experiments with I.

EXPERIMENTAL

Materials—Metoclopramide hydrochloride[1] (mol. wt. 336.31) (I) and deethyl metoclopramide[2] (II) were used. All chemicals were either official or reagent grade.

Animal Handling—Adult male Wistar rats, 225–275 g, were used in all experiments. All animals were maintained in metal cages, 6–8 per cage, in a controlled environment (22°C, 30% relative humidity, 14 h of light/d) for at least 3 d prior to experimentation. Food[3] and tap water were available *ad libitum*.

Urine Sample Collection—Rats were individually housed in stainless steel metabolism cages for the 48-h urine collection. The floors and sides of the cages were rinsed with deionized distilled water to maximize the drug recovery. The diluted urine samples were kept at −20°C until analyzed.

***In Vivo* Experiments**—*Two-Thirds Hepatectomy*—The animals were fasted overnight prior to the surgical removal of two-thirds of the liver using a method similar to that of Higgins and Anderson (8). Following ether anesthesia, a midline incision was made reaching 3–4 cm posteriorly from the xiphoid process of the sternum. Large portions of the median lobe together with the left lobe of the liver were securely ligated and then carefully excised. In this way, portions of the parenchyma ranging from 65 to 75% of the total liver were removed, leaving within the peritoneum, the right lateral, and small caudate lobes. The peritoneum and the abdominal muscles were sutured and the skin was closed; there was no special postoperative care.

For control rats, sham operations were carried out by making a similar midline incision. The peritoneal organs were gently disturbed with a cotton swab and the wound closed as previously described. One day following surgery, intraperitoneal administration of an isotonic solution (0.5 mL/250-g rat) of I, containing the equivalent to 15 mg/kg of base, was carried out in two-thirds hepatectomized as well as sham-operated rats. Urine was collected for 48 h after dosing and kept at −20°C until analyzed.

Carbon Tetrachloride Pretreatment—The animals were randomly selected and separated into two groups. The control and experimental group received an oral dose of 0.5 mL of normal saline or 1.0 mL/kg of carbon tetrachloride (9), respectively, followed by an overnight fast. On the following day, an intraperitoneal dose of the monohydrate hydrochloride salt of I equivalent to 1.0 mg/kg of base was administered to both

[1] Analysis No. 9207; A. H. Robins, Montreal, Can.
[2] AHR-3137; Robins Research Laboratories, Richmond, Va.
[3] Purina Laboratory Chow.

0022-3549/84/0200-0215$01.00/0
© 1984, American Pharmaceutical Association

Table I—Cumulative Urinary Excretion of I and II [a] in Two-Thirds Hepatectomized and Carbon Tetrachloride-Pretreated Rats

	Recovery, %[b]	
	Test	Control[c]
	Two-Thirds Hepatectomy	
I	32.20 ± 7.61 (5)[d]	14.01 ± 6.13 (5)
II	3.97 ± 1.90 (5)	3.65 ± 1.27 (5)
	Carbon Tetrachloride Pretreatment	
I	72.18 ± 13.43 (5)[d]	21.67 ± 7.14 (6)
II	9.79 ± 1.30 (5)[d]	3.44 ± 0.73 (6)

[a] Expressed as percent of dose of I after correction for the molecular weight difference. [b] Mean ± *SD*; number of animals in parentheses. [c] Sham-operated rats for hepatectomy and saline-pretreated for carbon tetrachloride pretreatment. [d] Statistically significantly different from the controls, $p = 0.05$.

groups. Food was limited to 2–3 pellets[3] per day and water was allowed *ad libitum*. Cumulative urine samples were collected up to 48 h postdose and stored at −20°C until analyzed.

***In Vitro* Metabolism Study**—A method similar to that used by Cowan *et al.* (10) was utilized to study the *in vitro* metabolism of I in the rat. The rats were stunned and sacrificed by decapitation, and their organs (liver, kidney, and lung) immediately were removed and placed in a fresh, ice-cold, isotonic (1.15% w/v) aqueous solution of potassium chloride. All subsequent operations were carried out at 0–4°C. The excised tissues were blotted dry, weighed, and minced with scissors. The liver tissue was homogenized in four volumes of fresh, ice-cold, isotonic potassium chloride using 4–5 passes with an homogenizer[4]. The lung and kidney tissues were homogenized separately in a similar manner. For lung and kidney tissues, a tissue–KCl solution ratio of 1:4 was also used. The homogenates were transferred to plastic tubes and centrifuged at 9000×*g* for 20 min to remove nuclei, mitochondria, and cell debris. Aliquots (0.5, 1.0, 1.5, and 2.0 mL) of supernatants as well as whole tissue homogenates were used for the incubation reactions.

The monohydrate hydrochloride salt of I (5 μmol/mL in deionized distilled water) was incubated in uncapped glass tubes at 37°C for 30 min with whole tissue homogenates (liver, kidney, and lung) as well with 9000×*g* tissue supernatant preparations. Each incubation tube contained 1.0 mL of substrate solution, one of the four volumes (0.5, 1.0, 1.5, and 2.0 mL) of whole tissue homogenate or 0.1 mL of 9000×*g* tissue supernatant, one of the corresponding volumes (3.5, 3.0, 2.5, and 2.0 mL) of 0.02 M pH 7.4 phosphate buffer, and 1 mL of cofactor solution (6 mg of glucose-6-phosphate, 3.4 mg of the monosodium salt of NADP, 0.2 mg of 0.1 M $MgCl_2 \cdot 6H_2O$, and 0.8 mL of deionized distilled water).

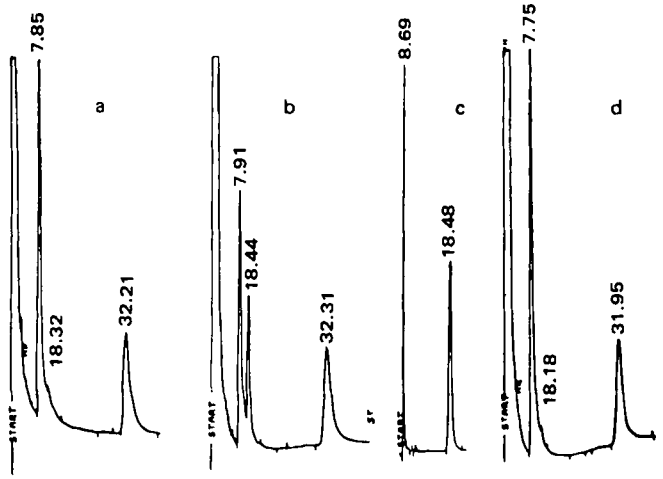

Figure 1—*Representative chromatograms showing the relative amounts of I obtained from various incubation mixtures at the end of each incubation reaction (initially, each incubation mixture contained an equal amount of I). Peaks with retention times of 7.85, 10.44, and 32.21 min represent heptafluorobutyryl derivatives of I, II, and diazepam (internal standard), respectively. Key: (A) in the absence of any tissue homogenate; (B) in the presence of 9000×g supernatant of liver homogenate (note the presence of peak for II); (C) representative chromatogram of II; (D) in the presence of 9000×g supernatant of kidney homogenate.*

[4] Polytron; International Equip. Co. (I.E.C.), Needham Hts., Mass.

Table II—*In Vitro* Metabolism of I in the Absence and Presence of 9000×*g* Supernatants from Liver, Kidney, and Lung Homogenates

Treatment	Area Ratios[a]	
	I	II
Control	1.65 ± 0.12(10)	ND[b]
Liver	0.90 ± 0.06(7)	0.49 ± 0.05(7)
Kidney	1.74 ± 0.20(7)	ND
Lung	1.62 ± 0.06(7)	ND

[a] Heptafluorobutyryl derivative of I or II/diazepam (internal standard) expressed as mean ± *SD*; number of incubation mixtures in parenthesis. [b] ND = not detected.

One milliliter of the substrate solution was replaced with 1 mL of 1.15% KCl in the control experiments, which were carried out concurrently. The incubation reactions were terminated by the addition of 0.5 mL of 3% trichloroacetic acid in all tubes. The tubes were then vortexed for 10 s and centrifuged (5 min at 2000 rpm) at room temperature. A similar experiment was also carried out with II (2.5 μmol/mL of deionized distilled water) using 0.5 mL of liver tissue homogenate only.

Bioavailability Experiments—Urinary excretion studies were carried out following intravenous and oral administrations of a range of doses of the monohydrate hydrochloride salt of I (equivalent to 0.1, 0.5, 1.0, and 5.0 mg of base/kg). Urine samples were collected as described previously.

Analyses—The urine samples and the various fractions of tissue homogenates were assayed for I and the metabolite (II) using a minor modification of a GC assay method of Tam and Axelson (11). The method involved an extraction procedure and the conversion of the drug and metabolite to their respective heptafluorobutyryl derivatives before analysis by electron-capture GC. A 1.8-m × 2-mm i.d. glass column packed with 3% Silar-9CP on Chromosorb-W (High Performance), 100–120 mesh, was used.

The bioavailability of I at different dose levels was calculated by comparing the percent of dose recovered as I in 48-h cumulative rat urine samples after equal oral and intravenous doses:

$$F = \frac{\left(\sum_0^{48} X_u\right)_{po}}{\left(\sum_0^{48} X_u\right)_{iv}}$$

where F is the systemic bioavailability, $(\Sigma_0^{48} X_u)_{po}$ and $(\Sigma_0^{48} X_u)_{iv}$ are the 48-h cumulative amounts of intact I excreted in the urine following administration of equal doses of I *via* oral and intravenous routes, respectively. The unpaired, two-tailed Student's t test was employed to statistically test the difference between groups of data; the level of significance was $p = 0.05$ for all analyses.

RESULTS

***In Vivo* Studies**—*Two-Thirds Hepatectomy*—The total percentages of I and II recovered in 48-h cumulative urine samples from two-third hepatectomized and sham-operated rats after intraperitoneal administration of the monohydrate hydrochloride salt of I (equivalent to 15 mg of base/kg) is shown in Table I. The levels of intact I recovered in the 48-h cumulative urine samples from two-thirds hepatectomized rats were significantly higher than those of sham-operated rats. There was no significant difference in the percentage of II recovered in the urine of two-third hepatectomized rats compared with that of sham-operated rats.

Carbon Tetrachloride Pretreatment—The results of carbon tetrachloride pretreatment study with respect to the percentage of intact I recovered from the 48-h cumulative urine samples were similar to that of the two-thirds hepatectomy study (Table II). The total amount of II recovered in the urine of carbon tetrachloride-pretreated rats was also significantly higher when compared with that of saline-pretreated rats.

***In Vitro* Studies**—*9000×g Liver, Kidney, and Lung Homogenate*—Figure 1 represents a series of chromatograms obtained from the extraction of various incubation mixtures, followed by heptafluorobutyric anhydride derivatization in the presence of the internal standard, diazepam (with retention time, $t_R = 32.2$ min). All mixtures contained an equal amount of I prior to initiating the incubation reaction. The first

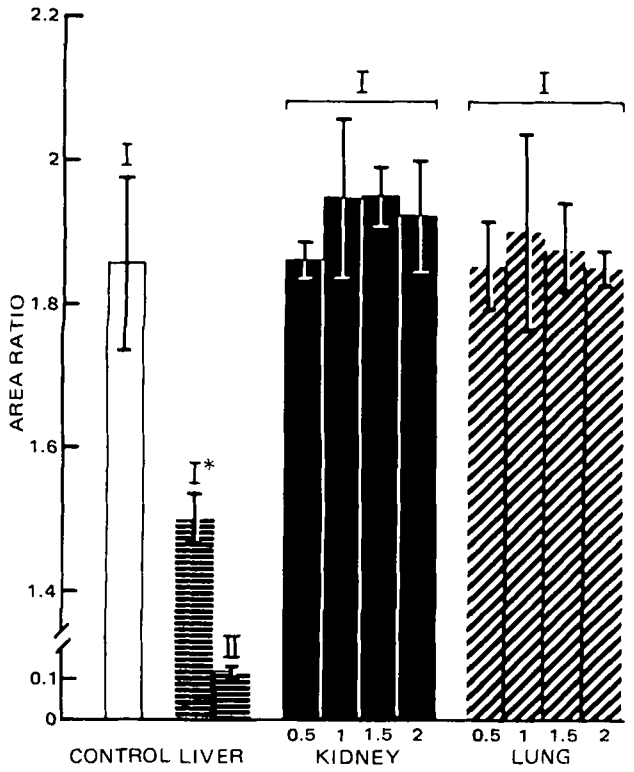

Figure 2—*Histograms representing the area ratios (heptafluorobutyryl derivative of I or II/diazepam) obtained from the* in vitro *metabolism of I in the absence and presence of different volumes of whole tissue homogenates of liver (2.0 mL), kidney (0.5, 1.0, 1.5, and 2.0 mL), and lung (0.5, 1.0, 1.5, and 2.0 mL). The asterisk signifies statistical significance,* $p < 0.05$.

chromatogram (a) reflects the relative amount of I (t_R = 7.85 min) present in the 9000×*g* supernatant after the incubation reaction in the absence of any tissue homogenate. The second chromatogram (b) represents the proportion of I present in the 9000×*g* supernatant of liver homogenate after the incubation reaction. There was an additional peak in this second chromatogram (t_R = 10.44 min) which was subsequently identified as the metabolite, II, as shown in the third chromatogram (c). The relative amount of I present in the mixture after the incubation reaction, in the presence of 9000×*g* supernatant of kidney homogenate only, is shown in the fourth chromatogram (d) in Fig. 1. The results of 9000×*g* supernatant of lung tissue were similar to those of kidney tissue.

Table II illustrates the relative amount of I remaining after various treatment procedures. Area ratios (heptafluorobutyryl derivative of I and II/diazepam as the internal standard in fixed amounts) were used for this purpose. The relative amount of I in the presence of liver tissue preparations was significantly lower than that of controls, as illustrated by the lower area ratio values. In addition, appreciable amounts of II were formed in the incubation mixture containing liver tissue. The relative amounts of I incubated in the presence of kidney and lung tissue preparations did not change significantly from controls, and metabolite II was absent.

Whole Fraction Tissue Homogenate—A study utilizing whole fraction tissue homogenates was conducted to examine the involvement of the lungs and/or kidneys in the metabolism of I. The results of the aforementioned experiment are shown in Fig. 2. There was no significant difference in the area ratios of lung and kidney tissue preparations compared with that of controls. The area ratios of liver homogenate preparations were significantly lower than the controls (Fig. 2).

***In Vitro* Metabolism of II**—The levels of II in the test incubation mixture containing 9000×*g* supernatant of liver tissue homogenate after the incubation reactions were significantly ($p < 0.05$) lower (heptafluorobutyryl derivative of II/diazepam = 1.199 ± 0.21, n = 6) compared with those of controls (without liver tissue) (1.96 ± 0.037, n = 6).

Bioavailability of I as a Function of Dose—The pharmacokinetic behavior of I in the rat was studied as a function of dose and route of administration. Forty-eight-hour cumulative urinary excretion data of intact I and II was utilized to study the effect of route of administration at different dose levels. Table III shows the percent recovery of intact I and II in 48-h cumulative urine samples after administration of equal doses of the monohydrate hydrochloride salt of I (equivalent to 5, 1.0, 0.5, and 0.1 mg of base/kg) *via* oral and intravenous routes in two randomly selected groups of rats. At the 5.0-mg/kg dose level the mean percent recovery of intact I (n = 9) following the oral route was lower than that of the intravenous route suggesting a slight hepatic first-pass effect, provided that complete absorption had occurred. The levels of II recovered were <5% for both routes. Statistically, the levels of both intact I as well as II recovered after oral administration were not significantly different from those of the intravenous route.

Table III—Percent of Dose Recovered as I and II [a] in Urine and Nonlinear Dose-Dependent Bioavailability of I [b]

Dose, mg/kg		Recovery, %[c] Oral	Intravenous	Bioavailability (F)
5.0	I	23.69 ± 7.81(9)	28.71 ± 6.09(8)	0.83
	II	3.43 ± 1.12(9)	4.12 ± 1.13(8)	
1.0	I	19.92 ± 5.27(6)	25.65 ± 6.21(6)	0.78
	II	3.20 ± 0.54(6)	4.40 ± 1.67(6)	
0.5	I	16.22 ± 2.03(6)[d]	21.89 ± 2.83(6)	0.75
	II	3.51 ± 1.21(6)	2.57 ± 1.62(6)	
0.1	I	9.75 ± 4.35(5)[d]	20.44 ± 5.02(5)	0.49
	II	1.14 ± 0.51(5)	1.51 ± 0.40(5)	
15.0				0.91[e]

[a] Expressed as percent of dose of I after correction for the molecular weight difference. [b] Bioavailability of I calculated as the ratio of 48-h cumulative urinary excretion data following oral and intravenous administration of different doses. [c] Mean ± *SD*; number animals in parentheses. [d] Statistically significantly different from the intravenous group, p = 0.05. [e] Calculated by comparing area under plasma concentration *versus* time curve after oral route to that of route of administration. Data taken from Ref. 1.

Similar results were obtained after a 1-mg/kg dose (Table III). The percent of dose recovered as intact I and II after the oral route was not significantly different from that seen after an intravenous route of administration. These results are consistent with the work done by previous investigators (1).

To test the hypothesis of temporary saturation of liver enzymes during the absorptive stage after relatively high doses (>1 mg/kg), the 48-h cumulative urinary excretion pattern at lower doses (<1 mg/kg) was studied. The results of the 0.5- and 0.1-mg/kg studies are also shown in Table III. In both cases, the total amounts of intact I recovered after oral dosing were significantly lower than those following intravenous administration. The total amount of II recovered was <5% by either route, and there was no significant difference between routes. Table III also represents the compilation of experimentally determined bioavailability data at different dose levels.

DISCUSSION

The two-thirds hepatectomy study assessed the involvement of the liver in the metabolism of I. The study was based on the assumption that surgical removal of two-thirds the liver of the rat would decrease hepatic function. If the liver is involved in metabolism of I, then one would expect increased amounts of intact drug in the cumulative urine of surgically altered rats as compared with normal rats. Surgical removal of two-thirds of the liver is a major operation, and ideally the rat should be allowed to recuperate from the surgically associated stress and trauma for at least 3 d prior to the beginning of an experiment. However, Higgins and Anderson (8) found that the regeneration of liver tissue in rats is very rapid. They reported that it took only 3 d after the surgery to restore the liver mass from 29% to ~70% of normal. Therefore, in the present study the animals were allowed to recuperate for only 1 d following surgery. Sham-operated rats were used for controls.

The intraperitoneal route of drug administration without ether anaesthesia, as stated earlier, was preferred over other routes (*i.e.*, intravenous or oral) which required the use of ether anesthesia. This was done to minimize mortality due to increased ether toxicity in two-third hepatectomized rats.

The total amount of intact I in urine samples at 48-h was significantly higher in two-third hepatectomized rats compared with that found in the urine from sham-operated rats (Table I). This strongly suggests that the liver is involved in the metabolism of I. The percentage of dose excreted as the metabolite (II) was too low (<5%) in both treatments to allow further interpretation of the effect of hepatectomy on the metabolism of I.

Carbon tetrachloride, a well-known hepatotoxin, has been widely used in experimental animals to produce varying degrees of liver impairment including necrosis (12), fatty infiltration (13), and decreased activity of

microsomal enzymes that catalyze the oxidation of drugs (14–16). Carbon tetrachloride impairs oxidative enzymes in liver microsomes by decreasing the amount of cytochrome P_{450} either due to an active metabolite (17) or free radical formation (18, 19).

Hepatotoxicity in rats is evident within 24 h of carbon tetrachloride treatment (1.0 mL/kg) (8). However, the toxic effects of carbon tetrachloride to other organs such as the kidney do not occur until many hours to several days after the exposure to the toxin (20–22). Therefore, rats pretreated with carbon tetrachloride 24 h prior to study were used to ensure minimal damage to other organs. The intraperitioneal route of drug administration, without ether anesthesia, was used as before to avoid ether toxicity.

The percentage of intact I recovered from the 48-h cumulative urine samples of carbon tetrachloride-pretreated rats is almost threefold higher (Table I) than that of saline-pretreated rats. This observation strongly suggests that the liver is a major organ for the metabolism of I in the rat.

A similar pattern of recovery of I was found by Tam *et al.* (2), who found no significant difference in the levels of II in the 48-h cumulative urine samples of carbon tetrachloride-pretreated rats as compared with the saline-pretreated rats. Based on the unchanged levels of II in both of these treatments, these investigators have speculated that extrahepatic metabolism of I is possible in the rat. But, in the present studies the levels of II in the 48-h cumulative urine samples of carbon tetrachloride-pretreated rats were higher than those of saline-pretreated rats. This observed difference may be a function of the dose of I, which was 1 mg/kg in the present study and 15 mg/kg for Tam *et al.* (2).

If the liver were the only metabolic organ for I, then during liver damage (*e.g.*, carbon tetrachloride pretreatment) metabolism would be impaired, the extent of impairment being a function of the hepatic injury. This damage should result in a greater proportion of parent drug being excreted unchanged and a lower fraction of metabolite in the urine of rats with hepatic injury as compared with the saline pretreated rats. The observation that the levels of II in our present study are higher, rather than lower, in the carbon tetrachloride-pretreated rat urine as compared with those of normal rats appears inconsistent. This can be rationalized from the *in vitro* metabolism studies of I and II. It has been found in our present *in vitro* studies that I is metabolized in the rat liver and one of its metabolites is II, which is then further metabolized in the liver. Therefore, during carbon tetrachloride pretreatment, the metabolism of both I and II are probably impaired resulting in higher overall levels of both of these compounds in the urine as compared with those in saline-pretreated rats.

The results of investigations using 9000×*g* homogenates suggest that the liver tissue is involved in the metabolism of I. The evidence of the presence of II in the incubation mixture containing liver homogenate (Fig. 1) suggests that microsomal oxidation of I had occurred. There was no such indication for the metabolism of I in the presence of kidney homogenate. The amount of I remaining in the incubation mixture containing kidney homogenate was similar to that of the control (Fig. 1d), suggesting that the kidney tissue is not involved in the metabolism of I in the rat. The results using lung homogenates are similar to those of the kidney homogenate study, indicating that lung tissue is not involved in significant metabolism of I in the rat (Table II).

Whole fraction tissue homogenate studies were performed because the exact location of I-metabolizing enzymes in the lung and/or kidney was not identified. Also, as the optimum tissue protein concentration for the metabolic reaction was not known, a wide range of whole tissue homogenate volumes (0.5, 1.0, 1.5, and 2.0 mL) was used. An incubation period of 30 min was chosen for the study of the *in vitro* metabolism of I (10). Evidence for the metabolism of I was found only with the whole liver tissue homogenate (Fig. 2). There was no indication of lung or kidney tissue involvement in the metabolism of I.

The results of both *in vivo* and *in vitro* experiments have clearly shown that the liver is the primary organ responsible for the metabolism of I in rats, essentially eliminating the hypothesis of significant extrahepatic metabolism. Based on this hypothesis, bioavailability studies involving urinary excretion patterns following oral and intravenous administration of various doses of I were characterized. These studies were undertaken to explore the possible reason(s) why I does not undergo hepatic first-pass metabolism following oral and intraperitoneal administration over the dose range studied (1) despite the fact that total body clearance of I approaches the hepatic blood flow. One of the hypotheses proposed by Tam *et al.* (1) to explain this phenomenon was that the concentration of I in the hepatoportal vein during the absorption phase is high enough to saturate the enzyme capacity of the liver at the dose range studied (1–35 mg/kg). To test this, the bioavailability (F) of I was determined at lower doses (0.1, 0.5, 1.0, and 5.0 mg/kg). The 48-h cumulative urinary excretion data obtained in our present studies showed significant hepatic first-pass metabolism of I at the 0.1- and 0.5-mg/kg doses, resulting in lower bioavailability values (Table III). A nonlinear, dose-dependent trend in the bioavailability values of I at different doses was evident. The bioavailability of I increased with increasing dose, suggesting that saturation of the liver enzyme capacity occurs at higher doses of I during GI absorption. This may explain why I does not undergo significant hepatic first-pass metabolism at doses >1.0 mg/kg. The phenomenon of dose-dependent bioavailability has also been exhibited by other high liver clearance drugs such as propranolol (23–29) and alprenolol (30, 31).

REFERENCES

(1) Y. K. Tam, J. E. Axelson, B. McErlane, R. Ongley, and J. D. E. Price, *J. Pharmacol. Exp. Ther.*, **217,** 764 (1981).

(2) Y. K. Tam, J. E. Axelson, B. McErlane, R. P. Kapil, K. W. Riggs, R. Ongley, and J. D. E. Price, *J. Pharmacol. Exp. Ther.*, **219,** 141 (1981).

(3) D. N. Bateman, C. Kahn, and D. S. Davies, *Br. J. Clin. Pharmacol.*, **9,** 371 (1980).

(4) D. N. Bateman, R. Gokal, T. R. P. Dodd, and P. G. Blain, *Eur. J. Clin. Pharmacol.*, **19,** 437 (1981).

(5) D. N. Bateman and R. Gokal, *Lancet* **i,** 982 (1980).

(6) C. Graffner, P. O. Lagerstrom, and P. Lundborg, *Br. J. Clin. Pharmacol.*, **8,** 469 (1979).

(7) L. Teng, R. B. Bruce, and L. K. Dunning, *J. Pharm. Sci.*, **66,** 1615 (1977).

(8) G. M. Higgins and R. M. Anderson, *Arch. Pathol.*, **12,** 186 (1931).

(9) K. Hirano, H. Matsumura, and Y. Imai, *J. Takeda Res. Lab.*, **34,** 1 (1975).

(10) D. A. Cowan, G. Huizing, and A. H. Beckett, *Xenobiotica*, **6,** 605 (1976).

(11) Y. K. Tam and J. E. Axelson, *J. Chromatogr.*, **170,** 157 (1979).

(12) G. H. Gallagher, *Austr. J. Exp. Biol. Med. Sci.*, **40,** 241 (1962).

(13) T. F. Slater, *Nature (London)*, **209,** 36 (1966).

(14) D. Neubert and D. Maibauer, *Naunyn-Schmiedeberg's Arch. Exp. Pathol. Pharmakol.*, **235,** 291 (1959).

(15) R. Kato, E. Chiesara, and P. Vasanelli, *Biochem. Pharmacol.*, **11,** 211 (1962).

(16) J. V. Dingell and M. Heimberg, *Biochem. Pharmacol.*, **17,** 1269 (1968).

(17) H. A. Sasame, J. A. Castro, and J. R. Gillette, *Biochem. Pharmacol.*, **17,** 1759 (1968).

(18) E. A. Glende, Jr., *Biochem. Pharmacol.*, **21,** 1697 (1972).

(19) E. A. Glende, Jr., *Biochem. Pharmacol.*, **21,** 2131 (1972).

(20) H. Smetana, *Arch. Int. Med.*, **63,** 760 (1939).

(21) H. D. Moon, *Am. J. Pathol.*, **26,** 1041 (1950).

(22) S. W. Zimmerman and D. H. Norbach, *Arch. Pathol. Lab. Med.*, **104,** 94 (1980).

(23) T. Suzuki, Y. Saitoh, S. Isozaki, and R. Ishida, *Chem. Pharm. Bull.*, **20,** 2731 (1972).

(24) T. Suzuki, S. Isozaki, R. Ishida, Y. Saitoh, and F. Nakagawa, *Chem. Pharm. Bull.*, **22,** 1639 (1974).

(25) G. H. Evans, G. R. Wilkinson, and D. G. Shand, *J. Pharmacol. Exp. Ther.*, **186,** 447 (1973).

(26) D. G. Shand, R. A. Branch, G. H. Evans, A. S. Nies, and G. Wilkinson, *Drug Metab. Dispos.*, **1,** 679 (1973).

(27) P. A. Routledge and D. G. Shand, *Clin. Pharmacokinet.*, **4,** 73 (1979).

(28) J. J. Mackichan, D. R. Pyszczynki, and W. J. Jusko, *Biopharm. Drug Dispos.*, **1,** 159 (1980).

(29) T. Rikihisa, T. Ohkuma, M. Mori, M. Otsuka, and T. Suzuki, *Chem. Pharm. Bull.*, **29,** 2035 (1981).

(30) B. Ablad, M. Ervik, J. Hallgren, G. Johnsson, and L. Solvell, *Eur. J. Clin. Pharmacol.*, **5,** 44 (1972).

(31) B. Ablad, B. O. Borg, G. Johnsson, C. G. Regardh, and L. Solvell, *Life Sci.*, **14,** 693 (1974).

ACKNOWLEDGMENTS

This work was supported by the Medical Research Council of Canada (MA-7027), the Kidney Foundation of Canada (65-4461), and the University of British Columbia.

The authors wish to thank Tracy Lakevold for assistance in manuscript preparation and Dr. Milo Gibaldi for advice during the composition of the manuscript.

Quantitative Evaluation of Topically Applied Pilocarpine in the Precorneal Area

AVINASH G. THOMBRE * and KENNETH J. HIMMELSTEIN *‡x

Received July 26, 1982, from the **Department of Chemical and Petroleum Engineering, University of Kansas, Lawrence, KS 66045.* Accepted for publication January 10, 1983. ‡Present address: Inter$_x$ Research Corporation, Merck Sharp & Dohme Research Laboratories, Lawrence, KS 66044.

Abstract □ The bioavailability of topically applied pilocarpine is poor due to various loss mechanisms that serve to lessen delivery of the drug to the aqueous humor. Precorneal drainage and other routes of loss have been investigated qualitatively as well as quantitatively. The mechanistic models proposed to date suffer from the drawback of being dependent on our understanding of the mechanism of drug transport through the corneal membrane. This report quantifies the initial disposition of topically applied drugs and their availability for systemic and local absorption. The rate constant for the conjunctival absorption is determined and is independent of the mechanism of transcorneal transport.

Keyphrases □ Pilocarpine—quantitative evaluation, topically applied in the precorneal area, bioavailability, disposition □ Bioavailability—quantitative evaluation of topically applied pilocarpine in the precorneal area, disposition □ Disposition, precorneal—quantitative evaluation of topically applied pilocarpine, bioavailability

The precorneal disposition of pilocarpine greatly influences its bioavailability. The factors that affect the concentration of a topically applied drug solution in the precorneal area are shown schematically in Fig. 1.

When a drug is instilled into the eye, a large loss occurs *via* drainage. The normal resident tear volume in rabbits is reported to be 7.5 μL (1), only slightly larger than that in humans. The normal dropper used commercially in ophthalmic drug solutions delivers ~40–50 μL. Since the cul-de-sac of the eye cannot hold such a large volume of liquid, a substantial portion of the drop is lost due to overflow. The remainder is immediately subjected to a physiological drainage mechanism. This drainage is proportional to the excess volume and continues until the total tear volume is restored to the normal lacrimal volume in ~5 min, independent of the drop size (1). Another route of drug loss in the precorneal area is the normal tear turnover which is ~15–16%/min in humans (2, 3) and ~9%/min in rabbits (1). Tear turnover serves to dilute the drug and hence, reduce the gradient for transport through the cornea. An additional, associated problem is that of induced lacrimation. For reasons of stability, most marketed pilocarpine solutions are at a pH of 4–5. The physiological pH of the tear fluid is much higher, ~7.47 (4). Since the average dose size is much greater than the volume of the tears, the drug solution overwhelms the buffering capacity of the tear film, resulting in an increased production of tears.

Other factors influencing the precorneal disposition of pilocarpine include drug–protein interactions (5). Although the protein binding is reversible, the tear turnover removes both free as well as bound drug. A factor that enhances bioavailability to some extent is the evaporation of tears. The rate of evaporation from the eye of the rabbit is 2.8 μL/h/cm^2 (6). Evaporation of tears serves to increase the concentration of the drug in the tear film and, hence, increase the gradient for productive absorption.

A precorneal factor of great importance with regard to the toxicological effects of topically applied drugs is the loss through the conjunctiva. The conjunctival area is ~6 times larger than the corneal area and is highly vascularized. Therefore, the conjunctiva can be a major route for entry of the drug into systemic circulation.

A mechanistic representation of the precorneal area, presented by Himmelstein *et al.* (7), took into account the volume-dependent drainage and the effect of tear turnover based on the work of Chrai *et al.* (1). The corneal transport of the drug was assumed to be *via* a linear diffusional first-order clearance parameter. Although conjunctival absorption was not considered, a framework was established for a mechanistic understanding of the drug disposition from topical instillation to reaching the aqueous humor. The model proposed by Makoid and Robinson (8) used a first-order elimination term to describe loss from the precorneal area. The major disadvantage of their model is that it does not consider volume-dependent drainage from the precorneal area; the cornea was assumed to be a homogeneous membrane. Lee and Robinson (9) extensively describe pilocarpine disposition in the precorneal area. They considered the corneal epithelium as a separate drug-containing tissue and included the stroma and the endothelium with the aqueous humor. This was done to incorporate the findings of Seig and Robinson (10) that the cornea acts as both a barrier as well as a depot for the drug. Miller (11) proposed a pharmacokinetic model to describe the fate of pilocarpine in the internal eye. The precorneal area in the model was not treated mechanistically. The concentration of pilocarpine in the tear film was measured experimentally and used as a forcing function for corneal transport. Mishima (12) has reviewed the literature on the topical administration of ocular drugs. The concentration of the drug in the tear film was assumed to decrease exponentially with time and the corneal uptake was assumed to be governed by either a first-order mass transfer coefficient or by partitioning of the drug into the epithelial barrier.

Due to the complex nature of the corneal membrane, a mechanistic understanding of the transport of ocular drugs through the cornea is severely limited. The *in vitro* ex-

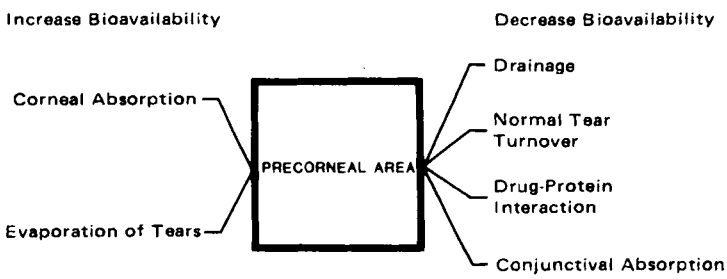

Figure 1—*Precorneal factors that influence bioavailability of topically applied ophthalmic drugs.*

0022-3549/84/0200-0219$01.00/0
© 1984, American Pharmaceutical Association

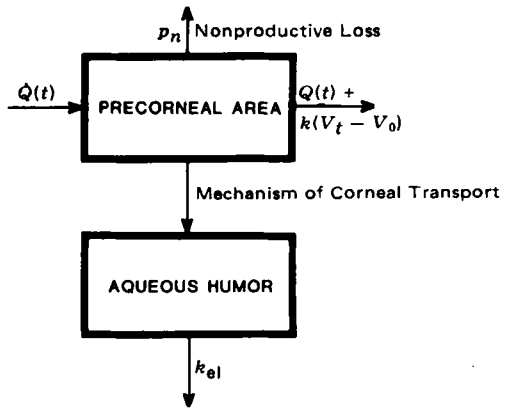

Figure 2—*Schematic diagram of the proposed model for drug disposition in the precorneal area.*

perimental data obtained by Mosher and Mikkelson (13) for the corneal transport of the *n*-alkyl *p*-aminobenzoates indicate that corneal transport is by diffusion through a trilaminate consisting of the epithelium, stroma, and the endothelium. Since the epithelium and the endothelium are more lipid in nature than the stroma, the partitioning and solubility of the drug in the individual laminates are important factors governing the transport. However, due to experimental difficulties, the individual resistances of the corneal membranes have not been estimated. In the pharmacokinetic models proposed to date, various simplifying assumptions have been made concerning the transport through the cornea. The rate constant describing the loss of drug through the conjunctiva is thus a function of these assumptions.

Here, a detailed model for the precorneal area is presented without making any assumptions about the mechanism of corneal transport. On the basis of the model, disposition of pilocarpine due to various factors are estimated quantitatively.

THEORETICAL

The proposed model for the precorneal area is shown schematically in Fig. 2. It can be considered as an extension of the model proposed by Himmelstein *et al.* (7) and Lee and Robinson (9), taking into account the volume-dependent drainage loss. The nonproductive loss is described by a first-order rate constant, p_n, and is primarily the conjunctival absorption. The analysis of the proposed model differs from previously reported analysis in the estimation of the corneal drug uptake, which is determined directly from experimentally reported pilocarpine levels in the aqueous humor (14).

The differential equation governing the concentrations of pilocarpine in the precorneal area is developed in a manner analogous to that of Himmelstein *et al.* (7). A mass balance for the amount of tear fluid in the precorneal area (Eq. 1) is made assuming that the solution has the density of water and that the nonproductive and productive loss of pilocarpine do not significantly affect the tear fluid volume:

$$\text{Rate of change in fluid volume} = \text{Rate of flow in} - \text{Rate of flow out} \quad \text{(Eq. 1)}$$

$$\frac{dV_t}{dt} = Q_t - [Q_t + K(V_t - V_0)] \quad \text{(Eq. 2)}$$

where V_t is the total volume in the precorneal area at any given time; V_0 is the normal resident tear volume; Q_t is the normal tear production rate; and K is a proportionality constant that is a function of the instilled drop size, V_d. Equation 2 has been solved analytically (1, 7) subject to the initial condition, $V_t = V_d + V_0$ at $t = 0$:

$$V_t = V_d \exp(-Kt) + V_0 \quad \text{(Eq. 3)}$$

Table I—Concentration of Pilocarpine in the Precorneal Area Following Topical Instillation of 25 μL of 1.00×10^{-2} M Pilocarpine Nitrate[a]

Minutes	Pilocarpine Concentration in Tears, μg/mL[b]
1	1690 (120)[c]
2	830 (220)
3	330 (90)
4	170 (40)
5	82 (26)

[a] Taken from Ref. 6. [b] Concentrations are based on pilocarpine alkaloid and are the average of seven determinations. Numbers in parentheses are the *SEM*.

The mass balance for pilocarpine in the tear fluid is given by:

$$\text{Rate of change of mass in tear fluid} = \text{Rate of transfer in by flow} - \text{Rate of loss by drainage} - \text{Rate of nonproductive loss} - \text{Rate of productive loss} \quad \text{(Eq. 4)}$$

The productive loss from the precorneal area is the drug transported to the aqueous humor. The rate of this productive loss is estimated as follows. Figure 3 shows the experimentally obtained levels of pilocarpine (14) in the aqueous humor after topical administration of 25 μL of a 1.00×10^{-2} M pilocarpine solution in the rabbit eye. It is seen from the figure that, for the first 5 min after instillation of the drug, the concentration in the aqueous humor increases approximately linearly with time. Thus, for the initial 5 min, the rate of productive loss is a constant. It should be noted that only the first 5 min postinstillation are critical with regard to defining the concentration gradient for drug between the precorneal area and the cornea. Table I shows the concentrations of pilocarpine in the tear film determined experimentally by Miller (6). It can be seen that the drug concentration drops to <4% of its initial value in 5 min. The initial concentration for a 25-μL dose of 1.00×10^{-2} M pilocarpine is 2083.5 μg/mL. Seig and Robinson (10) have also reported that rinsing the precorneal area 5 min after dosing has no effect on the ocular bioavailability of topically applied pilocarpine.

From Fig. 3, the slope of the aqueous humor concentration profile, assuming it to be linear for the first 5 min, was calculated to be 0.0960 μg/mL·min. Since the volume of the aqueous humor is 0.311 mL, the rate of loss of drug into the aqueous humor or the rate of productive loss in Eq. 4 is calculated to be 0.0299 μg/min. The assumption that the aqueous humor concentration profile is linear over the first 5 min is arbitrary and is justified on an empirical basis. In fact, this study attempts to obtain the precorneal factors without making any assumptions about the nature of transcorneal transport. Equation 4 can now be written as:

$$\frac{dV_tC_t}{dt} = 0 - [Q_t + k(V_t - V_0)]C_t - p_nC_t - 0.0299 \quad \text{(Eq. 5)}$$

By taking the indicated derivative and substituting the value of V_t from Eq. 3 into this expression, a simplified relationship is obtained:

$$\frac{dC_t}{dt} = \frac{-Q_tC_t - p_nC_t - 0.0299}{V_d \exp(-Kt) + V_0} \quad \text{(Eq. 6)}$$

Equation 6 can be solved analytically as:

$$-\frac{1}{(Q_t + p_n)} \ln\left(C_t + \frac{0.0299}{(Q_t + p_n)}\right) = \frac{t}{V_0} + \frac{1}{V_0K} \ln[V_0 + V_d \exp(-Kt)] + C \quad \text{(Eq. 7)}$$

where C is the constant of integration to be determined from the initial condition, *viz.*, $C_t = 2083.5$ μg/mL at $t = 0$.

Table II—Parameters of the Proposed Model

Parameter	Value	Reference
V_0	7.5 μL	1
V_d	25 μL	Experimental
V_{ah}[a]	311 μL	7
Q_t	0.66 μL/min	7
K	$(0.25 + 0.0113\ V_d)\ \text{min}^{-1}$	1
p_n	(estimated in terms of the model)	

[a] Volume in the aqueous humor.

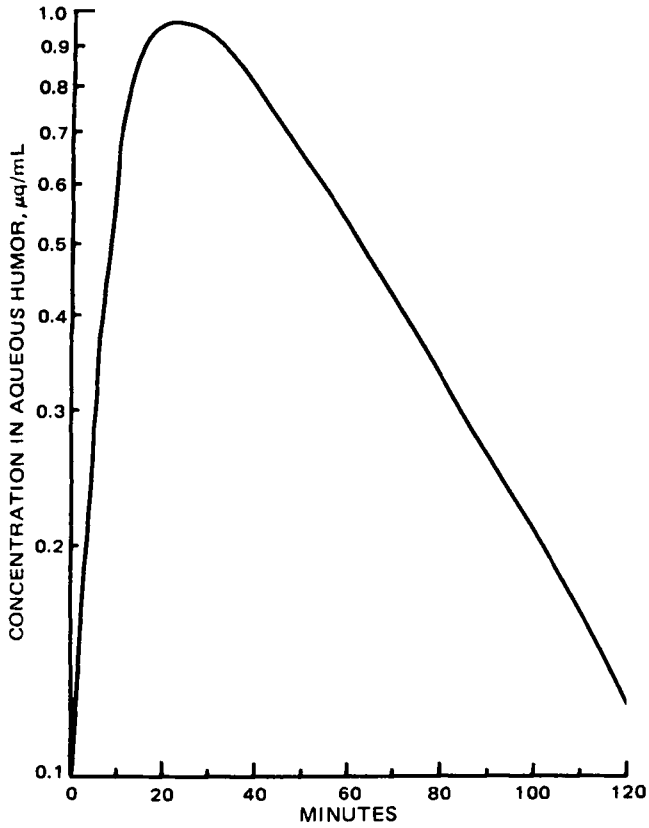

Figure 3—*Experimental Pilocarpine Concentrations in the Aqueous Humor (pH 6.24). Taken from Ref. 12.*

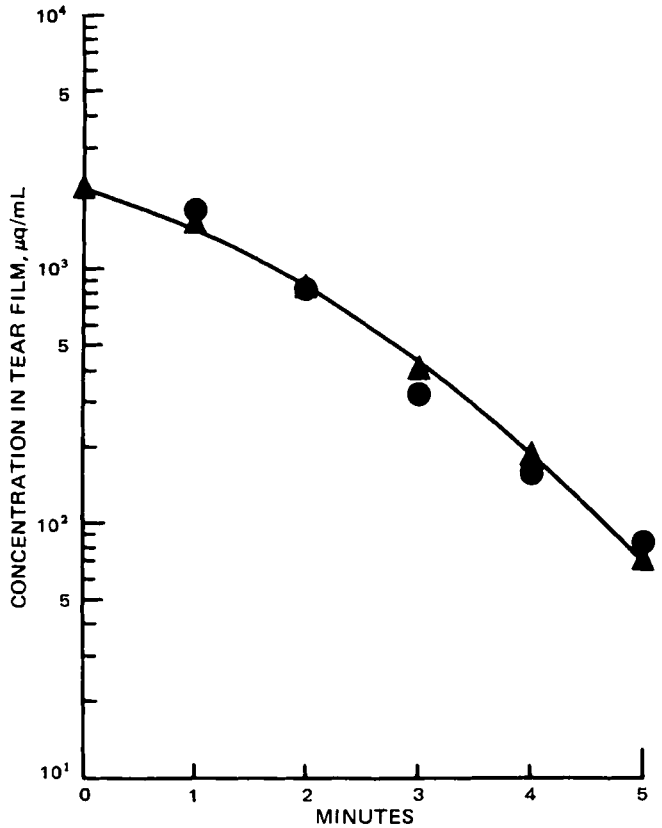

Figure 4—*Experimental [Lee and Robinson, 1979 (●); Miller, 1980 (▲)] and theoretical concentrations, according to the model (—), of pilocarpine in the tear film.*

RESULTS AND DISCUSSION

Except for the rate constant for nonproductive loss, p_n, all other parameters of the present model are known from experimental measurements. The value of K is taken as that obtained by Chrai *et al.* (1); the values used and their sources are given in Table II. The first-order rate constant for the nonproductive absorption, p_n, was evaluated in terms of the present model. Since Eq. 6 describing the concentration profile of pilocarpine in the precorneal area is nonlinear, the method of Pattern Search (15) was used to determine p_n. The objective function was formulated as:

$$J = \sum_{\text{all data}} (C_{t,\text{exp}} - C_{t,\text{model}})^2 \qquad \text{(Eq. 8)}$$

The experimental data obtained by Miller (6), presented in Table I, was used for $C_{t,\text{exp}}$. Since the concentration of pilocarpine in the precorneal area at $t = 0$ was used as the initial condition to numerically solve Eq. 6, the precorneal concentration profile is forced to pass through the point (0.0,2083.5). The value of p_n for which the objective function is minimum was found to be 8.84 μL/min.

The model-generated tear film pilocarpine concentration profile is plotted in Fig. 4. For comparison, the profiles obtained experimentally by Miller (6) and Lee and Robinson (9) have also been plotted in Fig. 4. Lee and Robinson simulated their profile with a value of 8.38 μL/min for the nonproductive loss parameter. It can be seen that the model predicts the experimental data very well. The slight curvature in the tear film pilocarpine concentration profile is also accounted for by the proposed model. This curvature indicates that the decline of pilocarpine concentration in the tear film is not a first-order process.

At this point, a distinction is made concerning the amount of pilocarpine in the precorneal area and the concentration of pilocarpine in the tear film. Evaluating the precorneal loss factors with respect to amount as well as concentration of the drug is important, since the concentration of the drug in the precorneal area determines the driving force for the corneal absorption and the amount of drug lost to the conjunctiva determines the amount that is available for systemic absorption leading to undesirable toxicological effects of the drug.

The relative amounts of loss of pilocarpine to the various loss mechanisms considered in the present model can be obtained by integration of each of the terms in the right-hand side of Eq. 4. This integration was done numerically using the composite Simpsons' rule (Table III). The above analysis shows that for 25 μL of a 0.01 M dose instilled into the eye, 52.2% is absorbed by the conjunctiva. It should be noted from Table III that up to 1 min postinstillation, the loss of pilocarpine *via* drainage is comparable with the loss due to conjunctival absorption. However, after 1 min postinstillation, the nonproductive loss is greater than that due to drainage. As mentioned earlier, drug absorbed by the conjunctiva gets into systemic circulation.

The contributions of the various precorneal factors to the decrease in the concentration of pilocarpine in the tear film is evaluated similarly by integrating the components on the right-hand side of Eq. 6 (Table IV). It is seen that the conjunctival absorption contributes 92.57% of the total decrease in pilocarpine concentration at the end of the first 5 min post-

Table III—Precorneal Disposition of Pilocarpine Following the Topical Instillation of 25 μL of 1.00×10^{-2} M Pilocarpine Nitrate

Minutes	Productive Loss	Loss Due to Tear Turnover, μg	Nonproductive Loss	Drainage Loss	Amount in Precorneal Area
0	0	0	0	0	67.7144
1	0.0299	1.1689	15.6574	18.5671	32.2911
2	0.0598	.9322	25.8825	25.7324	14.1074
3	0.0897	2.3579	31.5846	28.0953	5.5868
4	0.1196	2.5589	34.2767	28.7550	2.0042
5	0.1495	2.6398	35.3607	28.9120	0.6524

Table IV—Contributions of Precorneal Factors in the Decrease of Pilocarpine Concentration in the Tear Film Following Topical Instillation of 25 μL of 1.00×10^{-2} M Pilocarpine Nitrate

Minutes	Productive Loss	Loss Due to Tear Turnover, μg/mL	Nonproductive Loss	Concentration in Precorneal Area
0	0	0	0	2083.5198
1	1.1258	43.5164	582.9035	1455.9741
2	2.7230	83.7475	1121.8004	875.2490
3	4.8423	113.5022	1520.3654	444.8103
4	7.4670	130.9236	1753.7251	191.4049
5	10.5208	139.1052	1863.3178	70.5768

instillation. Thus, it should be noted that although drainage is responsible for 42.7% of the total amount of drug instilled, it is the conjunctival absorption that is primarily responsible for the dramatic fall in the tear film pilocarpine concentration. The tear turnover is next in importance, contributing 6.9% of the decrease of concentration. Due to the rapid decline of drug concentration in the tear film, there is considerable loss of the driving force for productive drug absorption resulting in the poor bioavailability of topically administered drugs. Thus, decreasing the nonproductive loss of drug through the conjunctiva is as important a consideration as is circumventing the drainage loss in attempts to increase the bioavailability.

CONCLUSIONS

A model has been presented to account for the precorneal disposition of topically applied pilocarpine solutions. Due to the unknown nature of transcorneal penetration, the precorneal model was solved without making any assumptions about the mechanism of corneal transport. Experimentally obtained aqueous humor pilocarpine concentrations were used to obtain the rate of productive absorption. The rate constant for nonproductive loss, p_n, was found to be 8.84 μL/min, comparable with that used by Lee and Robinson (9).

Analysis of the model leads to a clearer understanding of the relative importance of the precorneal factors in reducing both the amount of drug in the precorneal area and the concentration of the drug in the tear film. It was shown that the conjunctival absorption is an important factor in reducing the amount of drug in the precorneal area and is the single-most important factor responsible for the reduction of drug concentration in the tear film and, hence, affects the driving force for productive absorption.

REFERENCES

(1) S. S. Chrai, T. F. Patton, A. Mehta, and J. R. Robinson, *J. Pharm. Sci.*, **62**, 1112 (1973).

(2) S. Mishima, A. Gasset, S. D. Klyce, and J. L. Baum, *Invest. Ophthalmol.*, **5**, 264 (1966).

(3) M. J. Puffer, R. W. Nealt, and R. F. Brubaker, *Am. J. Ophthalmol.*, **89**, 369 (1980).

(4) A. Longwell, S. Birss, N. Keller, and D. Moore, *J. Pharm. Sci.*, **65**, 1654 (1976).

(5) T. J. Mikkelson, S. S. Chrai, and J. R. Robinson, *J. Pharm. Sci.*, **62**, 1648 (1973).

(6) S. C. Miller, Ph.D. Dissertation, University of Kansas (1980).

(7) K. J. Himmelstein, I. Guvenir, and T. F. Patton, *J. Pharm. Sci.*, **67**, 603 (1978).

(8) M. C. Makoid and J. R. Robinson, *J. Pharm. Sci.*, **68**, 435 (1979).

(9) V. H. Lee and J. R. Robinson, *J. Pharm. Sci.*, **68**, 673 (1979).

(10) J. W. Seig and J. R. Robinson, *J. Pharm. Sci.*, **65**, 1816 (1976).

(11) S. C. Miller, K. J. Himmelstein, and T. F. Patton, *J. Pharmaceut. Biopharm.*, **9**, 653 (1981).

(12) S. Mishima, *Invest. Ophthalmol. Visual Sci.*, **21**, 504 (1981).

(13) G. L. Mosher and T. J. Mikkelson, *Int. J. Pharmaceut.*, **2**, 239 (1979).

(14) T. F. Patton and J. R. Robinson, *J. Pharm. Sci.*, **65**, 1295 (1976).

(15) R. L. Fox, in "Optimization Methods for Engineering Design," Addison Wesley, 1971.

Antineoplastic Activity of Tetrakis-μ-(trimethylamine-boranecarboxylato)-*bis*(trimethylamine-carboxyborane)dicopper(II) in Ehrlich Ascites Carcinoma

I. H. HALL *, B. F. SPIELVOGEL ‡, and A. T. McPHAIL ‡

Received June 24, 1982, from the **Division of Medicinal Chemistry, School of Pharmacy, University of North Carolina, Chapel Hill, NC 27514* and the ‡*Paul M. Gross Chemical Laboratory, Duke University, Durham, NC 27706.* Accepted for publication December 12, 1982.

Abstract □ A binuclear copper(II) complex derived from trimethylamine carboxyborane [tetrakis-μ-(trimethylamine-boranecarboxylato)-*bis*-(trimethylamine-carboxyborane)dicopper(II)] was shown to have antineoplastic activity in the Ehrlich ascites carcinoma screen. Metabolic studies demonstrated that the compound suppressed DNA and protein syntheses. The inhibition of DNA synthesis appeared to be due to reduction of the DNA polymerase activity and the regulatory enzymes of *de novo* purine synthesis. Preliminary data suggest that the compound is an initiation inhibitor of protein synthesis in Ehrlich ascites cells.

Keyphrases □ Copper(II) complexes—with trimethylamine carboxyborane, antineoplastic activity, Ehrlich ascites carcinoma screen □ Trimethylamine carboxyborane—complex with copper(II), antineoplastic activity, Ehrlich ascites carcinoma screen □ Antineoplastic agents—potential, copper(II)–trimethylamine carboxyborane complex, Ehrlich ascites carcinoma screen

Previously, series of trimethylamine cyanoborane and trimethylamine carboxyborane derivatives were reported to be active as antineoplastic agents against Ehrlich ascites carcinoma, Walker 256 carcino-sarcoma, P388 lymphocytic leukemia, B16 melanoma, and Lewis lung carcinoma growth (1, 2). Trimethylamine cyanoborane in Ehrlich ascites cells effectively inhibited DNA and protein syntheses as well as DNA polymerase and thymidylate synthetase activities. Scheller *et al.* (3) have demonstrated that amine carboxyboranes in dilute solutions bind to metal ions such as Zn^{2+} and Cu^{2+} as simple carboxylates and not as chelates. The synthesis and antineoplastic ac-

0022-3549/84/0200-0222$01.00/0

© 1984, American Pharmaceutical Association

Table IV—Contributions of Precorneal Factors in the Decrease of Pilocarpine Concentration in the Tear Film Following Topical Instillation of 25 μL of 1.00×10^{-2} M Pilocarpine Nitrate

Minutes	Productive Loss	Loss Due to Tear Turnover, μg/mL	Nonproductive Loss	Concentration in Precorneal Area
0	0	0	0	2083.5198
1	1.1258	43.5164	582.9035	1455.9741
2	2.7230	83.7475	1121.8004	875.2490
3	4.8423	113.5022	1520.3654	444.8103
4	7.4670	130.9236	1753.7251	191.4049
5	10.5208	139.1052	1863.3178	70.5768

instillation. Thus, it should be noted that although drainage is responsible for 42.7% of the total amount of drug instilled, it is the conjunctival absorption that is primarily responsible for the dramatic fall in the tear film pilocarpine concentration. The tear turnover is next in importance, contributing 6.9% of the decrease of concentration. Due to the rapid decline of drug concentration in the tear film, there is considerable loss of the driving force for productive drug absorption resulting in the poor bioavailability of topically administered drugs. Thus, decreasing the nonproductive loss of drug through the conjunctiva is as important a consideration as is circumventing the drainage loss in attempts to increase the bioavailability.

CONCLUSIONS

A model has been presented to account for the precorneal disposition of topically applied pilocarpine solutions. Due to the unknown nature of transcorneal penetration, the precorneal model was solved without making any assumptions about the mechanism of corneal transport. Experimentally obtained aqueous humor pilocarpine concentrations were used to obtain the rate of productive absorption. The rate constant for nonproductive loss, p_n, was found to be 8.84 μL/min, comparable with that used by Lee and Robinson (9).

Analysis of the model leads to a clearer understanding of the relative importance of the precorneal factors in reducing both the amount of drug in the precorneal area and the concentration of the drug in the tear film. It was shown that the conjunctival absorption is an important factor in reducing the amount of drug in the precorneal area and is the single-most important factor responsible for the reduction of drug concentration in the tear film and, hence, affects the driving force for productive absorption.

REFERENCES

(1) S. S. Chrai, T. F. Patton, A. Mehta, and J. R. Robinson, *J. Pharm. Sci.*, **62**, 1112 (1973).

(2) S. Mishima, A. Gasset, S. D. Klyce, and J. L. Baum, *Invest. Ophthalmol.*, **5**, 264 (1966).

(3) M. J. Puffer, R. W. Nealt, and R. F. Brubaker, *Am. J. Ophthalmol.*, **89**, 369 (1980).

(4) A. Longwell, S. Birss, N. Keller, and D. Moore, *J. Pharm. Sci.*, **65**, 1654 (1976).

(5) T. J. Mikkelson, S. S. Chrai, and J. R. Robinson, *J. Pharm. Sci.*, **62**, 1648 (1973).

(6) S. C. Miller, Ph.D. Dissertation, University of Kansas (1980).

(7) K. J. Himmelstein, I. Guvenir, and T. F. Patton, *J. Pharm. Sci.*, **67**, 603 (1978).

(8) M. C. Makoid and J. R. Robinson, *J. Pharm. Sci.*, **68**, 435 (1979).

(9) V. H. Lee and J. R. Robinson, *J. Pharm. Sci.*, **68**, 673 (1979).

(10) J. W. Seig and J. R. Robinson, *J. Pharm. Sci.*, **65**, 1816 (1976).

(11) S. C. Miller, K. J. Himmelstein, and T. F. Patton, *J. Pharmaceut. Biopharm.*, **9**, 653 (1981).

(12) S. Mishima, *Invest. Ophthalmol. Visual Sci.*, **21**, 504 (1981).

(13) G. L. Mosher and T. J. Mikkelson, *Int. J. Pharmaceut.*, **2**, 239 (1979).

(14) T. F. Patton and J. R. Robinson, *J. Pharm. Sci.*, **65**, 1295 (1976).

(15) R. L. Fox, in "Optimization Methods for Engineering Design," Addison Wesley, 1971.

Antineoplastic Activity of Tetrakis-μ-(trimethylamine-boranecarboxylato)-*bis*(trimethylamine-carboxyborane)dicopper(II) in Ehrlich Ascites Carcinoma

I. H. HALL *, B. F. SPIELVOGEL ‡, and A. T. McPHAIL ‡

Received June 24, 1982, from the **Division of Medicinal Chemistry, School of Pharmacy, University of North Carolina, Chapel Hill, NC 27514* and the ‡*Paul M. Gross Chemical Laboratory, Duke University, Durham, NC 27706.* Accepted for publication December 12, 1982.

Abstract □ A binuclear copper(II) complex derived from trimethylamine carboxyborane [tetrakis-μ-(trimethylamine-boranecarboxylato)-*bis*-(trimethylamine-carboxyborane)dicopper(II)] was shown to have antineoplastic activity in the Ehrlich ascites carcinoma screen. Metabolic studies demonstrated that the compound suppressed DNA and protein syntheses. The inhibition of DNA synthesis appeared to be due to reduction of the DNA polymerase activity and the regulatory enzymes of *de novo* purine synthesis. Preliminary data suggest that the compound is an initiation inhibitor of protein synthesis in Ehrlich ascites cells.

Keyphrases □ Copper(II) complexes—with trimethylamine carboxyborane, antineoplastic activity, Ehrlich ascites carcinoma screen □ Trimethylamine carboxyborane—complex with copper(II), antineoplastic activity, Ehrlich ascites carcinoma screen □ Antineoplastic agents—potential, copper(II)–trimethylamine carboxyborane complex, Ehrlich ascites carcinoma screen

Previously, series of trimethylamine cyanoborane and trimethylamine carboxyborane derivatives were reported to be active as antineoplastic agents against Ehrlich ascites carcinoma, Walker 256 carcino-sarcoma, P388 lymphocytic leukemia, B16 melanoma, and Lewis lung carcinoma growth (1, 2). Trimethylamine cyanoborane in Ehrlich ascites cells effectively inhibited DNA and protein syntheses as well as DNA polymerase and thymidylate synthetase activities. Scheller *et al.* (3) have demonstrated that amine carboxyboranes in dilute solutions bind to metal ions such as Zn^{2+} and Cu^{2+} as simple carboxylates and not as chelates. The synthesis and antineoplastic ac-

0022-3549/84/0200-0222$01.00/0

© 1984, American Pharmaceutical Association

Table I—Antineoplastic Activity of I Against Ehrlich Ascites Carcinoma Growth in Male CF_1 Mice [a]

Group	Survival on Day 10	Ascites Fluid, mL	Ascrit[b]	Inhibition, %
Control (0.05% polysorbate 80)				
Treated	6	7.17	39.3	—
10 mg/kg/d of I	5	0.04	18.5	99.7
20 mg/kg/d of I	6	0.32	34.0	96.2
6-Mercaptopurine	6	0.10	2.5	99.9

[a] $n = 6$. [b] Packed-cell volume.

tivity of a binuclear copper(II) complex derived from trimethylamine carboxyborane [tetrakis-μ-(trimethylamine-boranecarboxylato)-*bis*(trimethylamine-carboxyborane)dicopper(II) $[Cu_2(Me_3NBH_2CO_2)4.2Me_3NBH_2CO_2H]$, henceforth referred to as I] is reported herein.

EXPERIMENTAL

Preparation of Tetrakis-μ-(trimethylamine-boranecarboxylato)-*bis*(trimethylamine-carboxyborane)dicopper(II)—Cupric chloride ($CuCl_2 \cdot 2H_2O$) was purchased commercially[1]. Trimethylamine carboxyborane was prepared as described previously (1). Trimethylamine carboxyborane (1.8703 g, 15.9 mmol) was dissolved in 1 M NaOH (16 mL) and water (20 mL). Dropwise addition of 23 mL of a solution of $CuCl_2 \cdot 2H_2O$ (1.36 g, 8 mmol) in water (40 mL) produced a dark green solution which was allowed to stand overnight. Subsequent filtration through a fine fritted funnel removed a greenish brown sludge and left a dark green filtrate which was allowed to evaporate in the atmosphere. After 6 d, the solution had evaporated, leaving many small green crystals in a clear liquor. These crystals were removed by filtration and washed with chloroform (40°C); no $(CH_3)_3N \cdot BH_2COOH$ crystals were evident. The green crystals were then washed with a minimal amount of cold water to ensure removal of any trace of sodium chloride and dried *in vacuo*. The yield was 0.49 g (28%), mp 165°C (dec.); IR: ν_{BH} 2350 and $\nu_{C=O}$ 1665 cm^{-1}. The structure has been determined by single crystal X-ray analysis (4).

Anal.—Calc. for $C_{24}H_{68}B_6Cu_2N_6O_{12}$: C, 34.95; H, 8.31; N, 10.19. Found: C, 35.00; H, 8.49; N, 10.15.

Biological Studies—Male CF_1 mice (~30 g) were implanted intraperitoneally with 2×10^6 Ehrlich ascites tumor cells on day 0. A homogeneous suspension of I in 0.05% polysorbate 80–water was administered intraperitoneally at 10 and 20 mg/kg for 9 d to determine the inhibition of tumor growth. Mice were sacrificed on day 10, and the ascites fluid was collected from the peritoneal cavity. The volume and ascrit (packed-cell volume) were determined for each animal, and the present inhibition of tumor growth was calculated (5). For the metabolic studies, mice were treated on days 8 and 9 with 10 mg/kg ip of I. The animal was sacrificed on day 10, and the ascites fluid was harvested. The *in vitro* metabolic studies were performed at 0.25, 0.50, and 1 mM final concentrations of I.

In vitro incorporation of [^{3}H]thymidine, [^{3}H]uridine, or [^{3}H]leucine was determined using 10^6 Ehrlich ascites cells, 1 μCi of labeled precursor, minimum essential medium, and final concentrations of drug from 0.25 to 1.0 mM. The mixtures were incubated at 37°C 60 min and inactivated by trichloroacetic acid. The acid-insoluble labeled DNA was collected on glass filter disks[2]; RNA and proteins were precipitated on nitrocellulose filters by vacuum suction (6). Results are expressed as dpm of incorporated precursor/h/10^6 cells.

For *in vivo* studies, incorporation of thymidine into DNA was determined by the method of Chae *et al.* (7). One hour prior to the animal sacrifice on day 10, 10 μCi of [6-^{3}H]thymidine (21.5 Ci/mmol) was injected intraperitoneally. The DNA was isolated, and the tritium content was determined in a toluene-based scintillation fluid[3]. The DNA concentration was determined by the diphenylamine reaction using calf thymus DNA as a standard. Uridine incorporation into RNA was determined using 10 μCi of [5,6-^{3}H]uridine (22.4 Ci/mmol). RNA was extracted by the method of Wilson *et al.* (8). Using yeast RNA as a standard, the RNA content was assayed by the orcinol reaction. Leucine incorporation into protein was determined by the method of Sartorelli (9) using 10 μCi of [4,5-^{3}H]leucine (52.2 Ci/mmol). Protein content was determined by the Lowry *et al.* procedure (10) using bovine serum albumin as a standard.

In vitro and *in vivo* nuclear DNA polymerase activity was determined on isolated Ehrlich ascites cell nuclei (11). The incubation was that described by Sawada *et al.* (12) except that [methyl-^{3}H]deoxythymidine triphosphate (82.4 Ci/mmol) was used. The acid-insoluble nucleic acid was collected on filters[2] and counted. Nuclear RNA polymerase activities were determined on enzymes isolated from the nuclei. mRNA, rRNA, and tRNA polymerase enzymes were isolated using, respectively, 0.3 M, 0.04 M, and 0.0 M ammonium sulfate in magnesium chloride. The incubation medium was that of Anderson *et al.* (13) using [^{3}H]UTP (23.2 Ci/mmol). The acid-insoluble RNA was collected on nitrocellulose filters and counted[3].

Deoxythymidine as well as deoxythymidylate monophosphate and diphosphate kinase activities were measured spectrophotometrically at 340 nm at 20 min using reduced NAD (0.1 μmol) (14). Thymidine incorporation (21.5 Ci/mmol) into nucleotides was measured using the medium of Maley and Ochoa (14). The reaction medium was extracted with ether, and the aqueous layer was plated on cellulose[4] plates and eluted with 0.5 M formic acid–0.6 M LiCl (1:1). Areas which correlated with the R_f values of thymidylate monophosphate, diphosphate, and triphosphate standards were scraped and counted[3].

Carbamyl phosphate synthetase activity was determined using the reaction medium of Kalman *et al.* (15) in the presence of of ornithine and ornithine transcarbamylase; citrulline formed from ornithine was measured at 490 nm by the method of Archibald (16). Aspartate transcarbamylase activity was assayed using the incubation medium of Kalman *et al.* (15). The colorimetric determination of carbamyl aspartate was conducted by the procedure of Koritz and Cohen (17). Orotidine monophosphate decarboxylase activity was assayed by the method of Appel (18) using 0.1 μCi of [^{14}C]orotidine monophosphate (34.9 mCi/mmol); the $^{14}CO_2$ generated in 15 min was trapped in 1 M KOH[5] and counted. Thymidylate synthetase activity was determined using a postmitochondrial supernatant (9000 × *g* for 10 min) and 5 μCi of [5-^{3}H]dUMP (14 Ci/mmol) according to the method of Kampf *et al.* (19).

[^{14}C]Formate incorporation into purines was determined by the method of Spassova *et al.* (20) using 0.5 μCi of [^{14}C]formic acid (52.0

Table II—*In Vivo* Effects of I on Ehrlich Ascites Carcinoma of Male CF_1 Mice [a]

Biochemical Parameter	Control (0.05% Polysorbate 80), % of control	Compound I[b] % of control
[^{3}H]Thymidine incorporation into DNA	100 ± 8	43 ● 5
[^{3}H]Uridine incorporation into RNA	100 ± 9	116 ± 10
[^{3}H]Leucine incorporation into protein	100 ± 8	48 ± 6[c]
[^{14}C]Formate incorporation into purines	100 ± 12	59 ± 6[c]
Number of cells/mL of ascites fluid (×10^6)		
Enzyme activities	100 ± 9	45 ● 4[c]
DNA polymerase	100 ± 6	38 ± 5[c]
mRNA polymerase	100 ± 8	96 ± 9
rRNA polymerase	100 ± 9	96 ± 11
tRNA polymerase	100 ± 10	63 ± 7[c]
Ribonucleotide reductase	100 ± 6	101 ● 8
Phosphoribosyl pyrophosphate amidotransferase	100 ± 9	41 ± 3[c]
Inosinic acid dehydrogenase	100 ± 10	100 ± 9
Dihydrofolate reductase	100 ± 8	75 ± 6[c]
Carbamyl phosphate synthetase	100 ± 10	77 ± 8[c]
Aspartate transcarbamylase	100 ± 9	89 ± 8
Orotidine monophosphate decarboxylase	100 ± 10	106 ± 9
Thymidylate synthetase	100 ± 9	102 ± 9
Thymidylase levels		
monophosphate	100 ± 10	43 ± 6[c]
diphosphate	100 ± 12	89 ± 11
triphosphate	100 ± 9	90 ± 10

[a] Mean ± *SD*; $n = 6$. [b] Dosed at 10 mg/kg/d on days 8 and 9. [c] Significantly different from the control group, $p \leq 0.001$.

[1] Allied Chemicals, Morristown, N.J.
[2] GF/F.
[3] Fisher Scintiverse.
[4] PEI cellulose F.
[5] Hyamine Hydroxide.

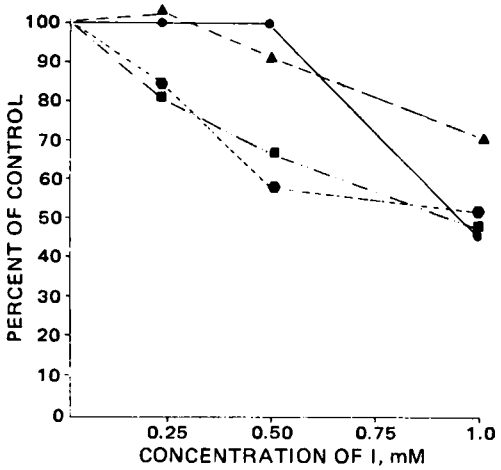

Figure 1—In vitro *effects of I on the incorporation of radiolabeled precursors into DNA, RNA, proteins, and purines of Ehrlich ascites cells. Key: (●) [^{3}H]thymidine incorporation into DNA; (▲) [^{3}H]uridine incorporation into RNA; (■) [^{3}H]leucine incorporation into proteins; (●) [^{14}C]formate incorporation into purines.*

mCi/mmol). Purines were separated on silica gel TLC plates eluted with *n*-butyl alcohol–acetic acid–water (4:1:5). After identifying R_f values consistent with the adenine and guanine standards, the plates were scraped and the radioactive content determined. Phosphoribosyl-1-pyrophosphate amidotransferase activity was determined on a supernatant fraction (600 × *g* for 10 min) measuring the reduction of 0.6 μmol of NAD at 340 nm for 30 min (21). Inosinic acid dehydrogenase activity was determined by the method of Becker and Löhr (22) using [8-^{14}C]IMP (61 mCi/mmol) and a 7000 × *g* supernatant. A sample of the reaction medium was plated on cellulose plastic-precoated TLC plates[4] and eluted with 0.5 M NH_4SO_4. The spot at the R_f value for xanthine monophosphate was scraped and counted. Dihydrofolate reductase activity was determined at 340 nm for 30 min as the oxidation of reduced NADP (23). Ribonucleotide reductase activity was determined by the method of Moore and Hurlbert (24) using [5-^{3}H]CDP (25 Ci/mmol). Ribose and deoxyribose nucleotides were separated on cellulose plastic-precoated TLC plates[4] eluted with 4% boric acid–4 M LiCl (4:3) and scraped at the R_f values consistent with the standard dCDP.

An *in vitro* method (25) was used to determine if I was an initiation or elongation inhibitor of Ehrlich ascites lysate protein synthesis by comparing with known inhibitors, pyrocatechol violet and emetine, using 1 μCi of [^{3}H]leucine (24.7 Ci/mmol). The reaction medium was spotted on filter paper[6] disks which, after drying, were treated for 10 min in boiling 5% trichloroacetic acid, for 10 min in cold 5% trichloroacetic acid, and washed with cold 5% trichloroacetic acid, ether–ethanol (4:1), and ether. The disks were dried and counted[3].

RESULTS

Compound I effectively inhibited Ehrlich ascites carcinoma growth at 10 and 20 mg/kg/d. The 10-mg/kg dose afforded greater inhibition of growth, *i.e.*, 99.7%, than the 20-mg/kg dose (Table I).

For the *in vivo* incorporation studies (Table II) the control values for thymidine incorporation into DNA for 60 min for day 10 Ehrlich ascites cells was 107,533 dpm/mg of isolated DNA, which was inhibited 57% by I. For uridine incorporation, the control was 51,193 dpm/mg of RNA isolated, which was unaffected by drug treatment. Leucine incorporation into protein for the control was 19,181 dpm/mg of isolated protein which was inhibited 52% by drug therapy. Formate incorporation into purine for the day 10 control was 28,786 dpm/mg of protein. *De novo* purine synthesis was inhibited 41% by I. It may be noted that drug administration for 2 d reduced the number of cells in the ascites fluid from 226 × 10^6 to 102 × 10^6 per milliliter.

Nuclear DNA polymerase activity for the control was 76,528 dpm/h/mg of nucleoprotein which was reduced 62% by administration of I. Nuclear mRNA polymerase activity for the control was 4867 dpm/h/mg of nucleoprotein, rRNA polymerase activity was 8751 dpm/h/mg of protein, and tRNA polymerase activity was 10,792 dpm/mg of protein. mRNA and rRNA polymerase activities were not affected by drug administration, but tRNA polymerase activity was suppressed 37%. Ribonucleotide reductase activity for the day 10 control was 153,791 dpm/mg of protein and was unaffected by drug administration.

[6] Whatman No. 3.

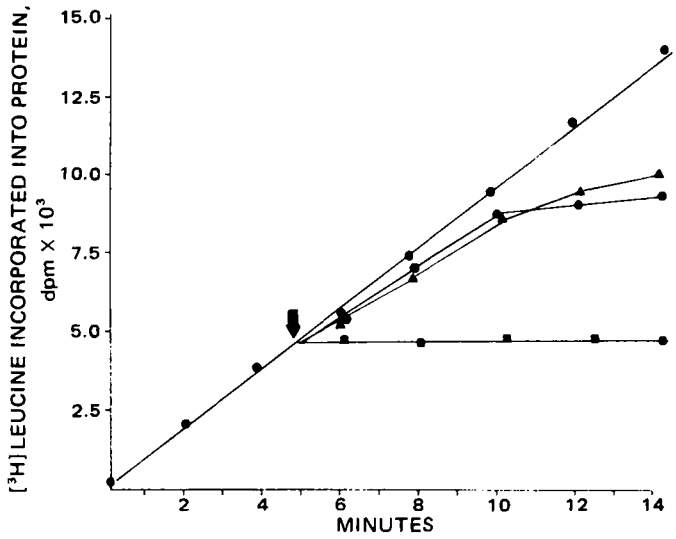

Figure 2—*Effects of I on the initiation and elongation of protein synthesis of Ehrlich ascites carcinoma cells. Key: (●) control; (●) pyrocatechol violet; (■) emetine; (▲) I; (⇓) drugs added at 100 μM concentrations.*

Phosphoribosyl pyrophosphate amidotransferase activity for the control resulted in a net change of 0.544 optical density units/h/mg of protein; drug administration for 2 d reduced the activity 59%. Inosinic acid dehydrogenase activity for the control was 36,530 dpm/mg of protein, which was essentially not affected by drug therapy. Dihydrofolate reductase activity for day 10 Ehrlich ascites cells was 0.514 optical density units/h/mg of protein; this was inhibited 25% by I. Carbamyl phosphate synthetase activity for the control was 0.128 mg of carbamyl phosphate formed/h/mg of protein, which was reduced 23% by I. Aspartate carbamyl transferase activity for the control was 7.526 mg of carbamyl aspartate formed/h/mg of protein, which was suppressed 11% by drug administration. Orotidine monophosphate decarboxylase activity for the control was 10,775 dpm of $^{14}CO_2$ generated in 15 min/mg of protein; this was not affected by drug administration. Thymidylate synthetase activity for the control was 103,328 dpm/mg of protein, which was not suppressed by I. [^{3}H]Thymidine incorporation into mono-, di-, and triphosphate pools were reduced 57, 19, and 10%, respectively. Deoxyribonuclease activity for the control was 247 μg of DNA hydrolyzed/h/mg of protein.

Preliminary whole cell *in vitro* incorporation studies demonstrated that I afforded an ID_{50} of 0.94 mM for the inhibition of DNA synthesis. For RNA synthesis the ID_{50} was 1.82 mM, and for the protein synthesis the ID_{50} was 0.863 mM. Using a supernatant fraction, the ID_{50} for formate incorporation into purine for I was 1.71 mM. Figure 1 demonstrates the *in vitro* effects of I on the incorporation studies for nucleic acid, protein, and purine biosyntheses.

DNA polymerase activity in isolated nuclei from Ehrlich ascites cells was inhibited significantly by I, with an ID_{50} of 0.454 mM. tRNA polymerase activity resulted in an ID_{50} of 0.433 mM. Phosphoribosyl pyrophosphate amidotransferase activity was also significantly inhibited by the copper complex with an ID_{50} of 0.523 mM. Deoxyribonuclease activity was inhibited significantly, with an ID_{50} of 0.682 mM. A number of other enzymes were not inhibited by I in the concentration range of 0.25–1.0 mM. These include carbamyl phosphate synthetase, aspartate carbamyl transferase, orotidine monophosphate decarboxylase, thymidylate synthetase, inosinic acid dehydrogenase, dihydrofolate reductase, ribonucleotide reductase, and mRNA and rRNA polymerase activities.

Figure 2 demonstrates that I does not immediately inhibit protein synthesis of Ehrlich ascites lysates, but rather there is a lag of several minutes before inhibition is observed. Protein synthesis inhibition by I resembles more closely the type of inhibition seen for pyrocatechol violet, an initiation inhibitor, rather than that by emetine, an elongation inhibitor of polypeptide synthesis.

DISCUSSION

The boron compounds were originally synthesized with the idea that they may act as antimetabolites of α-amino acids. They have been used

therapeutically in the past in neutron capture in cancer therapy. The parent compound, trimethylamine carboxyborane, at 20 mg/kg produced 82% inhibition of Ehrlich ascites growth. As can be seen, I is more potent, producing 96.2% inhibition at 20 mg/kg. Compound I significantly inhibited DNA and protein syntheses in Ehrlich ascites cells. The major sites in DNA synthesis that were inhibited include DNA polymerase and *de novo* purine syntheses. The regulatory enzyme of purine biosynthesis, phosphoribosyl pyrophosphate amidotransferase was significantly inhibited by I; the inhibition was of a magnitude to account for the observed inhibition of purine synthesis.

The trimethylamine cyanoboranes and carboxyboranes have been observed to inhibit DNA polymerase activity (1) in a similar manner as I. However, the former derivatives also significantly suppressed thymidylate synthetase activity. Compound I had no effect on thymidylate synthetase activity either *in vivo* or *in vitro*. It may be noted that heavy metals at low concentrations have been known to inhibit DNA polymerase activity by directly binding to the enzyme and form a stable complex with nucleotide triphosphates, polynucleotides, and DNA (26); however, in these studies the copper existed as an ion species. Further evidence indicates that metal ions are carcinogenic and mutagenic. The copper in I is securely bound to the molecule; thus, there is no reason to believe that it is in an ionic form.

Compound I moderately inhibited (23%) the regulatory enzyme of pyrimidine synthesis, *i.e.*, carbamyl phosphate synthetase. Moderate inhibition of dihydrofolate reductase by I was observed and may be important in one-carbon transfer in the synthesis of both purines and pyrimidines. Previous studies with trimethylamine cyanoboranes and carboxyboranes have shown that one-carbon transfer from *S*-adenosyl methionine was suppressed (1). Deoxyribonuclease activity was also suppressed, which indicates that I did not cause the release of hydrolytic enzymes from lysosomes and thus cause the degradation of nucleic acids.

The data for the protein experiment suggest that I is an initiation inhibitor of Ehrlich ascites protein synthesis. Compound I exhibited behavior similar to the initiation inhibitor pyrocatechol violet, which allows completion of the ongoing round of protein synthesis, rather than emetine (27), an elongation inhibitor which freezes the ribosome on the mRNA with an immediate cessation of polypeptide synthesis (28).

REFERENCES

(1) I. H. Hall, C. O. Starnes, B. F. Spielvogel, P. Wisian-Neilson, M. K. Das, and L. Wojnowich, *J. Pharm. Sci.*, **68**, 685 (1979).

(2) B. F. Spielvogel, in "Synthesis and Biological Activity of Boron Analogues of the α-Amino Acids and Related Compounds in Boron Chemistry," R. W. Parry and G. Kodama, Eds., Pergamon, New York, N.Y., 1980, p. 119.

(3) K. H. Scheller, R. B. Martin, B. F. Spielvogel, and A. T. McPhail, *Inorg. Chim. Acta*, **57**, 227 (1982).

(4) A. T. McPhail, M. Scheitlin, B. F. Spielvogel, and I. H. Hall, *J. Chem. Soc., Dalton Trans.*, in press.

(5) C. Piantadosi, C. S. Kim, and J. L. Irvin, *J. Pharm. Sci.*, **58**, 821 (1969).

(6) L. L. Liao, S. M. Kupchan, and S. B. Horwitz, *Mol. Pharmacol.*, **12**, 167 (1976).

(7) C. B. Chae, J. L. Irvin, and C. Piantadosi, *Proc. Am. Assoc. Cancer Res.*, **9**, 44 (1968).

(8) R. G. Wilson, R. H. Bodner, and G. E. MacHorter, *Biochim. Biophy. Acta*, **378**, 260 (1975).

(9) A. C. Sartorelli, *Biochim. Biophys. Res. Commun.*, **27**, 26 (1967).

(10) O. H. Lowry, N. J. Rosebrough, A. L. Farr, and R. J. Randall, *J. Biol. Chem.*, **193**, 265 (1951).

(11) W. C. Hymer and E. L. Kuft, *J. Histochim. Cytochem.*, **12**, 359 (1964).

(12) H. Sawada, K. Tatsum, M. Sasada, S. Shirakawa, T. Nakumura, and G. Wakisaka, *Cancer Res.*, **34**, 3341 (1974).

(13) K. M. Anderson, I. S. Mendelson, and G. Guzik, *Biochim. Biophy. Acta*, **383**, 56 (1975).

(14) F. Maley and S. Ochoa, *J. Biol. Chem.*, **233**, 1538 (1958).

(15) S. M. Kalman, P. H. Duffield, and T. Brzozuski, *Am. Biol. Chem.*, **24**, 1871 (1966).

(16) R. M. Archibald, *J. Biol. Chem.*, **156**, 121 (1944).

(17) S. B. Koritz and P. P. Cohen, *J. Biol. Chem.*, **209**, 145 (1954).

(18) S. H. Appel, *J. Biol. Chem.*, **243**, 3929 (1968).

(19) A. Kampf, R. L. Barfknecht, P. J. Schaffer, S. Osaki, and M. P. Mertes, *J. Med. Chem.*, **19**, 903 (1976).

(20) M. K. Spassova, G. C. Russev, and E. V. Colovinsky, *Biochem. Pharmacol.*, **25**, 923 (1976).

(21) J. B. Wyngaarden and D. M. Ashton, *J. Biol. Chem.*, **234**, 1492 (1959).

(22) H. J. Becker and G. W. Löhr, *Klin. Wochenschr.*, **57**, 1109 (1979).

(23) M. K. Ho, T. Hakalo, and S. F. Zakrzwski, *Cancer Res.*, **32**, 1023 (1972).

(24) E. G. Moore and R. B. Hurlbert, *J. Biol. Chem.*, **241**, 4802 (1966).

(25) L. L. Liao, S. M. Kupchan, and S. B. Horwitz, *Mol. Pharmacol.*, **12**, 167 (1976).

(26) E. A. Popenoe and M. A. Schmaeler, *Arch. Biochem. Biophys.*, **196**, 109 (1979).

(27) M. T. Huang and A. P. Grossman, *Biochem. Biophy. Res. Commun.*, **53**, 1049 (1976).

(28) A. P. Grollman and A. P. Huang, *Fed. Proc. Fed. Am. Soc. Exp. Biol.*, **32**, 1673 (1973).

ACKNOWLEDGMENTS

Support of the Army Research Office and the National Institutes of Health is gratefully acknowledged.

Ionization Constants by Curve Fitting: Application to The Determination of Partition Coefficients

FRANK H. CLARKE

Received March 18, 1982, from the *Research and Development Department, Pharmaceuticals Division, CIBA-GEIGY Corporation, Ardsley, NY 10502.* Accepted for publication January 6,1983.

Abstract □ A multiparametric curve-fitting technique for pK_a calculation has been adapted for use with a programmable calculator or microcomputer. This method provides for the convenient and accurate determination of the ionization constant in aqueous solution and of the apparent ionization constant in the presence of octanol. From these parameters, partition coefficients and apparent partition coefficients are easily calculated and agree with data reported using the shaker technique or HPLC. The curve-fitting method has been applied to the differential titration technique in which the solvent curve is subtracted from the solution curve before calculations are begun. This method has been applied to the potentiometric titration of aqueous solutions of the salts of bases with a very low solubility in water.

Keyphrases □ Partition coefficients—octanol–water, determination by a multiparametric curve-fitting technique, adaptation to a programmable calculator/microcomputer □ Curve fitting—multiparametric, octanol–water partition coefficient and pK_a determination, adaptation to a programmable calculator/microcomputer □ Differential titration—use with curve-fitting technique for the determination of pK_a and octanol–water partition coefficients, programmable calculator/microcomputer

Partition coefficients (P or log P), important physical properties of drugs, are useful for studies of quantitative structure–activity relationships (1, 2). For compounds that are ionized at physiological pH, the apparent partition coefficient (P′ or log P′) may be a more appropriate parameter (3). The variation of the apparent partition coefficient with pH has been used in various ways to measure the partition coefficient of the un-ionized compound (4–9). The method described by Kaufman *et al.* (9) is one of the simplest of these procedures. In this method the ionization constant (pK_a) and the apparent ionization constant (pK_a') are first obtained from the results of two potentiometric titrations, one without and one with the presence of octanol, respectively. The log P is calculated from the difference between the pK_a and pK_a' values and the volumes of water and octanol. The log P′ for any desired pH is calculated from the same data. We have modified this titration method and have shown it to be rapid and convenient and to provide reproducible results (10) which agree with those obtained using the shaker technique (1, 2) or HPLC (11–13). Recently, this modified titration method has been used successfully in other laboratories (14, 15) and its advantages described (15). Calculated aqueous–octanol titration curves are very similar to experimental curves (10) and lend support to the general application of the method (Fig. 1).

Since the measurement of partition coefficients by potentiometric titration depends on the ability to calculate the pK_a and pK_a' values from the titration curves, it is important to have a general procedure that is applicable in most instances. For strong acids or strong bases, for instance, there may be no inflection at one end of the aqueous titration curve. In these cases, when there is an appreciable difference between the pK_a and the pK_a', the two titration curves may be used together to provide the equivalent volume (10) (Fig. 1). Other methods of determining the end point in a potentiometric titration have been reviewed (16).

The method of Meites and his associates (17–20) uses a multiparametric curve-fitting technique involving an iterative computer program to compare the calculated pH with the experimental value for each point on a titration curve. Parameters are varied until the standard deviation (σ) of the difference between calculated and experimental values is a minimum. Using this criterion, the optimum equivalent volume (V_e) and the starting titrant volume (V_s) are located, and the mean pK_a is calculated using these values. Briggs and Stuehr (21) and Meites *et al.* (27) described a similar procedure in which the σ of the ionization constant (K_a) is minimized. The latter method has been characterized as being less reliable although it has the advantage of requiring less computer time (22). The method of Meites has been used to provide accurate results in automatic titrations (23, 24) using an on-line or laboratory computer.

We have modified the method of Briggs and Stuehr (21) so that the σ of the pK_a values is minimized and have adapted it for use with a programmable calculator (10). Originally only V_e was optimized (10), but now it has been found that the results are improved if optimization is carried out for both V_e and V_s. Running time is 1–2 h on the calculator, but equivalent results are obtained in a few minutes when a similar program is run on a microcomputer. With this iterative method of calculation, pK_a and pK_a' values are easily determined and the calculator or computer printout provides P, log P, P′, and log P′ as well as pertinent parameters used in the calculation.

The general method described above applies to most acids or bases which may be titrated in aqueous solution. However, it fails when the un-ionized compound precipitates early in the titration. For many drugs, such as chlorpromazine, the UV method (25) also fails because there is no change in the UV spectrum on ionization. The solubility method (26, 27) is cumbersome as are the methods involving nonlogarithmic linear titration curves (28) or titrations in solvent mixtures (16, 29–31). On the other hand, the differential potentiometric titration method (32) is applicable for very dilute solutions when the pK_a is in the range of 4–10 (33). In this method the titration curve obtained with solvent alone is subtracted from that of the solution. We have found that the iterative method gives excellent results when applied to the difference curve.

THEORETICAL

Equations—In the equations derived below, the following assumptions are made:

1. Only un-ionized compounds are soluble in octanol.

0022-3549/84/0200-0226$01.00/0
© 1984, American Pharmaceutical Association

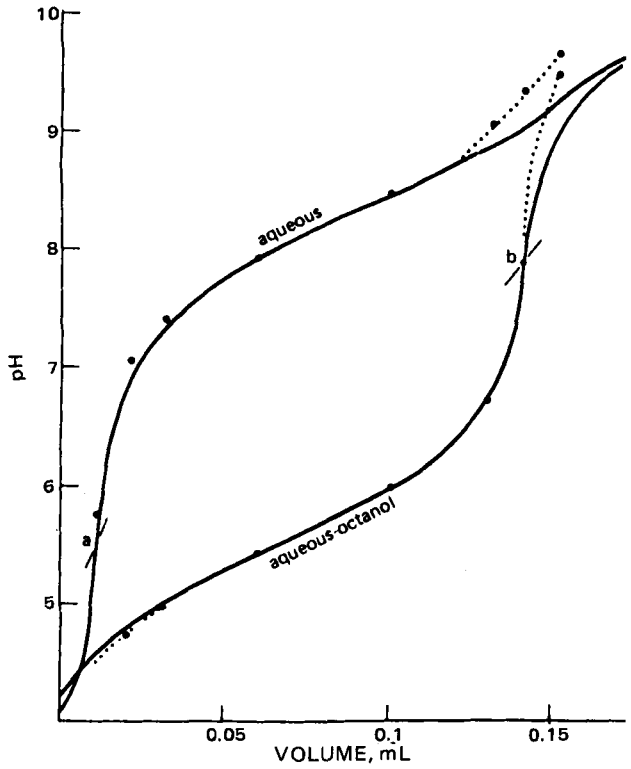

Figure 1—*Titration of an organic base in aqueous solution and in the presence of octanol. Inflections at a and b locate initial values of the starting titrant volume, V_s, and of the equivalent titrant volume, V_e. Key: (●) calculated values.*

2. All solutions are dilute (0.001 M) and the ionic strength is nearly constant (with added sodium chloride), so that it not necessary to consider activities.
3. Titrant volumes are small compared with the volume of titrated solution, so that the aqueous volume is considered constant for the calculation of the partition coefficient following a two-phase titration.

Concentration terms are indicated by square brackets, and the subscripts o and w refer to octanol and water phases, respectively. The following symbols are used: (M) molar amount of titrated compound; (m) molar amount of added titrant; (V_e) volume of titrant at the equivalence point; (V_i) volume of added titrant at the ith point; (V_w) total aqueous volume; (V_o) volume of octanol; (P) partition coefficient; (P′) apparent partition coefficient (at a given pH); (K_a) ionization constant; (K') apparent ionization constant (in the presence of octanol); (f) partition factor.

Consider the titration of the salt of a weak acid with a strong acid in the presence of octanol:

$$Na^+A^- + H^+Cl^- \rightleftarrows HA + Na^+ + Cl^- \qquad \text{(Eq. 1)}$$

By definition:

$$K_a = [H^+][A^-]/[HA] \qquad \text{(Eq. 2)}$$

$$P = \frac{[HA]_o}{[HA]_w} = \frac{HA_o \cdot V_w}{HA_w \cdot V_o} \qquad \text{(Eq. 3)}$$

$$P' = [HA]_o/([HA]_w + [A^-]_w) \qquad \text{(Eq. 4)}$$

Let f be a partition factor such that:

$$f = \frac{V_o \cdot P}{V_w} + 1 \qquad \text{(Eq. 5)}$$

Then, combining Eqs. 3 and 5:

$$HA_o + HA_w = f \cdot HA_w \qquad \text{(Eq. 6)}$$

At any point during the titration, material balance is maintained so that:

$$M = HA_o + HA_w + A^- \qquad \text{(Eq. 7)}$$

Table I—Raw Data for Computer Program [a] to Calculate pK_a and Log P

Symbol	Description
A$	Name of compound
B$	Source of compound
C$	Date
T$	Titrant: acid or base (A or B)
TX	Titrant increment
N	Normality of titrant
VI	Initial aqueous volume (mL)
VE	Estimated equivalent volume (mL)
Z$	Two-phase titration? (Y or N)
C	Volume of octanol (mL)
P$	Is the ion protonated? (Y or N)
A3	pK_a (when log P is calculated)
W$	Complete title? (Y or N) [b]
VI	First titrant volume
M	Number of data points
V(I)	Titrant volume at ith point
P(I)	pH at ith point

[a] A simplified, calculator version of the program is provided in Ref. 10. [b] A$, B$, and C$ are not repeated if both pK_a and log P results are printed at the same time.

Therefore:

$$M = f \cdot HA_w + A^- \qquad \text{(Eq. 8)}$$

Division by the aqueous volume converts amounts in the aqueous phase into concentration terms so that, after rearranging:

$$[HA]_w = \frac{1}{f}\left(\frac{M}{V_w} - [A^-]\right) \qquad \text{(Eq. 9)}$$

For ionic balance in the aqueous solution:

$$[H^+] + [Na^+] = [Cl^-] + [A^-] + [OH^-] \qquad \text{(Eq. 10)}$$

Since $[Na^+] = M/V_w$ and $[Cl^-] = [m]$ we may write:

$$[A^-] = \frac{M}{V_w} - [m] + [H^+] - [OH^-] \qquad \text{(Eq. 11)}$$

Hence:

$$K_a = f\left(\frac{[H^+]\left(\frac{M}{V_w} - [m] + [H^+] - [OH^-]\right)}{[m] - [H^+] + [OH^-]}\right) \qquad \text{(Eq. 12)}$$

$$K_a = f \cdot K', \quad pK_a = \log f + \log pK' \qquad \text{(Eq. 13)}$$

In the absence of octanol, $f = 1$ and:

$$pK_a = pH + \log\left(\frac{[m] - [H^+] + [OH^-]}{[M] - [m] + [H^+] - [OH^-]}\right) \qquad \text{(Eq. 14)}$$

In the presence of octanol:

$$pK' = pH + \log\left(\frac{[m] - [H^+] + [OH^-]}{\frac{M}{V_w} - [m] + [H^+] - [OH^-]}\right) \qquad \text{(Eq. 15)}$$

It can also be shown that:

$$P = \frac{V_w}{V_o}(10^{pK' - pK_a} - 1) \qquad \text{(Eq. 16)}$$

and:

$$P' = \frac{P}{1 + 10^{pH - pK_a}} \qquad \text{(Eq. 17)}$$

Corresponding expressions may be derived in an analogous fashion for the titration of the salt of a weak base with a strong base. In this case:

$$K_a = K'/f \qquad \text{(Eq. 18)}$$

$$pK_a = pH - \log\left(\frac{[m] + [H^+] - [OH^-]}{[M] - [m] - [H^+] + [OH^-]}\right) \qquad \text{(Eq. 19)}$$

Table II—Ionization Constants, Partition Coefficients, and Apparent Partition Coefficients

Curve No.	Compound	pK_a Found[a]	pK_a Lit.	pK_a Δ	Log P Found[a]	Log P Lit.	Log P Δ	Log P pH	Log P Found	Log P Lit.	Log P Δ
1	Pyridine	5.16	5.23[b]	0.07	0.63	0.65[c]	0.02	7.4	0.63		
2	*p*-Aminobenzoic Acid	4.71	4.67[d]	0.04	0.83	0.83[d]	0.00	7.4	0.83	0.85[e]	0.02
3	Benzoic Acid	4.08	4.17[b]	0.09	1.87	1.87[f]	0.00	7.4	1.87		
4	*p*-Toluic Acid	4.26	4.37[b]	0.11	2.34	2.27[f]	0.07	7.4	2.34		
5	Adamantanamine	10.49	10.63[g]	0.14	2.54	2.44[g]	0.10	7.4	−0.55		
6	*p*-Chlorobenzoic Acid	3.85	3.98[b]	0.13	2.66	2.65[f]	0.01	7.4	2.65		
7	Pyrilamine	8.91	8.85[h]	0.06	3.27	3.15[h]	0.12	7.4	1.74		
8	Chlorpheniramine	9.09	9.16[i]	0.07	3.39	3.38[j]	0.01	7.4	1.69	1.38[k]	0.31
9	Triprolidine	9.25	9.50[h]	0.25	3.87	3.92[h]	0.05	7.4	2.02		
10	Cyproheptadine	8.87			4.69			7.4	3.20	3.20[h]	0.00
										3.11[i]	0.09
11	Chlorpromazine	9.20	9.22[l]	0.01	5.25	5.32[h]	0.07	7.4	3.44	3.25[o]	0.19
			9.3[m]	0.1		5.55[n]	0.30	8.1	4.11	4.19[h]	0.08
								7.0	3.04	2.93[p]	0.11

[a] Mean value, $SD \pm 0.1$. [b] Ref. 1. [c] Ref. 2. [d] J. K. Seydel and W. Butte, *J. Med. Chem.*, **20**, 489 (1977). [e] H. P. A. Illing and D. Benford, *Biochim. Biophys. Acta*, **429**, 768 (1976). [f] T. Fugita, J. Iwasa, and C. Hansch, *J. Am. Chem. Soc.*, **86**, 5175 (1964). [g] J. G. Henkel, J. T. Lane, and G. Gianutsos, *J. Med. Chem.*, **25**, 51 (1982). [h] Ref. 1. [i] N. G. Lordi and J. E. Christian, *J Am. Pharm. Assoc. Sci. Ed.*, **45**, 300 (1956). [j] By HPLC Ref. 1. [k] By HPLC, S. H. Unger and G. H. Chiang, *J. Med. Chem.*, **24**, 262 (1981). [l] By extrapolation from aqueous-alcohol titrations, L. G. Chatten and L. E. Harris, *Anal. Chem.*, **34**, 1495 (1962). [m] By solubility method Ref. 19. [n] By potentiometric titration with large octanol-water ratio Ref. 8. [o] J. Krieglstein, W. Meiler and S. Staab, *Biochem. Pharmacol.*, **21**, 985 (1972). [p] M. Frisk-Holmberg and E. Kleijn, *Eur. J. Pharmacol.*, **18**, 139 (1972).

$$pK' = pH - \log\left(\frac{[m] + [H^+] - [OH^-]}{\frac{M}{V_w} - [m] - [H^+] + [OH^-]}\right) \quad \text{(Eq. 20)}$$

$$P = \frac{V_w}{V_o}(10^{pK_a - pK'} - 1) \quad \text{(Eq. 21)}$$

$$P' = \frac{P}{1 + 10^{pK_a - pH}} \quad \text{(Eq. 22)}$$

Curve Fitting—In the curve-fitting technique, the raw data and descriptive information (Table I) are entered into the calculator or computer as requested by the program. The calculator program has been described (10). In the case of the microcomputer[1] the raw data may be saved on a diskette. The program plots the titration curve on the monitor, locates one or two inflection points using the Kolthoff method (34), indicates these with vertical lines on the graph, and then makes a hard copy of the graph with the printer.

Iteration then begins. First V_e is varied systematically until the standard deviation (σ) is a minimum. Then, this V_e value is maintained and V_s is varied until σ is again minimized. Naturally an increment added to or subtracted from V_s must be added to or substracted from each V_i. The two-stage iterative process is repeated until successive σ values do not differ by more than 0.001. When this condition is met, iteration is complete if $SD < 0.008$.

If σ at this point exceeds 0.008, residuals are calculated for each pK_a value and compared (in absolute magnitude) with 2σ. Points at the beginning or end of the curve which do not meet this test are excluded and the entire iteration is repeated with the reduced number of points. This test approximates exclusion of points which lie outside the 95% confidence interval since $tS = X^* - \overline{X}$ and $t = 2.09$–2.13 for 15–20 DF (35).

When iteration is complete, a summary of titration conditions and results is printed together with a table of raw data and calculated pK_a values.

Differential Titration—The differential titration technique (32) succeeds in providing the pK_a of an aqueous solution for compounds with a very low solubility in water which form water-soluble salts. In this case, the titration curve of water is subtracted from that of the compound before the calculations are carried out. The equation is then a simple one:

$$pK_a = pH \pm \log\left(\frac{V_i}{V_e - V_i}\right) \quad \text{(Eq. 23)}$$

where V_i is the difference in titrant volumes for solution and solvent at each pH; the log term is added for an acid titrant and subtracted for a base titrant. The experiment is performed so that the conditions for the titration in solvent alone are as close as possible to those of the solution. The equation does not include concentration terms, so that neither the solution volume nor the titrant normality need to be known precisely provided conditions for the two titrations are the same. Impurities in the water, such as carbon dioxide, do not interfere. This is an important advantage for extremely dilute solutions.

EXPERIMENTAL

Apparatus—Potentiometric titrations were carried out with an automatic titrator[2], titration assembly[3], and an autoburet[4]. The titration assembly was fitted with a 40-mL water-jacketed sample cell kept at a constant temperature of 25°C with circulating water. A calomel reference electrode and a porous pin liquid junction electrode were used.

Aqueous solutions (10 mL) were titrated with 0.1 M standard HCl or NaOH delivered from a 0.25-mL microburet. Stirring was provided with a medium-size mechanical stirrer which emulsified two-phase octanol–water systems (15 mL and 10 mL, respectively). The solvents were boiled, deionized water and commercial-grade octanol[5]. Air was displaced from above the sample with a slow stream of nitrogen for a few minutes before stirring was begun, and the nitrogen stream was maintained during the titration.

Procedure—In a typical titration, water (9.0 mL), 0.02 M aqueous NaCl (0.5 mL), and a 0.5-mL aliquot of a stock solution containing 0.02 mM of the compound to be titrated were added to the titration vessel. For two-phase titrations, octanol (15 mL) was added. Aqueous and two-phase titrations were carried out in the same manner. Stirring and titrant addition were continuous while the titration curve was recorded on the servograph. The equilibrium titration mode provided smoother titration curves, especially for very dilute solutions, but the calculated results were equivalent without the step procedure, indicating that equilibrium is very rapid in the homogenized two-phase system.

Usually, the total volume of the stock solution was calculated from the sample weight and equivalent weight so that a 0.5-mL aliquot would require 0.2 mL of titrant. When the sample was available as its salt, a 20% excess of acid or base was added. Because the calculation finds both ends of the titration curve, it was not assumed that the original compound was exactly a 1:1 salt of acid and base. Weak bases were converted to their hydrochloride salts and weak acids to their sodium salts wilth a 20% excess of 0.1 M HCl or 0.1 M NaOH, respectively. Organic salts such as the maleate salt of a weak base or the dicyclohexylamine salt of a weak acid were converted to their hydrochloride or sodium salts, respectively, by passing the aqueous solution through a short column of an appropriate ion-exchange resin. Excess acid or base was added to the eluate before dilution to an appropriate volume in a volumetric flask. In these cases, the aliquot volume was calculated to require 0.2 mL of titrant and sufficient water was added to make the total aqueous volume of the titrated solution 10.0 mL.

An approximate value of one end of the titration curve may usually be obtained as the point along the curve where the slope changes sign [using parallel lines (10), the mathematical equation of Kolthoff (34), or the first

[1] Apple II Plus with 48K memory, disk drive, monitor, and Silentype printer; Apple Computer Inc., Cupertino, Calif.

[2] TTT60; Radiometer, Copenhagen, Denmark.
[3] TTA60; Radiometer, Copenhagen, Denmark.
[4] ABU 12; Radiometer, Copenhagen, Denmark.
[5] Aldrich Chemical Co., Milwaukee, Wis.

Table III—Influence of an Impurity (pK_a 6.4) on the Accuracy of pK_a Calculations

Curve No.	I, mEq	Titrant	pK_a (calc.)	Δ pK_a	×1000 *SD*	V_e[a]	Xs[b]	n[c]
1	0	A	7.00	0.00	4.10	0.200	0.000	19
2	0	B	7.00	0.00	4.10	0.200	0.000	19
3	0.005	A	6.99	0.01	5.04	0.204	0.000	19
4	0.005	B	6.98	0.02	7.72	0.204	0.000	20
5	0.01	A	6.98	0.02	6.65	0.209	0.000	20
6	0.01	B	6.97	0.03	9.38	0.210	−0.001	19
7	0.02	A	6.96	0.04	4.67	0.216	−0.001	18
8	0.02	B	6.95	0.05	6.32	0.217	0.001	19
9	0.02	B	6.954	0.046	6.32	0.217	0.002	19
10	0.02	B	6.959	0.041	3.86	0.216	0.001	18
11	0.02	B	6.94	0.06	6.71	0.216	0.000	37
12	0.01	B	3.05	0.05	8.93	0.192	−0.002	16
13	0.01	A	4.01	0.01	3.96	0.200	0.008	17
14	0.01	A	5.01	0.01	5.05	0.203	0.000	17
15	0.01	A	6.02	0.02	4.32	0.210	0.000	19
16	0.01	A	6.98	0.02	4.86	0.208	0.000	19
17	0.01	A	7.99	0.01	4.17	0.202	0.001	18
18	0.01	A	9.00	0.00	5.55	0.200	0.000	19
19	0.01	A	10.00	0.00	3.04	0.200	0.000	19
20	0.01	A	11.00	0.00	5.39	0.200	0.000	19
21	0.01	A	11.99	0.01	22.9	0.200	−0.006	17
22	0.02	A	6.04	0.04	5.95	0.219	0.000	20

[a] Calculated equivalent titrant volume. [b] Displacement of the starting titrant volume. [c] Number of data points used in the calculation.

derivative]. However, this point may not provide the most accurate pK_a because of the undetected presence of CO_2 or of titrated impurities in the solution. It has been shown that the most accurate pK_a values are provided by curve-fitting techniques (17–20).

At least one end of the titration curve may lack an inflection point because of the contribution of the dissociation of water to the pH. Approximate values of the equivalent titrant volume, V_e, and of the initial titrant volume, V_s, may often be obtained in such instances by carrying out the titration using the same aliquot volume in the presence of a water-immiscible solvent (such as octanol) or a water-miscible solvent (such as isopropyl alcohol or dimethyl sulfoxide) (10). Values of V_e and V_s obtained in this manner serve as initial estimates for the multiparametric curve-fitting technique.

Differential Titration—When a precipitate forms during the titration, it is often possible to use the curve-fitting technique to calculate the pK_a from the portion of the curve which preceded precipitation (10). For very insoluble acids or bases with water-soluble salts, a differential titration is often successful.

For this pK_a determination, 0.5 mL of a solution containing 0.002 mM of compound in water was added to 8.0 mL of water and 0.5 mL of a solution of 0.02 M NaCl. The solution was acidified with 5 μL of 0.1 M HCl and titrated with 0.001 M NaOH. A blank titration was carried out in the same manner except that 0.5 mL of water replaced the solution of compound. The titration curves were recorded using an expanded pH scale from 8.1 to 8.8. Titrant volumes were measured at pH intervals of 0.05 for both curves, and the differences were recorded as values of V_i. Using a microcomputer program V_e and V_i were varied until the σ of the calculated pK_a values was minimized. In contrast to a normal titration, there may not be an inflection in titration curves recorded on such an expanded scale. Accordingly, the computer program was designed to facilitate the initial trial and error process that is required to obtain optimum values of V_e and V_s. The pK_a results obtained in this way may have a larger experimental error because usually only a portion of the titration curve is available before errors in the measurement of V_i become large.

RESULTS AND DISCUSSION

Table II summarizes the results of pK_a and log P measurements for a series of 11 acids and bases which span the log P range from 0.63 to 5.33. These results were reproducible to within ≤0.06 of a pK_a or log P unit. These results for log P are in very close agreement with data reported using the classical shaker method or by chromatography. Apparent partition coefficients (pH 7.4) are automatically calculated by the program and may be calculated easily for any desired pH (no. 11). Log P calculations by potentiometric titration involve differences between pK_a measurements and appear in Table II to be closer to literature values than the pK_a determinations. However, it should be noted that there is a wide variation for most pK_a results in the literature (36) reflecting different experimental conditions. The pK_a values for cyproheptadine and chlorpromazine were determined using differential titration.

As an example, a very dilute solution of chlorpromazine [solubility of base, 6 μM (27)] was titrated with 0.001 M aqueous NaOH. An automatic titrator was used in which the pH scale was expanded so that no inflection appeared at either end of the titration curves. Application of the iterative procedure to the difference data optimized both V_e and V_s. The results of 9.20 and 5.33 for the pK_a and log P, respectively, are in close agreement with reported values of 9.22 (27) and 5.35 (1). In the calculation using this method, the solution volume and titrant normality are not involved and small amounts of carbon dioxide are compensated for by subtraction of the solvent curve.

The chlorpromazine value is unusual because the base is so insoluble that a potentiometric aqueous titration has been regarded as impossible (27). Previous results were obtained by extrapolation of results in aqueous–alcohol or by the solubility method (Table II).

Effect of Impurities—It was of interest to determine how an impurity such as carbon dioxide, with an effective pK_a of 6.4 (25), would affect the results of pK_a calculations by the curve-fitting method. Titration curves were calculated for mixtures of a major component and varying amounts (2.5, 5, and 10%) of an impurity (I) of pK_a 6.4 (to simulate carbon dioxide). In each case the solution volume was 10 mL, the titrant was 1 M acid or base, and the equivalent volume (V_e) of the major component was 0.2 mL. The data were used for calculations in the aforementioned manner. The raw data (19, 20, or 21 points, as appropriate) were entered into the computer and the program rejected points which failed to meet the standard criteria.

Table III provides the results of these calculations in which 5% of impurity (pK_a 6.4) was present. In these cases, the titration curves are smooth and do not indicate the presence of the impurity. Nevertheless the calculated pK_a is close to the theoretical value (the largest deviation is 0.06 pK unit). Furthermore, V_e is in error by ≤1% when the difference between the pK_a of the impurity and that of the major component is >2 pK_a units. When the difference between the two pK_a values is <2, the calculated V_e is closer to the sum of the two components. A similar calculation was performed for 10% of impurity. In these cases, the impurity is evident by an inflection in the curves when the pK_a values are quite different. However, in all cases the calculated pK_a is within 0.06 pK units of that of the major component. It is concluded from these results that curve fitting provides accurate data for the calculation of partition coefficients.

Raw data were calculated to four decimal places and rounded to two decimal places before entry into the computer. Curves 1 and 2 (Table III) for pure compounds show that a σ of 4.10×10^{-3} may be expected for data of such precision when there are no errors and no impurities. The maximum error in any of the curves is 0.06 pK_a unit. When the pK_a of the major component is close to that of the impurity (curves 3–8), the V_e reflects the sum of the two equivalent volumes, but the pK_a is very close to that of the major component. Curves 9 and 10 show that greater precision in the measurement of pH values (data rounded to three decimal places) does not increase the accuracy when there is titratable impurity present. Curve 11 shows that doubling the number of data points does

not improve the accuracy in the presence of an impurity. Curves 12 and 21 show that pK_a values of 3 and 12 are near the practical limits of this method of calculation. In fact, there was no convergence with curve 12 during the calculations when the titrant was an acid. When the impurity has a pK_a that is at least 2 pK_a units from the major component, this method of calculation will remove its influence completely. Curves 18–20 give the correct pK_a and the correct equivalent volume. Curve 22 has 10% of a titratable impurity and, although the V_e reflects both components, the pK_a is only 0.04 pK_a units in error.

CONCLUSIONS

It has been shown that the curve-fitting method for pK_a determination is easily adapted for the calculator and the microcomputer. The method provides a high degree of accuracy even in the presence of titratable impurity. When both the pK_a and the apparent pK_a are determined in this manner, accurate measures of the partition coefficient and the apparent partition coefficient are provided. It was surprising to find that pH measurement is so practical and convenient in emulsified aqueous–octanol mixtures and that equilibrium is reached so rapidly that titrant may be added continuously at a rate normal for an aqueous titration.

REFERENCES

(1) C. Hansch and A. Leo, "Substituted Constants for Correlation Analysis in Chemistry and Biology," Wiley Interscience, New York, N.Y., 1979.

(2) Y. C. Martin, "Quantitative Drug Design: A Critical Introduction," Dekker, New York, N.Y., 1978.

(3) R. A. Scherrer and S. M. Howard, *J. Med. Chem.*, **20,** 53 (1977).

(4) A. Bronstrom, *Acta Chem. Scand.*, **17,** 1218 (1963).

(5) S. S. Davis and G. Elson, *J. Pharm. Pharmacol.*, **26,** suppl., 903 (1974).

(6) K. Ezumi and T. Kubota, *Chem. Pharm. Bull.*, **29,** 85 (1980).

(7) K. J. Schaper, *J. Chem. Res. Synop.*, **(1979)** 357.

(8) P. Seiler, *Eur. J. Med. Chem.*, **9,** 663 (1974).

(9) J. J. Kaufman, N. M. Nemo, and W. S. Koski, *J. Med. Chem.*, **18,** 647 (1975).

(10) F. H. Clarke, "Calculator Programming for Chemistry and the Life Sciences," Academic, New York, N.Y., 1981.

(11) S. H. Unger, in "Drug Design IX," Academic, New York, N.Y., 1980, p. 102.

(12) S. H. Unger, J. R. Cook, and J. S. Hollenberg, *J. Pharm. Sci.*, **67,** 1364 (1978).

(13) S. H. Unger and T. F. Feuerman, *J. Chromatogr.*, **176,** 426 (1979).

(14) J. G. Henkel, J. T. Hane, and G. Gianutsos, *J. Med. Chem.*, **25,** 51 (1982).

(15) M. A. Pleiss, R. Pazhenchevsky, M. F. Rafferty, C. Gatchell, and G. L. Grunewald, "Abstracts," 184th National Meeting of the American Chemical Society, Kansas City, Mo., September, 1982; "Abstract MEDI 48," American Chemical Society, Washington, D.C., 1982.

(16) S. Ebel and A. Seuring, *Angew Chem. Int. Ed. Engl.*, **16,** 157 (1977).

(17) T. Meites and L. Meites, *Talanta*, **19,** 1131 (1972).

(18) D. M. Barry and L. Meites, *Anal. Chim. Acta*, **68,** 435 (1974).

(19) D. M. Barry, L. Meites, and B. H. Campbell, *Anal. Chim. Acta*, **69,** 143 (1974).

(20) D. Murtlow and L. Meites, *Anal. Chim. Acta*, **92,** 285 (1977).

(21) T. N. Briggs and J. E. Stuehr, *Anal. Chem.*, **46,** 1517 (1974).

(22) L. Meites, J. E. Stuehr, and T. N. Briggs, *Anal. Chem.*, **47,** 1485 (1975).

(23) M. Bos, *Anal. Chem.*, **90,** 61 (1977).

(24) G. Nowogrocki, J. Canarne, and M. Wozniak, *Anal. Chim. Acta*, **112,** 185 (1979).

(25) A. Albert and E. P. Serjeant, "Ionization Constants of Acids and Bases," Methuen and Co., Ltd., London, 1962.

(26) W. B. Roolvink and M. Bos, *Anal. Chim. Acta*, **122,** 81 (1980).

(27) A. L. Green, *J. Pharm. Pharmacol.*, **19,** 10 (1967).

(28) C. C. Peck and L. Z. Benet, *J. Pharm. Sci.*, **67,** 12 (1978).

(29) R. H. Levy and M. Rowland, *J. Pharm. Sci.*, **60,** 1155 (1971).

(30) J. Tencheva, G. Velinov, and O. Budevsky, *Arzneim.-Forsch.*, **29,** 1981 (1979).

(31) L. Z. Benet and J. E. Goyan, *J. Pharm. Sci.*, **56,** 665 (1967).

(32) H. L. J. Fleuren, C. A. M. von Genneken, and J. M. van Rosum, *J. Pharm. Sci.*, **68,** 105 (1979).

(33) E. R. Garrett, *J. Pharm. Sci.*, **52,** 401 (1963).

(34) I. M. Kolthoff and N. H. Furman, "Potentiometric Titration," Wiley, New York, N.Y., 1949, pp. 95, 96.

(35) T. R. Harshberger, "Introductory Statistics: A Decision Map," Macmillan, New York, N.Y., 1977.

(36) D. D. Perrin "Dissociation Constants of Organic Bases in Aqueous Solution," Butterworths, London, 1965.

ACKNOWLEDGMENTS

The author is grateful to Dr. Keith Chan and Mr. Kenneth Wnuck of the Drug Metabolism Department for helpful advice during the design of the computer program used in this work.

Improved Techniques for the Photometric Determination of Partition Coefficients, with Particular Reference to the Chloroform–Ammonia Solvent System

F. H. A. RUMMENS ˣ, R. F. BUJACZEK, M. PETERS, and R. D. GREEN

Received September 5, 1976, from the *Department of Chemistry, University of Regina, Regina, Saskatchewan, Canada S4S 0A2.* Accepted for publication April 6, 1977.

Abstract □ Accurate partition coefficients $K = C_{org}/C_{aq}$ in chloroform–ammonia can be obtained by measuring the absorbance of the aqueous layer, replenishing with fresh aqueous solvent, and remeasuring the absorption after reequilibration. Provided the solute has a reasonably strong UV absorption, only 0.1–5 mg of material is required. Neither the amount, the extinction coefficient, nor (in most cases) the purity of the substrate material need be known. In general, K values ranging from 100 to 0.01 can be measured with a precision of ≥10%. A detailed analysis of the absorbance and volumetric error sources permits the optimum combination of experimental conditions such as volume ratios, cell lengths, and absorbance (either direct or differential, or with scale expansion) to be predicted *a priori*. Quantitative estimates for all primary error sources, such as photometric precision, baseline error, stray light, and volumetric errors were also experimentally determined. The theoretical error model was tested by determining K for aniline under widely ranging experimental conditions and by comparing the experimental standard deviations with those calculated from the theoretical model. The agreement was found to be satisfactory. The method described appears to be of particular usefulness for the determination of extraction or chromatographic parameters of basic drugs.

Keyphrases □ Partition coefficients—photometric determination in two-solvent systems, application to aniline in chloroform–ammonia □ Aniline—chloroform–ammonia solvent system, partition coefficients, photometric determination □ Photometry—determination of partition coefficients in two-solvent systems, application to aniline in chloroform–ammonia

During investigations on the extraction of narcotic drugs from body fluids one is often confronted with poor extraction yields and reproducibility. Chloroform–ammonia is the two-phase system generally used for basic drugs. Very little is known about the partition coefficients of drugs in this system, although knowledge of such partition coefficients would seem to be a prerequisite before even attempting extraction from biological samples. Persson *et al.* (1, 2) have reported on partition coefficients of amine-type drugs in the chloroform–water system, but their method involves complexation with inorganic anions and consequently requires additional information such as dissociation and polymerization constants of the complexes. A series of papers by Kemula *et al.* (3), a review paper by Sandell (4), and several studies by Korenman *et al.* (5) contain useful information on the partition coefficients of amines (and other compounds) and the dependence of these on concentration, degree of dissociation of the conjugate acid, and their relationship to chemical structure. The applicability of these studies to amine-type drugs (such as amphetamines and morphines) is limited, however, mostly because they relate to relatively high concentrations or rely on analytical techniques that require fairly large amounts of solute, both of which are often impractical in drug studies. Partition coefficients of these types of basic drugs have been reported, notably by Barfknecht *et al.* (6), Leffler *et al.* (7), Leo *et al.* (8), Kakemi *et al.* (9), Vree *et al.* (10), and Ramses and Fujimoto (11). Most of these studies lack experimental detail, employ in part ill-defined experimental conditions, and generally do not provide estimates of the reliability. In fact, the mutual agreement between the results of various authors is poor, wherever such a check can be made.

This paper attempts to provide a detailed and quantitative discussion, based on theory and experimental observations, of all the factors that contribute to the errors in the photometric determination of partition coefficients. The photometric method was chosen because of its sensitivity (normally requiring around 1–3 mg of material) and because most, if not all, basic drugs do show a distinct UV-absorption band. Since this paper deals exclusively with methodology, any basic, UV-absorbing solute could be employed; we have chosen to use aniline for this purpose because it has average UV-absorbing characteristics and because it is probably a weaker base than any of the amphetamine or morphine basic drugs.

THEORETICAL

Relationships Between the Partition Coefficient and Measured Absorbances—Consider a two-phase system, consisting of an aqueous layer of volume V_{aq} and an organic layer of volume V_{org}. Let an amount x of a solute be partitioned between the two phases so that an amount px is in the organic and qx in the aqueous layer ($p + q = 1$). The partition coefficient K of the solute will then be given (assuming equal activity coefficients in the two solvents) by:

$$K = \frac{C_{org}}{C_{aq}} = \frac{px/V_{org}}{qx/V_{aq}} = \frac{pV_{aq}}{qV_{org}} \qquad \text{(Eq. 1)}$$

where C_i is the solute concentration in volume V_i of layer i.

If one further assumes that it is the aqueous solution which lends itself best to spectrophotometric measurement, then the basic partition coefficient measurement consists of taking an absorption measurement of the aqueous solution in a cell of length l_1 at a suitable wavelength (usually λ_{max} of the solute):

$$A_1 = \epsilon l_1 qx/V_{aq} \qquad \text{(Eq. 2)}$$

To obtain q from Eq. 2, it appears that it is necessary to know the extinction coefficient ϵ. This, however, may pose severe problems, particularly if the solute is not available in pure form. In addition, literature data on ϵ may not be applicable to the instrumental conditions at hand. To obviate the necessity of knowing ϵ one may, however, proceed as follows. Assume that the aqueous layer is removed after partitioning of the solute, fresh aqueous solvent of volume V_{aq} is added, new equilibrium established, and the absorption of the aqueous layer remeasured. Since an amount px remained in the organic phase this will now be divided as p^2x in the organic layer and pqx in the aqueous layer. Therefore:

$$A_2 = \epsilon l_2 pqx/V_{aq} \qquad \text{(Eq. 3)}$$

Elimination of ϵ from Eqs. 2 and 3, solution of the resulting equation for

0022-3549/84/0200-0231$01.00/0
© 1984, American Pharmaceutical Association

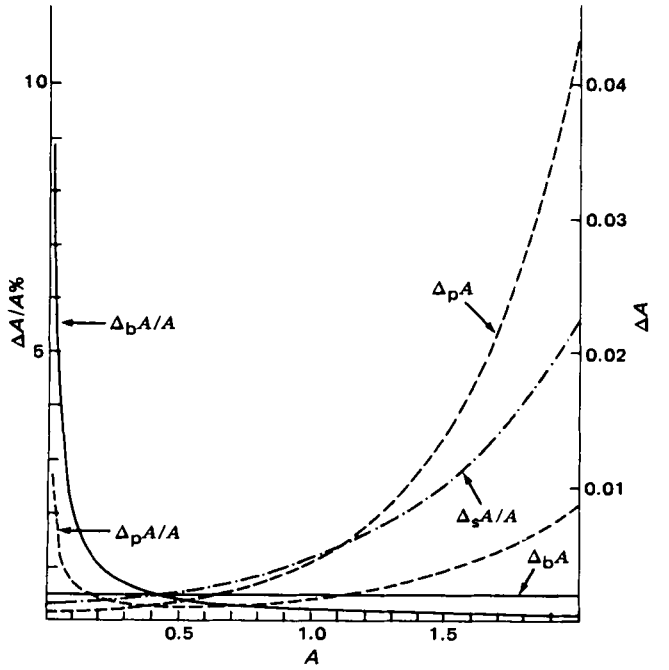

Figure 1—*Relative and absolute baseline absorbance errors based on* $\Delta_b A = 0.0020$, *relative and absolute photometric error based on* $\Delta_p T = 0.1\%$, *and relative stray light error based on* s = 0.003, *all as function of absorbance.*

p (and for $q = 1 - p$), and substitution into Eq. 1 gives:

$$K\frac{V_{org}}{V_{aq}} = \frac{A_2}{A_1 l_2/l_1 - A_2} = \frac{p}{q} \qquad \text{(Eq. 4)}$$

With this method there is the practical problem of removing all of the aqueous layer after the first equilibration. Even after centrifugation this is difficult to achieve, particularly since none of the organic layer should be removed in the process.

Experiments in our laboratory established that this problem was the one of the major causes of irreproducibility of K values determined with this method using Eq. 4. A considerable improvement can be obtained, however, by removing only a fraction, $(1 - f)V_{aq}$, of the aqueous layer. If, for example, V_{aq} was 5.00 mL only 4.00 or 4.50 mL was removed with a calibrated pipet, and the same volume of fresh solvent was added so as to restore the original volume, V_{aq}. Since an extra amount (fqx) of solute is left behind, Eq. 4 requires modification. It can be shown that for this method one has:

$$K\frac{V_{org}}{V_{aq}} = \frac{A_2 - fA_1 l_2/l_1}{A_1 l_2/l_1 - A_2} = \frac{p}{q} \qquad \text{(Eq. 5)}$$

A further possible improvement might be achieved by differential measurements. For example $A_1^o - A_2^o$ can be determined directly by measuring A_1^o relative to the A_2^o solution placed in the reference cell, both with cell length l^o. It is similarly possible to determine $A_2^* - fA_1^*$ directly, by diluting the A_1 solution $1/f$ times, and using this solution as the reference for the A_2 solution, with both cells having length l^*. Equation 5 can then be restated as:

$$K\frac{V_{org}}{V_{aq}} = \frac{(A_2^* - fA_1^*)/l^*}{(A_1 - A_2^o)l^o} = \frac{p}{q} \qquad \text{(Eq. 6)}$$

Sources of Error—*Optimization of* V_{org}/V_{aq} *and* f—A preliminary experiment should reveal the order of magnitude of K. As will be discussed below, the best results can be obtained when $KV_{org}/V_{aq} = p/q$ is between 1 and 10. If K is substantially different from this, V_{org}/V_{aq} should be adjusted to bring p/q into the proper range. For example, if $K = 50$ then a V_{org}/V_{aq} ratio of about 1:5 is in order. In practice, V_{org}/V_{aq} can be allowed to range between 1:5 and 5:1 without introducing any extra error. Beyond these ratios one needs careful mutual equilibration of the phases at a precisely controlled temperature so as not to cause appreciable volume changes due to changing mutual solubility of the solvents. With such precautions taken, ratios of 10:1 or even larger are quite practicable.

In general $f = 0.2$ is a good compromise for all circumstances. Not much can be gained by using smaller f values, because $A_2 - fA_1$ is almost insensitive to changes of f between 0.0 and 0.2. In practice the f factor is often determined by the choice of pipets employed.

Absorbance Errors—If it can be assumed that V_{org}/V_{aq}, l^*/l^o (or l_2/l_1), and f are accurately known, then the relative error in K is equal to that in p/q and is, therefore, determined by the errors in the absorbance measurements. The major sources of error are the photometric imprecision, $\Delta_p A$, the baseline error, $\Delta_b A$, and the stray light error, $\Delta_s A$. The photometric error function is given by (12):

$$\left(\frac{\Delta_p A}{A}\right)^2 = \left(\frac{0.434}{A}\right)^2 (1 + 10^{2A}) \left(\frac{\Delta I_0}{I_0}\right)^2 \qquad \text{(Eq. 7)}$$

where $\Delta I_0/I_0$ is the relative uncertainty of the signal strength in the reference beam; it is usually a constant for a given instrument. The validity of Eq. 7 is predicted on the condition that $\Delta I_0/I_0$ is determined by the detector and associated amplifier, and by implication that the contribution to $\Delta I_0/I_0$ of the readout device (meter, recorder, digital readout) is negligible in comparison. However, this condition must be fulfilled in any case; high damping and/or low gain may result in aesthetically more pleasing spectral curves or stable readouts, but the systematic errors incurred in this fashion usually are very large in comparison with the random error that results from allowing some "noise" to be visible. In Fig. 1 $\Delta_p A$ and $\Delta_p A/A$ as a function of A are given for a photometric precision $(\Delta I_0/I_0)$ of ±0.1%. The latter figure is typical for good instruments; for a low-price instrument this may be as high as ±1%. Figure 1 can actually be used for all $\Delta I_0/I_0$ values by using a different scale factor.

The baseline error $\Delta_b A$ is, in part, an instrument constant, but more often is determined by incomplete solvent compensation between the cells, variable scattering caused by the cells and their contents, variable amounts of impurities in solvents, blanks, or solutions, and the incomplete correction for the difference in absorption of the cells themselves. This type of error can be determined simply by measuring blanks relative to the same reference cell, and repeating this a number of times after emptying, refilling, and repositioning the sample cell. The average of these measurements gives the systematic baseline correction, which should be applied to all measurements, whereas the variation obtained gives the combined error:

$$\Delta_{pb} A = \sqrt{(\Delta_p A)^2 + (\Delta_b A)^2} \qquad \text{(Eq. 8)}$$

from which $\Delta_b A$ can be obtained if $\Delta_p A$ is known. The influence of $\Delta_b A/A$ as a function of A is also given in Fig. 1 for $\Delta_b A = 0.002$; for other $\Delta_b A$ errors, the corresponding errors can be found from Fig. 1 by using a suitable scale factor.

Differential measurements are often quoted (13) as giving much improved precision, because the exponent $2A$ in Eq. 7 is now replaced by $2(A_1 - A_2)$. However, this is only correct if the reference absorption is known beforehand in an absolute sense (by preparing standard solutions). Since this is something the present method deliberately has set out to avoid, the main advantage disappears; $(A_1 - A_2)$ has to be substituted for A in all places in Eq. 7 so that Eq. 7 is directly applicable. Some advantage may still accrue because $(A_1 - A_2)$ may correspond to a more favorable position on the error curve of Fig. 1 than A_1 or A_2 separately.

Scale expansion can similarly improve precision, particularly for high absorbances. For an n-fold scale expansion, the exponent $2A$ in Eq. 7 is replaced by $2(A - n/10)$. In practice it means increasing the detector amplifier gain n times when the sample is in the beam, but decreasing it to the normal level with the reference in the beam. It means also, however, that much wider slits must be used (by a factor of $n^{1/2}$), since otherwise the higher gain would result in an excessively high noise level, which would in part, if not entirely, offset the improvement in signal level. Since scale expansion is only helpful at high absorbance, stray light may then introduce a systematic error larger than the gain in precision (see below).

Stray light (*i.e.*, signal caused by light wavelengths other than the one selected) is a systematic error in that it always causes the apparent absorbance A_a to be smaller than the true absorbance A_t. If s is the fraction of unwanted stray signal (*i.e.*, $s = \Delta I_s/(I_0 + \Delta I_s)$ then the error $\Delta_s A$ is given by (12):

$$\frac{\Delta_s A}{A} = \frac{\log T_t - \log\{T_t(1 - s) + s\}}{A} \qquad \text{(Eq. 9)}$$

where T_t is the true transmittance. Figure 1 gives $\Delta_s A/A$ for $s = 0.003$ (0.3%). Such error curves for different s values are only approximately different by a scale factor. As can be seen, $\Delta_s A/A$ can be very large, even for low values of s. The error curve given applies only to individual total absorbances including the absorbance of solvent and cell. For differential

measurements the $\Delta_s A$ errors of the two absorbances have to be determined separately first and then subtracted.

Influence of Absorbance Errors on K—$\Delta_p A$ and $\Delta_b A$, being random errors, can be combined for any measurement by applying Eq. 8. If Eq. 5 is applicable, then one has for the uncertainty in K, as caused by absorbance errors:

$$\left(\frac{\Delta_{pb}K}{K}\right)^2 = \frac{(\Delta_{pb}A_2)^2 + (\Delta_{pb}A_1 f l_2/l_1)^2}{(A_2 - A_1 f l_2/l_1)^2} + \frac{(\Delta_{pb}A_2)^2 + (\Delta_{pb}A_1 l_2/l_1)^2}{(A_1 l_2/l_1 - A_2)^2} \quad \text{(Eq. 10)}$$

If differential measurements are made both on the numerator and denominator of Eq. 6, one has:

$$\left(\frac{\Delta_{pb}K}{K}\right)^2 = \frac{[\Delta_{pb}(A_2^* - fA_1^*)]^2}{(A_2^* - fA_1^*)^2} + \frac{[\Delta_{pb}(A_2^o - A_1^o)]^2}{(A_1^o - A_2^o)^2} \quad \text{(Eq. 11)}$$

If only $(A_2 - fA_1)$ or $(A_1 - A_2)$ is measured differentially, suitable changes in Eqs. 10 and 11 need to be made.

The error in K due to stray light is given by $\Delta_s K = K_a - K_t$, where the apparent partition coefficient K_a is determined using Eq. 5 or 6, with the apparent absorbances A_a, and where the true partition coefficient K_t is similarly related to the true absorbances. Since $\Delta_s A$ is a systematic error, it can be measured, at least in principle; appropriate corrections can then be made *via* Eq. 9.

Influence of Volumetric Errors Δ_vK—In the experimental procedure discussed herein (see *Experimental*), there are four volumetric transfers involved. Each of these carries a possible error, which influences the value of K through the volumetric parameters V_{aq}, V_{org}, and f (Eqs. 5 and 6). Following the recommended experimental procedure and applying standard rules for the propagation of random errors it can be shown that:

$$\left(\frac{\Delta_v K}{K}\right)^2 = \frac{A_2^2[(\Delta V_{aq})^2 + (\Delta V'_{aq})^2 + (\Delta V''_{aq})^2] + A_1^2[(\Delta V_{aq})^2 + (\Delta V'_{aq})^2]}{(A_2 - fA_1)^2 V_{aq}^2} + \frac{(A_1^2 + A_2^2)(\Delta V_{org})^2}{(A_1 - A_2)^2 (V_{org})^2} \quad \text{(Eq. 12)}$$

where V'_{aq} and $V''_{aq} = (1 - f)V_{aq}$ are the removed and replenished volumes of aqueous solvent, respectively.

If all volume errors (ΔV) are equal, a substantial simplification results:

$$\left(\frac{\Delta_v K}{K}\right)^2 \simeq \frac{(3A_2^2 + 2A_1^2)(\Delta V)^2}{(A_2 - fA_1)^2 V_{aq}^2} + \frac{(A_1^2 + A_2^2)(\Delta V)^2}{(A_1 - A_2)^2 V_{org}^2} \quad \text{(Eq. 13)}$$

On substitution of $A_2 = (p + qf)A_1$, this further reduces to:

$$\left(\frac{\Delta_v K}{K}\right)^2 = \frac{2 + 3(p + qf)^2}{p^2(1 - f)^2}\left(\frac{\Delta V}{V_{aq}}\right)^2 + \frac{1 + (p + qf)^2}{q^2(1 - f)^2}\left(\frac{\Delta V}{\Delta V_{org}}\right)^2 \quad \text{(Eq. 14)}$$

Eq. 14 shows that $\Delta_v K$ is fundamentally independent of the absorbances. It also shows why accurate K measurements are limited to a K range of 10 to 0.1; beyond these limits either of the denominator terms $p^2V_{aq}^2$ or $q^2V_{org}^2$ becomes very small. For example, if K is very large one needs a large V_{aq}/V_{org} ratio to keep $(A_1 - A_2)$ accurately measurable. Since the largest volume V_{aq} is limited by the physical dimensions of extraction and centrifugation equipment, a small V_{org} will have to be taken, combined with a small q value. The same reasoning applies for very small K values, with the roles of V_{aq} and V_{org} and of p and q interchanged.

Numerical Results—The implications of Eqs. 10–14 will be considered for three typical cases: $p/q = 10$, $p/q = 1.0$, and $p/q = 0.10$. The combined absorbance and volumetric errors in K can be calculated according to:

$$\left(\frac{\Delta K}{K}\right)^2 = \left(\frac{\Delta_{pb}K}{K}\right)^2 + \left(\frac{\Delta_v K}{K}\right)^2 \quad \text{(Eq. 15)}$$

The Case of p/q = *10*—Only a small fraction of the solute is extracted into the phase to be measured, and A_1 and A_2 will be fairly similar since $A_2 = l_2(10 + f)A_1/l_1$. For that reason equal cell lengths ($l_1 = l_2$) are used. K is likely to be >10 so that a ratio of V_{aq}/V_{org} larger than unity must be assumed to have been used to reduce p/q as much as possible. Typical volume parameters for this case are $V_{aq} = 8$ mL, $V'_{aq} = V''_{aq} = 6.4$ mL (*i.e.*, $f = 0.2$), and $V_{org} = 2$ mL. Most likely Mohr pipets have to be used throughout for which an average error of $\Delta V = \pm 0.012$ mL (see *Results*) can be taken. The first term of Eq. 12, 13, or 14 is negligible, and the second term gives a constant error of $(\Delta_v K)/K = 11.2\%$. With slightly different volume parameters (such as $V_{aq} = 10$ mL, $V'_{aq} = V''_{aq} = 8$ mL, and $V_{org} = 2$ ml), volumetric pipets could be used which have a typical error of $\Delta V = \pm 0.007$ mL. This would reduce $\Delta_v K/K$ to 7.1% (Fig. 2).

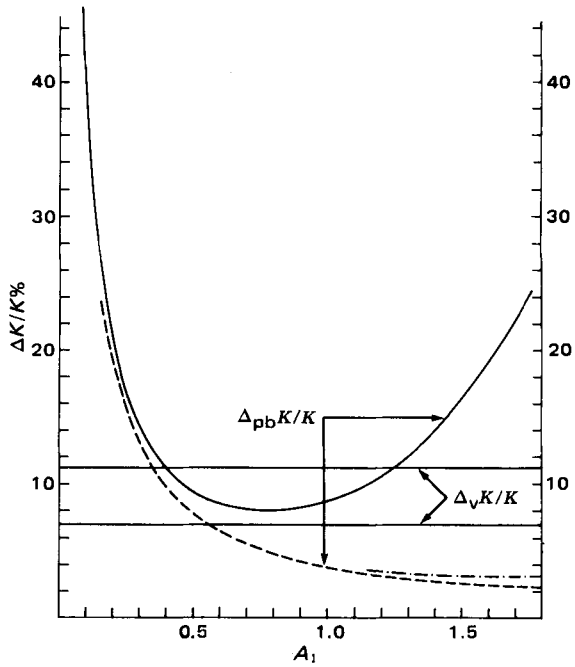

Figure 2—*Theoretical relative error in the partition coefficient* (K) *for the case* KV_{org}/V_{aq} = p/q = *10. Calculations are based on* $\Delta_b A$ = *0.0020,* $\Delta_p T$ = *0.1%,* f = *0.2, and* $l_1 = l_2$. *Calculations of* Δ_{pb}K/K *are for* A_1 *and* A_2 *separate (—);* A_1 *and* fA_2 *separate, but* $A_1 - A_2$ *measured in differential mode (- - - -); and for* A_1 *and* A_2 *measured with 10× scale expansion (- · - · -).* Δ_vK/K *is given for* ΔV = *0.012 mL (upper line) and* V_{org} = *2 mL,* ΔV = *0.007 mL (lower line). Total error* ΔK/K *can be calculated using Eq. 15.*

Figure 2 also shows the absorbance-related errors $\Delta_{pb}K$ based on $\Delta_b A = 0.0020$ and a photometric error of $\Delta_p T = 0.1\%$. It is seen that for $A_1 < 0.3$ the error in K is dominated by absorbance error, in particular $\Delta_b A$, whereas for $0.3 < A_1 < 1.0$ the $\Delta_p K$, $\Delta_b K$, and $\Delta_v K$ are of approximately the same magnitude. Differential measurement of $A_1 - A_2$ is only beneficial at $A_1 > 0.8$. Scale expansion measurement of A_1 and A_2 appears to give a similar improvement, but since this technique assumes that the scale expansion factor is errorless, the differential $(A_1 - A_2)$ technique should be preferred. The best overall result with $\Delta K/K = 8\%$ is obtainable for $1.0 < A_1 < 1.5$, using volumetric pipets and differential $(A_1 - A_2)$. No gain in accuracy is attainable at higher absorbance; $\Delta K/K$ is dominated by the constant $\Delta_v K/K$ term, and one would additionally run the risk of considerable stray light error.

The Case of p/q = *1*—A number of subcases arise in this situation. $K = 4$ with $V_{aq} = 8$ mL, $V_{org} = 2$ mL, and $V'_{aq} = V''_{aq} = 6.4$ mL requires Mohr pipets with $\Delta V = \pm 0.012$ mL. The second term in Eq. 14 is still dominant and $\Delta_v K/K = 1.9\%$. For $K = 1$, $V_{aq} = V_{org} = 5$ mL, $V'_{aq} = V''_{aq} = 4$ mL, and $\Delta V = 0.007$ mL, one finds $\Delta_v K/K = 1.2\%$, whereas for $K = 0.25$ with $V_{aq} = 2$ mL, $V_{org} = 8$ mL, and $V'_{aq} = V''_{aq} = 1.6$ mL with $\Delta V = \pm 0.012$ mL, one has $\Delta_v K/K = 2.5\%$. In either of these cases, however, the effect of volumetric errors on K is much smaller than with $p/q = 10$. The absorbance-caused errors in K are also substantially reduced because both p and q are relatively large ($p = q = 0.5$). Since A_2 is now about half that of A_1 (for $l_1 = l_2$), the use of a longer cell for A_2 ($l_2 = 2l_1$) might be contemplated. As Fig. 3 indicates this would indeed decrease $\Delta_{pb}K$ substantially at low A_1, but this improvement is illusory since one must assume that in practice a low A_1 is encountered despite having already used the longest available cells. Differential measurement of $(A_1 - A_2)$ is still of noticeable advantage, particularly at $A_1 > 1$, although the gain in precision is less than with $p/q = 10$. The optimum result will be around $\Delta K/K = 1.5\%$ and can be achieved at high A_1 ($1.0 < A_1 < 1.6$) with $(A_1 - A_2)$ in differential mode, provided $K = 1$ and provided all transfers can be done with volumetric pipets. Provided A_1 is at least 0.4, a precision of $\Delta K/K$ of 4% is always attainable. Scale expansion is of little use; it can be applied only to A_1 (because A_2 will always be smaller than unity); in Fig. 3 it would show predicted errors intermediate between those for A_1 and A_2 separately ($l_1 = l_2$ and without scale expansion) and for $(A_1 - A_2)$ in differential mode. Calculations show that an additional improvement results if $(A_1 - fA_1)$ is also measured differentially; but, this is almost quantitively balanced by a loss in precision due to the extra dilution required.

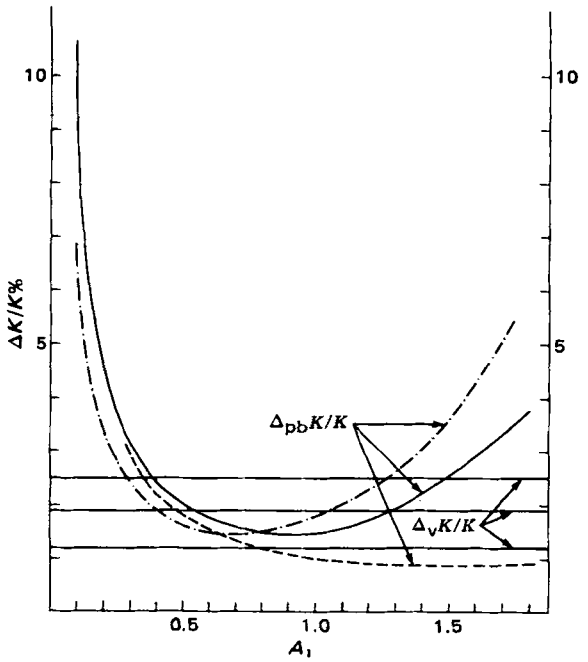

Figure 3—*Theoretical relative error in the partition coefficient (K) for the case* KV_{org}/V_{aq} = p/q = *1. Calculations are based on* $\Delta_b A$ = *0.0020,* $\Delta_p T$ = *0.1%, and* f = *0.2. Calculations of* $\Delta_{pb}K/K$ *are for* A_1 *and* A_2 *measured separately combined with* $l_2 = l_1$ *(—) and* $l_2 = 2l_1$ *(- · - · -), as well as for* $A_1 - A_2$ *measured in differential mode (- - - - -).* $\Delta_v K/K$ *is given for* V_{org} = *8 mL,* V_{aq} = *2 mL, and* ΔV = *0.012 mL (upper line), for* V_{org} = *2 mL,* V_{aq} = *2 mL, and* ΔV = *0.012 mL (middle line), and for* $V_{org} = V_{aq}$ = *5 mL and* ΔV = *0.007 mL (lower line). Total error* $\Delta K/K$ *can be calculated using Eq. 15.*

The Case of p/q = *0.1*—The phase to be measured has the smaller volume on this case. This, combined with the facts that p is also small and that the extra transfers required for the A_2 measurement are carried out on the small volume V_{aq}, means (Eq. 14) that the volumetric error $\Delta_v K/K$, even under the most careful experimental conditions will be very large and will dominate the total error (except for $A_1 \leq 0.2$). If accurate K values are required, all volumes need to be determined by weighing. If this is done, $\Delta_v K/K$ will be <1%, and the absorbance errors will become dominant. The absorbance A_1 is now much larger than A_2; as a result $(A_1 - A_2)$ is large, but $(A_2 - fA_1)$ is small so that the second term in Eq. 10 or 11 becomes negligible. There is, thus, no point in using a differential $(A_1 - A_2)$ measurement. Although A_2 and fA_1 are now of approximately the same magnitude, a differential measurement of $(A_2 - fA_1)$ does not give any improvement; on the contrary, careful analysis of the first terms of Eqs. 10 and 11 shows that for corresponding cell lengths (*i.e.*, $l^* = l_2$), the differential measurement of $(A_2 - fA_1)$ will, in fact, always produce larger errors. As Fig. 4 shows, some gain in precision can be obtained if l_2 is larger than l_1 at least for small A_1. Again, this is generally not a practical advantage: if A_1 is small, it will have to be measured in the largest available cell. Also, since V_{aq} is small there may not be enough liquid volume available to fill large cells. Without scale expansion, a best $\Delta_{pb}K/K$ of 3–4% can be obtained for $0.8 < A_1 < 1.6$. Scale expansion is useful in all cases where $A_1 > 1.0$, but to take full advantage of the technique, the l_2/l_1 ratio should be taken such that $A_1 = A_2$, so that both can be measured with scale expansion. Not only can $\Delta_{pb}K/K$ then be reduced to ~1%, but in addition, the stray light errors almost cancel if $A_1 = A_2$.

EXPERIMENTAL

A single-beam manual spectrophotometer of the electrical compensation type was used throughout[1]. It was equipped with one quartz glass prism and with a photomultiplier as detector. The slit width was set at 0.15 mm at λ = 239 nm; at other wavelengths, corresponding equal-energy slit widths were employed. Plastic-stoppered quartz glass cells of 10, 20, and 40 mm were used; the cell compartment was thermostated at 25°C. All photometer readings were repeated six times, and the average reading

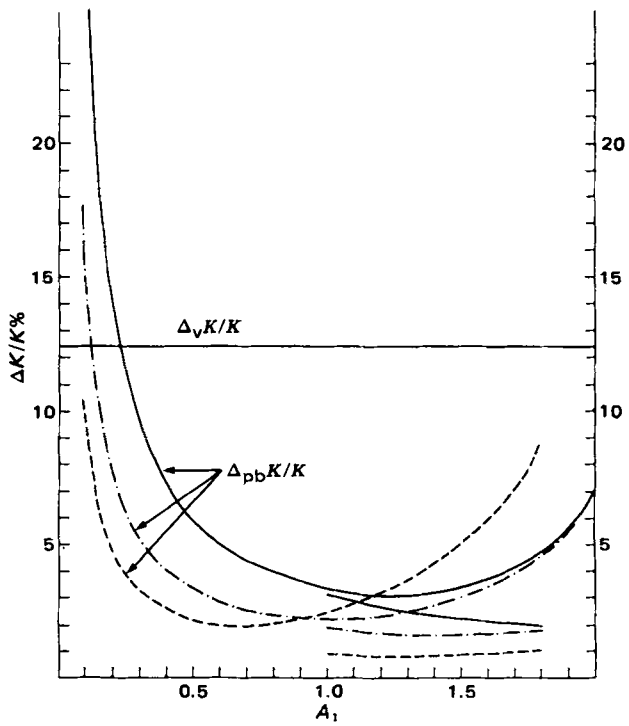

Figure 4—*Theoretical relative error in the partition coefficient (K) for the case* KV_{org}/V_{aq} = p/q = 0.1. Calculations of $\Delta_{pb}K/K$ *are based on* $\Delta_b A$ = *0.0020,* $\Delta_p T$ = *0.1%,* f = *0.2,* A_1 *and* A_2 *measured separately and for cell lengths* $l_2 = l_1$ *(—)* $l_2 = 2l_1$ *(- · - · -), and* $l_2 = 4l_1$ *(- - - - -); the extra curves for* $A_1 > 1.0$ *refer to the corresponding cell lengths ratios, but with a 10× scale expansion.* $\Delta_v K/K$ *is calculated for* V_{aq} = *2 mL and* ΔV = *0.005 mL. Total error* $\Delta K/K$ *can be calculated using Eq. 15.*

was calculated. The aniline absorbances were determined at λ = 281 nm. The instrument was equipped with a 10× scale expansion switch for measurements above A = 1.0.

A weighed amount of aniline hydrochloride was placed in a volumetric flask and dissolved in ammonia, the latter being presaturated with chloroform (IR spectrometric quality; *i.e.*, without ethyl alcohol) having a pH of 10.5. By adding ammonia (pH 11.5) the solution was brought to pH 10.5. To a standard 15-mL centrifuge tube[2] the appropriate volumes of aqueous solution and presaturated chloroform were added. The same volumes of chloroform and ammonia solvents were added to a second centrifuge tube to form the blank. Wherever necessary (particularly with the larger cells) two centrifuge tubes each for the solution and the blank were used. Plastic stoppers, designed specifically for this purpose with sides machined in such a way as to leave only three raised flanges in contact with the glass, were fitted into the centrifuge tubes ~2 cm. This guaranteed a tight fit with a minimum of liquid being trapped between the stopper and the glass wall of the centrifuge tube. The stoppered tubes were hand shaken for ~10 s, the stopper was then released, and the two phases were allowed to settle; this procedure was repeated three times. It was observed that with a 1:1 ratio of V_{aq}/V_{org} the two-phase system settled very quickly, whereas with other volume ratios a larger proportion of very fine droplets formed, requiring a much longer settling time. (These small droplets are more efficient in the extraction process as is evident from the results; with hindsight it can now be said that the above described extraction-by-shaking procedure is not adequate for volume ratios close to 1:1.) The tubes were then centrifuged at 2400 rpm for ~1 min. The second extraction (for the A_2 solution) was done in a similar fashion. Where possible, volumetric pipets were used, but for some volume ratios and for most removals and replenishing of volumes V'_{aq} and V''_{aq}, Mohr pipets were required. The extraction and centrifugation were carried out at room temperature (24–26° C).

RESULTS AND DISCUSSION

Error Determination—*Determination of the Photometric Error* $\Delta_p A$—Standard solutions of potassium chromate in 0.05 M NaOH, measured at the absorption maximum of ~230 nm, were used. Sixteen

[1] Unicam SP-500 series 2.

[2] Pyrex.

Table I—Random Baseline Absorbance Error $\Delta_b A$

Cell Length, mm	Number of Data Sets	Average Standard Error $\Delta_b A$
10	16	±0.0020
20	12	±0.0019
40[a]	9	±0.0043
40[b]	6	±0.0024

[a] Free-standing cell. [b] Positioned with spacer.

Table II—Random Errors of Volumetric Experiments

Type of Pipet	Average Standard Deviation ΔV, ml
1-mL Volumetric	0.0026
2-mL Volumetric	0.0038
5-mL Volumetric	0.0065
10-mL Volumetric	0.0090
2-mL Mohr	0.0057
5-mL Mohr	0.0079
10-mL Mohr	0.0110

different concentrations were used covering a range of 0.5–98% T. At each concentration six readings were taken, and the standard error was calculated. It was found that there was no correlation between these standard errors and the $\%T$, meaning that the photometric error $\Delta I/I$ is independent of $\%T$. The average of the individual standard errors was 100 $\Delta I/I = 100\ \Delta I_0/I_0 = 0.087\%\ T$. In all further calculations as well as in Figs. 1–4 this $\%T$ photometric error was rounded off to 0.1% T.

The scale readability standard error was found to be ~0.04% T so that Eq. 7 is still applicable for the calculation of $\Delta_p A$ or $\Delta_p A/A$; the latter are given in Fig. 1. For other instruments or for the same instrument under different energy conditions, the $\Delta_p A/A$ curve of Fig. 1 can be used by applying a simple scale factor; this is correct because of the proportionality between $\Delta_p A/A$ and $\Delta I_0/I_0$ (Eq. 7).

Determination of the Baseline Error Δ_bA—Systematic baseline errors were taken care of by running a blank sample (*i.e.*, one that did not contain the absorbing test compound, but was otherwise treated in identical fashion through the extraction and equilibrium procedures) with each test sample and by measuring its absorbance in the same cell as the test sample relative to the same reference cell. By subtracting the absorbance of the blank from that of the corresponding test sample, all absorbances were corrected for systematic differences between the measurement and reference cells, including their differing nonsolute contents.

There remains, however, the variability in the baseline correction, which is of a random nature and is caused by such things as variation in cell cleaning, drying efficiency, centrifugation efficiency, sample cleanliness (small particles, including small $CHCl_3$ bubbles, cause scattering and hence increase the apparent absorbance), and solvent composition. The determination of K for aniline automatically provided us with the necessary data. Since each K value was determined at least six times, the standard deviation in the baseline correction could be calculated from each six-fold set of absorbance measurements. These individual standard errors varied slightly, but their average value is thought to be a good measure of $\Delta_b A$ (Table I). Whereas the 10- and 20-mm cells were positioned with copper blade springs, the cell holder employed did not have the space to provide such a spring for the 40-mm cells. As Table I shows, tight cell positioning is necessary, as was found when a spacer was subsequently constructed to fit the 0.5-mm free space between the 40-mm cells and the cell holder rear wall. With this modification installed it appears that $\Delta_b A$ is virtually independent of cell length. In this case, therefore, the important contributor to $\Delta_b A$ can only have been variations in the cell cleaning efficiency. A value of $\Delta_b A = 0.0020$ has hence been taken for all further calculations (except for those referring to the free-standing 40-mm cells) and for Figs. 1–4.

The baseline variability $\Delta_b A$ is clearly an important source of error; it should be determined in conjunction with any absorbance measurements. The above determined baseline error also includes, in principle, the photometric error $\Delta_p A$. However, with $\Delta I_0/I_0 = 0.1\%$, the error $\Delta_p A$ is only equal to 0.0004 at the 99% T level which is relevant to the baseline measurements. This, however, is negligible compared with $\Delta_{pb} A = 0.0020$ in view of the quadratic progression of errors as given in Eq. 8.

Determination of the Scale Expansion Factor—On a total of 16 test samples with absorbance just over unity, the absorbance was measured (six times) with and without the 10× scale expansion. Both the average scale factors and their standard errors were then used to determine a weighted overall average and the overall uncertainty. It was found that the real scale factor was 10.11 (±0.02) which corresponds in absorbance to a scale term $\Delta A = 1.0047 \pm 0.0019$. Therefore, 1.0047 rather than unity was added to all absorbances measured with the 10× scale factor. Our impression is that the scale factor is not quite constant in time (presumably due to changes in contact resistance in the switch). The error given above includes both the photometric error and the possible nonconstancy of the scale factor itself.

Determination of the Stray Light Error Δ_sA—Since the chromate ion is known to accurately follow Beer's law (12), the stray light factor can be determined from an observed apparent nonlinearity of absorbance *versus* concentration (Eq. 9). Thirteen standard solutions of potassium

Table III—Partition Coefficient of Aniline in Chloroform–Ammonia at 25° C and its Experimental and Theoretical Standard Deviation as a Function of Experimental Conditions

	V_{aq}, mL	$V'_{aq} = V''_{aq}$, mL	V_{org}, mL	p/q	f	l_1, mm	l_2, mm	A_1	K	Standard Error, % Experimental	Standard Error, % Theoretical
1	5	4	5	20	0.2	10	10	0.10	22.4	62	79
2	6	4	6	20	0.33	10	20	0.10	16.6	46	63
3	10	8	10	20	0.2	10	40	0.10	14.3	41	63[a]
4	10	8	10	20	0.2	20	40	0.21	12.95	31	41[a]
5	10	8	10	20	0.2	20	20	0.19	12.9	25	35
6	10	8	10	20	0.2	40	40	0.38	12.4	53	44[a]
7	6	4	3	10	0.33	10	10	0.12	20.2	15	44
8	6	4.5	3	10	0.25	10	10	0.86	21.1	7.9	9.3
9	6	4.5	3	10	0.25	10	10	1.25	20.2	14.1	12.3
10	6	4.5	3	10	0.25	10	10	1.25[b]	20.8	12	5.7
11	6	4.5	3	10	0.25	10	10	1.35	18.9	9.7	14
12	6	4.5	3	10	0.25	10	10	1.35[b]	19.5	7.3	5.7
13	6	4.5	3	10	0.25	10	10	1.35[c]	19.5	6.4	5.4
14	6	4.5	3	10	0.25	10	10	1.75	22.5	28	26
15	6	4.5	3	10	0.25	10	10	1.75[b]	21.6	16	5.3
16	6	4.5	3	10	0.25	10	10	1.75[c]	25.4	7.3	5.8
17	6	4	3	10	0.33	10	20	0.13	18.2	30	28
18	12	9	6	10	0.25	10	40	0.16	19.2	33	24[a]
19	12	9	6	10	0.25	20	20	0.23	17.4	21	20
20	12	9	6	10	0.25	20	40	0.34	17.9	20	14[a]
21	12	9	6	10	0.25	40	40	0.50	26.2	15	19[a]
22	8	6	2	5	0.25	10	10	0.21	21.8	15	24
23	8	6	2	5	0.25	10	20	0.13	24.3	18	19
24	16	12	4	5	0.25	10	40	0.09	19.3	8.8	19[a]
25	16	12	4	5	0.25	20	20	0.21	21.0	6.1	12.3
26	16	12	4	5	0.25	20	40	0.24	20.2	81	10.3[a]
27	16	12	4	5	0.25	40	40	0.50	22.0	8.9	10.5[a]

[a] Calculated with $\Delta_b A$ (40 mm) = 0.0043 (Table II). [b] Scale expansion employed on A_1 and A_2. [c] Differential measurement on $(A_1 - A_2)$.

chromate in 0.05 M NaOH were prepared by dilution and weighing from a 0.003 M stock solution. In the conversion to mol/L units, corrections were applied for the varying density of the chromate solutions. Concentrations were such as to give absorbances at 230 nm in 10-mm cells ranging from 0.25 to 2.0. Where applicable (*i.e.*, $A = >1.0$) measurements were taken with and without 10-fold scale expansion. All readings were made sixfold, and at each concentration several completely separate measurements were made: 3 at absorbances ≤ 0.8, 6 between 0.9 and 1.8, and 12 for absorbances >1.8. For each concentration the average (baseline corrected) absorbance and its standard deviation were determined. With these data points a least-squares best straight line through the origin was fitted, with each point weighted according to the inverse of its relative standard error. With this best slope, absorbances at each of the actual concentrations were calculated and compared with those obtained experimentally. As it turned out each experimental point was on this straight line well within twice its own standard error, without any systematic deviation from linearity being apparent. Consideration of the standard errors in conjunction with Eq. 9 showed that the stray light must have been $\leq 0.03\%$. Stray light is wavelength dependent, but this result is likely correct for 220–300 nm. With other instruments or at wavelengths near the limit of the wavelength range of the instrument a much more severe stray light effect is possible. In all further calculations $s = 0.0003$ was used.

Volumetric Errors—These were determined experimentally by weighing and transferring water by pipet (for V_{aq} and V'_{aq}) and chloroform (for V_{org}) into an Erlenmeyer flask. For V'_{aq} water was transferred by pipet from out of an Erlenmeyer flask. The results are given in Table II. Each reported error ΔV is the average of at least four standard deviations, with each of the latter determined on six separate weighing experiments. There was no significant difference between water or chloroform.

Experimental Tests—The partition coefficient of aniline at 25°C and pH 10.5 was determined under a wide range of experimental conditions to test the theoretical error model developed herein (Table III). Each K value and its experimental standard deviation was determined from at least six independent determinations. The theoretical standard deviation was calculated according to Eqs. 10–15 with the numerical error data as given in the present section. Comparison of the experimental and theoretical standard errors indicates that, apart from the unavoidable statistical scatter, the agreement is good. In fact, the average ratio s(experimental)/s(theoretical) is 1.03, which proves that the error model is basically correct.

As predicted, the precision improves generally if p/q is lowered from 20 to 10 to 5 by changing the V_{aq}/V_{org} ratio. Also, as A_1 increases from 0.1, the precision first improves and then deteriorates (at high A_1), generally following the trend indicated by Fig. 2. Scale expansion on A_1 and A_2 does improve the precision, although not as much as predicted. This lends further credence to the aforementioned possibility that the scale factor is perhaps not constant. Differential ($A_1 - A_2$) measurement improves the precision approximately as predicted. Varying cell length has no effect other than that of varying the absorbances. Table III contains some data for $l_1 \neq l_2$. This, in itself, is not necessary for the $p/q = 10$ case; but, it is interesting to note that for, say $l_1 = 10$, $l_2 = 20$ mm, the resulting error (both experimental and theoretical) is intermediate between those for $l_1 = l_2 = 10$ mm and those for $l_1 = l_2 = 20$ mm. Several other such combinations yielded the same result.

The average K value for the $V_{aq}/V_{org} = 4$ case is 21.4 ± 1.7 and for the $V_{aq}/V_{org} = 2$ case, $K = 20.6 \pm 2.5$; for $V_{aq}V_{org} = 1$, $K = 15.2 \pm 4.9$. The decreasing K value with associated increase in standard error reveals a systematic error which was identified as being due to incomplete equilibration. Particularly a 1:1 chloroform–water system does not mix well; the phases separate immediately and completely when shaking is halted. With other mixing ratios one observes after shaking a mist of fine droplets in both phases, which clears up only slowly. Clearly, for $V_{aq} = V_{org}$ a much longer shaking period is required.

CONCLUSIONS

The above described technique and its error analysis indicates that K values ranging from 100 to 0.01 can be measured with an accuracy of $\geq 10\%$; in the K range of 10–0.1 an accuracy of 2% should be attainable. Several provisos must be made, however. First, the substrate of interest must have a reasonably strong absorption band in the UV or visible light region. For an extinction coefficient of ~10,000 (such as the p-band of aromatics in the 200–300 nm region) this translates to a requirement of ~1–5 mg if $K = 100$ and 0.01–0.05 mg if $K < 1$. The sample material need not be pure; impurities will cause erroneous results only if the following four conditions apply simultaneously: (*a*) the partition coefficient of the impurity is equal to or smaller than that of the compound of interest, (*b*) the impurity in question is present at a considerable level (*i.e.*, at least 10%), (*c*) the impurity has an extinction coefficient at the wavelength of maximum absorption of the compound of interest which is comparable in magnitude with that of the latter, and (*d*) the impurity has solubility in the two-phase system equal to or higher than that of the compound of interest. Second, to obtain accurate K values, careful attention has to be paid to the experimental conditions. Order-of-magnitude errors in the determination of K can easily occur if volumes, volume ratio, cell length, cell length ratio, initial absorbance, and photometric technique (separate, differential, and/or scale expansion) are not optimally chosen. In this regard, it is important to know the error characteristics of the photometric and volumetric equipment to be used. A final limitation to the use of this method may be posed by very low solubility of the substrate in either solvent. However, the method described is not limited to chloroform–ammonia. Any solvent pair will do, provided that at least one solvent is transparent at the wavelength to be used.

In applying this method there is no need for running multiple determinations. It may still be advisable to run duplicates in order to spot obviously erroneous results, but if an estimate of the accuracy of the partition coefficient is required, this can be calculated from the equations given in this paper. This is possibly even better than using experimental standard deviations, because the latter are not a reliable measure of imprecision for small numbers of repeated experiments.

REFERENCES

(1) G. Schill, R. Modin, and B.-A. Persson, *Acta Pharm. Suec.*, **2,** 119 (1965).

(2) B.-A. Persson and G. Schill, *Acta Pharm. Suec.*, **3,** 281 (1965).

(3) W. Kemula, H. Buchowski, *et al.*, *Bull. Acad. Poln, Sci., Ser. Sci. Chem.*, **12,** 267, 347, 491 (1964); **14,** 395 (1966).

(4) K. B. Sandell, *Monatsh. Chem.*, **89,** 36 (1958).

(5) I. M. Korenman, *Tr. Khim. Khim. Teknol.*, **1970,** 54; I. M. Korenman, N. Yu. Gurevich, and T. G. Kulagina, *Fhur. Priklad. Khim.*, **46,** 683 (1973); I. M. Korenman and Y. Yu. Gurevich; *Tr. Khim. Khim. Teknol.* **1972,** 120.

(6) C. F. Barfknecht, D. E. Nichols, and W. J. Dunn, *J. Med. Chem.*, **18,** 208 (1975).

(7) E. B. Leffler, H. M. Spencer, and A. Burger, *J. Am. Chem. Soc.*, **73,** 2611 (1951).

(8) A. Leo, C. Hansch, and D. Elkins, *Chem. Rev.*, **71,** 525 (1971).

(9) K. Kakemi, H. Sezaki, S. Muramishi, and Y. Tsujimura, *Chem. Pharm. Bull.*, **17,** 1641 (1969).

(10) T. B. Vree, A. Th. J. M. Muskens, and J. M. Van Rossum, *J. Pharm. Pharmacol.*, **21,** 774 (1969).

(11) H. Ramses and S. Fujimoto, *J. Pharm. Sci.*, **59,** 1783 (1970).

(12) G. Kortum, "Colorimetry, Photometry and Spectrometry," 4th ed., Springer Verlag, Heidelberg, 1962.

(13) G. W. Ewing, "Instrumental Methods of Chemical Analysis," 3rd ed., McGraw-Hill, New York, N.Y., 1969.

ACKNOWLEDGMENTS

The authors thank the Non-Medical Use of Drugs Directorate, Health and Welfare Canada, for the award of a generous research grant.

Quantitative Relationships Between Structure and Pharmacokinetic Parameters Using Molecular Connectivity Chi Indices I: Substituted 2-Sulfapyridines

K. REED, K. MEREISH ˣ, and B. JENSEN

Received December 6, 1982, from *The University of Nebraska Medical Center, College of Pharmacy, Department of Pharmaceutics, Omaha, NE 68105.* Accepted for publication January 10, 1983.

Abstract □ Quantitative relationships between the structure and pharmacokinetic parameters of several compounds have been derived using the molecular connectivity approach. The correlation coefficients of equations obtained using the Chi indices (χ) as predictor parameters were compared favorably with those obtained by the linear free energy approach, where physicochemical parameters have been used as predictor variables. High correlation coefficients (r) for the first-order elimination rate constant (r = 0.86), total body clearance (r = 0.89), and protein binding association constant (r = 0.78) for substituted 2-sulfapyridines were obtained. However, including the pK_a (indicative of electronic effects) of the compounds within the equation as a predictor variable caused an increase in the correlation coefficients.

Keyphrases □ Molecular connectivity—Chi indices, use in quantitative structure–pharmacokinetic relationships, substituted 2-sulfapyridines □ Pharmacokinetic parameters—quantitative relationship to structure, determination by molecular connectivity Chi indices, substituted 2-sulfapyridines □ Quantitative structure–pharmacokinetic relationships—application of molecular connectivity Chi indices, substituted 2-sulfapyridines

When considering the expense of synthesizing and testing compounds, it is economically advantageous to screen a few with high therapeutic potential rather than mass screening of a large number of compounds. With this goal in mind, medicinal chemists have applied quantitative structure activity relationships (QSAR) to drug design. In the free energy approach, Hansch (1) used physicochemical properties, *e.g.*, the partition coefficient and dissociation constant, as predictor variables in QSAR. These physicochemical properties were correlated with biological activity using regression analyses. The result of the treatment was an equation which describes, in a quantitative manner, the relationship between biological activity of a compound and its chemical structure.

An area which has been ignored until recently is the role of structural changes in altering pharmacokinetic parameters. It is known that alterations in the values of the pharmacokinetic parameters of a drug may result in critical changes in biological action (2). Recent successful work has been done deriving equations which relate various pharmacokinetic parameters of drug molecules to their corresponding physicochemical properties (3, 4). These derived equations, referred to as quantitative structure pharmacokinetic relationships (QSPR), offer promise for predicting pharmacokinetic parameters for compounds, given their physicochemical properties. In many studies, the physicochemical properties of the compounds must be determined experimentally. This limitation may be a serious disadvantage in using the free energy approach in deriving QSPR.

Kier and Hall (5, 6) have developed the methodology of molecular connectivity, which gives numerical values, Chi indices (χ), that are directly related to the molecular structure of the compound (5, 6). The χ indices of various molecules have been shown to have a high correlation with the corresponding boiling point, partition coefficient, and many other physical properties of the molecule (6, 7). Molecular connectivity indices are useful as input parameters in defining QSAR. QSAR of the antimicrobial activity of halogenated phenols, the hallucinogenic activity of amphetamines, the anesthetic activity of hydrocarbons, and various other biological activities have been derived (5, 6) using the molecular connectivity approach. It has been reported that the χ index compares favorably with other possible predictor variables in correlating structure to the duration of anesthesia of a series of barbiturates (8).

It would appear that molecular connectivity might be used in deriving QSPR. The objective of this study was to examine the potential ability of molecular connectivity to quantitatively relate pharmacokinetic parameters to structure. The main advantage of using molecular connectivity in QSPR studies, rather than the free energy approach, is that the χ indices can be calculated for compounds that have not yet been synthesized. Therefore, by using the molecular connectivity χ indices as the predictor variables, the investigator no longer needs to synthesize and determine the physicochemical properties of compounds with predicted undesirable pharmacokinetic characteristics.

Molecular connectivity χ values contain no information regarding electronic influences through bonds or across space (6). Electronic influences may be crucial in the correlation of structure and pharmacokinetic characteristics for certain series of compounds (4). An additional problem in using χ indices as predictor variables is the fact that molecular connectivity can not differentiate between stereoisomers (6). However, the number of therapeutic agents in which stereochemistry influences the pharmacokinetic parameters is minimal.

The free energy approach (Hansch) has been fairly successful in deriving QSPR, and one could refer to it as

Table I—Correlation Coefficients (r) of Equations Relating Structure to Pharmacokinetic Parameters for Various Compounds

Pharmacokinetic Parameter	r^g	r^h	r^i
Percent barbiturate absorbed[a]	0.98[j]	0.99	0.99
P.C.[e] of neutral compounds[b]	0.93[j]	0.90	0.98
P.C.[e] of acidic compounds[b]	0.90[j]	0.99	0.89
K_a of sulfonamides[c]	0.89[k]	0.88	0.99
Percent $\Sigma X_b{}^f$ of penicillins[d]	0.93[k]	0.96	0.99+

[a] Ref. 11. [b] Ref. 12. [c] Ref. 13. [d] Ref. 14. [e] Permeability coefficient. [f] Cumulative biliary excretion. [g] Correlation coefficient of equations in which the log of the pharmacokinetic parameters are correlated with physicochemical properties. [h] Correlation coefficient of equations in which the log of the pharmacokinetic parameters are correlated with χ indices. [i] Correlation coefficient in which the antilogs of pharmacokinetic parameters are correlated with χ indices. [j] Ref. 4. [k] Ref. 3.

0022-3549/84/0200-0237$01.00/0
© 1984, American Pharmaceutical Association

Table II—Correlation Coefficient (r) and the Sum of Residual Squared of Equations Relating Structure to Pharmacokinetic Parameters for Substituted 2-Sulfapyridines

Pharmacokinetic Parameter	R^b	S^{2a}	R^c	S^{2a}	R^d	S^2
K_{el}, h^{-1}	0.95[e]	0.29	0.83	11.09	0.86	0.22
CL_T, mL/min	0.96[e]	1.29	0.87	1.94	0.90	1.17
K_{assoc}, L/mol	0.85[e]	1.3×10^8	0.83	2.7×10^8	0.78	2.7×10^8
$t_{1/2}$, h	—	—	0.86	5.5×10^2	0.81	4.7×10^2
Vd, mL	—	—	0.88	1.1×10^4	0.87	1.2×10^4

[a] Using the antilog of the predicted values. [b] Values for equations in which the log of pharmacokinetic parameters are correlated with physicochemical properties. [c] Values for equations in which the log of the pharmacokinetic parameters are correlated with χ indices. [d] Values for the equations in which the antilog of pharmacokinetic parameters are correlated with χ indices. [e] Ref. 3.

Table III—Statistical Comparison of Equations With and Without pK_a for Substituted 2-Sulfapyridine[a] Compounds

Pharmacokinetic Parameter	χ Indices r	χ Indices + pK_a r
K_{el}, h^{-1}	0.86	0.92
$t_{1/2}$, h	0.81	0.89
CL_T, mL/min	0.90	0.91
Vd, mL	0.87	0.87
K_{assoc}, L/mol	0.78	0.92

[a] Ref. 3.

the "accepted method." We wished to compare the molecular connectivity approach, the "new method," to the "accepted method" in the ability to derive QSPR. Comparison between the two methods was based on the values of correlation coefficients of the corresponding derived equations.

A commonly encountered problem in studying QSAR is in choosing which computer-generated statistically significant equation best describes the relationship between structure and biological activity (7). Possessing the highest value for the correlation coefficient (r), does not ensure that the particular equation is the best equation. Adding an independent variable may slightly increase the r value without truly improving the practical predictor value of the equation. In general, the most practical equation is that which has a relatively large r value with a minimal number of predictor variables (7). A similar problem has been encountered in fitting data using linear pharmacokinetic models. A statistical method referred to as Akaike's Information Criteria (AIC) has been applied with success to indicate which pharmacokinetic model is more appropriate to describe the data (9). Additionally, Akaike (10) has indicated that this method should be applicable as a statistical identification procedure for prediction studies. Therefore, the Akaike statistical method was applied in this study to determine the equation that best describes the relationship of structure to pharmacokinetic parameters.

EXPERIMENTAL

Molecular connectivity χ values were calculated for the compounds listed in Tables I and II using the computer program written by Hall[1]. The pharmacokinetic parameters or the logarithm of the pharmacokinetic parameters were the dependent variables and the χ values were the independent predictor variables. The independent variables of the tested compounds were entered through stepwise inclusion into the multiple regression analysis subprogram of the Statistical Package for the Social Sciences (SPSS). Statistically significant equations, $p < 0.05$ according to the overall (F value) and DF, generated by the multiple regression program were compared using the AIC. The AIC was calculated according to $AIC = N \ln (S^2) + 2P$, where N is the number of experimental data points, P is the number of parameters, and S^2 is the residual sum of squares (8). The equation with the minimal value of AIC was considered as the best equation. The generated best equations and their associated statistical terms were provided in the output of the regression computer program. They are listed in Appendices I and II; terms are defined in Appendix III.

[1] Dr. L. H. Hall, Eastern Nazarene College, Quincy, Mass.

RESULTS AND DISCUSSION

The use of molecular connectivity χ indices as independent variables in equations defining QSPR compares favorably to those equations derived using physiochemical properties as independent variables, as shown in Tables I and II. The data indicate the potential of the molecular connectivity approach in establishing QSPR. The use of the logarithm of the pharmacokinetic parameters, rather than the use of the original values, did not result in a universal increase in the values of the correlation coefficients (Tables I and II). It was found in this study that the use of the logarithm of the pharmacokinetic parameters might give misleading results.

The mathematical transformation from normal values (antilog) to the log values is known to result in statistical compression of extreme points on both sides of the midpoint of the range. These extreme values are often of the most interest to the drug designer. The prediction capability of an equation can be measured by high r associated with a minimal S^2. We found in some cases, that the use of the logarithms of pharmacokinetic parameters caused an increase in r with an increase in S^2, when S^2 is calculated from the antilog of predicted values (Table II). Thus, the use of the log-dependent variable may result in equations with high r and low prediction capability.

The theoretical basis for the linear free energy approach dictates that the log dependent variable be used. The molecular connectivity approach, however, may use either the log or the antilog of the observed parameters in the regression equations. This added flexibility is an advantage of the molecular connectivity approach over the linear free energy approach in deriving QSPR.

It would seem reasonable that electronic effects would influence the pharmacokinetic parameters of compounds with ionizable groups. Molecular connectivity χ values do not include information concerning electronic effects (pK_a) (6). When the pK_a was included with χ indices as a possible predictor variable in the regression analysis of the antilog pharmacokinetic parameters of substituted 2-sulfapyridines, there was an improvement in r values for K_{el}, $t_{1/2}$, and K_{assoc}, while Vd was not affected (Table III).

It appears from this study that employing both χ indices and independent variables reflecting electronic effects may be useful in developing QSPR for compounds with ionizable groups. Kier has suggested that Hückel molecular orbital parameters or Hammett sigma values may be useful for this purpose (6).

In conclusion, the use of the molecular connectivity approach is a new method with a high applicability to QSPR studies. This method appears comparable with the linear free energy approach in predicting QSPR. Further work on the use of the molecular connectivity in QSPR studies for other series of compounds is presently in progress.

APPENDIX I

Equations of the pharmacokinetic parameters of substituted 2-sulfapyridines generated by multiregression analysis, where the χ indices were the independent variables, are given herein.

Antilog of the Pharmacokinetic Parameters

Total body clearance (CL_T) in mL/min:

$$CL_T = 1.18\chi_{PC5} - 2.03\chi_{PC4} + 1.05\chi_{PCV5} - 17.2\chi_{PCV4} + 51.4\chi_{CV5} + 13.14\chi_{CV3} + 7.84$$

$r = 0.90$; $SE = 0.31$; $F = 8.38$; $DF = 6, 12$ (Eq. 1)

Apparent volume of distribution (Vd) in L:

$$Vd = -145.64\chi_{PC5} - 15.70\chi_{C5} + 275.55\chi_{C3} - 986.92\chi_{CV5} + 429.06$$

$r = 0.87$; $SE = 28.8$; $F = 10.7$; $DF = 4, 14$ (Eq. 2)

Biological half life ($t_{1/2}$) in h:

$$t_{1/2} = -23.72\chi_{PC5} + 27.30\chi_{PC4} + 136.62\chi_{PCV4} - 592.4\chi_{CV5} - 85.09\chi_{CV3} - 31.04$$

$r = 0.81$; $SE = 6.01$; $F = 4.94$; $DF = 5, 13$ (Eq. 3)

Overall elimination rate constant (K_{el} in h^{-1}):

$$K_{el} = 0.66\chi_{PC5} - 0.93\chi_{PC4} - 2.89\chi_{PCV4} + 12.92\chi_{CV5} + 1.75\chi_{CV3} + 1.55$$

$r = 0.86$; $SE = 0.13$; $F = 7.53$; $DF = 5, 13$ (Eq. 4)

Affinity constant for protein binding (Kassoc) in L/mol:

$$K_{assoc} = 10^3(-55.51\chi_{t4} + 38.62\chi_{t3} + 33.65\chi_{t2} + 53.13\chi_{tV5} - 54.28\chi_{tV4} - 99.74)$$

$r = 0.78$; $SE = 4982$; $F = 3.48$; $DF = 5, 11$ (Eq. 5)

Log of the Pharmacokinetic Parameters.

$$\text{Log } CL_T = 1.22\chi_{PC5} - 1.76\chi_{PC4} - 10.34\chi_{PCV4} + 36.77\chi_{CV5} + 7.65\chi_{CV3} + 4.06$$

$r = 0.87$; $SE = 0.30$; $F = 8.00$; $DF = 5, 13$ (Eq. 6)

$$\text{Log } Vd = -0.36\chi_{PC5} - 0.48\chi_{PC4} + 1.37\chi_{C5} + 1.21\chi_{C3} - 3.09\chi_{CV5} + 2.92$$

$r = 0.88$; $SE = 0.08$; $F = 9.21$; $DF = 5, 13$ (Eq. 7)

$$\text{Log } t_{1/2} = -1.53\chi_{PC5} + 1.99\chi_{PC4} + 8.18\chi_{PCV4} - 35.46\chi_{CV5} - 5.19\chi_{CV3} - 2.36$$

$r = 0.86$; $SE = 0.31$; $F = 7.50$; $DF = 5, 13$ (Eq. 8)

$$\text{Log } K_{el} = 0.69\chi_{t5} + 0.86\chi_{t4} - 2.75\chi_{t3} + 0.34\chi_{t1} - 6.63\chi_{tV5} + 10.56\chi_{tV4} - 4.30\chi_{tV3} + 6.95$$

$r = 0.83$; $SE = 0.37$; $F = 3.60$; $DF = 7, 11$ (Eq. 9)

$$\text{Log } K_{assoc.} = 0.98\chi_{t5} - 3.47\chi_{t4} + 3.16\chi_{t2} - 0.01\chi_{tV4} + 4.60\chi_{tV3} - 3.72\chi_{tV2} - 3.54$$

$r = 0.83$; $SE = 0.24$; $F = 3.83$; $DF = 6, 10$ (Eq. 10)

Electronic Effect (pK_a) Included as Another Independent Parameter with the χ Indices.

$$CL_T = 0.20pK_a - 0.91\chi_{P5} + 2.17\chi_{P4} - 1.30\chi_{P2} + 3.24$$

$r = 0.91$; $SE = 0.28$; $F = 16.0$; $DF = 4, 14$ (Eq. 11)

$$Vd = -145.64\chi_{PC5} - 15.7\chi_{C5} + 275.55\chi_{C3} - 986.92\chi_{CV5} + 429.06$$

$r = 0.87$; $SE = 28.8$; $F = 10.68$; $DF = 3, 14$ (Eq. 12)

$$t_{1/2} = -4.82pK_a - 18.52\chi_{t5} + 13.90\chi_{t2} - 10.82\chi_{tV2} + 24.84$$

$r = 0.89$; $SE = 4.55$; $F = 12.92$; $DF = 4, 14$ (Eq. 13)

$$K_{el} = 0.10pK_a - 0.58\chi_{P5} + 0.99\chi_{P4} + 0.87\chi_{P3} - 1.00\chi_{P2} + 0.01$$

$r = 0.92$; $SE = 0.10$; $F = 13.5$; $DF = 5, 13$ (Eq. 14)

$$K_{assoc} = -10^2(38.99pK_a - 99.11\chi_{P5} + 44.96\chi_{P4} + 63.13\chi_{P3} - 15.76\chi_{P2} - 30.11\chi_{P0} - 69.70)$$

$r = 0.92$; $SE = 3359$; $F = 8.74$; $DF = 6, 10$ (Eq. 15)

APPENDIX II

Equations of the pharmacokinetic parameters of compounds listed in Table I, generated by the multiregression analysis, where the χ indices were the independent variables are presented herein.

Antilog of the Pharmacokinetic Parameters.

Percentage of barbiturates absorbed in the colon (%A):

$$\%A = -25.83\chi_{t5} + 34.97\chi_{t4} - 39.8\chi_{t3} + 44.65\chi_{t1} + 15.11\chi_{tV5} - 16.25\chi_{tV1} - 41.41$$ (Eq. 16)

$r = 0.99$; $SE = 2.19$; $F = 29.7$; $DF = 6, 2$

Permeability coefficients of neutral compounds ($P.C._{neutral}$):

$$P.C._{neutral} = -829.9\chi_{t4} + 2138\chi_{t1} - 1287\chi_{tV5} - 1271\chi_{tV1} - 418.6$$ (Eq. 17)

$r = 0.98$; $SE = 219.6$; $F = 45.6$; $DF = 4, 6$

Permeability coefficients of acidic compounds ($P.C._{acidic}$):

$$P.C._{acidic} = -1319\chi_{t5} + 1072\chi_{t4} + 905.1\chi_{t2} + 818.9\chi_{tV5} - 1148\chi_{tV3} + 704.8$$ (Eq. 18)

$r = 0.89$; $SE = 481.7$; $F = 5.22$; $DF = 5, 7$

Absorption rate of sulfonamides (K_a):

$$K_a = 0.06\chi_{t5} - 1.57\chi_{t4} + 2.18\chi_{t3} + 0.38\chi_{t1} - 0.22\chi_{tV5} + 4.08\chi_{tV3} - 6.41\chi_{tV2} + 1.19\chi_{tV1} + 1.77$$

$r = 0.99$; $SE = 0.10$; $F = 18.8$; $DF = 8, 3$ (Eq. 19)

Percent cumulative excreted amounts of penicillins in the bile (ΣX_b):

$$\Sigma X_b = 50.46\chi_{t4} - 64.59\chi_{t3} + 16.47\chi_{t2} - 30.52\chi_{t1} - 53.83\chi_{tV3} + 55.89\chi_{tV1} + 231.11$$

$r = 0.99$; $SE = 0.85$; $F = 183.1$; $DF = 6, 2$ (Eq. 20)

Log of the Pharmacokinetic Parameters

$$\text{Log } \%A = -0.29\chi_{t4} - 0.02\chi_{t3} - 0.20\chi_{t2} + 0.56\chi_{t1} + 0.57\chi_{tV4} - 0.48\chi_{tV3} - 0.02\chi_{tV1} + 0.85$$

$r = 0.99$; $SE = 0.01$; $F = 527.8$; $DF = 7, 1$ (Eq. 21)

$$\text{Log } P.C._{neutral} = -0.45\chi_{t5} + 0.50\chi_{t4} + 0.09\chi_{tV5} + 3.03$$

$r = 0.90$; $SE = 0.14$; $F = 12.4$; $DF = 3, 9$ (Eq. 22)

$$\text{Log } P.C._{acidic} = 2.30\chi_{PV5} - 2.37\chi_{PV4} + 0.20\chi_{PV0} + 3.07$$

$r = 0.99$; $SE = 0.04$; $F = 219.8$; $DF = 3, 7$ (Eq. 23)

$$\text{Log } K_a = 0.24\chi_{PC4} + 3.54\chi_{CV5} - 2.47\chi_{CV3} + 0.56$$

$r = 0.88$; $SE = 0.19$; $F = 9.15$; $DF = 3, 8$ (Eq. 24)

$$\text{Log } \Sigma X_b = -1.54\chi_{P5} + 1.16\chi_{P4} + 0.96\chi_{P3} - 1.19\chi_{P2} + 5.88$$

$r = 0.96$; $SE = 0.08$; $F = 12.03$; $DF = 4, 4$ (Eq. 25)

APPENDIX III: GLOSSARY

χ Molecular connectivity Chi index
DF Degrees of freedom
F Variance ratio
r Correlation coefficient
S^2 Residual sum squared
SE Standard error of the mean

Subscripts
- c Cluster subgraph
- p Path subgraph
- v Valence
- n An integer indicating the order of χ
- t Total sum of n-order χ indices

REFERENCES

(1) C. Hansch and T. Fujita, *J. Am. Chem. Soc.*, **86**, 1616 (1964).
(2) R. E. Notari, *J. Pharm. Sci.*, **62**, 865 (1973).
(3) J. K. Seydel and K. J. Schaper, in "Strategy in Drug Research," J. A. K. Busiman, Ed., Elsevier, Amsterdam, 1982, pp. 337, 354.

(4) E. J. Lien, *Ann. Rev. Pharmacol. Toxicol.*, **21**, 31 (1981).
(5) L. B. Kier and L. H. Hall, in "Chemistry and Drug Research," Academic, New York, N.Y., 1976.
(6) L. B. Kier, in "Physical Chemical Properties of Drugs," S. H. Yalkowsky, A. A. Sinkula, and S. C. Valvani, Eds., Dekker, New York, N.Y., 1980, pp. 277, 319.
(7) Y. C. Martin, "Quantitative Drug Design—A Critical Introduction," Dekker, New York, N.Y., 1978, pp. 167, 232.
(8) S. C. Basak, D. P. Gieschen, V. R. Magnuson, and D. K. Harriss, *IRC Med. Sci.*, **10**, 619 (1982).
(9) K. Yamaoka, T. Nakagawa, and T. Uno, *J. Pharmacokinet. Biopharm.*, **6**, 165 (1978).
(10) H. Akaike, *IEEE Trans. Automat. Control.*, **19**, 716 (1973).
(11) L. S. Schanker, *J. Med. Pharm. Chem.*, **2**, 343 (1960).
(12) N. F. H. Ho, J. Y. Park, W. Morozowich, and W. I. Higuchi, in "Design of Biopharmaceutical Properties Through Prodrugs and Analogs," E. B. Roche, Ed., APhA, Washington, D.C., 1977, pp. 136, 227.
(13) K. Kitao, K. Kubo, T. Morishita, N. Yata, and A. Kamada, *Chem. Pharm. Bull.*, **21**, 2417 (1973).
(14) A. Ryrfeld, *J. Pharm. Pharmacol.*, **23**, 463 (1971).

ACKNOWLEDGMENTS

We thank Douglas W. Litke for technical assistance.

Digitonin Derivatives of Low Toxicity: Potential Solubilizers for Lipophilic Compounds

JOSEF PITHA ˣ **and LAJOS SZENTE**

Received October 18, 1982, from the *Gerontology Research Center, National Institute on Aging, National Institutes of Health, Baltimore, MD 21224.* Accepted for publication January 10, 1983.

Abstract □ Digitoxin was modified by condensation with propylene oxide or with 1,4-butanediol diglycidyl ether in aqueous alkali, yielding products in which some of the CH_2OH groups of digitonin were converted to $CH_2OCH_2CHOHCH_3$ or to $CH_2OCH_2CHOHCH_2O(CH_2)_4O$-$CH_2CHOHCH_2OH$ groups, respectively. These modified digitonins were very soluble in water and chloroform and effectively solubilized lipophilic compounds into aqueous solutions; *e.g.*, 2 mg of vitamin A or 0.6 mg of cholecalciferol could be dissolved per 1 mL of 5% aqueous solutions of modified digitonins. Compared with the toxicity of digitonin (LD_{50} 4 mg/kg iv), the toxicity of modified digitonin was greatly reduced: doses of 500 mg/kg by intravenous infusion were not lethal for mice.

Keyphrases □ Digitonin—derivatives, potential use as solubilizers, lipophilic drugs, comparative toxicity □ Solubilizers—digitonin derivatives, potential use with lipophilic drugs □ Lipophilic drugs—potential use of digitonin derivatives as solubilizers, comparative toxicity

Solubilizing agents are widely used both in pharmacy and pharmacology, and there is a constant need for new compounds that have low toxicity and do not functionally interfere with biomolecules (1, 2). Saponins, which are steroid glycosides, have some of the desirable properties (3). Two saponins, tomatin and digitonin, are readily available. Commercial preparations of tomatin have reasonable purity but are expensive, whereas for digitonin, which is rather widely used, the situation is reversed (4). The commercial preparation of digitonin is an extract of saponins from seeds of *Digitalis purperea*, further purified by treatment with cholesterol, which precipitates digitonin and related compounds. Such preparations are described as containing digitonin (40%), digalonin (15%), desglucodigitonin (25%), gitonin (15%), tigonin (3%), and dig d′ (2%) (5). The content of digitonin in commercial preparations is given as 70–80% (6). In most applications, the mixture is used. Despite its complexity, this mixture has unique properties and has been used extensively in biochemical pharmacology (7–9). Digitonin, on the other hand, even in the pure state, has some undesirable properties—its solubility in water is low and variable depending on the sample used (7) and on whether the digitonin sample had been previously treated with solvents (10). Furthermore, digitonin forms a complex with cholesterol, a process which is bound to have toxic and denaturating effects. In this work the aim was to modify the digitonin mixture chemically to overcome these defects; attempts were also made to make the necessary chemical modifications simple and easy to perform even with large quantities of material.

EXPERIMENTAL

Synthesis of Digitonin Derivative 2—Digitonin[1] (1 g, 0.8 mmol) was suspended in a solution of sodium hydroxide (200 mg) in water (6.5 mL), and propylene oxide (1 mL, 15 mmol) was added. The mixture was then stirred at 60°C for 1 h and at room temperature overnight. The clear solution was then neutralized by hydrochloric acid and dialyzed for 1 d against distilled water. Dialysis tubing from regenerated cellulose[2] was used with a nominal molecular weight cutoff of 8000–12,000. Freeze-drying of the contents of dialysis tubing gave derivative 2 as a solid foam-like material (1 g).

The solubility of derivative 2 in water was ~21 g/100 mL at room temperature. This compound tended to occlude solvents and thus, elemental analysis could not be used to estimate the degree of substitution of derivative 2. Field-desorption mass spectrometry[3] was used for that purpose; analysis of the relative intensities of peaks (mass of digitonin derivative plus sodium ion) gave the following distribution at the molecular weight: unsubstituted (36%), monosubstituted (36%), disubstituted (19%), trisubstituted (6%), tetrasubstituted (2%), and pentasubstituted (1%). Thus, the average degree of substitution is ~1.4.

Synthesis of Digitonin Derivative 3—The same procedure as above using 1,4-butanediol diglycidyl ether[4] in place of propylene oxide yielded 6.9 g of derivative 3 from 8 g of digitonin. The solubility of derivative 3 in water at room temperature was 11 g/100 mL.

To estimate the degree of substitution in derivative 3, the compound was exhaustively methylated and then analyzed for the content of carbon and methoxy groups. Derivative 3 (1 g, ~1 mmol) was dissolved in dimethylformamide (10 mL), sodium hydride (0.4 g) was slowly added, and then the mixture was stirred at room temperature for 30 min. The viscous mixture was then cooled to 0°C, methyl iodide (4.5 g) was added in a dropwise manner, and stirring was continued for another 12 h. Methanol was added, and the mixture was dialyzed against water and freeze-dried. Product 4 was a white powder (0.92 g) which was hygroscopic; completion of methylation was established by absence of absorption in the region of the hydroxyl stretching vibration (3100–3600 cm^{-1}) in the IR spectrum[5]. Compound 4 was repeatedly dissolved in water and evaporated

[1] Sigma Chemical Co., St. Louis, Mo.
[2] A. H. Thomas Co., Philadelphia, Pa.
[3] NIHLB assembly, Bethesda, Md.
[4] Aldrich Chemical Co., Philadelphia, Pa.
[5] Beckman infrared spectrophotometer IR12.

0022-3549/84/0200-0240$01.00/0
© 1984, American Pharmaceutical Association

(4) E. J. Lien, *Ann. Rev. Pharmacol. Toxicol.*, **21**, 31 (1981).
(5) L. B. Kier and L. H. Hall, in "Chemistry and Drug Research," Academic, New York, N.Y., 1976.
(6) L. B. Kier, in "Physical Chemical Properties of Drugs," S. H. Yalkowsky, A. A. Sinkula, and S. C. Valvani, Eds., Dekker, New York, N.Y., 1980, pp. 277, 319.
(7) Y. C. Martin, "Quantitative Drug Design—A Critical Introduction," Dekker, New York, N.Y., 1978, pp. 167, 232.
(8) S. C. Basak, D. P. Gieschen, V. R. Magnuson, and D. K. Harriss, *IRC Med. Sci.*, **10**, 619 (1982).
(9) K. Yamaoka, T. Nakagawa, and T. Uno, *J. Pharmacokinet. Biopharm.*, **6**, 165 (1978).
(10) H. Akaike, *IEEE Trans. Automat. Control.*, **19**, 716 (1973).
(11) L. S. Schanker, *J. Med. Pharm. Chem.*, **2**, 343 (1960).
(12) N. F. H. Ho, J. Y. Park, W. Morozowich, and W. I. Higuchi, in "Design of Biopharmaceutical Properties Through Prodrugs and Analogs," E. B. Roche, Ed., APhA, Washington, D.C., 1977, pp. 136, 227.
(13) K. Kitao, K. Kubo, T. Morishita, N. Yata, and A. Kamada, *Chem. Pharm. Bull.*, **21**, 2417 (1973).
(14) A. Ryrfeld, *J. Pharm. Pharmacol.*, **23**, 463 (1971).

ACKNOWLEDGMENTS

We thank Douglas W. Litke for technical assistance.

Digitonin Derivatives of Low Toxicity: Potential Solubilizers for Lipophilic Compounds

JOSEF PITHA ˣ **and LAJOS SZENTE**

Received October 18, 1982, from the *Gerontology Research Center, National Institute on Aging, National Institutes of Health, Baltimore, MD 21224.* Accepted for publication January 10, 1983.

Abstract □ Digitoxin was modified by condensation with propylene oxide or with 1,4-butanediol diglycidyl ether in aqueous alkali, yielding products in which some of the CH_2OH groups of digitonin were converted to $CH_2OCH_2CHOHCH_3$ or to $CH_2OCH_2CHOHCH_2O(CH_2)_4O$-$CH_2CHOHCH_2OH$ groups, respectively. These modified digitonins were very soluble in water and chloroform and effectively solubilized lipophilic compounds into aqueous solutions; *e.g.*, 2 mg of vitamin A or 0.6 mg of cholecalciferol could be dissolved per 1 mL of 5% aqueous solutions of modified digitonins. Compared with the toxicity of digitonin (LD_{50} 4 mg/kg iv), the toxicity of modified digitonin was greatly reduced: doses of 500 mg/kg by intravenous infusion were not lethal for mice.

Keyphrases □ Digitonin—derivatives, potential use as solubilizers, lipophilic drugs, comparative toxicity □ Solubilizers—digitonin derivatives, potential use with lipophilic drugs □ Lipophilic drugs—potential use of digitonin derivatives as solubilizers, comparative toxicity

Solubilizing agents are widely used both in pharmacy and pharmacology, and there is a constant need for new compounds that have low toxicity and do not functionally interfere with biomolecules (1, 2). Saponins, which are steroid glycosides, have some of the desirable properties (3). Two saponins, tomatin and digitonin, are readily available. Commercial preparations of tomatin have reasonable purity but are expensive, whereas for digitonin, which is rather widely used, the situation is reversed (4). The commercial preparation of digitonin is an extract of saponins from seeds of *Digitalis purperea*, further purified by treatment with cholesterol, which precipitates digitonin and related compounds. Such preparations are described as containing digitonin (40%), digalonin (15%), desglucodigitonin (25%), gitonin (15%), tigonin (3%), and dig d′ (2%) (5). The content of digitonin in commercial preparations is given as 70–80% (6). In most applications, the mixture is used. Despite its complexity, this mixture has unique properties and has been used extensively in biochemical pharmacology (7–9). Digitonin, on the other hand, even in the pure state, has some undesirable properties—its solubility in water is low and variable depending on the sample used (7) and on whether the digitonin sample had been previously treated with solvents (10). Furthermore, digitonin forms a complex with cholesterol, a process which is bound to have toxic and denaturating effects. In this work the aim was to modify the digitonin mixture chemically to overcome these defects; attempts were also made to make the necessary chemical modifications simple and easy to perform even with large quantities of material.

EXPERIMENTAL

Synthesis of Digitonin Derivative 2—Digitonin[1] (1 g, 0.8 mmol) was suspended in a solution of sodium hydroxide (200 mg) in water (6.5 mL), and propylene oxide (1 mL, 15 mmol) was added. The mixture was then stirred at 60°C for 1 h and at room temperature overnight. The clear solution was then neutralized by hydrochloric acid and dialyzed for 1 d against distilled water. Dialysis tubing from regenerated cellulose[2] was used with a nominal molecular weight cutoff of 8000–12,000. Freeze-drying of the contents of dialysis tubing gave derivative 2 as a solid foam-like material (1 g).

The solubility of derivative 2 in water was ~21 g/100 mL at room temperature. This compound tended to occlude solvents and thus, elemental analysis could not be used to estimate the degree of substitution of derivative 2. Field-desorption mass spectrometry[3] was used for that purpose; analysis of the relative intensities of peaks (mass of digitonin derivative plus sodium ion) gave the following distribution at the molecular weight: unsubstituted (36%), monosubstituted (36%), disubstituted (19%), trisubstituted (6%), tetrasubstituted (2%), and pentasubstituted (1%). Thus, the average degree of substitution is ~1.4.

Synthesis of Digitonin Derivative 3—The same procedure as above using 1,4-butanediol diglycidyl ether[4] in place of propylene oxide yielded 6.9 g of derivative 3 from 8 g of digitonin. The solubility of derivative 3 in water at room temperature was 11 g/100 mL.

To estimate the degree of substitution in derivative 3, the compound was exhaustively methylated and then analyzed for the content of carbon and methoxy groups. Derivative 3 (1 g, ~1 mmol) was dissolved in dimethylformamide (10 mL), sodium hydride (0.4 g) was slowly added, and then the mixture was stirred at room temperature for 30 min. The viscous mixture was then cooled to 0°C, methyl iodide (4.5 g) was added in a dropwise manner, and stirring was continued for another 12 h. Methanol was added, and the mixture was dialyzed against water and freeze-dried. Product 4 was a white powder (0.92 g) which was hygroscopic; completion of methylation was established by absence of absorption in the region of the hydroxyl stretching vibration (3100–3600 cm^{-1}) in the IR spectrum[5]. Compound 4 was repeatedly dissolved in water and evaporated

[1] Sigma Chemical Co., St. Louis, Mo.
[2] A. H. Thomas Co., Philadelphia, Pa.
[3] NIHLB assembly, Bethesda, Md.
[4] Aldrich Chemical Co., Philadelphia, Pa.
[5] Beckman infrared spectrophotometer IR12.

0022-3549/84/0200-0240$01.00/0
© 1984, American Pharmaceutical Association

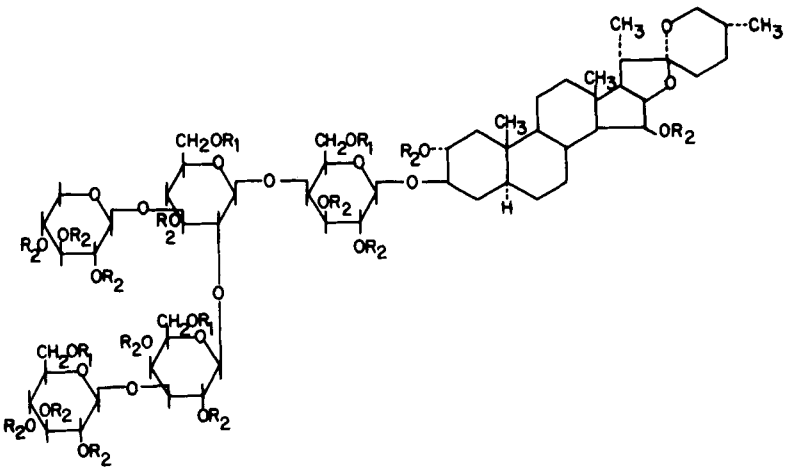

DIGITONIN R_1 = H, R_2 = H
DERIVATIVE 2, R_1 = —CH_2—CHOH—CH_3 or H; R_2 = H
DERIVATIVE 3, R_1 = —CH_2—CHOH—CH_2—O—CH_2—CH_2—CH_2—CH_2—O—CH_2—CHOH—CH_2OH or H; R_2 = H
DERIVATIVE 4, R_1 = —CH_2—CH(OCH_3)—CH_2—O—CH_2—CH_2—CH_2—CH_2—O—CH_2—CH(OCH_3)—CH_2—O—CH_3 or CH_3; R_2 = CH_3

to dryness *in vacuo* to eliminate all traces of organic solvents, and was then analyzed for carbon content and for content of methoxy groups (Zeissel method). In two separate preparations of product 4, these values were found to be 33.1 and 35.8% for methoxyl and 50.0 and 56.3% for carbon, respectively. From the ratio of methoxyl to carbon contents, the average degree of substitution was calculated to be ~1.

Control experiments, in which only digitonin or only 1,4-butanediol diglycidyl ether was treated with aqueous alkali, were performed with the following results. From self-condensation of digitonin, <1% of the water-soluble material could be isolated. If the products of self-condensation of digitonin were dissolved in 50% aqueous dimethylformamide, <1% was nondialyzable. The products of self-condensation of 1,4-butanediol diglycidyl ether were water soluble, but >97% was dialyzable.

Measurement of Micellar Space in Aqueous Solutions of Derivatives 2 and 3—The method (11, 12) is based on the color change of iodine that takes place when micelles are formed in the aqueous solution of iodine (30 mg/L). The absorbancy[6] at 385 nm, which is proportional to the micellar space, was measured as the function of concentration of derivatives 2 and 3 in solution.

Molecular Weight Determination by Vapor Pressure Osmometry—Chloroform (used as a solvent) was purified by washing with solutions of sulfuric acid, sodium hydroxide, and water, then dried and redistilled. The vapor pressure osmometer[7] was used for measurements; the osmometer was calibrated using pentaerythrityl tetrastearate (mol. wt. 1202) and polystyrene standard ($\overline{M}_w$:$\overline{M}_n$ = 1.04; $\overline{M}_w$ 9000). All measurements were performed at 29.9°C.

Precipitation of Digitonin and its Derivatives by Cholesterol—To a solution of a saponin (10 mg) in absolute ethanol (1 mL) was added a solution of cholesterol (40 mg) in ethanol (95%, 6.0 mL). The mixture was heated at 60°C for 10 min allowed to stand for 1 h and then the product was removed by filtration to give 41, 6, and 0 mg for digitonin and derivatives 2 and 3, respectively.

Binding of Cholesterol–Digitonin Derivatives by Equilibrium Dialysis—Dialysis tubing[2] was washed extensively with boiling water and with ethanol; dialyses were performed in ethanol (95%). The solution of digitonin derivative (1 mL) was placed inside of the dialysis tubing, and 2 mL of a solution of [^{14}C]cholesterol[8] was placed outside. After equilibration for 6 d, the concentration of radioactivity inside and outside of the dialysis bag was measured by liquid scintillation counting[9].

Solubilizing Effects of Digitonin Derivatives—Excess lipophilic compound (1.2 mL) was introduced into a stoppered polyethylene test tube containing phosphate-buffered isotonic saline (1 mL) without or with derivative 2 or 3 (50 mg). After equilibration by rotation overnight at 20–22°C, the suspension was centrifuged and the clear supernatant was used to measure spectrophotometrically[5] the concentration of the solubilized lipophilic compound.

Effects of Digitonin and its Derivatives on Cells in Culture—Friend erythroleukemia cells grown in Eagle's minimal essential medium with 10% calf serum were used (12) for the *in vitro* studies.

Toxicity of Digitonin Derivatives—Female C57B1/6J mice, ~9 weeks of age, were used for the experiments. The solution in phosphate-buffered saline was infused by peristaltic pump (0.12 mL/h) into the tail veins of animals for ~20 h. Five animals were used per group; these were followed for 3 weeks after treatment.

RESULTS AND DISCUSSION

Digitonin contains 17 hydroxyl groups; four of the groups are primary. Epoxides, which were used in the derivatization of digitonin, are known to react approximately one order of magnitude faster with primary hydroxyls than with secondary ones (13, 14); consequently, structures 2 and 3 are suggested for the products of the condensations of digitonin with propylene oxide or 1,4-butanediol diglycidyl ether, respectively. The average degree of substitution was found to be 1.4 and 1.0 for derivatives 2 and 3, respectively.

Since the commercial digitonin that was used in the condensation contains several other saponins, these were also derivatized. On the other hand, it was established that derivatives 2 and 3 were not contaminated with products of self-condensation reactions of either digitonin or epoxides. Derivatives 2 and 3, in spite of being mixtures, had uniform solubility properties. Digitonin dissolves in water only slightly, whereas derivatives 2 and 3 give solutions both in water and chloroform.

Derivatives 2 and 3 were found to be self-associated in aqueous solutions; that followed from the inability of these derivatives to dialyze. Self-association was also apparent from the concentration dependence of nonpolar (*i.e.*, micellar) space in aqueous solutions of derivatives 2 and 3. This space is relatively small when only nonassociated species of am-

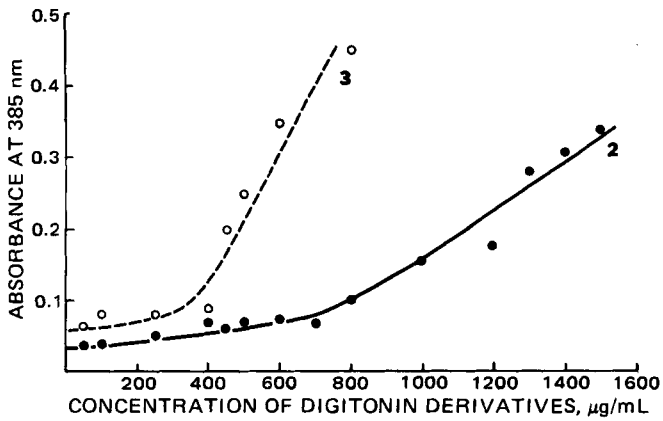

Figure 1—*Dependence of the absorbance at 385 nm of an aqueous solution of iodine (30 mg/L) on the concentration of derivatives 2 (●) and 3 (○). The absorbance at this wavelength is proportional to the concentration of iodine in nonpolar surroundings and, thus, to the amount of micelles present.*

[6] Cary 14 M recording ultraviolet spectrophotometer.
[7] Hitachi model 117.
[8] New England Nuclear, Boston, Mass.
[9] Beckman LS-250 Liquid Scintillation System.

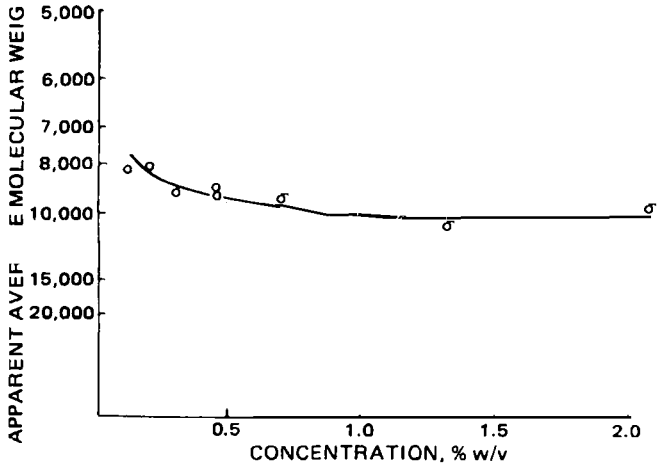

Figure 2—*Concentration dependence of apparent average molecular weight of derivative 3 as measured in chloroform by vapor pressure osmometry.*

phiphile are present in solution, but becomes prominent when the higher-order self-associated species (micelles) began to be formed; this occurred at concentrations of 700 μg/mL for derivative 2 and 300 μg/mL for derivative 3 (Fig. 1). Derivative 3 was also found to be strongly self-associated in chloroform solutions. Results of the concentration dependence of apparent molecular weight, as measured by vapor pressure osmometry, are in Fig. 2. Even at 0.1%, the measured molecular weight of derivative 3 is five to six times higher than that calculated for the monosubstituted product.

Digitonin forms insoluble complexes with cholesterol. The substitution of digitonin by epoxides apparently suppresses this complexation. Under the experimental conditions, when digitonin formed a precipitate with cholesterol in a relative amount of 100, derivatives 2 and 3 formed a precipitate in relative amounts of only 15 and 0, respectively.

Derivatives 2 and 3 did not permeate through the dialysis membrane; consequently, equilibrium dialysis could be used to study the potential interaction of cholesterol with derivative 3 in ethanol solutions, in which soluble complexes may be formed. The equilibrium concentrations of cholesterol found inside the dialysis tubing, which contained increasing amounts of derivative 3, were within experimental error and equal to those found in solutions outside the tubing, where there was no digitonin derivative present (Table I). Consequently, no complex formation was detected by this method.

The solubility of drugs and related compounds is of considerable theoretical and practical importance in the pharmaceutical sciences (1, 2, 15, 16), and development of effective solubilizing agents presents a useful complement to the development of new drugs. Derivatives 2 and 3 are very potent solubilizers of lipophilic compounds. Results of solubilization experiments are given in Table II; the solubility of some of the compounds in water was increased by two to three orders of magnitude even at moderate solubilizer concentrations. Derivative 3 seems to be a more potent solubilizer of vitamin A than any cyclodextrin or polymethionine sulfoxide previously tested (17, 18).

Although the mass spectra showed that compound 2 contained some unsubstituted digitonin, its presence could not be detected through the insolubility of digitonin in water or chloroform. Perhaps this behavior may be explained by a strong self-association of derivative 2. These self-associated species apparently have not only the capacity to complex and dissolve various lipophilic compounds, but also the contaminating digitonin.

Table I—Equilibrium Dialysis in the Cholesterol–Derivative 3 System

Conc. of Derivative 3[a], mg/mL	Distribution of [^{14}C]Cholesterol, cpm/mL[b]	
	Inside of Dialysis Tubing	Outside of Dialysis Tubing
0	13,820	13,940
2	13,980	14,020
10	14,380	14,920
50	14,940	14,680

[a] Inside the dialysis tubing. [b] Corrected for background counts.

Table II—Solubilization of Nonpolar Compounds by Derivatives of Digitonin in Phosphate-Buffered Isotonic Saline

Compound	Solubilization, μg/mL		
	No Agent	Derivative 2[a]	Derivative 3[a]
β-Ionone	7.3	2050	1820
Retinol	<4	1600	2500
β-Carotene	0	11	11
trans-β-Carotene	0	5	8
Cholecalciferol	0.2	190	640
Naphthalene	<0.5	850	1035
Anthracene	0	69	84
2,3-Benzanthracene	0	60	59

[a] 5% solutions.

The toxicity of derivatives 2 and 3 to cells grown in culture was tested by effects of these compounds on the growth curves of murine erythroleukemic cells for a 5-d growth period. A concentration of 0.1 mg/mL of derivative 3 added to the serum-supplemented medium allowed growth and cell division, whereas addition of 0.01 mg/mL of digitonin led to cell destruction. The onset of cell damage was also considerably slower for derivative 3 than for digitonin. When cells were treated with 0.1 mg/mL of digitonin in the absence of serum, even 30 min of treatment affected the cell growth that occurred later in serum-supplemented medium, whereas with derivative 3 at least 4 h of treatment was necessary to change the later growth (Fig. 3).

The toxicity of derivative 3 to animals was tested using intravenous infusions of derivative 3 into the tail veins of mice. Doses of 1000–2000 mg/kg of derivative 3 resulted in death, but doses of 500 mg/kg were without lethal effects.

When administered perorally, digitonin is toxic to mice (19) but nontoxic to rats (>50 mg/kg) (3), which tolerate even repeated applications (150 mg/kg/d) (19). Digitonin is also nontoxic to monkeys in amounts up to 0.4% in food (19). On the other hand, in all parenteral applications digitonin is rather toxic, producing acute inflammation when injected intramuscularly or subcutaneously (800-μg dose). This inflammation may be inhibited by anti-inflammatory drugs (20). Digitonin also has hemolytic effects (4). For digitonin given intravenously, the LD_{50} was found to be 4 mg/kg in rats (3). Since mice tolerated doses of 500 mg/kg iv by infusion of derivative 3, it is obvious that toxicity of digitonin was de-

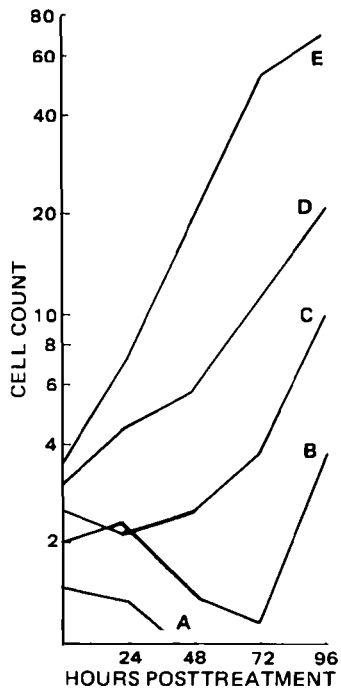

Figure 3—*Effects of treatment by digitonin and derivative 3 on the* in vitro *growth of Friend erythroleukemia cells. Cells were treated with 0.1 mg/mL of the compound in serum-free medium for the times indicated; thereafter, the cells were diluted into serum-supplemented medium. Key: (A) digitonin, 2 h; (B) digitonin, 1 h; (C) derivative 3, 4 h; (D) derivative 3, 2 h; (E) control.*

creased by at least two orders of magnitude on substitution by epoxides. Since the pharmacokinetics of parenterally applied lipophilic drugs are very strongly affected by their relative water solubility (21), derivatives 2 and 3 may be useful in modifying the effects of lipophilic drugs.

REFERENCES

(1) S. G. Frank, *J. Pharm. Sci.*, **64**, 1585 (1975).

(2) P. H. Elworthy, A. T. Florence, and C. B. Macfarlane, "Solubilization by Surface-Active Agents and Its Applications in Chemistry and the Biological Sciences," Chapman & Hall, Ltd., London, England, 1968.

(3) G. Vogel and M. L. Marek, *Arzneim.-Forsch.*, **12**, 815 (1962).

(4) J. G. R. Elferink, *Pharma. Weekbl.*, **112**, 1 (1977).

(5) R. Tschesche and G. Wulff, *Tetrahedron*, **19**, 621 (1963).

(6) M. Windholz (Ed.), "The Merck Index," 9th ed., Merck & Co., Rahway, N.J., 1976, p. 418.

(7) W. L. Strauss, G. Ghai, C. M. Fraser, and J. C. Venter, *Arch. Biochem. Biophys.*, **196**, 566 (1979).

(8) M. G. Caron, Y. Srinivasan, J. Pitha, K. Kociolek, and R. J. Lefkowitz, *J. Biol. Chem.*, **254**, 2923 (1979).

(9) G. Vauquelin, P. Geynet, J. Hanoune, and A. D. Strosberg, *Proc. Natl. Acad. Sci. USA*, **74**, 3710 (1977).

(10) G. R. Bauer and P. M. Breitenfeld, *Hoppe-Seyler's Z. Physiol. Chem.*, **302**, 111 (1955).

(11) S. Ross and J. P. Olivier, *J. Phys. Chem.*, **63**, 1671 (1959).

(12) J. Pitha, K. Kociolek, and M. G. Caron, *Eur. J. Biochem.*, **94**, 11 (1979).

(13) R. Uy and F. Wold, *Anal. Biochem.*, **81**, 98 (1977).

(14) G. Hilgetag and A. Martini (Eds.), "Weygand's Preparative Organic Chemistry," Wiley, New York, N.Y., 1972.

(15) T. Higuchi and K. A. Connors, *Adv. Anal. Chem. Instrum.*, **4**, 117 (1965).

(16) K. A. Connors and T. W. Rosanske, *J. Pharm. Sci.*, **69**, 173 (1980).

(17) J. Pitha, *Life Sci.*, **29**, 307 (1981).

(18) J. Pitha, L. Szente, and J. Greenberg, *J. Pharm. Sci.*, **72**, 665 (1983).

(19) M. R. Malinow, P. McLaughlin, and C. Stafford, *Am. J. Clin. Nutr.*, **31**, 814 (1978).

(20) E. M. Glenn, S. C. Lyster, and N. A. Rohloff, *Proc. Soc. Exp. Biol. Med.*, **130**, 110 (1969).

(21) K. Hirano and H. Yamada, *J. Pharm. Sci.*, **71**, 500 (1982).

ACKNOWLEDGMENTS

The authors appreciate the interest and help of Dr. Henry M. Fales who arranged for the mass spectra measurements and interpreted the results. For vapor pressure osmometry we thank Dr. K. Solc. The first attempts to synthesize derivative 3 were made by Dr. J. Zjawiony in this laboratory. For performance of cell culture experiments and for the equilibrium dialysis experiment we thank Mrs. B. A. Hughes.

Stability of the 6,14-*endo*-Ethanotetrahydrooripavine Analgesics: Acid-Catalyzed Rearrangement of Buprenorphine

E. J. CONE ˣ, C. W. GORODETZKY, W. D. DARWIN, and W. F. BUCHWALD

Received March 15, 1982, from the *National Institute on Drug Abuse, Division of Research, Addiction Research Center, Lexington, KY 40583.* Accepted for publication September 23, 1982

Abstract □ Buprenorphine (I), a member of the 6,14-*endo*-ethanotetrahydrooripavine series of analgesics, undergoes an acid-catalyzed rearrangement reaction when exposed to acid and heat. The product was shown by ^{1}H-NMR and GC–MS to have undergone overall elimination of a molecule of methanol with concurrent formation of a tetrahydrofuran ring at C(6)–C(7) of I. Short-term stability studies across a wide range of pH and temperature conditions indicate that I is stable in aqueous solution at pH > 3 for 24 h at 36–38°C. Under the more extreme conditions of the autoclave, significant loss of I occurred. Long-term stability studies (10 weeks) of I in aqueous solution (pH 1 and pH 5) at 0–4°C and 26–28°C indicate only minor conversion (4%) to the rearrangement product. Eight other 6,14-*endo*-ethanotetrahydrooripavine derivatives were subjected to extremes of acid (pH 0) and temperature (autoclave) to determine if similar rearrangement reactions occur. GC–MS indicated that hydrolysis products were produced whose spectra were consistent with the proposed rearrangement structures.

Keyphrases □ Buprenorphine—6,14-*endo*-ethanotetrahydrooripavine analgesics, stability, acid-catalyzed structural rearrangement □ Analgesics—6,14-*endo*-ethanotetrahydrooripavine series, buprenorphine, stability, acid-catalyzed structural rearrangement □ Stability—buprenorphine and other 6,14-*endo*-ethanotetrahydrooripavine analgesics, acid-catalyzed structural rearrangement

The 6,14-*endo*-ethanotetrahydrooripavine series of analgesics contains numerous potent narcotic agonist and antagonist derivatives including buprenorphine (I), diprenorphine (V), and etorphine (VI). These substances are highly lipophilic (1) and display limited solubility at physiological pH; however, at lower pH values their solubilities increase substantially. Members of the closely related 6,14-*endo*-ethanotetrahydrothebaine series of analgesics have been shown to undergo acid-catalyzed rearrangement under vigorous conditions (2). However, it was not apparent whether a similar rearrangement would be observed for the 6,14-*endo*-ethanotetrahydrooripavine series. Consequently, a study was made of the stability of I under a variety of conditions involving exposure to acid and heat. A rearrangement product of I was identified by mass spectrometry and ^{1}H-NMR. Evidence was obtained by GC–MS for the presence of similar rearrangement products from other 6,14-*endo*-ethanotetrahydrooripavine derivatives following acid hydrolysis.

EXPERIMENTAL

Materials—Compounds I–IX[1] (Table I) were used as received. Their structural identity and purity were confirmed by TLC and GC–MS. Tri-Sil Z[2], obtained in 1-mL sealed glass ampules, was used as supplied. All other chemicals were reagent-grade quality.

Instrumentation—GC was conducted on a gas chromatograph[3] equipped with a flame-ionization detector. The stationary liquid phase, 3% OV-210[4], was coated on 100–120 mesh Gas Chrom Q[5] and packed into a 0.36-m × 2-mm i.d. silanized glass column. The temperatures were:

[1] Reckitt and Coleman, Hull, England.
[2] Pierce, Rockford, Ill.
[3] Model 2700; Varian Associates, Palo Alto, Calif.
[4] Applied Science, State College, Pa.
[5] Supelco Inc., Bellefonte, Pa.

0022-3549/84/0200-0243$01.00/0

© 1984, American Pharmaceutical Association

creased by at least two orders of magnitude on substitution by epoxides. Since the pharmacokinetics of parenterally applied lipophilic drugs are very strongly affected by their relative water solubility (21), derivatives 2 and 3 may be useful in modifying the effects of lipophilic drugs.

REFERENCES

(1) S. G. Frank, *J. Pharm. Sci.*, **64**, 1585 (1975).

(2) P. H. Elworthy, A. T. Florence, and C. B. Macfarlane, "Solubilization by Surface-Active Agents and Its Applications in Chemistry and the Biological Sciences," Chapman & Hall, Ltd., London, England, 1968.

(3) G. Vogel and M. L. Marek, *Arzneim.-Forsch.*, **12**, 815 (1962).

(4) J. G. R. Elferink, *Pharma. Weekbl.*, **112**, 1 (1977).

(5) R. Tschesche and G. Wulff, *Tetrahedron*, **19**, 621 (1963).

(6) M. Windholz (Ed.), "The Merck Index," 9th ed., Merck & Co., Rahway, N.J., 1976, p. 418.

(7) W. L. Strauss, G. Ghai, C. M. Fraser, and J. C. Venter, *Arch. Biochem. Biophys.*, **196**, 566 (1979).

(8) M. G. Caron, Y. Srinivasan, J. Pitha, K. Kociolek, and R. J. Lefkowitz, *J. Biol. Chem.*, **254**, 2923 (1979).

(9) G. Vauquelin, P. Geynet, J. Hanoune, and A. D. Strosberg, *Proc. Natl. Acad. Sci. USA*, **74**, 3710 (1977).

(10) G. R. Bauer and P. M. Breitenfeld, *Hoppe-Seyler's Z. Physiol. Chem.*, **302**, 111 (1955).

(11) S. Ross and J. P. Olivier, *J. Phys. Chem.*, **63**, 1671 (1959).

(12) J. Pitha, K. Kociolek, and M. G. Caron, *Eur. J. Biochem.*, **94**, 11 (1979).

(13) R. Uy and F. Wold, *Anal. Biochem.*, **81**, 98 (1977).

(14) G. Hilgetag and A. Martini (Eds.), "Weygand's Preparative Organic Chemistry," Wiley, New York, N.Y., 1972.

(15) T. Higuchi and K. A. Connors, *Adv. Anal. Chem. Instrum.*, **4**, 117 (1965).

(16) K. A. Connors and T. W. Rosanske, *J. Pharm. Sci.*, **69**, 173 (1980).

(17) J. Pitha, *Life Sci.*, **29**, 307 (1981).

(18) J. Pitha, L. Szente, and J. Greenberg, *J. Pharm. Sci.*, **72**, 665 (1983).

(19) M. R. Malinow, P. McLaughlin, and C. Stafford, *Am. J. Clin. Nutr.*, **31**, 814 (1978).

(20) E. M. Glenn, S. C. Lyster, and N. A. Rohloff, *Proc. Soc. Exp. Biol. Med.*, **130**, 110 (1969).

(21) K. Hirano and H. Yamada, *J. Pharm. Sci.*, **71**, 500 (1982).

ACKNOWLEDGMENTS

The authors appreciate the interest and help of Dr. Henry M. Fales who arranged for the mass spectra measurements and interpreted the results. For vapor pressure osmometry we thank Dr. K. Solc. The first attempts to synthesize derivative 3 were made by Dr. J. Zjawiony in this laboratory. For performance of cell culture experiments and for the equilibrium dialysis experiment we thank Mrs. B. A. Hughes.

Stability of the 6,14-*endo*-Ethanotetrahydrooripavine Analgesics: Acid-Catalyzed Rearrangement of Buprenorphine

E. J. CONE ˣ, C. W. GORODETZKY, W. D. DARWIN, and W. F. BUCHWALD

Received March 15, 1982, from the *National Institute on Drug Abuse, Division of Research, Addiction Research Center, Lexington, KY 40583.* Accepted for publication September 23, 1982

Abstract □ Buprenorphine (I), a member of the 6,14-*endo*-ethanotetrahydrooripavine series of analgesics, undergoes an acid-catalyzed rearrangement reaction when exposed to acid and heat. The product was shown by ^{1}H-NMR and GC–MS to have undergone overall elimination of a molecule of methanol with concurrent formation of a tetrahydrofuran ring at C(6)–C(7) of I. Short-term stability studies across a wide range of pH and temperature conditions indicate that I is stable in aqueous solution at pH > 3 for 24 h at 36–38°C. Under the more extreme conditions of the autoclave, significant loss of I occurred. Long-term stability studies (10 weeks) of I in aqueous solution (pH 1 and pH 5) at 0–4°C and 26–28°C indicate only minor conversion (4%) to the rearrangement product. Eight other 6,14-*endo*-ethanotetrahydrooripavine derivatives were subjected to extremes of acid (pH 0) and temperature (autoclave) to determine if similar rearrangement reactions occur. GC–MS indicated that hydrolysis products were produced whose spectra were consistent with the proposed rearrangement structures.

Keyphrases □ Buprenorphine—6,14-*endo*-ethanotetrahydrooripavine analgesics, stability, acid-catalyzed structural rearrangement □ Analgesics—6,14-*endo*-ethanotetrahydrooripavine series, buprenorphine, stability, acid-catalyzed structural rearrangement □ Stability—buprenorphine and other 6,14-*endo*-ethanotetrahydrooripavine analgesics, acid-catalyzed structural rearrangement

The 6,14-*endo*-ethanotetrahydrooripavine series of analgesics contains numerous potent narcotic agonist and antagonist derivatives including buprenorphine (I), diprenorphine (V), and etorphine (VI). These substances are highly lipophilic (1) and display limited solubility at physiological pH; however, at lower pH values their solubilities increase substantially. Members of the closely related 6,14-*endo*-ethanotetrahydrothebaine series of analgesics have been shown to undergo acid-catalyzed rearrangement under vigorous conditions (2). However, it was not apparent whether a similar rearrangement would be observed for the 6,14-*endo*-ethanotetrahydrooripavine series. Consequently, a study was made of the stability of I under a variety of conditions involving exposure to acid and heat. A rearrangement product of I was identified by mass spectrometry and ^{1}H-NMR. Evidence was obtained by GC–MS for the presence of similar rearrangement products from other 6,14-*endo*-ethanotetrahydrooripavine derivatives following acid hydrolysis.

EXPERIMENTAL

Materials—Compounds I–IX[1] (Table I) were used as received. Their structural identity and purity were confirmed by TLC and GC–MS. Tri-Sil Z[2], obtained in 1-mL sealed glass ampules, was used as supplied. All other chemicals were reagent-grade quality.

Instrumentation—GC was conducted on a gas chromatograph[3] equipped with a flame-ionization detector. The stationary liquid phase, 3% OV-210[4], was coated on 100–120 mesh Gas Chrom Q[5] and packed into a 0.36-m × 2-mm i.d. silanized glass column. The temperatures were:

[1] Reckitt and Coleman, Hull, England.
[2] Pierce, Rockford, Ill.
[3] Model 2700; Varian Associates, Palo Alto, Calif.
[4] Applied Science, State College, Pa.
[5] Supelco Inc., Bellefonte, Pa.

0022-3549/84/0200-0243$01.00/0

© 1984, American Pharmaceutical Association

Table I—Structures of the 6,14-*endo*-Ethanotetrahydrooripavine Derivatives and Their Proposed Acid-Catalyzed Rearrangement Product

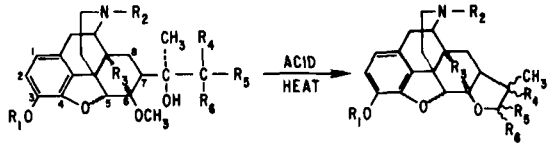

	Parent Compound	R_1	R_2	R_3	R_4	R_5	R_6
I	Buprenorphine; 21-cyclopropyl-7α-[(*S*)-1-hydroxy-1,2,2-trimethylpropyl]-6,14-*endo*-ethanotetrahydrooripavine	H	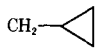	CH_2CH_2	CH_3	CH_3	CH_3
II	Norbuprenorphine; 17-Demethyl-7α-[(*S*)-1-hydroxy-1,2,2-trimethylpropyl]-6,14-*endo*-ethanotetrahydrooripavine	H	H	CH_2CH_2	CH_3	CH_3	CH_3
III	17-Demethyl-7α-[(*S*)-1-hydroxy-1,2,2-trimethylpropyl]-17-propyl-6,14-*endo*-ethanotetrahydrooripavine	H	$(CH_2)_2CH_3$	CH_2CH_2	CH_3	CH_3	CH_3
IV	17-Butyl-17-demethyl-7α-[(*S*)-1-hydroxy-1,2,2-trimethylpropyl]-6,14-*endo*-ethanotetrahydrooripavine	H	$(CH_2)_3CH_3$	CH_2CH_2	CH_3	CH_3	CH_3
V	Diprenorphine; 21-cyclopropyl-7α-(1-hydroxy-1-methylethyl)-6,14-*endo*-ethanotetrahydrooripavine	H	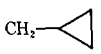	CH_2CH_2	H	H	H
VI	Etorphine; 7α-[(*R*)-1-hydroxy-1-methylbutyl]-6,14-*endo*-ethenotetrahydrooripavine	H	CH_3	CH=CH	H	H	CH_2CH_3
VII	7α-[(*R*)-1-Hydroxy-1-methylhexyl]-6,14-*endo*-ethenotetrahydrooripavine	H	CH_3	CH=CH	H	H	$(CH_2)_3CH_3$
VIII	7α-[(*R*)-2-Cyclohexyl-1-hydroxy-1-methylethyl]-6,14-*endo*-ethenotetrahydrooripavine	H	CH_3	CH=CH	H	H	C_6H_{11}
IX	22-Cyclopropyl-7α-(1-hydroxy-1-methylethyl)-6,14-*endo*-ethenotetrahydrothebaine	CH_3	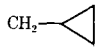	CH=CH	H	H	H

injector, 190°C; detector, 275°C; oven, programmed from 170°C to 260°C at 10°C/min. Nitrogen was the carrier gas at a flow rate of 20 mL/min.

Methane chemical-ionization mass spectral data were obtained on a quadrupole gas chromatograph–mass spectrometer[6]. The GC system was identical to that described. The temperature of the source was 260°C. The electron energy was 70 eV, and the multiplier voltage was 1.4 kV. Methane was used as reagent and carrier gas at a flow rate of 20 mL/min.

^{1}H-NMR[7] spectra were obtained on an NMR spectrometer operating in the Fourier-transform mode. Samples (60 mg) were dissolved in deuterated methanol (2 mL). Chemical shifts (δ) are expressed in ppm relative to tetramethylsilane.

Extraction—Aqueous aliquots (10 mL) of drug standards (5–10 μg/mL) were buffered to pH 9.5 with 2 mL of 3.3 M phosphate buffer. Sodium chloride (1 g) was added and a final adjustment of the pH was made with 2 M NaOH or 2 M HCl. Methylene chloride–isopropyl alcohol (70%, v/v) was added (15 mL) and the contents were shaken for 20 min. Following centrifugation, the aqueous layer was discarded, and 13 mL of the organic layer was transferred. The extract was evaporated to dryness under a stream of nitrogen, and the residue was dissolved in methanol and transferred quantitatively to an acylation tube[8] containing 50 μg of α-isocodeine (internal standard). The contents were evaporated to dryness under a nitrogen stream, and 100 μL of Tri-sil Z was added. The tube was sealed, vortexed, and allowed to remain at room temperature for 1 h. An aliquot (1–2 μL) was removed and analyzed by GC or GC–MS.

Stability Studies—Standard aqueous solutions of I (5–10 μg/mL) were prepared over the pH range of 0–12. The pH of the solutions was maintained constant by the use of saturated phosphate buffers (pH 2–12) or hydrochloric acid and sodium chloride (pH 0–2). Incubation studies were performed under the following conditions: 0–4°C, 24 h; 26–28°C, 24 h; 36–38°C, 24 h; autoclave at 112°C and 75.8 kN/m^2 for 30 min. Following the incubation period, the samples were neutralized and extracted as previously described.

A 10-week incubation study of I at pH 1.0 and 5.0 was performed at 0–4°C and at 26–28°C. Aliquots were removed at weekly intervals and analyzed for the rearrangement product. All samples were analyzed in triplicate, and the mean of the analyses is reported. Controls were included wherever appropriate to ensure that artifacts were not formed during the extraction and analysis procedures.

[6] Model 4021 Automated GC/MS/DS; Finnigan Corp., Sunnyvale, Calif.
[7] Model FT80A; Varian Associates, Palo Alto, Calif.
[8] Regis Chemical Co., Morton Grove, Ill.

RESULTS AND DISCUSSION

Structure of the Acid-Catalyzed Rearrangement Product of Buprenorphine (I)—Preliminary analytical and metabolic studies on the 6,14-*endo*-ethanotetrahydrooripavine derivatives indicated that they were unstable in the presence of acid and heat. When I was subjected to conditions commonly used for the acid-catalyzed cleavage of conjugated opiate metabolites (10% HCl, v/v; autoclave for 30 min at 112°C and 75.8 kN/m^2 steam pressure) (3), conversion was nearly complete to a hydrolysis product. Both I and the acid-hydrolysis product could be extracted from aqueous solution at pH 9.5 with methylene chloride–isopropyl alcohol (70%, v/v) with a 60–90% extraction efficiency. Extracts of I and the acid-hydrolysis product were analyzed by GC as the silyl derivatives. GC tracings are shown in Fig. 1 for standard I and extracts of I following various incubation conditions. The acid-hydrolysis product (R_t = 6.4 min) was not produced during incubation at pH 5 for 24 h (Fig. 1B), but appeared in the same incubation experiment at pH 0 (Fig. 1C). A nearly complete conversion occurred under autoclave conditions (Fig. 1D). Analytical quantities (100 mg) of the acid-hydrolysis product were produced for structural determination *via* the latter conditions and were isolated by precipitation at pH 9. The product was an amorphous white solid which, when converted to the hydrochloride salt, had a melting point range (uncorrected) of 250–268° dec. The methane chemical-ionization spectrum indicated a molecular weight of 435 AMU, representing a loss of 32 AMU from the parent substance. The most abundant ion was observed at *m/z* 436 [$(M + 1)^+$, pseudomolecular ion] and was accompanied by other ions at *m/z* (% relative abundance): 464(15), $(M + 29)^+$ ion; 437(29), isotopic ion; 435(32), M^+ ion; and 434(18), $(M - 1)^+$ ion.

Structural assignment of the acid-hydrolysis product of I was made by ^{1}H-NMR (Fig. 2). The singlets in the spectrum of I for the side-chain methyl groups at δ 1.0 and δ 1.3 ppm as well as the methoxyl group at δ 3.4 ppm are not present in the spectrum of the hydrolysis product. Instead, four new singlets of near equal intensity at δ 1.05, 1.15, 1.20, and 1.25 ppm are present, consistent with the proposed structure in which a new tetrahydrofuran ring is formed at C(6)–C(7). Similar products have been identified for tetrahydrothebaine analgesic derivatives following hydrolysis with formic acid under reflux conditions (2). The formation of the furan ring is speculated to occur following demethylation of the methoxyl group, acid-catalyzed elimination of the tertiary hydroxyl group, and a subsequent 1,2-shift of a substituent group on the C(7) side chain. The overall scheme results in the formation of a new ring with nonequivalent methyl groups on the basic skeleton of I and a net loss of a molecule of CH_3OH (32 AMU).

Stability of I in Aqueous Solution—The stability of I in aqueous

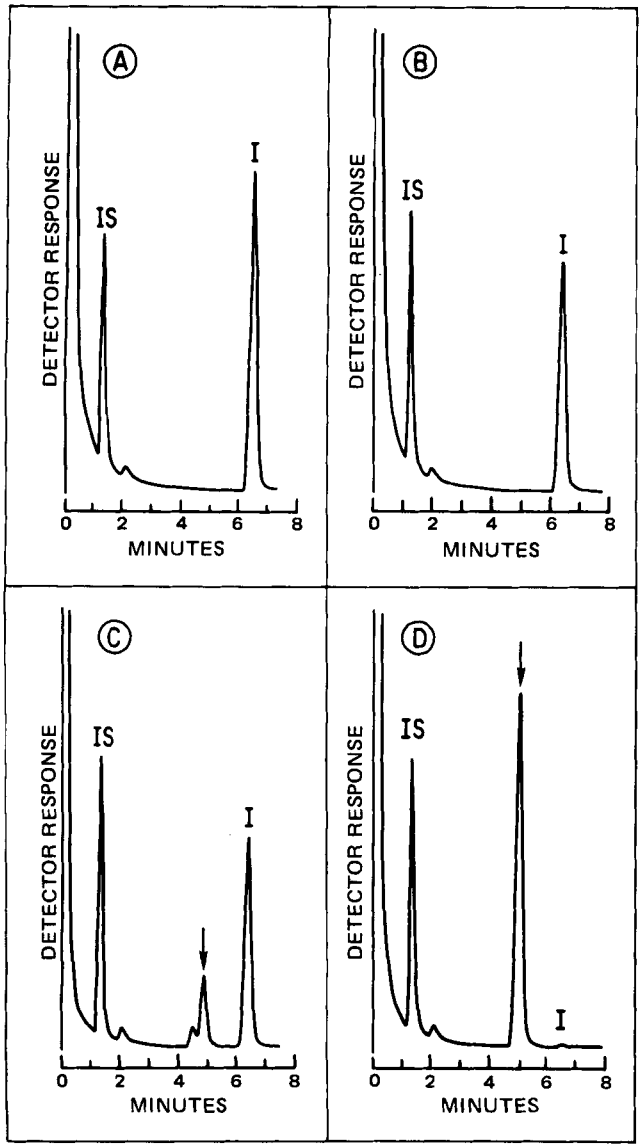

Figure 1—*Gas chromatograms of buprenorphine (I) and extracts following incubation under different conditions. Key: (A) standard I without extraction; (B) extract following incubation of I at pH 5 and 36–38°C for 24 h; (C) extract following incubation of I at pH 0 and 36–38°C for 24 h; (D) extract following incubation of I at pH 0 under autoclave conditions for 30 min; (IS) internal standard. The appearance of the rearrangement product of I is indicated by the arrow.*

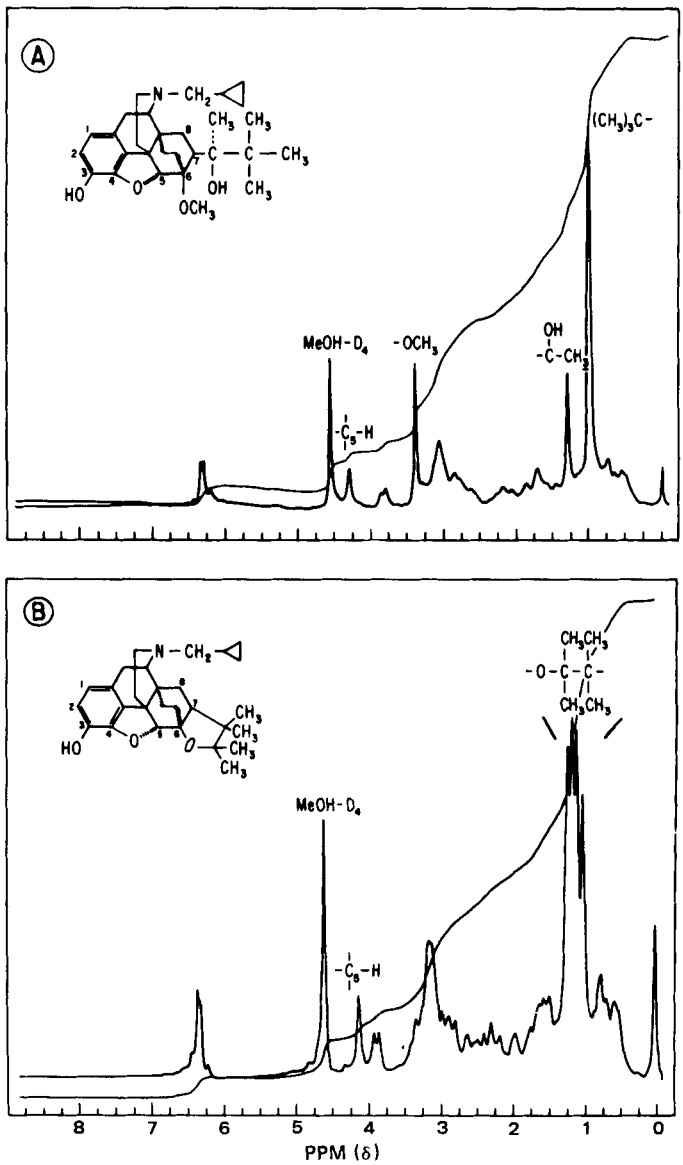

Figure 2—*^{1}H-NMR spectra of buprenorphine (A) and rearrangement product following acid hydrolysis (B).*

solution was studied over pH 0–12 under the following incubation conditions: 0–4°C, 24 h; 26–28°C, 24 h; 36–38°C, 24 h; 30 min, autoclave. Following incubation the samples were extracted and analyzed by GC for I and the rearrangement product. The percent recoveries of I were calculated from peak height ratios of I and the internal standard for extracted samples *versus* unextracted standards. Hence, percent recoveries reflect a combination of extraction efficiency and loss of I through rearrangement and other decomposition pathways. Calculations of percent rearrangement product were based on peak height ratios of rearrangement product to the sum of rearrangement product and parent compound. Therefore, percent rearrangement values are independent of the extraction efficiency of the solvent and reflect only the percentage of I converted to the rearrangement product.

Recoveries of I following incubation were consistently high (60–90%) at pH > 1 for all conditions except the autoclave (Table II). After incubation in the autoclave, recoveries generally fell and reached a low of 17% at pH 7.4, presumably reflecting decomposition *via* hydrolytic pathways other than rearrangement. The nature of these decomposition products is unknown. At pH 0 for all incubation conditions, rearrangement product was detectable, but the amount of rearrangement was clearly related to the temperature of incubation. Only a trace of rearrangement product was present in the 0–4°C samples, whereas a near quantitative conversion occurred under autoclave conditions. Rearrangement product was not detected in any sample at pH > 3.

Long-term incubation studies (10 weeks) were performed with aqueous solutions of I to determine if significant rearrangement occurred during storage at 0–4°C and 26–28°C. Solutions of I (50–100 μg/mL) were prepared for incubation at pH 1 and pH 5. Aliquots were withdrawn at weekly intervals and assayed by GC for I and the rearrangement product. The rearrangement product was first detected in week 2 samples (pH 1, 26–28°C) and represented ~1% of the parent compound. The amount of rearrangement product in these samples increased gradually to ~4% of I at week 10. Rearrangement product was detectable in the remaining solutions (pH 1, 0–4°C; pH 5, 0–4°C; and 26–28°C) only in trace amounts, ~0.1%, at week 10. Buprenorphine (I) was recovered in high yield (60–80%) from all samples throughout the incubation period, and products *via* other decomposition routes were not detected.

Acid-Hydrolysis of 6,14-*endo*-Ethanotetrahydrooripavine Derivatives—Other members of the oripavine series and related derivatives were subjected to autoclave conditions to determine if acid-catalyzed rearrangement occurs similar to that observed for I. The structures of the parent compounds and the potential rearrangement products are illustrated in Table I. Following autoclave incubation, the samples were allowed to cool and were extracted and analyzed by GC and GC–MS. Derivatization of a number of the compounds was found to be necessary for GC analysis. Recoveries of the compounds in Table I from aqueous solution ranged from 65–78% prior to autoclave incubation, but fell to

Table II—Recovery and Rearrangement of Buprenorphine Following Incubation Under Various pH Conditions [a]

pH	0–4°C Incubation [b]		26–28°C Incubation [b]		36–38°C Incubation [b]		Autoclave [c]	
	Recovery, %	Rearrangement, %	Recovery, %	Rearrangement, %	Recovery, %	Rearrangement, %	Recovery, %	Rearrangement, %
0	75.5 ± 6.8	0.7 ± 0.2	57.6 ± 4.5	3.3 ± 0.7	51.2 ± 2.4	18.4 ± 0.8	0.7 ± 0.1	99.3 ± 0.1
1	70.6 ± 5.1	0	63.0 ± 4.4	0	74.0 ± 5.7	0.9 ± 0.1	1.1 ± 0.1	98.7 ± 0.1
2	73.4 ± 1.8	0	72.9 ± 2.6	0	74.0 ± 0.4	0	78.1 ± 2.4	15.3 ± 0.5
2.5	68.6 ± 4.0	0	64.7 ± 2.8	0	76.3 ± 5.4	0	81.8 ± 2.7	4.1 ± 0.4
3	72.1 ± 2.0	0	71.1 ± 1.6	0	74.1 ± 1.4	0	89.4 ± 1.2	1.3 ± 0.3
4	71.9 ± 3.4	0	79.3 ± 5.2	0	73.0 ± 2.1	0	96.3 ± 3.6	0
5	74.9 ± 1.3	0	88.2 ± 2.6	0	71.1 ± 2.3	0	67.9 ± 2.3	0
6	78.3 ± 3.3	0	88.1 ± 5.7	0	70.5 ± 4.0	0	44.8 ± 2.3	0
7	75.4 ± 1.7	0	93.7 ± 4.4	0	73.9 ± 1.6	0	19.0 ± 1.4	0
7.4	71.5 ± 5.1	0	85.9 ± 5.4	0	70.5 ± 3.2	0	17.0 ± 0.3	0
8	91.0 ± 10.1	0	76.1 ± 0	0	76.6 ± 5.0	0	22.5 ± 1.6	0
9	92.5 ± 8.8	0	63.0 ± 3.2	0	76.4 ± 1.1	0	41.4 ± 1.1	0
10	91.2 ± 2.6	0	61.4 ± 6.0	0	77.1 ± 3.6	0	31.1 ± 3.0	0
12	88.9 ± 0.5	0	68.0 ± 4.8	0	80.7 ± 2.3	0	30.6 ± 1.2	0

[a] Decomposition by pathways other than rearrangement account for low recoveries under autoclave conditions and may have contributed to a lesser extent to the variability of recovery under all conditions. [b] For 24 h. [c] For 30 min.

Table III—Methane Chemical Ionization Spectra of 6,14-*endo*-Ethanotetrahydrooripavine Derivatives and Hydrolysis Products [a]

Compound	Standard				Hydrolysis Product		
	Mol. Wt.	$(M + 1)^+$	$(M - 17)^+$	Prominent Ions	Apparent Mol. Wt.	$(M + 1)^+$	Prominent Ions
I–Trimethyl silane	539	540(27)	522(100)	539(14), 538(12), 524(19), 523(39), 508(19), 506(31), 492(29), 490(22), 482(17)	507	508(100)	536(16), 509(39), 507(38), 506(15), 493(21), 492(51)
II–Trimethyl silane	485	486(23)	468(100)	470(19), 469(38), 454(22), 453(17), 452(33), 438(43), 436(34), 428(33), 396(15)	453	454(100)	482(17), 455(34), 453(39), 439(20), 438(58)
III–Trimethyl silane	527	528(21)	510(100)	512(25), 511(43), 496(20), 495(17), 494(34), 480(38), 478(27), 470(25), 438(15)	495	496(100)	524(17), 497(36), 495(37), 494(17), 481(24), 480(63)
IV–Trimethyl silane	541	542(19)	524(100)	541(17), 526(24), 525(43), 510(21), 509(17), 508(34), 498(18), 495(15), 494(38), 492(26), 484(26)	509	510(100)	538(18), 511(38), 509(38) 495(24), 494(62)
V	425	426(26)	408(100)	425(23), 409(31), 394(15), 376(33)	393 [b]	394(84)	448(19), 422(20), 421(25) 420(100), 419(25), 418(25), 395(21), 393(20)
VI	411	412(38)	394(100)	411(29), 410(16), 395(28), 298(18), 216(23)	379	380(100)	408(20), 381(26), 379(17)
VII	439	440(44)	422(100)	439(32), 438(21), 423(28), 298(17), 216(15)	407	408(100)	436(21), 409(26), 407(21), 252(19), 137(41)
VIII	451	452(44)	434(100)	480(18), 451(34), 450(28), 453(17), 435(32), 432(24) 298(40), 216(17), 191(19)	419	420(100)	448(19), 421(29), 419(18), 418(26), 408(20), 216(16), 137(16)
IX–Trimethyl silane	437	438(38)	420(100)	437(21), 421(32), 270(22)	405	406(100)	407(29), 405(17)

[a] *m/z* (percent relative abundance). Only ions ≥15% are reported. [b] Unresolved mixture.

zero following acid-hydrolysis in the autoclave. Compounds I–IV, VI, VII, and IX were converted to single major products, whereas two apparent isomeric products were present for VIII and a complex multicomponent mixture was obtained for V.

Methane chemical-ionization spectra are shown in Table III for I–IX and their major acid-hydrolysis products. The spectra present strong evidence for the formation of rearrangement products similar to that identified for I. The spectra of the parent compounds are characterized by a $(M + 1)^+$ ion (pseudomolecular ion) and a $(M - 17)^+$ ion (loss of —OH), the latter representing the most abundant ion in the spectrum of each compound. With the exception of III, which was a multicomponent mixture, the most abundant ions in the spectra of the acid-hydrolysis products were the $(M + 1)^+$ ions. The pseudomolecular ions were accompanied by corresponding $(M + 15)^+$ and $(M + C_2H_5)^+$ ions, thus supporting the molecular weight assignments of the hydrolysis products. Also, there was a notable lack of $(M - OH)^+$ ions in the spectra of the hydrolysis products. Overall, the mass spectral features of the acid-hydrolysis products of II–IX completely paralleled those observed for the rearrangement product of I and are entirely consistent with the structures of the proposed rearrangement products.

In summary, the acid and heat lability of the *endo*-ethanotetrahydrooripavines must be considered when these compounds are dissolved in aqueous media. Under conditions of high acidity (pH 0–1), heat accelerates an acid-catalyzed rearrangement reaction to yield an hydrolysis product. The structure of the acid-hydrolysis product of I contained a new tetrahydrofuran ring formed at C(6)—C(7) with a net loss of methanol from the parent compound. Evidence for similar acid-hydrolysis products arising from other members of the series (II–IX) was obtained by GC–MS. At higher pH (pH > 1) the rearrangement reaction of I was much slower or nonexistent. After 10 weeks incubation at pH 5 (26–28°C), I was recovered from aqueous solution in high yield with no evidence of decomposition. Significant loss of I *via* other decomposition pathways was apparent following exposure to the extreme conditions of the autoclave.

REFERENCES

(1) M. J. Rance and J. S. Shillingford, *Xenobiotica*, **7**, 529 (1977).

(2) K. W. Bentley, D. G. Hardy, B. Meek, J. B. Taylor, J. J. Brown, and G. O. Morton, *J. Chem. Soc.*, (C), **1969**, 2229.

(3) S. Y. Yeh and L. A. Woods, *J. Pharm. Sci.*, **59**, 380 (1970).

ACKNOWLEDGMENTS

Special thanks are given to Ms. W. M. Roberts and Ms. P. Settlemire for their assistance in preparing this manuscript.

Radioimmunoassay for Psychotropic Drugs III: Synthesis and Properties of Haptens for Trifluoperazine and Fluphenazine

E. M. HAWES, H. U. SHETTY, J. K. COOPER, G. RAUW, G. McKAY, and K. K. MIDHA ×

Received July 27, 1982, from the *College of Pharmacy, University of Saskatchewan, Saskatoon, Saskatchewan, Canada S7N 0W0.* Accepted for publication January 10, 1983.

Abstract □ For the development of radioimmunoassay procedures for trifluoperazine and fluphenazine, three haptens, *N*-(2-carboxyethyl)desmethyltrifluoperazine, *N*-(4-carboxybutyl)desmethyltrifluoperazine, and 10-[3-(4-carboxyethylpiperazinyl)-3-oxopropyl]-2-trifluoromethyl-10*H*-phenothiazine, were synthesized and characterized. Each hapten was coupled to bovine serum albumin, and the number of hapten residues per mole of bovine serum albumin was calculated by UV spectrophotometric methods. Antibodies to each hapten–protein conjugate were developed in rabbits, and titers of the antisera were checked by evaluating their binding characteristics to the tritiated drug.

Keyphrases □ Trifluoperazine—hapten synthesis, conjugation with bovine serum albumin, antisera production in rabbits, RIA □ Fluphenazine—hapten synthesis, conjugation with bovine serum albumin, antisera production in rabbits, RIA □ Psychotropic drugs—trifluoperazine, fluphenazine, hapten synthesis, conjugation with bovine serum albumin, antisera production in rabbits, RIA

Trifluoperazine (I), a piperazine-type phenothiazine, is widely used orally for the treatment of certain psychotic disorders. However, until recently there were no suitable sensitive and specific analytical methods available to quantitate this drug in the plasma of patients under treatment. This slow method development was primarily due to the reputed instability and adsorptive loss of phenothiazines in all stages of handling for analysis, the low plasma levels encountered (arising from such reasons as the low doses used), the probable significant first-pass metabolism, and extensive metabolism to numerous metabolites. The available reported chemical methods of analysis include GC–NPD (1–3) procedures sensitive to 0.5 ng/mL using a 2-mL plasma sample (1, 3) and a GC–MS method involving the use of a single-ion monitoring technique, which permitted the determination of 78 pg of trifluoperazine/mL of plasma using a 2-mL sample (4). Although of sufficient sensitivity to monitor plasma levels of patients under chronic treatment with normal therapeutic doses of trifluoperazine, these procedures are tedious, requiring extraction of the drug from the biological media, and are thus not easily amenable for routine clinical monitoring.

Radioimmunoassay (RIA) procedures, on the other hand, are simple, sensitive, require a small amount of plasma sample generally with no extraction, and are readily applicable to routine analysis with their ability to handle large numbers of samples with a short turnaround. In fact, an RIA procedure for trifluoperazine was recently reported from these laboratories, which can quantitate 0.25 ng/mL with a 200-μL plasma sample (5). This method is based on an antiserum developed to a protein conjugate (IIa), where the protein is linked to the side chain of the piperazine ring. This site was chosen since from previous experience, as with antibodies raised to chlorpromazine (6, 7), the antiserum raised to conjugates where the protein is coupled to carboxylic acid groups attached to the *N*-10 side-chain sites cross-reacted significantly less with phenothiazine ring metabolites (such as the sulfoxide and 7-hydroxy derivatives) than the antiserum raised to conjugates where the protein is coupled through carboxylic acid groups attached through other positions of the phenothiazine ring. Furthermore, antibodies have now been raised to the protein conjugates (IIb, III) of two other haptens, where the protein is also coupled through the side chain.

This paper describes the syntheses and characterizations of three drug–protein conjugates, the production of the antibodies to these conjugates in rabbits, and comparison of the titers of the antisera. Since fluphenazine only differs structurally from trifluoperazine in having a *N*-hydroxyethyl substituent on the piperazine ring in place of the *N*-methyl group shown in I, these antisera should be suitable for developing an RIA for fluphenazine as well as trifluoperazine.

RESULTS AND DISCUSSION

To modify the structure of trifluoperazine so as to contain an acid moiety in the side chain (*i.e.*, VII), 10-(3-chloropropyl)-2-trifluoromethylphenothiazine (V) was treated with carbomethoxyalkyl-substituted piperazines (IV), and the resultant esters (VI) subsequently hydrolyzed with base. The desired substituted piperazines were readily

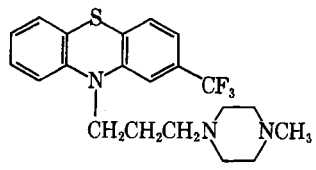

I

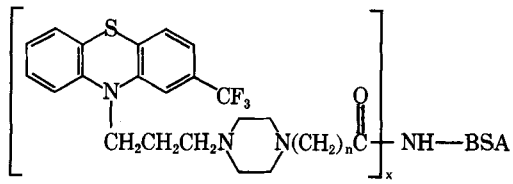

IIa: n = 2
IIb: n = 4

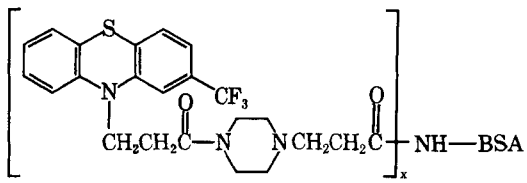

III

0022-3549/84/0200-0247$01.00/0
© 1984, American Pharmaceutical Association

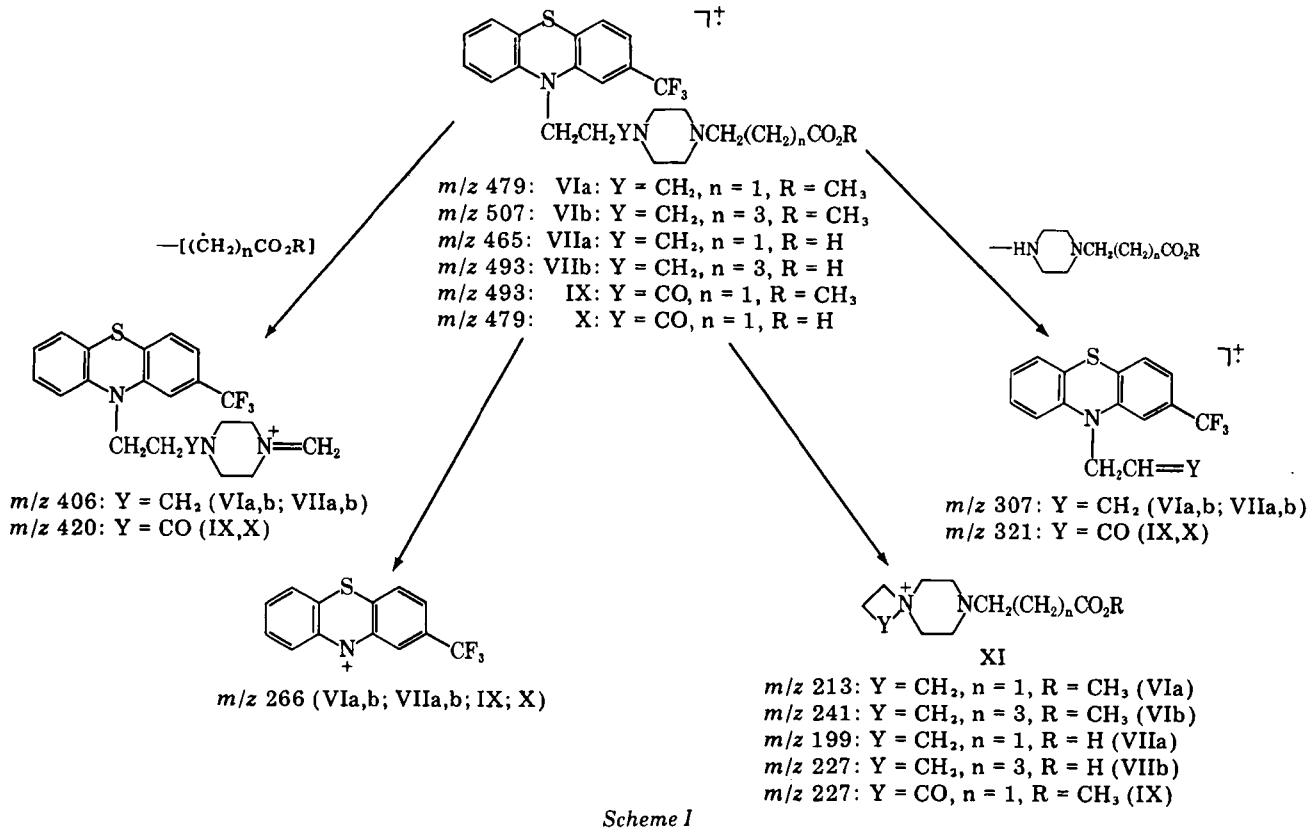

Scheme I

synthesized by treatment of piperazine with methyl acrylate or 5-bromovalerate. This approach to the synthesis of carboxyalkyl-substituted trifluoperazine differs from that initially reported for the synthesis of the analogous hapten of chlorpromazine (8), where *N*-desmethylchlorpromazine was reacted with methyl acrylate and the resultant ester of the desired hapten subsequently hydrolyzed (5). The lack of availability of *N*-desmethyltrifluoperazine and the simple synthetic accessibility of the chloropropyl starting material (V) prompted the approach reported here. Additionally, to investigate the effect that a carbonyl group in the side chain of the hapten has on the sensitivity and specificity of the antiserum raised to the protein conjugate, X was obtained by treatment of 3-[10-(2-trifluoromethylphenothiazinyl)]propionyl chloride (VIII) with 1-(2-methoxycarbonylethyl)piperazine (IVa) to yield the ester IX which was subsequently hydrolyzed to the desired acid (X).

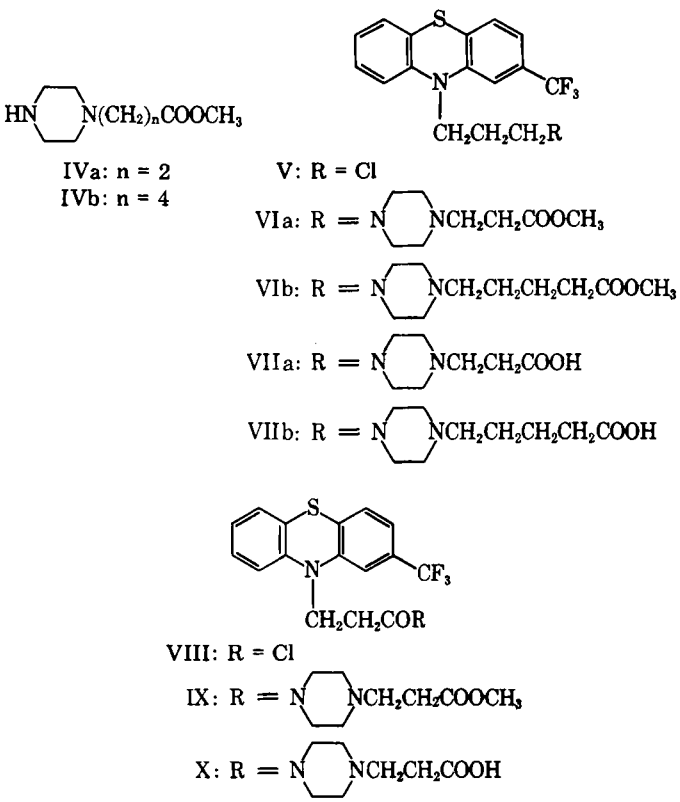

All three haptens and their methyl esters gave NMR and MS entirely consistent with the given structures. The mass spectra of the three esters (VIa, VIb, and IX) and their corresponding acids (VIIa, VIIb, and X) gave molecular ions in each case. The fragmentations of these esters and acids can be rationalized in terms of the structures of the compounds. Some of the major diagnostic ions of the mass spectra of all six compounds are shown in Scheme I, the origin of the various ions being indicated in parentheses. In each case, the loss of $(\dot{C}H_2)_nCO_2CH_3$ from the esters and the loss of $(\dot{C}H_2)_nCO_2H$ from the acids leads to the diagnostic ions at *m/z* 406 (VIa, VIb, VIIa, and VIIb) or *m/z* 420 (IX and X). Also, the loss of $NH(CH_2CH_2)NCH_2(CH_2)_nCO_2CH_3$ from the esters or $HN(CH_2CH_2)$-$NCH_2(CH_2)_nCO_2H$ from the acids, as a neutral molecule from the parent molecular ions, results in diagnostic ions at *m/z* 307 for VIa, VIb, VIIa, and VIIb and at *m/z* 321 for IX and X. The presence of the ion at *m/z* 266 in the mass spectra of all six compounds is due to the cleavage of the N—C bond between the ring and the side chain, with the charge being accommodated at the phenothiazine ring system (8). On the other hand, when the charge is accommodated in the side chain, then the diagnostic ions at *m/z* 213 (VIa), 241 (VIb), and 227 (IX) for esters and at *m/z* 199 (VIIa) and 227 (VIIb) for acids can be rationalized by the proposed structure for XI. Also, the ions due to XI can further fragment by loss of one or more of the neutral molecules, $CH{\equiv}CH$, $CH_2{=}CH_2$, $CH_2{=}C{=}O$, $CO(CH_2)_2$, $RN(CH_2)_2$, and $CH_3{-}N{=}CH_2$. The absence of the corresponding ion XI in the mass spectrum of X may be due to the fact that the charge is completely retained by the phenothiazine ring system (*m/z* 266, 100% relative abundance). The β-aminocarboxylic acids, VIIa and X, lose a neutral molecule of acrylic acid with a transfer of hydrogen as reported earlier (9). This results in the ions at *m/z* 393 and 407 for VIIa and X, respectively. However, in the mass spectrum of the γ-aminocarboxylic acid VIIb, the ion at *m/z* 393 was of low abundance, while the abundant ion at *m/z* 406 probably formed from the loss of $\dot{C}H_2CH_2CH_2CO_2H$ due to the bulkiness of the chain.

All attempts to find a suitable recrystallization solvent for the haptens failed and, thus, analytical figures were obtained for the hydrochloride salts of their methyl esters. Further confirmation of the integrity of the hapten was obtained by conversion of the acid group back to the methyl

ester by reaction with an ethereal solution of diazomethane (8). GC analysis of the crude methylated residue showed in each case only one peak, which gave on GC–MS the same electron-impact mass spectrum as the appropriate authentic hapten methyl ester.

The haptens were successfully coupled to bovine serum albumin by a modified mixed anhydride method (8, 10, 11). To investigate whether the number of moles of hapten coupled to one mole of the protein influences the quality of the antiserum in terms of specificity and sensitivity, both IIa and IIb were obtained with variation in the number of moles coupled to bovine serum albumin. Thus, while all three haptens were coupled with bovine serum albumin to produce an immunizing antigen with 15–30 hapten residues/mol of bovine serum albumin, IIa and IIb were also obtained with ~70 hapten residues/mol of bovine serum albumin.

Rabbits were immunized with each hapten–protein conjugate as described in the *Experimental* section. The preliminary assessment of the antisera so produced, together with the number of intravenous booster shots required, is presented in Table I. In the first experiments using at least five rabbits, operational titers were produced from all five conjugates. However, only the antisera produced from the conjugate with two carbon atoms between the piperazine ring and the amide linkage in structurally modified trifluoperazine (*i.e.*, IIa) gave titer values greater than 1:500. Thus, by comparison of the antisera produced from IIa and IIb it can be observed that on increasing the chain length between the piperazine ring and the amide linkage in the hapten–protein conjugate, the titer value did not increase. To check this important observation, two more rabbits each were immunized with IIa (X = 70) and IIb (X = 71) in a second experiment. Apart from a 1:500 titer in two of the rabbits, a 1:8000 titer was produced in one of the IIa rabbits, thus confirming the initial observation. It can also be deduced from the first experiments that since III only produced 1:500 titers, the insertion of a carbonyl group in the side chain of the hapten had a detrimental effect on the quality of the antisera raised to the resultant hapten–protein conjugate. Finally, from the initial experiments it was also observed that increasing the number of hapten residues per mole of bovine serum albumin did not have a dramatic effect on titer values. In the case of the two types of IIb (X = 27 and X = 71), there were virtually no differences with respect to the titer produced; however, in the case of IIa higher titers were produced from the antibodies raised to the high moles-coupled hapten–protein conjugate (*i.e.*, IIa, X = 70) than the low moles-coupled hapten–protein conjugate (*i.e.*, IIa, X = 27).

RIAs sensitive to the nanogram range have been developed for trifluoperazine using antibodies to IIa. The assays were not influenced by plasma and endogenous substances. A procedure using antibodies to the IIa (X = 27) conjugate has been previously published (5), where the antisera cross-reacted with the presumed major metabolites of trifluoperazine (the *N*-desmethyl, 7-hydroxy, and sulfoxide compounds) to the extent of 26, 24, and <1%, respectively. By comparison, the three 1:10,000 titer antisera raised to the IIa (X = 70) conjugate cross-reacted (12) with these same metabolites 12–14, <1–14, and <1%, respectively. These improved RIA procedures using the IIa (X = 70) conjugate are described in depth elsewhere (13). Also, these antisera raised to the IIa conjugates recognize especially well (100–143%, cross-reactivity) the side-chain-modified analogue of trifluoperazine, fluphenazine; therefore, RIA procedures are also being developed for fluphenazine using these same antisera.

Table I—Rabbit Antiserum Titers of Trifluoperazine Hapten–Protein Conjugates [a]

Immunizing Antigen[b]	No. of Positives/ No. Tested	No. of Intravenous Boosters	Titers[c]
IIa, X = 70	3/5	1	1:10,000 (3)
	2/2	4	1:500 (1)
		4	1:8000 (1)
IIa, X = 27	2/8	1	1:2000 (1)
		1	1:4000 (1)
IIb, X = 71	3/5	2–4	1:500 (3)
	1/2	4	1:500 (1)
IIb, X = 16	3/5	3–4	1:500 (3)
III, X = 24	6/8	3	1:500 (6)

[a] Titer values 1:250 or less are not recorded. [b] X = number of hapten residues per mole of bovine serum albumin. [c] Number of rabbits giving this titer in parentheses.

EXPERIMENTAL[1]

1-(4-Methoxycarbonylbutyl)piperazine (IVb) and 1,4-Bis(4-methoxycarbonylbutyl)piperazine—A stirred mixture of methyl 5-bromovalerate (7.80 g, 40 mmol) and anhydrous piperazine (6.88 g, 80 mmol) in 50 mL of dry benzene was heated under reflux for 4 h. The resulting piperazine hydrobromide was removed by filtration and washed with dry benzene (20 mL). The organic phase was evaporated, and the residue was distilled *in vacuo* to obtain 4.5 g (56%) of IVb as a colorless oil, bp 72–74°C/0.08 mm Hg; ^{1}H-NMR: δ 1.44–1.74 (m, 5, butyl central CH_2CH_2 and NH which exchanges with D_2O), 2.14–2.58 (m, 8, piperazine CH_2), 2.78–3.06 (m, 4, $CH_2CO_2CH_3$ and CH_2-piperazine), and 3.70 ppm (s, 3, CO_2CH_3); MS: m/z 200 (M^+, 21%), 169(34), 159(11), 158(81), 115(33), 100(13), 99(100), 98(13), 85(12), 84(23), and 83(15).

Anal.—Calc. for $C_{10}H_{20}N_2O_4$: C, 59.97; H, 10.07; N, 13.99. Found: C, 60.57; H, 10.40; N, 13.55.

The vacuum distillation also gave 1.5 g (12%) of the bis compound as a colorless oil, bp 134–136°C/0.08 mm Hg; ^{1}H-NMR: δ 1.30–1.80 (m, 8, butyl central CH_2CH_2), 2.17–2.57 (m, 16, piperazine CH_2, $CH_2CO_2CH_3$, and CH_2-piperazine), and 3.68 ppm (s, 6, CO_2CH_3); MS: m/z 314 (M^+, 11%), 283(17), 214(15), 213(100), 185(12), 158(16), 144(37), 115(19), 99(32), 98(35), 84(17), and 83(15).

***N*-(2-Methoxycarbonylethyl)desmethyltrifluoperazine (VIa)**—A mixture of 10-(3-chloropropyl)-2-trifluoromethylphenothiazine (V) (1.38 g, 4 mmol), mp 69–70°C [lit. (14) mp 70–71°C] synthesized by modification of a literature procedure (15), IVa (1.03 g, 6 mmol) (16), and sodium iodide (0.60 g, 4 mmol) in 20 mL of methyl ethyl ketone was refluxed with stirring for 20 h. The solvent was removed *in vacuo*, and the residue was extracted with 5% HCl (5 × 4 mL). The acidic extract was brought to pH 7.0 with sodium carbonate and extracted with ether (3 × 20 mL). The combined ether extract was dried (magnesium sulfate) and treated with dry hydrogen chloride in ether to afford 1.61 g (73%) of the dihydrochloride salt of the ester VIa as pale-yellow crystals from methanol–ether, mp 194–196°C; ^{1}H-NMR: δ 1.83–2.14 (m 2, propyl central CH_2), 2.34–2.81 (m, 14, piperazine CH_2, CH_2-piperazine, and $CH_2CH_2CO_2CH_3$), 3.74 (s, 3, CO_2CH_3), 4.04 (t, 2, J = 6.2 Hz, CH_2-phenothiazine ring), and 6.79–7.26 ppm (m, 7, aromatic); MS: m/z 479 (M^+, 37%), 406(10), 307(10), 280(28), 267(11), 266(15), 258(12), 248(14), 213(24), 199(42), 186(15), 185(100), 157(12), 142(14), 130(13), 116(28), 113(14), 111(16), 99(15), 98(35), 97(13), and 84(21).

Anal.—Calc. for $C_{24}H_{28}F_3N_3O_2S$·2HCl: C, 52.17; H, 5.11; N, 7.61. Found: C, 52.29; H, 5.29; N, 7.70.

***N*-(4-Methoxycarbonylbutyl)desmethyltrifluoperazine (VIb)**—This compound was synthesized from IVb (1.00 g, 5 mmol), V (1.38 g, 4 mmol), and sodium iodide (0.60 g, 4 mmol) in 20 mL of methyl ethyl ketone in the same manner as described for VIa. The yield was 65% of the dihydrochloride salt of VIb. recrystallized from methanol–ether, mp 235–236°C; ^{1}H-NMR: δ 1.36–2.57 (m, 20, side-chain CH_2 except CH_2-phenothiazine ring), 3.60 (s, 3, CO_2CH_3), 3.88 (t, 2, J = 6.2 Hz, CH_2-phenothiazine ring), and 6.80–7.23 ppm (m, 7, aromatic); MS: m/z 507 (M^+, 67%), 476(17), 406(28), 307(14), 306(11), 295(13), 281(21), 280(100), 267(26), 266(25), 248(27), 241(28), 228(15), 227(90), 214(18), 213(68), 203(21), 185(12), 170(11), 144(33), 115(12), 113(40), 99(17), 98(30), and 97(18).

Anal.—Calc. for $C_{26}H_{32}F_3N_3O_2S$·2HCl: C, 53.79; H, 5.90; N, 7.24. Found: C, 53.60; H, 6.04; N, 6.91.

***N*-(2-Carboxyethyl)desmethyltrifluoperazine (VIIa)**—A mixture of VIa as the dihydrochloride salt (0.55 g, 1 mmol), sodium hydroxide (0.16 g, 4 mmol), methanol (15 mL), and water (15 mL) was heated under gentle reflux for 1 h. The methanol was removed under reduced pressure, and a further 15 mL of water was added. After washing with ether (2 × 10 mL), the pH of the aqueous phase was adjusted to neutral with 1% HCl to yield an oily solid. The product was extracted with methylene chloride (3 × 10 mL), dried (magnesium sulfate), and concentrated under reduced pressure to give 0.41 g (88%) of pale-yellow scales; ^{1}H-NMR: δ 1.72–2.17 (m, 2, propyl central CH_2), 2.47–2.94 (m, 14, piperazine CH_2, $CH_2CH_2CO_2H$, and CH_2-piperazine), 4.00 (t, 2, J = 6.0 Hz, CH_2-phenothiazine ring), 6.94–7.43 (m, 7, aromatic), and 10.03 ppm (s, 1, acid H

[1] Melting points were determined in open-glass capillaries with a Gallenkamp melting point apparatus and are uncorrected. ^{1}H-NMR spectra were determined, with the free base in each case, on a Varian T-60 instrument in deuterochloroform with tetramethylsilane as internal reference. Low-resolution electron-impact mass spectra were recorded on a VG Micromass MM16F instrument at 70 eV, and except for base peak, diagnostic ion and parent ion peaks <m/z 75 or relative intensity <10% of the base peak were omitted. UV determinations were carried out using a Unicam SP 1700 instrument. Microanalyses for samples dried over phosphorus pentoxide at 60°C under reduced pressure were carried out by Mr. R. E. Teed, Department of Chemistry and Chemical Engineering, University of Saskatchewan.

which exchanges with D_2O); MS: *m/z* 465 ($M^{+\cdot}$, 23%), 406(2), 394(13), 393(49), 307(16), 306(17), 280(24), 267(22), 266(36), 248(28), 199(12), 185(12), 171(23), 127(36), 99(99), 97(17), 84(29), and 58(100).

***N*-(4-Carboxybutyl)desmethyltrifluoperazine (VIIb)**—This compound was synthesized from VIb by alkaline hydrolysis in the same manner as described for VIIa to yield 94% of pale-yellow scales; ^{1}H-NMR: 1.44–3.03 (m, 20, side-chain CH_2 except CH_2-phenothiazine ring), 3.97 (t, 2, J = 6.0 Hz, CH_2-phenothiazine ring), 6.78–7.41 (m, 7, aromatic), and 12.09 ppm (s, 1, acid H which exchanges with D_2O); MS: *m/z* 493 ($M^{+\cdot}$, 74%), 406(22), 393(2), 350(10), 307(17), 306(12), 294(16), 281(20), 280(100), 267(38), 266(36), 248(33), 227(37), 214(12), 213(78), 203(22), 200(17), 199(100), 197(10), 171(14), 156(17), 143(11), 139(10), 130(27), 113(45), 105(12), 99(29), 98(36), 97(22), 96(11), 85(12), 84(35), 83(18), 82(13), and 77(10).

10-[3-(4-Methoxycarbonylethylpiperazinyl)-3-oxopropyl]-2-trifluoromethyl-10*H*-phenothiazine (IX)—The propionyl acid chloride (VIII) (0.90 g, 2.5 mmol), prepared as previously reported (17), in 5 mL of dry benzene was added in a dropwise manner over a period of 1 h to a stirred solution of IVa (0.47 g, 2.75 mmol) and triethylamine (0.5 mL) in 10 mL of benzene at 5°C. After stirring at room temperature for an additional 2 h, the benzene layer was washed twice with water, dried over anhydrous magnesium sulfate, filtered, and evaporated *in vacuo* to leave an oily residue. Column chromatography with alumina as the adsorbent and benzene as the solvent gave, after evaporation of the solvent, 1 g (81%) of a colorless oil which yielded the hydrochloride salt as fine white crystals from methanol, mp 141–142°C; ^{1}H-NMR: δ 2.18–2.94 (m, 10, piperazine CH_2 and CH_2-piperazine), 3.17–3.73 (m, 7, CH_2CON, $CH_2CO_2CH_3$, and CO_2CH_3), 4.30 (t, 2, J = 7.0 Hz, CH_2-phenothiazine ring), and 6.77–7.40 ppm (m, 7, aromatic); MS: *m/z* 493 ($M^{+\cdot}$, 100%), 420(21), 321(13), 320(15), 280(66), 267(16), 266(42), 248(27), 227(55), 213(10), 210(17), 199(4), 185(3), 171(11), 142(49), 130(11), 127(16), 125(11), 116(13), 99(16), 98(10), and 97(11).

Anal.—Calc. for $C_{24}H_{26}F_3N_3O_3S$·HCl: C, 54.38; H, 5.14; N, 7.93. Found: C, 54.74; H, 5.12; N, 7.96.

10 - [3-(4-Carboxyethylpiperazinyl)-3-oxopropyl]-2-trifluoromethyl-10*H*-phenothiazine (X)—This compound was obtained from IX by alkaline hydrolysis in the same manner as described for VIIa to yield 86% of white scales; ^{1}H-NMR: δ 2.38–2.94 (m, 10, piperazine CH_2 and CH_2-piperazine), 3.22–3.87 (m, 4, CH_2CON and $CH_2CO_2H_3$), 4.31 (t, 2, J = 7.0 Hz, CH_2-phenothiazine ring), 6.91–7.37 (m, 7, aromatic), and 9.60 ppm (s, 1, acid H which exchanges with D_2O); MS: *m/z* 479 ($M^{+\cdot}$, 2%), 420(1), 408(10), 407(40), 340(12), 339(61), 321(2), 281(15), 280(78), 268(11), 267(50), 266(100), 248(39), 247(10), 141(46), 85(13), 79(10), 78(100), and 77(31).

Coupling of VIIa to Bovine Serum Albumin—Compound VIIa was coupled to bovine serum by a modified mixed anhydride method (8, 10, 11). Compound VIIa (0.20 g, 0.43 mmol) and isobutyl choroformate (56 μL, 0.43 mmol) were dissolved in freshly distilled dioxane (3 mL), and the solution was cooled to 15°C and allowed to stand for 20 min. The mixture was then slowly added in 0.5-mL aliquots to a stirred, cooled (4°C) solution of bovine serum albumin[2] (0.30 g, 0.0043 mmol) in a mixture of 20 mL of water and 6 mL of dioxane, which had been adjusted to pH 9.3 with 2 M NaOH. Throughout the addition, the pH was maintained at pH 9.3 with 2 M NaOH. After the addition was complete, the clear solution was allowed to stand at 4°C for 12 h with continuous stirring.

The solution was initially dialyzed[3] alternately every 15 min at room temperature against bicarbonate buffer (0.2 M, pH 8.0, 3 × 600 mL) and acetate buffer (0.2 M, pH 5.0, 3 × 600 mL), and then finally against distilled water continuously for 4 h. After lyophilization, the conjugate IIa was obtained as a white crystalline solid (0.48 g). A blank was prepared in the same manner, but without VIIa. The number of hapten residues per mole of bovine serum albumin was calculated by the UV method (10, 11) to be 70 (IIa, X = 70).

The procedure was repeated, decreasing by half the relative amount of VIIa (0.20 g, 0.43 mmol) used with bovine serum albumin (0.60 g, 0.0086 mmol). The conjugate (0.71 g) was determined to have 27 mol of hapten residues/mol of bovine serum albumin (IIa, X = 27).

Coupling of VIIb to Bovine Serum Albumin—Compound VIIb was coupled to bovine serum albumin by a modified mixed anhydride method (8, 10, 11) in the same manner as described for the coupling of VIIa. VIIb (0.20 g, 0.41 mmol) and bovine serum albumin[2] (0.29 g, 0.0041 mmol) gave 0.47 g of conjugate IIb, where the number of hapten residues per mole of bovine serum albumin was calculated by the UV method (10, 11) to be 71 (IIb, X = 71).

The procedure was repeated, decreasing by half the relative amount of VIIb (0.050 g, 0.10 mmol) used with bovine serum albumin (0.15 g, 0.00215 mmol). The conjugate (0.17 g) was determined to have 16 mol of hapten residues/mol of bovine serum albumin (IIb, X = 16).

Coupling of X to Bovine Serum Albumin—Compound X was coupled to bovine serum albumin by a modified mixed anhydride method (8, 10, 11) in the same manner as described for the coupling of VIIa. Compound X (0.080 g, 0.167 mmol) and bovine serum albumin (0.117 g, 0.00167 mmol) gave 0.15 g of conjugate III, where the number of hapten residues per mole of bovine albumin was calculated by the UV method (10, 11) to be 24 (III, X = 24).

Immunization—Each hapten–protein conjugate (4 mg) was dissolved in normal saline (2.0 mL) and emulsified with Freund's complete adjuvant[4] (2.0 mL). Each conjugate was administered to at least five New Zealand White female rabbits[5] by injection of 0.5 mL of the emulsion into each shoulder. At 2-week intervals thereafter, the injections were repeated with an emulsion prepared as described above, except that Freund's complete adjuvant was replaced by Freund's incomplete adjuvant. The antiserum titer of each rabbit was checked 1 week after the fifth injection, when the route of administration was changed to intravenous. In the experience of the authors (5, 7), selectivity does not change after five immunizations, whereas intravenous booster shots at this stage lead to improved sensitivity with maintained selectivity.

Serum was obtained from the marginal ear vein at 2-week intervals after the fifth injection. The antiserum titer of each rabbit was checked by evaluating the binding characteristics of tritiated trifluperazine[6] to each antiserum. After optimal titer values were achieved, blood was obtained from each rabbit by cardiac puncture. The harvested serum was immediately lyophilized in 1.0-mL samples and stored at −20°C.

REFERENCES

(1) T. J. Gillespie and I. G. Sipes, *J. Chromatogr.*, **223,** 95 (1981).

(2) J. I. Javaid, H. Dekirmenjian, and J. M. Davis, *J. Pharm. Sci.*, **71,** 63 (1982).

(3) R. M. H. Roscoe, J. K. Cooper, E. M. Hawes, and K. K. Midha, *J. Pharm. Sci.*, **71,** 625 (1982).

(4) K. K. Midha, R. M. H. Roscoe, K. Hall, E. M. Hawes, J. K. Cooper, G. McKay, and H. U. Shetty, *Biomed. Mass Spectrom.*, **9,** 186 (1982).

(5) K. K. Midha, J. W. Hubbard, J. K. Cooper, E. M. Hawes, S. Fournier, and P. Yeung, *Br. J. Clin. Pharmacol.*, **12,** 189 (1981).

(6) K. K. Midha, J. C. K. Loo, C. Charette, M. L. Rowe, J. W. Hubbard, and I. J. McGilveray, *J. Anal. Toxicol.*, **2,** 185 (1978).

(7) K. K. Midha, J. C. K. Loo, J. W. Hubbard, M. L. Rowe, and I. J. McGilveray, *Clin. Chem.*, **25,** 166 (1979).

(8) J. W. Hubbard, K. K. Midha, I. J. McGilveray, and J. K. Cooper, *J. Pharm. Sci.*, **67,** 1563 (1978).

(9) J. W. Hubbard, K. K. Midha, J. K. Cooper, and C. Charette, *Can. J. Pharm. Sci.*, **15,** 89 (1980).

(10) B. F. Erlanger, F. Borek, S. M. Beiser, and S. Lieberman, *J. Biol. Chem.*, **228,** 713 (1957).

(11) B. F. Erlanger, F. Borek, S. M. Beiser, and S. Lieberman, *J. Biol. Chem.*, **234,** 1090 (1959).

(12) G. E. Abraham, *J. Clin. Endocrinol. Metab.*, **29,** 866 (1969).

(13) K. K. Midha, E. M. Hawes, G. Rauw, G. McKay, J. K. Cooper, and H. U. Shetty, *J. Pharmacol. Meth.*, **9,** 283 (1983).

(14) H. L. Yale and F. Sowinski, *J. Am. Chem. Soc.*, **82,** 2039 (1960).

(15) Z. V. Zharavlev, A. N. Gritenko, and Z. I. Ermakova, *J. Gen. Chem. USSR (Engl. Transl.)*, **32,** 1889 (1962).

(16) O. Hromatka, R. Klink, and F. Sauter, *Monatsh. Chem.*, **93,** 1294 (1962).

(17) H. U. Shetty, E. M. Hawes, and K. K. Midha, *J. Labelled Comp. Radiopharm.*, **18,** 1633 (1981).

ACKNOWLEDGMENTS

The study was financially supported by the Medical Research Council of Canada (Development Grant 222). The authors are greatly indebted to K. Hall who measured the mass spectra and Mrs. Carol Constable for typing the manuscript.

[2] RIA Grade, Fraction V Powder; Sigma Chemical Co., St. Louis, Mo.

[3] Fisher dialyzer tubing (Size C); Fisher Scientific Co., Edmonton, Alberta, Canada.

[4] Grand Island Biological Co., Grand Island, N.Y.

[5] Mr. Avaldermeer, Sherwood Park, Alberta, Canada.

[6] Radioactive trifluoperazine, generally labeled with tritium, having a specific activity of 12.8 Ci/mmol; Nuclear Research Centre–Negev, Beer-Sheva, Israel. Radiochemical purity was checked by analytical TLC and HPLC.

Simultaneous Determination of Chloroprocaine Hydrochloride and Its Degradation Product 4-Amino-2-chlorobenzoic Acid in Bulk Drug and Injection Solutions by High-Performance Liquid Chromatography

G. MENON, B. NORRIS ˣ, and J. WEBSTER

Received November 19, 1982, from the *Department of Analytical Research, Abbott Laboratories, North Chicago, IL 60064.* Accepted for publication December 20, 1982.

Abstract □ A high-performance liquid chromatographic method has been developed for the simultaneous determination of chloroprocaine hydrochloride and its hydrolytic degradation product, 4-amino-2-chlorobenzoic acid. Separation is achieved using a μ-Bondapak C_{18} column and the eluant, water–acetonitrile–methanol–glacial acetic acid (74:20:5:1) containing 0.05–0.08% (w/v) sodium 1-heptanesulfonate, at a flow rate of 2 mL/min. Benzoic acid and *p*-nitroacetophenone were used as internal standards. A variable-wavelength UV detector (278 nm) was used for detection of the compounds. The method is simple, accurate, and precise.

Keyphrases □ Chloroprocaine hydrochloride—determination in bulk drug and injection formulations by HPLC separation from synthetic impurities

Chloroprocaine hydrochloride, a local anesthetic of the *para*-aminobenzoic ester class, is formulated as a 2 or 3% aqueous injection solution for caudal and epidural nerve blockage. Like other *para*-aminobenzoic esters, the drug is susceptible to hydrolysis, resulting in the formation of 4-amino-2-chlorobenzoic acid and diethylaminoethanol. The compendial assay (1) for chloroprocaine hydrochloride bulk drug is based on potentiometric titration with perchloric acid, after the addition of mercuric acetate to a glacial acetic acid solution of the drug. The assay is not specific, since any hydrochloride salts of the manufacturing precursors or free bases would also be titrated. The formulation is assayed by UV spectrophotometry following the extraction of the drug as the free base. Although the assay is stability indicating, numerous chloroform extractions of an alkaline sample solution are required. Since the drug is rapidly hydrolyzed in basic solutions, this assay is undesirable. The degradation product, 4-amino-2-chlorobenzoic acid, is determined in a limit test using the Bratton–Marshall reaction (2) of the 4-amino group.

The present study describes a high-performance liquid chromatographic (HPLC) method for the simultaneous determination of chloroprocaine hydrochloride and its potential degradation product, 4-amino-2-chlorobenzoic acid, in bulk drug and injection solutions. It is accurate, precise, and simple, with minimal sample manipulation.

EXPERIMENTAL

The chromatographic system was equipped with a dual piston reciprocating pump[1] at a flow rate of 2 mL/min, a universal injector[2] with 5-μL volume, and a variable-wavelength UV detector at 278 nm[3]. The separation was performed on a 30 cm × 4-mm i.d. column containing microparticulate (10 μm) bonded octadecylsilane material[4]. The chromatographic peaks were electronically integrated and recorded[5]. For quantitative analyses, peak area ratios of the sample preparation were compared with those of the standard preparations.

Materials—The eluant was water–acetonitrile[6]–methanol[6]–glacial acetic acid (74:20:5:1) containing 0.05–0.08% w/v sodium 1-heptanesulfonate[7], pH 3.1.

A 1-mg/mL benzoic acid[8] solution in 1:1 methanol–water was used as the internal standard for 4-amino-2-chlorobenzoic acid and a 5-mg/mL solution of *p*-nitroacetophenone[9] in methanol was used as the internal standard for chloroprocaine hydrochloride for the analysis of the bulk drug. The concentration of benzoic acid was increased to 4 mg/mL for the analysis of formulations.

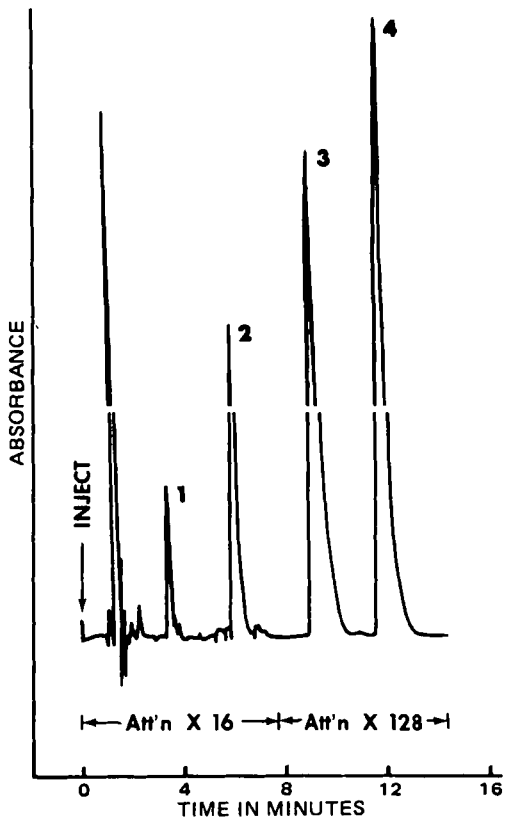

Figure 1—*HPLC analysis of 2% chloroprocaine hydrochloride injection exposed to artificial light for 1 month. Key: (1) 4-amino-2-chlorobenzoic acid; (2) benzoic acid; (3) chloroprocaine hydrochloride; and (4)* p-*nitroacetophenone.*

[1] Model 6000A, Waters Associates, Milford, MA 01757.
[2] Model U6K Universal Injector, Waters Associates, Milford, MA 01757.
[3] Model SF 770 Schoeffel, Westwood, NJ 07675 or Model LC-55, Perkin-Elmer, Norwalk, CT 06856
[4] μ-Bondapak C_{18}, Waters Associates, Milford, MA 01757.
[5] Model 3385A Automation System, Hewlett-Packard, Avondale, PA 19311.
[6] Distilled in Glass, Burdick and Jackson, Muskegon, MI 49442.
[7] Eastman Organic Chemicals, Rochester, NY 14650.
[8] Mallinckrodt, St. Louis, MO 63147.
[9] Aldrich Chemical Co., Milwaukee, WI 53233.

0022-3549/84/0200-0251$01.00/0
© 1984, American Pharmaceutical Association

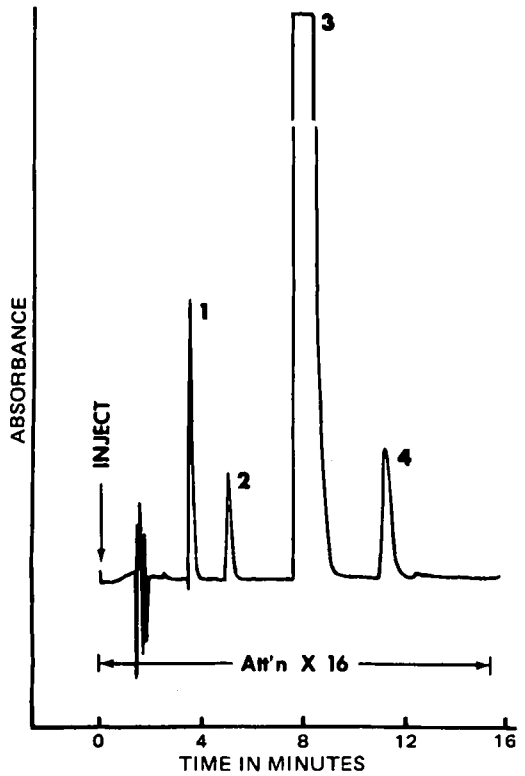

Figure 2—*HPLC analysis of a mixture of chloroprocaine hydrochloride bulk drug and the manufacturing precursors and 4-amino-2-chlorobenzoic acid each spiked at 1% level in the bulk drug. Key: (1) 4-Amino-2-chlorobenzoic acid; (2) 2-chloro-4-nitrobenzoic acid; (3) chloroprocaine hydrochloride; and (4) methyl-2-chloro-4-aminobenzoate.*

Standard Preparation—*4-Amino-2-chlorobenzoic Acid*—Ten milliliters of 0.1 mg/mL 4-amino-2-chlorobenzoic acid reference standard[10] in 1:1 methanol–water and 10.0 mL of 1 mg/mL benzoic acid internal standard solution were pipetted into a 100-mL volumetric flask and diluted to 100 mL with water; this solution was used for the analysis of the bulk drug. For the formulation assay, 20.0 mL of 0.1-mg/mL 4-amino-2-chlorobenzoic acid reference standard solution and 10.0 mL of 4-mg/mL benzoic acid solution were diluted to 100 mL with water.

Chloroprocaine Hydrochloride—One hundred milligrams of chloroprocaine hydrochloride USP reference standard was weighed into a 100-mL volumetric flask; 20.0 mL of *p*-nitroacetophenone internal standard solution was added and diluted to volume with water. This solution was used for the analyses of both bulk drug and injection formulation.

Sample Preparation—For the analysis of the bulk drug, 100 mg of the sample was mixed with 10.0 mL of 1-mg/mL benzoic acid solution and 20.0 mL of *p*-nitroacetophenone internal standard solution and diluted to 100 mL with water. For the formulation, an aliquot of the sample equivalent to 100–120 mg of chloroprocaine hydrochloride was mixed with 10.0 mL of 4-mg/mL benzoic acid internal standard solution and 20.0 mL of *p*-nitroacetophenone internal standard solution and diluted to 100 mL with water.

RESULTS AND DISCUSSION

The retention of chloroprocaine hydrochloride was found to increase with increasing concentration of the ion-pair reagent in the range of 0.02–0.10% in the mobile phase, while a decrease was observed with increase in acidity (1.0% acetic acid *versus* 0.05% sulfuric acid). Neither of the above changes caused any significant change in the retention volumes of 4-amino-2-chlorobenzoic acid and the internal standards.

Figure 1 shows a typical chromatogram of a sample preparation of the formulation exposed to artificial light for 1 month. Diethylaminoethanol is not detectable at the detector wavelength of 278 nm. Peak 1, which is due to 4-amino-2-chlorobenzoic acid, corresponds to ~0.7 mg in 100 mg of the drug (peak 3) in the sample preparation. The recorder has been attenuated after the elution of the benzoic acid peak to scale down the responses of the latter peaks. The concentration of ion-pair reagent in the eluant was 0.08%.

Table I—Statistical Data for the Analysis of Chloroprocaine Hydrochloride Bulk Drug and 2% Injection Solution

	Bulk Drug Purity, % w/w		Formulation, % of Label Claim	
	HPLC	USP XX	HPLC	USP XX
Number of Analyses	9	10	6	6
Chloroprocaine hydrochloride (Mean)	99.3	100.4	100.2	100.7
SD	±0.6%	±0.2%	±1.0%	±2.2%
RSD	±0.7%	±0.2%	±1.0%	±2.2%
4-Amino-2-chlorobenzoic acid	<0.1%	<0.625%[a]	0.67%	<3.0%[a]
SD	—	—	±0.05%	—
RSD	—	—	±7.2%	—

[a] USP XX Limit Test.

The trace component eluting between peaks 1 and 2 was identified as 2-chloro-4-nitrobenzoic acid[11], the starting material for the manufacture of chloroprocaine hydrochloride. Also, the trace component between peaks 3 and 4 was identified as methyl-2-chloro-4-aminobenzoate[11], a manufacturing intermediate. The only other intermediate in the manufacture of the bulk drug, methyl-2-chloro-4-nitrobenzoate[11] does not elute from the column during this chromatography. The levels of the two manufacturing impurities detected in the bulk drug were <0.5%, which was also confirmed by TLC.

Since the HPLC system separates all the manufacturing impurities from chloroprocaine hydrochloride, the procedure was also used for the analysis of the bulk drug. The concentration of the ion-pairing agent was reduced to 0.05% in the mobile phase to enhance the resolution of methyl-2-chloro-4-aminobenzoate from chloroprocaine hydrochloride. Figure 2 shows a chromatogram of the bulk drug spiked with the manufacturing precursors and 4-amino-2-chlorobenzoic acid (degradation product) each at the 1% level in the bulk drug.

The compendial limits for 4-amino-2-chlorobenzoic acid in the bulk drug and formulation are 0.625% and 3%, respectively, as determined by the Bratton–Marshall reaction. As low as 0.1% of the degradation product can be readily quantitated by the HPLC method. The bulk drug used in this study contained <0.1% of the degradation product. Since the drug degrades in solution, separate standard preparations of chloroprocaine hydrochloride and the degradation product are employed for quantitative analyses.

Acidic, basic, and neutral reflux studies of the drug showed 4-amino-2-chlorobenzoic acid as the only UV-active degradation product. The drug was degraded totally in 0.5 M sodium hydroxide, 3% in 0.5 M hydrochloric acid and 12% in water under reflux conditions for 1 h, with excellent material balance between the intact drug and degradation products.

Chloroprocaine hydrochloride formulations are discolored on prolonged storage under natural light. To study the nature of the photodegradation product, a formulation contained in a sealed vial was exposed to UV radiation for 45 min. A large peak was seen eluting at the same retention volume as the trace component seen between peaks 2 and 3 in Fig. 1. Preparative chromatography followed by mass spectrometry suggested the new component to be due to 2-hydroxyprocaine. This was confirmed by further hydrolyzing the UV degradation product in dilute carbonate solution to produce 4-aminosalicylic acid, the retention volume of which was in good agreement with that of an authentic material. The amount of the photodegradation product produced was found to be <0.1% after 1 month exposure to artificial light, as is apparent in Fig. 1, although the formulation was slightly discolored.

Linear detector responses were obtained when 50–200 mg of chloroprocaine hydrochloride and 0.25–5 mg of 4-amino-2-chlorobenzoic acid were analyzed. The correlation coefficients were 0.9999 in both cases, and the response *versus* concentration plots essentially passed through the origin.

A placebo formulation containing 0.4% sodium chloride and 0.2% sodium bisulfite in water for injection was spiked simultaneously with chloroprocaine hydrochloride at 12–28 mg/mL and 4-amino-2-chlorobenzoic acid at 0.2–1 mg/mL; 5 mL of each of the spiked solutions were taken through the procedure. The average recovery of chloroprocaine

[10] Pfaltz and Bauer, Inc., Stamford, CT 06902 (Characterized and designated Abbott House Reference Standard).

[11] Orgamol, S.A. Evionnaz (Valais) Suisse.

hydrochloride was found to be 99.8% ($n = 5$, $CV = \pm 0.7\%$) and that of 4-amino-2-chlorobenzoic acid, 101.0% ($n = 5$, $CV = \pm 0.7\%$). The reproducibility of the method was determined using a typical lot of bulk drug and a 2% formulation by three analysts over a 6-d period. The results and the statistical data are presented in Table I along with the results obtained by the corresponding assays prescribed by USP.

In conclusion, ion-pair reverse-phase chromatography permits the simultaneous analysis of chloroprocaine hydrochloride and its degradation product, 4-amino-2-chlorobenzoic acid, in bulk drug and injection formulations. The method is specific for the analysis of the bulk drug and stability indicating for the drug in injection solutions.

REFERENCES

(1) "U.S. Pharmacopeia XX; National Formulary XV," U.S. Pharmacopeial Convention, Rockville, Md., 1979, p. 135–136.

(2) A. C. Bratton and E. K. Marshall, *J. Biol. Chem.*, **128**, 537 (1939).

Adsorption of Sulfonylureas onto Activated Charcoal *In Vitro*

HANNU KANNISTO and PERTTI J. NEUVONEN ˣ

Received September 3, 1982, from the *Department of Clinical Pharmacology, University of Helsinki, Paasikivenkatu 4, SF-00250 Helsinki 25, Finland.* Accepted for publication December 23, 1982.

Abstract □ Adsorption of carbutamide, chlorpropamide, tolazamide, tolbutamide, glibenclamide (glyburide), and glipizide onto activated charcoal was compared *in vitro* using different charcoal-to-drug ratios. Maximal binding capacities of different sulfonylureas were 0.45–0.52 g/g of charcoal at pH 7.5. The affinity of the second generation derivatives, glibenclamide and glipizide, was considerably higher than that of the first generation derivatives. The affinity of sulfonylureas to charcoal was higher at pH 4.9 than at pH 7.5. Poor water solubility of sulfonylureas at pH 1 prevents the adequate testing in these conditions. Contrary to what has appeared previously, activated charcoal effectively adsorbs different sulfonylureas and can be used to possibly prevent their gastrointestinal absorption.

Keyphrases □ Activated charcoal—adsorption, sulfonylureas, carbutamide, chlorpropamide, tolazamide, tolbutamide, glibenclamide, glipizide □ Sulfonylureas—adsorption to activated charcoal □ Adsorption—sulfonylureas, activated charcoal

The capacity of activated charcoal to adsorb chemicals has been recognized for centuries, and in many countries charcoal is generally used as an antidote for intoxication. Maximal amounts of drugs adsorbed by charcoal of good quality are on the order of 100–1000 mg/g of charcoal (1–4). Decker *et al.* (4) have concluded from their *in vitro* studies that compounds insoluble in aqueous acidic solution, such as tolbutamide, are not adsorbed to any measurable extent onto activated charcoal. Others have cited this and extended the conclusions to include other sulfonylureas as well. Recently, claims have been made that activated charcoal is ineffective (5, 6) or even contraindicated (7) as an antidote in poisonings caused by tolbutamide or sulfonylureas in general. This paper reports the adsorption of six commonly used sulfonylureas onto activated charcoal *in vitro*.

EXPERIMENTAL

Material—Activated charcoal[1], carbutamide[2], chlorpropamide[3], tolazamide[4], tolbutamide[5], glibenclamide[2] (glyburide), and glipizide[4] were used as received. Dichlormethane, acetonitrile, isopropyl alcohol, and methanol were HPLC grade. All other reagents were analytical grade quality and were used as received.

Preparation of Drug Solutions—Solutions containing 700 mg/L of various sulfonylureas (or glipizide 360 mg/L, glibenclamide 100 mg/L) were prepared in 50 mM phosphate buffer as follows. The solutes were first dissolved in a small amount of 0.1 M NaOH, then phosphate buffer (pH 6.5) was added and the pH was adjusted to 7.5 with 1 M NaOH. Gilbenclamide, which is very sparingly soluble, was first dissolved in an ethanol–sodium hydroxide solution.

In addition, carbutamide and chlorpropamide were dissolved in two phosphate–acetate buffers, pH 7.5 and 4.9, containing 50 mM phosphate and 40 mM acetate. The sulfonylureas were maintained in the aforementioned solutions for several days at room temperature and at 4°C.

Adsorption Studies—The adsorption studies were carried out at room temperature (20–24°C) either at pH 7.5 or 4.9 (phosphate or phosphate–acetate buffers; see Preparation of Drug Solutions). A solution of 20 mL of sulfonylureas in different concentrations and 20 mg of charcoal were mixed in 30 mL stoppered glass tubes. When the effect of pH was studied, 16 mg of charcoal was added to 25 mL of the drug solution to achieve lower charcoal-to-drug ratios. The charcoal-to-drug ratio varied from 0.91:1 to 27:1. The tubes were shaken for 10 min, after which time the solutions were allowed to stand for an additional 10 min and then centrifuged (1800×*g* for 10 min). The drug concentration in the supernatant was determined.

Determination of Sulfonylurea Concentrations—The UV absorption of sulfonylureas could not be used for direct determination of these drugs because of the unpredictable amount of impurities absorbing at the UV range eluted from charcoal. The drug concentrations were therefore determined by HPLC[6] with some modification of the original procedure (8). The impurities from the charcoal did not interfere with the HPLC assay. Aliquots of the supernatant were diluted to constant volume with buffer and acidified with hydrochloric acid. The drugs were extracted with dichlormethane-containing internal standard (carbutamide or tolbutamide). The organic phase was separated and evaporated in a nitrogen stream. The residue was dissolved in methanol, and samples of this were injected into the chromatograph. The separation was performed with a C-18[7] column which was eluted with 50 mM phosphate buffer–acetonitrile, 55:45, pH 3.9 at a flow rate of 2.5 mL/min. For analysis of glibenclamide 10% isopropyl alcohol was added to the mobile phase to shorten the retention time. The sulfonylureas were monitored with a variable-wavelength UV detector[8] at 230–240 nm, depending on the optimal ratio of absorption of the derivatives and the internal standard.

The coefficient of variation between runs for the whole process comprising incubations with activated charcoal and drug determination was

[1] Carbomix (Norit A), Medica Ltd, Helsinki.
[2] Orion Ltd, Helsinki.
[3] Farmos Group Ltd, Turku.
[4] Medica Ltd, Helsinki.
[5] Hoechst AG, Frankfurt.

[6] HPLC: M6000A Chromatography pump and 6UK injector; Waters Associates, Milford, Mass.
[7] μBondapak C_{18}; Waters Associates, Milford, Mass.
[8] SF 770 Spectroflow; Schoeffel, Westwood, N.J.

0022-3549/84/0200-0253$01.00/0
© 1984, American Pharmaceutical Association

hydrochloride was found to be 99.8% ($n = 5$, $CV = \pm 0.7\%$) and that of 4-amino-2-chlorobenzoic acid, 101.0% ($n = 5$, $CV = \pm 0.7\%$). The reproducibility of the method was determined using a typical lot of bulk drug and a 2% formulation by three analysts over a 6-d period. The results and the statistical data are presented in Table I along with the results obtained by the corresponding assays prescribed by USP.

In conclusion, ion-pair reverse-phase chromatography permits the simultaneous analysis of chloroprocaine hydrochloride and its degradation product, 4-amino-2-chlorobenzoic acid, in bulk drug and injection formulations. The method is specific for the analysis of the bulk drug and stability indicating for the drug in injection solutions.

REFERENCES

(1) "U.S. Pharmacopeia XX; National Formulary XV," U.S. Pharmacopeial Convention, Rockville, Md., 1979, p. 135–136.

(2) A. C. Bratton and E. K. Marshall, *J. Biol. Chem.*, **128**, 537 (1939).

Adsorption of Sulfonylureas onto Activated Charcoal *In Vitro*

HANNU KANNISTO and PERTTI J. NEUVONEN ˣ

Received September 3, 1982, from the *Department of Clinical Pharmacology, University of Helsinki, Paasikivenkatu 4, SF-00250 Helsinki 25, Finland.* Accepted for publication December 23, 1982.

Abstract □ Adsorption of carbutamide, chlorpropamide, tolazamide, tolbutamide, glibenclamide (glyburide), and glipizide onto activated charcoal was compared *in vitro* using different charcoal-to-drug ratios. Maximal binding capacities of different sulfonylureas were 0.45–0.52 g/g of charcoal at pH 7.5. The affinity of the second generation derivatives, glibenclamide and glipizide, was considerably higher than that of the first generation derivatives. The affinity of sulfonylureas to charcoal was higher at pH 4.9 than at pH 7.5. Poor water solubility of sulfonylureas at pH 1 prevents the adequate testing in these conditions. Contrary to what has appeared previously, activated charcoal effectively adsorbs different sulfonylureas and can be used to possibly prevent their gastrointestinal absorption.

Keyphrases □ Activated charcoal—adsorption, sulfonylureas, carbutamide, chlorpropamide, tolazamide, tolbutamide, glibenclamide, glipizide □ Sulfonylureas—adsorption to activated charcoal □ Adsorption—sulfonylureas, activated charcoal

The capacity of activated charcoal to adsorb chemicals has been recognized for centuries, and in many countries charcoal is generally used as an antidote for intoxication. Maximal amounts of drugs adsorbed by charcoal of good quality are on the order of 100–1000 mg/g of charcoal (1–4). Decker *et al.* (4) have concluded from their *in vitro* studies that compounds insoluble in aqueous acidic solution, such as tolbutamide, are not adsorbed to any measurable extent onto activated charcoal. Others have cited this and extended the conclusions to include other sulfonylureas as well. Recently, claims have been made that activated charcoal is ineffective (5, 6) or even contraindicated (7) as an antidote in poisonings caused by tolbutamide or sulfonylureas in general. This paper reports the adsorption of six commonly used sulfonylureas onto activated charcoal *in vitro*.

EXPERIMENTAL

Material—Activated charcoal[1], carbutamide[2], chlorpropamide[3], tolazamide[4], tolbutamide[5], glibenclamide[2] (glyburide), and glipizide[4] were used as received. Dichlormethane, acetonitrile, isopropyl alcohol, and methanol were HPLC grade. All other reagents were analytical grade quality and were used as received.

Preparation of Drug Solutions—Solutions containing 700 mg/L of various sulfonylureas (or glipizide 360 mg/L, glibenclamide 100 mg/L) were prepared in 50 mM phosphate buffer as follows. The solutes were first dissolved in a small amount of 0.1 M NaOH, then phosphate buffer (pH 6.5) was added and the pH was adjusted to 7.5 with 1 M NaOH. Gilbenclamide, which is very sparingly soluble, was first dissolved in an ethanol–sodium hydroxide solution.

In addition, carbutamide and chlorpropamide were dissolved in two phosphate–acetate buffers, pH 7.5 and 4.9, containing 50 mM phosphate and 40 mM acetate. The sulfonylureas were maintained in the aforementioned solutions for several days at room temperature and at 4°C.

Adsorption Studies—The adsorption studies were carried out at room temperature (20–24°C) either at pH 7.5 or 4.9 (phosphate or phosphate–acetate buffers; see Preparation of Drug Solutions). A solution of 20 mL of sulfonylureas in different concentrations and 20 mg of charcoal were mixed in 30 mL stoppered glass tubes. When the effect of pH was studied, 16 mg of charcoal was added to 25 mL of the drug solution to achieve lower charcoal-to-drug ratios. The charcoal-to-drug ratio varied from 0.91:1 to 27:1. The tubes were shaken for 10 min, after which time the solutions were allowed to stand for an additional 10 min and then centrifuged (1800×*g* for 10 min). The drug concentration in the supernatant was determined.

Determination of Sulfonylurea Concentrations—The UV absorption of sulfonylureas could not be used for direct determination of these drugs because of the unpredictable amount of impurities absorbing at the UV range eluted from charcoal. The drug concentrations were therefore determined by HPLC[6] with some modification of the original procedure (8). The impurities from the charcoal did not interfere with the HPLC assay. Aliquots of the supernatant were diluted to constant volume with buffer and acidified with hydrochloric acid. The drugs were extracted with dichlormethane-containing internal standard (carbutamide or tolbutamide). The organic phase was separated and evaporated in a nitrogen stream. The residue was dissolved in methanol, and samples of this were injected into the chromatograph. The separation was performed with a C-18[7] column which was eluted with 50 mM phosphate buffer–acetonitrile, 55:45, pH 3.9 at a flow rate of 2.5 mL/min. For analysis of glibenclamide 10% isopropyl alcohol was added to the mobile phase to shorten the retention time. The sulfonylureas were monitored with a variable-wavelength UV detector[8] at 230–240 nm, depending on the optimal ratio of absorption of the derivatives and the internal standard.

The coefficient of variation between runs for the whole process comprising incubations with activated charcoal and drug determination was

[1] Carbomix (Norit A), Medica Ltd, Helsinki.
[2] Orion Ltd, Helsinki.
[3] Farmos Group Ltd, Turku.
[4] Medica Ltd, Helsinki.
[5] Hoechst AG, Frankfurt.

[6] HPLC: M6000A Chromatography pump and 6UK injector; Waters Associates, Milford, Mass.
[7] μBondapak C_{18}; Waters Associates, Milford, Mass.
[8] SF 770 Spectroflow; Schoeffel, Westwood, N.J.

0022-3549/84/0200-0253$01.00/0
© 1984, American Pharmaceutical Association

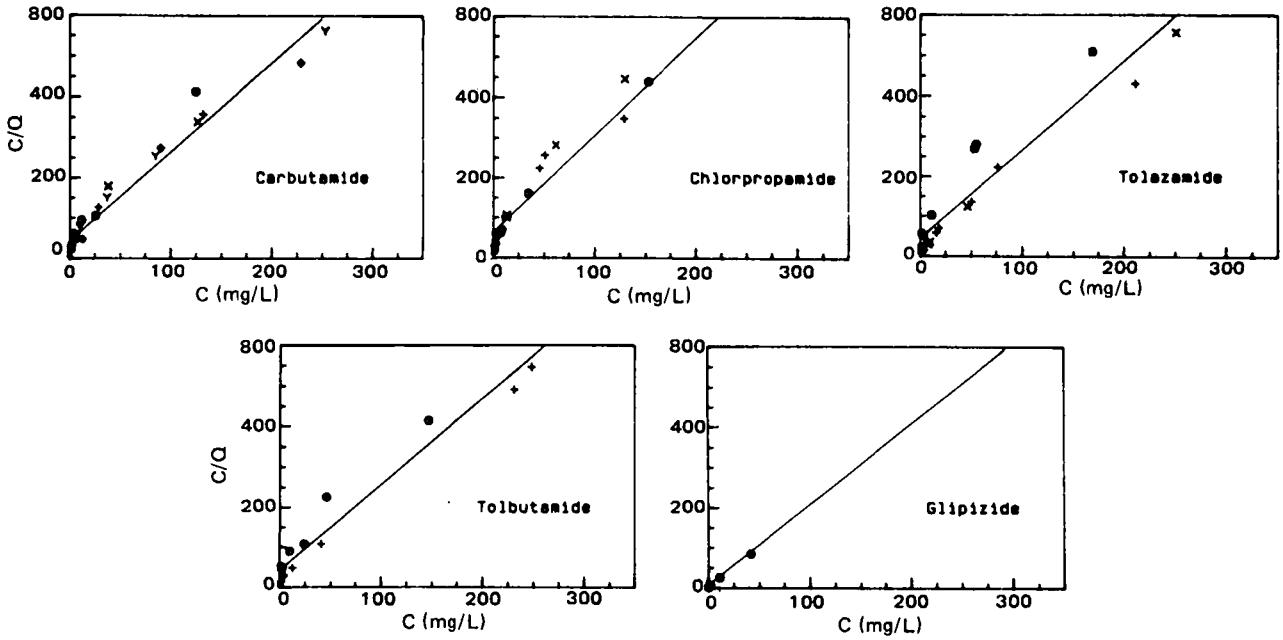

Figure 1—*Langmuir adsorption isotherms for sulfonylureas. Different symbols represent individual experiments. The correlation coefficients varied from 0.968 (tolazamide) to 1.00 (glipizide).*

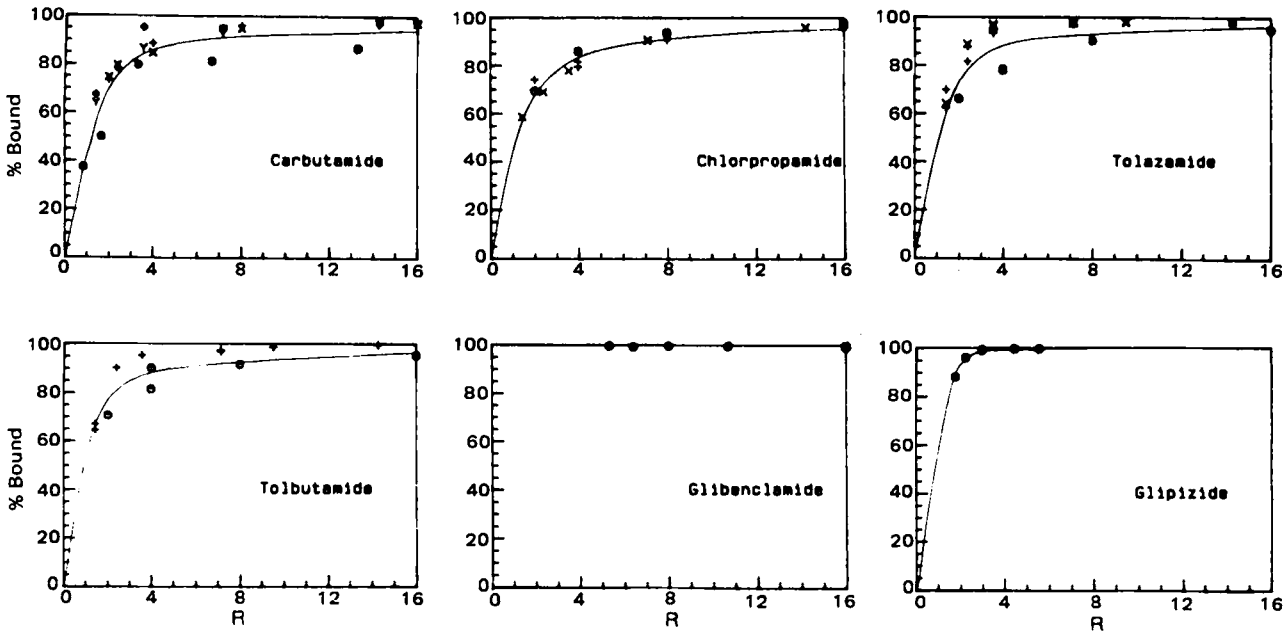

Figure 2—*Correlation of percentage adsorption of sulfonylureas to charcoal–drug ratio (R). Different symbols represent individual experiments.*

9.9% (N = 25). The coefficient of variation within run for drug determination only was 1.9% (N = 8).

Calculations—The Langmuir isotherm was constructed by the following equation (1):

$$\frac{C}{Q} = \frac{1}{KQ_m} + \frac{C}{Q_m}$$

where C is the concentration of free drug in the solution at equilibrium (mg/L), Q is the weight of drug (g) adsorbed per weight unit of charcoal (g), Q_m is the maximal adsorbing capacity, and K is a constant indicating the affinity of the drug to charcoal and physically represents the reciprocal of free drug concentration when half of the maximal binding capacity is used. The plot of C/Q *versus* C yields a straight line, and linear regression analysis was used to calculate the best line through the experimental data and to evaluate the adsorption parameters.

Table I—Parameters for Langmuir Adsorption Isotherm of Various Sulfonylureas, Phosphate Buffer pH 7.5

Parameter	Carbutamide	Chlorpropamide	Tolazamide	Tolbutamide	Glipizide
Q_m (g/g)	0.46	0.42	0.45	0.47	0.50
K (L/mg)	0.045	0.036	0.062	0.052	1.204

RESULTS

The Langmuir adsorption isotherms at pH 7.5 for carbutamide, chlorpropamide, tolazamide, tolbutamide, and glipizide are given in Fig. 1 and the calculated parameters in Table I. Due to the poor water solubility of glibenclamide the charcoal–drug ratio in the conditions used remained too high to allow the determination of its adsorption parameters.

Figure 2 shows the percentage adsorption of six sulfonylureas as a function of the charcoal–drug ratio. The adsorption of glibenclamide was

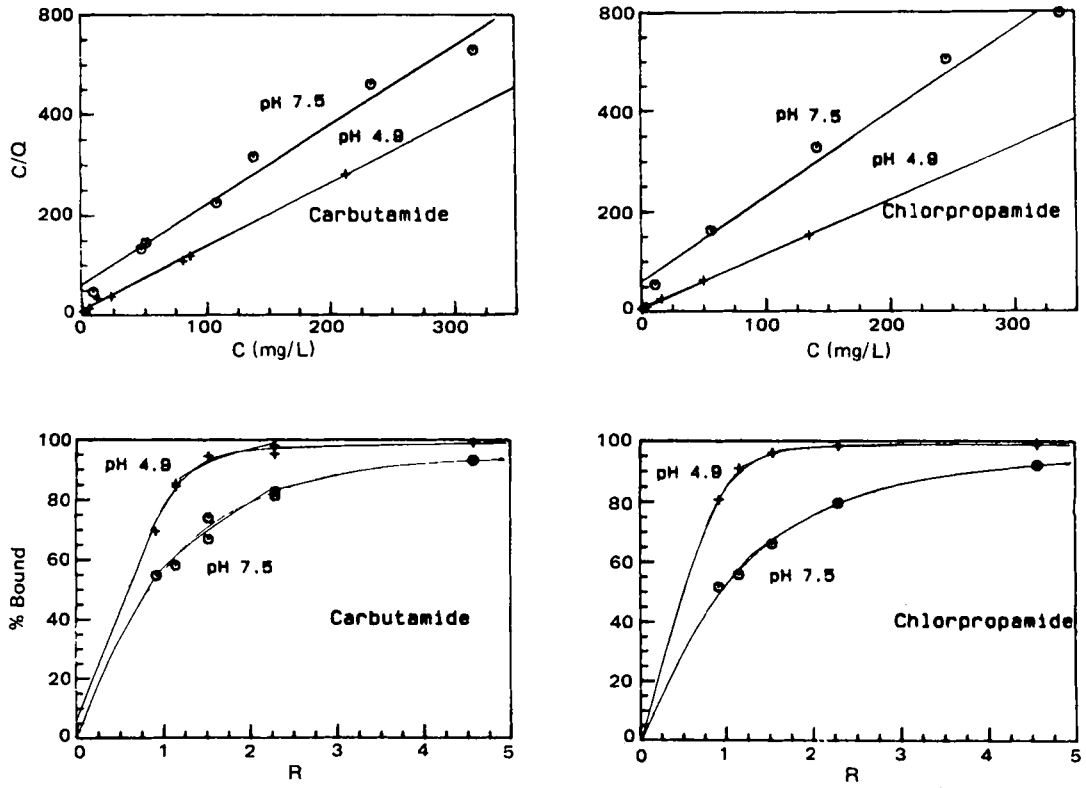

Figure 3—*Langmuir adsorption isotherms (top) and percentage adsorption (bottom) of carbutamide and chlorpropamide at pH 7.5 and 4.9.*

more than 99% at all charcoal–drug ratios tested (5.3:1–16:1). For other sulfonylureas the adsorption of 90% was attained at charcoal–drug ratios from ~2 (glipizide) to 6 (chlorpropamide).

As seen in Fig. 3 and Table II, the decrease of the incubation medium pH from 7.5 to 4.9 increased the affinity of carbutamide and chlorpropamide to charcoal. The differences of K were significant ($p < 0.001$), whereas the maximal binding capacities were only insignificantly increased ($p < 0.10$). The differences were tested by comparing the regression lines (9).

DISCUSSION

The adsorption of different drugs onto activated charcoal *in vitro* has been studied by several authors (1–4), but there have been no systematic studies on the adsorption of sulfonylureas. However, the statement, "The adsorptive capacity of activated charcoal for ferrous sulphate, sulfonylureas and organo-phosphorous insecticides is too low to be useful," has appeared (5), and activated charcoal has even been claimed to be contraindicated in poisonings caused by tolbutamide (7). To our knowledge, these conclusions are based on very limited *in vitro* studies in acidic conditions, in which the water solubility of tolbutamide was rather limited, so that its adsorption onto charcoal could not be measured (4).

Quite recently, the effect of activated charcoal on the absorption of tolbutamide and chlorpropamide has been studied in humans (10, 11). Activated charcoal (50 g), ingested 5 min after these drugs, reduced their absorption by ~90%. The charcoal–drug ratio was rather high in these two studies. However, *in vivo* the absolute amount of charcoal is probably more important than the charcoal–drug ratio, as has been demonstrated earlier (12, 13).

The present results demonstrate that sulfonylureas are adsorbed onto charcoal at pH 7.5 *in vitro*. In an acidic medium they seem to be even more effectively adsorbed, provided that they are soluble at that pH. The affinities of carbutamide and chlorpropamide were considerably higher at pH 4.9 than at pH 7.5, which was predictable because of the shift in equilibrium toward nondissociable, nonpolar species of these weak acids. Similar behavior of other acidic substances has been reported (6, 14).

Table II—Parameters for Langmuir Adsorption Isotherm of Carbutamide and Chlorpropamide, Phosphate–Acetate Buffer, pH 7.5 and 4.9

Parameter	Carbutamide		Chlorpropamide	
	pH 7.5	pH 4.9	pH 7.5	pH 4.9
Q_m (g/g)	0.62	0.78[a]	0.58	0.91[a]
K (L/mg)	0.028	0.160[b]	0.026	0.189[b]

[a] The differences from the respective value at pH 7.5, $p < 0.10$, [b] $p < 0.001$.

In the present study the adsorption isotherms in phosphate–acetate buffer, pH 7.5 differed from those in phosphate buffer, pH 7.5 (Tables I and II). This might be due to the buffers or to the fact that a different charcoal concentration (16 mg/25 mL instead of 20 mg/20 mL) was used in the experiments with phosphate–acetate buffer.

The affinity of the second generation sulfonylureas, glibenclamide and glipizide, to charcoal is considerably higher than that of the older derivatives (Table I, Fig. 2). Clinically used doses of glipizide and glibenclamide are only about $^1/_{100}$ of those of the first generation derivatives. Thus, most probably, the generally recommended doses of activated charcoal (50 g), given soon enough after the ingestion of glipizide and glibenclamide, would be effective in preventing their absorption. In massive intoxication caused by the older sulfonylureas, the adsorption capacity of charcoal may be saturated and the dose of charcoal should, therefore, be as high as possible.

Although poisoning due to oral hypoglycemic agents is relatively uncommon, several deaths and cerebral damage have been reported. Of 16 patients who had deliberately ingested toxic doses of a sulfonylurea, 6 died (15). The gastrointestinal absorption of many sulfonylureas is slow, at least partially due to their poor solubility at the gastric pH. Therefore, their absorption in acute intoxication may be delayed for several hours so that they may be adsorbed onto charcoal given even several hours later.

REFERENCES

(1) A. H. Andersen, *Acta Pharmacol.*, **2**, 69 (1946).

(2) T. Tsuchiya and G. Levy, *J. Pharm. Sci.*, **61**, 586 (1972).

(3) E. M. Sellers, V. Khuow, and L. Dolman, *J. Pharm. Sci.*, **66**, 1640 (1977).

(4) W. J. Decker, H. F. Combs, and D. G. Corby, *Toxicol. Appl. Pharmacol.*, **13**, 454 (1968).

(5) Editorial. *Drug Ther. Bull.*, **17**, 7 (1979).

(6) D. O. Cooney, in "Activated Charcoal, Antidotal and Other Medical Uses," Dekker, New York, Basle, 1980, p. 85.

(7) J. R. Boyd (Ed.), "Drug Facts and Comparisons," Lippincott, Philadelphia, Toronto, 1982, p. 1839.

(8) G. Raghow and M. C. Meyer, *J. Pharm. Sci.*, **70**, 1166 (1981).

(9) A. Held, "Statistical Theory with Engineering Applications," Wiley, New York, N.Y., 1952, pp. 571–579.
(10) P. J. Neuvonen, H. Kannisto, and E. L. Hirvisalo, *Eur. J. Clin. Pharmacol.*, **24**, 243 (1983).
(11) P. J. Neuvonen and S. Kärkkäinen, *Clin Pharmacol. Ther.*, **33**, 386 (1983).
(12) G. Levy and J. B. Houston, *Pediatrics*, **3**, 432 (1976).
(13) G. Levy and T. Tsuchiya, *Clin. Pharmacol. Ther.*, **13**, 317 (1972).
(14) A. H. Andersen, *Acta Pharmacol.*, **3**, 199 (1947).
(15) J. A. Vale and T. J. Meredith, "Poisoning—Diagnosis and Treatment," Update Books, London, Dordretch, Boston, 1981, p. 187.

Equilibrium Dialysis of Barbituric Acids up to High Concentrations of Aqueous Sodium Alkylsulfonate Solutions

CLAUDE TREINER *x, CATHERINE VAUTION ‡, and FRANCIS PUISIEUX ‡

Received March 17, 1982, from the **Laboratoire d'Electrochimie, Université Pierre et Marie Curie, 75230 Paris Cédex 05, France*, and the ‡ *Laboratoire de Pharmacie Galénique, Faculté de Pharmacie de Paris-Sud, 92290 Chatenay Malabry, France.* Accepted for publication January 14, 1983.

Abstract □ The partition coefficient K of four barbituric acids has been determined by the equilibrium dialysis method in aqueous solutions of sodium alkylsulfonate at 25°C. The results obtained from dilute solutions to 0.3 M surfactant concentration are compared with solubility data for the same systems. The K values as deduced from Langmuir or Freundlich isotherms decrease with increasing surfactant concentration. The detergent used was an impure commercial product of known composition, which could be considered as a mixed surfactant. The change of partition coefficient with surfactant concentration as obtained from equilibrium dialysis experiments has been interpreted by assuming a continuous change of micelle composition.

Keyphrases □ Barbituric acids—equilibrium dialysis up to high concentrations of aqueous sodium alkylsulfonate solutions, solubility □ Sodium alkylsulfonate—aqueous solutions, equilibrium dialysis of barbituric acids up to high concentrations, solubility □ Equilibrium dialysis—barbituric acids up to high concentrations of aqueous sodium alkylsulfonate solutions, solubility □ Solubility—equilibrium dialysis of barbituric acids up to high concentrations of aqueous sodium alkylsulfonate solutions

The solubility of 13 barbituric acids as a function of sodium alkylsulfonate concentration between 25°C and 55°C shows a rather sharp change in slope at low surfactant concentrations (~0.05 mol/L); the solubility increases less rapidly above this concentration than below it (1, 2). The ionic surfactant used was not pure but was a typical commercial product mixture consisting of 91% monosulfonated and 9% disulfonated ions. A model was suggested (1) to explain the solubility profile, which assumed two types of mixed micelles: predominantly monosulfonated mixed micelles at low surfactant concentration and predominantly disulfonated micelles at high concentrations. To further investigate this micellar system, we decided to study the solubilization behavior at 25°C of four typical barbituric acids (amobarbital, phenobarbital, secobarbital, and allobarbital) with the same surface-active agent using equilibrium dialysis instead of the solubility method.

Table I—Characteristics of Barbituric Acids

Barbituric Acid	Solubility, mol/L[a]	Melting Point, °C
Amobarbital	0.0022	157
Phenobarbital	0.0052	174
Allobarbital	0.0087	172
Secobarbital	0.0044	98

[a] Solubility in water at 25°C.

EXPERIMENTAL

Materials—The barbituric acids[1] were used without further purification. The melting points and the solubility in water at 25°C are presented in Table I. The sodium alkylsulfonate was a commercial product[2] containing monosulfonated ion–disulfonated ion–polysulfonated ion (90.7:8.8:0.5, v/v/v). The monosulfonated product was a mixture of $C_{14}H_{29}SO_3Na$ and $C_{15}H_{31}SO_3Na$, whose average molecular weight was 321.

Methods—The equilibrium dialysis experiments were performed using dilute to saturated solutions of barbituric acids at 25°C thermostatically controlled to within ±0.1°C with polytef cells and a cellulose acetate membrane. The equilibrium was attained in ~4 h. Barbituric acid concentrations were analyzed using a UV spectrophotometer. Each experiment was repeated five times, and at least six barbiturate concentrations were studied for each surfactant concentration.

The solubility of the barbituric acid is dependent on the pH of the medium. The pH of the solutions was measured at each concentration, and a correction applied to the concentration of barbituric acid on both sides of the dialysis using:

$$S_T = S_0(1 + 10^{pH-pK}) \qquad \text{(Eq. 1)}$$

where S_T and S_0 are the total concentration and the concentration of undissolved barbituric acid of a given pK, respectively.

RESULTS

Sodium alkylsulfonate showed a very high degree of adsorption onto the cellulose acetate membrane (Fig. 1). This adsorption was reproducible, and a systematic correction was applied. The barbituric acids were also partially adsorbed onto the membrane. A correction was also applied which amounted at most to 5% of the total concentration of the drug dissolved in the solution.

Two types of isotherms were used to obtain the partition constants. The Freundlich isotherm may be written as:

$$\log r = \log K + \frac{1}{n_f}\log B_{aq} \qquad \text{(Eq. 2)}$$

[1] Amobarbital and secobarbital obtained from: Expandia, 13 Avenue de l'Opéra, 75001 Paris, France. Allobarbital obtained from: Soprotec, 144 Avenue de Malakoff, 75116 Paris, France. Phenobarbital obtained from: Coopération Pharmaceutique Française, 66 Rue du Chemin Vert, 75001 Paris, France.

[2] Société des Produits Chimiques de la Montagne Noire, 81100 Castres, France.

0022-3549/84/0200-0256$01.00/0
© 1984, American Pharmaceutical Association

(9) A. Held, "Statistical Theory with Engineering Applications," Wiley, New York, N.Y., 1952, pp. 571–579.
(10) P. J. Neuvonen, H. Kannisto, and E. L. Hirvisalo, *Eur. J. Clin. Pharmacol.*, **24**, 243 (1983).
(11) P. J. Neuvonen and S. Kärkkäinen, *Clin Pharmacol. Ther.*, **33**, 386 (1983).
(12) G. Levy and J. B. Houston, *Pediatrics*, **3**, 432 (1976).
(13) G. Levy and T. Tsuchiya, *Clin. Pharmacol. Ther.*, **13**, 317 (1972).
(14) A. H. Andersen, *Acta Pharmacol.*, **3**, 199 (1947).
(15) J. A. Vale and T. J. Meredith, "Poisoning—Diagnosis and Treatment," Update Books, London, Dordretch, Boston, 1981, p. 187.

Equilibrium Dialysis of Barbituric Acids up to High Concentrations of Aqueous Sodium Alkylsulfonate Solutions

CLAUDE TREINER *x, CATHERINE VAUTION ‡, and FRANCIS PUISIEUX ‡

Received March 17, 1982, from the **Laboratoire d'Electrochimie, Université Pierre et Marie Curie, 75230 Paris Cédex 05, France*, and the ‡ *Laboratoire de Pharmacie Galénique, Faculté de Pharmacie de Paris-Sud, 92290 Chatenay Malabry, France.* Accepted for publication January 14, 1983.

Abstract □ The partition coefficient K of four barbituric acids has been determined by the equilibrium dialysis method in aqueous solutions of sodium alkylsulfonate at 25°C. The results obtained from dilute solutions to 0.3 M surfactant concentration are compared with solubility data for the same systems. The K values as deduced from Langmuir or Freundlich isotherms decrease with increasing surfactant concentration. The detergent used was an impure commercial product of known composition, which could be considered as a mixed surfactant. The change of partition coefficient with surfactant concentration as obtained from equilibrium dialysis experiments has been interpreted by assuming a continuous change of micelle composition.

Keyphrases □ Barbituric acids—equilibrium dialysis up to high concentrations of aqueous sodium alkylsulfonate solutions, solubility □ Sodium alkylsulfonate—aqueous solutions, equilibrium dialysis of barbituric acids up to high concentrations, solubility □ Equilibrium dialysis—barbituric acids up to high concentrations of aqueous sodium alkylsulfonate solutions, solubility □ Solubility—equilibrium dialysis of barbituric acids up to high concentrations of aqueous sodium alkylsulfonate solutions

The solubility of 13 barbituric acids as a function of sodium alkylsulfonate concentration between 25°C and 55°C shows a rather sharp change in slope at low surfactant concentrations (~0.05 mol/L); the solubility increases less rapidly above this concentration than below it (1, 2). The ionic surfactant used was not pure but was a typical commercial product mixture consisting of 91% monosulfonated and 9% disulfonated ions. A model was suggested (1) to explain the solubility profile, which assumed two types of mixed micelles: predominantly monosulfonated mixed micelles at low surfactant concentration and predominantly disulfonated micelles at high concentrations. To further investigate this micellar system, we decided to study the solubilization behavior at 25°C of four typical barbituric acids (amobarbital, phenobarbital, secobarbital, and allobarbital) with the same surface-active agent using equilibrium dialysis instead of the solubility method.

Table I—Characteristics of Barbituric Acids

Barbituric Acid	Solubility, mol/L[a]	Melting Point, °C
Amobarbital	0.0022	157
Phenobarbital	0.0052	174
Allobarbital	0.0087	172
Secobarbital	0.0044	98

[a] Solubility in water at 25°C.

EXPERIMENTAL

Materials—The barbituric acids[1] were used without further purification. The melting points and the solubility in water at 25°C are presented in Table I. The sodium alkylsulfonate was a commercial product[2] containing monosulfonated ion–disulfonated ion–polysulfonated ion (90.7:8.8:0.5, v/v/v). The monosulfonated product was a mixture of $C_{14}H_{29}SO_3Na$ and $C_{15}H_{31}SO_3Na$, whose average molecular weight was 321.

Methods—The equilibrium dialysis experiments were performed using dilute to saturated solutions of barbituric acids at 25°C thermostatically controlled to within ±0.1°C with polytef cells and a cellulose acetate membrane. The equilibrium was attained in ~4 h. Barbituric acid concentrations were analyzed using a UV spectrophotometer. Each experiment was repeated five times, and at least six barbiturate concentrations were studied for each surfactant concentration.

The solubility of the barbituric acid is dependent on the pH of the medium. The pH of the solutions was measured at each concentration, and a correction applied to the concentration of barbituric acid on both sides of the dialysis using:

$$S_T = S_0(1 + 10^{pH-pK}) \qquad \text{(Eq. 1)}$$

where S_T and S_0 are the total concentration and the concentration of undissolved barbituric acid of a given pK, respectively.

RESULTS

Sodium alkylsulfonate showed a very high degree of adsorption onto the cellulose acetate membrane (Fig. 1). This adsorption was reproducible, and a systematic correction was applied. The barbituric acids were also partially adsorbed onto the membrane. A correction was also applied which amounted at most to 5% of the total concentration of the drug dissolved in the solution.

Two types of isotherms were used to obtain the partition constants. The Freundlich isotherm may be written as:

$$\log r = \log K + \frac{1}{n_f}\log B_{aq} \qquad \text{(Eq. 2)}$$

[1] Amobarbital and secobarbital obtained from: Expandia, 13 Avenue de l'Opéra, 75001 Paris, France. Allobarbital obtained from: Soprotec, 144 Avenue de Malakoff, 75116 Paris, France. Phenobarbital obtained from: Coopération Pharmaceutique Française, 66 Rue du Chemin Vert, 75001 Paris, France.

[2] Société des Produits Chimiques de la Montagne Noire, 81100 Castres, France.

0022-3549/84/0200-0256$01.00/0
© 1984, American Pharmaceutical Association

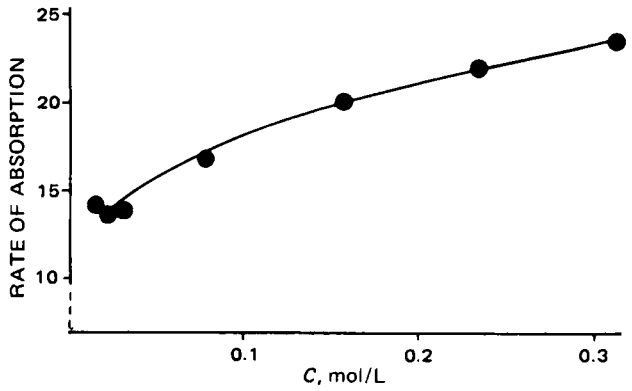

Figure 1—*Rate of adsorption of sodium alkylsulfonate onto the acetate cellulose membrane.*

where $r = B_{mic}/C$; B_{mic} and B_{aq} are the molar concentrations of barbituric acids within the micelles and in the aqueous phase, respectively; and C is the surfactant molar concentration. B_{aq} is assumed to be equal in both compartments of the cell. Figure 2A illustrates the corresponding curves for amobarbital. The Langmuir isotherm is presented for the same barbiturate in Fig. 2B:

$$\frac{1}{r} = \frac{1}{n} + \frac{1}{Kn}\left(\frac{1}{B_{aq}}\right) \qquad \text{(Eq. 3)}$$

Both isotherms suffer from a number of well-known deficiencies. They involve long linear extrapolations to obtain K or n, depending on which isotherm is used, although it is known at least in a few cases that they are not valid when a large concentration domain is investigated (3) (Freundlich isotherm). Furthermore, the intercept usually being very small, the n value of the Langmuir isotherm is known to have poor accuracy (4, 5). Finally, both equations are applicable only to dilute solutions. Thus, the slopes of Eqs. 2 and 3 can be better determined than their intercepts with the ordinate axis.

Table I compares, for the most dilute surfactant concentration studied, the values of the parameters obtained from the dialysis method according to the Freundlich and Langmuir methods, together with the solubility results at 25°C taken from our previous work. The apparent partition constant as obtained from the solubility data may be defined in dilute surfactant solutions by:

$$K = \frac{B_m - B_{aq}}{B_{aq} \cdot C} \qquad \text{(Eq. 4)}$$

There is no way of calculating with any confidence the individual values of n from the Langmuir isotherm. For each concentration of surface-active agent at least six dialysis experiments were performed ranging from very dilute to saturated concentrations of the barbituric acid. The correlation factors were excellent in all cases (in the range $0.994 < r^2 < 0.999$); thus, the intercepts and slopes were obtained with the highest accuracy compatible with the systems under investigation. This is the most complete set of data obtained from equilibrium dialysis experiments in the case of a single micellar system.

As can be seen from the data in Table II, n values ranging from 0.99 to 1.38 are necessary in order to match the solubility and dialysis results with the same isotherm. The n values are slightly >1 with the Freundlich isotherm, and the K values differ widely from those derived from the solubility data for those barbituric acids that showed good agreement

Table II—Comparison of Partition Constants as Deduced from Solubility or Equilibrium Dialysis Experiments at 25°C at Low Sodium Alkylsulfonate Concentrations [a]

Freundlich, K	n_F [b]	Langmuir, Kn	Solubility K	n_L [c]	Barbituric acid
27.4	1.07 ±0.02	51.5	51.6	0.99	Amobarbital
14.4	1.03 ±0.02	19.2	22.7	1.18	Phenobarbital
10.6	1.00 ±0.01	11.7	9.2	1.27	Allobarbital
82.4	1.04 ±0.01	119.9	80.6	1.38	Secobarbital

[a] $C = 0.0201$ mol/L. [b] Values of n deduced from the Freundlich isotherm. [c] Values of n deduced from the Langmuir isotherm.

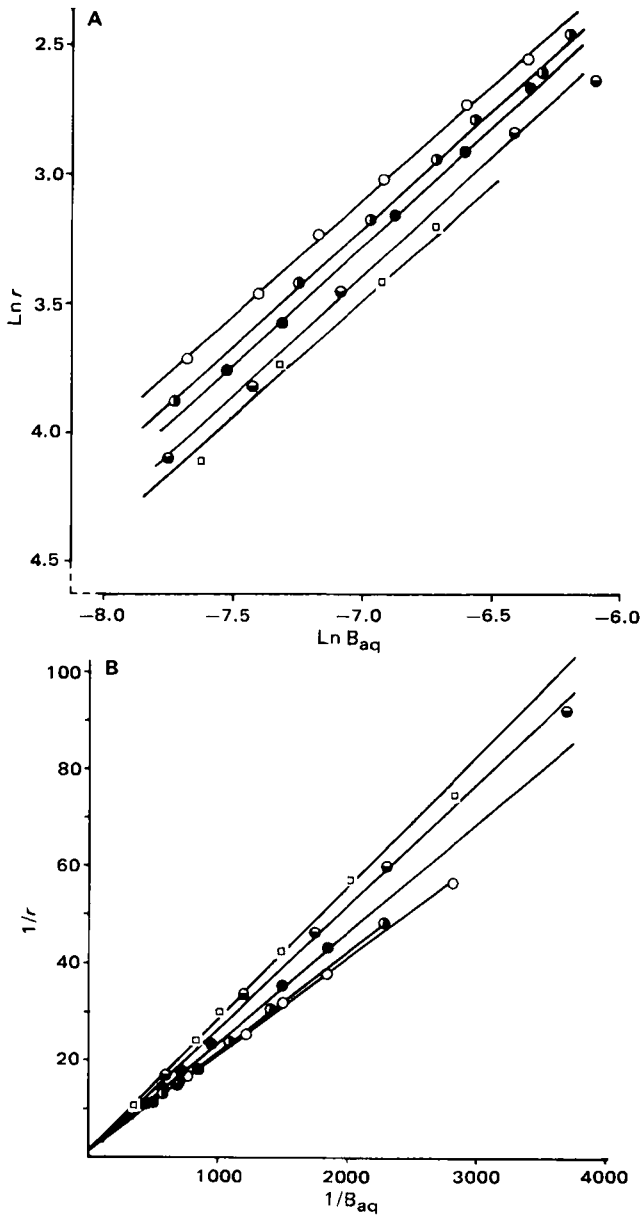

Figure 2—*Freundlich (A) and Langmuir (B) isotherms for amobarbital in aqueous sodium alkylsulfonate solutions. Key: (○) 0.020 mol/L; (◑) 0.065 mol/L; (●) 0.125 mol/L; (◒) 0.182 mol/L; (□) 0.239 mol/L.*

with the solubility results when using the Langmuir isotherm. The results are satisfactory in the other two cases.

The results of the analysis of the dialysis experiments with both kinds of isotherm do not agree with each other whatever barbituric acid is considered. Considerable care must be exercised when using these isotherms—the fact that $n \cong 1$ is obtained from the Freundlich plot does not ensure that the K values are necessarily correct. There is no reason for the n values obtained from the Freundlich or Langmuir isotherms to be equal, as can be inferred from their very different (3) theoretical derivation.

The Langmuir isotherm which has the soundest theoretical basis has been chosen (Table III). We think that the long extrapolation involved in the determination of K with the Freundlich isotherm is inappropriate. Table II shows the results obtained for all the solutions studied. It has been assumed that the n values are characteristic of the behavior of each barbituric acid. Thus, the K values have been calculated using the n values deduced from the comparison between the Langmuir isotherm and the solubility results at low surfactant concentrations.

DISCUSSION

It has been assumed previously (1) that the solubility profile for the barbituric acids in aqueous sodium alkylsulfonate solutions could be

Table III—Partition Constants of Barbituric Acids (Langmuir Isotherm) in Aqueous Sodium Alkylsulfonate Solutions

Barbituric Acid	Concentration of Sodium Alkylsulfonate, mol/L				
	0.0201	0.0646	0.1246	0.1822	0.2386
Amobarbital					
Kn	51.5	48.4	44.0	39.1	39.0
r^2	0.9996	0.9990	0.9998	0.9999	0.9968
Phenobarbital					
Kn	19.2	17.8	14.3	12.9	11.1
r^2	0.9893	0.9998	0.9986	0.9999	0.9999
Allobarbital					
Kn	11.7	8.0	6.9	5.8	5.3
r^2	0.9986	0.9997	0.9995	0.9999	0.9986
Secobarbital					
Kn	111.9	106.0	100.7	96.0	91.9
r^2	0.9992	0.9999	0.9996	0.9997	0.9999

described from dilute to concentrated surfactant solutions ($C \leq 0.3$ M or 10% w/v) by two partition coefficients, corresponding to two types of micelle. In the low concentration region, predominantly monosulfonated micelles would be formed, and a change in the slope of the solubility *versus* surfactant concentration curve might indicate the formation of disulfonated micelles.

The nonlinearity of a plot of the solubility of a solute *versus* surfactant concentration concerns only mixed systems, *e.g.*, 1-[(2-methylphenyl)-azo]-2-naphthylamine (Color Index No. 11390), in mixed anionic and nonionic surfactants (6, 7). Nishikido (7) attributed the nonlinear plot at low surfactant concentration to a variation of the micelle composition with the total surfactant concentration; the linearity observed at higher concentration was interpreted as evidence for a constant micelle composition. The previous model also assumed constant micelle composition (1). However, these conclusions were deduced solely from solubility measurements. The present equilibrium dialysis data suggest that these models might be too restrictive. In effect, a continuous change of the partition coefficient is observed from dilute to concentrated alkylsulfonate solutions with a levelling off at the highest concentrations (Fig. 3). The general pattern is observed whatever isotherm is employed to obtain the partition coefficients. Thus, the dialysis data are more compatible with a model of gradual change in micelle composition with total surfactant concentration.

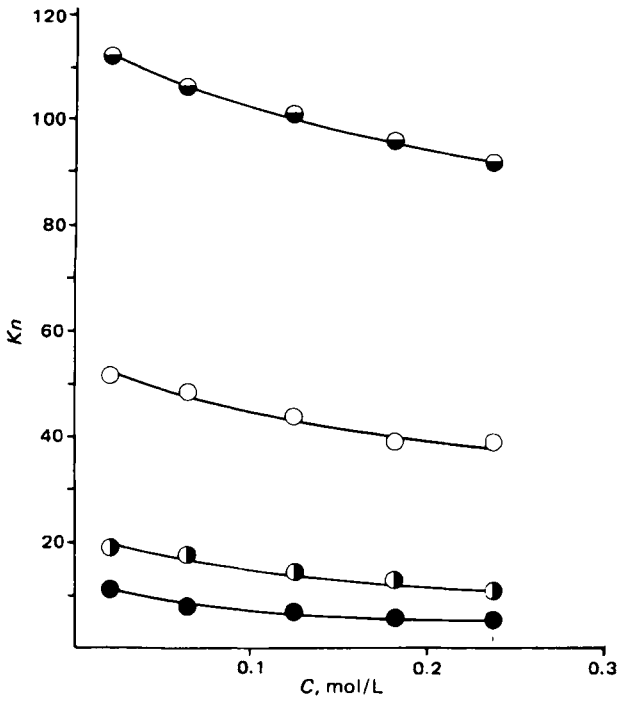

Figure 3—*Variation of partition constants with sodium alkylsulfonate concentration for different barbiturates. Key: (◒) secobarbital; (○) amobarbital; (◑) phenobarbital; (●) allobarbital.*

The following considerations indicate possible reasons for the decrease of K with surfactant concentration. It is known that the critical micelle concentration (CMC) of alkylsulfate surfactants increases when the sulfate group moves from the terminal to a median position along the hydrocarbon chain (8–10). In the case of the sodium tetradecanemonosulfate series quoted by Klevens (10), the CMC changes from 1.65×10^{-3} to 3.26×10^{-3} mol/L when the sulfonate group moves from the terminal position 1 to position 2. This situation is somewhat different from that of the present study, where the sulfonate group of the monosulfonated ions is on the terminal 1 position, while the second sulfonate group of the disulfonated ions is located somewhere on the hydrocarbon chain. However, a simple calculation may be used as a qualitative argument. The CMC of the compound used was 3.72×10^{-3} mol/L. Assuming an ideal behavior of the mixed micelles, the CMC of the pure sodium alkylmonosulfonated product would be 3.3×10^{-3} mol/L when taking into account the composition of the mixed surfactant. Thus, the CMC of the pure sodium alkyldisulfonated compound would be equal to 5.0×10^{-3} mol/L (the breaking point of the solubility curve is in most cases $\sim 5.0 \times 10^{-2}$ mol/L). Therefore, the progressive incorporation of the disulfonated ions in the monosulfonated micelles will increase the CMC of the mixed compound.

The increase in the CMC in a surfactant series is usually related to a decrease in the solubilization properties of the micelles. The appearance of mixed micelles with predominantly monosulfonated ions at low surfactant concentration with gradual incorporation of disulfonated ions at higher concentration may have the same effect: a decrease in the solubilization properties of the micellar solution; hence, the observed decrease of the partition coefficients with increasing surface active concentration for the four barbituric acids.

Finally, some aspects of the contradictions pointed out in this study between conclusions deduced from the solubility and from the equilibrium dialysis results have been discussed before, in particular by Donbrow *et al.* (3). It stresses the need for parallel studies using several solubilization methods to deduce nonequivocal conclusions about the behavior of complex molecules in micellar systems.

REFERENCES

(1) C. Vaution, J. Paris, F. Puisieux, and J. T. Carstensen, *Int. J. Pharm.*, **1**, 349 (1978).

(2) C. Vaution, C. Treiner, F. Puisieux, and J. T. Carstensen, *J. Pharm. Sci.*, **70**, 1238 (1981).

(3) J. J. Kipling, "Adsorption from Solutions of Non-Electrolyte," Academic, New York, N.Y., 1965.

(4) M. Donbrow, P. Molyneux, and C. T. Rhodes, *J. Chem. Soc. A.*, **1967**, 561.

(5) M. Donbrow, E. Azaz, and R. Hamburger, *J. Pharm. Sci.*, **59**, 1427 (1970).

(6) F. Tokiwa and K. Tsujii, *Bull. Chem. Soc. Jpn.*, **46**, 1338 (1973).

(7) N. Nishikido, *J. Colloid Interface Sci.*, **60**, 242 (1977).

(8) H. C. Evans, *J. Chem. Soc.*, **1956**, 579.

(9) P. A. Winsor, *Trans. Faraday Soc.*, **44**, 376 (1948).

(10) H. B. Klevens, *Chem. Rev.*, **47**, 1 (1950).

High-Performance Liquid Chromatographic Analysis of Nadolol and Bendroflumethiazide Combination Tablet Formulations

SOLOMON PERLMAN ˣ, MIRA SZYPER, and JOEL J. KIRSCHBAUM

Received July 21, 1982, from *The Squibb Institute for Medical Research, New Brunswick, NJ 08903.* Accepted for publication December 22, 1982.

Abstract □ A reverse-phase high-performance liquid chromatographic (HPLC) method was developed for the simultaneous assay of nadolol and bendroflumethiazide in tablet formulations. The tablets were extracted with methanol and, after centrifugation, were chromatographed. A phenyl column was used with a mobile phase of aqueous acetate buffer with sodium chloride–methanol (60:40); detection was at 270 nm. Linearity of both drugs was satisfactory. The procedure can be automated and also applied to bendroflumethiazide formulations and bulk material.

Keyphrases □ Nadolol—high-performance liquid chromatography with bendroflumethiazide, combination tablet formulations □ Bendroflumethiazide—high-performance liquid chromatography, with nadolol, combination tablet formulations

One of the principal uses of β-adrenergic-blocking drugs is for the control of hypertension (1). Accordingly, the β-blocker nadolol (2) has been formulated with the diuretic bendroflumethiazide since they work synergistically and need to be administered only once a day (3). A reverse-phase high-performance liquid chromatographic (HPLC) method for analyzing nadolol and other β-adrenergics has been developed in this laboratory (4). The USP methods for assaying bendroflumethiazide include UV spectrophotometry (for tablet content uniformity), nonaqueous titration (for bulk material), and Bratton–Marshall colorimetry (for tablet assay) (5).

The HPLC method for bendroflumethiazide described by Moskalyk *et al.* (6) uses an aqueous methanol mobile phase and may not be stability indicating since no mention is made of the disulfonamide degradation product. To simultaneously assay nadolol and bendroflumethiazide, a method was needed that would be rapid, stability indicating, and amenable to automation for unattended overnight analyses. Such a method is described in this report.

EXPERIMENTAL

Materials—Nadolol[1], bendroflumethiazide[1], and timolol[2] were used as received. Water was double-distilled and stored in glass. HPLC-grade methanol[3] and ACS reagent-grade sodium chloride[4], glacial acetic acid[4], and anhydrous sodium acetate[4] were obtained commercially.

Apparatus—A pump[5] capable of maintaining a constant flow at 200–3000 psig delivered deaerated mobile phase at a flow rate of 1.5–2.5 mL/min. A precision loop injector[6] with a nominal volume of 20 μL was attached to a prepacked reverse-phase medium-polarity column[7] (see *Discussion* section), containing 5- or 10-μm particles and 250–300 mm long × 4.6-mm i.d., through an inlet filter[8]. A saturator column, 50 × 0.2 cm packed with 37-μm silica, preceded the loop injector. This column saturates the mobile phase with silica and thus protects the analytical column. The analytical column was maintained above ambient temperature[9] (32°C) to avoid variations in retention time.

A variable-wavelength detector[10] was used, set at 270 nm. The 25-cm strip-chart recorders[11] had inputs compatible with the detector output. One recorder (or channel) was set to trace the nadolol and bendroflumethiazide peaks on scale. The other was set to be ~10 times more sensitive to detect possible impurities or degradation products. For automated, unattended analysis, an autosampler[12] was used in conjunction with a computing integrator[13].

The mobile phase was aqueous acetate buffer (0.029 M acetic acid, 0.01 M sodium acetate, 0.04 M sodium chloride)–methanol (6:4).

Tablet Analysis—Currently, there are three formulations containing 40, 80, or 160 mg of nadolol and 5 mg of bendroflumethiazide per tablet. These were extracted with 50, 100, and 150 mL of methanol, respectively, ultrasonicated for 15 min, and centrifuged for 15 min at 3000 rpm (~1200×*g*). For content uniformity, the whole, unground tablet was extracted; for average content (assay), 10–20 tablets were ground and the weight equivalent to one tablet of the powder was taken. Methanolic standard solutions were prepared by pipetting the appropriate amount of a stock methanolic bendroflumethiazide standard solution (1 or 0.5 mg/mL) into a volumetric flask containing a quantity of nadolol similar to that of the sample. All glassware containing bendroflumethiazide was low-actinic or covered with aluminum foil. A standard solution of the disulfonamide precursor (and degradation product) of bendroflumethiazide containing 2 μg/mL of methanol was also prepared.

System Suitability Test—A standard solution containing disulfonamide, nadolol, and bendroflumethiazide was injected into the system. The resolution of disulfonamide from the solvent front and of nadolol from disulfonamide were each >1.4, while the resolution of bendroflumethiazide from nadolol was >1.7. The resolution, R_s, is defined as $2(t_2 - t_1)/(W_1 + W_2)$, where t_1 and t_2 are the retention times and W_1 and W_2 are the respective peak widths of tangents to the base line expressed in the same units. Any column which passes this system suitability test can be used.

Solvent Suitability Test—Bendroflumethiazide has been shown to

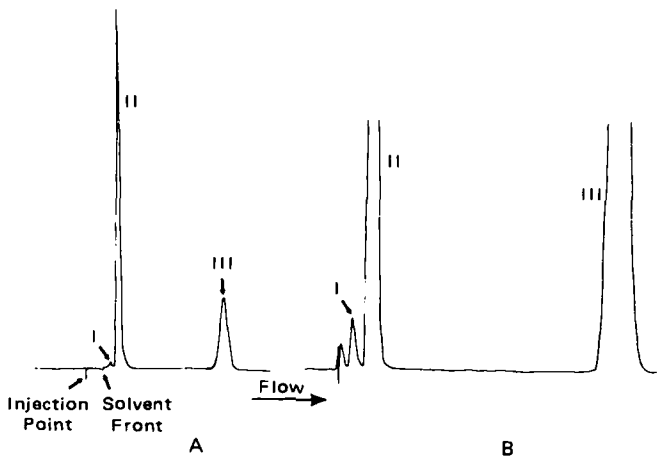

Figure 1—*Chromatogram of disulfonamide (I), nadolol (II), and bendroflumethiazide (III); Key: (A) on scale; (B) off scale. See text for details of the separation.*

[1] E. R. Squibb and Sons.
[2] Merck & Co.
[3] Baker.
[4] Fisher Scientific.
[5] Beckman-Altex 110A.
[6] Rheodyne 7010.
[7] Phenyl (Waters Associates or E.S. Industries).
[8] Rheodyne Model 7362.
[9] Bioanalytical Systems.
[10] Perkin-Elmer LC-75 or LC-85, or Schoeffel 770.
[11] Linear, Inc.
[12] Perkin-Elmer Model 420.
[13] Perkin-Elmer Sigma 10B.

0022-3549/84/0200-0259$01.00/0
© 1984, American Pharmaceutical Association

Table I—Recoveries from Placebo Formulation of Added Nadolol (80 mg), Bendroflumethiazide (5 mg), and Disulfonamide (0.05 mg) Using the Recommended Procedure

Compound	Recoveries, %	Mean	*RSD*, %
Nadolol	99.8, 99.0, 99.0 99.8, 99.8, 99.8	99.5	0.4
Bendroflumethiazide	100.4, 100.4, 100.2	100.3	0.1
Disulfonamide	100.2, 100.2, 100.0	100.1	0.1

react with even minute amounts of formaldehyde (7); thus, the methanol used to extract the tablets and to prepare the mobile phase must be free of formaldehyde. Therefore, when a fresh bottle of methanol is opened, it should be tested by preparing a standard solution of nadolol and bendroflumethiazide, as described above, injecting it after 24 h, and checking for the presence of a new peak eluting after bendroflumethiazide. If this peak is present, the methanol should not be used in the assay.

RESULTS AND DISCUSSION

Bendroflumethiazide, on hydrolysis or exposure to light, yields 2,4-disulfonamide-5′-trifluoromethylaniline, also referred to as free amine or (more correctly), as disulfonamide. Most compendia set limits on the disulfonamide content of bendroflumethiazide raw material. The USP (5) and BP (8) allow 1.5 and 1%, respectively. Thus, the system developed for assaying nadolol–bendroflumethiazide must be able to detect disulfonamide at these and lower concentrations. Furthermore, the sample preparation conditions must be designed so as to minimize or eliminate *in situ* formation of disulfonamide. The recommended system gave good separation of nadolol from bendroflumethiazide for all octadecylsilane columns tested (5–15% coverage). Separation of the disulfonamide peak from the solvent front was difficult. Accordingly, the system suitability test described in the *Experimental* section was devised. Any column that passes this test can be used. The mobile phase as described above has been optimized for high-efficiency phenyl columns (Fig. 1). Other columns which can be used on the basis of this test include trimethylsilane[14] and Partisil[15] 5 C8. However, the mobile phase would require slight modification to be optimized for these (and possibly other) columns. Changing the extracting solvent from methanol to mobile phase would, of course, eliminate the solvent front peak, but this has been shown to promote the degradation of bendroflumethiazide to disulfonamide at a rate of 40 μg/h/tablet.

The stability of bendroflumethiazide in methanol (in the dark) was confirmed by observing no change in the disulfonamide content after 60 h. A solution containing nadolol and bendroflumethiazide exposed to laboratory-intensity light showed increases in disulfonamide content corresponding to an average rate of formation of ~1.2 μg/h. In addition, the methanol must be free of formaldehyde which reacts with bendroflumethiazide (7) (*cf*, solvent suitability test in the *Experimental* section).

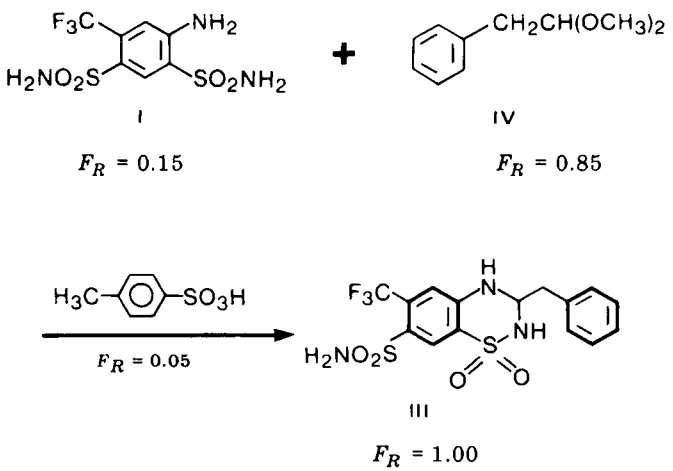

Scheme I—Synthetic intermediates in a synthesis of bendroflumethiazide showing relative retention times (F_R).

[14] Zorbax, DuPont.
[15] Whatman, Inc.

Table II—Assays of Typical Nadolol–Bendroflumethiazide (80:5) Tablets

Formulation	Nadolol, mg/tablet	Bendroflumethiazide, mg/tablet	Disulfonamide, mg/tablet
1	78.9	5.06	All
	80.1	5.08	<0.005
	78.2	5.08	
	82.4	4.92	
	79.3	5.08	
	81.8	5.04	
	80.5	5.08	
	80.6	5.02	
	80.9	4.93	
	81.2	5.07	
Mean	80.4	5.04	
RSD	1.3%	1.2%	
2	81.2	5.14	All
	78.9	5.07	<0.005
	79.4	5.14	
	81.1	5.13	
	79.4	5.07	
	80.6	5.07	
	83.1	5.00	
	81.8	5.04	
	79.0	5.11	
	81.2	4.85	
Mean	80.6	5.06	
RSD	1.7%	1.7%	

The precision of the method was confirmed by performing six injections of nadolol, bendroflumethiazide, and disulfonamide both alone and in the presence of each other. The relative standard deviation was always <0.7%. The plots of response *versus* concentration for all three compounds were linear and passed through the origin. The ranges for concentrations tested were 0–2000 μg/mL for nadolol, 0–250 μg/mL for bendroflumethiazide, and 0–200 μg/mL for disulfonamide. Table I lists the recoveries from spiked placebos of the three compounds both alone and combined, using amounts equivalent to the contents of a typical tablet. When placebo tablets were extracted and analyzed, no peak was seen corresponding to nadolol, bendroflumethiazide, or disulfonamide. Thus, the assay appears to be both accurate and precise. The potencies of two typical lots of tablets are shown in Table II. Disulfonamide results for various samples are all <0.005 mg/tablet (0.1%). The limit of detection is considered to be 0.005 (0.1%); better detectors give lower limits. The disulfonamide values for several experimental lots of bulk bendroflumethiazide as determined by this HPLC method are 0.15–0.25%.

The wavelength of 270 nm was selected because the peak heights of nadolol and bendroflumethiazide at the specified concentrations are relatively similar. If bendroflumethiazide raw material is being assayed, then 220 nm should be used and the samples and standards diluted accordingly. A synthetic route to bendroflumethiazide (9) (III) is shown in Scheme I. The relative retention times of the intermediates disulfonamide (I) and 1,1-dimethoxy-2-ethylbenzene (IV) and the catalyst, *p*-toluenesulfonic acid, indicate that they are resolved from each other and from bendroflumethiazide (III).

A commercially available formulation of timolol with bendroflumethiazide was injected into the system described herein. Both components and the disulfonamide were resolved from each other, indicating the potential of this method.

REFERENCES

(1) R. Clarkson, H. Tucker, and J. Wale, "Annual Reports in Medicinal Chemistry," Academic, New York, N.Y., 1975, pp. 10, 51.

(2) W. H. Frishman, *N. Engl. J. Med.*, **305**, 678 (1981).

(3) M. S. Kochar and J. S. Kalbfleisch, *Curr. Ther. Res.*, **31**, 573 (1982).

(4) B. R. Patel, J. J. Kirschbaum, and R. B. Poet, *J. Pharm. Sci.*, **70**, 336 (1981).

(5) "U.S. Pharmacopeia," 20th rev., U.S. Pharmacopeial Convention, Inc., Rockville, Md., 1980, p. 69.

(6) R. E. Moskalyk, R. A. Locock, L. G. Chatten, A. M. Veltman, and M. F. Bielech, *J. Pharm. Sci.*, **64**, 1406 (1975).

(7) J. Kirschbaum, S. Perlman, and R. B. Poet, *J. Chromatogr. Sci.*, **20**, (1982).

(8) "British Pharmacopoeia," Vol. 48, University Press, Cambridge, U.K. 1980, p. 47.

(9) W. O. Godtfredsen, F. Lund, and K. Lyngby, U.S. Patent 3392168 Leo Pharmaceuticals, 1968.

ACKNOWLEDGMENTS

The authors thank Rosemary Catena, Nancy Garside, Fred Hopps, and Harry Sambucini for performing the analyses; Dr. John M. Joseph for helpful discussions; and Mr. Raymond Poet, Dr. Glenn Brewer, and Dr. Klaus Florey for their critical reading of this manuscript. The talents of Sal Meloni in illustration, Joe Salenetri in photography, and Mrs. C. Saloom in typing are all gratefully appreciated.

Relative Bioavailability of a Commercial Trifluoperazine Tablet Formulation using a Radioimmunoassay Technique

K. K. MIDHA ˣ, E. D. KORCHINSKI, R. M. H. ROSCOE, E. M. HAWES, J. K. COOPER, and G. McKAY

Received July 15, 1982, from the *Colleges of Pharmacy and Medicine, University of Saskatchewan, Saskatoon, Saskatchewan, S7N OWO, Canada.* Accepted for publication January 26, 1983.

Abstract □ The relative bioavailability of a new conventional tablet formulation (5 mg) of trifluoperazine dihydrochloride was studied in 24 healthy volunteers. Using a sensitive radioimmunoassay technique, plasma trifluoperazine concentrations were measured up until 24 h following ingestion of single 5-mg doses of trifluoperazine. The mean ± *SD* for the peak concentration (C_{max}), time to C_{max}, area under the curve from 0 to 24 h (AUC_0^{24}), and terminal elimination half-life following the administration of the test formulation were 2.15 ± 1.07 ng/mL, 4.10 ± 1.38 h, 21.04 ± 11.92 ng·h/mL, and 9.5 ± 7 h, respectively. Following the ingestion of the original trifluoperazine tablet formulation (5 mg) these same parameters were estimated to be 1.92 ± 0.88 ng/mL, 4.02 ± 1.10 h, 18.03 ± 10.11 ng·h/mL, and 9.3 ± 7 h, respectively. Large intersubject variations in C_{max} and AUC_0^{24} were observed. The relative bioavailability of the test formulation was calculated to be 106.5 ± 25.5%.

Keyphrases □ Trifluoperazine—relative bioavailability, commercial tablet formulation, RIA technique □ Bioavailability—relative, commercial trifluoperazine tablet formulation, RIA technique □ Radioimmunoassay—relative bioavailability, commercial trifluoperazine tablet formulation

Trifluoperazine is an orally administered phenothiazine antipsychotic agent that has been in clinical use since 1958. Bioavailability studies of this drug have not been hitherto reported for a number of reasons. Trifluoperazine undergoes extensive metabolism to many metabolites which are formed from attack on both the phenothiazine ring and the side chain (1). Trifluoperazine is also known to undergo pronounced presystemic biotransformation in animals following oral administration (2). Phenothiazine drugs in general undergo significant first-pass effects in humans which contribute to large intersubject variability (3–5). Therefore, bioavailability studies require sensitive and specific analytical procedures. Recent analytical methods for trifluoperazine in plasma include GC–NPD (nitrogen-phosphorus detection) (6–8), GC–MS (9, 10), and radioimmunoassay (RIA) (11). Of these the GC–MS and RIA procedures have been used in single-dose pilot studies, where it was found that the bioequivalency parameters as determined by RIA were similar to those determined using GC–MS (12).

This study describes the estimation of the bioavailability of a new conventional trifluoperazine tablet formulation (5 mg)[1] relative to the original product[2]. Following single oral doses of 5 mg, the plasma concentration–time profiles of trifluoperazine were examined up to 24 h using RIA, which is sensitive to 0.25 ng/mL using a 200-μL plasma sample (11).

Table I—*In Vitro* Tablet Test Results

Test	Method	Test Product	Reference Product
Assay, mg (% potency)	USP XX	4.88 (97.6%)	5.23 (104.6%)
Disintegration[a], min	USP XX	5.5	7.0
Content uniformity, % (*RSD*, %)	USP XX	95.7 (3.04)	100.5 (1.69)
Dissolution, % (*RSD*, %)	(Gastric test solution, no enzyme)	100.7 (1.50)	80.7 (30.13)

[a] Gastric test solution.

EXPERIMENTAL

Tablet samples from production lots of two formulations of trifluoperazine were assigned as test[1] and reference[2]; standard *in vitro* tests were performed on both tablet formulations. The dissolution test was carried out on six individual tablets using apparatus 1, as described (13). The basket was rotated at 50 rpm, and the dissolution medium (900 mL) was 1% HCl (v/v) at 37 ± 0.5°C. At the end of 30 min, a suitable portion of the dissolution fluid was filtered. After discarding the first 20 mL of the filtrate, the absorbance of the standard and dissolution test preparations were determined in 1-cm cells at 255 (the wavelength of maximum absorbance) and 278 nm (the wavelength of minimum absorbance) using 1% HCl (v/v) as the blank.

Twenty-four healthy adult male volunteers, from whom written informed consent was obtained, were included in this study. With one exception, all were nonsmokers. The fitness of each subject was assessed by an independent physician who conducted complete physical examinations, reviewed medical histories and the results of clinical laboratory tests (hematology, SMA 12 biochemistry screen, and urinalysis), and monitored the health of the subjects throughout the study period. All subjects were drug free 30 d prior to the study and were asked to refrain from taking any drugs during the study, including abstaining from alcohol for 24 h, prior to and 24 h following each dose. The subjects were assigned randomly to receive the test or reference formulation for the first dose

[1] Trifluoperazine hydrochloride, lot #79-082, Cord Laboratories, Ltd., Broomfield, Colo.

[2] Stelazine, lot #2129S06, Smith Kline & French Ltd., Philadelphia, Pa.

0022-3549/84/0200-0261$01.00/0
© 1984, American Pharmaceutical Association

(9) W. O. Godtfredsen, F. Lund, and K. Lyngby, U.S. Patent 3392168 Leo Pharmaceuticals, 1968.

ACKNOWLEDGMENTS

The authors thank Rosemary Catena, Nancy Garside, Fred Hopps, and Harry Sambucini for performing the analyses; Dr. John M. Joseph for helpful discussions; and Mr. Raymond Poet, Dr. Glenn Brewer, and Dr. Klaus Florey for their critical reading of this manuscript. The talents of Sal Meloni in illustration, Joe Salenetri in photography, and Mrs. C. Saloom in typing are all gratefully appreciated.

Relative Bioavailability of a Commercial Trifluoperazine Tablet Formulation using a Radioimmunoassay Technique

K. K. MIDHA ˣ, E. D. KORCHINSKI, R. M. H. ROSCOE, E. M. HAWES, J. K. COOPER, and G. McKAY

Received July 15, 1982, from the *Colleges of Pharmacy and Medicine, University of Saskatchewan, Saskatoon, Saskatchewan, S7N OWO, Canada.* Accepted for publication January 26, 1983.

Abstract □ The relative bioavailability of a new conventional tablet formulation (5 mg) of trifluoperazine dihydrochloride was studied in 24 healthy volunteers. Using a sensitive radioimmunoassay technique, plasma trifluoperazine concentrations were measured up until 24 h following ingestion of single 5-mg doses of trifluoperazine. The mean ± *SD* for the peak concentration (C_{max}), time to C_{max}, area under the curve from 0 to 24 h (AUC_0^{24}), and terminal elimination half-life following the administration of the test formulation were 2.15 ± 1.07 ng/mL, 4.10 ± 1.38 h, 21.04 ± 11.92 ng·h/mL, and 9.5 ± 7 h, respectively. Following the ingestion of the original trifluoperazine tablet formulation (5 mg) these same parameters were estimated to be 1.92 ± 0.88 ng/mL, 4.02 ± 1.10 h, 18.03 ± 10.11 ng·h/mL, and 9.3 ± 7 h, respectively. Large intersubject variations in C_{max} and AUC_0^{24} were observed. The relative bioavailability of the test formulation was calculated to be 106.5 ± 25.5%.

Keyphrases □ Trifluoperazine—relative bioavailability, commercial tablet formulation, RIA technique □ Bioavailability—relative, commercial trifluoperazine tablet formulation, RIA technique □ Radioimmunoassay—relative bioavailability, commercial trifluoperazine tablet formulation

Trifluoperazine is an orally administered phenothiazine antipsychotic agent that has been in clinical use since 1958. Bioavailability studies of this drug have not been hitherto reported for a number of reasons. Trifluoperazine undergoes extensive metabolism to many metabolites which are formed from attack on both the phenothiazine ring and the side chain (1). Trifluoperazine is also known to undergo pronounced presystemic biotransformation in animals following oral administration (2). Phenothiazine drugs in general undergo significant first-pass effects in humans which contribute to large intersubject variability (3–5). Therefore, bioavailability studies require sensitive and specific analytical procedures. Recent analytical methods for trifluoperazine in plasma include GC–NPD (nitrogen-phosphorus detection) (6–8), GC–MS (9, 10), and radioimmunoassay (RIA) (11). Of these the GC–MS and RIA procedures have been used in single-dose pilot studies, where it was found that the bioequivalency parameters as determined by RIA were similar to those determined using GC–MS (12).

This study describes the estimation of the bioavailability of a new conventional trifluoperazine tablet formulation (5 mg)[1] relative to the original product[2]. Following single oral doses of 5 mg, the plasma concentration–time profiles of trifluoperazine were examined up to 24 h using RIA, which is sensitive to 0.25 ng/mL using a 200-μL plasma sample (11).

Table I—*In Vitro* Tablet Test Results

Test	Method	Test Product	Reference Product
Assay, mg (% potency)	USP XX	4.88 (97.6%)	5.23 (104.6%)
Disintegration[a], min	USP XX	5.5	7.0
Content uniformity, % (*RSD*, %)	USP XX	95.7 (3.04)	100.5 (1.69)
Dissolution, % (*RSD*, %)	(Gastric test solution, no enzyme)	100.7 (1.50)	80.7 (30.13)

[a] Gastric test solution.

EXPERIMENTAL

Tablet samples from production lots of two formulations of trifluoperazine were assigned as test[1] and reference[2]; standard *in vitro* tests were performed on both tablet formulations. The dissolution test was carried out on six individual tablets using apparatus 1, as described (13). The basket was rotated at 50 rpm, and the dissolution medium (900 mL) was 1% HCl (v/v) at 37 ± 0.5°C. At the end of 30 min, a suitable portion of the dissolution fluid was filtered. After discarding the first 20 mL of the filtrate, the absorbance of the standard and dissolution test preparations were determined in 1-cm cells at 255 (the wavelength of maximum absorbance) and 278 nm (the wavelength of minimum absorbance) using 1% HCl (v/v) as the blank.

Twenty-four healthy adult male volunteers, from whom written informed consent was obtained, were included in this study. With one exception, all were nonsmokers. The fitness of each subject was assessed by an independent physician who conducted complete physical examinations, reviewed medical histories and the results of clinical laboratory tests (hematology, SMA 12 biochemistry screen, and urinalysis), and monitored the health of the subjects throughout the study period. All subjects were drug free 30 d prior to the study and were asked to refrain from taking any drugs during the study, including abstaining from alcohol for 24 h, prior to and 24 h following each dose. The subjects were assigned randomly to receive the test or reference formulation for the first dose

[1] Trifluoperazine hydrochloride, lot #79-082, Cord Laboratories, Ltd., Broomfield, Colo.

[2] Stelazine, lot #2129S06, Smith Kline & French Ltd., Philadelphia, Pa.

0022-3549/84/0200-0261$01.00/0
© 1984, American Pharmaceutical Association

Table II—Mean Plasma Trifluoperazine Concentrations by Formulation

Formulation	Trifluoperazine Concentration, ng/mL									
	0.5 h	1.0 h	1.5 h	2.0 h	3.0 h	4.5 h	6.0 h	8.0 h	12 h	24 h
Test	0.18	0.55	1.04	1.43	1.93	1.89	1.36	1.03	0.84	0.35
(*SD*)	(0.23)	(0.65)	(0.72)	(0.83)	(1.06)	(1.03)	(0.86)	(0.61)	(0.41)	(0.35)
Reference	0.16	0.52	0.91	1.25	1.69	1.81	1.30	0.98	0.81	0.33
(*SD*)	(0.19)	(0.38)	(0.72)	(0.77)	(0.80)	(0.92)	(0.73)	(0.50)	(0.43)	(0.31)

Table III—Mean Values of Bioavailability Parameters of Trifluoperazine Formulations

Formulation	AUC_0^{24}, ng·h/mL	ln AUC_0^{24}, ng·h/mL	C_{max}, ng/mL	ln C_{max}	t_{max}, h	AUC_0^{24} Ratios, %[a]	C_{max} Ratios, %[a]	K_{el} (3–12 h), h^{-1}	K_{el} (12–24 h), h^{-1}
Test	20.54	2.86	2.10	0.61	4.10	106.54	108.39	0.1023	0.0729
(*SD*)	(11.63)	(0.61)	(1.04)	(0.55)	(1.38)	(25.46)	(25.50)	(0.0486)	(0.0330)
Reference	19.27	2.83	1.92	0.56	4.02	—	—	0.1013	0.0748
(*SD*)	(10.58)	(0.52)	(0.87)	(0.44)	(1.10)	—	—	(0.0455)	(0.0391)

[a] Test/reference formulation.

and then the respective alternate formulation for the second dose. There was a 2-week interval between treatments (balanced complete block). Single oral doses of trifluoperazine (5 mg) were administered with 100 mL of water to overnight-fasted subjects. Fluid and food intake were controlled for 4 h following each dose with a carbonated lemon-lime beverage (280 mL) and a standard lunch provided at 1.5 and 4 h, respectively. Blood samples were obtained by venipuncture immediately before and at 0.5, 1.0, 1.5, 2.0, 3.0, 4.5, 6.0, 8.0, 12, and 24 h after administration. During sampling, care was taken to prevent the blood from coming in contact with the rubber stopper of the heparinized evacuated sampling tubes[3] (14). The blood samples were centrifuged, and the separated coded plasma samples were stored at −20°C until analysis.

Three variables for bioequivalency, *i.e.*, area under the plasma concentration–time curve (AUC_0^{24}), maximum observed concentration (C_{max}), and time to C_{max} (t_{max}) were examined in this study. Plasma concentrations of trifluoperazine appeared to decline biexponentially, and elimination rate constants for trifluoperazine were calculated for the two phases (3–12 h and 12–24 h) employing least-squares linear regression analysis of the semilogarithmic data. The AUC_0^{24} was estimated using the trapezoidal rule to C_{max}, followed by the logarithmic trapezoidal rule (15) to 24 h. C_{max} and t_{max} were obtained directly from the raw data. The three-way analysis of variance of AUC_0^{24}, C_{max}, and t_{max} was carried out on the raw data. This analysis was also performed on natural logarithmic transformation of AUC_0^{24} and C_{max}. The subject effect, period effect, and the formulation effect were taken into account in each analysis. All results are reported as mean ± *SD* unless otherwise stated.

RESULTS AND DISCUSSION

Table I shows the results of the *in vitro* data for both the test and reference formulations of trifluoperazine. The assay results demonstrated that the test formulation was 97.6% and the reference formulation 104.6% of the label strength (5 mg).

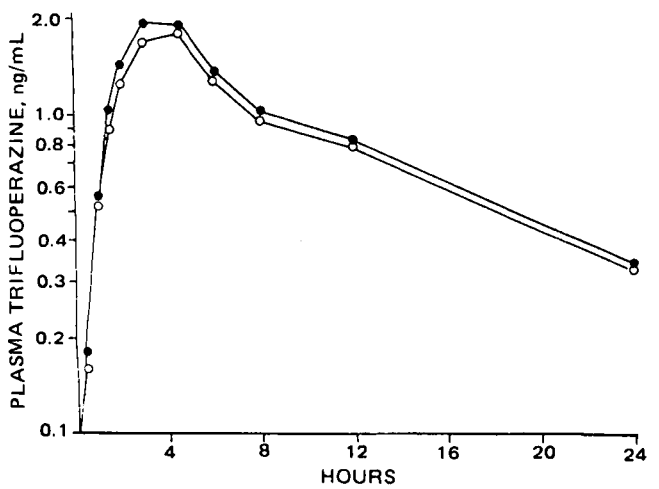

Figure 1—*Mean plasma trifluoperazine concentrations for test (●) and reference (○) formulations.*

[3] Vacutainer B. D., Becton, Dickinson & Co., Mississauga, Ont.

Figure 1 depicts the semilogarithmic mean plasma concentration–time profiles of trifluoperazine for the two formulations. The multicompartmental behavior of trifluoperazine and the limited number of correctly timed samples made it difficult to obtain meaningful estimates of the absorption, distribution, and elimination rate constants (16, 17).

Table II shows the mean plasma concentration–time data for the 24 subjects. Values reported <0.25 ng/mL are only estimates, as they fall below assay sensitivity (11). All other bioavailability data is presented in Table III. The AUC_0^{24} ranges for reference and test formulations were 6.3–53.3 and 3.9–55.5 ng·h/mL, respectively. The C_{max} values for reference and test formulations ranged from 0.67 to 4.28 and 0.43 to 4.64 ng/mL, respectively. The t_{max} ranged from 2 to 6 h for the reference formulation and from 2 to 8 h for the test formulation. The AUC_0^{24} (8- to 14-fold) and C_{max} (6- to 10-fold) ranges clearly demonstrated the large intersubject variability typical of the oral phenothiazine drugs (3–5), which is shown here for the first time for single doses of trifluoperazine.

The AUC_0^{24} and C_{max} ratios of test–reference formulation were 106.5 ± 25.5 and 108.4 ± 25.5, respectively, which demonstrates that the test product has acceptable relative bioavailability. This is further supported by the fact that 18/24 and 17/24 of the subjects who participated in this study had relative bioavailabilities of 100 ± 25% in terms of AUC and C_{max} ratios, respectively. This clearly establishes the bioequivalency of the test formulation.

Table IV presents the results of the analysis of variance. There are no statistically significant differences in the formulations in terms of AUC_0^{24}, ln AUC_0^{24}, and ln C_{max}, while there is statistically significant difference in C_{max}. However, this latter difference may not be of significance in the clinical situation. There is a subject effect on all of the parameters examined, and a period effect on AUC_0^{24}. The 95% confidence intervals for the test and reference formulations are summarized in Table V. It is clear that there is no detectable difference between the test and reference formulations for all the parameters examined. The narrow and overlapping confidence intervals for AUC_0^{24} and C_{max} further establish the bioequivalency of the test formulation as compared with the reference.

After reaching C_{max}, trifluoperazine plasma concentrations decline at least in a biphasic manner. The apparent terminal half-lives were unfortunately estimated from only two data points in each case (12 and 24 h). The mean values for apparent terminal half-lives for test and reference were 9.5 ± 7 and 9.3 ± 7 h, respectively. Information concerning trifluoperazine plasma concentrations in humans is scarce because of the lack of sensitive assay methods. In a patient under chronic treatment at various times with daily doses of 15, 30, and 80 mg, Curry *et al.* (18) was able to measure plasma trifluoperazine concentrations only at the 80-

Table IV—Three-way Analysis of Variance

	α-Values				
	AUC_0^{24}	ln AUC_0^{24}	C_{max}	ln C_{max}	t_{max}
Formulation	0.057	0.303	0.045*	0.219	0.606
Period	0.009[a]	0.010[a]	0.144	0.174	0.276
Subject	0.000[a]	0.000[a]	0.000*	0.000*	0.000[a]

[a] Significantly different from 100% at $\alpha = 0.05$, based on two-tailed t test.

Table V—Average Values of Bioavailability Parameters with 95% Confidence Intervals [a]

Formulation	AUC_0^{24}, ng-h/mL	C_{max}, ng/mL	t_{max}, h	Relative Bioavailability, %[b] AUC_0^{24}	C_{max}
Test	17.46	1.84	4.10	103.63	105.65
Confidence Intervals	(16.17–18.75)	(0.58–3.10)	(3.52–4.68)	(93.52–114.82)	(95.63–116.72)
Reference	16.95	1.75	4.02	—	—
Confidence Intervals	(15.70–18.20)	(0.55–2.95)	(3.56–4.48)	—	—

[a] These mean values are based on natural logarithm transformed data. [b] Test/reference formulations.

mg/d dose level. In the present study trifluoperazine plasma concentrations were followed for 24 h following a single 5-mg dose. The characteristic phenothiazine multicomponent elimination was demonstrated for trifluoperazine. The C_{max} to 12-h phase is clearly distinct from the 12–24-h elimination following cessation of dosing. Animal studies have indicated that trifluoperazine, like other phenothiazine antipsychotics, appears to be extensively biotransformed presystemically (2); most of this may occur during first passage through the liver or in the gut. This may explain the large intersubject variability seen here with trifluoperazine, which is very characteristic of a drug with a high hepatic extraction ratio (19–21). Alteration in the activity of drug metabolizing enzymes by factors such as diet and smoking (22) may produce significant variations in the plasma concentrations of trifluoperazine following oral administration.

The present study demonstrated that trifluoperazine plasma concentrations can be monitored for as long as 24 h following the oral administration of single 5-mg doses of trifluoperazine. The measurement of these plasma concentrations has allowed us to successfully establish the relative bioavailability of a newly developed trifluoperazine formulation. These results suggest that the available analytical methodology should be able to monitor plasma concentrations in patients under chronic treatment with even low doses of trifluoperazine so that plasma concentration *versus* clinical response correlations can be investigated.

REFERENCES

(1) U. Breyer and G. Schmalzing, *Drug Metab. Dispos.*, **5**, 97 (1977).

(2) G. Schmalzing, *Drug Metab. Dispos.*, **5**, 104 (1977).

(3) S. H. Curry, R. Whelpton, P. J. deSchepper, S. Vranckx, and A. A. Schiff, *Br. J. Clin. Pharmacol.*, **7**, 325 (1979).

(4) C. E. Hansen, T. R. Christensen, J. Elley, L. B. Hansen, P. Kragh-Sorensen, N. E. Larsen, J. Naestoft, and E. F. Hvidberg, *Br. J. Clin. Pharmacol.*, **3**, 915 (1976).

(5) J. C. K. Loo, K. K. Midha, and I. J. McGilveray, *Commun. Psychopharmacol.*, **4**, 121 (1980).

(6) T. J. Gillespie and I. G. Sipes, *J. Chromatogr.*, **223**, 95 (1981).

(7) J. I. Javaid, H. Dekirmenjian, and J. M. Davis, *J. Pharm. Sci.*, **71**, 63 (1982).

(8) R. M. H. Roscoe, J. K. Cooper, E. M. Hawes, and K. K. Midha, *J. Pharm. Sci.*, **71**, 625 (1982).

(9) K. K. Midha, R. M. H. Roscoe, E. M. Hawes, J. K. Cooper, G. McKay, and H. U. Shetty, *Biomed. Mass Spectrom.*, **9**, 186 (1982).

(10) R. Whelpton, S. H. Curry, and G. M. Watkins, *J. Chromatogr.*, **228**, 321 (1982).

(11) K. K. Midha, J. W. Hubbard, J. K. Cooper, E. M. Hawes, S. Fournier, and P. Yeung, *Br. J. Clin. Pharmacol.*, **12**, 189, (1981).

(12) K. K. Midha, E. M. Hawes, J. W. Hubbard, J. K. Cooper, and R. M. H. Roscoe, "Abstracts," 41st international conference of Pharmaceutical Sciences of FIP, Vienna, Austria, September 1981.

(13) "United States Pharmacopeia," 20th rev. United States Pharmacopeial Convention, Rockville, Md., 1980.

(14) K. K. Midha, J. K. Cooper, Y. D. Lapierre, and J. W. Hubbard, *Can. Med. Assoc. J.*, **124**, 263 (1981).

(15) W. L. Chiou, *J. Pharmacokinet. Biopharm.*, **6**, 539 (1978).

(16) H. G. Boxenbaum, S. Riegelman, and R. M. Elashoff, *J. Pharmacokinet. Biopharm.*, **2**, 123 (1974).

(17) H. I. Glass and A. C. deGarreta, *Phys. Med. Biol.*, **16**, 119 (1971).

(18) S. H. Curry, R. B. Stewart, P. K. Springer, and J. E. Pope, *Lancet*, **i**, 395 (1981).

(19) P. A. Routledge and D. G. Shand, *Annu. Rev. Pharmacol.*, **19**, 447 (1979).

(20) G. R. Wilkinson and D. G. Shand, *Clin. Pharmacol. Ther.*, **18**, 377 (1975).

(21) D. G. Shand, E. M. Nuckolls, and J. A. Oates, *Clin. Pharmacol. Ther.*, **11**, 112 (1970).

(22) W. J. Jusko, *J. Pharmacokinet. Biopharm.*, **6**, 7 (1978).

ACKNOWLEDGMENTS

Development Grant DG 222 to Dr. K. K. Midha and post doctoral fellowship to Dr. R. M. H. Roscoe both from MRC Canada, and expert technical assistance of Mrs. Janet Neilson and Mrs. Gail Rauw, are gratefully acknowledged. Dr. J. C. K. Loo, Bureau of Drug Research, Health and Welfare Canada, is thanked for helpful discussions.

Use of a *Lactobacillus casei* Assay as a Prescreen for Potential Anticancer Agents: An Update Study

THEODORE T. OTANI *x, MARY R. BRILEY *, and RUTH I. GERAN ‡

Received October 18, 1982, from the **Laboratory of Pathophysiology, Division of Cancer Biology and Diagnosis*, and the ‡*Drug Evaluation Branch, Developmental Therapeutics Program, Division of Cancer Treatment, National Cancer Institute, National Institutes of Health, Bethesda, MD 20205.* Accepted for publication December 15, 1982.

Abstract □ Updating an earlier report, 15 known antineoplastic agents, 11 of which are commercially available for treatment of human cancers, were tested for growth-inhibitory activity in a *Lactobacillus casei* system to determine if this microbial system could select them as "active." Although we previously reported that over 160 compounds tested in this assay were inactive, 11 of the 15 known antineoplastic agents tested here were inhibitory. Because of this observation and the advantage that the procedure is rapid and inexpensive, this microbiological assay is recommended for consideration as a prescreen for anticancer agents.

Keyphrases □ *Lactobacillus casei*—anticancer agents □ Anticancer agents—lactobacillus casei

The need for a simple, rapid, and inexpensive method of screening for potential anticancer agents has long been recognized. In 1958, an *ad hoc* committee[1] was organized by the National Cancer Institute Div. of Cancer Treatment to investigate the feasibility of using microbiological systems for such a purpose. As a result of the study, the committee published a comprehensive report in which it described 16 assays and the use of a set of four microbial systems capable of detecting 95% of 89 compounds from among some 200 compounds known at that time to be effective in *in vivo* assay against experimental neoplasms (1). Although certain limitations in the microbiological procedure were recognized, its possible role in the search for new agents was recognized.

In the present study 15 compounds currently being used for the treatment of human malignancies or being developed for clinical use by the National Cancer Institute were tested for growth-inhibitory activity in a *Lactobacillus casei* system.

EXPERIMENTAL

Fifteen anticancer agents[2] currently being used, clinically or in a developmental phase in the cancer treatment program, and soluble in aqueous systems were selected at random (Table I). Twenty milligrams of the test compound was dissolved in 10 mL of triple-distilled (in glass) water. In some cases sufficient amounts of 0.1 M sodium hydroxide were added to bring the test solution to pH 6.0 before bringing to volume. The solutions were sterilized by filtration through filter units[3] attached to a sterile 10-mL plastic syringe[4]. The test solutions were pipetted in graded volumes to contain 0.1, 0.5, and 1.0 mg/mL, final concentration, of the test compound. The volume was made to 2.5 mL by the addition of an appropriate volume of sterile water. The final volume of the assay system after the addition of the medium was 5.0 mL.

The assay procedure is that of Foley *et al.* (1) and is also described in our earlier paper (2).

A riboflavin assay medium[5] supplemented with a minimal quantity of riboflavin[6] to give maximal growth (0.03 μg/mL final concentration) was used. The period of medium autoclaving was monitored carefully to not exceed the 10-min period previously described (1).

The organism used was *Lactobacillus casei* ATCC 7469[7], which was carried on agar[8] as stab cultures, transferred monthly, incubated at 37°C for 24 h, and then stored at 4°C.

The inoculum for the assay was prepared by washing a 24-h broth[9] culture (grown at 37°C) in isotonic saline solution, suspending the bacterial pellet in 10 mL of isotonic saline by centrifugation, and from this making a 1:20 dilution suspension in isotonic saline.

An appropriate amount of the medium for the uninoculated control and the solution blank was removed, and the balance of the medium was inoculated with a sufficient volume of the 1:20 bacterial suspension so that each 5 mL contained 0.06 mL of the inoculum. Then 2.5 mL of the inoculated medium was added to each assay tube, which contained the graded amounts of the test solution. The sterility blank and reagent blank tubes containing the uninoculated medium were each treated with 0.06 mL of the isotonic saline solution that is used in washing the bacteria.

The pH of the assay system containing the highest concentration of the test compound determined in a parallel nonsterile system was within ±0.2 pH units of the control tubes containing an equal volume of water in place of the test solution.

The assay was incubated at 37°C for 19 h, after which growth was terminated by immersing the tubes in boiling water for 10 min. The extent of growth was determined turbidimetrically on a photoelectric colorimeter[10] equipped with a red filter (660 mμ). A positive control, consisting of 6-mercaptopurine at 0.1 mg/mL, a normal growth control, containing no test compound, and a sterility control were included routinely in all assays. An inhibition value of 52–56% by 6-mercaptopurine and a concurrent normal growth of 194–200 turbidity reading in the determination were the criteria of a valid assay. The figures shown in the table are typical values from at least three duplicate determinations.

RESULTS AND DISCUSSION

Fifteen compounds, most of which are currently being used clinically as antineoplastic agents, were tested for growth-inhibitory activity in a *Lactobacillus casei* system. The system was a portion of a set of 16 microbial systems selected by the Subcommittee on Microbiology (1), mentioned earlier, for the purpose of screening chemical compounds for potential antitumor activity. According to the study protocol compounds showing a growth inhibition of ≥50% at a concentration of 1 mg/mL were considered inhibitory.

As seen in Table I, 11 of the 15 compounds tested (73%) were inhibitory in the test system: the extent of inhibition was quite striking. Indeed, 10 of the 11 inhibitory compounds showed essentially complete inhibition at 0.5 mg/mL, and 6 of these showed essentially complete inhibition even at 0.1 mg/mL. The inhibition by phosphonoacetyl-L-aspartic acid (PALA) at 1 mg/mL (54%) is considered to be positive as defined by the protocol, even though the inhibition did not appear to be dose related.

The positive tests obtained from this series of compounds are somewhat lower than the 95% (using four microbial systems) or the 90% (using three microbial systems) described by Foley *et al.* (1). However, it is noteworthy that a single microbial system used here was capable of detecting a majority of the 15 selected antineoplastic compounds presently being used clinically or in the developmental phase of the cancer treatment program. The compounds run concurrently with these compounds and found to be negative in this system (*i.e.*, *N*-benzoyl-L-aspartic acid and *N*-propionyl-L-alanine) were also negative in mammalian *in vivo*

[1] Subcommittee on Microbiology, Screening Panel, Cancer Chemotherapy National Service Center, National Cancer Institute, Public Health Service, Bethesda, MD 20205.

[2] Obtained from Developmental Therapeutics Program, Division of Cancer Treatment, National Cancer Institute, Bethesda, MD 20205.

[3] Millex-GS 0.22 μm filter units, Millipore Corp., Bedford, MA 01730.

[4] BD Plastipak syringe, Becton, Dickinson and Co., Rutherford, NJ 07070.

[5] Difco Laboratories, Detroit, MI 48232.

[6] Calbiochem, San Diego, CA 92112.

[7] From American Type Culture Collection, Rockville, MD 20852.

[8] Micro Assay Culture Agar, Difco Laboratories, Detroit, MI 48232.

[9] Micro Inoculum Broth, Difco Laboratories, Detroit, MI 48232.

[10] Klett-Summerson.

0022-3549/84/0200-0264$01.00/0
© 1984, American Pharmaceutical Association

Table I—Effect of Some Antineoplastic Agents on the Growth of *L. casei* 7469

Compound	NSC[a] No.	Inhibition, %[b] 0.1 mg/mL[c]	0.5 mg/mL[c]	1.0 mg/mL[c]
Doxorubicin hydrochloride[d]	123127	90	—[e]	—[e]
Daunorubicin[d]	82151	99	—[e]	—[e]
Mitomycin[d]	26980	94	—[e]	—[e]
Streptozocin[d]	85998	100	100	100
Phosphonoacetyl-L-aspartic acid[f]	224131	42	50	54
Azaserine[f]	742	100	100	100
Alanosine[f]	153353	42	90	99
DON[f]	7365	100	100	100
Melphalan[d]	8806	0	0	8
Cyclophosphamide[d]	26271	1	0	2
Thiotepa[d]	6396	28	93	98
Cytarabine[d]	63878	59	97	98
Hydroxyurea[d]	32065	0	0	8
Procarbazine[d]	77213	0	−6[g]	−6[g]
6-Mercaptopurine[d]	755	55	100	100
N-α-Benzoyl-L-aspartic acid[h]	227406	0	0	0
N-Propionyl-L-alanine[h]	270569	2	2	2

[a] National Service Center number. The Cancer Chemotherapy National Service Center was the forerunner of the Developmental Therapeutics Program at the National Cancer Institute. [b] % Inhibition = (To − Tt)/To × 100, where To represents the turbidity reading of the system in the absence of the test compound and Tt represents the turbidity reading of the system in the presence of the test compound. The turbidity readings of the inoculated control tubes (containing no test compound) were 194–200 Klett units. At least three sets of duplicate determinations were made for each compound. The duplicate values in each determination agreed within ±5 Klett units. A positive control, 6-mercaptopurine, was run with each assay. An inhibition value of 52–56% by this compound at 0.1 mg/mL, and a concurrent normal growth (no inhibitor present) of 194–200 turbidity reading in the determination were criteria of a valid assay. [c] Final concentration in the assay system. [d] Commercially available. [e] Color interfered with Klett reading in higher concentrations of the test compound. However, the tubes were clear (no turbidity) upon visual examination. [f] Anticancer compounds in development in the Developmental Therapeutics Program, National Cancer Institute, Bethesda, MD. [g] Indicates stimulation of growth. [h] Negative control compounds: see text.

tumor systems (L1210[11] lymphoid and P388[12] lymphocytic leukemias). In addition, there are more than 160 compounds, including β-hydroxyamino acids (2, 3), *N*-chloroacetyl-β-hydroxyamino acids (2, 3), *N*-acetyl- and *N*-propionylamino acids (4), free amino acids (4), *N*-chloroacetyl amino acids (4), *N*-trifluoroacetyl amino acids (5), and certain *N*-benzoyl amino acids (6, 7) that exhibited no inhibition in this assay system. There are also ~30 compounds thus far reported (2–7) that showed considerable activity in this system. However, since these compounds, both active and inactive in the assay, have not been tested in human malignancies, no correlation between the *in vitro* data and the efficacy in human cancer can be made at this time.

Possibly the reason some of the antineoplastic compounds were "missed" in this test was due to the requirement for a metabolic conversion to an active form, and to the lack of an appropriate enzyme system in the test microorganism. For example, it has been reported that cyclophosphamide is activated by an enzymatic cleavage of the cyclic compound at the P—N-linkage (8–10) and procarbazine, upon metabolic conversion has been reported to depolymerize DNA (11). While some of the other compounds that require transformation to the active form showed inhibition in this system [such as 6-mercaptopurine (12), mitomycin (13), and cytarabine (14, 15)], the system apparently possessed the necessary mechanism to cause the transformation to the active form.

When designing prospective anticancer compounds, a simple and rapid assay procedure to follow the alteration of activity with modification in the molecular structure is necessary. Therefore, a procedure consisting of a single microbiological system was selected for studying the activity of the numerous compounds prepared in this laboratory. *Lactobacillus casei* ATCC 7469 in riboflavin assay media was selected because this system was rapid (with a 19-h incubation period) and was found to be the most sensitive among a set of three systems used in our earlier studies (2).

[11] Data obtained from Developmental Therapeutics Program, Division of Cancer Treatment, National Cancer Institute, Bethesda, MD 20205.

[12] Unpublished data; screening performed through Developmental Therapeutics Program, Division of Cancer Treatment, National Cancer Institute, Bethesda, MD 20205.

REFERENCES

(1) G. E. Foley, R. E. McCarthy, V. M. Binns, E. E. Snell, B. M. Guirard, G. W. Kidder, V. C. Dewey, and P. S. Thayer. *Ann. N.Y. Acad. Sci.*, **76**, 413 (1958).

(2) T. T. Otani, *Cancer Chemother. Rep.*, **38**, 25 (1964).

(3) T. T. Otani and M. R. Briley, *J. Pharm. Sci.*, **65**, 534 (1976).

(4) T. T. Otani and M. R. Briley, *J. Pharm. Sci.*, **67**, 520 (1978).

(5) T. T. Otani and M. R. Briley, *J. Pharm. Sci.*, **68**, 496 (1979).

(6) T. T. Otani and M. R. Briley, *J. Pharm. Sci.*, **68**, 260 (1979).

(7) T. T. Otani and M. R. Briley, *J. Pharm. Sci.*, **68**, 1366 (1979).

(8) E. S. Greenwald, M. Goldstein, and P. Barland. "Cancer Chemotherapy," 2nd ed., Medical Examination Publishing, New York, N.Y., 1973, p. 37.

(9) "Proceedings of the Symposium on the Metabolism and Mechanism of Action of Cyclophosphamide," *Cancer Treat. Rep.*, **60**, 299 (1976).

(10) S. K. Carter and K. B. Livingston, *Cancer Treat. Rep.*, **2**, 295 (1975).

(11) S. D. Spivack, *Ann. Intern. Med.*, **81**, 795 (1974).

(12) R. T. Dorr and W. B. Fritz, "Cancer Chemotherapy Handbook," Elsevier, New York, N.Y., 1980, p. 513.

(13) S. K. Carter, M. T. Bakowski, and K. Hellmann, "Chemotherapy of Cancer," 2nd ed. Wiley, New York, N.Y., 1981, p. 98.

(14) B. Chabner, C. E. Meyers, and V. T. Olivero, *Semin. Oncol.*, **4**, 165 (1977).

(15) W. B. Kremer, *Ann. Intern. Med.*, **82**, 684 (1975).

Synthesis and Evaluation of the Antitumor Properties of Esters of 2-Furoic Acid and 2-Furylacrylic Acid

ZIAODIN SAJADI *, MOHAMMAD M. ABRISHAMI *, PARICHER-MOHSENI *, JAMES M. CHAPMAN, JR.‡, and IRIS H. HALL ‡x

Received June 24, 1982, from the *Division of Medicinal Chemistry, School of Pharmacy, Ferdowsi University, Mashhad, Iran and the ‡Division of Medicinal Chemistry, School of Pharmacy, University of North Carolina, Chapel Hill, NC 27514. Accepted for publication December 7, 1982.

Abstract □ A series of activated and nonactivated esters of 2-furoic and 2-furylacrylic acids were synthesized and examined for antineoplastic activity in the Ehrlich ascites carcinoma screen at 20 mg/kg/d. 2-Furoic acid and 2-furylacrylic acid demonstrated potent activity, as did the methyl and cyanomethyl esters of each series. The vinyl ester of 2-furoic acid possessed antineoplastic activity. However, the ethyl and D,L-tetrahydropyranyl esters of each series were inactive in the tumor screen.

Keyphrases □ 2-Furoic acid—ester derivatives, synthesis, antitumor potential, Ehrlich ascites screen □ 2-Furylacrylic acid—ester derivatives, synthesis, antitumor potential, Ehrlich ascites screen

Activated esters such as vinyl, cyanomethyl, and dihaloethyl esters of amino acids have been shown to have antitumor properties in the Ehrlich ascites screen (1–4). Compounds containing furan moieties have similarly displayed antineoplastic activity (5). It was suggested by Cutting *et al.* (5) that the furan ring may compete for the pentoses in nucleotide synthesis. Such observations have stimulated interest in the synthesis and antineoplastic evaluation of several activated esters of 2-furoic and 2-furylacrylic acids. Reported at this time is the synthesis of vinyl, cyanomethyl, and pyranyl activated esters which were compared with similar nonactivated ethyl and methyl esters of 2-furoic acid and 2-furylacrylic acid for antineoplastic activity.

EXPERIMENTAL

Melting points were determined on an electro-thermal melting point apparatus and are uncorrected. IR spectra were determined in chloroform[1]. NMR spectra were determined in deuterochloroform[2], and chemical shifts are reported in ppm relative to internal tetramethylsilane. Silica gel G[3] was used for TLC, and compounds were visualized by charring with sulfuric acid. Silica gel (AR) CC, 200–325 mesh, was used for column chromatography[4]. 2-Furoic acid[4] (I), 3-furoic acid[4] (XIII), 2-furylacrylic acid[5] (VII), and 3,4-furandicarboxylic acid[4] (XIV) were purchased. Methyl 2-furoate (II), ethyl 2-furoate (III), methyl 2-furylacrylate (VIII), and ethyl 2-furylacrylate (IX) were prepared according to procedures described previously (6–11). Only NMR and IR data pertinent to structure determination are noted below for newly synthesized compounds.

Activated Esters of 2-Furoic Acids—*Vinyl 2-Furoate (IV)*—This compound was prepared by a modification of a procedure described by Weygand and Beryermann (12). To a solution of 1.20 g (10 mmol) of 2-furoic acid in 25 mL of vinyl acetate was added 20 mg of $PdCl_2$-NaCl. The solution was refluxed (70–75°C) for 5 h. After cooling and treating with 30 mg of activated charcoal, the resulting mixture was filtered and solvent was removed *in vacuo*. The residue was dissolved in 20 mg of vinyl acetate, 20 mg of $PdCl_2$-NaCl was added, and the entire procedure was repeated. Chromatography (chloroform) of the crude mixture gave 500 mg (40%) of a colorless oil. IR: 1755 (C=O str), 1648 (C=C str), and 900 cm^{-1} (C=C—H bend); ^{1}H-NMR: δ 4.70 (m, 2, CH_2).

Anal.—Calc. for $C_7H_6O_3$: C, 60.86; H, 4.34. Found: C, 60.90; H, 4.36.

Cyanomethyl 2-Furoate (V)—This material was prepared by treatment of the acid with chloroacetonitrile and triethylamine in ethyl acetate according to a procedure described by Morozova and Zhenodarova (13). The product was crystallized from ether–ligroine, to give ester V (35%), mp 30–31°C. IR: 1755 cm^{-1} (C=O str); ^{1}H-NMR: δ 4.4 (s, 2, OCH_2CN).

Anal.—Calc. for $C_7H_5NO_3$: C, 55.63; H, 3.31; N, 9.27. Found: C, 55.69; H, 3.34; N, 9.30.

Tetrahydropyranyl 2-Furoate (VI)—To a solution of 1.12 g (10 mmol) of 2-furoic acid in 30 mL of dry ether were added 50 mg of *p*-toluenesulfonic acid and 1.4 mL (20 mmol) 3,4-dihydropyran. The mixture was stirred at room temperature for ~4 h, filtered, and the filtrate was washed with 5% $NaHCO_3$ (3 × 5 mL) and water (3 × 5 mL) and dried over anhydrous magnesium sulfate. The solvent was removed at reduced pressure, to give 400 mg (20%) of an oily product. Chromatography ($CHCl_3$–EtOH, 95:5) on silica gel gave 250 mg (13%) of a colorless oil. IR: 1755 cm^{-1} (C=O str); ^{1}H-NMR: δ 1.4–2.0 (m, 6, C-3,-4,-5 tetrahydropyranyl protons).

Anal.—Calc. for $C_{10}H_{12}O_4$: C, 61.22; H, 6.12. Found: C, 61.22; H, 6.12.

Activated Esters of 2-Furylacrylic Acid—The vinyl (X), cyanomethyl (XI), and tetrahydropyranyl esters (XII) were synthesized according to the same procedures described for the analogous 2-furoic acid derivatives.

Vinyl 2-Furylacrylate (X)—Yield of 30%; chromatography ($CHCl_3$) on silica gel gave an oil.

Anal.—Calc. for $C_9H_8O_3$: C, 65.85; H, 4.87. Found: C, 65.90; H, 4.91.

Cyanomethyl 2-Furylacrylate (XI)—mp 46°C; 40% yield (ether–ligroine). IR: 2080 (C≡N str) and 1740 cm^{-1} (C=O str).

Anal.—Calc. for $C_9H_7NO_3$: C, 61.02; H, 3.98; N, 7.91. Found: C, 60.86; H, 4.06; N, 7.85.

Tetrahydropyranyl 2-Furylacrylate (XII)—Yield of ~10%; column chromatography, Florisil (ether), gave a colorless oil.

Anal.—Calc. for $C_{12}H_{14}O_4$: C, 64.86; H, 6.30. Found: C, 65.98; H, 6.35.

Repeated attempts at obtaining correct elemental analyses for chromatographically pure XII were unsuccessful. The structure was confirmed by ^{1}H- and ^{13}C-NMR spectra. ^{13}C-NMR: δ 20, 25, 28, 65 (C_3, C_4, C_5 and C_6 of tetrahydropyranyl), 95 (C_2), 165 (ester carbonyl), 125, 135 (C=C), 140, 118, 112, and 145 (C_2, C_3, C_4, C_5 of furyl). ^{1}H-NMR: 5.72 (s, 1, O_2CH), 3.69 (m, 2, C-6 tetrahydropyranyl protons), and 1.15–1.8 ppm (m, 6, C-3,-4,-5 tetrahydropyranyl protons).

Pharmacological Studies—The compounds were tested for antitumor activity in the Ehrlich ascites carcinoma screen in CF_1 male mice using a procedure described by Piantadosi *et al.* (14), with certain modifications. Eight days after tumor transplantation, donor mice were sacrificed, and ascites fluid was collected and diluted with isotonic saline. An aliquot was placed in a hemocytometer chamber, and the number of cells per milliliter was calculated. Then, 10^6 cells were injected intraperitoneally into each test animal using an 18-gauge needle. 6-Mercaptopurine was used as internal standard in the test. The test drugs were homogenized in 0.05% polysorbate 80 and administered intraperitoneally at 20 mg/kg/d for 9 d. After 10 d, the inoculated mice were sacrificed, and the ascitic fluid was collected. The volume (mL) of the ascitic fluid was measured, and the total packed ascites cell volume for each group was measured utilizing nonheparinized capillary tubes centrifuged at 3000

[1] With a PYE-Unicam SP/100 grating spectrophotometer.
[2] With a Varian T 60A spectrometer or JEOL FX-60 spectrometer.
[3] Merck.
[4] Elemental analyses were performed by Dorni U. Kolbe, West Germany.
[5] Aldrich Chemical Co.

0022-3549/84/0200-0266$01.00/0
© 1984, American Pharmaceutical Association

Table I—Antineoplastic Activity of 2-Furoic and 2-Furanacrylic Acids and Ester Derivatives in the Ehrlich Ascites Screen in CF_1 Male Mice at 20 mg/kg/d

Compound	R	mM/kg	Survival on Day 10	Ascrit (Packed Cell Volume), mL	Volume Ascites Fluid, mL	Inhibition, %
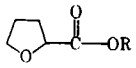						
I	—H	0.179	6/6	41.6	0.77	89.7
II	$-CH_3$	0.158	2/6	2.0	0.25	99.7
III	$-CH_2CH_3$	0.144	6/6	39.7	3.70	52.9
IV	$CH{=}CH_2$	0.145	7/8	25.1	0.21	98.3
V	CH_2CN	0.132	7/8	44.0	0.50	85.7
VI		0.075	6/6	505.6	3.73	39.5
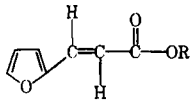						
VII	—H	0.145	6/6	28.4	0.08	99.3
VIII	$-CH_3$	0.132	6/6	28.3	0.66	94.0
IX	$-CH_2CH_3$	0.121	6/6	43.5	3.05	57.5
X	$CH{=}CH_2$	0.122	6/6	39.0	2.03	74.6
XI	CH_2CN	0.113	4/6	36.3	0.58	93.2
XII		0.090	4/6	37.5	3.58	56.1
XIII	—H	0.179	5/6	40.5	2.81	72.7
XIV	—H	0.128	5/6	38.9	2.10	72.7
6-Mercaptopurine	—	—	6/6	0.70	0.30	99.9
0.05% Polysorbate 80	—	—	6/6	32.4	9.62	—

rpm for 3–5 min. The control (C) value for the volume of tumor was 9.62 ± 0.48 (*SD*) mL; the ascrit (total packed cell volume) was 32.4 ± 1.69 mL at day 10. Percent inhibition of tumor growth was calculated by the following formula for the treated animals (T):

$$\% \text{ inhibition} = 100 - \frac{\text{volume}_T \times \text{ascrit}_T}{\text{volume}_C \times \text{ascrit}_C} \times 100$$

Any compound that exhibited 80% inhibition of tumor growth was considered significantly active (Table I).

RESULTS AND DISCUSSION

The 2-furoic and 2-furylacrylic acid derivatives that demonstrated potent activity in the Ehrlich ascites screen at 20 mg/kg/d were I, II, IV, V, VII, VIII, XI, and the standard (6-mercaptopurine). In the 2-furoic acid series, the methyl ester (II) derivative demonstrated the most potent activity demonstrating 99.7% inhibition. The activated vinyl (IV) and cyanomethyl esters (V) were also active, *i.e.*, 98.3% and 85.7% inhibition, respectively. The methyl ester (VIII) of the furylacrylic acid series, as well as the cyanomethyl ester (XI), demonstrated potent activity, *i.e.*, 94.0% and 93.2% inhibition of Ehrlich ascites carcinoma growth, respectively. The ethyl and tetrahydropyranyl esters of both series of acids proved to be inactive as antineoplastic agents in the Ehrlich ascites screen. Movement of the acid side chain on the furan ring from the 2-position (XIII and XIV) resulted in compounds which were not active in the Ehrlich ascites screen. These results suggest that activated esters of 2-furoic acid and 2-furylacrylic acid were not as active as the nonactivated methyl ester, but were more active than the ethyl ester derivatives.

REFERENCES

(1) L. J. Loeffler, Z. Sajadi, and I. H. Hall, *J. Med. Chem.*, **20**, 1578 (1977).

(2) L. J. Loeffler, Z. Sajadi, and I. H. Hall, *J. Med. Chem.*, **20**, 1584 (1977).

(3) I. H. Hall, Z. Sajadi, and L. J. Loeffler, *J. Pharm. Sci.*, **67**, 1726 (1978).

(4) W. Troll, A. Klassen, and A. Gunoff, *Science*, **169**, 1211 (1970).

(5) W. C. Cutting, R. H. Driesbach, and F. Matsushima, *Stanford Med. Bull.*, **10**, 304 (1952).

(6) J. P. Greenstein and M. Winitz, "Chemistry of the Amino Acids," Wiley, New York, N.Y., 1961, p. 1267.

(7) C. C. Vernon, E. F. Struss, and H. H. Ruwe, *Trans. Kentucky Acad. Sci.*, **9**, 23 (1941).

(8) A. A. Morton and G. H. Patterson, *J. Am. Chem. Soc.*, **65**, 1346 (1943).

(9) J. P. Trickey, *Ind. Eng. Chem.*, **19**, 643 (1927).

(10) F. F. Blicke, *Chem. Ber.*, **47**, 1355 (1914).

(11) T. Posner, *J. Prakt. Chem.*, **82**, 440 (1910).

(12) A. Weygand and M. W. Beryermann, *Recl. Trav. Chim. Pays-Bas*, **84**, 214 (1965).

(13) E. A. Morozova and S. M. Zhenodarova, *Zh. Obsch. Khim.*, **28**, 2661 (1958).

(14) C. Piantadosi, C. S. Kim, and J. L. Irvin, *J. Pharm. Sci.*, **58**, 821 (1969).

ACKNOWLEDGMENTS

Research sponsored by a grant from the Research Committee of Ferdowsi University to Ziaodin Sajadi.

Gas Chromatographic Determination of a Diuretic–Antihypertensive Agent, (±)-[[6,7-Dichloro-2-(4-fluorophenyl)-2-methyl-1-oxo-5-indanyl]oxy]acetic Acid, in Biological Fluids

LINDA L. WEIDNER and ANTHONY G. ZACCHEI ˣ

Received July 28, 1982, from the *Merck Sharp & Dohme Research Laboratories, Merck Institute for Therapeutic Research, West Point, PA 19486.* Accepted for publication December 17, 1982.

Abstract □ A method for the measurement of a potential diuretic–antihypertensive agent, (±)-[[6,7-dichloro-2-(4-fluorophenyl)-2-methyl-1-oxo-5-indanyl]oxy]acetic acid, in biological fluids is described. The procedure involves the addition of a related internal standard to the specimens followed by extraction of the acids into toluene at pH 1. The indanyloxyacetic acids, following back-extraction into base and reextraction into methylene chloride at an acidic pH, are converted to methyl esters by reaction with ethereal diazomethane for subsequent gas chromatographic analysis. The sensitivity of the method is such that 5 ng of drug in 1 mL of biological specimen can be quantitated using a ^{63}Ni electron-capture detector. The recovery from plasma in the 5–2000-ng/mL range (n = 53) was 97.0 ± 16.3%. Differences were noted in the disposition of the enantiomers of this agent in dogs following a pharmacologically active dose.

Keyphrases □ Diuretics—gas chromatographic determination of (±)-[[6,7 - dichloro-2-(4-fluorophenyl)-2-methyl-1-oxo-5-indanyl]oxy]-acetic acid in biological fluids □ Antihypertensives—gas chromatographic determination of (±)-[6,7-dichloro-2-(4-fluorophenyl)-2-methyl-1-oxo-5-indanyl]oxy]acetic acid in biological fluids □ (±)-[[6,7-Dichloro-2-(4-fluorophenyl)-2-methyl-1-oxo-5-indanyl]oxy]acetic acid—diuretic–antihypertensive, gas chromatographic determination, biological fluids

The search for potent diuretic–antihypertensive agents has led to the synthesis of a class of compounds known as the indanyloxyacetic acids (1). (±)-[[6,7-Dichloro-2-(4-fluorophenyl)-2-methyl-1-oxo-5-indanyl]oxy]acetic acid (I) and its enantiomers are examples of such compounds (2). Since disposition and metabolic differences have been reported (3–8) for the enantiomers of indacrinone (the defluoro analogue), studies were initiated on I to gain insight into the effects of blocking the primary site of metabolic transformation (9, 10).

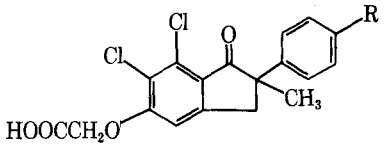

I R = F
II R = Cl

This report describes a sensitive electron-capture gas chromatographic (GC) method for the determination of I and its enantiomers in biological fluids. The method, which is similar to that reported for indacrinone (11, 12), does not differentiate between the enantiomers of I, but provides the methodology to study the disposition of these enantiomers separately following pharmacological doses.

EXPERIMENTAL

Chemicals and Instrumentation—The chemicals used were I and its enantiomers, the internal standard [(±)-[[6,7-dichloro-2-(4-chlorophenyl)-2-methyl-1-oxo-5-indanyl]oxy]acetic acid (II)], toluene[1], dichloromethane[2], and freshly prepared 0.5 M diazomethane (generated from N-nitroso-N-methylurea[3]). A gas chromatograph equipped with a data processor[4], a ^{63}Ni electron-capture detector, and a 122-cm × 4-mm (i.d.) glass column packed with 3% OV-17 on 80–100 mesh Gas Chrom Q was used in these studies. The column temperature was set at 280°C for the analysis of I and its enantiomers. The injection and detector temperatures were maintained at 300°C. Argon–methane (95:5) was used as the carrier gas at a flow rate of 34 mL/min.

Measurement of I in Biological Samples—The concentration of I or its enantiomers in biological samples was determined as follows. To 1.0 mL of plasma (0.1–0.5 mL of urine) in a 50-mL glass-stoppered centrifuge tube were added 1.0 μg of II (the internal standard), 1 mL of 2 M HCl, and 15 mL of toluene. The tube was shaken for 10 min, centrifuged, and the organic phase was transferred to a similar tube containing 2 mL of 0.1 M NaOH. After the tube was shaken for 10 min and centrifuged, the organic phase was removed by aspiration. The pH of the aqueous phase was adjusted to 1 by the addition of 0.25 mL of 2 M HCl, and the free acids were extracted into 5 mL of dichloromethane (agitated[5] for ~30 s). After centrifugation, the dichloromethane phase was transferred to a 13-mL centrifuge tube and treated with 100 μL of ethereal diazomethane at room temperature. The contents of the tube were evaporated to dryness[6]. The residue was dissolved in 1.5 mL of toluene, and a 4-μL aliquot was injected[7] into the chromatograph. The methyl esters of I and II exhibited retention times of 1.5 and 2.6 min, respectively, under the conditions of the analysis.

Standard recovery samples, which were run concurrently with the biological specimens, were prepared by spiking appropriate aliquots of control plasma or urine with 5–2000 ng of I and a constant amount (1000 ng) of internal standard. The samples were prepared for GC as described above. The standard curves were constructed by plotting area ratios of

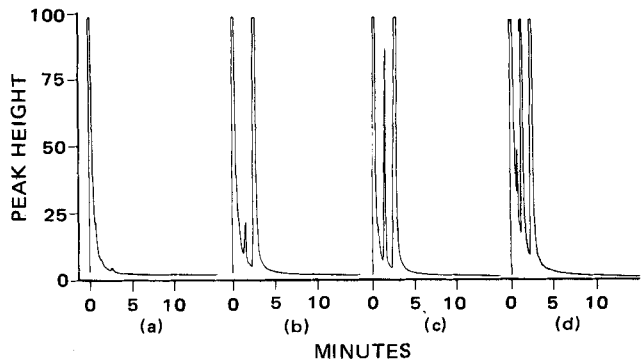

Figure 1—*Chromatograms of: (a) control dog plasma; (b) control dog plasma with 1000 ng of II added; (c) control dog plasma with 100 ng of I and 1000 ng of II added; and (d) dog plasma obtained 2 h after drug administration. All samples were carried through the electron-capture detection method. Four microliters was injected out of a 1.5-mL final volume.*

[1] Reagent Grade, Fisher Scientific.
[2] Nanograde, Mallinckrodt.
[3] ICN Pharmaceuticals.
[4] Hewlett-Packard Model 5840A.
[5] Vortex-Genie Model K-550-G.
[6] Buchler Vortex-Evaporator.
[7] Hewlett-Packard Automatic Sampler Model 7671A.

0022-3549/84/0200-0268$01.00/0
© *1984, American Pharmaceutical Association*

Table I—Recovery of I [a] from Plasma and Urine

Amount Added, ng	Amount Recovered[b], ng	
	Plasma	Urine
2000	1990 ± 104 (99.6 ± 5.3%)	1994 ± 44 (99.7 ± 2.2%)
1500	1477 ± 81 (98.5 ± 5.5%)	1500 ± 25[c] (100.0 ± 1.7%)
1000	997 ± 54 (99.7 ± 5.5%)	1004 ± 16 (100.4 ± 1.6%)
500	496 ± 34[c] (99.2 ± 7.0%)	502 ± 10 (100.5 ± 2.1%)
250	257 ± 25 (103.1 ± 10.1%)	
125	129 ± 16 (103.4 ± 13.5%)	
100	96.5 ± 11.4[c] (96.5 ± 11.4%)	116 ± 4 (116 ± 4.0%)
50	49.4 ± 7.2 (98.8 ± 14.5%)	61.8 ± 2.2 (123.6 ± 4.3%)
25	23.4 ± 3.2 (93.8 ± 12.9%)	
10	8.2 ± 2.7 (88.2 ± 27.3%)	
5	4.6 ± 1.8 (92.8 ± 37.3%)	5.8 ± 1.1 (116.0 ± 21.9%)
5–2000	97.0 ± 16.3% (n = 53)	108.3 ± 12.5% (n = 24)

[a] Represents racemic I and/or the enantiomers. [b] Means ± SD, n = 5 percent recovery is in parentheses. [c] n = 4.

I/II *versus* the amount of I added. The area ratio (I/II) of the unknown sample was then used to determine the amount of I present.

***In Vivo* Studies**—Three male beagle dogs, 8.8–10.0 kg, received either I or its enantiomers at a single oral dose of 2.5 mg/kg; 1 week later the same animals received the respective drugs intravenously in a crossover design. The animals were fasted overnight prior to drug administration. Blood was drawn into heparinized syringes, and the plasma separated by centrifugation prior to analysis. Urine specimens were frozen immediately on collection (dry ice) and kept frozen until analyzed. Animals were individually housed in metabolism cages. The specimens were analyzed for I or its enantiomers as described above.

RESULTS AND DISCUSSION

During the development of I and its enantiomers for potential use as a diuretic–antihypertensive agent, a method was needed to determine blood and urinary levels of the compound for absorption, excretion, and metabolism studies. Electron-capture GC of the methyl esters provided the sensitivity required for such studies following a pharmacologically active dose. Figure 1 presents chromatograms of control dog plasma, internal standard (II) added to control dog plasma, I and II added to control dog plasma, and dog plasma obtained 2 h after drug administration. Similar tracings were obtained during urinalysis. The retention times of the methyl esters of I and II were 1.5 and 2.6 min, respectively.

The small peak seen in Fig. 1b, which is present to the extent of ~2% of the internal standard peak, appears in all samples carried through the analytical procedure. This trace contaminant, which represented <2 ng/sample of biological specimen, limited the sensitivity of analysis for I to 5 ng/mL. The appropriate area ratio for this impurity was subtracted from all data values prior to linear regression analysis. A linear relationship was observed for all plasma samples containing amounts to 500 ng/sample: $y = 0.0028x + 0.003$ ($r = 0.973$). Above 500 ng, the standard curve exhibited a slight curvature. Regression analysis on this portion of the standard curve (500–2000 ng) gave $y = 0.0023x + 0.32$ ($r = 0.999$), which was used to calculate the results of the biological samples in this range. This equation was used whenever the area ratio was greater than that obtained with the 500-ng standard. Similar data were obtained on analysis of urine samples.

A summary of the results obtained following analysis of various amounts of I or its enantiomers in control dog plasma and urine is presented in Table I. In the 5–2000-ng range, the mean recovery of I from control plasma was 97.0 ± 16.3% (n = 53); the recovery from urine was 108.3 ± 12.5% (n = 34). The electron-capture GC method is extremely sensitive and exhibits a high degree of accuracy and precision over the entire range.

The values of I or its enantiomers in dog plasma and urine following single oral or intravenous administration of I as the racemate (±) or the (+)- or (−)-enantiomer at a dose of 2.5 mg/kg are presented in Tables II and III. Regardless of which enantiomer was given, peak plasma levels occurred within 0.5 h of dosing, suggesting rapid absorption. In addition, direct comparison of the respective oral *versus* intravenous areas under the curve (AUC) established that absorption was complete. Greater than 91% of the oral dose of either enantiomer was bioavailable. Although absorption was quantitative for each enantiomer, the absolute AUC values differed markedly between the enantiomers. Pharmacokinetic analyses using standard techniques previously described (3), established the fact that the (+)-enantiomer is cleared from the system twice as fast as the (−)-enantiomer (2.1 *versus* 1.1 mL/min·kg). This finding is consistent with the twofold difference in AUC values. The biexponential plasma profiles, which were observed for each enantiomer, exhibited

Table II—Plasma Levels of I [a] Following Administration of I to Dogs at a Dose of 2.5 mg/kg

	I, ng/mL					
	Oral			Intravenous		
Hours	(±) Dog 1	(+) Dog 2	(−) Dog 3	(±) Dog 1	(+) Dog 2	(−) Dog 3
0.08	N.S.[b]	N.S.	N.S.	13,400	13,500	13,180
0.25	3,995	4,425	4,050	7,795	7,200	9,710
0.5	3,990	4,520	5,710	5,920	4,925	7,275
1	2,960	3,500	5,400	4,325	3,620	5,100
1.5	3,190	2,110	4,950	N.S.	N.S.	N.S.
2	4,410	1,475	4,250	2,275	1,520	4,350
4	2,095	1,100	3,100	1,375	1,150	2,225
6	1,850	800	2,090	1,370	720	1,705
24	360	16	399	143	—	24
48	26	—[c]	—	21	—	—
72	—	—	—	—	—	—
AUC (0–24), ng·hr/mL	36,526	17,794	44,332	29,925	19,577	38,480

[a] Represents I and/or the enantiomers. [b] N.S. = no sample. [c] Less than detection limits.

Table III—Urinary Excretion of I [a] Following Administration of I to Dogs at a Dose of 2.5 mg/kg

	I, % of dose excreted					
	Oral			Intravenous		
Hours	(±) Dog 1	(+) Dog 2	(−) Dog 3	(±) Dog 1	(+) Dog 2	(−) Dog 3
0–24	17.97	9.73	13.00	16.46	14.30	11.62
24–48	2.69	0.82	3.60	1.99	3.36	1.52
48–72	0.51	0.35	0.11	0.33	0.50	0.10
Total	21.17	10.90	16.71	18.78	18.16	13.24

[a] Represents I and/or the entantiomers.

similar terminal half-lives, $t_{1/2,\beta} = 0.693/\lambda$ (2.5 *versus* 3.2 h). These minor differences were also noted in the volumes of distribution of the central compartment [139 *versus* 160 mL/kg for the (+)- and (−)-enantiomer, respectively]. Although these pharmacokinetic parameter values illustrate differences between the enantiomers of I, the data do not establish a definitive pharmacokinetic profile in view of the limited sample number.

REFERENCES

(1) E. J. Cragoe, Jr., E. M. Schultz, J. D. Schneeberg, G. E. Stokker, O. W. Woltersdorf, Jr., G. M. Fanelli, Jr., and L. S. Watson, *J. Med. Chem.*, **18**, 225 (1975).

(2) S. J. deSolms, O. W. Woltersdorf, Jr., E. J. Cragoe, Jr., L. S. Watson, and G. M. Fanelli, Jr., *J. Med. Chem.*, **21**, 437 (1978).

(3) A. G. Zacchei, M. R. Dobrinska, T. I. Wishousky, K. C. Kwan, and S. D. White, *Drug Metab. Dispos.*, **10**, 20 (1982).

(4) J. D. Irvin, P. H. Vlasses, P. B. Huber, J. A. Feinberg, R. K. Ferguson, J. J. Schrogie, and R. O. Davies, *Clin. Pharmacol. Ther.*, **27**, 260 (1980).

(5) A. G. Zacchei, M. R. Dobrinska, J. D. Irvin, K. C. Kwan, and P. H. Vlasses, *Abstr. World Conf. Clin. Pharmacol. Ther.*, No. 0793 (1980).

(6) P. H. Vlasses, J. D. Irvin, P. B. Huber, R. B. Lee, R. K. Ferguson, J. J. Schrogie, A. G. Zacchei, R. O. Davies, and W. B. Abrams, *Clin. Pharmacol. Ther.*, **29**, 798 (1981).

(7) J. A. Tobert, G. Hitzenberger, I. M. James, and J. S. Pryor, *Abstr. World Conf. Clin. Pharmacol. Ther.*, No. 0436 (1980).

(8) M. R. Dobrinska, A. G. Zacchei, J. J. Schrogie, R. K. Ferguson, and K. C. Kwan, *Abstr. World Conf. Clin. Pharmacol. Ther.*, No. 0762 (1980).

(9) A. G. Zacchei, T. I. Wishousky, B. H. Arison, and G. M. Fanelli, Jr., *Drug Metab. Dispos.*, **4**, 479 (1976).

(10) A. G. Zacchei and T. I. Wishousky, *Drug Metab. Dispos.* **4**, 490 (1976).

(11) A. G. Zacchei and T. I. Wishousky, *J. Pharm. Sci.*, **65**, 1770 (1976).

(12) A. G. Zacchei and T. I. Wishousky, *J. Pharm. Sci.*, **67**, 162 (1978).

ACKNOWLEDGMENTS

The authors thank J. D. Schneeberg and O. Woltersdorf for supplies of I and its enantiomers and S. White for the animal-related work.

Cytotoxic Effects of *Eleutherococcus senticosus* Aqueous Extracts in Combination with N^6-(Δ^2-Isopentenyl)-adenosine and 1-β-D-Arabinofuranosylcytosine Against L1210 Leukemia Cells

BRUCE HACKER and PHILIP J. MEDON ˣ

Received July 6, 1982, from the *Department of Pharmacology-Toxicology, Northeast Lousiana University, Monroe, LA 71209.* Accepted for publication November 22, 1982.

Abstract □ The use of the aqueous extracts of *Eleutherococcus senticosus* in combination with either cytarabine or N^6-(Δ^2-isopentenyl)-adenosine gave additive antiproliferative effects against L1210 murine leukemia. The ED_{50} for *E. senticosus* root extracts against L1210 cells was ~75 μg/mL. *E. senticosus* appears to be potentially useful for reducing the concentration of conventional antimetabolites used for their antiproliferative effects on tumor cells.

Keyphrases □ Cytarabine—*Eleutherococcus senticosus*, N^6-(Δ^2-isopentenyl) adenosine, L1210 leukemia □ *Eleutherococcus senticosus*—cytarabine, N^6-(Δ^2-isopentenyl) adenosine, L1210 leukemia

The Far Eastern plant *Eleutherococcus senticosus* (Rup. + Maxim.) Maxim. (Araliaceae or Ginseng family), formerly known as *Hedera senticosa* and *Acanthopanax senticosus*, is commonly known as "Siberian Ginseng," "Touch-me-not," "Devil's shrub," "Eleutherococc," and "Wild Pepper" (1). This plant, which has recently become an item for export from the People's Republic of China, is most abundant in the Khabarovsk and Primorsk Districts of the Soviet Union, with a distribution extending to the middle Amur region in the North, Sakhalin Island and Japan in the East, and South Korea and the Chinese Provinces of Shansi and Hopei in the South (1, 2). *E. senticosus* has been used extensively in the Soviet Union as an "adaptogen" (3), defined by these authors (4) as a nontoxic substance with so-called "normalizing" actions on a wide range of physical, chemical, and biochemical parameters. The effects of *E. senticosus*, as well as those of other natural products for alleviating numerous pathological changes when administered on a chronic basis, have been the subject of several recent reviews (2, 5–7).

There have been numerous reports suggesting that crude, unfractionated *E. senticosus per se* has cytostatic activity as well as metastasis-preventing effects against the following systems: Walker 256 and Ehrlich ascites tumor cells (8), and SSK sarcoma (9), spontaneous tumors in AKR mice (10), indole oil-induced leukemia (11), mammary tumors in C3H mice (12), as well as urethane-induced pulmonary tumors in CC57 mice (13). Moreover, the literature also suggested that *E. senticosus* extracts when administered in combination with thiotepa (14, 15), cyclophosphamide (14, 16), hydrocortisone (17), 6-mercaptopurine (18), or rubomycin-C (19) had a potentiating or enhancing effect on the parent agent. These data suggested the importance in evaluating the possible effects of *E. senticosus per se*, and its ability to enhance the antiproliferative property of two established cytotoxic agents: cytarabine hydrochloride (I) and N^6-(Δ^2-isopentenyl)-adenosine hemihydrate (II).

BACKGROUND

Cytarabine (I), an important pyrimidine antimetabolite used in combination chemotherapy for the treatment of acute myelocytic leukemia (20–22), has the potential for the treatment of chronic myelocytic leukemia as well, when given with the deaminase-inhibitor, tetrahydrouri-

0022-3549/84/0200-0270$01.00/0

© 1984, American Pharmaceutical Association

similar terminal half-lives, $t_{1/2,\beta} = 0.693/\lambda$ (2.5 *versus* 3.2 h). These minor differences were also noted in the volumes of distribution of the central compartment [139 *versus* 160 mL/kg for the (+)- and (−)-enantiomer, respectively]. Although these pharmacokinetic parameter values illustrate differences between the enantiomers of I, the data do not establish a definitive pharmacokinetic profile in view of the limited sample number.

REFERENCES

(1) E. J. Cragoe, Jr., E. M. Schultz, J. D. Schneeberg, G. E. Stokker, O. W. Woltersdorf, Jr., G. M. Fanelli, Jr., and L. S. Watson, *J. Med. Chem.*, **18**, 225 (1975).

(2) S. J. deSolms, O. W. Woltersdorf, Jr., E. J. Cragoe, Jr., L. S. Watson, and G. M. Fanelli, Jr., *J. Med. Chem.*, **21**, 437 (1978).

(3) A. G. Zacchei, M. R. Dobrinska, T. I. Wishousky, K. C. Kwan, and S. D. White, *Drug Metab. Dispos.*, **10**, 20 (1982).

(4) J. D. Irvin, P. H. Vlasses, P. B. Huber, J. A. Feinberg, R. K. Ferguson, J. J. Schrogie, and R. O. Davies, *Clin. Pharmacol. Ther.*, **27**, 260 (1980).

(5) A. G. Zacchei, M. R. Dobrinska, J. D. Irvin, K. C. Kwan, and P. H. Vlasses, *Abstr. World Conf. Clin. Pharmacol. Ther.*, No. 0793 (1980).

(6) P. H. Vlasses, J. D. Irvin, P. B. Huber, R. B. Lee, R. K. Ferguson, J. J. Schrogie, A. G. Zacchei, R. O. Davies, and W. B. Abrams, *Clin. Pharmacol. Ther.*, **29**, 798 (1981).

(7) J. A. Tobert, G. Hitzenberger, I. M. James, and J. S. Pryor, *Abstr. World Conf. Clin. Pharmacol. Ther.*, No. 0436 (1980).

(8) M. R. Dobrinska, A. G. Zacchei, J. J. Schrogie, R. K. Ferguson, and K. C. Kwan, *Abstr. World Conf. Clin. Pharmacol. Ther.*, No. 0762 (1980).

(9) A. G. Zacchei, T. I. Wishousky, B. H. Arison, and G. M. Fanelli, Jr., *Drug Metab. Dispos.*, **4**, 479 (1976).

(10) A. G. Zacchei and T. I. Wishousky, *Drug Metab. Dispos.* **4**, 490 (1976).

(11) A. G. Zacchei and T. I. Wishousky, *J. Pharm. Sci.*, **65**, 1770 (1976).

(12) A. G. Zacchei and T. I. Wishousky, *J. Pharm. Sci.*, **67**, 162 (1978).

ACKNOWLEDGMENTS

The authors thank J. D. Schneeberg and O. Woltersdorf for supplies of I and its enantiomers and S. White for the animal-related work.

Cytotoxic Effects of *Eleutherococcus senticosus* Aqueous Extracts in Combination with N^6-(Δ^2-Isopentenyl)-adenosine and 1-β-D-Arabinofuranosylcytosine Against L1210 Leukemia Cells

BRUCE HACKER and PHILIP J. MEDON ˣ

Received July 6, 1982, from the *Department of Pharmacology-Toxicology, Northeast Lousiana University, Monroe, LA 71209.* Accepted for publication November 22, 1982.

Abstract □ The use of the aqueous extracts of *Eleutherococcus senticosus* in combination with either cytarabine or N^6-(Δ^2-isopentenyl)-adenosine gave additive antiproliferative effects against L1210 murine leukemia. The ED_{50} for *E. senticosus* root extracts against L1210 cells was ~75 μg/mL. *E. senticosus* appears to be potentially useful for reducing the concentration of conventional antimetabolites used for their antiproliferative effects on tumor cells.

Keyphrases □ Cytarabine—*Eleutherococcus senticosus*, N^6-(Δ^2-isopentenyl) adenosine, L1210 leukemia □ *Eleutherococcus senticosus*—cytarabine, N^6-(Δ^2-isopentenyl) adenosine, L1210 leukemia

The Far Eastern plant *Eleutherococcus senticosus* (Rup. + Maxim.) Maxim. (Araliaceae or Ginseng family), formerly known as *Hedera senticosa* and *Acanthopanax senticosus*, is commonly known as "Siberian Ginseng," "Touch-me-not," "Devil's shrub," "Eleutherococc," and "Wild Pepper" (1). This plant, which has recently become an item for export from the People's Republic of China, is most abundant in the Khabarovsk and Primorsk Districts of the Soviet Union, with a distribution extending to the middle Amur region in the North, Sakhalin Island and Japan in the East, and South Korea and the Chinese Provinces of Shansi and Hopei in the South (1, 2). *E. senticosus* has been used extensively in the Soviet Union as an "adaptogen" (3), defined by these authors (4) as a nontoxic substance with so-called "normalizing" actions on a wide range of physical, chemical, and biochemical parameters. The effects of *E. senticosus*, as well as those of other natural products for alleviating numerous pathological changes when administered on a chronic basis, have been the subject of several recent reviews (2, 5–7).

There have been numerous reports suggesting that crude, unfractionated *E. senticosus per se* has cytostatic activity as well as metastasis-preventing effects against the following systems: Walker 256 and Ehrlich ascites tumor cells (8), and SSK sarcoma (9), spontaneous tumors in AKR mice (10), indole oil-induced leukemia (11), mammary tumors in C3H mice (12), as well as urethane-induced pulmonary tumors in CC57 mice (13). Moreover, the literature also suggested that *E. senticosus* extracts when administered in combination with thiotepa (14, 15), cyclophosphamide (14, 16), hydrocortisone (17), 6-mercaptopurine (18), or rubomycin-C (19) had a potentiating or enhancing effect on the parent agent. These data suggested the importance in evaluating the possible effects of *E. senticosus per se*, and its ability to enhance the antiproliferative property of two established cytotoxic agents: cytarabine hydrochloride (I) and N^6-(Δ^2-isopentenyl)-adenosine hemihydrate (II).

BACKGROUND

Cytarabine (I), an important pyrimidine antimetabolite used in combination chemotherapy for the treatment of acute myelocytic leukemia (20–22), has the potential for the treatment of chronic myelocytic leukemia as well, when given with the deaminase-inhibitor, tetrahydrouri-

0022-3549/84/0200-0270$01.00/0

© 1984, American Pharmaceutical Association

Table I—Antiproliferative Effects of *E. senticosus* Extracts Against L1210 Leukemia Cells [a]

Concentration[c], μg/mL	Time, h[b] 24 Cells/mL × 10^{-5}	24 Inhibition[d], %	48 Cells/mL × 10^{-5}	48 Inhibition, %	72 Cells/mL × 10^{-5}	72 Inhibition, %
0	18 ± 1.0	0	38 ± 2.0	0	44 ± 2.0	0
25	16 ± 1.0	11	31 ± 1.0	18	37 ± 1.0	16
50	9 ± 1.5	50	23 ± 2.0	39	24 ± 2.0	39
100	6 ± 2.0	67	16 ± 4.0	58	22 ± 2.5	50
200	7 ± 1.0	61	18 ± 2.0	53	23 ± 1.0	48
400	6 ± 2.0	67	16 ± 1.0	58	22 ± 1.5	49

[a] Each T-flask contained 5 mL of growth medium (RPMI-1640 plus 10% fetal calf serum) plus 1 × 10^5 L1210 leukemia cells. Incubations were conducted at 37°C in a 5% carbon dioxide environment as described previously (43). [b] After added to culture medium. Aliquots (0.20 mL) of each cell suspension were aseptically removed at the designated time for the determination of total and viable cell count (43). [c] Experiments conducted in triplicate were initiated (zero time) when lyophilized *E. senticosus* in RPMI 1640 without serum was added (0.1–0.2 mL) to each culture flask at the final designated concentrations. [d] Inhibition of L1210 proliferation was based on a comparison of treated cultures *versus* untreated cells in control cultures.

dine (23). In addition, cytarabine can be used in combination with other agents for the palliative treatment of large bowel and stomach cancer (22).

The primary biochemical site of action for cytarabine following its enzymatic phosphorylation to cytosine arabinoside-5′-triphosphate is thought to occur as an inhibitor of DNA synthesis during the S-phase of mitosis (24, 25). It inhibits formation of new DNA replicons as well as chain elongation in cultured human lymphoblasts (26), and can be lethally incorporated into low molecular weight species of RNA in L5178Y mouse leukemia cells (27).

Resistance to the antileukemic property of cytarabine has been attributed to diminished phosphokinase (28, 29) and/or enhanced deaminase activity (30–33).

N^6-(Δ^2-Isopentenyl)adenosine (II), a nucleoside previously shown to be both an inhibitor of growth and cytotoxic to human leukemic myeloblast and Sarcoma-180 cells (34), and also found by Hare and Hacker (35) and also in several isoaccepting species of tRNA, is capable of interfering with the transport of unmodified nucleosides through the cytoplasmic membranes of mouse embryo cells at the level of the transmembrane translocation function. This inhibition of membrane transport is believed to be responsible for the ability of nucleoside II to alter RNA synthesis in phytohemagglutinin-stimulated mouse spleen lymphocytes as well as to be immunosuppressive in its nature (36). In the latter context, it has been possible to prepare an antibody with serologic specificity for II (37). Previous studies by Hacker (38) have demonstrated that L1210 mouse leukemia cells do possess the necessary enzyme systems to phosphorylate I to the nucleotide level *in vitro*. It is not yet certain whether this biotransformation is a prerequisite for its antileukemic property.

Although II has antineoplastic and cytotoxic effects against leukemia cells when administered to humans, it is known to be susceptible to enzyme degradation. Results obtained by Chassy and Suhadolnik (39) indicated that adenosine deaminase catalyzes conversion of II to inosine. Hall and Mintsioulis (40) reported that elevated adenosine deaminase activity in human blood significantly facilitates the degradation of II. Chheda and Mittelman (41) have shown that the biological half-life of II after intravenous administration was 4 h. Compound II has also been prepared entrapped in a controlled-release polymeric delivery system using a silicone polymer monolithic disk to evaluate its relatively greater antineoplastic properties (42, 43). More recent studies by Hacker and Chang (44) using the adenosine deaminase inhibitor pentostatin, in combination with a silicone polymeric delivery system (45, 46) have led to a system for potentiating and prolonging the cytotoxic effects of II against L1210 leukemia cells in culture.

EXPERIMENTAL

The preparation of N^6-(Δ^2-isopentenyl)adenosine (i^6A) (II) was conducted as described previously (35, 36, 43). 1-β-D-Arabinofuranosylcytosine (cytarabine; Ara-C; NSC-63878) was supplied[1]. Aqueous extracts were prepared from *E. senticosus* roots by stirring for 10 min at 60°C followed by filtration, freezing, and lyophilization, as previously described (47).

L1210 lymphocytic leukemia cells were cultured to various densities as suspension cultures in fresh medium (RPMI-1640 plus L-glutamine and 10% fetal calf serum)[2] in plastic tissue culture flasks[3] at 37°C in a 5% carbon dioxide atmosphere (38, 42, 43). The technique for monitoring the progress of cell cultures by an inverted microscope–video system and the determination of total cell count and cell viability have been described earlier (42–44). The number of viable and/or total cell number monitored at various time periods before and during treatment was used as a measure of cytostatic or cytotoxic activity and is reported as percent inhibition in Tables I and II.

RESULTS AND DISCUSSION

This investigation sought to establish whether an extract of *E. senticosus* [with so-called "adaptogen" (3) and broad antitumor properties (4–19)] has cytotoxic effects on L1210 murine leukemia cells alone and in combination with two nucleoside antimetabolites (I and II) (20–44).

Inhibition of cellular proliferation by *E. senticosus* extract is seen to be concentration dependant between 25–100 μg/mL for a period up to 72 h following its addition to cultured L1210 leukemia cells (Table I). The magnitude of inhibition is greatest during the logarithmic or replicative phase of cellular growth, with diminished effects during the late-logarithmic and/or stationary stage. The ED_{50} is ~75 μg/mL. The maximal level of inhibition by *E. senticosus* extract alone is seen to occur at higher concentrations (200–400 μg/mL). The possibility exists that the crude extract of *E. senticosus* may contain multiple components which act to antagonize or negate the antiproliferative effects that have been observed against L1210 cells (Table I). This may account in part for the plateauing effect observed.

In those experiments where *E. senticosus* extracts were combined with I or II in varying concentrations, several salient features resulted (Table II). Nucleoside I (1 μg/mL) is equivalent in its antileukemic effect to nucleoside II (25 μg/mL) resulting in a 40% level of inhibition at those respective concentrations (Table II). A combination of *E. senticosus*

Table II—Antiproliferative Effects of *E. senticosus* Extract in Combination with N^6-(Δ^2-Isopentenyl)adenosine (I) and 1-β-D-Arabinofuranosylcytosine (II) Against L1210 Cells

Addition at Time Zero[a]	Cytotoxicity Level[b] (48 h) Cells/mL × 10^{-5}	Change in Total[c] Cell Number, %
None	38 ± 2.0	+53
E. senticosus (100 μg/mL)	16 ± 4.0	−58
E. senticosus (200 μg/mL)	18 ± 2.0	−53
I (1 μg/mL)	23 ± 1.0	−40
E. senticosus (200 μg/mL) + I (1 μg/mL)	10 ± 2.0	−74
II (10 μg/ml)	32 ± 1.0	−16
E. senticosus (100 μg/mL) + II (10 μg/mL)	8 ± 1.0	−78
II (25 μg/ml)	23 ± 1.0	−40
E. senticosus (200 μg/mL) + II (25 μg/mL)	0	−100

[a] Each T-flask contained 5 mL of growth medium (RPMI-1640 plus 10% fetal calf serum) plus 1 × 10^5 L1210 leukemia cells. The experiments were initiated (time zero) by the addition of each agent shown in RPMI-1650 without serum (0.05–0.10 mL) with prior sterile filtration before introduction into the cell culture. [b] Aliquots (0.20 mL) of each cell suspension were removed 72 h after the introduction of each agent for the determination of cell number, viability, and HPLC analyses for N^6-(Δ^2-isopentenyl)adenosine (I) and 1-β-D-arabinofuranosylcytosine (II). Values reflect 3–5 individual determinations using duplicate cultures. [c] Change in total cell number (%) for control cultures (no addition) represents increase in cell number (+ sign) compared with zero time. Inhibition in cell number (− sign) reflects cytotoxicity compared with value for 48-h control cultures.

[1] Natural. Products Br., Div. of Cancer Treatment, National Cancer Institute, Bethesda, Md.; or Cytosar-U or cytarabine, The Upjohn Co., Kalamazoo, Mich.

[2] Grand Island Biological Co., Grand Island, N.Y.

[3] Corning; no. 25100.

extract (100 μg/mL) and II (10 μg/mL) gave a similar level of inhibition (74–78%) compared with the arithmetic sum of their individual effects when used separately. Again, the most effective concentrations of *E. senticosus* extract appear to be in the 50–100 μg/mL range. Doubling the concentration of *E. senticosus* extract (200 μg/mL) in the presence of nucleoside II (25 μg/mL) resulted in an overall level of inhibition diminished by 20% when compared with the sum of their individual effects against L1210 cells. Again, this confirms our earlier suggestion that crude extracts of *E. senticosus* could contain components that interfere with its antiproliferative and "adaptogen" types of activity.

A combination of nucleoside I (1 μg/mL) plus *E. senticosus* extract (200 μg/mL), in contrast to the previous results, clearly resulted in a mutually additive antiproliferative effect on cultured L1210 cells. No synergistic effect was observed in the present investigation.

REFERENCES

(1) D. D. Soejarto and N. R. Farnsworth, *Bot. Mus. Leafl. Harv. Univ.*, **26**, 339 (1978).

(2) I. I. Brekhman, *U.S.S.R. Foreign Trade Publ.*, **28524**, 1 (1970).

(3) I. I. Brekhman, "First International Congress on Medicinal Plant Research," University of Munich, Munich, West Germany (1976).

(4) I. I. Brekhman and I. V. Dardymov, *Lloydia*, **32**, 46 (1969).

(5) G. F. Sandberg, *Planta Med.*, **24**, 392 (1973).

(6) G. P. Elyakov and V. S. Ovodov, *Khim. Prir. Soedin.*, **8**, 697 (1972).

(7) I. V. Dardymov, *Khim. Ahizm.*, **3**, 66 (1976).

(8) K. V. Yaremenko and K. G. Moskalik, *Vopr. Onkol.*, **17**, 66 (1971).

(9) L. Malyugina, *Acta Unio Int. Cancrum*, **20**, 199 (1964).

(10) A. N. Stukov, *Vopr. Onkol.*, **11**, 64 (1965).

(11) A. N. Stukov, *Vopr. Onkol.*, **13**, 94 (1967).

(12) L. L. Malyugina, *Vopr. Onkol.*, **12**, 53 (1966).

(13) F. K. Djioev, *Vopr. Onkol.*, **11**, 51 (1965).

(14) L. L. Malyugina, *Vopr. Onkol.*, **15**, 87 (1969).

(15) K. V. Yaremenko, *Lek. Sredtsva Dal'nago Vostoka*, **7**, 109 (1966).

(16) I. V. Monakhov, *Vopr. Onkol.*, **11**(12), 60 (1965).

(17) K. G. Moskalik, *Patol Fiziol. Eksp. Ter.*, **14**, 73 (1970).

(18) A. I. Mironova, *Vopr. Onkol.*, **9**(1), 42 (1963).

(19) E. D. Gol'berg, T. S. Shubina, and I. B. Shternberg, *Antibiotiki (Moscow)*, **16**(K), 113 (1971).

(20) G. P. Bodey, *et al.*, *Cancer Chemother. Rep.*, **53**, 59 (1969).

(21) R. R. Ellison, *et al.*, *Blood*, **32**, 507 (1968).

(22) I. H. Krakoff, in "Cancer Chemotherapeutic Agents," I. H. Krakoff, Ed., The American Cancer Society, Washington, D.C., 1977, pp. 1–15.

(23) D. H. W. Ho *et al.*, *Cancer Res.*, **40**, 2442 (1980).

(24) R. A. DiCioccio and B. I. S. Srivastava, *Eur. J. Biochem.*, **79**, 411 (1977).

(25) M. Strauss and R. Moran, *Cell Tissue Kinet.*, **11**, 529 (1978).

(26) D. E. Bell and A. Fridland, *Biochim. Biophys. Acta*, **606**, 57 (1980).

(27) M. Y. Chu, *Biochem. Pharmacol.*, **20**, 2057 (1971).

(28) D. Kessel, T. C. Hall, and D. Rosenthal, *Cancer Res.*, **29**, 459 (1969).

(29) M. H. N. Tattersall, K. Ganeshagurn, and A. V. Hoffbrand, *Br. J. Haematol.*, **27**, 39 (1974).

(30) B. A. Chabner, *et al.*, *J. Clin. Invest.*, **53**, 922 (1974).

(31) C. N. Coleman, D. G. Johns, and B. A. Chabner, *Ann. N.Y. Acad. Sci.*, **255**, 247 (1975).

(32) D. H. W. Ho, *Cancer Res.*, **33**, 2816 (1973).

(33) C. D. Steuart and P. J. Burke, *Nature (London)*, **233**, 109 (1971).

(34) J. T. Grace, M. T. Hakala, R. H. Hall, and J. Blakeslee, *Proc. Am. Assoc. Cancer Res.*, **8**, 23 (1967).

(35) D. Hare and B. Hacker, *Physiol. Chem. Phys.*, **4**, 275 (1972).

(36) B. Hacker and T. L. Feldbush, *Cancer*, **27**, 1384 (1971).

(37) B. Hacker, H. Van Vunakis, and L. Levine, *J. Immunol.*, **108**, 1726 (1972).

(38) B. Hacker, *Biochim. Biophys. Acta*, **224**, 635 (1970).

(39) B. M. Chassy and R. J. Suhadolnik, *J. Biol. Chem.*, **242**, 3655 (1967).

(40) R. H. Hall and G. Mintsioulis, *J. Biochem.*, **73**, 739 (1973).

(41) G. B. Chheda and A. Mittelman, *Biochem. Pharmacol.*, **21**, 27 (1972).

(42) B. Hacker and Y. Chang, *Proc. Am. Pharm. Assoc., Acad. Pharm. Sci.*, **11**, 136 (1981).

(43) Y. Chang and B. Hacker, *J. Pharm. Sci.*, **71**, 328 (1982).

(44) B. Hacker and Y. Chang, *Proc. Am. Assoc. Cancer Res.*, **23**, 161 (1982).

(45) B. Hacker and Y. Chang, *J. Pharm. Sci.*, **72**, 902 (1983).

(46) B. Hacker and Y. Chang, *J. Pharm. Sci.*, **72**, 1225 (1983).

(47) P. J. Medon, E. B. Thompson, and N. R. Farnsworth, *Acta Pharmacol. Sin.*, **2**, 281 (1981).

ACKNOWLEDGMENTS

English translations and reprints of References 2, 4, 6–19 are available from NAPRALERT Computer Retrieval Systems, Natural Products (World Health Organizations).

The authors thank Dr. Norman F. Farnsworth, Professor of Pharmacognosy, University of Illinois Medical Center, Chicago, Illinois for generously supplying the *Eleutherococcus senticosus* root extract.

Theorem on the Apparent Volume of Distribution and the Amount of Drug in the Body at Steady State

D. P. VAUGHAN

Received November 8, 1982, from the *Department of Pharmaceutics, Faculty of Pharmaceutical Sciences, Sunderland Polytechnic, Sunderland, Tyne & Wear SR1 3SD, UK.* Accepted for publication December 15, 1982.

Abstract □ For an N-compartmental system, with irreversible drug loss from the sampled compartment, the equilibrium concentration, $C(\infty)$, obtained with a zero-order drug input is related to the total amount of drug in the system, T, by $C(\infty)V = T$. The scalar V is the volume of distribution of the corresponding closed system. The moment functions of the open system define V, and hence T is directly calculable. The derivation is general in the sense that the topology of the system is not specified and no functional form for $C(t)$ is required.

Keyphrases □ Volume of distribution, apparent—theorem, amount of drug in the body at steady state, topology, moment functions □ Topology—apparent volume of distribution, amount of drug in the body at steady state, moment functions, theorem

The apparent drug distribution volume of an irreducible compartmental system, with a unit impulse drug input into a sampled compartment, is given by the ratio of the first statistical moment to the definite integral of the sampled concentration function (1). This apparent drug distribution volume is identical to the apparent volume of the corresponding closed system if drug elimination occurs exclusively from the sampled compartment (1).

In the present paper a relationship between the apparent volume of distribution of a compartmental system and the total amount of drug in the system, obtained with a zero-order drug input, is derived. The derivation does not require any conditions on (*a*) the eigenvalues of the system, (*b*) the topology of the system, or (*c*) the intercompartmental rate constants. However, it is assumed that drug input is into the sampled compartment and that drug elimination occurs only from the sampled compartment.

THEORETICAL

Consider an arbitrary set of N interconnected compartments in which it is possible for material in compartment j to reach each of i compartments ($i, j \epsilon 1, 2 \ldots N; i \neq j$). Such a compartmental system does not contain any sinks, disjointed sets of compartments, or subsystems. For such a system:

$$\begin{bmatrix} \dot{X}_1 \\ \dot{X}_2 \\ \dot{X}_3 \\ \vdots \\ \dot{X}_N \end{bmatrix} = \begin{bmatrix} -E_1 & k_{21} & k_{31} & \ldots & k_{N1} \\ k_{12} & -E_2 & k_{32} & \ldots & k_{N2} \\ k_{13} & k_{23} & -E_3 & \ldots & k_{N3} \\ & & & & \\ k_{1N} & k_{2N} & k_{3N} & \ldots & -E_N \end{bmatrix} \begin{bmatrix} X_1 \\ X_2 \\ X_3 \\ \vdots \\ X_N \end{bmatrix} \equiv \dot{\mathbf{X}} = \mathbf{AX} \qquad \text{(Eq. 1)}$$

where X_j ($j \epsilon 1,2 \ldots N$) is the amount of drug in compartment j, and $\dot{X}_j$ is the first derivative of X_j with respect to time. The off-diagonal elements of matrix A, k_{ji} and k_{ij}, are intercompartmental rate constants for drug transport from compartment j to compartment i and from compartment i to compartment j, respectively, j and $i \epsilon 1,2 \ldots N$ $i \neq j$. Both k_{ij} and k_{ji} are ≥ 0, and if a particular $k_{ij} = 0$ the status of k_{ji} cannot be inferred. Consequently, matrix **A** has no specified topological arrangement of the compartments. The diagonal elements of matrix **A** are defined by:

$$E_j = k_{j0} + \sum_{\substack{i=1 \\ j \neq i}}^{N} k_{ji} > 0 \qquad \text{(Eq. 2)}$$

$$(j \epsilon 1,2 \ldots N)$$

where k_{j0} ($k_{j0} \geq 0$) is the rate constant for irreversible drug loss from the system *via* compartment j. For an open compartmental system at least one k_{j0} is greater than zero, and for a closed compartmental system all values of k_{j0} are equal to zero.

For an open compartmental system the coefficient matrix **A** is a dominant diagonal matrix with respect to the columns and is an irreducible matrix (2, 3). Since the off-diagonal elements of **A** are non-negative, each $X_j(t)$ is greater than or equal to zero for all values of t for any set of non-negative initial conditions or any non-negative input function (4). Further, since matrix **A** is column dominant it follows from Gerschgorin's eigenvalue theorem (5) that all the characteristic values of **A** have negative real parts. Consequently, $X_j(\infty) = 0$, $j \epsilon 1,2 \ldots N$, for any set of non-negative initial conditions. Combining the non-negativity of $X_j(t)$ and the irreducibility of matrix A no $X_j(t)$ is zero for all values of t when the initial conditions are non-negative and at least one initial condition is >0. The latter conditions guarantee that $\int_0^\infty X_j(t)\,dt$ exists for all values of j and that each integral is greater than zero for any set of non-negative initial conditions with at least one positive initial condition. Theorems concerning the determinant of an irreducible matrix are known (6); thus, $|A| \neq 0$ if at least one $k_{j0} > 0$ and $|A| = 0$ if all $k_{j0} = 0$ for $j \epsilon 1,2 \ldots N$.

A special form of matrix **A** is one in which only one value of k_{j0} is greater than zero. Considering such a system, and without loss of generality, let $k_{10} > 0$ and $k_{j0} = 0$ for $j \epsilon 2,3 \ldots N$. In this case the apparent volume of distribution (V) of the irreducible compartmental system is given by:

$$V = \frac{D \int_0^\infty t\,C(t)\,dt}{\left(\int_0^\infty C(t)\,dt\right)^2} \qquad \text{(Eq. 3)}$$

where D is an impulse drug input into compartment 1 and $C(t)$ is the resulting drug concentration–time function observed in compartment 1 (1). This apparent volume is related to the total amount of drug in the body by the following theorem.

Theorem—For an irreducible compartmental system with irreversible drug loss from one compartment only, *e.g.*, compartment 1, and zero-order drug input K into this compartment, then the limiting concentration, $C_1(\infty)$ in the sampled compartment (compartment 1) is related to the total mass of drug in the system, $T(\infty)$, by:

$$C_1(\infty) \cdot V = T(\infty) \qquad \text{(Eq. 4)}$$

where V is the apparent volume of distribution of the compartmental system as defined by Eq. 3.

Proof—To establish a proof, an expression for the scalar volume ($\overline{V}$) that maps the limiting concentration, $C_1(\infty)$, in compartment 1 to the total mass of drug in the system as $t \to \infty$ is required. If this latter volume can be shown to be identical to V then a proof is established.

Expressions for $T(\infty)$ and $\overline{V}$ can be obtained as follows. By standard Laplace transform theory:

$$x_j(s) = \frac{K}{s} \cdot \frac{(-1)^{j+1}|s\mathbf{I} - \mathbf{M}_{1j}|}{|s\mathbf{I} - \mathbf{A}|} \qquad \text{(Eq. 5)}$$
$$(j \epsilon 1,2, \ldots N)$$

where $x_j(s)$ is the Laplace transform of $X_j(t)$, s the Laplace variable, $\mathbf{M}_{1j}$ the matrix obtained by deleting row 1 and column j from matrix **A**, and **I** is the identity matrix.

Expanding the polynomials in Eq. 5, then:

$$x_j(s) = \frac{K}{s} \cdot \frac{(-1)^{j+1}(s^{N-1} + a_1 s^{N-2} \ldots a_{N-2}s + (-1)^{N-1}|\mathbf{M}_{1j}|)}{(s^N + b_1 s^{N-1} \ldots b_{N-1}s + (-1)^N|\mathbf{A}|)} \qquad \text{(Eq. 6)}$$

0022-3549/84/0200-0273$01.00/0
© 1984, American Pharmaceutical Association

where b_i and a_i are $(-1)^i$ times the sum of the determinants of all the i-squared principle minors of matrix $\mathbf{A}$ and matrix $\mathbf{M}_{1j}$, respectively. The coefficients b_i ($i\epsilon 1,2 \ldots N-1$) and $(-1)^N|\mathbf{A}|$ are greater than zero (1).

Applying the final value theorem of Laplace transforms:

$$\underset{(j\epsilon 1,2 \ldots N)}{X_j(\infty)} = \underset{\text{Lim } s \to 0}{s \cdot x_j(s)} = \frac{K(-1)^{j+1}(-1)^{N-1}|\mathbf{M}_{1j}|}{(-1)^N|\mathbf{A}|} \quad \text{(Eq. 7)}$$

The numerator terms in Eq. 7 are all positive. The latter follows from the fact that $|-\mathbf{A}|$ has all positive cofactors (4), and since $-1^{(N-1)}|\mathbf{M}_{1j}| = |-\mathbf{M}_{1j}|$, the determinants $-1^{(j+1)}|-\mathbf{M}_{1j}|$ are cofactors of $|-A|$. Consequently $X_j(\infty) > 0$ for all values of ($j\epsilon 1,2 \ldots N$) when $K > 0$.

The total amount of drug in the system as $t \to \infty$ is given by $\Sigma_{j=1}^{N} X_j(\infty) = T(\infty)$ and $C_1(\infty) = X_1(\infty)/V_1$ where V_1 is the volume of compartment 1. Consequently, the scalar $\overline{V}$ that maps $C_1(\infty)$ to $T(\infty)$ is given by application of Eq. 7 as:

$$\overline{V} = \frac{\sum_{j=1}^{N}(-1)^{j+1}(-1)^{N-1}|\mathbf{M}_{1j}|}{(-1)^{N-1}|\mathbf{M}_{11}|} \cdot V_1 \quad \text{(Eq. 8)}$$

The latter scalar volume $\overline{V}$ is equivalent to the apparent volume of distribution (V). This identity can be established as follows. Consider the corresponding closed compartmental system ($k_{10} = 0$) with a unit impulse input into compartment 1. In this case, by standard Laplace transform theory:

$$\underset{(j\epsilon 1,2 \ldots N)}{\hat{X}_j(\infty)} = \underset{\text{Lim } s \to 0}{s \cdot \hat{x}_j(s)} = \lim_{s \to 0} \frac{s \cdot (-1)^{j+1}|sI - \mathbf{M}_{1j}|}{|sI - \hat{\mathbf{A}}|}$$

$$= \lim_{s \to 0} \frac{(-1)^{j+1} s\,[s^{N-1} + a_1 s^{N-2} \ldots . a_{N-2}s + (-1)^{N-1}|\mathbf{M}_{1j}|]}{[s^N + \hat{b}_1 s^{N-1} \ldots . \hat{b}_{N-1}s + (-1)^N|\hat{\mathbf{A}}|]} \quad \text{(Eq. 9)}$$

where $\hat{b}_i$ is $(-1)^i$ times the sum of the determinants of all the i-squared principal minors of $\hat{\mathbf{A}}$, $\hat{\mathbf{A}}$ is the coefficient matrix of the closed system (*i.e.*, all $k_{j0} = 0$) and $\hat{X}_j(\infty)$ is the mass of drug in compartment j of the closed system as $t \to \infty$. Since $|\hat{\mathbf{A}}| = 0$, the limits in Eq. 9 are obtained by the L'Hospital rule, and applying Eq. 9:

$$\sum_{j=1}^{N} \hat{X}_j(\infty) = \frac{\sum_{j=1}^{N}(-1)^{j+1}(-1)^{N-1}|\mathbf{M}_{1j}|}{\hat{b}_{N-1}} = 1 \quad \text{(Eq. 10)}$$

Since the system is closed the total amount of drug in the system at any time is unity, this gives the unity identity of Eq. 10.

Substituting Eq. 10 into Eq. 8 gives:

$$\overline{V} = \frac{\hat{b}_{N-1}}{(-1)^{N-1}|\mathbf{M}_{11}|} V_1 \quad \text{(Eq. 11)}$$

The quotient expressed in Eq. 11 has been shown previously (1) to be equivalent to the apparent volume of distribution of a compartmental system, whence $\overline{V} = V$, from which Eq. 4 follows and thus completes the proof.

DISCUSSION

The apparent volume of distribution specified by Eq. 3 does not assume any particular functional form for $C(t)$. After an impulse input (D), V can be calculated by standard numerical methods. Additionally, V can be calculated for any given input function into the central compartment and does not necessitate the use of an intravenous bolus drug dose (1).

As is stated in the given theorem the apparent volume can be used to calculate the total amount of drug in the system at steady state when a constant intravenous infusion is administered: conversely if the amount of drug in the system and $C(\infty)$ are known, then V can be calculated.

The volume of distribution of a compartmental system is the apparent volume of the completely closed system (*i.e.*, when no irreversible drug loss occurs). It is defined as that scalar quantity which maps the equilibrium concentration, in the sampled compartment of the closed system, to the amount of drug in the closed system after a finite drug input (1). For an open system with elimination occurring only from the observed compartment this volume is given by Eq. 3 when an impulse input (D) is used.

Riggs (7) introduced, but without reference to a closed system, the term steady-state distribution volume. This volume of distribution is defined specifically with respect to a two-compartment open model and it is the ratio of the total drug content in the system to the drug concentration in the central compartment, these measurements being taken at a time when the second compartment contains the maximum amount of drug. For a two-compartmental model with drug elimination occurring only from the central compartment the latter definition coincides with the definition based on a closed system. However, in an irreducible open compartmental system with more than two compartments, all of the peripheral compartments will not necessarily be in equilibrium with the central compartment at the same time. Consequently the steady-state distribution volume (7) cannot be arbitrarily extended to include a general N-compartmental system of unknown topology. For a two-compartmental model the use of permeability coefficients for drug transfer (8) or partition coefficients (9) also gives an identical distribution volume to that of the closed system. The concept of permeability and partition coefficients could be extended to larger compartmental models such as mammillary and catenary models. However, the notion of partitioning in systems containing irreversible drug cycles is inappropriate. No such difficulties arise when the closed system is used as the reference.

Since previous analyses are not general it is essential, for a clear understanding of drug distribution volume, to have a general theorem that relates the distribution volume to the total amount of drug in an open system of unknown topology at steady state. It could be argued that it is intuitively obvious that the volume of distribution of a closed system maps the equilibrium concentration of the sampled compartment obtained with a zero-order drug input to the total amount of drug in the system. However, the reverse opinion has been held previously (9, 10) and an erroneous proof has been presented to show that the distribution volume does not have a direct relationship to the total amount of drug in the system at steady state (10).

The derivation of the theorem presented in the text is general in the sense that no knowledge of the topology of the system is required and consequently no constraints on the eigenvalues of the system are required nor are any constraints on intercompartmental rate constants required. However, it is assumed that irreversible drug loss from the system occurs only from the sampled compartment.

Although the term compartment has been used in the derivation, the term is merely a convenience and should not be interpreted literally as a circumscribable region of space. Frequently the term noncompartmental is applied incorrectly to pharmacokinetic theory when topological independence is intended (11, 12).

REFERENCES

(1) D. P. Vaughan, *J. Pharm. Sci.*, **71**, 793 (1982).

(2) J. Z. Hearon, *Ann. N.Y. Acad. Sci.*, **108**, 36 (1963).

(3) C. D. Thorn, *Bull. Math. Biophys.*, **34**, 277 (1972).

(4) R. Bellman, "Introduction to Matrix Analysis," McGraw-Hill, New York, N.Y., 1960, chap. 13.

(5) S. Gerschgorin, *Izv. Akad. Nauk. SSSR Ser. Fiz-Mat*, **6**, 749 (1931).

(6) O. Taussky, *Am. Math. Mont.*, **56**, 672 (1949).

(7) D. S. Riggs, "The Mathematical Approach to Physiological Problems," Williams and Wilkins, Baltimore, Md., 1963, chap. 7 and 8.

(8) J. G. Wagner and J. I. Northam, *J. Pharm. Sci.*, **56**, 529 (1967).

(9) L. Z. Benet and R. A. Ronfeld, *J. Pharm. Sci.*, **58**, 639 (1969).

(10) S. Riegelman, J. Loo, and M. Rowland, *J. Pharm. Sci.*, **57**, 128 (1962).

(11) L. Z. Benet and R. L. Galeazzi, *J. Pharm. Sci.*, **68**, 1071 (1979).

(12) D. Perrier and M. Mayersohn, *J. Pharm. Sci.*, **71**, 372 (1982).

0022-3549/84/0200-0274$01.00/0

© 1984, American Pharmaceutical Association

New Compounds: Peptide Derivatives of the Antitumor Agent *N*-Phosphonoacetyl-L-aspartic Acid

DANIEL GIGOT and MICHEL PENNINCKX ×

Received March 3, 1982, from the *Laboratoire de Microbiologie, Université Libre de Bruxelles, c/o Institut de Recherches du Ceria B-1070 Brussels, Belgium.* Accepted for publication November 5, 1982.

Abstract □ Two peptide forms of the antitumor transition state analogue *N*-phosphonoacetyl-L-aspartic acid (N^2-phosphonoacetyl-N^4-glycylglycinamidoethyl-L-asparagine and N^1-glycylglycinamidoethyl-N^2-phosphonoacetyl-L-isoasparagine) have been synthesized to obtain potential medicinal agents useful as prodrugs or in a lysosomotropic carrier approach. The bridging unit, ethylenediamine, used for synthetic purposes might be of general interest.

Keyphrases □ *N*-Phosphonoacetyl-L-aspartic acid—peptide derivatives, synthesis, ethylenediamine bridging unit, potential prodrugs and lysosomal carriers □ Peptide derivatives—*N*-phosphonoacetyl-L-aspartic acid, synthesis, ethylenediamine bridging unit, potential prodrugs and lysosomal carriers □ Ethylenediamine—use as a bridging unit in syntheses of peptide derivatives, *N*-phosphonoacetyl-L-aspartic acid

Previous work (1, 2) showed that peptide derivatives of artificial inhibitors are useful alternatives for inhibiting the growth of cells having membrane systems unable to transport the free forms of these molecules. This paper describes the synthesis of two peptide derivatives of *N*-phosphonoacetyl-L-aspartic acid (I), a transition state inhibitor with antitumor activity (3, 4). The new compounds synthesized, N^2-phosphonoacetyl-N^4-glycylglycinamidoethyl-L-asparagine (VIII)[1] and N^1-glycylglycinamidoethyl-N^2-phosphonoacetyl-L-isoasparagine (XIII) are possible medical agents that could be used as prodrugs or in a lysosomotropic carrier approach (5). Two intermediates synthesized during this work, 1-*N*-(*tert*-butoxycarbonyl)ethylenediamine (II) and 1-*N*-(benzyloxycarbonylglycylglycyl)ethylenediamine (IX), might have numerous practical applications when bonding a drug to a peptide backbone is necessary.

DISCUSSION

Investigations in a model system (1) showed that peptide derivatives having a free *N*-terminal α-amino group were preferentially taken up by cells. The bonding of *N*-phosphonoacetyl-L-aspartic acid (I) to the C-terminal group of a peptide unit must, therefore, be carried out with the help of a bridge. Ethylenediamine was chosen as the bridging unit because the molecule bears two reactive amino groups and, due to its small size, was not expected to create major steric interferences in the intracellular transport of the bonded forms of I.

In the particular case of I, the two carboxyl functions appeared to be suitable attachment points. Because of this, isomeric forms of linked I were considered, since the ultimate biological response depends on the structure. In the synthesis of N^2-phosphonoacetyl-N^4-glycylglycinamidoethyl-L-asparagine (VII), the β-linked form of I (Scheme I), the bridging molecule was first connected to a precursor of the inhibitor. We synthesized 1-*N*-*tert*-butoxycarbonylethylenediamine (II) which was joined to *N*-benzyloxycarbonyl-L-aspartic acid α-*p*-nitrobenzyl ester to give N^2-benzyloxycarbonyl-N^4-(2-*tert*-butoxycarbonylaminoethyl)-L-asparagine *p*-nitrobenzyl ester (III). Compound III was partially unblocked with trifluoroacetic acid to unmask the amino group of the bridge. The resulting compound, N^2-benzyloxycarbonyl-N^4-(2-aminoethyl)-L-asparagine *p*-nitrobenzyl ester (IV), coupled with *N*-*tert*-butoxycarbonylglycylglycine (V) was then treated with hydrogen in the presence of Pd-C to give N^4-(*tert*-butoxycarbonylglycylglycinamidoethyl)-L-asparagine (VI). The final product (VIII) (26% yield) was obtained by phosphonoacetylation of VI, treatment with trifluoroacetic acid, and preparative TLC.

In the synthesis of N^1-(glycylglycinamidoethyl)-N^2-phosphonoacetyl-L-isoasparagine (XIII), the α-linked isomer of I (Scheme II), ethylenediamine was connected to *N*-benzyloxycarbonylglycylglycine to give 1-*N*-(benzyloxycarbonylglycylglycyl)ethylenediamine (IX). Compound IX coupled with *N*-*tert*-butoxycarbonyl-O^4-benzylhydrogen-L-aspartic acid gave N^1-benzyloxycarbonylglycylglycinamidoethyl-N^2-*tert*-butoxycarbonyl-O^4-benzylhydrogen-L-isoasparagine (X), which was then partially unblocked with trifluoroacetic acid. Compound XI, obtained in the previous step, was phosphonoacetylated and totally unblocked with hydrogen bromide in acetic acid (45%). A final preparative TLC gave XIII (32% yield).

It was found, using a paper disk assay (1, 2), that VIII and XIII did not inhibit the growth of *Escherichia coli*. Further investigations showed that the derivatives are actively transported into the microbial cells, but not cleaved[2].

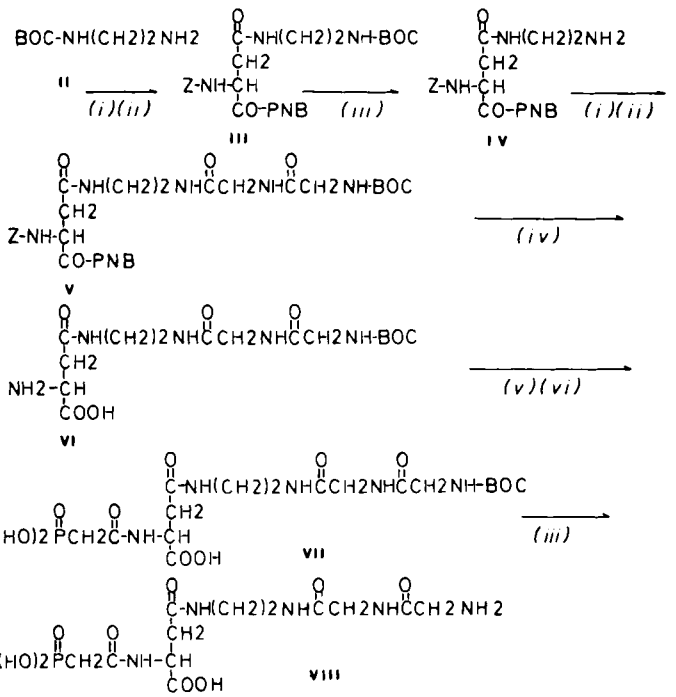

Scheme I

[1] Recommendations of the IUPA-IUB Commission of Biochemical Nomenclature [*J. Biol. Chem.*: **247**, 977 (1972); *Eur. J. Biochem.* **53**, 1 (1975)] have been followed for the biochemical names of the derivatives described in the text.

[2] D. Gigot and M. Penninckx, unpublished observations.

0022-3549/84/0200-0275$01.00/0
© 1984, American Pharmaceutical Association

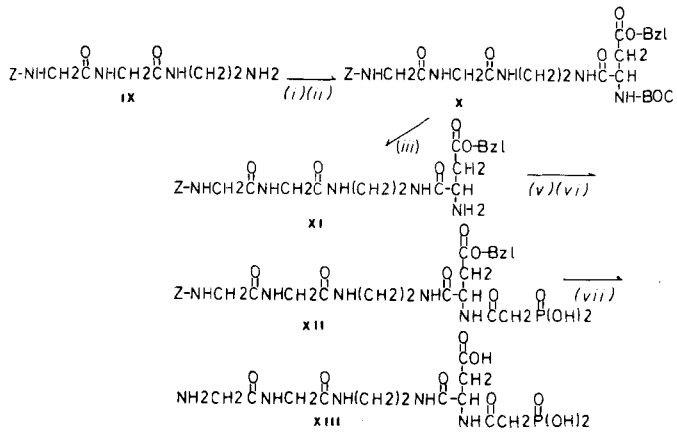

Scheme II

EXPERIMENTAL

For analytical purposes, ~50 μg of the products was spotted on silica gel plates[3]. Three elution systems, ethanol–25% aqueous ammonia (77:23) (system A), chloroform–methanol (2:1) (system B), and butanol–water (85:15) (system C), were used in this work. Spots were detected by ninhydrin and by chlorine and starch–iodine when applicable. Phosphorus-containing spots were detected by the Bandurski and Axelrod procedure (6). Free amino group analyses were made by the dansylation procedure (7). 1-*N*-dansyl-ethylenediamine was obtained by the labeling of *N*-(*tert*-butoxycarbonyl)ethylenediamine with dansyl chloride followed by acid hydrolysis (8). Resolution of the dansylation products was performed by TLC on polyamide sheets (9). High-voltage analytical paper electrophoresis (30 V/cm)[4] was carried out at pH 3.55 (pyridine–acetic acid–water, 1:10:289). Melting points are uncorrected.

1-*N*-(*tert*-Butoxycarbonyl)ethylenediamine (II)—Ethylenediamine (1.8 g, 0.03 mol) and 2-*tert*-butoxycarbonyloxyimino-2-phenylacetonitrile (10.4 g, 0.03 mol) were mixed in 50 mL of dry dioxane and cooled. The mixture was allowed to stand 2 h at room temperature, and the solvent was evaporated under reduced pressure; the residue was dissolved in 50 mL of ethyl acetate. The organic phase was extracted with 100 mL of hot water (50°C), and the aqueous layer was left overnight at 4°C. The resulting precipitate was removed by filtration and recrystallized from water to give II as white needles (0.6 g: 12%), mp 102–103°C; R_f: 0.87 (A), 0.15 (B), 0.05 (C); IR(KBr): 3350 (NH_2), 2940 (—CH_2—), 1690 [C=O (amide I)], 1620 (NH_2) 1535 [amide II (NH)], 1475 (—CH_2—), 1405–1395 (doublet), 1370 and 1255 [$C(CH_3)_3$], 1180 (C—O), 1030 (C—N), and 490 and 480 [$C(CH_3)$] cm^{-1}.

Anal.—Calc. for $C_7H_{16}N_2O_2$: C, 52.50; H, 10.00; N, 17.50; O, 20.00. Found: C, 52.32; H, 10.16; N 17.46.

N^2-Benzyloxycarbonyl-N^4-(2-*tert*-butoxycarbonylaminoethyl)-L-asparagine *p*-Nitrobenzyl Ester (III)—*N*,*N*′-dicyclohexylcarbodiimide (4.12 g, 0.02 mol) was added to a solution of *N*-hydroxysuccinimide (2.28 g, 0.02 mol) and 8.04 g (0.01 mol) of *N*-benzyloxycarbonyl-L-aspartic acid α-*p*-nitrobenzyl ester [obtained by the procedure of Schröder and Klieger (10)] in 40 mL of *N*,*N*-dimethylformamide and cooled. The mixture was allowed to stand at 4°C overnight. The dicyclohexylurea was removed by filtration and washed with 10 mL of *N*,*N*-dimethylformamide. To the filtrate, at room temperature, was added 1-*N*-*tert*-butoxycarbonylethylenediamine (3.2 g, 0.02 mol) in 30 mL of water containing sodium bicarbonate (3.36 g, 0.04 mol). After 12 h, the mixture was acidified to pH 5.0 at 4°C with citric acid and extracted twice with 25 mL of cold (5°C) ethyl acetate. The resulting organic phase was washed twice with 50 mL of saturated sodium chloride; a further concentration *in vacuo* gave a yellow clear oil which was triturated with ether. Recrystallization from ether–light petroleum (1:1) gave a white solid (8.06 g, 74%), mp 90–92°C; R_f: 0.94 (A), 0.69 (B), 0.48 (C); quantitative amino acid analysis of the hydrolyzed product (24 h in 5.7 M HCl at 105°C) gave 1.12 mol of aspartic acid/mol of the product.

Anal.—Calc. for $C_{26}H_{33}N_4O_9$: C, 57.25; H, 6.06; N, 10.28; O, 26.42. Found: C, 57.12; H, 6.12; N, 10.26.

N^2-Benzyloxycarbonyl-N^4-(2-aminoethyl)-L-asparagine *p*-Nitrobenzyl Ester (IV)—Compound III (5.45 g, 0.01 mol) was allowed to stand with 30 mL of anhydrous trifluoroacetic acid for 30 min at room temperature. The excess acid was removed under reduced pressure, and the oily residue was partitioned between 50 mL of cold (4°C) ethyl acetate and 50 mL of 1 *M* sodium carbonate. The organic layer was washed quickly with cold water until neutral and concentrated to dryness (35°C) to give a white solid (3.64 g; 82%), mp 98–100°C; R_f: 0.83 (A), 0.21 (B), 0.11 (C); quantitative amino acid analysis of the hydrolyzed peptide gave 0.97 mol of aspartic acid/mol of the product; amino group analysis by dansylation revealed a single fluorescent spot migrating to the same position as a sample of 1-*N*-dansyl-ethylenediamine.

Anal.—Calc. for $C_{21}H_{25}N_4O_7$: C, 56.63; H, 5.62; N, 12.58; O, 25.17. Found: C, 56.67; H, 5.65; N, 12.49.

N^2 - Benzyloxycarbonyl -N^4- (*tert*-butoxycarbonylglycylglycinamidoethyl)-L-asparagine *p*-Nitrobenzyl Ester (V)—*N*,*N*′-dicyclohexylcarbodiimide (2.06 g, 0.01 mol) was added to a solution of *tert*-butoxycarbonylglycylglycine (2.32 g, 0.01 mol) and 1.04 g (0.01 mol) of *N*-hydroxysuccinimide in 20 mL of *N*,*N*-dimethylformamide and cooled. The mixture was allowed to stand at 4°C overnight. The dicyclohexylurea was removed by filtration and washed with 5 mL of *N*,*N*-dimethylformamide. To the filtrate, at room temperature, was added 4.45 g (0.01 mol) of IV and 2.02 g (0.02 mol) of triethylamine. After standing for 24 h, 50 mL of water was added to the mixture, and the pH was adjusted to 5.0 with citric acid. The precipitated gum was extracted three times with 25 mL of cold (5°C) ethyl acetate. The organic layer was washed twice with 50 mL of saturated sodium chloride, and the solvent was evaporated under reduced pressure. The residue was crystallized from ether–light petroleum (1:1) to give a white solid (3.5 g, 53%), mp 137–139°C; R_f: 0.64 (A), 0.37 (B), 0.17 (C); quantitative amino acid analysis of the hydrolyzed peptide gave 1.04 mol of aspartic acid and 1.98 mol of glycine/mol of the product.

Anal.—Calc. for $C_{30}H_{38}N_6O_{11}$: C, 54.71; H, 5.77; N, 12.76; O, 26.74. Found: C, 54.71; H, 5.69; N, 12.74.

N^4-(*tert*-butoxycarbonylglycylglycinamidoethyl)-L-asparagine (VI)—Compound V (6.58 g, 0.01 mol) was dissolved in a 25-mL mixture of *N*,*N*-dimethylformamide–methanol (1:2) in the presence of 0.5 g of 10% Pd-C. The mixture was hydrogenated for 6 h at room temperature and atmospheric pressure. The catalyst was removed by filtration, and the solution concentrated to dryness under reduced pressure. The residue was dissolved in 20 mL of methanol, and the product precipitated by the addition of 100 mL of ether. Recrystallization from methanol–ether (1:1) gave a white solid (3.47 g; 89%), mp 192–194°C; R_f: 0.41 (A), 0.17 (B), 0.06 (C); amino acid analysis gave 0.95 mol of aspartic acid and 2.1 mol of glycine/mol of the product; amino group analysis by dansylation revealed only one spot migrating to the same position as *N*-dansyl-aspartic acid.

Anal.—Calc. for $C_{15}H_{27}N_5O_7$: C, 46.27; H, 6.94; N, 17.99; O, 28.79. Found: C, 46.17; H, 6.91; N, 18.04.

N^2-Phosphonoacetyl-N^4-glycylglycinamidoethyl-L-asparagine (VIII)—Triethylamine (1.2 g, 0.02 mol) was added to a solution of VI (3.89 g, 0.01 mol) in 20 mL of cold (4°C) dioxane–*N*,*N*-dimethylformamide (4:1). Phosphonoacetylchloride (1.51 g, 0.01 mol) in 15 mL of dioxane obtained by the method of Balsiger (11), was added with stirring to the aforementioned solution in a dropwise manner. After the addition was complete, the mixture was filtered. The precipitate was washed with 5 mL of dioxane–*N*,*N*-dimethylformamide (4:1). The filtrate was made alkaline with ammonia and extracted three times with 20 mL portions of ether. The aqueous layer was lyophilized, and the residue was treated during 1 h with 25 mL of anhydrous trifluoroacetic acid. The crude peptide salt was precipitated by the addition of 150 mL of anhydrous ether. The precipitate was decanted, transferred to a centrifuge tube, and repeatedly washed with ether, centrifuging each time.

Ten-milligram scale preparative fractionation of the material was performed by preparative TLC. The crude product contained in 100 μL of water was applied in a horizontal band near the base of the plate. Elution was performed using solvent system A. Under those conditions, the expected phosphonoacetylated product migrated slowly. The material was recovered by extraction of the desired gel portion with a solution of 5% ammonia. The aqueous phase was further lyophilized, and the final product was obtained as a white hygroscopic powder (1.22 g, 26.5% yield extrapolated); R_f: 0.06 (A).

The material migrated also as a single ninhydrin- and phosphorus-positive spot towards the anode when subjected to paper electrophoresis (0.3 cm for 2 h). Amino acid analysis gave 1.16 mol of aspartic acid and 2.07 mol of glycine/mol of the product. Amino group analysis revealed only one spot migrating to the same position as *N*-dansyl-glycine. The extent of racemization of the product was estimated by the enzymatic quantitative determination of L-aspartic acid released during the acid hydrolysis of the peptide. One mole of the product gave 0.95 mol of L-

[3] Merck Kieselgel 60-5721.
[4] Whatman 3-mm paper and Camag 67701 apparatus.

aspartic acid, as determined by conversion to ureidosuccinic acid with L-aspartate carbamoyltransferase (12).

Anal.—Calc. for $C_{12}H_{22}N_5O_9P \cdot 3NH_3$ (the triammonium salt of the peptide): C, 31.17; H, 6.71; N, 24.24; O, 31.17; P, 6.71. Found: C, 31.20; H, 6.76; N, 24.09; P, 6.83.

1-*N*-(Benzyloxycarbonylglycylglycyl)ethylenediamine (IX)—*N,N'*-dicyclohexylcarbodiimide (2.06 g, 0.01 mol) was added to a solution of *N*-benzyloxycarbonylglycylglycine (2.66 g, 0.01 mol) and 1.04 g (0.01 mol) of *N*-hydroxysuccinimide in 20 mL of *N,N*-dimethylformamide and cooled. After standing overnight at 4°C the mixture was filtered and the precipitate washed with 10 mL of *N,N*-dimethylformamide. To the filtrate was added a solution of 0.6 g (0.01 mol) of ethylenediamine in 10 mL of water adjusted to pH 8.5. The reaction mixture was allowed to stand overnight at room temperature and then was filtered. The filtrate was adjusted to pH 9.5 with 2 M NaOH and extracted three times with 25 mL of ethyl acetate. The organic layer was washed twice with 20 mL of saturated sodium chloride and concentrated *in vacuo*. The oily residue was mixed with 5 mL of absolute ethanol and three drops of 12 M HCl and allowed to crystallize in a desiccator under reduced pressure (1.24 g, 36%), mp 176–178°C; R_f: 0.61 (A), 0.11 (B), 0.06 (C); amino acid analysis gave 2.16 mol of glycine/mol of the product; amino group analysis gave one fluorescent spot running at the same position as 1-*N*-dansyl-ethylenediamine.

Anal.—Calc. for $C_{14}H_{20}N_4O_4 \cdot HCl$: C, 48.77; H, 6.10; N, 16.26; O, 18.58; Cl, 10.30. Found: C, 48.59; H, 6.04; N, 16.40.

N^1 - Benzyloxycarbonylglycylglycinamidoethyl - N^2 - *tert*-butoxycarbonyl-O^4-benzylhydrogen-L-isoasparagine (X)—*N,N'*-dicyclohexylcarbodiimide (2.06 g, 0.01 mol) was added to a solution of *N*-hydroxysuccinimide (1.04 g, 0.01 mol) and 3.27 g (0.01 mol) of *N*-*tert*-butoxycarbonyl-β-benzyl-L-aspartic acid [obtained by the procedure of Laufer and Blout (13)] in 20 mL of *N,N*-dimethylformamide and cooled, the mixture was allowed to stand at 4°C overnight and then was filtered. Compound IX (3.44 g, 0.01 mol) in 10 mL of water containing 2.02 g (0.02 mol) of triethylamine was added to the aforementioned mixture. After 12 h of reaction, at room temperature, the solution was acidified to pH 5.0 with citric acid, and the precipitate was extracted twice with 30 mL of cold (4°C) ethyl acetate; the organic layer was washed twice with 50 mL of saturated sodium chloride and concentrated *in vacuo*. Recrystallization of the residue from ether–light petroleum gave the product as a white powder (2.15 g; 62), mp 127–129°C; R_f: 0.83 (A), 0.71 (B), 0.54 (C); amino acid analysis gave 1.91 mol of glycine and 1.03 mol aspartic acid/mol of the product.

Anal.—Calc. for $C_{30}H_{39}N_5O_9$: C, 58.73; H, 6.36; N, 11.42; O, 23.49. Found: C, 58.62; H, 6.31; N, 11.44.

N^1 - Benzyloxycarbonylglycylglycinamidoethyl - O^4 - benzylhydrogen-L-isoasparagine (XI)—Compound X (5.9 g, 0.01 mol) was treated for 30 min at room temperature with 35 mL of anhydrous trifluoroacetic acid. The excess acid was removed under reduced pressure and the free base of the desired product was obtained by the same procedure as described for IV (3.4 g, 67%), mp 159–161°C; R_f: 0.44 (A), 0.36 (B), 0.25 (C); amino acid analysis gave 1.1 mol of aspartic acid and 1.98 mol of glycine/mol of the product; amino group analysis gave one single spot migrating at the same position as *N*-dansyl-aspartic acid.

Anal.—Calc. for $C_{25}H_{31}N_5O_7$: C, 58.48; H, 6.04; N, 13.65; O, 21.23. Found: C, 58.39; N, 5.93; N, 13.61.

N^1 - Glycylglycinamidoethyl - N^2 - phosphonoacetyl - L - isoasparagine (XIII)—Phosphonoacetylation of XI (2.56 g, 0.05 mol) was carried out by the same procedure as described for VI in the preparation of VII. The lyophilized intermediate (XII) was then treated with 15 mL of 35% hydrogen bromide in glacial acetic acid for 12 h at room temperature. The crude peptide salt was then precipitated by the addition of 100 mL of cold (4°C) anhydrous ether and further treated as in the preparation of VIII. After the final preparative TLC, XIII was obtained as a white hygroscopic powder (0.87 g, 38%); R_f: 0.10 (A). The material migrated also as a single ninhydrin- and phosphorus-positive spot toward the anode when subjected to paper electrophoresis (0.4 cm for 2 h). Amino acid analysis gave 0.98 mol of aspartic acid and 2.04 mol of glycine/mol of the product. Amino group analysis gave one single fluorescent spot migrating to the same position as *N*-dansyl-glycine. Extent of racemization of the product was determined using the procedure described for VIII; the aspartic acid residue of the product appears to be 97% under the L-form.

Anal.—Calc. for $C_{12}H_{31}N_8O_9P \cdot 3NH_3$, (the triammonium salt of the peptide): C, 31.17; H, 6.71; N, 24.24; O, 31.17; P, 6.71. Found: C, 31.24; H, 6.64; N, 24.32; P, 6.59.

REFERENCES

(1) M. Penninckx and D. Gigot, *J. Biol. Chem.*, **254,** 6392 (1979).

(2) M. Penninckx, *Trends Pharmacol. Sci.*, **1,** 271 (1980).

(3) E. E. Swyryd, S. S. Seaver, and G. R. Stark, *J. Biol. Chem.*, **249,** 6945 (1974).

(4) H. Koch, *Pharm. Int.*, **1,** 126 (1980).

(5) O. Vaizoglu and P. Speiser, *Trends Pharmacol. Sci.*, **3,** 28 (1982).

(6) R. S. Bandurski and B. Axelrod, *J. Biol. Chem.*, **193,** 405 (1951).

(7) W. R. Gray, *Methods Enzymol.*, **25** (part B) **121,** 333 (1972).

(8) G. Gros and B. Labouesse, *Eur. J. Biochem.*, **7,** 463 (1969).

(9) K. Narita, H. Matsuo, and T. Nakajima, *Mol. Biol. Biochem. Biophys.*, **8,** 52 (1975).

(10) E. Schröder and E. Klieger, *Justus Liebig Ann. Chem.*, **673,** 208 (1964).

(11) R. W. Balsiger, D. G. Jones, and J. A. Montgomery, *J. Org. Chem.*, **24,** 434 (1959).

(12) G. R. Jacobson and G. R. Stark, *Enzymes*, **9,** 225 (1973).

(13) D. A. Laufer and E. R. Blout, *J. Am. Chem. Soc.*, **89,** 1246 (1967).

Nucleoside Conjugates V: Synthesis and Biological Activity of 9-(β-D-Arabinofuranosyl)adenine Conjugates of Corticosteroids

CHUNG IL HONG ˣ, ALAN J. KIRISITS, ALEXANDER NECHAEV, DAVID J. BUCHHEIT, and CHARLES R. WEST

Received June 10, 1982, from the *Department of Neurosurgery, Roswell Park Memorial Institute, Buffalo, NY 14263.* Accepted for publication November 10, 1982.

Abstract □ Eight 5′-(steroid-21-phosphoryl)-9-(β-D-arabinofuranosyl)-adenines (IV–XI) have been prepared and evaluated against L1210 lymphoid leukemia in culture. These include the 9-(β-D-arabinofuranosyl)adenine conjugates of hydrocortisone (IV), cortisone (V), corticosterone (VI), cortexolone (VII), 11-deoxycorticosterone (VIII), prednisolone (IX), prednisone (X), and dexamethasone (XI). Conjugates IV, IX, X, and XI inhibited the *in vitro* growth of L1210 lymphoid leukemia cells by 50% (ED_{50}) at a concentration of 2.3–7.8 μM, while 9-(β-D-arabinofuranosyl)adenine (vidarabine, I) and its 5′-monophosphate (II) each showed ED_{50} value of 30 μM. All of the conjugates were enzymatically hydrolyzed to the corresponding steroid and II, the latter undergoing further hydrolysis to I, by phosphodiesterase I, 5′-nucleotidase, and acid phosphatase. However, these congugates were resistant to hydrolysis by alkaline phosphatase and adenosine deaminase.

Keyphrases □ 9-(β-D-arabinofuranosyl)adenine—conjugates with corticosteroids, synthesis, antileukemic activity □ Corticosteroids—conjugates with 9-(β-D-arabinofuranosyl)adenine, synthesis, antileukemic activity □ Antileukemic agents—potential, 9(β-D-arabinofuranosyl)adenine–corticosteroid conjugates, synthesis, L1210 screen

The therapeutic effectiveness of 9-(β-D-arabinofuranosyl)adenine (vidarabine, I) as an antitumor and antiviral agent is limited by poor solubility in water and by its metabolism to the less active 9-(β-D-arabinofuranosyl)hypoxanthine by adenosine deaminase (1). In an attempt to overcome these problems, a variety of analogues and prodrugs of I have been synthesized (2–6). In an effort to develop nucleoside conjugates as potential antitumor and antiviral agents, we reported the synthesis and antitumor activity of 1-(β-D-arabinofuranosyl)cytosine conjugates of corticosteroids, linked by a phosphodiester bond (7–9). Most of the conjugates showed superior antitumor activity and reduced toxicity based on 1-(β-D-arabinofuranosyl)-cytosine (cytarabine) content, and were resistant to enzymatic deamination by cytidine deaminase. Furthermore, the antiproliferative effects of corticosteroids on experimental cell systems (10, 11) and their sensitivity even in many nonlymphoid experimental and human tumors, including brain tumors (12–14), have been well demonstrated. In view of the success of the conjugation with corticosteroids, we synthesized 9-(β-D-arabinofuranosyl)adenine conjugates of corticosteroids linked through a naturally occurring phosphodiester bond. The advantages of this type of conjugate are (*a*) increased water solubility, (*b*) resistance to enzymatic deamination by adenosine deaminase, (*c*) biological activities from the steroid moiety after release from the conjugate, (*d*) increased lipophilicity, and (*e*) a possible target-specific carrier role by the steroid. This paper describes the synthesis and antitumor activity of eight I–corticosteroid conjugates.

EXPERIMENTAL[1]

9-(β-D-Arabinofuranosyl)adenine 5′-Monophosphate (II)—This compound was prepared by a previously published procedure (15) with some modification in the isolation procedure. To a cooled mixture (0°C) of 4 mL (44 mmol) of phosphorus oxychloride, 3.9 mL (48 mmol) of pyridine, and 10 mL of acetonitrile was added 0.5 mL of water in a dropwise manner, and the mixture was stirred at 0°C for 15 min, and then, 2.67 g (10 mmol) of I was added and the suspension was stirred at 0–5°C for 3 h. The solution was poured into 200 mL of ice water and neutralized to pH 7.0 with concentrated ammonium hydroxide solution. The mixture was then evaporated to dryness, and the residue was dissolved in 200 mL of water. The aqueous solution was applied to an AG1-X8 (formate) column (4 × 25 cm) prepacked in water. The column was eluted with water (500 mL) and then with 0.5 M formic acid (1000 mL). The 0.5 M formic acid eluate (first 600 mL) was evaporated to dryness, the residue was treated with acetone, and the resulting material removed by filtration and washed with acetone to give 2.62 g (76%) of II as a white solid. The chromatographic mobilities in various solvents and the IR spectrum were identical with those of authentic II; TLC: R_f(A) 0.21, R_f(B) 0.22, R_f(C) 0. Enzymatic hydrolysis with 5′-nucleotidase (EC 3.1.3.5) gave I.

N^6,2′,3′-Triacetyl-9-(β-D-arabinofuranosyl)adenine 5′-Monophosphate (III)—A mixture of 1.04 g (3 mmol) of dried II, 15 mL of acetic anhydride, and 30 mL of anhydrous pyridine was stirred at room temperature for 18 h, and then 10 mL of water was added to the ice-cooled mixture. After being stirred at room temperature for 2 h, the mixture was evaporated to dryness, and the last traces of water were removed by coevaporation 3 times with pyridine. The syrupy material was used in the next step without further purification.

TLC showed mainly one spot: R_f(A) 0.21, R_f(B) 0.23, and R_f(C) 0.44 (streak). The UV spectrum of the pyridine-free compound taken in 50% ethanol showed a maximum at 270.5 nm with a shoulder at 257 nm. The UV maximum was shifted to 277.5 and 290 nm in 0.1 M HCl and 0.1 M NaOH, respectively.

5′-(Prednisone-21-phosphoryl)-9-(β-D-arabinofuranosyl)adenine (X)—Compound III, prepared by acetylation of 1.04 g (3 mmol) of II with acetic anhydride (15 mL) and pyridine (30 mL) as described above, was stirred with 2.16 (6 mmol) of prednisone and 2.45 g (12 mmol) of *N,N′*-dicyclohexylcarbodiimide in 150 mL of anhydrous pyridine at room temperature for 2 d. The mixture was evaporated to dryness, and then the final traces of pyridine were removed by coevaporation with toluene (10 mL). The residue was treated with 100 mL of 50% ethanol, and the insoluble urea was removed by filtration. The filtrate was evaporated to dryness, and the residual material was stirred with 100 mL of 2 M methanolic ammonia at room temperature overnight. The solvent was removed by evaporation and the residue was dissolved in 100 mL of 50% ethanol, and then the solution was applied to a DE-52 (acetate) column (3.5 × 26 cm) prepacked in 50% ethanol. The material was then eluted

[1] Melting points were determined in capillary tubes using a Mel-Temp apparatus and are uncorrected. UV absorption spectra were obtained on a Beckman Acta V spectrophotometer. IR spectra were recorded on a Perkin-Elmer 297 IR spectrophotometer. ^{1}H-NMR spectra were obtained with a Varian EM-390 spectrometer using tetramethylsilane as internal standard. AG1-X8 (formate, Bio-Rad), diethylaminoethyl cellulose (DE-52, Whatman), and cellulose powder (CC-31, Whatman) were used for column chromatography. Evaporation was performed *in vacuo* at 30°C. TLC was performed on glass plates coated with a (0.25-mm layer of silica gel PF-254 (Brinkman) and on polygram sil G UV 254 plates (Brinkman) using the following solvent systems: (A) isopropyl alcohol–water–concentrated ammonium hydroxide (7:2:1), (B) ethanol–0.5 M ammonium acetate, pH 7.5 (5:2), and (C) chloroform–methanol–water–acetic acid (25:15:4:2). Elemental analyses were performed by Galbraith Laboratories, Inc., Knoxville, Tenn.

0022-3549/84/0200-0278$01.00/0
© 1984, American Pharmaceutical Association

Table I—Physical Data and Elemental Analysis for the Conjugates

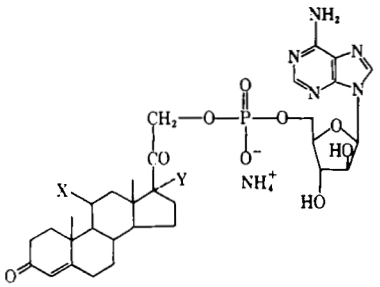

IV–VIII

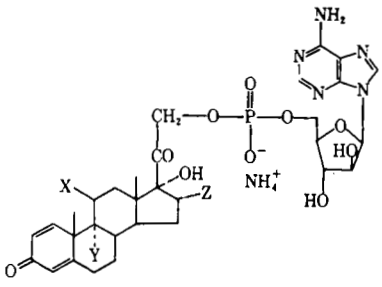

IX–XI

Compound	X	Y	Z	Melting Point[a], °C	Yield, %	Formula[b]	UV_{max}, nm ($\epsilon \times 10^{-3}$) H_2O	0.1 M HCl	0.1 M NaOH
IV	OH	OH	—	200–205 dec	14	$C_{31}H_{41}N_5O_{11}P \cdot NH_4 \cdot 3H_2O$	252 (22.5)	252 (22.7)	252 (22.1)
V	=O	OH	—	195–200 dec	16	$C_{31}H_{39}N_5O_{11}P \cdot NH_4 \cdot 2.5H_2O$	252 (23.9)	253 (23.9)	252 (23.0)
VI	OH	H	—	192–197 dec	11	$C_{31}H_{41}N_5O_{10}P \cdot NH_4 \cdot 3.5H_2O$	252 (21.1)	252 (21.2)	252 (21.2)
VII	H	OH	—	191–196 dec	21	$C_{31}H_{41}N_5O_{10}P \cdot NH_4 \cdot 3H_2O$	253 (24.0)	250 (24.9)	251 (24.0)
VIII	H	H	—	187–192 dec	16	$C_{31}H_{41}N_5O_9P \cdot NH_4 \cdot 2.5H_2O$	251 (24.1)	253 (24.8)	250 (24.2)
IX	OH	H	H	200–205 dec	21	$C_{31}H_{39}N_5O_{11}P \cdot NH_4 \cdot 5H_2O$	256 (19.5)	254 (20.2)	255 (19.9)
X	=O	H	H	205–215 dec	39	$C_{31}H_{37}N_5O_{11}P \cdot NH_4 \cdot 2.5H_2O$	253 (22.8)	252 (21.9)	254 (20.9)
XI	OH	F	CH_3	190–195 dec	11	$C_{32}H_{40}FN_5O_{11}P \cdot NH_4 \cdot 2H_2O$	251 (21.3)	251 (21.6)	250 (21.0)

[a] No distinct melting point. Slowly decomposed. [b] All compounds were analyzed for C, H, N, and P. Results were within ±0.4% of the theoretical values.

using a linear gradient of acetic acid in 50% ethanol (0–2.0 M, 1000 mL each). The fractions between 1250 and 1790 mL were pooled and evaporated to dryness. The residue was treated with acetone, the material removed by filtration, washed with acetone, and dried to give 798 mg (39%) of X. The analytical sample, as an ammonium salt was prepared as described previously (16), mp 205–215°C (slowly dec.). TLC R_f(A) 0.75, R_f(B) 0.71, R_f(C) 0.65; IR (KBr): 3300–3200 br, 2940, 1720, 1690, 1650, 1600, 1400, 1230, 1080, and 1040 cm^{-1}; ^1H-NMR (DMSO-d_6): δ 0.49 (s, 3, CH_3), 1.34 (s, 3, CH_3), 1.00–3.00 (br m, 13), 3.98 (d, 1, J = 4 Hz, C′4 H), 4.12 (d, 2, J = 4 Hz, C′5 H), 4.30–5.10 (br m, 7), 5.99 (d, 1, J = 3 Hz, C_4 H), 6.08 (d, 1, J = 10 Hz, C_2 H), 6.28 (d, 1, J = 5 Hz, C′1 H), 7.58 (d, 1, J = 10 Hz, C_1 H), 7.74 (br s, 2, NH_2), 8.19 (s, 1, adenine C_2 H), and 8.25 (s, 1, adenine C_8 H). Table I lists the conjugates prepared in an analogous manner.

Hydrolysis of the Conjugates with Barium Hydroxide—The conjugate (0.01 mmol) and barium hydroxide (0.1 mmol) in 1 mL of water were heated at 90–95°C in a stoppered vial for 15 min. Aliquots (0.1 mL) were removed at the designated time, treated with Dowex 50 (H^+) resin, and examined chromatographically in solvents A and B. Each band was extracted with 50% ethanol and quantitated by UV. Hydrolysis of the conjugate was completed in 5 min, and the products were the steroid 21-monophosphate and I. After standing at room temperature overnight, the steroid phosphate in the hydrolysate was further hydrolyzed to the corresponding steroid.

Solubility in Water—A mixture of the compound (20 mg) in 2 mL of water was vortex mixed at full speed at 25°C for 5 min and then filtered through a glass-fiber filter. The clear filtrate was quantitated by UV and the concentration was determined by using the molar extinction coefficient of the compound.

Antiproliferative Activity *In Vitro*—Compounds I, II, IV–XI, and mixtures of I with hydrocortisone, corticosterone, prednisolone, and prednisone were tested for growth-inhibitory activity against L1210 lymphoid leukemia in culture using the methodology described previously (8, 17).

Determination of Resistance of Adenosine Deaminase—Cytoplasmic adenosine deaminase (EC 3.5.4.4) of L1210 leukemia cells was prepared according to a published procedure (17). Assay of enzyme activity was performed in a UV spectrophotometer at 37°C in pH 7.3 phosphate buffer by determining the rate of change in absorbance at 265 nm, as previously described (17, 18). Activity of the enzyme with adenosine was 133.33 IU/L, and the protein concentration was 3.22 mg/mL. For assay of the conjugates, a mixture of compound (0.4 μmol) in 1 mL of water, 0.5 mL of enzyme preparation, and 0.5 mL of 0.18 M phosphate buffer (pH 7.5) was incubated at 37°C for 24 h. The mixture was then evaporated to a small volume and streaked on a TLC plate (0.1 × 20 × 20 cm), and the plate was developed with solvent A. The band matching with the conjugate was extracted with 50% ethanol and quantitated by UV. This was then further incubated with 5′-nucleotidase (EC 3.1.3.5) from *Crotalus adamanteus* in 0.1 M Tris-HCl (pH 9.0) and 0.005 M magnesium sulfate at 37°C for 24 h. The products were separated by TLC and characterized and quantitated by UV as described previously (8).

Enzymatic Hydrolysis—Enzymatic cleavage of the phosphodiester bond of the conjugates was studied by incubating the compounds (5 μmol) with phosphodiesterase I (EC 3.1.4.1), 5′-nucleotidase (EC 3.1.3.5), acid phosphatase (EC 3.1.3.2), and alkaline phosphatase (EC 3.1.3.1) in appropriate buffer (final volume 1.0 mL) as described previously (8). Aliquots (0.1 mL) of the incubation mixtures at various lengths of time were streaked on TLC plates (0.05 × 10 × 20 cm) with authentic markers, and the plates were developed with solvent A. Each band was extracted with 50% ethanol and quantitated by UV.

RESULTS AND DISCUSSION

Chemistry—The conjugates (IV–XI) were prepared by a method similar to that used for the preparation of the 1-(β-D-arabinofuranosyl)-cytosine conjugates (7–9). Phosphorylation of I with phosphorus oxychloride in the presence of water and pyridine in acetonitrile (15) afforded II in 76% yield. The latter compound was then acetylated with acetic anhydride in pyridine. Compound III showed one spot on TLC, and its observed UV maximum was 270.5 nm with a shoulder at 257 nm. Condensation of III with 2 molar equivalents of the various steriods in the presence of *N*,*N*′-dicyclohexylcarbodiimide and pyridine at room temperature for 2 d and the subsequent removal of the acetyl groups with 2 M methanolic ammonia gave the conjugates (IV–XI) in 10–40% yield after chromatography (Table I).

Table II—Effects of I, II, the Conjugates, and Mixtures of I and Steroids on the Viability of L1210 Lymphoid Leukemia Cells in Culture

Compound	ED_{50}, μM[a]
I	30
II	30
IV	4.3
V	61
VI	12
VII	25
VIII	42
IX	2.3
X	4.1
XI	7.8
I and hydrocortisone	52.7
I and corticosterone	48
I and prednisolone	52
I and prednisone	100

[a] Concentration for 50% loss of viability at 72 h.

Structures of the conjugates were verified by elemental analyses, UV, IR, and NMR spectroscopic methods, and chemical and enzymatic hydrolysis of the phosphodiester bond. The observed UV maxima in water for the conjugates were between 251–256 nm (ϵ ~21,000) (Table I), which were different from those for the steroids (237–242 nm) and I (259 nm). The strong IR absorption at 1720, 1690, 1650, and 1600 cm^{-1} supported the presence of the steroid (C=O) and the purine ring (C=C, C=N), and the strong absorptions at 1230 and 1040 cm^{-1} showed the presence of the phosphodiester bond (P=O, P—O—C). The presence of methyl groups of the steroids and the anomeric, C-2, and C-8 protons of the nucleoside (I) was also supported by the ^{1}H-NMR spectra of the conjugates. Like the 1-(β-D-arabinofuranosyl)cytosine conjugates (7–9), hydrolysis of the conjugates (IV–XI) by 0.05 M $Ba(OH)_2$ yielded I and the corresponding steroid 21-monophosphate, which was further hydrolyzed to the steroid. When enzymatic hydrolysis with phosphodiesterase I (EC 3.1.4.1) was used, the products were II and the steroid.

The conjugates were soluble in water (~5 mg/mL). For example, solubilities of IV and IX were 6.69 and 6.49 μmol/mL of water, respectively, while those of I and II were 3.38 and 13.2 μmol/mL of water.

Antiproliferative Activity *In Vitro*—Growth inhibition of L1210 lymphoid leukemia cells in culture by the compounds listed in Table II was measured by Trypan blue exclusion from the viable cells (17). The concentration of each drug which resulted in 50% inhibition (ED_{50}) of growth at 72 h is shown in Table II. The parent drugs, I and II, inhibited moderately the proliferation of L1210 cells in culture (ED_{50} = 30 μM each). Under the experimental conditions, only 11-deoxycorticosterone (among the steroids) used alone demonstrated an ED_{50} that was <100 μM (9). Mixtures of I and steroids showed an ED_{50} of 50–100 μM. Among the conjugates, IX, X, and IV were the most potent inhibitors with ED_{50} values of 2.3, 4.1, and 4.3 μM, respectively. The conjugates of dexamethasone (XI) and corticosterone (VI) were also active (ED_{50} = 7.8 and 12.0 μM, respectively); those of cortexolone (VII) and 11-deoxycorticosterone (VIII) were either as effective as I or II or nearly so. Only V was less inhibitory than the parent drugs. Thus, most of the conjugates we tested were found to be more inhibitory than I or II alone and mixtures of I and the steroids.

Resistance to Adenosine Deaminase—Using the adenosine deaminase (EC 3.5.4.4) from L1210 cells (17, 18), the observed K_m and V_{max} for adenosine was 63.07 μM and 4.92 μmol/L/min, while those of I were 87.33 μM and 1.32 μmol/L/min. However, the conjugates remained intact under the same experimental condition. In fact, they were found to be resistant to the adenosine deaminase even during a 24-h incubation period at 37°C.

Enzyme Hydrolysis—Enzymatic hydrolysis of the conjugates with purified phosphodiesterase I (EC 3.1.4.1), 5′-nucleotidase (EC 3.1.3.5) from *C. adamanteus*, and acid phosphatase (EC 3.1.3.2) from wheat germ showed that the products were the steroid and II. The latter was further hydrolyzed to I during a 24-h incubation period. For example, when IX was incubated with phosphodiesterase I, 50% of the conjugate was hydrolyzed within 60 min. However, the conjugate was almost intact after 60-min incubation with both 5′-nucleotidase and acid phosphatase, and 50% of the conjugate remained intact at the end of a 24-h incubation. All conjugates were found to be resistant to enzymatic hydrolysis by bacterial alkaline phosphatase (EC 3.1.3.1).

Under the conditions of the experimental procedures, the conjugates show strong antiproliferative activity against L1210 in culture. Furthermore, they are resistant to adenosine deaminase and water soluble. Thus, these findings will provide the bases for continued study of the effects of these conjugates *in vivo*. Moreover, as I is active in viral infections involving two groups of DNA viruses (herpes viruses and pox viruses) (19), the conjugates could be potential antiviral agents.

REFERENCES

(1) J. J. Brink and G. A. LePage, *Cancer Res.*, **24**, 312 (1964).

(2) J. A. Montgomery and K. Hewson, *J. Med. Chem.*, **12**, 498 (1969).

(3) R. Vince and S. Daluge, *J. Med. Chem.*, **20**, 612 (1977).

(4) G. A. LePage, Y.-T. Lin, R. E. Orth, and J. A. Gottleib, *Cancer Res.*, **32**, 2441 (1972).

(5) A. J. Repta, B. J. Rawson, R. D. Shaffer, K. B. Sloan, N. Bodor, and T. Higuchi, *J. Pharm. Sci.*, **64**, 392 (1975).

(6) T. Matsushita, E. K. Ryu, C. I. Hong, and M. MacCoss, *Cancer Res.*, **41**, 2707 (1981).

(7) C. I. Hong, A. Nechaev, and C. R. West, *Biochem. Biophys. Res. Commun.*, **88**, 1223 (1979).

(8) C. I. Hong, A. Nechaev, and C. R. West, *J. Med. Chem.*, **22**, 1428 (1979).

(9) C. I. Hong, A. Nechaev, A. J. Kirisits, D. J. Buchheit, and C. R. West, *J. Med. Chem.*, **23**, 1343 (1980).

(10) P. G. Braunschweiger and L. M. Schiffer, *Cancer Res.*, **41**, 3324 (1981).

(11) J. M. Harmon, M. R. Norman, B. J. Fowlkes, and E. D. Thompson, *J. Cell Physiol.*, **98**, 267 (1979).

(12) R. J. Grasso, J. F. Hackney, and N. J. Holbrook, "Proceedings International Symposium of Multidisciplinary Aspects of Brain Tumor Therapy," Elsevier/North-Holland Biomedical Press, Amsterdam, 1979, p. 45.

(13) C. B. Wilson, M. Barker, and T. Hoshino, "Steroids and Brain Edema," H. J. Reulen and K. Schurmann, Eds., Springer-Verlag, Berlin, 1973, p. 95.

(14) R. I. Freshney, A. Sherry, M. Hassanzadah, M. Freshney, P. Crilly, and D. Morgan, *Br. J. Cancer*, **41**, 857 (1980).

(15) T. Sowa and S. Ouchi, *Bull. Chem. Soc. (Jpn)*, **48**, 2084 (1975).

(16) C. I. Hong, G. L. Tritsch, A. Mittelman, P. Hebborn, and G. B. Chheda, *J. Med. Chem.*, **18**, 465 (1975).

(17) G. L. Tritsch, A. Nechaev, and A. Mittelman, *Cancer Biochem. Biophys.*, **2**, 87 (1977).

(18) G. L. Tritsch, P. R. Niswander, J. Rosenfeld, A. Nechaev, and A. Mittleman, *Mol. Cell. Biochem.*, **12**, 93 (1976).

(19) T. W. North and S. S. Cohen, *Proc. Natl. Acad. Sci. USA*, **75**, 4648 (1978).

ACKNOWLEDGMENTS

Presented in part at 181st National Meeting of the American Chemical Society in Atlanta, Ga., March 1981. Supported in part by National Cancer Institute Grant CA 26168 and contributions from the Alison Zach Memorial Fund and Health and Medical Research Foundation of Ancient Egyptian Order Nobles Mystic Shrine.

The authors thank Ms. M. J. Hardin and A. A. Bertuch, participants of the Summer Research Program for Students, for their technical assistance.

Noncompartmental Determination of the Steady-State Volume of Distribution During Multiple Dosing

Keyphrases □ Pharmacokinetics—noncompartmental determination of the steady-state volume of distribution during multiple dosing. □ Volume of distribution—steady-state, noncompartmental determination during multiple dosing

To the Editor:

A noncompartmental approach, based on statistical moment analysis, has been used by Benet and Galeazzi (1) to estimate the volume of distribution at steady-state, V_{ss}, following an intravenous bolus injection. This analysis is applicable at present to systems characterized by first-order kinetics, and assumes that drug elimination occurs exclusively from the central compartment. Exactly the same limitations apply to V_{ss} calculated from distributional rate constants (2) or from the coefficients and exponents of exponential equations (3). Perrier and Mayersohn (4) have extended the analysis of Benet and Galeazzi to allow the calculation of V_{ss} for other modes of drug administration. However, these methods can only be applied to single-dose concentration–time profiles. For multiple-dose data, V_{ss} will be overestimated. Straughn (5) has addressed this problem, but the area analysis is not valid in the situation where residual drug is present prior to data collection. This communication shows how, at steady-state, this difficulty can be overcome by using the identity:

$$\mathrm{AUC_{IV}}|_0^\infty = \mathrm{AUC_{ss}}|_0^\tau \qquad \text{(Eq. 1)}$$

The notation used expresses the area under the plasma concentration–time curve (AUC) after either a single intravenous bolus (IV) or a dose given at steady state (ss) over the time limits indicated. Area under the first moment curve (AUMC) is similarly denoted. The dosing interval is τ.

Following a single bolus dose, the mean residence time ($\bar{t}_{IV}$) for the drug in the body is given by:

$$\bar{t}_{IV} = \frac{\mathrm{AUMC_{IV}}|_0^\infty}{\mathrm{AUC_{IV}}|_0^\infty}$$

V_{ss} can be calculated from the product of total body clearance and $\bar{t}_{IV}$ (1, 6):

$$V_{ss} = \frac{\mathrm{A_{IV}}|_0^\infty}{\mathrm{AUC_{IV}}|_0^\infty}\left(\frac{\mathrm{AUMC_{IV}}|_0^\infty}{\mathrm{AUC_{IV}}|_0^\infty}\right) = \frac{\mathrm{Dose}\left(\sum_{i=1}^{n}\frac{C_i^0}{\lambda_1^2}\right)}{\left(\sum_{i=1}^{n}\frac{C_i^0}{\lambda_i}\right)^2} \qquad \text{(Eq. 2)}$$

$\mathrm{A_{IV}}|_0^\infty$ is the total amount of drug cleared, *i.e.*, the dose administered. C_i^0 and λ_i are the coefficients and exponents in a polyexponential equation.

Area under the moment curve for a single bolus dose until time τ, can be evaluated using:

$$\mathrm{AUMC_{IV}}|_0^\tau = \sum_{i=1}^{n}\left\{\frac{C_i^0}{\lambda_i^2} - \frac{C_i^0 e^{-\lambda_i\tau}}{\lambda_i^2} - \tau\frac{C_i^0 e^{-\lambda_i\tau}}{\lambda_i}\right\}$$

After multiple dosage at steady state:

$$\mathrm{AUMC_{ss}}|_0^\tau = \sum_{i=1}^{n}\left\{\left(\frac{1}{1-e^{-\lambda_i\tau}}\right) \times \left(\frac{C_i^0}{\lambda_i^2} - \frac{C_i^0 e^{-\lambda_i\tau}}{\lambda_i^2} - \tau\frac{C_i^0 e^{-\lambda_i\tau}}{\lambda_i}\right)\right\}$$

$$\mathrm{AUMC_{ss}}|_0^\tau = \sum_{i=1}^{n}\left\{\frac{C_i^0}{\lambda_i^2} - \tau\frac{C_i^0 e^{-\lambda_i\tau}}{\lambda_i(1-e^{-\lambda_i\tau})}\right\}$$

$$\mathrm{AUMC_{ss}}|_0^\tau = \mathrm{AUMC_{IV}}|_0^\infty - \tau\,\mathrm{AUC_{ss}}|_\tau^\infty$$

$$\mathrm{AUMC_{IV}}|_0^\infty = \mathrm{AUMC_{ss}}|_0^\tau + \tau\,\mathrm{AUC_{ss}}|_\tau^\infty \qquad \text{(Eq. 3)}$$

By analogy, it can be shown that for multiple infusions:

$$\mathrm{AUMC_{IV}}|_0^\infty = \mathrm{AUMC_{ss}}|_0^\tau - \frac{\mathrm{T}}{2}\mathrm{AUC_{ss}}|_0^\tau + \tau\,\mathrm{AUC_{ss}}|_\tau^\infty \qquad \text{(Eq. 4)}$$

where T is the duration of the infusion

V_{ss} can be determined by appropriate substitution of corrected area values, Eqs. 1, 3, and 4, into Eq. 2. If pharmacokinetic profiling is carried out during the last dose, then samples can be obtained until drug concentration is negligible, allowing $\mathrm{AUC_{ss}}|_\tau^\infty$ to be estimated by area analysis. Otherwise, when the concentration–time curve can only be characterized over a dosing interval, it is necessary to calculate an extrapolated area from the apparent terminal elimination rate. Although $\mathrm{AUC_{ss}}|_\tau^\infty$ may be numerically small, it should not be neglected as the product of $\mathrm{AUC_{ss}}|_\tau^\infty$ and τ will often contribute significantly to $\mathrm{AUMC_{IV}}|_0^\infty$.

It is recognized that in these situations, and often for the steady-state situation in general, mean residence time will be very closely approximated from the ratio of total AUMC to total AUC over a dosing interval with extrapolation to infinity. However, our method does offer an alternative and a more exact mathematical approach to estimating the apparent volume of distribution at steady-state during multiple dosing. We have applied this approach in our present pharmacokinetic studies (7, 8).

While this communication was under review, Bauer and Gibaldi (9) proposed the use of reverse superimposition to determine V_{ss} during multiple dosing. Unlike our analysis which assumes that steady state has been achieved, their method can be applied at any time during therapy. It should be noted, however, that the single-dose curve derived from data obtained during a dosing interval is dependent on the accuracy of the trough level for the previous dose. Therefore, both methods are likely to prove useful in the analysis of multiple-dose data but, as pointed out by Bauer and Gibaldi, are subject to computational errors.

(1) L. Z. Benet and R. L. Galeazzi, *J. Pharm. Sci.*, **68**, 1071 (1979).
(2) D. S. Riggs, "The Mathematical Approach to Physiological Problems," Williams and Wilkens, Baltimore, Md., 1963, chaps 7 and 8.
(3) J. G. Wagner, *J. Pharmacokinet. Biopharm.*, **4**, 443 (1976).
(4) D. Perrier and M. Mayersohn, *J. Pharm. Sci.*, **71**, 372 (1982).
(5) A. B. Straughn, *J. Pharm. Sci.*, **71**, 597 (1982).

0022-3549/84/0200-0281$01.00/0
© 1984, American Pharmaceutical Association

(6) J. H. ... Schwartz, and M. I. Surks, *J. Clin. Endocrinol. Me* ...1975).
(7) D. J. Swa... P. Reitberg, I. L. Smith, P. B. Wels, and J. J. Schentag, *J. Pharmacokinet. Biopharm*, in press (1984).
(8) D. P. Reitberg, T. J. Cumbo, I. L. Smith, and J. J. Schentag, *Clin. Pharmacol. Ther.*, in press (1984).
(9) L. A. Bauer and M. Gibaldi, *J. Pharm. Sci.*, **72**, 978 (1983).

*Ian L. Smith**x
Jerome J. Schentag‡
*The Clinical Pharmacokinetics Laboratory
Millard Fillmore Hospital
Buffalo, NY 14209
‡Division of Clinical Pharmacy Science
Department of Pharmaceutics
State University of New York at Buffalo
School of Pharmacy
Amherst, NY 14260

Received November 22, 1982.
Accepted for Publication November 16, 1983.

Transdermal Administration of (15*S*)-15-Methyl Prostaglandin $F_{2\alpha}$ Methyl Ester to Rhesus Monkeys

Keyphrases □ Drug delivery systems—controlled-release transdermal administration, prostaglandins, rhesus monkeys □ Prostaglandins—transdermal delivery system, controlled release

To the Editor:

Drug formulation technology has advanced dramatically in recent years. Controlled-release delivery systems offer a number of distinct advantages in therapeutics, one being the potential for designing delivery systems that release therapeutic agents at preselected rates such that in a given situation blood concentration of a drug can be maintained at the desired level for an extended period of time. This ability to control the rate of drug delivery aids in separating the beneficial effects of a drug from the undesirable side effects. Such delivery systems are particularly useful for drugs with short biological half-lives and/or narrow therapeutic indices. Transdermal delivery systems are one of the most exciting applications of controlled-release technology. We report here our preliminary experiments, which demonstrate that (15*S*)-15-methyl prostaglandin $F_{2\alpha}$ methyl ester (carboprost methyl) is readily absorbed when administered transdermally to rhesus monkeys using a polymeric controlled-release delivery system.

The transdermal delivery system consisted of laminated polymeric membranes with a surface area of 40 cm^2. Carboprost methyl was at a concentration of 16% (w/w) in the inner drug-bearing membrane. This membrane was covered with a rate-controlling membrane which allowed a steady-state release rate of 480 μg/h. Double-sided adhesive tape was applied to the periphery of the transdermal patches for attachment to the skin.

The transdermal patches were placed on the shaved chests of four third-trimester pregnant rhesus monkeys. The animals were anesthetized with ketamine hydrochloride[1], and uterine motility was recorded using a fluid-filled polyethylene catheter[2] inserted transabdominally which was attached to a polygraph[3] using a P-23 Dc transducer[4] (1). Peripheral blood samples were collected from the femoral vein and immediately placed in tubes containing heparin. The plasma was harvested and frozen at −20°C for subsequent determination of (15*S*)-15-methyl prostaglandin $F_{2\alpha}$ by radioimmunoassay (2).

The skin was hydrated prior to applying the transdermal delivery system in three animals: a hot towel compress was used on two animals and the skin was irrigated with water on the third animal. To evaluate the rate of drug absorption without prior hydration, the transdermal patch was applied to one animal immediately after shaving the skin.

Drug absorption was more rapid in those animals whose skin had been hydrated. A plasma prostaglandin concentration of ~1200 pg/mL was attained by 0.5 h after application of the transdermal delivery system in the water irrigated animal. In one animal in which a hot towel compress was used the plasma concentration of prostaglandin was ~2200 pg/mL by 0.5 h. The plasma prostaglandin concentration in the second animal similarly pretreated was ~1100 pg/mL by 1 h and 2300 pg/mL by 3 h. Thus, absorption of the drug was slightly slower in this animal even though the skin had been hydrated in a similar manner. When no attempt was made to hydrate the skin, prostaglandin was not detectable in the blood of the fourth monkey until 3 h after the transdermal delivery system had been applied. At this time the concentration was only 100 pg/mL. Thereafter there was a gradual increase in plasma concentration of prostaglandin to 490 pg/mL at 5 h when the delivery system was removed.

All four animals had an increase in the frequency and amplitude of uterine contractions following application of the transdermal delivery systems. In all cases uterine motility increased gradually without any evidence of a rapid onset of prostaglandin effects. The uterine motility tracing from one of these animals is shown in Fig. 1. The mean time to the initiation of stimulated uterine motility was 90 min (range = 45–150 min). The onset of increased uterine activity was temporally related to the increase in prostaglandin detected in the blood in three of the four animals. In one of the animals the rapid increase in blood prostaglandin (2200 pg/mL at 0.5 h) was not reflected in an immediate increase in uterine motility.

These preliminary results clearly demonstrate that carboprost methyl is readily absorbed transdermally in the rhesus monkey when administered using a polymeric controlled-release delivery system. This was particularly true when the skin was hydrated prior to application of the transdermal patch. It is known that hydration of the skin causes the stratum corneum to swell (3). Thus, the normally tight, dense packing of the cells in this layer is loosened. Presumably, this would facilitate movement of prostaglandin through the stratum corneum into the deeper epidermal and dermal layers. However, it is evident that prostaglandin can be absorbed when no effort is made to hydrate the skin, albeit, at a much slower initial rate.

Transdermal delivery systems are finding more and

[1] Vetalor, Parke-Davis and Co.

[2] PE60, Clay Adams.
[3] Grass.
[4] Strathan.

0022-3549/84/0200-0282$01.00/0
© 1984, American Pharmaceutical Association

(6) J. H. ... Schwartz, and M. I. Surks, *J. Clin. Endocrinol. Me* ...1975).
(7) D. J. Swa... P. Reitberg, I. L. Smith, P. B. Wels, and J. J. Schentag, *J. Pharmacokinet. Biopharm*, in press (1984).
(8) D. P. Reitberg, T. J. Cumbo, I. L. Smith, and J. J. Schentag, *Clin. Pharmacol. Ther.*, in press (1984).
(9) L. A. Bauer and M. Gibaldi, *J. Pharm. Sci.*, **72**, 978 (1983).

*Ian L. Smith**x
Jerome J. Schentag‡
*The Clinical Pharmacokinetics Laboratory
Millard Fillmore Hospital
Buffalo, NY 14209
‡Division of Clinical Pharmacy Science
Department of Pharmaceutics
State University of New York at Buffalo
School of Pharmacy
Amherst, NY 14260

Received November 22, 1982.
Accepted for Publication November 16, 1983.

Transdermal Administration of (15*S*)-15-Methyl Prostaglandin $F_{2\alpha}$ Methyl Ester to Rhesus Monkeys

Keyphrases □ Drug delivery systems—controlled-release transdermal administration, prostaglandins, rhesus monkeys □ Prostaglandins—transdermal delivery system, controlled release

To the Editor:

Drug formulation technology has advanced dramatically in recent years. Controlled-release delivery systems offer a number of distinct advantages in therapeutics, one being the potential for designing delivery systems that release therapeutic agents at preselected rates such that in a given situation blood concentration of a drug can be maintained at the desired level for an extended period of time. This ability to control the rate of drug delivery aids in separating the beneficial effects of a drug from the undesirable side effects. Such delivery systems are particularly useful for drugs with short biological half-lives and/or narrow therapeutic indices. Transdermal delivery systems are one of the most exciting applications of controlled-release technology. We report here our preliminary experiments, which demonstrate that (15*S*)-15-methyl prostaglandin $F_{2\alpha}$ methyl ester (carboprost methyl) is readily absorbed when administered transdermally to rhesus monkeys using a polymeric controlled-release delivery system.

The transdermal delivery system consisted of laminated polymeric membranes with a surface area of 40 cm^2. Carboprost methyl was at a concentration of 16% (w/w) in the inner drug-bearing membrane. This membrane was covered with a rate-controlling membrane which allowed a steady-state release rate of 480 μg/h. Double-sided adhesive tape was applied to the periphery of the transdermal patches for attachment to the skin.

The transdermal patches were placed on the shaved chests of four third-trimester pregnant rhesus monkeys. The animals were anesthetized with ketamine hydrochloride[1], and uterine motility was recorded using a fluid-filled polyethylene catheter[2] inserted transabdominally which was attached to a polygraph[3] using a P-23 Dc transducer[4] (1). Peripheral blood samples were collected from the femoral vein and immediately placed in tubes containing heparin. The plasma was harvested and frozen at −20°C for subsequent determination of (15*S*)-15-methyl prostaglandin $F_{2\alpha}$ by radioimmunoassay (2).

The skin was hydrated prior to applying the transdermal delivery system in three animals: a hot towel compress was used on two animals and the skin was irrigated with water on the third animal. To evaluate the rate of drug absorption without prior hydration, the transdermal patch was applied to one animal immediately after shaving the skin.

Drug absorption was more rapid in those animals whose skin had been hydrated. A plasma prostaglandin concentration of ~1200 pg/mL was attained by 0.5 h after application of the transdermal delivery system in the water irrigated animal. In one animal in which a hot towel compress was used the plasma concentration of prostaglandin was ~2200 pg/mL by 0.5 h. The plasma prostaglandin concentration in the second animal similarly pretreated was ~1100 pg/mL by 1 h and 2300 pg/mL by 3 h. Thus, absorption of the drug was slightly slower in this animal even though the skin had been hydrated in a similar manner. When no attempt was made to hydrate the skin, prostaglandin was not detectable in the blood of the fourth monkey until 3 h after the transdermal delivery system had been applied. At this time the concentration was only 100 pg/mL. Thereafter there was a gradual increase in plasma concentration of prostaglandin to 490 pg/mL at 5 h when the delivery system was removed.

All four animals had an increase in the frequency and amplitude of uterine contractions following application of the transdermal delivery systems. In all cases uterine motility increased gradually without any evidence of a rapid onset of prostaglandin effects. The uterine motility tracing from one of these animals is shown in Fig. 1. The mean time to the initiation of stimulated uterine motility was 90 min (range = 45–150 min). The onset of increased uterine activity was temporally related to the increase in prostaglandin detected in the blood in three of the four animals. In one of the animals the rapid increase in blood prostaglandin (2200 pg/mL at 0.5 h) was not reflected in an immediate increase in uterine motility.

These preliminary results clearly demonstrate that carboprost methyl is readily absorbed transdermally in the rhesus monkey when administered using a polymeric controlled-release delivery system. This was particularly true when the skin was hydrated prior to application of the transdermal patch. It is known that hydration of the skin causes the stratum corneum to swell (3). Thus, the normally tight, dense packing of the cells in this layer is loosened. Presumably, this would facilitate movement of prostaglandin through the stratum corneum into the deeper epidermal and dermal layers. However, it is evident that prostaglandin can be absorbed when no effort is made to hydrate the skin, albeit, at a much slower initial rate.

Transdermal delivery systems are finding more and

[1] Vetalor, Parke-Davis and Co.

[2] PE60, Clay Adams.
[3] Grass.
[4] Strathan.

0022-3549/84/0200-0282$01.00/0
© 1984, American Pharmaceutical Association

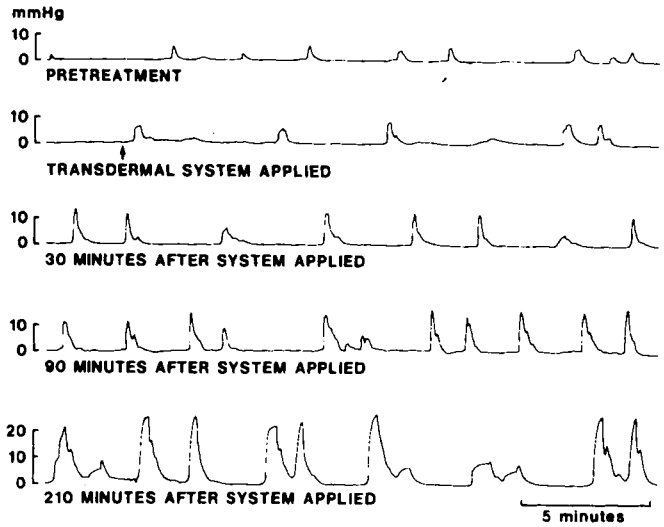

Figure 1—*Uterine motility tracing in a pregnant rhesus monkey (third trimester) treated with a transdermal delivery system containing (15S)-15-methyl prostaglandin $F_{2\alpha}$ methyl ester. Note the gradual increase in the frequency and amplitude of uterine contractions after the delivery system was applied.*

more application for the administration of therapeutic agents (4). A prostaglandin analogue has been shown to be hypotensive when administered transdermally (5). These systems may prove to be especially useful for the administration of prostaglandins for menses induction. The most commonly investigated route of administration for this indication is vaginal (6, 7). One disadvantage to the vaginal route of prostaglandin administration for menses induction is the fact that uterine bleeding is induced as a consequence of the therapy. The time of onset and the amount of uterine bleeding vary among patients. This creates a variable environment for the absorption of prostaglandin from the vagina, and can interfere with drug absorption (7). A transdermal controlled-release delivery system could alleviate these problems.

(1) C. H. Spilman and T. J. Roseman, *Contraception*, **11**, 409 (1975).

(2) J. C. Cornette, D. C. Beuving, and K. T. Kirton, *Prostaglandins*, 12 (Suppl), 53 (1976).

(3) P. Brisson, *Can. Med. Assoc. J.*, **110**, 1182 (1974).

(4) C. D. Black, *U.S. Pharmacist*, **November**, 49 (1982).

(5) J. E. Birnbaum, P. S. Chan, P. Cervoni, F. Dessy, and L. VanHumbeeck, *Prostaglandins*, **23**, 185 (1982).

(6) C. H. Spilman, G. D. Gutknecht, D. C. Beuving, and F. M. Southern, *Contraception*, **21**, 353 (1980).

(7) M. Bygdeman, N. Christenssen, K. Green, O. Vesterqvist, T. J. Roseman, M. E. Tuttle, and C. H. Spilman, *Contraception*, **27**, 141 (1983).

Charles H. Spilman ˣ
Diane C. Beuving
Adelbert D. Forbes
Theodore J. Roseman *
Robert M. Bennett
Fertility Research and Pharmacy Research
The Upjohn Company
Kalamazoo, MI 49001
* Present Address: Travenol Laboratories, Inc.
6301 Lincoln Avenue
Morton Grove, IL 60053

Received September 22, 1983.
Accepted for publication October 25, 1983.

Navel Absorption: Transdermal Bioavailability of Testosterone

Keyphrases □ Absorption—naval, transdermal, bioavailability of testosterone □ Testosterone—transdermal absorption *via* naval, bioavailability □ Bioavailability—transdermal via navel

To the Editor:

The navel (umbilicus) has for many years been widely used as the site for transdermal administration of a number of Chinese drugs, *e.g.*, *Mentha arvensis L.*[1], (1). No bioavailability data are yet available to justify the use of the navel as the site for drug administration.

Recently, a number of systemically active drugs, such as nitroglycerin and scopolamine, have been actively investigated and found to penetrate the skin tissues at a rate sufficient to achieve the therapeutic blood levels required for systemic effects (2–7).

We evaluated the transdermal bioavailability of testosterone through the skin tissues at the navel area[2] and compared the data with that obtained from the transdermal administration on the forearm area (dorsal surface) using four rhesus monkeys as the model animal. [^{14}C]-Testosterone [5 μCi (25 μg)], in 100 μL of acetone, was applied on a skin area (controlled at 0.2 cm^2 by a metal templet) for 5 d. The solvent was quickly evaporated, and the site of drug administration was then covered with a piece of plastic adhesive which remained intact throughout the study. Blood samples (2 mL) were collected in heparinized tubes at 30-min intervals for the first 6 h after administration and then every 24 h up to 9 d. Urine samples were collected daily. The systemic bioavailability and pharmacokinetic profile of [^{14}C]testosterone after topical administration on the navel and forearm skins were then compared using intravenous data as the reference.

The data generated (Fig. 1) suggest that administration *via* the navel yields a relatively faster absorption and also greater systemic bioavailability of [^{14}C]testosterone than administration *via* the forearm. Both routes of percutaneous absorption give well-defined first-order elimination kinetics, which is very much in parallel to that of intravenous administration. It is interesting to note that the systemic bioavailability of [^{14}C]testosterone by navel absorption is relatively close to the level obtained by the intravenous administration of an equivalent dose and is substantially greater than the level achieved by forearm administration. Calculated from Eq. 1, navel absorption of [^{14}C]testosterone has achieved a relative bioavailability of 79.9%, as compared with 49.9% by forearm administration.

$$\% \text{ relative bioavailability} = \frac{\left[\int_0^9 C_c dt\right]_p}{\left[\int_0^9 C_c dt\right]_i} \times 100 \qquad \text{(Eq. 1)}$$

[1] Chemical analysis indicated that it contains menthone, menthol, pinene, and methyl acetate.

[2] Navel area denotes the surface of the navel (Figure 329 in "Structure and Function in Man," 2nd ed., by S. W. Jacob and C. A. Francone, Saunders, Philadelphia, Pa., 1970).

0022-3549/84/0200-0283$01.00/0
© 1984, American Pharmaceutical Association

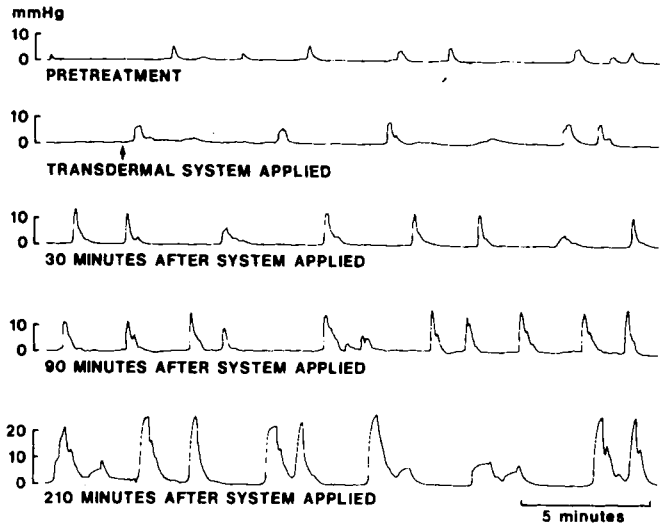

Figure 1—*Uterine motility tracing in a pregnant rhesus monkey (third trimester) treated with a transdermal delivery system containing (15S)-15-methyl prostaglandin $F_{2\alpha}$ methyl ester. Note the gradual increase in the frequency and amplitude of uterine contractions after the delivery system was applied.*

more application for the administration of therapeutic agents (4). A prostaglandin analogue has been shown to be hypotensive when administered transdermally (5). These systems may prove to be especially useful for the administration of prostaglandins for menses induction. The most commonly investigated route of administration for this indication is vaginal (6, 7). One disadvantage to the vaginal route of prostaglandin administration for menses induction is the fact that uterine bleeding is induced as a consequence of the therapy. The time of onset and the amount of uterine bleeding vary among patients. This creates a variable environment for the absorption of prostaglandin from the vagina, and can interfere with drug absorption (7). A transdermal controlled-release delivery system could alleviate these problems.

(1) C. H. Spilman and T. J. Roseman, *Contraception*, **11**, 409 (1975).

(2) J. C. Cornette, D. C. Beuving, and K. T. Kirton, *Prostaglandins*, 12 (Suppl), 53 (1976).

(3) P. Brisson, *Can. Med. Assoc. J.*, **110**, 1182 (1974).

(4) C. D. Black, *U.S. Pharmacist*, **November**, 49 (1982).

(5) J. E. Birnbaum, P. S. Chan, P. Cervoni, F. Dessy, and L. VanHumbeeck, *Prostaglandins*, **23**, 185 (1982).

(6) C. H. Spilman, G. D. Gutknecht, D. C. Beuving, and F. M. Southern, *Contraception*, **21**, 353 (1980).

(7) M. Bygdeman, N. Christenssen, K. Green, O. Vesterqvist, T. J. Roseman, M. E. Tuttle, and C. H. Spilman, *Contraception*, **27**, 141 (1983).

Charles H. Spilman ˣ
Diane C. Beuving
Adelbert D. Forbes
Theodore J. Roseman *
Robert M. Bennett
Fertility Research and Pharmacy Research
The Upjohn Company
Kalamazoo, MI 49001
* Present Address: Travenol Laboratories, Inc.
6301 Lincoln Avenue
Morton Grove, IL 60053

Received September 22, 1983.
Accepted for publication October 25, 1983.

Navel Absorption: Transdermal Bioavailability of Testosterone

Keyphrases □ Absorption—naval, transdermal, bioavailability of testosterone □ Testosterone—transdermal absorption *via* naval, bioavailability □ Bioavailability—transdermal via navel

To the Editor:

The navel (umbilicus) has for many years been widely used as the site for transdermal administration of a number of Chinese drugs, *e.g.*, *Mentha arvensis L.*[1], (1). No bioavailability data are yet available to justify the use of the navel as the site for drug administration.

Recently, a number of systemically active drugs, such as nitroglycerin and scopolamine, have been actively investigated and found to penetrate the skin tissues at a rate sufficient to achieve the therapeutic blood levels required for systemic effects (2–7).

We evaluated the transdermal bioavailability of testosterone through the skin tissues at the navel area[2] and compared the data with that obtained from the transdermal administration on the forearm area (dorsal surface) using four rhesus monkeys as the model animal. [^{14}C]-Testosterone [5 μCi (25 μg)], in 100 μL of acetone, was applied on a skin area (controlled at 0.2 cm^2 by a metal templet) for 5 d. The solvent was quickly evaporated, and the site of drug administration was then covered with a piece of plastic adhesive which remained intact throughout the study. Blood samples (2 mL) were collected in heparinized tubes at 30-min intervals for the first 6 h after administration and then every 24 h up to 9 d. Urine samples were collected daily. The systemic bioavailability and pharmacokinetic profile of [^{14}C]testosterone after topical administration on the navel and forearm skins were then compared using intravenous data as the reference.

The data generated (Fig. 1) suggest that administration *via* the navel yields a relatively faster absorption and also greater systemic bioavailability of [^{14}C]testosterone than administration *via* the forearm. Both routes of percutaneous absorption give well-defined first-order elimination kinetics, which is very much in parallel to that of intravenous administration. It is interesting to note that the systemic bioavailability of [^{14}C]testosterone by navel absorption is relatively close to the level obtained by the intravenous administration of an equivalent dose and is substantially greater than the level achieved by forearm administration. Calculated from Eq. 1, navel absorption of [^{14}C]testosterone has achieved a relative bioavailability of 79.9%, as compared with 49.9% by forearm administration.

$$\% \text{ relative bioavailability} = \frac{\left[\int_0^9 C_c dt\right]_p}{\left[\int_0^9 C_c dt\right]_i} \times 100 \qquad \text{(Eq. 1)}$$

[1] Chemical analysis indicated that it contains menthone, menthol, pinene, and methyl acetate.

[2] Navel area denotes the surface of the navel (Figure 329 in "Structure and Function in Man," 2nd ed., by S. W. Jacob and C. A. Francone, Saunders, Philadelphia, Pa., 1970).

0022-3549/84/0200-0283$01.00/0
© 1984, American Pharmaceutical Association

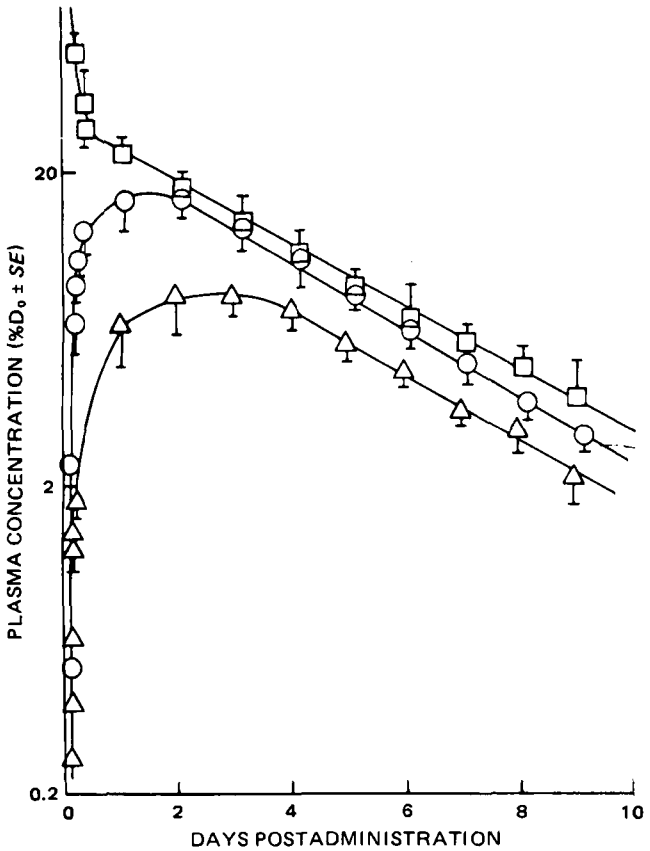

Figure 1—*Semilogarithmic relationship between the mean values (±SE) of plasma concentration (% of applied testosterone dose) and the time after various routes of administration of 5 μCi (25 μg) [^{14}C]-testosterone in four rhesus monkeys. Keys: (□) intravenous, drug in 2 mL saline solution; (○) navel, drug in 100 μL acetone; (△) forearm, drug in 100 μL acetone.*

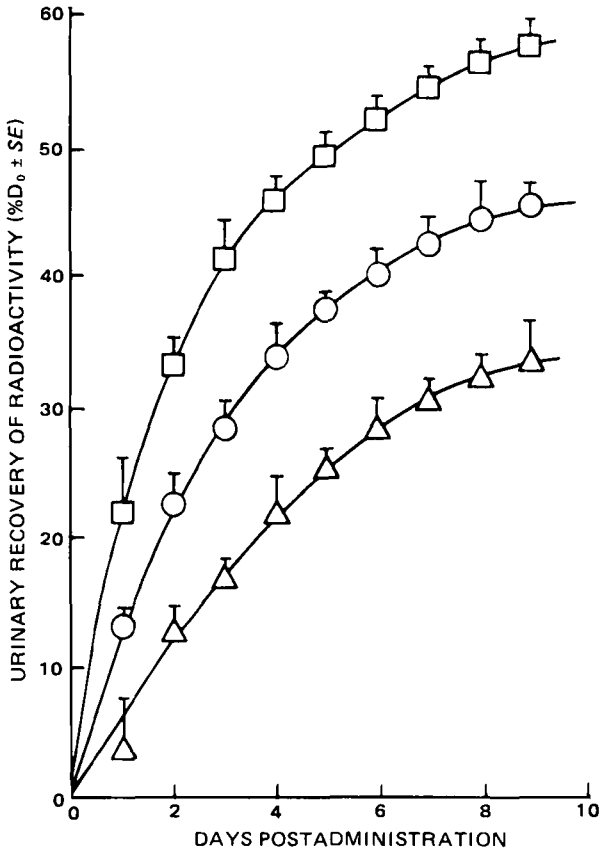

Figure 2—*Comparison of the time course of the cumulative urinary recovery of radioactive testosterone and metabolites [mean value (in % of applied dose) ±SE] following various routes of administration of 5 μCi (25 μg) [^{14}C]testosterone in four rhesus monkeys. Keys: (□) intravenous, drug in 2 mL saline solution; (○) navel, drug in 100 μL acetone; and (△) forearm, drug in 100 μL acetone.*

where $\int_0^9 C_c dt$ is the 9-day cumulative area under the plasma drug level *versus* time curve per unit dose applied (AUC/D_0) (8). And, the subscripts i and p denote, respectively, the administration of [^{14}C[testosterone *via* intravenous and percutaneous routes.

The relative bioavailability of [^{14}C]testosterone by navel and forearm absorption may also be compared using urinary recovery data. The results (Fig. 2) indicate that during a 5-day drug administration period a total of 57.3, 45.2, and 33.2% of the [^{14}C]testosterone dose administered had been recovered in urinary excretion, respectively, from intravenous, navel, and forearm administrations. Using the intravenous urinary recovery data (57.3%) as the reference for comparison, it is estimated that a relative bioavailability of 78.9% was achieved after navel administration and of 57.9% by forearm administration. The results are in good agreement with the plasma data reported (79.9 and 49.9%, respectively). Both plasma profiles and urinary recovery data demonstrate that navel absorption produces a greater transdermal bioavailability of [^{14}C]testosterone than forearm administration (79.9 and 78.9% *versus* 49.9 and 57.9%).

Additional studies were also conducted in four other rhesus monkeys with 24-h topical administration of [^{14}C]testosterone. Results (Table I) again confirmed the earlier observations that navel administration yields a higher systemic bioavailability than forearm administration (37.64 ± 3.62% *versus* 22.51 ± 1.72%).

The results lead us to conclude that a greater transdermal bioavailability of testosterone can be achieved by topical administration of drug *via* the navel route. This observation also paved the foundation for studying the feasibility of using the navel area as the site for long-term (*e.g.*, longer than 1 month) transdermal administration of testosterone *via* a controlled-release drug delivery device (9).

Table I—Comparison of the Fraction of Applied Dose Recovered in Urine after Transdermal Administration of [^{14}C]Testosterone [a]

Skin site	Monkeys	Fraction of Applied Dose Recovered in Urine, Percent[b]
Navel	#46	33.55
	#158	42.78
	#230	44.64
	#231	29.57
Mean ± *SE*		37.64 (±3.62)
Forearm	#46	18.42
	#158	21.40
	#230	23.71
	#231	26.51
Mean ± *SE*		22.51 (±1.72)

[a] 5 μCi (25 μg) of testosterone were dissolved in acetone and then applied, drop-by-drop, on either navel or forearm (0.2 cm^2). After 24 h application, the residual drug was washed off for correcting the total dose administered. [b] Calculated from: % applied dose = (Total radioactivity in the urine collected for 5 d)/(5 μCi − Residual radioactivity on the skin) × 100%.

(1) T. S. Chen, "Pharmacology Encyclopedia of Chinese Drugs," (in Chinese) Eastern Books, Taipei, Taiwan, Republic of China, 1958, p. 250.
(2) S. K. Chandrasekaran, W. Bayne, and J. E. Shaw, *J. Pharm. Sci.*, **67**, 1370 (1978).
(3) A. Karim, *Drug Dev. Ind. Pharm.*, **9**, 671 (1983).
(4) W. R. Good, *Drug Dev. Ind. Pharm.*, **9**, 647 (1983).
(5) Y. W. Chien, *Drug Dev. Ind. Pharm.*, **9**, 497 (1983).
(6) A. Gerardin, J. Hirtz, P. Frankhauser, and J. Moppert, "Abstracts," *APhA/APS 31st National Meeting Abstracts*, 11(2), 84 (1981).
(7) P. W. Armstrong, J. A. Armstrong, G. S. Marks, J. McKinven, and S. Slaughter, *Am. J. Cardiol.*, **46**, 670 (1980).
(8) G. A. Portmann, in "Current Concepts in Pharmaceutical Sciences—Biopharmaceutics," J. Swarbrick, Ed., Lea & Febiger, Philadelphia, Pa., 1970, chap. 1.
(9) Y. W. Chien, *J. Pharm. Sci.*, in press.

Yie W. Chien
Controlled Drug Delivery Research Center
Rutgers University
College of Pharmacy
Busch Campus
Piscataway, NJ 08854

Received on July 7, 1982.
Accepted for publication December 1, 1983.
The author wishes to extend his great appreciation to Dr. B. Nicolova, who believed in the idea and has worked diligently to make it possible. He also wishes to thank Mrs. E. Skurkay for manuscript preparation.

Variability in the Determination of Fraction Metabolized in a Triangular Metabolic Problem and Its Resolution with Stable Isotope Methodology

Keyphrases □ Cinromide—anticonvulsant, fraction metabolized □ Isotope methodology—administration of labeled metabolites □ Triangular metabolic pathway—fraction metabolized-cinromide, rhesus monkey

To the Editor:

A particular case of precursor–product relationship arises when one metabolite (metabolite II) of a parent drug is formed from two precursors, the parent drug as well as one of its proximal metabolites (metabolite I). The resolution of this metabolic problem is complicated by the fact that the fraction of parent drug metabolized directly to metabolite II can only be obtained indirectly from the following difference:

$$f_m(P \rightarrow MII, \text{direct}) = f_m(P \rightarrow MII, \text{total}) - f_m(P \rightarrow MI) \times f_m(MI \rightarrow MII) \quad \text{(Eq. 1)}$$

where f_m represents fraction metabolized, P refers to parent drug, and MI and MII refer to metabolites I and II, respectively. The classical approach to the determination of the fractions metabolized (Eq. 1) using blood data requires three separate studies: administration of parent drug, metabolite I, and metabolite II to the same subject at different times. This approach involves several assumptions of constancy of metabolite clearances among the three studies. As a result, estimates of the various fractions of Eq. 1 are subject to significant error. This type of metabolic problem arose during the elucidation of the pharmacokinetic profile of cinromide (3-bromo-*N*-ethylcinnamamide)(P), a new antiepileptic drug. This drug is metabolized by *N*-deethylation to 3-bromocinnamamide (I) and by amide hydrolysis to 3-bromocinnamic acid (II). However, I is also metabolized to II by amide hydrolysis. The resolution of this metabolic scheme prior to the efficacy evaluation of cinromide in the primate model (1, 2) was of particular significance because I was found to have anticonvulsant properties (3, 4) and II reached steady-state levels 10–20-fold higher than those of the parent drug (2). In an earlier study where the classical approach (administration of cinromide, I, and II separately) was used in a group of six rhesus monkeys, several unrealistic findings were obtained (5). The fraction of dose of cinromide metabolized directly to II ranged from 5 to 100% (mean ± *SD* = 48 ± 32%). Also, the sum of the two fractions (f_m(P → I) + f_m(P → II, direct)) ranged from 64 to 140% and was larger than 100% in three of six monkeys. This large variability was attributed to the intrasubject variability in clearances of I and II among the three studies. To test this hypothesis, a new approach using stable isotope methodology was devised. This approach involved the simultaneous administration of cinromide, and different stable isotope-labeled variants of I and II, in which case the clearances of I and II were obtained while these metabolites were formed *in situ*.

Five chaired normal male rhesus monkeys (chronically catheterized) were used in this study. Dideuterated I (I–d_2) and monodeuterated II (II–d_1) were administered along with the unlabeled parent drug (d_0). These were synthesized using the methods described for the corresponding unlabeled species (6–8). The deuterium labels were placed on the α, β ethylene carbons of I–d_2, and the β carbon of II–d_1 to minimize any possible isotope effect. Any secondary kinetic deuterium isotope effect on deethylation and amide hydrolysis or on epoxide formation and ring opening of the ethylene carbons would generally not be significant (9). Single intravenous doses of cinromide–d_0 (75 mg) and II–d_1 (80 mg) were administered consecutively to each monkey. I–d_2 (70 mg) was administered intravenously 2 h later such that the concentrations of II–d_2 would not be too far apart from those of II–d_0 and II–d_1 and could be analyzed at the same time. Solutions of cinromide–d_0, I–d_2, and II–d_1 were prepared in 60% polyethylene glycol 400 to concentrations of 25, 25, and 10 mg/mL, respectively. Blood samples (2 mL) were taken at 0.2, 0.5, 0.75, 1, 1.5, 2, 2.25, 2.5, 3, 4, 5, 6, 8, 10, 12, and 16 h after administration of II–d_1. EDTA was used as an anticoagulant in each blood sample. After the administration of cinromide–d_0, I–d_2 and II–d_1, six species were monitored in each blood sample: the three administered species as well as I–d_0 and II–d_0 formed from cinromide (d_0) and II–d_2 formed from I–d_2. Aliquots of 0.2 mL of each sample were used to analyze cinromide by HPLC (10). Aliquots of 0.5 to 0.8 mL of blood were used to analyze I and II by direct probe insertion chemical ionization mass spectrometry. Compounds I and II were separated by successive extractions at different pH. Blood samples were extracted with benzene under neutral conditions to extract I; the aqueous phases were acidified and extracted with benzene to recover II and benzene extracts containing I were washed with 0.1 M NaOH. Benzene extracts containing II were shaken with 0.1 M NaOH, then reacidified and extracted back into benzene. Chlorinated analogues of I and II were used as internal standards for

0022-3549/84/0200-0285$01.00/0
© 1984, American Pharmaceutical Association

(1) T. S. Chen, "Pharmacology Encyclopedia of Chinese Drugs," (in Chinese) Eastern Books, Taipei, Taiwan, Republic of China, 1958, p. 250.
(2) S. K. Chandrasekaran, W. Bayne, and J. E. Shaw, *J. Pharm. Sci.*, **67**, 1370 (1978).
(3) A. Karim, *Drug Dev. Ind. Pharm.*, **9**, 671 (1983).
(4) W. R. Good, *Drug Dev. Ind. Pharm.*, **9**, 647 (1983).
(5) Y. W. Chien, *Drug Dev. Ind. Pharm.*, **9**, 497 (1983).
(6) A. Gerardin, J. Hirtz, P. Frankhauser, and J. Moppert, "Abstracts," *APhA/APS 31st National Meeting Abstracts*, 11(2), 84 (1981).
(7) P. W. Armstrong, J. A. Armstrong, G. S. Marks, J. McKinven, and S. Slaughter, *Am. J. Cardiol.*, **46**, 670 (1980).
(8) G. A. Portmann, in "Current Concepts in Pharmaceutical Sciences—Biopharmaceutics," J. Swarbrick, Ed., Lea & Febiger, Philadelphia, Pa., 1970, chap. 1.
(9) Y. W. Chien, *J. Pharm. Sci.*, in press.

Yie W. Chien
Controlled Drug Delivery Research Center
Rutgers University
College of Pharmacy
Busch Campus
Piscataway, NJ 08854

Received on July 7, 1982.
Accepted for publication December 1, 1983.
The author wishes to extend his great appreciation to Dr. B. Nicolova, who believed in the idea and has worked diligently to make it possible. He also wishes to thank Mrs. E. Skurkay for manuscript preparation.

Variability in the Determination of Fraction Metabolized in a Triangular Metabolic Problem and Its Resolution with Stable Isotope Methodology

Keyphrases □ Cinromide—anticonvulsant, fraction metabolized □ Isotope methodology—administration of labeled metabolites □ Triangular metabolic pathway—fraction metabolized-cinromide, rhesus monkey

To the Editor:

A particular case of precursor–product relationship arises when one metabolite (metabolite II) of a parent drug is formed from two precursors, the parent drug as well as one of its proximal metabolites (metabolite I). The resolution of this metabolic problem is complicated by the fact that the fraction of parent drug metabolized directly to metabolite II can only be obtained indirectly from the following difference:

$$f_m(P \rightarrow MII, \text{direct}) = f_m(P \rightarrow MII, \text{total}) - f_m(P \rightarrow MI) \times f_m(MI \rightarrow MII) \quad \text{(Eq. 1)}$$

where f_m represents fraction metabolized, P refers to parent drug, and MI and MII refer to metabolites I and II, respectively. The classical approach to the determination of the fractions metabolized (Eq. 1) using blood data requires three separate studies: administration of parent drug, metabolite I, and metabolite II to the same subject at different times. This approach involves several assumptions of constancy of metabolite clearances among the three studies. As a result, estimates of the various fractions of Eq. 1 are subject to significant error. This type of metabolic problem arose during the elucidation of the pharmacokinetic profile of cinromide (3-bromo-*N*-ethylcinnamamide)(P), a new antiepileptic drug. This drug is metabolized by *N*-deethylation to 3-bromocinnamamide (I) and by amide hydrolysis to 3-bromocinnamic acid (II). However, I is also metabolized to II by amide hydrolysis. The resolution of this metabolic scheme prior to the efficacy evaluation of cinromide in the primate model (1, 2) was of particular significance because I was found to have anticonvulsant properties (3, 4) and II reached steady-state levels 10–20-fold higher than those of the parent drug (2). In an earlier study where the classical approach (administration of cinromide, I, and II separately) was used in a group of six rhesus monkeys, several unrealistic findings were obtained (5). The fraction of dose of cinromide metabolized directly to II ranged from 5 to 100% (mean ± *SD* = 48 ± 32%). Also, the sum of the two fractions (f_m(P → I) + f_m(P → II, direct)) ranged from 64 to 140% and was larger than 100% in three of six monkeys. This large variability was attributed to the intrasubject variability in clearances of I and II among the three studies. To test this hypothesis, a new approach using stable isotope methodology was devised. This approach involved the simultaneous administration of cinromide, and different stable isotope-labeled variants of I and II, in which case the clearances of I and II were obtained while these metabolites were formed *in situ*.

Five chaired normal male rhesus monkeys (chronically catheterized) were used in this study. Dideuterated I (I–d_2) and monodeuterated II (II–d_1) were administered along with the unlabeled parent drug (d_0). These were synthesized using the methods described for the corresponding unlabeled species (6–8). The deuterium labels were placed on the α, β ethylene carbons of I–d_2, and the β carbon of II–d_1 to minimize any possible isotope effect. Any secondary kinetic deuterium isotope effect on deethylation and amide hydrolysis or on epoxide formation and ring opening of the ethylene carbons would generally not be significant (9). Single intravenous doses of cinromide–d_0 (75 mg) and II–d_1 (80 mg) were administered consecutively to each monkey. I–d_2 (70 mg) was administered intravenously 2 h later such that the concentrations of II–d_2 would not be too far apart from those of II–d_0 and II–d_1 and could be analyzed at the same time. Solutions of cinromide–d_0, I–d_2, and II–d_1 were prepared in 60% polyethylene glycol 400 to concentrations of 25, 25, and 10 mg/mL, respectively. Blood samples (2 mL) were taken at 0.2, 0.5, 0.75, 1, 1.5, 2, 2.25, 2.5, 3, 4, 5, 6, 8, 10, 12, and 16 h after administration of II–d_1. EDTA was used as an anticoagulant in each blood sample. After the administration of cinromide–d_0, I–d_2 and II–d_1, six species were monitored in each blood sample: the three administered species as well as I–d_0 and II–d_0 formed from cinromide (d_0) and II–d_2 formed from I–d_2. Aliquots of 0.2 mL of each sample were used to analyze cinromide by HPLC (10). Aliquots of 0.5 to 0.8 mL of blood were used to analyze I and II by direct probe insertion chemical ionization mass spectrometry. Compounds I and II were separated by successive extractions at different pH. Blood samples were extracted with benzene under neutral conditions to extract I; the aqueous phases were acidified and extracted with benzene to recover II and benzene extracts containing I were washed with 0.1 M NaOH. Benzene extracts containing II were shaken with 0.1 M NaOH, then reacidified and extracted back into benzene. Chlorinated analogues of I and II were used as internal standards for

0022-3549/84/0200-0285$01.00/0
© 1984, American Pharmaceutical Association

Table I—Fraction Metabolized for the Various Pathways of the System Cinromide 3-Bromocinnamamide (I) 4-3-Bromocinnamic Acid (II)

Method	Monkey	Cinromide → II, Total	Cinromide → I	I → II	Cinromide → II, Direct	Cinromide (I + II
Stable isotope (1 study)	203	0.48	0.29	0.23	0.41	0.70
	514A	0.49	0.45	0.34	0.34	0.79
	712A	0.37	0.39	0.34	0.24	0.63
	79321	0.79	0.40	0.58	0.52	0.92
	79325	0.52	0.40	0.23	0.43	0.83
	Mean	0.53	0.39	0.34	0.39	0.77
	SD	0.16	0.06	0.14	0.10	0.11
Classical (3 studies)	Mean	0.73	0.53	0.53	0.48	1.01
	SD	0.35	0.24	0.21	0.32	0.34

Table II—Assumptions of Constancy Involved in Solving a Triangular Metabolite System Using the Classical Approach

	Studies		
	1	2	3
Species administered	Parent Drug	MI	MII
Species formed	MI, MII	MII	
Assumptions	ClMI (Study 1) = ClMI (Study 2)	ClMII (Study 2) = ClMII (Study 3)	
	ClMII (Study 1) = ClMII (Study 3)		
	Cl[MI → MII] (Study 1) = Cl[MI → MII] (Study 2)		

the assays. The MS (VG-7070)[1] was interfaced with a data system (VG-2035F/B)[1] and operated in the selected ion monitoring mode. Methane was used as reagent gas for chemical ionization. The source temperature was 190°C. The protonated molecular ions of internal standard, d_0, d_1, and d_2 were monitored (m/z 182, 226, 227, and 230 for the analysis of I; 183, 227, 228, and 231 for the analysis of II). To avoid the interference of ^{81}Br–d_0 and ^{79}Br–d_2, the ion of ^{81}Br–d_2 was monitored in each dideuterated metabolite. The natural abundance of carbon-13 in each species was taken into consideration in calculating concentrations.

The kinetic analysis of the data was aimed at the determination of the various fractions metabolized required in Eq. 1 and was based on area calculations (11). The fraction metabolized[2] was calculated by the following equation:

$$f_m = \frac{(AUC_{met})p/mol.\ wt._{met} \times CL_{met}}{Dose\ p/mol.\ wt.\ p} \quad \text{(Eq. 2)}$$

where $(AUC_{met})p$ represents the area under the metabolite concentration curve after a dose of the precursor, CL_{met} is the elimination clearance of the metabolite, and mol. wt. represents the molecular weight. The area under the blood concentration–time curve for each compound was measured by the trapezoidal rule with extrapolation to infinity using the last several points of each curve. On the average, the area obtained without extrapolation accounted for 83% of the total area. Clearance was calculated from dose–area ratio. In this study, both metabolites had low extraction ratios and, therefore, are not subject to hepatic sequential single pass metabolism (13).

The average clearances of cinromide, I–d_2 and II–d_1 were 8.04 ± 3.32, 0.91 ± 0.29, and 0.77 ± 0.3 L/h, respectively. Table I lists individual values of the fraction metabolized *via* the various pathways of the cinromide–metabolite I–metabolite II system. The fraction of dose of cinromide metabolized to II by all routes (directly and indirectly) was 53 ± 16%. The fraction of dose of cinromide metabolized to I was 39 ± 6%, while the fraction of dose of I metabolized to II was 34 ± 14%. The fraction of dose of cinromide metabolized directly to II calculated according to Eq. 1 was 39 ± 10%. Thus, as primary metabolites of cinromide, I and II together account for 77 ± 11% of a dose. The corresponding fractions metabolized obtained in a previous study by the classical approach are also given in Table I. Although the values obtained in the present study were generally smaller, comparison of the values obtained by both methods showed no statistically significant difference for any of the pathways (Mann–Whitney test). However, the variability in the various fractions metabolized determined in the present study was much smaller. There were significant decreases in variance in the fraction of cinromide metabolized to I, in the fraction of cinromide metabolized to II directly, and in the sum of these two fractions (variance ratio test, $p < 0.05$). The superiority of the stable isotope method is also supported by the fact that no unrealistic value, (larger than 100%) was obtained for the sum of the two fractions of cinromide metabolized to I and II (directly). The reduction in the coefficient of variation of the fraction cinromide → I (45% to 15%) is of particular interest. In the previous study, it was found that the half life of I was significantly longer after a dose of cinromide (5.8 ± 1.2 h) than after administration of I (4.4 ± 0.8 h) which suggested that the clearance of I measured when it is administered would be an overestimate of its clearance when formed *in situ*. In such a case, the stable isotope approach offers unique advantages since it allows an estimate of the clearance of the metabolite formed *in situ*.

The findings of the present study can be put in broader perspective if an analysis of the limitations inherent to the classical approach is considered. This approach requires three studies (1, 2, and 3) in which three species (cinromide, I, and II) are administered separately (Table II). To solve Eq. 1, four assumptions of constancy of clearance are

[1] VG-Analytical, Altrincham, Cheshire, U.K.

[2] In light of the experimental design (intravenous administration of parent drug and metabolites), this fraction refers to the fraction of total body clearances as well as the fraction of dose of parent drug (12).

required. Three clearances operating in study 1 are estimated in studies 2 and 3. Study 2 estimates the elimination clearance of I while study 3 estimates the elimination clearance of II. Studies 2 and 3 together estimate the formation clearance of II from I. Also, the elimination clearance of II operating in study 2 is measured in study 3. Intrasubject variability in any of these clearances leads to unrealistic values for the fraction of parent drug metabolized directly to metabolite II. This variability can be minimized by the simultaneous administration of metabolite(s) and precursor(s). This is possible with the use of stable isotope methodology.

(1) J. S. Lockard, R. H. Levy, L. L. DuCharme, and W. C. Congdon, *Epilepsia*, **20**, 339 (1979).

(2) A. J. Wilensky, E. A. Lane, R. H. Levy, L. M. Ojemann, and P. N. Friel, *Eur. J. Clin. Pharmacol.*, **21**, 149 (1981).

(3) J. A. Cramer and R. H. Mattson, American Epilepsy Society Meeting, San Diego, Calif., 1980.

(4) J. S. Lockard, R. H. Levy, L. L. DuCharme, and W. C. Congdon, *Epilepsia*, **21**, 177 (1980).

(5) E. A. Lane, "Study on Parent-Metabolite Relationships for Cinromide and Two Metabolites," Ph.D. thesis, University of Washington, 1981.

(6) R. P. Hatch, J. Shringapure, and S. M. Weinreb, *J. Org. Chem.*, **43**, 4175 (1978).

(7) E. J. Corey and J. W. Suggs, *Tetrahedron Lett.*, **31**, 2647 (1975).

(8) E. C. Horning, "Org. Syn., Coll." Vol. III, Wiley, New York, N.Y., 1955, p. 172.

(9) R. B. Westkaemper and R. P. Hanzlik, *Arch. Biochem. Biophys.*, **208**, 195 (1981).

(10) E. A. Lane and R. H. Levy, *J. Pharm. Sci.*, **72**, 493 (1983).

(11) S. A. Kaplan, M. L. Jack, S. Cotler, and K. Alexander, *J. Pharmacokinet. Biopharm.*, **1**, 201 (1973).

(12) K. S. Pang and K. C. Kwan, *Drug Metab. Dispos.*, **11**, 79 (1983).

(13) K. S. Pang and J. R. Gillette, *J. Pharmacokinet. Biopharm.*, **7**, 275 (1979).

Huey-shin Lin
Biochemicals Department
Stine Laboratories
E.I. Dupont de Nemours and Company
Newark, DE 19711

René H. Levy[x]
Departments of Pharmaceutics
and Neurological Surgery, BG-20
Schools of Pharmacy and Medicine
University of Washington
Seattle, WA 98195

Elizabeth A. Lane
Clinical Studies
National Institute of Alcohol Abuse and Alcoholism
Alcohol, Drug Abuse and Mental Health Administration
Bethesda, MD 20205

W. Perry Gordon
National Institute of Public Health
Geitmyrsvegen, 75-Oslo- Norway

Received June 6, 1983.
Accepted for publication November 28, 1983.
Supported by National Institutes of Health Contract N01-NS-1-2282, Grant NS-04053, and Biomedical Research Development Grant 1 S08 RR 09082.

BOOKS

Natural Product Chemistry—A Mechanistic and Biosynthetic Approach to Secondary Metabolism. By KURT B. G. TORSSELL. John Wiley & Sons, Inc., One Wiley Drive, Somerset, NJ 08873. 1983. 401 pp. 16 × 23 cm. Price $54.95.

This book presents an overview of the current known and postulated biosynthetic pathways of the secondary metabolites, those natural products whose precursors are the common α-amino acids, sugars, and low-molecular weight carboxylic acids of the Krebs cycle. Although the physiological functions of many of these natural products have not yet been established, some have been found to play important roles in the regulation of animal and insect social behavior and development, and plant protection mechanisms.

The contents of this volume are organized into eight chapters, each of which is subdivided into various topics. An overview of the natural products field and the importance of these metabolites are presented in the first chapter. The remaining chapters present the biosynthetic pathways for seven different classes of natural products in addition to a brief introduction about the general chemistry, nomenclature, and background of each class. In the second chapter on carbohydrates, photosynthesis, the Krebs or citric acid cycle, monosaccharides, and polysaccharides are among the topics discussed. The biosynthesis of shikimic acid; its conversion to aromatic amino acids, such as tryptophan, tyrosine, and phenylalanine; biological hydroxylation mechanisms, and the biosynthesis of aromatic carboxylic acids, coumarins, quinones, and lignins are included in the third chapter. Chapter 4 details the biosyntheses of compounds (such as saturated and unsaturated fatty acids and the aromatic anthraquinones, flavonoids, and tropolones) that originate from the polyketide pathway by condensation of acetyl CoA. The mevalonic acid pathway to the terpenes, squalene, steroids, and carotenes is the subject of the fifth chapter. In the sixth chapter, the biosyntheses of amino acids, peptides, and proteins are presented. The alkaloids derived from the amino acids ornithine, lysine, tyrosine, and tryptophan, from anthranilic acid, and from the amination of terpenes are found in the seventh chapter. In the last chapter, the *N*-heterocyclic aromatic compounds, including pyrimidines, purines, pteridines, pyrroles, porphyrins, and corrin ring-containing compounds, are discussed. Each chapter also includes historical and biological information about some of the metabolites. The inclusion of this material appreciably enhances reader interest. A set of biosynthetic mechanistic problems and a bibliography are presented at the end of each chapter. Answers to the problems and author and subject indices are included at the end of the volume.

On the basis of the table of contents, this work appears to be an informative and valuable text on natural product biosynthesis which emphasizes the biosynthetic pathways in an organic mechanistic approach. This book is recommended by the publishers as a text for undergraduates and graduate students and a reference work for researchers in the field. However, many mechanistic discussions are vague and not very clear. The internal organization of paragraphs is poor. For example, the section on the NIH shift is very confusing for a reader not familiar with this topic. This lack of clarity is found in many other areas of this book. The absence of numbered structures forces the reader to search each figure or reaction sequence for a particular compound that is being discussed in the text. The absence of carbon atom numbering on some of the structures is not helpful. In conclusion, only those scientists well-versed in biosynthetic pathways will find this an easily readable text. The literature cited is very current, and the notable accomplishments of workers in the area of metabolic biosynthetic pathways have been included. The mechanistic approach to biosynthetic processes used by the author is a valuable and informative one.

Reviewed by Marcia Dawson
Life Sciences Division
SRI International
Menlo Park, CA 94025

required. Three clearances operating in study 1 are estimated in studies 2 and 3. Study 2 estimates the elimination clearance of I while study 3 estimates the elimination clearance of II. Studies 2 and 3 together estimate the formation clearance of II from I. Also, the elimination clearance of II operating in study 2 is measured in study 3. Intrasubject variability in any of these clearances leads to unrealistic values for the fraction of parent drug metabolized directly to metabolite II. This variability can be minimized by the simultaneous administration of metabolite(s) and precursor(s). This is possible with the use of stable isotope methodology.

(1) J. S. Lockard, R. H. Levy, L. L. DuCharme, and W. C. Congdon, *Epilepsia*, **20**, 339 (1979).

(2) A. J. Wilensky, E. A. Lane, R. H. Levy, L. M. Ojemann, and P. N. Friel, *Eur. J. Clin. Pharmacol.*, **21**, 149 (1981).

(3) J. A. Cramer and R. H. Mattson, American Epilepsy Society Meeting, San Diego, Calif., 1980.

(4) J. S. Lockard, R. H. Levy, L. L. DuCharme, and W. C. Congdon, *Epilepsia*, **21**, 177 (1980).

(5) E. A. Lane, "Study on Parent-Metabolite Relationships for Cinromide and Two Metabolites," Ph.D. thesis, University of Washington, 1981.

(6) R. P. Hatch, J. Shringapure, and S. M. Weinreb, *J. Org. Chem.*, **43**, 4175 (1978).

(7) E. J. Corey and J. W. Suggs, *Tetrahedron Lett.*, **31**, 2647 (1975).

(8) E. C. Horning, "Org. Syn., Coll." Vol. III, Wiley, New York, N.Y., 1955, p. 172.

(9) R. B. Westkaemper and R. P. Hanzlik, *Arch. Biochem. Biophys.*, **208**, 195 (1981).

(10) E. A. Lane and R. H. Levy, *J. Pharm. Sci.*, **72**, 493 (1983).

(11) S. A. Kaplan, M. L. Jack, S. Cotler, and K. Alexander, *J. Pharmacokinet. Biopharm.*, **1**, 201 (1973).

(12) K. S. Pang and K. C. Kwan, *Drug Metab. Dispos.*, **11**, 79 (1983).

(13) K. S. Pang and J. R. Gillette, *J. Pharmacokinet. Biopharm.*, **7**, 275 (1979).

Huey-shin Lin
Biochemicals Department
Stine Laboratories
E.I. Dupont de Nemours and Company
Newark, DE 19711

René H. Levy[x]
Departments of Pharmaceutics
and Neurological Surgery, BG-20
Schools of Pharmacy and Medicine
University of Washington
Seattle, WA 98195

Elizabeth A. Lane
Clinical Studies
National Institute of Alcohol Abuse and Alcoholism
Alcohol, Drug Abuse and Mental Health Administration
Bethesda, MD 20205

W. Perry Gordon
National Institute of Public Health
Geitmyrsvegen, 75-Oslo- Norway

Received June 6, 1983.
Accepted for publication November 28, 1983.
Supported by National Institutes of Health Contract N01-NS-1-2282, Grant NS-04053, and Biomedical Research Development Grant 1 S08 RR 09082.

BOOKS

Natural Product Chemistry—A Mechanistic and Biosynthetic Approach to Secondary Metabolism. By KURT B. G. TORSSELL. John Wiley & Sons, Inc., One Wiley Drive, Somerset, NJ 08873. 1983. 401 pp. 16 × 23 cm. Price $54.95.

This book presents an overview of the current known and postulated biosynthetic pathways of the secondary metabolites, those natural products whose precursors are the common α-amino acids, sugars, and low-molecular weight carboxylic acids of the Krebs cycle. Although the physiological functions of many of these natural products have not yet been established, some have been found to play important roles in the regulation of animal and insect social behavior and development, and plant protection mechanisms.

The contents of this volume are organized into eight chapters, each of which is subdivided into various topics. An overview of the natural products field and the importance of these metabolites are presented in the first chapter. The remaining chapters present the biosynthetic pathways for seven different classes of natural products in addition to a brief introduction about the general chemistry, nomenclature, and background of each class. In the second chapter on carbohydrates, photosynthesis, the Krebs or citric acid cycle, monosaccharides, and polysaccharides are among the topics discussed. The biosynthesis of shikimic acid; its conversion to aromatic amino acids, such as tryptophan, tyrosine, and phenylalanine; biological hydroxylation mechanisms, and the biosynthesis of aromatic carboxylic acids, coumarins, quinones, and lignins are included in the third chapter. Chapter 4 details the biosyntheses of compounds (such as saturated and unsaturated fatty acids and the aromatic anthraquinones, flavonoids, and tropolones) that originate from the polyketide pathway by condensation of acetyl CoA. The mevalonic acid pathway to the terpenes, squalene, steroids, and carotenes is the subject of the fifth chapter. In the sixth chapter, the biosyntheses of amino acids, peptides, and proteins are presented. The alkaloids derived from the amino acids ornithine, lysine, tyrosine, and tryptophan, from anthranilic acid, and from the amination of terpenes are found in the seventh chapter. In the last chapter, the *N*-heterocyclic aromatic compounds, including pyrimidines, purines, pteridines, pyrroles, porphyrins, and corrin ring-containing compounds, are discussed. Each chapter also includes historical and biological information about some of the metabolites. The inclusion of this material appreciably enhances reader interest. A set of biosynthetic mechanistic problems and a bibliography are presented at the end of each chapter. Answers to the problems and author and subject indices are included at the end of the volume.

On the basis of the table of contents, this work appears to be an informative and valuable text on natural product biosynthesis which emphasizes the biosynthetic pathways in an organic mechanistic approach. This book is recommended by the publishers as a text for undergraduates and graduate students and a reference work for researchers in the field. However, many mechanistic discussions are vague and not very clear. The internal organization of paragraphs is poor. For example, the section on the NIH shift is very confusing for a reader not familiar with this topic. This lack of clarity is found in many other areas of this book. The absence of numbered structures forces the reader to search each figure or reaction sequence for a particular compound that is being discussed in the text. The absence of carbon atom numbering on some of the structures is not helpful. In conclusion, only those scientists well-versed in biosynthetic pathways will find this an easily readable text. The literature cited is very current, and the notable accomplishments of workers in the area of metabolic biosynthetic pathways have been included. The mechanistic approach to biosynthetic processes used by the author is a valuable and informative one.

Reviewed by Marcia Dawson
Life Sciences Division
SRI International
Menlo Park, CA 94025

Host Factors in Human Carcinogenesis. (IARC Scientific Publications, No. 30.) *Edited by* H. BARTSCH, B. ARMSTRONG, *and* W. DAVIS. International Agency for Research on Cancer, Health and Biomedical Information Programme, World Health Organization, Geneva 27, Switzerland. 1982. 581 pp. 17 × 24 cm. Price $50.00 (Sw. Fr. 100).

Current research on carcinogenesis from many laboratories is beginning to elucidate several facets of the complex cascade and progression of events that lead from the initiation of the biochemical lesions to the development of metastatic potential. Along with this progress in the areas of biochemistry and the molecular biology of cancer, other laboratories are reporting both human epidemiological and animal model studies which indicate that conditions within the individual at risk may influence the development of cancer and thereby susceptibility. A knowledge of the interactions between these "host factors" which influence susceptibility and the various stages of carcinogenesis will allow for the development of strategies to aid in the prevention of cancer.

The main goal of this book is to update the knowledge concerning the mechanisms by which various factors inherent in the host may alter the initiation and developmental progression of events leading to cancer. To meet this goal, the editors have drawn together investigators from the most promising research areas concerning host susceptibility to carcinogenesis.

The volume represents a compilation of papers presented at an international symposium and suffers from uneven presentation, as is often the case of such volumes. However, it does make the material presented available to a larger audience. The individual contributions take the format of either short reviews of the literature or reviews of the research efforts of a particular laboratory and presentations of specific research reports. Several of the latter lack sufficient introductory material to determine the significance of the studies in the overall field. This problem is somewhat overcome by the inclusion of a rapporteur's report summarizing and placing in perspective the individual presentations within each section. Most areas of the subject are given adequate coverage, with the exception of diet and nutrition. Only two reports are concerned with this topic (although it is mentioned in several others), which is rapidly being shown to be an important host factor in chemical carcinogenesis and which is generally under the control of the individual. It is hoped that this volume will inspire further studies to develop the mechanisms by which factors inherent within the host alter cancer susceptibility.

Overall, this volume makes a successful attempt to combine the divergent research interests concerned with the role of various host factors in altering susceptibility, and I can recommend it for those who are interested in developing more knowledge in this area. It will be useful for those considering this topic for the first time and even those whose individual research interest in host factors do not allow them to maintain current knowledge of the many areas of research concerned with this topic.

Reviewed by Johnnie R. Hayes
Department of Pharmacology and Toxicology
Medical College of Virginia
Virginia Commonwealth University
Richmond, VA 23298

Techniques of Solubilization of Drugs. (Drugs and the Pharmaceutical Sciences Series, Vol 12.) Edited by SAMUEL H. YALKOWSKY. Marcel Dekker, 270 Madison Avenue, New York NY 10016. 1981. 224 pp. 15 × 23 cm. Price $34.50 (20% higher outside the U.S.).

Techniques of Solubilization of Drugs is a very useful handbook for researchers involved in drug development. The problem and necessity of proper solubilization of drugs are nicely discussed in the two chapters by the editor, S. Yalkowsky. Of the other four chapters, the one on solubilization in surfactant systems by A. T. Florence deserves particular attention, as the author gives a rather complete overview of the subject. In the chapter on the solid-state manipulation, probably more attention should be given to the very important polymeric carriers and solid dispersions in matrices. The chapter on the use of complex formation for drug solubilization appears to use old literature data, and it seems that either the approach does not have much use or the field was not thoroughly searched for this review. The chapter on drug derivatization points out the importance and, in many ways, how to solve the problem of solubility by chemical means, such as prodrugs, but the examples seem to concentrate primarily on the potential usefulness of some amino acid esters. There are some misquotes from the literature.

Overall, the book is a very useful one and it defines the highly multidisciplinary field of effecting drug solubility by a variety of manipulations.

Reviewed by Nicholas Bodor
Department of Medicinal Chemistry
College of Pharmacy
J. Hillis Miller Health Center
University of Florida
Gainesville, FL 32610

Diuretics: Chemistry, Pharmacology, and Medicine. Edited by EDWARD J. CRAGOE, Jr. Wiley-Interscience, 605 Third Avenue New York, NY 10016. 1983. 694 pp. 15 × 23 cm. Price $80.00.

Diuretics: Chemistry, Pharmacology, and Medicine is the second volume in the "Chemistry and Pharmacology of Drugs" series. The series is edited by Daniel Lednicer, and this volume is edited by Edward J. Cragoe, Jr. The book has the following two goals: updating the field of diuretic research since the last comprehensive review was written by George deStevens in 1963 and laying the groundwork for the next era in diuretic research. It succeeds admirably on both counts by giving a balanced account of physiological principles, structure–activity relationships, mechanistic considerations, clinical data, and biochemical perspectives.

The book begins with a chapter on kidney physiology by Edward H. Blaine. Although not an exhaustive treatment, it is appropriate to the beginning of the book and serves as a useful digest of information with a good list of references. Nine subsequent chapters, describing the medical chemistry of diuretics, are divided according to chemical structure. Some decisions regarding chemical class were clearly difficult (4-anilino-3-pyridinosulfonamides are found under six-membered heterocycles rather than under sulfonamides), but any confusion is readily cleared up by consulting the index. The emphasis in these chapters is on structure–activity relationships: molecules have been dissected and the effect of substitution at each chemically accessible atom has been tabulated.

The chapter on sulfonamide diuretics by Richard C. Allen is a comprehensive and thorough treatment of the subject (153 pages). It is richly illustrated with figures and tables, and documents with over 700 references the 20 years of development in this area since the deStevens review. The chapters on (aryloxy)acetic acids and 2-aminomethylphenols have already appeared in large part in a 1978 ACS monograph, "Diuretic Agents," also edited by Dr. Cragoe. To their credit, the authors (Edward J. Cragoe and Robert L. Smith) have updated the tables on older chemical series with additional entries and have included new compounds that have appeared in the literature between 1978 and 1982. The next six chapters—covering pyrazine diuretics, three- and five-membered heterocyclic diuretics, tri- and tetracyclic heterocycles, six-membered monocyclic heterocycles, bicyclic heterocycles, and the inevitable "others"—were all written by Dr. Cragoe and maintain a standard of clarity and conciseness throughout.

The book concludes with a chapter on hormonal regulators of the kidney (R. L. Smith), which this reviewer found to be a lucid and scholarly synthesis of a large amount of diverse information (600 references). This chapter succeeds in bringing together the myriad effects and complex interrelationships among antidiuretic hormone, the renin–angiotensin–aldosterone system, the kallikrein–kinin system, and the prostaglandins, as well as considering the possible role of the hypothetical natriuretic hormone.

Throughout the book, tables have been effectively used to clarify structure–activity relationships, and the chapters have a logical organization, which is reinforced with a detailed outline at the beginning of each chapter. Inexplicably, the figures and tables are printed with a quality that varies from sharp to almost smudged. Although not a serious flaw, this reviewer found it an unfortunate distraction in a book that is otherwise crisply reproduced. Also distracting is the use of various scoring systems (rather than actual data) to present diuretic activity in several chapters. Although the format in which data were presented was clearly out of the authors' control in most cases, these scoring systems never-

Host Factors in Human Carcinogenesis. (IARC Scientific Publications, No. 30.) *Edited by* H. BARTSCH, B. ARMSTRONG, *and* W. DAVIS. International Agency for Research on Cancer, Health and Biomedical Information Programme, World Health Organization, Geneva 27, Switzerland. 1982. 581 pp. 17 × 24 cm. Price $50.00 (Sw. Fr. 100).

Current research on carcinogenesis from many laboratories is beginning to elucidate several facets of the complex cascade and progression of events that lead from the initiation of the biochemical lesions to the development of metastatic potential. Along with this progress in the areas of biochemistry and the molecular biology of cancer, other laboratories are reporting both human epidemiological and animal model studies which indicate that conditions within the individual at risk may influence the development of cancer and thereby susceptibility. A knowledge of the interactions between these "host factors" which influence susceptibility and the various stages of carcinogenesis will allow for the development of strategies to aid in the prevention of cancer.

The main goal of this book is to update the knowledge concerning the mechanisms by which various factors inherent in the host may alter the initiation and developmental progression of events leading to cancer. To meet this goal, the editors have drawn together investigators from the most promising research areas concerning host susceptibility to carcinogenesis.

The volume represents a compilation of papers presented at an international symposium and suffers from uneven presentation, as is often the case of such volumes. However, it does make the material presented available to a larger audience. The individual contributions take the format of either short reviews of the literature or reviews of the research efforts of a particular laboratory and presentations of specific research reports. Several of the latter lack sufficient introductory material to determine the significance of the studies in the overall field. This problem is somewhat overcome by the inclusion of a rapporteur's report summarizing and placing in perspective the individual presentations within each section. Most areas of the subject are given adequate coverage, with the exception of diet and nutrition. Only two reports are concerned with this topic (although it is mentioned in several others), which is rapidly being shown to be an important host factor in chemical carcinogenesis and which is generally under the control of the individual. It is hoped that this volume will inspire further studies to develop the mechanisms by which factors inherent within the host alter cancer susceptibility.

Overall, this volume makes a successful attempt to combine the divergent research interests concerned with the role of various host factors in altering susceptibility, and I can recommend it for those who are interested in developing more knowledge in this area. It will be useful for those considering this topic for the first time and even those whose individual research interest in host factors do not allow them to maintain current knowledge of the many areas of research concerned with this topic.

Reviewed by Johnnie R. Hayes
Department of Pharmacology and Toxicology
Medical College of Virginia
Virginia Commonwealth University
Richmond, VA 23298

Techniques of Solubilization of Drugs. (Drugs and the Pharmaceutical Sciences Series, Vol 12.) Edited by SAMUEL H. YALKOWSKY. Marcel Dekker, 270 Madison Avenue, New York NY 10016. 1981. 224 pp. 15 × 23 cm. Price $34.50 (20% higher outside the U.S.).

Techniques of Solubilization of Drugs is a very useful handbook for researchers involved in drug development. The problem and necessity of proper solubilization of drugs are nicely discussed in the two chapters by the editor, S. Yalkowsky. Of the other four chapters, the one on solubilization in surfactant systems by A. T. Florence deserves particular attention, as the author gives a rather complete overview of the subject. In the chapter on the solid-state manipulation, probably more attention should be given to the very important polymeric carriers and solid dispersions in matrices. The chapter on the use of complex formation for drug solubilization appears to use old literature data, and it seems that either the approach does not have much use or the field was not thoroughly searched for this review. The chapter on drug derivatization points out the importance and, in many ways, how to solve the problem of solubility by chemical means, such as prodrugs, but the examples seem to concentrate primarily on the potential usefulness of some amino acid esters. There are some misquotes from the literature.

Overall, the book is a very useful one and it defines the highly multidisciplinary field of effecting drug solubility by a variety of manipulations.

Reviewed by Nicholas Bodor
Department of Medicinal Chemistry
College of Pharmacy
J. Hillis Miller Health Center
University of Florida
Gainesville, FL 32610

Diuretics: Chemistry, Pharmacology, and Medicine. Edited by EDWARD J. CRAGOE, Jr. Wiley-Interscience, 605 Third Avenue New York, NY 10016. 1983. 694 pp. 15 × 23 cm. Price $80.00.

Diuretics: Chemistry, Pharmacology, and Medicine is the second volume in the "Chemistry and Pharmacology of Drugs" series. The series is edited by Daniel Lednicer, and this volume is edited by Edward J. Cragoe, Jr. The book has the following two goals: updating the field of diuretic research since the last comprehensive review was written by George deStevens in 1963 and laying the groundwork for the next era in diuretic research. It succeeds admirably on both counts by giving a balanced account of physiological principles, structure–activity relationships, mechanistic considerations, clinical data, and biochemical perspectives.

The book begins with a chapter on kidney physiology by Edward H. Blaine. Although not an exhaustive treatment, it is appropriate to the beginning of the book and serves as a useful digest of information with a good list of references. Nine subsequent chapters, describing the medical chemistry of diuretics, are divided according to chemical structure. Some decisions regarding chemical class were clearly difficult (4-anilino-3-pyridinosulfonamides are found under six-membered heterocycles rather than under sulfonamides), but any confusion is readily cleared up by consulting the index. The emphasis in these chapters is on structure–activity relationships: molecules have been dissected and the effect of substitution at each chemically accessible atom has been tabulated.

The chapter on sulfonamide diuretics by Richard C. Allen is a comprehensive and thorough treatment of the subject (153 pages). It is richly illustrated with figures and tables, and documents with over 700 references the 20 years of development in this area since the deStevens review. The chapters on (aryloxy)acetic acids and 2-aminomethylphenols have already appeared in large part in a 1978 ACS monograph, "Diuretic Agents," also edited by Dr. Cragoe. To their credit, the authors (Edward J. Cragoe and Robert L. Smith) have updated the tables on older chemical series with additional entries and have included new compounds that have appeared in the literature between 1978 and 1982. The next six chapters—covering pyrazine diuretics, three- and five-membered heterocyclic diuretics, tri- and tetracyclic heterocycles, six-membered monocyclic heterocycles, bicyclic heterocycles, and the inevitable "others"—were all written by Dr. Cragoe and maintain a standard of clarity and conciseness throughout.

The book concludes with a chapter on hormonal regulators of the kidney (R. L. Smith), which this reviewer found to be a lucid and scholarly synthesis of a large amount of diverse information (600 references). This chapter succeeds in bringing together the myriad effects and complex interrelationships among antidiuretic hormone, the renin–angiotensin–aldosterone system, the kallikrein–kinin system, and the prostaglandins, as well as considering the possible role of the hypothetical natriuretic hormone.

Throughout the book, tables have been effectively used to clarify structure–activity relationships, and the chapters have a logical organization, which is reinforced with a detailed outline at the beginning of each chapter. Inexplicably, the figures and tables are printed with a quality that varies from sharp to almost smudged. Although not a serious flaw, this reviewer found it an unfortunate distraction in a book that is otherwise crisply reproduced. Also distracting is the use of various scoring systems (rather than actual data) to present diuretic activity in several chapters. Although the format in which data were presented was clearly out of the authors' control in most cases, these scoring systems never-

Host Factors in Human Carcinogenesis. (IARC Scientific Publications, No. 30.) *Edited by* H. BARTSCH, B. ARMSTRONG, *and* W. DAVIS. International Agency for Research on Cancer, Health and Biomedical Information Programme, World Health Organization, Geneva 27, Switzerland. 1982. 581 pp. 17 × 24 cm. Price $50.00 (Sw. Fr. 100).

Current research on carcinogenesis from many laboratories is beginning to elucidate several facets of the complex cascade and progression of events that lead from the initiation of the biochemical lesions to the development of metastatic potential. Along with this progress in the areas of biochemistry and the molecular biology of cancer, other laboratories are reporting both human epidemiological and animal model studies which indicate that conditions within the individual at risk may influence the development of cancer and thereby susceptibility. A knowledge of the interactions between these "host factors" which influence susceptibility and the various stages of carcinogenesis will allow for the development of strategies to aid in the prevention of cancer.

The main goal of this book is to update the knowledge concerning the mechanisms by which various factors inherent in the host may alter the initiation and developmental progression of events leading to cancer. To meet this goal, the editors have drawn together investigators from the most promising research areas concerning host susceptibility to carcinogenesis.

The volume represents a compilation of papers presented at an international symposium and suffers from uneven presentation, as is often the case of such volumes. However, it does make the material presented available to a larger audience. The individual contributions take the format of either short reviews of the literature or reviews of the research efforts of a particular laboratory and presentations of specific research reports. Several of the latter lack sufficient introductory material to determine the significance of the studies in the overall field. This problem is somewhat overcome by the inclusion of a rapporteur's report summarizing and placing in perspective the individual presentations within each section. Most areas of the subject are given adequate coverage, with the exception of diet and nutrition. Only two reports are concerned with this topic (although it is mentioned in several others), which is rapidly being shown to be an important host factor in chemical carcinogenesis and which is generally under the control of the individual. It is hoped that this volume will inspire further studies to develop the mechanisms by which factors inherent within the host alter cancer susceptibility.

Overall, this volume makes a successful attempt to combine the divergent research interests concerned with the role of various host factors in altering susceptibility, and I can recommend it for those who are interested in developing more knowledge in this area. It will be useful for those considering this topic for the first time and even those whose individual research interest in host factors do not allow them to maintain current knowledge of the many areas of research concerned with this topic.

Reviewed by Johnnie R. Hayes
Department of Pharmacology and Toxicology
Medical College of Virginia
Virginia Commonwealth University
Richmond, VA 23298

Techniques of Solubilization of Drugs. (Drugs and the Pharmaceutical Sciences Series, Vol 12.) Edited by SAMUEL H. YALKOWSKY. Marcel Dekker, 270 Madison Avenue, New York NY 10016. 1981. 224 pp. 15 × 23 cm. Price $34.50 (20% higher outside the U.S.).

Techniques of Solubilization of Drugs is a very useful handbook for researchers involved in drug development. The problem and necessity of proper solubilization of drugs are nicely discussed in the two chapters by the editor, S. Yalkowsky. Of the other four chapters, the one on solubilization in surfactant systems by A. T. Florence deserves particular attention, as the author gives a rather complete overview of the subject. In the chapter on the solid-state manipulation, probably more attention should be given to the very important polymeric carriers and solid dispersions in matrices. The chapter on the use of complex formation for drug solubilization appears to use old literature data, and it seems that either the approach does not have much use or the field was not thoroughly searched for this review. The chapter on drug derivatization points out the importance and, in many ways, how to solve the problem of solubility by chemical means, such as prodrugs, but the examples seem to concentrate primarily on the potential usefulness of some amino acid esters. There are some misquotes from the literature.

Overall, the book is a very useful one and it defines the highly multidisciplinary field of effecting drug solubility by a variety of manipulations.

Reviewed by Nicholas Bodor
Department of Medicinal Chemistry
College of Pharmacy
J. Hillis Miller Health Center
University of Florida
Gainesville, FL 32610

Diuretics: Chemistry, Pharmacology, and Medicine. Edited by EDWARD J. CRAGOE, Jr. Wiley-Interscience, 605 Third Avenue New York, NY 10016. 1983. 694 pp. 15 × 23 cm. Price $80.00.

Diuretics: Chemistry, Pharmacology, and Medicine is the second volume in the "Chemistry and Pharmacology of Drugs" series. The series is edited by Daniel Lednicer, and this volume is edited by Edward J. Cragoe, Jr. The book has the following two goals: updating the field of diuretic research since the last comprehensive review was written by George deStevens in 1963 and laying the groundwork for the next era in diuretic research. It succeeds admirably on both counts by giving a balanced account of physiological principles, structure–activity relationships, mechanistic considerations, clinical data, and biochemical perspectives.

The book begins with a chapter on kidney physiology by Edward H. Blaine. Although not an exhaustive treatment, it is appropriate to the beginning of the book and serves as a useful digest of information with a good list of references. Nine subsequent chapters, describing the medical chemistry of diuretics, are divided according to chemical structure. Some decisions regarding chemical class were clearly difficult (4-anilino-3-pyridinosulfonamides are found under six-membered heterocycles rather than under sulfonamides), but any confusion is readily cleared up by consulting the index. The emphasis in these chapters is on structure–activity relationships: molecules have been dissected and the effect of substitution at each chemically accessible atom has been tabulated.

The chapter on sulfonamide diuretics by Richard C. Allen is a comprehensive and thorough treatment of the subject (153 pages). It is richly illustrated with figures and tables, and documents with over 700 references the 20 years of development in this area since the deStevens review. The chapters on (aryloxy)acetic acids and 2-aminomethylphenols have already appeared in large part in a 1978 ACS monograph, "Diuretic Agents," also edited by Dr. Cragoe. To their credit, the authors (Edward J. Cragoe and Robert L. Smith) have updated the tables on older chemical series with additional entries and have included new compounds that have appeared in the literature between 1978 and 1982. The next six chapters—covering pyrazine diuretics, three- and five-membered heterocyclic diuretics, tri- and tetracyclic heterocycles, six-membered monocyclic heterocycles, bicyclic heterocycles, and the inevitable "others"—were all written by Dr. Cragoe and maintain a standard of clarity and conciseness throughout.

The book concludes with a chapter on hormonal regulators of the kidney (R. L. Smith), which this reviewer found to be a lucid and scholarly synthesis of a large amount of diverse information (600 references). This chapter succeeds in bringing together the myriad effects and complex interrelationships among antidiuretic hormone, the renin–angiotensin–aldosterone system, the kallikrein–kinin system, and the prostaglandins, as well as considering the possible role of the hypothetical natriuretic hormone.

Throughout the book, tables have been effectively used to clarify structure–activity relationships, and the chapters have a logical organization, which is reinforced with a detailed outline at the beginning of each chapter. Inexplicably, the figures and tables are printed with a quality that varies from sharp to almost smudged. Although not a serious flaw, this reviewer found it an unfortunate distraction in a book that is otherwise crisply reproduced. Also distracting is the use of various scoring systems (rather than actual data) to present diuretic activity in several chapters. Although the format in which data were presented was clearly out of the authors' control in most cases, these scoring systems never-

theless make it difficult to compare data across chemical classes without excessive page flipping.

This book tries to offer something for the medicinal chemist, the renal pharmacologist and physiologist, and the physician. With its interdisciplinary approach it can be highly recommended to all three, but particularly to the medicinal chemist because of its emphasis on structure–activity relationships and possible future directions for diuretic research.

Reviewed by Gregory M. Shutske
Department of Chemical Research
Hoechst-Roussel Pharmaceuticals, Inc.
Somerville, NJ 08876

Polyether Antibiotics, Volume 2: Naturally Occurring Acid Ionophores. Edited by JOHN W. WESLEY. Marcel Dekker, 270 Madison Avenue, New York, NY 10016. 1983. 415 pp. 15 × 23 cm. Price $65.00 (20% higher outside the U.S. and Canada).

This work is the second of a two-volume set on polyether antibiotics. As the title indicates, it concentrates on the chemical aspects in this field whereas the microbiology, biosynthesis, pharmacology, and veterinary applications were covered in the first volume. The editor has chosen an excellent array of contributing authors, each of whom has done important original work in this field. The resulting volume therefore has the added advantage of being authoritative as well as informative.

The first chapter by Yoshito Kishi is an excellent review of the total synthesis of many of the polyethers which not only includes the author's own contributions, but also a critical view of other major contributors to this field. This is followed by a review of known chemical modifications of this class of antibiotics, which focuses attention on the lack of progress in this aspect of polyether chemistry in light of the high level of understanding brought to bear by X-ray crystallography. The remainder of this book covers the major contributions made to polyether chemistry by physical chemistry including X-ray crystallography, mass spectrometry, and ^{1}H- and ^{13}C-NMR. The authors of each of these sections used similar formats with illustrations, figures, and stereoviews. Each also tried to highlight the strengths and limitations of these various techniques.

The general tone of this book is to give the reader an overview and an exposition with an eye on future research. As such, this volume as well as the previous one, should prove useful as both a primer for the novice researcher and as a review and reference source for the established investigator. As the reviewer of Volume I noted in this journal, the subject index of Volume II is also somewhat inadequate and may prove a hindrance for those less familiar with this field. This book generally includes work up to 1980—only one author (Y. Kishi) attempted to update his chapter to cover work done in 1981.

In conclusion, this volume gives an excellent coverage of the subject matter it sets out to review. It has been well edited, is authoritative, and generally error free. It will surely be of great value to anyone interested in these fascinating antibiotics.

Reviewed by Manuel Debono
Lilly Research Laboratories
Microbiological and Fermentation Products Division
Indianapolis, IN 46285

Applied Statistics: A Handbook of Techniques, 5th Ed. By LOTHAR SACHS (translated by ZENON REYNAROWYCH). Springer-Verlag New York, Inc., 175 Fifth Avenue, New York, NY 10010. 1983. 706 pp. 16 × 24 cm.

This book was written "... both as an introductory and follow-up text ... and as a reference book with a collection of formulas and tables, numerous cross-references, and extensive bibliography." Satisfying such divergent purposes in one book is difficult, and the author does not entirely succeed. Although written at an introductory level, I found the organization of the material too confusing and the coverage too encompassing for an introductory text.

The book extensively covers the techniques relevant to most data analysis problems addressed in introductory texts in applied statistics. Chapter 0 covers arithmetic operations. Chapter 1 covers a wide variety of techniques relating to one variable. Chapter 2 suggests the diversity of specialized statistical problems and techniques arising in medicine and engineering and directs the reader to the relevant literature. Chapters 3–7 cover the comparison of two or more samples, correlation and regression, the analysis of contingency tables, and analysis of variance. In each case, most of the relevant parametric and nonparametric techniques are presented. Keeping with the introductory level of the book, general linear and categorical models are not discussed.

For a handbook, the inclusion of material could be better delineated. You might find a relatively unknown technique such as the minimum discrimination information statistic for analyzing multiway contingency tables or the Thorndike nomogram for evaluating Poisson probabilities. However, you will fail to find techniques for analyzing covariance studies, repeated measure studies, or studies with missing data. But, if the technique is there, its stepwise execution is lucidly illustrated. Assumptions are stated in practical terms and cross-referenced to techniques for testing their validity. The original and related references are always given. Statistical tables are readily accessible due to their placement in the text and convenient page referencing.

This easy use is one of the joys of this book. Another is the pleasure of perusing the book. To quote the author, "The numerous cross-references appearing throughout the text point out various *interconnections*. A serendipitous experience is possible." I concur.

Reviewed by Mark A. Johnson
The Upjohn Company
Kalamazoo, MI 49001

Structure–Activity Correlation as a Predictive Tool in Toxicology: Fundamentals Methods, and Applications. Edited by LEON GOLDBERG. Hemisphere Publishing Corp., 19 W. 44th St., New York, NY 10036. 330 pp. 16 × 23 cm. Price $49.50.

This book is a reasonably current review of the application of quantitative structure–activity relationships (QSAR) to problems in toxicology. Although the work is the result of a symposium which was held in February 1981, it is remarkably well-written and not at all like the usual symposia proceedings. The book is divided into four sections that, for the most part, are well-organized and show little evidence of overlap or duplication.

The first section covers biological activities and describes moderately well the problems that toxicologists have in defining and measuring the biological effects of toxic substances. Of particular interest are the examples in Chapter 2 on inhibition of chemical carcinogenisis by various factors which modify procarcinogen activation. The survey of literature and computer-accessible data bases for obtaining information on both toxicological responses and physical and chemical properties of toxicants is particularly helpful.

The second section contains a somewhat sketchy but suggestive survey of biochemical mechanisms underlying the toxic action of chemicals (Chapter 4) and an excellent historical overview of the physical and chemical parameters that have been correlated to biological activities (Chapter 5).

The third section, "Correlative Methods," contains the heart of the material presented in this book. An excellent review (Chapter 6) of multiple regression (Hansch) analysis by Y. C. Martin clearly states the fundamental assumptions that are frequently not met by the novice. Criteria for the acceptable quality of the biological data, for the selection of appropriate physiochemical parameters, and for the intellegent use of regression analysis methods are all succinctly stated. Chapter 7, by P. C. Jurs, contains a reasonably intelligible introduction to the use of pattern-recognition techniques for QSAR; however, the novice unfamiliar with the statistical basis for this method may find the discussion somewhat confusing. Finally, Chapter 8 contains a discussion of the application of quantum chemical methods to predicting the relative carcinogenicity of a series of polycyclic aromatic hydrocarbons.

The remainder of the book consists of examples of applications of QSAR methods to toxicological problems. Although the quality of those application reviews varies considerably, each topic is covered with sufficient depth such that these reviews should serve as a useful guide to the recent literature. Chapters 10 (Computer-Assisted Prediction of Me-

theless make it difficult to compare data across chemical classes without excessive page flipping.

This book tries to offer something for the medicinal chemist, the renal pharmacologist and physiologist, and the physician. With its interdisciplinary approach it can be highly recommended to all three, but particularly to the medicinal chemist because of its emphasis on structure–activity relationships and possible future directions for diuretic research.

Reviewed by Gregory M. Shutske
Department of Chemical Research
Hoechst-Roussel Pharmaceuticals, Inc.
Somerville, NJ 08876

Polyether Antibiotics, Volume 2: Naturally Occurring Acid Ionophores. Edited by JOHN W. WESLEY. Marcel Dekker, 270 Madison Avenue, New York, NY 10016. 1983. 415 pp. 15 × 23 cm. Price $65.00 (20% higher outside the U.S. and Canada).

This work is the second of a two-volume set on polyether antibiotics. As the title indicates, it concentrates on the chemical aspects in this field whereas the microbiology, biosynthesis, pharmacology, and veterinary applications were covered in the first volume. The editor has chosen an excellent array of contributing authors, each of whom has done important original work in this field. The resulting volume therefore has the added advantage of being authoritative as well as informative.

The first chapter by Yoshito Kishi is an excellent review of the total synthesis of many of the polyethers which not only includes the author's own contributions, but also a critical view of other major contributors to this field. This is followed by a review of known chemical modifications of this class of antibiotics, which focuses attention on the lack of progress in this aspect of polyether chemistry in light of the high level of understanding brought to bear by X-ray crystallography. The remainder of this book covers the major contributions made to polyether chemistry by physical chemistry including X-ray crystallography, mass spectrometry, and ^{1}H- and ^{13}C-NMR. The authors of each of these sections used similar formats with illustrations, figures, and stereoviews. Each also tried to highlight the strengths and limitations of these various techniques.

The general tone of this book is to give the reader an overview and an exposition with an eye on future research. As such, this volume as well as the previous one, should prove useful as both a primer for the novice researcher and as a review and reference source for the established investigator. As the reviewer of Volume I noted in this journal, the subject index of Volume II is also somewhat inadequate and may prove a hindrance for those less familiar with this field. This book generally includes work up to 1980—only one author (Y. Kishi) attempted to update his chapter to cover work done in 1981.

In conclusion, this volume gives an excellent coverage of the subject matter it sets out to review. It has been well edited, is authoritative, and generally error free. It will surely be of great value to anyone interested in these fascinating antibiotics.

Reviewed by Manuel Debono
Lilly Research Laboratories
Microbiological and Fermentation Products Division
Indianapolis, IN 46285

Applied Statistics: A Handbook of Techniques, 5th Ed. By LOTHAR SACHS (translated by ZENON REYNAROWYCH). Springer-Verlag New York, Inc., 175 Fifth Avenue, New York, NY 10010. 1983. 706 pp. 16 × 24 cm.

This book was written "... both as an introductory and follow-up text ... and as a reference book with a collection of formulas and tables, numerous cross-references, and extensive bibliography." Satisfying such divergent purposes in one book is difficult, and the author does not entirely succeed. Although written at an introductory level, I found the organization of the material too confusing and the coverage too encompassing for an introductory text.

The book extensively covers the techniques relevant to most data analysis problems addressed in introductory texts in applied statistics. Chapter 0 covers arithmetic operations. Chapter 1 covers a wide variety of techniques relating to one variable. Chapter 2 suggests the diversity of specialized statistical problems and techniques arising in medicine and engineering and directs the reader to the relevant literature. Chapters 3–7 cover the comparison of two or more samples, correlation and regression, the analysis of contingency tables, and analysis of variance. In each case, most of the relevant parametric and nonparametric techniques are presented. Keeping with the introductory level of the book, general linear and categorical models are not discussed.

For a handbook, the inclusion of material could be better delineated. You might find a relatively unknown technique such as the minimum discrimination information statistic for analyzing multiway contingency tables or the Thorndike nomogram for evaluating Poisson probabilities. However, you will fail to find techniques for analyzing covariance studies, repeated measure studies, or studies with missing data. But, if the technique is there, its stepwise execution is lucidly illustrated. Assumptions are stated in practical terms and cross-referenced to techniques for testing their validity. The original and related references are always given. Statistical tables are readily accessible due to their placement in the text and convenient page referencing.

This easy use is one of the joys of this book. Another is the pleasure of perusing the book. To quote the author, "The numerous cross-references appearing throughout the text point out various *interconnections*. A serendipitous experience is possible." I concur.

Reviewed by Mark A. Johnson
The Upjohn Company
Kalamazoo, MI 49001

Structure–Activity Correlation as a Predictive Tool in Toxicology: Fundamentals Methods, and Applications. Edited by LEON GOLDBERG. Hemisphere Publishing Corp., 19 W. 44th St., New York, NY 10036. 330 pp. 16 × 23 cm. Price $49.50.

This book is a reasonably current review of the application of quantitative structure–activity relationships (QSAR) to problems in toxicology. Although the work is the result of a symposium which was held in February 1981, it is remarkably well-written and not at all like the usual symposia proceedings. The book is divided into four sections that, for the most part, are well-organized and show little evidence of overlap or duplication.

The first section covers biological activities and describes moderately well the problems that toxicologists have in defining and measuring the biological effects of toxic substances. Of particular interest are the examples in Chapter 2 on inhibition of chemical carcinogenisis by various factors which modify procarcinogen activation. The survey of literature and computer-accessible data bases for obtaining information on both toxicological responses and physical and chemical properties of toxicants is particularly helpful.

The second section contains a somewhat sketchy but suggestive survey of biochemical mechanisms underlying the toxic action of chemicals (Chapter 4) and an excellent historical overview of the physical and chemical parameters that have been correlated to biological activities (Chapter 5).

The third section, "Correlative Methods," contains the heart of the material presented in this book. An excellent review (Chapter 6) of multiple regression (Hansch) analysis by Y. C. Martin clearly states the fundamental assumptions that are frequently not met by the novice. Criteria for the acceptable quality of the biological data, for the selection of appropriate physiochemical parameters, and for the intellegent use of regression analysis methods are all succinctly stated. Chapter 7, by P. C. Jurs, contains a reasonably intelligible introduction to the use of pattern-recognition techniques for QSAR; however, the novice unfamiliar with the statistical basis for this method may find the discussion somewhat confusing. Finally, Chapter 8 contains a discussion of the application of quantum chemical methods to predicting the relative carcinogenicity of a series of polycyclic aromatic hydrocarbons.

The remainder of the book consists of examples of applications of QSAR methods to toxicological problems. Although the quality of those application reviews varies considerably, each topic is covered with sufficient depth such that these reviews should serve as a useful guide to the recent literature. Chapters 10 (Computer-Assisted Prediction of Me-

theless make it difficult to compare data across chemical classes without excessive page flipping.

This book tries to offer something for the medicinal chemist, the renal pharmacologist and physiologist, and the physician. With its interdisciplinary approach it can be highly recommended to all three, but particularly to the medicinal chemist because of its emphasis on structure–activity relationships and possible future directions for diuretic research.

Reviewed by Gregory M. Shutske
Department of Chemical Research
Hoechst-Roussel Pharmaceuticals, Inc.
Somerville, NJ 08876

Polyether Antibiotics, Volume 2: Naturally Occurring Acid Ionophores. Edited by JOHN W. WESLEY. Marcel Dekker, 270 Madison Avenue, New York, NY 10016. 1983. 415 pp. 15 × 23 cm. Price $65.00 (20% higher outside the U.S. and Canada).

This work is the second of a two-volume set on polyether antibiotics. As the title indicates, it concentrates on the chemical aspects in this field whereas the microbiology, biosynthesis, pharmacology, and veterinary applications were covered in the first volume. The editor has chosen an excellent array of contributing authors, each of whom has done important original work in this field. The resulting volume therefore has the added advantage of being authoritative as well as informative.

The first chapter by Yoshito Kishi is an excellent review of the total synthesis of many of the polyethers which not only includes the author's own contributions, but also a critical view of other major contributors to this field. This is followed by a review of known chemical modifications of this class of antibiotics, which focuses attention on the lack of progress in this aspect of polyether chemistry in light of the high level of understanding brought to bear by X-ray crystallography. The remainder of this book covers the major contributions made to polyether chemistry by physical chemistry including X-ray crystallography, mass spectrometry, and ^{1}H- and ^{13}C-NMR. The authors of each of these sections used similar formats with illustrations, figures, and stereoviews. Each also tried to highlight the strengths and limitations of these various techniques.

The general tone of this book is to give the reader an overview and an exposition with an eye on future research. As such, this volume as well as the previous one, should prove useful as both a primer for the novice researcher and as a review and reference source for the established investigator. As the reviewer of Volume I noted in this journal, the subject index of Volume II is also somewhat inadequate and may prove a hindrance for those less familiar with this field. This book generally includes work up to 1980—only one author (Y. Kishi) attempted to update his chapter to cover work done in 1981.

In conclusion, this volume gives an excellent coverage of the subject matter it sets out to review. It has been well edited, is authoritative, and generally error free. It will surely be of great value to anyone interested in these fascinating antibiotics.

Reviewed by Manuel Debono
Lilly Research Laboratories
Microbiological and Fermentation Products Division
Indianapolis, IN 46285

Applied Statistics: A Handbook of Techniques, 5th Ed. By LOTHAR SACHS (translated by ZENON REYNAROWYCH). Springer-Verlag New York, Inc., 175 Fifth Avenue, New York, NY 10010. 1983. 706 pp. 16 × 24 cm.

This book was written "... both as an introductory and follow-up text ... and as a reference book with a collection of formulas and tables, numerous cross-references, and extensive bibliography." Satisfying such divergent purposes in one book is difficult, and the author does not entirely succeed. Although written at an introductory level, I found the organization of the material too confusing and the coverage too encompassing for an introductory text.

The book extensively covers the techniques relevant to most data analysis problems addressed in introductory texts in applied statistics. Chapter 0 covers arithmetic operations. Chapter 1 covers a wide variety of techniques relating to one variable. Chapter 2 suggests the diversity of specialized statistical problems and techniques arising in medicine and engineering and directs the reader to the relevant literature. Chapters 3–7 cover the comparison of two or more samples, correlation and regression, the analysis of contingency tables, and analysis of variance. In each case, most of the relevant parametric and nonparametric techniques are presented. Keeping with the introductory level of the book, general linear and categorical models are not discussed.

For a handbook, the inclusion of material could be better delineated. You might find a relatively unknown technique such as the minimum discrimination information statistic for analyzing multiway contingency tables or the Thorndike nomogram for evaluating Poisson probabilities. However, you will fail to find techniques for analyzing covariance studies, repeated measure studies, or studies with missing data. But, if the technique is there, its stepwise execution is lucidly illustrated. Assumptions are stated in practical terms and cross-referenced to techniques for testing their validity. The original and related references are always given. Statistical tables are readily accessible due to their placement in the text and convenient page referencing.

This easy use is one of the joys of this book. Another is the pleasure of perusing the book. To quote the author, "The numerous cross-references appearing throughout the text point out various *interconnections*. A serendipitous experience is possible." I concur.

Reviewed by Mark A. Johnson
The Upjohn Company
Kalamazoo, MI 49001

Structure–Activity Correlation as a Predictive Tool in Toxicology: Fundamentals Methods, and Applications. Edited by LEON GOLDBERG. Hemisphere Publishing Corp., 19 W. 44th St., New York, NY 10036. 330 pp. 16 × 23 cm. Price $49.50.

This book is a reasonably current review of the application of quantitative structure–activity relationships (QSAR) to problems in toxicology. Although the work is the result of a symposium which was held in February 1981, it is remarkably well-written and not at all like the usual symposia proceedings. The book is divided into four sections that, for the most part, are well-organized and show little evidence of overlap or duplication.

The first section covers biological activities and describes moderately well the problems that toxicologists have in defining and measuring the biological effects of toxic substances. Of particular interest are the examples in Chapter 2 on inhibition of chemical carcinogenisis by various factors which modify procarcinogen activation. The survey of literature and computer-accessible data bases for obtaining information on both toxicological responses and physical and chemical properties of toxicants is particularly helpful.

The second section contains a somewhat sketchy but suggestive survey of biochemical mechanisms underlying the toxic action of chemicals (Chapter 4) and an excellent historical overview of the physical and chemical parameters that have been correlated to biological activities (Chapter 5).

The third section, "Correlative Methods," contains the heart of the material presented in this book. An excellent review (Chapter 6) of multiple regression (Hansch) analysis by Y. C. Martin clearly states the fundamental assumptions that are frequently not met by the novice. Criteria for the acceptable quality of the biological data, for the selection of appropriate physiochemical parameters, and for the intellegent use of regression analysis methods are all succinctly stated. Chapter 7, by P. C. Jurs, contains a reasonably intelligible introduction to the use of pattern-recognition techniques for QSAR; however, the novice unfamiliar with the statistical basis for this method may find the discussion somewhat confusing. Finally, Chapter 8 contains a discussion of the application of quantum chemical methods to predicting the relative carcinogenicity of a series of polycyclic aromatic hydrocarbons.

The remainder of the book consists of examples of applications of QSAR methods to toxicological problems. Although the quality of those application reviews varies considerably, each topic is covered with sufficient depth such that these reviews should serve as a useful guide to the recent literature. Chapters 10 (Computer-Assisted Prediction of Me-

tabolism), 14 (Quantitative Structure–Mutagenicity Relationships), 18 (Molecular Basis for the Structure–Carcinogenicity Relationships of Polynuclear Aromatic Hydrocarbons), and 20 (Concept of the Integrated Approach)—the last a description of the EPA GENE-TOX program—provide some especially interesting applications to toxicological research.

QSAR methods should become increasingly important in toxicology, since the toxicologist is confronted with the problem of assessing the safety of millions of chemical entities which may cause injury or death to living organisms by only a reasonably small number of distinct toxic mechanisms. For example, genetic effects of toxic chemicals can be assessed by a half-dozen or so distinct classes of bioassays for different types of genetic damage. As the mechanisms underlying various types of toxic responses become better understood, QSAR methods will become more useful as a screening tool for predicting the adverse effects of new chemical entities. This book can serve as a useful introduction to the literature on QSAR for the practicing toxicologist and other scientists concerned with safety assessment of drugs and chemicals. The novice will find Chapters 5 and 6 particularly useful as an introduction to the field. Chemists who routinely use SAR approaches in research will find this work less helpful, since the problems of defining toxicological endpoints are not treated with the same standards of quality as the chapters on SAR methods. Nevertheless, this book is a valuable review.

Reviewed by William B. Porter
Center for Health Sciences
School of Pharmacy
University of Wisconsin—Madison
Madison, WI 53706

New Calcium Antagonists: Recent Developments and Prospects. Edited by A. FLECKENSTEIN, K. HASHIMOTO, M. HERRMANN, A. SCHWARTZ, and L. SEIPEL. Gustav Fischer Verlag, D-7000 Stuttgart 72, Postfach 720143, West Germany. 1983. 236 pp. 15 × 23 cm. Price DM 36.

This book represents the proceedings of a workshop on the calcium channel blocker diltiazem, held in May 1982 in honor of Professor A. Fleckenstein (the "father of calcium antagonists") on the occasion of his 65th birthday. Twenty-four international experts and their coworkers contributed chapters dealing almost exclusively with the authors' personal experimental findings. Of the 24 chapters in the book, only two are of a review nature. However, all the chapters provide recent and fascinating data on calcium antagonists. Although the focus of the workshop is on diltiazem, many other calcium antagonists are discussed throughout the book.

Eleven chapters are devoted to clinical experience with diltiazem and other calcium antagonists in the treatment of angina pectoris, coronary artery stenosis, coronary atherosclerosis, hypertension, and cardiac arrhythmias. The concensus from these chapters, is that the calcium antagonists are most valuable in treating all of these cardiovascular diseases.

Thirteen chapters deal with various aspects of the basic pharmacology of diltiazem and other calcium antagonists. Of these, nine chapters are concerned with the basic and applied pharmacology of calcium antagonists on the cardiovascular system. Among them, a notable chapter discussing the value of calcium antagonists in the prevention of arterial calcinosis provides tantalizing information and paves the way for future preventive clinical uses of this group of drugs. One chapter briefly suggests a therapeutic use for calcium antagonists in cerebrovascular disease, and another chapter details the molecular aspects (and pitfalls) of the binding properties of calcium antagonists to their presumptive membrane receptors and the relation of these receptors to the calcium channels which are blocked by these drugs. A review of the cellular mechanisms by which calcium antagonists preserve the integrity of myocardial cells and intracellular structures provides insightful reading. One chapter outlines the evidence for an interaction of calcium antagonists with presynaptic and postsynaptic α-adrenoreceptors, and serves to remind the reader of the complexity of the mechanism(s) of action of the calcium antagonists. Another reminder is provided in a chapter dealing with inhibition of adrenergic transmission by calcium antagonists at the vascular neuromuscular junction.

Despite the excellent scientific information provided in this book, a number of negative attributes are worth mentioning. The reader is repeatedly distracted by typographical errors which abound in virtually all chapters. Even the title on the front cover suffered from lack of proper proofreading. Furthermore, some chapters appear to have been transcribed from taped presentations, since incomplete sentences, verbless phrases, improper paragraph breakdown, and other miscellaneous grammatical oddities abound. A few chapters do not include a bibliography, and only one chapter was updated prior to publication. Finally, the absence of an index is unnerving, as is the absence of summaries or conclusions in a few chapters and English language summaries for two German language chapters.

In general, the book is most valuable to cardiovascular physiologists, pharmacologists, and clinicians who are involved in research aspects of calcium antagonists. It complements a half-dozen books on the same subject which appeared in the 1980's.

Reviewed by Ralf G. Rahwan
College of Pharmacy
The Ohio State University
Columbus, OH 43210

tabolism), 14 (Quantitative Structure–Mutagenicity Relationships), 18 (Molecular Basis for the Structure–Carcinogenicity Relationships of Polynuclear Aromatic Hydrocarbons), and 20 (Concept of the Integrated Approach)—the last a description of the EPA GENE-TOX program—provide some especially interesting applications to toxicological research.

QSAR methods should become increasingly important in toxicology, since the toxicologist is confronted with the problem of assessing the safety of millions of chemical entities which may cause injury or death to living organisms by only a reasonably small number of distinct toxic mechanisms. For example, genetic effects of toxic chemicals can be assessed by a half-dozen or so distinct classes of bioassays for different types of genetic damage. As the mechanisms underlying various types of toxic responses become better understood, QSAR methods will become more useful as a screening tool for predicting the adverse effects of new chemical entities. This book can serve as a useful introduction to the literature on QSAR for the practicing toxicologist and other scientists concerned with safety assessment of drugs and chemicals. The novice will find Chapters 5 and 6 particularly useful as an introduction to the field. Chemists who routinely use SAR approaches in research will find this work less helpful, since the problems of defining toxicological endpoints are not treated with the same standards of quality as the chapters on SAR methods. Nevertheless, this book is a valuable review.

Reviewed by William B. Porter
Center for Health Sciences
School of Pharmacy
University of Wisconsin—Madison
Madison, WI 53706

New Calcium Antagonists: Recent Developments and Prospects. Edited by A. FLECKENSTEIN, K. HASHIMOTO, M. HERRMANN, A. SCHWARTZ, and L. SEIPEL. Gustav Fischer Verlag, D-7000 Stuttgart 72, Postfach 720143, West Germany. 1983. 236 pp. 15 × 23 cm. Price DM 36.

This book represents the proceedings of a workshop on the calcium channel blocker diltiazem, held in May 1982 in honor of Professor A. Fleckenstein (the "father of calcium antagonists") on the occasion of his 65th birthday. Twenty-four international experts and their coworkers contributed chapters dealing almost exclusively with the authors' personal experimental findings. Of the 24 chapters in the book, only two are of a review nature. However, all the chapters provide recent and fascinating data on calcium antagonists. Although the focus of the workshop is on diltiazem, many other calcium antagonists are discussed throughout the book.

Eleven chapters are devoted to clinical experience with diltiazem and other calcium antagonists in the treatment of angina pectoris, coronary artery stenosis, coronary atherosclerosis, hypertension, and cardiac arrhythmias. The concensus from these chapters, is that the calcium antagonists are most valuable in treating all of these cardiovascular diseases.

Thirteen chapters deal with various aspects of the basic pharmacology of diltiazem and other calcium antagonists. Of these, nine chapters are concerned with the basic and applied pharmacology of calcium antagonists on the cardiovascular system. Among them, a notable chapter discussing the value of calcium antagonists in the prevention of arterial calcinosis provides tantalizing information and paves the way for future preventive clinical uses of this group of drugs. One chapter briefly suggests a therapeutic use for calcium antagonists in cerebrovascular disease, and another chapter details the molecular aspects (and pitfalls) of the binding properties of calcium antagonists to their presumptive membrane receptors and the relation of these receptors to the calcium channels which are blocked by these drugs. A review of the cellular mechanisms by which calcium antagonists preserve the integrity of myocardial cells and intracellular structures provides insightful reading. One chapter outlines the evidence for an interaction of calcium antagonists with presynaptic and postsynaptic α-adrenoreceptors, and serves to remind the reader of the complexity of the mechanism(s) of action of the calcium antagonists. Another reminder is provided in a chapter dealing with inhibition of adrenergic transmission by calcium antagonists at the vascular neuromuscular junction.

Despite the excellent scientific information provided in this book, a number of negative attributes are worth mentioning. The reader is repeatedly distracted by typographical errors which abound in virtually all chapters. Even the title on the front cover suffered from lack of proper proofreading. Furthermore, some chapters appear to have been transcribed from taped presentations, since incomplete sentences, verbless phrases, improper paragraph breakdown, and other miscellaneous grammatical oddities abound. A few chapters do not include a bibliography, and only one chapter was updated prior to publication. Finally, the absence of an index is unnerving, as is the absence of summaries or conclusions in a few chapters and English language summaries for two German language chapters.

In general, the book is most valuable to cardiovascular physiologists, pharmacologists, and clinicians who are involved in research aspects of calcium antagonists. It complements a half-dozen books on the same subject which appeared in the 1980's.

Reviewed by Ralf G. Rahwan
College of Pharmacy
The Ohio State University
Columbus, OH 43210

Having a Voice in APhA Scientific Policy

There is a familiar story that most of us have heard in one variation or another. Essentially, it is that people fall into one or another of three groups: (*a*) the great majority, who are doing well if they know what has occurred; (*b*) the relatively few, who are aware of what is presently happening; and (*c*) the very, very few, who are able to foresee where things are headed and what is likely to happen.

This classification has great relevance to policy establishment within the American Pharmaceutical Association. All too many APhA members—as in the case of most professional or scientific societies—learn belatedly of some position the organization has adopted. At that point their reaction is either "why wasn't I told?" or "when was this done?" or "how did that happen?" or "why didn't the leadership inform or consult the membership?"

No one wants to admit that he or she might have been "asleep at the switch," and that he or she has only one's own self to blame for being ignorant on the status of the subject.

At one time or another, we probably have all had this experience and the same reaction to it. Our point in discussing it in this column is simply to be sure that all our readers are aware that they can avoid this situation—at least as far as APhA policy positions that will be established by the Association's House of Delegates during the 1984 Annual Meeting this coming May.

Right now, the 1983–1984 Policy Committee reports, including the recommendations of the Policy Committees, are being released and publicized through APhA publications and *via* news releases to the pharmacy professional and trade press.

At this stage, the recommendations are only in a proposed status. They are open for review, debate, and consideration until early May when Reference Committee open hearings will be held to listen to verbal testimony and to review written comments that have been submitted. The Reference Committees will then make their recommendations to the House of Delegates for final action and policy establishment—but, again, only after further opportunity for debate on the issues within the full House of Delegates.

So, between now and early May, there is ample time for individual members to express their views and to offer their input before those proposals are acted upon. Consequently, everyone has plenty of opportunity to be numbered among the usually select few, who are in the category of knowing not only where we've been, and where we are, but even where we are going.

In addition to presenting this reminder, we would like to clarify another point. That is, the fact that APhA policy issues cover the full spectrum of concerns that are of interest to the membership. Four separate Policy Committees (and four similarly oriented Reference Committees) are appointed each year and are assigned topics considered most appropriate to their individual designations—which are, respectively, Educational Affairs, Professional Affairs, Public Affairs, and Scientific Affairs.

Hence, there is a committee specifically established to study, review, and recommend policy positions on scientific issues.

In recent years, the Association has formally adopted official policy positions emerging from its Policy Committee on Scientific Affairs on such diverse subjects as: (1) the pharmacist's role in postmarketing surveillance for approved drugs, (2) the utilization of institutional review boards (IRBs) for expediting new drug approval, (3) federal regulation of salt in processed foods, (4) the use of animals in drug research, (5) carcinogenicity testing, (6) needed drugs of limited commercial value (orphan drugs), (7) vaccine liability programs, (8) drug product therapeutic equivalence, (9) food labeling, (10) therapeutic orphans, and (11) the medicinal use of marijuana.

When many of these issues were originally debated and the policies established, there was relatively little public interest in those matters. At most, public awareness was just beginning to stir. But then, when the issue "caught fire" in the public eye and in the national political arena, APhA was ready with a well researched, thoughtfully considered, and clearly articulated policy position.

Two typical examples were the use of animals in research and the development of orphan drugs; both of these issues developed into hotly debated topics within the U.S. Congress over the past 2 years, and the Association was ideally positioned to influence the direction of legislation because of its already adopted policy statements.

Currently, APhA members have an opportunity to react to recommendations regarding four subjects, as just proposed by the 1983–1984 Policy Committee on Scientific Affairs. These are relative to: (1) abbreviated new drug applications (ANDAs) for post-1962 drugs, (2) a national center for human organ acquisition, (3) the freedom of scientific information, and (4) the availability of potassium iodide for nuclear accidents.

Moreover, many of the subjects that have been considered by the other three APhA Policy Committees have scientific-related aspects which make them of interest to pharmaceutical scientists.

Therefore, it behooves every member to take the time and effort to study these issues and their corresponding policy proposals. Having done so, any views—either pro or con—ought to be conveyed to the pertinent Reference Committee, either by letter or at the open hearing in May.

Obviously, everyone's wishes cannot be satisfied, particularly when different members will express diametrically opposite views. However, every voice will be heard and every opinion will be taken into consideration in formulating the ultimate policy statement.

And, in a democratic organization—as in a national democracy—that is what we can expect, and all that we can expect.

—EDWARD G. FELDMANN
American Pharmaceutical Association
Washington, DC 20037

A publication of the
American Pharmaceutical Association—
the National Professional Society
of Pharmacists

JOURNAL OF PHARMACEUTICAL SCIENCES

Volume 73, 1984

JPMSAE 73(1-12) 1-1910 (1984)
ISSN 0022-3549

Sharon G. Boots
Editor

Sue A. Kruger
Production Editor

Margaret M. Madeleine
Assistant Production Editor

Karen A. Blakney
Copy Editor

Edward G. Feldmann
Contributing Editor

Samuel W. Goldstein
Contributing Editor

Patricia A. Evich
Editorial Secretary

Editorial Advisory Board

Jordan L. Cohen
Kenneth A. Connors
Louis Diamond
Ho-Leung Fung
Milo Gibaldi
Everett N. Hiestand
W. Homer Lawrence
Ian W. Mathison
Carl M. Metzler
Robert E. Notari
Paul L. Schiff, Jr.
Jane E. Shaw

Published monthly under the supervision of the Board of Trustees

Having a Voice in APhA Scientific Policy

There is a familiar story that most of us have heard in one variation or another. Essentially, it is that people fall into one or another of three groups: (*a*) the great majority, who are doing well if they know what has occurred; (*b*) the relatively few, who are aware of what is presently happening; and (*c*) the very, very few, who are able to foresee where things are headed and what is likely to happen.

This classification has great relevance to policy establishment within the American Pharmaceutical Association. All too many APhA members—as in the case of most professional or scientific societies—learn belatedly of some position the organization has adopted. At that point their reaction is either "why wasn't I told?" or "when was this done?" or "how did that happen?" or "why didn't the leadership inform or consult the membership?"

No one wants to admit that he or she might have been "asleep at the switch," and that he or she has only one's own self to blame for being ignorant on the status of the subject.

At one time or another, we probably have all had this experience and the same reaction to it. Our point in discussing it in this column is simply to be sure that all our readers are aware that they can avoid this situation—at least as far as APhA policy positions that will be established by the Association's House of Delegates during the 1984 Annual Meeting this coming May.

Right now, the 1983–1984 Policy Committee reports, including the recommendations of the Policy Committees, are being released and publicized through APhA publications and *via* news releases to the pharmacy professional and trade press.

At this stage, the recommendations are only in a proposed status. They are open for review, debate, and consideration until early May when Reference Committee open hearings will be held to listen to verbal testimony and to review written comments that have been submitted. The Reference Committees will then make their recommendations to the House of Delegates for final action and policy establishment—but, again, only after further opportunity for debate on the issues within the full House of Delegates.

So, between now and early May, there is ample time for individual members to express their views and to offer their input before those proposals are acted upon. Consequently, everyone has plenty of opportunity to be numbered among the usually select few, who are in the category of knowing not only where we've been, and where we are, but even where we are going.

In addition to presenting this reminder, we would like to clarify another point. That is, the fact that APhA policy issues cover the full spectrum of concerns that are of interest to the membership. Four separate Policy Committees (and four similarly oriented Reference Committees) are appointed each year and are assigned topics considered most appropriate to their individual designations—which are, respectively, Educational Affairs, Professional Affairs, Public Affairs, and Scientific Affairs.

Hence, there is a committee specifically established to study, review, and recommend policy positions on scientific issues.

In recent years, the Association has formally adopted official policy positions emerging from its Policy Committee on Scientific Affairs on such diverse subjects as: (1) the pharmacist's role in postmarketing surveillance for approved drugs, (2) the utilization of institutional review boards (IRBs) for expediting new drug approval, (3) federal regulation of salt in processed foods, (4) the use of animals in drug research, (5) carcinogenicity testing, (6) needed drugs of limited commercial value (orphan drugs), (7) vaccine liability programs, (8) drug product therapeutic equivalence, (9) food labeling, (10) therapeutic orphans, and (11) the medicinal use of marijuana.

When many of these issues were originally debated and the policies established, there was relatively little public interest in those matters. At most, public awareness was just beginning to stir. But then, when the issue "caught fire" in the public eye and in the national political arena, APhA was ready with a well researched, thoughtfully considered, and clearly articulated policy position.

Two typical examples were the use of animals in research and the development of orphan drugs; both of these issues developed into hotly debated topics within the U.S. Congress over the past 2 years, and the Association was ideally positioned to influence the direction of legislation because of its already adopted policy statements.

Currently, APhA members have an opportunity to react to recommendations regarding four subjects, as just proposed by the 1983–1984 Policy Committee on Scientific Affairs. These are relative to: (1) abbreviated new drug applications (ANDAs) for post-1962 drugs, (2) a national center for human organ acquisition, (3) the freedom of scientific information, and (4) the availability of potassium iodide for nuclear accidents.

Moreover, many of the subjects that have been considered by the other three APhA Policy Committees have scientific-related aspects which make them of interest to pharmaceutical scientists.

Therefore, it behooves every member to take the time and effort to study these issues and their corresponding policy proposals. Having done so, any views—either pro or con—ought to be conveyed to the pertinent Reference Committee, either by letter or at the open hearing in May.

Obviously, everyone's wishes cannot be satisfied, particularly when different members will express diametrically opposite views. However, every voice will be heard and every opinion will be taken into consideration in formulating the ultimate policy statement.

And, in a democratic organization—as in a national democracy—that is what we can expect, and all that we can expect.

—EDWARD G. FELDMANN
American Pharmaceutical Association
Washington, DC 20037

JOURNAL OF PHARMACEUTICAL SCIENCES

MARCH 1984
VOLUME 73 NUMBER 3

RESEARCH ARTICLES

In Vivo and *In Vitro* Pharmacokinetics and Fate of Furaltadone in Meat- and Milk-Producing Animals

L. L. NG *§x, R. F. BEVILL, JR ‡, and E. G. PERKINS *

Received August 13, 1981, from the **Burnsides Research Laboratory* and the ‡*College of Veterinary Medicine, Department of Pharmacology, University of Illinois at Champaign–Urbana, Urbana, IL 61801.* Accepted for publication January 26, 1983. §Present address: Merck Sharp & Dohme, West Point, PA 19486.

Abstract □ The metabolism of furaltadone was examined by an *in vitro* hepatic study in cows and goats and an *in vivo* study in goats using ^{14}C-labeled and unlabeled drug. The half-life of furaltadone was 13 min in the homogenates of caprine and bovine liver and 35 min in the *in vivo* study of the goat. Less than 2% of the parent drug was present in the urine of animals dosed either intravenously or intramammarily. No furaltadone was detected in the milk after 24 h. Overall, the parent compound was rapidly absorbed, distributed, and widely degraded in the lactacting goat. The compound, labeled at the 2-formyl carbon of the furan ring, had a radioactivity recovery of 81% in the feces and urine. Of the total radioactivity, 99.4% infused into the udder had been absorbed after 72 h. Tissue distributions of radioactivity in decreasing order of abundance were: kidney, udder, liver, duodenum, muscular tissue, adipose tissue, and bile.

Keyphrases □ Furaltadone—*in vitro* and *in vivo* metabolism, fate in cattle and goats, pharmacokinetics □ Metabolism—furaltadone, *in vitro* and *in vivo*, fate in cattle and goats, pharmacokinetics □ Pharmacokinetics—furaltadone, *in vitro* and *in vivo* metabolism, fate in cattle and goats

The nitrofuran furaltadone, (±)-5-(morpholinomethyl)-3-[(5-nitrofurfurylidene)amino]-2-oxazolidinone (I), had been commonly administered intramammarily to lactating and dry cows for treatment against the micrococci in mastitis (1, 2). In 1973, Cohen *et al.* (3) reported that this nitrofuran had a strong carcinogenic response, and soon after, this compound was withdrawn from the market because of a lack of information on residues of the compound in animals. Paul *et al.* (4) demonstrated the presence of furaltadone in the bile of the chicken and dog and in the urine, but not the feces, of the rat. No furaltadone was found in animal tissues after oral administration, with sensitivity to 1 ppm. Other investigators were unable to detect the parent drug in milk 48 h after treatment using methods with detection limits at 10 ppb (5) and 5 ppm (6). Although these studies showed that furaltadone is biodegradable in mammals, an evaluation of its metabolsim and excretion in livestock and of residues in the blood, milk, and tissues has never been reported.

In the present study, the hepatic metabolism of furaltadone in goats and cattle are evaluated. Data from a pharmacokinetic study in lactating goats, as a model for the cow, are also presented. The distribution and metabolic fate of furaltadone, labeled at the 2-formyl carbon of the furan ring, and unlabeled drug administered intramammarily are compared.

EXPERIMENTAL

Materials—Unlabeled furaltadone was obtained from Norwich Pharmaceutical Co., Norwich, N.Y. [^{14}C]Furaltadone (0.106 μCi/mg) was synthesized in our laboratory[1]. The chemical purity of the compound was determined by TLC in acetone–chloroform (3:1, v/v) on a plate[2]. The spot corresponding to furaltadone in reference to a standard was cut from the plate and counted by liquid scintillation counting (LSC). Purity was >99%. Nonradioactive furaltadone was synthesized by the same preparative procedure. This product was compared with the commercial standard using melting point; elemental analysis; IR, UV, ^{1}H-NMR, ^{13}C-NMR, and MS spectrometry to support the identity of the [^{14}C]-furaltadone.

***In Vitro* Metabolism**—Fresh goat and cattle livers of known weights (~6 g) were homogenized[3] in 0.05 M sodium phosphate buffer, pH 7.4. The 125-mg/mL homogenate was centrifuged[4] at 5°C and 4500 × *g* (7000 rpm) for 10 min and then at 14,000 × *g* (12,500 rpm) for 30 min using a

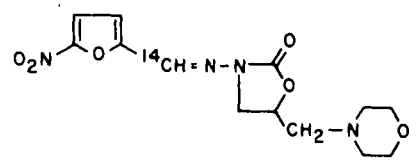

I

[1] Personal communications from Norwich Pharmaceutical Co., Norwich, N.Y.
[2] SAF; Gelman, Ann Arbor, Mich.
[3] Potter-Elvehjem Homogenizer.
[4] Ti-50 8-in. rotor, Model L2-65, Class D; Beckmann, Fullerton, Calif.

0022-3549/84/0300-0293$01.00/0
© 1984, American Pharmaceutical Association

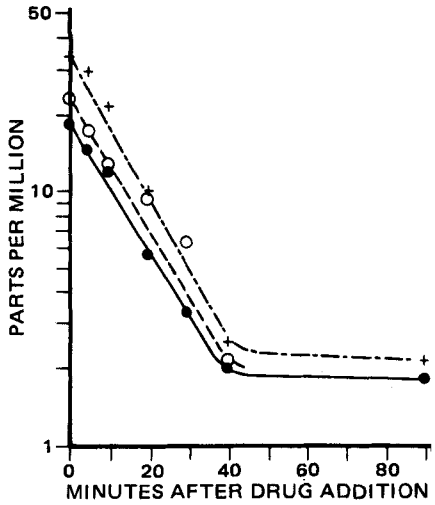

Figure 1—*Comparison of the metabolism of furaltadone in cattle and a goat. Key: (—) bovine liver, ^{14}C-labeled; (- - -) bovine liver, unlabeled; (-·-) caprine liver, unlabeled.*

fixed-angle rotor. The pellet containing the nuclei and mitochondria was discarded and the supernatant was saved.

In vitro experiments were carried out by adding the following ingredients in sequence into test tubes immersed in ice:

1. One milliliter of ^{14}C-labeled or unlabeled furaltadone (~2 μmol) and magnesium chloride (25 μmol) in water,
2. One milliliter of a tissue blank. For the control without furaltadone, magnesium chloride (25 μmol) in water was added.
3. Cofactor buffer mixture consisting of 0.65 μmol of NADP monosodium[5], 10.0 μmol of glucose-6-phosphate disodium[5], and 50.0 μmol of nicotinamide[5] dissolved in 3 mL of 0.5 M sodium phosphate buffer, pH 7.4.
4. Two milliliters of enzymes, containing microsomes equivalent to 250 mg of liver added while the tube was in the incubation bath. The resulting mixture in each test tube was incubated aerobically at 37°C with magnetic stirring in a water bath[6]. Samples in duplicate were removed from the water bath at 0, 5, 10, 20, 30, 40, and 90 min. The control containing no nitrofuran was incubated for 90 min.

***In Vivo* Metabolism with Unlabeled Furaltadone**—Two lactating goats, acclimatized in individual metabolism cages, were fitted with catheters[7] the evening before dosing, and control samples of urine and blood (10 mL) from the jugular vein were collected. A balanced diet consisting of alfalfa hay and water was provided *ad libitum* and a 12% concentrate[8] was given in limited amounts. The animals were milked once a day.

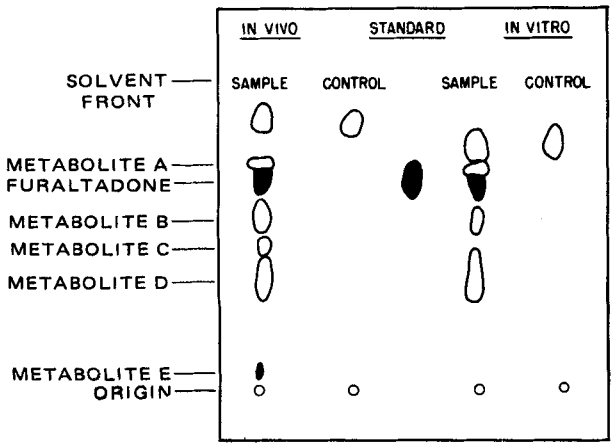

Figure 2—*Comparison of extracts of* in vivo *and* in vitro *metabolites of furaltadone by TLC in acetone–methanol–glacial acetic acid (50:50:1).*

[5] Calbiochem, San Diego, Calif.
[6] Landa MGW WB-20/R, West Germany.
[7] 16 FR Bardex Foley, Murray Hill, N.J.
[8] Illinois Calf 12, Ill.

Table I—*In Vivo* Metabolites of Furaltadone by TLC in Two Discrete Systems

Compound	Appearance Under UV Light	R_f Values: Acetone–Acetic Acid (100:1)	R_f Values: Acetone–Methanol–Acetic Acid (50:50:1)
Metabolite A	Bright yellow fluorescent	0.47	0.75
Furaltadone	Dark quenched	0.50	0.66
Metabolite B	Purple fluorescent	0.19	0.55
Metabolite C	Blue fluorescent	0.06	0.46
Metabolite D	Bright yellow fluorescent	0.00	0.42
Metabolite E	Dark quenched	0.00	0.05

Intravenous Dosing—Furaltadone dissolved in acidified water just before dosing was injected into the jugular vein utilizing an intravenous catheter[9] at a dose of 10 mg/kg of body weight immediately after the morning milking. Blood and urine samples were collected at 15, 30, 45, 60, 75, 90, 105, 120, 135, 150, 180, and 210 min.

Intramammary Dosing—The two goats were administered furaltadone equivalent to 37.5 mg/kg of body weight. The nitrofuran was suspended in pure peanut oil[10] using an ultrasonicator[11]. Blood and urine samples were collected at 0.5, 1, 2, 3, 4, 6, 8, 10, 12, 14, 16, 19 and 23 h.

***In Vivo* Metabolism with ^{14}C-Labeled Furaltadone**—A 31-kg milking goat was accommodated and fed under similar conditions as the goats in the unlabeled study. One day prior to treatment, control samples of feces, urine, milk, and blood were collected. The goat was dosed with 777 mg (82.6 μCi) of [^{14}C]furaltadone dispersed in an equal amount of pure peanut oil into the udders immediately after the morning milking. The goat was milked twice a day. Blood and urine were collected at 0.5, 1, 2, 3, 4, 6, 8, 10, 14, 24, 30, 36, 48, 54, 60, and 72 h. The goat was milked every 12 h after infusion for a total of 72 h. Feces were collected every 6 h for the first 12 h and every 12 h for the remainder of the experiment. Aliquots of urine were frozen at −40°C for later analysis. The goat was slaughtered 72 h after treatment. Selected tissue samples and organs were collected and frozen for subsequent analysis.

Analytical Methods—The *in vitro* incubation mixtures were analyzed for furaltadone by direct UV measurement[12] at 360 nm as well as by HPLC. An incubated control served as the background. No metabolite was detectable by HPLC at the concentrations used. All the *in vivo* samples were quantitated in duplicate on a reverse-phase column[13] by HPLC[14] (7) at 360 nm.

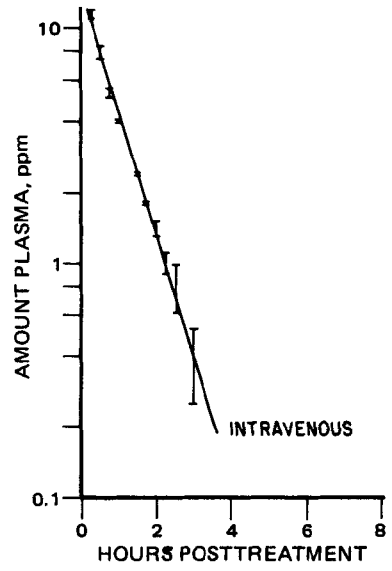

Figure 3—*Concentration of furaltadone in plasma in two intravenously dosed goats: $K_e = 1.17\ h^{-1}$; $t_{1/2} = 0.59\ h$; r = 0.996.*

[9] 16-Gauge, 8-in. Radiopaque Teflon Intravenous Placement; Sandy, Utah.
[10] Planters, Div. of Standard Brands, New York, N.Y.
[11] Branson Sonic Power Co., Danbury, Conn.
[12] Cary Model 11M UV Spectrophotometer, Pasadena, Calif.
[13] μ-Bondapak C_{18}, Waters Associates, Milford, Mass.
[14] Tracor, Austin, Tex.

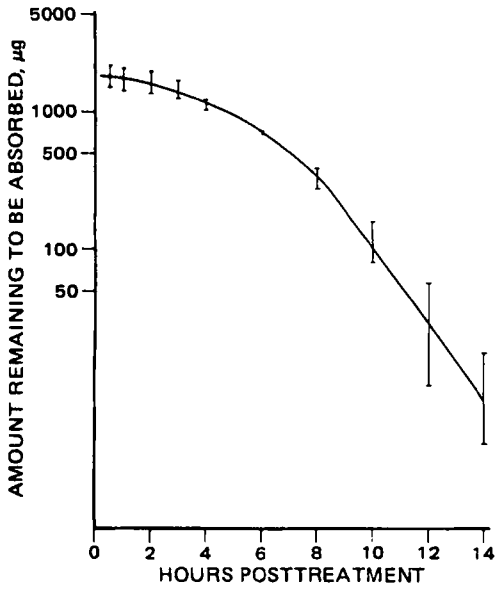

Figure 4—*Amount of furaltadone remaining to be absorbed at various times following its intramammary administration to two goats:* $K_a = 0.53\ h^{-1}$; $t_{1/2} = 1.31\ h$.

The *in vivo* radioactive urine samples were analyzed by TLC. Quantitation was as described for the chemical purity evaluation. Control urine served as the background.

Total Radioactivity Quantitation—Fecal pellets were blended with water (1:8, w/v) in a blender[15]. An aliquot of slurry, in triplicate, equivalent to ~50 mg of feces and 1.5 mL of solubilizer[16] was heated at 52°C for 90 min, cooled, and 0.5 mL of hydrogen peroxide added for decolorization. Radioactivity was determined by LSC[17] after the addition of 10 mL of a fluor[18] and 0.8 mL of 1 M HCl. Whole blood (0.2 mL) was swirled with 0.5 mL of solubilizer[16]–ethanol (1:2) at 60°C. After cooling, 0.5 mL of hydrogen peroxide was added. Whole milk was similarly treated with the elimination of the hydrogen peroxide step. Both milk and blood samples, each in triplicate, were mixed with 10 mL of the fluor and 0.5 mL of 0.5 M HCl and counted by LSC after dark adaptation. Radioactivity in the urine was determined by counting of a mixture containing 0.2 mL of urine, 0.2 mL of water, and 10 mL of fluor. These determinations were carried out at each time period. The level of radioactivity in

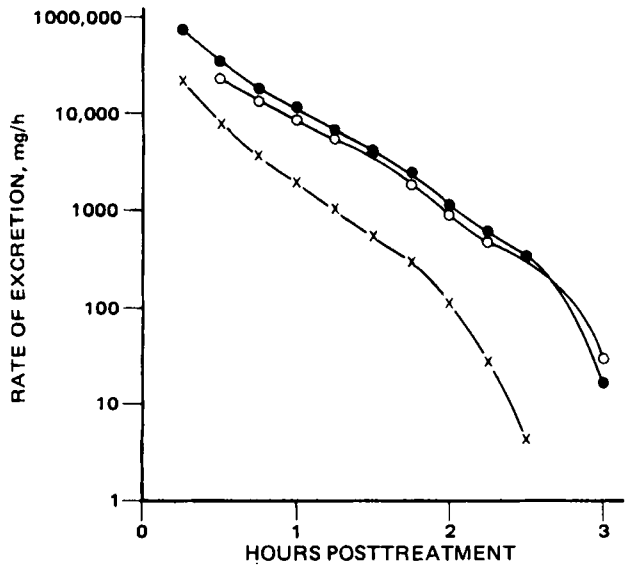

Figure 5—*Average rate of urinary excretion of furaltadone (X) and metabolites following intravenous administration to two goats. Values for metabolites A (●) and E (○) are as furaltadone equivalent.*

[15] Waring, Hartford, Conn.
[16] Protosol; New England Nuclear, Boston, Mass.
[17] Tricarb Model 3320; Packard, Downers Grove, Ill.
[18] Aquasol; New England Nuclear, Boston, Mass.

Table II—Radioactivity Distribution in a Goat Dosed Intramammarily with [^{14}C]Furaltadone [a]

Source	Recovery After 72 h, % of dose
Blood	0.093
Milk	0.76
Feces	25.11
Urine	56.01
Kidney	0.13
Liver	0.51
Total	82.61

[a] Dose: 82.57 µCi/776.97 mg of furaltadone.

the bile was quantitated by counting 0.2 mL of bile with 10 mL of fluor. Tissues, cut in small pieces, were quick-frozen and ground to a powder. An equivalent of 100 mg of tissue powder was mixed with 0.4 mL of water and 2 mL of solubilizer[16] and warmed at 52°C until dissolved. The total radioactivity was quantitated by LSC after the addition of 10 mL of the fluor and 0.8 mL of 1 M HCl and dark adaptation. Each tissue sample was counted in quadruplicate. The internal standard method with [^{14}C]toluene was employed for all samples. Counting efficiencies were 65–86% for urine, 49–64% for feces, 71–82% for blood, 84–88% for milk, and 73–85% for tissues.

Determination of Bound and Free Radioactivity in the Tissues—The powdered adipose tissue was extracted directly with chloroform (1:7, w/v). The fluor[18] was added to 1- and 2-mL aliquots of chloroform extracts from LSC. The liver, kidney, udder, duodenum, and muscular tissue powders were homogenized with water (1:5, w/v) and extracted with dichloromethane–isopropyl alcohol–water (75:25:2). Each tissue extraction was duplicated and subsequently counted as three phases: organic, aqueous, and a residue pellet. The tissue, expressed in gram-equivalent of protein, was determined by a modified Folin–Lowry assay (8).

Metabolites—A homogenate mixture incubated for 3 h at 37°C was extracted by chloroform and by dichloromethane–isopropyl alcohol–water (75:25:2). Urine from the *in vivo* experiment was extracted by the same solvents. Furaltadone and its metabolites were separated by TLC on silica gel G[19] and developed in discrete systems of acetone–methanol–glacial acetic acid (50:50:1) and acetone–acetic acid (100:1).

RESULTS AND DISCUSSIONS

The first-order disappearance of furaltadone and [^{14}C]furaltadone in supernatants obtained from cattle and goat livers is illustrated in Fig. 1. The half-life of furaltadone disappearance was 13 min during the first 40 min of incubation. Three metabolites (A, B, and D) of furaltadone were

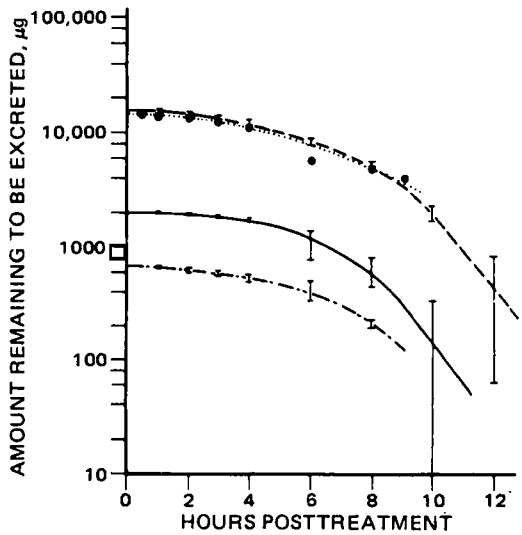

Figure 6—*Amount of furaltadone (– –) and metabolites remaining to be excreted at various times following intramammary administration to two goats. Values for metabolites A (—) and E (-·-) are as furaltadone equivalent. Key: (·····) [^{14}C]furaltadone.*

[19] Mallinckrodt, St. Louis, Mo.

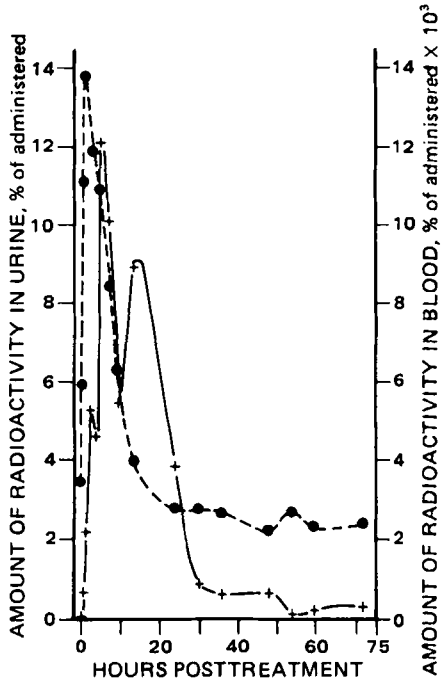

Figure 7—*Radioactive materials found in the urine and blood of a goat intramammarily infused with [¹⁴C]furaltadone. Key: (+) urine; (●) blood.*

isolated from the liver supernatant using TLC. The metabolites obtained from cattle and goats were similar. The metabolites obtained from the liver supernatant preparations were compared with those in the urine of animals dosed intravenously with furaltadone (Fig. 2 and Table I). Urine from furaltadone-treated animals contained two metabolites (C and E) not isolated from the *in vitro* liver preparations.

The metabolites of furaltadone and furaltadone isolated from liver supernatants failed to account for all the radioactivity present. An incubation mixture was fortified with 3.95 μg/mL of [¹⁴C]furaltadone. Following incubation the mixture contained 0.98 μg/mL. The postincubation supernatant was deproteinized and filtered. The filter cake contained 24.7% of the total radioactivity, the filtrate 72.6%. The presence

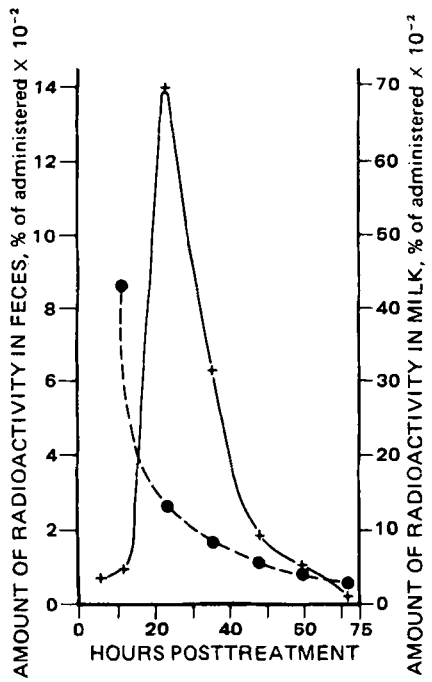

Figure 8—*Radioactive materials found in the feces and milk of a goat intramammarily dosed with [¹⁴C]furaltadone. Key: (+) feces; (●) milk.*

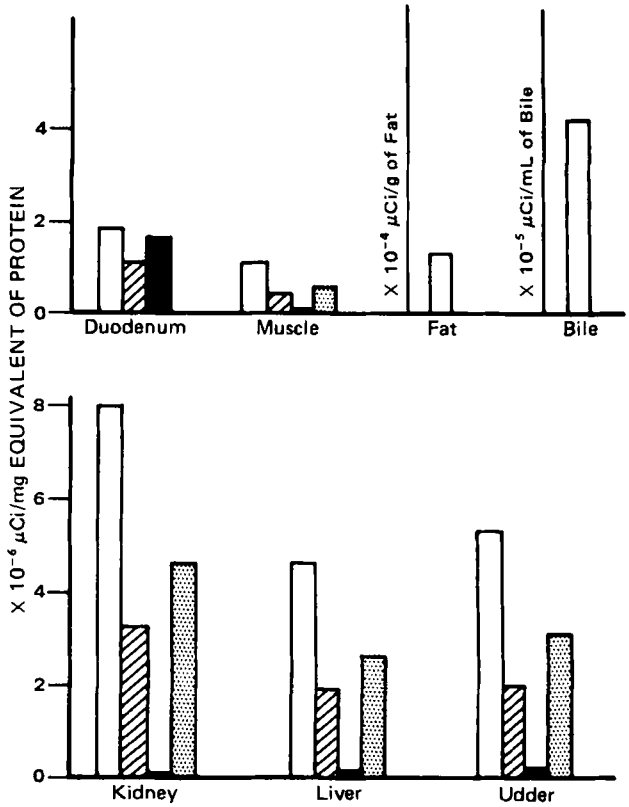

Figure 9—*Distribution of bound and free radioactivity in selected caprine tissues. Key: (□) before extraction; (▨) aqueous phase; (■) organic phase; (▩) residue.*

of carbon-14 in the filter cake indicated that nonextractable radioactivity from [¹⁴C]furaltadone was present. The bound material probably accounted for the persistence of the furaltadone in bovine and caprine liver during the 40–90-min incubation period, illustrated in Fig. 1. When the filtrate was extracted with dichloromethane–isopropyl alcohol–water the ratio of radioactivity in the organic extract to the aqueous filtrate was 1:1, which implied that polar metabolites were present. Similarly, in the *in vivo* study, chloroform and dichloromethane–isopropyl alcohol–water each extracted 13% of the radioactivity in urine.

An *in vivo* absorption, distribution, and elimination study was carried out with unlabeled furaltadone in two milking goats. The linear disappearance of furaltadone from plasma on a semilogarithmic plot of concentration *versus* time (Fig. 3) indicated that the data could be described by a one-compartment open kinetic model. The estimated half-life of furaltadone disappearance in goats was 35.4 min; this was comparable with 33 min in the rat and 37 min in the dog (9). At time zero, the plasma concentration was 14 mg/L. If the plasma occupied 5% of the body weight, the calculated concentration in plasma would have been 200 mg/L based on a dose of 10 mg/kg of body weight. This discrepancy between the observed and calculated concentrations of furaltadone in plasma indicated that furaltadone was rapidly distributed to and sequestered at an extracellular or intracellular site. Similar findings in rats were reported by Buzard and Conklin (9).

The amount of furaltadone remaining to be absorbed was calculated by the method reported previously by Wagner and Nelson (10). The calculated amount absorbed at each time period was plotted against time following drug administration (Fig. 4). The value of K used for calculation was the K_e determined in the intravenous study (1.17 h^{-1}). The half-life of absorption was determined from the linear segment of the curve and used for calculation of the absorption rate constant (10). A comparison of the doses administered and the calculated amounts of drug absorbed during a 14-h postdose period following intramammary drug infusion indicated that an average of 112.3% of the administered dose was absorbed. Although the calculated amount absorbed exceeded 100% and was therefore somewhat in error, the magnitude of the value indicated that furaltadone was almost totally absorbed from the udder. Further support for the almost complete absorption from the udder comes from results obtained following the intramammary infusion of [¹⁴C]furaltadone, where 99.4% of the infused dose was absorbed.

An examination of the rate of excretion of furaltadone and its metabolites in urine following intravenous administration (Fig. 5) indicated that the metabolites were excreted faster than the parent nitrofuran. Less than 2% of the furaltadone administered was recovered as such following intravenous and intramammary administration (Fig. 6).

The two metabolites that were quantitated accounted for <3%, expressed as furaltadone equivalent of the total administered dose. Similar recovery of furaltadone was observed following intramammary [^{14}C]-furaltadone administration to a lactating goat. The 5% recovered as unchanged drug and two metabolites is minor compared with the 56% radioactivity in the urine. Hence, the remainder of the radioactivity must be attributed to the presence of metabolites.

Of the 82.6% radioactivity accounted for in the [^{14}C]furaltadone study, 81% was present in the feces and urine (Table II). Within 48 h after administration, 99% of the radioactivity had been excreted in the urine, (Fig. 7), 95% in the feces, and only 0.06% of the radioactive dose was detectable in the milk (Fig. 8). Furaltadone was rapidly absorbed from the udder, as less than half the radioactivity was detected in the milk from the 12-h to the 24-h milkings. This was also supported in the unlabeled study by the absence of detectable furaltadone in milk 24 h after intramammary dosing.

Radioactive materials were present in decreasing levels of radioactivity in these tissues: kidney, udder, liver, duodenum, muscularis, and adipose tissues (Fig. 9). Of the total radioactivity administered, 1.16 ppm (expressed as furaltadone equivalent) was present per gram of fat, 2.1 ppm per gram of muscle, and 0.5 ppm per milliliter of bile. In the adipose tissue, no radioactivity was extractable with chloroform, which implied the absence of free furaltadone. In the organic solvent extract of the muscle, the equivalent of 0.19 ppm of the original radioactivity was recovered. The remainder of the radioactivity was bound to the tissue residue or was in the aqueous phase. Since furaltadone is lipophilic, and if the parent compound migrated to the tissues in its unchanged form, more radioactivity would be expected in the fatty tissues than in the lean meat. Labeling of normal body constituents as a result of metabolic degradation of furaltadone may explain why more radioactivity was present in the aqueous phase of the muscular tissue. The normal sites of absorption, metabolism, and excretion of furaltadone contained a relatively high amount of radioactivity. However, most of the radioactivity was retained in the aqueous and residue pellet of the udder, liver, and kidney tissue. In the duodenum, on the other hand, more radioactivity was present in the organic extract.

Radioactivity was found in the udder after 72 h, but since the majority of the activity was present in the unextractable residue and in the aqueous phase, it was presumed that furaltadone as such had disappeared from the udder. Of the total radioactivity. 99.4% infused into the udder had been absorbed. From the results obtained, it would appear that the absorption, distribution, and biotransformation of furaltadone in the goat is rapid and extensive.

REFERENCES

(1) S. J. Roberts, A. M. Meak, R. P. Natzke, R. S. Guthrie, L. E. Field, W. G. Merrill, G. H. Schmidt, and R. W. Everett, *J. Am. Vet. Med. Assoc.*, **155,** 157 (1969).

(2) R. G. Kingwill, F. K. Neave, F. H. Dodd, T. K. Griffin, D. R. Westgarth, and C. D. Wilson, *Vet. Rec.*, **87,** 94 (1970).

(3) S. M. Cohen, E. Erturk, A. M. von Esch, A. J. Crovetti, and G. T. Bryan, *J. Nat. Cancer Inst.*, **51,** 403 (1973).

(4) M. F. Paul, H. E. Paul, R. C. Bender, F. Kopke, C. M. Harrington, V. R. Ells, and J. A. Buzard, *Antibiot. Chemother.*, **10,** 287 (1959).

(5) P. L. Cox, and J. P. Heotis, *J. Agri. Food Chem.*, **11,** 499 (1963).

(6) G. Ziv, A. Savan-Rosenznaig, and R. Rizenberg, *Zentralbl. Veterinaermed. Reiche B.*, **20,** 415 (1973).

(7) L. L. Li, Ph.D. Thesis, University of Illinois. Champaign-Urbana, 1978.

(8) O. H. Lowry, N. J. Rosebrough, A. L. Farr, and R. J. Randall, *J. Biol. Chem.*, **193,** 265 (1951).

(9) J. A. Buzard and J. D. Conklin, *Antibiot. Chemother.*, **11,** 89 (1960).

(10) J. G. Wagner and E. Nelson, *J. Pharm. Sci.*, **52,** 610 (1963).

ACKNOWLEDGMENTS

Supported in part by NIH–FDA Contract 223-74-178 and the Illinois Agricultural Experimental Station.

Sincere thanks are extended to the Norwich Pharmaceutical Co., Norwich, N.Y. for supplying the furaltadone and to M. Limpoka for assistance in biological sample collection. Thanks also to the Research Art and Photography Department, Merck Sharp & Dohme and M. Sullivan for technical graphics, and to M. Gollon for typing of the manuscript.

Vaginal Absorption of a Potent Luteinizing Hormone-Releasing Hormone Analogue (Leuprolide) in Rats IV: Evaluation of the Vaginal Absorption and Gonadotropin Responses by Radioimmunoassay

HIROAKI OKADA ˣ, IWAO YAMAZAKI, TAKATSUKA YASHIKI, TSUGIO SHIMAMOTO, and HIROYUKI MIMA

Received October 12, 1982, from the *Central Research Division, Takeda Chemical Industries, Ltd., 2-17-85 Juso, Yodogawa, Osaka 532, Japan.* Accepted for publication January 11, 1983.

Abstract □ The vaginal absorption of leuprolide (a potent luteinizing hormone-releasing hormone analogue), which has the potential for producing regression of hormone-dependent tumors as well as high gonadotropin-releasing and ovulation-inducing activities, was evaluated in rats by radioimmunoassay. Gonadotropin (luteinizing hormone and follicle-stimulating hormone) release was concomitantly determined. Although leuprolide disappeared rapidly from the serum after intravenous administration (the biological half-lives were 8.4 min in the α-phase and 33.2 min in the β-phase), long-lasting serum levels were observed when the analogue was administered vaginally. The vaginal absorption was enhanced by adding citric acid to the test solution. The absolute bioavailability, estimated by the AUC of serum leuprolide levels, was 25.8% over 6 h and 38.0% over 12 h in the 5% citric acid solution (pH 3.5). The sustained release of gonadotropin was also obtained after vaginal administration of the analogue. A linear dose absorption correlation of leuprolide was obtained in the range of 10–1000 μg/kg in an aqueous solution or methylcellulose jelly. The release of gonadotropin showed a plateau level at >10 μg/kg, which corresponds to an effective dose for antitumor activity. The vaginal absorption of leuprolide varied with the estrous cycle, but this effect was eliminated by prior subcutaneous pretreatment with the analogue.

Keyphrases □ Leuprolide—vaginal absorption in rats, gonadotropin responses, effect of the estrous cycle, radioimmunoassay □ Gonadotropin response—leuprolide in rats, vaginal absorption, effect of the estrous cycle, radioimmunoassay □ Estrous cycle—effect on the vaginal absorption of leuprolide in rats, gonadotropin responses, radioimmunoassay

Leuprolide (I), a potent luteinizing hormone-releasing hormone (II) analogue (desGly^{10}-D-Leu^{6}-II ethylamide), has high gonadotropin-releasing and ovulation-inducing activities (1, 2). Recently, multiple high doses of leuprolide were found to effect regression of hormone-dependent mammary tumors (3, 4) and to have birth control potential in both sexes (5–8).

In our previous studies (9–11), investigations were conducted on the various routes of leuprolide administration for long-term therapy or convenient self-administration and on the absorption enhancement by assessing the ovulation-inducing activity in rats. We found that vaginal absorption was good and was enhanced by adding organic acids such as citric or succinic acid to the test solution. Although the estrous cycle influenced the vaginal absorption of phenolsulfonphthalein and insulin (used as hydrophilic markers), this influence was eliminated by a consecutive daily subcutaneous pretreatment with the analogue. Thus, the vaginal application of leuprolide was proposed as a practical route for long-term usage.

In the present study, we used a newly developed radioimmunoassay (RIA) for leuprolide (12) to investigate the pharmacokinetics of the analogue after intravenous administration, vaginal absorption, absorption enhancement, dose–absorption correlation, and the effect of the estrous cycle on vaginal absorption. Gonadotropin [luteinizing hormone (III) and follicle-stimulating hormone (IV)] release after vaginal administration of leuprolide was also determined by the RIA.

EXPERIMENTAL

Animals and Materials—Mature female Sprague–Dawley rats[1], 120–150 d of age, 250–330 g, which exhibited two or more consecutive 4-d estrous cycles were used. Leuprolide was administered to rats in the morning during the diestrus, except when studying the effect of the estrous cycle. Leuprolide was prepared as described previously (2) and was dried at 50°C under vacuum for 5 h before use. The analogue contained 6.2% acetic acid (as salt) and 2.5% water.

Radioimmunoassay of Leuprolide and Gonadotropin—Serum levels of leuprolide were determined in duplicate by the double-antibody RIA method reported previously (12). The serum sample or standard solution (0.2 mL) was mixed with 0.4 mL of 1% bovine serum albumin[2]–0.01 M phosphate-buffered saline (pH 7.0), 0.2 mL of rabbit anti-leuprolide serum diluted 1:10,000 in 1% bovine serum albumin–phosphate-buffered saline (pH 7.0) containing 0.05 M EDTA, and 0.1 mL of [^{131}I]leuprolide in 0.1% bovine serum albumin–phosphate-buffered saline (pH 7.0). After 48 h of incubation at 4°C, 0.2 mL of an appropriate dilution of goat anti-rabbit γ-globulin serum[3] (0.05 mL) and normal rabbit serum[3] (0.15 mL) in the buffered saline solution was added to each tube and the contents were mixed. Following an additional 24-h incubation at 4°C, the tube was centrifuged at 1000×g for 30 min, the supernatant aspirated, and the precipitate counted in an automatic gamma-counter[4].

Iodination of leuprolide was performed by the lactoperoxidase method (13). [^{131}I]Leuprolide was purified by gel filtration[5] with 0.2 M acetic acid as eluant. The specificity, sensitivity, and accuracy of the RIA for leuprolide have been described and characterized previously (12). The minimum measurable amount of the analogue using the antiserum was ~5 pg/tube (range: 5–10,000 pg/tube); the CV was <11.2% (50–1000 pg/tube) intra-assay and <19.2% (50–1000 pg/tube) interassay.

Gonadotropins (III and IV) in rat sera were also determined in duplicate by double-antibody RIA (14, 15) using kits[6]. Values are expressed in terms of the standard rat gonadotropins, NIAMDD-Rat-LH (RP-1) and NIAMDD-Rat-FSH (RP-1). The measurable range of both gonadotropins in this system was 1–800 ng/tube. The serum samples, stored at −20°C until assayed, were diluted to an adequate concentration with 0.01 M phosphate buffer (pH 7.0) before the assay.

Intravenous, Subcutaneous, and Vaginal Administration—Leuprolide was administered in the morning intravenously (100 μg/kg/0.1 mL of physiological saline), subcutaneously (100 μg/kg/0.1 mL of saline), and vaginally (500 μg/kg/0.2 mL) to diestrous rats under pentobarbital (50 mg/kg ip) and phenobarbital (100 mg/kg ip) anesthesia. For vaginal administration, leuprolide was dissolved in 5% citric acid solution at pH 3.5 (Solution A) and administered with a cotton ball (~12 mg) using a glass inserter (5-mm o.d.). After administration, the orifice of the vagina

[1] Clea Japan, Inc., Tokyo, Japan.
[2] Wako Pure Chemical Ind., Ltd., Osaka, Japan.
[3] Daiichi Radioisotope Laboratories, Ltd., Tokyo, Japan.
[4] Aloka Auto Well Gamma System, JDC-752; Aloka Co., Ltd., Tokyo, Japan.
[5] Sephadex G-10; Pharmacia Fine Chemicals AB, Uppsala, Sweden.
[6] Supplied by the National Institute of Arthritis, Metabolic, and Digestive Diseases, National Institutes of Health, Bethesda, Md.

0022-3549/84/0300-0298$01.00/0
© 1984, American Pharmaceutical Association

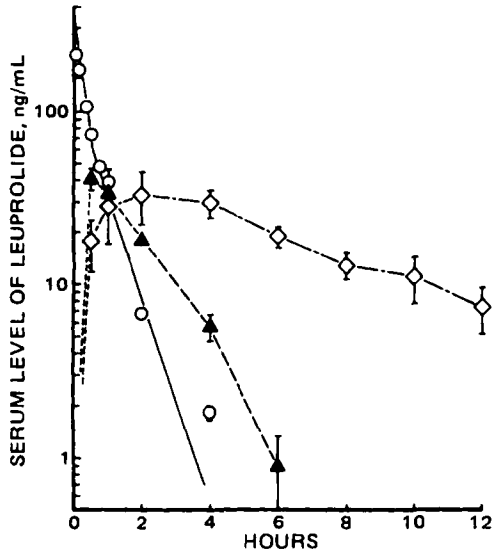

Figure 1—*Serum levels (log scale) of leuprolide after intravenous (○), subcutaneous (▲), and vaginal (◇) administration to diestrous rats. The analogue was administered intraveneously and subcutaneously at a dose of 100 μg/kg/mL in saline, and vaginally at 500μg/kg/0.2 mL in solution A, 5% citric acid solution (pH 3.5). Each point represents the mean ± SE of three or five (vaginal) rats.*

was sealed with a surgical adhesive agent. Blood (~0.5 mL) was collected from the tail vein at appropriate times during 12 h, and the serum was stored until assayed. In cases of intravenous administration, a group of three rats was used for blood collections (0.2–0.5 mL) at 5, 20, 45, 120, and 360 min postadministration and another group was used for collections at 10, 30, 60, and 240 min to prevent physiologically abnormal conditions (hypovolemia).

The pharmacokinetic parameters were obtained by fitting the individual rat data during 6 h to a two-compartment open model *via* the nonlinear least-squares regression computer program NONLIN (16). The

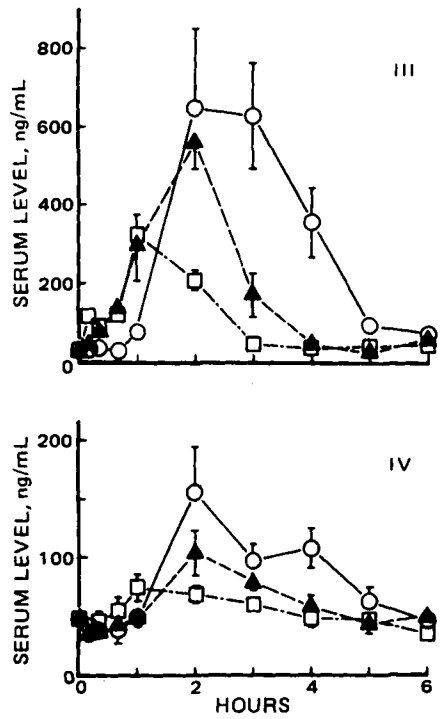

Figure 2—*Serum gonadotropin levels after intravenous (□), subcutaneous (▲), and vaginal (○) administration of leuprolide to diestrous rats. The analogue was administered at a dose corresponding to the ED_{50} of ovulation-inducing activity (38 ng/kg iv, 58 ng/kg sc, and 99 ng/kg) in 5% citric acid solution (pH 1.8) vaginally. Each point represents the mean ± SE of five rats.*

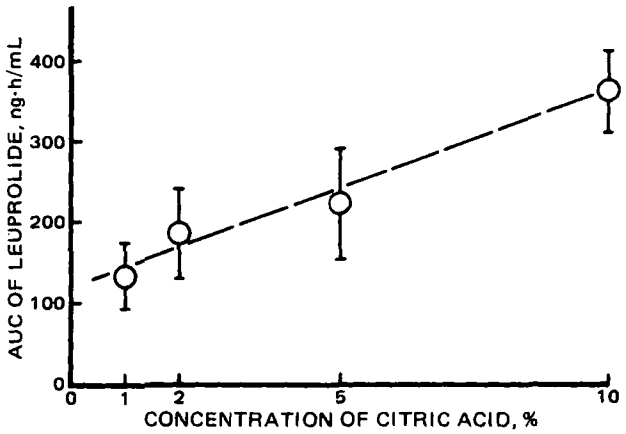

Figure 3—*AUC of leuprolide over 6 h after vaginal administration in the pH 3.5 aqueous solutions containing different concentrations of citric acid to diestrous rats. Dose of the analogue was 500 μg/kg/0.2 mL in the acid solution. Each point represents the mean ± SE of five rats.*

area under the serum level–time curve (AUC) of leuprolide was calculated by a trapezoidal method within the last collected time value, and the bioavailability was obtained using:

$$\text{Bioavailability (\%)} = \frac{AUC^{t}_{0,vag} \text{ or } AUC^{t}_{0,sc}}{AUC^{t}_{0,iv}} \times 100 \qquad \text{(Eq. 1)}$$

where t is the last collection time.

Gonadotropin release was determined after intravenous, subcutaneous, and vaginal administration of leuprolide at the dose corresponding to the ED_{50} of the ovulation-inducing activity [38, 58, and 99 ng/kg, respectively (9, 10)] in unanesthetized rats at diestrus. The analogue was dissolved in physiological saline containing 0.1% bovine serum albumin, 20 U/mL of aprotinin[7], and 0.01 M HCl for intravenous and subcutaneous administration, and in 5% citric acid solution (pH 1.8) for vaginal administration. Whole blood was taken from the abdominal aorta with the rats under ether anesthesia 10, 20, 40, 60, 120, 180, 240, 300, and 360 min after administration.

Enhancement of Vaginal Absorption—Aqueous solutions of leuprolide (500 μg/kg/0.2 mL) containing four different concentrations of citric acid were administered vaginally (cotton ball technique) to anesthetized diestrous rats. Each solution was previously adjusted to pH 3.5 by 10 M NaOH and 2 M HCl and to an isotonic preparation with sodium chloride. Blood was collected from the tail vein to determine the serum levels of leuprolide.

Dose-Absorption and Response Correlations—Four different doses (10–1000 μg/kg) of leuprolide in Solution A or 5% methylcellulose[8] jelly

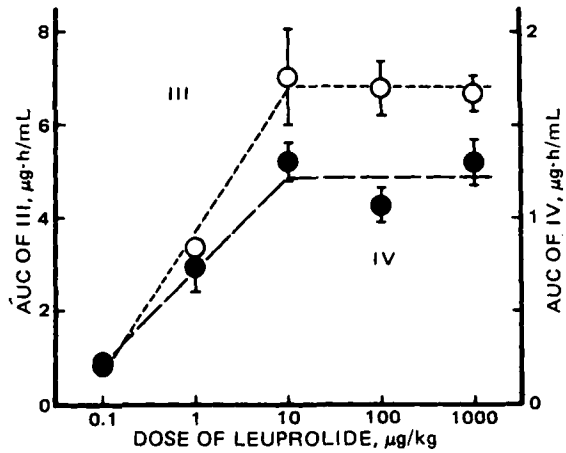

Figure 4—*Dose response (AUC of serum gonadotropin levels over 6 h) curves after vaginal administration of leuprolide to diestrous rats. The analogue was dissolved in solution A and administered at a dose of 0.1, 1, 10, 100 μg, and 1 mg/kg. Each point represents the mean ± SE of five rats.*

[7] Trasylol; Bayer AG, Leverkusen-Bayerwerk, W. Germany.
[8] Metolose 90SH4000; Shinetsu Chemicals Co., Tokyo, Japan.

Table I—AUC of Leuprolide after Vaginal Administration in Solution A[a] or 5% Methylcellulose Jelly Containing Solution A to Diestrous Rats

Dose, μg/kg	AUC of Leuprolide, ng·h/mL[b]	
	Aqueous Solution	Jelly
10	3.75 ± 0.82	—
50	19.3 ± 4.66	12.8 ± 1.56
100	34.6 ± 10.6	38.0 ± 7.43
500	222.0 ± 68.8	166.5 ± 19.1
1000	—	408.3 ± 33.7

[a] 5% citric acid solution, pH 3.5. [b] AUC was calculated from 0 to 6 h; each value represents the mean ± *SE* of five rats.

containing Solution A were administered vaginally to anesthetized diestrous rats to assay the serum levels of the analogue. Leuprolide was also administered vaginally at a dose range of 0.1–1000 μg/kg/0.2 mL in Solution A, and serum levels of gonadotropin were determined.

Effect of the Estrous Cycle—Leuprolide was administered vaginally at a dose of 500 μg/kg/0.2 mL in Solution A to proestrous, estrous, metestrous and diestrous rats under anesthesia, and the serum level of the analogue was determined. To determine the gonadotropin-releasing responses, an oleaginous suppository[9] containing 100 ng of leuprolide and 10% citric acid was administered vaginally to anesthetized rats exhibiting the four different stages of the estrous cycle.

For the determination of the effect of prior pretreatment of leuprolide on the vaginal absorption, 100 μg/kg of the analogue was given subcutaneously daily for 10 d to rats initially exhibiting the four different stages. The following morning, each rat received a single vaginal administration of 500 μg/kg of leuprolide in Solution A, and the serum levels of the analogue were assayed. Vaginal smears during the subcutaneous administration were examined daily to determine the change of the estrous cycle. The vagina and ovaries were removed for histological examination after taking the 6-h-blood samples.

RESULTS

Intravenous, Subcutaneous, and Vaginal Administration—Serum levels of leuprolide after intravenous, subcutaneous, and vaginal administration to diestrous female rats are shown in Fig. 1.

The pharmacokinetic parameters after intravenous administration were obtained by simulating to a two-compartment open model; the serum level (C_t) at time t was expressed by:

$$C_t = Ae^{-\alpha t} + Be^{-\beta t} \qquad \text{(Eq. 2)}$$

with A = 241.5 ± 99.6 ng/mL, B = 122.4 ± 43.1 ng/mL, α = 8.37 ± 4.12 h^{-1}, and β = 1.35 ± 0.23 hr^{-1}. Leuprolide rapidly disappeared from the serum: the half-lives were 8.4 ± 4.0 min in the α-phase and 33.2 ± 6.8 min in the β-phase. The transfer rate constants between central and tissue compartments were 2.99 ± 2.32 h^{-1} (from central to tissue) and 3.79 ± 1.35 h^{-1} (from tissue to central). The elimination rate constant from the central compartment was 2.94 ± 0.92 h^{-1}, and the volumes of distribution were 0.32 ± 0.07 L/kg for the central compartment and 1.31 ± 0.71 L/kg for the tissue compartment. Each value represents the mean ± *SE* of three rats.

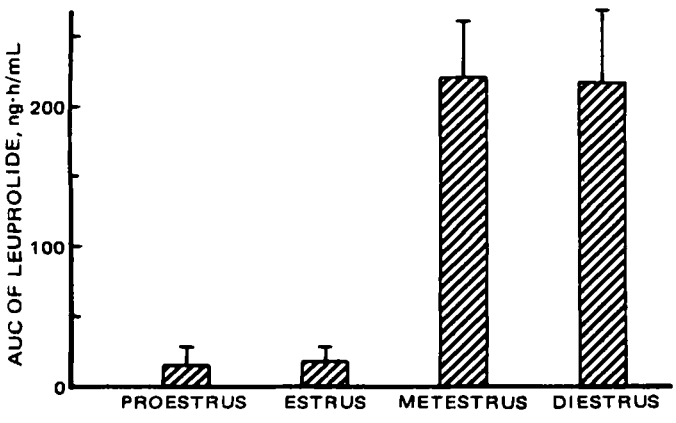

Figure 5—*AUC of leuprolide over 6 h after vaginal administration during different stages of the estrous cycle in rats. Dose of the analogue was 500 μg/kg/0.2 mL in solution A. Each bar represents the mean ± SE of five rats.*

[9] Witepsol S55; Dynamit Nobel Aktiengesellshaft, W. Germany.

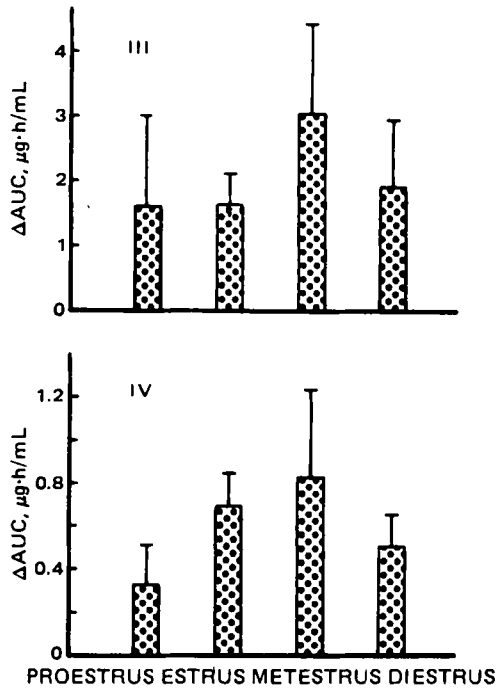

Figure 6—*AUC increment (ΔAUC) of serum gonadotropin levels over 6 h after vaginal administration of leuprolide during different stages of the estrous cycle in rats. The analogue was administered at a dose of 100 ng/rat in an oleaginous suppository containing 10% citric acid. Each bar represents the mean ± SE of three rats.*

The subcutaneous administration resulted in a sustained serum level: the serum level at 4 h after the administration was 3 times higher than that after the intravenous administration. The absolute bioavailability, determined by the AUC over 6 h, was 68.1%. In the case of vaginal administration, leuprolide was absorbed rapidly, and a long-lasting serum level was observed. The maximum serum level was observed 2 h after administration, but values were high and relatively constant over the 6-h period. The absolute bioavailability was 25.8% over 6 h and 38.0% over 12 h.

Gonadotropin-releasing responses to the analogue given by the three routes at doses corresponding to the ED_{50} of ovulation-inducing activity are shown in Fig. 2. The peak times of serum gonadotropin levels were the shortest after intravenous administration, whereas the serum levels after vaginal administration were the highest and had the longest duration. The total release of gonadotropin (which can be represented by the AUC values) after administration of leuprolide by the three routes were directly proportional to the doses given.

Enhancement of the Vaginal Absorption—Serum leuprolide levels after vaginal administration with four different concentrations of citric acid were determined, and the AUC over 6 h is shown in Fig. 3. The AUC increased progressively with the addition of citric acid up to 10%. The absolute bioavailability was 36.0% in the 5% citric acid solution and 58.7% in the 10% solution, which was 2.7 times larger than that in the 1% solution.

Dose Absorption and Response Correlations—Serum leuprolide levels after vaginal administration in either an aqueous solution or a methylcellulose jelly, both containing 5% citric acid, were determined at the dose range of 10–1000 μg/kg, and the AUC values were calculated (Table I). AUC values of serum gonadotropin levels after vaginal administration of leuprolide in Solution A are shown in Fig. 4. A linear relationship between the dose and AUC of leuprolide was observed over the entire range, whereas for the gonadotropin-releasing responses, a linear dose–response correlation was obtained only in the dose range of 0.1–10 μg/kg with a plateau at >10 μg/kg.

Effect of the Estrous Cycle—The AUC (mean ± *SE*) of leuprolide over 6 h after vaginal administration was 15.5 ± 13.0 ng·h/mL during proestrus, 17.4 ± 9.68 ng·h/mL during estrus, 221.3 ± 42.2 ng·h/mL during metestrus, and 218.8 ± 60.8 ng·h/mL during diestrus (Fig. 5). The AUC

values during metestrus and diestrus were 13 times higher than those during proestrus and estrus.

Gonadotropin release after vaginal administration of leuprolide during the four different stages of the cycle showed large variation, and the effect was not so clear as that seen for serum levels of the analogue (Fig. 6). However, the AUC increments of serum gonadotropin levels during metestrus and diestrus were larger than those seen during proestrus and estrus. The serum level of IV at estrus before vaginal administration was twice that seen at the other stages.

Vaginal absorption of leuprolide in rats pretreated with daily subcutaneous administrations of the analogue for 10 d was rapid and of increased magnitude; the maximum serum levels obtained between 1 and 2 h after vaginal administration were ~3 times larger than those in nontreated diestrous rats. The AUC values (mean ± *SE*) over 6 h after vaginal administration were 577.9 ± 59.0 ng·h/mL for proestrus (of the initial stage before cycle was disrupted due to the subcutaneous pretreatment), 530.4 ± 119.6 ng·h/mL for estrus, 571.0 ± 49.5 ng·h/mL for metestrus, and 550.0 ± 6.4 ng·h/mL for diestrus, respectively (Fig. 7).

Despite initiation of the pretreatment at different stages of the estrous cycle, the AUC values of leuprolide showed small fluctuations and were 2.5 times larger than that in nonpretreated diestrous rats. The examination of vaginal smears revealed that the estrous cycle was halted at diestrus in all rats as a result of subcutaneous pretreatment with the analogue. The histological observation after this experiment showed a thinner vaginal epithelium than that seen at normal diestrus, infiltration of neutrophil leucocytes in the vagina, and an increase in the number of corpora lutea with no Graafian follicles in the ovaries.

DISCUSSION

The disappearance of leuprolide from the serum of rats after intravenous administration was rapid; the biological half-lives were 8.4 min in the α-phase and 33.2 min in the β-phase. The half-life in the α-phase was identical to that of [^{3}H]II in female (17) and male rats (18). This result supports the idea that the potent and long-lasting activity of leuprolide is due not to the slow disappearance from the circulation, but rather to the high uptake in the anterior pituitary (19) or to a high receptor-binding affinity (20). The serum level of the analogue after subcutaneous administration was maintained for a longer period than that after intravenous administration, and the absolute bioavailability was 68.1%. After vaginal administration, high and long-lasting serum levels of leuprolide were observed with the absolute bioavailability up to 6 h being 25.8%. Although the true availability should be estimated to be much larger when sampling blood for a longer period, the bioavailability over 6 h paralleled the case of ovulation-inducing activity (10).

Gonadotropin release after leuprolide administration by the three routes, which was evaluated at the lowest dose exhibiting a linear dose–response correlation, was not identical, despite using doses corresponding to the ED_{50} of the ovulation-inducing activity. The different responses are possibly due to the lag time of distribution to the target organ (anterior pituitary), the releasing balance of gonadotropins III and IV, hormonal feedback, and sensitivity of the target cells. Nevertheless, these results do indicate that the vaginal absorption of leuprolide resulted in a maintenance of high serum levels and pituitary responses.

In our previous studies (9, 10) we demonstrated, by the determination of ovulation-inducing activity, that citric acid enhanced the vaginal absorption of leuprolide. In this study, it was directly confirmed that the acid progressively enhanced the vaginal absorption of the analogue at the concentrations used (Fig. 3).

Linear correlations between dose and vaginal absorption of leuprolide in an aqueous solution and methylcellulose jelly (as a practical dosage form) were obtained by determining the serum level of the analogue (Table I). However, both gonadotropin-releasing responses were proportional to the dose within 0.1–10 μg/kg and showed a plateau between 10–1000 μg/kg. Such saturation of the gonadotropin-releasing response at higher doses of II and its analogues has been reported (21–23) and is possibly due to the negative feedback effect of estrogen (24–26) or to the decrease of gonadotropin-releasing hormone receptor cells in the pituitary ("down regulation") (27–29). On the other hand, the minimum effective dose of leuprolide to produce regression of rat mammary tumors induced by 7,12-dimethylbenz[*a*]anthracene was ~100 μg/kg by vaginal administration[10], which is well within the dose range that caused a maximum pituitary stimulation in the present study.

In a previous study, we found that the estrous cycle of rats affected the vaginal absorption of insulin and phenolsulfonphthalein, used as markers

[10] Unpublished data.

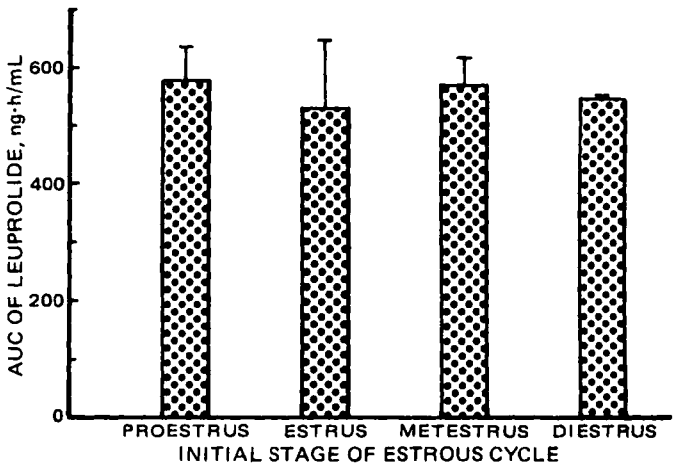

Figure 7—*AUC of leuprolide over 6 h after vaginal administration. Rats were pretreated subcutaneously with the analogue at a dose of 100 μg/kg/d for 10 d followed by a single vaginal dose of 500 μg/kg in solution A. Each bar represents the mean* ± SE *of three rats.*

of hydrophilic compounds (11). The vaginal absorption of leuprolide also was affected by the estrous cycle to the same degree as seen with phenolsulfonphthalein; the vaginal absorption during metestrus and diestrus was 13 times greater than that during proestrus and estrus. The effect of the estrous cycle can be explained by the change of pore-like pathways in the vaginal epithelium (11, 30), producing an unavoidable fluctuation in the vaginal absorption of drugs.

Gonadotropin release after vaginal administration of leuprolide throughout the estrous cycle has not been shown to be clearly dependent on the cycle, as is the case with the serum level of the analogue; high serum levels of gonadotropin were observed even during proestrus and estrus. This phenomenon is ascribed to increased absorbability due to alteration of the vaginal epithelium and to the pituitary responsiveness due to feed-back by progestins and estrogens (31–34) or due to regulation of gonadotropin-releasing hormone receptors (29, 35) during the estrous cycle. The responsiveness of III and IV to leuprolide is the highest at proestrus and estrus, respectively (36–38). Furthermore, the spontaneous surge is provoked in the afternoon of proestrus for III, and from the afternoon of proestrus to the morning of estrus for IV (35, 39). Nevertheless, the high serum levels of gonadotropin during metestrus and diestrus (with the lower pituitary responsiveness) should support the good vaginal absorption of the analogue.

Undue influence of the estrous cycle on the absorption of drugs is unfavorable for effective vaginal application. However, in the case of leuprolide, the pretreatment administration halted the cycle at diestrus, and resulted in a good vaginal absorption of the analogue with less variation. The augmented absorption compared with that in nonpretreated diestrous rats may be attributed to the thinner epithelium of the vagina, as seen histologically. Likewise, the enhancement of vaginal absorption of a hydrophilic marker compound by pretreatment with leuprolide was demonstrated in our previous study (11); cessation of the cycling at diestrus was also demonstrated by the vaginal smear examination and by histological observations.

In summary, leuprolide was absorbed sufficiently through the vagina in diestrous rats; prolonged serum levels of the radioimmunoreactive analogue and potent gonadotropin-releasing responses were observed, and the vaginal absorption of the analogue was enhanced by adding citric acid. Modifying effects of the estrous cycle on the vaginal absorption were observed, but such variations were eliminated by prior parenteral pretreatment with the analogue. From these results, we conclude that vaginal application of leuprolide can be a potentially effective method as self-administration or long-term treatment for anticancer or fertility control. Moreover, we propose that vaginal application of leuprolide be performed as a maintenance dose following consecutive parenteral administration, in order to terminate the menstrual cycle and provide a vaginal environment conducive to maximal analogue absorption with less variation.

REFERENCES

(1) J. A. Vilchez-Martinez, D. H. Coy, A. Arimura, E. J. Coy, Y. Hirotsu, and A. V. Schally, *Biochem. Biophys. Res. Commun.*, **59**, 1226 (1974).

(2) M. Fujino, T. Fukuda, S. Shinagawa, S. Kobayashi, I. Yamazaki, R. Nakayama, J. H. Seely, W. F. White, and R. H. Rippel, *Biochem. Biophys. Res. Commun.*, **60,** 406 (1974).
(3) E. S. Johnson, J. H. Seely, W. F. White, and E. R. DeSombre, *Science*, **194,** 329 (1976).
(4) E. R. DeSombre, E. S. Johnson, and W. F. White, *Cancer Res.*, **36,** 3830 (1976).
(5) A. Corbin, C. W. Beattie, J. Yardley, and T. J. Foell, *Endocrinol. Res. Commun.*, **3,** 359 (1976).
(6) R. F. Casper and S. S. C. Yen, *Science*, **205,** 408 (1979).
(7) C. Bergquist, S. J. Nillius, and L. Wide, *Lancet*, **ii,** 215 (1979).
(8) D. Heber and R. S. Swerdloff, *Science*, **209,** 936 (1980).
(9) H. Okada, I. Yamazaki, Y. Ogawa, S. Hirai, T. Yashiki, and H. Mima, *J. Pharm. Sci.*, **71,** 1367 (1982).
(10) H. Okada, I. Yamazaki, T. Yashiki, and H. Mima, *J. Pharm. Sci.*, **72,** 75 (1983).
(11) H. Okada, T. Yashiki, and H. Mima, *J. Pharm. Sci.*, **72,** 137 (1983).
(12) I. Yamazaki and H. Okada, *Endocrinol. Jpn.*, **27,** 593 (1980).
(13) Y. Miyachi, A. Chrambach, R. S. Mecklenburg, and M. B. Lipsett, *Endocrinology*, **92,** 1725 (1973).
(14) G. D. Niswender, A. R. Midgley, S. E. Monroe, and L. E. Reichert, *Proc. Soc. Exp. Biol. Med.*, **128,** 807 (1968).
(15) T. A. Daane and A. F. Parlow, *Endocrinology*, **88,** 653 (1971).
(16) C. M. Metzler, "NONLIN, (a computer program for parameter estimation in nonlinear situations), Technical Report 7292/69/7292/005, The Upjohn Co., Kalamazoo, Mich. (1969).
(17) T. W. Redding and A. V. Schally, *Life Sci.*, **12,** 23 (1973).
(18) A. Dupont, F. Labrie, G. Pelletier, R. Puviani, D. H. Coy, E. J. Coy, and A. V. Schally, *Neuroendocrinology*, **16,** 65 (1974).
(19) J. J. Reeves, G. K. Tarnavsky, S. R. Becker, D. H. Coy, and A. V. Schally, *Endocrinology*, **101,** 540 (1977).
(20) R. N. Clayton and K. J. Catt, *Endocrinology*, **106,** 1154 (1980).
(21) R. Rebar, S. S. C. Yen, G. Vandenberg, F. Naftolin, Y. Ehara, S. Engblom, K. J. Ryan, J. Rivier, M. Amoss, and R. Guillemin, *J. Clin. Endocrinol. Metab.*, **36,** 10 (1973).
(22) E. Friedrich, A. Etzrodt, H. Becker, J. P. Hanker, E. Keller, P. Kleisl, V. Pinto, A. E. Schindler, H. P. G. Schneider, O. Vanderbeke, H. Werder, and H. I. Wyss, *Acta Endocrinol.*, **87,** 19 (1978).
(23) L. Cusan, C. Auclair, A. Belanger, L. Ferland, P. A. Kelly, G. Seguin, and F. Labrie, *Endocrinology*, **104,** 1369 (1979).
(24) A. Negro-Vilar, R. Orias, and S. M. McCann, *Endocrinology*, **92,** 1680 (1973).
(25) C. Libertun, R. Orias, and S. M. McCann, *Endocrinology*, **94,** 1094 (1974).
(26) J. A. Vilchez-Martinez, A. Arimura, L. Debeljuk, and A. V. Schally, *Endocrinology*, **94,** 1300 (1974).
(27) C. Auclair, P. A. Kelly, F. Labrie, D. H. Coy, and A. V. Schally, *Biochem. Biophys. Res. Commun.*, **76,** 855 (1977).
(28) D. Heber and W. D. Odell, *Am. J. Physiol.*, **237,** E136 (1979).
(29) R. N. Clayton, A. R. Solano, A. Garcia-Vela, M. L. Dufau, and K. J. Catt, *Endocrinology*, **107,** 699 (1980).
(30) C. D. Turner and J. T. Bagnara, "General Endocrinology," 6th ed., Saunders, Philadelphia, Pa., 1976, p. 470.
(31) T. Yamaji, D. J. Dierschke, J. Hotchkiss, A. N. Bhattacharya, A. H. Surve, and E. Knobil, *Endocrinology*, **89,** 1034 (1971).
(32) M. S. Aiyer and G. Fink, *J. Endocrinol.*, **62,** 553 (1974).
(33) L. G. Nequin, J. Alvarez, and N. B. Schwartz, *J. Steroid Biochem.*, **6,** 1007 (1975).
(34) D. K. Sarkar and G. Fink, *J. Endocrinol.*, **80,** 303 (1979).
(35) R. T. Savoy-Moore, N. B. Schwartz, J. A. Duncan, and J. C. Marshall, *Science*, **209,** 942 (1980).
(36) J. E. Martin, L. Tyrey, J. W. Everett, and R. E. Fellows, *Endocrinology*, **94,** 556 (1974).
(37) K. J. Cooper, C. P. Fawcett, and S. M. McCann, *Endocrinology*, **95,** 1293 (1974).
(38) C. A. Blake, *Endocrinology*, **102,** 1043 (1978).
(39) K. Taya and M. Igarashi, *Endocrinol. Jpn.*, **20,** 199 (1973).

ACKNOWLEDGMENTS

We wish to thank the National Institute of Arthritis, Metabolic, and Digestive Diseases for supplying the radioimmunoassay kits for rat gonadotropin and H. Nakagawa for assistance with the experients, Y. Sakura for histological examination, and M. Ohara for comments on the manuscript.

In Vitro Release of Salicylic Acid from Lanolin Alcohols–Ethylcellulose Films

ARSHAD R. KHAN *§, BALASUBRAMANIAN V. IYER *‡, ROSETTA A. CIRELLI *, and RAVINDRA C. VASAVADA *x

Received March 11, 1982, from the **School of Pharmacy, University of the Pacific, Stockton, CA 95207* and ‡*Department 947, Lederle Laboratories Inc., Pearl River, NY 10965.* Accepted for publication February 1, 1983. §Present address: Agha Brothers, Karachi, Pakistan.

Abstract □ Lanolin alcohols–ethylcellulose films were investigated as a potential drug delivery system for the controlled release of salicylic acid. The effects of changes in film composition, drug concentration, drug solubility, and stirrer speed on the *in vitro* release of salicylic acid have been examined. The drug release has been found to obey a diffusion-controlled matrix model and square root of time release profile both in the suspension and solution cases.

Keyphrases □ Salicylic acid—*in vitro* release from lanolin alcohols–ethylcellulose films, drug diffusion □ Lanolin alcohols—films with ethyl cellulose, *in vitro* release of salicylic acid, drug diffusion □ Ethylcellulose—films with lanolin alcohols, *in vitro* release of salicylic acid, drug diffusion □ Drug diffusion—*in vitro* release of salicylic acid from lanolin alcohols–ethylcellulose films

The film-forming potential of nonpolymeric materials such as lanolin alcohols, which are extensively used in cosmetic and pharmaceutical formulations, has been recently investigated in our laboratory (1). Lanolin alcohols were found to form isolatable thin films on a mercury substrate. The incorporation of small percentages of ethylcellulose, a known film former (2), and a plasticizer such as propylene glycol with lanolin alcohols was found to give tack-free films of improved quality.

Effective utilization of nonpolymeric substances such as lanolin alcohols in film-forming composition holds considerable promise for a variety of reasons. Such delivery systems could be designed and formulated to provide sustained drug delivery. The potential hazards associated with monomeric impurities in polymers are avoided. Nonpolymeric materials are easy to manipulate and compound, and are relatively easy to obtain in a state of definable composition. They also can be washed from the skin with relative ease using soap and water.

0022-3549/84/0300-0302$01.00/0
© 1984, American Pharmaceutical Association

(2) M. Fujino, T. Fukuda, S. Shinagawa, S. Kobayashi, I. Yamazaki, R. Nakayama, J. H. Seely, W. F. White, and R. H. Rippel, *Biochem. Biophys. Res. Commun.*, **60,** 406 (1974).
(3) E. S. Johnson, J. H. Seely, W. F. White, and E. R. DeSombre, *Science*, **194,** 329 (1976).
(4) E. R. DeSombre, E. S. Johnson, and W. F. White, *Cancer Res.*, **36,** 3830 (1976).
(5) A. Corbin, C. W. Beattie, J. Yardley, and T. J. Foell, *Endocrinol. Res. Commun.*, **3,** 359 (1976).
(6) R. F. Casper and S. S. C. Yen, *Science*, **205,** 408 (1979).
(7) C. Bergquist, S. J. Nillius, and L. Wide, *Lancet*, **ii,** 215 (1979).
(8) D. Heber and R. S. Swerdloff, *Science*, **209,** 936 (1980).
(9) H. Okada, I. Yamazaki, Y. Ogawa, S. Hirai, T. Yashiki, and H. Mima, *J. Pharm. Sci.*, **71,** 1367 (1982).
(10) H. Okada, I. Yamazaki, T. Yashiki, and H. Mima, *J. Pharm. Sci.*, **72,** 75 (1983).
(11) H. Okada, T. Yashiki, and H. Mima, *J. Pharm. Sci.*, **72,** 137 (1983).
(12) I. Yamazaki and H. Okada, *Endocrinol. Jpn.*, **27,** 593 (1980).
(13) Y. Miyachi, A. Chrambach, R. S. Mecklenburg, and M. B. Lipsett, *Endocrinology*, **92,** 1725 (1973).
(14) G. D. Niswender, A. R. Midgley, S. E. Monroe, and L. E. Reichert, *Proc. Soc. Exp. Biol. Med.*, **128,** 807 (1968).
(15) T. A. Daane and A. F. Parlow, *Endocrinology*, **88,** 653 (1971).
(16) C. M. Metzler, "NONLIN, (a computer program for parameter estimation in nonlinear situations), Technical Report 7292/69/7292/005, The Upjohn Co., Kalamazoo, Mich. (1969).
(17) T. W. Redding and A. V. Schally, *Life Sci.*, **12,** 23 (1973).
(18) A. Dupont, F. Labrie, G. Pelletier, R. Puviani, D. H. Coy, E. J. Coy, and A. V. Schally, *Neuroendocrinology*, **16,** 65 (1974).
(19) J. J. Reeves, G. K. Tarnavsky, S. R. Becker, D. H. Coy, and A. V. Schally, *Endocrinology*, **101,** 540 (1977).
(20) R. N. Clayton and K. J. Catt, *Endocrinology*, **106,** 1154 (1980).
(21) R. Rebar, S. S. C. Yen, G. Vandenberg, F. Naftolin, Y. Ehara, S. Engblom, K. J. Ryan, J. Rivier, M. Amoss, and R. Guillemin, *J. Clin. Endocrinol. Metab.*, **36,** 10 (1973).
(22) E. Friedrich, A. Etzrodt, H. Becker, J. P. Hanker, E. Keller, P. Kleisl, V. Pinto, A. E. Schindler, H. P. G. Schneider, O. Vanderbeke, H. Werder, and H. I. Wyss, *Acta Endocrinol.*, **87,** 19 (1978).
(23) L. Cusan, C. Auclair, A. Belanger, L. Ferland, P. A. Kelly, G. Seguin, and F. Labrie, *Endocrinology*, **104,** 1369 (1979).
(24) A. Negro-Vilar, R. Orias, and S. M. McCann, *Endocrinology*, **92,** 1680 (1973).
(25) C. Libertun, R. Orias, and S. M. McCann, *Endocrinology*, **94,** 1094 (1974).
(26) J. A. Vilchez-Martinez, A. Arimura, L. Debeljuk, and A. V. Schally, *Endocrinology*, **94,** 1300 (1974).
(27) C. Auclair, P. A. Kelly, F. Labrie, D. H. Coy, and A. V. Schally, *Biochem. Biophys. Res. Commun.*, **76,** 855 (1977).
(28) D. Heber and W. D. Odell, *Am. J. Physiol.*, **237,** E136 (1979).
(29) R. N. Clayton, A. R. Solano, A. Garcia-Vela, M. L. Dufau, and K. J. Catt, *Endocrinology*, **107,** 699 (1980).
(30) C. D. Turner and J. T. Bagnara, "General Endocrinology," 6th ed., Saunders, Philadelphia, Pa., 1976, p. 470.
(31) T. Yamaji, D. J. Dierschke, J. Hotchkiss, A. N. Bhattacharya, A. H. Surve, and E. Knobil, *Endocrinology*, **89,** 1034 (1971).
(32) M. S. Aiyer and G. Fink, *J. Endocrinol.*, **62,** 553 (1974).
(33) L. G. Nequin, J. Alvarez, and N. B. Schwartz, *J. Steroid Biochem.*, **6,** 1007 (1975).
(34) D. K. Sarkar and G. Fink, *J. Endocrinol.*, **80,** 303 (1979).
(35) R. T. Savoy-Moore, N. B. Schwartz, J. A. Duncan, and J. C. Marshall, *Science*, **209,** 942 (1980).
(36) J. E. Martin, L. Tyrey, J. W. Everett, and R. E. Fellows, *Endocrinology*, **94,** 556 (1974).
(37) K. J. Cooper, C. P. Fawcett, and S. M. McCann, *Endocrinology*, **95,** 1293 (1974).
(38) C. A. Blake, *Endocrinology*, **102,** 1043 (1978).
(39) K. Taya and M. Igarashi, *Endocrinol. Jpn.*, **20,** 199 (1973).

ACKNOWLEDGMENTS

We wish to thank the National Institute of Arthritis, Metabolic, and Digestive Diseases for supplying the radioimmunoassay kits for rat gonadotropin and H. Nakagawa for assistance with the experients, Y. Sakura for histological examination, and M. Ohara for comments on the manuscript.

In Vitro Release of Salicylic Acid from Lanolin Alcohols–Ethylcellulose Films

ARSHAD R. KHAN *§, BALASUBRAMANIAN V. IYER *‡, ROSETTA A. CIRELLI *, and RAVINDRA C. VASAVADA *x

Received March 11, 1982, from the **School of Pharmacy, University of the Pacific, Stockton, CA 95207* and ‡*Department 947, Lederle Laboratories Inc., Pearl River, NY 10965.* Accepted for publication February 1, 1983. §Present address: Agha Brothers, Karachi, Pakistan.

Abstract □ Lanolin alcohols–ethylcellulose films were investigated as a potential drug delivery system for the controlled release of salicylic acid. The effects of changes in film composition, drug concentration, drug solubility, and stirrer speed on the *in vitro* release of salicylic acid have been examined. The drug release has been found to obey a diffusion-controlled matrix model and square root of time release profile both in the suspension and solution cases.

Keyphrases □ Salicylic acid—*in vitro* release from lanolin alcohols–ethylcellulose films, drug diffusion □ Lanolin alcohols—films with ethyl cellulose, *in vitro* release of salicylic acid, drug diffusion □ Ethylcellulose—films with lanolin alcohols, *in vitro* release of salicylic acid, drug diffusion □ Drug diffusion—*in vitro* release of salicylic acid from lanolin alcohols–ethylcellulose films

The film-forming potential of nonpolymeric materials such as lanolin alcohols, which are extensively used in cosmetic and pharmaceutical formulations, has been recently investigated in our laboratory (1). Lanolin alcohols were found to form isolatable thin films on a mercury substrate. The incorporation of small percentages of ethylcellulose, a known film former (2), and a plasticizer such as propylene glycol with lanolin alcohols was found to give tack-free films of improved quality.

Effective utilization of nonpolymeric substances such as lanolin alcohols in film-forming composition holds considerable promise for a variety of reasons. Such delivery systems could be designed and formulated to provide sustained drug delivery. The potential hazards associated with monomeric impurities in polymers are avoided. Nonpolymeric materials are easy to manipulate and compound, and are relatively easy to obtain in a state of definable composition. They also can be washed from the skin with relative ease using soap and water.

0022-3549/84/0300-0302$01.00/0
© 1984, American Pharmaceutical Association

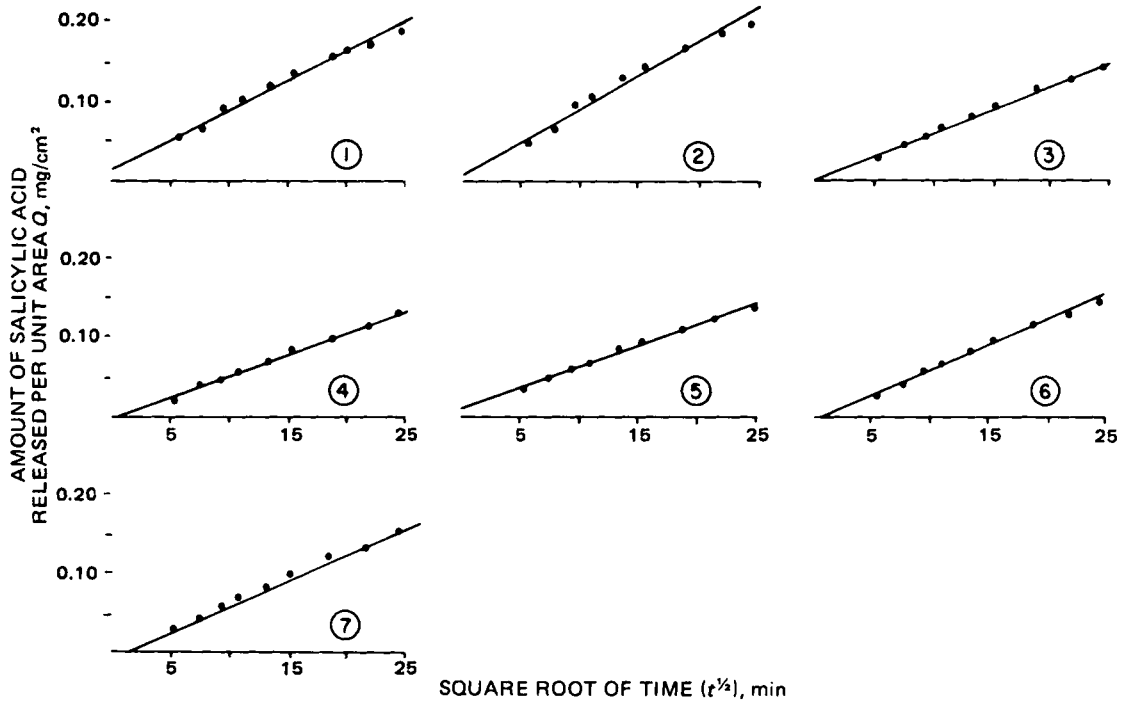

Figure 1—*Release of salicylic acid from films 1–7. Key: (1)* r = 0.992, b = 7.11; *(2)* r = 0.990, b = 7.82; *(3)* r = 0.998, b = 0.11; *(4)* r = 0.999, b = 5.76; *(5)* r = 0.993, b = 5.63; *(6)* r = 0.997, b = 6.34; *(7)* r = 0.999, b = 6.46.

It is the purpose of this study to investigate the *in vitro* release of salicylic acid (a known keratolytic agent) from selected lanolin alcohols–ethylcellulose film compositions with or without propylene glycol as a solvent–plasticizer.

THEORETICAL

In the present study, salicylic acid is assumed to be uniformly dispersed in the film matrix. The solubility of salicylic acid in lanolin alcohols or ethylcellulose is considered negligible based on preliminary work.

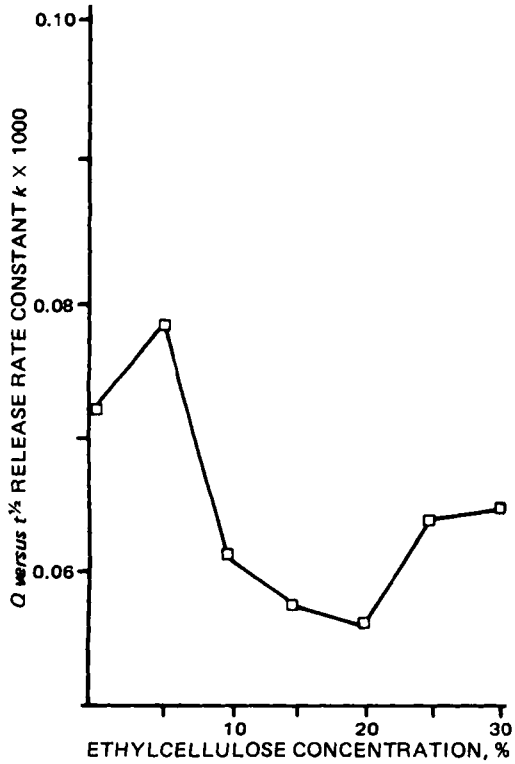

Figure 2—*Effect of vehicle composition on the release rate.*

The release from a planar system having a drug dispersed in a granular matrix has been shown by Higuchi (3) to follow a diffusion-controlled mechanism described by the relationship:

$$Q = \left[\frac{D}{\tau}(2A - \epsilon C_s)C_s \cdot t\right]^{1/2} \quad \text{(Eq. 1)}$$

where Q is the amount of drug released per unit area at time t, D and C_s refer to the diffusion coefficient and solubility of the drug in the permeating fluid, respectively, τ refers to the tortuosity and ϵ to the porosity of the matrix, and A is the amount of drug present in the matrix per unit volume. This equation describes drug release as being linear with the square root of time:

$$Q = kt^{1/2} \quad \text{(Eq. 2)}$$

where k is the rate constant of release:

$$k = \left[\frac{D\epsilon}{\tau}(2A - \epsilon C_s)C_s\right]^{1/2} \quad \text{(Eq. 3)}$$

The release of drug from a granular matrix in which the drug is present as a solution was shown by Desai *et al.* (4) to be:

$$Q = 2\epsilon C_0\left[\frac{Dt}{\tau\pi}\right]^{1/2} \quad \text{(Eq. 4)}$$

with the rate constant of release:

$$k = 2\epsilon C_0\left[\frac{D}{\tau\pi}\right]^{1/2} \quad \text{(Eq. 5)}$$

where C_0 is the solution concentration and the other parameters are as defined earlier. This equation is applicable when the drug released from the vehicle is <50%.

EXPERIMENTAL

Materials—Lanolin alcohols[1] (mp 61–64°C, *d* 0.98 g/mL), ethylcellulose[2] (*d* 1.38 g/mL), propylene glycol USP[3], and salicylic acid USP[4] (*d* 1.44 g/mL) were used as received. The solvents used were anhydrous methanol[5] (spectral grade) and isopropyl alcohol[5].

Solubility Studies—The solubility of salicylic acid in propylene glycol was determined at room temperature (22°C) and 37°C by adding excess

[1] Super Hartolan, Croda Inc., New York, N.Y.
[2] Ethyl Cellulose N-50; Hercules Inc. Wilmington, Del.
[3] Ruger Chemical Co., Irvington, N.J.
[4] Amend Drug and Chemical Co., Irvington, N.J.
[5] Mallinckrodt Chemical Works, St. Louis, Mo.

Table I—Calculated Values for Selected Parameters

Film	Film Composition[a]	Film Density[b], g/mL	Film Volume, mL	A, mg/mL	C_s, mg/mL
1	97.5:0:2.5	0.992	0.202	24.812	0.0167
2	92.5:5:2.5	1.012	0.205	25.324	0.0173
3	87.5:10:2.5	1.032	0.192	25.813	0.0165
4	82.5:15:2.5	1.052	0.186	26.300	0.0163
5	77.5:20:2.5	1.072	0.181	26.828	0.0162
6	72.5:25:2.5	1.092	0.176	27.300	0.0160
7	67.5:30:2.5	1.112	0.181	27.828	0.0168

[a] Proportion of lanolin alcohols, ethylcellulose, and salicylic acid expressed as % w/w. [b] Based on density (g/mL) of lanolin alcohols (0.98), ethylcellulose (1.38), and salicylic acid (1.44).

Table II—Release of Salicylic Acid from Lanolin Alcohols–Ethylcellulose Films

	Q versus $t^{1/2}$		
Film	Release Rate Constant (k) × 1000, mg/cm²·min$^{1/2}$	Intercept, min	r
1	7.11	−6.47	0.992
2	7.82	−2.80	0.990
3	6.11	1.06	0.998
4	5.76	4.87	0.999
5	5.63	−0.15	0.993
6	6.34	0.97	0.997
7	6.46	6.43	0.999

salicylic acid to 20 mL of propylene glycol contained in 50-mL screw-capped glass bottles. A polytef-coated magnetic bar was placed in each of the bottles prior to sealing. The contents of the bottle were then stirred in water baths for a period of 4 d to ensure attainment of equilibrium. All studies were conducted in triplicate.

Prior to sampling, the stirring was stopped and salicylic acid was allowed to settle. An aliquot was then filtered[6]. The filtration and sampling apparatus were equilibrated at 22°C or 37°C for a period of 48 h, and all operations were conducted in a constant-temperature room. Actual measurements of salicylic acid concentration were made using a scanning spectrophotometer[7] at 305 nm[8] after appropriate dilutions with anhydrous methanol to ensure compliance with Beer's Law.

Preparation of Solutions—Solutions containing appropriate amounts of lanolin alcohols, ethylcellulose, salicylic acid, and propylene glycol (if added) were prepared in the following manner. Weighed amounts of ethylcellulose were sprinkled onto 25 mL of isopropyl alcohol over a 2-h period with gentle stirring at 50–55°C. The lanolin alcohols were then dissolved in a similar manner. Prior to addition of the salicylic acid, the solutions were cooled to room temperature, transferred to a 50-mL volumetric flask, allowed to stand for 24 h, and the final volume was adjusted with isopropyl alcohol to give a 10% w/v solution.

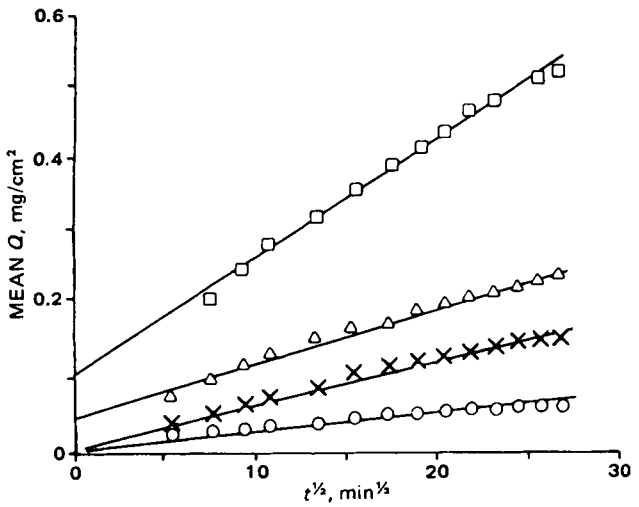

Figure 3—*Drug release from films containing lanolin alcohols–ethylcellulose (8.5:1.5) at different concentrations of salicylic acid. Key: (□) 9.09% w/w; (△) 4.76% w/w; (×) 2.91% w/w; and (○) 0.99% w/w.*

[6] Swinnex-25, 0.22-μm filter; Millipore Corp., Bedford, Mass.
[7] Perkin-Elmer model 202; Coleman Instruments Div., Oakbrook, Ill.
[8] Note that λ_{max} for the aqueous system was 297 nm.

Table III—Effect of Change in Drug Concentration on the Release Rate Constant for Films Containing Lanolin Alcohols and Ethylcellulose at a Ratio of 8.5:1.5

Drug Conc.[a], %	A, mg/cm³	Q versus $t^{1/2}$ [b] Intercept, min	r	$k \cdot 10^{-2}$, mg/cm³·min$^{1/2}$
0.99	10.25	0.20	0.985	0.189
2.91	30.74	0.44	0.991	0.576
4.76	51.23	−24.58	0.991	0.740
9.09	102.46	−35.00	0.990	1.642

[a] Weight of drug per weight of dry film. [b] All correlation coefficients and k values were computed from the regression line drawn from the data obtained by triplicate runs at each level by using the Tektronix (Model 4005-1) graphics terminal.

Preparation of Films—Two milliliters of an appropriate 10% w/v solution was transferred onto a preweighed glass petri dish (area = 18.1 cm²), placed on a flat surface at room temperature. The petri dishes were kept partially covered for 48 h to ensure slow and uniform evaporation of the solvent and to prevent blistering of the film, this also ensured uniform distribution of drug particles in the film matrix. Complete evaporation was ensured by drying to a constant weight. The film-coated petri dishes were stored in a desiccator (anhydrous calcium chloride) for at least 24 h prior to the release studies.

Release Studies—The release studies were conducted following the method reported previously (1), at 37 ± 0.5°C and a stirring rate of 40 rpm. Three-milliliter samples were drawn at definite intervals over a period of 10 h and, each time, replaced with an equal volume of distilled water. The salicylic acid concentrations were determined spectrophotometrically at 297 nm[9]. The unidirectional release of salicylic acid from the films was ensured by good adherence of the film to the bottom of the petri dish, as confirmed by frequent visual examinations during and at the termination of the release studies. No evidence of peeling was ever recorded. All release studies were conducted in triplicate.

RESULTS AND DISCUSSION

The solubility of salicylic acid in propylene glycol at 22°C and 37°C was found to be 0.481 ± 0.028 and 0.543 ± 0.025 g/mL, respectively; values are expressed as the mean ±SD of three measurements. The solubility of salicylic acid in lanolin alcohol or ethylcellulose was found to be negligible. The film compositions studied are described at appropriate locations in the text.

Release from Films Containing Solid Drug—Adherence of drug release to the Q *versus* $t^{1/2}$ relationship requires that the drug concentration in the film matrix far exceeds solution drug concentration at the interface ($A \gg C_s$ or $\epsilon\ C_s$). In the systems studied, this criterion was satisfied (Table I). The release data were examined in terms of the Higuchi model for a granular matrix. The correlation coefficient (r) for the regression line and the values of the intercept (time) were used as the principal criteria for evaluation.

Q *versus* $t^{1/2}$ plots for films 1–7 containing 2.5% w/w drug are shown in Fig. 1. On examination of the release data for compliance with the Higuchi model (Table II), it was observed that the correlation coefficients were consistently high (0.990–0.999). Three film compositions (*i.e.*, 1, 2, and 5) had negative intercepts, but the values were relatively small. Negative intercepts may be attributed to the immediate release of the drug present on the film surface. The calculated release rate constant

[9] Bausch and Lomb Spectronic 710.

Table IV—*Q versus* $t^{1/2}$ Treatment of Salicylic Acid Release Data from Films Containing Dissolved Drug in Solution

Film Composition[a]	Drug Conc.[b], %	C_0 mg/cm^3	t_{lag}, min	r	$k \cdot 10^{-2}$ [c], mg/cm^2·min$^{1/2}$
7.5:1.5:1.0	0.99	10.30	−0.04	0.996	0.180
7.5:1.5:1.0	2.91	30.90	−0.05	0.985	0.516
7.5:1.5:1.0	4.76	51.50	−12.22	0.982	0.776

[a] Proportion of lanolin alcohols, ethylcellulose, and propylene glycol expressed as % w/w. [b] Weight of drug per weight of dry film. [c] All correlation coefficients and k values were computed from the regression line drawn from the data obtained by triplicate runs at each level by using the Tektronix (Model 4005-1) graphics terminal.

represents the steady-state region. The variation of rate constant as a function of the film composition is shown in Fig. 2. Interestingly, the release rate constant increased at first with inclusion of ethylcellulose and then declined sharply with increases in ethylcellulose concentration, passing through a minimum value at ~15–20% ethylcellulose before increasing again. Increases in the concentration of ethylcellulose (>20% w/w) resulted in an increased rate of drug release, with a tendency to level off at ~30% ethylcellulose concentration.

Analysis of release data from films containing a fixed proportion of lanolin alcohol and ethylcellulose but varying drug concentrations of salicylic acid (Table III, Fig. 3) further supported earlier observations favoring the Higuchi model. A test previously used by Schwartz *et al.* (5) was then applied. By taking the logarithm, Eq. 2 can be rewritten as:

$$\log Q = \log k + \tfrac{1}{2}\log t \qquad \text{(Eq. 6)}$$

If the Higuchi model indeed described the release mechanism, the slope of log Q *versus* log t plots should be 0.5. The calculated values for the slope ranged from 0.42 to 0.53 with a mean of 0.49.

The effect of change in drug concentration on release rate constant, k, was tested using the four drug concentrations of salicylic acid for one film composition (Table III, Fig. 3). The k *versus* A plot was found to be more linear ($r = 0.996$) than k *versus* $A^{1/2}$ plot ($r = 0.850$). Although Eq. 1 predicts a linear relationship between k and $A^{1/2}$, the observed results could also be explained in terms of Eq. 1 if the initial porosity of the granular matrix was assumed to be very small. Higuchi (3) has shown that if the fraction of the matrix volume occupied by the drug is relatively large or if the initial porosity of the matrix is very small, $\epsilon = VA$ where V is the specific volume of the drug if A is expressed in terms of grams per milliliter. Eq. 3 then reduces to:

$$k = A\frac{DV}{\tau}(2 - VC_s)\,C_s \qquad \text{(Eq. 7)}$$

predicting a direct proportionality between k and A.

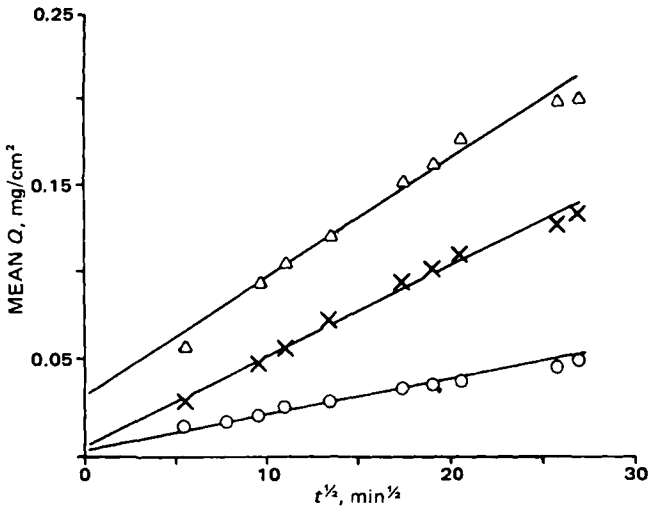

Figure 4—*Drug release from films containing lanolin alcohols–ethylcellulose–propylene glycol (7.5:1.5:1.0) at different concentrations of salicylic acid in solution. Key: (△) 4.76% w/w; (×) 2.91% w/w; and (○) 0.99% w/w.*

Drug Release from Film Matrices Containing the Drug in Solution—The release studies were conducted from lanolin alcohols–ethylcellulose films containing 10% w/w propylene glycol as solvent for the drug. The three drug concentrations examined were 0.99, 2.91, and 4.76% w/w, respectively. In each case the drug concentration was well below the saturation solubility of salicylic acid in propylene glycol. Furthermore, comparative examination of films with and without propylene glycol further established that the drug was in fact in solution.

The Q *versus* $t^{1/2}$ treatment of data showed linearity, but not as good as in the suspension case (Table IV, Fig. 4). It should be noted that the drug released rose to 71%, which was well above the constraints imposed on Eq. 5. The lag times were extremely small except in the case of films containing 4.76% w/w of drug. Equation 5 predicts a linear relationship between k and C_0 for the same system containing different concentrations of the drug in solution. Analysis of the data in Table IV revealed that there is an excellent linear correlation between k and C_0.

The release of both propylene glycol and salicylic acid is not predicted or accounted for by Eqs. 4 and 5. The square root of time dependency would be expected whether or not propylene glycol is released faster than the drug.

This study further demonstrated the potential application of lanolin alcohols–ethylcellulose films in controlled drug-delivery systems. Kinetic analysis suggests that the unidirectional release of salicylic acid from these films (whether the drug was suspended or in solution) follows a diffusion-controlled granular matrix model. The rate and extent of drug release from these films can be effectively manipulated by varying the drug concentration, film composition, and choice of solvent–plasticizer.

REFERENCES

(1) B. V. Iyer and R. C. Vasavada, *J. Pharm. Sci.*, **68**, 782 (1979).

(2) J. J. Sciarra and R. Gidwani, *J. Soc. Cosmet. Chem.*, **21**, 667 (1970).

(3) T. Higuchi, *J. Pharm. Sci.*, **52**, 1145 (1963).

(4) S. J. Desai, A. P. Simonelli, and W. I. Higuchi, *J. Pharm. Sci.*, **54**, 1459 (1965).

(5) J. B. Schwartz, A. P. Simonelli, and W. I. Higuchi, *J. Pharm. Sci.*, **57**, 274 (1968).

ACKNOWLEDGMENTS

Presented in part at the Basic Pharmaceutics Section, APhA Academy of Pharmaceutical Sciences meeting, San Antonio, Texas, November 1980. Abstracted in part from a thesis submitted by A. R. Khan to the School of Pharmacy, University of the Pacific, in partial fulfillment of the Master of Science degree requirements. Work done by R. A. Cirelli was supported by a faculty research grant from the University of the Pacific.

On the Mechanism of Dehydration of a β-Hydroxycyclopentanone Analogue of Prostaglandin E_1

HYUK-KOO LEE *x, **HOWARD J. LAMBERT** ‡, and **RICHARD L. SCHOWEN** §

Received August 17, 1978, from the *Pharmacy R&D Department, Ayerst Laboratories, Rouses Point, NY 12979, the ‡Product Development Department, Searle Laboratories, Skokie, IL 60076, and the §Department of Chemistry, University of Kansas, Lawrence, KS 66045. Accepted for publication January 25, 1983.

Abstract □ The dehydration of the β-hydroxycyclopentanone, 11,16-dihydroxy-16-methyl-9-oxo-13-*trans*-protenoic acid methyl ester, an analogue of prostaglandin E_1, proceeds with acid catalysis (pH < 3), by uncatalyzed routes (pH ≃ 4 and ≃ 7), and with base catalysis (pH ≃ 5–6 and > 8). Deuterium from the solvent is not introduced α to the reactant keto function at 60% reaction at pH ≃ 1, but ~30% exchange has occurred at pH ≃ 5, 50% at pH ≃ 7, and 80% at pH ≃ 9. The data are consistent with a mechanism in which the substrate is initially enolized with catalysis by acid, base, and water to a 1,3-enediol, which looses water with catalysis by acid, base, and water. The first stage is rate determining in very acidic solution, while the second stage assumes the limitation of rate to an ever greater degree as the solution becomes more basic.

Keyphrases □ Prostaglandin E_1—β-hydroxycyclopentanone analogue, dehydration kinetics, mechanism □ Kinetics—dehydration of the β-hydroxycyclopentanone analogue of prostaglandin E_1, mechanism □ Dehydration—β-hydroxycyclopentanone analogue of prostaglandin E_1, mechanism, kinetics

The prostaglandins are a structural class of compounds exhibiting the most diverse biological activities (1). Prostaglandin E_1 (alprostadil, Ia) possesses, among other capacities, the potential for inhibiting gastric secretion in humans (2). The analogue of prostaglandin E_1 (Ib) also possesses this activity and is in fact 30-fold more potent than the parent compound when administered orally (3).

E-type prostaglandins tend to undergo dehydration to yield the unsaturated A (II) and B (III) forms (4–6) (Scheme I). We report here some observations on the dehydration of Ib, which illuminate the mechanistic character of its degradation.

EXPERIMENTAL

Materials—Racemic mixtures of the 16α- and 16β-hydroxy epimers and their respective antipodes for 11,16-dihydroxy-16-methyl-9-oxo-13-*trans*-protenoic acid methyl ester (Ib, SC-29333) and its dehydration products, IIb and IIIb, were used as supplied[1].

Kinetics—The UV assay method developed by Monkhouse *et al.* (5) was adopted to follow the dehydration kinetics of Ib. Stock solutions of Ib (2.53×10^{-3} M in methanol) were diluted 50-fold with thermostated aqueous buffer (glycine–HCl, acetic acid–sodium acetate, sodium dihydrogen phosphate–sodium hydroxide, boric acid–sodium hydroxide), purged with nitrogen, and maintained at a constant temperature. Samples were withdrawn at measured intervals and spectra were recorded in Suprasil cells[2] from 200–350 nm. First-order rate constants were calculated; the pH values of the highly acidic solutions were calculated from the known concentrations of hydrochloric acid, with mean activity coefficients obtained or extrapolated from literature data (7). The pH values of the buffer solutions were read at the temperature of study with a pH-meter[3] standardized at the same temperature.

Deuterium Exchange—Exchange reactions were carried out to ~60% dehydration under each set of conditions, in a 44% (v/v) deuterated methanol–deuterated water solvent (CD_3OD–D_2O) of 4.5-mL volume, containing 20 mg of Ib. This solution was then extracted with 5 mL of $CDCl_3$; the extract was evaporated under nitrogen and reconstituted to 3 mL with $CDCl_3$. The NMR spectrum at 350–500 Hz downfield from tetramethylsilane was recorded with 150-Hz scale expansion and time averaging. The ratio of integrated peak areas for the α-H at C-10 (368 Hz) to that of the β-H at C-11 (448 Hz) was calculated.

Experiments were initiated by combining 2 mL of a CD_3OD solution of Ib with 2.5 mL of a D_2O solution of appropriate materials. The latter solutions were: (*a*) 0.1 M DCl in D_2O; (*b*) 29 mg of CH_3COONa and 0.1 mL of CD_3COOD in 10 mL of D_2O; (*c*) 68 mg of KH_2PO_4 and 1.49 mL of 0.2 M NaOD in 10 mL of D_2O; and (*d*) 31 mg of H_3BO_3 and 4.4 mL of 0.1 M NaOD in 10 mL of D_2O. The corresponding temperature and reaction times were: (*a*) 60°C, 3.5 h; (*b*) 70°C, 113 h; (*c*) 80°C, 6 h; and (*d*) 50°C, 2 h.

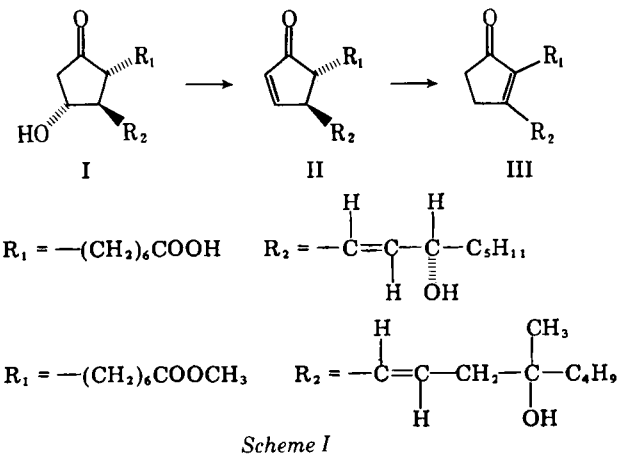

Scheme I

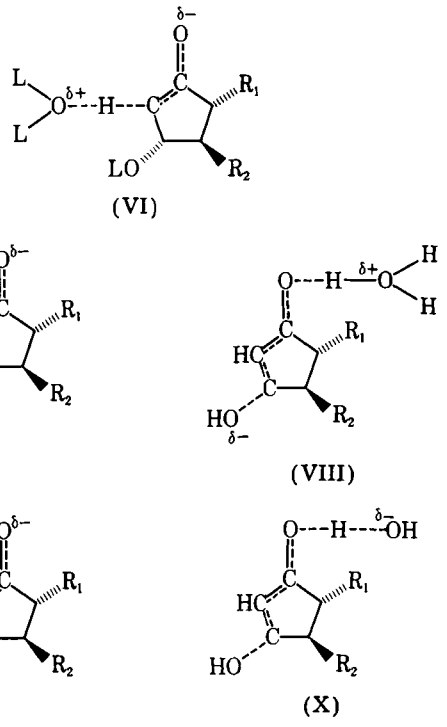

[1] Ib, IIb, and IIIb were provided by the Chemical Development and Chemical Research Departments of Searle Laboratories.
[2] Suprasil Cell; Scientific Products, McGaw Park, Ill.
[3] pH-Meter; Radiometer, Copenhagen, Denmark.

0022-3549/84/0300-0306$01.00/0
© 1984, American Pharmaceutical Association

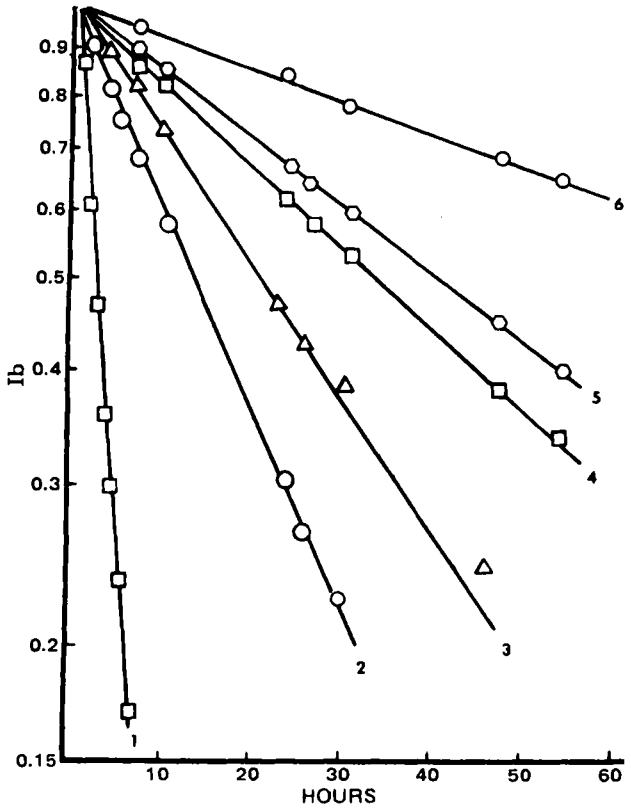

Figure 1—*Typical apparent first-order plots for the dehydration reaction of Ib at 60°C. Key: (1) 0.1 M HCl, pH 1.11; (2) 2.60 × 10^{-3} M KH_2PO_4-NaOH, pH 7.65; (3) 3.18 × 10^{-3} M KH_2PO_4-NaOH, pH 7.23; (4) 2.60 × 10^{-3} M KH_2PO_4-NaOH, pH 6.72; (5) 3.30 × 10^{-3} M KH_2PO_4-NaOH, pH 6.24; (6) 1.6 × 10^{-3} M CH_3COOH-CH_3COONa, pH 5.14.*

Solvent Isotope Effect—The solvent isotope effect in acidic solution was monitored at 80°C. This study utilized 0.01 M HCl (pH 2.0) with 1% methanol and ~0.01 M DCl (pD was adjusted to 2.0) with 1% CD_3OD.

RESULTS AND DISCUSSION

Stoichiometry—The dehydration of Ib was followed by the appearance of UV bands characteristic of IIb (λ_{max} 222 nm, ϵ 11,000) and IIIb (λ_{max} 288, ϵ 28,000), as shown by independent synthesis and spectral study of IIb and IIIb. Compound IIb appeared to be formed first and then converted to IIIb, which also decreased in concentration after some time. Small amounts of other products, including the 8-epimers of Ib and IIb, could be detected by HPLC, but were minor (<10%) in comparison with IIb and IIIb in 0.1 M HCl and pH 7.4 solutions at 60°C. It is very unlikely that the 8-epimer formation affects the rate of the dehydration reaction of Ib (I → II).

Another possible reaction intermediate, a prostaglandin C-type product (IV), could be formed (Scheme II). Jones (8) reported that prostaglandin C in methanol exhibits a UV λ_{max} at 234 nm (ϵ 21,000) with shoulders occurring at 228 and 243 nm. However, there was no indication of formation of this type of intermediate in the UV spectra throughout the course of the present kinetic studies. It may, of course, be formed but not accumulated in sufficient amounts to be detected because of the instability of this intermediate (8, 9).

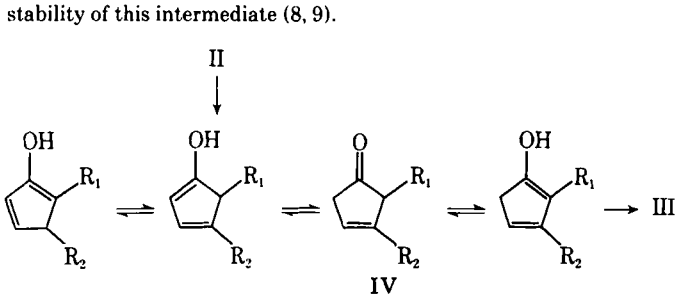

Scheme II

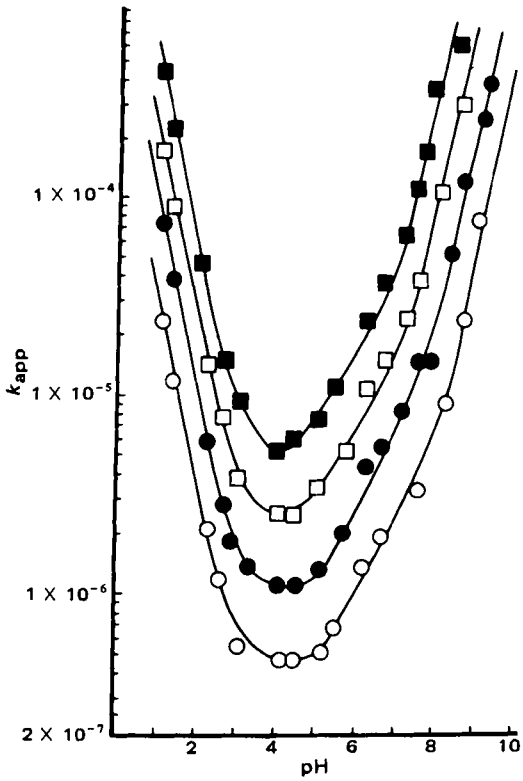

Figure 2—*Log k_{app}-pH profiles for the dehydration kinetics of Ib at several temperatures, where all points were experimentally obtained and the solid lines were fitted by Eq. 1. Key: (○) 50°C; (●) 60°C; (□) 70°C; (■) 80°C.*

When the concentration of Ib at any time was calculated from [Ib] = $[Ib]_0$ − ([IIb] + [IIIb]), with [IIb] and [IIIb] determined spectrophotometrically, first-order plots for loss of Ib were linear for two or more half-lives. Typical first-order plots at various pH values are given in Fig. 1. These data suggest that the major process under study is the irreversible conversion of Ib to IIb, which then proceeds to IIIb and other materials (Scheme I). Our observations do not bear on the conversion of IIb to IIIb or other products, although it is easy to see how IIIb might form from IIb by two simple proton-transfer reactions.

Effect of pH—The complete log k_{app}-pH profiles for the dehydration reaction of Ib at four temperatures are given in Fig. 2. Buffers were used to maintain the pH, but at a concentration of only 3 × 10^{-3} M so that the effects are essentially those of pH. The points of Fig. 2 are experimental; the lines are theoretical and are derived from:

$$k_{app} = k_H a_H + k_0 + k_B \frac{K_a}{K_a + a_H} + k_{OH} \frac{K_w}{a_H} \qquad \text{(Eq. 1)}$$

The rate constants k_H, k_0, k_B, and k_{OH}, as well as the apparent dissociation constant K_a, were shown to be a complex combination of rate constants (no simple definition of those empirical constants can reliably be made at the present stage; however, see Eqs. 13–17). These constant values were determined from the best fit of the log k_{app}-pH profiles in accordance with Eq. 1 (Table I).

Activation Parameters—The Arrhenius plots for the rate constants of Eq. 1 are shown in Fig. 3. The enthalpies and entropies of activation

Table I—Apparent Catalytic Rate Constants (k_H, k_0, k_B, and k_{OH}) and Kinetic Dissociation Constant (K_a) for the Dehydration of Ib in Aqueous Solution (1% Methanol) at Various Temperatures [a]

Temperature, °C	$k_H \times 10^3$, $M^{-1}\cdot s^{-1}$	$k_0 \times 10^6$, s^{-1}	$k_B \times 10^5$, s^{-1}	k_{OH}, $M^{-1}\cdot s^{-1}$	$K_a \times 10^6$, M
50 ± 0.5	0.29	0.46	0.03	0.69	0.21
60 ± 0.5	0.94	1.11	0.57	1.55	0.27
70 ± 0.5	2.16	2.47	0.75	4.27	1.27
80 ± 0.5	5.74	5.20	1.11	9.44	3.59

[a] Determined from the best fit of the log k_{app}-pH profiles in accordance with Eq. 1.

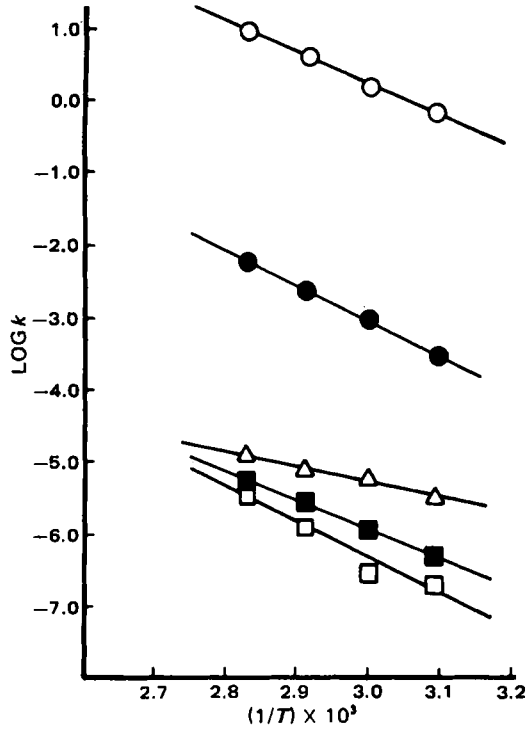

Figure 3—*Arrhenius plots for the apparent catalytic rate constants and the kinetic dissociation constant of dehydration kinetics of I, where each constant was defined by Eqs. 13–17 and each unit was shown as in Table I. Key:* (○) k_{OH}; (●) k_H; (△) k_B; (■) k_0; (□) K_a.

for each constant of Eq. 1 are shown in Table II.

Solvent Isotope Effect—At 80°C and pH (pD) 2.0, the ratio $k_H(H_2O)/k_H(D_2O)$ was found to be 0.8.

Deuterium Exchange at C-10 of Ib—It was possible to make an approximate determination of the degree of deuterium incorporation at the methylene carbon next to the keto function of Ib (C-10) by comparing the intensity of the NMR signal for the α-hydrogen at C-10 (368 Hz) to that of the β-hydrogen at C-11 (448 Hz). The NMR spectrum of IIb obtained from the dehydration reaction of Ib in a medium of 0.05 M DCl–45% CD_3OD showed that no incorporation occurred up to 60% reaction at 60°C. In deuterated acetate buffer in the same solvent at 70°C, ~30% of the C-10 hydrogen had been exchanged at 60°C reaction. A similar experiment with deuterated phosphate buffer showed 50% exchange at 80°C and with deuterated borate buffer 80% exchange at 50°C.

General base catalysis of enolization by buffers might give a larger ratio of exchange to dehydration at the higher buffer concentrations used in the exchange experiments in comparison with the kinetic experiments. However, it seems very unlikely that it could have resulted in an incorrect assignment of the rate-determining steps, since enolization seems clearly established as rate determining at low pH and the shape of the pH–rate profiles requires a partial change in the rate-determining step at pH >7 (*cf., Mechanistic Analysis*).

Formulation of the Rate Equation—A simple mechanism for loss of I, consistent with these findings, is shown in Scheme III. This postulates the conversion of I to its enolic form (V), which is assumed to be present in low steady-state concentrations, by pathways involving acid, base, and water catalysis (10). The enol V then decomposes by three similar pathways to II. Of course, V will be partly or wholly converted to enolate in the more basic solutions, but this will not affect the observable

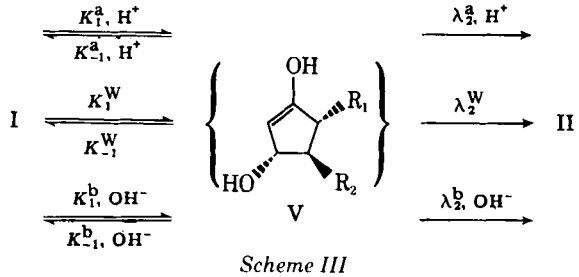

Scheme III

Table II—Activation Parameters[a] Associated with the Catalytic Constants for the Dehydration of Ib

Catalytic Constant[b]	$\Delta H^{\ddagger}$, kcal/mol	$\Delta S^{\ddagger}$, cal/K·mol
k_H	22 ± 1	−7 ± 3
k_0	18 ± 1	−31 ± 3
k_B	10 ± 1	−54 ± 3
k_{OH}	20 ± 1	+2 ● 3
K_a	19 ± 2[c]	+29 ± 6[c]

[a] Standard states of unit molarity at 80°C. [b] See Eq. 1. [c] These are properly $\Delta H°$ and $\Delta S°$ for interconversion of activated complexes.

kinetics (and cannot be deduced from the kinetics, only assumed on the basis of analogy).

In Scheme III, k_1^a, k_1^w, and k_1^b are the rate constants for hydronium ion-, neutral (water), and hydroxide ion-catalyzed enolization. The terms k_{-1}^a, k_{-1}^w, and k_{-1}^b are for the reverse enolization reaction. For dehydration, λ_2^a, λ_2^w, and λ_2^b are the rate constants for the hydronium ion-, neutral (water), and hydroxide ion-catalyzed dehydration reaction (V → II).

The rate of change in concentration of I, II, and V is described by:

$$-\frac{d[I]}{dt} = (k_1^a a_H + k_1^w + k_1^b K_w/a_H)[I] - (k_{-1}^a a_H + k_{-1}^w + k_{-1}^b K_w/a_H)[V] \quad \text{(Eq. 2)}$$

$$\frac{d[V]}{dt} = (k_1^a a_H + k_1^w + k_1^b K_w/a_H)[I] - (k_{-1}^a a_H + k_{-1}^w + k_{-1}^b K_w/a_H)[V] - (\lambda_2^a a_H + \lambda_2^w + \lambda_2^b K_w/a_H)[V] \quad \text{(Eq. 3)}$$

The steady-state kinetic law for this mechanism is:

$$k_{app} = \frac{(k_1^a a_H + k_1^w + k_1^b K_w/a_H)(\lambda_2^a a_H + \lambda_2^w + \lambda_2^b K_w/a_H)}{k_{-1}^a a_H + k_{-1}^w + k_{-1}^b K_w/a_H + \lambda_2^a a_H + \lambda_2^w + \lambda_2^b K_w/a_H} \quad \text{(Eq. 4)}$$

It is convenient to multiply the numerator and denominator of Eq. 4 by the equilibrium constant (K_1) for enolization of I:

$$K_1 = (k_1^a/k_{-1}^a) = (k_1^w/k_{-1}^w) = (k_1^b/k_{-1}^b) \quad \text{(Eq. 5)}$$

This yields Eq. 6, in which $k_2^a = K_1\lambda_2^a$, $k_2^w = K_1\lambda_2^w$, and $k_2^b = K_1\lambda_2^b$:

$$k_{app} = \frac{(k_1^a a_H + k_1^w + k_1^b K_w/a_H)(k_2^a a_H + k_2^w + k_2^b K_w/a_H)}{(k_1^a + k_2^a)a_H + (k_1^w + k_2^w) + (k_1^b + k_2^b)K_w/a_H} \quad \text{(Eq. 6)}$$

This formulation has the advantage that each rate constant has an initial reference state of I, rather than some referring to I (the K values) and some to V.

The mechanistic kinetic law of Eq. 6 can be related to the phenomenological law of Eq. 1 by expanding the numerator of Eq. 6. Each term in the expansion will be important in a particular pH region:

1. In acidic solution, only terms in a_H are important, and so Eq. 6 can be simplified to:

$$k_{app} \cong \frac{k_1^a k_2^a}{(k_1^a + k_2^a)} a_H \quad \text{(Eq. 7)}$$

2. In less acidic conditions (pH ~4), only k_1^w and k_2^w may be important, so that:

$$k_{app} \cong \frac{k_1^w k_2^w}{(k_1^w + k_2^w)} \quad \text{(Eq. 8)}$$

3. Near neutral pH, acid-catalytic terms are not important, so that:

$$k_{app} \cong \frac{k_1^w k_2^w (a_H)^2 + k_1^b k_2^b (K_w)^2 + k_1^w k_2^b K_w a_H + k_1^b k_2^w K_w a_H}{[(k_1^w + k_2^w)a_H + (k_1^b + k_2^b)K_w]a_H} \quad \text{(Eq. 9)}$$

where $k_1^w k_2^w (a_H)^2$ and $k_1^b k_2^b (K_w)^2$ are negligible, so that Eq. 9 gives:

$$k_{app} \cong \left(\frac{k_1^b k_2^w + k_2^b k_1^w}{k_1^b + k_2^b}\right) \frac{\left[\frac{(k_1^b + k_2^b)K_w}{k_1^w + k_2^w}\right]}{\left[\frac{(k_1^b + k_2^b)K_w}{k_1^w + k_2^w}\right] + a_H} \quad \text{(Eq. 10)}$$

4. At high pH (pH >9) only the k_1^b and k_2^b are important, so that Eq. 6 is simplified to:

$$k_{app} \cong \frac{k_1^b k_2^b}{(k_1^b + k_2^b)}\left(\frac{K_w}{a_H}\right) \quad \text{(Eq. 11)}$$

The overall rate expression, k_{app}, may be represented as the sum of Eqs. 7, 8, 10, and 11, because when one term is important, all the others are not:

$$k_{app} \cong \left(\frac{k_1^a k_2^a}{k_1^a + k_2^a}\right) a_H + \left(\frac{k_1^w k_2^w}{k_1^w + k_2^w}\right) + \left(\frac{k_1^b k_2^w + k_1^w k_2^b}{k_1^b + k_2^b}\right) \cdot \frac{\left[\frac{(k_1^b + k_2^b)K_w}{k_1^w + k_2^w}\right]}{\left[\frac{(k_1^b + k_2^b)K_w}{k_1^w + k_2^w}\right] + a_H} + \left(\frac{k_1^b k_2^b}{k_1^b + k_2^b}\right) \cdot \frac{K_w}{a_H} \quad \text{(Eq. 12)}$$

A comparison of Eqs. 1 and 12 reveals that both have the same mathematical form, so that Eq. 11 provides the correct log k_{app}–pH profiles for the dehydration of I. From Eqs. 1 and 12, the relationships shown in Eqs. 13–17 are obtained:

$$k_H = \frac{k_1^a k_2^a}{k_1^a + k_2^a} \quad \text{(Eq. 13)}$$

$$k_0 = \frac{k_1^w k_2^w}{k_1^w + k_2^w} \quad \text{(Eq. 14)}$$

$$k_B = \frac{k_1^b k_2^w + k_1^w k_2^b}{k_1^b + k_2^b} \quad \text{(Eq. 15)}$$

$$k_{OH} = \frac{k_1^b k_2^b}{k_1^b + k_2^b} \quad \text{(Eq. 16)}$$

$$K_a = \frac{(k_1^b + k_2^b)K_w}{k_1^w + k_2^w} \quad \text{(Eq. 17)}$$

Mechanistic Analysis—The deuterium exchange data and solvent isotope effect can aid in bringing out further detail. First, at low pH, as Eq. 13 emphasizes, either hydronium-catalyzed proton removal from I (k_1^a) or hydronium-catalyzed elimination of water from V (k_2^a) determines the rate. Lack of deuterium exchange suggests that $k_2^a > k_1^a$ (no reversion from V), so that $k_{app} \simeq k_1^a a_H$, with a rate-limiting transition state resembling VI (where L = H in H_2O, D in D_2O).

The solvent isotope effect at 25°C for such a transition state would be given (11) by $k_{H_2O}/k_{D_2O} = (0.69)^3/\phi_1\phi_2^2$, where ϕ_1 and ϕ_2 are isotopic fractionation factors relative to water for the hydrogen attached to the keto group (ϕ_1) and those of the reacting water molecule (ϕ_2). For a limiting reactant-like structure, $\phi_1 \sim 0.69$, $\phi_2 \sim 1.0$ and $k_{H_2O}/k_{D_2O} = 0.48$. For a limiting product-like structure, $\phi_1 \sim 1.0$, $\phi_2 \sim 0.69$, and $k_{H_2O}/k_{D_2O} = 0.69$. Rough correction to 80°C gives limiting predictions of 0.53 (reactant-like) and 0.73 (product-like). The latter is not far from the observed effect of 0.8 ± 0.1.

In acetate buffer, exchange of deuterium concurrently with reaction was observed, with ~30% exchange accompanying 60% dehydration. In this pH range, the dominant term is k_0 (Eq. 14). The exchange indicates some reversion from enol to reactant, so that apparently $k_2^w \gtrsim k_1^w$, with enol formation more important than elimination but not exclusively rate determining ($k_{app} \simeq k_1^w$).

Setting aside the phosphate buffer experiment momentarily, we can examine the borate buffer findings. These pertain to the high pH region governed by k_{OH} (Eq. 16). Since exchange exceeds dehydration (80% exchange, 60% dehydration), base-catalyzed decomposition of the enol dominates but does not wholly control rate limitation ($k_1^b \gtrsim k_2^b$, $k_{app} \simeq k_2^b K_w/a_H$).

Returning to the phosphate buffer exchange data, we note that these are related to the pH region of ~7, where:

$$k_{app} = k_B \frac{K_a}{K_a + a_H} \quad \text{(Eq. 18)}$$

with k_B given by Eq. 15 and K_a by Eq. 17. At low pH in this range, $k_{app} \simeq k_B K_a/a_H$ or:

$$k_{app} = \frac{(k_1^b k_2^w + k_1^w k_2^b)K_w}{(k_1^w + k_2^w)a_H} \quad \text{(Eq. 19)}$$

From arguments in the last two paragraphs, $k_1^b \gtrsim k_2^b$ and $k_2^w \gtrsim k_1^w$, so we can expect that $k_1^b k_2^w > k_1^w k_2^b$ in Eq. 19, or:

$$k_{app} = \frac{(k_1^b k_2^w)K_w}{(k_1^w + k_2^w)a_H} \simeq k_1^b K_w/a_H \quad \text{(Eq. 20)}$$

so that the main rate-limiting process at the acidic end of this pH range is base-catalyzed enolization (presumably proton abstraction from I by the hydroxide ion). At the high pH end of the range, $k_{app} \simeq k_B$ (*cf.* Eq. 15), and by the same arguments as just given:

$$k_{app} \simeq \frac{k_1^b k_2^w}{k_1^b + k_2^b} \simeq k_2^w \quad \text{(Eq. 21)}$$

so that the rate-determining step now tends toward water-catalyzed elimination from V. If enol formation truly determined the rate below pH 7, no exchange would be expected there, and if elimination from the enol truly determined the rate above pH ~7, then 100% exchange would be expected there. In fact, in a phosphate buffer, ~50% exchange was observed at 60% reaction.

We can compare finally the deductions made from the kinetics and the exchange experiments with the activation parameters for consistency. For example, we conclude that k_H is dominated by k_1^a with a transition-state structure like VI. From Table II, the formation of VI from I and hydronium ion is indicated to require $\Delta H^\ddagger \simeq 22$ kcal/mol, $\Delta S^\ddagger \simeq -7$ eu. These are acceptable in terms of the hypothesis, a small negative $\Delta S^\ddagger$ being consistent with a bimolecular process in which some solvation (presumably from the hydronium ion) is released.

For the region of pH 4–5 where k_0 rules, the most important rate constant was k_1^w with some contribution from k_2^w. Speculative structures for the transition state would be VII and VIII, respectively. According to Table II, conversion of I in aqueous solution to chiefly VII and some VIII is accompanied by $\Delta H^\ddagger = 18$ kcal/mol, $\Delta S^\ddagger = -31$ eu. The entropy change, in particular, is reasonable for the "freezing" of water molecules associated with proton transfer and development of change. Since k_B is roughly determined by k_2^w (see argument for Eq. 21), its activation parameters should also correspond to those expected for a transition state like VIII. Indeed the values found ($\Delta H^\ddagger = 10$ kcal/mol, $\Delta S^\ddagger = -54$ eu) are of the magnitudes anticipated.

For k_{OH}, determined chiefly by k_2^b with some contribution from k_1^b, the appropriate transition-state structures are IX and X. Here, as for formation of VI, the energy-requiring, entropy-producing release of water on binding of the strongly solvated hydroxide ion to generate a charge-delocalized transition state leads to relatively large $\Delta H^\ddagger$ (20 kcal/mol) and—from compensation with entropy loss in the bimolecular reaction—to a negligible $\Delta S^\ddagger$ (2 eu).

Lastly we have the equilibrium constant K_a, defined by Eq. 17. This equilibrium constant is for the reaction of Eq. 22; the reactant state for this equilibrium:

$$\begin{Bmatrix} \text{VII} \\ \text{VIII} \end{Bmatrix} \rightarrow H^+ + \begin{Bmatrix} \text{IX} \\ \text{X} \end{Bmatrix} \quad \text{(Eq. 22)}$$

is a weighted average of activated complexes VII and VIII (for water-catalyzed enolization and elimination, respectively), the more stable transition state contributing more to the average, while the product state is a similar weighted average of IX and X (for base-catalyzed formation and decomposition of enol). As the values of K_a in Table I show, the water-catalysis activated complexes are acids of $pK_a \simeq 5.4$–6.7 at 50–80°C, with pK_a estimated at 7.6 at 25°C. As anticipated, this is intermediate between values of 1.74 for H_3O^+ (product-like structure for VII–X) and 15.74 (reactant-like structure for VII–X).

On the other hand, the thermodynamic parameters of ionization are unlike those of stable acids, as judged by the very extensive collection of Izatt and Christensen (12). Most stable acids have smaller, positive ΔH (compared with 19 kcal/mol) and much more negative ΔS (*versus* 29 eu) of ionization than these activated complexes. Conceivably this is a reflection of a greater internal structural plasticity of activated complexes and the greater attendant release of solvation upon ionization.

REFERENCES

(1) T. K. Schaaf, *Annu. Rep. Med. Chem.*, **11**, 80 (1976).

(2) M. Classen, H. Koch, J. Bickhart, G. Topf, and L. Demling, *Digestion*, **4**, 333 (1971).

(3) E. Z. Dajemi, D. R. Driskill, R. G. Bianchi, P. W. Collins, and R. Pappo, *Digest. Dis.*, **21**, 1049 (1976).

(4) N. H. Andersen, *J. Lipid Res.*, **10**, 320 (1969).

(5) D. C. Monkhouse, L. Van Campen, and A. J. Aguiar, *J. Pharm. Sci.*, **62**, 576 (1973).

(6) G. F. Thompson, J. M. Collins, and L. Schmalzried, *J. Pharm. Sci.*, **62**, 1738 (1973).

(7) H. S. Harned and B. B. Owens, "The Physical Chemistry of Electrolytic Solutions," 3rd ed., Reinhold, New York, N.Y. 1958.

(8) R. L. Jones, *J. Lipid Res.*, **13**, 511 (1972).
(9) S. K. Perera and L. R. Fedor, *J. Am. Chem. Soc.*, **101**, 7390 (1979).
(10) D. J. Hupe, M. C. R. Kendall, G. T. Simner, and T. A. Spencer, *J. Am. Chem. Soc.*, **95**(7), 2260 (1973).
(11) R. L. Schowen, *Prog. Phys. Org. Chem.*, **9**, 275 (1972).
(12) R. M. Izatt and J. J. Christensen, in "Handbook of Biochemistry and Molecular Biology," Vol. I, 3rd ed., G. D. Fasman, Ed., CRC Press, Cleveland, Ohio, p. 151 ff.

ACKNOWLEDGMENTS

The authors thank Dr. Roy Bible and Mr. Arthur Ferreri for NMR studies and Ms. Lynelle Sachen for technical assistance.

α,α-Diphenylsuccinimide: Evaluation of Anticonvulsant and Hydrophobic Properties

GARY L. JONES **, ROBERT J. AMATO, and MARY F. JONES

Received December 13, 1982, from the *Department of Pathology, Texas College of Osteopathic Medicine, Fort Worth, TX 76107.* Accepted for publication January 13, 1983. *Present address: Physiology Department, University of Utah, Salt Lake City, UT 84117.

Abstract □ The anticonvulsant potencies (ED_{50}) of α,α-diphenylsuccinimide, phenytoin, and phenobarbital were evaluated in mice by a standard maximal electroshock technique. Potencies were expressed in terms of intraperitoneal dosage and blood and brain concentrations. Overt neurotoxicity (TD_{50}) was assessed by the rotorod method. These data were compared with relative hydrophobicities for the above compounds and three others [carbamazepine, cyheptamide, and (diphenylacetyl)urea] taken from the literature. An approximate parabolic dependence of anticonvulsant potency on hydrophobicity was observed regardless of the means of expressing potency (intraperitoneal dosage, blood concentration, or brain concentration); approximate optimal hydrophobicities were in the range of 2.18–2.23 (log P). Calculated therapeutic indices (TD_{50}/ED_{50}) also displayed a parabolic dependence on hydrophobicity, while toxic potency (TD_{50}) displayed a linear dependence (within the limited range of log P values studied). Implications of the parabolic dependence of anticonvulsant potency and linear dependence of toxic potency on hydrophobicity are discussed with respect to the possible mechanisms involved.

Keyphrases □ α,α-Diphenylsuccinimide—anticonvulsant potency, hydrophobic properties, overt neurotoxicity, maximal electroshock screen in mice □ Anticonvulsants—α,α-diphenylsuccinimide, hydrophobic properties, overt neurotoxicity, maximal electroshock screen in mice □ Hydrophobicity—α,α-diphenylsuccinimide, anticonvulsant potency, overt neurotoxicity, maximal electroshock screen in mice

The synthesis of α,α-diphenylsuccinimide (I) was reported by Miller and Long in 1951 (1). The anticonvulsant profile of the compound was evaluated in rats by a pentylenetetrazole model and in mice by a maximal electroshock (MES) model of epilepsy (1, 2). The compound was judged ineffective (500 mg/kg) in the prevention of pentylenetetrazole-induced seizures. However, sufficient dosage conferred complete protection against MES seizures; the ED_{50} (oral) in the MES model was 45 mg/kg (1, 2). A quantitative estimate of neurotoxicity was not provided. Since this early work, additional reports on the pharmacology of this compound have not appeared, and after three decades its profile remains unclear.

The present study was undertaken (*a*) to evaluate the anticonvulsant, neurotoxic, and hydrophobic properties of α,α-diphenylsuccinimide, phenytoin, and phenobarbital and (*b*) to compare these properties with the same properties for carbamazepine, cyheptamide, and (diphenylacetyl)urea (3, 4). Relative anticonvulsant potencies, determined using a standard MES model of epilepsy (5), are expressed in terms of intraperitoneal dose and blood and brain concentrations. Neurotoxicity was assessed using a rotorod method (6). Relative neurotoxicities and therapeutic indices are reported on the basis of intraperitoneal dose. Relative hydrophobicities were approximated using hydrophobic π-constants (7). Inspection of the data suggests that the potency of α,α-diphenylsuccinimide is subject to the same parabolic dependence on hydrophobicity already described for other compounds (8).

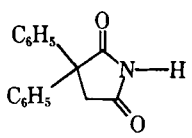

I

EXPERIMENTAL

Drugs—Phenytoin sodium[1] and phenobarbital sodium[2] were gifts. α,α-Diphenylsuccinimide was prepared utilizing a modification of a method described previously (1). The procedure involved the addition of ethyl bromoacetate to a mixture of diphenylacetonitrile in sodium ethoxide. The intermediate ethyl β-cyano-β,β-diphenylpropionate was hydrolyzed, initially in potassium hydroxide to β-cyano-β,β-diphenylpropionic acid and subsequently in concentrated hydrochloric acid to α,α-diphenylsuccinic acid. At this point the synthesis deviated from the published procedure. α,α-Diphenylsuccinic acid was heated at reflux in acetyl chloride to give the anhydride, an ethereal solution of which was treated with ammonia. The intermediate α,α-diphenylsuccinamic acid was removed by filtration and heated at reflux with acetyl chloride to give α,α-diphenylsuccinimide, which was recrystallized from methyl alcohol, mp 140–142°C (reported mp (1) 140–142°C). This material showed one spot on TLC (silica gel, alumina; chloroform). IR (chloroform): 1770 and 1740 cm^{-1} (5-membered ring, imide C=O's); ^1H-NMR (deuterochloroform): δ 3.38 (s, 2, CH_2), 7.16 (s, 10, ArH), and 8.84 ppm (s, 1, NH).

Animal Studies—Phenytoin sodium was suspended in 30% polyethylene glycol 400, and α,α-diphenylsuccinimide was suspended in 5% gum acacia. Phenobarbital sodium was dissolved in 0.9% NaCl. The suspensions were sonicated (probe-type) for ~5 min to produce a fine suspension. The drugs were administered intraperitoneally in a volume of 0.01 mL/g of body weight to male CF_1 mice[3], average weight 22 g. The mice, 30–32 d of age when received, were allowed several days to acclimatize before testing. Food and water were given *ad libitum*.

The anticonvulsant activity of each drug was evaluated by a standard MES test (5). A 60-Hz alternating current (50 mA) was applied for 0.2 s *via* corneal electrodes. Protection was defined as the absence of tonic

[1] Warner-Lambert Co., Morris Plains, N.J.
[2] Sterling-Winthrop Research Institute, New York, N.Y.
[3] Charles River Breeding Laboratories, Wilmington, Mass.

0022-3549/84/0300-0310$01.00/0
© 1984, American Pharmaceutical Association

(8) R. L. Jones, *J. Lipid Res.*, **13**, 511 (1972).
(9) S. K. Perera and L. R. Fedor, *J. Am. Chem. Soc.*, **101**, 7390 (1979).
(10) D. J. Hupe, M. C. R. Kendall, G. T. Simner, and T. A. Spencer, *J. Am. Chem. Soc.*, **95**(7), 2260 (1973).
(11) R. L. Schowen, *Prog. Phys. Org. Chem.*, **9**, 275 (1972).
(12) R. M. Izatt and J. J. Christensen, in "Handbook of Biochemistry and Molecular Biology," Vol. I, 3rd ed., G. D. Fasman, Ed., CRC Press, Cleveland, Ohio, p. 151 ff.

ACKNOWLEDGMENTS

The authors thank Dr. Roy Bible and Mr. Arthur Ferreri for NMR studies and Ms. Lynelle Sachen for technical assistance.

α,α-Diphenylsuccinimide: Evaluation of Anticonvulsant and Hydrophobic Properties

GARY L. JONES **, ROBERT J. AMATO, and MARY F. JONES

Received December 13, 1982, from the *Department of Pathology, Texas College of Osteopathic Medicine, Fort Worth, TX 76107.* Accepted for publication January 13, 1983. *Present address: Physiology Department, University of Utah, Salt Lake City, UT 84117.

Abstract □ The anticonvulsant potencies (ED_{50}) of α,α-diphenylsuccinimide, phenytoin, and phenobarbital were evaluated in mice by a standard maximal electroshock technique. Potencies were expressed in terms of intraperitoneal dosage and blood and brain concentrations. Overt neurotoxicity (TD_{50}) was assessed by the rotorod method. These data were compared with relative hydrophobicities for the above compounds and three others [carbamazepine, cyheptamide, and (diphenylacetyl)urea] taken from the literature. An approximate parabolic dependence of anticonvulsant potency on hydrophobicity was observed regardless of the means of expressing potency (intraperitoneal dosage, blood concentration, or brain concentration); approximate optimal hydrophobicities were in the range of 2.18–2.23 (log P). Calculated therapeutic indices (TD_{50}/ED_{50}) also displayed a parabolic dependence on hydrophobicity, while toxic potency (TD_{50}) displayed a linear dependence (within the limited range of log P values studied). Implications of the parabolic dependence of anticonvulsant potency and linear dependence of toxic potency on hydrophobicity are discussed with respect to the possible mechanisms involved.

Keyphrases □ α,α-Diphenylsuccinimide—anticonvulsant potency, hydrophobic properties, overt neurotoxicity, maximal electroshock screen in mice □ Anticonvulsants—α,α-diphenylsuccinimide, hydrophobic properties, overt neurotoxicity, maximal electroshock screen in mice □ Hydrophobicity—α,α-diphenylsuccinimide, anticonvulsant potency, overt neurotoxicity, maximal electroshock screen in mice

The synthesis of α,α-diphenylsuccinimide (I) was reported by Miller and Long in 1951 (1). The anticonvulsant profile of the compound was evaluated in rats by a pentylenetetrazole model and in mice by a maximal electroshock (MES) model of epilepsy (1, 2). The compound was judged ineffective (500 mg/kg) in the prevention of pentylenetetrazole-induced seizures. However, sufficient dosage conferred complete protection against MES seizures; the ED_{50} (oral) in the MES model was 45 mg/kg (1, 2). A quantitative estimate of neurotoxicity was not provided. Since this early work, additional reports on the pharmacology of this compound have not appeared, and after three decades its profile remains unclear.

The present study was undertaken (*a*) to evaluate the anticonvulsant, neurotoxic, and hydrophobic properties of α,α-diphenylsuccinimide, phenytoin, and phenobarbital and (*b*) to compare these properties with the same properties for carbamazepine, cyheptamide, and (diphenylacetyl)urea (3, 4). Relative anticonvulsant potencies, determined using a standard MES model of epilepsy (5), are expressed in terms of intraperitoneal dose and blood and brain concentrations. Neurotoxicity was assessed using a rotorod method (6). Relative neurotoxicities and therapeutic indices are reported on the basis of intraperitoneal dose. Relative hydrophobicities were approximated using hydrophobic π-constants (7). Inspection of the data suggests that the potency of α,α-diphenylsuccinimide is subject to the same parabolic dependence on hydrophobicity already described for other compounds (8).

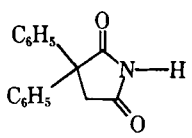

I

EXPERIMENTAL

Drugs—Phenytoin sodium[1] and phenobarbital sodium[2] were gifts. α,α-Diphenylsuccinimide was prepared utilizing a modification of a method described previously (1). The procedure involved the addition of ethyl bromoacetate to a mixture of diphenylacetonitrile in sodium ethoxide. The intermediate ethyl β-cyano-β,β-diphenylpropionate was hydrolyzed, initially in potassium hydroxide to β-cyano-β,β-diphenylpropionic acid and subsequently in concentrated hydrochloric acid to α,α-diphenylsuccinic acid. At this point the synthesis deviated from the published procedure. α,α-Diphenylsuccinic acid was heated at reflux in acetyl chloride to give the anhydride, an ethereal solution of which was treated with ammonia. The intermediate α,α-diphenylsuccinamic acid was removed by filtration and heated at reflux with acetyl chloride to give α,α-diphenylsuccinimide, which was recrystallized from methyl alcohol, mp 140–142°C (reported mp (1) 140–142°C). This material showed one spot on TLC (silica gel, alumina; chloroform). IR (chloroform): 1770 and 1740 cm^{-1} (5-membered ring, imide C=O's); ^1H-NMR (deuterochloroform): δ 3.38 (s, 2, CH_2), 7.16 (s, 10, ArH), and 8.84 ppm (s, 1, NH).

Animal Studies—Phenytoin sodium was suspended in 30% polyethylene glycol 400, and α,α-diphenylsuccinimide was suspended in 5% gum acacia. Phenobarbital sodium was dissolved in 0.9% NaCl. The suspensions were sonicated (probe-type) for ~5 min to produce a fine suspension. The drugs were administered intraperitoneally in a volume of 0.01 mL/g of body weight to male CF_1 mice[3], average weight 22 g. The mice, 30–32 d of age when received, were allowed several days to acclimatize before testing. Food and water were given *ad libitum*.

The anticonvulsant activity of each drug was evaluated by a standard MES test (5). A 60-Hz alternating current (50 mA) was applied for 0.2 s *via* corneal electrodes. Protection was defined as the absence of tonic

[1] Warner-Lambert Co., Morris Plains, N.J.
[2] Sterling-Winthrop Research Institute, New York, N.Y.
[3] Charles River Breeding Laboratories, Wilmington, Mass.

0022-3549/84/0300-0310$01.00/0
© 1984, American Pharmaceutical Association

hind limb extension greater than a 90° angle with the trunk. The time of peak anticonvulsant effect was determined as described previously (9). Complete dose-response profiles were determined for each drug at its time of peak effect.

Immediately after the MES test, 100 μL of blood was collected in 2% sodium fluoride, and the animal was decapitated. The entire brain was removed and blotted on filter paper. The specimens (including blood) were stored at −80°C until assayed. Blood and brains from 10 mice were pooled for each dose, and at least five doses were employed for each drug.

Relative neurotoxicity was assessed by the rotorod method (6) in which the rodent is placed on a 2.54-cm diameter knurled rod, rotating at 6 rpm. Minimal neurological deficit was defined as the inability of a mouse to remain on the rotating rod for 1 min in at least two of three trials.

The anticonvulsant and neurotoxicity data were evaluated with 95% confidence limits by a quantal statistical method (10). The relative anticonvulsant potencies (ED_{50}) are expressed in terms of blood and brain concentrations, as well as intraperitoneal dosage. The relative neurotoxicity data (TD_{50}) are expressed in terms of intraperitoneal dosage only.

Analytical Methods—The blood and brain concentrations for each drug were assayed by GC. The method for extraction from blood and brain is similar for all three compounds. Aqueous suspensions of blood and homogenized whole brain were saturated with ammonium sulfate and acidified with concentrated hydrochloric acid. These suspensions were extracted with toluene, and the toluene layer was back-extracted with tetramethylammonium hydroxide. The drugs were then derivatized with methyl iodide (11) and extracted into chloroform in the presence of excess 1 M monobasic potassium phosphate. 5-(*p*-Methylphenyl)-5-phenylhydantoin was used as internal standard for the analysis of phenytoin and α,α-diphenylsuccinimide, and 5-ethyl-5-tolylbarbituric acid was used for the phenobarbital assay. Phenytoin was recovered from brain and blood specimens with 77 and 86% efficiency, respectively. Phenobarbital and α,α-diphenylsuccinimide were recovered from either specimen with at least 86% efficiency. Each drug was chromatographed using Supelcoport, 80–100 mesh.

Blood and brain extracts of phenytoin were assayed isothermally at 230°C on 3% OV-17 (injector port and detector temperature 300°C). The retention times for phenytoin and its internal standard were 5.9 and 8.3 min, respectively. Phenobarbital was assayed isothermally in brain extracts at 210°C on 3% OV-17 (injector port temperature 280°C, detector temperature 300°C) and in blood extracts at 170°C on 3% OV-101 (injector port temperature 270°C, detector temperature 340°C). The retention times for phenobarbital and its internal standard were 2.3 and 3.3 min, respectively, for the brain extract, and 2.2 and 3.3 min, respectively, for the blood extract. α,α-Diphenylsuccinimide (I) in brain extracts was assayed with a programmed run from 170°C to 240°C (10°C/min) on 3% OV-17 (injector port and detector temperature 300°C). Assay of I in blood extracts was programmed as follows: 130°C held for 2 min, followed by a 10°C/min increase to 210°C, where it was held for a final 2 min (3% OV-101; injector port temperature 270°C, detector temperature 300°C). The retention times for α,α-diphenylsuccinimide and its internal standard were 8.3 and 3.1 min, respectively, for the brain extract, and 8.9 and 3.7 min, respectively, for the blood extract.

Each method employed flame-ionization detection. The carrier gas (nitrogen), flow rates (50 mL/min), and column dimensions (2-mm i.d. × 1.83 m) were also common for the three drugs, in both blood and brain extracts. An example of a typical chromatogram for α,α-diphenylsuccinimide extracted from brain tissue is depicted in Fig. 1.

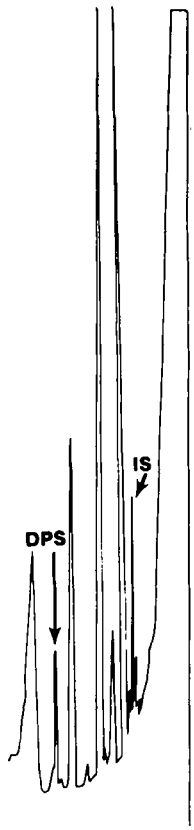

Figure 1—*Chromatogram of α,α-diphenylsuccinimide (DPS) from brain extract. Internal standard (IS) was 5-(p-methylphenyl)-5-phenylhydantoin. See text for methods.*

RESULTS AND DISCUSSION

α,α-Diphenylsuccinimide produced qualitatively the same alteration of MES-induced seizure pattern as that produced by phenytoin or phenobarbital; *i.e.*, the tonic hind limb extension was abolished with sufficient dosage of each drug. The ED_{50} (intraperitoneal dosage) for α,α-diphenylsuccinimide was 26.5 mg/kg (95% confidence limits: 23.4–30.0) (Table I). This is lower than the 45 mg/kg estimate reported for an oral dosage (1, 2). (The apparently greater potency by the intraperitoneal route can likely be ascribed to the greater surface area for absorption by this route.) In comparison, phenytoin and phenobarbital are more potent than α,α-diphenylsuccinimide when estimates are based on intraperitoneal dosage (Table I). However, the difference in potency among these drugs is much smaller when estimates are based on blood or brain concentrations. In fact, α,α-diphenylsuccinimide is more potent than phenobarbital when blood or brain concentration forms the basis of comparison (Table I).

Much of the variation in anticonvulsant potency among these drugs can be explained by a parabolic dependence of potency on hydrophobicity, already described for other agents (8). This is evident if one compares the potency and log P (logarithm of the partition coefficient) values of phenobarbital, carbamazepine, phenytoin, α,α-diphenylsuccinimide, cyheptamide, and (diphenylacetyl)urea (Table I). It will be seen that potency (expressed in terms of intraperitoneal dosage or blood concentrations) increases from phenobarbital to carbamazepine to phenytoin, with the increase of log P from 1.63 to 2.18 to 2.23, respectively. However, potency decreases from phenytoin to α,α-diphenylsuccinimide to cyheptamide to (diphenylacetyl)urea, with the continued increase of log P from 2.23 to 2.63 to 2.74 to 2.83, respectively. If expressed in terms of brain concentrations, potency increases from phenobarbital to carbamazepine with the increase of log P from 1.63 to 2.18, respectively; further increases in log P result in decreased potency. Thus, the optimal hydrophobicity among these compounds is expressed by log P values in the range of 2.18–2.23. This is not too different from the optimal hydrophobicities (log P_O) predicted by others for antielectroshock activity in rats (1.8) and mice (3.7) (12) and for hypnotic activity in rats and mice (2.0) (13). (The fact that log P_O for anticonvulsant activity does not differ significantly from log P_O for hypnotic activity indicates that changes in hydrophobicity alone may not result in more selective anticonvulsant agents.)

A conceptual explanation for the parabolic dependence of potency on hydrophobicity is that molecules must possess a certain degree of lipid solubility in order to "dissolve" in and penetrate the lipid matrix of membranes, and increases in lipophilicity (hydrophobicity) will, within limits, facilitate this process. However, increases beyond a certain optimal hydrophobicity (log P_O) result in lower potency because the molecules increasingly partition within the lipid matrix of the membrane. Because the probability of membrane penetration is thus diminished, higher concentrations of drug are necessary to permit an eventual efficacious engagement of receptors.

If the data in Table I are arranged to express brain–blood concentration ratios, it will be seen that the distribution of drug between the two compartments also follows an approximate parabolic relationship with hydrophobicity. The ratios increase from phenobarbital (0.87) to carbamazepine (2.04) to phenytoin (2.41) with increases in log P up to 2.23;

Table I—Anti-Maximal Electroshock Potency (ED_{50}), Overt Neurotoxicity (TD_{50}), and Calculated Log P of α,α-Diphenylsuccinimide, Phenytoin, Phenobarbital, Carbamazapine, Cyheptamide, and (Diphenylacetyl)urea

	Phenobarbital (III)	Carbamazepine	Phenytoin (II)	α,α-Diphenyl-succinimide (I)	Cyheptamide	(Diphenyl-acetyl)urea
ED_{50} intraperitoneal, mg/kg	19.0(17.1–21.2)	9.7(8.5–11.0)	7.1(6.5–7.8)	26.5(23.4–30.0)	81.0(52.0–127.0)	406(349–472)
blood, μg/mL	17.2(15.5–19.1)	2.4(2.2–2.7)	2.2(1.8–2.8)	5.0(3.4–7.2)	5.5(3.9–7.8)	23(12.6–42.1)
brain, μg/g	15.0(13.6–16.5)	4.9(4.1–5.7)	5.3(4.7–5.9)	8.4(6.4–11.1)	8.9(7.5–10.6)	40(25.5–62.8)
TD_{50}, mg/kg ip[a]	66(62–71)	71[b]	91(84–98)	220(200–241)	170[b]	—[c]
Therapeutic index[d] Log P	3.5(3.1–3.9)	7.6	12.8(11.4–14.3)	8.3(7.3–9.5)	2.1	—[c]
	1.63[e]	2.18[f]	2.23[f]	2.63[g]	2.74[f]	2.83[f]

[a] Overt toxicity was assessed by the rotorod method (Ref. 6). [b] Obtained from the literature (Refs. 15 and 16). [c] Not available from the literature. [d] Calculated for each drug as the ratio TD_{50}/ED_{50} with respect to the intraperitoneal dose (mg/kg). [e] Calculated by π (barbiturate function) + π (C_6H_5) + π (ethyl) = −1.35 (Ref. 13) + 1.96 (Ref. 7) + 1.02 = 1.63 (Ref. 7). The calculated log P was used in preference to the experimental value (1.42, Ref. 13) to maintain consistency among calculated values. [f] Obtained from the literature (Refs. 3 and 4). [g] Calculated by π (succinimide) + 2π(C_6H_5) = −1.29 (Ref. 12) + 3.92 = 2.63.

further increases in log P result in lower ratios. (The only compound which is in poor compliance with this relationship is (diphenylacetyl)-urea.) This, of course, is expected on the basis of the conceptual framework discussed above. Each membrane interposed along the pharmacokinetic path a drug might follow to its receptor will lessen the probability that the drug will ever engage its receptor. The greatest reduction in such probability occurs at extreme values of the partition coefficient. Since one or more membranes must separate the blood from the brain (and receptor) compartments, the decrease in the brain–blood ratios with either very low or very high log P values is likely the result of a failure to enter the lipid bilayer or a failure to penetrate once entry has been made, respectively.

After a comparison was made of the average potency ratios among the above drugs within each category (*i.e.*, intraperitoneal dosage, blood concentration, and brain concentration), it was found that the smallest average potency ratio (3.1, $SD = 2.2$, $n = 15$) was for potencies expressed in terms of brain concentrations; the largest average ratio was for potencies expressed in terms of intraperitoneal dosage (12.1, $SD = 16.5$, $n = 15$), and the average ratio in terms of blood concentrations (4.2, $SD = 3.1$, $n = 15$) was intermediate. This also can be explained within the conceptual framework already discussed. As the number of membranes a drug must penetrate increases, the probability of a particular molecule penetrating all of the membranes decreases; this decrease is disproportionately greater for drugs with hydrophobicities at either extreme. Hence, the smaller average potency ratios expressed on the basis of brain concentrations might simply be an expression of a smaller difference in probability permitted by fewer barriers separating the drug from its receptor. In the formalism of shallow *versus* deep compartmentalization (14), the receptors exist in a relatively more shallow compartment when potency is expressed in terms of brain concentrations than when expressed in terms of intraperitoneal dosage or blood concentration.

Another factor which might partially explain the larger average potency ratios for intraperitoneal dosage is limited aqueous solubility. The log P value is an index of relative solubility in a hydrophobic *versus* aqueous solvent; it is not a measure of the absolute aqueous solubility of a compound. Thus, the role that variance in log P might play in the parenteral absorption of the above drugs might be insignificant in comparison with the variance imposed by significant differences in absolute aqueous solubility. If the drug is not sufficiently soluble in water to permit intimate association with the membrane, the role of hydrophobicity in drug absorption will be minimized.

In contrast with the MES data, overt neurotoxicity assessed by the rotorod method did not exhibit an apparent parabolic dependence on log P. Neurotoxicity data are not available for (diphenylacetyl)urea, but the rotorod TD_{50} values for carbamazepine and cyheptamide in mice are 71 (15) and 170 mg/kg (16), respectively (the estimate for cyheptamide was based on oral dosage). Thus, neurotoxicity seems to be inversely related to log P; higher log P values are associated with lower toxic potency (*i.e.*, higher TD_{50} values). This observation is supported by regression analysis of 16 compounds (15) which provided the following:

$$\log 1/C = 15.94\log MW - 0.97\log P + 0.55\mu - 33.19 \quad \text{(Eq. 1)}$$

where C is the dose producing (in mice) measurable toxicity in 50% of the test population (*i.e.*, TD_{50}), MW is the molecular weight, and μ is the dipole moment. If one compares the above equation with one of several equations which have been written to characterize anti-MES potency, it becomes apparent that overt neurotoxicity is not simply an extension of anticonvulsant activity. For example, anti-MES potency in mice has been characterized by:

$$\log 1/C = -0.22(\log P)^2 + 1.15\log P - 0.37\mu + 2.99 \quad \text{(Eq. 2)}$$

where C is the dose conferring protection against seizures in 50% of the test population (*i.e.*, ED_{50}). Thus, there is considerable evidence for a linear dependence of neurotoxicity on log P (within the dosage range evaluated) and a parabolic dependence of anticonvulsant potency on log P. Furthermore, neurotoxic potency is directly proportional to μ, whereas anticonvulsant potency is inversely proportional to μ. Therefore, it is apparent that the mechanisms conferring toxicity are fundamentally different than those that confer an anticonvulsant effect.

This can also be rationalized if one compares the therapeutic indices (TD_{50}/ED_{50}) for the above drugs. These indices exhibit the same parabolic dependence on log P as does anticonvulsant potency. For example, the therapeutic indices increase from phenobarbital (3.5) to carbamazepine (7.6) to phenytoin (12.8) with successive increases in log P, but the indices decrease from phenytoin (12.8) to α,α-diphenylsuccinimide (8.3) to cyheptamide (2.1) with continued increases in log P (the therapeutic index is not yet known for (diphenylacetyl)urea). This parabolic dependence of therapeutic ratio would not be expected if the toxic and anticonvulsant actions were the result of identical mechanisms.

Although at first thought it might seem that the uniqueness of mechanisms involved might make it easier to design more selective (less toxic) anticonvulsant compounds, the parabolic dependence of therapeutic index on log P severely limits the utility of this parameter in such design. However, it is also apparent that other indices, such as dipole moment, should be explored more thoroughly. As is apparent from the above equations, larger dipole moments might be associated with lower anticonvulsant potency, but greater toxic potency. Thus, it might make sense to screen hypothetical compounds for dipole moment as well as hydrophobicity. Furthermore, as the quantitative structure–activity relationships (QSAR) of anticonvulsant compounds become more fully documented, it is distinctly possible that other physicochemical or empirical indices will contribute still more to rational drug design. The potency data provided herein should be useful in QSAR studies of anticonvulsant compounds, in particular because potency expressed in terms of brain concentration appears more suited for such analysis than potency expressed as parenteral dosage.

REFERENCES

(1) C. A. Miller and L. M. Long, *J. Am. Chem. Soc.*, **73**, 4895 (1951).

(2) G. Chen, R. Portman, C. R. Ensor, and A. C. Bratton, *J. Pharmacol. Exp. Ther.*, **103**, 54 (1951).

(3) G. L. Jones, R. J. Amato, G. H. Wimbish, and G. A. Peyton, *J. Pharm. Sci.*, **70**, 618 (1981).

(4) R. J. Amato and G. L. Jones, *Drug Dev. Res.*, **2**, 47 (1982).

(5) E. A. Swinyard, *Epilepsia*, **10**, 107 (1969).

(6) N. W. Dunham and T. S. Miya, *J. Am. Pharm. Assoc. Sci. Ed.*, **46**, 208 (1957).

(7) C. Hansch and A. Leo, "Substituent Constants for Correlation Analysis in Chemistry and Biology," Wiley, New York, N.Y., 1979.

(8) C. Hansch and J. M. Clayton, *J. Pharm. Sci.*, **62**, 1 (1973).

(9) J. G. Millichap, G. L. Pitchford, and M. G. Millichap, *Proc. Soc. Exp. Biol. Med.*, **127**, 1187 (1968).

(10) J. T. Litchfield and F. Wilcoxon, *J. Pharmacol. Exp. Ther.*, **96**, 99 (1949).

(11) G. F. Johnson, W. A. Dechtiaruk, and H. M. Solomon, *Clin. Chem.*, **21**, 144 (1975).

(12) E. J. Lien, *J. Med. Chem.*, 13, 1189 (1970).
(13) C. Hansch, A. R. Steward, S. M. Anderson, and D. Bentley, *J. Med. Chem.*, 11, 1 (1967).
(14) E. R. Garrett, *Drug Res.*, 21, 105 (1977).
(15) E. J. Lien, R. C. H. Liao, and H. G. Shinouda, *J. Pharm. Sci.*, 68, 463 (1979).
(16) A. B. H. Funcke, M. C. van Beek, G. van Hell, U. I. Lavy, H. Timmerman, and P. Zandberg, *Arch. Int. Pharmacodyn.*, 187, 174 (1970).

ACKNOWLEDGMENTS

Supported in part by grants from the Epilepsy Foundation of America and the Texas College of Osteopathic Medicine.

Pharmacokinetic Analysis of Concentration–Time Data Obtained Following Administration of Drugs that are Recycled in the Bile

WAYNE A. COLBURN

Received October 4, 1982, from the *Department of Pharmacokinetics and Biopharmaceutics, Hoffmann-La Roche Inc., Nutley, NJ 07110.* Accepted for publication January 18, 1983.

Abstract □ A pharmacokinetic model for calculating the pharmacokinetic parameters for a compound that is recycled in the bile is presented and tested using theoretical as well as experimental data. The results indicate that this method is stable and only slightly susceptible to sampling and recycling times. It is apparent from the present study that pharmacokinetic terms that have been used in classical situations are not directly applicable to drugs that enter the enterohepatic circulation. Effective half-life and effective clearance are used to describe the intrinsic ability of the eliminating organs to remove drug from the blood, whereas net half-life and net clearance are used to describe the irreversible elimination of the drug from the body.

Keyphrases □ Pharmacokinetics—biliary recycling of drugs, theoretical model, applications to cimetidine and isotretinoin □ Biliary excretion—incorporation in pharmacokinetics, model, applications to cimetidine and isotretinoin □ Mathematical models—incorporation of biliary recycling in pharmacokinetics, application to cimetidine and isotretinoin

The ability to predict plasma concentration–time profiles observed following repetitive doses from data obtained following a single dose is an important aspect of pharmacokinetic analysis. In most cases, drugs that follow linear pharmacokinetic models allow these predictions to be made with reasonable certainty. However, when plasma concentration–time data cannot be adequately described by classical pharmacokinetic equations, *i.e.*, saturable processes or enzyme induction, this predictive capability becomes impaired. When a compound is excreted in the bile and subsequently reabsorbed from the GI tract, a similar situation exists in that classical equations cannot be used to sufficiently characterize the erratic and fluctuating plasma concentration–time curves. The purpose of the present investigation was to develop a biliary recycling model, to test its susceptibility to sampling times and experimental error, and to apply it to experimental data from drugs that are known to recycle in the bile.

THEORETICAL

Two distinct types of compounds must be considered when discussing biliary excretion and enterohepatic circulation. In the first category, there are compounds that are recycled but still are eliminated in ≤24 h; indomethacin (1), cimetidine (2), and imipramine (3) are examples from this category. In the second category are compounds that persist for much longer than 24 h; isotretinoin (4), digitoxin (5), and phenprocoumon (6) are examples from this category of substances. For compounds that are eliminated from the body in ~24 h or less, extensive sampling of body fluids is required over the entire interval, whereas for compounds that take substantially longer than 24 h to be eliminated from the body, extensive sampling during the first 24 h and subsequent samples at 24-h intervals are required. The modeling procedure developed herein considers both types of compounds.

Model Development—The following compartmental models (Fig. 1) are among those applicable to the study of blood concentration–time data profiles of compounds that undergo enterohepatic circulation. The models differ only in the sites of elimination. It can be shown that models

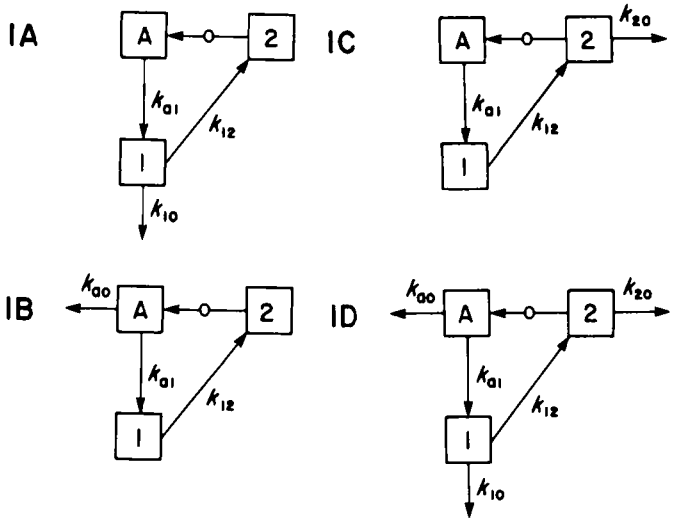

Figure 1—*Four possible enterohepatic recycling models. Compartment A is the absorption site, compartment 1 is the sampled blood compartment, and compartment 2 is the storage compartment that includes the gallbladder and the transit-time factor. The first-order rate constants* k_{a1} *and* k_{12} *represent the transfer of drug from the absorption site to the sampled blood compartment and from the sampled compartment to the gallbladder storage compartment whereas* k_{a0}, k_{10}, *and* k_{20} *are rate constants that represent first-order elimination from the absorption site, sampled compartment, and gallbladder storage compartment. The arrow between compartments 2 and A represent the discontinuous emptying process of the gallbladder such that the amount of drug in the gallbladder is transferred instantaneously to the absorption site at the time* (t_{bile}) *that reabsorption begins and V is the volume of the sampled compartment.*

0022-3549/84/0300-0313$01.00/0
© 1984, American Pharmaceutical Association

(12) E. J. Lien, *J. Med. Chem.*, 13, 1189 (1970).
(13) C. Hansch, A. R. Steward, S. M. Anderson, and D. Bentley, *J. Med. Chem.*, 11, 1 (1967).
(14) E. R. Garrett, *Drug Res.*, 21, 105 (1977).
(15) E. J. Lien, R. C. H. Liao, and H. G. Shinouda, *J. Pharm. Sci.*, 68, 463 (1979).
(16) A. B. H. Funcke, M. C. van Beek, G. van Hell, U. I. Lavy, H. Timmerman, and P. Zandberg, *Arch. Int. Pharmacodyn.*, 187, 174 (1970).

ACKNOWLEDGMENTS

Supported in part by grants from the Epilepsy Foundation of America and the Texas College of Osteopathic Medicine.

Pharmacokinetic Analysis of Concentration–Time Data Obtained Following Administration of Drugs that are Recycled in the Bile

WAYNE A. COLBURN

Received October 4, 1982, from the *Department of Pharmacokinetics and Biopharmaceutics, Hoffmann-La Roche Inc., Nutley, NJ 07110.* Accepted for publication January 18, 1983.

Abstract □ A pharmacokinetic model for calculating the pharmacokinetic parameters for a compound that is recycled in the bile is presented and tested using theoretical as well as experimental data. The results indicate that this method is stable and only slightly susceptible to sampling and recycling times. It is apparent from the present study that pharmacokinetic terms that have been used in classical situations are not directly applicable to drugs that enter the enterohepatic circulation. Effective half-life and effective clearance are used to describe the intrinsic ability of the eliminating organs to remove drug from the blood, whereas net half-life and net clearance are used to describe the irreversible elimination of the drug from the body.

Keyphrases □ Pharmacokinetics—biliary recycling of drugs, theoretical model, applications to cimetidine and isotretinoin □ Biliary excretion—incorporation in pharmacokinetics, model, applications to cimetidine and isotretinoin □ Mathematical models—incorporation of biliary recycling in pharmacokinetics, application to cimetidine and isotretinoin

The ability to predict plasma concentration–time profiles observed following repetitive doses from data obtained following a single dose is an important aspect of pharmacokinetic analysis. In most cases, drugs that follow linear pharmacokinetic models allow these predictions to be made with reasonable certainty. However, when plasma concentration–time data cannot be adequately described by classical pharmacokinetic equations, *i.e.*, saturable processes or enzyme induction, this predictive capability becomes impaired. When a compound is excreted in the bile and subsequently reabsorbed from the GI tract, a similar situation exists in that classical equations cannot be used to sufficiently characterize the erratic and fluctuating plasma concentration–time curves. The purpose of the present investigation was to develop a biliary recycling model, to test its susceptibility to sampling times and experimental error, and to apply it to experimental data from drugs that are known to recycle in the bile.

THEORETICAL

Two distinct types of compounds must be considered when discussing biliary excretion and enterohepatic circulation. In the first category, there are compounds that are recycled but still are eliminated in ≤24 h; indomethacin (1), cimetidine (2), and imipramine (3) are examples from this category. In the second category are compounds that persist for much longer than 24 h; isotretinoin (4), digitoxin (5), and phenprocoumon (6) are examples from this category of substances. For compounds that are eliminated from the body in ~24 h or less, extensive sampling of body fluids is required over the entire interval, whereas for compounds that take substantially longer than 24 h to be eliminated from the body, extensive sampling during the first 24 h and subsequent samples at 24-h intervals are required. The modeling procedure developed herein considers both types of compounds.

Model Development—The following compartmental models (Fig. 1) are among those applicable to the study of blood concentration–time data profiles of compounds that undergo enterohepatic circulation. The models differ only in the sites of elimination. It can be shown that models

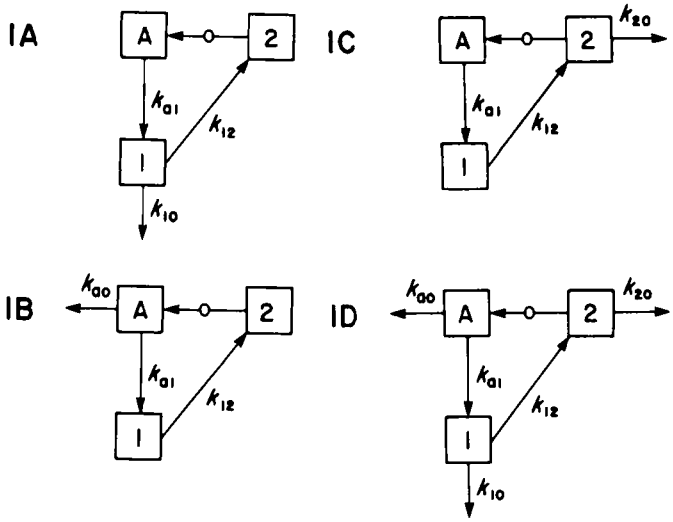

Figure 1—*Four possible enterohepatic recycling models. Compartment A is the absorption site, compartment 1 is the sampled blood compartment, and compartment 2 is the storage compartment that includes the gallbladder and the transit-time factor. The first-order rate constants* k_{a1} *and* k_{12} *represent the transfer of drug from the absorption site to the sampled blood compartment and from the sampled compartment to the gallbladder storage compartment whereas* k_{a0}, k_{10}, *and* k_{20} *are rate constants that represent first-order elimination from the absorption site, sampled compartment, and gallbladder storage compartment. The arrow between compartments 2 and A represent the discontinuous emptying process of the gallbladder such that the amount of drug in the gallbladder is transferred instantaneously to the absorption site at the time* (t_{bile}) *that reabsorption begins and V is the volume of the sampled compartment.*

0022-3549/84/0300-0313$01.00/0
© 1984, American Pharmaceutical Association

Table I—Schematic Representation of the Blood Sampling Schedules

Time, h	Schedule Designation A	B	C	D
0	+	+	+	+
1	+	+	+	+
2	+	+	+	+
3	+	+	+	+
4	+	+	+	+
5	+			
6	+	+	+	+
7	+			
8	+	+		
9	+		+	+
10	+	+		
11	+			
12	+	+	+	+
13	+			
14	+	+		
15	+		+	
16	+	+		
17	+			
18	+	+	+	+
19	+			
20	+	+		
21	+	+		
22	+	+		
23	+			
24	+	+	+	+

1A and 1B are pharmacokinetically differentiated from model 1C when recycling occurs at nonuniform intervals. However, within the limits of analytical precision and considering the biological variation that is associated with experimental data, the four models are not structurally identifiable when blood concentration–time data are evaluated. The four models are pharmacokinetically unique only if blood, urine, feces, and bile are collected following both intravenous and oral doses and analyzed for both parent drug and all metabolites.

One of these models (1A) has been previously described by Veng-Pedersen and Miller (7) and Steimer *et al.* (8), but the integrated equation derived in these manuscripts included only one recycling of bile during the experiment (7). For the purpose of testing the impact of sampling time and experimental error on the model predictions, data will be simulated assuming that the gallbladder empties at each meal ingestion (9) (e.g., at 0700, 1300, 1900 on each day of the study) and that drug is administered at 0700 on day 1 with no meal being ingested at that time. Therefore, the first gallbladder emptying occurs at 1300 on day 1. In the first example (case I) it is assumed that reabsorption begins each time (t_{bile}) that the gallbladder empties. However, in many cases, a conjugate of parent compound is excreted in the bile, deconjugated in the lower intestinal contents, then reabsorbed (10–12). This situation could result in substantial time delay between meal ingestion and subsequent reabsorption (13). For this purpose, blood concentration–time data were simulated after incorporating a 3-h (case II) or 6-h (case III) transit-time lag between gallbladder emptying and the onset of reabsorption (t_{bile}) such that the first reabsorption begins 9 or 12 h after the dose, respectively.

Model Testing—The ability of the recycling model to adequately describe simulated blood concentration–time data following a single dose of drug was tested under the following experimental conditions:

1. Ideal data sets (cases I–III) with four different sampling schedules (see Table I).
2. Ten errant data sets (case II only) with uniformly distributed random error using each of the four different sampling schedules.
3. Ten errant data sets assuming that gallbladder emptying occurred at 5 and 11 h and 10 errant data sets assuming gallbladder emptying occurred at 7 and 13 h during the first 24-h period after dosing to determine the effect of nonsampled recycling times.

In addition, two sets of experimental data were fitted with the model to assess the impact of repeated recycling during the experimental interval. In the first example, cimetidine concentration–time data (14) were *fitted with* model 1A. Patient data were obtained following a single 300-mg oral dose 3 h prior to breakfast (14); no mention was made of subsequent meal times. The results from the present curve-fitting technique are compared with previous attempts to fit the data with the single recycling technique (2). For the second example, blood concentration–time data from a recently completed single 100-mg oral dose pharmacokinetic study with isotretinoin (4) were fitted with model 1A.

Table II—Ideal Theoretical Data Sets Curve-Fitted Using the Different Sampling Schedules

	t_{bile}, h	k_a, h^{-1}	k_{12}, h^{-1}	k_{10}, h^{-1}	V, L
		Case I			
Ideal Schedule	6.00	0.693	0.420	0.0800	400
A	6.00	0.695	0.419	0.0801	401
B	6.00	0.694	0.420	0.0802	400
C	6.00	0.696	0.418	0.0800	401
D	6.00	0.696	0.419	0.0801	401
		Case II			
Ideal Schedule	9.00	0.693	0.420	0.0800	400
A	9.00	0.695	0.419	0.0800	401
B	9.00	0.694	0.420	0.0800	400
C	9.00	0.695	0.419	0.0801	401
D	9.00	0.706	0.411	0.0800	406
		Case III			
Ideal Schedule	12.0	0.693	0.420	0.0800	400
A	12.0	0.695	0.419	0.0801	400
B	12.0	0.695	0.419	0.0800	400
C	12.0	0.696	0.418	0.0800	401
D	12.0	0.695	0.419	0.0802	401

In this second example, it was assumed that the gallbladder emptied at meal ingestion and that the time to transit in the intestine to sites where deglucuronidation could occur was constant after each meal. In this way, a single recycling parameter could be estimated and used to calculate subsequent recycling times on the basis of meals ingested. All concentration (C_B) data were fitted with the differential equations required to describe model 1A in conjunction with the nonlinear least-squares regression program, NONLIN (15), using $1/C_B$ weighting[1].

In addition, a net elimination rate constant during recycling (β_R) can be determined by performing log-linear regression on concentration–time data at 24-h intervals during the elimination phase, *e.g.*, 24, 48, 72, and 96 h or 12, 36, 60, and 84 h. The determination of β_R is based on the assumption that gallbladder emptying and subsequent reabsorption occur at the same times each day. Therefore, if recycling occurs at the same time during each 24-h interval, the β_R obtained by fitting data points collected at 24-h intervals should reflect the true elimination rate since the concentration–time points fall on the same portion of the sinusoidal recycling curve. Experimentally, this can be achieved by controlling the time and type of food intake. This curve-fitting procedure was tested by introducing uniform random error into theoretical concentrations.

RESULTS

The parameters estimated for ideal theoretical data sets from cases I–III with the four different sampling schedules (Table I) are presented in Table II. The parameters estimated for 10 errant data sets from case II using the four different sampling schedules are presented in Table III. The parameters estimated for 10 errant data sets from 5- and 11-h recycling data and from 7- and 13-h recycling data are presented in Table IV.

It is apparent from the parameter estimates in Table II, that when no error is present in the data, the curve-fitting procedure is not dependent on either the times of recycling or sampling. Similarly, the mean parameter estimates presented in Tables III and IV would indicate that, on the average, the curve-fitting procedure is not strongly influenced by either recycling or sampling times. However, the variation around the mean values are greater for sampling schedules C and D than for schedules A and B, *i.e.*, when nonsampled intervals (Table I) become >2 h.

By introducing ±10% error into the 24-, 48-, 72-, 96-, and 120-h samples, it was possible to assess the impact of random error on the estimation of β_R. For the purpose of testing an extreme case, 10% error was added to the 24-h concentration and subtracted from either a 48-, 72-, 96-, or 120-h concentration. When 10% error was subtracted from the 48-, 72-, 96-, and 120-h concentration, the error introduced into β_R was 29.0, 14.5, 9.7, and 7.3%, respectively. It is apparent that the more time points and the longer the time used to calculate β_R, the more precise will be the estimate.

The results from curve-fitting the cimetidine blood concentration–time

[1] A listing of the FORTRAN program used in this study is available from the author on request.

Table III—Parameters Estimated from 10 Sets of Theoretical Concentration–Time Data Containing ±10% Uniformly Distributed Random Error and Simulated According to Case II

	Parameters				
	t_{bile}, h	k_a, h^{-1}	k_{10}, h^{-1}	k_{12}, h^{-1}	V, L
Ideal	9.00	0.693	0.0800	0.420	400
Schedule A					
Mean ± *SD*	9.04 ± 0.06	0.742 ± 0.095	0.0786 ± 0.0053	0.405 ± 0.036	418 ± 35.6
Range	(8.99–9.16)	(0.579–0.882)	(0.0714–0.0873)	(0.362–0.487)	(350–460)
Schedule B					
Mean ± *SD*	8.99 ± 0.13	0.749 ± 0.135	0.0774 ± 0.0057	0.407 ± 0.048	420 ± 43.3
Range	(8.78–9.12)	(0.565–0.972)	(0.0711–0.0879)	(0.337–0.501)	(343–486)
Schedule C					
Mean ± *SD*	9.11 ± 0.20	0.763 ± 0.149	0.0846 ± 0.0110	0.392 ± 0.058	430 ± 61.1
Range	(9.00–9.64)	(0.573–1.014)	(0.0640–0.0999)	(0.269–0.500)	(351–536)
Schedule D					
Mean ± *SD*	9.26 ± 0.24	0.747 ± 0.143	0.0865 ± 0.0122	0.402 ± 0.050	422 ± 53.9
Range	(9.00–9.67)	(0.553–0.988)	(0.0637–0.1090)	(0.319–0.491)	(349–494)

Table IV—Parameters Estimated from 10 Sets of Theoretical Concentration–Time Data Containing ±10% Uniformly Distributed Random Error and Simulated With Recycling Occurring at Nonsampled Times

	Parameters				
	t_{bile}, h	k_a, h^{-1}	k_{10}, h^{-1}	k_{12}, h^{-1}	V, L
Ideal	5.00	0.693	0.0800	0.420	400
Schedule D					
Mean ± *SD*	5.01 ± 0.14	0.735 ± 0.168	0.0790 ± 0.0177	0.421 ± 0.056	412 ± 59.6
Range	(4.71–5.18)	(0.570–0.954)	(0.0590–0.0950)	(0.338–0.496)	(346–487)
Ideal	7.00	0.693	0.0800	0.420	400
Schedule D					
Mean ± *SD*	7.09 ± 0.37	0.728 ± 0.166	0.0807 ± 0.0208	0.431 ± 0.057	408 ± 60.1
Range	(6.47–7.60)	(0.559–1.000)	(0.0510–0.1093)	(0.322–0.503)	(348–498)

data are presented in Table V, and a representative plasma concentration–time profile is presented in Fig. 2. Similarly, the results obtained by curve-fitting isotretinoin blood concentration–time data are presented in Table VI, and a representative curve is presented in Fig. 3. The parameter estimates determined by curve-fitting experimental data from the literature for cimetidine (14) and blood concentration–time data presently being generated in this laboratory for isotretinoin show the applicability of the procedure.

Comparing the results of the present analysis of cimetidine blood concentration–time data with those reported in the literature using the single-recycling model of Veng-Pedersen and Miller (2), it appears that the complexities associated with the previously reported model may not be required to fit the data. If one assumes that a second recycling occurs during the time-course of the study, one can adequately fit the data without having to involve the complexities inherent in the two-compartment distribution model of Veng-Pedersen and Miller. It is difficult to justify the more complex model when recycling occurs at 2–6 h intervals and sampling is not sufficiently frequent to differentiate biphasic distribution characteristics from the recycling characteristics. In fact, it can be shown that when sampling is infrequent a recycled drug that conforms to model 1A in Fig. 1 exhibits what appears to be a two-compartment model profile. In addition, when it is not possible to simultaneously fit data from several routes and modes of administration, parsimony dictates that the simplest model should be chosen.

DISCUSSION

A model-dependent method for calculating the pharmacokinetic parameters for a compound that is recycled in the bile has been presented and tested using simulated theoretical data as well as experimental data. The results indicate the the method is stable, only slightly susceptible to changes in sampling and recycling times, and adequate to describe the blood concentration–time profiles of drugs that recycle in the bile.

The results of the present analysis suggest that more explicit terms are required to describe the pharmacokinetic parameters of compounds that are recycled in the bile. The blood clearance (CL_B) determined by the classical method:

$$CL_B = \frac{\text{Dose}}{AUC_{0-\infty}} \qquad \text{(Eq. 1)}$$

does not reflect the *effective* clearance (CL_E) of the drug by the liver. From model 1A, it can be shown that:

$$CL_E = V \cdot K \qquad \text{(Eq. 2)}$$

where the *effective* elimination rate constant (K) is the sum of k_{10} and k_{12} in model 1A. However, the *net* clearance (CL_N) derived from model 1A according to the following equation:

$$CL_N = V \cdot k_{10} \qquad \text{(Eq. 3)}$$

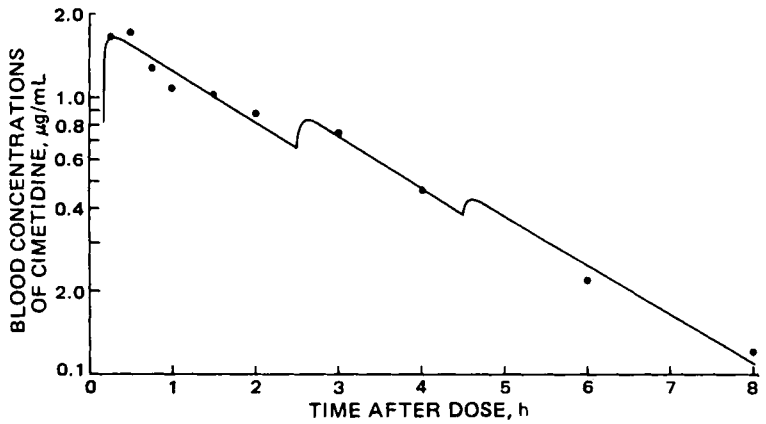

Figure 2—*Representative blood concentration–time profile of cimetidine along with the model-predicted line for subject 5.*

Table V—Parameters Estimated by Curve Fitting Cimetidine Blood Concentration–Time Data Following a Single 300-mg Oral Dose [a]

Subject	Parameters							
	t_{lag}, h	$t_{bile(1)}$ [b], h	$t_{bile(2)}$ [b], h	k_a, h^{-1}	k_{10}, h^{-1}	k_{12}, h^{-1}	V, L	r [c]
1	0.20	2.65	5.85	1.46	0.790	0.700	87.4	0.998
2	0.15	1.50	3.90	2.24	0.340	0.490	109	0.995
3	0.15	1.98	5.98	8.97	0.312	0.393	123	0.988
4	0.10	1.92	3.92	4.83	0.566	0.089	103	0.997
5	0.20	1.98	—	35.4	0.022	0.538	220	0.996
6	0.15	2.50	4.50	39.3	0.340	0.077	172	0.995
7	0.10	1.17	3.67	1.38	0.452	0.124	88.4	0.982
8	0.20	1.94	3.74	4.13	0.212	0.434	144	0.996
9	0.00	2.98	—	2.42	0.241	0.148	192	0.996
10	0.00	1.80	4.60	1.81	0.320	0.006	172	0.973
11	0.20	1.83	5.83	5.00	0.459	0.020	145	1.000
12	0.05	1.96	—	3.04	0.171	0.113	316	0.937
Mean	0.125	2.02	4.67	9.17	0.352	0.261	156	
SD	0.075	0.49	0.97	13.4	0.199	0.235	65.5	
Range	0–0.2	1.17–2.98	3.67–5.98	1.38–39.3	0.022–0.790	0.006–0.700	87.4–316	

[a] Concentration–time data obtained from Ref. 14. [b] $t_{bile(1)}$ and $t_{bile(2)}$ represent the times of the first and second recycling, respectively. [c] Correlation coefficient.

Table VI—Parameters Estimated by Curve Fitting Blood Concentrations of Isotretinoin Following a Single 100-mg Oral Dose to Five Normal Male Subjects

Parameter	Subject					Mean ± 1 *SD*
	1	2	3	4	5	
t_{lag}, h	1.95	0.71	0.10	0.87	0.77	0.88 ± 0.67
t_{bile}, h	7.83	11.8	9.53	9.83	17.9	11.4 ± 3.9
k_a, h^{-1}	1.33	0.609	0.635	0.456	0.825	0.771 ± 0.339
k_{10}, h^{-1}	0.182	0.099	0.052	0.072	0.087	0.098 ± 0.050
k_{12}, h^{-1}	0.333	0.478	0.125	0.152	0.299	277 ± 0.144
β_R, h^{-1}	0.0521	0.0206	0.0265	0.0312	0.0247	0.0310 = 0.0214
$t_{1/2\beta}$, h	13.3	33.6	26.2	22.2	28.1	22.4[a]
V/F, L	379	116	421	739	180	367 ± 245
AUC_D [b] ng·h/mL	1450	8708	4568	1879	6386	4598 ± 3057
r	1.000	.999	.999	.998	1.000	

[a] Harmonic mean. [b] Model-dependent area (AUC_D) calculated as $(F\cdot\text{Dose})/(V\cdot k_{10})$ and model.

is equivalent to CL_B. This distinction in clearance terms is similar to the approach previously employed by Kwan *et al.* (1) with indomethacin. However, it is a more unified approach which incorporates the differences in clearance into a single pharmacokinetic modeling technique.

Levy (16) has stated that fitting concentration–time data obtained following the administration of drugs that are involved in the enterohepatic circulation to classical pharmacokinetic models results in an overestimate of the true volume of distribution and an overestimation of the true half-life of the compound. In fact, curve-fitting data from compounds that are recycled to classical bi- or triexponential equations does overestimate the true volume of distribution and the *effective* elimination half-life ($t_{1/2E}$), derived from $0.693/K$. However, curve-fitting with classical equations may not, depending on the erratic nature of the blood concentration–time profile, overestimate the *net* elimination half-life ($t_{1/2N}$), derived from $0.693/\beta_R$ where β_R is the net elimination rate constant. β_R is related to the elimination rate constant (k_{10}) by:

$$\beta_R = F_1 \cdot k_{10} \qquad \text{(Eq. 4)}$$

where F_1 is the average fraction of the total amount of drug in the body that is in the blood compartment during any 24-h interval. This net elimination half-life ($t_{1/2N}$) is in fact the true elimination half-life, since it reflects the fraction of a dose that still remains to be irreversibly eliminated (17).

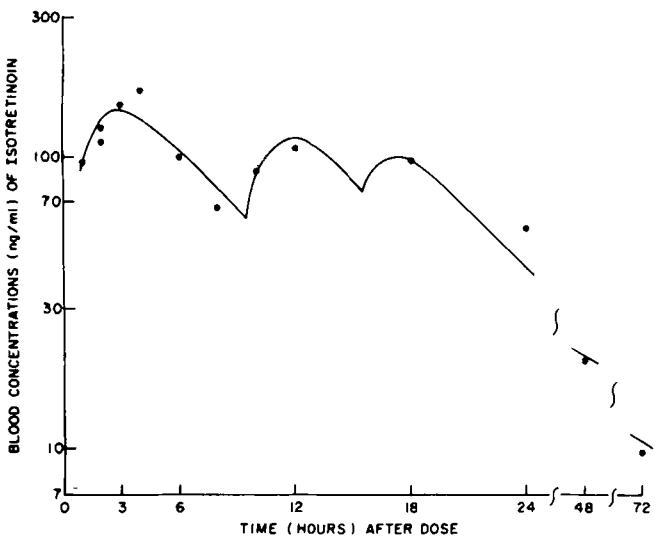

Figure 3—*Representative blood concentration–time profile of isotretinoin from subject 8 along with the model-predicted curve.*

If one applies these concepts to the data obtained for cimetidine and isotretinoin, interesting results are obtained. For cimetidine CL_E = 1393 mL/min (range 849–2170) and CL_N = 777 mL/min (range 81–1151), suggesting a first-pass effect ($E = CL_E/Q + CL_E$) of 0.36–0.59. However, using the net clearance to calculate the apparent first-pass effect ($E = CL_N/Q + CL_N$) yields values of 0.05–0.43, which are consistent with the conclusions from the original report (14). For isotretinoin, CL_E = 1906 mL/min (range 1116–3253) and CL_N = 571 mL/min (range 191–1150), suggesting a true first-pass effect of ~0.40. However, since isotretinoin is eliminated solely by liver clearance, 65–77% of the drug that is cleared by first-pass will be returned through enterohepatic circulation, resulting in an apparent first-pass effect of ~0.28. The average fraction (F_1) of the total amount of drug in the body that was in the blood compartment was 0.32.

It became apparent during these curve-fitting procedures that the pharmacokinetics of drugs that are incorporated into the enterohepatic circulation are complex, and development of their profiles will require specialized clinical studies. Two important aspects of performing clinical pharmacokinetic studies with compounds that recycle in the bile is to establish an appropriate experimental design and to maintain well-controlled conditions. Sufficient blood samples must be obtained to adequately characterize the recycling time course during a 24-h interval, and the time of meal ingestion must be controlled to ensure that the variation in recycling times is minimized.

In conclusion, a model-dependent method for analyzing pharmacokinetic data from drugs that are recycled in the bile has been developed and tested. It is apparent that the pharmacokinetic terms used in other situations are not directly applicable to drugs that enter the enterohepatic circulation. Effective half-life and effective clearance have been introduced to describe the intrinsic ability of the liver to remove drug from

the blood, whereas net half-life and net clearance have been used to describe the permanent elimination of the drug from the body.

REFERENCES

(1) K. C. Kwan, G. O. Breault, E. R. Umbenhauer, F. G. McMahon, and D. E. Duggan, *J. Pharmacokinet. Biopharm.*, **4**, 255 (1976).

(2) P. Veng-Pedersen and R. Miller, *J. Pharm. Sci.*, **69**, 394 (1980).

(3) H. Dencker, S. J. Dencker, A. Green, and A. Nagy, *Clin. Pharmacol. Ther.*, **19**, 384 (1976).

(4) K.-C. Khoo, D. Reik, and W. A. Colburn, *J. Clin. Pharmacol.*, **22**, 395 (1982).

(5) L. Storstein, *Clin. Pharmacol. Ther.*, **17**, 313 (1975).

(6) T. Meinertz, H.-J. Gilfeich, U. Groth, H. G. Jonen, and E. Janchen, *Clin. Pharmacol Ther.*, **21**, 731 (1977).

(7) P. Veng-Pedersen and R. Miller, *J. Pharm. Sci.*, **69**, 204 (1980).

(8) J.-L. Steimer, Y. Plusquellec, A. Guillaime, and J.-F. Boisveux, *J. Pharm. Sci.*, **71**, 297 (1982).

(9) E. A. Boyden, *Anat. Rec.*, **40**, 147 (1982).

(10) R. T. William, P. Millburn, and R. L. Smith, *Ann. N.Y. Acad. Sci.*, **123**, 110 (1965).

(11) S. M. Finegold, *Am. J. Clin. Nutr.*, **23**, 1466 (1970).

(12) P. C. Hirom, P. Millburn, and R. J. Parker, *Br. J. Pharmacol.*, **56**, 355P (1976).

(13) M. Kennedy, P. Chinwah, and D. N. Wade, *Br. J. Clin. Pharmacol.*, **8**, 372 (1979).

(14) S. S. Walkerstein, J. W. Dubb, W. C. Randolf, W. J. Westlake, R. M. Stote, and A. P. Intoccia, *Gastroenterology*, **74**, 360 (1978).

(15) C. M. Metzler, G. L. Elfring, and A. J. McEwen, *Biometrics*, **30**, 562 (1974).

(16) G. Levy, *Br. J. Clin. Pharmacol.*, **8**, 601 (1979).

(17) M. Gibaldi and D. Perrier, "Pharmacokinetics," Dekker, New York, N.Y., 1975, pp. 56–60.

Quantitative Determination of *N*-(*trans*-2-Dimethylaminocyclopentyl)-*N*-(3′,4′-dichlorophenyl)propanamide and Its *N*-Demethyl Metabolite in Dog Serum by Gas Chromatography

DUANE B. LAKINGS ˣ, RONALD P. STRYD, and TERRY J. GILBERTSON

Received July 23, 1982, from the *Pharmaceutical Research and Development, The Upjohn Company, Kalamazoo, MI 49001.* Accepted for publication February 17, 1983.

Abstract □ A gas chromatographic–electron capture (GC–EC) method has been developed for the determination of *N*-(*trans*-2-dimethylaminocyclopentyl)-*N*-(3′,4′-dichlorophenyl)propanamide, a potential antidepressant drug, and its *N*-demethyl metabolite in serum. The GC–EC system employed a 3% OV-17 on 100/120 mesh Supelcoport, 2-m × 2-mm i.d. glass column and an isothermal temperature of 195°C. The parent drug and metabolite were extracted from alkalinized serum (pH ~ 13) with toluene, back-extracted into an acidic solution (pH ~ 1), and finally, after adjusting to pH 13, extracted again with toluene. The extensive sample cleanup was necessary to remove serum components which interfered with the analysis. The analytical method was shown to give quantitative recovery of the drug and metabolite, to be linear over a 100-fold concentration range, and to have the necessary precision and sensitivity to detect and quantify as little as 1 ng/mL of the drug or its metabolite. The method has been employed to determine the serum level of drug and metabolite in dogs receiving a single oral dose and to determine the possible correlation between the administered dose and serum levels.

Keyphrases □ *N*-(*trans*-2-Dimethylaminocyclopentyl)-*N*-(3′,4′-dichlorophenyl)propanamide—quantitative determination, *N*-demethyl metabolite in dog serum, gas chromatography–electron capture □ Gas chromatography—electron capture, quantitative determination of *N*-(*trans*-2-dimethylaminocyclopentyl) -*N*- (3′,4′-dichlorophenyl) propanamide and its *N*-demethyl metabolite, dog serum

Some tricyclic antidepressants (*e.g.*, imipramine) used in the treatment of endogenous depression require an induction period of several days before improvement is noted and have been reported to have frequent side effects (1, 2). A potential antidepressant drug, *N*-(*trans*-2-dimethylaminocyclopentyl)-*N*-(3′,4′ - dichlorophenyl)propanamide (I) which may have a more rapid onset of therapeutic activity and fewer side effects was recently reported (3).

For definition of the pharmacokinetic and metabolic profiles of this potential antidepressant drug, a sensitive, precise, and specific analytical method is required. The presence of two chlorine moieties in the aromatic ring provides sufficient electronegativity for electron-capture (EC) detection after gas chromatographic (GC) separation. Initial studies[1] had shown that the drug was quickly demethylated at the dimethylamine functional group to give II. Also, a homologue of I with a cyclohexyl ring in place of the cyclopentyl ring was available (III) and was an ideal internal standard.

This report describes the GC–EC method for the quantitative determination of I, its *N*-demethyl metabolite, and the internal standard and the sample preparation procedure necessary to isolate the compounds from serum and to provide a sample amenable to GC–EC determination. Application of the methodology was demonstrated by the determination of serum levels of I and II in dogs

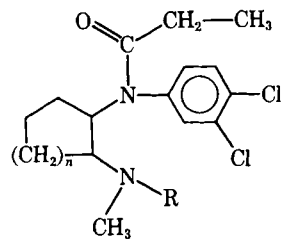

I: R = CH_3, n = 1
II: R = H, n = 1
III: R = CH_3, n = 2

[1] Unpublished data.

0022-3549/84/0300-0317$01.00/0

© 1984, American Pharmaceutical Association

the blood, whereas net half-life and net clearance have been used to describe the permanent elimination of the drug from the body.

REFERENCES

(1) K. C. Kwan, G. O. Breault, E. R. Umbenhauer, F. G. McMahon, and D. E. Duggan, *J. Pharmacokinet. Biopharm.*, **4**, 255 (1976).

(2) P. Veng-Pedersen and R. Miller, *J. Pharm. Sci.*, **69**, 394 (1980).

(3) H. Dencker, S. J. Dencker, A. Green, and A. Nagy, *Clin. Pharmacol. Ther.*, **19**, 384 (1976).

(4) K.-C. Khoo, D. Reik, and W. A. Colburn, *J. Clin. Pharmacol.*, **22**, 395 (1982).

(5) L. Storstein, *Clin. Pharmacol. Ther.*, **17**, 313 (1975).

(6) T. Meinertz, H.-J. Gilfeich, U. Groth, H. G. Jonen, and E. Janchen, *Clin. Pharmacol Ther.*, **21**, 731 (1977).

(7) P. Veng-Pedersen and R. Miller, *J. Pharm. Sci.*, **69**, 204 (1980).

(8) J.-L. Steimer, Y. Plusquellec, A. Guillaime, and J.-F. Boisveux, *J. Pharm. Sci.*, **71**, 297 (1982).

(9) E. A. Boyden, *Anat. Rec.*, **40**, 147 (1982).

(10) R. T. William, P. Millburn, and R. L. Smith, *Ann. N.Y. Acad. Sci.*, **123**, 110 (1965).

(11) S. M. Finegold, *Am. J. Clin. Nutr.*, **23**, 1466 (1970).

(12) P. C. Hirom, P. Millburn, and R. J. Parker, *Br. J. Pharmacol.*, **56**, 355P (1976).

(13) M. Kennedy, P. Chinwah, and D. N. Wade, *Br. J. Clin. Pharmacol.*, **8**, 372 (1979).

(14) S. S. Walkerstein, J. W. Dubb, W. C. Randolf, W. J. Westlake, R. M. Stote, and A. P. Intoccia, *Gastroenterology*, **74**, 360 (1978).

(15) C. M. Metzler, G. L. Elfring, and A. J. McEwen, *Biometrics*, **30**, 562 (1974).

(16) G. Levy, *Br. J. Clin. Pharmacol.*, **8**, 601 (1979).

(17) M. Gibaldi and D. Perrier, "Pharmacokinetics," Dekker, New York, N.Y., 1975, pp. 56–60.

Quantitative Determination of *N*-(*trans*-2-Dimethylaminocyclopentyl)-*N*-(3′,4′-dichlorophenyl)propanamide and Its *N*-Demethyl Metabolite in Dog Serum by Gas Chromatography

DUANE B. LAKINGS ˣ, RONALD P. STRYD, and TERRY J. GILBERTSON

Received July 23, 1982, from the *Pharmaceutical Research and Development, The Upjohn Company, Kalamazoo, MI 49001.* Accepted for publication February 17, 1983.

Abstract □ A gas chromatographic–electron capture (GC–EC) method has been developed for the determination of *N*-(*trans*-2-dimethylaminocyclopentyl)-*N*-(3′,4′-dichlorophenyl)propanamide, a potential antidepressant drug, and its *N*-demethyl metabolite in serum. The GC–EC system employed a 3% OV-17 on 100/120 mesh Supelcoport, 2-m × 2-mm i.d. glass column and an isothermal temperature of 195°C. The parent drug and metabolite were extracted from alkalinized serum (pH ~ 13) with toluene, back-extracted into an acidic solution (pH ~ 1), and finally, after adjusting to pH 13, extracted again with toluene. The extensive sample cleanup was necessary to remove serum components which interfered with the analysis. The analytical method was shown to give quantitative recovery of the drug and metabolite, to be linear over a 100-fold concentration range, and to have the necessary precision and sensitivity to detect and quantify as little as 1 ng/mL of the drug or its metabolite. The method has been employed to determine the serum level of drug and metabolite in dogs receiving a single oral dose and to determine the possible correlation between the administered dose and serum levels.

Keyphrases □ *N*-(*trans*-2-Dimethylaminocyclopentyl)-*N*-(3′,4′-dichlorophenyl)propanamide—quantitative determination, *N*-demethyl metabolite in dog serum, gas chromatography–electron capture □ Gas chromatography—electron capture, quantitative determination of *N*-(*trans*-2-dimethylaminocyclopentyl) -*N*- (3′,4′-dichlorophenyl) propanamide and its *N*-demethyl metabolite, dog serum

Some tricyclic antidepressants (*e.g.*, imipramine) used in the treatment of endogenous depression require an induction period of several days before improvement is noted and have been reported to have frequent side effects (1, 2). A potential antidepressant drug, *N*-(*trans*-2-dimethylaminocyclopentyl)-*N*-(3′,4′ - dichlorophenyl)propanamide (I) which may have a more rapid onset of therapeutic activity and fewer side effects was recently reported (3).

For definition of the pharmacokinetic and metabolic profiles of this potential antidepressant drug, a sensitive, precise, and specific analytical method is required. The presence of two chlorine moieties in the aromatic ring provides sufficient electronegativity for electron-capture (EC) detection after gas chromatographic (GC) separation. Initial studies[1] had shown that the drug was quickly demethylated at the dimethylamine functional group to give II. Also, a homologue of I with a cyclohexyl ring in place of the cyclopentyl ring was available (III) and was an ideal internal standard.

This report describes the GC–EC method for the quantitative determination of I, its *N*-demethyl metabolite, and the internal standard and the sample preparation procedure necessary to isolate the compounds from serum and to provide a sample amenable to GC–EC determination. Application of the methodology was demonstrated by the determination of serum levels of I and II in dogs

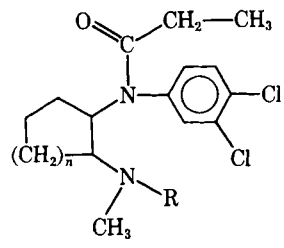

I: R = CH_3, n = 1
II: R = H, n = 1
III: R = CH_3, n = 2

[1] Unpublished data.

0022-3549/84/0300-0317$01.00/0

© 1984, American Pharmaceutical Association

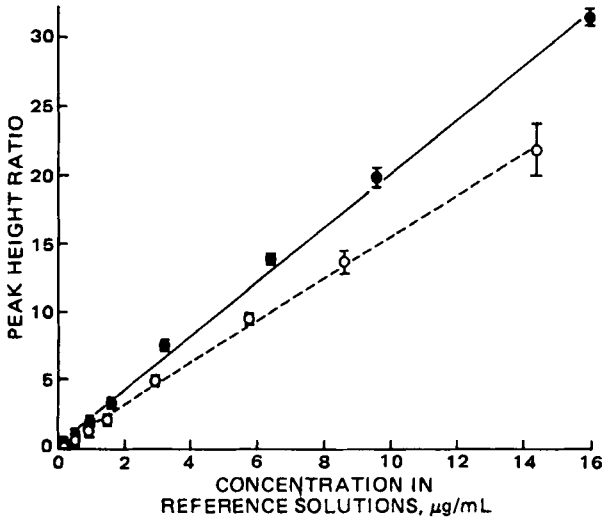

Figure 1—*Mean peak height ratio (n = 3) versus concentrations of I (●) and II (○) in the reference standard solutions. Concentrations ranged from 160 to 16,000 ng/mL for I and from 140 to 14,400 ng/mL for II. Bars represent ±2SD. Linear regression equations: (—) y = 1.97x + 0.42, r = 0.999; (- - -) y = 1.54x + 0.16, r = 0.996.*

administered a single oral dose of I and in dogs receiving different dose levels of I to determine the correlation between administered dose and serum levels.

EXPERIMENTAL

Apparatus and Reagents—The gas chromatograph[2] was equipped with a ^{63}Ni electron-capture detector. The toluene and methanol were distilled in glass[3]. Reference standards of the parent compound (I), the

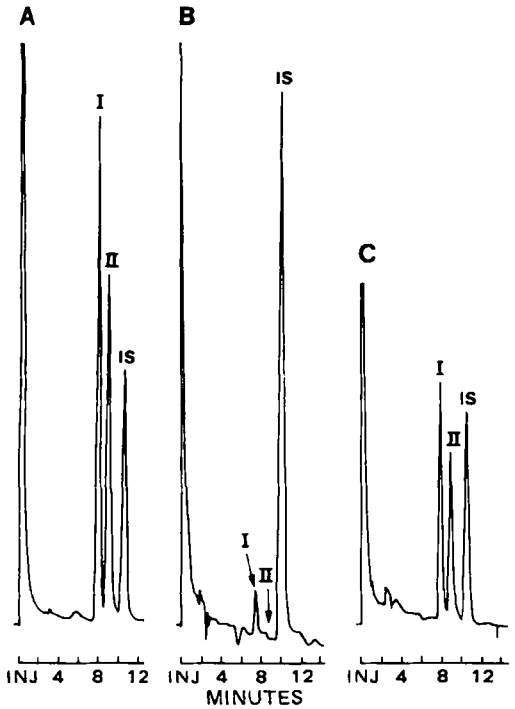

Figure 2—*Determination of I and II by GC-EC. Key: (A) reference standard solution containing 96 ng of I, 86 ng of II, and 61 ng of the internal standard; (B) extracted blank serum containing 60 ng of the internal standard (arrows indicate elution positions for I and II); (C) serum sample fortified with 64 ng/mL of I, 58 ng/mL of II, and 60 ng of the internal standard.*

[2] Model 222, Tracor Instruments, Austin, Tex.
[3] Burdick & Jackson Laboratories, Muskegon, Mich.

Table I—Recovery of I and II Added to Serum

Amount Added, ng/mL	Amount Found,[a] ng/mL	SD ±	RSD, %	Recovery, %
	I			
1602	1530	25	1.6	95.2
1202	1100	46	4.2	91.1
961	920	26	2.9	94.9
801	790	15	1.9	98.0
641	640	10	1.6	99.1
481	480	20	4.2	98.8
320	350	6	1.7	107.8
160[b]	175	22	12.4	106.2
128	117	15	10.2	87.5
96	81	14	17.3	79.2
80	76	2	2.7	88.8
64	61	8	13.9	87.5
48	45	5	11.0	83.3
32	34	2	4.5	90.6
16	21	2	7.3	100.0
8[c]	12	1	11.8	87.5
0	5	2	34.6	—
	II			
1438	1450	76	5.3	100.8
1079	1010	35	3.4	93.6
863	830	42	5.0	96.2
719	690	35	5.0	96.0
575	570	6	1.0	99.1
431	440	15	3.5	102.1
288	310	6	1.9	107.6
144[b]	151	18	11.9	104.9
115	96	21	2.2	83.5
86	74	2	3.1	86.0
72	76	6	8.0	105.6
58	49	8	14.1	84.5
43	40	3	7.5	93.0
29	28	4	14.4	96.6
14	14	1	4.1	100.0
7[c]	8	1	8.8	114.3
0	1	0	0	—

[a] Average value; $n = 3$ unless otherwise stated. [b] $n = 5$. [c] $n = 2$.

N-demethyl metabolite (II), and the internal standard (III) were used as obtained[4]. All other reagents and chemicals were of the highest quality available.

Chromatographic Conditions—A 3% (w/w) OV-17 on 100/120 mesh Supelcoport[5] in a 2-m × 2-mm i.d. glass column was used throughout these studies. The column was conditioned at 270°C for 24 h and deactivated by injecting 20 × 5 μL of bis(trimethylsilyl)trifluoroacetamide[6]. The conditioning and deactivation were necessary to prevent tailing by the compounds. The injector and detector temperatures were maintained at 300°C, and the column was isothermal at 195°C. The argon–methane (95:5, v/v) carrier gas flow rate was 25 mL/min, and the purge flow was 40 mL/min. The ^{63}Ni EC detector was operated in the pulse mode. All injections were made with a 10-μL syringe[7], and injection volumes varied from 2 to 5 μL.

Stock Solution Preparation—Stock solutions of I and II were prepared by accurately weighing 10.0 mg of I and II each into 100 mL of toluene–methanol (80:20, v/v), with concentrations of I and II at 100 μg/mL. Aliquots from this stock solution were diluted to give a working stock containing 1000 ng/mL of each compound. The working stock solution was used to prepare reference standard solutions and to fortify serum samples at various levels of I and II. An internal standard stock solution was prepared in a similar manner. The working internal standard stock solution concentration was 250 ng/mL.

Sample Preparation Procedure—The analysis of low levels, *i.e.*, nanograms per milliliter, of compounds in physiological fluids by GC–EC techniques requires that the compounds of interest be isolated from most components present in the sample and be dissolved in an organic solvent amenable to EC detection. The following sample preparation procedure employed liquid–liquid extraction to isolate I and II from serum components.

One milliliter of serum was transferred into a culture tube with a pol-

[4] Pharmaceutical Research and Development Laboratories, The Upjohn Co., Kalamazoo, Mich.
[5] Supelco, Inc., Bellefonte, Pa.
[6] Regis Chemical Co., Morton Grove, Ill.
[7] Hamilton, Reno, Nev.

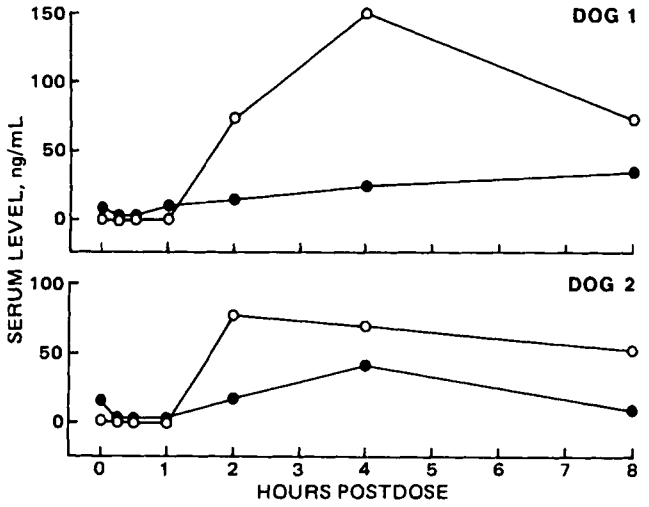

Figure 3—*Serum levels of I (●) and II (○) in dogs administered 10 mg/kg of I.*

ytef-lined screw cap. An equal volume of 1 M NaOH containing 100 mg/mL of NaCl was added, and the solution was mixed thoroughly. A 250-μL aliquot of the 250-ng/mL internal standard stock solution was added, followed by the addition of 4 mL of toluene–methanol (80:20, v/v). The solution was capped, vortexed for 45 s, and centrifuged at 2000 rpm for 10 min. The organic layer was transferred to a clean culture tube, and the extraction was repeated with 2 × 3 mL of toluene.

The organic phase was combined with the previous extract, and 2 mL of 1 M HCl was added. The solution was vortexed for 30 s, the organic phase was discarded, and the aqueous phase was washed by vortexing with 3 mL of toluene. The toluene was discarded, and the aqueous phase was made alkaline by adding 1 mL of 4 M NaOH containing 100 mg/mL of NaCl. This solution was extracted with 3 × 3 mL of toluene by vortexing for 30 s and centrifuged if necessary.

The toluene extracts were combined in a clean culture tube and evaporated to dryness at 40°C under a stream of nitrogen. The residue was dissolved in 100 μL of toluene–methanol (80:20, v/v); a 4-μL aliquot was injected into the chromatographic system.

Samples and Sample Handling—Serum levels of I and II were determined in two dogs, one male and one female, following oral administration of I. Blood samples were obtained prior to dosing and at 0.25, 0.5, 1, 2, 4, and 8 h after dosing. The blood was allowed to clot, and the serum was obtained by centrifugation. The serum was immediately frozen and maintained at −20 °C until sample preparation and analysis.

In addition, serum samples were obtained from a group of dogs being used in the evaluation of I. The dogs were a number of days into the evaluation, and thus, the samples that were collected were considered to be at steady state in relation to I. Four dogs, two male and two female, were selected from the 1-, 3-, and 10-mg/kg dosage levels and controls. Serum samples were obtained at 1 and 4 h after a daily dose. These sampling times were selected to provide samples at the expected highest serum concentration for I (1 h) and II (4 h). The serum samples were maintained at −20°C until sample preparation and analysis.

Calculations—The validation of the analytical method and the determination of I and II levels in dog serum were accomplished using the relative weight response (RWR) to an internal standard calculation method:

$$RWR_{Ref.\ Sol.} = \frac{PH_{cpd}}{PH_{IS}} \times \frac{ng_{IS}}{ng_{cpd}} \qquad \text{(Eq. 1)}$$

The average RWR of reference standard solutions of I and II analyzed with a sample set was employed to calculate the level of I and II in the samples:

$$ng_{cpd/sample} = \frac{PH_{cpd\ sample}}{PH_{IS}} \times \frac{ng_{IS\ sample}}{Avg.\ RWR_{Ref.\ Sol.}} \qquad \text{(Eq. 2)}$$

where PH_{cpd} and PH_{IS} are the peak heights of either I or II and the internal standard, and ng_{IS} and ng_{cpd} are the nanograms of internal standard and I or II in the reference solution or sample. For the serum samples, 1.0 mL of serum was used; thus, $ng_{cpd/sample}$ was equivalent to ng_{cpd}/mL of serum.

The reference standard solutions for each sample set were prepared over a concentration range equal to 15–300 ng/mL of I and II in serum. A minimum of five levels were selected for the reference standard solutions for each sample set. The recovery of I or II added to serum samples to validate the sample preparation procedure and to determine the accuracy of serum sample analyses was calculated as:

$$\%R = \frac{\text{ng of cpd in the fortified sample}}{\text{ng of cpd added + ng of cpd in the neat sample}} \times 100 \qquad \text{(Eq. 3)}$$

where %R is the percent recovery and the calculated amounts of I or II in the fortified and neat (unfortified) serum samples are in nanograms.

Table II—Serum Levels of I and II in Dogs Receiving Different Doses of I

Dose I, mg/kg	Compound	Time After Dose, h	Amount in Serum, ng/mL, Dog Group[a] A	B	C	D
10	I	1	17	13	4	11
		4	14	10	14	18
	II	1	226	53	19	60
		4	332	126	130	102
3	I	1	4	17	4	16
		4	4	5	3	4
	II	1	13	92	13	61
		4	24	64	17	21
1	I	1	2	2	5	3
		4	1	2	2	<1[b]
	II	1	7	3	6	<1
		4	2	4	6	<1
0	I	1	2	<1	~1	~1[c]
		4	<1	<1	<1	<1
	II	1	<1	<1	<1	<1
		4	<1	<1	<1	<1

[a] Dog groups A and B are female and groups C and D are male. [b] Below the detection limit (1 ng/mL) of the analytical method for I and II. [c] Small peak detected and calculated to be ~1 ng/mL.

RESULTS AND DISCUSSION

The GC–EC analytical technique was evaluated for linearity, precision, and sensitivity by analyzing triplicate reference solutions of I and II at eight concentration levels. The concentration levels ranged from 160 to 16,000 ng/mL for I and from 140 to 14,400 ng/mL for II. Figure 1 presents graphically the peak height ratio of I and II to the internal standard *versus* the concentrations of I and II. Linear regression equations and correlation coefficients for these data were $y = 1.97x + 0.42$ ($r = 0.999$) and $y = 1.54x + 0.16$ ($r = 0.996$) for I and II, respectively. The figure also shows two standard deviations around the average peak height ratio at each concentration. These data indicate the precision of the analytical

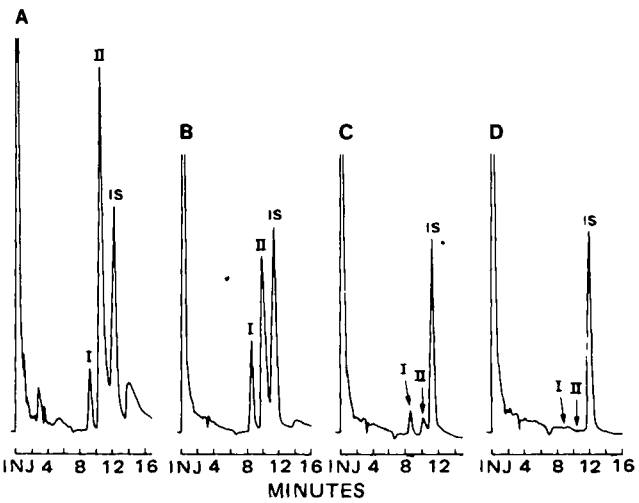

Figure 4—*GC–EC determination of I and II in serum from dogs receiving different doses of I. Key: (A) dose of 10 mg/kg; (B) dose of 3 mg/kg; (C) dose of 1 mg/kg; (D) control.*

technique. The sensitivity of the GC–EC (signal to noise ratio >5:1) was demonstrated to be <10 ng/mL for I and II. Assuming an initial serum volume of 1.0 mL and a final sample volume of 0.1 mL, the analytical technique can detect and quantify 1 ng/mL of serum for I and II.

The sample preparation procedure for the extraction of I and II from serum was developed through a series of experiments. The choice of toluene as the extraction solvent was made because of its low EC response and the high solubility of the compounds in this solvent. The serum samples were made alkaline to ensure a un-ionized species for extraction, and the addition of the salt to increase the ionic strength improved the extractability of the compounds. Initial studies indicated that stable emulsions formed when serum was extracted with toluene alone. By adding a small amount of methanol to the first toluene extraction, the emulsion problem was eliminated and the extraction efficiency was not affected. When only the first toluene extractions were employed to remove I and II from the serum, acceptable results were obtained for high levels, *i.e.*, >150 ng/mL, of I or II. However, interfering serum components at the GC elution positions of I and II prevented the single extraction technique from providing acceptable results below 150-ng/mL levels. Acidification of the toluene extracts from the serum removed I and II from the organic phase. The aqueous phase was alkalinized, and I and II were extracted with toluene. The double extraction gave very clean GC–EC chromatograms, and the recovery of I and II from the serum was high considering the extensive cleanup procedure employed. Figure 2 presents representative chromatograms of a reference solution, a blank serum sample, and a serum sample fortified with 64 ng/mL of I and 58 ng/mL of II.

The final sample preparation procedure was validated by preparing and analyzing replicate serum samples with added I and II at 16 concentration levels. The concentration ranges were 8–1600 and 7–1440 ng/mL for I and II, respectively. The results for these analyses are summarized in Table I. The average amount found for I and II at each concentration level and the standard deviation and relative standard deviation of the average are presented. Linear regression of the average amount found *versus* the amount added gave the following equations and correlation coefficients: $y = 0.947x + 8.5$, $r = 0.999$ for I and $y = 0.981x - 0.6$, $r = 0.999$ for II.

A small interfering serum component was observed at the elution position of I and gave a y-intercept of 8.5 ng/mL for I. The level of this unknown component in the blank serum was uniform and, thus, the level of I can be obtained by substracting the amount of the interfering component in blank serum from the level of I in the samples. However, serum levels of I <10 ng/mL must be considered questionable due to the possible presence of the unknown serum component. The percent recovery (%R) of I and II added to the serum gave average recoveries of 93.5 ± 7.9 for I and 97.7 ± 8.5 for II, indicating that the extraction efficiencies for I, II, and the internal standard were very similar and that no corrections for recovery of I and II from serum were necessary. These data demonstrate that the sample preparation procedure and analytical technique can provide reliable quantitative data over a large concentration range and that the recovery of I and II extracted from serum is quantitative.

The analytical method was utilized to determine the serum levels of I and II in two dogs administered a single oral 10-mg/kg dose of I. Blood samples were obtained before dosing and at 0.25, 0.5, 1, 2, 4, and 8 h after dosing. The serum from each dog was assayed for I and II, and the results are presented graphically in Fig. 3. Little or no compound was detected until 2 h after dosing. The level of the parent drug (I) in the serum was considerably lower than the *N*-demethyl metabolite (II), indicating possible extensive first-pass metabolism in the liver. Since both I and II have been reported to have similar therapeutic effects (3), the combination of the serum levels of I and II must be used to determine the concentration of active drug substance.

The method was also employed to assess if the serum levels of I and II correlated with the oral dose for dogs considered to be under steady-state conditions. Four dogs at each of three dose levels (10, 3, and 1 mg/kg) and four control dogs were evaluated; blood samples were obtained at 1 and 4 h after dosing. The data indicate that the serum levels of the parent drug and its *N*-demethyl metabolite may increase with increasing dose for the 10- and 3-mg/kg levels (Table II). At the 1-mg/kg dose, the levels of I and II in the serum approached the sensitivity limit of the method. Figure 4 presents representative chromatograms of serum samples from dogs at each dose level. The limited number of serum samples analyzed precludes statistical evaluation of the correlation of serum levels of I and II to the administered dose of I.

REFERENCES

(1) S. Fielding and H. Lai (Eds.), "Industrial Pharmacology," Vol. 2, Futura, Mount Kisco, N.Y., 1975.

(2) C. Kaiser and P. E. Setler in "Burger's Medicinal Chemistry," 4th ed., Part III, M. E. Wolff, Ed., Wiley-Interscience, New York, N.Y., 1981, p. 997.

(3) J. Szmuszkovicz, P. F. von Voigtlander, and M. P. Kane, *J. Med. Chem.*, **24**, 1230 (1982).

Effect of pH on Theophylline Transfer Across the Everted Rat Jejunum

DANA F. PERRY *, PHILIP D. WALSON ‡¶, and JAMES BLANCHARD §x

Received July 7, 1980, from the *Departments of *Pharmacology and Toxicology, ‡Pediatrics, and §Pharmaceutical Sciences, Colleges of Pharmacy and Medicine, University of Arizona, Tucson, AZ 85721.* Accepted for publication January 10, 1983. ¶Present address: Departments of Pediatrics and Pharmacology, Columbus Children's Hospital, Columbus, OH 43205.

Abstract □ The effect of pH on the cumulative transfer of theophylline across the everted rat jejunum *in vitro* was ihvestigated. Intestinal integrity was assessed by light and scanning electron microscopy, while the biochemical viability of the intestine was evaluated using glucose transfer measurements. The initial (0–30 min) clearance of theophylline was directly proportional to the fraction un-ionized at pH 5.5, 7.4, 8.0, and 10.0. Plots of cumulative theophylline transfer *versus* time over 60 min were nonlinear, but could be subdivided into two linear segments of 30-min duration. Due to this nonlinearity, differences in theophylline transfer with pH were significant only over the first 30 min of the experiment. Intestinal tissue integrity and viability correlated with the time at which the clearance (slope) increased, while the magnitude of the increase in clearance was proportional to the degree of ionization of theophylline.

Keyphrases □ Theophylline—transfer across the everted-jejunum, rats, effect of pH □ Jejunum—everted, effect of pH on theophylline transfer, rats, □ pH—effect on the theophylline transfer across the everted jejunum, rats

Theophylline, a bronchodilator widely used for treating chronic obstructive pulmonary diseases such as asthma or emphysema, may be given orally or parenterally in the form of various salts. Although theophylline is usually given orally, its absorption from the GI tract can be erratic. Nausea and gastric irritation often accompany the oral

0022-3549/84/0300-0320$01.00/0

© 1984, American Pharmaceutical Association

technique. The sensitivity of the GC–EC (signal to noise ratio >5:1) was demonstrated to be <10 ng/mL for I and II. Assuming an initial serum volume of 1.0 mL and a final sample volume of 0.1 mL, the analytical technique can detect and quantify 1 ng/mL of serum for I and II.

The sample preparation procedure for the extraction of I and II from serum was developed through a series of experiments. The choice of toluene as the extraction solvent was made because of its low EC response and the high solubility of the compounds in this solvent. The serum samples were made alkaline to ensure a un-ionized species for extraction, and the addition of the salt to increase the ionic strength improved the extractability of the compounds. Initial studies indicated that stable emulsions formed when serum was extracted with toluene alone. By adding a small amount of methanol to the first toluene extraction, the emulsion problem was eliminated and the extraction efficiency was not affected. When only the first toluene extractions were employed to remove I and II from the serum, acceptable results were obtained for high levels, *i.e.*, >150 ng/mL, of I or II. However, interfering serum components at the GC elution positions of I and II prevented the single extraction technique from providing acceptable results below 150-ng/mL levels. Acidification of the toluene extracts from the serum removed I and II from the organic phase. The aqueous phase was alkalinized, and I and II were extracted with toluene. The double extraction gave very clean GC–EC chromatograms, and the recovery of I and II from the serum was high considering the extensive cleanup procedure employed. Figure 2 presents representative chromatograms of a reference solution, a blank serum sample, and a serum sample fortified with 64 ng/mL of I and 58 ng/mL of II.

The final sample preparation procedure was validated by preparing and analyzing replicate serum samples with added I and II at 16 concentration levels. The concentration ranges were 8–1600 and 7–1440 ng/mL for I and II, respectively. The results for these analyses are summarized in Table I. The average amount found for I and II at each concentration level and the standard deviation and relative standard deviation of the average are presented. Linear regression of the average amount found *versus* the amount added gave the following equations and correlation coefficients: $y = 0.947x + 8.5$, $r = 0.999$ for I and $y = 0.981x - 0.6$, $r = 0.999$ for II.

A small interfering serum component was observed at the elution position of I and gave a y-intercept of 8.5 ng/mL for I. The level of this unknown component in the blank serum was uniform and, thus, the level of I can be obtained by substracting the amount of the interfering component in blank serum from the level of I in the samples. However, serum levels of I <10 ng/mL must be considered questionable due to the possible presence of the unknown serum component. The percent recovery (%R) of I and II added to the serum gave average recoveries of 93.5 ± 7.9 for I and 97.7 ± 8.5 for II, indicating that the extraction efficiencies for I, II, and the internal standard were very similar and that no corrections for recovery of I and II from serum were necessary. These data demonstrate that the sample preparation procedure and analytical technique can provide reliable quantitative data over a large concentration range and that the recovery of I and II extracted from serum is quantitative.

The analytical method was utilized to determine the serum levels of I and II in two dogs administered a single oral 10-mg/kg dose of I. Blood samples were obtained before dosing and at 0.25, 0.5, 1, 2, 4, and 8 h after dosing. The serum from each dog was assayed for I and II, and the results are presented graphically in Fig. 3. Little or no compound was detected until 2 h after dosing. The level of the parent drug (I) in the serum was considerably lower than the *N*-demethyl metabolite (II), indicating possible extensive first-pass metabolism in the liver. Since both I and II have been reported to have similar therapeutic effects (3), the combination of the serum levels of I and II must be used to determine the concentration of active drug substance.

The method was also employed to assess if the serum levels of I and II correlated with the oral dose for dogs considered to be under steady-state conditions. Four dogs at each of three dose levels (10, 3, and 1 mg/kg) and four control dogs were evaluated; blood samples were obtained at 1 and 4 h after dosing. The data indicate that the serum levels of the parent drug and its *N*-demethyl metabolite may increase with increasing dose for the 10- and 3-mg/kg levels (Table II). At the 1-mg/kg dose, the levels of I and II in the serum approached the sensitivity limit of the method. Figure 4 presents representative chromatograms of serum samples from dogs at each dose level. The limited number of serum samples analyzed precludes statistical evaluation of the correlation of serum levels of I and II to the administered dose of I.

REFERENCES

(1) S. Fielding and H. Lai (Eds.), "Industrial Pharmacology," Vol. 2, Futura, Mount Kisco, N.Y., 1975.

(2) C. Kaiser and P. E. Setler in "Burger's Medicinal Chemistry," 4th ed., Part III, M. E. Wolff, Ed., Wiley-Interscience, New York, N.Y., 1981, p. 997.

(3) J. Szmuszkovicz, P. F. von Voigtlander, and M. P. Kane, *J. Med. Chem.*, **24**, 1230 (1982).

Effect of pH on Theophylline Transfer Across the Everted Rat Jejunum

DANA F. PERRY *, PHILIP D. WALSON ‡¶, and JAMES BLANCHARD §x

Received July 7, 1980, from the *Departments of *Pharmacology and Toxicology, ‡Pediatrics, and §Pharmaceutical Sciences, Colleges of Pharmacy and Medicine, University of Arizona, Tucson, AZ 85721.* Accepted for publication January 10, 1983. ¶Present address: Departments of Pediatrics and Pharmacology, Columbus Children's Hospital, Columbus, OH 43205.

Abstract □ The effect of pH on the cumulative transfer of theophylline across the everted rat jejunum *in vitro* was ihvestigated. Intestinal integrity was assessed by light and scanning electron microscopy, while the biochemical viability of the intestine was evaluated using glucose transfer measurements. The initial (0–30 min) clearance of theophylline was directly proportional to the fraction un-ionized at pH 5.5, 7.4, 8.0, and 10.0. Plots of cumulative theophylline transfer *versus* time over 60 min were nonlinear, but could be subdivided into two linear segments of 30-min duration. Due to this nonlinearity, differences in theophylline transfer with pH were significant only over the first 30 min of the experiment. Intestinal tissue integrity and viability correlated with the time at which the clearance (slope) increased, while the magnitude of the increase in clearance was proportional to the degree of ionization of theophylline.

Keyphrases □ Theophylline—transfer across the everted-jejunum, rats, effect of pH □ Jejunum—everted, effect of pH on theophylline transfer, rats, □ pH—effect on the theophylline transfer across the everted jejunum, rats

Theophylline, a bronchodilator widely used for treating chronic obstructive pulmonary diseases such as asthma or emphysema, may be given orally or parenterally in the form of various salts. Although theophylline is usually given orally, its absorption from the GI tract can be erratic. Nausea and gastric irritation often accompany the oral

0022-3549/84/0300-0320$01.00/0

© 1984, American Pharmaceutical Association

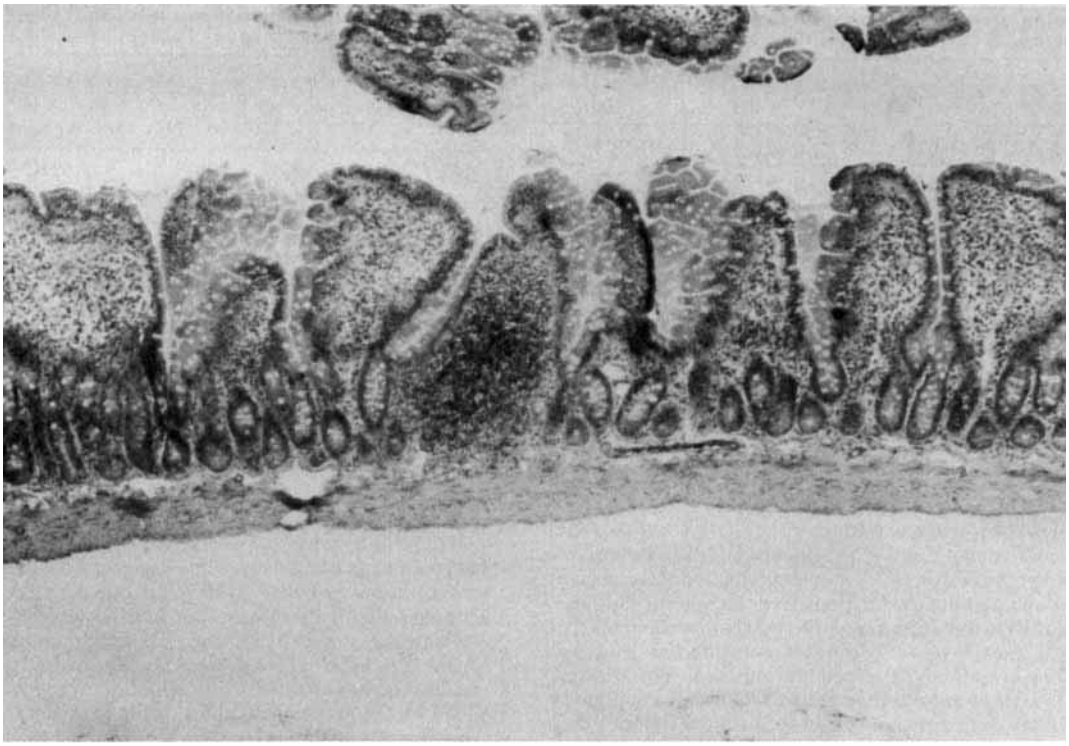

A

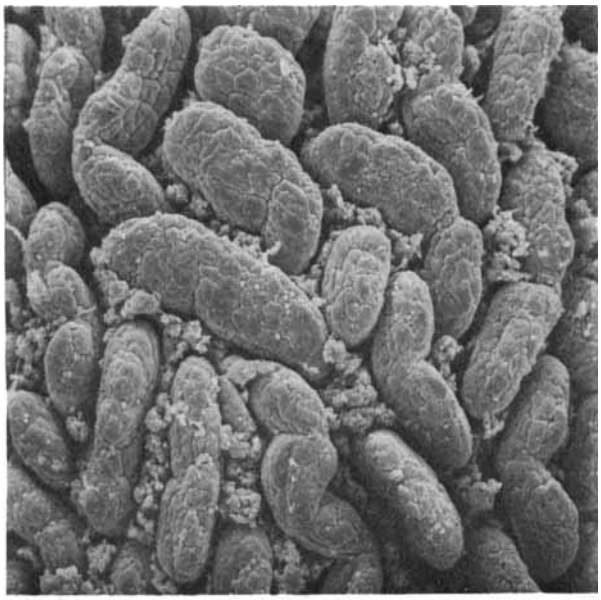

B

Figure 1—(*A*) *Details of intestinal villus immediately* (t = *0*) *following eversion (original magnification 800×). (B) Scanning electron micrograph showing surface detail of everted intestine* (t = *0*).

administration of theophylline, a condition which is frequently treated with antacids. A recent study by Shargel *et al.* (1) indicated that the concurrent administration of 15 mL of magnesium aluminum hydroxide antacid did not significantly affect the pharmacokinetics of theophylline. This result contrasts with the work of Arnold *et al.* (2) who reported that 30 mL of magnesium aluminum hydroxide suspension significantly decreased the absorption rate constant for theophylline. Furthermore, a study by Rohr *et al.* (3) indicated that theophylline may be adsorbed onto some antacid materials but not others. Since antacids can possibly alter the GI absorption (4) of drugs, it was of interest to determine how changes in the pH might alter the absorption of theophylline.

Several studies (5–7) have previously demonstrated the utility of everted intestinal preparations for evaluating the *in vitro* absorbability of drugs and nutrients and how various factors influence this process. In this report, cannulated everted jejunal segments of rat intestine (8) were used to evaluate the influence of pH on theophylline transfer. The structural integrity and biochemical viability of the intestinal segments were monitored by means of light and scanning electron microscopy and by measuring the rates of active glucose transfer, respectively.

EXPERIMENTAL

Reagents—The following reagent-grade chemicals were employed: theophylline[1], 1-[2-(β-D-glucopyranosyloxy)-4,6-dihydroxyphenyl]-3-

[1] Sigma Chemical Co., St. Louis, MO 63178.

Table I—Effect of pH on Theophylline Transfer Across the Everted Rat Jejunum

Time, min	pH 5.5	pH 7.4	pH 8.0	pH 10.0
10	0.117 ± 0.30[a]	0.099 ± .047	0.071 ± .016	0.052 ± .016
20	0.278 ± .030	0.256 ± .065	0.187 ± .034	0.137 ± .056
30	0.476 ± .074	0.443 ± .097	0.335 ± .062	0.264 ± .076
40	0.671 ± .118	0.653 ± .128	0.502 ± .083	0.446 ± .084
50	0.861 ± .166	0.879 ± .160	0.695 ± .102	0.668 ± 0.93
60	1.05 ± .217	1.10 ± .199	0.898 ± .130	0.910 ± .107

[a] Values represent the cumulative micrograms of theophylline transferred per unit mucosal concentration ±*SD*. All values represent the mean of six segments (proximal and distal combined) except at pH 7.4 and 8.0 where eight segments were used. A one-way analysis of variance was performed on the data to test for significant differences between means at a given time point. Bars enclosing values indicate means are not significantly different ($p > 0.05$). Means not connected are significantly different ($p < 0.05$) from each other.

(4-hydroxyphenyl)-1-propanone (phlorizin)[1], 3-*O*-methyl-D-[1-^{3}H]-glucose (I)[2], glucose[3], and acetonitrile[4]. Monobasic sodium phosphate monohydrate, anhydrous dibasic sodium phosphate, sodium carbonate, and sodium bicarbonate were used in preparing the isotonic buffers.

Preparation of Everted Jejunum—Everted jejunal segments from nonfasted Sprague–Dawley rats of both sexes, weighing 150–300 g, were prepared according to methods described previously (8). The intestines were removed from ether-anesthetized animals following a midline abdominal incision and transection of the intestine at the pyloric and ileocecal junctions. The proximal 30 cm of unstretched intestine was discarded to prevent inclusion of the bile duct. The next 30 cm was separated, rinsed in physiological saline at 37°C, then cut into two 15-cm segments designated as proximal and distal in reference to their original position relative to the pyloric junction.

The everted segments were positioned on the perfusion apparatus as described previously (8), and the total assembly time following removal was 7–10 min. The serosal surfaces were rinsed with 25 mL of serosal buffer solution prior to the first collection. Buffer pH was measured[5] before and after each experiment. Oxygen was bubbled through the mucosal solutions continually. Serosal and mucosal buffer solutions were warmed to 37°C prior to coming in contact with the tissue. Serosal buffer samples (5 mL) were collected at 10-min intervals for 1 h and replaced with fresh buffer within 20 s.

Buffer Composition—A Modified Krebs–Henseleit phosphate buffer was used for all experiments conducted at pH 5.5, 7.4, and 8.0 (9). This buffer was chosen instead of the Krebs bicarbonate, which reportedly provides the best environment for maintaining the viability of the intestine (10), because bicarbonate buffer does not function optimally over the pH range of 5.5–8.0. Experiments conducted at pH 10 used the same Krebs–Henseleit electrolyte solution except that the phosphate buffer was replaced by an equimolar amount of carbonate–bicarbonate buffer (9). Calcium ion was deleted from the buffer solution due to its tendency to precipitate in the presence of phosphate at pH >7.4. The absence of calcium ion was observed to have no effect on drug transfer. Glucose at a concentration of 130 mg% (7 mM) was added to the mucosal buffer only.

Preparation of Tissue Samples for Histological Evaluation—Histology was performed on jejunal segments immediately after eversion ($t = 0$ min) and after 60 min of incubation in a pH 7.4 phosphate buffer ($t = 60$ min). Everted intestinal segments were also examined using light microscopy after 30 min incubation at pH 5.5, 8, and 10. Specimens for light microscopy were fixed in 10% w/v buffered formalin, paraffin sectioned, and stained with hematoxylin and eosin. Specimens for scanning electron microscopy[6] were fixed in isotonic Karnofsky's solution and stained with 1% w/v osmium tetroxide prior to critical point drying from acetone. These specimens were sputter-coated with gold to a thickness of 300 Å and examined.

Transport of 3-*O*-Methyl-D-[1-^{3}H] glucose—The transport of tritiated 3-*O*-methyl-D-glucose (I), specific activity 2 Ci/mmol, was determined using liquid scintillation counting. Fifty microliters of 3-*O*-methyl-D-glucose (1 mCi/mL) was added to each 100 mL of buffer. This solution was used as the mucosal buffer for each intestinal segment. Two segments also has phlorizin (a specific inhibitor of glucose transport) added to give a final concentration of 1 mM, and two did not. The serosal and mucosal concentrations of I were measured by placing 1-mL aliquots of each solution into vials, adding 10 mL of liquid scintillation cocktail[7], and counting in a liquid scintillation counter[8] for 10 min. Intestinal tissue concentrations of I were measured by weighing accurately ~100 mg of jejunum (~1 cm) after rinsing and blotting with absorbant tissue. Samples were digested in a counting vial by the addition of 0.5 mL of 0.6 M NaOH. Ten milliliters of cocktail and 1 mL of water were then added, and the vial was counted for 10 min. Counting efficiencies were determined by the external standard method. Tissue radioactivity was expressed as disintegrations per min per mg of wet tissue (dpm/mg) divided by the mucosal concentrations of I in dpm/mL. D-glucose levels were determined in duplicate in an automated glucose analyzer[9] using the glucose oxidase method.

Table II—Ionization and Mean Intestinal Clearances (±*SD*) for Theophylline at Various pH Values

pH	Un-ionized[a], %	Clearance (mL/min) × 10^2 Period I (0–30 min)	Clearance (mL/min) × 10^2 Period II (30–60 min)	Clearance Ratio (Period II/Period I)
5.5	99.90	1.794 (0.38)	1.894 (0.50)	1.051 (0.11)
7.4	92.64	1.721 (0.31)	2.236 (0.43)	1.309 (0.18)
8.0	75.97	1.321 (0.25)	1.981 (0.27)	1.526 (0.24)
10.0	3.07	1.058 (0.30)	2.328 (0.36)	2.378 (0.82)

[a] The degree of ionization of theophylline was calculated from the Henderson–Hasselbalch equation, using a pK_a of 8.5 (20).

Theophylline Assay—Theophylline analyses were performed using an HPLC assay. A reverse-phase HPLC column[10], 4 mm i.d. × 30 cm, was used. The mobile phase of acetonitrile–water–acetic acid (10:89:1 v/v/v) was pumped[11] through the column at a flow rate of 3 mL/min. Detection of eluted theophylline was accomplished at 280 nm using a *fixed-wavelength detector*[12].

Aliquots (25 μL) of serosal buffer solution were injected directly onto the column. Quantitation was performed by comparing measured peak heights against a standard curve of theophylline peak height *versus* concentration. Samples were either assayed immediately or frozen at −20°C until analyzed. Theophylline concentrations were stable for 7–10 d under these storage conditions.

Measurement of Cumulative Transfer Rates—Theophylline transfer across the everted intestine was expressed as a cumulative mucosal to serosal clearance (transfer rate constant). In essence:

$$\text{Clearance (mL/min)} = \frac{\text{cumulative amount } (\mu g) \text{ transferred per } t \text{ min}}{\text{mucosal concentration } (\mu g/mL) \times t} \quad \text{(Eq. 1)}$$

The clearances were actually determined from the slopes of the plots of the cumulative amount of theophylline transferred per unit mucosal concentration *versus* time. The slopes of these plots were calculated using least-squares linear regression.

The average cumulative amount (μg) of theophylline transferred (±*SD*) was calculated at each 10-min interval throughout the course of the 60-min experiments for the various pH values tested, as shown in Table I. These data were subjected to a one-way analysis of variance (ANOVA) to detect any significant differences in clearance between the various pH values over a given time interval. The level of significance used for all analyses was $p < 0.05$. The Tukey test was employed *post hoc* to determine where pair-wise differences between means existed (11).

RESULTS AND DISCUSSION

The viability and structural integrity of an *in vitro* model must be considered when interpreting data from such a system (12, 13). Viability of the rat jejunal model has been characterized by many investigators.

[2] Amersham Radiochemical, Arlington Heights, IL 60006.
[3] Matheson, Coleman and Bell, Norwood, OH 45212.
[4] Burdick and Jackson Laboratories, Muskegon, MI 49422.
[5] pHasar Digital pH Meter, Beckman Instruments, Fullerton, CA 92634.
[6] ETEC Autoscan, ETEC Corp., Hayward, CA 94545.
[7] Beckman GP, Beckman Instruments, Fullerton, CA 92634.
[8] Model LS-3133P, Beckman Instruments, Fullerton, CA 92634.
[9] Glucose Analyzer I, Beckman Instruments, Fullerton, CA 92634.
[10] μBondapak-C_{18}, Waters Associates, Milford, MA 01757.
[11] Model 6000-A pump, Waters Associates, Milford, MA 01757.
[12] Model 400, Waters Associates, Milford, MA 01757.

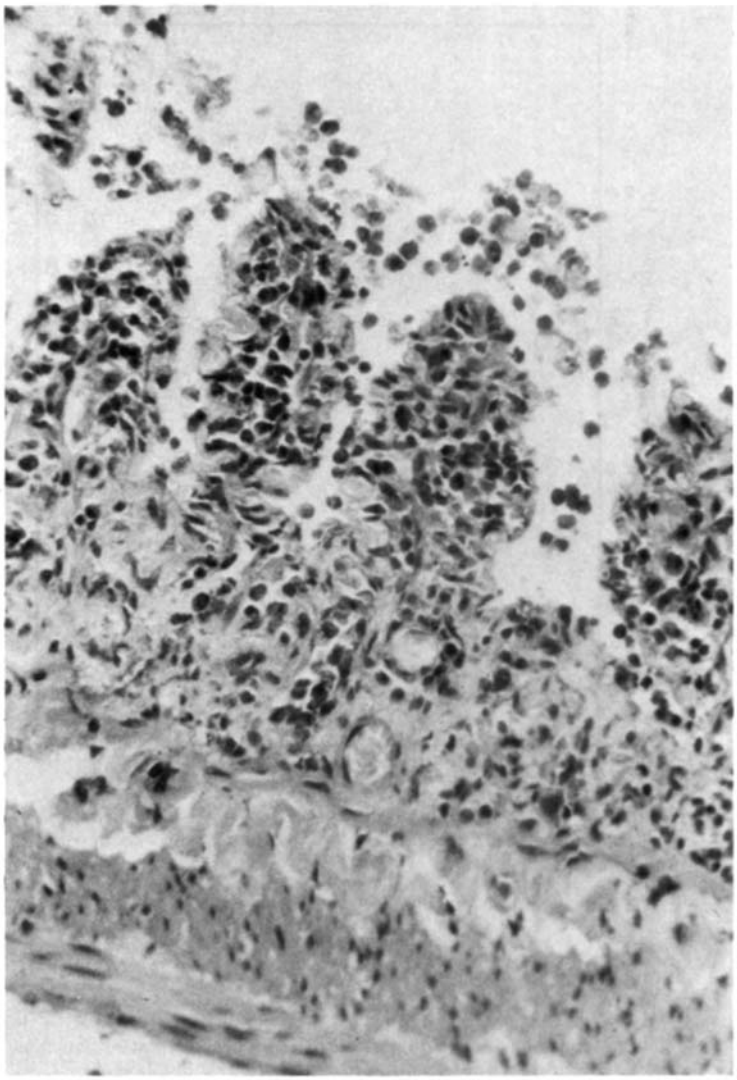

A

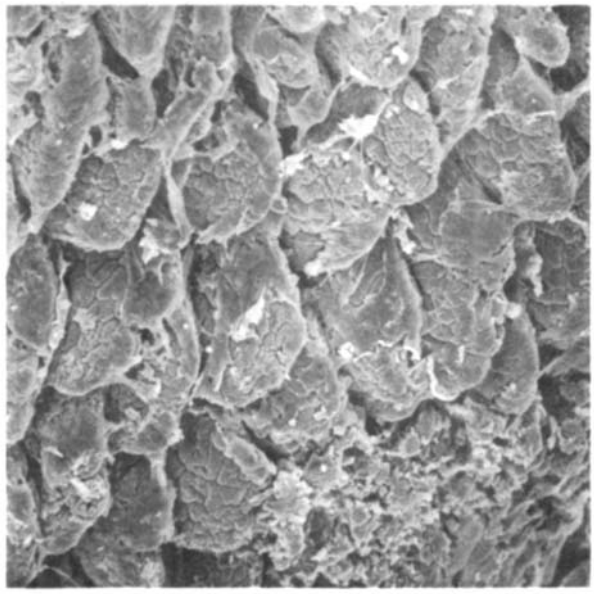

B

Figure 2—(*A*) *Appearance of intestinal villus after 60-min incubation at 37°C in pH 7.4 phosphate buffer (original magnification 800×). (B) Scanning electron micrograph of intestinal segment after 60-min incubation at 37°C in pH 7.4 phosphate buffer.*

It has been shown that oxygen uptake is linear for 1–3 h (14, 15), and that active uptake of L-histidine and iodine-131 (14), as well as linear active uptake of D-glucose, occur for up to 1 h (16).

In this study, the structural integrity of the everted rat jejunum was evaluated using both light and scanning electron microscopy. Intestinal segments were examined immediately after eversion (t = 0 min) and after 60 min of incubation in isotonic pH 7.4 phosphate buffer (t = 60 min). At t = 0 min, sections examined by light microscopy had good cytoplasmic and nuclear detail and good detail in submucosal structures (Fig. 1A). Examination by scanning electron microscopy also showed normal surface morphology with well-defined and well-separated villi and no evidence of gross damage (Fig. 1B). After a 60-min incubation, light microscopy revealed minimal disruption of submucosal or muscle layers, but a substantial disruption of the villous epithelium and areas where the basement membrane had separated from the lamina propria (Fig. 2A). Electron microscopy also demonstrated changes in villous structure (Fig. 2B). Everted intestinal segments incubated at pH 5.5, 8, and 10 for 30 min exhibited no gross morphological changes when examined using light microscopy.

The functional integrity of the everted rat jejunum was evaluated by determining the active transport of glucose and I. Since the active transport of glucose by the small intestine *in vitro* is known to require intact, functioning intestinal epithelial cells (17), the rate of appearance of glucose on the serosal side of the preparation over the 60-min incubation period was used as a measure of the biochemical and structural state of the epithelium.

The intestinal transport of glucose at pH 7.4 demonstrated that the amount of glucose appearing in the serosal fluid rose from an initial value at t = 0 min to a maximum at 30 min, then declined back to the initial value by 60 min. This coincides with the findings of Porteus and Pritchard (16) who observed that the rates of glucose transport by the intact intestine increased linearly to 30 min, then slowly decreased to zero by 60 min. The concentration gradient present in the direction of transport (*i.e.*, mucosal to serosal) was disregarded since the *in vitro* small intestine actively transports glucose 10–20 times faster than its rate of diffusion (18). Furthermore, at concentrations of ≤500 mg%, the rate of passive glucose transport up or down a concentration gradient is of the same order of magnitude (18).

The biphasic glucose transfer observed here was taken as evidence of a functioning active-transport system. This is supported by the fact that transport was eliminated when phlorizin, a specific inhibitor of active transport, was added to the mucosal solution. The rates of glucose transfer in the presence of phlorizin were considered to be those maximally obtainable by diffusion alone. Since there was no increase in transfer from 0 to 60 min, in the presence of phlorizin, it was concluded that the integrity of the intestinal membrane was not compromised to the extent of becoming "leaky" toward the relatively small (mol. wt. = 180), hydrophilic glucose molecule.

To examine the role of any metabolic utilization and/or transport of endogenous glucose stores by the intestine, experiments were conducted to measure the transport of I. This glucose analogue is actively transported by the same system that transports glucose across the intestine; however, it is not metabolized by the intestine (19). The transport of I showed a biphasic pattern similar to that found for glucose. In addition, the average tissue concentration of I in the presence of phlorizin was about one-seventh (0.5 *versus* 3.4 dpm/mg of tissue per 10^6 dpm in buffer) the control value. These data indicated that the biphasic nature of the transport curves was not due to the metabolism of glucose by the jejunal segments since I, which was not metabolized, exhibited a similar transport pattern. The histological studies and the biphasic transport of glucose

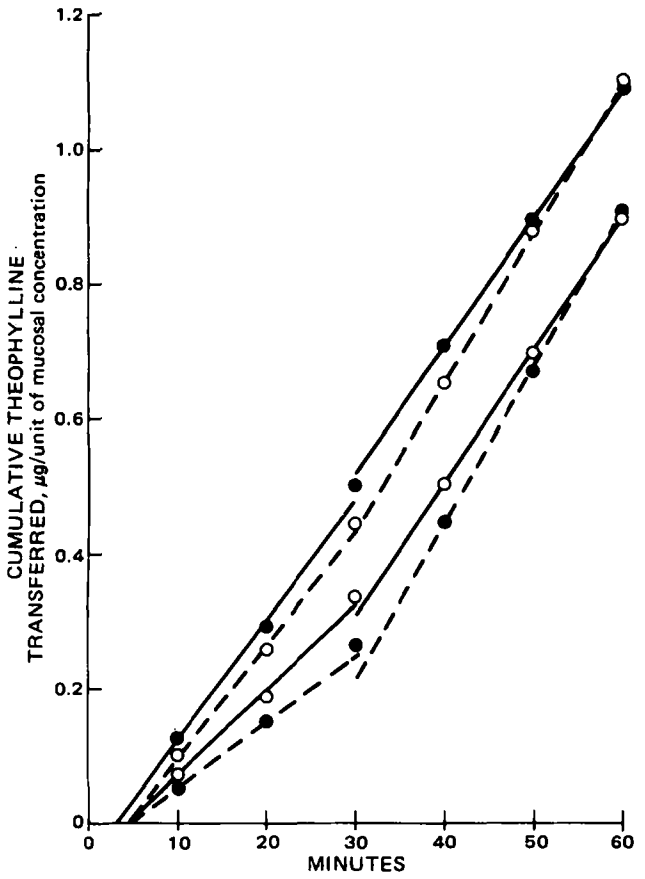

Figure 3—*Cumulative transfer of theophylline across the everted rat jejunum at various pH values as a function of time. All values represent the mean of six segments (proximal and distal combined) except at pH 7.4 and 8.0 where eight segments were used. Error bars are deleted for clarity. Key: (●—●) pH 5.5; (○- - -○) pH 7.4; (○—○) pH 8.0; (●- - -●) pH 10.0.*

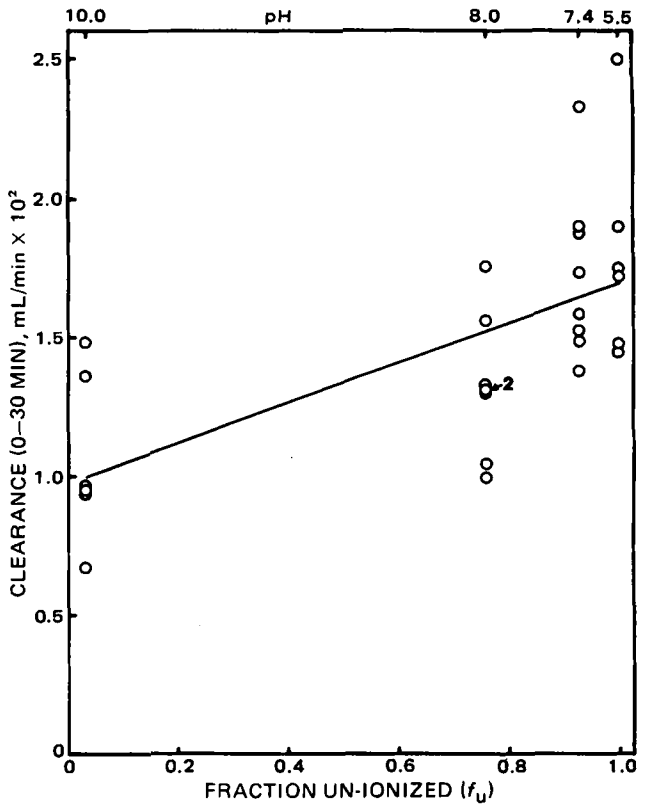

Figure 4—*Relationship between the initial (0–30-min) clearance of theophylline across the everted rat jejunum and its theoretical fraction un-ionized,* f_u *(r = 0.6375; p < 0.0005).*

and I, together with their inhibition by phlorizin, were taken as evidence that the preparation was biochemically intact up to 30 min, but that after 30 min the functional integrity was decreased, and by 60 min there were signs of both functional and structural disruption.

Effects of pH on Theophylline Transfer Rates—The transfer of theophylline appears to follow zero-order kinetics as is shown by the linear segments of the plots shown in Fig. 3. This linear transfer occurred because the concentration of theophylline in the mucosal solution remained essentially constant and was much higher than that in the serosal solution during the course of the experiment. This was achieved by replacing the serosal fluid at 10-min intervals and by using a large volume of mucosal solution relative to serosal solution. The intestinal clearances of theophylline at various pH values are shown in Table II.

Due to the biphasic nature of theophylline clearance over the 60-min time course of the experiments it was not possible to obtain the clearance at each experimental pH using transfer data from all the time points. Examination of Fig. 3 revealed that the slope of the clearance curve began to increase after 30 min for all pH values tested. This change in slope was such that transfer rates at different pH values were statistically nonsignificant ($p > 0.05$) after the first 40 min. Prior to the 30-min time point, the transfer of theophylline at all pH values tested was judged to be sufficiently linear (*i.e.*, all lines had $r^2 \geq 0.95$) to derive a clearance. Therefore, clearance values for all experiments were derived from the cumulative amount of theophylline transferred in the first 30 min. These initial theophylline clearances were directly proportional to the fraction un-ionized (f_u) as shown in Fig. 4.

If we assume that both the ionized and un-ionized forms of theophylline are capable of being transported across the everted rat jejunal membrane then the total clearance (CL_t) can be expressed as:

$$CL_t = f_i CL_i + f_u CL_u \qquad \text{(Eq. 2)}$$

wher CL_i and CL_u represent the clearances of the ionized and un-ionized species, respectively, and f_i and f_u are the fractions of the drug present in the ionized and un-ionized forms, respectively. Since:

$$f_i = (1 - f_u) \qquad \text{(Eq. 3)}$$

it follows that:

$$CL_t = CL_i + (CL_u - CL_i) f_u \qquad \text{(Eq. 4)}$$

Thus, from Eq. 4, it is evident that in a plot of CL_t *versus* f_u, such as Fig. 4, the intercepts at $f_u = 0$ and $f_u = 1$ will represent CL_i and CL_u, respectively.

Using this approach, linear regression of the data in Fig. 4 indicated that CL_u and CL_i were equal to 1.693×10^{-2} and 0.978×10^{-2} mL/min, respectively. Thus, the ratio of intrinsic clearances for these two species in the 0–30-min time period was $CL_u/CL_i = 1.732$. It is possible that undetected intestinal tissue damage may have occurred which could have artificially altered some of the clearance data in Fig. 4. However, the excellent agreement of the CL_u/CL_i ratio with the value recently reported by Crommelin *et al.* (21) for theophylline transfer across the rat rectum indicates that if such alterations did occur, their effects on theophylline transfer were minor. These authors reported values for the absorption rate constants of the un-ionized and ionized forms of theophylline which were very similar (*i.e.*, $K_u/K_i = 0.805$ and 1.13) and concluded that the absorption rates of the two forms "do not differ much." Our value is also similar in magnitude to the value (1.905) found for lidocaine at pH 6.4 and 7.4 by Cascella and Feldman (22) and to the values that Crouthamel *et al.* (23) calculated for sulfaethidole (5.56) and barbital (3.08) over the pH range of 5.15–8.52. The results indicate that the ionized forms of these compounds cross the *in vitro* rat intestine at a rate which is comparable with that of their un-ionized forms, a condition which may or may not exist *in vivo*. In fact, Turner *et al.* (24) noted that ionized species are more easily transferred across *in vitro* membrane systems, such as the one utilized here, than they are across *in vivo* membranes.

The use of the early time points to determine clearance values has been proposed by other authors (13) who recognized the phenomenon of increasing clearance with time. The assumption that the initial transfer rates are a more appropriate measure of clearance across the everted intestine than those obtained using the total amount of solute transferred over the course of a typical experiment (*i.e.*, 60 min) was also reached independently by Benet *et al.* (10) and is consistent with the assessment of the everted intestine as a method for studying drug transfer made by Levine *et al.* (12).

In our experiments, we observed that only the initial (0–30 min) transfer rates were pH dependent. Therefore, structural integrity of the everted intestine appeared to be necessary to demonstrate the effect of pH on theophylline transport. In contrast, the biochemical integrity of the intestinal segment was relatively unimportant in affecting the transfer of theophylline, since this compound is believed to be transported passively (25).

The change in theophylline clearance across the intestine was observed to increase as the pH increased, as shown by the data in Table II. There was also a time-dependent increase in the clearance at all pH values. This was believed to be due to a time-dependent degradation of the intestinal membrane, which resulted in an increased permeability of the membrane for theophylline, apparently due to a loss of structural integrity of the membrane.

One possible explanation for these observations is that the epithelial and the underlying connective and muscle tissue barriers are both intact only over the first 30 min of the experiment (26, 27), during which time the epithelial barrier is rate limiting (27). This is substantiated somewhat by Fig. 4, in which the initial clearance values are directly proportional to the fraction of theophylline un-ionized, which would be predicted from the pH-partition hypothesis (28). After 30-min incubation, the epithelial barrier may no longer be intact, with the result that the clearance in the 30–60-min time period (period II) is increased at all pH values relative to the corresponding 0–30-min (period I) clearance. Since the ionized form of the drug is less permeable than the un-ionized form, any disruption of the epithelial barrier would be expected to result in a more pronounced change in the clearance of this species. The relatively small effect of changes in the structural integrity of the intestinal membrane on the transfer rates of the un-ionized species over the 30–60-min period, observed at low pH, is consistent with previous suggestions that the epithelium is not the rate-limiting barrier to the transfer of nonpolar, lipid-soluble molecules (such as un-ionized theophylline) across this membrane model (13).

CONCLUSIONS

It has been shown that pH alters the initial (0–30-min) transfer of theophylline across the everted rat jejunum. The cumulative amount of theophylline transferred over the first 30 min was directly proportional to the calculated un-ionized fraction. A time-dependent change in transfer rate was also demonstrated which correlated with the structural integrity of the preparation. These results indicate that intestinal transfer rates measured during the first 30 min may be more valid than measurements taken over longer time periods. The ionized form of theophylline appears to be transported across the everted rat intestine *in vitro* at a rate comparable with that of the un-ionized form.

REFERENCES

(1) L. Shargel, J. A. Stevens, J. E. Fuchs, and A. B. C. Yu, *J. Pharm. Sci.*, **70,** 599 (1981).

(2) L. A. Arnold, G. H. Spurbeck, W. H. Shelver, and W. M. Henderson, *Am. J. Hosp. Pharm.*, **36,** 1059 (1979).

(3) W. J. Rohr, Jr., W. M. Henderson, and W. H. Shelver, *Am. J. Hosp. Pharm.*, **38,** 1779 (1981).

(4) J. A. Romankiewicz, *Primary Care*, **3,** 537 (1976).

(5) R. K. Crane and T. H. Wilson, *J. Appl. Physiol.*, **12,** 145 (1958).

(6) S. A. Kaplan and S. Cotler, *J. Pharm. Sci.*, **61,** 1361 (1972).

(7) D. S. Parsons, Methods for Investigation of Intestinal Absorption in "Handbook of Physiology," vol. 3, Sec. 6, C. F. Code, Ed., American Physiological Society, Washington, D.C., 1968, Chap. 64.

(8) J. Blanchard and A. Straussner, *Acta Pharm. Suecica*, **14,** 279 (1977).

(9) G. Gomori, in "Methods in Enzymology," S. P. Colowick and N. O. Kaplan, Eds., vol. 1, Academic, New York, N.Y., 1955, pp. 138–146.

(10) L. Z. Benet, J. M. Orr, R. H. Turner, and H. S. Webb, *J. Pharm. Sci.*, **60,** 234 (1971).

(11) B. J. Winer, "Statistical Principles in Experimental Design," 1st ed., McGraw-Hill, New York, N.Y., 1962, p. 80.

(12) R. R. Levine, W. F. McNary, P. J. Kornguth, and R. LeBlanc, *Eur. J. Pharmacol.*, **9,** 211 (1970).

(13) M. Gibaldi and B. Grundhofer, *J. Pharm. Sci.*, **61,** 116 (1972).

(14) D. R. Bamford, *Proc. R. Soc. London, Ser. B*, **166,** 30 (1966).

(15) T. H. Wilson and G. Wiseman, *J. Physiol. (London)*, **123,** 116 (1954).

(16) J. W. Porteus and P. Pritchard, *Proc. Biochem. Soc.*, **127,** 61P (1972).

(17) R. K. Crane and P. Mandelstam, *Biochim. Biophys. Acta*, **45,** 460 (1960).

(18) T. H. Wilson, "Intestinal Absorption," W. B. Saunders, Philadelphia, Pa., 1962, chap. 4.

(19) T. H. Wilson and T. N. Vincent, *J. Biol. Chem.*, **216,** 851 (1955).

(20) F. Bergmann, D. Lichtenberg, and Z. Neiman, in "The Jerusalem Symposia on Quantum Chemistry and Biochemistry," E. D. Bergmann and F. Pullman, Eds., vol. 4, Academic, New York, N.Y., 1972, pp. 264–276.

(21) D. J. A. Crommelin, J. Modderkolk, and C. J. de Blaey, *Int. J. Pharmaceut.*, **3,** 299 (1979).

(22) P. J. Cascella and S. Feldman, *J. Pharm. Sci.*, **69,** 643 (1980).

(23) W. G. Crouthamel, G. H. Tan, L. W. Dittert, and J. T. Doluisio, *J. Pharm. Sci.*, **60,** 1160 (1971).

(24) R. H. Turner, S. C. Mehta, and L. Z. Benet, *J. Pharm. Sci.*, **59,** 592 (1970).

(25) D. R. Sanvordeker, *J. Pharm. Sci.*, **67,** 1459 (1978).

(26) D. L. Wolfe, S. C. Forland, and L. Z. Benet, *J. Pharm. Sci.*, **62,** 200 (1973).

(27) R. K. Nayak and L. Z. Benet, *J. Pharm. Sci.*, **60,** 1508 (1971).

(28) C. A. M. Hogben, D. J. Tocco, B. B. Brodie, and L. S. Schanker, *J. Pharmacol. Exp. Ther.*, **125,** 275 (1959).

Relative Bioavailability and Pharmacokinetics: A Combination of Pentazocine and Acetaminophen

ALAN K. FRITZ, DAVID P. BENZIGER, JAMES E. PETERSON, GEORGE B. PARK, and JEROME EDELSON ˣ

Received November 15, 1982, from the *Department of Drug Metabolism, Sterling-Winthrop Research Institute, Rensselaer, NY 12144.* Accepted for publication January 26, 1983.

Abstract □ The relative bioavailability and pharmacokinetics of a combination product containing pentazocine and acetaminophen were studied in 20 healthy human males. Each subject, in a single-dose three-way crossover design, received two different preparations containing 50 mg of pentazocine (as base) and 1300 mg of acetaminophen either as capsule-shaped tablets or as a solution. Plasma concentrations of pentazocine and acetaminophen were determined from 0.25 to 12 h following oral administration. The plasma data for both compounds in the tablet formulation were described by an open one-compartment body model with first-order absorption. The average ($\pm SD$) bioavailability of the tablet relative to that of the solution was 85.0 ± 31.1 and 88.6 ± 13.1% for pentazocine and acetaminophen, respectively. The apparent first-order regression-dependent elimination rate constants for pentazocine from the tablet and solution preparations were 0.19 ± 0.08 and 0.20 ± 0.06 h^{-1}, respectively, while the rate constants for acetaminophen were 0.26 ± 0.03 and 0.25 ± 0.03 h^{-1} for the tablet and solution preparations, respectively. These rate constants correspond to terminal elimination half-lives of ~3.6 h for pentazocine and ~2.7 h for acetaminophen.

Keyphrases □ Pentazocine—relative bioavailability, pharmacokinetics, coadministration with acetaminophen □ Acetaminophen—relative bioavailability, pharmacokinetics, coadministration with pentazocine □ Bioavailability—relative, coadministered pentazocine and acetaminophen, pharmacokinetics □ Pharmacokinetics—coadministered pentazocine and acetaminophen, relative bioavailability

Pentazocine, a weak narcotic antagonist, is a potent analgesic in humans. The analgesic efficacy of both oral (1, 2) and parenteral (3–8) formulations of pentazocine is well documented. Acetaminophen is commonly used as a mild analgesic and antipyretic (9, 10). Both pentazocine and acetaminophen have low incidences of adverse side effects at therapeutic dosages (3, 9, 10).

Since pentazocine is thought to act centrally and acetaminophen acts primarily peripherally, the simple additive effect of a narcotic antagonist and an antipyretic–analgesic given together may be substantially greater than the analgesia obtained from each component separately (11, 12). In our investigation, the bioavailability and pharmacokinetic parameters of pentazocine and acetaminophen were determined in human subjects following administration of two different preparations of pentazocine combined with acetaminophen.

EXPERIMENTAL

Subjects—The subjects were 20 healthy male volunteers, ranging in age from 19 to 33 years and in weight from 53 to 104 kg. No subject had a clinical history or laboratory findings that were suggestive of renal, hepatic, or cardiac dysfunction. Appropriate institutional review and approval were obtained.

Drug Administration and Sampling—Each subject received two different preparations of pentazocine and acetaminophen in a single dose according to a randomized three-way crossover design. One dose was two capsule-shaped tablets[1], each containing 25 mg of pentazocine base and 650 mg of acetaminophen, and the other dose was a solution containing 50 mg of pentazocine base and 1300 mg of acetaminophen (prepared in-house). For the third dose, one-half of the subjects received a repeat dose of the solution and the other half of the subjects received a repeat dose of the tablets. There was a 1-week washout interval between medications. Blood samples were collected by venipuncture prior to drug administration and at 0.25, 0.50, 0.75, 1, 2, 4, 6, 7 and 12 h after treatment; potassium oxalate was used as the anticoagulant. All subjects were fasted for at least 8 h before treatment and 3 h afterwards. Blood samples were centrifuged, and the plasma was separated and frozen until it was assayed.

Analytical Methods—Pentazocine plasma concentrations were determined using a minor modification of the RIA procedure (13) developed in these laboratories; toluene was used for the extraction in place of benzene. The minimum quantifiable level of the assay was estimated as the concentration whose lower 95% confidence limit just encompassed zero and was ~0.4 ng/mL. Blind analyses of plasma samples spiked with pentazocine over the range of 0 and 0.4 to 100 ng/mL revealed a mean intraassay variation coefficient of 8.2% (n = 18) and a mean interassay coefficient of variation of 11.6% (n = 3).

Plasma concentrations of acetaminophen were determined by the HPLC method reported by Horwitz and Jatlow (14), with the following modifications. Plasma was extracted with 7 mL of diethyl ether instead of 5 mL. The residue remaining after evaporation of the solvent was dissolved in 200 μL of the mobile phase, and 50 μL were injected onto a 3.9-mm i.d. × 30-cm phenyl column[2] using a solvent system of 7% acetonitrile in 0.1 M KH_2PO_4 (v/v) adjusted to pH 2.4 with phosphoric acid. The flow rate was increased to 2.0 mL/min. The mean quantifiable level for acetaminophen was estimated by linear regression of the peak-height ratios as the concentration whose lower 80% confidence limit just encompassed zero (15) and was between 0.02 and 0.06 μg/0.5 mL. Blind analyses of acetaminophen standards prepared with human control plasma over the range of 0 and 0.1 to 15 μg/0.5 mL yielded an intraassay coefficient of variation (precision) of ±4.9% (n = 2). The accuracy of the assay, defined as the mean percent difference from a nominal value, ranged from −7.5 to 3.0% (n = 18).

Pharmacokinetic Calculations—Pharmacokinetic parameters for pentazocine and acetaminophen were derived by analysis of the plasma concentration data by means of a weighted nonlinear regression procedure (NLIN) using the Marquardt algorithm (16). The plasma concentrations were weighted as the squares of their reciprocals (17, 18). Where appropriate, results are expressed as the mean $\pm SD$.

The plasma data obtained for pentazocine (tablet and solution) and acetaminophen (tablet) was fitted to an open one-compartment body model with first-order absorption and was described by the following:

$$C = A[e^{-k_e(t-t_0)} - e^{-k_a(t-t_0)}] \qquad \text{(Eq. 1)}$$

where C is the plasma concentration at time, t, t_0 is the lag time (before absorption begins), A is a constant, and k_a and k_e are apparent first-order rate constants for absorption and elimination, respectively. Since the absorption of acetaminophen in solution is very rapid, the data from the analysis of the acetaminophen solution dose was fit to a one-compartment open model assuming instantaneous absorption (intravenous model) by means of a weighted regression analysis as above, and was described by the following:

$$C = B(e^{-k_e t}) \qquad \text{(Eq. 2)}$$

where B is a constant and the other terms are defined above.

The apparent volume of distribution (uncorrected for bioavailability), Vd/F, which relates the plasma concentration to the total amount of drug in the body, was calculated by the use of the following:

$$Vd/F = \frac{\text{Dose} \cdot k_a}{A(k_a - k_e)} \qquad \text{(Eq. 3)}$$

[1] Talacen; Winthrop Laboratories, New York, N.Y.

[2] μ-Bondapak CN; Waters Associates, Milford, Mass.

0022-3549/84/0300-0326$01.00/0
© 1984, American Pharmaceutical Association

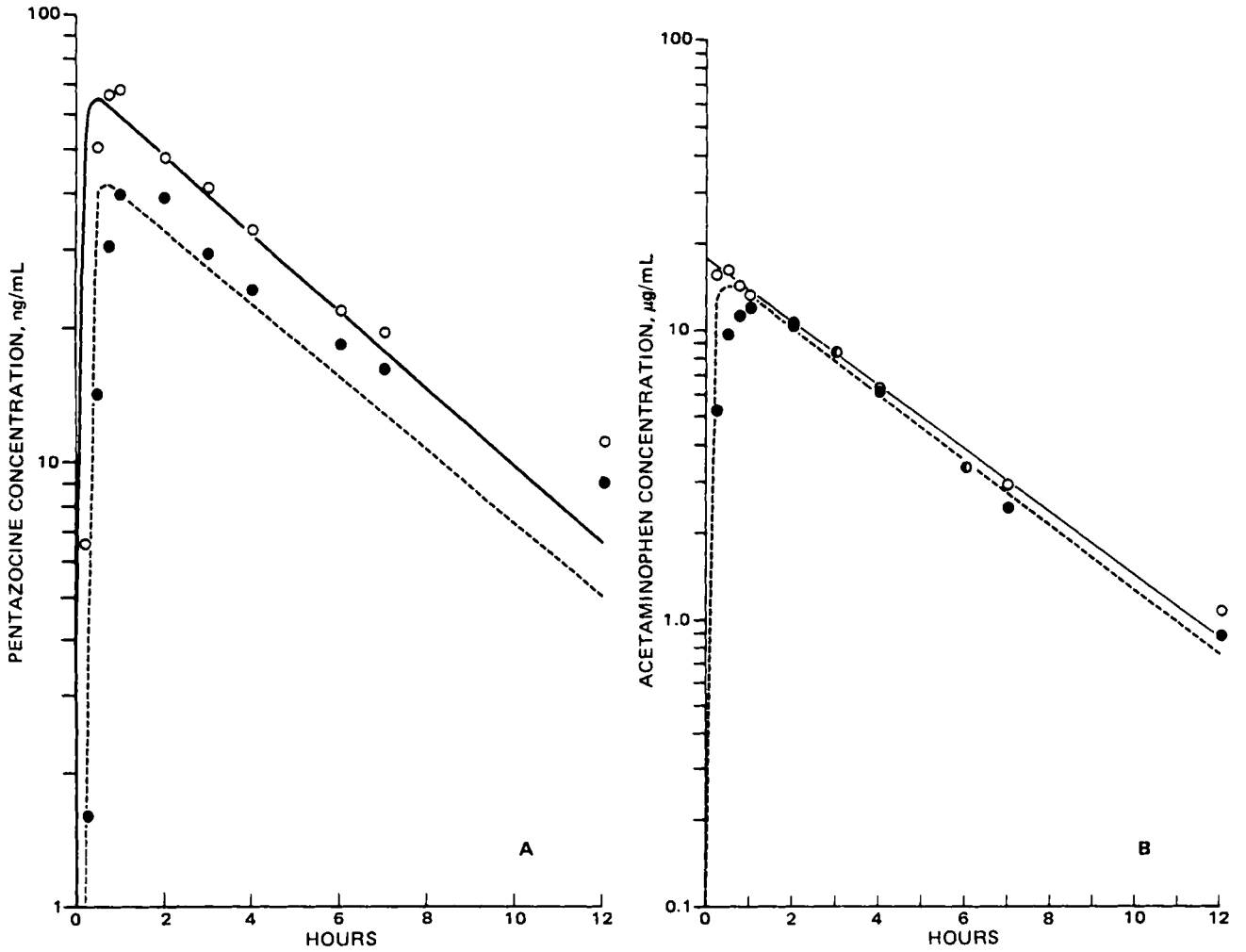

Figure 1—*Mean plasma concentrations of pentazocine (A) and acetaminophen (B) in 20 human volunteers after oral administration of either two tablets (●) or a solution (○) containing 50 mg of pentazocine and 1300 mg of acetaminophen. The lines represent the respective model-dependent curves derived from the mean pharmacokinetic parameters.*

$$Vd/F = \frac{\text{Dose}}{C_0} \qquad \text{(Eq. 4)}$$

where F is the fraction of the administered dose which is available to the systemic circulation; the other terms are defined above. The apparent total plasma clearance (CL_p) relates to drug availability (F) and was calculated from:

$$\frac{CL_p}{F} = \frac{\text{Dose}}{\text{AUC}_0^\infty} \qquad \text{(Eq. 5)}$$

The total area under the plasma concentration *versus* time curve (AUC_0^∞) for each subject was determined from the following:

$$\text{AUC}_0^\infty = \frac{A(k_a - k_e)}{k_a k_e} \qquad \text{(Eq. 6)}$$

$$\text{AUC}_0^\infty = \frac{F \cdot \text{Dose}}{Vd \cdot k_e} \qquad \text{(Eq. 7)}$$

In addition to the regression-dependent parameters (defined above), the plasma concentration data were analyzed with respect to the following regression-independent parameters: the maximum observed plasma concentration (C_{max}^{obs}), the time at which the maximum plasma concentration was observed (t_{max}^{obs}), and AUC_0^{12}. The latter was calculated by the trapezoidal rule, including all of the data for the study period. For those subjects who had detectable concentrations of pentazocine or acetaminophen in the last sample examined, the AUC was extrapolated to infinite time by use of the following:

$$\text{AUC}_0^\infty = \text{AUC}_0^{12} + \frac{C_p}{k_t} \qquad \text{(Eq. 8)}$$

where C_p was the pentazocine or acetaminophen concentration observed in the last measurable sample taken and k_t is the estimated apparent first-order terminal elimination rate constant; k_t was estimated by linear regression on the natural logarithms of the observed plasma concentration from t_{max} to the last data point.

The regression-independent volume of distribution (uncorrected for bioavailability), Vd/F, was determined by the following equation:

$$Vd/F = \frac{\text{Dose}}{k_t \cdot \text{AUC}_0^\infty} \qquad \text{(Eq. 9)}$$

The bioavailability of the tablet doses relative to that of the solution doses was determined from the ratio of their respective extrapolated AUC values:

$$\text{Relative bioavailability} = \frac{\text{AUC}_0^\infty \text{ (tablet)}}{\text{AUC}_0^\infty \text{ (solution)}} \times 100 \qquad \text{(Eq. 10)}$$

RESULTS

Pentazocine—The plasma levels of pentazocine for each subject declined exponentially with time and were best fit with an open one-compartment body model with first-order absorption. The mean plasma concentrations are shown in Fig. 1A. The mean apparent first-order elimination rates for the tablet and solution were 0.19 ± 0.08 and 0.20 ± 0.06 h^{-1}, respectively, which corresponds to a half-life of ~3.6 h for both the tablet and solution preparations. Results are shown in Tables I and II, respectively.

The apparent volume of distribution showed considerable variation between individuals for both preparations. The mean apparent Vd/F for the tablet was 1614 L, with a range of 495–4906 L, and the solution had a mean apparent Vd/F of 1177 L, with a range of 243–2865 L. Plasma clearance (CL_p) and the first-order absorption rate (k_a) demonstrated considerable intersubject variation. The mean AUC_0^∞ values for the tablet

Table I—Pharmacokinetic Parameters Derived from Pentazocine Plasma Data from Subjects Receiving Tablets Containing Pentazocine and Acetaminophen

	Model Independent						Regression Dependent						
Subject	t_{max}^{obs}, h	C_{max}^{obs}, ng/mL	Vd/F, L	CL_p/F, L·h^{-1}	AUC_0^{12}, ng·h/mL	k_t, h^{-1}	A, ng/mL	k_a, h^{-1}	k_e, h^{-1}	t_0, h	Vd/F, L	CL_p/F, L·h^{-1}	AUC_0^{∞}, ng·h/mL
101	2.0	86	645	148	306	0.23	68.3	1.24	0.21	0.24	879	183	273
101	1.0	35	1302	235	184	0.18	39.8	4.51	0.19	0.46	1311	244	205
102	2.0	94	549	27.5	821	0.05	79.1	52.7	0.03	0.25	633	19.8	2528
102	2.0	162	426	34.1	866	0.08	63.7	2.77	0.07	0.48	495	34.9	1432
103	2.0	21	2140	342	121	0.16	27.2	1.10	0.17	0.39	2165	360	139
103	0.75	41	1502	301	150	0.20	32.9	63.8	0.20	0.50	1525	301	166
104	1.5	24	1754	420	110	0.24	29.4	2.45	0.24	0.19	1887	459	109
104	1.0	62	926	222	208	0.24	55.3	1.25	0.24	0.24	1114	263	190
105	0.75	20	2591	521	86	0.20	20.8	2.51	0.21	0.24	2615	544	91.9
105	1.0	32	2088	481	95	0.23	21.3	52.9	0.23	0.47	2359	542	92.3
201	1.0	61	1129	237	188	0.21	39.3	2.32	0.19	0.48	1385	266	188
201	1.0	91	829	208	226	0.25	47.9	2.36	0.22	0.23	1152	256	195
202	0.5	52	1038	467	107	0.45	50.6	53.6	0.48	0.25	996	476	105
202	0.75	55	924	278	173	0.30	49.8	2.44	0.30	0.06	1144	342	146
203	7.0	38	740	118	316	0.16	25.1	52.8	0.02	0.49	1992	38.5	1300
203	1.0	62	963	202	218	0.21	45.4	6.43	0.21	0.49	1138	235	213
204	3.0	9.0	4386	526	70	0.12	12.2	1.25	0.11	—[a]	4498	510	98.1
204	0.75	8.0	5275	735	57	0.14	10.7	3.39	0.16	0.34	4906	780	64.1
205	3.0	63	764	99.4	357	0.13	61.4	1.27	0.14	0.48	918	133	376
205	3.0	45	824	140	304	0.17	63.5	1.51	0.17	0.47	889	153	327
301	1.0	25	1812	382	119	0.21	30.4	1.64	0.21	0.16	1894	406	123
302	1.0	38	1321	238	182	0.18	41.4	4.36	0.19	0.43	1263	244	205
303	1.0	121	448	49.3	688	0.11	107	1.53	0.11	0.24	503	55.9	895
304	2.0	28	1544	340	134	0.22	33.2	1.85	0.22	0.24	1711	382	131
305	1.0	61	1019	214	208	0.21	50.8	60.5	0.24	0.25	989	234	214
402	2.0	27	1600	305	144	0.19	33.9	1.42	0.19	0.42	1698	314	159
403	2.5	18	2154	345	122	0.16	28.1	1.31	0.18	0.46	2059	362	138
404	0.75	19	2796	336	114	0.12	17.9	59.5	0.12	0.48	2800	340	147
405	2.0	68	617	148	315	0.24	93.5	1.56	0.24	0.21	633	154	324
406	4.0	35	952	162	252	0.17	88.8	0.55	0.20	0.44	877	171	292
Mean	1.74	50.0	1502	275	238	0.19	45.6	14.9	0.19	0.35	1614	293	362
±*SD*	1.32	34.3	1105	164	211	0.07	24.2	23.5	0.08	0.13	1040	174	526

[a] No meaningful value; not included in the mean.

and solution preparations were 362 ± 526 and 404 ± 474 ng·h/mL, respectively. The calculated bioavailability of pentazocine in the tablet relative to the solution demonstrated considerable intrasubject variation, as well as significant interindividual variability, and ranged from 37.0 to 216% with a mean value of 85.0 ± 31.1%. Individual AUC_0^{∞} values and relative bioavailability data are presented in Table III.

The observed regression-independent parameters are in reasonable agreement with those estimated from the open one-compartment body

Table II—Pharmacokinetic Parameters Derived from Pentazocine Plasma Data from Subjects Receiving a Solution Containing Pentazocine and Acetaminophen

	Model Independent						Regression Dependent						
Subject	t_{max}^{obs}, h	C_{max}^{obs}, ng/mL	Vd/F, L	CL_p/F, L·h^{-1}	AUC_0^{12}, ng·h/mL	k_t, h^{-1}	A, ng/mL	k_a, h^{-1}	k_e, h^{-1}	t_0, h	Vd/F, L	CL_p/F, L·h^{-1}	AUC_0^{∞}, ng·h/mL
101	0.62	89	658	112	382	0.17	74.7	54.1	0.17	0.25	672	115	434
102	1.0	166	229	27	1055	0.12	99.8	5.39	0.04	0.24	505	21	2431
103	2.5	20	1921	327	129	0.17	31.5	1.29	0.19	0.45	1854	345	145
104	1.0	28	1749	333	131	0.19	28.7	2.31	0.19	0.23	1895	352	142
105	0.50	37	1869	485	96	0.26	24.6	56.0	0.26	0.25	2041	523	95.6
201	3.0	32	1082	216	202	0.20	48.8	1.27	0.19	0.23	1207	232	216
202	0.75	85	820	221	214	0.27	52.7	9.16	0.26	0.21	976	250	200
203	0.75	36	1279	255	174	0.20	44.0	3.98	0.28	0.20	1224	247	144
204	0.75	16	3173	413	95	0.13	18.3	2.03	0.15	0.20	2941	435	115
205	0.75	127	665	80	443	0.12	72.9	6.67	0.11	0.21	889	76	654
301	0.75	38	1279	320	148	0.25	38.0	56.9	0.25	0.25	1320	329	152
301	0.75	56	1348	300	155	0.22	34.0	56.6	0.21	0.48	1475	311	161
302	0.75	46	914	182	248	0.20	65.1	1.96	0.22	0.16	864	189	265
302	0.75	99	638	153	301	0.24	72.4	8.95	0.23	0.24	709	162	309
303	2.0	120	374	49	790	0.13	145	1.50	0.13	0.25	379	50	1000
303	0.75	203	254	38	1033	0.15	186	2.74	0.15	0.24	285	44	1136
304	0.50	83	1243	300	153	0.24	32.9	72.1	0.22	0.24	1524	340	147
304	0.87	53	1073	258	180	0.24	42.1	51.7	0.23	0.24	1192	273	183
305	1.0	58	855	171	262	0.20	55.2	17.5	0.19	0.23	917	177	283
305	1.0	131	549	143	327	0.26	94.3	52.4	0.31	0.25	533	166	301
402	2.5	34	1142	251	179	0.22	47.2	1.33	0.21	0.16	1260	267	187
402	1.0	54	1066	224	200	0.21	45.3	4.09	0.21	0.23	1163	238	210
403	0.75	35	1567	312	142	0.20	32.7	49.5	0.21	0.25	1535	318	157
403	0.50	42	1582	316	140	0.20	30.2	63.2	0.19	0.25	1661	320	156
404	2.0	26	1691	287	148	0.17	31.2	1.64	0.17	0.24	1787	303	165
404	0.75	21	2797	391	102	0.14	18.2	3.29	0.14	0.24	2865	397	126
405	0.75	162	275	66	707	0.24	187	5.36	0.25	0.21	280	69	727
405	1.0	219	236	61	768	0.26	222	3.78	0.27	0.23	243	65	772
406	1.0	49	792	127	335	0.16	79.7	1.07	0.19	0.20	761	142	351
406	0.75	214	285	60	744	0.21	147	61.5	0.20	0.25	342	67	746
Mean	1.06	79.3	1140	216	333	0.20	70.0	22.0	0.20	0.20	1177	227	404
±*SD*	0.65	61.1	721	123	283	0.04	54.4	25.9	0.06	0.06	128	129	464

Table III—Relative Bioavailability of Tablet Compared to Solution Based on Regression-Independent AUC_0^∞ Data

Subject	Pentazocine			Acetaminophen		
	AUC_0^∞, ng·h/mL		Relative	AUC_0^∞, μg·h/mL		Relative
	Tablet	Solution	Bioavailability	Tablet	Solution	Bioavailability
101	337	447	75.4	51.2	67.5	75.8
101	213	—	47.8	56.4	—	83.6
102	1821	1822	100	49.2	53.4	92.1
102	1466	—	80.5	56.9	—	107
103	146	153	95.4	88.5	89.9	98.5
103	166	—	109	93.4	—	104
104	118	150	78.9	53.6	55.3	96.9
104	225	—	120	60.9	—	110
105	96	103	93.8	45.7	54.1	84.4
105	104	—	101	51.2	—	94.7
201	211	231	91.3	71.6	75.8	94.6
201	241	—	104	93.0	—	123
202	107	226	47.4	65.8	74.4	88.4
202	180	—	79.8	59.5	—	80.0
203	422	196	216	61.4	66.7	92.1
203	248	—	127	66.7	—	100
204	95	122	78.2	56.7	59.5	95.3
204	68	—	55.7	60.8	—	102
205	503	626	80.3	40.6	66.2	61.0
205	357	—	57.0	41.2	—	62.2
301	131	156	84.0	63.2	67.4	93.6
301	—	169	77.9	—	73.9	85.4
302	210	274	76.9	57.2	68.9	83.1
302	—	327	64.4	—	83.6	68.5
303	1015	1028	98.7	54.1	60.3	89.7
303	—	1313	77.3	—	64.0	84.5
304	147	168	87.8	53.3	64.0	83.2
304	—	194	75.8	—	65.8	81.0
305	234	292	79.9	61.6	62.8	98.1
305	—	350	66.8	—	68.6	89.8
402	164	199	82.7	54.9	60.5	90.8
402	—	223	73.7	—	63.7	86.2
403	145	160	90.8	61.8	60.0	103
403	—	158	91.8	—	64.7	95.6
404	149	174	85.7	73.8	85.8	86.0
404	—	128	117	—	86.4	85.4
405	338	757	44.6	78.7	102	77.0
405	—	814	41.4	—	103	76.2
406	309	394	78.4	57.1	68.8	83.0
406	—	834	37.0	—	97.3	58.7
Mean	332	406	85.0	61.3	77.1	88.6
±*SD*	401	404	31.1	13.3	13.6	13.1

model with first-order absorption. The C_{max} values for the tablet and solution preparations were 50 ± 34.3 and 79.3 ± 61.1 ng/mL, respectively, and their respective t_{max} values occurred at 1.74 ± 1.32 and 1.06 ± 0.65 h. The regression-independent $t_{1/2}$ values for the tablet and solution preparation were identical to the regression-dependent $t_{1/2}$ values.

Acetaminophen—As seen in Fig. 1B, the plasma levels of acetaminophen in volunteers receiving the tablet declined exponentially with time, suggesting that an open one-compartment body model with first-order absorption would be appropriate. The plasma levels of acetaminophen in volunteers receiving the solution declined exponentially and were best described by a one-compartment body model assuming instantaneous absorption (intravenous model). The mean apparent first-order elimination rates for the tablet and solution were 0.26 ± 0.03 and 0.25 ± 0.03 h^{-1}, respectively, which corresponds to a $t_{1/2}$ of 2.7 h. The pharmacokinetic parameters are shown in Tables IV and V.

The mean apparent volume of distribution (Vd/F) for the tablet and solution were 90.3 ± 17.2 and 76.5 ± 14.7 L, respectively. Clearance of the tablet varied from 14.6 to 37.9 L·h^{-1}, while the plasma clearance of the solution ranged from 12.4 to 24.6 L·h^{-1}. The mean AUC_0^∞ values for the tablet and solution formulation were 57.5 ± 13.0 and 72.0 ± 14.4 μg·h/mL, respectively.

The observed, regression-independent parameters are in reasonable agreement with those calculated from the regression-dependent parameters. The mean apparent first-order terminal elimination rate constants were 0.25 ± 0.04 and 0.24 ± 0.03 h^{-1}, respectively, for the tablet and solution preparations. The C_{max}^{obs} for the tablet data was 13.6 ± 3.7 μg/mL, and the respective t_{max}^{obs} occurred at 0.95 ± 0.64 h.

The calculated bioavailability of the tablet relative to the solution ranged from 58.7 to 123%, with a mean value of 88.6 ± 13.1%. Individual AUC_0^∞ values and relative bioavailability are presented in Table III. The regression-independent AUC_0^∞ for the solution data was in close agreement to that of the AUC_0^∞ calculated from the regression-dependent parameters. This suggests that the model which assumed instantaneous absorption was appropriate for the available data.

DISCUSSION

Pentazocine—Pharmacokinetic parameters for each subject were estimated after computer-fitting of the data by a weighted iterative nonlinear least-squares regression technique. The plasma data from each subject was best fit by an open one-compartment body model with first-order absorption. Attempts to fit the data from each subject to an open two-compartment body model with first-order absorption yielded residual sum-of-squares values significantly greater than the comparable values for an open one-compartment body model. The half-lives for the capsule-shaped tablet and solution data, 3.65 and 3.46 h, respectively, are similar to those reported by Ehrnebo *et al.* (19): 3.38 ± 1.18 and 2.95 ± 0.57 h, following intravenous and oral administration, respectively. The present values are in very close agreement with the mean half-life of 3.83 ± 0.47 h reported by Neal *et al.* (20) for four normal subjects. The elimination half-lives for the urinary excretion rate of intact pentazocine for a period of 24 h ranged from 2.0 to 5.5 h (21, 22), which are in accordance with our plasma values. The mean apparent Vd/F for the tablet and solution preparations were 1610 and 1110 L, respectively, or, dividing by the mean body weight, 21.4 and 14.7 L/kg. These values suggest that pentazocine may be bound or partition favorably into tissues. Ehrnebo *et al.* (19) and studies conducted in our laboratories[3] have demonstrated that first-pass metabolism of pentazocine after oral administration was ~80%. Taking this into account, one obtains mean estimates of 222 and 322 L for the tablet and solution treatments, which are in reasonable agreement with the range of 251–548 L reported by Ehrnebo *et al.* (19)

[3] Unpublished data.

Table IV—Pharmacokinetic Parameters Derived from Acetaminophen Plasma Data from Subjects Receiving Tablet Containing Pentazocine and Acetaminophen

	Model Independent						Regression Dependent						
Subject	t_{max}^{obs}, h	C_{max}^{obs}, μg/mL	Vd/F, L	CL_p/F, L·h^{-1}	AUC_0^{12}, ng·h/mL	k_t, h^{-1}	A, μg/mL	k_a, h^{-1}	k_e, h^{-1}	t_0, h	Vd/F, L	CL_p/F, L·h^{-1}	AUC_0^{∞}, ng·h/mL
101	1.0	12	90.8	25.4	48.8	0.28	16.2	2.09	0.30	0.18	93.6	27.8	46.7
101	0.50	14	82.3	23.0	54.1	0.28	15.3	49.0	0.29	0.25	85.4	25.0	52.0
102	0.25	15	94.4	26.4	47.2	0.28	12.2	a	0.27	0.18	106	29.0	44.9
102	1.0	12	104	22.8	52.5	0.22	12.8	2.66	0.22	0.15	111	23.9	54.3
103	2.0	12	77.3	14.7	78.0	0.19	18.6	1.73	0.19	0.17	78.5	14.9	87.5
103	0.75	15	81.9	13.9	80.5	0.17	23.3	1.46	0.24	0.11	67.0	16.3	79.9
104	0.75	15	80.9	24.2	51.7	0.30	16.6	6.70	0.31	0.02	82.3	25.2	51.5
104	0.75	17	76.3	21.4	58.2	0.28	18.0	3.33	0.28	0.22	78.8	22.2	58.7
105	0.25	11	105	28.4	43.5	0.27	11.8	43.9	0.28	0.18	111	30.7	42.3
105	0.50	14	94.0	25.4	48.6	0.27	13.5	52.6	0.27	0.22	96.8	26.3	49.5
201	1.0	13	82.5	18.2	65.7	0.22	18.9	1.67	0.24	0.22	80.2	19.0	68.3
201	0.75	24	51.7	14.0	88.6	0.27	26.0	5.37	0.28	0.18	52.6	14.7	88.7
202	0.25	16	75.9	19.8	63.2	0.26	17.4	15.3	0.27	—[a]	75.9	20.2	64.4
202	1.0	15	72.8	21.8	57.4	0.30	18.6	2.98	0.29	0.21	77.2	22.1	58.9
203	0.75	17	75.6	21.2	58.4	0.28	14.0	8.45	0.28	0.23	95.7	26.4	49.2
203	1.0	17	74.9	19.5	62.9	0.26	17.7	3.64	0.26	0.19	79.0	20.7	62.9
204	0.50	12	95.5	22.9	52.6	0.24	14.3	7.81	0.28	0.21	94.6	26.8	48.6
204	0.50	12	93.0	21.4	56.6	0.23	13.7	8.74	0.23	0.22	97.2	22.3	58.2
205	2.0	10	110	32.0	38.6	0.29	13.1	1.29	0.30	0.23	128	37.9	34.3
205	3.0	7.6	105	31.6	39.4	0.30	13.6	1.54	0.28	0.22	117	33.2	39.2
301	1.0	11	103	20.6	56.2	0.20	13.1	3.36	0.21	0.23	106	22.4	58.1
302	2.0	12	75.7	22.7	55.1	0.30	20.4	1.58	0.30	0.14	78.7	23.8	54.5
303	0.75	10	109	24.0	50.2	0.22	11.9	5.10	0.22	—[a]	114	24.9	52.2
304	0.50	11	97.6	24.4	50.6	0.25	14.0	5.22	0.26	0.12	97.5	25.2	51.6
305	0.25	24	70.3	21.1	59.4	0.30	17.6	—[a]	0.31	0.25	73.9	22.6	57.6
402	1.0	10	103	23.7	50.9	0.23	13.7	3.04	0.24	0.21	103	24.5	53.1
403	1.0	11	95.5	21.0	56.4	0.22	17.8	0.96	0.24	0.15	97.8	23.7	54.9
404	1.0	13	76.5	17.6	69.1	0.23	18.7	2.84	0.24	0.22	75.9	18.0	72.3
405	0.50	15	66.1	16.5	75.1	0.25	20.9	4.11	0.26	—[a]	66.3	17.1	76.1
406	2.0	9.6	99.0	22.8	52.8	0.23	21.7	0.80	0.26	0.16	89.2	14.6	89.2
Mean	0.95	13.6	87.4	22.1	57.4	0.25	16.5	8.83	0.26	0.19	90.3	23.4	57.5
±*SD*	0.64	3.7	14.6	4.4	11.6	0.04	3.6	14.4	0.03	0.05	17.2	5.4	13.0

[a] No meaningful value; not included in the mean.

and similar to those of Neal *et al.* (20), 342 ± 188 L, following intravenous administration of 0.8 mg/kg.

The regression-independent bioavailability of the tablet relative to that of the solution was 85.0 ± 31.1%. The AUC_0^{∞} values varied considerably among these volunteers by a factor of 28 and 15 for the tablet and solution, respectively. The data obtained from the solution did not show the same degree of intrasubject variation as that of the tablet. Others have observed the same interindividual variation (19, 21). In general, it has

Table V—Pharmacokinetic Parameters Derived from Acetominophen Plasma Data from Subjects Receiving a Solution Containing Pentazocine and Acetaminophen

	Model Independent						Regression Dependent				
Subject	t_{max}^{obs}, h	C_{max}^{obs}, μg/mL	Vd/F, L	CL_p/F, L·h^{-1}	AUC_0^{12} μg·h/mL	k_t, h^{-1}	C_0, μg/mL	k_e, h^{-1}	Vd/F, L	CL_p/F, L·h^{-1}	AUC_0^{∞}, μg·h/mL
101	0.50	19	71.4	19.3	64.4	0.27	18.6	0.28	69.9	19.4	67.1
102	0.50	16	87.0	24.3	51.2	0.28	15.0	0.28	86.4	24.0	54.2
103	0.75	15	65.7	14.5	84.4	0.22	20.0	0.22	64.9	14.4	90.6
104	0.50	13	87.1	23.5	52.6	0.27	15.3	0.28	85.1	23.5	55.4
105	0.25	22	89.0	24.0	51.1	0.27	14.7	0.28	88.3	24.6	52.8
201	1.0	15	71.5	17.2	70.8	0.24	19.6	0.25	66.3	16.4	79.5
202	0.25	20	62.4	17.5	71.5	0.28	21.1	0.28	61.6	17.1	75.9
203	0.50	19	72.2	19.5	63.5	0.27	18.8	0.28	69.0	19.3	67.3
204	0.75	11	99.4	21.8	55.0	0.22	13.2	0.22	98.7	21.4	60.7
205	0.25	28	89.3	19.6	58.4	0.22	17.3	0.26	75.2	19.3	67.5
301	0.25	16	83.8	19.3	62.7	0.23	16.1	0.24	80.9	19.3	67.5
301	0.50	22	79.9	17.6	66.6	0.22	17.6	0.23	74.0	17.2	75.8
302	0.25	18	72.5	18.9	65.5	0.26	17.2	0.26	75.6	19.5	66.6
302	0.25	24	55.6	15.6	80.2	0.28	23.9	0.28	54.4	15.2	85.4
303	0.50	15	86.2	21.6	56.7	0.25	15.5	0.25	83.3	21.0	61.8
303	0.25	18	84.6	20.3	59.8	0.24	15.9	0.24	82.0	20.0	65.0
304	0.25	20	81.2	20.3	60.1	0.25	16.0	0.25	81.3	20.2	64.2
304	0.25	28	76.0	19.8	62.1	0.26	16.1	0.25	81.0	20.1	64.8
305	0.25	22	69.0	20.7	60.8	0.30	19.3	0.30	67.3	20.2	64.5
305	0.25	32	65.4	20.0	65.6	0.29	19.7	0.29	66.1	19.2	67.7
402	0.25	11	97.7	21.5	55.9	0.22	12.0	0.21	108	22.5	57.8
402	0.25	17	81.7	20.4	59.7	0.25	16.5	0.26	78.8	20.1	64.6
403	0.50	10	108	21.7	54.5	0.20	11.9	0.20	110	22.0	59.2
403	0.50	15	95.7	20.1	59.5	0.21	14.0	0.21	92.9	19.8	65.8
404	0.75	16	68.8	15.2	79.5	0.22	19.6	0.22	66.5	14.7	88.7
404	2.0	16	60.2	15.0	81.6	0.25	21.4	0.23	60.6	14.2	91.6
405	0.25	22	53.0	12.8	96.3	0.24	24.3	0.24	53.5	12.6	103
405	0.50	26	50.4	12.6	98.0	0.25	26.3	0.25	49.4	12.4	105
406	1.0	11	89.9	18.9	63.1	0.21	15.2	0.21	85.6	18.1	71.7
406	0.50	22	78.6	13.4	82.0	0.17	16.3	0.16	79.6	13.1	99.1
Mean	0.49	18.6	76.5	18.8	66.4	0.24	17.6	0.25	76.5	18.6	72.0
±*SD*	0.36	5.5	13.2	3.2	12.5	0.03	3.5	0.03	14.7	3.3	14.4

been observed that the AUC values vary substantially for drugs with pronounced hepatic clearance, such as nortriptyline (23) and imipramine (24); the data suggest this is also true for pentazocine. In addition, the oral bioavailability of pentazocine was significantly enhanced in patients with cirrhosis of the liver, due to reduction in hepatic clearance (20, 25).

Acetaminophen—The plasma data obtained from the solution was fit to a one-compartment body model assuming instantaneous absorption because the first blood sample obtained, in the majority of the subjects, contained the highest level of acetaminophen, while the data obtained from the tablet treatment was fit to a one-compartment body model with first-order absorption. The half-lives for the tablet and solution, 2.67 and 2.77 h, respectively, are in close agreement with those reported by Lee *et al.* (26): 2.6 h in both obese and nonobese subjects. Divoll *et al.* (27) and Rawlins *et al.* (28) found that the mean half-life was 2.7 and 2.8 h after intravenous administration of 650 mg and 500 mg of acetaminophen, respectively. Others have reported half-lives ranging from 2.24 to 3.0 h (17, 29–34). Sotiropoulus *et al.* (35), based on urinary elimination of acetaminophen, reported half-lives of 2.77, 3.14, and 4.12 h after oral administration of three different commercial tablets.

The apparent Vd/F of acetaminophen ranged from 52.6 to 128 L for subjects receiving the tablet and from 49.4 to 110 L for subjects receiving the solution. The mean apparent volumes of distribution, when corrected by the mean body weight, were 1.2 and 1.02 L/kg, respectively, for the tablet and solution suggesting that acetaminophen distributes into total body water. Divoll *et al.* (27) reported a mean value of 1.09 L/kg after intravenous administration of 650 mg of acetaminophen in young human males. As reported by others, the volume of distribution ranged from 0.60 to 1.36 L/kg (9, 18, 27, 29, 30). The regression-independent bioavailability of the tablet relative to that of the solution was 88.6 ± 13.1%.

In summary, the relative bioavailability of pentazocine and acetaminophen in the capsule-shaped tablet formulation proved to be equivalent to that of the solution. In addition, the pharmacokinetic parameters of pentazocine and acetaminophen were not altered after oral administration of the combination of both drugs.

REFERENCES

(1) W. T. Beaver, S. L. Wallenstein, R. W. Houde, and A. Rogers, *Clin. Pharmacol. Ther.*, **9,** 582 (1968).

(2) T. G. Kantor, A. Sunshine, E. Laska, M. Meisner, and M. Hopper, *Clin. Pharmacol. Ther.*, **7,** 447 (1966).

(3) W. T. Beaver, S. L. Wallenstein, R. W. Houde, and A. Rogers, *Clin. Pharmacol. Ther.*, **7,** 740 (1966).

(4) L. S. Cass, W. S. Frederick, and J. V. Teodoro, *J. Am. Med. Assoc.*, **188,** 112 (1964).

(5) A. S. Keats and J. Telford, *J. Pharmacol. Exp. Ther.*, **143,** 157 (1964).

(6) M. S. Sadove and R. C. Balagot, *J. Am. Med. Assoc.*, **193,** 887 (1965).

(7) M. S. Sadove, R. C. Balagot, and F. N. Pecora, *J. Am. Med. Assoc.*, **189,** 199 (1964).

(8) V. K. Stoelting, *Anesth. Anal.*, **44,** 769 (1965).

(9) B. Ameer and D. J. Greenblatt, *Ann. Intern. Med.*, **87,** 202 (1977).

(10) J. Koch-Weser, *Med. Intell.*, **295,** 1297 (1976).

(11) W. T. Beaver, *Arch. Intern. Med.*, **141,** 293 (1981).

(12) J. F. Calimlim, W. M. Wardell, D. M. Phil, H. T. Davis, L. Lasagna, and A. J. Gillies, *Clin. Pharmacol. Ther.*, **21,** 34 (1977).

(13) J. E. Peterson, M. Graham, W. F. Banks, D. P. Benziger, E. A. Rowe, S. Clemans, and J. Edelson, *J. Pharm. Sci.*, **68,** 626 (1979).

(14) R. A. Horwitz and P. I. Jatlow, *Clin. Chem.*, **23,** 1596 (1977).

(15) R. W. Ross and H. Stander, Paper presented at the Princeton Conference on Applied Statistics, December 1975.

(16) J. T. Helwig and K. A. Council (Eds), "SAS User's Guide," SAS Institute, Raleigh, N.C., 1979, pp. 317-329.

(17) K. S. Albert, A. J. Sedman, and J. G. Wagner, *J. Pharmacokinet. Biopharm.*, **2,** 381 (1974).

(18) J. A. Clements and L. F. Prescott, *J. Pharm. Pharmacol.*, **28,** 707 (1976).

(19) M. Ehrnebo, L. O. Boreus, and U. Lonroth, *Clin. Pharmacol. Ther.*, **22,** 888 (1977).

(20) E. A. Neal, P. J. Meffin, P. B. Gregory, and T. F. Blaschke, *Gastroenterology*, **77,** 96 (1979).

(21) A. H. Beckett, P. Kourounakis, D. P. Vaughan, and M. Mitchard, *J. Pharm. Pharmacol.*, **22** Suppl., 169s (1970).

(22) A. H. Beckett, J. F. Taylor, and P. Kourounakis, *J. Pharm. Pharmacol.*, **22,** 123 (1970).

(23) F. Sjoqvist, B. Alexanderson, M. Asberg, L. Bertilsson, O. Borga, B. Hamberger, and D. Tuck, *Acta Pharmacol. Toxicol.*, **29,** 255 (1971).

(24) L. F. Gram and J. Christiansen, *Clin. Pharmacol. Ther.*, **17,** 555 (1975).

(25) S. M. Pond, T. Tong, N. L. Benowitz, and P. Jacob, *Aust. N.Z. J. Med.*, **10,** 515 (1980).

(26) W. H. Lee, W. G. Kramer, and G. E. Granville, *J. Clin. Pharmacol.*, **21,** 284 (1981).

(27) M. Divoll, D. R. Abernethy, B. Ameer, and D. J. Greenblatt, *Clin. Pharmacol. Ther.*, **31,** 151 (1982).

(28) M. D. Rawlins, D. B. Henderson, and A. R. Hijab, *Eur. J. Clin. Pharmacol.*, **11,** 283 (1977).

(29) A. P. Douglas, R. L. Savage, and M. D. Rawlins, *Eur. J. Pharmacol.*, **13,** 209 (1978).

(30) S. Holt, R. C. Heading, J. A. Clements, F. Tothill, and L. F. Prescott, *Clin. Pharmacol. Ther.*, **30,** 232 (1981).

(31) R. P. Miller, R. J. Roberts, and L. J. Fischer, *Clin. Pharmacol. Ther.*, **19,** 284 (1976).

(32) E. Nelson and T. Morioka, *J. Pharm. Sci.*, **52,** 864 (1963).

(33) L. F. Prescott, P. Roscoe, N. Wright, and S. S. Brown, *Lancet* **i,** 519 (1971).

(34) R. A. Seymour and M. D. Rawlins, *Eur. J. Clin. Pharmacol.*, **20,** 215 (1981).

(35) J. B. Sotiropoulus, T. Deutsch, and F. M. Plakogiannis, *J. Pharm. Sci.*, **70,** 422 (1981).

ACKNOWLEDGMENTS

The authors are grateful to Cintest, Inc., Cincinnati, Ohio, for medicating the subjects and collecting the plasma samples, and to M. Graham, M. Brown, P. Kullberg, G. Freeman, and R. Brown for technical assistance.

Pharmacokinetics of the Antirheumatic Proquazone in Healthy Humans

PETER H. HINDERLING *x and ANDRÉ ROOS

Received August 5, 1980, from the *Department of Pharmacology, Biocenter, University of Basle, 4056 Basle, Switzerland.* Accepted for publication November 15, 1982. *Present address: F. Hoffmann-La Roche & Co. AG, Grenzacherstrasse 124, Basle CH-4002, Switzerland.

Abstract □ The pharmacokinetics of the antirheumatic proquazone and its conjugated and unconjugated *m*-hydroxy metabolites were investigated in five healthy male volunteers after both intravenous (75 and 122 mg) and peroral (300 and 900 mg *via* capsules) administration. For adequate intravenous dosing of the poorly water-soluble proquazone, advantage was taken of the high degree of protein binding of the drug. Proquazone was admixed with 40% sterile human albumin, and these proteinaceous drug-containing solutions were injected. The pharmacokinetics of proquazone and of the measured metabolites after intravenous administration and after the 300-mg po dose were first order, whereas deviations from linear kinetics were observed at the 900-mg dose level. The apparent half-lives of the α, β, and γ phases of proquazone in plasma were 2, 14, and 76 min, respectively, on intravenous administration. The total clearance of proquazone was 700 mL/min, which indicated a high hepatic extraction. The apparent volume of distribution at steady state was 40 L, implying extensive binding or partitioning of the lipophilic drug in the tissues. Unchanged proquazone (<0.001%), the *m*-hydroxy metabolite (<1.0%), and the conjugated *m*-hydroxy metabolite (20%) were renally excreted after intravenous administration. The extent of absorption of proquazone was ~7% and was entirely the result of a large first-pass effect. Digital computer analysis of the data after intravenous administration was performed with a linear three-compartment model. A model-independent approach was used in the analysis of the peroral data.

Keyphrases □ Proquazone—*m*-hydroxy metabolites, peroral and intravenous pharmacokinetics, humans, NONLIN, SAAM □ Pharmacokinetics—proquazone and its *m*-hydroxy metabolites, humans, oral and intravenous administration, NONLIN, SAAM □ Antirheumatics—proquazone and its *m*-hydroxy metabolites, oral and intravenous pharmacokinetics in humans, NONLIN, SAAM

Proquazone (I), a nonsteroidal anti-inflammatory drug (1, 2) which has been marketed in several countries in Europe since 1977[1], exhibits activities in animal models and humans comparable with those of classical nonsteroidal anti-inflammatory drugs (1–4). Its primary therapeutic indications are in the treatment of rheumatoid arthritis, osteoarthritis, and gouty arthritis (5, 6). Proquazone is very different chemically from other representatives of this class of drugs. It is a quinazolinone derivative and a weak base which is highly lipophilic and shows poor solubility in water (7).

The goal of this study was to delineate the pharmacokinetics of the parent proquazone and its primary metabolites in healthy humans after intravenous and oral administration. Preliminary pharmacokinetic experiments in healthy humans had been performed only after oral administration of the drug (8, 9). These studies indicated that the drug is extensively metabolized, and seven metabolites have been identified (8). Another investigation claimed an increased bioavailability of proquazone when the drug was administered concomitantly with food (9); first-order disposition kinetics for the drug were assumed in this study. Intravenous studies have not been executed with this drug. The sensitivity of the available assay methods and the poor water solubility of the drug necessitated either administration of too small a dosage in aqueous solution or of higher dosages dissolved in excessive volumes of solubilizers[2].

The study of the plasma protein binding of proquazone showed that the drug was highly bound to albumin (98%) (7). Subsequent experiments with human albumin indicated that the apparent solubility of proquazone was significantly increased in the presence of concentrated albumin solutions (7). Preliminary pharmacokinetic experiments showed that larger intravenous dosages could be administered by means of this "biological solubilizer" (7) and that a follow-up of the plasma concentrations and urinary excretion of proquazone and metabolites over sufficient time was possible with the available fluorometric and HPLC methods[2].

EXPERIMENTAL

Materials—The following were used: proquazone[3] (I), *n*-ethylproquazone[3], and *m*-hydroxyproquazone[3] (II). Proquazone in 4-hydroxymethyl-1,3-dioxolane–5-hydroxy 1,3-dioxane (1:2)[4] (7.5% w/v) was employed in the intravenous studies, and proquazone capsules[5] (300 mg) were administered in the oral studies. The dissolution characteristics of the capsules in 0.1 M HCl using the rotating basket method were 83.1, 93.4, and 97.5% of the drug dissolved after 15, 30, and 60 min postinitiation, respectively. Human albumin[6] (20% w/v) was employed as solubilizer for the intravenous dosages of proquazone; heparin[7] was used to prevent coagulation. β-Glucuronidase–sulfatase[8] was employed for enzymic hydrolysis of conjugated *m*-hydroxyproquazone (III).

Pharmacokinetic Procedures—Five nonsmoking, healthy, male volunteers (A–E), 22–24 years old, were selected for the study. Written

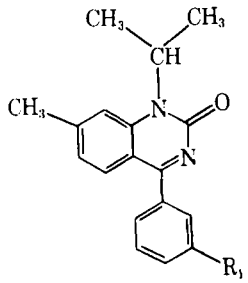

	R_1
I:	H
II:	OH
III:	O_{conj}

[1] Biarison; Sandoz Ltd., Basle and Wander Ltd., Berne, Switzerland.

[2] Unpublished data.
[3] Sandoz Ltd., Basle, Switzerland.
[4] Chemie Linz, Austria.
[5] Charge number 346 L 6.
[6] Human albumin SRK, Berne, Switzerland.
[7] Liquemin,Heparin; F. Hoffmann-La Roche Ltd., Basle, Switzerland.
[8] Glusulase: β-Glucuronidase (145,474 Fishman U) and arylsulfatase: (47,830 Roy U) Endo Laboratories, Inc., Garden City, N.Y.

0022-3549/84/0300-0332$01.00/0
© 1984, American Pharmaceutical Association

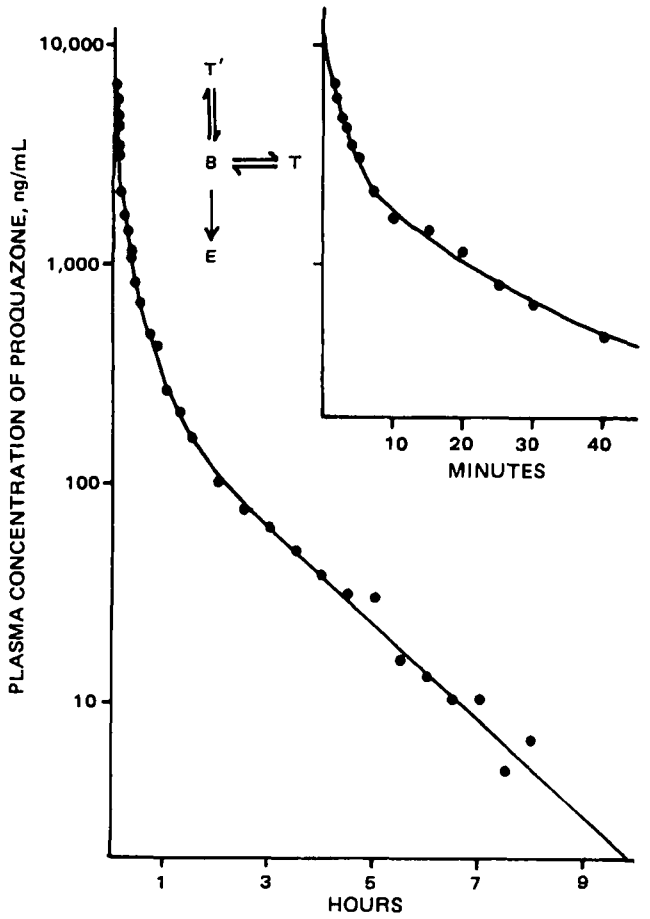

Figure 1—*Digital computer fitting (SAAM) of plasma data of I (●) in subject D after intravenous administration of 75 mg, in accordance with an intravenous infusion linear mamillary three-compartment body model. The inset is for an expanded time scale.*

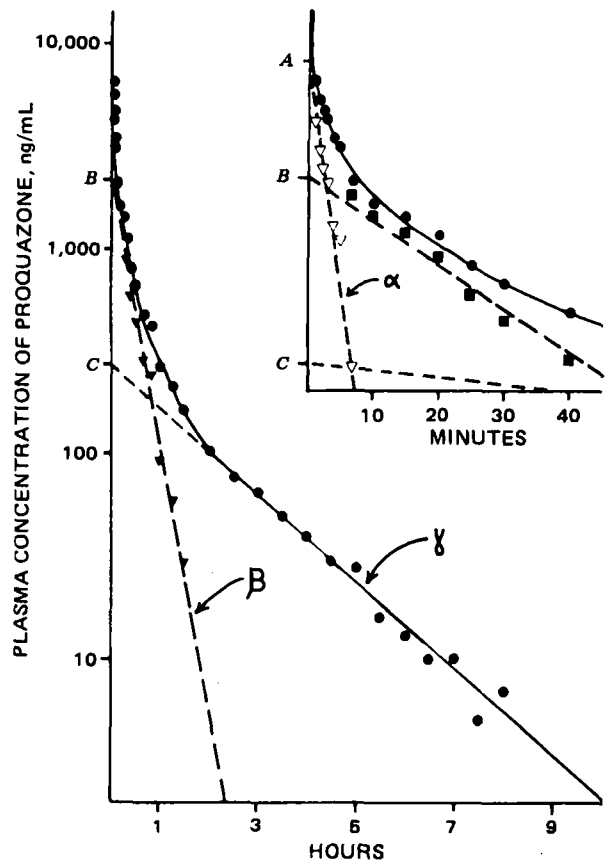

Figure 2—*Semilogarithmic plot against time of proquazone plasma concentrations following intravenous administration of 75 mg of the drug to subject D. The constants A, B, C, α, β, and γ were obtained by the method of residuals. The inset is for an expanded time scale. Key (△) original data; (▼,●,■) feathered values*

consent was obtained from all volunteers. An individual was considered healthy when he had a normal status, history, and laboratory checkup [complete blood count, hematocrit, sedimentation rate, serum electrophoresis, total proteins, creatinine clearance, urinalysis, bilirubin, serum glutamic oxaloacetic transaminase, serum glutamic pyruvic transaminase, alkaline phosphatase, and serum electrolytes (sodium, potassium, calcium, iron, inorganic phosphate)]. These tests were repeated prior to the second, third, and fourth study on each individual to determine possible adverse drug effects or changes due to the experimental procedures. Creatinine clearance of the individuals (117 ± 24 mL/min) was within the normal range (10).

Four different studies were performed in each of the selected volunteers: intravenous administration of 75 and 122 mg in human albumin solution and oral administration of 300 and 900 mg in capsules. The 122-mg iv dose corresponded to the largest amount of the drug that could safely be administered within 45 mL of human albumin solution. The 75-mg iv dose permitted a follow-up of the plasma concentrations and urinary excretion of proquazone and its main metabolite over sufficient time. The 300- and 900-mg po dosages corresponded, respectively, to a therapeutically effective maintenance dose and a cumulative daily dose during antirheumatic treatment. A total of 20 studies were conducted, and the design of the studies was identical for each volunteer. They first received the 900- and 300-mg po dosages and then the 122- and 75-mg iv dosages in that order. Preliminary experiments with other groups of volunteers had indicated that these dosages were well tolerated[2]. Intervals of at least 2 weeks were maintained between the studies to ensure washing out of the drug and to exclude any possible enzyme induction in the subjects due to repeated administration of the drug.

The volunteers were supine during the first 24 h after administration of the drug. Following this they were ambulatory, but no exercise was allowed. The individuals were fasted 12 h before drug administration in both the intravenous and oral studies. After drug administration, the volunteers fasted 6 h. Within the first 24 h after drug administration, the food intake was restricted to fluids, *e.g.*, soups, shakes, and other beverages. The fluid intake amounted to 3000 mL/24 h for the duration of the study. No beverage or food containing caffeine or other diuretically effective substances were allowed. Three hours prior to drug administration, the volunteers received a peroral water loading (10 mL/kg). One-half hour prior to administration of the drug, a catheter[9] was placed in a cubital vein and a constant drip of 0.45% NaCl[10] (flow rate 2.0 mL/min) was started. In the intravenous studies an additional catheter[9] was inserted in a contralateral cubital vein, and a constant drip of 0.9% NaCl[10] (flow rate, 2.5 mL/min) was started. Both infusion solutions contained 1 USP U of heparin/mL to prevent coagulation. Preliminary experiments had demonstrated, that the presence of heparin did not alter the plasma protein binding of I.

The second catheter was used for administering the drug in the intravenous studies and was removed 2 h after drug administration. The first catheter was employed for blood sampling and was removed 11 h after drug administration. Later blood samples were taken by venipuncture[11]. Blood samples (10 mL) were taken through the catheter with syringes using a three-way stopcock within 10 s at 0, 1.5, 2, 2.5, 3, 5, 7, 10, 15, 20, 25, 30, 40, 50, 60, 75, and 90 min, 2, 2.5, 3, 3.5, 4, 4.5, 5, 5.5, 6, 6.5, 7.5, 8, 9, and 10 h after intravenous administration of the drug and at 0, 2.5, 5, 7.5, 10, 15, 20, 30, 45, 60, 75, and 90 min, 2, 3, 4, 5, 6, 7, 8, 10, 15, 18, 24, 36, 42, and 48 h after oral administration. A total volume of approximately 1200 mL of blood was obtained from the volunteers in the four studies within a period of three months. The initial 2 mL of blood was discarded when blood was sampled through the catheters. The blood samples were immediately transferred to heparinized centrifuge tubes and subsequently centrifuged at 300 × *g* for 10 min. Centrifugation of the samples was always accomplished within 1 h after sampling. The plasma was then immediately transferred to storage tubes and kept at −20°C until assayed. In both intravenous and peroral experiments, total volumes of urine were obtained for the following collection periods: −3–0,

[9] Viggo Venflon; Viggo AB, Helsingborg, Sweden.
[10] Kantonsspital Basel, Switzerland.
[11] Vacutainer; Becton, Dickinson and Co., Rutherford, N.J.

Table I—Pharmacokinetic Parameters of Proquazone After Intravenous Administration Derived From the Best Fit by Digital Computer Programs [a]

Parameter	Subject A		B		C		D		E		Mean ± *SD* (n = 10)	
Weight, height [b]	70, 185		83, 184		68, 177		73, 174		82, 181			
Surface area, m^2	1.92		2.06		1.84		1.87		2.02			
Dose, mg iv	74.33	121.96	74.90	122.00	74.50	122.12	74.52	121.94	74.55	121.90		
α [c], 10^2 min^{-1}	48.6	86.8	17.6	26.9	14.6	16.7	44.0	59.2	30.9	32.1	36.7	23.1
	(1.48)	(0.96)	(4.78)	(0.96)	(0.87)	(2.11)	(1.04)	(1.00)	(1.48)	(0.68)	(1.54)	(1.21)
β [c], 10^2 min^{-1}	4.90	8.20	6.88	5.09	4.18	2.78	5.10	5.50	3.74	3.32	4.97	1.63
	(1.31)	(0.97)	(0.97)	(0.94)	(1.16)	(1.45)	(1.04)	(1.03)	(1.45)	(0.97)	(1.13)	(0.20)
γ [c], 10^2 min^{-1}	1.09	1.09	1.09	0.720	1.09	0.843	0.880	0.950	0.800	0.560	0.911	0.185
	(0.97)	(0.96)	(0.87)	(0.83)	(1.27)	(1.27)	(0.96)	(0.93)	(1.15)	(0.94)	(1.02)	(0.16)
A [c], % dose/L	12.7	11.6	1.15	4.47	1.48	3.93	13.2	8.91	9.35	6.13	7.29	4.49
	(1.59)	(0.96)	(6.25)	(1.03)	(1.29)	(1.38)	(1.02)	(1.01)	(1.32)	(1.00)	(1.69)	(1.62)
B [c], % dose/L	2.16	3.43	3.51	3.45	3.24	3.22	3.10	3.68	2.40	2.32	3.05	0.543
	(1.35)	(1.01)	(1.08)	(0.97)	(0.91)	(1.16)	(0.96)	(1.01)	(1.35)	(0.99)	(1.08)	(0.158)
C [c], % dose/L	0.747	0.900	0.846	0.229	0.599	0.372	0.395	0.699	0.472	0.237	0.550	0.224
	(1.05)	(0.96)	(0.86)	(0.91)	(1.59)	(2.11)	(1.01)	(0.92)	(1.40)	(0.92)	(1.17)	(0.41)
V [d], L	6.41	6.28	18.2	12.3	18.8	13.3	5.99	7.53	8.18	11.5	10.8	4.80
V_{ps} [d], L	66.1	66.6	67.9	120	62.6	64.7	83.7	67.7	81.5	136	81.6	25.6
V_{ss} [f], L	37.6	42.7	43.2	43.0	32.4	28.4	34.5	37.2	39.1	56.4	39.5	7.69
CL [g], mL/min	745	772	727	857	702	559	730	644	641	729	711	81.6
k_{BT} [h], min^{-1}	0.235	0.435	0.014	0.081	0.020	0.053	0.194	0.284	0.136	0.149	0.160	0.132
k_{TB} [h], min^{-1}	0.125	0.285	0.152	0.148	0.116	0.094	0.130	0.228	0.099	0.116	0.146	0.063
$k_{BT'}$ [h], min^{-1}	0.056	0.102	0.027	0.019	0.011	0.006	0.041	0.043	0.028	0.020	0.035	0.028
$k_{T'B}$ [h], min^{-1}	0.019	0.023	0.021	0.009	0.015	0.010	0.012	0.016	0.012	0.008	0.015	0.005
k_{BE} [i], min^{-1}	0.112	0.116	0.041	0.070	0.036	0.041	0.123	0.085	0.080	0.066	0.077	0.032

[a] NONLIN and SAAM. [b] Weight in kg; height in cm. [c] Parameters of the sum of the tri-exponential equations to express the plasma concentration of proquazone as a function of time as obtained using the digital computer programs NONLIN and SAAM. SAAM results expressed as fractions of the estimates by NONLIN are in parentheses. [d] Calculated from Eq. 2. [e] Obtained using Eq. 6. [f] Derived from Eq. 7. [g] Computed from Eq. 5; the plasma area was obtained using Eq. 3b. [h] Rate constants of distribution calculated using the method in Ref 28. [i] Rate constant of elimination obtained using the method in Ref. 28.

0–1, 1–2, 2–4, 4–6, 6–8, 8–10, 10–12, 12–18, 18–24, 24–36, 36–48, 48–60, 60–72, and 72–96 h after drug administration. The urinary pH was monitored, and aliquots of 20–30 mL were transferred to storage containers and kept at −20°C until assayed. Heart rate and blood pressure were monitored at hourly intervals in all the studies up to 10 h after administration.

Preliminary experiments investigated the possible binding of I to syringes, stopcocks, and urine containers. No significant drug binding was found for the drug with these materials.

Drug Administration—*Intravenous*—Freshly prepared sterile solutions of 1.6 and 1.0 mL of I in 4-hydroxymethyl-1,3-dioxolane-5-hydroxy 1,3-dioxane (1:2) (7.5% w/v) in 2-mL syringes were slowly added to 45 mL of human albumin solution kept in 50-mL syringes[12] using a three-way stopcock[13]. The solutions had been brought to a temperature of 37°C previously. After mixing the combined solutions thoroughly, 2-ml aliquots were taken for the determination of the dosages administered. The drug-containing albumin solutions were injected at a constant rate over a period of 60 ± 5 s through one of the catheters. The catheter was immediately flushed with 10 mL of blood which had been taken previously from the volunteer and had been heparinized subsequently. This time was considered as time zero.

Peroral—The capsules (1 or 3) were swallowed together with 100 mL of water. The time of swallowing was considered as time zero.

Analytical Procedures—Proquazone in plasma and urine was determined by a fluorometric method[2]. The main metabolite (II) and its conjugated product (III) were measured in urine by an HPLC assay[2].

The fluorometric assay involved extraction under alkaline conditions into n-heptane and back-extraction under acidic conditions into an aqueous phase. Fluorescence was determined at an emission wavelength of 510 nm (excitation at 326 nm). Unknown concentrations of I were determined by means of standard curves derived from samples spiked with known amounts of the drug. The individual time zero samples obtained from each volunteer served as blanks. The fluorometric assay was specific for I, and its lower level of sensitivity was at 10 ng/mL in plasma and urine. The mean percentage recovery (±*SD*) of the assay determined from samples which were spiked with known amounts of I was 108 ± 8% (n = 25) and 104 ± 5% (n = 7), respectively, for concentrations between 50 and 100 ng/mL in plasma and 95 ± 7% (n = 11) at a concentration of 50 ng/mL in urine. The mean percent precision (10^2 *SD*/Mean) of the fluorometric assay estimated from measurements of samples spiked with known amounts of I was 3% (n = 6) for the concentration range 10–1000 ng/mL in plasma and 9% (n = 6) for the concentration range 10–10,000 ng/mL in urine.

The HPLC method developed for the measurement of II in urine included an extraction into carbon tetrachloride–chloroform (1:1) prior to injection into the HPLC and measurement of the UV absorbance at 237 nm. HPLC conditions were as follows. A stainless steel column (25 × 0.4-cm i.d.)[14] prepacked with silica gel[15] was used for separation. It was protected by a stainless steel precolumn (4.0 × 0.4-cm i.d.) which was dry-packed with porous beads of silica gel[16]. A ternary mixture of isooctane–ether–ethoxyethanol (650:350:50, v/v/v) was employed as the mobile phase at flow rates of 1.6–2.0 mL/min. n-Ethylproquazone was used as internal standard. The respective retention times for II and n-ethylproquazone were 6.6 and 7.8 min.

For the determination of total [conjugated + unconjugated (II + III)] metabolites, the urine samples were exposed to enzymic hydrolysis at 37°C for 2 h at pH 5.35. The enzymic digests were then extracted into benzene–isopropyl alcohol (5:1) and subsequently injected into the HPLC. The amounts of III were obtained from the difference between the individually determined total metabolites and the amount of II. The lower level of sensitivity of the HPLC method in urine was 20 ng/mL. The mean percent recovery (±*SD*) for II plus III with this method was 98 ± 10 (n = 22) for the concentration range 0.2–1.0 μg/mL. The respective mean percent precisions of the method for II plus III and II obtained from samples spiked with known amounts of the metabolites were similar and were 7 and 11% (n = 6) for the above concentration ranges.

Estimates for the relative precision of the fluorometric and HPLC methods were also calculated from the replicate determinations of the samples obtained in the pharmacokinetic studies. In plasma the relative precision of the fluorometric method was constant over a large concentration range (8000–50 ng/mL) and was high (2%). In the lower concentration range (50–5 ng/mL), the relative precision of the method was clearly smaller (35%). In urine the variability of the fluorometric method for I in the concentration range of 50–5 ng/mL was large, and the relative precision was 60%. Similarly obtained estimates for the relative precision of II and III measurements by the HPLC method yielded average values of 7% (4.0–0.01 μg/mL) and 6% (250–0.01 μg/mL), respectively. All measurements in plasma and urine by fluorometry or HPLC were performed in duplicate. The means of these determinations were used for graphical and digital computer analyses.

Pharmacokinetic Data Analysis—*Proquazone*—The data analyses

[12] Disposable Syringes; ASIK I/S Hospital Supplies, Denmark.
[13] Pharmaseal Laboratories, Glendale, Calif.
[14] Hibar; Merck Ltd., Darmstadt, West Germany.
[15] Lickrosorb; Merck Ltd., Darmstadt, West Germany.
[16] Perisorb; Merck Ltd., Darmstadt, West Germany.

Table II—Urine Data of Proquazone and Its *m*-Hydroxy Metabolites

Subject	Dose, mg	$10^4\ U_\infty/D$[a]	$10^2\ U_\infty^{II}/D$[b]	$10^2\ U_\infty^{III}/D$[c]	$10^2\ U_\infty^{(II+III)}/D$[d]	$10^2\ U_\infty^{II}/U_\infty^{III}$[e]
A	75 iv				14.53	
	122 iv	0.616	0.201	14.36	14.56	1.40
	300 po		0.078	15.62	15.69	0.496
	900 po		0.068	10.35	10.42	0.657
B	75 iv				23.32	
	122 iv	1.749	0.176	18.75	18.93	0.936
	300 po		0.163	23.29	23.45	0.700
	900 po		0.040	11.05	11.11	0.391
C	75 iv				24.00	
	122 iv	0.346	0.363	27.85	28.21	1.30
	300 po		0.371	28.03	28.40	1.32
	900 po		0.116	19.35	19.46	0.598
D	75 iv				19.19	
	122 iv	0.733	0.358	18.78	19.14	1.91
	300 po		0.208	17.10	17.32	1.21
	900 po		0.150	10.68	10.84	1.40
E	75 iv				21.16	
	122 iv	0.600	0.149	18.28	18.43	0.815
	300 po		0.043	15.85	16.28	0.274
	900 po		0.049	13.55	13.61	0.359
Mean ± *SD* (*n* = 5)	75 iv				20.44 ± 3.80	
	122 iv	0.781 ± 0.492	0.250 ± 0.010	19.60 ± 4.97	19.85 ± 5.03	1.27 ± 0.430
	300 po		0.173 ± 0.129	19.97 ± 5.47	20.23 ± 5.50	0.800 ± 0.450
	900 po		0.085 ± 0.046	13.00 ± 3.77	13.08 ± 3.78	0.680 ± 0.420
Paired *t* test	300 po/900 po		$p < 0.14$	$p < 0.02$	$p < 0.02$	
	122 iv/300 po					$p < 0.05$
	122 iv/900 po					$p < 0.005$

[a] Fraction of dose renally excreted as unchanged proquazone at infinite time, obtained using Eq. 9. [b] Fraction of dose renally excreted as *m*-hydroxyproquazone at infinite time, obtained using Eq. 17. [c] Fraction of dose renally excreted as conjugated *m*-hydroxyproquazone at infinite time, obtained using Eq. 17. [d] Fraction of dose renally excreted at infinite time as the sum of unconjugated and conjugated *m*-hydroxyproquazone. [e] Ratio of the renally excreted amounts at infinite time of unconjugated to conjugated *m*-hydroxyproquazone.

on I after intravenous administration used graphical and digital computer methods. Initial (0–2.5 min) and terminal (10 h→∞) concentrations were not available. However determinations of clearance and volume of distribution parameters are based on plasma concentrations from time zero to infinity. Hence, plasma concentrations in the initial and terminal intervals were generated by fitting the experimentally determined plasma concentrations of I (C_p) after intravenous administration to polyexponential functions. The fittings were performed with the individual data using the nonlinear least-squares estimation programs SAAM (11) and NONLIN (12). Best results were obtained with both SAAM and NONLIN when the experimental data were fitted to the class (13) of three-compartment intravenous infusion models (without any assumptions regarding topology of the compartments) in accordance with:

$$C_p = A'e^{-\alpha t'} + B'e^{-\beta t'} + Ce^{-\gamma t'} \qquad \text{(Eq. 1)}$$

where A', B', and C' are the coefficients and α, β, and γ are exponents of the three-exponential equation and t' is the postinfusion time. Different weighting procedures were evaluated in preliminary fitting attempts with both programs. Weighting according to $w = 1/K \cdot C_p$, where K corresponds to a constant, and $w = 1/C_p$ was most adequate for the definitive fitting of the data by SAAM and NONLIN, respectively. The assumption of an intravenous infusion model was justified since the large value of the rate constant of the early disposition phase ($t_{1/2,\alpha}$ = 2 min) necessitated consideration of the 1-min infusion time. Fitting the data to a three-exponential equation, but not to a two-exponential equation, yielded random scatter of the data points about the regression line in all 10 data sets (by NONLIN and SAAM); a typical example (SAAM) is given in Fig. 1. Fitting the data to a four-exponential equation did not produce a significant reduction of the weighted sum of squared deviations (14), although four phases were separable by graphical analysis in some plots.

In fitting the data to the class of three-compartment models, no assumptions were made regarding the topology of the compartments. However, when clearance and steady-state volume of distribution values were derived from the coefficients and exponents of the fits, it was presumed that elimination of the drug occurred exclusively from the measured site, *i.e.*, plasma compartment (15). Only a few of the class of three-compartment models fulfill this requirement. Among those, a mamillary three-compartment model was arbitrarily chosen, and its volume and rate constant parameters calculated from the coefficients and exponents obtained in the fits. Mamillary models, which presume elimination to occur exclusively from the measured site, *i.e.*, the central compartment (15), represent the most often used model type in pharmacokinetic data analysis. The study of a particular type of model permits one to follow the time course of the drug in the tissue compartments and to evaluate depth and capacity of the different body compartments.

The peroral data were analyzed in a different way; they were not fitted to polyexponential equations. Only the terminal logarithmic linear phase plasma concentrations were fitted to obtain plasma concentrations over the entire time course. The plasma concentrations of I after peroral administration were much smaller and showed more scatter than the intravenous data. In addition, a possible deviation from first-order kinetics of I at the 900-mg dose level was implied by the metabolite data and could not be rejected.

m-Hydroxy Metabolites—The urinary data on metabolites II and III after both modes of administration were subjected to a model independent analysis.

Pharmacokinetic Calculations—*Proquazone*—The apparent volume of distribution of the central compartment, V, was estimated by:

$$V = D/C_0 = D/(A + B + C) \qquad \text{(Eq. 2)}$$

where D corresponds to the dose, C_0 is the drug concentration at time zero (intravenous bolus model), and A, B, and C represent the coefficients of the corresponding model equation (16). The total area under the plasma concentration time curve, AUC, was obtained from:

$$\text{AUC} = A/\alpha + B/\beta + C/\gamma \qquad \text{(Eq. 3a)}$$

$$\text{AUC} = \text{AUC}(t_0,t_1) + \text{AUC}(t_1,t_2) + \text{AUC}(t_2,t_\infty) \qquad \text{(Eq. 3b)}$$

where $\text{AUC}(t_0,t_1)$ and $\text{AUC}(t_1,t_2)$ correspond, respectively, to the partial area during the time of infusion and to the partial area during the time interval after the infusion was stopped to the last measured sample, and $\text{AUC}(t_2,t_\infty)$ is the partial area from the time of the last measured sample (10 h) to infinity on the presumption of terminal logarithmic linear decay. $\text{AUC}(t_0,t_1)$ and $\text{AUC}(t_1,t_2)$ were obtained by numerical integration (linear trapezoidal rule) after the plasma concentration at the end of infusion was estimated from Eq. 1. $\text{AUC}(t_2,t_\infty)$ was determined by algebraic integration in accordance with:

$$\text{AUC}(t_2,t_\infty) = C_{10\text{ h}}/\gamma \qquad \text{(Eq. 4)}$$

where $C_{10\text{ h}}$ corresponds to the concentration of the last measured sample. The ratio of the $\text{AUC}(t_0,t_1)$ to AUC was, on average, 0.04; the ratio of $\text{AUC}(t_2,t_\infty)$ to AUC was negligibly small (<0.004). The total clearance of drug, CL, was estimated according to:

$$CL = D/\text{AUC} \qquad \text{(Eq. 5)}$$

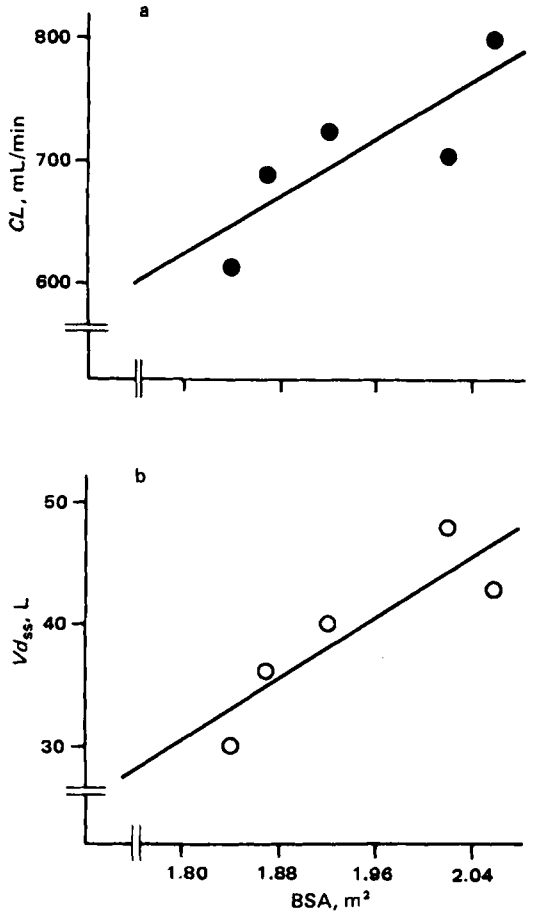

Figure 3—*Linear plots of the clearance (a) and steady-state volume of distribution (b) against body surface area in volunteers A–E, using the mean values obtained in the intravenous experiments for each individual. There are apparent linear relationships between* CL *and BSA [y = 435 (±440) + 588 (±226)·x, r = 0.832, p < 0.05] and* V_{ss} *and BSA [y = 83.6 (±38.5) + 63.4 (±19.8)·x, r = 0.880, p < 0.05].*

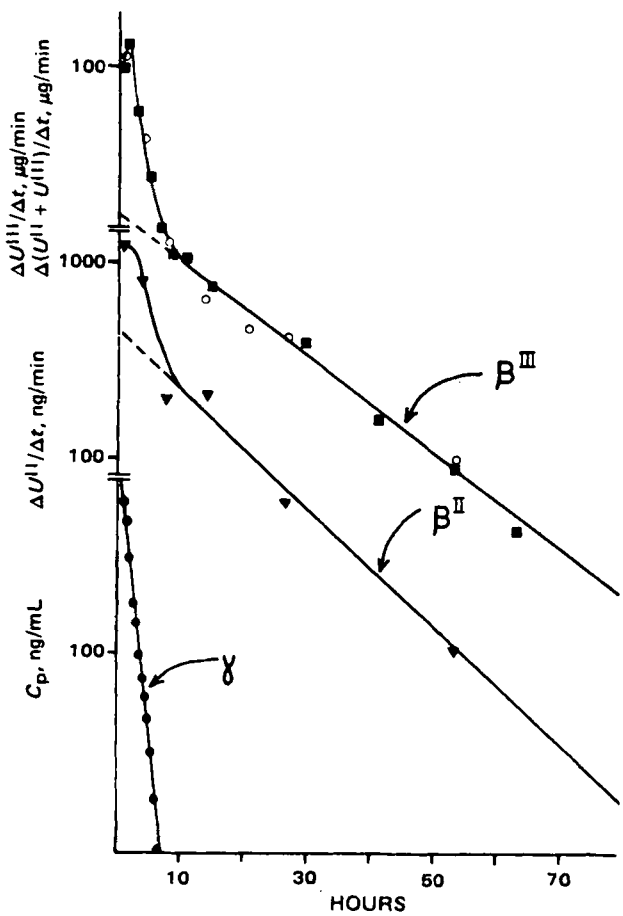

Figure 4—*Semilogarithmic plots against time after intravenous administration of the rates of urinary excretion per minute (*dU/dt*) for II (▼), III (○), and II plus III (■). A semilogarithmic plot of plasma concentration against time of I (●) is included for comparison. The metabolites II and III have similar triphasic profiles with peak rates at 1 h after administration and apparent terminal logarithmic linear phases with slopes of* $-\beta^{II,III}$. *Data were obtained in subject C after an intravenous dose of 122 mg.*

The apparent pseudo-steady-state volume of distribution, V_{ps}, was obtained from:

$$V_{ps} = CL/\gamma \qquad \text{(Eq. 6)}$$

The apparent steady-state volume of distribution was estimated according to:

$$V_{ss} = D\left(\frac{A}{\alpha^2} + \frac{B}{\beta^2} + \frac{C}{\gamma^2}\right) \Big/ \left(\frac{A}{\alpha} + \frac{B}{\beta} + \frac{C}{\gamma}\right)^2 \qquad \text{(Eq. 7)}$$

Amounts of unchanged drug excreted in urine at infinite time, U, were obtained from:

$$U = U_{6\text{ h}} + (dU/dt)_{6\text{ h}}/\gamma \qquad \text{(Eq. 8)}$$

where $U_{6\text{ h}}$ and $(dU/dt)_{6\text{ h}}$ correspond, respectively, to the amounts excreted up to 6 h and to the urinary excretion rate 6 h after drug administration; γ was estimated from semilogarithmic plots of the excretion rate against time. Renal clearance, CL_{ren}, was calculated according to:

$$CL_{ren} = U/\text{AUC} \qquad \text{(Eq. 9)}$$

Glomerular clearance, CL_{glom}, was predicted from:

$$CL_{glom} = CL_{cr} \cdot f_u \qquad \text{(Eq. 10)}$$

where CL_{cr} corresponds to the individually measured creatinine clearance, and f_u is the fraction of drug unbound in the plasma of the individual (7).

On the assumption that all nonrenal elimination occurred in the liver, the hepatic extraction efficiency (hepatic first-pass effect) was computed from:

$$\epsilon^{I,1} = \frac{CL_{hep}}{\hat{V}_{hep}} = \frac{CL - CL_{ren}}{\hat{V}_{hep}} \qquad \text{(Eq. 11)}$$

where CL_{hep} and $\hat{V}_{hep}$ correspond to the liver clearance and liver plasma flow [825 mL/min (17)], respectively.

The percentage of an oral dose of I that reached the systemic circulation unchanged [extent of absorption (18)], E, was estimated according to:

$$E = 10^2 \frac{(AUC/D)_{po}}{(AUC/D)_{iv}} \qquad \text{(Eq. 12)}$$

The fraction of the dose eliminated by first pass on oral administration, ϵ, was estimated from the urinary data of II and III using:

$$\epsilon^{II} = R^{II}\{(U^{II}/D)_{po} - [(U^{II}/D)_{iv} \cdot E/10^2]\} \qquad \text{(Eq. 13a)}$$

$$\epsilon^{III} = R^{III}\{(U^{III}/D)_{po} - [(U^{III}/D)_{iv} \cdot E/10^2]\} \qquad \text{(Eq. 13b)}$$

where $R^{II} = [(D - U^{I})/U^{II}]_{iv}$ and $R^{III} = [(D - U^{I})/U^{II}]_{iv}$ on the assumption that the ratio of drug metabolized to other metabolite(s) or eliminated by routes other than renal to the amount of II and III formed is invariant with route of administration. Estimates for ϵ were also obtained from proquazone data in accordance with:

$$\epsilon^{I,2} = 1 - (E/10^2) \qquad \text{(Eq. 14)}$$

The total extent of absorption of unchanged plus changed drug at the 300-mg dose level, E^{tot}, was estimated from:

$$E^{tot} = 10^2\epsilon^{I,1} + E \qquad \text{(Eq. 15)}$$

m-*Hydroxy Metabolites*—The respective amounts of II or III excreted in urine at infinite time, $U^{II,III}$, were obtained from:

$$U^{II,III} = [U_{72\text{ h}} + (dU/dt)_{72\text{ h}}/\beta]^{II,III} \qquad \text{(Eq. 16)}$$

where $U^{II,III}_{72\text{ h}}$ corresponds to the excreted amounts of II or III at 72 h and

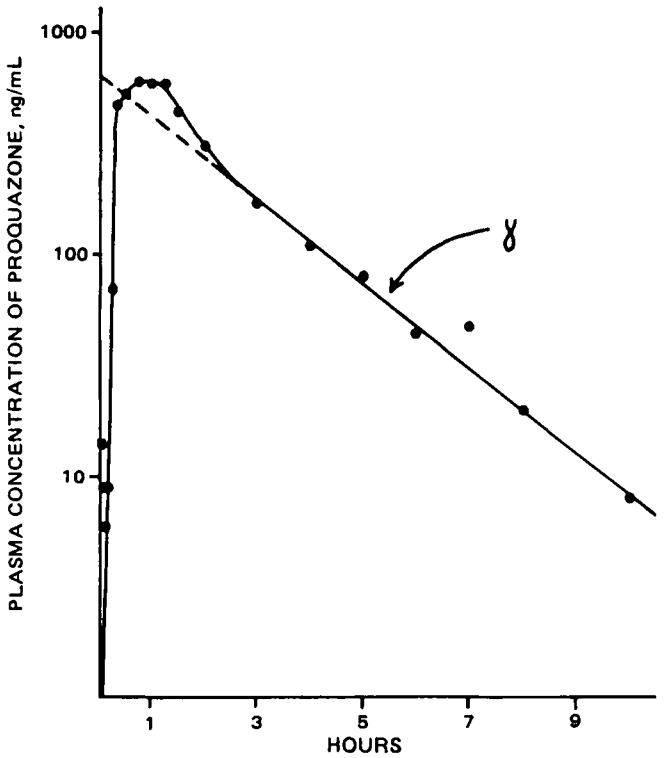

Figure 5—*Semilogarithmic plot against time of proquazone plasma concentration following administration of 900 mg po to subject A showing a triphasic profile. The apparent terminal logarithmic phase is linear with a slope of* $-\gamma$.

$(dU/dt)^{II,III}_{72\ h}$ to the excretion rates of II and III 72 h after drug administration; $\beta^{II,III}$ was estimated from semilogarithmic plots of the respective urinary excretion rates against time. The ratios of $(U_{72\ h-\infty}/U)^{II}$ and $(U_{72\ h-\infty}/U)^{III}$ were insignificant (<0.01).

Statistics—Paired *t* test statistics were performed with the proquazone and metabolite data after peroral administration of the drug.

RESULTS

Procedural and Adverse Effects—The values of the clinical laboratory data that were obtained prior to each of the four administrations of proquazone were always within the normal range for males of this age group (19). Proquazone at the four dosage levels was well tolerated, and no adverse drug effects were observed. Blood pressure and heart rate did not show significant changes in the interval up to 10 h after administration of the drug.

Pharmacokinetics of Proquazone and Its *m*-Hydroxy Metabolites—Mean values for the parameters as estimated by NONLIN are given hereafter in the text; the plus and minus values for these means refer to the standard deviation. The number of values considered was 10 unless otherwise specified. The volume and clearance parameters of I are referenced to total (bound plus unbound) drug concentration in plasma. It was assumed that the concentration ratio of total to unbound drug in plasma was maintained during the passage of I through the capillaries of the liver. Negligible concentrations of I were found in erythrocytes in whole blood (7).

Intravenous Administration—*Proquazone*—The NONLIN and SAAM estimates for the coefficients and exponents of the fitted three-exponential equation were equivalent (Table I). The values respectively obtained for A and α varied the most. There was good agreement between the estimated total clearance (NONLIN, 708 mL/min; SAAM, 689 mL/min) and steady-state volume of distribution (NONLIN, 39.5 L; SAAM, 39.7 L) obtained by the two programs.

The CL estimates by NONLIN and SAAM were close to those obtained by application of the trapezoidal rule (711 mL/min), suggesting that the polyexponential fittings by both programs were adequate. The dose-normalized plasma concentration–time data at the lower and higher dose levels were superimposable and indicated first-order kinetics of I. The dose percentages of unchanged I eliminated by the renal route were extremely small (<0.001%) and could be measured reliably only after the higher intravenous dose (Table II). Three phases with mean apparent half-lives of 2 (±1) min ($t_{1/2,\alpha}$), 14 (±5) min ($t_{1/2,\beta}$), and 76 (±15) min ($t_{1/2,\gamma}$) were separable in the curves in plasma (Fig. 2, Table I). The latter value was confirmed by $t_{1/2,\gamma}$ = 98 (±30) min (n = 5) estimated from semilogarithmic plots of the urinary excretion rates against time. In all the experiments, the plasma samples taken at 1.5 min after the end of the infusion yielded maximum concentrations and indicated fast initial mixing in plasma. The apparent volume of distribution of the central compartment (V) was, on average, 11 (±4.8) L (Table I) and exceeded the plasma volume [3 L (20)] significantly. This suggested fast extravascular distribution of the highly plasma protein-bound drug (7). Total clearance of I, CL, averaged 707 (±83.7) mL/min. The extraction efficiency of the liver for I (ϵ) was 0.86 (±0.101) and suggested that I can be classified as a highly extracted compound (21, 22). There was an apparent linear correlation between CL and body surface (BSA), but not between CL and weight, for the individuals (Fig. 3a). The renal clearance, CL_{ren}, averaged 0.06 (±0.05) mL/min and was smaller than the estimated glomerular clearance, CL_{glom} = 2.5 (±0.50) mL/min, indicating tubular reabsorption in excess of possible tubular secretion for the highly lipophilic drug.

Table III—Pharmacokinetic Parameters of Proquazone Derived from Plasma Data After Peroral Administration

Subject	Dose, mg	γ^a, 10^2 min^{-1}	$t_{max}{}^b$, min	$C_{max}{}^c$, % dose/L	$AUC_{0\text{-}10\ h}/D^d$, 10^2 min/L
A	300	0.75	45	0.087	10.45
	900	0.72	45	0.068	10.07
B	300	0.84	180	0.030	5.45
	900	0.81	240	0.016	4.14
C	300	0.65	90	0.027	8.44
	900	0.44	90	0.036	7.88
D	300	0.77	60	0.020	3.60
	900	1.24	30	0.056	3.94
E	300	0.87	60	0.088	13.77
	900	0.83	30	0.241	32.50
Mean ± *SD* (n = 5)	300	0.78 ± 0.08	87 ± 55	0.051 ± 0.034	8.43 + 4.02
	900	0.81 ± 0.29	87 ± 89	0.083 ± 0.090	11.71 ± 11.91

[a] Slopes of the apparent terminal logarithmic linear γ phase. [b] Times of the maximum plasma concentration of proquazone. [c] Maximum plasma concentration of proquazone at time t_{max} after peroral administration. [d] Dose corrected quasi total areas under the plasma concentration time curve from time zero to 10 h after administration, obtained using Eq. 3.

There was no indication for urine flow or urine pH dependency of the renal elimination of I. The volumes of distribution at pseudo-steady-state (V_{ps}) and at steady state (V_{ss}) were 82 (±26) and 39 (±7.7) L, respectively, (Table I). The large difference between these values indicated that the microscopic rate constants of distribution into the tissue compartment T′ ($k_{BT'}$ and $k_{T'B}$) were small relative to the rate constant of elimination (k_{BE}) (Table I). The slower equilibrating tissue compartment T′ (Fig. 1) must be regarded as a deep compartment. Its capacity for the drug is much larger than that of the shallow compartment T (Table I). The volume of distribution at steady state, V_{ss}, depended linearly on the BSA of the individuals (Fig. 3b). In contrast, no such correlation existed between V_{ss} and weight of the individuals, indicating that the widely used principle of weight normalization of kinetic parameters may be questionable.

m-Hydroxy Metabolites—Semilogarithmic plots against time of the urinary excretion rates of II and III showed triphasic profiles with terminal half-lives $t_{1/2\beta}$ of 6.7 (±3.1) h (n = 5) for II and 10.6 (±3.0) h (n = 5) for III (Fig. 4). This implied that the *m*-hydroxy metabolites have a considerably larger time of residence in the body than the parent drug. Metabolite II is reportedly pharmacologically active[2]. The percentages of the administered dose renally excreted as *m*-hydroxy metabolites (II plus III) were 20.4 ± 3.80% and 19.9 ± 5.03% (n = 5) (Table II) after the lower and higher intravenous dosages, respectively. This implied first-order kinetics of the metabolites. The combined urinary recoveries of I, II, and III amounted to 20%, indicating that 80% of the dose was eliminated by alternative routes. The renally recovered dose percentages of III [19.6 ± 4.97% (n = 5)] clearly exceeded those of II [0.25 ± 0.01% (n = 5)] (Table II).

A model comprising all the experimental findings after intravenous administration is given in Scheme I. As mentioned previously, a model-dependent data analysis was performed with the parent drug data,

Table IV—Extent of Absorption and First-Pass Effect of Proquazone

Subject	Dose mg	Extent of Absorption: Unchanged Drug E^a	Extent of Absorption: Unchanged + Changed Drug $E^{tot\ b}$	First-Pass Effect: $\epsilon^{I,1c}$	First-Pass Effect: $\epsilon^{III d}$	First-Pass Effect: $\epsilon^{II e}$	First-Pass Effect: $\epsilon^{I,2f}$
A	300	8.2	109	0.92	1.01	0.38	0.78
	900	7.7					
B	300	4.5	124	0.96	1.20	0.88	0.95
	900	3.3					
C	300	5.4	101	0.76	0.95	0.97	0.94
	900	5.1					
D	300	2.7	91	0.83	0.89	0.56	0.95
	900	2.7					
E	300	9.7	87	0.83	0.78	0.19	0.66
	900	22.4					
Mean ± *SD*	300	6.1 ± 2.8	103 ± 15	0.86 ± 0.13	0.96 ± 0.16	0.60 ± 0.33	0.86 ± 0.13
	900	8.2 ± 8.2					

[a] *Calculated from Eq. 12.* [b] *Computed according to Eq. 15.* [c] *Obtained using Eq. 11.* [d] *Estimated from Eq. 13a using III data.* [e] *Calculated from Eq. 13b using II data.* [f] Obtained in accordance with Eq. 14 after rearrangement.

whereas a model-independent approach was effected with the metabolite data. Scheme I reflects this approach. The model depicted is the most simple that can account for all the kinetic events observable with the type of data analysis chosen. The parent drug is represented by a three-compartment body model with extrarenal [formation of II, formation of unidentified metabolite(s), and biliary excretion (X)] and renal (U) elimination. The identified metabolites II and III are represented each by a body compartment (II, III) with renal (U_{II}, U_{III}) and extrarenal [formation of III, formation of unidentified metabolite(s), and biliary excretion (X)] elimination. As can be seen, the amounts of I, II, and III passing through all routes of elimination, which were not monitored directly, are lumped together (X).

Peroral Administration—*Proquazone*—Maximally, three (Fig. 5) or two phases were separable in the plasma concentration–time profiles of I after administration of the two peroral dosages. The triphasic profiles peaked earlier than the biphasic profiles. These findings indicated that absorption was faster than early disposition (β) in the former, but slower than early disposition in the latter experiments. The times of peak plasma concentration (t_{max}), the dose-normalized peak plasma concentrations ($10^2C_{max}/D$), and the dose-normalized areas under the plasma concentration time curves ($10^2AUC_{0-10\ h}/D$) were not significantly different for the two dose levels (Table III). The slopes of the terminal logarithmic linear phase (γ) after oral dosing agreed with those previously found after intravenous dosing. These results suggest that first-order kinetics were operative for I after oral dosing at both dosage levels. In four of the five individuals tested (A–D), the dose-normalized AUC values were remarkably similar at both dosage levels, whereas in one individual (E) this parameter was clearly larger after 900 mg than after 300 mg (Table III). The extent of absorption (18) averaged 6.1 ± 2.8% (n = 5) and did not differ significantly from E = 8.2 ± 8.2% (n = 5) after the 900-mg dose (Table IV). The small dose fractions of drug reaching the systemic circulation unchanged implied a poor absorption or a large first-pass effect for I.

m-*Hydroxy Metabolites*—Semilogarithmic plots of the urinary excretion rates against time after oral dosing showed profiles similar to those observed after intravenous administration except that they peaked later (Figs. 4 and 6). The percentages of the administered dose renally excreted as II and III after the 900-mg dose tended to be smaller than after the 300-mg dose, representing respectively 65 and 50% of the recoveries found at the lower dose level (Table II). The ratios of the urinary recoveries of II to III were equivalent after administration of the two peroral dosages (Table II), suggesting that the observed dose-dependent, nonlinear kinetics were associated with the formation of II. This was in contrast to the previously observed linear kinetics of disposition of I after peroral dosing, which implied linear kinetics of formation for II. When the dose fractions of I eliminated during first pass at the 300-mg dose level were estimated from II and III data assuming linear kinetics, average values of ϵ^{II} = 0.60 and ϵ^{III} = 0.96 were obtained (Table IV). Only the latter value was in accordance with ϵ estimates by proquazone data [$\epsilon^{I,1}$ = 0.86, $\epsilon^{I,2}$

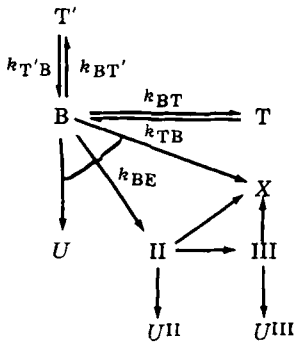

Scheme I—Model for intravenous administration of proquazone.

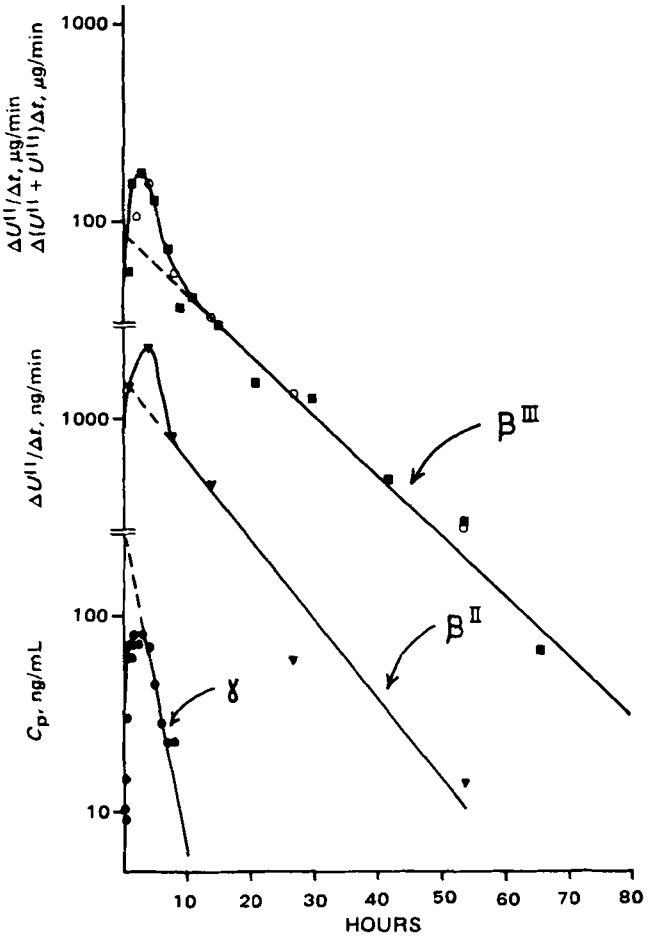

Figure 6—*Semilogarithmic plots against time after oral administration of the rates of urinary excretion per minute, (dU/dt) for II (▼), III (○), and II plus III (■). A semilogarithmic plot of plasma concentration against time of I (●) is included for comparison. The metabolites II and III have similar triphasic profiles with peak rates at 3 h after administration and apparent logarithmic linear phases with slopes of $-\beta^{II,III}$. Data were obtained in subject C after an oral dose of 300 mg.*

= 0.92, (Table IV)]. The underestimated values for ϵ obtained from II data (Table IV) implied that a significant percentage of I (~40%) was metabolized not only to II but subsequently to III during the first pass. The total extent of absorption (unchanged plus changed drug) of I was complete [E^{tot} = 103 ± 15% (n = 5), Table IV]. These results suggested that (*a*) the total first-pass effect should be assessed from III data, not from II data; (*b*) the low extent of absorption found for I was due to a large first-pass effect, and not due to poor absorption in accordance with the lipophilic nature of the compound; and (*c*) the assumption of first-order kinetics at the 300-mg dose level was reasonable.

DISCUSSION

The plasma and urinary data of proquazone and its *m*-hydroxy metabolites after administration of 75 and 122 mg iv and 300 mg po were indicative of first-order kinetics. Nonlinear, dose-dependent kinetics of formation for II were evident from the metabolite data at the 900-mg po dose level, whereas the parent drug data implied first-order kinetics of disposition for I (and hence first-order kinetics of generation for II) at this dose level. These findings were irreconcilable only if presystemic or systemic metabolism of I to II were the sole or major route of elimination for the parent drug, as equivalent 35% deviations from linear kinetics should then be found with both parent drug and metabolite data. However, if the percentage of I metabolized to II were smaller (≤40%), the parent drug data would deviate from linear kinetics by ≤14% (0.40·35%), whereas a unvariable 35% (1.0·35%) deviation from linear kinetics would be found with the metabolite data. Two other studies with administrations of 100 and 400 mg po of drug to 15 healthy volunteers determined quantitatively not only II and III, but all the metabolites which could be derivatives of II and III[2]. These studies used urinary data and permitted a quantitative assessment of the *m*-hydroxy pathway. The results showed that the percentage of I metabolized to II was ≤35%. Hence, the findings obtained at the 900-mg po dose level in the present study can be rationalized, and that the nonlinearity of the kinetics of I were recognized only with the metabolite data is reasonable. Considering the variability of the peroral plasma data of I, deviations on the order of ≤14% were too discrete to become apparent.

A major fraction of II (and III) after peroral administration of I was generated during first pass of drug through the liver; only a minor fraction of II (and III) was formed systemically from I (Table IV). The observed dose-dependent kinetics of formation of II (and III) at the 900-mg dose level was largely the result of a saturation of this first-pass effect. Whether or not the kinetics of systemically formed II (and III) were dose dependent at the higher peroral dose level could not be decided based on the available experimental evidence. A delineation as to the type of the nonlinear kinetics observed, *i.e.*, Michaelis–Menten kinetics (23), product inhibition kinetics (24), or blood flow-dependent kinetics (21, 22) (pharmacologically induced temporal decrease of the liver blood flow), was not possible with the available experimental data. However it is interesting to note that primarily hydroxy metabolites cause "product inhibition" (25).

The statistical design of the present study was not balanced. However, it is improbable that the nonlinearity of the kinetics observed at the 900-mg po dose level was a period- (procedure-) rather than a treatment- (dose-) related effect. First, the laboratory data gave no evidence for the existence of procedural effects. Second, the 900-mg dose was the first treatment given to the volunteers and procedural effects are more likely to become significant in the later experiments (300 mg po and 122 and 75 mg iv) as a result of a cumulative (carry over) effect. However, the kinetics of the parent drug and metabolites were first order in these experiments. Third, the intervals of at least 2 weeks which were maintained between the studies should have minimized possible carry-over effects.

Reports on data-fitting obtained by different computer programs can rarely be found in the literature (26, 27). The results of the present study indicated that there was reasonable agreement for the parameter estimates obtained by NONLIN and SAAM. There is a need for more of these comparative fitting efforts, so that the reliability and interchangeability of pharmacokinetic data obtained with different computer programs can be assessed definitively.

APPENDIX: GLOSSARY

D = Dose of proquazone (mg)
C_p = Concentration of proquazone in plasma (ng/mL)
C_0 = Concentration of proquazone in plasma at time zero after intravenous injection (ng/mL)
C_{max} = Maximum plasma concentration of proquazone at time t_{max} after peroral administration (ng/mL)
B = Amount of proquazone in the central compartment
T = Amount of proquazone in the shallow peripheral compartment
T′ = Amount of proquazone in the deep peripheral compartment
II = Amount of *m*-hydroxyproquazone in the body compartment
III = Amount of the conjugated *m*-hydroxyproquazone in the body compartment
U_t, U = Respective amounts of proquazone renally excreted unchanged at time t and at infinite time after administration
$U_t^{II,III}$, $U^{II,III}$ = Respective amounts of *m*-hydroxyproquazone and conjugated *m*-hydroxyproquazone renally excreted at time t and at infinite time
X = Amounts of proquazone, *m*-hydroxyproquazone, and conjugated *m*-hydroxyproquazone eliminated by routes that were not monitored directly: amounts of I, II, III excreted in bile and/or metabolized to unidentified metabolites
dU/dt = Amount of drug or metabolite excreted in urine, dU, (μg or ng) during a time interval, dt (min)
A', B', C', α, β, γ = Parameters of the three-exponential fit of the plasma concentrations of proquazone according to an intravenous infusion three-compartment model, where A', B', and C' are in ng/mL and α, β, and γ are in min
A, B, C = Parameters of the corresponding intravenous injection three-compartment model for proquazone, where A, B, and C are in % of dose/L
k_{ij} = Generalized form for the microscopic first-order rate constant from the ith to the jth compartment for proquazone (min^{-1})
$\beta^{II,III}$ = Slope of the apparent terminal logarithmic linear phase of *m*-hydroxyproquazone and conjugated *m*-hydroxyproquazone
V = Volume of distribution of proquazone in the central compartment (L)
V_{ps} = Apparent pseudo-steady-state volume of distribution of proquazone (L)
V_{ss} = Apparent steady-state volume of distribution of proquazone (L)
$AUC_{0-t'}$ AUC = Respective areas under the plasma concentration–time curve from time zero to time t and from time zero to infinity of proquazone
CL = Total clearance of proquazone (mL/min)
$\dot{V}_{hep}$ = Hepatic plasma flow (mL/min)
CL_{ren} = Renal clearance of proquazone (mL/min)
CL_{glom} = Glomerular clearance of proquazone (mL/min)
f_u = Fraction of proquazone in plasma unbound
E = Extent of absorption of unchanged proquazone
E^{tot} = Total extent of absorption of unchanged plus changed proquazone
ϵ^I, ϵ^{II}, ϵ^{III} = Respective estimates of first-pass effect (hepatic extraction efficiency) for proquazone from proquazone, *m*-hydroxy metabolite, and conjugated *m*-hydroxy metabolite data
t' = Postinfusion time (min)
BSA = Body surface area (m^2)

REFERENCES

(1) R. V. Coombs, R. P. Dauna, M. Denzer, G. E. Hardtmann, B. Huegi, G. Koletar, H. Ott, E. Junkiewicz, J. W. Perrine, and E. I. Takesue, *J. Med. Chem.*, **16**, 1237 (1973).

(2) G. E. Hardtmann, B. Huegi, G. Koletar, S. Kroin, J. W. Perrine, and E. I. Takesue, *J. Med. Chem.*, **17**, 636 (1974).

(3) E. I. Takesue, J. W. Perrine, and J. H. Trappold, *Arch. Int. Pharmacodyn.*, **221**, 122 (1976).

(4) U. Gubler and M. Baggiolini, *Scand. J. Rheum., Suppl.*, **21**, 8 (1978).

(5) R. Allan and M. Bleicher, *J. Int. Med. Res.*, **5**, 253 (1977).

(6) M. Nissilä and A. Kajander, *Scand. J. Rheum., Suppl.*, **21**, 36 (1978).

(7) A. Roos and P. H. Hinderling, *J. Pharm. Sci.*, **70**, 252 (1981).
(8) H. Ott and J. Meier, *Scand. J. Rheum., Suppl.*, **21**, 12 (1978).
(9) E. E. Ohnhaus, *Int. J. Clin. Pharmacol.*, **18**, 136 (1980).
(10) K. Siersbäck-Nielsen, J. Mølholm Hansen, J. Kampmann, and M. Kristensen, *Lancet*, **i**, 1133 (1971).
(11) M. Berman and M. F. Weiss, "User's Manual for SAAM," Public Service, Publication No. 1703, National Institutes for Health, Bethesda, Md. (1967).
(12) C. M. Metzler, "A User's Manual for NONLIN," The Upjohn Co., Technical Report 7292/69/7292/005, Kalamazoo, Mich. (1969).
(13) J. G. Wagner, *J. Pharmacokinet., Biopharm.*, **3**, 457 (1975).
(14) H. G. Boxenbaum, S. Riegelman, and R. M. Elashoff, *J. Pharmacokinet. Biopharm.*, **2**, 123 (1974).
(15) L. Z. Benet and R. L. Galeazzi, *J. Pharm. Sci.*, **68**, 1071 (1979).
(16) M. Gibaldi and D. Perrier, "Pharmacokinetics," Dekker, New York, N.Y., 1975, pp. 72–73.
(17) A. C. Guyton, "Textbook of Medical Physiology," 3rd ed., Saunders, Philadelphia, Pa., 1968, p. 325.
(18) M. Gibaldi and D. Perrier, "Pharmacokinetics," Dekkler, New York, N.Y., 1975, p. 145.
(19) K. Diem and C. Lentner (Eds), "Documenta Geigy, Scientific Tables," 7th ed. Geigy Pharmaceuticals, Division of Ciba-Geigy Corp., Ardsley, N.Y., 1975, pp. 617, 579.
(20) A. C. Guyton,"Textbook of Medical Physiology," 3rd ed., Saunders, Philadelphia, Pa., 1968, p. 419.
(21) A. S. Nies, D. G. Shand, and G. R. Wilkinson, *Clin. Pharmacokinet.*, **1**, 135 (1976).
(22) G. R. Wilkinson and D. G. Shand, *Clin. Pharmacol. Ther.*, **18**, 377 (1977).
(23) E. R. Garrett, J. Brés, K. Schnelle, and L. L. Rolf, *J. Pharmacokinet. Biopharm.*, **2**, 43 (1974).
(24) J. J. Ashley and G. Levy, *J. Pharmacokinet. Biopharm.*, **1**, 99 (1973).
(25) D. Perrier, J. J. Ashley, and G. Levy, *J. Pharmacokinet. Biopharm.*, **1**, 231 (1973).
(26) P. Veng Pedersen, *J. Pharmacokinet. Biopharm.*, **5**, 513 (1977).
(27) H. Wijnand and C. J. Timmer, *J. Pharmacokinet. Biopharm.*, **7**, 681 (1979).
(28) M. Gibaldi and D. Perrier, "Pharmacokinetics," Dekker, New York, N.Y. 1975, pp. 93–94.

ACKNOWLEDGMENTS

Supported in part by a grant provided by Sandoz Ltd., Basle, for which the authors are grateful.

We thank Ms. R. Leder and the nursing staff of the Merian Iselin Hospital in Basle for their expert technical assistance in performing the pharmacokinetic studies and Dr. W. Pacha, Dr. H. P. Keller, and the Sandoz Laboratories in Basle for performing the assays in plasma and urine.

Quantitative Determination of Captopril in Blood and Captopril and Its Disulfide Metabolites in Plasma by Gas Chromatography

M. S. BATHALA ˣ, S. H. WEINSTEIN, F. S. MEEKER, JR., S. M. SINGHVI, and B. H. MIGDALOF

Received December 8, 1982, from the *Department of Drug Metabolism, The Squibb Institute for Medical Research, Princeton, NJ 08540.* Accepted for publication February 11, 1983.

Abstract □ A sensitive, quantitative gas chromatographic–electron capture (GC–EC) method for the determination of captopril in blood and captopril and its disulfide metabolites (collectively) in plasma was developed. After addition of an internal standard and *N*-ethylmaleimide to the biological samples, excess *N*-ethylmaleimide and naturally occurring interfering substances were removed by extraction with benzene followed by acidification and extraction with hexane. The *N*-ethylmaleimide adducts of captopril and of the internal standard were then extracted with benzene and converted to their hexafluoroisopropyl esters. For the assay of captopril and its disulfide metabolites, tributylphosphine was used to reduce the disulfide metabolites to captopril prior to derivatization. The hexafluoroisopropyl esters of the *N*-ethylmaleimide adducts of captopril and of the internal standard, the 4-ethoxyproline analogue of captopril, were separated by GC on a column packed with 3% OV-101 on Chromosorb W-HP. The lower limits of sensitivity were 20 ng/mL for captopril in blood and 50 ng/mL for captopril and its disulfide metabolites in plasma. Linearity, precision, and accuracy were excellent. The method was validated by comparison of results obtained for total captopril in dog plasma by the GC–EC assay with results obtained by a published GC–MS method. The assay was applied to dog and human samples to explore its general utility.

Keyphrases □ Captopril—quantitative determination in blood and plasma, disulfide metabolites, gas chromatography □ Metabolites, disulfide—captopril, plasma, quantitative determination by gas chromatography □ Gas chromatography—captopril, quantitative determination in blood and plasma, disulfide metabolites

Captopril, 1-[(2*S*)-3-mercapto-2-methylpropionyl]-L-proline (I), the first orally active inhibitor of angiotensin-converting enzyme (peptidyl dipeptide hydrolase, kininase II, E.C. 3.4.15.1) to be used clinically, is a potent antihypertensive agent used to treat both renovascular and essential hypertension (1, 2). It is of particular value in treating hypertension resistant to conventional drugs (3), and shows great promise for use in congestive heart failure (2, 4).

The predominant route of excretion of captopril is *via* the kidneys (5–7). Since kidney function is often impaired in patients with hypertension, a sensitive assay for the drug in blood or plasma using readily accessible analytical equipment would be of value in optimizing dosage. Assays for both unchanged captopril and its disulfide metabolites would be useful, since interconversions occur among these compounds in rats, dogs, and humans (8–11). Metabolites of captopril include the symmetrical disulfide (IIA), captopril–L-cysteine mixed disulfide, captopril–glutathione mixed disulfide, and mixed disulfides of captopril with plasma proteins (IIB). Current methods for measurement of the drug in biological fluids are either not sensitive enough for monitoring therapeutic levels (12–14) or involve analytical equipment not available to the average clinical laboratory (15–17). Therefore, a sensitive method has been developed for quantifying captopril in blood and captopril

0022-3549/84/0300-0340$01.00/0
© 1984, American Pharmaceutical Association

(7) A. Roos and P. H. Hinderling, *J. Pharm. Sci.*, **70**, 252 (1981).
(8) H. Ott and J. Meier, *Scand. J. Rheum., Suppl.*, **21**, 12 (1978).
(9) E. E. Ohnhaus, *Int. J. Clin. Pharmacol.*, **18**, 136 (1980).
(10) K. Siersbäck-Nielsen, J. Mølholm Hansen, J. Kampmann, and M. Kristensen, *Lancet*, **i**, 1133 (1971).
(11) M. Berman and M. F. Weiss, "User's Manual for SAAM," Public Service, Publication No. 1703, National Institutes for Health, Bethesda, Md. (1967).
(12) C. M. Metzler, "A User's Manual for NONLIN," The Upjohn Co., Technical Report 7292/69/7292/005, Kalamazoo, Mich. (1969).
(13) J. G. Wagner, *J. Pharmacokinet., Biopharm.*, **3**, 457 (1975).
(14) H. G. Boxenbaum, S. Riegelman, and R. M. Elashoff, *J. Pharmacokinet. Biopharm.*, **2**, 123 (1974).
(15) L. Z. Benet and R. L. Galeazzi, *J. Pharm. Sci.*, **68**, 1071 (1979).
(16) M. Gibaldi and D. Perrier, "Pharmacokinetics," Dekker, New York, N.Y., 1975, pp. 72–73.
(17) A. C. Guyton, "Textbook of Medical Physiology," 3rd ed., Saunders, Philadelphia, Pa., 1968, p. 325.
(18) M. Gibaldi and D. Perrier, "Pharmacokinetics," Dekkler, New York, N.Y., 1975, p. 145.
(19) K. Diem and C. Lentner (Eds), "Documenta Geigy, Scientific Tables," 7th ed. Geigy Pharmaceuticals, Division of Ciba-Geigy Corp., Ardsley, N.Y., 1975, pp. 617, 579.
(20) A. C. Guyton,"Textbook of Medical Physiology," 3rd ed., Saunders, Philadelphia, Pa., 1968, p. 419.
(21) A. S. Nies, D. G. Shand, and G. R. Wilkinson, *Clin. Pharmacokinet.*, **1**, 135 (1976).
(22) G. R. Wilkinson and D. G. Shand, *Clin. Pharmacol. Ther.*, **18**, 377 (1977).
(23) E. R. Garrett, J. Brés, K. Schnelle, and L. L. Rolf, *J. Pharmacokinet. Biopharm.*, **2**, 43 (1974).
(24) J. J. Ashley and G. Levy, *J. Pharmacokinet. Biopharm.*, **1**, 99 (1973).
(25) D. Perrier, J. J. Ashley, and G. Levy, *J. Pharmacokinet. Biopharm.*, **1**, 231 (1973).
(26) P. Veng Pedersen, *J. Pharmacokinet. Biopharm.*, **5**, 513 (1977).
(27) H. Wijnand and C. J. Timmer, *J. Pharmacokinet. Biopharm.*, **7**, 681 (1979).
(28) M. Gibaldi and D. Perrier, "Pharmacokinetics," Dekker, New York, N.Y. 1975, pp. 93–94.

ACKNOWLEDGMENTS

Supported in part by a grant provided by Sandoz Ltd., Basle, for which the authors are grateful.

We thank Ms. R. Leder and the nursing staff of the Merian Iselin Hospital in Basle for their expert technical assistance in performing the pharmacokinetic studies and Dr. W. Pacha, Dr. H. P. Keller, and the Sandoz Laboratories in Basle for performing the assays in plasma and urine.

Quantitative Determination of Captopril in Blood and Captopril and Its Disulfide Metabolites in Plasma by Gas Chromatography

M. S. BATHALA ˣ, S. H. WEINSTEIN, F. S. MEEKER, JR., S. M. SINGHVI, and B. H. MIGDALOF

Received December 8, 1982, from the *Department of Drug Metabolism, The Squibb Institute for Medical Research, Princeton, NJ 08540.* Accepted for publication February 11, 1983.

Abstract □ A sensitive, quantitative gas chromatographic–electron capture (GC–EC) method for the determination of captopril in blood and captopril and its disulfide metabolites (collectively) in plasma was developed. After addition of an internal standard and *N*-ethylmaleimide to the biological samples, excess *N*-ethylmaleimide and naturally occurring interfering substances were removed by extraction with benzene followed by acidification and extraction with hexane. The *N*-ethylmaleimide adducts of captopril and of the internal standard were then extracted with benzene and converted to their hexafluoroisopropyl esters. For the assay of captopril and its disulfide metabolites, tributylphosphine was used to reduce the disulfide metabolites to captopril prior to derivatization. The hexafluoroisopropyl esters of the *N*-ethylmaleimide adducts of captopril and of the internal standard, the 4-ethoxyproline analogue of captopril, were separated by GC on a column packed with 3% OV-101 on Chromosorb W-HP. The lower limits of sensitivity were 20 ng/mL for captopril in blood and 50 ng/mL for captopril and its disulfide metabolites in plasma. Linearity, precision, and accuracy were excellent. The method was validated by comparison of results obtained for total captopril in dog plasma by the GC–EC assay with results obtained by a published GC–MS method. The assay was applied to dog and human samples to explore its general utility.

Keyphrases □ Captopril—quantitative determination in blood and plasma, disulfide metabolites, gas chromatography □ Metabolites, disulfide—captopril, plasma, quantitative determination by gas chromatography □ Gas chromatography—captopril, quantitative determination in blood and plasma, disulfide metabolites

Captopril, 1-[(2*S*)-3-mercapto-2-methylpropionyl]-L-proline (I), the first orally active inhibitor of angiotensin-converting enzyme (peptidyl dipeptide hydrolase, kininase II, E.C. 3.4.15.1) to be used clinically, is a potent antihypertensive agent used to treat both renovascular and essential hypertension (1, 2). It is of particular value in treating hypertension resistant to conventional drugs (3), and shows great promise for use in congestive heart failure (2, 4).

The predominant route of excretion of captopril is *via* the kidneys (5–7). Since kidney function is often impaired in patients with hypertension, a sensitive assay for the drug in blood or plasma using readily accessible analytical equipment would be of value in optimizing dosage. Assays for both unchanged captopril and its disulfide metabolites would be useful, since interconversions occur among these compounds in rats, dogs, and humans (8–11). Metabolites of captopril include the symmetrical disulfide (IIA), captopril–L-cysteine mixed disulfide, captopril–glutathione mixed disulfide, and mixed disulfides of captopril with plasma proteins (IIB). Current methods for measurement of the drug in biological fluids are either not sensitive enough for monitoring therapeutic levels (12–14) or involve analytical equipment not available to the average clinical laboratory (15–17). Therefore, a sensitive method has been developed for quantifying captopril in blood and captopril

0022-3549/84/0300-0340$01.00/0
© 1984, American Pharmaceutical Association

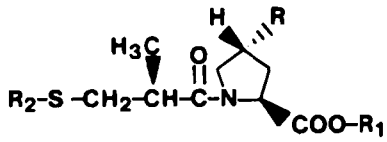

#	NAME	R	R_1	R_2
I	Captopril	H	H	H
IA	N-ethylmaleimide adduct of captopril	H	H	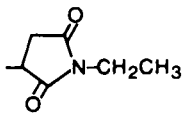
IB	Ester of N-ethylmaleimide adduct of captopril	H	$-CH(CF_3)_2$	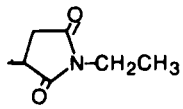
IIA	Captopril disulfide	H	H	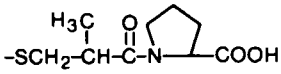
IIB	Mixed disulfides of captopril	H	H	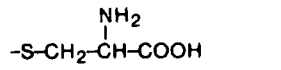
		H	H	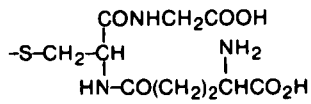
		H	H	-Plasma proteins
III	SQ 25,761	$-OC_2H_5$	H	H
IIIA	Ester of N-ethylmaleimide adduct of SQ 25,761	$-OC_2H_5$	$-CH(CF_3)_2$	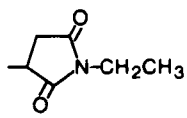

and its disulfide metabolites in plasma by gas chromatography with electron capture detection (GC–EC).

EXPERIMENTAL

Materials—*N*-Ethylmaleimide[1], hexafluoro-2-propanol[2], trifluoroacetic anhydride[2], sodium chloride[3], hydrochloric acid[3], and tributylphosphine[4] were obtained from commercial sources and used without further purification. Benzene, hexane, and methanol were suitable for HPLC analysis and used as supplied[5]. Captopril and the 4-ethoxyproline analogue of captopril (SQ 25,761, the internal standard) were of pharmaceutical quality and were used as received[6].

The chromatographic column was glass, 1.8 m × 2 mm i.d., packed with 3% methyl silicone on 100–120 mesh chromatographic (high-performance) diatomaceous earth[7]. Nitrogen and argon–methane (95:5) of the highest available[8] purity were used.

Equipment—GC was performed using an instrument[9] equipped with a nickel-63 electron-capture detector. All extractions were carried out by shaking the samples on a reciprocating shaker[10]. An analytical evaporator[11] was used for removing solvents from extracts with a nitrogen stream. The reduction of the biological samples with tributylphosphine and subsequent esterification with hexafluoro-2-propanol were performed by incubating in a heating block[12].

Extraction, Derivatization, and Chromatography of Unchanged Captopril in Blood—For spiking blood or plasma samples, separate stock solutions of captopril and the internal standard (III) were prepared in distilled water containing excess *N*-ethylmaleimide (1:5 molar ratio). Control dog or human blood (1 mL) containing 5 mg of *N*-ethylmaleimide was spiked with aqueous solutions of captopril containing *N*-ethylmaleimide to give standard solutions containing 20–200 ng/mL of captopril. The internal standard, 400 ng in 50 μL of aqueous solution, was added to each sample. All samples were extracted in acid-washed (16 × 125-mm) glass culture tubes. Twelve milliliters of benzene was added to each sample, and the samples were shaken on a reciprocating shaker for 10 min. After centrifuging the sample for 10 min at 3000×*g*, the benzene (upper) layer was removed by aspiration and discarded. One milliliter of 1 M HCl and 2 g of NaCl were added to each tube, and the contents of each tube was mixed on a vortex mixer for ~30 s. Ten milliliters of hexane was added to each sample, and the contents of each tube was again shaken for 10 min and then centrifuged for 10 min. The hexane (upper) layer was removed by aspiration and discarded. Each sample was then extracted with 12 mL of benzene by shaking for 20 min, followed by centrifugation for 10 min.

The organic layer was transferred to a clean tube and evaporated to dryness under a stream of nitrogen. The residue in each tube was derivatized with 100 μL of hexafluoro-2-propanol and 10 μL of trifluoroacetic anhydride at 50°C for 1 h. Excess reagents were removed by evaporation under a stream of nitrogen. Each residue, which contained derivatized captopril and internal standard, was reconstituted in 1 mL of benzene;

[1] Eastman Kodak Co., Rochester, N.Y.
[2] Pierce Chemical Co., Rockford, Ill.
[3] Mallinckrodt Inc., Paris, Ky.
[4] Aldrich Chemical Co., Milwaukee, Wis.
[5] Burdick and Jackson Laboratories, Muskegon, Mich.
[6] E. R. Squibb & Sons, Inc., Princeton, N.J.
[7] 3% OV-101 on Chromosorb W-HP (100–120 mesh); Alltech Assoc., Deerfield, Ill.
[8] Linde Corp., New York, N.Y.
[9] Model 5880A; Hewlett-Packard, Avondale, Pa.
[10] Eberbach Corp., Ann Arbor, Mich.
[11] N-Evap Model 112; Organomation Assoc., Northborough, Mass.
[12] Thermolyne Corp., Dubuque, Iowa.

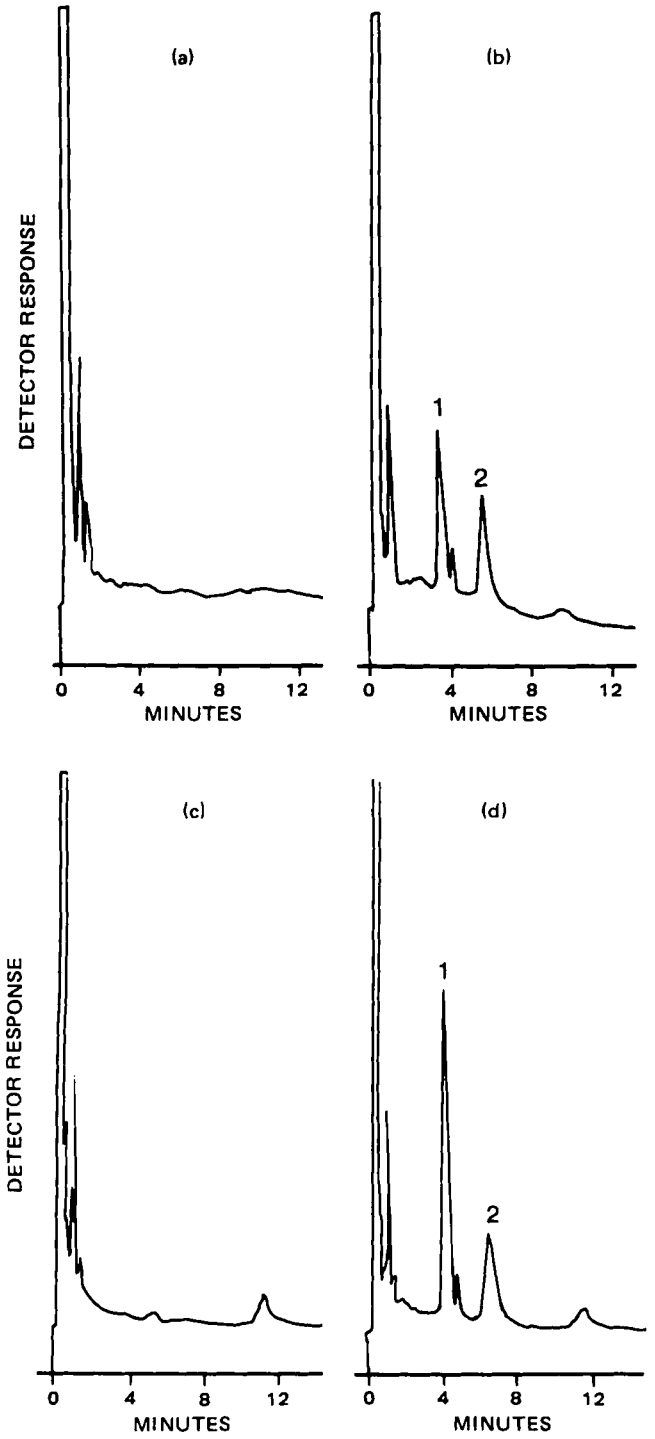

Figure 1—*Typical chromatograms of control human blood (a), control human blood containing derivatized captopril and internal standard (b), control dog plasma (c), and control dog plasma containing derivatized captopril and internal standard (d). Key: (1) captopril; (2) internal standard.*

an aliquot (≤5 μL) of each benzene solution was injected into the GC column. The column had been previously conditioned for 24 h at 250°C with the carrier gas (argon–methane, 95:5) at a flow rate of 10 mL/min. The detector and injector temperatures were 250°C and 225°C, respectively. The column operating temperature was 220°C, and the carrier gas flow rate was 40 mL/min.

Standard curves were constructed from spiked blood samples containing 0–200 ng/mL of captopril and a constant amount (400 ng/mL) of the internal standard. The peak height ratios of the unknown to the internal standard were plotted against concentrations. A new calibration curve was constructed daily. Comparison of peak height ratios from the unknown samples to those from the calibration curve permitted quantitation of the assayed samples.

Table I—Precision of the GC–EC Assay of Captopril and Captopril plus its Disulfide Metabolites

Actual Conc., ng/mL	Observed Conc., ng/mL	Mean ± *SD*	*CV*, %
	Captopril in Human Blood		
20	16	22 ± 4.5	20.5
	20		
	26		
	23		
	27		
100	112	101 ● 8.1	8.1
	94		
	96		
	102		
0200	196	204 ± 6.8	3.3
	201		
	207		
	214		
	203		
	Captopril and its Disulfide Metabolites in Dog Plasma		
50	55	49 ± 4.4	9.8
	45		
	49		
	52		
	45		
100	102	102 ± 3.7	3.7
	99		
	101		
	108		
	106		
500	464	491 ± 25.2	5.2
	465		
	502		
	521		
	504		
1000	1018	1023 ± 40.3	3.9
	1016		
	1027		
	927		

Extraction, Derivatization, and Chromatography for Quantitation of Captopril and its Disulfide Metabolites in Plasma—One-milliliter samples of plasma containing 800 ng of the internal standard (III) were transferred to acid-washed glass culture tubes (16 × 125 mm); 0.1 mL of a 2% solution of tributylphosphine in methanol was added to each sample. All tubes were mixed on a vortex mixer for ~30 s and then were heated for 30 min at 50°C. The samples were washed with 10 mL of hexane to remove excess tributylphosphine. The plasma layer was then mixed with 0.2 mL of a freshly prepared 2.5% aqueous solution of *N*-ethylmaleimide and allowed to stand for 15 min at room temperature. Further extraction, derivatization, and GC analyses then were performed as outlined for captopril in blood. Standard curves were constructed from spiked plasma samples containing 0–1000 ng/mL of captopril and 800 ng of the internal standard. Calibration curves, constructed on each day that analyses were performed, were used to quantitate the unknown samples.

Gas Chromatography–Mass Spectrometry—The derivatives of captopril and the internal standard were subjected to GC–MS analyses to confirm their structures. Mass spectra were obtained on a hyperbolic quadrupole mass spectrometer[13] in the electron-ionization mode.

RESULTS AND DISCUSSION

Derivatization of Captopril—Because of the reactivity of the thiol moiety of captopril, it was necessary to prevent oxidative degradation of captopril by adding *N*-ethylmaleimide to the samples of blood. *N*-Ethylmaleimide immediately reacts with captopril to form a stable thioalkyl derivative (IA) and prevents formation of the symmetrical (IIA) or mixed disulfides (IIB). The assay procedure for captopril and its disulfide metabolites is based on the quantitative reduction of its disulfide metabolites with tributylphosphine, as reported by Kawahara *et al.* (13).

[13] Hewlett-Packard, Palo Alto, Calif.

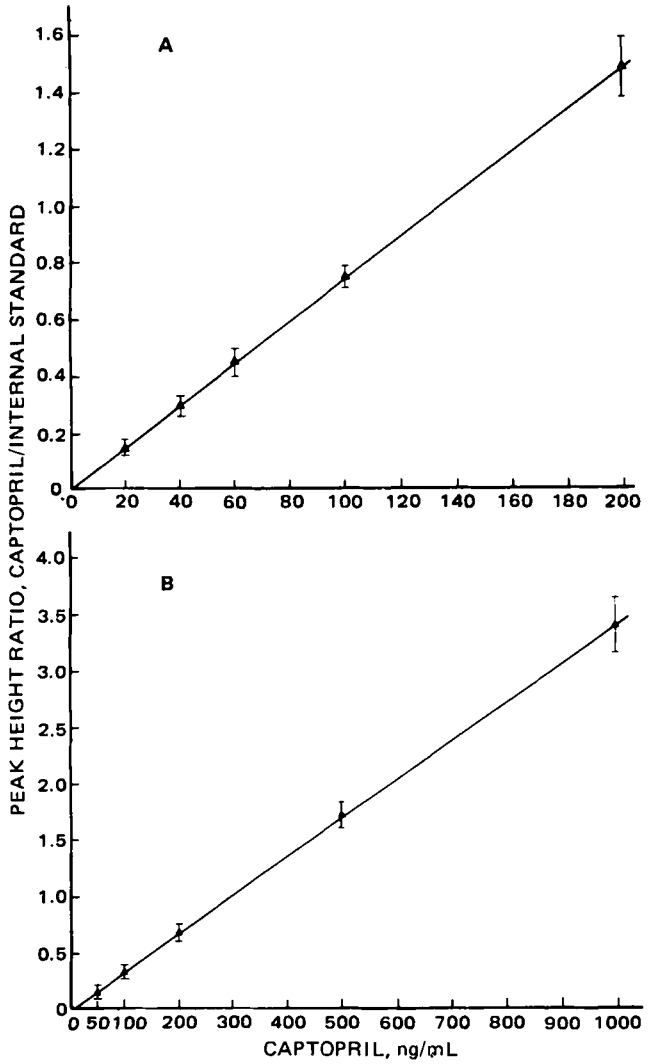

Figure 2—*Calibration curves for unchanged captopril in spiked human blood (A) and captopril and its disulfide metabolites measured as derivatized captopril in spiked dog plasma (B). Each point is the mean of six (A) or five (B) sets; the bars represent the ranges for each mean.*

The liberated captopril was treated with *N*-ethylmaleimide to form the stable derivative (IA). Compound IA formed from either unchanged captopril or captopril arising from reduced disulfides was further derivatized to give the hexafluoroisopropyl ester. The structures of the esters of the thioalkyl derivatives of both captopril (IB) and the internal standard (IIIA) were confirmed by GC–MS. The molecular ion peak (*m/z* 492), base peak (*m/z* 264), and other fragment ion peaks (*m/z* 366 and 228) obtained in the spectrum of derivatized captopril were in good agreement with those reported by Matsuke *et al.* (12). The characteristic fragmentation pattern of the derivatized internal standard (IIIA) agreed well with the known structure (*m/z* M^+ 536, 410, and 264).

The retention times of the derivatized captopril and internal standard were 3.4 and 5.8 min, respectively. No interfering peaks were observed in the extracts of the control human or dog blood. Typical chromatograms of an extract of human blood are shown in Fig. 1a and b. After treatment of plasma samples with tributylphosphine, no interfering peaks were observed in extracts of control human or dog plasma samples. Typical chromatograms of an extract of dog plasma are shown in Fig. 1c and d.

Linearity and Reproducibility—Known amounts of captopril and the internal standard were added to control dog or human blood to give standards suitable for captopril analysis. A plot of chromatographic peak height ratios *versus* concentrations was linear for captopril from 20 to 200 ng/mL (Fig. 2A); the linearity and reproducibility of the assay for captopril by the GC–EC method in human blood was demonstrated by six consecutive calibration curves. Linearity and reproducibility of the GC–EC method for captopril and its disulfide metabolites (50–1000 ng/mL) in dog plasma was demonstrated by five consecutive calibration curves (Fig. 2B). The correlation coefficient and the *y*-intercept for the straight lines were 0.999 and 0.004, respectively, for the captopril assay, and 0.999 and −0.001, respectively, for the assay of captopril and its disulfide metabolites. The average coefficient of variation (*CV*) for all the peak height ratios for both procedures was ±8%.

Table II—Analysis for Captopril and Captopril plus its Disulfide Metabolites in Spiked Human Blood and Plasma

Actual Conc., ng/mL	Observed Conc., ng/mL	Percent Deviation[a]
	Captopril in Human Blood	
0	0	—
50	52	+4.0
60	63	+5.0
70	71	+1.4
90	93	+3.3
100	111	+11.0
150	150	0
200	184	−8.0
500	512	+2.4
500	525	+5.0
	Captopril and its Disulfide Metabolites in Human Plasma	
0	0	—
67	68	+1.5
82	90	+9.7
96	98	+2.1
170	182	+7.1
202	167	−17.3
256	274	+7.0
287	286	−0.3
470	458	−2.5
690	682	−1.1
832	839	+0.8
878	967	+10.1

[a] Percent deviation = [(Observed Conc. − Actual Conc.)/Actual Conc.] × 100.

Precision and Accuracy—The precision of the method for captopril was determined by analysis of replicate human blood samples spiked at three concentrations (20, 100, and 200 ng/mL). Captopril and its disulfide metabolites were also assayed in replicate samples of dog plasma spiked at four concentrations (50, 100, 500, and 1000 ng/mL). For unchanged captopril assays, the *CV* was 20% at 20 ng/mL and 3% at 200 ng/mL; the *CV* for the assays of captopril and its disulfide metabolites was <10% (Table I).

To determine the relative accuracy of the methods, coded, spiked human blood and plasma samples were analyzed for captopril and captopril and its disulfide metabolites. The plasma samples spiked with various amounts of captopril (I), captopril disulfide (IIA), and captopril–L-cysteine mixed disulfide (IIB) were analyzed for captopril and its disulfide metabolites. Good agreement was observed between the actual concentrations and the experimentally determined concentrations for

Table III—Comparison of GC–MS and GC–EC Assays for Captopril and its Disulfide Metabolites in Dog Plasma After an Oral 2.5-mg/kg Dose of Captopril

Dog	Time After Dosing, h	Plasma Concentration, ng/mL GC–MS Method	Plasma Concentration, ng/mL GC–EC Method	Percent Deviation[a]
HO-56	0	0	0	—
	0.5	1551	1512	−2.5
	1	2955	3222	+9.0
	1.5	2122	1996	−6.9
	2	1633	1444	−11.6
	2.5	1038	1036	−0.2
	3.5	744	676	−9.1
	4.5	518	506	−2.3
	6	339	364	+7.4
HO-60	0	128	104	−18.8
	0.5	2946	2678	−9.1
	1	2465	2420	−1.8
	1.5	2057	2050	−0.3
	2	1532	1436	−6.3
	2.5	1005	978	−2.7
	3.5	734	738	+0.5
	4.5	487	482	−0.1
	6	578	322	−44.3

[a] Percent Deviation = [(GC–EC Value − GC–MS Value)/GC–MS Value] × 100.

both assays (Table II). The accuracy of the methods was further validated by comparing results from the assay of captopril and its disulfide metabolites by the GC–EC method with results from the GC–MS assay (15) in plasma from dogs that had been given oral doses of captopril (2.5 mg/kg). The generally excellent agreement obtained for the two methods is shown in Table III.

The GC–EC assay described appears suitable for determining blood concentrations of unchanged captopril and plasma concentrations of captopril and its disulfide metabolites in samples from dogs and humans. In the range of blood concentrations (captopril) from 20 to 200 ng/mL and plasma concentrations (captopril and its disulfide metabolites) from 50 to 1000 ng/mL, the linearity, reproducibility, precision, and accuracy of the assays were generally excellent. The lower limits for quantitation of captopril and its disulfide metabolites by the GC–EC method are comparable to the existing GC–MS (15) and liquid chromatography–electrochemical detector methods (16, 17). The thin-layer radiochromatographic method (18) is more sensitive when high specific activity [^{14}C]captopril is used. The GC–EC method is 4- to 10-fold more sensitive than the other quantitative methods (12, 14) previously reported.

REFERENCES

(1) M. A. Ondetti, B. Rubin, and D. W. Cushman, *Science*, **196**, 441 (1977).

(2) A. B. Atkinson and J. I. Robertson, *Lancet*, **ii**, 836 (1979).

(3) N. J. White and H. Yahya, *Lancet*, **ii**, 108 (1980).

(4) V. J. Dzau, W. S. Colucci, G. H. William, G. Curfman, L. Meggs, and N. K. Holkenberg, *N. Engl. J. Med.*, **302**, 1373 (1980).

(5) R. C. Heel, R. N. Brogdon, T. M. Speight, and G. S. Avery, *Drugs*, **20**, 409 (1980).

(6) K. J. Kripalani, D. N. McKinstry, S. M. Singhvi, D. A. Willard, R. A. Vukovich, and B. H. Migdalof, *Clin. Pharmacol. Ther.*, **27**, 636 (1980).

(7) S. M. Singhvi, D. N. McKinstry, J. M. Shaw, D. A. Willard, and B. H. Migdalof, *J. Clin. Pharmacol.*, **22**, 135 (1982).

(8) B. H. Migdalof, K. K. Wong, S. J. Lan, K. J. Kripalani, and S. M. Singhvi, *Fed. Proc. Fed. Am. Soc. Exp. Biol.*, **39**, 2589 (1980).

(9) K. K. Wong, S. J. Lan, and B. H. Migdalof, *Pharmacologist*, **21**, 173 (1979).

(10) K. J. Kripalani, A. V. Dean, and B. H. Migdalof, *Abstracts, APhA Acad. Pharm. Sci.*, **12**, 39 (1979).

(11) K. K. Wong and J. Dreyfuss, *Pharmacologist*, **20**, 213 (1978).

(12) Y. Matsuke, K. Fukuhara, T. Ito, H. Ono, N. Ohara, T. Yue, and T. Nambara, *J. Chromatogr.*, **188**, 177 (1980).

(13) Y. Kawahara, M. Hisaoka, Y. Yamazaki, A. Inaga, and T. Morioka, *Chem. Pharm. Bull.*, **29**, 150 (1981).

(14) B. Jarrott, A. Anderson, R. Hooper, and W. J. Louis, *J. Pharm. Sci.*, **70**, 665 (1981).

(15) P. T. Funke, E. Ivashkiv, M. F. Malley, and A. I. Cohen, *Anal. Chem.*, **52**, 1086 (1980).

(16) K. Shimada, M. Tanaka, T. Nambara, Y. Inai, K. Abe, and K. Yeshinagae, *J. Chromatogr.*, **227**, 445 (1982).

(17) D. Perrett and P. L. Drury, *J. Liq. Chromatogr.*, **5**, 97 (1982).

(18) B. H. Migdalof, S. M. Singhvi, and K. J. Kripalani, *J. Liq. Chromatogr.*, **3**, 857 (1980).

ACKNOWLEDGMENTS

The authors are grateful to Drs. P. T. Funke and A. I. Cohen of the Department of Analytical Research and Development for the mass spectrometric data presented in this paper. For editorial comments, we are grateful to Dr. J. Dreyfuss and Ms. H. M. Zarsky.

Cascade Impactor Method for the Droplet Size Characterization of a Metered-Dose Nasal Spray

CHENG DER YU ˣ, RICHARD E. JONES, and MAIDA HENESIAN

Received April 30, 1982, from the *Institute of Pharmaceutical Sciences, Syntex Research, Palo Alto, CA 94304.* Accepted for publication February 2, 1983.

Abstract □ A relatively rapid and simple method was developed to characterize the droplet size of a metered-dose nasal spray. The study primarily concerned the measurement of the relative proportion of small to large droplets. A small droplet could potentially reach bronchi or alveoli, depending on its size, and was therefore undesirable for the topical corticosteroid therapy of rhinal disease. The nasal spray was a solution of flunisolide, a topically active anti-inflammatory corticosteroid, administered by a manually operated, metered-dose pump spray system. The method utilized a cascade impactor fitted with a glass chamber; the cascade impactor collected and sized droplets into six fractions 0.5–16 μm in diameter, while the glass chamber collected droplets >16 μm in diameter as another fraction. Results showed that the majority of the spray droplets deposited in the glass chamber. Less than 0.5% by weight of the spray dose was delivered in droplets <8 μm aerodynamic diameter. These results are in good agreement with the droplet size distribution obtained by laser holography. The cascade impactor method showed that the number of undesirable small droplets produced by the flunisolide nasal spray unit was negligible. The method can be used with other aerosols where there is a similar concern for the inhalation of small particles.

Keyphrases □ Cascade impactor method—droplet-size characterization, metered-dose nasal spray □ Nasal spray—metered-dose, cascade impactor method for the droplet-size characterization □ Droplet-size characterization—cascade impactor method, metered-dose nasal spray

The particle or droplet size of an aerosol spray dosage form is important for both efficacy and toxicity. Inhalation aerosols intended for local activity in the lung must have the majority (by weight) of the particles in the size range of 2–6 μm in diameter to reach the terminal bronchi and alveoli (1). Particles <0.5 μm may fail to remain in this area (2), while particles >10 μm in diameter are mostly deposited in the upper respiratory tract (3).

In contrast, a nasal spray such as the metered-dose flunisolide nasal solution requires a majority of droplets having diameters >10 μm to localize delivery in the nose and to avoid possible undesired effects resulting from the material reaching the lung. It is therefore important, from an efficacy standpoint, to ensure that the nasal spray unit primarily produces droplets >10 μm in diameter. However, droplets <10 μm in diameter inevitably exist in small quantity in a spray. The ability of these small droplets to advance in the trachea–bronchi system depends on their

0022-3549/84/0300-0344$01.00/0

© 1984, American Pharmaceutical Association

both assays (Table II). The accuracy of the methods was further validated by comparing results from the assay of captopril and its disulfide metabolites by the GC–EC method with results from the GC–MS assay (15) in plasma from dogs that had been given oral doses of captopril (2.5 mg/kg). The generally excellent agreement obtained for the two methods is shown in Table III.

The GC–EC assay described appears suitable for determining blood concentrations of unchanged captopril and plasma concentrations of captopril and its disulfide metabolites in samples from dogs and humans. In the range of blood concentrations (captopril) from 20 to 200 ng/mL and plasma concentrations (captopril and its disulfide metabolites) from 50 to 1000 ng/mL, the linearity, reproducibility, precision, and accuracy of the assays were generally excellent. The lower limits for quantitation of captopril and its disulfide metabolites by the GC–EC method are comparable to the existing GC–MS (15) and liquid chromatography–electrochemical detector methods (16, 17). The thin-layer radiochromatographic method (18) is more sensitive when high specific activity [^{14}C]captopril is used. The GC–EC method is 4- to 10-fold more sensitive than the other quantitative methods (12, 14) previously reported.

REFERENCES

(1) M. A. Ondetti, B. Rubin, and D. W. Cushman, *Science*, **196**, 441 (1977).

(2) A. B. Atkinson and J. I. Robertson, *Lancet*, **ii**, 836 (1979).

(3) N. J. White and H. Yahya, *Lancet*, **ii**, 108 (1980).

(4) V. J. Dzau, W. S. Colucci, G. H. William, G. Curfman, L. Meggs, and N. K. Holkenberg, *N. Engl. J. Med.*, **302**, 1373 (1980).

(5) R. C. Heel, R. N. Brogdon, T. M. Speight, and G. S. Avery, *Drugs*, **20**, 409 (1980).

(6) K. J. Kripalani, D. N. McKinstry, S. M. Singhvi, D. A. Willard, R. A. Vukovich, and B. H. Migdalof, *Clin. Pharmacol. Ther.*, **27**, 636 (1980).

(7) S. M. Singhvi, D. N. McKinstry, J. M. Shaw, D. A. Willard, and B. H. Migdalof, *J. Clin. Pharmacol.*, **22**, 135 (1982).

(8) B. H. Migdalof, K. K. Wong, S. J. Lan, K. J. Kripalani, and S. M. Singhvi, *Fed. Proc. Fed. Am. Soc. Exp. Biol.*, **39**, 2589 (1980).

(9) K. K. Wong, S. J. Lan, and B. H. Migdalof, *Pharmacologist*, **21**, 173 (1979).

(10) K. J. Kripalani, A. V. Dean, and B. H. Migdalof, *Abstracts, APhA Acad. Pharm. Sci.*, **12**, 39 (1979).

(11) K. K. Wong and J. Dreyfuss, *Pharmacologist*, **20**, 213 (1978).

(12) Y. Matsuke, K. Fukuhara, T. Ito, H. Ono, N. Ohara, T. Yue, and T. Nambara, *J. Chromatogr.*, **188**, 177 (1980).

(13) Y. Kawahara, M. Hisaoka, Y. Yamazaki, A. Inaga, and T. Morioka, *Chem. Pharm. Bull.*, **29**, 150 (1981).

(14) B. Jarrott, A. Anderson, R. Hooper, and W. J. Louis, *J. Pharm. Sci.*, **70**, 665 (1981).

(15) P. T. Funke, E. Ivashkiv, M. F. Malley, and A. I. Cohen, *Anal. Chem.*, **52**, 1086 (1980).

(16) K. Shimada, M. Tanaka, T. Nambara, Y. Inai, K. Abe, and K. Yeshinagae, *J. Chromatogr.*, **227**, 445 (1982).

(17) D. Perrett and P. L. Drury, *J. Liq. Chromatogr.*, **5**, 97 (1982).

(18) B. H. Migdalof, S. M. Singhvi, and K. J. Kripalani, *J. Liq. Chromatogr.*, **3**, 857 (1980).

ACKNOWLEDGMENTS

The authors are grateful to Drs. P. T. Funke and A. I. Cohen of the Department of Analytical Research and Development for the mass spectrometric data presented in this paper. For editorial comments, we are grateful to Dr. J. Dreyfuss and Ms. H. M. Zarsky.

Cascade Impactor Method for the Droplet Size Characterization of a Metered-Dose Nasal Spray

CHENG DER YU ˣ, RICHARD E. JONES, and MAIDA HENESIAN

Received April 30, 1982, from the *Institute of Pharmaceutical Sciences, Syntex Research, Palo Alto, CA 94304.* Accepted for publication February 2, 1983.

Abstract □ A relatively rapid and simple method was developed to characterize the droplet size of a metered-dose nasal spray. The study primarily concerned the measurement of the relative proportion of small to large droplets. A small droplet could potentially reach bronchi or alveoli, depending on its size, and was therefore undesirable for the topical corticosteroid therapy of rhinal disease. The nasal spray was a solution of flunisolide, a topically active anti-inflammatory corticosteroid, administered by a manually operated, metered-dose pump spray system. The method utilized a cascade impactor fitted with a glass chamber; the cascade impactor collected and sized droplets into six fractions 0.5–16 μm in diameter, while the glass chamber collected droplets >16 μm in diameter as another fraction. Results showed that the majority of the spray droplets deposited in the glass chamber. Less than 0.5% by weight of the spray dose was delivered in droplets <8 μm aerodynamic diameter. These results are in good agreement with the droplet size distribution obtained by laser holography. The cascade impactor method showed that the number of undesirable small droplets produced by the flunisolide nasal spray unit was negligible. The method can be used with other aerosols where there is a similar concern for the inhalation of small particles.

Keyphrases □ Cascade impactor method—droplet-size characterization, metered-dose nasal spray □ Nasal spray—metered-dose, cascade impactor method for the droplet-size characterization □ Droplet-size characterization—cascade impactor method, metered-dose nasal spray

The particle or droplet size of an aerosol spray dosage form is important for both efficacy and toxicity. Inhalation aerosols intended for local activity in the lung must have the majority (by weight) of the particles in the size range of 2–6 μm in diameter to reach the terminal bronchi and alveoli (1). Particles <0.5 μm may fail to remain in this area (2), while particles >10 μm in diameter are mostly deposited in the upper respiratory tract (3).

In contrast, a nasal spray such as the metered-dose flunisolide nasal solution requires a majority of droplets having diameters >10 μm to localize delivery in the nose and to avoid possible undesired effects resulting from the material reaching the lung. It is therefore important, from an efficacy standpoint, to ensure that the nasal spray unit primarily produces droplets >10 μm in diameter. However, droplets <10 μm in diameter inevitably exist in small quantity in a spray. The ability of these small droplets to advance in the trachea–bronchi system depends on their

0022-3549/84/0300-0344$01.00/0

© 1984, American Pharmaceutical Association

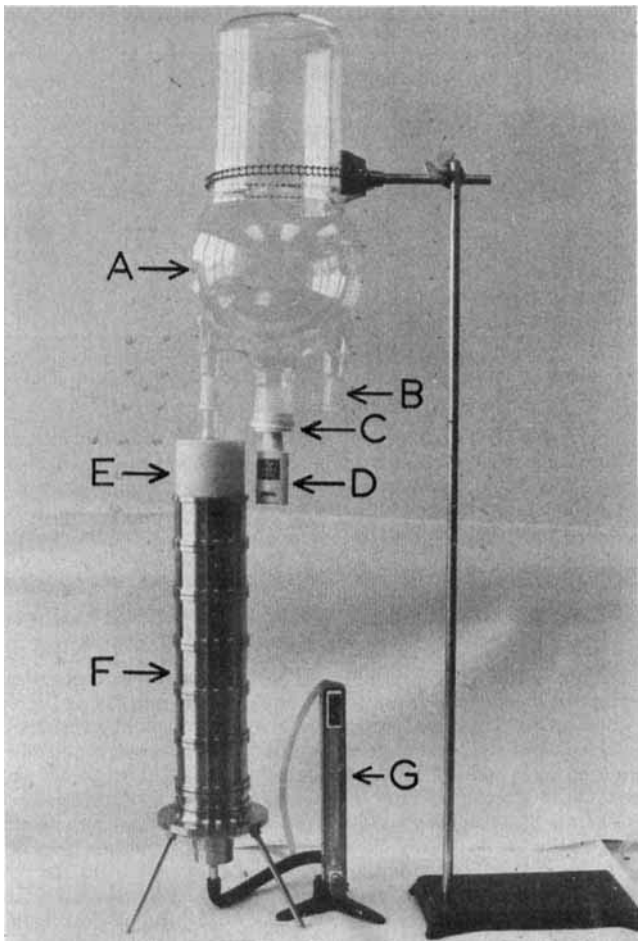

Figure 1—*Experimental setup for characterization of the droplet size of flunisolide nasal spray. Key: (A) glass chamber; (B) air inlet; (C) polytetrafluoroethylene stopper with a hole to fit the nasal spray unit; (D) flunisolide nasal spray unit; (E) polytetrafluoroethylene adaptor which has a conical cavity; (F) cascade impactor; (G) flow meter.*

sizes. Therefore, it is equally important, from a safety standpoint, to determine the amount and the size distribution of droplets <10 μm in diameter.

BACKGROUND

Numerous methods for sizing aerosol particles have been developed in the past (4–6), the most common of which are direct microscopy (7), light scattering (8), laser holography (9), and the impaction method (10–12). In the microscopic method, particles collected on a slide are counted and sized simultaneously. The method is simple, but tedious without the aid of an automatic image analyzer. Furthermore, in the case of liquid aerosols (as opposed to solid aerosols) the observed sizes need to be corrected for the spreading of the droplets. Light-scattering methods are based on the phenomenon that particles suspended in air are capable of scattering incident light. The method determines the particle size directly in the aerosol cloud. Laser holography employs a pulsed laser of short pulse duration to illuminate moving particles and consequently obtain the stop-action image of the droplets. The image is usually video-taped and replayed in slow motion for manual or automatic sizing. This method gives relatively accurate particle sizes and distributions, since the reconstructed hologram is essentially an undistorted image of

Table I—Total Recovery and Droplet Size Distribution of the Flunisolide Nasal Spray by Cascade Impactor

Spray Unit	Flunisolide Recovered, %			
	Stage 1	Stages 2–6	Glass Chamber	Total Recovery[a]
No. 1	1.20 (102.1)[b]	0.49 (104.7)	98.30 (101.4)	99.99
No. 2	1.75 (100.5)	0.55 (102.7)	97.70 (100.8)	99.50
No. 3	0.90 (102.1)	0.34 (106.0)	98.76 (101.4)	102.10
No. 4	0.33 (103.0)	0.19 (105.0)	99.48 (100.5)	99.50
No. 5	0.40 (102.0)	0.24 (105.0)	99.37 (99.0)	101.60
No. 6	0.38 (102.0)	0.20 (104.0)	99.42 (97.0)	102.10
Mean ± S.D.	0.83 ± 0.57	0.34 ± 0.15	98.84 ± 0.72	100.80 ± 1.28

[a] Percentage based on the weight difference of the spray unit before and after the experiment; converted to micrograms of flunisolide using density = 1.04 and concentration = 0.025% (w/v). [b] Number in parentheses is the recovery of the internal standard added into the washing solvent to quantitate the evaporation during washing.

particles in the aerosol cloud. However, the equipment is costly.

A cascade impactor, on the other hand, is relatively inexpensive. Various stages of the cascade impactor are capable of collecting and classifying particles ranging from 0.5–16 μm in diameter; a glass chamber can be employed to collect droplets >16 μm in diameter. The use of a cascade impactor fitted with a suitable glass chamber could therefore adequately provide the aforementioned critical droplet size information for the nasal spray product, namely the percentage of droplets >16 μm in diameter and the size distribution of the remaining small droplets. Although a 10-μm cutoff point is more desirable, the 16-μm cutoff point is dictated by the design of the cascade impactor. The six stages of the cascade impactor collect and size the droplets into 16-, 8-, 4-, 2-, 1-, and 0.5-μm diameter fractions. Nevertheless, since the primary concern about the particle size of a nasal spray is the relative proportion of small to large particles, the cascade impactor method is well suited for the purpose. This report describes the design of a glass chamber and its use with a cascade impactor for the droplet size characterization of a metered-dose nasal spray.

EXPERIMENTAL

Materials—The flunisolide nasal solution consisted of flunisolide[1] (0.25 mg/mL) in an aqueous vehicle containing propylene glycol, polyethylene glycol 3350, citric acid, sodium citrate, and benzalkonium chloride.

Assembly and Operation of the Nasal Spray—The nasal spray system consisted of four basic elements: a plastic bottle, a cap, a pump, and a shroud (plus its dust cap). Flunisolide nasal solution was packaged in the plastic bottle and capped, with the pump and shroud presented unassembled. Prior to the experiment, the original cap was removed from the bottle and discarded, and the pump/shroud system was assembled onto the bottle. During the experiment, the system was operated by rapid, firm finger and thumb pressure on the shroud and the base of the bottle, which forced a metered amount of drug solution up through the actuator to exit as a fine spray at the orifice. Metering was accomplished by the length of stroke of the pump piston, which forced the drug solution through the orifice. The meter chamber and the sealing action of the steel

[1] Flunisolide, (6α,11β,16α)-6-fluoro-11,21-dihydroxy-16,17-[(1-methylethylidene)bis(oxy)]-pregna-1,4-diene-3,20-dione; Institute of Organic Chemistry, Syntex Research, Palo Alto, Calif.

Table II—Recoveries of Flunisolide from Various Components of the Cascade Impactor and the Glass Chamber for Flunisolide Delivered by a Nebulizer

Stage	50% Cutoff Diameter[a], μm	Flunisolide Recovered[b], % Exp. 1	Exp. 2	Exp. 3
1	16.0	0.95	0.73	0.83
2	8.0	2.14	1.23	1.49
3	4.0	11.95	9.90	7.85
4	2.0	36.20	35.70	33.20
5	1.0	36.20	37.20	39.90
6	0.5	12.60	15.20	16.80
Glass chamber	—	0.00	0.00	0.00
Total	—	100.00	100.00	100.00

[a] Diameter of spherical particles of unit density for which 50% will impact on a given slide and 50% will pass around to a succeeding stage. [b] Recoveries of flunisolide from 20 sprays of the nebulizer.

ball on release of the actuator provided a fixed volume of drug solution for dosing. Each actuation of the pump system administered ~100 μL of the solution.

Assembly and Operation of the Cascade Impactor—The single-orifice metal cascade impactor[2] (10) was constructed of a succession of six jets, each followed by a glass impaction slide. It was based on the principle that particles in a moving air stream impacted on a slide placed in their path, if their momentum was sufficient to overcome the drag exerted by the air stream as it moved around the slide. As each jet was smaller than the preceding one, the velocity of the air stream, and therefore that of the dispersed particles, was increased as the aerosol advanced through the impactor. Consequently, small particles eventually acquired enough momentum to impact on a slide, and a complete particle sizing of the aerosol was achieved.

The air flow rate was maintained at 12.5 L/min in the system by applying a suitable vacuum at the impactor outlet and was monitored by a flow meter[3]. At this flow rate, the 50% cutoff diameters for each of the six jet stages were precalibrated[4] to be 16, 8, 4, 2, 1, and 0.5 μm. The 50% cutoff diameter is defined as the diameter of spherical particles of unit density for which 50% will impact on a given slide and 50% will pass around to a succeeding stage.

The impaction glass slide was attached to each of the six jets and the jets were assembled prior to the experiment. No entrapment was used for the impaction glass slide because flunisolide droplets remained liquid after spraying and, thereby, self-entrapping.

Glass Chamber—The design of the glass chamber for this study was similar to that of Sciarra *et al* (12). The glass chamber was made of a 5-L three-necked round-bottom flask with the bottom removed, and the remaining part of the flask joined to a 4-L beaker. The chamber was placed upside down on top of the cascade impactor with a ground glass joint and a polytetrafluoroethylene[5] adapter connecting a side-neck of the flask to the top stage of the impactor as depicted in Fig. 1. The other side-neck of the flask was left open for the air inlet, while the central neck of the flask was attached to the spray unit. Introduction of the spray mist into the chamber was accomplished by a vertical upward spraying at the central neck. A polytetrafluoroethylene[5] stopper with an opening to fit the head of the spray unit was employed to prevent the loss of the mist from the central neck.

Droplet Size Characterization Study—The glass chamber and cascade impactor were connected as shown in Fig. 1. After establishing an airflow of 12.5 L/min, the flunisolide nasal solution was sprayed into the glass chamber a total of 20 times at 10-s intervals. The glass chamber and its parts were removed and washed with the HPLC mobile phase. The impaction glass slide of stages 1–6 were detached and washed separately with the HPLC mobile phase. Washings from stages 2–6 were combined in certain experimental runs as indicated in the tabulated results. The amounts of flunisolide in the washings were then determined by HPLC.

Liquid Chromatographic Assay for Flunisolide—A high-performance liquid chromatograph[6] equipped with a variable-wavelength UV detector[7] and a 100-μL fixed-loop injector[8] was used for the quantitation of flunisolide. The wavelength chosen for detection was 240 nm. A commercially available microparticulate reverse-phase column[9] was operated at ambient temperature. A mixture of acetonitrile–water–acetic acid (35:64:1, v/v/v) was used as the mobile phase. Fluocinonide[10] was used as an internal standard. None of the excipients other than flunisolide and the internal standard appeared on the chromatogram.

Table III—Droplet Size Distribution of Flunisolide Nasal Spray by a Cascade Inpactor

Stage	50% Cutoff Diameter[a], μm	Flunisolide Recovered, % Exp. 1	Exp. 2[b]
1	16.0	1.30	1.14
2	8.0	0.38	0.20
3	4.0	0.29	0.13
4	2.0	0.12	0.04
5	1.0	0.07	0.01
6	0.5	0.00	0.00
Glass chamber	—	97.82	98.74

[a] Diameter of spherical particles of unit density for which 50% will impact on a given slide and 50% will pass around to a succeeding stage. [b] The same spray unit was used.

RESULTS AND DISCUSSION

Design of the Glass Chamber—The design of the glass chamber is critical for sizing aerosol sprays. Care must be taken to ensure that: (*a*) the aerosol cloud is carried through the cascade impactor by the imposed air flow and not by the imparted pumping force, in the case of a manually operated spray unit, or by the force of the propellant, in the case of a propellant-driven spray unit; (*b*) there is no dripping of the condensed liquid from the chamber wall into the cascade impactor and onto the first slide; (*c*) there is no retention of the small droplets, which are to be sized by the cascade impactor, by the glass chamber.

Sciarra *et al.* (12) studied several designs of glass chambers for sizing an aerosol hair spray. They claimed that a 1- or 2-L round-bottom flask with the bottom removed to fit the top stage of a cascade impactor, and the neck enlarged and extended at an angle 105° to the body was most suitable. However, in their design, the aerosol was sprayed into the chamber along with the imposed air flow at the neck which extended at an angle of 105° to the body of the cascade impactor. It is questionable that their design best fulfilled the aforementioned caution *a*. Furthermore, their design was not tested for fulfillment of caution *c*. Violation of caution *c* would result in a lower weight percentage of the impactor-detectable small droplets, which might lead to a misconception of product safety.

The glass chamber for the present study, to overcome the aforementioned shortcomings, was designed in such a manner that the mist produced by the spray unit would lose the momentum imparted by the pump operation and be carried into the cascade impactor by the imposed airflow. The large volume (9 L) of the chamber and the long distance (45 cm) between the tip of the spray unit and the top of the chamber helped to reduce the probability of droplets hitting the glass wall. The glass joint connecting the chamber and the cascade impactor aided in preventing the condensed liquid from dripping into the cascade impactor.

Total Recovery—The total recovery of the flunisolide sprayed into the system was checked by comparing the weights of the materials recovered from the various components of the system and the weight differences of the spray unit before and after the experiment, as shown in Table I. Of the six trials conducted, the total recoveries ranged from 99.50 to 102.10% with a mean value of 100.78%. The satisfactory total recovery indicated that there was no loss of the droplets through the open air inlet. Also listed in Table I are the recoveries (the numbers in parentheses) of the internal standard which was added to the washing solvent to determine the possible evaporation during washing. This procedure is necessary because only 1 mL of the HPLC mobile phase was used to wash an impaction slide plate of 3.8 cm in diameter. The increase in concentration

[2] Model CI-S-6; Sciotec Corp., Columbus, Ohio. It was originally designed by Mitchell and Pilcher of Battelle Memorial Institute, Columbus, Ohio.
[3] Precision flowmeter; Lab Crest Scientific, Warminster, Pa.
[4] Factory-precalibrated, at 12.5 L/min flow rate, using dibutyl phthalate droplets.
[5] Teflon, Du Pont.
[6] Altex model 110A; Altex, Berkeley, Calif.
[7] Schoeffel model 770; Schoeffel Instrument Corp., Westwood, N.J.
[8] Valco universal inlet; Altex.
[9] Spectra-Physics prepacked Spherisorb ODS 10 μm column; Spectra-Physics, Santa Clara, Calif.
[10] Fluocinonide, (6α,11β,16α(-21-(acetyloxy)-6,9-difluoro-11-hydroxy-16,17-[(1-methyl ethylidene)bis(oxy)]-pregna-1,4-diene-3,20-dione. Institute of Organic Chemistry, Syntex Research, Palo Alto, Calif.

Table IV—Effect of Emptying on the Droplet Size of Flunisolide Nasal Spray

Subject	Flunisolide Recovered, %							
	Stage 1		Stages 2–6		Glass Chamber		Total Recovery[a]	
	Day		Day		Day		Day	
	0	19[b]	0	19[b]	0	19[b]	0	19[b]
7	0.33	0.94	0.19	0.37	99.48	98.69	99.5	100.2
12	0.38	0.22	0.20	0.01	99.42	99.77	102.1	99.3
14	0.40	0.80	0.24	0.27	99.37	99.94	101.6	101.0

[a] Percentage based on weight difference of the bottle before and after the spray, converted to micrograms of flunisolide using density = 1.04 and concentration = 0.025% (w/v). [b] Nineteen days after the unit was used according to directions of four sprays, twice daily.

Table V—Droplet Size Distribution of Flunisolide Nasal Spray by Laser Holography

Diameter, μm	Flunisolide, %			
	Spray Unit No. 1		Spray Unit No. 2	
	2.54 cm[a]	7.62 cm[a]	2.54 cm[a]	7.62 cm[a]
0.5–1.0	0.000	0.001	0.000	0.000
1.0–5.0	0.000	0.051	0.001	0.000
5.0–10.0	0.003	0.435	0.008	0.003
10.0–20.0	0.053	11.917	0.173	0.079
20.0–30.0	0.191	11.379	0.514	0.105
30.0–40.0	0.294	19.870	1.071	0.075
40.0–50.0	0.417	10.055	1.665	0.187
50.0–60.0	0.729	14.686	1.216	0.097
60.0–70.0	0.628	6.060	1.840	0.241
70.0–80.0	0.563	0.000	3.083	0.741
80.0–90.0	0.468	0.000	2.618	0.000
90.0–100.0	0.980	0.000	3.133	0.251
100.0–110.0	0.662	25.547	0.705	0.000
110.0–120.0	1.159	0.000	1.853	0.000
120.0–130.0	0.744	0.000	1.190	0.000
130.0–140.0	0.938	0.000	2.997	0.000
140.0–150.0	1.162	0.000	3.714	0.000
150.0–160.0	2.129	0.000	4.536	0.000
160.0–170.0	3.425	0.000	2.736	0.000
170.0–180.0	1.021	0.000	0.000	0.000
180.0–190.0	1.207	0.000	0.000	0.000
190.0–200.0	0.000	0.000	0.000	0.000
>200.0	83.227	0.000	66.947	98.221
Total	100.0	100.0	100.0	100.0

[a] The sample was taken at either 2.54 or 7.62 cm downstream from the tip of the unit.

as a result of the evaporation was found to be only a few percent (Table I).

Condensation on the Chamber Wall—As discussed in the section on the design of the glass chamber, the condensation of droplets on the chamber wall could retain some small droplets which should have entered the cascade impactor. The relative proportion of small to large droplets determined by this device could potentially be biased if this phenomenon is not accounted for. The degree of condensation of the small droplets was therefore examined using a nebulizer[11] which generated primarily 1–2-μm size droplets[12]. The procedure was the same as that for the nasal spray. The nebulizer was equipped with a squeeze bulb. Each complete squeeze delivered approximately one one-hundredth of the amount delivered by one spray of the nasal unit. Table II lists the flunisolide recovered from various stages of the cascade impactor and the sampling chamber for three experiments with the nebulizer. The distribution patterns agreed well with one another. The majority of the droplets had diameters between 1 and 2 μm (Table II) which was consistent with the data from the manufacturer's technical report. As can be seen in Table II, the flunisolide retained by the glass chamber was essentially undetectable for a total of 20 squeezes. Evidently, the deposition of small droplets on the glass chamber is negligible.

Droplet Size Characteristics of the Nasal Spray—Results of the droplet size characterization are shown in Tables I and III. As can be seen in Table I, 98.84 ± 0.72% (mean ± *SD*) (by weight) of the spray was found in the glass chamber. The glass chamber was shown (Table II) not to retain droplets <16 μm in aerodynamic diameter, as discussed in the previous section. It is therefore believed that the nasal spray unit primarily produces droplets of >16-μm aerodynamic diameter.

The data in Table I were produced with six randomly selected spray units. The unit-to-unit variation was reasonably small, as shown by the standard deviation. The amounts of flunisolide found in stage 1 (16 μm) and in stages 2–6 combined (8–0.5 μm) were 0.83 and 0.34%, respectively (Table I). Details of the size distribution of this small droplet portion of the spray are shown in Table III. Only two experiments on one spray unit were performed because their purpose was to illustrate the size distribution obtained by the cascade impactor, not to show the within-unit variability. A clear trend can be seen, *i.e.*, the smaller the droplet size, the smaller their weight percentage.

Table IV shows the reproducibility among operators and the effect of emptying of the spray unit on the droplet size. The study was a part of a use test (13) in which 17 units were sprayed by 17 operators according to label instructions until the units ceased to deliver. Only three units were analyzed for the droplet size, among other parameters studied (13), because the assay reduced the availability of the nasal solution for other testings. It can be seen that the relative proportion of small to large droplets is reasonably consistent among the operators and between a full unit and an almost empty unit for each operator.

Table V lists results of the droplet size distribution[13] obtained independently by laser holography[14]. Examining Tables I, III, IV, and V, one can see that the relative proportion of small to large droplets obtained by the cascade impactor agrees well with that obtained by laser holography. The laser holographic results (Table V) reveal that the weight percentage of the small droplets between 0.5 and 10.0 μm in diameter is 0.13 ± 0.24% (mean ± *SD*). The weight percentage of the small droplets collected on stages 2–6 of the cascade impactor (i.e., droplets 0.5–8.0 μm in diameter) is 0.34 ± 0.15% (Table I). Evidently, there is no statistical difference between the two results.

CONCLUSION

Since concern for the droplet size of a nasal spray is primarily to ensure that the weight percentage of droplets <10 μm in diameter (and thereby potentially deliverable to the lower respiratory tract) produced by the spray unit is negligble, the cascade impactor method was demonstrated to be quite satisfactory for this purpose. The cascade impactor method developed here is a simple, economical, and reliable method for the droplet size characterization of a metered-dose flunisolide nasal spray. The method can be used for other aerosol products where there is a similar concern for the inhalation of small particles.

REFERENCES

(1) I. Porush, C. G. Thiel, and J. G. Young, *J. Am. Pharm. Assoc., Sci. Ed.*, **49**, 70 (1960).

(2) H. D. Landahl, T. Tracewell, and W. H. Lassen, *A.M.A. Arch. Ind. Hyg.*, **3**, 359 (1951).

(3) H. D. Landahl and R. Hermann, *J. Ind. Hyg.*, **30**, 181 (1948).

(4) M. Lefebvre and R. Tregan, *Aerosol Age*, **10**(7), 31 (1965); **10**(8), 32 (1965).

(5) J. L. Kanig, *J. Pharm. Sci.*, **52**, 513 (1963).

(6) W. B. Tarpley, *Aerosol Age*, **2**(12), 38 (1957).

(7) G. W. Hallworth and R. R. Hamilton, *J. Pharm. Pharmacol.*, **28**, 890 (1976).

(8) D. Sinclair and V. K. LaMer, *Chem. Rev.*, **44**, 245 (1949).

(9) B. J. Thompson and J. H. Ward, *Sci. Res.*, **1**(10), 37 (1966).

[11] DeVilbiss No. 40 Nebulizer, Health Care Division, DeVilbiss, Somerset, PA 15501.

[12] A technical report from DeVilbiss.

[13] Data were generated with randomly selected spray units, instead of those shown in Tables I, III, and IV.

[14] Contracted studies by Laser Holography Inc., Santa Barbara, Calif.

(10) R. I. Mitchell and J. M. Pilcher, *Ind. Eng. Chem.*, 51(9), 1039 (1959).
(11) W. M. Grim, J. B. Portnoff, F. A. Restaino, and R. V. Toberman, *Aerosol Age*, 13(3), 22 (1968).
(12) J. J. Sciarra, P. McGinley and L. Izzo, *J. Soc. Cosmet. Chem.*, **20**, 385 (1969).
(13) C. D. Yu, R. E. Jones, J. Wright, and M. Henesian, *Drug Dev. Ind. Pharm.*, **9**, 473 (1983).

ACKNOWLEDGMENTS

The authors thank Dr. B. J. Poulsen for his support.

Pharmacokinetics of Diazepam and Nordiazepam in the Cat

S. COTLER ˣ, J. H. GUSTAFSON, and W. A. COLBURN

Received May 11,1982, from the *Department of Pharmacokinetics and Biopharmaceutics, Hoffmann-La Roche Inc., Nutley, NJ 07110.* Accepted for publication February 1, 1983.

Abstract □ The cat has been used extensively as an experimental model for studying the pharmacology of compounds that exhibit CNS activity including diazepam and nordiazepam. However, since little is known about the distribution and elimination of diazepam in this species, the pharmacokinetics of diazepam and nordiazepam were studied in the cat following intravenous doses of 5, 10, and 20 mg/kg of diazepam and 5 and 10 mg/kg of nordiazepam. The disappearance of diazepam and nordiazepam from blood was fitted with classical equations. Theoretical and trapezoidal areas under the curve (AUC_{th} and AUC_{tr}) were calculated. The volumes of distribution (Vd_{β}) were calculated as model-independent parameters for diazepam and nordiazepam. Intrinsic hepatic clearance, extraction ratio, and tissue binding parameters were also calculated for diazepam. From the observed data, it is apparent that the blood concentrations and the resulting areas under the curves are proportional to the dose of diazepam administered and that the pharmacokinetics of diazepam were linear over the dose range studied. In addition, nordiazepam formed after diazepam administration appeared to be proportional to the dose of diazepam administered. The terminal elimination rate constant of nordiazepam remained constant over the dose range studied. It appears that both diazepam and nordiazepam are highly bound to tissue. The total body clearance of diazepam (4.72 ± 2.45 mL/min/kg) is approximately six times that of nordiazepam (0.85 ± 0.25 mL/min/kg). Approximately 50% of an administered dose of diazepam was biotransformed to nordiazepam in the cat.

Keyphrases □ Diazepam—pharmacokinetics in the cat, nordiazepam □ Nordiazepam—pharmacokinetics in the cat, diazepam □ Pharmacokinetics—diazepam and nordiazepam in the cat after intravenous doses

The benzodiazepines are centrally active compounds that reduce anxiety, produce sedation and sleep, have anticonvulsant effects, and may cause muscle relaxation. In addition, the benzodiazepine diazepam is also used in the treatment of alcohol abusers during potentially life-threatening withdrawal episodes (1). Diazepam has a long effective duration of action, probably due to slow elimination of parent compound and biotransformation to active metabolic products including nordiazepam (2). Many of the pharmacological properties of the benzodiazepines seen in humans are present in the cat (3–5). Diazepam has been shown to be effective in the cat in the control of seizures in experimental epilepsy (6) and with the sudden abstinence of alcohol after chronic use (5). Although the cat has been used extensively to study the effects of diazepam, little is known about the pharmacokinetics of diazepam and nordiazepam in this species. Morselli *et al.* (7) described the distribution of diazepam and its major metabolites in plasma and in several areas of the brain of the cat. A direct correlation was established between blood flow to various tissues of the brain and the diazepam found in these tissues. However, the accumulation of nordiazepam, the major blood metabolite, in the brain appeared to be inversely related to blood flow. Unfortunately, this data did not lend itself to an overall pharmacokinetic profile of diazepam or nordiazepam in this species.

The present study in the domestic short-hair cat was performed to (*a*) establish the pharmacokinetics of diazepam and nordiazepam following 5-, 10-, and 20-mg/kg iv doses of diazepam and (*b*) to compare the pharmacokinetic profile of nordiazepam after nordiazepam administration to its profile observed after the administration of diazepam in this species. These data will establish the fundamental pharmacokinetic profile of diazepam and nordiazepam in the cat.

EXPERIMENTAL

Animal Model—Domestic short-haired female cats (2.5–3.0 kg) were used for all experiments. Hematocrit values were determined before surgery and drug administration and were found to be within the normal range (8). Cats were anesthetized with 0.33–0.44 mL of a solution containing 100 mg/mL of ketamine and 7.5 mg/mL of promazine[1]. An incision was made in either the right or left leg exposing a branch of the femoral vein. A butterfly infusion set[2] with the needle removed, leaving the tubing and Luer fitting intact, was used as a cannula. The catheter was inserted into the vein, exteriorized, and the incision was closed with 000 surgical silk[3]. The catheter was cleared daily and kept patent with a sodium heparin flush. Diazepam or nordiazepam (10 mg/mL) was dissolved in dimethylacetamide[4] immediately prior to administration.

Study Design—Unanesthetized fasted cats, with a femoral vein catheter previously implanted to facilitate blood sampling, were administered 5-, 10-, and 20-mg/kg doses of diazepam or 10 mg/kg of nordiazepam intravenously as a short infusion (20 s) *via* a peripheral vein. Two weeks were allowed for recuperation between doses.

Sampling and Analysis—Blood specimens (0.5 mL) were obtained from the femoral vein catheter. The first specimen was obtained 2.5 min following intravenous administration and subsequent specimens were obtained for as long as 96 h. The blood specimens were collected in tubes containing dried heparin[5] and kept at −20°C until analyzed. The samples were analyzed simultaneously for diazepam and nordiazepam using the electron capture GC method of Weinfeld *et al.* (9) with the following modifications. Whole blood (0.1 mL) was extracted into 1 mL of benzene after adjusting the pH to 9.0 with a 1 M H_3BO_3–KCl–Na_2CO_3 buffer. The percent standard deviation for the intraassay variability averaged 3.6% for diazepam and 3.4% for nordiazepam over the range of 50–2000 ng/mL

[1] Ketaset Plus; Bristol Labs, Syracuse, N.Y.
[2] Model No. 44492; Abbott Laboratories, Chicago, Ill.
[3] Ethicon, New Brunswick, N.J.
[4] Model No. 4972, Eastman Kodak, Rochester, N.Y.
[5] Model No. 3206, Becton, Dickenson, Rutherford, N.J.

0022-3549/84/0300-0348$01.00/0
© 1984, American Pharmaceutical Association

(10) R. I. Mitchell and J. M. Pilcher, *Ind. Eng. Chem.*, 51(9), 1039 (1959).
(11) W. M. Grim, J. B. Portnoff, F. A. Restaino, and R. V. Toberman, *Aerosol Age*, 13(3), 22 (1968).
(12) J. J. Sciarra, P. McGinley and L. Izzo, *J. Soc. Cosmet. Chem.*, **20**, 385 (1969).
(13) C. D. Yu, R. E. Jones, J. Wright, and M. Henesian, *Drug Dev. Ind. Pharm.*, **9**, 473 (1983).

ACKNOWLEDGMENTS

The authors thank Dr. B. J. Poulsen for his support.

Pharmacokinetics of Diazepam and Nordiazepam in the Cat

S. COTLER ˣ, J. H. GUSTAFSON, and W. A. COLBURN

Received May 11,1982, from the *Department of Pharmacokinetics and Biopharmaceutics, Hoffmann-La Roche Inc., Nutley, NJ 07110.* Accepted for publication February 1, 1983.

Abstract □ The cat has been used extensively as an experimental model for studying the pharmacology of compounds that exhibit CNS activity including diazepam and nordiazepam. However, since little is known about the distribution and elimination of diazepam in this species, the pharmacokinetics of diazepam and nordiazepam were studied in the cat following intravenous doses of 5, 10, and 20 mg/kg of diazepam and 5 and 10 mg/kg of nordiazepam. The disappearance of diazepam and nordiazepam from blood was fitted with classical equations. Theoretical and trapezoidal areas under the curve (AUC_{th} and AUC_{tr}) were calculated. The volumes of distribution (Vd_{β}) were calculated as model-independent parameters for diazepam and nordiazepam. Intrinsic hepatic clearance, extraction ratio, and tissue binding parameters were also calculated for diazepam. From the observed data, it is apparent that the blood concentrations and the resulting areas under the curves are proportional to the dose of diazepam administered and that the pharmacokinetics of diazepam were linear over the dose range studied. In addition, nordiazepam formed after diazepam administration appeared to be proportional to the dose of diazepam administered. The terminal elimination rate constant of nordiazepam remained constant over the dose range studied. It appears that both diazepam and nordiazepam are highly bound to tissue. The total body clearance of diazepam (4.72 ± 2.45 mL/min/kg) is approximately six times that of nordiazepam (0.85 ± 0.25 mL/min/kg). Approximately 50% of an administered dose of diazepam was biotransformed to nordiazepam in the cat.

Keyphrases □ Diazepam—pharmacokinetics in the cat, nordiazepam □ Nordiazepam—pharmacokinetics in the cat, diazepam □ Pharmacokinetics—diazepam and nordiazepam in the cat after intravenous doses

The benzodiazepines are centrally active compounds that reduce anxiety, produce sedation and sleep, have anticonvulsant effects, and may cause muscle relaxation. In addition, the benzodiazepine diazepam is also used in the treatment of alcohol abusers during potentially life-threatening withdrawal episodes (1). Diazepam has a long effective duration of action, probably due to slow elimination of parent compound and biotransformation to active metabolic products including nordiazepam (2). Many of the pharmacological properties of the benzodiazepines seen in humans are present in the cat (3–5). Diazepam has been shown to be effective in the cat in the control of seizures in experimental epilepsy (6) and with the sudden abstinence of alcohol after chronic use (5). Although the cat has been used extensively to study the effects of diazepam, little is known about the pharmacokinetics of diazepam and nordiazepam in this species. Morselli *et al.* (7) described the distribution of diazepam and its major metabolites in plasma and in several areas of the brain of the cat. A direct correlation was established between blood flow to various tissues of the brain and the diazepam found in these tissues. However, the accumulation of nordiazepam, the major blood metabolite, in the brain appeared to be inversely related to blood flow. Unfortunately, this data did not lend itself to an overall pharmacokinetic profile of diazepam or nordiazepam in this species.

The present study in the domestic short-hair cat was performed to (*a*) establish the pharmacokinetics of diazepam and nordiazepam following 5-, 10-, and 20-mg/kg iv doses of diazepam and (*b*) to compare the pharmacokinetic profile of nordiazepam after nordiazepam administration to its profile observed after the administration of diazepam in this species. These data will establish the fundamental pharmacokinetic profile of diazepam and nordiazepam in the cat.

EXPERIMENTAL

Animal Model—Domestic short-haired female cats (2.5–3.0 kg) were used for all experiments. Hematocrit values were determined before surgery and drug administration and were found to be within the normal range (8). Cats were anesthetized with 0.33–0.44 mL of a solution containing 100 mg/mL of ketamine and 7.5 mg/mL of promazine[1]. An incision was made in either the right or left leg exposing a branch of the femoral vein. A butterfly infusion set[2] with the needle removed, leaving the tubing and Luer fitting intact, was used as a cannula. The catheter was inserted into the vein, exteriorized, and the incision was closed with 000 surgical silk[3]. The catheter was cleared daily and kept patent with a sodium heparin flush. Diazepam or nordiazepam (10 mg/mL) was dissolved in dimethylacetamide[4] immediately prior to administration.

Study Design—Unanesthetized fasted cats, with a femoral vein catheter previously implanted to facilitate blood sampling, were administered 5-, 10-, and 20-mg/kg doses of diazepam or 10 mg/kg of nordiazepam intravenously as a short infusion (20 s) *via* a peripheral vein. Two weeks were allowed for recuperation between doses.

Sampling and Analysis—Blood specimens (0.5 mL) were obtained from the femoral vein catheter. The first specimen was obtained 2.5 min following intravenous administration and subsequent specimens were obtained for as long as 96 h. The blood specimens were collected in tubes containing dried heparin[5] and kept at −20°C until analyzed. The samples were analyzed simultaneously for diazepam and nordiazepam using the electron capture GC method of Weinfeld *et al.* (9) with the following modifications. Whole blood (0.1 mL) was extracted into 1 mL of benzene after adjusting the pH to 9.0 with a 1 M H_3BO_3–KCl–Na_2CO_3 buffer. The percent standard deviation for the intraassay variability averaged 3.6% for diazepam and 3.4% for nordiazepam over the range of 50–2000 ng/mL

[1] Ketaset Plus; Bristol Labs, Syracuse, N.Y.
[2] Model No. 44492; Abbott Laboratories, Chicago, Ill.
[3] Ethicon, New Brunswick, N.J.
[4] Model No. 4972, Eastman Kodak, Rochester, N.Y.
[5] Model No. 3206, Becton, Dickenson, Rutherford, N.J.

0022-3549/84/0300-0348$01.00/0
© 1984, American Pharmaceutical Association

Table I—Diazepam Pharmacokinetic Parameters and Percent Coefficient of Variation [a] after Intravenous Administration of Diazepam to the Cat

Parameter	Cat										
	1		2			3			4	5	6
Dose, mg/kg	5	10	5	10	20	5	10	20	10	10	10
Weight, W kg	2.7	2.5	2.7	2.4	2.7	3.0	3.0	3.0	2.5	2.8	2.8
P, μg/mL				25.4 (9.90)							
π, h^{-1}				15.4 (12.7)							
A, μg/mL	4.43 (13.7)	28.8 (20.8)	9.28 (11.4)	7.40 (6.08)	24.2 (8.84)	4.55 (10.4)	10.4 (9.70)	18.1 (3.40)	12.4 (11.6)	8.99 (13.5)	
α, h^{-1}	2.30 (32.3)	1.44 (25.8)	2.56 (21.8)	.717 (14.2)	2.63 (16.8)	1.29 (21.0)	1.26 (20.5)	1.65 (6.86)	3.58 (21.4)	2.08 (29.3)	
B, μg/mL	2.58 (23.6)	3.15 (24.2)	2.77 (13.9)	1.30 (21.3)	8.08 (8.88)	1.25 (34.7)	2.09 (34.5)	3.85 (7.40)	2.41 (21.3)	2.06 (30.5)	6.98
β, h^{-1}	0.204 (22.8)	0.123 (10.9)	0.064 (33.6)	0.0125 (95.6)	0.048 (19.8)	0.120 (56.0)	0.111 (46.9)	0.077 (11.5)	0.149 (35.2)	0.096 (46.4)	0.397 8.39
V_c, mL/kg	713	313	416	293	618	862	800	911	675	905	
Vd_β, mL/kg	1684	1783	1668	6864	2345	2997	3327	4259	3418	4047	1432
V_c/Vd_β	0.42	0.18	0.25	0.043	0.26	0.29	0.24	0.21	0.20	0.22	
AUC_{th} μg·h	14.6	45.6	46.6	116	177	14.0	27.1	60.7	19.6	25.8	18.9
AUC_{tr} μg·h/mL	15.0	59.2	49.3	116	186	13.9	31.1	66.0	22.6	26.8	19.2
CL, mL/min/kg	5.70	3.65	1.78	1.43	1.88	5.95	6.17	5.48	8.48	6.47	8.76
CL_{tr}, mL/min/kg	5.55	2.80	1.68	1.43	1.78	6.00	5.35	5.05	7.38	6.20	8.68

[a] % CV in parentheses.

of blood for diazepam and 100–4000 ng/mL of blood for nordiazepam. The interassay variability for the same range was 6.0 and 8.9% for diazepam and nordiazepam, respectively.

Blood-to-plasma ratios were determined for diazepam and nordiazepam. Diazepam and nordiazepam (1500 ng) were added to 3-mL aliquots of blood, previously collected in a tube[5] containing dried heparin. The blood and the two components were gently shaken in a reciprocal shaker[6] at ~60 excursions per minute for 1.5 h. A 0.5-mL aliquot of whole blood was removed and the remainder was centrifuged for 30 min at 2500 rpm to separate the plasma from the red blood cells. A 0.5-mL volume of plasma was taken for each analysis. Both whole blood and plasma were analyzed for diazepam and nordiazepam by a specific and sensitive HPLC method (10).

Pharmacokinetic Analysis—Following rapid intravenous infusion of diazepam and nordiazepam, blood concentration–time curves were analyzed by a weighted iterative nonlinear least-squares regression technique (11). Data points were fitted with one of the following equations:

$$C_b = Be^{-\beta t} \quad \text{(Eq. 1)}$$

$$C_b = Ae^{-\alpha t} + Be^{-\beta t} \quad \text{(Eq. 2)}$$

$$C_b = Pe^{-\pi t} + Ae^{-\alpha t} + Be^{-\beta t} \quad \text{(Eq. 3)}$$

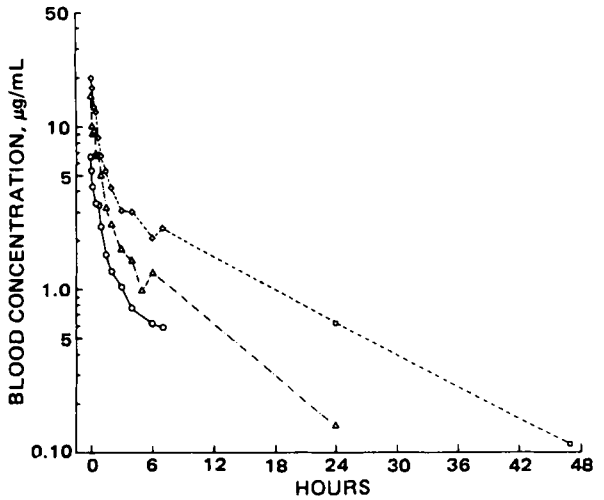

Figure 1—*Diazepam blood concentrations for Cat 3 after intravenous administration of 5- (○), 10- (△), and 20- (□) mg/kg doses of diazepam.*

[6] Eberbach Corp., Ann Arbor, Mich.

In all equations, C_b is the blood diazepam or nordiazepam concentration at time t after the dose. P, A, and B are coefficients and π, α, and β are hybrid rate constants that describe the disposition and elimination phases, respectively.

The equation selected for fitting the data was determined by comparing the sum of the squared deviations using the F-ratio test (12) and by scatter of the actual data points around the fitted function. Model-dependent pharmacokinetic parameters such as the theoretical areas under the blood concentration–time curves (AUC_{th}) were calculated from the following equations:

$$AUC_{th} = \frac{B}{\beta} \quad \text{(Eq. 4)}$$

$$AUC_{th} = \frac{A}{\alpha} + \frac{B}{\beta} \quad \text{(Eq. 5)}$$

$$AUC_{th} = \frac{P}{\pi} + \frac{A}{\alpha} + \frac{B}{\beta} \quad \text{(Eq. 6)}$$

The volume of the central compartment (V_c) was calculated by dividing the dose (mg/kg) by the sum of the coefficients, and the volume of distribution (Vd_β) was determined with the following:

$$Vd_\beta = \frac{\text{Dose}}{(AUC_{th}) \cdot \beta} \quad \text{(Eq. 7)}$$

where β is the terminal elimination rate constant. The theoretical total body clearance (TBC_{th}) was determined from the relationship of dose to the theoretical area under the curve:

$$TBC_{th} = \frac{\text{Dose}}{AUC_{th}} \quad \text{(Eq. 8)}$$

Table II—Pharmacokinetic Parameters for Nordiazepam after Intravenous Diazepam Administration to Cats

Cat	Dose, mg/kg	Wt, kg	β, h^{-1}	$AUC_{0-\infty}$, μg·h/mL	$\frac{(AUC_{nor})\ D}{(AUC_{nor})\ N}$ [a]
1	5	2.7	0.0424	47.2	0.45
	10	2.5	0.0356	108	0.79
2	5	2.7	0.0503	51.3	
	10	2.4	0.0239	105	0.69
	20	2.7	0.0329	188	
3	5	3.0	0.0135	97.0	
	10	3.0	0.0297	114	0.50
	20	3.0	0.0189	425	
4	10	2.5	0.119[b]	38.0	0.20
5	10	2.8	0.0501	87.8	0.37
6	10	2.8	0.0250	166	0.50

[a] Area under the nordiazepam blood concentration–time curve following diazepam administration divided by the area under the nordiazepam blood concentration–time curve following an equal dose of nordiazepam. [b] In Cat 4 of the series, β and AUC_{tr} of nordiazepam after diazepam administration were determined to be aberrant values and were not included in calculating the mean value of these parameters (26).

Table III—Pharmacokinetic Parameters and Percent Coefficient of Variation [a] for Nordiazepam after Intravenous Nordiazepam Administration to Cats

Cat	Wt, kg	Dose, mg/kg	A, μg/mL	α, h^{-1}	B, μg/mL	β, h^{-1}	$Area_{th}$, μg·h/mL	AUC_{tr}, μg·h/mL	CL_{tr}, mL/min/kg	V_c, mL/kg	Vd_β, mL/kg	V_c/Vd_β
1	2.7	5			4.31	0.0474	91	105	0.80		1004	
1	2.5	10	6.21 (23.5)	1.82 (43.6)	4.91 (10.7)	0.0389 (8.8)	130	136	1.23	899	1890	0.45
2	2.4	10	5.61 (27.0)	1.52 (45.0)	3.11 (11)	0.0236 (12)	136	152	1.08	1146	2754	0.37
3	3.0	10	4.81 (15)	0.957 (35)	6.24 (7.2)	0.0285 (10)	224	229	0.73	904	1543	0.58
4	2.5	10	15.6 (41)	8.26 (39)	5.51 (5.7)	0.0329 (11)	170	187	0.88	473	2217	0.26
5	2.8	10	27.9 (65)	7.95 (51)	4.75 (11)	0.0255 (17)	214	237	0.70	306	1647	0.16
6	2.8	10	4.19 (31.5)	0.776 (76)	6.09 (15)	0.0188 (28)	327	332	0.50	972	1602	0.60

[a] % *CV* in parentheses.

The model-independent areas under the blood concentration time curves were also calculated from time zero to infinity (AUC_{tr}) by adding the area from time t, of the final measurable concentration estimated by trapezoidal summation (AUC_{0-t}), to the area from time t to infinity ($AUC_{t-\infty}$) calculated with the following (13):

$$AUC_{t-\infty} = C_b{}^t/\beta \qquad \text{(Eq. 9)}$$

where $C_b{}^t$ is the observed blood concentration at time t and β is the terminal elimination rate constant estimated by nonlinear regression. The calculated total clearance (TBC_{tr}) was calculated as the dose divided by AUC_{tr}. In addition, the intrinsic clearance CL_I was calculated as:

$$CL_I = \frac{HBF \cdot CL_{tr}}{HBF - CL_{tr}} \qquad \text{(Eq. 10)}$$

where HBF is the hepatic blood flow. The extraction ratio (ER) was calculated as:

$$ER = \frac{CL_I}{HBF + CL_I} \qquad \text{(Eq. 11)}$$

as described by Wilkinson and Shand (14). The blood-to-plasma distribution ratio was calculated from the concentration of drug in whole blood divided by the concentration of drug in plasma.

RESULTS AND DISCUSSION

The mean ±*SD* blood-to-plasma distribution ratios for diazepam and nordiazepam in the cat were 0.56 ± 0.13 and 0.65 ± 0.19, respectively, which are similar to the 0.64 and 0.60 values observed for diazepam and nordiazepam in humans (15). From the blood-to-plasma distribution ratios, it is possible to estimate from blood concentration data the amount that would be in a corresponding plasma sample by simply dividing the blood concentration by the distribution ratio (16). In addition, it is possible to correct the pharmacokinetic parameters V and CL calculated from the blood concentration data for comparison with similar parameters calculated from plasma concentration data in other studies (16). Similarly, it was possible to calculate blood free fraction from known plasma free fraction values.

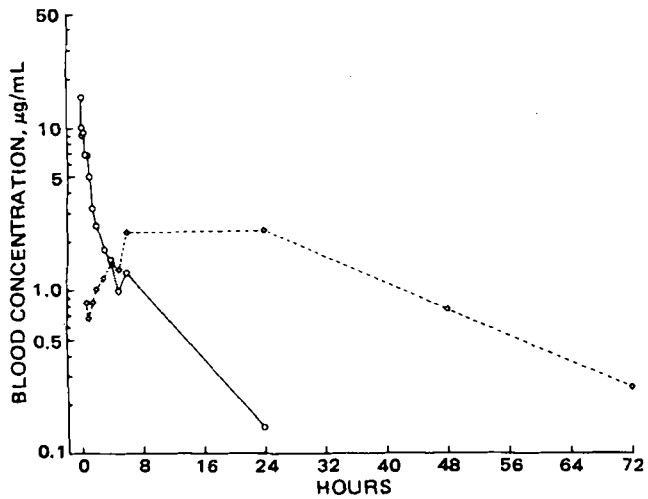

Figure 2—*Diazepam and nordiazepam blood concentrations after 10-mg/kg diazepam intravenous administration to Cat 5. Key: (○) diazepam; (◇) nordiazepam.*

Typical diazepam blood concentration–time curves following the administration of 5, 10, and 20 mg/kg of diazepam to a representative cat are presented in Fig. 1. The decline of diazepam blood concentrations were described by exponential functions. Visual inspection of the observed points about the fitted curve indicated a satisfactory randomness of scatter. Percent coefficients of variation of the parameters, P, π, A, α, B, and β were <50% (Table I), indicating that the good fit was dependent on each of these parameters. The disposition (α) phase was rapid with a harmonic mean half-life[7] of 0.35 h, and the harmonic mean terminal elimination half-life was 5.46 h.

The theoretical areas are virtually identical with the areas calculated from the trapezoidal rule. There is a proportional increase in diazepam blood concentrations between the 5-, 10-, and 20-mg/kg dose (Fig. 1). This relationship was supported by a doubling of the AUC_{tr} of diazepam with a doubling of the administered dose of diazepam (Table I). The mean ±*SD* total body clearance of diazepam is 4.72 ± 2.45 mL/min/kg, which represents an extraction ratio of 0.12 based on a total hepatic blood flow of 40 mL/min/kg (17) and assuming that diazepam is eliminated totally by hepatic clearance. The average intrinsic clearance (CL_I) is 5.35 mL/min/kg, which indicates that total body clearance is only slightly dependent on the hepatic blood flow. The total body clearance varied among cats, but for a single cat the clearance was constant over the dose range studied. It was concluded from the linear relationship of the blood concentrations and the areas under the blood concentration–time curves to the dose of diazepam administered, and the constant clearance within animals, that the pharmacokinetics of diazepam in the cat are linear over the dose range studied.

The mean ±*SD* of V_c and Vd_β were 651 ± 235 and 3075 ± 1603 mL/kg, respectively. The ratio of V_c/Vd_β (0.23 ± 0.094) suggests that ~23% of the dose of diazepam in the animal is in the central compartment available for elimination at any time, whereas ~77% of the dose is in a peripheral compartment unavailable for elimination. Distribution to a peripheral compartment tends to reduce the overall elimination of diazepam in humans, as previously observed by Kaplan *et al.* (18). The value for Vd_β was greater than total body water, which is generally indicative of extensive binding and/or localization in the tissue space. Previous studies with the cat also indicated that diazepam is highly bound to plasma protein (94%)[8].

From the following equation (19), one can estimate the average fraction (F_T) of diazepam in tissue space that is not bound to tissue:

$$F_T = \frac{V_T \cdot F_B}{Vd_\beta - V_B} \qquad \text{(Eq. 12)}$$

where the volume of distribution (Vd_β) was 3075 mL/kg, the volume of the blood (V_B) was 66.7 mL/kg (20), the average volume of the tissue (V_T) (21, 22) was 563 mL/kg, and the calculated fraction of the drug that is free in blood (F_B) was 0.11. Solving Eq. 12 for F_T yields a value of 0.019. Therefore, an estimate of the fraction of diazepam in the tissue that is bound to tissue protein is 0.981.

Figure 2 shows typical blood concentration–time curves for diazepam and its major blood metabolite, nordiazepam, observed after a 10-mg/kg iv dose of diazepam. The concentrations and the resulting AUC values of nordiazepam, the major blood metabolite seen after diazepam administration, appeared to increase in proportion to the dose of diazepam administered (Table II). Initially, the formation rate of nordiazepam after diazepam administration appeared to be rapid for 6–8 h and slower thereafter. Similar rate phenomena were observed in humans (18). The

[7] Since β rather than half-life appears to have a normal distribution, harmonic rather than arithmatic mean half-lives are reported. (P. R. Gwilt and S. P. Sytsma. Paper presented at 29th national meeting of the American Pharmaceutical Association, San Antonio, Texas, Nov. 1980.)

[8] Data on file, Hoffmann-La Roche, Nutley, NJ 07110.

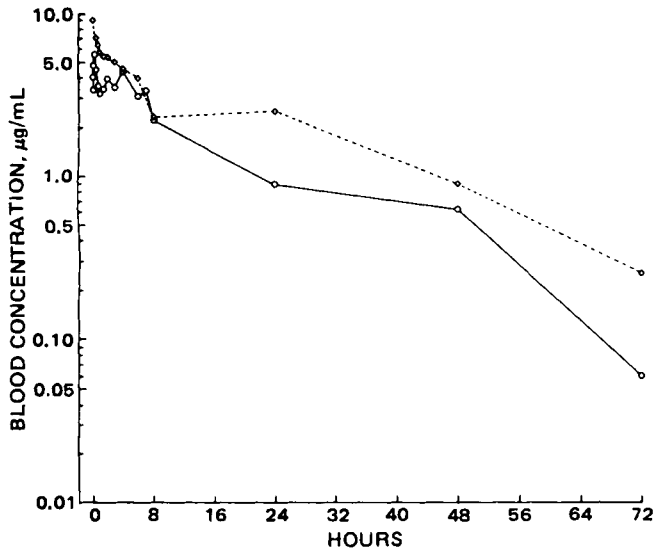

Figure 3—*Nordiazepam blood concentrations for Cat 1 after intravenous administration of 5- (○) and 10- (◇) mg/kg doses of nordiazepam.*

maximum blood concentrations of nordiazepam were generally observed at 24 h after diazepam administration. The value is only an approximation since no samples were obtained between 7 and 24 h after drug administration. The mean $\pm SD$ terminal elimination rate constant for nordiazepam was $0.032 \pm 0.012\ h^{-1}$, with a harmonic mean half-life of 21.3 h, which is 4.3 times slower than diazepam. From this data for nordiazepam after diazepam administration, it can be inferred that the amount of nordiazepam present is also directly proportional to the dose of diazepam administered and that the elimination of nordiazepam is not affected by the presence of diazepam over the dose range studied.

Corresponding nordiazepam data (Table III) were obtained following 10-mg/kg nordiazepam administration as a short (20-s) infusion to the same cats that received diazepam. In addition, one cat received 5 mg/kg of nordiazepam. Figure 3 is a typical nordiazepam blood concentration–time curve; the observed nordiazepam data could be satisfactorily described by a biexponential equation except for the cat that received 5 mg/kg, whose data appeared to be monoexponential. The disposition phase (α) for nordiazepam was rapid and variable (Table III). The terminal elimination phase (β) was much slower and less variable, with a harmonic mean elimination half-life of 21 h. The t test ($p < 0.05$) showed no significant difference between the terminal elimination half-lives of nordiazepam formed from diazepam and those for nordiazepam itself. This substantiates the earlier observation that the terminal elimination of nordiazepam after diazepam administration is not affected by the presence of diazepam nor by the rate of nordiazepam formation following diazepam administration.

The clearance of nordiazepam (mean $\pm SD = 0.85 \pm 0.24$ mL/min/kg) was approximately one-sixth the clearance of diazepam. This clearance value suggests a negligible potential for first-pass metabolism for nordiazepam. The model-independent value for the volume of distribution (Vd_β) for nordiazepam is also greater than total body water, which is generally indicative of extensive binding and/or localization in the tissue space as previously indicated for diazepam. As seen with diazepam (18), the distribution of nordiazepam into peripheral compartments reduces the overall elimination of nordiazepam from the cat.

Comparing the area of nordiazepam after nordiazepam administration to area of nordiazepam after the administration of an equivalent dose of diazepam (Table II), it was estimated that an average of 54% of the diazepam dose was biotransformed to nordiazepam in the cat. This observation of 54% conversion of diazepam to nordiazepam in the cat is in good agreement with the 50% fractional conversion of diazepam to nordiazepam observed in humans (23).

The observation that the pharmacokinetics in the cat were linear with respect to dose has been observed in humans. Greenblatt *et al.* (24) observed that in cases of diazepam overdose in humans, the terminal elimination half-lives for diazepam fell within the range observed in individuals after a therapeutic dose of diazepam. When the pharmacokinetic data in the cat are compared with those known for humans, a much more rapid elimination for diazepam and nordiazepam is apparent in the cat. The elimination half-lives of diazepam in humans are reported to be in the range of 24–48 h for adults (23) and 18 h for children, and the terminal elimination half-lives for nordiazepam are reported to be in the range of 51–120 h (25). It is apparent that nordiazepam has a longer elimination half-life than diazepam in humans; this relationship in the half-lives was also observed for the cats during this study. The first-pass effect of diazepam and nordiazepam in the cat and human is negligible compared with other animal species.

In conclusion, the cat has been previously used as an experimental model for studying the CNS pharmacology of diazepam and nordiazepam. The similarities between cat and human with respect to the pharmacokinetics of these compounds suggest that the cat may not only be a good model species for pharmacological studies but for pharmacokinetic studies as well.

REFERENCES

(1) S. M. Pond, M. Phillips, N. L. Bernowitz, R. E. Galinsky, T. G. Tong, and C. E. Becker, *Clin. Pharm. Ther.*, **25,** 832 (1979).

(2) D. J. Greenblatt and R. I. Shader, *South. Med. J.*, **71,** Suppl. 2 (1978).

(3) W. Schallek, W. Schosser, and L. Randal, in "Advances in Pharmacy and Chemotherapy," Vol. 10, S. Garattini, A. Goldin, F. Hawking, and J. Kopin, Ed., Academic, New York, N.Y., 1972, p. 119.

(4) R. H. de Jong and J. E. Heavner, *Anesthesiology*, **36,** 449 (1972).

(5) R. Guerrero-Figueroa, M. M. Rye, D. M. Gallant, and M. P. Bishop, *Neuropharmacology*, **9,** 143 (1968).

(6) G. G. Celesia, H. E. Booker, and S. Soto, *Epilepsia*, **15,** 417 (1974).

(7) P. L. Morselli, G. B. Cassana, G. F. Placidi, G. B. Muscettola, and M. Rizzo, in "The Benzodiazepines," S. Garattini, E. Mussini, and L. O. Randal, Eds., Raven, New York, N.Y. 1973, p. 129.

(8) P. P. Scott, in "The UFAW Handbook on the Care and Management of Laboratory Animals," Edited by UFAW, 330, Williams and Wilkins, Baltimore, Md., 5th ed., 1976.

(9) R. E. Weinfeld, H. H. Postmanter, K. C. Khoo, and C. V. Puglisi, *J. Chromatogr.*, **143,** 589 (1977).

(10) S. Cotler, C. V. Puglisi, and J. H. Gustafson, *J. Chromatogr.*, **222,** 95, (1981).

(11) C. M. Metzler, G. L. Elfring, and A. J. McEwen, *Biometrics*, **30,** 562 (1974).

(12) H. G. Boxenbaum, S. Riegelman, and R. M. Elsashoff, *J. Pharm. Biopharm.*, **2,** 123 (1974).

(13) M. Gibaldi and D. Perrier, in "Pharmacokinetics," Dekker, New York, N.Y., 1975.

(14) G. R. Wilkinson and D. G. Shand, *Clin. Pharm., Ther.*, **18,** 377 (1975).

(15) P. A. Routledge, B. B. Kitchell, T. D. Bjarnsson, T. Skinner, M. Linnoila, and D. G. Shand, *Clin. Pharm. Ther.*, **27,** 528, (1980).

(16) C. S. Lee, T. C. Marbury, and L. Z. Benet, *J. Pharmacokinet. Biopharm.*, **8,** 69, (1980).

(17) C. V. Greenway and R. D. Stark, *Physiol. Rev.*, **51,** 23 (1971).

(18) S. A. Kaplan, M. L. Jack, K. Alexander, and R. E. Weinfeld, *J. Pharm. Sci.*, **62,** 1789 (1973).

(19) J. R. Gillette, *Ann. N.Y. Acad. Sci.*, **179,** 43, (1971).

(20) R. E. Spink, R. L. Malvin, and B. J. Cohen, *Am. J. Vet. Res.*, **27,** 1041, (1966).

(21) M. Gibaldi and P. J. McNamara, *J. Pharm. Sci.*, **66,** 1211 (1977).

(22) "Biological Handbooks, Blood and Other Body Fluids," D. S. Dittmer, Ed., Federation of American Societies for Experimental Biology, Washington, D.C., 1961, p. 352.

(23) H. H. Dasberg, *Psychopharmacologie (Bul.)*, **43,** 191 (1975).

(24) D. J. Greenblatt, E. Woo, M. D. Allen, P. J. Orsulak, and R. I. Shader, *J. Am. Med. Assoc.*, **20,** 1872 (1978).

(25) M. Mandelli, G. Tognoni, S. Garatini, *Clin. Pharm.*, **3,** 72 (1978).

(26) W. Dixon and J. Masser, Jr., in "Introduction to Statistical Analysis," McGraw-Hill, New York, N.Y., 1969, p. 328.

ACKNOWLEDGMENTS

The authors wish to thank Mr. M. Cardinale for his technical assistance, Ms. A. Popick for supplying the plasma binding data in the cat, and Mrs. W. Morley for the preparation of this manuscript.

Structure–Activity Relationships of Sulfonamide Drugs and Human Carbonic Anhydrase C: Modeling of Inhibitor Molecules into the Receptor Site of the Enzyme with an Interactive Computer Graphics Display[1]

ANGELO VEDANI and EDGAR F. MEYER, JR. ˣ

Received October 15, 1982, from the *Biographics Laboratory, Department of Biochemistry and Biophysics, Texas A&M University, College Station, TX 77843.* Accepted for publication January 5, 1983.

Abstract □ We have analyzed the molecular interaction of 28 sulfonamide inhibitors with human carbonic anhydrase C (HCAC) using an interactive computer graphic display. Small aromatic sulfonamides gain most of their inhibitory power towards HCAC from the interaction of hydrogen bond acceptors at the *para* or *meta* positions with hydrophilic residues of the enzyme. Additional coordinated water molecules stabilize the complexes of heterocyclic sulfonamides (*i.e.*, thiophenes, 1,3-thiazoles, and 1,3,4-thiadiazoles) with HCAC. We propose two different modes of binding of the heterocyclic ring with respect to the active site cleft: the heterocyclic sulfur atom of a 3,4-unsubstituted thiophene approaches the oxygen atom of a coordinated water molecule (sulfur "out"), whereas in 3,4-unsubstituted 1,3,4-thiadiazoles, the sulfur is in contact with a hydrophobic part of the receptor site (sulfur "in"). This proposal is consistent with crystallographic evidence. Sulfonamides with two aromatic or heterocyclic rings also interact with a hydrophobic pocket of the enzyme located >10 Å away from the active site metal Zn^{2+}. We also discuss the possibility that the relative inactivity of thiazide diuretics is due to the steric interaction of the *ortho* chlorine atom with the enzyme receptor cavity.

Keyphrases □ Sulfonamides—structure–activity relationships with human carbonic anhydrase C, interactive computer graphic display □ Human carbonic anhydrase C—structure–activity relationships with sulfonamides, interactive computer graphic display □ Structure–activity relationships—enzyme–inhibitor complexes, modeling by interactive computer graphic display, sulfonamides with human carbonic anhydrase C

The isoenzymes of human carbonic anhydrase (HCAB, HCAC) reversibly catalyze the decomposition of carbonic acid into carbon dioxide and water at a remarkably fast rate (up to 1×10^6 s^{-1}). These zinc-containing enzymes consist of 260 amino acids with a molecular mass of ~30 kDa. The active site of human carbonic anhydrase contains a four-coordinated zinc ion: three nitrogen atoms (N—ϵ_2 of His 94, N—ϵ_2 of His 96, and N—δ of His 119) and one oxygen atom (coordinated water molecule, at higher pH values a hydroxide anion) leading to distorted tetrahedral metal coordination (1).

Aromatic and heterocyclic sulfonamides are very specific inhibitors of carbonic anhydrase when the sulfonamido group is unsubstituted. The inhibition of carbonic anhydrase was first reported by Keilin and Mann (2). Kinetic studies have shown sulfonamides to be competitive to the dehydration of carbonic acid as well as the hydration of carbon dioxide (3).

The detailed interaction of sulfanilamide, acetazolamide, and acetoxymercury sulfanilamide with HCAB and HCAC has been reported by Kannan *et al.* (4, 5). The sulfonamido group binds the metal ion at the fourth coordination site (replacing the water molecule from the native enzyme) through the nitrogen or oxygen atom of the sulfonamido moiety, probably through the amide nitrogen atom. This atom is also hydrogen-bonded to the hydroxyl group of Thr 199 in the same way as the fourth coordinated water molecule in the native enzyme. One of the two oxygen atoms is liganded to a fifth coordination site of the zinc. The sulfur atom (or carbon atoms) from the heterocyclic (or aromatic) ring interact with Ala 121 in HCAB and with Val 121 in HCAC, respectively.

Little attention has been paid thus far to enzyme–inhibitor interactions removed from the active site. Nevertheless, these interactions with protein side chains may contribute significantly to the stability of the enzyme–sulfonamide complex. While 4-methylbenzenesulfonamide forms an enzyme–inhibitor complex with a K value of 1.95×10^6 mol^{-1}, the complex formation constant of *p*-(salicyl-5-azo)-benzenesulfonamide is 2.38×10^8 mol^{-1}, two orders of magnitude greater. This is only explainable by the interaction of the salicyl group with side chains of the enzyme located >10 Å from the active site metal (*i.e.*, Ile 91, Trp 123, and Phe 131 in HCAC). We have, therefore, investigated sulfonamide–carbonic anhydrase (HCAC) interactions in an extended environment of the active site using original crystallographic coordinates and an interactive computer graphic display.

THEORETICAL

Several experimental and computational methods are now sufficiently developed to provide insight to the interaction of a small molecule with a macromolecule. Interactive computer graphic techniques are very useful for the study of molecular interactions characterized as recognition, binding, enzyme catalysis, and inhibition.

Basic adjustments of the model (*i.e.*, inhibitor molecule) to the receptor structure (*i.e.*, enzyme) on a 3-dimensional display are possible in real time (no intermediate keyboard commands) by means of the program FIT (6):

1. Model: (*a*) complete or subunit model translations relative to the receptor; (*b*) individual atom translation; (*c*) complete or subunit model rotation; (*d*) complete subunit rotation about a given bond; and (*e*) dihedral rotation before or after any selected bond.
2. Receptor: in principle the same as for the model, but due to the complexity of the protein only reorientations of amino acid side chains have been performed so far by dihedral rotation about single bonds.

In addition to the above functions, which are basic to any model-fitting method, several utility functions are furnished including (*a*) picture scale; (*b*) stereo image separation (right–left or top–bottom); (*c*) global picture translation and rotation; (*d*) receptor–model relative intensities; and (*e*) I/O functions to exchange or modify the receptor structure, exchange models, print any geometric information about the model (*i.e.*, atom identification, bond length, bond angles, dihedral angles), save the current picture and output the current model coordinates, calculate distances of enzyme–inhibitor interactions, and facilitate still or motion-picture photography.

[1] Dedicated to Professor J. D. Dunitz mentor and friend in honor of his 60th birthday.

0022-3549/84/0300-0352$01.00/0
© 1984, American Pharmaceutical Association

Table I—Enzyme–Inhibitor Complex Formation Constants K (mol^{-1}) for Sulfonamides with Human Carbonic Anhydrase

Inhibitor Molecule	Taylor *et al.* (9)[a] Stop Flow	Taylor *et al.* (9)[a] Affinity Titration	Taylor *et al.* (9)[a] Relative[d]	Kakeya *et al.* (10)[b] Calorimetry	Kakeya *et al.* (10)[b] Relative[d]	Sprague (11)[c] (Relative)[d]
Aromatic Sulfonamides						
Benzenesulfonamide Substituent						
4-H-	6.46×10^5	6.48×10^5	1.00	1.33×10^5	1.00	1.00
4-CH_3-	1.95×10^6	1.95×10^6	3.01	3.13×10^5	2.35	2.13
4-NH_2-				4.00×10^4	0.30	0.25
4-CO_2-	3.71×10^6	3.71×10^6	5.73			2.50
4-NO_2-	1.53×10^7	1.60×10^7	24.3	1.82×10^6	13.7	5.75
4-Cl-	8.27×10^6	8.27×10^6	12.8	9.09×10^5	6.83	4.50
4-N≡C-				1.54×10^6	11.6	3.75
4-SO_2NH_2-						10.0
3,4-di Cl-	1.56×10^7	1.56×10^7	24.1	3.33×10^6	25.0	14.0
3-SO_2NH_2, 4-Cl-						23.3
2,4,5-tri Cl-	6.78×10^6	6.80×10^6	10.5			
2,4,6-tri Cl-	4.57×10^6	4.57×10^6	7.05			
2,5-di NO_2, 4-Cl-	1.29×10^7	1.40×10^7	20.8			
3-SO_2NH_2, 4,5-di Cl-						43.8
3-SO_2NH_2, 4-Cl-6-NH_2-						0.93
H_3C—CO—NH—	1.60×10^6	1.60×10^6	2.47			3.75
Heterocyclic Sulfonamides						
Sulfonamide Substituent						
2-H-thiophene-						0.90
2-NO_2-thiophene	2.38×10^8	$>10^8$	368			
5-H-1,3-thiazole-2-						30.0
2-NH_2-1,3-thiazole-5-						0.75
4-CH_3-1,3-thiazole-2-						12.5
2-Acetamido-1,3-thiazole-5-						3.75
2-H-1,3,4-thiadiazole-5-						19.8
2-NH_2-1,3,4-thiadiazole-5-				1.85×10^6	13.9	
2-Acetamido-1,3,4-thiadiazole-5-	7.10×10^7	7.10×10^7	110	8.33×10^6	62.2	82.5
2-Propamido-1,3,4-thiadiazole-5-						99.0
2-Butamido-1,3,4-thiadiazole-5-						99.0
2-Acetimido-3-CH_3-1,3,4-thiadiazole-5-				1.00×10^7	75.2	132
Complex Sulfonamide						
p-(Salicyl-5-azo)-benzenesulfonamide	3.48×10^8	$>10^8$	526			
2-Benzenesulfonamido-1,3,4-thiadiazole-5-sulfonamide						421
2-(*p*-Chloro)-benzenesulfonamido-1,3,4-thiadiazole-5-sulfonamide						314
4-Chloro-*N*-furfuryl-5-sulfamoylanthranylic acid (furosemide)						0.3
5-Dimethylaminonaphthalene-1-sulfonamide	6.15×10^5	5.80×10^5	0.92			
2-(4-Sulfamylphenylazo)-1-hydroxonaphthalene-4,6-disulfonate	7.74×10^6	6.90×10^6	11.3			
6-Ethoxybenzothiazole-2-sulfonamide (ethoxzolamide)[e]		6.25×10^8				

[a] Using HCAC, pH 6.5, 25 °C. [b] Using HCAB and HCAC, pH 7.0 15 °C. [c] Using HCAB and HCAC, pH 5.5, 25 °C (50% inhibition). [d] Relative to benzenesulfonamide (H substituted at the 4-position). [e] See Ref. 13.

Thus, a flexible substrate may be fit into a relatively rigid receptor site. While potentially limiting, this assumption is reasonably valid for "lock and key"-type enzymes. These methods are entirely general in terms of the size and functionality of the receptor site and ligand. A number of advantages of graphically generated models (reproducibility, instant quantification of geometric parameters, and accessibility to refinement procedures) make this approach superior to desk-top modelling approaches.

EXPERIMENTAL[2]

Except for modified enzyme side-chain positions, the crystal structure parameters of the native human isoenzyme C were used [HCAC; Protein Data Bank 1976, 2.0-Å resolution (7)]. Individual side chains in the active site were repositioned, if necessary, by appropriate torsional rotations. The molecular coordinates (sulfonamides) were taken from crystal structure determinations or generated by the program PAD (8). To obtain a more realistic fitting, the side chains of the enzyme were not restricted to their native conformation. These dihedral rotations were also performed with the program FIT.

The starting coordinates for the sulfonamido group in the fitting routine were taken from the crystal structure determination of the HCAC–acetazolamide enzyme–inhibitor complex (5). The potency of some inhibitors can only be explained if one takes into account their interaction with additional coordinated water molecules; these were generated by PAD and inserted with FIT.

[2] The following standard designations for amino acids are used throughout this paper: (Ala) alanine; (Asn) asparagine; (Gln) glutamine; (Gly) glycine; (His) histidine; (Ile) isoleucine; (Leu) leucine; (Phe) phenylalanine; (Pro) proline; (Ser) serine; (Thr) threonine; (Trp) tryptophan; (Val) valine.

RESULTS AND DISCUSSION

A large number of sulfonamides have been examined by kinetic and thermoanalytical methods by Taylor *et al.* (9), Kakeya *et al.* (10), and Sprague (11); an abstract of these data is given in Table I. The general features of sulfonamide interactions with HCAC are presented in Table II.

Aromatic Sulfonamides—In addition to the interaction of the sulfonamido group with the enzyme, two additional types of interactions are observed for aromatic sulfonamides:

1. Hydrophobic interactions of the benzene ring and aliphatic substituents with nonpolar residues of the enzyme.
2. Hydrogen bonding involving hydrophilic substituents and polar residues of the enzyme.

The orientation of the benzene ring is very sensitive to the number and type of hydrogen bond interactions of its substituents and may be constrained in a less favorable position with respect to its hydrophobic contacts and *vice versa*. For example, 4-aminobenzenesulfonamide shows a threefold smaller inhibition constant than the unsubstituted 4-*H*-benzenesulfonamide (*cf.* Table I or Ref. 10). The crystal structure determination of the 4-aminobenzenesulfonamide–HCAC complex (5) shows that the interaction of the benzene ring with the hydrophobic part of the enzyme forces the amino group in the *para* position to a repulsive

Table II—General Features of Sulfonamide Interaction with HCAC

Functional Group of Inhibitor	Interaction with HCAC Residue	Type of Interaction
	Aromatic Sulfonamides	
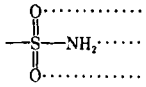	Zn^{2+}, (His 119)	coulombic[a]
	Zn^{2+}, Thr 199	coulombic, hydrogen bond[a]
	(NH of Thr 199 after small reorientation of the backbone of the enzyme)	
	Val 121, Leu 141 Val 143, Leu 198 Val 207	hydrophobic[a]
Ring Substituents		
para: aliphatic	Phe 131, (Ile 91)	hydrophobic
charged or hydrophilic	Gln 92, (Asn 67) solvent	hydrogen bonds[a]
meta: aliphatic	Val 121, (Pro 200, 201)	hydrophobic
charged or hydrophilic	His 64, Gln 92, O=C< of Pro 201, (Asn 67) solvent	hydrogen bonds
ortho: aliphatic	Leu 198, Val 121 Leu 141, Val 143 Val 207	hydrophobic
charged or hydrophilic	not very favorable	
	Heterocyclic Sulfonamides	
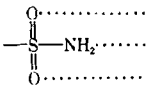	as above[b]	
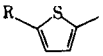 (S pointing out)	ring C: Val 121, Leu 141 ring S: H_2O...O=C< of Thr 200 and Pro 201	hydrophobic[c] hydrogen bonds[c]
(S pointing in)	ring C, N: H_2O...O=C< of Thr 200 or Pro 201 ring S: Val 121	repulsive ?, hydrogen bonds hydrophobic
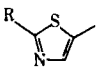 (S pointing out)	ring C, N: Val 121, Leu 141 ring S: H_2O...O=C< of Thr 200 and Pro 201	hydrophobic
(S pointing in)	ring S: Val 121 ring N: H_2O...O=C< of Thr 200 or Pro 201	hydrophobic[d] hydrogen bonds[d]
R: aliphatic	Phe 131, Ile 91 (Trp 123)	hydrophobic[b]
charged or hydrophilic	Gln 92, (Asn 67), His 64, solvent	hydrogen bonds[e]
	Complex Sulfonamides	
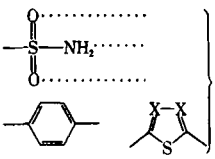	as above[a,b]	
—N=N—	Gln 92, solvent	hydrogen bonds[f]
—CO—NH—	Gln 92, solvent	hydrogen bonds
—CH_2—NH—	Gln 92, Phe 131	hydrogen bonds, hydrophobic[g]
—SO_2—NH—	Gln 92, His 64, Asn 67, solvent	hydrogen bonds
—S—NH—	Gln 92, solvent	hydrogen bonds
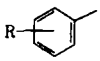	Phe 131, Ile 91 (Trp 123)	hydrophobic[f,g]
R = small aliphatic	Phe 131, Ile 91 (Trp 123)	hydrophobic
charged or hydrophilic	solvent	hydrogen bonds[f]

[a] See Fig. 1. [b] See Figs. 3–5. [c] See Fig. 3. [d] See Fig. 4. [e] See Figs. 3–6. [f] See Fig. 6. [g] See Fig. 7.

interaction with the amido group of Gln 92. (A reorientation of the amido moiety is not very probable, since its carbonyl oxygen atom is also hydrogen-bonded to the N—H of His 94).

Hydrogen bond acceptors are favorably oriented with respect to the *para* and *meta* positions, since more hydrophilic residues of HCAC are located in this region and the active site funnel is open to the solvent (hydrogen bonds to Asn 67 and Pro 201 through coordinated water molecules). 3-Sulfamoyl-4,5-dichlorobenzenesulfonamide is a very potent inhibitor of HCAC. The *ortho* position is not very favorable for hydrophilic or bulky hydrophobic substituents; steric hindrance with Leu 198 requires a rearrangement of the backbone of the enzyme. 4-Nitro-2-carboxybenzenesulfonamide inhibits HCAC three orders of magnitude less than 4-nitro-2*H*-benzenesulfonamide [$<10^4$ *versus* 1.60×10^7 (9)].

As an example, *p*-nitrobenzenesulfonamide will be discussed in detail (Fig. 1). The sulfonamido group has discrete interactions with the enzyme:

1. The amino group (2.14% ionized in free solution at pH 7.38) occupies the fourth coordination site at the Zn^{2+} ion (d = 2.5 Å) and is hydrogen-bonded to Thr 199 (d = 2.8 Å). This position is identical with the coordinated water molecule in the native enzyme.
2. O-1 occupies the fifth coordination site at the Zn^{2+} ion (d = 3.0 Å).

Table III—Main Interactions of Various Sulfonamides with HCAC[a]

Functional Group of Inhibitor	Atom	Enzyme Residue[b]	Atom	Distance, Å[c]
		p-Nitrobenzenesulfonamide		
SO_2NH_2	N	Het 301	Zn^{2+}	2.5
		Thr 199	O-γ	2.8
	O-1	Het 301	Zn^{2+}	3.0
	O-2	Leu 198	C-α	3.1
		Thr 199	NH	3.7
Benzene ring	C-2	Val 121	C-γ	4.1
			C-γ_2	3.6
	C-3	Val 121	C-γ	4.1
			C-γ_2	4.0
NO_2	O-2	Gln 92	N-ϵ_2	2.9
		2-Nitrothiophene-5-sulfonamide		
SO_2NH_2	N	Het 301	Zn^{2+}	2.4
		Thr 199	O-γ	3.4
	O-1	Het 301	Zn^{2+}	2.9
	O-2	Val 143	C-γ_2	3.4
Thiophene ring	S-1	Water	O	3.8
	C-3	Val 121	C-γ	3.2
		Leu 141	C-δ_2	3.5
	C-4	Val 121	C-γ	3.4
			C-γ_2	3.4
		Leu 141	C-δ_2	3.5
Nitro group	O-2	Gln 92	N-ϵ_2	2.8
		Acetazolamide		
SO_2NH_2	N	Het 301	Zn^{2+}	2.8 (2.5)
		Thr 199	O-γ	3.2 (3.2)
	O-1	Het 301	Zn^{2+}	3.0 (3.1)
	O-2	Val 143	C-γ_2	3.1 (3.0)
Thiadiazole ring	S-1	Val 121	C-γ	3.2 (3.4)
			C-γ_2	3.1 (2.9)
	N-3	Water	O	2.9
	N-4	Water	O	2.9
Acetamido group	N	Phe 131	C-ϵ_2	3.2 (3.0)
	O	Gln 92	N-ϵ_2	2.6 (1.7)
	C	Phe 131	C-ϵ_2	3.2 (3.1)
		Metazolamide		
SO_2NH_2	N	Het 301	Zn^{2+}	2.5
		Thr 199	O-γ	3.4
	O-1	Het 301	Zn^{2+}	3.0
	O-2	Val 143	C-γ_2	3.5
Thiadiazole ring	S-1	Val 121	C-γ	3.3
			C-γ_2	3.0
	Ring-CH_3	Phe 131	C-ϵ_2	4.1
		Leu 141	C-δ_2	3.9
		Leu 198	C-γ	3.8
Acetimido group	O	Gln 92	N-ϵ_2	2.7
	C	Ile 91	C-γ_2	3.6
		Phe 131	C-γ	3.1
			C-ϵ_2	2.7
			C-δ_2	2.7
		p-(Salicyl-5-azo)-benzenesulfonamide		
SO_2NH_2	N	Het 301	Zn^{2+}	2.7
		Thr 199	O-γ	3.4
	O-1	Het 301	Zn^{2+}	2.7
	O-2	Val 143	C-γ_2	3.4
Benzene ring	C-2	Val 121	C-γ	3.2
			C-γ_2	3.1
	C-3	Val 121	C-γ	2.5
	C-4	Val 121	C-γ	3.6
Azo bridge	N-1	Phe 131	C-ϵ_2	3.1
		Gln 92	N-ϵ_2	3.6
	N-2	Phe 131	C-ϵ_2	2.8
Salicyl ring	Since no relaxation of the backbone of HCAC was performed, these hydrophobic contacts with Ile 91 and Phe 131 turn out to be a little too short (<2 and 3 Å).			
		Furosemide		
SO_2NH_2	N	Het 301	Zn^{2+}	2.7
		Thr 199	O-γ	3.2

continued

Table III—*Continued*

Functional Group of Inhibitor	Atom	Enzyme Residue[b]	Atom	Distance, Å[c]
	O-1	Het 301	Zn^{2+}	3.4
	O-2	Val 143	C-γ_2	3.0
Benzene ring	C-2	Leu 141	C-δ_2	3.5
Ring substituents	CO_2:O-1	Gln 92	N-ϵ_2	2.6
	Cl	Leu 141	C-δ_2	2.5
Furfuryl group	C-3	Phe 131	C-ϵ_2	3.0
	C-4	Ile 91	C-δ	2.9
		Phe 131	C-γ	2.8
	C-5	Ile 91	C-δ	2.8
		Phe 131	C-γ	3.1

[a] Atomic coordinates for the inhibitors in the proposed model fits are available from the author on request. [b] Het = Protein Data Bank notation for any hetero atom or group. [c] Values in parentheses are calculated using atomic coordinates from the crystal structure determination of the HCAC–acetazolamide complex; taken from Ref. 5.

Because the dehydration of carbonic acid requires both the fourth and fifth coordination sites at the zinc, sulfonamides are competitive inhibitors to this reaction.

3. For O-2 no strong interaction could be found using the native conformation of the backbone of HCAC. However, it seems possible that a small reorientation of residues 196–200 would allow a better interaction of this oxygen atom with Thr 199 (NH of the backbone) and increase the distance to Leu 198 (Table III).

The benzene ring interacts with the hydrophobic part of the enzyme: C-2 and C-3 approach Val 121 at d = 3.6 Å and d = 4.0 Å, respectively. A hydrogen bond between the O-2 of the nitro group towards Gln 92 is present, d = 2.9 Å. Additional solvent molecules (H_2O) could be expected to bridge the oxygens of the nitro group with the carbonyl groups of Pro 201 and Asn 67. Since the most powerful aromatic inhibitors (*cf.* Table I) have good hydrogen bond acceptors in the *para* or *meta* position, these additional bridging water molecules may contribute significantly to the enzyme–inhibitor complex stability.

Heterocyclic Sulfonamides—*Participation of Solvent Molecules*—A 1,3,4-thiadiazole ring attached to the sulfonamido group facilitates sulfonamide–HCAC complex formation. Acetazolamide (2-acetamido-1,3,4-thiadiazole-2-sulfonamide) shows a 45-fold greater inhibition constant than 4-acetamidobenzenesulfonamide ($K = 7.1 \times 10^7$ *versus* 1.6×10^6 mol^{-1}). A crystal structure study of the acetazolamide–HCAC complex shows the heterocyclic sulfur atom of the 1,3,4-thiadiazole ring pointing towards Val 121. This interaction was reported to be the main reason why acetazolamide binds 10 times stronger to HCAC than to HCAB, where the ring sulfur atom approaches Ala 121.

We propose that in the acetazolamide–HCAC complex an additional significant contribution to the complex stability can be attributed to the interaction of the two heterocyclic nitrogen atoms through a coordinated water molecule with the backbone of Thr 200 or Pro 201 (Fig. 2). The structural rigidity of the portion of the receptor cavity occupied by Pro 201 and *cis*-Pro 202 should be noticed. The fixed backbone carbonyl groups, nevertheless, are well positioned for hydrogen bonding. Because this part of the enzyme is open to the solvent, the water molecule might be dynamically exchanged making it undetectable by X-ray diffraction analysis at ambient temperatures. In the receptor site of HCAB this coordinated water would interact in an unfavorable manner with His 200 (HCAC has a Thr residue at this position) and, thus, would be less probable.

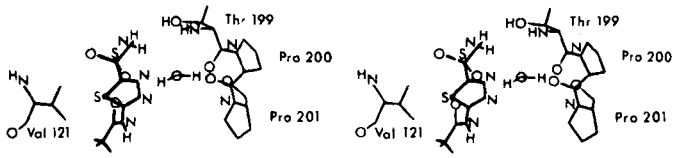

Figure 2—*H_2O molecule bridging the heterocyclic nitrogen atoms of the 1,3,4-thiadiazole ring of acetazolamide and the carbonyl group of Thr 200 or Pro 201.*

Such a coordinated water molecule is very probably present in all heterocyclic sulfonamides with a 3,4-unsubstituted 1,3,4-thiadiazole ring interacting with HCAC, as well as with thiophene ring systems (Fig. 3). Another water molecule may be expected to bridge the amino terminus of Asn 67 with the carbonyl function(s) of inhibitor molecules. Because no good interaction of O-4 of the sulfonamido group could be found with HCAC complexes, one might expect an additional water molecule between O-4 and an hydrophilic residue or the backbone in the vicinity (*i.e.*, Gly 196, Ser 197, Leu 198, Thr 199, Thr 200). With the coordinates of the native enzyme, however, no good site could be detected within the limits of the rigid receptor assumption.

Orientation of the Heterocyclic Ring—2-Nitrothiophene-5-sulfonamide is a very strong inhibitor for HCAC [$K = 2.38 \times 10^8$ *versus* 7.10×10^7 for acetazolamide (11)]. Assuming the same orientation as found in acetazolamide, the ring sulfur atom would point toward Val 121 and the 3,4-ring carbon atoms outward into the solvent. This would not contribute favorably to the binding energy of the enzyme–inhibitor complex and could not explain the large binding constant.

We therefore propose that 3,4-unsubstituted thiophenesulfonamides show an inverted binding to the active site cleft with respect to the orientation of the ring sulfur atom. 2-Nitrothiophenesulfonamide would thus achieve very good interactions of the ring carbon atoms with Val 121

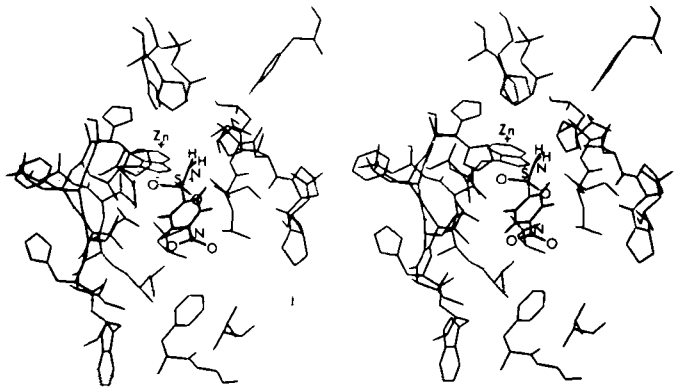

Figure 1—*Stereoprojection of the model fit of* p*-nitrobenzenesulfonamide in the receptor site of HCAC. The hydrogen atoms of the enzyme are not shown; the Zn^{2+} ion is represented by a cross (+).*

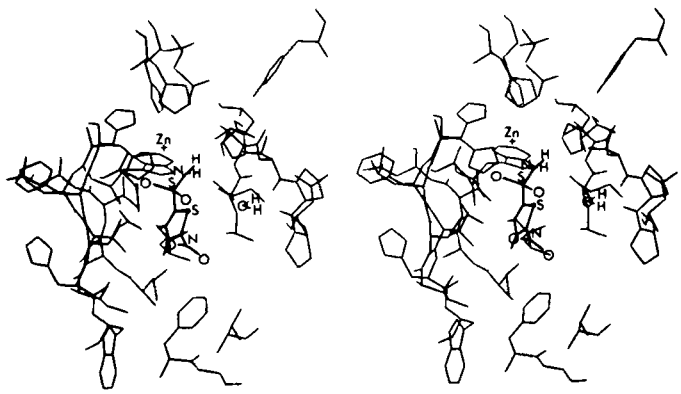

Figure 3—*Stereoprojection of the model fit of 2-nitrothiophene-5-sulfonamide into the receptor site of HCAC, with the bridging H_2O molecule to the right of the ring S atom.*

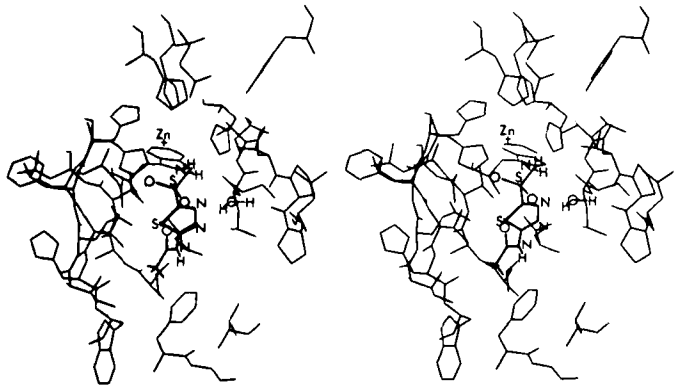

Figure 4—*Stereoprojection of the model fit of 2-acetamido-1,3,4-thiadiazole-5-sulfonamide (acetazolamide) into the receptor site of HCAC, with the bridging H_2O to the right of the ring N atoms.*

and Leu 141, and the sulfur atom would approach the oxygen atom of the coordinated water molecule (Fig. 3, Table III).

For 3,4-unsubstituted 1,3-thiazolesulfonamides, both orientations of the heterocyclic ring seem possible (Table II). This could also explain the unusually strong activity of 5-*H*-1,3-thiazole-2-sulfonamide *versus* 2-acetamido-1,3-thiazole-5-sulfonamide (Table I). For 3,4-unsubstituted 1,3,4-thiadiazolesulfonamides, an inverted binding of the heterocycle is very improbable, since the 3,4-ring nitrogen atoms would point into a hydrophobic part of the enzyme (*i.e.*, Val 121 and Leu 141).

The sulfonamido group of these inhibitors interacts with HCAC in the same manner as described for the aromatic sulfonamides. The main difference is that due to the lower pK value, heterocyclic sulfonamides may bind in the ionized form. At pH 7.38 (pH 6.50) acetazolamide is 49.9% (11.2%) deprotonated and metazolamide is 54.6% (13.7%) deprotonated.

With the inverted binding of the thiophene ring, 4-nitrothiophenesulfonamide achieves the following interactions with HCAC. The ring carbon atoms C-3 and C-4 are in contact with Val 121 and Leu 141 (d = 3.2 Å, d = 3.4 Å; d = 3.4 Å, d - 3.5 Å), whereas the ring sulfur atom approaches the oxygen atom of the postulated coordinated water molecule (d = 3.8 Å) which would be hydrogen bonded to the carbonyl group of Thr 200 (d = 3.0 Å) and Pro 201 (d = 2.7 Å). The nitro group would be hydrogen bonded to Gln 92 (d = 2.8 Å) and probably to the open solvent (Fig. 3, Table III).

The fit of acetazolamide, disregarding the additional water molecule bridging the heterocyclic ring with Thr 200 or Pro 201, is derived from crystal structure data reported by Kannan (5). Interactions include the heterocyclic sulfur atom with Val 121 (d = 3.1 Å and d = 3.2 Å), the acetamido oxygen with Gln 92 (d = 2.6 Å), and the methyl group with Phe 131 (d = 3.2 Å). The acetamido group is therefore tilted 74° out of the ring plane. In the crystal structure of molecular 2-acetamido-1,3,4-thiadiazole-5-sulfonamide (acetazolamide), this group is reported to be almost coplanar (4.9°) with the 1,3,4-thiadiazole ring, which allows an intramolecular S(ring)· · ·O(acetamido) contact of 2.75 Å (12). The two ring nitrogen atoms are located 2.9 Å from the water molecule (Fig. 4, and Table III), which is hydrogen bonded to Thr 200 (d = 3.4 Å) or Pro 201 (d = 3.1 Å).

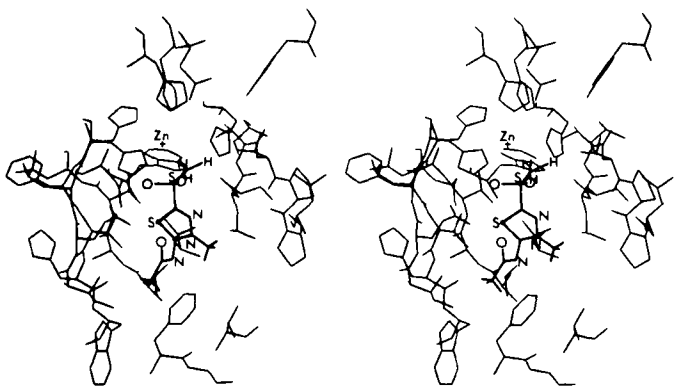

Figure 5—*Stereoprojection of the model fit of 2-acetamido-3-methyl-1,3,4-thiadiazole-5-sulfonamide (metazolamide) into the receptor site of HCAC.*

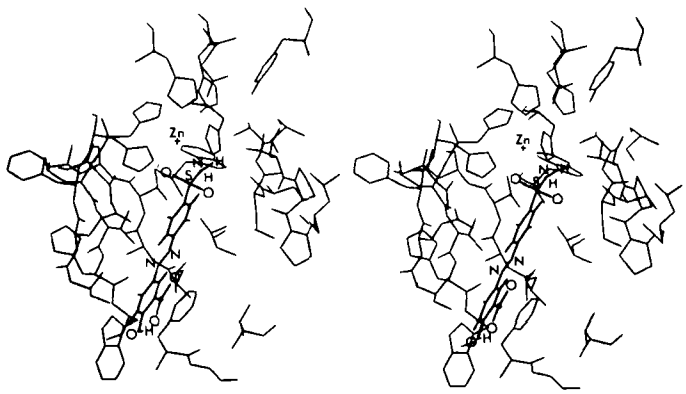

Figure 6—*Stereoprojection of the model fit of* p-*(salicyl-5-azo)-benzenesulfonamide into the receptor site of HCAC.*

The inhibitory power of metazolamide (2-acetamido-3-methyl-1,3,4-thiadiazole-5-sulfonamide) is reported to be 60% higher than in acetazolamide (11). This may be attributed to an additional interaction of either the 3-methyl group or the imido nitrogen atom of metazolamide with HCAC (Fig. 5). The heterocyclic sulfur atom is in contact with Val 121 (d = 3.0 Å, d = 3.3 Å). The ring methyl group is located in a hydrophobic pocket: Phe 131 (d = 4.1 Å), Leu 141 (d = 3.9 Å) and Leu 198 (d = 3.8 Å). The acetamido oxygen is hydrogen bonded to Gln 92 (d = 2.7 Å), whereas the methyl group is in contact with Ile 91 (d = 3.6 Å) and Phe 131 (d = 2.7 Å). The carbonyl group is tilted 35° out of the ring plane, and the intramolecular O(carbonyl)· · ·S(thiadiazole) distance is 3.27 Å.

Complex Sulfonamides—The interactions of *p*-(salicyl-5-azo)-benzenesulfonamide and furosemide (4-chloro-*N*-furfuryl-5-sulfamoylanthranylic acid) with HCAC will be discussed in detail. The benzene ring of *p*-(salicyl-5-azo)-benzenesulfonamide has close contacts to Val 121 (d = 2.5 Å, d = 3.1 Å, d = 3.2 Å, and d = 3.6 Å) (Fig. 6). The azo nitrogen atoms are 2.8 Å and 3.1 Å away from Phe 131, respectively. The amido nitrogen atom of Gln 92 interacts with the π-system of N-1 (d = 3.6 Å). The apparently short contacts of the salicyl group to Ile 91 and Phe 131 are not unrealistic if one takes into account that the backbone of the enzyme is not rigid and will relax to a more favorable conformation. (This additional degree of freedom is one of the subjects of our future investigations using force-field refinement.) The hydroxyl and carboxyl groups form hydrogen bonds with the surrounding solvent, which probably bridges these groups to the carbonyl group of Asn 67. A fit of the salicyl group into the hydrophobic pocket between Phe 131 and Val 135 was also investigated, but leads to less favorable contacts of the benzene ring.

Earlier investigations on aromatic sulfonamides indicated an enhancing effect of certain substituents (*i.e.*, halogens, trifluoromethyl, nitro, and methyl) *ortho* to the sulfonamido group with respect to diuretic activity. This structural alteration has decreased enzyme inhibitory activity and shifted the excretion pattern to a saluretic response. This separation of the two biological activities has been maintained and extended in the thiazide diuretics (11).

We therefore have investigated the steric interactions of such a sulfonamide drug, furosemide, with HCAC. With the native conformation of HCAC no favorable fit of furosemide could be obtained (Cl· · ·Leu 141: d = 2.5 Å). The chlorine in the *ortho* position of the benzene ring hinders

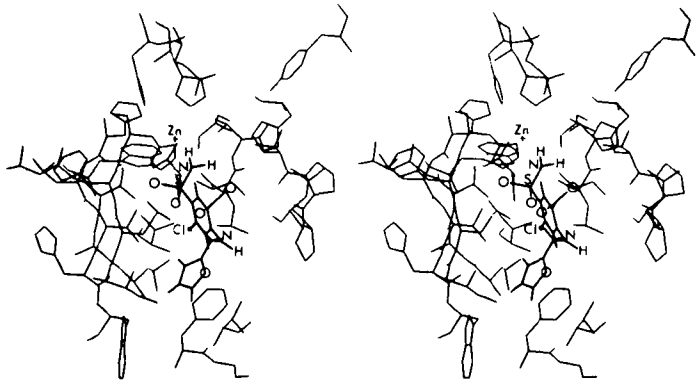

Figure 7—*Stereoprojection of the model fit of furosemide into the receptor site of HCAC.*

the molecule from entering deeply enough into the active site cleft to form good contacts (*i.e.*, sulfonamido group with Zn^{2+} and Thr 199, CO_2^- with Gln 92, furyl ring with Ile 91 and Phe 131). More drastic rearrangements of the hydrophobic part of the receptor site would be necessary in order to form good interactions. Therefore, simply for steric reasons, furosemide is expected to be a rather poor inhibitor of carbonic anhydrase; this is confirmed by *in vitro* measurements (11).

Figure 7 and Table III show that furosemide (without a chlorine atom in the *ortho* position) would be a good inhibitor of HCAC. The carboxyl group could hydrogen-bond to Gln 92 (d = 2.6 Å) and probably through a coordinated water molecule to the carbonyl groups of Pro 201. The furfuryl group would be located in the hydrophobic pocket between Ile 91 and Phe 131 (d = 2.8 Å through $d \approx 3.3$ Å), its oxygen atom pointing out into the solvent.

CONCLUSIONS

We have investigated 28 sulfonamide–HCAC complexes with interactive computer graphics in order to obtain a realistic starting conformation for force-field refinement. Aromatic sulfonamides gain most of their inhibitory power toward HCAC from the interaction of hydrogen bond acceptors in the *para* and *meta* positions with Gln 92 and Pro 201 and (*via* a coordinated water molecule) with Asn 67. No significant rearrangement of the backbone *versus* the conformation of native HCAC is expected, so long as the benzene ring is not substituted with bulky or multiple ligands.

In general, heterocyclic sulfonamides (*i.e.*, thiophenes, 1,3-thiazoles, and 1,3,4-thiadiazoles) are more potent inhibitors of HCAC than aromatic sulfonamides. This is due to the interaction of their heterocyclic ring with a hydrophobic part of the receptor site (Val 121$\cdots$S) and with Thr 200 and Pro 201 *via* a coordinated water molecule (S,N$\cdots H_2O\cdots$O=C$\langle$). We propose two different orientations of the heterocyclic ring with respect to the active site cleft:

1. The ring sulfur atom is in contact with Val 121, whereas the ring nitrogen atoms build hydrogen bonds to Thr 200 and Pro 201 (sulfur "in") for 3,4-unsubstituted 1,3,4-thiadiazoles. This is confirmed by the crystal structure determination of the acetazolamide–HCAC complex (5).
2. The ring sulfur atom is in contact with the oxygen atom of a coordinated water molecule, whereas the ring carbon atoms are located in a hydrophobic part of the receptor site such as Val 121 and Leu 143 (sulfur "out") for 3,4-unsubstituted thiophenes.

In addition to those interactions mentioned above, complex sulfonamides (two or more aromatic or heterocyclic rings) also show interactions of the "bridge" between the two ring systems (*e.g.*, —N=N—, —CO—NH—) with Gln 92 and the solvent. A significant contribution to the complex stability is derived from the interaction of aliphatic and aromatic substituents with the hydrophobic pocket around Ile 91, Trp 123, and Phe 131. Such sulfonamides, as well as aromatic or heterocyclic sulfonamides with larger substituents, may require a rearrangement of parts of the enzyme in order to bind. The hydrophobic pocket (Ile 91, Trp 123, Phe 131) for bulky aromatic or aliphatic parts of the inhibitor and the backbone around Leu 198 may need to be rearranged in order to obtain better interactions between the second sulfonamide oxygen atom and the enzyme.

Bulky ligands in the *ortho* position of the aromatic ring are not very favorable to inhibitory activity. Steric hindrance with Leu 141 and Leu 198 is the main reason why thiazide diuretics (Cl in the *ortho* position) are rather poor inhibitors of HCAC.

While crystallographic studies offer definitive information on the locus of binding and type of coordination of the sulfonamides with HCAB and HCAC, individual details cannot always be elucidated at the atomic level. By surveying the literature and applying known rules of stereochemistry and weak interactions, we have been able to propose alternative modes of binding of these small-molecule inhibitors that are consistent within the limits of the crystallographic studies and offer a better explanation for kinetic values. Interactive computer graphics, therefore, is a useful tool in surveying a broad literature data base to seek detailed correlations of structure and function. Such methods, when aided by the developing discipline of force-field refinement, offer the potential for detailed structure–activity studies. They may be extended by the intuitive chemist to include the prediction and design of novel drugs, inhibitors, and transition state analogues.

REFERENCES

(1) B. Notstrand, I. Vaara, and K. K. Kannan, in "The Isozymes," C. L. Markers, Ed., Academic, New York, N.Y., 1975, pp. 575–599.

(2) D. Keilin and T. Mann, *Nature (London)*, **146**, 164 (1940).

(3) S. Lindskog, H. E. Henderson, K. K. Kannan, A. Liljas, P. O. Nyman, and B. Strandberg, in "The Enzymes," Vol. V, P. Boyer, Ed., Academic, New York, N.Y., 1971, pp. 587–666.

(4) K. K. Kannan, in "Biophysics and Physiology of Carbon Dioxide," C. Bauer, G. Gros, and H. Bartels, Eds., Springer Verlag, Berlin, 1979, pp. 184–205.

(5) K. K. Kannan, I. Vaara, B. Notstrand, S. Lovgren, A. Borell, K. Fridborg, and M. Petef, in "Proceedings on Drug Action at the Molecular Level," G. C. K. Roberts, Ed., McMillan, London, 1977, pp. 73–91.

(6) C. N. Morimoto and E. F. Meyer, Jr., in "Crystallographic Computing Techniques," F. R. Ahmed, Ed., Munksgaard, Copenhagen, 1975, pp. 488–496.

(7) F. C. Bernstein, T. F. Koetzle, G. J. B. Williams, E. F. Meyer, Jr., M. D. Brice, J. R. Rodgers, O. Kennard, T. Shimanouchi, and M. Tasumi, *J. Mol. Biol.*, **112**, 535 (1977).

(8) W. G. White and E. F. Meyer, Jr., *J. Chem. Ed.*, **59**, 515 (1982).

(9) P. W. Taylor, R. W. King, and A. S. V. Burgen, *Biochemistry*, **9**, 13, 2638 (1970).

(10) N. Kakeya, M. Aoki, A. Kamada, and N. Yata, *Chem. Pharm. Bull.*, **17**, 1010 (1969).

(11) J. M. Sprague, in "Topics in Medicinal Chemistry," J. L. Rabinowitz and R. M. Myerson, Eds., Interscience, New York, N.Y., 1968, pp. 1–63.

(12) M. Mathew and G. J. Palenik, *J.C.S. Perkin II*, **1974**, 532.

(13) J. C. Kernohan, *Biochim. Biophys. Acta*, **81**, 346 (1964); **96**, 304 (1965); **118**, 405 (1966).

ACKNOWLEDGMENTS

This research was supported by the Swiss National Science Foundation and the Robert A. Welch Foundation. Funds for the purchase of the Biographics System were originally provided by the U.S. National Science Foundation.

The authors thank Dr. Stanley M. Swanson for programming assistance.

Bioavailability of Hydrochlorothiazide from Tablets and Suspensions

RAJNI B. PATEL *§, USHA R. PATEL *, MARK C. ROGGE *, VINOD P. SHAH ‡, VADLAMANI K. PRASAD ‡, ARZU SELEN *, and PETER G. WELLING *x

Received November 22, 1982, from the **School of Pharmacy, University of Wisconsin, Madison, WI 53706* and ‡*Division of Biopharmaceutics, Food and Drug Administration, Washington, DC 20204.* Accept for publication February 3, 1983. §Present address: Analytical R & D Subdivision, Wyeth Laboratories, Philadelphia, PA 19101.

Abstract □ The bioavailability of hydrochlorothiazide was determined following single oral 25-, 50-, 100-, and 200-mg tablet and suspension doses in 12 healthy male volunteers. Plasma and urine levels of hydrochlorothiazide were determined by HPLC. Plasma levels of hydrochlorothiazide were satisfactorily described by a triexponential function. Mean peak plasma levels, C_{max} (127–135, 270–280, and 437–490 ng/mL from the 25-, 50-, and 100-mg doses, respectively) were dose proportional, as were areas under plasma profiles, $AUC_{0-\infty}$. Mean percentage recovery of unchanged hydrochlorothiazide in 48-h urine samples accounted for 50–59, 54–55, 60–63, and 54–57% of the 25-, 50-, 100-, and 200-mg doses, respectively. There were no significant differences among these values. Correlation coefficients between 48-h urinary recovery of hydrochlorothiazide and the plasma values (C_{max} and AUC_{0-36}) for the 25-, 50-, and 100-mg doses were 0.73 and 0.84. There were no differences in the net increases in electrolyte excretion among the treatments during the 0–12-h postdose period. The systematic availability of hydrochlorothiazide, unlike that of chlorothiazide, is dose proportional in the therapeutic range.

Keyphrases □ Hydrochlorothiazide—bioavailability from tablets and suspensions, pharmacokinetics □ Bioavailability—hydrochlorothiazide, tablets and suspensions, pharmacokinetics □ Pharmacokinetics—hydrochlorothiazide, bioavailability from tablets and suspensions

Despite their close molecular similarity, the diuretics chlorothiazide and hydrochlorothiazide appear to have different absorption characteristics after oral dosing. It has been reported that chlorothiazide absorption is incomplete and dose dependent, being more efficient with decreasing dosage (1–4). On the other hand, preliminary studies have suggested that hydrochlorothiazide absorption is dose proportional (5). Hydrochlorothiazide is also absorbed more efficiently than chlorothiazide, but is administered at lower doses (6). At a dose of 50 mg, the bioavailabilities of chlorothiazide and hydrochlorothiazide are similar (4).

The objective of this study was to explore the preliminary observation that hydrochlorothiazide absorption is dose proportional (5). The previous observation was based on 25–100-mg tablet doses to two individuals. In the present study, both tablet and suspension dosage forms were administered at a range of 25–200 mg to 12 individuals.

EXPERIMENTAL

Protocol—Twelve healthy male volunteers[1], 22–29 years of age (mean 24 years) and weighing 67–84 kg (mean 78 kg) participated in the study after passing a physical examination and giving informed consent. Each subject was instructed to refrain from taking any other medication for 2 weeks prior to and during the study and caffeine-containing beverages were restricted for 24 h prior to and during the study.

Subjects were divided into six groups of two, and the single oral 25-, 50-, and 100-mg oral tablet[2] and suspension doses of hydrochlorothiazide were administered as a 6 × 6 crossover design. Doses were administered 1 week apart. All doses were given at 8 a.m. after overnight fast; no food was permitted until 4-h postdose. Tablets were administered with 240 mL of water. Suspension doses were prepared by grinding the appropriate tablet to a fine powder in a beaker, adding 50 mL of water, and administering directly from the beaker. Quantitative dosing was ensured by repeated washes of the beaker with water to complete intake of 240 mL. Additional 240-mL water volumes were administered at 2, 4, 6, 8, and 12 h after each drug dose to ensure adequate urine output. Total urine output during the 12-h period prior to dosing and aliquots of urine collected during the 12-h postdose period were retained for electrolyte (K^+, Na^+, Cl^-) analysis.

Urine for drug analysis was collected quantitatively through 48 h postdose. Twenty-milliliter urine aliquots were stored at −20°C until assayed. Heparinized blood samples (~8 mL) were obtained from a forearm vein immediately before and at 0.5, 1, 1.5, 2, 3, 4, 6, 8, 12, 24, and 36 h postdose. Plasma was separated and stored at −20°C until assayed. Plasma and urine were assayed within 2 weeks of sampling.

In a separate study, the same 12 subjects received single oral 200-mg doses of hydrochlorothiazide (2 × 100-mg tablets) under the same conditions as those described above. Urine was collected through 48 h to determine hydrochlorothiazide excretion. Plasma drug levels and electrolyte excretion were not determined in this study.

Analytical Procedures—Concentrations of hydrochlorothiazide in plasma and urine were determined by HPLC, as described previously (7). Assay response was linear for hydrochlorothiazide concentrations of 10–750 ng/mL in plasma and 1–100 μg/mL in urine, with correlation coefficients of 0.999 and 0.996, respectively. The coefficient of variation in assay response was <10%. Concentrations of K^+, Na^+, and Cl^- ions in urine were determined by direct potentiometry[3].

Data Analysis—Individual plasma hydrochlorothiazide concentration profiles following the 25-, 50-, and 100-mg doses were fitted to a triexponential function of the form:

$$C = xe^{-\alpha t} + ye^{-\beta t} + ze^{-\gamma t} \qquad \text{(Eq. 1)}$$

where C is the concentration of drug in plasma at any time t and other values are constants. Initial parameter estimates were obtained graphically. Improved estimates, with statistical analyses were obtained by nonlinear regression using the NREG computer program (8). Plasma and urine data were examined by ANOVA for crossover design. When significant treatment effects were observed, differences between specific dosages were examined by means of Tukey's test (9).

RESULTS

Mean plasma hydrochlorothiazide levels from the six treatments are given in Table I, the data are summarized in Fig. 1. Plasma pharmacokinetic values are given in Table II.

Absorption was rapid from all dosages, and peak drug levels in plasma occurred uniformly at ~2 h. Suspension doses tended to produce somewhat higher drug levels than the equivalent tablet doses at early sampling times and, with the 50- and 100-mg doses, somewhat lower values at later times. However, differences between the two dosage forms were significant ($p < 0.05$) only at 0.5 h. When plasma drug levels from all dosages were normalized for dose size, there were no significant treatment effects at sampling times after 0.5 h. The mean peak drug levels, C_{max}, were dose proportional: 127–134 ng/mL for the 25-mg doses, 270–280 ng/mL for the 50-mg doses, and 437–490 ng/mL for the 100-mg doses. Increasing the tablet dose from 25 to 100 mg resulted in a 3.4-fold increase in the

[1] Technical staff and graduate students.

[2] Hydrodiuril 25 mg (lot E0251), 50 mg (lot E0254), and 100 mg (lot E0509 tablets; Merck Sharp and Dohme, West Point, Pa.

[3] Technicon C800 System; Technicon Instruments Corp., Tarrytown, N.Y.

0022-3549/84/0300-0359$01.00/0
© 1984, American Pharmaceutical Association

Table I—Plasma Hydrochlorothiazide Levels Following Single Oral Doses to 12 Healthy Male Volunteers

Dosage, mg		Plasma Hydrochlorothiazide, ng/mL										
		0.5 h	1 h	1.5 h	2 h	3 h	4 h	6 h	8 h	12 h	24 h	36 h
Tablet												
25	Mean	22.8	71.6	97.9	107	115	92.6	54.2	39.3	23.3	9.0	4.6
	SD	21.9	32.4	39.1	36	29	21.1	11.6	9.5	11.9	6.3	5.2
50	Mean	49.5	184	232	251	212	178	113	80.7	44.3	19.7	8.7
	SD	38.6	125	92	102	57	28	16	13.5	10.5	7.7	4.6
100	Mean	115	284	354	368	401	353	206	142	84.3	32.2	12.5
	SD	113	150	148	138	90	99	60	35	16.2	10.4	5.4
Suspension												
25	Mean	41.7	103	122	123	118	96.5	51.4	37.5	20.3	10.6	7.4
	SD	29.4	52	45	44	35	26.9	15.4	9.4	7.3	5.5	6.0
50	Mean	105	213	257	227	208	173	103	67.0	42.1	17.0	8.1
	SD	51	79	84	67	50	34	21	18.4	11.0	7.6	7.1
100	Mean	125	341	451	460	401	344	197	139	68.5	28.4	12.0
	SD	12	151	124	117	113	94	57	32	22.9	10.4	9.0

Table II—Pharmacokinetic Parameter Values for Hydrochlorothiazide [a]

Parameter	Tablet			Suspension		
	25 mg	50 mg	100 mg	25 mg	50 mg	100 mg
C_{max}, ng/mL[b]	127 ± 34	280 ± 108	437 ± 105	134 ± 44	270 ± 76	490 ± 130
t_{max}, h[c]	2.4 ± 0.9	2.1 ± 1.0	2.3 ± 1.0	2.4 ± 0.9	1.8 ± 0.7	1.8 ± 0.3
$AUC_{0\text{-}36}$, ng·h/mL[d]	978 ± 237	1968 ± 390	3554 ± 779	1038 ± 282	1910 ± 344	3493 ± 735
CL_R, mL/min[e]	257 ± 83	222 ± 36	232 ± 52	232 ± 78	233 ± 83	256 ± 89

[a] Mean ± 1 *SD*; $n = 12$. [b] Maximum concentration of hydrochlorothiazide in plasma. [c] Time of C_{max}. [d] Area under hydrochlorothiazide concentration curve in plasma from 0 to 36 h, calculated by the trapezoidal rule. [e] Renal clearance of hydrochlorothiazide, calculated from $Au_{36}/AUC_{0\text{-}36}$ where Au_{36} is the 0–36-h urinary recovery. This parameter could not be calculated for the 200-mg dose.

Table III—Values of Rate Constants Obtained by Fitting Individual Plasma Hydrochlorothiazide Profiles to Eq. 1

Parameter	Tablet			Suspension		
	25 mg	50 mg	100 mg	25 mg	50 mg	100 mg
α, h^{-1}	0.40 ± 0.35	0.32 ± 0.28	0.32 ± 0.12	0.30 ± 0.07	0.29 ± 0.05	0.26 ± 0.05
β, h^{-1}	0.085 ± 0.084	0.082 ± 0.084	0.10 ± 0.11	0.060 ± 0.060	0.067 ± 0.031	0.081 ± 0.062
γ, h^{-1}	0.90 ± 0.30	0.99 ± 0.34	0.85 ± 0.77	0.94 ± 0.28	1.26 ± 0.63	0.98 ± 0.27
$t_{1/2\beta}$, h	8.2 ± 8.4	8.4 ± 5.4	12.1 ± 8.9	10.9 ± 9.6	10.4 ± 5.6	8.5 ± 6.4
r^2	0.97 ± 0.03	0.96 ± 0.03	0.97 ± 0.02	0.97 ± 0.01	0.98 ± 0.02	0.97 ± 0.02

[a] Mean ± *SD*; $n = 12$. [b] Half-life of the slowest rate constant β, calculated from $t_{1/2\beta} = \ln 2/\beta$. [c] Coefficient of determination, $r^2 = (\Sigma_{obs}^2 - \Sigma_{dev}^2)/\Sigma_{dev}^2$.

mean value of C_{max} and a 3.8-fold increase in the mean area under the drug plasma curve for 0 to 36 h, $AUC_{0\text{-}36}$. Increasing the suspension dose from 25 to 100 mg resulted in a 3.7-fold increase in C_{max} and a 3.5-fold increase in $AUC_{0\text{-}36}$.

Plasma levels from all dosages exhibited the familiar triphasic characteristic (3, 6, 7). After peak concentrations had been reached, drug levels declined rapidly through 12 h and then at a slower rate. In some subjects there was evidence of curvature in the logarithmic drug level *versus* time profiles throughout the postabsorptive period.

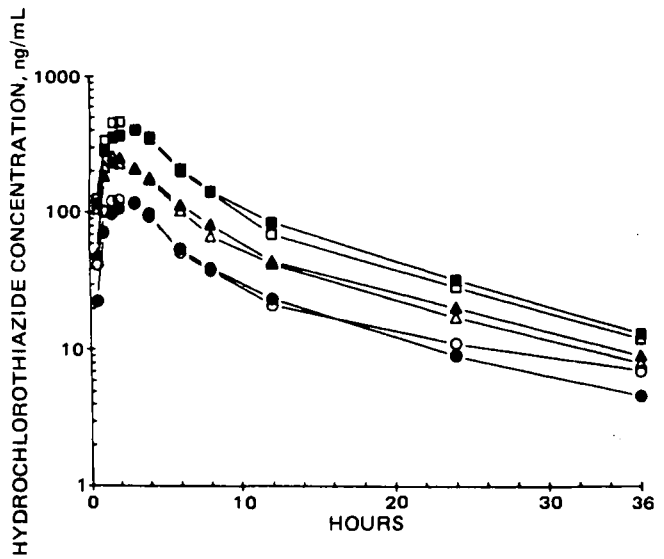

Figure 1—*Mean plasma levels of hydrochlorothiazide following single 25- (●), 50- (▲), and 100-mg (■) tablet and 25- (○), 50- (△), and 100-mg (□) suspension doses (n = 12).*

Analysis of individual drug curves in terms of Eq. 1 yielded the numerical values for the first-order rate constants α, β, and γ shown in Table III. The value of each constant was similar for all treatments, and no significant treatment effects were detected by ANOVA. The uniformly high coefficients of determination (r^2) show that individual drug profiles are satisfactorily described by a triexponential function. The mean half-life of the slowest rate constant β, which represents the terminal drug elimination half-life in plasma, ranged from 8.2 to 12.1 h; this is consistent with previously reported values (6, 7).

The mean cumulative recovery of hydrochlorothiazide in urine at 6, 24, and 48 h is summarized in Fig. 2. Recovery was markedly consistent between dose levels at each collection interval. The mean percentage urinary recoveries from the 25-, 50-, 100-, and 200-mg tablet doses were 62.9, 54.5, 50.3, and 54.0%, respectively. From equivalent suspension doses, the percentage recovery was 60.2, 54.1, 59.0, and 57.3%. There were no significant dosage or formulation effects in the percentage recovery at any collection time. The mean renal clearance of chlorothiazide (Table II), 222–257 ng/mL, was similar from all treatments for which this parameter could be calculated and is in close agreement with values reported earlier (6, 7).

The mean net increases in electrolyte excretion during the 0–12-h post-dose period following the 25-, 50-, and 100-mg doses, compared with the 12–0-h predose period are summarized in Table IV. There was considerable individual variation in these values. The mean net increases were 93–140 mmol for Na^+, 15.2–23.0 mmol for K^+, and 132–176 mmol for Cl^-. The increases were independent of dose size and formulation. Similar observations to these have been made with chlorothiazide administered over a 125–500-mg dosage range (2).

DISCUSSION

Previous studies have shown that the absorption efficiency of orally administered chlorothiazide is dose dependent over a dosage range of

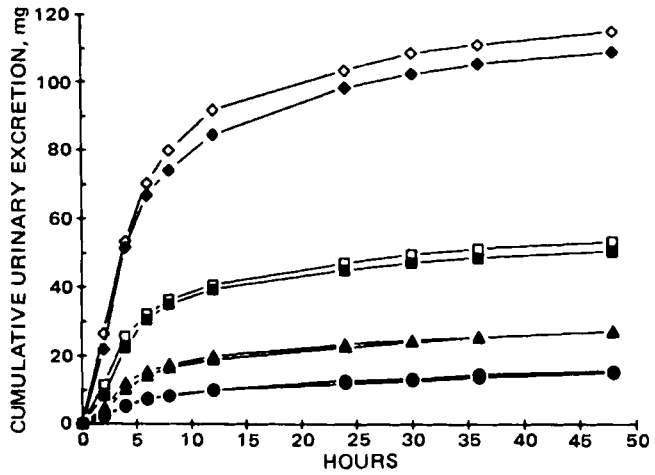

Figure 2—*Mean cumulative urinary recovery of hydrochlorothiazide following 25- (●), 50- (▲), 100- (■), and 200-mg (◆) tablet and 25- (○), 50- (△), 100- (□), and 200-mg (◇) suspension doses (n = 12).*

50–500 mg, the efficiency decreasing with increasing dose (1–4). The results of this study confirm the previous suggestion that the absorption efficiency of oral hydrochlorothiazide, unlike that of chlorothiazide, is independent of dose size (5).

The original objectives of this study were (*a*) to examine the absorption efficiency of hydrochlorothiazide from tablets and suspension doses within the normal therapeutic range of 25- 100 mg, (*b*) to compare urinary excretion and plasma levels, and (*c*) to evaluate the effect of dose size on electrolyte excretion. Mean plasma levels of hydrochlorothiazide were independent of formulation and proportional to dose size, and mean urinary recovery accounted for 50–60% of all dosages.

To determine whether hydrochlorothiazide absorption continued to be dose proportional at dose levels similar to those of chlorothiazide, and also in view of the good agreement between urinary excretion of hydrochlorothiazide and plasma levels, an additional dose of 200 mg was administered to the same subjects and absorption efficiency was assessed from urinary recovery alone. The percent urinary recovery of hydrochlorothiazide from this dose was the same as from the lower doses. The absorption efficiency of oral hydrochlorothiazide is thus independent of dose size over an eight-fold dosage range, which extends into the therapeutic dosage range for chlorothiazide.

These data show that hydrochlorothiazide and chlorothiazide exhibit different absorption characteristics. Whereas chlorothiazide exhibits a marked saturation or "absorption window" effect, hydrochlorothiazide absorption is constant over a wide dosage range. The absorption efficiency of chlorothiazide approaches that of hydrochlorothiazide only at the 50-mg dose level (4).

The reason for the different absorption behavior of the two thiazides is uncertain. The small differences in their molecular structure and physical and chemical characteristics should not cause differences in their absorption if both drugs are absorbed by passive mechanisms.

A possible explanation for their different behavior is that hydrochlorothiazide is efficiently absorbed by a passive process, while chlorothiazide absorption is controlled by an active, saturable component, together with a passive component which is less efficient than that of hydrochlorothiazide. Alternatively, chlorothiazide availability may be influenced by an "absorption window" to a far greater extent than that of hydrochlorothiazide.

Table IV—Net Increase in Electrolyte Excretion in Urine During the 12-h Interval Following All Hydrochlorothiazide Administrations

Dosage, mg	Increase in Electrolyte Excretion, mmol		
	Na^+	K^+	Cl^-
Tablet			
25	102 ± 64	20.2 ± 17.9	136 ± 71
50	93 ± 62	23.0 ± 12.5	132 ± 66
100	109 ± 76	15.2 ± 20.3	142 ± 85
Suspension			
25	103 ± 57	15.3 ± 21.3	137 ± 61
50	125 ± 58	20.7 ± 19.3	160 ± 67
100	140 ± 95	20.4 ± 16.6	176 ± 106

[a] Mean ± *SD*.

Whereas other studies in this laboratory and elsewhere have reported poor correlations between plasma levels and urinary excretion of hydrochlorothiazide (6, 10, 11), good agreement was obtained between these parameters over the dosage range used in this study. Typically, linear regressions of 48-h urinary recovery against AUC_{0-36} and C_{max} values for the combined 25-, 50-, and 100-mg tablet and suspension dosages yielded quite high correlation coefficients of 0.84 and 0.73, respectively. Thus, both plasma level and urinary data may be suitable for determining hydrochlorothiazide bioavailability, but the relative ease of obtaining urine data makes this the method of choice.

The electrolyte excretion data indicate that regardless of the absorption efficiency of hydrochlorothiazide, the maximum pharmacological effect occurs at low doses. There were no increases in net electrolyte excretion as doses were increased from 25 to 100 mg. These results are similar to those reported elsewhere (12, 13). Whether the plateau in pharmacological effect is due to maximal response at lower doses or to an inhibition effect at higher doses (13) cannot be ascertained from our data. Whatever the reason for the plateau effect it is evident that the therapeutic effectiveness of both chlorothiazide and hydrochlorothiazide may be limited at high doses, but for different reasons.

The mechanism causing biphasic elimination of hydrochlorothiazide is uncertain; the prolonged α phase of decline, extending to 12 h postdose, is probably too long to explain in terms of tissue uptake or redistribution according to usual two-compartment model concepts (14). A factor common to studies in which this phenomenon has been reported is water loading during the initial 12 h postdose in order to ensure adequate urine output (4, 5). This may influence hydrochlorothiazide elimination by a variety of mechanisms, including decreased reabsorption of drug from the bladder (15).

REFERENCES

(1) M. C. Meyer and A. B. Straughn, *Curr. Ther. Res.*, **22**, 573 (1972).

(2) V. P. Shah, J. Lee, J. P. Hunt, V. K. Prasad, B. E. Cabana, and T. Foster, *Curr. Ther. Res.*, **29**, 823 (1981).

(3) P. G. Welling and R. H. Barbhaiya, *J. Pharm. Sci.*, **71**, 32 (1982).

(4) M. A. Osman, R. B. Patel, D. S. Irwin, W. A. Craig, and P. G. Welling, *Biopharm. Drug. Dispos.*, **3**, 89 (1982).

(5) V. P. Shah, J. Lee, V. K. Prasad, and B. E. Cabana, "Abstracts," 27th APS National Meeting, Kansas City, Nov. 1979, p. 123.

(6) R. H. Barbhaiya, W. A. Craig, H. P. Corrick-West, and P. G. Welling, *J. Pharm. Sci.*, **71**, 245 (1982).

(7) R. H. Barbhaiya, T. A. Phillips, and P. G. Welling, *J. Pharm. Sci.*, **70**, 291 (1981).

(8) MACC Nonlinear Regression Routines, Academic Computer Center, University of Wisconsin, Madison, 1972.

(9) J. Neter and W. Wasserman, "Applied Linear Statistical Models," Richard D. Irwin, Homewood, Ill., 1974, p. 275.

(10) B. Beermann, M. Groschinsky-Grind, and B. Lindström, *Eur. J. Clin. Pharmacol.*, **11**, 203 (1977).

(11) V. P. Shah, J. P. Hunt, V. K. Prasad, and B. E. Cabana, *J. Pharm. Sci.*, **70**, 833 (1981).

(12) B. Beermann and M. Groschinsky-Grind, *Eur. J. Clin. Pharmacol.*, **12**, 297 (1977).

(13) R. L. Williams, R. O. Davies, R. S. Berman, G. I. Holmes, P. Huber, W. L. Gee, E. T. Lin, and L. Z. Benet, *J. Clin. Pharmacol.*, **22**, 32 (1982).

(14) M. Gibaldi and D. Perrier, "Pharmacokinetics," Dekker, New York, N.Y., 1975, p. 48.

(15) J. H. Wood and T. W. Leonard, "Abstracts," 33rd National Meeting of the Academy of Pharmaceutical Sciences, San Diego, Nov. 14-18, 1982, p. 169.

ACKNOWLEDGMENTS

Funds for this study were provided from Contract No. 223-78-3006, Food and Drug Administration, and from Grant No. GM 20327, National Institutes of Health.

Determination and Prediction of Tissue Binding of Prednisolone in the Rabbit

NAWAL KHALAFALLAH [‡] **and WILLIAM J. JUSKO** [*x]

Received December 27, 1982, from the [*]*Department of Pharmaceutics, School of Pharmacy, State University of New York at Buffalo, Buffalo, NY 14260* and the [‡]*Department of Pharmaceutics, Faculty of Pharmacy, University of Alexandria, Alexandria, Egypt.* Accepted for publication February 25, 1983.

Abstract □ Binding of prednisolone to rabbit tissue was determined experimentally and by computation to assess factors and proteins responsible for tissue distribution of this corticosteroid. Binding in tissue slices ranged from 36% in the lung to 83% in the liver. The results obtained were compared with steady-state tissue distribution data generated *in vivo* in the rabbit. Linear uptake with good agreement between the two sets of data was observed for the skeletal muscle and kidney, but not for the liver and lung. *In vivo* uptake of prednisolone in the liver is severely affected by metabolism and biliary excretion, while *in vitro* distribution into liver slices showed a pattern typical of saturation of a low-capacity site followed by linear nonspecific binding at higher concentrations. Specific saturable binding ($K_1 = 1.95 \times 10^7\ M^{-1}$) accounted for 74% of drug bound at a steroid concentration in the liver of 0.3×10^{-6} M, but its contribution decreased to 5% at a concentration of 20×10^{-6} M. Expected prednisolone binding in rabbit tissue was calculated based on various effective protein concentrations in tissues and binding parameters of prednisolone to rabbit plasma. The use of total Lowry protein concentrations markedly overestimates, while albumin (and transcortin) concentrations severely underestimate the tissue binding of prednisolone. The thiopental effective protein fraction best approximates the *in vivo* and tissue slice binding of prednisolone. Metabolism and saturable binding in liver complicate the otherwise relatively linear uptake of prednisolone into various tissues where macromolecules other than albumin dominate in tissue binding of the steroid.

Keyphrases □ Prednisolone—pharmacokinetics, tissue distribution, tissue binding, rabbits □ Tissue binding—prednisolone in the rabbit, liver, muscle, kidney, lung, albumin, effective protein fractions

Current interest in tissue binding stems partly from its uncertain nature and a growing recognition of the magnitude of effect on drug pharmacokinetics exerted by this process. The volume of distribution (1), biological half-life (2), and, of course, total tissue concentrations (3) are influenced by, and respond linearly in some cases to, changes in the fraction bound in tissue. Simulations and limited experimental evidence suggest a stronger influence of tissue binding on these aspects of drug pharmacokinetics compared with plasma binding (3). Occasionally, evidence of saturable tissue uptake invalidates or complicates the assumptions implied in linear pharmacokinetic models (4). Accurate estimates of individual tissue binding parameters over the therapeutic range of concentration are usually required as direct input data in mass-balance equations of physiological pharmacokinetic models (5).

From a pharmacodynamic point of view, the effect elicited by many drugs, including steroids, is a function of the amount of drug bound to receptors in tissues (6). In characterizing receptor binding as a unique type of tissue binding, it is important to be aware of the influence of methodological and pathophysiological factors on both specific and nonspecific tissue binding.

Several approaches have emerged for generating tissue binding data. *In vivo* methods involve measurement of drug uptake in mammalian tissue, with drug gaining access to the tissue while the animal is alive. Drug in tissue, in excess of that diffused into the tissue water, is considered bound to cellular constituents in the absence of time factors, metabolism, active transport, and pH effects. Steady-state conditions are necessary to be certain of the true degree of tissue binding or distribution.

A semiphysiological approach involves the use of perfused animal organs such as kidney, liver, and lung tissues (7, 8). However, the limited duration of organ viability may limit this approach, and it is best used for examining clearance processes.

In vitro determination of tissue binding requires tissue reduction to a near-liquid state manageable in equilibrium dialysis and ultrafiltration procedures (9, 10). The question is often raised, however, as to the degree that the intact tissue characteristics are retained in the homogenate. A milder alternative method is to measure drug uptake into tissue slices suspended in a physiological medium (11, 12). However, as with many other methods, the net drug uptake into slices may be the sum of several processes (transport, metabolism, and ion trapping) including binding.

Prednisolone, a synthetic corticosteroid, is used under various dosage regimens, during which body tissues are exposed to a wide range of concentrations. Specific glucocorticoid receptors have been identified in numerous tissues (6). However, little information is available in the literature concerning binding to mammalian tissues over the therapeutic plasma concentration range. We have found that this steroid is taken up by the majority of tissues of the rabbit in amounts exceeding the diffusion of free drug into tissue water (13). This species also appears to handle prednisolone pharmacokinetically in a manner similar to humans (14).

The aim of the present study was to determine prednisolone binding to rabbit tissue *in vitro* using tissue slices and to compare it with data obtained *in vivo* in rabbits (13). Further comparison will be made with predictions based on various effective (15) protein concentrations of rabbit tissues.

EXPERIMENTAL

Materials—Female New Zealand White rabbits, weighing 3.6–4.2 kg, were used. The animals were sacrificed with ether, and blood was drained from the abdominal aorta. Skeletal muscle, liver, kidney, and lung samples were obtained, washed with ice-cold saline, blotted dry, wrapped in aluminum foil, and frozen. The steroids used were prednisolone[1], prednisone[1], hydrocortisone[1], and dexamethasone[1].

Binding to Tissue Slices—The frozen tissues were cut with a razor blade into slices ~0.5 mm thick, weighing 500 mg. Slices were blotted, weighed, and placed in stoppered vials containing 3.0 mL of steroid solution in isotonic phosphate-buffered saline, pH 7.4. The vials were oscillated at 37°C for 3 h, which was predetermined to be adequate for equilibrium uptake of drug in the tissue slices. At equilibrium, slices were removed, washed quickly with 3 mL of ice-cold saline, blotted, weighed,

[1] *Sigma Chemical Co., St. Louis, Mo.*

0022-3549/84/0300-0362$01.00/0
© 1984, American Pharmaceutical Association

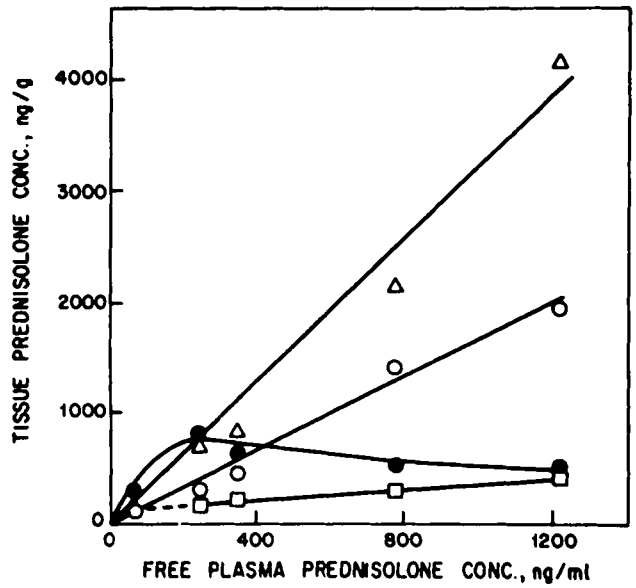

Figure 1—*Uptake of prednisolone in rabbit heart (△), skeletal muscle (○), liver (●), and fat (□) showing the relationships to free concentrations in plasma.*

and homogenized (1:5) with water in a cell disrupter. Vials containing steroid solution but devoid of tissue slices were included in all runs. Initial solutions, solutions remaining at equilibrium, and tissue homogenates were analyzed by HPLC, as described elsewhere (13). The assay yielded equilibrium drug concentrations in the slice (S) and medium (M). Percent bound in tissue (% TB) was calculated from:

$$\%TB = \frac{S - M \cdot f_w}{S \cdot 0.01} \quad \text{(Eq. 1)}$$

where f_w is the fractional tissue water, determined by drying tissue slices to a constant weight (13).

Distribution to Rabbit Tissues *In Vivo*—Distribution data were obtained in an *in vivo* study of prednisolone pharmacokinetics in the rabbit (13). Briefly, the study involved administration of a zero-order intravenous infusion of prednisolone and measurement of the steady-state uptake of the steroid in rabbit tissues and plasma. Apparent percent binding was calculated for each tissue concentration (C_{tissue}) and unbound plasma concentration (C_f) from:

$$\%TB = \frac{C_{tissue} - C_f \cdot f_w}{C_{tissue} \cdot 0.01} \quad \text{(Eq. 3)}$$

It follows that:

$$\%TB = \frac{K_p - f_w}{K_p \cdot 0.01} \quad \text{(Eq. 4)}$$

where K_p is the tissue–free plasma distribution ratio as reported previously (13).

Prediction of Binding to Rabbit Tissues—The *in vivo* tissue distribution data obtained previously in the rabbit (13), indicated linear binding of prednisolone in most rabbit tissues over the concentration range examined. Hence, bound (C_b) and free (C_f) concentrations are related by:

$$C_b = nK \cdot P \cdot C_f \quad \text{(Eq. 5)}$$

and the fraction bound (f_b) is:

$$f_b = \frac{nK \cdot P}{1 + nK \cdot P} \quad \text{(Eq. 6)}$$

where nK is the composite binding parameter (number of binding sites × association constant) and P is the effective protein concentration in tissue. The assumption was then made that the nK value obtained from binding of prednisolone to rabbit plasma can characterize its binding to other tissue proteins. The value of nK was calculated from steady-state plasma *Pn* binding, determined *in vivo* (13), using (16):

$$nK = \frac{1}{[Prot]} \cdot \frac{\beta_0}{1 - \beta_0} \quad \text{(Eq. 7)}$$

where β_0 is the extrapolated fraction bound in the linear binding range

Table I—Binding of Prednisolone to Rabbit Tissue Slices

Tissue	Medium Prednisolone Concentration at Equilibrium, ng/mL	Recovery[a] (*SD*), %	Bound[a] (*SD*), %
Lung	439	91.1 (1.3)	35.86 (10.5)
Skeletal muscle	90–8000	92.8 (7.7)	60.91 (3.1)
Skeletal muscle[b]	458	91.9 (1.8)	52.64 (4.0)
Liver	30–8000	50.8 (11.3)	82.6–54.7[c]
Kidney	399	85.1 (1.5)	61.87 (2.7)

[a] Mean of 6–16 slices. [b] Uptake of prednisolone was measured in the presence of an equal initial prednisolone and hydrocortisone concentration in the medium of 500 ng/mL. [c] Decreasing with increasing concentration.

and [Prot] is the molar concentration of binding proteins in plasma, calculated from the sum of albumin and transcortin concentrations reported in rabbit plasma (14).

Fraction bound in tissue was then predicted (Eq. 6) using P values corresponding to total protein concentrations in tissue (17), albumin concentrations in tissue (18), and effective tissue protein concentrations reported for thiopental (15). The protein values used were reported as fractions of tissue weight and were converted to molar concentration assuming a molecular weight of 69,000 and tissue density of unity. For tissue albumin content, we employed the extravascular albumin spaces determined in rats by Studer and Potchen (18), except in the case of liver where data from dogs (19) were used because of inaccuracy in the rat value.

RESULTS

***In Vivo* Distribution of Prednisolone**—Steady-state tissue-to-plasma distribution of prednisolone was measured in five rabbits. Confirmation of assay methodology, stability, recovery data, and other experimental results are provided elsewhere (13). The equilibrium tissue–unbound prednisolone in plasma ratios for four tissues is shown in Fig. 1. All tissues except the liver showed linear distribution ratios.

Binding in Tissue Slices—Steroid recoveries and percent tissue binding for the tissue slices are reported in Table I. Recovery data were generated by comparing the amount of prednisolone found in tissue slices and medium at equilibrium to the amount of drug initially added to the medium. Both liver and kidney slices generated prednisone when incubated with prednisolone. The recovery values and standard deviations indicate good reproducibility of the data, with marked loss of drug occurring only in the liver.

Binding Kinetics in Muscle and Liver Slices—Uptake of prednisolone into muscle and liver slices was examined over a wide range of

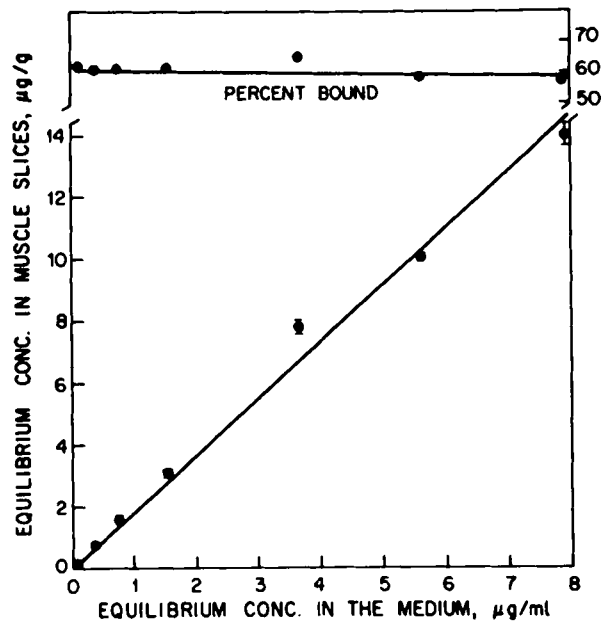

Figure 2—*Uptake of prednisolone in rabbit skeletal muscle slices at 37°C. Verticle lines denote 1* SD. *Percentage binding was calculated using Eq. 1.*

Table II—Protein Fractions Used to Predict the Binding of Prednisolone to Rabbit Tissue

Tissue	Solid (Non-water) Fraction[a]	Effective Protein Fraction		
		Total Protein Fraction[b]	Thiopental Fraction[c]	Albumin Fraction[d]
Lung	0.217	—	—	0.0040
Heart	0.210	0.144	0.0301	0.0022
Skeletal muscle	0.235	0.195	0.0175	0.0036
Brain	0.260	0.108	0.0212	0.0004
Liver	0.298	0.190	0.0362	0.0014[e]
Spleen	0.245	—	—	—
Kidney	0.207	0.152	0.0237	0.0048
Small intestine	0.177	—	—	0.0056
Skin	—	—	—	0.0072

[a] Data in the rabbit, Ref. 13. [b] Data in the rabbit, Ref. 17. [c] Data in the rabbit, Ref. 15. [d] Data in the rat, calculated from *EV* albumin space × 0.04, Ref. 18. [e] Data in the dog, uncorrected for plasma space (Ref. 19).

Table III—Binding of Prednisolone to Rabbit Tissue Determined *In Vivo*, *In Vitro*, and by Prediction

Tissue	Prednisolone Bound, %				
			Predicted Using		
	In Vivo	*In Vitro*	Total Protein Conc.	Effective Thiopental Binding Protein	Albumin Conc.
Lung	72.6	35.9	—	—	25.4
Heart	73.0	—	92.4	71.9	15.8
Skeletal muscle	50.3	60.9	94.3	59.8	23.4
Brain	59.3[a]	—	90.2	64.3	3.3
Liver	84.3– <58.7	82.6–54.7	94.2	75.5	10.6
Spleen	34.9	—	—	—	—
Kidney	72.8	61.9	92.8	66.8	29.0
Small intestine	87.6	—	—	—	32.2
Skin	—	—	—	—	38.0

[a] Based on brain to CSF ratios (Ref. 13).

concentrations (Figs. 2 and 3). Linear binding to the muscle was evident throughout the concentration range examined. Binding to liver slices was nonlinear in the low concentration range but progressed linearly beyond that. The insert in Fig. 3 is a Scatchard plot of the binding data. Drug bound in the liver (D_b) at each concentration was calculated from S − M·f_w, while M·f_w yielded free drug (D_f) in the tissue. The shape of the plot suggests both nonlinear (subscript 1) and linear (subscript 2) binding in accordance with:

$$\frac{D_b}{D_f} = \frac{n_1K_1P_1}{1 + k_1D_f} + n_2K_2P_2 \qquad \text{(Eq. 8)}$$

Individual parameters were calculated as follows. At high drug concentration the first term in Eq. 8 could be neglected and $n_2K_2P_2$ was calculated from the slope of a plot of D_b *versus* D_f. For each data point, drug bound nonspecifically (D_{bNS}) was calculated using $D_{bNS} = n_2K_2P_2 \cdot D_f$. Subtracting this term from the total drug bound yielded D_{bSP}. Plotting D_{bSP}/D_f *versus* D_{bSP} gave a straight line with an abscissa intercept of n_1P_1, and a slope of $-K_1$. The parameters generated were: $n_2K_2P_2 = 1.23$ (no units); $n_1P_1 = 0.142$ μg/g of liver; and $K_1 = 54.2$ g/μg or 1.95×10^7 M^{-1}.

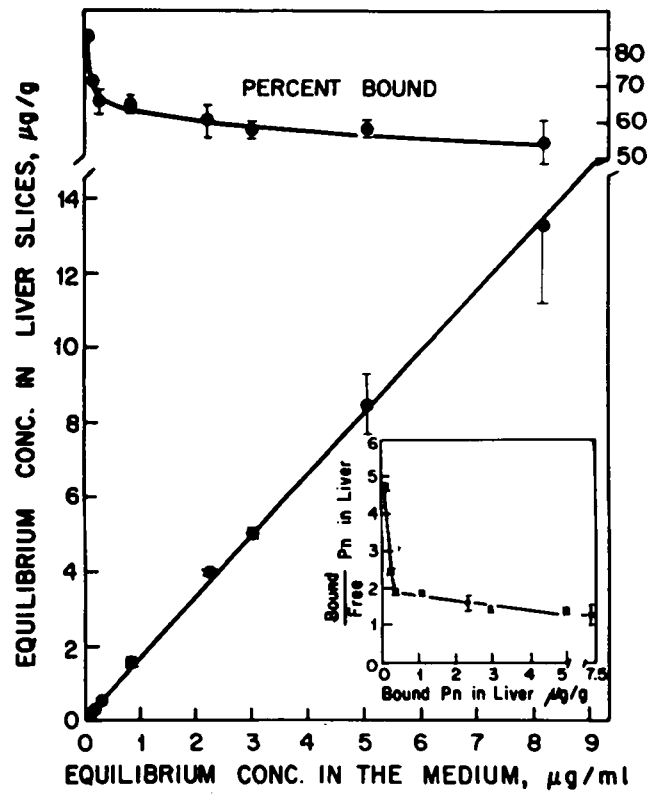

Figure 3—*Uptake of prednisolone in rabbit liver slices at 37°C. The insert is a Scatchard plot of the binding data.*

Calculated Tissue Binding—The protein fractions of the rabbit tissues, obtained from three literature sources, are listed in Table II. Of the total solids of the various rabbit tissues measured in our previous study (13), the Lowry assay-reactive proteins comprise 64–83%, except for brain (42%). The albumin fraction is extremely small and does not change perceptibly when transcortin is included. The effective protein fraction with respect to thiopental binding generally reflects 1.8–3.6% of the tissue weights.

The calculated percentage binding of prednisolone using the three protein fractions are compared with the *in vivo* and *in vitro* tissue binding values in Table III. The use of total protein concentrations markedly overestimates, while albumin concentrations severely underestimate, the tissue binding of prednisolone. The effective protein fraction best approximates both the *in vivo* and tissue slice binding of prednisolone.

DISCUSSION

The present study reports tissue binding data for prednisolone in the rabbit, obtained using different methods. The binding data were generated over a range of steroid concentrations where linear tissue uptake was evident in most tissues both *in vivo* and *in vitro*. The range of concentrations investigated in tissue slices reached an equilibrium medium concentration of 8 μg/mL, which exceeds human plasma exposure to free drug at usual therapeutic doses. However, some corticosteroids such as hydrocortisone and methylprednisolone are sometimes prescribed in large

doses, resulting in plasma levels of 1 mg/mL of total (bound and free) steroid (20, 21), and it is of interest to investigate the manner by which mammalian tissues handle high steroid concentrations.

Binding to Slices Compared with *In Vivo* Data—There was good agreement between slice uptake and *in vivo* distribution of prednisolone in the case of skeletal muscle and kidney. This permits some speculation concerning the mode of entry of the drug into rabbit tissue. The fact that *in vivo* uptake of prednisolone in tissues such as the skeletal muscle was linear and could be quantitatively reproduced in slices under the conditions described, suggests the absence of an active transport process. If the latter occurs *in vivo*, but only partly *in vitro*, drug uptake in slices may underestimate *in vivo* distribution, as reported for the tetraethylammonium ion (22).

Uptake of prednisolone into lung slices markedly differed from the *in vivo* situation. Many aspects of *in vivo* drug localization in lung tissue are not well understood, and underestimation of *in vivo* drug binding when using lung homogenates has been reported (23, 24).

Prednisolone Binding in the Liver—The liver showed a strikingly different uptake pattern *in vivo* compared with the other tissues (Fig. 1). We thus chose to further examine the uptake over a wide range of concentrations in both liver and a tissue such as skeletal muscle using the slice technique. The *in vivo* and *in vitro* data indicated a disparate type of nonlinear binding or uptake of the steroid to the liver tissue. *In vitro*, the results showed a pattern typical of saturation of a low-capacity site followed by linear, nonspecific binding at higher concentrations. The *in vivo* data showed the opposite saturation pattern in the high concentration range. However, these data were probably confounded by rapid metabolism and appreciable excretion in the bile (13) resulting in gross underestimation of the true tissue binding (5). In this respect, the slice technique offers the advantage of measuring drug uptake in the liver in the absence of total expression of its metabolic activity. However, judging by the relatively low recovery values of prednisolone from liver slices compared with other tissues (Table I), steroid metabolism in liver slices cannot be ruled out and may consequently have resulted in some underestimation of binding in the liver.

In generating binding data, part of the information sought is identification of the binding constituent, usually protein, and characterization of the ligand–protein reaction by numerical parameters. Binding data in liver slices yielded an apparent association constant (K_1) for specific nonlinear binding ($1.95 \times 10^7\ M^{-1}$), while for linear binding, only a value for percent bound (59.6%) could be calculated.

The association constant of the liver protein, exhibiting high affinity but low capacity for prednisolone, fits within the range reported for the glucocorticoid receptor, but is also compatible with steroid affinities of other liver proteins such as ligandin and transcortin. Values reported for liver receptor binding range between $5–74 \times 10^7\ M^{-1}$ for dexamethasone in humans (25), rabbits (26), and rats (27), and for hydrocortisone and corticosterone in rats (28, 29). The ligandin association constants for steroids are in the range of $10^5\ M^{-1}$ for purified ligandin, but native cytosol binding may be greater (30). Receptors have been identified in numerous rabbit tissues including the skeletal muscle (31). Prednisolone uptake in muscle slices showed no evidence of high-affinity–low-capacity binding in the low concentration range, which suggests that the corresponding binding seen in liver slices may not necessarily be to the glucocorticoid receptors.

Whatever the identity of the liver protein exhibiting high affinity for prednisolone, and whether or not it is directly involved in expression of steroid activity, it contributed significantly to drug uptake. The percent prednisolone bound specifically (related to total drug bound in liver slices) was as high as 74% at a total drug concentration of 0.3×10^{-6} M, but decreased to 5% at a corresponding concentration of 20×10^{-6} M. The activity of this protein, ($K_1 = 1.95 \times 10^7\ M^{-1}$) is higher than that of albumin in plasma ($nK = 6 \times 10^3\ M^{-1}$) and is as high as that of transcortin in plasma ($K = 2 \times 10^7\ M^{-1}$) (14). It may thus be an important factor in the mechanism of uptake and concentration of prednisolone in liver cells.

Predicted Tissue Binding Data Compared with *In Vivo* Results—The possibility of predicting prednisolone binding to rabbit tissue, based on parameters obtained for binding to rabbit plasma and an estimate of effective protein concentration, was explored in the present study (Table III). Only a portion of tissue proteins are effective in drug binding (32); hence, the observation that total tissue protein binding overestimates prednisolone binding is not unexpected. Albumin, by virtue of its high concentration, is a major binding species in plasma, but apparently assumes a less significant role in tissues. Binding of prednisolone to albumin accounts for less than half of the calculated and measured *Pn* binding in the rabbit tissues (Table III). Owing to the extremely low tissue concentrations, the addition of tissue transcortin to this calculation barely affects the binding values based on albumin alone.

It was intriguing to note that the effective protein fraction calculated for thiopental from binding data to rabbit tissue homogenates (15) yielded good estimates of prednisolone binding in the same species (Table III). Values of the effective protein fraction for prednisolone, and possibly other drugs, may be similar to those reported for thiopental. The concept of a common array of tissue binding proteins for certain types of drugs in various species is worth contemplating, bearing in mind that the binding data presented in this study correspond to a concentration range governed mainly by nonspecific binding, a likely situation for most therapeutic agents.

Recently, some criticism has been raised regarding the assumptions made when utilizing the concept of effective protein fraction in predicting tissue binding. Particularly strong are arguments against extrapolation of binding data from one species or from one protein concentration to another with the inherent assumptions that binding is independent of these factors. Experimental data and simulations have appeared which invalidate these assumptions (32, 33). Furthermore, the effective protein fraction was shown to vary with drug concentration in some of the protein media examined (33). In the present study, mingling of data from different species was minimal. The data presented, whether determined experimentally or predicted (apart from tissue albumin concentration) all pertain to the rabbit. Furthermore, the composite binding parameter, nK (Eq. 7), was determined over the same range of plasma concentration used in the determination of tissue binding *in vivo*. Hence, it is felt that the present data provided a good opportunity to test the usefulness of the effective thiopental protein fraction in predicting the tissue binding of other drugs.

REFERENCES

(1) M. Gibaldi and P. J. McNamara, *Eur. J. Clin. Pharmacol.*, **13,** 373 (1978).

(2) M. Gibaldi, G. Levy, and P. J. McNamara, *Clin. Pharmacol. Ther.*, **24,** 1 (1978).

(3) W. A. Craig and P. J. Welling, *Clin. Pharmacokinet.*, **2,** 252 (1977).

(4) J. G. Wagner, *J. Pharmacokinet. Biopharm.*, **1,** 363 (1973).

(5) H.-S. G. Chen and J. F. Gross, *J. Pharmacokinet. Biopharm.*, **7,** 117 (1979).

(6) A. Munck and K. Leung, "Modern Pharmacology—Toxicology," Vol. 8, part II, J. R. Pasqualini, Ed., Dekker, New York, N.Y., 1977, p. 311.

(7) R. Stegmann and M. H. Bickel, *Xenobiotica*, **7,** 737 (1977).

(8) K. Okumura, H. Yoshida, and R. Hori, *J. Pharm. Dyn.*, **1,** 230 (1978).

(9) C. M. Kunin, *J. Infect. Dis.*, **121,** 55 (1970).

(10) B. Fichtl, B. Bondy, and H. Kurtz, *J. Pharmacol. Exp. Ther.*, **215,** 248 (1980).

(11) T. M. Ludden, L. S. Schanker, and R. C. Lanman, *Drug Metab. Dispos.*, **4,** 8 (1976).

(12) C. Post, R. G. G. Andersson, A. Ryrfeldt, and E. Nilsson, *Acta Pharmacol. Toxicol.*, **43,** 156 (1978).

(13) N. Khalafallah and W. J. Jusko, in press.

(14) M. L. Rocci, Jr., N. F. Johnson, and W. J. Jusko, *J. Pharm. Sci.*, **69,** 977 (1980).

(15) R. L. Dedrick and K. B. Bischoff, *Chem. Eng. Prog. Symp. Ser.*, **64,** 32 (1968).

(16) I. Odar-Cederlof and O. Borga, *Clin. Pharmacol. Ther.*, **20,** 36 (1976).

(17) O. H. Lowry, N. J. Rosebrough, A. L. Farr, and R. J. Randall, *J. Biol. Chem.*, **193,** 265 (1951).

(18) R. Studer and J. Potchen, *Microvas. Res.*, **3,** 35 (1971).

(19) J. Wetterfors, *Acta Med. Scand.*, **177,** 243 (1965).

(20) J. C. Melby, *Ann. Int. Med.*, **81,** 505 (1974).

(21) H. S. Jacob, P. R. Craddock, D. E. Hammerschmidt, and C. F. Moldow, *N. Engl. J. Med.*, **302,** 789 (1980).

(22) M. Mintun, K. J. Himmelstein, R. L. Schroder, M. Gibaldi, and D. D. Shen, *J. Pharmacokinet. Biopharm.*, **8,** 373 (1980).

(23) J. R. Gillette, *J. Pharmacokinet. Biopharm.*, **1,** 497 (1973).

(24) R. Kuntzman, I. Tsai, and J. J. Burns, *J. Pharmacol. Exp. Ther.*, **158,** 332 (1962).

(25) H. Bojar, S. Westerkamp, W. Staib, and Ch. Broelch, *Gastroenterology*, **27,** 176 (1980).

(26) P. L. Ballard, J. D. Baxter, S. J. Higgins, G. G. Rousseau, and G. M. Tomkins, *Endocrinology*, **94,** 998 (1974).

(27) M. Beato and P. Feigelson, *J. Biol. Chem.*, **247**, 7890 (1972).
(28) B. S. Roth, *Endocrinology*, **94**, 82 (1974).
(29) Zs. Ács, E. Stark, and G. Folly, *J. Steroid Biochem.*, **6**, 1127 (1975).
(30) B. Ketterer and E. Tipping, *Biochem. Soc. Trans.*, **3**, 626 (1975).
(31) P. L. Ballard and R. A. Ballard, *Proc. Natl. Acad. Sci., USA*, **69**, 2668 (1972).
(32) D. Shen and M. Gibaldi, *J. Pharm. Sci.*, **63**, 1698 (1974).
(33) Y. Igari, Y. Sugiyama, S. Awazu, and M. Hanano, *J. Pharm. Sci.*, **70**, 1049 (1981).

ACKNOWLEDGMENTS

Supported in part by Grant No. 24211 from the National Institute of General Medical Sciences, N.I.H., and by a grant for Dr. Khalafallah from the Egyptian government.

Deaza Analogues of Adenosine as Inhibitors of Blood Platelet Aggregation

IPPOLITO ANTONINI *, GLORIA CRISTALLI *, PALMARISA FRANCHETTI *, MARIO GRIFANTINI *x, SANTE MARTELLI *, and FRANCO PETRELLI ‡

Received May 24, 1982, from the **Institute of Pharmaceutical and Organic Chemistry* and ‡*Institute of Physiology, University of Camerino, 62032 Camerino (MC) Italy.* Accepted for publication December 22, 1982.

Abstract □ A number of deaza analogues of adenosine were prepared and tested as inhibitors of platelet aggregation induced by ADP and collagen to investigate the structure–activity relationships in this class of nucleoside analogues. The results showed that the presence of a 6-amino group and nitrogen atoms at positions 3 and 7 of the purine moiety are required for inhibitory activity.

Keyphrases □ Adenosine—deaza analogues, inhibition of ADP- and collagen-induced platelet aggregation □ Platelet aggregation—induction by ADP and collagen, inhibition by deaza analogues of adenosine □ Nucleoside analogues—deazaadenosines, inhibition of ADP- and collagen-induced platelet aggregation

Blood platelets seem to play a dominant role in both the physiological and pathological events of hemostasis (1). In fact, platelet aggregation leads to the formation of either hemostatic plugs or thrombi. Several tissue constituents can give rise to platelet aggregation (2, 3). Among these substances, adenosine diphosphate (ADP) has been shown to be important as it can initiate aggregation (4) and can also mediate aggregation induced by other agents (3, 5).

Adenosine, a structural analogue of ADP, is a powerful inhibitor of platelet aggregation induced by ADP (6). A number of adenosine derivatives and analogues have been synthesized and tested in an attempt to clarify the structure–activity relationships in this class of platelet-aggregation inhibitors (6–9). The present paper investigates the influence of the purine nitrogen atoms on adenosine activity. Some deaza analogues of adenosine and purine riboside have been prepared and tested *in vitro* as inhibitors of platelet aggregation induced by ADP and collagen.

DISCUSSION AND RESULTS

Adenosine[1] (Ia), 7-deazaadenosine[2] (Ie), and purine riboside[2] (Ig) were purchased from commercial sources. 3-Deazaadenosine (Ic) was synthesized using a method previously described (10). 1-Deazaadenosine (Ib) was synthesized using a modification of previous methods (11–14) (Scheme I). Imidazo[4,5-*b*]pyridine (II) (11) was prepared in a 73% yield by the condensation of 2,3-diaminopyridine with triethyl orthoformate.

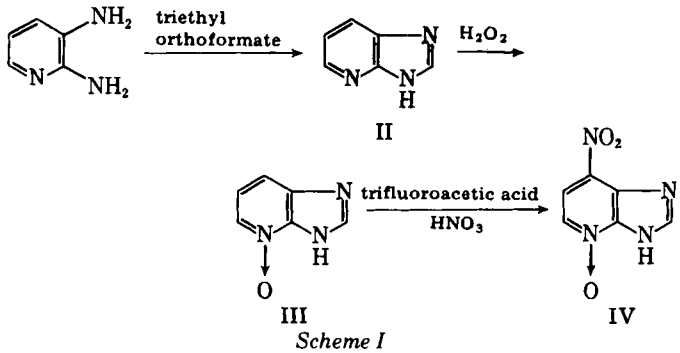

Scheme I

Nitration of *N*-oxide III, employing a nitric acid–trifluoroacetic acid mixture instead of a nitric acid–acetic acid mixture (12), gave 7-nitroimidazo[4,5-*b*]pyridine-4-oxide (IV) in good yield. The other steps involved following known procedures (13, 14). 1,3-Dideazaadenosine (Id) was synthesized as shown in Scheme II instead of the method reported

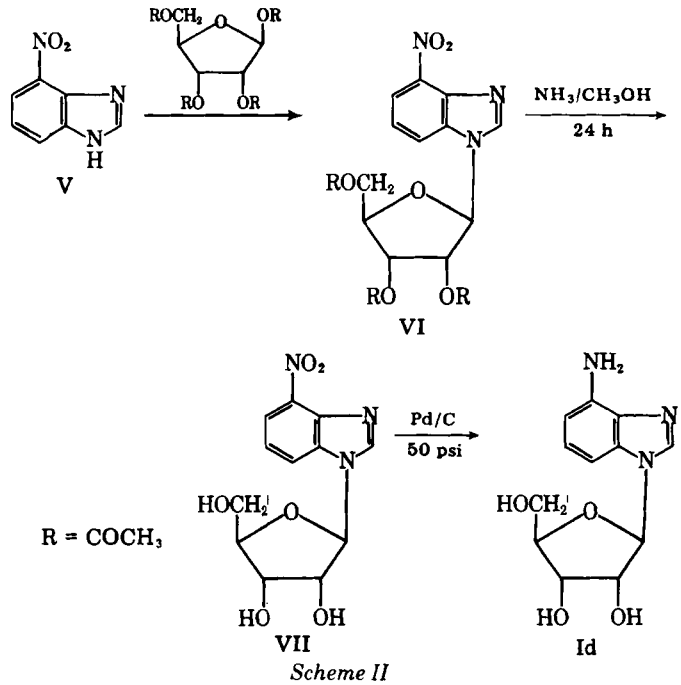

Scheme II

[1] Fluka.
[2] Sigma Chemical Co.

0022-3549/84/0300-0366$01.00/0
© 1984, American Pharmaceutical Association

(27) M. Beato and P. Feigelson, *J. Biol. Chem.*, **247**, 7890 (1972).
(28) B. S. Roth, *Endocrinology*, **94**, 82 (1974).
(29) Zs. Ács, E. Stark, and G. Folly, *J. Steroid Biochem.*, **6**, 1127 (1975).
(30) B. Ketterer and E. Tipping, *Biochem. Soc. Trans.*, **3**, 626 (1975).
(31) P. L. Ballard and R. A. Ballard, *Proc. Natl. Acad. Sci., USA*, **69**, 2668 (1972).
(32) D. Shen and M. Gibaldi, *J. Pharm. Sci.*, **63**, 1698 (1974).
(33) Y. Igari, Y. Sugiyama, S. Awazu, and M. Hanano, *J. Pharm. Sci.*, **70**, 1049 (1981).

ACKNOWLEDGMENTS

Supported in part by Grant No. 24211 from the National Institute of General Medical Sciences, N.I.H., and by a grant for Dr. Khalafallah from the Egyptian government.

Deaza Analogues of Adenosine as Inhibitors of Blood Platelet Aggregation

IPPOLITO ANTONINI *, GLORIA CRISTALLI *, PALMARISA FRANCHETTI *, MARIO GRIFANTINI *x, SANTE MARTELLI *, and FRANCO PETRELLI ‡

Received May 24, 1982, from the **Institute of Pharmaceutical and Organic Chemistry* and ‡*Institute of Physiology, University of Camerino, 62032 Camerino (MC) Italy.* Accepted for publication December 22, 1982.

Abstract □ A number of deaza analogues of adenosine were prepared and tested as inhibitors of platelet aggregation induced by ADP and collagen to investigate the structure–activity relationships in this class of nucleoside analogues. The results showed that the presence of a 6-amino group and nitrogen atoms at positions 3 and 7 of the purine moiety are required for inhibitory activity.

Keyphrases □ Adenosine—deaza analogues, inhibition of ADP- and collagen-induced platelet aggregation □ Platelet aggregation—induction by ADP and collagen, inhibition by deaza analogues of adenosine □ Nucleoside analogues—deazaadenosines, inhibition of ADP- and collagen-induced platelet aggregation

Blood platelets seem to play a dominant role in both the physiological and pathological events of hemostasis (1). In fact, platelet aggregation leads to the formation of either hemostatic plugs or thrombi. Several tissue constituents can give rise to platelet aggregation (2, 3). Among these substances, adenosine diphosphate (ADP) has been shown to be important as it can initiate aggregation (4) and can also mediate aggregation induced by other agents (3, 5).

Adenosine, a structural analogue of ADP, is a powerful inhibitor of platelet aggregation induced by ADP (6). A number of adenosine derivatives and analogues have been synthesized and tested in an attempt to clarify the structure–activity relationships in this class of platelet-aggregation inhibitors (6–9). The present paper investigates the influence of the purine nitrogen atoms on adenosine activity. Some deaza analogues of adenosine and purine riboside have been prepared and tested *in vitro* as inhibitors of platelet aggregation induced by ADP and collagen.

DISCUSSION AND RESULTS

Adenosine[1] (Ia), 7-deazaadenosine[2] (Ie), and purine riboside[2] (Ig) were purchased from commercial sources. 3-Deazaadenosine (Ic) was synthesized using a method previously described (10). 1-Deazaadenosine (Ib) was synthesized using a modification of previous methods (11–14) (Scheme I). Imidazo[4,5-*b*]pyridine (II) (11) was prepared in a 73% yield by the condensation of 2,3-diaminopyridine with triethyl orthoformate.

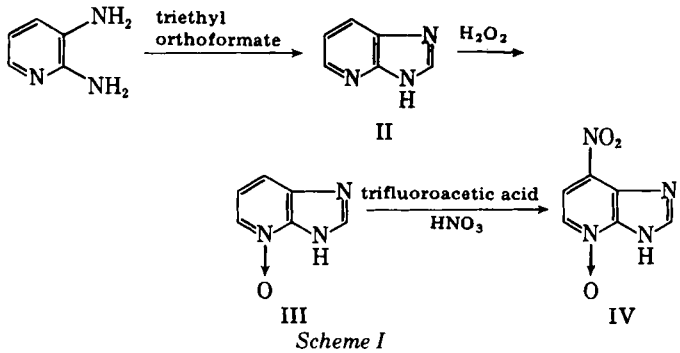

Scheme I

Nitration of *N*-oxide III, employing a nitric acid–trifluoroacetic acid mixture instead of a nitric acid–acetic acid mixture (12), gave 7-nitroimidazo[4,5-*b*]pyridine-4-oxide (IV) in good yield. The other steps involved following known procedures (13, 14). 1,3-Dideazaadenosine (Id) was synthesized as shown in Scheme II instead of the method reported

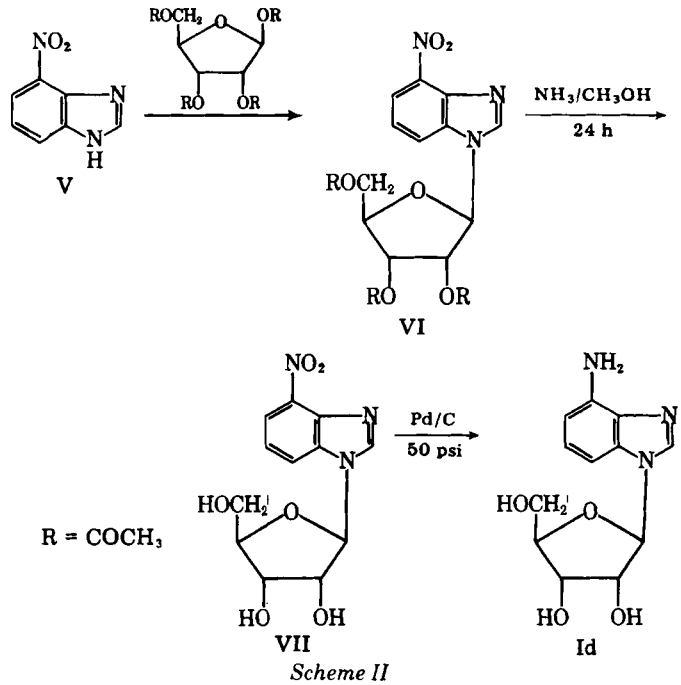

Scheme II

[1] Fluka.
[2] Sigma Chemical Co.

0022-3549/84/0300-0366$01.00/0
© 1984, American Pharmaceutical Association

Table I—Effect of Deaza Analogues of Adenosine on Human Platelet Aggregation

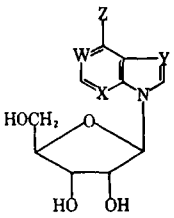

	Compound	W	X	Y	Z	Inhibition of Aggregation[a] ADP Induced %	ADP Induced RAD[b]	Collagen Induced %	Collagen Induced RAD[b]
Ia	Adenosine	N	N	N	NH_2	93	1	97	1
Ib	1-Deazaadenosine	CH	N	N	NH_2	82	0.88	87	0.89
Ic	3-Deazaadenosine	N	CH	N	NH_2	<10	<0.1	<10	<0.1
Id	1,3-Dideazaadenosine	CH	CH	N	NH_2	<10	<0.1	<10	<0.1
Ie	7-Deazaadenosine (tubercidin)	N	N	CH	NH_2	<10[c]	<0.1	<10	<0.1
If	1,7-Dideazaadenosine	CH	N	CH	NH_2	<10	<0.1	<10	<0.1
Ig	Purine riboside	N	N	N	H	<10[c]	<0.1	<10	<0.1
Ih	1-Deazapurine riboside	CH	N	N	H	<10	<0.1	<10	<0.1

[a] Compounds were tested at 1.10^{-4} M final concentration. [b] RAD is the relative potency of the compounds to adenosine tested at the same conditions. [c] Values obtained for Ie and Ig are in agreement with literature data (6, 8).

by Mizuno *et al.* (15). Fusion of 4(7)-nitrobenzimidazole (V) (16) with tetra-*O*-acetyl-β-ribofuranose followed by deacetylation with methanolic ammonia at room temperature gave VII in good yield. Ribonucleoside Id was then obtained by catalytic hydrogenation of VII with palladium-on-carbon (17). The same synthetic procedure was followed to prepare 1-deazapurine riboside (Ih) as shown in Scheme III, instead of the syntheses previously described (18, 19). The synthesis 1,7-dideazaadenosine (If) has been described elsewhere (20).

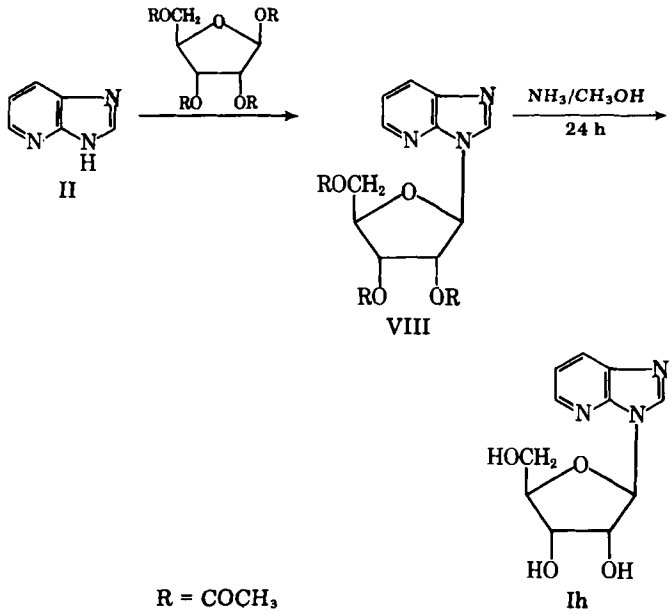

Scheme III

The compounds in Table I were tested as inhibitors of ADP- and collagen-induced human platelet aggregation *in vitro* according to the method of Born and Cross (6). The inhibitory activity of each compound was estimated by the extent of the decrease in optical density after the addition of ADP and collagen and compared with adenosine activity (RAD). 7-Deazaadenosine (Ie) and purine riboside (Ig) were tested previously and found to be ~1% as active as adenosine (6, 8). The results of the aggregation tests are shown in Table I.

1-Deazaadenosine (Ib) proved to be the only deaza analogue of adenosine showing significant inhibitory activity at 1×10^{-4} M concentration. When 1-deazaadenosine was tested at different concentrations between 5×10^{-6} M and 1×10^{-4} M, its effect on platelet aggregation induced by ADP and collagen was dose dependent, as shown in Fig. 1. The activity, also affected by the incubation period, was maximal after 7.5 min of preincubation (Fig. 2).

When adenosine and 1-deazaadenosine were coadministered, the cumulative effect was almost equal to the sum of the effects elicited by the substances separately. The results of aggregation tests clearly indicated that the nitrogen atoms at positions 3 and 7 of the purine ring are required for inhibitory activity. In fact 3-deazaadenosine (Ic), 7-deazaadenosine (Ie), 1,3-dideazaadenosine (Id), and 1,7-dideazaadenosine (If) did not show any significant inhibitory activity at a concentration of 1×10^{-4} M.

Elimination of the 6-amino group both in adenosine and 1-deazaadenosine resulted in loss of activity, as shown by the fact that purine riboside (Ig) and 1-deazapurine riboside (Ih) did not inhibit platelet aggregation induced by ADP and collagen (Table I). On the other hand, the nitrogen atom at position 1 of the purine ring appeared to be less critical than the other nitrogen atoms suggesting that some substituent changes can be made without loss of the inhibitory activity against platelet aggregation.

EXPERIMENTAL[3]

Imidazo[4,5-*b*]pyridine (II)—A mixture of 20 g (0.183 mol) of 2,3-diaminopyridine[1] and 400 mL of triethyl orthoformate was heated at reflux for 3 h. The solution was evaporated to dryness *in vacuo*, and then the residue was heated at reflux with 200 mL of concentrated hydrochloric acid for 1 h. The mixture was allowed to cool, neutralized with solid Na_2CO_3, and extracted with ethyl acetate. The combined extracts were dried (Na_2SO_4), and the solvent was removed at reduced pressure. The residue was dissolved in absolute ethanol, treated with charcoal, filtered, and then the solvent was evaporated to give 16 g of II as colorless needles (73% yield), mp 152–153°C [lit. (11) mp 153–154°C]; ^{1}H-NMR (DMSO-d_6): δ 7.3 (m, 1, 6-H), 8.11 (d, 1, J = 8 Hz, 7-H), 8.45 (d, 1, J = 5 Hz, 5-H), and 8.54 ppm (s, 1, 2-H).

7-Nitroimidazo[4,5-*b*]pyridine-4-oxide (IV)—To a cold (0°C) solution of 13.6 g (0.1 mol) of imidazo[4,5-*b*]pyridine-*N*-oxide (III) (12) in 100 mL of trifluoroacetic acid was added, in a dropwise manner, 65 mL of 90% fuming nitric acid. The mixture was heated at 90°C for 3 h, cooled, and then poured into crushed ice. The mixture was neutralized with concentrated ammonium hydroxide while maintaining the temperature below 30°C. The resulting solid was filtered, washed with ice water, and dried to give 13.5 g of IV as light-yellow needles (75% yield). The structure of IV was confirmed by comparison of the data obtained with that in the literature (12).

1-(2′,3′,5′-Tri-*O*-acetyl-β-D-ribofuranosyl)-4-nitrobenzimidazole (VI)—A mixture of 4(7)-nitrobenzimidazole (1g, 6.13 mmol) (17), 1,2,3,5-tetra-*O*-acetyl-β-D-ribofuranose (3.9 g, 12.25 mmol) and *p*-toluenesulfonic acid (50 mg) was heated at 160°C with stirring *in vacuo* (25 mm) for 20 min. The mixture was cooled, and the resulting solid was neutralized with a saturated Na_2CO_3 solution and extracted with chloroform. The organic layers were dried (Na_2SO_4), filtered, and evaporated to dryness. The residue was chromatographed on silica gel (ethyl acetate) to give 1.6 g (60%) of VI as light-yellow needles, mp 75–77°C; ^{1}H-NMR ($CDCl_3$): δ 2.08–2.15 (m, 9, 3 CH_3), 4.4–4.63 (m, 3, 4′-H and 5′-CH_2), 5.36–5.63 (m, 2, 2′-H and 3′-H), 6.16 (d, 1, J = 5 Hz, 1′-H), 7.3 (t, 1, 6-H),

[3] The melting points were determined with a Büchi apparatus and are uncorrected. The NMR spectra were obtained with a Varian EM-390 90-MHz spectrometer, using tetramethylsilane as the internal standard. For column chromatography silica gel 60 Merck was used.

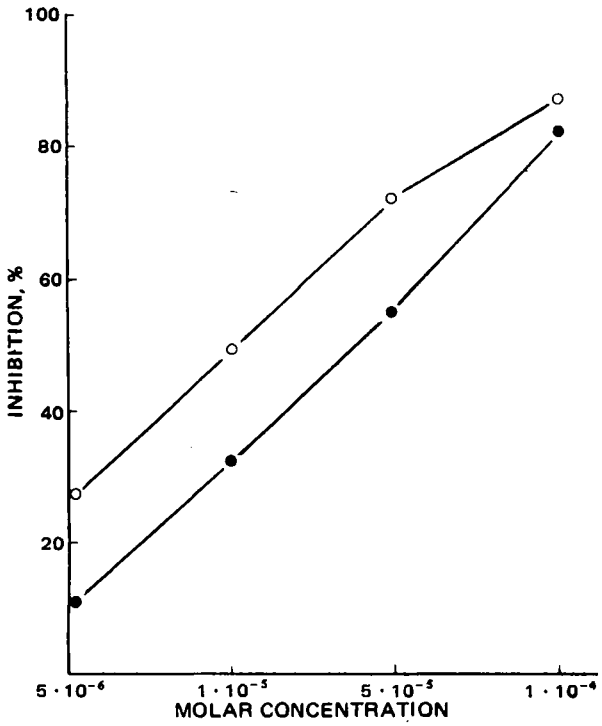

Figure 1—*Inhibitory effects of 1-deazaadenosine (Ib) at different concentrations on human platelet aggregation induced by ADP (●) and collagen (○). Ib was incubated in platelet-rich plasma at 37°C for 5 min before the addition of ADP and collagen.*

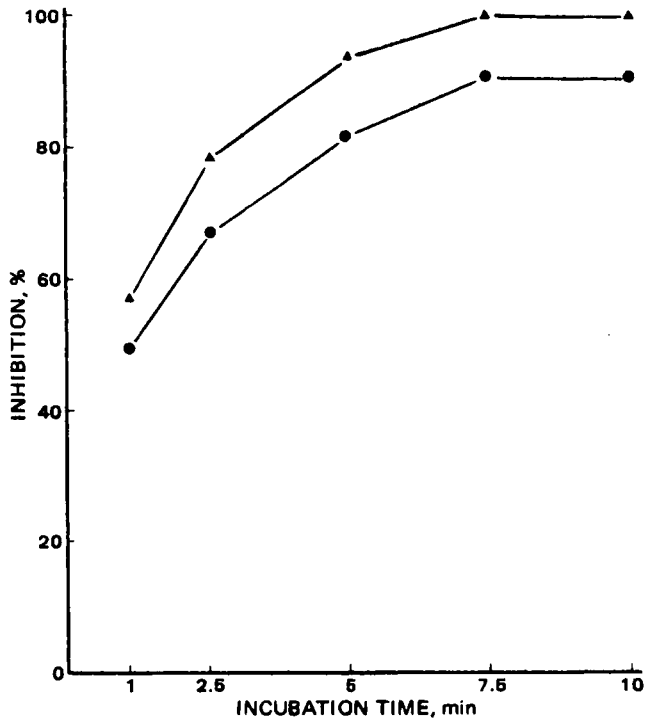

Figure 2—*Effect of 1-deazaadenosine (Ib) (●) and adenosine (Ia) (▲) on ADP-induced human platelet aggregation. The compounds were added to platelet-rich plasma at 1 × 10⁻⁴ M concentration and incubated at 37°C for increasing intervals before the addition of ADP.*

7.98 (d, 1, J = 8 Hz, 7-H), 8.17 (d, 1, J = 5 Hz, 6-H), and 8.41 ppm (s, 1, 2-H).

Anal.—Calc. for $C_{18}H_{19}N_3O_9$: C, 51.31; H, 4.55; N, 9.97. Found: C, 51.18; H, 4.59; N, 10.06.

3 - (2',3',5'-Tri -*O*- acetyl-β-D-ribofuranosyl)-3*H*-imidazo-[4,5-*b*]pyridine (VIII)—An intimate mixture of II (200 mg, 1.66 mmol), 1,2,3,5-tetra-*O*-acetyl-β-D-ribofuranose (1 g, 3.3 mmol), and *p*-toluenesulfonic acid (20 mg) was heated at 160°C with stirring *in vacuo* (25 mm) for 20 min. The solid was neutralized with a saturated Na_2CO_3 solution and extracted several times with ethyl acetate. The combined extracts were concentrated *in vacuo* to dryness, and the residue was chromatographed on silica gel (ethyl acetate–methanol, 9:1) to give 320 mg (50%) of VIII as a vitreous solid.

Anal.—Calc. for $C_{17}H_{19}N_3O_7$: C, 54.11; H, 5.08; N, 17.28. Found: C, 53.98; H, 5.11; N, 17.42.

3-β-D-Ribofuranosyl-3*H*-imidazo[4,5-*b*]pyridine (Ih)—A solution of VIII (280 mg, 0.74 mmol) in methanol saturated with ammonia (15 mL) was set aside at room temperature for 24 h. The solvent was removed *in vacuo*, and the residue was crystallized from water to yield 160 mg (85%) of Ih, mp 220–221°C [lit. (18) mp 220–222°C]. ^{1}H-NMR (DMSO-d_6): δ 3.65 (m, 2, 5'-CH_2), 4.02 (m, 1, 4'-H), 4.22 (t, 1, 3'-H), 4.7 (t, 1, 2'-H), 6.1 (d, 1, J = 5.5 Hz, 1'-H), 7.36 (m, 1, 6-H), 8.16 (d, 1, J = 8 Hz, 7-H), 8.4 (d, 1, J = 4 Hz, 5-H), and 8.72 ppm (s, 1, 2-H).

Inhibition of Platelet Aggregation—Platelet aggregation was measured by the method of Born and Cross (5), using a platelet aggregation meter[4]. The aggregative agents ADP and collagen were purchased[5]; blood was obtained by venipuncture in the forearms of apparently healthy humans and collected in polyethylene tubes containing a 1:9 volume of 3.8% sodium citrate. Platelet-rich plasma was obtained by centrifugation at 1200 rpm for 10 min, while platelet-poor plasma was obtained by centrifugation at 4500 rpm for 20 min. The platelet-rich plasma was adjusted to ~250,000 platelets/mL by adding platelet-poor plasma.

A 50-μL aliquot of the test sample dissolved in Michaelis buffer was added to a cuvette containing 0.5 mL of platelet-rich plasma, and a 50-μL aliquot of Michaelis buffer was added to the test control. The cuvette was placed in the aggregation meter and allowed to incubate at 37°C for 5 min, after which 50 μL of ADP or collagen was added to the platelet-rich plasma. The final concentration of each sample is reported in Table I and in Figs. 1 and 2. The percent inhibition of aggregation by a test compound was calculated by dividing the maximal deflection in the optical density curve in the presence of the compound by that observed in the control, then multiplying by 100. As inhibition percentage differed from preparation to preparation of platelet-rich plasma, relative potency (RAD) to a reference standard (adenosine) in the same concentration was a direct measure of the potency of inhibition.

[4] 1060 S Elvi 840 platelet aggregation meter.
[5] Centropa A6P test; Mascia Brunelli.

REFERENCES

(1) K. M. Brinkhous, R. W. Shermer, and F. K. Mostofi (Eds.), "The Platelet," Williams and Wilkins, Baltimore, Md., 1971.

(2) J. F. Mustard and M. A. Packham, *Pharm. Rev.*, **22**, 97 (1970).

(3) B. B. Vargaftig, M. Chignard, and J. Benveniste, *Biochem. Pharmacol.*, **30**, 263 (1981).

(4) A. Gaarder, J. Jonsen, S. Laland, A. J. Hellem, and P. A. Owren, *Nature (London)*, **192**, 531 (1961).

(5) R. J. Haslam, *Nature (London)*, **202**, 765 (1969).

(6) G. V. R. Born and M. J. Cross, *J. Physiol.*, **168**, 178 (1963).

(7) S. Clayton, G. V. R. Born, and M. J. Cross, *Nature (London)*, **200**, 138 (1963).

(8) G. V. R. Born, J. Haslam, and M. Goldman, *Nature (London)*, **205**, 678 (1965).

(9) K. C. Agarwal, R. E. Parks, Jr., and L. B. Townsend, *Biochem. Pharmacol.*, **28**, 501 (1979).

(10) J. A. Montgomery, A. T. Shortnacy, and S. D. Clayton, *Biochem. Pharmacol.*, **14**, 195 (1977).

(11) V. Petrow and J. Saper, *J. Chem. Soc.*, **1948**, 1389.

(12) P. C. Jain, S. K. Chatteryee, and N. Anond, *Indian J. Chem.*, **4**, 403 (1966).

(13) R. W. Middleton and D. G. Wibberly, *J. Heterocycl. Chem.*, **17**, 1757 (1980).

(14) T. Itoh, S. Kitano, and Y. Mizuno, *J. Heterocycl. Chem.*, **9**, 465 (1972).

(15) Y. Mizuno, M. Ikehara, F. Ishikowa, and H. Ikehara, *Chem. Pharm. Bull.*, **10**, 762 (1962).

(16) J. L. Rahinowitz and E. C. Wagner, *J. Am. Chem. Soc.*, **73**, 3030 (1951).

(17) S. R. Jenkins, F. W. Holly, and R. K. Robins, *J. Med. Chem.*, **11**, 910 (1968).

(18) Y. Mizuno, M. Ikehara, T. Itoh, and K. Saito, *J. Org. Chem.*, **28**, 1837 (1963).

(19) P. Jain and N. Anand, *Indian J. Chem.*, **6**, 616 (1968).

(20) I. Antonini, F. Claudi, G. Cristalli, P. Franchetti, M. Grifantini, and S. Martelli, *J. Med. Chem.*, **25**, 1258 (1982).

ACKNOWLEDGMENTS

This paper, number 3 in a series on platelet aggregation inhibitors, was presented in part at the VII International Symposium on Medicinal Chemistry in Torremolinos (Malaga), Spain, September 1980 (Abstract P40).

The authors thank A. Biondi for elemental analysis, F. Lupidi for NMR spectra, and I. Pennacchioli for typing the manuscript.

Degradation and Epimerization Kinetics of Moxalactam in Aqueous Solution

NAOFUMI HASHIMOTO ˣ, TAKENOBU TASAKI, and HIROYOSHI TANAKA

Received September 7, 1982, from the *Shionogi Research Laboratories, Shionogi & Co., Ltd., Fukushima-ku, Osaka 553, Japan.* Accepted for publication January 26, 1983.

Abstract □ The kinetics of epimerization and degradation of moxalactam in aqueous solution was investigated by HPLC. The pH–rate profiles of the degradation and epimerization were determined separately over the pH range of 1.0–11.5 at 37°C and constant ionic strength 0.5. The degradation and simultaneous epimerization were followed by measuring both of the residual *R*- and *S*-epimers of moxalactam and were found to follow pseudo-first-order kinetics. The degradation was subjected to hydrogen ion and hydroxide ion catalyses and influenced by the dissociation of the side chain phenolic group. The epimerization rates were influenced significantly in the acidic region by the dissociation of the side chain carboxylic acid group and in the basic region by hydroxide ion catalysis. The pH–degradation rate profile of moxalactam showed a minimum degradation rate constant between pH 4.0 and 6.0. The pH–epimerization rate profiles of moxalactam showed minimum epimerization rate constants at pH 7.0. The epimerization rate constants of the *R*- and *S*-epimers were not very different.

Keyphrases □ Moxalactam—degradation and epimerization in aqueous solutions, kinetics, HPLC □ Degradation—moxalactam in aqueous solutions, kinetics, epimerization □ Epimerization—moxalactam in aqueous solutions, kinetics, degradation □ Kinetics—moxalactam degradation and epimerization in aqueous solutions, HPLC

Stereoisomers, occurring widely in nature, display different biological and pharmacological effects than their racemic mixtures. Many β-lactam antibiotics have stereoisomers with different antibacterial activities (1). Few reports (2, 3) describe the kinetics of the epimerization of β-lactam antibiotics, a process which should offer valuable information for predicting and improving antibacterial activity.

Moxalactam (6059-S)[1] is a new semisynthetic (4), broad-spectrum (5) 1-oxacephalosporin which exists as the *R*- and *S*-epimers, epimeric at C-7. The *in vitro* activity of the *R*-epimer is twice that of the *S*-epimer (1). In the present study, the epimerization and degradation of moxalactam were investigated kinetically.

EXPERIMENTAL

Materials—*R*- and *S*-epimers of moxalactam disodium and decarboxy-moxalactam monosodium (decarboxylated in the 7-side chain)[1] were used as obtained. All other chemicals were of reagent grade. Water was purified with an ion-exchange column and distilled before being used.

pH—The pH of the solution was controlled throughout the reaction by a pH-stat[2]. The titrated volume of diluted hydrochloric acid or sodium hydroxide solution was at most 2% of the reaction volume. The ionic strength was adjusted to 0.5 by the addition of potassium chloride. No significant pH change was observed throughout the reaction. The pH meter[3] was standardized with the combination of standard buffer solutions of pH 4 and 7 or pH 7 and 9 at the temperature of the kinetic experiments.

Analytical Procedures—HPLC[4] was used to determine the concentrations of *R*- and *S*-epimers of moxalactam and decarboxy-moxalactam. Quantification was based on integration of peak areas using an integrator[5]. The elution was carried out on a 4.0 × 250-mm stainless steel column packed with octadecylsilane chemically bonded on silica gel[6] at room temperature. The mobile phase employed to resolve *R*- and *S*-epimers in the HPLC operation consisted of 0.05 M ammonium acetate–methanol (50:3). The mobile phase employed to resolve the decarboxy-moxalactam consisted of a solution containing 5.2 g of tetra-*n*-butylammonium hydroxide (10% in water), 6.1 g of tetra-*n*-propylammonium hydroxide (10% in water), 1.0 g of dibasic sodium phosphate, and 1.0 g of monobasic sodium phosphate, adjusted to pH 6.0 by acetic acid, and methanol (7:3). The mobile phases were prepared by micropore filtration[7] and deaerated. No difference in absorbance between *R*- and *S*-epimers was observed at any wavelength of the UV spectrum (6). Accordingly, the peak areas of *R*- and *S*-epimers represent their intact concentrations. The calibration curves of the peak area against the concentration of moxalactam was satisfactorily linear.

Kinetic Procedure—All kinetic experiments were carried out at 37

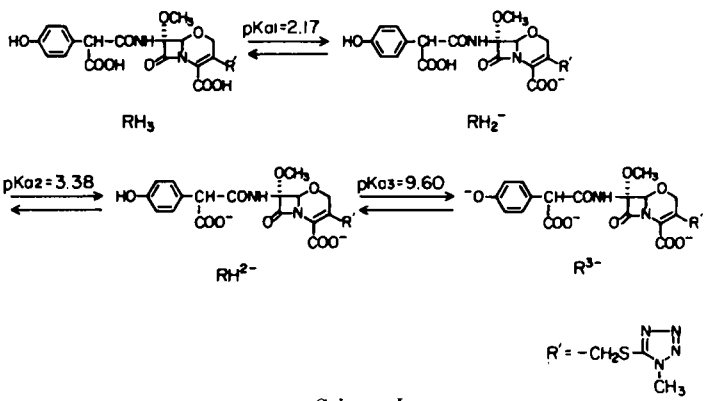

Scheme I

[1] Latamoxef; Shionogi & Co., Ltd., Osaka, Japan.

[2] pH-Stat titrator assembly consisting of TTT80 titrator, ABS80 autoburet, PHM84 research pH meter, REC80 servo graph, TTT81 digital titrator, and TIK801 titration keyboard; Radiometer, Copenhagen, Denmark.

[3] Radiometer PHM84 research pH meter.

[4] Waters ALC/GPC 204 series with U6K universal injector, Model 440 absorbance detector (254 nm), and Model M6000A pump, Waters Associates, Milford, Mass.

[5] Chromatopac C-E1B; Shimadzu, Kyoto, Japan.

[6] Nucleosil $7C_{18}$, particle size 5 μm; Macherey-Nagel Co., Düren, West Germany.

[7] 0.45 μm HAWP; Millipore Corp., Bedford, Mass.

0022-3549/84/0300-0369$01.00/0
© 1984, American Pharmaceutical Association

(20) I. Antonini, F. Claudi, G. Cristalli, P. Franchetti, M. Grifantini, and S. Martelli, *J. Med. Chem.*, **25**, 1258 (1982).

ACKNOWLEDGMENTS

This paper, number 3 in a series on platelet aggregation inhibitors, was presented in part at the VII International Symposium on Medicinal Chemistry in Torremolinos (Malaga), Spain, September 1980 (Abstract P40).

The authors thank A. Biondi for elemental analysis, F. Lupidi for NMR spectra, and I. Pennacchioli for typing the manuscript.

Degradation and Epimerization Kinetics of Moxalactam in Aqueous Solution

NAOFUMI HASHIMOTO ˣ, TAKENOBU TASAKI, and HIROYOSHI TANAKA

Received September 7, 1982, from the *Shionogi Research Laboratories, Shionogi & Co., Ltd., Fukushima-ku, Osaka 553, Japan.* Accepted for publication January 26, 1983.

Abstract □ The kinetics of epimerization and degradation of moxalactam in aqueous solution was investigated by HPLC. The pH–rate profiles of the degradation and epimerization were determined separately over the pH range of 1.0–11.5 at 37°C and constant ionic strength 0.5. The degradation and simultaneous epimerization were followed by measuring both of the residual *R*- and *S*-epimers of moxalactam and were found to follow pseudo-first-order kinetics. The degradation was subjected to hydrogen ion and hydroxide ion catalyses and influenced by the dissociation of the side chain phenolic group. The epimerization rates were influenced significantly in the acidic region by the dissociation of the side chain carboxylic acid group and in the basic region by hydroxide ion catalysis. The pH–degradation rate profile of moxalactam showed a minimum degradation rate constant between pH 4.0 and 6.0. The pH–epimerization rate profiles of moxalactam showed minimum epimerization rate constants at pH 7.0. The epimerization rate constants of the *R*- and *S*-epimers were not very different.

Keyphrases □ Moxalactam—degradation and epimerization in aqueous solutions, kinetics, HPLC □ Degradation—moxalactam in aqueous solutions, kinetics, epimerization □ Epimerization—moxalactam in aqueous solutions, kinetics, degradation □ Kinetics—moxalactam degradation and epimerization in aqueous solutions, HPLC

Stereoisomers, occurring widely in nature, display different biological and pharmacological effects than their racemic mixtures. Many β-lactam antibiotics have stereoisomers with different antibacterial activities (1). Few reports (2, 3) describe the kinetics of the epimerization of β-lactam antibiotics, a process which should offer valuable information for predicting and improving antibacterial activity.

Moxalactam (6059-S)[1] is a new semisynthetic (4), broad-spectrum (5) 1-oxacephalosporin which exists as the *R*- and *S*-epimers, epimeric at C-7. The *in vitro* activity of the *R*-epimer is twice that of the *S*-epimer (1). In the present study, the epimerization and degradation of moxalactam were investigated kinetically.

EXPERIMENTAL

Materials—*R*- and *S*-epimers of moxalactam disodium and decarboxy-moxalactam monosodium (decarboxylated in the 7-side chain)[1] were used as obtained. All other chemicals were of reagent grade. Water was purified with an ion-exchange column and distilled before being used.

pH—The pH of the solution was controlled throughout the reaction by a pH-stat[2]. The titrated volume of diluted hydrochloric acid or sodium hydroxide solution was at most 2% of the reaction volume. The ionic strength was adjusted to 0.5 by the addition of potassium chloride. No significant pH change was observed throughout the reaction. The pH meter[3] was standardized with the combination of standard buffer solutions of pH 4 and 7 or pH 7 and 9 at the temperature of the kinetic experiments.

Analytical Procedures—HPLC[4] was used to determine the concentrations of *R*- and *S*-epimers of moxalactam and decarboxy-moxalactam. Quantification was based on integration of peak areas using an integrator[5]. The elution was carried out on a 4.0 × 250-mm stainless steel column packed with octadecylsilane chemically bonded on silica gel[6] at room temperature. The mobile phase employed to resolve *R*- and *S*-epimers in the HPLC operation consisted of 0.05 M ammonium acetate–methanol (50:3). The mobile phase employed to resolve the decarboxy-moxalactam consisted of a solution containing 5.2 g of tetra-*n*-butylammonium hydroxide (10% in water), 6.1 g of tetra-*n*-propylammonium hydroxide (10% in water), 1.0 g of dibasic sodium phosphate, and 1.0 g of monobasic sodium phosphate, adjusted to pH 6.0 by acetic acid, and methanol (7:3). The mobile phases were prepared by micropore filtration[7] and deaerated. No difference in absorbance between *R*- and *S*-epimers was observed at any wavelength of the UV spectrum (6). Accordingly, the peak areas of *R*- and *S*-epimers represent their intact concentrations. The calibration curves of the peak area against the concentration of moxalactam was satisfactorily linear.

Kinetic Procedure—All kinetic experiments were carried out at 37

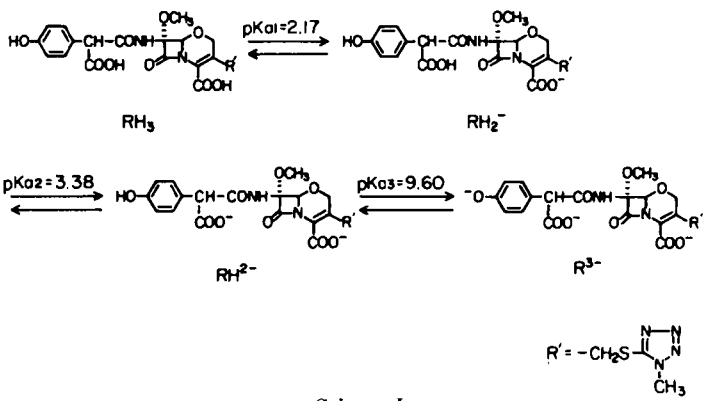

Scheme I

[1] Latamoxef; Shionogi & Co., Ltd., Osaka, Japan.

[2] pH-Stat titrator assembly consisting of TTT80 titrator, ABS80 autoburet, PHM84 research pH meter, REC80 servo graph, TTT81 digital titrator, and TIK801 titration keyboard; Radiometer, Copenhagen, Denmark.

[3] Radiometer PHM84 research pH meter.

[4] Waters ALC/GPC 204 series with U6K universal injector, Model 440 absorbance detector (254 nm), and Model M6000A pump, Waters Associates, Milford, Mass.

[5] Chromatopac C-E1B; Shimadzu, Kyoto, Japan.

[6] Nucleosil $7C_{18}$, particle size 5 μm; Macherey-Nagel Co., Düren, West Germany.

[7] 0.45 μm HAWP; Millipore Corp., Bedford, Mass.

0022-3549/84/0300-0369$01.00/0
© 1984, American Pharmaceutical Association

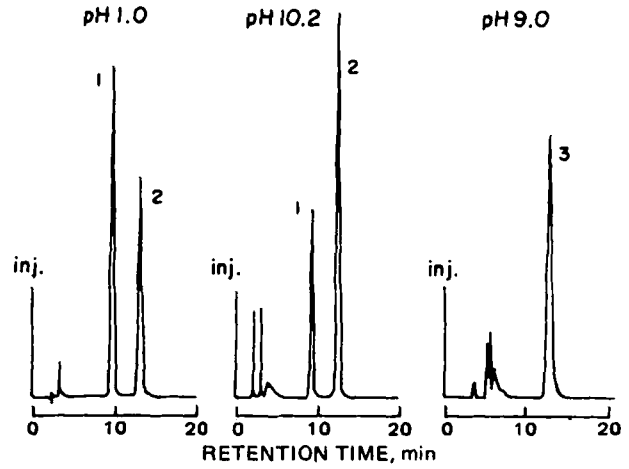

Figure 1—*Chromatograms at 254 nm for the reaction mixtures of moxalactam at pH 1.0 and 10.2 and the decarboxy-moxalactam at pH 9.0. Key: (1) R-epimer; (2) S-epimer; (3) decarboxy analogue.*

± 0.1°C and ionic strength 0.5 unless otherwise stated. The accurately weighed sample (*R*-epimer, *S*-epimer, or decarboxy-moxalactam) was dissolved in 1 mL of 0.5 M KCl and immediately diluted with 20 mL of 0.5 M KCl adjusted to the appropriate pH by the pH-stat and preheated to 37°C by a thermoregulator[8] with ±0.1°C precision. The final sample concentration was between 1×10^{-4} and 1×10^{-3} M. Portions were removed from the reaction solution at appropriate intervals and quickly frozen in a solid carbon dioxide–acetone bath. These were thawed just before HPLC analysis, and the remaining substances were determined.

Determination of Ionization Constants—The apparent ionization constants of moxalactam were determined potentiometrically (7) at ionic strength 0.5 and 37°C. The apparent ionization constants pK_{a1}, pK_{a2}, and pK_{a3}, which refer to the dissociation of the 4-carboxylic acid, the

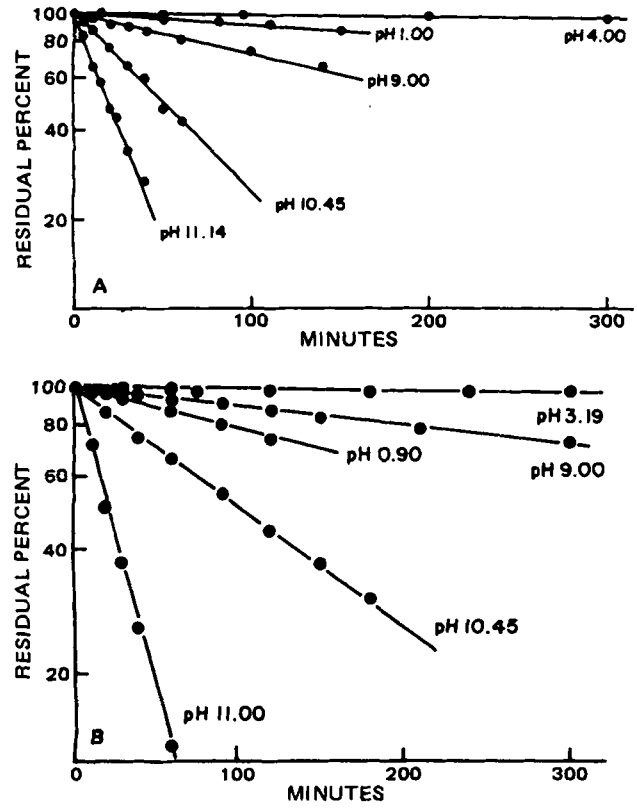

Figure 2—*Apparent first-order plots for moxalactam (A) and decarboxy-moxalactam (B) degradation at various pH values, 37°C, and ionic strength 0.5.*

[8] Taiyo Thermo Unit C-550; Taiyo Kagaku Kogyo Co., Ltd., Tokyo, Japan.

Table I—Rate Constants for Epimerization and Degradation of Moxalactam at 37°C and Ionic Strength 0.5

k_{pH}, h^{-1}	k_H, $M^{-1}h^{-1}$	k_a[a], h^{-1}	10^2k_b[a], h^{-1}	10^2k_c[b], h^{-1}	k_d[b], h^{-1}	k_{OH}, $M^{-1}h^{-1}$
k_1		2.37	0.61			3689
k_2		3.02	0.82			4127
k_3	0.477			0.42	0.584	210

[a] Rate constants defined in Eq. 6. [b] Rate constants defined in Eq. 7.

7-side chain carboxylic acid, and the phenol group, were 2.17, 3.38, and 9.60, respectively (Scheme I).

RESULTS AND DISCUSSION

Order of Degradation and Observed Rate Constants—Typical chromatograms of acidic (pH 1.0) and basic (pH 10.2) reaction mixtures, sampled at suitable times, are shown in Fig. 1, indicating that the *R*-epimer, the *S*-epimer, and the degradation products can be reasonably separated from one another. The chromatogram taken at pH 1.0 shows the reaction mixture which started with the *R*-epimer and that taken at pH 10.2 shows the reaction mixture which started with the *S*-epimer. Decarboxy-moxalactam, one of the degradation products, was found as a single broad peak with a longer retention time under the HPLC conditions which separated the *R*- and *S*-epimers. So, decarboxy-moxalactam is not shown in the chromatograms of the reaction mixtures starting with the *R*- and *S*-epimers in Fig. 1. Figure 1 also shows a typical chromatogram of the basic (pH 9.0) reaction mixture of the decarboxy-moxalactam. The parent compound can be separated from the degradation products.

As shown in Fig. 2, the semilogarithmic plots of the percent residual total moxalactam and the percent residual decarboxy-moxalactam *versus* time were reasonably linear and indicated that the degradation of the drug and its analogue followed pseudo-first-order kinetics at constant pH, temperature, and ionic strength 0.5 under various pH conditions. The disappearance of the *R*-epimer and the appearance of the *S*-epimer and *vice versa* were measured under various pH conditions. Figure 3 shows typical plots of the percent residual *R*- and *S*-epimers of the initial concentration of moxalactam, which is the total concentration of *R*- and *S*-epimers at the time when the first portion was removed, at pH 2.32, 2.36 and 10.20. A reversible epimerization was found to occur between *R*- and *S*-epimers. Furthermore, since the total amount of *R*- and *S*-epimers decreased in a semilogarithmic linear fashion with time as shown in Figs. 2A and 3, the *R*- and *S*-epimers probably decompose to other products with almost the same degradation rate constant. If either the *R*- or *S*-epimer decomposes faster than the other, the semilogarithmic plots of the percent residual moxalactam *versus* time must curve at the early stage of the decomposition.

From these results, the concentration–time profiles at various pH values are thought to be a consequence of the reaction illustrated in Scheme II, where k_1 is the epimerization rate constant from *R*-epimer to *S*-epimer, k_2 is the reverse, and k_3 is the degradation rate constant of moxalactam (*R*- and *S*-epimers).

According to Scheme II, the following kinetic equations can be written for the *R*- and *S*-epimers:

$$d(R)/dt = -k_1(R) + k_2(S) - k_3(R) \quad \text{(Eq. 1)}$$

$$d(S)/dt = k_1(R) - k_2(S) - k_3(S) \quad \text{(Eq. 2)}$$

The differential equations for *R*- and *S*-epimers (Eqs. 1 and 2) can be solved using Laplace transforms. The solutions of Eqs. 1 and 2 are:

$$(R) = \frac{(R_0)k_2 + (S_0)k_2}{k_1 + k_2} \cdot e^{-k_3 t} + \frac{(R_0)k_1 - (S_0)k_2}{k_1 + k_2} \cdot e^{-(k_1+k_2+k_3)t} \quad \text{(Eq. 3)}$$

$$(S) = \frac{(R_0)k_1 + (S_0)k_1}{k_1 + k_2} \cdot e^{-k_3 t} - \frac{(R_0)k_1 - (S_0)k_2}{k_1 + k_2} \cdot e^{-(k_1+k_2+k_3)t} \quad \text{(Eq. 4)}$$

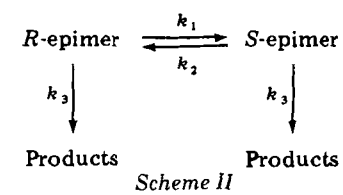

Scheme II

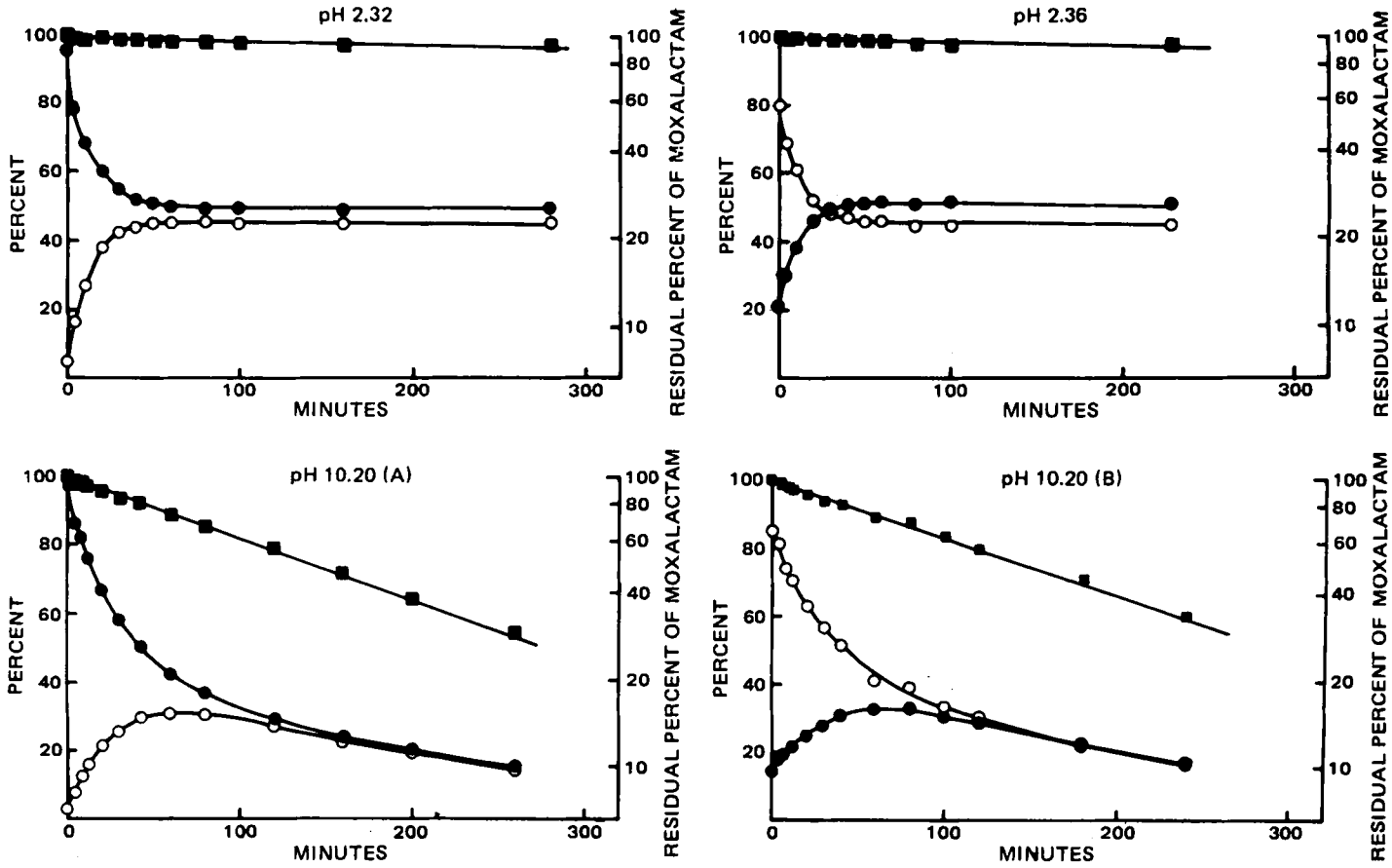

Figure 3—*Time courses for the* R-*epimer* (●), S-*epimer* (○), *and moxalactam (total of* R- *and* S-*epimers,* ■) *at pH 2.32 (disappearance of* R-*epimer and appearance of* S-*epimer), pH 2.36 (disappearance of* S-*epimer and appearance of* R-*epimer), and pH 10.2 [disappearance of* R-*epimer and appearance of* S-*epimer (A) and vice versa (B)], 37°C, and ionic strength 0.5. Moxalactam is semilogarithmically plotted* versus *time. The solid lines are the least-square fit (NONLIN) of the experimental data shown.*

$$(R) + (S) = [(R_0) + (S_0)]e^{-kst} \qquad \text{(Eq. 5)}$$

where (R) and (S) represent the concentrations of the R- and S-epimers at time t, and (R_0) and (S_0) represent the initial concentrations of R- and S-epimers, respectively. The experimental data, typified in Fig. 3, were fitted using the integrated forms of the equations through nonlinear regression analysis (NONLIN) (8) and yielded excellent fits to the theoretical solid lines calculated from Eqs. 3 and 4.

Primary Salt Effects—The primary salt effects on the epimerization of R- and S-epimers were studied at pH 3.50 and 37°C. The ionic strength was varied by adding potassium chloride. Figure 4 shows semilogarithmic plots of the apparent epimerization rate constant, k_{pH}, *versus* the square root of ionic strength ($\sqrt{\mu}$) based on an extended and modified form of the Debye–Hückel equation (9). Plots based on this equation should yield a linear relationship with a slope proportional to the product of the charges carried by the reactive species forming the activated complex. Although this modified equation holds, in theory, only up to an ionic strength of ~0.01, it has been shown to predict the kinetic salt effect reliably in some pharmaceutical systems to as high as an ionic strength of unity.

The slopes of the regression lines in Fig. 4 fitted to the data at pH 3.50 were slightly negative, −0.08 and −0.19 for k_1 and k_2, respectively. Neither of these slopes exactly fits any theoretical model predicted by the equation used, but their relatively low values are probably more consistent with the absence of ionic charge on at least one reactant rather than charges on all reactants.

Dissociation Equilibrium—In the pH range studied, moxalactam exists in four different forms: as free RH_3, a monoanion RH_2^-, a dianion RH^{2-}, and a trianion R^{3-}. Some reports indicate that the pK_a value of the carboxylic acid group at the 4-position of cephalosporins is between 1.9 and 2.9 (10, 11).

These results support the assignment of $pK_{a1} = 2.17$ to the carboxylic acid group at the 4-position of the drug. Accordingly, the value of $pK_{a2} = 3.38$ can be attributed to the carboxylic acid group in the 7-side chain. The apparent pK_a values of RH_3, RH_2^-, and RH^{2-} are 2.17, 3.38, and 9.60, respectively (Scheme I).

pH–Rate Profile—The pH dependencies of overall first-order rate constants k_1 and k_2 of moxalactam epimerization and k_3 of moxalactam degradation at 37°C and ionic strength 0.5, are shown in Figs. 5 and 6. Figure 5 shows that the observed rates of the epimerization increased rapidly and uniformly with increasing pH above pH 7.5. Since the slopes of these straight-line portions of log k_{pH} *versus* pH profiles are unity, it is likely that dissociation of the phenolic group has no effect on the epimerization, and the specific hydroxide ion-catalyzed reactions of RH^{2-} and R^{3-} take place at almost the same rate in this pH region.

The profiles bent over to constant rates at pH values lower than pH 4, indicating that a dissociation constant, pK_{a2}, affected the epimerization rates. But the two reaction mechanisms, the hydrogen ion-catalyzed epimerization reaction of RH^{2-} and the water-catalyzed epimerization

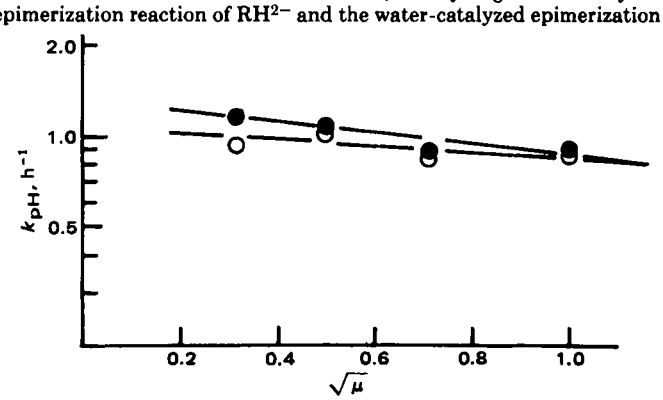

Figure 4—*Semilogarithmic plots of* k_{pH} versus *the square root of ionic strength* ($\sqrt{\mu}$) *for the epimerization of moxalactam at pH 3.50 and 37°C. Key:* (○) k_1; (●) k_2.

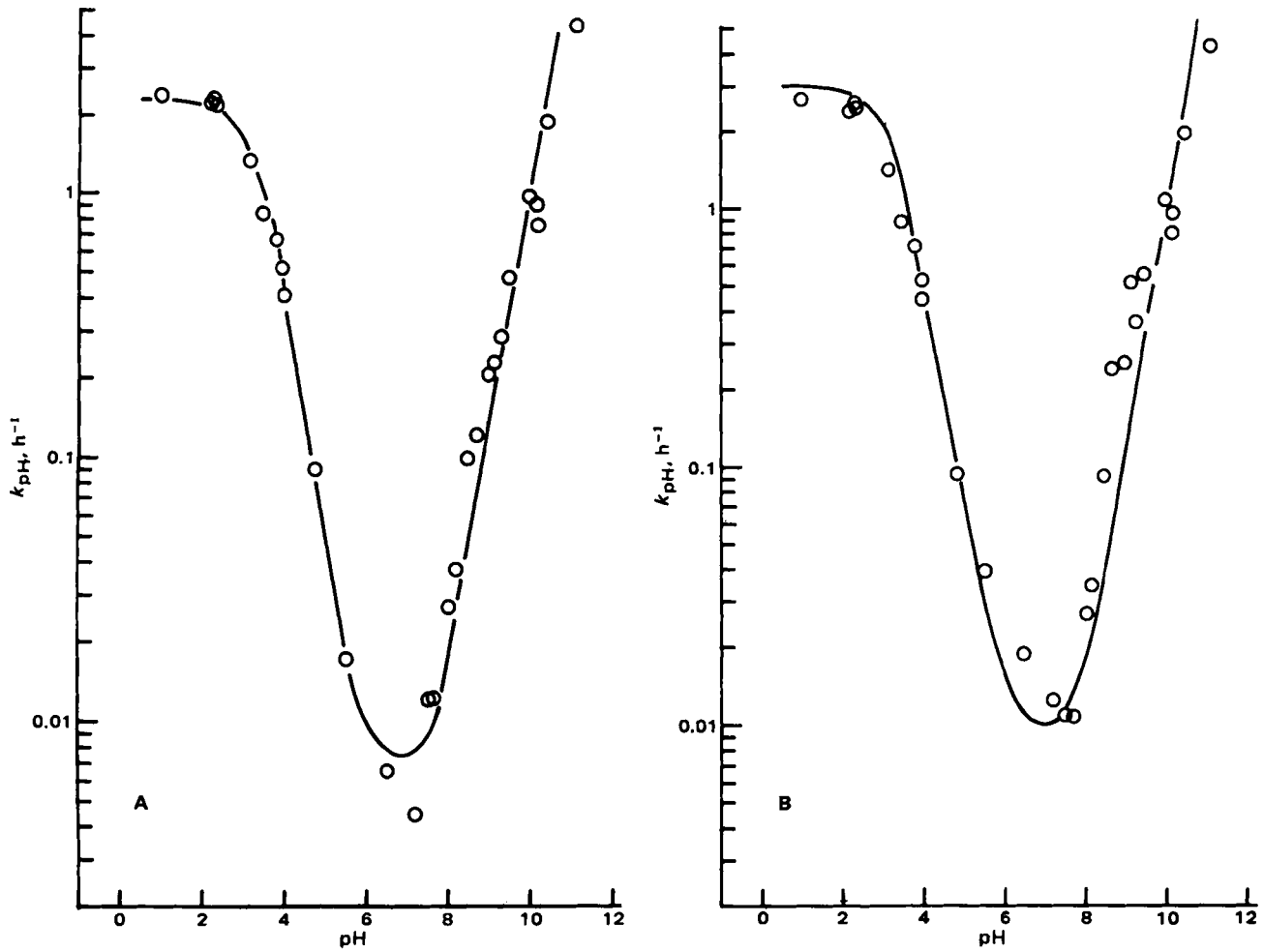

Figure 5—*Log k_{pH}–pH profile for moxalactam epimerization in aqueous solution at 37°C and ionic strength 0.5. The points are experimental values and the solid line is the theoretical curve calculated from Eq. 6 and the constants in Table I. Key: (A) k_1; (B) k_2.*

reactions of RH_3 and RH_2^- (undissociated moxalactam of the 7-side chain carboxylic acid group), give the same pH–rate profile and are kinetically equivalent in this pH range. However, it is possible to distinguish between the two reaction mechanisms according to the results of the primary salt effect of *R*- and *S*-epimers. The near lack of the primary salt effect at pH 3.50, where the concentrations of the undissociated and dissociated forms of the 7-side chain carboxylic acid group are almost the same (Fig. 4) indicates that the water-catalyzed epimerization reactions may occur below pH 6. Proton abstraction, which is important for epimerization, by the water-catalyzed reaction is more likely to occur than the hydrogen ion-catalyzed reaction due to water having stronger basicity than the hydrogen ion.

The total shape of log *k versus* pH profiles of moxalactam epimerization (k_1 and k_2) can be expressed by the following rate law:

$$k_{pH} = k_a\left(\frac{a_H}{K_{a2} + a_H}\right) + k_b + k_{OH}\left(\frac{K_w}{a_H}\right) \qquad \text{(Eq. 6)}$$

where k_a and k_b are the first-order rate constants of the undissociated and dissociated forms of the 7-side chain carboxylic acid group for the water-catalyzed epimerization, respectively, k_{OH} is the second-order rate constant for the hydroxide ion-catalyzed epimerization, and a_H and K_{a2} are the activity of hydrogen ion measured by the glass electrode and the dissociation constant of the 7-side chain carboxylic acid group, respectively. The value for the autoprotolysis constant of water, K_w, at 37°C is 2.38×10^{-14} (12). The solid lines in Fig. 5 represent the theoretical curves calculated by NONLIN and the points are the experimental results. The rate constants k_1 and k_2 with the best fits of the observed rate–pH profiles are given in Table I.

Figure 6 shows the log k_{pH}–pH profile for the degradation of moxalactam (k_3). The observed rate of the degradation decreased uniformly with increasing pH, and the slope of the straight-line portion of the log k_{pH} *versus* pH curve is negative unity below pH 2.5. The degradation rate of moxalactam between pH 4 and 6 showed pH independence, although there was a little dispersion. This implies that the overall degradation consists of the water-catalyzed or spontaneous reactions of moxalactam. Such a pH-independent degradation is known to be a common feature for the degradation of the β-lactam moiety of cephalosporins (10). There was a sigmoid dependence of k_{pH} on pH at pH values near pK_{a3}, followed by a rapid decrease of almost positive unity as the pH decreased. This inflection indicates that the degradation rate was influenced by the dissociation equilibria of the 7-side chain phenolic group (pK_{a3}). The observed rate of the degradation increased by positive unity with increasing pH above pH 10.5, which shows the hydroxide ion-catalyzed degradation.

The total shape of the log k_{pH}–pH profile of moxalactam degradation can be expressed by the following rate law:

$$k_{pH} = k_H a_H + k_c + k_d\left(\frac{K_{a3}}{K_{a3} + a_H}\right) + k_{OH}\left(\frac{K_w}{a_H}\right) \qquad \text{(Eq. 7)}$$

where k_c and k_d represent the first-order rate constants for the water-catalyzed degradation of dianionic and trianionic moxalactam, k_H and k_{OH} represent the second-order rate constants for the specific hydrogen ion-catalyzed and specific hydroxide ion-catalyzed degradation, and K_{a3} is the dissociation constant of the 7-side chain phenolic group.

In Fig. 6, the solid line represents the theoretical curve calculated by NONLIN. The rate constants in Eq. 7 that produced the best fit to the observed rate–pH profile are given in Table I; the white circles show the experimental results. The good agreement indicates that this equation adequately describes the kinetics of moxalactam degradation. The solid circles in Fig. 6 show the degradation rates of the decarboxy-moxalactam obtained from the slopes in Fig. 2B. The degradation rate of the drug is 1.5–3 times as large as the degradation rate of the decarboxy-moxalactam at pH 7.5 and 9.0, and little difference exists between the degradation rates at pH 0.9, 3.1, 10.2, and 11.0. These results suggest that a sigmoidal dependency of the degradation rate on pH below pH 10 comes from the spontaneous decarboxylation reaction of the dissociated moxalactam of

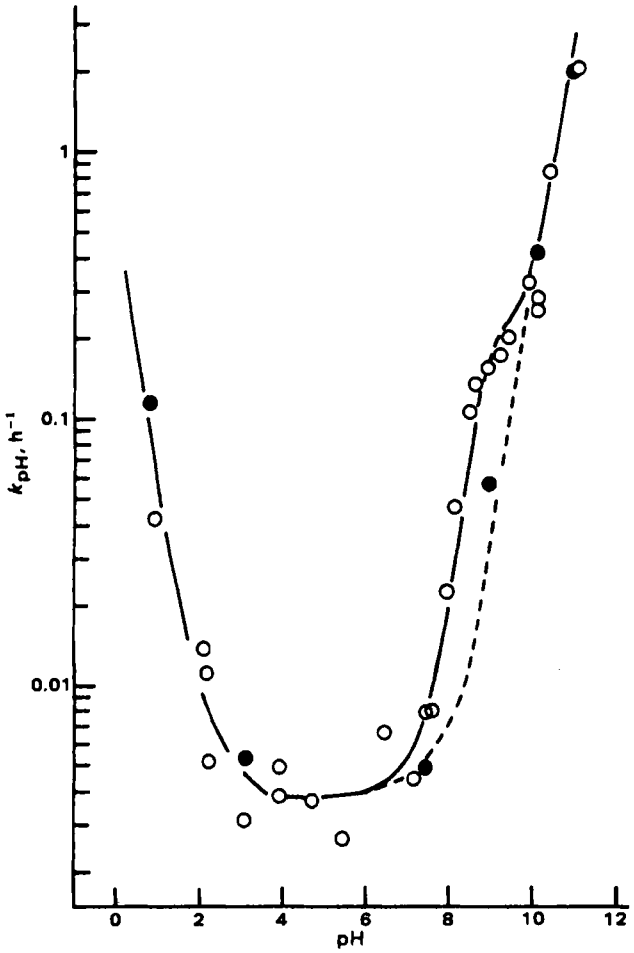

Figure 6—*Log k_{pH}–pH profiles for moxalactam (○) degradation (k_3) and the decarboxy-moxalactam (●) in aqueous solution at 37°C and ionic strength 0.5. The points are experimental values, and the solid line is the theoretical curve of moxalactam calculated from Eq. 7 and the constants in Table I.*

the 7-side chain phenolic group in parallel with the specific hydroxide ion-catalyzed degradation of the drug.

Epimerization Mechanism—The pH–epimerization rate profiles yielded straight lines with a slope of unity verifying first-order dependence on hydroxide ion in the basic region. The mechanism for the epimerization reaction can be written in terms of the abstraction of the α-proton by hydroxide ion leading to the formation of a planar carbanion (2). The mechanism for the epimerization reaction in the acidic region can be explained by the abstraction of the α-proton by water mainly from the undissociated moxalactam of the 7-side chain carboxylic acid group to the formation of a planar carbanion.

The relative order of k_a and k_b in Table I agrees with the decrease in electron-withdrawing by the dissociation of the 7-side chain carboxylic acid group attached to the α-carbon and causes a corresponding decrease in the rate of epimerization. On the other hand, the dissociation of the 7-side chain phenolic group had little influence on the epimerization rates. This is because the contribution of hydroxide ion toward the α-proton abstraction dominates in the basic region, and the influence of the dissociation of the phenolic group may disappear. However, factors other than the inductive effect of the substituents attached to the α-carbon may be considered in determining the rate of epimerization, as the stability of an enolate intermediate consisting of an amido or a carboxylic acid group resulting from the α-proton abstraction.

REFERENCES

(1) R. Wise, P. J. Wills, and K. A. Bedford, *Antimicrob. Agents Chemother.*, **20**, 30 (1981).

(2) A. Tsuji, Y. Itatani, and T. Yamana, *J. Pharm. Sci.*, **66**, 1004 (1977).

(3) H. Bundgaard, *Int. J. Pharm.*, **5**, 257 (1980).

(4) M. Narisada, T. Yoshida, H. Onoue, M. Ohtani, T. Okada, T. Tsuji, I. Kikkawa, N. Haga, H. Satoh, H. Itani, and W. Nagata, *J. Med. Chem.*, **22**, 757 (1979).

(5) T. Yoshida, S. Matsuura, M. Mayama, Y. Kameda, and S. Kuwahara, *Antimicrob. Agents Chemother.*, **17**, 302 (1980).

(6) R. Konaka, K. Kuruma, R. Nishimura, Y. Kimura, and T. Yoshida, *J. Chromatogr.*, **225**, 169 (1981).

(7) A. Albert and E. P. Serjeant, "The Determination of Ionization Constants," Chapman and Hall, London, England, 1971, chaps. 2 and 3.

(8) C. M. Metzler, "NONLIN, A Computer Program for Parameter Estimation in Nonlinear Situations," The Upjohn Co., Kalamazoo, Mich., 1969.

(9) A. N. Martin, J. Swarbrick, and A. Cammarata, "Physical Pharmacy," Lea & Febiger, Philadelphia, Pa., 1969, pp. 380, 381.

(10) T. Yamana and A. Tsuji, *J. Pharm. Sci.*, **65**, 1563 (1976).

(11) E. C. Rickard and G. C. Cooke, *J. Pharm. Sci.*, **66**, 379 (1977).

(12) H. S. Harned and W. J. Hamer, *J. Am. Chem. Soc.*, **55**, 2194 (1933).

ACKNOWLEDGMENTS

The authors thank Professor Akira Tsuji, Faculty of Pharmaceutical Science of Kanazawa University, for his generous support and timely advice and Drs. Kaoru Kuriyama and Hiroshi Tanida for their helpful discussions.

Structure–Activity Studies on Antihyperlipidemic *N*-Benzoylsulfamates, *N*-Benzylsulfamates, and Benzylsulfonamides

STEVEN D. WYRICK *x, IRIS H. HALL *, and AGNES DUBEY ‡

Received November 19, 1982, from the **Division of Medicinal Chemistry, School of Pharmacy, University of North Carolina, Chapel Hill, NC 27514* and the ‡*Chemistry and Life Sciences Group, Research Triangle Institute, Research Triangle Park, NC 27709.* Accepted for publication February 1, 1983.

Abstract □ A series of aryl substituted *N*-benzoyl- and *N*-benzylsulfamic acid sodium salts and benzylsulfonamide sodium salts have been prepared and examined for antihyperlipidemic activity in male CF_1 mice at a dose level of 20 mg/kg/d ip for 16 d. These substances were also subjected to toxicological evaluation and chemical stability studies. In general, both series of sulfamates and sulfonamides significantly lowered serum cholesterol and triglyceride levels in mice. The compounds were nonmutagenic, showed no acute toxicity or impaired liver or kidney function in male mice, and were chemically stable both as the monohydrates and in aqueous solution over a pH range of 3.5–7.4. While both series of sulfamates and sulfonamides lowered serum cholesterol and triglyceride levels, the sulfamates were relatively more potent with regard to decreasing cholesterol levels, while the sulfonamides were more effective in lowering serum triglyceride levels in mice.

Keyphrases □ *N*-Benzoylsulfamates—potential antihyperlipidemic agents, structure–activity relationships, mutagenicity, toxicity in mice □ *N*-Benzylsulfamates—potential antihyperlipidemic agents, structure–activity relationships, mutagenicity, toxicity in mice □ Benzylsulfonamides—potential antihyperlipidemic agents, structure–activity relationships, mutagenicity, toxicity in mice

Cardiovascular disease is currently a major cause of death of males in Western civilized societies. Atherosclerosis is characterized by partial or complete occlusion of the vessels that supply blood to the myocardial tissues, due primarily to the formation of the fibrous lesion known as a sclerotic plaque within the vessel lumen (1). Elevated levels of cholesterol and triglycerides have been detected in plaque cells, and there appears to be a link between plaque formation and long-term elevated serum lipids (2, 3). Therefore, lowering of elevated serum lipid levels either by dietary restriction or chemotherapy appears desirable.

It has been demonstrated that a wide structural variety of chemical agents are active as antihyperlipidemics (1) including the synthetic sweetening agent, saccharin (4). Saccharin has demonstrated significant antihyperlipidemic activity in male mice, with the optimum dose level of 20 mg/kg/d ip affording serum cholesterol levels 67 ± 10% of control values after 16 d of administration and triglyceride levels 51 ± 16% of control values after 14 d. A series of *N*-benzoylsulfamic acid sodium salts as acyclic analogues of saccharin were prepared in an attempt to improve the antihyperlipidemic activity while eliminating the undesirable effects which are associated with saccharin (5, 6). Also prepared were two other structurally related classes of compounds, *N*-benzylsulfamates and benzylsulfonamides. Structural modifications among the series include aromatic substitutions with groups that vary in their lipophilicity, electronic character, and steric parameters. In addition, replacement of the carbonyl function (*N*-benzoylsulfamates) by a methylene group (*N*-benzylsulfamates) and alteration of the relative position of the nitrogen atom with regard to the aromatic and sulfonyl functions (benzylsulfonamides) were examined.

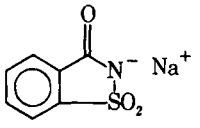

Saccharin (sodium salt)

$C_6H_5CH_2NHSO_3^-Na^+$

N-Benzylsulfamic Acid (sodium salt)

$C_6H_5CONHSO_3^-Na^+$

N-Benzoylsulfamic Acid (sodium salt)

$C_6H_5CH_2SO_2NH^-Na^+$

Benzylsulfonamide (sodium salt)

BACKGROUND

Few reports exist concerning the synthesis of *N*-benzoylsulfamates. The unsubstituted prototype was prepared by Baumgarten and Marggraff (7) by heating benzamide and pyridine–sulfur trioxide complex (pyr·SO_3) to the melting point with subsequent conversion to the sodium salt with aqueous sodium hydroxide. In our hands, this procedure afforded extremely low yields of the prototype and no product for any aryl-substituted derivative. Dipyridinium imidodisulfonate (8) has also been employed for the sulfonation of benzamide but, again, yields are on the order of 5–10%. Two procedures have been developed in this laboratory which permit the preparation of the series of aryl-substituted *N*-benzoyl- and *N*-benzylsulfamic acid sodium salts in significantly greater yields. The appropriate benzamide or benzylamine was treated with pyr·SO_3 in pyridine solution for 3–5 h at 80–90°C. The product was isolated as the ammonium salt and converted to the sodium salt by ion-exchange chromatography (Scheme I). In addition, the *N*-benzoylsulfamates may also be prepared by benzoylation of pyridinium sulfamate with the acid chloride in pyridine.

The benzylsulfonamides were prepared from the corresponding sulfonyl chlorides, which were obtained by treatment of the benzylisothioureas with chlorine at 0–10°C (9) (Scheme II). This procedure is satisfactory for derivatives that are substituted with electron-withdrawing groups or hydrogen atoms on the aromatic ring, whereas strong electron-releasing substituents (*i.e.*, OCH_3) induce chlorination of the aromatic ring during conversion to the sulfonyl chloride as evidenced by ^{1}H-NMR and MS data. This problem was circumvented by obtaining the nitrobenzylsulfonamide by the above procedure followed by introduction of the methoxy substituent *via* the diazonium tetrafluoroborate salt. The compounds prepared were examined for chemical stability at room temperature, both as the monohydrates and in aqueous solution, over a pH range of 3.5–7.4 using both reverse-phase HPLC and TLC to detect the formation of hydrolysis products (*i.e.*, benzamides and benzylsulfonic acids).

RESULTS AND DISCUSSION

Chemical stability studies using reverse-phase HPLC revealed that all of the compounds except VI were stable at room temperature both

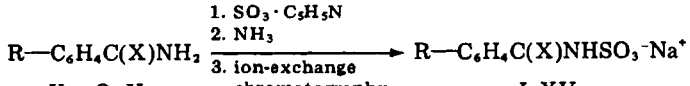

$R—C_6H_4C(X)NH_2$ → $R—C_6H_4C(X)NHSO_3^-Na^+$

X = O, H_2 I–XV

Scheme I

0022-3549/84/0300-0374$01.00/0
© 1984, American Pharmaceutical Association

as the monohydrate and in aqueous solution over a pH range of 3.5–7.4 for a period of at least 60 d. Compound VI underwent 55–60% hydrolysis in solution after 30 d and was completely degraded after 60 d. This compound was also found to be completely hydrolyzed after 3 months when stored in solid form, and was therefore not evaluated biologically.

None of the compounds were found to be mutagenic in the Ames assay; however, all of the compounds exhibited toxicity to bacteria at the high-dose level of 3000 μg/plate. It is advisable to include one toxic dose level when testing unknown compounds for mutagenicity (10). The toxicity assay indicated essentially no cell death; therefore, the toxic effect at 3000 μg/plate was not due to cell death, but rather to the inhibition of revertent colony growth *via* another mechanism. Results of acute toxicity testing in male mice indicated that none of the compounds tested produced abnormal levels of alanine amino transferase (ALT) activity or urea nitrogen, nor were any signs of toxicity or abnormal behavior observed during the 14-d period. No abnormalities or irregular fluctuations in body weight were observed on termination of the study and gross necropsy. Likewise, no toxicity was observed during the course of the antihyperlipidemic study.

Of the two series, the *N*-benzoylsulfamates appear to be the more potent antihypercholesteremic agents with the *o*- and *p*-chloro derivatives (IV, II) being the most active (Table I). As indicated in Table II, electron-withdrawing substituents on the aromatic ring lend slightly greater activity to the series than do electron-releasing substituents. Activity decreases somewhat with increasing substituent size. In general, activity within the series does not appear to be heavily dependent on the size, electronic properties, or lipophilicity of the aromatic substituents as the unsubstituted prototype (VII) is also quite active. A significantly greater structural dependence within this series resides in the side-chain

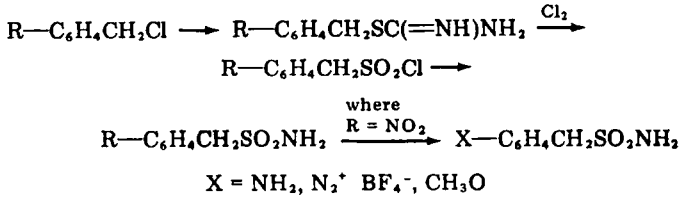

Scheme II

requirement for the carbonyl function. By comparison of the *p*-Cl, *o*-Cl, *p*-OCH_3, and unsubstituted derivatives (II, IV, I, and VII, respectively) with their carbonyl-reduced counterparts among the *N*-benzylsulfamates (XV, XIV, XII, and XIII, respectively), it is evident that antihypercholesteremic activity is markedly reduced in the absence of the carbonyl function. This structural requirement for antihyperlipidemic activity has also been noted for saccharin as well as other imides (11).

Serum triglyceride levels are moderately reduced by the *N*-benzoylsulfamates, with the exception of the *p*-Cl (II) and *p*-isopropyl (XI) derivatives, which lower serum triglyceride levels to 55 ± 7% and 49 ± 8% of control values, respectively, by day 16. As in the case of antihypercholesteremic activity, the dependence on the presence of the side-chain carbonyl for antihypertriglyceridemic activity appears evident when comparing I, II, and VII with XII, XV, and XIII, respectively. However, *N*-benzylsulfamate (XIV) showed increased antihypertriglyceridemic activity compared with *N*-benzoylsulfamate (IV). Each of the *N*-benzoylsulfamates shows greater antihypercholesteremic activity than clofibrate, which is not active at 20 mg/kg, requiring dose levels of 150–200 mg/kg to reduce serum cholesterol ~15% in rodents. Saccharin at 20 mg/kg/d lowered serum cholesterol levels 35% and serum triglyceride

Table I—*N*-Benzoyl- and *N*-Benzylsulfamic Acid Sodium Salts

$R—C_6H_4C(X)NHSO_3^-Na^+$

Compound	R	X	^{1}H-NMR (DMSO-d_6), (δ) ppm	Synthetic Procedure or Literature Reference	Yield, %	Formula
I	*p*-OCH_3	O	7.3 (q, 4, ArH) 10.1 (s, 1, —NH—) 3.7 (s, 3, —OCH_3)	8	7	$C_8H_8NO_5SNa·H_2O$
II	*p*-Cl	O	7.6 (q, 4, ArH) 10.4 (s, 1, —NH—)	8	11	$C_7H_5ClNO_4SNa·H_2O$
III	*m*-Cl	O	7.5 (m, 4, ArH) 10.3 (s, 1, —NH—)	8	21	$C_7H_5ClNO_4SNa·H_2O$
IV	*o*-Cl	O	7.3 (m, 4, ArH) 10.3 (s, 1, —NH—)	A	50	$C_7H_5ClNO_4SNa·H_2O$
V	*m*-OCH_3	O	7.2 (m, 4, ArH) 10.2 (s, 1, —NH—) 3.7 (s, 3, —OCH_3)	8	26	$C_8H_8NO_5SNa·H_2O$
VI	*o*-OCH_3	O	7.5 (m, 4, ArH) 9.7 (s, 1, —NH—) 3.7 (s, 3, —OCH_3)	B	42	$C_8H_8NO_5SNa·H_2O$
VII	H	O	7.6 (m, 5, ArH) 10.4 (s, 1, —NH—)	8	4	$C_7H_6NO_4SNa·H_2O$
VIII	*p*-Br	O	10.56 (s, 1, NH) 7.76 (q, 4, ArH)	A	31	$C_7H_5BrNO_4SNa·H_2O$
IX	*p*-CH_3	O	10.35 (s, 1, NH) 7.4 (s, 4, ArH) 2.35 (s, 3, CH_3)	A	39	$C_8H_8NO_4SNa·H_2O$
X	*p*-CH_3C	O	10.58 (s, 1, NH) 8.04 (s, 4, ArH) 2.68 (s, 3, CH_3)	A	28	$C_9H_8NO_5SNa·H_2O$
XI	*p*-iso-C_3H_7	O	7.6 (q, 4, ArH) 10.54 (s, 1, NH) 3.0 [m, 1, $(CH_3)_2CH$] 1.23 [d, 6, $(CH_3)_2$]	A	23	$C_{10}H_{12}NO_4SNa·H_2O$
XII	*p*-OCH_3	H_2	6.95 (q, 4, ArH) 3.85 (d, 2, —CH_2) 3.70 (s, 3, —OCH_3) 4.45 (t, 1, —NH)	A	36	$C_8H_{10}NO_4SNa$
XIII	H	H_2	7.3 (s, 5, ArH) 4.0 (d, 2, —CH_2) 4.7 (t, 1, —NH)	A	23	$C_7H_8NO_3SNa$
XIV	*o*-Cl	H_2	7.3 (m, 4, ArH) 4.0 (d, 2, —CH_2) 4.8 (t, 1, —NH)	A	18	$C_7H_7ClNO_3SNa$
XV	*p*-Cl	H_2	7.25 (s, 4, ArH) 3.8 (d, 2, —CH_2) 4.75 (t, 1, —NH)	A	21	$C_7H_7ClNO_3SNa$

Table II—Benzylsulfonamide Sodium Salts

	$R—C_6H_4CH_2SO_2NH^-Na^+$			
Compound	R	^{1}H-NMR (DMSO-d_6), (δ) ppm	Yield, %	Formula
XVI	*o*-Cl	7.25 (m, 4, ArH) 3.9 (s, 2, $—CH_2$) 3.0 (broad, 1, NH)	83	$C_7H_7ClNO_2SNa·H_2O$
XVII	*o*-OCH_3	6.95 (m, 4, ArH) 3.8 (s, 2, CH_2) 3.65 (s, 3, $—OCH_3$)	15 (Overall)	$C_8H_{10}NO_3SNa·2H_2O$
XVIII	*m*-OCH_3	6.85 (m, 4, ArH) 3.7 (s, 2, $—CH_2$) 3.6 (s, 3, $—OCH_3$)	8 (Overall)	$C_8H_{10}NO_3SNa·1½H_2O$
XIX	*p*-OCH_3	6.9 (q, 4, ArH) 3.7 (s, 2, $—CH_2$) 3.7 (s, 3, $—OCH_3$)	20 (Overall)	$C_8H_{10}NO_3SNa·½H_2O$
XX	H	7.2 (m, 5, ArH) 3.7 (s, 2, CH_2)	37	$C_7H_8NSO_2Na·H_2O$
XXI	*m*-Cl	7.2 (m, 4, ArH) 3.8 (s, 2, CH_2)	66	$C_7H_7ClNO_2SNa·H_2O$
XXII	*p*-Cl	7.1 (m, 4, ArH) 3.7 (s, 2, CH_2)	22	$C_7H_7ClNO_2SNa·H_2O$

levels 46% in mice. Compounds I, II, III, IV,and VII are more active than saccharin in lowering serum cholesterol levels, but less active in lowering triglyceride levels.

Within the benzylsulfonamide series (Table III), the *o*-OCH_3 derivative (XVII) was the most active antihypercholesteremic agent, being equal in activity to saccharin. In general, moderate antihypercholesteremic activity is displayed by this series, whereas antihypertriglyceridemic activity surpasses that of the *N*-benzoylsulfamates and clofibrate. The *p*-Cl derivative (XXII) is equally active with saccharin in this respect. Compounds XVIII and XX are more active than saccharin, lowering serum triglyceride levels to 42% of control values. Comparing the activities of XVI, XVIII, XX, and XXII, the most active antihypertriglyceridemic agents in the series, no dependence on substituent parameters is evident.

EXPERIMENTAL

All chemicals were used as received from the manufacturer[1]. Melting points were obtained on a capillary melting point apparatus[2]. ^{1}H-NMR spectra[3] were obtained for all novel products. Elemental analyses[4] of all products were within ±0.4% of the theoretical values. Ion-exchange chromatography was performed using sodium-form resin[5]. Reverse-phase HPLC was performed on a gradient programmable high-pressure liquid chromatograph[6] with a C_{18} column[7] and radial compression module. Male CF_1 mice[8] were used for antihyperlipidemic testing.

Aryl-Substituted Benzamides—According to the procedure of Vogel (12), the appropriate benzoyl chloride was treated with cold concentrated NH_4OH. The product was filtered, dried, and recrystallized from ethanol–water.

***N*-Benzoyl- and *N*-Benzylsulfamic Acid Sodium Salts (I–XV)**—*General Procedure A*—The appropriate benzamide or benzylamine (5.0 g) and 1.1 equivalents of pyridine–sulfur trioxide complex were dissolved with warming in 50 mL of dry pyridine under nitrogen. The reaction was stirred at 80–90°C for 3–5 h, at which time TLC (ethyl acetate–acetic acid–water, 6:3:1) showed no further reaction. The solution was cooled in ice, and the excess precipitated pyridine–sulfur trioxide was removed by filtration and washed with cold pyridine. The filtrate was treated with gaseous ammonia for 10 min, concentrated *in vacuo* to approximately one-third its volume, and poured into ether–methanol (4:1) with vigorous stirring. The precipitated ammonium salt was collected, washed with ether, and dried. Conversion to the sodium salt was effected by dissolving the crude ammonium salt in the least amount of water (warming if necessary) followed by rapid elution with water from an ion-exchange resin (sodium ion form). The aqueous eluant was concentrated *in vacuo*, and the resulting crystals were stored at 3–5°C. The product was collected, washed with cold water, dried, and recrystallized from methanol to give material melting at ~100°C up to ~200°C (Table I).

General Procedure B—Pyridinium sulfamate (4–7 g) was suspended in 25 mL of dry pyridine under nitrogen. The appropriate benzoyl chloride (1.2 equivalents) was added dropwise, followed by stirring at 60°C for 3–4 h. Methanol (3.0 mL) was added, and the mixture was stirred for an additional 30 minutes, cooled to room temperature, treated with gaseous ammonia for 10 min; the sodium salt was prepared as in procedure A (Table I).

Aryl-Substituted Benzyl Chlorides—According to the procedure of Brooks and Snyder (13), the appropriate benzyl alcohol was treated with thionyl chloride in pyridine at room temperature and the product was distilled.

S-(*Substituted Benzyl*) *Isothiourea Hydrochlorides*—The procedure of Johnson and Sprague (9) was utilized. The appropriate benzyl chloride (0.05–0.2 mol) and one equivalent of thiourea were stirred under reflux in absolute ethanol (25 mL/0.05 mol of benzyl chloride) for 3–4 h. On cooling, the product crystallized in 85% yield. This material was used in the next step.

Substituted Benzylsulfonyl Chlorides—The appropriate *S*-(substi-

Table III—Antihyperlipidemic Effects of Test Compounds in Male CF_1 Mice [a]

Compound	Serum Cholesterol Day 9	Serum Cholesterol Day 16	Serum Triglycerides Day 16
I	63 ± 6[b]	60 ± 7[b]	65 ± 8[b]
II	57 ± 5[b]	52 ± 6[b]	55 ± 7[b]
III	72 ± 5[b]	64 ± 6[b]	97 ± 7
IV	78 ± 6[b]	51 ± 5[b]	86 ± 8
V	86 ± 7	72 ± 5[b]	80 ± 7[c]
VII	74 ± 6[b]	57 ± 5[b]	70 ± 6[b]
VIII	75 ± 4[b]	73 ± 7[b]	88 ± 3
IX	70 ± 3[b]	63 ± 3[b]	82 ± 4
X	95 ± 3	72 ± 4[b]	69 ± 6[b]
XI	90 ± 6	77 ± 6[b]	49 ± 8[b]
XII	88 ± 4	87 ± 2[b]	91 ± 9
XIII	94 ± 7	88 ± 2[a]	97 ± 8
XIV	84 ± 8	78 ± 2[b]	75 ± 2[b]
XV	94 ± 2	93 ± 4	79 ± 7[b]
XVI	99 ± 8	73 ± 6[b]	52 ± 6[b]
XVII	69 ± 4[b]	68 ± 7[b]	58 ± 6[b]
XVIII	84 ± 6[c]	79 ± 7[b]	42 ± 4[b]
XIX	74 ± 8[b]	70 ± 5[b]	76 ± 7[b]
XX	95 ± 8	75 ± 5[b]	42 ± 3[b]
XXI	92 ± 7	77 ± 5[b]	71 ± 5[b]
XXII	94 ± 7	78 ± 8[b]	48 ± 4[b]
Saccharin	77 ± 6[b]	65 ± 7[b]	54 ± 6[b]
Clofibrate	98 ± 7	97 ± 9	95 ± 7
1% Carboxymethylcellulose (Control)	100 ± 7	100 ± 6	100 ± 7

[a] Mean ± *SD* as percent of control; $n = 6$. [b] Significantly different, $p < 0.001$. [c] Significantly different, $p < 0.005$.

[1] Aldrich Chemical Co.
[2] Thomas Hoover.
[3] Either on a Varian EM360 or JOEL FX 60 FT.
[4] Galbraith Laboratories, Knoxville, Tenn. All compounds were tested for C and H; I–VII and XII–XXII were tested for N.
[5] Bio-Rad AG50W-X8.
[6] Waters Associates.
[7] Radial-Pak, Waters Associates.
[8] Jackson Laboratories.

tuted benzyl) isothiourea hydrochloride was dissolved in water (600–700 mL/0.2 mol depending on solubility) and cooled in ice to 0–10°C. The solution was then treated with gaseous chlorine for 30 min while maintaining the temperature <10°C. The solid or oily product was extracted into ether, and the ether extracts were dried (sodium sulfate) and evaporated *in vacuo* to afford the product which was sufficiently pure for conversion to the sulfonamide.

Substituted Benzylsulfonamides (XVI, XX, XXI, and XXII)—The appropriate benzylsulfonyl chloride was dissolved in liquid ammonia, the resulting yellow solution was kept at −78°C for 1 h, and then the excess ammonia was allowed to evaporate. The residue was dissolved in chloroform and filtered. The filtrate was dried (sodium sulfate) and evaporated to afford the crude sulfonamide which was either recrystallized from ethanol or column chromatographed[9]. This material was converted to the sodium salt by treating an ethanolic solution with 1.0 equivalent of 12 M aqueous NaOH. On cooling, the precipitated salt was collected and dried *in vacuo*. These products were obtained in varying degrees of hydration (Table II). Melting points were >250°C.

Catalytic Reduction of Nitrobenzylsulfonamides—A solution of the appropriate nitro-substituted benzylsulfonamide (prior to sodium salt formation) was dissolved in absolute ethanol (1600 mL/34 g of substrate) and was shaken for 6–8 h at 40°C[10] with 1.0 g of 5% palladium-on-charcoal under 60 psi of hydrogen. When the reaction was complete by TLC, the catalyst was removed by filtration, and the filtrate was evaporated *in vacuo* to afford an essentially quantitative yield of the aniline compound.

Diazotization of Aminobenzylsulfonamides (14)—A 24% solution of fluoroboric acid (0.12 mol) was added dropwise with cooling and stirring to 9–10 g of the aniline. The resulting solution was maintained at 0–5°C while an aqueous solution of $NaNO_2$ (0.048 mol) was added dropwise with stirring, and then the mixture was stirred at 0–5°C for 1.5 h. The precipitated salt was collected by filtration, washed with 5% HBF_4, cold methanol, and cold ether, and then was dried *in vacuo* to afford light-tan crystals.

Methoxybenzylsulfonamides (15) (XVII, XVIII, and XIX)—A solution of the above diazonium fluoroborate salt in methanol (1200 mL/10 g) was heated at 50°C for 5 h. The orange solution was then evaporated to dryness *in vacuo*, and the residue was column chromatographed[11] to afford material which was converted to the sodium salt as described above (Table II).

Ames Mutagenicity Assay (16, 17)—Compounds I–V, VII, and XII–XXII were each added to test culture plates in triplicate with and without mammalian microsomal activator S-9 present in the culture medium at dose levels of 0.3, 3, 30, 300, and 3000 μg/plate. Each compound was tested with five strains of non-histidine-producing *Salmonella typhimurium*. A threefold increase in the number of colonies per plate over background control constituted a positive mutagenic result. Control groups were treated only with the dosing vehicle (dimethyl sulfoxide).

Acute Toxicity Studies—Compounds I–V, VII, and XII–XXII were subjected to acute toxicity studies in male CD-1 mice (20–30 g)[12] in full compliance with the Food and Drug Administration Good Laboratory Practices Regulations for Nonclinical Laboratory Studies (18). Blood samples were taken by tail vein bleeding 3 d before dosing and at sacrifice on day 14 to be used for biochemical testing of liver and kidney function. Animals were weighed on days 0, 7, and 14. A single 100-mg/kg dose as a 1% solution in sterile water was administered by oral intubation on day 0. At this time and at various times throughout the day for 14 d, the animals were observed for signs of toxicity and/or abnormal behavior. Six animals were used per test compound. The animals were maintained on rodent diet[13] and water *ad libitum*. On day 14, the animals were weighed, sacrificed, and gross necropsies performed. The blood samples were assayed for alanine amino transferase activity as a test for liver function and urea nitrogen as a test for kidney function. The tests were performed on a miniature centrifugal fast analyzer. Each individual assay included 1 blank, 13 samples, and 2 controls (commercial sera samples of normal and abnormal alanine amino transferase and urea nitrogen levels). Abnormal values were defined as being >2 *SD* from untreated group values.

Assay for Antihyperlipidemic Activity—Compounds I–V and VII–XXII, as well as saccharin and clofibrate, were administered daily to male CF_1 mice (~28 g) as a 1% carboxymethylcellulose suspension at 20 mg/kg/d ip. On days 9 and 16, blood was obtained by tail vein bleeding and, after centrifugation to obtain serum, 25-μL samples were assayed for total cholesterol by the procedure of Ness *et al.* (19). Serum triglycerides were assayed using a commercial kit[14] on blood collected on the 16th day. By comparison to standards, the amounts of cholesterol (mg %) and triglycerides (mg/dL) were calculated. Treated values were expressed as percent of control (Table III).

Chemical Stability Studies—A 1% solution of each compound prepared in pH 3.5 citrate buffer, distilled water, and phosphate buffer (pH 7.4) was allowed to stand at room temperature. These solutions, as well as a 1% solution in distilled water of each compound which had been stored in solid form at room temperature, were analyzed directly by reverse-phase HPLC (C_{18}, 254 nm, 10% aqueous acetonitrile) for the presence of benzamides, benzylsulfonic acids, or other decomposition products on days 2, 6, 18, 30, and 60. These studies were paralleled using reverse-phase TLC plates[15] with methanol–water (9:1).

REFERENCES

(1) E. M. Jepson, in *Advances in Drug Research*, A. B. Simmonds, Ed., Vol. 9, Academic, London, 1974, p. 1.

(2) J. Horsey, B. Livesby, and J. W. T. Dickerson, *Age Aging*, **9**, 154 (1980).

(3) J. D. Bronzell, *N. Engl. J. Med.*, **303**, 1060 (1980).

(4) I. H. Hall, J. M. Chapman, and G. H. Cocolas, *J. Pharm. Sci.*, **70**, 326 (1981).

(5) "Need to Resolve Safety Questions on Saccharin," Report to the Comptroller General of the United States, HRD-76-156, Washington, D.C. (1976).

(6) M. O. Tisdel, P. O. Nees, D. L. Harris, and P. H. Derse, in "Symposium: Sweeteners," G. E. Inglett, Ed., AVI Publishing, Westport, Conn., 1974, p. 145.

(7) P. Baumgarten and I. Marggraff, *Chem. Ber.*, **64B**, 1582 (1931).

(8) K. Nakano, H. Yamaguchi, and K. Yazawa, Nitto Chem. Ind. Co., Ltd., Japanese Patent 2857 (1964).

(9) T. B. Johnson and J. M. Sprague, *J. Am. Chem. Soc.*, **58**, 1348 (1936).

(10) F. deSerres and M. Shelby, *Science*, **203**, 563 (1979).

(11) I. H. Hall, J. M. Chapman, and G. H. Cocolas, *J. Med. Chem.*, **28**, 243 (1983).

(12) A. I. Vogel, "A Textbook of Practical Organic Chemistry," 3rd ed., 1962, p. 797.

(13) L. A. Brooks and H. R. Snyder, *Org. Synth., Coll.*, **3**, 698 (1955).

(14) A. Roe, *Org. React.*, **5**, 205 (1960).

(15) D. F. Detar and T. Kosuge, *J. Am. Chem. Soc.*, **80**, 6072 (1958).

(16) B. N. Ames, in "Chemical Mutagens: Principles and Methods for Their Detection," Vol. 1, A. Hollander, Ed., Plenum, New York, N.Y., 1971, p. 267.

(17) B. N. Ames, F. Lee, and W. Durston, *Proc. Natl. Acad. Sci. USA*, **70**, 782 (1973).

(18) Fed. *Regist.*, December 22, 1978, pp. 60013–60025.

(19) A. T. Ness, J. V. Pastewka, and A. C. Peacock, *Clin. Chem. Acta*, **10**, 229 (1964).

ACKNOWLEDGMENTS

This work was supported by National Institute of Dental Research Contract N01-DE-02428, American Heart and Lung Association Grant HL25680-02, and University of North Carolina Research Council Grant VF737.

We wish to thank Mr. Thomas J. Hughes and Dr. R. Wayne Hendren at the Research Triangle Institute, Research Triangle Park, N.C., for performing the Ames and acute toxicity assays.

[9] Silica gel 60, methylene chloride–methanol (9:1).
[10] Parr shaker apparatus.
[11] Silica gel 60, methylene chloride–acetone (9:1), (8:2).
[12] Acute toxicity studies and Ames assays were performed at the Research Triangle Institute, Research Triangle Park, N.C.
[13] Purina Certified Rodent Chow.
[14] Bio Dynamics/nm.
[15] Whatman C_{18}.

Antihyperlipidemic Activity of *o*-Chlorobenzylsulfonamide in Rodents

IRIS H. HALL *, STEVEN D. WYRICK *x, P. JOSÉE VOORSTAD *, and AGNES DUBEY ‡

Received November 19, 1982, from the **Division of Medicinal Chemistry, School of Pharmacy, University of North Carolina, Chapel Hill, NC 27514* and ‡*Research Triangle Institute, Research Triangle Park, NC 27709.* Accepted for publication February 1, 1983.

Abstract □ *o*-Chlorobenzylsulfonamide was observed to be a potent hypolipidemic agent in rodents, reducing serum cholesterol levels 71% and triglyceride levels 49% at 60 mg/kg/d. The agent was effective both in normal and hyperlipidemic mice and was active both orally and intraperitoneally. *o*-Chlorobenzylsulfonamide significantly inhibited phosphatidate phosphohydrolase activity and marginally inhibited *sn*-glycerol-3-phosphate acyl transferase activity both *in vitro* and *in vivo*. The lowering of serum cholesterol levels appeared to be correlated with the accelerated excretion of cholesterol *via* the bile into the feces, with a marginal reduction of cholesterol absorption from the intestine. Reduced concentrations of lipids, *e.g.*, cholesterol, triglycerides, and neutral lipids, were observed in the liver, small intestine, and blood lipoprotein fractions of rats.

Keyphrases □ *o*-Chlorobenzylsulfonamide—antihyperlipidemic activity, rodents, cholesterol, triglycerides □ Antihyperlipidemic agents—potential, *o*-chlorobenzylsulfonamide, activity in rodents, cholesterol, triglycerides

Recently a series of *N*-benzoylsulfamates, *N*-benzylsulfamates, and benzylsulfonamides were shown to be potent hypolipidemic agents in mice (1). These agents were examined for hypolipidemic activity because of their structural resemblance to saccharin, which has been shown to lower serum cholesterol levels 33% and serum triglyceride levels 49% in mice (2) at a dose of 20 mg/kg/d for 16 d. *o*-Chlorobenzylsulfonamide was observed to lower serum cholesterol levels 27% and serum triglyceride levels 48% after dosing for 16 d at 20 mg/kg/d in mice (1). This series of compounds was nonmutagenic and demonstrated no acute toxicity or impaired liver or kidney functions in male mice (1). Since the saccharin moiety has been associated with potential carcinogenicity, and consequently may not be a desirable hypolipidemic agent, we decided to investigate the effects of *o*-chlorobenzylsulfonamide on lipid metabolism to assess the possibility of this compound being a more feasible therapeutic agent.

EXPERIMENTAL

Source of Compound—The sodium salt of *o*-chlorobenzylsulfonamide was prepared as described previously (1).

Antihyperlipidemic Screens in Normal Rodents—The sodium salt of *o*-chlorobenzylsulfonamide was suspended in 1% carboxymethylcellulose–water and administered to male CF_1 mice (~25 g) intraperitoneally for 15 d or male Holtzman rats (~350 g) orally by an intubation needle for 14 d. On days 9 and 14 or 15, blood was obtained by tail vein bleeding, and the serum was separated by centrifugation for 3 min. The serum cholesterol levels were determined by a modification of the Liebermann–Burchard reaction (3). Serum was also collected on day 14 or 15 and the triglyceride content was determined by a commercial kit[1].

Testing in Atherogenic Mice—Male CF_1 mice (~25 g) were placed on a commercial diet[2] which contained butterfat (400 g), cellulose[3] (60 g), cholesterol (53 g), choline dihydrogen citrate (4 g), salt mixture oil[4] (40 g), sodium cholate (20 g), sucrose (223 g), vitamin-free casein (200 g), and total vitamin supplement for 10 d. After the cholesterol and triglyceride levels were assayed and observed to be elevated, the mice were administered test drugs at 20 mg/kg/d ip for an additional 12-d period. Serum cholesterol and triglyceride levels were measured after 12 d of drug administration.

Animal Weights and Food Intake—Periodic animal weights were obtained during the experiments and expressed as a percentage of the animal's weight on day 0. After dosing for 14 d with test drugs, selected organs were excised, trimmed of fat, and weighed.

Toxicity Studies—The acute toxicity (LD_{50} value) (4) was determined in male CF_1 mice by administering test drugs intraperitoneally from 100 mg to 2 g/kg as a single dose. The number of deaths were recorded over a 7-d period for each group.

Enzymatic Studies—*In vitro* enzymatic studies were determined using 10% homogenates of male CF_1 mouse liver with 2.5–10 μmol of the test drugs. *In vivo* enzymatic studies were determined using 10% homogenates of liver from male CF_1 mice obtained after administering the agents for 15 d at a dose ranging from 10–60 mg/kg/d ip. The liver homogenates for both *in vitro* and *in vivo* studies were prepared in 0.25 mM EDTA [(ethylenedinitrilo)tetraacetic acid].

Acetyl-CoA synthetase (5) and adenosine triphosphate-dependent citrate lyase (6) activities were determined spectrophotometrically at 540 nm as the hydroxamate of acetyl CoA formed after 30 min at 37°C. Mitochondrial citrate exchange was determined by the procedure of Robinson *et al.* (7, 8) using sodium [^{14}C]bicarbonate (41 mCi/mmol) incorporated into mitochondrial [^{14}C]citrate after isolating rat mitochondria (9000×*g* for 10 min) from the homogenates. The exchange of the [^{14}C]citrate was determined after incubating the mitochondrial fraction, which was loaded with labeled citrate and test drugs, for 10 min. Radioactivity was measured in the mitochondrial and supernatant fractions in scintillation fluid[5] and expressed as a percentage. Cholesterol side-chain oxidation was determined by the method of Kritchevsky and Tepper (9) using [26-^{14}C]cholesterol (50 mCi/mmol) and mitochondria isolated from rat liver homogenates. After an 18-h incubation at 37°C with the test drugs, the generated $^{14}CO_2$ was trapped in the center well in {2-[2-(*p*-1,1,3,3-tetramethylbutylcresoxy)ethoxy]ethyl}dimethylbenzylammonium hydroxide[6] and counted[5]. 3-Hydroxy-3-methylglutaryl CoA reductase (HMG-CoA reductase) was measured using [1-^{14}C]acetate (56 mCi/mmol) and a postmitochondrial supernatant (9000×*g* for 20 min) incubated for 60 min at 37°C (10). The digitonide derivative of cholesterol was isolated and counted (11). Acetyl-CoA carboxylase activity was measured by the method of Greenspan and Lowenstein (12). Initially, the subunits of the enzyme had to be polymerized for 30 min at 37°C, and then the assay mixture containing sodium [^{14}C]bicarbonate (41.0 mCi/mmol) was added and incubated for 30 min at 37°C with test drugs. Fatty acid synthetase activity was determined by the method of Brady *et al.* (13) using [2-^{14}C]malonyl CoA (37.5 mCi/mmol), which was incorporated into newly synthesized fatty acids that were extracted with ether and counted[5]. *sn*-Glycerol-3-phosphate acyl transferase activity was determined with glycerol-3-phosphate [2-^{3}H] (7.1 Ci/mmol) and the microsomal fraction of the liver homogenates (14). The reaction was terminated after 10 min, and the lipids were extracted with chloroform–methanol (1:2) containing 1% concentrated HCl and counted. Phosphatidate phosphohydrolase activity was measured as the inorganic phosphate released after 30 min from phosphatidic acid by the method of Mavis *et al.* (15). The released inorganic phosphate after development with ascorbic acid and ammonium molybdate was determined at 820 nm.

Liver, Small Intestine and Fecal Lipid Extraction—In male CF_1 mice that had been administered test drugs for 15 d, the liver, small intestine, and fecal materials (24-h collection) were removed and a 10%

[1] Hycel Triglyceride Test Kit; Fisher Scientific Co.
[2] Basal Atherogenic Test Diet; U.S. Biochemical Corp.
[3] Celufil.
[4] Wesson.

[5] Fisher Scintiverse in a Packard Scintillation Counter.
[6] Hyamine Hydroxide; New England Nuclear.

0022-3549/84/0300-0378$01.00/0
© 1984, American Pharmaceutical Association

Table I—Effects of *o*-Chlorobenzylsulfonamide on Serum Cholesterol and Triglycerides in Mice and Rats [a]

Compound	Mouse [b]			Rat [c]		
	Serum Cholesterol		Serum Triglyceride	Serum Cholesterol		Serum Triglyceride
	Day 9	Day 15	Day 15	Day 9	Day 14	Day 14
Control (1% Carboxymethylcellulose)	100 ± 5[d]	100 ± 6[e]	100 ± 6[f]	100 ± 9[g]	100 ± 7[h]	100 ± 8[i]
o-Chlorobenzylsulfonamide						
10 mg/kg	77 ± 4[j]	70 ± 2[j]	89 ± 6	—	—	—
20 mg/kg	90 ± 3[k]	70 ± 6[j]	48 ± 3[j]	84 ± 7	71 ± 6[j]	51 ± 6[j]
40 mg/kg	86 ± 4[j]	62 ± 3[j]	45 ± 4[j]	—	—	—
60 mg/kg	70 ± 3[j]	56 ± 5[j]	29 ± 2	—	—	—

[a] Expressed as percentage of control (mean ± *SD*). [b] Administered intraperitoneally as a suspension of the sodium salt in 1% carboxymethylcellulose. [c] Administered orally as a suspension of the sodium salt in 1% carboxymethylcellulose. [d] 125 mg%. [e] 122 mg%. [f] 137 mg/dL. [g] 75 mg%. [h] 78 mg%. [i] 110 mg/dL. [j] $p \leq 0.001$. [k] $p \leq 0.005$.

Table II—*In Vitro* Enzymatic Inhibition by *o*-Chlorobenzylsulfonamide of Liver Lipid-Synthesized Enzymes [a]

	Inhibition % of Control			
	Control	50 μM	100 μM	200 μM
Mitochondrial citrate exchange	100 ± 10[b]	88 ± 3	88 ± 5	87 ± 3
Citrate lyase	100 ± 9[c]	100 ± 8	100 ± 7	100 ± 4
Acetyl-CoA synthetase	100 ± 8[d]	100 ± 9	100 ± 8	100 ± 6
HMG-CoA reductase	100 ± 7[e]	80 ± 7	80 ± 6[k]	100 ± 8
Cholesterol side-chain oxidation	100 ± 8[f]	—	58 ± 5[k]	—
Acetyl-CoA carboxylase	100 ± 6[g]	70 ± 6[k]	86 ± 5	103 ± 7
Fatty acid synthetase	100 ± 7[h]	76 ± 5[k]	80 ± 6[k]	70 ± 7[k]
Phosphatidate phosphohydrolase	100 ± 7[i]	22 ± 3[k]	22 ± 5[k]	24 ± 4[k]
Acyl transferase	100 ± 8[j]	78 ± 6[k]	73 ± 7[k]	61 ± 5[k]

[a] Mean ± *SD*; the compound was administered as a suspension of the sodium salt in 1% carboxymethylcellulose. [b] 30.8 ± 3.1 mg% exchange in mitochondrial citrate. [c] 30.5 ± 2.74 mg if citrate hydrolyzed/g of wet tissue/30 min. [d] 28.5 ± 3.14 mg of acetyl CoA formed/g of wet tissue/30 min. [e] 384,900 ± 26,943 dpm of cholesterol formed/g of wet tissue/60 min. [f] 6980 ± 558 dpm of CO_2 formed/g of wet tissue/18 h. [g] 32,010 ± 1921 dpm/g of wet tissue/30 min. [h] 37,656 ± 2635 dpm/g of wet tissue/30 min. [i] 16.70 ± 1.16 μg Pi/g of wet tissue/15 min. [j] 537,800 ± 43,024 dpm of triglyceride formed/g of wet tissue/10 min. [k] $p \leq 0.001$.

homogenate in 0.25 M sucrose plus 0.001 M EDTA was prepared. A 2-mL aliquot of the homogenate was extracted by the methods of Folch *et al.* (16) and Bligh and Dyer (17) and the milligrams of lipid were determined. The lipid was taken up in methylene chloride and the cholesterol level (3), triglyceride levels[7], neutral lipid content (18), and phospholipid content (19) were determined.

[^{3}H]Cholesterol Distribution in Rats—Male Holtzman rats (~350 g) were administered test agents orally for 14 d. On day 13, 10 μCi of [^{3}H]cholesterol was administered intraperitoneally to mice and orally to rats, and feces were collected after 24 h. Twenty-four hours after cholesterol administration, the major organs were excised and samples of blood, chyme, and urine were obtained. Homogenates (10%) of the tissues were prepared, combusted[8], and counted[5]. Some tissue samples were plated on filter paper[9], dried, and digested for 24 h in base[6] at 40°C and counted[5]. Results were expressed as dpm per total organ.

Cholesterol Absorption Study—Male Holtzman rats (~400 g) were administered test drug intraperitoneally for 14 d at 20 mg/kg/d. On day 13, 10 μCi of [1,2-^{3}H]cholesterol (40.7 Ci/mmol) was administered to the rat orally. Twenty-four hours later, blood was collected and the serum separated by centrifugation (20). Both the serum and the precipitate were counted[5].

Bile Cannulation Study—Male Holtzman rats (~400 g) were treated with test drugs at 20 mg/kg/d orally for 14 d. The rats were anesthetized with chlorpromazine[10] at 25 mg/kg followed after 30 min by pentobarbital[11] (22 mg/kg ip). The duodenum of the small intestine was isolated and ligatures were placed around the pyloric sphincter and distally to a site approximately one-third of the way down the duodenum. Sterile isotonic saline was injected into the sectioned off duodenal segment. The saline expanded the duodenum and the common bile duct. Once the bile duct was identified, a loose ligature was placed around it, an incision was made, and plastic tubing[12] was introduced into the duct. Once past the ligature, the tubing was tied in place, and the ligatures around the duodenum were removed. Once bile was freely moving down the cannulated tube, [1,2-^{3}H]cholesterol (40.7 mCi/mmol) was injected subcutaneously into the rats. The bile was collected over the next 6 h and measured (in milliliters). Aliquots were counted[5] as well as analyzed for cholesterol content (3).

[7] Bio-Dynamics/bmc Triglyceride Kit.
[8] Packard Tissue Oxidizer.
[9] Whatman No. 1.
[10] Thorazine, chlorpromazine hydrochloride; Smith, Kline & French Laboratories.
[11] Nembutal, sodium pentobarbital; Abbott Laboratories.
[12] PE-10 Intramedic polyethylene tubing.

Plasma Lipoprotein Fractions—Male Holtzman rats (~400 g) were administered test drugs at 20 mg/kg/d for 14 d. On day 14, blood was collected from the abdominal aorta. Serum was separated from whole blood by centrifugation at 3500 rpm. Aliquots (3 mL) were separated by density gradient ultracentrifugation into the chylomicrons, very low-density lipoproteins, high-density lipoproteins, and low-density lipoproteins according to the methods of Hatch and Lees (21) and Havel *et al.* (22). Each of the fractions was analyzed for cholesterol (3), triglyceride[7], neutral lipids (18), phospholipids (19), and protein levels (23).

RESULTS

Data in the tables are expressed as the mean percent of control ± the standard deviation. The probable significant level (p) between each test group and the control group was determined by the Student's t test.

o-Chlorobenzylsulfonamide was found to effectively lower serum cholesterol and triglyceride levels in rats and mice (Table I). In mice, the agent lowered serum cholesterol levels after intraperitoneal administration in a dose-dependent manner with 60 mg/kg/d affording 44% reduction, the maximum effect observed. Serum triglyceride levels were also reduced in a dose-dependent manner, with 60 mg/kg/d resulting in 71% reduction on day 15. After 14 d of oral administration at 20 mg/kg/d to rats, *o*-chlorobenzylsulfonamide reduced serum cholesterol levels 29% and serum triglyceride levels 49%, comparable to the same reductions observed in mice at 20 mg/kg/d. Subsequent to inducing a hyperlipidemic state in mice, in which case serum cholesterol levels were elevated 183% (354 mg%) above normal control values (125 mg%), the agent reduced serum cholesterol levels to 76% (220 mg%) above normal serum cholesterol levels. Serum triglyceride levels were elevated 168% (367 mg/dL) above the control value (137 mg/dL) by the high lipid diet; however, drug administration reduced the serum triglyceride levels to 40% (192 mg/dL) above control triglyceride values. Whereas the agent did not lower serum lipids absolutely to the normal value in male CF_1 mice, a significant reversal of the induced hyperlipidemic state was observed by drug administration for 12 d. The LD_{50} value for the agent was 400 mg/kg.

In vitro mouse liver enzymatic studies (Table II), with *o*-chlorobenzylsulfonamide at 50–200 μM final concentration, showed that citrate lyase and acetyl CoA synthetase activities were not inhibited by the agent. Mitochondrial citrate exchange and HMG-CoA reductase activity were marginally inhibited by the agent (0–20%). Acetyl-CoA carboxylase activity was reduced 30% at 50 μM, and fatty acid synthetase was inhibited 20–30%. *sn*-Glycerol-3-phosphate acyl transferase activity was reduced in a dose-dependent manner, with 200 μM affording 39% inhibition. Phosphatidate phosphohydrolase activity was markedly inhibited

Table III—Effects of *o*-Chlorobenzylsulfonamide on *In Vivo* CF_1 Mouse Liver Enzyme Activities Involved in Lipid Synthesis After 15 d of Intraperitoneal Administration [a]

Compound	Citrate Lyase	Acetyl-CoA Synthetase	HMG-CoA Reductase
Control (1% Carboxymethylcellulose)	100 ± 10	100 ± 8	100 ± 8
o-Chlorobenzylsulfonamide			
10 mg/kg	90 ± 6	84 ± 7	103 ± 3
20 mg/kg	92 ± 4	85 ± 6	101 ± 5
40 mg/kg	96 ± 4	78 ± 7[b]	101 ± 8
60 mg/kg	97 ± 7	100 ± 9	97 ± 6

	Acetyl-CoA Carboxylase	Fatty Acid Synthetase	*sn*-Glycerol-3-P Acyl Transferase	Phosphatidate Phosphohydrolase
Control (1% Carboxymethylcellulose)	100 ± 7	100 ± 8	100 ± 6	100 ± 7
o-Chlorobenzylsulfonamide				
10 mg/kg	85 ± 9	94 ± 7	78 ± 7[b]	54 ± 5[b]
20 mg/kg	87 ± 4[c]	92 ± 7	73 ± 4[b]	32 ± 4[b]
40 mg/kg	93 ± 3	77 ± 6[b]	77 ± 5[b]	28 ± 2[b]
60 mg/kg	93 ± 5	87 ± 8	90 ± 6	28 ± 3[b]

[a] Expressed as percentage of control (mean ± *SD*). The compound was administered as a suspension of the sodium salt in 1% carboxymethylcellulose. [b] $p \leq 0.001$. [c] $p \leq 0.005$.

Table IV—Effects of *o*-Chlorobenzylsulfonamide on Lipid Distribution of Rat Organs After 14 d of Administration at 20 mg/kg [a]

	Amount of Lipid, mg	Cholesterol	Neutral Lipids	Triglycerides	Phospholipids	Protein
Liver						
Control	100 ± 6	100 ± 7[b]	100 ± 4[c]	100 ± 5[d]	100 ± 8[e]	100 ± 8[f]
Treated	87 + 3	73 ± 4*	55 ± 5*	64 ± 4*	84 ± 4**	102 ± 6
Small Intestine						
Control	100 ± 5	100 ± 7[g]	100 ± 5[h]	100 ± 6[i]	100 ± 8[j]	100 ± 5[k]
Treated	31 ± 4*	40 ± 3*	41 ± 6*	20 ± 3*	101 ± 7	84 ± 6
Feces						
Control	100 ± 8	100 ± 8[l]	100 ± 6[m]	100 ± 7[n]	100 ± 5[o]	100 ± 7[p]
Treated	70 ± 6	116 ± 9	77 ± 5*	89 ± 5	165 ± 9*	96 ± 6
Blood Lipoproteins						
Chylomicrons						
Control		100 ± 9[q]	100 ± 8[r]	100 ± 6[s]	100 ± 10[t]	100 ± 7[u]
Treated		71 ± 6*	48 ± 4*	55 ± 6*	102 ± 6	101 ± 6
Very low-density lipoprotein						
Control		100 ± 8[v]	100 ± 9[w]	100 ± 7[x]	100 ± 8[y]	100 ± 8[z]
Treated		100 ± 9	49 ± 5*	37 ± 3*	122 ± 3*	87 ± 8
Low-density lipoprotein						
Control		100 ± 9[aa]	100 ± 7[bb]	100 ± 8[cc]	100 ± 7[dd]	100 ± 8[ee]
Treated		85 ± 7	46 ± 6*	86 ± 4	189 ± 11*	100 ± 6
High-density lipoprotein						
Control		100 ± 8[ff]	100 ± 9[gg]	100 ± 4[hh]	100 ± 6[ii]	100 ± 8[jj]
Treated		73 ± 5*	43 ± 2*	52 ± 5*	126 ± 7*	100 ± 6
Rat Bile						
Control		100 ± 7[kk]	100 ± 4[ll]	100 ± 6[mm]	100 ± 4[nn]	100 ± 8[oo]
Treated		129 ± 5*	108 ± 3**	126 ± 7*	122 ± 8*	166 ± 12*

[a] Expressed as percentage of control (mean ± *SD*); asterisks indicate statistical significance at $p \leq 0.001$ double asterisks at $p \leq 0.010$. The compound was administered as a suspension of the sodium salt in 1% carboxymethylcellulose. [b] 24.03 mg/g. [c] 44.11 mg/g. [d] 6.37 mg/g. [e] 7.19 mg/g. [f] 4.5 mg/g. [g] 7.82 mg/g. [h] 6.98 mg/g. [i] 1.12 mg/g. [j] 2.06 mg/g. [k] 42 mg/g. [l] 28.47 mg/g. [m] 33.94 mg/g. [n] 1.86 mg/g. [o] 1.39 mg/g. [p] 6.99 mg/g. [q] 337 mg/mL. [r] 67 mg/mL. [s] 420 mg/mL. [t] 149 mg/mL. [u] 3 mg/mL. [v] 190 mg/mL. [w] 98 mg/mL. [x] 22 mg/mL. [y] 26 mg/mL. [z] 50 mg/mL. [aa] 210 mg/mL. [bb] 10 mg/mL. [cc] 45 mg/mL. [dd] 41 mg/mL. [ee] 0.681 mg/mL. [ff] 544 mg/mL. [gg] 620 mg/mL. [hh] 27 mg/mL. [ii] 153 mg/mL. [jj] 5.677 mg/mL. [kk] 118 mg%. [ll] 5 mg/dL. [mm] 170 mg/mL. [nn] 1.75 mg/mL. [oo] 1.29 mg/ml.

(76–78%) by *o*-chlorobenzylsulfonamide from 50–200 μM. Cholesterol side-chain oxidation was reduced 52% at 100 μM.

In vivo enzymatic studies (Table III) in mice showed similar patterns of inhibition by *o*-chlorobenzylsulfonamide. Citrate lyase, HMG CoA reductase, and acetyl CoA carboxylase activities were essentially unaffected by drug administration. Acetyl-CoA synthetase and fatty acid synthetase activities were inhibited 22 and 23%, respectively, at 40 mg/kg/d after 15 d of drug administration. Acyl transferase activity was inhibited 22–27% at doses from 20–60 mg/kg/d.

Phosphatidate phosphohydrolase activity was inhibited 72% at 10 and 20 mg/kg/d, 68% at 40 mg/kg/d, and 46% at 60 mg/kg/d. The inhibition of phosphatidate phosphohydrolase activity was of a magnitude to account for the degree of reduction of serum triglyceride levels observed after *o*-chlorobenzylsulfonamide treatment. However, the enzymes involved in cholesterol synthesis were essentially unaffected by the agent. Thus, it seemed important to examine the effect of the agent on cholesterol distribution and excretion (Tables IV and V).

o-Chlorobenzylsulfonamide markedly accelerates the movement of cholesterol through the normal excretion routes, *i.e.*, high values of [^{3}H]cholesterol content were observed in fecal and urine collections. Both kidney and urine showed increases (16% and 40%, respectively) of [^{3}H]-cholesterol content after drug administration. The small intestine (115%), large intestine (71%), chyme (77%), and feces (185%) all demonstrated increases of [^{3}H]cholesterol content in the respective organs above that of the control. Studies of the actual lipid content of the liver and small intestine of the rats showed a decrease in cholesterol, triglycerides, and neutral lipid levels compared with the control. The reduction of small intestine lipids was greater than that observed in liver. Feces showed an increase in cholesterol and phospholipid levels, but a reduction in triglyceride and neutral lipid levels. The bile cholesterol, triglyceride, and phospholipid levels were increased, with neutral lipid levels being affected the least. Marginal inhibition (20%) by the agent of cholesterol absorption from the intestine after oral administration of [^{3}H]cholesterol was observed.

The lipoprotein fractions were also examined for cholesterol content, which was lower in the chylomicron, low-density, and high-density fractions. All four fractions were reduced in triglyceride and neutral lipid content; however, phospholipid content was elevated in all four fractions after drug administration. Protein content of the lipoprotein fractions was not altered by drug administration.

Table V—Rat Organ Weights and Radioactivity Distribution of 10 μCi of [^{3}H]Cholesterol After 14 d of Dosing with *o*-Chlorobenzylsulfonamide at 20 mg/kg/d[a]

	Organ Weight		dpm/Total Organ	
	Control	Treated	Control	Treated
Liver	14.466	12.667	47429	46375
Brain	1.966	1.966	5877	5292
Spleen	0.667	0.767	2315	6339
Lung	2.600	1.700	7069	7073
Kidney	3.367	3.134	8170	9482
Heart	1.334	1.200	4004	4338
Stomach	2.967	2.433	11375	7077
Small intestine	10.167	6.333	41656	89703
Large intestine	4.100	3.566	14104	24116
Chyme	2.567	7.583	9226	16309
Feces	2.634	5.033	8349	23779
			dpm/mL	
Urine			281	393
Bile			1016	1257
Serum			648	523

[a] Administered as a suspension of the sodium salt in 1% carboxymethylcellulose.

DISCUSSION

o-Chlorobenzylsulfonamide appears to be active in a safe therapeutic range. Whereas it was more effective in lowering serum triglycerides, significant effects were also observed for serum cholesterol. The agent was active orally and intraperitoneally in both normal and hyperlipidemic mice and was shown to be a more potent hypolipidemic agent than clofibrate. Clofibrate at 150–200 mg/kg lowers rat cholesterol levels 15% maximally and serum triglyceride levels 25% (24). *o*-Chlorobenzylsulfonamide did not suppress *de novo* cholesterol synthesis in a manner similar to clofibrate at HMG CoA reductase, the regulatory site. However, like clofibrate, *o*-chlorobenzylsulfonamide did accelerate cholesterol excretion *via* the bile and feces. The lipids removed from the blood compartment were not deposited in the major organs. This can be observed from three different types of studies: (*a*) there was no increase in organ weight, (*b*) lipid content of the organs examined was reduced, and (*c*) the [^{3}H]cholesterol distribution studies showed lower content in the treated animals than the normal tissue.

The reduction of serum triglyceride levels can be explained by the observed reduction of phosphatidate phosphohydrolase and *sn*-glycerol-3-phosphate acyl transferase activities by *o*-chlorobenzylsulfonamide. There appears to be a positive correlation between the two events, since clofibrate (14), saccharin (2), and phthalimide (25) all reduce the activity of these two enzymes and reduce serum triglyceride levels in rodents. Both enzymes play a major regulatory role in the synthesis of triglycerides.

The effects of *o*-chlorobenzylsulfonamide on the lipid content of lipoprotein fractions were varied. Nevertheless, a marked reduction of triglyceride content of chylomicrons and very low-density lipoproteins (*i.e.*, the lipoproteins which have the highest triglyceride content), as well as minor reduction of low- and high-density lipoprotein triglyceride content, were observed after drug treatment. Cholesterol content was marginally reduced (29–15%) in the chylomicron and high-density fractions. Whereas it is difficult to extrapolate observations of lipid reduction of rat lipoprotein fractions by an agent to human lipoproteins, these studies do indicate that *o*-chlorobenzylsulfonamide has the capability to modulate lipid content of lipoprotein fractions and may have the potential to affect the lipoprotein lipid levels of humans.

REFERENCES

(1) S. D. Wyrick, I. H. Hall, and A. S. Dubey, *J. Pharm. Sci.* **73,** 374 (1984).

(2) I. H. Hall, P. J. Voorstad, J. M. Chapman and G. H. Cocolas, *J. Pharm. Sci.*, **72,** 1192 (1983).

(3) A. T. Ness, J. V. Pastewka, and A. C. Peacock, *Clin. Chim. Acta*, **10,** 229 (1964).

(4) J. T. Litchfield, Jr. and F. Wilcoxon, *J. Pharmacol. Exp. Ther.*, **96,** 99 (1949).

(5) A. G. Goodridge, *J. Biol. Chem.*, **248,** 4218 (1973).

(6) M. Hoffman, L. Weiss, and O. H. Wieland, *Anal. Biochem.*, **84,** 441 (1978).

(7) B. H. Robinson, G. R. Williams, M. L. Halperin, and C. C. Leznoff, *Eur. J. Biochem.*, **15,** 263 (1970).

(8) B. H. Robinson and G. R. Williams, *Biochim. Biophys. Acta*, **216,** 63 (1970).

(9) D. Kritchevsky and S. A. Tepper, *Atherosclerosis*, **18,** 93 (1973).

(10) G. T. Haven, J. R. Krzemien, and T. T. Nguyen, *Res. Commun. Chem. Pathol. Pharmacol.*, **6,** 253 (1973).

(11) F. Wada, K. Hirata, and Y. Sakameto, *J. Biochem. (Tokyo)*, **65,** 71 (1969).

(12) M. D. Greenspan and J. M. Lowenstein, *J. Biol. Chem.*, **243,** 6273 (1968).

(13) R. O. Brady, R. M. Bradley, and E. G. Trams, *J. Biol. Chem.*, **235,** 3093 (1960).

(14) R. G. Lamb, S. D. Wyrick, and C. Piantadosi, *Atherosclerosis*, **27,** 147 (1977).

(15) R. D. Mavis, J. N. Finkelstein, and B. P. Hall, *J. Lipid Res.*, **19,** 467 (1978).

(16) J. Folch, M. Lees, and G. H. C. Stanley, *J. Biol. Chem.*, **226,** 497 (1957).

(17) E. G. Bligh and W. J. Dyer, *Can. J. Biochem. Physiol.*, **37,** 911 (1957).

(18) J. H. Bragdon, *J. Biol. Chem.*, **190,** 513 (1951).

(19) C. P. Stewart and E. B. Henday, *Biochem. J.*, **29,** 1683 (1935).

(20) A. Adam, J. van Cantfort and J. Gielen, *Lipids*, **11,** 610 (1976).

(21) F. T. Hatch and R. S. Lees, *Adv. Lipid Res.*, **6,** 33 (1968).

(22) R. J. Havel, H. A. Eder, and J. H. Bragdon, *J. Clin. Invest.*, **34,** 1395 (1955).

(23) O. H. Lowry, N. J. Rosebrough, A. L. Farr, and R. J. Randall, *J. Biol. Chem.*, **193,** 265 (1951).

(24) J. M. Thorp and W. S. Waring, *Nature (London)*, **194,** 948 (1962).

(25) I. H. Hall, P. J. Voorstad, J. M. Chapman, and G. H. Cocolas, *J. Pharm. Sci.*, **72,** 845 (1983).

Inclusion Complexation of Prostaglandin $F_{2\alpha}$ with γ-Cyclodextrin in Solution and Solid Phases

KANETO UEKAMA *x, FUMITOSHI HIRAYAMA *, AKIHIKO FUJISE *, MASAKI OTAGIRI *, KOHJI INABA ‡, and HAZIME SAITÔ §

Received October 25, 1982, from the *Faculty of Pharmaceutical Sciences, Kumamoto University, Kumamoto, 862, Japan, ‡Research Institute, Ono Pharmaceutical Co., Ltd., Osaka, 618, Japan, and §Biophysics Division, National Cancer Research Institute, Tokyo, 104, Japan. Accepted for publication January 27, 1983.

Abstract □ A solid complex of prostaglandin $F_{2\alpha}$ (dinoprost) with γ-cyclodextrin in a molar ratio of 1:1 was obtained on the basis of the B_S-type phase solubility diagram. The mode of interaction in the solid state was studied by powder X-ray diffractometry, thermal analysis, and carbon-13 cross polarization/magic angle spinning nuclear magnetic resonance (^{13}C-CP/MAS-NMR) spectrometry. The X-ray diffraction and NMR data suggested that prostaglandin $F_{2\alpha}$ is included in the cylindrical channels formed by coaxial alignment of γ-cyclodextrin molecules to give a channel type structure. Dissolution and thermal behaviors of the prostaglandin $F_{2\alpha}$–γ-cyclodextrin complex were examined and compared with the drug itself. The result indicated that the γ-cyclodextrin complex may have great utility as a rapidly dissolving form of prostaglandin $F_{2\alpha}$ with improved thermal stability.

Keyphrases □ Prostaglandin $F_{2\alpha}$—inclusion complex with γ-cyclodextrin, solution and solid phases, solubility, dissolution behavior □ γ-Cyclodextrin—inclusion complex with prostaglandin $F_{2\alpha}$, solution and solid phases, solubility, dissolution behavior □ Solubility—prostaglandin $F_{2\alpha}$–γ-cyclodextrin inclusion complex, dissolution behavior □ Dissolution—prostaglandin $F_{2\alpha}$–γ-cyclodextrin complex, solubility

Prostaglandins are essentially long-chain fatty acids containing a substituted cyclopentane ring system. The relative hydrophobic environment of the cyclodextrin cavity seems to be particularly favorable for inclusion of the highly hydrophobic prostaglandin molecules. The complexation of α- and β-cyclodextrins with some prostaglandin analogues including prostaglandin $F_{2\alpha}$ (dinoprost)[1] have been reported (1–3). Frank and Cho have recently reported the complexing behavior of dinoprostone (prostaglandin E_2) with β-cyclodextrin in water (4). Unfortunately, an attempt to isolate the solid complex from α- or β-cyclodextrin solution was unsuccessful because the prostaglandin molecule is too bulky to be completely included into the cavities of α- and β-cyclodextrins.

Continuing these investigations, we now report an inclusion complexation of prostaglandin $F_{2\alpha}$ with γ-cyclodextrin, which has a larger hydrophobic cavity than α- and β-cyclodextrins [internal diameters of α-, β-, and γ-cyclodextrins are 5.0, 6.2, and 7.9 Å, respectively (5)]. Solubility analysis, X-ray diffractometry, and thermal analysis were used in the present study, and in addition carbon-13 cross polarization/magic angle spinning nuclear magnetic resonance (^{13}C-CP/MAS-NMR) spectrometry was employed to gain insight into the mode of interaction in the solid phase. Furthermore, the dissolution and thermal behaviors of the complex were examined.

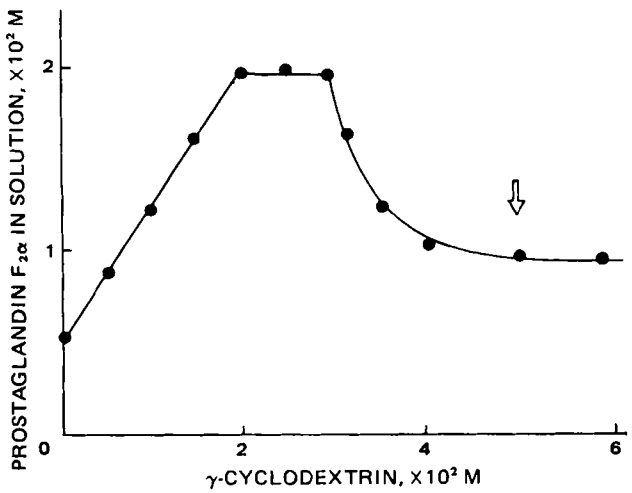

Figure 1—*Phase solubility diagram of the prostaglandin $F_{2\alpha}$–γ-cyclodextrin system in water at 25°C. The arrow shows the experimental condition of the preparation of the solid complex (see text).*

EXPERIMENTAL

Materials—Prostaglandin $F_{2\alpha}$[2] and γ-cyclodextrin[3] were used as supplied. All other materials and solvents were of analytical reagent grade. Deionized, double-distilled water was used.

Solubility Studies—Solubility measurements were carried out according to Higuchi and Lach (6). Excess amounts of prostaglandin $F_{2\alpha}$ were added to aqueous solutions containing various concentrations of γ-cyclodextrin and were shaken at 25 ± 0.5°C. After equilibration was attained (~2 d), an aliquot was centrifuged and pipetted through a cotton filter. A 0.5-mL aliquot of the sample solution was extracted with 5 mL of ether from acidified media, and 3 mL of the ether phase was evaporated to dryness under reduced pressure. The concentration of prostaglandin

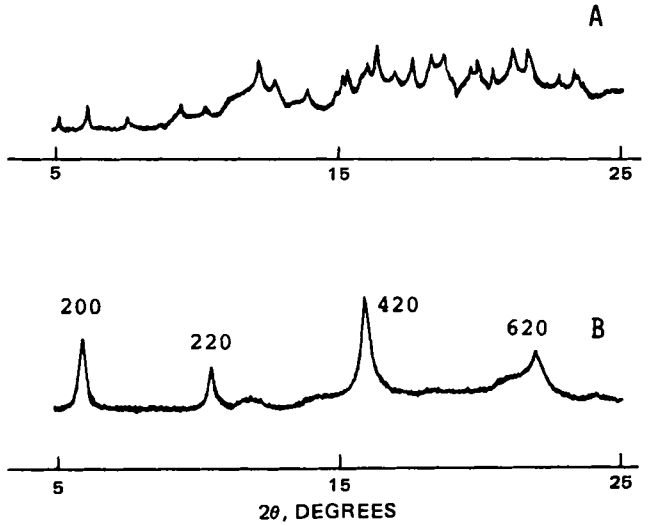

Figure 2—*Powder X-ray diffraction patterns of the prostaglandin $F_{2\alpha}$–γ-cyclodextrin system. Key: (A) γ-cyclodextrin; (B) prostaglandin $F_{2\alpha}$–γ-cyclodextrin complex. The reflection peaks of the complex were indexed according to Ref. 9.*

[1] (5Z,9α,11α,13E,15S)-9,11,15-Trihydroxyprosta-5,13-dien-1-oic acid.

[2] Ono Pharmaceutical Co. Ltd., Osaka, Japan.

[3] Nippon Shokuhin Kako, Tokyo, Japan.

0022-3549/84/0300-0382$01.00/0
© 1984, American Pharmaceutical Association

Table I—Diffraction Data for Prostaglandin $F_{2\alpha}$–γ-Cyclodextrin Complex

hkl[a]	d, Å Observed	d, Å Calculated
200	14.68	14.68
220	8.47	8.48
420	5.54	5.55
620	4.07	4.07

[a] Hexagonal indices.

$F_{2\alpha}$ was determined by GC according to the method of Roseman and Yalkowsky (7). The chromatographic conditions were the same as those reported previously (1). The apparent 1:1 stability constant (K') was calculated from the slope and intercept of the initial straight-line portion of the phase solubility diagram according to the following (8):

$$K' = \frac{\text{slope}}{\text{intercept}\,(1 - \text{slope})}$$

Preparation of the Solid Complex—The solid complex was derived by mixing appropriate amounts of prostaglandin $F_{2\alpha}$ and γ-cyclodextrin in water. The amounts were calculated from the descending curvature of the phase solubility diagram. For example, 100 mg of prostaglandin $F_{2\alpha}$ and 650 mg of γ-cyclodextrin were added to 10 mL of water, sealed in a flask, and stirred at 25°C for 2 d. The complex, which precipitated as a microcrystalline powder, was filtered and dried under vacuum at room temperature for 2 d. This powder corresponded to a complex of prostaglandin $F_{2\alpha}$–γ-cyclodextrin, in a molar ratio of 1:1 which had a molecular weight of 1652 (±5%).

X-Ray Diffractometry—The powder X-ray diffractometer[4] was operated under the following conditions: X-ray, Ni-filtered Cu-K_α radiation; voltage, 30 kV; current, 20 mA; time constant, 2 s; scanning speed, 1°/min.

Differential Thermal Analysis (DTA)—The thermometer[5] was operated at a scanning rate of 10°C/min over the temperature range of 10–350°C. The sample weight was 2–10 mg.

^{13}C-NMR Spectrometry—Single-contact ^{13}C-CP/MAS measurements[6] were obtained at 75.46 MHz with a spectrometer equipped with a CP/MAS accessory. The sample (~300 mg) was placed in a Andrew–Beams-type rotor machined from perdeuterated poly(methyl methacrylate) and spun as fast as 3–4 kHz. The contact time was chosen as 1 ms (not optimized, but chosen to avoid buildup of strong signals from residual signals from the rotor and probe assembly), and repetition time was 2 s. The spectral width and data points were 30 kHz and 4K, respectively. Carbon-13 chemical shifts were calibrated indirectly through external benzene (128.5 ppm from tetramethylsilane).

Dissolution Studies—The dissolution behaviors of prostaglandin $F_{2\alpha}$ and its γ-cyclodextrin complex in water were compared at the same concentration of prostaglandin $F_{2\alpha}$ according to the dispersed-amount method (9). An 850-mg sample of the complex as a 100-mesh powder was weighed and put in a dissolution cell. Because prostaglandin $F_{2\alpha}$ is easy to melt at room temperature (the melting temperature is ~30°C), an ether solution containing 182 mg of the drug was placed in the dissolution cell and evaporated to dryness. The dissolution medium (25 mL) was maintained at 25°C and stirred at 91 rpm. At an appropriate interval, 0.5 mL of solution was sampled by a pipet with a cotton filter. The assay procedure for prostaglandin $F_{2\alpha}$ was the same as that used in the solubility studies.

RESULTS AND DISCUSSION

Figure 1 shows the equilibrium phase solubility diagram obtained for prostaglandin $F_{2\alpha}$ with γ-cyclodextrin in water. The plot shows a typical B_S-type solubility curve (8). The initial rising portion is followed by a plateau region and then decreases in total concentration of prostaglandin $F_{2\alpha}$ with precipitation of a microcrystalline complex at high γ-cyclodextrin concentration. In sharp contrast, the phase solubility diagrams of prostaglandin $F_{2\alpha}$ with α- and β-cyclodextrins showed an A_L-type curve, and no precipitation of the complexes was observed (1). The apparent 1:1 stability constant (K') of the γ-cyclodextrin complex was calculated to be 480 M^{-1} from the initial straight-line portion of the solubility diagram in Fig. 1. The K' value of the γ-cyclodextrin complex was found to be intermediate between the α-cyclodextrin complex (254 M^{-1}) and the β-cyclodextrin complex (1240 M^{-1}) values reported previously (1). The 1:1 stoichiometry of the γ-cyclodextrin complex in the solid phase was ascertained on the basis of data in the plateau region of the solubility diagram. The result was in good agreement with that obtained by isolation and analysis of the solid complex. Thus, the 1:1 solid complex isolated from the descending curvature of the B_S-type solubility diagram was used for further study.

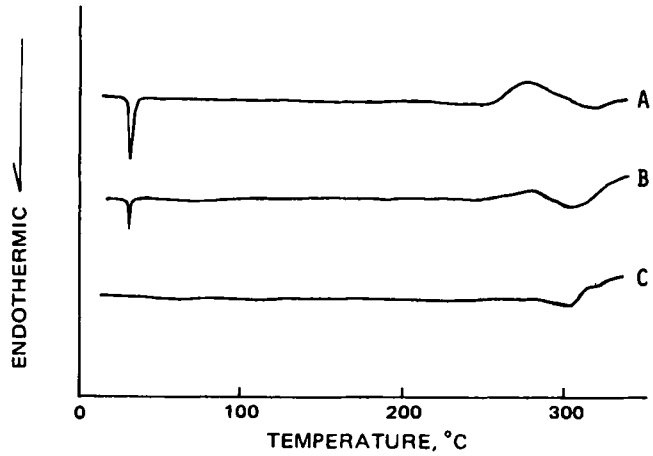

Figure 3—*DTA thermograms of prostaglandin $F_{2\alpha}$–γ-cyclodextrin system. Key: (A) prostaglandin $F_{2\alpha}$; (B) physical mixture of prostaglandin $F_{2\alpha}$ and γ-cyclodextrin in a molar ratio of 1:1; (C) prostaglandin $F_{2\alpha}$–γ-cyclodextrin complex.*

Figure 2 shows the powder X-ray diffraction pattern of the prostaglandin $F_{2\alpha}$–γ-cyclodextrin complex, comparing with that of γ-cyclodextrin itself. It was difficult to obtain the diffraction pattern of prostaglandin $F_{2\alpha}$ under these experimental conditions because of the low melting temperature. The diffraction pattern of the complex was apparently different from that of γ-cyclodextrin, indicating the constitution of a new solid phase. It was noted that the diffraction diagram of the complex in Fig. 2 showed a hexagonal nature of pattern similar to that observed for the *n*-propyl alcohol–γ-cyclodextrin complex (10). The *n*-propyl alcohol–γ-cyclodextrin complex is known to have a channel structure (10, 11) with a hexagonal close packing of the cylinders of γ-cyclodextrin molecules. Therefore, the diffraction pattern of the complex was indexed on the basis of a two-dimensional hexagonal unit cell having $a = b = 33.90$ Å, where *d*-spacing for the 200 reflection peak on the diagram was used to calculate the unit cell dimensions (10). As shown in Table I, the calculated *d*-spacing was in excellent agreement with that observed. This suggests that prostaglandin $F_{2\alpha}$ is included

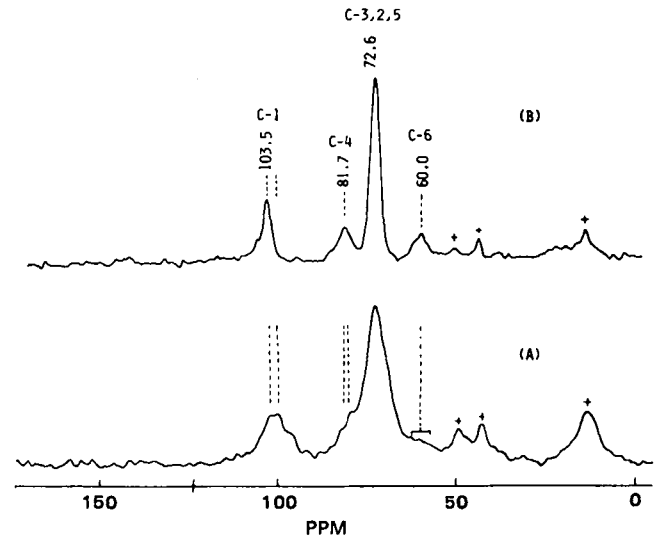

Figure 4—*^{13}C-CP/MAS-NMR spectra of prostaglandin $F_{2\alpha}$–γ-cyclodextrin system in solid state. Key: (A) γ-cyclodextrin; (B) prostaglandin $F_{2\alpha}$–γ-cyclodextrin complex.*

[4] Geiger Flex-2012 diffractometer; Rigaku Denki, Tokyo, Japan.
[5] Model DT-20B thermal analyzer; Shimadzu, Kyoto, Japan.
[6] CXP-300 spectrometer; Bruker, Silber-Streifen, West Germany.

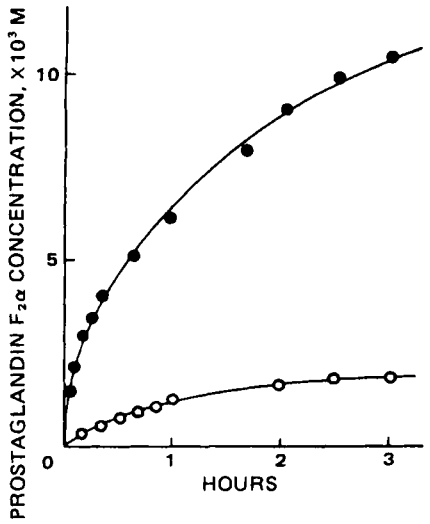

Figure 5—*Dissolution profiles of prostaglandin $F_{2\alpha}$ and its γ-cyclodextrin complex in water at 25°C. Key: (○) prostaglandin $F_{2\alpha}$; (●) prostaglandin $F_{2\alpha}$–γ-cyclodextrin complex.*

within the cylindrical channels formed by coaxial alignment of γ-cyclodextrin molecules to give a channel type structure.

Figure 3 shows DTA thermograms of the prostaglandin $F_{2\alpha}$–γ-cyclodextrin system. In the cases of prostaglandin $F_{2\alpha}$ and its physical mixture with γ-cyclodextrin (1:1 molar ratio), an endothermic peak due to the melting was observed around 30°C. In sharp contrast, the complex showed no appreciable endothermic peak within the degradation temperature of γ-cyclodextrin (~290°C) (12), suggesting that the complexed form of prostaglandin $F_{2\alpha}$ is considerably stable compared with the drug itself.

^{13}C-CP/MAS-NMR techniques were employed to gain further insight into the mode of interaction between prostaglandin $F_{2\alpha}$ and γ-cyclodextrin in the solid state. Figure 4 shows the ^{13}C-CP/MAS-NMR spectra of γ-cyclodextrin and its inclusion complex with prostaglandin $F_{2\alpha}$. The signals are readily assigned to the individual carbons of the glucose residues, as indicated in Fig. 4 [signals marked by the + are ascribed to the residual signals from the rotor of magic angle spinning machined from perdeuterated poly(methyl methacrylate)]. In the case of the complex, no appreciable signal from the guest molecule was observed under the experimental conditions used. Carbon-13 signals from guest molecules are known to be, in many instances, lost or obscured because the amount of the guest molecules is usually low compared with that of the glucose residues; also, buildup of the ^{13}C-magnetization might be strongly influenced by plausible molecular motions within the cavity (13, 14). Nevertheless, it is clearly seen that the complex formation resulted in the substantial reduction of the line widths of the glucose residues, especially in the C-1, C-4, and C-6 region, as well as the significant displacement of these signals. The distinct spectral change on complex formation might arise from a macrocyclic conformational change associated with the inclusion of the guest molecule.

In this connection, it is emphasized that the C-1 and C-X carbon-13 shifts at the glycosidic linkages for a number of polysaccharides (15, 16) are substantially displaced depending on their conformations. In particular, such displacements of the C-1 and C-4 shifts of α-D-(1,4)-linked glucans are well related to the dihedral angles ϕ and ψ for the C(1)—O_{gly} and O_{gly}—C(4) rotations (13, 14), respectively, which characterize the conformation of the individual glucose residues, as manifested from the previous ^{13}C-CP/MAS-NMR studies on polymorphs of amylose and various types of cyclodextrin complexes (13, 14). Therefore, broad carbon-13 signals in the γ-cyclodextrin are explained in terms of superposition of slightly displaced signals from glucose residues whose dihedral angles are distributed to some extent because of distorted macrocyclic conformation (15). It should be also noted that the ^{13}C-chemical shift changes of this complex are identical to those of γ-cyclodextrin–*n*-propyl alcohol complex within the experimental error (±1 ppm) (13, 14). Obviously, this finding is consistent with the X-ray diffraction study described above and also with the work by Lindner and Saenger (11).

The dissolution behavior of the γ-cyclodextrin complex was examined in anticipation of improved dissolution characteristics of prostaglandin $F_{2\alpha}$. It would be interesting to compare the effect of complexation on the dissolution rate for the three cyclodextrins, but an attempt to isolate the solid complexes of prostaglandin $F_{2\alpha}$ with α- and β-cyclodextrins was unsuccessful.

Figure 5 shows the dissolution profiles of prostaglandin $F_{2\alpha}$ and its γ-cyclodextrin complex in water. It was found that the complex dissolved much more rapidly (>10-fold) than prostaglandin $F_{2\alpha}$ itself. The observed increase in the rate may be due to the increase in solubility, as expected from Fig. 1, although other factors such as diffusion coefficient, wettability, and the dissociation of the complex in the dissolution medium (17) should be considered in the rate enhancement.

Thus, the increased dissolution rate suggests that prostaglandin $F_{2\alpha}$–γ-cyclodextrin complex may have great utility in the development of fast-dissolving dosage forms with improved bioavailability. Furthermore, the increased melting temperature and/or thermal stability of prostaglandin $F_{2\alpha}$ by γ-cyclodextrin complexation may facilitate the ease of handling the pharmaceutical preparations.

REFERENCES

(1) K. Uekama and F. Hirayama, *Chem. Pharm. Bull.*, **26**, 1195 (1978).

(2) K. Uekama, F. Hirayama, and T. Irie, *Chem. Lett.*, **1978**, 661.

(3) F. Hirayama, K. Uekama, and H. Koinuma, *Chem. Pharm. Bull.*, **28**, 1975 (1980).

(4) S. G. Frank and M. J. Cho, *J. Pharm. Sci.*, **67**, 1665 (1978).

(5) W. Saenger, *Angew. Chem. Int. Ed. Engl.*, **19**, 344 (1980).

(6) T. Higuchi and J. L. Lach, *J. Am. Pharm. Assoc., Sci. Ed.*, **43**, 349 (1954).

(7) T. J. Roseman and S. H. Yalkowsky, *J. Pharm. Sci.*, **62**, 1680 (1973).

(8) T. Higuchi and K. A. Connors, *Adv. Anal. Chem. Inst.*, **4**, 117 (1965).

(9) H. Nogami, T. Nagai, and Y. Yotsuyanagi, *Chem. Pharm. Bull.*, **17**, 499 (1969).

(10) K. Takeo and T. Kuge, *Agr. Biol. Chem.*, **34**, 568 (1970).

(11) K. Lindner and W. Saenger, *Biochem. Biophys. Res. Commun.*, **92**, 933 (1980).

(12) K. Uekama, T. Fujinaga, F. Hirayama, M. Otagiri, and Y. Yamasaki, *Int. J. Pharm.*, **10**, 1 (1982).

(13) H. Saitô, G. Izumi, T. Mamizuka, S. Suzuki, and R. Tabeta, *J. C. S. Chem. Commun.*, **1982**, 1386.

(14) H. Saitô, G. Izumi, and R. Tabeta, "Abstracts of Papers," 21st Symposium on NMR, Nagoya, 1982, p 37.

(15) H. Saitô and R. Tabeta, *Chem. Lett.*, **1981**, 713.

(16) H. Saitô, R. Tabeta, and S. Hirano, *Chem. Lett.*, **1981**, 1479.

(17) M. Donbrow and E. Touitou, *J. Pharm. Sci.*, **67**, 95 (1978).

ACKNOWLEDGMENTS

This work was supported in part by a grant from the Ministry of Education, Science and Culture, Japan.

Improved Delivery Through Biological Membranes XIV: Brain-Specific, Sustained Delivery of Testosterone Using a Redox Chemical Delivery System

NICHOLAS BODOR [x] **and HASSAN H. FARAG** *

Received July 6, 1982, from the *Department of Medicinal Chemistry, College of Pharmacy, J. Hillis Miller Health Center, Gainesville, FL 32610.* Accepted for publication February 24, 1983. *Permanent address: Faculty of Pharmacy, University of Assiut, Egypt.

Abstract □ The dihydropyridine ⇌ pyridinium salt redox delivery system was used for the specific delivery and sustained release of testosterone in the brain. Administration of the *N*-methyl-1,4-dihydro nicotinate ester of testosterone in female rats gave high and sustained brain levels of the corresponding quaternary ester, testosterone trigonellinate. This contrasted with rapid elimination from the general circulation. Release of testosterone "locked into" brain as the quaternary salt was sustained, $t_{1/2}$ = 20 h.

Keyphrases □ Testosterone—brain-specific delivery, redox chemical delivery system, rats □ Delivery systems—redox chemical, brain-specific sustained delivery of testosterone, rats □ Tissue-specific drug delivery—testosterone in brain tissues, rats, redox chemical delivery system

Our earlier studies with phenylethylamine and dopamine (1–5)[1] established the feasibility of using the biological oxidation of dihydropyridine derivatives to the corresponding quaternary salts as the basis for a potentially selective drug-delivery system. We now report further investigation of this redox delivery concept as it applies to the selective retention and subsequent release of testosterone in the brain. One objective was to extend the redox concept to a larger molecule, testosterone, representative of a biologically important class of compounds, the steroids. A second objective was to study the effects of an ester linkage on the redox properties, distribution, and site-specific delivery of the target drug testosterone. Finally, it is suggested that this type of drug delivery system would also be useful for specific and/or enhanced delivery of drugs to the testes.

BACKGROUND

The selection of testosterone as the target drug and brain as target organ was motivated by our earlier work with phenylethylamine and dopamine derivatives (1–3) and by other considerations, both theoretical and practical. The potentially practical value of selective delivery and sustained release of testosterone in the brain resides in its physiological and biochemical roles in reproductive functions. It has been suggested that testosterone controls male sexual behavior by direct action on the brain (6, 7), and evidence indicates that gonadal steroids are concentrated in brain tissue relative to plasma (8). It has been shown that brains of mammals concentrate sex-related steroids in cells that form a stable core for a hormone-concentrating neural structure (9, 10) and that androgens influence male reproductive behavior by direct action on these discrete areas of the brain known as the anterior hypothalamic–preoptic complex. There is substantial evidence (11, 12) that estradiol is formed from testosterone by aromatization in the preoptic region and that it is the principal, centrally acting steroid in the maintenance of copulatory behavior. The use of androgen to treat breast cancer cases that respond to male hormones is well known (13), but despite the reported antiestrogenic action of testosterone (14), the exact mechanism through which advanced postmenopausal breast cancer responds to testosterone is unknown. A sustained-action form of testosterone that selectively concentrates in brain tissue clearly would be of value in studying the mechanisms through which testosterone exerts its effects on sexual behavior, sexual development, and reproduction. Similarly, it would be of value in studying any possible central role of androgens in the control of breast cancer.

The existence of a blood–testis barrier (BTB) by which some substances are prevented from being carried into the seminiferous tubules long has been suspected (15–18), and some investigators have suggested a similarity between the blood–brain barrier (BBB) and the BTB (19–22). Fawcette *et al.* (23) suggested that the permeability barrier is not in the testis capillary walls because these more closely resemble the capillaries of muscle than those involved in the BBB. Dym and Fawcette (24) concluded that the epithelioid contractile layer around the seminiferous tubules constitutes a significant permeability barrier augmented by an apparently more efficient barrier involving tight cell-to-cell junctions between Sertoli cells that inhibits penetration of substances through the germinal epithelium. Despite such histological differences, pharmacokinetic studies (25, 26) have demonstrated that the functional BTB resembles the BBB in transport characteristics, both depending on lipid solubility and molecular size.

As will be apparent from subsequent considerations, concentration of testosterone in the brain tissues of female rats by biological quaternization is accomplished without significant elevation of serum testosterone levels. The low serum levels would allow one to use such a drug in prepubertal hypoganodism tests, without fear of epiphyseal closure. Similarly, if androgens exert antineoplastic and other effects through central actions, concentration in the brain without elevated peripheral circulatory levels would minimize peripheral side effects such as edema and masculinization.

Our earlier work with phenylethylamine and dopamine derivatives (1–3) led us to conclude that the 17-β(1,4-dihydrotrigonelline) ester of testosterone (I) would, by virtue of its good lipid solubility, cross both the BBB and the BTB (in male rats). As shown in Scheme I, it was also anticipated that biological oxidation to the corresponding quaternary derivative would follow, causing a "lock in" of the corresponding ionic, hydrophilic product in the brain and in the testes in male animals. Conversely, oxidation in locales not involving a permeability barrier would favor rapid clearance from blood because the quaternary derivative (II) is excreted more rapidly than the unoxidized form (I). Thus, oxidation would favor the accumulation of II in the brain while yielding minimal blood levels. A subsequent slow hydrolysis to free testosterone in the brain, therefore, would provide a site-specific, prolonged testosterone action and minimal peripheral effects. In a systematic study of some trigonelline and dihydrotrigonelline esters (III, IV), where R = C_nH_{2n-1} and n = 1–10 (5), we have demonstrated that the quaternary esters (III) hydrolyze in different biological media at rates much slower than those of the uncharged analogues. Esters IV also are very difficult to hydrolyze, and although it was expected that $K_8 \gg K_9$ and $K_5 \gg K_4$, the slow rates of quaternary hydrolysis were expected to ensure a sustained release of testosterone in both testes and brain while yielding minimal levels in blood and other tissues. Earlier studies (1, 2) also led us to expect that trigonelline released in the brain by the hydrolytic process would be excreted easily and at comparable rates (25)[1].

EXPERIMENTAL

All melting points were taken on a melting point apparatus[2] and are uncorrected. Elemental analyses were performed at Atlantic Microlabs, Inc., Atlanta, Georgia. IR spectra were determined using a double-beam recording spectrophotometer[3]. ^{1}H-NMR spectra were determined using a spectrometer[4]. All chemical shifts reported are in δ units (ppm) relative

[1] N. Bodor and M. E. Brewster; unpublished results.

[2] Mel-Temp.
[3] Beckman Acculab 1.
[4] Varian T60A or FX100.

0022-3549/84/0300-0385$01.00/0
© 1984, American Pharmaceutical Association

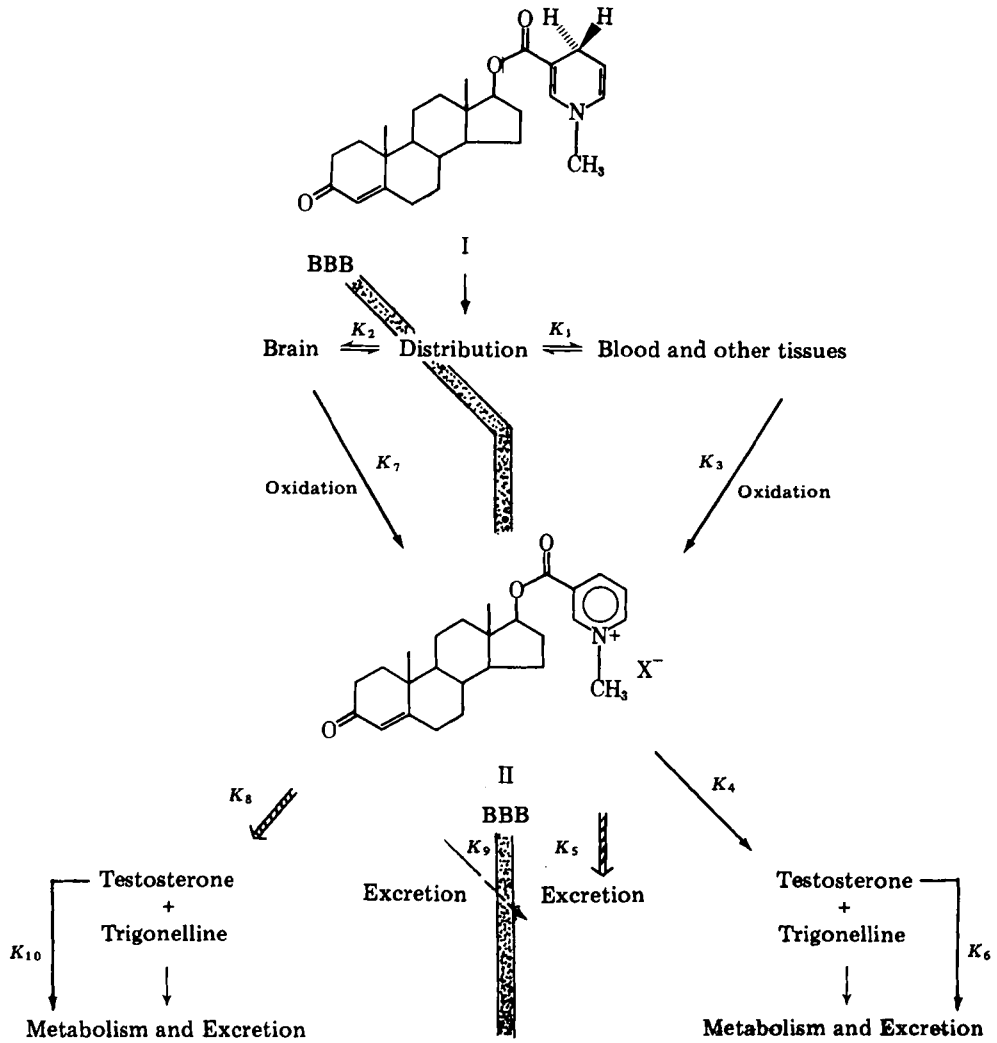

Scheme I

to tetramethylsilane. UV absorbance spectra were determined using a spectrophotometer[5]. HPLC analyses were performed on a ternary liquid chromatograph[6] with a solvent delivery system[7], injector[8], absorbance detector[9], and controller[10].

Testosterone Nicotinate (V)—Thionyl chloride (2.mL) was added to 0.7 g (5.7 mmol) of nicotinic acid[11] and the mixture was refluxed for 3 h. The excess thionyl chloride was removed under reduced pressure, and 10 mL of dry pyridine was then added to the cold residue followed by 1.44 g (5.0 mmol) of testosterone[11]. The mixture was heated with continuous stirring at 100°C for 4 h. The pyridine was removed *in vacuo*, and 5 mL of methanol was added to the oily residue. The mixture was cooled, and the solid that crystallized was filtered and recrystallized from methanol–acetone to give 1.4 g of V as white crystals (yield 71%), mp 187–188°C. This material was used without further purification.

17β-[(1-Methyl-3-pyridiniumcarbonyl) oxy] androst-4-en-3-one Iodide (II)—To a solution of 1.0 g (2.5 mmol) of the aforementioned

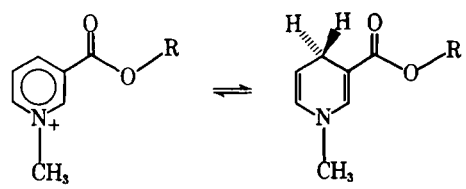

III IV

testosterone nicotinate (V) in 15 mL of acetone was added 1 mL of methyl iodide, and the mixture was heated at reflux overnight. The yellow material that separated was removed by filtration, washed with acetone, and crystallized from methanol–ether to yield 1.25 g (92%) of II as yellow crystals, mp 215–220°C (dec.). UV (CH_3OH): λ 270 nm (shoulder), ε = 4579; 240 nm (shoulder), ε = 19,375. ^{1}H-NMR ($CDCl_3$): δ 10.0–8.3 (m, 4, C_5H_5N), 5.73 (s, 1, C_4 vinyl H), 4.86 (s, 3, N—CH_3), and 2.40–1.06 ppm (m, 26, methylene H).

Anal.—Calc. for $C_{26}H_{34}INO_3$: C, 58.32; H, 6.40; N, 2.62. Found: C, 58.17; H, 6.48; N, 2.60.

17β-[(1,4-Dihydro-1-methyl-3-pyridinylcarbonyl)oxy]androst-4-en-3-one (I)—To an ice-cold solution of 1.1 g (2 mmol) of testosterone nicotinate-*N*-methyl iodide (II) in 150 mL of deaerated 10% aqueous methanol were added 0.67 g (8 mmol) of sodium bicarbonate and 1.37 g (8 mmol) of sodium dithionite. The mixture was stirred for 20 min at room temperature, and the separated pale-yellow material was removed by filtration, washed with water, and dried over P_2O_5 under vacuum to yield 0.82 g (98%) of I, mp 172–175°C. UV (CH_3OH): λ 356 nm, ε = 9511. IR (KBr): 1700 and 1660 cm^{-1} (C=O). ^{1}H-NMR (DMSO-d_6): δ 6.90 (br s, 1, C_2 dihydropyridine H), 5.83–5.70 (m, 1, C_6 dihydropyridine H), 5.56 (s, 1, C_4 vinyl H), 4.7–4.33 (m, 1, C_5 dihydropyridine H), 3.26 (br s, 2, C_4 dihydropyridine H), 2.93 (s, 3, N—CH_3), and 2.5–0.83 ppm (m, 26, methylene H with CH_3's at 1.16 and 0.83).

Anal.—Calc. for $C_{26}H_{35}NO_3$: C, 76.25; H, 8.61; N, 3.42. Found: C, 76.07; H, 8.65; N, 3.38.

Analytical Methods—An HPLC method was developed for the studies of the degradation of the quaternary (II) and dihydropyridine derivatives (I) using the system described earlier. The absorbance detector was operated at 254 nm. A 15-cm × 4.6-mm i.d., 5-μm particle size, Ultrasphere reverse-phase C_{18} column[12], operated at ambient tempera-

[5] Model 210; Cary.
[6] Model 345; Beckman.
[7] Model 112; Beckman.
[8] Model 210; Beckman.
[9] Model 160; Beckman.
[10] Model 421; Beckman.
[11] Aldrich Chemical Co., Milwaukee, Wis.
[12] Altex.

Table I—Kinetics of *In Vitro* Oxidation of the Dihydropyridine Ester I to the Quaternary Derivative II in Biological Fluids [a]

Medium	k, s^{-1}	$t_{1/2}$, min	r	Method [b]
80% Plasma	8.12×10^{-5}	142	0.959	A
20% Brain homogenate	1.72×10^{-4}	67	0.997	A
Whole blood	1.74×10^{-4}	66	0.997	A, B

[a] At 37°C, initial concentration of I = 2.4×10^{-4} M. [b] Method A: following appearance of [II]; Method B: following disappearance of [I].

ture, was used for all separations. The mobile phase used for the separation of the dihydropyridine derivative, its degradation products, and oxidation products consisted of a 0.002 M solution of 1-heptanesulfonic acid sodium salt[13] in CH_3CN–0.01 M aqueous Na_2HPO_4 (7:3). At a flow rate of 2.0 mL/min, II has a retention time of 12 min and I has a retention time of 5 min. For the analysis of testosterone in the *in vivo* brain delivery studies, the solvent consisted of a 0.002 M solution of 1-heptanesulfonic acid sodium salt in CH_3CN–0.01 M aqueous Na_2HPO_4 (1:1). At a flow rate of 2.0 mL/min, testosterone has a retention time of 3.3 min and II has a retention time of 36.5 min (very broad peak).

Chemical Oxidation Studies—*By Silver Nitrate*—One milliliter of a 5% methanolic solution of the dihydropyridine derivative (I) was added to 5 mL of saturated methanolic $AgNO_3$ solution. The mixture was shaken, left 10 min for complete oxidation, centrifuged, and the UV spectrum checked.

By Hydrogen Peroxide—To a standardized solution of H_2O_2 (0.18 M) contained in a UV cuvette equilibrated at 37°C was added a solution of dihydropyridine derivative (I) to make a concentration of $\sim 5 \times 10^{-6}$ M. The mixture was thoroughly mixed and monitored for the disappearance of the dihydropyridine maximum at 356 nm using a spectrophotometer[5] interfaced with microprocessor[14] with an enzyme kinetic software package.

By Diphenylpicrylhydrazyl Free Radical—To 2 mL of a 9.3×10^{-5} M solution of 2,2-diphenyl-1-picrylhydrazyl free radical in acetonitrile, equilibrated at 26°C, was added 20 μL of a 1.5×10^{-2} M solution of the dihydropyridine derivative in acetonitrile to make a final concentration of 1.48×10^{-4} M. The mixture was monitored at 515 nm using the same instrumentation as for the hydrogen peroxide method against a reference cuvette containing the same mixture in exactly the same concentrations which was previously prepared and left for at least 10 min (reference for A_∞).

Determination of *In Vitro* Rates of Oxidation of I in Biological Media—*Human Plasma*—The freshly collected plasma used was obtained at the Civitan Regional Blood Center, Inc. (Gainesville, Fla.) and contained ~80% plasma diluted with the anticoagulant citrate phosphate dextrose solution USP. The plasma was stored in a refrigerator and used the next day. One hundred microliters of a freshly prepared 0.024 M solution of I in dimethyl sulfoxide was added to 10 mL of plasma, previously equilibrated to 37°C in a water bath, and mixed thoroughly to result in an initial concentration of 2.4×10^{-4} mol/L. One-milliliter samples of plasma were withdrawn every 20 min from the test medium, added immediately to 5 mL of ice-cold acetonitrile, shaken vigorously, and placed in a freezer. When all samples had been collected, they were centrifuged and the supernatants were filtered through nitrocellulose membrane filters (0.45 μm pore size) and analyzed by HPLC, following the appearance of II (method A).

Human Blood—The freshly collected heparinized blood was obtained at the Civitan Regional Blood Center, Inc. (Gainesville, Fla.). The blood was stored in a refrigerator and used the next day. One hundred microliters of a freshly prepared 0.048 M solution of I in dimethyl sulfoxide was added to 20 mL of blood, previously equilibrated to 37°C in a water bath, and mixed thoroughly to result in an initial concentration of 2.4×10^{-4} mol/L. One-milliliter samples of blood were withdrawn from the test medium every 10 min, added immediately to 5 mL of ice-cold acetonitrile, shaken vigorously, and placed in a freezer. When all samples had been collected, they were centrifuged and the supernatants were filtered using nitrocellulose membrane filters (0.45-μm pore size) and analyzed by HPLC following the appearance of II (method A) and the disappearance of I (method B).

Rat Brain Homogenate—Five female Sprague–Dawley rats were decapitated, and the brains were removed, pooled, weighed (total weight 9.2 g), and homogenized in 36.8 mL of aqueous 0.11 M phosphate buffer, pH 7.4. One hundred microliters of a 0.024 M solution of I in dimethyl sulfoxide was mixed with 20 mL of the homogenate, previously equilibrated to 37°C in a water bath, to result in an initial concentration of 2.4×10^{-4} mol/L. Samples of 1.0 mL were withdrawn every 10 min from the test medium, added immediately to 5 mL of ice-cold acetonitrile, shaken vigorously, and placed in a freezer. When all samples had been collected, they were centrifuged and the supernatants were filtered through nitrocellulose membrane filters (0.45-μm pore size) and analyzed by HPLC (method A).

***In Vitro* Determination of the Site-Specific Conversion of II to Testosterone**—A fresh brain homogenate was prepared as previously described. One hundred microliters of a 0.017 M solution of the quaternary compound (II) in methanol was mixed with 10 mL of the brain homogenate, previously equilibrated to 37°C, to result in an initial concentration of 1.7×10^{-4} M. Samples of 1.0 mL were withdrawn every 20 min from the test medium, added immediately to 5 mL of ice-cold acetonitrile, and placed in a freezer. When all samples had been collected, they were centrifuged, and the supernatant was filtered through a nitrocellulose membrane filter (0.45 μm pore size) and analyzed for the quaternary compound II.

***In Vivo* Brain Delivery of Testosterone Following its Administration**—Female Sprague–Dawley rats with an average weight of 225 ± 10 g were injected intravenously with testosterone at a dose level of 28.2 mg/kg. Samples of brain and blood were collected as previously described (1, 3, 4) and were analyzed for testosterone using HPLC.

Distribution of II after Intravenous Administration—Following the same procedure, female Sprague–Dawley rats were injected intravenously with quaternary solution (0.18%) in dimethyl sulfoxide at a dose level of 13.0 mg/kg. The brain samples collected were analyzed for the presence of quaternary II using HPLC.

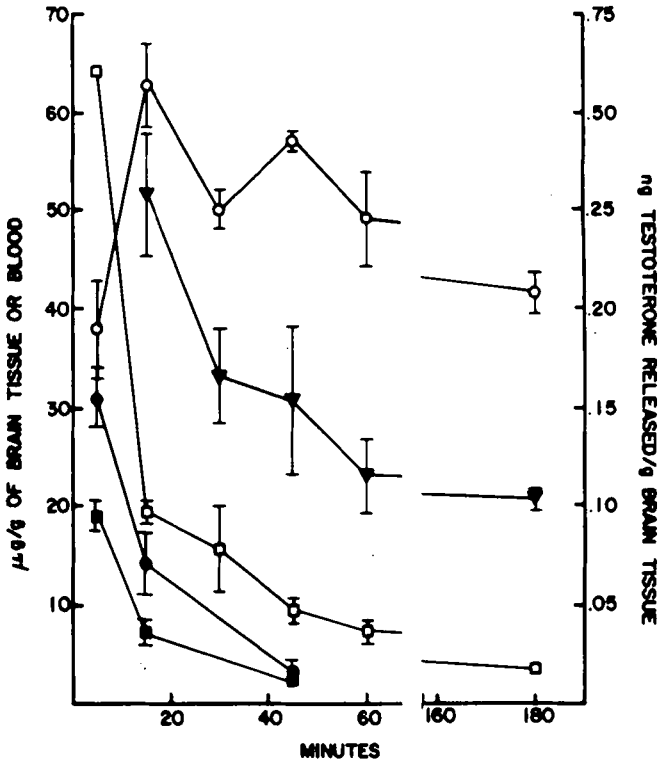

Figure 1—*Concentrations against time for the testosterone-17-nicotinate-N-methyl cation, calculated as iodide, in brain (○) and in blood (□) and concentration of released testosterone (ng/g) in brain (▼) following administration of the corresponding dihydropyridine derivative I. Concentrations of testosterone in brain (●) and blood (■) following administration of testosterone are also included. Bars represent the standard errors.*

RESULTS AND DISCUSSION

Compound I was prepared *via* quaternization of testosterone nicotinate (V) with methyl iodide followed by reduction of the quaternary salt II

[13] PIC B-7; Eastman Kodak Co.
[14] Apple II computer.

using sodium dithionite. The rates of oxidation of the dihydro derivative (I) with silver nitrate, hydrogen peroxide, and diphenylpicrylhydrazyl free radical ($DPP^{\cdot}$) were determined. The reactions were carried out under pseudo-first-order conditions, either with higher concentrations of the oxidant in the case of hydrogen peroxide or higher concentrations of I in the case of the picryl reagent. With $DPP^{\cdot}$ a reference sample was made using the same amounts as the test sample, but prepared 10 min before mixing and monitoring the test sample. This reference is used as a measure of A_∞, and these were the data used to calculate the kinetic parameters. The *in vitro* rates of oxidation of the dihydro derivative were also determined in biological fluids, *e.g.*, 80% plasma, whole blood, 20% brain homogenate, and 20% liver homogenate. The rate of disappearance of the ester II and appearance of testosterone in medium was also determined. Finally, the *in vivo* brain delivery and blood concentration profile of the quaternary derivative and testosterone released, against time, was determined following a single injection of the dihydropyridine derivative (I) to female rats. These results were compared with the blood and brain kinetics of testosterone following administration of the hormone itself.

Chemical Oxidation of the Dihydropyridine Derivative I—*By Silver Nitrate*—It was observed that this dihydro derivative is more stable towards oxidation than the previously studied analogous (1, 3, 4) derivatives containing amido functions; it takes a few minutes standing for the silver to form. The product is exclusively the quaternary salt II, as verified by the change in the UV and NMR spectra.

By Hydrogen Peroxide—Using low concentrations of the dihydro derivative I (5×10^{-6} M) and higher concentrations of the peroxide (0.18 M), the oxidation proceeds according to a first-order kinetics: $k = 2.7 \pm 0.3 \times 10^{-3}\ s^{-1}$; $t_{1/2} = 3.98 \pm 0.7$ min; $r = 0.995$. At higher concentrations I is insoluble in H_2O_2.

By Diphenylpicrylhydrazyl Free Radical—The reaction was carried out under pseudo-first-order conditions using excess dihydropyridine derivative. With the concentrations used, all of the runs gave first-order plots every 3 half-lives, with a correlation coefficient of >0.9998: $k = 4.87 \pm 0.31 \times 10^{-2}$; s^{-1} $t_{1/2} = 14.1 \pm 0.6$ s.

***In Vitro* Oxidation and Hydrolysis in Biological Media**—Table I shows the rates, half-lives, and correlation coefficients for the process of oxidation of the 1,4-dihydropyridine derivative I in different biological media. The rate of hydrolysis of the quaternary II in 20% brain homogenate was also determined, and it was found to be $3.6 \times 10^{-5}\ s^{-1}$, corresponding to a half-life, $t_{1/2}$, of 5.16 h.

***In Vivo* Administration of I and Testosterone**—Figure 1 illustrates the concentrations of quaternary derivative II in brain and blood and the concentration of testosterone released in the brain following intravenous administration of the 1,4-dihydropyridine derivative I. Also, it shows the concentration of testosterone in the brain and blood following administration of testosterone.

17β-[(1,4-Dihydro-1-methyl-3-pyridinylcarbonyl)oxy]androst-4-en-3-one (I) could be obtained in a high yield, >90%, from testosterone 17β-nicotinate by simple chemical procedures. The dihydro product obtained directly from the reduction reaction medium was found to be quite pure by HPLC, and a single crystallization from hot methanol afforded an analytically pure product. No signs of oxidation were observed during crystallization (even from hot methanol), filtration, or drying. The crystalline solid dihydro compound did not show signs of oxidation, decomposition, or polymerization when tested by HPLC during the 2-month shelf storage at ambient temperature under nitrogen. This compound (I) was found to be quantitatively oxidizable to the corresponding quaternary derivative (II), as identified by UV spectrometry, whether by silver nitrate or hydrogen peroxide. The process of oxidation with silver nitrate is slower than that with the dihydropyridine derivatives of phenylethylamine (3) or dopamine (4). Oxidation with hydrogen peroxide or $DPP^{\cdot}$, under pseudo-first-order conditions, was found to take place at measurable rates ($t_{1/2} = 3.98 \pm 0.7$ min and 14.1 ± 0.6 s, respectively) compared with the rates of oxidation of the corresponding phenylethylamine and dopamine derivatives, which were found to be too fast to be monitored using the same procedure. The *in vitro* investigation in biological fluids indicated a facile oxidative conversion of the dihydro form (I) to the corresponding quaternary (II), but at a slower rate than that of the analogous amides of phenylethylamine or dopamine.

For the *in vivo* studies of I, female Sprague–Dawley rats were chosen because the concentration of endogenous testosterone in the blood and brain of these animals is below the range of sensitivity of the procedure used for its analysis. The results shown in Fig. 1 indicate that the dihydro derivative penetrates the BBB and is readily oxidized in the brain to the quaternary precursor II. The *in vivo* rate of oxidation of the dihydro derivative seems faster than that obtained from the *in vitro* experiment. No dihydro derivative could be detected in the brain within the sensitivity limits of the procedure. After II reaches its maximum concentration, within ~15 min, its concentration starts a decline phase corresponding to overall excretion and/or metabolism–hydrolysis. The overall rate of this phase was calculated to be $2 \times 10^{-3}\ min^{-1}$ ($t_{1/2} = 5.7$ h). In the same time the concentration of II in blood was decreasing progressively from the beginning at a rate $1.27 \times 10^{-2}\ min^{-1}$ or with a half-life of 54 min.

Equimolar administration of testosterone using the same solvent (dimethyl sulfoxide) and the same route of administration showed a rapid absorption of testosterone into the brain, reaching a maximum concentration within 5 min, followed by fast clearance from both brain and blood ($t_{1/2}$ = 12.6 and 14.5 min, respectively). The ratio of brain/blood concentration for testosterone was found to be 1.6 at 5 min and 1.8 at 15 min postadministration. The ratio of brain/blood concentration of the quaternary II was found to increase progressively with time (3.23 at 15 min, 6.33 at 45 min, and 12 at 3 h postadministration). This indicates the predicted "lock in" property for the quaternary II.

Testosterone was found to be released from the quaternary ester II and could be detected in the brain following administration of the dihydro derivative I. Analysis of the time concentration curve for release of testosterone (Fig. 1) indicated two-phase kinetics for disappearance from the brain. The first is a fast descending phase at a rate of $1.2 \times 10^{-2}\ min^{-1}$ followed by a slow clearance phase with a rate of $5.8 \times 10^{-4}\ min^{-1}$ and a half-life of ~20 h, which corresponds to ~130 h for complete clearance from the brain. This result, if compared with that obtained by Frey *et al.* (27), for the clearance of testosterone from plasma after oral administration (~6 h), is very promising. Although the concentrations of testosterone in the brain following administration of I are low compared with that following administration of testosterone, this is by no means a disadvantage, because such high concentration of testosterone may not be needed for receptor saturation. By dose manipulation of the dihydro derivative, a concentration of testosterone just sufficient for receptor saturation for a delayed period could be attained.

REFERENCES

(1) N. Bodor, H. H. Farag, and M. E. Brewster, *Science*, **214**, 1370 (1981).

(2) N. Bodor, G. Roller, and S. J. Selk, *J. Pharm. Sci.*, **67**, 685 (1978).

(3) N. Bodor and H. H. Farag, *J. Med. Chem.*, **26**, 313 (1983).

(4) N. Bodor and H. H. Farag, *J. Med. Chem.*, **26**, 528 (1983).

(5) N. Bodor and M. E. Brewster, *Pharmacol. Therap.*, **19**, 337 (1983).

(6) J. B. Hutchison, *Adv. Study Behav.*, **6**, 159 (1976).

(7) B. B. Kelley and D. W. Pfaff, "Biological Determinants of Sexual Behavior," J. B. Hutchison Ed., Wiley, Bath, 1978.

(8) W. M. Pardridge, T. L. Moeller, L. J. Mietus, and W. H. Olendorf, *Am. J. Physiol.*, **239**, E96 (1980).

(9) R. B. Michael, *Ber. Med. Bul.*, **21**, 87 (1965).

(10) C. Anderson, *Anat. Rec.*, **181**, 287 (1975).

(11) M. J. Baum and J. T. M. Vreeburg, *Science*, **182**, 283 (1973).

(12) B. S. McEwen, P. G. Davis, P. H. Jellinck, L. C. Krey, I. L. Lieberburg, V. N. Luine, N. J. MacLusky, B. Parsons, and E. J. Roy, *Adv. Biochem. Psychopharmacol.*, **21**, 383 (1980).

(13) H. Vorherr, "Breast Cancer, Epidemiology, Endocrinology, Biochemistry and Pathology," Urban & Schwarzenberg, Baltimore, Md., 1980, pp. 248–281.

(14) C. W. Emmens and B. G. Miller, *Steroids*, **13**, 725 (1969).

(15) P. P. H. Bruyn, R. C. Robertson, and R. S. Farr, *Anat. Rec.*, **108**, 279 (1950).

(16) R. J. Goldacre and B. Sylven, *Nature (London)*, **184**, 63 (1959).

(17) R. J. Goldacre and B. Sylven, *J. Cancer*, **16**, 306 (1962).

(18) T. S. Ro and H. Busch, *Biochim. Biophys. Acta*, **108**, 317 (1965).

(19) A. T. Cowie, A. K. Lascelle, and J. C. Wallace, *J. Physiol. (London)*, **171**, 1976 (1964).

(20) R. E. Mancini, O. Vilar, B. Alvarez, and A. C. Seiguer, *J. Histochem. Cytochem.*, **13**, 376 (1965).

(21) M. Kormano, *Acta Physiol. Scand.*, **71**, 125 (1967).

(22) M. Kormano, *Histochemie*, **g**, 327 (1967).

(23) D. W. Fawcette, L. V. Leak, and P. M. Heidger, Jr., *J. Reprod. Fertil. Suppl.*, **10**, 105 (1970).

(24) M. Dym and D. W. Fawcette, *Biol. Reprod.*, **3**, 308 (1970).

(25) K. O. Kumora, I. P. Lee, and R. L. Dixon, *J. Pharmacol. Exp. Ther.*, **194**, 89 (1975).
(26) I. P. Lee and R. L. Dixon, *Environ. Health*, **24**, 117 (1978).
(27) H. Frey, A. Aadvaag, D. Saahum, and J. Falch, *Eur. J. Clin. Pharmacol.*, **16**, 345 (1979).

ACKNOWLEDGMENTS

This research was supported by Grant GM 27167 from the National Institutes of Health. The technical assistance of N. Gildersleeve and M. E. Brewster is gratefully acknowledged.

Angular Dependence of the Interaction Energy Between the N Lone Pair of Amines and a Proton: Relevance to Drug–Receptor Systems

VERA M. KOLB ˣ and STEVE SCHEINER

Received October 8, 1982, from the *Department of Chemistry and Biochemistry, Southern Illinois University, Carbondale, IL 62901.* Accepted for publication February 11, 1983.

Abstract □ *Ab initio* molecular orbital calculations with a 4-31G basis set have been performed to study the angular dependence of the interaction energy between a lone electron pair of nitrogen and a proton. In this study ammonia and trimethylamine were used as models of biologically active amines. A proton was used as a model of an electrophilic site at the receptor. Results obtained confirm previous indications that the energy required to bend the proton from the lone pair direction decreases markedly as the two species are further separated from one another. Implications regarding the interactions of drugs and hormones at specific receptors are discussed.

Keyphrases □ Interaction energy—nitrogen lone electron pair of amines and a proton, angular dependency, drug–receptor systems □ Drug–receptor systems—interaction energy of the nitrogen lone electron pair of amines and a proton, angular dependency □ Amines—biologically active, interaction energy of the lone electron pair and a proton, angular dependency

Many hormones and drugs elicit their biological response through interactions with specific receptors (1–10). These interactions are typically weak, reversible, and specific (11) and, in addition, do not involve covalent bonding (1, 2, 8, 9). Many such interactions are of the electrophile–nucleophile type between sterically fixed groups. Because the nucleophilic pharmacophore frequently contains nitrogen at a critical position, we focus here specifically on the nature of the interaction of nitrogen with an electrophile.

One way nitrogen could interact with the specific electrophilic center at the receptor is *via* its lone electron pair. Such a mechanism has been suggested for opiate–receptor interactions (12–15). The influence of the directionality of the lone pair of biologically active amines on their activity has been demonstrated experimentally in some cases (12). One may envisage the most productive interaction as that in which the N lone pair is aligned exactly in the direction of the electrophilic site. This concept of amine–receptor interaction is illustrated in Fig. 1, which schematically depicts the binding of a (tertiary) amine to its receptor. Both the amine molecule and the electrophilic site are visualized as being sterically fixed at the receptor. We consider the distance between the N lone pair and the electrophilic site as longer than the normal bonding distance, since covalent bonding of nitrogen to the receptor does not occur (1). Figure 1A shows a perfect fit between the N lone pair and the electrophilic site. Figure 1B depicts a case of a substituted amine whose substituent (shown as a "bump" at the left-hand side of the molecule) interferes with the proper fit with the receptor cavity. There may of course be other factors leading to poor fit, and the effect shown in Fig. 1B is used only as an example. The repulsion between the substituent and the receptor cavity causes a small tilting of the molecule, which changes the position of the nitrogen atom and, therefore, its lone electron pair, relative to the electrophilic site. The N lone pair forms a "bent" complex with the electrophilic site.

Since the activity of the amine depends on the nucleophile–electrophile complexation, it is very important to learn about the energetics of the "bent" complexation of

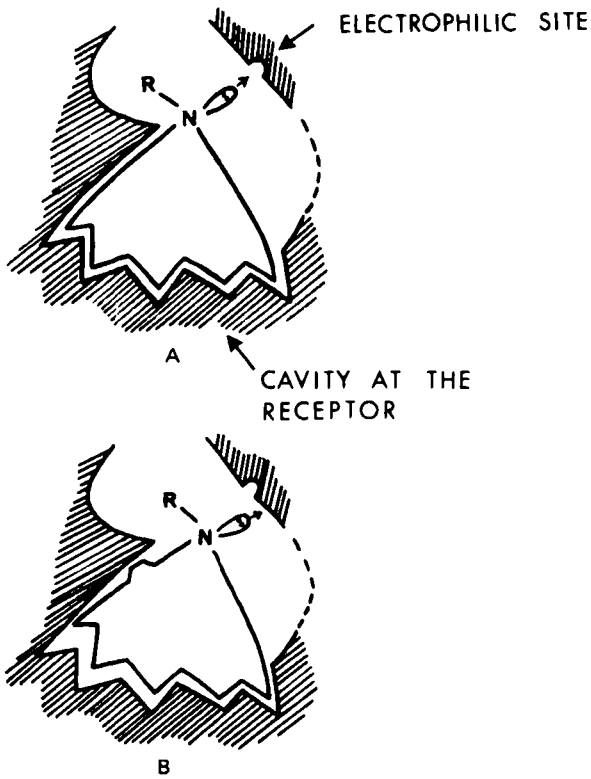

Figure 1—*Schematic representation of the binding of a biologically active (tertiary) amine to its receptor. Key: (A) perfect fit between the amine and its receptor; (B) less than perfect fit due to presence of a substituent (shown as bump on left of molecule).*

0022-3549/84/0300-0389$01.00/0
© 1984, American Pharmaceutical Association

(25) K. O. Kumora, I. P. Lee, and R. L. Dixon, *J. Pharmacol. Exp. Ther.*, **194**, 89 (1975).
(26) I. P. Lee and R. L. Dixon, *Environ. Health*, **24**, 117 (1978).
(27) H. Frey, A. Aadvaag, D. Saahum, and J. Falch, *Eur. J. Clin. Pharmacol.*, **16**, 345 (1979).

ACKNOWLEDGMENTS

This research was supported by Grant GM 27167 from the National Institutes of Health. The technical assistance of N. Gildersleeve and M. E. Brewster is gratefully acknowledged.

Angular Dependence of the Interaction Energy Between the N Lone Pair of Amines and a Proton: Relevance to Drug–Receptor Systems

VERA M. KOLB ˣ and STEVE SCHEINER

Received October 8, 1982, from the *Department of Chemistry and Biochemistry, Southern Illinois University, Carbondale, IL 62901.* Accepted for publication February 11, 1983.

Abstract □ *Ab initio* molecular orbital calculations with a 4-31G basis set have been performed to study the angular dependence of the interaction energy between a lone electron pair of nitrogen and a proton. In this study ammonia and trimethylamine were used as models of biologically active amines. A proton was used as a model of an electrophilic site at the receptor. Results obtained confirm previous indications that the energy required to bend the proton from the lone pair direction decreases markedly as the two species are further separated from one another. Implications regarding the interactions of drugs and hormones at specific receptors are discussed.

Keyphrases □ Interaction energy—nitrogen lone electron pair of amines and a proton, angular dependency, drug–receptor systems □ Drug–receptor systems—interaction energy of the nitrogen lone electron pair of amines and a proton, angular dependency □ Amines—biologically active, interaction energy of the lone electron pair and a proton, angular dependency

Many hormones and drugs elicit their biological response through interactions with specific receptors (1–10). These interactions are typically weak, reversible, and specific (11) and, in addition, do not involve covalent bonding (1, 2, 8, 9). Many such interactions are of the electrophile–nucleophile type between sterically fixed groups. Because the nucleophilic pharmacophore frequently contains nitrogen at a critical position, we focus here specifically on the nature of the interaction of nitrogen with an electrophile.

One way nitrogen could interact with the specific electrophilic center at the receptor is *via* its lone electron pair. Such a mechanism has been suggested for opiate–receptor interactions (12–15). The influence of the directionality of the lone pair of biologically active amines on their activity has been demonstrated experimentally in some cases (12). One may envisage the most productive interaction as that in which the N lone pair is aligned exactly in the direction of the electrophilic site. This concept of amine–receptor interaction is illustrated in Fig. 1, which schematically depicts the binding of a (tertiary) amine to its receptor. Both the amine molecule and the electrophilic site are visualized as being sterically fixed at the receptor. We consider the distance between the N lone pair and the electrophilic site as longer than the normal bonding distance, since covalent bonding of nitrogen to the receptor does not occur (1). Figure 1A shows a perfect fit between the N lone pair and the electrophilic site. Figure 1B depicts a case of a substituted amine whose substituent (shown as a "bump" at the left-hand side of the molecule) interferes with the proper fit with the receptor cavity. There may of course be other factors leading to poor fit, and the effect shown in Fig. 1B is used only as an example. The repulsion between the substituent and the receptor cavity causes a small tilting of the molecule, which changes the position of the nitrogen atom and, therefore, its lone electron pair, relative to the electrophilic site. The N lone pair forms a "bent" complex with the electrophilic site.

Since the activity of the amine depends on the nucleophile–electrophile complexation, it is very important to learn about the energetics of the "bent" complexation of

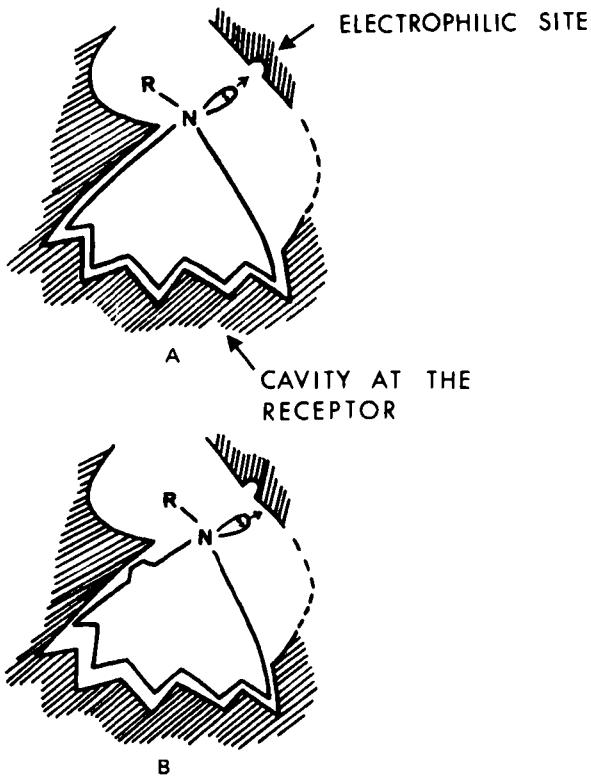

Figure 1—*Schematic representation of the binding of a biologically active (tertiary) amine to its receptor. Key: (A) perfect fit between the amine and its receptor; (B) less than perfect fit due to presence of a substituent (shown as bump on left of molecule).*

0022-3549/84/0300-0389$01.00/0
© 1984, American Pharmaceutical Association

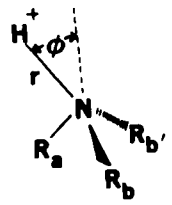

R = H , CH_3

Scheme I

the N lone pair (Fig. 1B) as compared with the "straight" complexation (Fig. 1A). The knowledge acquired about this problem may help to predict the activity of the derivatives of active amines and to understand better the mechanism of action of biologically active amines in situations where they are sterically restricted at the receptors.

Specifically, we wanted to determine the effects of the relative steric disposition of the nitrogen lone electron pair and an electrophilic site on the energetics of the interaction at distances longer than the normal bonding distance. Quantum chemical methods are particularly well suited for this purpose, since the relative orientations of molecules may be precisely specified. In addition, the wave functions may be analyzed to determine electron densities at various regions in the space between the two molecules to provide insights concerning the interaction. To perform *ab initio* calculations it was necessary to model the usually large biomolecules by smaller representative systems. Ammonia and trimethylamine were chosen as models of the nitrogen-containing portion of a biologically active amine. The proton, a spherically symmetrical species with no intrinsic steric requirements, was chosen as the simplest model for an electrophilic site at the receptor (the nature of such sites is generally poorly understood).

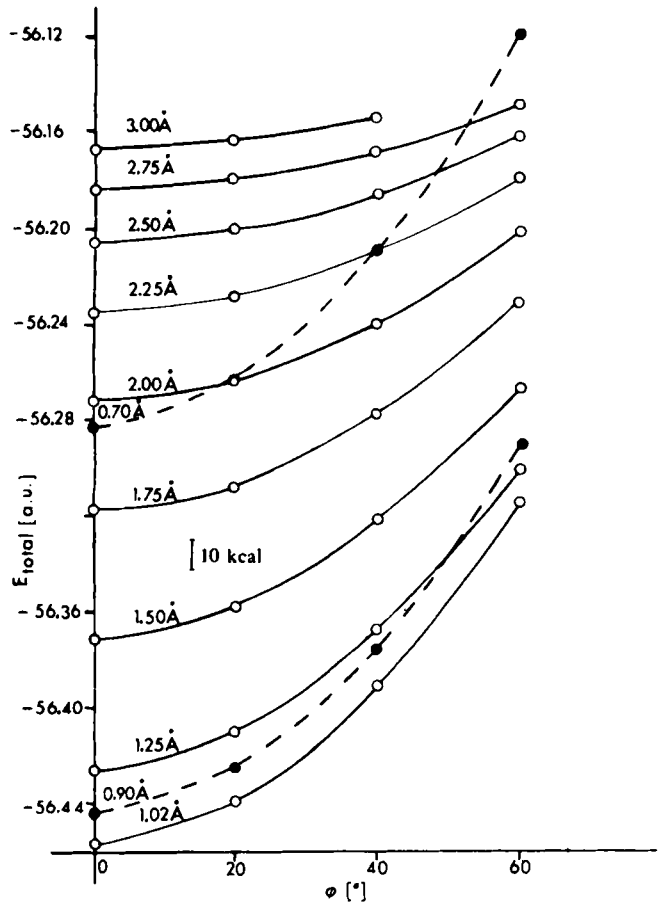

Figure 2—*Dependence of total energy* E *of the* $(H_3N\cdots H)^+$ *system on angle* ϕ *for various distances* r. *Filled circles and dashed lines indicate that* r *is shorter than the equilibrium distance* r = 1.02 Å. E(r = ∞) = −56.10249 a.u.

Table I—Angular Dependence of the Total Energy of the $(H_3N\cdots H)^+$ and $((CH_3)_3N\cdots H)^+$ Systems

r, Å	φ, °	ΔE, kcal/mol[a] $(H_3N\cdots H)^+$	ΔE, kcal/mol[a] $((CH_3)_3N\cdots H)^+$
1.02	20.0	11.6	
	40.0	42.2	
	60.0	90.8	
1.20	20.0	10.4	11.5
	40.0	38.4	46.3
	60.0	81.1	
	−20.0	6.5	11.0
1.50	20.0	8.4	
	40.0	31.4	
	60.0	66.0	
1.75	20.0	6.9	8.8
	40.0	25.8	35.3
	60.0	54.7	
	−20.0	4.3	8.3
2.00	20.0	5.6	
	40.0	20.8	
	60.0	44.5	
2.25	20.0	4.5	6.1
	40.0	16.6	
	60.0	35.7	
	−20.0	2.9	5.7
2.50	20.0	3.6	
	40.0	13.3	
	60.0	28.5	
2.75	20.0	2.9	
	40.0	10.6	
	60.0	22.8	
	−20.0	1.9	
3.00	20.0	2.4	
	40.0	8.5	

[a] $\Delta E = E(\phi) - E(0)$.

EXPERIMENTAL

Molecular orbital calculations were carried out within the *ab initio* restricted Hartree–Fock formalism. The GAUSSIAN-70 package of computer codes (16) was used to construct molecular orbitals as linear combination of atomic orbitals. The split valence–shell 4-31G basis set (17) was used rather than a minimal basis set, since the former provides greater flexibility to the valence orbitals and is expected to furnish a more realistic picture of long-range interactions between the amine and the proton than would the latter.

The experimentally determined geometries of ammonia (18) and trimethylamine (19) were used in our calculations. Ammonia belongs to the C_{3v} point group and has r(N—H) = 1.01 Å and θ(HNH) = 106.7°. The N—C bond distances in trimethylamine are 1.45 Å and the θ(CNC) is 110.9°. Each methyl group is staggered with respect to the other two C—N bonds.

A proton was placed at various positions relative to the amines. As shown in Scheme I, these positions are characterized by the N—H^+ distance r and ϕ, the angle between the N—H^+ axis and the C_{3v} symmetry axis of the R_3N molecule. (The latter axis coincides with the expected direction of the N lone pair.) A positive value of ϕ, shown in Scheme I, indicates a bend of H^+ toward R_a, while a negative value corresponds to a bend in the opposite direction.

The variation of the total energy of the $(H_3N\cdots H)^+$ system with changing ϕ is illustrated in Fig. 2 for values of r between 0.70 and 3.0 Å. Dashed lines represent curves for $r < 1.02$ Å, the equilibrium N—H bond length. For each value of r, the lowest energy structure is that with ϕ = 0°, in which the proton lies directly along the C_3 symmetry axis of NH_3. Increasing ϕ results in a monotonic increase in the energy corresponding to a less stable complex. The sensitivity of the energy to ϕ decreases as r is increased. For example, for r = 1.02 Å the $(H_3N\cdots H)^+$ complex with

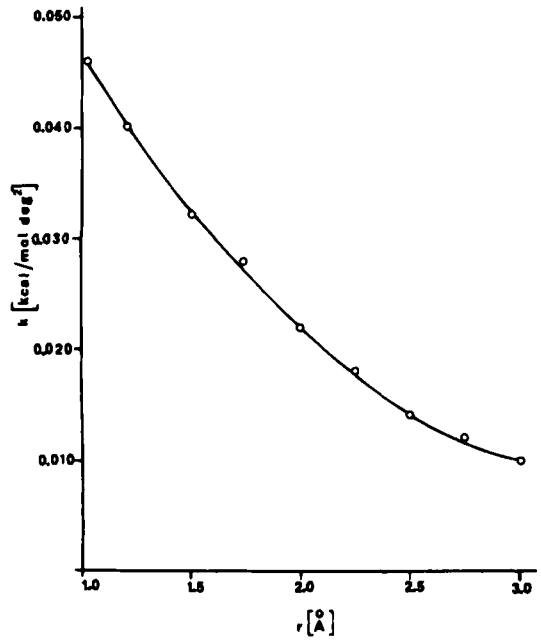

Figure 3—*Dependence of the bending force constant* k *on distance* r *for the* $(H_3N\cdots H)^+$ *system.*

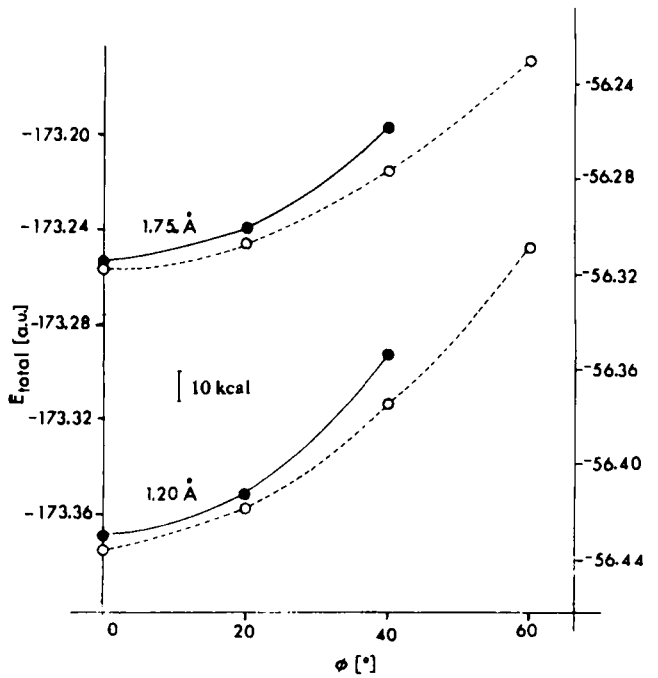

Figure 4—*Dependence of total energy* E *of the* $((CH_3)_3N\cdots H)^+$ *system on angle* ϕ *for two distances* r (● *and* —, *left ordinate). Also shown are the corresponding values for* $(H_3N\cdots H)^+$ *for the same distances* r (○ *and* - - -, *right ordinate). For the* $((CH_3)_3N\cdots H)^+$ *system* E (r = ∞) = −173.00797 *a.u.*

the proton bent 20° off the C_3 axis is 11.6 kcal/mol less stable than that for $\phi = 0°$, whereas the analogous quantity is only 2.4 kcal/mol for r = 3.0 Å. Additional data concerning the energetics of deformation for angles $\phi = 20°$, 40°, and 60° are presented in Table I. Each value of ΔE is defined as the difference in energy between the indicated value of ϕ and that for $\phi = 0°$. Fitting these data to a parabola for each value of r *via* least-squares analysis yields the bending force constants, k ($\Delta E = 0.5k\phi^2$). Figure 3 shows how these bending force constants decrease with increasing r.

Deformation energies for selected conformations of $((CH_3)_3N\cdots H)^+$ are listed in the final column of Table I. Figure 4 shows a comparison of the results for the latter system (solid line) with those for the $(H_3N\cdots H)^+$ system (dashed line) at r = 1.20 and 1.75 Å. A strong similarity is clearly evident for the energetics of bending in the two amine systems. For values of $\phi > 20°$, we note that the energy for $((CH_3)_3N\cdots H)^+$ rises somewhat faster with increasing ϕ than does $(H_3N\cdots H)^+$. This difference is probably a result of steric repulsion between the incoming proton and the methyl hydrogen atoms of trimethylamine, which are not present in NH_3.

The deformation energy for trimethylamine is quite uniform in the + and − direction of ϕ, as indicated by similar ΔE values for $\phi = 20°$ and $-20°$. This is contrary to the $(H_3N\cdots H)^+$ case, where the deformation energy for positive ϕ is noticeably greater than for negative angles. In the latter case the proton fits "in between" (in a staggered manner) two ammonia hydrogen atoms (H_b and $H_{b'}$; see Scheme I) while for positive ϕ, the proton is eclipsed with one hydrogen (H_a). Thus, the three H^+—H distances for $\phi = 20°$ and r = 1.75 Å are 2.02, 2.44, and 2.44 Å, as compared with 2.52, 2.20, and 2.20 Å for $\phi = -20°$. For trimethylamine the hydrogen atoms are more uniformly distributed around the central nitrogen. The four shortest H^+—H distances in the $((CH_3)_3N\cdots H)^+$ system, again for r = 1.75 Å, are 2.33, 2.33, 2.81, and 2.81 Å for $\phi = 20°$, which is very similar to the corresponding values of 2.37, 2.37, 2.73, and 2.73 Å for $\phi = -20°$.

DISCUSSION

We have presented calculated results of the energetics of deformation of the amine–proton system. The preferred or lowest energy structure in each case is one in which the proton lies directly along the lone pair direction of the amine. (A similar conclusion was reached by Baird (20) for the interaction of NH_3 with both NH_4^+ and NH_3.) Calculated bending energies extended over a wide range of values, varying up to 90 kcal/mol for 60° bends at the equilibrium r(NH) distance of 1.02 Å for the $(H_3N\cdots H)^+$ system.

Our calculated results show a greatly diminished sensitivity of the amine–electrophile interaction energy to angular deformation as the distance between the two species is increased. Qualitatively similar conclusions may be reached by examination of the molecular electrostatic potentials in the vicinity of the amine group of morphines (21, 22). Although these potential maps include only nonperturbing effects of a unit charge and thereby neglect polarization, charge transfer, and exchange terms, the results indicate preferred binding of a positive charge along the lone pair direction of nitrogen. The maps (21, 22) further suggest that the decreasing sensitivity of the binding energy to angle at longer distances, found here for simple amines, is common to morphines as well. Thus, the formation of a bent complex may be only a little less favorable energetically than a "straight" complex at separations of perhaps 2.5 or 3.0 Å. For example, while a bend of 20° in the $(H_3N\cdots H)^+$ system leads to a deformation energy of 11.6 kcal/mol at 1.02 Å, the strain energy for a similar bend is only 2.4 kcal/mol at r = 3.0 Å.

It is therefore important to consider what might be expected for the distance between the nucleophile and the electrophile at the receptor when the (noncovalent) interaction occurs. A distance of 2 Å was used in the "transition-state complex" between the propene nucleophile and a proton by Caramella *et al.* (23). Distances between nucleophiles and electrophiles of as long as 3 Å have been observed in crystal structure studies (24). Bürgi *et al.* interpreted these long distances as indicating nonbonded interactions of the donor–acceptor and dipole–dipole types (24). Therefore, distances between the amine nucleophile and electrophile of ≥2 Å at the receptor would not be an unreasonable estimate.

At interaction distances >2 Å, the lone pair and electrophile may be significantly misaligned without large deformation energies. For example, for the $(H_3N\cdots H)^+$ system, at r = 2.0 Å, a bend of 15° from optimal orientation produces an energy increase of 3 kcal/mol, while the analogous bend yielding a similar increase at r = 3.0 Å is 24°.

While it would be presumptuous to generalize our data on the $(H_3N\cdots H)^+$ and $((CH_3)_3N\cdots H)^+$ systems and claim that they are directly applicable to all nitrogen-containing drugs and hormones, we believe that our findings should be considered qualitatively when picturing the interaction of the N lone pair of biologically active amines with an electrophilic site at the receptor.

The fact that the difference in energy between a "bent" and "straight" complex may become very small for longer r values does not support the orbital steering concept (25). The experimental (26) and theoretical (*e.g.*, 27) work of other investigators has already provided evidence which is not in agreement with the orbital steering concept.

Finally, we may note that our studies on angular dependence of the interaction between the N lone pair of amines with a proton complement

previous studies of the angular dependence of the interaction between nucleophiles and certain electrophiles which possess intrinsic steric requirements (27, 28), as well as electrophiles in general (20, 29–32).

REFERENCES

(1) A. Korolkovas, "Essentials of Molecular Pharmacology," Wiley Interscience, New York, N.Y., 1970, pp. 137–178; references therein.

(2) R. R. Levine, "Pharmacology, Drug Actions and Reactions," Little, Brown, Boston, Mass., 1973, pp. 40–44.

(3) W. I. P. Mainwaring, in "Cellular Receptors for Hormones and Neurotransmitters," D. Schulster and A. Levitzki, Eds., Wiley, New York, N.Y., 1980, pp. 91–126.

(4) R. J. B. King and W. I. P. Mainwaring, "Steroid-Cell Interactions," University Park Press, Baltimore, Md., 1974, pp. 288–378.

(5) F. J. Zeelen, in "Biological Activity and Chemical Structure," J. A. Kaverling Buisman, Ed., Elsevier, New York, N.Y., 1977, pp. 147–160.

(6) S. H. Snyder and S. Matthysse, "Opiate Receptor Mechanisms," MIT Press, Cambridge, Mass., 1975, pp. 9–13.

(7) S. H. Snyder, S. R. Childers, and I. Creese, in "Neurochemical Mechanisms of Opiates and Endorphins," H. H. Loh and D. H. Ross, Eds., Raven, New York, N.Y., 1979, pp. 543–552.

(8) P. S. Portoghese, *J. Pharm. Sci.*, **55**, 865 (1966).

(9) V. Höllt and A. Herz, *Fed. Proc. Fed. Am. Soc. Exp. Biol.*, **37**, 158 (1978).

(10) J. E. Leysen, W. Gommeren, and P. Laduron, *Arch. Intern. Physiol. Biochim.*, **86**, 874 (1978).

(11) Y. F. Jacquet, W. A. Klee, K. C. Rice, I. Iiijima, and J. Minamikawa, *Science*, **198**, 842 (1977).

(12) B. Belleau, T. Conway, F. R. Ahmed, and A. D. Hardy, *J. Med. Chem.*, **17**, 907 (1974).

(13) B. Belleau and P. Morgan, *J. Med. Chem.*, **17**, 908 (1974).

(14) V. M. Kolb, *J. Pharm. Sci.*, **67**, 999 (1978).

(15) C. Humblet and G. R. Marshall, *Ann. Rep. Med. Chem.*, **15**, 267 (1980) (see p. 273).

(16) W. J. Hehre, W. A. Lathan, R. Ditchfield, M. D. Newton, and J. A. Pople, *GAUSSIAN-70*, QCPE No. 236 (1974).

(17) R. Ditchfield, W. J. Hehre, and J. A. Pople, *J. Chem. Phys.*, **54**, 724 (1971).

(18) W. S. Benedict and E. K. Plyler, *Can. J. Phys.*, **35**, 1235 (1957).

(19) J. E. Walrab and V. W. Laurie, *J. Chem. Phys.*, **51**, 1580 (1969).

(20) N. C. Baird, *Int. J. Quantum Chem., Quantum Biol. Symp.*, **1**, 49 (1974).

(21) J. J. Kaufman, P. C. Hariharan, F. L. Tobin, and C. Petrongolo in "Chemical Applications of Atomic and Molecular Electrostatic Potentials," P. Politzer and D. G. Truhlar, Eds., Plenum, New York, N.Y., 1981, pp. 335–380.

(22) J. J. Kaufman, P. C. Hariharan, H. E. Popkie, C. Petrongolo, *Ann. N.Y. Acad. Sci.*, **367**, 452 (1981).

(23) P. Caramella, N. C. Rondan, M. N. Paddon-Row, and K. N. Houk, *J. Am. Chem. Soc.*, **103**, 2438 (1981).

(24) H. B. Bürgi, J. D. Dunitz, and E. Shefter, *J. Am. Chem. Soc.*, **95**, 5065 (1973).

(25) D. R. Storm and D. E. Koshland, Jr., *J. Am. Chem. Soc.*, **94**, 5815 (1972).

(26) F. M. Menger and L. E. Glass, *J. Am. Chem. Soc.*, **102**, 5404 (1980).

(27) S. Scheiner, W. N. Lipscomb, and D. A. Kleier, *J. Am. Chem. Soc.*, **98**, 4770 (1976).

(28) A. J. Stone and R. W. Erskine, *J. Am. Chem. Soc.*, **102**, 7185 (1980).

(29) R. Taylor, *J. Mol. Struct.*, **71**, 311 (1981).

(30) R. Taylor, *J. Mol. Struct.*, **73**, 125 (1981).

(31) G. A. Jeffrey and S. Tagaki, *Acct. Chem. Res.*, **11**, 264 (1978).

(32) P. Dauber and A. T. Hagler, *Acct. Chem. Res.*, **13**, 105 (1980).

ACKNOWLEDGMENTS

A generous allocation of computer time from the Academic Computing Center of Southern Illinois University is gratefully acknowledged. This work was supported in part by grants from the University Research Foundation, La Jolla, Calif., to V. M. Kolb and from the National Institute of General Medical Sciences and the Research Corporation to S. Scheiner. S. Scheiner is also a recipient of a Research Career Development Award from NIH.

NOTES

Determination of the Average Molecular Weight of Nonionic Emulsifiers by Vapor-Phase Osmometry

FRANCE GUAY and SUZANNE BISAILLON ˣ

Received October 5, 1982, from the *Faculty of Pharmacy, University of Montreal, Montreal, Quebec, H3C 3J7, Canada.* Accepted for publication January 10, 1983.

Abstract □ Standard nonionic emulsifiers are heterogenous by nature. Their reported molecular weight is unreliable, especially when several lots of the product are used in a study. The number-average molecular weights of two nonionic emulsifiers, poloxamer 188 and polyoxyethylene(23) lauryl ether were determined by vapor-phase osmometry. This determination is essential when the concentration should be given in molarity rather than in weight per volume. A discrepancy was noted between the number-average molecular weights of two lots of poloxamer 188. That difference is taken into account prior to the establishment of any comparison of the behavior of the emulsifiers.

Keyphrases □ Poloxamer 188—number-average molecular weight, vapor-phase osmometry □ Polyoxyethylene(23) lauryl ether—number-average molecular weight, vapor-phase osmometry □ Vapor-phase osmometry—determination of number-average molecular weights, poloxamer 188, polyoxyethylene(23) lauryl ether

Standard nonionic emulsifiers are chemically impure, with a composite nature that confers specific properties which render them suitable for numerous applications such as emulsification, wetting, foaming, *etc.* Because of this particular feature, determination of the molecular weight of nonionic emulsifiers is complicated and the analytical

0022-3549/84/0300-0392$01.00/0

© 1984, American Pharmaceutical Association

previous studies of the angular dependence of the interaction between nucleophiles and certain electrophiles which possess intrinsic steric requirements (27, 28), as well as electrophiles in general (20, 29–32).

REFERENCES

(1) A. Korolkovas, "Essentials of Molecular Pharmacology," Wiley Interscience, New York, N.Y., 1970, pp. 137–178; references therein.

(2) R. R. Levine, "Pharmacology, Drug Actions and Reactions," Little, Brown, Boston, Mass., 1973, pp. 40–44.

(3) W. I. P. Mainwaring, in "Cellular Receptors for Hormones and Neurotransmitters," D. Schulster and A. Levitzki, Eds., Wiley, New York, N.Y., 1980, pp. 91–126.

(4) R. J. B. King and W. I. P. Mainwaring, "Steroid-Cell Interactions," University Park Press, Baltimore, Md., 1974, pp. 288–378.

(5) F. J. Zeelen, in "Biological Activity and Chemical Structure," J. A. Kaverling Buisman, Ed., Elsevier, New York, N.Y., 1977, pp. 147–160.

(6) S. H. Snyder and S. Matthysse, "Opiate Receptor Mechanisms," MIT Press, Cambridge, Mass., 1975, pp. 9–13.

(7) S. H. Snyder, S. R. Childers, and I. Creese, in "Neurochemical Mechanisms of Opiates and Endorphins," H. H. Loh and D. H. Ross, Eds., Raven, New York, N.Y., 1979, pp. 543–552.

(8) P. S. Portoghese, *J. Pharm. Sci.*, **55**, 865 (1966).

(9) V. Höllt and A. Herz, *Fed. Proc. Fed. Am. Soc. Exp. Biol.*, **37**, 158 (1978).

(10) J. E. Leysen, W. Gommeren, and P. Laduron, *Arch. Intern. Physiol. Biochim.*, **86**, 874 (1978).

(11) Y. F. Jacquet, W. A. Klee, K. C. Rice, I. Iiijima, and J. Minamikawa, *Science*, **198**, 842 (1977).

(12) B. Belleau, T. Conway, F. R. Ahmed, and A. D. Hardy, *J. Med. Chem.*, **17**, 907 (1974).

(13) B. Belleau and P. Morgan, *J. Med. Chem.*, **17**, 908 (1974).

(14) V. M. Kolb, *J. Pharm. Sci.*, **67**, 999 (1978).

(15) C. Humblet and G. R. Marshall, *Ann. Rep. Med. Chem.*, **15**, 267 (1980) (see p. 273).

(16) W. J. Hehre, W. A. Lathan, R. Ditchfield, M. D. Newton, and J. A. Pople, *GAUSSIAN-70*, QCPE No. 236 (1974).

(17) R. Ditchfield, W. J. Hehre, and J. A. Pople, *J. Chem. Phys.*, **54**, 724 (1971).

(18) W. S. Benedict and E. K. Plyler, *Can. J. Phys.*, **35**, 1235 (1957).

(19) J. E. Walrab and V. W. Laurie, *J. Chem. Phys.*, **51**, 1580 (1969).

(20) N. C. Baird, *Int. J. Quantum Chem., Quantum Biol. Symp.*, **1**, 49 (1974).

(21) J. J. Kaufman, P. C. Hariharan, F. L. Tobin, and C. Petrongolo in "Chemical Applications of Atomic and Molecular Electrostatic Potentials," P. Politzer and D. G. Truhlar, Eds., Plenum, New York, N.Y., 1981, pp. 335–380.

(22) J. J. Kaufman, P. C. Hariharan, H. E. Popkie, C. Petrongolo, *Ann. N.Y. Acad. Sci.*, **367**, 452 (1981).

(23) P. Caramella, N. C. Rondan, M. N. Paddon-Row, and K. N. Houk, *J. Am. Chem. Soc.*, **103**, 2438 (1981).

(24) H. B. Bürgi, J. D. Dunitz, and E. Shefter, *J. Am. Chem. Soc.*, **95**, 5065 (1973).

(25) D. R. Storm and D. E. Koshland, Jr., *J. Am. Chem. Soc.*, **94**, 5815 (1972).

(26) F. M. Menger and L. E. Glass, *J. Am. Chem. Soc.*, **102**, 5404 (1980).

(27) S. Scheiner, W. N. Lipscomb, and D. A. Kleier, *J. Am. Chem. Soc.*, **98**, 4770 (1976).

(28) A. J. Stone and R. W. Erskine, *J. Am. Chem. Soc.*, **102**, 7185 (1980).

(29) R. Taylor, *J. Mol. Struct.*, **71**, 311 (1981).

(30) R. Taylor, *J. Mol. Struct.*, **73**, 125 (1981).

(31) G. A. Jeffrey and S. Tagaki, *Acct. Chem. Res.*, **11**, 264 (1978).

(32) P. Dauber and A. T. Hagler, *Acct. Chem. Res.*, **13**, 105 (1980).

ACKNOWLEDGMENTS

A generous allocation of computer time from the Academic Computing Center of Southern Illinois University is gratefully acknowledged. This work was supported in part by grants from the University Research Foundation, La Jolla, Calif., to V. M. Kolb and from the National Institute of General Medical Sciences and the Research Corporation to S. Scheiner. S. Scheiner is also a recipient of a Research Career Development Award from NIH.

NOTES

Determination of the Average Molecular Weight of Nonionic Emulsifiers by Vapor-Phase Osmometry

FRANCE GUAY and SUZANNE BISAILLON ˣ

Received October 5, 1982, from the *Faculty of Pharmacy, University of Montreal, Montreal, Quebec, H3C 3J7, Canada.* Accepted for publication January 10, 1983.

Abstract □ Standard nonionic emulsifiers are heterogenous by nature. Their reported molecular weight is unreliable, especially when several lots of the product are used in a study. The number-average molecular weights of two nonionic emulsifiers, poloxamer 188 and polyoxyethylene(23) lauryl ether were determined by vapor-phase osmometry. This determination is essential when the concentration should be given in molarity rather than in weight per volume. A discrepancy was noted between the number-average molecular weights of two lots of poloxamer 188. That difference is taken into account prior to the establishment of any comparison of the behavior of the emulsifiers.

Keyphrases □ Poloxamer 188—number-average molecular weight, vapor-phase osmometry □ Polyoxyethylene(23) lauryl ether—number-average molecular weight, vapor-phase osmometry □ Vapor-phase osmometry—determination of number-average molecular weights, poloxamer 188, polyoxyethylene(23) lauryl ether

Standard nonionic emulsifiers are chemically impure, with a composite nature that confers specific properties which render them suitable for numerous applications such as emulsification, wetting, foaming, *etc.* Because of this particular feature, determination of the molecular weight of nonionic emulsifiers is complicated and the analytical

0022-3549/84/0300-0392$01.00/0

© 1984, American Pharmaceutical Association

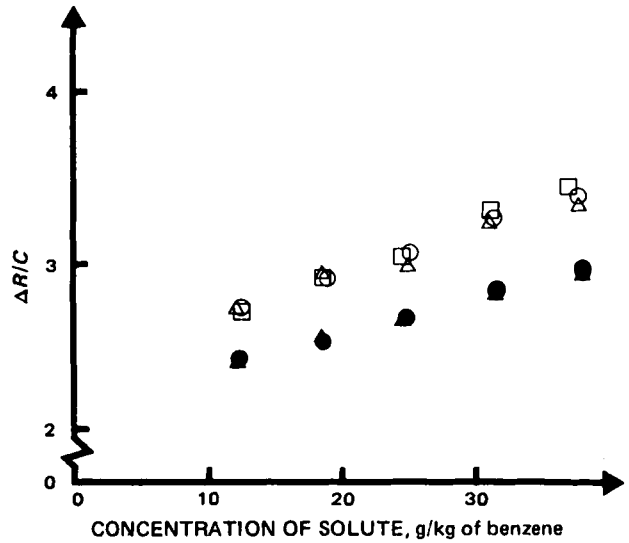

Figure 1—*Sample calculation curves of two lots of poloxamer 188. Key: (□, ○, △) three sets of data for lot WPTY 175B; (▲, ●) two sets of data for lot WXPG 112.*

method chosen must overcome the heterogeneity of the product, which renders impossible the consideration of the reported molecular weight. Methods involving the measurement of colligative properties are extensively used for estimating number-average molecular weights <20,000 (1–3). A prime interest in this area is directed toward vapor-phase osmometry as a rapid and reliable technique (4).

The number-average molecular weights of poloxamer 188 (I) and polyoxyethylene(23) lauryl ether (II) were determined by vapor-phase osmometry. Even if an estimation of the number-average molecular weights can be done from their formulas, a more systematic procedure should be employed to confirm the uniformity of the product, which can vary from lot to lot. These determinations were undertaken on both substances prior to their use in a study dealing with emulsifier behavior at the air–water and soybean oil–water interfaces.

EXPERIMENTAL

Two lots of I (WPTY 175B and WXPG 112)[1] and one lot of II (667)[2] were studied. The emulsifiers were dissolved in benzene (ACS grade) previously dried over calcium sulfate and filtered through a 0.45-μm cellulose membrane. Benzil (practical grade, mol. wt. 210.23) was used as the standard for calibration.

The measurements were performed on a molecular weight apparatus[3]. Since the accurate measurement of vapor pressure is difficult, the determination of the number-average molecular weights is based on the temperature difference between a solution and its solvent at the same vapor pressure. The apparatus consists of a thermostated chamber containing two thermistors where a pool of pure solvent is maintained at equilibrium with the environment. When a drop of solvent is placed on each thermistor, the rates of evaporation and condensation are equal in all parts of the system and the temperature is constant. When a drop of solution is placed on one thermistor, this equilibrium is upset and a change of temperature for one thermistor is reflected by a change in the resistance (ΔR) of the system. The calibration and calculation curves were obtained under the following experimental conditions: main oven temperature, 40.1 ± 0.1°C; sub-oven temperature, 35.3 ● 0.15°C; room temperature, 22°C; and equilibration time, 10 min.

[1] Pluronic-F_{68} (BASF-Wyandotte), a block copolymer containing 80% of polyoxyethylene units and 20% of polyoxypropylene units.
[2] Brij-35, Atlas Chemicals Div., ICI America, Inc.
[3] Hitachi/Perkin-Elmer Molecular Weight Apparatus, model 115.

Table I—Comparison of Reported and Experimentally Determined Number-Average Molecular Weights

	Number-Average Molecular Weight	
	Literature Value	Estimated by Vapor-Phase Osmometry
Poloxamer 188		
Lot WPTY 175B	8350[a]	7448.1 ± 95.8
Lot WXPG 112		8246.9 ± 4.8
Polyoxyethylene (23) lauryl ether (lot 667)	1200[b]	1264.4 ± 33.5

[a] Taken from Ref. 5. [b] Taken from Ref. 6.

RESULTS AND DISCUSSION

Determination of the Instrument Constant (K)—This constant is the same as the slope of the calibration curve showing the change in the ΔR values for the standard substance (benzil) in benzene at different concentrations (C). The range of concentration was chosen to generate ΔR values from 50 to 150. K was calculated using four sets of data. No significant difference has been noted between the slopes obtained from each set of data based on the Student's t test. Since the origin is included within the confidence limits (1%) of each intercept, the equation of the calibration curve can be represented as follows:

$$\Delta R = KC + b \qquad \text{(Eq. 1)}$$

where $b = 0$. The slope is calculated as the sum of ΔR values divided by the sum of the concentrations obtained for the four sets of data. Accordingly, the instrument constant (K) is equal to 18,000.150.

Determination of the Number-Average Molecular Weights—Sample calculation curves were obtained by plotting $\Delta R/C$ as a function of C for different concentrations of a sample dissolved in benzene (g of sample/kg of benzene). Figures 1 and 2 show the curves obtained for the two lots of I and for II. The number-average molecular weight is calculated using the following equation[4]:

$$\text{Number-average mol. wt.} = \frac{\text{Instrument constant } (K)}{\text{Intercept of the sample calculation curve}} \qquad \text{(Eq. 2)}$$

Table I shows the number-average molecular weights determined for each sample; these results are close enough to those reported, except for one lot of I. This difference may have a twofold significance. This particular lot was stored in our laboratory for over 3 years at room temperature in an air-tight container. One can suppose that the two lots of I were

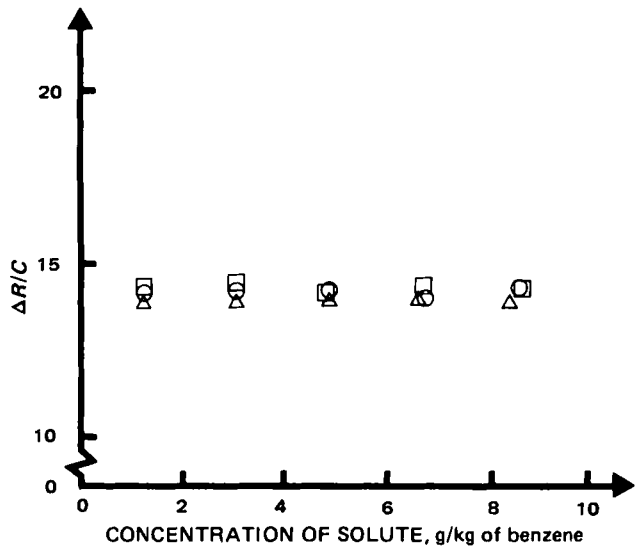

Figure 2—*Sample calculation curves of polyoxyethylene 23 lauryl ether. Key: (□, ○, △) three sets of data for lot 667.*

[4] Since the sample calculation curves were made in duplicate or triplicate, the mean intercept was used in each case for the calculation.

composed of different fractions or that "degradation" occurred during the storage period of lot WPTY 175B. No matter which hypothesis is retained, the product has not lost its activity as far as emulsifying or surface-active properties are concerned.

Nevertheless, the average molecular weight of an emulsifier ought to be known in order to determine its surface excess and to produce the curve of the surface pressure *versus* "molecular" cross-sectional area of the emulsifier (7). Relying on the reported molecular weight can generate misleading values for the aforementioned parameters, especially if the data are obtained from different batches of the same emulsifier. No comparison can be made between the behavior of different lots of one product unless a correction is made for the difference in their molecular weights.

REFERENCES

(1) G. Champetier, L. Monnerie, "Introduction à la Chimie Macromoléculaire," Masson & Cie., Paris, 1969, p. 206.

(2) K. E. Chung, L. L. Anderson, and W. H. Wiser, *Fuel*, **58**, 847 (1979).

(3) J. Zynger and A. D. Kossoy, *Anal. Chem.*, **52**, 1538 (1980).

(4) R. V. Figini, *Makromol. Chem.*, **181**, 2409 (1980).

(5) "The Wonderful World of Pluronic Polyols," BASF-Wyandotte, Mich., 1973.

(6) J. L. Woodhead, J. A. Lewis, G. N. Malcolm, and I. D. Watson, *J. Colloid Interface Sci.*, **79**, 454 (1981).

(7) F. Guay and S. Bisaillon, *J. Colloid Interface Sci.*, **93**, 25 (1983).

ACKNOWLEDGMENTS

The authors acknowledge the award of a studentship and a research grant from the Medical Research Council of Canada and from C.A.F.I.R. (University of Montreal). We are also grateful to BASF-Wyandotte and Atlas Chemical Industries for providing the surface-active agents, and wish to thank Ginette Giasson-Gagnon for her technical assistance.

Alloxan Analogues as Potential Pancreatic-Imaging Radiopharmaceuticals

WILLIAM E. ADAMS *, NED D. HEINDEL *x, GENE TUTWILER ‡, and HENRY FAWTHROP ‡

Received August 19, 1982, from the **Center for Health Sciences, Lehigh University, Bethlehem, PA 18015* and the ‡*Biochemistry Department, McNeil Laboratories, Spring House, PA 19477.* Accepted for publication January 10, 1983.

Abstract □ Three families of alloxan derivatives, 5-arylthiobarbituric, 5-aryliminobarbituric, and 5-aryldialuric acids, were prepared as prospective radioiodine-transporting radiopharmaceuticals for the delineation of pancreatic insulinomas. Members of each class were screened for effects on blood sugar levels in a rat glucose tolerance assay. Transient hyperglycemia was observed with 5-(2,4-dichlorophenyl)iminobarbituric acid. No agent evaluated induced permanent diabetes at the doses tested.

Keyphrases □ Alloxan—analogues, potential tumor-imaging agents, pancreatic insulinomas, effect on blood glucose levels, rats □ Tumor-imaging agents—alloxan analogues, pancreatic insulinomas, effect on blood glucose levels, rats

Alloxan and several of its derivatives are diabetogenic (1–3). While no definitive structure–activity studies have been reported, it appears that alloxan, alloxan monohydrate (II), alloxantin (I), and dialuric acid (III), without bulky substituents on nitrogen, are all able to induce frank diabetes (1–3). Some evidence supports a direct effect on the pancreas, for degranulation of β-cells is observed; [^{14}C]alloxan was shown to concentrate in the islet cells by autoradiography (4–7).

Development of radiopharmaceuticals for the scintigraphic imaging of occult pancreatic malignancies has been a goal of these laboratories for several years (8–11). In at least one previous study, it has been shown that substances with direct effects on serum glucose levels can, if radioisotopically labeled, preferentially delineate insulinomas (12, 13). Alloxan analogues would appear worthy of investigation in this regard.

Three classes of alloxan derivatives have been prepared which differ from the parent molecule by possessing an aryl moiety at C-5. This pendant aromatic ring would provide a suitable locus for the attachment of radioiodine in the chemical agent actually selected for the tumor-imaging study. As an initial screen to select analogues for isotopic labeling, a glucose tolerance test was performed to assay diabetogenic potential. This procedure has been described previously (14). Candidates were selected from the three classes synthesized: 5-arylthiobarbituric acids (IV), 5-aryliminobarbituric acids (V), and 5-aryldialuric acids (VI).

A new and more facile synthesis of 5-arylthiobarbituric acids (IVa–c) was developed from triphenylphosphine–alloxan adducts (VII), whose synthesis was described in an earlier publication (15), and aromatic thiols (Scheme

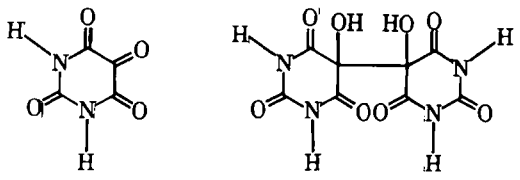

alloxan

I

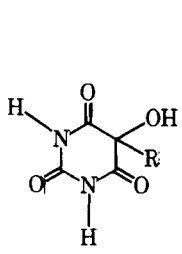

II: R = OH
III: R = H

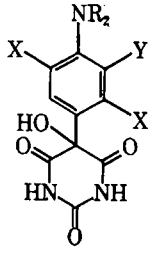

VIa: R = X = Y = H
VIb: R = Me, X = Y = H
VIc: R = Y = H, X = OMe
VId: R = Y = H, X = OEt

0022-3549/84/0300-0394$01.00/0

© 1984, American Pharmaceutical Association

composed of different fractions or that "degradation" occurred during the storage period of lot WPTY 175B. No matter which hypothesis is retained, the product has not lost its activity as far as emulsifying or surface-active properties are concerned.

Nevertheless, the average molecular weight of an emulsifier ought to be known in order to determine its surface excess and to produce the curve of the surface pressure *versus* "molecular" cross-sectional area of the emulsifier (7). Relying on the reported molecular weight can generate misleading values for the aforementioned parameters, especially if the data are obtained from different batches of the same emulsifier. No comparison can be made between the behavior of different lots of one product unless a correction is made for the difference in their molecular weights.

REFERENCES

(1) G. Champetier, L. Monnerie, "Introduction à la Chimie Macromoléculaire," Masson & Cie., Paris, 1969, p. 206.

(2) K. E. Chung, L. L. Anderson, and W. H. Wiser, *Fuel*, **58**, 847 (1979).

(3) J. Zynger and A. D. Kossoy, *Anal. Chem.*, **52**, 1538 (1980).

(4) R. V. Figini, *Makromol. Chem.*, **181**, 2409 (1980).

(5) "The Wonderful World of Pluronic Polyols," BASF-Wyandotte, Mich., 1973.

(6) J. L. Woodhead, J. A. Lewis, G. N. Malcolm, and I. D. Watson, *J. Colloid Interface Sci.*, **79**, 454 (1981).

(7) F. Guay and S. Bisaillon, *J. Colloid Interface Sci.*, **93**, 25 (1983).

ACKNOWLEDGMENTS

The authors acknowledge the award of a studentship and a research grant from the Medical Research Council of Canada and from C.A.F.I.R. (University of Montreal). We are also grateful to BASF-Wyandotte and Atlas Chemical Industries for providing the surface-active agents, and wish to thank Ginette Giasson-Gagnon for her technical assistance.

Alloxan Analogues as Potential Pancreatic-Imaging Radiopharmaceuticals

WILLIAM E. ADAMS *, NED D. HEINDEL *x, GENE TUTWILER ‡, and HENRY FAWTHROP ‡

Received August 19, 1982, from the **Center for Health Sciences, Lehigh University, Bethlehem, PA 18015* and the ‡*Biochemistry Department, McNeil Laboratories, Spring House, PA 19477.* Accepted for publication January 10, 1983.

Abstract □ Three families of alloxan derivatives, 5-arylthiobarbituric, 5-aryliminobarbituric, and 5-aryldialuric acids, were prepared as prospective radioiodine-transporting radiopharmaceuticals for the delineation of pancreatic insulinomas. Members of each class were screened for effects on blood sugar levels in a rat glucose tolerance assay. Transient hyperglycemia was observed with 5-(2,4-dichlorophenyl)iminobarbituric acid. No agent evaluated induced permanent diabetes at the doses tested.

Keyphrases □ Alloxan—analogues, potential tumor-imaging agents, pancreatic insulinomas, effect on blood glucose levels, rats □ Tumor-imaging agents—alloxan analogues, pancreatic insulinomas, effect on blood glucose levels, rats

Alloxan and several of its derivatives are diabetogenic (1–3). While no definitive structure–activity studies have been reported, it appears that alloxan, alloxan monohydrate (II), alloxantin (I), and dialuric acid (III), without bulky substituents on nitrogen, are all able to induce frank diabetes (1–3). Some evidence supports a direct effect on the pancreas, for degranulation of β-cells is observed; [^{14}C]alloxan was shown to concentrate in the islet cells by autoradiography (4–7).

Development of radiopharmaceuticals for the scintigraphic imaging of occult pancreatic malignancies has been a goal of these laboratories for several years (8–11). In at least one previous study, it has been shown that substances with direct effects on serum glucose levels can, if radioisotopically labeled, preferentially delineate insulinomas (12, 13). Alloxan analogues would appear worthy of investigation in this regard.

Three classes of alloxan derivatives have been prepared which differ from the parent molecule by possessing an aryl moiety at C-5. This pendant aromatic ring would provide a suitable locus for the attachment of radioiodine in the chemical agent actually selected for the tumor-imaging study. As an initial screen to select analogues for isotopic labeling, a glucose tolerance test was performed to assay diabetogenic potential. This procedure has been described previously (14). Candidates were selected from the three classes synthesized: 5-arylthiobarbituric acids (IV), 5-aryliminobarbituric acids (V), and 5-aryldialuric acids (VI).

A new and more facile synthesis of 5-arylthiobarbituric acids (IVa–c) was developed from triphenylphosphine–alloxan adducts (VII), whose synthesis was described in an earlier publication (15), and aromatic thiols (Scheme

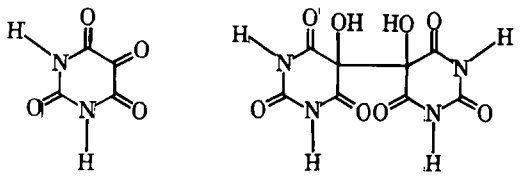

alloxan

I

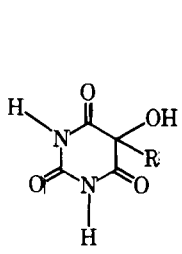

II: R = OH
III: R = H

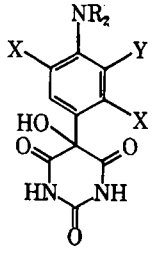

VIa: R = X = Y = H
VIb: R = Me, X = Y = H
VIc: R = Y = H, X = OMe
VId: R = Y = H, X = OEt

0022-3549/84/0300-0394$01.00/0

© 1984, American Pharmaceutical Association

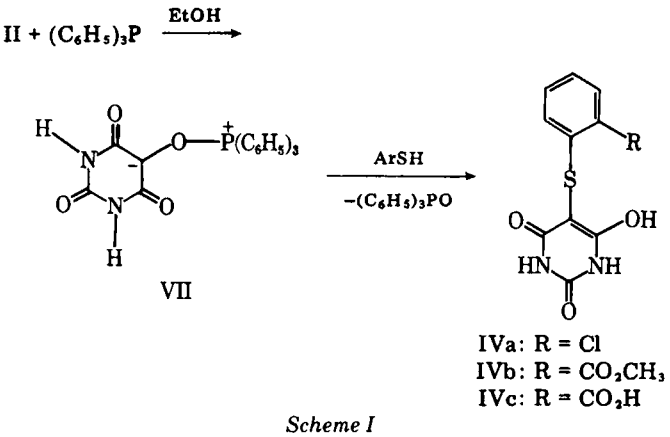

Scheme I

I). The mercapto function displaces the triphenylphosphine oxide to generate the arylthiobarbiturates. Since the alloxan–triphenylphosphine adduct is available in nearly quantitative yield, the overall conversion to the desired products (IVa–c) is more convenient than the published route, which requires the preparation and purification of 5-chlorobarbituric acid and subsequent nucleophilic displacement of the chloro group by an arylthiolate anion (16).

5-Aryliminobarbituric acids have been previously prepared from alloxan anhydride, which was obtained by dehydration of the alloxan monohydrate (II) (17). Here, the alloxan anhydride, generated *in situ* by treatment of the monohydrate with glacial acetic acid, was trapped by the aromatic amine (Scheme II).

The dialuric acids (VIa–g) were generated by condensation of anilines, possessing an unsubstituted *para*-position, with alloxan monohydrate in glacial acetic acid. Even primary aromatic amines with open *para*-positions condense preferentially at the *para* site (to form dialuric acids) rather than at the amino group (to form iminobarbiturates) (17–20).

EXPERIMENTAL[1]

5-Arylthiobarbituric Acids (IVa–c)—Equimolar amounts (5.0 mmol) of the triphenylphosphine–alloxan adduct (VII) (15) and the requisite aromatic thiol (see Scheme I) were refluxed for 2 h in 50 mL of 1:1 glacial acetic acid–absolute ethanol. The solvent was evaporated *in vacuo* to approximately one-half the original volume, the mixture was chilled, and the product was removed by filtration. The resulting thiobarbiturates were recrystallized by dissolution in a minimal quantity of boiling ethanol and reprecipitation by dropwise addition of 1:3 benzene–petroleum ether (60–110°C). The 5-arylthiobarbituric acids were characterized by broad—OH and —NH absorption in the IR between 2800 and 3300 cm^{-1} and by carbonyl absorption at 1725 ± 5, 1705 ± 5, and 1645 ± 5 cm^{-1}. Yields are reported in Table I.

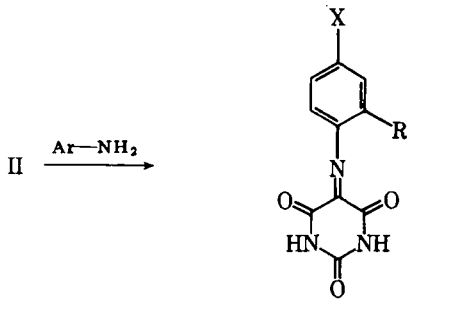

Scheme II

5-Aryliminobarbituric Acids (Va–d)—Equimolar amounts (6.25 mmol) of alloxan monohydrate (II) and the requisite aniline (see Scheme II) were heated at reflux in 15 mL of glacial acetic acid for 0.5 h. The mixture was cooled (0°C); Vb–d crystallized as red-purple solids and Va separated as an oil (crystallized from dioxane–benzene). The solids, Vb–d, were washed with a minimum of warm benzene, filtered, and dried *in vacuo* to yield analytical specimens. The 5-aryliminobarbituric acids were characterized by composite —OH and —NH absorption between 2820 and 3380 cm^{-1} and by carbonyl and imine absorption at 1750 ± 5, 1720 ± 5, and 1680 ± 5 cm^{-1}. Yields are reported in Table I.

5-Aryldialuric Acids (VIa–d)—The dialuric acids were prepared by a previously described method (20) from equimolar amounts (6.25 mmol) of alloxan monohydrate and an aniline with an unsubstituted *para*-position in 20 mL of glacial acetic acid at 25°C. The mixture was stirred at ambient temperature for 30 min, chilled, and the product removed by filtration. The resulting crystalline material was washed with 2 × 10-mL portions of cold glacial acetic acid and then dried (0.01 mm). Yields are reported in Table I. The IR spectra displayed —OH and —NH absorption between 3100 and 3600 cm^{-1} and carbonyl absorption at 1730 ± 5 and 1710 ± 5 cm^{-1}.

[1] Analyses were performed by Dr. G. I. Robertson, Florham Park, N.J. Melting points were determined between glass disks on a Fisher-Johns Apparatus and are reported uncorrected. NMR spectra were obtained on a Perkin-Elmer Hitachi R20A spectrometer and are calibrated against tetramethylsilane. Infrared spectra were taken in 1–2% KBr disks on a Perkin-Elmer Model 257 infrared spectrometer.

Table I—Alloxan Analogues Investigated as Potential Pancreatic Radiopharmaceuticals

Compound	Formula[a]	mp, °C dec.	Yield, %
IVa	$C_{10}H_7ClN_2O_3S$	268.0–268.5	34
IVb	$C_{12}H_{10}N_2O_5S \cdot \frac{3}{4}H_2O$	235	17
IVc	$C_{11}H_8N_2O_5S \cdot \frac{1}{2}H_2O$	247–248	39
Va	$C_{10}H_5Cl_2N_3O_3$	251–253	40
Vb	$C_{10}H_6BrN_3O_3 \cdot \frac{1}{4}H_2O$	234	64
Vc	$C_{10}H_7N_3O_4 \cdot \frac{1}{4}H_2O$	>300	94
VIa		252–253[b]	67
VIb		232–233[c]	72
VIc	$C_{12}H_{13}N_3O_6$	267–270	83
VId	$C_{14}H_{17}N_3O_6$	225–226	85

[a] Elemental analyses for C, N, and H were within 0.4% of the theoretical values for all compounds. [b] Lit. mp 248°C (dec.) (ref. 19). [c] Lit. mp 230°C (dec.) (ref. 19).

RESULTS AND DISCUSSION

Six of the materials prepared in this study, including representatives of each of the three compound classes, underwent a rat glucose tolerance screen. The assay was performed as previously described (14) on sets of three male Sprague–Dawley (210–250 g) rats fasted for 48 h prior to intraperitoneal injection of the test compound as a suspension in 0.5% methylcellulose. Animals were administered glucose (1.0 g/kg of body weight) orally 30 min after injection of the test compound. Blood, withdrawn from the tail vein at the time of glucose administration and at 1, 2, 3, 4, 5, 6, 24, and 48 h postdose, was analyzed for glucose by a previously described method (21). The maximum percent rise in blood glucose and any permanent glycosuria were the test observations made on the candidate agents.

The two dialuric acid derivatives, VIa and b, were inactive at 50 mg/kg ip; VIc was evaluated at 100 mg/kg and was similarly inactive. The thiobarbiturate IVb was inactive at 43 mg/kg, and the iminobarbiturate Vd was inactive at 50 mg/kg. However, the 5-(2,4-dichlorophenyl)iminobarbituric acid (Va) was toxic to all three rats at 100 mg/kg and produced a marked, but transient, rise (*i.e.*, 48% at 2 h) in blood glucose with no permanent hyperglycemia and no toxic deaths at 25 mg/kg ip.

The doses employed in this study were below the diabetogenic levels usually reported for alloxan-induced diabetes in rats (22), but they were in vast excess of the levels which would be employed in radiolabeled, carrier-free, radiopharmaceuticals. The absence of any permanent glycosuria at 48 h postdose and the transient rise in blood glucose (for Va) indicate that at these concentration levels, the alloxan derivatives are probably not cytotoxic to sufficient β-cells to be diabetogenic. The one active imine (Va) may, in fact, induce hyperglycemia by an *in vivo* hy-

drolytic scission to alloxan itself; electron-withdrawing halogens on the aryl ring would be anticipated to activate the anil to hydrolysis. Compound Va would appear to be an attractive candidate for radiohalogenation and study as an insulinoma-imaging agent with the caveat that *in vivo* hydrolysis may separate the label-bearing aniline and thwart target uptake of the tracer.

REFERENCES

(1) G. Brückmann and E. Wertheimer, *J. Biol. Chem.*, **168**, 241 (1947).

(2) P. H. Hidy, *J. Biol. Chem.*, **163**, 307 (1946).

(3) H. R. Jacobs, *Proc. Soc. Exp. Biol. Med.*, **37**, 407 (1935).

(4) J. L. Webb, "Enzyme and Metabolic Inhibitors," Vol. III, Academic, New York, N.Y., 1966, pp. 367–419.

(5) D. Watkins, S. J. Cooperstein, and A. Lazarow, *Am. J. Physiol.*, **207**, 431 (1964).

(6) S. J. Cooperstein, D. Watkins, and A. Lazarow, "Structure and Metabolism of Pancreatic Islets," Proc. 3rd International Symposium, Uppsalla and Stockholm, Sweden, 1963, p. 389.

(7) L. Hammarström, B. Hellman, and S. Ullberg, *Diabetologia*, **3**, 340 (1967).

(8) N. D. Heindel, V. R. Risch, H. D. Burns, T. Honda, L. W. Brady, and M. Micalizzi, *J. Pharm. Sci.*, **64**, 687 (1975).

(9) N. D. Heindel, V. R. Risch, W. E. Adams, T. Honda, and L. W. Brady, *Int. J. Appl. Radiat. Isot.*, **27**, 621 (1976).

(10) A. M. Markoe, V. R. Risch, N. D. Heindel, J. Emrich, W. Lippincott, T. Honda, and L. W. Brady, *J. Nucl. Med.*, **20**, 753 (1979).

(11) V. R. Risch, T. Honda, N. D. Heindel, J. Emrich, and L. W. Brady, *Radiology*, **124**, 837 (1977).

(12) N. D. Heindel, H. D. Burns, R. Schneider, and N. Foster, in "Structure-Activity Relationships in Radiopharmaceuticals," R. Spencer, Ed., Grune and Stratton, New York, N.Y., 1981, pp. 101–128.

(13) N. D. Heindel, V. R. Risch, H. D. Burns, E. G. Corley, E. Michener, and T. Honda, "Proc. 2nd International Symposium on Radiopharmacy," V. Sodd, D. Hoogland, D. Allen and R. Ice, Eds., Society Nuclear Medicine, New York, N.Y., 1979, pp. 697–707.

(14) G. F. Tutwiler, G. J. Bridi, T. J. Kirsch, H. D. Burns, and N. D. Heindel, *Proc. Soc. Exp. Bio. Med.*, **152**, 195 (1976).

(15) W. E. Adams and N. D. Heindel, *J. Heterocycl. Chem.*, **17**, 559 (1980).

(16) H. Fenner, R. W. Grauert, and P. Hemmerich, *Justus Liebigs Ann. Chem.*, **1978**, 193.

(17) J. W. Clark-Lewis and J. A. Edgar, *J. Chem. Soc.*, **1965**, 5551.

(18) Chemische Fabrik Boehringer and Sohne, Ger. Pat. 112,174 (1900); see also Chem. Zentralblatt, **II**, 789 (1900).

(19) G. Pellizzari, *Gaz. Chim. Ital.*, **17**, 409 (1887); see also *J. Chem. Soc.*, **54**, 142 (1888).

(20) J. W. Clark-Lewis and K. Moody, *Aust. J. Chem.*, **23**, 1229 (1970).

(21) G. F. Tutwiler, *Int. J. Biochem.*, **5**, 107 (1974).

(22) E. H. Kass and B. A. Waisbren, *Proc. Soc. Exp. Bio. Med.*, **60**, 303 (1945).

ACKNOWLEDGMENTS

This study was supported by grants from the Elsa U. Pardee Foundation and the W. W. Smith Foundation.

Analysis of Gossypol and Gossypol–Acetic Acid by High-Performance Liquid Chromatography

GUIDO B. MARCELLE, MOHAMED S. AHMED *, JOHN M. PEZZUTO, GEOFFREY A. CORDELL ˣ, DONALD P. WALLER, D. D. SOEJARTO, and H. H. S. FONG

Received September 16, 1982, from the *Department of Pharmacognosy and Pharmacology, College of Pharmacy, University of Illinois at the Medical Center, Chicago, IL 60612.* Accepted for publication January 10, 1983. *Present Address: Faculty of Pharmacy, Cairo University, Cairo, Egypt.

Abstract □ Gossypol, a bis-sesquiterpenoid cotton pigment, is of current interest as a male fertility-regulating agent. For the purposes of analyzing material to be studied biologically, a method is described for the analysis of gossypol by high-performance liquid chromatography. This has been used for examining the purity of gossypol–acetic acid using a UV-absorbance ratio technique.

Keyphrases □ Gossypol—analysis, gossypol–acetic acid, high-performance liquid chromatography □ Contraceptives, male—gossypol–acetic acid, analysis, high-performance liquid chromatography

Gossypol (I), one of several pigments isolated from *Gossypium* (Malvaceae) (1, 2), is found in concentrations of up to 1.7% in cotton seeds (*G. hirsutum* L.). Because of the toxicity of gossypol, cotton seed flour has limited use for humans and domestic animals; the upper limit of gossypol concentration for human consumption has been set at 0.045% (3). Gossypol is reported to be unstable and is, therefore, usually available as the 1:1 complex with acetic acid (1, 2, 4, 5)[1].

Several analyses of gossypol have been described, including complexation with aromatic amines followed by UV analysis (6, 7), GC analysis of the trimethylsilyl ether (8) and *N,O*-bis(trimethylsilyl) acetamide derivatives (9), paper chromatography (10), and TLC (11). A recent (12) communication describing the high-performance liquid chromatographic (HPLC) analysis of gossypol prompts us to report our own efforts in this area[2].

Our interest in gossypol was stimulated by reports that it possessed *in vitro* spermicidal activity (13, 14) and *in*

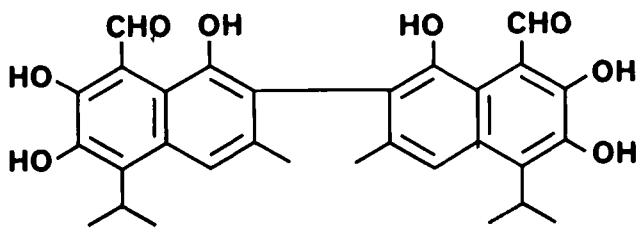

I

[1] For an extensive review of early chemical work on gossypol see Ref. 1; for a broader discussion of gossypol see Ref. 2.

[2] This work was first presented at a meeting of the Core Group of Advisors to the Chemical Synthesis Programme, Task Force on Long-Acting Agents for the Regulation of Fertility, World Health Organization, held in Bethesda, Md., November 1980.

0022-3549/84/0300-0396$01.00/0

© 1984, American Pharmaceutical Association

drolytic scission to alloxan itself; electron-withdrawing halogens on the aryl ring would be anticipated to activate the anil to hydrolysis. Compound Va would appear to be an attractive candidate for radiohalogenation and study as an insulinoma-imaging agent with the caveat that *in vivo* hydrolysis may separate the label-bearing aniline and thwart target uptake of the tracer.

REFERENCES

(1) G. Brückmann and E. Wertheimer, *J. Biol. Chem.*, **168**, 241 (1947).

(2) P. H. Hidy, *J. Biol. Chem.*, **163**, 307 (1946).

(3) H. R. Jacobs, *Proc. Soc. Exp. Biol. Med.*, **37**, 407 (1935).

(4) J. L. Webb, "Enzyme and Metabolic Inhibitors," Vol. III, Academic, New York, N.Y., 1966, pp. 367–419.

(5) D. Watkins, S. J. Cooperstein, and A. Lazarow, *Am. J. Physiol.*, **207**, 431 (1964).

(6) S. J. Cooperstein, D. Watkins, and A. Lazarow, "Structure and Metabolism of Pancreatic Islets," Proc. 3rd International Symposium, Uppsalla and Stockholm, Sweden, 1963, p. 389.

(7) L. Hammarström, B. Hellman, and S. Ullberg, *Diabetologia*, **3**, 340 (1967).

(8) N. D. Heindel, V. R. Risch, H. D. Burns, T. Honda, L. W. Brady, and M. Micalizzi, *J. Pharm. Sci.*, **64**, 687 (1975).

(9) N. D. Heindel, V. R. Risch, W. E. Adams, T. Honda, and L. W. Brady, *Int. J. Appl. Radiat. Isot.*, **27**, 621 (1976).

(10) A. M. Markoe, V. R. Risch, N. D. Heindel, J. Emrich, W. Lippincott, T. Honda, and L. W. Brady, *J. Nucl. Med.*, **20**, 753 (1979).

(11) V. R. Risch, T. Honda, N. D. Heindel, J. Emrich, and L. W. Brady, *Radiology*, **124**, 837 (1977).

(12) N. D. Heindel, H. D. Burns, R. Schneider, and N. Foster, in "Structure-Activity Relationships in Radiopharmaceuticals," R. Spencer, Ed., Grune and Stratton, New York, N.Y., 1981, pp. 101–128.

(13) N. D. Heindel, V. R. Risch, H. D. Burns, E. G. Corley, E. Michener, and T. Honda, "Proc. 2nd International Symposium on Radiopharmacy," V. Sodd, D. Hoogland, D. Allen and R. Ice, Eds., Society Nuclear Medicine, New York, N.Y., 1979, pp. 697–707.

(14) G. F. Tutwiler, G. J. Bridi, T. J. Kirsch, H. D. Burns, and N. D. Heindel, *Proc. Soc. Exp. Bio. Med.*, **152**, 195 (1976).

(15) W. E. Adams and N. D. Heindel, *J. Heterocycl. Chem.*, **17**, 559 (1980).

(16) H. Fenner, R. W. Grauert, and P. Hemmerich, *Justus Liebigs Ann. Chem.*, **1978**, 193.

(17) J. W. Clark-Lewis and J. A. Edgar, *J. Chem. Soc.*, **1965**, 5551.

(18) Chemische Fabrik Boehringer and Sohne, Ger. Pat. 112,174 (1900); see also Chem. Zentralblatt, **II**, 789 (1900).

(19) G. Pellizzari, *Gaz. Chim. Ital.*, **17**, 409 (1887); see also *J. Chem. Soc.*, **54**, 142 (1888).

(20) J. W. Clark-Lewis and K. Moody, *Aust. J. Chem.*, **23**, 1229 (1970).

(21) G. F. Tutwiler, *Int. J. Biochem.*, **5**, 107 (1974).

(22) E. H. Kass and B. A. Waisbren, *Proc. Soc. Exp. Bio. Med.*, **60**, 303 (1945).

ACKNOWLEDGMENTS

This study was supported by grants from the Elsa U. Pardee Foundation and the W. W. Smith Foundation.

Analysis of Gossypol and Gossypol–Acetic Acid by High-Performance Liquid Chromatography

GUIDO B. MARCELLE, MOHAMED S. AHMED *, JOHN M. PEZZUTO, GEOFFREY A. CORDELL ˣ, DONALD P. WALLER, D. D. SOEJARTO, and H. H. S. FONG

Received September 16, 1982, from the *Department of Pharmacognosy and Pharmacology, College of Pharmacy, University of Illinois at the Medical Center, Chicago, IL 60612.* Accepted for publication January 10, 1983. *Present Address: Faculty of Pharmacy, Cairo University, Cairo, Egypt.

Abstract □ Gossypol, a bis-sesquiterpenoid cotton pigment, is of current interest as a male fertility-regulating agent. For the purposes of analyzing material to be studied biologically, a method is described for the analysis of gossypol by high-performance liquid chromatography. This has been used for examining the purity of gossypol–acetic acid using a UV-absorbance ratio technique.

Keyphrases □ Gossypol—analysis, gossypol–acetic acid, high-performance liquid chromatography □ Contraceptives, male—gossypol–acetic acid, analysis, high-performance liquid chromatography

Gossypol (I), one of several pigments isolated from *Gossypium* (Malvaceae) (1, 2), is found in concentrations of up to 1.7% in cotton seeds (*G. hirsutum* L.). Because of the toxicity of gossypol, cotton seed flour has limited use for humans and domestic animals; the upper limit of gossypol concentration for human consumption has been set at 0.045% (3). Gossypol is reported to be unstable and is, therefore, usually available as the 1:1 complex with acetic acid (1, 2, 4, 5)[1].

Several analyses of gossypol have been described, including complexation with aromatic amines followed by UV analysis (6, 7), GC analysis of the trimethylsilyl ether (8) and *N,O*-bis(trimethylsilyl) acetamide derivatives (9), paper chromatography (10), and TLC (11). A recent (12) communication describing the high-performance liquid chromatographic (HPLC) analysis of gossypol prompts us to report our own efforts in this area[2].

Our interest in gossypol was stimulated by reports that it possessed *in vitro* spermicidal activity (13, 14) and *in*

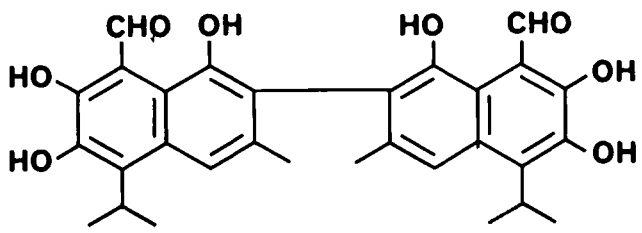

I

[1] For an extensive review of early chemical work on gossypol see Ref. 1; for a broader discussion of gossypol see Ref. 2.

[2] This work was first presented at a meeting of the Core Group of Advisors to the Chemical Synthesis Programme, Task Force on Long-Acting Agents for the Regulation of Fertility, World Health Organization, held in Bethesda, Md., November 1980.

0022-3549/84/0300-0396$01.00/0

© 1984, American Pharmaceutical Association

Table I—Analytical Solvent Systems Used for the HPLC Separation of Gossypol

Solvent	Column			
	μ-Porasil	μ-Styragel 500	μ-Bondapak Cyano	μ-Bondapak C_{18}
CCl_4		X		
$CHCl_3$				
alone	X	X	X	X
containing 0.01 M HOAc	X			
$CHCl_3$–MeOH (99:1)		X		
CH_2Cl_2		X		
CH_2Cl_2–isopropyl alcohol–H_2O (96:4:0.5)	X			
CH_2Cl_2–MeOH				
10:90			X	X
25:75			X	X
25:75, containing 0.001 M HOAc			X	X
95:5	X			
99:1		X		
CH_3CN				
alone			X	X
containing 0.01 M HOAc			X	X
containing 0.001 M HOAc			X	X
CH_3CN–H_2O (90:10)			X	X
CH_3CN–H_2O–HOAc				
35:65:0.1			X	X
70:20:10			X	X
CH_3CN–H_2O–MeOH (25:30:45)			X	X
MeOH			X	X
MeOH–H_2O (7:3)			X	X
MeOH–0.01 M K_3PO_4 (1:1)			X	X
MeOH–0.01 M KH_2PO_4 (85:15)			X	X
MeOH–0.025 M NaH_2PO_4 (40:60)			X	X
n-Propyl alcohol			X	X
Tetrahydrofuran		X		

vivo antifertility activity in several male mammalian species (rats, hamsters, and rhesus monkeys) (15, 16) including humans (17–19). A preliminary report of our work (20) indicates that gossypol, but not its chemically related impurities, has antifertility activity in male hamsters. A critical basis for these pharmacological experiments was the need to have highly purified gossypol available to be able, categorically, to indicate the nature of the material used for dosing. In this paper we report our efforts on the analysis of gossypol and a determination of the purity of gossypol–acetic acid by a combination of quantitative HPLC and HPLC–UV absorbance ratio techniques (21, 22).

EXPERIMENTAL

Materials—Gossypol [2,2′-bis(1,6,7-trihydroxy-3-methyl-5-isopropylnaphthalene-8-carboxaldehyde), (I)] was supplied as the acetic acid complex[3]. Gossypol, mp 182–184°C, was liberated from the complex by the procedure of Campbell *et al.* (23), followed by crystallization from petroleum ether–ether. Concordance with previously reported physical and spectroscopic data for gossypol (24) was established. A highly purified sample of gossypol–acetic acid[4] was recrystallized three times from methyl ethyl ketone–acetic acid (3:1).

All chemicals and solvents used in this investigation were reagent grade and when used for HPLC were redistilled in glass or were HPLC grade[5]. The melting point was determined using a Kofler hot-stage instrument and is uncorrected.

Equipment—The initial separations were conducted using a liquid chromatograph[6] equipped with a syringe-loading sample injector with

[3] Kindly supplied by Dr. V. Graci, Southern Regional Research Center, ARS, USDA, New Orleans, La.

[4] Kindly supplied by Dr. H. K. Kim, National Institute of Child Health and Human Development, National Institutes of Health, Bethesda, MD 20205.

[5] Fisher Scientific Co., Pittsburgh, PA 15219.

[6] Model 6000A; Waters Associates, Milford, MA 01757.

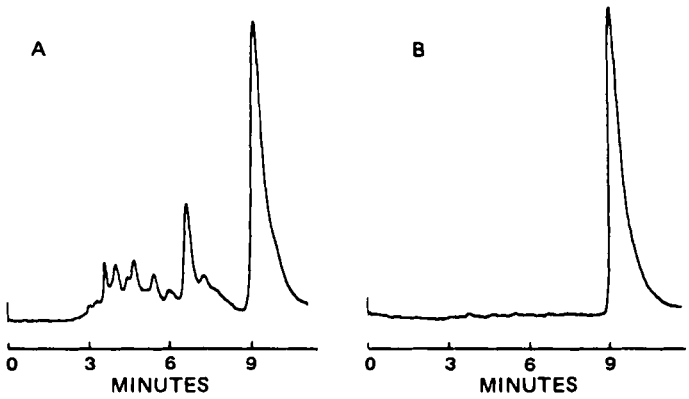

Figure 1—*Typical chromatograms of impure (A) and recrystallized (B) gossypol–acetic acid. For conditions see footnote 17.*

20-μL sample loop[7], a variable-wavelength UV spectrophotometer[8] at 285 nm, and a 25.4-cm strip-chart recorder[9]. Separations were carried out using 30 × 0.39-cm i.d. prepacked columns with a typical flow rate of 1 mL/min[10]. For subsequent analysis of gossypol–acetic acid, the HPLC apparatus used was a combination instrument consisting of a system controller[11], pumps[9] with an added stop–flow valve, a variable-wavelength UV spectrophotometric detector[12] with an automated control[13], an integrator–recorder[14], and an injector[15].

Separation of Gossypol—Table I indicates the analytical solvent systems which were used in a preliminary attempt to separate gossypol from its impurities. Thus, four systems were used with μ-Styragel 500[10], 17 with μ-Bondapak cyano[10], and 17 with μ-Bondapak C_{18} columns[10]. Only one of these systems [μ-Bondapak C_{18} column, CH_3CN:H_2O:HOAc (7:2:1)] was found to be effective for the required separation. Detection was carried out at 254 nm. Gossypol and gossypol–acetic acid had identical retention times in this system.

Purity of Gossypol–Acetic Acid—To examine the purity of gossypol–acetic acid by HPLC, the best wavelength(s) for its detection were first established. Using the analytical solvent system described above, UV spectra of gossypol–acetic acid were obtained on a grating spectrophotometer[16] [complex dissolved in CH_3CN–H_2O–HOAc (7:2:1)] and using a variable-wavelength UV spectrophotometric detector[11] (directly on the solution eluting from the reverse-phase column). Maxima were observed at 254, 263 (sh), 283, 293, and 371 nm. When the absorbance was monitored at 254 nm[17], 260 nm[17], and 290 nm[17], gossypol–acetic acid eluted as a single peak (retention time, 9.18 min), and integration of the area under the peak indicated a minimum purity of 99.90%[18].

RESULTS AND DISCUSSION

Figure 1 shows typical chromatograms of impure gossypol–acetic acid (A) and the recrystallized gossypol–acetic acid (B) used as a standard. The lower limit of detection was 5 μg at 0.04 AUFS and 5 ng at 0.01 AUFS.

For the chromatographic conditions used, the peak representing gossypol–acetic acid has some tailing. To demonstrate that this peak was intrinsically a single peak and to further substantiate the purity of the gossypol–acetic acid sample, an absorbance ratio technique was utilized (21, 22). In this experiment, the flow of the eluting peak was stopped at the leading edge (point 1), and crest (point 2), and the trailing edge (point 3), as illustrated in Fig. 2. Based on the UV-absorption spectra of gossypol–acetic acid taken in CH_3CN–H_2O–HOAc (7:2:1), absorbancy was

[7] Rheodyne model T120; Waters Associates, Milford, MA 01757.

[8] Model 450; Waters Associates, Milford, MA 01757.

[9] Beckman Instruments, Fullerton, CA 92634.

[10] Waters Associates, Milford, MA 01757.

[11] Model 21421; Beckman Instruments, Fullerton, CA 92634.

[12] Model LC85; Perkin-Elmer Corp., Norwalk, CT 06856.

[13] Autocontrol, Model LC75; Perkin-Elmer Corp., Norwalk, CT 06856.

[14] Model C-R1A; Altex Scientific, Inc., Berkeley, CA 94710.

[15] Model 210; Altex Scientific, Inc., Berkeley, CA 94710.

[16] Model DB-G; Beckman Instruments, Fullerton, CA 92634.

[17] Conditions: μBondapak C_{18} (10-μm particle size) column (3.9 mm × 30 cm); eluant CH_3CN:H_2O:HOAc (7:2:1); flow rate, 1.0 mL/min; temperature, 26°C; sample concentration, 0.27 mg/mL; injection volume, 4 μL; sensitivity, 0.04 AUFS; inlet pressure, 1057 psi; chart speed, 10 mm/min.

[18] The chromatographic profile generally indicated a single peak eluting at 9.18 min. Occasionally, a small peak (≤0.3%) eluted at the solvent front (3.42 min) which could be attributed to a system artifact.

Table II—Absorbance Ratios for Gossypol–Acetic Acid

Stopping Point	Absorbance Readings				Absorbance Ratios, λ_1/λ_2					
	254 nm	260 nm	290 nm	370 nm	254/260 nm	254/290 nm	254/370 nm	260/290 nm	260/370 nm	290/370 nm
1. Leading edge	0.063	0.054	0.056	0.031	1.167	1.125	2.032	0.964	1.742	1.806
	0.083	0.071	0.074	0.041	1.169	1.122	2.024	0.959	1.732	1.805
	0.057	0.049	0.051	0.028	1.163	1.117	2.036	0.961	1.750	1.821
	0.064	0.055	0.057	0.031	1.164	1.122	2.064	0.965	1.774	1.838
2. Crest	0.105	0.090	0.094	0.049	1.167	1.117	2.100	0.958	1.837	1.918
	0.106	0.091	0.095	0.051	1.165	1.116	2.078	0.958	1.784	1.863
	0.105	0.090	0.094	0.049	1.167	1.117	2.100	0.958	1.837	1.918
	0.106	0.091	0.095	0.051	1.165	1.116	2.078	0.958	1.784	1.863
3. Trailing edge	0.049	0.042	0.044	0.023	1.167	1.114	2.130	0.955	1.826	1.913
	0.032	0.028	0.029	0.015	1.143	1.103	2.133	0.965	1.866	1.933
	0.043	0.037	0.039	0.021	1.162	1.103	2.048	0.948	1.762	1.857
	0.043	0.037	0.039	0.021	1.162	1.103	2.048	0.948	1.762	1.857
Mean					1.164	1.115	2.073	0.958	1.788	1.866
SD					0.007	0.008	0.037	0.006	0.043	0.045
RSD, %					0.60	0.72	1.78	0.42	1.85	2.41

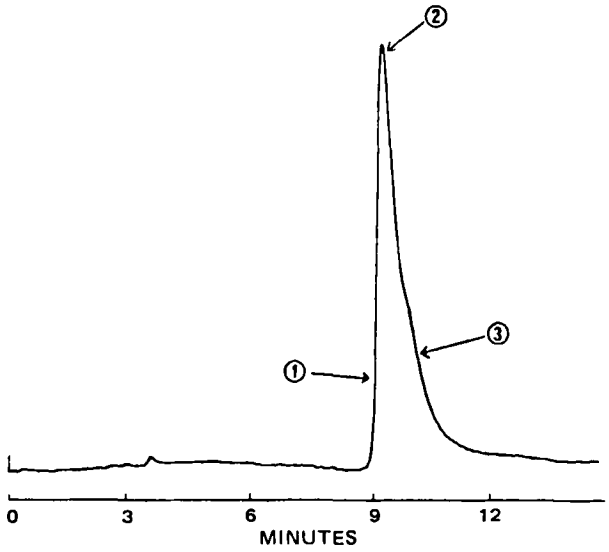

Figure 2—*Points of eluting HPLC peak of gossypol–acetic acid at which absorbance measurements were made at preselected wavelengths. Key: (1) leading edge, (2) crest, (3) trailing edge.*

determined at four preselected wavelengths (254, 260, 290, and 370 nm) each time the flow was stopped. The sensitivity was reduced for higher absorbance readings. Absorbance ratios were then calculated for (λ_1/λ_2) 254/260, 254/290, 254/370, and 290/370 nm. The experiment was done in replicate. The results (Table II) strongly indicate that the chromatographic peak for gossypol–acetic acid consists of a single, spectroscopically (UV, IR, ^{1}H-NMR, ^{13}C-NMR, and MS) pure substance, since the absorbance ratios at the various points of the peak did not differ significantly.

From these results the most consistent and reliable ratios are those involving wavelengths of 254, 260, and 290 nm. From an analysis of variance of the calculated absorbance ratios taking the leading edge, the crest, and the trailing edge as three distinct populations, the results were $F_{2,69} = 0.03$; the reference shows $F_{0.005,2,60} = 5.80$. The three sets of ratios are therefore similar with a 99.5% degree of confidence. This method appears to be a highly effective HPLC technique for the analysis of gossypol–acetic acid, which is superior to those reported previously.

REFERENCES

(1) R. Adams, T. A. Geissman, and J. D. Edwards, *Chem. Rev.*, **60**, 555 (1960).

(2) A. L. Markman and V. P. Rzhekhin, "Gossypol and Its Derivatives," Israel Program for Scientific Translations, Jerusalem, 1969.

(3) L. C. Bocardi and L. A. Goldblatt, "Toxic Constituents of Plant Foodstuffs," Academic, New York, N.Y., 1969, p. 211.

(4) J. O. Halverson and F. H. Smith, *Ind. Eng. Chem.*, **5**, 29 (1953).

(5) C. L. Hoffpauir, J. A. Harris, and J. P. Hughes, *J. Assoc. Off. Agric. Chem.*, **43**, 329 (1960).

(6) F. H. Smith, *J. Am. Oil Chem. Soc.*, **35**, 261 (1958).

(7) W. A. Pons, Jr., C. L. Hoffpauir, and R. T. O'Connor, *J. Am. Oil Chem. Soc.*, **27**, 390 (1950).

(8) P. I. Raju and C. M. Cater, *J. Am. Oil Chem. Soc.*, **44**, 465 (1967).

(9) M. A. McClure, *J. Chromatogr.*, **54**, 25 (1971).

(10) G. Schramm and J. H. Benedict, *J. Am. Oil Chem. Soc.*, **35**, 371 (1958).

(11) M. B. Abou-Donia and J. W. Dieckart, *Toxicol. Appl. Pharmacol.*, **31**, 32 (1975).

(12) S. A. Abou-Donia, J. M. Lasker, and M. B. Abou-Donia, *J. Chromatogr.*, **206**, 606 (1981).

(13) D. P. Waller, L. J. D. Zaneveld, and H. H. S. Fong, *Contraception*, **22**, 183 (1980).

(14) H. Poso, K. Wichmann, J. Janne, and T. Luukkainen, *Lancet*, **i**, 885 (1980).

(15) M. C. Chang, Z. P. Gu, and S. K. Saksena, *Contraception*, **21**, 461 (1980).

(16) Y. C. Lin, M. A. Hadley, D. Klingener, and M. Dym, *Abstr. Soc. Study Reprod.*, Ann Arbor, Mich., Aug. 1980, p. 149.

(17) Anonymous, *Chin. Med. J.*, **4**, 417 (1978).

(18) Anonymous, *Gynecol. Obstet. Invest.*, **10**, 163 (1979).

(19) S. P. Xie, *Symp. Rec. Adv. Fert. Reg.*, Beijing, China, Sept. 1980.

(20) D. P. Waller, H. H. S. Fong, G. A. Cordell, and D. D. Soejarto, *Contraception*, **23**, 653 (1981).

(21) R. Yost, J. Stoveken, and W. MacLean, *J. Chromatogr.*, **134**, 73 (1977).

(22) A. F. Poile and R. D. Conlon, The Pittsburgh Conference on Analytical Chemistry and Applied Spectroscopy, March (1979), paper no. 252.

(23) K. N. Campbell, R. C. Morris, and R. Adams, *J. Am. Chem. Soc.*, **59**, 1723 (1980).

(24) R. D. Stipanovic, A. A. Bell, M. E. Mace, and C. R. Howell, *Phytochemistry*, **14**, 1077 (1975).

ACKNOWLEDGMENTS

This investigation was supported in part by funds from the Special Programme of Research, Development and Research Training in Human Reproduction, World Health Organization (HRP Project 77918C).

Noninteraction of Temazepam and Cimetidine

DAVID J. GREENBLATT ˣ, DARRELL R. ABERNETHY, MARCIA DIVOLL, ANN LOCNISKAR, JEROLD S. HARMATZ, and RICHARD I. SHADER

Received October 6, 1982, from the *Division of Clinical Pharmacology, Departments of Psychiatry and Medicine, Tufts-New England Medical Center, Boston, MA 02111.* Accepted for publication February 11, 1983.

Abstract □ The possible kinetic interaction of the hypnotic temazepam and the H_2-receptor antagonist cimetidine was evaluated. Nine healthy male and female volunteers received a 30-mg oral dose of temazepam on two occasions in random sequence, separated by at least 1 week. On one occasion, temazepam was given in the otherwise drug-free state; on the other, temazepam was given with concurrent administration of cimetidine, 300 mg every 6 h. Mean pharmacokinetic parameters for temazepam in control *versus* cimetidine trials were: peak plasma concentration, 560 *versus* 498 ng/mL; time of peak concentration, 2.0 *versus* 2.1 h after the dose; volume of distribution, 1.30 *versus* 1.39 L/kg; elimination half-life, 9.9 *versus* 11.4 h; total clearance, 1.59 *versus* 1.60 mL/min/kg; free fraction of temazepam in plasma, 4.1 *versus* 3.8% unbound. Cimetidine has been shown to reduce the metabolic clearance of the benzodiazepines that are biotransformed by oxidative mechanisms. Temazepam, transformed by conjugation, appears unaffected by the coadministration of cimetidine.

Keyphrases □ Temazepam—noninteraction with cimetidine, pharmacokinetics □ Cimetidine—noninteraction with temazepam, pharmacokinetics □ Pharmacokinetics—noninteraction of temazepam and cimetine

Temazepam (I) is a 3-hydroxybenzodiazepine derivative utilized in clinical practice as an hypnotic (1). Previous studies have suggested that the widely prescribed antiulcer agent cimetidine (2, 3) may have the additional capacity to impair hepatic microsomal oxidizing capacity and thereby impair the metabolic clearance of certain benzodiazepine derivatives when the two are administered together. Cimetidine coadministration reduces the metabolic clearance of the oxidatively biotransformed benzodiazepines chlordiazepoxide, diazepam, desmethyldiazepam, alprazolam, and triazolam (4–9). However, cimetidine has very little influence on the clearance of benzodiazepines transformed by glucuronide conjugation, including oxazepam and lorazepam (8–10). Since temazepam is also metabolized by glucoronide conjugation (11), the present study was undertaken to test the hypothesis that cimetidine coadministration would similarly have little effect on the metabolic clearance of temazepam.

EXPERIMENTAL

Subjects and Procedure—Nine healthy male and female volunteers, aged 21–67 years, participated after giving written informed consent. All were healthy, active, ambulatory adults with no evidence of medical disease and were taking no other medications.

All subjects received a 30-mg oral dose of temazepam[1] on two occasions in random sequence separated by at least 1 week. On one occasion, temazepam was given in the control state without coadministration of other drugs. For the other trial, temazepam was administered during concurrent treatment with cimetidine[2], 300 mg taken every 6 h beginning 12 h prior to temazepam dosage and continuing for the entire 48-h duration of the temazepam kinetic study.

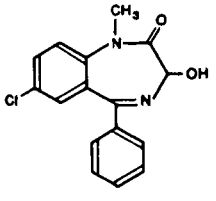

TEMAZEPAM

After an overnight fast, a single 30-mg oral dose of temazepam was administered with 100–200 mL of tap water. Subjects were tested for an additional 3 h after the dose. Venous blood samples were drawn into heparinized tubes prior to temazepam administration and at the following postdosage times: 5, 10, 15, 30, and 45 min, 1, 1.5, 2, 2.5, 3, 4, 6, 8, 12, 24, 32, and 48 h. Blood samples were centrifuged and the plasma separated and frozen until the time of assay.

Analysis of Samples—Plasma concentrations of temazepam were determined by electron-capture GC using a previously described method (12) with minor modifications. The analytical instrument[3] was a gas chromatograph equipped with a 15-mCi electron-capture detector, an automatic sampler, and an electronic data processor–integrator. The column was coiled glass, 183 cm in length by 2-mm i.d., packed with 1% OV-17 on 80/100 Chromosorb WHP. The column temperature was 270°C, and the injection port and detection temperatures were 310°C. The carrier gas was argon–methane (95:5) at 30 mL/min. After addition of 3-hydroxyprazepam as the internal standard, calibration standards and unknown plasma samples were extracted once with benzene–dichloromethane (80:20). After mixing and centrifugation, the organic extract was separated, evaporated to dryness, reconstituted, and injected into the chromatograph using the automatic sampler. Sensitivity, replicability, and linearity were as described previously (12). All samples

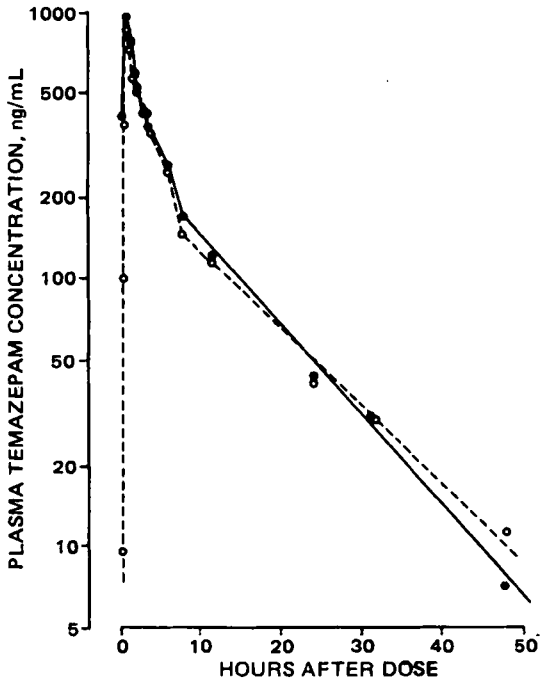

Figure 1—*Plasma temazepam concentrations in a representative volunteer after administration of 30 mg of temazepam in the control state and during concurrent treatment with cimetidine. Key: (●) control; (○) with cimetidine.*

[1] Restoril (C-IV) capsules; Sandoz Pharmaceuticals, East Hanover, N.J.

[2] Tagamet; Smith Kline and French, Philadelphia, Pa.

[3] Model 5830A or 5840A; Hewlett-Packard.

0022-3549/84/0300-0399$01.00/0
© 1984, American Pharmaceutical Association

Table I—Effect of Cimetidine on Temazepam Kinetics

	Mean (with Range) Values		Value of Student's *t* test
	Control	With Cimetidine	
Peak plasma concentration, ng/mL	560 (326–1002)	498 (367–849)	1.46 (NS)[a]
Time to peak concentration, h, postdose	2.1 (1.0–4.0)	2.0 (0.75–6.0)	0.14 (NS)
Volume of distribution, L/kg	1.30 (0.72–2.15)	1.39 (0.90–2.06)	0.81 (NS)
Elimination half-life, h	9.9 (5.6–17.7)	11.4 (5.5–21.4)	1.53 (NS)
Total clearance, mL/min/kg	1.59 (0.92–2.40)	1.60 (0.87–2.61)	0.11 (NS)
Free fraction, % unbound	4.1 (3.2–5.6)	3.8 (2.8–4.8)	1.99 (NS)

[a] NS = not significant.

from a given subject's two trials were extracted and analyzed on the same day using the same calibration standards.

For each subject the influence of cimetidine on temazepam plasma protein binding was determined using a 6-mL sample of plasma obtained in the nonfasting state during the control temazepam trial (without cimetidine treatment). Cimetidine (5 μg/mL) was added to one 3-mL plasma aliquot; no cimetidine was added to the other. Both aliquots were then spiked to contain 3.2 nCi/mL of [^{14}C]temazepam (specific activity: 11 μCi/mg). The extent of temazepam protein binding in each sample was determined in duplicate by equilibrium dialysis for 18 h at 37°C (13, 14). Compliance with the prescribed cimetidine regimen during the temazepam–cimetidine trial was verified by measurement of plasma cimetidine concentrations by HPLC (15) in samples drawn prior to temazepam dosage and at 12, 24, 32, and 48 h after the dose.

Kinetic Analysis—The apparent elimination half-life of temazepam was determined using the slope of the terminal log-linear plot of the plasma concentration curve (Fig. 1). The area under the curve from time zero until the final detectable concentration was determined using the trapezoidal method. To this was added the residual area extrapolated to infinity, calculated as the final concentration divided by the terminal rate constant (β). The sum of these two areas represents the total area under the plasma concentration curve (AUC). The total clearance of temazepam was calculated as dose/AUC, assuming that the entire 30-mg dose was available to the systemic circulation. Likewise, the apparent volume of distribution was calculated as clearance/β. Differences between control and cimetidine treatment conditions were analyzed by the Student's paired *t* test.

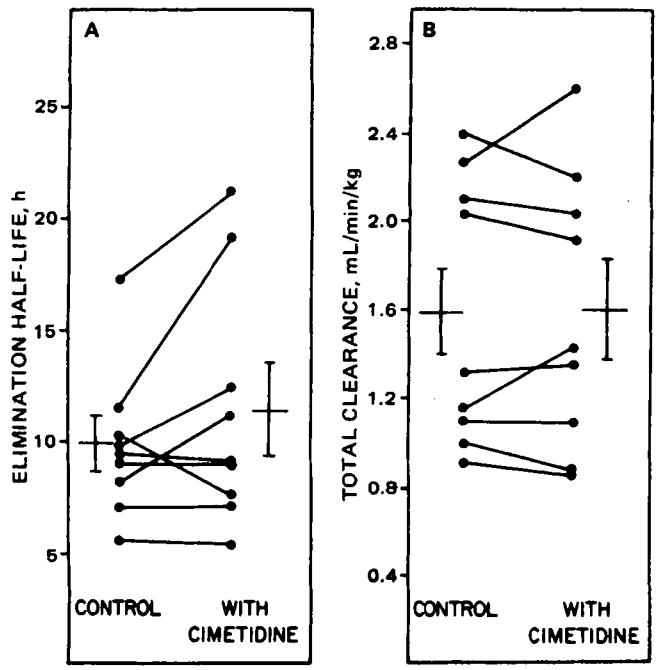

Figure 2—*Temazepam elimination half-life (A) and total metabolic clearance of temazepam (B) in the control state and during coadministration with cimetidine. Individual and mean (±SE) values are shown.*

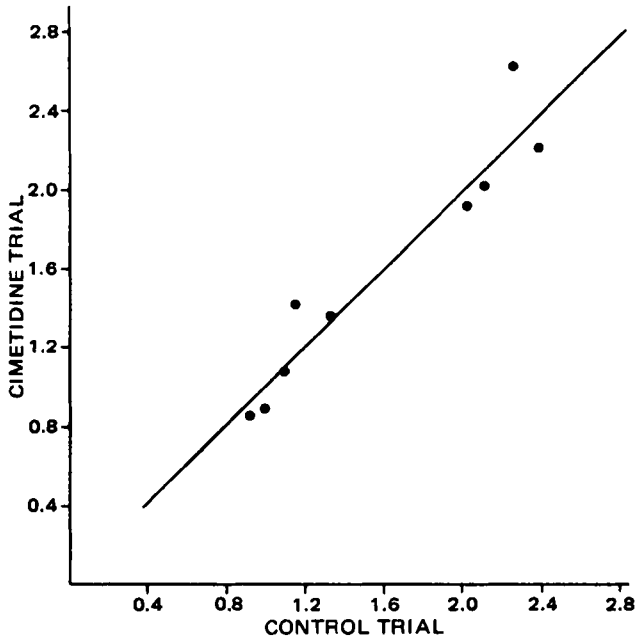

Figure 3—*Values of temazepam clearance (●) in mL/min/kg for the nine individuals during the control trial (x axis) and during coadministration with cimetidine (y axis). Solid line was determined by least-squares regression analysis. Note the high correlation and the regression line slope, which is not significantly different from unity. Slope = 0.98; r = 0.96.*

RESULTS

Compliance with the prescribed cimetidine regimen was acceptable in all subjects. Mean (±*SE*) plasma cimetidine concentrations were: prior to temazepam dosage, 1.43 (±0.32) μg/mL; 12 h postdose, 1.23 (±0.39) μg/mL; 24 h, 2.05 (±0.44) μg/mL; 32 h, 1.06 (±0.23) μg/mL; 48 h, 1.76 (±0.45) μg/mL.

Absorption of temazepam was not significantly influenced by cimetidine. The peak plasma concentration in control and cimetidine treatment conditions averaged 560 and 498 ng/mL, respectively, and the times of peak concentration averaged 2.0 and 2.1 h after the dose. Neither of these differences approached significance (Table I).

Temazepam volume of distribution, elimination half-life, and total clearance were similar between control and cimetidine treatment conditions (Table I, Figs. 1 and 2). Mean half-life values were 9.9 and 11.4 h, respectively, in the two conditions, with an overall range of 6–21 h. None of the differences approached statistical significance. Furthermore, for any given individual, temazepam clearance was highly reproducible between the two trials (Fig. 3). Temazepam free fraction in plasma averaged 4.1 and 3.8% in the two conditions; again the difference did not approach significance.

DISCUSSION

Cimetidine, an H_2-receptor antagonist that is extensively used in the treatment of peptic ulcer disease (2, 3), also has the secondary pharmacological property of impairing hepatic microsomal oxidizing capacity. Previous studies have indicated that benzodiazepines biotransformed by oxidative mechanisms, including diazepam, chlordiazepoxide, desmethyldiazepam, alprazolam, and triazolam, have reduced metabolic clearance during coadministration of cimetidine as opposed to the drug-free control state (4–9). This interaction appears not to occur for benzodiazepines biotransformed by conjugation as opposed to oxidation, including oxazepam and lorazepam (8–10). Temazepam is a 3-hydroxybenzodiazepine biotransformed by conjugation at the 3-position to glucuronic acid, yielding a water-soluble glucuronide metabolite that is excreted in the urine (11). The present study indicated that coadministration of temazepam with cimetidine had no influence on the pattern of temazepam absorption, distribution, or clearance. Consistent with

previous reports (16), absorption of temazepam from the hard gelatin capsule utilized in the United States occurs relatively slowly, with peak plasma concentrations an average of 2.0–2.1 h after dosage. Temazepam elimination half-lives ranged from 6 to 21 h, and total metabolic clearances ranged from 0.9 to 2.6 mL/min/kg. None of these kinetic variables were significantly influenced by cimetidine coadministration, nor was the extent of temazepam binding to plasma protein altered by cimetidine. Furthermore, for any given individual, the kinetic profile for temazepam was highly consistent between the two treatment trials.

The clinical implications of an interaction or noninteraction with cimetidine for any particular benzodiazepine cannot at present be determined. The present study nonetheless suggests that, consistent with its biotransformation pathway mainly involving glucuronide conjugation, the pharmacokinetic profile of temazepam is not influenced by concurrent treatment with cimetidine.

REFERENCES

(1) M. M. Mitler, *Pharmacotherapy*, **1**, 3 (1981).

(2) W. Finkelstein and K. J. Isselbacher, *N. Engl. J. Med.*, **299**, 992 (1978).

(3) R. N. Brogden, R. C. Heel, T. M. Speight, and G. S. Avery, *Drugs*, **15**, 93 (1978).

(4) U. Klotz and I. Reimann, *N. Engl. J. Med.*, **302**, 1012 (1980).

(5) P. V. Desmond, R. V. Patwardhan, S. Schenker, and K. V. Speeg, *Ann. Intern. Med.*, **93**, 266 (1980).

(6) D. R. Abernethy, D. J. Greenblatt, M. Divoll, L. J. Moschitto, J. S. Harmatz, and R. I. Shader, *Psychopharmacology*, **80**, 275 (1983).

(7) M. Divoll, D. J. Greenblatt, D. R. Abernethy, and R. I. Shader, *J. Am. Geriat. Soc.*, **30**, 684 (1982).

(8) U. Klotz and I. Reimann, *Eur. J. Clin. Pharmacol.*, **18**, 517 (1980).

(9) D. R. Abernethy, D. J. Greenblatt, M. Divoll, B. Ameer, and R. I. Shader, *J. Pharmacol. Exp. Ther.*, **224**, 508 (1983).

(10) R. V. Patwardhan, G. W. Yarborough, P. V. Desmond, R. F. Johnson, S. Shenker, and K. V. Speeg, *Gastroenterology*, **79**, 912 (1980).

(11) H. J. Schwarz, *Br. J. Clin. Pharmacol.*, **8**, 23s, (1979).

(12) M. Divoll and D. J. Greenblatt, *J. Chromatogr.*, **222**, 125 (1981).

(13) E. Woo and D. J. Greenblatt, *J. Pharm. Sci.*, **68**, 466 (1979).

(14) M. Divoll and D. J. Greenblatt, *J. Pharm. Pharmacol.*, **34**, 122 (1982).

(15) B. Lorenzo and D. E. Drayer, *J. Lab. Clin. Med.*, **97**, 545 (1981).

(16) M. Divoll, D. J. Greenblatt, J. S. Harmatz, and R. I. Shader, *J. Pharm. Sci.*, **70**, 1104 (1981).

ACKNOWLEDGMENTS

Supported in part by United States Public Health Service Grant MH-34223, by a Clinical Pharmacology Developmental Grant from The Pharmaceutical Manufacturers' Association Foundation, and by a Grant-in-Aid from Sandoz, Inc.

We are grateful for the assistance of Rita Matlis, Dr. William R. Sterling, and the Staff of the Clinical Study Unit, New England Medical Center Hospital. (Supported by USPHS Grant RR-24040).

Dissolution Rates of Corticoid Solutions Dispersed on Silicas

CHI-CHOW LIAO and C. I. JAROWSKI ˣ

Received July 21, 1982, from the *College of Pharmacy and Allied Health Professions, St. John's University, Jamaica, NY 11439.* Accepted for publication January 27, 1983.

Abstract □ Two nonporous and three porous amorphous silicas were used as dispersion media to convert corticoid solutions into free-flowing powders. The corticoids (prednisone, prednisolone, and hydrocortisone) were dissolved in *N,N*-dimethylacetamide–polyethylene glycol 400 (7:3 v/v) and their 10% (w/v) solutions were mixed with the silicas (1:3 v/w). Dissolution rates of the corticoids from such powdered solutions were more rapid than their micronized powders in various aqueous media.

Keyphrases □ Dissolution rate—corticoid solutions dispersed on silicas, prednisone, prednisolone, hydrocortisone, free-flowing powders □ Corticoids—solutions dispersed on silicas, dissolution rates, prednisone, prednisolone, hydrocortisone, free-flowing powders □ Powders, free-flowing—corticoid solutions dispersed on silicas, dissolution rates, prednisone, prednisolone, hydrocortisone

The USP (1) requires that ≥60% of the prednisone or prednisolone from their respective tablets must dissolve within 20 min in deaerated water. These water-insoluble neutral drug molecules could exhibit poor dissolution rates from improperly prepared capsule or tablet dosage forms. Oral absorption efficiency of the corticoids from such solid dosage forms could be impaired.

Concentrated solutions of three corticoids (prednisone, prednisolone, and hydrocortisone) had been prepared in *N,N*-dimethylacetamide, a high-boiling, water-miscible liquid (2). These earlier studies had shown that the addition of 30% (v/v) polyethylene glycol 400 to the *N,N*-dimethylacetamide would prevent the softening effect of the latter on hard gelatin capsules. As a consequence, this mixture of solvents was used to prepare 10% (w/v) solutions of the three corticoids.

Simple admixture of the corticoid solutions with amorphous, porous, or nonporous silicas converted them to free-flowing powders. The corticoids in such powdered solutions are thus in a molecular state of subdivision. Dissolution rates of such water-insoluble, neutral compounds should be instantaneous if localized dilution with simulated GI media does not cause their precipitation.

The purpose of this study was to convert solutions of corticoids to free-flowing powders by dispersing them on various silicas. Dissolution rates in simulated GI media are compared with those of micronized powders. A comparison of the dissolution rate with ball-milled or solvent-deposited prednisone–silica dispersions is also presented (3).

Table I—UV Wavelengths Used in the Development of Calibration Curves for the Three Drugs in Various Solvents

Solvent	Wavelength of Light, nm I	II	III
Simulated gastric fluid (without pepsin)	248	243	247
Simulated intestinal fluid (without pancreatin)	248	243	247
Ethanol	248	243	247

0022-3549/84/0300-0401$01.00/0

© 1984, American Pharmaceutical Association

previous reports (16), absorption of temazepam from the hard gelatin capsule utilized in the United States occurs relatively slowly, with peak plasma concentrations an average of 2.0–2.1 h after dosage. Temazepam elimination half-lives ranged from 6 to 21 h, and total metabolic clearances ranged from 0.9 to 2.6 mL/min/kg. None of these kinetic variables were significantly influenced by cimetidine coadministration, nor was the extent of temazepam binding to plasma protein altered by cimetidine. Furthermore, for any given individual, the kinetic profile for temazepam was highly consistent between the two treatment trials.

The clinical implications of an interaction or noninteraction with cimetidine for any particular benzodiazepine cannot at present be determined. The present study nonetheless suggests that, consistent with its biotransformation pathway mainly involving glucuronide conjugation, the pharmacokinetic profile of temazepam is not influenced by concurrent treatment with cimetidine.

REFERENCES

(1) M. M. Mitler, *Pharmacotherapy*, **1**, 3 (1981).

(2) W. Finkelstein and K. J. Isselbacher, *N. Engl. J. Med.*, **299**, 992 (1978).

(3) R. N. Brogden, R. C. Heel, T. M. Speight, and G. S. Avery, *Drugs*, **15**, 93 (1978).

(4) U. Klotz and I. Reimann, *N. Engl. J. Med.*, **302**, 1012 (1980).

(5) P. V. Desmond, R. V. Patwardhan, S. Schenker, and K. V. Speeg, *Ann. Intern. Med.*, **93**, 266 (1980).

(6) D. R. Abernethy, D. J. Greenblatt, M. Divoll, L. J. Moschitto, J. S. Harmatz, and R. I. Shader, *Psychopharmacology*, **80**, 275 (1983).

(7) M. Divoll, D. J. Greenblatt, D. R. Abernethy, and R. I. Shader, *J. Am. Geriat. Soc.*, **30**, 684 (1982).

(8) U. Klotz and I. Reimann, *Eur. J. Clin. Pharmacol.*, **18**, 517 (1980).

(9) D. R. Abernethy, D. J. Greenblatt, M. Divoll, B. Ameer, and R. I. Shader, *J. Pharmacol. Exp. Ther.*, **224**, 508 (1983).

(10) R. V. Patwardhan, G. W. Yarborough, P. V. Desmond, R. F. Johnson, S. Shenker, and K. V. Speeg, *Gastroenterology*, **79**, 912 (1980).

(11) H. J. Schwarz, *Br. J. Clin. Pharmacol.*, **8**, 23s, (1979).

(12) M. Divoll and D. J. Greenblatt, *J. Chromatogr.*, **222**, 125 (1981).

(13) E. Woo and D. J. Greenblatt, *J. Pharm. Sci.*, **68**, 466 (1979).

(14) M. Divoll and D. J. Greenblatt, *J. Pharm. Pharmacol.*, **34**, 122 (1982).

(15) B. Lorenzo and D. E. Drayer, *J. Lab. Clin. Med.*, **97**, 545 (1981).

(16) M. Divoll, D. J. Greenblatt, J. S. Harmatz, and R. I. Shader, *J. Pharm. Sci.*, **70**, 1104 (1981).

ACKNOWLEDGMENTS

Supported in part by United States Public Health Service Grant MH-34223, by a Clinical Pharmacology Developmental Grant from The Pharmaceutical Manufacturers' Association Foundation, and by a Grant-in-Aid from Sandoz, Inc.

We are grateful for the assistance of Rita Matlis, Dr. William R. Sterling, and the Staff of the Clinical Study Unit, New England Medical Center Hospital. (Supported by USPHS Grant RR-24040).

Dissolution Rates of Corticoid Solutions Dispersed on Silicas

CHI-CHOW LIAO and C. I. JAROWSKI ˣ

Received July 21, 1982, from the *College of Pharmacy and Allied Health Professions, St. John's University, Jamaica, NY 11439.* Accepted for publication January 27, 1983.

Abstract □ Two nonporous and three porous amorphous silicas were used as dispersion media to convert corticoid solutions into free-flowing powders. The corticoids (prednisone, prednisolone, and hydrocortisone) were dissolved in *N,N*-dimethylacetamide–polyethylene glycol 400 (7:3 v/v) and their 10% (w/v) solutions were mixed with the silicas (1:3 v/w). Dissolution rates of the corticoids from such powdered solutions were more rapid than their micronized powders in various aqueous media.

Keyphrases □ Dissolution rate—corticoid solutions dispersed on silicas, prednisone, prednisolone, hydrocortisone, free-flowing powders □ Corticoids—solutions dispersed on silicas, dissolution rates, prednisone, prednisolone, hydrocortisone, free-flowing powders □ Powders, free-flowing—corticoid solutions dispersed on silicas, dissolution rates, prednisone, prednisolone, hydrocortisone

The USP (1) requires that ≥60% of the prednisone or prednisolone from their respective tablets must dissolve within 20 min in deaerated water. These water-insoluble neutral drug molecules could exhibit poor dissolution rates from improperly prepared capsule or tablet dosage forms. Oral absorption efficiency of the corticoids from such solid dosage forms could be impaired.

Concentrated solutions of three corticoids (prednisone, prednisolone, and hydrocortisone) had been prepared in *N,N*-dimethylacetamide, a high-boiling, water-miscible liquid (2). These earlier studies had shown that the addition of 30% (v/v) polyethylene glycol 400 to the *N,N*-dimethylacetamide would prevent the softening effect of the latter on hard gelatin capsules. As a consequence, this mixture of solvents was used to prepare 10% (w/v) solutions of the three corticoids.

Simple admixture of the corticoid solutions with amorphous, porous, or nonporous silicas converted them to free-flowing powders. The corticoids in such powdered solutions are thus in a molecular state of subdivision. Dissolution rates of such water-insoluble, neutral compounds should be instantaneous if localized dilution with simulated GI media does not cause their precipitation.

The purpose of this study was to convert solutions of corticoids to free-flowing powders by dispersing them on various silicas. Dissolution rates in simulated GI media are compared with those of micronized powders. A comparison of the dissolution rate with ball-milled or solvent-deposited prednisone–silica dispersions is also presented (3).

Table I—UV Wavelengths Used in the Development of Calibration Curves for the Three Drugs in Various Solvents

Solvent	Wavelength of Light, nm I	II	III
Simulated gastric fluid (without pepsin)	248	243	247
Simulated intestinal fluid (without pancreatin)	248	243	247
Ethanol	248	243	247

0022-3549/84/0300-0401$01.00/0

© 1984, American Pharmaceutical Association

Table II—Dissolution in Simulated Gastrointestinal Media of Solutions of Prednisolone, Prednisone, and Hydrocortisone Dispersed on Various Silicas

Sample	Solvent: Simulated Gastric	Solvent: Simulated Intestinal	Amount Dissolved, %: 5 min	10 min	20 min	30 min	45 min	60 min	75 min	90 min	105 min	120 min
1. I[a]	+		62.0	74.7	79.5	81.9	84.8	86.4	88.6	88.7	90.0	90.0
2. I[a]		+	67.9	79.0	83.1	85.7	87.5	89.4	90.3	91.2	92.5	93.1
3. I–IV	+		87.5	97.0	99.8	100						
4. I–V	+		92.1	95.1	96.4	96.4	96.5	97.0	97.0	97.3	97.8	97.8
5. I–VI	+		91.5	94.9	96.0	96.5	97.5	97.6	98.0	98.0	98.4	98.4
6. I–VII	+		84.2	86.5	89.5	90.1	91.1	91.6	91.8	92.0	92.2	92.5
7. I–VIII	+		84.2	86.5	89.5	90.1	91.1	91.6	91.8	92.0	92.2	92.5
8. I–IV		+	85.0	86.2	89.5	90.1	90.8	91.9	92.3	94.1	—	95.0
9. I–V		+	84.8	88.8	92.0	93.2	94.1	94.1	94.8	95.1	95.3	95.3
10. I–VI		+	89.3	93.6	94.2	94.5	94.9	95.1	95.2	96.2	96.6	96.6
11. I–VII		+	75.3	86.8	91.7	94.9	96.2	96.8	97.0	97.3	97.6	98.1
12. I–VIII		+	87.7	93.8	96.6	97.6	99.1	100				
13. I–VI[b]	+		80.2	87.2	91.5	92.5	93.6	93.8	94.2	94.6	94.6	94.7
14. I–V[b]	+		74.5	80.9	85.1	86.9	89.7	91.2	92.1	93.2	92.8	92.8
15. I–VI[b]	+		74.0	79.1	82.6	87.6	89.5	89.5	89.8	90.8	91.8	93.1
16. I–IV[b]		+	51.5	57.9	64.5	67.9	71.2	73.8	83.3	86.3	87.7	88.9
17. I–V[b]		+	60.2	68.4	73.3	77.0	80.2	81.8	83.2	84.7	86.2	87.5
18. I–VI[b]		+	61.5	66.7	73.1	75.0	77.2	79.7	80.3	81.0	82.3	83.0
19. II[a]	+		22.6	36.8	55.1	62.5	68.5	73.3	76.9	79.4	81.6	83.3
20. II[a]		+	19.5	30.0	57.3	65.4	71.1	73.3	75.9	81.4	83.1	85.1
21. II–IV	+		73.7	79.3	86.4	93.7	95.3	96.6	98.9	99.0	99.2	99.4
22. II–V	+		76.0	84.0	89.4	93.5	95.9	97.8	99.4	99.6	100	
23. II–VI	+		70.8	75.6	82.0	91.4	95.7	96.1	96.7	97.6	99.3	99.3
24. II–VII	+		48.4	58.7	63.1	67.7	72.1	73.9	76.1	78.2	79.7	80.2
25. II–VIII	+		43.0	49.9	59.9	65.3	68.4	71.7	75.6	78.3	79.3	80.6
26. II–IV		+	62.4	71.6	80.7	86.2	91.6	93.5	96.5	98.6	99.0	100
27. II–V		+	70.5	83.9	91.5	92.7	96.0	97.1	97.8	98.3	99.1	99.8
28. II–VI		+	57.9	68.5	81.5	84.9	90.5	93.9	96.6	98.7	99.9	100
29. II–VII		+	48.4	58.7	63.1	67.7	72.1	73.9	76.1	78.2	79.7	80.2
30. II–VIII		+	43.9	49.9	58.5	64.4	69.1	74.9	84.0	87.9	91.3	93.1
31. III[a]	+		25.0	34.9	52.5	59.4	66.1	77.7	82.8	86.7	89.5	91.6
32. III[a]		+	60.5	72.4	80.0	84.9	88.6	89.8	91.3	91.8	92.8	92.8
33. III–IV	+		96.9	100								
34. III–V	+		96.4	100								
35. III–VI	+		98.5	100								
36. III–VII	+		98.2	99.6	100	100						
37. III–VIII	+		94.3	98.3	98.3	98.3	98.4	98.4	99.0	99.1	100	
38. III–IV		+	81.8	93.0	98.3	99.1	100					
39. III–V		+	94.8	98.3	99.3	99.7	99.9	100				
40. III–VI		+	90.2	95.9	98.5	99.2	99.7	99.7	100			
41. III–VII		+	90.2	93.8	96.6	96.7	96.8	96.8	96.8	96.8	96.8	96.8
42. III–VIII		+	92.8	96.9	97.3	97.5	97.5	97.5	97.5	97.5	97.5	97.5

[a] Micronized powder. [b] Corticoid was solvent-deposited on the surface of the silica by the method of Yang *et al.* (3).

EXPERIMENTAL

Materials—The following were obtained from commercial sources: anhydrous micronized prednisolone[1] (I); micronized prednisone, USP[1] (II); micronized hydrocortisone[2] (III); three grades of porous silicas[3]; two types of nonporous silicas[4]; *N,N*-dimethylacetamide[5]; polyethylene glycol 400[6]; anhydrous ethanol (UV grade)[7]; hydrochloric acid[7]; sodium chloride[7]; monobasic potassium phosphate (AR)[7]; sodium hydroxide pellets[7]; phosphate buffer, pH 7[8]; phosphate buffer, pH 4[8]; and distilled water. The following equipment was used: double-beam spectrophotometer[9]; pH meter (Model DB-GT)[8]; analytical balance[10]; USP XIX dissolution test basket assembly[11]; polytherm constant-temperature water bath[12]; 13-mm Swinny adapter[13]; filter paper, 0.45-μm porosity[13]; plastic syringe[13]; and quartz electric stopwatch[14].

Methods—Corticoid solutions were prepared by dissolving 1 g of corticoid in a sufficient quantity of *N,N*-dimethylacetamide–polyethylene glycol 400 (7:3 v/v) to make 10 mL of solution. The weights of mixed solvent used are: for I, 9.2031 g; for II, 9.2067 g; for III, 9.2086 g.

Corticoid–silica dispersions were prepared by placing 1 mL of corticoid solution (1 mL of prednisolone solution weighs 1.01 g) in a mortar and adding 3 g of silica. Simple admixture with a pestle produced a homogeneous free-flowing powder. Aliquots of 0.401 g should contain 10 mg of prednisolone. All corticoid solution–silica samples were prepared in duplicate.

Spectrophotometric absorption and calibration curves were obtained by diluting the corticoid solutions with simulated GI media, without enzymes (4), and wavelengths for maximum absorbance were determined (Table I). Absorbance *versus* concentration plots (concentration range 3–12 μg/mL) revealed that Beer's law was followed (regression coefficient, 0.999). To blank out interference from the organic solvents present, stock solutions of simulated GI fluids were used which contained identical quantities of mixed solvent without the corticoid.

The assay of the corticoid solution–silica dispersions involved the extraction of 1 g of corticoid solution–silica dispersion with 15 mL of ethanol four times. The ethanol extracts were combined and centrifuged. Three milliliters of supernatant was diluted to 200 mL with ethanol, and the absorbance was measured at the wavelength shown in Table I.

Dissolution rates of the corticoid solution–silica dispersions were determined by the USP basket method (1) using 1000 mL of simulated gastric juice without pepsin (pH 1.2) or simulated intestinal fluid without pancreatin (pH 7.4). Dispersions which contained the equivalent of 10 mg of corticoid were placed in the basket, which was lowered to a depth 2 cm from the bottom of the vessel and rotated at 150 rpm. All dissolution studies were conducted at 37 ± 0.5°C.

Five-milliliter aliquots were withdrawn midway between the surface

[1] Lots 314GR (prednisolone) and 7A566 (prednisone); The Upjohn Co., Kalamazoo, Mich.
[2] Lot 8X371; Pfizer Inc., New York, N.Y.
[3] Syloid 63 (IV), Syloid 72 (V), and Syloid 244 (VI); Davison Chemical Div., W. R. Grace & Co., Baltimore, Md.
[4] Cab-O-Sil EH-5 (VII); Cabot Corp., Boston, Mass. Aerosil 380 (VIII); Degussa Inc., Pigments Div., New York, N.Y.
[5] Eastman Kodak Co., Rochester, N.Y.
[6] Ruger Chemical Co., Inc., Irvington, N.J.
[7] J. T. Baker Chemical Co., Phillipsburg, N.J.
[8] Beckman Instruments, Fullerton, Calif.
[9] Model 124; Coleman Instruments Div., Maywood, Ill.
[10] Mettler Instrument Corp., Hightstown, N.J.
[11] Hanson Research Corp., Northridge, Calif.
[12] Bench Scale Equipment Co., Inc., Dayton, Ohio.
[13] Millipore Corp., Bedford, Mass.
[14] Citizen Watch Corp., Tokyo, Japan.

of the dissolution medium and the bottom of the vessel, filtered through 0.45-μm membrane, and assayed spectrophotometrically. The volume of the dissolution medium was maintained at 1000 mL by the addition of the appropriate medium and cumulative corrections were made for the previously removed samples in determining the total amount of drug in solution. The results of all the dissolution studies, which were run in duplicate, are shown in Table II.

RESULTS AND DISCUSSION

The data in Table II clearly show the more rapid presence of I, II, or III in either dissolution medium when the corticoid solutions were dispersed on the five silicas used. As a micronized powder, II (samples 19 and 20) dissolved very slowly in either GI medium; after 20 min <60% had dissolved. However, when a solution of II was dispersed on IV, V, or VI, >70% of II was in solution within 5 min (samples 21, 22, and 23) in simulated gastric juice. In simulated intestinal juice, the rate was not as large; within 10 min >68.5% of II had dissolved (samples 26, 27, and 28).

Silicas IV, V, and VI were consistently more efficient in releasing the drug solutions dispersed on them than were VII and VIII. When silicas VII and VIII were used with a solution of II <100% of II had dissolved in the simulated GI media after 120 min (samples 24, 25, 29, and 30).

A comparison of solvent-deposited I with its silica-dispersed solution is also of interest. In every instance the silica-dispersed solutions were superior (samples 3 *versus* 13, 4 *versus* 14, 5 *versus* 15; 8 *versus* 16, 9 *versus* 17, and 10 *versus* 20). Ball-milled samples were not prepared. However, Yang *et al.* (3) reported that after ball-milling prednisone with a 20-fold excess of IV, V, or VI, a maximum of 65% of II had dissolved after 120 min in simulated GI media. Their dissolution studies were conducted at 100 rpm. Narurkar and Jarowski (5) also reported similar slow dissolution rates for I that had been ball-milled with various ratios of IV, V, VI, or VII. When solutions of I or II were dispersed on IV, V, VI, VII, or VIII and their dissolution rates studied at 100 rpm, all but one sample released 83–99% within 120 min. The exception was a solution of II dispersed on VI; only 60% had dissolved in simulated intestinal fluid after 120 min.

Such reduction in dissolution rate resulting from reduced basket speed is of concern since the anticipated superiority in the *in vivo* performance of silica-dispersed solutions over micronized powders is suspect. A preliminary *in vivo* experiment with salicylamide indicates that more rapid oral absorption does occur when the compound is dissolved and dispersed on silica. This data will be published elsewhere.

REFERENCES

(1) "The United States Pharmacopeia," 19th rev., U.S. Pharmacopeial Convention, Rockville, Md., 1975, pp. 398, 404.

(2) T. H. Nguyen, Master's Thesis, St. John's University (1978).

(3) K. Y. Yang, R. Glemza, and C. I. Jarowski, *J. Pharm. Sci.*, **68**, 560 (1979).

(4) "The United States Pharmacopeia," 19th rev., U.S. Pharmacopeial Convention, Rockville, Md., 1975, p. 765.

(5) A. N. Narurkar, Doctoral Thesis, St. John's University (1979).

Synthesis of New 8-(5-Substituted Amino-1,3,4-oxadiazol-2-yl) and 8-(5-Substituted Amino-1,3,4-thiadiazol-2-yl) Methoxyquinolines with Antibilharzial Activity

RAAFAT SOLIMAN *§x, HASSAN M. MOKHTAR ‡, and SAMIR K. EL SADANY ‡

Received November 8, 1982, from the **Department of Pharmaceutical Chemistry, Faculty of Pharmacy* and the ‡*Department of Chemistry, Faculty of Science, University of Alexandria, Alexandria, Egypt.* Accepted for publication February 1, 1983. §Present address: College of Pharmacy, University of Florida, J. Hillis Miller Health Center, Gainesville, FL 32610.

Abstract □ Several 5-substituted amino-1,3,4-oxadiazol-2-yl and 5-substituted amino-1,3,4-thiadiazol-2-yl derivatives with different 8-hydroxyquinoline moieties in the 2-position were prepared and tested for their antiparasitic activity. Preliminary biological tests on mice experimentally infested with *Schistosoma mansoni* revealed that the new compounds show moderate schistosomicidal activity.

Keyphrases □ 8-(5-Substituted amino-1,3,4-oxadiazol-2-yl) methoxyquinolines—synthesis, antibilharzial activity against *Schistosoma mansoni* □ 8-(5-Substituted amino-1,3,4-thiadiazol-2-yl) methoxyquinolines—synthesis, antibilharzial activity against *Schistosoma mansoni* □ Antischistosomal agents—synthesis of 8-(5-substituted amino-1,3,4-oxadiazol-2-yl) and 8-(5-substituted amino-1,3,4-thiadiazol-2-yl) methoxyquinolines

The fact that lucanthone (1) and its active metabolite hycanthone (2) were the first metal-free compounds to show clinical activity against bilharziasis initiated the synthesis of a distantly related compound 6-chloro-5-(2-diethylaminoethylamino)-8-methylquinoline. The latter exhibited outstanding activity against experimental schistosomiasis (3, 4). Unfortunately, preclinical toxicity studies indicated wide differences among various species of laboratory animals, precluding early clinical trials of this compound (3). A new entry in bilharzial chemotherapy is 1,2,3,4-tetrahydro-2-[[(1-methylethyl)amino]methyl]-7-nitro-6-quinolinemethanol (oxamniquine). It has potent schistosomicidal activity against *Schistosoma mansoni* by causing worms to shift from the mesenteric veins to the liver, where they are destroyed (5).

In our previous work (6) several 3-mercaptotriazoles with the 8-hydroxyquinoline moiety were prepared by cyclization of their corresponding substituted thiosemicarbazides by the action of hot sodium hydroxide solution. Preliminary biological tests revealed that those mercaptotriazoles showed potent schistosomicidal activity. These observations prompted the synthesis of several 5-substituted amino-1,3,4-oxadiazol-2-yl and 5-substituted amino-1,3,4-thiadiazol-2-yl derivatives with different 8-hydroxyquinoline moieties in the 2-position. Contrary to the mercaptotriazoles, the incorporation of the potent antiparasitic drug iodochlorhydroxyquinoline in the 2-oxadiazole or 2-thiadiazole rings produced compounds with moderate or low schistosomicidal activity.

0022-3549/84/0300-0403$01.00/0

© 1984, American Pharmaceutical Association

of the dissolution medium and the bottom of the vessel, filtered through 0.45-μm membrane, and assayed spectrophotometrically. The volume of the dissolution medium was maintained at 1000 mL by the addition of the appropriate medium and cumulative corrections were made for the previously removed samples in determining the total amount of drug in solution. The results of all the dissolution studies, which were run in duplicate, are shown in Table II.

RESULTS AND DISCUSSION

The data in Table II clearly show the more rapid presence of I, II, or III in either dissolution medium when the corticoid solutions were dispersed on the five silicas used. As a micronized powder, II (samples 19 and 20) dissolved very slowly in either GI medium; after 20 min <60% had dissolved. However, when a solution of II was dispersed on IV, V, or VI, >70% of II was in solution within 5 min (samples 21, 22, and 23) in simulated gastric juice. In simulated intestinal juice, the rate was not as large; within 10 min >68.5% of II had dissolved (samples 26, 27, and 28).

Silicas IV, V, and VI were consistently more efficient in releasing the drug solutions dispersed on them than were VII and VIII. When silicas VII and VIII were used with a solution of II <100% of II had dissolved in the simulated GI media after 120 min (samples 24, 25, 29, and 30).

A comparison of solvent-deposited I with its silica-dispersed solution is also of interest. In every instance the silica-dispersed solutions were superior (samples 3 *versus* 13, 4 *versus* 14, 5 *versus* 15; 8 *versus* 16, 9 *versus* 17, and 10 *versus* 20). Ball-milled samples were not prepared. However, Yang *et al.* (3) reported that after ball-milling prednisone with a 20-fold excess of IV, V, or VI, a maximum of 65% of II had dissolved after 120 min in simulated GI media. Their dissolution studies were conducted at 100 rpm. Narurkar and Jarowski (5) also reported similar slow dissolution rates for I that had been ball-milled with various ratios of IV, V, VI, or VII. When solutions of I or II were dispersed on IV, V, VI, VII, or VIII and their dissolution rates studied at 100 rpm, all but one sample released 83–99% within 120 min. The exception was a solution of II dispersed on VI; only 60% had dissolved in simulated intestinal fluid after 120 min.

Such reduction in dissolution rate resulting from reduced basket speed is of concern since the anticipated superiority in the *in vivo* performance of silica-dispersed solutions over micronized powders is suspect. A preliminary *in vivo* experiment with salicylamide indicates that more rapid oral absorption does occur when the compound is dissolved and dispersed on silica. This data will be published elsewhere.

REFERENCES

(1) "The United States Pharmacopeia," 19th rev., U.S. Pharmacopeial Convention, Rockville, Md., 1975, pp. 398, 404.

(2) T. H. Nguyen, Master's Thesis, St. John's University (1978).

(3) K. Y. Yang, R. Glemza, and C. I. Jarowski, *J. Pharm. Sci.*, **68**, 560 (1979).

(4) "The United States Pharmacopeia," 19th rev., U.S. Pharmacopeial Convention, Rockville, Md., 1975, p. 765.

(5) A. N. Narurkar, Doctoral Thesis, St. John's University (1979).

Synthesis of New 8-(5-Substituted Amino-1,3,4-oxadiazol-2-yl) and 8-(5-Substituted Amino-1,3,4-thiadiazol-2-yl) Methoxyquinolines with Antibilharzial Activity

RAAFAT SOLIMAN *§x, HASSAN M. MOKHTAR ‡, and SAMIR K. EL SADANY ‡

Received November 8, 1982, from the **Department of Pharmaceutical Chemistry, Faculty of Pharmacy* and the ‡*Department of Chemistry, Faculty of Science, University of Alexandria, Alexandria, Egypt.* Accepted for publication February 1, 1983. §Present address: College of Pharmacy, University of Florida, J. Hillis Miller Health Center, Gainesville, FL 32610.

Abstract □ Several 5-substituted amino-1,3,4-oxadiazol-2-yl and 5-substituted amino-1,3,4-thiadiazol-2-yl derivatives with different 8-hydroxyquinoline moieties in the 2-position were prepared and tested for their antiparasitic activity. Preliminary biological tests on mice experimentally infested with *Schistosoma mansoni* revealed that the new compounds show moderate schistosomicidal activity.

Keyphrases □ 8-(5-Substituted amino-1,3,4-oxadiazol-2-yl) methoxyquinolines—synthesis, antibilharzial activity against *Schistosoma mansoni* □ 8-(5-Substituted amino-1,3,4-thiadiazol-2-yl) methoxyquinolines—synthesis, antibilharzial activity against *Schistosoma mansoni* □ Antischistosomal agents—synthesis of 8-(5-substituted amino-1,3,4-oxadiazol-2-yl) and 8-(5-substituted amino-1,3,4-thiadiazol-2-yl) methoxyquinolines

The fact that lucanthone (1) and its active metabolite hycanthone (2) were the first metal-free compounds to show clinical activity against bilharziasis initiated the synthesis of a distantly related compound 6-chloro-5-(2-diethylaminoethylamino)-8-methylquinoline. The latter exhibited outstanding activity against experimental schistosomiasis (3, 4). Unfortunately, preclinical toxicity studies indicated wide differences among various species of laboratory animals, precluding early clinical trials of this compound (3). A new entry in bilharzial chemotherapy is 1,2,3,4-tetrahydro-2-[[(1-methylethyl)amino]methyl]-7-nitro-6-quinolinemethanol (oxamniquine). It has potent schistosomicidal activity against *Schistosoma mansoni* by causing worms to shift from the mesenteric veins to the liver, where they are destroyed (5).

In our previous work (6) several 3-mercaptotriazoles with the 8-hydroxyquinoline moiety were prepared by cyclization of their corresponding substituted thiosemicarbazides by the action of hot sodium hydroxide solution. Preliminary biological tests revealed that those mercaptotriazoles showed potent schistosomicidal activity. These observations prompted the synthesis of several 5-substituted amino-1,3,4-oxadiazol-2-yl and 5-substituted amino-1,3,4-thiadiazol-2-yl derivatives with different 8-hydroxyquinoline moieties in the 2-position. Contrary to the mercaptotriazoles, the incorporation of the potent antiparasitic drug iodochlorhydroxyquinoline in the 2-oxadiazole or 2-thiadiazole rings produced compounds with moderate or low schistosomicidal activity.

0022-3549/84/0300-0403$01.00/0

© 1984, American Pharmaceutical Association

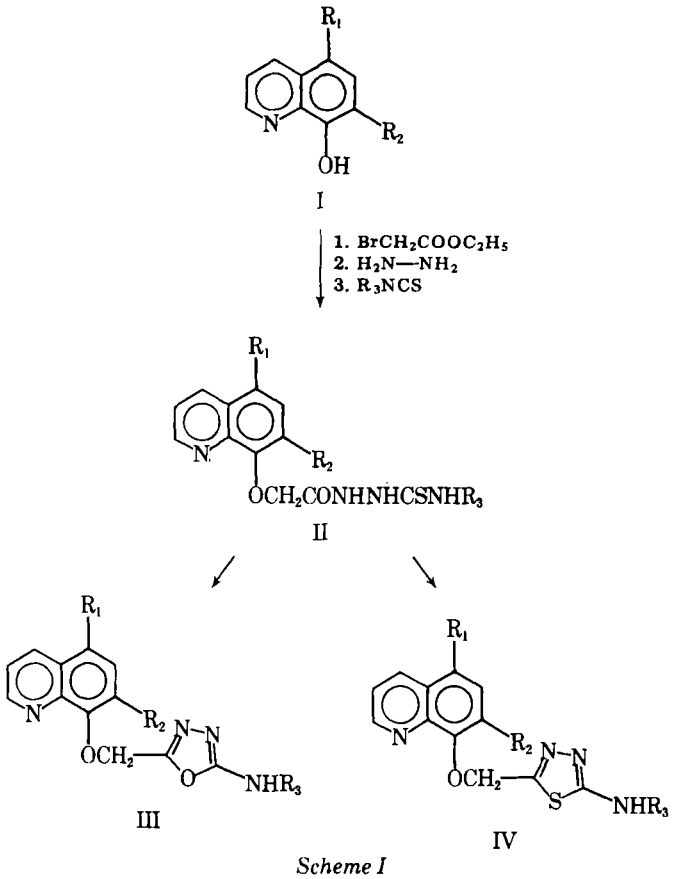

Scheme I

EXPERIMENTAL[1]

The various 1,3,4-oxadiazoles and 1,3,4-thiadiazoles were synthesized by reactions outlined in Scheme I. Conversion of the 8-hydroxyquinoline derivative (I) to the 8-quinolinoxyacetic acid hydrazide was effected by treating the corresponding ethyl ester with 99–100% hydrazine hydrate.

Substituted thiosemicarbazides (II), prepared by the reaction of 8-quinolinoxyacetic acid hydrazide with the appropriate isothiocyanate, were cyclized to the corresponding 8-(5-substituted amino-1,3,4-oxadiazol-2-yl)methoxyquinoline (III) in 4 M NaOH and 5% iodine in potassium iodide solution, and to the corresponding 8-(5-substituted amino-1,3,4-thiadiazol-2-yl)methoxyquinoline (IV) by the action of cold concentrated sulfuric acid (7). All compounds were characterized by their melting points, elemental analysis, and IR and ^{1}H-NMR spectra.

1-(8-Quinolinoxyacetyl)-4-substituted Thiosemicarbazides (II)—Series II compounds were prepared as mentioned previously (6), by refluxing equimolar quantities of 8-quinolinoxyacetic acid hydrazides with the appropriate isothiocyanate in dry benzene.

8-(5-Substituted Amino-1,3,4-oxadiazol-2-yl) Methoxyquinolines (III)—To a suspension of the appropriate 1-(8-quinolinoxyacetyl)-4-substituted thiosemicarbazide (II, 0.01 mol) in water (10 mL) was added a cold solution of sodium hydroxide (4 M, 5 mL) with stirring. When a clear solution was obtained, iodine in potassium iodide solution (5%) was then added in a dropwise manner with stirring until the color of iodine persisted at room temperature. Thereafter, the reaction mixture was heated at reflux on a boiling-water bath, and more iodine solution was carefully added until a permanent tinge of excess iodine remained. After cooling the mixture was poured into ice-cold water, and the precipitated solid was removed by filtration, washed with a dilute solution of sodium thiosulfate and then washed with water, dried, and crystallized from a suitable solvent (Table I).

IIId—^{1}H-NMR ($CDCl_3$): δ 7.2–8.9 (m, ArH), 5.2 (s, 2, OCH_2), and 4.5 ppm (d, N*H*-Ar).

[1] Melting points were determined in open glass capillaries and are uncorrected. IR spectra were determined as Nujol mulls with Beckman IR-4210; ^{1}H-NMR spectra were recorded on a Varian EM-360 60-Hz NMR spectrophotometer in $CDCl_3$ with TMS as internal standard. Microanalyses were performed by the Microanalytical Unit, Faculty of Science, University of Cairo, Cairo, Egypt.

Table I—8-(5-Substituted Amino-1,3,4-oxadiazol-2-yl) Methoxyquinolines (III) and 8-(5-Substituted Amino-1,3,4-thiadiazol-2-yl) Methoxyquinolines (IV) [a]

Compound	R_1	R_2	R_3	Yield, %	Melting Point, °C	Formula
IIIa	H	H	$-CH_2CH=CH_2$	65	154	$C_{15}H_{14}N_4O_2$
IIIb	H	H	$-(CH_2)_3CH_3$	70	175	$C_{16}H_{18}N_4O_2$
IIIc	H	H	$-C_6H_{11}$	68	160	$C_{18}H_{20}N_4O_2$
IIId	H	H	$-C_6H_5$	65	219	$C_{18}H_{14}N_4O_2$
IIIe						
IIIf	H	H	$-C_6H_4$-*p*-CH_3	73	218	$C_{19}H_{16}N_4O_2$
IIIg	Cl	I	$-CH_2CH=CH_2$	70	150	$C_{15}H_{12}ClIN_4O_2$
IIIh	Cl	I	$-(CH_2)_3CH_3$	66	135	$C_{16}H_{16}ClIN_4O_2$
IIIi	Cl	I	$-C_6H_{11}$	70	150	$C_{18}H_{18}ClIN_4O_2$
IIIj	Cl	I	$-C_6H_5$	68	120	$C_{18}H_{12}ClIN_4O_2$
IIIk	Cl	I	$-CH_2C_6H_5$	72	156	$C_{19}H_{14}ClIN_4O_2$
IIIl	Cl	I	$-C_6H_4$-*p*-CH_3	75	170	$C_{19}H_{14}ClIN_4O_2$
IVa	H	H	$-CH_2CH=CH_2$	70	250	$C_{15}H_{14}N_4OS$
IVb	H	H	$-(CH_2)_3CH_3$	68	160	$C_{16}H_{18}N_4OS$
IVc	H	H	$-C_6H_{11}$	73	200	$C_{18}H_{20}N_4OS$
IVd	H	H	$-C_6H_5$	65	225	$C_{18}H_{14}N_4OS$
IVe	H	H	$-CH_2C_6H_5$	66	195	$C_{19}H_{16}N_4OS$
IVf	H	H	$-C_6H_4$-*p*-CH_3	70	208	$C_{19}H_{16}N_4OS$
IVg	Cl	I	$-CH_2CH=CH_2$	65	140	$C_{15}H_{12}ClIN_4OS$
IVh	Cl	I	$-(CH_2)_3CH_3$	70	127	$C_{16}H_{16}ClIN_4OS$
IVi	Cl	I	$-C_6H_{11}$	74	132	$C_{18}H_{18}ClIN_4OS$
IVj	Cl	I	$-C_6H_5$	67	136	$C_{18}H_{12}ClIN_4OS$
IVk	Cl	I	$-CH_2C_6H_5$	70	130	$C_{19}H_{14}ClIN_4OS$
IVl	Cl	I	$-C_6H_4$-*p*-CH_3	72	160	$C_{19}H_{14}ClIN_4OS$

[a] All compounds were recrystallized from ethanol and showed absorption in the IR range at 3200–3095 cm^{-1} (NH). Elemental analyses (C, H, N, and S for all compounds, I for compounds with R_2 = I) were within ±0.4% from theoretical for all of the methoxyquinolines.

IIIh—^{1}H-NMR ($CDCl_3$): δ 7.0–8.2 (m, ArH), 5.2 (s, 2, OCH_2), 4.1 (t, 2, N—CH_2), 1.8 (m, CH_2), 1.4 (m, CH_2), and 1.0 ppm (t, CH_3).

8-(5-Substituted Amino-1,3,4-thiadiazol-2-yl) Methoxyquinolines (IV)—1-(8-Quinolinoxyacetyl)-4-substituted thiosemicarbazide (II, 0.01 mol) was added in small portions to concentrated sulfuric acid (25 mL) with stirring, maintaining the temperature below 0°C during addition for 1 h. The reaction mixture was allowed to stand at room temperature overnight and then warmed to 50°C. It was then cooled and poured onto crushed ice. The solid product was removed by filtration, washed with water, treated with dilute ammonia to remove any sulfonated product, again washed with water, dried, and crystallized from a suitable solvent (Table I). ^{1}H-NMR ($CDCl_3$) for IVf: δ 7.1–9.0 (m, ArH), 5.7 (s, 2, OCH_2), 5.1 (d, N*H*-Ar), and 2.3 ppm (s, Ar-C*H*$_3$).

Antibilharzial Activity—Swiss albino mice were inoculated with 100 cercariae of *S. mansoni* by the tail immersion technique (8). Eight weeks after infestation, the animals were divided into seven groups: an untreated control group, a group for each of the new drugs to be tested (IIId, IIIh, IVf, IVh, and IVj), and hycanthone as a positive control group. The drugs were given orally as a single 100-mg/kg dose in suspension of 1% carboxymethylcellulose. Hycanthone was given as a single injection, 70 mg/kg im in 0.1 mL of distilled water. Oogram studies of the liver and intestine were made every third day on five animals from each group, (3, 6, 9, and 12 d posttreatment). Table II shows the average oogram pattern in the liver and small intestine during the period of maximum drug effect (9 d), which was usually at the end of the first week, compared with hycanthone (9).

RESULTS AND DISCUSSION

The efficiency of a new antischistosomal drug was assessed in experimentally infested mice by the oogram changes, which were said to be caused by loss of schistosoma worm muscle tone, during action on the parasite reproductive organs, and death of the worms (10). Deviation of the oogram picture from normal was considered to be an absence of any immature stages or when the number of mature ova exceeded 50% (10). Results obtained showed small deviation of the oogram picture from normal. Compounds IVf, IVh, and IVj showed moderate activity, while the others showed only mild activity.

Table II—Oogram Findings in Liver and Small Intestine of Infested Mice 9 d After Treatment with Experimental Compounds

Compound	Liver				Small Intestine			
	Mean Eggs/ Mouse (Range)	Total Immature Eggs, %	Mature Eggs, %	Dead Eggs %	Mean Eggs/ Mouse (Range)	Total Immature Eggs, %	Mature Eggs, %	Dead Eggs, %
Control	25–30	76	18	6	27–31	70	28	2
Hycanthone	23–29	—	—	—	25–30	0	48	52
IIId	26–31	35	30	35	28–32	16	34	50
IIIh	28–30	32	38	30	24–30	20	60	20
IVf	25–30	20	40	40	25–31	2	55	43
IVh	27–32	15	47	38	26–30	13	60	27
IVj	26–30	10	42	48	25–32	2	68	30

REFERENCES

(1) W. Kikuth and R. Connert, *Ann. Trop. Med. Parasitol.*, **42**, 256 (1948).

(2) D. Rosi, G. Peruzzotti, E. W. Dennis, D. A. Berberian, H. Freele, and S. Archer, *Nature (London)*, **208**, 1005 (1965).

(3) N. W. Bristow, B. Lessel, H. C. Richards, and G. A. Williams, *Nature (London)*, **216**, 282 (1967).

(4) J. Pellegrino, N. Katz, and J. F. Scherrer, *J. Parasitol.*, **53**, 1225 (1967).

(5) P. Schmidt and M. Wilhelm, *Angew. Chem. Int. Ed.*, **5**, 857 (1966).

(6) R. Soliman and N. A. Hammouda, *J. Pharm. Sci.*, **68**, 1377 (1979).

(7) S. N. Sawhney, J. Singh, and O. P. Bansal, *Ind. J. Chem.*, **13**, 804 (1975).

(8) J. M. Watson and M. Abdel Azim, *Ann. Trop. Med. Parasitol.*, **43**, 41 (1949).

(9) H. F. Farag, M. Youssef, N. A. Hammouda, and H. N. Awadalla, *Egypt. J. Soc. Parasitol.*, **8**, 1 (1978).

(10) J. Pellegrino, C. A. Oliveira, J. Faria, and A. Cunha, *Am. J. Trop Med. Hyg.*, **11**, 201 (1962).

ACKNOWLEDGMENTS

The authors are indebted to Dr. N. A. Hammouda for the biological screening of the new compounds at the Department of Parasitology, Faculty of Medicine, University of Alexandria, Alexandria, Egypt.

Synthesis and Anticonvulsant Evaluation of *N*-Aminosuccinimides

MILTON J. KORNET

Received December 20, 1982, from the *College of Pharmacy, University of Kentucky, Lexington, KY 40536-0053.* Accepted for publication January 24, 1983.

Abstract □ Twelve new *N*-aminosuccinimides were synthesized by the condensation of hydrazines with succinic anhydrides in glacial acetic acid. The compounds were evaluated in the maximal electroshock seizure and subcutaneous pentylenetetrazol seizure threshold tests for anticonvulsant activity and in the rotorod test for neurotoxicity in mice. The lowest dose at which several of the compounds exhibited anticonvulsant activity was 300 mg/kg.

Keyphrases □ *N*-Aminosuccinimides—synthesis, anticonvulsant and neurotoxic potential, mice □ Anticonvulsants—potential, *N*-aminosuccinimides, synthesis, neurotoxicity, mice

Potential anticonvulsants and hydrazine-derived drugs in general have been a principal interest of ours over several years. Anticonvulsant activity has been found among the 3,5-pyrazolidinediones (1), semicarbazides (2–4), and hydrazino urethans (5, 6). Because of the effectiveness of the succinimides such as phensuximide, methsuximide, and ethosuximide for the treatment of the petit mal condition and the paucity of information (7) concerning *N*-aminosuccinimides, an investigation in this area appeared warranted. A related compound, *N*-amino-3-(*m*-bromophenyl)succinimide, has been shown to possess potent maximal electroshock seizure activity (8). A decrease in spontaneous motor activity by *N*-arylaminosuccinimides has been noted (9).

This paper reports on the synthesis and anticonvulsant activity of a series of *N*-aminosuccinimides. The compounds vary in the nature of the amino nitrogen (alkylated or arylated) and in the α-position of the succinimide ring (unsubstituted, methyl, or phenyl).

RESULTS AND DISCUSSION

The synthesis of the aminosuccinimides (III) was accomplished by treating various succinic anhydrides (I) with substituted hydrazines (II) in glacial acetic acid (Scheme I) (Table I). Others (10) have used a mixture of equal volumes of glacial acetic acid and concentrated sulfuric acid to effect this condensation.

Compounds IIIa–IIIn were tested in the maximal electroshock seizure and subcutaneous pentylenetetrazol seizure threshold tests for anticonvulsant activity and in the rotorod test for neurotoxicity in male mice[1] by reported procedures (2). None of the compounds showed activity at 100 mg/kg in either test. In the maximal electroshock seizure test, IIIc, IIId, IIIf, IIIk, and IIIm exhibited activity at 300 mg/kg at 30 min with no indication of toxicity. One compound, IIIg, showed activity at this same dose at 4 h. In the pentylenetetrazol seizure test, IIIb, IIIl, and IIIm displayed activity at 300 mg/kg at 30 min with no toxicity. Overall, this

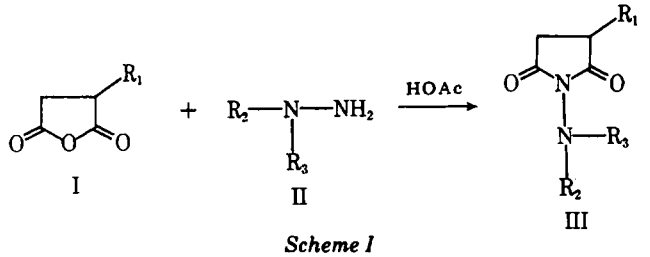

Scheme I

[1] No. 1, Carworth Farms.

0022-3549/84/0300-0405$01.00/0

© 1984, American Pharmaceutical Association

Table II—Oogram Findings in Liver and Small Intestine of Infested Mice 9 d After Treatment with Experimental Compounds

Compound	Liver				Small Intestine			
	Mean Eggs/ Mouse (Range)	Total Immature Eggs, %	Mature Eggs, %	Dead Eggs %	Mean Eggs/ Mouse (Range)	Total Immature Eggs, %	Mature Eggs, %	Dead Eggs, %
Control	25–30	76	18	6	27–31	70	28	2
Hycanthone	23–29	—	—	—	25–30	0	48	52
IIId	26–31	35	30	35	28–32	16	34	50
IIIh	28–30	32	38	30	24–30	20	60	20
IVf	25–30	20	40	40	25–31	2	55	43
IVh	27–32	15	47	38	26–30	13	60	27
IVj	26–30	10	42	48	25–32	2	68	30

REFERENCES

(1) W. Kikuth and R. Connert, *Ann. Trop. Med. Parasitol.*, **42**, 256 (1948).

(2) D. Rosi, G. Peruzzotti, E. W. Dennis, D. A. Berberian, H. Freele, and S. Archer, *Nature (London)*, **208**, 1005 (1965).

(3) N. W. Bristow, B. Lessel, H. C. Richards, and G. A. Williams, *Nature (London)*, **216**, 282 (1967).

(4) J. Pellegrino, N. Katz, and J. F. Scherrer, *J. Parasitol.*, **53**, 1225 (1967).

(5) P. Schmidt and M. Wilhelm, *Angew. Chem. Int. Ed.*, **5**, 857 (1966).

(6) R. Soliman and N. A. Hammouda, *J. Pharm. Sci.*, **68**, 1377 (1979).

(7) S. N. Sawhney, J. Singh, and O. P. Bansal, *Ind. J. Chem.*, **13**, 804 (1975).

(8) J. M. Watson and M. Abdel Azim, *Ann. Trop. Med. Parasitol.*, **43**, 41 (1949).

(9) H. F. Farag, M. Youssef, N. A. Hammouda, and H. N. Awadalla, *Egypt. J. Soc. Parasitol.*, **8**, 1 (1978).

(10) J. Pellegrino, C. A. Oliveira, J. Faria, and A. Cunha, *Am. J. Trop Med. Hyg.*, **11**, 201 (1962).

ACKNOWLEDGMENTS

The authors are indebted to Dr. N. A. Hammouda for the biological screening of the new compounds at the Department of Parasitology, Faculty of Medicine, University of Alexandria, Alexandria, Egypt.

Synthesis and Anticonvulsant Evaluation of *N*-Aminosuccinimides

MILTON J. KORNET

Received December 20, 1982, from the *College of Pharmacy, University of Kentucky, Lexington, KY 40536-0053.* Accepted for publication January 24, 1983.

Abstract □ Twelve new *N*-aminosuccinimides were synthesized by the condensation of hydrazines with succinic anhydrides in glacial acetic acid. The compounds were evaluated in the maximal electroshock seizure and subcutaneous pentylenetetrazol seizure threshold tests for anticonvulsant activity and in the rotorod test for neurotoxicity in mice. The lowest dose at which several of the compounds exhibited anticonvulsant activity was 300 mg/kg.

Keyphrases □ *N*-Aminosuccinimides—synthesis, anticonvulsant and neurotoxic potential, mice □ Anticonvulsants—potential, *N*-aminosuccinimides, synthesis, neurotoxicity, mice

Potential anticonvulsants and hydrazine-derived drugs in general have been a principal interest of ours over several years. Anticonvulsant activity has been found among the 3,5-pyrazolidinediones (1), semicarbazides (2–4), and hydrazino urethans (5, 6). Because of the effectiveness of the succinimides such as phensuximide, methsuximide, and ethosuximide for the treatment of the petit mal condition and the paucity of information (7) concerning *N*-aminosuccinimides, an investigation in this area appeared warranted. A related compound, *N*-amino-3-(*m*-bromophenyl)succinimide, has been shown to possess potent maximal electroshock seizure activity (8). A decrease in spontaneous motor activity by *N*-arylaminosuccinimides has been noted (9).

This paper reports on the synthesis and anticonvulsant activity of a series of *N*-aminosuccinimides. The compounds vary in the nature of the amino nitrogen (alkylated or arylated) and in the α-position of the succinimide ring (unsubstituted, methyl, or phenyl).

RESULTS AND DISCUSSION

The synthesis of the aminosuccinimides (III) was accomplished by treating various succinic anhydrides (I) with substituted hydrazines (II) in glacial acetic acid (Scheme I) (Table I). Others (10) have used a mixture of equal volumes of glacial acetic acid and concentrated sulfuric acid to effect this condensation.

Compounds IIIa–IIIn were tested in the maximal electroshock seizure and subcutaneous pentylenetetrazol seizure threshold tests for anticonvulsant activity and in the rotorod test for neurotoxicity in male mice[1] by reported procedures (2). None of the compounds showed activity at 100 mg/kg in either test. In the maximal electroshock seizure test, IIIc, IIId, IIIf, IIIk, and IIIm exhibited activity at 300 mg/kg at 30 min with no indication of toxicity. One compound, IIIg, showed activity at this same dose at 4 h. In the pentylenetetrazol seizure test, IIIb, IIIl, and IIIm displayed activity at 300 mg/kg at 30 min with no toxicity. Overall, this

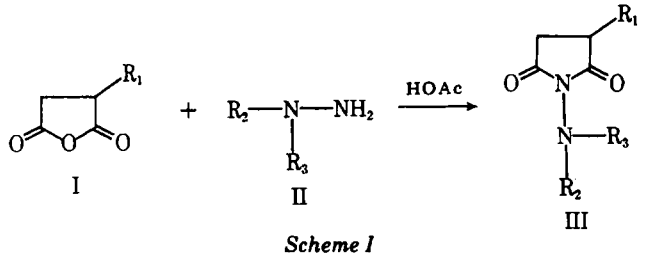

Scheme I

[1] No. 1, Carworth Farms.

0022-3549/84/0300-0405$01.00/0

© 1984, American Pharmaceutical Association

Table I—Physical Properties of *N*-Aminosuccinimides

Compound	R_1	R_2	R_3	Melting Point, °C	Yield, %	Formula
IIIa	H	H	$C(CH_3)_3$	98–99.5[a]	22	$C_8H_{14}N_2O_2$
IIIb	C_6H_5	CH_3	CH_3	86–87[b]	70	$C_{12}H_{14}N_2O_2$
IIIc	C_6H_5	H	$C(CH_3)_3$	123–124[b]	64	$C_{14}H_{18}N_2O_2$
IIId	C_6H_5	—$CH_2(CH_2)_3CH_2$—		101–102[c]	80	$C_{15}H_{18}N_2O_2$
IIIe	C_6H_5	—$CH_2CH_2OCH_2CH_2$—		152.5–153.5[b]	50	$C_{14}H_{16}N_2O_3$
IIIf	H	H	C_6H_5	160–161.5[d,e]	37	$C_{10}H_{10}N_2O_2$
IIIg	H	H	p-ClC_6H_4	155–157[d]	29	$C_{10}H_9ClN_2O_2$
IIIh	H	H	p-$O_2NC_6H_4$	268–270[f]	59	$C_{10}H_9N_3O_4$
IIIi	H	H	o-$O_2NC_6H_4$	203.5–205[f,g]	68	$C_{10}H_9N_3O_4$
IIIj	H	CH_3	C_6H_5	150–151[d]	50	$C_{11}H_{12}N_2O_2$
IIIk	H	H	o-$CH_3C_6H_4$	138–139.5[d]	44	$C_{11}H_{12}N_2O_2$
IIIl	H	H	2,4-$Cl_2C_6H_3$	156–157[h]	75	$C_{10}H_8Cl_2N_2O_2$
IIIm	CH_3	H	C_6H_5	111–112[i]	63	$C_{11}H_{12}N_2O_2$
IIIn	C_6H_5	H	o-$CH_3C_6H_4$	121–122[d]	73	$C_{17}H_{16}N_2O_2$

[a] Cyclohexane–toluene. [b] 70% Ethanol. [c] 60% Ethanol. [d] 95% Ethanol. [e] Reported mp 158°C [A. Michaelis and R. Hermens, *Chem. Ber.*, **25**, 2750 (1892)]. [f] Glacial acetic acid. [g] Reported mp 206–208°C (Ref. 9). [h] 80% Ethanol. [i] Toluene.

group of compounds does not display anticonvulsant activity comparable with currently available drugs.

EXPERIMENTAL[2]

Compound IIId was prepared by the dropwise addition of 3.15 g (0.0315 mol) of *N*-aminopiperidine to a solution of 5.28 g (0.030 mol) of phenylsuccinic anhydride (11) in 15 mL of glacial acetic acid. The initially exothermic reaction mixture was refluxed under nitrogen for 1.5 h, and the acetic acid was evaporated under reduced pressure. Water (10 mL) was added to the residue, and the pH was adjusted to 8 by addition of 5% NaOH solution. The product was extracted into chloroform, dried over magnesium sulfate, the solvent evaporated, and the residue recrystallized from 60% ethanol, affording 6.11 g (79%) of white crystals, mp 101–102°C. The reflux period for arylhydrazines was 3 h, and the NaOH neutralization in the workup was omitted.

[2] Melting points were determined on a Thomas-Hoover melting point apparatus and are uncorrected. The IR spectra were taken on a Perkin-Elmer 700 spectrophotometer as either liquid films or as potassium bromide pellets. NMR spectra were recorded on a Varian EM-360 or T-60 spectrometer, using tetramethylsilane as the internal reference. Mass spectra were obtained on a RMU-7 double-focusing spectrometer by Hitachi/Perkin-Elmer. Elemental analyses for C, H, and N were performed by Baron Consulting Co., Orange, Conn.; values for all compounds were within ± 0.4% of theoretical. All compounds exhibited ^{1}H-NMR and mass spectra consistent with the structures shown.

REFERENCES

(1) M. J. Kornet, J. H. Thorstenson, and W. C. Lubawy, *J. Pharm. Sci.*, **63**, 1090 (1974).

(2) M. J. Kornet, *J. Pharm. Sci.*, **67**, 1471 (1978).

(3) M. J. Kornet and J. Chu, *J. Heterocycl. Chem.*, **18**, 293 (1981).

(4) M. J. Kornet and J.Y-R. Chu, *J. Heterocycl. Chem.*, **19**, 697 (1982).

(5) M. J. Kornet, *J. Pharm. Sci.*, **69**, 729 (1980).

(6) M. J. Kornet, *J. Heterocycl. Chem.*, **17**, 975 (1980).

(7) J. Lapszewicz, J. Lange, S. Rump, and K. Walczyna, *Eur. J. Med. Chem.*, **13**, 465 (1978).

(8) S. Rump, I. Ilczuk, and K. Walczyna, *Arzneim.-Forsch/Drug Res.*, **29**, 290 (1979).

(9) Z. Kleinrok, E. Jagiello-Wojtowicz, and Z. Choma, *Acta Pol. Pharm.*, **33**, 265 (1976); through *Chem. Abstr.*, **86**, 297c (1977).

(10) S. Baloniak, *Rocz. Chem.*, **40**, 1567 (1966); through *Chem. Abstr.*, **67**, 32411j (1967).

(11) M. J. Kornet and H. S. I. Tan, *J. Pharm. Sci.*, **61**, 1781 (1972).

ACKNOWLEDGMENTS

The author is grateful to the Antiepileptic Drug Development Program of the National Institutes of Health for the anticonvulsant activity data and to Mr. Walter Beaven and Mrs. Tarla Varia for technical assistance.

Synthesis and Antibacterial Activity of Some 5-Nitro-3-phenyliminoindol-2(3*H*)-ones and Their *N*-Mannich Bases

ROY W. DAISLEY ˣ **and VASANTI K. SHAH**

Received November 23, 1982, from the *Department of Pharmacy, Brighton Polytechnic, Brighton, BN2 4GJ, England.* Accepted for publication January 13, 1983.

Abstract □ The antimicrobial and antifungal activities of a series of 5-nitro-3-phenyliminoindol-2(3*H*)-ones and their 1-piperidinomethyl analogues (*N*-Mannich bases) were investigated. Growth inhibition of Gram-positive bacteria was observed with little or no activity against Gram-negative bacteria. Antifungal activity was absent. The syntheses were accomplished from 5-nitroindol-2,3-dione by condensation with the appropriate aniline followed by formation of the *N*-Mannich base.

Keyphrases □ 5-Nitro-3-phenyliminoindol-2(3*H*)-ones—synthesis, antimicrobial and antifungal activity □ *N*-Mannich bases—5-nitro-3-phenyliminoindol-2(3*H*)-ones, synthesis, antimicrobial and antifungal activity □ Antimicrobial agents—potential, 5-nitro-3-phenyliminoindol-2(3*H*)-ones and their *N*-Mannich bases, synthesis

Interest in biologically active indol-2,3-dione (isatin) derivatives has increased rapidly over the past few years. Mannich bases derived from indol-2,3-diones have shown antimicrobial (1, 2), antiviral (3), cytostatic, and antimitotic (4, 5) activities. The corresponding substituted 3-thiosemicarbazones or 3-hydrazones have similarly shown antimicrobial (2), antiviral (6), cytostatic, and antimitotic (4, 5) activities. Recently a series of 3-aryliminoindol-2(3*H*)-ones and their *N*-Mannich bases have been shown to possess antibacterial and antifungal (7) activity and have shown promise as excystment and cysticidal agents against *Schizopyrenus russelli* (8, 9). CNS activity has recently been demonstrated for some *N*,*N*-disubstituted 1-(aminomethyl)-5-alkyl-3-(aryloxyacetylhydrazono)indol-2(3*H*)-ones (10).

The 3-*o*-nitrophenylhydrazone of indol-2,3-dione has shown activity against Walker carcinosarcoma 256 (11). Because of the well-known antibacterial activity of other nitro heterocycles (12) and our interest in this area (13), we decided to prepare and test a series of 5-nitro substituted 3-phenyliminoindol-2(3*H*)-ones and their *N*-Mannich bases for antimicrobial activity.

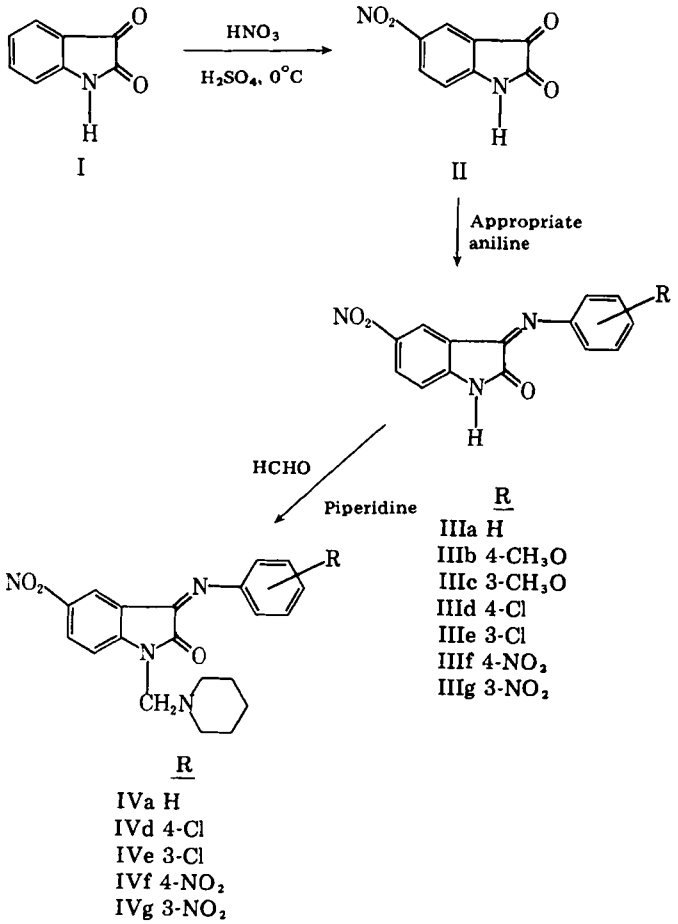

Scheme I—Synthesis of 5-nitro-3-phenylimino-1-piperidinomethylindol-2(3H)-ones.

RESULTS AND DISCUSSION

The synthetic procedure followed is outlined in Scheme I. The starting material was 5-nitroindol-2,3-dione (II) prepared by the nitration of indol-2,3-dione (I) using a modification of the method reported by Calvery (14) which prevented the formation of resinous side products. Direct condensation of the appropriate aniline with 5-nitroindol-2,3-dione (II) in a boiling mixture of ethanol and dimethyl sulfoxide furnished the corresponding 3-phenylimino derivatives (IIIb–d). The remaining compounds (IIIa, e–f) were prepared similarly, but required the addition of a few drops of glacial acetic acid to the reaction medium. Using dimethyl sulfoxide containing a few drops of glacial acetic acid as solvent allowed the reaction to proceed to completion by standing at room temperature overnight.

The 1-piperidinomethyl derivatives (*N*-Mannich bases) (IVa, d–g) were prepared from the 3-phenylimino derivatives using standard methods (7). The reaction failed for IVb and IVc.

All compounds gave satisfactory elemental analysis for C, H, and N (within ±0.4%), the UV, IR, ^{1}H-NMR, and mass spectra were consistent with the assigned structures. Physical constants of the 3-phenylimino

Table I—Physical Properties of 5-Nitro-3-phenyliminoindol-2(3*H*)-ones (III) and 5-Nitro-3-phenylimino-1-piperidinomethylindol-2(3*H*)-ones (IV)

Compound	R	Method	Yield, %	mp, °C	Formula
IIIa	H	C	90	242–243[a]	$C_{14}H_9N_3O_3$
IIIb	4-CH_3O	A	91	222–224[a]	$C_{15}H_{11}N_3O_4$
IIIc	3-CH_3O	A	62	168–170	$C_{15}H_{11}N_3O_4 \cdot H_2O$
IIId	4-Cl	A	77	220–221[a]	$C_{14}H_8ClN_3O_3 \cdot H_2O$
IIIe	3-Cl	B	89	130–131	$C_{14}H_8ClN_3O_3$
IIIe	3-Cl	C	83	129–131	—
IIIf	4-NO_2	B	77	151–152	$C_{14}H_8N_4O_5 \cdot H_2O$
IIIf	4-NO_2	C	80	151–153	—
IIIg	3-NO_2	B	51	235–237	$C_{14}H_8N_4O_5$
IIIg	3-NO_2	C	64	237–238	—
IVa	H	–	66	145–147	$C_{20}H_{20}N_4O_3$
IVd	4-Cl	–	68	165–167	$C_{20}H_{19}ClN_4O_3$
IVe	3-Cl	–	66	174–176	$C_{20}H_{19}ClN_4O_3$
IVf	4-NO_2	–	24	185–187	$C_{20}H_{19}N_5O_5$
IVg	3-NO_2	–	31	188–189	$C_{20}H_{19}N_5O_5$

[a] Kallmayer (15) reports mp 245–247°C for IIa, and 266–270°C and 238–240°C, respectively, for the anhydrous forms of IIIb and IIId.

0022-3549/84/0300-0407$01.00/0
© 1984, American Pharmaceutical Association

Table II—Antibacterial and Antifungal Activities of 5-Nitro-3-phenyliminoindol-2(3*H*)-ones (III) and 5-Nitro-3-phenylimino-1-piperidinomethylindol-2(3*H*)-ones (IV)

Compound	Diameter of Inhibition Zones[a], mm × 10					
	E. Coli (NCTC 5933)		*S. aureus* (NCTC 8532)		*C. albicans* (NCTC 45348)	
	Carpet	Pour	Carpet	Pour	Carpet	Pour
II	–	–	–	–	–	–
IIIa	–	–	–	–	–	–
IIIb	–	–	±	±	–	–
IIIc	–	–	130	120	–	–
IIId	–	–	170	142	–	–
IIIe	–	–	186	162	–	–
IIIf	–	–	–	–	–	–
IIIg	–	–	170	150	–	–
IVa	–	–	–	–	–	–
IVd	±	±	250	240	–	–
IVe	–	–	170	142	–	–
IVf	–	–	–	–	–	–
IVg	–	–	202	176	–	–
Dimethyl sulfoxide	–	–	–	–	–	–

[a] Average of six determinations. Key: (–) no inhibition; (±) minimally observable inhibition.

and corresponding 1-piperidinomethyl derivatives are listed in Table I.

All the compounds synthesized were evaluated for potential antimicrobial activity against Gram-negative *Escherichia coli*, Gram-positive *Staphylococcus aureus*, and *Candida albicans* using the cup–plate technique with either a pour plate or surface-innoculated (carpet) plate. None of the compounds tested showed any activity against *C. albicans*, and only IVd exhibited slight activity against *E. coli* (Table II). Compounds II, IIIa, IIIf, IVa, and IVf were inactive and IIIb showed only slight inhibitory activity against *S. aureus*. However, IIIc–e, IIIg, IVd–e, and IVg were active, with IVd the most active, followed by IVg.

The Mannich bases were usually more active than the 3-phenylimino compounds, with the exception that IIIe was more active than IVe. This is consistent with the observation of Varma (7) and demonstrates the necessity of the 3-phenylimino group, as 5-nitro-3-piperidinomethylindol-2,3-dione has been shown to be devoid of antimicrobial activity (2).

EXPERIMENTAL

Antimicrobial Evaluation—The organisms used were *E. coli* (NCTC 5933), *S. aureus* (NCTC 8532), and *C. albicans* (NCTC 45348). The cup–plate technique was used with either a pour plate or a surface-innoculated (carpet) plate using nutrient agar for the bacteria and malt extract for *C. albicans*.

The compounds were tested at 1 mg/mL in dimethyl sulfoxide, and 100-μl portions were transferred to 9-mm diameter holes cut into the plates. The agar plates were then incubated at 37°C for 24 h and the malt extract plates at 25°C for 72 h, after which the zones of inhibition around each hole were measured. Table II shows the average of six determinations for each zone of inhibition. Dimethyl sulfoxide showed no inhibitory effects on the test organisms.

Chemistry—Melting point values were determined[1] and are corrected. The ^{1}H-NMR[2] spectra were obtained in DMSO-d_6 using 1% tetramethylsilane as internal standard. IR[3] and UV[4] spectra were recorded on double-beam spectrophotometers. Mass spectra[5] were also recorded. TLC was carried out using plates coated with silica gel, and products were visualized with UV light at 254 nm. All compounds submitted for elemental analysis[6] gave spectral data consistent with the proposed structure and were pure by TLC.

5-Nitroindol-2,3-dione (II)—Indol-2,3-dione (44.2 g, 0.33 mol) was dissolved in concentrated sulfuric acid (208 mL), and the solution was kept at 0°C while nitric acid (d = 1.50, 15.5 mL, 0.34 mol) was added dropwise over a period of 3 h. After the addition was complete, the solution was allowed to stand for 1 h and then poured into ice (1.5 kg). The yellow precipitate was collected and recrystallized from aqueous methanol to yield 5-nitroindol-2,3-dione (II), 48.3 g (85%), mp 254–255°C [lit. (14) mp 254–255°C].

5-Nitro-3-phenyliminoindol-2(3H)-ones (III)—Compounds IIIa–g were prepared by one of the following methods:

1. 5-Nitroindol-2,3-dione (1.92 g, 0.01 mol) and the appropriate aniline (0.01 mol) were suspended in a mixture of ethanol (15 mL) and dimethyl sulfoxide (15 mL). The mixture was heated at reflux for 1 h, an equal volume of warm water was added, and the mixture was allowed to stand at room temperature overnight. The material was removed by filtration, washed with aqueous ethanol (50% v/v), and dried. Analytical and microbiological samples were recrystallized from aqueous methanol (50% v/v) (method A).

2. Identical to method A except that a few drops of glacial acetic acid were added to the reaction mixture (method B).

3. 5-Nitroindol-2,3-dione (1.92 g, 0.01 mol) and the appropriate aniline (0.01 mol) were stirred overnight in dimethyl sulfoxide (25 mL) containing a few drops of glacial acetic acid. The products were isolated by dilution with an equal quantity of warm water as described for method A (method C).

5-Nitro-3-phenylimino-1-piperidinomethylindol-2(3H)-ones (IV)—The appropriate 5-nitro-3-phenyliminoindol-2(3*H*)-one (0.01 mol) was treated with piperidine (0.01 mol), formaldehyde solution (2 mL, 37% w/v), ethanol (10 mL), and dimethyl sulfoxide (10 mL). The mixture was then heated on a water bath until a clear solution was obtained. An equal volume of warm water was then added and the resulting mixture was allowed to stand at room temperature overnight; the product was removed by filtration and then recrystallized from aqueous methanol (50% v/v).

REFERENCES

(1) R. S. Varma and W. L. Nobles, *J. Pharm. Sci.*, **64**, 881 (1975).

(2) M. Kupinic, M. Medić-Šarić, M. Movrin, and D. Maysinger, *J. Pharm. Sci.*, **68**, 459 (1979).

(3) R. S. Varma and W. L. Nobles, *J. Med. Chem.*, **10**, 510 (1967).

(4) D. Maysinger, J. Ban, and M. Movrin, *Arzneim.-Forsch.*, **30**(I), 6, 932 (1980).

(5) D. Maysinger and M. Movrin, *Arzneim.-Forsch.*, **30**(II), 11, 1839 (1980).

(6) R. S. Varma and W. L. Nobles, *J. Med. Chem.*, **10**, 972 (1967).

(7) R. S. Varma, *Pol. J. Pharmacol. Pharm.*, **27**, 641 (1975).

(8) S. A. Imam and R. S. Varma, *Experientia*, **31**, 1287 (1975).

(9) R. S. Varma and I. A. Khan, *Pol. J. Pharmacol. Pharm.*, **29**, 549 (1977).

(10) R. Agarwal, S. Misra, R. K. Satsangi, and S. S. Tiwari, *Arch. Pharm.*, **315**, 142 (1982).

(11) F. D. Popp, *J. Med. Chem.*, **12**, 182 (1969).

(12) C. L. K. Lins, J. H. Block, and R. F. Doerge, *J. Pharm. Sci.*, **71**, 556 (1982).

(13) R. W. Daisley and J. Walker, *Eur. J. Med. Chem. Chim. Ther.*, **14**, 47 (1979) and references therein.

(14) H. O. Calvery, C. R. Noller, and R. Adams, *J. Am. Chem. Soc.*, **47**, 3059 (1925).

(15) H. J. Kallmayer, *Arch. Pharm.*, **308**, 752 (1975).

[1] Mettler model FP61.
[2] Perkin-Elmer model R32.
[3] Perkin-Elmer model 157G in KBr disks.
[4] Perkin-Elmer model 554.
[5] VG MM 16F spectrometer with DS 2135 data system.
[6] Carried out by Dr. J. Baker, Department of Pharmacy, Brighton Polytechnic.

Stability Kinetics of Ginsenosides in Aqueous Solution

ETSUKO MIYAMOTO *, SHIZUO ODASHIMA ‡x, ISAO KITAGAWA §, and AKIRA TSUJI ¶

Received July 7, 1982, from the **School of Pharmacy, Hokuriku University, Kanagawa-machi, Kanazawa 920-11, Japan,* ‡*the Department of Pathology, Kanazawa Medical University, Uchinada-machi, Kahoku-gun 920-02, Japan,* §*the Faculty of Pharmaceutical Sciences, Osaka University, 1-6, Yamada-oka Suita, Osaka 565, Japan, and* ¶*the Faculty of Pharmaceutical Sciences, Kanazawa University, Takara-machi, Kanazawa 920, Japan.* Accepted for publication December 21, 1982.

Abstract □ The stability of ginsenosides (Rb_1, Rb_2, and Rg_1) in aqueous solutions of varying pH was studied kinetically at 37°C and an ionic strength of 0.15, using reverse-phase high-performance liquid chromatography. Degradation readily occurred by a proton-catalyzed reaction, the half-lives being only ~30 min at pH 1. However, under neutral intestinal pH conditions, the degradation was almost negligible throughout the experimental period (~40 h).

Keyphrases □ Ginsenosides—stability kinetics, aqueous solutions of varying pH □ Stability—ginsenosides in aqueous solutions of varying pH, kinetics □ Ginseng—stability kinetics of ginsenosides in aqueous solutions of varying pH

Ginseng has been used as a folkloric medicine in traditional herbal remedies for a long time. It has several noteworthy properties such as an antistress or rehabilitative action (1, 2). Many studies suggest that the pharmacological effects of ginseng come from the ginsenosides. Recently, Odashima *et al.* (3) reported the interesting finding that ginsenosides induced morphological changes and phenotypic transformations in cultured Morris Hepatoma cells (MH_1C_1), calling this "reverse transformation."

We have investigated the stability of the ginsenosides in both water and GI fluid since many herbal medicines seem to be effective when given orally. The ginsenosides have been known to degrade in the presence of acid, and the degradation mechanism and structures of the products have been described (4, 5). However, the detailed stability kinetics of ginsenosides have not been investigated. The present study reports the kinetics of degradation of the ginsenosides Rg_1, as 20*S*-panaxatriol, and Rb_1 and Rb_2, as 20*S*-panaxadiol, in water.

EXPERIMENTAL

Materials—The ginsenosides used in this study were prepared from the dried roots of *Panax ginseng* C. A. Meyer (Araliaceae), which were obtained from a commercial source[1], according to the usual procedures (6). The purity of the ginsenosides was confirmed by TLC (6). All other chemicals were of reagent grade and were used without further purification.

Ginsenosides Hydrolysis—Kinetic studies were carried out at 37 ± 0.1°C, at various pH values, and an ionic strength of 0.15. Each ginsenoside was dissolved in buffer solution preheated at 37°C to give a final concentration of 1×10^{-4} to 4×10^{-4} M. The buffer solutions employed were hydrochloric acid and phosphate (NaH_2PO_4) buffer systems, which were adjusted to a constant ionic strength of 0.15 with potassium chloride. The artificial GI fluids of pH 1.22 and pH 6.84 described in the Japanese Pharmacopeia X were also used. At appropriate intervals, aliquots were withdrawn, cooled, neutralized as necessary to quench the reaction with the same volume of phosphate (NaH_2PO_4–Na_2HPO_4) buffer solution (0.1 M, pH 6.8), and then analyzed. The pH of the reaction mixture was measured[2] both before use and at the end of the experiments. No significant change was observed.

Analytical Procedures—The reaction samples were assayed by reverse-phase HPLC. The liquid chromatograph[3] was equipped with a UV detector[4] set at 207 nm and a radial compression system[5] with an inserted reverse-phase cartridge[6]. The mobile phase was 70% (v/v) methanol–water. The instrument was operated at ambient temperature and a flow rate of 1.0 mL/min. A 100-μL sample was injected through an injector[7] on flow; the samples were filtered through a 0.45-μm membrane filter[8] before injection. Peak heights were used for quantification, and the coefficient of variation (*CV*) was 2.9%.

RESULTS AND DISCUSSION

Figures 1 and 2 show typical chromatograms of intact Rg_1 in the reaction mixture at 37°C, an ionic strength of 0.15, and pH 1.81. The peak of Rg_1 (peak 1) with a retention time (t_R) of 9 min decreased as a function of time and several peaks of degradation products appeared as the degradation reaction proceeded (Fig. 2).

All reactions were followed for 1–3 half-lives. The degradation of Rg_1, Rb_1, and Rb_2 followed first-order kinetics. Furthermore, in the pH range studied (pH 1–3), the rate of degradation was found to be first order with respect to hydrogen ion activity and independent of buffer concentration.

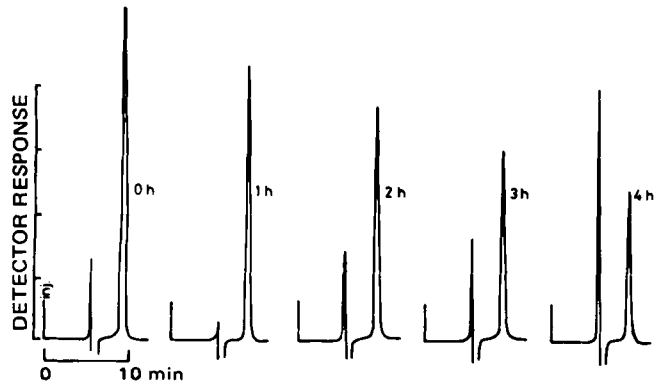

Figure 1—*Chromatograms of Rg_1 in 0.15 M phosphate buffer solution (pH 1.81) at 37°C and an ionic strength of 0.15 with time. t_R in minutes.*

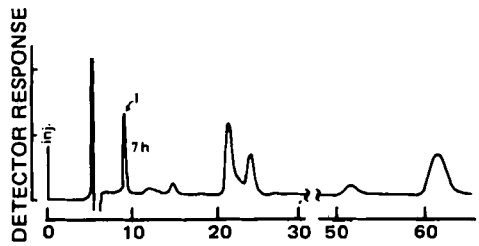

Figure 2—*Typical chromatogram of 80% degraded Rg_1 under the same conditions as in Fig. 1. t_R in minutes.*

[1] Japan and Research Laboratory, C. Koshiro and Co. Ltd., Osaka, Japan.
[2] pH meter, Model HM-18E; TOA Electronics Ltd., Tokyo, Japan.
[3] Waters analytical liquid chromatograph, model 244; Waters Associates, Milford, Mass.
[4] UVIDEC-100-III, UV spectrophotometer; Japan Spectroscopic Co., Tokyo, Japan.
[5] Model RCM-100; Waters Associates, Milford, Mass.
[6] Radial-Pak A cartridge (8 mm i.d. × 10 cm long); Waters Associates, Milford, Mass.
[7] Model U6K; Waters Associates, Milford, Mass.
[8] Sartorious-membranfilter, GmbH; 34 Göttingen, West Germany.

0022-3549/84/0300-0409$01.00/0
© 1984, American Pharmaceutical Association

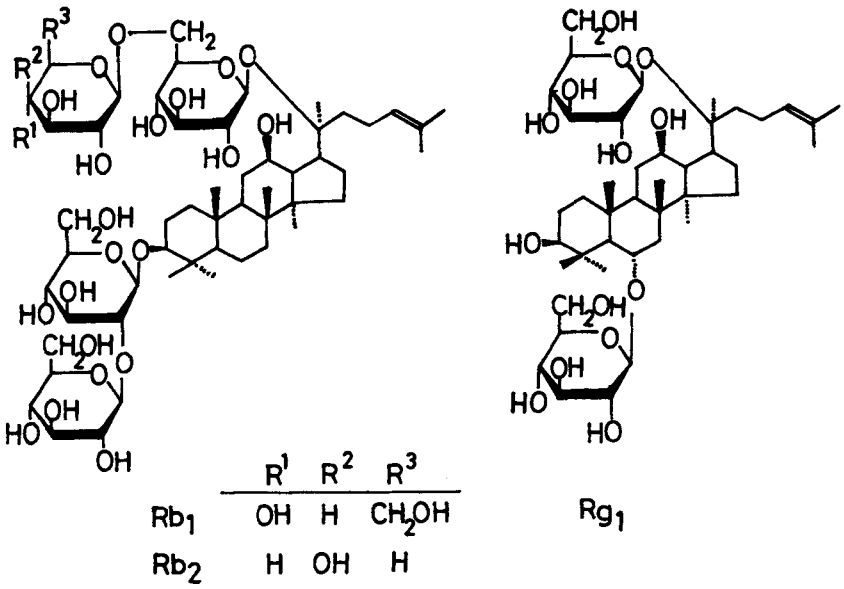

The pH dependency of the Rg_1 degradation in the acidic region can therefore be represented by the following:

$$k_{obs} = k_H a_{H^+}$$

where k_{obs} is the observed first-order rate constant, k_H is the specific proton-catalyzed rate constant, and a_{H^+} is the hydrogen ion activity as determined with a glass electrode. The k_H value for each ginsenoside was calculated from the kinetic data, and the observed rate constants and the values of k_H for the respective ginsenosides are listed in Table I. No significant difference among the catalyzed rate constants was observed. If these catalyzed rate constants can be employed to predict the stability of the ginsenosides at constant pH in nonbuffered solution, the half-life at 37°C and pH 1 would be 30 min. At neutral pH, Rg_1 is very stable and the degradation is negligible overnight.

These results suggest that chemical degradation of ginsenosides in the acidic pH region, such as in the stomach, could proceed readily by producing many products (see Fig. 2). On the other hand, the degradation under intestinal pH conditions was negligible.

Table I—Apparent First-Order Rate Constants, k_{obs}, at Various pH Values and Rate Constants, k_H, for the Acid Degradation of Ginsenosides at 37°C and Ionic Strength of 0.15

Ginsenoside	pH	k_{obs} (±*SD*), h^{-1}	k_H, $M^{-1}\,h^{-1}$
Rg_1	0.85[a]	2.096[b]	15.0[c]
	1.22[a]	0.924 (0.012)[d]	
	1.48[a]	0.552[b]	
	1.81[e]	0.224 (0.012)[f]	
	2.04[e]	0.131 (0.006)[f]	
	2.34[e]	0.055 (0.002)[f]	
Rb_1	1.81[g]	0.218[b]	14.0[h]
Rb_2	1.81[g]	0.231[b]	14.9[h]

[a] Hydrochloric acid was used as a buffer solution. [b] Observed value, calculated by the least-squares method using the experimental data. [c] Calculated according to the equation, obtained by the least-squares method using k_{obs} at varying pH. [d] Averaged value, calculated using k_{obs} under the experimental condition of three different initial concentrations of Rg_1. [e] Phosphate buffer solution was used. [f] Averaged value, calculated using k_{obs} under the experimental condition of at least three different buffer concentrations. [g] Phosphate buffer solution (0.15 M) was used. [h] Calculated according to the equation using k_{obs}.

REFERENCES

(1) W. Petkov and D. Staneva, *Arzneim.-Forsch.*, **13**, 1078 (1963).

(2) I. I. Brekhman and I. V. Dardymov, *Annu. Rev. Pharmacol.*, **9**, 419 (1969).

(3) S. Odashima, Y. Nakayabu, N. Honjo, H. Abe, and S. Arichi, *Eur. J. Cancer*, **15**, 885 (1979).

(4) O. Tanaka, M. Nagai, T. Ohsawa, N. Tanaka, K. Kawai, and S. Shibata, *Chem. Pharm. Bull. (Tokyo)*, **20**, 1204 (1972).

(5) M. Nagai, T. Ando, N. Tanaka, O. Tanaka, and S. Shibata, *Chem. Pharm. Bull. (Tokyo)*, **20**, 1212 (1972).

(6) S. Sanada, N. Kondo, J. Shoji, O. Tanaka, and S. Shibata, *Chem. Pharm. Bull. (Tokyo)*, **22**, 421 (1974).

ACKNOWLEDGMENTS

The data reported here were presented in part at the 15th Symposium on Wakan-yaku, Toyama, Japan, August 1981.

Plant Anticancer Agents XXX: Cucurbitacins from *Ipomopsis aggregata* (Polemoniaceae)

MUNEHISA ARISAWA *, JOHN M. PEZZUTO, A. DOUGLAS KINGHORN ˣ, GEOFFREY A. CORDELL, and NORMAN R. FARNSWORTH

Received January 11, 1983, from the *Department of Pharmacognosy and Pharmacology, College of Pharmacy, University of Illinois at the Medical Center, Chicago, IL 60612.* Accepted for publication February 25, 1983. *Present address: Faculty of Pharmaceutical Sciences, Toyama Medical and Pharmaceutical University, Sugitani 2630, Toyama 930-01, Japan.

Abstract □ Isocucurbitacin B (I), 3-epi-isocucurbitacin B (II), and cucurbitacin B (III) were identified as the principal cytotoxic constituents of *Ipomopsis aggregata* (Pursh) V. Grant (Polemoniaceae). The structure of the new compound, II, was determined through analysis of its spectrometric characteristics.

Keyphrases □ *Ipomopsis aggregata* (Polemoniaceae)—isolation and identification of cytotoxic constituents □ Cucurbitacins—cytotoxic principles from *Ipomopsis aggregata* □ 3-Epi-isocucurbitacin B—novel cytotoxic constituent of *Ipomopsis aggregata*

Ipomopsis aggregata represents a small New World genus of herbs in the family Polemoniaceae (1). This species is the most wide-ranging member of the genus, extending in distribution from British Columbia to northwest Mexico (2). In previous phytochemical work, an uncharacterized saponin was isolated from an extract of the entire plant of *I. aggregata* (3), but there appear to have been no prior studies to determine the biological activity of extracts and isolates derived from this taxon.

In a continuing search for tumor inhibitors of plant origin[1], we found that a chloroform extract of the combined roots, stems, leaves, flowers, and fruits of *I. aggregata* exhibited significant cytotoxic activity against Eagle's carcinoma of the nasopharynx in cell culture (KB), but no activity when tested at a dose range of 1.87–15.0 mg/kg (ip) against the P388 lymphocytic leukemic system in mice[2]. In the present contribution we wish to report the isolation of three cytotoxic cucurbitacins from this plant, namely, isocucurbitacin B (I), a new compound 3-epi-isocucurbitacin B (II), and cucurbitacin B (III).

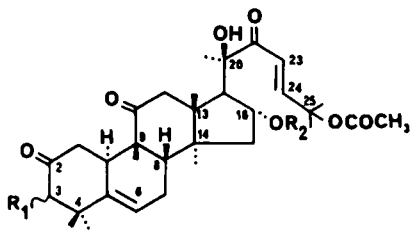

I R_1 = α-OH; R_2 = H
II R_1 = β-OH; R_2 = H
IV R_1 = α-$OCOCH_3$; R_2 = $COCH_3$
V R_1 = β-$OCOCH_3$; R_2 = $COCH_3$

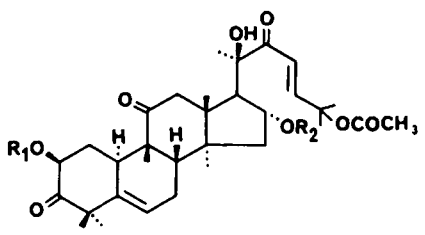

III R_1 = H; R_2 = H
VI R_1 = $COCH_3$; R_2 = $COCH_3$

EXPERIMENTAL[3]

Plant Material—The combined roots–stems–leaves–flowers–fruits of *Ipomopsis aggregata* (Pursh) V. Grant (Polemoniaceae) were collected in Idaho during July 1980[4].

KB Cell Culture Assays—Substances were evaluated for cytotoxic activity essentially by the procedure of Geran *et al.* (5), as described previously (6). All assays were performed in duplicate, and the results were expressed as the effective dose to inhibit 50% of the growth observed in control tubes which were treated with solvent only. Mithramycin was used as a positive cytotoxic control substance (ED_{50} = 0.1 μg/mL).

Extraction and Fractionation—The air-dried, milled plant material (10 kg) was extracted sequentially with petroleum ether (bp 60–80°C) and methanol. The methanol extract was concentrated *in vacuo* to yield a residue (1.57 kg), which was partitioned between 3-L portions of chloroform and water. Cytotoxic activity was found to be concentrated in the chloroform fraction (ED_{50} = 0.64 μg/mL), which was further partitioned between petroleum ether (2 L) and methanol–water (9:1, 2 L). After removal of the solvent, the cytotoxic aqueous methanol extract (600 g, ED_{50} = 0.30 μg/mL) was chromatographed over silica gel[5] (5 kg), by elution with chloroform and mixtures of chloroform–methanol of increasing polarity. A total of 22 fractions (2-L each) were collected. Fractions 9–11, eluted from this column with chloroform–methanol (99:1), were cytotoxic (ED_{50} = 0.27, 0.01, and 0.10 μg/mL, respectively). These combined fractions were chromatographed over a Florisil[6] column that was eluted with chloroform. Fractions eluted with this solvent were combined to afford a cytotoxic residue (1.32 g, ED_{50} = 0.05 μg/mL). Final purification of the cytotoxic constituents was achieved by preparative TLC on silica

[1] For the previous article in this series, see Ref. 4.

[2] Plant extracts and certain fractions were tested under the auspices of the Research and Development Program of the National Cancer Institute. The remaining fractions prepared from this plant, as well as the isolates that are the subject of this paper, were tested at our in-house facilities, as described under *Experimental*. A compound is considered active *in vivo* if it exhibits a prolongation of life >125%, and is regarded as cytotoxic if the ED_{50} is ≤4 μg/mL. For *in vivo* testing, samples were administered intraperitoneally to six male CD_2F_1 P388-infected mice daily for a 10-d period. Evaluation was carried out by comparison of survival times with control tumor-bearing animal groups.

[3] Melting points were determined by means of a Koffler hot-plate apparatus and are uncorrected. Specific rotations were measured on a Perkin-Elmer 241 polarimeter. The UV spectra were obtained with a Beckman DB-G spectrophotometer, and IR spectra on a Beckman model 118-A spectrophotometer, with polystyrene calibration at 1601 cm^{-1}. ^1H-NMR spectra were recorded in $CDCl_3$ with a Varian T-60A instrument operating at 60 MHz, equipped with a Nicolet TT-7 Fourier Transform attachment. Tetramethylsilane was used as internal standard, and chemical shifts are reported on the δ (ppm) scale. Low-resolution mass spectra were obtained with a Varian MAT 112S double-focusing mass spectrometer, operating at 70 eV, and the high-resolution mass spectrum was obtained by peak matching using an AEI MS-902 instrument.

[4] The plant material was collected and identified by staff of the Economic Botany Laboratory, BARC-East, USDA, Science and Education Administration, Beltsville, Md. A voucher specimen representing this collection has been deposited in the Herbarium of the National Arboretum, Washington, D.C.

[5] E. Merck, Darmstadt, W. Germany.

[6] Fisher Scientific Co., Itasca, Ill.

0022-3549/84/0300-0411$01.00/0
© 1984, American Pharmaceutical Association

gel GHLF[7] plates, using cyclohexane–ether–ethyl acetate (1:1:1) and chloroform–acetone–methanol (14:1:2) as solvents. Compounds I (33 mg), II (31 mg), and III (120 mg) were obtained from preparative TLC zones found to be cytotoxic, by crystallization from methanol.

Characterization of Biologically Active Isolates—Isocucurbitacin B (I, 33 mg, 0.00033%) crystallized in the form of colorless needles, mp 220–222°C, $[\alpha]_D^{25}$ +38° (*c* 0.2, $CHCl_3$) [lit. (7) mp 223–223.5°C, $[\alpha]_D$ +43° (*c* 1.61, $CHCl_3$)]; IR ν_{max} (KBr): 3550, 3450, 2950, 1720, 1680, 1620, 1440, 1360, 1230, 1170, 1120, 1090, 1030, and 980 cm^{-1}; UV λ_{max} (MeOH) (log ϵ): 232 (4.32) nm; ^{1}H-NMR (60 MHz): δ 0.81 and 0.96 (two s, 6, 9-CH_3 and 13-CH_3), 1.18 and 1.26 [two s, 6, 4-$(CH_3)_2$], 1.32 (s, 3, 14-CH_3), 1.41 (s, 3, 20-CH_3), 1.54 [s, 6, 25-$(CH_3)_2$], 2.00 (s, 3, 25-$OCOCH_3$), 3.89 (br s, 1, 3-H), 4.25 (br s, 1, 20-OH exchangeable with D_2O), 4.33 (m, 1, 16-H), 5.92 (m, 1, 6-H), 6.42 (d, 1, J = 15.6 Hz, 23-H), and 7.07 ppm (d, 1, J = 15.6 Hz, 24-H); MS *m/z* (70 eV) (relative intensity): 498 (M^+ −60, 2%), 386 (1), 385 (1), 369 (1), 219 (1), 203 (2), 164 (4), 137 (3), 135 (3), 113 (6), 112 (9), 111 (8), 109 (8), 97 (10), and 96 (100). These data (IR, UV, and ^{1}H-NMR) are in agreement with those previously reported for isocucurbitacin B (I) (7, 8), although no mass spectral data for this compound appear to have been published. Identity was established as isocucurbitacin B by direct comparison with an authentic sample[8] (MS, co-TLC).

Isocucurbitacin B (I, 10 mg) was treated with acetic anhydride–pyridine (1:1, 1 mL) at room temperature overnight. Workup in the usual manner afforded a triacetate (IV, 8 mg) as colorless needles, mp 120–123°C; ^{1}H-NMR (60 MHz): δ 0.97 and 1.01 (two s, 6, 9-CH_3 and 13-CH_3), 1.18 (s, 3, 4-CH_3), 1.22 (s, 6, 4-CH_3 and 14-CH_3), 1.39 (s, 3, 20-CH_3), 1.57 [s, 6, 25-$(CH_3)_2$], 1.85 (s, 3, 16-$OCOCH_3$), 2.01 (s, 3, 25-$OCOCH_3$), 2.17 (s, 3, 3-$OCOCH_3$), 4.25 (br s, 1, 20-OH exchangeable with D_2O), 4.93 (s, 1, 3-H), 5.17 (m, 1, 16-H), 5.90 (m, 1, 6-H), 6.37 (d, 1, J = 15.6 Hz, 23-H), and 7.16 ppm (d, 1, J = 15.6 Hz, 24-H); MS *m/z* (70 eV) (relative intensity): 582 (M^+ −60, 1%), 522 (1), 507 (1), 487 (2), 427 (1), 411 (2), 385 (1), 383 (1), 368 (2), 367 (4), 279 (3), 219 (3), 177 (3), 166 (8), 150 (3), 135 (4), 113 (8), 112 (6), 111 (6), 109 (6), 97 (11), and 96 (100).

3-Epi-isocucurbitacin B (II, 31 mg, 0.00031%) was obtained in the form of a white powder, mp 92–98°C, $[\alpha]_D^{25}$ −28.5° (*c* 0.2, $CHCl_3$); IR ν_{max} ($CHCl_3$): 3450, 2960, 2920, 1720, 1690, 1630, 1450, 1360, 1250, 1130, 1090, 980, and 940 cm^{-1}; UV λ_{max} (MeOH) (log ϵ): 229 (4.47) nm; ^{1}H-NMR (60 MHz): δ 0.85 and 0.96 (two s, 6, 9-CH_3 and 13-CH_3), 1.07 and 1.25 [two s, 6, 4-$(CH_3)_2$], 1.31 (s, 3, 14-CH_3), 1.41 (s, 3, 20-CH_3), 1.55 [s, 6, 25-$(CH_3)_2$], 2.00 (s, 3, 25-$OCOCH_3$), 4.11 (s, 1, 3-H), 4.24 (br s, 1, 20-OH exchangeable with D_2O), 4.36 (t, 1, J = 7.4 Hz, 16-H), 5.90 (m, 1, 6-H), 6.44 (d, 1, J = 15.6 Hz, 23-H), and 7.06 ppm (d, 1, J = 15.6 Hz, 24-H); MS *m/z* (70 eV) (relative intensity): 498 (M^+ −60, 2%), 385 (1), 327 (2), 287 (2), 286 (7), 285 (3), 271 (4), 266 (4), 253 (9), 187 (4), 185 (7), 175 (11), 173 (25), 159 (6), 147 (5), 131 (5), 129 (16), 115 (22), 113 (7), 112 (11), 111 (8), 101 (13), 97 (16), and 96 (100); mass measurement: calc. for $C_{30}H_{42}O_6$, 498.2981; observed, 498.2986.

3-Epi-isocucurbitacin B (II, 10 mg) was acetylated as described for I, and the triacetate V (7 mg) obtained after workup was found to exhibit the following data: colorless needles, mp 103–107°C; ^{1}H-NMR (60 MHz): δ 1.05 and 1.10 (two s, 6, 9-CH_3 and 13-CH_3), 1.17 and 1.26 [two s, 6, 4-$(CH_3)_2$], 1.30 (s, 3, 14-CH_3), 1.41 (s, 3, 20-CH_3), 1.58 [s, 6, 25-$(CH_3)_2$], 1.86 (s, 3, 16-$OCOCH_3$), 2.03 (s, 3, 25-$OCOCH_3$), 2.18 (s, 3, 3-$OCOCH_3$), 4.26 (br s, 1, 20-OH exchangeable with D_2O), 5.13 (s, 1, 3-H), 5.19 (m, 1, 16-H), 5.85 (m, 1, 6-H), 6.38 (d, 1, J = 15.5 Hz, 23-H), and 7.16 ppm (d, 1, J = 15.5 Hz, 24-H); MS *m/z* (70 eV) (relative intensity): 582 (M^+ −60, 1%), 522 (1), 487 (4), 427 (4), 411 (9), 385 (3), 367 (6), 325 (4), 219 (4), 189 (5), 187 (7), 177 (6), 171 (5), 161 (4), 159 (7), 137 (5), 135 (9), 133 (6), 121 (5), 113 (14), 112 (41), 111 (30), 109 (9), 105 (9), 97 (19), and 96 (100).

Cucurbitacin B (III, 120 mg, 0.0012%) was obtained in the form of a white powder, mp 160–162°C, $[\alpha]_D^{25}$ +44° (*c* 0.1, $CHCl_3$) [lit. (7) mp 184–186°C, crystallized from EtOH; $[\alpha]_D^{25}$ +87° (EtOH)]; IR ν_{max} (KBr): 3550, 3400, 2950, 1720, 1680, 1620, 1450, 1360, 1230, 1120, 1050, 1020, and 980 cm^{-1}; UV λ_{max} (MeOH) (log ϵ): 229 (4.47) nm; ^{1}H-NMR (60 MHz): δ 0.97 and 1.07 (two s, 6, 9-CH_3 and 13-CH_3), 1.25 and 1.29 [two s, 6, 4-$(CH_3)_2$], 1.34 (s, 3, 14-CH_3), 1.43 (s, 3, 20-CH_3), 1.56 [s, 6, 25-$(CH_3)_2$], 2.01 (s, 3, 25-$OCOCH_3$), 4.25 (t, 1, J = 7.4 Hz, 16-H), 4.28 (br s, 1, 20-OH exchangeable with D_2O), 4.43 (dd, 1, J = 12.8 and 5.7 Hz, 2-H), 5.76 (m, 1, 6-H), 6.49 (d, 1, J = 15.6 Hz, 23-H), and 7.08 ppm (d, 1, J = 15.6 Hz, 24-H); MS *m/z* (70 eV) (relative intensity): 498 (M^+ −60, 4%), 480 (1), 385 (1), 299 (1), 285 (1), 219 (1), 203 (1), 187 (2), 175 (3), 173 (3), 133 (3), 121 (3), 115 (3), 113 (4), 112 (8), 111 (7), 109 (5), 105 (4), 97 (11), and 96 (100). The above spectral data are consistent with those published previously for cucurbitacin B (7–15). Identity as cucurbitacin B was established by direct comparison with an authentic sample[8] (MS, co-TLC).

Cucurbitacin B (III, 15 mg) was acetylated as described for I, and the triacetate VI (9 mg) obtained after workup was found to exhibit the following data: colorless needles, mp 114–117°C; ^{1}H-NMR (60 MHz): δ 1.03 and 1.10 (two s, 6, 9-CH_3 and 13-CH_3), 1.32 [s, 9, 4-$(CH_3)_2$ and 14-CH_3], 1.42 (s, 3, 20-CH_3), 1.58 [s, 6, 25-$(CH_3)_2$], 1.87 (s, 3, 16-$OCOCH_3$), 2.03 (s, 3, 25-$OCOCH_3$), 2.13 (s, 3, 2-$OCOCH_3$), 4.27 (br s, 1, 20-OH exchangeable with D_2O), 5.20 (t, 1, J = 7.3 Hz, 16-H), 5.48 (dd, 1, J = 13.4 and 5.7 Hz, 2-H), 5.77 (m, 1, 6-H), 6.42 (d, 1, J = 15.6 Hz, 23-H), and 7.18 ppm (d, 1, J = 15.6 Hz, 24-H); MS *m/z* (70 eV) (relative intensity): 582 (M^+ −60, 1%), 522 (1), 487 (4), 427 (5), 411 (4), 385 (1), 367 (5), 325 (4), 219 (3), 189 (6), 187 (6), 177 (6), 159 (5), 137 (5), 111 (12), 109 (9), 107 (6), 105 (7), 97 (19), and 96 (100).

Biological Activity of the Isolates—Isocucurbitacin B (I, NSC-106400), 3-epi-isocucurbitacin B (II, NSC-359240), and cucurbitacin B (III, NSC-049451) exhibited ED_{50} values of 0.016, 0.050, and 0.032 μg/mL, respectively, in the KB cell culture system.

DISCUSSION

The known tetracyclic triterpenes isocucurbitacin B (I) and cucurbitacin B (III) were isolated and identified in the present study from a cytotoxic fraction of *I. aggregata* whole flowering plants. The molecular ions of both compounds were characteristically absent from their electron-impact mass spectra (10), so that the highest fragment peaks observed occurred at *m/z* 498, representing in each case a loss of one acetate unit from the parent ion. In its ^{1}H-NMR spectrum, I was typified by the presence of a singlet assignable for the C-3 methine proton at δ 3.89, which, since it was shifted downfield in isocucurbitacin B diacetate (IV) to δ 4.93, suggested the presence of a 2-keto-3-hydroxy ring A moiety in I (8, 15). Isocucurbitacin B (I) is a relatively rare compound, previously being reported only from three species of two Cucurbitaceae genera (9). Cucurbitacin B (III), on the other hand, appears to be the most widely distributed cucurbitacin known, since it occurs in more than 15 genera of the Cucurbitaceae, and in species of the Begoniaceae, Cruciferae, and Euphorbiaceae (9, 12, 16, 17). Cucurbitacins have not previously been reported from the family Polemoniaceae.

The spectrometric parameters (IR, UV, ^{1}H-NMR, and MS) of II were very similar to those observed for isocucurbitacin B (I). Thus, comparable with I, no molecular ion was evident in the mass spectrum of II, with the highest observable fragment peak occurring at *m/z* 498, of elemental composition $C_{30}H_{42}O_6$, as determined by high-resolution MS. In its ^{1}H-NMR spectrum, signals indicating the presence of eight quaternary attached C-methyl groups, one acetate methyl group, two methine protons on carbons bearing hydroxyl groups, and three olefinic protons were observed. Following mild acetylation, triacetate V was produced from II, for which paramagnetic C-3 and C-16 methine proton shifts occurred from δ 4.11 and 4.36, respectively, in II, to δ 5.13 and 5.19 in V. By analogy to conclusions reached on the basis of almost identical C-3 ^{1}H-NMR assignments made for isocucurbitacin D (the C-25 deacetyl derivative of I) and 3-epi-isocucurbitacin D (7), II could therefore be assigned a 2-keto-3-hydroxy ring A moiety, and is the C-3 epimer of I.

The role of cucurbitacin B (III) in nature has been partially characterized. For example, III has been shown to stimulate feeding by the spotted cucumber (18) and diabroctic beetles (19). Further, it acts as an antigibberellin (20). In regard to antitumor activity, both isocucurbitacin B (I) and cucurbitacin B (III) have been shown in earlier work to demonstrate significant inhibitory activity against cultured KB cells (7, 12, 21, 22). We presently extend these results through the demonstration of the cytotoxic activity of II. Previous studies have also shown III to be active *in vivo* against the Walker 256 (im) carcinosarcoma and Lewis lung carcinoma in rats (7). The therapeutic index, however, appears too low for use as a clinical agent (7), and it is likely that the same would be found for I and II. An additional biological activity demonstrated by III, however, which may be worthy of additional investigation, is the prevention of experimentally induced hepatitis and cirrhosis (23).

Interestingly, it has been observed previously that cucurbitacin D, a constituent of *Phormium tenax* Forst. (Liliaceae) is degraded to isocucurbitacin D and 3-epi-isocucurbitacin D as a result of lengthy passage over silica gel during column chromatography (8). Therefore, since large-scale gravity column chromatography was employed in this study to obtain I–III from *I. aggregata*, it is possible that I and II are progeny of III and are not indigenous to this plant. For studies concerned primarily with chemotaxonomic relationships, it may be suggested that rapid techniques of isolation, preferably avoiding the use of silica gel, should be used to obtain cucurbitacins from plants.

[7] Analtech, Inc., Newark, Del.

[8] Authentic samples of isocucurbitacin B and cucurbitacin B were generously provided by Professor J. M. Cassady, Purdue University.

REFERENCES

(1) J. C. Willis in "A Dictionary of Flowering Plants and Ferns," 8th ed., H. K. Airy-Shaw, Ed., University Press, Cambridge, England, 1973, p. 594.

(2) C. L. Lundell and collaborators, "Flora of Texas," vol. 1, part III, Texas Research Foundation, Renner, Tex., 1966, p. 285.

(3) M. E. Wall and K. H. Davis, Jr., in "Toxins of Animal and Plant Origin," A. de Vries and E. Kochra, Eds., Grodon and Breach, New York, N.Y., 1972, p. 597.

(4) M. Arisawa, S. S. Handa, D. D. McPherson, G. A. Cordell, H. H. S. Fong, and N. R. Farnsworth, *J. Nat. Prod.*, in press.

(5) R. I. Geran, N. H. Greenberg, M. M. McDonald, A. M. Schumacher, and B. J. Abbott, *Cancer Chemother. Rep.*, 3(3), 1 (1972).

(6) J. M. Pezzuto, S. K. Antosiak, W. M. Messmer, M. B. Slaytor, and G. R. Honig, *Chem.-Biol. Interactions*, **43**, 323 (1983).

(7) S. M. Kupchan, A. H. Gray, and M. D. Grove, *J. Med. Chem.*, **10**, 337 (1967).

(8) S. M. Kupchan, H. Meshulam, and A. T. Sneden, *Phytochemistry*, **17**, 767 (1978).

(9) W. O. Eisenhut and C. R. Noller, *J. Org. Chem.*, **23**, 1984 (1958).

(10) H. E. Audier and B. C. Das, *Tetrahedron Lett.*, **1966**, 2205.

(11) R. W. Doskotch, M. V. Malik, and J. L. Beal, *Lloydia*, **32**, 115 (1969).

(12) D. Lavie and E. Glotter, *Prog. Chem. Org. Nat. Prod.*, **29**, 307 (1971).

(13) P. J. Curtis and P. M. Meade, *Phytochemistry*, **10**, 3081 (1971).

(14) J. Konopa, J. Zieliński, and A. Matuszkiewicz, *Arzneim.-Forsch.*, **24**, 1554 (1974).

(15) C. A. Rice, K. S. Rymal, O. L. Chambliss, and F. A. Johnson, *J. Agr. Food. Chem.*, **29**, 194 (1981).

(16) P. R. Enselin, C. W. Holzapfel, K. B. Norton, and S. Rehm, *J. Chem. Soc. (C)*, **1967**, 964.

(17) A. M. Tessier, A. Bouquet, and R. R. Paris, *Plant. Méd. Phytothér.*, **9**, 328 (1975).

(18) G. C. Sharma and C. V. Hall, *J. Am. Soc. Hort. Sci.*, **96**, 750 (1971).

(19) R. L. Metcalf, R. A. Metcalf, and A. M. Rhodes, *Proc. Natl. Acad. Sci. USA*, **77**, 3769 (1980).

(20) J. Guha and S. P. Sen, *Nature (New Biol.)*, **244**, 223 (1973).

(21) J. Konopa, J. Zieliński, A. Matuszkiewicz, and M. Hrabowska, *Adv. Antimicrob. Antineoplast. Chemother., Proc. Int. Congr. Chemother., 7th 1971*, (Pub. 1972), **2**, 163; through *Chem. Abstr.*, **79**, 73776y, 1973.

(22) J. Konopa, A. Matuszkiewicz, M. Hrabowska, and K. Onoszka, *Arzeim.-Forsch.*, **24**, 1741 (1974).

(23) T.-W. Han, H.-H. Ma, Y.-C. Chao, and L.-M. Chou, *Chung-hua I Hsueh Tsa Chih (Peking)*, **59**, 206 (1979); through *Chem. Abstr.* **92**, 209055r, 1980.

ACKNOWLEDGMENTS

This study was carried out under contract CM-97295 with the Division of Cancer Treatment, National Cancer Institute, Department of Health and Human Services, Bethesda, Md. We would like to thank the Economic Botany Laboratory, BARC-East, USDA, Science and Education Administration, Beltsville, Md. (funded by the National Cancer Institute) for the provision and identification of plant material.

We also wish to thank Dr. J. M. Cassady, Purdue University, West Lafayette, Ind., for reference samples of isocucurbitacin B and cucurbitacin B; Dr. W. Lichter, University of Miami School of Medicine, Miami, Fla., for the supply of a KB cell-line; Dr. M. Wani and Mr. F. Williams, Research Triangle Institute, Research Triangle Park, N.C., for the high-resolution mass spectrum; and Ms. L.-J. Lin and Mr. G. T. Marshall, of this department, for the ^{1}H-NMR and mass spectral data, respectively.

Assay of Benzenoid Drugs in Tablet and Capsule Formulations by Second-Derivative Ultraviolet Spectrophotometry

A. G. DAVIDSON ˣ and S. M. HASSAN *

Received December 8, 1982, from the *Department of Pharmacy, University of Strathclyde, Glasgow, G1 1XW, United Kingdom.* Accepted for publication February 2, 1983.

*Present address: Analytical Chemistry Department, Faculty of Pharmacy, Mansoura University, Mansoura, Egypt.

Abstract □ Rapid second-derivative assay procedures are described for tablet and capsule formulations of benzenoid drugs, which eliminate the interference of the formulation excipients in simple UV spectrophotometric methods. Accuracy, precision, and selectivity of the technique are discussed. The general application of the procedures for the batch assay of tablet and capsule dosage forms containing ≥2 mg of a benzenoid drug is indicated by the results obtained for 18 such formulations, in good agreement with pharmacopeial assay results and/or declared amounts. The procedures are sufficiently sensitive to permit unit dose assays of these formulations.

Keyphrases □ Benzenoid drugs—tablet and capsule formulations, second-derivative UV spectrometry □ Formulations—benzenoid drugs, second-derivative UV spectrometry, tablets and capsules □ UV spectrometry, second-derivative—benzenoid drugs, tablet and capsule formulations

The interference of formulation excipients in the conventional ultraviolet (UV) spectrophotometric procedures for certain formulated drugs is well recognized. It is a particular problem in the assay of tablets and capsules of benzenoid drugs, which, in general, are both weakly absorbing and also formulated at a relatively low dosage level (typically 1–50 mg/unit dose). The high excipient–drug ratio and high sample weight required for these formulations result in background-irrelevant absorption of a sufficiently high intensity to possibly prohibit the application of simple spectrophotometric methods.

Techniques that reduce or eliminate matrix interference in the assay of formulated drugs include the Morton–Stubbs (1) correction procedure, which requires that the irrelevant absorption is linear over the wavelength range of the absorption band of the drug; orthogonal polynomials, which can cope with nonlinear irrelevant absorption if the correct choice of the polynomial order, wavelength range, and interval is made (2, 3); compensation spectrophotometry, in which the reference solution contains the matrix or sample at the same concentration present in the sample solution (4, 5); and difference spectrophotometry, which may be applied if an absorbance difference can be

0022-3549/84/0300-0413$01.00/0

© 1984, American Pharmaceutical Association

REFERENCES

(1) J. C. Willis in "A Dictionary of Flowering Plants and Ferns," 8th ed., H. K. Airy-Shaw, Ed., University Press, Cambridge, England, 1973, p. 594.

(2) C. L. Lundell and collaborators, "Flora of Texas," vol. 1, part III, Texas Research Foundation, Renner, Tex., 1966, p. 285.

(3) M. E. Wall and K. H. Davis, Jr., in "Toxins of Animal and Plant Origin," A. de Vries and E. Kochra, Eds., Grodon and Breach, New York, N.Y., 1972, p. 597.

(4) M. Arisawa, S. S. Handa, D. D. McPherson, G. A. Cordell, H. H. S. Fong, and N. R. Farnsworth, *J. Nat. Prod.*, in press.

(5) R. I. Geran, N. H. Greenberg, M. M. McDonald, A. M. Schumacher, and B. J. Abbott, *Cancer Chemother. Rep.*, 3(3), 1 (1972).

(6) J. M. Pezzuto, S. K. Antosiak, W. M. Messmer, M. B. Slaytor, and G. R. Honig, *Chem.-Biol. Interactions*, **43**, 323 (1983).

(7) S. M. Kupchan, A. H. Gray, and M. D. Grove, *J. Med. Chem.*, **10**, 337 (1967).

(8) S. M. Kupchan, H. Meshulam, and A. T. Sneden, *Phytochemistry*, **17**, 767 (1978).

(9) W. O. Eisenhut and C. R. Noller, *J. Org. Chem.*, **23**, 1984 (1958).

(10) H. E. Audier and B. C. Das, *Tetrahedron Lett.*, **1966**, 2205.

(11) R. W. Doskotch, M. V. Malik, and J. L. Beal, *Lloydia*, **32**, 115 (1969).

(12) D. Lavie and E. Glotter, *Prog. Chem. Org. Nat. Prod.*, **29**, 307 (1971).

(13) P. J. Curtis and P. M. Meade, *Phytochemistry*, **10**, 3081 (1971).

(14) J. Konopa, J. Zieliński, and A. Matuszkiewicz, *Arzneim.-Forsch.*, **24**, 1554 (1974).

(15) C. A. Rice, K. S. Rymal, O. L. Chambliss, and F. A. Johnson, *J. Agr. Food. Chem.*, **29**, 194 (1981).

(16) P. R. Enselin, C. W. Holzapfel, K. B. Norton, and S. Rehm, *J. Chem. Soc. (C)*, **1967**, 964.

(17) A. M. Tessier, A. Bouquet, and R. R. Paris, *Plant. Méd. Phytothér.*, **9**, 328 (1975).

(18) G. C. Sharma and C. V. Hall, *J. Am. Soc. Hort. Sci.*, **96**, 750 (1971).

(19) R. L. Metcalf, R. A. Metcalf, and A. M. Rhodes, *Proc. Natl. Acad. Sci. USA*, **77**, 3769 (1980).

(20) J. Guha and S. P. Sen, *Nature (New Biol.)*, **244**, 223 (1973).

(21) J. Konopa, J. Zieliński, A. Matuszkiewicz, and M. Hrabowska, *Adv. Antimicrob. Antineoplast. Chemother., Proc. Int. Congr. Chemother., 7th 1971*, (Pub. 1972), **2**, 163; through *Chem. Abstr.*, **79**, 73776y, 1973.

(22) J. Konopa, A. Matuszkiewicz, M. Hrabowska, and K. Onoszka, *Arzeim.-Forsch.*, **24**, 1741 (1974).

(23) T.-W. Han, H.-H. Ma, Y.-C. Chao, and L.-M. Chou, *Chung-hua I Hsueh Tsa Chih (Peking)*, **59**, 206 (1979); through *Chem. Abstr.* **92**, 209055r, 1980.

ACKNOWLEDGMENTS

This study was carried out under contract CM-97295 with the Division of Cancer Treatment, National Cancer Institute, Department of Health and Human Services, Bethesda, Md. We would like to thank the Economic Botany Laboratory, BARC-East, USDA, Science and Education Administration, Beltsville, Md. (funded by the National Cancer Institute) for the provision and identification of plant material.

We also wish to thank Dr. J. M. Cassady, Purdue University, West Lafayette, Ind., for reference samples of isocucurbitacin B and cucurbitacin B; Dr. W. Lichter, University of Miami School of Medicine, Miami, Fla., for the supply of a KB cell-line; Dr. M. Wani and Mr. F. Williams, Research Triangle Institute, Research Triangle Park, N.C., for the high-resolution mass spectrum; and Ms. L.-J. Lin and Mr. G. T. Marshall, of this department, for the ^{1}H-NMR and mass spectral data, respectively.

Assay of Benzenoid Drugs in Tablet and Capsule Formulations by Second-Derivative Ultraviolet Spectrophotometry

A. G. DAVIDSON ˣ and S. M. HASSAN *

Received December 8, 1982, from the *Department of Pharmacy, University of Strathclyde, Glasgow, G1 1XW, United Kingdom.* Accepted for publication February 2, 1983.

*Present address: Analytical Chemistry Department, Faculty of Pharmacy, Mansoura University, Mansoura, Egypt.

Abstract □ Rapid second-derivative assay procedures are described for tablet and capsule formulations of benzenoid drugs, which eliminate the interference of the formulation excipients in simple UV spectrophotometric methods. Accuracy, precision, and selectivity of the technique are discussed. The general application of the procedures for the batch assay of tablet and capsule dosage forms containing ≥2 mg of a benzenoid drug is indicated by the results obtained for 18 such formulations, in good agreement with pharmacopeial assay results and/or declared amounts. The procedures are sufficiently sensitive to permit unit dose assays of these formulations.

Keyphrases □ Benzenoid drugs—tablet and capsule formulations, second-derivative UV spectrometry □ Formulations—benzenoid drugs, second-derivative UV spectrometry, tablets and capsules □ UV spectrometry, second-derivative—benzenoid drugs, tablet and capsule formulations

The interference of formulation excipients in the conventional ultraviolet (UV) spectrophotometric procedures for certain formulated drugs is well recognized. It is a particular problem in the assay of tablets and capsules of benzenoid drugs, which, in general, are both weakly absorbing and also formulated at a relatively low dosage level (typically 1–50 mg/unit dose). The high excipient–drug ratio and high sample weight required for these formulations result in background-irrelevant absorption of a sufficiently high intensity to possibly prohibit the application of simple spectrophotometric methods.

Techniques that reduce or eliminate matrix interference in the assay of formulated drugs include the Morton–Stubbs (1) correction procedure, which requires that the irrelevant absorption is linear over the wavelength range of the absorption band of the drug; orthogonal polynomials, which can cope with nonlinear irrelevant absorption if the correct choice of the polynomial order, wavelength range, and interval is made (2, 3); compensation spectrophotometry, in which the reference solution contains the matrix or sample at the same concentration present in the sample solution (4, 5); and difference spectrophotometry, which may be applied if an absorbance difference can be

0022-3549/84/0300-0413$01.00/0

© 1984, American Pharmaceutical Association

Table I—Assay Results

Drug	Analytical Concentration, mg/mL	Measured[a] Amplitude	Specific[b] Amplitude	Formulation[c]	Stated Amount per Unit, mg	Found, % of Declared Amount: Derivative Method	BP[d] Method	Uncorrected Absorbance
Trihexiphenidyl hydrochloride	0.6	257_S	0.86	T	2	97.4	95.7	179.9
Benztropine mesylate	0.65	258_S	0.80	T	2	100.6	98.7	167.2
Bethanidine sulfate	0.5	257_S	1.06	T	10	99.8	99.2	136.2
Bretylium tosylate	0.2	278_S	2.51	T	50	101.4	NA	115.6
Chlorcyclizine hydrochloride	0.25	268_L	2.26	T	50	96.7	97.3	106.0
Cyclizine hydrochloride	0.11	270_S	4.78	T	50	102.5	99.6	107.0
Debrisoquin sulfate	0.25	268_L	2.21	T	20	99.8	101.4	105.2
Diphenhydramine hydrochloride	0.5	258_S	1.20	C	25	96.2	95.4	97.9
Diphenylpyraline hydrochloride	0.5	257_S	1.14	C	5	102.0	NA	124.2
Hydroxyzine hydrochloride	0.3	270_L	1.70	T	10	96.4	NA	139.5
Scopolamine butylbromide	0.8	257_S	0.66	T	10	97.7	95.1	129.3
Meclizine hydrochloride	0.25	272_L	2.35	T	25	101.8	103.2	106.5
Methadone hydrochloride	0.65	260_S	0.81	T	5	101.4	100.2	121.1
Orphenadrine hydrochloride	0.40	270_L	1.51	T	50	100.2	99.9	106.8
Oxyphenonium bromide	0.8	257_S	0.64	T	5	97.2	NA	111.2
Meperidine hydrochloride	0.5	257_S	1.04	T	25	96.9	97.0	102.3
Phenelzine sulfate	0.5	258_S	1.01	T	25.8	99.1	100.5	226.0
Tolazoline hydrochloride	0.35	256_S	1.63	T	25	97.1	98.5	100.2

[a] Wavelength of minimum (nanometers) measured to the shorter (S) or longer (L) satellite. [b] See text for definition. [c] T = tablet, C = capsule. [d] NA = not applicable.

induced between equimolar solutions of the drug by the addition of reagents to one or both of the solutions, provided the matrix absorbance is unaffected by the reagents (6). The accuracy and specificity of UV absorption methods may also be considerably improved by conversion of the normal zero-order spectrum into a higher order (usually second or fourth) derivative spectrum. The improved resolution of overlapping absorption bands and the discrimination in favor of narrow bands against broader bands, which are the principal characteristics of derivative spectrophotometry (7, 8), can result in the complete elimination of both nonspecific matrix interference (8, 9) and specific interference from coformulated compounds (10–12).

The benzenoid drugs are ideal candidates for derivative measurements, as the narrow absorption bands of the fine structure in the 250–270-nm region give derivative bands of greater amplitudes than many of the more strongly absorbing drugs, which have a wider spectral band width. Several applications of derivative spectrophotometry in the assay of individual benzenoid compounds in formulations have been published (11–13). The purpose of this paper is to report the general application of the technique to a much wider range of these drugs in tablet and capsule formulations.

EXPERIMENTAL

Drug Substances—Scopolamine butylbromide[1], orphenadrine hydrochloride[2], bethanidine sulfate[3], bretylium tosylate[3], chlorcyclizine hydrochloride[3], cyclizine hydrochloride[3], methadone hydrochloride[3], trihexiphenidyl hydrochloride[4], benztropine mesylate[5], debrisoquin sulfate[6], meperidine hydrochloride[6], diphenhydramine hydrochloride[7], diphenylpyraline hydrochloride[8], meclizine hydrochloride[9], hydroxyzine hydrochloride[10], oxyphenonium bromide[11], tolazoline hydrochloride[11], and phenelzine sulfate[12] were used.

[1] Sigma London Chemical Co. Ltd., Poole, Dorset, U.K.
[2] Aldrich Chemical Co. Inc., Gillingham, Dorset, U.K.
[3] The Wellcome Foundation Ltd., Crewe, Cheshire, U.K.
[4] Lederle Laboratories, Gosport, Hants., U.K.
[5] Merck Sharp and Dohme, Ltd., Hoddesdon, Herts., U.K.
[6] Roche Products Ltd., Welwyn Garden City, Herts., U.K.
[7] Park Davis and Co., Pontypool, Gwent, U.K.
[8] Smith Kline and French Laboratories Ltd., Welwyn Garden City, Herts., U.K.
[9] BDH Pharmaceuticals Ltd., Alton, Hants., U.K.
[10] Pfizer Ltd., Sandwich, Kent, U.K.
[11] Ciba Laboratories, Horsham, West Sussex, U.K.
[12] Charles R. Warner and Co. Ltd., Pontypool, Gwent, U.K.

Spectrophotometry—Second-derivative absorption spectra of standard and sample solutions, equilibrated to room temperature were recorded in 1-cm silica quartz cells using a double-beam UV–visible recording spectrophotometer[13]. The scan speed was 60 nm/min, the spectral slit width 1 nm, response (time constant) 0.5 s, and the maximum and minimum ordinate settings +0.5 and −0.5, respectively. The unit dose assays of trihexiphenidyl hydrochloride, benzotropine mesylate, methadone hydrochloride, and oxyphenonium bromide required more sensitive ordinate settings of ±0.15, ±0.15, ±0.4, and ±0.3 respectively.

Standard Solutions—The second-derivative absorption spectrum was recorded from 290 to 230 nm for a standard solution of the drug, accurately prepared at the analytical concentration specified in Table I. For the unit dose assays of trihexiphenidyl hydrochloride, benztropine mesylate, methadone hydrochloride, and oxyphenonium bromide, standard solutions of 0.2, 0.2, 0.5, and 0.5 mg/mL, respectively, were prepared.

Sample Solutions—Twenty tablets or the contents of 20 capsules were weighed and powdered. A quantity of powder which gave an extract of the drug at the concentration, based on the declared strength of the formulation, that is specified for the drug in Table I was weighed into a 50-mL volumetric flask. The powder was shaken with 0.1 M HCl (40 mL) for 20 min and diluted to 50.0 mL with 0.1 M HCl. The extract was filtered through filter paper[14], the first 10 mL of filtrate was discarded to avoid problems arising from adsorption of the drug to the filter, and the second-derivative absorption spectrum of the filtrate was recorded.

For unit dose assays, a tablet or the contents of a capsule were powdered in a beaker with a glass rod. A suitable volume of 0.1 M HCl, 10.0–500.0 mL (given by declared unit dose in mg/analytical concentration in mg/mL), was added which yielded an extract containing the specified analytical concentration of the drug. Small volume extracts, <20 mL, were filtered through a membrane filter[15] and larger volume extracts through filter paper[14], as described above, and the second-derivative spectrum of the filtrate was recorded. For the unit dose assays of trihexiphenidyl hydrochloride, benztropine mesylate, methadone hydrochloride, and oxyphenonium bromide, 10.0 mL of 0.1 M HCl was used.

RESULTS AND DISCUSSION

Experimental Parameters—The zero-order and second-derivative absorption spectra of meperidine hydrochloride (pethidine hydrochloride), as an example of a benzenoid drug displaying characteristic fine structure in the region of 250—270 nm, are shown in Fig. 1A and B, respectively. The wavelengths of the minima of the inverted bands (a, b, c, and d) in the second-derivative spectrum correspond, after correction for displacement of the spectrum in the direction of the scan (14, 15), with the λ_{max} value (a, b, and c) at 251, 257, and 262.5 nm and shoulder at 268 nm in the zero-order spectrum. The second-derivative spectra of the other

[13] Perkin-Elmer 552 Spectrophotometer, Perkin-Elmer Corp., Norwalk, Conn.
[14] Whatman No. 1.
[15] Millipore Filter, 0.45 μm, 25-mm dia.

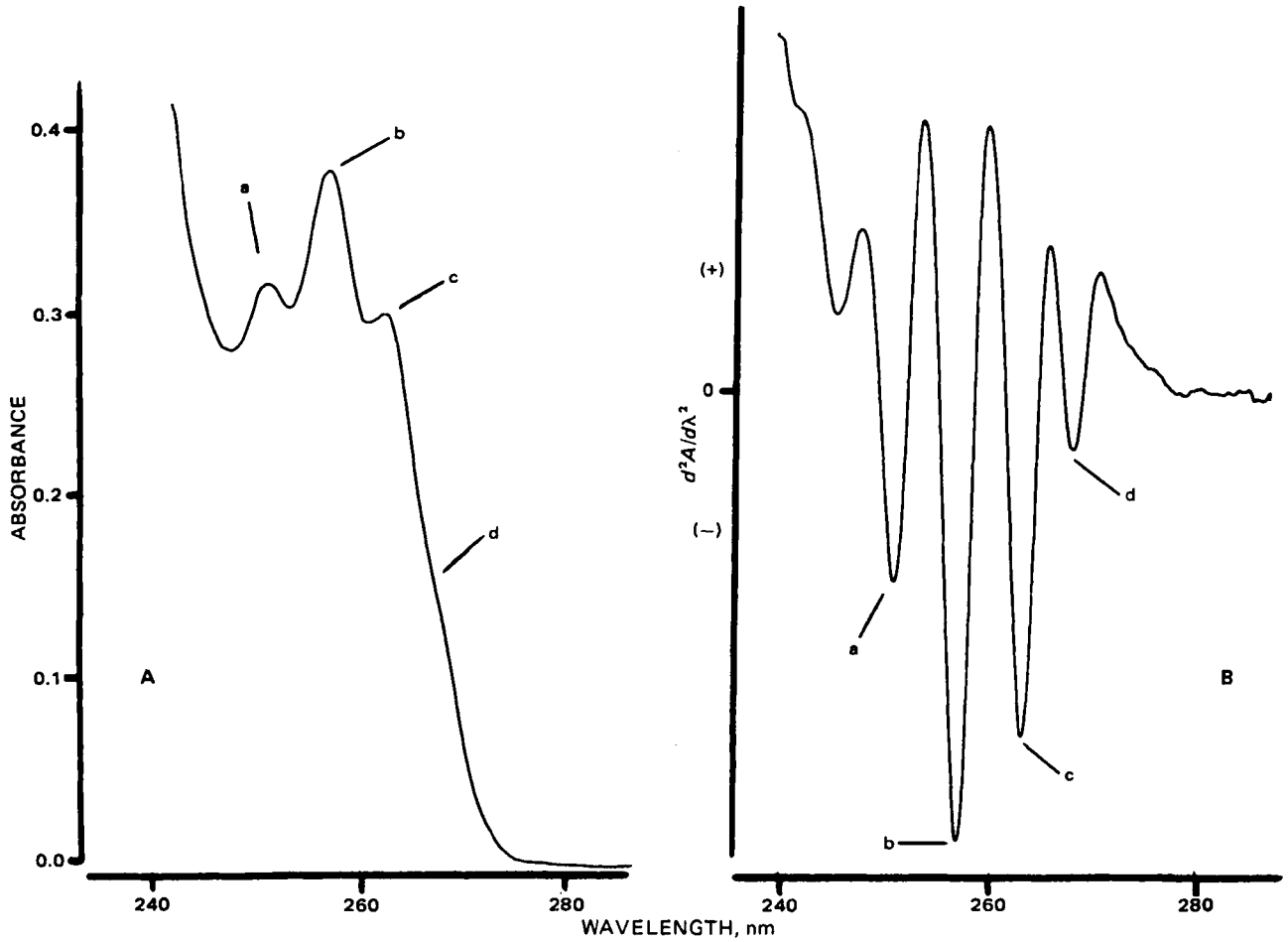

Figure 1—*Zero-order (A) and second-order derivative (B) spectra of meperidine hydrochloride (0.5 mg/mL in 0.1 M HCl).*

benzenoid drugs are similar to that of meperidine, differing only in the relative amplitudes of the vibrational bands and the wavelengths at which they occur. The amplitude of the largest band in the derivative spectrum of each drug (*e.g.*, for meperidine at 257 nm measured to its shorter wavelength satellite), providing the greatest sensitivity, was chosen for the analytical measurement.

The solvent used throughout was 0.1 M HCl, which is a satisfactory extracting solvent for these basic drugs, maintaining them substantially in the protonated form. It has been observed during the present work that certain drugs which show a barely discernible difference between the protonated and nonprotonated forms in the zero-order spectra display considerably larger differences in the derivative spectra. For example, the absorbance at λ_{max} 262.5 nm of meperidine is only 2.6% greater in 0.1 M HCl than in 0.1 M NaOH, whereas the amplitude of the second derivative minimum at 262.5 nm measured to its longer wavelength satellite is 26.3% greater in 0.1 M HCl than in 0.1 M NaOH.

The instrumental variables (absorbance range, spectral band pass, time constant, scan speed, and recorder voltage) were held constant for all the drugs, and the analytical concentration of each drug was selected as that giving the largest derivative amplitude at 50–60% of the chart full range. This approach enabled a direct comparison of the derivative responses at a constant instrumental damping and noise level to be made. Table I lists the analytical concentration together with the specific amplitude of the largest band, calculated as the amplitude, in millimeters, of a 1-mg/mL solution of the drug at 20°C as a ratio of the full chart width (250 mm) of the recorder on the 1-V range, and given by:

$$\text{Specific amplitude} = \frac{\text{Amplitude (mm)}}{\text{Concentration of drug (mg/mL)} \times 250}$$

Validation—The proportionality of the measured amplitude and concentration was checked for each drug by means of a six-point calibration graph at concentrations of 0, 25, 50, 75, 100, and 125% of the analytical concentration. In all cases, a proportional relationship was found to exist, with correlation coefficients ≥0.9996 and intercepts ≤ ±1% of the analytical concentration.

The precision of the amplitude measurements under the instrumental conditions was determined by recording the second-derivative spectra of five drug solutions, at their analytical concentrations, 10 times. The replicate measurements were each made after refilling the cell with fresh solution at room temperature to avoid an increase in the temperature of the solution in the cell compartment, which may reduce the measured amplitude (16). The relative standard deviations of the amplitudes of bethanidine, diphenhydramine, hydroxyzine, cyclizine, and diphenylpyraline all fell in the range of 0.42–0.59%. The similarity of these values is undoubtedly due to the similarity of the measured amplitudes (50–60% of the recorder scale) achieved by the selection of the analytical concentration.

As instrumental noise is a major factor affecting the reproducibility of spectra, the constant instrumental parameters adopted throughout this work would be expected to give constant noise levels, similar signal-to-noise ratios, and simllar satisfactory precision for the other drugs. Furthermore, the sampling procedure for most of the drug formulations may be readily modified to cope with unit dose assays using the same instrumental parameters without loss of precision of the measurement.

Unit dose assays may be carried out by crushing the formulation unit and extracting the drug with a suitable volume of 0.1 M HCl, as little as 10.0 mL if necessary, to obtain the desired analytical concentration, followed by filtration of the extract through a membrane filter or filter paper. It is considered that the systematic error incurred in this procedure by the increase in volume due to the dissolved components of the formulation is negligible.

The only formulations for which the normal instrumental parameters had to be modified for the unit dose assays were of those drugs having small specific amplitude (<1.0) and which are formulated in low dosage (≤5 mg/unit dose), *viz.*, trihexiphenidyl hydrochloride, benztropine mesylate, methadone hydrochloride, and oxyphenonium bromide. The unit dose assay of these formulations required the extraction of a dose unit with 10.0 mL of 0.1 M HCl, membrane filtration, and an increase in the sensitivity of the ordinate scales by factors of 3.33, 3.33, 1.25, and 1.67, respectively, of that of the normal scale. The relative standard deviations of the measurements for those drugs for which the unit dose assay re-

quired the ordinate scale expansion were 0.96, 0.91, 0.62, and 0.58% for trihexiphenidyl hydrochloride, benztropine mesylate, methadone hydrochloride, and oxyphenonium bromide, respectively.

Assay Results—Table I records the results obtained for 18 solid dosage formulations of benzenoid drugs which, with the exception of four, are official in the British Pharmacopoeia 1980 (17). The analytical concentration for each drug is given, and the measured amplitude is specified by the wavelength of the minimum in the derivative spectrum, after correction for scan speed effects (14, 15), measured either to its shorter or longer wavelength satellite. The specific amplitude is included to indicate the relative derivative responses of the drugs on a weight basis.

The presence of irrelevant absorption in all the sample extracts was confirmed by the observation of nonspecific absorption above 285 nm (where the drugs, except methadone, have zero absorptivity) and of the increasing distortion of the spectra toward lower wavelengths. The extent of the interference in the sample extracts is evident from the results (in the last column of Table I) showing the assay results calculated from the absorbance of the extracts at the λ_{max} in the region of 255–270 nm, uncorrected for irrelevant absorption. The background absorption at the λ_{max} of one drug formulation, that of phenelzine sulfate, exceeded the absorbance of the drug itself and many formulations showed interference >10% of that of the drug. The derivative spectra of the sample extracts, however, showed no apparent distortion and were identical in shape to the corresponding standard solutions, indicating the elimination of the broad-band irrelevant absorption of the formulation excipients from the derivative spectra of the sample solutions. In the case of two benzenoid drugs, atropine sulfate and scopolamine hydrobromide, formulated at very low doses (0.3 and 0.6 mg/tablet), there was unacceptable distortion of the second- and even of the fourth-derivative spectra by the tablet excipients. The derivative spectrophotometric assay of these very low-dose formulations by an alternative procedure is the subject of another report (18).

The assay results for the formulations, obtained by the derivative procedure, are in excellent agreement with the declared amount and, where appropriate, with the results given by official procedures of the BP 1980 (17), confirming that second-derivative spectrophotometry is a simple, rapid, and selective technique which has general application in the assay of tablet and capsule formulations containing a single benzenoid drug. The specificity of the procedures for drugs in the presence of degradation products has not been investigated in the present study. It is likely, however, that degradation products will contribute to the derivative spectrum of the sample solution and therefore interfere in the assay, if their zero-order UV spectra, like that of the parent drug, show fine structure in the 250–270-nm region.

REFERENCES

(1) R. A. Morton and A. L. Stubbs, *Analyst*, **71**, 348, (1946).

(2) A. L. Glenn, *J. Pharm. Pharmacol., Suppl.*, **15**, 123T, (1963).

(3) H. Abdine, A. M. Wahbi, and K. A. Korany, *J. Pharm. Pharmacol.*, **23**, 444 (1971).

(4) J. H. Jones, G. R. Clark, and L. S. Harrow, *J. Assoc. Off. Agr. Chem.*, **34**, 135 (1951).

(5) C. F. Hiskey, *Anal. Chem.*, **33**, 927 (1961).

(6) T. D. Doyle and F. R. Fazzari, *J. Pharm. Sci.*, **63**, 1921 (1974).

(7) T. C. O'Haver and G. L. Green, *Int. Lab.*, **5**, 11 (1975).

(8) A. F. Fell, *Proc. Anal. Div. Chem. Soc.*, **15**, 260 (1978).

(9) J. Traveset, V. Such, R. Gonzalo, and E. Gelpi, *J. Pharm. Sci.*, **69**, 629 (1980).

(10) A. F. Fell, D. R. Jarvie, and M. J. Stewart, *Clin. Chem.*, **27**, 286 (1981).

(11) A. F. Fell and G. Smith, *Anal. Proc.* **19**, 28 (1982).

(12) A. G. Davidson and H. Elsheik, *Analyst*, **107**, 879, (1982).

(13) R. Jones and G. Marnham, *J. Pharm. Pharmacol.*, **33**, 458 (1981).

(14) G. Talsky, L. Mayring, and H. Kreuzer, *Angew. Chem. Int. Ed. Engl.*, **17**, 785 (1978).

(15) "Perkin-Elmer Model 552 UV-VIS Spectrophotometer Operator's Manual," Perkin-Elmer Corp., Norwalk, Conn.

(16) A. G. Davidson, *Analyst*, **108**, 728 (1983).

(17) "British Pharmacopoeia," Her Majesty's Stationery Office, London, U.K., 1980.

(18) S. M. Hassan and A. G. Davidson, *J. Pharm. Pharmacol.*, **36**, 7 (1984).

Estrogenic and Antiestrogenic Activity of Novel Selenosteroids

SAMY A. SADEK *x, J. THOMAS PENTO ‡, and GARO P. BASMADJIAN ‡

Received November 22, 1982, from the **Faculty of Medicine, Kuwait University, Kuwait*, and the ‡ *College of Pharmacy, The University of Oklahoma, Oklahoma City Campus Health Science Center, Oklahoma City, OK 73190.* Accepted for publication February 8, 1983.

Abstract □ An assay for estrogenic and antiestrogenic activity of seven selenoestrogens has been carried out in immature female rats. The estrogenic activity was compared to the *in vitro* binding affinity data. The study reveals that introduction of selenium substituents on C-16 or C-17 of the steroid nucleus produced a marked reduction in the estrogenic activity. The selenium analogues of ethynylestradiol produced the highest estrogenic activity. None of the compounds produced antiestrogenic activity.

Keyphrases □ Selenoestrogens—estrogenic and antiestrogenic activity in immature rats, comparison with *in vitro* binding affinity □ Estrogens—selenium substituted, estrogenic and antiestrogenic activity in immature rats, comparison with *in vitro* binding affinity □ Binding affinity, *in vitro*—selenium-substituted estrogens, correlation with *in vivo* estrogenic and antiestrogenic activity, rats

The differentiation between estrogen receptor-negative and receptor-positive breast tumors and their metastases is important in the management and treatment of such tumors (1, 2). Present techniques are based on the *in vitro* measurement of estrogen receptors in freshly obtained biopsies of breast tissue. Therefore, a radiopharmaceutical which could be used to image estrogen-dependent breast tumors and metastatic foci by external detection could be a useful diagnostic tool. A number of investigators have attempted to develop such a radiopharmaceutical using radiohalogenated (*e.g.*, iodine-125, bromine-77) estrogens (3, 4). However, most of these studies have met with limited success. Although selenium-75 may not be an ideal radionuclide for diagnostic use, it offers the following advantages (5, 6): (*a*) its long half-life (120 d) allows enough time for synthesis and handling; (*b*) it can be incorporated into organic molecules with minimal difficulty; (*c*) the organoselenium compounds are more stable *in vivo* than the corresponding halogenated derivatives; and (*d*) preliminary studies with selenium-75 could determine the feasibility of using the potentially more useful ^{73}Se-labeled compounds ($t_{1/2}$ = 7 h).

0022-3549/84/0300-0416$01.00/0

© 1984, American Pharmaceutical Association

quired the ordinate scale expansion were 0.96, 0.91, 0.62, and 0.58% for trihexiphenidyl hydrochloride, benztropine mesylate, methadone hydrochloride, and oxyphenonium bromide, respectively.

Assay Results—Table I records the results obtained for 18 solid dosage formulations of benzenoid drugs which, with the exception of four, are official in the British Pharmacopoeia 1980 (17). The analytical concentration for each drug is given, and the measured amplitude is specified by the wavelength of the minimum in the derivative spectrum, after correction for scan speed effects (14, 15), measured either to its shorter or longer wavelength satellite. The specific amplitude is included to indicate the relative derivative responses of the drugs on a weight basis.

The presence of irrelevant absorption in all the sample extracts was confirmed by the observation of nonspecific absorption above 285 nm (where the drugs, except methadone, have zero absorptivity) and of the increasing distortion of the spectra toward lower wavelengths. The extent of the interference in the sample extracts is evident from the results (in the last column of Table I) showing the assay results calculated from the absorbance of the extracts at the λ_{max} in the region of 255–270 nm, uncorrected for irrelevant absorption. The background absorption at the λ_{max} of one drug formulation, that of phenelzine sulfate, exceeded the absorbance of the drug itself and many formulations showed interference >10% of that of the drug. The derivative spectra of the sample extracts, however, showed no apparent distortion and were identical in shape to the corresponding standard solutions, indicating the elimination of the broad-band irrelevant absorption of the formulation excipients from the derivative spectra of the sample solutions. In the case of two benzenoid drugs, atropine sulfate and scopolamine hydrobromide, formulated at very low doses (0.3 and 0.6 mg/tablet), there was unacceptable distortion of the second- and even of the fourth-derivative spectra by the tablet excipients. The derivative spectrophotometric assay of these very low-dose formulations by an alternative procedure is the subject of another report (18).

The assay results for the formulations, obtained by the derivative procedure, are in excellent agreement with the declared amount and, where appropriate, with the results given by official procedures of the BP 1980 (17), confirming that second-derivative spectrophotometry is a simple, rapid, and selective technique which has general application in the assay of tablet and capsule formulations containing a single benzenoid drug. The specificity of the procedures for drugs in the presence of degradation products has not been investigated in the present study. It is likely, however, that degradation products will contribute to the derivative spectrum of the sample solution and therefore interfere in the assay, if their zero-order UV spectra, like that of the parent drug, show fine structure in the 250–270-nm region.

REFERENCES

(1) R. A. Morton and A. L. Stubbs, *Analyst*, **71**, 348, (1946).

(2) A. L. Glenn, *J. Pharm. Pharmacol., Suppl.*, **15**, 123T, (1963).

(3) H. Abdine, A. M. Wahbi, and K. A. Korany, *J. Pharm. Pharmacol.*, **23**, 444 (1971).

(4) J. H. Jones, G. R. Clark, and L. S. Harrow, *J. Assoc. Off. Agr. Chem.*, **34**, 135 (1951).

(5) C. F. Hiskey, *Anal. Chem.*, **33**, 927 (1961).

(6) T. D. Doyle and F. R. Fazzari, *J. Pharm. Sci.*, **63**, 1921 (1974).

(7) T. C. O'Haver and G. L. Green, *Int. Lab.*, **5**, 11 (1975).

(8) A. F. Fell, *Proc. Anal. Div. Chem. Soc.*, **15**, 260 (1978).

(9) J. Traveset, V. Such, R. Gonzalo, and E. Gelpi, *J. Pharm. Sci.*, **69**, 629 (1980).

(10) A. F. Fell, D. R. Jarvie, and M. J. Stewart, *Clin. Chem.*, **27**, 286 (1981).

(11) A. F. Fell and G. Smith, *Anal. Proc.* **19**, 28 (1982).

(12) A. G. Davidson and H. Elsheik, *Analyst*, **107**, 879, (1982).

(13) R. Jones and G. Marnham, *J. Pharm. Pharmacol.*, **33**, 458 (1981).

(14) G. Talsky, L. Mayring, and H. Kreuzer, *Angew. Chem. Int. Ed. Engl.*, **17**, 785 (1978).

(15) "Perkin-Elmer Model 552 UV-VIS Spectrophotometer Operator's Manual," Perkin-Elmer Corp., Norwalk, Conn.

(16) A. G. Davidson, *Analyst*, **108**, 728 (1983).

(17) "British Pharmacopoeia," Her Majesty's Stationery Office, London, U.K., 1980.

(18) S. M. Hassan and A. G. Davidson, *J. Pharm. Pharmacol.*, **36**, 7 (1984).

Estrogenic and Antiestrogenic Activity of Novel Selenosteroids

SAMY A. SADEK *x, J. THOMAS PENTO ‡, and GARO P. BASMADJIAN ‡

Received November 22, 1982, from the **Faculty of Medicine, Kuwait University, Kuwait*, and the ‡ *College of Pharmacy, The University of Oklahoma, Oklahoma City Campus Health Science Center, Oklahoma City, OK 73190.* Accepted for publication February 8, 1983.

Abstract □ An assay for estrogenic and antiestrogenic activity of seven selenoestrogens has been carried out in immature female rats. The estrogenic activity was compared to the *in vitro* binding affinity data. The study reveals that introduction of selenium substituents on C-16 or C-17 of the steroid nucleus produced a marked reduction in the estrogenic activity. The selenium analogues of ethynylestradiol produced the highest estrogenic activity. None of the compounds produced antiestrogenic activity.

Keyphrases □ Selenoestrogens—estrogenic and antiestrogenic activity in immature rats, comparison with *in vitro* binding affinity □ Estrogens—selenium substituted, estrogenic and antiestrogenic activity in immature rats, comparison with *in vitro* binding affinity □ Binding affinity, *in vitro*—selenium-substituted estrogens, correlation with *in vivo* estrogenic and antiestrogenic activity, rats

The differentiation between estrogen receptor-negative and receptor-positive breast tumors and their metastases is important in the management and treatment of such tumors (1, 2). Present techniques are based on the *in vitro* measurement of estrogen receptors in freshly obtained biopsies of breast tissue. Therefore, a radiopharmaceutical which could be used to image estrogen-dependent breast tumors and metastatic foci by external detection could be a useful diagnostic tool. A number of investigators have attempted to develop such a radiopharmaceutical using radiohalogenated (*e.g.*, iodine-125, bromine-77) estrogens (3, 4). However, most of these studies have met with limited success. Although selenium-75 may not be an ideal radionuclide for diagnostic use, it offers the following advantages (5, 6): (*a*) its long half-life (120 d) allows enough time for synthesis and handling; (*b*) it can be incorporated into organic molecules with minimal difficulty; (*c*) the organoselenium compounds are more stable *in vivo* than the corresponding halogenated derivatives; and (*d*) preliminary studies with selenium-75 could determine the feasibility of using the potentially more useful ^{73}Se-labeled compounds ($t_{1/2}$ = 7 h).

0022-3549/84/0300-0416$01.00/0

© 1984, American Pharmaceutical Association

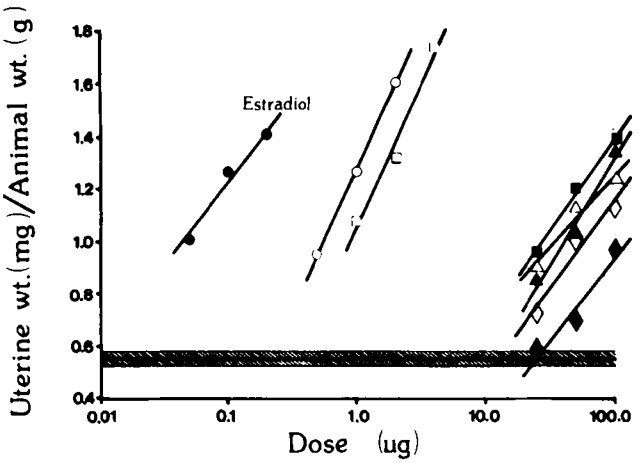

Figure 1—*Dose–uterotropic response curves of the selenosteroids. The horizontal bar represents the mean ± SEM of the control group. Key: (◆) I; (▲) II; (○) III; (□) IV; (△) V; (◇) VI; (■) VII.*

In previous studies (7, 8) we reported the synthesis and the relative binding affinity of various selenosteroids to the cytoplasmic estrogen receptor of rat uteri *in vitro*. In the present study, the uterotropic activity of these selenosteroids was examined and a correlation made between the *in vivo* uterotropic activity and *in vitro* receptor affinity.

EXPERIMENTAL

The uterotropic assay for estrogenic activity was a modification (9) of the original method of Rubin *et al.* (10). Immature female Sprague–Dawley rats weighing 40–50 g (~21 d old) were randomly distributed into groups containing five rats each. Estradiol and the test compounds were dissolved separately in corn oil and administered subcutaneously in a volume of 0.1 mL. Control animals were treated with the same volume of corn oil alone.

All animals were treated daily for three consecutive days with the same test compounds. On the fourth day the animals were sacrificed, and the uteri were carefully dissected, blotted lightly, and weighed to the nearest 0.1 mg; body weights were also recorded. Estradiol was used in a dosage range of 0.5–2 μg (total dose) as the assay standard. Each compound was examined over a dosage range of 5–100 μg (total dose).

The uterotropic assay was also used to evaluate the antiestrogenic activity of the test compounds. The antiestrogenic assay was conducted as described above for estrogenic activity except that each animal in the selenosteroid treatment groups received a standard stimulating dose of estradiol (2 μg). A separate control group which was treated with estradiol alone (2 μg) was also included in this assay. The test compounds and estradiol were administered separately at different injection sites to minimize possible physical interaction or reduce absorption of either compound. The antiestrogenic activity was measured as a decrease in estradiol-stimulated uterotropic response in groups which received both the test compound and estradiol as compared with the control group, which was treated with estradiol alone.

A line of best fit was plotted for each compound that produced an estrogenic response. Regression analysis was used to determine the dose–response line for each test compound. The slope of the response to each

Table I—Relative Uterotropic Activity of the Selenosteroids

Compound	Relative Uterotropic Activity[a]	RBA × 100[b]
Estradiol	100.00	100.00
I	0.06	1.0
II	0.14	5.1
III	10.46	2.0
IV	6.44	18.7
V	0.14	2.8
VI	0.11	0.1
VII	0.17	1.3

[a] Expressed as percentage of estradiol activity according to the method of Bliss (Ref. 11). [b] Ratio of the concentration of nonradioactive estradiol required to inhibit 50% of [^{3}H]estradiol binding to that of the competitor multiplied by 100 (from Ref. 8).

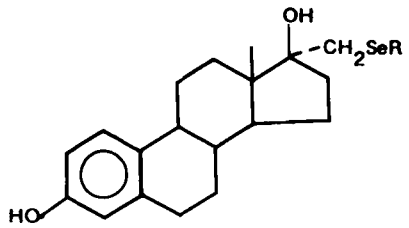

I : R = Ph
II : R = CH_3

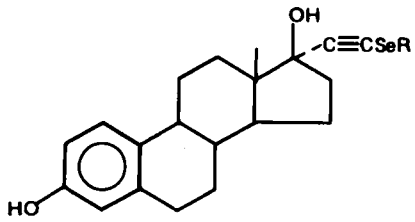

III : R = Ph
IV : R = CH_3

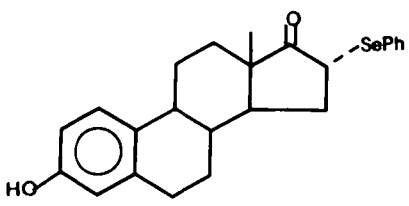

V

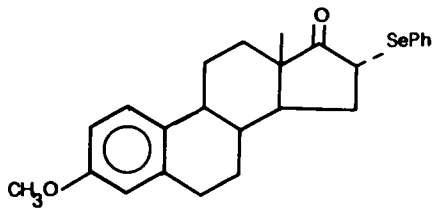

VI

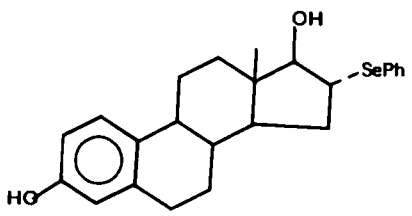

VII

analogue was compared with the slope of the estradiol response to determine parallelism in this assay system. The relative uterotropic activity of each compound was expressed as a percentage of estradiol activity according to the method of Bliss (11).

RESULTS

The dose–response curve produced by each of the selenium analogues is presented in Fig. 1. The potency of each compound relative to estradiol is summarized in Table I.

Among the selenosteroids that were examined in this study, III produced the greatest uterotropic activity while I produced the least activity. The selenoanalogues of ethynylestradiol (III and IV) were more active than those of estradiol or estrone. This may be due to the differences in the activity of the parent compounds (12). None of the test compounds produced a significant degree of antiestrogenic activity in this study.

DISCUSSION

In Table I the relative binding affinity of the test compounds was compared with the uterotropic activity. The potency estimates were in good agreement with the relative binding affinities with few exceptions. To correlate *in vitro* and *in vivo* results, metabolism has to be taken into consideration. Even though VI demonstrated a low *in vitro* binding affinity, its *in vivo* potency is almost equal to that of V. This could be as a result of demethylation *in vivo*. Sulfur-containing organic compounds are metabolized to sulfoxides (13); analogously, selenides are expected to oxidize to selenoxides *in vivo*. Reports indicate that aromatic selenoxides are less stable than the aliphatic derivatives (14–16). Therefore, we assume that the greater activity of III as compared with IV, despite a lower affinity for estrogen receptors, is due to the degradation of III to the more potent ethynylestradiol.

It is reasonable to assume that VII has a greater *in vivo* uterotropic activity than V because estradiol (the parent compound of analogue VII) is more potent than estrone (the parent compound of analogue V) (12).

This study indicates that increasing the size of the substituent on C-17 decreases the *in vitro* binding and the *in vivo* potency. These data confirm the importance of the β-hydroxyl group on C-17 to retain the estrogenic activity (17). Since these selenosteroids retain a high degree of estrogenic activity (especially III and IV) *in vivo*, as shown in the present study, and display potent receptor binding *in vitro* (8), it is possible that one of these derivatives might be a suitable imaging agent for estrogen-dependent tumors and metastatic foci. Selenium-75 labeling of II has been accomplished utilizing newly developed methodology (18). Biodistribution studies of this ^{75}Se-labeled compound in tumor-bearing animals are underway.

REFERENCES

(1) W. L. McGuire, K. L. Horwitz, D. T. Zava, R. E. Garola, and G. C. Chamness, *Metabolism*, **27**, 487 (1978).

(2) C. K. Osborne and W. L. McGuire, *Bull. Cancer (Paris)*, **66**, 203 (1979).

(3) J. A. Katzenellenbogen, K. D. McElvany, S. G. Senderoff, K. E. Carlson, S. W. Landvatter, M. J. Welch, and the Los Alamos Medical Radioisotope Group, *J. Nucl. Med.*, **23**, 411 (1982).

(4) R. N. Hanson, D. E. Seitz, and J. C. Botarro, *J. Nucl. Med.*, **23**, 431 (1982).

(5) G. P. Basmadjian, R. R. Hetzel, and R. D. Ice, *Int. J. Appl. Radiat. Isotopes*, **26**, 695 (1975).

(6) F. F. Knapp, in "Radiopharmaceuticals: Structure Activity Relationships," R. P. Spencer, Ed., Grune & Stratton, New York, N.Y., 1981, p. 345.

(7) S. A. Sadek, S. M. Shaw, W. V. Kessler, and G. C. Wolf, *J. Org. Chem.*, **46**, 3259 (1981).

(8) S. A. Sadek, W. V. Kessler, S. M. Shaw, J. N. Anderson, and G. C. Wolf, *J. Med. Chem.*, **25**, 1488 (1982).

(9) J. T. Pento, R. A. Magarian, R. T. Wright, M. M. King, and E. T. Benjamin, *J. Pharm. Sci.*, **70**, 399 (1981).

(10) B. L. Rubin, A. S. Dorfman, L. Black, and R. I. Dorfman, *Endocrinology*, **49**, 429 (1951).

(11) C. I. Bliss, "The Statistics of Bioassay," Academic, New York, N.Y., 1952.

(12) J. P. Raynaud, M. M. Bouton, D. Gallet-Bourguin, D. Philibert, C. Tournemine, and G. Azadian-Barlanger, *Mol. Pharmacol.*, **9**, 520 (1973).

(13) N. P. Salzman and B. B. Brodie, *J. Pharmacol. Exp. Ther.*, **118**, 46 (1956).

(14) R. Walter and J. Roy, *J. Org. Chem.*, **36**, 2561 (1971).

(15) K. B. Sharpless, M. W. Young, and R. F. Lauer, *Tetrahedron Lett.*, **1973**, 1979.

(16) G. Ayrey, D. Barnard, and D. T. Woodbridge, *J. Chem. Soc.*, **1962**, 2089.

(17) S. G. Korenman, *Steroids*, **13**, 163 (1969).

(18) S. A. Sadek, G. P. Basmadjian, and R. D. Ice, *Nucl. Med. Commun.*, **3**, 247 (1982).

Diaspirins of Methylenecitric Acid

SOLOMON E. MASSIL, GUEY-YUEH SHI, and IRVING M. KLOTZ ˣ

Received October 25, 1982, from the *Department of Chemistry, Northwestern University, Evanston, IL 60201.* Accepted for publication January 19, 1983.

Abstract □ A series of bissalicylic esters of methylenecitric acid have been prepared and, as a probe of their potential as antisickling agents, tested for their ability to modify hemoglobin. Substantial acylation of hemoglobin was obtained with these dicarboxylate esters at 1–5 mM concentrations.

Keyphrases □ Methylenecitric acid—bissalicylic esters, synthesis, hemoglobin-modifying potential □ Antisickling agents—potential, bissalicylic esters of methylenecitric acid, synthesis, hemoglobin-modifying ability

Diaspirins have been found (1) to modify hemoglobin S and to change its solubility markedly. Consequently, this class of compounds may provide promising antisickling agents. Just as aspirin is an acetate of salicylic acid, so are diaspirins the alkanedioates of salicylic acid. Alkanedioic acids of 4–5 carbon chain length seem to be optimal in modification of hemoglobins, probably because they can readily span the β-cleft of the hemoglobin molecule and form a covalent bridge between the two Lys 82 residues. Such a bridge evidently locks the protein into a conformation out of register for the aggregation that occurs in sickling.

The modified pentanedioic acid, 4-oxo-1,3-dioxolane-5,5′-diacetic acid, also known as methylenecitric acid (A), is a five-carbon span dicarboxylic acid whose monoesters have been examined previously for pharmacological ac-

0022-3549/84/0300-0418$01.00/0

© 1984, American Pharmaceutical Association

analogue was compared with the slope of the estradiol response to determine parallelism in this assay system. The relative uterotropic activity of each compound was expressed as a percentage of estradiol activity according to the method of Bliss (11).

RESULTS

The dose–response curve produced by each of the selenium analogues is presented in Fig. 1. The potency of each compound relative to estradiol is summarized in Table I.

Among the selenosteroids that were examined in this study, III produced the greatest uterotropic activity while I produced the least activity. The selenoanalogues of ethynylestradiol (III and IV) were more active than those of estradiol or estrone. This may be due to the differences in the activity of the parent compounds (12). None of the test compounds produced a significant degree of antiestrogenic activity in this study.

DISCUSSION

In Table I the relative binding affinity of the test compounds was compared with the uterotropic activity. The potency estimates were in good agreement with the relative binding affinities with few exceptions. To correlate *in vitro* and *in vivo* results, metabolism has to be taken into consideration. Even though VI demonstrated a low *in vitro* binding affinity, its *in vivo* potency is almost equal to that of V. This could be as a result of demethylation *in vivo*. Sulfur-containing organic compounds are metabolized to sulfoxides (13); analogously, selenides are expected to oxidize to selenoxides *in vivo*. Reports indicate that aromatic selenoxides are less stable than the aliphatic derivatives (14–16). Therefore, we assume that the greater activity of III as compared with IV, despite a lower affinity for estrogen receptors, is due to the degradation of III to the more potent ethynylestradiol.

It is reasonable to assume that VII has a greater *in vivo* uterotropic activity than V because estradiol (the parent compound of analogue VII) is more potent than estrone (the parent compound of analogue V) (12).

This study indicates that increasing the size of the substituent on C-17 decreases the *in vitro* binding and the *in vivo* potency. These data confirm the importance of the β-hydroxyl group on C-17 to retain the estrogenic activity (17). Since these selenosteroids retain a high degree of estrogenic activity (especially III and IV) *in vivo*, as shown in the present study, and display potent receptor binding *in vitro* (8), it is possible that one of these derivatives might be a suitable imaging agent for estrogen-dependent tumors and metastatic foci. Selenium-75 labeling of II has been accomplished utilizing newly developed methodology (18). Biodistribution studies of this ^{75}Se-labeled compound in tumor-bearing animals are underway.

REFERENCES

(1) W. L. McGuire, K. L. Horwitz, D. T. Zava, R. E. Garola, and G. C. Chamness, *Metabolism*, **27**, 487 (1978).

(2) C. K. Osborne and W. L. McGuire, *Bull. Cancer (Paris)*, **66**, 203 (1979).

(3) J. A. Katzenellenbogen, K. D. McElvany, S. G. Senderoff, K. E. Carlson, S. W. Landvatter, M. J. Welch, and the Los Alamos Medical Radioisotope Group, *J. Nucl. Med.*, **23**, 411 (1982).

(4) R. N. Hanson, D. E. Seitz, and J. C. Botarro, *J. Nucl. Med.*, **23**, 431 (1982).

(5) G. P. Basmadjian, R. R. Hetzel, and R. D. Ice, *Int. J. Appl. Radiat. Isotopes*, **26**, 695 (1975).

(6) F. F. Knapp, in "Radiopharmaceuticals: Structure Activity Relationships," R. P. Spencer, Ed., Grune & Stratton, New York, N.Y., 1981, p. 345.

(7) S. A. Sadek, S. M. Shaw, W. V. Kessler, and G. C. Wolf, *J. Org. Chem.*, **46**, 3259 (1981).

(8) S. A. Sadek, W. V. Kessler, S. M. Shaw, J. N. Anderson, and G. C. Wolf, *J. Med. Chem.*, **25**, 1488 (1982).

(9) J. T. Pento, R. A. Magarian, R. T. Wright, M. M. King, and E. T. Benjamin, *J. Pharm. Sci.*, **70**, 399 (1981).

(10) B. L. Rubin, A. S. Dorfman, L. Black, and R. I. Dorfman, *Endocrinology*, **49**, 429 (1951).

(11) C. I. Bliss, "The Statistics of Bioassay," Academic, New York, N.Y., 1952.

(12) J. P. Raynaud, M. M. Bouton, D. Gallet-Bourguin, D. Philibert, C. Tournemine, and G. Azadian-Barlanger, *Mol. Pharmacol.*, **9**, 520 (1973).

(13) N. P. Salzman and B. B. Brodie, *J. Pharmacol. Exp. Ther.*, **118**, 46 (1956).

(14) R. Walter and J. Roy, *J. Org. Chem.*, **36**, 2561 (1971).

(15) K. B. Sharpless, M. W. Young, and R. F. Lauer, *Tetrahedron Lett.*, **1973**, 1979.

(16) G. Ayrey, D. Barnard, and D. T. Woodbridge, *J. Chem. Soc.*, **1962**, 2089.

(17) S. G. Korenman, *Steroids*, **13**, 163 (1969).

(18) S. A. Sadek, G. P. Basmadjian, and R. D. Ice, *Nucl. Med. Commun.*, **3**, 247 (1982).

Diaspirins of Methylenecitric Acid

SOLOMON E. MASSIL, GUEY-YUEH SHI, and IRVING M. KLOTZ ˣ

Received October 25, 1982, from the *Department of Chemistry, Northwestern University, Evanston, IL 60201.* Accepted for publication January 19, 1983.

Abstract □ A series of bissalicylic esters of methylenecitric acid have been prepared and, as a probe of their potential as antisickling agents, tested for their ability to modify hemoglobin. Substantial acylation of hemoglobin was obtained with these dicarboxylate esters at 1–5 mM concentrations.

Keyphrases □ Methylenecitric acid—bissalicylic esters, synthesis, hemoglobin-modifying potential □ Antisickling agents—potential, bissalicylic esters of methylenecitric acid, synthesis, hemoglobin-modifying ability

Diaspirins have been found (1) to modify hemoglobin S and to change its solubility markedly. Consequently, this class of compounds may provide promising antisickling agents. Just as aspirin is an acetate of salicylic acid, so are diaspirins the alkanedioates of salicylic acid. Alkanedioic acids of 4–5 carbon chain length seem to be optimal in modification of hemoglobins, probably because they can readily span the β-cleft of the hemoglobin molecule and form a covalent bridge between the two Lys 82 residues. Such a bridge evidently locks the protein into a conformation out of register for the aggregation that occurs in sickling.

The modified pentanedioic acid, 4-oxo-1,3-dioxolane-5,5′-diacetic acid, also known as methylenecitric acid (A), is a five-carbon span dicarboxylic acid whose monoesters have been examined previously for pharmacological ac-

0022-3549/84/0300-0418$01.00/0

© 1984, American Pharmaceutical Association

Table I—Modification of Hemoglobin by Bissalicylic Esters of Methylenecitric Acid

Compound	Melting Point, °C	Yield, %	Formula[a]	Conc., mM	Modification of Oxyhemoglobin A, %[b]
I	155–157	72	$C_{21}H_{16}O_{11}$	5	34
				1	20
II	153–155	54	$C_{21}H_{14}F_2O_{11}$	5	46
				1	24
III	161–163	51	$C_{21}H_{14}Cl_2O_{11}$[d]	5	70
				1	35
IV	168–169	45	$C_{21}H_{14}Br_2O_{11}$[e]	5	74
				1	38
V	167–168	53	$C_{21}H_{14}I_2O_{11}$	5	83
				1	42
VI	165–166	45	$C_{21}H_{14}Cl_2O_{11}$[f]	5	69
				1	35
VII[c]	155–157	69	$C_{21}H_{12}Cl_4O_{11}$[g]	1	27
VIII[c]	183–185	53	$C_{21}H_{12}Br_4O_{11}$[h]	1	32
IX[c]	146–148	76	$C_{21}H_{12}I_4O_{11}$[i]	1	35
X	[Bis(4,6-dibromo-*z*-carboxyphenol)fumarate]			1	87
				1[j]	88

[a] Compounds I–IX underwent elemental analyses for C, H, and the appropriate halogen. Unless otherwise noted, all analyses were within ±0.4% of the theoretical values. [b] Hemoglobin concentration, 1 mM. [c] Unstable compared with the monosubstituted compounds; they hydrolyzed slowly on standing. Repeated recrystallization did not improve the analysis. [d] Calc. for Cl, 13.82; found, 13.21. [e] Calc. for Br, 26.54; found, 26.04. [f] Calc. for Cl, 13.82; found, 12.98. [g] Calc. for H, 2.08; Cl, 24.36. Found for H, 2.72; Cl, 19.75. [h] Calc. for Br, 42.06; found, 39.06. [i] Calc. for I, 53.55; found, 48.62. [j] In aqueous solution containing 2.6% ethanol to aid in solubilizing the compound.

tivity (2, 3). It seemed interesting, therefore, to prepare salicylic derivatives (B) of this diacid and to examine their effects on hemoglobin. The significant parts of B for its chemical and biological activity are the three C—O—C moieties designated O(1), O(2), and O(3). Classification of the functionality of the C—O—C at O(1) is acid anhydride, at O(2) acetal, and at O(3) acylal, and their relative reactivities toward amino groups are O(1) > O(3) > O(2).

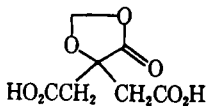

A

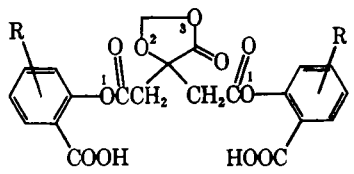

B′

I: R = H
II: R = 5-F
III: R = 5-Cl
IV: R = 5-Br
V: R = 5-I
VI: R = 4-Cl
VII: R = 3,5-Cl_2
VIII: R = 3,5-Br_2
IX: R = 3,5-I_2

EXPERIMENTAL[2]

To a stirred mixture of salicylic acid (2.00 mmol) or its halogen derivatives and dimethylaniline (4.13 mmol) in 100 mL of dry benzene was added in a dropwise manner 4-oxo-1,3-dioxolane-5,5-bis(acetylchloride) (methylene-citroyl dichloride, 1.02 mmol) dissolved in 20 mL of benzene. After 0.5 h at room temperature, the mixture was further warmed on a water bath (at 60–70°C) for ~10 min and then stirred overnight at room temperature. The solvent was removed *in vacuo*; the residue was suspended in 100 mL of ethyl acetate and then extracted twice with ice-cold 1 M aqueous H_2SO_4 (50 mL) and once with water (50 mL). After the organic layer had been dried ($MgSO_4$), filtered, and evaporated (*in vacuo*), the residue was triturated with several milliliters of petroleum ether to give solid material. Recrystallization either from benzene or a mixture of chloroform–petroleum ether (30–60°C) provided purified bis(substituted 2-carboxyphenyl)4-oxo-1,3-dioxolane-5,5′-diacetates, commonly known as bis(substituted salicyl)anhydromethylene citrates.

The compounds were identified by elemental analysis (Table I), IR, and ^{1}H-NMR spectrometry (1). The C=O stretching vibration of esters occurs in the range 1690–1770 cm^{-1}. NMR data were consistent with the proposed structures. The NMR spectra (DMSO-d_6 tetramethylsilane as internal standard) showed the following common absorption peaks: δ 3.3–3.5 (s, —C—CH_2—CO), 5.4–5.52 (s, O—CH_2—O), and 7.2–8.2 ppm (ArH).

Isoelectric focusing (6, 7) was used to assess the extent of modification of oxyhemoglobin. The acylated protein was separated from the parent protein in a flat gel by electrophoresis[3]. Minor alterations (8) were made in the procedures described by the manufacturer. Before application to the gel surface (on small pieces of filter paper) all hemoglobin samples were saturated with carbon monoxide and made to 0.01 M in NaCN. After focusing had been achieved, the gel was fixed (8) and dried overnight, and a densitometric scan was made with a soft laser scanning densitometer[4] and integrator. From this pattern the extent of modification was calculated.

RESULTS AND DISCUSSION

The extent of modification of oxyhemoglobin by these diesters is shown in Table I. The prototype of this series, the diester with unsubstituted salicylate (I), shows significant modification of the protein even at concentrations as low as 1 mM. The effectiveness increases progressively as one proceeds from the fluoro to the chloro, bromo, and iodo monosubstituted salicylates (II–V). With the monochlorosalicylate, a comparison was also made of the 4-substituted (VI) with the 5-substituted derivative (III), but the difference in behavior is insignificant. Derivatives with disubstituted halosalicylates (VII–IX) are not more effective as acylating agents for hemoglobin than are the monosubstituted derivatives.

Using [^{14}C]acetyl-labeled salicylate, we established previously (8) that acylation of hemoglobin occurs on lysine side chains. Subsequently, with the "double-headed" aspirins, chemical work supplemented by X-ray diffraction (9, 10), showed that the β-subunits of hemoglobin were cross-linked by —C(=O)—CH_2—CH_2—C(=O)— or —C(=O)—CH=CH—C(=O)— bridges connecting β_1 Lys 82 to β_2 Lys 82. Similar cross linking has been observed with five-atom bridges (11). Thus, the methylene citric acid series became a natural candidate for the extension of these structure-function investigations.

At first glance one would have expected (1) the dihalosalicylate diesters to be more effective than the monohalo ones since the additional halogen substituents should increase binding to hemoglobin. However, one must recognize that the extra electron-withdrawing substituents also activate the ester bond and make the compound more sensitive to hydrolysis. Such effects have already been observed (11, 12) with derivatives containing polar substituents on a four-carbon bridge; oxygen moieties adjacent to the carbonyl groups decrease the stability of the bis(dibromo)salicylate

[1] Numbering of substituents in structure B is in terms of salicylate ring.

[2] Elemental analyses were performed by Micro-Tech Laboratories of Skokie, Ill. IR spectra (in KBr pellets) were obtained with a Perkin-Elmer 283 spectrometer. ^{1}H-NMR spectra were obtained with Varian EM-360 (60 MHz) and JEOL FX-270 spectrometers. Melting points were taken in open capillary tubes and are uncorrected. Salicylic acids used herein were purchased from the Aldrich Chemical Co. Methylenecitric acid was prepared from citric acid and paraformaldehyde, and its subsequent conversion into dichloride was by treatment with PCl_5. The physical properties in all cases were in close agreement with those cited in the literature (2, 4, 5).

[3] LKB 2117 Multiphor with a Savant power source.

[4] Zeineh.

esters. Corresponding results have also been evident when electron-withdrawing groups were placed on the salicylate ring (13). The doubly halogenated salicylate derivatives of methylenecitric acid have activating groups both on the aromatic rings and on the middle carbon of the five-carbon bridge so that hydrolytic instabilities are magnified. Even in the solid state, traces of moisture lead to slow cleavage of these esters. Thus, as has been emphasized previously (11, 12) a careful balance between stability and reactivity is essential for optimal activity of the double-headed aspirins.

REFERENCES

(1) I. M. Klotz, D. N. Haney, and L. C. King, *Science*, **213**, 724 (1981).

(2) A. Dulin and J. W. Martin, Jr., *J. Am. Pharm. Assoc., Sci. Ed.*, **47**, 851 (1958).

(3) R. J. Warren, R. W. Gardier, A. B. Richards, and W. M. Alexander, *J. Am. Pharm. Assoc., Sci. Ed.*, **47**, 853 (1958).

(4) C. A. Nau, E. B. Brown, and J. R. Bailey, *J. Am. Chem. Soc.*, **47**, 2596 (1925).

(5) Ger. pat. 185,800, 1906; *Chem. Abstr.*, **2**, 351 (1908); Ger. pat. 186,659, 1906; *Chem. Abstr.*, **2**, 354 (1908).

(6) H. F. Bunn, *Ann. N.Y. Acad. Sci.*, **209**, 345 (1973).

(7) P. G. Righetti and J. W. Drysdale, in "Laboratory Techniques in Biochemistry and Molecular Biology," Vol. 5, Part 2, T. S. Work and E. Work, Eds., Elsevier, Amsterdam, 1976.

(8) M. Shamsuddin, R. G. Mason, J. M. Ritchey, G. R. Honig, and I. M. Klotz, *Proc. Natl. Acad. Sci. USA*, **71**, 4693 (1974).

(9) J. A. Walder, R. Y. Walder, A. Arnone, and I. M. Klotz, *Fed. Proc. Fed. Am. Soc. Exp. Biol.*, **38**, 461 (1979).

(10) J. A. Walder, R. Y. Walder, and A. Arnone, *J. Mol. Biol.*, **141**, 195 (1980).

(11) L. E. Wood, D. N. Haney, J. R. Patel, S. E. Clare, G.-Y. Shi, L. C. King, and I. M. Klotz, *J. Biol. Chem.*, **256**, 7046 (1981).

(12) E. J. Delaney, S. E. Massil, G.-Y. Shi, and I. M. Klotz, *Arch. Biochem. Biophys.*, in press.

(13) R. H. Zaugg, J. A. Walder, R. Y. Walder, J. M. Steele, and I. M. Klotz, *J. Biol. Chem.*, **255**, 2816 (1980).

ACKNOWLEDGMENTS

This work was supported in part by Grant No. HL22719 from the National Heart, Lung, and Blood Institute of the National Institutes of Health. We are also very grateful to Professor C. D. Hurd for his advice on proper nomenclature of the compounds studied and his helpful comments on this manuscript.

COMMUNICATIONS

Computer-Interfaced Capacitive Sensor for Monitoring the Granulation Process

Keyphrases □ Granulation—computer-interfaced capacitive sensor, high-intensity mixer, moisture measurement, instrumentation, process control

To the Editor:

Wet granulation of powders is a fundamental process in pharmaceutical technology. The phenomenon of granulation, however, is not well understood because of the many variables involved in the process. The need for a better understanding and control of wet granulation has increased in recent years because greater utilization of high-intensity mixers has dramatically reduced the total time required to reach or exceed a proper granulation end point. Several workers have reported results from studies of the granulation process using instrumented mixers (1–8). These studies have shown that measurements of power consumption by the mixer, torque on the mixer shaft, change in rotation-rate of the mixer shaft, or the force with which granules deflect a strain-gauged beam, provided insight into the changes that occur as a powder is massed.

We wish to report a new approach to study the dynamics of wet granulation, which uses a computer-interfaced capacitive sensor that has been designed in our laboratories. The sensor is constructed from a polytetrafluoroethylene cylinder 1.5 cm in diameter, to which two insulated stainless steel electrodes are attached. The sensor is threaded to fit the existing thermocouple port in the wall of a high-intensity mixer[1]. The sensor extends into the mixer a distance of 5 cm and is 12 cm below the mixer center, with the distal 3 cm of each electrode exposed.

The two electrical leads from the sensor are connected to a moisture analyzer[2] which acts as the interface to the computer. The electronics of the moisture analyzer have been modified to filter signal noise caused by the rotation of the mixer plowshares and to allow for initial baseline adjustments. The moisture analyzer with sensor operates on the principle of power loss from a tuned radio-frequency (R/F) circuit as the dielectric of the medium surrounding the sensor changes. The analog DC voltage output of the moisture analyzer is converted to a digital value by an A/D converter and is fed to a 16-bit microprocessor[3] which is used for data processing and system control. System software is stored in a nonvolatile form in an onboard, programmable, read-only memory and allows for operator control of data sampling rate and text information for hard-copy output. Each data point, taken at 4-s intervals, is the average of 5000 A/D conversions.

Granulations were prepared by charging the mixer with 20 kg of lactose powder and using only the plowshare mixing action. Figure 1 shows the resulting voltage *versus* mixing time profile as incremental additions of water were made to the lactose[4]. The decreases in voltage are the result of rapid moisture distribution throughout the powder after each addition. The plateau reached between each addition is an equilibrium voltage value that is a function of the amount of water in the moist powder. The granules formed with this simple lactose water system, however, were not of good quality.

Figure 2 shows the voltage response when 2.5 kg of a 4% w/w methylcellulose 15 cps[5] aqueous solution was added to 20 kg of lactose at time zero. A similar voltage response

[1] Model FM-50, Littleford-Lödige, Florence, Ky.

[2] Moisture Register Model G8R, Moisture Register Co., Berwind Instruments Group, North Hollywood, Calif.

[3] iSBC 88/25, Intel Inc., Santa Clara, Calif.

[4] Lactose Hydrous USP, No. 80M, Sheffield Products, Memphis, Tenn.

[5] Methocel A 15 Premium, The Dow Chemical Co., Midland, Mich.

0022-3549/84/0300-0420$01.00/0

© 1984, American Pharmaceutical Association

esters. Corresponding results have also been evident when electron-withdrawing groups were placed on the salicylate ring (13). The doubly halogenated salicylate derivatives of methylenecitric acid have activating groups both on the aromatic rings and on the middle carbon of the five-carbon bridge so that hydrolytic instabilities are magnified. Even in the solid state, traces of moisture lead to slow cleavage of these esters. Thus, as has been emphasized previously (11, 12) a careful balance between stability and reactivity is essential for optimal activity of the double-headed aspirins.

REFERENCES

(1) I. M. Klotz, D. N. Haney, and L. C. King, *Science*, **213**, 724 (1981).

(2) A. Dulin and J. W. Martin, Jr., *J. Am. Pharm. Assoc., Sci. Ed.*, **47**, 851 (1958).

(3) R. J. Warren, R. W. Gardier, A. B. Richards, and W. M. Alexander, *J. Am. Pharm. Assoc., Sci. Ed.*, **47**, 853 (1958).

(4) C. A. Nau, E. B. Brown, and J. R. Bailey, *J. Am. Chem. Soc.*, **47**, 2596 (1925).

(5) Ger. pat. 185,800, 1906; *Chem. Abstr.*, **2**, 351 (1908); Ger. pat. 186,659, 1906; *Chem. Abstr.*, **2**, 354 (1908).

(6) H. F. Bunn, *Ann. N.Y. Acad. Sci.*, **209**, 345 (1973).

(7) P. G. Righetti and J. W. Drysdale, in "Laboratory Techniques in Biochemistry and Molecular Biology," Vol. 5, Part 2, T. S. Work and E. Work, Eds., Elsevier, Amsterdam, 1976.

(8) M. Shamsuddin, R. G. Mason, J. M. Ritchey, G. R. Honig, and I. M. Klotz, *Proc. Natl. Acad. Sci. USA*, **71**, 4693 (1974).

(9) J. A. Walder, R. Y. Walder, A. Arnone, and I. M. Klotz, *Fed. Proc. Fed. Am. Soc. Exp. Biol.*, **38**, 461 (1979).

(10) J. A. Walder, R. Y. Walder, and A. Arnone, *J. Mol. Biol.*, **141**, 195 (1980).

(11) L. E. Wood, D. N. Haney, J. R. Patel, S. E. Clare, G.-Y. Shi, L. C. King, and I. M. Klotz, *J. Biol. Chem.*, **256**, 7046 (1981).

(12) E. J. Delaney, S. E. Massil, G.-Y. Shi, and I. M. Klotz, *Arch. Biochem. Biophys.*, in press.

(13) R. H. Zaugg, J. A. Walder, R. Y. Walder, J. M. Steele, and I. M. Klotz, *J. Biol. Chem.*, **255**, 2816 (1980).

ACKNOWLEDGMENTS

This work was supported in part by Grant No. HL22719 from the National Heart, Lung, and Blood Institute of the National Institutes of Health. We are also very grateful to Professor C. D. Hurd for his advice on proper nomenclature of the compounds studied and his helpful comments on this manuscript.

COMMUNICATIONS

Computer-Interfaced Capacitive Sensor for Monitoring the Granulation Process

Keyphrases □ Granulation—computer-interfaced capacitive sensor, high-intensity mixer, moisture measurement, instrumentation, process control

To the Editor:

Wet granulation of powders is a fundamental process in pharmaceutical technology. The phenomenon of granulation, however, is not well understood because of the many variables involved in the process. The need for a better understanding and control of wet granulation has increased in recent years because greater utilization of high-intensity mixers has dramatically reduced the total time required to reach or exceed a proper granulation end point. Several workers have reported results from studies of the granulation process using instrumented mixers (1–8). These studies have shown that measurements of power consumption by the mixer, torque on the mixer shaft, change in rotation-rate of the mixer shaft, or the force with which granules deflect a strain-gauged beam, provided insight into the changes that occur as a powder is massed.

We wish to report a new approach to study the dynamics of wet granulation, which uses a computer-interfaced capacitive sensor that has been designed in our laboratories. The sensor is constructed from a polytetrafluoroethylene cylinder 1.5 cm in diameter, to which two insulated stainless steel electrodes are attached. The sensor is threaded to fit the existing thermocouple port in the wall of a high-intensity mixer[1]. The sensor extends into the mixer a distance of 5 cm and is 12 cm below the mixer center, with the distal 3 cm of each electrode exposed.

The two electrical leads from the sensor are connected to a moisture analyzer[2] which acts as the interface to the computer. The electronics of the moisture analyzer have been modified to filter signal noise caused by the rotation of the mixer plowshares and to allow for initial baseline adjustments. The moisture analyzer with sensor operates on the principle of power loss from a tuned radio-frequency (R/F) circuit as the dielectric of the medium surrounding the sensor changes. The analog DC voltage output of the moisture analyzer is converted to a digital value by an A/D converter and is fed to a 16-bit microprocessor[3] which is used for data processing and system control. System software is stored in a nonvolatile form in an onboard, programmable, read-only memory and allows for operator control of data sampling rate and text information for hard-copy output. Each data point, taken at 4-s intervals, is the average of 5000 A/D conversions.

Granulations were prepared by charging the mixer with 20 kg of lactose powder and using only the plowshare mixing action. Figure 1 shows the resulting voltage *versus* mixing time profile as incremental additions of water were made to the lactose[4]. The decreases in voltage are the result of rapid moisture distribution throughout the powder after each addition. The plateau reached between each addition is an equilibrium voltage value that is a function of the amount of water in the moist powder. The granules formed with this simple lactose water system, however, were not of good quality.

Figure 2 shows the voltage response when 2.5 kg of a 4% w/w methylcellulose 15 cps[5] aqueous solution was added to 20 kg of lactose at time zero. A similar voltage response

[1] Model FM-50, Littleford-Lödige, Florence, Ky.

[2] Moisture Register Model G8R, Moisture Register Co., Berwind Instruments Group, North Hollywood, Calif.

[3] iSBC 88/25, Intel Inc., Santa Clara, Calif.

[4] Lactose Hydrous USP, No. 80M, Sheffield Products, Memphis, Tenn.

[5] Methocel A 15 Premium, The Dow Chemical Co., Midland, Mich.

0022-3549/84/0300-0420$01.00/0

© 1984, American Pharmaceutical Association

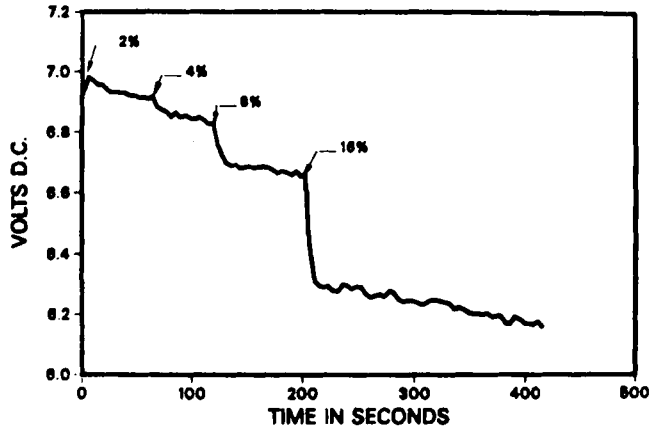

Figure 1—*Voltage response curve when water is added in incremental portions to 20 kg of lactose. Amount of water is shown as cumulative percent based on the weight of lactose.*

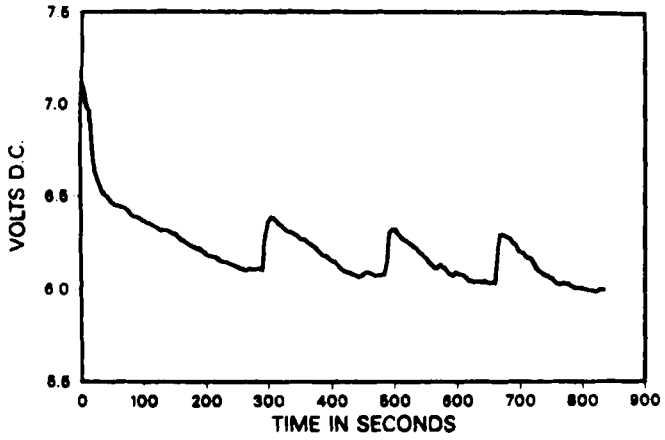

Figure 2—*Voltage response curve when 2.5 kg of an aqueous methylcellulose (4% w/w) granulating solution is added at time zero to 20 kg of lactose.*

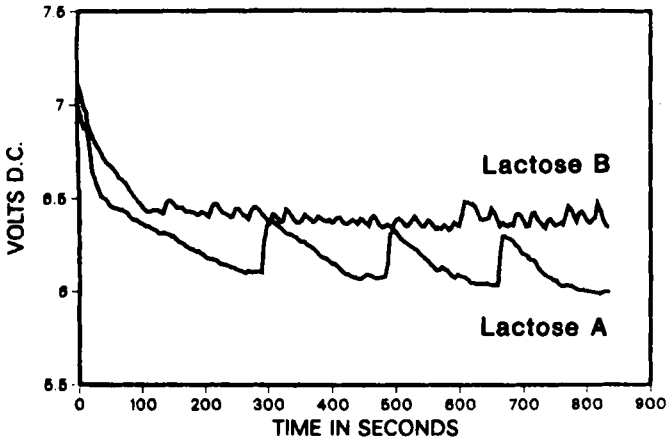

Figure 3—*Voltage response curves for smaller particle lactose A and larger particle lactose B when 20 kg of each is granulated with 2.5 kg of an aqueous methylcellulose (4% w/w) solution added at time zero.*

is seen; however, after the initial distribution phase, periodic voltage increases are observed. The difference in voltage response when a granulating agent is used in place of water indicates that the system, as designed, is sensing granule formation as well as moisture distribution. These voltage fluctuations have also been observed with other granulating agents when granules are formed. The height and periodicity of these voltage spikes seem to be associated with granule quality. The favored explanation for these observations is that the apparent density of the moist powder bed fluctuates in a periodic manner as agglomeration and deagglomeration occur during the mixing process. The changes in bed porosity around the sensor are reflected in a greater or lesser power-loss from the tuned R/F circuit.

Table I—Sieve Analysis Comparison of Lactose from Two Sources

	Lactose A[a]	Lactose B[b]
Weight % > 200 mesh	16.2	41.8
Weight % on 325 mesh	33.9	35.5
Weight % < 325 mesh	49.9	22.7

[a] Lactose hydrous USP, No. 80M, Sheffield Products, Memphis, Tenn. [b] Lactose hydrous USP, 310/Regular Grind, Foremost-McKesson, Inc., San Francisco, Calif.

Figure 3 illustrates the difference in sensor response when two lots of lactose having different particle sizes are granulated using the identical procedure described above for Fig. 2. The lower curve is the granulation response seen with fine particle lactose, while the upper curve is that observed with a more coarse lactose. A comparison of results from sieve analyses[6] conducted on the two lots of lactose is given in Table I. It is hypothesized that the finer lactose, because of its smaller particle diameter, forms more stable agglomerates that tend to deagglomerate less readily; therefore, the voltage spikes are fewer and more widely spaced. Conversely, the coarser lactose does not agglomerate as well and tends to deagglomerate rather quickly as indicated by the smaller and more closely spaced voltage spikes. Moreover, the granulation produced from the finer lactose was of better quality than that produced from the coarser lactose.

The dynamic granulation monitor using a computer-interfaced capacitive sensor shows promise both as a research tool to gain better understanding of the granulation phenomenon and as a control system to obtain better reproduction of granulations made in high-intensity mixers. In future communications, we will discuss the system and its applications in greater detail.

(1) B. M. Hunter and D. Ganderton, *J. Pharm. Pharmacol.*, **25**, 71P (1973).

(2) N.-O. Lindberg, L. Leander, L. Wenngren, H. Helgeson, and B. Reenstierna, *Acta Pharm. Suecica*, **11**, 603 (1974).

(3) D. N. Travers, A. G. Rogerson, and T. M. Jones, *J. Pharm. Pharmacol.*, **27**, 3P (1975).

(4) D. Kay and P. C. Record, *Mfg. Chemist*, 48(9), 45 (1978).

(5) H. P. Bier, H. Leuenberger, and H. Sucker, *Pharm. Ind.*, **41**, 375 (1979).

(6) H. Leuenberger, *Pharm. Acta Helv.*, **57**, 72 (1982).

(7) N.-O. Lindberg, L. Leander, and B. Reenstierna, *Drug Dev. Ind. Pharm.*, **8**(5), 775 (1982).

(8) N.-O. Lindberg and C. Jönsson, *Drug Dev. Ind. Pharm.*, **9**(6), 959 (1983).

William C. Fry
William C. Stagner
Kenneth C. Wichman [x]
Merrell Dow Pharmaceuticals Inc.
Indianapolis, IN 46268

Received November 7, 1983.
Accepted for publication January 13, 1984.

[6] ATM Sonic Sifter, Model L3, Allen-Bradley Co., Milwaukee, Wis.

Hepatic Tissue Binding and the Oral First-Pass Effect

Keyphrases □ Oral bioavailability—influence of hepatic tissue binding on first-pass effect □ Lidocaine—oral availability in healthy subjects and epileptic patients compared □ Hepatic tissue binding—effect on oral availability of lidocaine, healthy subjects and epileptic patients compared

To the Editor:

The development in recent years of physiological pharmacokinetic models has provided valuable quantitative insights into factors determining drug disposition. This is particularly so for the process of elimination by either a single (1–3) or a series of multiple organs (4, 5). A seminal contribution was that of Rowland and colleagues (1) who conceptualized the quantitative interrelationship between organ clearance and certain determinants:

$$CL = Q\left[\frac{k_m K_P V_E}{Q + k_m K_P V_E}\right] \qquad \text{(Eq. 1)}$$

where Q is the organ blood flow, k_m is the first-order rate constant for drug elimination, K_P is the apparent partition coefficient of total drug between the eliminating organ and the emergent venous blood, and V_E is the actual tissue volume of the eliminating organ. Subsequent refinement of what has become known as the "venous equilibration" or "well-stirred" model of elimination (3) led to the concept of intrinsic clearance of either total (CL_{int}^{tot}) or unbound (CL_{int}^{u}) drug, and the definition of organ clearance in these terms and the other physiological determinants. Namely, organ blood flow and the unbound fraction of drug in the blood (f_B):

$$CL = Q\left[\frac{CL_{int}^{tot}}{Q + CL_{int}^{tot}}\right] = Q\left[\frac{f_B CL_{int}^{u}}{Q + f_B CL_{int}^{u}}\right] \qquad \text{(Eq. 2)}$$

For a drug that is metabolized under linear conditions, free intrinsic clearance is equivalent to the ratio of the net maximal rate of metabolism from liver water, *i.e.*, nonproteinaceous fluid of the liver (V_{max}) to the Michaelis–Menten constant (K_m) for the involved enzyme(s) (6). It is readily apparent, therefore, that organ clearance, *i.e.*, irreversible drug removal, is independent of the extent of tissue binding in the organ, as reflected by the unbound fraction in the tissue. Nevertheless, some confusion over this matter appears to exist (7) presumably because of the apparent involvement of tissue uptake in Eq. 1. This misconception arises because of the failure to recognize the equivalence of the clearance terms $k_m K_P V_E$ (Eq. 1) and $f_B CL_{int}^{u}$ (Eq. 2), and the inverse relationship between the first-order rate constant (k_m) and effective volume of distribution ($K_P V_E$) when clearance is constant. Such equivalence is readily apparent if K_P is expressed according to its physiological determinants, *i.e.*, the ratio of the unbound fractions of drug present in the blood and the liver (f_B/f_L), and CL_{int}^{u} is equated in the conventional fashion to the product of the rate constant (k_m) and the volume of distribution of unbound drug (V_E/f_L).

The conclusion that tissue binding could affect drug clearance by an organ was based on an analysis (7) of data obtained following oral and intravenous administration of lidocaine to normal volunteers and patients who were receiving chronic anticonvulsant therapy with known enzyme-inducing agents (8). In essence, a simple three-compartmental physiological model was postulated to include rapidly and slowly equilibrating noneliminating tissue pools and the hepatoportal system. By assigning parameter values to tissue volumes, partition coefficients between serum and the tissue (referred to as retention factors in Ref. 7), tissue flow rates, and total intrinsic clearance, the study in the normal subjects was simulated with good agreement between the experimental data and the model. Parameter adjustment then permitted a reasonably good simulation of the different pharmacokinetic findings obtained in the epileptic patients, *i.e.*, a significantly reduced area under the serum concentration–time profile following oral but not intravenous administration with essentially no change in the elimination half-lives. It was indicated in the text and in the legend of Fig. 1 of Ref. 7 that the only difference between the two simulations was an increase in the effective liver volume ($V_H R_H$, equivalent to $V_E K_p$ of Eq. 1). However, examination of the parameters provided in Table I of Ref. 7 indicates that the successful simulation of the data from the epileptic patients required modification of *both* the effective liver volume *and* the total intrinsic clearance (referred to as CL_H in Ref.

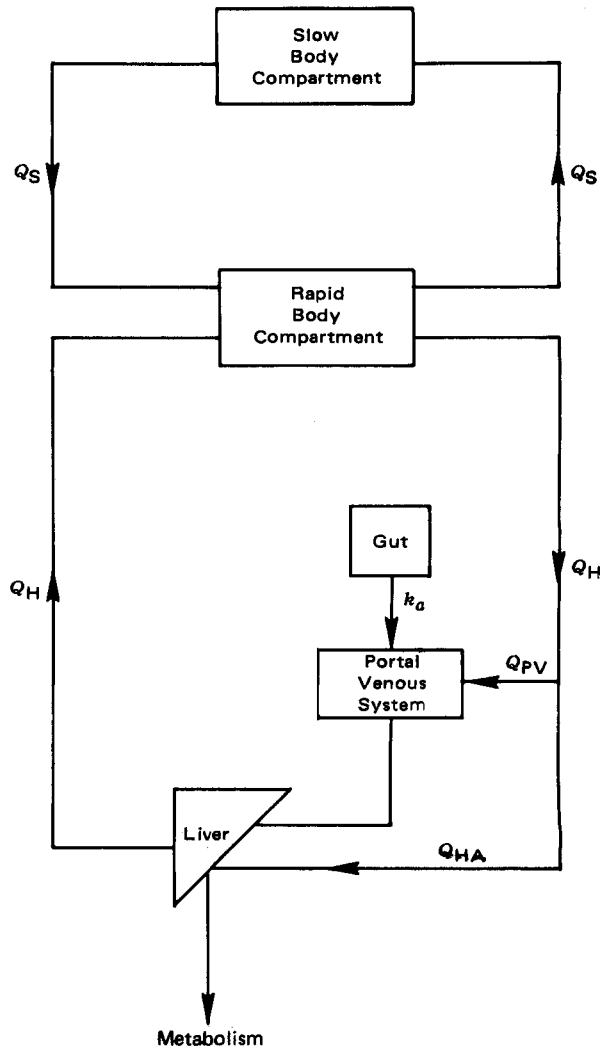

Figure 1—*Physiological model for evaluating the first-pass effect when the body has the characteristics of a two-compartmental system.*

0022-3549/84/0300-0422$01.00/0
© 1984, American Pharmaceutical Association

Table I—Model Parameters for Lidocaine

Volume, L	
V_B	5.0
V_L	1.5
V_{PV}	1.0
V_T^R	11.47
V_T^S	23.0
Flow rate, L/h	
Q_{HA}	18.0
Q_{PV}	72.0
Q_S	198.0
Unbound fraction	
f_B	0.40
f_L	0.65
f_T^R	0.176
f_T^S	0.176
Free intrinsic clearance, L/h	390
Absorption rate constant, h^{-1}	1.75

7). It is, therefore, impossible to conclude that the changes in the pharmacokinetics of lidocaine produced by enzyme-inducing agents was caused solely by an increase in the effective volume of the liver. An additional problem with the simulations is the parameter values chosen for the effective liver volumes: 50 and 150 L for the normal and epileptic subjects, respectively; the physiological basis and appropriateness of these values were not indicated.

To clarify the findings with lidocaine in normal and epileptic subjects, and to specifically examine the role of tissue binding in organ clearance and elimination, a number of simulations were performed based on the physiological model shown in Fig. 1 and described by the following mass balance equations.

Rapidly equilibrating compartment:

$$\frac{dA_T^R}{dt} = (Q_{PV} + Q_{HA})\left(C_L\frac{f_L}{f_B} - C_B\right) + Q_T^S\left(C_T\frac{f_T^S}{f_B} - C_B\right) \quad \text{(Eq. 3)}$$

Slowly equilibrating compartment:

$$\frac{dA_T^S}{dt} = Q_T^S\left(C_B - C_T\frac{f_T^S}{f_B}\right) \quad \text{(Eq. 4)}$$

Liver:

$$\frac{dA_L}{dt} = Q_{PV}C_{PV} + Q_{HA}C_B - (Q_{HA} + Q_{PV})C_L\frac{f_L}{f_B} - CL_{int}^u C_L f_L \quad \text{(Eq. 5)}$$

Metabolism:

$$\frac{dM}{dt} = -CL_{int}^u C_L f_L \quad \text{(Eq. 6)}$$

Portal vein:

$$\frac{dA_{PV}}{dt} = k_a G + Q_{PV}C_B - Q_{PV}C_{PV} \quad \text{(Eq. 7)}$$

Gut:

$$\frac{dG}{dt} = -kaD \quad \text{(Eq. 8)}$$

where C_B, C_T, C_L, and C_{PV} refer to the total drug concentrations in the arterial blood, slowly equilibrating tissue, liver, and portal vein, respectively; Q_T^S, Q_{PV}, and Q_{HA} are the blood flows to the slowly equilibrating tissue, portal vein, and hepatic artery; f_B, f_T^R, f_T^S, and f_L are the unbound fractions of drug in the blood, the rapidly equilibrating tissue, the slowly equilibrating tissue, and the liver; CL_{int}^u is the free intrinsic clearance; D is the oral dose; and k_a is the first-order rate constant for oral absorption.

Furthermore, the effective volumes of the various "organs" may be defined assuming equilibration of the emergent and tissue concentrations of unbound drug.

Rapidly equilibrating compartment:

$$V_R = V_B + V_T^R\frac{f_B}{f_T^R} \quad \text{(Eq. 9)}$$

Slowly equilibrating compartment:

$$V_S = V_T^S\frac{f_B}{f_T^S} \quad \text{(Eq. 10)}$$

Liver:

$$V_L = V_T^L\frac{f_B}{f_L} \quad \text{(Eq. 11)}$$

where V_B, V_T^R, V_T^S, and V_T^L correspond to the actual physiological volumes of the blood, the other rapidly equilibrating tissues, the slowly equilibrating tissues, and the liver, respectively.

The present model is essentially the same as that used by Colburn (7) except that the hepatoportal system is separated into its component organs and the apparent partition coefficient of the drug between the blood and tissue is identified by its physiological determinants, namely the ratio of the unbound fractions of drug in the blood and the tissue. Accordingly, Eq. 5 which describes the mass balance relationship in the liver is mathematically equivalent to Eq. 5 of Ref. 7.

Parameter values for the model (Table I) were selected on the basis of standard values of blood volume, hepatic blood flow, liver weight, and portal venous system volume for a 70-kg man. Other values were based on the known disposition characteristics of lidocaine, for example, the unbound fraction in the blood was taken to be 0.4 (9). The liver/emergent venous plasma partition coefficient of lidocaine at steady state has been experimentally determined to be 0.61 ± 0.16 in the rhesus monkey (10). Based on a blood–plasma concentration ratio in the monkey of 0.8 and an unbound fraction in the plasma of 0.4 (10), this partition ratio provided an estimate of the unbound fraction of lidocaine in the liver of 0.65. To investigate the effect of altering such binding and, therefore, changing the effective volume of the liver, values of f_L ranging from 0.002 to 1.0 were also used. The values of V_T^R and f_T^R and V_T^S and f_T^S were arbitrarily selected to provide the appropriate effective tissue volumes according to preliminary conventional compartmental analysis based on the first-pass model described by Gibaldi and Feldman (11). This analysis also provided an estimate of the blood flow to the slowly equilibrating compartment. The estimate of free intrinsic clearance was based on the mean value reported by Perucca and Richens (8) in the control subjects after taking into account the extent of binding in the blood. Finally, to compare the simulations based on blood concentrations with the experimental serum concentration, the theoretical data was corrected by the blood–serum concentration of lidocaine using a value of 0.88 (8).

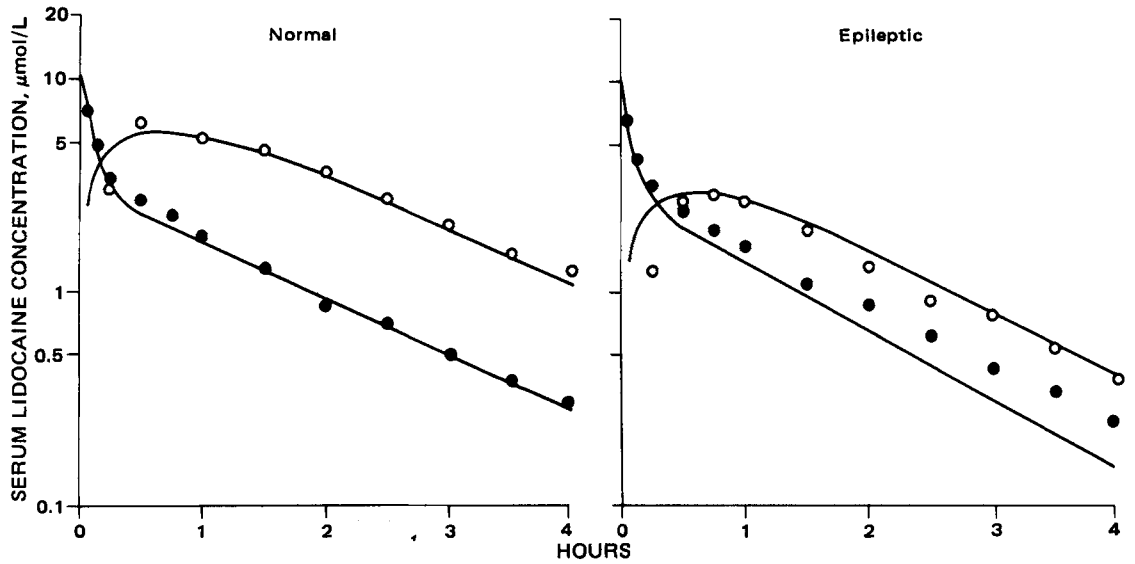

Figure 2—*Simulated and mean observed serum concentrations of lidocaine in normal subjects and epileptic patients following intravenous (●) and oral (○) doses of lidocaine. The solid lines represent the theoretical curves according to the model in Fig. 1 and parameter values in Table I; in the simulation of the epileptic patients only the free intrinsic clearance value was increased.*

Excellent agreement was obtained between the simulation using the parameter values in Table I and the experimental data from the normal subjects (Fig. 2). To test the hypothesis that the altered pharmacokinetics of lidocaine in the epileptic patients was solely due to an increase in hepatic drug-metabolizing ability, as suggested by Perucca and Richens (8), the value of free intrinsic clearance was increased from 390 to 930/h. Again, excellent agreement was obtained with the experimental observations (Fig. 2).

The effect of altering hepatic tissue binding on the oral disposition of lidocaine was examined by altering the unbound fraction over a 500-fold range (0.002–1.0) equivalent to changing the effective liver volume from 0.6 to 300 L. As shown in Fig. 3, this had essentially no effect on the serum concentration–time profile other than a small reduction in the peak serum level and a modest prolongation of the elimination half-life at very high levels of hepatic binding ($f_L < 0.01$). At such extreme values, about 20–70% of drug in the body during the terminal elimination phase would be present in the liver. Importantly, the changes in hepatic tissue binding had no effect on the total area under the oral serum concentration–time curve. Additional simulations indicated that these effects were independent of the value of the free intrinsic clearance, *i.e.*, they applied equally to low- and high-extraction drugs.

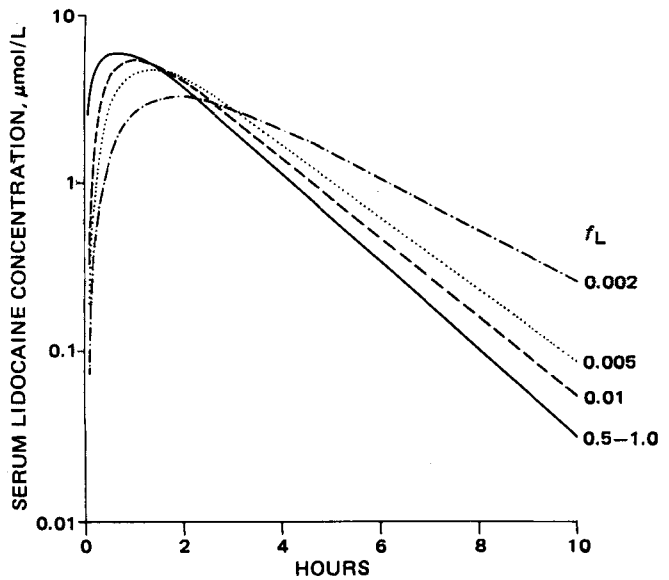

Figure 3—*The effects of the fraction of lidocaine not bound to liver tissue (f_L) on the serum concentrations of lidocaine following oral administration.*

The major experimental finding concerning the effect of chronic anticonvulsant therapy on the disposition of lidocaine was a reduction in the areas under the serum concentration–time curve to about 40% of that determined in subjects not receiving such medication. The elimination half-life and disposition profile following intravenous administration were, however, largely unaffected. It was concluded that these differences were consistent with enzyme induction leading to a two- to threefold increase in the hepatic drug metabolizing activity of a drug that is well extracted by the liver and, therefore, undergoes a large first-pass effect (8). The present analysis based on physiological modeling completely supports this conclusion using parameters consistent with the known disposition of lidocaine. Moreover, the simulations indicate that changes in hepatic tissue binding leading to alterations in the effective volume of the liver have no effect on oral clearance. This is not unexpected, since the total area under the curve following oral administration is equal to the ratio of the absorbed dose to the total intrinsic clearance (2). The major effects of increasing liver binding is to modestly reduce the peak serum concentration and prolong the elimination half-life, as would be predicted from the increased total volume of distribution of the drug.

Considerable insights have been obtained in recent years concerning the quantitative disposition of drugs and the factors controlling important processes such as elimination. In particular, the oral first-pass effect is well understood, especially under linear conditions. While hepatic

tissue binding contributes to the initial uptake and storage of drug in the liver, except in unusual situations, this is a reversible process, and such binding does not affect the irreversible removal of drug by the clearance processes. Accordingly, such a mechanism does not need to be invoked to explain the increased first-pass effect of drugs, including lidocaine, produced by the administration of enzyme-inducing agents.

(1) M. Rowland, L. Z. Benet, and G. G. Graham, *J. Pharmacokinet. Biopharm.*, **1**, 123 (1973).

(2) G. R. Wilkinson and D. G. Shand, *Clin. Pharmacol. Ther.*, **18**, 377 (1975).

(3) K. S. Pang and M. Rowland, *J. Pharmacokinet. Biopharm.*, **5**, 625 (1977).

(4) J. R. Gillette and K. S. Pang, *Clin. Pharmacol. Ther.*, **22**, 623 (1977).

(5) J. R. Gillette, *J. Pharm. Sci.*, **71**, 673 (1982).

(6) A. Rane, G. R. Wilkinson, and D. G. Shand, *J. Pharmacol. Exp. Ther.*, **200**, 420 (1977).

(7) W. A. Colburn, *J. Pharm. Sci.*, **70**, 969 (1981).

(8) E. Perucca and A. Richens, *Br. J. Clin. Pharmacol.*, **8**, 21 (1979).

(9) G. T. Tucker and L. E. Mather, *Br. J. Anaestheol.*, **47** (Suppl.), 213 (1975).

(10) N. Benowitz, R. P. Forsyth, K. L. Melmon, and M. Rowland, *Clin. Pharmacol. Ther.*, **16**, 87 (1974).

(11) M. Gibaldi and S. Feldman, *J. Pharm. Sci.*, **58**, 1477 (1969).

P. J. Wedlund
G. R. Wilkinson[x]
Department of Pharmacology
Vanderbilt University
Nashville, Tennessee 37232

Received January 4, 1983.
Accepted for publication June 16, 1983.
Supported in part by USPHS Grant GM 31304.

OPEN FORUM

Aspirin Prodrug Studies: Lack of Proper Literature Citation

I read with great interest the recent article by Hussain *et al.*, *J. Pharm. Sci.*, **72**, 1093 (1983), which contradicts the observations of Amidon *et al.*, *J. Pharm. Sci.*, **70**, 1299 (1981), concerning the question of aspirin phenylalanine ethyl ester as an aspirin prodrug.

Although the former article unequivocally demonstrates the inadequacies of the latter, it appears that both senior authors have been remiss in acknowledging the important contributions of other investigators in the development of aspirin prodrugs.

In particular, the aspirin triglyceride works of Paris *et al.*, *J. Med. Chem.*, **22**, 683 (1979) and *Agents and Actions*, **10**, 240 (1980) are never cited. More importantly, the only published article which describes the detection of aspirin in the plasma after *in vivo* administration of a prodrug of aspirin is conspicuously absent, Bodor *et al.*, *J. Pharm. Sci.*, **70**, 743 (1981).

The lack of proper literature citation by these authors is a poor reflection of the care taken by them in the preparation of their manuscripts, and is also a reflection on the quality of the reviewers who would allow such an obvious lack of citation to occur.

James J. Kaminski
Schering Corporation
Bloomfield, NJ 07003

Received December 22, 1983.

tissue binding contributes to the initial uptake and storage of drug in the liver, except in unusual situations, this is a reversible process, and such binding does not affect the irreversible removal of drug by the clearance processes. Accordingly, such a mechanism does not need to be invoked to explain the increased first-pass effect of drugs, including lidocaine, produced by the administration of enzyme-inducing agents.

(1) M. Rowland, L. Z. Benet, and G. G. Graham, *J. Pharmacokinet. Biopharm.*, **1**, 123 (1973).

(2) G. R. Wilkinson and D. G. Shand, *Clin. Pharmacol. Ther.*, **18**, 377 (1975).

(3) K. S. Pang and M. Rowland, *J. Pharmacokinet. Biopharm.*, **5**, 625 (1977).

(4) J. R. Gillette and K. S. Pang, *Clin. Pharmacol. Ther.*, **22**, 623 (1977).

(5) J. R. Gillette, *J. Pharm. Sci.*, **71**, 673 (1982).

(6) A. Rane, G. R. Wilkinson, and D. G. Shand, *J. Pharmacol. Exp. Ther.*, **200**, 420 (1977).

(7) W. A. Colburn, *J. Pharm. Sci.*, **70**, 969 (1981).

(8) E. Perucca and A. Richens, *Br. J. Clin. Pharmacol.*, **8**, 21 (1979).

(9) G. T. Tucker and L. E. Mather, *Br. J. Anaestheol.*, **47** (Suppl.), 213 (1975).

(10) N. Benowitz, R. P. Forsyth, K. L. Melmon, and M. Rowland, *Clin. Pharmacol. Ther.*, **16**, 87 (1974).

(11) M. Gibaldi and S. Feldman, *J. Pharm. Sci.*, **58**, 1477 (1969).

P. J. Wedlund
G. R. Wilkinson[x]
Department of Pharmacology
Vanderbilt University
Nashville, Tennessee 37232

Received January 4, 1983.
Accepted for publication June 16, 1983.
Supported in part by USPHS Grant GM 31304.

OPEN FORUM

Aspirin Prodrug Studies: Lack of Proper Literature Citation

I read with great interest the recent article by Hussain *et al.*, *J. Pharm. Sci.*, **72**, 1093 (1983), which contradicts the observations of Amidon *et al.*, *J. Pharm. Sci.*, **70**, 1299 (1981), concerning the question of aspirin phenylalanine ethyl ester as an aspirin prodrug.

Although the former article unequivocally demonstrates the inadequacies of the latter, it appears that both senior authors have been remiss in acknowledging the important contributions of other investigators in the development of aspirin prodrugs.

In particular, the aspirin triglyceride works of Paris *et al.*, *J. Med. Chem.*, **22**, 683 (1979) and *Agents and Actions*, **10**, 240 (1980) are never cited. More importantly, the only published article which describes the detection of aspirin in the plasma after *in vivo* administration of a prodrug of aspirin is conspicuously absent, Bodor *et al.*, *J. Pharm. Sci.*, **70**, 743 (1981).

The lack of proper literature citation by these authors is a poor reflection of the care taken by them in the preparation of their manuscripts, and is also a reflection on the quality of the reviewers who would allow such an obvious lack of citation to occur.

James J. Kaminski
Schering Corporation
Bloomfield, NJ 07003

Received December 22, 1983.

The Total Synthesis of Natural Products, Vol. 5. Edited by JOHN ApSIMON. John Wiley and Sons, One Wiley Drive, Somerset, NJ 08873. 1983. 550 pp. 15 × 23 cm. Price $60.00

Volume 5 of this series is devoted entirely to a review of sesquiterpene total synthesis from 1971 to 1979. Those familiar with the literature on synthesis will appreciate the enormity of this task. In Volume 2 a single chapter covered sesquiterpene synthesis through 1970; that an entire volume is now required attests to the explosion of research in this area during the past decade. The Heathcock group has assembled a lucid and readable account of modern sesquiterpene synthesis which can be heartily recommended to students and practicing chemists alike.

The authors have done a creditable job of organizing over 250 total syntheses. The volume is grouped into sesquiterpenes of increasing connective complexity (*i.e.*, acyclic, monocyclic, bicyclic) and includes a chapter on alkaloid sesquiterpenes. This organizational scheme facilitates the location of specific structural classes in addition to permitting the reader to digest the synthetic efforts toward a specific class of compounds in one sitting. A notable improvement over previous volumes is a closer correlation between the text and the reaction schemes, greatly improving the readability of the former. Each synthesis is accompanied by a detailed discussion, with special attention given to key steps. The syntheses of selected compounds are subjected to comparative analysis, including tabulated information on the number of steps, separations, and overall efficiency. The authors wisely refrain from the obvious temptation to use this interesting data to rate the individual syntheses. References to the isolation and activity of compounds are not included, but should be readily available through the papers on synthesis, making Volume 5 a useful reference to those involved in natural products chemistry. Practitioners of organic synthesis will find this volume of *The Total Synthesis of Natural Products* an enlightened and indispensable resource.

Reviewed by James Kallmerten
Department of Chemistry
Syracuse University
Syracuse, NY 13210

Deposition of Toxic Drugs and Chemicals in Man, 2nd Ed. By RANDALL C. BASELT. Biomedical Publications, P.O. Box 495, Davis, CA 95617. 1983. 795 pp. 15 × 23 cm. Price $49.50.

This compilation of important and useful information about common drugs and chemicals offers an excellent "one-stop" general reference for toxicologists, pharmacologists, and clinical chemists. This edition is organized in a format easier to read and contains considerably more information than the first edition.

Dr. Baselt devotes individual attention to 305 substances including drugs, pesticides, metals, and commonly used solvents to which humans are frequently exposed. He dedicates a section to each compound, showing the chemical structure and, when available, the volume of distribution, plasma protein binding, plasma half-life of drugs, and pK_a of compounds. Individual paragraphs describe concisely the drug as it relates to occurrence and usage, blood concentration, metabolism and excretion, toxicity, and analytical procedures. The references listed are plentiful in most cases, especially in each section on analytical methods.

In presenting data for the "metabolism and excretion" sections, the author made an effort to profile the metabolic process with both descriptive information and chemical structure. The reader should find this useful, considering the increased understanding of the role metabolites play in the human response to drugs. Each section on "toxicity" includes brief case histories and literature references of fatalities, relating the concentrations of the substance as found in blood and other body tissues.

With the overwhelming amount of information being generated on the fate of drugs and chemicals in the human body, it is almost a relief to see such data capsulized and presented in a useful source for the practicing scientist. This reference book certainly should have a spot reserved for it on the shelf of all analytical and clinical toxicologists who function in hospital laboratories.

Review by Gary L. Lensmeyer
University of Wisconsin Hospitals
Toxicology Laboratory
Madison, WI 53792

Recent Advances in Clinical Therapeutics, Vol. II: Psychopharmacology, Neuropharmacology, and Gastrointestinal Therapeutics. Edited by JACK Z. YETIV and JOSEPH R. BIANCHINE. Grune and Stratton, Inc., 111 Fifth Avenue, New York, NY 10003. 1983. 290 pp. 16.5 × 24 cm. Price $32.50.

As the Preface states, this volume "is an outgrowth of a symposium held annually at the Ohio State University College of Medicine under the cosponsorship of the Departments of Pharmacology, Medicine, and Family Practice. The majority of the topics in this book were presented at the Fourth Annual Symposium on Recent Advances in Clinical Therapeutics held in September 1981. Several additional chapters were commissioned to round out the general focus of this volume." While fearing another random collection of disjointed lectures from 21 contributors, this volume was a pleasant surprise.

For each section, chapters are devoted to updates in general therapeutic principles as well as new drugs. Thus, the 25 newly approved or promising investigational drugs in this book are discussed in the context of their value in the overall management of the particular disease state. The table of contents is very detailed, and the index is more than adequate to help find desired information. Most chapters are well referenced.

The psychopharmacology section contains five chapters, covering neuroleptics, antidepressants, lithium, and phencyclidine. An excellent chapter on psychopharmacological classification of depressive disorders consolidates and clearly explains controversial and confusing literature. The lithium chapter focuses on new and important information, including renal effects and drug interaction concerns. The only chapter suffering from the 2½ year lag-time from presentation to publication is the chapter on antidepressants. So much has happened in the last 2½ years with newer antidepressants that this chapter is significantly out of date.

The neuropharmacology section contains chapters updating antiepileptic drugs, newer muscle-relaxant drugs, aging and neuropsychopharmacology, and the benzodiazepines. Each chapter is current and relevant. The aging and neuropsychopharmacology chapter is a concise summary of clinically useful information.

The gastrointestinal therapeutics section contains five very specific chapters. The histamine H_2-receptor antagonists chapter provides a useful discussion of cimetidine and ranitidine as well as their value for various indications. Other chapters include new therapeutics of reflux esophagitis, nonsteroidal anti-inflammatory drugs and the stomach, effects of GI and hepatic pathology on human drug responses, and chenodeoxycholic acid in the management of gallstones. The final miscellaneous section contains chapters on the treatment of sexually transmitted diseases, therapeutic use of marijuana derivatives, and management of bronchial asthma in the ambulatory patient.

For the pharmaceutical scientist interested in a concise update in clinical therapeutics, this volume will be helpful. It also provides some insight into the relative value of newly introduced drugs, as well as the remaining need for even better medicines.

Reviewed by Glen L. Stimmel
School of Pharmacy
University of Southern California
Los Angeles, CA 90033

The Total Synthesis of Natural Products, Vol. 5. Edited by JOHN ApSIMON. John Wiley and Sons, One Wiley Drive, Somerset, NJ 08873. 1983. 550 pp. 15 × 23 cm. Price $60.00

Volume 5 of this series is devoted entirely to a review of sesquiterpene total synthesis from 1971 to 1979. Those familiar with the literature on synthesis will appreciate the enormity of this task. In Volume 2 a single chapter covered sesquiterpene synthesis through 1970; that an entire volume is now required attests to the explosion of research in this area during the past decade. The Heathcock group has assembled a lucid and readable account of modern sesquiterpene synthesis which can be heartily recommended to students and practicing chemists alike.

The authors have done a creditable job of organizing over 250 total syntheses. The volume is grouped into sesquiterpenes of increasing connective complexity (*i.e.*, acyclic, monocyclic, bicyclic) and includes a chapter on alkaloid sesquiterpenes. This organizational scheme facilitates the location of specific structural classes in addition to permitting the reader to digest the synthetic efforts toward a specific class of compounds in one sitting. A notable improvement over previous volumes is a closer correlation between the text and the reaction schemes, greatly improving the readability of the former. Each synthesis is accompanied by a detailed discussion, with special attention given to key steps. The syntheses of selected compounds are subjected to comparative analysis, including tabulated information on the number of steps, separations, and overall efficiency. The authors wisely refrain from the obvious temptation to use this interesting data to rate the individual syntheses. References to the isolation and activity of compounds are not included, but should be readily available through the papers on synthesis, making Volume 5 a useful reference to those involved in natural products chemistry. Practitioners of organic synthesis will find this volume of *The Total Synthesis of Natural Products* an enlightened and indispensable resource.

Reviewed by James Kallmerten
Department of Chemistry
Syracuse University
Syracuse, NY 13210

Deposition of Toxic Drugs and Chemicals in Man, 2nd Ed. By RANDALL C. BASELT. Biomedical Publications, P.O. Box 495, Davis, CA 95617. 1983. 795 pp. 15 × 23 cm. Price $49.50.

This compilation of important and useful information about common drugs and chemicals offers an excellent "one-stop" general reference for toxicologists, pharmacologists, and clinical chemists. This edition is organized in a format easier to read and contains considerably more information than the first edition.

Dr. Baselt devotes individual attention to 305 substances including drugs, pesticides, metals, and commonly used solvents to which humans are frequently exposed. He dedicates a section to each compound, showing the chemical structure and, when available, the volume of distribution, plasma protein binding, plasma half-life of drugs, and pK_a of compounds. Individual paragraphs describe concisely the drug as it relates to occurrence and usage, blood concentration, metabolism and excretion, toxicity, and analytical procedures. The references listed are plentiful in most cases, especially in each section on analytical methods.

In presenting data for the "metabolism and excretion" sections, the author made an effort to profile the metabolic process with both descriptive information and chemical structure. The reader should find this useful, considering the increased understanding of the role metabolites play in the human response to drugs. Each section on "toxicity" includes brief case histories and literature references of fatalities, relating the concentrations of the substance as found in blood and other body tissues.

With the overwhelming amount of information being generated on the fate of drugs and chemicals in the human body, it is almost a relief to see such data capsulized and presented in a useful source for the practicing scientist. This reference book certainly should have a spot reserved for it on the shelf of all analytical and clinical toxicologists who function in hospital laboratories.

Review by Gary L. Lensmeyer
University of Wisconsin Hospitals
Toxicology Laboratory
Madison, WI 53792

Recent Advances in Clinical Therapeutics, Vol. II: Psychopharmacology, Neuropharmacology, and Gastrointestinal Therapeutics. Edited by JACK Z. YETIV and JOSEPH R. BIANCHINE. Grune and Stratton, Inc., 111 Fifth Avenue, New York, NY 10003. 1983. 290 pp. 16.5 × 24 cm. Price $32.50.

As the Preface states, this volume "is an outgrowth of a symposium held annually at the Ohio State University College of Medicine under the cosponsorship of the Departments of Pharmacology, Medicine, and Family Practice. The majority of the topics in this book were presented at the Fourth Annual Symposium on Recent Advances in Clinical Therapeutics held in September 1981. Several additional chapters were commissioned to round out the general focus of this volume." While fearing another random collection of disjointed lectures from 21 contributors, this volume was a pleasant surprise.

For each section, chapters are devoted to updates in general therapeutic principles as well as new drugs. Thus, the 25 newly approved or promising investigational drugs in this book are discussed in the context of their value in the overall management of the particular disease state. The table of contents is very detailed, and the index is more than adequate to help find desired information. Most chapters are well referenced.

The psychopharmacology section contains five chapters, covering neuroleptics, antidepressants, lithium, and phencyclidine. An excellent chapter on psychopharmacological classification of depressive disorders consolidates and clearly explains controversial and confusing literature. The lithium chapter focuses on new and important information, including renal effects and drug interaction concerns. The only chapter suffering from the 2½ year lag-time from presentation to publication is the chapter on antidepressants. So much has happened in the last 2½ years with newer antidepressants that this chapter is significantly out of date.

The neuropharmacology section contains chapters updating antiepileptic drugs, newer muscle-relaxant drugs, aging and neuropsychopharmacology, and the benzodiazepines. Each chapter is current and relevant. The aging and neuropsychopharmacology chapter is a concise summary of clinically useful information.

The gastrointestinal therapeutics section contains five very specific chapters. The histamine H_2-receptor antagonists chapter provides a useful discussion of cimetidine and ranitidine as well as their value for various indications. Other chapters include new therapeutics of reflux esophagitis, nonsteroidal anti-inflammatory drugs and the stomach, effects of GI and hepatic pathology on human drug responses, and chenodeoxycholic acid in the management of gallstones. The final miscellaneous section contains chapters on the treatment of sexually transmitted diseases, therapeutic use of marijuana derivatives, and management of bronchial asthma in the ambulatory patient.

For the pharmaceutical scientist interested in a concise update in clinical therapeutics, this volume will be helpful. It also provides some insight into the relative value of newly introduced drugs, as well as the remaining need for even better medicines.

Reviewed by Glen L. Stimmel
School of Pharmacy
University of Southern California
Los Angeles, CA 90033

The Total Synthesis of Natural Products, Vol. 5. Edited by JOHN ApSIMON. John Wiley and Sons, One Wiley Drive, Somerset, NJ 08873. 1983. 550 pp. 15 × 23 cm. Price $60.00

Volume 5 of this series is devoted entirely to a review of sesquiterpene total synthesis from 1971 to 1979. Those familiar with the literature on synthesis will appreciate the enormity of this task. In Volume 2 a single chapter covered sesquiterpene synthesis through 1970; that an entire volume is now required attests to the explosion of research in this area during the past decade. The Heathcock group has assembled a lucid and readable account of modern sesquiterpene synthesis which can be heartily recommended to students and practicing chemists alike.

The authors have done a creditable job of organizing over 250 total syntheses. The volume is grouped into sesquiterpenes of increasing connective complexity (*i.e.*, acyclic, monocyclic, bicyclic) and includes a chapter on alkaloid sesquiterpenes. This organizational scheme facilitates the location of specific structural classes in addition to permitting the reader to digest the synthetic efforts toward a specific class of compounds in one sitting. A notable improvement over previous volumes is a closer correlation between the text and the reaction schemes, greatly improving the readability of the former. Each synthesis is accompanied by a detailed discussion, with special attention given to key steps. The syntheses of selected compounds are subjected to comparative analysis, including tabulated information on the number of steps, separations, and overall efficiency. The authors wisely refrain from the obvious temptation to use this interesting data to rate the individual syntheses. References to the isolation and activity of compounds are not included, but should be readily available through the papers on synthesis, making Volume 5 a useful reference to those involved in natural products chemistry. Practitioners of organic synthesis will find this volume of *The Total Synthesis of Natural Products* an enlightened and indispensable resource.

Reviewed by James Kallmerten
Department of Chemistry
Syracuse University
Syracuse, NY 13210

Deposition of Toxic Drugs and Chemicals in Man, 2nd Ed. By RANDALL C. BASELT. Biomedical Publications, P.O. Box 495, Davis, CA 95617. 1983. 795 pp. 15 × 23 cm. Price $49.50.

This compilation of important and useful information about common drugs and chemicals offers an excellent "one-stop" general reference for toxicologists, pharmacologists, and clinical chemists. This edition is organized in a format easier to read and contains considerably more information than the first edition.

Dr. Baselt devotes individual attention to 305 substances including drugs, pesticides, metals, and commonly used solvents to which humans are frequently exposed. He dedicates a section to each compound, showing the chemical structure and, when available, the volume of distribution, plasma protein binding, plasma half-life of drugs, and pK_a of compounds. Individual paragraphs describe concisely the drug as it relates to occurrence and usage, blood concentration, metabolism and excretion, toxicity, and analytical procedures. The references listed are plentiful in most cases, especially in each section on analytical methods.

In presenting data for the "metabolism and excretion" sections, the author made an effort to profile the metabolic process with both descriptive information and chemical structure. The reader should find this useful, considering the increased understanding of the role metabolites play in the human response to drugs. Each section on "toxicity" includes brief case histories and literature references of fatalities, relating the concentrations of the substance as found in blood and other body tissues.

With the overwhelming amount of information being generated on the fate of drugs and chemicals in the human body, it is almost a relief to see such data capsulized and presented in a useful source for the practicing scientist. This reference book certainly should have a spot reserved for it on the shelf of all analytical and clinical toxicologists who function in hospital laboratories.

Review by Gary L. Lensmeyer
University of Wisconsin Hospitals
Toxicology Laboratory
Madison, WI 53792

Recent Advances in Clinical Therapeutics, Vol. II: Psychopharmacology, Neuropharmacology, and Gastrointestinal Therapeutics. Edited by JACK Z. YETIV and JOSEPH R. BIANCHINE. Grune and Stratton, Inc., 111 Fifth Avenue, New York, NY 10003. 1983. 290 pp. 16.5 × 24 cm. Price $32.50.

As the Preface states, this volume "is an outgrowth of a symposium held annually at the Ohio State University College of Medicine under the cosponsorship of the Departments of Pharmacology, Medicine, and Family Practice. The majority of the topics in this book were presented at the Fourth Annual Symposium on Recent Advances in Clinical Therapeutics held in September 1981. Several additional chapters were commissioned to round out the general focus of this volume." While fearing another random collection of disjointed lectures from 21 contributors, this volume was a pleasant surprise.

For each section, chapters are devoted to updates in general therapeutic principles as well as new drugs. Thus, the 25 newly approved or promising investigational drugs in this book are discussed in the context of their value in the overall management of the particular disease state. The table of contents is very detailed, and the index is more than adequate to help find desired information. Most chapters are well referenced.

The psychopharmacology section contains five chapters, covering neuroleptics, antidepressants, lithium, and phencyclidine. An excellent chapter on psychopharmacological classification of depressive disorders consolidates and clearly explains controversial and confusing literature. The lithium chapter focuses on new and important information, including renal effects and drug interaction concerns. The only chapter suffering from the 2½ year lag-time from presentation to publication is the chapter on antidepressants. So much has happened in the last 2½ years with newer antidepressants that this chapter is significantly out of date.

The neuropharmacology section contains chapters updating antiepileptic drugs, newer muscle-relaxant drugs, aging and neuropsychopharmacology, and the benzodiazepines. Each chapter is current and relevant. The aging and neuropsychopharmacology chapter is a concise summary of clinically useful information.

The gastrointestinal therapeutics section contains five very specific chapters. The histamine H_2-receptor antagonists chapter provides a useful discussion of cimetidine and ranitidine as well as their value for various indications. Other chapters include new therapeutics of reflux esophagitis, nonsteroidal anti-inflammatory drugs and the stomach, effects of GI and hepatic pathology on human drug responses, and chenodeoxycholic acid in the management of gallstones. The final miscellaneous section contains chapters on the treatment of sexually transmitted diseases, therapeutic use of marijuana derivatives, and management of bronchial asthma in the ambulatory patient.

For the pharmaceutical scientist interested in a concise update in clinical therapeutics, this volume will be helpful. It also provides some insight into the relative value of newly introduced drugs, as well as the remaining need for even better medicines.

Reviewed by Glen L. Stimmel
School of Pharmacy
University of Southern California
Los Angeles, CA 90033

The Total Synthesis of Natural Products, Vol. 5. Edited by JOHN ApSIMON. John Wiley and Sons, One Wiley Drive, Somerset, NJ 08873. 1983. 550 pp. 15 × 23 cm. Price $60.00

Volume 5 of this series is devoted entirely to a review of sesquiterpene total synthesis from 1971 to 1979. Those familiar with the literature on synthesis will appreciate the enormity of this task. In Volume 2 a single chapter covered sesquiterpene synthesis through 1970; that an entire volume is now required attests to the explosion of research in this area during the past decade. The Heathcock group has assembled a lucid and readable account of modern sesquiterpene synthesis which can be heartily recommended to students and practicing chemists alike.

The authors have done a creditable job of organizing over 250 total syntheses. The volume is grouped into sesquiterpenes of increasing connective complexity (*i.e.*, acyclic, monocyclic, bicyclic) and includes a chapter on alkaloid sesquiterpenes. This organizational scheme facilitates the location of specific structural classes in addition to permitting the reader to digest the synthetic efforts toward a specific class of compounds in one sitting. A notable improvement over previous volumes is a closer correlation between the text and the reaction schemes, greatly improving the readability of the former. Each synthesis is accompanied by a detailed discussion, with special attention given to key steps. The syntheses of selected compounds are subjected to comparative analysis, including tabulated information on the number of steps, separations, and overall efficiency. The authors wisely refrain from the obvious temptation to use this interesting data to rate the individual syntheses. References to the isolation and activity of compounds are not included, but should be readily available through the papers on synthesis, making Volume 5 a useful reference to those involved in natural products chemistry. Practitioners of organic synthesis will find this volume of *The Total Synthesis of Natural Products* an enlightened and indispensable resource.

Reviewed by James Kallmerten
Department of Chemistry
Syracuse University
Syracuse, NY 13210

Deposition of Toxic Drugs and Chemicals in Man, 2nd Ed. By RANDALL C. BASELT. Biomedical Publications, P.O. Box 495, Davis, CA 95617. 1983. 795 pp. 15 × 23 cm. Price $49.50.

This compilation of important and useful information about common drugs and chemicals offers an excellent "one-stop" general reference for toxicologists, pharmacologists, and clinical chemists. This edition is organized in a format easier to read and contains considerably more information than the first edition.

Dr. Baselt devotes individual attention to 305 substances including drugs, pesticides, metals, and commonly used solvents to which humans are frequently exposed. He dedicates a section to each compound, showing the chemical structure and, when available, the volume of distribution, plasma protein binding, plasma half-life of drugs, and pK_a of compounds. Individual paragraphs describe concisely the drug as it relates to occurrence and usage, blood concentration, metabolism and excretion, toxicity, and analytical procedures. The references listed are plentiful in most cases, especially in each section on analytical methods.

In presenting data for the "metabolism and excretion" sections, the author made an effort to profile the metabolic process with both descriptive information and chemical structure. The reader should find this useful, considering the increased understanding of the role metabolites play in the human response to drugs. Each section on "toxicity" includes brief case histories and literature references of fatalities, relating the concentrations of the substance as found in blood and other body tissues.

With the overwhelming amount of information being generated on the fate of drugs and chemicals in the human body, it is almost a relief to see such data capsulized and presented in a useful source for the practicing scientist. This reference book certainly should have a spot reserved for it on the shelf of all analytical and clinical toxicologists who function in hospital laboratories.

Review by Gary L. Lensmeyer
University of Wisconsin Hospitals
Toxicology Laboratory
Madison, WI 53792

Recent Advances in Clinical Therapeutics, Vol. II: Psychopharmacology, Neuropharmacology, and Gastrointestinal Therapeutics. Edited by JACK Z. YETIV and JOSEPH R. BIANCHINE. Grune and Stratton, Inc., 111 Fifth Avenue, New York, NY 10003. 1983. 290 pp. 16.5 × 24 cm. Price $32.50.

As the Preface states, this volume "is an outgrowth of a symposium held annually at the Ohio State University College of Medicine under the cosponsorship of the Departments of Pharmacology, Medicine, and Family Practice. The majority of the topics in this book were presented at the Fourth Annual Symposium on Recent Advances in Clinical Therapeutics held in September 1981. Several additional chapters were commissioned to round out the general focus of this volume." While fearing another random collection of disjointed lectures from 21 contributors, this volume was a pleasant surprise.

For each section, chapters are devoted to updates in general therapeutic principles as well as new drugs. Thus, the 25 newly approved or promising investigational drugs in this book are discussed in the context of their value in the overall management of the particular disease state. The table of contents is very detailed, and the index is more than adequate to help find desired information. Most chapters are well referenced.

The psychopharmacology section contains five chapters, covering neuroleptics, antidepressants, lithium, and phencyclidine. An excellent chapter on psychopharmacological classification of depressive disorders consolidates and clearly explains controversial and confusing literature. The lithium chapter focuses on new and important information, including renal effects and drug interaction concerns. The only chapter suffering from the 2½ year lag-time from presentation to publication is the chapter on antidepressants. So much has happened in the last 2½ years with newer antidepressants that this chapter is significantly out of date.

The neuropharmacology section contains chapters updating antiepileptic drugs, newer muscle-relaxant drugs, aging and neuropsychopharmacology, and the benzodiazepines. Each chapter is current and relevant. The aging and neuropsychopharmacology chapter is a concise summary of clinically useful information.

The gastrointestinal therapeutics section contains five very specific chapters. The histamine H_2-receptor antagonists chapter provides a useful discussion of cimetidine and ranitidine as well as their value for various indications. Other chapters include new therapeutics of reflux esophagitis, nonsteroidal anti-inflammatory drugs and the stomach, effects of GI and hepatic pathology on human drug responses, and chenodeoxycholic acid in the management of gallstones. The final miscellaneous section contains chapters on the treatment of sexually transmitted diseases, therapeutic use of marijuana derivatives, and management of bronchial asthma in the ambulatory patient.

For the pharmaceutical scientist interested in a concise update in clinical therapeutics, this volume will be helpful. It also provides some insight into the relative value of newly introduced drugs, as well as the remaining need for even better medicines.

Reviewed by Glen L. Stimmel
School of Pharmacy
University of Southern California
Los Angeles, CA 90033

A publication of the
American Pharmaceutical Association—
the National Professional Society
of Pharmacists

JOURNAL OF PHARMACEUTICAL SCIENCES

Volume 73, 1984

JPMSAE 73(1-12) 1-1910 (1984)
ISSN 0022-3549

Sharon G. Boots
Editor

Sue A. Kruger
Production Editor

Margaret M. Madeleine
Assistant Production Editor

Karen A. Blakney
Copy Editor

Edward G. Feldmann
Contributing Editor

Samuel W. Goldstein
Contributing Editor

Patricia A. Evich
Editorial Secretary

Editorial Advisory Board

Jordan L. Cohen
Kenneth A. Connors
Louis Diamond
Ho-Leung Fung
Milo Gibaldi
Everett N. Hiestand
W. Homer Lawrence
Ian W. Mathison
Carl M. Metzler
Robert E. Notari
Paul L. Schiff, Jr.
Jane E. Shaw

Published monthly under the supervision of the Board of Trustees

Observations on the Selection of Our Professional Leaders

We are indebted to a fellow editor—who is also a current member of the APhA Academy of Pharmaceutical Science's Executive Committee—for the "idea germ" that triggered this month's editorial. We refer specifically to Professor Joseph R. Robinson of the School of Pharmacy, University of Wisconsin.

Among his many concurrent responsibilities, Dr. Robinson serves as Editor of the *Journal of Parenteral Science and Technology*, and he authors the editorial column that regularly appears in that bimonthly periodical.

His column—or more precisely, the "Editor's Page," as it is actually headed—in the January-February 1984 issue, is entitled "Leading Versus Managing." We recommend that the article be read in its entirety to get the benefit of Professor Robinson's full message. However, for our purposes here, we will briefly summarize his points as: (*a*) bringing out the important distinction between leadership and managership; (*b*) noting that a good manager is not necessarily a good leader, and in fact only rarely does a single individual possess both attributes; (*c*) observing that it is easier to be a good manager than it is to be a good leader; (*d*) pointing out that new executives often start out as good leaders but then gradually drift into an operating style wherein managing replaces leadership; and (*e*) concluding that the awareness of the value of, and the need for, leadership represents a vital first step in developing this very rare quality in one's self.

We would now like to take Professor Robinson's thoughts and observations a bit further.

Granted, virtually all of us profess to want leaders in our positions of authority, and we profess to want them to lead in a forceful and effective manner. But although we profess these desires, are they truly what we want or only what we have deluded ourselves into believing that we want?

These thoughts particularly come to mind as the American Pharmaceutical Association is currently in the throes of selecting a new President and chief executive officer. The criteria mentioned by all involved or in any way interested—from the APhA Board of Trustees, to the general membership, to the professional press—universally include "strong leadership" as a prime qualification for the person to be chosen for the office.

Certainly, the person who held the position for the past twenty-five years—the late William S. Apple—was unquestionably one of the strongest leaders that the entire health care community has ever produced. He was acknowledged by fan and critic alike as a dynamic, forceful personality who was able to achieve a level of success in his objectives far beyond normal expectations—and that this was primarily due to his strong leadership, his political astuteness, and his forceful personality.

Indeed, except perhaps for a few isolated criticisms in his later years, never did anyone fault either Dr. Apple or the organization he led, as being inactive, lethargic, unimaginative, or inflexible. When Dr. Apple took the reins at APhA, it had an image of being a conservative, outdated, and stodgy organization. He quickly reversed that perception, and by the early 1960s APhA was acknowledged as the frontrunner organization in pharmacy and among the forefront of all health care organizations.

But interestingly, criticism of Apple and APhA grew proportionately with their leadership influence. It appears that many members down deep really prefer the *status quo*. They want the appearance of activity, but they don't want change. The new APhA policy positions and initiatives were unpopular among many of the "rank and file" within the profession. Drug product selection, patient consultation, and clinical roles for the pharmacist were just some of the policies that APhA espoused first within organized pharmacy and which were vigorously resisted for a long time by much of the profession itself.

The role of APhA as an organizational "leader" for the profession—rather than simply a "protector" or "caretaker" for the profession—meant that, as an organization, it was out in front of the general membership and the profession as a whole. But the reaction of many pharmacists to APhA and Apple suggested that they didn't really want leadership. When they called for *a strong leader*, they really meant to say that they wanted *a dynamic manager*.

We see this same phenomenon repeated time-after-time in other areas. Journal subscribers and authors also profess to want a strong leader as the periodical's Editor. However, when changes are initiated, innovative approaches are established, or new policies are adopted, these developments are usually met with shocked disbelief if not outright resistance.

Scientific societies, including the APhA Academy of Pharmaceutical Sciences, almost universally will contend that they want an established, prominent scientist as their chief executive officer. Purportedly, this is so that the individual can serve with a high profile for the group in its dealings with other scientific organizations, with government agency officials, with the press, and with the general public.

But in contrast to industry and trade groups, experience shows that scientific societies and professional associations usually prefer to retain the leadership visability role for their chief elected officers or for some comparable elected officials.

Although the motivating reasons are natural and quite understandable, this sort of *modus operandi* is bound to impede the full exercise of the most effective leadership for the organization.

Consequently, we felt that Professor Robinson's observations have special relevance and application to the pharmaceutically related organizations, groups, and institutions with which we are involved or in which we participate.

If it is strong leadership that we truly want from those we select to staff and run those operations, then we must be prepared to accept the "fall-out" associated with new ideas, new directions, and new approaches. If we are not willing to do so, then let us be honest and admit candidly that what we really desire is simply good *managers*—and not good *leaders*.

—EDWARD G. FELDMANN
American Pharmaceutical Association
Washington, DC 20037

0022-3549/84/0400-0427$01.00/0
© 1984, American Pharmaceutical Association

JOURNAL OF PHARMACEUTICAL SCIENCES

APRIL 1984
VOLUME 73 NUMBER 4

RESEARCH ARTICLES

Comparative Study of Lipophilicity *versus* Topological Molecular Descriptors in Biological Correlations

S. C. BASAK, D. K. HARRISS, and V. R. MAGNUSON ˣ

Received September 7, 1982, from the *Department of Chemistry, University of Minnesota-Duluth, Duluth, MN 55812.* Accepted for publication February 15, 1983

Abstract □ This paper analyzes the relative efficacies of lipophilicity *vis-à-vis* topological indices in the correlation of the biological properties of four groups of bioactive molecules: alcohols, barbiturates, triazinones, and ketobemidones. Wiener number (W), information-theoretic topological parameters (IC, SIC, CIC, I_D^w, and $\bar{I}_D^w$), and molecular connectivity indices ($^1\chi$, $^1\chi^v$) were used as the molecular descriptors. Results show that theoretical indices are comparable or superior to log P in biological correlations.

Keyphrases □ Lipophilicity—correlations with topological molecular descriptors, assessment of the biological activity of diverse molecules □ Biological activity—comparison of lipophilicity with topological molecular descriptors, diverse molecules □ Topology—molecular descriptors, comparison with lipophilicity, assessment of the biological activity of diverse molecules

In contemporary biomedicinal chemistry, quantum chemical (1–4), physicochemical (5–7), and topological (8–21) parameters have been extensively utilized in the prediction of biological activity of molecules. While quantum chemical descriptors provide the most accurate numerical information regarding molecular architecture, the complexity of many bioactive molecules precludes the possibility of the extensive use of these methods in drug design (8). The problem reaches a staggering dimension when one considers the enormous number of candidate structures derivable from a pharmacological "lead" by means of probable molecular manipulations (22).

To resolve this impasse attempts have been directed at developing methods that contribute reasonably accurate and practical information at a level less comprehensive than the quantum chemical treatment (8). The extrathermodynamic linear free energy relationship (LFER) approach, derived from physical organic chemistry, and topological indices defined on the chemical graph of the molecule, appear to provide convenient model systems in relating chemical structure to biological functions.

The LFER approach, usually termed Hansch analysis, relies on the basic premise that complex physicochemical interactions between pharmacological and biological targets under *in vitro* and *in vivo* conditions can be quantitatively expressed in terms of multiparametric regression models involving steric, electronic, hydrophobic, and other substituent constants (6, 7). The outcome of a large number of quantitative structure–activity relationship (QSAR) studies of the Hansch type indicates the predominant role of hydrophobicity (log P or π) in determining the action of a large variety of nonspecific bioactive molecules. On the other hand, stereoelectronic variables seem to be crucial for the physiological action of molecules that act *via* specialized enzyme or receptor systems (23). However, a number of studies show that steric, electronic, and hydrophobic factors have an appreciable degree of interdependence on each other. For a group of aromatic molecules, Rogers and Cammarata (24) found log P to be positively correlated with ΣS_r, the sum of the electrophilic superdelocalizabilities for the aryl atoms, and negatively correlated with $\Sigma|Q_r|$, the sum of the π-electron charge densities. Fujita (25) discussed the inherent difficulty in the complete separation of the hydrophobic and steric effects of substituents arising out of the internal correlation between these two classes of substituent constants. Van der Waals' volume (V_w), a steric factor, is well correlated with log P for a wide variety of compounds (26). Also, the different topological steric descriptors have appreciable correlation with log P (8, 15, 17, 20). These studies indicate that some common structural features affect the steric, electronic, and hydrophobic factors in an unknown manner. Moreover, it has been pointed out that although the Hansch approach is a valid QSAR model for the closely related congeners, it cannot account for the common biological properties of molecules with considerable structural diversity (27).

These considerations necessitated the development of substructural (27–29) and topological methods (8) to determine a direct relationship between chemical structure and biological action. In particular, QSAR literature of recent years shows

0022-3549/84/0400-0429$01.00/0
© 1984, American Pharmaceutical Association

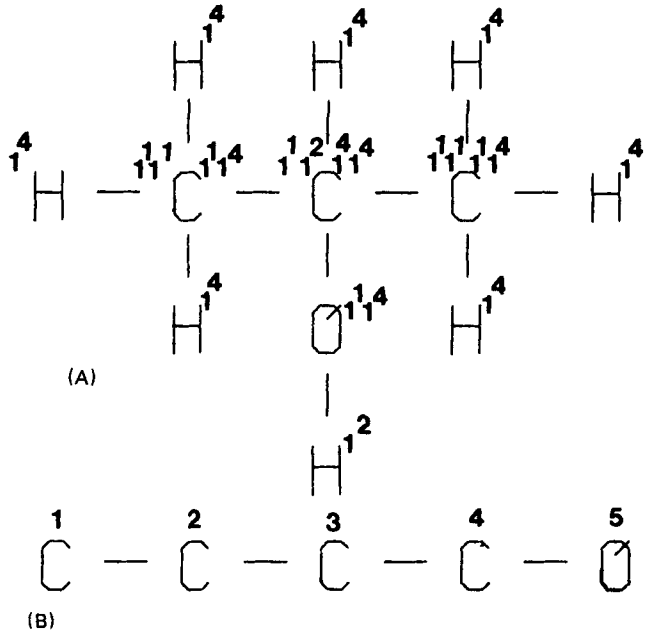

Figure 1—*(A) Coordinate-attached structure for 2-propanol. The coordinate notation $1^1 1^2 1^4 1^4$ for C-2 means that this carbon atom is singly bonded to four atoms whose valences are 1, 2, 4, and 4. (B) The labeled graph for 1-butanol.*

the progressive reliance on various topological indices as convenient structural parameters for correlational studies in chemistry (8, 30) and biology (8–21). Although a topological index is likely to be inherently steric in nature by virtue of being a numerical descriptor of molecular shape and size (8, 21), the most important progress in this area has been the development of topological structural parameters capable of expressing the electronic properties of molecules (31, 32).

One of the necessary preconditions of successful QSAR analysis is the availability of a set of parameters with minimum overlap profile (21, 33). Therefore, it seemed fitting to study the relative efficacies of lipophilicity *vis-à-vis* steric descriptors in rationalizing pharmacological and toxicological properties. With this purpose we have investigated the utility of log P (octanol-water), information-theoretic topological indices (IC, SIC, CIC, I_D^v, $\bar{I}_D^w$), Wiener number (W), and molecular connectivity indices ($^1\chi$, $^1\chi^v$) in the quantitative correlation of the toxicity of alcohols, the analgesic property of ketobemidones, Hill reaction inhibitory potencies of triazinones, and the anesthetic action of three different groups of barbiturates.

EXPERIMENTAL

Source of the Hydrophobic Parameter (log P, Octanol-Water)—Log P values for the various congeneric series were taken either from the literature or calculated according to the method of Hansch and Leo (34).

Table I—Partitioning and Calculation of Information Indices (IC, SIC, and CIC) for 2-Propanol [a]

Partition Class with Coordinate	Number of Atoms in the Partitioned Class[b] (n_i)	Probability ($p_i = n_i/n$)
I 1^4	7	7/12
II 1^2	1	1/12
III $1^1 1^4$	1	1/12
IV $1^1 1^1 1^1 1^4$	2	2/12
V $1^1 1^4 1^4 1^2$	1	1/12

[a] $IC = 7/12 \log_2(12/7) + 2/12 \log_2(12/2) + 3 \times 1/12 \log_2(12) = 1.7807$ bits; $SIC = IC/\log_2(12) = 0.4967$; $CIC = 1/12[7 \log_2(7) + 2 \log_2(2) + 1 \log_2(1)] = 1.8043$ bits. [b] Total number of atoms in the molecule (n) = 12.

Table II—Distance Matrix D(G) of the Hydrogen-Suppressed Graph G of 1-Butanol

Atom	1	2	3	4	5
1	0	1	2	3	4
2	1	0	1	2	3
3	2	1	0	1	2
4	3	2	1	0	1
5	4	3	2	1	0

Calculation of Molecular Connectivity ($^1\chi$)—To each atom of the hydrogen-suppressed molecular graph, a δ value is assigned corresponding to the number of nonhydrogen atoms bonded to it. A connectivity value for a bond C_k (connecting atoms i and j) is computed as follows (8):

$$C_k = (\delta_i \delta_j)^{-1/2} \qquad \text{(Eq. 1)}$$

And finally, $^1\chi$ is calculated as the sum of all the individual connectivity terms:

$$^1\chi = \sum_k C_k \qquad \text{(Eq. 2)}$$

Calculation of Valence Molecular Connectivity ($^1\chi^v$)—To each atom of the hydrogen-depleted molecular skeleton, a δ^v value is assigned according to the formulation:

$$\delta^v = Z_i^v - h_i \qquad \text{(Eq. 3)}$$

where Z_i^v represents the number of valence electrons and h_i denotes the number of bonded hydrogen atoms for the ith atom in the labeled graph. Thereafter, $^1\chi^v$ is calculated as in the case of $^1\chi$ by substituting δ^v for δ in Eq. 1.

Calculation of Information-Theoretic Indices from the Molecular Graph—The statistical treatment of chemical structure by means of information theory relies on the basic premise that each structure contains a finite set of elements (n) that could be decomposed into disjoint subsets n_i ($i = 1, 2, \ldots, k$) by means of selected equivalence relations defined on the set. A probability scheme may then be attached to this distribution:

$$\begin{pmatrix} n_1, n_2, \ldots, n_k \\ p_1, p_2, \ldots, p_k \end{pmatrix}$$

where $p_i = n_i/n$ is the probability that a randomly selected element will lie in the ith subset. The entropy (or complexity) of the probability distribution of the elements of the set (or structure) can then be computed by means of Shannon's formula (35):

$$\text{Information Content} = -\sum_i p_i \cdot \log_2 p_i \text{ bits} \qquad \text{(Eq. 4)}$$

where the logarithm is taken at a basis 2 in order to measure the information in bits. Following the pioneering studies of Rashevsky (36) and Trucco (37, 38) on the topological information content of chemical graphs, various authors have defined information-theoretic indices and applied them to structure-property (15, 30, 39, 40) and structure-activity (15–20, 40) correlations.

In the formalism developed by Sarker *et al.* (41), Basak *et al.* (19, 42), and Raychaudhury *et al.* (43) the total (nonhydrogen-suppressed) molecular graph is used to define the various topological indices, and the method is sufficiently general to include linear graphs as well as multigraphs. On the basis of a first-order topological neighborhood, Sarker *et al.* (41) defined an equivalence relation which decomposes the vertex set $\mathbf{X}(G)$ of the molecular graph G into disjoint subsets, whereby the information content (IC) of the graph is computed as:

$$IC(\mathbf{X}(G)) = -\sum_i p_i \cdot \log_2 p_i \text{ bits}$$

Subsequently, Basak *et al.* (42) defined another information-theoretic index, structural information content (SIC):

$$SIC(\mathbf{X}(G)) = IC/\log_2 n \qquad \text{(Eq. 5)}$$

where n is the cardinality of $\mathbf{X}(G)$. In continuation of this work Raychaudhury *et al.* (43) developed another information-theoretic topological index, *viz* complementary information content (CIC):

$$CIC(\mathbf{X}(G)) = \frac{1}{n}\sum_{i=1}^{k} n_i \cdot \log_2 n_i \text{ bits} \qquad \text{(Eq. 6)}$$

The equivalence relation is a relation (defined on a set) that has the property of being reflexive, symmetric, and transitive. Such a relation partitions a set into nonempty and disjoint subsets. The probability scheme attached to such

Table III—Hydrophobicity, Toxicity (log LC_{50}), and Molecular Descriptors for Aliphatic Alcohols

Compound	log LC_{50}	log P	IC	SIC	CIC	$^1\chi$	$^1\chi^v$	W	I_D^w	$\bar{I}_D^w$
Methanol	−0.06	−0.77	1.7925	0.6934	0.7925	1.0000	0.4472	1	0.00	0.00
Ethanol	−0.51	−0.32	1.8800	0.5931	1.2900	1.4142	1.0233	4	6.00	1.50
2-Propanol	−0.80	0.14	1.7807	0.4967	1.8043	1.7320	1.4129	9	22.53	2.50
1-Butanol	−1.63	0.88	1.8716	0.4790	2.0353	2.4142	2.0233	20	62.93	3.15
1-Hexanol	−3.02	2.03	1.7206	0.3917	2.6717	3.4142	3.0233	56	233.46	4.17
1-Octanol	−4.00	3.15	1.6069	0.3379	3.1480	4.4142	4.0233	120	590.03	4.92
1-Nonanol	−4.40	3.65	1.5615	0.3182	3.3454	4.9142	4.5233	165	862.59	5.23
1-Decanol	−4.84	4.15	1.5220	0.3017	3.5224	5.4142	5.0233	220	1211.77	5.51
1-Undecanol	−5.22	4.65	1.4874	0.2877	3.6825	5.9142	5.5233	286	1648.26	5.76
1-Dodecanol	−5.27	5.15	1.4568	0.2756	3.8286	6.4142	6.0233	364	2183.03	6.00

Table IIIa—Correlation of the log LC_{50} with log P and Topological Indices (log $LC_{50} = a + bx + cx^2$)[a]

x	a	b	c	r	s	F
IC	−23.0	12.0	—	0.94	0.75	58.8
	−40.6	33.2	−6.34	0.94	0.80	26.4
SIC	−8.75	13.8	—	0.96	0.58	104
	−15.0	43.2	−31.3	0.99	0.21	422
CIC	1.98	−1.90	—	0.99	0.32	355
	0.730	−0.601	−0.272	0.99	0.23	353
$^1\chi$	0.839	−1.03	—	0.99	0.26	551
	1.64	−1.63	0.0822	0.99	0.13	1090
$^1\chi^v$	0.398	−1.02	—	0.99	0.26	544
	0.839	−1.44	0.0650	0.99	0.19	512
W	−1.19	−1.43E-2	—	0.91	0.91	37.7
	−0.585	−3.40E-2	5.97E-5	0.98	0.43	98.7
I_D^w	−1.39	−2.32E-3	—	0.88	1.03	27.5
	−0.822	−5.78E-3	1.77E-5	0.97	0.57	54.3
$\bar{I}_D^w$	0.842	−0.986	—	0.97	0.53	128
	.00776	−0.105	−0.138	0.99	0.20	456
log P	−0.842	−0.939	—	0.99	0.21	875
	−0.826	−1.14	4.75E-2	0.99	0.14	911

[a] In all cases the number of data points = 10.

decompositions of a set is, therefore, very much dependent on the nature of the equivalence relation. So, the information indices (IC, SIC, and CIC) of a chemical graph are not unique; rather the values of such indices are dependent on the mode of partition of the vertex set $\mathbf{X}(G)$ of the corresponding molecular graph G. In this paper we have computed IC, SIC, and CIC indices from the corresponding chemical graphs using an equivalence relation which is a slightly modified form of that used by Sarkar *et al.* (41). According to the equivalence relation used in this paper, two vertices of a chemical graph are said to be equivalent if they have similar edge multiplicity and the same number of first-order neighbors that have identical degrees (valence). If x represents an arbitrary element of the vertex set $\mathbf{X}(G)$ of a molecular graph G and r is a real number satisfying the relation $1 < r \leq 2$, then the open sphere $S(x,r)$ is given by:

$$S(x,r) = (x) \cup S_x^1 \qquad \text{(Eq. 7)}$$

where $S_x^1 = \{y \epsilon \mathbf{X}(G), d(x,y) = 1\}$ and (x) is the one-point set consisting of x only. If N be a set consisting of all such open spheres $S(x,r)$, where x runs over the whole set $\mathbf{X}(G)$, then N represents a collection of the first-order neighborhoods of all the vertices belonging to $\mathbf{X}(G)$.

Two vertices x and y of the vertex set $\mathbf{X}(G)$ will be called equivalent with respect to the first-order topological neighborhood if and only if:

1. $\mathbf{O}(S_x^1) = \mathbf{O}(S_y^1)$, where $\mathbf{O}(S_x^1)$ and $\mathbf{O}(S_y^1)$ represent the cardinalities of S_x^1 and S_y^1, respectively.
2. Corresponding to each element $x^i \epsilon S_x^1$ there exists an element $y^i \epsilon S_y^1$ such that $E[x,x^i] = E[y,y^i]$, where $E[x,x^i]$ denotes the number of edges connecting x and x^i, while $E[y,y^i]$ represents the number of edges of G connecting y and y^i; and
3. x^i and y^i have the same degrees (valence) for all i.

This theoretical scheme for the realization of the partition of atoms is exemplified along with the coordinate-attached structure of 2-propanol (Fig. 1A) and the calculation of its IC, SIC, and CIC indices (Table I) from the consideration of first-order topological neighborhood.

The Wiener number (W), proposed by Wiener (44), was the first topological index and represents the sum of all possible topological distances of a hydrogen-suppressed molecular graph. W can be conveniently calculated from the distance matrix $\mathbf{D}(G)$ of any graph G. It is a square $N \times N$ matrix, where N is the number of vertices in the hydrogen-depleted graph, the entries of the matrix being $d_{ij} = d_{ji}$, d_{ij} representing the number of bonds between vertices i and j by the shortest path. Table II shows the distance matrix of the labeled graph of 1-butanol (Fig. 1B). From the distance matrix, W is computed as:

$$W = \sum_{ij} d_{ij}/2 \qquad \text{(Eq. 8)}$$

The information indices from the distance matrix arise out of the statistical treatment of the topological distances of the chemical graph through the formalism of information theory (39). The index (I_D^w) is defined as:

$$I_D^w = W \cdot \log_2 W - \sum(k_d)(d \cdot \log_2 d) \qquad \text{(Eq. 9)}$$

where the distance d appears k_d times in the partition. The mean information index ($\bar{I}_D^w$) is calculated as:

$$\bar{I}_D^w = I_D^w / W \qquad \text{(Eq. 10)}$$

Statistical Analysis—Regression analysis was carried out according to the method of Nie *et al.* (45).

RESULTS AND DISCUSSION

Toxicity of Alcohols—The characteristic toxic action of aliphatic alcohols probably is narcosis (46). Veith *et al.* (47) reported that the aquatic toxicity (96 h LC_{50}) of alkanols in *Pimephales promelas* is highly correlated with log P (octanol-water) in terms of a bilinear model (48). However, Basak and Magnuson (19) showed that CIC can account for the toxicity of alcohols in a significant manner. It was of interest, therefore, to carry out a comparative study of log P *vis-à-vis* various structural parameters in the correlation of the LC_{50} of alcohols.

Table III shows the log LC_{50}, log P, IC, SIC, CIC, $^1\chi$, $^1\chi^v$, W, I_D^w, and $\bar{I}_D^w$ values for a series of 10 alkanols; the experimental log LC_{50} values were taken from Veith *et al.* (47). Table IIIa summarizes the results of the statistical analysis in an attempt to correlate log LC_{50} with log P and the different topological indices; r is the correlation coefficient, s the standard deviation, and F the F-ratio between the variances of observed and calculated values.

It appears from the results that a nonlinear fit shows significant improvement in the correlation coefficients as compared with the linear fits. The extent of fit of log LC_{50} values with log P and other structural parameters indicate that the topological indices (SIC, CIC, $^1\chi$, $^1\chi^v$, $\bar{I}_D^w$) are capable of explaining the properties of alcohols almost as efficiently as log P.

Analgesic Property of Ketobemidones—The opiate group of drugs is thought to bring about analgesia through the perturbation of certain types of specific receptors (49). The importance of lipophilicity for analgesic action is evident from the sharp decrease in the agonistic potency concomitant with quaterni-

Table IV—Hydrophobicity, Analgesic Potency (A-ED_{50}), and Molecular Descriptors for Ketobemidones (I)

R	A-ED_{50}, mM	log P	IC	SIC	CIC	$^1\chi$	$^1\chi^v$	W	I_D^w	$\bar{I}_D^w$
Methyl[a]	2.10	1.22	2.2949	0.4179	3.1970	8.5814	7.4814	558	3950.76	7.08
Ethyl	67.20	1.76	2.2305	0.3994	3.3544	9.1194	8.0575	662	4785.09	7.23
Propyl	16.00	2.30	2.1830	0.3848	3.4894	9.6194	8.5575	785	5781.87	7.36
Butyl	4.60	2.84	2.1385	0.3716	3.6164	10.1194	9.0575	928	6954.56	7.49
Pentyl	0.78	3.38	2.0970	0.3595	3.7359	10.6194	9.5575	1092	8316.82	7.62
Hexyl	7.50	3.92	2.0581	0.3484	3.8488	11.1194	10.0575	1278	9882.44	7.73
Heptyl	9.00	4.46	2.0218	0.3382	3.9555	11.6194	10.5575	1487	11665.27	7.84
Octyl	26.50	5.00	1.9878	0.3289	4.0566	12.1194	11.0575	1720	13679.22	7.95
Nonyl[a]	Inactive	5.54	1.9558	0.3202	4.1527	12.6194	11.5575	1978	10217.71	5.16

[a] Not included in the regression analysis.

Table IVa—Correlation of A-ED_{50} with log P and Topological Indices (A-$ED_{50} = a + bx + cx^2$)[a]

x	a	b	c	r	s	F
IC	$-2.54E+2$	$1.30E+2$	—	0.50	22	1.6
	$1.36E+4$	$-1.30E-4$	$3.11E+3$	0.97	7.2	29
SIC	$-1.48E+2$	$4.63E+2$	—	0.51	22	1.8
	$4.70E+3$	$-2.63E+4$	$3.67E+4$	0.97	6.5	36
CIC	$1.84E+2$	−44.5	—	0.49	22	1.6
	$5.28E+3$	$-2.80E+3$	$3.72E+2$	0.96	7.4	27
$^1\chi$	$1.20E+2$	−9.51	—	0.44	22	1.2
	$2.40E+3$	$-4.44E+2$	20.4	0.94	9.1	17
$^1\chi^v$	$1.10E+2$	−9.51	—	0.45	22	1.2
	$1.96E+3$	$-4.00E+2$	20.4	0.94	9.1	17
W	43.1	$-2.14E-2$	—	0.36	24	0.73
	$2.47E+2$	−0.400	$1.60E-4$	0.88	13	7.1
I_D^w	40.4	$-2.48E-3$	—	0.35	24	0.68
	$2.09E+2$	$-4.38E-2$	$2.25E-6$	0.88	14	6.6
$\bar{I}_D^w$	$3.42E+2$	−42.5	—	0.48	22	1.5
	$2.05E+4$	$5.35E+3$	$3.50E+2$	0.96	7.6	25
log P	48.6	−8.81	—	0.45	22	1.2
	$2.28E+2$	$-1.27E+2$	17.5	0.94	9.1	17

[a] In all cases, the number of data points = 7.

zation (50). It is proposed that hydrophobicity is critically important for the passage of opiates through the blood–brain barrier (51). In view of the fact that the mode of action for opiates is complicated by participation of various biogenic amine systems, different neuronal subpopulations, and multiple receptor types (52, 53), substituted ketobemidones (I) provide a convenient class of compounds for the study of the structure–activity relationships of opiates because the molecular manipulations within the group involve minimal alterations in the molecular electronic characteristics.

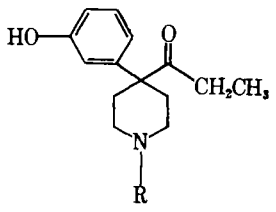

I

In an earlier study, Ray *et al.* (17) reported that SIC could correlate the analgesic potency (A-ED_{50}) of ketobemidones in mice. In view of the reportedly important role of lipophilicity in opiate pharmacology, we decided to study the relative efficacies of log P *vis-à-vis* other structural parameters in the correlation of the analgesic action of ketobemidones.

Table IV depicts the hot-plate analgesic potencies (A-ED_{50}) in mice, log P values, and the topological descriptors for a series of nine ketobemidones; the experimental A-ED_{50} values were taken from Wilson *et al.* (54). A look at the A-ED_{50} values indicates that there are two peaks of agonist activity in the series, namely when the side chain in the nitrogen atom is either methyl or amyl. Some of the higher homologues (hexyl, heptyl, and octyl) have measurable antagonist potencies (50), while the nonyl derivative has no analgesic property in the *in vivo* test. Under these circumstances we decided to delete the methyl and nonyl homologues of Table IV from the regression analysis. Table IVa represents the outcome of nonlinear regression analysis using log P as well as the topological indices. The linear correlations were not appreciable with any of the parameters. It is evident from the statistical analysis that the topological parameters IC, SIC, CIC, and $\bar{I}_D^w$ are superior to log P in the correlation of analgesic action while $^1\chi$ and $^1\chi^v$ appear to be as correlated as log P.

Herbicidal Action of Triazinones—Most herbicides are thought to exert their characteristic action through the blocking of the electron-transfer step in the oxygen-evolving photosynthesis process (55, 56). Therefore, in an attempt to design more effective herbicides, various authors have studied the effects of molecular manipulations on the Hill reaction inhibitory potencies of these compounds in isolated chloroplasts (55–59).

For a group of 1,2,4-triazinones, Hansch analysis revealed that lipophilicity (log P) alone was able to correlate the Hill reaction inhibitory potency (pI_{50}) in a significant manner (59). On the other hand, Ray *et al.* (17) reported that the information-theoretical topological index SIC could adequately account for the pI_{50} of triazinones. So it was deemed desirable to undertake a comparative study of log P and other theoretical parameters in the QSAR study of this class of herbicides.

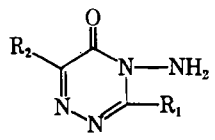

II

The pI_{50}, log P, $^1\chi$, $^1\chi^v$, IC, SIC, CIC, W, I_D^w, and $\bar{I}_D^w$ values for a series of 11 triazinone derivatives (II) are presented in Table V; the log P and experimental pI_{50} values were taken from Draber *et al.* (59). Table Va reveals the outcome of statistical analysis in an attempt to correlate pI_{50} with log P and other descriptors. It is clear that all the parameters correlate significantly with experimental pI_{50} values. In all cases the parabolic relationship results in significant improvement in the fit with respect to the linear one. It is noteworthy that the theoretically derived indices IC, SIC, CIC, $^1\chi$, and $\bar{I}_D^w$ are almost as effective as log P in the correlation of pI_{50} values of the herbicides.

Narcotic Property of Barbiturates—Barbiturates are widely used in the treatment of several convulsive disorders (60). Although the precise mechanism of action of barbiturates is still not clear, attenuation of excitatory synaptic transmission (61, 62), potentiation of inhibitory synaptic transmission (61, 63), and blockage of electrically excitable membranes (64) are tentatively considered to be the causative factors behind the biological action of these compounds. Some recent studies, however, demonstrated the interaction of barbiturates with benzodiazepine receptors (65).

The high correlations of the physiological action of barbiturates with log P are the crucial factors for the assignment of a nonspecific mode of action to

Table V—Hydrophobicity, Hill Reaction Inhibitory Potency (pI_{50}), and Molecular Descriptors for Triazinones (II)

R_1	R_2	pI_{50}	IC	SIC	CIC	$^1\chi$	$^1\chi^v$	W	I_D^w	$\bar{I}_D^w$	log P
SCH_3	Methyl	3.88	3.2211	0.7583	1.0268	5.1639	4.1393	146	821.30	5.62	−0.16
$NHCH_3$	Isopropyl	5.79	3.0860	0.6565	1.6144	6.0746	4.0001	236	1442.11	6.11	0.30
SCH_3		5.38	3.1144	0.6347	1.7925	7.7364	6.3606	428	2868.80	6.70	0.38
SCH_3	Ethyl	5.27	3.1867	0.7146	1.2727	5.7019	7.4000	190	1115.97	5.87	0.46
SCH_3	Propyl	5.70	3.0751	0.6622	1.5688	6.2019	5.2000	246	1499.30	6.09	0.93
SCH_3	Isopropyl	6.24	3.0751	0.6622	1.5688	6.0746	5.0827	236	1442.11	6.11	1.01
SCH_3	Isobutyl	6.15	3.0567	0.6358	1.7507	5.5558	4.3356	304	1918.55	6.31	1.39
SCH_3	*tert*-Butyl	6.63	2.9583	0.6154	1.8491	6.3752	5.3893	284	1798.44	6.33	1.70
SCH_3	3-Methylbutyl	6.40	2.9767	0.6008	1.9775	7.0577	6.0558	386	2507.45	6.50	1.85
SCH_3	Cyclohexyl	6.60	2.8465	0.5693	2.1535	7.7364	6.7445	428	2868.80	6.70	2.14
SCH_3	Hexyl	6.43	2.7460	0.5398	2.3415	7.7019	6.7000	496	3302.79	6.66	2.68

Table Va—Correlation of pI_{50} with Hydrophobicity and Topological Indices ($pI_{50} = a + bx + cx^2$)[a]

x	a	b	c	r	s	F
IC	19.3	−4.42	—	0.77	0.54	13
	$-1.67E+2$	$1.21E+2$	−20.9	0.95	0.29	35
SIC	13.0	−11.1	—	0.85	0.45	23
	−12.8	69.1	−61.9	0.92	0.35	22
CIC	2.79	1.78	—	0.83	0.48	19
	−2.13	7.90	−1.81	0.91	0.38	19
$^1\chi$	2.19	0.558	—	0.60	0.68	5.2
	−31.5	10.9	−0.779	0.89	0.41	15
$^1\chi^v$	3.10	0.508	—	0.60	0.68	5.0
	−3.99	3.20	−0.249	0.64	0.69	2.9
W	4.54	$4.30E-3$	—	0.60	0.68	5.0
	0.548	$3.21E-2$	$-4.30E-5$	0.82	0.52	8.2
I_D^w	4.71	$5.85E-4$	—	0.59	0.70	4.7
	1.43	$4.26E-3$	$-8.81E-7$	0.82	0.51	8.4
$\bar{I}_D^w$	−4.31	1.62	—	0.71	0.60	9.0
	$-1.53E+2$	49.5	−3.85	0.91	0.37	19
log P	4.98	0.760	—	0.83	0.48	20
	4.58	1.97	−0.490	0.94	0.32	28

[a] In all cases the number of data points = 11.

Table VI—Lipophilicity, Duration of Anesthesia (log T), Induction Time for Anesthesia (log t), and Molecular Descriptors for Barbiturates (III)

R_1	R_2	R_3	log T^a, h	log t^b, min	IC	SIC	CIC	log P	$^1\chi$	$^1\chi^v$	W	$\bar{I}_D^w$	I_D^w
Methyl	Ethyl	Methyl	0.0000	1.2041	2.8397	0.5845	2.0183	1.15	6.9238	4.5593	340	2224.00	6.5410
Ethyl	Ethyl	Methyl	−0.3979	0.9542	2.7871	0.5574	2.2129	1.65	7.4844	5.3271	398	2684.00	6.7430
Propyl	Ethyl	Methyl	−0.5229	0.8451	2.7217	0.5306	2.4076	2.15	7.9844	5.8271	472	3268.00	6.9240
Isopropyl	Ethyl	Methyl	−0.5229	0.6021	2.7648	0.5390	2.3645	1.95	7.8672	5.7098	458	3174.00	6.9300
Methyl	Methyl	Ethyl	0.0000	1.3222	2.8397	0.5845	2.0183	1.15	6.9618	4.7890	330	2164.00	6.5570
Ethyl	Methyl	Ethyl	−0.1549	1.0792	2.7871	0.5574	2.2129	1.65	7.5224	5.3497	387	2165.00	6.7570
Propyl	Methyl	Ethyl	−0.3979	0.7782	2.7271	0.5306	2.4076	2.15	8.0224	5.8497	460	3191.00	6.9360
Isopropyl	Methyl	Ethyl	−0.5229	0.6990	2.7648	0.5390	2.3645	1.95	7.9052	5.7324	446	3105.00	6.9620
Methyl	Propyl	Methyl	0.0000	0.7782	2.7871	0.5574	2.2129	1.65	8.4238	5.2664	423	2840.00	6.7130
Ethyl	Propyl	Methyl	0.0792	0.4771	2.7217	0.5306	2.4076	2.15	7.9844	5.8271	488	3374.00	6.9140
Methyl	Isopropyl	Methyl	−0.2218	0.7782	2.7482	0.5496	2.2518	1.45	7.2796	5.1391	410	2758.00	6.7270
Methyl	Butyl	Methyl	−0.3979	0.7782	2.7217	0.5306	2.4076	2.15	7.9238	5.7664	522	3588.00	6.8730
Ethyl	Butyl	Methyl	−1.0000	0.9031	2.6540	0.5057	2.5939	2.65	8.4844	6.3271	595	4197.00	7.0540
Ethyl	Ethyl	Propyl	−1.0000	0.9031	2.6540	0.5057	2.5939	2.65	8.5224	6.3877	551	3909.00	7.0950

[a] Logarithm of the duration of anesthesia in hours after intraperitoneal injection at the AD_{100} dose level. [b] Logarithm of the induction time for anesthesia in minutes after intraperitoneal injection at the AD_{100} dose level.

this class of drugs (23, 66, 67). On the other hand, Kier and Hall (8) found the action of congeneric series of barbiturates to be well correlated with connectivity-type steric parameters. Raychaudhury *et al.* (68) reported significant linear correlations of the *in vivo* stability of barbiturates with IC and SIC indices. In a further study, Basak *et al.* (20) showed that steric parameters like V_w, CIC, $^1\chi^v$, and $\bar{I}_D^w$ are superior to log P in rationalizing the duration of physiological action of the barbiturate group of drugs. The above considerations necessitate a comparative study of lipophilic and steric parameters in the quantitative prediction of the phenomenology of barbiturate action.

To illustrate the relative efficacies of log P *vis-à-vis* topological descriptors in the analysis of the narcotic action of barbiturates, a QSAR study was carried out with three different groups of barbituric acid derivatives, where the structural variations in the side chains include elongation of the carbon skeleton, branching, and unsaturation. Table VI presents the duration of anesthesia (T in hours) and the logarithm of the induction time for anesthesia (t in minutes) after administration of the drugs at AD_{100} dose levels, log P, $^1\chi$, $^1\chi^v$, IC, SIC, CIC, W, I_D^w, and $\bar{I}_D^w$ values for a series of 14 barbiturates (III) with variously modified side chains. The experimental T and t values (determined after the intraperitoneal injection of the compounds to albino mice) were taken from Cope and Hancock (69), and the log P values were taken from Hansch (23).

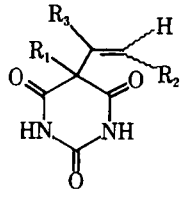

III

Table VIa shows the correlations of log T values with lipophilicity and the theoretically computed descriptors. None of the parameters used show excellent correlations with the T values. However, $\bar{I}_D^w$, $^1\chi$, and CIC exhibit correlations comparable or superior to that with log P values. Table VIa depicts the correlation of the induction time for anesthesia (log t) with log P and other theoretical structural parameters. It is noteworthy that the correlations of log t

Table VIa—Correlation of log T and log t with log P and Topological Indices [a]

x	a	b	c	r	s	F
			$\log T = a + bx + cx^2$			
IC	$-0.132E+02$	$0.467E+01$	—	0.77	0.23	17
	$-0.169E+03$	$0.118E+03$	$-0.207E+02$	0.80	0.22	9.8
CIC	$0.324E+01$	$-0.155E+01$	—	0.80	0.22	21
	$-0.115E+02$	$0.113E+02$	$-0.280E+01$	0.85	0.20	14
SIC	$-0.648E+01$	$0.113E+02$	—	0.79	0.22	20
	$-0.500E+02$	$0.171E+03$	$-0.147E+03$	0.84	0.21	13
W	$0.120E+01$	$-0.348E-02$	—	0.76	0.23	16
	$-0.666E+00$	$0.489E-02$	$-0.914E-05$	0.78	0.24	8.5
I_D^w	$0.925E+00$	$-0.422E-03$	—	0.76	0.23	17
	$-0.824E+00$	$0.757E-03$	$-0.191E-06$	0.80	0.23	9.6
$\bar{I}_D^w$	$0.108E+02$	$-0.163E+01$	—	0.80	0.22	21
	$-0.168E+03$	$0.508E+02$	$-0.385E+01$	0.86	0.19	16
$^1\chi$	$0.281E+01$	$-0.406E+00$	—	0.61	0.28	7.0
	$-0.468E+01$	$0.154E+01$	$-0.126E+00$	0.61	0.30	3.3
$^1\chi^v$	$0.254E+01$	$-0.522E+00$	—	0.79	0.22	20
	$-0.740E+01$	$0.313E+01$	$-0.333E+00$	0.85	0.20	14
log P	$0.724E+00$	$-0.574E+00$	—	0.78	0.22	19
	$-0.512E+00$	$0.814E+00$	$-0.367E+00$	0.82	0.21	12
			$\log t = a + bx + cx^2$			
IC	$-0.450E+01$	$0.195E+01$	—	0.49	0.20	3.8
	$0.311E+03$	$-0.228E+03$	$0.418E+02$	0.85	0.13	14
SIC	$-0.214E+01$	$0.553E+01$	—	0.59	0.19	6.4
	$0.600E+02$	$-0.223E+03$	$0.209E+03$	0.86	0.13	15
CIC	$0.262E+01$	$-0.756E+00$	—	0.59	0.19	6.5
	$0.235E+02$	$-0.190E+02$	$0.396E+01$	0.86	0.13	15
W	$0.158E+01$	$-0.161E-02$	—	0.54	0.20	4.9
	$0.661E+01$	$-0.242E-01$	$0.247E-04$	0.89	0.11	22
I_D^w	$0.148E+01$	$-0.202E-03$	—	0.56	0.19	5.4
	$0.486E+01$	$-0.248E-02$	$0.370E-06$	0.88	0.12	20
$\bar{I}_D^w$	$0.646E+01$	$-0.819E+00$	—	0.62	0.18	7.3
	$0.204E+03$	$-0.590E+02$	$0.427E+01$	0.82	0.14	11
$^1\chi$	$0.282E+01$	$-0.251E+00$	—	0.57	0.19	5.9
	$0.319E+02$	$-0.781E+01$	$0.489E+00$	0.81	0.14	10
$^1\chi^v$	$0.220E+01$	$-0.241E+00$	—	0.56	0.19	5.4
	$0.136E+02$	$-0.444E+01$	$0.383E+00$	0.77	0.16	8.0
log P	$0.134E+01$	$-0.294E+00$	—	0.52	0.20	4.5
	$0.334E+01$	$-0.250E+01$	$0.596E+00$	0.82	0.14	11

[a] In all cases, the number of data points = 14.

Table VII—Lipophilicity, Minimum Anesthetic Dose (MAD, log $1/c$), and Topological Descriptors for a Set of 16 Barbiturate Derivatives (IV)

R_1	log P	MAD (log $1/c$)	IC	SIC	CIC	W	I_D^w	$\bar{I}_D^w$	$^1\chi$	$^1\chi^v$
Ethyl	1.15	3.23	2.8397	0.5845	2.0183	334	2189.41	6.5551	6.9196	4.7504
Propyl	1.65	3.27	2.7871	0.5574	2.2129	402	2711.99	6.7462	7.4196	5.2504
Isopropyl	1.45	3.35	2.7482	0.5496	2.2518	389	2627.46	6.7544	7.3023	5.1331
Butyl	2.15	3.38	2.7217	0.5306	2.4076	486	3361.64	6.9170	7.9196	5.7504
Isobutyl	1.95	3.36	2.7649	0.5390	2.3644	472	3269.89	6.9277	7.7754	5.6062
sec-Butyl	1.95	3.42	2.7649	0.5390	2.3644	460	3189.83	6.9344	7.8403	5.6711
Amyl	2.65	3.26	2.6540	0.5057	2.5939	587	4151.26	7.0720	8.4196	6.2504
sec-Amyl	2.45	3.62	2.7265	0.5195	2.5214	548	3888.54	7.0959	8.3403	6.1711
2-Methylbutyl	2.45	3.34	2.7265	0.5195	2.5214	559	3964.27	7.0917	8.3134	6.1442
3-Methylbutyl	2.45	3.36	2.7265	0.5195	2.5214	572	4051.54	7.0831	8.2754	6.1062
1-Ethylpropyl	2.45	3.50	2.7265	0.5195	2.5214	535	3802.09	7.1067	8.3783	6.2091
Hexyl	3.15	3.18	2.5878	0.4830	2.7697	706	5094.11	7.2155	8.9196	6.7504
2-Ethylbutyl	2.95	3.25	6.6759	0.4995	2.6817	650	4713.39	7.2514	8.8514	6.6822
Cyclopentyl	2.29	3.40	2.8156	0.5446	2.3543	530	3763.10	7.1002	8.4641	6.2949
Allyl	1.35	3.44	2.7974	0.5701	2.1095	402	2711.99	6.7462	7.4196	4.8891
2-Methylallyl	1.65	3.37	2.7396	0.5431	2.3048	472	3269.89	6.9277	7.7754	5.2671
Phenyl	1.92	3.24	3.0659	0.5761	2.2560	726	5368.42	7.3945	9.3579	6.8696

with I_D^w, $\bar{I}_D^w$, $^1\chi$, W, CIC, SIC, and IC are superior or comparable to that with log P (Table VIa).

Table VII summarizes the minimal anesthetic dose (MAD, log $1/c$) levels, log P, molecular connectivity, Wiener number, and the different information-theoretic indices for a series of 17 barbiturates (IV); the experimental MAD (log $1/c$) values were taken from Doran and Shoule (70). In an earlier study Hansch *et al.* (67) showed that log P correlates more or less satisfactorily with the experimental log $1/c$ values of this set of compounds. The results of regression analysis, depicted in Table VIIa, show that some of the topological descriptors (SIC, CIC, W, I_D^w, $\bar{I}_D^w$, $^1\chi$, and $^1\chi^v$) are superior to log P in the correlation of the anesthetic concentrations of this congeneric series of compounds.

Table VIII represents the anesthetic concentrations (AD_{50}, log $1/c$), log P,

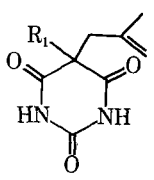

IV

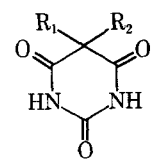

V

Table VIIa—Correlation of MAD (Rats) with log P and Molecular Descriptors, [log (1/c) = a + bx + cx²][a]

x	a	b	c	r	s	F
IC	0.348E + 01	−0.450E − 01	—	0.04	0.11	0.025
	−0.218E + 02	0.179E + 02	−0.316E + 01	0.52	0.10	2.6
SIC	0.334E + 01	0.204E − 01	—	0.005	0.11	0.00
	−0.201E + 01	0.878E + 02	−0.819E + 02	0.64	0.090	5.0
CIC	0.340E + 01	−0.218E − 01	—	0.040	0.11	0.023
	−0.392E + 01	0.613E + 01	−0.128E + 01	0.54	0.099	2.9
W	0.348E + 01	−0.251E − 03	—	0.25	0.11	1.0
	0.206E + 01	0.528E − 02	−0.518E − 05	0.68	0.086	6.0
I_D^w	0.346E + 01	−0.308E − 04	—	0.25	0.11	0.97
	0.240E + 01	0.561E − 03	−0.782E − 07	0.66	0.088	5.5
$\bar{I}_D^w$	0.357E + 01	−0.319E − 01	—	0.062	0.11	0.058
	−0.480E + 02	0.148E + 02	−0.106E + 01	0.54	0.099	2.8
$^1\chi$	0.354E + 01	−0.238E − 01	—	0.14	0.11	0.30
	−0.512E + 01	0.212E + 01	−0.132E + 00	0.59	0.095	3.7
$^1\chi^v$	0.349E + 01	−0.236E − 01	—	0.14	0.11	0.30
	−0.170E + 01	0.178E + 01	−0.155E + 00	0.57	0.096	3.4
log P	0.338E + 01	−0.148E − 01	—	0.075	0.11	0.086
	0.266E + 01	0.717E + 00	−0.172E + 00	0.53	0.099	2.7

[a] In all cases, the number of data points = 17.

Table VIII—Lipophilicity, Anesthetic Dose (AD_{50}, log 1/c), and Topological Indices for a Set of Barbituric Acid Derivatives (V)

R_1	R_2	log P	AD_{50} (log 1/c)	IC	SIC	CIC	W	I_D^w	$\bar{I}_D^w$	$^1\chi$	$^1\chi^v$
Propyl	1-Propenyl	1.35	3.12	2.7968	0.5757	2.0612	338	2215.24	6.5540	7.0637	4.8724
Isopropyl	1-Propenyl	1.15	3.28	2.7708	0.5704	2.0872	326	2139.91	6.5641	6.9464	4.7551
Butyl	1-Propenyl	1.85	3.31	2.7246	0.5449	2.2754	415	2794.55	6.7338	7.5637	5.3724
Ethyl	1-Butenyl	1.35	3.37	2.7968	0.5757	2.0612	346	2262.81	6.5399	7.0637	4.9104
Propyl	1-Butenyl	1.85	3.31	2.7246	0.5449	2.2754	415	2794.55	6.7338	7.5637	5.4104
Isopropyl	1-Butenyl	1.65	3.57	2.7871	0.5574	2.2129	402	2709.65	6.7404	7.4464	5.2931
Butyl	1-Butenyl	2.35	3.56	2.6506	0.5168	2.4787	500	3453.76	6.9075	8.0637	5.9104
Ethyl	2-Methyl-1-propenyl	1.15	2.56	2.8397	0.5845	2.0183	334	2189.41	6.5551	6.9196	4.7504
Ethyl	1-Pentenyl	1.85	3.45	2.7246	0.5449	2.2754	431	2892.67	6.7115	7.5637	5.4104
Isopropyl	1-Pentenyl	2.15	3.50	2.7433	0.5348	2.3860	494	3409.09	6.9010	7.9464	5.7931
Ethyl	3-Methyl-1-butenyl	1.65	3.51	2.7871	0.5574	2.2129	418	2811.32	6.7257	7.4196	5.2831
Propyl	3-Methyl-1-butenyl	2.15	3.32	2.7433	0.5348	2.3860	494	3413.36	6.9096	7.9196	5.7831
Isopropyl	3-Methyl-1-butenyl	1.95	3.68	2.6506	0.5168	2.4787	480	3318.94	6.9145	7.8023	5.6658

Table VIIIa—Correlation of AD_{50} (Mice) with log P and Molecular Descriptors [log (1/c) = a + bx + cx²][a]

x	a	b	c	r	s	F
IC	0.124E + 02	−0.329E + 01	—	0.65	0.22	8.2
	−0.200E + 03	0.153E + 03	−0.283E + 02	0.74	0.21	6.1
SIC	0.822E + 01	−0.885E + 01	—	0.69	0.21	10
	−0.491E + 02	0.200E + 03	−0.190E + 03	0.76	0.20	6.6
CIC	0.630E + 00	0.121E + 01	—	0.68	0.22	9.4
	−0.179E + 02	0.177E + 02	−0.367E + 01	0.73	0.21	5.8
W	0.222E + 01	0.272E − 02	—	0.62	0.23	6.9
	−0.170E + 01	0.221E − 01	−0.234E − 04	0.68	0.23	4.2
I_D^w	0.236E + 01	0.354E − 03	—	0.62	0.23	6.8
	−0.780E + 00	0.266E − 02	−0.412E − 06	0.68	0.23	4.2
$\bar{I}_D^w$	−0.375E + 01	0.120E + 01	—	0.62	0.23	7.0
	−0.173E + 03	0.511E + 02	−0.371E + 01	0.66	0.23	3.8
$^1\chi$	−0.837E − 01	0.459E + 00	—	0.64	0.23	7.6
	−0.412E + 02	0.115E + 02	−0.740E + 00	0.72	0.21	5.4
$^1\chi^v$	0.958E + 00	0.449E + 00	—	0.64	0.22	7.8
	−0.178E + 02	0.758E + 01	−0.673E + 00	0.72	0.21	5.3
log P	0.258E + 01	0.446E + 00	—	0.62	0.23	6.7
	0.670E + 00	0.280E + 01	−0.690E + 00	0.70	0.22	4.8

[a] In each case, the number of data points = 13.

$^1\chi$, $^1\chi^v$, W, I_D^w, $\bar{I}_D^w$, IC, SIC, and CIC values) for a set of 13 barbiturates (V). The experimental log 1/c data were taken from the work of Cope *et al.* (71). The outcome of regression analysis indicates that log P and the various molecular descriptors correlate significantly with the AD_{50} values of this group of analogues (Table VIIIa). It is evident from the statistical analysis that IC, SIC, CIC, and $^1\chi$ are superior and I_D^w as well as $\bar{I}_D^w$ are slightly inferior to log P in accounting for the AD_{50} values of this group of barbiturates.

CONCLUSIONS

We have analyzed the relative roles of hydrophobicity (log P, octanol–water) *vis-à-vis* several topological parameters in the QSAR study of diverse sets of bioactive molecules that vary considerably with respect to chemical structure and physiological function. While alcohols and ketobemidones are simple homologous series, triazinones and barbiturates represent considerable structural diversity. At the biochemical level, alcohols and barbiturates are thought to be narcotic agents that act through nonspecific perturbation of cellular proteins or lipoprotein complexes (46, 47, 66, 72, 73). On the other hand, triazinones and ketobemidones act *via* specific mechanisms where well-defined biotargets are involved (54, 59). Yet it is interesting to note that certain graph theoretic invariants like CIC, $^1\chi$, $^1\chi^v$, W, and $\bar{I}_D^w$ could predict these dissimilar biological phenomena as efficiently as hydrophobicity.

From QSAR studies of different series of bioactive molecules, Hansch (23) pointed out that lipophilicity alone is sufficient to account for the action of

nonspecific bioactive molecules. On the other hand, stereoelectronic factors are deemed to be critical for molecules with specialized mechanism of action at the biochemical level (23, 74). However, the results of this paper indicate that topological steric parameters can correlate the action of both specific (triazinones and ketobemidones) and nonspecific (alcohol and barbiturates) bioactive agents. These findings could be rationalized in terms of the studies of Nemethy and Scheraga (75–77) where a "steric basis of hydrophobicity" is proposed on theoretical grounds. Alternatively, some recent studies highlight that certain so called "nonspecific" compounds may have specific physiological receptors (65, 78, 79) which could conceivably be sensitive to the steric factors associated with the effector molecule.

Finally, from the QSAR of these diverse series of bioactive molecules, the easily calculable molecular descriptors like CIC, $^1\chi$, $^1\chi^v$, W, and $\bar{I}_D^w$ appear to be as effective as log P in the rationalization of biological action. Of these five topological descriptors, only CIC and $\bar{I}_D^w$ are highly correlated with biological response for all six sets of compounds tested; accordingly, either CIC or $\bar{I}_D^w$ is the best single choice for a molecular descriptor.

REFERENCES

(1) L. B. Kier, "Molecular Orbital Theory in Drug Research," Academic, New York, N.Y., 1971.

(2) W. P. Purcell and J. M. Clayton, in "Molecular Orbital Studies in Chemical Pharmacology," L. B. Kier, Ed., Springer-Verlag, New York, Heidelberg, London, 1970.

(3) J. J. Kaufman, *Int. J. Quant. Chem., Quant. Biol. Symp.*, **4,** 375 (1977).

(4) W. G. Richards, "Quantum Pharmacology," Butterworths, London, UK, 1977.

(5) C. Hansch, in "Drug Design," vol. I, E. J. Ariens, Ed., Academic, New York, London, 1971.

(6) T. Fujita, in "Biological Correlations—The Hansch Approach," R. F. Gould, Ed., Advances in Chemistry Series 114, American Chemical Society, Washington D.C., 1972.

(7) C. Hansch, in "Correlation Analysis in Chemistry," N. B. Chapman and J. Shorter, Eds., Plenum, New York, N.Y., 1978.

(8) L. B. Kier and L. H. Hall, "Molecular Connectivity in Chemistry and Drug Research," Academic, New York, N.Y., 1976.

(9) L. B. Kier and L. H. Hall, *J. Med. Chem.*, **20,** 1631 (1977).

(10) J. S. Millership and A. D. Woolfson, *J. Pharm. Pharmacol.*, **30,** 483 (1978).

(11) L. B. Kier, R. J. Simons, and L. H. Hall, *J. Pharm. Sci.*, **67,** 725 (1978).

(12) B. K. Evans, K. C. James, and D. K. Luscombe, *J. Pharm. Sci.*, **68,** 370 (1979).

(13) B. van't Riet, L. B. Kier, and H. L. Elford, *J. Pharm. Sci.*, **69,** 856 (1980).

(14) L. B. Kier and L. H. Hall, *Eur. J. Med. Chem.*, **12,** 307 (1977).

(15) S. K. Ray, S. C. Basak, C. Raychaudhury, A. B. Roy, and J. J. Ghosh, *Ind. J. Chem.*, **20B,** 894 (1981).

(16) S. C. Basak, S. K. Ray, C. Raychaudhury, A. B. Roy, and J. J. Ghosh, *IRCS Med. Sci.*, **10,** 145 (1982).

(17) S. K. Ray, S. C. Basak, C. Raychaudhury, A. B. Roy, and J. J. Ghosh, *Arzneim.-Forsch.*, **32,** 322, (1982).

(18) S. C. Basak, D. P. Gieschen, D. K. Harriss, and V. R. Magnuson, *J. Pharm. Sci.*, **72,** 934 (1983).

(19) S. C. Basak and V. R. Magnuson, *Arzneim.-Forsch.*, **33,** 501 (1983).

(20) S. C. Basak, D. P. Gieschen, V. R. Magnuson, and D. K. Harriss, *IRCS Med. Sci.*, **10,** 619 (1982).

(21) A. T. Balaban, A. Chiriac, I. Motoc, and Z. Simon, "Steric Fit in Quantitative Structure-Activity Relations," Lecture Notes in Chemistry, vol. 15, Springer-Verlag, Berlin, W. Germany, 1980.

(22) C. Hansch, in "Biological Correlations—The Hansch Approach," R. F. Gould, Ed., Advances in Chemistry Series 114, American Chemical Society, Washington D.C., 1972.

(23) C. Hansch, *Drug Metab. Rev.*, **1,** 1 (1972).

(24) K. S. Rogers and A. Cammarata, *J. Med. Chem.*, **12,** 692 (1969).

(25) T. Fujita, *Pure Appl. Chem.*, **50,** 987 (1978).

(26) I. Moriguchi, Y. Kanada, and K. Komatsu, *Chem. Pharm. Bull.*, **24,** 1799 (1976).

(27) A. J. Stuper, W. E. Brugger, and P. C. Jurs, "Computer Assisted Studies of Chemical Structure and Biological Function," Wiley, New York, N.Y., 1979.

(28) K. Enslein and P. N. Craig, *J. Environ. Pathol. Toxicol.*, **2,** 115 (1978).

(29) P. N. Craig and K. Enslein, in "Safe Handling of Chemical Carcinogens, Mutagens, Teratogens, and Highly Toxic Substances," Vol. 2, D. B. Walters, Ed., Ann Arbor Science Publishers, Ann Arbor, Mich., 1980.

(30) O. Mekenyan, D. Bonchev, and N. Trinajstic, *Int. J. Quant. Chem.*, **18,** 369 (1980).

(31) L. B. Kier and L. H. Hall, *J. Pharm. Sci.*, **70,** 583 (1981).

(32) S. P. Gupta and P. Singh, *Bull. Chem. Soc. Jpn.*, **52,** 2745 (1979).

(33) A. Verloop, in "Drug Design," vol. III, E. J. Ariens, Ed., Academic, New York, N.Y., 1972.

(34) C. Hansch and A. J. Leo, "Substituent Constants for Correlational Analysis in Chemistry and Biology," Wiley, New York, N.Y., 1979.

(35) C. E. Shannon, *Bell System Tech. J.*, **27,** 379 (1948).

(36) N. Rashevsky, *Bull. Math. Biophys.*, **17,** 229 (1955).

(37) E. Trucco, *Bull. Math. Biophys.*, **18,** 129 (1956).

(38) E. Trucco, *Bull. Math. Biophys.*, **18,** 237 (1956).

(39) D. Bonchev and N. Trinajstic, *J. Chem. Phys.*, **67,** 4517 (1977).

(40) L. B. Kier, *J. Pharm. Sci.*, **69,** 807 (1980).

(41) R. Sarkar, A. B. Roy, and P. K. Sarkar, *Math. Biosci.*, **39,** 299 (1978).

(42) S. C. Basak, A. B. Roy, and J. J. Ghosh, "Proceedings of the II International Conference on Mathematical Modelling," vol. 2, University of Missouri-Rolla, 1979, p. 851.

(43) C. Raychaudhury, S. C. Basak, S. K. Ray, A. B. Roy, and J. J. Ghosh, "Abstract, Proceedings of the 19th Annual Meeting, Society of Engineering Sciences Inc.," University Missouri-Rolla, Missouri, 1982.

(44) H. Wiener, *J. Am. Chem. Soc.*, **69,** 17 (1947).

(45) N. H. Nie, C. C. Hull, J. G. Jenkins, K. Steinbrenner, and D. H. Bent, "Statistical Package for Social Sciences," McGraw-Hill, New York, N.Y., 1975.

(46) L. J. Mullins, *Chem. Rev.*, **54,** 289 (1954).

(47) G. D. Veith, D. J. Call, and L. T. Brooke, in "Aquatic Toxicology and Hazard Assessment: Sixth Symposium," W. E. Bishop, R. D. Cardwell, and B. B. Heidolph, Eds., American Society for Testing and Materials, Philadelphia, Pa., 1983, p. 90.

(48) H. Kubinyi and O. H. Kehrhahn, *Arzneim.-Forsch.*, **28,** 598, 1978.

(49) C. B. Pert and S. H. Snyder, *Science*, **179,** 1011 (1973).

(50) H. W. Kosterlitz and A. A. Waterfield, *Annu. Rev. Pharmacol.*, **15,** 29 (1975).

(51) S. H. Snyder, *Neurosci. Res. Prog. Bull.*, **13,** (Suppl.), 5 (1975).

(52) P. Dole, *Annu. Rev. Biochem.*, **39,** 821 (1970).

(53) J. A. H. Lord, A. A. Waterfield, J. Hughes, and H. W. Kosterlitz, *Nature (London)*, **267,** 495 (1977).

(54) R. M. Wilson, M. E. Rogers, C. B. Pert, and S. H. Snyder, *J. Med. Chem.*, **18,** 40 (1975).

(55) N. D. Camper and D. E. Moreland, *Biochim. Biophys. Acta*, **94,** 383 (1965).

(56) M. Kamrin, W. F. Bertsch, and R. F. Wood, *Proc. Natl. Acad. Sci., USA*, **53,** 1118 (1965).

(57) C. Hansch and E. W. Deutsch, *Biochim. Biophys. Acta*, **112,** 381 (1966).

(58) D. E. Moreland, *Progr. Photosyn. Res.*, **3,** 1693 (1969).

(59) W. Draber, K. H. Buchel, H. Timmler, and A. Trebst, "Mechanism of Pesticide Action," G. K. Kohn, Ed., American Chemical Society, Washington, D.C., 1974, p. 100.

(60) S. C. Harvey, in "The Pharmacological Basis of Therapeutics," L. S. Goodman and A. Gilman Eds., 5th ed., Macmillan, New York, N.Y., 1975.

(61) R. A. Nicoll and J. M. Wojtowicz, *Brain Res.*, **191,** 225 (1980).

(62) C. D. Richards, *J. Physiol. (London)*, **227,** 749 (1972).

(63) L. Y. M. Huang and J. L. Barker, *Science*, **207,** 195, (1980).

(64) M. P. Blaustein, *J. Gen. Physiol.*, **51,** 293 (1968).

(65) F. Leeb-Lundberg and R. W. Olsen, *Mol. Pharmacol.*, **21,** 320 (1982).

(66) C. Hansch and S. M. Anderson, *J. Med. Chem.*, **10,** 745 (1967).

(67) C. Hansch, A. R. Steward, S. M. Anderson, and D. J. Bentley, *J. Med. Chem.*, **11,** 1 (1968).

(68) C. Raychaudhury, S. C. Basak, A. B. Roy, and J. J. Ghosh, *Indian Drugs*, **18,** 97 (1980).

(69) A. C. Cope and E. M. Hancock, *J. Am. Chem. Soc.*, **61,** 776 (1939).

(70) W. J. Doran and H. A. Shonle, *J. Am. Chem. Soc.*, **59,** 1625 (1937).

(71) A. C. Cope, W. H Hartung, E. M. Hancock, and F. S. Crossley, *J. Am. Chem. Soc.*, **62,** 1199 (1940).

(72) K. W. Miller, W. D. M. Paton, E. B. Smith, and R. A. Smith, *Anesthesiology*, **36,** 339 (1972).

(73) S. H. Roth, *Fed. Proc. Fed. Am. Soc. Exp. Biol.*, **39,** 1595 (1980).

(74) E. J. Ariens (Ed.), in "Drug Design," vol. I, Academic, New York, N.Y., 1971.
(75) G. Nemethy and H. A. Scheraga, *J. Chem. Phys.*, **36**, 3382 (1962).
(76) G. Nemethy and H. A. Scheraga, *J. Chem. Phys.*, **41**, 680 (1964).
(77) G. Nemethy and H. A. Scheraga, *J. Phys. Chem.*, **66**, 1773 (1962).
(78) F. S. LaBella, *Perspect. Biol. Med.*, **25**, 323 (1982).
(79) C. D. Richards, K. Martin, S. Gregory, C. A. Keightley, T. K. Hesketh, G. A. Smith, G. B. Warren, and J. C. Metcalfe, *Nature (London)*, **276**, 775 (1978).

ACKNOWLEDGMENTS

The authors express their appreciation to the U.S. Environmental Protection Agency (Contract CR 807566) for support of this work and to the University of Minnesota, Duluth Computer Center for partial financial assistance.

Comparative Bioavailability of Two Furosemide Formulations in Humans

B. K. MARTIN *, M. UIHLEIN §, R. M. J. INGS ‡, L. A. STEVENS ‡, and J. McEWEN ‡x

Received September 8, 1980, from **BIOS (Consultancy and Contract Research) Ltd., Pinewood, College Ride, Bagshot, Surrey, GU19 5ER, England,* §*Pharma-Forschung, Hoechst AG, Postfach 80 03 20, D-6230 Frankfurt (Main) 80, West Germany, and* ‡*Hoechst UK, Walton Manor, Milton Keynes, Buckinghamshire, MK7-7AJ, England.* Accepted for publication February 10, 1983.

Abstract □ Twelve healthy male volunteers participated in a balanced crossover comparison of a brand-name and generic furosemide formulations. Each treatment was given as a single 40-mg tablet following an overnight fast. Furosemide concentrations in plasma and urine were determined up to 24 h after treatment; urine output and urinary sodium excretion were also measured. In comparison with the brand-name tablets, generic furosemide was significantly less bioavailable. Using a 95% confidence interval approach, generic furosemide gave up to 66% lower maximum furosemide plasma levels, up to 52% less area under the plasma level curve to infinite time, and up to 37% less urinary recovery of furosemide. Comparison of the effect of the two treatments was a less sensitive measurement of bioequivalence. Confidence intervals for differences in urinary output and sodium excretion over the period of maximum effect (0–4 h) were, however, asymmetrical, and pharmacodynamic differences between treatments were significant at the 10% level.

Keyphrases □ Furosemide—comparative bioavailability, brand-name and generic formulations, humans, plasma and urine □ Bioavailability—comparative, furosemide formulations in humans, plasma and urine □ Formulations—comparative bioavailability, brand-name and generic furosemide in humans, plasma and urine

During 1979, generic formulations of furosemide tablets which were not legally marketed became available to U.S. physicians. Shortly after these tablets were introduced, reports began to appear of diuretic ineffectiveness of some of the products. The Food and Drug Administration became aware of the problem and took steps to prevent further clinical use of unauthorized furosemide tablets (1).

With the above background in mind, it was felt that it would be useful to compare the relative bioavailability of the brand-name tablet formulation of furosemide available in the United States and one of the abovementioned generic furosemide tablets. This paper presents the results of a crossover study in healthy volunteers with comparative pharmacokinetic and pharmacodynamic measurements.

EXPERIMENTAL

Subjects—Twelve healthy male volunteers aged 18–42 years, within 10% of ideal body weight, received treatment on two occasions with 1-week between doses. A comprehensive checkup, including clinical examination, clinical chemistry/hematology evaluation, and urinalysis revealed no evidence of cardiac, respiratory, hepatic, or renal disease. The project was subject to ethics review, and each subject gave his signed informed consent.

Treatment—Furosemide (40 mg) was administered as a single tablet on two occasions 1 week apart to each subject, according to a balanced crossover design. Treatments were designated product I[1] and product II[2] respectively. Product I (the brand-name tablet) contained an average of 39.6 mg of furosemide/tablet; product II (the generic tablet) contained an average of 40.3 mg of furosemide/tablet. Therapy was given by mouth with 100 mL of water following an overnight fast, 1 h before a standard tea/toast breakfast. Oral fluid supplements (150 mL of water) were given at 1, 2, 3, 4, and 6 h after treatment.

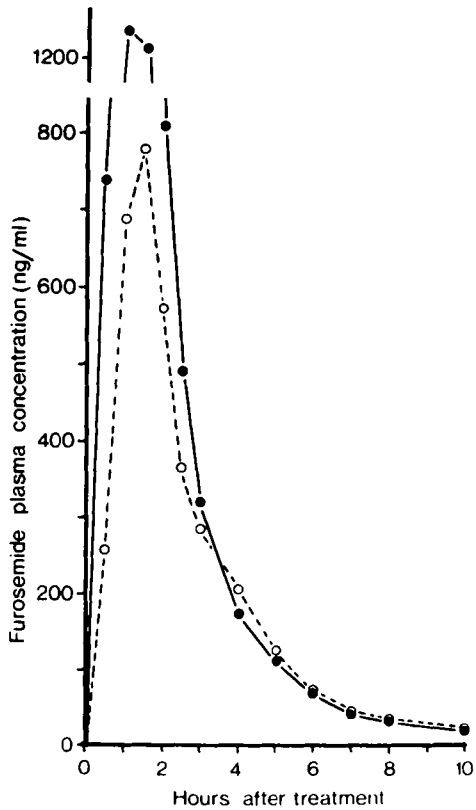

Figure 1—*Mean furosemide plasma concentration following oral treatment with product I (●) and product II (○).*

[1] Lasix, lot 600229; Hoechst-Roussel Pharmaceuticals, Inc., Somerville, N.J.
[2] Furosemide lot 8137-07; Pharmadyne Laboratories Inc., Elmwood Park, N.J.

0022-3549/84/0400-0437$01.00/0
© 1984, American Pharmaceutical Association

(74) E. J. Ariens (Ed.), in "Drug Design," vol. I, Academic, New York, N.Y., 1971.
(75) G. Nemethy and H. A. Scheraga, *J. Chem. Phys.*, **36**, 3382 (1962).
(76) G. Nemethy and H. A. Scheraga, *J. Chem. Phys.*, **41**, 680 (1964).
(77) G. Nemethy and H. A. Scheraga, *J. Phys. Chem.*, **66**, 1773 (1962).
(78) F. S. LaBella, *Perspect. Biol. Med.*, **25**, 323 (1982).
(79) C. D. Richards, K. Martin, S. Gregory, C. A. Keightley, T. K. Hesketh, G. A. Smith, G. B. Warren, and J. C. Metcalfe, *Nature (London)*, **276**, 775 (1978).

ACKNOWLEDGMENTS

The authors express their appreciation to the U.S. Environmental Protection Agency (Contract CR 807566) for support of this work and to the University of Minnesota, Duluth Computer Center for partial financial assistance.

Comparative Bioavailability of Two Furosemide Formulations in Humans

B. K. MARTIN *, M. UIHLEIN §, R. M. J. INGS ‡, L. A. STEVENS ‡, and J. McEWEN ‡x

Received September 8, 1980, from **BIOS (Consultancy and Contract Research) Ltd., Pinewood, College Ride, Bagshot, Surrey, GU19 5ER, England,* §*Pharma-Forschung, Hoechst AG, Postfach 80 03 20, D-6230 Frankfurt (Main) 80, West Germany, and* ‡*Hoechst UK, Walton Manor, Milton Keynes, Buckinghamshire, MK7-7AJ, England.* Accepted for publication February 10, 1983.

Abstract □ Twelve healthy male volunteers participated in a balanced crossover comparison of a brand-name and generic furosemide formulations. Each treatment was given as a single 40-mg tablet following an overnight fast. Furosemide concentrations in plasma and urine were determined up to 24 h after treatment; urine output and urinary sodium excretion were also measured. In comparison with the brand-name tablets, generic furosemide was significantly less bioavailable. Using a 95% confidence interval approach, generic furosemide gave up to 66% lower maximum furosemide plasma levels, up to 52% less area under the plasma level curve to infinite time, and up to 37% less urinary recovery of furosemide. Comparison of the effect of the two treatments was a less sensitive measurement of bioequivalence. Confidence intervals for differences in urinary output and sodium excretion over the period of maximum effect (0–4 h) were, however, asymmetrical, and pharmacodynamic differences between treatments were significant at the 10% level.

Keyphrases □ Furosemide—comparative bioavailability, brand-name and generic formulations, humans, plasma and urine □ Bioavailability—comparative, furosemide formulations in humans, plasma and urine □ Formulations—comparative bioavailability, brand-name and generic furosemide in humans, plasma and urine

During 1979, generic formulations of furosemide tablets which were not legally marketed became available to U.S. physicians. Shortly after these tablets were introduced, reports began to appear of diuretic ineffectiveness of some of the products. The Food and Drug Administration became aware of the problem and took steps to prevent further clinical use of unauthorized furosemide tablets (1).

With the above background in mind, it was felt that it would be useful to compare the relative bioavailability of the brand-name tablet formulation of furosemide available in the United States and one of the abovementioned generic furosemide tablets. This paper presents the results of a crossover study in healthy volunteers with comparative pharmacokinetic and pharmacodynamic measurements.

EXPERIMENTAL

Subjects—Twelve healthy male volunteers aged 18–42 years, within 10% of ideal body weight, received treatment on two occasions with 1-week between doses. A comprehensive checkup, including clinical examination, clinical chemistry/hematology evaluation, and urinalysis revealed no evidence of cardiac, respiratory, hepatic, or renal disease. The project was subject to ethics review, and each subject gave his signed informed consent.

Treatment—Furosemide (40 mg) was administered as a single tablet on two occasions 1 week apart to each subject, according to a balanced crossover design. Treatments were designated product I[1] and product II[2] respectively. Product I (the brand-name tablet) contained an average of 39.6 mg of furosemide/tablet; product II (the generic tablet) contained an average of 40.3 mg of furosemide/tablet. Therapy was given by mouth with 100 mL of water following an overnight fast, 1 h before a standard tea/toast breakfast. Oral fluid supplements (150 mL of water) were given at 1, 2, 3, 4, and 6 h after treatment.

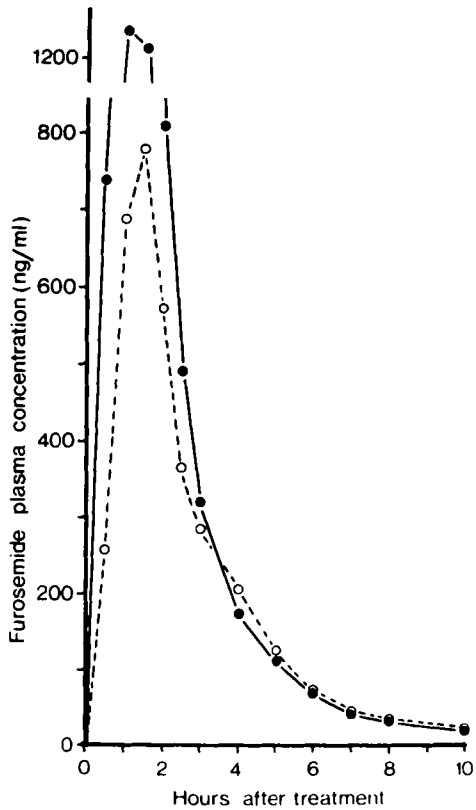

Figure 1—*Mean furosemide plasma concentration following oral treatment with product I (●) and product II (○).*

[1] Lasix, lot 600229; Hoechst-Roussel Pharmaceuticals, Inc., Somerville, N.J.
[2] Furosemide lot 8137-07; Pharmadyne Laboratories Inc., Elmwood Park, N.J.

0022-3549/84/0400-0437$01.00/0
© 1984, American Pharmaceutical Association

Table I—Plasma Furosemide Concentration, ng/mL

Time, h	Subject 1	2	3	4	5	6	7	8	9	10	11	12	Mean ± *SD*
						Product I							
0.5	1000	1180	1610	90	1190	2950	25	100	70	105	145	400	739 ± 893
1	1650	1560	970	1810	1630	2010	75	1870	165	130	740	2240	1236 ± 787
1.5	1110	1650	430	1460	1080	1490	1060	1710	550	1380	1500	1150	1214 ± 404
2	670	1150	340	800	570	830	720	820	430	1360	1040	940	806 ± 292
2.5	420	730	220	470	330	530	460	570	380	930	480	370	491 ± 188
3	240	460	140	290	240	380	270	370	250	630	360	220	321 ± 130
4	115	230	60	160	145	250	130	210	160	280	220	140	175 ± 63
5	50	125	50	115	70	140	50	100	230	190	145	80	112 ± 58
6	30	75	45	65	35	95	25	60	120	135	95	60	70 ± 35
7	20	45	20	40	15	50	15	40	75	110	70	30	44 ± 29
8	15	35	15	40	15	35	20	35	55	65	45	30	34 ± 16
10	<15	20	20	25	0	20	<15	25	40	45	25	20	21 ± 13
24	0	<15	0	20	0	<15	0	0	25	<15	<15	<15	— —
						Product II							
0.5	135	200	880	45	670	30	30	65	30	570	15	420	258 ± 301
1	1800	1350	740	90	1010	135	45	280	60	1580	20	1140	688 ± 665
1.5	910	1350	490	210	730	1340	380	770	105	1400	600	1080	780 ± 446
2	660	850	420	180	490	1100	420	630	100	800	620	590	572 ± 278
2.5	390	440	260	180	340	700	240	480	100	450	400	420	367 ± 158
3	300	260	185	155	280	560	160	450	95	330	330	350	288 ± 132
4	200	130	105	175	135	330	100	250	190	160	540	165	207 ± 123
5	85	65	80	120	95	150	75	160	240	105	290	80	129 ± 71
6	65	50	50	45	60	100	40	105	90	80	140	55	73 ± 30
7	45	25	35	35	45	60	30	70	65	55	75	45	49 ± 16
8	35	<15	25	20	30	40	30	55	50	40	50	30	34 ± 15
10	25	20	20	20	25	15	20	35	40	25	25	20	24 ± 7
24	<15	0	<15	0	<15	0	<15	<15	25	0	<15	<15	— —

Table II—Urinary Furosemide Excretion, mg/Sample

Time, h	Subject 1	2	3	4	5	6	7	8	9	10	11	12	Mean ± *SD*
						Product I							
0–1	6.51	3.34	5.66	1.53	5.11	5.11	0.25	1.73	—	0.23	0.84	3.41	3.07 ± 2.28
1–2	8.12	5.79	4.46	5.32	4.67	2.89	6.37	5.43	1.23	3.91	7.85	5.49	5.13 ± 1.93
2–3	2.34	2.77	1.14	1.97	4.54	1.67	2.90	1.71	2.03	2.87	2.99	1.94	2.40 ± 0.87
3–4	0.86	1.00	0.68	0.93	0.67	0.80	0.56	0.85	—	1.37	1.80	0.93	0.95 ± 0.35
4–6	0.75	—	0.44	0.52	0.85	0.63	0.75	—	3.03	0.87	1.51	0.75	1.01 ± 0.77
6–8	0.43	1.63	0.77	0.56	0.42	0.39	0.52	1.26	0.91	0.74	0.75	0.40	0.65 ± 0.37
8–10	0.20	0.45	0.27	0.17	0.29	0.20	0.29	0.25	0.47	0.38	0.29	0.20	0.29 ± 0.10
10–24	0.38	0.57	0.76	0.20	0.64	0.42	0.64	0.47	0.28	1.00	0.52	0.28	0.51 ± 0.23
						Product II							
0–1	2.53	1.43	2.54	—	2.49	—	0.05	0.45	0.09	6.13	0.05	2.48	1.82 ± 1.88
1–2	6.75	5.98	3.72	0.83	4.92	2.75	1.88	3.09	5.24	4.80	1.69	3.66	3.78 ± 1.82
2–3	1.53	1.49	1.16	0.92	1.56	2.40	1.83	2.26	1.07	2.52	2.69	1.97	1.78 ± 0.59
3–4	1.02	1.01	0.70	0.71	0.89	0.69	—	1.42	0.41	1.23	1.90	1.18	1.01 ± 0.41
4–6	0.91	0.98	0.74	1.13	0.93	0.69	1.80	1.69	1.90	1.01	2.39	0.98	1.26 ± 0.54
6–8	0.46	0.42	0.42	0.49	0.56	0.56	0.43	0.71	0.44	0.44	0.95	0.52	0.53 ± 0.16
8–10	0.29	0.30	0.25	—	0.34	0.36	0.32	0.10	0.69	0.26	0.37	0.32	0.33 ± 0.14
10–24	0.49	0.61	0.70	0.77	0.60	0.75	0.94	0.75	0.13	0.59	0.75	0.78	0.66 ± 0.20

Collection of Samples—Blood samples were taken by direct venipuncture at 0, 0.5, 1, 1.5 2, 2.5, 3, 4, 5, 6, 7, 8, 10, and 24 h and placed in heparinized tubes[3]. Following centrifugation, the plasma were stored in the deep-freeze until analyzed. A predose 24-h urine collection was made; after treatment complete urine samples were collected over the intervals of 0–1, 1–2, 2–3, 3–4, 4–6, 6–8, 8–10, and 10–24 h. The volume of each sample was recorded; aliquots were stored in the deep-freeze for electrolyte and drug assay. Urinary sodium was measured by flame photometry.

Furosemide Assay—Furosemide concentrations in plasma and urine were fluorometrically determined following HPLC separation. Urine was directly chromatographed after centrifugation. Following an initial 5-mL ether extraction of 0.25 mL of plasma plus 0.25 mL of phosphate buffer (pH 7.0) (with the ether layer discarded), the plasma was acidified with 50 μL of 5 M HCl and furosemide was extracted into 5 mL of ether. The ether layer was separated and evaporated under nitrogen; the residue was taken up with 0.1 mL of pH 7.0 phosphate buffer. An internal standard (100 ng of the phenyl analogue of furosemide) was simultaneously taken through the plasma procedure.

The chromatographic apparatus consisted of an automatic sampler[4], a solvent delivery pump[5], and a fluorometric detector with automatic overload reset[6]. The extracts were separated on a 12-cm × 4.3-mm column packed with 5-μm reverse-phase irregular organically modified silica[7]. The eluant was methanol–0.1 M H_3PO_4 (53:47). The excitation wavelength was 233 nm, and the emission wavelength was 370 nm (sharp-cut filter, with additional blue filter[8]).

The method was found to be linear over the concentration ranges of 10–1000 ng/mL for plasma and 0.5–10 μg/mL for urine. Assay precision for the plasma method was ± (7.7 + 0.039 C_p) ng/mL, where C_p is the plasma concentration; for urine, precision was ± (0.5 + 0.013 C_u) μg/mL, where C_u is urine concentration.

Pharmacokinetic Analysis—Initial estimates of furosemide elimination half-lives were calculated, using urinary data, by linear regression analysis of the logarithm of rate of urinary furosemide excretion against time (2). These estimates were employed as the starting values in an iterative least-squares curve-fitting program developed for a minicomputer[9], which generated a series of fitted coefficients and exponential constants. Most profiles fitted a model

[3] Li-Heparin; Walter Sarstedt Ltd., Leicester, U.K.
[4] WISP 710A; Waters Associates, Milford, Mass.
[5] M 6000A; Waters Associates, Milford, Mass.
[6] SF 970; Kratos Schoeffel Instruments, Westwood, N.J.
[7] LichroSorb RP-18; H. Knauer GmbH, 1000 Berlin 37, W. Germany.
[8] CS 5-61; Corning Optical Products Dept., Corning, N.Y.
[9] HP 1000 MX(E); Hewlett-Packard Ltd., Winnersh, Wokingham, Berks, U.K.

Table III—Results of Curve-Fitting [a]

	Subject											
	1	2	3	4	5	6	7	8	9	10	11	12
						Product I						
A, ng/mL	9677	9508	2840	7113	19340	5030	9867	24380	2865	15970	2393	6570
B, ng/mL	235.3	289.5	254.7	226.5	1045	758.2	112.5	143.4	308.7	480.8	718.8	171.6
C, ng/mL	10590	10490	3102	8710	20480	5790	10980	26200	5136	22280	4117	7627
α, h^{-1}	1.216	1.018	1.374	1.073	1.678	1.153	1.073	1.188	0.959	1.159	0.847	1.149
β, h^{-1}	0.355	0.271	0.350	0.223	0.569	0.374	0.294	0.174	0.201	0.238	0.343	0.218
γ, h^{-1}	1.974	1.678	13.42	1.896	1.968	4.957	1.469	1.458	1.623	1.755	1.981	2.257
r	0.985	0.991	0.995	0.913	0.983	0.998	0.915	0.933	0.956	0.993	0.908	0.903
						Product II						
A, ng/mL	9599	7312	2111	9137	16530	87980	77.32	3986	200.8	11190	—	11220
B, ng/mL	138.1	2138	399.7	1402	178.1	3504	3761	567.5	1229	402.3	7318	159.4
C, ng/mL	10350	10150	2515	10540	16840	91400	4957	5233	1466	12730	7776	12270
α, h^{-1}	1.069	1.633	1.249	1.089	1.225	3.380	1.003	0.817	0.356	1.285	—	1.134
β, h^{-1}	0.171	0.646	0.348	0.498	0.204	0.576	0.135	0.293	0.327	0.279	0.551	0.199
γ, h^{-1}	1.458	1.928	2.885	1.022	1.405	3.070	1.524	1.164	0.431	1.844	0.700	1.525
r	0.913	0.903	0.998	0.959	0.992	0.954	0.949	0.957	0.851	0.959	0.901	0.975

[a] $C_p = Ae^{-\alpha t} + Be^{-\beta t} - Ce^{-\gamma t}$.

Table IV—Urine Output, mL

Time, h	Subject												Mean ± *SD*
	1	2	3	4	5	6	7	8	9	10	11	12	
							Product I						
Predose (24 h)	685	1130	672	2650	1222	2560	1300	1320	1252	2000	1220	1283	1441 ± 638
0-1	885	785	790	343	684	662	116	376		143	258	447	457 ± 298
1-2	821	573	533	650	413	315	950	605	387	695	1141	595	640 ± 238
2-3	237	207	108	242	378	159	362	122	384	658	426	201	290 ± 158
3-4	67	48	37	92	26	105	44	45		243	107	59	73 ± 62
4-6	60	—	26	46	45	48	81	—	233	113	111	46	67 ± 63
6-8	58	140	84	127	54	67	105	218	219	96	148	92	117 ± 56
8-10	52	82	54	82	57	67	79	120	109	123	108	84	85 ± 25
10-24	360	420	475	380	450	400	410	550	1470	615	410	1200	595 ± 358
							Product II						
Predose (24 h)	830	1136	725	1310	1060	2000	1453	1040	1702	1508	1250	1620	1303 ± 373
0-1	360	319	452	—	450	—	75	176	255	905	55	433	290 ± 259
1-2	905	649	500	148	638	780	527	538	633	596	410	477	567 ± 189
2-3	168	134	100	186	142	278	428	255	293	430	544	296	271 ± 138
3-4	73	52	40	256	42	54	—	82	128	151	276	85	103 ± 86
4-6	68	65	55	254	51	62	238	85	198	115	256	61	126 ± 85
6-8	64	80	69	106	62	77	177	155	98	97	148	88	102 ± 38
8-10	78	78	72		60	95	144	38	246	110	119	85	94 ± 61
10-24	390	630	880	790	350	410	645	510	1090	650	595	440	615 ± 220

with two elimination phases following absorption. The half-lives were calculated from each declining exponential term; the areas under the plasma level time curve to 10 h ($AUC_{0\ 10\ h}$) and to infinite time ($AUC_{0\ \infty}$) for each subject were calculated from the fitted equation by integration. Maximum plasma concentration (C_{max}) and time to maximum concentration (t_{max}) were taken directly from the observed data.

Statistical Analysis—Analysis of variance (ANOVA) was used to test for significant subject, treatment, or week differences (3) for each pharmacokinetic or pharmacodynamic parameter. Missing data were estimated using Yates' method (4). Before analysis, a normality test was carried out (5). If necessary, the results were logarithmically transformed to normalize the distribution of data and to stabilize the variance. The 95% confidence limits of Shirley (6) were applied to the mean treatment differences for each parameter. This gave a measure of precision and established whether the limits were symmetrical about a mean distribution of zero. The results for generic furosemide (product II) were expressed as a percentage of those for brand-name furosemide (product I).

The split-plot analysis of Westlake (7) was also used. This examined the data in two ways: (*a*) giving a measurement of quantitative differences in overall mean plasma concentrations for each treatment, and (*b*) giving an evaluation of the relative shapes of the plasma concentration-time profiles of the two treatments.

RESULTS

Table I shows the individual plasma levels of furosemide associated with each treatment. Mean plasma concentration with time is plotted in Fig. 1. Table II shows the amount of furosemide in each urine collection. The results of pharmacokinetic curve-fitting appear in Table III. Table IV gives the individual urine volumes, and Table V gives the individual urinary sodium data. The key pharmacokinetic and pharmacodynamic results are summarized in Table VI, and a summary of statistical analyses with 95% confidence limits is shown in Table VII.

Pharmacokinetics—For one individual (subject 9) following product II, the curve-fit was unacceptable (Table III, $r = 0.851$). In this case, derived pharmacokinetic values ($t_{1/2}$ and AUC terms) were estimated by Yates' method (5).

Following product I administration, the mean maximum plasma furosemide concentration (C_{max}) was 1658 ng/mL (range 550–2950 ng/mL). Following product II administration, the values were significantly lower ($p < 0.01$) with a mean C_{max} of 947 ng/mL (range 210–1800 ng/mL). There was no significant difference in time to maximum concentration (t_{max}), although there was a trend toward later values following product II treatment (*i.e.*, an asymmetrical confidence limit).

The overall bioavailability judged from AUC values followed the same trend as that shown by C_{max}, with a highly significant ($p < 0.01$) difference between treatments in values both to 10 h and to infinite time. Product I gave a mean $AUC_{0-\infty}$ of 3066 ng·h/mL (range 1362–5223 ng·h/mL), whereas product II gave a mean $AUC_{0-\infty}$ of 2098 ng·h/mL (range 891–3252 ng·h/mL). Figure 2 shows the individual $AUC_{0-\infty}$ values diagrammatically, and illustrates that despite some interindividual variability in plasma level profiles, subjects tended to keep a similar rank order of bioavailability following each preparation of furosemide.

Urinary elimination of unchanged furosemide accounted for between 17–50% of the administered dose. Again, a significant difference ($p = 0.02$) was observed between formulations in respect of the cumulative 0-24-h urinary furosemide, with product I giving a mean value of 13.6 mg (range 8.0–19.6 mg) and product II giving a mean value of 10.8 mg (range 4.9–17.0 mg).

Table V—Urinary Sodium Output, mmol

Time, h	Subject 1	2	3	4	5	6	7	8	9	10	11	12	Mean ± *SD*
						Product I							
Predose (24 h)	199	113	108	305	141	269	156	119	144	230	195	103	174 ± 67
0–1	137	86	99	46	82	60	20	36	—	17	40	58	57 ± 39
1–2	111	57	72	85	52	35	138	67	45	45	154	83	82 ± 36
2–3	37	23	15	31	49	14	52	13	50	79	62	30	38 ± 21
3–4	11	4	4	10	2	6	4	4	—	27	15	8	8 ± 7
4–6	11	—	3	3	3	1	10	—	41	7	19	5	9 ± 12
6–8	16	11	10	8	6	3	16	22	37	5	32	12	15 ± 11
8–10	9	6	7	5	7	4	12	14	20	9	24	12	11 ± 6
10–24	59	13	71	25	59	40	62	50	29	55	68	60	49 ± 18
						Product II							
Predose (24 h)	100	91	83	144	80	240	189	125	60	241	206	105	139 ± 64
0–1	50	33	52	—	45	—	17	17	8	122	12	63	35 ± 35
1–2	127	81	55	19	77	66	79	62	66	86	55	64	70 ± 25
2–3	25	17	11	25	18	29	68	33	13	60	73	49	35 ± 22
3–4	11	6	2	18	5	5	—	9	5	20	30	13	10 ± 9
4–6	10	6	2	24	4	5	45	11	24	8	35	8	15 ± 14
6–8	9	8	3	16	7	7	42	23	9	9	25	18	15 ± 11
8–10	13	9	5	—	7	7	31	3	22	12	20	15	12 ± 9
10–24	45	50	35	103	42	51	94	51	11	68	95	81	61 ± 28

Table VI—Summary of Kinetic and Dynamic Results

Parameter	Subject 1	2	3	4	5	6	7	8	9	10	11	12	Mean ± *SD*
						Product I							
C_{max}, ng/mL	1650	1650	1610	1810	1630	2950	1060	1870	550	1380	1500	2240	1658 ± 585
t_{max}, h	1.0	1.5	0.5	1.0	1.0	0.5	1.5	1.0	1.5	1.5	1.5	1.0	1.1 ± 0.4
$t_{1/2,\alpha}$, h	0.55	0.68	0.51	0.65	0.41	0.60	0.65	0.58	0.72	0.60	0.82	0.60	0.6 ± 0.1
$t_{1/2,\beta}$, h	1.95	2.56	1.98	3.11	1.22	1.85	2.36	3.99	3.45	2.91	2.02	3.19	2.55 ± 0.70
AUC_{0-10h}, ng·h/mL	2933	4085	2542	2922	2951	5175	2084	3222	1127	2889	2771	3033	2977 ± 981
$AUC_{0-\infty}$, ng·h/mL	2943	4159	2564	3037	2964	5223	2102	3373	1362	3099	2845	3125	3066 ± 959
0–24-h urinary furosemide, mg	19.6	15.6	14.2	11.2	17.2	12.1	12.3	11.7	8.0	11.4	16.5	13.4	13.6 ± 3.2
Urine volume, mL													
0–4 h	2010	1613	1468	1327	1501	1241	1472	1148	771	1739	1932	1302	1460 ± 343
0–24 h	2540	2255	2107	1962	2107	1823	2147	2036	2802	2685	2709	2724	2325 ± 345
Sodium output, mmol													
0–4 h	296	170	190	172	185	115	214	120	95	168	271	179	181 ± 59
0–24 h	391	200	281	213	260	163	314	206	222	244	414	268	264 ± 76
						Product II							
C_{max}, ng/mL	1800	1350	880	210	1010	1340	420	770	240	1580	620	1140	947 ± 518
t_{max}, h	1.0	1.5	0.5	1.5	1.0	1.5	2.0	1.5	5.0	1.0	2.0	1.0	1.6 ± 1.2
$t_{1/2,\alpha}$, h	0.65	0.43	0.56	0.64	0.57	0.21	0.69	0.85	1.95	0.54	—	0.61	0.70 ± 0.44
$t_{1/2,\beta}$, h	4.05	1.07	1.99	1.39	3.39	1.20	5.14	2.37	2.12	2.49	1.26	3.48	2.50 ± 1.28
AUC_{0-10h}, ng·h/mL	2537	2519	1932	871	2268	2327	911	2204	705	3158	2113	2532	2006 ± 772
$AUC_{0-\infty}$, ng·h/mL	2687	2525	1968	891	2382	2346	1070	2321	918	3252	2167	2646	2098 ± 756
0–24-h urinary furosemide, mg	14.0	12.2	10.2	4.9	12.3	8.2	7.3	10.5	10.0	17.0	10.8	11.9	10.8 ± 3.1
Urine volume, mL													
0–4 h	1506	1154	1092	590	1272	1112	1030	1051	1309	2082	1285	1291	1231 ± 349
0–24 h	2106	2007	2168	1740	1795	1756	2234	1839	2941	3054	2403	1965	2167 ± 438
Sodium output, mmol													
0–4 h	213	137	120	62	145	100	164	121	92	288	170	189	150 ± 61
0–24 h	290	210	165	205	205	170	376	209	158	385	345	311	252 ± 84

Split-plot analysis showed highly significant ($p < 0.01$) differences between formulations both in the overall mean plasma values and in the treatment–time shape of the curves.

Pharmacodynamics—The missing values in the urinary tables reflect the fact that not all subjects were able to micturate on demand. Prior to statistical evaluation of pharmacodynamic data, estimates of the "missing" values were made by assuming that the urine eventually collected was actually produced at a constant rate over both "observed" and "missing" time periods.

The pharmacodynamic measurements presented for analysis in Tables VI and VII are those from the 0–4- and 0–24-h urine collection periods; the former covered the period of maximum diuresis (Tables IV and V) and was considered to be the most appropriate measure of meaningful pharmacodynamic effect. The mean 0–4-h urine volume following product I was 1460 mL (range 771–2010 mL); the equivalent mean result for product II was 1231 mL (range 590–2082 mL). The mean 0–4-h urine sodium output following product I was 181 mmol (range 95–296 mmol), and the mean 0–4-h urine sodium output following generic furosemide was 150 mmol (range 62–288 mmol). Most subjects showed less diuresis following product II; however, for the 0–4-h urine volume this trend was clearly reversed in subjects 9 and 10. With respect to urinary sodium, subject 10 again reversed the general trend toward diminished natriuresis following product II; subject 9 showed little difference between treatments in this respect.

Statistical analysis of these pharmacodynamic results (Table VII), in contrast with the corresponding analysis of pharmacokinetic data, did not show any significant differences between the effects of the two furosemide preparations. However, the 95% confidence intervals, especially for 0–4-h data, were asymmetrical with product II giving between −33% and 2% ($p = 0.07$) of the 0–4-h urine output of product I and between −38% and 4% ($p = 0.08$) of the 0–4-h sodium output of product I, reflecting the general trend for the generic formulation to show a diminished effect.

DISCUSSION

This study has shown statistically significant differences in the bioavailability of two furosemide formulations, the generic tablet giving up to 66% lower C_{max} values, up to 52% lower $AUC_{0-\infty}$ values, and up to 37% less urinary elimination of furosemide over 24 h. Although not statistically significant, there was also a trend toward later t_{max} values following the generic treatment. However, simultaneous analysis of drug effect did not give correspondingly significant differences in urine output and sodium excretion. Nevertheless,

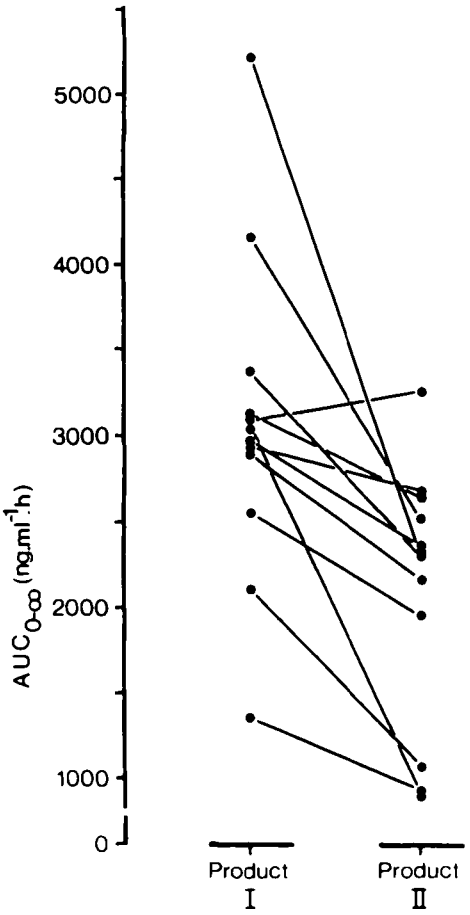

Figure 2—*Comparative bioavailability of the two furosemide formulations.*

pharmacodynamic differences between formulations over 0–4-h collection periods were significant at the 10% level, and the 95% confidence intervals were clearly asymmetrical; therefore, biological equivalence of these two formulations cannot be assumed.

The analysis of pharmacodynamic effects has concentrated on 0–4-h data rather than the complete collection interval of the experiment, since following acute diuresis and natriuresis in normal subjects, homeostatic mechanisms can result in compensatory "rebound" conservation of salt and water by 24 h. This tendency is shown by the diminished significance of 0–24-h statistical analysis in comparison with that for 0–4 h, especially with respect to urinary sodium excretion. The inherent logarithmic shape of the classical dose–response curve in pharmacology makes any pharmacodynamic measurement a less sensitive measure of formulation differences, since a given percentage change in drug concentration will give a smaller percentage change in drug effect: a linear change on the latter scale corresponds to a logarithmic change on the former scale.

This study supports the clinical observations of diuretic ineffectiveness which led to the withdrawal of this generic furosemide product. Since it has been reported that the absorption of furosemide is impaired in the presence of edema (8), it is possible that unequivalent furosemide formulations may show proportionately greater pharmacokinetic and pharmacodynamic differences in patients with cardiac failure than in normal subjects.

Kelly *et al.* (9) have previously shown that the bioavailability of brand-name furosemide tablets was similar to that of an aqueous solution. A comparative bioavailability study from Sweden (10) which included pharmacokinetic and pharmacodynamic observations revealed no significant differences between brand-name furosemide tablets and a generic tablet; however, a study from Israel (11) demonstrated statistically significant pharmacokinetic and pharmacodynamic differences between two other furosemide products. A preliminary observation from investigators in New Zealand (12) suggested that there may be clinically important differences in the response to brand-name and generic furosemide tablets, although a later more formal study (13) reported that the two furosemide products in question were in fact bioequivalent. However, it should be noted that this last study consisted only of urinary pharmacodynamic measurements, and our present investigation has shown that this may not be a sufficiently sensitive technique. Investigators in Australia (14) reported bioequivalence of yet another generic furosemide product basing their conclusions on measurements of urine volume and urine electrolytes.

Table VII—Summary of Statistical Results

Parameter	Overall Differences (ANOVA)[a] Subject Treatment Week 1	2	3	95% Confidence Interval (Generic as % of Standard)
C_{max}	NS	**	NS	−66% to −21%
t_{max}	NS	NS	NS	− 8% to +82%
$t_{1/2\alpha}$	NS	NS	NS	−18% to +21%
$t_{1/2\beta}$	NS	NS	•	−24% to +37%
$AUC_{0-10\ h}$	*	**	NS	−50% to −14%
$AUC_{0-\infty}$	•	**	NS	−52% to −15%
0–24 h urinary furosemide	NS	*	NS	−37% to − 5%
Urine volume				
0–4 h	NS	NS	NS	−33% to + 2%
0–24 h	NS	NS	NS	−15% to + 2%
Sodium output				
0–4 h	*	NS	NS	−38% to + 4%
0–24 h	**	NS	*	−19% to +10%

[a] Key: (NS) = not significant; (*) = significant at the 5% level; (**) = significant at the 1% level.

Furosemide can be used in clinical circumstances where a prompt diuresis is essential. While it is clear from the above discussion that some generic formulations are equivalent to brand-name tablets, it is also evident that other products may not be adequate. Alternative furosemide formulations should be carefully evaluated, preferably by means of full pharmacokinetic and pharmacodynamic investigations in humans.

In the absence of greater detail, it is difficult to comment on any pharmaceutical factors which may have contributed to inequivalence of these furosemide formulations. However, calcium and phosphate were detected in product II and not in product I following the application of standard National Formulary methods[10]. Residue analysis also showed differences in the amounts of inorganic excipients (4% for product I and 37% for product II)[10]. These observations appear to be in keeping with the findings of Rubinstein (15) who reported that the bioavailability of experimental batches of furosemide was considerably influenced by the choice of excipient. He also found a poor correlation between dissolution rate and drug bioavailability.

REFERENCES

(1) "HEW News P79-6," U.S. Department of Health, Education and Welfare, March, 30, 1979, p. 1.

(2) N. R. Draper and H. Smith, "Applied Regression Analysis," Wiley, New York, N.Y., 1966, p. 7.

(3) W. G. Cochran and G. M. Cox, "Experimental Designs," Wiley, New York, N.Y., 1957, p. 127.

(4) F. Yates, *Emp. J. Exp. Agr.*, **1**, 129 (1933).

(5) W. J. Dixon and F. J. Massey, "Introduction to Statistical Analysis," McGraw-Hill, New York, N.Y., 1969, p. 63.

(6) E. Shirley, *J. Pharm. Pharmacol.*, **28**, 312, (1976).

(7) W. J. Westlake, "Current Concepts in the Pharmaceutical Sciences," Lea and Febiger, Philadelphia, Pa., 1973, p. 150.

(8) B. J. Odlind and B. Beermann, *Br. Med. J.*, **i**, 1577 (1980).

(9) M. R. Kelly, R. E. Cutler, A. W. Forey, and B. M. Kimpel, *Clin. Pharmacol. Ther.*, **15**, 178 (1974).

(10) B. Beerman, E. Dalen, and B. Lindstrom, *Br. J. Clin. Pharmacol.*, **6**, 537 (1978).

(11) A. Danon and J. Kaplanski, *Therapiewoche*, **29**, 1887 (1979).

(12) R. Bailey, *N. Z. Med. J.*, **90**, 30 (1979).

(13) D. M. Paton, *N. Z. Med. J.*, **91**, 208 (1980).

(14) J. J. McNeil, F. J. E. Vajda, V. Vijayasekaran, and W. J. Louis, *Med. J. Austr.*, **2**, 505 (1977).

(15) M. H. Rubinstein, *Drug. Dev. Ind. Pharm.*, **6**, 105 (1980).

[10] H. B. Lassman, Hoechst-Roussel Pharmaceuticals, Inc., personal communication.

pK_a Determination of Verapamil by Liquid–Liquid Partition

JIRO HASEGAWA *x, TAKESHI FUJITA *, YAYOI HAYASHI ‡, KIKUO IWAMOTO ‡, and JUN WATANABE ‡

Received August 13, 1982, from the *Department of Drug Metabolism and Biopharmaceutics, Eisai Co. Ltd., 6-10, Koishikawa 4-chome, Bunkyo-ku, Tokyo 112, Japan and the ‡ Department of Biopharmaceutics, Faculty of Pharmaceutical Sciences, Nagoya City University, Mizuho-ku, Nagoya 467, Japan. Accepted for publication January 10, 1983.

Abstract □ The pK_a of verapamil was determined by measuring the partition coefficient of verapamil between *n*-heptane and aqueous buffer solution at various pH values. The magnitude of the effects of ionic strength or temperature on the pK_a of verapamil was in agreement with those reported previously. The estimated pK_a of verapamil in human plasma was 8.75. The pK_a of 2,4,6-trimethylpyridine measured by means of the present partition method was in good agreement with that determined by UV spectrophotometry.

Keyphrases □ Verapamil—pK_a determination, liquid–liquid partition coefficients, effects of ionic strength and temperature □ Partition coefficients—liquid–liquid, use in determining the pK_a of verapamil, effects of ionic strength and temperature □ Dissociation constants—verapamil, determination using liquid–liquid partition coefficients, effects of ionic strength and temperature

Verapamil, an effective antiarrhythmic agent, exerts its effect through selective inhibition of slow inward transport of calcium across cell membranes. Although the drug was first introduced in 1962 in Germany, no report on the pK_a value of verapamil, a weakly basic compound, has yet appeared. We required this information to analyze our results on the mechanism of salivary excretion of verapamil in humans and dogs.

Potentiometric or UV spectrophotometric methods are generally most useful for the accurate and reproducible determination of aqueous dissociation constants of organic compounds. However, these methods are not applicable for the determination of the pK_a of verapamil because the drug is insufficiently soluble in aqueous media to give a reliable titration curve and also because of the lack of a significant pH-dependent change in the absorption spectra. Several alternative methods exist for the determination of pK_a values of such compounds (1). For instance, mixed aqueous solvents can be used for the titration of sparingly soluble compounds.

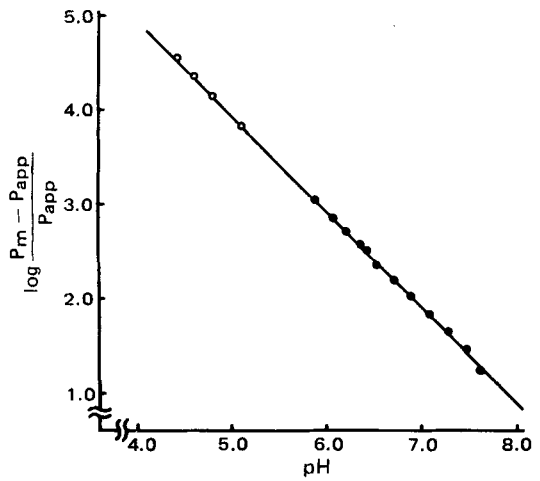

Figure 1—*Plot of log* $[(P_m - P_{app})/P_{app}]$ versus *pH. Initial concentration of verapamil in* n*-heptane, 0.003 M; ionic strength, 0.0315; temperature, 25°C. Key: (○) in phosphate buffer; (●) in acetate buffer.*

However, there is no completely satisfactory method for converting the results to the aqueous pK_a scale (2). The solubility (3, 4) and modified titration (5) methods are also unsuitable for verapamil, since it is difficult to determine the aqueous solubility of the un-ionized form of the compound with sufficient accuracy because of the extremely low solubility.

In the present study, we attempted to determine the pK_a of verapamil by a partition method based on measurement of the partition coefficient between water and an immiscible organic solvent at various pH values of the aqueous phase. Although this method was first proposed several decades ago (6, 7), it has not been generally recognized as a useful method for the pK_a determination of sparingly soluble compounds. Recently, Ezumi and Kubota extended this method to determine pK_a values of weak organic bifunctional acids and bases (8), but their proposed equation cannot be applied to the pK_a determination of verapamil because of the extremely high partition coefficient of this drug. To test the general applicability of the partition method, the effects of organic solvent, ionic strength, temperature, and concentration of verapamil on the pK_a value of verapamil were also studied. Furthermore, to confirm the validity of this method, the pK_a value of 2,4,6-trimethylpyridine was measured by means of both the partition and the UV spectrophotometric methods.

EXPERIMENTAL

Materials—Verapamil hydrochloride[1] and 2,4,6-trimethylpyridine were used as received. Organic solutions of the free base of verapamil or 2,4,6-trimethylpyridine were prepared by extracting alkaline solutions of these compounds (pH 11.0) with the appropriate organic solvent, followed by adjustment of the volume to 100 mL. *n*-Heptane[2], *n*-hexane[2], and carbon tetrachloride[2] were of spectroscopic grade, and other reagents[3] were of analytical grade.

Equipment—The pH values of aqueous buffer solutions were measured with a pH meter[4] with an accuracy of 0.01 pH unit. UV absorption measurements relevant to the determination of partition coefficients and the pK_a determination of 2,4,6-trimethylpyridine by the UV method were made using a spectrophotometer[5]. A spectrofluorophotometer[6] was used for the determination of verapamil in the low concentration range.

Determination of Partition Coefficient—Five milliliters of organic solvent containing verapamil or 2,4,6-trimethylpyridine and 5 mL of phosphate buffer or sodium hydroxide solution were added to a screw-capped vial and incubated for 2 h in a temperature-controlled incubator (±0.1°C) with occasional vigorous shaking by hand. The tube was centrifuged for 5 min at 3000 rpm, then immersed in the incubator again and allowed to stand for 30 min. Aliquots of both phases were withdrawn and subjected to analyses, and the pH of the aqueous phase was measured immediately.

Analytical Procedure—For verapamil, the concentration in the aqueous phase was determined either spectrophotometrically (λ_{max} = 277 nm) or spectrofluorophotometrically (excitation at 275 nm, emission at 339 nm) after appropriate dilution of the solution with 0.5 M HCl depending on the con-

[1] Knoll A. G., Ludwigshafen, West Germany.
[2] Dojin Chemical Co., Ltd., Tokyo, Japan.
[3] Wako Chemicals, Co., Ltd., Osaka, Japan.
[4] Model HM-5B with a type GST 155C glass electrode; Toa Electric Co., Ltd.
[5] UV 300; Shimadzu Co., Ltd., Kyoto, Japan.
[6] Model RF 502; Shimadzu Co., Ltd., Kyoto, Japan.

0022-3549/84/0400-0442$01.00/0
© 1984, American Pharmaceutical Association

Table I—Effect of pH on P_m [a]

Conc. of NaOH[b]	pH	P_m[c]
0.01 M	11.85	487 ± 12
0.03 M	12.38	523 ± 18
0.10 M	12.89	492 ± 15

[a] Organic solvent, *n*-heptane; initial concentration of verapamil in *n*-heptane, 0.001 M; temperature, 25°C. [b] Ionic strength was adjusted to 0.1 with sodium chloride. [c] Mean ± *SD* of three experiments.

Table II—Effect of Ion Species on P_m [a]

Salt[b]	pH[c]	P_m[d]
KCl	11.90	434 ± 21
NaCl	11.95	467 ± 6
Na_2SO_4	11.92	426 ± 6

[a] Organic solvent, *n*-heptane; initial concentration of verapamil in *n*-heptane, 0.001 M; temperature, 25°C. [b] Ionic strength was adjusted to 0.03 with the indicated salt. [c] Concentration of sodium hydroxide was 0.01 M. [d] Mean ± *SD* of three experiments.

centration of verapamil present. The organic phase was evaporated to dryness under a nitrogen stream at 40°C, and the residue was dissolved in 0.1 M HCl for spectrophotometric measurement. For 2,4,6-trimethylpyridine, concentrations in the aqueous and *n*-heptane phases were determined spectrophotometrically (λ_{max} = 266 nm and 263 nm, respectively) after appropriate dilution with 0.5 M HCl and *n*-heptane, respectively.

Preparation of Buffer Solution—All buffer solutions were prepared using monobasic potassium phosphate and dibasic sodium phosphate. The ionic strength of the aqueous phase after the partition experiment was calculated by means of the following:

$$I = \frac{1}{2}\left\{\frac{4[P]}{1 + 10^{7.21\text{-pH}}} + [P]\left(1 - \frac{1}{1 + 10^{7.21\text{-pH}}}\right) + [K] + [Na] + [V]\frac{1}{1 + P_{app}}\right\} \quad \text{(Eq. 1)}$$

where I is the ionic strength of the aqueous phase; [P], [V], [K], and [Na] are the molar concentrations of total phosphate, verapamil, potassium, and sodium, respectively; and P_{app} is the apparent partition coefficient of verapamil. The calculated ionic strength in the aqueous phase after partition varied appreciably with pH because of the differences in the concentration of verapamil in the aqueous solution. However, since deviations in ionic strength of this magnitude were estimated to change the pK_a value by no more than 0.01 pK_a unit, the variation of ionic strength with pH was disregarded and the ionic strength was expressed as the mean value.

Calculation of pK_a from Apparent Partition Coefficient—During partitioning of a weak base between organic and aqueous phases, the distribution of each species can be described by Scheme I: where, K_a and K_a' are the stoichiometric ionization constants of BH^+ in the aqueous and organic phases, respectively; P_m and P_i are the partition coefficients of un-ionized and ionized molecules, respectively; $[B]_o$ and $[B]_w$ are the molar concentrations of un-ionized molecules in the organic and aqueous phases, respectively; and $[BH^+]_o$ and $[BH^+]_w$ are the molar concentrations of ionized molecules in the organic and aqueous phases, respectively.

If the concentration of the ionized molecule is far less than that of the un-ionized molecule in the organic phase, that is $[BH^+]_o \ll [B]_o$, the apparent partition coefficient can be expressed by:

$$P_{app} = \frac{[B]_o}{[B]_w + [BH^+]_w} \quad \text{(Eq. 2)}$$

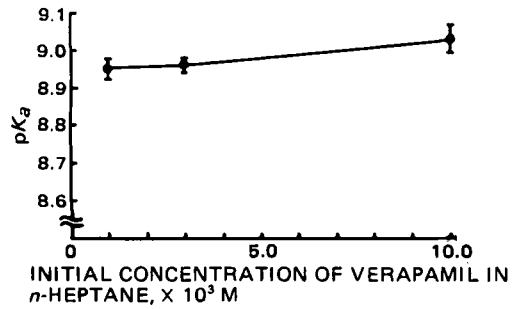

Figure 2—*Effect of concentration of verapamil on* pK_a. *Each point represents the mean* ± SD *of 10 experiments. Ionic strength, 0.1050–0.1005; temperature, 25°C.*

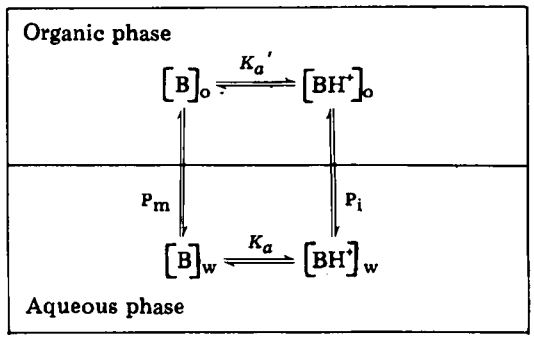

Scheme I

From the definition:

$$P_m = \frac{[B]_o}{[B]_w} \quad \text{(Eq. 3)}$$

$$K_a = \frac{[B]_w[H^+]}{[BH^+]_w} \quad \text{(Eq. 4)}$$

$$pK_a = pH + \log\frac{[BH^+]_w}{[B]_w} \quad \text{(Eq. 5)}$$

From Eqs. 2, 3, and 5:

$$pK_a = \log\frac{P_m - P_{app}}{P_{app}} + pH \quad \text{(Eq. 6)}$$

Equation 6 can be rearranged to:

$$P_{app} = P_m - \frac{1}{K_a}[H^+]\,P_{app} \quad \text{(Eq. 7)}$$

By plotting P_{app} *versus* $[H^+]\,P_{app}$, K_a, and P_m can be obtained simultaneously from the slope and the intercept of the plot, respectively. However, for a compound with a large P_m value, such as verapamil, this plot gives inaccurate results. Instead, by measuring P_m at a pH which is higher than the pK_a value of the compound by 2.0 pH units and P_{app} at a pH where the P_{app} value is ~1.0, the pK_a value can be calculated from Eq. 6.

Measurement of pK_a of 2,4,6-Trimethylpyridine by UV Spectrophotometry—The UV absorbances of 1×10^{-4} M 2,4,6-trimethylpyridine in phosphate buffer (from pH 6.98 to pH 7.57, I = 0.03), and in 0.1 M HCl and 0.1 M NaOH were measured at 266 nm and at 25°C. The pK_a value was calculated by using:

$$pK_a = pH + \log\frac{d - d_M}{d_I - d} \quad \text{(Eq. 8)}$$

where d, d_I, and d_M are the absorbances in buffer solution, 0.1 M HCl solution (where 2,4,6-trimethylpyridine exists predominantly as the ionized form), and 0.1 M NaOH solution (where it exists predominantly as the un-ionized form), respectively.

RESULTS AND DISCUSSION

Estimation of P_m—The present method inherently requires the measurement of the P_m value. Since the ion composition of the solution used for the measurement of P_m is inevitably different from that of the buffer solution used for the measurement of P_{app}, it is necessary to estimate the effect of ion species on the P_m value. As shown in Tables I and II, the observed P_m values change appreciably with change of pH or of the kind of neutral salts added to the solution. This discrepancy in P_m value results in a variation in the calculated

Table III—Effect of Organic Solvents on pK_a [a]

Solvent	pK_a[b]	P_m[c]
n-Heptane	8.93 ± 0.001	479 ± 5
	8.92 ± 0.001	448 ± 5
	8.90 ± 0.003	460 ± 2
Mean ± *SD*	8.92 ± 0.01	
n-Hexane	8.89 ± 0.02	561 ± 17
	8.88 ± 0.01	632 ± 18
Mean ± *SD*	8.89 ± 0.01	
n-Pentane	8.93 ± 0.02	486 ± 4
Carbon tetrachloride	8.54 ± 0.02	$3.63 \times 10^4 \pm 0.13 \times 10^4$

[a] Initial concentration of verapamil in organic solvent, 0.003 M; ionic strength, 0.0315; temperature, 25°C. [b] Mean ± *SD* of seven experiments; different values for the same solvent show results obtained on different days. [c] Mean ± *SD* of three experiments; different values for the same solvent show results obtained on different days.

Table IV—pK_a Values of 2,4,6-Trimethylpyridine Determined by the UV Spectrophotometric Method [a]

pH	Absorbance[b]	pK_a[c]
6.98	0.694	7.50
7.09	0.678	7.52
7.19	0.653	7.49
7.28	0.634	7.49
7.38	0.610	7.48
7.48	0.592	7.51
7.57	0.574	7.51
Mean ± *SD*		7.50 ± 0.01
0.1 M HCl	0.788	
0.1 M KOH	0.384	

[a] Concentration of 2,4,6-trimethylpyridine, 1×10^{-4} M; ionic strength, 0.03; temperature, 25°C. [b] Absorbance was measured at 266 nm. [c] $pK_a = pH + \log (d - d_M)/(d_I - d)$, where d, d_I, and d_M are the absorbances in solutions of the indicated pH, in 0.1 M HCl, and in 0.1 M KOH, respectively.

pK_a of up to 0.03 pK_a unit depending on the salt used; this possible deviation of the pK_a values obtained by the present method must be borne in mind. P_m measurements in the following experiments were carried out in 0.01 M NaOH solution whose ionic strength had been adjusted to 0.03 with sodium chloride.

Validity of Equation 6—To test the validity of Eq. 6 for the pK_a determination of verapamil, the apparent partition coefficients of verapamil between *n*-heptane and aqueous buffer solution at pH from 4.42 to 7.64 were obtained. The resultant log $[(P_m - P_{app})/P_{app}]$ *versus* pH plot was linear with a slope of −1.016 (r = 0.9999) (Fig. 1). This means that Eq. 6 is applicable to the calculation of pK_a from partition coefficients obtained under the proposed experimental conditions. There should be no appreciable effect of buffer composition on the resultant pK_a value, since the results obtained in acetate and phosphate buffers as the aqueous phase are essentially on the same regression line.

Effect of Verapamil Concentration—To determine the effect of verapamil concentration, pK_a values were measured at three different initial verapamil concentrations. As shown in Fig. 2, the obtained pK_a values increased slightly with increase of the verapamil concentration; in particular, the results at 0.01 M gave a significantly higher pK_a value than those at the lower concentrations.

One possible reason for this finding might be the self-association of verapamil in the solution, although extensive studies would be necessary to elucidate the actual reason. At the initial concentrations of 0.001 and 0.003 M, the obtained pK_a values were 8.95 and 8.96, respectively. These values are essentially identical, especially when the experimental error is taken into account. In the following experiment, the initial concentration of verapamil in *n*-heptane was fixed at 0.003 M.

Effect of Organic Solvent—If the theories and assumptions in the proposed method are valid, the pK_a values obtained by this method should be independent of the kind of organic solvent used for the determination of the partition coefficient. One possible source of error in determining the true pK_a value would be partial miscibility of the organic solvent with the aqueous phase during the partition experiment, which might interfere with the dissociation reaction in the aqueous phase. To minimize the extent of contamination of the aqueous phase with the organic solvent, paraffinic hydrocarbons were chosen as organic solvents for the partition experiment in view of their low water solubility. The pK_a values obtained with various organic solvents are presented in Table III. Three highly nonpolar solvents gave comparable pK_a values (*n*-heptane, 8.92; *n*-hexane, 8.89; and *n*-pentane, 8.93) even though they differ in water solubility by a factor of four (9, 10).

On the other hand, carbon tetrachloride gave a fairly low pK_a value compared with those obtained with paraffins. This result is consistent with those reported by Irving and Bell (7), who showed that the pK_a value of dithizone as determined by the partition method using carbon tetrachloride was smaller than that determined using cyclohexane by 0.4 pK_a unit. *n*-Heptane was chosen in the following experiments to minimize organic solvent contamination in the aqueous layer as well as to minimize evaporation, which may lead to volume loss of the organic phase during the partition experiment.

Table V—pK_a Values of 2,4,6-Trimethylpyridine Determined by the Partition Method

pH	P_{app}[a]	pK_a
5.88	0.276	7.53
6.08	0.433	7.53
6.20	0.579	7.51
6.38	0.835	7.53
6.42	0.929	7.52
6.55	1.165	7.54
6.71	1.718	7.51
Mean ± *SD*		7.52 ± 0.01
0.01 M NaOH	12.5[b]	

[a] Initial concentration of 2,4,6-trimethylpyridine in *n*-heptane, 0.003 M; ionic strength, 0.0315; temperature, 25°C. [b] Mean ± *SD* of three experiments.

Table VI—Temperature Dependency of pK_a^T of Verapamil

Temp.	Observed pK_a[a]	pK_a^T	
25°C	8.92[b]	8.84[c]	
31°C	8.79	8.71[c]	8.73[d]
37°C	8.68	8.60[c]	8.61[d]

[a] Initial concentration of verapamil in *n*-heptane, 0.003 M. [b] Mean of three experiments carried out on different days. [c] Calculated using Eq. 10 and the observed pK_a. [d] Calculated by the method of Albert and Sergent (14).

Comparison of the Partition Method with the UV Spectrophotometric Method—To confirm the reliability of the partition method, the pK_a value of 2,4,6-trimethylpyridine was determined by means of both the partition and UV spectrophotometric methods. As shown in Tables IV and V, the results obtained by the two methods were almost identical (7.52 and 7.50, respectively); the thermodynamic pK_a value (pK_a^T), calculated by subtracting the value of $-\log \gamma^{\pm}$ (*cf.*, Eq. 10) from the mean pK_a value to correct for the activity coefficient of the aqueous solvent, was 7.43, identical with the reported value (11). This result strongly supports the reliability of this method.

Effect of Ionic Strength—Methods to correct for ionic strength and obtain the pK_a^T value are well documented (1, 2). One method is to subtract the following log $\gamma^{\pm}$ value from the experimentally determined pK_a value:

$$-\log \gamma^{\pm} = \frac{AZ^+Z^-\sqrt{I}}{1 + Ba_i\sqrt{I}} \qquad \text{(Eq. 9)}$$

where I is the ionic strength of the solvent, $\gamma^{\pm}$ is the ionic activity coefficient, A and B are constants dependent on the dielectric constant of the solvent and the temperature, Z^+ and Z^- are the charge of the ion ($Z^+ = Z^- = 1$ for verapamil), and a_i is the ion size parameter. Since a_i for most electrolytes used in this experiment is equal to $3\text{–}4.5 \times 10^{-8}$ (12) and B changes only from 0.330×10^8 to 0.333×10^8 with the change of temperature from 25°C to 40°C, Eq. 9 can be simplified (13)[7]:

$$-\log \gamma^{\pm} = \frac{A\sqrt{I}}{1 + \sqrt{I}} \qquad \text{(Eq. 10)}$$

An alternative method is to determine pK_a at several different ionic strengths and then to plot pK_a *versus* $\sqrt{I}/(1 + \sqrt{I})$ and extrapolate the plot to infinite dilution (2). Figure 3 is the obtained pK_a *versus* $\sqrt{I}/(1 + \sqrt{I})$ plot for verapamil at 25°C. The intercept was 8.85 and is very close to the calculated value obtained from Eq. 10 (8.84). Although accurate and theoretically sound, this method is tedious. Therefore, since the two methods gave almost identical pK_a^T values at 25°C, Eq. 10 seems to be satisfactory for the determination of the pK_a^T of verapamil.

Temperature Dependency of pK_a^T—Determination of the pK_a is usually performed at 25°C. However, to interpret the absorption, distribution, metabolism, and excretion of drugs in terms of pK_a, one must obtain the pK_a value at 37°C experimentally or by calculation. Several equations have been proposed to express the variation of pK_a with temperature (1). Albert and Sergent proposed a temperature coefficient of pK_a of organic nitrogenous bases in the range of 0–40°C (14), but it is generally recognized that compounds vary somewhat in the sensitivity of their acidity constants to temperature changes. Therefore, the pK_a^T values of verapamil of 25°C, 31°C, and

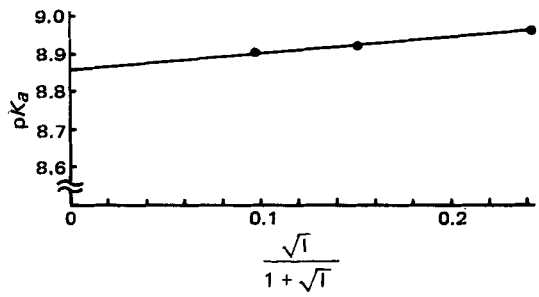

Figure 3—*Plot of* pK_a versus $\sqrt{I}/(1 + \sqrt{I})$. *Initial concentration of verapamil in organic solvent, 0.003 M; temperature, 25°C.*

[7] A = 0.488 at 0°C, 0.500 at 15°C, 0.509 at 25°C, 0.524 at 45°C.

Table VII—pK_a of Verapamil Under Various Conditions

Temp.	pK_a[a]				
	I = 0.00	I = 0.01	I = 0.03	I = 0.05	I = 0.10
5°C	9.28	9.32	9.35	9.37	9.40
10°C	9.16	9.21	9.23	9.25	9.28
15°C	9.05	9.10	9.12	9.14	9.17
20°C	8.94	8.99	9.01	9.03	9.06
25°C	8.84	8.89	8.92	8.93	8.96
30°C	8.74	8.79	8.82	8.83	8.86
37°C	8.60	8.65	8.68	8.70	8.73

[a] These values were calculated using Eqs. 10 and 12.

37°C were calculated, using Eq. 10, from the experimentally determined pK_a values at these temperatures. Experimentally obtained pK_a and pK_a^T values as well as pK_a^T values estimated using the temperature coefficients reported by Albert and Sergent are shown in Table VI.

Since the pK_a^T values calculated by the method of Albert and Sergent were close to the experimentally obtained values, their method seems to be applicable for the rough estimation of the pK_a^T of verapamil at various temperatures. On the other hand, the variation of pK_a^T with temperature can be expressed by (1):

$$pK_a^T = \frac{\Delta H^\circ}{2.303RT} - \frac{\Delta S^\circ}{2.303R} \qquad \text{(Eq. 11)}$$

where ΔH° is the enthalpy change under standard conditions, ΔS° is the entropy change under standard conditions, R is the gas constant, and T is the absolute temperature. As shown in Fig. 4, a plot of experimentally obtained pK_a^T values *versus* $1/T$ gave a straight line and could be expressed by Eq. 12. The pK_a^T values at arbitrary temperatures can be calculated by using:

$$pK_a^T = 1.833 \times 1/T \times 10^3 + 2.696 \qquad \text{(Eq. 12)}$$

CONCLUSIONS

The pK_a values of verapamil at various temperatures and ionic strengths can be estimated by means of Eqs. 10 and 12. The resultant values are presented in Table VII. On the assumption that sodium chloride is the main ionized component in plasma, the pK_a of verapamil in human plasma at 37°C can be calculated to be ~8.75.

Subject to the following restrictions, the present method should be applicable to the determination of pK_a of weak organic bases or acids[8], whose aqueous solubility is too low to give concentrations adequate for the determination of pK_a by the titration method:

1. A paraffinic hydrocarbon should be used as the organic solvent for the partition experiment to prevent the contamination of the aqueous phase with organic solvent.

[8] For acidic compounds, use $pK_a = \log [P_{app}/(P_m - P_{app})] + pH$ in place of Eq. 6 and add the $-\log \gamma^{\pm}$ value to the obtained pK_a in order to get pK_a^T.

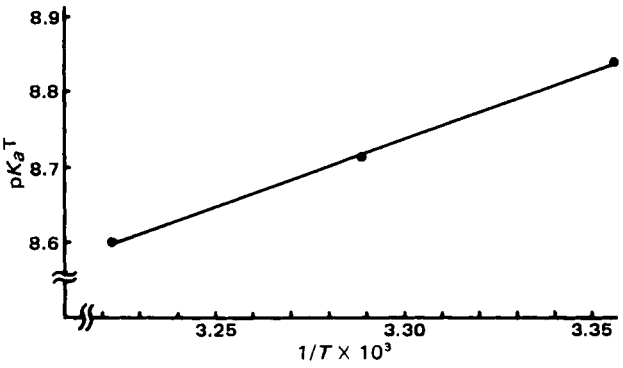

Figure 4—*Plot of* pK_a^T versus 1/T. *Initial concentration of verapamil in organic solvent, 0.003 M; temperature, 25°C; ionic strength, 0.0315.*

2. A P_m value of 1.0–1000 is advisable from the standpoint of accuracy.

3. The concentration of the drug in the partition experiment should be as low as possible.

4. Low buffer concentration is advisable to make the correction for the activity coefficient of ions simple. A swamping electrolyte such as sodium chloride should be added to adjust the ionic strength to a certain value (such as 0.05) to minimize the contribution of drug concentration change in the aqueous phase to the ionic strength.

REFERENCES

(1) R. F. Cookson, *Chem. Rev.*, **74,** 5 (1974).

(2) L. Z. Benet and J. E. Goyan, *J. Pharm. Sci.*, **56,** 665 (1967).

(3) H. A. Krebs and J. C. Speakman, *J. Chem. Soc.*, **1945,** 593.

(4) C. C. Peck and L. Z. Benet, *J. Pharm. Sci.*, **67,** 12 (1978).

(5) R. H. Levy and M. Rowland, *J. Pharm. Sci.*, **60,** 1155 (1971).

(6) C. Golumbic, M. Orchin, and S. Weller, *J. Am. Chem. Soc.*, **71,** 2624 (1949).

(7) H. Irving and C. F. Bell, *J. Chem. Soc.*, **1952,** 1216.

(8) K. Ezumi and T. Kubota, *Chem. Pharm. Bull.*, **28,** 85 (1980).

(9) S. Asahara, "Handbook of Solvents," Kyoritsu Shuppan, Tokyo, Japan, 1976.

(10) S. Musha, "Dictionary of Analytical Chemistry," Kyoritsu Shuppan, Tokyo, Japan, 1971.

(11) E. M. Arnet, R. P. Quirk, and J. J. Burk, *J. Am. Chem. Soc.*, **92**(3), 1260 (1970).

(12) J. Kieland, *J. Am. Chem. Soc.*, **59,** 1675 (1937).

(13) A. N. Martin, J. Swarbrick, and A. Cammarata," Physical Pharmacy," 2nd ed., Lea & Febiger, Philadelphia, Pa., 1970.

(14) A. Albert and E. P. Sergent, "Ionization Constants of Acids and Bases," Wiley, New York, N.Y., 1962.

Quantitative Determination of Dexamethasone in Human Plasma by Stable Isotope Dilution Mass Spectrometry

YASUJI KASUYA *§, JAMES R. ALTHAUS *, JAMES P. FREEMAN*, RONALD K. MITCHUM*x, and JEROME P. SKELLY ‡

Received November 24, 1982, from the *Department of Health and Human Services, Food and Drug Administration, National Center for Toxicological Research, Jefferson, AR 72079, and the ‡Division of Biopharmaceutics, Department of Health and Human Services, Food and Drug Administsration, 5600 Fishers Lane, Rockville, MD 20857. Accepted for publication February 8, 1983. §Present address: Tokyo College of Pharmacy, 1432-1 Horinouchi, Hachioji, Tokyo 192-03, Japan.

Abstract □ An analytical method for the quantitation of nanogram to subnanogram amounts of dexamethasone is described. Dexamethasone was isolated from human plasma using a C_{18}-bonded reverse-phase cartridge, purified by subsequent normal-phase HPLC, and the corresponding trimethylsilyl derivative analyzed by gas chromatography–mass spectrometry (GC–MS). The quantitation by isotope-dilution MS was carried out by selected-ion monitoring on the $(M + 1)^+$ ion of the trimethylsilyl derivative of dexamethasone and its stable isotopically labeled diluent, [$^{13}C_6$,$^2H_3$]dexamethasone (681 and 690 *m/z*, respectively). Methane was used as the GC carrier gas and as the chemical-ionization reagent gas. The sensitivity of the method, judged from the lower limit of detection of the mass spectrometer, was at ~100 pg. The inter- and intraassay coefficients of variation (CV) determined at two different concentrations were 3.83 and 3.78% for 2 ng/mL and 2.64 and 1.29% for 5 ng/mL, respectively. Plasma concentration profiles for dexamethasone following a single 1-mg iv and a 2-mg oral dose of dexamethasone administered 24 h apart to two healthy volunteers are presented. The mass fragmentographic method described here is useful for bioavailability and pharmacokinetic studies of the synthetic glucocorticoid.

Keyphrases □ Dexamethasone—quantitative determination in human plasma, stable isotope dilution mass spectrometry □ Stable isotope mass spectrometry—quantitative determination of dexamethasone in human plasma

The assay of steroid hormones in biological fluids has been greatly simplified with the development of highly sensitive RIA techniques. RIA methods were developed for the estimation of plasma dexamethasone (1–3) and used to follow plasma levels of dexamethasone to determine the bioavailability of oral dexamethasone (4) and intravenous dexamethasone esters (5). Bioavailability studies of prednisone tablets have also been performed by an RIA method (6). There are often, however, serious restrictions to the use of RIA techniques in that cross-reactivity with other steroids is a serious problem in achieving acceptable specificity.

More specific and precise HPLC methods have been widely used in determining natural and synthetic corticosteroids in biological fluids. The methods have been applied to bioavailability and pharmacokinetic studies of synthetic corticosteroids such as prednisone, prednisolone (7, 8), and budesonide (9). A test method for determining content uniformity by HPLC has also been described for fludrocortisone acetate (10). The HPLC method offers the advantage that the corticosteroids can be analyzed without derivatization, unlike GC. However, the HPLC method lacks sensitivity and cannot be used to make accurate determinations of plasma concentrations in the nanogram-to-subnanogram range. Moreover, analytical methods such as RIA and HPLC do not have the advantage of the isotope dilution technique in that the correction for losses of a particular substance in various biological samples in the extraction and purification procedure cannot be easily made.

The use of gas chromatography–mass spectrometry (GC–MS) and isotopically labeled drugs as diluents has found broad application in pharmacological studies (11, 12). In this technique, stable isotopically labeled carriers serve as the ideal internal standard to correct for losses of a substance under study in the initial isolation procedures. Pharmacokinetic studies represent one field in which the sensitivity and specificity of GC–MS techniques offer an advantage. The present paper describes the development of an analytical method which involves stable isotope dilution mass spectrometry to follow plasma concentrations of dexamethasone after the administration of a therapeutic dose. The internal standard used was dexamethasone M+9 ([$^{13}C_6$,$^2H_3$]dexamethasone). The method has been applied to the bioavailability study of a commonly used tablet formulation of dexamethasone.

EXPERIMENTAL

Chemicals—Methanol[1] (HPLC grade), methylene dichloride[2] (distilled in glass), hexane[2] (UV grade, distilled in glass), and glacial acetic acid[3] (AR grade) were used without further purification. *N,O*-bis(Trimethylsilyl)trifluoroacetamide[4] (BSTFA) was commercially available, and dexamethasone[5] was a gift. Stable isotopically labeled dexamethasone, [1,2,3,4,10,19-$^{13}C_6$,19,19,19-$^2H_3$]dexamethaone, was synthesized under an FDA contract[6].

Mass Fragmentography—Mass fragmentographic determinations were made with a gas chromatograph–mass spectrometer fitted with a chemical-ionization source and a data system[7]. Methane was used as the GC carrier (15 mL/min) and as the chemical-ionization reagent gas. The chemical-ionization source pressure was maintained at ~0.21 torr, and electron energy of 70 eV. The trimethylsilyl derivatives were monitored at *m/z* values of 681 (nonlabeled dexamethasone) and 690 (labeled dexamethasone) by multiple-ion detection with an integration time of 0.839 s each.

GLC was performed on a glass column (60.96 cm × 2 mm i.d.) packed with 3% SP-2100[8] on Supelcoport[8] (80–100 mesh). The column temperature was 270°C and the temperature of the injector was 285°C. The temperature of the ion source was 270°C.

In the electron-impact mode of operation, the electron energy was set to 70 eV and the multiple-ion detection program was set to monitor the ions at *m/z* 680 and 689. The GC column was the same as described above. Helium (20 mL/min) was used as the carrier gas. The column temperature was 240°C, the injector was at 255°C, and the jet separator was at 250°C. The temperature of the ion source was 250°C.

Sample Preparation for Mass Fragmentography—To 1.0 mL of plasma was added 20 ng of dexamethasone M+9 dissolved in 10 μL of methanol, and the plasma was allowed to stand for 30 min. The plasma sample was applied to a C_{18} bonded reverse-phase cartridge[9]. The cartridge was washed with 4 mL of water and then eluted with 5 mL of methanol. The methanol eluate was evaporated to dryness under a stream of nitrogen. To the residue was added 100 μL of the HPLC solvent and the sample was injected with a syringe-loading sample injector[10] into a liquid chromatograph[11] equipped with a

[1] Fisher Scientific Co., Fair Lawn, N.J.
[2] Burdick & Jackson Laboratories, Inc., Muskegon, Mich.
[3] Mallinckrodt, Inc., St. Louis, Mo.
[4] Pierce Chemical Co., Rockford, Ill.
[5] U.S. Pharmacopeial Convention, Inc., Rockville, Md.
[6] Contract No. 223-79-3011; SRI International, Palo Alto, Calif.
[7] Finnigan Model 4023 with INCOS data system; Finnigan Corp., San Jose, Calif.
[8] Supelco, Inc., Bellefonte, Pa.
[9] C_{18} Sep-Pak Cartridge; Waters Associates, Milford, Mass.
[10] Rheodyne, Inc., Berkeley, Calif.
[11] Waters Model 6000.

0022-3549/84/0400-0446$01.00/0
© 1984, American Pharmaceutical Association

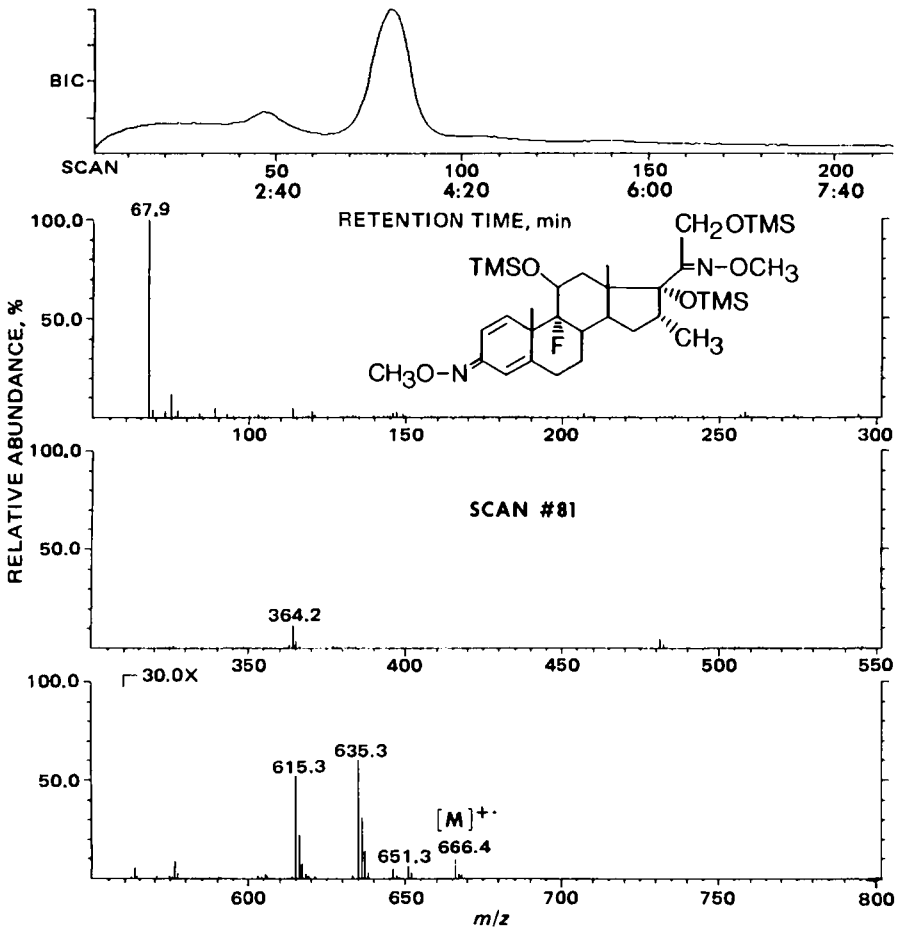

Figure 1—*Mass chromatogram (upper) and mass spectrum (lower) of MO-TMS dexamethasone.*

UV-visible detector[12]. The normal-phase HPLC column[13] (0.25 m × 4.6 mm i.d.) was eluted with 30% methylene dichloride-4% methanol-0.2% acetic acid in *n*-hexane (13) at the rate of 2.5 mL/min, and the column effluent was monitored at 240 nm. Approximately 5 mL of HPLC eluate of the appropriate fraction was collected. The solvent was evaporated to dryness under a stream of nitrogen. The trimethylsilyl derivative was formed by reacting the residue with 30 μL of BSTFA in the presence of 10 μg of potassium acetate as a base catalyst (14, 15). The reaction was completed in 0.5–1 h at 80°C. Excess BSTFA was removed under a stream of nitrogen, and the residue was dissolved in 30 μL of *n*-hexane. A 5–10-μL volume of the above *n*-hexane solution was analyzed by GC–MS. In addition, a methoxime-trimethylsilyl (MO-TMS) derivative of dexamethasone was prepared for GC–MS analysis according to a reported method (16).

Preparation of Calibration Curve—To each of 10 standards containing 0.5–200 ng of dexamethasone in 10 μL of methanol was added 20 ng of dexamethasone M+9 in 10 μL of methanol and 10 μg of potassium acetate in 10 mL of methanol. After evaporation of the solvent to dryness under a stream of nitrogen, 30 μL of BSTFA was added to each sample to form the TMS (trimethylsilyl) derivative as described above. A 5–10-μL aliquot of the sample was subjected to GC–MS.

Determination of Accuracy—Dexamethasone in amounts of 2.02, 5.05, and 10.10 ng dissolved in 10 μL of methanol was added to 1.0-mL aliquots of pooled plasma. After preparation of the sample for mass fragmentography as described above, the observed area ratio of *m/z* 681 to *m/z* 690 was determined in triplicate.

Drug Administration—The two healthy adult male volunteers, 39 (subject 1) and 56 (subject 2) years old, weighed 64 and 77 kg, respectively. As a part of the experiment, a complete blood count, urinalysis, and screening blood chemistry battery (SMA) was performed. The laboratory results were found to be within normal limits. After an overnight fast, subjects 1 and 2 received three 0.75-mg dexamethasone tablets[14] orally with 250 mg of water and 1 mg of dexamethasone in its phosphate ester form[15] in 5 mL of saline intravenously over 5 min (1 mL/min), respectively, on the first day. No food was permitted for 4 h after drug administration. On the second day, the drug administration was repeated with each subject receiving the reverse treatment.

On the first day, 20-mL heparinized blood samples were taken from both subjects immediately before drug administration. At the end of injection and 5 min after injection, 10-mL heparinized blood samples were taken from subject 2. At 15, 30, 45, 60, 90, 120, 180, 240, 360, 480, 600, 1200, and 1420 min after dosing, 10-mL heparinized blood samples were taken from both subjects. On the second day, 5-mL blood samples were taken rather than 10 mL. The samples were centrifuged at 2000 rpm for 15 min. The plasma samples were placed in culture tubes with plastic caps and stored at −20°C until the time of assay.

RESULTS

Prerequisites for Mass Fragmentographic Analysis—*Derivative Formation*—In the electron-impact or chemical-ionization mass spectrum of dexamethasone, the relative abundance of the molecular or $(M+1)^+$ ion was very small and, unless derivatized, the ionization efficiency of the compound was not sufficient to make possible the analysis of nanogram amounts of dexamethasone. The 3,20-diMO-11β,17α,20-triTMS (MO-TMS) derivative (16) and 11β,17α,20,21-tetraTMS derivative (15) possessed good GC properties and were suitable for use in GC–MS analysis. The electron-impact mass spectra shown in Figs. 1 and 2 indicate that a much higher molecular ion intensity was observed for the tetra TMS derivative at *m/z* 680 than for the MO-TMS derivative at *m/z* 666. When the molecular ion of the tetra TMS derivative was monitored, the sensitivity limit of the assay by GC–MS (electron-impact) was found to be 10 ng of dexamethasone/sample for a standard solution with a signal-to-noise ratio of ~2.5.

Figure 3 shows the chemical-ionization mass spectrum of tetra TMS dexamethasone. An intense $(M+1)^+$ ion was observed at *m/z* 681, with three other predominant peaks in the high mass region >*m/z* 450. This was accomplished by using the chemical-ionization mode for MS analysis and methane as the GC carrier and chemical-ionization reagent gas. The GC effluent was introduced *via* the direct inlet of an MS interface. When the $(M+1)^+$ ion at *m/z* 681 was monitored, the sensitivity limit by GC–MS (chemical-ionization) was found to be 100 pg of dexamethasone for a standard

[12] Tracor 970A.
[13] Spherisorb 5-μm Silica; Phase Sep, Hauppauge, N.Y.
[14] Decadron, 0.75 mg, Lot D0257; Merck Sharp & Dohme.
[15] Decadron phosphate injection, 4 mg/mL, Lot 2371F; Merck Sharp & Dohme.

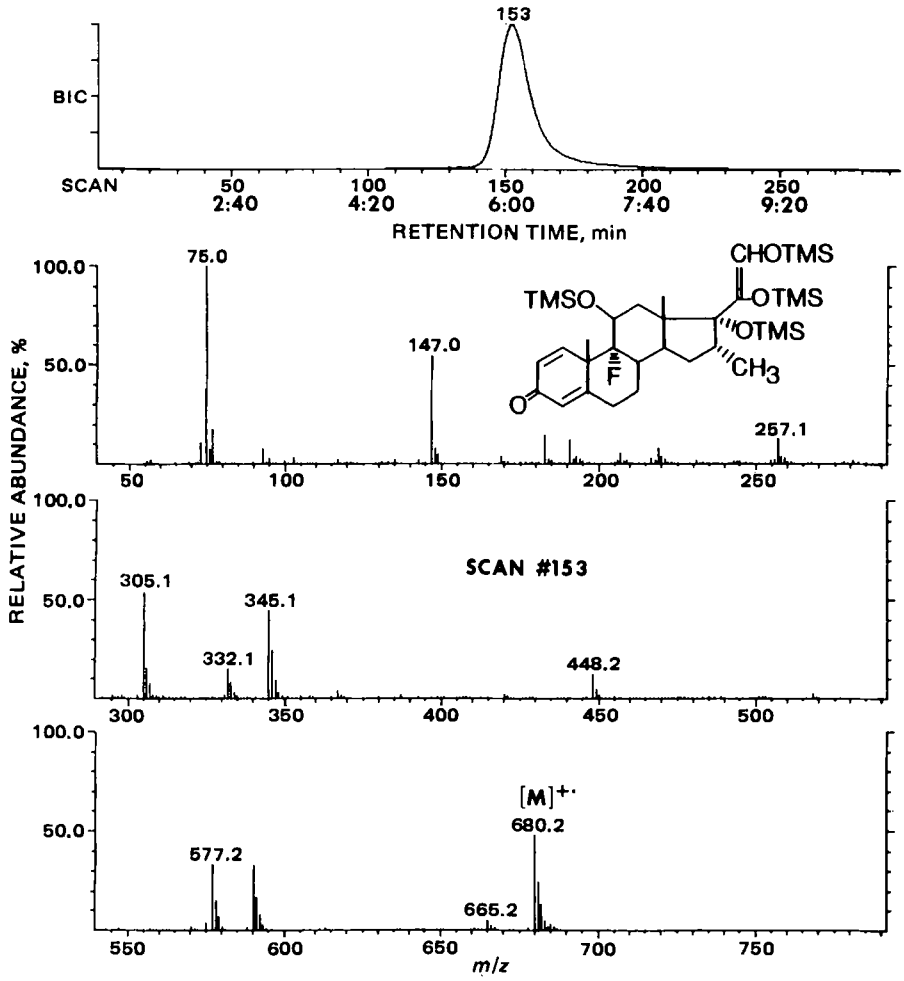

Figure 2—*Mass chromatogram (upper) and mass spectrum (lower) of tetra TMS dexamethasone.*

solution (equivalent to 300 pg/mL of plasma) when a signal-to-noise ratio of ≥2.5:1 was used as a criterion for a significant response.

Selective-ion recordings of tetra TMS dexamethasone showed that no contaminating byproducts with retention times close to that of the TMS derivative were present. After the initial purification procedures, there was no interference with the dexamethasone $(M+1)^+$ ion of the TMS derivative from endogenous compounds in the plasma extract.

Calibration Curve—Dexamethasone M+9 was used as the internal standard in the MS analysis of dexamethasone. The tetra TMS ether of dexamethasone M+9 gave the same fragmentation pattern as the TMS derivative of nonlabeled dexamethasone with the expected mass shifts of 9 amu (Fig. 4). Known mixtures of dexamethasone and dexamethasone M+9 were prepared so that the sample size (5–10 μL) injected into the GC–MS covered the dexamethasone calibrations range of 0.5–200 ng with a fixed amount (20 ng) of dexamethasone M+9. Each mixture was then anlayzed as the TMS derivative, monitoring the $(M+1)^+$ ions at *m/z* 681 for dexamethasone and *m/z* 690 for dexamethasone M+9. There was a good correlation between the mixed molar ratio and the observed peak area ratio. Least-squares analysis of the observed ratio gave a regression line with a slope coefficient of 0.9997.

Accuracy—The accuracy of measurements was determined for dexamethasone added to 1.0-mL aliquots of pooled plasma. The plasma samples contained 20 ng of the internal standard and different amounts (2.02, 5.05, and 10.10 ng) of dexamethasone. The amounts of dexamethasone were measured by the described GC–MS (chemical-ionization) method. The amounts of dexamethasone added were determined and were in good agreement with the amounts of the dexamethasone spiked, the relative error being <3% (Table I).

Precision—As determined by assaying in triplicate six 1.0-mL plasma samples with a dexamethasone concentration of either 2 or 5 ng/mL (Table II), the intraassay coefficients of variation were 3.78% for 2 ng/mL and 1.29% for 5 ng/mL. The interassay coefficients of variation at these two concentrations were 3.83% for 2 ng/mL and 2.64% for 5 ng/mL.

Pharmacokinetics and Bioavailability of Dexamethasone—A single oral dose of three 0.75-mg dexamethasone tablets and a single intravenous dose of 1 mg of dexamethasone in its phosphate ester form were administered 24 h apart to two healthy male volunteers (subjects 1 and 2). Time courses of dexamethasone concentrations in plasma were followed for 24 h by the present

Table I—Accuracy of Mass Fragmentographic Analysis of Dexamethasone in Plasma

Amount Added, ng	Amount Measured, ng				Relative Error, %
	Individual Values[a]			Mean ± *SD*	
2.02	1.96	2.01	1.94	1.97 ± 0.03	−2.47
5.05	5.11	4.97	4.86	4.98 ± 0.10	−1.39
10.10	10.41	9.73	10.08	10.07 ± 0.28	−0.30

[a] Each value represents the mean of triplicate measurements.

Table II—Precision of Mass Fragmentographic Analysis of Dexamethasone in Plasma

Run No.	Amount Determined, ng				*CV*, %
	Individual Values			Mean ± *SD*	
	Amount Added, 2 ng				
1	2.30	2.05	2.12	2.16 ± 0.11	5.09
2	1.96	2.08	2.03	2.02 ± 0.05	2.48
3	1.90	1.96	2.14	2.00 ± 0.10	5.10
4	2.22	2.16	2.11	2.16 ± 0.05	2.32
5	1.88	2.00	2.04	1.97 ± 0.07	3.55
6	1.92	1.86	2.05	1.94 ± 0.08	4.12
				Mean 2.04	3.78
				CV (%) 3.83	
	Amount Added, 5 ng				
1	5.40	5.53	5.34	5.42 ± 0.08	1.48
2	5.08	5.02	5.16	5.08 ± 0.05	0.98
3	5.14	5.26	5.12	5.17 ± 0.07	1.35
4	5.02	5.12	4.95	5.03 ± 0.07	1.39
5	4.94	4.87	4.99	4.93 ± 0.05	1.01
6	5.32	5.10	5.18	5.20 ± 0.08	1.54
				Mean 5.14	1.29
				CV (%) 2.64	

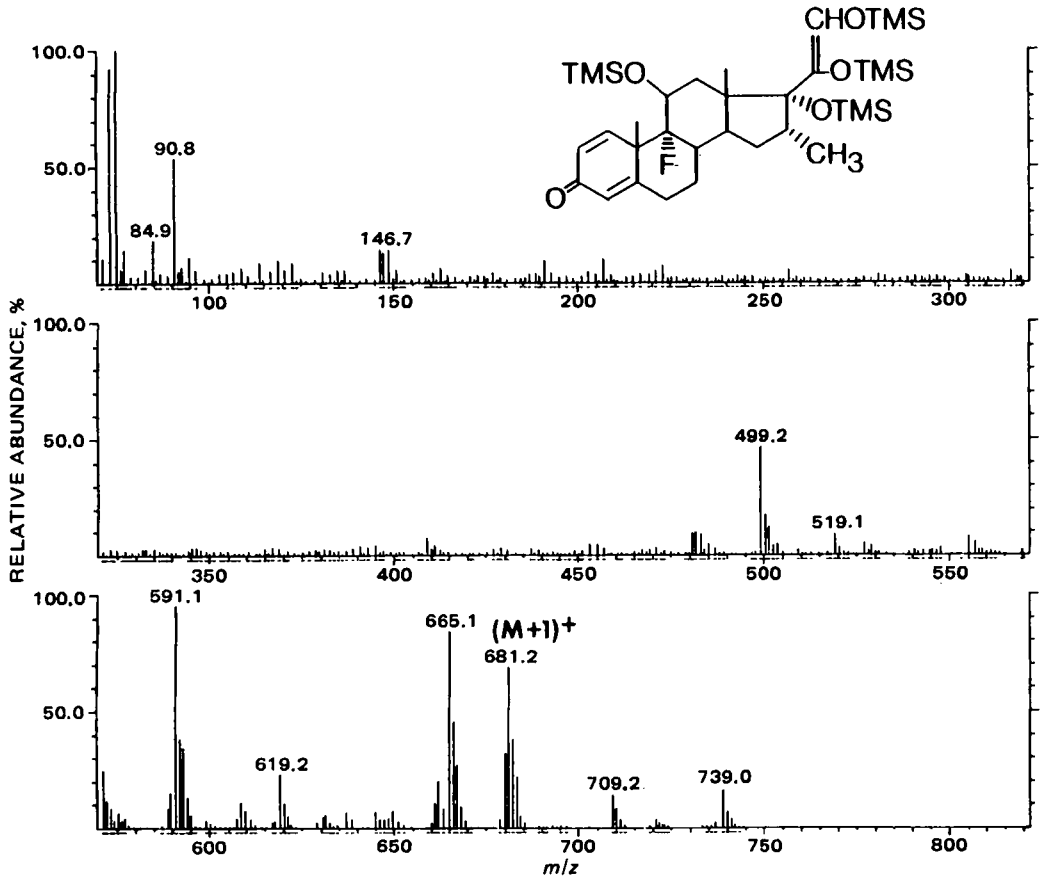

Figure 3—*Chemical-ionization mass spectrum of tetra TMS dexamethasone.*

method. Figure 5 shows a typical example of the selected-ion chromatogram for dexamethasone from the plasma sample.

Plasma concentrations of dexamethasone after intravenous administration appeared to decrease in a biexponential fashion (Fig. 6). The terminal phase of plasma concentrations of dexamethasone after oral administration paralleled that after intravenous administration in each subject. After oral administration the appearance of dexamethasone in the plasma was very rapid. The peak dexamethasone concentrations (15.4 ng/mL for subject 1 and 14.1 ng/mL for subject 2) were observed at 45 and 60 min, respectively, after a single oral dose of 2.25 mg. Semilogarithmic plots of the plasma concentration *versus* time (Fig. 6) indicate that after absorption, a distribution phase was observed in both subjects. The terminal decline phase was monoexponential at time points later than 2 h for subjects 1 and 2.

The observed set of plasma data was fitted to the polyexponential equation ($C_p = \Sigma C_i e^{-\lambda_i t}$) describing the plasma concentration–time curves and parameters characterizing the absorption and disposition of oral and intravenous dexamethasone were obtained *via* a computer[16] by a least-squares estimation using the steepest descent method. The estimate of the elimination half-life ($t_{1/2}$) was obtained from the terminal slope (λ_i): $t_{1/2} = 0.693/\lambda_i$. The total plasma clearance (CL_{pl}) was expressed as the intravenous dose divided by the area under the plasma concentration–time curve (AUC). The AUC from t = 0–10 h ($AUC_{10\ h}$) or t = 0 to infinity (AUC_∞) was measured by the trapezoidal rule. In the case of intravenous administration, the time point of 15 min was taken to be the first data point to measure the AUC. The AUC beyond the last detectable plasma dexamethasone concentration was calculated by dividing the last detectable plasma concentration (10-h point) by the terminal elimination rate constant, λ_i. The volume of distribution (Vd, area) was calculated by dividing the clearance by the terminal rate constant: Vd, area = CL_{pl}/λ_i. These pharmacokinetic parameters are summarized in Table III.

Bioavailability—The absolute bioavailability of oral dexamethasone was calculated from a comparison of dexamethasone concentrations after oral dexamethasone and intravenous dexamethasone-21-phosphate administration based on the AUC. It was assumed that after intravenous injection dexamethasone-21-phosphate rapidly and quantitatively hydrolyzed to its free alcohol (5). The calculated values for bioavailability were 54.7% ($AUC_{10\ h}$) and 54.9% (AUC_∞) for subject 1 and 71.7% ($AUC_{10\ h}$) and 71.2% (AUC_∞) for subject 2.

[16] CBM Model 2001-32.

DISCUSSION

The use of isotope dilution techniques coupled with isotope ratio determination by MS is rapidly becoming the method of choice in the analysis of steroids in biological samples (17–19). Since bioavailability and pharmacokinetic studies of synthetic corticosteroids require sensitive, specific, and reproducible analytical techniques, attempts were made in the present study to devise procedures that would allow analysis of nanogram-to-subnanogram amounts of dexamethasone in human blood by isotope dilution MS.

Generally, the MS analysis of corticosteroids in biological extracts is difficult due to their thermal instability and the problems associated with isolating sufficiently pure material for analysis. Recently, sample purification procedures using a C_{18} bonded reverse-phase cartridge for the quantitative analysis of corticosteroids in adrenal cell cultures by HPLC or GC–MS have been described (20). The present isotope-dilution MS method involves spiking the plasma sample with stable isotopically labeled dexamethasone M+9 and then purifying it by the use of a C_{18} bonded reverse-phase cartridge and normal-

Table III—Parameters Characterizing the Disposition of Dexamethasone

Parameter	Subject 1	Subject 2
	Intravenous Administration	
C_1, mg/mL	481.6	155.8
λ_1, h^{-1}	15.17	10.37
C_2, ng/mL	12.2	8.2
λ_2, h^{-1}	0.38	0.18
$t_{1/2}$, h	1.82	3.85
$AUC_{10\ h}$, h·ng/mL	29.85	34.26
AUC h·ng/mL	30.68	39.21
CL_{pl}, L/h	33.9 (0.53 L/h/kg)	21.82 (0.28 L/h/kg)
Vd, L	89.2 (1.4 L/kg)	121.2 (1.5 L/kg)
	Oral Administration	
C_1, ng/mL	−292.5	−76.4
λ_1, h^{-1}	1.60	2.05
C_2, ng/mL	278.4	52.6
λ_2, h^{-1}	1.54	1.38
C_3, ng/mL	14.1	11.7
λ_3, ng/mL	0.35	0.18
$t_{1/2}$, h	1.98	3.85
$AUC_{10\ h}$, h·ng/mL	35.24	55.95
AUC, h·ng/mL	36.45	63.10

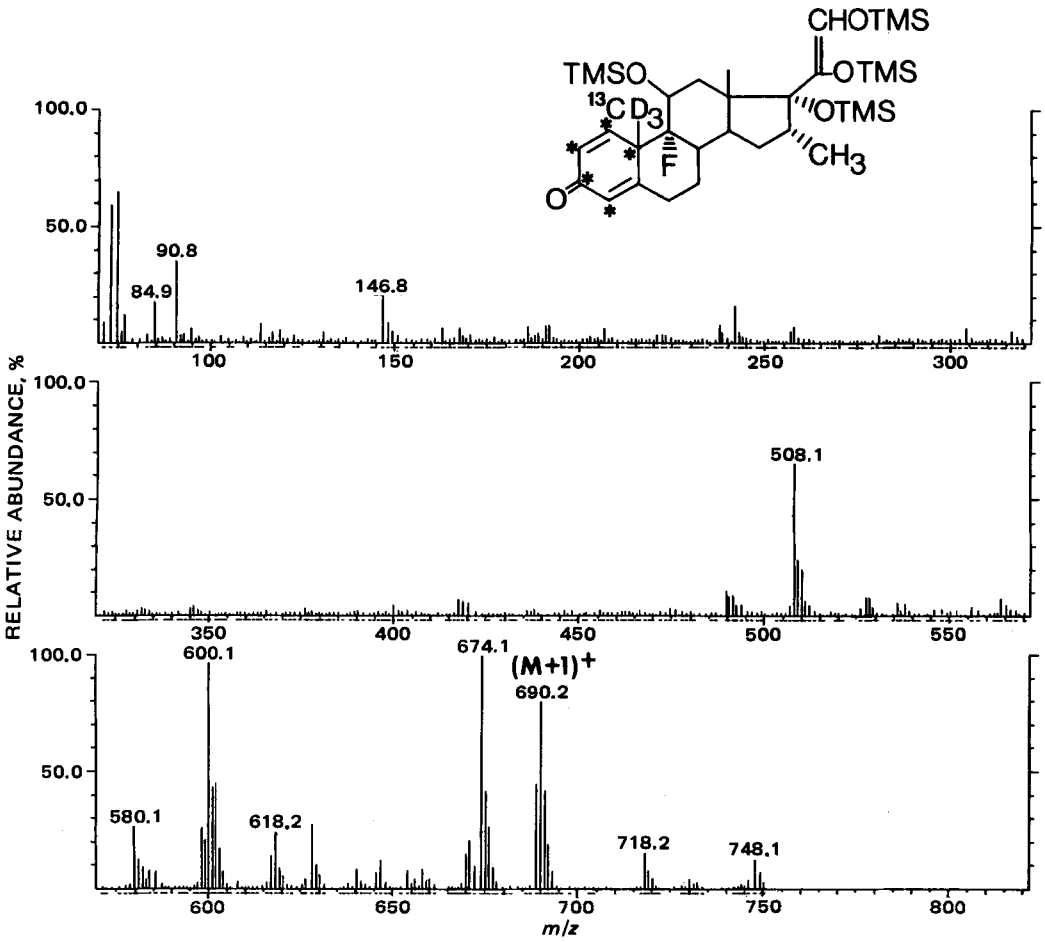

Figure 4—*Chemical-ionization mass spectrum of tetra TMS dexamethasone M+9.*

phase HPLC. The steroid sample was then derivatized and analyzed by GC–MS. The absolute recovery of the purification procedures varied from 80 to 90%, and coextracted endogenous material did not present any problems in the final GC–MS analysis.

For each MS method developed, the choice of derivative and mode of MS analyses must be made to reduce the possibility of interferences and enhance the sensitivity. Several derivatives of corticosteroids for GC analysis have been introduced in the past (14, 21–24), and from a quantitative point of view the double MO-TMS derivative has been shown to be the most satisfactory (23). MO-TMS derivatives have been used for the quantitative determination of prednisolone and prednisone in human plasma using GC–MS (chemical-ionization) with methane as the chemical-ionization reagent gas (25).

It has also been suggested that in order to produce stable silylated derivatives of corticosteroids it is necessary first to protect the ketone groups at C-3 and C-20 (26–28). This step has now, however, been shown not to be necessary in the case of dexamethasone when the silylation reaction was carried out with BSTFA in the presence of a base catalyst such as anhydrous potassium or sodium acetate (15). In the present study potassium acetate was used as a base catalyst, the C-20 ketone group of dexamethasone was converted to an enol ether, and all hydroxyl groups were converted to TMS ether groups under reaction with BSTFA at 80°C for 0.5–1 h. A single product was obtained, and the tetra TMS derivative showed excellent thermal stability and good GC behavior. The MO-TMS derivative of dexamethasone was also thermally stable and suitable for GC analysis. This derivative was recently used for the qualitative determination of dexamethasone along with other synthetic corticosteroids in horse urine samples by combined HPLC-negative-ion chemical-ionization MS using ammonia as the reagent gas (29).

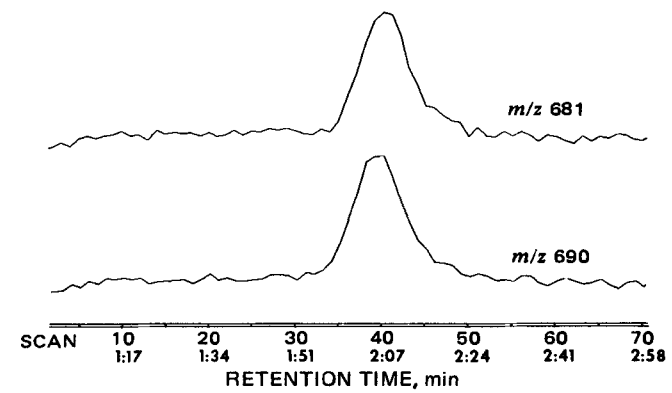

Figure 5—*Mass fragmentograms of tetra TMS dexamethasone and tetra TMS dexamethasone M+9 after processing from a plasma sample.*

Quantitation by MS requires the availability of isotopically labeled compounds to function as internal standards. It was expected that the molecular ion for tetra TMS dexamethasone would have a significant contribution to M+1, M+2, and M+3 because of the presence of four TMS groups. This multiplicity of the molecular ion imposes certain restrictions on the choice of a GC–MS internal standard. For a stable isotopically labeled dexamethasone to serve as an internal standard in the present study, it must be substituted with a large number of stable isotopes so that its molecular ion cluster will not overlap with the molecular ion cluster of nonlabeled dexamethasone.

Dexamethasone M+9, used as the internal standard, was suitable for the present purpose. The standard curve prepared by plotting the peak area ratio of the $(M+1)^+$ ions of the tetra TMS derivatives *versus* the amount of nonlabeled dexamethasone added to 20 ng of dexamethasone M+9 was linear at a concentration range of 0–200 ng, a concentration range commensurate with the clinical levels in the bioavailability study of dexamethasone. Furthermore, accuracy and precision provided by the present method were satisfactory.

The applicability of the method was shown by the determination of plasma dexamethasone levels in two healthy human volunteers after administration of a 2-mg oral or 1-mg iv dose of dexamethasone. This study indicated that most of orally administered dexamethasone was absorbed within 60 min. The terminal half-lives ($t_{1/2}$) calculated from plasma concentration data after oral and intravenous administration were in close agreement in both subjects. The half-life was somewhat short in subject 1 (~2 h) and was ~3.5 h in subject 2. These values were similar to results reported by other workers, who measured total plasma radioactivity after administering radiolabeled dexamethasone intravenously (30) or plasma levels by RIA (4).

An assumption was made that the total plasma clearance (CL_{pl}) was constant for each subject from oral to intravenous dose or *vice versa*, and the values for bioavailability of the oral preparation were estimated by a model-

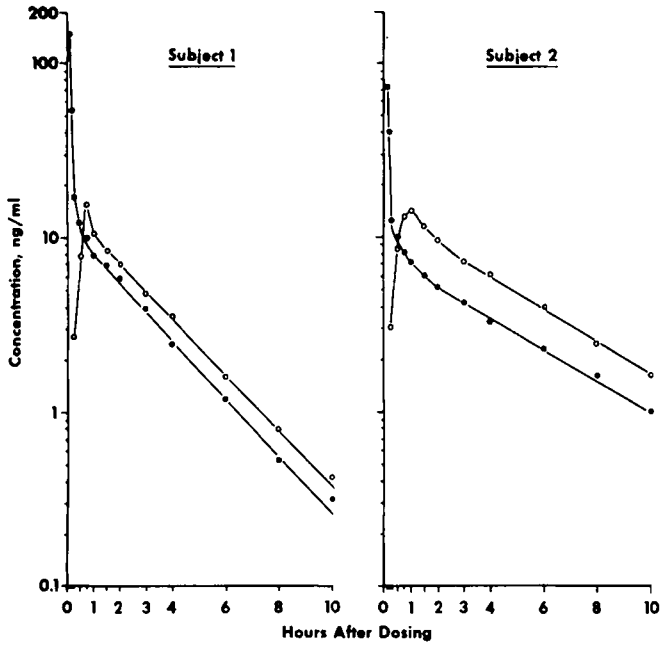

Figure 6—*Semilogarithmic plot of plasma concentrations of dexamethasone* versus *time after single 1-mg iv (●) and 2-mg oral (○) doses of dexamethasone.*

independent comparison of dexamethasone levels after oral and intravenous administration based on the $AUC_{10\ h}$ values of ~55 and 71% for subjects 1 and 2, respectively. A comparison of AUC_{∞} resulted in only a small difference in the bioavailability values from those obtained above.

CONCLUSION

The isotope dilution MS method described here afforded a sensitive and reliable technique to measure nanogram-to-subnanogram amounts of dexamethasone in plasma. Specificity was high because the GC–MS system was used to separate and to detect the specific compound in question after initial purification by a C_{18} bonded reverse-phase cartridge and normal-phase HPLC. It was possible to apply the present method for the accurate determination of low concentrations of dexamethasone in human plasma after administering only a few milligrams of the drug.

REFERENCES

(1) A. W. Meikle, L. G. Lagerquist, and F. H. Tyler, *Steroids*, **22,** 193 (1973).

(2) M. C. Dumasia, D. I. Chapman, M. S. Moss, and C. O'Connor, *Biochem. J.*, **133,** 401 (1973).

(3) M. Hichens and A. F. Hogans, *Clin. Chem.*, **20,** 266 (1974).

(4) D. E. Duggan, K. C. Yeh, N. Matalia, C. A. Ditzler, and F. G. McMahon, *Clin. Pharm. Ther.*, **18,** 205 (1975).

(5) S. Miyabo, T. Nakamura, S. Kuwajima, and S. Kishida, *Eur. J. Clin. Pharmacol.*, **20,** 277 (1981).

(6) T. J. Sullivan, M. R. Hallmark, E. Sakmar, D. J. Weidler, R. H. Earhart, and J. G. Wagner, *J. Pharmacokinet. Biopharm.*, **4,** 157 (1976).

(7) J. Q. Rose, A. M. Yruchak, and W. J. Jusko, *Biopharm. Drug Dispos.*, **1,** 247 (1980).

(8) J. Q. Rose, A. M. Yruchak, and W. J. Jusko, *J. Pharmacokinet. Biopharm.*, **9,** 389 (1981).

(9) A. Ryrfeldt, M. Tonnesson, E. Nelson, and A. Wibby, *J. Steroid Biochem.*, **10,** 317 (1979).

(10) T. M. Ast and H. M. Absou, *J. Pharm. Sci.*, **68,** 421 (1979).

(11) T. A. Baillie, *Pharmacol. Rev.*, **33,** 81 (1981).

(12) W. A. Garland and M. L. Powell, *J. Chromatogr. Sci.*, **19,** 392 (1981).

(13) J. C. K. Loo and N. Jordan, *J. Chromatogr.*, **143,** 314 (1977).

(14) E. M. Chambaz, G. Defaye, and C. Madani, *Anal. Chem.*, **45,** 1090 (1973).

(15) H. Tokunaga, T. Kimura, and J. Kawamura, *Yakugaku Zasshi*, **99,** 800 (1979).

(16) J-P. Thenot and E. C. Horning, *Anal. Lett.*, **5,** 905 (1972).

(17) I. Björkhem, R. Blomstrand, O. Lantto, A. Lof, and L. Svesson, *Clin. Chim. Acta*, **56,** 241 (1974).

(18) S. Baba, Y. Shinohara, and Y. Kasuya, *J. Chromatogr.*, **162,** 529 (1979).

(19) C. Lindberg, S. Jonsson, P. Hender, and A. Gustafsson, *Clin. Chem.*, **28,** 174 (1982).

(20) L. C. Ramirez, C. Millot, and B. F. Maume, *J. Chromatogr.*, **229,** 267 (1982).

(21) N. Sakauchi and E. C. Horning, *Anal. Lett.*, **4,** 41 (1971).

(22) J-P. Thenot and E. C. Horning, *Anal. Lett.*, **5,** 21 (1972).

(23) T. A. Baillie, C. J. W. Brooks, and B. S. Middleditch, *Anal. Chem.*, **44,** 30 (1972).

(24) P. M. Simpson, *J. Chromatogr.*, **77,** 161 (1973).

(25) S. B. Matin and B. Amos, *J. Pharm. Sci.*, **67,** 923 (1978).

(26) W. L. Gardiner and E. C. Horning, *Biochim. Biophys. Acta*, **115,** 524 (1966).

(27) S. Hara, T. Watabe, and Y. Ike, *Chem. Pharm. Bull. (Tokyo)*, **14,** 1311 (1966).

(28) W. J. A. VandenHeuvel, J. L. Patterson, and K. L. K. Braly, *Biochim. Biophys. Acta.*, **144,** 691 (1967).

(29) E. Houghton, M. C. Dumasia, and J. K. Wellby, *Biomed. Mass Spectrom.*, **8,** 558 (1981).

(30) N. Haque, K. Thrasher, E. E. Werk, H. C. Knowles, and L. J. Sholiton, *J. Clin. Endocrinol. Metab.*, **34,** 44 (1972).

ACKNOWLEDGMENTS

The authors are grateful to Drs. J. G. Harter and T. Cairns, of the United States Food and Drug Administration, for helpful discussions and for the performance of the study in humans. We also thank Dr. N. Castagnoli, School of Pharmacy, University of California, San Francisco, for his suggestions concerning this publication.

Comparative Disposition Kinetics of Two Diastereomeric Pairs of Cinchona Alkaloids in the Dog

ISAAC ABRAHAM * and CLARENCE T. UEDA ˣ

Received April 5, 1982, from the *Department of Pharmaceutics, College of Pharmacy, University of Nebraska Medical Center, Omaha, NE 68105.* Accepted for publication February 25, 1983. *Present Address: College of Pharmacy, Dalhousie University, Halifax, Nova Scotia.

ABSTRACT □ The comparative disposition kinetics of quinidine, quinine, cinchonine, and cinchonidine were investigated in five male, mongrel dogs after intravenous bolus injections of a 9.2-mmol/kg dose of each alkaloid base. Blood and plasma specimens were obtained at various times up to 6 h postdose and assayed for quinidine and quinine with a TLC–fluorometric procedure and for cinchonine and cinchonidine by HPLC. The plasma alkaloid concentration–time data were analyzed by weighted, nonlinear least-squares regression analysis to obtain the central compartment volume (V_c), disposition rate constants (α and β), and corresponding half-life values ($t_{1/2}$). Total body clearance (CL) and apparent volume of distribution (Vd) were estimated by nonparametric analysis. In this study, the highest plasma alkaloid concentrations were reached with quinidine and the lowest concentrations with the quinidine congener, cinchonine. The other congeneric pair, quinine and cinchonidine, exhibited plasma alkaloid concentrations that were comparable and intermediate to those of quinidine and cinchonine. With cinchonine and cinchonidine, the plasma and blood concentration–time curves were virtually superimposable. However, with quinidine and quinine, the plasma alkaloid concentrations of these diastereomers were approximately twice the corresponding blood concentrations. The total body clearance rate of quinidine was significantly slower than quinine and cinchonine clearance. No difference in clearance was observed between cinchonine and cinchonidine. The β and $t_{1/2\beta}$ for quinidine were significantly smaller and larger, respectively, than the corresponding values obtained with the other alkaloids. No significant differences in α or V_c and Vd were found between and within the two diastereomeric pairs of alkaloids. The differences in disposition kinetics observed in this study were attributable to an interaction of stereochemical and 6′-methoxy group substitution effects.

Keyphrases □ Quinine—comparative disposition kinetics in the dog, effects of stereochemistry and 6′-methoxy group substitution □ Quinidine—comparative disposition kinetics in the dog, effects of stereochemistry and 6′-methoxy group substitution □ Cinchonine—comparative disposition kinetics in the dog, effects of stereochemistry and 6′-methoxy group substitution □ Cinchonidine—comparative disposition kinetics in the dog, effects of stereochemistry and 6′-methoxy group substitution

Optical isomers as well as congeners of various drugs have been shown to exhibit different pharmacokinetic and/or pharmacological properties. Stereoselective behavior has been demonstrated for a number of drugs including disopyramide (1), fenfluramine (2), propoxyphene (3), propranolol (4, 5), quinidine/quinine (6–8), thyroxine (9), and warfarin (10). For optical isomers, the asymmetry in their molecular structure (and the resultant effects) clearly account for the differences in properties observed between isomers. Drug congeners, on the other hand, possess different properties because of the presence of different group substituents on the parent drug molecule. The various tetracycline, penicillin, and phenothiazine derivatives are well-known examples of drug congeners possessing different pharmacokinetic and pharmacological activities.

In this investigation, quinidine, quinine, cinchonine, and cinchonidine, two diastereomeric pairs of cinchona alkaloids, were used to evaluate the effects of stereochemistry and group substitution on drug disposition kinetics. Quinidine, quinine, cinchonine, and cinchonidine are the four principal naturally occurring alkaloids isolated from the bark of trees and shrubs of various species of the *Cinchona* and *Remijia* genera. Stereochemically, quinidine, quinine, cinchonine, and cinchonidine fall into two configurational and polarimetric groups. Cinchonine and its 6′-methoxy congener, quinidine, are dextrorotatory and have the same configuration at C-9. The other congeneric pair, cinchonidine and quinine, are levorotatory and have the opposite configuration at C-9 when compared with the dextrorotatory isomers.

The diastereomeric pairs, quinidine/quinine and cinchonine/cinchonidine, do not form racemates and are substances with distinct physicochemical properties (11) and therapeutic uses (7, 8). The purpose of this paper is to report our results on the disposition kinetics of quinidine, quinine, cinchonine, and cinchonidine in dogs.

EXPERIMENTAL

Materials—Quinine, cinchonine, and cinchonidine bases were obtained commercially[1] and used without further purification. Chromatographic analysis of these substances revealed the presence of trace amounts (<7%) of materials that were most likely the corresponding dihydro derivatives of these alkaloids. Quinidine, free of dihydroquinidine, was prepared from quinidine sulfate USP[2] according to the method of Thron and Dirscherl (12). The separated and purified dihydroquinidine was used as the internal standard for the assay of cinchonine and cinchonidine described below.

Drug solutions suitable for parenteral administration were prepared by dissolving the alkaloid base in dilute sulfuric acid (pH 4) and aseptically filtering each solution through a 0.45-μm membrane filter[3]. All other reagents and chemicals were analytical reagent grade.

Intravenous Drug Administration and Blood Sampling—Five male mongrel dogs (15–22 kg) were used in a crossover study with a 7–10-d washout period between drug treatments. During the study, the animals were housed in separate cages with free access to water and they were fed commercial dog food[4]. Food was withheld during the actual experiments.

After placing the dog in a sling support, vein infusion sets[5] with 19-gauge hypodermic needles were inserted into a leg vein of a fore- and hindlimb to facilitate intravenous drug administration and sampling of blood for drug analysis. Patency of the blood catheter was maintained by intermittent flushing with heparinized normal saline (100 IU/mL).

Prior to drug administration, 5 mL of blood was removed as a control sample and for the determination of the hematocrit. A 9.2-mmol/kg dose of alkaloid base was given by rapid intravenous injection *via* the infusion set. Each dose was followed by 3–5 mL of normal saline to ensure complete delivery of the intended dose.

Following drug administration, 3-mL blood samples for drug analysis were obtained at 5, 10, 15, 30, 60, 90, 120, 180, 240, 300, and 360 min, using the second infusion set, and placed in 10-mL heparinized tubes[6]. Approximately 1 mL of blood was reserved for the determination of drug concentrations in whole blood. The remaining sample was centrifuged to obtain the plasma fraction. The blood and plasma samples were stored at −10°C until analyzed.

Analysis of Alkaloids in Blood and Plasma—The concentrations of quinidine and quinine in blood and plasma were determined with the TLC-fluorometric method previously described for quinidine (13).

The samples containing cinchonine and cinchonidine were extracted with benzene in the same manner as quinidine and quinine and assayed using an adaptation of the liquid chromatographic procedure for quinidine described by Drayer and associates (14). After evaporating the benzene extract to

[1] Fluka AG, Buchs SG, Switzerland.
[2] New York Quinine and Chemical Works, New York, N.Y.
[3] Millipore; Gelman Instrument Co., Ann Arbor, Mich.
[4] Wayne Pro-Mix; Applied Mills, Inc., Chicago, Ill.
[5] Travenol Laboratories, Inc., Deerfield, Ill.
[6] Becton, Dickinson and Co., Rutherford, N.J.

0022-3549/84/0400-0452$01.00/0
© 1984, American Pharmaceutical Association

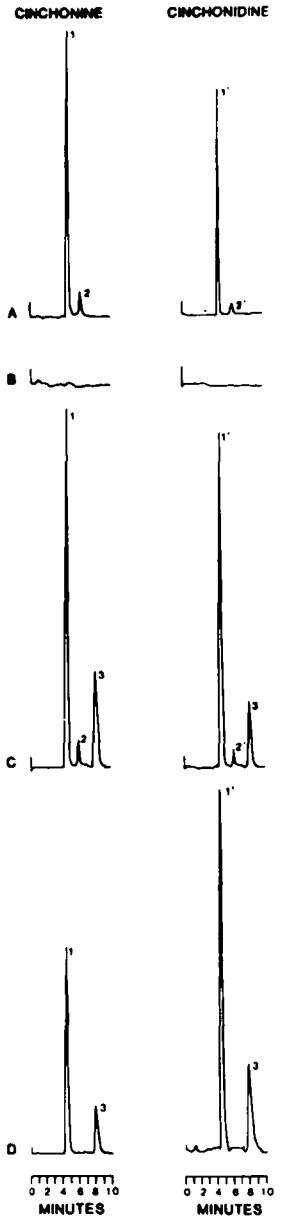

Figure 1—*Chromatograms for cinchonine and cinchonidine obtained under the following test conditions: (A) parenteral drug solutions; (B) plasma blank obtained from an untreated dog; (C) plasma blank spiked with the drug and internal standard; (D) plasma sample obtained from a treated dog, with added internal standard. Peaks 1 and 1′ are cinchonine and cinchonidine, respectively; peaks 2 and 2′ are the corresponding unknown impurities found in the respective drug samples. Peak 3 is the internal standard, dihydroquinidine.*

dryness under a stream of nitrogen, the residue was reconstituted with 25 μL of mobile phase containing 40 ng of dihydroquinidine as the internal standard. An aliquot of this solution was injected into a liquid chromatograph[7] equipped with a loop injector, a C_{18} reverse-phase μ-Bondapak column[8] (3.9 mm × 30 cm; 10-μm particles), and a variable-wavelength fluorescence detector[9]. The mobile phase consisted of 15% (v/v) acetonitrile in 2.5% acetic acid, which was delivered at a rate of 2 mL/min (~2000 psi), and monitored with an excitation wavelength of 315 nm using a 418-nm cutoff filter.

Figure 1 shows the chromatographic characteristics of cinchonine and cinchonidine, as well as the internal standard, obtained under various test conditions with the assay procedure used. As shown in this figure, excellent separation and resolution of the two cinchona alkaloid peaks were achieved. Cinchonine and cinchonidine both eluted with a retention time of 4.3 min. The

[7] Model 2/2; Perkin-Elmer, Norwalk, Conn.
[8] Waters Associates, Millford, Mass.
[9] Schoeffel Model FS 970, Kratos, Inc., Westwood, N.J.

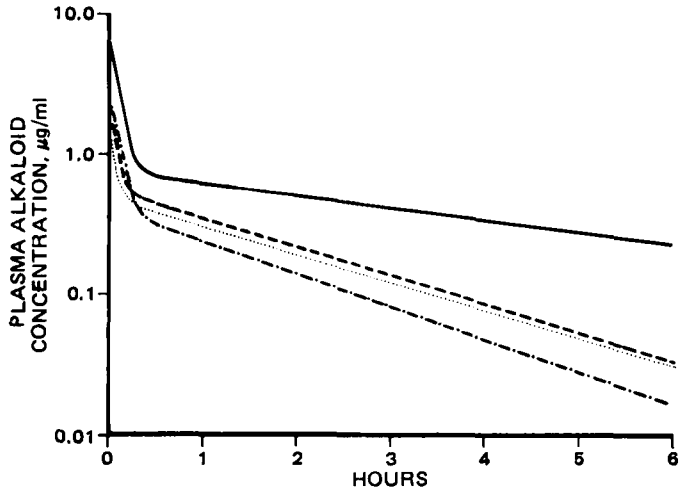

Figure 2—*Semilogarithmic graphs of the plasma alkaloid concentration–time curves for quinidine (—), quinine (· · · ·), cinchonine (- - - -), and cinchonidine (- · - · -) obtained after a 9.2 mmol/kg iv bolus dose of each alkaloid base in dog E. Each graph is the best-fit curve for each alkaloid obtained by nonlinear least-squares regression analysis of the experimental data.*

internal standard, dihydroquinidine, eluted in 8.1 min. The unidentified impurities in the drug samples eluted with an intermediate retention time of 6.0 min and, therefore, did not interfere with the assay for either drug.

Standard samples containing known concentrations of cinchonine and cinchonidine were prepared using blood obtained from untreated animals. They were processed concurrently with the plasma and blood samples to be analyzed and were used to prepare standard calibration curves using the peak height ratio of cinchonine or cinchonidine to internal standard. The unknown drug concentrations in plasma or blood were determined from the best-fit equation of the calibration curves obtained by linear regression analysis after blank correction. In all cases, the correlation coefficients were ≥0.995.

In the concentration range of 0.1–10 μg/mL for cinchonine and cinchonidine in blood and plasma, the relative standard deviations for the respective fluids were ≤7% and ≤5% for cinchonine and ≤8% and ≤5% for cinchonidine.

Data Analysis—The plasma drug concentration–time curves obtained with the bolus injections were fitted to a biexponential equation by weighted ($1/C^2$), nonlinear least-squares regression analysis using the NONLIN program (15):

$$C = Ae^{-\alpha t} + Be^{-\beta t} \qquad \text{(Eq. 1)}$$

Initial estimates of A, B, α, and β were obtained with the program CSTRIP (16); C is the plasma concentration of alkaloid at any time t, α, and β are first-order rate constants for the fast and slow disposition processes, respectively, and A and B are the corresponding ordinate intercepts for each exponential term.

Central compartment volumes (V_c) were estimated by:

$$V_c = \frac{\text{Dose}}{A + B} \qquad \text{(Eq. 2)}$$

The total body clearance rate (CL) was calculated for each alkaloid using:

$$CL = \frac{Dose}{\int_0^\infty C\,dt} \qquad \text{(Eq. 3)}$$

where $\int_0^\infty C\,dt$ is the total area under the plasma drug concentration–time curve, which was estimated by the trapezoidal rule to obtain the area up to the last measured concentration (C^*) and computing the area beyond C^* by dividing C^* by the terminal rate constant β.

The apparent volume of distribution (Vd) was determined by the relationship:

$$Vd = \frac{\text{Dose}}{\int_0^\infty C\,dt \cdot \beta} \qquad \text{(Eq. 4)}$$

Half-life values ($t_{1/2}$) were calculated as:

$$t_{1/2} = 0.693/\alpha \text{ or } \beta \qquad \text{(Eq. 5)}$$

Table I—Values for the Disposition Constants Obtained after a 9.2-mmol/kg iv Bolus Injection[a]

Parameter	Quinidine	Quinine	Cinchonine	Cinchonidine
A, mg/L	2.51 ± 0.56	2.95 ± 1.53	0.61 ± 0.20	0.66 ± 0.20
α, h^{-1}	14.2 ± 4.4	14.3 ± 7.1	14.4 ± 6.6	20.6 ± 3.4
$t_{1/2\alpha}$, h	0.09 ± 0.05	0.12 ± 0.04	0.08 ± 0.02	0.04 ± 0.01
B, mg/L	1.95 ± 0.99	1.33 ± 0.46	0.81 ± 0.21	1.05 ± 0.27
β, h^{-1}	0.179 ± 0.014	0.311 ± 0.059	0.500 ± 0.021	0.424 ± 0.024
$t_{1/2\beta}$, h	4.91 ± 0.95	2.24 ± 0.28	1.40 ± 0.06	1.86 ± 0.20
V_c, L/kg	1.10 ± 0.30	2.01 ± 0.85	2.22 ± 0.43	2.07 ± 0.51
Vd, L/kg	2.78 ± 0.69	3.93 ± 1.38	3.72 ± 0.78	3.04 ± 0.66
CL, L/h/kg	0.499 ± 0.111	1.435 ± 0.405	2.140 ± 0.436	1.333 ± 0.345

[a] Mean ± SEM; n = 5.

The two-way ANOVA test method was used to evaluate the significance of the differences observed between the four alkaloids in this study. This statistical procedure provided a means to evaluate the effects of stereochemistry, 6′-methoxy group substitution, and an interaction of both factors on drug disposition kinetics. A 0.05 significance level was used; the data are reported as the mean ±1 SE.

RESULTS AND DISCUSSION

A comparison of the plasma concentrations of quinidine, quinine, cinchonine, and cinchonidine obtained after intravenous administration of equimolar bolus doses is shown in Fig. 2 for a representative dog. In all dogs, the plasma concentration–time curves for each alkaloid declined biexponentially according to Eq. 1. A rapid distribution phase followed by a slower, terminal disposition phase was observed with all four alkaloids following the bolus injections. It was also noted in all animals studied that the highest plasma concentrations of alkaloid observed were achieved with quinidine. On the other hand, of the four alkaloids studied, the lowest plasma concentrations were always seen with the quinidine congener, cinchonine. The two remaining congeneric pair of alkaloids, quinine and cinchonidine, exhibited plasma concentrations that were comparable and intermediate between those of quinidine and cinchonine.

The rapid and brief distribution phase seen in this study in dogs with the four alkaloids ($t_{1/2\alpha} \simeq 5$ min) has also been observed for quinidine in rabbits (17, 18) and monkeys (19). Moreover, a similar distribution characteristic has been found with quinidine in humans (20–22).

Analysis of the plasma concentration-time data for each drug indicated that the relative differences in plasma alkaloid concentrations seen in this study were attributable to differences in total body clearance rates (CL) for the four alkaloids (Table I). Total body quinidine clearance (0.499 ± 0.111 L/h/kg) was significantly slower than the observed clearance rates of quinine and cinchonine of 1.435 ± 0.405 and 2.140 ± 0.436 L/h/kg, respectively. Interestingly, while there was a difference in CL between quinidine and quinine, it was observed that the cinchonine/cinchonidine diastereomers had similar clearance rates.

The terminal first-order elimination rate constant obtained for quinidine of 0.179 ± 0.014 h^{-1} was significantly smaller than the observed values for the remaining alkaloids ($p < 0.01$), which included the l-isomer of the diastereomeric pair, quinine (Table I). This finding indicated that the fractional removal rate of quinidine was the slowest of the four alkaloids studied. Further analysis of the results revealed that, while there was no difference in β between the cinchonine and cinchonidine diastereomers (0.500 ± 0.021 and 0.424 ± 0.024 h^{-1}), the terminal rate constants for this diastereomeric pair were significantly greater than the rate constant of quinine (0.311 ± 0.059 h^{-1}).

With the corresponding elimination half-life determinations (Table I), the cinchonine/cinchonidine pair were eliminated with similar $t_{1/2\beta}$ values of 1.40 ± 0.06 and 1.86 ± 0.20 h, respectively. On the other hand, the elimination half-lives of the quinidine/quinine diastereomers of 4.91 ± 0.95 and 2.24 ± 0.28 h, respectively, were significantly different ($p < 0.01$).

The results of the volume measurements are also summarized in Table I. In this study, no significant differences were observed between or within the two diastereomeric pairs of alkaloids in their central compartment volumes or overall apparent volumes of distribution.

In a recent investigation, Clohisy and Gibson (6) also observed that the total body clearance rate of quinidine was slower than the clearance rate of quinine in dogs. They found that the clearance of quinidine of 0.215 L/h/kg was about 44 or 56% slower than the quinine clearance rate of 0.487 L/h/kg. Although these clearance rates are less than the respective values observed in the present study, the results of the two studies are in agreement in that we observed a clearance rate of quinidine that was 63% slower than the corresponding rate of quinine clearance.

A possible explanation for these discrepancies could be the different dosages

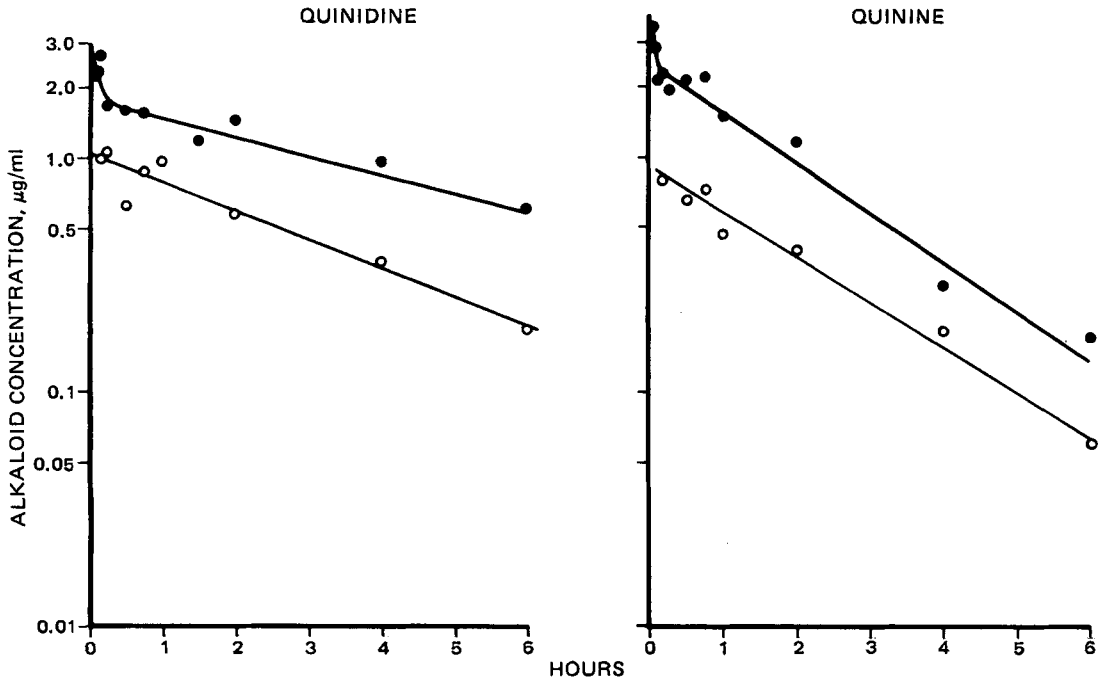

Figure 3—*Semilogarithmic graphs comparing the blood and plasma drug concentration–time curves of quinidine and quinine obtained after a 9.2 mmol/kg iv bolus dose of alkaloid base to dog C. The solid lines are the best-fit curves.*

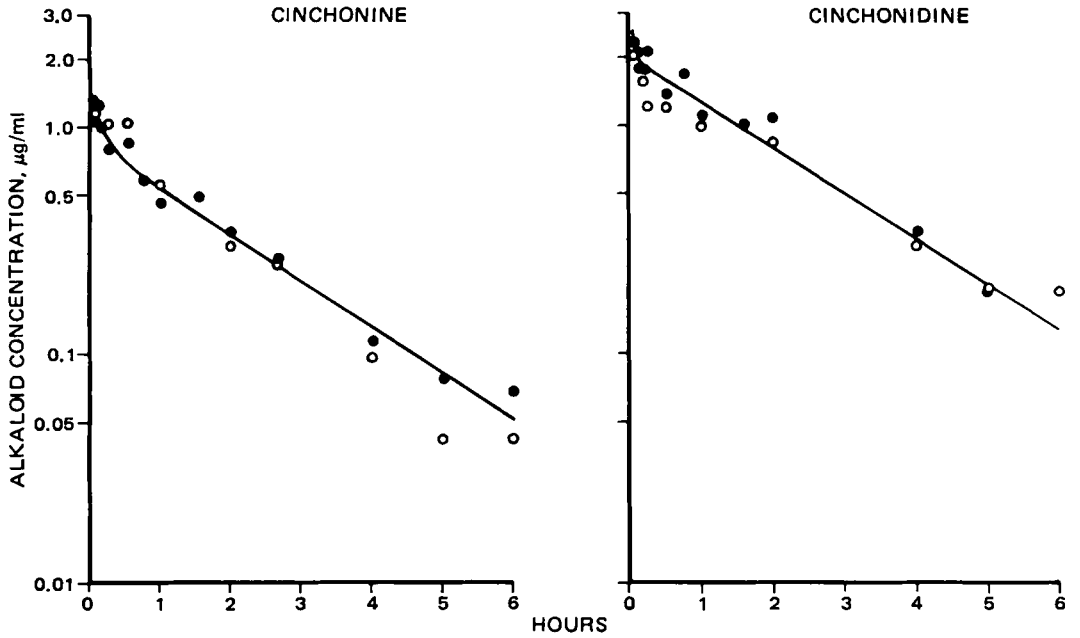

Figure 4—*Semilogarithmic graphs comparing the blood and plasma drug concentration-time curves of cinchonine and cinchonidine obtained after a 9.2 mmol/kg iv bolus dose of alkaloid base to dog C. The solid lines are the best-fit plasma curves.*

that were used in the two studies. In 1948, the findings of Taggart *et al.* (23) suggested that the disposition kinetics of all of the four alkaloids examined in this study were dose dependent. For quinidine, quinine, cinchonine, and cinchonidine, they reported that there was a disproportionate relationship between dose and mean plasma drug concentration attained. More recently, Bolme and Otto (24) also suggested that the pharmacokinetics of quinidine in humans is dose dependent. Thus, dose-dependent pharmacokinetics for quinidine and quinine in the dog is a distinct possibility. In this investigation, quinidine and quinine doses of 3 mg of alkaloid base/kg of body weight were given. Clohisy and Gibson (6) administered doses of the two alkaloids of 6.5 mg/kg. In support of the present findings, after the administration of a quinidine dose of 2.5 mg/kg, the estimated rate of quinidine clearance observed in dogs by Jellett *et al.* (25) was 0.435 L/h/kg (compared with 0.499 ± 0.111 L/h/kg in this study).

The observed difference in clearance between quinidine and quinine suggests that the disposition characteristics of these two diastereomers are stereoselective, as recently reported by Clohisy and Gibson (6). With the similarities in the apparent distribution volumes of these two alkaloids that were observed, these findings suggest that the stereoselective disposition behavior of quinidine and quinine is most likely associated with mechanisms for the metabolism and/or excretion of these drugs rather than a distribution process. In support of this conclusion, it was demonstrated in this study that the other diastereomers, cinchonine and cinchonidine, exhibited similar total body clearance rates. The two diastereomeric pair of alkaloids differ only in the 6′-position of the quinoline ring system, quinidine and quinine having a methoxy group in this position. Drayer *et al.* (26) have shown that a minor metabolite of quinidine in humans is the *o*-demethylated derivative of the drug. Therefore, the present data suggest that the 6′-position might be a site on the drug molecule that is involved in the stereoselective clearance of the quinidine/quinine diastereomers.

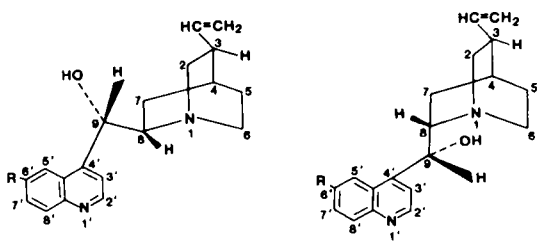

	R	
CINCHONINE	-H	CINCHONIDINE
QUINIDINE	$-OCH_3$	QUININE

With the observation that quinidine, quinine, cinchonine, and cinchonidine exhibited similar volumes of distribution, the differences in terminal rate constants and corresponding elimination half-lives found between quinidine and quinine were expressions of the differences in total body clearance rates that these diastereomers possess. A similar observation has been seen recently with the optical isomers of disopyramide (1) as well as by Clohisy and Gibson (6) in their study with quinidine and quinine.

In this study, there was no apparent effect of stereochemistry or the presence of the methoxy group in the 6′-position of the quinoline nucleus on the two measured volumes (V_c and Vd). *A priori*, this finding was quite unexpected since the 6′-methoxy group would have been expected to increase the volume of distribution by imparting greater lipid solubility to the parent drug molecule[10]. It is possible that the distribution volumes of the four alkaloids are similar because the stereochemical difference and 6′-methoxy substitution do not materially affect the manner and extent to which these alkaloids interact with tissue proteins.

In the present investigation, corresponding blood samples were collected and analyzed for their alkaloid content to evaluate the relative differences in drug concentrations between plasma and whole blood. It was reasoned that this information might give some insight into how the four drugs might differ in disposition in the body. With the quinidine/quinine diastereomers, after pseudodistribution equilibrium conditions were achieved, the blood concentrations of both diastereomers were demonstrably lower than the corresponding alkaloid concentrations in the plasma (Fig. 3). Nevertheless, the terminal disposition rate constants assessed with the blood and plasma data were similar for the respective isomers and, therefore, the blood and plasma elimination curves were parallel. For cinchonine and cinchonidine, the blood and plasma concentration-time curves were virtually superimposable after distribution equilibrium conditions were reached (Fig. 4).

In the plasma alkaloid concentration range of ~0–5 μg/mL, the overall plasma-to-blood concentration ratios observed for quinidine, quinine, cinchonine, and cinchonidine were 2.15 ± 0.26, 2.11 ± 0.28, 0.92 ± 0.10, and 1.26 ± 0.13, respectively. From these results and Fig. 4 it can be seen that the cinchonine/cinchonidine diastereomers are essentially distributed and cleared to the same extent whether assessed by measuring blood or plasma concentrations of these two alkaloids in the dog. On the other hand, the plasma-to-blood concentration ratios for quinidine and quinine suggest that these diastereomers are cleared twice as fast from the blood as from the plasma. In addition, based on blood quinidine and quinine concentration determinations, the apparent volumes of distribution for both of the diastereomers are twice as large as the corresponding plasma-estimated values.

Two possible explanations would account for the differences in plasma and blood concentrations observed for the two pairs of structurally related diastereomers in this investigation. First, quinidine and quinine may have had a higher affinity and/or capacity for binding to plasma proteins. In the vas-

[10] In three different solvent systems, 1-octanol, chloroform, and benzene–0.1 M phosphate buffer (pH 7.4), the partition coefficients of the methoxy diastereomers were significantly greater than the corresponding cinchonine/cinchonidine diastereomers in each of these systems (27).

cular system, a drug that is highly bound to plasma proteins will tend to remain in the plasma fraction. In separate *in vitro* experiments, the binding of quinidine, quinine, cinchonine and cinchonidine to bovine serum albumin was studied by equilibrium dialysis (28). In these studies, the bound fraction was highest for quinidine (followed by cinchonine > quinine > cinchonidine) when the plasma alkaloid concentrations were in the range of $0\text{-}25 \times 10^{-6}$ M. Moreover, the affinity constant (K_A) of quinidine for bovine serum albumin was three times greater than the K_A of quinine, and the affinity constants for the methoxy-substituted diastereomers were found to be 4–8 times larger than the corresponding unsubstituted diastereomers. It is possible that qualitatively similar conditions exist for the interactions of the four alkaloids to plasma proteins in the dog.

Alternatively, the differences in the relationship between blood and plasma alkaloid concentrations for the two diastereomeric pairs may have been due to differences in the binding to the red blood cell membrane and/or relative affinity for components within the erythrocytes (*e.g.*, hemoglobin). A lower affinity for erythrocytes could also result in a lower overall concentration of an alkaloid in the blood. The red blood cell/plasma ratios (K_r) were estimated for each alkaloid with the following expression:

$$K_r = \frac{K_b - (1 - H)}{H} \qquad \text{(Eq. 6)}$$

where K_b is the ratio of the concentration of drug in the blood to the corresponding plasma drug concentration and H is the hematocrit. According to Eq. 6, it was observed that the ratios of the cinchonine/cinchonidine diastereomers were significantly larger than the ratios obtained with the quinidine/quinine diastereomers.

Stereoselective drug disposition kinetics have been seen with a number of different optical isomers including disopyramide (1), propranolol (4,5), and warfarin (9). These differences in disposition kinetics undoubtedly affect the quantitative differences in pharmacological activities observed between isomers. In this study with the quinidine/quinine and cinchonine/cinchonidine diastereomers, the two-way ANOVA test method indicated that the disposition characteristics of these alkaloids were due to an interaction of stereochemical and 6′-methoxy group substitution effects and could not be attributed to a single effect. However, the stereochemical influences on the disposition kinetics of these four alkaloids appeared to be weaker than the effects contributed by the 6′-methoxy substitution.

REFERENCES

(1) K. M. Giacomini, J. C. Giacomini, S. E. Swezey, D. C. Harrison, W. L. Nelson, T. R. Burke, Jr., and T. F. Blaschke, *J. Cardiovasc. Pharmacol.*, **2,** 825 (1980).

(2) A. Jori, P. DePonte, and S. Caccia, *Xenobiotica*, **8,** 538 (1978).

(3) J. H. Jaffe and W. R. Martin, in "The Pharmacological Basis of Therapeutics," A. G. Gilman, L. S. Goodman, and A. Gilman, Eds., Macmillan, New York, N.Y., 1980, pp. 520–521.

(4) M. L. Powell, R. R. Wagoner, C. H. Chen, and W. L. Nelson, *Res. Commun. Chem. Pathol. Pharmacol.*, **30,** 387 (1980).

(5) K. Tawara, K. Kawashima, H. Ishikawa, K. Yamamoto, K. Saito, A. Ebihara, and S. Yoshida, *Eur. J. Clin. Pharmacol.*, **19,** 197 (1981).

(6) D. R. Clohisy and T. P. Gibson, *J. Cardiovasc. Pharmacol.*, **4,** 107 (1982).

(7) J. T. Bigger and B. F. Hoffman, in "The Pharmacological Basis of Therapeutics," A. G. Gilman, L. S. Goodman, and A. Gilman, Eds., Macmillan, New York, N.Y., 1980, pp. 768–774.

(8) I. M. Rollo, in "The Pharmacological Basis of Therapeutics," A. G. Gilman, L. S. Goodman, and A. Gilman, Eds., Macmillan, New York, N.Y., 1980, pp. 1054–1057.

(9) R. C. Haynes and F. Murad, in "The Pharmacological Basis of Therapeutics," A. G. Gilman, L. S. Goodman, and A. Gilman, Eds., Macmillan, New York, N.Y., 1980, pp. 1397–1408.

(10) A. Yacobi and G. Levy, *J. Pharmacokinet. Biopharm.*, **2,** 239 (1974).

(11) W. Solomon, in "Chemistry of the Alkaloids," S. W. Pelletier, Ed., Van Nostrand Reinhold, New York, N.Y., 1970, pp. 301–353.

(12) H. Thron and W. Dirscherl, *Justus Liebigs Ann. Chem.*, **515,** 252 (1935).

(13) C. T. Ueda, B. J. Williamson, and B. S. Dzindzio, *Clin. Pharmacol. Ther.*, **20,** 260 (1976).

(14) D. E. Drayer, K. Restivo, and M. M. Reidenberg, *J. Lab. Clin. Med.*, **90,** 816 (1977).

(15) C. M. Metzler, G. L. Elfring, and A. J. McEwen, *Biometrics*, **30,** 562 (1974).

(16) A. J. Sedman and J. G. Wagner, *J. Pharm. Sci.*, **65,** 1006 (1976).

(17) C. T. Ueda and J. G. Nickols, *J. Pharm. Sci.*, **69,** 1400 (1980).

(18) T. W. Guentert, J. D. Huang, and S. Øie, *J. Pharm. Sci.*, **71,** 812 (1982).

(19) C. T. Ueda, B. E. Ballard, and M. Rowland, *J. Pharmacol. Exp. Ther.*, **200,** 459 (1977).

(20) C. T. Ueda, D. S. Hirschfeld, M. M. Scheinman, M. Rowland, B. J. Williamson, and B. S. Dzindzio, *Clin. Pharmacol. Ther.*, **19,** 30 (1976).

(21) D. J. Greenblatt, H. J. Pfeifer, H. R. Ochs, K. Franke, D. S. MacLaughlin, T. W. Smith, and J. Koch-Weser, *J. Pharmacol. Exp. Ther.*, **202,** 365 (1977).

(22) T. W. Guentert, N. H. G. Holford, P. E. Coates, R. A. Upton, and S. Riegelman, *J. Pharmacokinet. Biopharm.*, **7,** 315 (1979).

(23) J. V. Taggart, D. P. Earle, Jr., R. W. Berliner, C. G. Zubrod, W. J. Welch, N. B. Wise, E. F. Schroeder, I. M. London, and J. A. Shannon, *J. Clin. Invest.*, **27,** 80 (1948).

(24) P. Bolme and U. Otto, *Eur. J. Clin. Pharmacol.*, **12,** 73 (1977).

(25) L. B. Jellett, B. L. Lloyd, R. R. Taylor, and K. F. Ilett, *Pharmacol. Res. Commun.*, **9,** 455 (1977).

(26) D. E. Drayer, D. T. Lowenthal, K. M. Restivo, A. Schwartz, C. E. Cook, and M. M. Reidenberg, *Clin. Pharmacol., Ther.*, **24,** 31 (1978).

(27) I. Abraham, Ph.D. Dissertation, University of Nebraska Medical Center, Omaha, Neb., 1980, p. 72.

(28) I. Abraham, Ph.D. Dissertation, University of Nebraska Medical Center, Omaha, Neb., 1980, p. 77.

ACKNOWLEDGMENTS

This study was supported in part by a grant-in-aid from the American Heart Association, Nebraska Affiliate.

Leucine Enkephalin Analogues Containing a Conformationally Restrained *N*-Terminal Amino Acid Residue

TREVOR DEEKS, PETER A. CROOKS *x, and ROGER D. WAIGH

Received December 2, 1982, from the *Department of Pharmacy, University of Manchester, Manchester, M13 9PL, UK.* Accepted for publication January 24, 1983. *Present address: Division of Medicinal Chemistry and Pharmacognosy College of Pharmacy, University of Kentucky, Lexington, KY 40506.

Abstract □ Three analogues of leucine enkephalin, in which the terminal tyrosine-1 residue has been replaced by conformationally restrained aromatic amino acids, have been synthesized by classical solution methods. Their opiate agonist potencies on electrically stimulated guinea pig ileum and mouse vas deferens preparations were determined and compared with morphine, Met enkephalin, and Leu enkephalin. None of these analogues had analgesic properties when evaluated on the above tissue preparations or when evaluated by the hot-plate test in mice after subcutaneous and intracerebroventricular administration.

Keyphrases □ Leucine enkephalin—conformationally restrained analogues, synthesis, analgesic activity □ Analgesics—evaluation of conformationally restrained leucine enkephalin derivatives, synthesis

A milestone in neurochemical research during the last decade has been the elucidation of the role of enkephalins as natural endogenous ligands for the opiate receptor (1, 2). Since this discovery, the synthesis of a multitiude of structural analogues of leucine and methionine enkephalins (Ig and Ih, respectively) have been reported (recent review, 3), some of which are more potent analgesics and/or possess greater *in vivo* stability than the natural opiate ligands. These synthetic analogues have resulted from modifications of the parent molecules, such as shortening or lengthening of the pentapeptide chain (4, 5), substitution of individual amino acids by other amino acids (5–11), and chemical modification of individual amino acids (12–14).

Preferred conformations of enkephalin molecules at analgesic receptors have been suggested, based on data from conformational studies involving both spectroscopic measurements and structure–activity considerations (15–33). These studies have attempted to relate the structure of the terminal tyrosine residue in the enkephalin molecule to the tyramine moiety present in the morphine molecule. Since morphine is a conformationally rigid molecule, this implies that the conformationally "loose" tyrosine residue in the enkephalin may interact at opiate receptors in a specific conformation which is related, stereochemically, to the rigid tyramine moiety present in the morphine molecule.

As part of a study designed to evaluate the importance of the tyrosine conformation in the enkephalins on analgesic activity and receptor recognition, we have initiated a preliminary investigation into the synthesis of Leu enkephalin derivatives in which the terminal tyrosine unit has been replaced by a variety of conformationally restrained aromatic amino acids and in which the terminal leucine-5 residue has been esterified to aid passage into the central nervous system. The investigations described in this report are restricted to the preparation of Leu enkephalin analogues containing a nonhydroxylated aromatic amino acid in place of the tyrosine-1 residue in order to initially determine the feasibility of preparing pentapeptides such as IIe–Ve, with a bulky terminal amino acid unit, *via* classical solution methods, before embarking on the preparation of the synthetically more difficult aromatic hydroxy derivatives IIf–Vf, which were regarded as the ultimate target compounds.

We now report the synthesis of the Leu enkephalin analogues IIe–IVe and their evaluation as analgesic agents on isolated guinea pig ileum myenteric plexus muscle, mouse vas deferens tissue, and by the hot-plate test in mice after subcutaneous and intracerebroventricular administration.

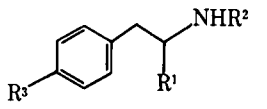

I

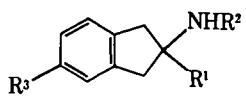

II

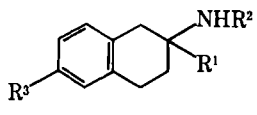

III

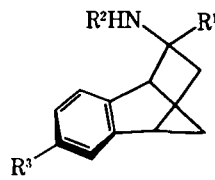

IV

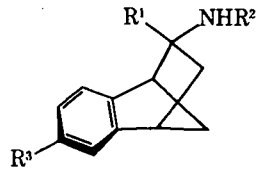

V

a R^1 = COOH, R^2 = R^3 = H.
b R^1,R^2 = CO—NHCO—, R^3 = H.
c R^1 = COOH, R^2 = CO—O—CH_2Ph, R^3 = H.
d R^1 = CONHGlyGlyL—PheL—LeuOCH$_3$,
R^2 = CO—OCH_2Ph, R^3 = H.
e R^1 = CONHGlyGlyL—PheL—LeuOCH$_3$, R^2 = R^3 = H.
f R^1 = CONHGlyGlyL—PheL—LeuOCH$_3$, R^2 = H, R^3 = OH.
g R^1 = CONHGlyGlyL—PheL—LeuOH, R^2 = H, R^3 = OH.
h R^1 = CONHGlyGlyL—PheL—MetOH, R^2 = H, R^3 = OH.

H_2NGlyGlyL—PheL—LeuOCH$_3$

VI

EXPERIMENTAL

Melting points were determined on a hot-stage microscope[1] and are uncorrected. Microanalyses were performed by the Micro-analytical Laboratory, Department of Chemistry, University of Manchester, analytical results obtained for all compounds were within ±0.4% of the theoretical value unless otherwise stated. ^{1}H-NMR spectra were recorded on a spectrometer[2] and are quoted in ppm on the δ scale. ^{13}C-NMR spectra were recorded on a spectrometer[3]. IR spectra were recorded as KCl disks, nujol mulls, or liquid films

[1] Reichert.
[2] Model HR 220 or SC 300; Varian Instruments.
[3] Model WP 80; Bruker.

0022-3549/84/0400-0457$01.00/0
© 1984, American Pharmaceutical Association

on a spectrophotometer[4]. Mass spectra were determined on a spectrometer[5] operating at a probe temperature of 250°C. TLC separations were carried out on 0.25-mm silica gel[6]. 2-Aminoindan-2-carboxylic acid (34) and (±) 2-aminotetralin-2-carboxylic acid (35) were prepared by literature procedures. Amino acids and peptides with free amino functions were visualized by spraying with 1% ninhydrin in ethanol. *N*-Protected amino acids and peptides were visualized with 5% potassium dichromate in concentrated H_2SO_4; other compounds were visualized in iodine vapor. Hydrogenations were carried out on a hydrogenator[7] operating at atmospheric pressure and room temperature.

Ion-exchange chromatographic separations of *N*-deprotected pentapeptides were carried out on carboxymethylcellulose[8], prewashed with 0.5 M sulfuric acid followed by 0.2 M ammonium acetate buffer adjusted to pH 5.1 with 0.88 M ammonium hydroxide or glacial acetic acid and measured using a pH meter[9] fitted with a combined electrode[10]. Ion-exchange columns were run under slight pressure using a peristaltic pump set for an effluent output of 100 mL/h. Column effluents were monitored by UV spectrophotometry at 280 nm using a spectrophotometer[11] fitted with a 10-mm path length flow-through cell. Columns were eluted with 0.005–0.5 M gradient ammonium acetate buffer solutions at pH 5.1, and fractions were collected on an automatic fraction collector.

Amino acid analyses of peptides were performed on an amino acid analyzer[12] using ninhydrin as visualizer. The peptides were hydrolyzed in 6 M HCl at 110°C for 24 h in a sealed, evacuated tube.

Synthesis of *endo*-2-Aminobenzonorbornen-2-carboxylic Acid (IVa)—*Spiro[benzonorbornen-2,5′-hydantoin] (IVb)*—A solution of ammonium carbonate (28.6 g, 0.18 mol) in 50% aqueous ethanol (200 mL) was added to benzonorbornen-2-one (36) (11.1 g, 0.07 mol) in 50% aqueous ethanol (40 mL). The mixture was warmed to 50°C and a solution of potassium cyanide (4.6 g, 0.072 mol) in water (40 mL) was added in small portions over a 1-h period. The mixture was stirred at 58–60°C for 5 h. The ethanol was removed under reduced pressure, and the aqueous residue was extracted with ethyl acetate (3 × 200 mL). The combined organic extracts were dried, filtered, and evaporated to dryness, and the residue was triturated with ether to afford white crystals of IVb mp 225–229°C. The aqueous layer was acidified to pH 2 with concentrated sulfuric acid to afford an additional product for a total of 12.07 g 76%). This compound had identical spectrometric properties (IR, NMR) to an authentic sample recently prepared *via* a Strecker synthesis (48).

endo-*2-Aminobenzonorbornen-2-carboxylic Acid (IVa)*—A mixture of spiro[benzonorbornen-2,5′-hydantoin] (IVb) (6.63 g, 0.029 mol), barium hydroxide [$Ba(OH)_2{\cdot}8H_2O$, 17.6 g, 0.056 mol], and water (100 mL) was heated under reflux, in an atmosphere of nitrogen, for 70 h and then filtered while hot. The collected solid was washed with an equal volume of water, and the combined filtrate and washings were saturated with carbon dioxide, heated to boiling point, and refiltered. The filtrate (on cooling) afforded white crystals of IVb (140 mg, 2% recovery). The mother liquors were evaporated to ~50 mL to afford white crystals of IVa (4.69 g, 79%), mp 227.0–229.5°C [lit. (48) mp 227.5–229.5°C]. The hydrochloride salt was prepared from a portion of the product and had mp 228–231°C (dec.). ^{13}C-NMR (CH_3OH): 173.8 (s, CO_2H), 149.5 and 141.8 (2 × s, C-4a and C-8a), 129.5, 128.0, 125.2, and 123.1 (4 × d, ArC), 65.1 (s, C-2), 53.9 (d, C-4), 51.1 (d, C-1), 44.9 (t, C-9), and 39.8 (t, C-3); *m/z* 203 (M^+).

Preparation of *N*-Benzyloxycarbonyl Amino Acids—As a general method, the appropriate amino acid (0.011 mol) suspended in 2 M NaOH solution (100 mL) was heated on a steam bath to dissolve the amino acid and then cooled in an ice bath to 0–5°C, which caused the sodium salt of the amino acid to precipitate. Carbobenzyloxy chloride (2.11 g, 0.012 mol) was added in a dropwise manner to the cooled, stirred mixture over 40 min. The ice bath was then removed, and the mixture was stirred at room temperature for 30 h. The mixture was cooled to 0–5°C, and a further 2.11 g (0.012 mol) of carbobenzyloxy chloride added in a dropwise manner. After 60 h the mixture was carefully adjusted to pH 1 with 5 M HCl and extracted with ether (2 × 100 mL). The combined organic extracts were dried, filtered, and evaporated to dryness, and the residue was crystallized from ether–petroleum ether (bp 30–40°C) to afford the appropriate *N*-benzyloxycarbonyl amino acid.

2-Benzyloxycarbamidoindan-2-carboxylic acid (IIc)—This compound was prepared as described above from IIa in 32% yield, mp 46.5–53.0°C. IR (Nujol): 1748, 1663, 1545, and 1532 cm^{-1}; ^{1}H-NMR (DMSO-d_6): δ 3.48 (m, 4, C-1 and C-3 H), 5.04 (s, 2, benzyloxy CH_2), 7.05–7.45 (m, 9, ArH), 7.88 (s, 1, exchangeable with D_2O, NH), and 9.10 ppm (br s, 1, exchangeable with D_2O, COOH); *m/z* 311 (M^+).

Anal.—Calc. for $C_{18}H_{17}NO_4$: C, 69.5; H, 5.5; N, 4.5. Found: C, 69.9; H, 5.8; N, 4.2.

2-Benzyloxycarbamidotetralin-2-carboxylic Acid (IIIc)—Compound IIIc was prepared as described above from IIIa in 19% yield, mp 131.0–137.5°C. IR (KCl): 1772, 1728, 1688, 1680, 1580, and 1526 cm^{-1}; ^{1}H-NMR ($CDCl_3$): δ 2.24 (m, 2, C-3 H), 2.80 (m, 2, C-4 H), 3.18 (m, 2, C-1 H), 5.05 (s, 2, benzyloxy CH_2), 5.30 (br s, 1, exchangeable with D_2O, NH), 6.90–7.50 (m, 9, ArH), and 10.32 (br s, 1, exchangeable with D_2O, COOH); *m/z* 325 (M^+).

Anal.—Calc. for $C_{19}H_{19}NO_4$: C, 70.2; H, 5.8; N, 4.3. Found: C, 70.1, H, 5.9, N, 4.0.

endo-*2-Benzyloxycarbamidobenzonorbornene-2-carboxylic Acid (IVc)*—This compound was prepared as described above from IVa in 27% yield, mp 90–93°C. IR (KCl): 1742, 1686, 1641, 1600, and 1582 cm^{-1}; ^{1}H-NMR ($CDCl_3$): δ 1.28 (d of d, 1, J = 3 and 12 Hz, C-3 *endo*-H), 1.91 and 2.26 (2 × d, AB, J = 9 Hz, C-9 H), 2.95 (d of d, 1, J = 4 and 12 Hz, C-3 *exo*-H), 3.37 (m, 1, C-4 H), 3.84 (m, 1, C-1 H), 4.80 (br s, 1, exchangeable with D_2O, NH), 5.00 (d, 2, J = 4 Hz, benzyloxy CH_2), 6.95–7.50 (m, 9, ArH), and 11.05 ppm (s, 1, exchangeable with D_2O, COOH).

Anal.—Calc. for $C_{20}H_{25}NO_5$: C, 71.2; H, 5.6; N, 4.2. Found: C, 71.6; H, 5.8; N, 4.0.

Preparation of *N*-Protected Pentapeptides—As a general method, a solution of the appropriate *N*-benzyloxycarbonyl amino acid (1.9 mmol), glycylglycyl-L-phenylalanyl-L-leucine methyl ester (VI) (37) (1.9 mmol), and triethylamine (2.2 mmol) in CH_2Cl_2 (50 mL) was cooled in an ice bath, and 1-hydroxybenzotriazole (3.9 mol) in CH_2Cl_2 (10 mL) was added in a dropwise manner. The mixture was stirred for 5 min before adding *N,N′*-dicyclohexylcarbodiimide (2.1 mol) in CH_2Cl_2 (20 mL) in one portion. The ice bath was removed, the reaction was stirred at room temperature for 56 h, the precipitated dicyclohexylurea was removed by filtration, and the filtrate was evaporated to a volume of 10 mL and then refiltered. The resulting filtrate was evaporated to dryness, dissolved in ethyl acetate (50 mL) and washed with 1 M HCl (50 mL), saturated $NaHCO_3$ solution (50 mL), and finally water (50 mL). The organic layer was then dried, filtered, and evaporated to dryness. The resulting gummy residue was triturated with ether to afford the appropriate *N*-protected pentapeptide as a buff-colored, amorphous solid.

{[(*2 - Benzyloxycarbamido) -2- indanyl]carbonyl}glycylglycyl-L-phenylalanyl-L-leucine Methyl Ester (IId)*—Compound IId was prepared as above from IIc in 61% yield, mp 134–138°C. TLC (silica, ethyl acetate–methanol, 40:60): R_f 0.60; IR (KCl): 1726, 1675, 1665, 1650, 1595, 1532, and 1520 cm^{-1}; ^{1}H-NMR ($CDCl_3$): δ 0.81 [d, 6, leucine δ-$(CH_3)_2$], 1.51 (m, 2, leucine β-CH_2), 1.78 (m, 1, leucine γ-CH), 3.07 (d of d, 4, indane 1- and 3-H), 3.09 (m, 2, phenylalanine β-CH_2), 3.55 and 3.57 (2 × s, 3, conformational forms of leucine OCH_3), 3.72 (m, 2, one of glycine α-CH_2's), 3.92 (m, 2, one of glycine α-CH_2's), 4.49 (m, 1, leucine α-CH), 4.71 (m, 1, phenylalanine α-CH), 4.99 (d, 2, $C_6H_5OCH_2$—O), 6.28 (d, 1, exchangeable with D_2O, NH), 7.03 (t, 2, exchangeable with D_2O, 2 × NH), 7.08–7.35 (m, 14, ArH), and 7.66 ppm (m, 2, exchangeable with D_2O, 2 × NH).

Anal.—Calc. for $C_{38}H_{45}N_5O_8$: C, 65.2; H, 6.2; N, 10.0. Found: C, 65.3; H, 6.2; N, 10.0.

{[(*2-Benzyloxycarbamido)-2-tetralyl]carbonyl} glycylglycyl-L-phenylalanyl-L-leucine Methyl Ester (IIId)*—This compound was prepared as above from IIIc in 91% yield, mp 86–90°C. TLC (silica, chloroform–methanol–acetic acid, 120:90:5): R_f 0.62; IR (KCl): 1740, 1725, 1704, 1690, 1675, 1660, 1564, and 1530 cm^{-1}; ^{1}H-NMR ($CDCl_3$): δ 0.87 [d, 6, leucine δ-$CH_3)_2$], 1.55 (m, 2, leucine β-CH_2), 2.22 (m, 1, leucine γ-CH), 2.41 (m, 2, tetralin 3-H), 2.60–3.80 (m, 4, tetralin 1- and 4-H), 3.32 (m, 2, phenylalanine β-CH_2), 3.52 and 3.54 (2 × s, 3, leucine OCH_3's), 3.80 (m, 2, one of glycine α-CH_2's), 3.91 (m, 2, one of glycine α-CH_2's), 4.54 (m, 1, leucine α-CH), 4.73 (m, 1, phenylalanine α-CH), 5.02 (d, 2, benzyloxy CH_2), 6.78–7.70 (m, 14, ArH), 6.83 (d, 1, exchangeable with D_2O, NH), 7.16 (t, 2, exchangeable with D_2O, 2 × NH), 7.78 (m, 1, exchangeable with D_2O, NH), and 7.89 ppm (m, 1, exchangeable with D_2O, NH).

Anal.—Calc. for $C_{39}H_{47}N_5O_8$: C, 65.6; H, 6.6; N, 9.8. Found: C, 65.2; H, 6.7; N, 10.1.

{[(endo-*2-Benzyloxycarbamido) -2- benzonorbornenyl]carbonyl}glycylglycyl-L-phenylalanyl-L-leucine Methyl Ester (IVd)*—Compound IVd was prepared as above from IVc in 43% yield, mp 118–121°C. TLC (silica, chloroform–methanol–acetic acid, 120:90:5): R_f 0.72; IR (KCl): 1740, 1705, 1690, 1660, 1632, 1565, 1545, and 1520 cm^{-1}; ^{1}H-NMR ($CDCl_3$): δ 0.84 [d, 6, leucine δ-$(CH_3)_2$], 1.30 (m, 1, benzonorbornenyl C-3 *exo*-H), 1.53 (m, 2, leucine β-CH_2), 1.94 (m, 1, leucine γ-CH), 1.98 (m, 2, benzonorbornenyl C-9 H), 2.64 (m, 1, benzonorbornenyl C-3 *endo*-H), 3.09 (m, 2, phenylalanine

[4] Model 237; Perkin-Elmer.
[5] A.E.I. model M59.
[6] Polygram silica gel UV_{254}.
[7] Gallenkampf.
[8] Whatman CMC 52.
[9] Model PW 9418; Pye Unicam.
[10] Pye Unicam 401.
[11] Cecil CE 202.
[12] *Model 123*; Beckmann SPINCO.

β-CH_2), 3.62 (s, 3, leucine OCH_3), 3.63 (m, 2, benzonorbornenyl C-1 and C-4 H), 3.72 (m, 2, one of glycine α-CH_2's), 3.94 (m, 2, one of glycine α-CH_2's), 4.52 (m, 1, leucine α-CH), 4.69 (m, 1, phenylalanine α-CH), 5.17 (d, 2, benzyloxy CH_2), 6.38 (m, 1, exchangeable with D_2O, NH), 6.70–7.55 (m, 16, ArH and 2 exchangeable × NH), 7.60 (m, 1, exchangeable with D_2O, NH), and 7.70 ppm (m, 1, exchangeable with D_2O, NH).

Anal.—Calc. for $C_{40}H_{47}N_5O_8$: C, 66.2; H, 6.5, N, 9.2. Found: C, 65.8; H, 6.6; N, 8.9.

Synthesis of Unprotected Pentapeptides—As a general method, the appropriate *N*-protected pentapeptide (16 nmol) was dissolved in absolute ethanol (100 mL), 5% palladium-on-charcoal catalyst (0.5 g) was added, and the mixture was hydrogenated with stirring at room temperature and atmospheric pressure for 20 h. The catalyst was then removed by filtration, the filtrate evaporated to dryness, and the residue dissolved in ethyl acetate (50 mL). The organic solution was extracted with 1 M HCl (2 × 50 mL), followed by water (1 × 30 mL). The combined aqueous extracts were basified to pH 9 with solid sodium bicarbonate and back-extracted with ethyl acetate (2 × 50 mL). The combined ethyl acetate extracts were dried, filtered, and evaporated to dryness, and the residue was purified on a carboxymethylcellulose column, eluting with ammonium acetate buffer, as previously described, to afford the appropriate *N*-deprotected pentapeptide in buffer solution. The water and buffer salts were removed by freeze-drying, redissolving the residue in water (200 mL), and redrying on a freeze-drying apparatus[13] at 10^{-1}–10^{-2} torr.

[*(2-Aminoindanyl)carbonyl*]*glycylglycyl -L- phenylalanyl -L- leucine Methyl Ester (IIe)*—This compound was prepared as above from IId in 17% yield, mp 93–95°C. TLC (silica, chloroform–methanol–acetic acid, 120:90:5): R_f 0.69; IR (KCl): 1740, 1686, 1672, 1650, 1580, 1562, 1545, and 1525 cm^{-1}; ^{1}H-NMR ($CDCl_3$): δ 0.85 and 0.93 [t and d, 6, leucine δ-$(CH_3)_2$], 1.60 (m, 2, leucine β-CH_2), 2.12 (m, 1, leucine γ-CH), 2.82 (d of d, 4, indane 1- and 3-H), 3.08, (m, 2, phenylalanine β-CH_2), 3.65 and 3.70 (2 × s, 3, leucine OCH_3), 3.81 (s, 2, exchangeable with D_2O, NH_2), 3.95 (d of d, 2, one of glycine α-CH_2's), 4.06 (d of d, 2, one of glycine α-CH_2's), 4.48 (m, 1, leucine α-CH), 4.92 (t, 1, phenylalanine α-CH), 7.00–7.31 (m, 9, ArH), 7.26 (d, 1, exchangeable with D_2O, NH), 7.49 (d, 1, exchangeable with D_2O, NH), 7.63 (m, 1, exchangeable with D_2O, NH), and 8.45 ppm (m, 1, exchangeable with D_2O, NH); amino acid analysis (after acidic hydrolysis): 2d 0.95, Gly 1.97, Phe 1.00, and Leu 1.01.

Anal.—Calc. for $C_{30}H_{39}N_5O_6 \cdot H_2O$: C, 61.7; H, 7.1; N, 12.0. Found: C, 61.7; H, 6.8; N, 11.6.

[*(2-Aminotetralyl)carbonyl*] *glycylglycyl -L- phenylalanyl -L- leucine Methyl Ester (IIIe)*—Compound IIIe was prepared as above from IIId in 11% yield, mp 165–170°C. TLC (silica, chloroform–methanol–acetic acid, 120:90:5): R_f 0.61; IR (KCl): 1740, 1690, 1678, 1655, 1550, and 1522 cm^{-1}; ^{1}H-NMR ($CDCl_3$): δ 0.92 [m, 6, leucine δ-$(CH_3)_2$], 1.39 (m, 2, leucine β-CH_2), 1.58 (m, 2, tetralin 3-H), 1.82 (br s, 2, exchangeable with D_2O, NH_2), 1.92 (m, 1, leucine γ-CH), 3.01 (m, 4, tetralin 1- and 4-H), 3.38 (m, 2, phenylalanine β-CH_2), 3.70 and 3.72 (2 × s, 3, leucine OCH_3), 3.98 (m, 2, one of glycine α-CH_2's), 4.05 (m, 2, one of glycine α-CH_2's), 4.46 (m, 1, leucine α-CH), 4.82 (m, 1, phenylalanine α-CH), 6.88 (m, 1, exchangeable with D_2O, NH), 6.90–7.45 (m, 9, ArH), 7.54 (m, 1, exchangeable with D_2O, NH), 7.64 (m, 1, exchangeable with D_2O, NH), and 8.64 ppm (m, 1, exchangeable with D_2O, NH); amino acid analysis (after acidic hydrolysis): 3d 0.92, Gly 2.02, Phe 1.00, and Leu 1.12.

Anal.—Calc. for $C_{31}H_{41}N_5O_6 \cdot H_2O$: C, 62.3; H, 7.2; N, 11.7. Found: C, 62.8; H, 6.7; N, 11.2.

[(endo-*2-Aminobenzonorbornenyl)carbonyl*] *glycylglycyl -L- phenylalanyl-L-leucine Methyl Ester (IVe)*—This compound was prepared as above from IVd in 31% yield, mp 113–116°C. TLC (silica, chloroform–methanol–acetic acid, 120:90:5): R_f 0.78; IR (KCl): 1742, 1703, 1688, 1657, 1560, 1545, and 1520 cm^{-1}; ^{1}H-NMR ($CDCl_3$): δ 0.85 [m, 6, leucine δ-$(CH_3)_2$], 1.32 (m, 2, leucine β-CH_2), 1.52 (d of d, 1, benzonorbornene C-3 *endo*-H), 1.60 (m, 1, leucine γ-CH), 1.70 (m, 2, benzonorbornene C-9 H), 1.92 (m, 2, benzonorbornene C-3 *exo*-H), 2.47 (m, 2, benzonorbornene 1- and 4-H), 3.08 (m, 2, phenylalanine β-CH_2), 3.34 (br s, 2, exchangeable with D_2O, NH_2), 3.65 (m, 3, leucine OCH_3), 3.90 (m, 2, one of glycine α-CH_2's), 4.04 (m, 2, one of glycine α-CH_2's), 4.52 (m, 1, leucine α-CH), 4.76 (m, 1, phenylalanine α-CH), 6.80–7.56 (m, 9, ArH), 7.02 (m, 1, exchangeable with D_2O, NH), 7.63 (m, 1, exchangeable with D_2O, NH), 7.77 (m, 1, exchangeable with D_2O, NH), and 8.70 ppm (m, 1, exchangeable with D_2O, NH); amino acid analysis (after acidic hydrolysis): 4d 0.91, Gly 2.4, Phe 1.00, and Leu 1.01.

Anal.—Calc. for $C_{32}H_{41}N_5O_6 \cdot H_2O$: C, 63.1; H, 7.1; N, 11.5. Found: C, 62.9; H, 7.4; N, 11.5.

Pharmacology—Compounds were evaluated for analgesic properties in albino mice (Tuck, TFW strain) by the following procedures. *In vitro* testing was carried out by measuring the inhibition of electronically stimulated contractions of the guinea pig ileum myenteric plexus muscle using the method of Kosterlitz and Watt (38) and by measuring the inhibition of mouse vas deferens tissue after stimulation with twin rectilinear pulses 10 ms apart (39). *In vivo* evaluation was carried out using the mouse hot-plate test (40).

[13] Model EF03; Edwards.

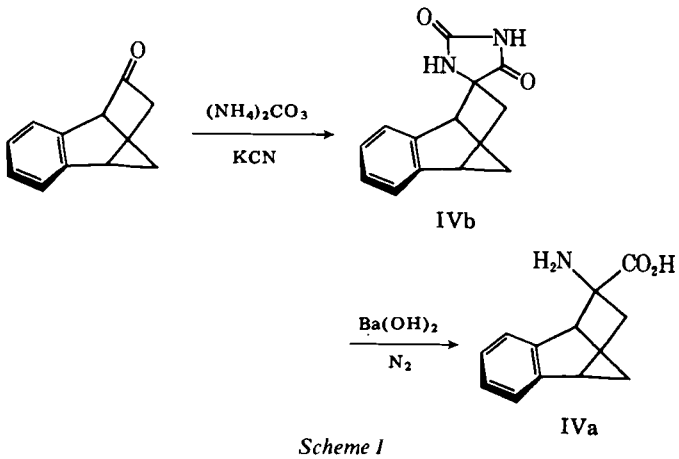

Scheme I

RESULTS

Chemistry—The amino acids IIa and IIIa were prepared by literature methods (34, 35). Synthetic routes to IVa and Va were designed based on the stereochemistry of the products that have been obtained from Strecker and Bucherer reactions on norbornane-2-one and related compounds (41–47). Reaction of benzonorbornen-2-one with ammonium carbonate and KCN afforded exclusively the expected spirohydantoin, IVb, which could be hydrolyzed with barium hydroxide to the *endo*-amino acid, IVa (Scheme I). The unequivocal structural assignment of IVa was determined from data obtained from ^{1}H- and ^{13}C-NMR spin-spin coupling data and from two-dimensional ^{1}H-NMR studies, both of which are reported by us elsewhere (48). Attempted synthesis of Va from benzonorbornen-2-one *via* a modified Strecker synthesis resulted in formation of only the *endo*-amino acid IVa (48).

The amino acids IIa, IIIa, and IVa were each *N*-protected with carbobenzoxy chloride in base and coupled with tetrapeptide VI (37) using the *N,N'*-dicyclohexylcarbodiimide-1-hydroxybenztriazole method. Hydrogenolysis of the protected pentapeptides IId, IIId, and IVd and purification of the resulting deprotected products by gradient buffer elution from carboxymethylcellulose at pH 5.1 afforded the pentapeptide methyl esters IIe, IIIe, and IVe.

Pharmacology—Compound IIe exhibited only weak analgesic properties when evaluated on electrically stimulated guinea pig ileum, showing an ID_{50} of 3.8 μm (ID_{50} values for morphine, Met enkephalin, and Leu enkephalin on the same preparation are 90.5, 86.8, and 450 nM, respectively), whereas compounds IIIe and IVe were inactive. None of the pentapeptides were active analgesics in the mouse vas deferens preparation or in the hot-plate test in mice after subcutaneous and intracerebroventricular injection.

CONCLUSIONS

This study has developed synthetic routes, based on classical solution techniques, which can be used to prepare Leu enkephalin derivatives in which the terminal tyrosine-1 residue has been replaced by a variety of conformationally restrained amino acid moieties, as represented in structures IIe, IIIe, and IVe. None of these pentapeptides possess any significant analgesic activity, both *in vitro* and *in vivo*, which is consistent with the observation that enkephalins lacking an aromatic *para*-hydroxy group in the tyrosine-1 moiety are inactive as analgesics (4, 7). The synthetic procedures developed in this study should be of value in the preparation of Leu enkephalin derivatives incorporating aromatic hydroxylated derivatives of IIa, IIIa, and IVa in place of the tyrosine-1 moiety.

REFERENCES

(1) J. A. H. Lord, A. A. Waterfield, J. Hughes, and H. W. Kosterlitz, "Opiates and Endogenous Opioid Peptides," H. W. Kosterlitz, Ed. North-Holland, Amsterdam, 1976.

(2) S. H. Snyder, *Sci. Am.*, **236**, 44 (1977).

(3) J. Morley, *Annu. Rev. Pharmacol. Toxicol.*, **20**, 81 (1980) and references cited therein.

(4) L. Terenius, A. Wahlström, G. Lindenberg, S. Karlsson, and U. Ragnarsson, *Biochem. Biophys. Res. Commun.*, **71,** 175 (1976).
(5) N. S. Agarwal, V. J. Houby, R. Katz, W. Klee, and M. Nierenberg, *Biochem. Biophys. Res. Commun.*, **76,** 129 (1977).
(6) C. R. Bedell, R. B. Clark, G. W. Hardy, L. A. Lowe, F. B. Ubatuba, J. R. Vane, S. Wilkinson, K-L Chang, P. Cuatreacasas, and R. J. Miller, *Proc. R. Soc. London B*, **198,** 249 (1977).
(7) D. H. Coy, A. J. Kastin, A. V. Schally, O. Morin, N. G. Caron, F. Labrie, J. M. Walker, R. Fertel, G. G. Berntson, and C. A. Sandman, *Biochem. Biophys. Res. Commun.*, **73,** 632 (1976).
(8) J. S. Shaw and M. J. Turnbull, *Eur. J. Pharmacol.*, **49,** 313 (1978).
(9) S. Bajusz, A. Z. Ronai, J. I. Szekely, L. Graf, Z. Dunai-Kovacs, and I. Berzetei, *FEBS Lett.*, **76,** 91 (1977).
(10) E. T. Wei, L. F. Tseng, H. H. Loh, and C. H. Li, *Life Sci.*, **21,** 321 (1977).
(11) D. Yamashiro, L. F. Tseng, and C. H. Li, *Biochem. Biophys. Res. Commun.*, **78,** 1124 (1977).
(12) A. S. Dutta, J. J. Gormley, C. F. Hayward, J. S. Morley, J. S. Shaw, G. J. Stacey, and M. J. Turnbull, *Life Sci.*, **21,** 559 (1977).
(13) P. W. Schiller, C. F. Yam, and M. Lis, *Biochemistry*, **16,** 1831 (1977).
(14) J-K Chang, B. T. W. Fong, A. Pert, and C. B. Pert, *Life Sci.*, **18,** 1473 (1976).
(15) S. Combrisson, B. P. Roques, and R. Oberlin, *Tetrahedron Lett.*, **1976,** 3455.
(16) H. E. Bleich, J. D. Cutnell, A. R. Day, R. J. Freer, J. A. Glasel, and J. F. McKelvy, *Proc. Natl. Acad. Sci. USA*, **73,** 2589 (1976).
(17) J. L. De Coen, C. Humblett, and M. H. J. Koch, *FEBS Lett.*, **73,** 38 (1977).
(18) B. E. Maryanoff and M. J. Zelesko, *J. Pharm. Sci.*, **67,** 590 (1978).
(19) R. H. B. Galt, *J. Pharm. Pharmacol.*, **29,** 711 (1977).
(20) A. S. Horn and J. R. Rodgers, *Nature (London)*, **260,** 795 (1976).
(21) W. A. Klis, E. Nawrocka, T. Z. Siemon, A. P. Plech, Z. Stachura, and Z. S. Herman, *Biorg. Chem.*, **8,** 255 (1979).
(22) F. A. Gorin and G. R. Marshall, *Proc. Natl. Acad. Sci. USA*, **74,** 5179 (1977).
(23) B. P. Roques, C. Garby-Jaureuiberry, and R. Oberlin, *Nature (London)*, **262,** 778 (1976).
(24) C. R. Jones, W. A. Gibbons, and V. Garskey, *Nature (London)*, **262,** 779 (1976).
(25) E. R. Stimson, Y. C. Meinwald, and H. A. Scheraga, *Biochemistry*, **18,** 1661 (1979) and references cited therein.
(26) J. DiMaio, P. W. Schiller, and B. Belleau, "Proceedings American Peptide Symposium," Vol. 6, E. Gross and J. Meienhofer, Eds., Pierce Chem. Co., Rockford, Ill., 1979, p. 889.
(27) M. C. Summers and R. J. Hayes, *FEBS Lett.*, **113,** 99 (1980).
(28) D. Hudson, R. Sharpe, and M. Szelke, *Int. J. Pept. Protein Res.*, **15,** 122 (1980).
(29) B. P. Roques, G. Gacel, M.-C. Fournie-Zaluski, B. Senault, and J.-M. Lecomte, *Eur. J. Pharmacol.*, **69,** 109 (1979).
(30) J. DiMaio and P. W. Schiller, *Proc. Natl. Acad. Sci. USA*, **77,** 7162 (1980).
(31) G. D. Smith and J. F. Griffin, *Science*, **199,** 1214 (1978).
(32) T. L. Blundell, L. Hearn, I. J. Tickle, R. A. Palmer, B. A. Morgan, G. D. Smith, and J. F. Griffin, *Science*, **205,** 220 (1979).
(33) D. M. Rice, R. J. Wittebort, R. G. Griffin, E. Meirovitch, E. R. Stimson, Y. C. Meinwald, J. H. Freed, and H. A. Scheraga, *J. Am. Chem. Soc.*, **103,** 7707 (1981).
(34) H. Fletcher, P. B. Russel, and H. E. Album, *U.S. Pat.*, 3,532,744; 1970; *Chem. Abstr.*, **74,** P42218k (1971).
(35) R. M. Render, B. H. Butcher, D. A. Buxton, and D. J. Howells, *J. Med. Chem.*, **14,** 892 (1971).
(36) D. J. Sandman, K. Mislow, W. P. Giddings, J. Dirlam, and G. C. Hanson, *J. Am. Chem. Soc.*, **90,** 4877 (1968).
(37) E. Vilkas, M. Vilkas, and J. Sainton, *Int. J. Pept. Protein Res.*, **15,** 29 (1980).
(38) H. W. Kosterlitz and A. J. Watt, *Br. J. Pharmacol. Chemother.*, **33,** 266 (1963).
(39) J. Hughes, H. W. Kosterlitz, and F. M. Leslie, *Br. J. Pharmacol.*, **53,** 371 (1975).
(40) N. B. Eddy and D. Leimbach, *J. Pharmacol. Exp. Ther.*, **107,** 385 (1953).
(41) S. N. Rastogi, J. S. Bindra, and N. Anand, *Indian J. Chem.*, **9,** 1175 (1971).
(42) Y. Maki, T. Masugi, and K. Ozeki, *Chem. Pharm. Bull.*, **21,** 2466 (1973).
(43) H. S. Trager and H. N. Christensen, *J. Am. Chem. Soc.*, **94,** 968 (1972).
(44) Y. Maki and T. Masugi, *Chem. Pharm. Bull.*, **21,** 685 (1973).
(45) Y. Maki, M. Sato, and K. Obata, *Chem. Pharm. Bull.*, **13,** 1377 (1965).
(46) G. G. Trigo, C. Avendano, S. Emila, J. T. Edward, and S. Wong, *Can. J. Chem.*, **57,** 1456 (1979).
(47) G. L. Grunewald, S. H. Kuttab, M. A. Pleiss, J. B. Mangold, and P. Soine, *J. Med. Chem.*, **23,** 754 (1980).
(48) W. J. Layton, and S. L. Smith, P. A. Crooks, T. Decks, and R. D. Waigh, *J. Chem. Soc. Perk. Trans.* I, in press.

ACKNOWLEDGMENTS

We gratefully acknowledge the support of the Wellcome Research Laboratories in carrying out and releasing results of the biological testing and the Pharmaceutical Society of Great Britain for providing a research studentship for one of us (T.D.)

Percutaneous Absorption: A New Physicochemical Predictive Model for Maximum Human *In Vivo* Penetration Rates

H. Y. ANDO [x], T. W. SCHULTZ, R. L. SCHNAARE, and E. T. SUGITA

Received December 18, 1981, from the *Department of Pharmacy, Philadelphia College of Pharmacy and Science, Philadelphia, PA 19104.* Accepted for publication February 7, 1983.

Abstract □ A diffusion model for stratum corneum-limited percutaneous absorption based on the interaction of the diffusate with the stratum corneum was derived. Two types of interactions were proposed, ion-dipole and lipid-lipid, based on current knowledge of the stratum corneum and on irreversible thermodynamic arguments. The resulting flux equations predict a linear dependence of flux on the dipole moment and ln X of the diffusates, where X is the mole fraction solubility. These flux equations were tested on 21 different diffusates whose human percutaneous absorption rates *in vivo* had been previously determined. A solubility method was used to classify the interaction pathway for each diffusate. Correlation of the maximum absorption rate for the lipid and polar pathways give correlation coefficients of 0.946 and 0.998, respectively. It is believed that these studies provide a starting point for the ultimate goal of percutaneous absorption research: to be able to bypass *in vivo* and *in vitro* studies and to predict absorption solely on the basis of the physicochemical properties of the diffusates.

Keyphrases □ Absorption, percutaneous—maximum *in vivo* penetration rates, humans, physicochemical predictive model □ Penetration rates—maximum, *in vivo* percutaneous absorption in humans, physicochemical predictive model □ Diffusion model—physicochemical, predictive, stratum corneum-limited percutaneous absorption, maximum *in vivo* penetration rates in humans

The ultimate goal of percutaneous penetration research is to predict the permeability of structurally unrelated compounds from physical properties, thereby eliminating the need for studies in humans or animals (1). Stoughton *et al.* (2) examined a series of nicotinic acid esters and correlated absorption with the oil-water partition coefficient of the molecules. Similar studies were carried out by Katz and Shaikh (3), Durrheim *et al.* (4), and Roberts *et al.* (5) for a series of corticosteroids, alcohols, and phenols, respectively. Lien and Tong (6) attempted to use multiple regression analysis to correlate absorption with steric factors, molar refraction, Taft's polar substituent constant, and molecular weight. In all of these studies, the correlation had to be limited to a series of closely related compounds. The goal of this study is to develop a model that can be used to predict human percutaneous absorption of any molecule from only its physicochemical properties.

THEORETICAL

Diffusion - In 1855, Fick (7) formulated a set of diffusion equations by direct analogy with the equations of heat conduction, which have come to be known as Fick's First and Second Laws, respectively:

$$J = -D \text{ grad } C \qquad \text{(Eq. 1)}$$

$$\partial C/\partial t = D \text{ div grad } C \qquad \text{(Eq. 2)}$$

where J is the flux in mol/cm^2/s, D is the diffusion coefficient in cm^2/s, and C is the molar concentration of the diffusate. Equations 1 and 2 only describe ideal diffusion. In most real systems, the driving force for diffusion is the gradient of the chemical potential, μ, and not the gradient of the concentration. Thus, the most general forms of the diffusion equations are (8):

$$J = -(C \cdot u/N) \text{ grad } \mu \qquad \text{(Eq. 3)}$$

$$\partial C/\partial t = \text{div } [(C \cdot u/N) \text{ grad } \mu] \qquad \text{(Eq. 4)}$$

where u is the mobility and N is Avogadro's number. Because Eqs. 2 and 4 are not invariant with respect to time inversion, one characteristic of diffusion so described is that it is an irreversible process in which chemical equilibrium is approached in such a way that free energy is minimized and entropy is maximized. Classical thermodynamics deals mainly with closed systems at equilibrium; irreversible thermodynamics copes with open systems that are not at equilibrium.

Irreversible Thermodynamics - This discipline is almost exclusively concerned with the analysis of entropy production, entropy flow, and the possible coupling of entropy production between different processes. In Fig. 1, a model irreversible system applied to percutaneous absorption is shown. System I is composed of the stratum corneum, which is generally considered the rate-limiting skin barrier for passive diffusion. System II contains system I and the applied drug, the rest of the organism, and its excretory products. In this model, system I is *open* to exchange mass with system II. The global system containing I and II is isolated.

For a continuous open system, such as system I, in which the only change in entropy is due to exchange of matter by diffusion, entropy is a function of the spatial coordinates. If s denotes entropy per unit volume for system I, then (9):

$$\partial s/\partial t = -\text{div } \Phi + \sigma \qquad \text{(Eq. 5)}$$

where Φ is the flow of entropy due to the interactions of system I with system II and σ is the entropy production per unit volume and time due to changes within system I. One of the fundamental postulates of irreversible thermodynamics is that:

$$\sigma > 0 \qquad \text{(Eq. 6)}$$

for irreversible processes like diffusion.

For a multicomponent system of γ elements with no temperature gradients, σ is given by (9):

$$\sigma = \sum_{\gamma} \sum_{i} \frac{1}{T}\left[F^i - T\frac{\partial \mu/T}{\partial x^i}\right] \rho_\gamma u_\gamma{}^i + \frac{A \cdot v}{T} \qquad \text{(Eq. 7)}$$

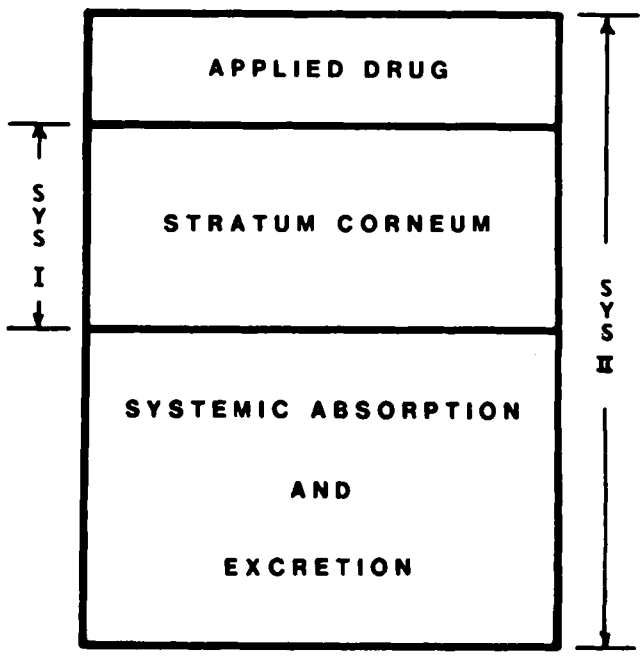

Figure 1—*A model thermodynamic system for percutaneous absorption.*

0022-3549/84/0400-0461$01.00/0
© 1984, American Pharmaceutical Association

where F is the force/mass acting on the component γ; μ is the free energy/mass for the component γ; ρ_γ is the density of component γ; u_γ is the diffusion velocity of component γ; A is the affinity of chemical reaction; v is the rate of chemical reaction/unit volume; and i is the index for spacial coordinates. If consideration is limited to a two-component system in which a diffusing chemical ($\gamma = 2$) moves in the x direction through a stratum corneum ($\gamma = 1$) stationary with respect to the coordinate system, then σ becomes:

$$\sigma = (F_2 - \text{grad } \mu_2)\frac{\rho_2\Delta_2}{T} + \frac{A \cdot v}{T} \qquad \text{(Eq. 8)}$$

where Δ_2 is the diffusion velocity with respect to the velocity of the center of gravity. The first term represents the diffusion contribution to σ, the second, the chemical reaction.

When:

$$A \cdot v < 0, \textit{ i.e.}, \text{ an endothermic reaction} \qquad \text{(Eq. 9)}$$

$$A \cdot v > 0, \textit{ i.e.}, \text{ an exothermic reaction} \qquad \text{(Eq. 10)}$$

where A is the affinity of the reaction (9) and v is the rate of the reaction per unit volume. The chemical potential, μ_2, can be written as:

$$\mu_2 = \mu_2^\circ + RT \cdot ln\ \gamma_2^\circ C_2 \qquad \text{(Eq. 11)}$$

$$\mu_2 = RT \cdot \ln \gamma_2 C_2 \qquad \text{(Eq. 12)}$$

where:

$$RT \cdot \ln \gamma_2 = \mu_2^\circ + RT \cdot \ln \gamma_2^\circ \qquad \text{(Eq. 13)}$$

Using Eq. 12, we can rewrite Eq. 8 as:

$$\sigma = \sigma_d + \sigma_f + \sigma_i + \sigma_x \qquad \text{(Eq. 14)}$$

where:

$$\sigma_d = -(\rho_2\Delta_2/T)RT \text{ grad ln } C_2 \qquad \text{(Eq. 15)}$$

$$\sigma_f = (\rho_2\Delta_2 F_2)/T \qquad \text{(Eq. 16)}$$

$$\sigma_i = -(\rho_2\Delta_2/T)RT \text{ grad ln } \gamma_2 \qquad \text{(Eq. 17)}$$

$$\sigma_x = A \cdot v/T \qquad \text{(Eq. 18)}$$

Equation 14 expresses the fact that the local entropy production rate within system I can be attributed to at least four additive factors. The first factor is due to ideal diffusion as described by Fick's Law, while the third factor accounts for the interaction of the diffusate within the stratum corneum. These terms will be the subject of further discussion in the next section.

With regard to the σ_f and the σ_x terms, it is possible that under some circumstances they might be important in understanding *in vivo* percutaneous absorption. Since there is a sizable electric potential across the stratum corneum of ~−30 mV (10), certain highly polar diffusates might be affected by this force field; σ_f is the predicted manifestation of this effect. Such an effect would not be expected *in vitro* since the skin potential disappears when the animal dies. At this time, it is not clear how large or significant this effect might be. However, it was noted by Anjo *et al.* (11) that while the correlation between *in vivo* and *in vitro* penetration is good, any individual component may deviate significantly. With regard to σ_x, if a substance reacts within the stratum corneum, σ_x will be altered. There are many enzymes in the stratum corneum which might facilitate this process. This would affect σ_i and σ_d since the character of the diffusing substance would be changed.

The total entropy production rate, σ, must be positive in every macroscopic region of system I. This local formulation of the second law is the fundamental postulate of irreversible thermodynamics. This does not mean, however, that each individual term in Eq. 14 must be positive. Since the concentration gradient for passive diffusion is always negative, σ_d must always be positive. The other two terms that are of most interest are σ_i and σ_x. For σ_i, the gradient of the activity coefficient could be positive or negative; the same is true for σ_x. Therefore, the type of gradient and the kind of chemical reaction can influence whether these terms increase or decrease the total entropy production rate.

Physicochemical Predictive Model—Equation 1 has been used to confirm the passive diffusion properties of the stratum corneum (12). It implies, however, that the activity coefficient of the diffusate in the stratum corneum is unity. This is not likely. Higuchi (13) has written Eq. 1 in a form equivalent to:

$$J = -(D/\gamma) \text{ grad } a \qquad \text{(Eq. 19)}$$

where γ and a are the activity coefficient and the activity, respectively, in the stratum corneum. Although Eq. 18 formally appears more correct than Eq. 1, it is difficult to experimentally distinguish D from D/γ. This equation also assumes that grad γ is zero, *i.e.*, it is not a function of the space coordinates.

To account for the contribution of activity gradients in our model, Eq. 3 will be used as the description of diffusion in which the driving force is the gradient of the chemical potential, μ. The stationary component (stratum corneum) will be denoted by the subscript 1 in this model; the diffusate, by the subscript 2. Since Eq. 12 can be written as:

$$\mu_2 = RT \cdot \ln C_2 + RT \cdot \ln \gamma_2 \qquad \text{(Eq. 20)}$$

Eq. 3 can be written as:

$$J_2 = J_2^i - J_{21} \qquad \text{(Eq. 21)}$$

where:

$$J_2^i = -(C_2u_2/N)RT \text{ grad ln } C_2 \qquad \text{(Eq. 22)}$$

$$J_{21} = (C_2u_2/N)RT \text{ grad ln } \gamma_2 \qquad \text{(Eq. 23)}$$

and N is Avogadro's number.

Equation 21 is the fundamental equation in our model. It says that the flux of a diffusate through the stratum corneum is dependent on two terms. The first term, J_2^i, is a restatement of Fick's Law for ideal diffusion since Eq. 22 is identical to Eq. 1 where:

$$D = u_2RT/N \qquad \text{(Eq. 24)}$$

The second term, J_{21}, depends on the interaction between the stratum corneum and the diffusing molecules. This interaction is expressed in the γ_2 factor. If biological gradients exist in the stratum corneum with respect to keratin hydration of the fixed amino acid ions and with respect to lipid composition, γ_2 would be expected to be a function of the spacial coordinate in the direction of diffusion, chosen here to be x.

Polar Gradients—Consider first the interaction of the fixed ions of the amino acids in the stratum corneum keratin with *polar* diffusants: ln γ_2 can be expressed as (14):

$$\ln \gamma_2 = (A/RT)(w_{11} + w_{22} - 2w_{21}) \qquad \text{(Eq. 25)}$$

where A is constant, w_{11} and w_{22} are the cohesive energies of the stratum corneum and the diffusate, respectively, and w_{21} is the interaction energy of the stratum corneum and the diffusate.

The simplest interpretation of w_{11} and w_{22} is in terms of the solubility parameters δ_1 and δ_2 (15) where $\delta_1 = (w_{11})^{1/2}$ and $\delta_2 = (w_{22})^{1/2}$. For the lipoidal barrier model, in the absence of a gradient, the closer δ_2 matches δ_1, the faster the diffusate permeates through the membrane (16). The gradient of w_{21} accounts for a deviation from this ideality. The interpretation of δ_1 for the ion–dipole interaction could be made in terms of cross-linkings of keratin by disulfide and ϵ-(γ-glutamyl)lysine bonds (17).

If constant cohesive energies are assumed, then Eq. 23 can be written as:

$$J_{21} = -L_{21} \text{ grad } w_{21} \qquad \text{(Eq. 26)}$$

where $L_{21} = 2C_2u_2A/N$. For the percutaneous absorption, the positive x coordinate direction will be chosen as increasing from the skin surface into the deeper layers of the skin.

Water gradients in fixed-charge systems of proteins have been proposed by Ling (18, 19) as a mechanism for the selective permeability of nonelectrolytes into the cells. Such multilayer gradients can exist when fixed negative charges alternate with positive charges in a checkerboard-like arrangement of the right dimension (19). More recently, Flagg-Newton and Loewenstein (20) have argued that the directional "permselectivity" channels that they found between asymmetric cell junctions of two different cell types could only result from an interaction of the permeating species with the channel. The effects of the interaction of the stratum corneum with a diffusate in terms of irreversible thermodynamics have been discussed. For a continuous system, the total entropy production per unit volume per unit time is given by Eq. 14. The importance of activity gradients can be seen from Eq. 17.

From skin resistance data, a linear hydration gradient of the stratum corneum keratin with respect to depth has been shown to exist, the innermost layer being the most hydrated (21). Water adsorption occurs at the polarized amino acid fixed ions of the polypeptide chain in keratin, which are then surrounded by a maximum of four water molecules (22). A linear increase of the dielectric isotherm up to 8% water suggests that there is a well-defined contribution for each newly added water molecule to the total polarization. For increasing positive values of x, such a reduction of the effective charge of the z_ith ion due to increasing hydration with depth can be expressed as $Z_{ix}e = Z_ie(1 - x/b)$,

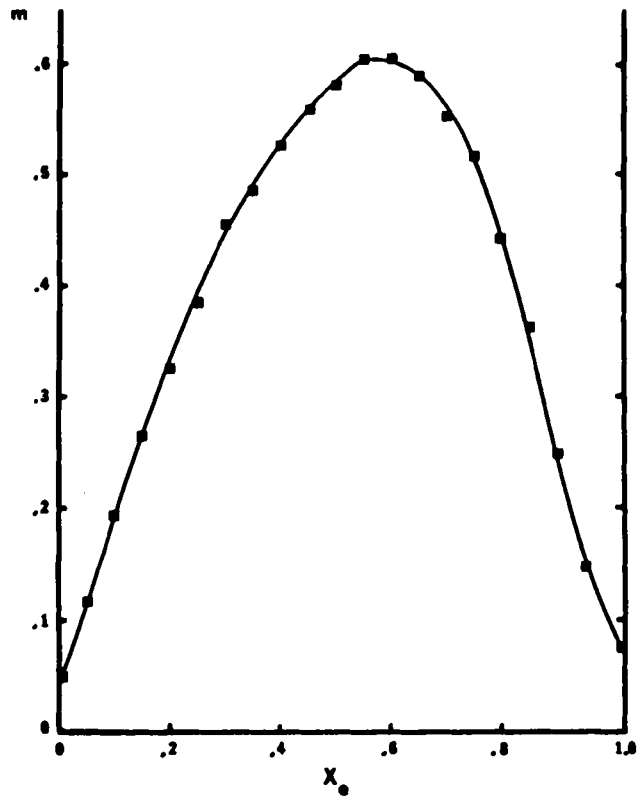

Figure 2—*Determination of the maximum solubility for cholesterol in the* n-*heptane-ethanol cosolvent system. Key:* (m) *molal solubility;* (X_e) *mole fraction ethanol.* m_{max} *occurs at* $X_e = 0.575$.

where b is the thickness of the stratum corneum. Therefore, replacing $Z_i e$ by $Z_{ix} e$ in the ion-dipole interaction energy expression (23) gives:

$$w_{21} = \sum_i (Z_i e \cos\theta\, \mu_2 / r_i^2)(1/D_s - (x/b)/D_s) \qquad \text{(Eq. 27)}$$

for $x \leq b$, where $Z_i e$ is the charge on the ions in the stratum corneum a distance r_i from the diffusate of dipole moment μ_2, D_s is the aqueous dielectric saturation value (24, 25), and b is the asymptotic value of r_i when the dielectric constant equals that of liquid water. Equation 26 can now be written as:

$$J_{21} = \Delta_p \mu_2 \qquad \text{(Eq. 28)}$$

where:

$$\Delta_p = L_{21} \sum_i (Z_i e \cos\theta)/(D_s b \cdot r_i^2) \qquad \text{(Eq. 29)}$$

Using Eq. 28, Eq. 21 can be written for ion-dipole interactions as:

$$J_2 = J_2^i - \Delta_2 \mu_2 \qquad \text{(Eq. 30)}$$

For the polar diffusing species in our study, it will be shown that a plot of J_2 *versus* μ_2 is linear.

Lipid Gradients—Recent freeze-fracture electron microscopic studies by Elias *et al.* (26) have shown that within the stratum corneum there is a gradient of lipid coalescence from the innermost layer to the surface. Odland bodies (membrane-coating granules), which are extruded into the intercellular spaces of the stratum granulosum, aggregate in the lower reaches of the stratum corneum. However, in the middle and upper reaches, all membrane-associated particles are absent. Studies with essential fatty acid-deficient mice (27) have shown that when these particles fail to coalesce into normal neutral lipid-rich sheets in the upper stratum corneum, a defective barrier results. Recent studies in humans stress the importance of these lipids as a major determinant of percutaneous absorption (28). Onken and Moyer made similar observations many years ago (29).

At this time, the exact profile of the lipid gradient is not known. However, it is likely that it will have exponential character for the following reasons. For phospholipid membranes, like the Odland bodies, the bimolecular leaflet is thermodynamically the most stable configuration (30, 31). Such membranes do not coalesce under normal conditions; according to Lucy (32), coalescence will only occur when two adjoining membranes both take on micellar character. In the micellar configuration, coalescence can occur when adjacent micelles mutually interdigitate.

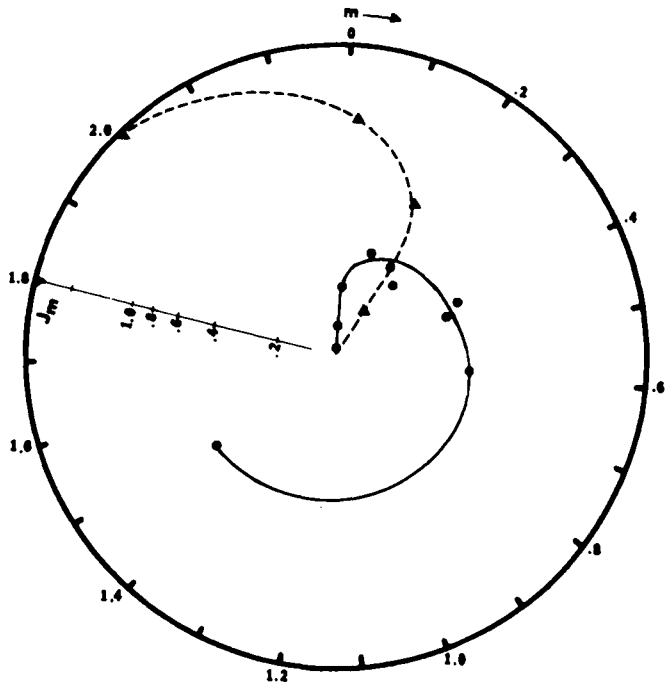

Figure 3—*Absorption patterns for proposed dipole and lipid pathway. Key:* (J_m) *maximum percutaneous absorption rate (%/h) (46);* (m) *molal solubility in the* n-*heptane-ethanol cosolvent,* $X_e = 0.575$; *(---) proposed polar pathway for* ▲ *diffusates; (—) proposed lipid pathway for* ● *diffusates.*

Certain agents cause micellar configurations in membranes, including the biologically significant lysolecithin (33). In the stratum corneum, lysolecithin is released when the phospholipase A enzymes decompose phospholipids (34). This byproduct of enzyme metabolism is an excellent detergent (35), which, because of its wedge shape, easily forms micelles (32). Studies have shown that treatment of whole cells with lysolecithin causes membrane fusion and disintegration (33). The action of phospholipase A on red blood cells (36) and rat liver cells (37) *in vitro* is the same as its action on lipid extracts, except higher concentrations of the enzyme are required for extracts (37). Evidently, surface phospholipids are more available to the enzyme. Whole cells, therefore, have a higher effective enzyme/phospholipid molar ratio. For the release of lysolecithin in the stratum corneum from the Odland bodies, this means that enzyme kinetics is most likely carried out in the linear Michaelis-Menten region. Since the release of lysolecithin would be expected to be the rate-limiting step in initiating coalescence of the Odland bodies, coalescence would be expected to have an exponential time dependence. The gradient would also be expected to have an exponential dependence, since the stratum corneum squames are shed at a uniform rate from the innermost layer to the surface (38, 39).

For diffusates with lipid-like character, interaction with the lipid stratum corneum gradient would be expected to occur through dispersion or van der Waals forces (40). Using Hildebrand's thermodynamic interpretation of such interactions in terms of solubility parameters (40), Khalil and Martin (41) have argued that permeation is optimal when the solubility parameter of the diffusate, δ_2, is as close to the solubility parameter of the lipid barrier, δ_1. Therefore, ln γ_2 in Eq. 25 would be expressed as (14):

$$-\ln \gamma_2 = (A/RT)(\delta_1 - \delta_2)^2 \qquad \text{(Eq. 31)}$$

where δ_1 and δ_2 are the solubility parameters of the barrier and the diffusate, respectively. Therefore:

$$\text{grad} \ln \gamma_2 = -(2A/RT)(\delta_1 - \delta_2)\, \text{grad}\, (\delta_1 - \delta_2) \qquad \text{(Eq. 32)}$$

From our discussion above, if the lipid gradient has the general exponential character:

$$\delta_1 - \delta_2 = E\text{-}\exp\,(g_{np} x) \qquad \text{(Eq. 33)}$$

then:

$$\text{grad} \ln \gamma_2 = 2g_{np}(A/RT)(\delta_1 - \delta_2)^2 \qquad \text{(Eq. 34)}$$

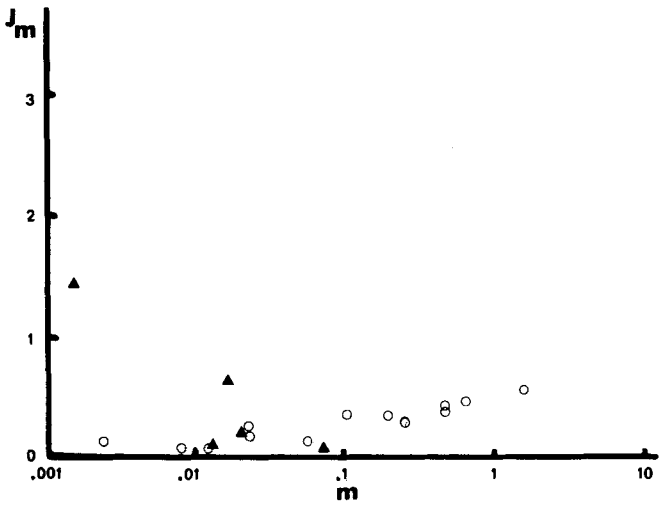

Figure 4—*Log-linear plot of absorption patterns for proposed dipole and lipid pathway. Key: (J_m) maximum percutaneous absorption rate (%/h) (46); (m) molal solubility in the* n*-heptane–ethanol cosolvent, X_e = 0.575; (▲) proposed polar pathway diffusates; (○) proposed lipid pathway diffusates.*

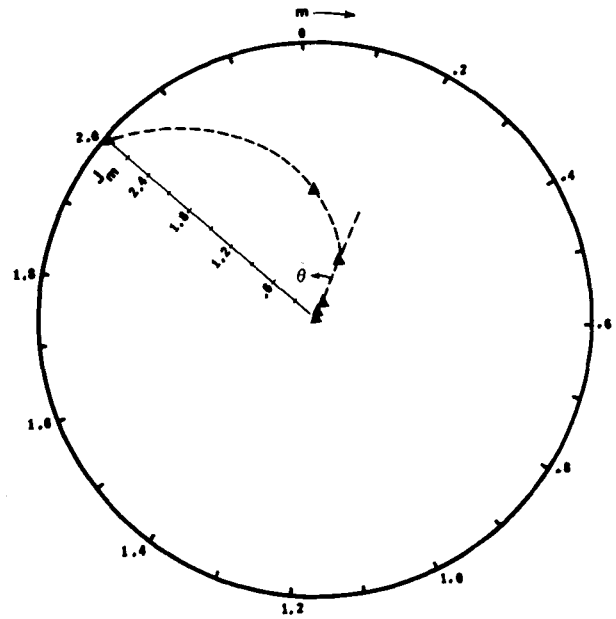

Figure 5—*Absorption pattern for proposed dipole pathway. Key: (J_m) maximum percutaneous absorption rate (%/h) (46); (m) molal solubility in the* n*-heptane–ethanol cosolvent, X_e = 0.575; (θ) positive azimuthal angle in the counterclockwise direction from m = 0.16; (▲) diffusate outward along the spiral: thiourea, urea, nicotinamide,* p*-aminobenzoic acid, caffeine, and benzoic acid.*

But from regular solution theory (13):

$$(A/RT)(\delta_1 - \delta_2)^2 = ln\, X_2^i - \ln X_2 \qquad \text{(Eq. 35)}$$

where X_2^i and X_2 are the ideal and the measured solubilities of the diffusates. Therefore, Eq. 21 can be expressed as:

$$J_2 = J_2^i - \Delta_{np}(\ln X_2^i - \ln X_2) \qquad \text{(Eq. 36)}$$

where $\Delta_{np} = 2C_2u_2RTg_{np}/N_2$ and the ideal solubility, X_2^i, can be determined from (18):

$$\ln X_2^i = (\Delta H_f/RT)[(T_m - T)/T_m] \qquad \text{(Eq. 37)}$$

where ΔH_f is the molar heat of fusion of the diffusate and T_m is the melting point in degrees Kelvin. Equation 36 is the lipid–lipid interactional diffusion equation that is analogous to Eq. 30 for the polar gradient. This equation can also be expressed as:

$$J_2 = J_2^i - \frac{\Delta_{np} \cdot A}{RT}(\delta_1 - \delta_2)^2 \qquad \text{(Eq. 38)}$$

Resolution of Diffusional Pathways—In the stratum corneum, both lipid and protein interactional pathways have been hypothesized by Higuchi (13) and Scheuplein (42). The nonideal portion of Eq. 21 (Eq. 23) has, therefore, been expressed in a form which reflects such pathways. Equation 30 is based on an ion–dipole interaction, Eq. 36, on van der Waals interaction. To experimentally identify those solutes that might interact with the stratum corneum lipids by van der Waals forces during diffusion, a plot of flux *versus* the molal solubility of the diffusate in a cosolvent system in which the polarity could be varied over a wide range was proposed. Since the cholesterol/phospholipid (C/P) molar ratio increases 1700-fold from the basal layer to the stratum corneum (43) due to the near complete catabolism of the phospholipids, cholesterol was hypothesized to be the major lipid which interacts with the diffusing solutes. The proposed composition of the cosolvent, therefore, was chosen to be that in which cholesterol has a maximum solubility. At this composition, $w_{11} = w_{22}$, *i.e.* the difference in solubility parameters of the solvent and the lipid approaches zero (44, 45).

EXPERIMENTAL

Solutes—The following solutes were used as provided by the manufacturer: acetylsalicylic acid[1], androstenedione[1], benzoic acid[1], caffeine[1], corticosterone[1], cortisone[1], dehydroepiandrosterone[1], estradiol[1], hydrocortisone[1], hydrocortisone acetate[1], nicotinamide[1], *p*-aminobenzoic acid[1], progesterone[1], testosterone[1], testosterone acetate[1], testosterone propionate[1], salicylic acid[1], thiourea[1], urea[1], 17-hydroxyprogesterone[2], deoxycorticosterone[2], and cholesterol[3].

Solubility Determination—All solubility determinations were carried out in cosolvent mixtures of absolute ethanol[4] and *n*-heptane[3], which were miscible in all proportions. To obtain a saturated solution, 5 mL of solvent was added to a 7-mL liquid scintillation vial[5] containing an excess amount of solute and a 6-mm glass bead. The bead ensured good mixing of the solute and the solvent when the vials were placed on a linear reciprocating agitator[6]. A temperature of 27°C was maintained during agitation by placing a plastic heating pad[7] underneath the vial holders. Dissolution studies showed that agitation at 180 cpm for 48 h was sufficient to ensure that a saturated solution was formed for the most insoluble solute–solvent combinations: that of caffeine or thiourea in *n*-heptane. These agitation conditions, therefore, were used for all solutes.

After agitation, the vials were centrifuged in a clinical centrifuge[8] at 4000 rpm for 5 min. During this centrifugation, a hair dryer[9] was used to maintain the temperature of the vials >27°C. The vials were then allowed to equilibrate at 25°C in a water bath for 24 h before solubility determinations of the saturated supernatant were carried out gravimetrically in aluminum foil planchets[10]

RESULTS

Diffusional Pathways—The molal solubility of cholesterol in an *n*-heptane–ethanol cosolvent system is shown in Fig. 2. These data show that the maximum solubility occurs at an ethanol mole fraction (X_e) of 0.575. Since cholesterol was chosen as our model stratum corneum interactional lipid, all subsequent solubility determinations were carried out at X_e = 0.575. Such data were used, first, to discriminate the lipid and polar pathways.

In Fig. 3, the molal solubilities of the solutes that were studied are plotted as the azimuthal coordinate in a polar coordinate system. The maximum percutaneous absorption rates, J_m, for these solutes determined by Feldmann and Maibach (1, 46) are plotted as the radial coordinate on a logarithmic scale. Two distinct trends for these data are depicted by the dotted and solid lines. The dotted line describes a curve that spirals out from the origin in the positive azimuthal direction (counterclockwise) from the initial ray, m = 0.19. The solid line, on the other hand, describes a curve that spirals out from the initial ray, m = 0, in the negative azimuthal direction. In the strictest sense, these logarithmic curves are not true spirals. However, it will be shown presently that each curve, plotted with respect to a rectilinear radial coordinate, can

[1] Sigma Chemical Co., St. Louis, Mo.
[2] Research Plus Steroid Laboratory, Bayonne, N.Y.
[3] Fisher Scientific, Fair Lawn, N.J.
[4] Publicker Industries, Linfield, Pa.
[5] Kimble, Toledo, Ohio.
[6] Eberbach, Ann Arbor, Mich.
[7] Walker Co., Middleboro, Mass.
[8] Model CL, IEC, Needham Heights, Mass.
[9] Osler Corp., Milwaukee, Wis.
[10] A. H. Thomas, Philadelphia, Pa.

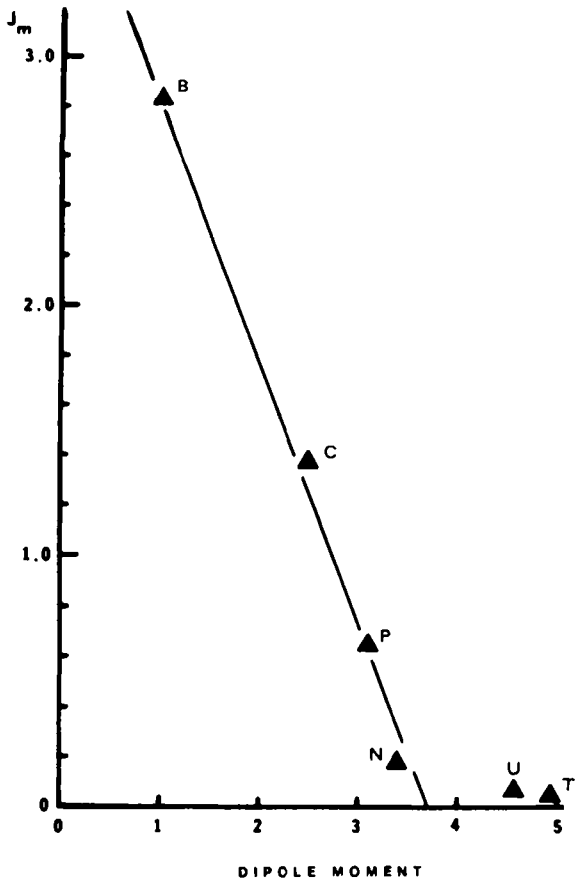

Figure 6—*Regression of dipole moment* versus *absorption rate. Key: (J_m) maximum percutaneous absorption rate (%/h)(46); (B) benzoic acid dipole moment (47); (C) caffeine dipole moment (51); (P)* p*-aminobenzoic acid dipole moment (48); (N) nicotinamide dipole moment (52); (U) urea dipole moment (49); (T) thiourea dipole moment (50).*

be represented by a modified Archimedean spiral[11] and that each spiral is consistent with one of the proposed mechanisms. Figure 4 shows how a similar pathway designation on a log-linear plot would be much more difficult to ascertain for the solid triangles. These points are the same as the triangles on the counterclockwise spiral in Fig. 3.

Polar Mechanism—In Fig. 5, J_m for the diffusates along the dotted line of Fig. 3 are plotted on a rectilinear scale. The diffusates lie on a path described by a modified Archimedean spiral:

$$J_m = J_i + a \cdot \theta \qquad \text{(Eq. 39)}$$

where the initial ray is defined by:

$$J_i = 1.1; \qquad m = 0.16 \qquad \text{(Eq. 40)}$$

θ is the angular molal increment in the positive azimuthal direction from the initial ray, and the slope a is given by:

$$a = 8.3 \qquad \text{(Eq. 41)}$$

This spiral is defined as a modified Archimedean spiral since some of the diffusates lie on the initial ray before θ evolves. Thus, for $\theta = 0$, thiourea, urea, nicotinamide, and *p*-aminobenzoic acid (from the origin outward) lie on the initial ray. For increasing values of θ (counterclockwise direction), the radial component of each diffusing species is located on the spiral by adding a times θ to J_i. Caffeine and then benzoic acid lie on the spiral as θ increases.

Figure 6 shows a plot of J_m *versus* μ_2, the dipole moment of the diffusates (47–52) in Fig. 4. The first four points agree with the linear relationship

[11] Archimedes described in his book *On Spirals* a plane spiral as the locus of points described by the polar coordinate equation $\rho = a \cdot \theta$, where θ = angular (azimuthal) coordinate and ρ = radial coordinate. Such a spiral could be formed, mechanically, in the following way. Imagine a machine that could move a pen along a straight line at a uniform rate. If the pen were placed at the center of a rotating turntable and pulled outward along this line, the curve that would be traced out on the turntable would be an Archimedean spiral. The line would be called the initial line; the center, the origin. The modified Archimedean spiral we defined spirals out from some point along the initial line rather than from the origin.

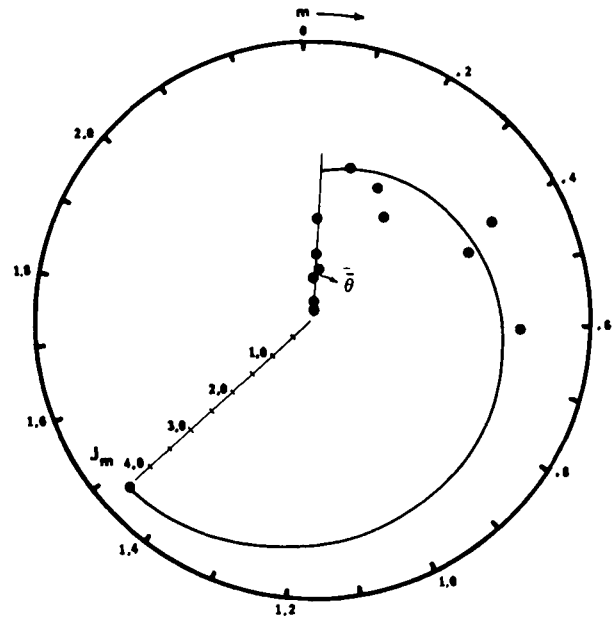

Figure 7—*Absorption pattern for proposed lipid pathway. Key: (J_m) maximum percutaneous absorption rate (%/h) (46); (*m*) molal solubility in the* n*-heptane–ethanol cosolvent. $X_e = 0.575$; ($\bar{\theta}$) negative azimuthal angle from* m *= 0.03; (●) diffusates outward along the spiral: hydrocortisone, cortisone, hydrocortisone acetate, estradiol, corticosterone, 17-hydroxyprogesterone, androstenedione, deoxycorticosterone, progesterone, acetylsalicylic acid, testosterone, dehydroepiandrosterone, salicylic acid.*

predicted by the polar pathway of Eq. 30. The linear regression equation for J_m *versus* μ_2 is:

$$J_m = 4.25 - 1.18 \cdot \mu_2 \qquad \text{(Eq. 42)}$$

with a linear regression coefficient of −0.998. It is also evident from Fig. 6 that there is a limit beyond which further increases in the dipole moment, μ_2, cannot continue to cause a linear reduction in J_m. This, evidently, is the situation with urea and thiourea.

Nonpolar Mechanism—The data along the solid line spiral are plotted in Fig. 7 on a rectilinear radial scale. This modified Archimedean spiral can be described by:

$$J_m = J_i + a \cdot \bar{\theta} \qquad \text{(Eq. 43)}$$

where the initial ray is defined as:

$$J_i = 2.7; \qquad m = 0.3, \qquad \text{(Eq. 44)}$$

$\bar{\theta}$ is the angular molal increment in the negative azimuthal direction from the initial ray, and the slope a is given by:

$$a = 1.22 \qquad \text{(Eq. 45)}$$

Along the initial ray of this spiral, from the origin outward, are hydrocortisone, cortisone, hydrocortisone acetate, estradiol, corticosterone, and 17-hydroxyprogesterone. For increasing values of $\bar{\theta}$ (clockwise direction), androstenedione, deoxycorticosterone, progesterone, acetylsalicylic acid, testosterone, dehydroepiandrosterone, and salicylic acid are found on the spiral. In Fig. 8, J_m *versus* $-\ln X$ is plotted assuming that the nonpolar mechanism of Eq. 36 would describe this spiral, since all of the diffusates are steroids except for salicylic acid. The linear regression equation for this plot is:

$$J_m = 0.73 + (9.3 \times 10^{-2}) \cdot \ln X_2 \qquad \text{(Eq. 46)}$$

with a linear regression coefficient of −0.945.

DISCUSSION

The existence of gradients in the stratum corneum were suspected over 17 years ago. Kligman (53) argued that even though the stratum corneum appears to be a homogeneous structure from its innermost layer to its outer surface, there must be a stratification of the keratinization process within the structure, at least at the chemical level. Believing that biochemical and biophysical events of this magnitude could take place so abruptly, in Kligman's opinion, is tantamount to believing in a biological miracle. It has been only recently, however, that experimental evidence for such gradients has been

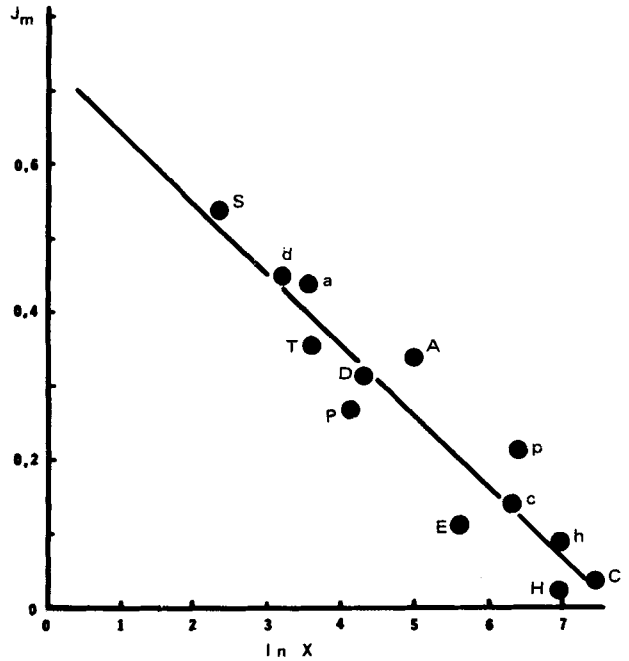

Figure 8—*Regression of ln* X versus *absorption rate. Key: (X) mole fraction solubility; (J_m) maximum absorption rate (%/h.) (46); (S) salicylic acid; (d) dehydroepiandrosterone; (T) testosterone; (a) acetylsalicylic acid; (P) progesterone; (D) deoxycorticosterone; (A) androstenedione; (E) estradiol, (p) 17-hydroxyprogesterone; (c) corticosterone; (h) hydrocortisone acetate; (H) hydrocortisone; (C) cortisone.*

confirmed. Elias *et al.* (26) have demonstrated a lipid gradient of coalescence and Tagami *et al.* (21, 54), a hydration gradient of the stratum corneum keratin. Based on reasonable physical assumptions concerning the mathematical form of these gradients, a physical model predicting the dependence of solute transport through the stratum corneum on the dipole moment, μ_2, and the logarithm of the mole fraction solubility, ln X_2, have been derived.

To test this model, a solubility method, using a polar coordinate plot, has been developed to separate those diffusates that would be most affected by the lipophilicity of the stratum corneum from those that would be more affected by its ionic components. However, it is not clear what the "effective" lipophilicity of the stratum corneum might be. Most likely it is different between different animal species. This may be the reason why human penetration data often differ from animal data, even after corrections are made for the stratum corneum thickness (55).

Classically, the oil–water partition coefficient has been used as a measure of lipophilicity. The relationship of octanol–water partition coefficients to biological activity has proven to be of value in predicting quantitative structure–activity relationships (56). However, application of this approach to percutaneous absorption has not been completely successful, we believe, because lipophilicity differs from tissue to tissue depending on the relative composition of neutral to polar lipids. One reason diffusion in nervous tissue is slower than in liver tissue is because the cholesterol/phospholipid molar ratio of nerve cell plasma membranes is much higher than in liver cells. Mammalian cells appear to control membrane permeability by varying the relative amounts of cholesterol and phospholipids in their membranes (57, 58).

For these reasons, use of 1-octanol which has a solubility parameter of 10.3 and the 1-octanol–water partition coefficient may not accurately represent the lipophilicity of the stratum corneum. In these studies, an *n*-heptane–ethanol cosolvent system that spans a solubility parameter range from 7.5 to 13 was used. Since cholesterol is one of the dominant neutral lipids in the stratum corneum (59), the cosolvent composition (or solubility parameter) at which cholesterol had an optimum was chosen to represent the lipophilicity of the stratum corneum, other lipids such as ceramide not being readily available in sufficient quantities. In this sense, then, these studies should be viewed only as a first attempt to evaluate stratum corneum lipophilicity. Conceptually a distribution function, $X(\delta)$, could be determined for each compound by determining its mole fraction solubility, X, over a range of solvent polarities. Chertkoff and Martin (44) and others have shown that $X(\delta)$ will have a maximum value when δ for the solute equals δ for the cosolvent. Experimental data for these bell-shaped distribution functions could then be fitted by nonlinear regression to a mathematical function so that for each solute $X_j(\delta_i)$ for any δ_i could be generated. For a given δ_i, ln X_j for all of the diffusates in the van der Waal group could then be determined. The linear regression coefficient r_i for the regression over j of ln X *versus* the percutaneous absorption rate for the jth drug, J_j, would then be possible. δ_i could then be varied to optimize r_i. The value of δ, δ_{pa}, which corresponds to the largest value of r_i might then be designated the "effective" lipophilicity for percutaneous absorption. If such studies should come to pass, it is possible that separate δ_{pa} values for humans and animals could be determined, thus providing a quantitative parameter for human–animal correlations.

The penetration data of Feldmann and Maibach (1, 46) was used because these data represent the most complete set of human *in vivo* studies ever attempted using a common methodology and have provided the human *in vivo* comparison for most animal models (60–63). Maximum absorption rates were chosen because they are the only unique characteristics of these absorption curves, since half-lives or absorption constants could not be determined due to the sampling intervals.

A classification based on modified Archimedean spiral pattern formation was used to determine which regression expression should be used. To date, 21 different diffusates have been studied. Nineteen of these solutes correlate with one of the two mechanisms developed in the *Theoretical* section. The permeability of two solutes, testosterone acetate and testosterone propionate, cannot be explained on the basis of either mechanism. Parenthetically, these solutes were not predicted to correlate with either mechanism, *i.e.*, they did not fall on either the polar or nonpolar spirals. On the other hand, it was extremely gratifying that the percutaneous absorption of diffusates of such differing structure could be explained in terms of two physical properties.

Since the net flux in Eq. 21 is a function of the ideal flux and the interaction flux, the good correlation between the net flux and μ_2 or ln X_2 may indicate that the ideal fluxes of the different solutes within the stratum corneum are of the same order of magnitude. This would differ from diffusion in liquids, where the mobility is a function of the reciprocal of the frictional resistance, which is in turn a function of the viscosity of the media and the size of the molecule (64). In the stratum corneum, specific physical interactions may control diffusion.

Finally, this physicochemical model does not attempt to explain percutaneous absorption in terms of different structural components of the epidermis. Michaels *et al.* (65) have described one such model in which the stratum corneum is conceived of as proteinaceous bricks held together by interstitial lipid mortar. For the model developed here, only the properties of the physical components are accounted for, because it is extremely difficult to unambiguously discriminate structural pathways. On the other hand, the parameters that have been chosen are open to future verification. If on further testing, deviations from the predicted model expressions are found, an analysis can be carried out to determine whether the form of the gradient or the polarity of the solvent system that has been chosen to represent the stratum corneum can explain this deviation. In some situations, neither approach may suffice because the stratum corneum may not be rate limiting. In summary, the physicochemical model presented here is only meant to represent the current state of knowledge; it may need modifications in the future based on new evidence. It is hoped, however, that it provides a measurable framework for the future testing of its validity.

REFERENCES

(1) R. J. Feldmann and H. I. Maibach, *J. Invest. Dermatol.*, **52,** 89 (1969).

(2) R. B. Stoughton, W. E. Clendening, and D. Kruse, *J. Invest. Dermatol.*, **35,** 337 (1960).

(3) M. Katz and Z. I. Shaikh, *J. Pharm. Sci.*, **54,** 591 (1965).

(4) H. Durrheim, G. L. Flynn, W. I. Higuchi, and C. R. Behl, *J. Pharm. Sci.*, **69,** 781 (1980).

(5) M. S. Roberts, R. A. Anderson, and J. Swarbrick, *J. Pharm. Pharmacol.*, **29,** 677 (1977).

(6) E. J. Lien and G. L. Tong, *J. Soc. Cosmet. Chem.*, **24,** 371 (1973).

(7) A. Fick, *Poggendortts Ann.*, **94,** 59 (1855).

(8) W. Jost, "Diffusion," Academic, New York, N.Y., 1960, p. 156.

(9) I. Prigogine, "Introduction to Thermodynamics of Irreversible Processes," 3rd ed., Interscience, New York, N.Y., 1967, pp. 14, 54.

(10) N. Melczer, in "Cancer of the Skin," vol. I, R. Andrade, Ed., Saunders, Philadelphia, Pa., 1976, pp. 293, 313.

(11) D. M. Anjo, R. J. Feldmann, and H. I. Maibach, in "Percutaneous Absorption of Steroids," P. Mauvais-Jarvis, C. F. H. Vickers, and J. Wepierry, Eds., Academic, New York, N.Y., 1980, pp. 31–51.

(12) R. J. Scheuplein, *J. Invest. Dermatol.*, **67,** 31 (1976).

(13) T. Higuchi, *J. Soc. Cosmet. Chem.*, **11,** 85 (1960).

(14) A. N. Martin, J. Swarbrick, and A. Cammarata, "Physical Pharmacy," 2nd ed., Lea and Febiger, Philadelphia, Pa., 1969, p. 300.

(15) J. H. Hildebrand and R. L. Scott, in "The Solubility of Nonelectro-

lytes," Dover, New York, N.Y., 1964, p. 124.
(16) S. A. Khalil and A. N. Martin, *J. Pharm. Sci.*, **56,** 1225 (1967).
(17) T. T. Sun and H. Green, *J. Biol. Chem.*, **253,** 2053 (1953).
(18) G. N. Ling, "A Physical Theory of the Living State: The Association-Induction Hypothesis," Blaisdell, Waltham, Mass., 1962, pp. 343, 352.
(19) G. N. Ling, in "Cell-Associated Water," W. Drost-Hansen and J. S. Clegg, Eds., Academic, New York, N.Y., 1979, pp. 261, 269.
(20) J. L. Flagg-Newton and W. R. Loewenstein, *Science*, **207,** 771 (1980).
(21) H. Tagami, M. Ohi, K. Iwatsuki, Y. Kanamuru, M. Yamada, and B. Ichijo, *J. Invest. Dermatol.*, **75,** 500 (1980).
(22) H. J. von Reim, "Mol. Strukt. Strahlenwirking, Jahrestag, Deut. Ges. Giophy. Tagungaber," H. Glubrecht, Ed., Georg Thieme Verlag, Stuttgart, 1968, pp. 36, 39.
(23) E. S. Amis, *J. Chem. Ed.*, **30,** 351 (1953).
(24) J. B. Hasted, D. M. Ritson, and C. H. Collie, *J. Chem. Phys.*, **16,** 1 (1948).
(25) D. C. Grahame, *J. Chem. Phys.*, **18,** 903 (1950).
(26) P. M. Elias, J. Goerke, and D. S. Friend, *J. Invest. Dermatol.*, **69,** 535 (1977).
(27) P. M. Elias, B. E. Brown, and V. A. Ziboh, *J. Invest. Dermatol.*, **74,** 230 (1980).
(28) P. M. Elias, E. R. Cooper, A. Korc, and B. E. Brown, *J. Invest. Dermatol.*, **76,** 297 (1981).
(29) H. D. Onken and C. A. Moyer, *Arch. Dermatol.*, **87,** 90 (1963).
(30) D. A. Haydon and J. Taylor, *J. Theor. Biol.*, **4,** 281 (1963).
(31) J. F. Danielli, in "Formation and Fate of Cell Organelles" (Symp. Intern. Soc. Cell Biol.), Vol. 6, K. B. Warren, Ed., Academic, New York, N.Y., 1967, p. 239.
(32) J. A. Lucy, *Nature (London)*, **227,** 815 (1970).
(33) A. R. Poole, J. I. Howell, and J. A. Lucy, *Nature (London)*, **227,** 810 (1970).
(34) R. K. Freinkel and T. N. Traczyk, *J. Invest. Dermatol.*, **74,** 169 (1980).
(35) A. White, P. Handler, and E. L. Smith, "Principles of Biochemistry," 4th ed., McGraw-Hill, New York, N.Y., 1968, p. 472.
(36) A. T. Tu, R. B. Passey, and P. M. Toom, *Arch. Biochem. Biophys.*, **140,** 96 (1970).
(37) J. Gallai-Hatchard and G. M. Gary, *Eur. J. Biochem.*, **4,** 35 (1968).
(38) A. M. Kligman, in "The Epidermis," W. Montagna and W. C. Lobitz, Jr., Eds., Academic, New York, N.Y., 1964, p. 397.
(39) E. Christophers and E. B. Laurence, *Curr. Probl. Dermatol.*, **6,** 87 (1976).
(40) J. H. Hildebrand and R. L. Scott, "The Solubility of Nonelectrolytes," Dover, New York, N.Y., 1964, pp. 48–61.
(41) S. A. Khalil and A. N. Martin, *J. Pharm. Sci.*, **56,** 1225 (1967).
(42) R. J. Scheuplein, in "Advances in the Biology of the Skin XII," W. Montagna, E. J. Van Scott, and R. B. Stoughton, Eds., Appleton-Century-Croft, New York, N.Y., 1972, p. 125.
(43) G. M. Gray and H. J. Yardley, *J. Lipid Res.*, **16,** 434 (1975).
(44) M. J. Chertkoff and A. Martin, *J. Am. Pharm. Assoc., Sci. Ed.*, **49,** 444 (1960).
(45) F. A. Restaino and A. Martin, *J. Pharm. Sci.*, **53,** 636 (1964).
(46) R. J. Feldmann and H. I. Maibach, *J. Invest. Dermatol.*, **54,** 399 (1970).
(47) A. L. McClellan, "Table of Experimental Dipole Moments," W. H. Freeman, San Francisco, Calif., 1963, p. 240.
(48) A. L. McClellan, "Table of Experimental Dipole Moments," W. H. Freeman, San Francisco, Calif., 1963, p. 247.
(49) A. L. McClellan, "Table of Experimental Dipole Moments," W. H. Freeman, San Francisco, Calif., 1963, p. 45.
(50) A. L. McClellan, "Table of Experimental Dipole Moments," W. H. Freeman, San Francisco, Calif., 1963, p. 46.
(51) H. Wollmann, B. Skaletzki, and A. Schaaf, *Pharmazie*, **29,** 708 (1974).
(52) J. Kuthan, L. Musil, and V. Jehlicka, *Collection Czechoslov. Chem. Commun.*, **42,** 283 (1977).
(53) A. M. Kligman, in "The Epidermis," W. Montagna and W. C. Lobitz, Jr., Eds., Academic, New York, N.Y., 1964, p. 397.
(54) H. Tagami, Y. Kanamaru, K. Inoue, S. Suehisa, F. Inoue, K. Iwatsuki, K. Yoshikuni, and M. Yamada, *J. Invest. Dermatol.*, **78,** 425 (1982).
(55) H. Y. Ando, E. T. Sugita, R. L. Schnaare, and L. Bogdanowich, *J. Pharm. Sci.*, in press.
(56) C. Hansch, in "Drug Design," vol. 1, E. J. Ariens, Ed., Academic, New York, N.Y., 1971, pp. 242–271.
(57) R. A. Demel and B. De Kruyff, *Biochim. Biophy. Acta*, **457,** 109 (1976).
(58) K. Block, in "Membranes and Transport," vol. 1, A. N. Martonosi, Ed., Plenum, New York, N.Y., 1982, pp. 25–35.
(59) H. J. Yardley and R. Summerly, *Pharmacol. Ther.*, **13,** 357 (1981).
(60) M. J. Bartek and J. A. La Budde, in "Animals Models in Dermatology," H. I. Maibach, Ed., Churchill Livingstone, New York, N.Y., 1975, pp. 103–120.
(61) R. C. Wester and H. I. Maibach, *Toxicol. Appl. Pharmacol.*, **32,** 394 (1975).
(62) K. E. Andersen, H. I. Maibach, and M. D. Anjo, *Br. J. Dermatol.*, **102,** 447 (1980).
(63) R. C. Wester, P. K. Noonan, and H. I. Maibach, *Arch. Dermatol.*, **116,** 186 (1980).
(64) T. Erdey-Gruz, "Transport Phenomenon in Aqueous Solutions," Halsted, New York, N.Y., 1974, pp. 149–156.
(65) A. S. Michaels, S. K. Chandrasekaran, and J. E. Shaw, *Am. Inst. Chem. Eng. J.*, **21,** 985 (1975).

Viscosity of Xanthan Gum Solutions at Low Shear Rates

JOEL L. ZATZ ˣ and STEVEN KNAPP

Received September 3, 1982, from the *Rutgers College of Pharmacy, Piscataway, NJ 08854.* Accepted for publication November 30, 1982.

Abstract □ The viscosity of xanthan gum solutions in the low shear region was investigated with the aid of a Couette instrument. All solutions were highly pseudoplastic. Solutions containing 0.3–0.5% of the gum exhibited a highly ordered phase at very low shear. Viscosity, the degree of pseudoplasticity, and the value of the transition from soft gel to pseudoplastic behavior were directly related to gum concentration. The effect of the addition of a salt on viscosity depended on the xanthan gum concentration. The viscosity of a 0.3% xanthan gum solution was practically unaffected by the salts. Higher gum concentrations exhibited a viscosity increase when salt was present. Concentrations <0.3% exhibited a viscosity decrease in the presence of a salt. All viscosity effects seemed to reach limiting values at $\sim 10^{-3}$ to 3.3×10^{-3} *N* salt. No major differences were observed between sodium chloride, calcium chloride, and sodium citrate in their influence on xanthan gum viscosity.

Keyphrases □ Viscosity—xanthan gum in aqueous solutions, low shear rates, effect of added salts □ Xanthan gum—aqueous solutions, viscosity at low shear rates, effect of added salts □ Shear rate—low range, viscosity of xanthan gum in aqueous solutions, effect of added salts

Xanthan gum, an extracellular polysaccharide of the bacterium *Xanthamonas campestris* which was originally isolated and characterized by Jeanes and coworkers (1), has a wide variety of uses in the pharmaceutical, cosmetic, oil, and food industries. The polymer is an efficient thickening agent whose aqueous solutions are shear thinning (2, 3).

Examination of the molecular structure of xanthan gum offers insight into the basis for much of the physicochemical behavior of the substance in solution. Xanthan gum is structurally very complex. As proposed by Jansson and coworkers (4), the backbone of the molecule is a cellulose chain composed of [β(1→4)-D-glucose]. Every second residue of the chain has a β(1→3) substituted trisaccharide side chain of the [β-D-mannopyranosyl - (1→4)-α-D-glucopyranosyl-(1→2)-β-D-mannopyranoside-6-*O*-acetate] variety. Further, pyruvic acid substitution on the terminal mannose residue of the side chain (to the degree of 25–50%) has been reported and probably plays a key role in the molecular properties of xanthan gum in solution (5). The proposed structure of xanthan gum also suggests that the substituted trisaccharide side chains may lie close to the cellulose backbone at room temperature in some ordered, rod-like conformation held together loosely by short range van der Waals forces (6). At elevated temperatures, however, it has been shown, *via* NMR relaxation procedures and optical methods such as circular dichroism and optical rotation, that there is a temperature-induced rearrangement within the molecular structure of the gum (7). It has been suggested that "chain melting" occurs, and the ordered, rod-like helix may become more flexible at elevated temperatures, with the trisaccharide side chains extending outward from the cellulose backbone. This structural change may be responsible for a sudden drop in viscosity of a 1% aqueous xanthan gum solution at elevated temperature (7).

The addition of salt to a water solution of purified xanthan gum raises the temperature at which structural rearrangement takes place, as shown by optical rotation and viscosity measurements (8). Calcium chloride was effective in much lower concentrations than sodium chloride, suggesting that stabilization of the helical, rod-like confirmation was due to reduction in charge repulsion between the backbone and the side chains (8). The response of xanthan gum to variations of ionic strength is unlike that of most other polyelectrolytes. Normally, polyelectrolytes exhibit an expanded structure under conditions of low ionic strength as the result of neighboring group electrostatic charge repulsion. The addition of a salt results in a screening of the neighboring group repulsive forces and causes the molecule to collapse into a compact coil. Studies of the effects of salts on xanthan gum viscosity have produced somewhat contradictory results. In one case, the viscosity of a dilute xanthan gum solution was increased in the presence of sodium chloride (3). Another report shows a moderate decrease in viscosity under similar conditions (9), although the extent of viscosity reduction was not as pronounced as for typical polyelectrolytes. Symes (10) showed that the effect of 0.1 M KCl on xanthan gum solution viscosity depended on the gum concentration. At gum concentrations <0.25%, viscosity of aqueous solutions without added salt were higher than those containing potassium chloride. The reverse was true for solu-

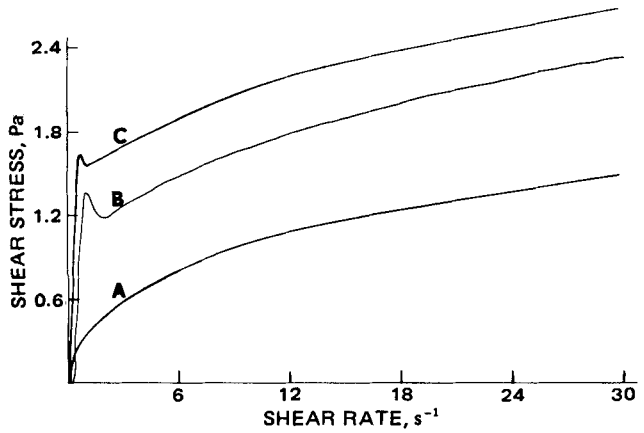

Figure 1—*Shear stress* versus *shear rate for three aqueous xanthan gum solutions with a scan time of 4 min. Key: (A) 0.133%; (B) 0.3%; (C) 0.5%.*

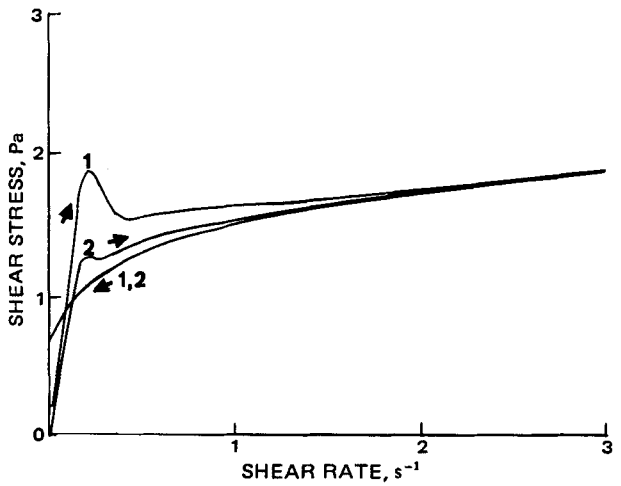

Figure 2—*Shear stress* versus *shear rate for a 0.5% aqueous xanthan gum solution. Scan time for a complete cycle was 8 min. Numbers indicate the order of execution of the shearing cycles, and arrows indicate the direction of shear rate change.*

0022-3549/84/0400-0468$01.00/0
© 1984, American Pharmaceutical Association

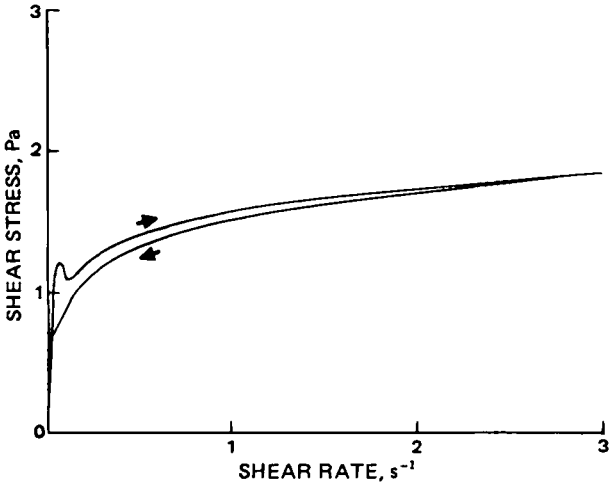

Figure 3—*Shear stress* versus *shear rate for a 0.5% aqueous xanthan gum solution. Scan time for the complete cycle was 2 h. Arrows indicate the direction of shear rate change.*

tions containing >0.25% xanthan gum. The relative stability of viscosity of xanthan gum solutions to ionic strength, temperature, and pH variation (11) has been ascribed to the rod-like shape of the molecule and the importance of hydrogen bonding in intermolecular interaction (12).

In considering the application of xanthan gum as a suspending agent and emulsion stabilizer, viscosity characteristics in the very low shear region are of great importance. The only previous investigation in which very low shear viscosity was studied (2, 3) utilized a purified xanthan gum preparation. In the present study, a new instrument based on the Couette principle and capable of measurements at very low shear was utilized to investigate the rheological behavior of solutions prepared from commercial food-grade xanthan gum. The influence of several salts on solutions containing various xanthan gum concentrations was also studied.

EXPERIMENTAL

Xanthan gum[1] was utilized as received. All salts and preservatives were reagent or USP grade. Deionized water was used in the preparation of solutions.

Xanthan gum solutions (2%) containing 0.1% methylparaben and 0.03% propylparaben served as a stock preparation of the gum. Desired electrolyte

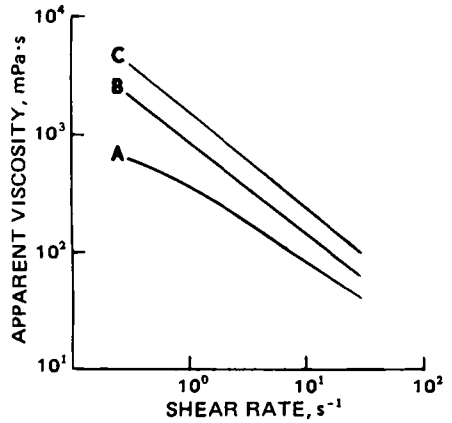

Figure 4—*Logarithm of apparent viscosity as a function of the logarithm of shear rate for xanthan gum solutions. Key: (A) 0.133%; (B) 0.3%; (C) 0.5%.*

[1] KELTROL; Kelco, Div. Merck and Co., Inc., San Diego, Calif.

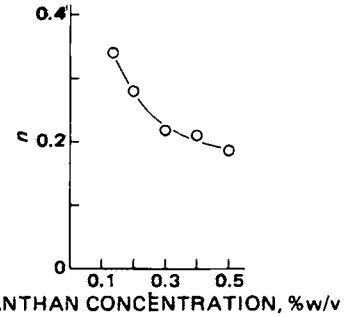

Figure 5—*Power low constant, n, as a function of xanthan gum concentration in aqueous solution.*

concentrations were obtained by dilution of 0.1 *N* stock solutions containing the parabens. Dilutions were made with deionized water containing methyl- and propylparabens. The diluted solutions were mixed using a low-torque mixer until they were homogeneous. Several samples were taken at various locations in the solution and examined rheologically to assure homogeneity of the mixed solutions. It was found that a 2-min mixing time, even at the highest concentration of xanthan gum used, was sufficient to ensure solution homogeneity.

Rheological measurements were made with a commercial instrument[2] that utilizes the Couette principle, with an air bearing to maintain the position of an inner cylinder while the outer cylinder rotates. The torque on the inner cylinder is measured. Both shear rate and shear stress are determined with high precision and plotted automatically as a flow curve (shear stress *versus* shear rate) while the properties of the sample are explored. Sensitivity and scaling factors are adjustable to cover a wide range of shear rates and material characteristics. Sample properties can be measured by increasing shear rate, decreasing shear rate, or cycling back and forth, and the time period during which these measurements are made may be selected from within a wide range.

RESULTS AND DISCUSSION

Flow curves for aqueous solutions containing three xanthan gum concentrations are presented in Fig. 1. To obtain these curves the instrument was set so that scanning of the shear rates covered (0–30 s^{-1}) took 4 min. The curve for 0.133% xanthan gum solution exhibited continuous curvature with no evidence of a yield point or discontinuity. The pseudoplastic behavior of the solution is evident. At 0.3% xanthan gum the flow curve rises steeply at first, reaches a peak, drops sharply, and then rises smoothly again. The abrupt change in slope signals a different type of behavior than that observed at lower concentrations. At shear values beyond the discontinuity, the 0.3% solution exhibits typical pseudoplastic behavior. Shear stress values for the 0.5% xanthan gum solution fall above that of the 0.3% solution, indicating that the apparent viscosity is higher at all values of shear rate. However, the flow curves for the 0.3 and 0.5% solutions are qualitatively similar.

The effect of changing the direction of shear rate change and of a second shearing cycle on the flow curve of a 0.5% xanthan gum solution are shown in Fig. 2. A complete shear cycle consists of having the shear rate increase from zero to a preset value (in this case, 3 s^{-1}) and then decrease again to zero. Arrows in Fig. 2 indicate whether a curve was generated from left to right (increasing shear rate) or right to left (decreasing shear rate). The instrument was programmed so that each complete cycle was executed during 8 min. A 1-min rest period separated the onset of the second shearing cycle (cycle 2 in Fig. 2) from completion of the initial cycle (cycle 1). The initial scan (cycle 1 going from 0 to 3 s^{-1}) was not retraced by the return curve (cycle 1 from 3 to 0 s^{-1}). Also, when the sample was sheared a second time (cycle 2) only the return curve coincided with that from the first shearing cycle. The curve generated by increasing the shear rate during cycle 2 fell between that of the initial trace in the same direction and the return curves, although closer to the latter. The behavior of 0.3% xanthan gum solutions was similar to that of the 0.5% solution, but the difference in magnitude between the various curves was smaller.

Several conclusions may be drawn from the data in Fig. 2 and similar data for 0.3% solutions:

1. Initial disturbance of a sample encounters high resistance. This is shown by the high slope found in the flow curve when shear is first applied.
2. A transition in behavior is found when the shear rate is increased to slightly higher values (but the shear rate at which this transition occurs is still quite small).

[2] Haake RV 100/CV100; Haake, Saddle Brook, N.J.

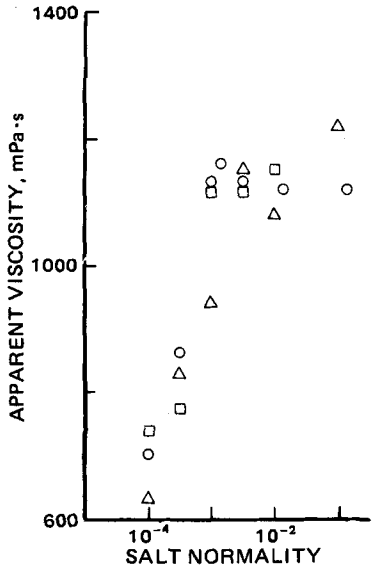

Figure 6—*Effect of various salts on the apparent viscosity of 0.5% solutions of xanthan gum at a shear rate of 3.0 s^{-1}. Key: (○) calcium chloride; (△) sodium chloride; (□) sodium citrate.*

3. Viscosity in the low shear region is dependent on the recent history of the sample. In other words, some thixotropy is evident.

Figure 3 shows results for a single shearing cycle of a 0.5% xanthan gum solution in which the low shear rates were scanned at a rate equal to 1/15 that used in the previous experiments. Comparison of the curve in Fig. 3 arising from increasing the shear rate with that of the corresponding curve for cycle 1 in Fig. 2 shows that although there are some differences in magnitude in the very low shear rate area, the same general pattern is found. After a sharp increase in shear stress, the curve in Fig. 3 peaks, drops, and then follows the pattern of a psuedoplastic material as the shear rate rises. The return curve (3 to 0 s^{-1}) in Fig. 3 does not coincide with the initial tracing. In fact it is identical to the return curves obtained at the faster scan rate (Fig. 2).

Using the same scan rate as for the work in Fig. 3, the discontinuity in the flow curve of a 0.4% xanthan gum solution was still quite marked. With a 0.3% solution it was not so sharp, but still discernable. Reducing the rate of change of the shear rate increased the extent to which the structural architecture could adjust in response to changing shear conditions. Although the difference in magnitude between the two curves that comprise a complete shear cycle was reduced at the slower scan rate, the existence of a structural change at very low shear was still evident.

The viscosity behavior of xanthan gum solutions must be described in terms of intermolecular networks formed by the extremely long, rigid, highly asymmetric polymer molecules (10). At concentrations of 0.3–0.5% (in aqueous solution), network formation results in a system that may be described as a "soft gel" which persists as long as the system is not disturbed. At extremely low shear stress, particles of gel are the unit of flow, and the resistance

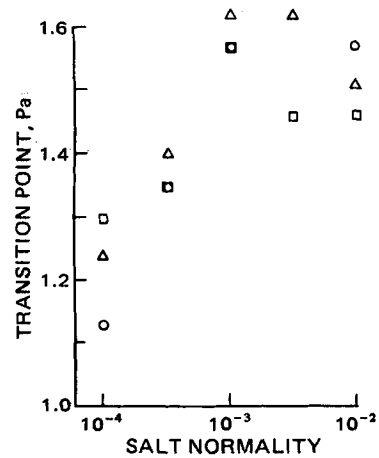

Figure 7—*Effect of various salts on the gel transition point of 0.5% solutions of xanthan gum. Key: (○) calcium chloride; (△) sodium chloride; (□) sodium citrate.*

Table I—Effect of Salts on the Apparent Viscosity of Xanthan Gum Solutions at a Shear Rate of 3.0 s^{-1}

Xanthan Gum Concentration, % w/v	Apparent Viscosity, mPa·s					
	No Added Salt	10^{-4} M NaCl	10^{-3} M NaCl	10^{-2} M NaCl	10^{-3} M $CaCl_2$	10^{-2} M $CaCl_2$
0.133	186	—	—	80	83	76
0.2	340	265	210	220	—	—
0.3	414	460	430	450	415	410
0.4	580	670	670	740	—	—
0.5	620	630	940	1080	1160	1120

to deformation is very high. After the transition point, structure within the gel particles is affected. Partial breakdown of intermolecular linkages and spatial rearrangement of the polymer molecules accounts for the pseudplastic behavior at shear rates higher than that at which the transition occurs. From the breaks in the consistency curves, the transition shear stress was estimated to be 1.1 Pa for the 0.5% solution, 0.9 Pa for the 0.4% solution, and 0.4 Pa for the 0.3% solution.

At xanthan gum concentrations >0.5%, gel strength would be expected to increase. A yield value was reported for a 1% xanthan gum solution, but not for lower concentrations (2, 3). At concentrations < ~0.3%, measurements in our laboratory failed to show a definite gel-like region and then a transition to a less-ordered state.

Apparent viscosity (shear stress/shear rate) was calculated for the xanthan gum solutions from first cycle flow curves using fresh solutions. Flow curves in which the maximum shear rate scanned was 3.0 s^{-1} were used to calculate apparent viscosity for shear rates ranging from 0.3 to 3.0 s^{-1}. All values calculated were for shear rates higher than those at which the transition from a gel state took place. Apparent viscosity for shear rates from 3.0 to 30 s^{-1} were obtained from flow curves for which the maximum shear rate setting was 30 s^{-1}. The logarithm of apparent viscosity is plotted as a function of the logarithm of shear rate in Fig. 4. These plots are linear for the 0.3 and 0.5% xanthan gum solutions; the 0.133% solution also exhibits a linear relationship except for the lowest shear rate values. The curves in Fig. 4, which follow the same general pattern as plots shown previously for other xanthan gum concentrations (2), indicate that the power law equation is applicable:

$$\eta = KD^{(n-1)}$$

where η is apparent viscosity, D is shear rate, K is the viscosity at 1 s^{-1}, and n is a constant that indicates the degree of pseudoplasticity. The minimum possible value of n, corresponding to the highest degree of pseudoplasticity, is zero (13). Values of n, calculated from the linear portion of log viscosity–log shear rate relations, are plotted as a function of xanthan gum concentration in Fig. 5. From Figs. 4 and 5, it is evident that an increase in xanthan gum concentration results in an increase in both viscosity and the degree of pseudoplasticity.

The addition of various salts to a 0.5% xanthan gum solution brought about an increase in apparent viscosity. Results for one shear rate, 3.0 s^{-1}, are shown in Fig. 6. Similar relationships were found by making comparisons at other shear rate values. The increase in viscosity reached a limiting value with increasing salt concentration, which was about the same for the three salts studied. Furthermore, the three salts appeared to be nearly equally effective. A concentration of 10^{-3} N $CaCl_2$ or NaCl brought viscosity to the plateau level. Sodium citrate required a concentration of 3.3×10^{-3} N to reach the same viscosity.

These salts also increased the magnitude of the shear stress at which the low shear transition from a gel state took place (Fig. 7). Transition points were estimated from the low shear range flow curves obtained under the same conditions as those shown in Fig. 3. The error in reading the transition points from the graphs was ~0.1 Pa. The addition of a salt increases the magnitude of shear stress at which the transition from a gel occurs, and, as with the effect on viscosity, the transition shear stress reaches a limiting value with increasing salt concentration. All salts appear to be equally effective, reaching maximal shear stress at a concentration of 10^{-3} N.

Although the most extensive salt studies were performed on 0.5% xanthan gum solutions, some data were obtained with lower gum concentrations (Table I). The dependence of apparent viscosity on salt concentration varied with the xanthan gum concentrations. In a 0.5% xanthan gum solution, the addition of a salt nearly doubled the viscosity. The viscosity of a 0.4% xanthan gum solution was also increased by salt, but to a smaller extent. The viscosity of a 0.3% xanthan gum solution was hardly affected by salt, while solutions containing ≤0.2% of the gum showed a decrease in viscosity. The decrease in viscosity was more pronounced at the lower xanthan gum concentration (0.133%). Sodium chloride and calcium chloride seemed to have equal effect on viscosity at all xanthan gum concentrations, suggesting that reduction of

intramolecular charge repulsion is not a primary factor in these salt effects on viscosity. However, interpretation of these results is complicated by the fact that xanthan gum, as supplied by the manufacturer, contains some cellular material and ions. Typically, monovalent cations, (principally sodium and potassium) amount to 3–6% (w/w) of the finished product[3]. Divalent cations, principally calcium and magnesium, make up ~0.15–0.35% by weight of the commercial polymer[3]. For the same reason, it is difficult to compare results of this study with many previous reports for which purified gum was utilized.

The utility of xanthan gum as a stabilizer of aqueous suspensions and other disperse systems is due, in part, to the pseudoplastic nature of gum solutions. At high shear the viscosity is quite low, permitting shaking, pouring, and pumping without high resistance. On the other hand, the high viscosity augmented by existence of a gel-like state at very low shear accounts for the high resistance to particle sedimentation. Viscosity, the degree of pseudoplasticity, and the value of the transition from gel-like to pseudoplastic behavior are dependent on xanthan gum concentration. The effect of addition of a salt on viscosity of xanthan gum solutions is complex. A 0.3% xanthan gum solution exhibits negligible viscosity changes when a salt is added. Higher concentrations of xanthan gum show increased viscosity, and lower xanthan gum concentrations undergo a reduction in viscosity. All of these effects seem to reach limiting values at $\sim 10^{-3}$ *N* to 3.3×10^{-3} *N* salt concentration. Based on the small number of salts studied, viscosity changes appear to be independent of the salt. However, certain ions in particular pH ranges exhibit more specific effects on viscosity (11).

[3] J. Baird, Kelco Division of Merck and Co., Inc., personal communication.

REFERENCES

(1) A. Jeanes, J. E. Pittsley, and F. R. Senti, *Appl. Polymer Sci.*, **5**, 519 (1961).

(2) P. J. Whitcomb, B. J. Ek, and C. W. Macosko, *Am Chem. Soc. Symp. Ser.*, **45**, 160 (1977).

(3) P. J. Whitcomb and C. W. Macosko, *J. Rheol.*, **22**, 493 (1978).

(4) P. E. Jansson, L. Keene, and B. Lindberg, *Carbohydr. Res.*, **45**, 275 (1975).

(5) P. A. Sandford, J. E. Pittsley, C. A. Knutson, P. R. Watson, M. C. Cadmus, and A. Jeanes, *Am. Chem. Soc. Symp. Ser.*, **45**, 192 (1977).

(6) R. Moorhouse, M. D. Walkinshaw, and S. Arnott, *Am. Chem. Soc. Symp. Ser.*, **45**, 90 (1977).

(7) E. R. Morris, D. A. Rees, G. Young, M. D. Walkinshaw, and A. Darke, *J. Mol. Biol.*, **110**, 1 (1977).

(8) G. Holzwarth, *Biochemistry*, **15**, 4333 (1976).

(9) M. Rinaudo and M. Milas, *Biopolymers*, **17**, 2663 (1978).

(10) K. C. Symes, *Food Chem.*, **6**, 63 (1980).

(11) "Xanthan Gum," 2nd ed., Kelco Co., San Diego, Calif., 1978.

(12) J. G. Southwick, H. Lee, A. M. Jamieson, and J. Blackwell, *Carbohydr. Res.*, **84**, 287 (1980).

(13) J. R. Van Wazer, J. W. Lyons, K. Y. Kim, and R. E. Colwell, "Viscosity and Flow Measurement," Interscience, New York, N.Y., 1963, pp. 15, 16.

ACKNOWLEDGMENTS

The authors thank the Kelco Division of Merck and Co., Inc. for grant support and samples of KELTROL® xanthan gum, and Haake, Inc. for the use of the Rotovisco viscometer.

Syntheses and Evaluation of Some Mannich Bases Derived from Acetophenones Against P388 Lymphocytic Leukemia and Toxicological Assessment of 3-Dimethylamino-2-dimethylaminomethyl-1-(4-methoxyphenyl)-1-Propanone Dihydrochloride in Rats

J. R. DIMMOCK *[x], K. SHYAM *, B. M. LOGAN *, P. J. SMITH [‡], and B. M. CROSS [§]

Received September 7, 1982, from the **College of Pharmacy*, [‡]*Department of Chemistry, College of Arts and Science* and [§]*Department of Veterinary Pathology, Western College of Veterinary Medicine, University of Saskatchewan, Saskatoon, Saskatchewan S7N 0W0 Canada.* Accepted for publication January 18, 1983.

Abstract □ A number of analogues of 3-dimethylamino-2-dimethylaminomethyl-1-(4-methoxyphenyl)-1-propanone dihydrochloride (IIa) and related compounds which showed activity against P388 lymphocytic leukemia were prepared, and of the 16 analogues, three met the criterion for activity in this screen. The toxicity of IIa was examined in rats and either a single dose of 25 mg/kg or nine daily doses of 12.5 mg/kg administered by the intraperitoneal route produced marked irritation and damage to the tissue with which it came into contact. Compound IIa did not show significant activity against eight other tumor systems.

Keyphrases □ Mannich bases—derived from acetophenones, antileukemic activity in the P388 screen, toxicological assessment in rats □ Antileukemic agents—potential, Mannich bases derived from acetophenones, P388 screen, toxicological assessment in rats □ 3-Dimethylamino-2-dimethylaminomethyl-1-(4-methoxyphenyl)-1-propanone dihydrochloride—synthesis, antileukemic activity in the P388 screen, toxicological assessment in rats

A number of Mannich bases have been synthesized and evaluated against murine P388 lymphocytic leukemia (1–3). Under certain conditions, Mannich bases undergo elimination leading to the formation of the corresponding α,β-unsaturated ketones (4, 5), which have a marked affinity for nucleophiles (6, 7). This property may account for certain of the biological properties of Mannich bases (8, 9).

Series I was recently evaluated against P388 leukemia in mice and shown to be inactive (10). However, if a second dimethylaminomethyl group is inserted into the molecule, as in IIa, the deamination product would retain a dimethylaminomethyl function attached to the olefinic carbon atom α to the carbonyl group. Since, on occasions, the pH of tumor cells has been claimed to be more acidic than normal cells (11–13), deamination of IIa could give rise, possibly preferentially in malignant tissue, to a compound bearing a protonated nitrogen atom. Hence nucleophilic attack by cellular macromolecules would be enhanced since the intermediate formed as a result of Michael addition would be stabilized by two electron-withdrawing functions, namely the carbonyl group and the positively charged nitrogen atom.

A representative compound, IIa, was synthesized and shown to increase the median survival time in mice with P388 lymphocytic leukemia by 28 and 24% at dose levels of 25 and 12.5 mg/kg, respectively. A comparison of the bioactivities of IIb–f

0022-3549/84/0400-0471$01.00/0

© 1984, American Pharmaceutical Association

intramolecular charge repulsion is not a primary factor in these salt effects on viscosity. However, interpretation of these results is complicated by the fact that xanthan gum, as supplied by the manufacturer, contains some cellular material and ions. Typically, monovalent cations, (principally sodium and potassium) amount to 3–6% (w/w) of the finished product[3]. Divalent cations, principally calcium and magnesium, make up ~0.15–0.35% by weight of the commercial polymer[3]. For the same reason, it is difficult to compare results of this study with many previous reports for which purified gum was utilized.

The utility of xanthan gum as a stabilizer of aqueous suspensions and other disperse systems is due, in part, to the pseudoplastic nature of gum solutions. At high shear the viscosity is quite low, permitting shaking, pouring, and pumping without high resistance. On the other hand, the high viscosity augmented by existence of a gel-like state at very low shear accounts for the high resistance to particle sedimentation. Viscosity, the degree of pseudoplasticity, and the value of the transition from gel-like to pseudoplastic behavior are dependent on xanthan gum concentration. The effect of addition of a salt on viscosity of xanthan gum solutions is complex. A 0.3% xanthan gum solution exhibits negligible viscosity changes when a salt is added. Higher concentrations of xanthan gum show increased viscosity, and lower xanthan gum concentrations undergo a reduction in viscosity. All of these effects seem to reach limiting values at $\sim 10^{-3}$ *N* to 3.3×10^{-3} *N* salt concentration. Based on the small number of salts studied, viscosity changes appear to be independent of the salt. However, certain ions in particular pH ranges exhibit more specific effects on viscosity (11).

[3] J. Baird, Kelco Division of Merck and Co., Inc., personal communication.

REFERENCES

(1) A. Jeanes, J. E. Pittsley, and F. R. Senti, *Appl. Polymer Sci.*, **5**, 519 (1961).

(2) P. J. Whitcomb, B. J. Ek, and C. W. Macosko, *Am Chem. Soc. Symp. Ser.*, **45**, 160 (1977).

(3) P. J. Whitcomb and C. W. Macosko, *J. Rheol.*, **22**, 493 (1978).

(4) P. E. Jansson, L. Keene, and B. Lindberg, *Carbohydr. Res.*, **45**, 275 (1975).

(5) P. A. Sandford, J. E. Pittsley, C. A. Knutson, P. R. Watson, M. C. Cadmus, and A. Jeanes, *Am. Chem. Soc. Symp. Ser.*, **45**, 192 (1977).

(6) R. Moorhouse, M. D. Walkinshaw, and S. Arnott, *Am. Chem. Soc. Symp. Ser.*, **45**, 90 (1977).

(7) E. R. Morris, D. A. Rees, G. Young, M. D. Walkinshaw, and A. Darke, *J. Mol. Biol.*, **110**, 1 (1977).

(8) G. Holzwarth, *Biochemistry*, **15**, 4333 (1976).

(9) M. Rinaudo and M. Milas, *Biopolymers*, **17**, 2663 (1978).

(10) K. C. Symes, *Food Chem.*, **6**, 63 (1980).

(11) "Xanthan Gum," 2nd ed., Kelco Co., San Diego, Calif., 1978.

(12) J. G. Southwick, H. Lee, A. M. Jamieson, and J. Blackwell, *Carbohydr. Res.*, **84**, 287 (1980).

(13) J. R. Van Wazer, J. W. Lyons, K. Y. Kim, and R. E. Colwell, "Viscosity and Flow Measurement," Interscience, New York, N.Y., 1963, pp. 15, 16.

ACKNOWLEDGMENTS

The authors thank the Kelco Division of Merck and Co., Inc. for grant support and samples of KELTROL® xanthan gum, and Haake, Inc. for the use of the Rotovisco viscometer.

Syntheses and Evaluation of Some Mannich Bases Derived from Acetophenones Against P388 Lymphocytic Leukemia and Toxicological Assessment of 3-Dimethylamino-2-dimethylaminomethyl-1-(4-methoxyphenyl)-1-Propanone Dihydrochloride in Rats

J. R. DIMMOCK *[x], K. SHYAM *, B. M. LOGAN *, P. J. SMITH [‡], and B. M. CROSS [§]

Received September 7, 1982, from the **College of Pharmacy*, [‡]*Department of Chemistry, College of Arts and Science* and [§]*Department of Veterinary Pathology, Western College of Veterinary Medicine, University of Saskatchewan, Saskatoon, Saskatchewan S7N 0W0 Canada.* Accepted for publication January 18, 1983.

Abstract □ A number of analogues of 3-dimethylamino-2-dimethylaminomethyl-1-(4-methoxyphenyl)-1-propanone dihydrochloride (IIa) and related compounds which showed activity against P388 lymphocytic leukemia were prepared, and of the 16 analogues, three met the criterion for activity in this screen. The toxicity of IIa was examined in rats and either a single dose of 25 mg/kg or nine daily doses of 12.5 mg/kg administered by the intraperitoneal route produced marked irritation and damage to the tissue with which it came into contact. Compound IIa did not show significant activity against eight other tumor systems.

Keyphrases □ Mannich bases—derived from acetophenones, antileukemic activity in the P388 screen, toxicological assessment in rats □ Antileukemic agents—potential, Mannich bases derived from acetophenones, P388 screen, toxicological assessment in rats □ 3-Dimethylamino-2-dimethylaminomethyl-1-(4-methoxyphenyl)-1-propanone dihydrochloride—synthesis, antileukemic activity in the P388 screen, toxicological assessment in rats

A number of Mannich bases have been synthesized and evaluated against murine P388 lymphocytic leukemia (1–3). Under certain conditions, Mannich bases undergo elimination leading to the formation of the corresponding α,β-unsaturated ketones (4, 5), which have a marked affinity for nucleophiles (6, 7). This property may account for certain of the biological properties of Mannich bases (8, 9).

Series I was recently evaluated against P388 leukemia in mice and shown to be inactive (10). However, if a second dimethylaminomethyl group is inserted into the molecule, as in IIa, the deamination product would retain a dimethylaminomethyl function attached to the olefinic carbon atom α to the carbonyl group. Since, on occasions, the pH of tumor cells has been claimed to be more acidic than normal cells (11–13), deamination of IIa could give rise, possibly preferentially in malignant tissue, to a compound bearing a protonated nitrogen atom. Hence nucleophilic attack by cellular macromolecules would be enhanced since the intermediate formed as a result of Michael addition would be stabilized by two electron-withdrawing functions, namely the carbonyl group and the positively charged nitrogen atom.

A representative compound, IIa, was synthesized and shown to increase the median survival time in mice with P388 lymphocytic leukemia by 28 and 24% at dose levels of 25 and 12.5 mg/kg, respectively. A comparison of the bioactivities of IIb–f

0022-3549/84/0400-0471$01.00/0

© 1984, American Pharmaceutical Association

with Ia–e was made in order to explore the generality of this molecular modification on antileukemic activity. It was found that IIb–f increased the median survival time by 36, 38, 17, 16, and 8%, respectively, and this gradation in biological activity followed, in general, the values of the Hammett σ constants of −0.27, −0.17, 0.00, 0.23, and 0.60 for the nuclear substituents of IIb–f, respectively (10). The stabilities of representative compounds in I and II which possessed extremes of Hammett σ values (Ia,e and IIb,f) were examined under simulated physiological conditions (phosphate buffer, pH 7.4, at 37°C). While I was stable for at least 1.5 h, IIb and f broke down to the corresponding olefinic ketones at rates which seemed to suggest that elimination was favored by electron-withdrawing substituents on the aromatic ring. It was considered possible that an optimal rate of breakdown was associated with anticancer activity, *i.e.*, if decomposition was too rapid (as in the case of IIf), then the α,β-unsaturated ketone generated was sequestered prior to interaction with leukemia cells, whereas if it was too slow or even refractory to deamination (as suggested by the data for I), there would be insufficient α,β-unsaturated ketone present for presumed nucleophilic attack.

The aims of the present investigation were twofold. First, since the promising lead compounds IIa–c possessed nuclear methoxyl and methyl groups with Hammett σ values of $\sim$−0.2, it was proposed to synthesize III, which principally contained these groups and in which the Hammett σ value for the substituents on the aromatic ring for IIIa–f were +0.12, −0.15, −0.03, −0.37, −0.07, and −0.24, respectively. Thus, the rate of release of the α,β-unsaturated ketone would be expected to vary, and the validity of the rate of breakdown of III with antileukemic activity could be explored further. However, the rate of release of the conjugated styryl ketones *in vivo* could also be influenced by the pK_a of the basic group and, hence, the preparation of IV was envisaged. The pK_a values for dimethylamine, pyrrolidine, piperidine, morpholine, and trimethylamine are 10.77, 11.27, 11.22, 8.70, and 9.80, respectively (14), and thus the rate of decomposition predicted is IVd > IVe > IVa > IVb,c. Since the dibasic compounds in II were, in general, more active *versus* P388 lymphocytic leukemia than I, a comparison of the antineoplastic activities of III and IV with the monobasic derivatives V and VI was deemed profitable to shed more light on the generality of this observation. Second, IIa has been designated a Selected Agent Compound by the National Cancer Institute, and it seemed of importance, therefore, to explore the toxicity of IIa in order to further evaluate its potential as a candidate anticancer drug.

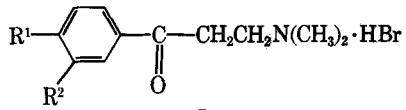

I

a. $R^1 = OCH_3$; $R^2 = H$
b. $R^1 = CH_3$; $R^2 = H$
c. $R^1 = R^2 = H$
d. $R^1 = Cl$; $R^2 = H$
e. $R^1 = R^2 = Cl$

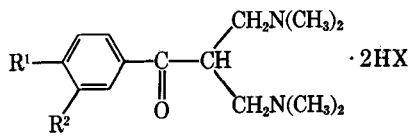

II

a. $R^1 = OCH_3$; $R^2 = H$; X = Cl
b. $R^1 = OCH_3$; $R^2 = H$; X = Br
c. $R^1 = CH_3$; $R^2 = H$; X = Br
d. $R^1 = R^2 = H$; X = Br
e. $R^1 = Cl$; $R^2 = H$; X = Br
f. $R^1 = R^2 = Cl$; X = Br

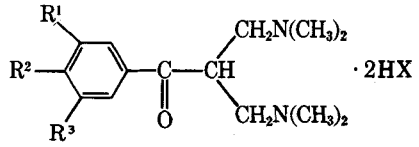

III

a. $R^1 = OCH_3$; $R^2 = R^3 = H$; X = Cl
b. $R^1 = R^2 = OCH_3$; $R^3 = H$; X = Br
c. $R^1 = R^2 = R^3 = OCH_3$; X = Br
d. $R^1 = R^3 = H$; $R^2 = OH$; X = Br
e. $R^1 = CH_3$; $R^2 = R^3 = H$; X = Br
f. $R^1 = R^2 = CH_3$; $R^3 = H$; X = Br

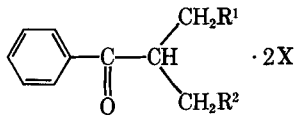

IV

a. $R^1 = N(CH_3)_2$; $R^2 =$; X = HBr
b. $R^1 = R^2 =$; X = HBr
c. $R^1 = R^2 =$; X = HBr
d. $R^1 = R^2 =$; X = HBr
e. $R^1 = R^2 = \overset{(+)}{N}(CH_3)_3$; X = $\overset{(-)}{Br}$

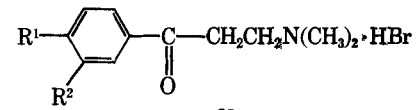

V

a. $R^1 = H$; $R^2 = OCH_3$
b. $R^1 = OH$; $R^2 = H$
c. $R^1 = H$; $R^2 = CH_3$

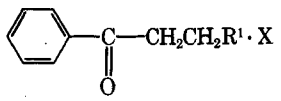

VI

a. $R^1 =$; X = HBr
b. $R^1 =$; X = HBr
c. $R^1 =$; X = HBr
d. $R^1 = \overset{(+)}{N}(CH_3)_3$; X = $\overset{(-)}{Br}$

RESULTS AND DISCUSSION

Compounds IIa, IIIa–c, e, f, and IVb–d were prepared by treating acetophenone or a substituted acetophenone with an excess of formaldehyde and amine and converting the products into the corresponding dihydrohalide salts. Utilization of this general procedure in attempting to prepare IIId gave rise to the nuclear bis(aminomethyl) product, VII (Scheme I). To obtain exclusively side chain aminomethylation, the nuclear hydroxyl group of *p*-hydroxyacetophenone was protected by a tetrahydropyranyl function (15), and TLC of the product of a Mannich reaction with this ketone showed a mixture of diamines was formed in which both protected and free hydroxyl groups were present. The mixture was then treated with hydrogen bromide to give the desired product IIId (Scheme I).

The mass spectrum of this compound was of interest insofar as the base peak

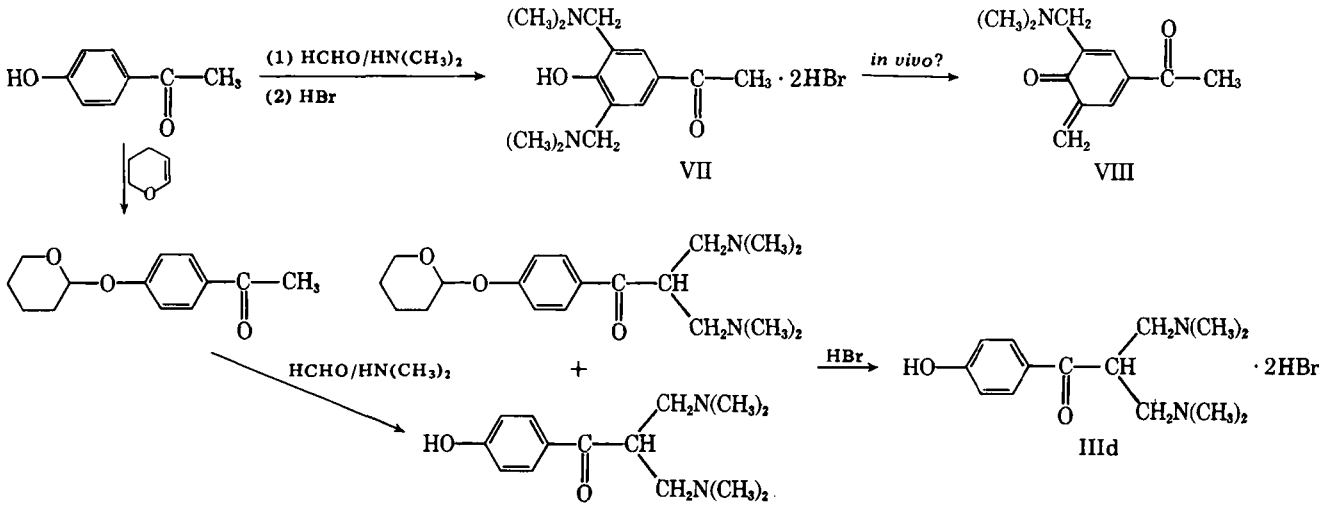

Scheme I

differed from four related compounds IIb and d–f, although common fragmentation pathways were found in all five compounds (Table I; Scheme II). The peak due to the dimethyl(methylene)ammonium ion (f, *m/z* 58) is the base peak except for IIId, in which case it is the acylium ion (g) *m/z* 121. Stabilization of the positive charge in the acylium ion by the powerful electron-releasing mesomeric effect of the hydroxyl group ($\sigma_p^+ = -0.85$) (16) could account for this phenomenon (Scheme III). It is of interest to note that a major ion in the fragmentation pattern of IIb is *m/z* 135, due to the related *p*-methoxy acylium ion. Other observations of interest from Scheme II are as follows.

1. The radical ion of the free diamine (a) which could be formed is absent in all five cases. On the other hand, each spectrum shows peaks of equal intensity at *m/z* 80 and 82 due to $[HBr]^+$ and also at *m/z* 79 and 81 due to Br^+.

2. The peak due to the radical ion of 1-aryl-2-dimethylaminomethyl-2-propen-1-one (b), which could arise from loss of dimethylamine from a, is also absent. This pathway, however, cannot be ruled out since the data obtained suggest that ion b is formed, but is of low intensity because of its fragmentation to give c, *m/z* 84.

3. The carbocation (d) may account for the peak having the highest mass-charge ratio in each case. Homolytic fission of the bond γ to the carbonyl function in d gives the radical ion of the acrylophenone (e).

Compound IVa was prepared by Mannich condensation of Ic with pyrrolidine and formaldehyde, and quaternization of the free base of IId and Ic with methyl bromide gave IVe and VId, respectively. The remaining compounds in series V and VI were prepared essentially by the method of Maxwell (17). The physical data of IIa and III–VII and the efficacy of most of the compounds against P388 lymphocytic leukemia are given in Table II.

Compounds IIIb, d, and f, like the active diamines IIb and c, have nuclear substituents with an average Hammett σ value of ~−0.25, and both IIIb and f are active against P388 lymphocytic leukemia while IIId possesses marginal activity. It is conceivable that facile *O*-glucuronidation minimizes the antileukemic efficacy of IIId. The remaining three compounds IIIa, c, and e, with an average nuclear Hammett σ value of 0.02, were inactive. There was slightly higher activity in the case of IIIa, d, and e (average T/C% = 115) than with their monobasic counterparts Va–c (average T/C% = 105). No correlation between the predicted ease of breakdown in series IV with anticancer activity was apparent, and compounds VIa, b, and d were inactive. However, two

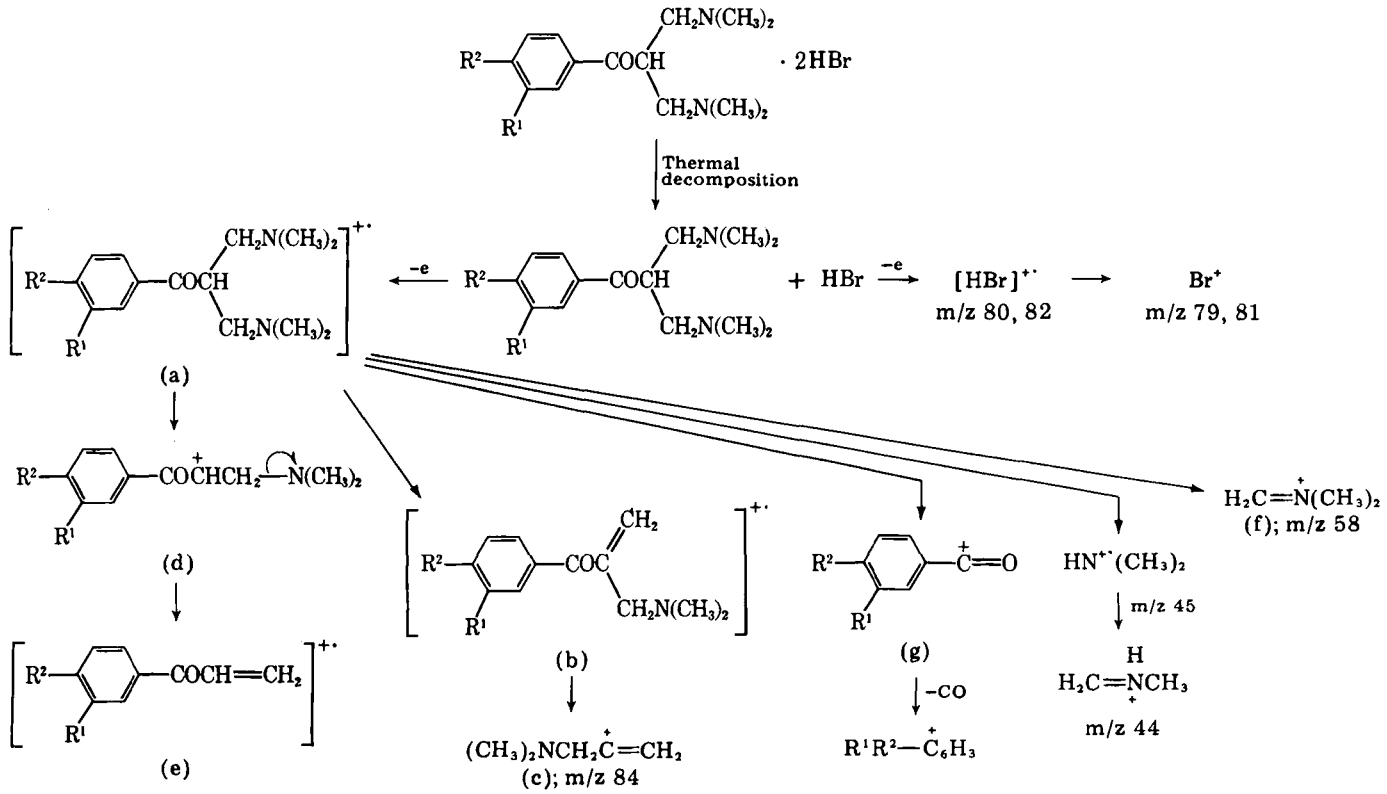

Scheme II

Table I—*m/z* (Relative Intensity) Values of the Principal Ions Observed in the 70-eV Mass Spectra of the 1-Aryl-3-dimethylamino-2-dimethylaminomethyl-1-propanone Dihydrobromides IIb, d–f, and IIId

Compound	*m/z* (Relative Intensity) of Principal Ions
IIb	206(18), 202(6), 162(35), 135(78), 107(11), 92(18), 84(12), 82(28), 81(11), 80(28), 79(11), 77(24), 58(100), 45(16), 44(32)
IId	176(23), 172 (4), 132(18), 105(44), 84(13), 82(24), 81(8), 80(24), 79(8), 77(33), 58(100), 45(11), 44(21)
IIe	212(3), 210(9), 206(6), 141(18), 139(53), 113(7), 111(22), 84(8), 82(18), 81(6), 80(20), 79(7), 75(15), 58(100), 45(14), 44(27)
IIf	246(3), 244(6), 240(3), 202(9), 200(14), 117(4), 175(27), 173(42), 149(2), 147(11), 145(16), 109(10), 84(9), 82(21), 81(8), 80(22), 79(8), 75(6), 74(8), 58(100), 45(15), 44(27)
IIId	192(11), 188(4), 148(41), 121(100), 93(22), 84(8), 82(21), 81(8), 80(21), 79(8), 65(23), 58(93), 45(24), 44(44)

compounds (IVa and d) increased the median survival time in mice with P388 lymphocytic leukemia by ~20%. It was hoped that VII would give rise to the *ortho* quinone VIII *in vivo* (Scheme I), but the lack of both antineoplastic activity and marked murine toxicity suggested that this pathway did not materialize. The screening results observed in this study reveal a continuation of a trend observed earlier (10) that, in general, higher anticancer activity is found among dibasic derivatives of substituted acetophenones than with the corresponding monobasic analogues.

The second phase of this investigation was to examine the disposition of IIa. As mentioned earlier, significant antineoplastic activity was found at dose levels of 12.5 and 25 mg/kg. During the first trial with IIa, a single 12.5-mg/kg ip injection was administered to rats. Three test and one control rats were killed 2, 4, 6, 8, 10, and 15 d postinjection. During the second trial, three rats were given a single 25-mg/kg injection of IIa. The rats were closely observed, and one rat was killed 5, and two others at 30, and 48 h postinjection, Following this, a single 12.5-mg/kg injection of IIa was repeated in three animals. One of the test rats and one control were killed 24, 48, and 84 after the injection. In the final trial, it was proposed to give nine daily injections of IIa (12.5 mg/kg) to nine rats and to examine the animals 3, 8, and 15 after the ninth injection.

The results obtained were as follows. On both occasions a single 12.5-mg/kg injection of IIa produced no gross or microscopic lesions in the rats. After the single 25-mg/kg injection of IIa, the rats appeared very depressed, were reluctant to move and were "hunched over." One rat (no. 1) was killed 5 h after injection. Twenty-four hours after injection, the remaining rats (nos. 2 and 3) were depressed and reluctant to move. Porphyrin stained the forelimbs, faces, and heads; the hair coats were rough and spiky. The abdomen of one animal was tense and contracted.

At necropsy, all three rats were observed to have hydroperitoneum. The proximal intestine was flaccid, dilated, and fluid filled. The contents of the distal jejunum, ileum, and large intestine were very dry. Numerous white opaque areas of coagulation necrosis and saponification were scattered throughout the abdominal fat and the fat associated with the spermatic cords in rats 2 and 3. The cecal wall of rat 1 was edematous and contained a perforated ulcer at the distal end. Microscopic examination revealed interlobular pancreatic edema and edema of the colonic muscularis. Rat 2 was killed 30 h after the injection. Opaque areas present in the pancreas represented acute necrosis of the peripheral lobules. The subserosal longitudinal muscle of the stomach, small intestine, and colon had also undergone acute necrosis. The myonecrosis ranged from focal to diffuse; in places it extended through the circular muscle into the submucosa and was accompanied by hemorrhage. The walls of the seminal vesicles and coagulating glands were similarly affected, with the necrosis extended through the entire wall in areas. Rat 3 was killed 48 h after injection. A fibrinous peritonitis was present with fibrinous adhesions joining the liver to the diaphragm and the pancreas to the stomach, and fibrin coated the seminal vesicles, coagulating glands, and the mesentery. Petechial hemorrhages were visible on the serosa of the cecum, colon, and rectum. The histopathological lesions were similar to those of rat 2. The necrosis and hemorrhage in the wall of the stomach and intestine were more diffuse and often extended into the lamina propria. Small ulcers were present in the squamous portion of the stomach.

Table III indicates the changes in weight resulting from the multiple-injection trial of the animals surviving this treatment regimen; a marked weight

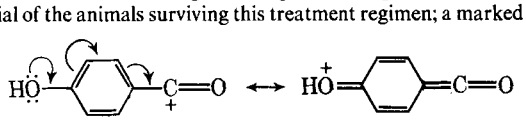

Scheme III

Table II—Physical Data on the Mannich Bases IIa and III–VII and Activity Against P388 Lymphocytic Leukemia in Mice

Compound	Yield, %	Melting Point, °C	Formula[a]	Maximum C%[b]	Toxicity in mice[c]
IIa	31	175–177	$C_{15}H_{26}Cl_2N_2O_2$	128(25)	0/6(100), 2/6(50), 6/6(25)
IIIa	21	161–163	$C_{15}H_{26}Cl_2N_2O_2$	114(12.5)	0/6(50), 6/6(25)
IIIb	58	200–203	$C_{16}H_{28}Br_2N_2O_3$	124(12.5)	0/6(100, 4/6(50), 6/6(25)
IIIc	61	208–211	$C_{17}H_{30}Br_2N_2O_4$	111(50)	0/6(100), 5/5(50)
IIId	34	193–195	$C_{14}H_{24}Br_2N_2O_2$[d]	118(6.25)	0/5(50), 6/6(25)
IIIe	28	196–198	$C_{15}H_{26}Br_2N_2O$	114(25)	0/5(100), 1/6(50), 6/6(25)
IIIf	59	205–207	$C_{16}H_{28}Br_2N_2O$	128(12.5)	0/5(50), 6/6(25)
IVa	41	191–192	$C_{16}H_{26}Br_2N_2O$	121(12.5)	0/6(100), 6/6(50)
IVb	43	177–179	$C_{18}H_{28}Br_2N_2O$[e]	102(50)	0/6(100), 6/6(50)
IVc	19	184	$C_{20}H_{32}Br_2N_2O$	—	—
IVd	54	188	$C_{18}H_{28}Br_2N_2O_3$	119(50)	0/6(200), 6/6(100)
IVe	64	208–211	$C_{16}H_{28}Br_2N_2O$[f]	108(12.5)	0/6(50), 3/6(25), 6/6(12.5)
Va	50	147	$C_{12}H_{18}BrNO_2$	106(50)	1/6(200), 6/6(100)
Vb	58	192–193	$C_{11}H_{16}BrNO_2$	106(200)	6/6(200)
Vc	41	164–166	$C_{12}H_{18}BrNO$	103(50)	0/6(200), 4/6(100), 6/6(50)
VIa	63	187–188	$C_{13}H_{18}BrNO$	100(25)	0/6(100), 3/6(50), 6/6(25)
VIb	54	194–195[g]	$C_{14}H_{20}BrNO$	95(25)	0/6(100), 4/6(50), 6/6(25)
VIc	67	191–192[h]	$C_{13}H_{18}BrNO_2$	—	—
VId	48	197–198[i]	$C_{12}H_{18}BrNO$	99(12.5)	0/6(100), 3/6(50), 5/5(25)
VII	43	225	$C_{14}H_{24}Br_2N_2O_2$	101(50)	5/5(200)

[a] Elemental analyses for C, H, and N were conducted for all compounds. Unless otherwise noted, all values were within ±0.4% of the theoretical values. [b] Ratios of the survival time of the treated (T) to control (C) animals expressed as a percentage. Compounds were initially screened at 200, 100, and 50 mg/kg; if mortalities occurred at these doses, they were reduced to nonlethal levels. A compound should increase the median survival time by at least 20% to be considered active. The dose in mg/kg is in parentheses. [c] Numbers of survivors 5 d after commencement of the dosage schedule of nine daily doses, except for IIIb–f, IVb, IVe (50-mg/kg dose), and VII in which cases five daily doses were administered. [d] Calc. for C, 40.79; found, 39.96. [e] Calc. for C, 48.23; found 47.77. [f] Calc. for C, 45.30; found 44.88. [g] Lit. (18) mp 197.0–197.5°C. [h] Lit. (19) mp 189.5–190.5°C. [i] Lit. (20) mp 238°C.

loss was observed after completing the injection schedule, although 15 d after the last injection, some weight gain was noted (rats 5 and 6).

Four animals (nos. 4 and 7–9) died before the termination of the multiple-injection trial. Porphyrin staining of the faces was marked in all the rats. Necropsy revealed mild hydroperitoneum, a dilated fluid-filled proximal small intestine, and a large intestine filled with dry ingesta. Rat 7 was killed after it had received its second 12.5-mg/kg injection of IIa. The animal was very quiet, reluctant to move, had a tense contracted abdomen and a spiky coat. Histopathological examination revealed acute degeneration and necrosis of the subcapsular muscle fibers of the seminal vesicles with infiltration by granulocytes. The bladder wall was edematous, and the subserosal myofibers had undergone acute necrosis. The intestinal serosal mesothelium was hypertrophied.

A second rat (no. 8) died after it had received its second injection. In addition to those necropsy findings previously mentioned, all serosal blood vessels were very congested. Areas of necrosis were scattered throughout the abdominal fat and the fat associated with the reproductive organs. Numerous small ulcers extended into the submucosa of the squamous stomach. Throughout the intestine and bladder there was necrosis of subserosal muscle. Fibers were eosinophilic and shrunken. Nuclei were absent, pycnotic, and karyorrhectic. Peripheral pancreatic acini had undergone acute necrosis, and granulocytes had infiltrated the affected areas.

A third test rat (no. 9) died after receiving its fifth injection of IIa. Hematuria had been reported on the previous day. In addition to heavy porphyrin staining of the face and forepaws, blood stained the fur around the prepuce.

Table III—Weight Changes of Male Wistar Rats after Intraperitoneal Injection of IIa and Saline for Nine Consecutive Days

Rat[a]	Day 1	Day 2	Day 3	Day 4	Day 5	Day 6	Day 7	Day 8	Day 9	Weight Difference Between Days 1 and 9, g	Weight, g Day 12	Day 17	Day 24	Weight Difference Between Day 1 Day of Examination, g
1	350	340	330	325	320	305	290	300	295	−55	295			−55
2	348	328	315	328	325	305	295	290	295	−53	285			−63
3	360	345	340	315	310	300	310	295	305	−55		305		−55
4	380	368	355	340	340	355	335	330	325	−55		[b]		
5	334	315	320	305	292	275	270	270	270	−64			335	+ 1
6	380	370	365	360	355	330	320	300	315	−65			375	− 5
7	350	330	[c]											
8	354	335	[d]											
9	342	335	325	305	290	[e]								
Control 1	358	352	355	355	355	350	335	350	355	− 3	360			+ 2
Control 2	330	340	345	340	335	330	335	335	335	+ 5		340		+10
Control 3	355	340	330	315	320	335	340	345	340	−15			375	+20

[a] Rats 1-9 were injected with IIa at 12.5 mg/kg, while controls 1-3 were injected with 0.9% NaCl (saline). [b] Rat 4 died on Day 14. [c] Rat 7 was killed after receiving a second injection. [d] Rat 8 died after receiving a second injection. [e] Rat 9 died after a fifth injection.

The fluid contained in the stomach, duodenum, and jejunum was blood stained. There were areas of hemorrhage and necrosis in the pancreas, circular hemorrhages in the cecal mucosa, and blood in the urinary bladder. Histopathological examination revealed an acute diffuse peritonitis, characterized by the presence of fibrin and granulocytes on the intestinal serosa and in the connective tissue and fat associated with the seminal vesicles, coagulating glands, and the right spermatic cord. The duodenal serosa was coated with granulocytes, which extended through the edematous muscularis in some areas to the submucosa. Acute myonecrosis was noted in the duodenal wall. Similar lesions were scattered throughout the wall of the intestine and bladder. An ulcerative cystitis consisted of areas of mucosal necrosis, granulocyte infiltration into an edematous submucosa, and necrosis of single mucosal cells which sloughed into a blood-filled lumen.

The fourth animal (no. 4) died 5 d after the ninth injection of IIa. The animal was autolyzed; however, a large area of necrosis bounded by hemorrhage was noticed in the right inguinal subcutis and body wall.

Two test animals (nos. 1 and 2) and one control (no. 1) were killed 3 d after the ninth injection. One of the test animals was lame in the right hind limb. In both test animals, fibrous adhesions joined large areas of the subcutaneous tissue and body wall in the right inguinal region. In each rat, an area of necrosis, 1-1.5 cm in diameter, in the body wall was bounded by a distinct red line; grossly, the viscera appeared normal. The coagulation necrosis extended through the body wall to the peritoneum. Many of the necrotic muscle fibers were calcified. Granulation tissue has replaced much of the necrotic tissue, and muscle fibers bordering the areas of necrosis showed signs of regeneration with very long, plump nuclei and multinucleate areas. The necrotic subcutaneous fat had been replaced with granulation tissue. In the intestine and bladder, areas of the serosa and outermost muscularis had been replaced by regenerating muscle fibers, fibroblasts, and capillaries. The orientation of the regenerating fibers was irregular. Areas of mesenteric fat necrosis had been replaced by granulation tissue and lymphocytes.

One rat (no. 3) was killed 8 d after the last injection. This rat was also lame in the right hind limb. During necropsy, a large area of necrosis was found in the subcutis of the right inguinal area. A severe chronic peritonitis was present; all intestine loops were tightly adhered to each other, the bladder, seminal vesicles, and sublumbar musculature. The intestines were dilated and contained fluid. Normal fecal pellets were present in the rectum. Areas of the intestinal wall were thickened; however, the intestine was patent although the lumen was greatly reduced. A mass 1.5 cm in diameter occupied a position in the dorsal body wall midway between the right kidney and the bladder. The mass had a fibrous wall, was filled with clear fluid, and involved the right ureter and sublumbar muscles. The right ureter proximal to the mass was dilated with clear fluid. There was hydronephrosis of an enlarged right kidney. The right seminal vesicle was shrunken; atrophy of the right testis was seen during microscopic examination. Few spermatogonia were present in the seminal tubules; however, spermatozoa were present in the epididymal tubules. The walls of the intestines, seminal vesicles, and coagulating glands were thickened with a layer of granulation tissue. Areas of abdominal fat necrosis had been walled off with fibrous tissue; many of these areas had calcified. Fibrous tissue thickened the pancreatic capsule and extended between acini. Gastric ulcers extended into the muscularis mucosa. Beneath the ulcers, the muscularis and submucosa were infiltrated by fibroblasts, angioblasts, and numerous eosinophils. The medulla of the right kidney was compressed, and there was perivascular and cortical edema.

The thick fibrous wall of the fluid-filled mass extended into the adipose tissue and the muscles of the dorsal abdominal wall. It surrounded blood vessels, nerves, and sublumbar lymph nodes. Areas of mineralizing necrotic muscle were present in the mass; lymphocytes and multinucleate giant cells were prominently associated with these areas. Thrombosed blood vessels and areas of fat necrosis were also trapped in the mass. The central cavity appeared to be lined by fibroblasts.

The last two test animals (nos. 5 and 6) were sacrificed 15 d after the ninth injection. Hematuria had been reported in one of these animals after the eighth and ninth injections. Diarrhea was reported at the same time for the other rat. An ulcer 1 cm long was present in one animal in the skin fold between the right stifle and right inguinal area. Further examination revealed ulceration, necrosis, and replacement with granulation tissue that extended through the dermis and subcutis and into the body wall. Fibrous adhesions between abdominal viscera were extensive in both rats; adhesions trapped the right testes, epididymes, and spermatic cords in the scrotal sacs. The right testis from one rat was extremely small and lacked spermatogonia. The seminal vesicles and bladder were adhered together. Areas of necrotic seminal vesicle had undergone mineralization. Epididymal fibrosis was prominent in the rat no. 6; no spermatozoa were present in the epididymal or seminal tubules. Large numbers of abnormal cells, including multinucleate giant cells, were present in the seminal tubules. Sertoli cells were very prominent.

One may summarize these disposition studies by noting that when the rats received a single 25-mg/kg injection of IIa, it appeared that any portion of the abdominal viscera coming into contact with the substance underwent necrosis. Adynamic ileus, produced by peritonitis and pain, resulted in a large volume of fluid pooling in the anterior intestine and probably caused severe electrolyte imbalance. Acute gastric ulceration was probably also a manifestation of the stress produced by abdominal pain. Although a single dose of 12.5 mg/kg produced no gross or light microscopic lesions, nine daily doses at the same level resulted in severe myonecrosis and peritonitis. Throughout the series of injections, the rats exhibited behavioral manifestations of stress and pain and lost a significant amount of weight. After cessation of injections there was tissue healing; however, the permanent damage produced would interfere with intestinal, reproductive, and (in one instance) renal function. It must be concluded that the compound, at a single 25-mg/kg dose or a series of 12.5-mg/kg doses, is very irritating and severely damages any tissue with which it comes into contact.

Finally, the screening of the Selected Agent Compound IIa *versus* a number of tumors (21) was undertaken (Table IV). In tumor systems 3-8 inclusive, IIa was inactive and although some reduction in tumor weight was found in the colon and lung xenografts, it was insufficient to meet the criteria for activity.

EXPERIMENTAL

Melting points are uncorrected. Elemental analyses were undertaken locally[1], and organic extracts were dried with anhydrous magnesium sulfate. TLC was carried out using sheets of silica gel with fluorescent indicator[2] and a solvent mixture of toluene–methanol (9:1). Mass spectra[3] were run at 70 eV, and the 60-MHz NMR spectra[4] were determined in deuterochloroform or deuterium oxide using internal standards of tetramethylsilane and sodium 2,2-dimethyl-2-silapentane-5-sulfonate, respectively.

Syntheses of Compounds—*1-Aryl-3-dimethylamino-2-dimethylamino-*

[1] Mr. R. E. Teed, Department of Chemistry, College of Arts and Science, University of Saskatchewan, Saskatoon.
[2] Eastman-Kodak Co.
[3] VG Micromass MM16F mass spectrometer with 2025 data system.
[4] Varian T-60 spectrometer.

Table IV—Evaluation of IIa Against Various Tumors in Mice

Tumor	Treatment Schedule	Maximum T/C%[a]	Toxicity[b]
CX-1 Colon xenograft	Four daily injections	38(25)	0/6(100), 3/6(50), 6/6(25)
LX-1 Lung xenograft	One injection every 4 d; total of three injections	64(50)	0/6(100), 6/6(50)
MX-1 Breast xenograft	One injection every 4 d; total of four injections	101(12.5)	0/6(100), 5/6(50), 6/6(25)
$CD8F_1$ Mammary tumor	One injection	103(7.81)	1/10(125), 3/10(62.5), 10/10(31.25)
Colon 38	One injection every 7 d; total of two injections	102(25)	0/10(100), 1/10(50), 10/10(25)
B16 Melanocarcinoma	Nine daily injections	102(25)	0/10(50), 10/10(25)
L 1210 Lymphoid leukemia	Nine daily injections	110(25)	1/6(50), 6/6(25)
Lewis lung carcinoma	Nine daily injections	105(12.5)	1/10(50), 10/10(25)
P388 Lymphocytic leukemia	Nine daily injections	128(25)	0/6(100), 2/6(50), 6/6(25)

[a] Figures for tumors 1–5 are the weight differences of the treated animals compared with controls expressed as a percentage. A value of <20 for the first four tumors indicates activity; values of <42 in the case of the colon 38 tumor are considered active. The figures for tumors 6–9 are the ratios of the median survival time of treated animals compared with controls expressed as a percentage. A compound should increase the survival time by 25, 25, 40, and 20%, respectively, to be considered active. Doses in mg/kg are in parentheses. [b] At day 5; doses are in parentheses.

methyl-1-propanone Dihydrohalides (*IIa*, *IIIa–c,e,f*)—A mixture of the substituted acetophenone (0.05 mol), aqueous solutions of formaldehyde (37% w/v, 0.15 mol) and dimethylamine (25% w/v, 0.15 mol), and ethanol (25 mL) was heated under reflux for 3 h (IIa, IIIa,e), 24 h (IIIb,f), or 30 h (IIIc). The solvent was removed *in vacuo*, and the mixture was extracted with ether (3 × 20 mL). The combined ethereal extracts were washed with water, dried, and then the solvent was removed under reduced pressure to give the Mannich base, which was dissolved in acetone and treated with either hydrogen chloride or hydrogen bromide. The colorless solid which precipitated was removed by filtration, dried, and recrystallized from methanol to give the desired Mannich base salts.

3-Dimethylamino-2-dimethylaminomethyl-1-(4-hydroxyphenyl)-1-propanone Dihydrobromide (*IIId*)—A mixture of 4-hydroxyacetophenone (13.6 g, 0.1 mol), 2,3-dihydro-4*H*-pyran (10.4 g, 0.12 mol), an acidic ion-exchange resin[5] (1.5 g), and benzene (125 mL) was stirred vigorously at room temperature for 24 h. The reaction was monitored by following the disappearance of 4-hydroxyacetophenone (R_f 0.65) using TLC. After removal of the resin by filtration, the mixture was passed through a column of silica gel (60–200 mesh, benzene). The resultant yellow solution was washed with aqueous sodium hydroxide solution (10% w/v, 3 × 20 mL) and then with water (4 × 20 mL). After drying, the benzene was removed *in vacuo* to give a yellow solid, which was recrystallized from *n*-hexane to give 4-(2-tetrahydropyranyloxy)-acetophenone (15.6 g, 71%) as yellow crystals, mp 84–86°C [lit. (22) mp 89.5–91.0°C]; R_f 0.82; ^{1}H-NMR ($CDCl_3$): δ 7.82 (d, 2, ArH at C_2 and C_6), 7.00 (d, 2, ArH at C_3 and C_5), 5.45 (t, 1, tetrahydropyranyl H at C_2), 3.68 (m, 2, tetrahydropyranyl H at C_6), 2.54 (s, 3, CH_3), and 2.20–1.40 ppm (m, 6, tetrahydropyranyl H at C_3, C_4, and C_5).

A mixture of 4-(2-tetrahydropyranyloxy)-acetophenone (2.2 g, 0.01 mol), an aqueous solution of formaldehyde (37% w/v, 2.4 mL, 0.03 mol), dimethylamine (25% w/v, 4.5 mL, 0.025 mol), and ethanol (10 mL) was heated at reflux for 30 h. The ethanol was removed *in vacuo*, the mixture was extracted with ether (2 × 10 mL), and the combined organic extracts were washed with water (3 × 5 mL) and dried. After filtration, an additional quantity of anhydrous ether (10 mL) was added, and the solution was treated with hydrogen bromide to give a light-yellow solid, which was recrystallized from methanolic hydrogen bromide (1% w/v) and then from methanol to give IIId (1.4 g) as a bright-yellow solid. ^{1}H-NMR (D_2O): δ 8.04 (d, 2, ArH at C_2 and C_6), 7.04 (d, 2, ArH at C_3 and C_5), 4.04–3.20 [m, 5, $C_2H(CH_2)_2$], and 2.95 ppm [s, 12, $2N(CH_3)_2$]. The yield is based on the use of 4-(2-tetrahydropyranyloxy)-acetophenone as the starting material.

3-Dimethylamino-1-phenyl-2-(1-pyrrolidinylmethyl)-1-propanone Dihydrobromide (*IVa*)—A mixture of 3-dimethylamino-1-phenyl-1-propanone hydrochloride (5.35 g, 0.025 mol) (17), an aqueous solution of formaldehyde (37% w/v, 24 mL, 0.03 mol), pyrrolidine (2.5 mL, 0.03 mol), and ethanol (35 mL) was heated at reflux for 3 h. The solvent was removed *in vacuo*, and water (40 mL) followed by excess aqueous sodium hydroxide (40% w/v) were added to the crude mixture; the aqueous phase was then extracted with ether (50 mL). The organic extract was dried, and removal of the ether gave an oil, which was dissolved in acetone and treated with hydrogen bromide. The resultant crude dihydrobromide salt was recrystallized from ethanol to give IVa as colorless prisms (4.3 g). The yield was based on the use of 3-dimethylamino-1-phenyl-1-propanone hydrochloride as starting material.

3-Amino-2-aminomethyl-1-phenyl-1-propanone Dihydrobromides (*IVb–d*)—These compounds were prepared using the general procedure described for the synthesis of IIa, IIIa–c, e, and f *vide supra*. In the synthesis of IVb–d, the time of heating at reflux in ethanol was 24, 3, and 24 h, respectively.

3-Dimethylamino-2-dimethylaminomethyl-1-phenyl-1-propanone Dimethobromide (*IVe*)—3-Dimethylamino-2-dimethylaminomethyl-1-phenyl-1-propanone dihydrochloride was prepared as colorless crystals, mp 163–164°C [lit. (23) mp 164–165°C] in 20% yield by a reported procedure (10), except that hydrogen chloride was passed through a solution of the free base in acetone and not hydrogen bromide. An aqueous solution of the diamine dihydrochloride (5.8 g, 0.02 mol) was cooled to 5°C and rendered basic to litmus with triethylamine. The mixture was stirred with ice-cooling for 15 min and extracted with ether (3 × 15 mL). The combined organic extracts were washed with water (3 × 10 mL) and dried, and then the solvent was removed under reduced pressure to give a pale-yellow oil, which was dissolved in dry acetone and treated with excess methyl bromide. The solid was removed by filtration, washed with dry acetone, dried, and recrystallized from acetone–methanol to give IVe as a colorless solid (5.4 g).

3-Dimethylamino-1-aryl-1-propanone Hydrobromides (*V*)—The substituted 1-propanone hydrochlorides were prepared by a literature method (17) and then converted into the hydrobromide salts by a reported procedure (10). The crude hydrobromides were recrystallized from acetone–methanol (Va and c) or methanol (Vb). The percentage yields listed in Table II are based on syntheses from the appropriate substituted acetophenone and not from the crude hydrochloride.

3-Amino-1-phenyl-1-propanone Hydrobromides (*VIa–c*)—The appropriate 1-propanone hydrochlorides were prepared essentially by a literature method (17) using the required amine hydrochloride in place of dimethylamine hydrochloride. The times of heating the reactants at reflux were 2 h (VIa and c) and 3 h (VIb). The hydrobromides were obtained from the hydrochloride salts by a literature method (10) and purified by recrystallization from acetone–methanol. The percentage yields in Table II are based on the quantity of acetophenone used.

3-Dimethylamino-1-phenyl-1-propanone Methobromide (*VId*)—Aqueous sodium carbonate solution (10% w/v) was added to an aqueous solution of crude 3-dimethylamino-1-phenyl-1-propanone hydrochloride (17) (4.27 g, 0.02 mol) in water until basic to litmus, and the mixture was extracted with chloroform (4 × 15 mL). After the combined organic extracts were washed with water (3 × 5 mL) and dried, the chloroform was removed *in vacuo* to give a pale-yellow oil, which was dissolved in anhydrous ether (15 mL) and treated with methyl bromide (1.6 mL, 2.77 g, 0.029 mol). The solution was cooled to −4°C for 3 h, and the precipitate was removed by filtration, washed with dry ether, dried, and recrystallized from methanol–acetone (4:1) to give VId as colorless crystals. The yield recorded in Table II was based on the quantity of acetophenone used.

3,5-Bis(dimethylaminomethyl)-4-hydroxyacetophenone Dihydrobromide (*VII*)—A mixture of *p*-hydroxyacetophenone (6.8 g, 0.05 mol), an aqueous solution of formaldehyde (37% w/v, 8.9 mL, 0.11 mol), dimethylamine (5.0 g, 0.11 mol), and ethanol (50 mL) was heated at reflux for 20 h. After removal of the ethanol and water *in vacuo*, the resultant viscous oil was dissolved in acetone and treated with hydrogen bromide. The precipitate was removed by filtration, washed with acetone, dried, and recrystallized from methanol to give VII as colorless prisms (8.8 g). ^{1}H-NMR (D_2O): δ 8.00 (s, 2, ArH at C_2 and C_6), 4.45 (s, 4, 2 × CH_2N), 2.98 [s, 12, 2 × $N(CH_3)_2$], and 2.62 ppm (s, 3, $COCH_3$).

Biological Evaluations—*Screening of Compounds*—The antineoplastic evaluation of the compounds described herein was undertaken by the National Cancer Institute, Bethesda, Maryland, using their protocols (24). The compounds listed in Table II were injected by the intraperitoneal route into male or female Swiss, $B_6D_2F_1$, or CD_2F_1 mice. The derivatives were dissolved in saline prior to injection, except for IVe and VId which were administered in hydroxypropyl cellulose; VIb was injected in both saline and saline containing polysorbate 80[6]. Compounds IVc and VI had been previously assessed by the

[5] Amberlyst H-15; Rohm and Haas, Philadelphia, Pa.

[6] Tween 80; Atlas Chemical Industries.

National Cancer Institute, although not against P388 lymphocytic leukemia.

The data in Table IV was generated as follows. Compound IIa was dissolved in saline and administered to mice hosting tumors 1–3 by the subcutaneous route and intraperitoneally in the remaining cases. The xenografts (tumors 1–3) were inoculated into NU/NU athymic Swiss mice by subcutaneous injection. The activity recorded is the mean tumor weight change between day 0 and the final evaluation days which were 15, 11, and 11 d, respectively. The $CD8F_1$ mammary and colon 38 tumors in $CD8F_1$ and $B_6C_3F_1$ mice, respectively, were evaluated after 34 and 20 d. The activity noted for the $CD8F_1$ mammary tumor was the median tumor weight change, and for the colon 38 tumor, the median tumor weight was estimated from the diameter of the tumor. The B16 melanocarcinoma was injected intraperitoneally into $B_6C_3F_1$ mice and evaluated on day 60. Both L1210 and P388 leukemias were injected by the intraperitoneal route into CD_2F_1 mice and evaluated on day 30. The Lewis lung carcinoma was injected intravenously into $B_6C_3F_1$ mice and evaluated on day 60. The activity of the last four tumors is expressed as the effect on median survival time. The toxicity of IIa *versus* the nine tumors listed in Table IV was evaluated on days 15, 11, 11, 34, 20, 5, 5, 5, and 5, respectively.

Disposition Studies with IIa—Dosed male Wistar rats, weighing 220–250 g (first trial), 285–300 g (second trial), and 240–250 g (third trial) were injected with IIa dissolved in sterile saline (0.9% w/v) by the intraperitoneal route, while control animals received sterile saline (0.9% w/v). All animals were necropsied after sacrifice, and the following tissues were fixed in 10% buffered formalin: lung, heart, thymus, trachea, thyroid, liver, spleen, pancreas, kidney, adrenal, stomach, duodenum, jejunum, ileum, cecum, colon, rectum, lymph nodes, bladder, and reproductive organs. Tissues were processed routinely, sectioned at 5 μm, and stained with hematoxylin and eosin.

REFERENCES

(1) J. R. Dimmock, C. B. Nyathi, and P. J. Smith, *J. Pharm. Sci.*, **67**, 1543 (1978).

(2) J. R. Dimmock, G. B. Baker, and R. G. Sutherland, *Can. J. Pharm. Sci.*, **10**, 53 (1975).

(3) J. R. Dimmock and W. G. Taylor, *J. Pharm. Sci.*, **64**, 241 (1975).

(4) F. A. Carey and R. J. Sundberg, "Advanced Organic Chemistry, Part B: Reactions and Synthesis," Plenum, New York, N.Y., 1977, pp. 44, 46.

(5) F. F. Blicke, in "Organic Reactions," Vol. 1, R. Adams, Ed., Wiley, New York, N.Y., 1942, p. 303.

(6) F. W. Menger and J. H. Smith, *J. Am. Chem. Soc.*, **91**, 4211 (1969).

(7) C. E. Lough, D. J. Currie, and H. L. Holmes, *Can. J. Chem.*, **46**, 771 (1968).

(8) P. N. Gordon, J. D. Johnston, and A. R. English in "Antimicrobial Agents and Chemotherapy," G. L. Hobby, Ed., American Society for Microbiology, Ann Arbor, Mich., 1965, p. 165.

(9) H. Schönenberger, T. Bastug, L. Bindl, A. Adam, D. Adam, A. Petter, and W. Zwez, *Pharm. Acta. Helv.*, **44**, 691 (1969).

(10) J. R. Dimmock, K. Shyam, N. W. Hamon, B. M. Logan, S. K. Raghavan, D. J. Harwood, and P. J. Smith, *J. Pharm. Sci.*, **72**, 887 (1983).

(11) M. Eden, B. Haines, and H. Kahler, *J. Natl. Cancer Inst.*, **16**, 541 (1955).

(12) H. Kahler and W. v B. Robertson, *J. Natl. Cancer Inst.*, **3**, 495 (1943).

(13) K. A. Meyer, E. M. Kammerling, L. Amtman, M. Koller, and S. J. Hoffman, *Cancer Res.*, **8**, 513 (1948).

(14) A. Albert and E. J. Serjeant, "Ionisation Constants of Acids and Bases," Methuen, London, 1962, pp. 140–141.

(15) A. Bongini, G. Cardillo, M. Orena, and S. Sandri, *Synthesis*, **1979**, 618.

(16) F. A. Carey and R. J. Sundberg, "Advanced Organic Chemistry, Part A: Structure and Mechanisms," Plenum, New York, N.Y., 1977, p. 145.

(17) C. E. Maxwell, *Org. Syn.*, **23**, 30 (1943).

(18) A. H. Land, C. Ziegler, and J. M. Sprague, *J. Am. Chem. Soc.*, **69**, 125 (1947).

(19) A. L. Williams and A. R. Day, *J. Am. Chem. Soc.*, **74**, 3875 (1952).

(20) O. R. Hansen and R. Hammer, *Acta. Chim. Scand.*, **7**, 1331 (1953).

(21) A. Goldin, S. A. Schepartz, J. M. Vendetti, and V. T. DeVita, Jr., "Methods in Cancer Research," Vol. XVI Part A, Academic, New York, N.Y., 1979, p. 165.

(22) J. H. Burkhalter, W. D. Dixon, M. L. Black, R. D. Westland, L. M. Werbel, H. A. DeWald, J. D. Rice, G. Rodney, and D. H. Kaump, *J. Med. Chem.*, **10**, 567 (1967).

(23) H. A. Albrecht, J. T. Plati, and W. Wenner, U.S. Pat. 3,058,987, Oct. 6, 1962; Chem. Abstr., **58**, 5644c (1963).

(24) R. I. Geran, N. H. Greenberg, M. M. MacDonald, A. M. Schumacher, and B. J. Abbott, *Cancer Chemother. Rep.* (Part 3), **3** (Sept. 1972).

ACKNOWLEDGMENTS

The authors thank the Medical Research Council of Canada for the award of an operating grant (MA-5538) to J. R. Dimmock and the University of Saskatchewan for the award of a Graduate Scholarship to K. Shyam. Appreciation is recorded to the National Cancer Institute, Bethesda, Md., who undertook the antineoplastic evaluation of most of the compounds reported in this investigation.

Tack Behavior of Coating Solutions II

S. K. CHOPRA and R. TAWASHI ˣ

Received November 17, 1982, *from the Faculty of Pharmacy, University of Montreal, Case Postale 6128, Succursale "A", Montreal, Quebec, H3C 3J7 Canada.* Accepted for publication March 9, 1983.

Abstract □ The tackiness of coating solutions containing high concentrations of polymers was determined using a parallel plate technique. Kinematics of the film-splitting process was also investigated using a high-speed movie camera. The results showed that the impulse required to split a liquid film of highly concentrated polymer solution (semisolid), in contrast to a dilute solution is related not to viscosity, but to the internal structures of the system. Evidence has been found that the materials that are considered to be tacky in practice, display "delayed elastic effects" and require far larger impulses than nontacky materials.

Keyphrases □ Film-coating solutions—tablets, tack behavior, viscosity, concentrated polymer solutions □ Viscosity—film-coating solvents for tablets, tack behavior, concentrated polymer solutions □ Polymers—concentrated solutions, viscosity, tack behavior, film-coating of tablets

The technique of film-coating solid dosage forms has grown at an accelerating rate, employing a wide variety of materials and coating systems (1–3). One of the factors affecting the tablet-coating process is the tackiness of the coating formulations. The concentration of the film formers used in these coating formulations depends on the molecular weight, grade, and chemical structure of the polymers (4). Generally, the concentration of a polymer used in a film-coating formulation ranges from 2 to 10% (5). During the drying phase of the coating process, evaporation of the solvent occurs. Consequently, the concentration of the polymer increases, giving rise to increasing tackiness until the deposited film is essentially

© 1984, American Pharmaceutical Association

National Cancer Institute, although not against P388 lymphocytic leukemia.

The data in Table IV was generated as follows. Compound IIa was dissolved in saline and administered to mice hosting tumors 1–3 by the subcutaneous route and intraperitoneally in the remaining cases. The xenografts (tumors 1–3) were inoculated into NU/NU athymic Swiss mice by subcutaneous injection. The activity recorded is the mean tumor weight change between day 0 and the final evaluation days which were 15, 11, and 11 d, respectively. The $CD8F_1$ mammary and colon 38 tumors in $CD8F_1$ and $B_6C_3F_1$ mice, respectively, were evaluated after 34 and 20 d. The activity noted for the $CD8F_1$ mammary tumor was the median tumor weight change, and for the colon 38 tumor, the median tumor weight was estimated from the diameter of the tumor. The B16 melanocarcinoma was injected intraperitoneally into $B_6C_3F_1$ mice and evaluated on day 60. Both L1210 and P388 leukemias were injected by the intraperitoneal route into CD_2F_1 mice and evaluated on day 30. The Lewis lung carcinoma was injected intravenously into $B_6C_3F_1$ mice and evaluated on day 60. The activity of the last four tumors is expressed as the effect on median survival time. The toxicity of IIa *versus* the nine tumors listed in Table IV was evaluated on days 15, 11, 11, 34, 20, 5, 5, 5, and 5, respectively.

Disposition Studies with IIa—Dosed male Wistar rats, weighing 220–250 g (first trial), 285–300 g (second trial), and 240–250 g (third trial) were injected with IIa dissolved in sterile saline (0.9% w/v) by the intraperitoneal route, while control animals received sterile saline (0.9% w/v). All animals were necropsied after sacrifice, and the following tissues were fixed in 10% buffered formalin: lung, heart, thymus, trachea, thyroid, liver, spleen, pancreas, kidney, adrenal, stomach, duodenum, jejunum, ileum, cecum, colon, rectum, lymph nodes, bladder, and reproductive organs. Tissues were processed routinely, sectioned at 5 μm, and stained with hematoxylin and eosin.

REFERENCES

(1) J. R. Dimmock, C. B. Nyathi, and P. J. Smith, *J. Pharm. Sci.*, **67**, 1543 (1978).

(2) J. R. Dimmock, G. B. Baker, and R. G. Sutherland, *Can. J. Pharm. Sci.*, **10**, 53 (1975).

(3) J. R. Dimmock and W. G. Taylor, *J. Pharm. Sci.*, **64**, 241 (1975).

(4) F. A. Carey and R. J. Sundberg, "Advanced Organic Chemistry, Part B: Reactions and Synthesis," Plenum, New York, N.Y., 1977, pp. 44, 46.

(5) F. F. Blicke, in "Organic Reactions," Vol. 1, R. Adams, Ed., Wiley, New York, N.Y., 1942, p. 303.

(6) F. W. Menger and J. H. Smith, *J. Am. Chem. Soc.*, **91**, 4211 (1969).

(7) C. E. Lough, D. J. Currie, and H. L. Holmes, *Can. J. Chem.*, **46**, 771 (1968).

(8) P. N. Gordon, J. D. Johnston, and A. R. English in "Antimicrobial Agents and Chemotherapy," G. L. Hobby, Ed., American Society for Microbiology, Ann Arbor, Mich., 1965, p. 165.

(9) H. Schönenberger, T. Bastug, L. Bindl, A. Adam, D. Adam, A. Petter, and W. Zwez, *Pharm. Acta. Helv.*, **44**, 691 (1969).

(10) J. R. Dimmock, K. Shyam, N. W. Hamon, B. M. Logan, S. K. Raghavan, D. J. Harwood, and P. J. Smith, *J. Pharm. Sci.*, **72**, 887 (1983).

(11) M. Eden, B. Haines, and H. Kahler, *J. Natl. Cancer Inst.*, **16**, 541 (1955).

(12) H. Kahler and W. v B. Robertson, *J. Natl. Cancer Inst.*, **3**, 495 (1943).

(13) K. A. Meyer, E. M. Kammerling, L. Amtman, M. Koller, and S. J. Hoffman, *Cancer Res.*, **8**, 513 (1948).

(14) A. Albert and E. J. Serjeant, "Ionisation Constants of Acids and Bases," Methuen, London, 1962, pp. 140–141.

(15) A. Bongini, G. Cardillo, M. Orena, and S. Sandri, *Synthesis*, **1979**, 618.

(16) F. A. Carey and R. J. Sundberg, "Advanced Organic Chemistry, Part A: Structure and Mechanisms," Plenum, New York, N.Y., 1977, p. 145.

(17) C. E. Maxwell, *Org. Syn.*, **23**, 30 (1943).

(18) A. H. Land, C. Ziegler, and J. M. Sprague, *J. Am. Chem. Soc.*, **69**, 125 (1947).

(19) A. L. Williams and A. R. Day, *J. Am. Chem. Soc.*, **74**, 3875 (1952).

(20) O. R. Hansen and R. Hammer, *Acta. Chim. Scand.*, **7**, 1331 (1953).

(21) A. Goldin, S. A. Schepartz, J. M. Vendetti, and V. T. DeVita, Jr., "Methods in Cancer Research," Vol. XVI Part A, Academic, New York, N.Y., 1979, p. 165.

(22) J. H. Burkhalter, W. D. Dixon, M. L. Black, R. D. Westland, L. M. Werbel, H. A. DeWald, J. D. Rice, G. Rodney, and D. H. Kaump, *J. Med. Chem.*, **10**, 567 (1967).

(23) H. A. Albrecht, J. T. Plati, and W. Wenner, U.S. Pat. 3,058,987, Oct. 6, 1962; Chem. Abstr., **58**, 5644c (1963).

(24) R. I. Geran, N. H. Greenberg, M. M. MacDonald, A. M. Schumacher, and B. J. Abbott, *Cancer Chemother. Rep.* (Part 3), **3** (Sept. 1972).

ACKNOWLEDGMENTS

The authors thank the Medical Research Council of Canada for the award of an operating grant (MA-5538) to J. R. Dimmock and the University of Saskatchewan for the award of a Graduate Scholarship to K. Shyam. Appreciation is recorded to the National Cancer Institute, Bethesda, Md., who undertook the antineoplastic evaluation of most of the compounds reported in this investigation.

Tack Behavior of Coating Solutions II

S. K. CHOPRA and R. TAWASHI ˣ

Received November 17, 1982, *from the Faculty of Pharmacy, University of Montreal, Case Postale 6128, Succursale "A", Montreal, Quebec, H3C 3J7 Canada.* Accepted for publication March 9, 1983.

Abstract □ The tackiness of coating solutions containing high concentrations of polymers was determined using a parallel plate technique. Kinematics of the film-splitting process was also investigated using a high-speed movie camera. The results showed that the impulse required to split a liquid film of highly concentrated polymer solution (semisolid), in contrast to a dilute solution is related not to viscosity, but to the internal structures of the system. Evidence has been found that the materials that are considered to be tacky in practice, display "delayed elastic effects" and require far larger impulses than nontacky materials.

Keyphrases □ Film-coating solutions—tablets, tack behavior, viscosity, concentrated polymer solutions □ Viscosity—film-coating solvents for tablets, tack behavior, concentrated polymer solutions □ Polymers—concentrated solutions, viscosity, tack behavior, film-coating of tablets

The technique of film-coating solid dosage forms has grown at an accelerating rate, employing a wide variety of materials and coating systems (1–3). One of the factors affecting the tablet-coating process is the tackiness of the coating formulations. The concentration of the film formers used in these coating formulations depends on the molecular weight, grade, and chemical structure of the polymers (4). Generally, the concentration of a polymer used in a film-coating formulation ranges from 2 to 10% (5). During the drying phase of the coating process, evaporation of the solvent occurs. Consequently, the concentration of the polymer increases, giving rise to increasing tackiness until the deposited film is essentially

© 1984, American Pharmaceutical Association

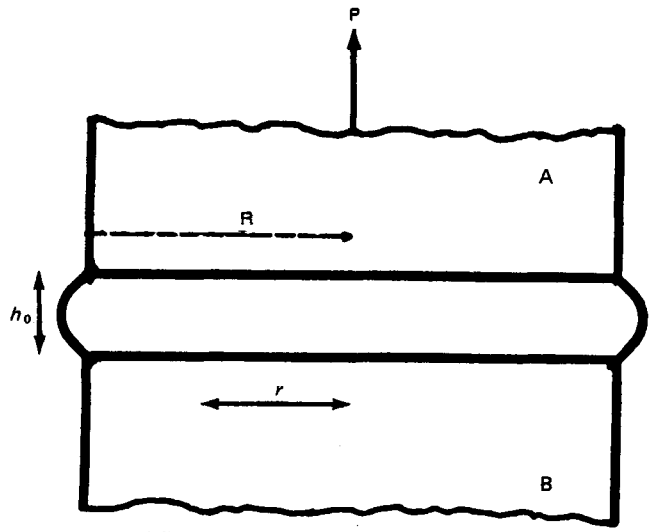

Figure 1—*Liquid flow between parallel plates.*

free of solvent (6). The tackiness of various coating solutions containing relatively low concentrations of polymers has been measured using a parallel-plate technique (7). The present study quantifies the tackiness of coating solutions containing high concentrations of polymers, *i.e.*, high-viscosity solutions.

BACKGROUND

In a previous communication (7), it was suggested that the relationship between tackiness and viscosity of coating solutions is nonlinear, and the following modified Stefan equation was proposed:

$$ft = \frac{3}{4} r^2 k' \eta^{0.67} \left[\frac{1}{h_1^2} - \frac{1}{h_2^2}\right] \qquad \text{(Eq. 1)}$$

where ft (tack) is the impulse per unit area required to separate two planes, initially in contact, through an intervening liquid; η is the viscosity (in poises) of the liquid; r is the radius (in centimeters) of the plates; h_1 and h_2 are the initial and final thickness (in centimeters) of the liquid film; and k' is the instrumental factor.

The above relationship was found to be satisfactory, provided that the rate of separation of plates joined with a liquid of given viscosity was below a certain limit. The upper limit of the speed of separation beyond which the experimental tack values obtained are lower than those predicted by Eq. 1 decreases with increase in the viscosity of a solution. An earlier study (8) on the tackiness of inks suggested that a rapid film separation does not occur by liquid flow, but is the result of a viscoelastic response of the liquid, which may react as a solid towards rapidly applied stress. This theory was later supported by another study performed on the kinematics of liquid film separation (9). Other studies (10, 11) acknowledged the existence of limits beyond which obedience to:

$$F = \frac{3\pi\eta r^4}{4t} \left[\frac{1}{h_1^2} - \frac{1}{h_2^2}\right] \qquad \text{(Eq. 2)}$$

by Stefan may not be expected, but the authors rejected the basic tenets of the viscoelastic theory in their explanation of film splitting at high rates of separation. These authors suggested that at high rates of separation, the flow conditions consistant with the above equation are upset by the onset of cavitation, which sets upper limits to the force of separation. On this basis the limiting force should be independent of the liquid and the initial distance between the plates. This is contrary to the results obtained experimentally. In the present study, an attempt is made to clarify the aforementioned discrepancies.

Consider two flat circular plates of radius R arranged parallel to each other

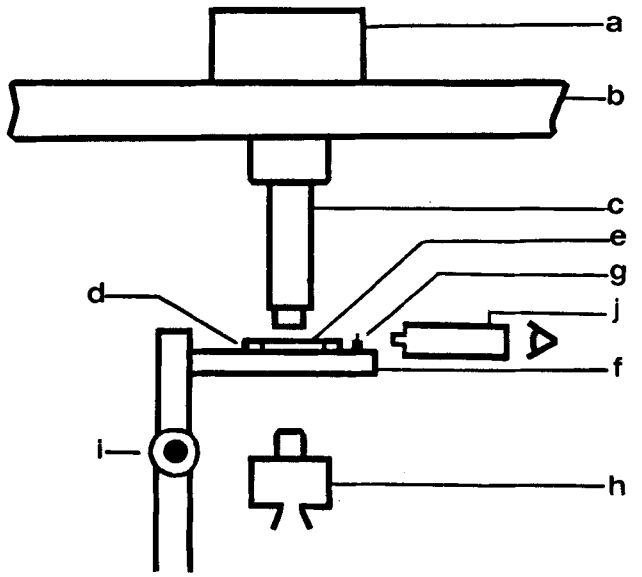

Figure 2—*Schematic diagram of tack measuring assembly in conjunction with a high-speed movie camera. Key: (a) load cell 500- or 5000-g capacity; (b) crosshead bar; (c) stainless steel probe r = 0.5642 cm; (d) stainless steel ring; (e) circular space; (f) glass plate; (g) pin; (h) high-speed movie camera; (i) knob for moving stage; (j) telemicroscope.*

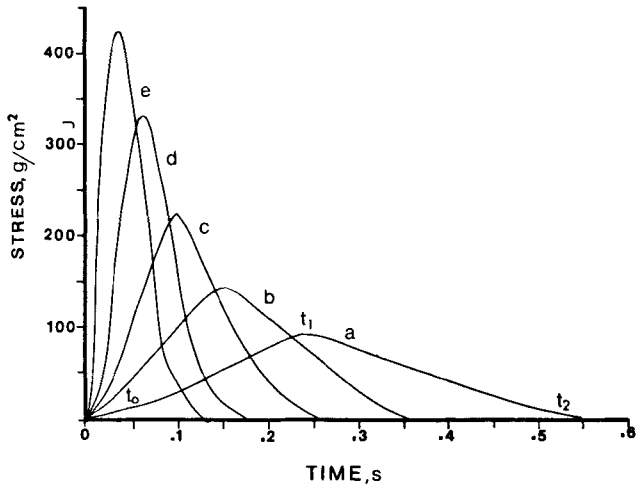

Figure 3—*Stress–time oscillograms at various rates of separation for 30% (w/w) aqueous solution of povidone. Key: (a) 8.33 × 10^{-3} cm/s; (b) 1.66 × 10^{-2} cm/s; (c) 3.33 × 10^{-2} cm/s; (d) 8.33 × 10^{-2} cm/s; (e) 1.66 × 10^{-1} cm/s.*

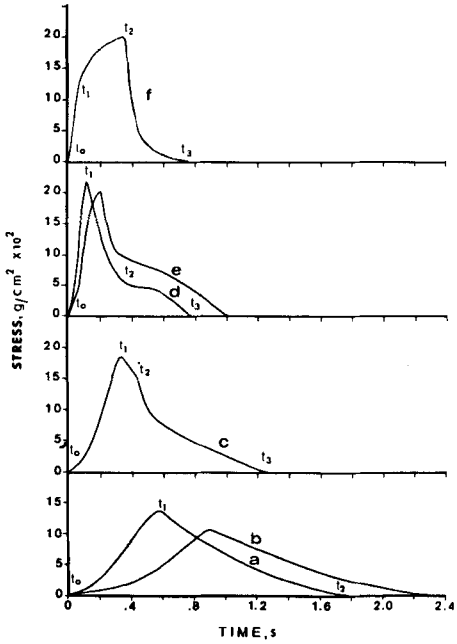

Figure 4—*Stress–time oscillograms at various rates of separation for 60% (w/w) aqueous solution of povidone. Key: (a) 3.33 × 10^{-3} cm/s; (b) 8.33 × 10^{-3} cm/s; (c) 1.66 × 10^{-2} cm/s; (d) 3.33 × 10^{-2} cm/s; (e) 8.33 × 10^{-2} cm/s; (f) 1.66 × 10^{-1} cm/s.*

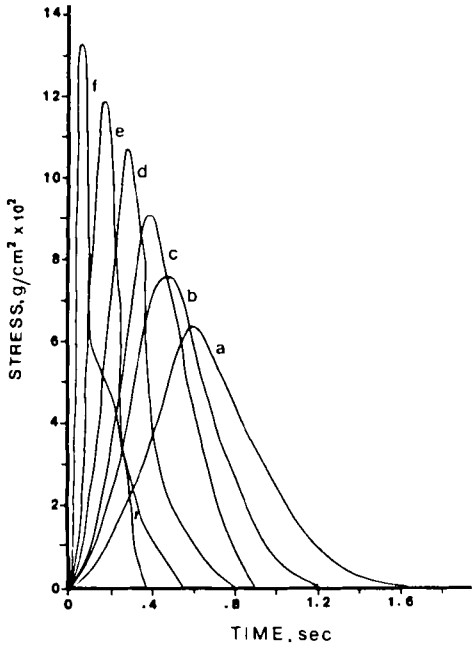

Figure 5—*Stress-time oscillograms at various rates of separation for lecithin. Key: (a) 3.33×10^{-3} cm/s; (b) 8.33×10^{-3} cm/s; (c) 1.66×10^{-2} cm/s; (d) 3.33×10^{-2} cm/s; (e) 8.33×10^{-2} cm/s; (f) 1.66×10^{-1} cm/s.*

and initially in contact through an interlayer of liquid of thickness h_0 (Fig. 1). When the plates are separated, the liquid from the periphery moves toward the center of the plates. This centripetal flow of the liquid is directly caused by the pressure difference between the peripheral and the central portion of the liquid layer (12).

When the distance h_0 between the plates increases by dh_0 in dt seconds, the volume of an imaginary cylinder of a radius r between the plates, increases by $\pi r^2 dh_0$. This volume increase is equal to the volume of liquid that must flow from the periphery into the above cylindrical space within the same time interval. The viscous force acting on the above volume of liquid of viscosity η is given by $\eta \cdot d^2u/dh^2 \cdot 2\pi \cdot r dr \cdot dh$. Here u is the linear viscosity of flow at the point (r,h). Therefore, the force F needed to separate the plates must be equal to the above viscous force. If the volume of liquid flowing at time dt into the cylindrical space $\pi r^2 dh_0$ is less than the latter, then the force F needed to separate the plates will be a fraction of the theoretical value.

With the increase in the concentration of a polymer in solution due to evaporation of the solvent during the coating process, a transition from low-viscosity solution to high-viscosity solution, followed by highly viscous solutions (semisolids) occurs, until a solid state is reached. In other words, the fluidity of the solution decreases with the increase in the concentration of the polymer. Therefore, it may be difficult for highly concentrated solutions of polymers to flow into the cylindrical space between the parallel plates according to the conditions described earlier. Furthermore, it is also likely that no flow occurs at all in the case of semisolids. Therefore, for highly concentrated solutions, the film separation process may be different from the one described above for the tack equation. Based on these considerations, experiments were designed to study simultaneously the kinematics and dynamics of the film separation process.

EXPERIMENTAL

Materials—Polymers used in this study were hydroxypropyl methylcellulose (5 cps)[1], hydroxypropyl cellulose[2], and povidone[3]. Solutions of polymers were prepared in distilled water. Lecithin[4], a Newtonian liquid, and white petrolatum[5], a semisolid gel, were also used.

Preparation of Solutions—The solutions of hydroxypropyl methylcellulose (5 cps) and hydroxypropyl cellulose were prepared by first dispersing the polymers in distilled water at 70°C and 50°C, respectively, and then cooling the dispersions with ice-cold water to 25°C to obtain clear solutions. The solutions of povidone were prepared by simply dissolving the polymer in water at 70°C. All solutions were allowed to stand at 25°C until free of air bubbles.

[1] Methocel "E" Premium (USP); The Dow Chemical Co., Midland, Mich.
[2] Klucel L F; Hercules, Wilmington, Del.
[3] Polyvinylpyrrolidone; Plasdone K 29-32; GAF Corp., Linden, N.J.
[4] Lecithin Technical; Anachemia Chemicals Ltd., Montréal, Canada.
[5] Ointment base No. 6; Penreco, Butler, Pa.

Table I—Tack Values of 30 and 60% (w/w) Aqueous Solutions of Povidone and Lecithin at Various Rates of Separation [a]

Rate of Separation, cm/s	ft, g/cm/s: Aqueous Solution of Povidone, 30% (w/w) (η = 0.93 poise)	Aqueous Solution of Povidone, 60% (w/w) (Pseudoplastic)	Lecithin (η = 62 poises)
3.33×10^{-3}	-	9.02×10^5	3.88×10^5
8.33×10^{-3}	2.30×10^4	9.45×10^5	3.87×10^5
1.66×10^{-2}	2.40×10^4	8.40×10^5	3.86×10^5
3.33×10^{-2}	2.45×10^4	7.65×10^5	3.75×10^5
8.33×10^{-2}	2.35×10^4	5.32×10^5	2.65×10^5
1.66×10^{-1}	2.42×10^4	6.28×10^5	1.87×10^5

[a] h_1 = 0.00108 cm.

Measurement of Viscosity—All measurements were made on a rotational cup-and-bob viscometer[6] in conjunction with a strip-chart recorder[7]. The temperature of solutions was held constant at 25°C. The cup-and-bob geometry was varied according to the viscosity of the sample.

Tack Measurement Assembly—Tack measurements were made using a tensile testing machine[8]. A schematic diagram of the tack measurement assembly has been described in our previous report (7).

Assembly for Kinematic Study—Figure 2 illustrates the setup of a 16-mm high-speed motion picture camera[9] in conjunction with the tack measuring assembly. The movie camera is capable of taking 4000 frames/s. A mechanical switching device simultaneously starts the movie camera and the upward movement of the crosshead bar (b) of the tensile tester.

Measurement of Film Thickness and Tack—The method for measuring the thickness of the liquid film has been described in our previous report (7). After adjustment of the thickness of the test liquid, the crosshead bar was allowed to move upward at a specified speed. The film separation events were recorded on a storage-type oscilloscope[10], where the separation force (F) was displayed as a function of time. All measurements were made at 25°C, and a minimum of six measurements were taken for every test solution at each separation rate. The experimental tack values were within a margin of error of ±6%.

RESULTS AND DISCUSSION

Tack Behavior of Solutions Containing High Concentrations of Polymers (High-Viscosity Liquids)—Rheograms of 30 and 60% (w/w) aqueous solutions of povidone revealed the former to be Newtonian, whereas the latter is pseudoplastic in nature. The stress-time oscillograms obtained at various rates of separation of these solutions are shown in Figs. 3 and 4, respectively, and show that as the time of separation decreases, the peak force of separation increases. This response by the above liquids is similar to the one reported for the solutions containing relatively low concentration of various polymers (7). The oscillograms for the 60% solution of povidone at rates of separation $\leq 8.33 \times 10^{-3}$ cm/s, are similar in shape to those for the 30% povidone solution at all rates of separation studied in this investigation. However, the oscillograms obtained for the 60% polymer solution vary in shape when the rates of separation are $>8.33 \times 10^{-3}$ cm/s. This change in shape of the oscillograms at higher rates of separation was also observed in the case of lecithin, a high-viscosity Newtonian liquid. In this case, the upper limit of the rate of separation beyond which the oscillograms begin to vary in shape is 1.66×10^{-2} cm/s (Fig. 5).

The tack values of the above solutions are given in Table I. The tack was calculated by dividing the area under the curves of the stress-time oscillograms by the surface area of the probe. Table I shows that for a 30% (w/w) aqueous solution of povidone, tack is independent of the rate of separation. This is in agreement with Eq. 1. However, the tackiness of the 60% polymer solution decreased with an increase in separation rates at $>8.33 \times 10^{-3}$ cm/s. This decrease in tack values cannot be attributed solely to the pseudoplastic nature of the above solution, since the tackiness of lecithin, a Newtonian liquid, also decreased at rates of separation $>1.66 \times 10^{-2}$ cm/s (Table I).

The above results suggest that there is an upper limit to the rate of separation beyond which the shapes of the oscillograms begin to vary, regardless

[6] Rotovisco; Brinkmann Instruments, Inc., Westbury, N.Y.
[7] Honeywell Electronik 194 Recorder; Honeywell Ltd., Montréal, Québec, Canada.
[8] Instron Tensile Tester Model 1122; Instron Canada, Burlington, Ontario, Canada.
[9] Hycam, Model #K20S4E; Kifer Industrial Park, Santa Clara, Calif.
[10] Model 5113 with 5B12N time base and two 5A26 dual differential amplifiers; Tektronix Inc., Beaverton, Ore.

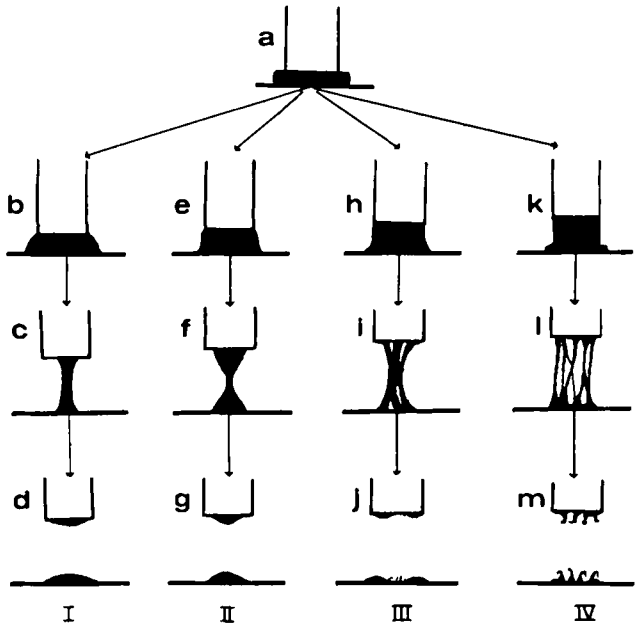

Figure 6—*Types of liquid flow patterns during film separation.*

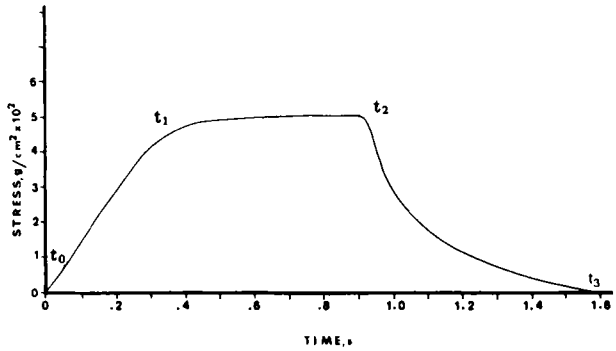

Figure 7—*Stress-time oscillogram at rate of separation of 8.33 × 10^{-2} cm for a 70% (w/w) aqueous solution of povidone;* h_1 = *0.00216 cm.*

of the flow behavior of the liquid. However, there is one noticeable difference between the shape of the oscillogram of lecithin and that of the 60% povidone solution obtained at a rate of separation of 1.66 × 10^{-1} cm/s. The slope of the ascending portion of the oscillogram (Fig. 5f) of lecithin is constant, whereas that for povidone solution (Fig. 4f) decreases gradually. The reason for this difference can be explained by simultaneously studying the kinematics and dynamics of the film-splitting process.

Kinematics of Film Splitting—The high-speed motion picture of the film separation process revealed four main patterns of liquid film splitting. The schematic diagrams of the film-splitting patterns as observed by projecting the high-speed movie are illustrated in Fig. 6.

Type I—Figure 6a–d represents the various stages of type I film-splitting pattern. The shapes of the oscillograms obtained for this pattern of film splitting are similar to those presented in Fig. 3. The first portion, *i.e.*, from t_0 to t_1 of the oscillogram (Fig. 3a), displays an increase in force which reaches a maximum. This is due to upward movement of the probe, which produces an increasing tension in the liquid until it begins to flow toward the center of the probe in order to relieve its strain (see Fig. 6b). The force required to maintain the centripetal flow is represented by the portion t_1 to t_2 of the oscillogram (Fig. 3a). This portion shows a gradual decrease in force from peak to zero. At t_2, the diameter of the base of the liquid column as seen from the bottom of the glass plate is at its minimum. Any further increase in the gap between the probe and the plate does not lead to further centripetal movement of the liquid, but rather to a necking-down of the column which eventually splits (see Fig. 6d). In cases such as above, the experimental *ft* is equal to that calculated using Eq. 1. Therefore, this pattern of liquid film splitting is in accordance with the theoretical consideration.

Type II—The various stages followed by the type II pattern of liquid film splitting are shown sequentially in Fig. 6e–g. The corresponding oscillogram is presented in Fig. 4c. The increase in force exhibited by the oscillogram from t_0 to t_1 is due to the increase in strain in the liquid before it begins to flow. The initial velocity of centripetal flow of the liquid is slower than the corresponding vertical movement of the probe. During this period a rapid decrease in force occurs. This is represented by the oscillogram (Fig. 4c) from t_1 to t_2. From t_2 to t_3, the velocity of the centripetal flow of the liquid increases, but does not keep pace with the rate of increase in the gap between the probe and the plate. During this time interval, the force gradually decreases to zero. At t_3, the diameter of the base of the liquid column is larger than that shown in Fig. 6f. The final separation takes place by necking-down of the hourglass column (Fig. 6g). The above observations clearly show that the centripetal flow of the liquid is not achieved within the time of creation of the cylindrical space between the probe and the plate. This means that the conditions described for the tack equation are not met. Therefore, in this type of film separation pattern, the value of experimental *ft* is less than that predicted by Eq. 1.

Type III—The oscillogram (Fig. 4d) corresponds to the film separation sequence shown in Figs. 6h–j. As soon as the tension in the liquid reaches its maximum, *i.e.*, at t_1 in Fig. 4d, the liquid begins to move centripetally but in irregular fashion. This type of movement leads to "channeling" of the liquid and produces a rapid decrease in force as shown by the portion t_1 to t_2 of the oscillogram. The liquid in channel form continues to move toward the a[x]is of the plate. This results in a gradually decreasing force as depicted by t[h]e portion t_2 to t_3 of the trace. The column arising out of the channeled liqu[id] is not cylindrical (Fig. 6i). The channel formation of the liquid (Fig. 6j) c[an] be seen even after film splitting. As in type II, the value of the experimen[tal] *ft* is lower than the predicted value.

Type IV—The oscillogram (Fig. 4f) corresponds to the film-splitting sequence shown in Figs. 6k–m. When the strain in the liquid is increased, a rapid linear increase in force from t_0 to t_1 is recorded. From t_1 to t_2, an increase in force continues but with decreasing slope. Since no centripetal flow occurs from t_0 to t_2, the decreasing slope of the increasing stress from t_1 to t_2 could be attributed to the orientation of polymer molecules toward the direction of flow, thereby reducing the internal resistance of the material until the flow begins (12). With the further increase in the gap between the probe and the plate, the liquid moves toward several points instead of moving toward the center of the plate. This eventually leads to the formation of several filaments (Fig. 6m). During this time, the separation force decreases, first rapidly and then gradually until it reaches zero, at t_3.

The increase in force with decreasing slope as shown by the portion t_1 to t_2 of the oscillogram for povidone (Fig. 4f) was also observed in the case of 30% (w/w) aqueous solution of hydroxypropyl methylcellulose (5 cps) and 30% (w/w) aqueous solution of hydroxypropyl cellulose. However, in the case of lecithin, the ascending portion of the oscillogram (Fig. 5) showed a linear increase in force at all rates of separation.

The results of this simultaneous kinematic and dynamic study of the film separation process suggest that the separation force reaches a maximum before the centripetal flow of the liquid takes place. The rate of increase in force during this time, remains constant if the resistance is purely viscous. A decrease in the rate of increase in force occurs in the case of highly concentrated polymer solutions and is probably due to the rearrangement of the internal structure of the system. The portion of the oscillogram representing maximum to zero separation force is dependent on the centripetal flow of the liquid during film separation. The shape of this region of the oscillogram changes with the change in pattern of the centripetal flow, which in turn is dependent on the viscosity of the liquid and the rate of film separation.

Tack Behavior of Highly Concentrated Polymer Solutions (Semisolids)—The stress-time oscillogram for a 70% (w/w) aqueous solution of povidone obtained at a rate of separation of 8.33 × 10^{-2} cm/s is shown in Fig. 7. The film separation process indicated that no centripetal movement of the liquid occurs and that film splitting proceeds by simple stretching and thinning-down of the filaments. Therefore, the film-separation process is different from that described for low- and high-viscosity solutions.

The stress-time oscillogram obtained is to a certain extent close to the stress-strain curve exhibited by the ductile response of plastics at high rates of separation (13). It can be divided into three regions. The first region represented by the portion t_0 to t_1 of the oscillogram (Fig. 7) is predominently due to the elastic forces of the liquid. In this region, the force first rises proportionally to the elongation and then rises less rapidly until it reaches "yield point" at t_1. In the second region following the "yield point," the specimen offers a pull resistance which is constant over a long period of time: t_1–t_2. Since no centripetal flow takes place during this time, the force is mainly due to the resistance to elongation of the filament beyond the elastic limit. This second region of the curve has been suggested to be due to the "delayed elastic deformation" effects (14). In the third region, t_2–t_3, "necking" and eventually splitting of the filaments occur. In Fig. 7, the *ft*, 9.80 × 10^4 g/cm/s for thinning and final rupture of the filament is only 20% of the total 4.81 × 10^5 g/cm/s required for the separation of the film. The bulk of the *ft*, 3.83 × 10^5 g/cm/s is devoted to the process of film elongation.

Tack experiments performed with petrolatum, a highly viscous semisolid did not show the region of "delayed elastic effects." This resulted in a rather short duration for filament elongation; hence the ft was relatively small.

The above observations suggest that the response of the concentrated polymer solutions (semisolids) to applied pull stress is a combination of viscous and elastic forces. The "delayed elastic effects" observed are the result of configurational elasticity, which is a process associated with orientation, alignment, and elongation by the uncurling of large chain molecules. Therefore, the ft required for the elongation of the filament will not only depend on the viscosity of the liquid, but also on the internal structure of the system.

Earlier investigators (10–12) suggested that tackiness is related to the geometry of the system and the rheological characteristics of the liquid. Therefore, according to this definition, lecithin, petrolatum, and even water added with high concentration of finely divided solids will be considered tacky, since these liquids or dispersions do offer resistance to flow. In actual practice, the above materials, unlike povidone solution, are not known to be tacky even though impulse for liquid film separation is required in both cases. Based on these observations, it can be concluded that a tacky material is one that displays "delayed elastic effects," and because of these effects it requires a long period of time for filament elongation. This provides a rather large impulse for a given force of separation.

Tack Effects in Tablet Coating—Coating solutions, when applied to the tablets during the coating process, are dilute solutions of polymers of low-viscosity grade. Separation of tablets stuck together by a freshly applied coating solution will occur by viscous flow. Therefore, the ft required will be equal for solutions of similar viscosity. As the solvent evaporates during the drying phase of the coating process, the solution will reach a semisolid state. At this point, resistance to filament elongation will depend on the molecular structure of the polymer.

Tablet coating solutions usually contain opacifier, plasticizers, and colorants to modify the physical characteristics and improve the film-forming properties of the polymers. The effect of these additives on the tack behavior of coating solutions is under investigation.

REFERENCES

(1) S. C. Porter, *Pharm. Tech.*, **4**(3), 67 (1980).

(2) H. A. Lieberman and L. Lachman, "Pharmaceutical Dosage Forms: Tablets," Vol. 3, Dekkar, New York, N.Y., 1982, pp. 73–117.

(3) J. Cooper and J. E. Rees, *J. Pharm. Sci.*, **61**, 1511 (1972).

(4) J. R. Cloche, *Labo-Pharma*, **157**, 41 (1967).

(5) "Cellulose Ethers in Aqueous System for Tablet Coating," Dow Chemical Co., Midland, Mich., 1977, p. 4.

(6) N. O. Lindberg and E. Jonsson, *Acta Pharm. Suecica*, **9**, 589 (1972).

(7) S. K. Chopra and R. Tawashi, *J. Pharm. Sci.*, **71**, 907 (1982).

(8) A. Voet and C. F. Geffken, *Ind. Eng. Chem.*, **43**, 1614 (1951).

(9) R. A. Erb and R. S. Hanson, *Trans. Soc. Rheal.*, **1**, 3 (1957).

(10) W. H. Bank and C. C. Mill, *J. Colloid Sci.*, **8**, 137 (1953).

(11) H. Strasburger, *J. Colloid Sci.*, **13**, 218 (1958).

(12) J. J. Bikerman, *J. Colloid Sci.*, **2**, 163 (1947).

(13) S. S. Voyutskii, "Autohesion and Adhesion of High Polymers," Interscience, New York, N.Y., 1963, pp. 235–248.

(14) A. D. Jenkins, "Polymer Science," American Elsevier, New York, N.Y., 1972, pp. 775–800.

ACKNOWLEDGMENTS

This work was supported by the Medical Research Council of Canada.

Phase Diagram and Aqueous Solubility of the Lidocaine–Prilocaine Binary System

A. BRODIN *x, A. NYQVIST-MAYER *, T. WADSTEN ‡, B. FORSLUND ‡, and F. BROBERG *

Received December 28, 1982, from the **Astra Läkemedel AB, Research and Development Laboratories, Pharmaceutics, S-151 85 Södertalje* and the ‡*Arrhenius Laboratory, University of Stockholm, Fack, S-106 91 Stockholm, Sweden.* Accepted for publication February 17, 1983.

Abstract □ The phase behavior of the lidocaine–prilocaine binary system has been studied by X-ray diffraction, differential thermal analysis, hot-stage microscopy, and IR spectrometry. No intermediate compounds or solid solubilities have been detected. The eutectic composition is close to 1:1, and the eutectic temperature is 18 ± 1°C. Aqueous solubility studies show that the lidocaine heat of solubility from the eutectic mixture is different from that of the pure drug, whereas it is the same for prilocaine. Investigations of various lidocaine–prilocaine ratios indicate that the two local anesthetics decrease the solubility of each other. The total solubility, however, is affected only to a minor extent.

Keyphrases □ Lidocaine—binary system with prilocaine, phase diagram and aqueous solubility □ Prilocaine—binary system with lidocaine, phase diagram and aqueous solubility □ Solubility—phase diagram of the lidocaine–prilocaine binary system in water □ Phase diagram—lidocaine–prilocaine binary system, aqueous solubility

Solid–solid interactions are of great interest in the development of pharmaceutical preparations. Dissolution rates, and thus bioavailability, of poorly soluble drugs can be enhanced by their fusion with water-soluble carriers such as urea or polyethylene glycol, which form solid solutions with drugs (1, 2). Eutectic mixtures may even be used to prevent freeze–thaw coagulation of suspensions (3). In powder technology, on the other hand, a eutectic interaction between substances may be considered as an incompatibility, making it necessary to use some auxiliary substance to inhibit adhesion of the powders (4). The physical state in which the drugs are present in such fused mixtures is debatable. The dispersion of phenylbutazone in urea represents a "plug compound" (5). Such solid dispersions are known to age (6, 7).

Studies on eutectic combinations of two drugs are rare (8). Recently, lidocaine and prilocaine have been reported to form a eutectic mixture (9). Since this mixture is liquid at room temperature, it has been possible to formulate an effective local anesthetic preparation for topical application. The purpose of this investigation is to characterize the lidocaine–prilocaine system from a physical point of view and to study its aqueous solubility.

EXPERIMENTAL

Materials—Lidocaine[1] and prilocaine[1] were used as obtained. To prepare the eutectic mixture (EMLA), 49.6% lidocaine and 50.4% prilocaine by weight were mixed and heated gently until liquefaction occurred.

X-Ray Diffraction—An X-ray powder diffraction camera[2] with a 50-mm diameter and strictly monochromatized Cu$K\alpha_1$ radiation was used. A small amount of the powder was spread out on the glue side of ordinary tape. The tape was attached to a thin metal plate, 30 mm in diameter, with an 8-mm

[1] Astra Pharmaceutical Production AB, Sweden.

[2] Guinier-Hägg.

0022-3549/84/0400-0481$01.00/0

© 1984, American Pharmaceutical Association

Tack experiments performed with petrolatum, a highly viscous semisolid did not show the region of "delayed elastic effects." This resulted in a rather short duration for filament elongation; hence the ft was relatively small.

The above observations suggest that the response of the concentrated polymer solutions (semisolids) to applied pull stress is a combination of viscous and elastic forces. The "delayed elastic effects" observed are the result of configurational elasticity, which is a process associated with orientation, alignment, and elongation by the uncurling of large chain molecules. Therefore, the ft required for the elongation of the filament will not only depend on the viscosity of the liquid, but also on the internal structure of the system.

Earlier investigators (10–12) suggested that tackiness is related to the geometry of the system and the rheological characteristics of the liquid. Therefore, according to this definition, lecithin, petrolatum, and even water added with high concentration of finely divided solids will be considered tacky, since these liquids or dispersions do offer resistance to flow. In actual practice, the above materials, unlike povidone solution, are not known to be tacky even though impulse for liquid film separation is required in both cases. Based on these observations, it can be concluded that a tacky material is one that displays "delayed elastic effects," and because of these effects it requires a long period of time for filament elongation. This provides a rather large impulse for a given force of separation.

Tack Effects in Tablet Coating—Coating solutions, when applied to the tablets during the coating process, are dilute solutions of polymers of low-viscosity grade. Separation of tablets stuck together by a freshly applied coating solution will occur by viscous flow. Therefore, the ft required will be equal for solutions of similar viscosity. As the solvent evaporates during the drying phase of the coating process, the solution will reach a semisolid state. At this point, resistance to filament elongation will depend on the molecular structure of the polymer.

Tablet coating solutions usually contain opacifier, plasticizers, and colorants to modify the physical characteristics and improve the film-forming properties of the polymers. The effect of these additives on the tack behavior of coating solutions is under investigation.

REFERENCES

(1) S. C. Porter, *Pharm. Tech.*, **4**(3), 67 (1980).

(2) H. A. Lieberman and L. Lachman, "Pharmaceutical Dosage Forms: Tablets," Vol. 3, Dekkar, New York, N.Y., 1982, pp. 73–117.

(3) J. Cooper and J. E. Rees, *J. Pharm. Sci.*, **61**, 1511 (1972).

(4) J. R. Cloche, *Labo-Pharma*, **157**, 41 (1967).

(5) "Cellulose Ethers in Aqueous System for Tablet Coating," Dow Chemical Co., Midland, Mich., 1977, p. 4.

(6) N. O. Lindberg and E. Jonsson, *Acta Pharm. Suecica*, **9**, 589 (1972).

(7) S. K. Chopra and R. Tawashi, *J. Pharm. Sci.*, **71**, 907 (1982).

(8) A. Voet and C. F. Geffken, *Ind. Eng. Chem.*, **43**, 1614 (1951).

(9) R. A. Erb and R. S. Hanson, *Trans. Soc. Rheal.*, **1**, 3 (1957).

(10) W. H. Bank and C. C. Mill, *J. Colloid Sci.*, **8**, 137 (1953).

(11) H. Strasburger, *J. Colloid Sci.*, **13**, 218 (1958).

(12) J. J. Bikerman, *J. Colloid Sci.*, **2**, 163 (1947).

(13) S. S. Voyutskii, "Autohesion and Adhesion of High Polymers," Interscience, New York, N.Y., 1963, pp. 235–248.

(14) A. D. Jenkins, "Polymer Science," American Elsevier, New York, N.Y., 1972, pp. 775–800.

ACKNOWLEDGMENTS

This work was supported by the Medical Research Council of Canada.

Phase Diagram and Aqueous Solubility of the Lidocaine–Prilocaine Binary System

A. BRODIN *x, A. NYQVIST-MAYER *, T. WADSTEN ‡, B. FORSLUND ‡, and F. BROBERG *

Received December 28, 1982, from the **Astra Läkemedel AB, Research and Development Laboratories, Pharmaceutics, S-151 85 Södertalje* and the ‡*Arrhenius Laboratory, University of Stockholm, Fack, S-106 91 Stockholm, Sweden.* Accepted for publication February 17, 1983.

Abstract □ The phase behavior of the lidocaine–prilocaine binary system has been studied by X-ray diffraction, differential thermal analysis, hot-stage microscopy, and IR spectrometry. No intermediate compounds or solid solubilities have been detected. The eutectic composition is close to 1:1, and the eutectic temperature is 18 ± 1°C. Aqueous solubility studies show that the lidocaine heat of solubility from the eutectic mixture is different from that of the pure drug, whereas it is the same for prilocaine. Investigations of various lidocaine–prilocaine ratios indicate that the two local anesthetics decrease the solubility of each other. The total solubility, however, is affected only to a minor extent.

Keyphrases □ Lidocaine—binary system with prilocaine, phase diagram and aqueous solubility □ Prilocaine—binary system with lidocaine, phase diagram and aqueous solubility □ Solubility—phase diagram of the lidocaine–prilocaine binary system in water □ Phase diagram—lidocaine–prilocaine binary system, aqueous solubility

Solid–solid interactions are of great interest in the development of pharmaceutical preparations. Dissolution rates, and thus bioavailability, of poorly soluble drugs can be enhanced by their fusion with water-soluble carriers such as urea or polyethylene glycol, which form solid solutions with drugs (1, 2). Eutectic mixtures may even be used to prevent freeze–thaw coagulation of suspensions (3). In powder technology, on the other hand, a eutectic interaction between substances may be considered as an incompatibility, making it necessary to use some auxiliary substance to inhibit adhesion of the powders (4). The physical state in which the drugs are present in such fused mixtures is debatable. The dispersion of phenylbutazone in urea represents a "plug compound" (5). Such solid dispersions are known to age (6, 7).

Studies on eutectic combinations of two drugs are rare (8). Recently, lidocaine and prilocaine have been reported to form a eutectic mixture (9). Since this mixture is liquid at room temperature, it has been possible to formulate an effective local anesthetic preparation for topical application. The purpose of this investigation is to characterize the lidocaine–prilocaine system from a physical point of view and to study its aqueous solubility.

EXPERIMENTAL

Materials—Lidocaine[1] and prilocaine[1] were used as obtained. To prepare the eutectic mixture (EMLA), 49.6% lidocaine and 50.4% prilocaine by weight were mixed and heated gently until liquefaction occurred.

X-Ray Diffraction—An X-ray powder diffraction camera[2] with a 50-mm diameter and strictly monochromatized Cu$K\alpha_1$ radiation was used. A small amount of the powder was spread out on the glue side of ordinary tape. The tape was attached to a thin metal plate, 30 mm in diameter, with an 8-mm

[1] Astra Pharmaceutical Production AB, Sweden.

[2] Guinier-Hägg.

0022-3549/84/0400-0481$01.00/0

© 1984, American Pharmaceutical Association

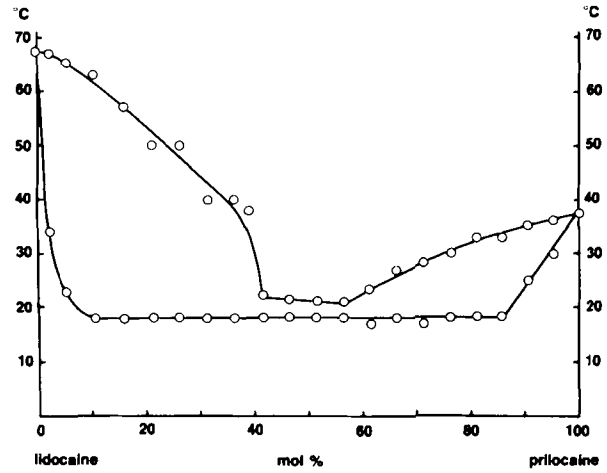

Figure 1—*Phase diagram of the nonequilibrated lidocaine-prilocaine system determined by hot-stage microscopy.*

central hole. This hole was covered with the tape and sample, and the X-ray was passed through; the exposure time was ~45 min. To obtain very accurate diffraction data, an internal standard of potassium chloride was added to the specimens.

One exposure was performed at 4–5°C. The composition was 1:1, and the mixture was kept at 4–5°C for 10 d after having reacted at room temperature to form a viscous homogeneous mass. The material was spread out on extra-thin foil[3] covered with a thin layer of high-vacuum grease to avoid the influence of water. The sample holder was very rapidly transferred from the storing room to the camera. In this case, the internal standard was elemental silicon. No X-ray diffraction lines were registered from the grease-covered foil.

Differential Thermal Analysis (DTA)—A low-temperature instrument that covers the interval of 100–600 K (10) was used. Six different samples can be run simultaneously.

A rather unusual strategy was used to reach equilibrium, since a long time period was involved (several days). Different amounts of the components were weighed and mixed at room temperature in individual glass cups. After a few days, 20-mg portions were transferred to the DTA sample holders. These were

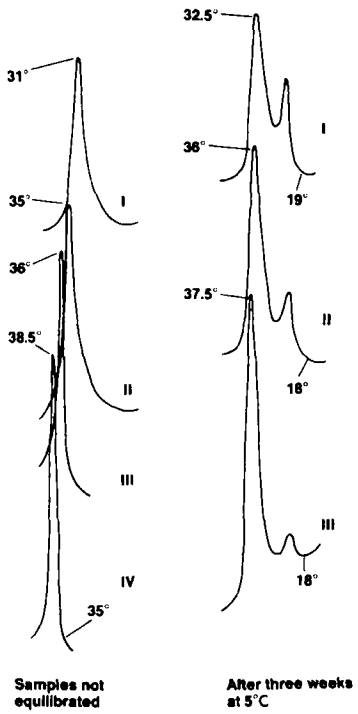

Figure 2—*Some typical examples of the DTA registrations of ~20 mg lidocaine plus prilocaine on heating showing the endothermic peaks. Prilocaine concentration (mol%): (I) 85; (II) 90; (III), 95; (IV) 100.*

[3] Mylar.

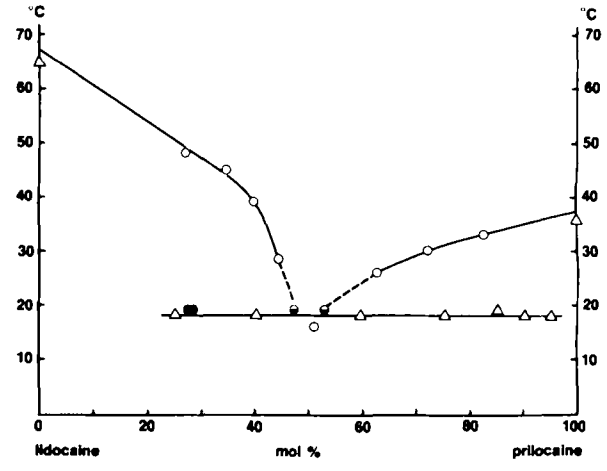

Figure 3—*Phase diagram of the equilibrated lidocaine-prilocaine system determined by hot-stage microscopy (○), long-time storage in a thermostat at 19°C. Key: (●) solid but no observed liquid phase; (◒) liquid phase clearly observed over solid; (△) DTA.*

stored at 4–5°C for different periods of time. The temperature was chosen to avoid ice formation. Just before a specific registration was to take place, the whole DTA measuring head was also cooled to 4–5°C. The filled sample holders were then rapidly moved from refrigeration to the instrument, which was evacuated and further cooled to ~−20°C before the heating program (3°C/min) was started in dry air at atmospheric pressure.

The accuracy of the temperature reading is estimated to be ±1°C according to the calibrating procedure performed with standard samples[4]. The time to obtain equilibrium was found to be longer in the lidocaine-rich part of the system than in the prilocaine-rich part.

Hot-Stage Microscopy—*Nonequilibrium Conditions*—Weighed amounts of lidocaine and prilocaine in various ratios were mixed thoroughly and heated until melting occurred. The melts were cast on watch glasses and allowed to congeal at 5°C. The solidified mixtures were crushed and then homogenized with a mortar and pestle.

A binocular microscope with a hot stage and a control unit was used[5]. Phase transitions of the specimens were observed between crossed polars, both visually and by using a photoelectric sensor to record the changes in light transmission.

A proper amount of specimen was placed on a cooled slide. The specimen was observed from 5°C, with a heating rate of 1°C/min. The temperature at which the crystals just started to melt, or when using the photoelectric sensor the recorded curve started to change, was taken as the eutectic temperature. The temperature at which the whole field became dark was considered the melting point.

Equilibrium Conditions—To determine the liquidus curves of the lidocaine-prilocaine system and to supplement the results gained by the dynamic thermoanalytical methods, a number of equilibration experiments were undertaken. For these experiments, similar to those performed on ternary transition-metal oxide systems (11, 12), a simple microscope hot-stage device comprised of a copper reaction cell (Φ = 5 cm, height = 2 cm) and two 1-mm transparent quartz glass plates were used. The sample was held on the bottom plate, which was in direct contact with a copper block supporting the reaction cell, tempered by means of a circulating-water thermostat. Continuous observation of the sample with the help of a stereo microscope (40×) was made through the upper silica plate, and the temperature (5–75°C) of the sample was checked by a chromel-alumel thermocouple fixed in the copper block close to the sample. The melting temperatures of pure lidocaine, prilocaine, and ice (67°C, 37°C, and 0°C, respectively) served as calibration points in the temperature determinations. The gas-tight reaction cell was also provided with a gas inlet and outlet and a simple manipulator.

A typical run on this hot-stage was performed in the following way. A weighed mixture of lidocaine and prilocaine (in total ~5 mg) was kept at an appropriate temperature for enough time (~1 d) to get a homogeneous melt with a remaining solid phase centered in the droplet. The temperature during this primary stage must be low enough to preserve both kinds of crystals observed: thin platelets (lidocaine) and needles (prilocaine). When the coarse-grained original mixture finally was transformed into a more homogeneous crystalline mass of lidocaine or prilocaine, the temperature was raised in steps until very little solid phase was left in the melt droplet. During this second

[4] NBS-ICTA, Standard Reference Material 758.
[5] Mettler FP52 + FP5.

stage, lasting 1–2 d, checks for equilibrium attainment between solid and liquid were made by observing the growth-dissolution response of the crystals to small temperature changes. Finally, the highest temperature for a solid-liquid equilibrium, *i.e.*, the melting point, for the mixture was noted as that temperature at which the smallest solid residue to be observed in the microscope persisted and showed response to temperature changes.

For some mixtures the primary crystals were grown after the melting point determination by slow cooling and separated for subsequent X-ray analysis from the mother liquor by absorbing the liquor on a piece of porous filter paper. This was brought in contact with the melt by means of the manipulator. Albeit he equilibration experiments were performed in a dynamic atmosphere argon, ~10 mL/min) and lasted for long periods, no changes in size and color f the melt droplets were observed, thus indicating that evaporation losses were egligible.

IR Studies—The IR spectra of lidocaine, prilocaine, and EMLA were re-ɔrded using an IR spectrophotometer[6]. The EMLA samples were prepared : −6°C, and the resulting crystals were spread on potassium bromide disks. MLA was studied both in crystalline form at low temperatures and in liquid ɪrm at room temperature. The spectrum of each sample was recorded 3–4 mes in succession while its physical condition was observed.

Solubility Determination—The solubilities in 1 mM NaOH were deter-ıined for lidocaine, prilocaine, and EMLA at 25°C, 32°C, 37°C, and 45°C. ther combinations of lidocaine and prilocaine were studied in distilled water. quilibrated mixtures of the local anesthetics and water were filtered through ass wool and 0.1-μm polycarbonate filters[7]. The concentrations in the filtrate were determined by UV spectrophotometry[8] at 230 nm. The filtrate was analyzed at fixed time intervals until a constant concentration was obtained.

In the case of EMLA and the other combinations of lidocaine and prilocaine, HPLC was used to analyze the two concentrations separately. For the HPLC method, a 20-μL loop injection valve and a column (200 mm × 3.0 i.d.) packed with Lichrosorb RP-8 (10-μm particles) were connected to an 8-μL flow cell in a spectrophotometer[9]. The column was eluted at ambient temperature with a methanol-phosphate buffer (70:30 v/v, pH 8.0, I = 0.05) at a rate of 1 mL/min. The eluant was monitored at 246 mm with a recorder setting of 0.05 AUFS. Before injection, the samples were diluted with eluant to a concentration of 120 to 140 μg/mL of lidocaine and prilocaine. The peak heights were compared with those of standards chromatographed under similar conditions. Doubling the excess of a mixture did not affect the individual solubilities.

RESULTS AND DISCUSSION

Phase Diagram—The phase diagram for the lidocaine–prilocaine system obtained by hot-stage microscopy is shown in Fig. 1. In the extreme regions, <25% on both sides, visual observations were necessary to estimate the initial melting temperature, while the photoelectric sensor could be used in between. The results obtained with the two methods were in agreement. In the regions of the higher concentrations of lidocaine and prilocaine, respectively, the diagram indicates the existence of solid solutions.

To investigate this further, ~0–15% on both sides were analyzed by X-ray diffraction. A solid solubility may be observed as a shift in the line positions according to changes of the unit cell dimensions if the second component is located in the interstitial spaces of the crystal lattice of the first component. Different amounts of the starting materials were observed, and no interstitial solid solubility between the components could be detected. This may not exclude the existence of noncrystalline solid solutions in which the one component replaces molecules from the crystal lattice of the other component. The formation of substitutional solid solutions is favored if the molecular sizes of the two substances are similar.

Another complication in the phase diagram is the shape of the melting point curve in the 40–60% prilocaine range. Instead of coming to a distinctive eutectic point, the curve only approaches, without touching, the line representing the eutectic temperature. This and the relatively poor reproducibility of the curve on the lidocaine side, may be due to interactions between lidocaine and prilocaine and/or to a very slow process to obtain equilibrium between the melted and solid phases. The latter may also explain the discrepancy between the phase diagram and the X-ray diffraction data about the existence of solid solutions.

Comparing the IR spectrum of crystalline EMLA with those of the single components, no significant difference was detected, which indicates that no chemical interaction takes place between lidocaine and prilocaine. When EMLA melts, the absorbance of some bands are changed in the manner expected in the solid to fluid transition. The characteristic X-ray diffraction lines

[6] Perkin-Elmer Model 298.
[7] Nuclepore Corp., Pleasanton, Calif.
[8] Zeiss DM4.
[9] Perkin-Elmer Model LC 75.

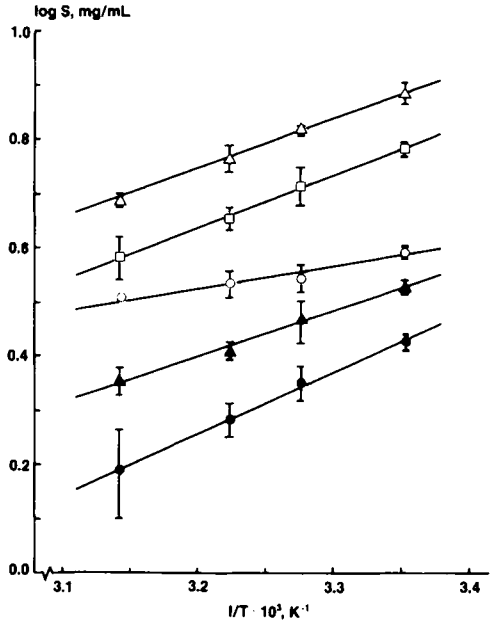

Figure 4—*Solubilities (S) in 1 mM NaOH plotted according to the van't Hoff equation (mean values and their 95% confidence intervals). Key: (△) pure prilocaine; (□) lidocaine plus prilocaine from EMLA; (○) pure lidocaine; (▲) prilocaine from EMLA; (●) lidocaine from EMLA.*

obtained at low temperature showed that EMLA contained nothing but the two single components. By slowly raising the temperature to room level, all lines completely disappeared and only an amorphous liquid remained.

Since both IR spectrometry and X-ray diffraction indicated that no chemical interaction existed between lidocaine and prilocaine, the effects of prolonged equilibration times were investigated. As can be seen from Fig. 2, in the region of high prilocaine content, DTA of nonequilibrated samples only showed a single peak. After equilibration of the samples for 3 weeks at 5°C, another peak corresponding to the eutectic melting point appeared. It was also observed that when crystals from a lidocaine–prilocaine mixture (55:45) stored for a long time at 5°C were analyzed after being washed with cold water and dried, only lidocaine was found. The analysis was made by IR spectrometry and by melting point determination. This, plus the results from the DTA and X-ray diffraction studies, strongly suggests that no solid solutions exist on either side of the phase diagram. These regions seem to be due to the formation of a metastable product during the fusion process. Thus, in an equilibrated system, the eutectic consists of a mixture of the pure components, not a mixture of two solid solutions.

To locate more accurately the eutectic point, a set of lidocaine–prilocaine samples (~5 g) were kept for several weeks at temperatures below the liquidus. Results of the 19°C runs are shown in Fig. 3.

Hot-stage microscopy was also performed under equilibrium conditions. From these results, giving the liquidus curves, and the DTA information, mainly giving the eutectic temperature, we arrived at a tentative temperature-composition diagram (Fig. 3) very similar to that constructed on the basis of the nonequilibrium experiments (Fig. 1). The main differences are in the extreme regions and next to the eutectic composition.

Solubilities—Both lidocaine and prilocaine decrease the surface tension of water very little and do not form micelles (13). However, to determine the extent of interaction between the two local anesthetics in aqueous solution, equilibrium solubility experiments were conducted. As can be seen from Fig. 4, the temperature dependence is smaller for pure lidocaine [$\Delta H = -7.6 \pm 0.69$ (12) kJ/mol, $\pm SE$ (df)] than for pure prilocaine [$\Delta H = -17.5 \pm 0.58$ (13) kJ/mol]. The lidocaine solubilities are in agreement with those reported previously (14), $\Delta H = -8.9$ kJ/mol. The total solubility of lidocaine and prilocaine when equilibrating water with EMLA has a ΔH value of -18.2 ± 0.80 (10) kJ/mol.

Analyzing the water for lidocaine and prilocaine separately showed that lidocaine, in this case, had a slightly higher heat of solubility than prilocaine, -21.5 ± 1.25 (10) and -15.8 ± 0.78 (10) kJ/mol, respectively. The different ΔH value of lidocaine in the presence of prilocaine and the lower individual solubilities of the combined substances demonstrate that solute–solute–solvent interactions take place in the aqueous solution. These interactions are also seen when the solubilities are determined from different mixtures of the two local anesthetics (Fig. 5). In one series of experiments, solidified melts of lidocaine and prilocaine were studied. Enough mixture to assure saturation

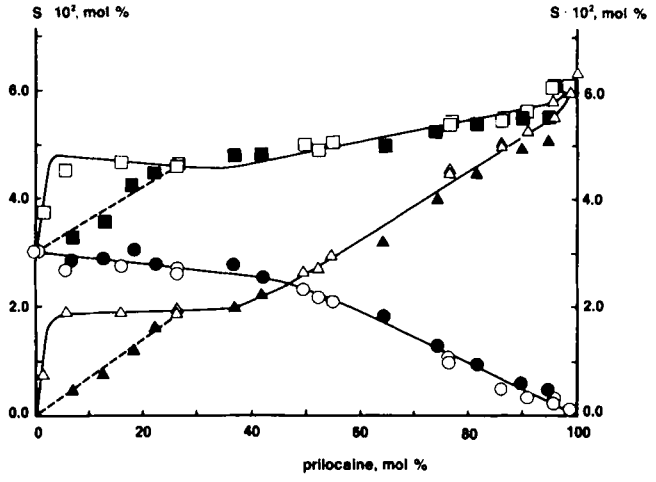

Figure 5—*Solubilities of lidocaine (○), prilocaine (△), and lidocaine plus prilocaine (□) from mixtures of the two local anesthetics at 25°C. Filled symbols represent experiments where the component with <50 mol% was initially dissolved in the water.*

with both components was used. After an initial increase due to a change in prilocaine solubility, the total solubility of the local anesthetics is affected very little compared with the solubilities of the individual substances when the molar ratio of the mixture is changed.

To obtain solutions saturated by only one of the substances, the substance with <50 mol% was dissolved in water before the other was added in excess. It was possible to make solutions where the prilocaine concentration did not reach its saturation level (Fig. 5). Due to the low saturation concentration and the relatively high molar ratio needed, this could not be achieved for lidocaine. In this case, the already dissolved lidocaine started to precipitate on the addition of prilocaine. The values for systems saturated with both substances simultaneously, *i.e.*, the first series of experiments, represent the highest obtainable solubilities. Concentrations lower than the solubility of prilocaine at <30 mol% in Fig. 5 do not influence the lidocaine solubility differently. Only the total amount of local anesthetics is changed. It can be noted that the total concentration of the local anesthetics only varies within 30% of the maximum concentration (that of pure prilocaine), in the range of 2–100 mol% prilocaine in the mixture.

Depending on the influence of additives, especially of salts, on the structure of water or their ability to compete with solvent water molecules, additives will affect the solubility of a solute. To quantify the effect of salts, the empirical Setschenov equation is convenient to use (15):

$$\ln (S_0/S) = k_s C$$

where S and S_0 are the solubilities with and without additive, respectively. The Setschenov coefficient, k_s, measures the sensitivity of the activity coefficient of the solute towards the additive. The concentration of additive, C, is expressed in moles per liter.

To illustrate the aqueous interactions between lidocaine and prilocaine further, the data were plotted according to the equation (Fig. 6). Data from both series of solubility experiments coincided. The Setschenov equation could be applied to prilocaine up to a lidocaine concentration of 0.013 M, with a k_s value of 0.68 obtained by linear regression through the origin. This corresponds to the linear part of Fig. 5 at >50 mol% prilocaine. As lidocaine approaches its highest value of saturation, ln (S_0/S) increases toward infinity. For lidocaine, k_s = 0.09; however, a second linear part with a slope of 1.88 seems to exist. The two linear parts correspond to those of lidocaine in Fig. 5. Since the intersection points in Fig. 5 at a prilocaine concentration of ~0.013 M do not coincide, an intermediate sensitivity of lidocaine to prilocaine might exist. This may also be the case for prilocaine. However, the experimental results do not permit any further evaluation of the intermediate regions using the simple Setschenov equation. As with prilocaine, ln (S_0/S) of lidocaine approaches infinity when the prilocaine concentration gets closer to the maximum saturation concentration. Other empirical expressions can be used to take this into account.

From a pharmaceutical point of view, the maximum aqueous total solubility of the local anesthetics is of interest. In nearly the entire range of lidocaine–prilocaine ratios studied, this solubility is ≥70% of that of pure prilocaine. Thus, the different pharmacological profiles of the two local anesthetics are more important than the aqueous solubility in selecting a suitable ratio for a pharmaceutical preparation. However, the eutectic mixture has the major advantage of being liquid at room temperature. For a preparation such as an oil-in-water cream for topical use, it is possible to emulsify the eutectic mixture directly without first dissolving the drugs in an inert oil.

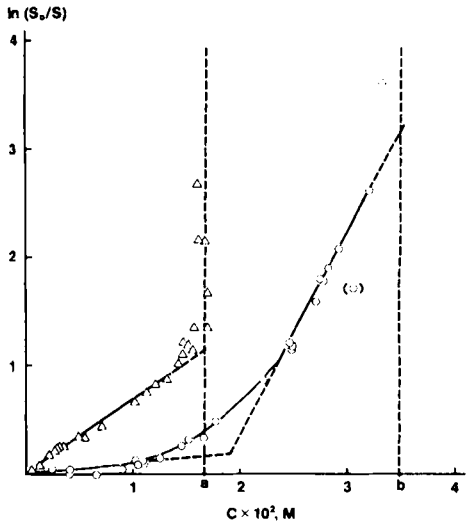

Figure 6—*Setschenov plots for lidocaine (○) and prilocaine (△) in solutic of the other component. Key: (a) solubility of lidocaine, 1.66 × 10⁻² M; solubility of prilocaine, 3.47 × 10⁻² M.*

CONCLUSION

The lidocaine–prilocaine binary system is a simple eutectic containing no intermediate compounds. The eutectic composition is close to 1:1, and the eutectic temperature is 18 ± 1°C. No solid solubility could be detected.

The temperature dependence of the individual solubilities of lidocaine and prilocaine from the eutectic mixture compared with that of the pure substances was higher for lidocaine and the same for prilocaine. For both substances, the individual solubilities from the mixture are lower than those obtained using the single components in the temperature range studied. This was also found for mixtures other than the eutectic. Complex aqueous interactions take place between lidocaine and prilocaine. These interactions depend on the initial ratio of the two drugs.

REFERENCES

(1) W. L. Chiou and S. Riegelman, *J. Pharm. Sci.*, **60,** 1281 (1971).

(2) J. L. Ford and M. H. Rubinstein, *Pharm. Acta Helv.*, **53,** 93 (1978).

(3) A. Nakamura and R. Okada, *Coll. Polymer Sci.*, **255,** 362 (1977).

(4) M. Kata and M. Wayer, *Pharmazie*, **30,** 382 (1975).

(5) K. Kreuschner, K-H. Frömming, and R. Hosemann, *Acta Pharm. Tech.*, **26,** 159 (1980).

(6) S. S. El-Gamal, V. F. B. Naggar, and A. M. Motawi, *Sci. Pharm.*, **49,** 20 (1981).

(7) J. L. Ford and M. H. Rubinstein, *Int. J. Pharm.*, **8,** 311 (1981).

(8) H. M. El-Banna, S. A. Khalil, and M. W. Gouda, *J. Pharm. Sci.*, **67,** 1112 (1978).

(9) B. F. J. Broberg and H. C. A. Evers, *European Pat.* no. 0,002,425, (1981).

(10) T. Hörlin, T. Niklewski, and M. Nygren, *Chem. Commun. Univ. Stockholm*, **No 9,** 1975.

(11) B. Forslund, *Chemica Scripta*, **11,** 93 (1977).

(12) B. Forslund and B. Jelinski, *Chemica Scripta*, **15,** 13 (1980).

(13) K. Thoma and C. D. Herzfeldt, in "Proceeding, 1st International Conference on Pharmaceutical Technology," Paris, May 31–June 2, 1977, pp. 157–166.

(14) N. I. Nakano, *J. Pharm. Sci.*, **68,** 667 (1979).

(15) B. E. Conway, "Ionic Hydration in Chemistry and Biophysics," Elsevier, Amsterdam-Oxford-New York, 1981, p. 444.

ACKNOWLEDGMENTS

We are grateful to Bohdan Jelinski at the Arrhenius Laboratory and to Wiia Steenhoff, Kjell Mattsson, and Ann-Charlotte Dahlquist at Astra Läkemedel AB for their skillful technical assistance. Bo Runesson, at the same company, is acknowledged for the IR investigations.

Absorption of Phenobarbital from Tablets and Elixir

MARVIN C. MEYER *x, ARTHUR B. STRAUGHN *, GURSHARAN RAGHOW *, WILLIAM L. SCHARY ‡§, and KEITH S. ROTENBERG ‡‖

Received November 19, 1982, from the *Department of Pharmaceutics, College of Pharmacy, University of Tennessee Center for the Health Sciences, Memphis, TN 38163 and the ‡Division of Biopharmaceutics, Food and Drug Administration, Rockville, MD 20857. Accepted for publication March 7, 1983. Present addresses: §Endo Pharmaceuticals, Inc., Du Pont Co., Wilmington, DE 19898 and ‖Pennwalt Corporation, Rochester, NY 14623.

Abstract □ A three-way crossover study was conducted with 24 healthy male volunteers to determine the relative bioavailability of four different 100-mg phenobarbital tablets compared with a reference elixir. Each subject received two of the tablets and the elixir at 30-d intervals. Blood samples were collected daily for 19 d after each dose. Plasma phenobarbital concentrations achieved with the five dosage forms differed by <20% within 2–3 h after dosing. The extent of absorption for all dosage forms, as determined from area under the plasma concentration-time profiles, were within 10% of each other. The peak plasma concentration was the greatest and the time to peak concentration was the shortest for the elixir. One of the tablets exhibited a time to peak concentration of 8.6 h, which was significantly longer than any of the other dosage forms. The time to peak concentration correlated with the percent of drug dissolved in 60 min, as determined in 0.1 M HCl, using the USP XX paddle method at 50 rpm.

Keyphrases □ Phenobarbital—relative bioavailability, tablets and elixir, pharmacokinetics in humans □ Bioavailability—relative, phenobarbital tablets and elixir, pharmacokinetics in humans □ Pharmacokinetics—phenobarbital tablets and elixir in humans, relative bioavailability

Phenobarbital, used as a sedative-hypnotic and as an anticonvulsant, has an aqueous solubility of only 1 mg/mL, and differences have been reported in the dissolution rates of different polymorphic forms of the drug (1). Because of its clinical indications and physicochemical properties, it is important to establish the bioavailability of dosage forms of phenobarbital. A recent brief clinical report indicated significantly different plasma phenobarbital concentrations in patients who were receiving 32-mg tablets from two manufacturers (2). However, a bioavailability study of a 30-mg tablet indicated better absorption from the tablet than from an intramuscular dose, which was only 80% absorbed (3). In another study (4) the absolute bioavailability of 60-mg tablets was determined, and the extent of absorption averaged 95%. In the most extensive study to date, five healthy subjects were given seven 100-mg tablets from different manufacturers (5). A noncrossover design was employed, and blood samples were obtained for only 64 h, although half-lives ranged from 41–220 h. Further, the doses were administered every 6 d, and no correction for residual drug from preceding doses was noted in the report. The time of maximum plasma concentration was the only parameter that exhibited statistically significant differences among the test products. There did not appear to be any correlation between the blood level-time profiles and the results of *in vitro* dissolution testing.

The present study employed 24 healthy subjects, four different 100-mg tablet dosage forms, and a reference elixir. Blood samples were obtained for 19 d following dose administration. Attempts were made to relate parameters obtained *in vivo* to those seen using an *in vitro* dissolution system.

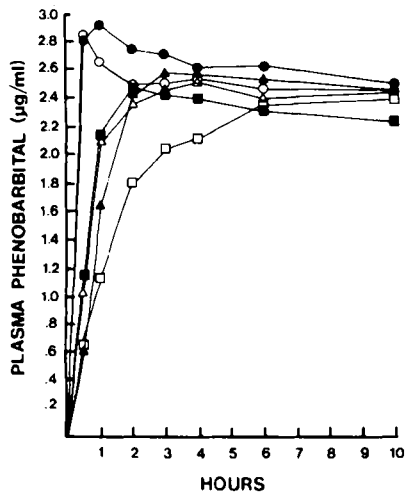

Figure 1—*Mean phenobarbital plasma concentrations during the initial 10 h after dosing* (n = 12). *Key: group I—product 1* (○); *product 2* (□); *product 3* (△); *group II—product 1* (●); *product 4* (■); *product 5* (▲).

EXPERIMENTAL

Dosage Forms—Four tablet products, containing between 97.2 and 100 mg of phenobarbital, were obtained from four manufacturers[1]. The products were selected from the numerous available sources on the basis of preliminary dissolution testing. An elixir[2] containing 100 mg of phenobarbital/25 mL was employed as a reference dosage form. Calculations were based on the labeled drug content of each of the five dosage forms.

Clinical Protocol—Twenty four male subjects (23–30 years, 53–100 kg) were randomly divided into two groups of 12. All subjects underwent urinalysis and hematological and blood chemistry[3] determinations, as well as a physical examination and an ECG, to ensure they were in good health. All subjects provided written informed consent. The subjects had not taken any known enzyme inducers for at least 3 months, any medication for 14 d, or any alcohol for 7 d prior to the start of the study.

Using a crossover design, group I received a 100-mg dose of the elixir (product 1) and two of the test tablets (products 2 and 3). The subjects in group II also received the elixir and the other two tablets (products 4 and 5). The three dosings were each separated by a 30-d period. The doses were administered after an overnight fast, along with 240 mL of water. No food or liquid

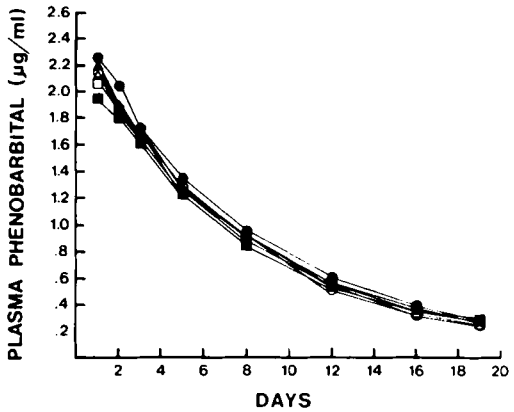

Figure 2—*Mean phenobarbital plasma concentrations 1–19 d after dosing* (n = 12). *Key: group I—product 1* (○); *product 2* (□); *product 3* (△); *group II—product 1* (●); *product 4* (■); *product 5* (▲).

[1] Parke-Davis, Lot WC187, 100 mg, Exp. 1/83 (product 2); Lannett, Lot 19806, 100 mg, Exp. 5/82 (product 3); Wyeth, Lot 1772455, 100 mg, Exp. 1/82 (product 4); West-Ward, Lot 42342, 97.2 mg, Exp. 12/82 (product 5).
[2] Parke-Davis, Lot YJ200, 20 mg/5 mL, Exp. 7/84 (product 1).
[3] SMA 18/90.

0022-3549/84/0400-0485$01.00/0
© 1984, American Pharmaceutical Association

Table I—Plasma Concentrations (μg/mL) at Each Sampling Time [a]

Group	Product No.	0.5	1 h	2 h	3 h	4 h	6 h	10 h	24 h	48 h	72 h	120 h	192 h	288 h	384 h	456 h
I	1	2.86	2.66	2.49	2.50	2.53	2.46	2.43	2.15	1.87	1.63	1.26	0.88	0.52	0.32	0.23
		(17)	(20)	(35)	(24)	(20)	(19)	(19)	(19)	(19)	(20)	(21)	(25)	(24)	(30)	(35)
	2	0.63	1.12	1.79	2.03	2.11	2.33	2.37	2.06	1.86	1.66	1.28	0.91	0.55	0.35	0.24
		(92)	(52)	(22)	(17)	(19)	(19)	(17)	(22)	(19)	(26)	(29)	(27)	(30)	(34)	(38)
	3	1.07	2.09	2.35	2.45	2.51	2.38	2.44	2.14	1.89	1.63	1.27	0.85	0.54	0.33	0.24
		(72)	(52)	(29)	(22)	(19)	(20)	(19)	(22)	(20)	(23)	(25)	(27)	(30)	(40)	(41)
Percent Difference [b]		78.0	57.9	28.1	18.8	16.6	5.3	2.9	4.2	1.6	1.8	1.6	6.6	5.5	8.6	4.2
II	1	2.81	2.93	2.75	2.71	2.61	2.62	2.48	2.26	2.05	1.72	1.35	0.96	0.61	0.40	0.28
		(25)	(19)	(18)	(18)	(19)	(20)	(20)	(21)	(21)	(24)	(26)	(43)	(61)	(72)	(80)
	4	1.14	2.14	2.48	2.42	2.38	2.29	2.21	1.95	1.80	1.61	1.23	0.84	0.55	0.38	0.29
		(62)	(32)	(23)	(20)	(21)	(26)	(23)	(25)	(20)	(21)	(22)	(30)	(46)	(57)	(60)
	5	0.60	1.64	2.43	2.57	2.55	2.51	2.42	2.19	1.88	1.68	1.27	0.89	0.53	0.35	0.27
		(96)	(61)	(24)	(14)	(15)	(18)	(16)	(18)	(15)	(17)	(24)	(28)	(37)	(48)	(56)
Percent Difference [b]		78.6	44.0	11.6	10.7	8.8	12.6	10.9	13.7	12.2	6.4	8.9	12.5	13.1	12.5	6.9

[a] Each value (μg/mL) represents the mean of the 12 subjects. The relative standard deviations are given in parentheses ($SD \times 100$/mean). [b] Percent difference = (100) (highest − lowest)/(highest).

other than water was permitted for 4 h following dosing. A standard meal[4] was provided 4 and 8 h after dosing. Ten-milliliter blood samples were obtained *via* a catheter or venipuncture just prior to the dose and 0.5, 1, 3, 4, 6, 10 h and 1, 2, 3, 5, 8, 12, 16, and 19 d after each dose using heparin as the anticoagulant. The blood samples were immediately centrifuged, and the plasma was stored frozen until the time of assay.

Plasma Assay—Plasma phenobarbital concentrations were determined using a slightly modified HPLC procedure previously employed in a study of ethotoin (6). A 1-μg/mL aqueous solution of phenytoin was used as the internal standard. The ether extraction of the plasma was adjusted to pH 11.2, and the chromatographic conditions were essentially as previously reported. The only modifications involved the reconstitution of the dried extract with 100 μL of mobile phase, the use of a 15-μL injection volume, and a mobile phase of 40% acetonitrile in 0.1 M sodium phosphate buffer (pH 7). Quantitation was accomplished with standard curves of peak height ratio (phenobarbital/phenytoin) *versus* phenobarbital concentration, prepared with pooled human plasma. The assay was linear over a concentration range of at least 0.25–3.0 μg/mL. The retention times for phenobarbital and phenytoin were 1.7 and 2.4 min, respectively. No interfering peaks were noted in blank plasma extracts. Duplicate determinations differed by <6% at the lowest standard concentration and by <3% at the highest value.

Data Analysis—The time of maximum plasma concentration (t_{max}) and maximum plasma concentration (C_{max}) were determined by inspection of individual subject data. The elimination rate constant (k) for each dose was determined by least-squares fitting of the postabsorption concentration–time data. The area under the plasma concentration–time curve (AUC) from 0 to 456 h was calculated using the trapezoidal method, while the $AUC_{0-\infty}$ was calculated by addition of the $AUC_{(456\ h-\infty)}$ to the $AUC_{(0-456\ h)}$. The $AUC_{(456\ h-\infty)}$ was determined by dividing the 456-h plasma concentration by k.

The statistical analysis was first performed separately on data from groups I and II. Analysis of variance was used to evaluate statistically significant differences ($p < 0.05$) at each sampling time, as well as values for t_{max}, C_{max}, and AUC. In cases where significant differences occurred, the Newman–Keuls *a posteriori* test was used to evaluate which subjects, treatment sequence, or dosage forms were different. To make comparisons of all four tablet formulations across both groups, a one-way analysis of variance and the Newman–Keuls *a posteriori* test were used to evaluate C_{max}, t_{max}, and relative $AUC_{(0-\infty)}$ for each tablet, adjusted for half-life differences. This latter value was determined as the product of the individual observed $AUC_{(0-\infty)}$ and k, divided by the product of $AUC_{(0-\infty)}$ and k for the elixir dose in each subject, to adjust for intrasubject differences in k. A power analysis (7) was used to evaluate the potential for statistical errors based on $\alpha = 0.05$ and $\beta = 0.2$. Because of an analytical failure, the data for one subject in group II (product 4) were lost. All concentrations and other parameters were estimated using a statistical method (8) based on the performance of the other two dosage forms in this subject and the data obtained for the other subjects within this group.

***In Vitro* Dissolution**—The dissolution of six tablets of each of the four tablet dosage forms was determined using the USP XX paddle method at 50 rpm. Deionized water and 0.1 M HCl at 37°C were employed as the dissolution media, using a volume of 1000 mL. Samples of the media were periodically withdrawn over a 90-min period.

[4] Content of each meal available on request.

RESULTS AND DISCUSSION

Although all subjects were instructed to avoid other drugs during the 3-month study, it was anticipated that some subjects might require minor medication. Thirteen of the subjects took at least one dose of some additional drug, with the majority of these being either acetaminophen for headache or antihistamines for rhinitis. Acetaminophen was previously shown not to interfere in the assay, and the basic antihistamines were not extracted during the assay. Further, inspection of time zero chromatograms and individual plasma concentration–time data did not reveal any effects of the other medications on the phenobarbital plasma concentration–time profiles.

Plasma Concentrations at Each Sampling Time—The mean plasma concentrations at each sampling time for both groups are summarized in Table I. The mean plasma concentrations at each sampling time from 0 to 10 h and from 24 to 456 h are illustrated in Figs. 1 and 2, respectively. Statistically significant differences among products in each study group are summarized in Table II. The rapidly absorbed elixir (product 1) resulted in the highest plasma phenobarbital concentrations for the first 6 h in group I and the highest concentrations at all but the 456-h time in group II. The actual difference among the products was <20% after the 2- and 1-h samples for the groups I and II studies, respectively. The intersubject variability, as reflected by the relative standard deviations, was much less for the elixir during the first hour, which is consistent with a rapidly absorbed dosage form.

The analysis of variance indicated that significant differences among the products occurred at 0.5, 1.0, 2.0, 3.0, and 4.0 h in group I and at 0.5 and 1.0 h in group II. In group I the Newman–Keuls *a posteriori* test (Table II) showed product 2 to have significantly lower concentrations than the elixir during the first 4 h. Product 2 was also significantly lower than product 3 in that group at 1, 3, and 4 h. Product 3 was significantly lower in concentration than the elixir at 0.5, 1, and 2 h. At the remainder of the sampling times product 2 had the lowest concentration at sampling times up to 48 h and slightly higher concentrations at the remainder of the sampling times.

In group II the Newman–Keuls *a posteriori* test indicated a significant difference among all the products at the 0.5-h sampling time, with product 5 having the lowest concentration and the elixir having the highest concentration. At 1 h the ranking of the products was identical to the ranking at 0.5 h, but the only significant difference was between the elixir and the two tablets. From 2 to 456 h no significant difference was observed among the three products.

Peak Concentration, Time of Peak Concentration, k, and AUC Values—

Table II—Newman-Keuls *a Posteriori* Test for Significant Product Differences

Observation	Product Ranking (Lowest to Highest) [a] Group I	Group II
Concentration		
0.5 h	2 3 1	5 4 1
1 h	2 3 1	5 4 1
2 h	2 3 1	5 4 1
3 h	2 3 1	4 5 1
4 h	2 3 1	4 5 1
C_{max}	2 3 1	4 5 1
t_{max}	1 3 2	1 4 5

[a] Dosage forms underlined by a common line show no significant differences ($p > 0.05$).

Table III—Phenobarbital Bioavailability Parameters [a]

Group	Product	C_{max}, μg/mL	t_{max}, h	$AUC_{(0-19d)}$, μg·d/mL	k, h^{-1}	$AUC_{(0-\infty)}$, μg·d/mL
I	1	3.01	1.0	17.54	0.00529	19.49
		(16)	(82)	(21)	(15)	(23)
	2	2.44	8.6	17.66	0.00522	19.73
		(16)	(68)	(24)	(15)	(26)
	3	2.70	2.6	17.46	0.00510	19.80
		(23)	(51)	(24)	(15)	(26)
	Percent Difference[b]	18.9	88.4	1.1	3.6	1.6
II	1	3.15	1.0	19.17	0.00500	22.16
		(17)	(75)	(34)	(22)	(46)
	4	2.57	3.2	17.27	0.00452	20.70
		(22)	(79)	(26)	(31)	(35)
	5	2.69	4.2	17.75	0.00478	20.53
		(14)	(59)	(22)	(23)	(29)
	Percent Difference[b]	18.4	76.2	9.9	9.6	7.4

[a] Each value represents the mean of the 12 subjects. The relative standard deviations are given in parentheses. [b] Percent difference = (100)(highest − lowest)/(highest).

Table III summarizes the mean values for the peak plasma concentration, time of peak concentration, $AUC_{(0-456\ h)}$, $AUC_{(0-\infty)}$, and the terminal elimination rate constant. The statistical analysis of differences among these values are given in Table II.

In group I the mean peak concentration (C_{max}) ranged from 3.01 μg/mL (product 1) to 2.44 μg/mL (product 2). This difference of 18.9% was significant ($p < 0.001$), and each product was significantly different from the other two products. The differences in C_{max} in group II was 18.4% with a range of 2.57 μg/mL (product 4) to 3.15 μg/mL (product 1). This difference was also significant ($p < 0.01$), with the elixir showing a higher concentration than the two tablets, which were not significantly different from each other.

The time of peak concentration (t_{max}) for the elixir (product 1) was 1 h in both groups. In group I, product 2 had a significantly longer t_{max} of 8.6 h compared with the elixir and product 3, which did not differ from each other. The significantly lower peak concentration and longer time to reach peak concentration for product 2 are indicative of a slower rate of absorption for this tablet. In group II, the elixir peaked sooner than the two tablets.

In group I the $AUC_{(0-456\ h)}$ ranged from 17.46 (product 3) to 17.66 μg·d/mL (product 2). This 1.1% difference was not significant. Extrapolation of the AUC to infinity resulted in AUC values ranging from 19.49 (product 1) to 19.80 μg·d/mL (product 3). Although extrapolation changed the ranking of the products, the 1.6% difference was not significant. The AUC values for the group II products were very similar to those in group I, with a range in $AUC_{(0-456\ h)}$ from 17.27 (product 4) to 19.17 μg·d/mL (product 1). The $AUC_{(0-\infty)}$ ranged from 20.53 (product 5) to 22.16 μg·d/mL (product 1). No significant differences in these values were noted ($p > 0.05$).

Sequence and Subject Differences—Significant differences among administration sequences (phases) were observed for several of the parameters. Generally, the ranking of the phases showed increases in plasma concentrations, with phase I < phase II < phase III. These differences were not significant ($p > 0.05$) for group II. Further, for group I the differences between phase I and phase III data were only ~10% for C_{max}, AUC, and k values. The slightly higher phenobarbital plasma concentrations obtained during phase III indicated that one dose per month did not result in any enzyme induction. Further, there was no progressive change in the apparent first-order elimination rate constant (k). Others have similarly found no apparent autoinduction of phenobarbital metabolism (4, 9). A decrease in the apparent volume of distribution over the 3-month testing period cannot be ruled out as a potential explanation for the slightly elevated plasma concentrations during phase III.

Significant subject differences were noted for all the parameters except the 0.5-h concentration and t_{max} in group I, and all but the 0.5-, 1.0-, 3.0-, 4.0- and 10.0-h concentrations and t_{max} in group II. Among the subjects, the C_{max} values ranged from 2.06 to 3.90 μg/mL and the mean $AUC_{(0-\infty)}$ ranged from 12.72 to 40.30 μg·d/mL. Mean terminal elimination rate constants for the subjects ranged from 0.0025 to 0.0064 h^{-1}, with an overall mean elimination rate constant for all dose administrations of 0.0050 h^{-1}.

Power Analysis—A power analysis (7) was also conducted utilizing an α level of 0.05 and a β level of 0.2. In group I, 12 subjects were sufficient to detect a 20% difference in products as being significant for the majority of the parameters. In those instances where >12 subjects were necessary, the actual difference in the products was greater than the percent difference required for significance to be detected. The statistical power for group II was not as great as in group I. However, it was sufficient to detect a 20% difference among the products in terms of 8 of the 15 sampling times, the C_{max}, and AUC values.

Comparisons Across Groups I and II—Table IV summarizes the one-way analysis of variance for comparison of products 2–5 in terms of C_{max}, t_{max}, and relative $AUC_{(0-\infty)}$. This table also includes the Newman–Keuls analysis of these parameters. The time of peak concentration ranged from 2.6 (product 3) to 8.6 h (product 2). Product 2 showed a significantly longer time to reach peak than the other three tablet products, which were not significantly different from each other. The peak plasma concentrations, which ranged from 2.44 to 2.70 μg/mL for the four tablet products, were not significantly different ($p > 0.05$). The relative $AUC_{(0-\infty)}$ ranged from 88 to 100% for the four tablets relative to the elixir. This difference among products was not significant ($p > 0.05$).

***In Vivo–In Vitro* Relationships**—Using the USP XIX basket method at 50 rpm, with pH 1.2 simulated gastric fluid as the dissolution media, Sylvestri

Table IV—Summary of Statistical Analysis Across Groups

Parameter	Mean Values: Product 2	Product 3	Product 4	Product 5	p Value
t_{max} (h)	8.60	2.60	3.20	4.20	<0.001
C_{max} (μg/mL)	2.44	2.70	2.57	2.69	0.532
Relative[a] $AUC_{(0-\infty)}$	1.01	0.98	0.88	0.95	0.515

Newman–Keuls Ranking[b]

Parameter	Product Ranking (Lowest to Highest)
t_{max}	3 4 5 2
C_{max}	2 4 5 3
Relative $AUC_{(0-\infty)}$	4 5 3 2

[a] See text for calculation. [b] Products underlined by a common line show no significant difference ($p > 0.05$).

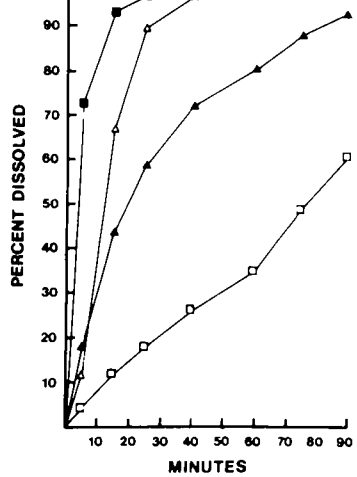

Figure 3—*Dissolution of four phenobarbital tablets in 0.1 M HCl using the USP XX paddle method at 50 rpm. Each value represents the mean of six determinations. Key: product 2 (□); product 3 (△); product 4 (■); product 5 (▲).*

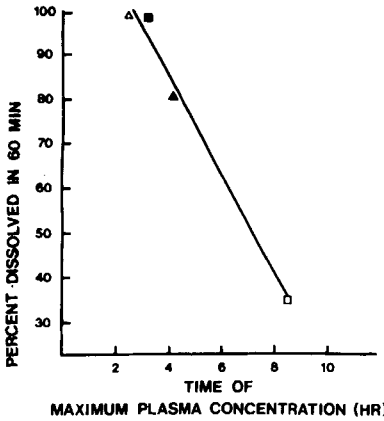

Figure 4—In vitro-in vivo *correlation for four phenobarbital tablets. Each* t_{max} *value represents the mean of 12 subjects and each* in vitro *value is the mean of six determinations. Key: product 2* (□); *product 3* (△); *product 4* (■); *product 5* (▲).

and Ueda (5) did not observe any correlation between the dissolution properties and the *in vivo* performance of seven different 100-mg phenobarbital tablets. Two of the products were different lots of products 2 and 4 employed in the present study. The results of the present study are shown in Fig. 3 for dissolution in 0.1 M HCl. Product 2 dissolved much slower than the other three tablets. The results were similar using deionized water, except for product 3 which dissolved slightly more slowly than product 5 in water. Since significant differences were noted among the products in terms of t_{max}, which reflects the rate of drug absorption, attempts were made to correlate the dissolution in acid with the mean values of t_{max} for the four tablets. Figure 4 illustrates the good relationship ($r = -0.995$) found between t_{max} and the percent of drug dissolved at 60 min. Whether the previously reported (5) lack of *in vitro–in vivo* correlation was due to differences between the two studies in the *in vivo* study design, in the *in vitro* methodology, and/or in the test tablets cannot be determined from the available data. In the present study there were no significant differences among the four tablets in terms of AUC, and the C_{max} values differed by <10%. Thus, it was not unexpected that the observed differences in dissolution rates could not be related to these *in vivo* parameters.

Clinical Implications—Since there were no significant differences in either C_{max} or AUC values, it can be concluded that the extent of absorption of phenobarbital was similar for the elixir and the four tablet products. However, there were significant differences among the tablet products in terms of rate of absorption, with product 2 showing the longest t_{max}. Because of the long half-life for phenobarbital in humans, differences in the rate of absorption should not have much effect on the steady-state phenobarbital plasma concentrations when the drug is employed on a chronic basis as an anticonvulsant. Projections of steady-state concentrations using a one-compartment model with first-order absorption suggest only minor differences in maximum and minimum plasma concentrations, comparing two dosage forms with an elimination half-life of 130 h and with absorption rate constants differing 10-fold. However if the drug is employed on an acute basis as a hypnotic, it is possible the onset of action could be delayed with product 2. In such an instance a patient could potentially ingest additional doses in an attempt to achieve the desired effect. Depending on the number of doses taken, there exists the possibility of excessive ingestion of the more slowly absorbed product resulting in undesirable side effects or toxicity. Thus, on the basis of rate of absorption, the four tablet products cannot be considered bioequivalent.

REFERENCES

(1) J. A. Clements and D. Stanski, *Can J. Pharm. Sci.*, **6**, 9 (1971).

(2) N. Alvarez, E. Hartford, and E. Cavalleri, *Ann. Neurol.*, **9**, 309 (1981).

(3) C. T. Viswanathan, H. E. Booker, and P. G. Welling, *J. Clin. Pharmacol.*, **18**, 100 (1978).

(4) E. Nelson, J. R. Powell, K. Conrad, K. Likes, J. Byers, S. Baker, and D. Perrier, *J. Clin. Pharmacol.*, **22**, 141 (1982).

(5) M. F. Sylvestri and C. T. Ueda, *Intl. J. Clin. Pharmacol. Biopharm.*, **17**, 492 (1979).

(6) M. C. Meyer, B. J. Holcombe, G. J. Burckart, G. Raghow, and M. K. Yau, *Clin. Pharm. Ther.*, **33**, 329 (1983).

(7) E. Purich, in "Drug Absorption and Disposition: Statistical Considerations," K. S. Albert, Ed., American Pharmaceutical Association, Washington, D.C., 1980, p. 123.

(8) W. G. Cochran and G. M. Cox, "Experimental Designs," 2nd ed., Wiley, New York, N.Y., 1957, p. 125.

(9) C. T. Viswanathan, H. E. Booker, and P. G. Welling, *J. Clin. Pharmacol.*, **19**, 282 (1979).

ACKNOWLEDGMENTS

Supported in part by the U.S. Food and Drug Administration (FDA No. 223-77-3011) and the Tennessee Department of Public Health. The medical supervision provided by Dr. Phillip Lieberman is gratefully acknowledged.

Use of Hexadeuterated Valproic Acid and Gas Chromatography–Mass Spectrometry to Determine the Pharmacokinetics of Valproic Acid

ANDREW A. ACHEAMPONG, FRANK S. ABBOTT ˣ, JAMES M. ORR, SHEILA M. FERGUSON, and ROLAND W. BURTON

Received July 19, 1982, from the *Faculty of Pharmaceutical Sciences, University of British Columbia, Vancouver, B.C., Canada V6T 1W5.* Accepted for publication February 18, 1983.

Abstract □ Di-([3,3,3-$^2H_3$]propyl)acetic acid, a hexadeuterated analogue of valproic acid, was synthesized and its pharmacokinetic properties compared with valproic acid. Concentrations of valproic acid and [^{2}H]valproic acid in serum and saliva were determined by GC–MS using selected-ion monitoring. Saliva drug levels were measured with good precision down to 0.1 μg/mL. Kinetic equivalence of valproic acid and [^{2}H]valproic acid was demonstrated in a single-dose study in a human volunteer. An isotope effect was observed for ω-oxidation, but the difference in metabolism was not sufficient to make [^{2}H]valproic acid biologically nonequivalent. The application of [^{2}H]valproic acid to determine the kinetics of valproic acid under steady-state concentrations was evaluated in the same volunteer. The kinetic data obtained with [^{2}H]valproic acid was consistent with previously reported values for valproic acid including kinetic differences observed between single-dose and steady-state experiments. Saliva levels of valproic acid were found to give a good correlation (r = 0.953) with total serum valproic acid under multiple-dose conditions. A concentration dependence was found for the ratio of saliva valproic acid to free valproic acid in serum, low ratios being observed at high serum concentrations of valproic acid.

Keyphrases □ Valproic acid—hexadeuterated analogue, gas chromatography–mass spectrometry, pharmacokinetics single- and multiple-dose regimes □ Pharmacokinetics—valproic acid, hexadeuterated, analogue, single- and multiple-dose regimens, gas chromatography–mass spectrometry

Valproic acid (I), an anticonvulsant drug that is effective in the treatment of absence seizures, is also used to treat primary and generalized tonic-clonic seizures (1, 2). The pharmacokinetics of valproic acid have been studied extensively in patients who also receive other antiepileptic drugs (3–6). As a consequence, little is known about the basic elimination kinetics of valproic acid during multiple dosing with valproic acid alone. Only a few studies have reported multiple-dose kinetics of valproic acid given as a single agent to normal volunteers (7–9).

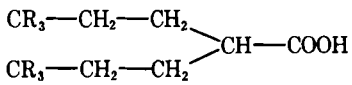

I R = H
II R = ^{2}H

One method of determining changes in the kinetic parameters of a drug in patients on multiple-dose therapy is the use of a pulse-dose of a stable-isotope-labeled drug (10, 11). Application of this method to antiepileptic drug studies allows the elimination kinetics of the drug to be determined without discontinuing therapy and risking the exacerbation of seizures. The labeled-drug elimination phase can be followed for 3–4 half-lives during subsequent uninterrupted multiple dosing of unlabeled drug. This technique has been used by Von Unruh *et al.* (6) to study the elimination kinetics of valproic acid under steady-state conditions in patients on combined antiepileptic drug therapy using di-([2,3-$^2H_2$]propyl)acetic acid.

The purpose of this study was to synthesize a deuterium analogue of valproic acid, namely, di-([3,3,3-$^2H_3$]-propyl)-acetic acid (II) and to undertake a preliminary evaluation of its pharmacokinetics. The location of the deuterium atoms only on the terminal carbons of the propyl chains of II was thought to be ideal since ω-oxidation of valproic acid is a minor metabolic pathway (3).

To demonstrate the applicability of labeled valproic acid for determining the steady-state kinetics of valproic acid without interruption of drug administration, the pharmacokinetics of II were compared with I under both single- and multiple-dose situations in a healthy human volunteer. To achieve this, a selective and sensitive assay for II acid using GC–MS was required. The application of this technique to the measurement of salivary levels of valproic acid and [^{2}H]valproic acid was also investigated.

EXPERIMENTAL

Chemicals and Reagents—Valproic acid[1] and 1-bromo[3,3,3-$^2H_3$]propane[2] were obtained commercially. Octanoic acid[3] and diethyl malonate[4] were redistilled before use. Ethyl acetate[5], hexane[5], and methanol[5] were distilled-in-glass grade. All other chemicals were analytical grade.

Synthesis of Di-([3,3,3-$^2H_3$]propyl)acetic Acid (II)—Diethyl malonate (2.88 g, 0.018 mol) was added dropwise to a solution of sodium ethoxide (0.44 g of sodium in 11.0 mL of absolute ethanol). The mixture was heated at reflux for 20 min, cooled, and then 1-bromo[3,3,3-$^2H_3$]propane (2.5 g, 0.02 mol) was introduced in a dropwise manner. The mixture was stirred at reflux for 2 h. For the second alkylation step, the same amounts, of sodium ethoxide solution and 1-bromo[3,3,3-$^2H_3$]propane as used previously were added, and the reaction mixture was heated at reflux for an additional 3 h.

Sodium hydroxide solution (5.5 g in 16 mL of water) was added to the reaction mixture containing diethyl [$^2H_6$]dipropylmalonate and the mixture was refluxed for 8 h. After removing the ethanol by distillation at atmospheric pressure, the solution was diluted and cooled in an ice-water bath. A solution of 9 M sulfuric acid was added in a dropwise manner until the pH of the resulting solution fell to 2.5 (monitored with a pH meter[6]). A white precipitate of [^{2}H]dipropylmalonic acid was collected by filtration, washed with water, and dried *in vacuo* for 6 h (mp[7] 156–158°C). The [^{2}H]dipropylmalonic acid was heated at 190–200°C until evolution of carbon dioxide had ceased. The residue was distilled *in vacuo* to give 1.39 g of [^{2}H]valproic acid (50% yield based on diethyl malonate), bp 71–72°C, 0.5 mm Hg [lit. (12) bp 221°C, 760 mm Hg for valproic acid]. ^{1}H-NMR[8] ($CDCl_3$) relative to tetramethylsilane: δ 1.1–1.9 (m, 8), 2.2–2.5 (m, 1), and 10.5–11.5 ppm (br s, 1, COOH). The deuterium label was >97% as determined by GC–MS analysis of the *tert*-butyldimethylsilyl ester of the product as compared with derivatized unlabeled valproic acid.

Gas Chromatography–Mass Spectrometry— The instrument used for the ion-monitoring assay was a gas chromatograph[9] interfaced to a mass spec-

[1] K and K Fine Chemicals, ICN Pharmaceuticals, Plainview, N.Y.
[2] Purity 98 atom %D; Merck Sharp and Dohme Canada Ltd.
[3] Nutritional Biochemical Corp., Cleveland, Ohio.
[4] British Drug House Ltd, Poole, U.K.
[5] Caledone, Georgetown, Canada.
[6] Model 220 pH meter; Fisher Scientific, Fair Lawn, N.J.
[7] Thomas Hoover Apparatus; Arthur H. Thomas Co., Philadelphia, Pa.
[8] Spectrum recorded with an XL-100 spectrometer; Varian Associates, Palo Alto, Calif.
[9] Model 5700A; Hewlett-Packard, Avondale, Pa.

0022-3549/84/0400-0489$01.00/0
© 1984, American Pharmaceutical Association

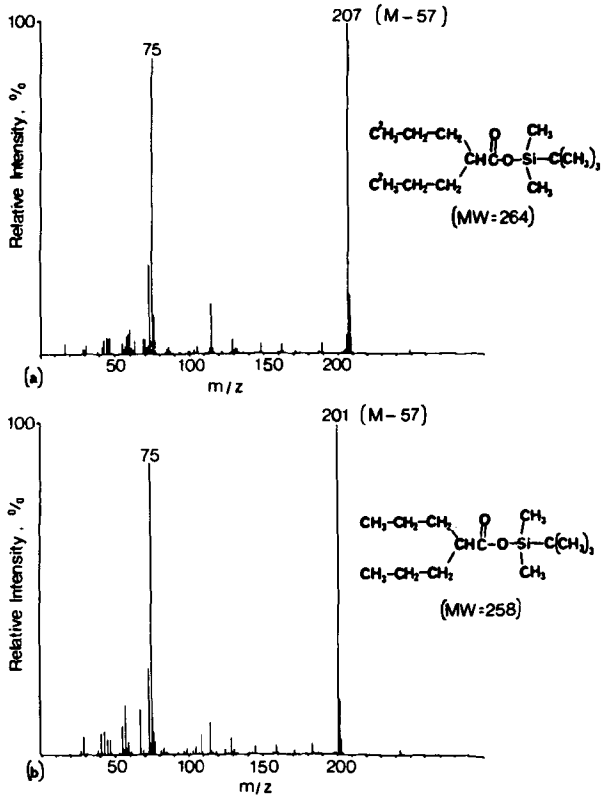

Figure 1—*Electron-impact mass spectra of the* tert-*butyldimethylsilyl esters of (a) [²H]valproic acid and (b) valproic acid.*

trometer[10] *via* a variable-slit separator and connected to an on-line data system[11]. The 1.8-m × 2-mm i.d. glass column was packed with 3% Dexsil 300 on 100–120 mesh Supelcoport[12]. Injection into the system was accomplished with an automatic sampler[13]. Operating conditions were: injection port temperature, 250°C; inlet line temperature, 250°C; column temperature, 135°C; and helium (carrier gas) flow rate of 25 mL/min. The mass spectrometer was operated with an electron-ionization energy of 80 eV, trap current of 300 μA, and ion source pressure of 5.0×10^{-6} Torr.

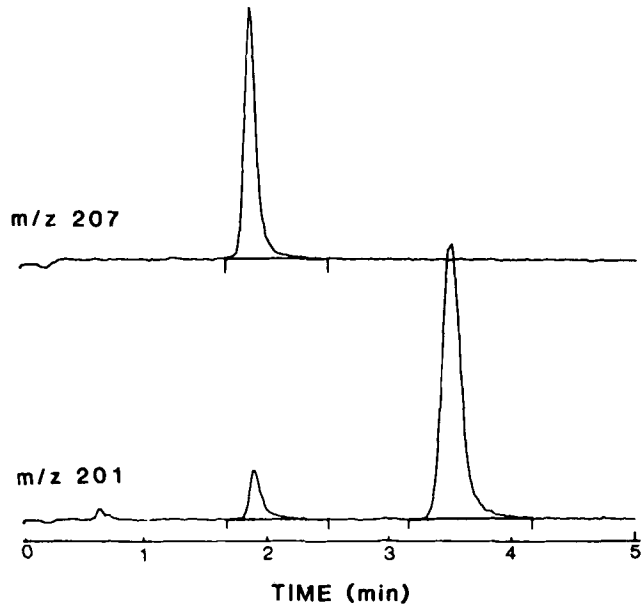

Figure 2—*Selected-ion chromatograms of an extracted saliva sample. Key: (m/z 207) [²H]valproic acid; (m/z 201) valproic (1.90 min) and octanoic (3.55 min) acids.*

[10] Model MAT-111; Varian Associates.
[11] Model 620L Computer; Varian Associates.
[12] Supelco, Inc., Bellefonte, Pa.
[13] Model 761A; Hewlett-Packard.

Table I—Calibration Curve Data of the *tert*-Butyldimethylsilyl Ester of [²H]Valproic Acid in Biological Samples

Concentration, μg/mL	Mean Peak Area Ratio[a] (*RSD*)	Linear Regression Parameters[b]
	Saliva	
0.10	0.20 (6.67%)	
0.25	0.045 (3.77%)	$a^0 = -0.008$
0.50	0.085 (0.79%)	
1.00	0.186 (1.89%)	$a_1 = 0.185$
1.50	0.238 (0.92%)	
3.00	0.546 (1.02%)	$r^2 = 0.9986$
6.00	1.108 (1.45%)	
	Serum	
10	0.350 (1.75%)	$a^0 = -0.0349$
20	0.705 (2.68%)	
40	1.295 (0.77%)	$a_1 = 0.0358$
60	2.130 (0.57%)	
80	2.880 (0.31%)	$r^2 = 0.9981$
100	3.525 (0.44%)	

[a] $n = 4$. Peak area ratio is the ratio of *m/z* 207 of hexadeuterated valproic acid ester to *m/z* 201 of octanoic acid ester. [b] r^2 is the coefficient of determination, a_1 is the slope, and a^0 is the intercept. Equation for the line is $y = a_1x + a^0$ where y is the peak area ratio mean and x is drug concentration.

Single-Dose Study—A healthy male volunteer, 41 years of age (weight, 63.64 kg), who had not taken any drugs during the month prior to the experiment, participated in both the single- and multiple-dose studies. A single oral dose was prepared by dissolving 372 mg of valproic acid (I) and 182 mg of [²H]valproic acid (II) in 100 mL of water, and the pH of the resulting solution was adjusted to 7.4 using 1 M NaOH. The oral dose was taken in the morning after an overnight fast; food was not allowed until 3 h after dosing. Blood samples (5 mL) were taken at 0, 0.5, 1, 1.5, 2, 2.5, 3, 4, 5, 6, 7, 8, 12, 24, and 48 h, using an indwelling catheter (flushed with heparin solution) for the first 4 h and thereafter by venipuncture. Serum was prepared immediately after blood sampling. Saliva samples (2–5 mL) were obtained coincident to blood sample collections *via* expectoration into clean scintillation vials. Urine was collected at the following times: 0, 1, 2, 3, 4, 5, 6, 7, 8–12, 12–24, and 24–48 h after dosing. The serum, saliva, and urine samples were kept at −20°C until they were analyzed.

Multiple-Dose Study—A 600-mg oral dose of valproic acid syrup[14] (50 mg/mL) was given to the volunteer, who participated in both dosing studies, at 8 p.m. on day 1. The same dose of valproic acid was administered twice a day 12 h apart for the next 3 d. On day 5 (84 h after the initial dose) 600 mg of [²H]valproic acid dissolved in 100 mL of water (pH 7.4) was substituted for the valproic acid as the eighth dose. This dose was taken at the usual time in the morning after an overnight fast (all morning doses were following an

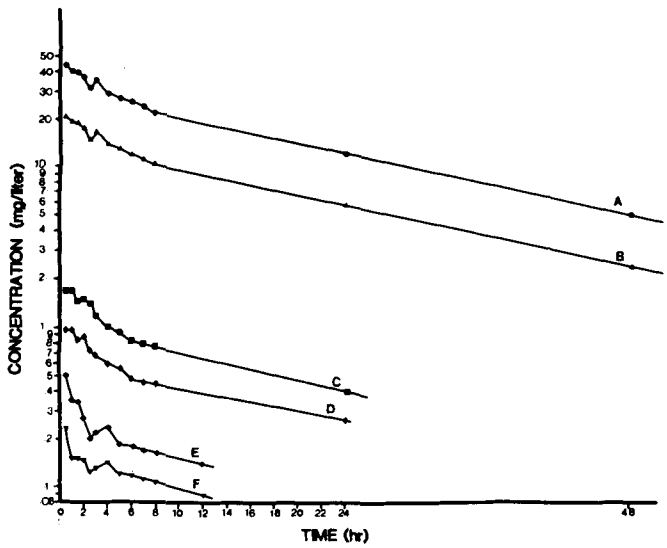

Figure 3—*Time course of valproic acid (I) and [²H]valproic acid (II) in saliva and serum following a single oral dose of 372 mg of I plus 182 mg of II. Key: (A) serum total I; (B) serum total II; (C) serum free I; (D) serum free II; (E) saliva I; (F) saliva II.*

[14] Depakene; Abbott Laboratories Ltd., Montreal, Canada.

Table II—Pharmacokinetic Parameters for Valproic Acid (I) and [^{2}H]-Valproic Acid (II) Under Single-Dose and Steady-State Conditions in a Healthy Male Volunteer [a]

Biophase	$t_{1/2}$,h	K_E, h^{-1}	CL[b], L/h/kg	Vd (area)	AUC, mg·h/L
Single-Dose Conditions (372 mg of I and 182 mg of II)					
Serum					
Total I	18.6	0.0372	0.0070	0.188	841.3
Total II	18.7	0.0371	0.0075	0.202	379.1
Free I	16.8	0.0413	0.20	4.84	29.27
Free II	18.3	0.0378	0.17	4.50	16.83
Saliva					
I	17.4	0.0398	1.1	27.6	5.23
II	15.4	0.0451	0.88	19.5	3.25
Steady-State Conditions (Multiple Doses of I, 600 mg of II)					
Serum					
Total II[c]	14.3	0.0485	0.010	0.206	900
Total (I + II)[d]	13.5	0.0513	0.011	0.214	872
Free II	13.2	0.0525	0.12	2.29	79.48
Free (I + II)	14.8	0.0468	0.13	2.78	72.52
Saliva					
II	16.5	0.0420	0.88	20.9	10.66
(I + II)	13.1	0.0529	1.1	20.8	8.86

[a] Weight = 63.64 kg. [b] Oral bioavailability is assumed to be unity. [c] Parameters for II are calculated from $t = 0$–∞. [d] Parameters for (I + II) are calculated from steady-state I and II concentrations summed during the dosing interval of 12 h following the dose of II.

overnight fast). Thereafter, valproic acid syrup (600 mg) was administered every 12 h for a further period of 3 d.

During the multiple-dose study, blood samples (5 mL) were withdrawn periodically (usually at the trough levels) prior to the administration of the labeled valproic acid. Following the [^{2}H]valproic acid dose, blood samples were taken at various times. Serum was prepared from each sample, and the pH was measured immediately using a pH meter[6]. Serum samples were stored at −20°C until analyzed.

Saliva samples (2–5 mL) were obtained with and without stimulation with sucrose. For the correlation study of saliva and serum drug levels, unstimulated saliva samples were collected 5 min before each blood sampling time and a stimulated saliva sample was obtained 5 min following the blood sample collection. Saliva samples were also obtained at times not coincident with blood sampling times. The pH of the saliva sample was determined immediately following collection using a pH meter[6]. Saliva samples were stored at −20°C until analyzed.

Serum and Saliva Standards—The valproic acid assay used has been described previously in detail (13). Serum standards of labeled and unlabeled valproic acid were prepared by the addition of 0.1 mL of appropriate stock solutions in methanol into 5-mL volumetric flasks. Drug-free serum was added to the 5-mL mark to provide [^{2}H]valproic acid concentrations of 10, 20, 40, 60, 80, and 100 μg/mL and valproic acid concentrations of 20, 40, 60, 80, 100, and 120 μg/mL.

Saliva standards were prepared similarly, but with [^{2}H]valproic acid concentrations of 0.1, 0.25, 0.5, 1.0, 1.5, 3.0, and 6.0 μg/mL and valproic acid concentrations of 0.25, 0.5, 1.0, 1.5, 3.0, and 6.0 μg/mL.

Extraction and Derivatization—Serum standard or sample (50 μL) was pipetted into a 1.0-mL conical reaction vial[15]. Internal standard (200 μL of a solution of 10 mg/L octanoic acid in 1 M HCl) was added, followed by 200 μL of solvent (10% ethyl acetate in *n*-hexane), and the mixture was vortex mixed for 60 s. After centrifuging at 1000×*g* for 20 min, 150 μL of the solvent layer was transferred to a second vial and 7 μL of *tert*-butyldimethylchlorosilane reagent[16] was added. The mixture was vortex mixed for 30 s and then centrifuged for 5 min. A 5-μL aliquot of the organic layer was injected into the GC–MS system.

For saliva drug analysis, 200-μL saliva samples were treated in a manner similar to the serum samples, except that the internal standard concentration was 6.5 mg/L in 1 M HCl.

Selected-Ion Monitoring—Labeled and unlabeled valproic acids were quantitated in serum and saliva by selected-ion monitoring with the GC–MS system operated in the EI-mode. The very intense ions *m/z* 201 from the *tert*-butyldimethylsilyl derivatives of valproic acid and octanoic acid and the corresponding *m/z* 207 from the derivative of [^{2}H]valproic acid were monitored continuously. The retention times for the *tert*-butyldimethylsilyl derivatives of valproic acid (or [^{2}H]valproic acid) and octanoic acid on the Dexsil 300 column were 2.0 and 3.6 min, respectively.

[15] Reacti-vial with teflon-lined cap; Pierce Chemical Co., Rockford, Ill.

[16] 1 mmol of *tert*-butyldimethylchlorosilane and 2.5 mmol of imidazole dissolved in 1 mL of dimethylformamide; Applied Science Lab. Inc., State College, Pa.

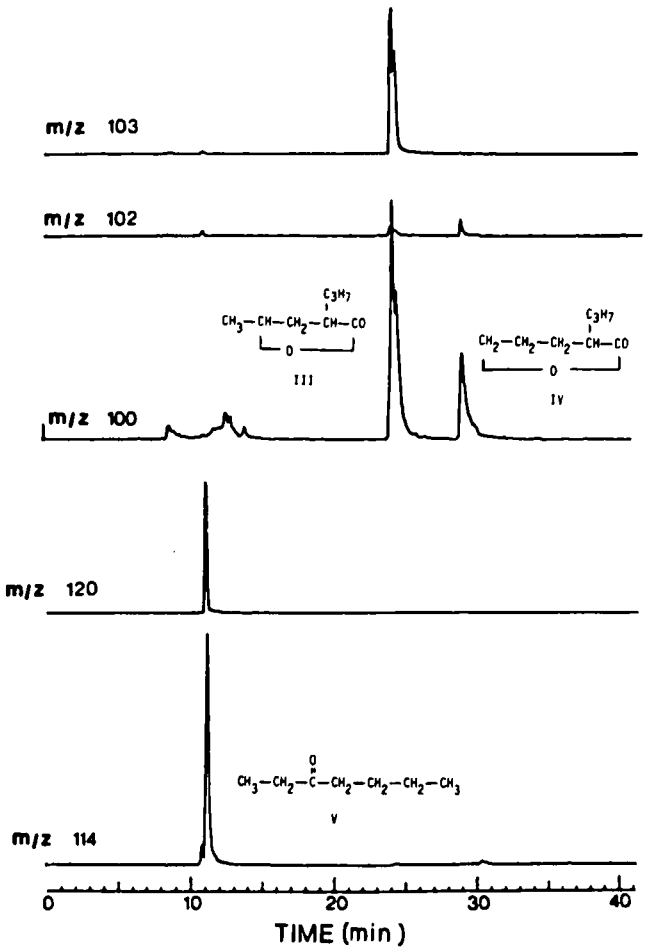

Figure 4—*Mass chromatograms of metabolites isolated from a urine sample following a single oral dose containing both valproic acid and [^{2}H]valproic acid. The* m/z *100 ion fragment peaks at 24 and 29 min are from the lactones of 4-hydroxyvalproic acid (III) and 5-hydroxyvalproic acid (IV), respectively. Corresponding peaks at* m/z *103 and* m/z *102 are the tri- and di- deuterated-analogues of the lactones. The lactones are formed during the acid extraction of the urine. Isomer separation is observed for the 4-hydroxyvalproic acid lactone (*m/z *100,* m/z *103 peaks);* m/z *114 and* m/z *120 peaks are 3-heptanone (V) and 3-[^{2}H]heptanone, respectively. The heptanone arises from acidic decarboxylation of 3-ketovalproic acid during the extraction.*

Calibration curves for valproic acid and [^{2}H]valproic acid were prepared by plotting the ion area ratios of drug to internal standard against the known drug concentrations. For valproic acid, the *m/z* 201 area ratios were used while the *m/z* 207 to *m/z* 201 area ratios were used for [^{2}H]valproic acid.

Plasma Protein Binding Studies—Free drug levels in serum were determined by equilibrium dialysis. The procedure has been described in a previous study (13). The serum and buffer samples from the two compartments were analyzed by GC–MS for free levels of valproic acid and [^{2}H]valproic acid. The extraction and derivatization procedures used were the same as for total drug quantitation in serum. The concentrations of free drug were determined using standard curves (1–10 μg/mL) prepared from buffer solutions to which valproic acid or [^{2}H]valproic acid had been added.

Pharmacokinetic Analysis—The elimination rate constants (K_E) of both valproic acid and [^{2}H]valproic acid were determined by least-squares regression analysis of the terminal log-linear part of the decay curves. The kinetic parameters, elimination half-life ($t_{1/2}$), area under the curve (AUC), total body clearance (CL), and apparent volume of distribution (Vd) were calculated by standard methods (14).

RESULTS AND DISCUSSION

Synthesis—[^{2}H]Valproic acid (II) was obtained *via* malonic ester synthesis according to the method of Adams and Kamm (15). The deuterated product had a high isotopic purity, as shown by comparison of the mass spectra of the

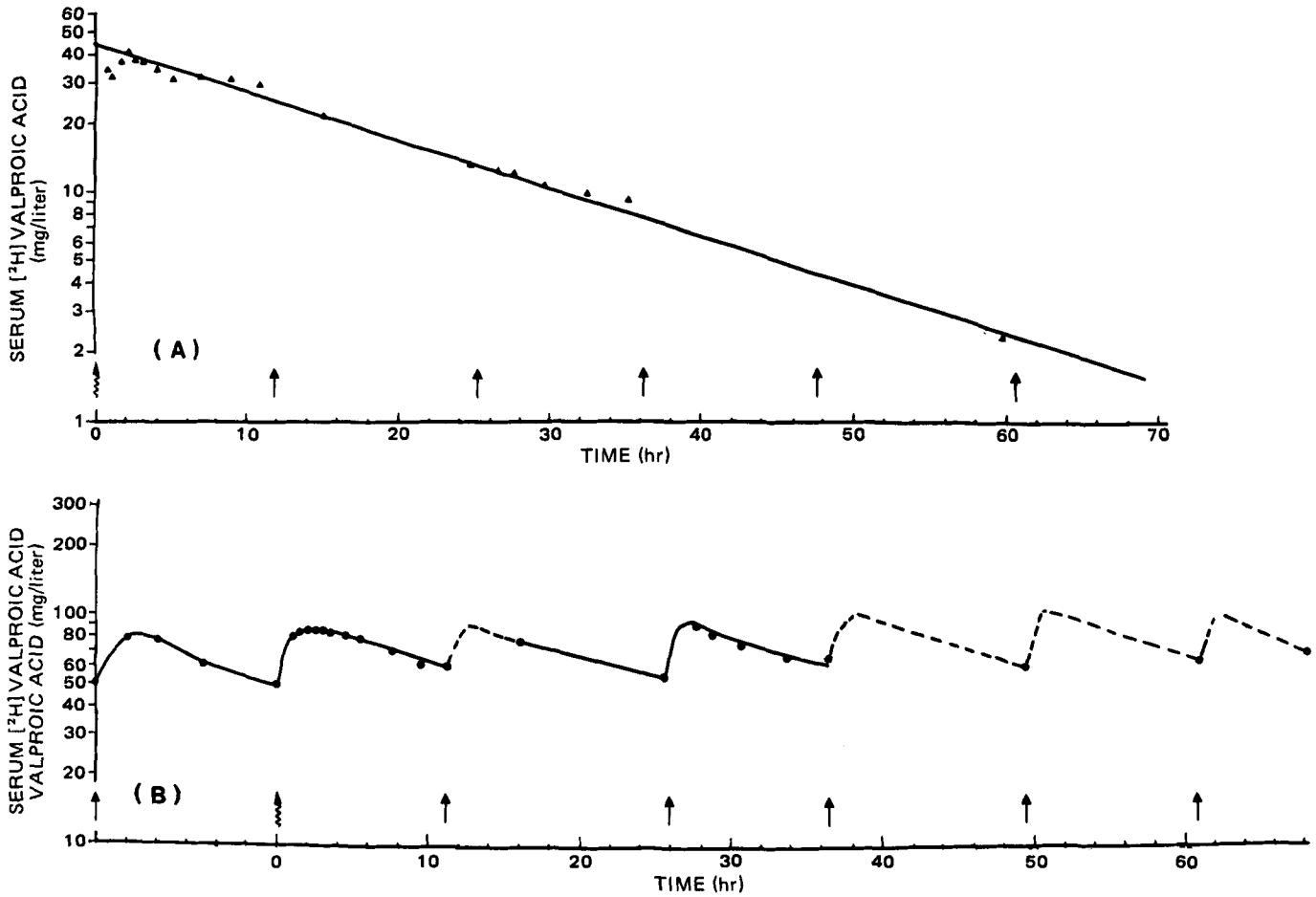

Figure 5—*(A) Time course of serum total [²H]valproic acid given as a substitute dose (600 mg) during multiple dosing with valproic acid. (B) Time course of serum total valproic acid + [²H]valproic acid beginning 12 h prior to and continuing for 60 h after the [²H]valproic acid dose. Key: (↕) time of dose of [²H]valproic acid; (↑) times when valproic acid (600 mg) was given.*

tert-butyldimethylsilyl derivatives of [²H]valproic acid and valproic acid (Fig. 1).

Assay—In this study it was imperative to develop a specific and sensitive assay to measure both valproic acid and [²H]valproic acid in serum and saliva. Quantitation was accomplished by monitoring the highly intense $[M-57]^+$ ions of the *tert*-butyldimethylsilyl derivatives (Fig. 1). The advantages of using the *tert*-butyldimethylsilyl derivatives compared with the trimethylsilyl and methyl esters of valproic acid have been discussed previously (13). The assay procedure used has resulted in clean mass chromatograms. Figure 2 shows a typical selected-ion chromatogram from a saliva sample. The recoveries of [²H]valproic acid from spiked serum and saliva samples were found to be 100%. The calibration curves constructed for valproic acid and [²H]valproic acid in serum and saliva were linear within the concentration ranges used and gave high correlation coefficients. Table I shows typical standard curves for [²H]valproic acid in serum and saliva. Calibration curves for valproic acid in serum and saliva were similar to that of a previous study (13). The relative standard deviations were generally <5%, attesting to the reproducibility of the assay.

Table III—Relationship of Saliva Concentrations of Valproic Acid and [²H]Valproic Acid and Serum Total or Serum Free Drug Levels in the Single- and Multiple-Dose Studies

Parameters[a]	Valproic Acid	[²H]Valproic Acid
Single-Dose Conditions		
Mean ratio, saliva/total serum	0.007	0.009
SD	0.001	0.001
r	0.926	0.901
Mean ratio, saliva/free serum	0.196	0.200
SD	0.027	0.033
r	0.863	0.850
Steady-State Conditions		
Mean ratio, saliva/total serum	0.009	0.011
SD	0.002	0.002
r	0.953	0.956
Mean ratio, saliva/free serum	0.112	0.138
SD	0.021	0.031
r	0.939	0.916

[a] Steady-state concentrations were measured during the first three dosing intervals following labeled-drug administration ($n = 17$); single-dose concentrations cover a period of 24 h ($n = 10$).

Pharmacokinetics of the Single- and Multiple-Dose Studies—Stable-isotope-labeled drugs have been used in different areas of pharmacokinetics including steady-state kinetics (10, 11), bioavailability studies (16), drug interaction studies (6), and drug metabolism studies (17). A stable-isotope-labeled drug which shows a significant biological isotope effect is not appropriate for use in a pharmacokinetic study. To examine the suitability of [²H]valproic acid for pharmacokinetic studies, (*i.e.*, lack of significant isotope effects), a single oral dose consisting of a 2:1 molar ratio of valproic acid to [²H]valproic acid was administered to a healthy human subject. The concentration–time curves of valproic acid and [²H]valproic acid for both serum and saliva describe the same constant 2:1 ratio of areas (Table II) as in the dose. The parallelism between the elimination phases of serum total valproic acid and serum total [²H]valproic acid (Fig. 3) strongly demonstrated that there was no significant isotope effect on the elimination kinetics of valproic acid after incorporation of six deuterium atoms onto the terminal carbon atoms of the propyl chains.

Additional evidence for the absence of a major isotope effect came from the analysis of urinary metabolites, where the major metabolites [valproic acid glucuronide, 3-ketovalproic acid, and 4-hydroxyvalproic acid (3)] showed the consistent 2:1 molar ratio of unlabeled to labeled metabolite (Fig. 4). An isotope effect was observed for the formation of the minor metabolite, 5-hydroxyvalproic acid. Because of the small proportion of 5-hydroxyvalproic acid relative to the other metabolites, a decrease in the formation of 5-hydroxy[$^2H_5$]valproic acid does not markedly affect the elimination kinetics of [²H]valproic acid.

The serum concentration–time curves of both valproic acid and [²H]valproic

acid after a single oral dose were biphasic, similar to those described by Gugler *et al.* (7) and as previously reported by Abbott *et al.* (13). Peak levels of valproic acid and [^{2}H]valproic acid were observed at 0.5 h in serum and saliva.

Following the dose of [^{2}H]valproic acid at steady state, absorption of this deuterated analogue was rapid with peak serum levels appearing within 2–3 h (Fig. 5). Biphasic elimination was not evident for either valproic acid in the 12-h dosing intervals or for [^{2}H]valproic acid as observed over 72 h. All decay curves appeared to be monoexponential.

Table II summarizes the pharmacokinetic data derived from the single-dose and steady-state experiments. The single-dose serum elimination half-life values observed for valproic acid and [^{2}H]valproic acid are practically identical and are comparable with the 15.9 ± 2.6 h value reported by Gugler *et al.* (7). Under multiple-dose conditions, the similar half-life values observed for serum total [^{2}H]valproic acid (14.3 h) and serum total valproic acid plus [^{2}H]valproic acid (13.5 h) was further evidence that [^{2}H]valproic acid is assimilated by the body in a manner identical to the unlabeled valproic acid. As an additional test, the serum total half-life values of valproic acid and valproic acid plus [^{2}H]valproic acid were compared over three consecutive days beginning the day prior to the deuterated dose. No significant change in half-life values was observed. Identical kinetic behavior of the two valproic acid species under multiple-dose conditions is also evident from the AUC data; the serum total $AUC_{0-\infty}$ for [^{2}H]valproic acid (900 mg·h/L) is essentially identical to the valproic acid plus [^{2}H]valproic acid $AUC_{\tau 1-\tau 2}$ (872 mg·h/L) as is expected from application of the principle of superposition where $AUC_{0-\infty}$ after first dose is equivalent to $AUC_{\tau 1-\tau 2}$ at steady state (14).

The elimination half-life of serum total [^{2}H]valproic acid of 14.3 h in this individual under multiple-dose conditions was shorter than the half-life observed in the single-dose study. The apparent volume of distribution of [^{2}H]valproic acid at steady state was not different from the single-dose value. However, the total body clearance of [^{2}H]valproic acid increased by 33% over the single-dose value. The observed increase in total body clearance may better reflect the change in valproic acid elimination kinetics from single- to multiple-dose conditions, since it is a parameter that is model independent (18). The change in total body clearance is not likely due to a reduction in the amount of drug absorbed, since the oral bioavailability is nearly 100% (19, 20). There is the possibility that the 33% increase in total body clearance is due to either an enzyme-inducing effect of valproic acid or a change in binding of valproic acid to serum proteins or both.

On the enzyme-inducing property of valproic acid, several investigators (21, 22) have reported that the half-life of antipyrine and D-glucaric acid urinary excretion in patients treated with sodium valproate were not different from those in drug-free controls. There has been one study (23) that reported that valproic acid increased D-glucaric acid urinary excretion significantly but not serum γ-glutamyltranspeptidase activity in epileptic children.

Valproic acid is cleared by metabolism and has a low extraction ratio (19); its rate of metabolism is proportional to the free serum concentrations. Total body clearance (CL_T) is a function of the free fraction of valproic acid (fu) and the intrinsic clearance (CL'_{int}) through the expression:

$$CL_T = CL'_{int} \cdot fu$$

where fu is the ratio of free drug to the total drug in serum and CL'_{int} is the inherent activity of the liver to metabolize unbound valproic acid (free clearance of valproic acid). In theory, a decrease in plasma protein binding (increase in fu) should increase total body clearance and decrease total serum concentrations of valproic acid or [^{2}H]valproic acid, but should have no effect on the free serum concentration of valproic acid or [^{2}H]valproic acid (18, 24).

In the present study total body clearance increased at steady state compared with the single-dose study (Table II), while the average free fraction in serum (fu) increased from 0.05 (±0.01 *SD*) under single-dose conditions to 0.09 (±0.01 *SD*) at steady-state serum total valproic acid plus [^{2}H]valproic acid concentrations of 50–100 μg/mL. Unless the liver enzyme activity was affected, one would not expect CL_{free} (CL'_{int}) to change between single-dose and steady-state conditions. The clearance of the free drug, however, was seen to decrease (*e.g.*, single dose for [^{2}H]valproic acid = 0.17 L/h/kg; steady state for [^{2}H]valproic acid = 0.12 L/h/kg; see Table II) under steady-state conditions, suggesting possible inhibition of metabolism of valproic acid or saturation of drug-metabolizing enzymes in this subject. Similar decreases in clearance of the free drug (CL_{free}) at steady state were observed by Bowdle *et al.* (8) for a group of normal volunteers on a multiple-dose schedule with valproic acid.

Saliva Valproic Acid Measurement—The saliva levels of valproic acid and [^{2}H]valproic acid were measured to determine if a significant correlation exists between serum total or serum free drug concentrations and saliva drug concentrations. The GC–MS method used here for measuring saliva valproic acid levels is highly sensitive and proved more than adequate to obtain precise data for the saliva concentrations in pharmacokinetic studies.

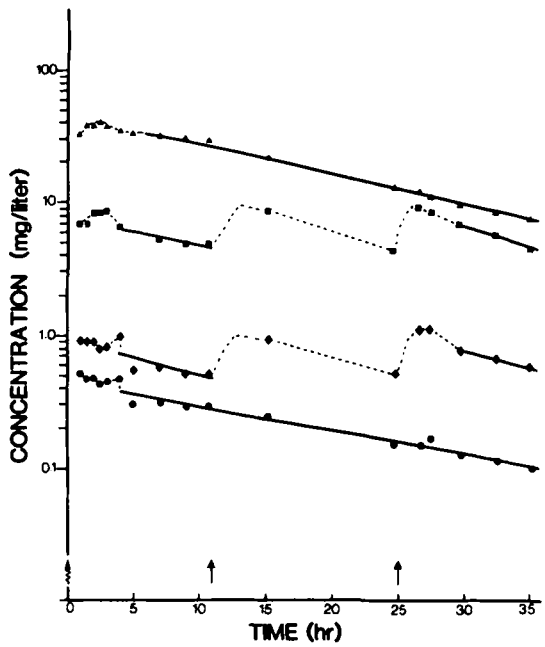

Figure 6—*Concentration–time curves of valproic acid (I) and [^{2}H]valproic acid (II) in serum and saliva following a 600-mg dose of II during the multiple-dose study. Key: (▲) serum total II; (■) serum free (I + II); (◆) saliva (I + II); (●) saliva II; (‡) time of dose of II; (↑) times when I (600 mg) was given.*

Sucrose-stimulated saliva samples had consistently lower pH (5.85 ± 0.48, n = 25) than unstimulated saliva samples (6.98 ± 0.29, n = 25) at similar sampling times. The greater variation in stimulated saliva pH may explain the greater fluctuations observed in the stimulated saliva drug concentrations compared with unstimulated saliva drug concentrations. Sucrose-stimulated saliva valproate levels during the multiple-dose study were higher (mean = 0.684 mg/L) than unstimulated saliva valproic acid levels (mean = 0.609 mg/L), and the difference was significant (pairwise t test, p = 0.013, n = 22).

The time course of unstimulated saliva valproic acid and [^{2}H]valproic acid concentrations at steady state are presented in Fig. 6 together with that of serum total [^{2}H]valproic acid concentrations and serum free valproic acid plus [^{2}H]valproic acid concentrations. Table III summarizes the relationship of drug levels found in saliva and serum.

The mean saliva to serum drug ratios are comparable with values obtained by Gugler *et al.* (7, 25). The correlation between saliva and serum total drug levels was fairly high (Table III) and is, in part, due to the precision of the assay (13). The low correlation values (0.11–0.64) reported in previous studies (9, 26, 27) may be due in part to the GC assays used in measuring saliva levels <1 μg/mL (7, 27). Another factor is the pooled human data analyzed in these studies, since interindividual variability is greater than intraindividual variability (7, 20).

The saliva levels of valproic acid were 20% of the serum free valproic acid concentration under single-dose conditions. Under a multiple-dose regimen, saliva valproate decreased to ~12% of the free serum drug concentrations (Table III). The increase in the serum free fraction under the multiple-dose conditions accounts for the observed decrease in the saliva to free serum valproate ratio.

REFERENCES

(1) D. Simon and J. K. Penry, *Epilepsia*, **16**, 549 (1975).

(2) R. M. Pinder, R. N. Brogden, T. M. Speight, and G. S. Avery, *Drugs*, **13**, 81 (1977).

(3) R. Gugler and G. E. Von Unruh, *Clin. Pharmacokinet.*, **5**, 67 (1980).

(4) J. Bruni, B. J. Wilder, L. J. Wilmore, R. J. Perchalski, and H. J. Villareal, *Clin. Pharmacol. Ther.*, **24**, 324 (1978).

(5) E. Perucca, G. Gatti, G. M. Frigo, A. Crema, S. Calzetti, and D. Visintini, *Br. J. Clin. Pharmacol.*, **5**, 495 (1978).

(6) G. E. Von Unruh, B. C. Jancik, and F. Hoffmann, *Biomed. Mass Spectrom.*, **7**, 164 (1980).

(7) R. Gugler, A. Schell, M. Eichelbaum, W. Froscher, and H-U. Schultz, *Eur. J. Clin. Pharmacol.*, **12**, 125 (1977).

(8) T. A. Bowdle, I. H. Patel, R. H. Levy, and A. J. Wilensky, *Clin. Pharmacol. Ther.*, **28**, 486 (1980).
(9) V. Nitsche and H. Mascher, *Epilepsia*, **23**, 152 (1982).
(10) H. R. Sullivan, F. J. Marshall, R. E. McMahon, E. Anggard, L.-M. Gunne, and J. H. Holmstrand, *Biomed. Mass Spectrom.*, **2**, 197 (1975).
(11) I. M. Kapetanovic and H. J. Kupferberg, *Biomed. Mass Spectrom.*, **7**, 47 (1980).
(12) V. V. Ranade and A. Alter, *J. Labelled Compd. Radiopharmaceut.*, **17**, 733 (1980).
(13) F. S. Abbott, R. Burton, J. Orr, D. Wladichuk, S. Ferguson, and T. H. Sun, *J. Chromatogr.*, **227**, 433 (1982).
(14) M. Gibaldi and D. Perrier, "Pharmacokinetics," J. Swarbrick, Ed., Dekker, New York, N.Y., 1975, pp. 1–118.
(15) R. Adams and R. M. Kamm, "Organic Syntheses," Coll. vol. I, Wiley, New York, N.Y., 1941, p. 250.
(16) J. M. Strong, J. S. Dutcher, W. K. Lee, and A. J. Atkinson Jr., *Clin. Pharmacol. Ther.*, **18**, 613 (1975).
(17) R. Roncucci, M. J. Simon, G. Jacques, and G. Lambelin, *Eur. J. Drug Metab. Pharmacokinet.*, **2**, 9 (1976).
(18) G. R. Wilkinson and D. G. Soha, *Clin. Pharmacol. Ther.*, **18**, 377 (1975).
(19) U. Klotz and K. H. Antonin, *Clin. Pharmacol. Ther.*, **21**, 736 (1977).
(20) E. Perucca, G. Gatti, G. M. Frigo, and A. Crema, *Br. J. Clin. Pharmacol.*, **5**, 313 (1978).
(21) B. J. Jordan, J. S. Shillingford, and K. P. Steed, in "Clinical and Pharmacological Aspects of Sodium Valproate (Epilim) in the Treatment of Epilepsy," N. J. Legg, Ed., M. C. S. Consultant, Tunbridge Wells, U.K., 1976, pp. 112–116.
(22) E. Perucca, A. Hedges, K. A. Makki, J. Hebridge, J. Wadsworth, and A. Richens, *Br. J. Clin. Pharmacol.*, **7**, 414P (1979).
(23) F. A. De Wolff, A. C. B. Peters, and G. M. J. Van Kempen, *Lancet*, **i**, 843 (1981).
(24) M. Rowland, *Ther. Drug Monit.*, **2**, 29 (1980).
(25) R. Gugler, M. Eichelbaum, A. Schell, W. Froscher, H. Kiefer, H-U. Schultz, and G. Muller in "Antiepileptic Therapy: Advances in Drug Monitoring," S. I. Johannessen, P. L. Morselli, C. E. Pippenger, A. Richens, A. Schmidt, and H. Meinardi, Eds., Raven, New York, N.Y., 1980, p. 121.
(26) G. F. Blom, and P. J. M. Guelen in "Antiepileptic Drug Monitoring," C. Gardner-Thorpe, D. Janz, and H. Meinardi, Eds., Pitman Medical, Tunbridge Wells, U.K., 1977, p. 287.
(27) E. Monaco, S. Piredda, R. Mutani, C. Mastropaolo, and M. Tondi, *Epilepsia*, **23**, 23 (1982).

ACKNOWLEDGMENTS

Supported in part by a grant from the British Columbia Health Care Research Foundation. Abstracted from the Master of Science thesis of Andrew A. Acheampong, 1982. Presented in part at the 28th IUPAC Congress, Vancouver, B.C., August 1981.

The technical assistance of Ting-Hui Sun, Visiting Scientist, The People's Republic of China, is gratefully acknowledged.

Pharmacokinetics of Nicorandil, a New Coronary Vasodilator, in Dogs

TAKASHI ISHIZAKI *x, KAN CHIBA *, TOSHIYUKI SUGANUMA *, TOMIO SASAKI *, HIROSHI KAMIYAMA ‡, and HIDEKI NAKANO ‡

Received April 12, 1982, from the **Division of Clinical Pharmacology, Clinical Research Institute, National Medical Center, Toyama 1-21-2, Shinjuku-ku,* and the ‡*Central Research Institute, Chugai Pharmaceutical Co., Ltd., Tokyo, Japan.* Accepted for publication March 3, 1983.

Abstract □ The kinetic disposition of nicorandil, *N*-[2-(nitroxy)ethyl]-3-pyridinecarboxamide (I), and its main metabolic product, *N*-[2-(hydroxy)-ethyl]-3-pyridinecarboxamide (II), was studied after administering intravenous and oral doses (2.5 mg/kg) of nicorandil to the same beagle dogs. The plasma concentrations were measured using a high-performance liquid chromatographic method. The pharmacokinetic data derived from intravenous administration of nicorandil were: $t_{1/2}$, 0.73 ± 0.11 h; Vd_{area}, 0.67 ± 0.04 L/kg; and total plasma clearance, 13.50 ± 1.05 mL/min/kg. After oral administration, nicorandil was rapidly absorbed (t_{max}, 0.58 ± 0.11 h). The oral bioavailability was calculated as 0.72 ± 0.07. The metabolic formation of the corresponding alcohol after intravenous and oral administration of the parent compound appeared to occur quite efficiently, and its elimination half-life (3.09 ± 0.25 and 3.69 ± 0.88 h after intravenous and oral administration of nicorandil, respectively) was longer than that of the parent compound. Since the dose employed in this study was much higher than the expected therapeutic doses, whether such a good bioavailability after a lower dose of the drug would be obtained in humans remains unanswered.

Keyphrases □ Nicorandil—metabolism in dogs, pharmacokinetics, detection in plasma by HPLC □ Vasodilators, coronary—nicorandil, metabolism in dogs, pharmacokinetics, detection in plasma by HPLC □ Bioavailability—nicorandil in dogs, oral and intravenous administration, pharmacokinetics, detection in plasma by HPLC

Nicorandil[1] (*N*-[2-(nitroxy)ethyl]-3-pyridinecarboxamide, I) a new coronary vasodilator has been shown to produce a potent coronary vasodilating effect, virtually without affecting cardiac contraction, heart rate, or myocardial oxygen consumption in anesthetized dogs (1–3). The pharmacological profile appears to be somewhat similar to that of nitroglycerin (2–4). However, except for one study where the metabolic disposition of nicorandil was qualitatively examined in rats (5), the pharmacokinetics and bioavailability of this drug have not been investigated. The lack of a sensitive and specific method for measurement of nicorandil in the blood has precluded any quantitative pharmacokinetic analysis.

In this study we describe a high-performance liquid chromatographic (HPLC) method for determining nicorandil levels in canine plasma. Using this method, we attempted to study the kinetic disposition of nicorandil (I) administered intravenously and orally on two separate occasions in the same dogs. Some pharmacokinetic variables of *N*-[2-(hydroxy)-ethyl]-3-pyridinecarboxamide (II), a primary metabolite of nicorandil, were also estimated.

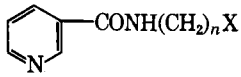

I X = ONO_2, n = 2
II X = OH, n = 2
III X = ONO_2, n = 3

EXPERIMENTAL

Materials and Procedures—Six adult beagle dogs weighing 8.2–9.9 kg were used for the study. They were fasted overnight; water was supplied *ad libitum*.

[1] The generic name was published in the *Supplement to WHO Chronicle*, **34**(9), 18 (1980). Lot R9B09, synthesized at the Organic Chemistry Research Laboratory, Chugai Pharmaceutical Co., Ltd., Tokyo, Japan, was used throughout.

0022-3549/84/0400-0494$01.00/0
© 1984, American Pharmaceutical Association

(8) T. A. Bowdle, I. H. Patel, R. H. Levy, and A. J. Wilensky, *Clin. Pharmacol. Ther.*, **28**, 486 (1980).
(9) V. Nitsche and H. Mascher, *Epilepsia*, **23**, 152 (1982).
(10) H. R. Sullivan, F. J. Marshall, R. E. McMahon, E. Anggard, L.-M. Gunne, and J. H. Holmstrand, *Biomed. Mass Spectrom.*, **2**, 197 (1975).
(11) I. M. Kapetanovic and H. J. Kupferberg, *Biomed. Mass Spectrom.*, **7**, 47 (1980).
(12) V. V. Ranade and A. Alter, *J. Labelled Compd. Radiopharmaceut.*, **17**, 733 (1980).
(13) F. S. Abbott, R. Burton, J. Orr, D. Wladichuk, S. Ferguson, and T. H. Sun, *J. Chromatogr.*, **227**, 433 (1982).
(14) M. Gibaldi and D. Perrier, "Pharmacokinetics," J. Swarbrick, Ed., Dekker, New York, N.Y., 1975, pp. 1–118.
(15) R. Adams and R. M. Kamm, "Organic Syntheses," Coll. vol. I, Wiley, New York, N.Y., 1941, p. 250.
(16) J. M. Strong, J. S. Dutcher, W. K. Lee, and A. J. Atkinson Jr., *Clin. Pharmacol. Ther.*, **18**, 613 (1975).
(17) R. Roncucci, M. J. Simon, G. Jacques, and G. Lambelin, *Eur. J. Drug Metab. Pharmacokinet.*, **2**, 9 (1976).
(18) G. R. Wilkinson and D. G. Soha, *Clin. Pharmacol. Ther.*, **18**, 377 (1975).
(19) U. Klotz and K. H. Antonin, *Clin. Pharmacol. Ther.*, **21**, 736 (1977).
(20) E. Perucca, G. Gatti, G. M. Frigo, and A. Crema, *Br. J. Clin. Pharmacol.*, **5**, 313 (1978).
(21) B. J. Jordan, J. S. Shillingford, and K. P. Steed, in "Clinical and Pharmacological Aspects of Sodium Valproate (Epilim) in the Treatment of Epilepsy," N. J. Legg, Ed., M. C. S. Consultant, Tunbridge Wells, U.K., 1976, pp. 112–116.
(22) E. Perucca, A. Hedges, K. A. Makki, J. Hebridge, J. Wadsworth, and A. Richens, *Br. J. Clin. Pharmacol.*, **7**, 414P (1979).
(23) F. A. De Wolff, A. C. B. Peters, and G. M. J. Van Kempen, *Lancet*, **i**, 843 (1981).
(24) M. Rowland, *Ther. Drug Monit.*, **2**, 29 (1980).
(25) R. Gugler, M. Eichelbaum, A. Schell, W. Froscher, H. Kiefer, H-U. Schultz, and G. Muller in "Antiepileptic Therapy: Advances in Drug Monitoring," S. I. Johannessen, P. L. Morselli, C. E. Pippenger, A. Richens, A. Schmidt, and H. Meinardi, Eds., Raven, New York, N.Y., 1980, p. 121.
(26) G. F. Blom, and P. J. M. Guelen in "Antiepileptic Drug Monitoring," C. Gardner-Thorpe, D. Janz, and H. Meinardi, Eds., Pitman Medical, Tunbridge Wells, U.K., 1977, p. 287.
(27) E. Monaco, S. Piredda, R. Mutani, C. Mastropaolo, and M. Tondi, *Epilepsia*, **23**, 23 (1982).

ACKNOWLEDGMENTS

Supported in part by a grant from the British Columbia Health Care Research Foundation. Abstracted from the Master of Science thesis of Andrew A. Acheampong, 1982. Presented in part at the 28th IUPAC Congress, Vancouver, B.C., August 1981.

The technical assistance of Ting-Hui Sun, Visiting Scientist, The People's Republic of China, is gratefully acknowledged.

Pharmacokinetics of Nicorandil, a New Coronary Vasodilator, in Dogs

TAKASHI ISHIZAKI *x, KAN CHIBA *, TOSHIYUKI SUGANUMA *, TOMIO SASAKI *, HIROSHI KAMIYAMA ‡, and HIDEKI NAKANO ‡

Received April 12, 1982, from the **Division of Clinical Pharmacology, Clinical Research Institute, National Medical Center, Toyama 1-21-2, Shinjuku-ku,* and the ‡*Central Research Institute, Chugai Pharmaceutical Co., Ltd., Tokyo, Japan.* Accepted for publication March 3, 1983.

Abstract □ The kinetic disposition of nicorandil, *N*-[2-(nitroxy)ethyl]-3-pyridinecarboxamide (I), and its main metabolic product, *N*-[2-(hydroxy)-ethyl]-3-pyridinecarboxamide (II), was studied after administering intravenous and oral doses (2.5 mg/kg) of nicorandil to the same beagle dogs. The plasma concentrations were measured using a high-performance liquid chromatographic method. The pharmacokinetic data derived from intravenous administration of nicorandil were: $t_{1/2}$, 0.73 ± 0.11 h; Vd_{area}, 0.67 ± 0.04 L/kg; and total plasma clearance, 13.50 ± 1.05 mL/min/kg. After oral administration, nicorandil was rapidly absorbed (t_{max}, 0.58 ± 0.11 h). The oral bioavailability was calculated as 0.72 ± 0.07. The metabolic formation of the corresponding alcohol after intravenous and oral administration of the parent compound appeared to occur quite efficiently, and its elimination half-life (3.09 ± 0.25 and 3.69 ± 0.88 h after intravenous and oral administration of nicorandil, respectively) was longer than that of the parent compound. Since the dose employed in this study was much higher than the expected therapeutic doses, whether such a good bioavailability after a lower dose of the drug would be obtained in humans remains unanswered.

Keyphrases □ Nicorandil—metabolism in dogs, pharmacokinetics, detection in plasma by HPLC □ Vasodilators, coronary—nicorandil, metabolism in dogs, pharmacokinetics, detection in plasma by HPLC □ Bioavailability—nicorandil in dogs, oral and intravenous administration, pharmacokinetics, detection in plasma by HPLC

Nicorandil[1] (*N*-[2-(nitroxy)ethyl]-3-pyridinecarboxamide, I) a new coronary vasodilator has been shown to produce a potent coronary vasodilating effect, virtually without affecting cardiac contraction, heart rate, or myocardial oxygen consumption in anesthetized dogs (1–3). The pharmacological profile appears to be somewhat similar to that of nitroglycerin (2–4). However, except for one study where the metabolic disposition of nicorandil was qualitatively examined in rats (5), the pharmacokinetics and bioavailability of this drug have not been investigated. The lack of a sensitive and specific method for measurement of nicorandil in the blood has precluded any quantitative pharmacokinetic analysis.

In this study we describe a high-performance liquid chromatographic (HPLC) method for determining nicorandil levels in canine plasma. Using this method, we attempted to study the kinetic disposition of nicorandil (I) administered intravenously and orally on two separate occasions in the same dogs. Some pharmacokinetic variables of *N*-[2-(hydroxy)-ethyl]-3-pyridinecarboxamide (II), a primary metabolite of nicorandil, were also estimated.

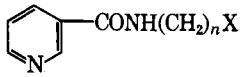

I X = ONO_2, n = 2
II X = OH, n = 2
III X = ONO_2, n = 3

EXPERIMENTAL

Materials and Procedures—Six adult beagle dogs weighing 8.2–9.9 kg were used for the study. They were fasted overnight; water was supplied *ad libitum*.

[1] The generic name was published in the *Supplement to WHO Chronicle*, **34**(9), 18 (1980). Lot R9B09, synthesized at the Organic Chemistry Research Laboratory, Chugai Pharmaceutical Co., Ltd., Tokyo, Japan, was used throughout.

0022-3549/84/0400-0494$01.00/0
© 1984, American Pharmaceutical Association

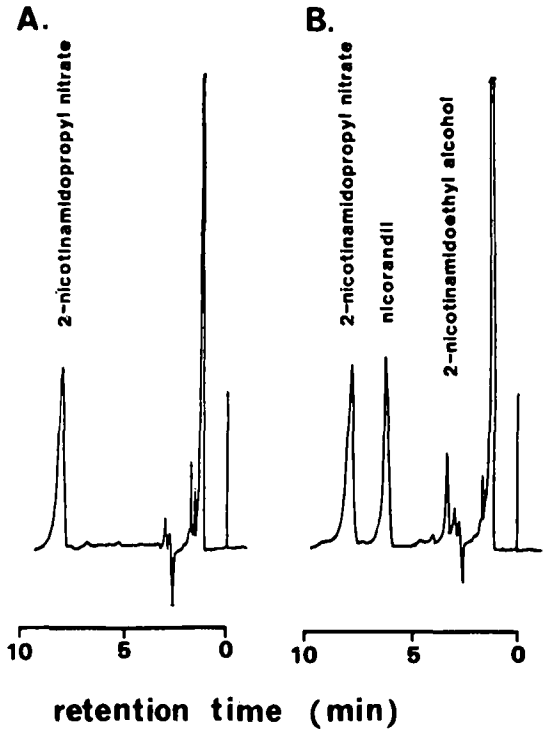

Figure 1—*Chromatograms of 10-μL canine plasma extracts. Key: (A) blank plasma spiked with 1.0 μg/mL of III (internal standard); (B) plasma spiked with 1 μg/mL of nicorandil and each of its analogues.*

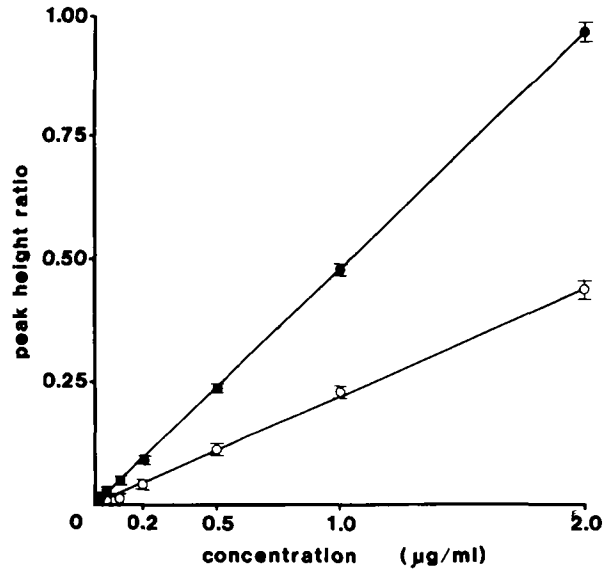

Figure 2—*Calibration curves for nicorandil and alcohol II in canine plasma. A four-point standard curve was prepared by plotting the ratio of the peak height of each compound to that of the internal standard, as mean ± SEM. Linear regression analysis of calibration curve data indicated no significant deviation from linearity for both compounds:* y = 0.4768x + 0.0031, r = 0.9997 *for nicorandil (●);* y = 0.2225x + 0.0006, r = 0.9970 *for alcohol II (○). In addition, intercept values did not significantly differ from zero.*

The dogs were examined during a 7-d acclimation period prior to the experiment, and showed no apparent hepatic or renal dysfunction. No anesthetic was administered during the experiments.

The dogs received 2.5 mg/kg of nicorandil (I) intravenously and orally on two occasions, separated by a 2-week wash-out period. The study was carried out in a randomized crossover fashion: three dogs received the intravenous dose first, while the oral dose was administered to the remaining three; the group given the intravenous dose in the first experiment was given the oral dose in the second and *vice versa*. Nicorandil was dissolved at a concentration of 10.0 mg/mL in 0.9% NaCl for intravenous injection (infused into the antebrachial vein over 30 s) or in distilled water for oral administration. The solutions were prepared just prior to administration. Oral dosing was accomplished with the aid of a rubber catheter (6.5 mm i.d., 9.5 mm o.d.) which was inserted ~40 cm through the mouth into the esophagus.

Blood samples (5 mL) for drug assay were withdrawn into heparinized syringes from the antebrachial vein opposite to where nicorandil was intravenously administered prior to and at 1, 2, 4, 10, 15, 20, 30, and 45 min and 1, 1.5, 2, 3, 4, 5, 6, 7, 8, 9, and 12 h after administration by either route. Immediately after blood collection, the plasma was separated and stored at −20°C until assayed.

Assay Method—The nitrate III[2] was used as the internal standard. Two milliliters of the plasma was transferred to a 15-mL stoppered conical-tip glass tube to which 1 mL of distilled water, 1 mL of internal standard solution (1 mL of distilled water contained 2.5 μg of internal standard III), two drops of 1 M NaOH, and 6.5 mL of ethyl acetate were added. The mixture was vigorously shaken in a mechanical shaker for 10 min. The upper ethyl acetate layer was removed after centrifugation at 3 × 10 rpm for 10 min, and the extraction procedure was repeated. The ethyl acetate layers were combined, transferred to a 30-mL pear-shaped glass flask, and evaporated to dryness. Immediately after evaporation, 0.5 mL of distilled water was added to dissolve the residue.

Ten-microliter samples were injected into an HPLC system[3] with a 30-cm × 4-mm i.d. stainless steel column[4]. The flow rate of the solvent, 25% methyl alcohol and 7% ethyl alcohol in distilled water, was 1.1 mL/min; the operating temperature was 25 ± 2°C. Successive eluates were checked by means of a UV absorption detector (254 nm with 0.01 AUFS) and recorded on a chart recorder at a rate of 0.5 cm/min. Under these conditions, the retention times were 6.0, 3.5, and 8.0 min for I, II, and III, respectively (Fig. 1).

Standard curves for nicorandil (I) and alcohol II in canine plasma were prepared as follows. One milliliter of a solution containing the equal amounts of both compounds in distilled water and 1 mL of a solution of III (2.5 μg) were added to the control canine plasma (2.0 mL) to give duplicate standards. An equal volume of distilled water was added to the control plasma (blank). The prepared standard plasma samples were treated in the same manner as the test samples.

The calibration curves (Fig. 2) were linear, passing through the origin, at concentrations ranging from 0.025 to 4.0 μg/mL for I and from 0.2 to 4.0 μg/mL for II. The coefficients of a linear regression analysis of the calibration values were found to be 0.9997 for I and 0.9970 for II. The reproducibility of the analysis, as determined by quadruplicate assays of plasma with known concentrations of both compounds, was examined on different days over a 3-week period. The coefficients of variation found at concentrations of 0.5 and 2.0 μg/mL were 5.7 and 2.7% for I and 4.2 and 2.0% for II, respectively. Within-day assays gave the following coefficient of variation values for both compounds: 3.3 and 1.8% at concentrations of 0.5 and 2.0 μg/mL for I, respectively, and 9.7 and 3.8% at concentrations of 0.5 and 2.0 μg/mL for II, respectively. The recovery rate for nicorandil was 92.0 ± 4.1 (mean ± *SD*), 91.3 ± 2.7, 99.5 ± 3.5, and 98.0 ± 3.6% at concentrations of 0.5, 1.0, 2.0, and 4.0 μg/mL of canine plasma (from 10 determinations at each concentration); the value for II was quite low, yielding 13.2 ± 2.6, 12.6 ± 2.3, 14.3 ± 1.6, and 14.6 ± 1.9%, respectively, at the same concentrations as for I. The sensitivity limits were ~0.025 μg/mL for I and ~0.2 μg/mL for II.

The stability of the test compounds in frozen plasma was also examined. Standard solutions containing 1, 2, and 4 μg of I, II, and III, respectively, were added to 2.0-mL aliquots of canine plasma, and the mixtures were stored at −20°C; the respective compounds were assayed on days 18 and 40 of storage. The mean ±*SD* recovery rates on day 18 relative to the same standard solutions freshly prepared were 101.5 ± 3.7% for I, 94.8 ± 2.6% for II, and 96.0 ± 3.5% for III; the respective values for the three compounds on day 40 were 95.0 ± 4.5, 94.0 ± 3.7, and 94.7 ± 3.5%. These compounds are considered to be stable in plasma kept at −20°C for a period of ≥40 d.

Concentrations of I and II reported in this study were the values measured within 20 d after the blood collection. Duplicate analyses were done on all samples with the average values reported.

Pharmacokinetic and Statistical Calculations—Model-independent pharmacokinetic parameters were estimated throughout the study. The terminal elimination rate constant of nicorandil (K) and its metabolite (K_{met}) was calculated from the least-squares regression slope of the terminal log-linear phase of the phase concentration–time data. The elimination half-life ($t_{1/2}$) was calculated as $t_{1/2}$ or $t_{1/2met} = 0.693/K$ or K_{met}.

The area under the curve against time (AUC) for nicorandil was estimated

[2] Chugai Pharmaceutical Co., Ltd., Tokyo, Japan.

[3] The HPLC system consisted of a model U6K injector, a model 6000A high-pressure pump, and a model 440 absorbance detector, all from Waters Associates, Milford, Mass.

[4] μ Bondapak C_{18}; Water Associates, Milford, Mass.

Table I—Pharmacokinetic Parameters of Nicorandil Following a 2.5-mg/kg iv Dose of Nicorandil

Dog	Weight, kg	K, h^{-1}	$t_{1/2}$, h	Vd_{area}, L/kg	CL_{tot}, mL/min/kg	AUC_0^∞, μg·h/mL
1	8.8	0.56	1.23	0.67	12.37	3.37
2	8.2	1.54	0.45	0.67	17.76	2.35
3	9.1	0.93	0.74	0.73	12.93	3.22
4	9.3	1.29	0.54	0.59	14.00	2.98
5	9.2	0.89	0.78	0.82	14.01	2.97
6	9.9	1.08	0.64	0.56	9.94	4.19
Mean	9.1	1.05	0.73	0.67	13.50	3.18
SEM	±0.2	±0.14	±0.11	±0.04	±1.05	±0.25

Table II—Pharmacokinetic Parameters of Nicorandil Following a 2.5-mg/kg Oral Dose of Nicorandil

Dog[a]	K, h^{-1}	$t_{1/2}$, h	C_{max}, μg/mL	t_{max}, h	AUC_0^∞, μg·h/mL	F	F'	F'/F[b]
1	0.86	0.81	1.9	0.75	2.23	0.66	0.69	1.05
2	0.69	1.00	0.9	0.50	1.69	0.72	0.56	0.78
3	0.60	1.16	0.7	0.50	1.92	0.60	0.68	1.13
4	0.80	0.86	0.8	0.50	1.54	0.52	0.65	1.25
5	1.01	0.69	2.1	0.25	2.94	0.99	0.65	0.66
6	0.80	0.87	1.6	1.00	3.65	0.87	0.75	0.86
Mean	0.79	0.90	1.3	0.58	2.33	0.72	0.66	0.95
SEM	±0.06	±0.07	±0.2	±0.11	±0.33	±0.07	±0.03	±0.09

[a] Each number of animals is the same as that given in Table I. [b] The mean ± *SEM* value is 1.01 ± 0.09 when dog 5 is excluded.

according to $AUC_0^\infty = AUC_0^T + C_p^T/K$. The AUC_0^T was calculated using the trapezoidal method, where T is the time of the last measured plasma concentration of nicorandil (C_p^T). The apparent volume of distribution (Vd_{area}) of nicorandil was obtained from the equation, Vd = intravenous dose/(intravenous $AUC_0^\infty \cdot K$). The apparent total body clearance (CL_{tot}) of nicorandil was calculated from CL_{tot} = intravenous dose/intravenous AUC_0^∞.

The absolute bioavailability of nicorandil (F) after oral administration was determined from F = oral AUC_0^∞/intravenous AUC_0^∞, where the oral AUC_0^∞ is defined as $AUC_0^T + C_p^T/K$. The maximal plasma nicorandil concentration (C_{max}) after oral administration and the time to peak concentration (t_{max}) were read from the concentration-time data of each animal.

We also predicted the theoretical value for oral bioavailability (F') of nicorandil using the following equation (6): F' = 1 − intravenous dose/(intravenous $AUC_0^\infty \cdot \lambda \cdot Q$), where Q is the liver blood flow of 41.0 mL/min/kg in the dog (7) and λ is the blood-plasma concentration ratio of nicorandil in the dog, which is known to be close to unity (1.01 ± 0.05, n = 10)[5]. This F' value was compared with the calculated value (F) for each dog.

Such pharmacokinetic variables as Vd_{area} and CL_{tot} were normalized for the body weight of the animal and expressed as liters per kilogram and milliliters per minute per kilogram, respectively. All average data are given as the mean ± *SEM*. All the pharmacokinetic and statistical calculations were done with a computer[6]. Statistical comparison of the data obtained using the two different routes of drug administration was made by a paired Student's t test, with a significance level of $p < 0.05$.

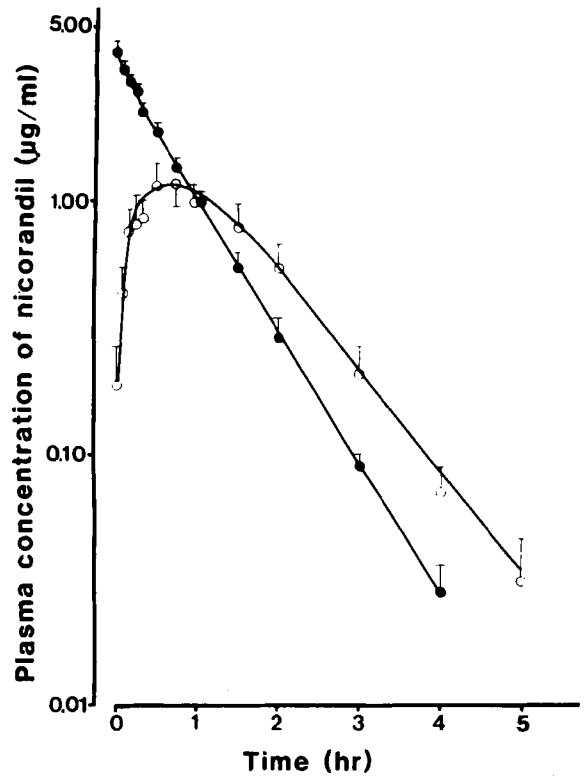

Figure 3—*Average concentration-time profile of nicorandil in plasma after intravenous (●) or oral (○) administration of a 2.5-mg/kg dose of nicorandil to six dogs, mean* ± SEM.

RESULTS

Semilogarithmic plots of nicorandil plasma concentrations against time after intravenous and oral administrations of the same dose of nicorandil (2.5 mg/kg) are shown in Fig. 3. Pharmacokinetic parameters of nicorandil related to intravenous and oral dosing are summarized in Tables I and II, respectively.

Following intravenous administration, the elimination phase had a $t_{1/2}$ of 0.73 ± 0.11 h. No nicorandil could be detected in the plasma 5 h after dosage with this HPLC method. The AUC_0^∞ values ranged from 2.35 to 4.19 μg·h/mL. The weight-normalized volume of distribution (Vd_{area}) and total body (plasma) clearance (CL_{tot}) was 0.67 ± 0.04 L/kg and 13.50 ± 1.05 mL/min/kg, respectively.

After oral administration, nicorandil in plasma was detected within 10 min of dosing and reached peak concentrations between 0.25 and 1.0 h (t_{max}, Table II). The mean peak plasma concentration (C_{max}) was 1.3 ± 0.2 μg/mL at ~0.58 h. After 6 h, no drug could be detected in the plasma with the HPLC method used. The interindividual variation in oral AUC_0^∞ (≃2.4-fold) was larger than that of intravenous AUC_0^∞ (≃1.8-fold) for the six dogs. The mean AUC_0^∞ was statistically different ($p < 0.02$) for the two different routes of nicorandil administration. The mean bioavailability (F), calculated from oral AUC_0^∞/intravenous AUC_0^∞, was 0.72 (Table II). The value (F') predicted the equation (6) was fairly consistent with that of F in all but one dog (no. 5). This dog showed the greatest C_{max} (2.1 μg/mL) with the shortest t_{max} (0.25 h), which may seemingly diminish the hepatic first-pass effect for orally administered nicorandil. Except for this dog, the ratio of F'/F ranged from 0.78 to 1.25 (mean = 1.01; Table II).

Semilogarithmic plots of plasma concentration-time data of alcohol II following intravenous and oral administration of nicorandil are shown in Fig. 4. The mean value for the oral AUC_0^∞ (13.0 ± 1.7 μg·h/mL) was identical with that for the intravenous AUC_0^∞ (13.5 ± 0.1 μg·h/mL). The mean terminal half-life of the metabolite (Table III) was much longer than that of the parent drug (Tables I and II).

[5] H. Kamiyama, Chugai Pharmaceutical Co., Ltd., Tokyo, Japan, unpublished data.

[6] M100 Ace Mark IV; SORD Computer Systems, Inc., Tokyo, Japan.

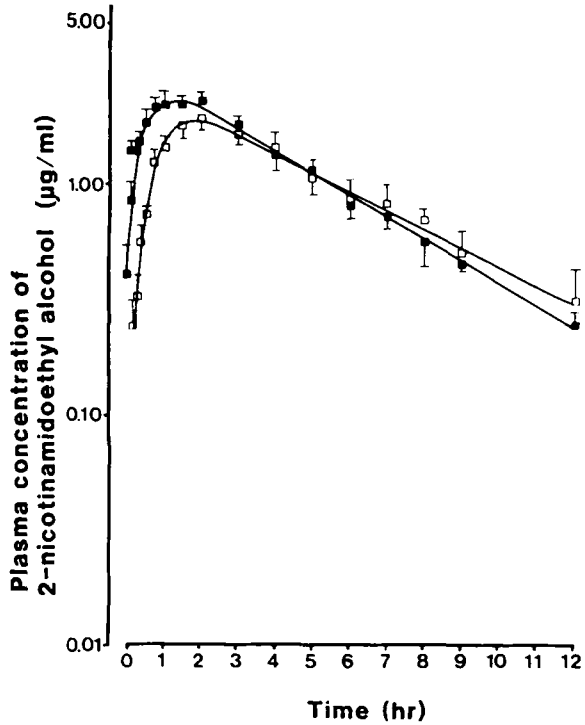

Figure 4—*Average concentration-time profile of alcohol II in plasma after intravenous (■) or oral (□) administration of a 2.5-mg/kg dose of nicorandil to six dogs, mean* ± SEM

DISCUSSION

The elimination half-life observed for nicorandil in this study appears to be longer than the respective values of conventional coronary vasodilators such as glyceryl trinitrate (nitroglycerin), isosorbide dinitrate, and pentaerythritol trinitrate, which are on the order of minutes in animals (including dogs) and humans (8–10). Previous workers (9) noted a plasma half-life for unchanged isosorbide dinitrate of ~7 min in dogs, while others (10) observed a plasma half-life for nitroglycerin of 4.4 min in normal volunteers. A preliminary clinical study (11) showed that the mean elimination half-life observed in 10 patients with heart disease after a single 20-mg oral administration of nicorandil was ~52 min (≃0.87 h).

It is noteworthy that the fraction available in the systemic circulation (*F*) for nicorandil, a mononitrate compound, was ~70% with a long elimination half-life (0.90 ± 0.07 h) after oral administration to dogs (Table II). This seems to be in marked contrast to the di- and trinitrate compounds in various animal species, including dogs (8, 9, 12). Studies conducted in animals (8, 9, 13–16) and humans (17) have suggested that the di- and trinitrates are rapidly and extensively degraded in the liver. On the other hand, isosorbide-5-mononitrate, a major metabolite of isosorbide dinitrate in dogs (9, 12) and humans (18–20), has recently been reported to be completely bioavailable after a single oral dose of 20 mg (21); the elimination half-life of isosorbide-5-mononitrate is ~8 times that of isosorbide dinitrate (20, 22).

We are tempted to speculate that the mononitrate forms of coronary vasodilators (*e.g.*, nicorandil) are resistant to metabolic breakdown and will attain higher plasma concentrations, resulting in greater bioavailability after oral administration. As our bioavailability data on nicorandil were obtained from only one species, however, it must be interpreted with caution. There are several other agents whose systemic availability is not proportional to the dose administered. For example, single-oral-dose studies using propranolol (23) have shown that as large doses of the drug are ingested, the hepatic extraction becomes saturated, allowing more of the drug to reach the systemic circulation. Since the oral dose of nicorandil administered to the dogs was ~3.3- to 10-fold greater than that recently tested (5–15 mg/d TID) in patients with angina pectoris (24), whether a similar bioavailability after a lower dose of nicorandil would have been obtained remains unanswered; a dose-ranging pharmacokinetic study would be required. It is likely that the degradation rate of nicorandil may vary from species to species, and that the bioavailability data from an animal species can not directly be translated into human terms.

Concerning the formation of the main metabolic product of nicorandil, the alcohol II, the low recovery of this metabolite from canine plasma using this HPLC method hampers discussion on its quantitative disposition. Bearing this limitation in mind, however, the formation of this metabolite appears to occur quite efficiently in dogs after both intravenous and oral administrations of the parent compound (Fig. 4). The metabolite has a longer half-life (Table III) compared with the parent compound (Tables I and II), and plasma concentrations were maintained at higher levels for a longer period of time following intravenous or oral administration of nicorandil (Fig. 4). One may question if the metabolite would affect the disposition of the parent compound, thereby modifying the cardiovascular effects of nicorandil. However, previous workers (1, 3, 5) have demonstrated that alcohol II is pharmacologically inactive and has no influence on the cardiovascular effects of nicorandil. Nevertheless, whether the alcohol can distort the disposition of nicorandil remains totally unknown.

Table III—Apparent Pharmacokinetic Parameters of Alcohol II Following a 2.5-mg/kg iv or Oral Dose of Nicorandil

Dog	Intravenous Study		Oral Study	
	K_{met}, h^{-1}	$t_{1/2met}$, h	K_{met}, h^{-1}	$t_{1/2met}$, h
1	0.18	3.76	0.26	2.68
2	0.28	2.50	0.23	3.05
3	0.20	3.43	0.34	2.05
4	0.22	3.15	0.10	6.93
5	0.31	2.18	0.36	1.94
6	0.20	3.50	0.14	4.90
Mean	0.23	3.09	0.24	3.60
SEM	±0.02	±0.25	±0.04	±0.80

In summary, nicorandil has a longer elimination half-life, and its oral bioavailability appears considerably greater than conventional nitrate compounds. However, before nicorandil becomes a therapeutic agent for the treatment of angina pectoris, its disposition and metabolic fate in the human body must be elucidated. Undoubtedly, this requires a more sensitive and specific assay method. Thus, the results reported herein using this HPLC method, which is sensitive enough to detect nicorandil only in the plasma of dogs administered a relatively large dose of nicorandil, should be viewed as a basis for further studies.

REFERENCES

(1) N. Taira, K. Satoh, T. Yanagisawa, Y. Imai, and M. Hiwatari, *Clin. Exp. Pharmacol. Physiol.*, **6**, 301 (1979).

(2) K. Sakai, J. Aono, and K. Haruta, *Jpn. J. Pharmacol.*, **31**, 281 (1981).

(3) K. Sakai, Y. Shiraki, and H. Nabata, *J. Cardiovasc. Pharmacol.*, **3**, 139 (1981).

(4) K. Furukawa, T. Itoh, K. Kajiwara, K. Kitamura, H. Suzuki, Y. Itoh, and H. Kuriyama, *J. Pharmacol. Exp. Ther.*, **218**, 248 (1981).

(5) K. Sakai, Y. Ohba, M. Akima, H. Kamiyama, Y. Hinohara, and H. Nakano, *Jpn. J. Pharmacol.*, **30**, 881 (1980).

(6) M. Gibaldi, R. N. Boyes, and S. Feldman, *J. Pharm. Sci.*, **60**, 1338 (1971).

(7) H. Boxenbaum, *J. Pharmacokinet. Biopharm.*, **8**, 165 (1980).

(8) P. Needleman, *Annu. Rev. Pharmacol. Toxicol.*, **16**, 81 (1976).

(9) S. F. Sisenwine and H. W. Ruelius, *J. Pharmacol. Exp. Ther.*, **176**, 296 (1971).

(10) P. W. Armstrong, J. A. Armstrong, and G. S. Marks, *Circulation*, **59**, 585 (1979).

(11) Y. Oyama, H. Nakaya, and K. Kanda, "Abstracts in Eighth International Congress of Pharmacology," Tokyo, Japan, 1981, p. 716.

(12) D. E. Reed, J. F. May, L. G. Hart, and D. H. McCurdy, *Arch. Int. Pharmacodyn.*, **191**, 318 (1971).

(13) P. Needleman, S. Lang, and E. M. Johnson, Jr., *J. Pharmacol. Exp. Ther.*, **181**, 489 (1972).

(14) P. Needleman and F. E. Hunter, Jr., *Mol. Pharmacol.*, **1**, 77 (1965).

(15) P. Needleman and J. C. Krantz, Jr., *Biochem. Pharmacol.*, **14**, 1225 (1965).

(16) S. Lang, E. M. Johnson, Jr., and P. Needleman, *Biochem. Pharmacol.*, **21**, 422 (1972).

(17) J. W. F. Davidson, H. S. Millar, Jr., and F. J. Di Carlo, *J. Pharm. Sci.*, **60**, 274 (1971).

(18) M. Rosseel and M. G. Bogaert, *J. Pharm. Sci.*, **62**, 754 (1973).

(19) W. H. Down and L. F. Chasseaud, *J. Pharm. Sci.*, **63**, 1147 (1974).

(20) S. Spörl-Radun, G. Betzien, B. Kaufmann, V. Liede, and U. Abshagen, *Eur. J. Clin. Pharmacol.*, **18**, 237 (1980).

(21) U. Abshagen, G. Betzien, R. Endele, and B. Kaufmann, *Eur. J. Clin. Pharmacol.*, **20**, 269 (1981).
(22) U. Abshagen and S. Spörl-Radun, *Eur. J. Clin. Pharmacol.*, **19**, 423 (1981).
(23) D. G. Shand and R. E. Rangno, *Pharmacology*, **1**, 195 (1972).
(24) S. Murao and E. Kimura, *Jpn. J. Clin. Pharmacol.*, **13**, 311 (1982).

ACKNOWLEDGMENTS

This work was supported in part by a grant-in-aid from the Ministry of Health and Welfare, Japan. The preliminary account of this study was presented at the Eighth International Congress of Pharmacology, Tokyo, July 19–24, 1981.

The authors thank Mrs. Akiko Kuramoto, Miss Kaori Narita, and Miss Junko Taki for their secretarial assistance.

Isolation and Identification of Piperacillin Amide as an Impurity in Piperacillin

MARSHALL M. SIEGEL *x, RICHARD MILLS *†, LANE GEHRLEIN *, WILLIAM E. GORE *, GEORGE MORTON *, T. CHANG ‡, DONNA COSULICH *, JEFFREY MEDWID *, and P. MIRANDO *

Received November 1, 1982, from the *American Cyanamid Company*, **Medical Research Division, Lederle Laboratories, Pearl River, NY 10965* and the ‡*Chemical Research Division, Stamford, CT 06904.* Accepted for publication March 11, 1983. † Deceased.

Abstract □ Piperacillin amide (IV) was successfully identified as the predominant impurity in commercial lots of piperacillin monohydrate (III). The impurity was isolated *via* a preparative liquid chromatographic scheme utilizing Florisil as the adsorbent and a mobile phase of water–acetonitrile (4:96, v/v). The isolated component had nearly the same reverse-phase HPLC properties as piperacillin and was chemically and thermally unstable. This labile impurity was spectroscopically identified by field desorption (FD), fast atom bombardment (FAB) with collision activation decomposition (CAD), and desorption chemical ionization (DCI) mass spectrometries, and NMR and IR spectrometries. Identity was confirmed on comparison of the chromatographic and spectrometric data of the impurity with an independently synthesized sample of piperacillin amide.

Keyphrases □ Piperacillin amide—impurity in piperacillin, isolation, identification using soft-ionization mass spectra, high-field NMR, and IR spectrometry □ Piperacillin—isolation of an amide impurity by column chromatography, identification using soft-ionization mass spectra, high-field NMR, and IR spectrometry, antibiotic activity

Piperacillin[1] is a third generation semisynthetic penicillin antibiotic with a broad spectrum of antimicrobial activity against both Gram-positive and Gram-negative organisms (1). As shown in Scheme I, piperacillin (III) is produced from the reaction of ampicillin (I) with 4-ethyl-2,3-dioxo-1-piperazinecarbonyl chloride (II). Five low-level components, each ≤0.6% w/w, were observed in the final piperacillin product. Two of these components were related to the starting materials: ampicillin and 1-ethyl-2,3-piperazinedione (2). Two components were expected process impurities: the β-lactam hydrolysis product of piperacillin (3) and the condensation product of piperacillin with ampicillin (2). The isolation and identification of the fifth component is the subject of this paper. This component, referred to as the "unknown piperacillin impurity," constituted the major impurity in commercial lots of piperacillin, 0.2–0.4% w/w[2]. This impurity proved to be difficult to isolate chromatographically and to characterize spectrometrically.

Two main factors which complicated the development of a reverse-phase HPLC method for isolating the unknown piperacillin impurity from piperacillin in quantities large enough for spectrometric analysis are:

1. the difficulty in resolving the major impurity from piperacillin because the impurity eluted as a shoulder on the high retention time side of piperacillin;
2. the chemical instability of the unknown material in normal HPLC reverse-phase solvents, *viz.*, methanol and aqueous media, at other than neutral pH for extended periods.

For these reasons, a unique preparative column chromatographic method using an isocratic normal phase was developed which was successful in resolving the unknown piperacillin impurity from piperacillin.

Identification of the isolated impurity was not routine, since it was highly polar and chemically and thermally unstable. The unknown impurity was characterized by mass spectrometry using soft-ionization conditions, *i.e.*, field desorption (FD) (4, 5), fast atom bombardment (FAB) (6, 7), and desorption chemical ionization (DCI) (8, 9). High-field NMR and Fourier transform IR spectrometries were also used to elucidate the structure of the unknown piperacillin impurity. The spectrometric data suggested that the unknown was piperacillin amide (IV). This hypothesis was confirmed by compar-

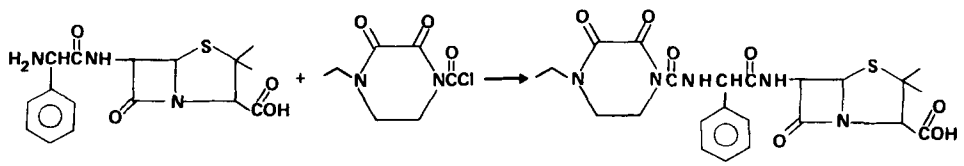

(I) (II) (III)

Scheme I

[1] Marketed by Lederle Laboratories in the U.S. as Pipracil and in Europe as Pipril.

[2] Penticillin (Toyama Chemicals Co., Ltd. brand of piperacillin marketed in Japan) also contains piperacillin amide, but the quantity is negligible.

0022-3549/84/0400-0498$01.00/0
© 1984, American Pharmaceutical Association

(21) U. Abshagen, G. Betzien, R. Endele, and B. Kaufmann, *Eur. J. Clin. Pharmacol.*, **20**, 269 (1981).
(22) U. Abshagen and S. Spörl-Radun, *Eur. J. Clin. Pharmacol.*, **19**, 423 (1981).
(23) D. G. Shand and R. E. Rangno, *Pharmacology*, **1**, 195 (1972).
(24) S. Murao and E. Kimura, *Jpn. J. Clin. Pharmacol.*, **13**, 311 (1982).

ACKNOWLEDGMENTS

This work was supported in part by a grant-in-aid from the Ministry of Health and Welfare, Japan. The preliminary account of this study was presented at the Eighth International Congress of Pharmacology, Tokyo, July 19–24, 1981.

The authors thank Mrs. Akiko Kuramoto, Miss Kaori Narita, and Miss Junko Taki for their secretarial assistance.

Isolation and Identification of Piperacillin Amide as an Impurity in Piperacillin

MARSHALL M. SIEGEL *x, RICHARD MILLS *†, LANE GEHRLEIN *, WILLIAM E. GORE *, GEORGE MORTON *, T. CHANG ‡, DONNA COSULICH *, JEFFREY MEDWID *, and P. MIRANDO *

Received November 1, 1982, from the *American Cyanamid Company*, **Medical Research Division, Lederle Laboratories, Pearl River, NY 10965* and the ‡*Chemical Research Division, Stamford, CT 06904.* Accepted for publication March 11, 1983. † Deceased.

Abstract □ Piperacillin amide (IV) was successfully identified as the predominant impurity in commercial lots of piperacillin monohydrate (III). The impurity was isolated *via* a preparative liquid chromatographic scheme utilizing Florisil as the adsorbent and a mobile phase of water–acetonitrile (4:96, v/v). The isolated component had nearly the same reverse-phase HPLC properties as piperacillin and was chemically and thermally unstable. This labile impurity was spectroscopically identified by field desorption (FD), fast atom bombardment (FAB) with collision activation decomposition (CAD), and desorption chemical ionization (DCI) mass spectrometries, and NMR and IR spectrometries. Identity was confirmed on comparison of the chromatographic and spectrometric data of the impurity with an independently synthesized sample of piperacillin amide.

Keyphrases □ Piperacillin amide—impurity in piperacillin, isolation, identification using soft-ionization mass spectra, high-field NMR, and IR spectrometry □ Piperacillin—isolation of an amide impurity by column chromatography, identification using soft-ionization mass spectra, high-field NMR, and IR spectrometry, antibiotic activity

Piperacillin[1] is a third generation semisynthetic penicillin antibiotic with a broad spectrum of antimicrobial activity against both Gram-positive and Gram-negative organisms (1). As shown in Scheme I, piperacillin (III) is produced from the reaction of ampicillin (I) with 4-ethyl-2,3-dioxo-1-piperazinecarbonyl chloride (II). Five low-level components, each ≤0.6% w/w, were observed in the final piperacillin product. Two of these components were related to the starting materials: ampicillin and 1-ethyl-2,3-piperazinedione (2). Two components were expected process impurities: the β-lactam hydrolysis product of piperacillin (3) and the condensation product of piperacillin with ampicillin (2). The isolation and identification of the fifth component is the subject of this paper. This component, referred to as the "unknown piperacillin impurity," constituted the major impurity in commercial lots of piperacillin, 0.2–0.4% w/w[2]. This impurity proved to be difficult to isolate chromatographically and to characterize spectrometrically.

Two main factors which complicated the development of a reverse-phase HPLC method for isolating the unknown piperacillin impurity from piperacillin in quantities large enough for spectrometric analysis are:

1. the difficulty in resolving the major impurity from piperacillin because the impurity eluted as a shoulder on the high retention time side of piperacillin;
2. the chemical instability of the unknown material in normal HPLC reverse-phase solvents, *viz.*, methanol and aqueous media, at other than neutral pH for extended periods.

For these reasons, a unique preparative column chromatographic method using an isocratic normal phase was developed which was successful in resolving the unknown piperacillin impurity from piperacillin.

Identification of the isolated impurity was not routine, since it was highly polar and chemically and thermally unstable. The unknown impurity was characterized by mass spectrometry using soft-ionization conditions, *i.e.*, field desorption (FD) (4, 5), fast atom bombardment (FAB) (6, 7), and desorption chemical ionization (DCI) (8, 9). High-field NMR and Fourier transform IR spectrometries were also used to elucidate the structure of the unknown piperacillin impurity. The spectrometric data suggested that the unknown was piperacillin amide (IV). This hypothesis was confirmed by compar-

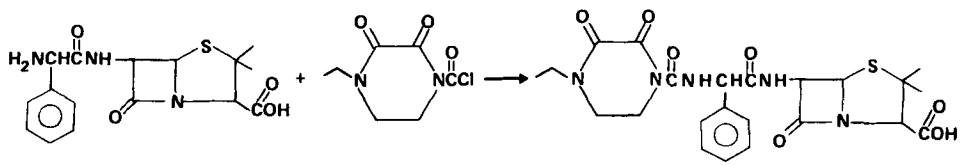

(I) (II) (III)

Scheme I

[1] Marketed by Lederle Laboratories in the U.S. as Pipracil and in Europe as Pipril.

[2] Penticillin (Toyama Chemicals Co., Ltd. brand of piperacillin marketed in Japan) also contains piperacillin amide, but the quantity is negligible.

0022-3549/84/0400-0498$01.00/0
© 1984, American Pharmaceutical Association

ison of the chromatographic and spectrometric data with that of an authentic piperacillin amide sample prepared in an unambiguous organic synthesis. These results demonstrate that the combination of soft-ionization mass spectral techniques, high-field NMR, and IR are exceptionally effective for identifying small amounts of nonvolatile components.

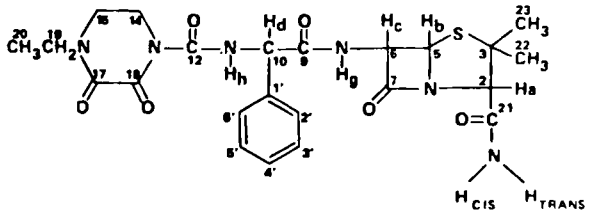

(IV)

EXPERIMENTAL

Chromatography—A column chromatographic procedure was followed for isolating the unknown piperacillin impurity. The chromatographic column was 80 × 5.2 cm and was packed with 1 kg of Florisil[3], 60–100 mesh. Twenty grams of bulk piperacillin monohydrate were dissolved in 200 mL of acetonitrile and loaded on to the column. The elution solvent consisted of acetonitrile–water (96:4, v/v) with a flow rate of 35 mL/min. The detector was a UV spectrophotometer[4] fitted with a variable-volume flow cell set to monitor at 220 nm. This system operated at ambient temperature. The elution volume of the piperacillin impurity was 2100–4000 mL. This experiment was repeated three times before discarding the column packing. The eluant containing the impurity from three runs was combined, distilled *in vacuo*, and freeze-dried to produce 84 mg of white solid.

Analytical reverse-phase HPLC[5] with UV detection[6] at 220 nm was used for the analysis of bulk piperacillin and the isolated impurity components. A 250 × 4.6-mm column packed with silica gel chemically bonded with octadecylchlorosilane[7] was maintained at 35°C. The mobile phase consisted of methanol–water–0.2 M Na_2HPO_4 (45:34:10, v/v/v) adjusted to pH 6.5 with 0.33 M phosphoric acid. The injection volume of samples was 20 μL, made up in the mobile phase.

Although dimethyl sulfoxide (Me_2SO) is the solvent of choice for the unknown piperacillin impurity, methanol was used even though the impurity underwent a chemical transformation when dissolved in the latter solvent for an extended period (>1 d) at room temperature. At elevated temperatures the reaction rate is enhanced considerably. However, by limiting the contact time to <30 min, this problem was circumvented.

Spectrometry—FD mass spectra were obtained with a double-focusing high-performance mass spectrometer[8]. The FD emitter consisted of a 10-μm tungsten wire with microneedles of pyrolytic carbon grown to a length of ~30 μm. The FD emitter was coated with a Me_2SO solution of the unknown piperacillin impurity sample. On application of the emitter current, very weak signals were observed due to a high sodium ion content contaminating the sample and emitter. The original sample was washed in the following fashion to remove inorganic salts. Approximately 20 mg of the trapped piperacillin impurity was partially dissolved in 5 mL of acetonitrile. On addition of 5 mL of distilled water a white precipitate formed, which was collected on a filter and washed with 1 mL of distilled water. The filtrate was then dried *in vacuo* and analyzed in the FD mode. The sodium signal of the washed sample was reduced considerably, and relatively intense FD signals were produced by the sample. Low-resolution FD data were acquired at a resolution of 1000.

Exact mass measurements in the FD mode were made at a resolution of 6000 in the following fashion. A reference peak in the electron-impact (EI) mode (PFK[9] fragment: $C_{13}F_{19}$, *m/z* 516.9697) was sequentially peak matched against the molecular ion of the unknown piperacillin impurity in the FD mode. The experimental mass difference between the FD and EI modes was measured with a known reference compound peak in both the field ionization (FI) and EI modes [tris(pentafluoroethyl)-*s*-triazine[9]: $C_9F_{15}N_3$, *m/z* 434.9853]. Using this mass difference, the exact mass of the unknown was corrected.

FAB spectra were obtained with a double-focusing high-performance mass spectrometer[8] and with a triple-stage quadrupole mass spectrometer[10]. Collision-activation decomposition (CAD) of selected FAB ions was performed on the latter instrument (10). The fast atom reagent gas was xenon, and the collision gas was argon. The samples for FAB ionization were either mixed directly with glycerol or dissolved in Me_2SO and then mixed with glycerol. FAB spectra of the unknown piperacillin impurity were obtained in both the positive- and negative-ionization modes. FAB/CAD spectra in the positive-ionization mode were obtained on the protonated molecular ion and the sodium adduct molecular ion of the unknown piperacillin impurity and synthetic piperacillin amide (neat and spiked with sodium chloride).

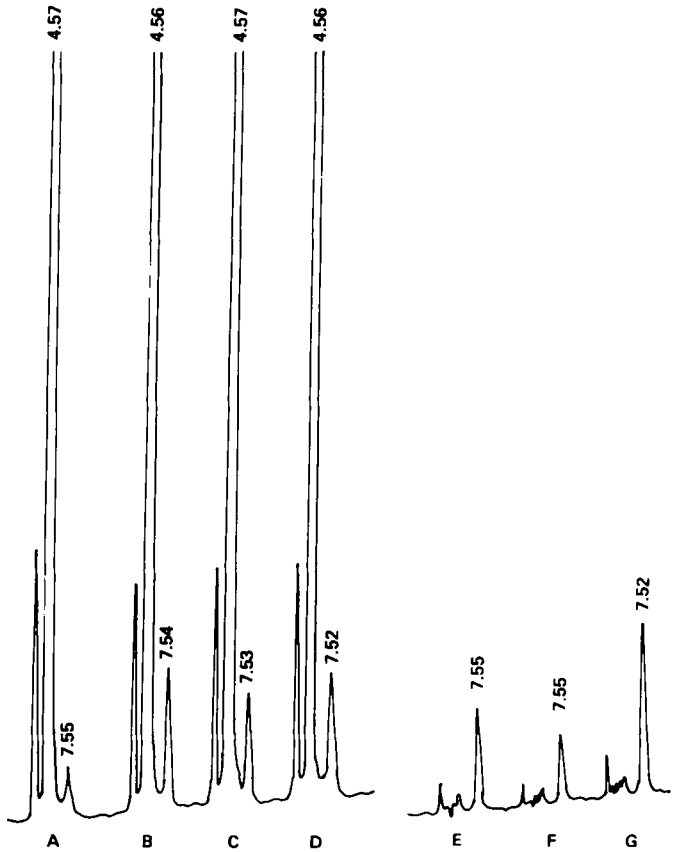

Figure 1—*HPLC chromatograms with retention times (min). Key: (A) bulk piperacillin; (B) bulk piperacillin spiked with unknown piperacillin impurity; (C) bulk piperacillin spiked with synthetic piperacillin amide; (D) bulk piperacillin spiked with unknown piperacillin impurity and synthetic piperacillin amide; (E) unknown piperacillin impurity; (F) synthetic piperacillin amide; (G) unknown piperacillin impurity spiked with synthetic piperacillin amide.*

Desorption chemical ionization (DCI) was performed on a quadrupole mass spectrometer[11] in the positive- and negative-ionization modes with methane and ammonia as the reagent gases. The sample was rubbed onto the surface of one end of a gold wire, ~1 cm long, and the other end was inserted into the tip of the direct insertion probe. This gold wire effectively extended the probe length so that the sample was inserted directly in the ion plasma region of the source. The thermal energy of the ion plasma and rapid heating of the probe gently desorbed the sample from the gold wire surface generating ions of diagnostic interest in the negative-ion mode. The DCI mass spectral data reported in this paper correspond to the first signal in the reconstructed total ion current profile, as the samples were rapidly heated.

The ^1H- and ^{13}C-NMR spectra were obtained on a high-field NMR spectrometer[12] operating in the pulsed Fourier transform mode at 250.13 and 62.89 MHz, respectively. The samples were dissolved in Me_2SO-d_6, and the spectra were referenced to tetramethylsilane. The IR spectra were recorded in 100 scans on a Fourier transform IR system[13] using samples pressed into potassium bromide pellets.

Preparation of Piperacillin Amide—To a solution of isobutyl chloroformate (13.6 g, 100 mmol) in chloroform (100 mL) at −30°C under argon was added a cold solution of piperacillin monohydrate (53.5 g, 100 mmol) in a mixture

[3] Floridin Co., Pittsburgh, Pa.
[4] Model DU; Beckman Instruments, Fullerton, Calif.
[5] Model M6000A HPLC Pump; Waters Associates, Milford, Mass.
[6] Model SF 770 Spectroflow Monitor; Schoeffel Instrument Corp., Westwood, N.J.
[7] Partisil 10/25 ODS; Whatman, Inc., Clifton, N.J.
[8] Model MS-50; Kratos Instrument Corp., Manchester, England.
[9] PCR Research Chemicals, Inc., Gainesville, Fla.
[10] Model TSQ; Finnigan Corp., Sunnyvale, Calif.
[11] Model 4021T and Incos Model 2000 Data System; Finnigan Corp., Sunnyvale, Calif.
[12] Model WM-250; Brucker Instruments Inc., Billerica, Mass.
[13] Model 7199; Nicolet Instrument Corp., Madison Wis.

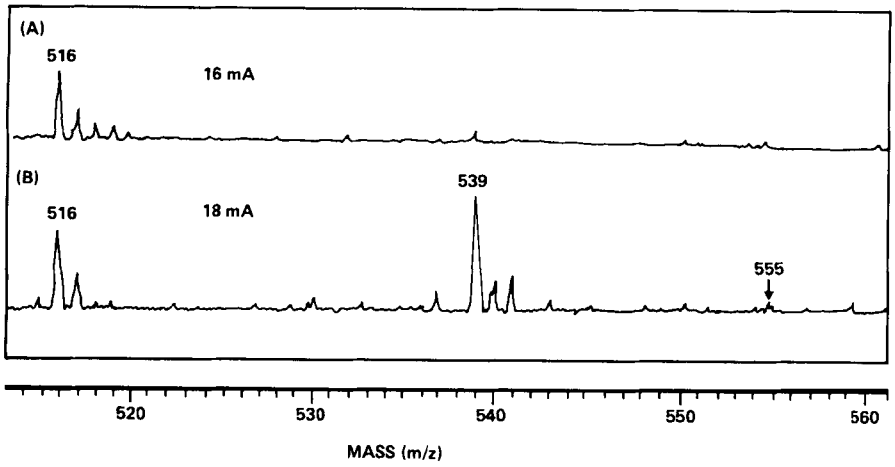

Figure 2—*Molecular ion region of the field desorption mass spectrum of the unknown piperacillin impurity with emitter current at 16 (A) and 18 mA (B).*

of chloroform (500 mL) and triethylamine (10.1 g, 100 mmol, 14 mL) over a 40-min period. The mixture was stirred an additional 1.5 h at 0°C. Ammonia was bubbled through the mixture (a white precipitate formed immediately) in a steady stream for 25 min. The thick white suspension was diluted with 1 L of chloroform and then filtered. The white filter cake was washed with chloroform (2 × 200 mL) and dried *in vacuo* to afford 49 g of crude piperacillin amide, which contained a considerable amount of ammonium chloride.

The aforementioned crude product (30 g) was suspended in 150 mL of distilled water and stirred vigorously for 2 h. The white solid was filtered, washed with acetone (2 × 50 mL) and anhydrous ether (2 × 100 mL), and dried *in vacuo* to afford 24 g of piperacillin amide (78% yield), mp 217–220°C dec[14].

Anal.—Calc. for $C_{23}H_{28}N_6O_6S \cdot 0.2H_2O$: C, 53.13; H, 5.49; N, 16.16; S, 6.17. Found[15]: C, 52.97; H, 5.27; N, 16.12; S, 6.17. KF[16] = 0.66% (which equals $0.2H_2O$).

Spectral Data—All the spectral data listed below were identical for both the unknown piperacillin impurity and the synthetic piperacillin amide unless noted otherwise. FD-MS *m/z* (%) for the piperacillin impurity: 555, 539, 517, 516, 375, 374, 373, 143, 142, and 141; for piperacillin amide: 516(18), 375(18), 359(18), 274(12), 160(8), 159(14), 158(12), 144(20), 143(100), and 142(100). +FAB-MS *m/z* for the piperacillin impurity and amide spiked with sodium chloride: 539, 519, 518, 517, 397, 359, 333, 241, 159, and 143. −FAB-MS *m/z* for the piperacillin impurity: 517, 516, 515, and 373. +FAB/CAD(517)-MS *m/z* (%): 359(13), 274(12), 186(20), 175(3.5), 174(4), 159(100), 143(82), 132(4), 115(5), and 114(6). +FAB/CAD(539)-MS *m/z* (%): 475(11), 397(100), 181(2), and 165(20). +DCI-MS *m/z* (%): 375(15), 159(60), and 143(100). −DCI-MS *m/z* (%); 516(22), 374(100), 341(35), 331(35), 330(45), 233(85), 175(77), 174(62), 173(50), and 155(35). ^{1}H-NMR (Me_2SO-d_6): δ 1.18 (t, NCH_2CH_3, J = 7.5 Hz), 1.39 (s, CH_3), 1.53 (s, CH_3), 3.32 (q, NCH_2CH_3, J = 5.0 Hz), 3.56 (m, CH_2), 3.90 (m, CH_2), 4.10 (s, CH_a), 5.36 (d, CH_b, J = 3.5 Hz), 5.46 (dd, CH_c), 5.72 (d, CH_d, J = 7.0 Hz), 7.2–7.5 (m, 5 ArH; s, NH_{cis}), 7.58 (s, NH_{trans}), 9.35 (d, NH_g, J = 7.0 Hz), and 9.84 ppm (d, NH_h, J = 7.5 Hz). ^{13}C-NMR (Me_2SO-d_6): δ 11.9 (q, C-20), 26.5 (q, C-22), 30.0 (q, C-23), 40.3 (t, C-19), 41.6 (t, C-15), 42.8 (t, C-14), 56.5 (d, C-6), 57.7 (d, C-10), 63.9 (s, C-3), 66.7 (d, C-5), 70.6 (d, C-2), 126.5 (d, C-3′ and C-5′), 127.8 (d, C-4′), 128.3 (d, C-2′ and C-6′), 137.8 (s, C-1′), 151.8 (s, C-12), 155.3 (s, C-18), 159.4 (s, C-17), 168.8 (s, C-7), 169.3 (s, C-9), and 173.4 ppm (s, C-21).

RESULTS AND DISCUSSION

Florisil was chosen as the adsorbent because it almost irreversibly adsorbs acidic materials (11). Since this material should adsorb piperacillin acid irreversibly, it should be possible to elute the more chemically neutral piperacillin impurity selectively. The resolution of the two components on Florisil was accomplished using an elution solvent mixture containing an unusually high water concentration in acetonitrile, *i.e.*, water–acetonitrile (4:96, v/v). The high water content of the elution solvent did not degrade the Florisil adsorption properties for these very polar materials. Only very low levels of piperacillin were detected in the trapped piperacillin impurity sample using the analytical reverse-phase HPLC conditions described in the *Experimental* section.

Bulk piperacillin (monohydrate) and the trapped unknown piperacillin impurity component, when analyzed under the analytical HPLC conditions, produced the chromatograms illustrated in Fig. 1a and e, respectively. The components eluting at 4.57 and 7.55 min correspond to piperacillin and the unknown piperacillin impurity, respectively.

Similarly, the analytical HPLC chromatograms of the synthetic piperacillin amide and piperacillin spiked with the synthetic piperacillin amide are illustrated in Fig. 1f and c, respectively. In addition, experiments were performed in which piperacillin was spiked with the unknown piperacillin impurity (Fig. 1b) or both the unknown impurity and the synthetic piperacillin amide (Fig. 1d). In all cases, the retention times of the synthetic piperacillin amide and the unknown piperacillin impurity either individually or in the spiking experiments were identical, *i.e.*, within the experimental errors associated with the reproducibility of the HPLC experiment.

The mass spectral properties exhibited by the piperacillin impurity, even under soft-ionization conditions, included (*a*) the difficulty in generating intense molecular and fragment ions of long enough duration for accurate measurement and (*b*) the lability of the chemical bond between the piperazine moiety and the rest of the piperacillin molecule. These mass spectral properties of the piperacillin impurity were similar to those of piperacillin.

The FD mass spectra of the washed piperacillin impurity are illustrated in Fig. 2 as a function of increasing emitter current. At 16 mA (Fig. 2a) an intense ion cluster at *m/z* 516 appears, to which is added at 18 mA (Fig. 2b) an intense ion cluster at *m/z* 539 and a weak peak at *m/z* 555. The ion cluster at *m/z* 539 and the weak peak at *m/z* 555 correspond to the sodium and potassium adducts of the molecular ion, respectively, of the unknown piperacillin impurity. This confirms that *m/z* 516 is $M^{+\cdot}$ and not $[M + H]^+$.

The molecular ion of the unknown piperacillin impurity was peak-matched in the FD mode and had an exact mass of 516.1882. This value is within 9.1 millimass units of $C_{23}H_{28}N_6O_6S$ (516.1791), the corresponding elemental formula of piperacillin amide.

The FD mass spectrum of the synthetic piperacillin amide produced a relatively intense molecular ion as well as a number of fragment ions consistent with its structure. No sodium or potassium adduct molecular ions were observed due to the absence of the cations.

The molecular weight of 516 for the unknown piperacillin impurity as well as its identity as piperacillin amide were confirmed by positive and negative FAB ionization and DCI mass spectrometries. The FAB ionization mass spectra of the unknown piperacillin impurity contained the quasimolecular ions $[M + H]^+$, $[M + Na]^+$, and $[M - H]^-$ at *m/z* 517, 539, and 515, respectively. Weak fragment ions were produced as well and often were difficult to distinguish from the glycerol background spectrum. The identity of the impurity with that of piperacillin amide was confirmed on comparison of the nearly identical ions and intensities produced in the FAB/CAD spectra from the *m/z* 517 and 539 ions for the two materials.

Similarly, the positive and negative DCI spectra of the unknown piperacillin impurity and the synthetic piperacillin amide were identical. The positive DCI spectrum obtained no molecular ion and resembled the spectrum produced under electron-impact conditions. The negative DCI spectrum contained a molecular ion, $M^{-\cdot}$, and diagnostic ions characteristic of the molecule.

The ^{1}H-NMR spectrum of the unknown piperacillin impurity is nearly identical to that of piperacillin except for additional absorption observed in the aromatic proton region, which correspond to two additional protons. These two uncoupled nonequivalent protons correspond to the *cis* and *trans* amide protons of piperacillin amide. Synthetic piperacillin amide gave a NMR spectrum identical with that of the unknown impurity with the exception of the *trans* amide proton chemical shift, 7.58 ppm in piperacillin amide *versus*

[14] Melting points were determined on a Melt-Temp Melting Point Apparatus.

[15] Micro analytical elemental analyses were performed on a Model 240 Elemental Analyzer; Perkin-Elmer Corp., Norwalk, Conn.

[16] Karl Fisher analyses were performed on a Methohm Herisau-K.F. Automate E547 and Dosmat E535.

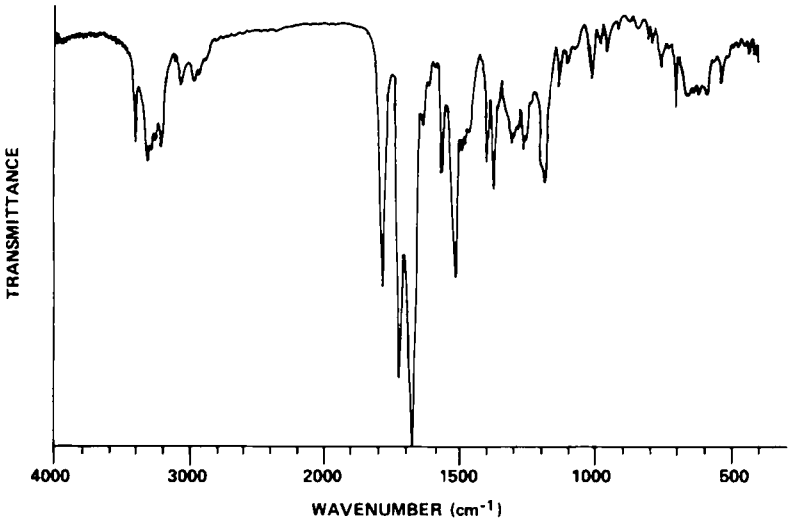

Figure 3—*IR spectrum of the unknown piperacillin impurity and synthetic piperacillin amide.*

7.72 ppm in the unknown piperacillin impurity. These differences in chemical shift, attributed to differences in concentration between the two samples, were verified in a NMR spiking experiment of synthetic piperacillin amide into the piperacillin impurity. Chemical shifts of amide protons undergo large variations when the hydrogen bonding interactions are modified by concentration, pH, temperature, and solvent changes.

The ^{13}C-NMR spectrum of the unknown piperacillin impurity is identical (within experimental error) to that of piperacillin; hence, piperacillin and the unknown impurity have identical carbon backbone structures. The ^{13}C-NMR chemical shifts and intensities of the synthetic piperacillin amide were identical to that of the unknown impurity.

The IR spectrum of the unknown piperacillin impurity and that of the synthetic piperacillin amide were identical (Fig. 3). The characteristic absorption band assigned to the carbonyl stretching mode of the β-lactam ring is at 1780 cm^{-1}.

The unknown piperacillin impurity is structurally very similar to piperacillin, *viz.*, the β-lactam group is intact (IR) and the major NMR absorptions of piperacillin and the piperacillin impurity are nearly identical, with the exception of two proton resonances at 7.72 and ~7.3 ppm. The MS data indicate that the unknown structure has a molecular weight of 516, one mass unit less than piperacillin, and based on this even mass has an elemental composition of an even number of nitrogen atoms. The unknown piperacillin impurity has been shown, based on the comparison of liquid chromatographic and MS, NMR, and IR spectrometric data, to be identical with *bona fide* piperacillin amide. The origin of the piperacillin amide is unknown.

Piperacillin amide was tested for biological activity in an *in vitro* spectrum assay against 27 bacteria. It lacked antimicrobial activity.

REFERENCES

(1) *Drugs Future*, **5**, 585 (1980); *Drugs Today*, **17**, 29 (1981); I. Saikawa, N. Matsubara, S. Minami, and S. Mitsuhashi, in "β-Lactam Antibiotics: Mode of Action, New Developments, and Future Prospects," M. R. J. Salton and G. D. Shockman, Eds., Academic, New York, N.Y., 1981, p. 353.

(2) I. Saikawa, S. Takano, C. Yoshida, O. Takashima, K. Momoni, T. Yasuda, K. Kasuya, and M. Komatsu, *J. Pharm. Soc. Jpn.*, **97**, 980 (1977).

(3) S. Takano, C. Yoshida, H. Sakai, Y. Yamamoto, M. Tai, T. Yasuda and I. Saikawa, *J. Pharm. Soc. Jpn.*, **97**, 1064 (1977).

(4) H.-R. Schulten, *Int. J. Mass Spectrom Ion Phys.*, **32**, 97 (1979).

(5) M. Shimizu, H. Matsumoto, A. Koda, T. Ichimura, and Y. Kobayashi, *Yamanouchi Seiyaku Kenkyu Hokoku*, **4**, 112 (1980).

(6) M. Barber, R. S. Bordoli, R. D. Sedgwick, and A. N. Tyler, *JCS Chem. Commun.*, **1981**, 325.

(7) M. Barber, R. S. Bordoli, R. D. Sedgwick, A. N. Tyler, B. N. Green, V. C. Parr, and J. L. Gower, *Biomed. Mass Spectrom.*, **9**, 11 (1982).

(8) R. J. Cotter, *Anal. Chem.*, **52**, 1592A (1980).

(9) J. L. Gower, C. Beaugrand, and C. Sallot, *Biomed. Mass Spectrom.*, **8**, 36 (1981).

(10) D. F. Hunt, W. M. Bone, J. Shabanowitz, J. Rhodes, and J. M. Ballard, *Anal. Chem.*, **53**, 1704 (1981).

(11) P. A. Mills, *J. Assoc. Off. Anal. Chem.*, **51**, 29 (1968).

ACKNOWLEDGMENTS

This paper is dedicated to the memory of Richard Mills. The authors appreciate the assistance of Professor K. Nakanishi and the fine work performed by Mr. J. James in obtaining the high-field NMR data at Columbia University; the microanalysis work of Mr. L. Brancone and the Lederle Laboratories microanalysis staff; the staff of the Middle Atlantic Mass Spectroscopy Center, Johns Hopkins University and J. Shabanowitz, University of Virginia (Charlottesville), for generating the FAB spectra; and Peter J. Peterson for the microbiological work.

Excretion, Distribution, and Metabolism of Primaquine in Rats

ALICE M. CLARK *x, JOHN K. BAKER ‡, and JAMES D. McCHESNEY *

Received April 4, 1982, from the *Department of Pharmacognosy and the ‡Department of Medicinal Chemistry, School of Pharmacy, The University of Mississippi, University, MS 38677. Accepted for publication February 7, 1983.

Abstract □ The metabolism of the 8-aminoquinoline antimalarial drug, primaquine (I) was studied using rats. The drug was administered intravenously, intraperitoneally, and orally, and blood samples were collected at various time intervals. Primaquine was metabolized by oxidative deamination to give 8-(3-carboxy-1-methylpropylamino)-6-methoxyquinoline (III). The plasma levels of both primaquine and its metabolite were determined by HPLC. The tissue distributions of radioactive primaquine after intravenous, intraperitoneal, and oral administrations were also determined. Significant concentrations of radioactivity were found in the lungs, adrenal glands, and liver. In addition, a significant portion of the dose was found to be excreted in the feces within 24 h after administration of the drug by either of the three routes.

Keyphrases □ Primaquine—excretion, distribution, and metabolism in rats □ 8-(3-Carboxy-1-methylpropylamino)-6-methoxyquinoline—primaquine metabolite, excretion and distribution in rats □ Metabolism—primaquine in rats, excretion and distribution

Primaquine (I), an 8-amino-6-methoxyquinoline derivative used for the treatment of malaria, is active against the exoerythrocytic forms of *Plasmodium vivax* and *Plasmodium ovale* and against the gametocytes of *Plasmodium falciparum*, thus inhibiting sporogony (1). Primaquine has a low chemotherapeutic index, therefore greatly limiting its prophylactic and therapeutic applications. It is known to induce hemolytic lesions in patients suffering from a deficiency in glucose 6-phosphate dehydrogenase, a genetic condition most common among inhabitants of regions in which malaria is endemic.

Although earlier workers suggested that one or more metabolites of primaquine may be responsible for its toxicity and/or antimalarial activity, very little has actually been accomplished in identifying the metabolite(s) of primaquine. Studies with other 8-aminoquinolines such as pamaquine and pentaquine have indicated that these drugs are metabolized very rapidly (2–6); it was speculated that primaquine might undergo a similar fate. Based on earlier work with pentaquine (6) and pamaquine (7), it was proposed that primaquine underwent metabolic degradation by *O*-demethylation of the 6-methoxy group followed by hydroxylation at the 5-position and oxidation to give a 5,6-quinone derivative. It was further speculated that this product was capable of oxidation–reduction activity and, therefore, may account for the hemolytic activity of primaquine (8). None of these proposed metabolites have actually been characterized from humans or animals; however, 6-methoxy-8-aminoquinoline (II) was identified as a metabolite of primaquine in the urine of humans (9).

We have recently reported the identification of 8-(3-carboxy-1-methylpropylamino)-6-methoxyquinoline (III) as the major metabolite of primaquine in rat plasma after intravenous injection (10); this is also the major metabolite in several species of fungi (11). We report herein further studies on the metabolism and distribution of primaquine after intravenous, intraperitoneal, and oral administrations.

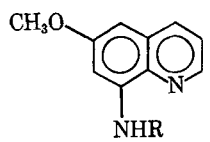

I: R = —$CH(CH_3)CH_2CH_2CH_2NH_2$
II: R = H
III: R = —$CH(CH_3)CH_2CH_2CO_2H$

EXPERIMENTAL

Source of Compounds—Commercially available primaquine diphosphate (I) was used as received[1]. [2,4-^{14}C]Primaquine diphosphate[2] had a specific activity of 1.55 mCi/mmol. 8-(3-Carboxy-1-methylpropylamino)-6-methoxyquinoline (III) was prepared by microbial transformation of primaquine as previously described (11).

Determination of Plasma Levels of Primaquine and Its Metabolite—Male Wistar rats (200–300 g) were anesthetized with sodium pentobarbital (30 mg/kg ip). Primaquine diphosphate was administered either intravenously (10 or 20 mg/kg), intraperitoneally (20 mg/kg), or orally (20 mg/kg) as an aqueous solution in distilled water (40 mg/mL). Multiple blood samples were collected from the intraorbital sinus vein in two 50-μL heparanized capillary tubes at 1, 3, 15, 30 min, and 1, 3, 6, 12, and 24 h after dosing.

After centrifugation in a hematocrit centrifuge for 2 min, the plasma was analyzed using an HPLC procedure shown to be specific for III and primaquine (10). HPLC analyses utilized a C_{18} reverse-phase column[3] (10 μm) with a mobile phase consisting of 6.6 g of K_2HPO_4, 8.4 g of KH_2PO_4, 2.4 L of methanol, 1.6 L of water, and 4 g of *N,N*-dimethyloctylamine (flow rate = 1 mL/min) (10). The sample size consisted of 20 μL of plasma, and detection was accomplished using a dual-wavelength UV detector (254 and 280 nm). For pharmacokinetic studies, the carboxylic acid metabolite (III) was injected at a dosage of 12 mg/kg iv, the molar equivalent to the primaquine diphosphate dosage of 20 mg/kg. Blood samples were collected from the intraorbital sinus vein at 1, 3, 15, 30 min, and 1, 3, 6, 12, and 24 h postadministration. After centrifugation, the plasma samples (20 μL) were analyzed directly by HPLC.

Tissue Distribution of [2,4-^{14}C]Primaquine Diphosphate—Fifty-four male Wistar rats (200–300 g) were anesthetized with sodium pentobarbital (30 mg/kg of body weight ip). An aqueous solution consisting of a 9:1 mixture of primaquine diphosphate and [^{14}C]primaquine diphosphate was administered intravenously (10 mg/kg), intraperitoneally (20 mg/kg), and orally (20

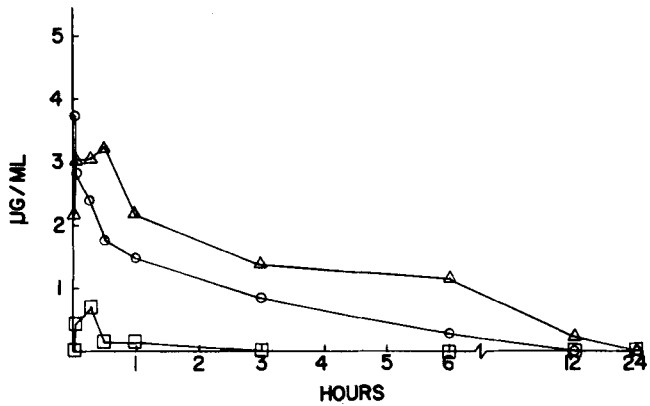

Figure 1—*Plasma concentration of primaquine diphosphate after intravenous (○), intraperitoneal (△), and oral (□) administrations of primaquine diphosphate. Each value represents the average of two animals.*

[1] Aldrich Chemical Co., Milwaukee, Wis.
[2] New England Nuclear, Boston, Mass.
[3] μ-Bondapak; Waters Associates, Milford, Mass.

0022-3549/84/0400-0502$01.00/0
© 1984, American Pharmaceutical Association

Table I—Area Under the Plasma Concentration *versus* Time Curve (AUC) for Primaquine Diphosphate after a 20-mg/kg Dose

Route	Subject	AUC[a], μg/mL·h	Amount Absorbed[b], %
Intravenous	A	9.11	
	B	3.94	
	C	7.98	
	D	4.14	
Mean ± *SD*		6.29 ± 2.6	
Oral	E	3.51	56
	F	0.55	8
	G	0.77	12
Mean ± *SD*		1.61 ± 1.64	25 ± 26

[a] AUC for primaquine diphosphate. [b] Percent absorption as determined from the AUC when primaquine diphosphate was administered orally compared with the AUC when it was administered intravenously.

mg/kg). The rats were sacrificed at 1, 3, 15, 30 min, and 1, 3, 6, 12, and 24 h after administration; two rats were used for the determination of each time point for each route of administration. A blood sample was collected by cardiac puncture and the following organs and tissues were removed: lungs, kidneys, adrenal glands, heart, liver, spleen, pancreas, brain, abdominal muscle, abdominal fat, small intestine, large intestine, testes, and stomach. After the total wet weight of each organ was determined, a portion (100–200 mg) was taken for combustion. The tissue samples were burned in a sample oxidizer[4] and the [^{14}C]carbon dioxide was trapped with a carbon dioxide absorber[5]. The trapped [^{14}C]carbon dioxide was diluted in an organic scintillation cocktail[6], and the radioactivity of each sample was measured in a liquid scintillation counter[7]. Radioactivity in the various tissues was expressed as

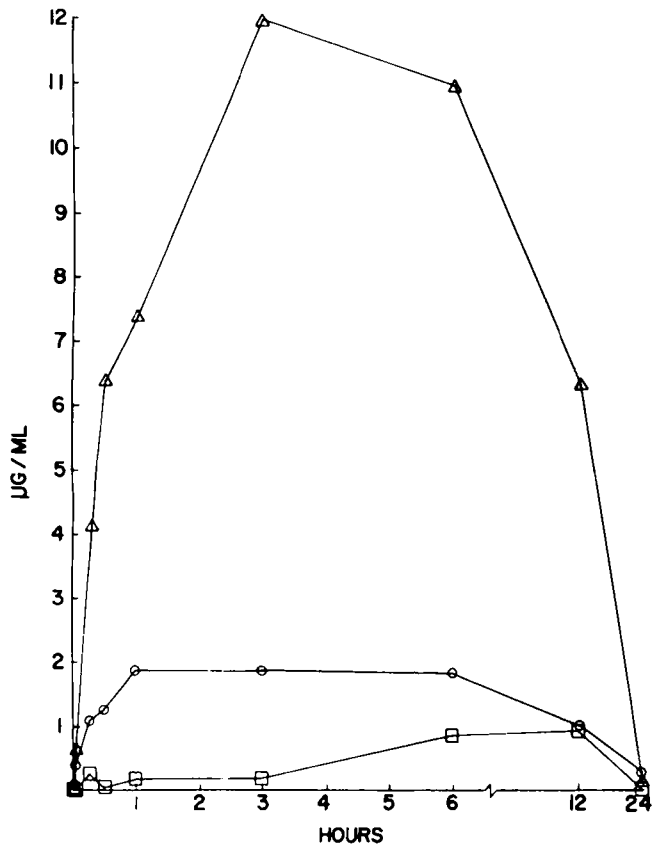

Figure 2—*Plasma concentrations of 8-(3-carboxy-1-methylpropylamino)-6-methoxyquinoline (III) after intravenous (○), intraperitoneal (△), and oral (□) administrations of primaquine diphosphate. Each value represents the average of two animals.*

[4] Packard Tri-Carb Sample Oxidizer Model 306; Packard Instrument Co., Downers Grove, Ill.
[5] Carbosorb; Packard Instrument Co., Downers Grove, Ill.
[6] Perma-Fluor V; Packard Instrument Co., Downers Grove, Ill.
[7] Packard Tri-Carb Liquid Scintillation Spectrometer Model 3255; Packard Instrument Co., Downers Grove, Ill.

Table II—Area Under the Plasma Concentration *versus* Time Curves for 8-(3-Carboxy-1-methylpropylamino)-6-methoxyquinoline (III)

Drug Given	Dose, mg/kg	Subject	AUC[a], μg/mL·h	Conversion to Metabolite[b], %
Primaquine diphosphate	20 iv	H	166	63.6
		I	14.7	5.63
		J	28.5	10.9
		K	22.6	8.67
Mean ± *SD*			57.9 ± 72	22 ± 28
Primaquine diphosphate	10 iv	L	20.2	15.5
		M	25.6	19.6
		N	21.3	16.3
Mean ± *SD*			22.4 ± 2.9	17.1 ± 2.2
Primaquine diphosphate	20 ip	O	56.4	21.6
		P	106.3	40.7
		Q	192.9	73.9
Mean ± *SD*			118.5 ± 69.1	45 ± 26
Primaquine diphosphate	20 po	R	7.08	2.71
		S	7.55	2.89
		T	17.95	6.88
Mean ± *SD*			10.8 ± 6.1	4.2 ± 2.4
Carboxylic acid	12[c] iv	U	216	
		V	298	
		W	270	
Mean ± *SD*			261 ± 42	

[a] Area under the plasma concentration *versus* time curve for metabolite III. [b] Percent conversion as determined from the curve area of III when primaquine diphosphate was administered and curve area when III was administered directly (iv). [c] Molar equivalent to 20 mg/kg of primaquine diphosphate.

the relative concentration (12), defined as (counts of radioactivity in an organ/total radioactivity dose) × (weight of animal/weight of organ).

Determination of Radioactivity in Plasma After Administration of [^{14}C]-Primaquine Diphosphate—[^{14}C]Primaquine diphosphate (1.55 mCi/mmol) was injected intravenously into a single rat at a dose of 10 mg/kg. After 3 h, a blood sample was collected by cardiac puncture, and the rat was sacrificed. The blood was centrifuged, and a portion of the plasma (20 μL) was injected into the HPLC. A total of 16 fractions (1 mL each) were collected, and each fraction was diluted with 15 mL of scintillation cocktail[8]. The radioactivity of each fraction was measured using a liquid scintillation counter[7]. To determine the total radioactivity, a 20-μL portion of the plasma was also diluted with 1 mL of the HPLC mobile phase and 15 mL of scintillation cocktail, and the radioactivity was measured.

RESULTS AND DISCUSSION

Primaquine diphosphate was administered intravenously, intraperitoneally, and orally to male rats, blood was collected at various time intervals, and the plasma was analyzed by HPLC for primaquine (I) and its metabolite (III). After intravenous injection of primaquine diphosphate, the drug disappeared very rapidly from the blood ($t_{1/2} \sim 1$ min). Within 1 min after administration of the dose, the plasma concentration was only 1–5% of the value one would expect if there were an even distribution of the drug in the blood (Fig. 1). This extremely rapid fall in plasma concentration was also observed using ^{14}C-labeled primaquine, where at 1 min after intravenous administration, the relative concentration in blood was 0.22 and in the lung a value of 4.90 was observed. These observations were consistent with the observations of other workers (13, 14) using structurally related drugs, who found that if a given drug contained a basic aliphatic amino group ($pK_a > 8.5$) that was joined to a lipophilic aromatic ring system, the drug would rapidly ($t_{1/2} < 3$ min) accumulate in the lung tissue. Primaquine also contains an aliphatic amine side chain ($pK_a = 10.39$) with a very lipophilic aromatic ring system, which probably accounted for its rapid disappearance from plasma and accumulation in the lung tissue.

After intravenous administration of primaquine diphosphate (20 mg/kg), an initial rapid drop in plasma concentration of primaquine was observed, followed by a considerably slower fall in the plasma level ($t_{1/2} = 2.24 \pm 0.82$ h). When the animals were dosed at a lower level (10 mg/kg), essentially the same half-life was observed ($t_{1/2} = 1.88 \pm 0.35$ h). After intraperitoneal administration of primaquine diphosphate, the plasma levels of primaquine reached a maximum ~30 min (Fig. 1) after administration of the dose, then began to fall at about the same rate that was observed for the intraveneous dose. Following oral administration of primaquine diphosphate (20 mg/kg), the plasma level of primaquine (Fig. 1) never rose above 1.0 μg/mL. From

[8] Insta-gel; Packard Instrument Co., Downers Grove, Ill.

Table III—Relative Concentration of Radioactivity in Tissues after Intravenous Administration of [^{14}C]Primaquine Diphosphate [a]

Tissue	1 min	3 min	15 min	30 min	1 h	3 h	6 h	12 h	24 h	AUC
Lungs	4.90	4.97	4.88	2.69	2.33	1.39	0.28	0.15	0.06	12.12
Adrenal glands	2.39	8.27	3.81	2.15	3.96	1.35	0.87	2.58	0.35	40.23
Liver	1.02	1.55	3.47	1.08	1.92	0.99	0.47	0.20	0.16	11.13
Spleen	0.88	1.10	2.01	0.96	1.01	0.34	0.17	0.58	0.12	9.77
Small intestine[b]	0.50	0.50	0.77	0.68	1.00	4.68	11.23	1.69	0.33	50.88
Large intestine[b]	0.28	0.24	0.26	0.15	0.25	0.09	8.06	7.00	2.07	112.37
Kidney	1.95	3.56	2.56	0.76	0.78	0.57	0.37	0.42	0.37	11.37
Heart	2.43	2.35	1.08	0.40	0.58	0.24	0.17	0.12	0.08	4.36
Stomach[b]	0.11	0.05	0.84	0.55	1.22	0.78	0.18	0.86	0.05	12.73
Blood	0.22	0.19	0.27	0.12	0.28	0.21	0.19	0.08	0.06	2.94
Pancreas	0.77	1.26	0.42	0.56	0.56	0.15	0.12	0.16	0.06	3.88
Abdominal muscle	0.35	0.56	0.62	0.46	0.31	0.08	0.08	0.19	0.05	3.34
Abdominal fat	0.30	0.24	0.29	0.21	0.14	0.18	0.15	0.09	0.05	2.59
Brain	0.13	0.27	0.22	.09	0.24	0.13	0.03	0.05	0.03	1.51
Testes	0.06	0.12	0.16	0.07	0.16	0.17	0.15	0.12	0.06	2.82

[a] Values represent the average obtained from two animals (dosage, 10 mg/kg) per data point. [b] Contents.

Table IV—Relative Concentration of Radioactivity in Tissues after Intraperitoneal Administration of [^{14}C]Primaquine Diphosphate [a]

Tissue	1 min	3 min	15 min	30 min	1 h	3 h	6 h	12 h	24 h	AUC
Lungs	2.21	1.89	5.45	4.08	4.24	3.80	0.53	0.75	0.07	27.37
Adrenal glands	1.16	1.93	5.70	3.19	5.48	2.03	0.74	0.29	0.31	21.77
Liver	3.07	3.38	5.73	1.94	3.06	1.26	0.65	0.24	0.12	15.24
Spleen	3.52	1.30	1.47	1.92	3.45	1.50	0.29	0.14	0.10	12.49
Small intestine[b]	2.22	2.20	0.75	1.07	1.13	1.65	17.25	0.90	0.23	93.51
Large intestine[b]	2.43	1.00	0.31	0.29	0.37	0.22	7.71	1.35	1.56	57.55
Kidney	0.58	1.48	1.90	1.54	1.43	1.12	0.45	0.25	0.14	10.89
Heart	0.59	0.38	0.44	0.61	0.59	0.48	0.21	0.14	0.06	4.88
Stomach[b]	0.28	0.36	0.18	1.04	0.76	1.59	0.81	0.04	0.02	9.53
Blood	0.22	0.10	0.18	0.18	0.33	0.34	0.36	0.08	0.05	4.03
Pancreas	2.75	2.77	0.72	2.18	1.27	0.69	0.22	0.18	0.06	7.63
Abdominal muscle	3.42	0.29	1.61	0.32	0.31	0.34	0.18	0.04	0.04	3.22
Abdominal fat	2.61	0.56	0.30	0.48	0.37	0.31	0.27	0.13	0.08	4.46
Brain	0.06	0.05	0.04	0.05	0.11	0.10	0.05	0.04	0.02	1.13
Testes	0.20	0.05	0.20	0.07	0.14	0.15	0.15	0.13	0.02	2.60

[a] Values represent the average obtained from two animals (dosage, 20 mg/kg) per data point. [b] Contents.

Table V—Relative Concentration of Radioactivity in Tissues after Oral Administration of [^{14}C]Primaquine Diphosphate [a]

Tissue	1 min	3 min	15 min	30 min	1 h	3 h	6 h	12 h	24 h	AUC
Lungs	0.46	0.16	0.40	0.51	0.24	1.20	0.19	0.23	0.04	6.772
Adrenal glands	0.11	0.32	1.32	0.50	0.37	0.98	0.54	0.98	0.41	17.15
Liver	0.03	0.04	0.14	0.71	0.73	1.15	0.43	0.39	0.06	9.90
Spleen	0.06	0.19	0.09	0.29	0.14	0.51	0.08	0.16	0.03	3.582
Small intestine[b]	0.04	0.03	0.06	0.11	1.35	13.44	4.87	0.87	0.08	65.571
Large intestine[b]	0.04	0.02	0.02	0.04	0.03	0.48	0.84	2.15	0.30	26.190
Kidney	0.03	0.04	0.14	0.20	0.15	0.55	0.16	0.17	0.07	4.344
Heart	0.06	0.05	0.16	0.12	0.09	0.21	0.06	0.07	0.03	1.81
Stomach[b]	0.57	11.98	41.30	53.17	19.14	13.71	8.40	2.48	0.04	149.20
Blood	0.02	0.03	0.02	0.04	0.04	0.08	0.04	0.05	0.03	1.08
Pancreas	0.47	0.11	0.05	0.33	0.13	0.26	0.08	0.08	0.03	2.23
Abdominal muscle	0.14	0.04	0.13	0.10	0.09	0.10	0.07	0.06	0.06	1.651
Abdominal fat	0.19	0.08	0.07	0.05	0.06	0.18	0.03	0.09	0.10	2.12
Brain	0.03	0.02	0.02	0.03	0.02	0.05	0.02	0.05	0.02	0.83
Testes	0.04	0.01	0.03	0.04	0.02	0.06	0.03	0.09	0.02	1.26

[a] Values represent the average obtained from two animals (dosage, 20 mg/kg) per data point. [b] Contents.

a comparison of the area under the primaquine concentration *versus* time curves of the oral and intravenous routes of administration (Table I), it was found that only 25% (range 8–56%) of the primaquine diphosphate was available to the central compartment.

Following intravenous or intraperitoneal administration of primaquine diphosphate (20 mg/kg), the plasma level of the carboxylic acid metabolite (III) was found to increase very rapidly, and after 1 h the concentration of metabolite III was far greater than that of primaquine (Fig. 2). When a pure sample of III was given at a dose equivalent on a molar basis to 20 mg/kg of primaquine diphosphate, the initial concentration of III was much greater (Fig. 3) than had been observed for primaquine. Therefore, it would appear that once the basic amino group is metabolically removed from the side chain of primaquine, the metabolite no longer has a high affinity for the lung and other tissues. In addition, the half-life of III ($t_{1/2} = 4.38 \pm 0.26$ h) was found to be twice as long as that of primaquine itself. The very high plasma concentration of the metabolite compared with primaquine (Figs. 1 and 2) could be a result of the much lower tissue affinity and longer half-life of the metabolite compared with that of the parent drug.

Following intravenous administration of primaquine diphosphate (20 mg/kg, Table II) it was found that 22% (range 5.63–63.6%) of the dose was converted to the metabolite (III). When the dose was reduced by half, essentially the same extent of conversion was observed (mean 17.1%; range 15.5–19.6%). When the primaquine diphosphate was administered intraperitoneally, the percent conversion to the metabolite was slightly higher (mean 45%, range 21.6–73.9%); however, the difference was not statistically significant at the 95% level.

Following oral administration of primaquine diphosphate (20 mg/kg, Table II), it was found that the percent of metabolite III that ultimately reached the plasma (mean 4.2%, range 2.71–6.88%) was significantly lower than that seen in the other routes of administration. Since only 25% of the primaquine that was administered orally actually reached the plasma, it would also be anticipated that the amount of the metabolite formed would be correspondingly lower if the primaquine was poorly absorbed or if the primaquine was being excreted in the bile following a first pass through the liver.

From a comparison of the HPLC analyses of the plasma of primaquine-treated animals and plasma blanks, only metabolite III and primaquine were

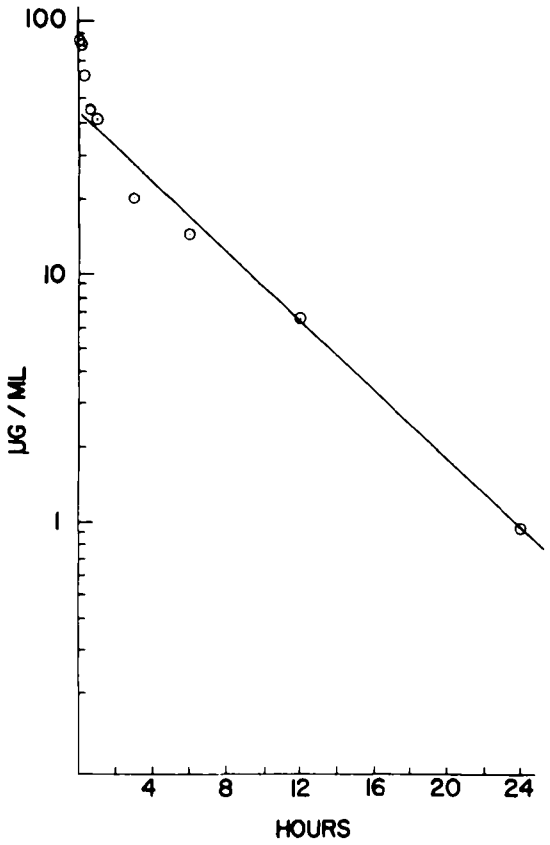

Figure 3—*Plasma concentration of 8-(3-carboxy-1-methylpropylamino)-6-methoxyquinoline (III) after an intravenous injection of III. Each value represents the average of three animals. Metabolite III showed a half-life of 4.38 ± 0.26 h.*

detected. To determine if other metabolites might have gone undetected in the plasma, a rat was administered [^{14}C]primaquine diphosphate (10 mg/kg iv; 1.55 mCi/mmol). The rat was sacrificed 3 h after administration of the labeled primaquine, and a blood sample was taken by cardiac puncture. A portion of the plasma was injected into the HPLC, and 1-mL fractions were collected. Each of the fractions was diluted with scintillation cocktail and the radioactivity was measured. It was found that 59% of the total radioactivity in the plasma could be accounted for in fractions containing the carboxylic acid metabolite (III) and 5% as unchanged primaquine.

An investigation of the tissue distribution of primaquine in rats was undertaken using ^{14}C-labeled primaquine diphosphate. While this work was in progress, Holbrook *et al.* reported on the tissue distribution of labeled primaquine in rats using [6-*O*-methyl-^{3}H]primaquine (15). In that report, the distribution of primaquine was measured in seven rat tissues (lung, liver, kidney, spleen, heart, brain, and blood) at 15–180 min after intraperitoneal administration (15). We report herein the distribution of primaquine in 15

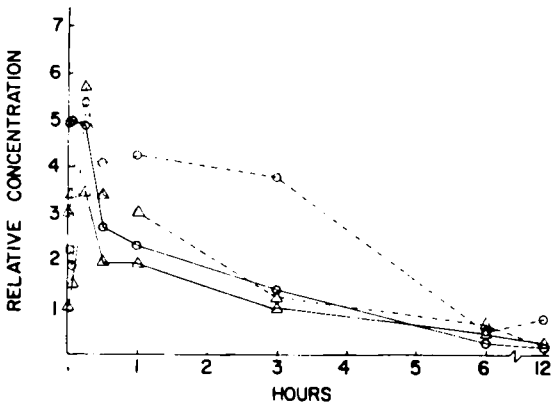

Figure 4—*Relative concentration of radioactivity in the lung (○) and liver (△) after intravenous (—) and intraperitoneal (---) administrations of [^{14}C]primaquine diphosphate. Each value represents the average of two animals.*

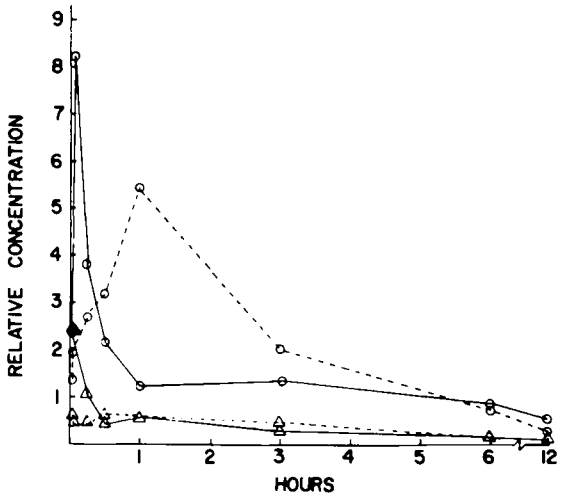

Figure 5—*Relative concentration of radioactivity in the adrenal gland (○) and heart (△) after intravenous (—) and intraperitoneal (---) administrations of [^{14}C]primaquine diphosphate. Each value represents the average of two animals.*

tissues at nine intervals from 1 min to 24 h after intravenous, intraperitoneal, and oral administration using ring-labeled [^{14}C]primaquine rather than the methyl-labeled [^{3}H]primaquine previously used. Although there appears to be wide distribution of primaquine throughout the body tissues, it is apparent that the radioactivity is concentrated in certain tissues, as determined by relative concentration (12).

At 1 min after intravenous administration of [^{14}C]primaquine diphosphate, the lungs contained the highest concentration of radioactivity (relative concentration = 4.90; Table III). Radioactivity was also concentrated in the heart, adrenal glands, kidneys, and liver. The adrenal glands and lungs contained the highest concentrations of radioactivity until 3 h after injection, when the contents of the small intestine showed the highest concentration of radioactivity. The contents of both the small and large intestines continued to contain the highest relative amount of radioactivity at 6, 12, and 24 h after injection. It appears, therefore, that there is extensive recirculation of radiolabeled material through the intestinal system after intravenous injection.

Following intraperitoneal administration of labeled primaquine, a number of tissues showed a selective concentration of the radioactivity (Table IV). Significant uptake was observed for the lung (Fig. 4), liver (Fig. 4), adrenal (Fig. 5), and spleen (Fig. 6) tissues. Large quantities of the radioactivity were also found in the contents of the large and small intestines in the later time periods following the intraperitoneal dosage (Fig. 7). Although the time course of the intraperitoneal and intravenous routes were different, there were no significant differences in the tissue distribution.

Following oral administration of labeled primaquine, a significantly different distribution of the radioactivity was observed (Table V). The areas under the curves (AUC) for the lung, adrenal, spleen, kidney, heart, blood, and pancreas tissues were found to be only 22 ± 4% (range 19–29%) of the dose-adjusted AUC values obtained after intravenous administration. However, the AUC for the liver was found to be 45% of that obtained after intravenous administration. These findings suggest that a major portion of the primaquine reaches the liver; however, metabolism and excretion into the bile prevents the major portion of the dose from reaching the plasma and other tissues.

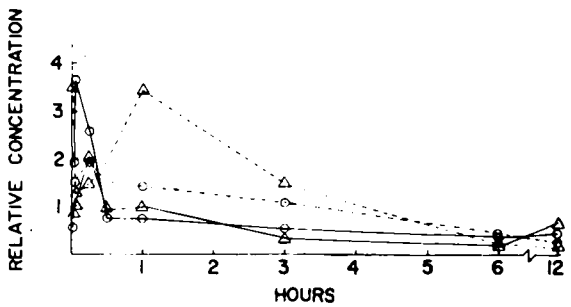

Figure 6—*Relative concentration of radioactivity in kidney (○) and spleen (△) after intravenous (—) and intraperitoneal (---) administrations of [^{14}C]primaquine diphosphate. Each value represents the average of two animals.*

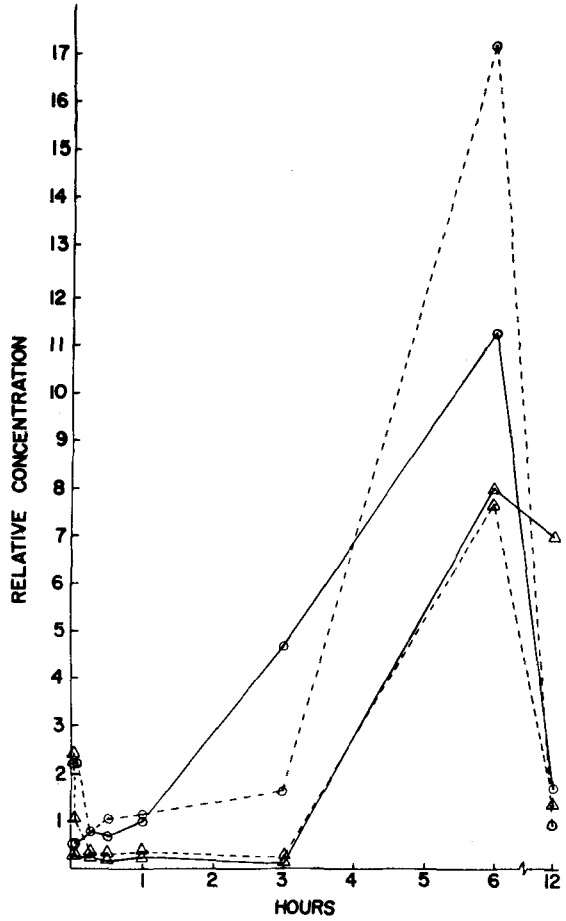

Figure 7—*Relative concentration of radioactivity in the contents of the small intestine (○) and large intestine (△) after intravenous (—) and intraperitoneal (---) administrations of [^{14}C]primaquine diphosphate. Each value represents the average of two animals.*

Consistent with these findings was the observation that a significant portion of the radioactivity was found in the feces following intravenous or intraperitoneal administrations (Table VI). Since the percentages of the dose found in the feces after intravenous, intraperitoneal, and oral administrations are all nearly the same, it would appear that primaquine is fairly well absorbed when given orally, but that only a small portion (25% by HPLC analysis) of the primaquine actually reaches the plasma because of first-pass metabolism and enterohepatic circulation.

CONCLUSIONS

The results of these studies show that primaquine was rapidly metabolized after intravenous and intraperitoneal injection and a major metabolite (mean 28%, range 5.6–74%) was found to be the carboxylic acid product (III) resulting from oxidative deamination. At 3 h after administration of the dose, this metabolite accounted for almost 60% of the total radioactivity in rat plasma, as shown by HPLC fractionation of radioactive blood samples. These findings were consistent with those of Holbrook *et al.* (15), which indicated that the majority of the radioactivity in the blood samples was not extractable into heptane under alkaline conditions.

A significant finding of the current distribution studies was that a large portion of the carbon-14 was found in the intestinal tract and feces following intravenous or intraperitoneal administration. Of the label excreted during the first 24 h following intravenous or intraperitoneal administration, approximately one-third was found in the feces, which would suggest that enterohepatic circulation may be involved in the distribution and metabolism of primaquine.

When primaquine was given orally, only 25% (range 5–56%) of the dose ultimately reached the plasma, while 18% of the dose was excreted in the feces during the first 24 h. These observations would suggest that first-pass metabolism and enterohepatic circulation may be involved in the systemic availability of primaquine following oral dosing. When labeled primaquine was administered intravenously, the major portion of the dose was found in highly perfused tissues such as the lungs, adrenal glands, liver, spleen, and heart, while little remained in the plasma. This rapid uptake by lung tissue has also been reported for similar aromatic compounds containing a very basic aliphatic amino group (13, 14).

When the labeled primaquine was administered orally, the tissue distribution was found to be significantly different because of enterohepatic recirculation and first-pass metabolism. Following oral administration, the amount of label reaching most tissues was reduced to 22% of that obtained after intravenous administration. However, the amount reaching the liver remained fairly high following oral administration, which was significant considering that primaquine is normally administered orally to suppress the malaria organisms residing in the liver.

Table VI—Percentage of Radioactive Dose Excreted in Urine and Feces after Intravenous, Intraperitoneal, and Oral Administrations of [^{14}C]-Primaquine Diphosphate [a]

Route of Administration	Radioactive Dose Recovered, %	
	Urine (0–24 h)	Feces (0–24 h)
Intravenous	26%	18%
Intraperitoneal	37%	14%
Oral	11% (17%)[b]	16% (20%)[b]

[a] Each value represents the average from two animals. [b] Values reported by Ryer *et al.* (16).

REFERENCES

(1) D. F. Clyde, *Bull. WHO*, **59**(3), 391 (1981).

(2) E. S. Josephson, J. Greenberg, D. J. Taylor, and H. L. Bami, *J. Pharmacol. Exp. Ther.*, **103**, 7 (1951).

(3) E. S. Josephson, D. J. Taylor, J. Greenberg, and A. P. Ray, *Proc. Soc. Exp. Biol. Med.*, **76**, 700 (1951).

(4) B. B. Brodie and S. Udenfriend, *Proc. Soc. Exp. Biol. Med.*, **74**, 845 (1950).

(5) R. C. Elderfield and L. L. Smith, *J. Am. Chem. Soc.*, **75**, 1022 (1953).

(6) C. C. Smith, *J. Pharmacol. Exp. Ther.*, **116**, 67 (1956).

(7) F. Schonhofer, *Hoppe-Seyler's Z. Physiol. Chem.*, **274**, 1 (1942).

(8) A. R. Tarlov, G. J. Brewer, P. E. Carson, and A. S. Alving, *Arch. Intern. Med.*, **109**, 209 (1962).

(9) J. D. Baty, D. A. Price Evans, and P. A. Robinson, *Biomed. Mass Spectrom.*, **2**, 304 (1975).

(10) J. K. Baker, J. D. McChesney, C. D. Hufford, and A. M. Clark, *J. Chromatogr.*, **230**, 69 (1982).

(11) A. M. Clark, C. D. Hufford, and J. D. McChesney, *Antimicrob. Agents Chemother.*, **19**, 337 (1981).

(12) H. Q. Woodard, R. E. Bigler, and B. Freed, *J. Nucl. Med.*, **16**, 958 (1975).

(13) T. C. Orton, M. W. Anderson, R. D. Pickett, T. E. Eling, and J. R. Fouts, *J. Pharmacol. Exp. Ther.*, **186**, 482 (1973).

(14) A. G. E. Wilson, R. D. Pickett, T. E. Eling, and M. W. Anderson, *Drug Metab. Dispos.*, **7**, 420 (1979).

(15) D. J. Holbrook, J. B. Griffin, L. Fowler, and B. R. Gibson, *Pharmacology*, **22**, 330 (1981).

(16) F. H. Ryer, *Fed. Proc. Fed. Am. Soc. Exp. Biol.*, **30**, 335 (1971).

ACKNOWLEDGMENTS

This investigation received the financial support of the UNDP/World Bank/World Health Organization Special Program for Research and Training in Tropical Diseases.

The authors thank Karen Varner, John Williamson, Michael King, and Robert Pridgen for excellent technical assistance and Dr. Anthony J. Verlangieri, Associate Professor, Department of Pharmacology, School of Pharmacy, University of Mississippi for many helpful suggestions and advice.

Characterization of Microenvironments of 2-(4′-Hydroxyphenylazo)benzoic Acid Bound to Bovine Serum Albumin by Studying the Solvent Effects

TAMIKO SAKURAI ˣ **and SEISHI TSUCHIYA**

Received September 10, 1982, from the *Tokyo College of Pharmacy, 1432-1, Horinouchi, Hachioji, Tokyo, Japan.* Accepted for publication February 11, 1983.

Abstract □ The binding and thermodynamic parameters of the two binding forms of 2-(4′-hydroxyphenylazo)benzoic acid to bovine serum albumin were estimated. The number of the binding sites of the azo form was 3.2 and that of the hydrazone form was 0.7. The binding of the hydrazone form was affected only by enthalpy changes, in contrast to that of the azo form which was affected by both enthalpy and entropy changes. To estimate the complex microenvironments of 2-(4′-hydroxyphenylazo)benzoic acid molecules on bovine serum albumin, the solvent effects were studied. The 2-carboxyl group of 2-(4′-hydroxyphenylazo)benzoic acid participates in the azo–hydrazone tautomerism. The 2-carboxylate ion forms an ion pair with triethylamine in ethylene dichloride, chloroform, and benzene, resulting in the appearance of the hydrazone form. The hydrazone formation in the system of 2-(4′-hydroxyphenylazo)benzoic acid–triethylamine (1:1) in chloroform was affected only by enthalpy changes, in the same manner as in the system of 2-(4′-hydroxyphenylazo)benzoic acid–bovine serum albumin. We speculate the presence of the two kinds of ion pairs on the basis of the changes of the azo–hydrazone tautomerism in chloroform, and that the azo form takes the contact ion pair and the hydrazone form takes the solvent-separated ion pair. A new possible model for the interaction of the azo and hydrazone forms and bovine serum albumin is proposed.

Keyphrases □ Microenvironments—2-(4′-hydroxyphenylazo)benzoic acid bound to bovine serum albumin, solvent effects, characterization □ 2-(4′-Hydroxyphenylazo)benzoic acid—binding to bovine serum albumin, solvent effects, characterization of microenvironments □ Protein binding—microenvironments of 2-(4′-hydroxyphenylazo)benzoic acid bound to bovine serum albumin, solvent effects

In a previous paper (1), it was shown that 2-(4′-hydroxyphenylazo)benzoic acid binds to two different classes of binding sites on bovine serum albumin. This binding can be distinguished spectrally since it involves the preferential binding of either the azo or hydrazone forms of this molecule to these sites. 2-(4′-Hydroxyphenylazo)benzoic acid has therefore become a useful probe when studying drug affinities and competitive binding of drugs at the two classes of binding sites (2).

To investigate the circumstances of the two classes of binding sites, the thermodynamic parameters of the azo and the hydrazone forms bound to bovine serum albumin in pH 7.40 phosphate buffer were sought. It was found that the binding of the hydrazone form was affected by the contribution of enthalpy changes only ($\Delta H°$), in contrast with that of the azo form which was affected by both enthalpy ($\Delta H°$) and entropy ($\Delta S°$) changes.

We attempted to simulate the situation leading to the hydrazone stabilization in the binding sites by measuring the changes of the azo–hydrazone tautomerism in various solvents with different dielectric constants. Baxter (3) observed the spectral change of 2-(4′-hydroxyphenylazo)benzoic acid in some organic solvents containing small amounts of the aqueous solution or in the cationic detergent. His observation has been taken to suggest the importance of the hydrophobic environments in development of the hydrazone form. However, this interpretation obscures the explanation of the thermodynamic parameters mentioned above. This paper reveals the participation of the 2-carboxyl group of 2-(4′-hydroxyphenylazo)-benzoic acid, rather than of the dielectric constant of the solvent, to the azo–hydrazone tautomerism and discusses a new possible model for the interaction of the azo and hydrazone forms in two classes of binding sites on bovine serum albumin.

EXPERIMENTAL

Materials—Bovine serum albumin (fraction V[1]) was used without further purification. 2-(4′-Hydroxyphenylazo)benzoic acid was recrystallized. Methanol, ethanol, and isopropyl alcohol were dried with molecular sieves and distilled. *tert*-Butyl alcohol, benzene, chloroform, and ethylene dichloride were refluxed over calcium hydride and distilled. Dimethyl sulfoxide and dimethylformamide were dried with molecular sieves, followed by distillation under nitrogen and reduced pressure. *n*-Butyl alcohol and isobutyl alcohol were redistilled. Triethylamine dried with calcium hydride was distilled under nitrogen and reduced pressure.

Apparatus—The visible[2], UV[2], and IR spectra[3] were obtained by spectrophotometers. Conductivity measurements[4] were made at 25°C (cell constant, 1 mho/cm).

Binding Constants of the Azo and Hydrazone Forms—Five milliliters of the solution containing 2-(4′-hydroxyphenylazo)benzoic acid (0.2×10^{-4} M–4.0×10^{-4} M) and 0.3% bovine serum albumin was dialyzed against 15 mL of the buffer solution, (0.067 M phosphate buffer, pH 7.40) for 20 h at 20°C or 37°C. After equilibration, the concentration of the total bound 2-(4′-hydroxyphenylazo)benzoic acid was determined by analyzing the free concentration in 15 mL of buffer solution. The analysis of the concentration of the azo and hydrazone forms has been described previously (1). The binding of the azo form, the hydrazone form, and total 2-(4′-hydroxyphenylazo)-benzoic acid was drawn in Scatchard plots; the binding constants were obtained from the slopes of these plots.

Equilibrium Constants of Azo–Hydrazone Tautomerism—2-(4′-Hydroxyphenylazo)benzoic acid and triethylamine were mixed at the same concentration (0.5×10^{-4} M) in the solvent, and the absorption spectra were measured at 0°C, 10°C, 20°C, and 30°C. The equilibrium constant (K) of the azo–hydrazone tautomerism is obtained by the concentration ratio (4):

$$K = \frac{(\text{hydrazone})}{(\text{azo})} = \frac{A_h/E_h}{A_a/E_a} = \frac{A_h}{A_a} \cdot \frac{E_a}{E_h} \qquad \text{(Eq. 1)}$$

where A_h, A_a, E_h, and E_a are the absorbances of the hydrazone form at 480 nm, that of the azo form at 350 nm, the molar extinction coefficient of the hydrazone form, and that of the azo form, respectively. The decrease of the concentration of the azo form, $\Delta A_a/E_a$, equals the increase of that of the hydrazone form, $\Delta A_h/E_h$. Therefore:

$$\Delta A_a/E_a = \Delta A_h/E_h \qquad \text{(Eq. 2)}$$

$$E_a/E_h = \Delta A_a/\Delta A_h \qquad \text{(Eq. 3)}$$

As E_a/E_h was 0.5 by Eq. 3 in this experiment, K was obtained by substituting this value and A_h/A_a at each temperature into Eq. 1.

pK_a of the 2-Carboxyl Group by Conductivity Measurements—The conductivity water was obtained by passing water through ion-exchange resin, followed by distillation (relative conductivity $< 1 \times 10^{-6}$ mho/cm). As the first step, 1×10^{-4} M 2-(4′-hydroxyphenylazo)benzoic acid solution was prepared under nitrogen, and the equivalent conductances ($\Lambda_{I(C)}$) at the acid

[1] Armour Co.
[2] Hitachi 557 spectrophotometer.
[3] JASCO IRA-1 spectrophotometer.
[4] Model CA-2A; Toa Denpa Kogyo Co. Ltd.

0022-3549/84/0400-0507$01.00/0
© 1984, American Pharmaceutical Association

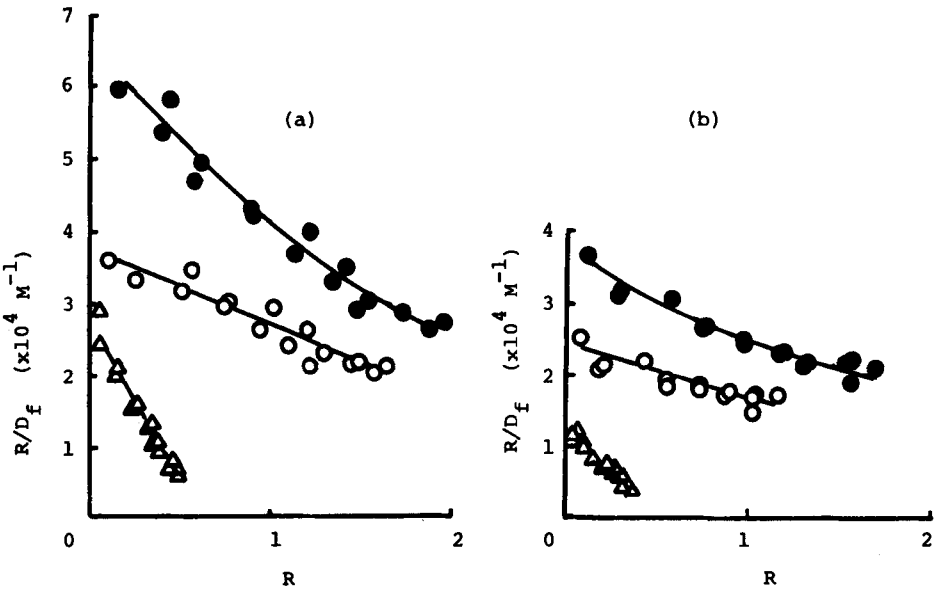

Figure 1—*Scatchard plots of the binding of the azo form (○), hydrazone form (△), and total (●) 2-(4′-hydroxyphenylazo)benzoic acid to 0.3% bovine serum albumin at 20°C (a) and 37°C (b). R represents the molar ratio of the bound form to bovine serum albumin; D_f is the concentration of the free form.*

concentrations (C) of 0.9×10^{-4}, 1.05×10^{-4}, 1.2×10^{-4}, 1.35×10^{-4}, and 1.5×10^{-4} M were measured twice. As the second step, the limiting conductance of 2-(4′-hydroxyphenylazo)benzoic acid ($\mathring{\Lambda}_I$) was obtained as follows. A solution of the sodium salt of 2-(4′-hydroxyphenylazo)benzoic acid (5×10^{-3} M) was prepared by dissolving the acid in 0.005 M NaOH ($f = 0.98$), and the equivalent conductances of the sodium salt of 2-(4′-hydroxyphenylazo)benzoic acid ($\Lambda_{I\text{-}Na}$) were measured twice for each concentration using the diluted solution (0.2×10^{-3}–5×10^{-3} M). The limiting conductance of the sodium salt of the acid ($\mathring{\Lambda}_{I\text{-}NA}$) was graphically estimated by plotting $\Lambda_{I\text{-}Na}$ against the square root of the concentration of the sodium salt of 2-(4′-hydroxyphenylazo)benzoic acid and was found to be 70.3. $\mathring{\Lambda}_I$ was then calculated as 370.3, taking the limiting conductance of Na^+ and that of H^+ as 50 and 350, respectively (5).

The degree of ionization (α) is equal to $(\Lambda_{I(C)})/(\mathring{\Lambda}_I)$, and the ionization constant (K_a) can be obtained by the following Ostwald's equation, taking C as the concentration of 2-(4′-hydroxyphenylazo)benzoic acid:

$$K_a = \frac{\alpha^2 \cdot C}{1 - \alpha}$$

The pK_a value of the 2-carboxyl group of 2-(4′-hydroxyphenylazo)benzoic acid was estimated to be 3.66 at 25°C by averaging the values obtained from the aforementioned five concentrations.

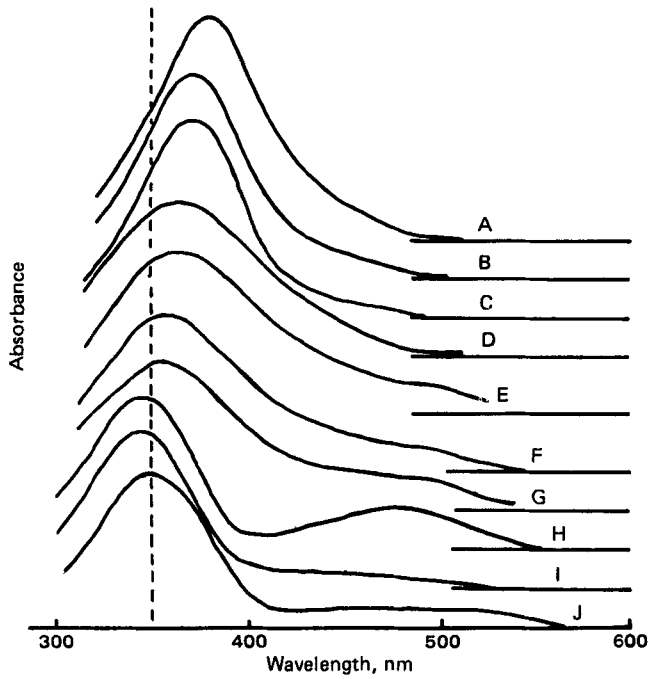

Figure 2—*Absorption spectra of 2-(4′-hydroxyphenylazo)benzoic acid (0.5×10^{-4} M) in various solvents. The ordinate is arbitrary; the broken line represents 350 nm; the solid lines to the right of the diagram are the baselines for each solvent. Key for solvents (dielectric constant): (A) chloroform (4.8 at 20°C); (B) ethylene dichloride (9.1 at 20°C); (C) benzene (2.3 at 20°C); (D) tert-butyl alcohol (10.9 at 30°C); (E) n-butyl alcohol (17.1 at 25°C); (F) isopropyl alcohol (18.3 at 25°C); (G) isobutyl alcohol (17.7 at 25°C); (H) ethanol (24.3 at 25°C); (I) methanol (32.6 at 25°C); (J) dimethyl sulfoxide (48.9 at 20°C).*

RESULTS AND DISCUSSION

Thermodynamics of the Azo and Hydrazone Forms—Figure 1 shows the Scatchard plots of the binding of the azo form, the hydrazone form, and total 2-(4′-hydroxyphenylazo)benzoic acid with bovine serum albumin at 20°C and 37°C. In this concentration range, the plots of both the azo and hydrazone forms showed straight lines and were extrapolated to 3.2 and 0.7 on the x-axis, respectively, which corresponds to the number of the binding sites. On the other hand, the binding of total 2-(4′-hydroxyphenylazo)benzoic acid showed a curvature; this binding curve satisfactorily corresponded to the line obtained by the graphical summation of the plots of the azo and hydrazone forms according to the method described by Rosenthal (6).

The thermodynamic parameters are shown in Table I. The binding of both forms shows an exothermic reaction, as has been reported for many protein bindings. However, the negative value of free energy changes ($\Delta G°$) of the hydrazone form was derived from the contribution of $\Delta H°$ only, in contrast with the concentration of both $\Delta H°$ and $\Delta S°$ in that of the azo form. Therefore, the binding of the hydrazone form is entropically unstable, but energetically stable. On the other hand, the binding of the azo form is stable both entropically and energetically. These facts show that two different microenvironments of 2-(4′-hydroxyphenylazo)benzoic acid molecules produced two binding forms, the azo and the hydrazone.

Solvent Effects of the Azo–Hydrazone Tautomerism—To consider the situation leading to the hydrazone stabilization, the solvent effects of the azo–hydrazone tautomerism were investigated. Figure 2 shows the absorption spectra of 2-(4′-hydroxyphenylazo)benzoic acid in various solvents. In

Table I—Thermodynamic Parameters for Azo and Hydrazone Forms Bound to Bovine Serum Albumin at pH 7.40

Form	Temp.	log K^a	$\Delta G°$, kcal/M	$\Delta H°$, kcal/M	$\Delta S°$, eu
Azo	20°C	4.01	−5.37	−3.02	7.88
	37°C	3.87	−5.49	−3.02	7.96
Hydrazone	20°C	4.47	−6.30	−7.99	−5.97
	37°C	4.11	−5.87	−7.99	−6.97

[a] Binding constant.

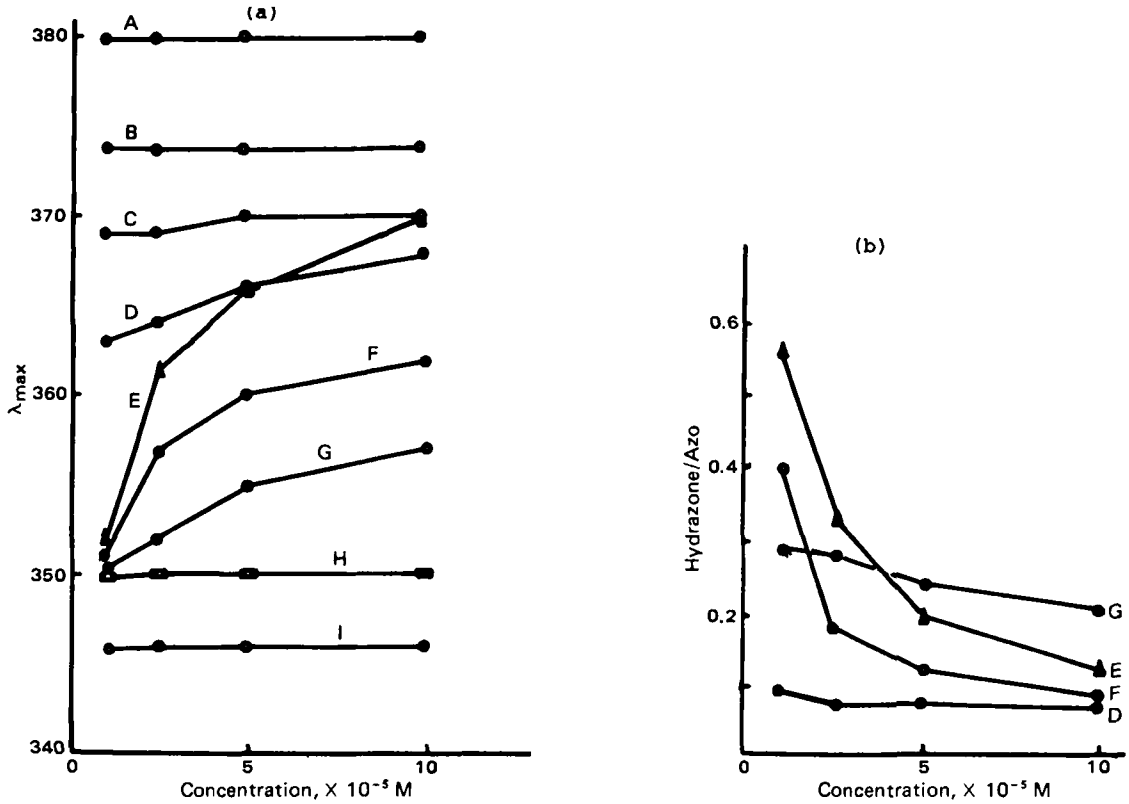

Figure 3—*Concentration dependence of the absorption spectra of 2-(4′-hydroxyphenylazo)benzoic acid utilizing λ_{max} (a) and the expedient concentration ratio of hydrazone to azo forms (b). Key: (A) chloroform; (B) ethylene dichloride; (C) benzene; (D)* tert*-butyl alcohol; (E)* n*-butyl alcohol; (F) isopropyl alcohol; (G) isobutyl alcohol; (H) dimethyl sulfoxide; (I) methanol and ethanol.*

methanol, ethanol, isopropyl alcohol, *n*-butyl alcohol, and isobutyl alcohol, λ_{max} was observed at ~350 nm with the shoulder or broad peak at ~500 nm; in *tert*-butyl alcohol λ_{max} was at 365 nm without a shoulder.

According to the calculation by means of Hückel molecular orbital by Moriguchi (7), $\pi \rightarrow \pi^*$ transition of the azo and the hydrazone forms of 4-hydroxyazobenzene shows λ_{max} at 350 and 458 nm, respectively. Terada *et al.* (8) reported that the absorption spectra with λ_{max} at ~350 nm and at ~480 nm in the aqueous solutions of 2-(4′-hydroxyphenylazo)benzoic acid under the different conditions are the azo and hydrazone forms on the basis of the resonance Raman spectra. We considered the λ_{max} values at ~350 nm and the broad peak at ~500 nm observed in the solvents as the azo and hydrazone forms, respectively.

In the solvents with low dielectric constants (ethylene dichloride, chloroform, and benzene), λ_{max} was observed at 374, 380, and 370 nm, shifting to a longer wavelength than in alcoholic solvents with higher dielectric constants. As a general rule, the absorption spectrum due to the $\pi \rightarrow \pi^*$ transition shifts to the shorter wavelength in the solvent with the lower polarity. To determine which of the absorption spectra in the solvents with low dielectric constants are assigned to the azo and hydrazone forms respectively, the IR spectra were measured. In the IR spectra of 2-(4′-hydroxyphenylazo)benzoic acid in eth-

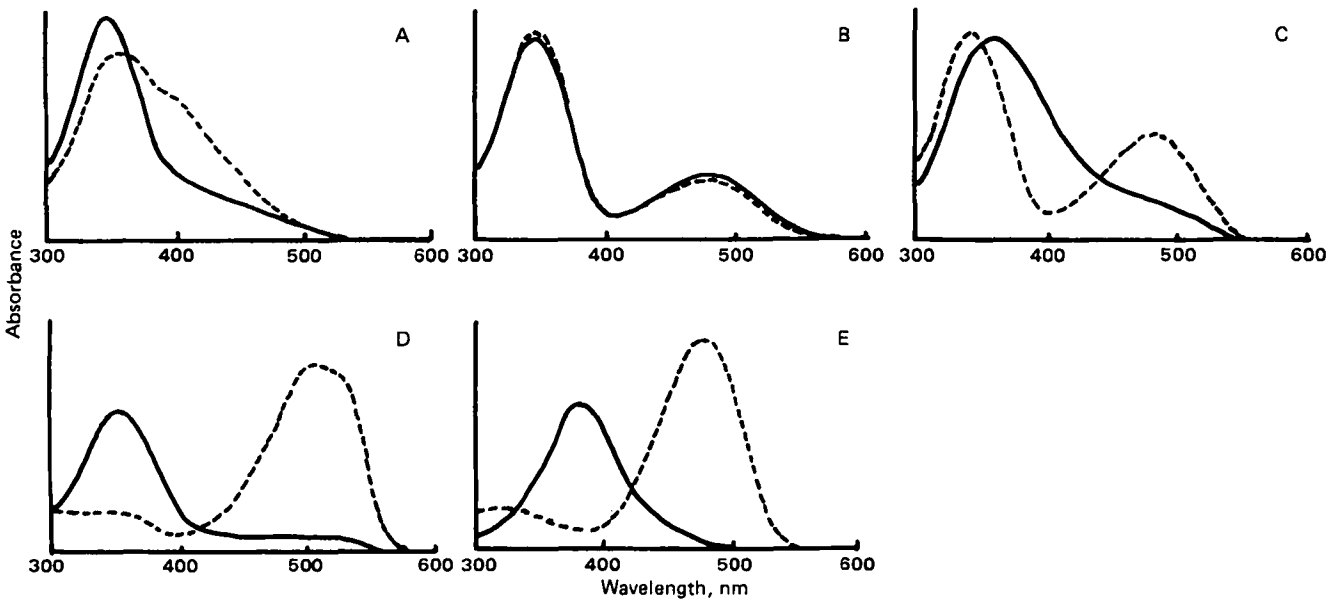

Figure 4—*Absorption spectra of 2-(4′-hydroxyphenylazo)benzoic acid in solvents with (----) or without (—) 0.1 M triethylamine. Key: (A) methanol; (B) ethanol; (C) isopropyl alcohol; (similar change observed with* n*-butyl and isobutyl alcohols); (D) dimethylformamide (similar change observed with dimethyl sulfoxide); (E) chloroform (similar change observed with ethylene dichloride and benzene).*

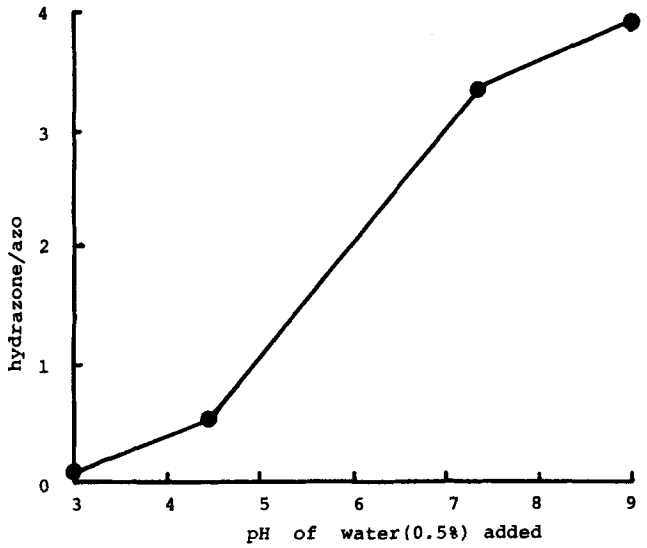

Figure 5—*Effects of the pH of water added to dimethylformamide on hydrazone formation. The ordinate was obtained as the ratio of the absorbance at 510 nm to that at 350 nm.*

ylene dichloride and chloroform, there was an absorption maximum at 3670 cm^{-1} due to ν_{OH} of the 4′-hydroxy group monomer, but no appearance of a peak at ~1660 cm^{-1} due to $\nu_{C=O}$ of the conjugated ketone group. Therefore, 2-(4′-hydroxyphenylazo)benzoic acid takes the azo form in ethylene dichloride and chloroform. As the solvent effects of the absorption spectra of 4-hydroxyazobenzene obeyed the ordinary rule in this experiment, it seems that the 2-carboxyl group in the 2-(4′-hydroxyphenylazo)benzoic acid molecule takes part in the unusual spectral shift to the longer wavelength in the solvents with lower dielectric constants.

So, to investigate the intra- or intermolecular interaction, the effects of the concentration of 2-(4′-hydroxyphenylazo)benzoic acid on the absorption spectra were examined. As shown in Fig. 3a λ_{max} shifted to the longer wavelength with the increase of the concentrations of 2-(4′-hydroxyphenylazo)-benzoic acid in isobutyl, isopropyl, *n*-butyl, and *tert*-butyl alcohols, indicating the presence of the intermolecular interaction (9), while no shift was observed in chloroform, ethylene dichloride, benzene, dimethyl sulfoxide, ethanol, and methanol.

It seems that dimethyl sulfoxide, ethanol, and methanol with relatively high dielectric constants can solvate the hydroxy moiety of the 2-carboxyl group easily. On the other hand, chloroform, ethylene dichloride, and benzene could not solvate the hydroxy moiety of the 2-carboxyl group easily. Therefore, it is suggested that in these solvents the intramolecular interaction stabilizes the azo form (I). Figure 3b shows the concentration dependence of the ratio of the maximum absorbance at ~500 nm to that at ~350 nm, which expediently corresponds to the concentration ratio of the hydrazone form to the azo form. The increase of the intermolecular interaction in isobutyl, isopropyl, *n*-butyl, and *tert*-butyl alcohols with the increase of the concentration of 2-(4′-hydroxyphenylazo)benzoic acid resulted in the decrease in the hydrazone form. This may indicate the stabilization of the azo form due to the dimerization of the 2-carboxyl group.

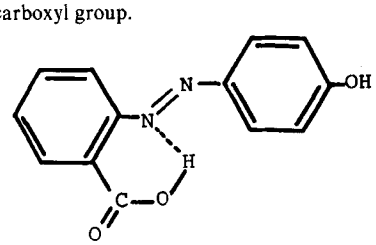

I

Solvent Effects on the 2-Carboxylate Ion—As mentioned above, the formation of the hydrazone form in various solvents cannot be estimated only from the dielectric constants of the solvents, but depends on their solvation to 2-(4′-hydroxyphenylazo)benzoic acid molecules and the intra- or intermolecular interaction of the 2-carboxyl group.

As the 2-carboxyl group dissociates in the pH 7.40 phosphate buffer used in the study of the binding of 2-(4′-hydroxyphenylazo)benzoic acid with bovine serum albumin, the participation of the 2-carboxylate ion in the azo–hydrazone tautomerism in various solvents was investigated. Figure 4 shows the absorption spectra at the addition of 0.1 M triethylamine to 2-(4′-hydroxyphenylazo)benzoic acid in some solvents. In the IR spectra, the addition of triethylamine to 2-(4′-hydroxyphenylazo)benzoic acid in all the solvents caused the disappearance of the peak at ~1700 cm^{-1} due to the carboxyl group and the appearance of the peak at ~1600 cm^{-1} due to the carboxylate ion, indicating the dissociation of the 2-carboxyl group. The absorption spectra in methanol showed the spectrum similar to that in the alkaline aqueous solution assigned to the azo form (10), and in ethanol the spectral change was not observed. In dimethylformamide, with a high dielectric constant, the hydrazone form predominated. On the other hand, in chloroform, with a low dielectric constant, the same change was observed as in dimethylformamide. However, the addition of 0.1 M triethylamine to 4-hydroxyazobenzene did not cause the spectral change in any solvent.

Table II—Direct Conductivity Measurements of 2-(4′-Hydroxyphenylazo)-benzoic Acid–Triethylamine (1×10^{-3}M:0.1 M) at 25°C

Solvent	0.1 M Triethylamine, μmho/cm[a]	2-(4′-Hydroxyphenylazo)benzoic Acid–Triethylamine System, μmho/cm
Dimethyl sulfoxide	1.2[b]	17.6
Methanol	49.7[b]	123.5
Ethanol	8.0[b]	24.7
Isopropyl alcohol	<1	2.3
tert-Butyl alcohol	<1	<1
Ethylene dichloride	<1	<1
Chloroform	<1	<1
Benzene	<1	<1

[a] Triethylamine only was added to the solvent. [b] This indicates the ionization of triethylamine.

Moreover, to estimate the participation of the 2-carboxylate ion in the formation of the hydrazone form, aqueous solutions at four pH values were all added to dimethylformamide at a concentration of 0.5% (Fig. 5). According to the principle of the specific sorting of solvents, a component with a stronger solvating power in the mixtures of solvents selectively solvates the solute. So, in the dimethylformamide–water mixtures, water solvates the 2-carboxyl group. Therefore, the pH of a small quantity of water may significantly affect the ionization of the 2-carboxyl group. With pH >3.66 (the pK_a value obtained by conductivity measurements), the ratio of the hydrazone form increased. These facts show that the ionization of the 2-carboxyl group resulted in the accelerated formation of the hydrazone form.

Next, conductivity measurements were carried out on the system of 1×10^{-3} M 2-(4′-hydroxyphenylazo)benzoic acid–0.1 M triethylamine in some solvents (Table II). In the 2-(4′-hydroxyphenylazo)benzoic acid–triethylamine system, the conductivity was not observed in *tert*-butyl alcohol, ethylene dichloride, chloroform, and benzene. This observation indicates that 2-carboxylate ion exists as an ion pair with a triethylammonium ion exclusively in these solvents. In the other solvents, the free ions and ion pair are in equilibrium. Therefore, the predominant appearance of the hydrazone form in such solvents as ethylene dichloride, chloroform, and benzene after the addition of triethylamine (Fig. 4) is attributed to the formation of ion pairs.

Table III shows the thermodynamic parameters for hydrazone formation in the system of 2-(4′-hydroxyphenylazo)benzoic acid–amines (1:1) in chloroform. When the temperature was lowered, the hydrazone form increased. Only $\Delta H°$ contributed to the hydrazone formation (−4130 cal·M^{-1} in triethylamine and −5880 cal·M^{-1} in diethylamine), in the same manner as in the system of 2-(4′-hydroxyphenylazo)benzoic acid–bovine serum albumin (Table I). The same result was obtained in ethylene dichloride and benzene. It seems that this change of the azo–hydrazone tautomerism depending on temperature reflects the presence of two species of ion pairs. One ion pair takes the azo form and the other the hydrazone form. Hogen-Esch and Smid (11) presented evidence for two kinds of ion pairs for 9-fluorenyl-alkali metal, *viz.*, the contact ion pair and the solvent-separated ion pair, which were distin-

Table III—Thermodynamic Parameters for Hydrazone Formation in Chloroform

Amine	Temp., °C	K^a	$\Delta G°$, cal/M	$\Delta H°$, cal/M	$\Delta S°$, eu
Triethylamine	0	0.356	560	−4130	−17.2
	10	0.270	737	−4130	−17.2
	20	0.232	852	−4130	−17.0
	30	0.164	1087	−4130	−17.2
Diethylamine	0	0.197	883	−5880	−24.8
	10	0.135	1123	−5880	−24.8
	20	0.102	1326	−5880	−24.6
	30	0.078	1530	−5880	−24.5

[a] Equilibrium constants of azo–hydrazone tautomerism.

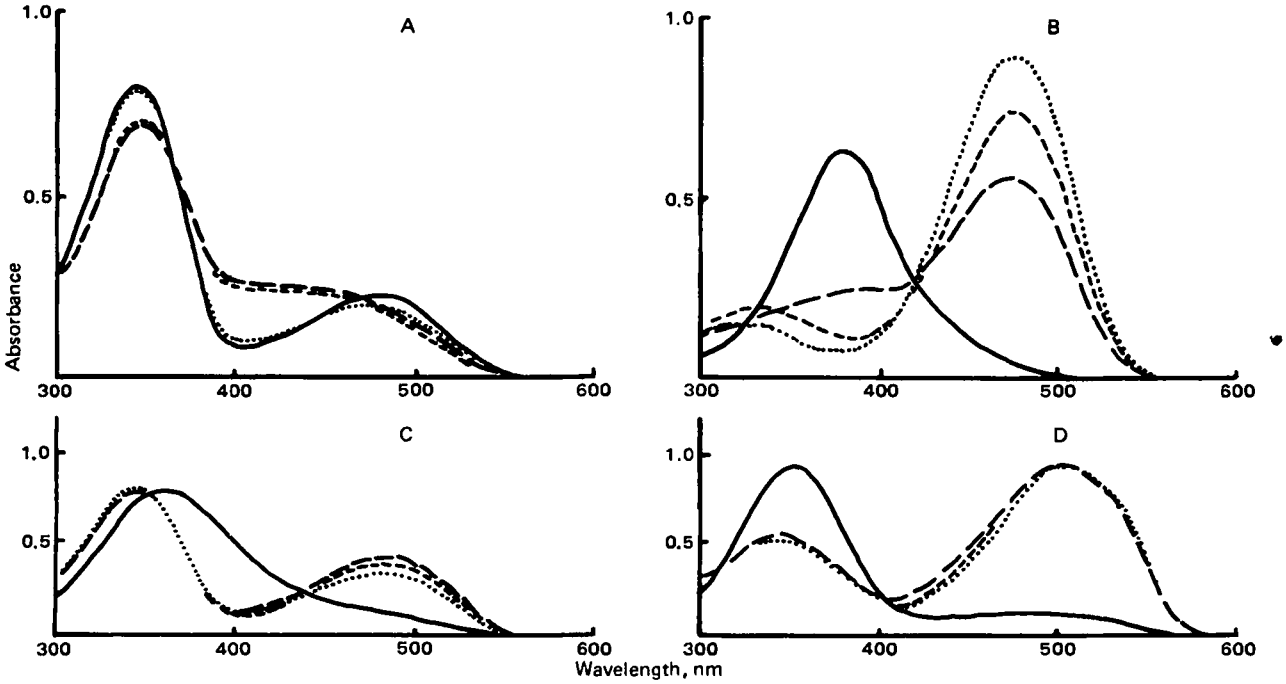

Figure 6—*Effects of* n*-butylamine (—), diethylamine (---), piperidine (---), and triethylamine (·····) on the absorption spectra of 2-(4′-hydroxyphenylazo)benzoic acid (0.5 × 10⁻⁴ M). Piperidine induced the same change as diethylamine. The solid line represents no addition of amines. Key: (A) ethanol; (B) chloroform; (C) isopropyl alcohol; (D) dimethyl sulfoxide.*

guishable by the absorption spectra. The relative amounts of these two kinds of ion pairs were found to be the sensitive functions for the solvating power, temperature of the medium, and for the types of anion and cation. In the same solvent, an ion pair of any ion with a counterion with a larger molecular volume is likely to take the form of the solvent-separated ion pair (12). According to Grunwald's description (13), the distance between a cation and an anion is ~3 Å for a contact ion pair and ~6 Å for a solvent-separated ion pair.

Investigation was carried out on the effects of some amines, which dissociated the 2-carboxyl group of 2-(4′-hydroxyphenylazo)benzoic acid in methanol, ethanol, isopropyl alcohol, dimethyl sulfoxide, benzene, ethylene dichloride, and chloroform, but are considered to have different steric hindrances in forming ion pairs. Figure 6 shows the absorption spectra of 2-(4′-hydroxyphenylazo)benzoic acid with four amines. Among the solvents investigated, triethylamine, with a larger molecular volume, induced the hydrazone formation more strongly than the other amines only in ethylene dichloride, chloroform, and benzene.

Solvent-separated ion pairs become stable when the temperature is lowered due to the large gain of solvation enthalpy (11). Therefore, the hydrazone formation in chloroform (Table III) is attributed to the solvent-separated ion pairs. At the same temperature, as diethylamine more easily introduces the contact ion pairs than triethylamine because of a small steric hindrance, the hydrazone formation decreases (Table III). From these considerations, the origin of the hydrazone formation is speculated to be the formation of the solvent-separated ion pairs, in which the 2-carboxylate ion may take an energetically stable form due to the intramolecular hydrogen bond (Scheme I).

It seems that the accelerated formation of the hydrazone form was not observed (Fig. 4) in methanol and ethanol, because of the easy solvation of 2-carboxylate ion. These facts imply that 2-(4′-hydroxyphenylazo)benzoic acid molecules do not take the hydrazone form in the solvents in which the contact ion pairs can be formed or the free ions can solvate easily.

On the other hand, that the hydrazone form predominated in dimethyl sulfoxide or dimethylformamide (Fig. 4) in spite of the high dielectric constants of these solvents can be interpreted by the solvating power of these solvents. Because these solvents are powerful solvating agents to a cation, but not to an anion (14), no contact ion pairs may be formed. The fact that no difference was observed among the four amines in their effects in dimethyl sulfoxide (Fig. 6) may prove the predominant presence of the solvent-separated ion pairs.

Thomas and Merlin (15) inferred from their resonance Raman spectroscopic study that hydrazone formation on protein binding is stabilized by the intermolecular hydrogen bond between the —NH— group of the hydrazone form and the carboxylate of a suitable amino acid residue in the binding sites. Unlike that of Thomas and Merlin, another possible model can be proposed for the 2-(4′-hydroxyphenylazo)benzoic acid–bovine serum albumin interaction. The 2-carboxyl group of the 2-(4′-hydroxyphenylazo)benzoic acid dissociated at pH 7.40 may be attracted by a long-range electrostatic force due to the arginine or lysine residues in the proposed binding sites (16) of Brown's model (17). At the binding sites of the azo form, 2-(4′-hydroxyphenylazo)benzoic acid may be able to form contact ion pairs with the basic amino acid residues. On the other hand, at the binding sites of the hydrazone form, the microenvironment of 2-(4′-hydroxyphenylazo)benzoic acid molecules may structurally restrict the proximity of the 2-carboxylate ion to the amino acid residues, resulting in no formation of the contact ion pairs. Consequently, the distance between the 2-carboxylate ion and the basic amino acid residue may be similar to that between the two counterions of the solvent-separated ion pair, *viz.*, 6 Å. This speculation may be corroborated by the fact that the binding capacity of bovine serum albumin to the hydrazone

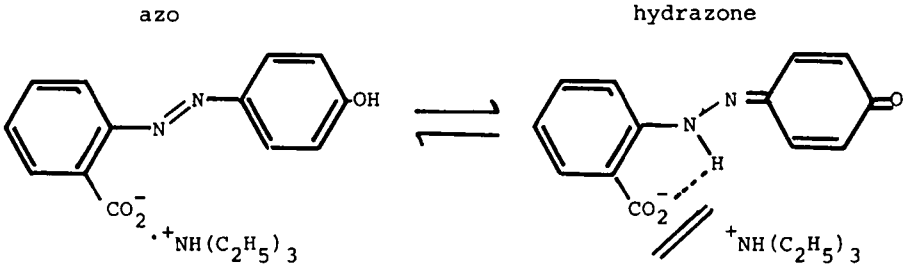

Scheme I

form is smaller than that to the azo form (Fig. 1); *i.e.*, the number of the binding sites of the former is 0.7, although that of the latter is 3.2. Moreover, as was shown previously (18), the circular dichroism spectra of the azo form induced by bovine serum albumin was larger than that of the hydrazone form. Taking into consideration this result and the theory of Takenaka *et al.* (19) that the contact ion pair formation between unchiral benzoic acid derivatives and chiral amines introduces the larger circular dichroism, the azo form may be present as the contact ion pairs in the 2-(4′-hydroxyphenylazo)benzoic acid–bovine serum albumin interaction.

REFERENCES

(1) T. Sakurai, S. Tsuchiya, and H. Matsumaru, *J. Pharm. Dyn.*, **4**, 65 (1981).

(2) T. Sakurai, S. Tsuchiya, and H. Matsumaru, *J. Pharm. Dyn.*, **4**, 345 (1981).

(3) J. H. Baxter, *Arch. Biochem. Biophys.*, **108**, 375 (1964).

(4) J. G. Dawber and M. M. Crane, *J. Chem. Educ.*, **44**, 150 (1967).

(5) A. Albert and E. P. Serjeant, "Ionization Constants of Acids and Bases; A Laboratory Manual," The Great Britain, Methuen, 1962; Japanese Edition, Maruzen, Tokyo, 1963, p. 93.

(6) H. E. Rosenthal, *Anal. Biochem.*, **20**, 525 (1967).

(7) I. Moriguchi, S. Fushimi, and C. Ohshima, *Chem. Pharm. Bull.*, **18**, 2447 (1970).

(8) H. Terada, B-K. Kim, Y. Sato, and K. Machida, *Spectrochim. Acta*, **31A**, 945 (1975).

(9) W. F. Forbes and A. R. Knight, *Can. J. Chem.*, **37**, 334 (1959).

(10) J. C. Merlin and E. W. Thomas, *Spectrochim. Acta*, **35A**, 1243 (1979).

(11) T. E. Hogen-Esch and J. Smid, *J. Am. Chem. Soc.*, **88**, 307 (1966).

(12) N. Tokura, "Solvation," Kagakudohzin, Kyoto, Japan, 1972, p. 131.

(13) E. Grunwald, *Anal. Chem.*, **26**, 1696 (1954).

(14) N. Tokura, "Solvation," Kagakudohzin, Kyoto Japan, 1972, p. 34.

(15) E. W. Thomas and J. C. Merlin, *Spectrochim. Acta*, **35A**, 1251 (1979).

(16) K. J. Fehske, W. E. Muller, and U. Wollert, *Biochem. Pharmacol.*, **30**, 687 (1981).

(17) J. M. Brown, "Albumin Structure, Function and Uses," V. M. Rosenoer, M. Oratz, and M. A. Rothchild, Eds., Pergamon, New York, N.Y., 1977, p. 36.

(18) T. Sakurai, S. Tsuchiya, and H. Matsumaru, *J. Pharm. Dyn.*, **4**, 451 (1981).

(19) S. Takenaka, K. Kondo, and N. Tokura, *J. Chem. Phys., Perkin II*, **1974**, 1749.

ACKNOWLEDGMENTS

The authors are grateful to Dr. K. Tabei, Tokyo College of Pharmacy, for helpful discussions about the IR spectra.

Polymorphism of Butyrophenones Related to Haloperidol

M. AZIBI, M. DRAGUET-BRUGHMANS ˣ, and R. BOUCHE

Received June 28, 1982, from the *Laboratoire d'Analyse des Médicaments, Université Catholique de Louvain, BP 7340 1200 Bruxelles, Belgium.* Accepted for publication March 31, 1983.

Abstract □ A comparison of X-ray powder diffraction patterns, IR spectra, and crystal structures of structurally related compounds belonging to the butyrophenone family has been undertaken to obtain information about the elements of chemical structure which predispose a substance to exhibit polymorphism. Five butyrophenones, differing by the nature of only one substituent, were selected. After crystallization from 15 solvents, it appears that two compounds of the group exhibit more than one crystalline form. An explanation of the absence of polymorphism in the other compounds of the group is proposed and discussed.

Keyphrases □ Polymorphism—disubstituted butyrophenones, comparison of IR spectra, X-ray diffraction patterns, and crystal structures □ Haloperidol—polymorphism, comparison of IR spectra, X-ray diffraction patterns, and crystal structures □ Moperone—polymorphism, comparison of IR spectra, X-ray diffraction patterns, and crystal structures □ Bromperidol—polymorphism, comparison of IR spectra, X-ray diffraction patterns, and crystal structures

Many papers have been published in the past 10 years about drug polymorphism, generally describing the way of obtaining the polymorphs of a given substance (1–3); their IR spectra (2, 4, 5), thermal behaviors (6–8), and X-ray diffraction patterns (3, 8, 9); their dissolution and solubility profiles (2, 8, 10, 11); and more rarely their *in vivo* rates of release (12–15). Studies of polymorphism are thus often empirical. Few studies attempted to determine what structural characteristics predispose an organic compound to exhibit polymorphism; in a paper concerning the polymorphism of sulfamides, Yang and Guillory (16) investigated that problem.

This work was undertaken to study the polymorphism of closely related compounds belonging to the butyrophenone family; to compare their IR spectra, X-ray diffraction patterns, and crystal structures; and to correlate, if possible, the frequency of polymorphism occurrence and chemical structure. The substances were chosen because of their therapeutic importance, structural simplicity, and crystalline nature (17–21).

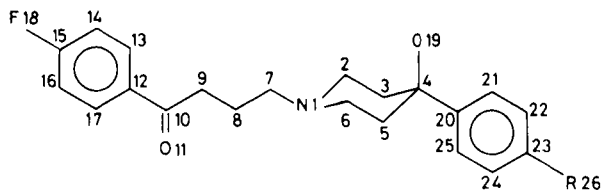

HALOPERIDOL: R = Cl
BROMPERIDOL: R = Br
I: R = F
II: R = H
MOPERONE: R = CH_3

EXPERIMENTAL

Materials—Five butyrophenones were selected for study: haloperidol[1], bromperidol[2], 4-[4-hydroxy-4-(4-fluorophenyl)-1-piperidinyl]-1-(4-fluorophenyl)-1-butanone[3] (I), moperone[4], and 4-(hydroxy-4-phenyl-1-piperidinyl)-1-(4-fluorophenyl)-1-butanone[5] (II). The difference between these substances lies only in the nature of the substituent at the 26 position.

[1] Haloperidol: 4-[4-(4-chlorophenyl)-4-hydroxy-1-piperidinyl]-1-(4-fluorophenyl)-1-butanone.

[2] Bromperidol: 4-[4-(4-bromophenyl)-4-hydroxy-1-piperidinyl]-1-(-4-fluorophenyl)-1-butanone.

[3] I: 4-[4-(4-fluorophenyl)-4-hydroxy-1-piperidinyl]-1-(4-fluorophenyl)-1-butanone (no generic name).

[4] Moperone: 4′-fluoro-4(4-hydroxy-4-*p*-tolylpiperidino)butyrophenone.

[5] II: 4-(4-hydroxy-4-phenyl-1-piperidinyl)-1-(4-fluorophenyl)-1-butanone (no generic name).

0022-3549/84/0400-0512$01.00/0

© 1984, American Pharmaceutical Association

form is smaller than that to the azo form (Fig. 1); *i.e.*, the number of the binding sites of the former is 0.7, although that of the latter is 3.2. Moreover, as was shown previously (18), the circular dichroism spectra of the azo form induced by bovine serum albumin was larger than that of the hydrazone form. Taking into consideration this result and the theory of Takenaka *et al.* (19) that the contact ion pair formation between unchiral benzoic acid derivatives and chiral amines introduces the larger circular dichroism, the azo form may be present as the contact ion pairs in the 2-(4′-hydroxyphenylazo)benzoic acid–bovine serum albumin interaction.

REFERENCES

(1) T. Sakurai, S. Tsuchiya, and H. Matsumaru, *J. Pharm. Dyn.*, **4**, 65 (1981).

(2) T. Sakurai, S. Tsuchiya, and H. Matsumaru, *J. Pharm. Dyn.*, **4**, 345 (1981).

(3) J. H. Baxter, *Arch. Biochem. Biophys.*, **108**, 375 (1964).

(4) J. G. Dawber and M. M. Crane, *J. Chem. Educ.*, **44**, 150 (1967).

(5) A. Albert and E. P. Serjeant, "Ionization Constants of Acids and Bases; A Laboratory Manual," The Great Britain, Methuen, 1962; Japanese Edition, Maruzen, Tokyo, 1963, p. 93.

(6) H. E. Rosenthal, *Anal. Biochem.*, **20**, 525 (1967).

(7) I. Moriguchi, S. Fushimi, and C. Ohshima, *Chem. Pharm. Bull.*, **18**, 2447 (1970).

(8) H. Terada, B-K. Kim, Y. Sato, and K. Machida, *Spectrochim. Acta*, **31A**, 945 (1975).

(9) W. F. Forbes and A. R. Knight, *Can. J. Chem.*, **37**, 334 (1959).

(10) J. C. Merlin and E. W. Thomas, *Spectrochim. Acta*, **35A**, 1243 (1979).

(11) T. E. Hogen-Esch and J. Smid, *J. Am. Chem. Soc.*, **88**, 307 (1966).

(12) N. Tokura, "Solvation," Kagakudohzin, Kyoto, Japan, 1972, p. 131.

(13) E. Grunwald, *Anal. Chem.*, **26**, 1696 (1954).

(14) N. Tokura, "Solvation," Kagakudohzin, Kyoto Japan, 1972, p. 34.

(15) E. W. Thomas and J. C. Merlin, *Spectrochim. Acta*, **35A**, 1251 (1979).

(16) K. J. Fehske, W. E. Muller, and U. Wollert, *Biochem. Pharmacol.*, **30**, 687 (1981).

(17) J. M. Brown, "Albumin Structure, Function and Uses," V. M. Rosenoer, M. Oratz, and M. A. Rothchild, Eds., Pergamon, New York, N.Y., 1977, p. 36.

(18) T. Sakurai, S. Tsuchiya, and H. Matsumaru, *J. Pharm. Dyn.*, **4**, 451 (1981).

(19) S. Takenaka, K. Kondo, and N. Tokura, *J. Chem. Phys., Perkin II*, **1974**, 1749.

ACKNOWLEDGMENTS

The authors are grateful to Dr. K. Tabei, Tokyo College of Pharmacy, for helpful discussions about the IR spectra.

Polymorphism of Butyrophenones Related to Haloperidol

M. AZIBI, M. DRAGUET-BRUGHMANS ˣ, and R. BOUCHE

Received June 28, 1982, from the *Laboratoire d'Analyse des Médicaments, Université Catholique de Louvain, BP 7340 1200 Bruxelles, Belgium.* Accepted for publication March 31, 1983.

Abstract □ A comparison of X-ray powder diffraction patterns, IR spectra, and crystal structures of structurally related compounds belonging to the butyrophenone family has been undertaken to obtain information about the elements of chemical structure which predispose a substance to exhibit polymorphism. Five butyrophenones, differing by the nature of only one substituent, were selected. After crystallization from 15 solvents, it appears that two compounds of the group exhibit more than one crystalline form. An explanation of the absence of polymorphism in the other compounds of the group is proposed and discussed.

Keyphrases □ Polymorphism—disubstituted butyrophenones, comparison of IR spectra, X-ray diffraction patterns, and crystal structures □ Haloperidol—polymorphism, comparison of IR spectra, X-ray diffraction patterns, and crystal structures □ Moperone—polymorphism, comparison of IR spectra, X-ray diffraction patterns, and crystal structures □ Bromperidol—polymorphism, comparison of IR spectra, X-ray diffraction patterns, and crystal structures

Many papers have been published in the past 10 years about drug polymorphism, generally describing the way of obtaining the polymorphs of a given substance (1–3); their IR spectra (2, 4, 5), thermal behaviors (6–8), and X-ray diffraction patterns (3, 8, 9); their dissolution and solubility profiles (2, 8, 10, 11); and more rarely their *in vivo* rates of release (12–15). Studies of polymorphism are thus often empirical. Few studies attempted to determine what structural characteristics predispose an organic compound to exhibit polymorphism; in a paper concerning the polymorphism of sulfamides, Yang and Guillory (16) investigated that problem.

This work was undertaken to study the polymorphism of closely related compounds belonging to the butyrophenone family; to compare their IR spectra, X-ray diffraction patterns, and crystal structures; and to correlate, if possible, the frequency of polymorphism occurrence and chemical structure. The substances were chosen because of their therapeutic importance, structural simplicity, and crystalline nature (17–21).

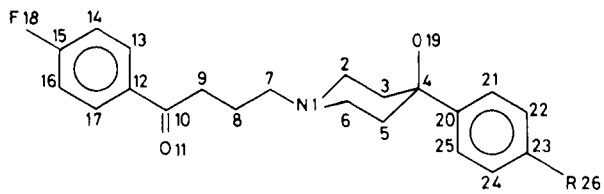

HALOPERIDOL: R = Cl
BROMPERIDOL: R = Br
I: R = F
II: R = H
MOPERONE: R = CH_3

EXPERIMENTAL

Materials—Five butyrophenones were selected for study: haloperidol[1], bromperidol[2], 4-[4-hydroxy-4-(4-fluorophenyl)-1-piperidinyl]-1-(4-fluorophenyl)-1-butanone[3] (I), moperone[4], and 4-(hydroxy-4-phenyl-1-piperidinyl)-1-(4-fluorophenyl)-1-butanone[5] (II). The difference between these substances lies only in the nature of the substituent at the 26 position.

[1] Haloperidol: 4-[4-(4-chlorophenyl)-4-hydroxy-1-piperidinyl]-1-(4-fluorophenyl)-1-butanone.

[2] Bromperidol: 4-[4-(4-bromophenyl)-4-hydroxy-1-piperidinyl]-1-(-4-fluorophenyl)-1-butanone.

[3] I: 4-[4-(4-fluorophenyl)-4-hydroxy-1-piperidinyl]-1-(4-fluorophenyl)-1-butanone (no generic name).

[4] Moperone: 4′-fluoro-4(4-hydroxy-4-*p*-tolylpiperidino)butyrophenone.

[5] II: 4-(4-hydroxy-4-phenyl-1-piperidinyl)-1-(4-fluorophenyl)-1-butanone (no generic name).

0022-3549/84/0400-0512$01.00/0

© 1984, American Pharmaceutical Association

Table I—X-ray Powder Diffraction Data of Moperone

Form I		Form II		Hydrated	
d, Å	I/I_1	d, Å	I/I_1	d, Å	I/I_1
8.75	22	8.98	24	9.78	14
5.33	90	6.67	11	6.78	13
5.08	14	5.30	66	5.79	39
4.80	34	5.04	14	5.34	53
4.70	46	4.75	25	5.14	48
4.51	14	4.63	22	4.98	41
4.32	21	4.38	22	4.88	78
4.20	20	4.32	20	4.74	40
4.05	27	4.00	100	4.66	45
3.98	100	3.49	18	4.55	21
3.66	12			4.34	26
3.60	10			4.12	100
3.46	16			4.04	18
3.12	11			3.66	14
3.08	10			3.60	35
				3.42	11
				3.37	11
				3.25	30

Thermal Analysis—Thermal behavior was studied on a differential scanning calorimeter[6] (DSC) at a heating rate of 4°C/min. Temperatures of fusion were measured at the onset point of each peak. A thermogravimetric analyzer[7] (TGA) was used for distinguishing between polymorphs and solvates and for determining the stoichiometry of the solvates.

Infrared Spectrometry[8]—IR spectra were recorded in potassium bromide[9] pellets (0.5 % w/w) and in *n*-hexane or carbon tetrachloride solution[10] (1 mg/mL).

X-ray Diffraction[11]—X-ray powder diffraction patterns were recorded using a powder camera. The incident beam was CuKα with λ = 1.5406 Å. The interplanar spacing (d values) were obtained by direct measurement on the films, and the corresponding intensities were estimated using a densitometer[12].

Crystallizations—Crystallizations of the five selected compounds were performed in analytical-grade[13] acetone, benzene, 1-butanol, carbon tetrachloride, chloroform, cyclohexane, dichloromethane, ether, dimethyl sulfoxide, ethanol, *n*-heptane, *n*-hexane, isopropyl alcohol, methanol, and petroleum ether either by slow evaporation at room temperature or by slow cooling of hot saturated solutions.

RESULTS AND DISCUSSION

Three polymorphic forms of moperone, including a monohydrated form, were observed and characterized. At ~70°C, the hydrated form undergoes dehydration, which generates polymorph III. This form melts at 96°C; it is very unstable and cannot be isolated. Forms I and II are stable. Form II undergoes a solid–solid transition to form I at 110°C; form I melts at 124°C. X-ray powder diffraction patterns (Table I) and IR spectra in potassium bromide pellets (Table II) exhibit significative differences between the three forms. In the spectrum of form II, only one —OH stretching vibration band appears at 3180 cm^{-1}. The IR spectrum of form I presents two —OH stretching vibration bands: a large one at 3100 cm^{-1} and a narrow and very strong one at 3560 cm^{-1}. Comparison with spectra obtained in carbon tetrachloride solution allows assignment of the 3560 cm^{-1} band to the vibration of weakly bonded —OH group; the 3180 and 31,000 cm^{-1} bands correspond to hydrogen-bonded hydroxyl groups (22).

Two polymorphs of II were obtained by recrystallization. They are easily identified by DSC (Fig. 1): form II melts at 112°C (ΔH_{fusion} = 35 kJ/mol) and form I melts at 140°C (ΔH_{fusion} = 43 kJ/mol). The data from X-ray diffraction patterns show great differences between the two forms (Table III). The IR spectra in potassium bromide pellets also have obvious differences, especially in the region of the —OH, —CH, and CO stretching vibrations (Table IV). The band of the —OH stretching appears as at 3180 cm^{-1} in the two spectra, but it is broader for form II. As the —OH stretching frequency of II in carbon tetrachloride solution is observed at 3620 cm^{-1}, it can be concluded that the two polymorphs are hydrogen bonded. The stability of form II is poor.

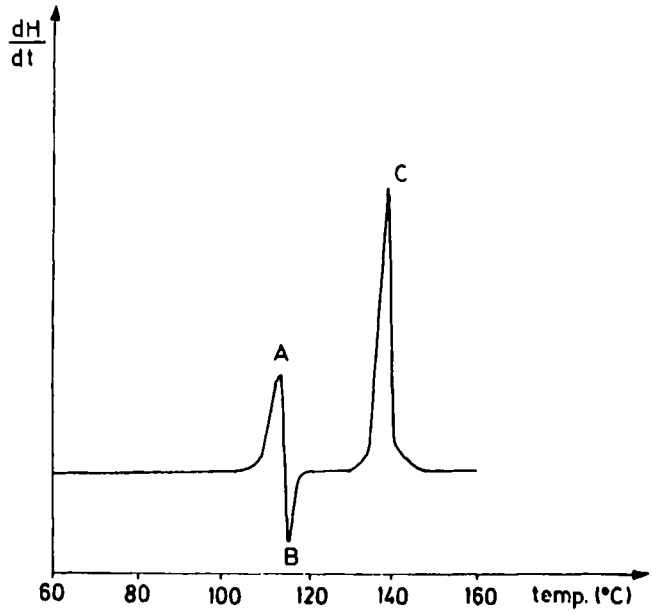

Figure 1—*Thermogram of a mixture of two polymorphs of II. Key: (A) melting of form II; (B) recrystallization of form I from the melt; (C) melting of form I.*

Despite repeated crystallizations from 15 solvents at room temperature and in a water bath, we find no evidence of polymorphism in haloperidol, bromperidol, and I. All crystallization batchs give the same X-ray powder diffraction patterns, the same DSC thermograms, and the same spectra (Table V). Temperatures and heats of fusion of haloperidol, bromperidol, and I are, respectively, 150°C and 48 kJ/mol, 158°C and 51 kJ/mol, 123°C and 34 kJ/mol. Thus, it appears that the three dihalosubstituted compounds do not exhibit polymorphism, whereas moperone and II occur as two or more polymorphs or pseudopolymorphs.

To obtain a better understanding of the phenomenon of polymorphism and to confirm the influence of the substituent on the occurrence of polymorphism in this family, the crystal structure of each polymorph must be investigated. Instability of moperone form II and II form II produces poor quality monocrystals and did not allow determination of their crystal structures. Nevertheless, considering the crystal structure of polymorph I and using the data of the IR spectra of form II of both compounds, the solid structures of moperone form II and II form II can be approached.

The main differences between the crystal structures of haloperidol, bromperidol, I, and moperone forms I and II lie in the nature and strength of the intermolecular hydrogen bonds and in intermolecular van der Waals contacts. Crystal structures show that haloperidol, bromperidol, and I are isomorphs (2-4). Their molecules are bonded together by a strong intermolecular O(19)—N(1) hydrogen bond. The length of that bond is, respectively, 2.84, 2.86, and 2.84 Å (Table VI). The energy of the hydroxyl group stretching vibrations in the IR spectra is in good agreement with these data. The intermolecular van der Waals contacts are the same in the three substances. Dipole–dipole F(18)—C(15) interactions and R(26)—R(26) contacts hold the molecules end to end (Table VII).

Molecules of II form I are also held together by a O(19)—N(1) bond, but in this case the bond is longer (2.94 Å) (Table VI). The position of the —OH stretching vibration band at 3180 cm^{-1} indicates a bond weaker than in the first group of substances. An F(18)—C(19) van der Waals contact stabilizes the crystal lattice (Table VII).

The crystal structure of II form II was not resolved. Meanwhile, considering the crystallographic data of form I, the enlargement of the νOH band and the lowering (15 cm^{-1}) of the νCO band in form II (Table IV) can be attributed to the existence of a O(19)—O(11) bond. Hydrogen bonding is thus different between the two forms.

Moperone form I presents a very peculiar crystal structure: its asymmetric unit is made up by two independent molecules, A and B (Table VI). Molecules of type A are held together by a short O(10)—N(1) hydrogen bond. The two absorption bands at 3100 and 3560 cm^{-1} can now be explained (Table II): the first arises from the strong O(19)—N(1) hydrogen bond, and the second can be attributed to the stretching of a hydroxyl group included in a cyclic dimeric structure. The narrowness of the band at 3560 cm^{-1} supports this interpretation. The van der Waals contacts between molecules A and B con-

[6] DSC model 1B; Perkin-Elmer.
[7] TGA model 951; Du Pont.
[8] Model 580 IR spectrophotometer; Perkin-Elmer.
[9] IR quality potassium bromide; Merck, Darmstadt, West Germany.
[10] Spectroscopic quality solvents; Merck, Darmstadt, West Germany.
[11] Philips PW 1720 diffraction equipment with a model XDC 700 Guinier-Hägg camera.
[12] Home-made densitometer.
[13] Merck, Darmstadt, West Germany.

Table II—IR Spectra of Moperone: Observed Frequencies (cm^{-1}) and Their Assignments

Form I	Form II	Hydrated	Assignments
3560 (strong, narrow)			ν OH
			ν OH (water)
3350	3350	3350	2ν CO
		3230	ν OH (moperone)
	3180		ν OH
3100			ν OH
3080, 3060, 3030	3080, 3060, 3030	3080, 3060, 3030	ν CH (aromatic)
2960, 2930, 2980	2960, 2930, 2980	2970, 2950, 2930, 2900	ν CH (nonnitrogen-bonded methylenic CH)
2820(sh), 2790	2840, 2790	2830, 2790	ν CH (Bohlman's bands)[a]
1685	1685	1685	ν CO
1600, 1510, 1472	1600, 1510, 1475	1600, 1510, 1475	aromatic ring
1370, 1345, 1315, 1300, 1275	1370, 1345, 1320, 1300, 1275	1370, 1350, 1320, 1300	δ CH (methylenic CH bending)
1235 (sh)	1235	1235 (sh)	ν CF
1155 (sh)	1155	1160	δ CH (in-plane aromatic CH bending)
840	835	835	γ CH (out-of-plane fluorophenyl CH bending)
820	845	825	γ CH (out-of-plane benzyl CH bending)

[a] See Ref. 23.

tribute to the building of the crystal lattice. The main intermolecular contacts are F(18)—C(2) and F(18A—C26)B. Knowing the crystal structure of moperone form I and the IR spectra of moperone form II, it is possible to infer the existence of only one type of hydrogen bond, O(19)—N(1), in moperone form II (Tables II and VI).

Table III—X-ray Powder Diffraction Data of II

Form I		Form II	
d, Å	I/I_1	d, Å	I/I_1
7.70	22	6.26	11
7.45	18	5.06	16
7.17	35	4.82	19
6.78	23	4.76	22
5.85	16	4.66	49
5.74	18	4.49	59
5.45	100	4.31	100
4.74	23	4.25	65
4.63	44	4.17	38
4.56	42	4.04	54
4.25	40	3.34	14
4.14	63	2.96	19
4.01	11	2.18	21
3.94	11		
3.88	48		
3.85	45		
3.79	11		
3.59	10		
3.42	55		
3.14	32		
2.92	18		

Table IV—IR Spectra of II: Observed Frequencies (cm^{-1}) and Their Assignments

Form I	Form II	Assignments
3350	3330	2ν CO
3180	3180 (larger)	ν OH
3080, 3050, 3020	3080, 3060, 3030	ν CH (aromatic CH)
2980, 2960, 2950, 2930, 2920, 2900	2960, 2950, 2920	ν CH (nonnitrogen-bonded methylenic CH)
2920, 2800, 2770	2890, 2870, 2850	ν CH (Bohlman's bands)[a]
1685	1670	ν CO
1600, 1505, 1490, 1470, 1460, 1445, 1410	1600, 1505, 1445, 1410	aromatic ring
1365, 1340, 1310	1375, 1340	δ CH (methylenic CH bending)
1230 (sh)	1230	ν CF
1155	1155	δ CH (in-plane aromatic CH bending)
830	830	γ CH (out-of-plane fluorophenyl CH bending)
765	760, 705	γ CH (out-of-plane phenyl CH bending)

[a] See Ref. 23.

Comparison of the crystallographic data of haloperidol, bromperidol, I, moperone form I, and II form I shows differences of molecular conformation in the crystal lattices (17–21). The side chain of the three dihalosubstituted compounds is in a TTGT conformation, while it is in a TTTT conformation in moperone form I and II form I. The latter is the most frequent among the five isoenergetic confirmations showed by PCILO calculations (25). The piperidine ring is in the usual chair form encountered in the butyrophenones, the hydroxyl group is axial, and the phenyl ring equatorial. The torsion angle along the C(4)—C(20) bond takes a relatively constant value, except in molecule B of moperone form I (17–21).

The three dihalosubstituted substances (haloperidol, bromperidol, and I) are thus isomorphs. Their crystals are monoclinic, with a $P2_1/C$ spatial grouping and four molecules per unit cell. The molecules are packed into parallel layers, which are built up by the intermolecular van der Waals contacts between the R-26 substituents of two molecules put end to end and by dipole–dipole F(18)—C(15) contacts. The layers are linked together by the strong O(19)—N(1) hydrogen bond, and they generate areas of high halogen concentration. From these observations, it is apparent that electrostatic forces, caused by the presence of the halogens and acting at the extremities of each molecule, play a significant role in the building of the crystal structure. In the process of crystal growth, a molecule reaching the surface of a crystal is influenced predominantly by the halogens of the molecule extremities located on the faces of the growing crystal. Bernstein *et al.* (26–28), working on dihalosubstituted substances, have made the same observations. The van der Waals contacts and the hydrogen bonds give a great stability to the crystal building. The observed crystal packing therefore depicts the highest probabilities of occurrence, which elucidate the absence of polymorphism of haloperidol, bromperidol, and I.

Moperone and II exhibit polymorphism. Moreover, they present a very different crystalline structure from the other three substances. In II form II and molecule B of moperone form I, peculiar hydrogen bonds appear: O(19)—O(11) and O(19)—C(22). The absence of halogen in the R-26 position leads to more disordered crystal structures, and the linear packing of haloperidol, bromperidol, and I disappears. During the crystallization, the

Table V—IR Spectra of Haloperidol, Bromperidol, and I: Observed Frequencies (cm^{-1}) and Their Assignments

Haloperidol	Bromperidol	I	Assignments
3350	3350	3350	2ν CO
3130	3130	3120	ν OH
2960, 2930	2970, 2960	2960, 2950	ν CH (nonnitrogen-bonded methylenic CH)
2850, 2830	2850, 2830	2840, 2820	ν CH (Bohlman's bands)[a]
1685	1685	1685	ν CO
1600, 1510, 1470, 1410	1600, 1510, 1480, 1410	1600, 1510, 1480, 1410	aromatic ring
1375, 1365, 1300	1365, 1365, 1300	1365, 1300	δ CH (methylenic CH bending)
1225	1225	1240	ν CF
1160	1160	1160	δ CH (in-plane aromatic CH bending)
	1070		ν CBr
1090			ν CCl
830	830	830 (sh)	γ CH (out-of-plane aromatic bending)

[a] See Ref. 23.

Table VI—Nature and Strength of the Hydrogen Bonds [a]

	Bromperidol	Haloperidol	I	II		Moperone		
				Form I	Form II[b]	Form I		Form II[b]
						Molecule A	Molecule B	
Type	O(19)—N(1)	O(19)—N(1)	O(19)—N(1)	O(19)—N(1)	O(10)—O(11)	O(19)—N(1)	O(19)—C(22)	O(10)—N(1)
Length, Å[c]	2.86	2.84	2.84	2.94	—	2.85	3.37	—
νO-H, cm^{-1}	3130	3130	3120	3180	3180	3100	3560	3180
δH[d], kcal/mol	7.40	7.40	7.55	6.64	8.56	7.85	0.91	6.64

[a] SD on bond lengths: 0.01 Å. [b] Crystal structure not resolved. [c] From Refs. 17-21. [d] Values calculated from Ref. 24.

Table VII—van der Waals Contacts Observed in the Crystal Structures [a]

	Bromperidol	Haloperidol	I	II, Form I	Moperone, Form I
Type	F(18)—C(15)	F(18)—C(15)	F(18)—C(15)	—	—
Length, Å	3.11	3.07	3.10		
Sum of van der Waals radii, Å	3.20	3.20	3.20		
Type	Br(26)—Br(26)	Cl(26)—Cl(26)	F(26)—F(26)[b]	—	—
Length, Å	3.60	3.52	4.24		
Sum of van der Waals radii, Å	3.90	3.60	2.70		
Type	—	—	—	F(18)—C(19)	F(18)A—C(2)B
Length, Å				3.28	3.38
Sum of van der Waals radii, Å				3.35	3.35
Type	—	—	—	—	F(18)A—C(26)B
Length, Å					3.17
Sum of van der Waals radii, Å					3.35

[a] From Refs. 17-21. SD on bond lengths: 0.01 Å. [b] Reported in this table for information and comparison, although the distance between fluorine atoms is longer than the sum of their van der Waals radii.

molecules have a greater freedom and several crystal structures are possible; this explains why moperone and II exhibit more than one crystalline form. In this limited group of butyrophenones, it can be concluded that the substituent at the 26 position predominantly influences the occurrence or absence of polymorphism.

REFERENCES

(1) D. Jordan and J. E. Carless, *J. Pharm. Pharmacol.*, **28,** 410 (1976).

(2) H. G. Ibrahim, F. Pisano, and A. Bruno, *J. Pharm. Sci.*, **66,** 669 (1977).

(3) J. Piccolo, *Can. J. Pharm. Sci.*, **14,** 99 (1979).

(4) A. R. Ebian and N. A. El-Gindy, *Sci. Pharm.*, **46,** 1 (1978).

(5) R. J. Mesley and E. E. Houghton, *J. Pharm. Pharmacol.*, **19,** 295 (1967).

(6) M. Himmelreich, B. J. Rawson, and T. R. Watson, *Aust. J. Pharm. Sci.*, **6,** 123 (1977).

(7) K. C. Lee and J. A. Hersey, *Acta Pharm. Suec.*, **14,** 213 (1977).

(8) W. C. Stagner and J. K. Guillory, *J. Pharm. Sci.*, **68,** 1005 (1979).

(9) M. L. Huang and S. Niazi, *J. Pharm. Sci.*, **66,** 608 (1977).

(10) N. A. El-Gindy and A. R. Ebian, *Sci. Pharm.*, **46,** 8 (1978).

(11) M. Muramatsu, M. Iwahashi, and V. Takeuchi, *J. Pharm. Sci.*, **68,** 175 (1979).

(12) A. J. Aguiar, K. J. John, A. W. Kinkel, and J. C. Samyn, *J. Pharm. Sci.*, **56,** 847 (1967).

(13) A. J. Aguiar and J. E. Zelmer, *J. Pharm. Sci.*, **58,** 983 (1969).

(14) I. S. Gibbs, A. Heald, H. Jacobson, D. Wadke, and I. Weliky, *J. Pharm. Sci.*, **65,** 1381 (1976).

(15) T. Yokoyama, T. Umeda, K. Kuroda, K. Sato, and Y. Takagismi, *Chem. Pharm. Bull.*, **27,** 1476 (1979).

(16) S. S. Yang and J. K. Guillory, *J. Pharm. Sci.*, **61,** 26 (1972).

(17) M. H. J. Koch and G. Germain, *Acta Crystallogr.*, **B28,** 121 (1972).

(18) B. Tinant, G. Germain, J. P. Declercq, M. Van Meerssche, M. Azibi, M. Draguet-Brughmans, and R. Bouche, *Cryst. Struct. Commun.*, **11,** 633 (1982).

(19) L. L. Read and J. P. Schaefter, *Acta Crystallogr.*, **B29,** 1886 (1973).

(20) B. Tinant, G. Germain, J. P. Declercq, M. Van Meerssche, M. Azibi, M. Draguet-Brughmans, and R. Bouche, *Bull. Soc. Chim. Belg.*, **91,** 283 (1982).

(21) B. Tinant, G. Germain, J. P. Declercq, M. Van Meerssche, M. Azibi, M. Draguet-Brughmans, and R. Bouche, *Cryst. Struct. Commun.*, **11,** 639 (1982).

(22) L. J. Bellamy, "The Infrared Spectra of Complex Molecules," vol. 1, 3rd ed., Chapman and Hall, London, 1975, p. 108.

(23) F. Bohlman, *Chem. Ber.*, **91,** 2157 (1958).

(24) Th. Zeegers-Huyskens, *Bull. Soc. Chim. Belg.*, **86,** 823 (1977).

(25) J. P. Tollenaere, H. Moereels, and M. H. J. Koch, *Eur. J. Med. Chem.*, **12,** 199 (1977).

(26) J. Bernstein and G. M. T. Schmidt, *J. Chem. Soc. Perkin II*, **1972,** 951.

(27) J. Bernstein and I. Izak, *J. Chem. Soc. Perkin II*, **1976,** 429.

(28) J. Bernstein and I. Izak, *J. Crystallogr. Mol. Struct.*, **5,** 257 (1975).

ACKNOWLEDGMENTS

The authors thank the Fonds de la Recherche Scientifique Medicale (FRSM) for supporting the project and Janssen Pharmaceutica (Beerse, Belgium) for providing the studied substances.

Gas Chromatographic Determination of Quazepam and Two Major Metabolites in Human Plasma

JAMES M. HILBERT ˣ, JAMES M. NING, GREGORY MURPHY, ANGEL JIMENEZ, and NICOLA ZAMPAGLIONE

Received January 7, 1983, from *Schering Corporation, Bloomfield, NJ 07003.* Accepted for publication March 29, 1983.

Abstract □ Two rapid, sensitive, and specific gas chromatographic (GC) methods for the quantitative determination of quazepam (I), 7-chloro-5-(2-fluorophenyl-1,3-dihydro-1-(2,2,2-trifluoroethyl)- 2*H* -1,4-benzodiazepine-2-thione, and its major active plasma metabolites, the 2-oxo compound (II) and the dealkylated oxo compound (III), have been developed; the first measures I and II and the second measures III. The compounds are extracted from plasma with toluene and quantitated by electron-capture detection using the internal standard method. The methods are capable of quantitating plasma levels of I and II as low as 0.75 ng/mL and plasma levels of III as low as 1.5 ng/mL. Correlation coefficients of standard curves were >0.9995 for all compounds. Precision of the methods was measured at two different concentrations for each compound; the *CV* values were 3–6% for all three compounds. The recovery of all compounds was >80%, and the ratio of recovery of each compound to that of its internal standard did not vary at different concentrations, indicating appropriate internal standards have been selected for the methods. Quazepam metabolites, other benzodiazepines, and drugs which are potential comedication do not interfere with either method. The methods were shown to be suitable for investigating the bioavailability and pharmacokinetics of quazepam at therapeutic doses.

Keyphrases □ Quazepam—gas chromatography two major metabolites, human plasma □ Gas chromatography—quazepam and two major metabolites in human plasma □ Metabolites—quazepam, human plasma, gas chromatography

Quazepam, 7-chloro-5-(2-fluorophenyl)-1,3-dihydro-1-(2,2,2-trifluoroethyl)-2*H*-1,4-benzodiazepine-2-thione, a novel benzodiazepine which has been reported to have good sedative and hypnotic activity (1, 2), is extensively metabolized in humans. Two major active metabolites have been identified in plasma (Scheme I), the 2-oxo compound II [7-chloro-5-(2-fluorophenyl) -1,3-dihydro-1-(2,2,2-trifluoroethyl)-2*H*-1,4-benzodiazepin-2-one] and III [7-chloro-5-(2-fluorophenyl)-1,3-dihydro-2*H*-1,4-benzodiazepin-2-one] (2). To fully evaluate the bioavailability and pharmacokinetics of quazepam, two sensitive and specific gas chromatographic (GC) assays have been developed to measure the unchanged drug and the two major metabolites in plasma; one method measures I and II, and the other measures III.

Polarographic (3) and GC methods (4–6) have been published for III. However, these methods either lack sensitivity or involve derivatization. The methods described in this report require simple extraction procedures, no derivatization, and are more sensitive than previously reported chromatographic assays.

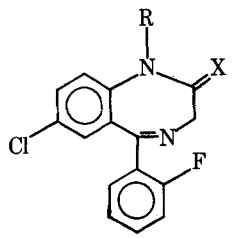

I: X = S, R = —CH_2CF_3
II: X = O, R = —CH_2CF_3
III: X = O, R = H

EXPERIMENTAL

Chemicals and Reagents—Quazepam[1] (I), II[1], 7,9-dibromo-1,3-dihydro-5-phenyl-2*H*-1,4-benzodiazepin-2-one (IV)[1] (the internal standard for the assay of III), III[2], and diazepam[2] (the internal standard for the assay for I and II) were used. A stock solution of I and II (0.75 mg/mL) was prepared by accurately weighing 75 mg each of I and II into a 100-mL volumetric flask and dissolving them in toluene. The standard solution of the two compounds (1.5 μg/mL) was prepared by diluting 0.20 mL of the stock solution to 100 mL with toluene. A stock solution of III (1 mg/mL) was prepared by weighing accurately 10 mg of III into a 10-mL volumetric flask and dissolving the compound in toluene. The standard solution of III (1.5 μg/mL) was prepared by diluting 0.15 mL of the stock solution to 100 mL with toluene.

Both standard solutions of the internal standards (diazepam and IV) were prepared by accurately weighing 10 mg of each compound, dissolving it in 10 mL with toluene, and diluting 1 mL of the resulting stock solution to 100 mL of toluene. Toluene[3] and cyclohexane[3] were glass distilled.

Chromatographic Conditions for the Assay of I and II—The chromatograph[4] was equipped with a ^{63}Ni pulse-modulated electron-capture detector, an automatic injector[5], and a data system for measuring peak heights and calculating concentrations[6]. The coiled glass column (1.83 m × 2 mm i.d.) was silanized[7] and then packed with 3% OV-25 on 80–100 mesh Supelcoport[8]. The temperatures of the column, injector, and detector were maintained at 220°C, 280°C, and 350°C, respectively. Ultra-high purity nitrogen was used as the carrier gas with a flow rate of 28 mL/min.

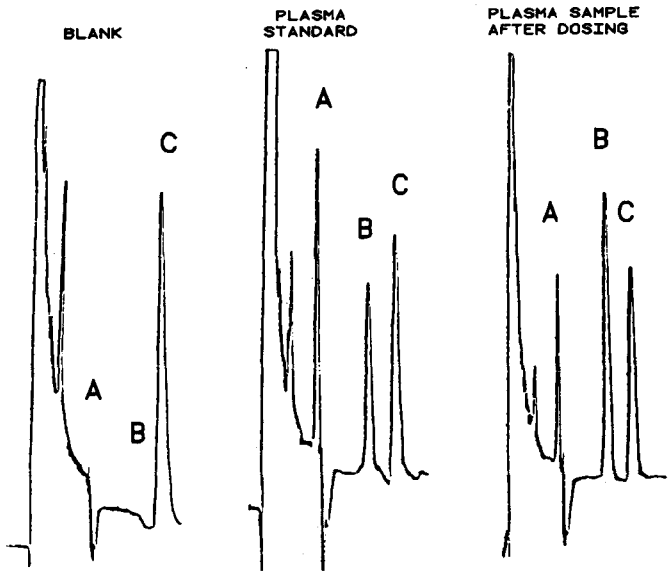

Figure 1—*Typical gas chromatograms of blank plasma, a standard concentration of 12 ng/mL of quazepam and II plasma, and human plasma withdrawn at 1.5 h after an oral dose of 15 mg of quazepam. Chromatography was on OV-25 at 220°C with electron-capture detection. Key: (A) II; (B) quazepam; (C) diazepam.*

[1] Synthesized at Schering Corporation.
[2] Gifts from Hoffmann-La Roche, Nutley, N.J.
[3] Burdick and Jackson, Muskegon, Mich.
[4] Model 3700; Varian Associates, Palo Alto, Calif.
[5] Model 8000; Varian Associates, Palo Alto, Calif.
[6] HP 3353A Data System; Hewlett Packard, Co., Paramus, N.J.
[7] Silyl-8; Pierce Chemical Co., Rockford, Ill.
[8] Supelco, Inc., Bellefonte, Pa.

0022-3549/84/0400-0516$01.00/0
© 1984, American Pharmaceutical Association

Table I—Standard Curves for Quazepam and Its Two Plasma Metabolites

Amount Added to Plasma, ng/mL	Amount Found in Plasma, ng/mL[a]	Linear Regression Equation
	Quazepam	
0.75	0.881	
1.50	1.636	
3.00	3.461	
6.00	6.365	$y = 1.043(0.003)x$
12.00	12.667	$+ 0.193(0.093)$
24.00	25.533	$r^2 = 0.9999$
48.00	50.636	
96.00	100.123	
	Compound II	
0.75	0.853	
1.50	1.389	
3.00	3.074	
6.00	5.537	$y = 0.979(0.007)x$
12.00	12.373	$- 0.001(0.265)$
24.00	23.895	$r^2 = 0.9996$
48.00	45.600	
96.00	94.542	
	Compound III	
1.50	1.531	
3.00	3.008	
6.00	6.095	$y = 1.004(0.004)x$
12.00	12.737	$+ 0.109(0.140)$
24.00	23.829	$r^2 = 0.9999$
48.00	48.602	
96.00	96.455	

[a] Values are the average of duplicate determinations.

Sample Preparation for the Assay of I and II—Aliquots (0.5 mL) of plasma samples were pipetted in a glass centrifuge tube, mixed with 6 μL of the 10-μg/mL solution of diazepam, and extracted with 0.5 mL of toluene. Following centrifugation[9] at 1500 rpm, 1.0 μL of the toluene extract was injected into the gas chromatograph.

Chromatographic Conditions for the Assay of III—The chromatograph[4] was equipped with a ^{63}Ni pulse-modulated electron-capture detector, an automatic injector[5], and a data system for measuring peak heights and calculating concentrations[6]. The coiled glass column (1.83 m × 2 mm i.d.) was silanized[7] and then packed with 3% SP-2250 DB on 100–120 mesh Supelcoport[8]. The temperature of the column, injector, and detector were maintained at 235°C, 250°C, and 350°C, respectively. Ultra-high purity nitrogen was used as the carrier gas with a flow rate of 43 mL/min.

Sample Preparation for the Assay of III—Aliquots (0.25 mL) of plasma samples were prepared in a glass centrifuge tube and extracted twice with 0.25 mL of cyclohexane. The cyclohexane layer was discarded; 0.2 mL of the extracted plasma was transferred to a centrifuge tube and mixed with 0.25 mL of toluene and 6 μL of the 10-μg/mL toluene solution of IV. Following centrifugation at 1500 rpm for 5 min, 3 μL of the toluene extract was injected into the gas chromatograph.

Table II—Accuracy and Precision of the Assays for Quazepam and Its Two Metabolites

Compound	Plasma Concentration, ng/mL[a]	Mean Concentration Found, ng/mL	*CV*, %
Quazepam	1.5	1.50	2.94
	12.0	12.27	5.80
Compound II	1.5	1.51	6.25
	12.0	11.65	5.34
Compound III	3.0	2.97	6.19
	24.0	23.86	2.54

[a] Five replicate determinations were performed for each compound at each plasma concentration.

[9] Size 2 Model K Centrifuge; International Equipment Co., Needham Heights, Mass.

Table III—Retention Times of Quazepam Metabolites, Benzodiazepines, and Other Drugs on the GC Columns Used in the Assays

	Retention Time, min	
	3% OV-25[a]	3% SP-2250 DB[b]
Quazepam	6.8	2.0
Compound II	3.5	1.9
Compound III	13.2	5.9
Compound IV	NP[c]	10.3
Diazepam	8.7	4.3
3-Hydroxy derivative of III	4.4	2.6
3-Hydroxy derivative of II	6.0	8.4
Flurazepam	18.2	10.8
Halazepam	3.4	2.0
N-Demethyldiazepam	14.0	7.4
Oxazepam	5.4	7.6
Nitrazepam	NP	19.7
Chlorpromazine	6.4	3.4
Perphenazine	4.0	2.5
Chlorimipramine[d]	NP	NP
Chlorpheniramine	NP	NP

[a] Used for the assay of I and II. [b] Used for the assay of III. [c] No peak observed for the compound. [d] 3-Chloro-10,11-dihydro- *N*,*N*-dimethyl-5*H*-dibenz[6,*F*]azepine-5-propanamine.

Standard Curves, Reproducibility, and Recovery Studies—A standard curve was prepared for each compound by adding aliquots of each stock solution to a series of control human plasma samples. A set of standard plasma concentrations were made for each of these compounds ranging from 0.75 to 96 ng/mL for I and II and from 1.5 to 96 ng/mL for III. The samples were carried through the respective assay procedures, and the concentration values obtained from the data system were plotted against the actual concentrations.

To demonstrate the precision and accuracy of I–II assay, 10 plasma samples were spiked with I and II, five samples at 1.5 ng/mL and five samples at 12 ng/mL. Similarly five plasma samples were spiked with III at 3 ng/mL and five samples at 24 ng/mL. Then, the plasma samples were carried through the respective assay procedures, and the means, standard deviations, and coefficients of variation calculated.

For determination of recoveries from plasma, the peak heights of extracted standards of each compound at 3 and 48 ng/mL were compared with those of the respective unextracted standards. The unextracted standards were made

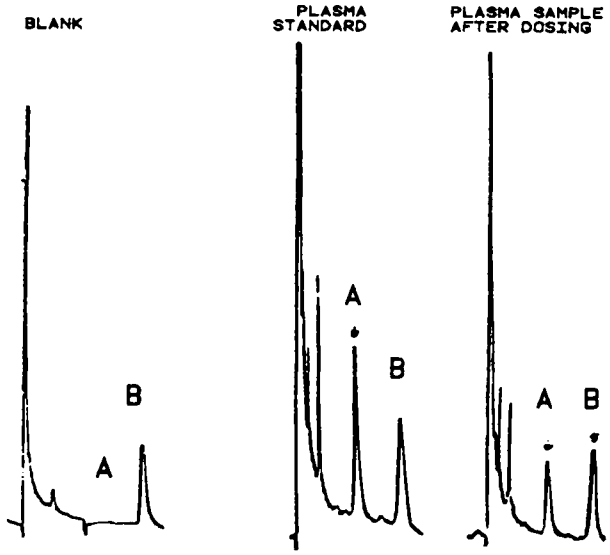

Figure 2—*Typical gas chromatograms of blank plasma, a standard concentration of 24 ng/mL of III in human plasma, and human plasma withdrawn 48 h after an oral dose of 15 mg of quazepam. Chromatography was on SP-2250 DB at 235°C with electron-capture detection. Key: (A) III; (B) IV.*

Table IV—Recoveries of I, II, III, and the Internal Standards From Plasma [a]

Amount Added to Plasma, ng/mL	Assay for I and II: Recovery, % Quazepam	Compound II	Diazepam	Ratio of Recovery: Quazepam/ Diazepam	Compound II Diazepam
3	96.5 ± 7.9	94.7 ± 3.4	99.3 ± 3.6	0.898 ± 0.04	0.954 ± 0.01
48	88.8 ± 8.3	99.2 ± 8.5	102.0 ± 8.6	0.869 ± 0.05	0.971 ± 0.05

Amount Added to Plasma ng/mL	Assay for III: Recovery, % Compound III	Compound IV	Ratio of Recovery
3	78.3 ± 1.1	85.8 ± 5.1	0.915 ± 0.05
48	84.0 ± 5.0	93.5 ± 3.2	0.898 ± 0.04

[a] Values are the mean of five determinations ±*SD*.

by adding the compounds to toluene which had been previously extracted with an equal volume of plasma.

RESULTS AND DISCUSSION

As shown in Fig. 1, I, II, and the internal standard (diazepam) were well separated from one another on the OV-25 stationary phase. The respective retention times of I, II, and diazepam were 6.8, 3.5, and 8.7 min.

Compound III could not be analyzed under the conditions used for I and II due to poor sensitivity and excessive tailing of its peaks on OV-25 and similar stationary phases. It was found that III could be analyzed on SP-2250 DB, a stationary phase deactivated for bases. This packing gave excellent symmetrical peak shapes (Fig. 2) and much higher sensitivity. Compound III and the internal standard IV had retention times of 5.9 and 10.3 min, respectively, on the SP-2250 DB column.

Table I shows that the standard curves were linear for quazepam and both metabolites ($r^2 > 0.9995$) throughout the entire range investigated. The smallest concentration of each compound used in the standard curves, 0.75 ng/mL for I and II and 1.5 ng/mL for III, exhibited acceptable chromatographic peaks which were clearly within the linear range of the GC response. Therefore, the assays are sensitive enough to detect and quantitate concentrations of 0.75 ng/mL for I and II and 1.5 ng/mL for III.

The results of replicate analyses indicate that the methods have a high degree of accuracy, since the mean concentration values determined were very close to known concentrations. The coefficient of variation was 3–6% for the three compounds at each concentration, indicating the assays are very precise (Table II).

To determine the specificity of the methods, possible interferences from two other quazepam metabolites, the 3-hydroxy derivative of II, and the 3-hydroxy derivative of III (7), other benzodiazepines, and drugs that might be used as comedication were checked by chromatographing solutions of pure standards. None of these compounds (with the exception of halazepam, which was not completely resolved from II) had a retention time similar to those compounds being analyzed in either system (Table III). Thus, the assays are specific for quazepam and its two metabolites, II and III, in the presence of these compounds. Furthermore, the assays should be specific for quazepam and its metabolites in the presence of compounds which do not contain a nitro or halogen moiety, since these compounds do not respond to electron-capture detection.

Both assays are rapid, since, unlike the extraction procedures in previous assays of III and benzodiazepines similar to I and II (3–6, 8–12), no buffering of the plasma is needed to extract all the compounds with recoveries >80% (Table IV). However, in the assay of III, it is necessary to first wash the plasma with cyclohexane to selectively remove an unidentified plasma constituent which gives a chromatographic peak that interferes with the peak of III.

In addition to good recoveries, the data in Table IV show that the ratio of recoveries of I, II, and III to the respective internal standards were very similar at each concentration examined, indicating that appropriate internal standards have been selected for the methods.

The application of these methods is shown in the mean plasma level–time profile of quazepam and its two metabolites in 12 subjects following administration of a 15-mg quazepam tablet (Fig. 3). Clearly, the described methods are suitable for investigating the bioavailability and pharmacokinetics of quazepam at therapeutic doses.

In summary, rapid, sensitive, specific, and reproducible methods for quazepam and its two metabolites have been developed. The methods are capable of quantitating plasma levels of I and II as low as 0.75 ng/mL and plasma levels of III as low as 1.5 ng/mL. Pharmacokinetic studies which have been conducted utilizing these methods will be reported elsewhere.

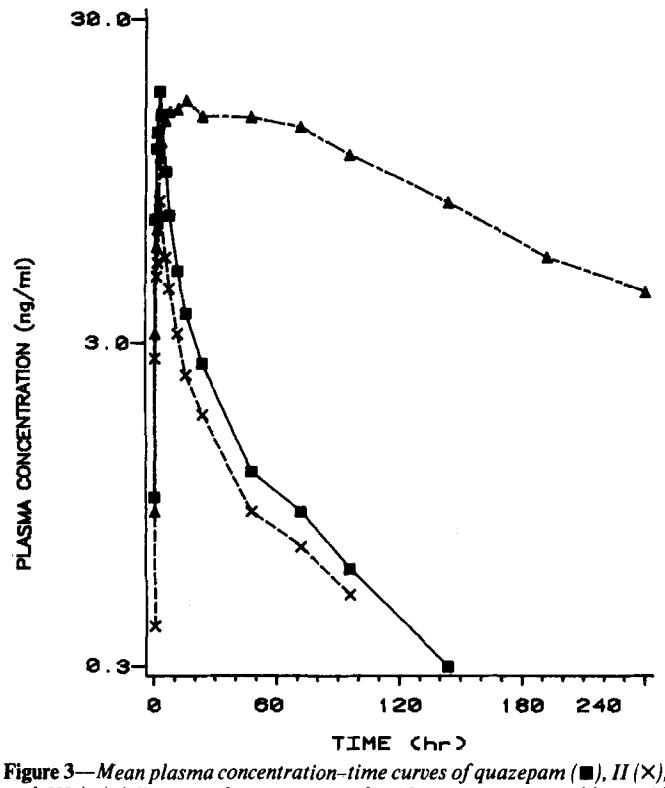

Figure 3—*Mean plasma concentration–time curves of quazepam (■), II (×), and III (▲) following administration of a 15-mg quazepam tablet to 12 subjects.*

REFERENCES

(1) A. Kales, M. B. Scharf, E. O. Bixler, P. K. Schweitzer, J. A. Jacoby, and C. R. Soldatos, *Clin. Pharmacol. Ther.*, **30**, 194 (1981).

(2) A. Kales, M. B. Scharf, C. R. Soldatos, and E. O. Bixler, *J. Clin. Pharmacol.*, **20**, 184 (1980).

(3) J. A. F. de Silva, C. V. Puglisi, M. A. Brooks, and M. R. Hackman, *J. Chromatogr.*, **99**, 461 (1974).

(4) M. Hasegawa and I. Matsubara, *Chem. Pharm. Bull.*, **23**, 1826 (1975).

(5) W. F. Smyth and J. A. Groves, *Anal. Chim. Acta*, **123**, 175 (1981).
(6) R. Riva, M. De Anna, F. Albani, and A. Baruzzi, *J. Chromatogr. Biomed. Appl.*, **222**, 491 (1981).
(7) J. Hilbert, S. Symchowicz, and N. Zampaglione, *Pharmacologist*, **23**, 196 (1981).
(8) J. A. F. de Silva and C. V. Puglisi, *Anal. Chem.*, **42**, 1725 (1970).
(9) J. A. F. de Silva and I. Bekersky, *J. Chromatogr.*, **99**, 447 (1974).
(10) M. T. Smith, *et al.*, *Eur. J. Clin. Pharmacol.*, **16**, 141 (1979).
(11) B. J. Miwa, W. A. Garland, and P. Blumenthal, *Anal. Chem.*, **53**, 793 (1981).
(12) A. K. Dhar and H. Kutt, *J. Chromatogr. Biomed. Appl.*, **222**, 203 (1981).

ACKNOWLEDGMENTS

The authors thank Mr. Barry Bravette for technical assistance.

Use of the Fluorescence Probe 1-Anilino-8-naphthalenesulfonate in Predicting Interindividual Differences in the Plasma Protein Binding of Acidic Drugs in Rats

JUN SATO, YUICHI SUGIYAMA ˣ, and MANABU HANANO

Received September 10, 1979, from the *Faculty of Pharmaceutical Sciences, University of Tokyo, Hongo, Bunkyo-ku, Tokyo 113, Japan.* Accepted for publication March 24, 1983.

Abstract □ The possibility that the fluorescence probe, 1-anilino-8-naphthalenesulfonate (I), might be used for predicting the interindividual differences in the plasma protein binding of acidic drugs was examined. The interindividual differences in the free fraction of I (f_I) were found not to be due to corresponding differences in plasma albumin concentration, but to those differences in binding constant. The binding constant of I to the plasma of 18 individual rats ranged from 1.75×10^6 M^{-1} to 2.3×10^7 M^{-1}. The free fraction of I had a highly significant statistical correlation with plasma concentration of free fatty acids, but had no significant correlation with the infinite fluorescence of I or the degree of the polarization of I. Each free fraction of five acidic drugs (warfarin, phenylbutazone, salicylic acid, indomethacin, and sulfaphenazole) was correlated with f_I with high statistical significance. Therefore, the simple and convenient method using I may predict the interindividual differences in the plasma protein binding of acidic drugs in rats.

Keyphrases □ 1-Anilino-8-naphthalenesulfonate—fluorescence probe, prediction of interindividual differences in plasma protein binding, acidic drugs, rats □ Fluorescence probe—1-anilino-8-naphthalenesulfonate, prediction of interindividual differences in plasma protein binding, acidic drugs, rats □ Binding, plasma protein—1-anilino-8-naphthalenesulfonate, prediction of interindividual differences, acidic drugs, rats

Serum (or plasma) protein binding can have pronounced effects on the pharmacodynamic and toxicological actions of drugs, as well as on their elimination kinetics. This effect is particularly striking with respect to the elimination of the extensively serum protein-bound drugs such as anticoagulants (warfarin, dicoumarol) by rats and humans, since there are pronounced interindividual differences in the free fraction of these drugs (1, 2). Minor interindividual changes in the degree of binding of such highly protein-bound drugs can produce significant changes in the amount of unbound drug. Differences in the structure of albumin or in the plasma concentration of endogenous inhibitory agents were suggested to be alternative reasons for such pronounced interindividual differences in the free fraction of these drugs (1); however, the details are, as yet, unresolved. Based on these facts, Levy and Yacobi (3) suggested that *in vitro* plasma protein binding tests with blood samples prior to drug administration might be useful for predicting quantitatively unusual distribution, elimination, and pharmacological effect characteristics of certain highly plasma protein-bound drugs.

It was previously reported that there are pronounced interindividual differences in binding of the anionic fluorescence probe 1-anilino-8-naphthalenesulfonate (I) to rat plasma (4). Free fatty acids were found to be one of the endogenous inhibitors, and there was a highly significant correlation between the free fractions of I and phenylbutazone (4).

In the present study, we investigated further the correlation between the free fraction of I and those of various acidic drugs extensively bound to plasma protein, and suggested the possibility that I might be used clinically for predicting the interindividual differences in the plasma protein binding of acidic drugs. Furthermore, we tried to examine whether or not differences in the structure of albumin are associated with differences in the free fraction of I.

EXPERIMENTAL

Materials—The following analytical-grade materials were used: 1-anilino-8-naphthalenesulfonate (I) as the sodium salt[1], warfarin[2], indomethacin[3], sulfaphenazole[4], sodium salicylate[5], sodium laurate[6], sodium palmitate[6], sodium stearate[6], sodium oleate[6], and rat serum albumin (fraction V)[7]. The rat serum albumin was defatted by the method of Chen (5).

Plasma Preparation—Adult male Wistar rats, weighing 290–340 g, were used. Approximately 10 min after heparinizing, blood was collected from the carotid artery under light ether anesthesia, and the plasma was obtained by centrifugation (3000 rpm for 10 min). Prepared plasma (2.5 mL) was used on the same day for measuring the bindings of drugs, and the remaining plasma (2 mL) was divided into the three aliquots, which were stored at −40°C and used within 1 week for the measurements of the concentrations of albumin, free fatty acids, and total bilirubin.

Equilibrium Dialysis—The 2-mL fresh plasma sample was diluted to 25% by the addition of 6 mL of Tris-HCl buffer (50 mM, pH 7.4). The bindings of four acidic drugs (sulfaphenazole, salicylic acid, indomethacin, and phenylbutazone) to the dilute plasma were measured by equilibrium dialysis (25°C). The details of the equilibrium dialysis techniques were described previously (4, 6).

[1] Tokyo Chemical Industries, Co., Tokyo, Japan.
[2] Eizai Co., Tokyo, Japan.
[3] Merck Banyu Co., Tokyo, Japan.
[4] Dainippon Seiyaku Co., Tokyo, Japan.
[5] Koso Chemical Co., Tokyo, Japan.
[6] Tokyo Kasei Industries, Co., Tokyo, Japan.
[7] Sigma Chemical Co., St. Louis, Mo.

0022-3549/84/0400-0519$01.00/0
© 1984, American Pharmaceutical Association

(5) W. F. Smyth and J. A. Groves, *Anal. Chim. Acta*, **123**, 175 (1981).
(6) R. Riva, M. De Anna, F. Albani, and A. Baruzzi, *J. Chromatogr. Biomed. Appl.*, **222**, 491 (1981).
(7) J. Hilbert, S. Symchowicz, and N. Zampaglione, *Pharmacologist*, **23**, 196 (1981).
(8) J. A. F. de Silva and C. V. Puglisi, *Anal. Chem.*, **42**, 1725 (1970).
(9) J. A. F. de Silva and I. Bekersky, *J. Chromatogr.*, **99**, 447 (1974).
(10) M. T. Smith, *et al.*, *Eur. J. Clin. Pharmacol.*, **16**, 141 (1979).
(11) B. J. Miwa, W. A. Garland, and P. Blumenthal, *Anal. Chem.*, **53**, 793 (1981).
(12) A. K. Dhar and H. Kutt, *J. Chromatogr. Biomed. Appl.*, **222**, 203 (1981).

ACKNOWLEDGMENTS

The authors thank Mr. Barry Bravette for technical assistance.

Use of the Fluorescence Probe 1-Anilino-8-naphthalenesulfonate in Predicting Interindividual Differences in the Plasma Protein Binding of Acidic Drugs in Rats

JUN SATO, YUICHI SUGIYAMA ˣ, and MANABU HANANO

Received September 10, 1979, from the *Faculty of Pharmaceutical Sciences, University of Tokyo, Hongo, Bunkyo-ku, Tokyo 113, Japan.* Accepted for publication March 24, 1983.

Abstract □ The possibility that the fluorescence probe, 1-anilino-8-naphthalenesulfonate (I), might be used for predicting the interindividual differences in the plasma protein binding of acidic drugs was examined. The interindividual differences in the free fraction of I (f_I) were found not to be due to corresponding differences in plasma albumin concentration, but to those differences in binding constant. The binding constant of I to the plasma of 18 individual rats ranged from 1.75×10^6 M^{-1} to 2.3×10^7 M^{-1}. The free fraction of I had a highly significant statistical correlation with plasma concentration of free fatty acids, but had no significant correlation with the infinite fluorescence of I or the degree of the polarization of I. Each free fraction of five acidic drugs (warfarin, phenylbutazone, salicylic acid, indomethacin, and sulfaphenazole) was correlated with f_I with high statistical significance. Therefore, the simple and convenient method using I may predict the interindividual differences in the plasma protein binding of acidic drugs in rats.

Keyphrases □ 1-Anilino-8-naphthalenesulfonate—fluorescence probe, prediction of interindividual differences in plasma protein binding, acidic drugs, rats □ Fluorescence probe—1-anilino-8-naphthalenesulfonate, prediction of interindividual differences in plasma protein binding, acidic drugs, rats □ Binding, plasma protein—1-anilino-8-naphthalenesulfonate, prediction of interindividual differences, acidic drugs, rats

Serum (or plasma) protein binding can have pronounced effects on the pharmacodynamic and toxicological actions of drugs, as well as on their elimination kinetics. This effect is particularly striking with respect to the elimination of the extensively serum protein-bound drugs such as anticoagulants (warfarin, dicoumarol) by rats and humans, since there are pronounced interindividual differences in the free fraction of these drugs (1, 2). Minor interindividual changes in the degree of binding of such highly protein-bound drugs can produce significant changes in the amount of unbound drug. Differences in the structure of albumin or in the plasma concentration of endogenous inhibitory agents were suggested to be alternative reasons for such pronounced interindividual differences in the free fraction of these drugs (1); however, the details are, as yet, unresolved. Based on these facts, Levy and Yacobi (3) suggested that *in vitro* plasma protein binding tests with blood samples prior to drug administration might be useful for predicting quantitatively unusual distribution, elimination, and pharmacological effect characteristics of certain highly plasma protein-bound drugs.

It was previously reported that there are pronounced interindividual differences in binding of the anionic fluorescence probe 1-anilino-8-naphthalenesulfonate (I) to rat plasma (4). Free fatty acids were found to be one of the endogenous inhibitors, and there was a highly significant correlation between the free fractions of I and phenylbutazone (4).

In the present study, we investigated further the correlation between the free fraction of I and those of various acidic drugs extensively bound to plasma protein, and suggested the possibility that I might be used clinically for predicting the interindividual differences in the plasma protein binding of acidic drugs. Furthermore, we tried to examine whether or not differences in the structure of albumin are associated with differences in the free fraction of I.

EXPERIMENTAL

Materials—The following analytical-grade materials were used: 1-anilino-8-naphthalenesulfonate (I) as the sodium salt[1], warfarin[2], indomethacin[3], sulfaphenazole[4], sodium salicylate[5], sodium laurate[6], sodium palmitate[6], sodium stearate[6], sodium oleate[6], and rat serum albumin (fraction V)[7]. The rat serum albumin was defatted by the method of Chen (5).

Plasma Preparation—Adult male Wistar rats, weighing 290–340 g, were used. Approximately 10 min after heparinizing, blood was collected from the carotid artery under light ether anesthesia, and the plasma was obtained by centrifugation (3000 rpm for 10 min). Prepared plasma (2.5 mL) was used on the same day for measuring the bindings of drugs, and the remaining plasma (2 mL) was divided into the three aliquots, which were stored at −40°C and used within 1 week for the measurements of the concentrations of albumin, free fatty acids, and total bilirubin.

Equilibrium Dialysis—The 2-mL fresh plasma sample was diluted to 25% by the addition of 6 mL of Tris-HCl buffer (50 mM, pH 7.4). The bindings of four acidic drugs (sulfaphenazole, salicylic acid, indomethacin, and phenylbutazone) to the dilute plasma were measured by equilibrium dialysis (25°C). The details of the equilibrium dialysis techniques were described previously (4, 6).

[1] Tokyo Chemical Industries, Co., Tokyo, Japan.
[2] Eizai Co., Tokyo, Japan.
[3] Merck Banyu Co., Tokyo, Japan.
[4] Dainippon Seiyaku Co., Tokyo, Japan.
[5] Koso Chemical Co., Tokyo, Japan.
[6] Tokyo Kasei Industries, Co., Tokyo, Japan.
[7] Sigma Chemical Co., St. Louis, Mo.

0022-3549/84/0400-0519$01.00/0
© 1984, American Pharmaceutical Association

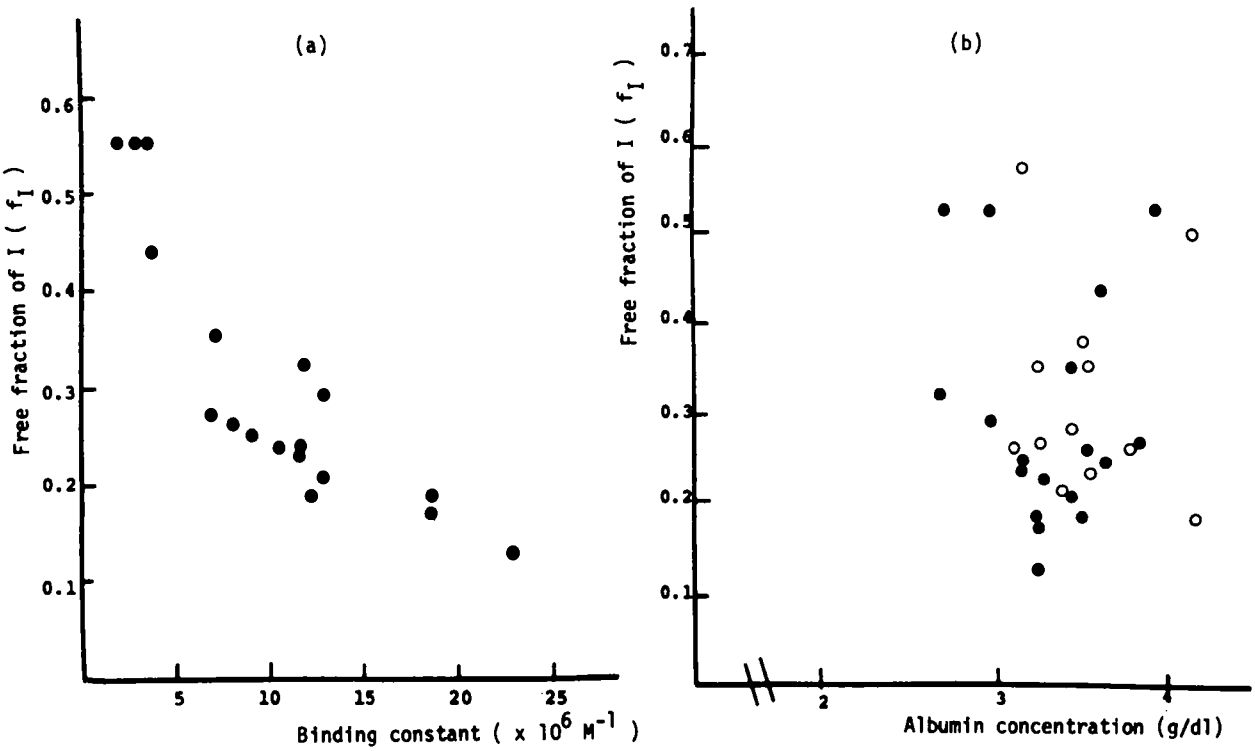

Figure 1—*Relationship between the free fraction of I and the binding constant (a) and albumin concentration (b) in the plasma of individual rats. Rat plasma diluted to 0.2% was used for the determination of f_I at a I concentration of 1 μM using the fluorescence method as described in the text. Correlation coefficient for the binding constant = −0.858, $p < 0.001$. Correlation coefficient for the albumin concentration = −0.072 (not significant). Key: (●) rats 1–18; (○) rats 19–32.*

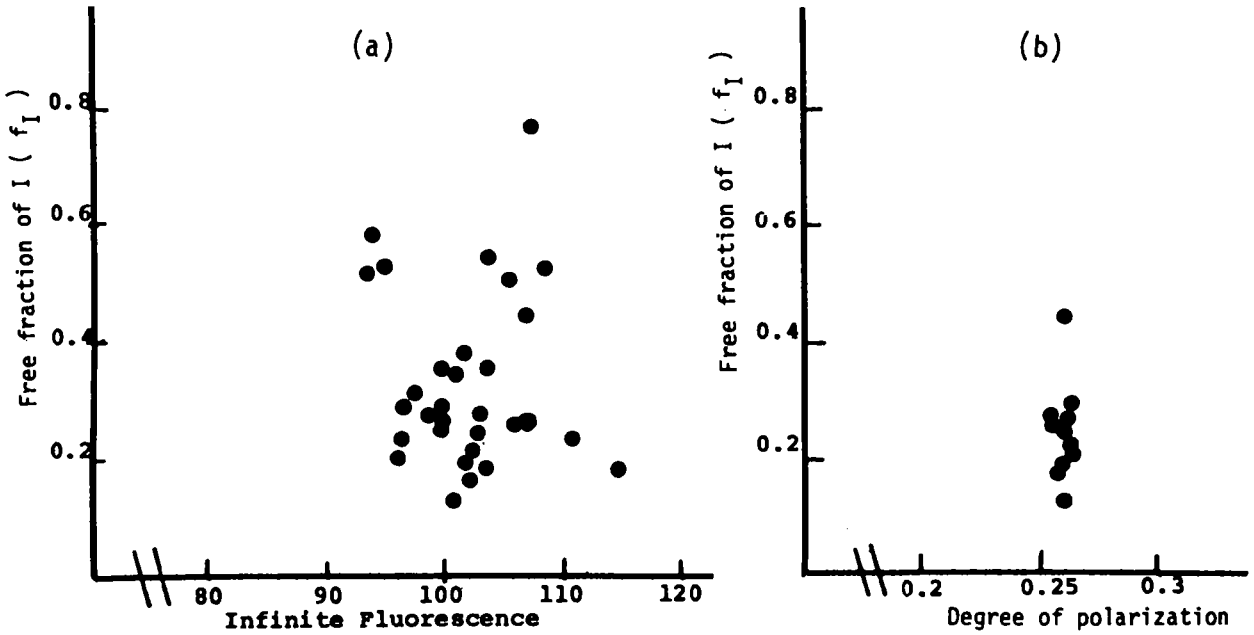

Figure 2—*Relationship between f_I and the infinite fluorescence of I (a) and the degree of polarization (b) in the plasma of individual rats. (See text for details.) Correlation coefficient for infinite fluorescence = −0.368 (not significant), using rats 1–32; correlation coefficient for degree of polarization = 0.258 (not significant), using rats 8–18.*

Fluorescence Measurement—Fluorometric measurements[8] were performed in the same buffer as above at room temperature (19–23°C). The bindings of I and warfarin to plasma were measured by the fluorescence method.

Binding of I.—The excitation and emission wavelengths were 400 and 480 nm, respectively. Titration of 1 μM of I with plasma was used to determine the infinite fluorescence when this concentration of I was completely bound. The infinite fluorescence thus obtained shows the fluorescence quantum yield of bound I and may reflect the changes in the environment at the binding site.

A reverse titration of 0.3% plasma with I was then carried out to obtain the binding parameters. Details of this titration procedure have been described previously (4, 6). The bound fraction of I (X_1) was given by:

$$X_1 = F_{obs}/F_{bound} \quad \text{(Eq. 1)}$$

where F_{obs} is the observed fluorescence and F_{bound} is the infinite fluorescence when a given concentration of I is completely bound. The free fraction of I (f_I) was then calculated by:

$$f_I = 1 - X_I \quad \text{(Eq. 2)}$$

[8] Hitachi MPF-4 fluorescence spectrometer.

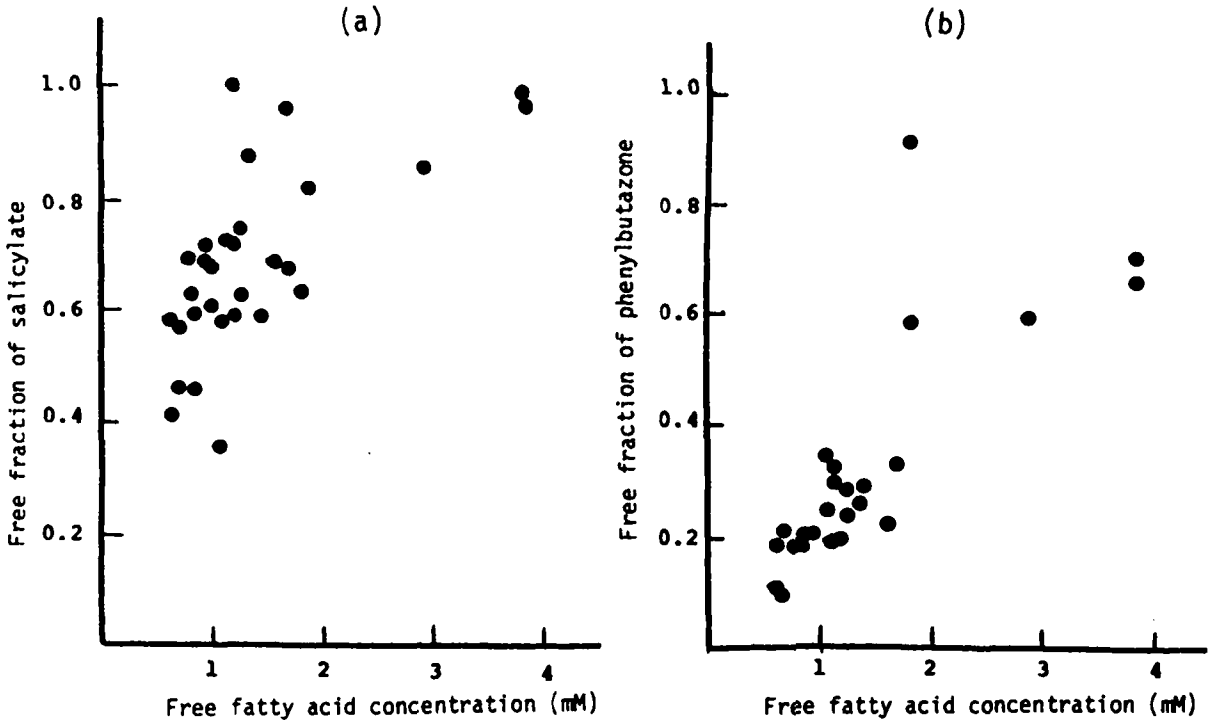

Figure 3—*Relationship between free fatty acid concentration and the free fractions of salicylate (a) and phenylbutazone (b) in the plasma of individual rats, determined by equilibrium dialysis using rat plasma diluted to 25% and initial drug concentrations of 0.1 mM. Correlation coefficient for salicylate = 0.661 ($p < 0.001$) using rats 3–32; correlation coefficient for phenylbutazone = 0.761 ($p < 0.001$) using rats 8–32.*

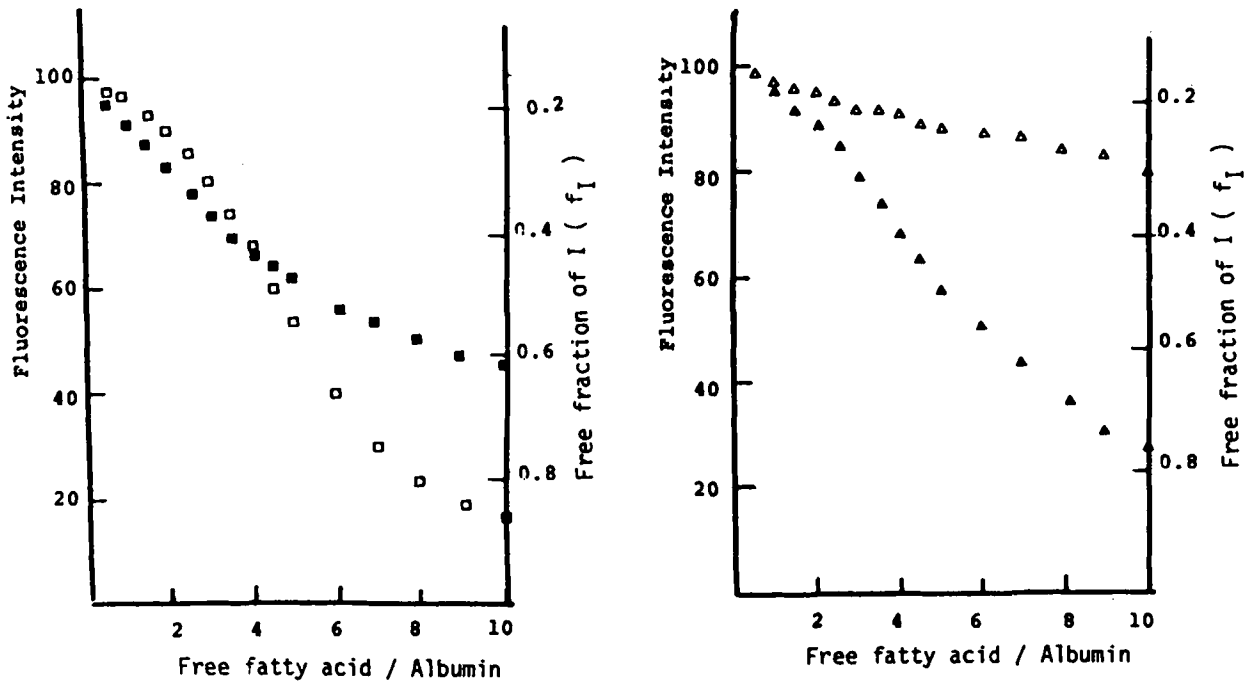

Figure 4—*Effect of various free fatty acids on the fluorescence of I with 1 μM defatted rat albumin and 1 μM of I. The fluorescence intensity in the absence of free fatty acids was set at 100 U. Fluorescence intensities (left ordinate) were converted to free fractions of I (right ordinate). Key: (□) oleic acid; (■) lauric acid; (△) stearic acid; (▲) palmitic acid.*

To study the conformational changes in the structure of plasma proteins, the polarization of the fluorescence of I bound to plasma proteins (mainly albumin) was measured using excitation and emission wavelengths of 380 and 480 nm, respectively. The degree of polarization, P, was calculated as:

$$P = (F_{par} - hF_{per})/(F_{par} - hF_{per}) \quad \text{(Eq. 3)}$$

where F_{par} and F_{per} refer to the intensity of the fluorescence light polarized parallel and perpendicular to the exciting light, respectively, and h is a correction factor which accounts for the selective transmission of the monochromatic light and the selective reflection of the sample tubes. Two film-type polarizers were used for the polarization measurements.

Warfarin Binding—The binding of warfarin to plasma was also measured by the fluorescence method previously adopted by Chakrabarti *et al.* (7, 8). The excitation and emission wavelengths were 320 and 390 nm, respectively. The bound fraction of warfarin (X_{II}) was calculated as:

$$X_{II} = (F_{obs} - F_{free})/(F_{bound} - F_{free}) \quad \text{(Eq. 4)}$$

where F_{obs} is the observed fluorescence corrected for the protein blank, F_{free}

Table I—Correlation Coefficients Between Free Fatty Acid Concentration and the Free Fractions of Various Acidic Drugs in Rat Plasma

Drug	n	Correlation Coefficient[a] (r)	Free Fatty Acid Level	
			Mean, mM	Range, mM
1-Anilino-8-naphthalenesulfonate (I)	32	0.609*[b]	1.35	0.43–3.78
Warfarin (II)	21	0.609**	1.14	0.62–1.80
Phenylbutazone (III)	25	0.761*[c]	1.14	0.62–3.78
Salicylate (IV)	30	0.661*[c]	1.39	0.62–3.78
Sulfaphenazole (V)	30	0.551** (0.687)*[d]	1.39	0.62–3.78
Indomethacin (VI)	15	0.536***	1.72	0.62–3.78

[a] Key for statistical significance: (*) $p < 0.001$; (**) $p < 0.01$; (***) $p < 0.05$. [b] Previously reported in Ref. 4. [c] Experimental data are shown in Fig. 3. [d] Among the 30 rats studied, one (rat 28) showed an abnormal free fraction (0.773), as indicated by an asterisk in Fig. 6. The correlation coefficient in parentheses was calculated excluding this abnormal datum point.

is the fluorescence of warfarin in the buffer at a given concentration, and F_{bound} is the fluorescence in the presence of a large excess of plasma proteins. The X_{II} value was obtained using 10 μM warfarin and 2% plasma, which corresponded to ~10 μM albumin.

Analytical Method—In the equilibrium dialysis experiments, the determination of drug at the buffer side was carried out spectrofluorometrically[8] or spectrophotometrically[9].

Indomethacin—The concentration was directly measured spectrophotometrically (λ_1 = 370 nm, λ_2 = 320 nm). The blank value which came from the membrane-permeable components was subtracted.

Phenylbutazone—After addition of 0.5 mL of 1 M HCl to 0.5 mL of sample, the mixture was extracted with 4 mL of *n*-heptane, and the 2.5-mL organic layer was reextracted with 2 mL of 4% sodium carbonate. The sodium carbonate layer was measured spectrophotometrically (λ_1 = 330 nm, λ_2 = 270 nm).

Salicylic Acid—After addition of 0.5 mL of 1 M HCl to 0.5 mL of sample, the mixture was extracted with 6 mL of dichloroethane, and the 4-mL organic layer was reextracted with 4 mL of 4% sodium carbonate. The drug concentration of the aqueous layer was measured spectrofluorometrically (λ_{ex} = 300 nm, λ_{em} = 410 nm) using a 390-nm cut-off filter at the emission side.

Sulfaphenazole—The concentration was determined colorimetrically (λ_1 = 650 nm, λ_2 = 550 nm) according to the method of Tsuda and Matsunaga (9). The determinations of free fatty acids[10], total bilirubin[11] (conjugated plus unconjugated), and albumin[12] in the plasma were performed using kits.

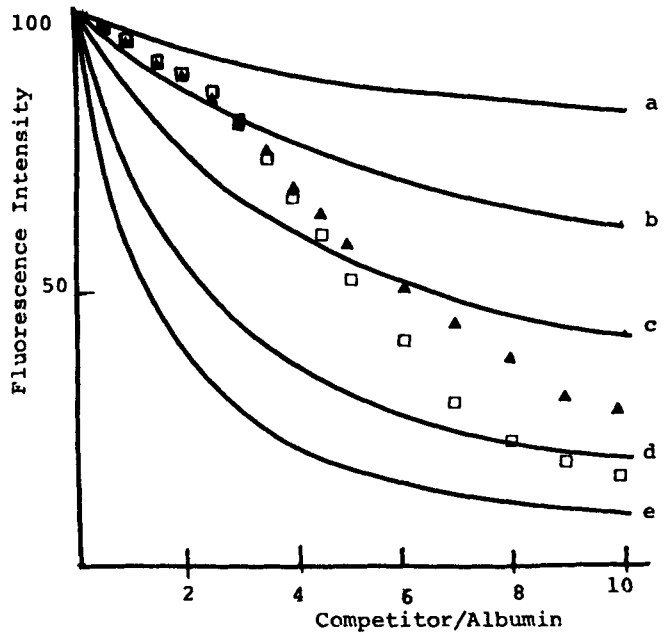

Figure 5—*Simulation of inhibition of the binding of I to rat albumin based on the assumption of simple competition. The solid lines were calculated with Eq. 5, using* $T_A = 1\ \mu M$, $P = 1\ \mu M$, $n = 1$, $K_A = 2.2 \times 10^7\ M^{-1}$, *and* K_B: *(a)* $0.3 \times 10^6\ M^{-1}$, *(b)* $1 \times 10^6\ M^{-1}$, *(c)* $3 \times 10^6\ M^{-1}$, *(d)* $10 \times 10^6\ M^{-1}$, *and (e)* $30 \times 10^6\ M^{-1}$. *(See text for details.) Data for oleic (□) and palmitic (▲) acids from Fig. 4 are shown for comparison.*

[9] Hitachi 356 dual-type spectrophotometer.
[10] Nefatest; Wako Pure Chemical Industries Co., Tokyo, Japan.
[11] Bil Set "Daiichi"; Daiichi Pure Chemical Co., Tokyo, Japan.
[12] Diagnotesta-A; Daiichi Pure Chemical Co., Tokyo, Japan.

RESULTS AND DISCUSSION

Interindividual Differences in the Plasma Binding of I—It was previously reported that the free fraction of I (f_I) showed pronounced interindividual differences ranging from 0.126 to 0.777 (4). To determine whether these interindividual differences were due to differences in the binding constant or to those in albumin concentration, the correlations between f_I and these two factors were examined. Using plasma of 18 rats, binding kinetics with changing concentration of I were examined. Although the binding constant for the high-affinity site shows some interindividual differences (ranging from $1.75 \times 10^6\ M^{-1}$ to $2.3 \times 10^7\ M^{-1}$), the number of binding sites on albumin gives values $\simeq 1$. As shown in Fig. 1a, there is a highly statistically significant negative correlation between f_I and the binding constant for the high-affinity site ($r = -0.858$, $p < 0.001$); no significant correlation between f_I and the albumin concentration was seen (Fig. 1b). Figure 2 shows the correlation between f_I and the infinite fluorescence of I and the degree of polarization, both of which have been used as indices of the conformational changes of plasma albumin (7, 10, 11). No significant correlation was observed in either case. Consequently, the conformational changes of albumin might not be associated with the interindividual differences in f_I. On the other hand, it was previously found that there was a significant positive correlation between f_I and free fatty acid concentration in plasma, which was considered to be one of the endogenous displacing agents (4). However, the correlation coefficient was not so high ($r = 0.609$) that the interindividual differences could be explained only by free fatty acids (4).

Correlation Between the Free Fractions of Various Acidic Drugs and the Free Fatty Acid Concentration—Correlations between the free fatty acid concentrations in rat plasma and the free fractions of five acidic drugs (warfarin, phenylbutazone, salicylic acid, sulfaphenazole, and indomethacin) were investigated. Results in the case of phenylbutazone and salicylic acid are shown in Fig. 3; the correlation coefficients obtained are listed in Table I. Statistically significant positive correlations were observed between the free fatty acid concentration and the free fractions of all the drugs.

Plasma albumin is generally thought to play a major role in the binding of acidic drugs to plasma. To evaluate the extent of the potency of various free fatty acids to inhibit the binding of I to albumin, the titrations of the mixture of I (1 μM) and defatted rat albumin (1 μM) with various free fatty acids were carried out (Fig. 4). If it is assumed that the quantum yield of bound I (infinite fluorescence) is not altered by the binding of free fatty acid to albumin, the decrease in the fluorescence would represent the decrease in the concentration of bound I (see Eq. 1). The free fraction of I in the absence of free fatty acids under this condition was calculated to be 0.14 using Eq. 1. This value was essentially the same as the smallest free fraction of I (0.126) among those obtained using rat plasma.

Table II—Matrix of the Correlation Coefficients Between the Free Fractions of Six Acidic Drugs[a]

Drug	I	II	III	IV	V	VI
I		0.944*[b]	0.896*[c]	0.701*[b]	0.548**[b] (0.715*)[d]	0.808*[b]
II			0.911*	0.641*	0.422[ns] (0.561**)[d]	0.797*
III				0.732*	0.721* (0.655*)[d]	0.830*
IV					0.405*** (0.638*)[d]	0.605**
V						0.810* (0.775*)[d]

[a] Key for statistical significance: (*) $p < 0.001$; (**) $p < 0.01$; (***) $p < 0.05$; (ns) not significant ($p > 0.05$). [b] Experimental data are shown in Fig. 6. [c] Previously reported in Ref. 4. [d] The explanation for the values in parentheses is given in Table I, footnote *d*.

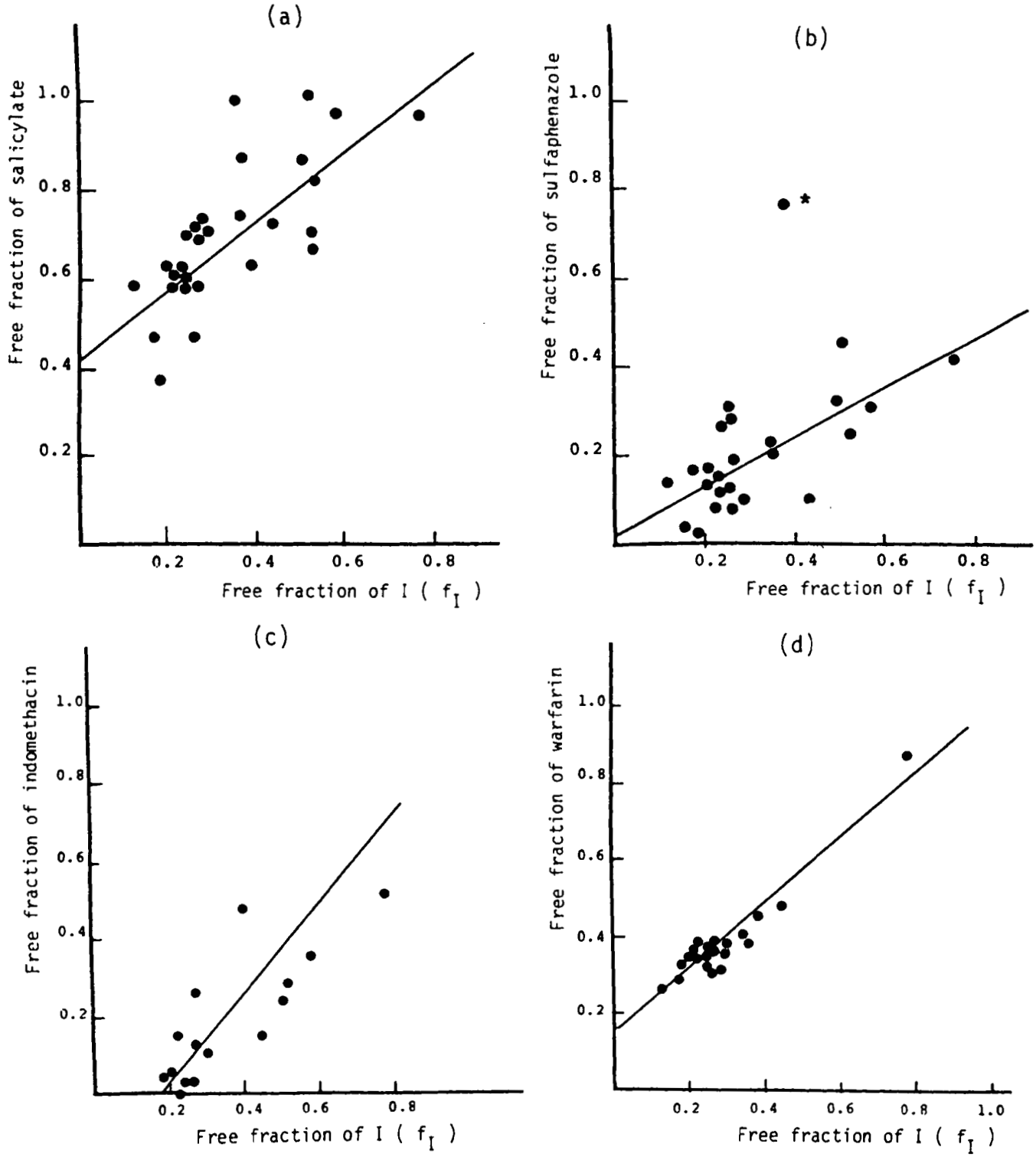

Figure 6—*Relationship between* f_I *and the free fractions of salicylate (a), sulfaphenazole (b), indomethacin (c), and warfarin (d) in the plasma of individual rats. Least-squares fits of the data yielded the solid lines. The experimental conditions are the same as described in Fig 3, and the correlation coefficients were summarized in Table II.*

Among the four free fatty acids studied, stearic acid is a weak inhibitor, while oleic acid and palmitic acid are relatively strong inhibitors. The latter acids have a similar pattern of inhibition, in which the fluorescence decrease is slow up to a free fatty acid/albumin ratio of 2 and faster thereafter. If simple competition by two ligands (I and free fatty acid in this case) for equal and independing binding sites is assumed, the following equation holds (12):

$$T_B = \left[n - r_A - \frac{r_A}{(T_A - P \cdot r_A)K_A}\right] \times \left[P + \frac{K_A(T_A - P \cdot r_A)}{r_A \cdot K_B}\right] \quad \text{(Eq. 5)}$$

where T_A and T_B are the total concentrations of I and the competitor (free fatty acid), respectively, P is the albumin concentration, r_A is the number of I molecules bound per mole of albumin, n is the number of binding sites, and K_A and K_B are the binding constants of I and competitor, respectively. In the present case, parameters used in this calculation are $T_A = 1\ \mu M$, $P = 1\ \mu M$, $n = 1$, $K_A = 2.2 \times 10^7\ M^{-1}$ (4).

Since the fluorescence intensity (F) of I is proportional to r_A, F can be calculated as a function of T_B using Eq. 5, when K_B is given. Figure 5 shows the simulation curves thus calculated. The simulation curve at any K_B value never reproduces the anomalous patterns obtained in the titration with oleic

and palmitic acids. Therefore, the slow fluorescence decrease up to the free fatty acid/albumin ratio of ~2 and the faster decrease after that could not be explained by the simple competition. Santons and Spector (13, 14) investigated the effects of free fatty acids on the binding of I to human or bovine serum albumin. They found that the fluorescence of I was enhanced when ≤2 mol of palmitate were added to 1 mol of human albumin, but larger amounts of palmitate produced a reduction in the fluorescence of I; with bovine and rabbit albumins, palmitate in all concentrations only reduced the fluorescence of I. The present result with rat albumin is similar to those with bovine and rabbit albumin.

Correlation Between the Free Fraction of I and those of Various Acidic Drugs—Figure 6 shows the correlation between f_I and the free fractions of various acidic drugs. There are highly statistically significant positive correlations in all cases. Warfarin and phenylbutazone were especially well correlated with I, $r \geq 0.9$. Such high correlations are reasonable when considering that warfarin and phenylbutazone reportedly competitively inhibit the binding of I to bovine serum albumin (15). The correlation coefficients between the free fractions of all drugs are listed in Table II; there is a statistically significant positive correlation between the free fraction of any pair of drugs.

This finding suggests that we can probably estimate the degree of plasma binding of such acidic drugs by knowing that of I. However, it must be kept in mind that the free fractions of various drugs obtained in the present study using dilute plasma samples do not necessarily represent the *in vivo* free fraction. To be able to employ this method using I as a clinical test, therefore, it would be necessary to determine the plasma bindings of various drugs using undiluted human plasma and examine the correlations between the free fractions of these drugs and that of I. However, the fluorescence method using I, which we have presented herein, has the advantages that it takes a short time (5–10 min) and needs a very small amount of plasma (<0.1 mL) to measure the free fraction of I.

Note added in proof: Heparin was used to prepare rat plasma in this study. The effect of heparin injection on plasma protein binding of I was subsequently studied and was reported (16).

REFERENCES

(1) G. Levy, "The Effect of Disease States on Drug Pharmacokinetics," L. Z. Benet, Ed., Academy of Pharmaceutical Sciences, American Pharmaceutical Association, Washington, D.C. 1976, pp. 137–151.

(2) A. Yacobi and G. Levy. *J. Pharm. Sci.*, **66**, 567 (1977).

(3) G. Levy and A. Yacobi, *J. Pharm. Sci.*, **63**, 805 (1974).

(4) Y. Sugiyama, J. Sato, and M. Hanano, *J. Pharmacobio. Dyn. (Tokyo)*, **2**, 403 (1979).

(5) R. F. Chen, *J. Biol. Chem.*, **242**, 173 (1967).

(6) Y. Sugiyama, T. Iga, S. Awazu, and M. Hanano, *Chem. Pharm. Bull.*, **26**, 199 (1978).

(7) S. K. Chakrabarti, R. Laliberte, and J. Brodeur. *Biochem. Pharmacol.*, **25**, 2515 (1976).

(8) S. K. Chakrabarti, *Biochem. Pharmacol.*, **27**, 739 (1978).

(9) K. Tsuda and S. Matsunaga, *Yakugaku Zasshi*, **62**, 362 (1942).

(10) R. F. Chen and R. L. Bowman, *Science*, **147**, 729 (1965).

(11) G. Weber and L. B. Young, *J. Biol. Chem.*, **239**, 1415 (1964).

(12) E. Tipping, B. Ketterer, L. Christodoulides, and G. Enderby, *Eur. J. Biochem.*, **67**, 583 (1976).

(13) E. C. Santons and A. A. Spector, *Mol. Pharmacol.*, **10**, 519 (1973).

(14) E. C. Santons and A. A. Spector, *Biochemistry*, **11**, 2299 (1972).

(15) H. W. Jun, L. A. Luzzi, and P. L. Hsu, *J. Pharm. Sci.*, **61**, 1835 (1972).

(16) J. Sato, Y. Sawada, Y. Sugiyama, T. Iga, and M. Hanano, *J. Pharmacobio. Dyn. (Tokyo)*, **3**, 720 (1980).

Interaction of Doxorubicin with Nuclei Isolated from Rat Liver and Kidney

TETSUYA TERASAKI, TATSUJI IGA ˣ, YUICHI SUGIYAMA, and MANABU HANANO

Received April 1, 1982, from the *Faculty of Pharmaceutical Sciences, University of Tokyo, Hongo, Bunky-ku, Tokyo, 113, Japan.* Accepted for publication March 24, 1983.

Abstract □ The interaction of doxorubicin with nuclei isolated from rat liver and kidney was studied by fluorospectrometry. The nuclei had at least two different types of binding sites for the drug. Both Mg^{2+} and Ca^{2+} competitively inhibited the binding of doxorubicin to the nuclei, which showed a remarkable temperature dependency. No significant difference was observed between the numbers of binding sites ($n = 6.70 \times 10^{-2}$ mol/mol of DNA for liver; 6.41×10^{-2} mol/mol of DNA for kidney) or the affinity constants ($K_a = 4.85 \times 10^5$ M^{-1} for liver; 5.41×10^5 M^{-1} for kidney) under quasi-physiological conditions. These results obtained from *in vitro* binding experiments support previous suggestions that the differences in the *in vivo* distribution of doxorubicin among tissues are not due to differences in the nuclear binding of the drug. The amount of nuclei per gram of tissue is the primary determinant of the characteristic tissue distribution of doxorubicin.

Keyphrases □ Doxorubicin—interaction with nuclei isolated from rat liver and kidney, binding, distribution □ Binding—interaction of doxorubicin with nuclei isolated from rat liver and kidney, distribution □ Nuclei, liver and kidney—interaction with doxorubicin, rats, binding, distribution □ Distribution—interaction of doxorubicin with nuclei isolated from rat liver and kidney, binding

Doxorubicin, an anthracycline antibiotic, has cytotoxic and antineoplastic activities and inhibits both enzymatic RNA and DNA synthesis by intercalating with DNA (1). The tissue distribution of doxorubicin has been studied extensively in humans and laboratory animals, but the mechanism of its distribution in such tissues as liver, kidney, and muscle has not been elucidated (2–6). The tissue distribution of this drug is generally thought to be related to the affinity for the tissue binder, the concentration of binder, and the permeability across the plasma membrane.

The interaction of doxorubicin and other derivatives with DNA or chromatins isolated from tumor cells, calf thymus, and cultured lung cells has been studied by several methods (7–10). Although the binding of the drug to native DNA has been extensively studied, little information has been obtained on its intercalation with nuclei isolated from normal tissues. Moreover, it has been suggested that doxorubicin also interacts strongly with the negatively charged phospholipid, cardiolipin (11). In addition, it was revealed that tumor cells may have a carrier-mediated influx system and an active efflux mechanism (12). Previously, a good correlation between the *in vivo* tissue-to-plasma partition coefficients for doxorubicin in several tissues and the amounts of nuclei per gram of tissue in rats and rabbits was demonstrated, suggesting that there is little or no difference in the nuclear binding of the drug among tissues (13).

The purpose of this study was to determine the *in vitro* binding characteristics of doxorubicin with isolated nuclei from rat liver and kidney in an attempt to elucidate the mechanisms by which the *in vivo* tissue distribution of the drug occurs.

0022-3549/84/0400-0524$01.00/0

© 1984, American Pharmaceutical Association

and palmitic acids. Therefore, the slow fluorescence decrease up to the free fatty acid/albumin ratio of ~2 and the faster decrease after that could not be explained by the simple competition. Santons and Spector (13, 14) investigated the effects of free fatty acids on the binding of I to human or bovine serum albumin. They found that the fluorescence of I was enhanced when ≤2 mol of palmitate were added to 1 mol of human albumin, but larger amounts of palmitate produced a reduction in the fluorescence of I; with bovine and rabbit albumins, palmitate in all concentrations only reduced the fluorescence of I. The present result with rat albumin is similar to those with bovine and rabbit albumin.

Correlation Between the Free Fraction of I and those of Various Acidic Drugs—Figure 6 shows the correlation between f_I and the free fractions of various acidic drugs. There are highly statistically significant positive correlations in all cases. Warfarin and phenylbutazone were especially well correlated with I, $r \geq 0.9$. Such high correlations are reasonable when considering that warfarin and phenylbutazone reportedly competitively inhibit the binding of I to bovine serum albumin (15). The correlation coefficients between the free fractions of all drugs are listed in Table II; there is a statistically significant positive correlation between the free fraction of any pair of drugs.

This finding suggests that we can probably estimate the degree of plasma binding of such acidic drugs by knowing that of I. However, it must be kept in mind that the free fractions of various drugs obtained in the present study using dilute plasma samples do not necessarily represent the *in vivo* free fraction. To be able to employ this method using I as a clinical test, therefore, it would be necessary to determine the plasma bindings of various drugs using undiluted human plasma and examine the correlations between the free fractions of these drugs and that of I. However, the fluorescence method using I, which we have presented herein, has the advantages that it takes a short time (5–10 min) and needs a very small amount of plasma (<0.1 mL) to measure the free fraction of I.

Note added in proof: Heparin was used to prepare rat plasma in this study. The effect of heparin injection on plasma protein binding of I was subsequently studied and was reported (16).

REFERENCES

(1) G. Levy, "The Effect of Disease States on Drug Pharmacokinetics," L. Z. Benet, Ed., Academy of Pharmaceutical Sciences, American Pharmaceutical Association, Washington, D.C. 1976, pp. 137–151.

(2) A. Yacobi and G. Levy. *J. Pharm. Sci.*, **66**, 567 (1977).

(3) G. Levy and A. Yacobi, *J. Pharm. Sci.*, **63**, 805 (1974).

(4) Y. Sugiyama, J. Sato, and M. Hanano, *J. Pharmacobio. Dyn. (Tokyo)*, **2**, 403 (1979).

(5) R. F. Chen, *J. Biol. Chem.*, **242**, 173 (1967).

(6) Y. Sugiyama, T. Iga, S. Awazu, and M. Hanano, *Chem. Pharm. Bull.*, **26**, 199 (1978).

(7) S. K. Chakrabarti, R. Laliberte, and J. Brodeur. *Biochem. Pharmacol.*, **25**, 2515 (1976).

(8) S. K. Chakrabarti, *Biochem. Pharmacol.*, **27**, 739 (1978).

(9) K. Tsuda and S. Matsunaga, *Yakugaku Zasshi*, **62**, 362 (1942).

(10) R. F. Chen and R. L. Bowman, *Science*, **147**, 729 (1965).

(11) G. Weber and L. B. Young, *J. Biol. Chem.*, **239**, 1415 (1964).

(12) E. Tipping, B. Ketterer, L. Christodoulides, and G. Enderby, *Eur. J. Biochem.*, **67**, 583 (1976).

(13) E. C. Santons and A. A. Spector, *Mol. Pharmacol.*, **10**, 519 (1973).

(14) E. C. Santons and A. A. Spector, *Biochemistry*, **11**, 2299 (1972).

(15) H. W. Jun, L. A. Luzzi, and P. L. Hsu, *J. Pharm. Sci.*, **61**, 1835 (1972).

(16) J. Sato, Y. Sawada, Y. Sugiyama, T. Iga, and M. Hanano, *J. Pharmacobio. Dyn. (Tokyo)*, **3**, 720 (1980).

Interaction of Doxorubicin with Nuclei Isolated from Rat Liver and Kidney

TETSUYA TERASAKI, TATSUJI IGA ˣ, YUICHI SUGIYAMA, and MANABU HANANO

Received April 1, 1982, from the *Faculty of Pharmaceutical Sciences, University of Tokyo, Hongo, Bunky-ku, Tokyo, 113, Japan.* Accepted for publication March 24, 1983.

Abstract □ The interaction of doxorubicin with nuclei isolated from rat liver and kidney was studied by fluorospectrometry. The nuclei had at least two different types of binding sites for the drug. Both Mg^{2+} and Ca^{2+} competitively inhibited the binding of doxorubicin to the nuclei, which showed a remarkable temperature dependency. No significant difference was observed between the numbers of binding sites ($n = 6.70 \times 10^{-2}$ mol/mol of DNA for liver; 6.41×10^{-2} mol/mol of DNA for kidney) or the affinity constants ($K_a = 4.85 \times 10^5$ M^{-1} for liver; 5.41×10^5 M^{-1} for kidney) under quasi-physiological conditions. These results obtained from *in vitro* binding experiments support previous suggestions that the differences in the *in vivo* distribution of doxorubicin among tissues are not due to differences in the nuclear binding of the drug. The amount of nuclei per gram of tissue is the primary determinant of the characteristic tissue distribution of doxorubicin.

Keyphrases □ Doxorubicin—interaction with nuclei isolated from rat liver and kidney, binding, distribution □ Binding—interaction of doxorubicin with nuclei isolated from rat liver and kidney, distribution □ Nuclei, liver and kidney—interaction with doxorubicin, rats, binding, distribution □ Distribution—interaction of doxorubicin with nuclei isolated from rat liver and kidney, binding

Doxorubicin, an anthracycline antibiotic, has cytotoxic and antineoplastic activities and inhibits both enzymatic RNA and DNA synthesis by intercalating with DNA (1). The tissue distribution of doxorubicin has been studied extensively in humans and laboratory animals, but the mechanism of its distribution in such tissues as liver, kidney, and muscle has not been elucidated (2–6). The tissue distribution of this drug is generally thought to be related to the affinity for the tissue binder, the concentration of binder, and the permeability across the plasma membrane.

The interaction of doxorubicin and other derivatives with DNA or chromatins isolated from tumor cells, calf thymus, and cultured lung cells has been studied by several methods (7–10). Although the binding of the drug to native DNA has been extensively studied, little information has been obtained on its intercalation with nuclei isolated from normal tissues. Moreover, it has been suggested that doxorubicin also interacts strongly with the negatively charged phospholipid, cardiolipin (11). In addition, it was revealed that tumor cells may have a carrier-mediated influx system and an active efflux mechanism (12). Previously, a good correlation between the *in vivo* tissue-to-plasma partition coefficients for doxorubicin in several tissues and the amounts of nuclei per gram of tissue in rats and rabbits was demonstrated, suggesting that there is little or no difference in the nuclear binding of the drug among tissues (13).

The purpose of this study was to determine the *in vitro* binding characteristics of doxorubicin with isolated nuclei from rat liver and kidney in an attempt to elucidate the mechanisms by which the *in vivo* tissue distribution of the drug occurs.

0022-3549/84/0400-0524$01.00/0

© 1984, American Pharmaceutical Association

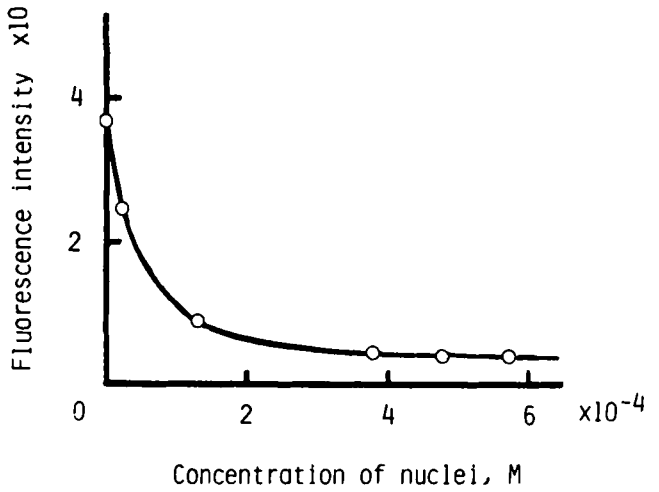

Figure 1—*Effect of nuclear binding on the fluorescence intensity of doxorubicin. The concentration of nuclei is expressed in terms of a nucleotide. A nucleotide molecular weight of 330.9 was used to determine DNA concentration (as nucleotide) as the sodium salt.*

EXPERIMENTAL

Materials—Doxorubicin hydrochloride[1] was stored in the dark in a desiccator at 4°C. Solutions of the drug (2×10^{-6}–5×10^{-4} M) in 405 mM sucrose were freshly prepared immediately before use. Calf thymus DNA[2] and yeast RNA[2] (type XI) were used as standards for the determination of DNA and RNA concentrations in the tissue and nuclei. Micrococcal nuclease[3] was used for the preparation of chromatin. All other reagents were commercial products of analytical grade.

Preparation of Nuclei and Chromatin—Male Wistar rats[4], weighing 250–270 g, were used as liver and kidney donors. Nuclei and chromatin were prepared essentially according to the procedure of Sugano *et al.* (14), except that 1 mM magnesium chloride was added to the isolation buffer to prevent the aggregation of nuclei. No detergent was added to the buffer. The resulting nuclear pellet was suspended in buffer (pH 7.4) containing 340 mM sucrose, 60 mM potassium chloride, 15 mM Tris, 15 mM 2-mercaptoethanol, 1 mM calcium chloride, 1 mM magnesium chloride, and 0.1 mM α-toluenesulfonyl fluoride. The integrity of isolated nuclei was examined microscopically after staining with 1.0% orcein-45% acetic acid solution. The yield of nuclei was 20–30%.

Binding Experiments—The binding studies of doxorubicin to nuclei were performed by spectrofluorometric titration in a fluorospectrometer[5]. Aliquots (2–10 μL) of freshly prepared doxorubicin stock solution (2×10^{-6}–5×10^{-4} M), up to a 150-μL total sample volume, were added to the cuvette filled with 3 mL of nuclei (2×10^{-5}–5×10^{-5} M as DNA) in a quasi-physiological buffer (pH 7.0) solution containing 135 mM sucrose (which was added to inhibit the swelling of nuclei), 20 mM Tris, 50 mM sodium chloride, 100 mM potassium chloride, 1 mM magnesium chloride, and 1 mM calcium chloride (15, 16). The solution was stirred with a glass rod after each addition, and the fluorescence was measured at 590 nm (excitation at 500 nm) at 10 min (at 37°C) or 30 min (at 7°C) after the addition of the drug. The fluorescence intensity of doxorubicin decreased with increasing amount of nuclei added (Fig. 1), as reported for the interaction of anthracycline antibiotics with DNA and chromatins (7), and the fluorescence intensity (I) of the drug binding to the nuclei can be expressed by:

$$I = q_f C_f + q_b C_b \qquad \text{(Eq. 1)}$$

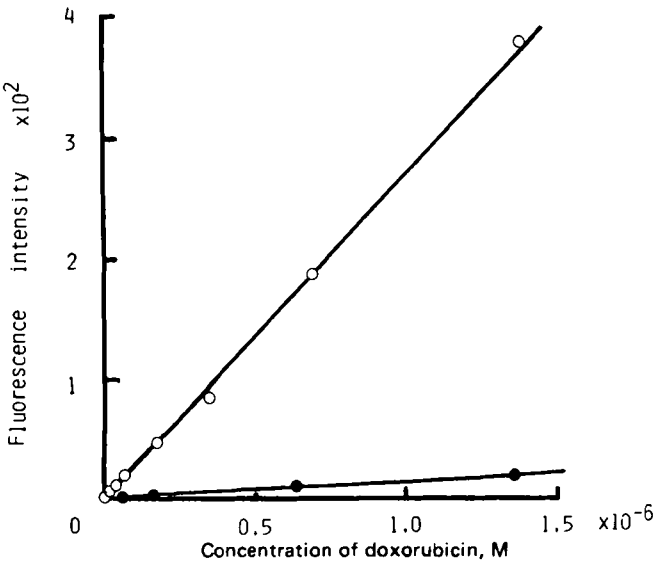

Figure 2—*Representative calibration curves for the binding of doxorubicin to nuclei isolated from rat liver. Key: (○) without nuclei; (●) with nuclei.*

[1] Adriamycin; Kyowa Hakko Kogyo Co., Ltd., Tokyo.
[2] Sigma Co., Ltd., Chicago, Ill.
[3] Boehringer Mannheim GmbH, Mannheim, West Germany.
[4] Nihon Ikagaku Dobutsu Co., Tokyo.

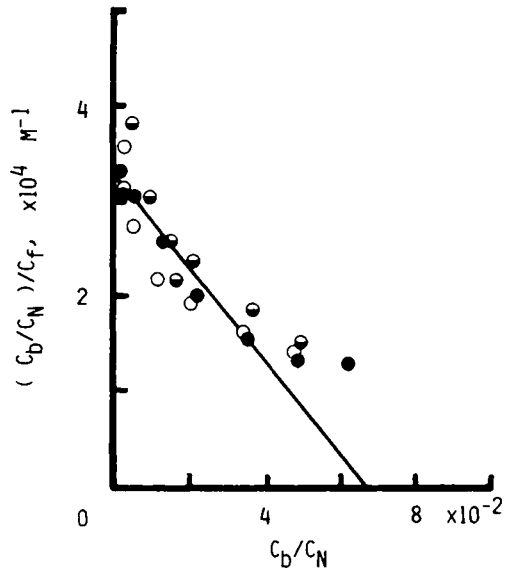

Figure 3—*Scatchard plot of data for the binding of doxorubicin to nuclei isolated from the rat liver. The binding study was performed at 37°C in quasi-physiological buffer. The concentration of nuclei was 4.0×10^{-5}–4.6×10^{-5} M as DNA. The line was calculated for the high-affinity binding site by the SALS method using a digital computer (see text). Key: (●, ⊖, ○) observed values from three independent experiments.*

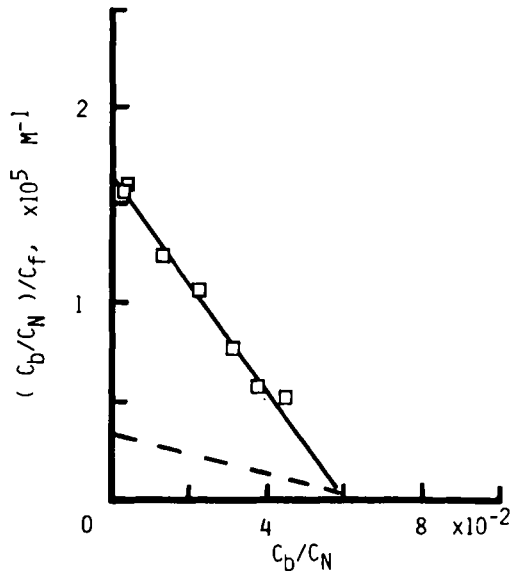

Figure 4—*Scatchard plot for the effect of temperature on the binding of doxorubicin to isolated liver nuclei. The concentration of nuclei was 2.2×10^{-5} M as DNA. Lines were fitted by the SALS method using a digital computer. Key: (□) observed values at 7°C; (- - -) calculated line at 37°C from Fig. 3 for comparison.*

[5] Hitachi MPF-4.

Table I—Characterization of Nuclei Isolated from Rat Liver and Kidney

	Liver			Kidney		
	Homogenate	Nuclei[a]	Ratio of Nuclei/ Homogenate	Homogenate	Nuclei[a]	Ratio of Nuclei/ Homogenate
RNA[b]/DNA[c]	7.36	0.289	0.039	3.04	0.132	0.043
Protein[d]/DNA[c]	108.0	2.95	0.027	68.0	1.93	0.028
Yield (%)		25.8			21.6	

[a] Obtained from four independent experiments. [b] RNA was extracted by the method of Schneider (17) and determined by the orcinol method (19). [c] DNA was extracted in the same manner as described for RNA and determined by the method of Burton (18). [d] Protein was determined according to Lowry *et al.* (20) with bovine serum albumin (Fraction V) as the standard.

where q_f and q_b are the quantum yields of free and bound doxorubicin and C_f and C_b are the concentrations of free and bound drug, respectively. The total concentration (C_t) of doxorubicin is given by:

$$C_t = C_f + C_b \quad \text{(Eq. 2)}$$

The procedure for estimating the quantum yield of drug bound to nuclei is presented in the *Appendix*. Representative calibration curves, determined for each experiment, are shown in Fig. 2.

The apparent binding constants were calculated by means of the following equation using C_f and C_b obtained from Eqs. 1 and 2:

$$(C_b/C_N)/C_f = nK_a - K_a(C_b/C_N) \quad \text{(Eq. 3)}$$

where C_N is the concentration of nuclei as DNA, n is the number of binding sites, and K_a is the affinity constant. To check the degradation of doxorubicin during the binding experiments, the amount of drug in the nuclear suspension before and after incubation was determined by TLC scanning, as reported previously (13).

Analytical Methods—The concentration of nuclei was expressed as that of nucleotide. The molecular weight of 330.9 (the average molecular weight for a nucleotide) was used to determine DNA concentration as the sodium salt. DNA in the tissue and isolated nuclei was extracted according to the procedure of Schneider (17) and determined colorimetrically by the method of Burton (18). RNA was extracted in the same manner as described for DNA and was determined by the orcinol method (19). Protein was determined according to the procedure of Lowry *et al.* (20) with bovine serum albumin[6] as the standard.

Data Analysis—The data were analyzed by a least-squares method using a digital computer[7]. The SALS program (21) was used for the calibration curves and the calculation of the binding parameters of the Scatchard plots.

RESULTS

Characterization of Isolated Nuclei—From microscopic observations of nuclei prepared from the liver and kidney, both preparations were confirmed to be unaffected by the isolation procedure, and only slight cytoplasmic contamination was observed. The RNA/DNA and protein/DNA ratios of tissue homogenate and isolated nuclei were compared (Table I). Since no significant metabolism of doxorubicin was observed during the period of the spectrophotometric study, contamination of nuclei with microsomal and/or cytoplasmic enzymes appeared to be negligible.

Scatchard Analysis of Doxorubicin Binding to Liver Nuclei—A Scatchard plot of doxorubicin binding to liver nuclei based on three independent experiments is shown in Fig. 3; reproducibility was good. The curvature of the plot suggests the existence of at least two classes of binding sites. The binding parameters for the high-affinity sites obtained in the lower drug concentration range (9×10^{-8}–4×10^{-6} M) by the least-squares method were $K_a = 4.85 \times 10^5\ M^{-1}$ and $n = 6.70 \times 10^{-2}$ mol/mol of DNA. However, it was difficult to calculate meaningful binding parameters for the low-affinity sites, since the high inner filter effect of doxorubicin made it difficult to use higher drug concentrations in the binding experiments. The number of high-affinity binding sites is comparable to the value of 8×10^{-2} for the binding of daunomycin to chromatin prepared from Ehrlich ascites tumor cells, as reported by Sabeur *et al.* (7). However, the affinity constant obtained for nuclei showed a large difference from their value ($5 \times 10^6\ M^{-1}$) (2), which might be due to differences in both temperature and buffer composition.

Effect of Temperature—Figure 4 shows Scatchard plots of the temperature dependency of doxorubicin binding to nuclei. The calculated binding constant at 7°C was $K_a = 2.76 \times 10^6\ M^{-1}$, and the number of binding sites was $n = 5.97 \times 10^{-2}$ mol/mol of DNA. This number of binding sites is similar to that observed at 37°C (6.70×10^{-2}), but there appeared to be a remarkable temperature dependency of the affinity constant, K_a. The calculated enthalpy change was −10 kcal/mol.

Effect of Magnesium and Calcium Ions—To examine the effect of divalent metal ions on doxorubicin binding to liver nuclei, the binding was studied in the absence of 1 mM Mg^{2+} or Ca^{2+} in the buffer. The Scatchard plots of doxorubicin binding to liver nuclei are shown in Fig. 5a for Mg^{2+} and in Fig. 5b for Ca^{2+}. Both divalent metal ions decreased the affinity constant, but did not change the number of binding sites. The affinity constant and the number of binding sites, calculated by the least-squares method, for the high-affinity binding sites in divalent metal ion-free buffer were $K_a = 8.39 \times 10^5\ M^{-1}$ and $n = 6.03 \times 10^{-2}$ mol/mol of DNA, respectively, without Mg^{2+}, and $K_a = 6.67 \times 10^5\ M^{-1}$ and $n = 6.44 \times 10^{-2}$ mol/mol of DNA, respectively, without Ca^{2+}. No remarkable decrease in K_a was observed at two- or threefold higher concentrations of these divalent ions.

Effect of pH—Since different intracellular pH values (pH 6.8–7.4) among various tissues have been reported (22), the effect of the buffer pH on doxorubicin binding to liver nuclei was studied over the pH range of 6.4–8.0. As shown in Fig. 6, a small difference appears to exist, but this may not be significant.

Comparison of Doxorubicin Binding to Nuclei and Chromatin Isolated from Liver—Figure 7 shows the Scatchard plots of drug binding to nuclei and chromatin prepared from the liver nuclei. The affinity constant for chromatin in 10 mM Tris buffer at 37°C (pH 7.0) was $2.65 \times 10^6\ M^{-1}$, and the number of binding sites was 7.59×10^{-2} mol/mol of DNA. The numbers of binding sites to nuclei (Fig. 3) and to chromatin (Fig. 7) are very similar. When doxorubicin binding to chromatin was examined under the same conditions as employed for nuclei (Fig. 3), aggregations of chromatin occurred which might be caused by the high cation concentration (23). Since a homogenous dispersion of chromatin could not be obtained in the physiological buffer, the Tris buffer was used. However, there seemed to be little difference in the binding characteristics of the drug between nuclei and chromatin.

Comparison of Doxorubicin Binding to Nuclei Isolated from Liver and Kidney—To determine whether the binding characteristics of doxorubicin to nuclei are different among different tissues, the binding of the drug to nuclei isolated from kidney, as well as liver, was examined. The results of the antibiotic binding to kidney nuclei are shown in Fig. 8. The calculated affinity constant was $5.41 \times 10^5\ M^{-1}$, and the number of binding sites was 6.41×10^{-2} mol/mol of DNA. Little difference was observed in these parameters between nuclei isolated from the liver ($K_a = 4.85 \times 10^5\ M^{-1}$, $n = 6.70 \times 10^{-2}$ mol/mol of DNA; Fig. 3) and kidney under the same conditions.

DISCUSSION

It is well known that the concentrations of doxorubicin after intravenous administration show large differences among tissues (2–6). We have studied the mechanisms of this characteristic tissue distribution on the basis of the working hypothesis that the amount of nuclei per gram of tissue is the predominant factor and, therefore, the differences in the binding characteristics among tissues are probably negligible (13). In this study, the *in vitro* binding characteristics of doxorubicin to nuclei isolated from the rat liver and kidney were examined in an attempt to prove that these assumptions are valid.

Both the integrity and purity of nuclei are known to be important determinants of the *in vitro* binding of doxorubicin. In this study, the ratios of RNA/DNA and protein/DNA (Table I) are comparable to those reported for liver chromatin by Spelsberg and Hnilica (RNA/DNA ratio = 0.1; protein/DNA ratio = 2.2) (24), and no significant aggregation of the isolated nuclei was observed by microscopic examination. Thus, the nuclei prepared in this study were thought to be suitable for the binding study of doxorubicin. Moreover, the chromosomal proteins, which were suggested to inhibit the interaction of homidium bromide and dactinomycin, bind tightly to DNA (25, 26). Therefore, the release of those important proteins might be negligible in this mild isolation procedure. Since nuclei are the dominant organelles

[6] Fraction V; Sigma Chemical Co., St. Louis, Mo.
[7] HITAC M-200H; Hitachi, Tokyo, Japan.

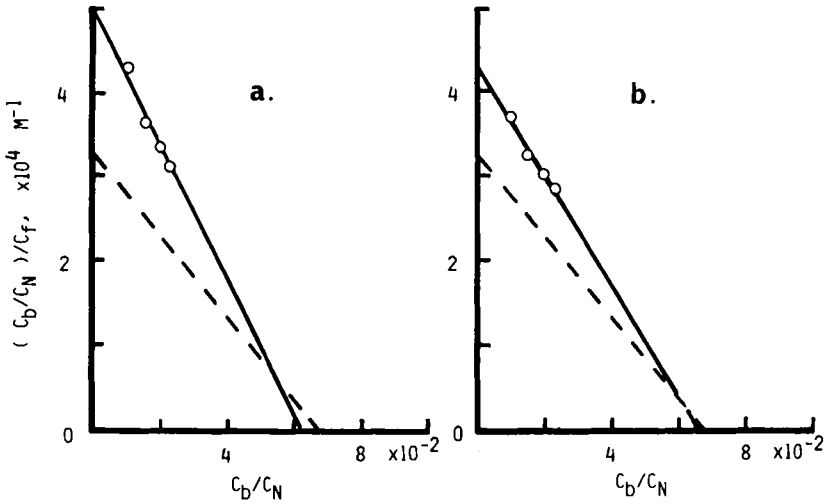

Figure 5—*Scatchard plots for the effects of Mg^{2+} (a) and Ca^{2+} (b) on the binding of doxorubicin to nuclei isolated from the rat liver at 37°C. The concentration of nuclei was 4.3 × 10^{-5} M as DNA in each study. Lines were fitted by the SALS method using a digital computer. Key: (○) in the buffer without Mg^{2+} or Ca^{2+}; (---) calculated line from Fig. 3 for comparison.*

associated with the intracellular localization of doxorubicin (27), slight contamination by cytoplasm might not affect the binding parameters.

The results obtained from the nuclei and chromatin binding studies (Figs. 3–8), suggest that both the temperature and buffer contents are more important determinants than is the medium pH. Two binding sites have been reported for daunomycin binding to DNA; one site is a hydrophobic site which binds the antibiotic aglycone with successive base pairs of the double helix, the other site binds daunomycin by an electrostatic interaction involving the DNA phosphate groups and the daunomycin amino group. Data in Fig. 3 also support the existence of at least two binding sites. Another possible interaction by means of hydrogen bonding has also been proposed (28). It has been reported that divalent cations such as Mg^{2+} and Ca^{2+} interact with the phosphate groups of DNA (29). In this study, typical competitive inhibition by both Mg^{2+} and Ca^{2+} was observed in the nuclear binding of doxorubicin (Fig. 5). Accordingly, the present results support the proposed mechanism that the drug binds predominantly to DNA by an electrostatic interaction with phosphate groups.

No significant pH dependency of doxorubicin binding to nuclei was observed over the pH range studied (pH 6.4–8.0) (Fig. 6), which might be due to the complete ionization of the primary phosphate groups of DNA over this pH range. This result is in agreement with the finding that Ca^{2+} showed a constant binding to DNA over the pH range of 5.0–9.5 (29). Consequently, it is considered that doxorubicin binding to nuclei might not be affected by the tissue differences of intracellular pH in the physiological region (22).

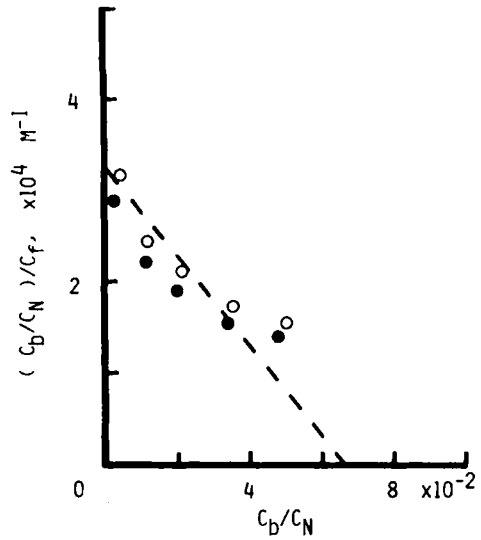

Figure 6—*Scatchard plots of the effect of pH on the binding of doxorubicin to nuclei isolated from the rat liver. The binding study was performed at 37°C in quasi-physiological buffer. The concentration of nuclei was 4.6 × 10^{-5} M as DNA in each study. Key: (○) pH 8.0; (●) pH 6.4; (---) pH 7.0, taken from Fig. 3 for comparison.*

A previous study (13) demonstrated that the *in vivo* tissue-to-plasma partition coefficient of the kidney was 1.5 times greater than that of the liver. However, in the current study no significant difference was observed between the numbers of binding sites (n = 6.70 × 10^{-2} mol/mol of DNA for liver, 6.41 × 10^{-2} mol/mol of DNA for the kidney) or the affinity constants (K_a = 4.85 × 10^5 M^{-1} for the liver, 5.41 × 10^5 M^{-1} for the kidney). Thus, the working hypothesis that the binding of doxorubicin per nuclei is constant among various tissues is supported.

As shown in Fig. 7, the degree of drug binding was similar to nuclei and chromatin. Since chromatin prepared by the procedure employed in this study had a negligible amount of nuclear membrane (14), it is probable that the binding to nuclei reflects the binding characteristics to nuclear DNA rather than to nuclear membranes. Furthermore, the nuclear membrane has numerous nuclear pores (average diameter, 90 nm) (30), so it is unlikely that the membrane permeability is an important determinant of doxorubicin binding either *in vivo* or *in vitro*, in view of the molecular weight of the drug.

A quasi-physiological buffer, which has been proposed to provide the best possible conditions on the basis of morphological examination of isolated nuclei and the intracellular concentrations of ions (15, 16), was used as the buffer for the binding study. Thus, the values of nuclear binding parameters (Figs.

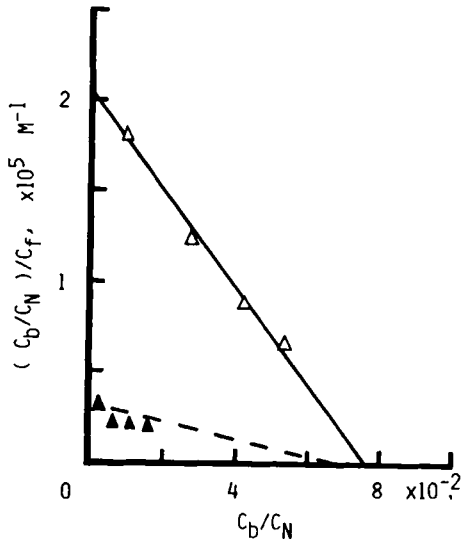

Figure 7—*Scatchard plots for the binding of doxorubicin to nuclei and chromatin prepared from rat liver nuclei. The binding was studied in two different concentrations of buffer at 37°C. The solid line was fitted by the SALS method using a digital computer. Key: (△) 10 mM Tris (pH 7.0, concentration of nuclei was 2.2 × 10^{-5} M as DNA); (▲) 135 mM sucrose, 10 mM Tris, 50 mM sodium chloride, 100 mM potassium chloride, 1 mM magnesium chloride, and 1 mM calcium chloride (concentration of nuclei was 6.5 × 10^{-5} as DNA); (---) binding curve for liver nuclei, taken from Fig. 3.*

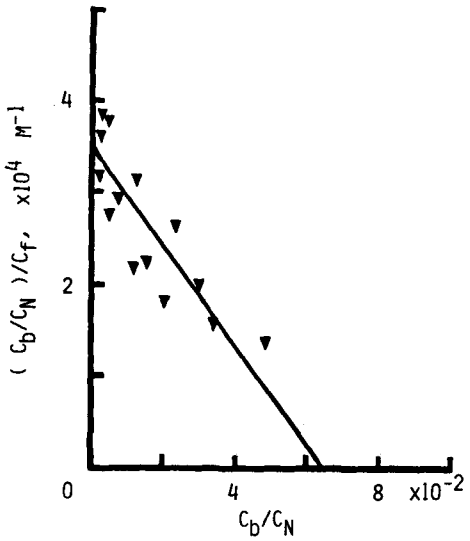

Figure 8—*Scatchard plot of data for the binding of doxorubicin to nuclei isolated from the rat kidney. The concentration of nuclei was 3.7 × 10^{-5} M as DNA. The line was fitted by the SALS method using a digital computer.*

3 and 8) obtained in this *in vitro* study might be comparable with those under *in vivo* conditions. However, further detailed study would be necessary to elucidate whether these results on *in vitro* nuclei actually reflect the *in vivo* binding.

In conclusion, no difference in the nuclear binding of doxorubicin was demonstrated between the liver and kidney, suggesting that the amount of nuclei per gram of tissue is the primary determinant of the characteristic tissue distribution of this drug.

APPENDIX: Estimation of Quantum Yield of Doxorubicin Binding to Nuclei

Rearranging Eq. 3 gives:

$$(C_b/C_f) = nK_aC_N/(1 + K_aC_f) \quad \text{(Eq. 4)}$$

According to Eq. 4, in the presence of an excess amount of nuclei doxorubicin is bound completely to nuclei.

Since the fluorescence intensity (I) of doxorubicin decreases with increasing amount of nuclei added, I gives the minimum value (I_{min}) when the drug is bound completely to nuclei, and the maximum value (I_{max}) is obtained in the absence of nuclei. The quantum yields of free (q_f) and bound (q_b) drug are defined as:

$$q_f = I_{max}/C_t \quad \text{(Eq. 5)}$$

$$q_b = I_{min}/C_t \quad \text{(Eq. 6)}$$

where C_t is the total concentration of doxorubicin. Substituting Eqs. 5 and 6 into Eq. 1 gives:

$$I = (I_{max}C_f + I_{min}C_b)/C_t \quad \text{(Eq. 7)}$$

When $K_aC_f \ll 1$, Eq. 4 is reduced to:

$$(C_b/C_f) = nK_aC_N \quad \text{(Eq. 8)}$$

Substituting Eqs. 2 and 8 into Eq. 7 gives:

$$I = (I_{max} + I_{min}nK_aC_N)/(1 + nK_aC_N) \quad \text{(Eq. 9)}$$

Thus, rearranging Eq. 9 gives:

$$I = I_{min} + (1/nK_a) \times (I_{max} - I)/C_N \quad \text{(Eq. 10)}$$

A plot of I *versus* $(I_{max} - I)/C_N$ should yield a straight line. The intercept of the ordinate gives I_{min}, and the reciprocal of the slope gives nK_a. Accordingly, the quantum yield of bound doxorubicin (q_b) can be calculated from Eq. 6.

REFERENCES

(1) A. D. Marco, F. Arcamone, and F. Zunino, in "Mechanism of Action of Antimicrobial and Antitumor Agents," Vol. 3, (J. W. Corcoran and F. E. Hahn, Eds.), Springer-Verlag, New York, N.Y., 1975, pp. 101–128.

(2) D. W. Yesair, E. Schwartzbach, D. Shuck, E. P. Denine, and M. A. Asbell, *Cancer Res.*, **32,** 1177 (1972).

(3) K. Harrison and H. N. Wagner, Jr., *J. Nucl. Med.*, **19,** 84 (1978).

(4) N. Tavoloni and A. M. Guarino, *Pharmacology*, **21,** 244 (1980).

(5) P. A. Harris and J. F. Gross, *Cancer Chemother. Rep.*, Part 1, **59,** 819 (1975).

(6) K. K. Chan, J. L. Cohen, J. F. Gross, K. J . Himmelstein, J. R. Bateman, Y. Tsu-Lee, and A. S. Marlis, *Cancer Treat. Rep.*, **62,** 1161 (1978).

(7) G. Sabeur, D. Genest, and G. Aubel-Sadron, *Biochem. Biophys. Res. Commun.*, **88,** 722 (1979).

(8) F. Zunino, R. Gambetta, A. D. Marco, and A. Zaccara, *Biochim. Biophys. Acta*, **277,** 489 (1972).

(9) F. Zunino, A. D. Marco, A. Zaccara, and R. A. Gambetta, *Biochim. Biophys. Acta*, **607,** 206 (1980).

(10) H. Waldes and M. S. Center, *Biochem. Biophys. Res. Commun.*, **98,** 95 (1981).

(11) E. Goormaghtigh, P. Chatelain, J. Caspers, and J. M. Ruysschaert, *Biochim. Biophys. Acta*, **597,** 1 (1980).

(12) T. Skovsgaard, *Biochem. Pharmacol.*, **27,** 1221 (1978).

(13) T. Terasaki, T. Iga, Y. Sugiyama, and M. Hanano, *J. Pharm. Pharmacol.*, **34,** 597 (1982).

(14) N. Sugano, Y. Gobou, and K. Shimizu, *J. Biochem.*, **86,** 1651 (1979).

(15) A. I. Lishanskaya and M. I. Mosevitsky, *Biochem. Biophys. Res. Commun.*, **62,** 822 (1975).

(16) D. Veloso, R. W. Guynn, M. Oskarsson, and R. L. Veech, *J. Biol. Chem.*, **248,** 4811 (1973).

(17) W. C. Schneider, *J. Biol. Chem.*, **164,** 747 (1946).

(18) K. Burton, *Biochem. J.*, **62,** 315 (1956).

(19) W. Meybaum, *Z. Physiol. Chem.*, **258,** 117 (1939).

(20) O. H. Lowry, N. J. Rosebrough, A. L. Farr, and R. J. Randall, *J. Biol. Chem.*, **193,** 265 (1951).

(21) T. Nakagawa, Y. Koyanagi, and H. Togawa, "SALS, a Computer Program for Statistical Analysis with Least-Squares Fitting," Library Program of the University of Tokyo Computer Center, Tokyo, Japan.

(22) A. Roos and W. F. Boron, *Physiol. Rev.*, **61,** 296 (1981).

(23) A. Jerzmanowski, K. Staron, B. Tyniec-Kroenke, and K. Toczko, *Biochim. Biophys. Acta*, **565,** 356 (1979).

(24) T. C. Spelsberg and L. S. Hnilica, *Biochim. Biophys. Acta*, **228,** 202 (1971).

(25) H. L. Rue and D. Pallotta, *Nucl. Acids Res.*, **3,** 2193 (1976).

(26) L. Kleiman and R. C. C. Huang, *J. Mol. Biol.*, **55,** 503 (1971).

(27) M. J. Egorin, R. C. Hildebrand, E. F. Cimico, and N. R. Bachur, *Cancer Res.*, **34,** 2243 (1974).

(28) W. J. Pigram, W. Fuller, and L. D. Hamilton, *Nature New Biol.*, **235,** 17 (1972).

(29) K. Y. Chang and C. W. Carr, *Biochim. Biophys. Acta*, **157,** 127 (1968).

(30) A. L. Lehninger, in "Principles of Biochemistry," Part I, Worth Publishers, New York, N.Y., 1982, pp. 15–44.

ACKNOWLEDGMENTS

This work is taken in part from a dissertation submitted by T. Terasaki to the Graduate School, Division of Pharmaceutical Sciences, University of Tokyo, Tokyo, Japan, in partial fulfillment of the requirement for the degree of Doctor of Philosophy.

This work was supported by a Grant-in-Aid for Scientific Research provided by the Ministry of Education, Science and Culture of Japan. The authors are grateful to Kyowa Hakko Co., Ltd. for the gift of the drug.

In Vivo Competition Studies with Analogues of 3-Quinuclidinyl Benzilate

WILLIAM C. ECKELMAN *§x, M. GRISSOM ‡, J. CONKLIN ‡, W. J. RZESZOTARSKI *, R. E. GIBSON *, B. E. FRANCIS *, E. M. JAGODA *, R. ENG ‡, and R. C. REBA *

Received December 16, 1982, from the *Section of Radiopharmaceutical Chemistry, The George Washington University Medical Center, Washington, DC 20037 and ‡Nuclear Sciences Division, Armed Forces Radiobiology Research Institute, Bethesda, MD 20814. Accepted for publication March 17, 1983. §Present address: National Institutes of Health, Building 10, Rm 1C488, Bethesda, MD 20205.

Abstract □ Among ligands that bind to the α- and β-adrenoceptors and to the muscarinic acetylcholine receptor (m-AChR), those that bind to the latter have the best properties for external detection of receptor sites by gamma-camera imaging. To develop the optimal radiotracer, nonradioactive analogues of 3-quinuclidinyl benzilate (I) were tested in *in vivo* displacement studies with (−)-[^{3}H]I to determine their ability to compete with (−)-[^{3}H]I for the muscarinic acetylcholine receptor. There is a linear correlation between the ability to compete with (−)-[^{3}H]I for the m-AChR and the affinity constant of the analogue as determined by *in vitro* assay, suggesting that the test is a valid indicator of *in vivo* distribution. One radioiodinated analogue, 3-quinuclidinyl *p*-iodobenzilate, bound to m-AChR in the heart and brain of rats.

Keyphrases □ 3-Quinuclidinyl benzilate—analogues, binding to α- and β-adrenoceptors and the muscarinic acetylcholine receptor, gamma-camera imaging □ Radioligand binding—3-quinuclidinyl benzilate analogues to the muscarinic acetylcholine receptor, gamma-camera imaging □ Radiotracers—development of 3-quinuclidinyl benzilate analogues for gamma-camera imaging, binding to α- and β-adrenoceptors and muscarinic acetylcholine receptor

We have attempted to develop an effective strategy for the design, synthesis, *in vitro* analysis, animal distribution studies, and clinical evaluation of receptor binding radiotracers. Because of the special requirements for receptor binding radiotracers (high effective specific activity, high chemical and radiochemical purity, low nonreceptor binding, and low rate of metabolism) the choice is crucial (1). A large investment of research effort is needed to produce a radiolabeled receptor-binding ligand; only one receptor-binding radiotracer, 16α-[^{77}Br]bromoestradiol, is presently in the clinical trial phase (2)*.

To prepare a gamma-emitting receptor-binding radiotracer we have investigated several tritium-labeled compounds that bind to the α- and β-adrenoceptor and to the muscarinic acetylcholine receptor (m-AChR). The results, both *in vitro* and *in vivo*, using the tritium-labeled compounds led us to synthesize a number of nonradioactive derivatives of I substituted with stable isotopes of the routinely used gamma-emitting radionuclides iodine-123, bromine-77 and -75, and fluorine-18 (3). These stable halogenated derivatives of I were used in *in vivo* competition studies with (−)-[^{3}H]I to determine their ability to compete with the parent structure for m-AChR and, thus, give an indication of their own distribution.

Because making each derivative with iodine-123, bromine-77, or fluorine-18 would be an overwhelming task given the requirements mentioned previously, we thought that this approach—*in vivo* competition studies—would be an efficient strategy to determine which radiotracer to pursue. We also prepared and tested a number of other receptor-binding ligands to determine the structural requirements for binding to the receptor.

EXPERIMENTAL

Radioligands—(−)-3-[^{3}H]Quinuclidinyl benzilate (I)[1], (±)-4-(3-*tert*-butylamino-2-hydroxypropoxy)-1-*H*-2-cyano-3-[^{125}I]iodoindole (II)[2], and [^{3}H]prazosin (III)[1] were used without further purification. (±)-4-(3-*tert*-Butylamino-2-hydroxypropoxy)-1-*H*-3-[^{125}I]iodoindole (IV) was prepared according to the method of Barovsky and Brooker (4). Each was determined to be >95% radiochemically pure.

Preparation of Nonradioactive Compounds—*N*-Methyl scopolamine (V)[3], scopolamine (VI)[3], benactyzine (VII)[4], α-(hydroxymethyl) 4-bromobenzeneacetic acid 8-methyl-8-azabicyclo[3.2.1]oct-3-yl ester (4-bromoatropine; VIII)[5], benztropine (IX)[6], carbetapentane (X)[7], carazolol (XI)[8], phentolamine (XII)[9], propranolol (XIII)[10], and pindolol (XIV)[11] were obtained commercially. Other compounds were prepared and purified as previously published (3). Each derivative (3 μmol) was dissolved in 3 mL of EtOH without heat. At the time of use, 3 mL of saline was added, and 2 mL of this solution was mixed with 0.075–0.100 mL of (−)-[^{3}H]I at a final concentration of 37–50 μCi/mL. A 0.1-mL aliquot was injected per animal. Each compound was analyzed by HPLC before and after use by published techniques (3) and found to be chemically pure. Each analogue of I is a mixture of the four diastereomers.

Animal Studies—The *in vivo* distribution was determined in male Sprague–Dawley rats weighing 250–300 g at the time of study. The thyroid was not blocked. Under light halothane anesthesia, 0.1 mL of radiopharmaceutical solution (3–5 μCi in 50% ethanol) was injected into an exposed femoral vein. At selected times after the injection, the animals were killed and samples of blood, ventricular muscle, lung, liver, pancreas, midbrain, and cerebellum tissues were taken. The midbrain included the corpus striatum and hippocampus along with a portion of the brain stem. No cerebral cortex or pineal gland tissue was sampled. Small samples of solid tissue (100–200 mg) and blood (25 μL) were processed overnight in tissue solubilizer and then counted after the addition of liquid scintillation cocktail. Replicate counts separated by 24 h were taken to verify the absence of chemiluminescence. The results are expressed as the percentage of the injected dose per gram of wet tissue with 95% confidence limits. This allows direct comparison to determine if differences are significant at the 95% level.

RESULTS AND DISCUSSION

From our previous survey of various receptor systems in the heart such as the α- and β-adrenoceptors and the muscarinic acetylcholine receptor (m-AChR), it became obvious that the m-AChR system has the greatest potential. From a simple biomolecular model (5) and from distribution studies using commercially available tritium-labeled ligands, 3-quinuclidinyl benzilate (I) appeared to be the best radioligand (6).

Distribution of α- and β-Adrenoceptor Binding Radiotracer—The high-affinity β-adrenoceptor ligand XI and the high affinity α-adrenoceptor ligand III showed displaceable binding in the rat heart and lung, but XI gave

[1] New England Nuclear, Boston, Mass.
[2] ^{125}ICYP; Amersham, Arlington Height, Ill.
[3] Sigma Chemical Co., St.Louis, Mo.
[4] Aldrich Chemical Co., Milwaukee, Wis.
[5] 4-Bromoatropine; Smith Kline and French, Philadelphia, Pa.
[6] Merck Sharp & Dohme, West Point, Pa.
[7] Armour Pharmaceutical, Phoenix, Ariz.
[8] Boehringer Mannheim GmbH, Mannheim, West Germany.
[9] CIBA Pharmaceutical Co., Summit, N.J.
[10] Ayerst Lab Inc., New York, N.Y.
[11] Sandoz Pharmaceutical Laboratories, Hanover, N.J.

* Note added in proof: Two additional studies in humans have appeared: H. N. Wagner, Jr., H. D. Burns, R. F. Daniels, *et al.*, *Science*, **221**, 1262 (1983) and W. C. Eckelman, R. C. Reba, W. J. Rzeszotarski *et al.*, *Science*, **223**, 291 (1984).

0022-3549/84/0400-0529$01.00/0
© 1984, American Pharmaceutical Association

Table I—Distribution of Selected α- and β-Adrenoceptor Radioligands in the Rat

	Time, h	Percent of Dose/g (95% Confidence Limits) Blood	Lung	Heart	Liver	Midbrain
[^{3}H]III						
Alone	2	0.052 (0.039–0.065)	0.301 (0.285–0.317)	0.880 (0.703–1.06)	1.80 (1.68–1.92)	0.056 (0.051–0.061)
+ 530 nmol of XII[a]	2	0.076 (0.071–0.082)	0.234 (0.206–0.263)	0.464 (0.441–0.487)	1.96 (1.71–2.21)	0.055 (0.049–0.061)
[^{3}H]XI						
Alone	2	0.175 (0.158–0.193)	4.49 (3.50–5.48)	0.392 (0.339–0.446)	0.525 (0.440–0.610)	0.090 (0.075–0.107)
+ 100 nmol of XIII[a]	2	0.097 (0.086–0.107)	1.26 (1.07–1.44)	0.201 (0.184–0.218)	0.497 (0.432–0.566)	0.080 (0.066–0.094)
[^{125}I]IV	0.25	0.494 (0.450–0.538)	2.09 (1.62–2.57)	0.326 (0.295–0.357)	—	0.054 (0.042–0.067)
	2	0.322 (0.283–0.361)	0.501 (0.371–0.632)	0.132 (0.106–0.158)	—	0.031 (0.026–0.036)
[^{125}I]II						
Alone	0.25	0.178 (0.137–0.220)	5.14 (2.40–7.88)	0.949 (0.606–1.29)	0.560 (0.334–0.787)	0.020 (0.012–0.029)
+ 100 nmol of XIV[a]	0.25	0.067 (0.053–0.080)	1.25 (0.627–1.87)	0.844 (0.380–1.31)	0.647 (0.355–0.939)	0.013 (0.001–0.024)
Alone	2	0.169 (0.139–0.199)	5.68 (5.00–6.38)	0.638 (0.498–0.777)	0.178 (0.149–0.207)	0.016 (0.012–0.020)
+ 100 nmol of XIV[a]	2	0.062 (0.052–0.069)	0.658 (0.532–0.785)	0.139 (0.108–0.168)	0.243 (0.204–0.283)	0.012 (0.007–0.018)

[a] Amount of nonradioactive compound coinjected per animal, six animals per group.

heart-to-blood (H/B) ratios of <5 (Table I) and III was not displaceable in guinea pig and rabbit (6). (±)-[^{3}H]I showed H/B ratios of >25 and displaceable binding in two species (6, 7).

Recently, three iodinated β-adrenoceptor ligands became available commercially. The first, iodohydroxybenzylpindolol (XV) gave low H/B ratios but displaceable binding in the lung (6). Two other compounds, II and IV, have also been prepared (8). Compound IV does not give high H/B ratios in the rat, but II does and also shows displaceable binding in the heart and lung (Table I). This compound appears to be useful for studying the change in concentration of β-adrenoceptors in both the heart and lung.

Very little uptake in the midbrain is observed so that this interesting location of α- and β-adrenoceptors cannot be studied with these agents (Table I). (−)-[^{3}H]I, on the other hand, shows not only high displaceable binding in the heart but also in the striatum (9). There is, therefore, an opportunity to study the change in m-AChR in these tissues if an appropriate gamma-emitting analogue of I can be prepared.

Proof of m-AChR Binding—The binding of (−)-[^{3}H]I to m-AChR in the heart and brain *in vitro* has been well documented. The burden of proof for m-AChR binding is based on the pharmacological profile whereby various agonists and antagonists are used in the *in vitro* assay, and the relative binding affinities are compared with physiological responses (10–13). We have added to this another test of binding to the m-AChR: stereospecificity. *In vitro*, the *R* and *S* isomers of I were shown to have affinity constants that differ by a factor of 58 in caudate putamen and 153 in ventricular muscle preparations (Table II). The evidence that (−)-[^{3}H]I is binding to the m-AChR *in vivo* is shown by the difference in competition of (−)-[^{3}H]I by the *R* and *S* isomers of I (Table III). The specific receptor binding relative to the nonreceptor binding can be determined in each case by comparing the concentration of (−)-[^{3}H]I in the presence and absence of an excess of competing nonradioactive ligand. Again the competition appeared to be stereoselective, with the more active isomer causing the greater displacement. We therefore conclude that we are studying binding to the m-AChR both *in vitro* and *in vivo*.

Table II—Relative Binding Index (RBI) of Derivatives of I[a]

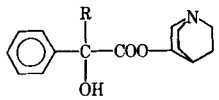

R	RBI Heart	Midbrain
C_6H_5	100	100
c-C_5H_9	155	99
c-C_6H_{11}	66	70
n-C_4H_9	55	95
4-FC_6H_4	57	110
3-FC_6H_4	95	116
4-BrC_6H_4	11	69
3-BrC_6H_4	8	84
2-BrC_6H_4	8	18
4-IC_6H_4	23	65
3-IC_6H_4	9	32
4-$NH_2C_6H_4$	6	16
(*R*)-C_6H_5	184	230
(*S*)-C_6H_5	2	4
Propargyl	1	3
C_6H_5, *N*-methyl	15	—
3-Quinuclidinyl xanthene-9-carboxylate	4	98
Atropine	3	20
Scopolamine	3	22

[a] Calculated from data in Refs. 3 and 11. The RBI is the affinity constant of each compound relative to that of (±)-I as determined by *in vitro* assay where (±)-I is 100.

Competitive Binding of Muscarinic Antagonist—Fifty nmole of each halogen analogue of I was coinjected with (−)-[^{3}H]I to determine the distribution of these nonradioactive derivatives indirectly. In the heart and midbrain the fluoro analogues are the most potent, followed by the bromo analogues, and finally the iodo analogues (Table III).

We also prepared a number of alkyl derivatives that contain a cyclohexyl, a cyclopentyl, or an *n*-butyl group in place of one aromatic ring (3) (Table IV). The cyclopentyl derivative has a higher affinity than I for the m-AChR in the heart, and this is reflected in the *in vivo* competition study (Fig. 1). This study shows that these structural changes do not adversely affect *in vivo* m-AChR binding and indicates alternate pathways to radiolabeling.

The remaining compounds are drugs that are thought to interact with the m-AChR (Table V). Compound VI is used for the relief of pylorospasm, peptic ulcer, and spastic colon. It is not as effective as I in inhibiting (−)-[^{3}H]I. The *N*-methyl quaternary derivative (V) is more potent than VI in *in vivo* displacement in the heart, but does not displace (−)-[^{3}H]I in the brain because the quaternary salt does not cross the blood–brain barrier. Compound VII is a mild antidepressant and anticholinergic agent; from the *in vivo* displacement studies it is indeed a weak displacer. Likewise VIII, a halogenated derivative of atropine, IX, an anticholinergic and antihistaminic derivative of tropine, and X, a sympathomimetic agent used in cough medicine, all are weak inhibitors of (−)-[^{3}H]I binding in all organs studied.

Correlation of *In Vitro* and *In Vivo* Results—These values for competitive blockade are in general agreement with the affinity constants determined by *in vitro* assay in our laboratory (Table II). The *in vitro* relative binding affinity was correlated with the *in vivo* displacement data using the logit–log plot (Fig. 1) (14). The logit–log plot was chosen because it uses experimental values, *i.e.*, B/B_0 (the amount of (−)-[^{3}H]I bound in the presence of nonradioactive inhibitor divided by the amount bound in the absence of inhibitor) and usually the log of the concentration of inhibitor (h):

$$\text{Logit } B/B_0 = -\log h - \log \frac{K_h}{1 + K_a L_0} \qquad \text{(Eq. 1)}$$

Since in our case the amount of (−)-[^{3}H]I injected (L_0), the affinity (K_a), and h are constant, we have chosen to plot the log of the relative binding index

Table III—Displacement of (−)-[^{3}H]I by I and Halogenated Derivatives at 2 h in the Rat

Derivative (R)[a]	Percent of Dose/g (95% Confidence Limits)					
	Blood	Lung	Heart	Liver	Midbrain	Cerebellum
3-FC_6H_4	0.085 (0.079–0.091)	0.285 (0.226–0.344)	0.284 (0.263–0.305)	0.270 (0.244–0.297)	0.508 (0.418–0.598)	0.164 (0.153–0.175)
4-FC_6H_4	0.074 (0.071–0.078)	0.277 (0.210–0.345)	0.363 (0.308–0.419)	0.215 (0.202–0.228)	0.455 (0.422–0.488)	0.170 (0.157–0.183)
3-BrC_6H_4	0.026 (0.006–0.046)	0.286 (0.216–0.356)	1.23 (1.09–1.37)	0.191 (0.164–0.218)	0.515 (0.424–0.606)	0.335 (0.289–0.382)
4-BrC_6H_4	0.060 (0.048–0.071)	0.395 (0.269–0.521)	1.86 (1.64–2.08)	0.206 (0.180–0.232)	0.462 (0.362–0.562)	0.381 (0.322–0.441)
3-IC_6H_4	0.077 (0.069–0.086)	0.462 (0.348–0.576)	2.78 (2.37–3.18)	0.214 (0.190–0.237)	0.580 (0.465–0.695)	0.474 (0.404–0.543)
4-IC_6H_4	0.091 (0.066–0.115)	0.426 (0.370–0.482)	2.12 (1.63–2.61)	0.260 (0.189–0.330)	0.722 (0.582–0.863)	0.555 (0.459–0.651)
Saline	0.063 (0.052–0.074)	0.510 (0.443–0.577)	3.99 (3.76–4.22)	—	—	—
Compound I						
0.5 nmol	0.092 (0.074–0.111)	0.364 (0.278–0.449)	1.65 (1.47–1.83)	0.243 (0.205–0.281)	0.674 (0.483–0.865)	0.481 (0.400–0.562)
5 nmol	0.092 (0.078–0.107)	0.356 (0.213–0.500)	0.409 (0.379–0.439)	0.261 (0.214–0.308)	0.659 (0.591–0.727)	0.236 (0.207–0.265)
50 nmol	0.085 (0.071–0.098)	0.346 (0.227–0.465)	0.186 (0.165–0.207)	0.289 (0.244–0.334)	0.389 (0.322–0.457)	0.121 (0.109–0.133)
500 nmol	0.136 (0.097–0.174)	0.296 (0.223–0.369)	0.120 (0.112–0.128)	0.269 (0.243–0.296)	0.092 (0.085–0.099)	0.078 (0.74–0.085)
(*R*)-I, 50 nmol	0.090 (0.067–0.114)	0.458 (0.298–0.619)	0.228 (0.199–0.257)	0.325 (0.250–0.400)	0.378 (0.305–0.451)	0.144 (0.121–0.168)
(*S*)-I, 50 nmol	0.092 (0.075–0.109)	0.571 (0.342–0.801)	3.79 (2.97–4.60)	0.306 (0.243–0.369)	0.601 (0.243–0.369)	0.527 (0.436–0.618)

[a] 50 nmol per animal of each halogenated derivative was coinjected; in the case of I the indicated amount was coinjected; six rats per group.

Table IV—Displacement of (−)-[^{3}H]I by Alkyl Derivatives at 2 h in the Rat

QNB Derivative (R)[a]	Percent of Dose/g (95% Confidence Limits)					
	Blood (B)	Lung	Heart (H)	H/B	Liver	Midbrain
c-C_6H_{11}	0.082 (0.074–0.091)	0.312 (0.236–0.338)	0.398 (0.371–0.426)	4.8	0.266 (0.218–0.314)	0.430 (0.402–0.457)
c-C_5H_9	0.072 (0.061–0.082)	0.319 (0.252–0.386)	0.206 (0.186–0.226)	2.9	0.177 (0.130–0.224)	0.210 (0.188–0.232)
n-C_4H_9	0.076 (0.062–0.091)	0.381 (0.257–0.505)	0.378 (0.281–0.475)	4.9	0.258 (0.181–0.334)	0.336 (0.278–0.393)
Propargyl	0.068 (0.058–0.078)	0.303 (0.251–0.355)	2.68 (2.39–2.97)	39.2	0.222 (0.189–0.255)	0.579 (0.532–0.627)
4-$NH_2C_6H_4$	0.081 (0.072–0.089)	0.423 (0.260–0.587)	1.64 (1.26–2.03)	20.4	0.275 (0.231–0.318)	0.515 (0.420–0.609)
3-Quinuclidinyl xanthene-9-carboxylate	0.063 (0.047–0.078)	0.351 (0.286–0.416)	3.10 (2.79–3.40)	49.4	0.201 (0.167–0.236)	0.526 (0.463–0.590)

[a] 50 nmol of the I derivative per animal was coinjected with 3.5–5 μCi (−)-[^{3}H]I [15–20 μCi/kg]; six rats per group.

Table V—Displacement of (−)-[^{3}H]I by Other Muscarinic Antagonists at 2 h in the Rat

Displacer[a]	Percent of Dose/g (95% Confidence Limits)					
	Blood (B)	Lung	Heart (H)	H/B	Liver	Midbrain
N-Methyl scopolamine	0.074 (0.068–0.081)	0.286 (0.236–0.335)	0.453 (0.400–0.507)	6.1	0.236 (0.207–0.266)	0.641 (0.547–0.736)
Scopolamine	0.104 (0.094–0.114)	0.339 (0.274–0.403)	1.79 (1.53–2.05)	17.2	0.253 (0.227–0.278)	0.546 (0.493–0.599)
Benactyzine	0.062 (0.052–0.072)	0.390 (0.336–0.443)	3.92 (3.53–4.31)	63.2	0.201 (0.165–0.237)	0.542 (0.494–0.590)
4-Bromoatropine	0.061 (0.048–0.074)	0.436 (0.340–0.533)	2.75 (1.49–4.01)	53.3	0.191 (0.165–0.218)	0.517 (0.429–0.605)
Benztropine	0.058 (0.050–0.066)	0.492 (0.399–0.586)	4.31 (3.94–4.67)	74.1	0.177 (0.123–0.231)	0.656 (0.592–0.720)
Carbetapentane	0.048 (0.044–0.053)	0.717 (0.450–0.985)	5.01 (4.62–5.41)	103.2	1.105 (0.091–0.119)	0.507 (0.448–0.566)

[a] 50 nmol of the antagonist per rat was coinjected with 3.5 to 5 μCi (−)-[^{3}H]I [15–20 μCi/kg]; six rats per group.

(RBI). The RBI is defined as the affinity of the analogue (K_h) relative to that of (±)-I as determined by *in vitro* assay, where (±)-I is 100 (Table II). Another advantage of the logit plot is the linear relationship between the logit B/B_0 and the log RBI; this linear relationship allows easier statistical analysis.

Although 50 nmol of each nonradioactive compound (h) was coinjected with the (−)-[^{3}H]I, the actual concentration of material at the receptor site is unknown. The uptake of I in the target tissues is rapid (Table VI), and therefore coinjection of the displacer with the radioligand should allow competitive binding without complications due to differing pharmacokinetics (15). This competition has been demonstrated independently by Maziere *et al.* (16) who showed that atropine could increase the washout of ^{11}C-labeled *N*-methyl-I. If irreversible binding occurred or excretion was faster than rebinding, then these results would not be possible (17). If the concentration of inhibitor is similar, the various compounds should compete with (−)-[^{3}H]I in relation to their affinities for the m-AChR provided that receptor binding is the dominant factor controlling the *in vivo* distribution.

The linear correlation equation for the heart is logit $y = 1.28 - 0.777$ ln RBI ($r^2 = 0.70$) and for the midbrain, logit $y = 3.54 - 0.679$ ln RBI ($r^2 = 0.60$), where logit y is ln $[(B/B_0)/(1 - B/B_0)]$. The correlations are reasonably good

Table VI—Pharmacokinetics of (−)-[^{3}H]I [a]

Time, min	Percent of Dose/g (95% Confidence Limits)				
	Blood	Lung	Heart	Liver	Midbrain
5	0.080 (0.47–0.114)	2.51 (1.85–3.17)	2.53 (1.51–3.56)	0.304 (0.200–0.409)	0.237 (0.147–0.326)
30	0.046 (0.041–0.050)	0.903 (0.751–1.05)	3.54 (2.93–4.16)	0.261 (0.211–0.311)	0.399 (0.270–0.528)
60	0.059 (0.053–0.065)	0.759 (0.615–0.904)	4.12 (3.30–4.93)	0.468 (0.117–1.05)	0.401 (0.319–0.484)
90	0.061 (0.049–0.073)	0.602 (0.535–0.668)	4.43 (3.75–5.12)	0.231 (0.117–0.346)	0.534 (0.425–0.644)
120	0.035 (0.030–0.040)	0.355 (0.296–0.413)	3.16 (2.91–3.41)	0.121 (0.105–0.137)	0.412 (0.353–0.471)

[a] Six rats per group.

considering the assumptions of uniform pharmacokinetics. We suggest that these results, therefore, imply the validity of these assumptions. The *p*-iodo derivative is not as potent as it ought to be based on the correlation in the midbrain (not shown in Fig. 1B, $B/B_0 = 1.07$). This suggests that iodinated I is not as available as the other derivatives for receptor binding in the brain. In general, all iodinated and brominated derivatives lie above the correlation line, indicating that they are not as readily transported to the receptor. However, the high correlation in both the heart and brain indicate that the major factor controlling the *in vivo* distribution in the target organs is the affinity for the m-AChR.

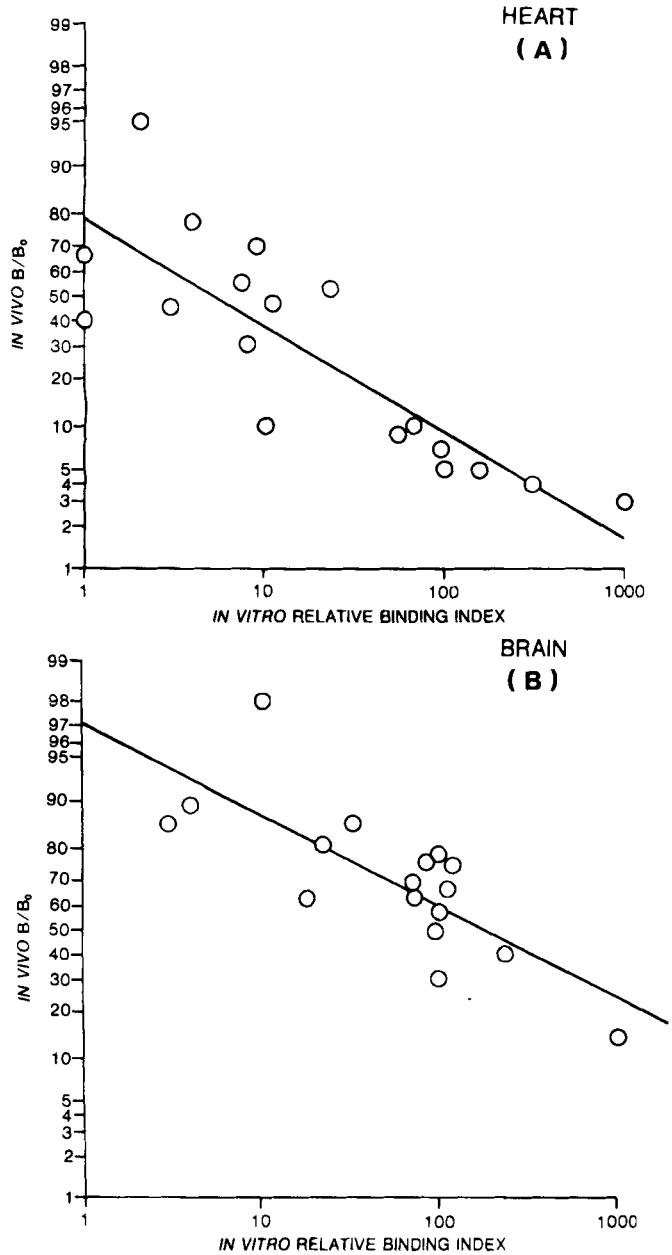

Figure 1—*Plot of logit* B/B_0 *calculated from the ratio of the percent of dose/g bound in the heart (A) and brain (B) in the presence of 50 nmol of nonradioactive analogue per animal to the percent of dose/g bound in the absence of the analogue* versus *the relative bonding index (RBI) determined by* in vitro *assay.*

Relative Displacement in the Heart and Brain—At the same concentration of nonradioactive I, more (−)-[^{3}H]I binding is inhibited in the heart than in the striatum. This could be due to either a higher concentration of m-AChR in the midbrain compared with the heart or to a decreased concentration of nonradioactive compound in the midbrain compared with the heart. From the pharmacokinetic data in Table VI, it is clear that a higher concentration (percent of dose/g) of I is obtained in the heart than in the midbrain by a factor of ≥10 despite the fact that the receptor concentration is considered greater in the striatum (12). Since amines such as I are only transported across the blood–brain barrier as the uncharged species, the differences in uptake between the heart and midbrain could be expected.

The heart-to-blood ratios for (−)-[^{3}H]I (Table VI) are significantly higher than those published for (±)-[^{3}H]I (6, 7). This shows the importance of using the highest affinity stereoisomer of the receptor ligand.

Relative Competition in the Midbrain and Cerebellum—The effect of a difference in m-AChR concentration can best be investigated by comparing the uptake of (−)-[^{3}H]I in the cerebellum and the midbrain (Table III). At maximum specific activity for (−)-[^{3}H]I (33 Ci/mmol), the uptake in the midbrain (MB) and cerebellum (C) is 0.67 and 0.48% of the dose/g, respectively, for a MB/C ratio of 1.40. As the specific activity is decreased by coinjection of I, the percent of dose/g is decreased more rapidly in the cerebellum than in the midbrain. This has the effect of producing higher MB/C ratios as the specific activity is decreased. Finally, with coinjection of 500 nmol of I the ratio is again reduced to 1.2. This can be explained by the cubic equation describing displacement (18):

$$R^2 + R(1 + K^*p^* - K^*q) - K^*q + \frac{hK_h(R+1)R}{(K_h/K^*)R + 1} = 0 \quad \text{(Eq. 2)}$$

where R is the bound/free ratio, K^* is the equilibrium affinity constant of p^*, p^* is the total concentration of radioligand, K_h is the equilibrium affinity constant of h, h is the total concentration of displacer, and q is the total concentration of receptor, provided that the midbrain contains more m-ACh receptor than the cerebellum as the *in vitro* data indicate (12). Examples of the effect of the change in conditions on the bound/free ratio are given in Table VII. It is interesting to note that Yamamura *et al.* (10) using 15 nmol of (±)-[^{3}H]I at 5 Ci/mmol suggested that the MB/C ratio of tritium was indicative of the receptor concentration, but it appears to be fortuitous that the MB/C ratio of 6 approximated the receptor concentration in their experiments. The relative displacement from the two organs appears to be a better explanation than distribution based on receptor concentration. The 2-h distribution of (−)-[^{3}H]I appears to be unrelated to receptor concentration at high specific activity of (−)-[^{3}H]I.

Distribution of Radioiodinated 3-Quinuclidinyl *p*-Iodobenzilate (XVI)—The distribution of XVI labeled with iodine-125 was studied to determine the correlation between the *in vivo* competition study and radiolabeled distribution studies (Table VIII). Four distribution studies at slightly different specific activities show that XVI does give reasonable heart-to-brain (H/B) ratios, but high lung concentration is also evident. The radioactivity is inhibited in the heart and striatum by 50 nmol of I, indicating that XVI is binding to receptor at least in part in these organs. The specific activities were determined by comparing (−)-[^{3}H]I and [^{125}I]XVI binding curves. Setting the receptor concentration equal for both curves permits the calculation of the specific activity of [^{125}I]XVI (19). Another method (20, 21) of adding nonradioactive XII (p) to [^{125}I]XII (p^*) was not sensitive to changes in the specific activity. It is only useful for low specific activity radioligands when the concentration of p and p^* are similar at receptor saturation.

Table VII—Effect of Receptor, Radioligand, and Inhibitor Concentrations on the Bound to Free Drug Ratio (B/F)

	Effect of Concentration on Calculated B/F[a]							
p^*	1.4 nM	1.4 pM	1.4 pM	1.4 nM	1.4 nM	1.4 pM	1.4 pM	1.4 nM
h	25 nM	25 nM	2.5 nM	2.5 nM	25 nM	25 nM	2.5 nM	2.5 nM
q	10 nM	10 nM	10 nM	10 nM	100 nM	100 nM	100 nM	100 nM
B/F								
Calculated	≤1	≤1	96	79	921	938	121	1201
Maximum[b]	125	125	125	125	1250	1250	1250	1250

[a] Calculated from the Cubic Equation (18) using $K^* = 12.5 \times 10^9 M^{-1}$, $K_h = 12.5 \times 10^9 M^{-1}$ for I displacing [^{3}H]I at a typical concentration of p^* (1.4 pM for iodine-125 and 1.4 nM for tritium, h, and q). [b] Calculated from $B/F = K^*q$ (5).

Table VIII—Distribution of 3-Quinuclidinyl-*p*-[^{125}I] Iodobenzilate (XVI)[a]

Displacer	Time, h	Specific Activity, kCi/mol	Percent of Dose/g (95% Confidence Limits)				
			Blood	Lung	Heart	Midbrain	Cerebellum
Saline	0.25	1195	0.118 (0.109-0.128)	5.57 (4.72-6.42)	1.03 (0.782-1.28)	0.222 (0.173-0.271)	0.180 (0.136-0.224)
I[b]	0.25	1195	0.064 (0.056-0.071)	5.66 (4.79-6.54)	0.50 (0.474-0.533)	0.200 (0.142-0.258)	0.156 (0.128-0.185)
Saline	0.25	1214	0.043 (0.035-0.051)	3.93 (2.41-5.45)	0.675 (0.530-0.820)	0.216 (0.182-0.250)	0.150 (0.120-0.179)
Saline	2	1214	0.049 (0.039-0.059)	1.43 (1.00-1.85)	0.274 (0.207-0.342)	0.333 (0.235-0.432)	0.080 (0.055-0.105)
I[b]	2	1214	0.038 (0.035-0.042)	0.961 (0.779-1.14)	0.124 (0.110-0.138)	0.069 (0.064-0.074)	0.030 (0.028-0.033)
Saline	2	—	0.026 (0.024-0.029)	0.977 (0.669-1.28)	0.190 (0.155-0.225)	—	—
I[b]	2	—	0.034 (0.029-0.039)	1.17 (0.922-1.41)	0.142 (0.117-0.167)	—	—
Saline	2	1060	0.038 (0.030-0.047)	1.07 (0.70-1.45)	0.163 (0.117-0.210)	0.176 (0.134-0.219)	0.018 (0.011-0.025)
I[b]	2	1060	0.024 (0.018-0.030)	0.88 (0.55-1.21)	0.094 (0.075-0.112)	0.049 (0.033-0.065)	0.007 (0.002-0.012)

[a] Mixture of four diastereomers. [b] 50 nmol of I per animal coinjected with [^{125}I]XVI; six rats per group.

The higher lipophilicity of XVI when compared with (−)-[^{3}H]I causes higher lung concentration and greater nonreceptor binding to tissue. This may be the cause of the lower displacing power of the nonradioactive compound in the brain. It is also of interest that XVI gives a MB/C ratio of ≥4 at high specific activity. Although it appears that XVI is distributed according to receptor concentration in the brain, recent studies suggest that the ratio is the result of more rapid washout from the cerebellum (9). Using ^{123}I-labeled XVI we were able to visualize the heart and cerebrum of the dog (22). Just as increased uptake in the receptor-containing organs was observed when we used (−)-[^{3}H]I instead of (±)-[^{3}H]I, we also expect in the case of XVI (a mixture of four disastereomers) that the percent of the dose in the receptor-containing organ will increase when the highest affinity isomer is used.

CONCLUSIONS

The *in vivo* displacement experiments show that the relative uptake is correlated with the affinity constant of all derivatives except the *p*-iodo derivative in the brain. The *m*-fluoro derivative is more potent than the *p*-fluoro derivative *in vitro* and *in vivo*. Both bromo derivatives are equally weak receptor binders *in vitro* and *in vivo*. Because of its increased concentration in nontarget organs such as the lung, the *p*-iodo derivative does not inhibit (−)-[^{3}H]I from the midbrain to the same extent as derivatives with comparable m-AChR affinities. Nevertheless, ^{125}I-labeled XVI is taken up by the m-AChR in the heart and brain, although to a lesser extent than (−)-[^{3}H]I. Images of the dog heart and midbrain have been obtained using ^{123}I-labeled XVI (22).

It appears that radioiodinated derivatives are now available for the imaging of β-adrenoceptors in the heart and lung (II) and for the imaging of m-AChR in the heart and brain (XVI). With these agents, changes in receptor concentration as a function of disease may be evaluated *in vivo* (23).

REFERENCES

(1) W. C. Eckelman (Ed.), "Receptor Binding Radiotracers," vols. I and II, CRC Press, Boca Raton, Fla., 1982.

(2) K. D. McElvany, J. A. Katzenellenbogen, S. G. Senderoff, *et al.*, *J. Nucl. Med.*, **22**, P19 (1981).

(3) W. J. Rzeszotarski, R. E. Gibson, W. C. Eckelman, *et al.*, *J. Med. Chem.*, **25**, 1103 (1982).

(4) K. Barovsky and G. Brooker, *J. Cyclic Nucleotide Res.*, **6**, 297 (1980).

(5) W. C. Eckelman, R. C. Reba, R. E. Gibson, *et al.*, *J. Nucl. Med.*, **20**, 350 (1979).

(6) B. E. Francis, W. C. Eckelman, M. Grissom, *et al.*, *Int. J. Nucl. Med. Biol.*, **9**, 173 (1982).

(7) R. E. Gibson, W. C. Eckelman, and F. Vieras, *J. Nucl. Med.*, **20**, 865 (1979).

(8) G. Engel, D. Hoyer, R. Berthold, *et al.*, *NS Arch. Pharmacol.*, **317**, 277 (1981).

(9) R. E. Gibson, E. M. Jagoda, E. M. Weckstein, *et al.*, *J. Nucl. Med.*, **23**, P104 (1982).

(10) H. I. Yamamura, M. J. Kuhar, and S. H. Snyder, *Brain Res.*, **80**, 170 (1974).

(11) H. I. Yamamura and S. H. Snyder, *Mol. Pharmacol.*, **10**, 861 (1974).

(12) R. M. Kobayashi, M. Palkovits, R. E. Hruska, *et al.*, *Brain Res.*, **154**, 13 (1978).

(13) J. A. Fields, W. J. Rocske, E. Morkin, *et al.*, *J. Biol. Chem.*, **253**, 3251 (1978).

(14) D. Rodbard, P. K. Rayford, J. A. Cooper, *et al.*, *J. Clin. Endocrinol.*, **28**, 1412 (1968).

(15) R. J. Tallarida, A. Cowan, and M. W. Adler, *Life Sci.*, **25**, 637 (1979).

(16) M. Maziere, D. Comar, J. M. Godot, *et al.*, *Life Sci.*, **29**, 2391 (1981).

(17) J. J. Frost, "Receptor Binding Radiotracers," vol. II, W. C. Eckelman, Ed., CRC Press, Boca Raton, Fla., 1982, p. 25.

(18) R. P. Ekins, G. B. Newman, and J. L. H. O'Riordan, "In Vitro Studies," R. L. Hayes, Ed., U.S. Atomic Energy Commission, Oak Ridge, Tenn., 1968, p. 59.

(19) R. E. Gibson, W. C. Eckelman, B. E. Francis, *et al.*, *Int. J. Nucl. Med. Biol.*, **9**, 245 (1982).

(20) B. T. Morris, *Clin. Chim. Acta*, **73**, 213 (1976).

(21) J. E. Roulston, *Ann. Clin. Biochem.*, **16**, 26 (1979).

(22) J. J. Conklin, M. P. Grissom, R. R. Eng, *et al.*, *J. Nucl. Med.*, **23**, P22 (1982).

(23) R. E. Gibson, "Receptor Binding Radiotracers," vol. II, W. C. Eckelman, Ed., CRC Press, Boca Raton, Fla., 1982, p. 185.

ACKNOWLEDGMENTS

This work was supported at The George Washington University Medical

Center by Grant No. HL19127 awarded by the Heart, Lung and Blood Institute, at the Armed Forces Radiobiology Research Institute by Research Work Unit 7452-00056 and 7452-00084, and by Grant No. ER60039 awarded by the Department of Energy. We appreciate the technical assistance of Mr. Ralph Will at GWU and E. Barron, N. Fleming, M. Flynn, J. Josza, J. Warrenfeltz, and M. Corral of the AFRRI. Animal research at AFRRI was conducted according to the principles enunciated in the "Guide for the Care and Use of Laboratory Animals," prepared by the Institute of Laboratory Animal Resources, National Research Council.

We would like to thank Dr. Carl Kaiser of Smith Kline and French Laboratories for 4-bromoatropine; Dr. J. W. Bastian of Armour Pharmaceutical Co. for carbetapentane; Dr. W. Bartsch of Boehringer Mannheim for carazolol; and Dr. D. J. Marshall of Ayerst for propranolol. We would also like to thank G. Rosen for preparing the manuscript.

Percutaneous Absorption of Alkanoic Acids I: A Study of Operational Conditions

ZVI LIRON and SASSON COHEN ˣ

Received December 27, 1982, from the *Department of Physiology and Pharmacology, Tel Aviv University, Sackler School of Medicine and Institute for Biological Research, Ness Ziona, Israel.* Accepted for publication October 11, 1983.

Abstract □ The rate of penetration of propionic and butyric acids through excised porcine skin was determined *in vitro* in specific apparatus allowing optimal control of operational conditions. In one technique, the rate was followed by continuous pH-stat titration of acid appearing in the perfusate, in another, by periodic monitoring of [^{14}C]propionic acid in the perfusate. With the assumption that Fick's equation applies to the process of penetration, it was found that the permeability coefficient, K_p, increases with increasing mass of neat penetrant applied per unit area to the donor side, increases with increasing concentration of penetrant in *n*-heptane as vehicle, increases with increasing temperature, E_a = 11.4 kcal/mol, and decreases with decreasing perfusion rate of the acceptor side when this rate is smaller than 60 mL/h.

Keyphrases □ Absorption, percutaneous—alkanoic acids *in vitro*, porcine skin, permeability coefficients, operational conditions □ Alkanoic acids—percutaneous absorption *in vitro*, porcine skin, permeability coefficients, operational conditions □ Permeability coefficients—alkanoic acids through porcine skin, *in vitro* percutaneous absorption, operational conditions

The process of transdermal drug absorption is a subject of current interest in the areas of pharmaceutics, applied pharmacology, and toxicology. For passage through the skin, the penetrating molecule must move first through the stratum corneum, then into the viable epidermis, the papillary dermis, and the capillary walls into the bloodstream. Scheuplein and Blank (1) analyzed the diffusional resistance of the different skin layers, and it was shown clearly that the stratum corneum is overwhelmingly dominant.

This and the passive nature of the stratum corneum enabled application of Fick's equation to the transport process across the skin. A passive system has two main characteristics: (*a*) a delay period following contact of the penetrant with the surface, during which time the membrane itself becomes charged with the penetrant and (*b*) flow across the bulk of the membrane barrier at a steady rate, which lasts as long as the penetrant remains in adequate supply on one side and is being removed from the other. The steady-state flux of penetration, J_s, is given by:

$$J_s = \frac{K_m D(C_I - C_{II})}{X} = K_p \Delta C_s \qquad \text{(Eq. 1)}$$

where $K_p = K_m D/X$. K_p is the permeability coefficient, D is the diffusion coefficient, K_m is the membrane–solution partition coefficient, and X is the thickness of the membrane. ΔC_s expresses the concentration difference under steady-state conditions between the two phases at either side of the membrane. The permeability coefficient, K_p, is physically equivalent to the solute permeability coefficient at zero-volume flow, ω, as shown by Kedem and Katchalsky (2); the relationship is given by $K_p = RT\omega$. It was shown by many workers (1) that Fick's law holds fairly well for skin whether the penetrating substance is a gas, an ion, or a nonelectrolyte.

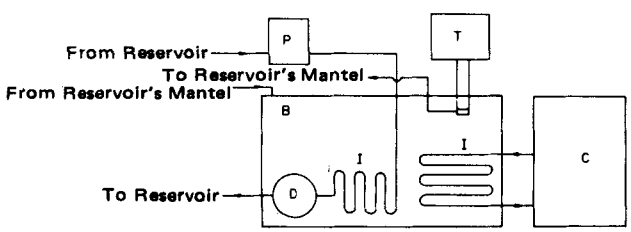

Figure 1—*Schematic representation of the pH-stat assembly. Key: (B) bath; (C) cooler; (D) diffusion cell; (I) immersion coil; (P) peristaltic pump; (T) thermostat.*

For optimal control of operational conditions, the penetration process is usually studied *in vitro*. Excised skin is used in diffusion cells in which a barrier of animal or human skin is interposed between two compartments, and the passage of compounds is measured from the epidermal surface on one side into a bathing fluid on the other side.

The present work is a pilot study of operational factors that affect the percutaneous absorption of propionic and butyric acids through excised porcine skin *in vitro*. Its main objective has been the generation of adequate knowledge to allow a systematic investigation of the permeation process by these and other members of this class of compounds. Concern with the alkanoic acids stems from an interest in the applicability of regular solution theory (3) to pharmaceutical sciences in general and to percutaneous drug application in particular. Recent accurate data (4) on the solubility parameter and molal volumes of a wide range of alkanoic acids suggested their use as candidates of choice in such a study, in preference to other potential permeating species, such as the series of alcohols used by Scheuplein (5). Compliance of the alkanoic acids with this theory is being presented in the second paper of this series (6).

The methodology used in this study is a modified extension of procedures that had been adequately described by earlier workers in this field, notably Ainsworth (7), Blank (8, 9), Wurster and Kramer (10), Scheuplein (5), Polano and Ponec

0022-3549/84/0400-0534$01.00/0
© 1984, American Pharmaceutical Association

Center by Grant No. HL19127 awarded by the Heart, Lung and Blood Institute, at the Armed Forces Radiobiology Research Institute by Research Work Unit 7452-00056 and 7452-00084, and by Grant No. ER60039 awarded by the Department of Energy. We appreciate the technical assistance of Mr. Ralph Will at GWU and E. Barron, N. Fleming, M. Flynn, J. Josza, J. Warrenfeltz, and M. Corral of the AFRRI. Animal research at AFRRI was conducted according to the principles enunciated in the "Guide for the Care and Use of Laboratory Animals," prepared by the Institute of Laboratory Animal Resources, National Research Council.

We would like to thank Dr. Carl Kaiser of Smith Kline and French Laboratories for 4-bromoatropine; Dr. J. W. Bastian of Armour Pharmaceutical Co. for carbetapentane; Dr. W. Bartsch of Boehringer Mannheim for carazolol; and Dr. D. J. Marshall of Ayerst for propranolol. We would also like to thank G. Rosen for preparing the manuscript.

Percutaneous Absorption of Alkanoic Acids I: A Study of Operational Conditions

ZVI LIRON and SASSON COHEN ˣ

Received December 27, 1982, from the *Department of Physiology and Pharmacology, Tel Aviv University, Sackler School of Medicine and Institute for Biological Research, Ness Ziona, Israel.* Accepted for publication October 11, 1983.

Abstract □ The rate of penetration of propionic and butyric acids through excised porcine skin was determined *in vitro* in specific apparatus allowing optimal control of operational conditions. In one technique, the rate was followed by continuous pH-stat titration of acid appearing in the perfusate, in another, by periodic monitoring of [^{14}C]propionic acid in the perfusate. With the assumption that Fick's equation applies to the process of penetration, it was found that the permeability coefficient, K_p, increases with increasing mass of neat penetrant applied per unit area to the donor side, increases with increasing concentration of penetrant in *n*-heptane as vehicle, increases with increasing temperature, E_a = 11.4 kcal/mol, and decreases with decreasing perfusion rate of the acceptor side when this rate is smaller than 60 mL/h.

Keyphrases □ Absorption, percutaneous—alkanoic acids *in vitro*, porcine skin, permeability coefficients, operational conditions □ Alkanoic acids—percutaneous absorption *in vitro*, porcine skin, permeability coefficients, operational conditions □ Permeability coefficients—alkanoic acids through porcine skin, *in vitro* percutaneous absorption, operational conditions

The process of transdermal drug absorption is a subject of current interest in the areas of pharmaceutics, applied pharmacology, and toxicology. For passage through the skin, the penetrating molecule must move first through the stratum corneum, then into the viable epidermis, the papillary dermis, and the capillary walls into the bloodstream. Scheuplein and Blank (1) analyzed the diffusional resistance of the different skin layers, and it was shown clearly that the stratum corneum is overwhelmingly dominant.

This and the passive nature of the stratum corneum enabled application of Fick's equation to the transport process across the skin. A passive system has two main characteristics: (*a*) a delay period following contact of the penetrant with the surface, during which time the membrane itself becomes charged with the penetrant and (*b*) flow across the bulk of the membrane barrier at a steady rate, which lasts as long as the penetrant remains in adequate supply on one side and is being removed from the other. The steady-state flux of penetration, J_s, is given by:

$$J_s = \frac{K_m D(C_I - C_{II})}{X} = K_p \Delta C_s \qquad \text{(Eq. 1)}$$

where $K_p = K_m D/X$. K_p is the permeability coefficient, D is the diffusion coefficient, K_m is the membrane–solution partition coefficient, and X is the thickness of the membrane. ΔC_s expresses the concentration difference under steady-state conditions between the two phases at either side of the membrane. The permeability coefficient, K_p, is physically equivalent to the solute permeability coefficient at zero-volume flow, ω, as shown by Kedem and Katchalsky (2); the relationship is given by $K_p = RT\omega$. It was shown by many workers (1) that Fick's law holds fairly well for skin whether the penetrating substance is a gas, an ion, or a nonelectrolyte.

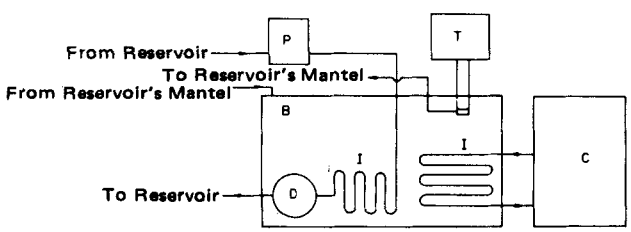

Figure 1—*Schematic representation of the pH-stat assembly. Key: (B) bath; (C) cooler; (D) diffusion cell; (I) immersion coil; (P) peristaltic pump; (T) thermostat.*

For optimal control of operational conditions, the penetration process is usually studied *in vitro*. Excised skin is used in diffusion cells in which a barrier of animal or human skin is interposed between two compartments, and the passage of compounds is measured from the epidermal surface on one side into a bathing fluid on the other side.

The present work is a pilot study of operational factors that affect the percutaneous absorption of propionic and butyric acids through excised porcine skin *in vitro*. Its main objective has been the generation of adequate knowledge to allow a systematic investigation of the permeation process by these and other members of this class of compounds. Concern with the alkanoic acids stems from an interest in the applicability of regular solution theory (3) to pharmaceutical sciences in general and to percutaneous drug application in particular. Recent accurate data (4) on the solubility parameter and molal volumes of a wide range of alkanoic acids suggested their use as candidates of choice in such a study, in preference to other potential permeating species, such as the series of alcohols used by Scheuplein (5). Compliance of the alkanoic acids with this theory is being presented in the second paper of this series (6).

The methodology used in this study is a modified extension of procedures that had been adequately described by earlier workers in this field, notably Ainsworth (7), Blank (8, 9), Wurster and Kramer (10), Scheuplein (5), Polano and Ponec

0022-3549/84/0400-0534$01.00/0
© 1984, American Pharmaceutical Association

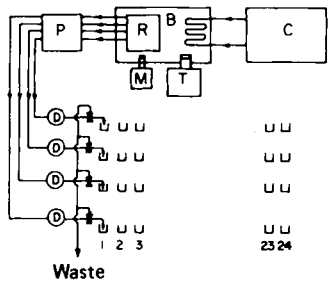

Figure 2—*Schematic representation of the automatic sampling skin penetration system, using radioisotope-labeled penetrant. Key: (B) bath; (C) cooler; (D) diffusion cell; (I) immersion coil; (M) centrifugal pump, (P) peristaltic pump; (R) perfusate reservoir; (T) thermostat; (⋈) T-valve, time actuated; (⊔) collecting vial.*

(11), and others (12). The main improvements over earlier procedures consisted in the design of the diffusion cells, which allowed much flexibility in the choice of experimental conditions, and in the automation of the perfusate sampling procedure, which was based on either of two independent methods: pH-stat titration of acid or the monitoring of isotope-labeled acid in the perfusate. Occasionally, both sampling procedures were used jointly, with remarkable agreement.

EXPERIMENTAL

Apparatus—Two procedures were used in the skin penetration studies. In one the penetration process could be followed directly by recording the titration of the acid appearing in the perfusate over a given period. This procedure however, was limited to relatively high concentrations of penetrants and to one diffusion cell at a time. In the automatic sampling system, using a radioisotope-labeled penetrant, one could use four diffusion cells in parallel and much lower concentrations of penetrant. The diffusion cells used in either procedure were almost identical, differing only in some external features.

pH-Stat System—This consisted of the diffusion cell assembly and the analyzing or titration assembly. The diffusion cell assembly is schematically shown in Fig. 1. The diffusion cell (D) was immersed in a thermostatic bath (B). The perfusate was made to flow in a closed circuit, being continuously sucked from the reservoir by a peristaltic pump (P), through an immersion coil (I), into the lower entrance of the diffusion cell, and through the exit of the diffusion cell, back to the reservoir. The flow rate in all these experiments

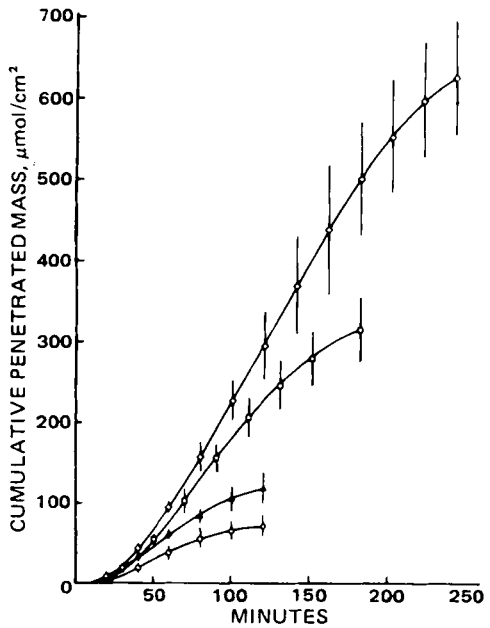

Figure 3—*Penetration of butyric acid through porcine skin at 37°C by the pH-stat procedure showing acid mass effect. Points and bars are means and* SE *from 3–5 runs. Key: (◇) 80 μL, 860 μmol; (□) 40 μL, 430 μmol; (△) 20 μL, 215 μmol; (○) 10 μL, 112 μmol.*

Table I—Penetration of Neat Butyric Acid Through Porcine Skin at 37°C [a]

Acid Applied, μL	Flux at Steady State (J_s), μmol/cm²/min	Permeability Coefficient ($K_p \times 10^3$), cm/min	Breakthrough Time, min
10	0.95	0.09	10
20	1.33	0.12	10
40	2.68	0.25	10
80	3.50	0.33	10

[a] Applied amount effect, determined by the titrimetric procedure.

was 1 mL/min. The temperature of the bath was controlled by a thermostat (T), equipped with a pump which was connected to the heating mantle of the reservoir. In cases where the room temperature was higher than the working temperature, a cooler (C) was used. The temperature in the bath was measured with a Brand thermometer, 0.1°C scale division.

The titration assembly was used in its pH-stat mode of operation. At that mode, the apparatus recorded the supply of the corresponding base required to keep the reservoir at a constant pH as a function of time. The equipment[1] included the following parts: recorder, pH meter, titrator, autoburet, stirring motor, and a reservoir equipped with a heating mantle and a combined microelectrode[2]. Nitrogen was bubbled into the reservoir to minimize access to atmospheric carbon dioxide.

The diffusion cell was of polytef and consisted of two parts assembled together to hold the skin sample. The lower part had a cylindrical hollow 1-cm² cross-circular area and 1-mL volume. Two stainless steel pipes of 1 mm i.d. entered the hollow, one at the bottom and one at the upper edge of the cylinder. Buffered solution flowing from the reservoir entered the diffusion cell through the lower pipe and left the cell, now with penetrant, through the upper pipe and back to the reservoir for titration. The skin to be tested was mounted on needle tips so that it constituted a tight barrier between the two compartments of the diffusion cell. The upper part of the diffusion cell contained suitable holes through which the needles passed, leading metal pins for convenience and accurate closing of the cell, and three screws for tightening the two parts of the cell to each other. The upper part was equipped also with a screw cap and a neoprene O-ring which enabled water-tight closure and immersion of the whole diffusion cell in the thermostatic bath.

Automatic Radioisotope Sampling System—A diagram of this system is shown in Fig. 2. The perfusate was contained in the reservoir (R) at a constant temperature maintained by the thermostat (T). When working at lower temperatures, the cooler (C) was used. The perfusate was sucked in parallel through four channels by the peristaltic pump and it was delivered into the lower entrance of each of the four diffusion cells. The perfusate containing the penetrant left each cell through the upper exit tube into the proper collecting vial. When working at high perfusate flow rates, the effluent from each diffusion cell was divided by a T-valve, electro-pneumatic actuated in a predetermined time cycle so that the proper amounts were in the vials and the rest was discarded. The 4-mL collecting vials were held in a special tray, in four rows of 24 vials each. The tray was shifted to each of its 24 positions, according to a predetermined time cycle. The tray shifting was activated by an electro-pneumatic system composed of a solenoid valve, a feeder, and two synchronic motors of 1 and 2 rph. When the tray reached its last position the whole system, including the peristaltic pump, was automatically switched off.

This experimental system was planned to work also at low perfusate flow rates and it became important to shorten, as much as possible, the distance from the exit of the diffusion cell to the sampling vial. This requirement could not be fulfilled when the cells had to be dipped into a thermostated bath. Therefore, it was decided to use diffusion cells of similar construction and design, but also equipped with a jacket for temperature control. To achieve good heat transfer, and yet work with noninteracting materials, the diffusion cells were made of stainless steel. In principle, each of the two parts of the diffusion cell could be temperature controlled independently, simulating the condition of the skin *in vivo*. In experiments in which the whole cell was kept at a single temperature, the jackets of the two parts of the diffusion cell were connected in series. The thermostatic fluid flowing through two diffusion cells was driven by the pump of the thermostat (T). The two other cells got their thermostatic fluid through the pump (M). The four diffusion cells were placed on a special tray, over and near the sampling vials tray.

Skin Samples—Intact porcine skin was used in all the experiments. Skin was clipped from the backs of male minipigs (Kibbutz Lahav strain) weighing

[1] Radiometer, Copenhagen.
[2] Ingold,type 2293.

Table II—Penetration of Propionic Acid (1 M *n*-Heptane Solution) Through Porcine Skin

Temperature[a], °C	Permeability Coefficient ($K_p \times 10^3$), cm/min	Breakthrough Time, min
50	6.72	4
37	3.00	8
30	1.64	10
25	1.25	20
15	0.81	40

[a] Temperature effect determined by titrimetric procedure.

~15 kg each. The skin was fastened to a hard board, enclosed in a plastic bag, and stored at ~−20°C until used. In preliminary tests, it was found that storage under these conditions for 2 months did not affect the penetration rate of propionic acid through the skin. The fat was carefully removed with a scalpel just before the skin sample was fastened in the diffusion cell. All samples of new skin were standardized before use by running a penetration experiment with 1 M propionic acid in *n*-heptane and by measuring the thickness of the stratum corneum, using the frozen-section technique (13).

Materials—All the compounds used in this study were of the highest analytical grade available commercially. The specific activity of [^{14}C]propionic acid was about 55 mCi/mmol; as a marker, it was diluted with "cold" propionic acid, to suitable working concentrations. The scintillation medium was prepared by mixing the following reagents, all scintillation grade: xylene (1 L), triton X-100 (0.5 L), 2,5-diphenyloxazole (6 g), and 1,4-bis-2-(4-methyl-5-phenyloxazolyl)benzene (0.15 g). The perfusate medium was phosphate buffer, pH 7.4, composed of 140 mM NaCl, 0.4 mM KH_2PO_4, and 2 mM K_2HPO_4.

Operating Procedure—At the beginning of each experiment the titration assembly was calibrated with two buffer solutions, pH 7.0 and 4.0. A 25.0-mL volume of the corresponding phosphate buffer solution was introduced into the reservoir, and *via* the peristaltic pump the buffer solution flowed into the open diffusion cell and created a dome over the cylindrical hollow. The skin was mounted on the needles, pressed by the upper part of the diffusion cell, and fastened by screws into the proper position. In mounting the skin into the diffusion cell, care was taken to exclude air bubbles. The diffusion cell was then closed by its screw cap, dipped into the thermostatic bath, and preconditioned for 2 h to wash away the intrinsic acidity of the skin. This point, when reached, could be inspected easily from the trace of the recorder. In general, during the last half-hour of the preconditioning time no acid entered the perfusate.

After the preconditioning period, the diffusion cell was taken out of the bath, the cap was removed, and the proper amount of penetrant was applied to the skin. In all experiments except those in which the influence of the neat acid was studied, the penetrating medium was applied in a volume of 0.3 mL. The cap was replaced and the diffusion cell was returned to the thermostatic bath. As the penetrating acid entered the titration reservoir, it was automatically measured by titration with base. This allowed for direct recording of the penetration curve. In experiments where titration and radioactive analysis were simultaneously performed as a cross-check, 100-μL samples were taken from the reservoir at half-hour intervals. A 3-mL volume of scintillation medium was added, and the samples were counted in a scintillation counter. Triplicate runs were made for a given set of penetration conditions.

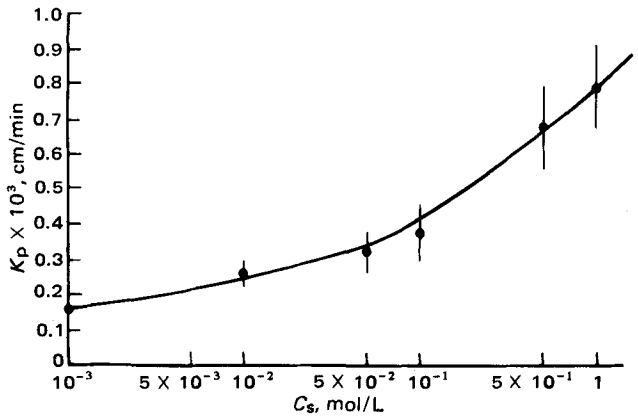

Figure 4—*Penetration of propionic acid from* n*-heptane solution through porcine skin at 25°C and at a perfusate flow rate of 3 mL/h by the radioisotope and pH-stat procedures, showing concentration effect. Points and bars are mean and* SE *from 3–5 runs.*

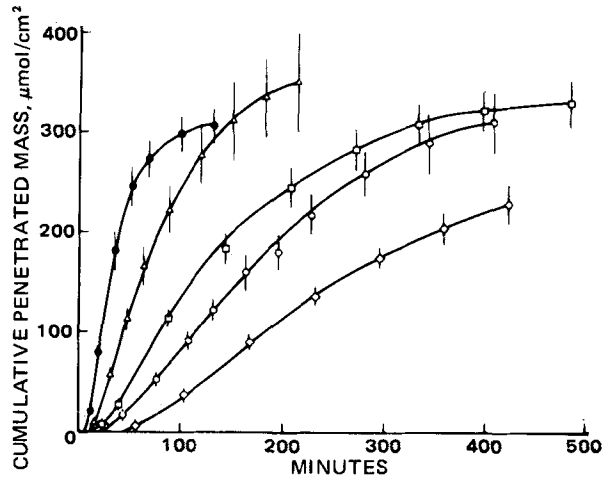

Figure 5—*Penetration of propionic acid (1 M* n*-heptane solution) through porcine skin by the pH-stat procedure, showing temperature effect. Points and bars are mean and* SE *from 3–5 runs. Key: (◇) 15°C; (○) 25°C; (□) 30°C; (△) 37°C; (●) 50°C.*

In the automatic sampling system the main procedure was essentially similar. The four diffusion cells were connected to the perfusate reservoir and the thermostatic fluid *via* flexible tygon tubing. The skin samples were mounted into the diffusion cell, the system was equilibrated for 2 h, and the penetrant was added to each of the diffusion cells. At the end of the penetration process the sampling vials were removed, and their contents were mixed with scintillation medium and counted. A 10-mL aliquot of scintillation liquid was added to 3 mL of sample; these proportions were found to give reproducible counting efficiencies. The first two samples were used as blanks for background counting immediately after the preconditioning period and before application of the penetrant.

The two techniques gave almost identical penetration curves and were complementary to each other. The titration assembly offered the advantage of direct recording of a continuous breakthrough curve and the convenience of following the penetration process in "real time." The system was simple to operate, but required use of relatively high donor phase concentrations.

In the automatic sampling system, use of radiolabeled penetrant increased the sensitivity of detection and estimation, making possible operation at low concentrations of the penetrant in the donor medium. But in this case, penetration analysis was not a continuous process as in the titration method. Samples of the perfusate were taken at distinct time intervals for analysis, the cumulative penetrating mass was calculated, and the penetration curve was drawn accordingly.

RESULTS AND DISCUSSION

Applied Mass Effect—The influence of the applied mass of the neat acid on the penetration characteristics was tested with butyric acid at 37°C. Experiments were done with 10, 20, 40, and 80 μL applied to the upper part of the skin; the corresponding penetration curves are shown in Fig. 3. The rates of penetration at steady state (J_s) and the corresponding permeability coefficients (K_p) are given in Table I; the values of K_p were calculated from Eq. 1 setting ΔC_s equal to the reciprocal molal volume of the neat acid. Breakthrough time was defined as the period taken for the first detectable penetrating molecules to appear in the perfusate.

With penetrating agents that do not interact with the skin membrane, it would be reasonable to assume that as long as the exposed skin area in the diffusion cell was covered with penetrant, the amount applied would not change the penetration curve. However, if the penetration rate depended on the amount of penetrant, as was indeed observed, then it could be reasoned that there occurred an interaction between the stratum corneum and the penetrant. From Fig. 3 it can be clearly seen that, in the early phase of penetration, the breakthrough time was similar for all amounts of acid applied. But as the process of penetration advanced further, the rate of penetration appeared to increase with the amount applied to the donor side. It is conceivable that butyric acid eventually affected the integrity of the stratum corneum barrier, which became less resistant as a barrier to the flow of the penetrant. The present finding agrees with those of Allenby *et al.* (14) who measured skin impedance changes after applying neat acids. Changes in impedance were found for neat acids, but almost no change was found for formic acid aqueous solutions (<80%).

Further insight into the effect of neat acid may be sought from a careful

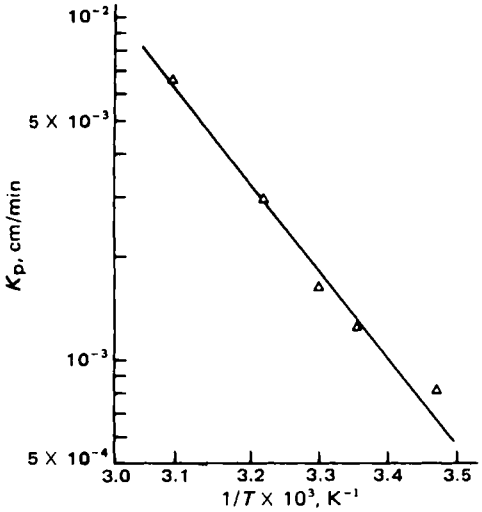

Figure 6—*Arrhenius plot of the dependence on temperature of the penetration of propionic acid (1 M n-heptane solution) through porcine skin: log* $K_p = 6.69 - 2.87 \times 10^3/T$ *(r = 0.99).*

consideration of the penetration curves (Fig. 3). There is first an exponential transient region, followed by a steady-state region, then an exponential decay region. The relative length of time for each region appears to depend on the amount of applied acid.

From the recovered fraction of the amount applied at the end of the steady-state region, it is conceivable that the eventual decline in penetration rate was due to the combined effect of depletion and a water back-diffusion process through which the acid on the donor side had become diluted to an extent that decreased its penetration. Such a process could also explain the apparent dependence of the penetration curves on the amount of compound applied, because it is expected to have a greater effect for smaller amounts of applied penetrant.

Concentration Effect—The effect of concentration was studied in the automatic sampling system using labeled propionic acid. The experiments were done at 25°C and at a perfusate flow rate of 3 mL/h; *n*-heptane solutions in the range of 0.001–1 M were used. Typical penetration curves were obtained, and the permeability coefficients, K_p, were calculated and plotted as a function of the penetrant concentration (Fig. 4). For convenience, the concentrations were drawn on a log scale. It can be seen that there is a smooth increase in the permeability coefficient as the concentration is increased. The increase in the permeability coefficient over a concentration range of three orders of magnitude is ~4.5.

The effect of concentration has been reported in many papers, but not much fundamental work has been done. It is generally taken as obvious that as the concentration increases, the flux also increases. Scheuplein and Blank (1) measured the penetration of butanol from aqueous solutions, in a concentration range of 0.01–0.3 M, and their results are consistant with the present findings; namely, there was a slight but continuous increase in the permeability coefficient as the penetrant concentration in the donor phase increased. The rate of change in K_p was larger for the higher concentrations. This change could be ascribed to altered barrier function as presumed to occur with large amounts of applied acid.

Temperature Effect—The effect of temperature on skin penetrations was studied for 1 M propionic acid in *n*-heptane. The experiments were carried out at 15°C, 25°C, 30°C, 37°C, and 50°C. The corresponding permeability coefficients are listed in Table II, and the penetration curves at these temperatures are shown in Fig. 5. A plot of log permeability coefficients against the absolute temperature reciprocal (Fig. 6) gave a straight line, the slope of which was used to derive the corresponding Arrhenius activation energy. The activation energy for propionic acid was found to be 11.4 kcal/mol. For comparison, Scheuplein and Blank (1) found values of 16.5 and 10 kcal/mol for the polar and nonpolar alcohols, respectively. It should be recalled that

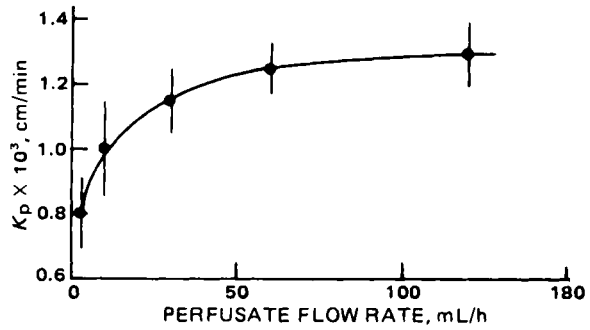

Figure 7—*Penetration of propionic acid (1 M n-heptane solutions) through porcine skin at 25°C by the pH-stat procedure, showing the effect of perfusion flow rate. Points and bars represent the mean and* SE *of 3–5 runs.*

they used a single membrane for the whole range of temperatures studied, in a procedure that took as long as 2 weeks to perform. In the present procedure, use was made of new skin samples for each experiment. The fit of results to a straight line (Fig. 6) is very good ($r = 0.99$).

This relationship, while useful, does not allow direct extrapolation to conditions that occur *in vivo*, where there is a temperature gradient across the skin. The sharp dependence of K_p on temperature implies a corresponding dependence of either K_m or D or both (Eq. 1) on the same variable. A temperature rise (or drop) across the skin may have a differential effect on each of the partitioning and diffusion steps in the overall permeation process.

Perfusate Flow Rate Effect—The perfusate flow rate is an operational factor which must be considered, especially if one intends to extrapolate from *in vitro* to *in vivo* conditions and also for a proper comparison of experimental data obtained from different sources. In a transport process where the diffusion through the membrane is the rate-limiting factor, it would be reasonable to assume that the penetration profile would not be affected by a change in the perfusate flow rate. But this would be true only for a certain range; the situation would change when the perfusate flow rate approaches zero, especially for the fast penetrants. In view of this, the effect of perfusate flow rate was considered in more detail. Accordingly, a study was made of the effect of the perfusate flow rate in the range of 3–120 mL/h, on the penetration rate of propionic acid (1 M in *n*-heptane). The results are shown in Fig. 7. As expected, the effect was pronounced at the lower perfusate flow rates, but at a flow rate of ~60 mL/h there was no further effect on permeability. Similar results were obtained by Tregear (15) for the penetration of tri-*n*-butyl phosphate through perfused porcine skin.

REFERENCES

(1) R. J. Scheuplein and I. H. Blank, *Physiol. Rev.*, **51**, 702 (1971).

(2) O. Kedem and A. Katchalsky, *J. Gen. Physiol.*, **45**, 143 (1961).

(3) J. H. Hildebrand, J. M. Pausnitz, and R. S. Scott, "Regular and Related Solutions," Van Nostrand-Reinhold, New York, N.Y., 1970.

(4) Z. Liron and S. Cohen, *J. Pharm. Sci.*, **72**, 499 (1983).

(5) R. J. Scheuplein, *J. Invest. Dermatol.*, **45**, 334 (1965).

(6) Z. Liron and S. Cohen, *J. Pharm. Sci.*, **73**, 538 (1984).

(7) M. Ainsworth, *J. Soc. Cosmet. Chem.*, **11**, 69 (1960).

(8) I. H. Blank, *J. Occup. Med.*, **2**, 6 (1960).

(9) I. H. Blank, *J. Invest. Dermatol.*, **43**, 415 (1964).

(10) D. E. Wurster and S. F. Kramer, *J. Pharm. Sci.*, **50**, 288 (1961).

(11) M. K. Polano and M. Ponec, *Arch. Dermatol.*, **112**, 675 (1976).

(12) W. Montagna, E. J. Van Scott, and R. B. Stoughton (Eds.), "Pharmacology and the Skin," Appleton-Century-Crofts, New York, N.Y., 1969.

(13) C. Blair, *Br. J. Dermatol.*, **80**, 430 (1968).

(14) A. C. Allenby, J. Fletcher, C. Schock, and T. F. S. Tees, *Br. J. Dermatol. Suppl.*, **4**, 81, 31 (1969).

(15) R. T. Tregear, "Physical Functions of the Skin," Academic, New York, N.Y., 1966.

Percutaneous Absorption of Alkanoic Acids II: Application of Regular Solution Theory

ZVI LIRON and SASSON COHEN ˣ

Received December 27, 1982, from the *Department of Physiology and Pharmacology, Tel Aviv University, Sackler School of Medicine and Institute for Biological Research, Ness Ziona, Israel.* Accepted for publication February 10, 1983.

Abstract □ The permeability coefficient, K_p, of pure unbranched alkanoic acids (C_2-C_7) applied to isolated porcine skin, reached a maximum in the solubility parameter (δ_2) range of 9.7–10 $cal^{1/2}/cm^{3/2}$. When these and other penetrants were delivered from a solvent vehicle, the following linear relationships could be demonstrated: (*a*) between log K_p and the molar attraction constant of the penetrant [$\delta_2 v_2$ or $(-Ev)^{1/2}$] for six unbranched and six branched acids delivered from 1 M solution in *n*-heptane; (*b*) between K_p and the partial molal volume difference in *n*-heptane ($\bar{v}_2 - v_2^0$) for the unbranched acids; and (*c*) between K_p and ($\bar{v}_2 - v_2^0$) for propionic acid delivered from 1 M solutions in nine solvents having δ_1 values in the range 7.4–12.7 $cal^{1/2}/cm^{3/2}$. Drug penetrability in a given series could be assessed from knowledge of the excess free energy of the penetrant in the delivery system used.

Keyphrases □ Absorption, percutaneous—alkanoic acids *in vitro*, porcine skin, permeability coefficients, application of regular solution theory □ Alkanoic acids—percutaneous absorption *in vitro*, porcine skin, permeability coefficients, application of regular solution theory □ Permeability coefficients—alkanoic acids through porcine skin, *in vitro* percutaneous absorption, application of regular solution theory

Percutaneous absorption is determined by two major processes: dissolution and diffusion. The contribution of each of these in the overall process is expressed in Fick's equation in terms of the partition coefficient and the diffusion coefficient (1). Both of these factors are affected by the molecular characteristics of the penetrant, such as solubility, size, and shape.

Solubility is dominant in skin penetration. Its importance was recognized early when it was found that compounds with both lipid and water solubilities penetrate better than substances with either high water or high lipid solubility. This led many workers to seek a correlation between skin penetrability and the partition coefficient of the penetrating compound between two reference solvents, such as ether–water (2), olive oil–water (3), benzene–water (4), and others. Later, it was recognized (3) that such partition coefficients may be misleading, since none represent the true partitioning between the penetrant and the stratum corneum.

The situation is even more complex when a vehicle is used. To ensure penetration from a vehicle, one approach utilizes the differences in thermodynamic activities of the penetrant between the vehicle and membrane phases. Ideally, such vehicles or formulations "push" the drug into the skin without causing detectable injury to the skin membrane. Intuitively, one would choose a vehicle that does not bind the incorporated drug too strongly; *i.e.*, the thermodynamic activity of the active ingredient in the vehicle should be relatively high. On the other hand, the flux is proportional to the drug concentration, and these two opposing factors lead to the conclusion that for each drug an optimal delivery system could be designed through a judicious combination of vehicle and concentration. Poulsen (5) analyzed vehicle effects for some theoretical cases in which one vehicle system, composed of two components, was used. The change in flux, related to the change in the partition coefficient and the drug concentration, was illustrated as a function of the change in the vehicle composition. The use of such an analysis in an experimental system is laborious and difficult to apply to practical problems. Thus, a more straightforward measure of vehicle effect on drug penetrability seems necessary.

Little is known about the effect of molecular size and shape on penetration through skin. An inverse relationship appears to exist between absorption rate and molecular weight (6). Small molecules penetrate more rapidly than large molecules, but within a narrow range of molecular size, there is little correlation between size and penetration rate. It has not been easy to separate the contribution of the size factor in the overall process when there is also a simultaneous change in solubility. For example, in a study of the percutaneous absorption of closely related compounds in human skin, Feldman and Maibach (7) found wide differences in penetration which could not be explained on a strict basis.

The present work deals with the application of regular so-

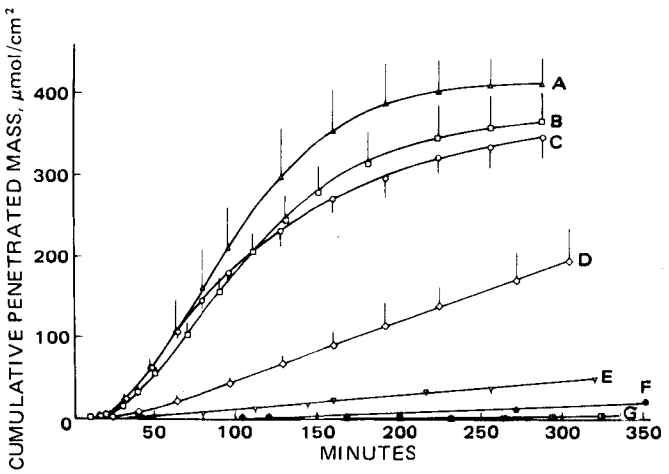

Figure 1—*Penetration of pure straight-chain alkanoic acids (430 μmol) through porcine skin at 37°C, determined by titrimetry. Number of carbon atoms: (A) 3; (B) 4; (C) 2; (D) 5; (E) 6; (F) 7; (G) 8.*

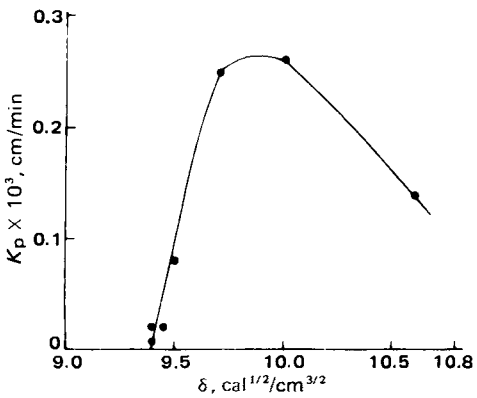

Figure 2—*Relationship between the permeability coefficient and the solubility parameter of pure straight-chain alkanoic acids.*

0022-3549/84/0400-0538$01.00/0
© 1984, American Pharmaceutical Association

Table I—Penetration of Pure Straight-Chain Alkanoic Acids Through Porcine Skin at 37°C [a]

Carbon Atoms in Molecule	Flux at Steady Rate (J_s) μmol/cm²/min	Permeability Coefficient ($K_p \times 10^3$) cm/min	Solubility[b] Parameter (δ) cal$^{1/2}$/cm$^{3/2}$
2	2.46	0.14	10.6
3	3.27	0.26	10.0
4	2.68	0.25	9.7
5	0.74	0.08	9.5
6	0.19	0.02	9.5
7	0.15	0.02	9.4
8	0.04	0.006	9.4

[a] Determined by the titrimetric procedure. [b] From Ref. 14.

lution theory (8) to the percutaneous absorption of alkanoic acids as model penetrants. This theory provides for the contribution of both solubility and size in the dissolution process.

THEORETICAL

Solubility and Molal Volume—Fick's equation was originally formulated using penetrant concentrations within the membrane:

$$J_s = \frac{D_m \Delta C_m}{X} \qquad \text{(Eq. 1)}$$

where the subscript m refers to the membrane. In the extreme case where the solubility of the penetrant in the membrane is nil, $\Delta C_m = 0$, and the flux (J_s) must vanish. The concentrations within the membrane can be related to the concentrations in the donor and receptor phases using the partition coefficient term. Fick's law is then expressed in its more familiar form; hence, knowledge of D_m and K_m should allow the prediction of drug penetrability, but these two constants are usually not accessible.

Scheuplein and Blank (3) studied the penetrability of straight-chain alcohols, members of an homologous series. They found that homologues from methanol to octanol had almost the same diffusion coefficient. Therefore, any change in the permeability coefficient could be related directly to the change in the partition coefficient or the solubility of a particular homologue. In view of this, one expects to find for members of an homologous series a correlation between the permeability coefficient K_p and K_m or its equivalent in terms of regular solution. A necessary oversimplification is the consideration of the admittedly complex structure of the skin as an homogenous phase. Such an approach would be justified if the analysis of skin penetration data could be simplified, or at least correlated with parameters predicted from regular solution theory. In this theory, the heat of mixing ΔH^M was given by Hildebrand *et al.* (9) as:

$$\Delta H^M = (X_1 v_1 + X_2 v_2)(\delta_1 - \delta_2)^2 \phi_1 \phi_2 \qquad \text{(Eq. 2)}$$

where X is the mole fraction, ϕ is the volume fraction, v is the molal volume,

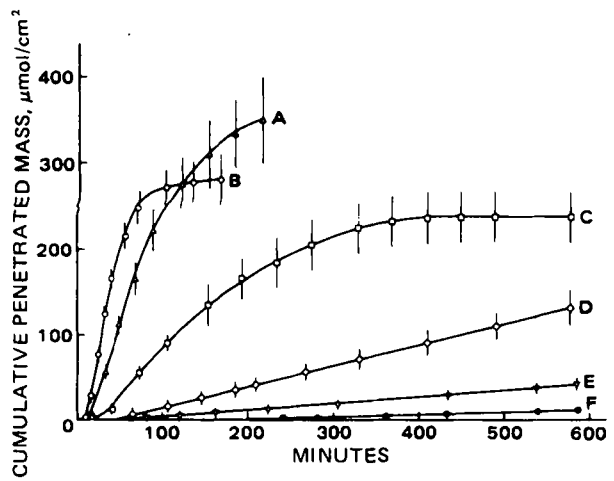

Figure 3—*Penetration of straight-chain alkanoic acids (300 μL of 1 M solutions in* n*-heptane) through porcine skin at 37°C, determined by titrimetry. Number of carbon atoms: (A) 3; (B) 2; (C) 4; (D) 5; E (6); (F) 7.*

Table II—Penetration of Straight-Chain Alkanoic Acids in Solution Through Porcine Skin at 37°C [a]

Carbon Atoms in Molecule	Permeability Coefficient $K_p \times 10^3$, cm/min	Permeability Coefficient log K_p	Difference in Partial Molal Volume at 25°C $\bar{v}_2 - v_2^0$, mL/mol	$\delta_2 v_2 = (-Ev)^{1/2}$, kcal-L$^{1/2}$/mol
2	5.86	−2.23	5.57	0.61
3	3.00	−2.52	2.90	0.75
4	1.00	−3.00	1.94	0.89
5	0.25	−3.60	0.84	1.04
6	0.08	−4.10	0.72	1.19
7	0.03	−4.52	0.05	1.35

[a] Determined by the titrimetric procedure using 300 μL of 1 M solutions in *n*-heptane.

and subscripts 1 and 2 relate to the solute and solvent, respectively[1]. The Gibbs free energy change in the mixing process is given by:

$$\Delta F^M = \Delta H^M - T\Delta S^M \qquad \text{(Eq. 3)}$$

The smaller ΔF^M the more compatible the elements being mixed. This means that the best mixing conditions will be achieved when δ_2 approaches δ_1. If we consider the stratum corneum membrane as a solvent having an average solubility parameter δ_1, different molecules will dissolve and penetrate through this medium in accordance with their specific solubility parameter, δ_2.

Davis (10) expressed the relationship between solubility parameter and partition coefficient, and later Srebrenik and Cohen (11) developed a more refined expression that takes into account partial molal volume changes. The partition coefficient was given by:

$$\ln K_m = \frac{-2\delta_1\delta_2}{RT} v_2 + \frac{\delta_1^2}{RT}\bar{v}_{21} - \frac{\bar{v}_{21}}{v_1} - \left(-2\frac{\delta_3\delta_2}{RT} v_2 + \frac{\delta_3^2}{RT}\bar{v}_{23} - \frac{\bar{v}_{23}}{v_3}\right) \qquad \text{(Eq. 4)}$$

where K_m is the partition coefficient, subscript 2 refers to solute which partitions between two phases (subscripts 1 and 3), and $\bar{v}_{21}$ and $\bar{v}_{23}$ are the partial molal volumes of solute 2 in phase 1 and phase 3, respectively. The application of Eq. 4 to skin transport analysis is not straightforward, but nevertheless it could be used with approximation, as will be shown later. A dissolution process is accompanied by a change in the molal volume of the solute. The degree of this change depends on the similarity between the solute-solvent pair; for low solute concentrations it is given by:

$$\frac{\bar{v}_2 - v_2^0}{v_2^0} = \frac{(\delta_1 - \delta_2)^2}{(\partial E/\partial v)_T} \qquad \text{(Eq. 5)}$$

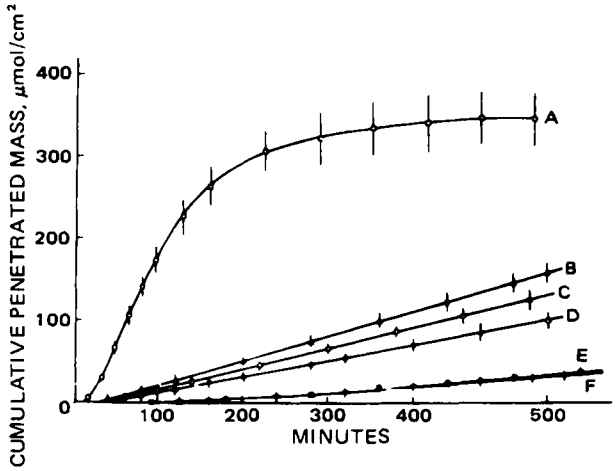

Figure 4—*Penetration of branched alkanoic acids (300 μL of 1 M solutions in* n*-heptane) through porcine skin at 37°C, determined by titrimetry. Key: (A) Cyclopropane carboxylic; (B) 3-methylbutyric; (C) 2-methylbutyric; (D) pivalic; (E) 3,3-dimethylbutyric; (F) 2-ethylbutyric, superimposed on (E).*

[1] For the sake of consistency with previous publications and throughout this article, the subscript 2 refers only to solute or penetrant, subscripts 1 or 3 refer to solvents or biophase.

Table III—Penetration of Branched-Chain Alkanoic Acids in Solution Through Porcine Skin at 37°C [a]

Acid	Permeability Coefficient $K_p \times 10^3$, cm/min	Permeability Coefficient log K_p	Solubility[b] Parameter (δ), cal$^{1/2}$/cm$^{3/2}$	$\delta_2 v_2 = (-Ev)^{1/2}$, kcal·L$^{1/2}$/mol
Butyric	1.00	−3.00	9.7	0.89
Cyclopropane-carboxylic	2.28	−2.64	9.5	0.76
3-Methylbutyric	0.31	−3.51	9.6	1.06
2-Methylbutyric	0.26	−3.59	9.3	1.02
Pivalic	0.20	−3.70	10.3	1.13
3,3-Dimethylbutyric	0.08	−4.10	9.3	1.19
2-Ethylbutyric	0.07	−4.15	9.5	1.20

[a] Determined by the titrimetric procedure using 300 μL of 1 M solutions in *n*-heptane. [b] From Ref. 14.

For solutions obeying regular solution theory, the solute excess free energy is directly proportional to the change in the solute partial molal volume (12):

$$\Delta F_2^{ex} = (\bar{v}_2 - v_2^0)(\partial E/\partial v)_T \qquad \text{(Eq. 6)}$$

The excess free energy of the solute in the donor phase is an important parameter that may be considered as the driving force for the penetration process through the skin membrane. Since the value of the excess free energy is higher, the flux (and hence the permeability coefficient) is increased. In principle, knowledge of δ_2 and v_2^0 of a particular homologue in a given series should allow the prediction of its relative penetrability through a common membrane, in this case the stratum corneum.

EXPERIMENTAL

The experimental system used has been described in detail in the previous paper (1). All skin penetration experiments were done on excised porcine skin maintained at 37.0°C or 25.0°C on either side of the membrane. Pure penetrants were applied to the donor side in a constant mass. Solutions of penetrants in *n*-heptane (1 M) were applied in a constant volume. The total penetrated mass over time was determined either by automatic titration of acid appearing in the perfusate or by scintillation counting of the carbon-14 radioisotope label added to the penetrant (1).

The effect on the skin of the pure solvent as vehicle was studied by simulating penetration experiments in diffusion cells with no penetrant added. The skin was removed after 5 and 20 h, and the condition and thickness of the stratum corneum were examined using the paraffin and frozen-section techniques (13). No significant changes were observed from untreated skin.

Partial molal volumes of penetrants ($\bar{v}_2$) at high dilution in a given solvent were determined by a previously described densitometric procedure (14). All

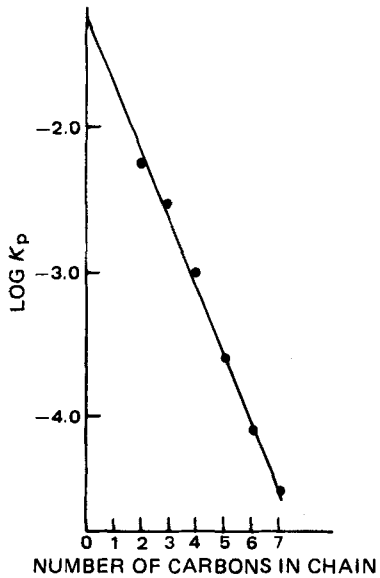

Figure 5—*Penetration of straight-chain alkanoic acids (1 M in* n*-heptane) through porcine skin at 37°C. Permeability coefficient as a function of the number of carbons in the chain; log* $K_p = -1.17 - 0.48n$ *(r = 1.00).*

Table IV—Vehicle Effect on the Penetration of Propionic Acid from 1 M Solutions Through Porcine Skin at 25°C [a]

Solvent	Permeability Coefficient $K_p \times 10^3$, cm/min	Permeability Coefficient log K_p	Solubility[b] Parameter of Solvent (δ_1), cal$^{1/2}$/cm$^{3/2}$	Partial Molal Volume Change ($\bar{v}_2 - v_2^0$), mL/mol
Heptane	1.25	−2.90	7.4	2.90
Cyclohexane	1.67	−2.78	8.2	4.84
Carbon Tetrachloride	0.92	−3.04	8.6	1.83
Toluene	0.88	−3.06	8.9	0.83
Chlorobenzene	0.80	−3.10	9.5	0.49
o-Dichloroben-zene	0.69	−3.16	10.0	0.41
Bromonaph-thalene	0.41	−3.39	10.6	0.02
Nitroethane	0.10	−4.00	11.1	−0.82
Acetonitrile	0.006	−5.22	11.9	−1.47
Nitromethane	0.007	−5.15	12.7	−1.15

[a] Determined by the radioisotope procedure. [b] Taken from Ref 17.

chemicals and solvents were of the highest analytical grade available commercially.

RESULTS AND DISCUSSION

Pure Straight-Chain Alkanoic Acids—The donor phase consisted of 430 μmol of each tested compound. The acids may be classified into two main groups according to the rate of penetration (Fig. 1; Table I). The faster penetrants were the acetic–butyric acids; the slower ones were hexanoic–octanoic acids; valeric acid had an intermediate penetration rate. The slower penetrants showed a steady penetration rate over the entire experimental period, whereas the more rapid penetrants showed a characteristic curve (1) with a lag phase region, a steady-state region, and a decay region. The latter could be due to the decline in penetrant mass at the donor side or its dilution with water through back-diffusion. Propionic acid, rather than acetic acid, had the highest rate of penetration. A plot of the permeability coefficients of these acids as a function of their solubility parameter (Fig. 2), shows a maximum at $\delta_2 = 9.7 - 10.0$ cal$^{1/2}$/cm$^{3/2}$. This range could be taken to represent the solubility parameter of the stratum corneum, but with the reservation that the lower acids could considerably alter this parameter with increasing applied mass, as observed earlier for butyric acid (1).

Straight and Branched-Chain Alkanoic Acids—*n-Heptane Solution Experiments*—The problem encountered in the use of the pure penetrants could be minimized by studying penetration rates from dilute solutions in a relatively "inert" solvent, in this case *n*-heptane. The penetration of the straight-chain alkanoic acids, delivered from 300 μL of 1 M solutions in this solvent, is shown in Fig. 3. From the penetration curves thus obtained, the permeability coefficients were calculated and tabulated with the corresponding values of the partial molal volume differences, ($\bar{v}_2 - v_2^0$ determined at 25°C) and the values of the square root of the volume–cohesive energy product or $\delta_2 v_2^0$ (Table II). The value ($\bar{v}_2 - v_2^0$) is proportional to excess free energy ΔF_2^{ex} at infinite dilution in *n*-heptane (Eq. 6); $\delta_2 v_2^0$ is the molar attraction constant of the penetrant, irrespective of vehicle used. On theoretical grounds (Eq. 4), there should exist a correlation between K_m (and hence K_p) and each of these parameters. The penetration data of some branched alkanoic acids are given separately (Fig. 4, Table III). Cyclopropane carboxylic acid was the fastest penetrant, whereas the isomeric 3,3-dimethylbutyric and 2-ethylbutyric acids were the slowest, both showing a similar penetration profile.

From Fig. 5, the correlation between log K_p and the number of carbon atoms in the molecule of unbranched acids is very good ($r = 1.00$). A similar result was obtained by Scheuplein and Blank (3) for normal alcohols in aqueous solution.

In view of the linear relationship between the number of carbon atoms in the molecule and log K_p on the one hand, and the number of carbon atoms and the square root of the volume–cohesive energy product $(-Ev)^{1/2}$ or $\delta_2 v_2^0$ (14) on the other, one expects to find a linear relationship between $(-Ev)^{1/2}$ and log K_p. Such a plot is shown in Fig. 6 where K_p had been derived from data at 37°C, but $(-Ev)^{1/2}$ from data at 25°C. The linearity of the plot should not be affected by this difference in temperature since it can be demonstrated (15) that in related compounds with an almost common thermal expansion coefficient:

$$(\delta v)_T = (\delta v)_{T^0} \cdot \text{constant} \qquad \text{(Eq. 7)}$$

Remarkably, the branched-chain homologues follow the same relationship. The fit to a straight line [$\log K_p = -0.16 - 3.26(-Ev)^{1/2}$] is very good ($r =$

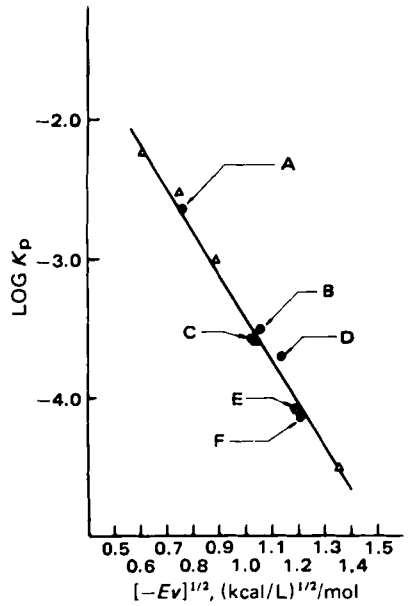

Figure 6—*Penetration of alkanoic acids through porcine skin at 37°C. Permeability coefficient as a function of the square root of the volume cohesive energy product: log* $K_p = -0.16 - 3.26(-Ev)^{1/2}$, (r = 0.99). *See Fig. 4 for key; Δ refers to straight-chain acids.*

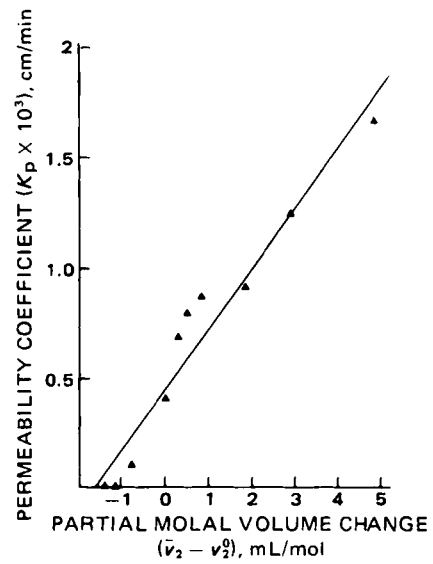

Figure 7—*Penetration of propionic acid from 1 M solutions through porcine skin at 25°C showing vehicle effect.* $K_p = 4.57 \times 10^{-4} + 2.75 \times 10^{-4}(\bar{v}_2 - v_2^0)$.

0.99). This relationship is important because it enables one to evaluate the permeability coefficient of an untested acid from its solubility parameter (δ_2) and molal volume (v_2^0). In this context, there is some analogy between the present findings and the demonstration by Ostrenga (16) of the relationship between the molal attraction constant and the relative degree of drug-receptor interaction for several different groups of structurally related compounds.

From Fig. 6 and Eq. 4 one can derive the following empirical relationship (see the *Appendix*):

$$\ln K_p \simeq \frac{-2(\delta_1 - \delta_3)}{RT}\delta_2 v_2^0 + b \qquad \text{(Eq. 8)}$$

where $\delta_1 = \delta_m$, the solubility parameter of the stratum corneum; $\delta_3 = 7.4$, the solubility parameter of *n*-heptane; and *b* (constant) = −0.16. From the slope (−3.26), temperature (310 K), and any given value of $\delta_2 v_2^0$, it can be shown that $\delta_1 \simeq 9.7$. This value is compatible with the rapid penetration rates found for pure propionic and butyric acids (Figs. 1 and 2), which have comparable δ_2 values.

In an alternative approach, a plot of K_p at 37°C as a function of the net molal expansion ($\bar{v}_2 - v_2^0$), at infinite dilution in *n*-heptane at 25°C (Table II) gave a straight line (not shown) with an acceptable correlation coefficient ($r = 0.97$) for this type of experiment. This means that permeability could be related to excess free energy (Eq. 6). As this last function becomes larger for a given solvent-solute system the permeability coefficient of the penetrant through the skin should increase.

Vehicle Effect—The vehicle effect was studied for 1 M propionic acid solutions in the solvents listed in Table IV. The penetration experiments with *n*-heptane through bromonaphthalene were done in the titration assembly system, whereas those with nitroethane through nitromethane were done in the automatic radioisotope sampling system. Experiments with *n*-heptane were also carried out in the last system as a cross-check.

If regular solution behavior were to hold throughout the whole range of solvents used, Eqs. 5 and 6 predict a parabolic relationship between K_p and δ_1, with a minimum in penetration rate for the solvent having the closest solubility parameter to that of propionic acid. However, the experimental data show a steady decrease in K_p as one moves from *n*-heptane to nitromethane (a monotonous increase in the solubility parameter). The reason for this phenomenon might be due to the breakdown of regular solution behavior beyond a certain polarity ($\delta_1 > 10$).

Irrespective of this apparent discrepancy it is still possible to analyze the vehicle effect by use of the excess free energy approach. Figure 7 is a plot of the permeability coefficient K_p as a function of the partial molal volume change; the fit, over this wide range, is very good ($r = 0.97$). This function also accounts for the higher permeability coefficient of the penetrant in cyclohexane ($\delta_1 = 8.2$) relative to *n*-heptane ($\delta_1 = 7.4$). Negative values of $\bar{v}_2 - v_2^0$ for nitroethane, acetonitrile, and nitromethane are also well correlated with the change in the permeability coefficient. The excess free energy is a measure of the force driving the penetrant molecule from its solution in a given vehicle. The determination of the partial molal volume of the penetrant in a given solvent affords an excellent means for the assessment of its delivery into the skin.

APPENDIX

The following applies to penetrants that are members of an homologous series delivered from a common solvent vehicle into a common skin sample. Under these conditions, δ_1, δ_3, v_1, and v_3 become constant and Eq. 4 can be written:

$$\ln K_m = \frac{-2(\delta_1 - \delta_3)}{RT}\delta_2 v_2^0 + \bar{v}_{21}a_1 - \bar{v}_{23}a_2 \qquad \text{(Eq. 9)}$$

where a_1 and a_2 are constants.

If the differences between the partial molal volumes of the solute in each of the three phases considered is negligible, then:

$$v_2^0 \simeq \bar{v}_{21} \simeq \bar{v}_{23} \qquad \text{(Eq. 10)}$$

For an homologous series:

$$v_2^0 = a_3 + a_4 \cdot n \qquad \text{(Eq. 11)}$$

where a_3 and a_4 are constants and $n = 0,1,2,3\ldots$ Eq. 9 now becomes:

$$\ln K_m = \frac{-2(\delta_1 - \delta_3)}{RT}\delta_2 v_2^0 + (a_1 - a_2)(a_3 + a_4 \cdot n) \qquad \text{(Eq. 12)}$$

For low *n* values $a_3 > a_4 \cdot n$, and the expression $(a_1 - a_2)(a_3 + a_4 \cdot n)$ is practically constant. Even at $n = 5$ (equivalent to heptanoic acid), the change in the value $(a_1 - a_2)(a_3 + a_4 \cdot n)$ is still small compared with the value of $-2(\delta_1 - \delta_3)/RT\ \delta_2 v_2^0$, so that:

$$\ln K_m \simeq \frac{-2(\delta_1 - \delta_3)}{RT}\delta_2 v_2^0 + a_5 \qquad \text{(Eq. 13)}$$

where a_5 is a constant.

In an homologous series, D_m is almost constant, therefore:

$$\ln K_p \simeq \ln K_m + \text{constant} \qquad \text{(Eq. 14)}$$

or

$$\ln K_p \simeq \frac{-2(\delta_1 - \delta_3)}{RT}\delta_2 v_2^0 + \text{constant} \qquad \text{(Eq. 8)}$$

REFERENCES

(1) Z. Liron and S. Cohen, *J. Pharm. Sci.*, **73**, 534 (1984).

(2) C. F. Vickers, in "Modern Trends in Dermatology," R. M. B. McKenne, Ed., Butterworths, London, 1966, chap. 4.

(3) R. J. Scheuplein and I. H. Blank, *Physiol. Rev.*, **51**, 702 (1971).

(4) R. B. Stoughton, W. E. Clendenning, and D. Kruse, *J. Invest. Dermatol.*, **31**, 255 (1959).
(5) B. J. Poulsen, in "Advances in Biology of Skin Vol. XII," W. Montagna, E. J. Van Scott, and R. B. Stoughton, Ed., Appleton-Century-Crofts, New York, N.Y., 1969.
(6) R. T. Tregear, "Physical Functions of the Skin," Academic, New York, N.Y., 1966.
(7) R. J. Feldman and H. I. Maibach, *J. Invest. Dermatol.*, **54**, 399 (1970).
(8) J. H. Hildebrand, J. M. Prausnitz, and R. S. Scott, "Regular and Related Solutions," Van Nostrand-Reinhold, New York, N.Y., 1970.
(9) J. H. Hildebrand, J. M. Prausnitz, and R. S. Scott, "Regular and Related Solutions," Van Nostrand-Reinhold, New York, N.Y., 1970 p. 86.
(10) S. S. Davis, *Experientia*, **26**, 671 (1970).
(11) S. Srebrenik and S. Cohen, *J. Phys. Chem.*, **80**, 996 (1976).
(12) J. H. Hildebrand, J. M. Prausnitz, and R. S. Scott, "Regular and Related Solutions," Van Nostrand-Reinhold, New York, N.Y., 1970 p. 185.
(13) C. Blair, *Br. J. Dermatol.*, **80**, 430 (1968).
(14) Z. Liron and S. Cohen, *J. Pharm. Sci.*, **72**, 499 (1983).
(15) J. H. Hildebrand and R. L. Scott, "Solubility of Nonelectrolytes," 3rd ed., Reinhold, New York, N.Y., 1950; p. 434.
(16) J. A. Ostrenga, *J. Med. Chem.*, **12**, 349 (1968).
(17) A. F. Barton, *Chem. Rev.*, **75**, 731 (1975).

ACKNOWLEDGMENTS

The authors thank Dr. Alfred Martin, Drug Dynamics Institute of the University of Texas School of Pharmacy, for reading the original text and making helpful criticism.

Quantitative Analysis of Trimethobenzamide Hydrochloride by Ion-Pair Column Chromatography and Semiquantitative Analysis of 3,4,5-Trimethoxybenzoic Acid by Thin-Layer Chromatography

HELEN NAVIASKY

Received November 23, 1982, from the *Food and Drug Administration, Baltimore, MD 21201.* *Accepted for publication March 29, 1983.*

Abstract □ An ion-pair column chromatographic/UV spectrophotometric method for assaying trimethobenzamide hydrochloride in capsules and injections is presented, as well as a method for the detection of 3,4,5-trimethoxybenzoic acid in trimethobenzamide hydrochloride bulk drug and dosage forms. Results obtained by the USP XX, Pharmacopeial Forum, and ion-pair column assay procedures are compared, and results of a collaborative study of the proposed assay and impurity detection methods are presented.

Keyphrases □ Trimethobenzamide hydrochloride—quantitative analysis by ion-pair column chromatography, semiquantitative analysis of 3,4,5-trimethoxybenzoic acid □ 3,4,5-Trimethoxybenzoic acid—semiquantitative analysis by thin-layer chromatography, quantitative analysis of trimethobenzamide hydrochloride □ Ion-pair column chromatography—quantitative analysis of trimethobenzamide hydrochloride, semiquantitative analysis of 3,4,5-trimethoxybenzoic acid by thin-layer chromatography

Monographs (1, 2) for trimethobenzamide hydrochloride (I) in capsules and injections have several shortcomings. The USP (1) assay method for the capsules involves direct dilution in 0.1 M HCl and UV spectrometric comparison with the USP reference standard. This procedure does not separate possible impurities, such as 3,4,5-trimethoxybenzoic acid (II), or interfering excipients. The *Pharmacopeial Forum* (PF) assay for injection preparations (2) also involves a UV assay which has several shortcomings.

This paper describes an ion-pair column chromatographic assay procedure, in which I is quantitatively removed from an aqueous acidic chloride column with a chlorinated organic solvent. Ether is used to remove phenolic ingredients and breakdown products prior to the elution of I.

Also, a TLC procedure is reported for the detection of II in amounts as low as 0.25% of the weight of I. Compound II is both a synthetic precursor and a breakdown product of I and could be encountered as a contaminant in drug preparations.

Table I—Recovery Data for I using the Proposed Ion-Pair, USP, and PF Injection Assay Methods

	Column Ion Pair	USP Injection	PF Injection
I, mg	8	200	200
Number of assays	10	10	10
Mean amount recovered, %	99.4	96.6	97.6
Range, %	98.3–101.0	95.4–98.1	96.1–98.4
SD	0.81	0.91	0.68
CV, %	0.82	0.94	0.70

EXPERIMENTAL

Reagents—Trimethobenzamide hydrochloride USP reference standard[1] was dried at 105°C for 4 h prior to use. Methylene chloride[2], pentane[2], and ether[2] were commercial distilled-in-glass grade. Compounds I[3] and II[3], chromatographic diatomaceous earth[4], glass wool, and the other reagents were used as received.

Apparatus—An ultrasonic bath, chromatographic tubes[5], a tamping rod[5], commercial TLC plates coated with a 250-μm layer of silica gel with a fluorescent indicator, a suitable TLC developing chamber, and a recording UV spectrophotometer were used.

Standard Preparation—Approximately 10 mg of trimethobenzamide hydrochloride USP reference standard was accurately weighed and transferred to a 100-mL volumetric flask. Methylene chloride (70 mL) was added, and the mixture was sonicated. The resulting solution was diluted to volume with methylene chloride. A 20-μg/mL solution was obtained by diluting quantitatively and stepwise with methylene chloride.

Chromatographic Column—A pledget of fine glass wool was packed in the base of a chromatographic column. A flexible spatula was used to mix 1 g of chromatographic diatomaceous earth with 500-μL of 1 M HCl in a 50-mL beaker. The mixture was transferred to a column and tamped.

Capsule Assay Preparation—The contents of ≥20 capsules were transferred to a tared container, and the average weight/capsule was determined. The

[1] USP Reference Standards; U.S. Pharmacopeial Convention, Rockville, Md.
[2] Burdick and Jackson Laboratories, Muskegon, Mich.
[3] Hoffmann-LaRoche, Inc., Nutley, N.J.
[4] Celite; Johns Manville Corp, New York, N.Y.
[5] *AOAC Book of Methods 13th Ed.*, 37.002(a) and (b) (3).

0022-3549/84/0400-0542$01.00/0
© 1984, American Pharmaceutical Association

(4) R. B. Stoughton, W. E. Clendenning, and D. Kruse, *J. Invest. Dermatol.*, **31**, 255 (1959).
(5) B. J. Poulsen, in "Advances in Biology of Skin Vol. XII," W. Montagna, E. J. Van Scott, and R. B. Stoughton, Ed., Appleton-Century-Crofts, New York, N.Y., 1969.
(6) R. T. Tregear, "Physical Functions of the Skin," Academic, New York, N.Y., 1966.
(7) R. J. Feldman and H. I. Maibach, *J. Invest. Dermatol.*, **54**, 399 (1970).
(8) J. H. Hildebrand, J. M. Prausnitz, and R. S. Scott, "Regular and Related Solutions," Van Nostrand-Reinhold, New York, N.Y., 1970.
(9) J. H. Hildebrand, J. M. Prausnitz, and R. S. Scott, "Regular and Related Solutions," Van Nostrand-Reinhold, New York, N.Y., 1970 p. 86.
(10) S. S. Davis, *Experientia*, **26**, 671 (1970).
(11) S. Srebrenik and S. Cohen, *J. Phys. Chem.*, **80**, 996 (1976).
(12) J. H. Hildebrand, J. M. Prausnitz, and R. S. Scott, "Regular and Related Solutions," Van Nostrand-Reinhold, New York, N.Y., 1970 p. 185.
(13) C. Blair, *Br. J. Dermatol.*, **80**, 430 (1968).
(14) Z. Liron and S. Cohen, *J. Pharm. Sci.*, **72**, 499 (1983).
(15) J. H. Hildebrand and R. L. Scott, "Solubility of Nonelectrolytes," 3rd ed., Reinhold, New York, N.Y., 1950; p. 434.
(16) J. A. Ostrenga, *J. Med. Chem.*, **12**, 349 (1968).
(17) A. F. Barton, *Chem. Rev.*, **75**, 731 (1975).

ACKNOWLEDGMENTS

The authors thank Dr. Alfred Martin, Drug Dynamics Institute of the University of Texas School of Pharmacy, for reading the original text and making helpful criticism.

Quantitative Analysis of Trimethobenzamide Hydrochloride by Ion-Pair Column Chromatography and Semiquantitative Analysis of 3,4,5-Trimethoxybenzoic Acid by Thin-Layer Chromatography

HELEN NAVIASKY

Received November 23, 1982, from the *Food and Drug Administration, Baltimore, MD 21201.* *Accepted for publication March 29, 1983.*

Abstract □ An ion-pair column chromatographic/UV spectrophotometric method for assaying trimethobenzamide hydrochloride in capsules and injections is presented, as well as a method for the detection of 3,4,5-trimethoxybenzoic acid in trimethobenzamide hydrochloride bulk drug and dosage forms. Results obtained by the USP XX, Pharmacopeial Forum, and ion-pair column assay procedures are compared, and results of a collaborative study of the proposed assay and impurity detection methods are presented.

Keyphrases □ Trimethobenzamide hydrochloride—quantitative analysis by ion-pair column chromatography, semiquantitative analysis of 3,4,5-trimethoxybenzoic acid □ 3,4,5-Trimethoxybenzoic acid—semiquantitative analysis by thin-layer chromatography, quantitative analysis of trimethobenzamide hydrochloride □ Ion-pair column chromatography—quantitative analysis of trimethobenzamide hydrochloride, semiquantitative analysis of 3,4,5-trimethoxybenzoic acid by thin-layer chromatography

Monographs (1, 2) for trimethobenzamide hydrochloride (I) in capsules and injections have several shortcomings. The USP (1) assay method for the capsules involves direct dilution in 0.1 M HCl and UV spectrometric comparison with the USP reference standard. This procedure does not separate possible impurities, such as 3,4,5-trimethoxybenzoic acid (II), or interfering excipients. The *Pharmacopeial Forum* (PF) assay for injection preparations (2) also involves a UV assay which has several shortcomings.

This paper describes an ion-pair column chromatographic assay procedure, in which I is quantitatively removed from an aqueous acidic chloride column with a chlorinated organic solvent. Ether is used to remove phenolic ingredients and breakdown products prior to the elution of I.

Also, a TLC procedure is reported for the detection of II in amounts as low as 0.25% of the weight of I. Compound II is both a synthetic precursor and a breakdown product of I and could be encountered as a contaminant in drug preparations.

Table I—Recovery Data for I using the Proposed Ion-Pair, USP, and PF Injection Assay Methods

	Column Ion Pair	USP Injection	PF Injection
I, mg	8	200	200
Number of assays	10	10	10
Mean amount recovered, %	99.4	96.6	97.6
Range, %	98.3–101.0	95.4–98.1	96.1–98.4
SD	0.81	0.91	0.68
CV, %	0.82	0.94	0.70

EXPERIMENTAL

Reagents—Trimethobenzamide hydrochloride USP reference standard[1] was dried at 105°C for 4 h prior to use. Methylene chloride[2], pentane[2], and ether[2] were commercial distilled-in-glass grade. Compounds I[3] and II[3], chromatographic diatomaceous earth[4], glass wool, and the other reagents were used as received.

Apparatus—An ultrasonic bath, chromatographic tubes[5], a tamping rod[5], commercial TLC plates coated with a 250-μm layer of silica gel with a fluorescent indicator, a suitable TLC developing chamber, and a recording UV spectrophotometer were used.

Standard Preparation—Approximately 10 mg of trimethobenzamide hydrochloride USP reference standard was accurately weighed and transferred to a 100-mL volumetric flask. Methylene chloride (70 mL) was added, and the mixture was sonicated. The resulting solution was diluted to volume with methylene chloride. A 20-μg/mL solution was obtained by diluting quantitatively and stepwise with methylene chloride.

Chromatographic Column—A pledget of fine glass wool was packed in the base of a chromatographic column. A flexible spatula was used to mix 1 g of chromatographic diatomaceous earth with 500-μL of 1 M HCl in a 50-mL beaker. The mixture was transferred to a column and tamped.

Capsule Assay Preparation—The contents of ≥20 capsules were transferred to a tared container, and the average weight/capsule was determined. The

[1] USP Reference Standards; U.S. Pharmacopeial Convention, Rockville, Md.
[2] Burdick and Jackson Laboratories, Muskegon, Mich.
[3] Hoffmann-LaRoche, Inc., Nutley, N.J.
[4] Celite; Johns Manville Corp, New York, N.Y.
[5] *AOAC Book of Methods 13th Ed.*, 37.002(a) and (b) (3).

0022-3549/84/0400-0542$01.00/0
© 1984, American Pharmaceutical Association

Table II—Linearity of Recoveries for I using Ion-Pair and PF Injection Assay Methods

	Column Ion Pair		PF	
	I, mg	Amount Recovered, %	I, mg	Amount Recovered, %
	4.0	98.1	122	97.3
	6.0	97.8	162	98.1
	8.0	98.6	203	97.5
	10.0	98.3	243	97.5
	12.0	99.0	284	98.2
Mean (n = 15)		98.4		97.7
Range	6.0-12.0	96.2-99.4	122-162	97.0-98.9
SD (n = 15)		0.77		0.52
CV, % (n = 15)		0.78		0.54

contents were finely powdered and mixed, and an accurately weighed portion of powder equivalent to 200 mg of I was transferred to a 50-mL volumetric flask. Thirty milliliters of water was added, the mixture was shaken mechanically for 10 min, and then diluted to volume with water. The mixture was filtered (the first 10 mL was discarded).

Injection Assay Preparation—An accurately measured volume of injection solution, equivalent to 200 mg of I, was transferred to a 50-mL volumetric flask, then diluted to volume with water.

Procedure—Assay preparation (2 mL) was tranferred to a 100-mL beaker, 200 μL of hydrochloric acid was added, and the mixture was swirled gently. Three grams of chromatographic diatomaceous earth was added, mixed well with a flexible spatula, and transferred to the column. The beaker was scrubbed with 1 g of diatomaceous earth, which was added to the column, and tamped with a pledget of glass wool. Fifty milliliters of water-saturated ether then four 50-mL portions of water-saturated methylene chloride were passed through the column. The methylene chloride eluants were combined; a 25 mL portion was diluted to 50 mL with methylene chloride.

The absorbance of this solution and the standard preparation were concomitantly determined in 1-cm cells at the wavelength of maximum absorbance, 261 nm, with a spectrophotometer, using methylene chloride as the blank. The quantity (in mg) of I in the portion of the capsules was calculated by $10C(A_u/A_s)$. The quantity (in mg) of I/mL of injection taken was calculated by $(10C/V)(A_u/A_s)$. C is the exact concentration in μg/mL) of I in the standard preparation; V is the volume (in mL) of the injection solution; and A_u and A_s are the absorbances of the sample solution and the standard preparation, respectively.

Assay for 3,4,5-Trimethoxybenzoic Acid (4)—The standard solution was prepared by diluting 25 mg of 3,4,5-trimethoxybenzoic acid to 50 mL with methanol. The bulk drug samples were prepared by transferring 400 mg of I, accurately weighed, to a 10-mL volumetric flask. Methanol was added to volume, and the contents were mixed until a solution was obtained.

Capsule Sample Preparation—An accurately weighed portion of the capsule contents equivalent to 400 mg of I was transferred to a 10-mL volumetric flask. Methanol (~7 mL) was added, and the flask was shaken for ~5 min. The solution was diluted to volume with methanol, mixed, and centrifuged or let stand until the precipitate settled.

Injection Sample Preparation—An accurately measured volume of injection solution equivalent to 200 mg of I was transferred to a separator containing 5 mL of water and 3 mL of 1 M HCl and extracted with two 20-mL portions of ether. The ether extracts were combined and extracted with 10 mL of water. The aqueous layer was discarded, the ether layer was filtered through cotton premoistened with ether into a small glass-stoppered flask and evaporated under a stream of nitrogen, and the residue was dissolved in 2.0 mL of methanol.

Procedure—A 25.0-μL aliquot of bulk drug or capsule sample preparation, or 10.0 μL of injection sample preparation, and 10.0 μL of standard prepa-

Table III—Results for Commercial I Capsules Using the Column Ion-Pair and USP Assay Procedures

Code	Column Ion Pair[a]		USP XX[b]	
	mg/Capsule	Percent of Label	mg/Capsule	Percent of Label
		100-mg Capsule		
A				
Mean	100.8	100.8	103.5	103.5
SD	0.32	0.32	0.31	0.31
CV, %	0.32	0.32	0.30	0.30
High	101.2	101.2	103.8	103.8
Low	100.1	100.1	103.2	103.2
B				
Mean	100.5	100.5	101.6	101.6
SD	0.35	0.35	0.67	0.67
CV, %	0.34	0.34	0.66	0.66
High	101.3	101.3	102.0	102.0
Low	100.1	100.1	100.8	100.8
C				
Mean	99.8	99.8	101.8	101.8
SD	0.37	0.37	0.59	0.59
CV, %	0.37	0.37	0.58	0.58
High	100.4	100.4	102.2	102.2
Low	99.3	99.3	101.1	101.1
		250-mg Capsule		
D				
Mean	255.8	102.3	260.1	104.0
SD	1.59	0.64	1.73	0.70
CV, %	0.62	0.63	0.67	0.67
High	258.1	103.2	261.1	104.4
Low	253.1	101.2	258.1	103.2
E				
Mean	253.6	101.4	255.2	102.1
SD	1.58	0.61	1.60	0.65
CV, %	0.62	0.60	0.63	0.64
High	255.6	102.2	256.8	102.7
Low	250.9	100.4	253.6	101.4
F				
Mean	250.8	100.3	258.1	103.3
SD	1.79	0.72	3.35	1.35
CV, %	0.71	0.72	1.30	1.39
High	253.2	101.3	261.4	104.6
Low	248.1	99.2	254.7	101.9

[a] n = 10. [b] n = 3.

Table IV—Results for Commercial I Injections Using the Column Ion-Pair, PF, and USP XX Assay Procedures [a]

Container and Code	Column Ion Pair[b]		PF[b]		USP XX[c]	
	mg/2 mL	Percent of Label	mg/2 mL	Percent of Label	mg/2 mL	Percent of Label
Ampule						
A						
Mean	202.8	101.4	200.5	100.2	195.0[d]	97.5
Range	200.7–205.4	100.4–102.7	198.6–201.5	99.3–100.8	192.8–196.8	96.4–98.4
SD	1.69	0.82	0.86	0.44	1.78	0.89
CV, %	0.83	0.81	0.43	0.44	0.91	0.91
B						
Mean	201.0	100.5	200.8	100.4	196.2	98.1
Range	199.9–204.1	100.0–102.0	200.3–201.4	100.2–100.7	195.5–197.3	97.8–98.6
SD	1.46	0.70	0.40	0.19	0.95	0.42
CV, %	0.72	0.69	0.20	0.19	0.48	0.42
C						
Mean	199.3	99.7	198.6	99.3	193.3	96.6
Range	197.6–201.5	98.8–100.8	196.9–200.6	98.4–100.3	192.9–193.6	96.4–96.8
SD	1.60	0.82	1.12	0.58	0.35	0.20
CV, %	0.81	0.83	0.56	0.59	0.18	0.21
Syringe						
A						
Mean	206.1	103.1	201.1	100.5	198.2[d]	99.4
Range	203.1–209.0	101.6–104.5	199.7–203.7	99.8–101.8	196.8–200.1	98.4–100.0
SD	2.00	0.99	1.20	0.61	1.48	0.72
CV, %	0.97	0.96	0.60	0.60	0.74	0.72
B						
Mean	204.3	102.2	202.1	101.1	196.1	98.0
Range	202.8–206.3	101.4–103.2	199.9–203.9	100.0–102.0	195.8–196.2	97.9–98.1
SD	1.10	0.57	1.39	0.71	0.23	0.11
CV, %	0.54	0.56	0.69	0.70	0.12	0.12
C						
Mean	200.9	100.4	203.1	101.6	196.4	98.2
Range	199.1–202.6	99.6–101.3	202.8–203.9	101.4–102.0	195.4–197.3	97.7–98.6
SD	1.37	0.66	0.47	0.26	0.95	0.45
CV, %	0.68	0.66	0.23	0.25	0.49	0.46
Vial						
A						
Mean	201.5	100.8	200.5	100.2	195.0[d]	97.5
Range	198.7–203.0	99.4–101.5	194.9–202.3	97.4–101.2	191.8–196.4	95.9–98.2
SD	1.51	0.73	2.12	1.09	2.15	1.09
CV, %	0.75	0.73	1.06	1.09	1.10	1.12
B						
Mean	199.4	99.7	201.4	100.7	197.2	98.6
Range	197.2–200.3	98.6–100.2	199.4–203.1	99.7–101.6	195.7–197.9	97.8–99.0
SD	0.87	0.45	0.94	0.49	1.27	0.69
CV, %	0.44	0.46	0.47	0.48	0.64	0.70
C						
Mean	200.9	100.5	196.4	98.2	192.7	96.3
Range	198.3–202.7	99.2–101.4	194.4–198.1	97.2–99.0	190.4–194.0	95.2–97.0
SD	1.44	0.72	1.08	0.52	2.00	0.99
CV, %	0.72	0.72	0.55	0.53	1.04	1.02

[a] Labeled to contain 200 mg of trimethobenzamide HCl/2 mL. [b] $n = 10$. [c] $n = 3$. [d] $n = 4$.

ration were applied ~2.5 cm from the bottom of a TLC plate coated with a 250-μm layer of fluorescent silica gel. The plate was developed in a mixture of pentane–acetic acid (88:12) in a suitable unlined chamber until the solvent had ascended 10 cm above the spotting line. The plate was removed, dried in air, and observed under short-wavelength UV light. The R_f value of II is ~0.3; I remains on the spotting line.

RESULTS AND DISCUSSION

Assay Method—The compositing method herein includes a "finely powder" step not usually included for capsules. This was necessary because the varying particle sizes of the components caused stratification of the composite, resulting in nonuniform sample portions.

Methylene chloride was chosen as the eluting solvent rather than chloroform, even though the solubility of I is over fourfold greater in chloroform than in methylene chloride[6]. Because the UV cutoff of $CHCl_3$ is at ~245 nm, it is a poor solvent for the UV determination of I, whose maximum and minimum are at 261 and 240 nm, respectively. If chloroform were used as an eluting solvent and then evaporated so that the residue could be dissolved in methanol or 0.1 M HCl, breakdown could occur during heating and evaporating, catalyzed by traces of HCl eluting from the column with the $CHCl_3$. The UV cutoff of CH_2Cl_2 is ~230 nm, and by using it as the eluant, the evaporation and redissolution steps are eliminated, as is the opportunity for decomposition. The FDA Compendial Monograph Evaluation and Development (CMED) program guidelines require that at least 95% of the drug be eluted in the first half of the eluate when column chromatography is used. Analysis of fractions of eluate of bulk I taken through the column ion-pair elution show that methylene chloride is a satisfactory solvent for meeting this requirement.

Statistical results comparing replicate recoveries of bulk I using the column ion-pair, PF, and the USP injection assay procedures are shown in Table I. Recoveries average 99.4% for the column ion-pair procedure, which is ~2–3% higher than recoveries by the PF and USP methods. Linearity of the column ion-pair and PF techniques are shown in Table II. Both methods were found to be equally linear throughout the ranges tested, *i.e.*, 4–12 mg for the column ion-pair and 122–284 mg for the PF methods. Assay results for commercial capsules are shown in Table III, with statistical comparison of the proposed and USP methods. Results are higher using the USP method, but since this is a direct dilution with no cleanup other than filtration, it was expected. Table IV shows results of injection preparation assays by the ion-pair, USP, and PF methods. Both the column ion-pair and PF results are higher than those for the USP method for all lots tested, indicating improved recoveries.

Collaborative Study—All samples for the study were distributed as coded, blind duplicates. Capsule samples were sent to the collaborators as powders. Capsule sample A was prepared by finely powdering and blending 240 commercial I capsules[7] labeled to contain 250 mg of I/capsule. Capsule sample B was composited by finely powdering and blending the contents of 390 capsules[7] of I labeled to contain 100 mg of I/capsule. Capsule sample C was an "authentic" mixture prepared by finely powdering and blending I with the

[6] Unpublished results.

[7] Beecham–Massengill, Inc., Bristol, Tenn.

Table V—Collaborative Capsule Assay Results Using the Ion-Pair Method

Lab.	Composite A, % of Label[b]		Composite B, % of Label[c]		Composite C, % Theoretical[d]	
1	101.8	101.4	100.6	100.5	98.1	98.5
2	98.3	98.4	97.5	94.5	96.7	98.3
3	100.5	101.6	120.2[a]	99.9[a]	100.0[a]	99.9[a]
4	98.0	99.4	98.8	98.7	97.9	98.1
5	99.9	103.0	100.7	100.1	97.8	97.1
6	102.5	102.0	101.3	98.0	98.0	96.9
Mean	100.5		99.1		97.7	
SD	1.75		2.05		0.62	
CV	1.74		2.07		0.63	

[a] Outliers by Dixon test; not included in mean, *SD*, or *CV* calculations (5). [b] Commercial 250-mg capsule. [c] Commercial 100-mg capsule. [d] Authentic sample, 480 mg of I/g.

Table VI—Collaborative Injection Assay Results Using the Ion-Pair Method [a]

Lab.	Ampule, % of Theoretical[b]		Vial, % of Label[c]		Syringe, % of Label[d]	
1	98.9	99.3	99.8	101.2	102.7	102.9
2	96.9	97.1	97.7	97.3	100.1	98.9
3	97.6	98.6	97.7	99.4	102.2	101.6
4	101.0	101.3	102.6	103.1	104.1	105.1
5	99.0	98.6	99.3	99.7	101.9	103.1
6	98.7	100.6	100.8	100.8	103.9	102.5
Mean	99.0		100.0		102.4	
SD	1.42		1.86		1.70	
CV	1.43		1.86		1.66	

[a] Labeled as containing 200 mg of I/2 mL. [b] Authentic sample, composite A. [c] Commercial sample, composite B. [d] Commercial sample, composite C.

manufacturer's designated excipients to achieve a concentration of ~450 mg of I/g and an amount of II equal to 0.25% of the weight of I. Injection solution sample A was an authentic mixture simulating the ampule formulation of I plus II equal to 0.25% of the weight of I. Injection solution samples B and C were composites of 22 20-mL vials[7] and 168 2-mL disposable syringes[7], respectively, each labeled to contain 100 mg of I/mL. Bulk drug samples contained I with 0.8% of added II, I with 0.25% of II, or I alone.

Collaborative assay results are presented in Tables V and VI. Average results for both capsules and injection solutions ranged from 97.7 to 102.4% (recovered or of theoretical) with coefficients of variation of ≤2.07%, indicating good recovery and reproducibility.

None of the commercial lots of the bulk drug, capsules, or injection preparations of I were found to contain II, but the TLC impurity test was developed and included in the collaborative study because it is a rapid and sensitive method for detecting degradation of I. Collaborators reported results on a basis of ≥0.5% of the amount of I, <0.5% of the amount of I, and no II. One collaborator reported incorrectly that one of the 0.8% bulk drug samples was <0.5% and another analyst incorrectly reported that both authentic injection samples had ≥0.5%. Otherwise, the results correlated well.

CONCLUSIONS

The back-extraction method was studied by the author prior to its publication in PF and was found to be a definite improvement over the USP injection assay method. However, a method was desired that would be specific and stability indicating for I, be applicable to assays of capsule as well as injection formulations, and eliminate the problems inherent in separator extractions with ether. The ion-pair chromatography method has been demonstrated by both statistical and collaborative studies to have achieved these purposes. In addition, the proposed TLC procedure has been shown to be a rapid, sensitive, and reliable method for detecting the presence of II, an impurity of I, in bulk drug and formulations.

REFERENCES

(1) "United States Pharmacopeia," 20th rev., U.S. Pharmacopeial Convention, Inc., Rockville, Md., 1980, pp. 827–828.

(2) *Pharm. Forum*, **8**, 1907 (1982).

(3) "Official Methods of Analysis," 13th ed., AOAC, Washington, D.C., 1980, sec. 37.002.

(4) H. Naviasky, *Pharm. Forum*, **7**, 1444 (1981).

(5) S. Sherken, *Pharm. Forum*, **7**, 1449 (1981).

ACKNOWLEDGMENTS

This work was researched and collaborated under the FDA Compendial Monograph Evaluation and Development (CMED) Program.

The author thanks the following people who have contributed to the completion of this project: William M. Adams, Beverly A. Ebaugh, Richard L. Everett, Dr. Catherine Fenselau, Michael Gurbarg, Thomas Knott, Dr. S. Edward Krikorian, George Mack, William M. Ment, John G. Meyer, Buford Poet, Mary Ellen Richelieu, Frank J. Schenck, Stephen Sherken, William M. Smith, Don W. Thompson, John H. Turner, and Norlin Tymes, all of the Food and Drug Administration, R. Mostillo and Dr. Jane Sheridan of Hoffmann-La Roche, Inc., and Dr. David Walters of Beecham-Massengill Pharmaceuticals.

Bromperidol Radioimmunoassay: Human Plasma Levels

JOHN TISCHIO ˣ, NANCY HETYEI, and JAMES PATRICK *

Received July 6, 1982, from the *Research Laboratories, Ortho Pharmaceutical Corporation, Raritan, NJ 08869.* Accepted for publication March 9, 1983. *Present address: Schering Corporation, Bloomfield, NJ 07003.

Abstract □ A sensitive radioimmunoassay (RIA) procedure was developed to assay for bromperidol levels in human plasma after therapeutic drug administration. The antisera used in the RIA procedure was generated in rabbits against a haloperidol–bovine serum albumin conjugate. Tritiated haloperidol was used as the radioligand in the assay. A single ether extraction of alkalinized plasma was used to separate bromperidol from its more polar metabolites and to reduce assay variability encountered with a direct plasma assay. The lower limit of detection was ~0.5 ng/mL of parent drug in plasma. The assay exhibited within- and between-assay variabilities of ~9 and 14%, respectively. A 103–106% recovery of bromperidol from quality control plasma samples was observed over the concentration range of 1–150 ng/mL. A correlation coefficient of 0.9999 with respect to measured *versus* expected bromperidol content in the quality control plasma samples was exhibited. Cross-reactivity characteristics of the antisera indicated that dehydrobromperidol could significantly interfere (~25% cross-reactivity) with the RIA procedure. However, biotransformation studies have not suggested this compound as a metabolite of bromperidol. Predose (C_{min}) plasma levels of bromperidol in schizophrenic patients maintained on drug therapy are also reported.

Keyphrases □ Bromperidol—radioimmunoassay, human plasma levels, haloperidol-bovine serum albumin conjugate □ Radioimmunoassay—bromperidol, human plasma levels, haloperidol-bovine serum albumin conjugate

Bromperidol (I), 4-[4-(*p*-bromophenyl)-4-hydroxypiperidino]-4′-fluorobutyrophenone, the bromo analogue of haloperidol (II), is a potent neuroleptic agent which has been under clinical investigation for the treatment of psychoses such as schizophrenia. The bioavailability and pharmacokinetics of this drug in dogs under steady-state conditions following multiple-dose oral administration have been reported (1). A limited study comparing preliminary pharmacokinetic results from dogs and humans was also reported (2). In general, relating pharmacokinetics of the psychotropic agents with effective treatment of psychiatric disorders is difficult partly due to the lack of a sensitive and reliable analytical methodology. This problem can be aggravated by the different neuroleptic plasma levels observed in patients receiving concurrent medication (3).

A radioimmunoassay (RIA) method was developed in our laboratory and was used to measure levels of bromperidol in human plasma (4, 5). With this methodology the bioavailability and pharmacokinetics of bromperidol in patients chronically receiving drug therapy was studied (5). This paper describes the RIA procedure used to measure bromperidol plasma levels in schizophrenic patients. Also reported are mean C_{min} drug plasma levels from 15 schizophrenic patients maintained on various drug regimens.

EXPERIMENTAL

Materials—Antisera[1] used in the RIA procedure was generated in rabbits against a haloperidol hapten chemically linked to bovine serum albumin *via* the tertiary alcohol functional group. Tritiated haloperidol[1], specific activity ~14 Ci/mmol, was used as the radioligand in the RIA procedure and to determine extraction efficiencies of drug material in the biological sample extraction procedure.

Radioimmunoassay—A bromperidol standard RIA curve was routinely generated from a series of test tubes (12 × 75 mm) prepared to contain an extract of control plasma sample (50 μL), unlabeled competitor (bromperidol, 0.02–10.0 ng in 50 μL of buffer), [^{3}H]haloperidol (50 μL containing ~6600 cpm), haloperidol antisera (50 μL, final antisera dilution of 1:1800), and RIA buffer (0.1 M sodium phosphate, 0.9% NaCl, 0.1% bovine IgG, and 0.1% sodium azide, pH 7.0) to achieve a final volume of 600 μL/tube. The contents were then mixed and incubated[2] at room temperature (~21°C) for ~18 h. (Note that this incubation period was chosen for convenience, since equilibrium of the radioligand binding to the antisera was demonstrated for an incubation period of 6 h.) Bound and free [^{3}H]haloperidol were separated by adsorption of free radioligand using dextran-coated charcoal (200 μL of a suspension containing 1 g of charcoal[2] and 100 mg of dextran[3] in 50 mL of RIA buffer). The charcoal suspension was incubated for 1.5 h, at room temperature. Centrifugation at ~330×*g* for 15 min adequately separated the charcoal-adsorbed material from that bound to the antisera. The supernatants were decanted into scintillation vials containing 15 mL of liquid scintillation cocktail[4] and 600 μL of water to aid dissolution of the sample. Bound radioactivity for each sample was determined using a liquid scintillation counter[5].

Quality control plasma samples were prepared to contain known amounts of bromperidol ranging from 1 to 150 ng/mL. These samples were prepared at the start of the study, stored at ~−20°C, and assayed throughout the study period (~6 months). Data from these analyses provided a measure of the drug stability in the biological matrix, as well as information from which assay statistics were calculated.

Patient plasma samples and quality control plasma samples were extracted according to the procedure outlined in Scheme I. This extraction procedure

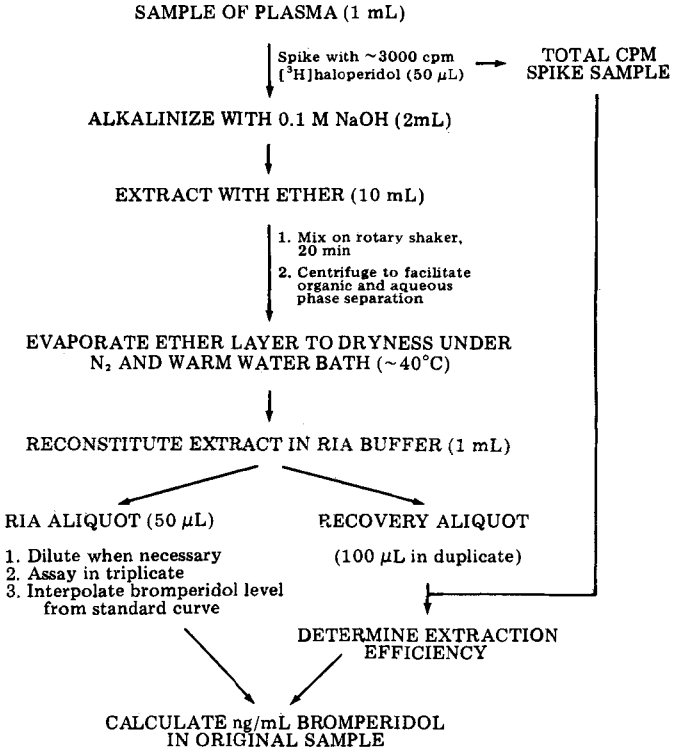

Scheme I—Plasma sample extraction procedure and assay protocol for the bromperidol RIA.

[1] Janssen Pharmaceutica, Beerse, Belgium. The haloperidol contained one tritium atom *ortho* to the chlorine atom.

[2] Norite SG Extra; J. T. Baker Chemical Co., Phillipsburg, N.J.
[3] Dextran T-70; Pharmacia Fine Chemicals, Piscataway, N.J.
[4] Biofluor; New England Nuclear Corp., Boston, Mass.
[5] Model SL4000; Intertechnique Corp., IN/US, Fairfield, N.J.

0022-3549/84/0400-0546$01.00/0
© 1984, American Pharmaceutical Association

Table I—Compounds Examined for Cross-Reactivity Characteristics

Compound	Structure	D_{50}[a], ng	Relative Percent Cross-Reactivity[b]
I	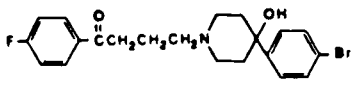	0.26	100.0%
II	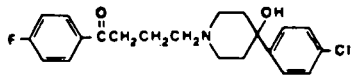	0.28	92.9%
III	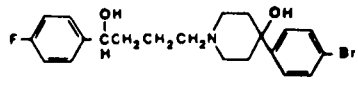	277.4	0.1%
IV	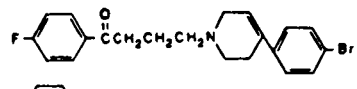	1.07	24.3%
V	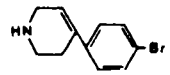	>1000	N.D.I.[c]
VI	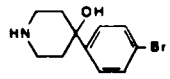	>1000	N.D.I.
VII	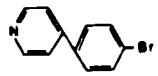	5.76	4.5%
VIII		>1000	N.D.I.
IX		>1000	N.D.I.
X		>1000	N.D.I.

[a] D_{50} is the amount of compound required to depress the radioligand binding to the antisera 50%. [b] (D_{50} bromperidol/D_{50} competitor) × 100. [c] No detectable interference.

was required in order to remove potential interferences (presumably conjugates of bromperidol). The reconstituted extracts, or dilutions thereof, were assayed in replicate (3 × 50-μL aliquots) for drug content as described for the standard curve.

Data Processing—The standard curve and plasma bromperidol levels were determined using the logit-log computer program of Frazier and Rodbard (6).

Antisera Selectivity—The cross-reactivity of the compounds in Table I was determined by competing the individual substances, over a range of 0.05–1000 ng, with a fixed amount of radioligand and antisera. A 50% displacement value (D_{50}, amount of compound required to displace the radioligand binding to the antisera by 50%) was determined for each compound. The ratio of D_{50} observed for bromperidol to the D_{50} observed for the other compounds was used to determine a relative percent cross-reactivity.

Patient Samples—Schizophrenic patients (n = 15) were maintained on bromperidol therapy given in tablet form[6] once daily. Whole blood samples were collected by venipuncture using heparinized evacuated blood collection tubes (10–15 mL) prior to medication over a period of several days (n = 4–10, Table II). Each whole blood sample was centrifuged (~500×g for 10 min at 4°C), and the plasma was separated and frozen. At an appropriate time the plasma samples were thawed, and aliquots (1 mL) were transferred to test tubes and sealed with a polytef screw cap. The aliquots were refrozen and maintained at ~ −20°C until analysis could be performed (usually within 4 weeks) by the RIA procedure. Duplicate 1-mL aliquots of selected plasma samples were assayed in parallel to estimate between-sample variability.

RESULTS AND DISCUSSION

A history of standard curve parameters for the bromperidol RIA was compiled. The mean (±SD) B_0 value[7], slope, intercept, D_{50}, and minimal detectable amount, as described by the data handling computer program (6) calculated from 10 assays, were 39.8% (5.1%), −1.06 (0.06), −1.13 (0.19), 0.35 ng (0.06 ng), and 0.03 ng (0.01 ng), respectively. The mean extraction efficiency for the quality control plasma samples (n = 227) assayed in the 10 assays was 84.6 ± 7.3%. This sample extraction step was necessary to reduce the variability observed when the plasma sample was assayed directly and to separate bromperidol from its polar metabolites. A similar extraction procedure was used by Van den Eeckhout *et al.* (2) to eliminate interfering plasma constituents.

[6] In house, bromperidol, Cilag-Chemie, Schaffhausen, Switzerland.

[7] B_0 is the amount of radioactivity bound to the antisera when no unlabeled drug is present.

Table II—Patient Plasma Bromperidol Levels

Patient	Dose mg/kg	Daily Dose[a], mg	Mean ± SD[b], ng/mL	CV[c], %	N[d]
A	0.15	10	3.73 ± 0.94	25.1	9
B	0.10	10	1.65 ± 0.97	58.5	5
C	0.14	12	6.67 ± 1.31	19.6	10
D	0.23	18	8.25 ± 1.83	22.2	9
E	0.35	20	12.02 ± 5.06	42.1	4
F	0.33	20	7.62 ± 3.13	41.0	4
G	0.26	20	7.14 ± 1.19	16.7	10
H	0.51	30	10.15 ± 4.48	44.1	9
I	0.44	30	10.36 ± 1.44	13.9	10
J	0.44	30	12.77 ± 5.19	42.7	7
K	0.55	50	9.20 ± 0.42	4.6	4
L	0.93	50	10.72 ± 0.94	8.8	10
M	0.55	50	20.24 ± 2.11	10.4	7
N	0.91	60	55.13 ± 14.85	26.9	9
O	1.00	60	32.23 ± 4.12	12.8	9

[a] Administered once a day in tablet form. [b] Determined from plasma samples collected prior to dose administration (C_{min}). [c] Determined as follows: 100 × (SD/mean). [d] Number of days C_{min} blood samples were collected.

The RIA procedure for the measurement of bromperidol levels in human plasma was demonstrated by investigating the following criteria: (*a*) accuracy—correlating measured bromperidol in human plasma samples (quality control plasma samples) containing known amounts of drug (*i.e.*, 1, 5, 10, 25, 50, 100, and 150 ng/mL of bromperidol; (*b*) precision—determining replicate, within-assay, and between-assay variability statistics; and (*c*) selectivity—determining cross-reactivity characteristics of several structurally related compounds and potential metabolites of bromperidol. Table III summarizes the results obtained from the analysis of approximately five samples of each quality control human plasma specimen in several different assays performed over a 6-month period. (Note that not all quality control plasma concentrations were analyzed in every assay.) The mean values of the observed bromperidol content and between-assay variation, as well as the within-assay and replicate variations for each of the quality control plasma samples, are shown.

The quality control plasma sample concentrations of 1–50 ng/mL (reported in Table III) were compared with the expected (theoretical) values. Linear regression of the observed *versus* expected data yielded $y = 1.026x + 1.317$, with a correlation coefficient of 0.9994. If the 100- and 150-ng/mL quality control plasma results were included in this correlation, linear regression yielded $y = 1.051x + 0.889$, with a correlation coefficient of 0.9999. (Note that there were a limited number of assays, n = 3 and 2, which included the 100- and 150-ng/mL samples, respectively.)

The mean coefficient of variation [CV = 100 × (SD/mean)] observed between sample replicates (triplicate) for the seven quality control plasma concentrations ranged from 6 to 9.6%. Likewise, the mean CV observed between samples within an assay ranged from 5.4 to 12.4%, and the CV between assays ranged from 2.1 to 21.4% for the seven quality control plasma concentrations. In both instances, the within- and between-assay precision was greatest at the higher bromperidol concentrations and lowest at the 1-ng/mL concentration. These results demonstrate the stability of bromperidol in the biological matrix under the storage conditions and reasonable reproducibility of the RIA throughout the study.

The selectivity of the RIA for bromperidol is summarized in Table I, which lists the compounds examined for cross-reactivity characteristics with the haloperidol antisera. As can be seen, bromperidol (I) and haloperidol (II) show almost identical cross-reactivity characteristics with the antisera. Of the remaining compounds examined, only dehydrobromperidol (IV) showed appreciable cross-reactivity with the antisera (~25%). However, interference of dehydrobromperidol with the analysis of bromperidol in plasma is not likely to occur since there is no suggestion that this compound is a metabolite of bromperidol[8].

[8] Bromperidol is extensively metabolized in humans with the major metabolite being an *O*-glucuronide conjugate of the intact drug. Oxidative-*N*-dealkylation does not appear to be a major metabolic pathway of the drug in humans. These results have been presented at the 23rd Annual American Society of Pharmacognosy Meeting in Pittsburgh, Pa., August 1982.

Table III—Radioimmunoassay Statistics for Bromperidol Determination in Human Plasma Quality Control Samples

	Bromperidol Concentration ng/ml						
	1[a]	5[a]	10[a]	25[b]	50[b]	100[c]	150[c]
Number of assays	7	10	10	10	10	3	2
Total number of samples	22	46	46	46	46	13	8
Bromperidol concentration							
Mean ± *SD*	1.49 ± 0.32	6.38 ± 0.99	12.60 ± 1.52	27.14 ± 3.80	52.37 ± 3.89	105.35 ± 4.51	159.14 ± 3.27
n	7	10	10	10	10	3	2
Between-assay *CV*[d], %	21.2	15.6	12.1	14.0	7.4	4.3	2.1
Within-assay sample variation *CV*[e], %							
Mean ± *SD*	12.2 ± 9.4	10.3 ± 4.4	7.1 ± 4.1	7.7 ± 3.8	8.91 ± 3.8	8.2 ± 4.3	5.4 ± 0.5
n	7	10	10	10	10	3	2
Sample replicate variation *CV*[f], %							
Mean ± *SD*	9.6 ± 5.9	6.0 ± 3.8	6.0 ± 3.4	7.1 ± 4.5	8.8 ± 4.4	6.0 ± 5.1	8.1 ± 6.3
n	22	46	46	46	46	13	8

[a] Quality control plasma samples were reconstituted to original sample volume (1 mL) with RIA buffer and assayed directly by RIA method. [b] Quality control plasma samples were diluted 1:2 after reconstitution with RIA buffer prior to being assayed by RIA method. [c] Quality control plasma samples were diluted either 1:2, 1:3, or 1:9 after reconstitution with RIA buffer prior to being assayed by RIA method. [d] The mean (±*SD*) and CV of the bromperidol concentration was calculated averaging the mean bromperidol concentration of each assay for each quality control plasma concentration. [e] The mean ± *SD* of the CV observed between samples within an assay was calculated averaging the mean CV between samples of each assay for each quality control plasma concentration. [f] The mean ± *SD* of the CV of the replicates of all samples assayed for each quality control plasma concentration.

Bromperidol levels (C_{min}) determined in the patient plasma samples are summarized in Table II. These data represent the mean bromperidol concentrations determined in samples collected immediately before the daily medication (n = 4–10 d) was administered. The patient plasma samples generally demonstrated the same degree of precision described for the quality control plasma samples with regard to replicate and within-assay variability. These variabilities (*CV*) were 7.1 ± 3.9 (n = 101) and 6.6 ± 4.6 (n = 45), respectively. However, intrasubject variability, the variability observed between the C_{min} values of an individual, ranged from 4.6 to 58.5% with no apparent correlation between the *CV* and the level of drug measured (Table II). In addition, comparison of the mean C_{min} drug levels from subjects receiving approximately the same dose per body weight demonstrated substantial intersubject variability. Specifically, patients A and C (dose, 0.14–0.15 mg/kg) had mean C_{min} levels of 3.73 and 6.67 ng/mL, respectively; patients K and M (dose, 0.55 mg/kg) had mean C_{min} levels of 9.20 and 20.24 ng/mL, respectively; and patients L, N, and O (dose, 0.91–1.00 mg/kg) had mean C_{min} levels of 10.72, 55.13, and 32.23, respectively. Realistically, this intra- and interindividual variability observed in mean C_{min} bromperidol levels cannot be explained solely by assay variability. Rather a combination of metabolism, elimination, and possibly concurrent medication may significantly influence the scatter in these single time point determinations.

In conclusion, this report describes an RIA procedure used to assay the bromperidol content of human plasma samples. Predose plasma samples, obtained from schizophrenic patients chronically receiving bromperidol therapy, were assayed using this RIA method. Substantial intra- and intersubject variabilities in the C_{min} drug levels were demonstrated. The bioavailability and pharmacokinetic information of bromperidol in schizophrenic patients will be reported elsewhere.

REFERENCES

(1) L. Abrams, P. Chaikin, J. Tischio, J. Killinger, and H. Weintraub, "Abstracts," American Pharmaceutical Association Academy of Pharmaceutical Sciences, 29th Nat'l. Meeting., San Antonio, Texas, Nov., 1980.

(2) E. Van den Eeckhout, F. M. Belpaire, M. G. Bogaert, and P. De Moerloose, *Eur. J. Drug Metab. Pharmacol.*, **5**, 45 (1980).

(3) J. Gautier, A. Jus, A. Villeneuve, K. Jus, P. Pires, and R. Villeneuve, *Biol. Psychiatry*, **12**, 389 (1977).

(4) J. Tischio, N. Hetyei, J. Patrick, and J. Killinger, *Clin. Chem.*, **27**(6), 1102 (1981) (Abstract).

(5) J. Tischio, P. Chaikin, L. Abrams, N. Hetyei, J. Patrick, H. Weintraub, D. Collins, M. Chasin, D. Wesson, and F. Abuzzahab, *J. Clin. Pharmacol.*, **22**(4), 16A (1982) (Abstract).

(6) G. R. Frazier and D. Rodbard, "A Logit-Log RIA Program; Radioimmunoassay Data Processing," 3rd ed., vol. 1, Reproduction Research Branch, National Institutes of Health, Bethesda, Md., 1972.

Novel Concept for a Mucosal Adhesive Ointment

K.-D. BREMECKER *[x], H. STREMPEL [‡], and G. KLEIN [‡]

Received December 14, 1982, from the *Institut für Pharmazeutische Technologie der Philipps Universität Marburg/Lahn, Ketzerbach 63, 3550 Marburg*, and the [‡]*Hautabteilung des Luisen-Hospitals, Aachen, West Germany.* Accepted for publication March 8, 1983.

Abstract □ Conventional adhesive ointments cause irritation to the mucous membranes. Therefore, a novel mucosal adhesive ointment based partly on neutralized polymethacrylic acid methyl ester was formulated. The flow curves of the ointment vehicle showed pseudoplastic properties. The rheological behavior as well as the adhesion on the mucosal membrane could be varied by the type and concentration of the polymer used and the base used for neutralization. During clinical studies, the ointment vehicle as well as a tretinoin (vitamin A acid) preparation for the treatment of lichen planus did not cause any local irritation or systemic side effects. Both vehicle and preparation were found to be pleasant for the patients to use. The new system of the mucosal adhesive ointment is not limited to the incorporation of tretinoin as the active agent; combined with other drugs the system could be applied to all types of mucosal membranes.

Keyphrases □ Adhesive ointment, mucosal—tretinoin, irritation-free formulation, clinical assessment □ Lichen ruber planus—treatment with tretinoin, irritation-free formulation, mucosal adhesive ointment □ Tretinoin—mucosal adhesive ointment, irritation-free formulation, clinical testing for lichen ruber planus

Ointments employed for the treatment of the mucous membranes of the mouth must be suited to the special conditions pertaining to that particular site of application. The flow of saliva and the mechanical stress generated by the continuous movements of the buccal cavity prevent any long-term adhesion of the ointment subsequent to its application. The quantity

0022-3549/84/0400-0548$01.00/0

© 1984, American Pharmaceutical Association

Table III—Radioimmunoassay Statistics for Bromperidol Determination in Human Plasma Quality Control Samples

	Bromperidol Concentration ng/ml						
	1[a]	5[a]	10[a]	25[b]	50[b]	100[c]	150[c]
Number of assays	7	10	10	10	10	3	2
Total number of samples	22	46	46	46	46	13	8
Bromperidol concentration							
Mean ± *SD*	1.49 ± 0.32	6.38 ± 0.99	12.60 ± 1.52	27.14 ± 3.80	52.37 ± 3.89	105.35 ± 4.51	159.14 ± 3.27
n	7	10	10	10	10	3	2
Between-assay *CV*[d], %	21.2	15.6	12.1	14.0	7.4	4.3	2.1
Within-assay sample variation *CV*[e], %							
Mean ± *SD*	12.2 ± 9.4	10.3 ± 4.4	7.1 ± 4.1	7.7 ± 3.8	8.91 ± 3.8	8.2 ± 4.3	5.4 ± 0.5
n	7	10	10	10	10	3	2
Sample replicate variation *CV*[f], %							
Mean ± *SD*	9.6 ± 5.9	6.0 ± 3.8	6.0 ± 3.4	7.1 ± 4.5	8.8 ± 4.4	6.0 ± 5.1	8.1 ± 6.3
n	22	46	46	46	46	13	8

[a] Quality control plasma samples were reconstituted to original sample volume (1 mL) with RIA buffer and assayed directly by RIA method. [b] Quality control plasma samples were diluted 1:2 after reconstitution with RIA buffer prior to being assayed by RIA method. [c] Quality control plasma samples were diluted either 1:2, 1:3, or 1:9 after reconstitution with RIA buffer prior to being assayed by RIA method. [d] The mean (±*SD*) and CV of the bromperidol concentration was calculated averaging the mean bromperidol concentration of each assay for each quality control plasma concentration. [e] The mean ± *SD* of the CV observed between samples within an assay was calculated averaging the mean CV between samples of each assay for each quality control plasma concentration. [f] The mean ± *SD* of the CV of the replicates of all samples assayed for each quality control plasma concentration.

Bromperidol levels (C_{min}) determined in the patient plasma samples are summarized in Table II. These data represent the mean bromperidol concentrations determined in samples collected immediately before the daily medication (n = 4–10 d) was administered. The patient plasma samples generally demonstrated the same degree of precision described for the quality control plasma samples with regard to replicate and within-assay variability. These variabilities (*CV*) were 7.1 ± 3.9 (n = 101) and 6.6 ± 4.6 (n = 45), respectively. However, intrasubject variability, the variability observed between the C_{min} values of an individual, ranged from 4.6 to 58.5% with no apparent correlation between the *CV* and the level of drug measured (Table II). In addition, comparison of the mean C_{min} drug levels from subjects receiving approximately the same dose per body weight demonstrated substantial intersubject variability. Specifically, patients A and C (dose, 0.14–0.15 mg/kg) had mean C_{min} levels of 3.73 and 6.67 ng/mL, respectively; patients K and M (dose, 0.55 mg/kg) had mean C_{min} levels of 9.20 and 20.24 ng/mL, respectively; and patients L, N, and O (dose, 0.91–1.00 mg/kg) had mean C_{min} levels of 10.72, 55.13, and 32.23, respectively. Realistically, this intra- and interindividual variability observed in mean C_{min} bromperidol levels cannot be explained solely by assay variability. Rather a combination of metabolism, elimination, and possibly concurrent medication may significantly influence the scatter in these single time point determinations.

In conclusion, this report describes an RIA procedure used to assay the bromperidol content of human plasma samples. Predose plasma samples, obtained from schizophrenic patients chronically receiving bromperidol therapy, were assayed using this RIA method. Substantial intra- and intersubject variabilities in the C_{min} drug levels were demonstrated. The bioavailability and pharmacokinetic information of bromperidol in schizophrenic patients will be reported elsewhere.

REFERENCES

(1) L. Abrams, P. Chaikin, J. Tischio, J. Killinger, and H. Weintraub, "Abstracts," American Pharmaceutical Association Academy of Pharmaceutical Sciences, 29th Nat'l. Meeting., San Antonio, Texas, Nov., 1980.

(2) E. Van den Eeckhout, F. M. Belpaire, M. G. Bogaert, and P. De Moerloose, *Eur. J. Drug Metab. Pharmacol.*, **5**, 45 (1980).

(3) J. Gautier, A. Jus, A. Villeneuve, K. Jus, P. Pires, and R. Villeneuve, *Biol. Psychiatry*, **12**, 389 (1977).

(4) J. Tischio, N. Hetyei, J. Patrick, and J. Killinger, *Clin. Chem.*, **27**(6), 1102 (1981) (Abstract).

(5) J. Tischio, P. Chaikin, L. Abrams, N. Hetyei, J. Patrick, H. Weintraub, D. Collins, M. Chasin, D. Wesson, and F. Abuzzahab, *J. Clin. Pharmacol.*, **22**(4), 16A (1982) (Abstract).

(6) G. R. Frazier and D. Rodbard, "A Logit-Log RIA Program; Radioimmunoassay Data Processing," 3rd ed., vol. 1, Reproduction Research Branch, National Institutes of Health, Bethesda, Md., 1972.

Novel Concept for a Mucosal Adhesive Ointment

K.-D. BREMECKER *[x], H. STREMPEL [‡], and G. KLEIN [‡]

Received December 14, 1982, from the *Institut für Pharmazeutische Technologie der Philipps Universität Marburg/Lahn, Ketzerbach 63, 3550 Marburg*, and the [‡]*Hautabteilung des Luisen-Hospitals, Aachen, West Germany.* Accepted for publication March 8, 1983.

Abstract □ Conventional adhesive ointments cause irritation to the mucous membranes. Therefore, a novel mucosal adhesive ointment based partly on neutralized polymethacrylic acid methyl ester was formulated. The flow curves of the ointment vehicle showed pseudoplastic properties. The rheological behavior as well as the adhesion on the mucosal membrane could be varied by the type and concentration of the polymer used and the base used for neutralization. During clinical studies, the ointment vehicle as well as a tretinoin (vitamin A acid) preparation for the treatment of lichen planus did not cause any local irritation or systemic side effects. Both vehicle and preparation were found to be pleasant for the patients to use. The new system of the mucosal adhesive ointment is not limited to the incorporation of tretinoin as the active agent; combined with other drugs the system could be applied to all types of mucosal membranes.

Keyphrases □ Adhesive ointment, mucosal—tretinoin, irritation-free formulation, clinical assessment □ Lichen ruber planus—treatment with tretinoin, irritation-free formulation, mucosal adhesive ointment □ Tretinoin—mucosal adhesive ointment, irritation-free formulation, clinical testing for lichen ruber planus

Ointments employed for the treatment of the mucous membranes of the mouth must be suited to the special conditions pertaining to that particular site of application. The flow of saliva and the mechanical stress generated by the continuous movements of the buccal cavity prevent any long-term adhesion of the ointment subsequent to its application. The quantity

0022-3549/84/0400-0548$01.00/0

© 1984, American Pharmaceutical Association

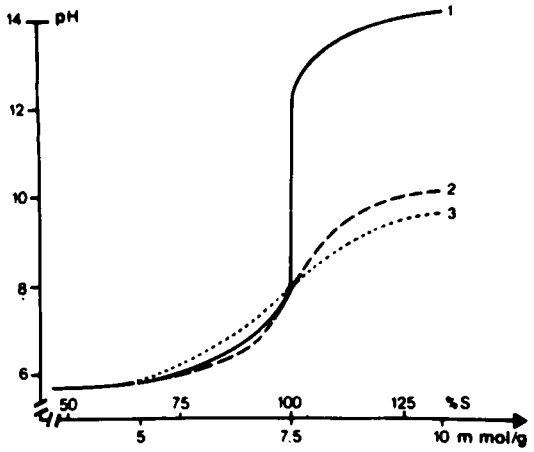

Figure 1—*pH value of polymethyl methacrylate preparations using various bases. Key: (1) NaOH; (2) triethanolamine; (3) diisopropanolamine.*

of saliva produced each day ranges from 0.5 to 1.5 L (1, 2); with suitable stimulation, transient flow rates of up to 10 mL/min have been found (3, 4). On the one hand, therefore, mucosal adhesive ointments should be sufficiently hydrophilic to permit intimate contact with and adhesion to the skin surface; on the other hand, they should include a lipophilic component to prevent the ointment base from being washed away, or at least to delay this process. It is for this reason that such ointments frequently contain a hydrogel constituent suspended in a lipophilic base, which swells and exhibits its adhesive characteristics only after contact with mucous membranes and saliva. Typical ointments that have been developed in this way are a polyacrylate[1]-calcium carbonate–liquid paraffin suspension (5) and a sodium carboxymethylcellulose, pectin, and gelatin combination in a polyethylene–paraffin base[2]. In some cases, highly viscous solutions or hydrogels with no lipophilic admixtures are also used for this purpose, in which case natural and synthetic macromolecular compounds such as tragacanth alginates, pectin, methylcellulose, and polyacrylate[1] are incorporated.

The intended objective, apart from good mucosal adhesion over as long a period as possible, is for the ointment base to be as free from mechanical, physical, and chemical irritant properties as is practical, depending on the indication. Any

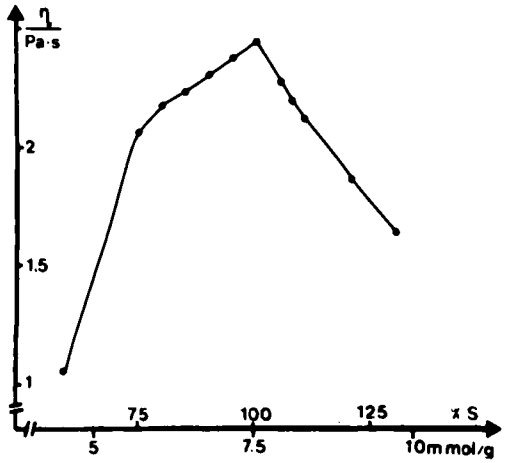

Figure 2—*Viscosity dependence on the stoichiometric saturation of the carboxyl groups (5% polymethyl methacrylate hv neutralized with NaOH; shear rate* $D = 90\ s^{-1}$).

[1] Carbopol; Goodrich, Cleveland Ohio.
[2] Orabase; Squibb Pharmaceuticals, Mooton, England.

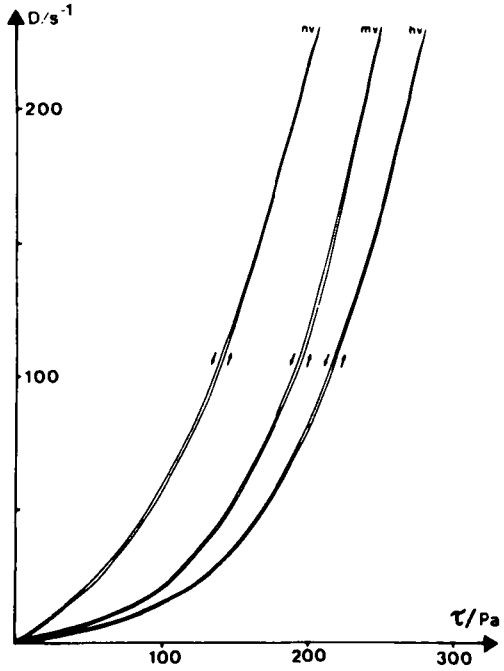

Figure 3—*Flow curves of polymethyl methacrylate-Na (100% S) using 5% polymethyl methacrylate nv, mv, and hv.*

irritation of the oral mucosa should be strictly avoided, as it is extremely sensitive. This whole problem has to be faced, for example, in developing a mucosal adhesive ointment for the treatment of lichen planus mucosae oris with tretinoin (vitamin A acid). Tretinoin, described by Günther (6) in 1972 in the treatment of lichen ruber planus, has been employed with great success by many clinicians. However a number of patients have complained of reddening of the mucosa, pain, burning sensations, and maceration (7–10); the ointment bases were considered to have caused irritation to the sensitized oral mucosa. Therefore, there has been a need to formulate a nonirritating mucosal adhesive ointment containing tretinoin.

Polymethyl methacrylate[3] would seem to be a logical candidate for these tests, as it is a polymer with lipophilic methyl groups and hydrophilic carboxyl and ester groups. Both of these components were mentioned earlier as being essential for a mucosal adhesive ointment. The solubility of this polymer in water and its adhesiveness and viscidity can be varied, within certain limits, by using different degrees of neutralization (11). However, as polymethyl methacrylate has not previously been used as a mucosal adhesive ointment, the drug-free ointment base was first clinically investigated in volunteers. For dermatological reasons, no preservations, surfactants, stabilizers, or taste adjusters were added either to the ointment base or to the final tretinoin preparation, because of their potential irritant and allergenic effects.

EXPERIMENTAL

Production of the Polymethyl Methacrylate Base—Dilute polymethyl methacrylate salt solutions (<10%) were produced from concentrated master batches (≥10%) and, following the neutralization reaction (~1 h), made up to the required end concentration with water. For the master batch, polymethyl methacrylate was steeped for 10 min in 3–4 times its volume of cold water (20°C), and the amount of base required for neutralization was added cold with the remaining water (20°C) with continuous stirring. A 7.5-mmol volume of base/g of polymethyl methacrylate is needed for complete neutralization

[3] Eudispert hv; Röhm Pharma, Darmstadt, West Germany.

Table 1—Tretinoin Grain Size Distribution as a Function of Storage Temperature and Time

Storage Temp.	Particle Size, μm	Storage Time		
		Nil	3 months	6 months
8°C	10	97%	98%	97%
	10-20	2.8%	1.7%	2.7%
	20	0.2%	0.2%	0.3%
25°C	10	98%	97%	98%
	10-20	1.8%	2.7%	1.7%
	20	0.2%	0.3%	0.3%

(Fig. 1). It was possible to accelerate the reaction by heating the mixture to ~ 60°C *in vacuo*. A detailed procedure has been described previously (11). The final stage in preparing the ointment base involved its sterilization for 20 min at 121°C in a steam autoclave.

Production of the Adhesive Ointment Base—The following quantities were used to prepare a 1-kg batch: 50 g of polymethyl methacrylate in 200 g of water and 12 g of NaOH in 238 g of water. The sterilized polymethyl methacrylate ointment base was produced from the above ingredients, into which the following components were incorporated under aseptic conditions: 1 g of tretinoin[4], 200 g of glycerol (85%)[5], and 299 g of water. The tretinoin was micronized with the aid of a high-efficiency mill[6] and a three-roller mill[7]. The ointment was placed into 20-g tubes for the clinical tests.

Flow Characteristics—The flow characteristics of the aqueous polymethyl methacrylate solutions were investigated with a rotational viscometer[8] at 25°C. The number of rpm was changed by 25 s^{-1}. The pH value was measured with a digital pH meter[9].

Tretinoin Determination—The tretinoin content in the finished preparation was determined with a UV-visual spectrophotometer at 351 nm ($E^{1\%}_{1cm}$ = 1500). For this purpose, 1 g of ointment was dissolved in 50 mL of water, brought to 100 mL with isopropyl alcohol, and measured against a blank made from drug-free ointment base, water, and isopropyl alcohol. This complies essentially with the requirement described in the USP XX (12). The particle size of the active agent in the ointment was determined microscopically immediately after manufacture and after 3 and 6 months of storage at room temperature and at 8°C. The drug content was also checked after storage.

Clinical Testing—Clinical testing was carried out in three sections: study

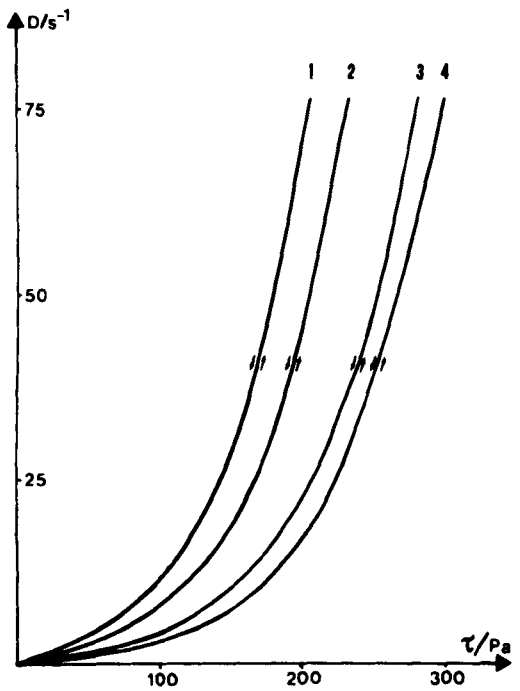

Figure 4—*Flow curves of 5% polymethyl methacrylate hv (100% S) neutralized with $Na_2B_4O_7$ (1), NaOH (2), triethanolamine (3), and diisopropanolamine (4).*

[4] Fa. Hoffmann-La Roche, Basle, Switzerland.
[5] Merck, Darmstadt, West Germany.
[6] Ultra-Turrax TP 18/10: Janke und Kunkel, Stauffen, West Germany.
[7] Kupper, Troisdorf, West Germany.
[8] Model RV 12 with MV-System; Haake, Karlsruhe, West Germany.
[9] Model 532; Metrohm, Herisau, Switzerland.

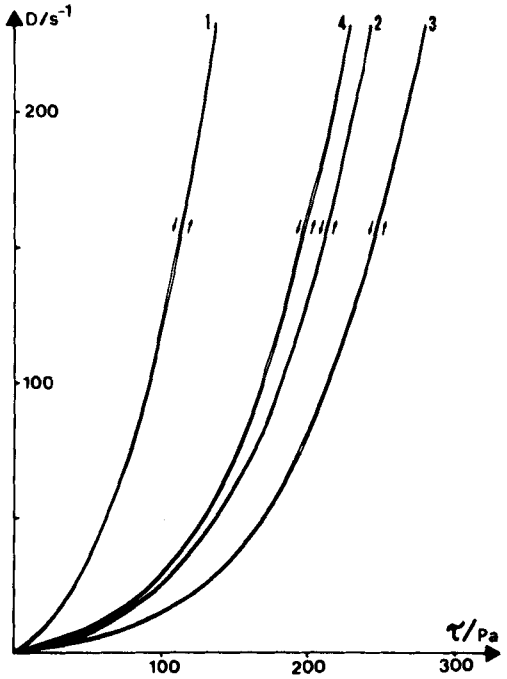

Figure 5—*Flow curves of 5% polymethyl methacrylate hv neutralized with NaOH. Key: (1) 50% S; (2) 75% S; (3) 100% S; (4) 125% S.*

of the ointment base on (A) skin and (B) mucous membranes and (C) application of the tretinoin adhesive ointment.

Section A: Patch Testing of the Polymethyl Methacrylate Ointment Base—A nonallergenic test patch[10] to which the ointment base under investigation had been applied was affixed to the flexor surface of the right forearm of each of 16 subjects, aged 17 to 43 years (10 females and 6 males), with no skin or mucosal disorders. The patch was removed after 24 h. The skin reaction was read after 24, 48, and 72 h and once again after 1 week, in accordance with the procedure of Bandmann and Dohn (13).

Section B: Application of the Polymethyl Methacrylate Ointment Base to the Oral Mucosa—The same ointment base was then tested on the oral mucosa of the same 16 subjects. The test was carried out over a period of 14 d in each case. The subjects were each provided with a 20-g tube of ointment base and were instructed to apply the ointment four times daily to the same area of the oral mucosa. They were reexamined and questioned after 1 and 2 weeks. Fifteen of the subjects completed the study; one dropped out prematurely due to a recurrence of perlèche, which was apparently associated with poorly fitting dentures.

Section C: Application of the Tretinoin Adhesive Ointment to the Oral Mucosa—A total of 18 patients (7 females and 11 males) with lichen ruber planus, confirmed histologically in each case, were treated over a nearly 2-year period. The changes in the mucous membranes had first appeared on the average 20.8 months earlier and had been treated, unsuccessfully, with adhesive ointments and lozenges containing such active ingredients as cortisone, psychopharmacological drugs, external agents with a local anesthetic action, and antimycotics. The condition affecting 17 of the patients was a striate or reticular form of lichen ruber planus, while one patient had lichen planus annularis of the mucosa, which manifested the same kind of changes found on the skin. No erosive or verrucose lesions were observed. While two patients were found to have eruptions on the tongue in addition to buccal changes, only the upper surface of the tongue was affected in two others.

RESULTS AND DISCUSSION

One of the most important criteria in assessing the consistency of ointments is the flow behavior. Among other factors the rheological behavior of aqueous polymethyl methacrylate preparations was influenced by the degree of the neutralization. Strong bases such as sodium hydroxide produced a sharp rise in the pH at the end point corresponding to 7.5 mmol of base/g of the polymer. Weaker bases produced a flatter curve (Fig. 1). The neutralization characteristics of polymethyl methacrylate were similar to those of a weak acid. Maximal viscosity was achieved on the stoichiometric neutralization (100% S) of the carboxyl groups (Fig. 2).

[10] Fin Chambers on Scanpor; Hermal Chemie, Hamburg, West Germany.

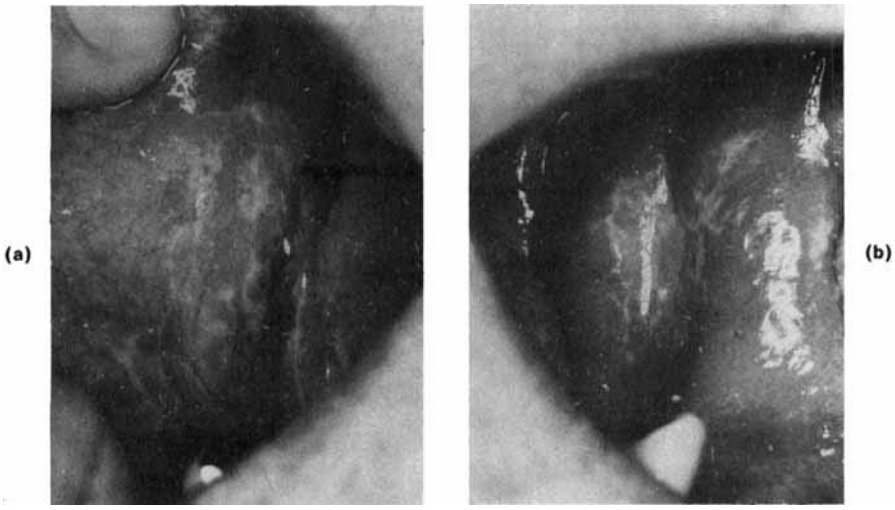

Figure 6—*Buccal mucosa of a patient with lichen planus mucosae oris, right (a) and left (b) sides.*

Admittedly, rheological measurements of polymethyl methacrylate had already been carried out by various researchers (14–16), but these were mainly discontinuous measurements which had lent themselves to widely differing interpretations. To obtain some unequivocal evidence, therefore, it would seem advisable to repeat an investigation of the flow characteristics of the polymethyl methacrylate preparations with a modern rotational viscometer. For this purpose the three standardly marketed types of polymethyl methacrylate (nv, low; mv, medium; hv, high viscidity) were investigated as 5% solutions neutralized with sodium hydroxide. Viscous texture flow curves typical of macromolecular disperse systems were obtained.

The flow characteristics were pseudoplastic; no pronounced thixotropic effect was observed. The highest viscosity was found with polymethyl methacrylate hv (Fig. 3), in line with the molecular weight which, according to the type, varied between 5×10^5 and 2×10^6 (17). In addition to the molecular weight, the solvation status of the polymer coil is also a significant factor in the viscosity of the solution.

The type and concentration of the base (degree of neutralization) can influence the viscosity of the polymer solution. This influence exerted by the base was investigated with sodium tetraborate, sodium hydroxide, triethanolamine, and diisopropanolamine. Relatively small cations, such as sodium ions, afforded relatively low viscosities; sterically expansive cations such as those of the amines, afforded higher viscosities (Fig. 4).

Different concentrations of the base influenced the viscosity of the polymer solution equally (Fig. 5). Fully neutralized carboxyl groups, corresponding to a 100% S (100% saturation) degree of neutralization, resulted in a high viscosity. A probable explanation of this behavior may be the degree of solvation of the polymer. Polymethyl methacrylate as a weak acid is badly dissociated and insoluble in aqueous systems (11). After neutralization of the polymer it can be assumed that nearly all acid groups are dissociated and the polymer is completely solvated, resulting in a viscous solution. Partly neutralized preparations as well as those with an excess of base were less viscous; in the first case, not all the carboxyl groups were completely solvated, and in the second, free cations interfered with complete solvation.

The polymethyl methacrylate preparations became increasingly tacky as the degree of neutralization was reduced, which is a desirable feature for good mucosal adhesion. Since saliva is weakly acidic—the values quoted in the literature vary between pH 5.8 and 7.8 (18–20), with average normal saliva at pH 6.4—only partly neutralized polymethyl methacrylate (80% S) was used for the mucosal adhesive ointment. The resulting ointment was free of irritation due to isohydria and had good mucosal adhesion, due to partial neutralization. The active substance, tretinoin, is stable in the weakly acidic milieu afforded by the ointment base.

Solubilizers and organic solvents such as those in tretinoin preparations for external application (21) should not be used to incorporate the active substances for mucosal ointments. Consequently, the micronized drug could only be suspended in the ointment base. Hence, there is a possibility of sedimentation due to the base lacking any thixotropic effect; in addition, crystal growth is possible and had to be tested for. To that end, the fineness and degree of dispersion of the active substance were determined as a function of storage conditions. The majority of the particles were <10 μm. Larger particles up to 60 μm were observed sporadically. Table I shows that there is no appreciable recrystallization as judged by the grain size distribution as a function of storage time.

If due allowance is made for the variations that occur with the analytical method, it will be seen that the drug content was practically constant over the observation period (Table II). Neither sedimentation nor any loss of active substance occurred during storage. These qualities go far beyond the requirements of the USP XX with regard to tretinoin ointments, which allow contents to vary between 90 and 130% (12). For the clinical tests, the ointment was supplied to the patients in 20-g tubes. This was at most a 2-week supply.

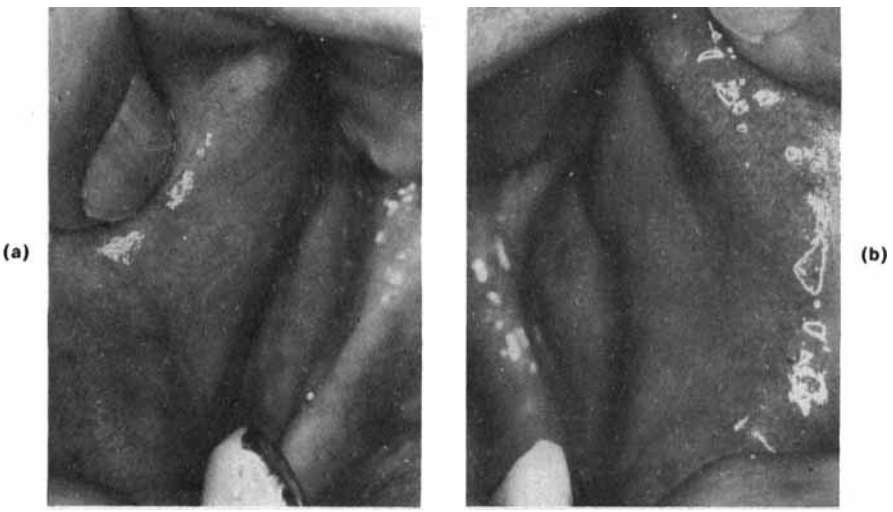

Figure 7—*Buccal mucosa of the same patient after treatment with the tretinoin adhesive ointment, right (a) and left (b) sides.*

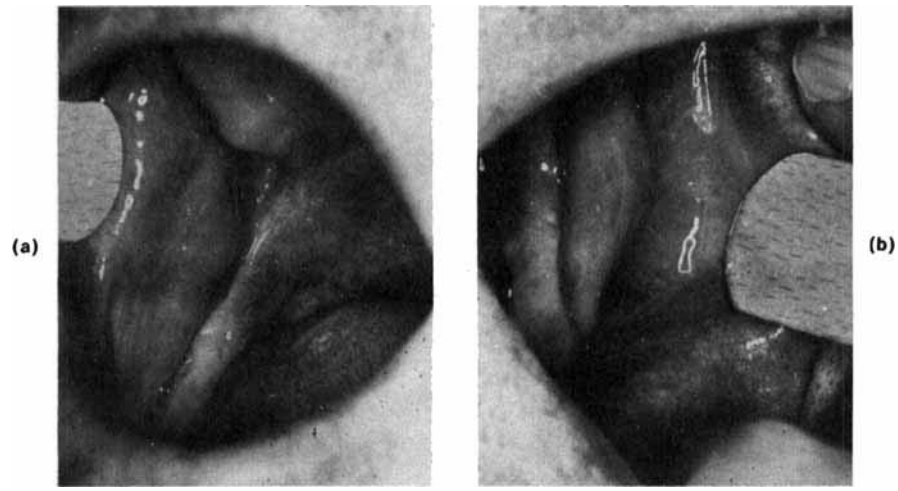

Figure 8—*Buccal mucosa of the same patient 20 months after completing a 3-week course of treatment with the tretinoin adhesive ointment, right (a) and left (b) sides.*

The use of this package size reduced to a low level the risk of any secondary contamination of the ointment.

No positive skin reaction was found in any of the subjects when the patch test was evaluated. No observable objective changes in either the treated or untreated areas were found when the oral mucosa of the subjects remaining in the trial were examined macroscopically with illumination of the buccal cavity. Subjectively, a feeling of "numbness" or of "stickiness" at the site of application lasting some 10–15 min after application of the ointment was reported.

With twice-daily treatment with tretinoin mucosal adhesive ointment, the macroscopic lesions disappeared after an average of 3.12 weeks in 15 of 18 patients (Figs. 6 and 7). This observation was also in accordance with the histological findings in two patients who agreed to an exploratory excision of tissue after completing therapy. To examine the long-term effect, the patients returned for a checkup 11.4 months (on average) after discontinuing therapy; this revealed that none had suffered a relapse (Fig. 8). The two patients who had lesions on the tongue only were among the three subjects in whom therapy was unsuccessful. The tongue lesions of one patient who had buccal changes as well also failed to respond to treatment. However, other authors have also reported that tongue changes in lichen ruber planus exhibit similar resistance to therapy (22). No undesirable side effects of the oral mucosa occurred in any of our cases. The ointment caused no unpleasant sensations and had good adhesive qualities.

As a novel concept, aqueous polymethyl methacrylate preparations can be employed as extremely well-tolerated ointment bases for use in mucous membranes. These ointment bases are characterized by an excellent adhesion. A description of a model for the determination of the adhesive time of mucosal adhesive ointments *in vitro* will be published elsewhere. The preparation of the polymethyl methacrylate ointment base as well as the incorporation of the active agent is easily carried out. The system can be utilized for other drugs, other symptoms, and all mucous membranes, with possible application to oral and vaginal mycoses, herpes labialis, pyoderma, and aphthosis.

Table II—Percentage of Tretinoin in Polymethyl Methacrylate Mucosal Adhesive Ointment as a Function of Storage Temperature and Time

Storage Temp.	Storage Time		
	Nil	3 months	6 months
8°C	0.102%	0.101%	0.100%
25°C	0.101%	0.098%	0.099%

REFERENCES

(1) D. Afonsky, "Saliva and Its Relation to Oral Health," University of Alabama Press, Drawer, Ala., 1961.

(2) J. E. Eastoe, in, "Biochemists' Handbook," C. King, E. J. King, and W. M. Sperry, Eds., Spon, London, 1961, p. 907.

(3) S. Dreizen, J. S. Goodrich, and B. M. Levy, *Arch. Oral. Biol.*, **13,** 229 (1968).

(4) C. Dawes, *Arch. Oral Biol.*, **14,** 277 (1968).

(5) H. Sucker, P. Fuchs, and P. Speiser, "Pharmazeutische Technologie," Georg Thieme Verlag, Stuttgart, 1978, p. 656.

(6) M. S. H. Günther, *Bull. Derm.*, **79,** 477 (1972).

(7) K. Sloberg, K. Hersle, H. Mobacken, and H. Thilander, *Arch. Dermatol.*, **115,** 716 (1979).

(8) A. R. Shalita, *Int. J. Dermatol.*, **15,** 182 (1976).

(9) S. H. Günther, *Arch. Dermatol.*, **107,** 277 (1973).

(10) S. Günther, *Dermatologica*, **147,** 130 (1973).

(11) K.-D. Bremecker, *Acta Pharm. Technol.*, **26,** 231 (1980).

(12) U.S. Pharmacopeia, 20th rev., U.S. Pharmacopeial Convention, Rockville, Md., 1980, p. 809.

(13) H. J. Bandmann and W. Dohn, "Die Epicutantestung," Verlag Bergmann, München, 1967.

(14) J. Smid-Korbar and J. Kristl, *Parfuem. Kosmet.*, **59,** 188 (1978).

(15) S. Srcic, J. Smid-Korbar, and J. Kristl, *Acta Pharm. Technol.*, **26,** 121 (1980).

(16) S. Srcic, I. Erös, and J. Smid-Korbar, *Acta Pharm. Technol.*, **27,** 243 (1981).

(17) Information Sheet, Röhm Pharma, Darmstadt.

(18) W. Kreusser, A. Heidland, H. Hennemann, M. E. Wigand, and H. Knauf, *Eur. J. Clin. Invest.*, **2,** 398 (1972).

(19) D. B. Ferguson and A. Fort, *Arch. Oral Biol.*, **19,** 47 (1974).

(20) C. Dawes, *Arch. Oral Biol.*, **19,** 887 (1974).

(21) D. A. Schlichting, W. M. Wooding, and M. Brown, *J. Pharm. Sci.*, **62,** 388 (1973).

(22) S. Günther, *Z. Hautkr.*, **50,** 41 (1975).

Examination of the Interrelationship Between Aliphatic Group Dipole Moment and Polar Substituent Constants

WEN-YEN LI, ')NG-RU GUO, and ERIC J. LIEN ˣ

Received February 1 83, from the *Section of Biomedicinal Chemistry, School of Pharmacy, University of Southern California, Los Angeles, CA 90033.* Acceptec ublication March 29, 1983.

Abstract □ The relationships between 210 aliphatic group dipole moments (μ) and Taft polar constants (σ^*) are explored, and they are shown to be correlated by a general equation: $\mu = -a\cdot\sigma^* - b\cdot n' - c$, where a, b, and c are constants. The value n' is a parameter reflecting the attenuating factor due to the number and electronic nature of the interval atoms between the most electronegative atom and the first atom connected to the acetate in the measurement of σ^*. The μ and σ^* values of over 214 aliphatic substituents are compiled for future correlation studies. Comparative examples using σ^* and μ in quantitative structure-activity relationships are presented.

Keyphrases □ Dipole moment—aliphatic group, correlation with Taft polar substituent constants, quantitative structure-activity relationships □ Taft polar substituent constants—correlation with aliphatic group dipole moment, quantitative structure-activity relationships □ Quantitative structure-activity relationships—interrelationships between aliphatic group dipole moment and Taft polar substituent constants, applications

In addition to the electronic parameters like the Hammett σ constant and Taft polar constant (σ^*), the group dipole moment, a free energy-related parameter, has been used to study drug-receptor interactions and quantitative structure-activity relationships, especially if σ or other electronic parameters fail to give meaningful correlations (1). It has been reported (1) that the correlation between the aromatic group dipole moment (μ) and σ_m or σ_p varies drastically, or fails completely, if noncongeneric groups are pooled together.

The Taft polar constant (σ^*), which describes mainly the magnitude of inductive electron-withdrawing power of the substituent in the aliphatic system X—CH_2COOR on the reactive center, is defined by (1):

$$\sigma^* = (1/2.48)[\log (K_X/K_0)_B - \log (K_X/K_0)_A] \quad \text{(Eq. 1)}$$

in which B and A designate base- and acid-catalyzed hydrolyses of the ester with the substituent α to the carbonyl group. Although there are problems associated with the definition of σ^*, it is a reasonably accurate measure of the inductive effect, *i.e.*, the inductive electron-withdrawing power of an atom or group of atoms in a molecule. One may expect a better correlation between the aliphatic dipole moment μ, a measure of the charge separation in the group, and σ^* than that of μ and σ_m or σ_p. There have been some reports about the correlation of σ^* values with dipole moments (2), but they mainly involve some limited congeneric series of substituents. The present report attempts to make a wider exploration of the problem and to compile a table of aliphatic group dipole moments and σ^* for future use in correlation studies.

EXPERIMENTAL

A total of 214 substituent groups (for which both μ and σ^* were available) were analyzed to examine the relationship between μ and σ^*. Taft polar constants (σ^*) were taken from Hansch and Leo (3) and Perrin (4). The aliphatic group dipole moments (μ) were taken from the corresponding aliphatic molecular dipole moments (5), where the group is attached to an alkyl group, $CH_3(CH_2)_n$ — X (n = 0–6), assuming the dipole moment value of the alkyl group to be zero. The sign is assigned by comparison of the electronegativities between the substituent and the alkyl group to which the substituent group is connected. A negative sign indicates an electron-withdrawing group. All the regression lines were derived by a computer[1] *via* the method of nonweighted least-squares fit.

RESULTS AND DISCUSSION

Equation 2 shows the overall correlation between σ^* and μ of 214 substituent groups:

$$\mu = -0.676\sigma^* - 1.055$$

$$n = 214 \quad r = 0.583 \quad s = 1.031 \quad \text{(Eq. 2)}$$

It is obvious that the correlation is not good, and only 34% ($r^2 = 0.34$) of the variance in the data can be explained by this equation. Since the exact number of n in $CH_3(CH_2)_nR$ will not affect the dipole moment, but will affect the σ^* value of such an $R(CH_2)_n$ group attached to an acetate used in the acid- and base-catalyzed hydrolyses, the attenuated polar effect due to different n values needs to be corrected.

According to an alternative approach to the definition of localized effect, a new parameter σ' was proposed by Roberts and Moreland (6) using the pK_a of 4-substituted bicyclo[2.2.2]octane-1-carboxylic acids:

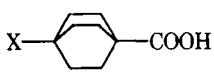

where

$$\sigma'X = \frac{-pK_X + pK_H}{\rho'} \quad \text{(Eq. 3)}$$

Kirkwood and Westheimer used Eq. 4 to describe the effect of the substituent on the acid strength of a series of XG—COOH (7):

$$\log K_X/K_H = \frac{c\mu_x\cdot\cos\theta}{2.303\cdot RTD\cdot r^2} \quad \text{(Eq. 4)}$$

where e is the electric charge on the proton, μ_x is the moment of the X—G bond, r is the distance between the proton and the center of the dipole, θ is the angle made by the distance r and the X—G bond, and D is the dielectric constant.

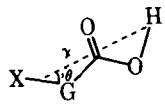

Combining Eq. 4 with the Hammett equation, one obtains (7):

$$\rho'\cdot\sigma_x = \frac{c\mu_x\cdot\cos\theta}{2.303\cdot RTD\cdot r^2} \quad \text{(Eq. 5)}$$

Equation 5 indicates that the localized effect of the constituent group is not only dependent on its dipole moment, but also inversely proportional to the square of the distance from the center of the dipole to the reaction site. Accurately determining the distance and the electrical effect of G between X and the reaction site is not easy. The polar effect of the substituent group is some combination of the inductive (through a bond) and field (through space) effects; therefore, the interval atom number between the most electronegative atom (where the negative inductive effect predominates) and the first atom of the group connecting the reaction site in the measurement of σ^*, as well as their electronic character, need to be considerd to fully reflect the effect of G on the magnitude of σ^*. This requires the addition of an attenuating parameter in correlating μ with σ^*.

Each interval atom exerts a shielding effect to transmit the inductive electron-withdrawing power as measured by σ^*. The higher the interval atom number (n), the greater will be the total shielding effect. When going over three —CH_2— the inductive effect of the group becomes insignificant.

[1] Model 370/185; IBM.

0022-3549/84/0400-0553$01.00/0
© 1984, American Pharmaceutical Association

Table I—Correlation Equations for Anticonvulsant Activity of Substituted Benzyl *N,N*-Dimethyl Carbamates

a	*b*	*c*	Constant	*n*	*r*	*s*	$F_{1,x}$[a]	Eq. No.
$-\log ED_{50} = -a(\log p)^2 + b(\log p) + c\cdot\sigma$ + constant								
0.191	0.795		2.541	20	0.702	0.212		12
0.200	0.836	−0.150	2.252	20	0.720	0.213	$F_{1,16} < 0$	13
0.217	0.905		2.481	18	0.814	0.175		14
0.245	1.040	−0.324	2.392	18	0.876	0.150	$F_{1,14} = 6.3$	15
$-\log ED_{50} = -a(\log p)^2 + b(\log p) + c\cdot\mu_{ph}$ + constant								
0.219	0.898	0.077	2.565	20	0.801	0.183	$F_{1,16} = 6.4$	16
0.213	0.882		2.499	18	0.800	0.182		17
0.262	1.077	0.102	2.486	18	0.940	0.106	$F_{1,14} = 29.4$	18
$-\log ED_{50} = -a(\log p)^2 + b(\log p) + c\cdot\sigma^*$ + constant								
0.212	0.895	−0.208	2.575	20	0.740	0.206	$F_{1,16} = 2.08$	19
0.217	0.905		2.481	18	0.814	0.175		20
0.250	1.058	−0.253	2.501	18	0.860	0.158	$F_{1,14} = 4.42$	21
$-\log ED_{50} = -a(\log p)^2 + b(\log p) + c\cdot\mu$ + constant								
0.205	0.758	0.129	2.965	20	0.891	0.139	$F_{1,16} = 22.4$	22
0.217	0.905		2.481	18	0.814	0.175		23
0.226	0.861	0.118	2.863	18	0.946	0.102	$F_{1,14} = 30.8$	24

[a] $F_{1,16;0.95} = 4.49$; $F_{1,14;0.95} = 4.60$; $F_{1,16;0.99} = 8.53$; $F_{1,14;0.99} = 8.86$.

However, different types or locations of the interval atom will have different electronic environments which may produce different shielding effects. Thus, n' as an attenuating parameter reflecting the environmental factor of G should not only be the atom number, but be determined on the basis of its contribution to the electron-withdrawing power. Among the environmental factors contributing appreciably to the electron-withdrawing power, the intrinsic electronegativity of the atoms is the most important. If the interval atoms are such that their electronegativity is higher than an sp^3-hybrid carbon atom (—CH_2—) such as O, N, S, sp^2-, sp-hybrid carbon atom, or the sp^3-carbon atom attached by two electronegative atoms (—CCl_2—, —CBr_2—) or groups like NO_2, —C_6H_5, their shielding effect is smaller than that of —CH_2—. This is not only due to electron delocalization of p or d orbitals formed for transmission of inductive action, but also the additive inductive effect on their neighboring atom. Generally, this effect can be shown by causing a downfield shift in NMR spectrum of the proton attached to these atoms. Daily and Shoolery (8) have proposed a scale of electronegativity of substituent groups obtained from shifts in the NMR spectra of ethyl and methyl derivatives; it was strikingly demonstrated that the electronegativities obtained in this manner are essentially equal to the electronegativities of the Pauling scale of the first atom in the group.

For the reasons mentioned above, the following rough rules are suggested as an initial premise to determine the n' values introduced into the regression analysis as a parameter:

1. For each —CH_2— and other atom that has less electronegativity than a carbon atom, $n' = 1$.

2. For N, S, —CH=CH—, —C≡C—, =C=O, and carbon atoms to which two halogen atoms or electronegative groups are attached simultaneously, $n' = 0.5$ each. For the conjugated system —C_6H_4—, —CH=CH—CH=CH—, and —CH=CH—, $n' = 1$.

3. Carbon or other atoms to which three or more oxygen or halogen atoms are attached are assigned $n' = 0$, for example, —CCl_3, —SO_3R.

The above method is employed to determine the n' values of each group. For example, with a *p*-nitrophenyl sulfide group, the —NO_2 withdraws electrons from all atoms, the negative pole of this group is toward oxygen atoms, the interval atoms include one sulfur atom ($n' = 0.5$), one benzine ring ($n' = 1$), and a nitrogen atom ($n' = 0.5$); therefore, the total $n' = 0.5 + 1 + 0.5 = 2.0$.

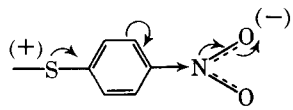

By introducing the n' into the regression analysis together with σ^* values, Eq. 6 was obtained:

$$\mu = -0.853\sigma^* - 1.045n' - 0.160$$
$$n = 214 \quad \gamma = 0.801 \quad s = 0.762 \qquad \text{(Eq. 6)}$$

Comparison with Eq. 2 shows that the correlation coefficient is markedly improved. An *F*-test indicates that the interval atom factor n' is statistically highly significant ($F_{1,211} = 171$) for studying the relationship between σ^* and μ.

By deleting those groups which deviate greater than 2 *SD* from this regression and by dividing the 210 substituents into two subgroups, the following equations were obtained. For subgroup I:

$$\mu = -0.687\sigma^* - 0.760$$
$$n = 177 \quad r = 0.686 \quad s = 0.755 \qquad \text{(Eq. 7)}$$
$$\mu = -0.853\sigma^* - 0.942n' - 0.028$$
$$n = 177 \quad r = 0.921 \quad s = 0.406 \qquad \text{(Eq. 8)}$$

Table II—Anticonvulsant Activity and Physicochemical Parameters of Substituted Benzyl *N,N*-Dimethyl Carbamates

X	$\log 1/ED_{50}$[a] Obs.	Calc.	log p[a]	σ[a]	μ_{ph}[b]	σ^*[c]	μ[c]
H	3.71	3.67	2.16	0.00	0.03	0.75	−0.38
p-CH_3	3.58	3.55	2.63	−0.15	0.36	0.59	−0.10
p-F	3.50	3.44	2.30	0.17	−1.43	0.81	−1.78
m-OCH_3	3.49	3.53	2.09	0.13	−0.65	0.62	−1.25
p-OCH_3	3.46	3.52	2.20	−0.12	−1.30	0.42	−1.23
m-NH_2	3.45	3.35	1.06	−0.14	0.80	0.16	−1.44
m-Cl	3.41	3.28	2.82	0.37	−0.80	0.85	−1.82
p-Cl	3.35	3.22	2.93	0.27	−1.59	0.92	−1.90
m-$N(CH_3)_2$	3.29[d]	3.46	2.28	−0.15	0.80	0.16	−1.60
m-O-*i*-Pr	3.21	3.35	2.80	0.04	−0.65	0.62	−1.25
p-OCH_2Ph	3.19[d,e]	3.09	3.27	−0.42	−1.35	0.42	−1.23
p-NO_2	3.19	3.16	1.95	0.82	−4.13	1.14	−4.43
p-CN	3.16	3.15	1.67	0.69	−4.08	1.05	−4.41
p-Br	3.15	3.18	3.01	0.26	−1.57	0.90	−1.91
p-I	3.14	3.02	3.32	0.27	−1.36	0.87	−1.76
p-CF_3	3.10	3.14	3.08	0.53	−2.61	0.96	−1.94
m-OPh	2.92	2.91	3.55	0.25	−0.58	0.35	−1.38
p-*tert*-Bu	2.47	2.55	4.14	−0.17	0.52	0.43	0.00
p-$OCON(CH_3)_2$	3.09	3.21	1.59	0.22	−3.70	1.40[f]	−3.90
p-SCH_3	2.88[e]	3.19	2.12	0.08	−1.34	0.66	−4.08

[a] Taken from Ref. 11; $\log 1/ED_{50}$ calculated using Eq. 24. [b] Value along the *para*-direction. [c] The value of substituent 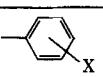 [d] Outliers in Eq. 16. [e] Outliers in Eqs. 13, 19, and 22. [f] Calculated from Eq. 10.

Table III—Antifungal Activity and Physicochemical Parameters

R	pI_{50} Obs.[a]	pI_{50} Calc.[b]	Log MW	Log p[a]	μ
	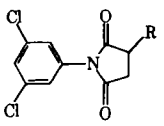				
H	5.58	5.63	2.39	1.90	−0.02
Me	5.62	5.69	2.41	2.22	0.00
Et	5.73	5.77	2.44	2.76	0.00
n-Pr	5.83	5.85	2.46	3.30	0.08
Isopr	5.89	5.83	2.46	3.17	0.08
n-Bu	5.99	5.94	2.49	3.84	0.08
Ph	6.00	5.89	2.51	3.36	−0.38
S—Me	5.49	5.52	2.46	1.28	−1.45
S—Et	5.68	5.58	2.48	1.82	−1.47
S—*n*-Pr	5.70	5.64	2.50	2.36	−1.47
S—*n*-Bu	5.79	5.69	2.52	2.90	−1.47
S—*n*-Pent	5.65	5.75	2.54	3.44	−1.47
CH_2—S—Et	5.48	4.64	2.50	2.36	−1.47
CH_2—S—*n*-Pr	5.62	5.69	2.52	2.90	−1.47
CH_2—S—Isopr	5.68	5.69	2.52	2.77	−1.47
SOMe	5.06	5.10	2.49	−0.94	−3.88
SO—*n*-Pr	5.25	5.21	2.53	0.14	−3.88
SO_2Me	5.11	5.07	2.51	−1.37	−4.26
SO_2Et	5.27	5.13	2.53	−0.83	−4.26
SO_2—*n*-Pr	4.92	5.19	2.55	−0.29	−4.26
SO_2—*n*-Bu	5.15	5.22	2.56	0.25	−4.26
CH_2-SO_2-Et	5.38	5.19	2.55	−0.29	−4.26
	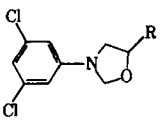				
H	5.47	5.63	2.39	2.77	−0.02
Me	5.80	5.69	2.41	3.09	0.00
Et	5.95	5.77	2.44	3.63	0.00
Isopr	5.83	5.83	2.46	4.04	0.08
tert-Bu	5.90	5.92	2.49	4.45	0.08
Ph	5.79	5.89	2.51	4.23	−0.38

[a] Taken from Ref. 12. [b] Calculated from Eq. 31.

For subgroup II:

$$\mu = -0.635\sigma^* - 2.666$$

$$n = 33 \quad r = 0.787 \quad s = 0.648 \qquad \text{(Eq. 9)}$$

$$\mu = -0.763\sigma^* - 0.853n' - 1.820$$

$$n = 33 \quad r = 0.940 \quad s = 0.366 \qquad \text{(Eq. 10)}$$

The first subgroup includes 180 substituent groups of no distinct structural relationship, but the second subgroup includes 33 substituent groups characterized structurally as amido, sulfonyl, sulfone, nitrophenyl, and amino groups.

All the equations have very similar slopes, and n' shows similar contribution to the overall correlation. Thus, the relationship between the dipole moment and polar substituent constant σ^* may be presented by the following:

$$\mu = -a\cdot\sigma^* - b\cdot n' - c \qquad \text{(Eq. 11)}$$

n' is a complex factor including the number and electronic nature of the interval atoms. Whether n' can be expressed more accurately by the chemical shift values of these atoms in ^{1}H- or ^{13}C-NMR remains to be studied. Careful examination of the data shows that for practical application of the equation, the range of the value of n' is limited to 0–2.5, and the total value of n' generally should not be greater than the value of σ^* or μ to obtain a reasonable result (*Appendix*).

In Eq. 11, c is a constant representing the types of substituent groups. Substituents in the second subgroup, like amido, sulfonyl, sulfone, amino, and nitrophenyl groups, have considerably larger μ values with relatively small σ^* values. For amines and amides this may be due to the lone pair electron on the nitrogen atom decreasing the inductive electron-withdrawing power of C=O and SO_2—, while at the same time increasing the dipole moment through its resonance effect. For sulfonyl and sulfone groups, the relatively large dipole moment values may be due to presence of much larger mesomeric moments (9, 10).

On the basis of the correlations obtained, σ^* expresses the total electronic effect of the substituent, including the X and G in the group. Thus if interaction between drug and receptor is controlled by the total electronic nature (X + G) of the substituent through transmission toward the reactive site, σ^* constants may be a suitable descriptor of electronic effects for QSAR. If, on the other hand, the interaction is intermolecular in nature and is controlled directly by the electronic nature of the X portion of the substituent, then dipole moment μ as a measure of the charge separation in the group may give a more meaningful correlation.

For instance, Eqs. 12–24 (Table I) show the QSAR between the anticonvulsant activity and physicochemical parameters (Table II) of substituted benzyl *N*,*N*-dimethyl carbamates reported by Yamauea *et al.* (11):

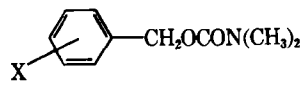

Equations 13 and 15 were obtained by using simultaneously Hammett σ constant and Hansch's π, but in Eqs. 16 and 18, the aromatic group dipole moment μ_{ph} was used as an electronic parameter instead of σ. When the substituted benzene is regarded as an aliphatic substituent group of CH_3—$OCON(CH_3)_2$, Eqs. 19 and 21, and 22 and 24 are obtained by using the Taft polar constant σ^* and aliphatic group dipole moment μ as the electronic parameters, respectively.

According to the correlation coefficient and *F*-test, the dipole moment (whether aromatic group moment μ_{ph} or aliphatic group moment μ) gives a statistically more significant correlation than the Hammett σ or Taft σ^*. Among these electronic parameters used, the aliphatic group dipole moment seems to be the best, giving the highest degree of correlation in the case examined (Eq. 24).

Takayama *et al.* (12) reported the QSAR of antifungal 1-(3,5-dichlorophenyl)-2,5-pyrrolidinediones and 3-(3,5-dichlorophenyl)-2,4-oxazolidinediones and showed that the activity becomes greater with the increasing hydrophobicity of the substituents on the imido ring, independent of the electronic (σ^*) and steric effects (E_s) (Table III). Reexamination with aliphatic group dipole moment μ as an electronic parameter and log MW as a measure of bulk is shown by Eqs. 25–31 (Table IV). The correlation with μ or log p alone is statistically significant, although the improvement in regression with log p by introducing μ or log MW is generally not very significant ($F_{1,25}$ = 2.58 or 0.25, respectively) because of considerable covariance between log p and μ or μ and log MW. Among the two parameter equations, the combination of log MW and μ gives the highest correlation (Eq. 31), and the combination of log p and μ gives a slightly lower correlation (Eq. 30). The addition of log MW is statistically significant at the 99.9% level, as indicated by an *F*-test ($F_{1,25}$ = 21.80). This suggests that both the size of the molecule (13) and the dipole moment of the substituent group are important in determining the antifungal activity of the compounds examined.

The existence of the covariance among log p, log MW, and μ is shown in the following squared correlation matrix:

	log MW	log p	μ
log MW	1	0.13	0.50
log p		1	0.81
μ			1

Use of these three parameters simultaneously or the addition of $(\log p)^2$ does not result in a further improvement in correlation.

Table IV—Equations Correlating Antifungal Activity with Physicochemical Constants

Equation	*n*	*r*	*s*	$F_{1,25}$	Eq. No.
$pI_{50} = -2.352(\log MW) + 11.442$	28	0.378	0.281		25
$pI_{50} = 0.153\mu + 2.582$	28	0.871	0.145		26
$pI_{50} = 0.158(\log p) + 5.258$	28	0.907	0.128		27
$pI_{50} = (\log p)^2 + 0.159(\log p) + 5.258$	28	0.907	0.130		28
$pI_{50} = -0.350(\log MW) + 0.155(\log p) + 6.133$	28	0.908	0.130	0.25	29
$pI_{50} = 0.113(\log p) + 0.050\mu + 5.428$	28	0.915	0.125	2.58	30
$pI_{50} = 2.879(\log MW) + 0.212\mu - 1.252$	28	0.934	0.111	21.80	31

Appendix Aliphatic Dipole Moments and Taft Polar Constants (σ^*)
$CH_3(CH_2)_nR$, where n = 0–6

No.	Formula	R	n'	μR, Debye	σ^*	WLN	Solvent[a]	Temp., °C
1	BH_2O_2	—$B(OH)_2$	0.5	−1.16	0.95	*BQQ	G	115
2	Br	—Br	0.0	−1.97	2.84	*E	CCl_4	25
3	Cl	—Cl	0.0	−1.93	2.68	*G	CCl_4	25
4	ClO_2S[b]	—SO_2Cl	0.0	−2.28	5.00	*SWG	B	25
5	Cl_2PS	—$PSCl_2$	0.0	−3.00	3.70	*PS&GG	B	20
6	ClS	—SCl	0.5	−2.00	2.50	*SG	G	—
7	F	—F	0.0	−1.90	3.21	*F	G	NS
8	FO_2S	—SO_2F	0.0	−3.39	4.70	*SWF	B	25
9	F_4P	—PF_4	0.0	−2.55	2.80	*PFFFF	G	31–70
10	I	—I	0.0	−1.79	2.46	*I	CCl_4	25
11	NHCHO	—NHCHO	1.0	−3.86	1.62	*MVH	B	25
12	NCO	—NCO	1.0	−2.81	2.25	*NCO	B	20
13	H_2NO	—NHOH	0.5	−0.80	0.30	*MQ	B	25
14	NH_2	—NH_2	0.0	−1.35	0.62	*Z	B,CHx	25
15	NO	—NO	0.5	−2.30	2.08	*NO	G	NS
16	NO_2	—NO_2	0.5	−3.59	4.25	*NW	G	20
17	NH_2O_2S	—SO_2NH_2	0.5	−4.60	2.61	*SWZ	D	30
18	NO_3	—ONO_2	0.5	−3.08	3.86	*ONW	G	−78
19	N_2H_3	—$NHNH_2$	0.5	−1.82	0.40	*MZ	G	25
20	N_3	—N=N=N	0.0	−2.17	2.62	*NNN	G	NS
21	OH	—OH	0.0	−1.66	1.55	*Q	B	25
22	SH	—SH	0.0	−1.51	1.68	*SH	B	25
23	SO_2CH_3	—$S(O)OCH_3$	0.5	−2.83	2.84	*SO&O1	B	25
24	SO_3CH_3	—SO_2CH_3	0.0	−4.16	3.62	*OSWI	D	25
25	$SeCH_3$	—$SeCH_3$	1.0	−1.41	0.95	*-Se-1	G	NS
26	CClO	—COCl	0.5	−2.48	1.81	*VG	CCl_4	25
27	CCl_3	—CCl_3	0.0	−1.84	2.65	*XGGG	CHx	25
28	CF_3	—CF_3	0.0	−1.94	2.61	*XFFF	B	25
29	CN	—CN	0.5	−3.63	3.30	*CN	B	30
30	CNS	—SCN	1.0	−3.89	3.43	*SCN	B	25
31	CNSe	—SeCN	1.5	−3.91	3.61	*-Se-CN	B	25
32	$CHBr_2$	—$CHBr_2$	0.5	−1.90	1.90	*YEE	CHx	25
33	$CHCl_2$	—$CHCl_2$	0.5	−1.96	1.94	*YGG	B	25
34	CHO	—CHO	0.5	−2.58	2.15	*VH	B	25
35	CHO_2	—COOH	0.5	−1.65	2.08	*VQ	B	30
36	CH_2Br	—CH_2Br	1.0	−1.97	1.00	*1E	CCl_4	25
37	CH_2Cl	—CH_2Cl	1.0	−1.93	1.05	*1G	CCl_4	25
38	CH_2I	—CH_2I	1.0	−1.79	0.85	*1I	CCl_4	25
39	CH_2NO	—$CONH_2$	0.5	−3.73	1.68	*VZ	B	25
40	CH_2NO_2	—CH_2NO_2	1.5	−3.29	1.73	*1NW	B	25
41	CH_2ClO	—OCH_2Cl	0.0	−1.90	2.56	*01G	B	0
42	CH_2SH	—CH_2SH	1.0	−1.52	0.62	*1SH	G	−50
43	CH_3	—CH_3	0.0	0.0	0.0	*1	G	—
44	CH_3N_2S[b]	—$NHCSNH_2$	0.0	−0.16	1.80	*MYZUS	B	25
45	CH_3O	—OCH_3	0.0	−1.27	1.81	*01	B	25
46	CH_3OS	—$S(O)CH_3$	0.5	−3.88	2.88	*SO&1	B	20
47	CH_3O_2S	—SO_2CH_3	0.5	−4.26	3.68	*SW1	B	25
48	CH_3O_3S	—SO_2OCH_3	0.0	−4.18	3.62	*SW01	D	25
49	CH_3S	—SCH_3	0.0	−1.45	1.56	*S1	B	25
50	CH_4N	—$NHCH_3$	0.0	−1.01	−0.81	*M1	G	NS
51	CH_4N	—CH_2NH_2	1.0	−1.35	0.50	*1Z	B,CHx	25
52	C_2H	—C≡CH	0.0	−0.78	1.30	*1UU1	NS	NS
53	C_2HS	—SCCH	0.0	−1.69	2.00	*S1UU1	G	−53
54	C_2H_2Cl	—CHCHCl	1.0	−1.64	0.87	*1U1G	G	—
55	$C_2H_2NO_2$	—$CHCHNO_2$	1.5	−3.99	1.75	*1U1NW	B	20
56	$C_2H_2Cl_3$	—CH_2CCl_3	1.0	−1.84	0.75	*1XGGG	CHx	25
57	C_2H_2OCl	—$COCH_2Cl$	0.5	−2.27	2.50	*V1G	CCl_4	25
58	C_2H_3	—$CH=CH_2$	0.0	−0.40	0.56	*1U1	G	−78
59	$C_2H_3Br_2$	—$CHBrCH_2Br$	1.0	−1.43	1.38	*YE1E	B	25
60	$C_2H_2Cl_3$	—$CHClCHCl_2$	1.0	−2.07	1.08	*YGYGG	—	—
61	$C_2H_3Cl_2$	—CCl_2CH_3	0.5	−2.33	1.53	*XGG1	I	31–55
62	C_2H_3O	—CH_2CHO	1.5	−2.23	0.62	*1VH	B	25
63	C_2H_3O	—$COCH_3$	0.5	−2.77	1.81	*V1	B	30
64	$C_2H_3O_2$	—CH_2COOH	1.5	−1.68	1.08	*1VQ	B	25
65	$C_2H_3O_2$	—$COOCH_3$	0.5	−1.75	2.00	*V01	B	25
66	$C_2H_3O_2$	—$OCOCH_3$	0.0	−1.81	2.56	*OV1	B	25
67	C_2H_3S	—$SCH=CH_2$	0.0	−1.38	1.31	*S1U1	B	25
68	C_2H_4Br	—$CHBrCH_3$	1.0	−2.08	1.25	*YE	CCl_4	25
69	C_2H_4Br	—CH_2CH_2Br	2.0	−1.97	0.44	*2E	CCl_4	25
70	C_2H_4Cl	—$CHClCH_3$	1.0	−2.05	1.00	*YG	CCl_4	25
71	C_2H_4Cl	—CH_2CH_2Cl	2.0	−1.93	0.41	*2G	CCl_4	25
72	C_2H_4I	—CH_2CH_2I	2.0	−1.79	0.41	*2I	CCl_4	25
73	C_2H_4NO	—$NHCOCH_3$	1.0	−3.81	1.40	*MV1	B	25
74	C_2H_4NO	—CH_2CONH_2	1.5	−3.75	0.31	*1VZ	B	25
75	$C_2H_4NO_2$	—$CH_2CH_2NO_2$	2.5	−2.69	0.50	*2NW	B	30
76	C_2H_5	—C_2H_5	0.0	0.0	−0.10	*2	G	NS
77	C_2H_5O	—OC_2H_5	0.0	−1.27	1.68	*02	B	25
78	C_2H_5O	—CH_2OCH_3	1.0	−1.32	0.66	*101	CCl_4	25
79	C_2H_5O	—$CH(OH)CH_3$	1.0	−1.69	0.46	*YQ	CHx	25

continued

Appendix (continued)

No.	Formula	R	n'	μR, Debye	σ^*	WLN	Solvent[a]	Temp., °C
80	C_2H_5O	$-CH_2CH_2OH$	2.0	−1.66	0.21	*2Q	B	25
81	$C_2H_5O_2S$	$-S(O)OC_2H_5$	0.5	−2.84	2.84	*SO&O2	B	25
82	$C_2H_5O_2S$	$-CH_2SO_2CH_3$	1.5	−4.40	1.32	*1SW1	B	25
83	C_2H_6N	$-N(CH_3)_2$	0.0	−1.26	−0.62	*N1&1	B	25
84	$C_2H_6NO_2S$	$-SO_2N(CH_3)_2$	0.5	−4.71	2.62	*SWN1&1	B	25
85	$C_2H_6NO_2S$	$-NCH_3SO_2CH_3$	1.0	−4.71	2.10	*N1&SW1	B	25
86	C_2H_6OP	$-PO(CH_3)_2$	1.0	−4.20	2.81	*PO&1&1	B	25
87	C_3H_3	$-CCCH_3$	0.0	−0.84	1.20	*1UU2	G	—
88	C_3H_3	$-CH_2CCH$	1.0	−0.84	0.81	*2UU1	G	35
89	$C_3H_4F_3$	$-CH_2CH_2CF$	2.0	−1.94	0.32	*2XFFF	—	—
90	C_3H_4N	$-CH_2CH_2CN$	2.5	−3.51	0.49	*2CN	CCl_4	20
91	C_3H_5	$-C(CH_3)CH_2$	0.0	−0.34	0.48	*YU1	B	25
92	C_3H_5	$-CH_2CHcH_2$	1.0	−0.35	0.0	*2U1	G	−78
93	C_3H_5	$-CHCHCH_3$	0.0	−0.25	0.36	*1U2	G	NS
94	C_3H_5	—cyclo-C_3H_5	0.0	−0.14	0.15	*AL3TJ	G	—
95	C_3H_5O	$-COC_2H_5$	0.5	−2.79	1.61	*V2	B	25
96	C_3H_5O	$-CH_2CH_2CHO$	2.5	−2.23	0.29	*2VH	B	25
97	C_3H_5O	$-CH_2COCH_3$	1.5	−2.80	0.62	*1V1	B	25
98	$C_3H_5O_2$	$-CH_2OCOCH_3$	1.0	−1.84	1.06	*10V1	B	25
99	$C_3H_5O_2$	$-COOC_2H_5$	0.5	−1.81	2.26	*V02	B	25
100	$C_3H_5O_2$	$-CH_2COOCH_3$	1.5	−1.84	1.00	*1V01	B	25
101	C_3H_6NO	$-CON(CH_3)_2$	0.5	−3.81	1.94	*VN1&1	B	25
102	C_3H_6NO	$-NHCOC_2H_5$	1.0	−3.55	1.56	*MV2	G	110
103	C_3H_6NO	$N(CH_3)COCH_3$	1.0	−3.86	2.25	*N1&V1	B	25
104	C_3H_6NO	$-CH_2CH_2CONH_2$	2.5	−3.78	0.19	*2VZ	B	25
105	C_3H_6NO	$-CH_2NHCOCH_3$	2.0	−3.55	0.43	*1MV1	G	110
106	$C_3H_6NO_2$	$-NHCOOC_2H_5$	1.0	−3.80	1.99	*MV02	/	20
107	$C_3H_6NO_2$	$-OCON(CH_3)_2$	0.0	−3.80	2.87	*OVN1&1	/	20
108	C_3H_7	$-CH(CH_3)_2$	0.0	0.08	−0.19	*Y	/	—
109	C_3H_7	$-C_3H_7$	0.0	0.08	−0.12	*3	/	—
110	C_3H_7O	$-OCH(CH_3)_2$	0.0	−1.32	1.62	*0Y	B	25
111	C_3H_7O	$CH_2OC_2H_5$	1.0	−1.27	0.58	*102	B	25
112	C_3H_7O	$-OC_3H_7$	0.0	−1.32	1.68	*03	CCl_4	25
113	C_3H_7O	$-CH_2CH(OH)CH_3$	2.0	−1.77	0.16	*1YQ	D	25
114	C_3H_7O	$-CH_2CH_2OCH_3$	2.0	−1.27	0.24	*201	B	25
115	C_3H_7O	$-C(OH)(CH_3)_2$	1.0	−1.72	0.35	*XQ	D	25
116	C_3H_7S	$-SC_3H_7$	0.0	−1.63	1.38	*S3	B	19
117	C_3H_7S	$-SCH(CH_3)_2$	0.0	−1.61	1.49	*SY	B	20
118	$C_3H_7O_2S$	$-SO_2CH(CH_3)_2$	0.5	−4.50	3.68	*SWY	B	25
119	C_4H_7	$-CHCHC_2H_5$	0.0	−0.34	0.31	*1U3	B	25
120	C_4H_7	$-CHC(CH_3)_2$	0.0	−0.34	0.19	*1UY	B	25
121	C_4H_7	$-CH_2CHCHCH_3$	1.0	−0.34	0.0	*2U2	B	25
122	C_4H_9	$-C_4H_9$	0.0	0.08	0.25	*4	B	25
123	C_4H_9O	$-OC_4H_9$	0.0	−1.26	1.68	*04	B	25
124	$C_4H_{10}N$	$-NHC_4H_9$	0.0	−1.27	−1.08	*M4	B	20
125	$C_4C_{10}O_3P$	$-OP(OC_2H_5)_2$	0.0	−2.88	3.02	*PO&O2&02	B	25
126	C_5H_9O	—O-cyclo-C_5H_9	0.0	−1.60	1.62	*OAL5TJ	B	25
127	C_5H_{11}	$-C_5H_{11}$	0.0	0.10	−0.23	*5	/	NS
128	$C_5H_{11}O$	$-O(CH_2)_4CH_3$	0.0	−1.32	1.52	*05	B	25
129	$C_5H_{11}S$	$-S(CH_2)_4CH_3$	0.0	−1.63	1.35	*S5	D	25
130	$C_5H_{11}O_2$	$-CH(OC_2H_5)_2$	0.5	−1.27	1.14	*Y02&02	B	25
131	$C_5H_8O_2$	$-CHCHCOOC_2H_5$	1.5	−1.95	1.12	*1U1V02	B	24
132	$C_6H_2N_3O_6$	$-C_6H_2$—2,4,6-$(NO_2)_3$	0.0	−1.19	1.62	*R BNW DNW FNW	B	25
133	$C_6H_3Cl_2O$	$-OC_6H_3$—2,4-Cl_2	0.0	−2.77	3.17	*OR BG DG	B	20
134	C_6H_4Br	$-C_6H_4$—4-Br	1.0	−1.91	0.86	*R DE	B	25
135	C_6H_4Cl	$-C_6H_4$—2-Cl	1.0	−1.34	1.05	*R BG	HP	20
136	C_6H_4Cl	$-C_6H_4$—4-Cl	1.0	−1.90	0.92	*R DG	B	25
137	C_6H_4Cl	$-C_6H_4$—3-Cl	1.0	−1.82	0.85	*R CG	B	25
138	C_6H_4F	$-C_6H_4$ 3-F	1.0	−1.78	0.82	*R CF	B	25
139	C_6H_4F	$-C_6H_4$—4-F	1.0	−1.78	0.81	*R DF	B	25
140	C_6H_4I	$-C_6H_4$—4-I	1.0	−1.76	0.87	*R DI	B	25
141	$C_6H_4NO_2$	$-C_6H_4$—2-NO_2	1.5	−3.60	1.14	*R BNW	/	9–25
142	$C_6H_4NO_2$	$-C_6H_4$—3-NO_2	1.5	−3.40	1.21	*R CNW	B	25
143	$C_6H_4NO_2$	$-C_6H_4$—4-NO_2	1.5	−4.43	1.26	*R DNW	B	25
144	C_6H_4BrO	$-OC_6H_4$—2-Br	0.0	−2.50	2.45	*OR BE	CCl_4	20
145	C_6H_4BrO	OC_6H_4—3-Br	0.0	−2.05	2.48	*OR CE	B	25
146	C_6H_4BrO	$-OC_6H_4$—4-Br	0.0	−2.37	2.44	*OR DE	B	25
147	C_6H_4ClO	$-OC_6H_4$—3-Cl	0.0	−2.06	2.57	*OR CG	B	25
148	C_6H_4ClO	$-OC_6H_4$—4-Cl	0.0	−2.30	2.62	*OR DG	B	25
149	C_6H_4IO	$-OC_6H_4$—2-I	0.0	−2.25	2.38	*OR BI	CCl_4	20
150	C_6H_4IO	$-OC_6H_4$—4-I	0.0	−2.14	2.39	*OR DI	CCl_4	20
151	$C_6H_4NO_3$	$-OC_6H_4$—2-NO_2	2.0	−4.05	2.78	*OR BNW	B	30, 50
152	$C_6H_4NO_3$	$-OC_6H_4$—3-NO_2	2.0	−4.00	2.76	*OR CNW	B	20
153	$C_6H_4NO_3$	OC_6H_4—4-NO_2	2.0	−4.00	2.91	*OR DNW	B, D	30, 60
154	C_6H_4BrS	$-SC_6H_4$—3-Br	0.0	−1.83	1.84	*SR CE	B	30
155	C_6H_4BrS	$-SC_6H_4$—4-Br	0.0	−1.80	1.83	*SR DE	B	25
156	C_6H_4ClS	$-SC_6H_4$—3-Cl	0.0	−1.83	2.02	*SR CG	B	30
157	C_6H_4ClS	$-SC_6H_4$—4-Cl	0.0	−1.81	1.97	*SR DG	B	30
158	C_6H_4FS	$-SC_6H_4$—4-F	0.0	−1.64	1.77	*SR DF	B	30
159	$C_6H_4NO_2S$	$-SC_6H_4$—2-NO_2	2.5	−4.93	2.47	*SR BNW	B	NS
160	$C_6H_4NO_2S$	$-SC_6H_4$—4-NO_2	2.5	−4.43	2.33	*SR DNW	B	25

Continued on next page

Appendix (continued)

No.	Formula	R	n'	μR, Debye	σ^*	WLM	Solvent[a]	Temp., °C
161	C_6H_4NOSe	$-SeC_6H_4-4-NO_2$	2.5	−4.38	1.83	*SeR DNW	B	NS
162	$C_6H_4NO_4S$	$-SO_2C_6H_4-4-NO_2$	0.0	−2.80	3.63	*SWR DNW	D	25
163	C_6H_4BrOS	$-S(O)C_6H_4-4-Br$	0.5	−3.26	3.14	*SO&R DE	B	20
164	C_6H_4ClOS	$-S(O)C_6H_4-4-Cl$	0.5	−3.08	3.14	*SO&R DG	B	20
165	C_6H_5	$-C_6H_5$	0.0	−0.38	0.75	*R	CHx	25
166	C_6H_5O	$-OC_6H_5$	0.0	−1.38	2.43	*OR	B	25
167	$C_6H_5O_2$	$-OC_6H_4-2-OH$	0.0	−2.46	2.60	*OR BQ	B	60
168	$C_6H_5O_2S$	$-OSOC_6H_5$	0.0	−3.48	3.25	*OSO&R	B	25
169	$C_6H_5O_2S$	$-SO_2C_6H_5$	0.5	−4.75	3.55	*SWR	B	25
170	$C_6H_5O_3S$	$-OSO_2C_6H_5$	0.0	−4.99	3.62	*OSWR	D	25
171	C_6H_5S	$-SC_6H_5$	0.0	−1.29	1.87	*SR	B	25
172	C_6H_5S	$-C_6H_4-2-SH$	1.0	−1.16	0.72	*R BSH	B	25
173	$C_6H_6NO_2S$	$-NHSO_2C_6H_5$	1.0	−4.62	1.99	*MSWR	B	25–55
174	C_6H_{11}	−cyclohexyl	0.0	0.00	0.18	*AL6TJ	CCl_4	25
175	$C_6H_{11}O$	−O-cyclohexyl	0.0	−1.68	1.81	*O AL6TJ	B	25
176	$C_6H_{13}S$	$-S(CH_3)_5CH_3$	0.0	−1.56	1.33	*S6	B	25
177	C_7H_4NO	$-O-C_6H_4-4-CN$	0.0	−4.39	2.73	*OR DCN	B	20
178	C_7H_4ClO	$-OCO(C_6H_4-4-Cl)$	0.0	−1.94	2.63	*OVR DG	B	25
179	$C_7H_4NO_4$	$-OCO(C_6H_4-4-NO_2)$	0.0	−3.48	2.73	*OVR DNW	B	25
180	C_7H_5O	$-CO(C_6H_5)$	0.5	−2.90	2.26	*VR	B	20
181	C_7H_5O	$-OCOC_6H_5$	0.0	−1.94	2.57	*OVR	B	20
182	C_7H_5O	$-COOC_6H_5$	0.0	−1.69	2.57	*VOR	B	25
183	C_7H_6NO	$-CONHC_6H_5$	1.0	−3.62	1.68	*VNR	B	25
184	C_7H_7	$-CH_2C_6H_5$	1.0	−0.39	0.27	*1R	CHx	25
185	C_7H_7	$-C_6H_5-2-CH_3$	0.0	−0.54	0.62	*R B1	CHx	25
186	C_7H_7	$-C_6H_5-4-CH_3$	0.0	−0.10	0.59	*R D1	*l*	25
187	C_7H_7O	$-CH_2O-C_6H_5$	1.0	−1.38	0.87	*1OR	B	25
188	C_7H_7O	$-OC_6H_4-2-CH_3$	0.0	−1.09	2.29	*OR B1	B	20
189	C_7H_7O	$-OC_6H_4-3-CH_3$	0.0	−1.25	2.33	*OR C1	B	20
190	C_7H_7O	$-OC_6H_4-4-CH_3$	0.0	−1.23	2.30	*OR D1	B	20
191	C_7H_7O	$-C_6H_4-4-OCH_3$	1.0	−1.23	0.42	*R D01	B	20
192	$C_7H_7O_2$	$-OC_6H_4-2-OCH_3$	0.0	−1.26	2.29	*OR B01	B	20
193	$C_7H_7O_2$	$-OC_6H_4-3-OCH_3$	0.0	−1.58	2.42	*OR C01	B	20
194	$C_7H_7O_2$	$-OC_6H_4-4-OCH_3$	0.0	−1.72	2.32	*OR D01	B	20
195	C_7H_7S	$-SCH_2C_6H_5$	0.0	−1.46	1.56	*S1R	D	25
196	C_7H_7S	$-SC_6H_4-3-CH_3$	0.0	−1.38	1.89	*SR C1	B	30
197	C_7H_7S	$-SC_6H_4-4-CH_3$	0.0	−1.49	1.80	*SR D1	B	30
198	C_7H_7OS	$-SC_6H_4-3-OCH_3$	0.0	−1.74	1.89	*SR C01	B	30
199	C_7H_7OS	$-SC_6H_4-4-OCH_3$	0.0	−1.98	1.66	*SR D01	B	30
200	$C_7H_7O_2S$	$-S(O)C_6H_4-4-OCH_3$	0.5	−4.24	3.00	*SO&R D01	B	20
201	$C_7H_7O_2S$	$-SO_2C_6H_4-4-CH_3$	0.5	−5.08	3.32	*SWR D1	D	25
202	$C_7H_7S_2$	$-SC_6H_4-4-SCH_3$	0.0	−1.81	1.69	*SR DS1	B	30
203	C_7H_7Se	$-SeC_6H_4-4-CH_3$	1.0	−1.46	1.23	*-Se^- R D1	B	NS
204	$C_7H_{13}O$	$-OCH_2-cyclo-C_6H_{11}$	0.0	−1.41	1.31	*01 A16TJ	B	20
205	C_8H_7	$-CH=CHC_6H_5$	0.0	−0.77	0.41	*1U1R	B	25
206	C_8H_9	$-CH(CH_3)C_6H_5$	1.0	−0.40	0.37	*YR	CHx	25
207	$C_8H_7O_2$	$-OC_6H_4-4-COCH_3$	0.0	−3.04	2.91	*OR DV1	B	25
208	C_8H_8NO	$-N(COCH_3)C_6H_5$	1.0	−3.63	1.37	*NR&V1	B	25
209	$C_8H_9O_3S$[b]	$-CH_2OSO_2C_6H_4-4-CH_3$	1.0	−5.30	1.44	*10SWR D1	D	25
210	C_9H_{11}	$-C_6H_4-4-CH(CH_3)_2$	0.0	−0.15	0.56	*R DY	*l*	25
211	$C_{10}H_{13}$	$-C_6H_4-4-C(CH_3)_3$	0.0	0.0	0.52	*R DX	CCl_4	25
212	$C_{12}H_{10}P$	$-P(C_6H_5)_2$	0.5	−1.39	1.06	*PR&R	B	20
213	$C_{12}H_{10}OP$	$-PO(C_6H_5)_2$	1.0	−4.66	1.71	*PO&R&R	B	20
214	$C_{13}H_{11}S_2$	$-CH(SC_6H_5)_2$	0.5	−1.72	1.56	*YSR&SR	B	25

[a] Key: (B) benzene; (D) dioxane; (G) gaseous phase; (CHx) cyclohexane; (HP) heptane; (*l*) liquid; (NS) not stated. [b] Omitted in equations 8 and 10.

REFERENCES

(1) E. J. Lien, Z. R. Guo, R. L. Li, and C. T. Su, *J. Pharm. Sci.*, **71**, 641 (1982).

(2) M. S. Newman, "Steric Effects in Organic Chemistry," Wiley, New York, N.Y., 1956, p. 614.

(3) C. Hansch and A. Leo, "Substituent Constants for Correlation Analysis in Chemistry and Biology," Wiley, New York, N.Y., 1979.

(4) D. D. Perrin, in "Physical Chemical Properties of Drugs," S. H. Yalkowsky, A. A. Sinkula, and S. C. Valvani, Eds., Decker, New York, N.Y., 1980, pp. 1–48.

(5) A. L. McClellan, "Tables of Experimental Dipole Moments," Vol. 2, Rahara Enterprises, El Cerrito, Calif., 1974.

(6) J. D. Roberts and W. T. Moreland, Jr., *J. Am. Chem. Soc.*, **75**, 2167 (1953).

(7) M. Charton, in "Progress in Physical Organic Chemistry," vol. 13, R. W. Taft, Ed., Wiley, New York, N.Y., 1981, p. 122.

(8) B. P. Daily and J. N. Shoolery, *J. Am. Chem. Soc.*, **77**, 3977 (1955).

(9) C. P. Smyth, "Dielectric Behavior and Structure," New York, N.Y., 1955, pp. 254–255.

(10) E. A. Braude and F. C. Machod, "Determination of Organic Structures by Physical Methods," Academic, New York, N.Y., 1955.

(11) C. Yamauea, C. Sonota, T. Tako, M. Tanaka, J. Yamada, C. Horizaka, and T. Fujita, "8th Symposium on Structure-Activity Relationships," Tokyo, 1981, pp. 31–35.

(12) C. Takayama, A. Fujinami, O. Kirino, and Y. Hisada, *Agri. Biol. Chem.* **46**(11), 2755 (1982).

(13) E. J. Lien and P. H. Wang, *J. Pharm Sci.*, **69**, 648 (1980).

Synthesis and Evaluation of *N*-Alkanoyl-*S*-benzyl-L-cysteinylglutamic Acid Esters as Glyoxalase I Inhibitors and Anticancer Agents

WILLIAM O. FOYE ˣ and CHAUR-MING JAN ‡

Received October 14, 1982, from the *Samuel M. Best Research Laboratory, Massachusetts College of Pharmacy and Allied Health Sciences, Boston, MA 02115.* Accepted for publication February 3, 1983. ‡ Present address: G. D. Searle and Company, Chicago, IL 60680.

Abstract □ Esters of several glutathione analogues have been synthesized in which the glycine moiety was replaced by straight-chain fatty acids and the mercapto group was benzylated. Two of the derivatives (sufficiently water-soluble for the assay) were found to inhibit glyoxalase I to a greater extent than did *S*-methylglutathione. The two glyoxalase I inhibitors did not inhibit P388 lymphocytic leukemia in mice, however.

Keyphrases □ *N*-Alkanoyl-*S*-benzyl-L-cysteinylglutamic acid esters—synthesis, anticancer activity in the P388 leukemia screen, glyoxalase I inhibition □ Anticancer agents—potential, *N*-alkanoyl-*S*-benzyl-L-cysteinylglutamic acid esters, activity in the P388 leukemia screen, glyoxalase I inhibition

S-Alkyl and *S*-aryl glutathiones are potent competitive inhibitors of glyoxalase (1). The glyoxalase enzyme system converts methylglyoxal to lactic acid in the presence of the cofactor glutathione (2). Since methylglyoxal and other α-keto aldehydes are known to be carcinostatic (3), it was suggested that inhibitors of the glyoxalase system may create a build-up of methylglyoxal in the cells and thus inhibit cellular growth (4). The fact that glutathione concentration in the cells is rapidly increased (5) just prior to cell division suggests that the glyoxalase system is involved in the regulation of cell growth by maintaining a proper concentration of methylglyoxal (1). The high concentration of lactic acid (6) and deficiency of methylglyoxal (7) in cancer cells suggests further that such cells, having lost the ability to maintain the necessary balance of methylglyoxal, continue to grow at an uncontrolled rate. Inhibitors of the glyoxalase system that result in a build-up of cellular methylglyoxal could, therefore, function as anticancer agents. To some extent this has been realized. Some of the *S*-alkyl and *S*-aryl glutathione inhibitors of the glyoxalase system exhibited cytotoxic activity against L1210 leukemia and KB cells in tissue culture (8). However, α-hydroxy thiol esters of glutathione inhibited glyoxalase I but lacked antileukemic activity against L1210 lymphoid leukemia (9).

The rapid metabolism of *S*-substituted glutathiones by glutathionase rendered the *S*-alkyl and *S*-aryl glutathiones inactive when tested *in vivo* (10). Glutathione and *S*-substituted derivatives are rapidly hydrolyzed by two enzymes, glutathionase and cysteinylglycinase (11). In an attempt to find glutathione analogues that might be resistant to enzymatic hydrolysis, a series of analogues (I) having the glycine residue replaced by a fatty acid was synthesized. The diester function was not successfully converted to the carboxyl function, however. It was also considered possible that such a derivative would have greater lipophilicity and possibly provide a more strongly bound enzyme-inhibitor complex. A series of *S*-(ω-phthalimidoalkyl)glutathiones and *S*-(ω-aminoalkyl)-glutathiones, for instance, showed greater inhibition of glyoxalase I with greater lipophilicity (12).

Table I—Physical Properties of the *N*-Alkanoyl-*S*-benzyl-L-cysteines [a]

R	Formula	Reaction Time, h	Yield, %	Melting Point, °C
C_2H_5	$C_{13}H_{17}NO_3S$	30	69	86.0–86.5
C_3H_7	$C_{14}H_{19}NO_3S$	40	63	115–116
C_5H_{11}	$C_{16}H_{23}NO_3S$	96	52	83–84
C_8H_{17}	$C_{18}H_{27}NO_3S$	96	51	88–89
$C_{10}H_{21}$	$C_{20}H_{31}NO_3S$	144	18 [b]	73–74
Dimethyl *N*-Alkanoyl-*S*-benzyl-L-cysteinylglutamates (I)				
C_2H_5	$C_{20}H_{28}N_2O_6S$	2	61	113–114
C_3H_7	$C_{21}H_{30}N_2O_6S$	2	59	93–94
C_8H_{17}	$C_{25}H_{38}N_2O_6S$	2	50	107–108

[a] Elemental analyses for C, H, N, and S were within ± 0.4% of the theoretical values for all compounds. [b] Recrystallized from *n*-hexane.

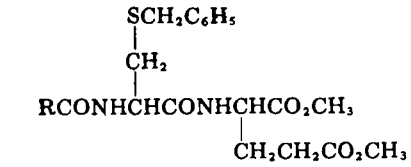

I: R = C_3H_7—$C_{10}H_{21}$

DISCUSSION

Chemistry—*S*-Benzyl-L-cysteine was readily converted to fatty acid amides (11) by reaction of the pyridinium salt of *S*-benzyl-L-cysteine with the fatty acid chloride in excess pyridine at 0°C. Yields of 18–69% were realized, with chain lengths ranging from 3 to 10 carbons with the longer chain acids giving progressively lower yields. Physical properties of the *N*-alkanoyl-*S*-benzyl-L-cysteines are recorded in Table I.

Condensation of the *N*-alkanoyl-*S*-benzyl-L-cysteines with dimethyl glutamate was carried out by conversion of the cysteine moiety to a mixed anhydride with isobutyl chlorocarbonate in the presence of *N*-methylmorpholine. Condensation with dimethyl glutamate hydrochloride in the presence of triethylamine took place readily at −10–0°C giving reasonable yields (50–61%) of I, in the case of the propanoyl, butanoyl, and octanoyl derivatives. Attempts to hydrolyze the methyl ester functions were unsuccessful. The reaction sequence is shown in Scheme I, and physical properties of I are listed in Table I.

Biological Testing—The method of Racker (13) for measuring inhibition of glyoxalase I was used. This was based on the formation of *S*-lactoylglutathione, catalyzed by glyoxalase I, which has high optical density at 240 nm. The rate of increase in absorption at 240 nm was measured, and the ratio of inhibitor concentration to substrate concentration at 50% inhibition was used to compare relative inhibitory properties of the compounds. To determine the concentration of inhibitor required for 50% inhibition, a plot of v_0/v_i *versus*

0022-3549/84/0400-0559$01.00/0
© 1984, American Pharmaceutical Association

Table II—Inhibition of Glyoxalase I

Compound	ID_{50}, mM	$[I/S]_{50}$[a]
S-Methylglutathione	6.10	9.84
Dimethyl *N*-propanoyl-*S*-benzyl-L-cysteinylglutamate	1.95	3.15
Dimethyl *N*-butanoyl-*S*-benzyl-L-cysteinylglutamate	1.90	3.06

[a] Ratio of inhibitor concentration to substrate concentration at 50% inhibition.

Table III—Antileukemic Activities in Mice[a]

Compound	Dose, mg/kg[b]	Weight Difference (T − C)	Median Survival Time (T/C), %[c]
Dimethyl *N*-propanoyl-*S*-benzyl-L-cysteinylglutamate	200	0.8	97
	100	0.3	100
	50	−0.2	110
Dimethyl *N*-butanoyl-*S*-benzyl-L-cysteinylglutamate	200	−0.2	96
	100	1.4	104
	50	1.1	104

[a] CDF_1 mice were inoculated (5×10^6 cells) with P388 lymphocytic leukemia. [b] Drugs were administered intraperitoneally daily for 9 d; observations were continued for 30 d. [c] A T/C% value of >125 is considered a positive result.

[I] was made, where v_0 is the initial velocity of the uninhibited enzymatic reaction and v_I is the initial velocity of the inhibited reaction at various concentrations of inhibitor (Table II). The *N*-propanoyl- and *N*-butanoyl-*S*-benzyl-L-cysteinylglutamic acid esters both showed better inhibitory activities than did *S*-methylglutathione. The longer-chain amide proved to be too insoluble in water to be measured by this method.

Antileukemia testing[1] of the propanoyl and butanoyl amides was carried out in mice against P388 lymphocytic leukemia, according to the NCI protocol (14). Details regarding dose and survival times are listed in Table III. Neither of the compounds showed positive activity in this screen.

EXPERIMENTAL[2]

S-Benzyl-L-cysteine—L-(+)-Cysteine hydrochloride (36.0 g, 0.229 mol) was dissolved in a small amount of water, and 27.5 g (0.687 mol) of sodium hydroxide was added. Benzyl bromide (38.9 g, 0.229 mol) was added in a dropwise manner to the solution, and the mixture was shaken vigorously for 1 h. The unreacted benzyl bromide and benzyl alcohol were extracted with ether. The aqueous solution was acidified with 20% acetic acid, and the white crystals were collected and recrystallized from water, yielding 36.5 g (75%); mp 215–217°C [lit. (15) mp 213–214°C].

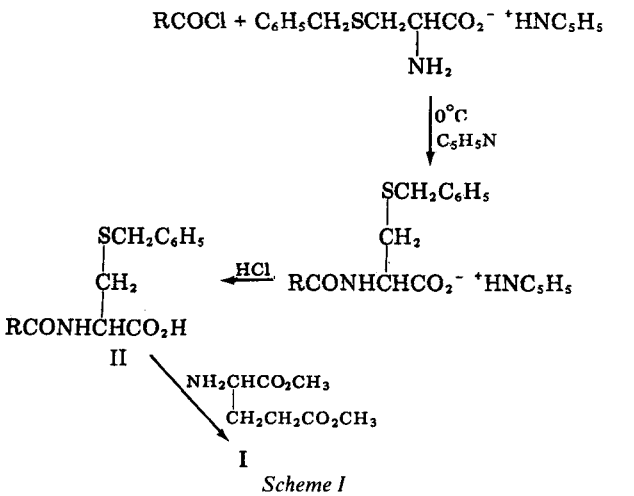

Scheme I

***N*-Alkanoyl-*S*-benzyl-L-cysteines**[3]—*S*-Benzyl-L-cysteine (31.65 g, 0.15 mol) in 180 mL of pyridine was cooled to 0°C. After 30 min, 13.02 mL (0.15 mol) of propanoyl chloride was added in a dropwise manner with vigorous shaking and ice cooling during 30 min. The mixture was shaken mechanically for 30 h at room temperature, and the excess pyridine was removed under reduced pressure. The syrupy residue was acidified with 10% HCl (Congo Red endpoint), and the oily product was extracted three times with ethyl acetate. The extract was dried (Na_2SO_4) and concentrated to a small volume using a rotary evaporator. The residual solution was treated with petroleum ether and stored at 0°C; recrystallization of the product from benzene gave 27.6 g (69%) of white needles, mp 86.0–86.5°C; IR(KBr): 3380 (N—H), 1735 (C=O), 1600 (C=O), and 1525 cm^{-1} (CNH).

***N*-Alkanoyl-*S*-benzyl-L-cysteinylglutamic Acid Dimethyl Esters**[3]—A solution of 5.35 g (0.02 mol) of *N*-propanoyl-*S*-benzyl-L-cysteine in 60 mL of dry tetrahydrofuran containing 2.20 mL (0.02 mol) of *N*-methylmorpholine was cooled to −15°C, and 2.80 mL (0.021 mol) of isobutyl chlorocarbonate was added with stirring. After 15 min, 4.66 g (0.022 mol) of L-glutamic acid dimethyl ester hydrochloride was added, followed by 3.0 mL (0.021 mol) of triethylamine in 60 mL of cold tetrahydrofuran. Stirring was continued at −10–0°C for 30 min and at 0°C for 1.5 h. The reaction mixture was diluted with 300 mL of cold water, and a yellow-green oil separated and was extracted three times with ethyl acetate. The extract was dried (Na_2SO_4) and concentrated to a small volume using a rotary evaporator. Crystallization resulted on storage at 0°C, and recrystallization from absolute ethanol gave 5.2 g (61% yield) of white crystals, mp 113–114°C; IR (KBr): 3300 (N—H), 1755 (C=O), 1735 (C=O), 1660 (C=O), 1640 (C=O), and 1545 cm^{-1} (CNH).

Inhibition of Glyoxalase I—The enzymatic reactions were carried out at room temperature in 0.05 M phosphate buffer, pH 6.6. A fresh solution of glutathione in distilled water was made before each assay. For each assay, the spectrophotometer cell contained a total volume of 3.0 mL, which was 5.0 mM in methylglyoxal and 0.869 mM in glutathione.

A commercial 40% (w/v) solution (10 mL) of methylglyoxal was diluted to 50 mL with distilled water, and the acidic components were removed by a Dowex 1-X8 (200–400 mesh, carbonate form) column. The solution was standardized by the method of Friedemann (16). Glyoxalase I was diluted to a concentration of 40 μg of protein/mL with 0.05 M phosphate buffer (pH 6.6) containing 0.1% bovine serum albumin.

Sufficient amounts of glyoxalase I were employed to give an easily measurable initial rate, which was followed by increase in absorption at 240 nm. Methylglyoxal, glutathione, and buffer were added to the cell and allowed to equilibrate for exactly 6 min before addition of the enzyme. The ratio of the inhibitor concentration to that of the substrate for 50% inhibition, $[I/S]_{50}$ was determined for each compound measured. To determine the concentration of inhibitor required for 50% inhibition (ID_{50}), a plot of v_0/v_I *versus* [I] was made, where v_0 is the initial velocity of the uninhibited reaction and v_I is the initial velocity of the inhibited reaction at various inhibitor (I) concentrations (17). At least two of the points on the plot were in the 30–70% inhibition range. Initial velocity measurements were determined by the change in absorbance, ΔO.D./time with readings at 1-min intervals for 3 min.

REFERENCES

(1) R. Vince, S. Daluge, and W. B. Wadd, *J. Med. Chem.*, **14,** 402 (1971).

(2) E. Bricas and C. Fromageot, *Adv. Protein Chem.*, **8,** 1 (1953); W. E. Knox, *Enzymes*, **2,** 253 (1960).

(3) F. A. French and B. L. Freedlander, *Cancer Res.*, **18,** 172 (1958).

(4) R. Vince and W. B. Wadd, *Biochem. Biophys. Res. Commun.*, **35,** 593 (1969).

(5) H. Stern, *Science*, **124,** 1292 (1956).

(6) B. Issekutz, "The Chemotherapy of Cancer," Akademiai Kiado, Budapest, 1969, pp. 17–19.

(7) K. F. Lewis, E. H. Majane, and S. Weinhouse, *Cancer Res.*, **19,** 97 (1959).

(8) R. Vince and S. Daluge, *J. Med. Chem.*, **14,** 35 (1971).

(9) S. S. Hall, L. M. Doweyko, A. M. Doweyko, and J. S. R. Zilenovski, *J. Med. Chem.*, **20,** 1239 (1977).

(10) R. Vince, M. Wolf, and C. Sanford, *J. Med. Chem.*, **16,** 951 (1973).

(11) J. J. Clapp and L. Young, *Biochem. J.*, **118,** 765 (1970).

(12) M. V. Kester, J. A. Reese, and S. J. Norton, *J. Med. Chem.*, **17,** 413 (1974).

[1] Testing was done at the National Cancer Institute; results were made available through the courtesy of Dr. Harry B. Wood, Jr.

[2] Melting points were taken in capillaries with a Mel-Temp block and are uncorrected. IR spectra were obtained with a Perkin-Elmer model 457 A grating spectrophotometer. The glyoxalase inhibition assay was determined with a Beckman model DB spectrophotometer. Elemental analyses were done by Dr. F. B. Strauss, Oxford, England. TLC was carried out using silica gel plates, and products were detected by exposure to iodine vapor. Organic reagents were supplied by J. T. Baker Laboratory Chemicals and Products, Eastman Organic Chemicals, or Fisher Scientific Co. Glyoxalase I, L-glutamic acid dimethyl ester hydrochloride, *S*-methyl-glutathione, and methylglyoxal were supplied by Sigma Chemical Co.

[3] Representative procedure.

(13) E. Racker, *J. Biol. Chem.*, **190**, 685 (1951).
(14) R. I. Geran, N. H. Greenberg, M. M. MacDonald, A. M. Schumacher, and B. J. Abbott, *Cancer Chemother. Rep.*, Part 3, **3**, 1 (1972).
(15) R. A. Gortner and W. F. Hoffman, *J. Biol. Chem.*, **72**, 444 (1927).
(16) T. E. Friedemann, *J. Biol. Chem.*, **73**, 331 (1927).
(17) B. R. Baker and H. S. Sachdev, *J. Pharm. Sci.*, **52**, 933 (1963).

ACKNOWLEDGMENTS

Abstracted from a thesis submitted by C.-M. Jan to the Massachusetts College of Pharmacy and Allied Health Sciences in partial fulfillment of Master of Science degree requirements. Supported by funds from the John R. and Marie K. Sawyer Memorial Fund, Massachusetts College of Pharmacy and Allied Health Sciences.

Simple Radioligand Binding Assay for the Determination of Urinary Scopolamine

M. SCHEURLEN *x, H. BITTIGER ‡, and BIRGIT AMMANN *

Received November 2, 1982, from the **Human Pharmacology Institute, Ciba-Geigy, Tübingen, Federal Republic of Germany* and the ‡*Research Department of the Pharmaceutical Division, Ciba-Geigy, Basel, Switzerland.* Accepted for publication March 29, 1983.

Abstract □ A sensitive radioligand binding assay is described for the determination of scopolamine in human urine. As a measure for the drug concentration, the quantitative displacement of scopolamine of tritiated quinuclidinyl benzylate from rat brain receptors was used. The assay is sensitive to concentrations as low as 1.2 ng/mL, surpassed only by GC–MS techniques. It can be performed easily and quickly and does not include extraction procedures. Scopoline and scopine, possible metabolites of scopolamine, do not interfere with the assay. After transdermal administration of scopolamine, 34% of the drug is found in the urine. Of the total scopolamine excreted, 79% is conjugated to glucuronic and/or sulfuric acid and 21% is excreted in the unbound form.

Keyphrases □ Scopolamine—urinary determination, radioligand binding assay, □ Radioligand binding—simple assay, determination of urinary scopolamine □ Excretion, urinary—scopolamine, determination by radioligand binding assay

The lack of suitable methods for measuring low concentrations of scopolamine and other strongly acting parasympatholytic substances in biological fluids after therapeutic dosages in humans makes it difficult to obtain exact pharmacokinetic data on these drugs. Several methods exist for the determination of scopolamine, but these do not allow a rapid and sensitive measurement of low drug concentrations. GC (1) or acid–dye techniques (2) are not sensitive enough, while a GC–MS method (3) is not specific and involves difficult extraction procedures.

The development of radioligand binding techniques for studies of drug interactions with cholinergic receptors, using tritiated quinuclidinyl benzylate (I) as the radioligand (4), allows (analogous to RIA) the measurement of drugs having strong affinity to muscarinic receptors. Using tritiated I we developed a radioligand binding assay for the determination of the very low urinary concentrations of scopolamine that are found after transdermal administration of the drug.

EXPERIMENTAL

Preparation of Rat brain Homogenate—Male rats (Tif RAI f SPF) of 150–250-g body weight were used. After being sacrificed by decapitation, the brains were removed and the cerebral cortices dissected on ice and homogenized[1] for 30 s, at position 5, in 20 volumes of ice-cold 50 mM Tris-HCl buffer (pH 7.3). The homogenate was centrifuged at 26,000×*g* for 10 min, and the pellet was resuspended in the same volume of fresh buffer; this step was repeated three times. All procedures were performed at 4°C. The final pellet was suspended in 20 volumes of Tris-HCl and divided into 1-mL aliquots, which were rapidly frozen in liquid propane (~−160°C) and stored at −30°C. (After storage at −30°C for up to 3 months no loss of binding capacity was observed.) For the radioreceptor assay, the 1-mL aliquots were thawed for 5 min in a water bath (37°C) and diluted 17-fold by addition of ice-cold Tris-HCl. Membrane suspensions were not used in the assay for longer than 12 h after thawing.

Radioligand Binding Assay—The radioreceptor assay was performed at room temperature in 5-mL polystyrene tubes in a total volume of 2 mL of Tris-HCl containing brain membranes [~100 μg of protein as determined according to Lowry *et al.* (5)], 0.2 nM [^{3}H]-I[2] (33 Ci/mmol), and a 50-μL urine sample.

After 30 min, the incubation was terminated by filtration through a glass-fiber filter (2.4 cm diameter[3]) under reduced pressure. The filters were rinsed twice with 5-mL ice-cold Tris-HCl. After incubation of the filters for 30 min with 1-mL of tissue solubilizer[4] (diluted 1:1 with propanol), 10 mL of acidified scintillation fluid[5] was added and the radioactivity was determined in a liquid scintillation counter[6]. Nonspecific binding was defined by 10^{-7} M unlabeled I[7]. Scopolamine hydrobromide trihydrate[8] was used as a standard.

For the calibration curve, different concentrations of scopolamine were added to blank urine and tested as described above. The displacement (in percent) of ^{3}H-QNB from the muscarinic receptors in the brain homogenate was plotted on logit–log scale against the scopolamine concentration. Unknown urinary scopolamine concentrations were calculated from the calibration curve. To determine the total scopolamine (conjugated and free drug), urine samples were incubated at 37°C for 3 h with an equal volume of 1 M acetate buffer (pH 4.75) and 7.5 μL of β-glucuronidase–sulfatase[9]/mL of the mixture. The pH was adjusted to 7.3 with NaOH before the binding assay was performed.

Scopolamine Medication and Collection of Urine—Scopolamine was administered transdermally to nine healthy volunteers as a transdermal therapeutic system with scopolamine[10]. The drug system was applied on the skin surface behind the ear. Each system contains 1.5 mg of scopolamine base and can deliver ~0.5 mg of drug over 72 h. The system is programmed to release 0.15 mg as a loading dose during the first few hours; afterward, ~5 μg of scopolamine/h pass through the skin into the blood circulation. The drug system was applied for 64 h, delivering ~0.45 mg of scopolamine. Urine was collected in plastic bottles before the medication, in 12-h periods during the application, and for 8 × 6 h after removal of the drug. Aliquots were stored at −20°C in plastic tubes until assayed. For each subject, an individual urine blank for the calibration of the assay was collected before the medication.

[1] Polytron; Kinematika, Luzern, Switzerland.

[2] New England Nuclear, Boston, Mass.
[3] GF/B; Whatman.
[4] Soluene; Packard.
[5] Aquasol; Packard.
[6] Tri-Carb 460C; Packard.
[7] Synthesized by Dr. A. Storni, Ciba-Geigy, Basel, Switzerland.
[8] EGA Chemie, Steinheim, West Germany.
[9] Calbiochem.
[10] Scopoderm TTS; Ciba-Geigy.

0022-3549/84/0400-0561$01.00/0
© 1984, American Pharmaceutical Association

(13) E. Racker, *J. Biol. Chem.*, **190**, 685 (1951).
(14) R. I. Geran, N. H. Greenberg, M. M. MacDonald, A. M. Schumacher, and B. J. Abbott, *Cancer Chemother. Rep.*, Part 3, **3**, 1 (1972).
(15) R. A. Gortner and W. F. Hoffman, *J. Biol. Chem.*, **72**, 444 (1927).
(16) T. E. Friedemann, *J. Biol. Chem.*, **73**, 331 (1927).
(17) B. R. Baker and H. S. Sachdev, *J. Pharm. Sci.*, **52**, 933 (1963).

ACKNOWLEDGMENTS

Abstracted from a thesis submitted by C.-M. Jan to the Massachusetts College of Pharmacy and Allied Health Sciences in partial fulfillment of Master of Science degree requirements. Supported by funds from the John R. and Marie K. Sawyer Memorial Fund, Massachusetts College of Pharmacy and Allied Health Sciences.

Simple Radioligand Binding Assay for the Determination of Urinary Scopolamine

M. SCHEURLEN *x, H. BITTIGER ‡, and BIRGIT AMMANN *

Received November 2, 1982, from the **Human Pharmacology Institute, Ciba-Geigy, Tübingen, Federal Republic of Germany* and the ‡*Research Department of the Pharmaceutical Division, Ciba-Geigy, Basel, Switzerland.* Accepted for publication March 29, 1983.

Abstract □ A sensitive radioligand binding assay is described for the determination of scopolamine in human urine. As a measure for the drug concentration, the quantitative displacement of scopolamine of tritiated quinuclidinyl benzylate from rat brain receptors was used. The assay is sensitive to concentrations as low as 1.2 ng/mL, surpassed only by GC–MS techniques. It can be performed easily and quickly and does not include extraction procedures. Scopoline and scopine, possible metabolites of scopolamine, do not interfere with the assay. After transdermal administration of scopolamine, 34% of the drug is found in the urine. Of the total scopolamine excreted, 79% is conjugated to glucuronic and/or sulfuric acid and 21% is excreted in the unbound form.

Keyphrases □ Scopolamine—urinary determination, radioligand binding assay, □ Radioligand binding—simple assay, determination of urinary scopolamine □ Excretion, urinary—scopolamine, determination by radioligand binding assay

The lack of suitable methods for measuring low concentrations of scopolamine and other strongly acting parasympatholytic substances in biological fluids after therapeutic dosages in humans makes it difficult to obtain exact pharmacokinetic data on these drugs. Several methods exist for the determination of scopolamine, but these do not allow a rapid and sensitive measurement of low drug concentrations. GC (1) or acid–dye techniques (2) are not sensitive enough, while a GC–MS method (3) is not specific and involves difficult extraction procedures.

The development of radioligand binding techniques for studies of drug interactions with cholinergic receptors, using tritiated quinuclidinyl benzylate (I) as the radioligand (4), allows (analogous to RIA) the measurement of drugs having strong affinity to muscarinic receptors. Using tritiated I we developed a radioligand binding assay for the determination of the very low urinary concentrations of scopolamine that are found after transdermal administration of the drug.

EXPERIMENTAL

Preparation of Rat brain Homogenate—Male rats (Tif RAI f SPF) of 150–250-g body weight were used. After being sacrificed by decapitation, the brains were removed and the cerebral cortices dissected on ice and homogenized[1] for 30 s, at position 5, in 20 volumes of ice-cold 50 mM Tris-HCl buffer (pH 7.3). The homogenate was centrifuged at 26,000×*g* for 10 min, and the pellet was resuspended in the same volume of fresh buffer; this step was repeated three times. All procedures were performed at 4°C. The final pellet was suspended in 20 volumes of Tris-HCl and divided into 1-mL aliquots, which were rapidly frozen in liquid propane (~−160°C) and stored at −30°C. (After storage at −30°C for up to 3 months no loss of binding capacity was observed.) For the radioreceptor assay, the 1-mL aliquots were thawed for 5 min in a water bath (37°C) and diluted 17-fold by addition of ice-cold Tris-HCl. Membrane suspensions were not used in the assay for longer than 12 h after thawing.

Radioligand Binding Assay—The radioreceptor assay was performed at room temperature in 5-mL polystyrene tubes in a total volume of 2 mL of Tris-HCl containing brain membranes [~100 μg of protein as determined according to Lowry *et al.* (5)], 0.2 nM [^{3}H]-I[2] (33 Ci/mmol), and a 50-μL urine sample.

After 30 min, the incubation was terminated by filtration through a glass-fiber filter (2.4 cm diameter[3]) under reduced pressure. The filters were rinsed twice with 5-mL ice-cold Tris-HCl. After incubation of the filters for 30 min with 1-mL of tissue solubilizer[4] (diluted 1:1 with propanol), 10 mL of acidified scintillation fluid[5] was added and the radioactivity was determined in a liquid scintillation counter[6]. Nonspecific binding was defined by 10^{-7} M unlabeled I[7]. Scopolamine hydrobromide trihydrate[8] was used as a standard.

For the calibration curve, different concentrations of scopolamine were added to blank urine and tested as described above. The displacement (in percent) of ^{3}H-QNB from the muscarinic receptors in the brain homogenate was plotted on logit–log scale against the scopolamine concentration. Unknown urinary scopolamine concentrations were calculated from the calibration curve. To determine the total scopolamine (conjugated and free drug), urine samples were incubated at 37°C for 3 h with an equal volume of 1 M acetate buffer (pH 4.75) and 7.5 μL of β-glucuronidase–sulfatase[9]/mL of the mixture. The pH was adjusted to 7.3 with NaOH before the binding assay was performed.

Scopolamine Medication and Collection of Urine—Scopolamine was administered transdermally to nine healthy volunteers as a transdermal therapeutic system with scopolamine[10]. The drug system was applied on the skin surface behind the ear. Each system contains 1.5 mg of scopolamine base and can deliver ~0.5 mg of drug over 72 h. The system is programmed to release 0.15 mg as a loading dose during the first few hours; afterward, ~5 μg of scopolamine/h pass through the skin into the blood circulation. The drug system was applied for 64 h, delivering ~0.45 mg of scopolamine. Urine was collected in plastic bottles before the medication, in 12-h periods during the application, and for 8 × 6 h after removal of the drug. Aliquots were stored at −20°C in plastic tubes until assayed. For each subject, an individual urine blank for the calibration of the assay was collected before the medication.

[1] Polytron; Kinematika, Luzern, Switzerland.

[2] New England Nuclear, Boston, Mass.
[3] GF/B; Whatman.
[4] Soluene; Packard.
[5] Aquasol; Packard.
[6] Tri-Carb 460C; Packard.
[7] Synthesized by Dr. A. Storni, Ciba-Geigy, Basel, Switzerland.
[8] EGA Chemie, Steinheim, West Germany.
[9] Calbiochem.
[10] Scopoderm TTS; Ciba-Geigy.

0022-3549/84/0400-0561$01.00/0
© 1984, American Pharmaceutical Association

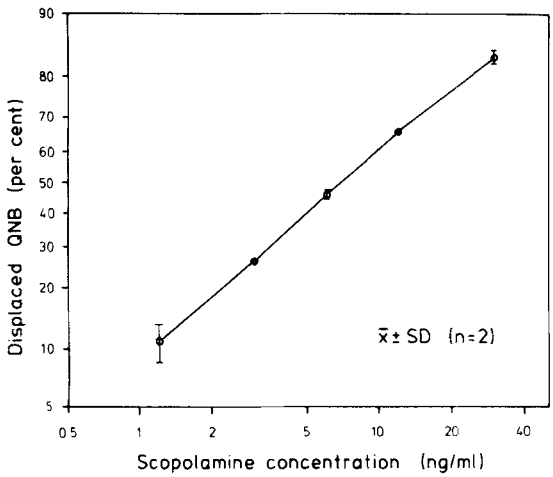

Figure 1—*Displacement of tritiated quinuclidinyl benzylate (QNB) from rat brain membranes by scopolamine (logit-log scale). Different concentrations of scopolamine were added to blank urine. The displacement of the labeled I from rat brain membranes was determined under the assay conditions described in* Experimental. *The values are means* ±SD *of two measurements.*

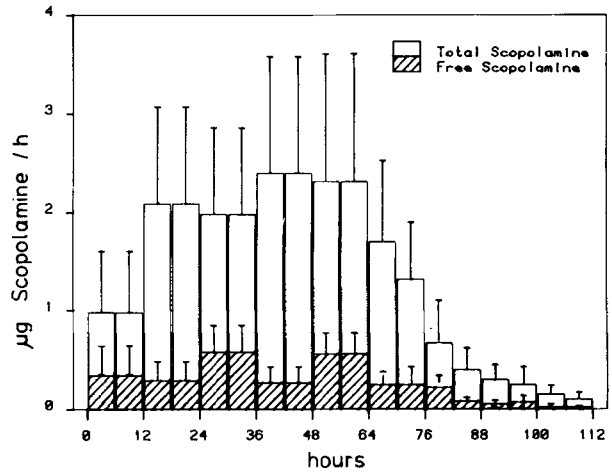

Figure 2—*Urinary excretion of scopolamine after transdermal administration. Application time was 64 h. Urine was collected as described under* Experimental. *The values are means* ±SD *from nine volunteers.*

RESULTS AND DISCUSSION

Under the test conditions selected, there was a linear correlation on logit-log scale between inhibition of [^{3}H]-I binding and scopolamine concentration in the range of 10^{-10}–2.5×10^{-9} M. This corresponds to a 1.2–30-ng/mL scopolamine concentration in 0.05-mL urine samples (Fig. 1). The IC_{50} value was 4.7×10^{-10} M.

To test the intra- and interassay reproducibility of the binding assay, blank urine samples containing 2, 10, and 25 ng/mL of scopolamine, respectively, were assayed repeatedly on a single day or different days. The results of these measurements are shown in Table I.

To exclude interference of the radioligand binding assay by scopoline and scopine, possible degradation products of scopolamine, these two substances were added to the urine blank in different concentrations (10^{-10}, 10^{-9}, and 10^{-8} M in the incubation mixture). Under these conditions, no displacement of [^{3}H]-I from brain membranes was observed.

The radioligand binding assay was used to measure the urinary excretion of scopolamine after administration of the transdermal system for 64 h. During the time of medication and 48 h thereafter, a total urinary excretion of 156 µg (80–276 µg) of scopolamine was observed (mean of nine volunteers). Steady state was reached after ~12 h of medication, lasting until the removal of the drug system (Fig. 2).

Scopolamine is excreted mainly in its conjugated form (79% *versus* 21% in unbound form), as determined after β-glucuronidase–sulfatase incubation. Assuming a total delivery of 0.45 mg of scopolamine to the circulatory system, an average of 34% (17–60%) of the administered scopolamine can be detected in the urine. Scopolamine, in very small amounts, was recovered from the urine even in the last collection period [42–48 h after the removal of the system (Fig. 2].

The use of radioligand binding techniques was originally established for studies of drug–receptor interactions *in vitro*. Radioreceptor assays were also exploited to measure concentrations of hormones (6), neurotransmitters (7, 8), or drugs (9) in biological fluids (10). Recently, such an assay for the measurement of atropine in plasma was published (11).

Table I—Intra- and Interassay Reproducibility of the Radioligand Binding Assay [a]

n	Conc. Given, ng/mL	Conc. Found, ng/mL	CV, %	Recovery, %
		Within Day		
10	2	2.3	13.7	113
10	5	5.5	5.0	109
10	10	11.7	8.0	117
10	25	27.8	7.9	111
		Day-to-Day		
11	2	2.3	32.1	114
10	5	5.7	11.3	115
20	10	10.3	12.1	103
21	25	25.6	12.6	103

[a] Scopolamine was added to the urine blank in different concentrations (2, 5, 10, and 25 ng/mL). The samples were assayed as described in the text either in one series or on different days.

The method described here was developed to determine the very low amounts of scopolamine excreted in the urine after transdermal administration of the drug. In spite of similar detection limits with this method (1.2 ng/mL) and that of Metcalfe (0.9 ng/mL) (11), scopolamine concentrations in plasma could not be measured after application of a transdermal delivery system. This could be explained by the different amounts of drug administered. While Metcalfe injected 2 mg im of atropine, the transdermal system only delivers 0.5 µg of drug/h to the blood.

The sensitivity of the radioligand binding method is only surpassed by the GC–MS technique (3), which has a detection limit of 50 pg/mL. However, this GC–MS assay has several disadvantages compared with the radioligand binding test. First, deuterated scopolamine has to be synthesized as an internal standard. Second, the method includes a complicated and time-consuming extraction procedure. Third, scopolamine is hydrolyzed to scopoline in this method, and the latter substance would be detected under the same peak. Additionally, the authors state that scopine and apo-scopolamine (possible metabolites of scopolamine) would also interfere with their assay.

The radioligand binding assay is easily and quickly performed; 50 samples can be determined in half a day, because no extraction is needed. The assay also shows good reproducibility (Table I). Measurements of the urinary excretion of scopolamine after administration of the transdermal system indicate that only 21% of scopolamine is excreted in free form, while 79% is conjugated to glucuronic and/or sulfuric acid. This confirms similar observations from animal studies (12), where the 9′-glucuronide was found to be the main metabolite of scopolamine in the mouse.

If one assumes that during a 64-h period 0.45 mg of scopolamine is absorbed through the skin, then an average of 7% of the total drug is excreted in the urine. This agrees with the results of Bayne *et al.* (3) and with those of Shaw *et al.* (13), both using a GC–MS method. Bayne *et al.* (3) recovered 4–5% of an oral dose unchanged in the urine, while Shaw *et al.* (13) measured 10% of the drug as free scopolamine given either intravenously or intramuscularly. Comparable results from this study, therefore, show the suitability of the radioligand binding technique.

Up to 48 h after removal of the drug system, scopolamine can still be detected in urine, despite its short elimination half-life of ~1 h (14). Similar results were obtained by Shaw and Urquhart (15), who assumed that an intradermal reservoir continues to deliver scopolamine to the circulation even after termination of the transdermal medication.

REFERENCES

(1) H. Kolb and P. W. Patt, *Arzneim.-Forsch.*, **15,** 924 (1965).

(2) Z. I. ElDarawy and S. L. Tompsett, *Analyst*, **81,** 601 (1956).

(3) W. F. Bayne, F. T. Tao, and N. Crisologo, *J. Pharm. Sci.*, **64,** 288 (1975).

(4) H. I. Yamamura and S. H. Snyder, *Proc. Natl. Acad. Sci. USA*, **71,** 1725 (1974).

(5) O. H. Lowry, N. J. Rosebrough, A. L. Farr, and R. J. Randall, *J. Biol. Chem.*, **193,** 265 (1951).

(6) R. Lefkowitz, J. Roth, and I. Pastan, *Science*, **170,** 633 (1970).

(7) S. Y. Enna and S. H. Snyder, *J. Neurochem.*, **26,** 221 (1976).

(8) R. Bernasconi, H. Bittiger, J. Heid, and P. Martin, *J. Neurochem.*, **34**, 614 (1980).
(9) J. Creese and S. H. Snyder, *Nature*, **270**, 261 (1977).
(10) S. Y. Enna, in "Neurotransmitter Receptor Binding," H. I. Yamamura, S. J. Enna, M. J. Kuhar, Eds., 1st ed., Raven, New York, N.Y., 1978.
(11) R. F. Metcalfe, *Biochem. Pharmacol.*, **30**, 209 (1981).
(12) G. Werner and K.-H. Schmidt, *Hoppe-Seyler's Z. Physiol. Chem.*, **349**, 741 (1968).
(13) J. E. Shaw, S. K. Chandrasekaran, P. S. Campbell, and L. G. Schmitt, in "Cutaneous Toxicity," V. A. Drill and P. Lazar, Eds., Academic, New York, N.Y., 1977.
(14) S. K. Chandrasekaran, W. Bayne, and J. Shaw, *J. Pharm. Sci.*, **67**, 1370 (1978).
(15) J. Shaw and J. Urquhart, *TIPS*, **1**, 208 (1980).

ACKNOWLEDGMENTS

This article is dedicated to Professor Dr. W. Dölle, University Tübingen, on his 60th birthday.

We would like to thank Drs. P. Bieck and K.-H. Antonin for their cooperation and helpful discussion. We are grateful for the assistance of Ms. M. Hügler and J. Fischer.

Determination of 17β-Hydroxy-1α-methyl-17α-propyl-5-α-androstan-3-one in Plasma by Gas Chromatography–Mass Spectrometry with Single-Ion Detection

WERNER KRAUSE ˣ **and UWE JAKOBS**

Received June 16, 1982, from the *Department of Pharmacokinetics, Schering Berlin/Bergkamen, Müllerstrasse 170-178, 1000 Berlin 65, West Germany.* Accepted for publication March 30, 1983.

Abstract □ The topical anti-androgen 17β-hydroxy-1α-methyl-17α-propyl-5α-androstan-3-one is determined in plasma samples by extracting with ether and subsequent mass fragmentography with single-ion detection at *m/z* 303. 17β-Hydroxy-1α-methyl-17α-pentyl-5α-androstan-3-one, added to the samples before extraction, is used as the internal standard. Reproducibility was calculated to be ±5.9% at the 5-ng/mL level and 0.4% at the 20-ng/mL level. The limit of detection is ~1 ng/mL. Total gas chromatography–mass spectrometry analysis time is ~10 min/sample.

Keyphrases □ 17β- Hydroxy -1α-methyl-17α- propyl -5α- androstan -3-one—determination in plasma, gas chromatography—mass spectrometry, single-ion detection □ Mesterolone—17α-propyl analogue, determination in plasma, gas chromatography–mass spectrometry, single-ion detection

17β-Hydroxy-1α-methyl-17α- propyl -5α-androstan-3-one, the 17α-propyl analogue of mesterolone, is currently under investigation as a topical anti-androgen for the treatment of acne and seborrhea. Pharmacological data of this compound, which may act similarly to the 17α-propyl analogue of testosterone (1), have been reported earlier (2).

Topical anti-androgens act locally in the skin, and the systemic availability of this class of compounds should be as low as possible in order to avoid endocrinological disorders. Therefore, any analytical method applied to the determination of these drugs in plasma must be very sensitive to be able to detect very small portions of absorbed substances. Because the drug molecule may be metabolized during passage through the skin, there are also certain requirements regarding specificity of the assay. In the present report an analytical method for the determination of plasma concentrations of 17β-hydroxy-1α-methyl-17α-propyl-5α-androstan-3-one (I) is described, which is devoid of tedious extraction or derivatization procedures and may, therefore, be useful in clinical tolerance studies of this compound when relatively high doses of drug are administered. Furthermore, it may serve for controlling the specificity of an RIA procedure.

EXPERIMENTAL

Subjects and Medication—Two healthy male volunteers (40 and 31 years of age, and 88 and 70 kg, respectively) were treated topically two times daily with 10 mL of a 3% solution of I in 70% aqueous ethanol. The drug was spread over the total body of the volunteers. During the first week the skin area to which the drug has been applied was kept under occlusion for 22 h/d. Blood was drawn into heparinized syringes before the treatment and in weekly intervals up to 8 weeks after the beginning of the 6-week treatment. The samples were immediately centrifuged, and the plasma stored frozen until analysis.

Chemicals—All solvents (ethanol, *n*-hexane, and ether) were of analytical reagent grade[1] and were used without further purification.

Extraction Procedure—Fifty nanograms of the internal standard (17β-hydroxy-1α-methyl-17α-pentyl-5α-androstan-3-one) dissolved in 50 μL of *n*-hexane was transferred into a 15-mL stoppered test tube and evaporated to dryness under a stream of nitrogen. One milliliter of plasma was added, followed after a short mixing time by 3 mL of ether. After thoroughly mixing on a vortex mixer for 1 min and centrifugation at 1200×*g* for 5 min, the organic phase was transferred to another test tube and evaporated to give a final volume of ~10 μL. One microliter of this solution was analyzed by gas chromatography–mass spectrometry (GC–MS). The recovery of the extraction procedure was determined by spiking 1-mL plasma samples with either 20 or 50 ng of radiolabeled I, with subsequent determination of the radioactivity in the organic phase.

Gas Chromatography–Mass Spectrometry—A GC–MS system[2] with the following components was used: a gas chromatograph[3], a quadrupole mass spectrometer[4], and a data system[5]. The gas chromatograph was equipped with a CP-SiL 5-coated open-tubular glass column (25 m × 0.25 mm) used in the direct-coupling mode or, alternatively, a CP-SiL 5 CB wall-coated open-tubular fused silica column (25 m × 0.23 mm), which was directly introduced into the ion source.

The temperature program applied to the column was 240°C for 1 min, then rising to a final temperature of 260°C at a rate of 10°C/min. Using the fused silica column the program was 200°C for 2 min, then 10°C/min up to 300°C. The injector was kept at 290°C, the direct coupling device at 280°C. Helium was used as carrier gas with a pressure of 14 psi in front of the column. The split ratio was 1:5.

Calibration Curve—The standard curve was constructed with 1-mL blank plasma samples containing 0, 5, 10, 15, 20, and 50 ng of I and 50 ng of the internal standard. These samples were extracted by the method described above. The peak areas of the internal standard and drug were measured, and the calibration curve (peak area ratio of drug/standard *versus* the concentration of I) was constructed. The precision of the assay was calculated from consecutive determinations of the drug within 1 d and by comparison with the results obtained on different days.

[1] E. Merck, Darmstadt, West Germany.
[2] Finnigan 4021.
[3] Finnigan 9610.
[4] Finnigan 4000.
[5] Incos-type 2100.

0022-3549/84/0400-0563$01.00/0
© 1984, American Pharmaceutical Association

(8) R. Bernasconi, H. Bittiger, J. Heid, and P. Martin, *J. Neurochem.*, **34**, 614 (1980).
(9) J. Creese and S. H. Snyder, *Nature*, **270**, 261 (1977).
(10) S. Y. Enna, in "Neurotransmitter Receptor Binding," H. I. Yamamura, S. J. Enna, M. J. Kuhar, Eds., 1st ed., Raven, New York, N.Y., 1978.
(11) R. F. Metcalfe, *Biochem. Pharmacol.*, **30**, 209 (1981).
(12) G. Werner and K.-H. Schmidt, *Hoppe-Seyler's Z. Physiol. Chem.*, **349**, 741 (1968).
(13) J. E. Shaw, S. K. Chandrasekaran, P. S. Campbell, and L. G. Schmitt, in "Cutaneous Toxicity," V. A. Drill and P. Lazar, Eds., Academic, New York, N.Y., 1977.
(14) S. K. Chandrasekaran, W. Bayne, and J. Shaw, *J. Pharm. Sci.*, **67**, 1370 (1978).
(15) J. Shaw and J. Urquhart, *TIPS*, **1**, 208 (1980).

ACKNOWLEDGMENTS

This article is dedicated to Professor Dr. W. Dölle, University Tübingen, on his 60th birthday.

We would like to thank Drs. P. Bieck and K.-H. Antonin for their cooperation and helpful discussion. We are grateful for the assistance of Ms. M. Hügler and J. Fischer.

Determination of 17β-Hydroxy-1α-methyl-17α-propyl-5-α-androstan-3-one in Plasma by Gas Chromatography–Mass Spectrometry with Single-Ion Detection

WERNER KRAUSE ˣ **and UWE JAKOBS**

Received June 16, 1982, from the *Department of Pharmacokinetics, Schering Berlin/Bergkamen, Müllerstrasse 170-178, 1000 Berlin 65, West Germany.* Accepted for publication March 30, 1983.

Abstract □ The topical anti-androgen 17β-hydroxy-1α-methyl-17α-propyl-5α-androstan-3-one is determined in plasma samples by extracting with ether and subsequent mass fragmentography with single-ion detection at *m/z* 303. 17β-Hydroxy-1α-methyl-17α-pentyl-5α-androstan-3-one, added to the samples before extraction, is used as the internal standard. Reproducibility was calculated to be ±5.9% at the 5-ng/mL level and 0.4% at the 20-ng/mL level. The limit of detection is ~1 ng/mL. Total gas chromatography–mass spectrometry analysis time is ~10 min/sample.

Keyphrases □ 17β- Hydroxy -1α-methyl-17α- propyl -5α- androstan -3-one—determination in plasma, gas chromatography—mass spectrometry, single-ion detection □ Mesterolone—17α-propyl analogue, determination in plasma, gas chromatography–mass spectrometry, single-ion detection

17β-Hydroxy-1α-methyl-17α- propyl -5α-androstan-3-one, the 17α-propyl analogue of mesterolone, is currently under investigation as a topical anti-androgen for the treatment of acne and seborrhea. Pharmacological data of this compound, which may act similarly to the 17α-propyl analogue of testosterone (1), have been reported earlier (2).

Topical anti-androgens act locally in the skin, and the systemic availability of this class of compounds should be as low as possible in order to avoid endocrinological disorders. Therefore, any analytical method applied to the determination of these drugs in plasma must be very sensitive to be able to detect very small portions of absorbed substances. Because the drug molecule may be metabolized during passage through the skin, there are also certain requirements regarding specificity of the assay. In the present report an analytical method for the determination of plasma concentrations of 17β-hydroxy-1α-methyl-17α-propyl-5α-androstan-3-one (I) is described, which is devoid of tedious extraction or derivatization procedures and may, therefore, be useful in clinical tolerance studies of this compound when relatively high doses of drug are administered. Furthermore, it may serve for controlling the specificity of an RIA procedure.

EXPERIMENTAL

Subjects and Medication—Two healthy male volunteers (40 and 31 years of age, and 88 and 70 kg, respectively) were treated topically two times daily with 10 mL of a 3% solution of I in 70% aqueous ethanol. The drug was spread over the total body of the volunteers. During the first week the skin area to which the drug has been applied was kept under occlusion for 22 h/d. Blood was drawn into heparinized syringes before the treatment and in weekly intervals up to 8 weeks after the beginning of the 6-week treatment. The samples were immediately centrifuged, and the plasma stored frozen until analysis.

Chemicals—All solvents (ethanol, *n*-hexane, and ether) were of analytical reagent grade[1] and were used without further purification.

Extraction Procedure—Fifty nanograms of the internal standard (17β-hydroxy-1α-methyl-17α-pentyl-5α-androstan-3-one) dissolved in 50 μL of *n*-hexane was transferred into a 15-mL stoppered test tube and evaporated to dryness under a stream of nitrogen. One milliliter of plasma was added, followed after a short mixing time by 3 mL of ether. After thoroughly mixing on a vortex mixer for 1 min and centrifugation at 1200×*g* for 5 min, the organic phase was transferred to another test tube and evaporated to give a final volume of ~10 μL. One microliter of this solution was analyzed by gas chromatography–mass spectrometry (GC–MS). The recovery of the extraction procedure was determined by spiking 1-mL plasma samples with either 20 or 50 ng of radiolabeled I, with subsequent determination of the radioactivity in the organic phase.

Gas Chromatography–Mass Spectrometry—A GC–MS system[2] with the following components was used: a gas chromatograph[3], a quadrupole mass spectrometer[4], and a data system[5]. The gas chromatograph was equipped with a CP-SiL 5-coated open-tubular glass column (25 m × 0.25 mm) used in the direct-coupling mode or, alternatively, a CP-SiL 5 CB wall-coated open-tubular fused silica column (25 m × 0.23 mm), which was directly introduced into the ion source.

The temperature program applied to the column was 240°C for 1 min, then rising to a final temperature of 260°C at a rate of 10°C/min. Using the fused silica column the program was 200°C for 2 min, then 10°C/min up to 300°C. The injector was kept at 290°C, the direct coupling device at 280°C. Helium was used as carrier gas with a pressure of 14 psi in front of the column. The split ratio was 1:5.

Calibration Curve—The standard curve was constructed with 1-mL blank plasma samples containing 0, 5, 10, 15, 20, and 50 ng of I and 50 ng of the internal standard. These samples were extracted by the method described above. The peak areas of the internal standard and drug were measured, and the calibration curve (peak area ratio of drug/standard *versus* the concentration of I) was constructed. The precision of the assay was calculated from consecutive determinations of the drug within 1 d and by comparison with the results obtained on different days.

[1] E. Merck, Darmstadt, West Germany.
[2] Finnigan 4021.
[3] Finnigan 9610.
[4] Finnigan 4000.
[5] Incos-type 2100.

0022-3549/84/0400-0563$01.00/0
© 1984, American Pharmaceutical Association

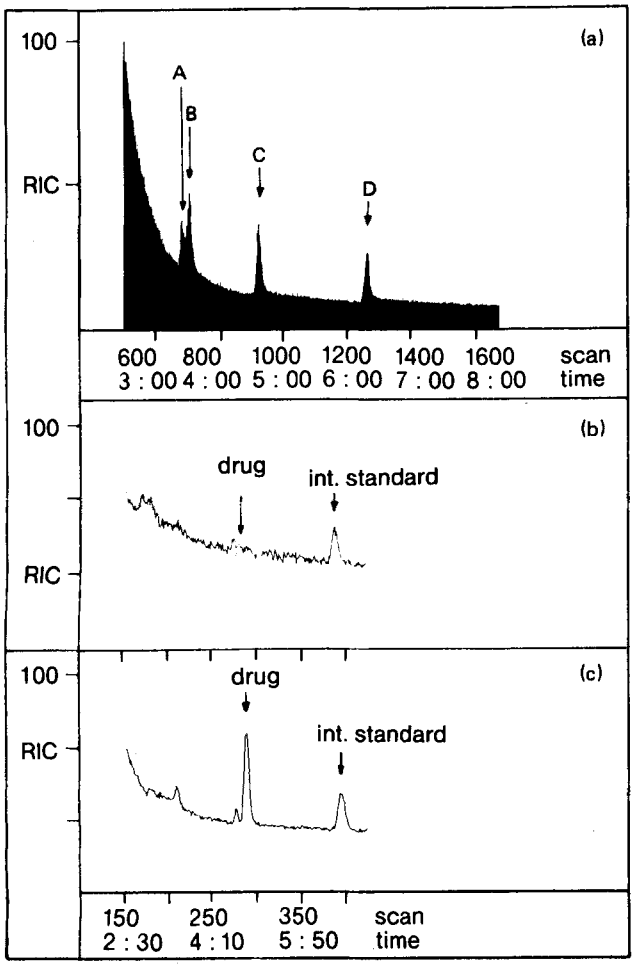

Figure 1—*Mass fragmentograms of (a) a mixture of mesterolone (A) and its 17α-methyl- (B), 17α-propyl- (C), and 17α-pentyl (D) analogues; (b) a plasma extract containing 5 ng of internal standard; and (c) a plasma extract with 7.5 ng of I and 5 ng of internal standard. The chromatograms were obtained with a CP-SiL 5 glass capillary column.*

RESULTS AND DISCUSSION

Assay—This report describes a sensitive and highly selective method for the determination of I in plasma utilizing GC–MS with single-ion detection. Plasma samples are extracted with ether after the addition of the internal standard, and the extract is evaporated to dryness, taken up in *n*-hexane, and injected directly into the GC–MS system.

Detection of the substances eluted from the chromatographic column is performed by means of single-ion measurements at *m/z* 303. This mass constitutes the base peak of the spectrum of both the drug and the internal standard, and it probably results from cleavage at the propyl and pentyl side chains.

The retention times of I and the internal standard using the glass column were 4.8 and 6.7 min, respectively. Figure 1 shows chromatograms of a blank plasma sample, of a sample containing drug and internal standard, and of some reference compounds.

Plasma concentrations of I were determined by comparing the peak areas of the drug and the internal standard added to the plasma before extraction.

Table I—Calibration Curves of the Assay Obtained on Five Different Days

Day	Calibration Curve[a]	Correlation Coefficient (r)
1	$y = -0.020 + 0.022x$	0.9990
2	$y = 0.001 + 0.019x$	0.9995
3	$y = 0.005 + 0.020x$	0.9997
4	$y = -0.007 + 0.021x$	0.9990
5	$y = -0.006 + 0.021x$	0.9997
Mean	$y = -0.005 + 0.021x$	0.9994

[a] Data obtained with the fused silica column; y = peak area of the drug/peak area of the internal standard and x = concentration of the drug (ng/mL).

Table II—Interassay Variation of Different Concentrations of I Using the Fused Silica Column

Amount Added ng/mL	Peak Area Ratio (Drug/Standard)	n	*RSD*, %
5	0.100 ± 0.016	5	16.0
10	0.201 ± 0.012	10	5.7
15	0.300 ± 0.011	5	3.7
20	0.394 ± 0.009	14	2.2

Table III—Plasma Concentrations of I Determined After Repeated Daily Topical Applications of 600 mg of Drug to Two Male Volunteers

Week	Subject 1	Subject 2	Mean ± *SD*
0	0	0	0 ± 0
1	16	14	15 ± 1
2	—	8	—
3	18	12	15 ± 4
4	20	15	18 ± 4
5	12	11	12 ± 1
6	11	11	11 ± 0
7	0	0	0 ± 0
8	0	0	0 ± 0

Typical calibration curves of the assay are described in Table I. The recovery of the extraction process was determined by measuring the radioactivity in the organic phase of samples spiked with ^{3}H-labeled drug. With 20 and 50 ng/mL, 83 ± 4 and 80 ± 1% were recovered in the ether phase (n = 5 each), respectively.

The recovery of the internal standard was identical with that of I, as could be demonstrated by establishing a calibration curve of unextracted drug. The data obtained were identical with that described in Table I.

The overall accuracy of the assay, expressed as the standard deviation of seven consecutive plasma determinations of 5 ng/mL, was 5.9%. With 20 ng/mL, an accuracy of 0.4% was calculated. The interassay variation, determined by comparing peak area ratios on different days, is given in Table II. The limit of detection was found to be ~1 ng/mL.

Plasma Concentrations—After daily repeated topical applications of 600 mg of I to two male volunteers, plasma levels of the drug were <20 ng/mL (Table III). During the first week of treatment the body was kept under occlusion for 22 h/d, while in the following weeks there was no occlusion. However, there were no differences in plasma levels between the two parts of the study. One week after the last treatment, the concentration of I had dropped below the limit of detection of ~1 ng/mL.

The analytical assay described differs from other methods for the detection of steroids by its simple extraction and, more importantly, lack of derivatization for a GC analysis. For similar molecules, such as testosterone and dihydrotestosterone, less simple procedures have been described in the literature (3–6). These compounds are extracted with ether, purified on Sephadex LH 20 and Lipidex 5000, derivatized with silylating agents, and finally detected in a high-resolution mass spectrometer either by single-ion monitoring or by metastable peak determination.

In the present report, on the other hand, ether extracts are taken to dryness, the residue is dissolved in *n*-hexane, centrifuged, and the supernatant injected onto the column; the drug concentration is assayed by single-ion detection in a quadrupole mass spectrometer. Deterioration of the capillary column, either the glass or the fused silica columns used, was not observed as might be expected from the very simple extraction procedure. The column was heated every evening at 300°C for 1 h. Therefore, we were able to analyze >300 plasma samples without any loss of resolution. The method described, therefore, seems to be suitable for routine analysis of I in clinical studies.

REFERENCES

(1) R. A. Ferrari, K. Chakrabarty, A. L. Beyler, and J. Wiland, *J. Invest. Dermatol.*, **71**, 320 (1978).

(2) A. Schleusener, M. Albring, and F. Neumann, *Curr. Topics Repro. Endrocinol.* **1**, 71 (1982).

(3) S. J. Gaskell and A. W. Pike, *Quant. Mass Spectrom. Life Sci.*, **2**, 181 (1978).

(4) S. J. Gaskell and D. S. Millington, *Quant. Mass Spectrom. Life Sci.*, **2**, 135 (1978).

(5) S. J. Gaskell and A. W. Pike, *Adv. Mass Spectrom.*, **8A**, 279 (1980).

(6) D. S. Millington and V. C. Parr, *Ann. Chim.* (*Rome*), **69**, 629 (1979).

Stability of Cefotaxime Sodium as Determined by High-Performance Liquid Chromatography

V. DAS GUPTA

Received December 3, 1982, from the *Department of Pharmaceutics, College of Pharmacy, University of Houston, Houston, TX 77030.* Accepted for publication February 24, 1983.

Abstract □ The stability of cefotaxime sodium in water (with either hydrochloric acid, phosphate buffers, or other ingredients) dextrose, and sodium chloride has been studied using a stability-indicating high-performance liquid chromatographic method with a relative standard deviation of 1.9% based on six injections. The optimum pH range of stability was determined to be ~4.3–6.2. In this pH range, the decomposition process was catalyzed only by the solvent. At pH ≤3.4, the hydrogen ion also catalyzed the reaction while at pH >6.2, the hydroxyl ion hastened the process of decomposition. The solutions in 5% dextrose and 0.9% NaCl injections were stable for at least 1, 22, and 112 d at 24°C, 4°C, and −10°C, respectively. For both solutions, the loss in potency was <5% at −10°C in 224 d, <9% at 4°C in 42 d, and <3.1% at 24°C in 1 d.

Keyphrases □ Cefotaxime sodium—stability as determined by high-performance liquid chromatography □ Stability—cefotaxime sodium, determined by high-performance liquid chromatography

Cefotaxime sodium, a new semisynthetic cephalosporin antibiotic, is effective against a wide variety of microorganisms when administered intravenously. Stability studies (1) indicate that solutions for intravenous use are stable for 24 h at 25°C, 10 d under refrigeration (<5°C) and for at least 13 weeks in the frozen state. It also appears that cefotaxime solutions exhibit maximum stability in the pH range of 5–7 and that it is not advisable to prepare solutions with diluents having a pH >7.5 (1). In general, cephalosporins have been reported to be stable (2).

Elrod *et al.* (3) reported the various methods available for the quantitation of β-lactam antibiotics, including microbiological (4), iodometric (5), colorimetric (6–8), and high-performance liquid chromatographic (HPLC) (9–12) assays. The two official procedures often specified for cephalosporins are the microbiological agar diffusion (13) and hydroxylamine (14) methods. An HPLC procedure for the quantitation of cefotaxime in serum (15) has been reported.

The purpose of this investigation was to study the stability of cefotaxime sodium at various pH values and in intravenous admixtures. A stability-indicating HPLC method is described which is rapid, accurate, and sensitive.

EXPERIMENTAL

Materials—All chemicals and reagents were either USP, NF, or ACS quality and were used without further purification. Cefotaxime sodium[1] powder was used as received. The high-pressure liquid chromatograph[2] was equipped with a multiple-wavelength detector[3], a recorder[4], and an integrator[5]. A semipolar[6] column (30 cm long × 4 mm i.d.) was used.

The mobile phase for method A contained 0.02 M ammonium acetate and 18% v/v of methanol in water. The flow rate was 2.5 mL/min, the sensitivity was 0.1 AUFS (254 nm), and the chart speed 30.5 cm/h. The temperature was ambient. Chromatographic conditions were the same for method B except that the mobile phase contained 9% v/v of acetonitrile instead of methanol and the sensitivity was 0.04 AUFS.

Methods—A stock solution was prepared fresh daily by dissolving 100 mg of cefotaxime sodium in enough water to make 100 mL of the solution. The stock solution was diluted further with water as needed. The standard solution contained 100 μg/mL of cefotaxime sodium. All the antibiotic solutions were prepared using a simple solution method (Table I). After the initial data (physical appearance, pH values[7], and assays) were obtained, the solutions were stored either at room temperature (24 ± 1°C), under refrigeration (4 ± 1°C), in the freezer (−10 ± 1°C), or at all the three temperatures.

At appropriate intervals, solutions of cefotaxime were assayed using the HPLC method. Before analysis, all solutions were diluted with water to an appropriate concentration (identical to the standard solution based on the label claim). Before dilution, the solutions were always brought to room temperature by putting the bags/bottles in tap water.

A 20-μL aliquot of the assay solution was injected into the chromatograph using the described conditions. For comparison, an identical volume of the standard solution was injected after the assay solution eluted. The concentration of cefotaxime sodium in the standard solution was identical to label claim of the assay solution.

Since preliminary investigations indicated that the peak heights were related directly to the concentrations (range tested was 0.3–2.4 μg), the results were calculated using:

$$\frac{(Ph)_a}{(Ph)_s} \times 100 = \text{percent of label claim} \qquad \text{(Eq. 1)}$$

where $(Ph)_a$ is the peak height of the assay solution and $(Ph)_s$ is the peak height of the standard solution of an identical concentration based on the label claim.

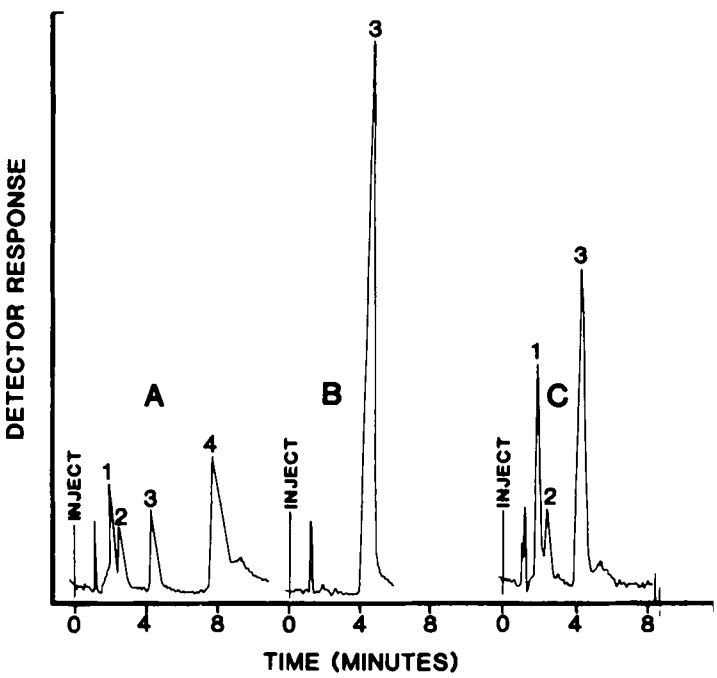

Figure 1—*Typical chromatograms; peak 3 is from cefotaxime and all others are from the decomposition products. Chromatograms A–C are from a 3-d old solution (pH 1.5), a standard solution, and 3-d old solution (pH 8.5), respectively. Chromatographic method A was used (see text).*

[1] Hoechst-Roussel Pharmaceuticals, Somerville, N.J.
[2] Model ALC 202 equipped with U6K universal injector; Waters Associates, Milford, Mass.
[3] Spectroflow monitor SF770; Schoeffel Instrument Corp., Westwood, N.J.
[4] Omniscribe 5313-12; Houston Instruments, Austin, Tx.
[5] Autolab minigrator; Spectra-Physics, Santa Clara, Calif.
[6] μBondapak phenyl (Catalog No. 27198); Waters Associates.
[7] All pH values were measured using Beckman Zeromatic SS-3, pH meter.

0022-3549/84/0400-0565$01.00/0
© 1984, American Pharmaceutical Association

Table I—Cefotaxime Solutions Prepared for the Stability Studies

Solution	Conc. of Cefotaxime Sodium, mg/mL	pH, Initial	Other Ingredients	Ionic Strength[a]	Storage Container
1	10.0	4.7	5% Dextrose	[b]	Plastic Bag[c]
2	10.0	4.6	0.9% NaCl	[b]	Plastic Bag[c]
3	1.0	1.5	0.1 M HCl	0.3	Bottle[d]
4	1.0	2.8	0.1 M Phosphate	0.3	Bottle
5	1.0	3.4	0.1 M Phosphate	0.3	Bottle
6	1.0	4.3	0.1 M Phosphate	0.3	Bottle
7	1.0	4.3	0.2 M Phosphate	0.3	Bottle
8	1.0	4.3	0.1 M Phosphate	0.6	Bottle
9	1.0	5.4	0.1 M Phosphate	0.3	Bottle
10	1.0	6.2	0.1 M Phosphate	0.3	Bottle
11	1.0	7.5	0.1 M Phosphate	0.3	Bottle
12	1.0	8.5	0.1 M Phosphate	0.3	Bottle

[a] Adjusted with KCl. [b] Ionic strength of this solution was not adjusted. [c] The original plastic Viaflex PL 146 bags (Travenol Laboratories), from which either 5% dextrose or 0.9% NaCl injection in water was withdrawn to make the solutions. [d] All bottles are 60-mL amber colored glass; Brockway Glass Co., Brockway, Pa.

RESULTS AND DISCUSSION

Assay Method—The method developed is reproducible with a relative standard deviation of 1.9% based on six injections. The developed procedure separated a number of decomposition products (Fig. 1A–C) from the intact drug (peak 3 in Fig. 1).

The HPLC methods developed are stability indicating (Fig. 1). In a solution of pH 1.5, there was no intact drug present after 7 d of storage. Instead there were four new peaks from the decomposition products. The author feels that the HPLC method may be better, since the results are more accurate and precise compared with the microbiological assay method. Moreover, the decomposition products, especially when only the 3-acetoxy group may have been hydrolyzed, could interfere with the microbiological assay technique, since the intact β-lactam moiety is expected to be active against the bacteria. With the HPLC procedure, this interference is not expected, due to separation of the decomposition products.

Effect of pH and Order of Reaction—The decomposition was first order (Fig. 2). The optimum pH range of stability (Fig. 3) was in the 4.3–6.2 range. At pH values of 3.4 and 7.5, the decomposition was ~10% faster than in the 4.3–6.2 pH range. At pH 1.5, the degradation was the fastest (~11 times faster than in the optimum range), and at pH 8.5 the K_{obs} was ~3 times faster than the K_{obs} between pH 4.3 and pH 6.2. The increase in buffer concentration (phosphate) and the ionic strength (solutions 6–8 in Table I) did not affect the decomposition constant. Since pH had very little effect on K_{obs} the pH range of 4.2–6.2 and reaction was catalyzed only by water, it can be assumed that K_w in Eq. 2 is 0.056 d^{-1} (K_{obs} in the pH range of 4.3–6.2):

$$K_{obs} = K_H(H^+) + K_w + K_{OH}(OH^-) \qquad \text{(Eq. 2)}$$

Neglecting the effect of OH^- at pH 1.5 and that of H^+ at pH 8.5, the K_H and K_{OH} values were estimated to be 18.0 and 3.3×10^4 $M^{-1} \cdot d^{-1}$, respectively.

Decomposition of Cefotaxime—It is well documented (2) that at lower pH, the β-lactam moiety undergoes hydrolysis (K_1 step in Scheme I, *cf.* Ref. 2), and at higher pH (~8), the side chain undergoes hydrolysis (K_2 step). In Fig. 1A (as compared with Fig. 1B) the additional unidentified peaks are from the hydrolysis of side chain (peaks 1–2) and lactonization (peaks 4–5) of the β-lactam ring. In Fig. 1C, the additional peaks (peaks 1 and 2) are from the hydrolysis of the 3-acetoxy group (side chain). The decomposition of cefotaxime in this assay solution of pH 1.5 was fast. It is obvious that decomposition products from the side chain elute immediately after the solvent, while those from the β-lactam lactonization elute after the intact drug (Fig. 1A). This was expected, since the hydrolysis of the 3-acetoxy group produced more polar product(s) while lactonization produced less polar product(s). Lactonization predominates only in the acidic medium (2). In these investigations, peaks 3–4 were small in solutions of pH 2.8 and 3.4 and absent in others (pH 4.3–8.5). The absence of lactonization in neutral and basic solutions was expected. Obviously, lactonization does not proceed even under weakly acidic conditions. Peaks 1–2 were larger in pH 8.5 solution, since hydrolysis of the 3-acetoxy group was fastest at this pH (highest in the series of solutions studied).

Stability of Intravenous Solutions—The testing results of intravenous solutions indicate (Table II) that the manufacturer-recommended (1) expiration date of 24 h at room temperature is reasonable. However, cefotaxime sodium solutions were stable for 22 d at 4°C *versus* the manufacturer-recommended expiration date of 10 d. Even in 35 d, the loss in potency was <5%. The frozen

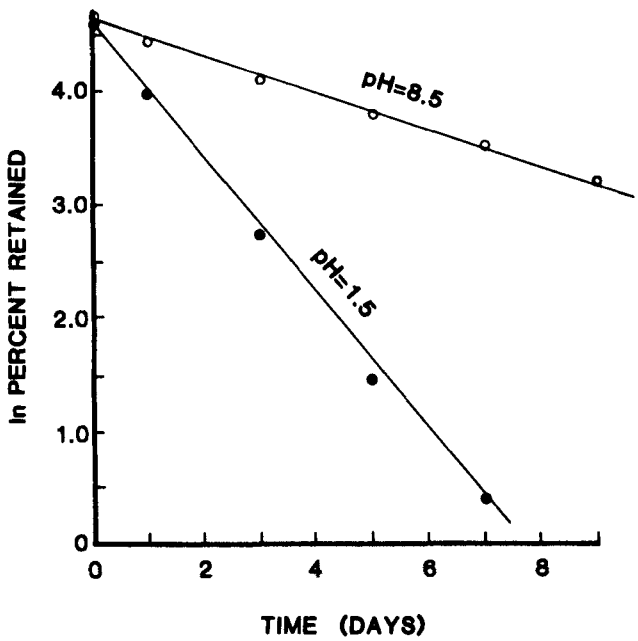

Figure 2—*First-order plots of the degradation of cefotaxime in solutions of pH 1.5 and 8.5.*

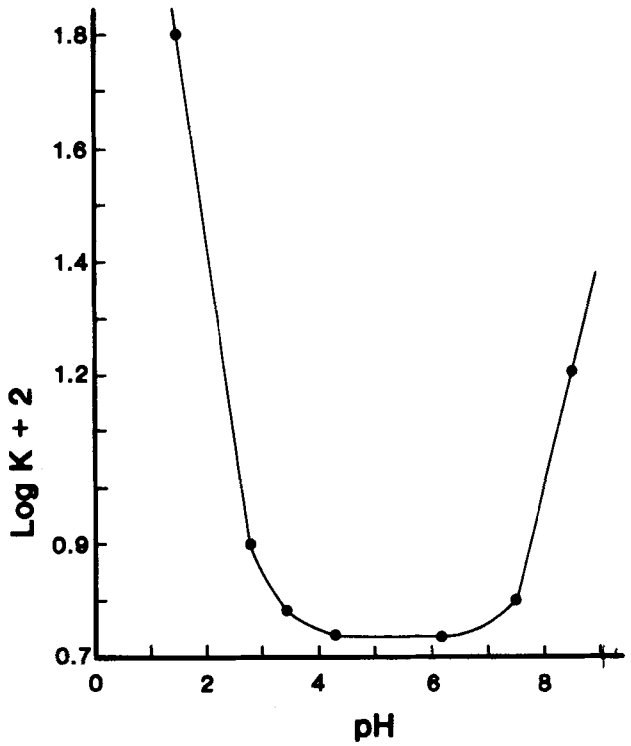

Figure 3—*A pH-rate profile curve from data of solutions 3–12 (Table I).*

Table II—Assay Results and pH Values of the Solutions at Various Temperatures [a]

Vehicle	Amount Retained[b] Based on the Label Claim, %			
	24 ± 1°C			
	0 d	1 d	3 d	7 d
5% Dextrose	100.2 (4.7)	97.0 (4.5)	75.9 (4.5)	60.4 (4.4)
0.9% NaCl	100.8 (4.6)	98.0 (4.4)	76.7 (4.4)	59.0 (4.2)

	4 ± 1°C					
	0 d	11 d	17 d	22 d	35 d	42 d
5% Dextrose	100.2 (4.7)	101.2 (4.7)	101.2 (4.7)	100.8 (4.7)	96.1 (4.5)	92.5 (4.7)
0.9% NaCl	100.8 (4.6)	99.6 (4.6)	100.2 (4.6)	99.2 (4.6)	95.2 (4.5)	91.7 (4.6)

	−10 ± 1°C				
	0 d	28 d	63 d	112 d	224 d
5% Dextrose	100.2 (4.7)	100.2 (4.7)	100.4 (4.7)	99.8 (4.7)	95.3 (4.6)
0.9% NaCl	100.8 (4.6)	100.8 (4.6)	100.2 (4.6)	99.6 (4.6)	95.6 (4.5)

[a] Results (using chromatographic method A) of buffered solutions are presented in Figs. 2 and 3. The increase in buffer concentration and the ionic strength (solutions 6-8, Table I) did not affect the K_{obs} value. All solutions containing 1.0 mg/mL of cefotaxime sodium were clear and pH values were constant to the last day of these investigations. The solutions containing 1% cefotaxime sodium were very slightly yellow in color on day 0. The intensity of color increased after 1, 25, and 112 d of storage at 24°C, 4°C, and −10°C, respectively. [b] These were determined using chromatographic method B. The results obtained on selected samples with chromatographic method A were similar. The pH value is in parentheses.

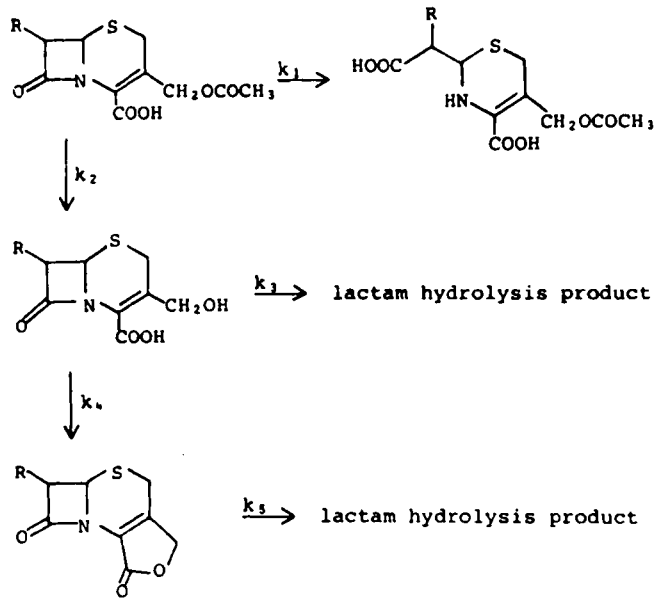

Scheme I—Decomposition of Cefotaxime. R represents the amide side chain.

solutions were stable for at least 16 weeks. In 32 weeks, the loss in potency was <5%, and the change in pH was negligible. However, an additional important factor must be considered, *e.g.*, a poor mixing technique could contaminate the admixture and make it unsuitable for use.

REFERENCES

(1) Hoechst-Roussel Pharmaceuticals, Claforan Insert 71789, Somerville, N.J., Rev. 1981.

(2) K. A. Connors, G. L. Amidon, and L. Kennon, "Chemical Stability of Pharmaceuticals," Wiley, New York, N.Y., 1979 p. 195.

(3) L. Elrod, Jr., L. B. White, D. C. Wimer, and R. D. Cox, *J. Chromatogr.*, **237**, 515 (1982).

(4) J. V. Bennett, J. L. Brodie, E. J. Benner, and W. M. M. Kirby, *Appl. Microbiol.*, **14**, 170 (1966).

(5) J. F. Alicino, *Anal. Chem.*, **33**, 648 (1961).

(6) J. W. Munson, D. Papadimitriou, and P. P. Deluca, *J. Pharm. Sci.*, **68**, 1333 (1979).

(7) L. P. Merrelli, *J. Pharm. Sci.*, **57**, 2172 (1968).

(8) L. P. Merrelli in "Cephalosporins and Penicillins," E. H. Flynn, Ed., Academic, New York, N.Y., 1972 pp. 617-619.

(9) E. R. White, M. A. Carroll, and J. E. Zarembo, *J. Antibiot.*, **30**, 811 (1977).

(10) M. G. Young, *J. Chromatogr.*, **150**, 221 (1978).

(11) J. M. Indelicato, B. A. Steward, and G. L. Engel, *J. Pharm. Sci.*, **69**, 1183 (1980).

(12) V. D. Gupta and K. R. Stewart, *J. Pharm. Sci.*, **69**, 1264 (1980).

(13) Code of Federal Regulations, Title 21, U.S. Govt. Printing Office, Washington, D.C., 1980, Part 436.105.

(14) Code of Federal Regulations, Title 21, U.S. Govt. Printing Office, Washington, D.C., 1980, Part 436.205.

(15) T. Bergan and R. Solberg, *Chemotherapia*, **27**, 155 (1981).

Serotonergic Receptor Antagonist from *Nandina domestica* Thunberg

N. SHOJI *, A. UMEYAMA *, T. TAKEMOTO *, and Y. OHIZUMI ‡x

Received May 10, 1982, from the **Faculty of Pharmacy, Tokushima-Bunri University, Tokushima-shi, Tokushima 770*, and the ‡*Mitsubishi-Kasei Institute of Life Sciences, 11 Minamiooya, Machida-shi, Tokyo 194, Japan.* Accepted for publication March 21, 1983.

Abstract □ A crude methanolic extract of the fruit of *Nandina domestica* Thunberg strongly inhibits serotonin-induced contractions of the rabbit aorta. The extract of the fruit has been fractionated to afford nantenine (*O*-methyldomesticine) as the active agent.

Keyphrases □ *Nandina domestica* Thunberg—nantenine, extraction, serotonergic receptor antagonist, isolated rabbit aorta □ Nantenine—serotonergic receptor antagonist extracted from *Nandina domestica* Thunberg, isolated rabbit aorta □ Serotonergic receptor antagonist—nantenine, extracted from *Nandina domestica* Thunberg, isolated rabbit aorta

The fruit of *Nandina domestica* Thunberg (Berberidaceae) has been used to treat asthma, whooping cough, pharynx tumor, and uterine bleeding in Japan for many years (1). Chemical studies on the constituents of the plant have revealed that presence of numerous alkaloids in this species (1–18). Initially, it was found that the crude methanolic extract of the fruit selectively inhibited serotonin-induced contractions of isolated rabbit aorta without producing inhibitory effects on contractions induced by potassium chloride or histamine. In this paper, the isolation and the determination of the chemical structure of the antiserotonergic substance from the fruit are described.

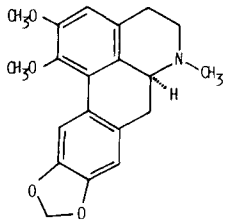

Fruits of *Nandina domestica* Thunberg (4 kg)
↓ extracted with methanol
Methanolic extract (729 g) (+)
↓ partitioned between ethyl acetate and water

- Ethyl acetate-soluble portion (136 g) (−)
- Water-soluble portion (+) → extracted with *n*-butyl alcohol
  - *n*-Butyl alcohol-soluble portion (158 g) (+) → chromatographed on silica gel (chloroform-methanol)
    - Fraction I (37 g) (−)
    - Fraction II (44 g) (+) → chromatographed on silica gel (chloroform-methanol)
      - Fraction A (12.8 g) (+) → recrystallized (ethyl acetate) → nantenine (8.0 g) (+)
      - Fraction B (0.4 g) (−)
      - Fraction C (20.0 g) (−)
    - Fraction III (22 g) (−)
    - Fraction IV (26 g) (−)
  - Water-soluble portion (428 g) (−)

Scheme I—Procedure for the isolation of the serotonergic receptor antagonist from Nandina domestica *Thunberg. Key: (+) active; (−) inactive.*

0022-3549/84/0400-0568$01.00/0
© 1984, American Pharmaceutical Association

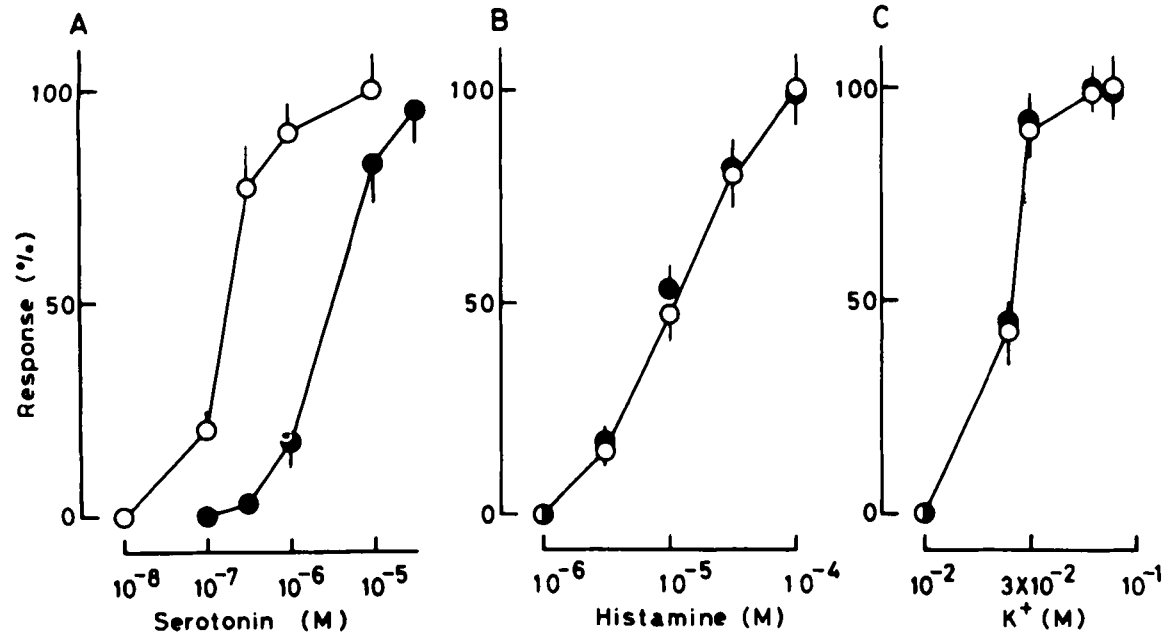

Figure 1—*Effect of nantenine on the dose-response curve for serotonin (A), histamine (B) and potassium chloride (K^+) (C) added 15 min after administration of nantenine to isolated rabbit aorta. The maximum response to serotonin (3×10^{-6} M), histamine (10^{-4} M), and K^+ (8×10^{-2} M) is expressed as 100%. Vertical lines indicate* SEM (n = 6). *Key: (○) control; (●) treatment with nantenine (3×10^{-6} M).*

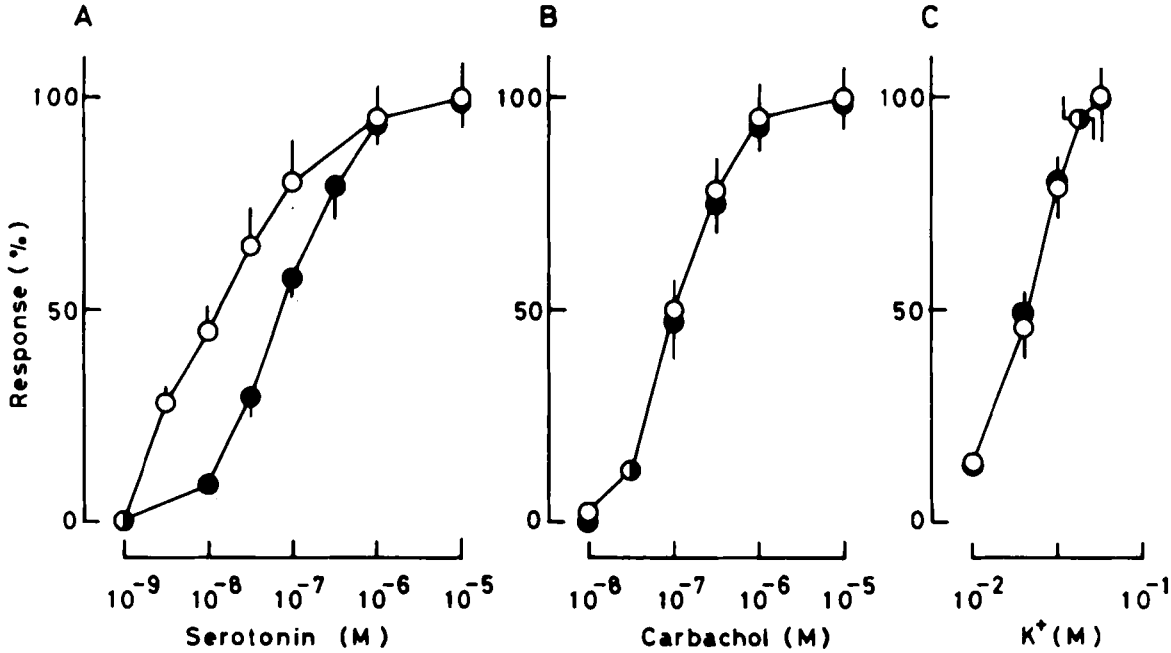

Figure 2—*Effect of nantenine on the dose-response curve for serotonin (A), carbachol (B), and potassium chloride (K^+) (C) added 15 min after administration of nantenine to isolated rat stomach. The maximum response to serotonin (10^{-5} M), carbachol (10^{-5} M), and K^+ (8×10^{-2} M) is expressed as 100%. Vertical lines indicate* SEM (n = 6). *Key: (○) control; (●) treatment with nantenine (3×10^{-6} M).*

EXPERIMENTAL[1]

Isolation—The dried, powdered fruit[2] (4 kg) of *N. domestica* were extracted with methanol (3 × 6 L) at room temperature yielding an extract (729 g), which was fractionated and monitored for inhibitory effects on the serotonin-induced contraction of rabbit aorta, as shown in Scheme I. The pharmacologically active *n*-butyl alcohol fraction was evaporated to dryness *in vacuo*, the residue (158 g) was chromatographed on silica gel[3] eluted with chloroform–methanol mixtures of increasing polarity, and fractionated successively. Each fraction was monitored by TLC[4] with chloroform–methanol–water (65:30:4) as the developing solvent and Dragendorf reagent as the detecting spray. The active second fraction (fraction II) was evaporated to dryness *in vacuo*, and the residue (44 g) was rechromatographed on silica gel using the chloroform–methanol solvent system. The active fraction (12.8 g) from the first eluate (fraction A) was recrystallized from ethyl acetate to give 8.0 g of nantenine as colorless needles ($C_{20}H_{21}NO_3$), mp 140–141°C [lit. (2) mp 139°C], $[\alpha]_D$ + 102.0° (*c* 1.0, $CHCl_3$) [lit. (2) $[\alpha]_D$ + 101.7°]; ^{1}H-NMR (pyridine-d_5): δ 2.43 (s, 3, N—CH_3), 3.72 (s, 3, C(1)—OCH_3), 3.76 (s, 3, C(2)—OCH_3), 6.00 (s, 2, O—CH_2—O), 6.66 (s, 1, C(3)—H), 6.87 (s, 1, C(8)—H), and 8.20 ppm (s, 1, C(11)—H); ^{13}C-NMR (pyridine-d_5): δ 29.66 (t, C-4), 35.52 (t, C-5), 44.03 (q, N—CH_3), 53.47 (t, C-7), 55.86 (d, C-6a), 60.06 (q, C(1)—OCH_3), 63.02 (q, C(2)—OCH_3), 101.47 (t, O CH_2—O), 108.95 (d, C-3), 109.22 (d, C-8), 111.80 (d, C-11), 126.21 (s, C-11b), 127.28

[1] Melting points were obtained on a Yanagimoto micro melting point apparatus and are uncorrected. Optical rotation was recorded on a Jasco DIP-180 digital polarimeter. UV spectra were obtained with a Hitachi 200-20 spectrophotometer. IR spectra were obtained on a Hitachi R-22 spectrometer. ^{1}H- and ^{13}C-NMR spectra were recorded on a Shimadzu LKB-9000B.

[2] Purchased from Nippon Hunmatsu Yakuhin, Ltd.

[3] Silica gel 60, Merck.

[4] TLC plates silica gel 60 F_{254} (0.25 mm), Merck.

(s, C-11c), 128.25 (s, C-7a), 129.44 (s, C-3a), 131.68 (s, C-11a), 145.24 (s, C-2), 147.01 (s, C-9*), 147.13 (s, C-10*), and 152.60 ppm (s, C-1). Assignments are interchangeable between carbons with an asterisk. The MS and UV spectra were identical with published spectra (11, 13).

Bioassay—Male albino rabbits (2–3 kg) were killed by cervical dislocation. The aortae were removed and cut into helical strips. The strips were mounted vertically in a 20-mL organ bath containing Krebs–Ringer bicarbonate solution (pH 7.4) of the following composition (in mmoles): sodium chloride, 120; potassium chloride, 4.8; calcium chloride, 1.2; magnesium sulfate, 1.3; monobasic potassium phosphate, 1.2; sodium bicarbonate, 25.2; and glucose, 5.8. The solution was bubbled with a gas mixture of oxygen–carbon dioxide (95:5, v/v) and maintained at 37°C. A resting tension of 1 g was applied to the strips and isometric contractions were recorded with a force displacement transducer.

Male Wistar rats (300–350 g) were killed by a blow on the neck and the stomach was removed. The fundus was cut longitudinally into strips (20 × 2 mm) as described by Offermeiser and Ariens (19). The strips were suspended in a 20-mL organ bath containing Krebs–Ringer bicarbonate solution. The solution was aerated with oxygen–carbon dioxide (95:5 v/v) and maintained at 37°C. A resting tension of 0.5 g was applied to the strips. Mechanical responses were recorded isotonically on a pen recorder through an isotonic transducer.

RESULTS AND DISCUSSION

A methanolic extract of the fruit of *N. domestica* almost completely inhibited the serotonin-induced contractions of isolated rabbit aorta and had no effect on contractions induced by potassium chloride or histamine. To isolate the active substance, fractionation of the methanolic extract of the fruits were performed (Scheme 1), accompanied by a bioassay using isolated rabbit aorta. Silica gel chromatography of the *n*-butyl alcohol-soluble portion of the methanolic extract afforded the active substance as colorless crystals (8.0 g, 0.2% dry weight of the fruit). The compound showed a positive Dragendorff test and its physicochemical properties (*i.e.*, melting point, specific optical rotation, UV absorption, and mass spectrum) agreed with those of nantenine (1, 5, 6, 11, 13), which was previously isolated as a major alkaloid of the same material. Furthermore, the ^{1}H- and ^{13}C-NMR spectra also supported the identity of the active substance as nantenine (see *Experimental*).

In isolated rabbit aorta, nantenine (3×10^{-6} M) produced a parallel, right shift of the dose–response curve for the contractile effect of serotonin, but had no effect on the dose–response curves for histamine and potassium chloride (Fig. 1), indicating competitive antagonism. Furthermore, in rat stomach strips, nantenine (3×10^{-6} M) shifted the dose–contractile response curve for serotonin to the right in a similar manner, but the dose–response curves for carbachol and potassium chloride were not affected by nantenine (Fig. 2). These results suggest that nantenine selectively inhibits the contractile response of these tissues to serotonin. On the basis of the present results, it is concluded that *N. domestica* Thunberg has a serotonergic receptor blocking action in the isolated rabbit aorta, and that the main active compound is nantenine.

REFERENCES

(1) T. Takase and H. Ohashi, *J. Pharm. Soc., Jpn.*, **535,** 742 (1926).
(2) Z. Kitasato, *J. Pharm. Soc. Jpn.*, **522,** 695 (1925).
(3) Z. Kitasato, *J. Pharm. Soc. Jpn.*, **523,** 791 (1925).
(4) Z. Kitasato, *J. Pharm. Soc. Jpn.*, **534,** 653 (1926).
(5) Z. Kitasato, *J. Pharm. Soc. Jpn.*, **536,** 843 (1926).
(6) H. Maniwa, R. Sakae, and I. Kan, *J. Pharm. Soc. Jpn.*, **536,** 833 (1926).
(7) H. Maniwa and R. Sakae, *J. Pharm. Soc. Jpn.*, **536,** 874 (1926).
(8) J. Ohta, *Yakugaku Zasshi*, **69,** 502 (1949).
(9) M. Tomita, Y. Inubushi, S. Ishii, and M. Yamagata, *Yakugaku Zasshi*, **71,** 381 (1951).
(10) M. Tomita and T. Kugo, *Yakugaku Zasshi*, **76,** 751 (1956).
(11) M. Tomita and T. Kitamura, *Yakugaku Zasshi*, **79,** 1092 (1959).
(12) M. Chikamatsu, M. Tomita, and M. Kotake, *Nippon Kagaku Zasshi*, **82,** 1708 (1961).
(13) M. Ohashi, J. M. Wilson, H. Budzikiewicz, W. A. Slusarchyk, and C. Djerassii, *J. Am. Chem. Soc.*, **85,** 2807 (1963).
(14) J. Kunitomo, K. Morimoto, S. Tanaka, and S. Hayata, *Yakugaku Zasshi*, **92,** 207 (1972).
(15) J. Kunitomo, M. Ju-ichi, Y. Yoshikawa, and H. Chikamatsu, *Yakugaku Zasshi*, **94,** 97 (1974).
(16) J. Kunitomo, M. Ju-ichi, Y. Yoshikawa, Y. Masada, K. Hashimoto, T. Inoue, and M. Fujioka, *Yakugaku Zasshi*, **94,** 1149 (1974).
(17) J. Kunitomo, J. Ju-ichi, Y. Ando, Y. Yoshikawa, S. Nakamura, and T. Shingu, *Yakugaku Zasshi*, **95,** 445 (1975).
(18) J. Kunitomo and Y. Murakami, *Shoyakugaku Zasshi*, **33,** 84 (1979).
(19) J. Offermeiser and E. J. Ariens, *Arch. Int. Pharmacodyn.*, **164,** 192 (1966).

ACKNOWLEDGMENTS

The authors are extremely grateful to A. Kajiwara, K. Takeda, Y. Doi, and M. Yoshimura for their technical assistance.

COMMUNICATIONS

Computation of Model-Independent Pharmacokinetic Parameters During Multiple Dosing

Keyphrases □ Pharmacokinetic parameters—model independent, multiple dosing

To the Editor:

In a recent article, Bauer and Gibaldi (1) reported an alternate, noncompartmental method to calculate pharmacokinetic parameters during multiple dosing. The method was based on reverse superposition from which a single-dose drug concentration–time curve was derived from data obtained at steady state. The following method would be a more general approach for computation of model-independent pharmacokinetic parameters during multiple dosing. The plasma drug concentration–time curve after the Nth dose (C_N) of a fixed dose of a drug at a given dosing interval of τ can be described by Eq. 1, when a drug obeys linear pharmacokinetics:

$$C_N = \sum_{i=1}^{n} A_i \frac{1 - \exp(-Nk_i\tau)}{1 - \exp(-k_i\tau)} \exp(-k_i t) = \sum_{i=1}^{n} I_i \exp(-k_i t) \quad \text{(Eq. 1)}$$

where A_i and I_i are the coefficients of the specific first-order rate constant, k_i, after a single dose and the Nth dose, respectively; t is the time after each drug administration. The total area under the plasma drug concentration–time curve (AUC) from the time after the Nth dose is given to time infinity, $\text{AUC}(\infty)_N$ can be obtained as follows:

0022-3549/84/0400-0570$01.00/0

© 1984, American Pharmaceutical Association

(s, C-11c), 128.25 (s, C-7a), 129.44 (s, C-3a), 131.68 (s, C-11a), 145.24 (s, C-2), 147.01 (s, C-9*), 147.13 (s, C-10*), and 152.60 ppm (s, C-1). Assignments are interchangeable between carbons with an asterisk. The MS and UV spectra were identical with published spectra (11, 13).

Bioassay—Male albino rabbits (2–3 kg) were killed by cervical dislocation. The aortae were removed and cut into helical strips. The strips were mounted vertically in a 20-mL organ bath containing Krebs–Ringer bicarbonate solution (pH 7.4) of the following composition (in mmoles): sodium chloride, 120; potassium chloride, 4.8; calcium chloride, 1.2; magnesium sulfate, 1.3; monobasic potassium phosphate, 1.2; sodium bicarbonate, 25.2; and glucose, 5.8. The solution was bubbled with a gas mixture of oxygen–carbon dioxide (95:5, v/v) and maintained at 37°C. A resting tension of 1 g was applied to the strips and isometric contractions were recorded with a force displacement transducer.

Male Wistar rats (300–350 g) were killed by a blow on the neck and the stomach was removed. The fundus was cut longitudinally into strips (20 × 2 mm) as described by Offermeiser and Ariens (19). The strips were suspended in a 20-mL organ bath containing Krebs–Ringer bicarbonate solution. The solution was aerated with oxygen–carbon dioxide (95:5 v/v) and maintained at 37°C. A resting tension of 0.5 g was applied to the strips. Mechanical responses were recorded isotonically on a pen recorder through an isotonic transducer.

RESULTS AND DISCUSSION

A methanolic extract of the fruit of *N. domestica* almost completely inhibited the serotonin-induced contractions of isolated rabbit aorta and had no effect on contractions induced by potassium chloride or histamine. To isolate the active substance, fractionation of the methanolic extract of the fruits were performed (Scheme 1), accompanied by a bioassay using isolated rabbit aorta. Silica gel chromatography of the *n*-butyl alcohol-soluble portion of the methanolic extract afforded the active substance as colorless crystals (8.0 g, 0.2% dry weight of the fruit). The compound showed a positive Dragendorff test and its physicochemical properties (*i.e.*, melting point, specific optical rotation, UV absorption, and mass spectrum) agreed with those of nantenine (1, 5, 6, 11, 13), which was previously isolated as a major alkaloid of the same material. Furthermore, the ^{1}H- and ^{13}C-NMR spectra also supported the identity of the active substance as nantenine (see *Experimental*).

In isolated rabbit aorta, nantenine (3×10^{-6} M) produced a parallel, right shift of the dose–response curve for the contractile effect of serotonin, but had no effect on the dose–response curves for histamine and potassium chloride (Fig. 1), indicating competitive antagonism. Furthermore, in rat stomach strips, nantenine (3×10^{-6} M) shifted the dose–contractile response curve for serotonin to the right in a similar manner, but the dose–response curves for carbachol and potassium chloride were not affected by nantenine (Fig. 2). These results suggest that nantenine selectively inhibits the contractile response of these tissues to serotonin. On the basis of the present results, it is concluded that *N. domestica* Thunberg has a serotonergic receptor blocking action in the isolated rabbit aorta, and that the main active compound is nantenine.

REFERENCES

(1) T. Takase and H. Ohashi, *J. Pharm. Soc., Jpn.*, **535,** 742 (1926).
(2) Z. Kitasato, *J. Pharm. Soc. Jpn.*, **522,** 695 (1925).
(3) Z. Kitasato, *J. Pharm. Soc. Jpn.*, **523,** 791 (1925).
(4) Z. Kitasato, *J. Pharm. Soc. Jpn.*, **534,** 653 (1926).
(5) Z. Kitasato, *J. Pharm. Soc. Jpn.*, **536,** 843 (1926).
(6) H. Maniwa, R. Sakae, and I. Kan, *J. Pharm. Soc. Jpn.*, **536,** 833 (1926).
(7) H. Maniwa and R. Sakae, *J. Pharm. Soc. Jpn.*, **536,** 874 (1926).
(8) J. Ohta, *Yakugaku Zasshi*, **69,** 502 (1949).
(9) M. Tomita, Y. Inubushi, S. Ishii, and M. Yamagata, *Yakugaku Zasshi*, **71,** 381 (1951).
(10) M. Tomita and T. Kugo, *Yakugaku Zasshi*, **76,** 751 (1956).
(11) M. Tomita and T. Kitamura, *Yakugaku Zasshi*, **79,** 1092 (1959).
(12) M. Chikamatsu, M. Tomita, and M. Kotake, *Nippon Kagaku Zasshi*, **82,** 1708 (1961).
(13) M. Ohashi, J. M. Wilson, H. Budzikiewicz, W. A. Slusarchyk, and C. Djerassii, *J. Am. Chem. Soc.*, **85,** 2807 (1963).
(14) J. Kunitomo, K. Morimoto, S. Tanaka, and S. Hayata, *Yakugaku Zasshi*, **92,** 207 (1972).
(15) J. Kunitomo, M. Ju-ichi, Y. Yoshikawa, and H. Chikamatsu, *Yakugaku Zasshi*, **94,** 97 (1974).
(16) J. Kunitomo, M. Ju-ichi, Y. Yoshikawa, Y. Masada, K. Hashimoto, T. Inoue, and M. Fujioka, *Yakugaku Zasshi*, **94,** 1149 (1974).
(17) J. Kunitomo, J. Ju-ichi, Y. Ando, Y. Yoshikawa, S. Nakamura, and T. Shingu, *Yakugaku Zasshi*, **95,** 445 (1975).
(18) J. Kunitomo and Y. Murakami, *Shoyakugaku Zasshi*, **33,** 84 (1979).
(19) J. Offermeiser and E. J. Ariens, *Arch. Int. Pharmacodyn.*, **164,** 192 (1966).

ACKNOWLEDGMENTS

The authors are extremely grateful to A. Kajiwara, K. Takeda, Y. Doi, and M. Yoshimura for their technical assistance.

COMMUNICATIONS

Computation of Model-Independent Pharmacokinetic Parameters During Multiple Dosing

Keyphrases □ Pharmacokinetic parameters—model independent, multiple dosing

To the Editor:

In a recent article, Bauer and Gibaldi (1) reported an alternate, noncompartmental method to calculate pharmacokinetic parameters during multiple dosing. The method was based on reverse superposition from which a single-dose drug concentration–time curve was derived from data obtained at steady state. The following method would be a more general approach for computation of model-independent pharmacokinetic parameters during multiple dosing. The plasma drug concentration–time curve after the Nth dose (C_N) of a fixed dose of a drug at a given dosing interval of τ can be described by Eq. 1, when a drug obeys linear pharmacokinetics:

$$C_N = \sum_{i=1}^{n} A_i \frac{1 - \exp(-Nk_i\tau)}{1 - \exp(-k_i\tau)} \exp(-k_i t) = \sum_{i=1}^{n} I_i \exp(-k_i t) \quad \text{(Eq. 1)}$$

where A_i and I_i are the coefficients of the specific first-order rate constant, k_i, after a single dose and the Nth dose, respectively; t is the time after each drug administration. The total area under the plasma drug concentration–time curve (AUC) from the time after the Nth dose is given to time infinity, $\text{AUC}(\infty)_N$ can be obtained as follows:

0022-3549/84/0400-0570$01.00/0

© 1984, American Pharmaceutical Association

$$\mathrm{AUC}(\infty)_N = \int_0^{\infty} C_N dt = \sum_{i=1}^{n} \frac{I_i}{k_i} = \mathrm{AUC}(\infty) + \sum_{i=1}^{n} \frac{A_i[1 - \exp(-(N-1)k_i\tau)\exp(-k_i\tau)]}{k_i[1 - \exp(-k_i\tau)]} = \mathrm{AUC}(\infty)_{ss} - \sum_{i=1}^{n} \frac{A_i \exp(-Nk_i\tau)}{k_i[1 - \exp(k_i\tau)]} \quad \text{(Eq. 2)}$$

When the dosing interval is located in the terminal phase, Eq. 2 can be approximated by Eq. 2a:

$$\mathrm{AUC}(\infty)_N = \mathrm{AUC}(\infty) + C_{\min N-1}/k_n = \mathrm{AUC}(\infty)_{ss} - (C_{\min ss} - C_{\min N-1})/k_n \quad \text{(Eq. 2a)}$$

where $\mathrm{AUC}(\infty)$ and $\mathrm{AUC}(\infty)_{ss}$ are the total areas after a single dose and at steady state, respectively; $C_{\min N-1}$ and $C_{\min ss}$ are the plasma drug concentrations at the dosing interval after the $(N-1)$th dose and at steady state, respectively; k_n is the terminal phase disposition rate constant.

The $\mathrm{AUC}(\infty)_N$ can be obtained by numerical integration using the trapezoidal rule from the time course data of plasma drug concentrations:

$$\mathrm{AUC}(\infty)_n = \int_0^{t^*} C_N dt + \int_{t^*}^{\infty} C_N dt = \sum_{i=1}^{n} \frac{1}{2}(C_{Ni} + C_{Ni-1})(t_i - t_{i-1}) + \sum_{i=1}^{n} \frac{I_i \exp(-k_i t^*)}{k_i} \quad \text{(Eq. 3)}$$

The residual area from t^* (usually the last sampling time point) to infinity is usually approximated by C_N^*/k_n, where C_N^* is the estimated drug concentration at time t^* after the Nth dose.

The total area under the first moment of the plasma drug concentration–time curve after the Nth dose, $\mathrm{AUMC}(\infty)_N$ can be calculated as follows:

$$\mathrm{AUMC}(\infty)_N = \int_0^{\infty} tC_N dt = \sum_{i=1}^{n} \frac{I_i}{k_i^2} = \mathrm{AUMC}(\infty) + \sum_{i=1}^{n} \frac{A_i[1 - \exp(-(N-1)k_i\tau)\exp(-k_i\tau)]}{k_i^2[1 - \exp(-k_i\tau)]} = \mathrm{AUMC}(\infty)_{ss} - \sum_{i=1}^{n} \frac{A_i \exp(-Nk_i\tau)}{k_i^2[1 - \exp(-k_i\tau)]} \quad \text{(Eq. 4)}$$

When the τ is located in the terminal phase, Eq. 4 can be approximated by Eq. 4a:

$$\mathrm{AUMC}(\infty)_N = \mathrm{AUMC}(\infty) + C_{\min N-1}/k_n^2 = \mathrm{AUMC}(\infty)_{ss} - (C_{\min ss} - C_{\min N-1})/k_n^2 \quad \text{(Eq. 4a)}$$

where $\mathrm{AUMC}(\infty)$ and $\mathrm{AUMC}(\infty)_{ss}$ are the total area moments after a single dose and at steady state, respectively. The $\mathrm{AUMC}(\infty)_N$ can also be obtained as follows:

$$\mathrm{AUMC}(\infty)_N = \sum_{i=1}^{n} \frac{1}{2}(t_i C_{Ni} + t_{i-1}C_{Ni-1})(t_i - t_{i-1}) + \sum_{i=1}^{n} \frac{I_i}{k_i^2}(1 + k_i t^*)\exp(-k_i t^*) \quad \text{(Eq. 5)}$$

The residual area moment from t^* to infinity is usually approximated by:

$$\frac{C_N^*}{k_n^2} + \frac{t^* C_N^*}{k_n}$$

According to the statistical concept of moments for pharmacokinetics, the mean residence time of a drug in the body (MRT) after a single dose is defined as follows (2):

$$\mathrm{MRT} = \frac{\mathrm{AUMC}(\infty)}{\mathrm{AUC}(\infty)} = \frac{\sum_{i=1}^{n} A_i/k_i^2}{\sum_{i=1}^{n} A_i/k_i} \quad \text{(Eq. 6)}$$

This concept can be extended to the observed data after the Nth dose and at steady state by applying Eqs. 2a and 4a as follows:

$$\mathrm{MRT} = \frac{k_n^2\,\mathrm{AUMC}(\infty)_N - C_{\min N-1}}{k_n[k_n\mathrm{AUC}(\infty)_N - C_{\min N-1}]} = \frac{k_n^2\mathrm{AUMC}(\infty)_{ss} - C_{\min ss}}{k_n[k_n\mathrm{AUC}(\infty)_{ss} - C_{\min ss}]} \quad \text{(Eq. 7)}$$

For the data obtained during the dosing interval:

$$\mathrm{MRT} = \frac{k_n^2\mathrm{AUMC}(\tau)_N + k_n\tau C_{minN} + C_{minN} - C_{minN-1}}{k_n[k_n\mathrm{AUC}(\tau)_N + C_{minN} - C_{minN-1}]} = \frac{k_n\mathrm{AUMC}(\tau)_{ss} + \tau C_{\min ss}}{k_n\mathrm{AUC}(\tau)_{ss}} = \frac{\mathrm{AUMC}(\tau)_{ss}}{\mathrm{AUC}(\tau)_{ss}} + \frac{\tau C_{\min ss}}{k_n\mathrm{AUC}(\tau)_{ss}} \quad \text{(Eq. 8)}$$

Although Bauer and Gibaldi (1) stated that the apparent volume of distribution at steady state, Vd_{ss}, cannot be calculated directly from steady-state data, Vd_{ss} can be calculated from the MRT (using Eq. 7 or Eq. 8) after multiple intravenous bolus dosing of a drug as (3):

$$Vd_{ss} = \mathrm{TBC}\cdot\mathrm{MRT} \quad \text{(Eq. 9)}$$

where total body clearance (TBC) after the Nth dose and at steady state can be calculated as:

$$\mathrm{TBC} = \frac{k_n\cdot\mathrm{Dose}}{k_n\mathrm{AUC}(\infty)_N - C_{\min N-1}} = \frac{\mathrm{Dose}}{\mathrm{AUC}(\tau)_{ss}} \quad \text{(Eq. 10)}$$

No model has to be assumed to calculate MRT, Vd_{ss}, and TBC after multiple dosing. This method can be applied to data obtained from any number of doses including steady state and does not require the plasma drug concentrations derived by means of reverse superposition. The method describes an exact solution and its approximation. The approximation requires an assumption that doses must be administered during the terminal phase. This assumption is generally valid. When the assumption is not valid, one may use the exponential equations to calculate the residual area and area moment.

(1) L. A. Bauer and M. Gibaldi, *J. Pharm. Sci.*, **72**, 978 (1983).
(2) K. Yamaoka, T. Nakagawa, and T. Uno, *J. Pharmacokinet. Biopharm.*, **6**, 547 (1978).
(3) L. Z. Benet and R. L. Galeazzi, *J. Pharm. Sci.*, **68**, 1071 (1979).

Menger Chung
Department of Drug Metabolism and Pharmacokinetics
Schering-Plough Research Division
Bloomfield, NJ 07003

Received September 26, 1983.
Accepted for publication January 19, 1984.

Analytical Profiles of Drug Substances, Vol. 12. Edited by KLAUS FLOREY. Academic Press, 111 Fifth Avenue, New York, NY 10003. 1983. 735 pp. 15 × 23 cm. Price $47.00.

Continuing the yearly volumes in the series, analytical profiles of 17 drug substances are given in 713 pages. These are: amantadine, amikacin sulfate, benzocaine, dibucaine and dibucaine hydrochloride, estrone, etomidate, heparin sodium, hydrocortisone, metoprolol tartrate, phenylpropanolamine hydrochloride, pilocarpine, pyrazinamide, pyrimethamine, quinidine sulfate, quinine hydrochloride, rutin, and trimipramine maleate. There are also two profile supplements: dioctyl sodium sulfosuccinate (8 pp.) and isopropamide (12 pp.). The main profiles for each of these are in Volume 2.

This volume follows the pattern set in Volume 11. It has all of the strengths of the extensive data given in an analytical profile (including structures, spectra, tables of properties and chromatographic systems, and extensive references) and the lack of consistency inherent in having different authorships of each profile [see review of Vol. 11, *J. Pharm. Sci.*, **72,** 582 (1983)]. One reference which was looked for was found as reference 69 under pilocarpine; however, the authors listed are not correct. This volume, like the others in the series, is a valuable reference for those engaged in pharmaceutical formulation and quality control and those needing information on drug metabolism, biopharmaceutics, and pharmacokinetics.

Reviewed by Murray M. Tuckerman
School of Pharmacy
Temple University
Philadelphia, PA 19140

Cell Surface Receptors. Edited by P. G. STRANGE. John Wiley and Sons, Inc., One Wiley Drive, Somerset, NJ 08873. 1983. 298 pp. 16 × 24 cm. Price $79.95.

Dr. Strange has assembled a collection of some 15 reviews, average length 20 pages, dealing with a variety of membrane receptors and approaches to the study of receptor structure and function. Included are chapters on α_2-adrenoceptors, opiate, benzodiazepine, dopamine, and calcium receptors, focusing largely on structure–activity relationships seen through pharmacological and radioligand binding studies. Other chapters discuss receptor changes and regulation including neuroleptic–dopamine interactions, biogenic amine changes in schizophrenia, regulation of GnRH receptors, cyclase defects in pseudohypoparathyroidism, and the implications of coexistence of amine and peptide transmitters. Coupling mechanisms are considered in chapters on phospholipids and adenylate cyclase. Final chapters discuss the gene coding of the nicotinic acetylcholine receptor and radioreceptor assays in quantitative drug assay.

Despite the necessary brevity of the chapters, there is material of interest to expert and nonexpert alike. Each chapter is, at least, adequately written with decent illustrations and few misprints. Few will leave the book without both gaining some useful insights and a deepened appreciation for the rapid pace of development of the study of pharmacological receptors. However, it is difficult to determine the primary audience for this book. To the nonexpert, graduate student, or new worker in the field, the volume is simply not systematic enough; however, the volume could certainly be a helpful supplementary volume accompanying a more basic course. For this purpose, the book is highly priced. To the expert, the volume may be useful in providing brief reviews in a number of receptor areas, but probably not to the extent of individual purchase.

In summary, I enjoyed reading this book and obtained some useful insights into a number of receptor areas. I do not recommend it for individual purchase, but an institutional purchase would certainly be appropriate.

Reviewed by David J. Triggle
Department of Biochemical Pharmacology
State University of New York at Buffalo
Amherst, NY 14260

Manufacturing Processes for New Pharmaceuticals. By MARSHALL SITTIG. Noyes Publications, Mill Road at Grand Avenue, Park Ridge, NJ 07656. 1983. 612 pp., 15 × 23 cm. Price $84.00.

This is Chemical Technology Review No. 220 from Noyes Publications. The book describes the processes for the manufacture of nearly 500 new-chemical-entity pharmaceuticals. The great majority of the compounds are undergoing some level of FDA review, with approval as new drugs being the ultimate goal. The author states in the foreword to the book that the information used in the reviews was obtained from the patent literature, and that the new drugs described have attained generic name status, but in most cases have not yet received trade names.

The arrangement within the reference is alphabetical by generic name. There is no index or cross-index of the compounds listed in the book by chemical name. The lack of such a chemical name index detracts from the value of the book, since its not possible to conveniently determine whether or not a particular compound is listed in the book, unless the generic name is known.

Under each entry in the book, the generic name is given first, followed by the therapeutic function of the compound, the chemical name, the empirical chemical formula, the structural formula, in some cases a product description (usually limited to the melting point), the code number of the compound, the manufacturer and country, the manufacturing process, and references. The manufacturing processes are described in detail. In some cases, several alternative syntheses are given. Where intermediates are involved, the syntheses of the intermediates are given. In addition to the one or more patent references given with each compound, other references are frequently given, where results of pharmacological studies or other data on therapeutic uses, adverse effects, or precautions may be found.

The book is intended as a guide to future drugs. The book should thus be of interest to scientists engaged in the design and development of new drugs. Furthermore, some of the chemical synthesis manufacturing methods reported for the wide range of compounds in the book will be of interest to medicinal and organic chemists.

Reviewed by Gilbert S. Banker
Industrial and Physical Pharmacy Department
School of Pharmacy and Pharmacal Sciences
Purdue University
West Lafayette, IN 47907

Antibiotics: An Introduction. By ROLAND REINER. Thieme-Stratton Inc., 381 Park Avenue South, New York, NY 10016. 1982. 172 pp. 12 × 19 cm. Price $9.95.

This small volume is intended to provide "a condensed introduction to the chemistry, biochemistry, biology, pharmacy, and medical usage of antibiotics." The book begins with a brief historical outline in tabular form of the discovery of important chemotherapeutic agents. This is followed by very brief discussions concerning the detection and determination of antibiotic activity and the production and isolation of antibiotics. The chapter entitled "Chemistry of Antibiotics" includes a limited discussion of the structure proof of penicillin and oxytetracycline, followed by a series of schemes illustrating the partial and total synthesis of several antibiotics. The synthetic pathways are not discussed. The chapter on "Mechanism of Action of Antibiotics" is presented in tabular form listing the antibiotic class and site of action with minimal discussion. A chapter entitled "Chemotherapeutic Properties of Antibiotics" provides a brief overview of the clinical use, antibacterial spectrum, administration and dosage, and bacterial resistance of important antibiotics. The information is presented primarily in tabular form. The final chapter, about one-third of the book, is entitled "Structural Formulas and Main Properties of Individual Antibiotics." This chapter consists primarily of the structural and empirical formulas and molecular weight of over 100 antibiotics. A bibliography containing an extensive listing of mono-

Analytical Profiles of Drug Substances, Vol. 12. Edited by KLAUS FLOREY. Academic Press, 111 Fifth Avenue, New York, NY 10003. 1983. 735 pp. 15 × 23 cm. Price $47.00.

Continuing the yearly volumes in the series, analytical profiles of 17 drug substances are given in 713 pages. These are: amantadine, amikacin sulfate, benzocaine, dibucaine and dibucaine hydrochloride, estrone, etomidate, heparin sodium, hydrocortisone, metoprolol tartrate, phenylpropanolamine hydrochloride, pilocarpine, pyrazinamide, pyrimethamine, quinidine sulfate, quinine hydrochloride, rutin, and trimipramine maleate. There are also two profile supplements: dioctyl sodium sulfosuccinate (8 pp.) and isopropamide (12 pp.). The main profiles for each of these are in Volume 2.

This volume follows the pattern set in Volume 11. It has all of the strengths of the extensive data given in an analytical profile (including structures, spectra, tables of properties and chromatographic systems, and extensive references) and the lack of consistency inherent in having different authorships of each profile [see review of Vol. 11, *J. Pharm. Sci.*, **72,** 582 (1983)]. One reference which was looked for was found as reference 69 under pilocarpine; however, the authors listed are not correct. This volume, like the others in the series, is a valuable reference for those engaged in pharmaceutical formulation and quality control and those needing information on drug metabolism, biopharmaceutics, and pharmacokinetics.

Reviewed by Murray M. Tuckerman
School of Pharmacy
Temple University
Philadelphia, PA 19140

Cell Surface Receptors. Edited by P. G. STRANGE. John Wiley and Sons, Inc., One Wiley Drive, Somerset, NJ 08873. 1983. 298 pp. 16 × 24 cm. Price $79.95.

Dr. Strange has assembled a collection of some 15 reviews, average length 20 pages, dealing with a variety of membrane receptors and approaches to the study of receptor structure and function. Included are chapters on α_2-adrenoceptors, opiate, benzodiazepine, dopamine, and calcium receptors, focusing largely on structure–activity relationships seen through pharmacological and radioligand binding studies. Other chapters discuss receptor changes and regulation including neuroleptic–dopamine interactions, biogenic amine changes in schizophrenia, regulation of GnRH receptors, cyclase defects in pseudohypoparathyroidism, and the implications of coexistence of amine and peptide transmitters. Coupling mechanisms are considered in chapters on phospholipids and adenylate cyclase. Final chapters discuss the gene coding of the nicotinic acetylcholine receptor and radioreceptor assays in quantitative drug assay.

Despite the necessary brevity of the chapters, there is material of interest to expert and nonexpert alike. Each chapter is, at least, adequately written with decent illustrations and few misprints. Few will leave the book without both gaining some useful insights and a deepened appreciation for the rapid pace of development of the study of pharmacological receptors. However, it is difficult to determine the primary audience for this book. To the nonexpert, graduate student, or new worker in the field, the volume is simply not systematic enough; however, the volume could certainly be a helpful supplementary volume accompanying a more basic course. For this purpose, the book is highly priced. To the expert, the volume may be useful in providing brief reviews in a number of receptor areas, but probably not to the extent of individual purchase.

In summary, I enjoyed reading this book and obtained some useful insights into a number of receptor areas. I do not recommend it for individual purchase, but an institutional purchase would certainly be appropriate.

Reviewed by David J. Triggle
Department of Biochemical Pharmacology
State University of New York at Buffalo
Amherst, NY 14260

Manufacturing Processes for New Pharmaceuticals. By MARSHALL SITTIG. Noyes Publications, Mill Road at Grand Avenue, Park Ridge, NJ 07656. 1983. 612 pp., 15 × 23 cm. Price $84.00.

This is Chemical Technology Review No. 220 from Noyes Publications. The book describes the processes for the manufacture of nearly 500 new-chemical-entity pharmaceuticals. The great majority of the compounds are undergoing some level of FDA review, with approval as new drugs being the ultimate goal. The author states in the foreword to the book that the information used in the reviews was obtained from the patent literature, and that the new drugs described have attained generic name status, but in most cases have not yet received trade names.

The arrangement within the reference is alphabetical by generic name. There is no index or cross-index of the compounds listed in the book by chemical name. The lack of such a chemical name index detracts from the value of the book, since its not possible to conveniently determine whether or not a particular compound is listed in the book, unless the generic name is known.

Under each entry in the book, the generic name is given first, followed by the therapeutic function of the compound, the chemical name, the empirical chemical formula, the structural formula, in some cases a product description (usually limited to the melting point), the code number of the compound, the manufacturer and country, the manufacturing process, and references. The manufacturing processes are described in detail. In some cases, several alternative syntheses are given. Where intermediates are involved, the syntheses of the intermediates are given. In addition to the one or more patent references given with each compound, other references are frequently given, where results of pharmacological studies or other data on therapeutic uses, adverse effects, or precautions may be found.

The book is intended as a guide to future drugs. The book should thus be of interest to scientists engaged in the design and development of new drugs. Furthermore, some of the chemical synthesis manufacturing methods reported for the wide range of compounds in the book will be of interest to medicinal and organic chemists.

Reviewed by Gilbert S. Banker
Industrial and Physical Pharmacy Department
School of Pharmacy and Pharmacal Sciences
Purdue University
West Lafayette, IN 47907

Antibiotics: An Introduction. By ROLAND REINER. Thieme-Stratton Inc., 381 Park Avenue South, New York, NY 10016. 1982. 172 pp. 12 × 19 cm. Price $9.95.

This small volume is intended to provide "a condensed introduction to the chemistry, biochemistry, biology, pharmacy, and medical usage of antibiotics." The book begins with a brief historical outline in tabular form of the discovery of important chemotherapeutic agents. This is followed by very brief discussions concerning the detection and determination of antibiotic activity and the production and isolation of antibiotics. The chapter entitled "Chemistry of Antibiotics" includes a limited discussion of the structure proof of penicillin and oxytetracycline, followed by a series of schemes illustrating the partial and total synthesis of several antibiotics. The synthetic pathways are not discussed. The chapter on "Mechanism of Action of Antibiotics" is presented in tabular form listing the antibiotic class and site of action with minimal discussion. A chapter entitled "Chemotherapeutic Properties of Antibiotics" provides a brief overview of the clinical use, antibacterial spectrum, administration and dosage, and bacterial resistance of important antibiotics. The information is presented primarily in tabular form. The final chapter, about one-third of the book, is entitled "Structural Formulas and Main Properties of Individual Antibiotics." This chapter consists primarily of the structural and empirical formulas and molecular weight of over 100 antibiotics. A bibliography containing an extensive listing of mono-

Analytical Profiles of Drug Substances, Vol. 12. Edited by KLAUS FLOREY. Academic Press, 111 Fifth Avenue, New York, NY 10003. 1983. 735 pp. 15 × 23 cm. Price $47.00.

Continuing the yearly volumes in the series, analytical profiles of 17 drug substances are given in 713 pages. These are: amantadine, amikacin sulfate, benzocaine, dibucaine and dibucaine hydrochloride, estrone, etomidate, heparin sodium, hydrocortisone, metoprolol tartrate, phenylpropanolamine hydrochloride, pilocarpine, pyrazinamide, pyrimethamine, quinidine sulfate, quinine hydrochloride, rutin, and trimipramine maleate. There are also two profile supplements: dioctyl sodium sulfosuccinate (8 pp.) and isopropamide (12 pp.). The main profiles for each of these are in Volume 2.

This volume follows the pattern set in Volume 11. It has all of the strengths of the extensive data given in an analytical profile (including structures, spectra, tables of properties and chromatographic systems, and extensive references) and the lack of consistency inherent in having different authorships of each profile [see review of Vol. 11, *J. Pharm. Sci.*, **72,** 582 (1983)]. One reference which was looked for was found as reference 69 under pilocarpine; however, the authors listed are not correct. This volume, like the others in the series, is a valuable reference for those engaged in pharmaceutical formulation and quality control and those needing information on drug metabolism, biopharmaceutics, and pharmacokinetics.

Reviewed by Murray M. Tuckerman
School of Pharmacy
Temple University
Philadelphia, PA 19140

Cell Surface Receptors. Edited by P. G. STRANGE. John Wiley and Sons, Inc., One Wiley Drive, Somerset, NJ 08873. 1983. 298 pp. 16 × 24 cm. Price $79.95.

Dr. Strange has assembled a collection of some 15 reviews, average length 20 pages, dealing with a variety of membrane receptors and approaches to the study of receptor structure and function. Included are chapters on α_2-adrenoceptors, opiate, benzodiazepine, dopamine, and calcium receptors, focusing largely on structure–activity relationships seen through pharmacological and radioligand binding studies. Other chapters discuss receptor changes and regulation including neuroleptic–dopamine interactions, biogenic amine changes in schizophrenia, regulation of GnRH receptors, cyclase defects in pseudohypoparathyroidism, and the implications of coexistence of amine and peptide transmitters. Coupling mechanisms are considered in chapters on phospholipids and adenylate cyclase. Final chapters discuss the gene coding of the nicotinic acetylcholine receptor and radioreceptor assays in quantitative drug assay.

Despite the necessary brevity of the chapters, there is material of interest to expert and nonexpert alike. Each chapter is, at least, adequately written with decent illustrations and few misprints. Few will leave the book without both gaining some useful insights and a deepened appreciation for the rapid pace of development of the study of pharmacological receptors. However, it is difficult to determine the primary audience for this book. To the nonexpert, graduate student, or new worker in the field, the volume is simply not systematic enough; however, the volume could certainly be a helpful supplementary volume accompanying a more basic course. For this purpose, the book is highly priced. To the expert, the volume may be useful in providing brief reviews in a number of receptor areas, but probably not to the extent of individual purchase.

In summary, I enjoyed reading this book and obtained some useful insights into a number of receptor areas. I do not recommend it for individual purchase, but an institutional purchase would certainly be appropriate.

Reviewed by David J. Triggle
Department of Biochemical Pharmacology
State University of New York at Buffalo
Amherst, NY 14260

Manufacturing Processes for New Pharmaceuticals. By MARSHALL SITTIG. Noyes Publications, Mill Road at Grand Avenue, Park Ridge, NJ 07656. 1983. 612 pp., 15 × 23 cm. Price $84.00.

This is Chemical Technology Review No. 220 from Noyes Publications. The book describes the processes for the manufacture of nearly 500 new-chemical-entity pharmaceuticals. The great majority of the compounds are undergoing some level of FDA review, with approval as new drugs being the ultimate goal. The author states in the foreword to the book that the information used in the reviews was obtained from the patent literature, and that the new drugs described have attained generic name status, but in most cases have not yet received trade names.

The arrangement within the reference is alphabetical by generic name. There is no index or cross-index of the compounds listed in the book by chemical name. The lack of such a chemical name index detracts from the value of the book, since its not possible to conveniently determine whether or not a particular compound is listed in the book, unless the generic name is known.

Under each entry in the book, the generic name is given first, followed by the therapeutic function of the compound, the chemical name, the empirical chemical formula, the structural formula, in some cases a product description (usually limited to the melting point), the code number of the compound, the manufacturer and country, the manufacturing process, and references. The manufacturing processes are described in detail. In some cases, several alternative syntheses are given. Where intermediates are involved, the syntheses of the intermediates are given. In addition to the one or more patent references given with each compound, other references are frequently given, where results of pharmacological studies or other data on therapeutic uses, adverse effects, or precautions may be found.

The book is intended as a guide to future drugs. The book should thus be of interest to scientists engaged in the design and development of new drugs. Furthermore, some of the chemical synthesis manufacturing methods reported for the wide range of compounds in the book will be of interest to medicinal and organic chemists.

Reviewed by Gilbert S. Banker
Industrial and Physical Pharmacy Department
School of Pharmacy and Pharmacal Sciences
Purdue University
West Lafayette, IN 47907

Antibiotics: An Introduction. By ROLAND REINER. Thieme-Stratton Inc., 381 Park Avenue South, New York, NY 10016. 1982. 172 pp. 12 × 19 cm. Price $9.95.

This small volume is intended to provide "a condensed introduction to the chemistry, biochemistry, biology, pharmacy, and medical usage of antibiotics." The book begins with a brief historical outline in tabular form of the discovery of important chemotherapeutic agents. This is followed by very brief discussions concerning the detection and determination of antibiotic activity and the production and isolation of antibiotics. The chapter entitled "Chemistry of Antibiotics" includes a limited discussion of the structure proof of penicillin and oxytetracycline, followed by a series of schemes illustrating the partial and total synthesis of several antibiotics. The synthetic pathways are not discussed. The chapter on "Mechanism of Action of Antibiotics" is presented in tabular form listing the antibiotic class and site of action with minimal discussion. A chapter entitled "Chemotherapeutic Properties of Antibiotics" provides a brief overview of the clinical use, antibacterial spectrum, administration and dosage, and bacterial resistance of important antibiotics. The information is presented primarily in tabular form. The final chapter, about one-third of the book, is entitled "Structural Formulas and Main Properties of Individual Antibiotics." This chapter consists primarily of the structural and empirical formulas and molecular weight of over 100 antibiotics. A bibliography containing an extensive listing of mono-

Analytical Profiles of Drug Substances, Vol. 12. Edited by KLAUS FLOREY. Academic Press, 111 Fifth Avenue, New York, NY 10003. 1983. 735 pp. 15 × 23 cm. Price $47.00.

Continuing the yearly volumes in the series, analytical profiles of 17 drug substances are given in 713 pages. These are: amantadine, amikacin sulfate, benzocaine, dibucaine and dibucaine hydrochloride, estrone, etomidate, heparin sodium, hydrocortisone, metoprolol tartrate, phenylpropanolamine hydrochloride, pilocarpine, pyrazinamide, pyrimethamine, quinidine sulfate, quinine hydrochloride, rutin, and trimipramine maleate. There are also two profile supplements: dioctyl sodium sulfosuccinate (8 pp.) and isopropamide (12 pp.). The main profiles for each of these are in Volume 2.

This volume follows the pattern set in Volume 11. It has all of the strengths of the extensive data given in an analytical profile (including structures, spectra, tables of properties and chromatographic systems, and extensive references) and the lack of consistency inherent in having different authorships of each profile [see review of Vol. 11, *J. Pharm. Sci.*, **72,** 582 (1983)]. One reference which was looked for was found as reference 69 under pilocarpine; however, the authors listed are not correct. This volume, like the others in the series, is a valuable reference for those engaged in pharmaceutical formulation and quality control and those needing information on drug metabolism, biopharmaceutics, and pharmacokinetics.

Reviewed by Murray M. Tuckerman
School of Pharmacy
Temple University
Philadelphia, PA 19140

Cell Surface Receptors. Edited by P. G. STRANGE. John Wiley and Sons, Inc., One Wiley Drive, Somerset, NJ 08873. 1983. 298 pp. 16 × 24 cm. Price $79.95.

Dr. Strange has assembled a collection of some 15 reviews, average length 20 pages, dealing with a variety of membrane receptors and approaches to the study of receptor structure and function. Included are chapters on α_2-adrenoceptors, opiate, benzodiazepine, dopamine, and calcium receptors, focusing largely on structure–activity relationships seen through pharmacological and radioligand binding studies. Other chapters discuss receptor changes and regulation including neuroleptic–dopamine interactions, biogenic amine changes in schizophrenia, regulation of GnRH receptors, cyclase defects in pseudohypoparathyroidism, and the implications of coexistence of amine and peptide transmitters. Coupling mechanisms are considered in chapters on phospholipids and adenylate cyclase. Final chapters discuss the gene coding of the nicotinic acetylcholine receptor and radioreceptor assays in quantitative drug assay.

Despite the necessary brevity of the chapters, there is material of interest to expert and nonexpert alike. Each chapter is, at least, adequately written with decent illustrations and few misprints. Few will leave the book without both gaining some useful insights and a deepened appreciation for the rapid pace of development of the study of pharmacological receptors. However, it is difficult to determine the primary audience for this book. To the nonexpert, graduate student, or new worker in the field, the volume is simply not systematic enough; however, the volume could certainly be a helpful supplementary volume accompanying a more basic course. For this purpose, the book is highly priced. To the expert, the volume may be useful in providing brief reviews in a number of receptor areas, but probably not to the extent of individual purchase.

In summary, I enjoyed reading this book and obtained some useful insights into a number of receptor areas. I do not recommend it for individual purchase, but an institutional purchase would certainly be appropriate.

Reviewed by David J. Triggle
Department of Biochemical Pharmacology
State University of New York at Buffalo
Amherst, NY 14260

Manufacturing Processes for New Pharmaceuticals. By MARSHALL SITTIG. Noyes Publications, Mill Road at Grand Avenue, Park Ridge, NJ 07656. 1983. 612 pp., 15 × 23 cm. Price $84.00.

This is Chemical Technology Review No. 220 from Noyes Publications. The book describes the processes for the manufacture of nearly 500 new-chemical-entity pharmaceuticals. The great majority of the compounds are undergoing some level of FDA review, with approval as new drugs being the ultimate goal. The author states in the foreword to the book that the information used in the reviews was obtained from the patent literature, and that the new drugs described have attained generic name status, but in most cases have not yet received trade names.

The arrangement within the reference is alphabetical by generic name. There is no index or cross-index of the compounds listed in the book by chemical name. The lack of such a chemical name index detracts from the value of the book, since its not possible to conveniently determine whether or not a particular compound is listed in the book, unless the generic name is known.

Under each entry in the book, the generic name is given first, followed by the therapeutic function of the compound, the chemical name, the empirical chemical formula, the structural formula, in some cases a product description (usually limited to the melting point), the code number of the compound, the manufacturer and country, the manufacturing process, and references. The manufacturing processes are described in detail. In some cases, several alternative syntheses are given. Where intermediates are involved, the syntheses of the intermediates are given. In addition to the one or more patent references given with each compound, other references are frequently given, where results of pharmacological studies or other data on therapeutic uses, adverse effects, or precautions may be found.

The book is intended as a guide to future drugs. The book should thus be of interest to scientists engaged in the design and development of new drugs. Furthermore, some of the chemical synthesis manufacturing methods reported for the wide range of compounds in the book will be of interest to medicinal and organic chemists.

Reviewed by Gilbert S. Banker
Industrial and Physical Pharmacy Department
School of Pharmacy and Pharmacal Sciences
Purdue University
West Lafayette, IN 47907

Antibiotics: An Introduction. By ROLAND REINER. Thieme-Stratton Inc., 381 Park Avenue South, New York, NY 10016. 1982. 172 pp. 12 × 19 cm. Price $9.95.

This small volume is intended to provide "a condensed introduction to the chemistry, biochemistry, biology, pharmacy, and medical usage of antibiotics." The book begins with a brief historical outline in tabular form of the discovery of important chemotherapeutic agents. This is followed by very brief discussions concerning the detection and determination of antibiotic activity and the production and isolation of antibiotics. The chapter entitled "Chemistry of Antibiotics" includes a limited discussion of the structure proof of penicillin and oxytetracycline, followed by a series of schemes illustrating the partial and total synthesis of several antibiotics. The synthetic pathways are not discussed. The chapter on "Mechanism of Action of Antibiotics" is presented in tabular form listing the antibiotic class and site of action with minimal discussion. A chapter entitled "Chemotherapeutic Properties of Antibiotics" provides a brief overview of the clinical use, antibacterial spectrum, administration and dosage, and bacterial resistance of important antibiotics. The information is presented primarily in tabular form. The final chapter, about one-third of the book, is entitled "Structural Formulas and Main Properties of Individual Antibiotics." This chapter consists primarily of the structural and empirical formulas and molecular weight of over 100 antibiotics. A bibliography containing an extensive listing of mono-

graphs is provided. However, failure to reference the material in the individual chapters is a serious omission.

This book may serve as a quick reference for chemical structures and chemotherapeutic properties of a large number of antibiotics. However, the handbook approach used to present the material makes this book unsuitable as a text.

Reviewed by Marvin R. Boots
Department of Pharmaceutical Chemistry
Medical College of Virginia
Virginia Commonwealth University
Richmond, VA 23298

Solid-State Chemistry of Drugs. By STEPHEN R. BYRN. Academic Press, 111 Fifth Avenue, New York, NY 10003. 1982. 346 pp. 15 × 23 cm. Price $55.00.

The literature on solid-state chemistry is not abundant, and the topic of solid-state chemistry of drugs *per se* has not been treated previously in book form. (Granted, chapters in books and reviews in journals have appeared.) Dr. Byrn's book hence fills a void. It is refreshing to note, at the onset, that it does this very well.

The book is, first of all, self-contained. It commences with morphological descriptions and definitions, followed by a broad overview of what actually happens in a solid when the molecules contained in it (or some of them) undergo chemical change. It then gives examples of the various types of solid-state reactions documented in the literature (and of pharmaceutical interest).

A chapter is devoted to methods of analysis, in a somewhat different way than the casual reader might expect. The tools of trade in this field, if mechanistic understanding is the goal, are X-ray, spectroscopy, and thermal methods. In other words, the analysis section is not cluttered with specific assay methods, but rather with the specific tools. It might have been instructive to have a section dealing with high-vacuum techniques of gas analysis, since these are frequently used in solid-state kinetics in isothermal studies of gas-producing reactions.

The chapter on solid-state kinetics is excellent and covers all essential principles. Particularly useful is Table I, where one particular reaction is treated by a large number of different mechanistic models, leading to the conclusion (not surprisingly) that simply fitting the data to a model will not, in itself, serve as a selection criterion. That philosophy is true in general, but is well stated.

A large chapter is devoted to polymorphism, an important aspect not often thought of as "chemistry" (as implied in the title of the book). But, it certainly belongs in the book and should be of great usefulness to those working in this particular field.

The book contains a wealth of examples. It is written in a very pleasant style. A must for the pharmaceutical scientist involved in solid dosage forms.

Reviewed by J. T. Carstensen
School of Pharmacy
University of Wisconsin,
Madision, WI 53706

Dermatological Formulations: Percutaneous Absorption. By BRIAN W. BARRY. Marcel Dekker, 270 Madison Avenue, New York, NY 10016. 1983. 479 pp. 16 × 23.5 cm. Price $55.00 (20% higher outside the U.S. and Canada).

This is a concise, single-authored overview of percutaneous penetration as it relates to dermatological formulations. Demonstrating the breadth and depth of his personal reading and experience, Dr. Barry singlehandedly tackles many different areas. He starts with a brief overview of the structure, function, diseases, and topical treatment of human skin. The second chapter is a classical review of the principles of diffusion through membranes. He next discusses the facts and theory related to skin transport and properties influencing percutaneous absorption. Following a brief review of methods for quantitating absorption, he ends with two strong chapters on formulation and rheology of dermatological vehicles.

This book is heartily recommended for the novitiate as well as the expert. Being a personal statement, you will enjoy the author's strengths and weaknesses in terms of understanding the field. The index is unique in that it allows you to find the primary places where each author is mentioned throughout the book. In the short time that I have had it, I easily justified the cost of the book by rapidly finding author references.

Reviewed by Howard Maibach
University of California
Medical School
San Francisco, CA 94143

Alkaloids, Volume 1: Chemical and Biological Perspectives. Edited by S. WILLIAM PELLETIER. Wiley-Interscience, 605 Third Avenue, New York, NY 10158. 1983. 398 pp. 16 × 24 cm. Price $60.00.

Alkaloids never seem to cease attracting the interest of chemists. Since the turn of the century, numerous books and series have been published on the subject. This is another ambitious, comprehensive treatise intending to add new perspectives to the subject. The series takes a new topic-oriented approach, departing from the traditional descriptive system based on the class of compounds.

The first volume begins with the nature and definition of an alkaloid by the editor and includes such mixed topics as "Arthropod Alkaloids: Distribution, Functions, and Chemistry," by T. H. Jones and M. S. Blum; "Biosynthesis and Metabolism of the Tobacco Alkaloids," by E. Leete; "The Toxicology and Pharmacology of Diterpenoid Alkaloids," by M. H. Benn and J. M. Jacyno; and "A Chemotaxonomic Investigation of the Plant Families of Apocynaceae, Loganiaceae, and Rubiaceae by Their Indole Alkaloid Content," by M. V. Kisakurek, A. J. M. Leeuwenberg, and M. Hesse. All were written by unquestionable experts in their particular field and provide not only first-hand information by researchers themselves, but also deep insights into the individual subjects.

Dr. Pelletier's devotion to the chemistry of alkaloids, especially diterpenoid alkaloids, is widely known, and his ability to cover this broad topic is also well-proven by his earlier publication in *The Royal Society of Chemistry—Specialist Periodical Reports* on alkaloids. In the first volume he has certainly exercised his knowledge of the topics and taken advantage of his close acquaintance with top researchers in the individual fields. However, it remains to be seen in future volumes how successful the series will be in raising the interest of interdisciplinary readers in such diversified areas as medicinal chemistry, natural products chemistry, pharmacology, pharmacognosy, biochemistry, phytochemistry, plant taxonomy, oncology, forensic science, and medicine as originally intended. At any rate, in conjunction with recent research interest in natural products chemistry, books taking the multidisciplinary approach as, for example, a series on marine natural products with the same subtitle (*Marine Natural Products: Chemical and Biological Perspectives*, P. J. Scheuer, Ed., Academic Press, Volumes I–V), are seen more and more on the bookshelves.

Reviewed by Yuzuru Shimizu
Department of Pharmacognosy and
Environmental Health Sciences
College of Pharmacy
University of Rhode Island
Kingston, RI 02881

Annual Review of Pharmacology and Toxicology, Volume 23. Edited by ROBERT GEORGE, RONALD OKUN, and ARTHUR K. CHO. Annual Reviews Inc., 4139 El Camino Way, Palo Alto, CA 94306. 1983. 713 pp. 15 × 22 cm. Price $27.00.

This review of pharmacology and toxicology continues a successful series of monographs in these areas. The book contains 27 different reviews and a review of the reviews. Each of the reviews is written by a person familiar with the area of research. The reviews are normally concise and well referenced; important tables and figures are included in many of the reviews. The initial review by Leslie Iversen on "Nonopioid Neuropeptides in Mammalian CNS" provides some insight into the re-

graphs is provided. However, failure to reference the material in the individual chapters is a serious omission.

This book may serve as a quick reference for chemical structures and chemotherapeutic properties of a large number of antibiotics. However, the handbook approach used to present the material makes this book unsuitable as a text.

Reviewed by Marvin R. Boots
Department of Pharmaceutical Chemistry
Medical College of Virginia
Virginia Commonwealth University
Richmond, VA 23298

Solid-State Chemistry of Drugs. By STEPHEN R. BYRN. Academic Press, 111 Fifth Avenue, New York, NY 10003. 1982. 346 pp. 15 × 23 cm. Price $55.00.

The literature on solid-state chemistry is not abundant, and the topic of solid-state chemistry of drugs *per se* has not been treated previously in book form. (Granted, chapters in books and reviews in journals have appeared.) Dr. Byrn's book hence fills a void. It is refreshing to note, at the onset, that it does this very well.

The book is, first of all, self-contained. It commences with morphological descriptions and definitions, followed by a broad overview of what actually happens in a solid when the molecules contained in it (or some of them) undergo chemical change. It then gives examples of the various types of solid-state reactions documented in the literature (and of pharmaceutical interest).

A chapter is devoted to methods of analysis, in a somewhat different way than the casual reader might expect. The tools of trade in this field, if mechanistic understanding is the goal, are X-ray, spectroscopy, and thermal methods. In other words, the analysis section is not cluttered with specific assay methods, but rather with the specific tools. It might have been instructive to have a section dealing with high-vacuum techniques of gas analysis, since these are frequently used in solid-state kinetics in isothermal studies of gas-producing reactions.

The chapter on solid-state kinetics is excellent and covers all essential principles. Particularly useful is Table I, where one particular reaction is treated by a large number of different mechanistic models, leading to the conclusion (not surprisingly) that simply fitting the data to a model will not, in itself, serve as a selection criterion. That philosophy is true in general, but is well stated.

A large chapter is devoted to polymorphism, an important aspect not often thought of as "chemistry" (as implied in the title of the book). But, it certainly belongs in the book and should be of great usefulness to those working in this particular field.

The book contains a wealth of examples. It is written in a very pleasant style. A must for the pharmaceutical scientist involved in solid dosage forms.

Reviewed by J. T. Carstensen
School of Pharmacy
University of Wisconsin,
Madision, WI 53706

Dermatological Formulations: Percutaneous Absorption. By BRIAN W. BARRY. Marcel Dekker, 270 Madison Avenue, New York, NY 10016. 1983. 479 pp. 16 × 23.5 cm. Price $55.00 (20% higher outside the U.S. and Canada).

This is a concise, single-authored overview of percutaneous penetration as it relates to dermatological formulations. Demonstrating the breadth and depth of his personal reading and experience, Dr. Barry singlehandedly tackles many different areas. He starts with a brief overview of the structure, function, diseases, and topical treatment of human skin. The second chapter is a classical review of the principles of diffusion through membranes. He next discusses the facts and theory related to skin transport and properties influencing percutaneous absorption. Following a brief review of methods for quantitating absorption, he ends with two strong chapters on formulation and rheology of dermatological vehicles.

This book is heartily recommended for the novitiate as well as the expert. Being a personal statement, you will enjoy the author's strengths and weaknesses in terms of understanding the field. The index is unique in that it allows you to find the primary places where each author is mentioned throughout the book. In the short time that I have had it, I easily justified the cost of the book by rapidly finding author references.

Reviewed by Howard Maibach
University of California
Medical School
San Francisco, CA 94143

Alkaloids, Volume 1: Chemical and Biological Perspectives. Edited by S. WILLIAM PELLETIER. Wiley-Interscience, 605 Third Avenue, New York, NY 10158. 1983. 398 pp. 16 × 24 cm. Price $60.00.

Alkaloids never seem to cease attracting the interest of chemists. Since the turn of the century, numerous books and series have been published on the subject. This is another ambitious, comprehensive treatise intending to add new perspectives to the subject. The series takes a new topic-oriented approach, departing from the traditional descriptive system based on the class of compounds.

The first volume begins with the nature and definition of an alkaloid by the editor and includes such mixed topics as "Arthropod Alkaloids: Distribution, Functions, and Chemistry," by T. H. Jones and M. S. Blum; "Biosynthesis and Metabolism of the Tobacco Alkaloids," by E. Leete; "The Toxicology and Pharmacology of Diterpenoid Alkaloids," by M. H. Benn and J. M. Jacyno; and "A Chemotaxonomic Investigation of the Plant Families of Apocynaceae, Loganiaceae, and Rubiaceae by Their Indole Alkaloid Content," by M. V. Kisakurek, A. J. M. Leeuwenberg, and M. Hesse. All were written by unquestionable experts in their particular field and provide not only first-hand information by researchers themselves, but also deep insights into the individual subjects.

Dr. Pelletier's devotion to the chemistry of alkaloids, especially diterpenoid alkaloids, is widely known, and his ability to cover this broad topic is also well-proven by his earlier publication in *The Royal Society of Chemistry—Specialist Periodical Reports* on alkaloids. In the first volume he has certainly exercised his knowledge of the topics and taken advantage of his close acquaintance with top researchers in the individual fields. However, it remains to be seen in future volumes how successful the series will be in raising the interest of interdisciplinary readers in such diversified areas as medicinal chemistry, natural products chemistry, pharmacology, pharmacognosy, biochemistry, phytochemistry, plant taxonomy, oncology, forensic science, and medicine as originally intended. At any rate, in conjunction with recent research interest in natural products chemistry, books taking the multidisciplinary approach as, for example, a series on marine natural products with the same subtitle (*Marine Natural Products: Chemical and Biological Perspectives*, P. J. Scheuer, Ed., Academic Press, Volumes I–V), are seen more and more on the bookshelves.

Reviewed by Yuzuru Shimizu
Department of Pharmacognosy and
Environmental Health Sciences
College of Pharmacy
University of Rhode Island
Kingston, RI 02881

Annual Review of Pharmacology and Toxicology, Volume 23. Edited by ROBERT GEORGE, RONALD OKUN, and ARTHUR K. CHO. Annual Reviews Inc., 4139 El Camino Way, Palo Alto, CA 94306. 1983. 713 pp. 15 × 22 cm. Price $27.00.

This review of pharmacology and toxicology continues a successful series of monographs in these areas. The book contains 27 different reviews and a review of the reviews. Each of the reviews is written by a person familiar with the area of research. The reviews are normally concise and well referenced; important tables and figures are included in many of the reviews. The initial review by Leslie Iversen on "Nonopioid Neuropeptides in Mammalian CNS" provides some insight into the re-

graphs is provided. However, failure to reference the material in the individual chapters is a serious omission.

This book may serve as a quick reference for chemical structures and chemotherapeutic properties of a large number of antibiotics. However, the handbook approach used to present the material makes this book unsuitable as a text.

Reviewed by Marvin R. Boots
Department of Pharmaceutical Chemistry
Medical College of Virginia
Virginia Commonwealth University
Richmond, VA 23298

Solid-State Chemistry of Drugs. By STEPHEN R. BYRN. Academic Press, 111 Fifth Avenue, New York, NY 10003. 1982. 346 pp. 15 × 23 cm. Price $55.00.

The literature on solid-state chemistry is not abundant, and the topic of solid-state chemistry of drugs *per se* has not been treated previously in book form. (Granted, chapters in books and reviews in journals have appeared.) Dr. Byrn's book hence fills a void. It is refreshing to note, at the onset, that it does this very well.

The book is, first of all, self-contained. It commences with morphological descriptions and definitions, followed by a broad overview of what actually happens in a solid when the molecules contained in it (or some of them) undergo chemical change. It then gives examples of the various types of solid-state reactions documented in the literature (and of pharmaceutical interest).

A chapter is devoted to methods of analysis, in a somewhat different way than the casual reader might expect. The tools of trade in this field, if mechanistic understanding is the goal, are X-ray, spectroscopy, and thermal methods. In other words, the analysis section is not cluttered with specific assay methods, but rather with the specific tools. It might have been instructive to have a section dealing with high-vacuum techniques of gas analysis, since these are frequently used in solid-state kinetics in isothermal studies of gas-producing reactions.

The chapter on solid-state kinetics is excellent and covers all essential principles. Particularly useful is Table I, where one particular reaction is treated by a large number of different mechanistic models, leading to the conclusion (not surprisingly) that simply fitting the data to a model will not, in itself, serve as a selection criterion. That philosophy is true in general, but is well stated.

A large chapter is devoted to polymorphism, an important aspect not often thought of as "chemistry" (as implied in the title of the book). But, it certainly belongs in the book and should be of great usefulness to those working in this particular field.

The book contains a wealth of examples. It is written in a very pleasant style. A must for the pharmaceutical scientist involved in solid dosage forms.

Reviewed by J. T. Carstensen
School of Pharmacy
University of Wisconsin,
Madision, WI 53706

Dermatological Formulations: Percutaneous Absorption. By BRIAN W. BARRY. Marcel Dekker, 270 Madison Avenue, New York, NY 10016. 1983. 479 pp. 16 × 23.5 cm. Price $55.00 (20% higher outside the U.S. and Canada).

This is a concise, single-authored overview of percutaneous penetration as it relates to dermatological formulations. Demonstrating the breadth and depth of his personal reading and experience, Dr. Barry singlehandedly tackles many different areas. He starts with a brief overview of the structure, function, diseases, and topical treatment of human skin. The second chapter is a classical review of the principles of diffusion through membranes. He next discusses the facts and theory related to skin transport and properties influencing percutaneous absorption. Following a brief review of methods for quantitating absorption, he ends with two strong chapters on formulation and rheology of dermatological vehicles.

This book is heartily recommended for the novitiate as well as the expert. Being a personal statement, you will enjoy the author's strengths and weaknesses in terms of understanding the field. The index is unique in that it allows you to find the primary places where each author is mentioned throughout the book. In the short time that I have had it, I easily justified the cost of the book by rapidly finding author references.

Reviewed by Howard Maibach
University of California
Medical School
San Francisco, CA 94143

Alkaloids, Volume 1: Chemical and Biological Perspectives. Edited by S. WILLIAM PELLETIER. Wiley-Interscience, 605 Third Avenue, New York, NY 10158. 1983. 398 pp. 16 × 24 cm. Price $60.00.

Alkaloids never seem to cease attracting the interest of chemists. Since the turn of the century, numerous books and series have been published on the subject. This is another ambitious, comprehensive treatise intending to add new perspectives to the subject. The series takes a new topic-oriented approach, departing from the traditional descriptive system based on the class of compounds.

The first volume begins with the nature and definition of an alkaloid by the editor and includes such mixed topics as "Arthropod Alkaloids: Distribution, Functions, and Chemistry," by T. H. Jones and M. S. Blum; "Biosynthesis and Metabolism of the Tobacco Alkaloids," by E. Leete; "The Toxicology and Pharmacology of Diterpenoid Alkaloids," by M. H. Benn and J. M. Jacyno; and "A Chemotaxonomic Investigation of the Plant Families of Apocynaceae, Loganiaceae, and Rubiaceae by Their Indole Alkaloid Content," by M. V. Kisakurek, A. J. M. Leeuwenberg, and M. Hesse. All were written by unquestionable experts in their particular field and provide not only first-hand information by researchers themselves, but also deep insights into the individual subjects.

Dr. Pelletier's devotion to the chemistry of alkaloids, especially diterpenoid alkaloids, is widely known, and his ability to cover this broad topic is also well-proven by his earlier publication in *The Royal Society of Chemistry—Specialist Periodical Reports* on alkaloids. In the first volume he has certainly exercised his knowledge of the topics and taken advantage of his close acquaintance with top researchers in the individual fields. However, it remains to be seen in future volumes how successful the series will be in raising the interest of interdisciplinary readers in such diversified areas as medicinal chemistry, natural products chemistry, pharmacology, pharmacognosy, biochemistry, phytochemistry, plant taxonomy, oncology, forensic science, and medicine as originally intended. At any rate, in conjunction with recent research interest in natural products chemistry, books taking the multidisciplinary approach as, for example, a series on marine natural products with the same subtitle (*Marine Natural Products: Chemical and Biological Perspectives*, P. J. Scheuer, Ed., Academic Press, Volumes I–V), are seen more and more on the bookshelves.

Reviewed by Yuzuru Shimizu
Department of Pharmacognosy and
Environmental Health Sciences
College of Pharmacy
University of Rhode Island
Kingston, RI 02881

Annual Review of Pharmacology and Toxicology, Volume 23. Edited by ROBERT GEORGE, RONALD OKUN, and ARTHUR K. CHO. Annual Reviews Inc., 4139 El Camino Way, Palo Alto, CA 94306. 1983. 713 pp. 15 × 22 cm. Price $27.00.

This review of pharmacology and toxicology continues a successful series of monographs in these areas. The book contains 27 different reviews and a review of the reviews. Each of the reviews is written by a person familiar with the area of research. The reviews are normally concise and well referenced; important tables and figures are included in many of the reviews. The initial review by Leslie Iversen on "Nonopioid Neuropeptides in Mammalian CNS" provides some insight into the re-

graphs is provided. However, failure to reference the material in the individual chapters is a serious omission.

This book may serve as a quick reference for chemical structures and chemotherapeutic properties of a large number of antibiotics. However, the handbook approach used to present the material makes this book unsuitable as a text.

Reviewed by Marvin R. Boots
Department of Pharmaceutical Chemistry
Medical College of Virginia
Virginia Commonwealth University
Richmond, VA 23298

Solid-State Chemistry of Drugs. By STEPHEN R. BYRN. Academic Press, 111 Fifth Avenue, New York, NY 10003. 1982. 346 pp. 15 × 23 cm. Price $55.00.

The literature on solid-state chemistry is not abundant, and the topic of solid-state chemistry of drugs *per se* has not been treated previously in book form. (Granted, chapters in books and reviews in journals have appeared.) Dr. Byrn's book hence fills a void. It is refreshing to note, at the onset, that it does this very well.

The book is, first of all, self-contained. It commences with morphological descriptions and definitions, followed by a broad overview of what actually happens in a solid when the molecules contained in it (or some of them) undergo chemical change. It then gives examples of the various types of solid-state reactions documented in the literature (and of pharmaceutical interest).

A chapter is devoted to methods of analysis, in a somewhat different way than the casual reader might expect. The tools of trade in this field, if mechanistic understanding is the goal, are X-ray, spectroscopy, and thermal methods. In other words, the analysis section is not cluttered with specific assay methods, but rather with the specific tools. It might have been instructive to have a section dealing with high-vacuum techniques of gas analysis, since these are frequently used in solid-state kinetics in isothermal studies of gas-producing reactions.

The chapter on solid-state kinetics is excellent and covers all essential principles. Particularly useful is Table I, where one particular reaction is treated by a large number of different mechanistic models, leading to the conclusion (not surprisingly) that simply fitting the data to a model will not, in itself, serve as a selection criterion. That philosophy is true in general, but is well stated.

A large chapter is devoted to polymorphism, an important aspect not often thought of as "chemistry" (as implied in the title of the book). But, it certainly belongs in the book and should be of great usefulness to those working in this particular field.

The book contains a wealth of examples. It is written in a very pleasant style. A must for the pharmaceutical scientist involved in solid dosage forms.

Reviewed by J. T. Carstensen
School of Pharmacy
University of Wisconsin,
Madision, WI 53706

Dermatological Formulations: Percutaneous Absorption. By BRIAN W. BARRY. Marcel Dekker, 270 Madison Avenue, New York, NY 10016. 1983. 479 pp. 16 × 23.5 cm. Price $55.00 (20% higher outside the U.S. and Canada).

This is a concise, single-authored overview of percutaneous penetration as it relates to dermatological formulations. Demonstrating the breadth and depth of his personal reading and experience, Dr. Barry singlehandedly tackles many different areas. He starts with a brief overview of the structure, function, diseases, and topical treatment of human skin. The second chapter is a classical review of the principles of diffusion through membranes. He next discusses the facts and theory related to skin transport and properties influencing percutaneous absorption. Following a brief review of methods for quantitating absorption, he ends with two strong chapters on formulation and rheology of dermatological vehicles.

This book is heartily recommended for the novitiate as well as the expert. Being a personal statement, you will enjoy the author's strengths and weaknesses in terms of understanding the field. The index is unique in that it allows you to find the primary places where each author is mentioned throughout the book. In the short time that I have had it, I easily justified the cost of the book by rapidly finding author references.

Reviewed by Howard Maibach
University of California
Medical School
San Francisco, CA 94143

Alkaloids, Volume 1: Chemical and Biological Perspectives. Edited by S. WILLIAM PELLETIER. Wiley-Interscience, 605 Third Avenue, New York, NY 10158. 1983. 398 pp. 16 × 24 cm. Price $60.00.

Alkaloids never seem to cease attracting the interest of chemists. Since the turn of the century, numerous books and series have been published on the subject. This is another ambitious, comprehensive treatise intending to add new perspectives to the subject. The series takes a new topic-oriented approach, departing from the traditional descriptive system based on the class of compounds.

The first volume begins with the nature and definition of an alkaloid by the editor and includes such mixed topics as "Arthropod Alkaloids: Distribution, Functions, and Chemistry," by T. H. Jones and M. S. Blum; "Biosynthesis and Metabolism of the Tobacco Alkaloids," by E. Leete; "The Toxicology and Pharmacology of Diterpenoid Alkaloids," by M. H. Benn and J. M. Jacyno; and "A Chemotaxonomic Investigation of the Plant Families of Apocynaceae, Loganiaceae, and Rubiaceae by Their Indole Alkaloid Content," by M. V. Kisakurek, A. J. M. Leeuwenberg, and M. Hesse. All were written by unquestionable experts in their particular field and provide not only first-hand information by researchers themselves, but also deep insights into the individual subjects.

Dr. Pelletier's devotion to the chemistry of alkaloids, especially diterpenoid alkaloids, is widely known, and his ability to cover this broad topic is also well-proven by his earlier publication in *The Royal Society of Chemistry—Specialist Periodical Reports* on alkaloids. In the first volume he has certainly exercised his knowledge of the topics and taken advantage of his close acquaintance with top researchers in the individual fields. However, it remains to be seen in future volumes how successful the series will be in raising the interest of interdisciplinary readers in such diversified areas as medicinal chemistry, natural products chemistry, pharmacology, pharmacognosy, biochemistry, phytochemistry, plant taxonomy, oncology, forensic science, and medicine as originally intended. At any rate, in conjunction with recent research interest in natural products chemistry, books taking the multidisciplinary approach as, for example, a series on marine natural products with the same subtitle (*Marine Natural Products: Chemical and Biological Perspectives*, P. J. Scheuer, Ed., Academic Press, Volumes I–V), are seen more and more on the bookshelves.

Reviewed by Yuzuru Shimizu
Department of Pharmacognosy and
Environmental Health Sciences
College of Pharmacy
University of Rhode Island
Kingston, RI 02881

Annual Review of Pharmacology and Toxicology, Volume 23. Edited by ROBERT GEORGE, RONALD OKUN, and ARTHUR K. CHO. Annual Reviews Inc., 4139 El Camino Way, Palo Alto, CA 94306. 1983. 713 pp. 15 × 22 cm. Price $27.00.

This review of pharmacology and toxicology continues a successful series of monographs in these areas. The book contains 27 different reviews and a review of the reviews. Each of the reviews is written by a person familiar with the area of research. The reviews are normally concise and well referenced; important tables and figures are included in many of the reviews. The initial review by Leslie Iversen on "Nonopioid Neuropeptides in Mammalian CNS" provides some insight into the re-

graphs is provided. However, failure to reference the material in the individual chapters is a serious omission.

This book may serve as a quick reference for chemical structures and chemotherapeutic properties of a large number of antibiotics. However, the handbook approach used to present the material makes this book unsuitable as a text.

Reviewed by Marvin R. Boots
Department of Pharmaceutical Chemistry
Medical College of Virginia
Virginia Commonwealth University
Richmond, VA 23298

Solid-State Chemistry of Drugs. By STEPHEN R. BYRN. Academic Press, 111 Fifth Avenue, New York, NY 10003. 1982. 346 pp. 15 × 23 cm. Price $55.00.

The literature on solid-state chemistry is not abundant, and the topic of solid-state chemistry of drugs *per se* has not been treated previously in book form. (Granted, chapters in books and reviews in journals have appeared.) Dr. Byrn's book hence fills a void. It is refreshing to note, at the onset, that it does this very well.

The book is, first of all, self-contained. It commences with morphological descriptions and definitions, followed by a broad overview of what actually happens in a solid when the molecules contained in it (or some of them) undergo chemical change. It then gives examples of the various types of solid-state reactions documented in the literature (and of pharmaceutical interest).

A chapter is devoted to methods of analysis, in a somewhat different way than the casual reader might expect. The tools of trade in this field, if mechanistic understanding is the goal, are X-ray, spectroscopy, and thermal methods. In other words, the analysis section is not cluttered with specific assay methods, but rather with the specific tools. It might have been instructive to have a section dealing with high-vacuum techniques of gas analysis, since these are frequently used in solid-state kinetics in isothermal studies of gas-producing reactions.

The chapter on solid-state kinetics is excellent and covers all essential principles. Particularly useful is Table I, where one particular reaction is treated by a large number of different mechanistic models, leading to the conclusion (not surprisingly) that simply fitting the data to a model will not, in itself, serve as a selection criterion. That philosophy is true in general, but is well stated.

A large chapter is devoted to polymorphism, an important aspect not often thought of as "chemistry" (as implied in the title of the book). But, it certainly belongs in the book and should be of great usefulness to those working in this particular field.

The book contains a wealth of examples. It is written in a very pleasant style. A must for the pharmaceutical scientist involved in solid dosage forms.

Reviewed by J. T. Carstensen
School of Pharmacy
University of Wisconsin,
Madision, WI 53706

Dermatological Formulations: Percutaneous Absorption. By BRIAN W. BARRY. Marcel Dekker, 270 Madison Avenue, New York, NY 10016. 1983. 479 pp. 16 × 23.5 cm. Price $55.00 (20% higher outside the U.S. and Canada).

This is a concise, single-authored overview of percutaneous penetration as it relates to dermatological formulations. Demonstrating the breadth and depth of his personal reading and experience, Dr. Barry singlehandedly tackles many different areas. He starts with a brief overview of the structure, function, diseases, and topical treatment of human skin. The second chapter is a classical review of the principles of diffusion through membranes. He next discusses the facts and theory related to skin transport and properties influencing percutaneous absorption. Following a brief review of methods for quantitating absorption, he ends with two strong chapters on formulation and rheology of dermatological vehicles.

This book is heartily recommended for the novitiate as well as the expert. Being a personal statement, you will enjoy the author's strengths and weaknesses in terms of understanding the field. The index is unique in that it allows you to find the primary places where each author is mentioned throughout the book. In the short time that I have had it, I easily justified the cost of the book by rapidly finding author references.

Reviewed by Howard Maibach
University of California
Medical School
San Francisco, CA 94143

Alkaloids, Volume 1: Chemical and Biological Perspectives. Edited by S. WILLIAM PELLETIER. Wiley-Interscience, 605 Third Avenue, New York, NY 10158. 1983. 398 pp. 16 × 24 cm. Price $60.00.

Alkaloids never seem to cease attracting the interest of chemists. Since the turn of the century, numerous books and series have been published on the subject. This is another ambitious, comprehensive treatise intending to add new perspectives to the subject. The series takes a new topic-oriented approach, departing from the traditional descriptive system based on the class of compounds.

The first volume begins with the nature and definition of an alkaloid by the editor and includes such mixed topics as "Arthropod Alkaloids: Distribution, Functions, and Chemistry," by T. H. Jones and M. S. Blum; "Biosynthesis and Metabolism of the Tobacco Alkaloids," by E. Leete; "The Toxicology and Pharmacology of Diterpenoid Alkaloids," by M. H. Benn and J. M. Jacyno; and "A Chemotaxonomic Investigation of the Plant Families of Apocynaceae, Loganiaceae, and Rubiaceae by Their Indole Alkaloid Content," by M. V. Kisakurek, A. J. M. Leeuwenberg, and M. Hesse. All were written by unquestionable experts in their particular field and provide not only first-hand information by researchers themselves, but also deep insights into the individual subjects.

Dr. Pelletier's devotion to the chemistry of alkaloids, especially diterpenoid alkaloids, is widely known, and his ability to cover this broad topic is also well-proven by his earlier publication in *The Royal Society of Chemistry—Specialist Periodical Reports* on alkaloids. In the first volume he has certainly exercised his knowledge of the topics and taken advantage of his close acquaintance with top researchers in the individual fields. However, it remains to be seen in future volumes how successful the series will be in raising the interest of interdisciplinary readers in such diversified areas as medicinal chemistry, natural products chemistry, pharmacology, pharmacognosy, biochemistry, phytochemistry, plant taxonomy, oncology, forensic science, and medicine as originally intended. At any rate, in conjunction with recent research interest in natural products chemistry, books taking the multidisciplinary approach as, for example, a series on marine natural products with the same subtitle (*Marine Natural Products: Chemical and Biological Perspectives*, P. J. Scheuer, Ed., Academic Press, Volumes I–V), are seen more and more on the bookshelves.

Reviewed by Yuzuru Shimizu
Department of Pharmacognosy and
Environmental Health Sciences
College of Pharmacy
University of Rhode Island
Kingston, RI 02881

Annual Review of Pharmacology and Toxicology, Volume 23. Edited by ROBERT GEORGE, RONALD OKUN, and ARTHUR K. CHO. Annual Reviews Inc., 4139 El Camino Way, Palo Alto, CA 94306. 1983. 713 pp. 15 × 22 cm. Price $27.00.

This review of pharmacology and toxicology continues a successful series of monographs in these areas. The book contains 27 different reviews and a review of the reviews. Each of the reviews is written by a person familiar with the area of research. The reviews are normally concise and well referenced; important tables and figures are included in many of the reviews. The initial review by Leslie Iversen on "Nonopioid Neuropeptides in Mammalian CNS" provides some insight into the re-

markable changes that have taken place in understanding chemical substances that are important in the central nervous system over the past ten years. Cannon's review on "Structure–Activity Relationships of Dopamine Agonists" is well illustrated with chemical formulas, which is an important aid in following the discussion. The chapter on "Recent Developments in Mass Spectrometry for the Analysis of Complex Mixtures" provides some very basic and informative material on how the new techniques in this area are being used. The volume provides a number of other very timely reviews; they seem to be well written and could provide the reader with some initial leads to more in-depth studies that have been carried out.

The indexing for the volume is very complete, both by author and subject, for rapid access to the desired material. Each of the reviews ends with a Conclusion or Summary section which distills each review to some very basic points and areas of interest for the future.

Because of the nature of the series, this would be a good volume to have present in the library so that individuals could easily read a review in one of the areas covered. I would recommend that the volume be acquired for a School of Pharmacy library or Health Science library or in a general reading room facility for faculty and graduate students. The volume provides a valuable resource for a reasonable cost, in that the authors of the various sections have provided good coverage of findings that have taken place in recent years in pharmacology and toxicology.

Reviewed by Duane D. Miller
College of Pharmacy
Division of Medicinal Chemistry and Pharmacognosy
The Ohio State University
Columbus, OH 43210

FREE RADICALS AND CANCER. Edited by ROBERT A. FLOYD. Marcel Dekker, Inc., 270 Madison Avenue, New York, NY 10016. 1982. 541 pp. 16 × 23.5 mm. Price $69.75 (20% higher outside the U.S. and Canada).

The role of free radicals in cancer development has been of concern to, and studied by, many investigators in the past three decades. Up to the present, however, there is as yet no clear-cut settlement of this seemingly simple but actually complicated problem and probably there never will be. This is perhaps one of the main reasons that the editor is compiling the thoughts of many investigators from all over the world into one volume.

Thirteen groups of researchers contributed their findings and interpretations. These include (titles abbreviated): C. Nagata *et al.* (Free Radicals from Chemical Carcinogens and Significance in Carcinogenesis) from Japan; [illegible] *et al.* (Nitroxide Metabolism in Liver Microsomes) from the Federal Republic of Germany; H. M. Swartz (ESR Studies of Cancer) of Illinois; E. Cavalieri *et al.* (Multiple Activation Mechanisms in Aromatic Hydrocarbon Carcinogenesis) of Nebraska; A. M. Bobst (Spin Bioassays with Nucleic Acids) of Ohio; J. Cadet and R. Téoule (Binding of Radiosensitizing Drugs to DNA) from France; F. R. DeRubertis and P. A. Craven (Activation of Guanylate Cyclase and Evidence for a Free Radical Mechanism) of Pennsylvania; N. M. Emanuel (Free Radicals and Growth of Tumors) from the U.S.S.R.; R. Sridhar (Radiation Sensitizers in Therapy) of Oklahoma; R. A. Floyd (Free Radicals and Arylamine Carcinogenesis) of Oklahoma; E. G. Janzen and E. R. Davis (Detection of Free Radicals by Spin-Trapping) from Canada; J. A. Hinson *et al.* (Role of Free Radicals in the Mutagenicity of *N*-Hydroxy-2-acetylaminofluorene) of Maryland; and J. E. Biaglow *et al.* (Metabolic Activation of Carcinogenic Nitro Compounds to Oxygen-Reactive Intermediates) from the U.S. and Canada. It is probably unavoidable that writings which came from such a variety of sources would contain material with duplicate or even contradictory information. Actually this is perhaps a clever way to inform the readers of the vastness and the uncertainties of this field of study.

Aside from the key question raised at the beginning of this review, there are other points that deserve to be mentioned. Although free radicals have been detected in many carcinogens with or without enzymatic action, they have also been detected in normal and pathological tissues. Throughout this book it is reported that even some compounds possessing recognized antineoplastic action, such as doxorubicin hydrochloride (Adriamycin), or prophylactic property against cancer information, such as ascorbic acid, produce free radicals in ESR measurements. To make the situation even more complicated, some carcinogens do not produce free radicals. Free radicals generally are defined as species having ESR signals in the g = 2.00 region with line shapes and power-saturation characteristics typical of organic free radicals (the latter exclude paramagnetic metals). However, measurement of free radicals depends on a number of variable experimental conditions, including the preparation of samples, the temperature during measurement, the solvent used, the type of tissue examined, and animal species differences. Therefore, one should be extremely careful and cautious in making empirical and qualitative correlations and straightforward interpretations.

The relationship of free radicals to cancer can perhaps be approached in another aspect. That is, to study the quantitative rather than the qualitative characteristics of free radicals in certain types of cancer detection, diagnosis, and response to treatment. There are already indications in this book that an in-depth study of ESR signals may reveal characteristic information in the development and progression of certain types of tumors and tumor response to therapeutic treatment. Studies along this line should be extremely useful in cancer research.

After reading all of the material presented in this book, one may assume that free radical formation may well be just a phenomenon observed during the cellular proliferation (rather than limited to only during the cancer growth) or a phenomenon observed as formation of intermediates during metabolic activation of many chemical compounds (not necessarily limited to mutagens, carcinogens, or antineoplastic agents). The situation is analogous to that of the numerous studies on drug–DNA intercalation: that the observed phenomenon may not be the real, or the major, or even the minor, mode of biological action.

This book is recommended to those scientists who are interested in these aspects of biology and medicine, as well as to oncologists and physicians who are forever searching for the fundamental knowledge of the secret of life.

Reviewed by C. C. Cheng
Department of Pharmacology, Toxicology, and Therapeutics
University of Kansas Medical Center
Kansas City, KS 66103

Current Trends in Organic Synthesis. Proceedings of the Fourth International Conference on Organic Synthesis. Edited by HITOSI NOZAKI. Pergamon Press, Maxwell House, Fairview Park, Elmsford, NY 10523. 1983. 429 pp. 18.5 × 27.5 cm. Price $90.00 (£45.00).

The 30 lectures compiled from the talks presented at the 1982 IUPAC meeting in Tokyo (August 1982) constitute an impressive review of the current state of the art in the field of organic synthesis. Because the book is a reproduction of the authors' manuscripts, there are a few typographical errors and unclear figures, but these minor shortcomings in no way detract from the overall appeal of this volume. As outlined in the Preface, the book is divided into four areas: synthesis of natural products, methods for achieving stereoselectivity, new synthetic methodology, and new reactions.

The group of lectures on natural product synthesis begins with a presentation by E. J. Corey on his work in the leukotriene field, which includes synthetic methodology developed for use in this area, but with applications throughout organic synthesis, as well as total syntheses of LTB and several rationally designed inhibitors of lipoxygenase enzymes. The next lecture, by W. Bartmann, discusses the synthesis of stable analogues of PGI2, illustrating the intimate connection between chemical synthesis, biological testing, and development of commercially feasible syntheses characteristic of industry. C. Heathcock then describes the efforts of his group in the area of stereoselective aldol condensation reactions and their application to his ongoing total synthesis of erythromycin. B. M. Trost outlines the observations that lead to the development of the total synthesis of verrucarol as well as continuing work on its elaboration to verrucarin A. A review of the numerous examples of the Diels–Alder reaction developed by the group of M. E. Jung and their application to steroid and anthracycline natural products is offered next. Highly selective protecting group chemistry is the focus of a lecture by C. B. Reese on the total synthesis of yeast alanine tRNA, a nonadecaribonucleotide. W. Nagata presents the work that led to the first industrially feasible synthesis of a 1-oxacephem, illustrating the multiplicity of routes attempted and new methodology that had to be developed along

markable changes that have taken place in understanding chemical substances that are important in the central nervous system over the past ten years. Cannon's review on "Structure–Activity Relationships of Dopamine Agonists" is well illustrated with chemical formulas, which is an important aid in following the discussion. The chapter on "Recent Developments in Mass Spectrometry for the Analysis of Complex Mixtures" provides some very basic and informative material on how the new techniques in this area are being used. The volume provides a number of other very timely reviews; they seem to be well written and could provide the reader with some initial leads to more in-depth studies that have been carried out.

The indexing for the volume is very complete, both by author and subject, for rapid access to the desired material. Each of the reviews ends with a Conclusion or Summary section which distills each review to some very basic points and areas of interest for the future.

Because of the nature of the series, this would be a good volume to have present in the library so that individuals could easily read a review in one of the areas covered. I would recommend that the volume be acquired for a School of Pharmacy library or Health Science library or in a general reading room facility for faculty and graduate students. The volume provides a valuable resource for a reasonable cost, in that the authors of the various sections have provided good coverage of findings that have taken place in recent years in pharmacology and toxicology.

Reviewed by Duane D. Miller
College of Pharmacy
Division of Medicinal Chemistry and Pharmacognosy
The Ohio State University
Columbus, OH 43210

FREE RADICALS AND CANCER. Edited by ROBERT A. FLOYD. Marcel Dekker, Inc., 270 Madison Avenue, New York, NY 10016. 1982. 541 pp. 16 × 23.5 mm. Price $69.75 (20% higher outside the U.S. and Canada).

The role of free radicals in cancer development has been of concern to, and studied by, many investigators in the past three decades. Up to the present, however, there is as yet no clear-cut settlement of this seemingly simple but actually complicated problem and probably there never will be. This is perhaps one of the main reasons that the editor is compiling the thoughts of many investigators from all over the world into one volume.

Thirteen groups of researchers contributed their findings and interpretations. These include (titles abbreviated): C. Nagata *et al.* (Free Radicals from Chemical Carcinogens and Significance in Carcinogenesis) from Japan; [illegible] *et al.* (Nitroxide Metabolism in Liver Microsomes) from the Federal Republic of Germany; H. M. Swartz (ESR Studies of Cancer) of Illinois; E. Cavalieri *et al.* (Multiple Activation Mechanisms in Aromatic Hydrocarbon Carcinogenesis) of Nebraska; A. M. Bobst (Spin Bioassays with Nucleic Acids) of Ohio; J. Cadet and R. Téoule (Binding of Radiosensitizing Drugs to DNA) from France; F. R. DeRubertis and P. A. Craven (Activation of Guanylate Cyclase and Evidence for a Free Radical Mechanism) of Pennsylvania; N. M. Emanuel (Free Radicals and Growth of Tumors) from the U.S.S.R.; R. Sridhar (Radiation Sensitizers in Therapy) of Oklahoma; R. A. Floyd (Free Radicals and Arylamine Carcinogenesis) of Oklahoma; E. G. Janzen and E. R. Davis (Detection of Free Radicals by Spin-Trapping) from Canada; J. A. Hinson *et al.* (Role of Free Radicals in the Mutagenicity of *N*-Hydroxy-2-acetylaminofluorene) of Maryland; and J. E. Biaglow *et al.* (Metabolic Activation of Carcinogenic Nitro Compounds to Oxygen-Reactive Intermediates) from the U.S. and Canada. It is probably unavoidable that writings which came from such a variety of sources would contain material with duplicate or even contradictory information. Actually this is perhaps a clever way to inform the readers of the vastness and the uncertainties of this field of study.

Aside from the key question raised at the beginning of this review, there are other points that deserve to be mentioned. Although free radicals have been detected in many carcinogens with or without enzymatic action, they have also been detected in normal and pathological tissues. Throughout this book it is reported that even some compounds possessing recognized antineoplastic action, such as doxorubicin hydrochloride (Adriamycin), or prophylactic property against cancer information, such as ascorbic acid, produce free radicals in ESR measurements. To make the situation even more complicated, some carcinogens do not produce free radicals. Free radicals generally are defined as species having ESR signals in the g = 2.00 region with line shapes and power-saturation characteristics typical of organic free radicals (the latter exclude paramagnetic metals). However, measurement of free radicals depends on a number of variable experimental conditions, including the preparation of samples, the temperature during measurement, the solvent used, the type of tissue examined, and animal species differences. Therefore, one should be extremely careful and cautious in making empirical and qualitative correlations and straightforward interpretations.

The relationship of free radicals to cancer can perhaps be approached in another aspect. That is, to study the quantitative rather than the qualitative characteristics of free radicals in certain types of cancer detection, diagnosis, and response to treatment. There are already indications in this book that an in-depth study of ESR signals may reveal characteristic information in the development and progression of certain types of tumors and tumor response to therapeutic treatment. Studies along this line should be extremely useful in cancer research.

After reading all of the material presented in this book, one may assume that free radical formation may well be just a phenomenon observed during the cellular proliferation (rather than limited to only during the cancer growth) or a phenomenon observed as formation of intermediates during metabolic activation of many chemical compounds (not necessarily limited to mutagens, carcinogens, or antineoplastic agents). The situation is analogous to that of the numerous studies on drug–DNA intercalation: that the observed phenomenon may not be the real, or the major, or even the minor, mode of biological action.

This book is recommended to those scientists who are interested in these aspects of biology and medicine, as well as to oncologists and physicians who are forever searching for the fundamental knowledge of the secret of life.

Reviewed by C. C. Cheng
Department of Pharmacology, Toxicology, and Therapeutics
University of Kansas Medical Center
Kansas City, KS 66103

Current Trends in Organic Synthesis. Proceedings of the Fourth International Conference on Organic Synthesis. Edited by HITOSI NOZAKI. Pergamon Press, Maxwell House, Fairview Park, Elmsford, NY 10523. 1983. 429 pp. 18.5 × 27.5 cm. Price $90.00 (£45.00).

The 30 lectures compiled from the talks presented at the 1982 IUPAC meeting in Tokyo (August 1982) constitute an impressive review of the current state of the art in the field of organic synthesis. Because the book is a reproduction of the authors' manuscripts, there are a few typographical errors and unclear figures, but these minor shortcomings in no way detract from the overall appeal of this volume. As outlined in the Preface, the book is divided into four areas: synthesis of natural products, methods for achieving stereoselectivity, new synthetic methodology, and new reactions.

The group of lectures on natural product synthesis begins with a presentation by E. J. Corey on his work in the leukotriene field, which includes synthetic methodology developed for use in this area, but with applications throughout organic synthesis, as well as total syntheses of LTB and several rationally designed inhibitors of lipoxygenase enzymes. The next lecture, by W. Bartmann, discusses the synthesis of stable analogues of PGI2, illustrating the intimate connection between chemical synthesis, biological testing, and development of commercially feasible syntheses characteristic of industry. C. Heathcock then describes the efforts of his group in the area of stereoselective aldol condensation reactions and their application to his ongoing total synthesis of erythromycin. B. M. Trost outlines the observations that lead to the development of the total synthesis of verrucarol as well as continuing work on its elaboration to verrucarin A. A review of the numerous examples of the Diels–Alder reaction developed by the group of M. E. Jung and their application to steroid and anthracycline natural products is offered next. Highly selective protecting group chemistry is the focus of a lecture by C. B. Reese on the total synthesis of yeast alanine tRNA, a nonadecaribonucleotide. W. Nagata presents the work that led to the first industrially feasible synthesis of a 1-oxacephem, illustrating the multiplicity of routes attempted and new methodology that had to be developed along

markable changes that have taken place in understanding chemical substances that are important in the central nervous system over the past ten years. Cannon's review on "Structure–Activity Relationships of Dopamine Agonists" is well illustrated with chemical formulas, which is an important aid in following the discussion. The chapter on "Recent Developments in Mass Spectrometry for the Analysis of Complex Mixtures" provides some very basic and informative material on how the new techniques in this area are being used. The volume provides a number of other very timely reviews; they seem to be well written and could provide the reader with some initial leads to more in-depth studies that have been carried out.

The indexing for the volume is very complete, both by author and subject, for rapid access to the desired material. Each of the reviews ends with a Conclusion or Summary section which distills each review to some very basic points and areas of interest for the future.

Because of the nature of the series, this would be a good volume to have present in the library so that individuals could easily read a review in one of the areas covered. I would recommend that the volume be acquired for a School of Pharmacy library or Health Science library or in a general reading room facility for faculty and graduate students. The volume provides a valuable resource for a reasonable cost, in that the authors of the various sections have provided good coverage of findings that have taken place in recent years in pharmacology and toxicology.

Reviewed by Duane D. Miller
College of Pharmacy
Division of Medicinal Chemistry and Pharmacognosy
The Ohio State University
Columbus, OH 43210

FREE RADICALS AND CANCER. Edited by ROBERT A. FLOYD. Marcel Dekker, Inc., 270 Madison Avenue, New York, NY 10016. 1982. 541 pp. 16 × 23.5 mm. Price $69.75 (20% higher outside the U.S. and Canada).

The role of free radicals in cancer development has been of concern to, and studied by, many investigators in the past three decades. Up to the present, however, there is as yet no clear-cut settlement of this seemingly simple but actually complicated problem and probably there never will be. This is perhaps one of the main reasons that the editor is compiling the thoughts of many investigators from all over the world into one volume.

Thirteen groups of researchers contributed their findings and interpretations. These include (titles abbreviated): C. Nagata *et al.* (Free Radicals from Chemical Carcinogens and Significance in Carcinogenesis) from Japan; [illegible] *et al.* (Nitroxide Metabolism in Liver Microsomes) from the Federal Republic of Germany; H. M. Swartz (ESR Studies of Cancer) of Illinois; E. Cavalieri *et al.* (Multiple Activation Mechanisms in Aromatic Hydrocarbon Carcinogenesis) of Nebraska; A. M. Bobst (Spin Bioassays with Nucleic Acids) of Ohio; J. Cadet and R. Téoule (Binding of Radiosensitizing Drugs to DNA) from France; F. R. DeRubertis and P. A. Craven (Activation of Guanylate Cyclase and Evidence for a Free Radical Mechanism) of Pennsylvania; N. M. Emanuel (Free Radicals and Growth of Tumors) from the U.S.S.R.; R. Sridhar (Radiation Sensitizers in Therapy) of Oklahoma; R. A. Floyd (Free Radicals and Arylamine Carcinogenesis) of Oklahoma; E. G. Janzen and E. R. Davis (Detection of Free Radicals by Spin-Trapping) from Canada; J. A. Hinson *et al.* (Role of Free Radicals in the Mutagenicity of *N*-Hydroxy-2-acetylaminofluorene) of Maryland; and J. E. Biaglow *et al.* (Metabolic Activation of Carcinogenic Nitro Compounds to Oxygen-Reactive Intermediates) from the U.S. and Canada. It is probably unavoidable that writings which came from such a variety of sources would contain material with duplicate or even contradictory information. Actually this is perhaps a clever way to inform the readers of the vastness and the uncertainties of this field of study.

Aside from the key question raised at the beginning of this review, there are other points that deserve to be mentioned. Although free radicals have been detected in many carcinogens with or without enzymatic action, they have also been detected in normal and pathological tissues. Throughout this book it is reported that even some compounds possessing recognized antineoplastic action, such as doxorubicin hydrochloride (Adriamycin), or prophylactic property against cancer information, such as ascorbic acid, produce free radicals in ESR measurements. To make the situation even more complicated, some carcinogens do not produce free radicals. Free radicals generally are defined as species having ESR signals in the g = 2.00 region with line shapes and power-saturation characteristics typical of organic free radicals (the latter exclude paramagnetic metals). However, measurement of free radicals depends on a number of variable experimental conditions, including the preparation of samples, the temperature during measurement, the solvent used, the type of tissue examined, and animal species differences. Therefore, one should be extremely careful and cautious in making empirical and qualitative correlations and straightforward interpretations.

The relationship of free radicals to cancer can perhaps be approached in another aspect. That is, to study the quantitative rather than the qualitative characteristics of free radicals in certain types of cancer detection, diagnosis, and response to treatment. There are already indications in this book that an in-depth study of ESR signals may reveal characteristic information in the development and progression of certain types of tumors and tumor response to therapeutic treatment. Studies along this line should be extremely useful in cancer research.

After reading all of the material presented in this book, one may assume that free radical formation may well be just a phenomenon observed during the cellular proliferation (rather than limited to only during the cancer growth) or a phenomenon observed as formation of intermediates during metabolic activation of many chemical compounds (not necessarily limited to mutagens, carcinogens, or antineoplastic agents). The situation is analogous to that of the numerous studies on drug–DNA intercalation: that the observed phenomenon may not be the real, or the major, or even the minor, mode of biological action.

This book is recommended to those scientists who are interested in these aspects of biology and medicine, as well as to oncologists and physicians who are forever searching for the fundamental knowledge of the secret of life.

Reviewed by C. C. Cheng
Department of Pharmacology, Toxicology, and Therapeutics
University of Kansas Medical Center
Kansas City, KS 66103

Current Trends in Organic Synthesis. Proceedings of the Fourth International Conference on Organic Synthesis. Edited by HITOSI NOZAKI. Pergamon Press, Maxwell House, Fairview Park, Elmsford, NY 10523. 1983. 429 pp. 18.5 × 27.5 cm. Price $90.00 (£45.00).

The 30 lectures compiled from the talks presented at the 1982 IUPAC meeting in Tokyo (August 1982) constitute an impressive review of the current state of the art in the field of organic synthesis. Because the book is a reproduction of the authors' manuscripts, there are a few typographical errors and unclear figures, but these minor shortcomings in no way detract from the overall appeal of this volume. As outlined in the Preface, the book is divided into four areas: synthesis of natural products, methods for achieving stereoselectivity, new synthetic methodology, and new reactions.

The group of lectures on natural product synthesis begins with a presentation by E. J. Corey on his work in the leukotriene field, which includes synthetic methodology developed for use in this area, but with applications throughout organic synthesis, as well as total syntheses of LTB and several rationally designed inhibitors of lipoxygenase enzymes. The next lecture, by W. Bartmann, discusses the synthesis of stable analogues of PGI2, illustrating the intimate connection between chemical synthesis, biological testing, and development of commercially feasible syntheses characteristic of industry. C. Heathcock then describes the efforts of his group in the area of stereoselective aldol condensation reactions and their application to his ongoing total synthesis of erythromycin. B. M. Trost outlines the observations that lead to the development of the total synthesis of verrucarol as well as continuing work on its elaboration to verrucarin A. A review of the numerous examples of the Diels–Alder reaction developed by the group of M. E. Jung and their application to steroid and anthracycline natural products is offered next. Highly selective protecting group chemistry is the focus of a lecture by C. B. Reese on the total synthesis of yeast alanine tRNA, a nonadecaribonucleotide. W. Nagata presents the work that led to the first industrially feasible synthesis of a 1-oxacephem, illustrating the multiplicity of routes attempted and new methodology that had to be developed along

the way. S. Wolfe's lecture shows how an academic laboratory can branch out into exploration of combining chemical with enzymatic reactions to fashion new and important compounds in the β-lactam field, including the commercial product ceftizoxime. Finally, Y. Kishi discusses his group's efforts toward the determination of the stereochemistry of the *entire palytoxin* molecule, mentioning numerous synthetic methods developed in the pursuit of this gargantuan task.

The next group of lectures discusses the development of methodology for achieving stereoselectivity in synthetic reactions. W. Oppolzer begins by describing his work using chiral precursors to direct carbon–carbon bond-forming reactions and his exploitation of the metallo-ene reaction to construct complex carbon skeletons. D. Enders continues with a discussion of his work on the use of metallated chiral hydrazones to form carbon–carbon bonds with high stereoselectivity. Y. Ito next illustrates applications of the intramolecular Diels–Alder reaction of *o*-quinodimethanes to the construction of steroidal and alkaloidal skeletons. G. Posner discusses his results in stereoselective carbon–carbon bond formation *via* conjugate addition of Grignard reagents to chiral 2-sulfinylcycloalkenones. P. Bartlett shows the potential of his iodolactonization chemistry for controlling the stereochemistry along a carbon chain. An elegant stereocontrolled synthesis of the side chains of two vitamin D3 metabolites *via* remote asymmetric induction during a nitrone cycloaddition reaction is presented next by M. Uskokovic. B. Fraser-Reid then discusses his progress toward the ansa chain of rifamycin starting from readily available chiral precursors. S. Hanessian continues this theme of chiral templates with an in-depth look at the strategy and chemistry he is employing in an assault on boromycin. E. Vedejs next discusses the importance of local conformational effects which he has used in conjunction with his sulfur-mediated ring expansion strategy to approach erythronolide. Finally, W. C. Still illustrates his application of molecular mechanics calculations to the determination of macrocycle conformations with the syntheses of eucannibinolide and rosaramicin.

Nine lectures demonstrate the role of organometallic reagents in the development of new synthetic methodology. H. C. Brown provides a thorough review and update on hydroborating reagents which can achieve remarkable chemical selectivity. E. Negishi next discusses the allylation and vinylation of organometallics, especially metal enolates, *via* nickel and palladium catalysis. H. Yamamoto shows how oxime sulfonates can be used with organoaluminum reagents to provide α-alkylated amines or as precursors for intramolecular cyclization to interesting heterocycles. Additions of organometallic reagents to acetylenes and vinyl halides for the preparation of conjugated dienes is the theme of a lecture by J. Normant. M. Semmelhack next illustrates some interesting applications of nickel and chromium chemistry to the synthesis of quinone natural products. I. Kuwajima discusses several features of his trimethylsilyl enol ether chemistry culminating in a synthesis of showdomycin. The preparation and functionalization of various heterocyclic systems by using the trimethylsilyl group for activation is presented by H. Vorbruggen. The array of functionality available from the ring-opening reactions of cyclopropanes generated by the addition of carbenes to silyl enol ethers is outlined by J. Conia. Finally, M. Mikolajczyk demonstrates the utility of sulfur-substituted Wittig reagents for the formation of five-membered ring systems.

The last group of lectures describes much new chemistry which should see widespread application in future synthetic work. G. Stork begins by presenting his recent work on radical cyclization reactions, stressing the power of his methodology for generating pentacyclic systems. H. Musso next discusses rules governing the direction of hydrogenolytic cleavage of cyclopropane bonds. E. Vogel reviews the chemistry developed in the pursuit of various novel annulene structures. M. Makosza demonstrates the versatility of nitroarene substitution reactions by carbanions containing a leaving group at the carbanionic site for the construction of various aromatic and heteroaromatic systems. Finally, D. J. Sam concludes by outlining the potential of dichlorine monoxide as a powerful yet selective chlorinating reagent.

While much of the above material has appeared in print since this meeting was held, readers will still find this book a useful compendium of the work currently being pursued at the frontiers of organic synthesis. It may thus be useful to students as an introduction and overview of the field and to long-time practitioners of the art of synthesis as a review and indication of trends for the future. It is a worthwhile investment for both academic and industrial chemistry libraries.

Reviewed by John A. Lowe III
Central Research Division
Pfizer, Inc.
Groton, CT 06340

NOTICES

Apartheid and Health. World Health Organization, 1121 Geneva 27, Switzerland, 1983. 258 pp. 16 × 24 cm. Price Sw. Fr. 29.

Approved Prescription Drug Products, with Therapeutic Equivalence Evaluations, 4th Ed. U.S. Dept. of Health and Human Services, Public Health Service, Food and Drug Administration, Rockville, MD 20857. 1983. 190 pp. 22 × 28 cm. Price $67.00 ($83.75 outside the U.S.).

Arzneiformenlehre: Ein Lehrbuch für Pharmazeuten. By PAUL HEINZ LIST. Wissenschaftliche Verlagsgesellschaft mbH Stuttgart, Birkenwaldstrasse 44, 7000 Stuttgart 1, West Germany. 1982. 605 pp. 17 × 24.5 cm. Price DM 68.

Biochemistry: A Functional Approach. By ROBERT W. McGILVERY. Saunders, West Washington Square, Philadelphia, PA 19105. 1983. 909 pp. 19 × 27 cm. Price $39.95.

Cancer Statistics. By RICHARD F. MOULD. Heyden & Son, 247 South 41st Street, Philadelphia, PA 19104. 1983. 230 pp. 16 × 24 cm. Price $29.00.

Chromatographic Analysis of the Environment, 2nd Ed. Edited by ROBERT L. GROB. Dekker, 270 Madison Avenue, New York, NY 10016. 1983. 724 pp. 15.5 × 23.5 cm. Price $95.00.

Clinical Toxicology of Drugs: Principles and Practice. By VASILIOS A. SKOUTAKIS. Lea and Febriger, 600 Washington Square, Philadelphia, PA 19106. 1982. 293 pp. 13 × 25 cm. Price $25.50 ($30.50 in Canada).

Controlling Medicaid Costs: Federalism, Competition, and Choice. By THOMAS W. GRANNEMANN and MARK V. PAULY. American Enterprise Institute for Public Policy Research, 1150 17th Street N.W., Washington, DC 20036. 1983. 112 pp. 15 × 23 cm. Price $4.95 (paperback), $13.95 (cloth).

An Eight Peak Index of Mass Spectra of Compounds of Forensic Interest. Edited by R. E. ARDREY, C. BROWN, A. R. ALLAN, T. S. BAL, and A. C. MOFFAT. Scottish Academic Press, 33 Montgomery Street, Edinburgh EH7 5JX, U.K. 1983. 281 pp. 21 × 30.5 cm. Price $50.00.

Enzyme Technology: Preparation, Purification, Stabilization, Immobilization. Recent Advances. (Biotechnology Review No. 2, Chemical Technology Review No. 222). Edited by S. TORREY. Noyes, Mill Road at Grand Avenue, Park Ridge, NJ 07656. 1983. 308 pp. 26 × 24 cm. Price $42.00.

Ethics and Animals. Edited by HARLAN B. MILLER and WILLIAM H. WILLIAMS. The Humana Press, P.O. Box 2148, Clifton, NJ 07015. 1983. 400 pp. 15.5 × 23.5 cm. Price $39.50 ($49.50 outside the U.S.).

The GABA Receptors. Edited by S. J. ENNA. The Humana Press, P.O. Box 2148, Clifton, NJ 07015. 1983. 341 pp. 15.5 × 23.5 cm. Price $49.50 ($59.50 outside the U.S.).

Gaussian Basis Sets for Molecular Calculations. (Physical Sciences Data 16). Edited by S. HUZINAGA, J. ANDZELM, M. KLOBUKOWSKI, E. RADZIO-ANDZELM, Y. SAKAI, and H. TATEWAKI. Elsevier, P.O. Box 300, 1000 AH Amsterdam, The Netherlands. 1984. 426 pp. Price $102.00 (Dfl. 265.00).

Handbook of Tropical Foods. (Food Science Series, Vol. 9). Edited by HARVEY T. CHAN, JR. Dekker, 270 Madison Avenue, New York, NY 10016. 1983. 639 pp. 15.5 × 23.5 cm. Price $75.00 (20% higher outside the U.S. and Canada).

High-Performance Liquid Chromatography in Forensic Chemistry. (Chromatographic Sciences Series Vol. 24). Edited by IRA S. LURIE and JOHN D. WITTWER, JR. Dekker, 270 Madison Ave., New York, NY 10016. 1983. 439 pp. 16 × 23.5 cm. Price $65.00 (20% higher outside the U.S. and Canada).

Hyperbilirubinemia in the Newborn. (Report on the 85th Ross Conference on Pediatric Research). Edited by RODNEY L. LEVINE and M. JEFFREY MAISELS. Ross Laboratories, Columbus, OH 42316. 1983. 138 pp. 14 × 22 cm.

Information Resources Guide to Words and Phrases Used in the Pharmaceutical Industry. Edited by PETER HAMILTON. Gothard House, Henley-on-Thames, Oxon, RG9 1AJ, U.K. 1983. 43 pp. 9.5 × 21 cm. Price £6.70.

Laboratory Biosafety Manual. Health and Biomedical Information Programme, World Health Organization, 1211 Geneva 27, Switzerland. 1983. 123 pp. 16 × 24 cm. Price Sw. Fr. 14.

Laboratory Manual for Medical Microbiology. (Microbiology Series, Vol. 11). Edited by the Faculty of the Department of Microbiology, Schools

of Medicine and Dentistry, State University of New York at Buffalo. Dekker, 270 Madison Avenue, New York, NY 10016. 1983. 177 pp. 18 × 25 cm. Price $16.75 (20% higher outside the U.S. and Canada).

Learning to Live with Osteoarthritis. By SARAH JEFFRIES and CYNTHIA B. WONG. Pfizer Pharmaceuticals, 235 East 42nd Street, New York, NY 10017. 1983. 62 pp. 15 × 23 cm. Free.

Leukotrienes and Other Lipoxygenase Products. Edited by PRISCILLA J. PIPER. Research Studies Press, div. Wiley, One Wiley Drive, Somerset, NJ 08873. 1983. 353 pp. 15.5 × 23.5 cm. Price $61.95.

Liquid Chromatography Detectors. (Chromatographic Science Series Vol. 23). Edited by THOMAS M. VICKERY. Dekker, 270 Madison Avenue, New York, NY 10016. 1983. 434 pp. 16 × 23 cm. Price $57.50 (20% higher outside the U.S. and Canada).

Management of Hazardous Waste. Policy Guidelines and Code of Practice. (WHO Regional Publications, European Series No. 14). Edited by M. J. SUESS and J. W. HUISMANS. Health and Biomedical Information Programme, World Health Organization, 1211 Geneva 27, Switzerland. 1983. 100 pp. 16 × 24 cm. Price Sw. Fr. 10.

Mass Catering. (WHO Regional Publications, European Series No. 15.) Edited by R. H. G. CHARLES. Health and Biomedical Information Programme, World Health Organization, 1211 Geneva 27, Switzerland. 1983. 70 pp. 16 × 24 cm. Price Sw. Fr. 13.

Methods for Cohort Studies of Chronic Airflow Limitation. (WHO Regional Publications, European Series No. 12.). By C. DU V. FLOREY and S. R. LEEDER. World Health Organization, Copenhagen, Denmark. 1982. 134 pp. 16 × 24 cm. Price Sw. Fr. 19.

Neurobiology of the Trace Elements, Vol. 1: Trace Element Neurobiology and Deficiencies. Edited by IVOR E. DREOSTI and RICHARD M. SMITH. The Humana Press, P.O. Box 2148, Clifton, NJ 07015. 1983. 16 × 23.5 cm. Price $49.50 ($59.50 outside the U.S.).

Neurobiology of the Trace Elements, Vol. 2: Neurotoxicology and Neuropharmacology. Edited by IVOR E. DREOSTI and RICHARD M. SMITH. The Humana Press, P.O. Box 2148, Clifton, NJ 07015. 1983. 320 pp. 16 × 23.5 cm. Price $49.50 ($59.50 outside the U.S.).

Organic Electrochemistry: An Introduction and a Guide. Edited by MANUEL M. BAIZER and HENNING LUND. Dekker, 270 Madison Avenue, New York, NY 10016. 1983. 1166 pp. 18.5 × 26 cm. Price $155.00 (20% higher outside the U.S. and Canada).

Peptide and Protein Reviews, Vol. 1. Edited by MILTON T. W. HEARN. Dekker, 270 Madison Avenue, New York, NY 10016. 1983. 244 pp. 15.5 × 23.5 cm. Price $35.00 (20% higher outside the U.S. and Canada).

Planning the Finances of the Health Sector. A Manual for Developing Countries. By E. P. MACH and B. ABEL-SMITH. Health and Biomedical Information Programme, World Health Organization, 1211 Geneva 27, Switzerland. 1983. 124 pp. 16 × 24 cm. Price Sw. Fr. 14.

Preventing Adolescent Drug Abuse: Intervention Strategies (NIDA Research Monograph Series 47). Edited by THOMAS J. GLYNN, CARL G. LEUKEFELD, and JACQUELINE P. LUDFORD. U.S. Dept. of Health and Human Services, Public Health Service, Alcohol, Drug Abuse, and Mental Health Administration, Rockville, MD 20857. 1983. 261 pp. 14.5 × 23 cm.

Primary Health Care: The Chinese Experience. World Health Organization, 1121 Geneva 27, Switzerland. 1983. 105 pp. 16 × 24 cm. Price Sw. Fr. 14.

Progestogens in Therapy. (Serono Symposia Publications from Raven Press, Vol. 3). Edited by GIUSEPPE BENAGIANO. PIETRO ZULLI, and EGON DICZFALUSY. Raven, 1140 Avenue of the Americas, New York, NY 10036. 1983. 270 pp. 16 × 24 cm. Price $55.00.

Psychosocial Constructs of Alcoholism and Substance Abuse. Edited by BARRY STIMMEL. Haworth, 28 East 22 Street, New York, NY 10010. 1983. 110 pp. 14.5 × 22.5 cm. Price $14.95.

Public Health Reports. (Promoting Health/Preventing Disease, Public Health Service Implementation Plans for Attaining the Objectives for the Nation). U.S. Department of Health and Human Services. Superintendent of Documents, U.S. Goverment Printing Office, Washington DC 20402. 1983. 178 pp. 20 × 26 cm. Price $5.50 ($6.50 outside the U.S.).

Secondary Metabolism and Differentiation in Fungi. (Mycology Series Vol. 5). Edited by J. W. BENNETT and ALEX CIEGLER. Dekker, 270 Madison Avenue, New York, NY 10016. 1983. 478 pp. 16 × 23.5 cm. Price $69.75 (20% higher outside U.S. and Canada).

Stimulants: Neurochemical, Behavioral, and Clinical Perspectives. Edited by IAN CREESE. Raven, 1140 Avenue of the Americas, New York, NY 10036. 1983. 350 pp. 16 × 24 cm. Price $45.00.

Treatise on Analytical Chemistry, 2nd Ed. Edited by I. M. KOLTHOFF and PHILIP J. ELVING. Wiley, One Wiley Drive, Somerset, NJ 08873. 1983. 592 pp. 17 × 24 cm. Price $70.00.

Understanding Anorexia Nervosa and Bulimia (Report of the Fourth Ross Conference on Medical Research). Ross Laboratories, Columbus, OH 43216. 1983. 84 pp. 17.5 × 23 cm.

NEW JOURNALS

Lens Research, (Vol. 1: 1983). Editor-in-Chief: SIDNEY LERMAN. Dekker, 270 Madison Ave., New York, NY 10016. 220 pp. 18 × 25.5 cm. Price $125.00 (institutional), $62.50 (individual). Add postage ($16.10, surface; $28.42, airmail Europe; $35.42, airmail Asia) outside the U.S.

A publication of the
American Pharmaceutical Association—
the National Professional Society
of Pharmacists

JOURNAL OF PHARMACEUTICAL SCIENCES

Volume 73, 1984

JPMSAE 73(1-12) 1-1910 (1984)
ISSN 0022-3549

Sharon G. Boots
Editor

Sue A. Kruger
Production Editor

Margaret M. Madeleine
Assistant Production Editor

Karen A. Blakney
Copy Editor

Edward G. Feldmann
Contributing Editor

Samuel W. Goldstein
Contributing Editor

Patricia A. Evich
Editorial Secretary

Editorial Advisory Board

Jordan L. Cohen
Kenneth A. Connors
Louis Diamond
Ho-Leung Fung
Milo Gibaldi
Everett N. Hiestand
W. Homer Lawrence
Ian W. Mathison
Carl M. Metzler
Robert E. Notari
Paul L. Schiff, Jr.
Jane E. Shaw

Published monthly under the supervision of the Board of Trustees

Putting an End to Secret Formulations

"Secret nostrums" were a scourge of the past that pharmacy, medicine, and the general public had to deal with in their collective efforts to advance rational therapy. From the medical scientist's viewpoint, it is basic, elementary, and essential that, if at all possible, one knows exactly what it is that is being used as an agent of treatment. Without complete composition information, how else is it possible to practice either good medicine or good pharmacy?

We recently attended a scientific conference at which University of California Pharmacy School Dean—and former Food and Drug Commissioner—Jere E. Goyan was a featured speaker. During his presentation, he observed that in the former dark days of science, "magic was medicine"; but in the present, enlightened period of science, "medicine is magic."

It is wonderful if medicine is able to produce results that can be described as "magical." However, it is in no one's best interest—and certainly not in the patient's nor in the practitioners' who are treating that patient—for the product used in treatment to be a secret formula: a sort of "magic potion," if you will.

But yet, that is still what prevails to a large degree even today.

Granted, drug manufacturers are required by law and regulation to make known the identity and quantity of the medicinally active ingredients in their products. However, they are not required to do so with respect to the so-called "inactive" ingredients. This despite the fact that these "inactive" ingredients may pose a serious health hazard to many patients. For reasons of safety, patients either may need to avoid, or may wish to avoid, such ingredients as lactose, tartrazine, cyclamates, saccharin, monosodium glutamate, sulfites, nitrites, as well as miscellaneous other preservatives, colors, or flavoring agents.

Yet, most drug manufacturers not only are unwilling to list such inactive ingredients in the labeling or advertising of their products, but adamantly refuse to divulge the information in response to specific requests.

When queried as to the basis for this policy, the usual response is "trade secrets." To which we can only retort: "Baloney!"

Every manufacturer must surely realize that the sophistication of trained laboratory personnel and the instruments and advanced equipment available today would enable any competition to "crack" a product's formula, both qualitatively and quantitatively with relative ease and speed. Competent pharmaceutical analysts would find such a task to be only a moderate challenge at most. And when we have stated this view to our industrial scientist colleagues, they have generally admitted—although usually "off the record"—that such is indeed the case.

So what is the real reason for this carefully maintained cloak of secrecy?

In our opinion, it has virtually nothing to do directly with competitors—any real trade secrets are much more likely to be involved in how the product is put together, than what is in it. No, we believe that the underlying reason for this policy on the part of so many drug firms is simply due to their desire to maintain an aura of the unknown, of magic, and of mystique surrounding their products. And this is not done out of concern about competing firms, but rather for the effect they believe it has on physicians, pharmacists, and patients.

As early as 1970, the American Pharmaceutical Association, by formal action of its House of Delegates, adopted a policy statement that "the Association seek legislation or regulations to require a full disclosure of therapeutically inactive as well as active ingredients of all drug products."

Subsequently, this official APhA policy position was broadened and strengthened on several occasions: most notably in 1980, when it was explicitly clarified that the policy was intended to cover both prescription and nonprescription drugs, and that disclosure included not only a passive willingness to reveal the information, but also an active listing of the information in product labeling and advertising.

Regrettably, however, the "proponents of magic" prevailed in the policy-making offices of corporate drugdom, and few companies have been willing to break with the operating policy of composition secrecy.

In recent months, however, the issue has heated up considerably. *First*, Ralph Nader's Health Research Group filed a "citizens' petition" with the Food and Drug Administration seeking new regulations to require that inactive ingredient information be listed on labels, in package inserts, and in the *Physician's Desk Reference*. *Second*, Jeffrey L. Brown, chairman of pediatrics at United Hospital in New York, filed suit in Washington, DC, federal court to force FDA to divulge the names of all approved drug products containing lactose as an ingredient. *Third*, Congressman Richard L. Ottinger (D.-NY) introduced legislation (H.R. 4126) to require disclosure of both active and inactive drug ingredients.

FDA initially refused freedom-of-information and similar efforts to get it to reveal the requested composition information. But then the agency notified the industry that, in effect, it would no longer serve as the industry's guardian angel; it would not defend against trade secret lawsuits unless the companies themselves defended against those suits.

How each individual drug company decides to act remains to be seen. But for the prescription drug industry's major trade group, the Pharmaceutical Manufacturers Association, this clearly presented a serious dilemma: is their primary concern to protect patients' lives or company dollars?

In rapid succession, the PMA first jumped in, and then scrambled out. Indeed, PMA's retreat was so hasty that the trade press was still carrying reports about PMA's February 27 decision to intervene in the case even after PMA actually withdrew from the lawsuit on March 14.

But, embodied in PMA's announcement to the press that it decided to withdraw from the case was an explanatory statement that, in our view, was most gratifying: "PMA withdrew . . . because it concluded that, while the identity of inactive ingredients is legally a trade secret, the medical justification for disclosure of the presence of lactose nevertheless warrants release of that information . . . . PMA recognizes the concerns of those who favor disclosure of inactive ingredients generally and intends to work with all interested parties toward a fair and equitable solution to the overall problem."

It appears that a new day has dawned, and that human lives rather than dollars may yet prevail as the subject of principal industry concern. Welcome aboard, PMA!

—EDWARD G. FELDMANN
American Pharmaceutical Association
Washington, DC 20037

0022-3549/84/0500-0577$01.00/0
© 1984, American Pharmaceutical Association

JOURNAL OF PHARMACEUTICAL SCIENCES

MAY 1984
VOLUME 73 NUMBER 5

LITERATURE SURVEY

Novel Anti-Inflammatory Agents

ERNEST CULLEN

Received October 12, 1982 from *Boehringer Ingelheim Ltd., Ridgefield, CT 06877.*

Keyphrases □ Literature survey—anti-inflammatory agents □ Anti-inflammatory agents—literature survey

The nonsteroidal anti-inflammatory (NSAI) drugs currently in use are characterized by their ability to relieve the pain, fever, and inflammation associated with inflammatory disorders; to inhibit the synthesis of endogenous prostaglandins (PG's) by blocking the action of the cyclooxygenase (CO) enzyme; and, in relation with this inhibition, to cause GI irritation. As useful as they are, they do not interfere fundamentally with the progression of the disease. The question of the relevance of PG's on the course and/or the regulation of the disease has not been settled [for review see (1, 2)].

In the past few years, anti-inflammatory (AI) compounds having a profile of action on the arachidonic acid cascade metabolism distinct from that of the classical NSAI drugs have been reported. Some affect both pathways of arachidonic acid metabolism, while others have no effect on these endogenous mediators.

A nonexhaustive survey of these nonclassical NSAI agents along with the recently disclosed AI immunomodulators and of the classical agents currently in clinical trial is presented. Excluded are the steroids, the disease-modifying antirheumatic drugs (DMARD) such as penicillamine and gold salts, and the cytotoxic agents such as cyclophosphamide.

NONCLASSICAL, NONSTEROIDAL ANTI-INFLAMMATORY AGENTS

Inhibitors of Both Pathways of Arachidonic Acid Metabolism—3-Amino-1-[(*m*-trifluoromethyl)phenyl]-2-pyrazoline (I)[1] (3, 4), timegadine (5), and benoxaprofen (6) (Fig. 1) have in common AI activity and the capacity to inhibit both the cyclooxygenase (CO) pathway leading to the PG's and the lipoxygenase (LO) pathway leading *inter alia* to 5,12-dihydroxy-eicosatetraenoic acid (5,12-HETE), a potent chemotactic agent for polymorphonuclear leukocytes (7). The dual inhibition property of compound I, is reported to be of the same order both for CO and LO, while timegadine shows superior inhibitory activity for the CO system (5, 8). In the case of benoxaprofen, published data indicate a lower inhibition for CO and actually the low ulcerogenic activity of this product was related to this finding (9).

The activity profile of substances blocking both pathways of arachidonic acid should in some respects at least parallel that of the steroids. In fact, like dexamethasone, I was found to cause a dose-dependent reduction in leukocyte migration into inflammatory sponge exudate (3, 10). Benoxaprofen also inhibits migration of cells into inflammatory sites (6, 11). Moreover, the latter was found equipotent with hydrocortisone in the granuloma pouch test—in contrast to most NSAI agents (9) which are not active or weakly active in that test.

According to a recent paper (12), the action of I on the CO enzyme is selective: it inhibits PG production in inflammatory exudate but not in the GI tract—thus explaining its nonulcerogenicity as compared with aspirin and indomethacin.

Benoxaprofen, it is claimed, has the convenience of once-a-day dosage. It has been launched in Great Britain, Germany, and France (13), and it was currently being introduced in the United States when it was voluntarily recalled by the manufacturer after reports of deaths associated with the drug (14). The product, it was reported, induced photosensitivity and onycholysis in 10% of the patients (15).

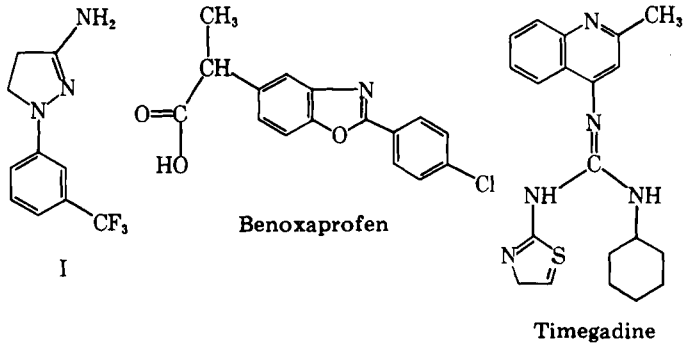

Figure 1.

[1] Code name: BW-755.

0022-3549/84/0500-0579$01.00/0
© 1984, American Pharmaceutical Association

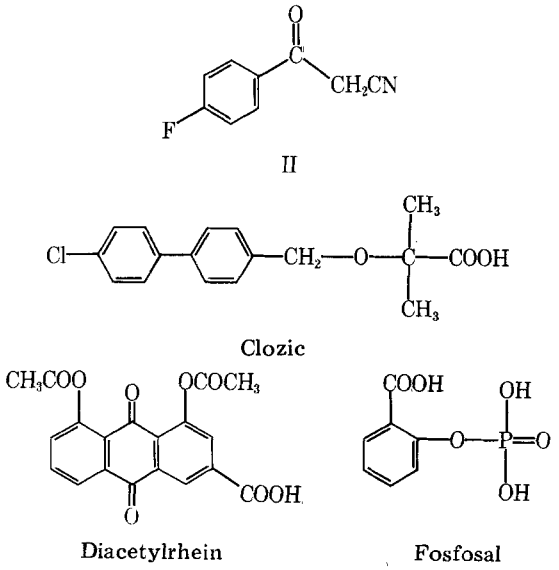

Figure 2.

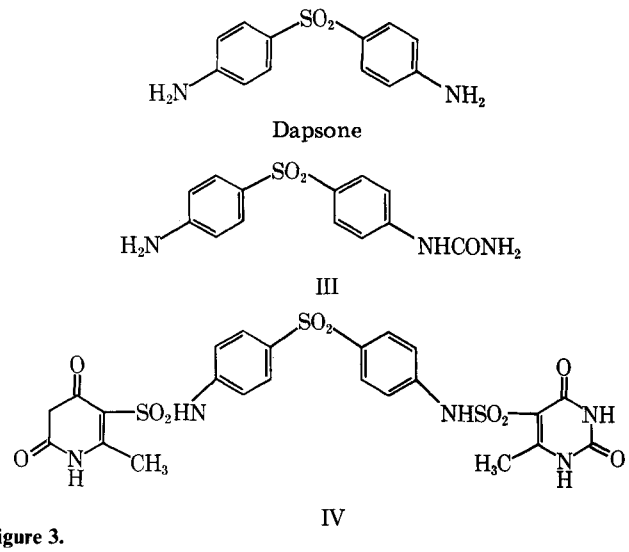

Figure 3.

Timegadine, which had been chosen out of a series of more than 100 guanidine derivatives, has only recently been submitted for clinical evaluation. In animal studies it showed low acute toxicity, low gastroulcerogenic effect, and high AI activity in both acute and chronic assays (16). Noteworthy is the fact that it can suppress the development of secondary lesions in the adjuvant arthritis (AA) screen when given only for a short period after the adjuvant injection (17). The tuberculin hypersensitivity reaction is enhanced by timegadine. Experimental allergic encephalomyelitis (EAE) (a model for cell-mediated immune response) is not inhibited by this product. Because of these results, it was concluded that the effect of timegadine in AA is not due to an immunosuppressive action (17).

Agents Having AI Effects not Mediated through Inhibition of Prostaglandins—*p*-Fluorobenzylacetonitrile (II)[2], (18, 19), clozic (20) and diacetylrhein (21) (Fig. 2) are novel agents which have in common, as opposed to the classical NSAI drugs, a markedly reduced potency in blocking the synthesis of PG's.

The acetonitrile II and clozic possess minimal acute AI or analgesic activity but are reported to be very potent in chronic assays. They produce little or no GI irritation in laboratory animals. For clozic, activity in type II collagen-induced arthritis is also claimed (22).

Clozic has been compared with penicillamine and gold salt clinically in a double-blind study testing 30 and 40 rheumatic patients, respectively, over a 6-month period. Similar activity to gold and penicillamine was found with substantial lowering of the biochemical markers of disease activity and with no serious side effects (23). If this result is confirmed in a long-term, larger clinical trial, then clozic would be the first example of a penicillamine-like drug susceptible to detection by conventional screening in animal models.

Diacetylrhein does not block PG production, on the contrary, it stimulates its synthesis. In *in vivo* experiments with rat inflamed exudate it produced, at 4 mg/kg po, an increase (69%) in total PG-like substances, while indomethacin, at 0.2 mg/kg, under the same conditions, produced a decrease (−72%) of the same substances. A confirmation of this is the ability of diacetylrhein to counteract indomethacin-induced gastric damage in a dose-dependent manner. The product has the same AI potency as aspirin in experimental animal models. In the retinoic acid-induced rabbit ear cartilage degeneration assay, it was shown to have the potency of hydrocortisone (21). In a short-term clinical study it was found to be well tolerated and effective, the therapeutic effect persisting for several weeks after suspension of therapy (24, 25). A controlled double-blind clinical evaluation confirmed the therapeutic value of this drug in the treatment of osteoarthritis of the hip and knee (26). It is assumed that the drug exerts its action through its ability to inhibit the release of proteases (21). It also forms water soluble Cu-complexes, and this may also contribute to its mode of action (25).

Another drug potentially belonging to this group is fosfosal, a compound analogous to aspirin except for the acetyl function, which has been replaced by a phosphono group. This results in substantial modification of the activity profile. Indeed, contrary to aspirin, fosfosal does not inhibit PG synthetase even at very high doses, and probably because of that, produces no significant ulcerogenic effect in rats in spite of its very high acidity. In animal models it was found equipotent to aspirin in analgesic assays and slightly less so in AI tests (27). In a double-blind clinical study with 60 patients, the AI action was confirmed with no sign of serious side effects and good tolerance (28). The compound is reported to produce negligible effect on platelet aggregation induced by ADP (a much smaller effect than aspirin). Another facet of fosfosal is the fact that it is 6 times more potent than aspirin in inhibiting phosphodiesterase activity (27).

Dapsone and Derivatives—It was observed in a clinical study that dapsone (Fig. 3), a well-established antileprotic drug, given at 100 mg/d improved the clinical state of RA patients while reducing some of the biomedical markers of the disease (C-reactive protein and erythrocyte sedimentation rate). Compared with gold, its efficacy was judged slightly less pronounced and its toxic side effects were less severe [for review see (29)]. The fact that dapsone has apparently no effect on the immune system, and that its experimental AI profile is akin to that of the classical NSAI drugs, does not concur with the above findings (30). However, doses at which activity was seen in animals were much higher than the ones used clinically [NB: results of two different assays in AA regarding activity and toxicity are at odds in the literature (30, 31)]. Also,

[2] Code name: CL-224385.

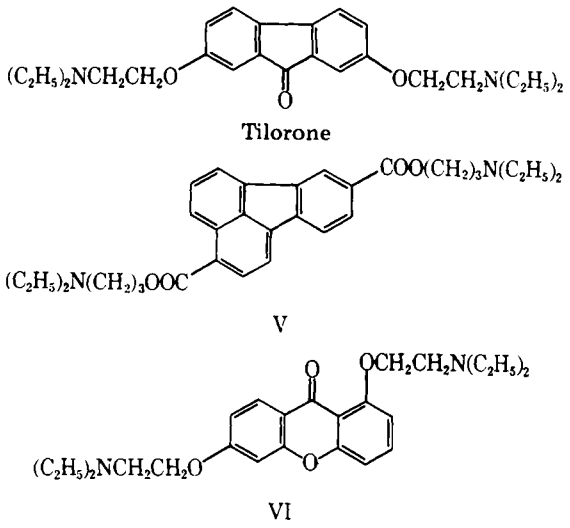

Figure 4.

contrary to the classical drugs, dapsone does not inhibit the PG-dependent ultraviolet-induced erythema, nor does it induce GI irritation in rats. The product has activity in zymosan, anti-IgG, and reversed passive Arthus models of inflammation, and in relation to these effects, it was suggested that dapsone could exert its AI effect by inhibiting complement activation. On the other hand, part of its mode of action must be related to its ability to inactivate the release (and the activity) of lysosomal enzymes from macrophages. It has been reported that dapsone and its urea derivative, (1-[4-(4-sulfanilyl)phenyl]-urea)[3] (III), specifically block *in vitro* incorporation of choline into phosphotidylcholine (lecithin) (32).

In clinical tests with 69 RA patients, 4,4′-bis-[(6-methyluracyl-5-sulfonyl)aminophenyl]sulfone (IV) led to a reduction of morning torpidity, after oral administration of 100–200 mg doses, and to the disappearance of pain syndrome after 10–12 d of treatment, for the majority of the patients (33).

IMMUNOMODULATORS

There seems to be little doubt that RA diseases are directly related to a deficiency in the regulation of the immune system (34). Substances capable of affecting any part of the complicated immunological network may present a potential for more efficacious treatment.

Tilerone-Like Agents—One of the first agents that demonstrated that selective manipulation of the two limbs of the immune system was possible is tilerone (35). A few laboratories have looked upon this interferon inducer as a worthwhile lead. Two examples of this line of research are bis-[3-(diethylamino)propyl] fluoranthene-3,9-dicarboxylate (V)[4] and 1,6-bis[2-(diethylamino)ethoxy]-9H-xanthen-9-one (VI)[5] (Fig. 4).

Like tilerone, these two compounds are able to suppress cell-mediated immune responses and, at the same time, to enhance antibody production (36, 37). Both compounds are effective in several of the cell-mediated immune response assays (EAE, tuberculin skin reaction, developing adjuvant-induced arthritis (D-AA), *etc.*). However, only compound VI is active orally in these tests. Another difference is the fact that VI is devoid of activity in the acute models of inflammation

[3] Code name: MK 241.
[4] Code name: RMI-9563.
[5] Code name: WY-15297.

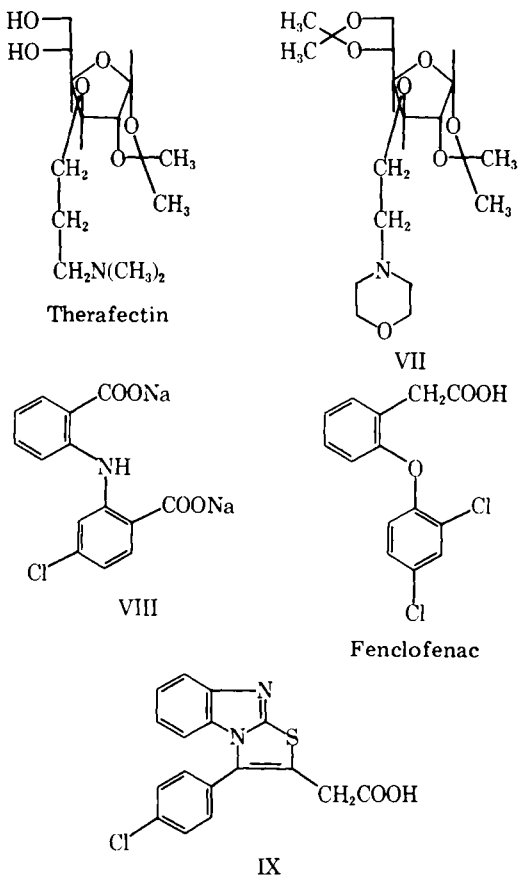

Figure 5.

(carrageenan-induced paw edema (CPE), Na urate, Randall-Sellito yeast tests), while V is active.

Like the steroids and the NSAI drugs, but contrary to immunosuppressive agents, VI is active in established adjuvant arthritis (E-AA) and also in the early phase of D-AA. However in E-AA, unlike the steroids and NSAI drugs, no rebound is observed up to 24 d after the last dosing. The product on the other hand, like the immunosuppressive drugs, is highly active in the EAE (a model in which the NSAI drugs are not active). This agent, it seems, does not fit the standard pattern of either the classical NSAI drugs nor the immunosuppressive agents. This mode of action might reflect selective stimulation of B-cells and suppression of T-cells (37).

Other Compounds—Novel compounds of various chemical classes, unrelated to tilerone, have also been recognized as immunomodulators. Drugs such as the anthelmintic levamisol (38) and more recently the H_2-antagonist cimetidine (39, 40), used in the treatment of peptic ulcers, have been found more or less by serendipity to have an effect on rheumatoid arthritis.

Other agents like therafectin (Fig. 5) first claimed as antiviral, antibacterial, and/or antitumor agents (41) were later discovered to respond positively to AI screening in animal models. Still others, which one would have classified as classical NSAI agents on the basis of their chemical structures, such as Chugai's *N*-(2-carboxyphenyl)-4-chloroanthranilic acid disodium salt (VIII) (42) and fenclofenac (44), were found in fact to have immunomodulating capability.

Therafectin is currently in Phase II of clinical trials in this country. The product is practically devoid of toxicity (in rats $LD_{50} > 10$ g/kg) and active in both the acute and chronic

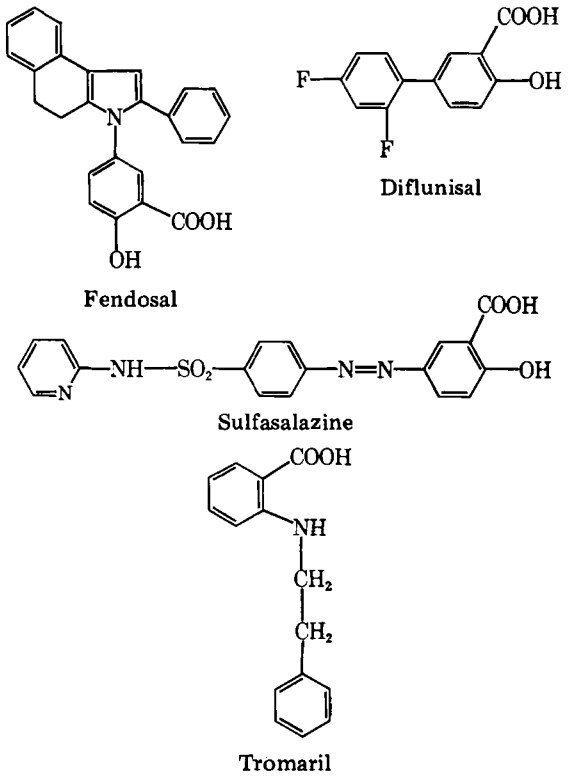

Figure 6.

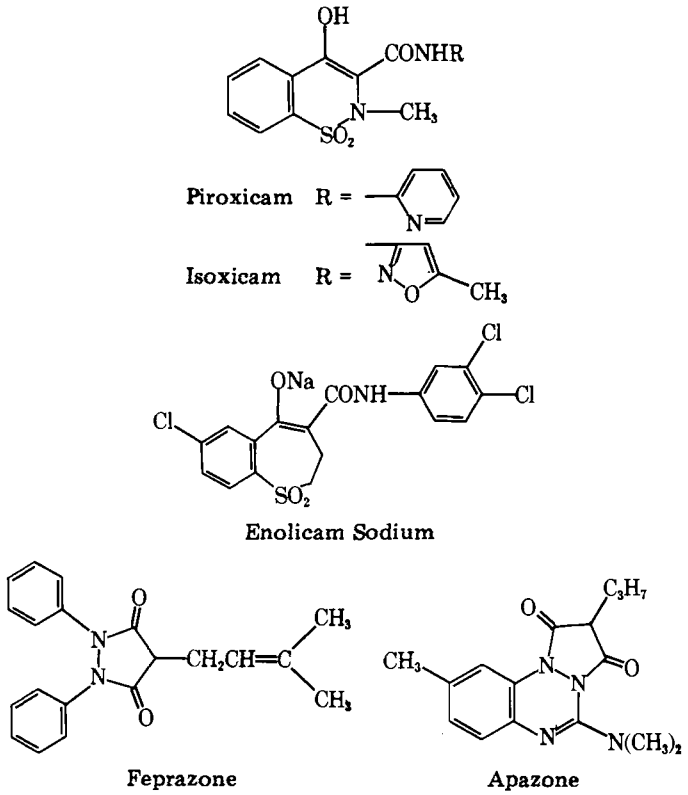

Figure 7.

animal assays of inflammation (CPE, D-AA and E-AA). It is an immunomodulator which primarily stimulates the activity of macrophages (45, 46). Another closely related glucofuranose in which the 5,6-dihydroxy functions are still protected with the isopropylidene group and described as 3-*O*-(2-morpholinoethyl)-1,2,5,6-di-*O*-isopropylidene-α-D-glucofuranose (VII) (47) has been claimed to have immunomodulatory properties.

Contrary to diclofenac sodium (to which it is closely related) the anthranilic acid (VIII) shows no activity in the acute assays, has no effect on tuberculin skin reaction, and no effect on passive cutaneous anaphylaxis in rats. The product is, however, quite active in the D-AA and E-AA assays. It has no immunosuppressive activity, but it enhances antibody levels in immune-deficient animals (42, 48).

As mentioned before, fenclofenac [a close analogue of fenoprofen (Lilly)], first thought to be of the classical type (49) has now been found to modulate the immune system (43). Again in animal studies, this product was found to have minimal activity in the acute but strong activity in the chronic assays. In AA the suppression of edema was seen to persist after treatment was discontinued. The product is 8 times as potent as aspirin in inhibiting PG synthetase. In a 1-year clinical study with 54 rheumatic patients, the effect of fenclofenac was compared with those of penicillamine and placebo (44). It was concluded that fenclofenac can indeed alter the disease profile of rheumatoid arthritis (RA) and, that on the basis of this result, a larger long-term study was warranted. An NDA for this compound has been filed recently in the United States (50).

In the same line, according to recent results of clinical trials, the NSAI agents sulfasalazine (51, 52) (Fig. 6), proquazone (53–55), and diftalone (56) (Fig. 13) would also have some of the characteristics of the disease-modifying agents, since besides improvement in the patient's physical condition, reduction in the RA abnormal parameters was observed. However, these claims have yet to be substantiated. As exemplified in the case of alclofenac (57), preliminary observations are not necessarily confirmed through long-term clinical studies (58–60).

3-(*p*-Chlorophenyl)thiazolo[3,2-*a*]benzimidazole-2-acetic acid (IX)[6] (Fig. 5), contrary to its immediate precursor the 3-hydroxy-2,3-dihydro compound (61), was not transformed *in vivo* to toxic metabolites. Although the product elicited weak inhibition of rat CPE (ED_{50} 200 mg/kg) (inhibition which was not abolished in adrenalectomized animals), it was found to be twice as active as aspirin in inhibiting PGE_2 biosynthesis in sheep seminal vesicles. In the rat AA model, it paralleled levamisole in enhancing the secondary paw edema on days 2–4, but it differs in being quite effective when given therapeutically (on days 16–28) (62).

CLASSICAL NONSTEROIDAL ANTI-INFLAMMATORY AGENTS

Including fenclofenac, sulfasalazine, proquazone, and diftalone [which may be working at a more fundamental level than most of the NSAI drugs in current use (*vide supra*)], there are at present, in clinical trials at one stage or another, more than 40 compounds related to the classical type of AI drugs. The unifying claim here is an improved therapeutic ratio. Several of these new agents are prodrugs of known substances.

Carboxylic Acids—Fendosal (Fig. 6), an indole derivative of salicylic acid, is undergoing Phase III clinical evaluation (63). In animal models this drug was 7–9 times more active than aspirin in the chronic assays (D- and E-AA). It was only slightly more active in the acute tests, but the duration of action was substantially longer than with aspirin (64).

[6] Code name: WY-18251.

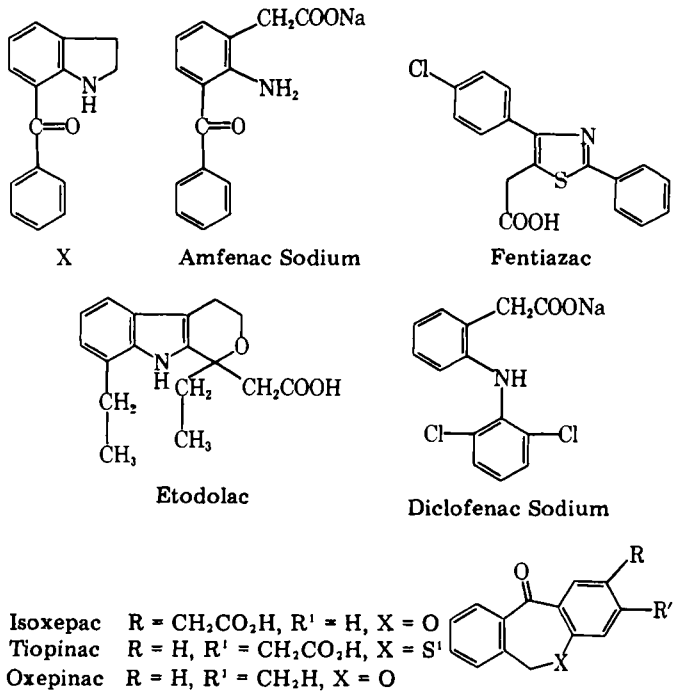

Figure 8.

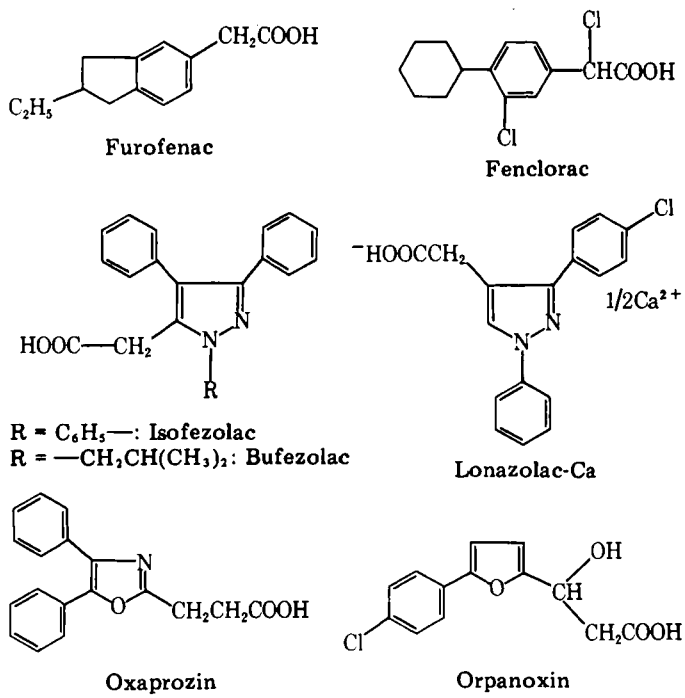

Figure 9.

Diflunisal, a follow-up of flunisal recalled from the clinic (65), was chosen out of more than 500 salicylates. The product is more potent, longer acting, and less toxic than aspirin. Its analgesic potency is about 4 times greater than aspirin. It does not affect platelet aggregation and bleeding time at therapeutic doses in humans. In animal models it was shown to have 7–9 times greater potency than aspirin both in acute and chronic assays (66). Already introduced in 17 countries, diflunisal has recently been approved for marketing in the United States under the analgesic indication (67, 68).

Sulfasalazine was introduced in Great Britain around 1940. Subsequently, on the basis of an unfavorable report, it was abandoned. Later (1965) it was proven effective against ulcerative colitis. Lately this product has been reexamined for the treatment of RA and the results were found particularly encouraging (51, 52). As mentioned earlier, sulfasalazine might have immunological activity.

Tromaril, an anthranilic acid derivative, is reported to be an effective agent in the treatment of rheumatoid disorders. Like the fenamates its side effects were skin rashes, itching, and diarrhea. The product inhibits platelet aggregation without affecting coagulation (69, 70).

Enolic Acids—The enolic acid type of AI drugs, of which butazolidine (PB) is the prototype, has been revived lately by the success story of piroxicam (Pfizer) (Fig. 7). This drug [already approved in 21 countries (71) and recently launched in the United States (68)] has a remarkably long plasma half-life, allowing a once-a-day (20 mg recommended) dose. The compound has high potency and its side effects are confined to the GI tract (72). An analogue, isoxicam, is undergoing Phase III evaluation in the United States (73), while quite a few more are currently in preclinical studies (74).

A new group in this class of products comprise the 1-benzothiepin analogues, some of which showed activity in rats at doses as low as 1 mg/kg/d (75). A representative of this group, enolicam sodium, is currently being evaluated in animals (76).

Replacing the *n*-butyl moiety of phenylbutazone (PB) by a prenyl group gave a compound comparable, in animal models, to PB in efficacy, but with fewer side effects on the hematopoietic system and the GI tract. Clinical evaluation, on the whole, indicated the same trend. At present this drug, feprazone, has been introduced in five countries abroad (77). Another congener of PB, apazone, was recalled recently from Phase III clinical trials (78).

Aryl and Heteroaryl Alkanoic Acids—Amphenac sodium (Fig. 8), originally discovered as the metabolite of 7-benzoylindoline (X), has potent AI activity against acute inflammation and comparable or superior activity to PB in suppressing chronic inflammation in rats (79). The product possesses strong analgesic and antipyretic activity. In pyloric-ligated rats or Heidenhain pouch dogs, the compound did not produce gastric mucosal damage; in chronic administration to rats, intestinal lesions were produced at 10 times the rate of PB (80). Relative to aspirin, the inhibition of CO enzymes by this product is about 600 times more efficient (81). Amphenac sodium is currently in Phase II of clinical trials (82).

Contrary to myalex which turned out to be hepatotoxic in humans (83), fentiazac, a close analogue, seems to undergo a metabolic detoxification process (84). In AA tests the product is 5 times more effective than PB (85). It has analgesic and antipyretic activity and the ability to decrease macrophage migration (86). The drug is already marketed in more than 15 countries; in the United States, it is undergoing Phase II evaluation (87).

Isoxepac (Hoechst) which is in late clinical trials (88) was reported to have high levels of gastric intestinal tolerance, its therapeutic index in dogs being 10–12 times that of indomethacin (89). According to the same source, the effective dose in AA rats is 39–78 times lower than the ulcerogenic dose. The Japanese firm Diichi Seiyaku is currently investigating oxepinac, the corresponding analogue with the acetic acid chain at position 3 of the dibenz[*b*,*e*]oxepin system. In animal models this product exhibits potency similar to that of indomethacin both in the acute and chronic assays (90). Syntex has been developing tiopinac, the sulfur analogue of oxepinac, for which

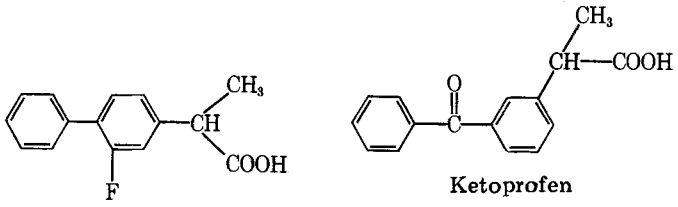

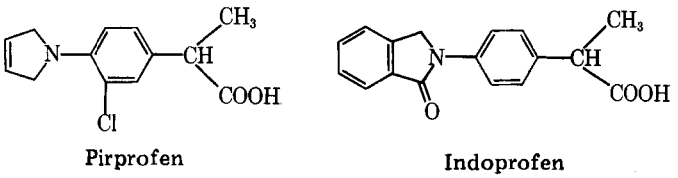

Figure 10.

activity equal to or greater than PB and/or indomethacin was reported. As an analgesic the product is said to be particularly effective against the pain of inflammed joints (91).

Etodolac is structurally related to prodolic acid, and like this compound, which for a while was considered for clinical trials (92), it is more active against the chronic than against the acute model of inflammation (93). The product is a good analgesic and its therapeutic index is 3 and 4 times higher than that of PB and indomethacin (94). It is now in Phase III of clinical assay (95).

Diclofenac sodium[7] is currently undergoing Phase II evaluation in this country (96). Structurally it is close to meclofenamic acid, the first fenamate approved for distribution in the United States. The drug was shown to be equipotent to indomethacin in the CPE, the rat AA, and the mouse writhing phenyl-*p*-benzoquinone assays. Moreover it possesses, as compared with indomethacin, a favorable therapeutic index and the ability to normalize the erythrocyte sedimentation rate (ESR) (97).

Furofenac (Fig. 9) was reported to have marked AI and antiplatelet aggregation activity, low toxicity, and weak ulcerogenicity. It is a PG and thromboxane synthetase inhibitor. In anticipation of clinical trials a metabolic study in animals and in humans has been conducted (98).

Fenclorac presents the singularity of having a chlorine atom α to the carboxy function. The product is in Phase II of clinical evaluation in the United States (99). In animal models its potency lies between aspirin and indomethacin. Its therapeutic ratio, however, is 3–9 times higher than indomethacin. It is also nonulcerogenic in rats at doses less than the LD_{50} (100).

In terms of the AI activity profile, bufezolac is about half as active as indomethacin, while isofezolac is equipotent. The

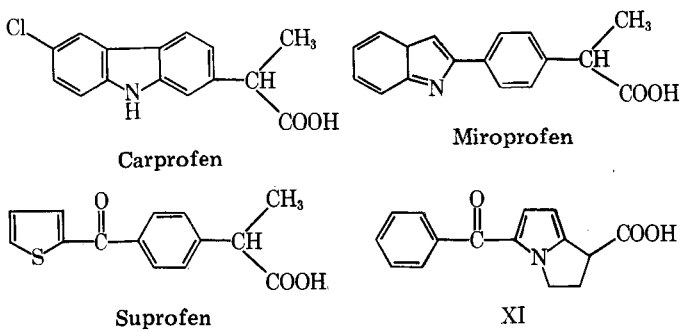

Figure 11.

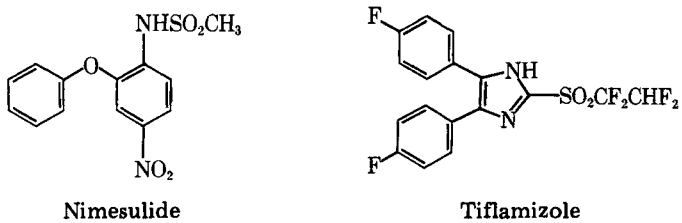

Figure 12.

latter is also more potent in inhibiting the biosynthesis of PG's than indomethacin while the former is much weaker, thus explaining the greater gastric tolerance of bufezolac as compared with isofezolac and/or indomethacin. Results of the analgesic assays as well as the acute toxicity determinations are quite different depending on the animal species tested, thus showing for these two pyrazole derivatives different species sensitivities or a difference in pharmacokinetics between species. These two substances have been considered for clinical trials (101). Structurally they are related to lonazolac calcium[8], which is sold in Germany as an AI drug (102, 103).

Both oxaprozin and orpanoxin have potent analgesic, antipyretic, and AI activity in animal screens (104, 105). The former compared favorably in terms of efficacy with aspirin in clinical studies. It was found to cause significantly less tinnitus and no significant toxic effects (106). The drug is highly protein bound (107) and has a long half-life allowing a once-a-day dosing regimen (108). Regarding orpanoxin, it was speculated that its nonulcerogenicity in rats ($\leq$2 g/kg) was due to its selective lack of effect on stomach PG biosynthesis (105). Clinical work on this substance has recently been deemphasized (109).

Chemically, oxaprozin and orpanoxin are unusual in that they are β-substituted propionic acids. This breaks the unwritten rule that AI activity is restricted to an acetic, α-methylacetic, or again, butyric acid residue which can be transformed to an acetic acid function by β-oxidation.

Flurbiprofen, ketoprofen, pirprofen, and indoprofen (Fig. 10) are either currently in advanced stages of clinical testing or awaiting FDA approval for marketing (110–113). Except for pirprofen, these drugs have already been introduced in several countries abroad for treatment of rheumatoid arthritis and other related diseases. In the classical AI screen, potencies equal to or greater than indomethacin and/or PB have been demonstrated for these compounds (114–117).

Flurbiprofen is well tolerated in humans. In the treatment of RA disease, 100–300 mg was reported to be equivalent to 75–100 mg of indomethacin (110). The product is also being evaluated as an ophthalmic AI agent (118). Ketoprofen was shown in a double-blind crossover study to be equipotent to indomethacin (119). Compared with aspirin, 240 mg of the compound, given daily, had the same effectiveness as 4 g of aspirin, with less side effects (111). Several clinical trials have determined the potency of pirprofen to be the same as aspirin in RA and higher in osteoarthritis (116). It was also found to be a good analgesic agent in the treatment of postoperative pain. Likewise indoprofen (100 and 200 mg) was evaluated in oral and other surgical procedures and found to have superior analgesic activity when compared with aspirin (600 mg) (120). In another clinical study involving RA patients, no difference was seen between indoprofen and indomethacin (121).

[7] Used extensively in Europe, Voltaren.

[8] Active ingredient of Irritren.

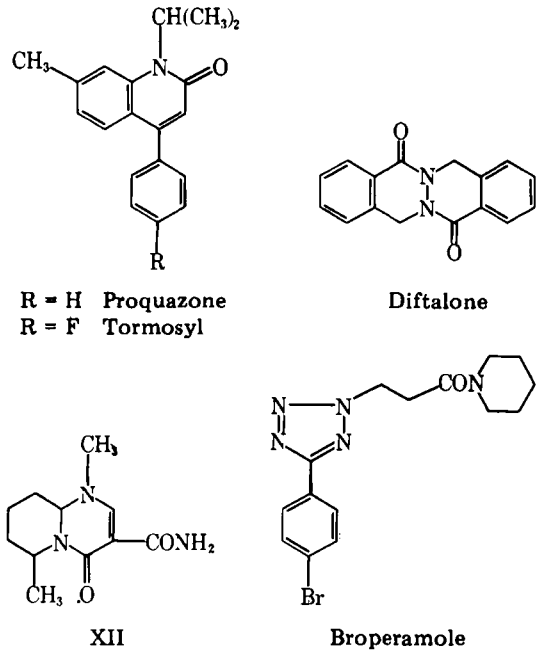

Figure 13.

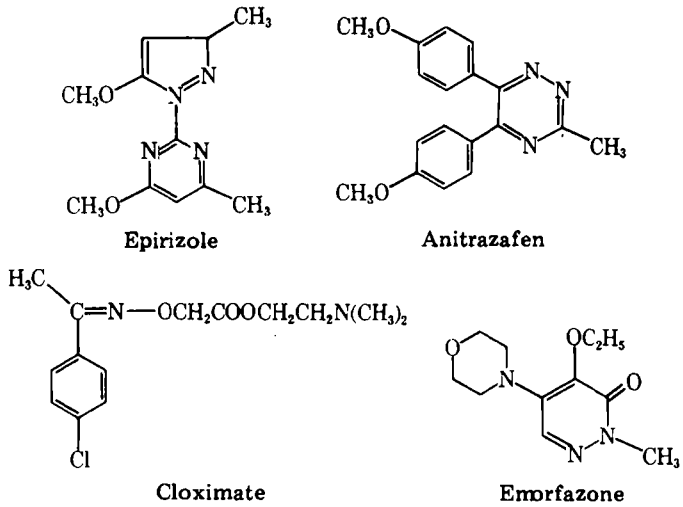

Figure 14.

Double-blind studies comparing carprofen (Fig. 11), indomethacin, ibuprofen, and oxyphenbutazone have been reported. The compound proved highly effective, but it induced GI irritation more often than indomethacin (122). Animal studies, in parallel with indomethacin, had indicated equipotent AI activity, lower potency (10–25 times) in inhibiting PG synthesis, and lower ulcerogenic activity (123, 124).

Miroprofen, a strong analgesic, specifically inhibits pain responses and acute inflammation associated with increased vascular permeability. The substance also has AI activity, being as potent as PB in inhibiting rat AA. Its ulcerogenic potential also compares well with that of PB. Its efficacy in relieving gingivitis was demonstrated in a clinical study (125).

In the rat D-AA screen, suprofen was found to have the highest safety margin when compared with PB, tolmetin, indomethacin, and aspirin: 48:20:16:8:2, respectively. Also observed in the rats undergoing that test was a reduction of bone erosion at 10–40 mg/kg (126). Moreover it was shown that suprofen is a potent antagonist of acetic acid-induced writhing in rats (127) of ultraviolet erythema in guinea pigs (128), and of sodium urate crystal-induced arthritis in dogs (129). In the clinic, drowsiness was observed as one of its side effects (130).

(±)-5-Benzoyl -3*H*- 1,2-dihydropyrrolo[1,2-*a*]pyrrole-1-carboxylic acid (XI) has in lieu of an α-methyl substituent to the carboxylic acid rest, an α-methylene group fixed in a pentacyclic ring (131). This product, which is undergoing phase I clinical trial, is a potent platelet inhibitor with strong analgesic and AI activities (132).

Miscellaneous Acidic Compounds—Nimesulide (Fig. 12), an acidic compound by virtue of its sulfonamide functional group, was reported to respond quite effectively in acute and chronic animal AI assays and to present a marked superiority in the therapeutic index to most reference NSAI drugs (133). Compared with indomethacin, its AI potency was of the same order; however, the product was 10 times less effective in suppressing PG *in vitro* (134). In clinical studies, nimesulide was evaluated in 70 patients with rheumatic disorders for a mean duration of 26 d. A complete cure or significant improvement in 86% of patients was reported. Side effects were mainly GI disturbances (135).

Another nonalkanoic acidic drug is the hexafluoroimidazole derivative tiflamizole. In animal studies, the product was about 10 times as potent as indomethacin in D-AA and E-AA screens (ED_{50} 0.03 mg/kg/d). An unusual feature was the duration of the therapeutic effect following daily oral doses of 0.09 mg/kg for 7 d. The inhibition persisted for more than 70 d when, in the case of indomethacin, there was a flare up after 2–3 days. The drug had a long half-life, was rapidly absorbed, and slowly excreted in various animal species. There was apparently no evidence of metabolites. Tiflamizole strongly suppressed bovine seminal vesicle PG synthetase (IC_{50} $4 \cdot 10^{-7}$ mol/L); nevertheless, its ulcerogenic activity in rats, was found to be weaker than that of the regular AI drugs in use (136–138). This compound is currently in Phase II of clinical evaluation (139).

Nonacidic NSAI Drugs—There are not many nonacidic NSAI drugs available for the treatment of RA. Benzydamine (mostly an analgesic agent) and tiaramide (sold in Japan) are two examples of this class of product. Also, relatively few novel compounds of this type have been developed to the point of clinical trial. Proquazone (Fig. 13), which is sold in Germany and in Switzerland, is actually in Phase II of clinical trials in the United States (140). Like the acidic NSAI drugs, the compound blocks the CO pathway of the arachidonic cascade. It is particularly effective in inhibiting collagen-induced platelet aggregation (141). In clinical tests, proquazone was found to be comparable with indomethacin in terms of efficacy and tolerance (142). Evaluated in postoperative dental pain, it was found to have 5–6 times the potency of aspirin (143). Some lower intestinal intolerance appears to be the main problem. Recent reports would attribute disease-modifying capability to this drug (53–55). Tormosyl, the corresponding fluoro analogue of proquazone, has been evaluated as an analgesic in humans (144).

The phthalazine derivative, diftalone, had AI potency in animal models approximately equal to that of PB, while gastro-ulcerogenic activity (in rats) and manifestations of acute toxic effects were practically absent (145). In the clinic it was found effective for the treatment of RA and comparable with indomethacin. Suppression of the ESR was also reported (56).

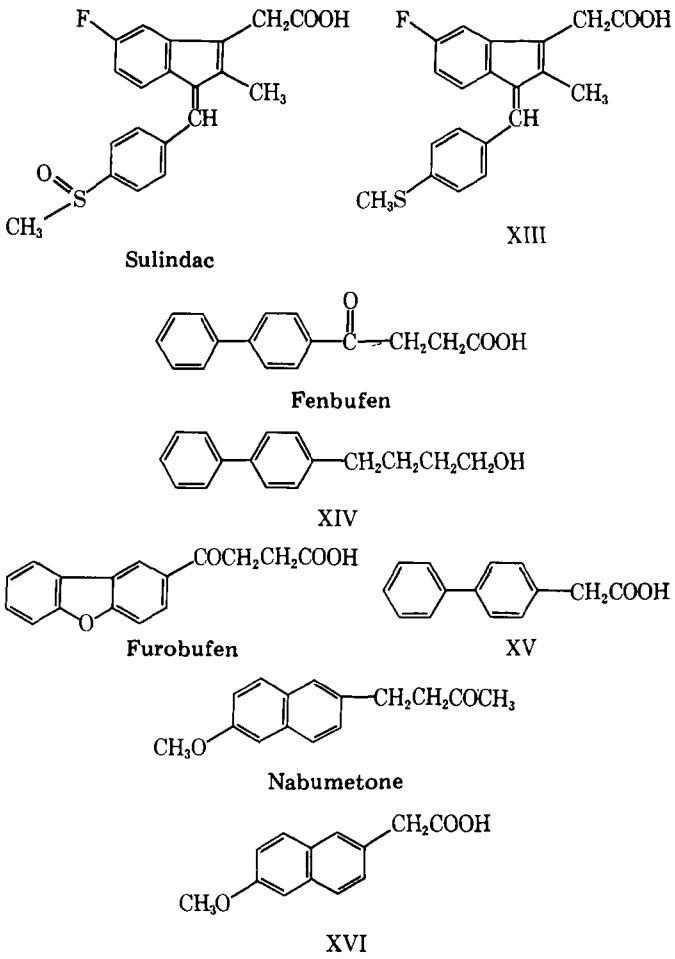

Figure 15.

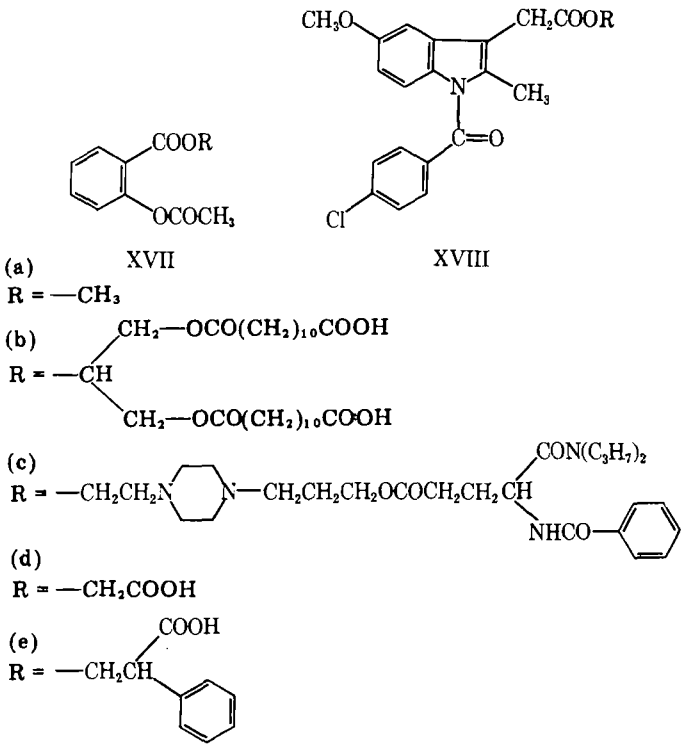

Figure 16.

Antipyretic, analgesic, and AI activity combined with a high therapeutic index as compared with indomethacin have been reported for 1,6-dimethyl-4-oxo-1,6,8,9,9a-hexahydro-4H-pyrido[1,2-*a*]pyrimidine-3-carboxamide (XII)[9]. A marked synergistic effect was observed in the reduction of rat CPE when a low dose of XII was coadministered with indomethacin. It is assumed that the product will be examined clinically and this synergistic effect evaluated (146).

Broperamole showed systemic AI activity 5–6 times that of PB in acute assays, and 10 times in the case of chronic assays. The product caused gastric irritation only at very high doses (147). It had topical AI activity, but less than that of hydrocortisone. The product is undergoing preclinical testings (148).

Epirizole (Fig. 14), a Japanese drug having higher analgesic activity than aminopyrine with less toxicity, is being evaluated for clinical trials in this country (149). Apparently this product can inhibit gastric lesions induced by acidic NSAI drugs (150).

The triazine anitrazafen is 50–100 times more potent than indomethacin in inhibiting fatty acid CO. It was found inactive in rat CPE and AA when given orally, but topically, it inhibited or reversed the formation of erythema induced by ultraviolet light (151). The development of this product, under evaluation for some time, may have been deemphasized (152).

In addition to showing good inhibiting activity in the usual assays of experimental inflammation, cloximate, an oxime ether derivative, showed marked activity in traumatic edema and in the Arthus antigen-antibody assay. Tested in acute and chronic experiments in rats and dogs, it had practically no harmful effect in the gastrointestinal mucosa. It is reported to be as potent as aspirin in blocking the biosynthesis of PGE_2. The product has been submitted to a first clinical trial (153).

Emorfazone, evaluated in acute models of inflammation showed analgesic and AI activity similar to PB (154). It was found to inhibit compound 48/80[10]- induced histamine release from mast cells and from rat skin, to have no effect on the immune system, and not to suppress PG synthesis. The main site of its anti-nociceptive activity was suggested to be in the periphery (155). Treatment of a group of patients with acute cystitis resulted in good to excellent remission of micturition pain in 14 of the 15 cases (156).

Prodrugs—Sulindac (Fig. 15), an indene isostere of indomethacin, was recently introduced in the United States. It is a prodrug for the active corresponding sulfide metabolite XIII. It has longer duration of action, fewer side effects than indomethacin, and it is claimed to be free of GI problems (157).

Fenbufen is characterized by its high analgesic activity, the sustained duration of its analgesic and AI action relative to the other known drugs, and the fact that it does not directly inhibit fatty acid CO. Its activity is due mainly to its main metabolite, biphenylacetic acid (BAA) (XV) which, in this case, must be obtained by quite an unusual transformation. This acid is a potent inhibitor of PG biosynthesis. The low potency of fenbufen to induce gastric irritation can be explained by the fact that BAA is not directly in contact with the GI tract (158, 159). Fenbufen is currently sold in more than 14 countries. Its introduction in the United States is expected in the near future (160).

The fluorene analogue, furobufen, has recently been recalled

[9] Code name: Chinoin-127.

[10] Mixture of polymeric amines; see W. D. M. Paton, *Br. J. Pharmacol.*, **6**, 499 (1951).

from clinical testing (161). In AA assays furobufen elicited similar activity to PB. The product has analgesic but no antipyretic activity (162). Thomae's butyryl alcohol derivative, 4-(4-biphenyl)butanol (XIV)[11], is also metabolized to XV and it presents, not unexpectedly, an activity profile similar to fenbufen[12].

Biotransformation of nabumetone to the active metabolite, 6-methoxynaphthalene acetic acid (XVI), is also responsible for the much reduced ability of this compound to induce gastric lesions as compared with standard drugs such as naproxen and/or indomethacin. The product is now being evaluated clinically (163, 164).

Most attempts to prepare AI prodrugs have revolved around modification of the acidic function, through esterification and/or amide formation, of known inflammation inhibitors. One of the most expedient ways would be esterification with methanol. Indeed, according to a recent report (165), the methyl esters of acidic NSAI drugs were found far less ulcerogenic than the acids, yet their AI activities were not changed appreciably. In the case of the methyl ester of aspirin (XVIIa) (Fig. 16) it was established that the toxicity after long-term oral administration to rats and guinea pigs was less than aspirin. Another study with radiolabeled salicylate derivatives showed that the methyl ester group did not quantitatively change the biodistribution of the active form generated *in vivo* (166).

On the basis that triglycerides are able to pass through the stomach without undergoing hydrolysis and then to be absorbed in the intestines, it was assumed that NSAI drugs incorporated in the triglyceride structure would bypass the stomach and then be metabolized to provide free drug delivery.

In the case of the triglycerides of aspirin (XVIIIb) it was found that the therapeutic ratio was improved 80-fold over aspirin. However, with indomethacin (XVIIb) only a threefold improvement was experienced. It was concluded that GI damage due to indomethacin is mainly produced systematically by the circulating drug, whereas in the case of aspirin the irritation is primarily the result of local action on the gastric mucosa (167–170). It was shown with the use of radiolabeled compounds that effective therapeutic concentration of the free active salicylate was easily obtained after ingestion of the triglycerides of aspirin (171).

The isoglutaminyl moiety of proglumetacin (XVIIIc) is said to procure protective activity to the gastric mucosa, while the presence of the piperazine nucleus seems important for providing a favorable therapeutic ratio (172). The product caused GI tract damage (in rats) only at dose levels close to the LD_{50} (173).

Acemetacin (XVIIId) was chosen from a series of more than 100 compounds, mostly esters and amides of indomethacin. In animal tests it was found to be more active than indomethacin (in acute and chronic assays), and to be equipotent with corticosteroid in the granuloma pouch test (cotton pellet). It is a weaker inhibitor of PG synthesis than indomethacin and, apparently in connection with that, it causes less damage to the mucous membrane of the gastrointestinal tract (174, 175). In a multicenter long-term study with 200 outpatients, the efficacy of acemetacin was assessed as good to very good in 75% of the cases. Only 3% of the patients gave preference to

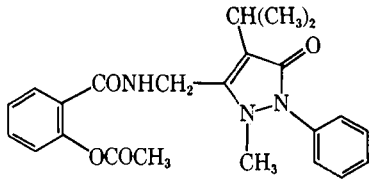

XIX

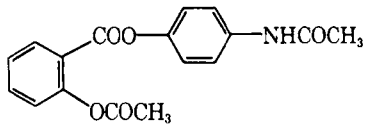

Benorylate

Figure 17.

indomethacin in this study. Damage to the GI tract was observed but in general it was much reduced (176, 177).

Among a large series of esters of indomethacin, tropesin (XVIIIe) had the slowest rate of cleavage by action of serum esterases *in vitro*. Compared with indomethacin, the product exhibited the same AI efficacy, in acute and chronic models of inflammation, and a much lower tendency to induce gastric damage (UD_{50} 50 mg/kg *versus* 1 mg/kg for indomethacin). In a first clinical trial, symptoms of intolerance were not observed with daily doses of tropesin up to 210 mg (178).

The antiarthritic and analgesic activity of the double prodrug of aspirin and isopropylantipyrine (AIA)—*N*-(4-propyphenazon-5-yl)-2-acetoxybenzamide (XIX)—(Fig. 17), was found to have about the same potency as that of each moiety taken separately, but with the difference that the gastric ulcerogenic activity was much less pronounced. This product also showed practically no acute toxicity as shown by the LD_{50} values: 5 g/kg orally and subcutaneously, and 3.68 g/kg intraperitoneally in mice (179).

Benorylate, another example of a double prodrug (aspirin and paracetamol), is now marketed in Europe (180). It is believed that paracetamol, by stimulating stomach PG synthetase, inhibits the erosive action of aspirin (181).

CONCLUSION

Most of the compounds currently under investigation are CO inhibitors and as such are analogues of aspirin and/or indomethacin. Yet these may be justified as useful alternatives in view of individual diversity in response to treatment, if not as offering greater tolerance and, in some cases, the convenience of a once-a-day medication. More importantly, however, is the fact that a few of these may influence some of the more fundamental mechanisms of the disease, overlapping, it would seem, with the newer types of compounds whose mode of action is related either to their capacity to inhibit the chemotaxis of cells perpetuating the disease at the site of inflammation and/or to their selective control of the body's immune system.

REFERENCES

(1) I. L. Bonta and M. J. Parhnam, *Biochem. Pharmacol.*, **27**, 1611 (1978).

(2) S. A. Metz, *Med. Clin. North Am.*, **65**, 713 (1981).

(3) R. W. Randall, K. E. Eakins, G. A. Higgs, J. A. Salmon, and J. E. Tateson, *Agents Actions*, **10**, 553 (1980).

(4) G. A. Higgs, R. J. Flower, and J. R. Vane, *Biochem. Pharmacol.*, **28**, 1959 (1979).

[11] Code name: CO-893.

[12] Personal communication.

(5) I. Ahnfelt-Rønne and E. Arrigoni-Martelli, *Biochem. Pharmacol.*, **29,** 3265 (1980).
(6) J. R. Walker and W. Dawson, *J. Pharm. Pharmacol.*, **31,** 778 (1979).
(7) A. W. Ford-Hutchison, *Agents Actions*, Suppl. 12, 154 (1982).
(8) I. Ahnfelt-Rønne and E. Arrigoni-Martelli, *Biochem. Pharmacol.*, **31,** 2619 (1982).
(9) C. H. Cashin, W. Dawson, and E. A. Kitchen, *J. Pharm. Pharmacol.*, **29,** 330 (1977).
(10) K. E. Eakins, G. A. Higgs, S. Moncada, K. G. Mugridge, and J. R. Vane, *Br. J. Pharmacol.*, **69,** 270P (1979).
(11) S. C. R. Meacock and E. A. Kitchen, *J. Pharm. Pharmacol.*, **31,** 366 (1979).
(12) K. E. Eakins, G. A. Higgs, and B. J. R. Whittle, *Br. J. Pharmacol.*, **70,** 82P (1980).
(13) New Drug Comment., **7**(64), 20 (1980).
(14) New Drug Comment., **9**(91) 49 (1982).
(15) A. Von Wiskemann, *Arzneim.-Forsch.*, **31**(I), 730 (1981).
(16) S. Rachlin, E. Bramm, I. Ahnfelt-Rønne, and E. Arrigoni-Martelli, *J. Med. Chem.*, **23,** 13 (1980).
(17) E. Bramm, L. Binderup, and E. Arrigoni-Martelli, *Agents Actions*, **11,** 402 (1981).
(18) D. N. Ridge, J. W. Hanifin, L. A. Harten, B. D. Johnson, J. Menschik, G. Nicolau, A. E. Sloboda, and E. D. Watts, *J. Med. Chem.*, **22,** 1385 (1979).
(19) J. W. Hanifin, B. D. Johnson, J. Menschik, D. N. Ridge, and H. E. Sloboda, *J. Pharm. Sci.*, **68,** 536 (1979).
(20) M. E. J. Billingham, *Br J. Pharmacol.*, **72,** 523P (1981).
(21) P. Pomarelli, M. Berti, M. T. Gatti, and P. Mosconi, *Il Farmaco Ed. Sci.*, **35,** 836 (1980).
(22) M. E. J. Billingham, R. B. Clague, K. Morgan, and M. N. Smith *Br. J. Pharmacol.*, **72,** 551P (1981).
(23) *Drugs Future*, **7,** 428 (1982).
(24) M. Neuman, *Drugs Exp. Clin. Res.*, **6,** 53 (1980).
(25) *Drugs Future*, **4,** 445 (1979).
(26) M. Lingetti, P. L. D'Ambrosio, F. Di Grezia, P. Sorrentino, and E. Lingetti, *Curr. Ther. Res.*, **31,** 408 (1982).
(27) J. G. Rafanell, L. Bellés, M. S. Sánchez, and J. Forn, *Arzneim.-Forsch.*, **30**(11), 1091 (1980).
(28) *Drugs Future*, **5,** 290 (1980).
(29) I. M. Hunneyball, "Progress in Drug Research," vol. 24, E. Jucker, Ed., Berkhaüser Verlag Basel, Switzerland 1980 p. 192.
(30) A. J. Lewis, D. K. Gemmell, and W. H. Stimson, *Agents Actions*, **8,** 578 (1978).
(31) K. Williams, R. B. Capstick, D. A. Lewis, and R. Best, *J. Pharm. Pharmacol.*, **28,** 555 (1976).
(32) R. J. Bonney, P. D. Wightman, and P. Davies, *Biochem. Pharmacol.*, **28,** 2471 (1979).
(33) N. M. Goloshchapov, Ya. A. Sigidin, E. S. Tsvekova, I. L. Bilich, V. S. Reznik, N. G. Pashkurov, G. F. Zaika, and A. A. Muslinkin, U.S. Patent 4,151,281; *Chem. Abstracts*, **91,** 44522e (1979).
(34) T. Azumat, *Drugs Exp. Clin. Res.*, **5,** 139 (1979).
(35) H. Megel, A. Raychaudhuri, I. Shemano, T. H. Beaver, and L. L. Thomas, *Proc. Soc. Exp. Biol. Med.*, **145,** 513 (1974).
(36) H. Megal, A. Raychaudhuri, M. Bayer, and T. H. Beaver, *Agents Actions*, **8,** 218 (1978).
(37) W. E. Rosenthale, A. A. Santilli, A. C. Scotese, S. C. Bell, and B. A. Rubin, *J. Immunopharm.*, **2,** 257 (1980).
(38) E. C. Huskisson, J. Scott, H. W. Balme, P. A. Dieppe, J. Trapnell, and D. A. Willoughby, *Lancet*, **i,** 393 (1976).
(39) S. Norm, H. Permin, and P. S. Skov, *Allergy*, **35,** 357 (1980).
(40) H. A. Al-Haboubi and I. J. Zeitlin, *Br. J. Pharmacol.*, **67,** 446P (1979).
(41) P. Gordon, *Chem. Abstracts*, **83,** 147697e (1975).
(42) Y. Ohsugi, S. I. Hata, M. Tanemura, T. Nakano, T. Matsuno, Y. Takagaki, Y. Nishu, and M. J. Shindo, *Pharm. Pharmacol.*, **29,** 636 (1977).
(43) N. C. Phillips, *Fenclofenac, Int. Congr. Symp. Ser.-R. Soc. Med.*, Academic Press No. 28, 1980, p. 83.
(44) A. V. Camp, D. Heywood, H. Berry, M. G. Molloy, D. W. James, E. B. D. Hamilton, and A. W. Ford-Hutchinson, *Int. Congr. Symp. Ser.-R. Soc. Med.*, Academic Press No. 28, 1980, p. 95.
(45) P. Gordon, in Inflammation: Mechanisms and Treatment," Proceedings 4th International Meeting, D. A. Willoughby and J. P. Giroud, Eds. University Park Press, Baltimore, Md., 1980, p. 169.
(46) *New Drug Comment.*, **8**(76), 30 (1981).
(47) A. Goi, T. Bruzzese, A. F. Notarianni, M. Riva, and A. Ronchini, *Arzneim.-Forsch.*, **29**(11), 986 (1979).
(48) *Drugs Future*, **6,** 313 (1981).
(49) D. C. Atkinson and E. C. Leach, *Agents Actions*, **8,** 438 (1978).
(50) *New Drug Comment.*, **8**(79), 26 (1981).
(51) B. McConkey, R. S. Amos, E. P. Butler, R. A. Crockson, A. P. Crockson, and L. Walsh, *Agents Actions*, **8,** 438 (1978).
(52) H. A. Bird, J. S. Dixon, M. E. Pickup, V. M. Rhind, J. R. Lowe, M. E. Lee, and V. Wright, *J. Rheumatol.*, **9,** 36 (1982).
(53) G. E. Ehrlich, *Infect. Dis.*, **June,** 12 (1981).
(54) B. Skrifvars and M. Nissilä, *Scand. J. Rheumatol.*, **9,** 33 (1980).
(55) B. Skrifvars and M. Nissilä, *Scand. J. Rheumatol.*, Suppl. **21** (1978) (review of proquazone).
(56) A. Bremová, E. Pěgřímová, V. Rejholec, A. Šusta, P. Truhlář, and M. Vykydal, *Scand J. Rheumatol.*, Suppl., **17,** 1 (1977).
(57) R. S. Brogden, R. C. Heel, T. M. Speight, and G. S. Avery, *Drugs*, **14,** 241 (1977).
(58) H. Berry, L. Ferwandes, A. W. Ford-Hutchinson, S. J. W. Evans, and E. B. D. Hamilton, *Ann. Rheum. Dis.*, **37,** 93 (1978).
(59) E. C. Huskisson, in "Inflammation: Mechanism and Treatment," Proceedings 4th International Meeting, D. A. Willoughby, and J. P. Giroud, Eds. Univ. Park Press, Baltimore, Md., 1980, p. 55.
(60) H. A. Bird, J. S. Dixon, M. E. Pickup, M. R. Lee, and V. Wright, *Ann. Rheum. Dis.*, **39,** 281 (1980).
(61) S. C. Bell and P. H. L. Wei, *J. Med. Chem.*, **19,** 524 (1976).
(62) A. J. Lewis, J. DiLuigi, J. Parker, L. Datko, and R. P. Carlton, *Fed. Proc.*, **40,** Abst. 4395 (1981).
(63) *New Drug Comment.*, **7**(72), 7 (1980).
(64) H. B. Lassman, J. C. Wilker, V. B. Anderson, M. N. Agnew, R. C. Allen, and W. J. Novick, Jr., *Agents Actions*, **8,** 209 (1978).
(65) S. S. Bloomfield, T. P. Barden, and R. Hille, *Clin. Pharmacol. Ther.*, **11,** 747 (1970).
(66) J. Hannah, W. V. Ruyle, H. Jones, A. R. Matzuk, K. W. Kelly, B. E. Witzel, W. J. Holtz, R. A. Houser, T. Y. Shen, L. H. Sarett, V. J. Lotti, E. A. Risley, C. G. Van Arman, and C. A. Winter, *J. Med. Chem.*, **21,** 1093 (1978).
(67) *New Drug Comment.*, **8**(79), 6 (1981).
(68) *New Drug Comment.*, **9**(88), 3 (1982).
(69) N. A. Kshirsagar, T. Paul, and U. K. Sheth, *Br. J. Clin. Pharmacol.*, **9,** 530 (1980).
(70) D. P. Jindal and T. R. Bhardwaj, *Pharmacos*, **24,** 13 (1980).
(71) *New Drug Comment.*, **8**(79), 13 (1981).
(72) P. Schiantarelli and S. Cadel, *Arzneim.-Forsch.*, **31**(I), 87 (1981).
(73) *New Drug Comment.*, **7**(70), 12 (1980).
(74) J. G. Lombardino and E. H. Wiseman, *Trends Pharmacol. Sci.*, **1981,** 132.
(75) M. H. Rosen, *Chem. Abstracts*, **93,** 46451w (1982).
(76) *New Drug Comment.*, **9**(89), 8 (1982).
(77) "Feprazone, New Biological and Clinical Aspects," The IX European Congress of Rheumatology, Weisbaden, Sept. 1979.
(78) *New Drug Comment.*, **7**(70), 11 (1980).
(79) W. Welstead Jr., H. W. Moran, J. F. Stauffer, L. B. Turnbull, and L. Sancilio, *J. Med. Chem.*, **22,** 1074 (1979).
(80) *Drugs Future*, **3,** 340 (1978).
(81) *Drugs Future*, **5,** 417 (1980).
(82) *New Drug Comment.*, **7**(67), 5 (1980).
(83) *Lancet*, **i,** 662 (1970).
(84) S. Fumero, A. Mondino, S. Silvestri, G. Zanolo, G. De Marchi, and S. Pedrazzini, *Arzneim.-Forsch.*, **30**(II), 1253 (1980).
(85) K. Brown, P. D. Cater, J. F. Cavalla, D. Green, R. A. Newberry, and A. B. Wilson, *J. Med. Chem.*, **17,** 1177 (1974).
(86) E. Galimberti, S. Cerutti, A. Forlani, and G. D'Atri, *Arzneim.-Forsch.*, **26,** 392 (1976).
(87) *New Drug Comment.*, **7**(72), 27 (1980).
(88) *New Drug Comment.*, **7,** 9 (1980).
(89) D. E. Aultz, C. Helsley, D. Hoffman, A. R. McFadden, H. B. Lassman, and J. C. Wilker, *J. Med. Chem.*, **20,** 66 (1977).
(90) T. Yoshioka, M. Kitagawa, M. Oki, S. Kubo, H. Tagawa, K. Ueno, W. Tsukada, M. Tsubokawa, and A. Kasahara, *J. Med. Chem.*, **21,** 633 (1978).
(91) W. H. Rooks II, A. J. Tomolonis, P. J. Maloney, A. Roszkowski, and M. B. Wallach, *Agents Actions*, **10,** 266 (1980).
(92) *New Drug Comment.*, **7**(72), 17 (1980).
(93) R. R. Martel, J. Klicius, and F. Herr, *Agents Actions*, **4,** 370 (1974).
(94) R. R. Martel and J. Klicius, *Can. J. Physiol. Pharmacol.*, **54,** 245 (1976).

(95) *New Drug Comment.*, **8**(76) 32 (1981).
(96) *New Drug Comment.*, **7**(62) 13 (1980).
(97) P. J. Krupp, R. Menassé-Gdynia, A. Sallmann, G. Wilhelmi, R. Zeil, and R. Jaques, *Experientia*, **29,** 450 (1973).
(98) C. Casalini, G. Mascellani, G. Tamagnone, G. Cesarano, and A. Giumanini, *J. Pharm. Sci.*, **69,** 164 (1980).
(99) *New Drug Comment.*, 7(67), 9 (1980).
(100) G. W Nuss, R. D. Smyth, C. H. Breder, M. J. Hitchings, N. G. Mir, and N. H. Reaveycantwell, *Agents Actions*, **6,** 735 (1976).
(101) J. Mizoule, G. Le Fur, and A. Uzan, *Arch Int. Pharmacodyn.*, **238,** 305 (1979).
(102) G. Rainer, U. Krüeger, and K. Klemm, *Arzneim.-Forsch*, **31,** 649 (1981).
(103) R. Riedel, *Arzneim.-Forsch.*, **31,** 655 (1981).
(104) K. Brown, J. F. Cavalla, D. Green, and A. B. Wilson, *Nature (London)*, **219,** 164 (1968).
(105) M. M. Goldenberg, K. L. Boise, and A. C. Ilse, *Arch. Int. Pharmacodyn.*, **243,** 331 (1980).
(106) J. A. Hubsher, I. M. Ballard, B. R. Walker, and J. A. Gold, *J. Int. Med. Res.*, **7,** 69 (1979).
(107) *Drugs Future*, **4,** 450 (1981).
(108) W. J. Reynolds, S. F. Shaar, A. Buik, and W. J. Lancee, *J. Rheumatol.*, **6,** 345 (1979).
(109) *New Drug Comment.*, **7**(65), 30 (1980).
(110) *New Drug Comment.*, **7**(69) 20 (1980.
(111) *New Drug Comment.*, **7**(72) 21 (1980).
(112) *New Drug Comment.*, **8**(76) 11 (1981).
(113) *New Drug Comment.*, 7(71) 14 (1980).
(114) S. S. Adams, K. F. McCullough, and J. S. Nicholson, *Arzneim.-Forsch.*, **25,** 1786 (1975).
(115) L. Julou, J. C. Gayonnet, R. Ducrot, C. Garret, M. C. Bardone, G. Maignan, and J. Pasquet, *J. Pharmacol.*, **2,** 259 (1971).
(116) *Drugs Future*, **5,** 52 (1980).
(117) G. Nannini, P. N. Giraldi, G. Molgora, G. Biasoli, F. Spinelli, W. Logemann, E. Dradi, G. Zanni, A. Buttinoni, and R. Tommasini, *Arzneim.-Forsch.*, **23,** 1090 (1973).
(118) *New Drug Comment.*, **8**(82), 9 (1981).
(119) A. N. Gyory, M. Bloch, H. C. Burry, and R. Grahame, *Br. Med. J.*, **4,** 398 (1972).
(120) R. Okun, J. K. Green, and R. W. Shackleford, *J. Clin. Pharmacol.*, **19,** 487 (1979).
(121) G. C. Saba and G. Orlandi, *Curr. Ther. Res.*, **25,** 260 (1979).
(122) *Drugs Future*, **5,** 47 (1980).
(123) Z. N. Gaunt, H. Baruth, L. O. Randall, C. Ashley, and J. R. Paulsrud, *Prostaglandins*, **10,** 59 (1975).
(124) E. T. Stiller, P. A. Diassi, D. Gerschutz, D. Meikle, J. Moetz, P. A. Principe, and S. D. Levine, *J. Med. Chem.*, **15,** 1029 (1972).
(125) Y. Maroyama, K. Anami, M. Terasawa, K. Goto, T. Imayoshi, Y. Kadobe, and Y. Mizushima, *Arnzeim.-Forsch.*, **31**(III), 1111 (1981).
(126) F. Awouters, C. J. E. Niemegeers, P. M. H. Lenaerts, and P. A. J. Janssen, *Arnzeim.-Forsch.*, **25,** 1526 (1975).
(127) C. J. E. Niemegeers, J. A. A. Van Bruggen, and P. A. J. Janssen, *Arnzeim.-Forsch.*, **25,** 1505 (1975).
(128) F. Awouters, C. J. E. Niemegeers, P. M. H. Lenaerts, and P. A. J. Janssen, *Arnzeim.-Forsch.*, **25,** 1509 (1975).
(129) C. J. E. Niemegeers and P. A. J. Janssen, *Arnzeim.-Forsch.*, **25,** 1512 (1975).
(130) *New Drug Comment.*, **7**(64), 18 (1980).
(131) *Ger. Offen.*, 2,731,678; *Chem. Abstracts*, **89,** 6215h (1978).
(132) *New Drug Comment.*, **8**(80), 32 (1981).
(133) K. F. Swingle, G. G. I. Moore, and T. J. Grant, *Arch. Int. Pharmacodyn.*, **221,** 132 (1976).
(134) R. L. Vigdahl and R. H. Tukey, *Biochem. Pharmacol.*, **26,** 307 (1977).
(135) R. Weissenbach, *J. Int. Med. Res.*, **9,** 349 (1981).
(136) W. E. Henes, D. C. Rakestraw, C. C. Whitney, and V. G. Vernier, *Pharmacologist*, **24,** 129 (1982), Abst. 199.
(137) G. S. Shotzberger, W. E. Hewes, W. Galbraith, and V. G. Vernier, *Pharmacologist*, **24,** 129 (1982), Abst. 200.
(138) D. C. Rakestraw, C. C. Whitney, and V. G. Vernier, *Pharmacologist*, **24,** 129 (1982), Abst. 201.
(139) *New Drug Comment.*, **9**(89), 27 (1982).
(140) *New Drug Comment.*, **7**(67), 14 (1980).
(141) I. B. Hoomes, *Arch. Int. Pharmacodyn.*, **228,** 136 (1977).
(142) M. Schattenkirchner and Z. Fryda-Kaurimski, *Curr. Ther. Res.*, **24,** 905 (1978).
(143) J. A. Forbes, F. W. White, E. H. White, and M. K. Hughes, *J. Clin. Pharmacol.*, **20,** 465 (1980).
(144) O. Kranz, *Drugs in Germany*, **1981,** 81.
(145) P. Schiatti, D. Selva, E. Arrigoni-Martelli, L. J. Lerner, A. Diena, A. Sardi, and G. Maffi, *Arnzeim.-Forsch.*, **24,** 2003 (1974).
(146) J. Knoll, K. Gyires, and A. Mészáros, *Arnzeim.-Forsch.*, **29**(I), 766 (1979).
(147) J. Leeling, B. Phillips, and O. Lorenzetti, *Arnzeim.-Forsch.*, **30**(II), 1109 (1980).
(148) *New Drug Comment.*, **8**(73), 11 (1981).
(149) *New Drug Comment.*, **7**(65), 6 (1980).
(150) K. Kobayashi, S. Chono, and H. Yamada, *Gastroenterol. Jpn.*, **15,** 427 (1980); *Chem. Abstracts*, **94,** 96048m (1981).
(151) P. P. K. Ho, Don N. Benslay, W. B. Lacefield, and W. Pfeider, ACS/CSJ Chem. Cong. (April, Honolulu), MEDI 59 (1979).
(152) *New Drug Comment.*, **8**(76), 6 (1981).
(153) J. van Dijk and J. M. A. Zwagemakers, *J. Med Chem.*, **20,** 1199 (1977).
(154) M. Takaya, M. Sato, K. Terashima, H. Tanizawa, and Y. Maki, *J. Med. Chem.*, **22,** 53 (1979).
(155) *Drugs Future*, **6,** 651 (1981).
(156) *Drugs Future*, **9,** 522 (1980).
(157) T. Y. Shen and C. A. Winter, "Advances in Drug Research," vol. 12, J. Harpern and S. A. B. Simmond, Eds., Academic, New York, N.Y., 178, p. 90.
(158) A. E. Sloboda and A. C. Osterberg, *Inflammation*, **1,** 415 (1976).
(159) A. E. Sloboda, E. L. Tolman, A. C. Osterberg, and J. Panagides, *Arnzeim.-Forsch.*, **30**(I), 716 (1980).
(160) *New Drug Comment.*, **7**(71), 21 (1980).
(161) *New Drug Comment.*, **7**(72), 15 (1980).
(162) R. R. Martel, J. C. Rochefort, J. Klicius, and T. A. Dobson, *Can. J. Physiol. Pharmacol.*, **52,** 669 (1974).
(163) A. C. Goudie, L. M. Gaster, W. A. Lake, C. J. Rose, P. C. Freeman, B. O. Hughes, and D. Miller, *J. Med. Chem.*, **21,** 1260 (1978).
(164) *Drugs Future*, **6,** 35 (1981).
(165) M. W. Whitehouse and K. D. Rainsford, *J. Pharm. Pharmacol.*, **32,** 795 (1980).
(166) K. D. Rainsford, A. Schweitzer, P. Green, M. W. Whitehouse, and K. Brune, *Agents Actions*, **10,** 457 (1980).
(167) G. Y. Paris, D. L. Garmaise, D. G. Cimon, L. Swett, G. W. Carter, and P. Young, *J. Med. Chem.*, **22,** 683 (1979).
(168) G. Y. Paris, D. L. Garmaise, D. G. Cimon, L. Swett, G. W. Carter, and P. Young, *J. Med. Chem.*, **23,** 79 (1980).
(169) G. W. Carter, P. R. Young, L. R. Sweet, and G. Y. Paris, *Agents Actions*, **10,** 240 (1980).
(170) G. Jones, *Chem. Ind.*, **1980,** 452.
(171) R. Kumar and J. D. Billimoria, *J. Pharm. Pharmacol.*, **30,** 754 (1978).
(172) F. Makovec, P. Senin, P. L. Casula, R. R. Vidal y Plana, and A. L. Rovati, *Eur. J. Med. Chem.*, **14,** 447 (1979).
(173) R. R. Vidal y Plana, A. Cifarelli, D. Bizzarri, P. Senin, and F. Makovec, *Arnzeim.-Forsch.*, **29**(II), 1126 (1979).
(174) K.-H. Boltze, O. Brendler, H. Jacobi, W. Opitz, S. Raddatz, P.-R. Seidel, and D. Vollbrecht, *Arnzeim.-Forsch.*, **30**(II) 1314 (1980).
(175) H. von Jacobi, P. Beirer, and H.-D. Dell, *Arnzeim.-Forsch.*, **30**(II), 1326 (1980).
(176) W. von Blumberger, H. Reichziegler, and H. Spechtmeyer, *Arnzeim.- Forsch.*, **30**(II), 1463 (1980).
(177) A. von Heiter, G. Tausch, and R. Erbel, *Arnzeim.-Forsch.*, **30**(II), 1460 (1980).
(178) J. Grimová, L. Fišnerová, Z. Roubal, J. Němec, Z. Tranvská, and O. Němecěk, "Inflammation: Mechanism and Treatment," Proceedings 4th International Meeting, D. A. Willoughby and J. P. Giroud, Eds. University Park Press, Baltimore, Md., 1980, p. 143.
(179) S. Aonuma, Y. Kohama, Y. Komiyama, and S. Fujimoto, *Chem. Pharm. Bull.*, **28,** 1237 (1980).
(180) *New Drug Commun.*, **7**(68), 29 (1980).
(181) A. J. M. Seegers, L. P. Jager, and J. van Norrdwijk, "Advances in Prostaglandin and Thromboxane Research," vol. 8, B. Samuelson, P. W. Ramwell, and R. Paoletti, Eds., Raven, New York, N.Y., 1980, p. 1547.

ACKNOWLEDGMENTS

The writer is very grateful to Dr. K. Freter of Boehringer Ingelheim Ltd. USA for his enlightened guidance and advice as well as for his assistance in reviewing this article.

Application of Dynamic Mechanical Testing to Characterize the Viscoelastic Properties of Powder-Filled Semisolids

GALEN W. RADEBAUGH * and ANTHONY P. SIMONELLI ˣ

Received January 14, 1983, from the *College of Pharmacy and Institute of Materials Science, University of Connecticut, Storrs, CT 06268.* Accepted for publication May 6, 1983. *Present address: McNeil Consumer Products Co., Exploratory Research and Development, Camp Hill Road, Fort Washington, PA 19034.

Abstract □ A nondestructive technique, dynamic mechanical testing, was used to characterize the viscoelastic properties of dispersions of powdered starch in anhydrous lanolin. The elastic shear modulus (G'), viscous shear modulus (G''), and loss tangent (damping; tan δ) were determined as a function of shear frequency, temperature, and the volume fraction of starch. The results of these studies show that constitutive mathematical models, derived to predict the mechanical behavior of solid-filled polymeric materials, can be applied to solid-filled semisolid pharmaceuticals. In particular, the Kerner equation was useful in describing the influence of starch on the G' of the dispersions. Even though the Kerner equation was unable to predict viscoelastic behavior at all shear frequencies, temperatures, and starch volume fractions, it proved beneficial in postulating mechanisms for starch–starch and starch–anhydrous lanolin interactions within the dispersions. In addition, damping was able to differentiate the influence of temperature. Data obtained from three temperature ranges, where anhydrous lanolin exists in three different structural states, shows that the influence of starch on damping is dictated by the structural state of anhydrous lanolin.

Keyphrases □ Dynamic mechanical testing—viscoelastic properties of powder-filled semisolids, starch–anhydrous lanolin model, Kerner equation □ Viscoelasticity—powder-filled semisolids, starch–anhydrous lanolin model, dynamic mechanical testing, Kerner equation □ Kerner equation—dynamic mechanical testing, application to the viscoelasticity of powder-filled semisolids, starch–anhydrous lanolin model

Pharmaceutical and cosmetic products are commonly heterogeneous dispersions of solid particles in liquid or semisolid vehicles. Usually, their rheology is studied with rotational, continuous shear viscometers (1–4). But unfortunately, continuous shear viscometers destroy the microcrystalline or amorphous three-dimensional networks that determine basic rheological properties and introduce the parameter of variation of structure with time. These viscometers are capable of determining the viscosity of Newtonian systems, but they are unable to determine fundamental viscoelastic parameters such as elastic or viscous moduli (5).

Semisolids in particular have been shown to exhibit complex rheological behavior and are generally classified as viscoelastic (6), *i.e.*, they exhibit spontaneously reversible deformation called elasticity and irreversible deformation called flow. To accurately characterize the viscoelasticity of a semisolid, the method of testing must minimize damage to structure that determines rheological properties. One such nondestructive method, dynamic mechanical testing, has been successfully used to characterize the viscoelastic properties of the heterogeneous semisolid anhydrous lanolin as a function of temperature and shear frequency (7, 8).

Because of the extensive use of solids suspended in ointments in the past and present, it would be invaluable to know the effect of suspended particles on the apparent viscoelastic properties of the ointment and to understand the phenomena associated with any observed changes. Despite the obvious importance of this type of information, there has been, up to now, a lack of information in the literature that examines the effects of powdered fillers on the viscoelastic properties of pharmaceutical semisolids.

This study was therefore initiated and showed that powdered fillers can have a significant influence on the viscoelastic properties of pharmaceutical semisolids. Data that relate temperature, shear frequency, and the volume fraction of starch to changes in viscoelastic moduli are presented for dispersions of starch in anhydrous lanolin. In addition, it is shown that mathematical models, which have been successfully used to predict viscoelastic moduli of powder-filled high polymers, can also be applied to powder-filled pharmaceutical semisolids to interpret changes in viscoelastic moduli in terms of interactions between the powder and the surrounding semisolid phase.

BACKGROUND

Unfortunately, the viscoelastic and mechanical properties of powder-filled pharmaceutical semisolids are not well understood, especially when the particles of powder interact among themselves or with the surrounding semisolid. Therefore, it is pertinent to this report that selected literature dealing with the rheological aspects and mechanical properties of suspensions of solid particles in nonaqueous media be reviewed first. In particular, emphasis will be placed on literature that deals with the mechanical properties of suspensions of solid particles in polymeric materials.

The flow behavior of suspensions of rigid particles in liquids is important because most theories of the moduli of composites have their origin in the theory of the viscosity of suspensions. Einstein's equation for the viscosity of a suspension of spherical particles is fundamental to the theory (9, 10):

$$\eta/\eta_1 = 1 + k_e\phi_2 \qquad \text{(Eq. 1)}$$

The apparent viscosity, η, is related to the viscosity of the suspending media, η_1, the Einstein coefficient, k_e, and the volume fraction of the suspended phase, ϕ_2[1]. When $\phi_2 \ll 1$ and the spheres are noninteractive, $k_e = 2.5$. Equation 1 holds only for very dilute suspensions. Attempts to extend the validity of this equation are numerous (11).

One of the most useful extensions is the Mooney equation (12):

$$\ln(\eta/\eta_1) = k_e\phi_2[1/(1 - \phi_2/\phi_m)] \qquad \text{(Eq. 2)}$$

where ϕ_m is the maximum volume fraction that the particles can attain when packed[2]. Equation 2 is a constitutive equation which adequately describes the viscosity of many kinds of suspensions over a wide range of concentrations.

[1] ϕ_2 is equal to the volume occupied by the particles divided by the total volume of the suspension.

[2] ϕ_m is equal to the true volume of the particles divided by the apparent volume occupied by particles.

0022-3549/84/0500-0590$01.00/0
© 1984, American Pharmaceutical Association

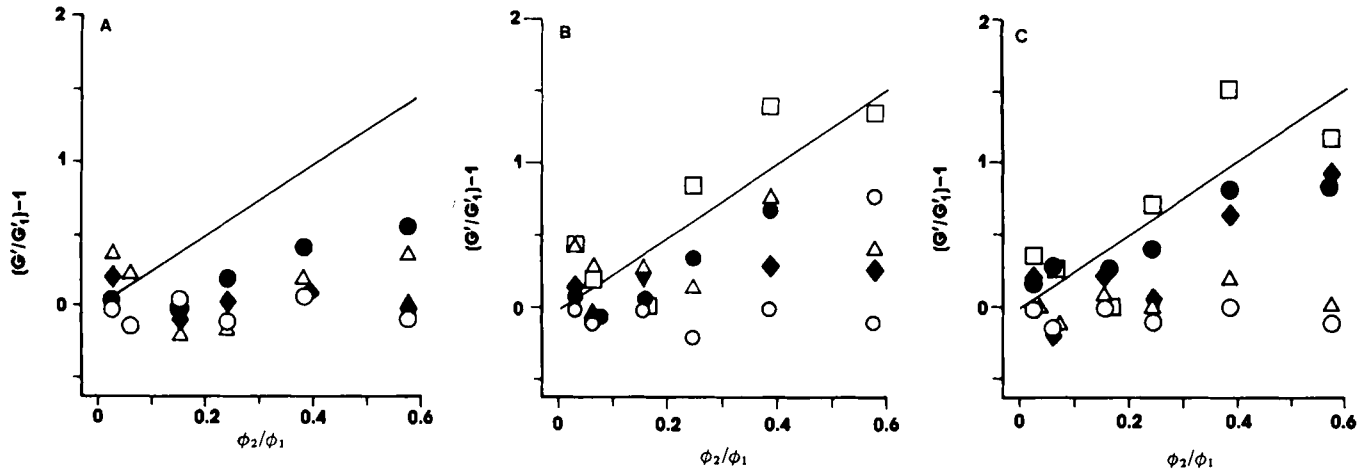

Figure 1—*Effect of the volume fraction of starch on the elastic moduli of starch-filled anhydrous lanolin USP dispersions, plotted on Kerner axes, at 3.54% strain and 0.0464 (A), 0.464 (B), and 4.64 (C) Hz. Key: (○) 0°C; (△) 10°C; (◆) 15°C; (●) 20°C; (—) ideal Kerner equation prediction when $\mu_1 = 0.5$.*

Theoretically, ϕ_m is 0.74 for spheres in hexagonal close packing, but generally the value is much less because of irregularities in particle shape and particle-particle interactions. Viscosity generally increases rapidly with concentration and state of aggregation. The Einstein coefficient has been estimated for shapes other than nonagglomerated spheres, including roughly spherically shaped agglomerates of rigid spheres (13). Irregularities in shape generally increase k_e values.

With high concentrations of particles, suspensions become non-Newtonian and viscosity becomes a function of shear rate, $\dot{\gamma}$. For non-Newtonian suspensions that show a decrease in η with an increase in $\dot{\gamma}$, the Cross equation:

$$\eta = \eta_\infty + (\eta_0 - \eta_\infty)[1/(1 + \Omega\dot{\gamma}m)] \qquad \text{(Eq. 3)}$$

often holds (14, 15). The constants Ω and m depend on the system, while η_0 is the viscosity at zero shear rate and η_∞ is the viscosity at high shear rates. It is generally assumed that the shear rate dependence of viscosity seen in these systems is due to structural changes in the suspension, such as the breaking up of agglomerates by shearing forces. Other shear-dependent theories have been proposed by Krieger and Dougherty (16) and Gillespie (17, 18).

For a given instrument, the theoretical equations for shear viscosity and shear modulus should be of the same form for a given instrument geometry (19, 20). Therefore, shear strain in the modulus equation replaces shear rate in the viscosity equation. For a dispersion of a rigid filler in a viscoelastic matrix phase with a Poisson's ratio[3], μ, equal to 0.5, the relationship between relative viscosities and relative shear moduli can be expressed as:

$$\eta/\eta_1 = G/G_1 \qquad \text{(Eq. 4)}$$

where G is the shear modulus of the disperse system and G_1 is the shear modulus of the unfilled matrix phase. Consequently, the same theory that is used to determine the viscosity of a disperse system can be used to estimate its shear modulus. For example, G/G_1 can be substituted for η/η_1 in Eqs. 1 or 2 to yield corresponding equations for the relative shear modulus. It should be noted that the correlation between the relative viscosities and relative shear moduli expressed by Eq. 4 breaks down when μ is <0.5. Fortunately, a theoretical equation has been developed which compensates for this condition (22). In addition, if the rigidity of the dispersed phase is not much greater than that of the matrix, Eq. 4 is not applicable, as the modulus ratio will be substantially less than the viscosity ratio. Actual moduli, lower than predicted, can occur because (*a*) the Poisson's ratio of the matrix is <0.5, (*b*) thermal stresses reduce the apparent modulus, or (*c*) the modulus of the filler is not significantly greater than the modulus of the matrix. On the other hand, when the matrix is a rigid material, the Mooney equation (Eq. 2) predicts shear moduli which are too high (23).

Another constitutive equation that can be used to predict the modulus of a dispersion is the Kerner equation (24). When the dispersed particles are more rigid than the bulk polymer and deformation occurs by shear, the Kerner equation can be written as:

$$\frac{G}{G_1} = 1 + \frac{15(1 - \mu_1)}{8 - 10\mu_1} \cdot \frac{\phi_2}{\phi_1} \qquad \text{(Eq. 5)}$$

where μ_1 is Poisson's ratio of the bulk phase and ϕ_1, the volume fraction of the bulk phase, equals $(1 - \phi_2)$. This equation assumes the particles dispersed in the bulk polymer phase are spherical and that there is good adhesion between the particles and the bulk polymer. Good adhesion between the dispersed phase and the matrix or bulk phase is assumed to exist if the externally applied stress does not exceed the frictional forces between the phases. In many cases where adhesion is poor, Eq. 5 holds because there is little if any relative motion across the dispersed particle-matrix interface. Viscoelastic response can vary dramatically from the case of perfect adhesion to that of no adhesion. Weak agglomerates which break under applied stress show many of the characteristics of poor adhesion.

According to theory, the elastic modulus of a composite system is independent of the size of the filler particles, but experimental data indicates that there is an inverse proportionality between particle size and modulus (23). When the dispersed phase volume fraction is held constant, an increase in the elastic modulus of the dispersion may be attributed to an increase in total particle surface area when particle size is reduced. As particle size decreases, the tendency for particle agglomeration increases, which causes a corresponding decrease in maximum packing volume and a resultant increase in the elastic modulus.

It has also been demonstrated that the distribution of particle sizes has an effect on the moduli and viscosity of suspensions (25–28). Dispersions of

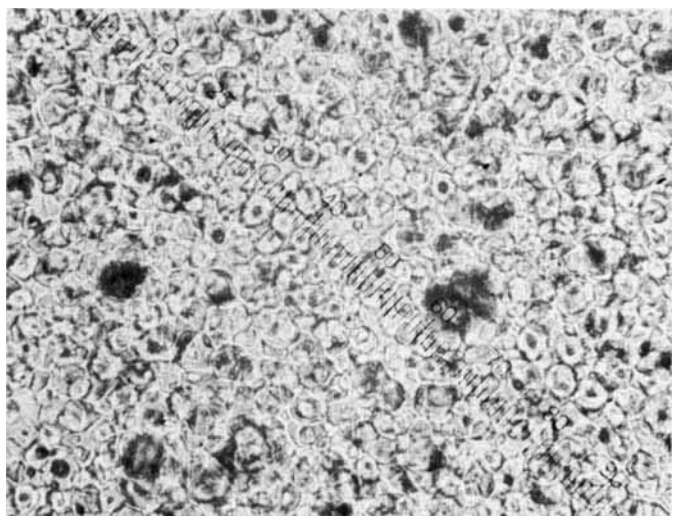

Figure 2—*Photomicrograph of a poured thin film of a starch-filled anhydrous lanolin USP dispersion, $\phi_1 = 0.802$. Original magnification 400×; 1 small division = 3.3 μm.*

[3] Poisson's ratio, μ, is an elastic constant which is defined for small elongations as the decrease in width of the specimen per unit width divided by the increase in length per unit length on the application of a tensile force. It can be shown that the relationship between μ and change in volume of the specimen, ΔV, can be expressed as: $\mu = 0.5 - (\Delta V/2\epsilon V_0)$, where V_0 is the original volume of the specimen and ϵ is the tensile force. When ΔV is sufficiently close to zero, the term $\Delta V/(2\epsilon V_0)$ is insignificant and equals 0.5. This condition holds for materials such as liquids and ideal rubbers. But when ΔV is positive, μ decreases to <0.5; and when ΔV is negative, μ increases to >0.5. Although the equation indicates that μ can be negative when the term $\Delta V/(2\epsilon V_0)$ is >0.5, this does not occur under conditions of small strain testing because ΔV is small compared to V_0 (21).

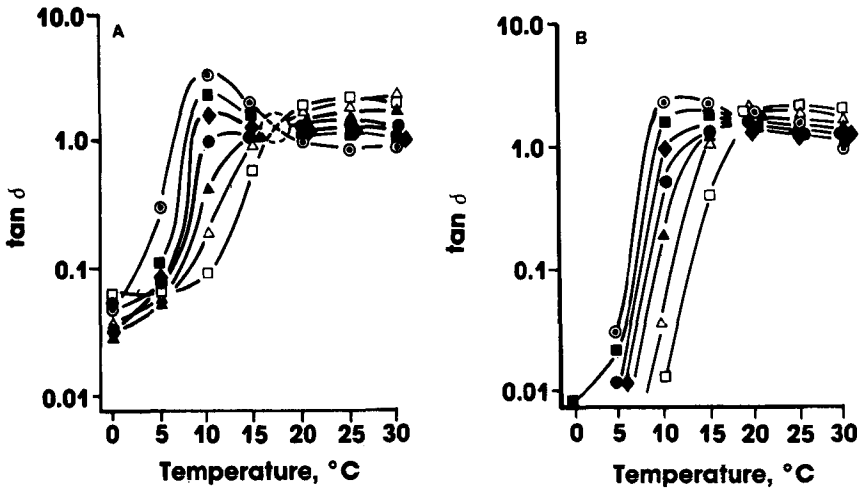

Figure 3—*Effect of temperature on the loss tangent of starch-filled anhydrous lanolin USP, at ϕ_1 equal to 0.802 (A) and 0.586 (B), and 3.54% strain. Key: (⊙) 0.0464 Hz; (■) 0.10 Hz; (◆) 0.215 Hz; (●) 0.464 Hz; (▲) 1.0 Hz, (△) 2.15 Hz; (□) 4.64 Hz.*

various particle sizes can pack more closely than monosized particles. Consequently, there is a larger maximum packing fraction and, hence, a lower modulus at a given concentration of dispersed phase.

In summary, the modulus of the disperse system (or composite) is dependent on the ratio of the moduli of the dispersed phase and matrix phase. The larger the modulus ratio, the greater is the modulus of the disperse system. This is especially true for high concentrations of particles.

EXPERIMENTAL

Materials—Anhydrous lanolin USP from the same production lot was used in all experiments[4]. It is a heterogeneous wax designated by the USP to contain not more than 0.25% water (25), the chemical composition of which has been examined extensively (26, 27). Potato starch[5], USP grade, was used to make the dispersions. When dispersed in anhydrous lanolin, 1 g of starch occupies an ~0.66-mL volume.

Apparatus—The viscoelastic properties of the starch dispersed in anhydrous lanolin were determined with a mechanical spectrometer, equipped with 50-mm cone and plate text fixtures[6]. Samples were oscillated sinusoidally by the output of a digital function generator and phase analyzer[7]. Temperature was controlled by enclosing the mounted sample in an environmental chamber[8]. A functional description of the apparatus, procedures for maintaining sample temperature and calculating the dynamic moduli, and data reproducibility have been previously given (7, 28).

Sample Preparation—Dispersions were prepared in 30-g lots. To prepare the dispersions, the appropriate weighed amounts of anhydrous lanolin and desiccator-dried starch were manually levigated together using a spatula and ointment tile. When the starch particles appeared to be completely coated, the mixture was transferred to a beaker and placed into a water bath at 50°C. After melting, the molten mixtures were gently stirred and placed into a desiccator. The desiccator was then evacuated by a filter pump, which acted to pull entrapped air from the molten mixtures. Deaerated samples were then gently stirred and poured onto the flat test fixture, while preventing air pocket formation. After 30 min at room temperature, the plate was mounted and the cone lowered to the preset gap. The extruded material was removed, and the sample was allowed to equilibrate at the test temperature for 15 min. Dispersions were made that contained the following volume fractions of starch (ϕ_2): 0.0295, 0.0604, 0.126, 0.198, 0.278, 0.366, and 0.414.

Description of Experiments—Samples were tested at 0°C, 5°C, 10°C, 15°C, 20°C, 25°C, and 30°C. At each T, all samples were oscillated over three decades of ν, 0.01–10.0 Hz, at a shear strain (γ) of 3.54%. The γ of 3.54% was the lowest obtainable strain with the equipment used (7). The moduli, G' and G'', and damping, tan δ, are calculated as a function of ν, T, and ϕ_2. In addition, photomicrographs[9] of thin poured films of the dispersions were taken to gain insight into the morphology of the dispersions.

RESULTS AND DISCUSSION

Kerner Equation Predictions—As previously discussed, many empirically derived equations are used to predict the viscoelastic behavior of powder-filled polymeric systems. Most of these equations are similar, but Kerner's equation is most useful (Eq. 5). For dispersions which undergo dynamic mechanical testing, the Kerner equation takes on the form:

$$\frac{G'}{G'_1} = 1 + \frac{15(1-\mu_1)}{8-10\mu_1} \cdot \frac{\phi_2}{\phi_1} \qquad \text{(Eq. 6)}$$

where G' is the elastic modulus of the dispersion, G'_1 is the elastic modulus of the unfilled bulk phase, and ϕ_1 and ϕ_2 are the volume fractions of the bulk phase and filler, respectively. It generally holds when there is adhesion between the phases and the dispersed particles are nearly spherical. If Poisson's ratio, μ_1, equals 0.5, then the slope of the line predicted by a plot of $[(G'/G'_1) - 1]$ *versus* (ϕ_2/ϕ_1) is 2.5.

Deviations from a slope of 2.5 suggest that one or more assumptions on which the equation is based do not hold. For example, slopes of >2.5 could be due to strong interactions between particles, which causes an increase in elastic structure. In contrast, slopes of <2.5 could be caused by slippage at the particle–bulk phase interface, which gives an apparent loss in elastic structure. Other deviations from a slope of 2.5 could be due to irregularities in the shapes of the particles or variations in μ_1.

Experimentally determined elastic moduli, G', of starch-filled anhydrous lanolin dispersions are plotted on Kerner axes for three test frequencies, 0.0464, 0.464, and 4.64 Hz, in Fig. 1. These frequencies are representative of the three decades of shear frequency examined in these experiments. For comparison, a line equal to the "ideal" Kerner equation prediction (slope = 2.5) is presented in each plot.

An examination of the plots shows that at temperatures ≥10°C, an increase in ϕ_2 and ν causes an increase in G', up to a ϕ_2 of ~0.4. The plots also show that the effects of ϕ_2 on G' are enhanced as T and ν increase. An increase in G' occurs with increasing ν because the molecules of anhydrous lanolin do not have time to rearrange themselves within the time frame of straining.

An increase in G' with increasing T can also be explained in terms of particle interaction with anhydrous lanolin. The starch particles tie up anhydrous lanolin molecules by adhesion, thereby providing a more elastic structure. At T = 0°C, G' of the disperse systems do not change with ν and ϕ_2. Each dispersion has the same limiting elastic modulus, G_E, as unfilled anhydrous lanolin. The modulus contribution of the starch to the modulus of the dispersion is apparently shielded by the "frozen" structure of the anhydrous lanolin phase. The shielding action may result from a fluid component of the anhydrous lanolin, or air, adsorbing on the surface of the starch particles.

An increase in G' would also be expected from increasing particle–particle contact. A representative photomicrograph of a starch-filled anhydrous lanolin

Table I—Experimentally Determined Loss Tangents of Unfilled Anhydrous Lanolin USP at 3.54% Strain

Shear Frequency, Hz	$(G''/G')_1$ Unfilled Anhydrous Lanolin[a] 0°C	10°C	20°C
0.0464	0.0478	2.67	0.785
0.100	0.0337	2.20	0.827
0.215	0.0247	1.63	0.884
0.464	0.0220	1.09	0.985
1.00	0.0118	0.613	1.13
2.15	0.0139	0.184	1.32
4.64	0.0101	0.075	1.49

[a] ϕ_1 equals 1.00.

[4] Ruger Chemical Co., Irvington-on-Hudson, N.Y.
[5] J. T. Baker Chemical Co., Phillipsburg, N.J.
[6] Model RMS-7200; Rheometrics, Inc., Union, N.J.
[7] Model SA-2200; Rheometrics, Inc., Union, N.J.
[8] Model EC-1000; Rheometrics, Inc., Union, N.J.
[9] Olympus BH.

Table II—Theoretically Predicted and Experimentally Determined Loss Tangents of Starch-Filled Anhydrous Lanolin USP at 3.54% Strain

Shear Frequency, Hz	$(G''/G')_1 \cdot \phi_1$ Starch-Filled Anhydrous Lanolin[a]					
	0°C		10°C		20°C	
	Theory[b]	Exp.[c]	Theory	Exp.	Theory	Exp.
0.0464	0.0383	0.0448	2.14	3.30	0.630	1.08
0.100	0.0270	0.0399	1.76	2.41	0.663	1.01
0.215	0.0198	0.0348	1.30	1.62	0.709	1.08
0.464	0.0176	0.0540	0.874	0.969	0.790	1.16
1.00	0.00946	0.0310	0.492	0.517	0.906	1.30
2.15	0.0111	0.0358	0.148	0.208	1.05	1.48
4.64	0.00810	0.0559	0.060	0.091	1.19	1.64

[a] ϕ_1 equals 0.802. [b] Calculated using Eq. 7 and data in Table I. [c] Experimentally determined.

dispersion shows a packed network of starch particles (Fig. 2). Two physical mechanisms can be postulated to explain the increase in G' from increasing particle-particle contact. The first is a phenomenon known as bridging. Bridging occurs when the ends of molecules in the disperse phase interact with the surfaces of suspended particles, linking different particles together. As the volume fraction of starch increases, particle density and the probability of particle-particle contact increase. Therefore, it is probable that anhydrous lanolin molecules will bridge more particles, provide more structure, and increase G' because the particles are generally closer to one another. This phenomenon is well illustrated by the interaction of rubber with suspended particles of carbon black (29).

The second mechanism that could cause an increase in G' with increasing particle-particle contact is volumetric dilation. As particle density increases, suspended particles are forced past one another during shear. In the process, there is a dilation in the volume of the dispersion. Resistance to volumetric dilation appears as an increase in G'. The degree of dilation and resultant increase in G' is, therefore, proportional to ϕ_2. This postulate is supported by the Kerner equation (Eq. 6). In this equation, μ_1 compensates for changes in volume of the matrix phase. When there is no change in volume, $\mu_1 = 0.5$, but when volumetric dilation occurs, μ_1 decreases[3]. Therefore, a decrease in μ_1 would be reflected as an increase in G'.

The Kerner equation has proved beneficial for postulating a general mechanism for the influence of starch particles on the elastic modulus of dispersions of starch in anhydrous lanolin, but it must be emphasized that the "ideal" Kerner prediction does not correlate with experimentally determined moduli at all ν and T. As evidenced by Fig. 1, the "ideal" Kerner prediction is approximated only at $\nu \geq 0.464$ Hz and $T = 30$°C. One would intuitively expect ν and T to affect G'/G'_1 because of their demonstrated influence on the viscoelastic properties of anhydrous lanolin. The shapes of the Kerner plots presented in this study may be due to nonlinear viscoelastic behavior. Nonlinear behavior results from testing at strains in excess of that necessary for linear viscoelasticity. The effects of ν and T on G' will subsequently be discussed further in this report. To further study the effects of powdered starch on the viscoelastic properties of anhydrous lanolin, it was decided to examine energy dissipation (7) by measuring damping, tan δ, as a function of volume fraction.

Energy Dissipation Considerations—Like the Kerner equation, the ratio of G'' to G', tan δ, is also an indicator of structural changes. To illustrate, the damping curves for the two volume fractions of starch used in these experiments, 0.198 and 0.414 ($\phi_1 = 0.802$ and 0.586, respectively), are presented in Fig. 3. When the shapes of these curves are compared with those of unfilled anhydrous lanolin in Fig. 4, noticeable differences occur at 0°C, 5°C, 10°C, and 20°C. Essentially, at these temperatures the range of tan δ obtained from 4.64 to 0.464 Hz is narrower for the starch-filled anhydrous lanolin dispersions, which indicates that the internal structure created by the starch tends to dominate the contribution of the anhydrous lanolin.

Changes in the dynamic mechanical properties of polymers as a function of ϕ_2 are often most evident in damping (30). The change in tan δ of solid-filled polymers can be approximated by a volume averaging relation (31, 32):

$$(G''/G') = (G''/G')_1 \cdot \phi_1 + (G''/G')_2 \cdot \phi_2 \qquad \text{(Eq. 7)}$$

where $(G''/G') = \tan \delta$, the damping of the filled polymer; $(G''/G')_1$ and $(G''/G')_2$ are the damping of the pure polymer and pure filler, respectively; and ϕ_1 and ϕ_2 are the volume fractions of the pure polymer and pure filler, respectively. Since the damping of most rigid fillers is very small compared with that of the polymeric bulk phase, the term $(G''/G')_2 \cdot \phi_2$ is almost zero and can be neglected.

Experimentally determined damping values of unfilled anhydrous lanolin, at 0°C, 10°C, and 20°C, are given in Table I. These data represent three temperature ranges where anhydrous lanolin is in three different viscoelastic states (7). The glassy state of anhydrous lanolin is represented by 0°C, while 10°C is within the transition zone from a glassy to a rubbery state, and 20°C is within the region just beyond the transition zone. In Tables II and III, theoretical and experimentally determined damping values of two starch-filled anhydrous lanolin dispersions, $\phi_1 = 0.802$ and 0.586, respectively, are given. The theoretically predicted values were calculated by substituting the values from Table I into Eq. 7.

It is apparent that predicted damping does not equal that determined experimentally. In Table II, where $\phi_1 = 0.802$, it can be seen that the presence of starch increases damping over the temperature range of 0–20°C and over the entire test frequency range. The increases are probably caused by newly introduced damping mechanisms that are not present in anhydrous lanolin alone. The new damping mechanisms may include (*a*) particle-particle friction, where particles touch each other as in weak agglomeration, (*b*) particle-anhydrous lanolin friction, where there is little or no adhesion at the interface, and (*c*) excess damping in anhydrous lanolin near the interface because of induced thermal stresses or changes in anhydrous lanolin molecular conformation. Each of these mechanisms cause the elastic modulus to decrease and the viscous modulus to increase, which both independently give higher damping. An increase in damping indicates that these damping mechanisms cause an increase in energy dissipation during deformation of the dispersion.

In Table III, where $\phi_1 = 0.586$, the presence of starch increases or decreases damping of anhydrous lanolin depending on the temperature. At 0°C, where anhydrous lanolin exists in the glassy state, the experimentally determined damping of this dispersion is lower than that predicted by Eq. 7. At 10°, where anhydrous lanolin is in the transition zone from a glassy to a rubbery state, results are mixed. At low ν, experimental results are higher, while at higher ν experimental results are lower. At 20°C, a temperature just above the transition zone, experimental results are higher at all ν. Damping values lower than those predicted by Eq. 7 can be explained in terms of particle-particle interactions and particle-bulk phase interactions that result in a structure that is not easily deformed or broken by applied stress. These interactions result in increased elasticity and a consequent increase in G'. The viscous modulus, G'', also increases but not as greatly as the rate of increase in G'. Hence, the net result of changes in G' and G'' is a lower tan δ (the ratio of G'' to G').

For dispersions of starch in anhydrous lanolin, it would be appropriate to modify Eq. 7 to the form:

$$(G''/G') = (G''/G')_1 \cdot \phi_1 + (G''/G')_2 \cdot \phi_2 + \text{Interaction Term} \qquad \text{(Eq. 8)}$$

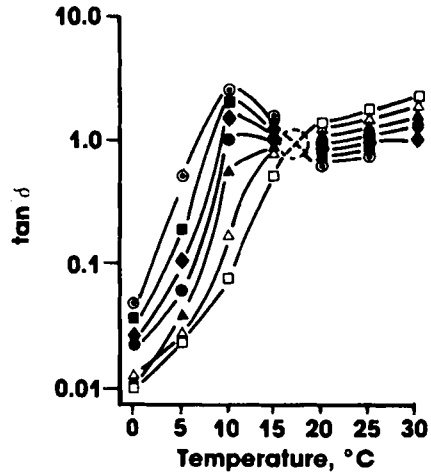

Figure 4—*Effect of temperature on the loss tangent of unfilled anhydrous lanolin USP, at 3.54% strain. Key: (⊙) 0.0464 Hz; (■) 0.10 Hz; (◆) 0.215 Hz; (●) 0.464 Hz; (▲) 1.0 Hz; (△) 2.15 Hz (□) 4.64 Hz.*

Table III—Theoretically Predicted and Experimentally Determined Loss Tangents of Starch-Filled Anhydrous Lanolin USP at 3.54% Strain

Shear Frequency, Hz	$(G''/G')_1 \cdot \phi_1$ Starch-Filled Anhydrous Lanolin[a]					
	0°C		10°C		20°C	
	Theory[b]	Exp.[c]	Theory	Exp.	Theory	Exp.
0.0464	0.0285	0.00681	1.59	2.25	0.468	1.34
0.100	0.0201	0.00797	1.31	1.58	0.493	1.28
0.215	0.0147	0.00677	0.971	0.964	0.527	1.27
0.464	0.0131	0.00294	0.650	0.508	0.587	1.30
1.00	0.00703	0.00498	0.365	0.207	0.673	1.38
2.15	0.00828	0.00288	0.110	0.0370	0.787	1.56
4.64	0.00602	0.00291	0.0447	0.0128	0.888	1.68

[a] ϕ_1 equals 0.586. [b] Calculated using Eq. 7 and data in Table I. [c] Experimentally determined.

where the interaction term accounts for deviations from idealized behavior. The interaction term would be negative when experimentally observed damping is lower than that predicted by Eq. 7. Conversely, the interaction term would be positive when experimentally observed damping is higher than that predicted by Eq. 7.

As previously mentioned, Figs. 3 and 4 illustrate the relationships between tan δ, T, and ϕ_2 for starch-filled and unfilled anhydrous lanolin. A comparison of Fig. 3 to Fig. 4 shows the maxima in the damping curves at the lowest ν all occur at 10°C. Overall, there appears to be no significant difference between Fig. 4 and Fig. 3A. This is a good indication that starch, up to $\phi_2 = 0.198$, does not shift the mechanical transition temperature (analog of T_g) of anhydrous lanolin. There also appears to be no significant shift in the crossover region of the damping curves. But when ϕ_2 reaches 0.414, there is a significant difference in appearance in the damping curves, as evidenced by a comparison of Figs. 4 and 3B. Even though the damping curve generated by a ν of 0.0464 Hz has its maximum at 10°C, its magnitude has been reduced, as is also the case at each ν at ≤10°C. At >10°C, the curves are closer together and most noticeably, the crossover region has shifted from 17°C to ~20°C. These plots suggest that the degree of influence on the transition temperature of anhydrous lanolin is proportional to the volume fraction of starch.

CONCLUSION

Dynamic mechanical testing has been shown to be a sensitive tool to examine the effects of a powdered filler on the viscoelastic properties of a pharmaceutical semisolid. Viscoelastic parameters give insight into fine structural changes of the dispersions that cannot be observed with conventional steady shear rheometers. Even though the widely used Kerner equation was unable to predict the elastic moduli of starch-filled anhydrous lanolin dispersions at all ν, T, and ϕ_2, it did prove useful in postulating mechanisms of interaction between the filler and the bulk phase. One probable reason for the limited applicability of the Kerner equation is the nonlinear viscoelastic effects caused by the introduction of starch into anhydrous lanolin. It must be noted, however, that damping was an effective indicator of the degree of influence starch had on the mechanical transition of anhydrous lanolin from the rubbery state to the glassy state.

APPENDIX: Glossary

G = shear modulus (dyne cm^2 or Pa: N m^2)
G_1 = shear modulus of the unfilled matrix phase
G' = dynamic shear storage modulus (same units as G)
G'' = dynamic shear loss modulus (same units as G)
G_E = limiting value of G'
T = temperature
V_0 = original volume of test specimen
ΔV = change in volume of specimen
T_g = glass transition temperature
k_e = Einstein coefficient
ϵ = tensile force
m = exponent of shear rate in Cross equation
δ = phase angle between stress and strain vectors
γ = strain
$\dot{\gamma}$ = rate of strain
η = shear viscosity (Poise: dyne s cm^{-2} or Pascal seconds: N s m^{-2})
η_0 = shear viscosity at zero shear rate
η_1 = shear viscosity of the suspending media
η_∞ = shear viscosity at very high shear rates
μ = Poisson's ratio (dimensionless)
μ_1 = Poisson's ratio of the bulk phase
ϕ_1 = volume fraction of bulk phase
ϕ_2 = volume fraction of dispersed phase
ϕ_m = volume fraction of maximally packed particles
ν = shear frequency (Hz)
Ω = constant in the Cross equation

REFERENCES

(1) G. W. Scott Blair, *J. Soc. Cosmet. Chem.*, **11**, 181 (1960).
(2) P. Sherman, *J. Soc. Cosmet. Chem.*, **17**, 439 (1966).
(3) M. H. Wohl, *Chem. Eng.*, **75**(7), 99 (1968).
(4) A. N. Martin, G. S. Banker, and A. H. C. Chun, in "Advances in Pharmaceutical Sciences," vol. 1, H. S. Bean, A. H. Beckett, and J. E. Carless, Eds., Academic, New York, N. Y., 1964, pp. 1–85.
(5) S. S. Davis, E. Shotton, and B. Warburton, *J. Pharm. Pharmacol.*, **20**, 157s (1968).
(6) B. W. Barry, in "Advances in Pharmaceutical Sciences," vol. 4, H. S. Bean, A. H. Beckett, and J. E. Carless, Eds., Academic, New York, N.Y., 1974, pp. 1–72.
(7) G. W. Radebaugh and A. P. Simonelli, *J. Pharm. Sci.*, **72**, 415 (1983).
(8) G. W. Radebaugh and A. P. Simonelli, *J. Pharm. Sci.*, **72**, 422 (1983).
(9) A. Einstein, *Ann. Phys. (Paris)*, **19**, 289 (1906).
(10) A. Einstein, *Ann. Phys. (Paris)*, **24**, 591 (1911).
(11) I. R. Rutgers, *Rheol. Acta*, **2**, 305 (1962).
(12) M. Mooney, *J. Colloid Sci.*, **6**, 162 (1951).
(13) T. B. Lewis and L. E. Nielsen, *Trans. Soc. Rheol.*, **12**, 421 (1968).
(14) M. M. Cross, *J. Appl. Polym. Sci.*, **13**, 765 (1969).
(15) M. M. Cross, *J. Colloid Interface Sci.*, **33**, 30 (1970).
(16) I. M. Krieger and T. J. Dougherty, *Trans. Soc. Rheol.*, **3**, 137 (1959).
(17) T. Gillespie, *J. Colloid Interface Sci.*, **22**, 554 (1966).
(18) T. Gillespie, *J. Colloid Interface Sci.*, **22**, 563 (1966).
(19) H. M. Smallwood, *J. Appl. Phys.*, **15**, 758 (1944).
(20) E. Guth, *J. Appl. Phys.*, **16**, 20 (1945).
(21) L. E. Nielsen, "Mechanical Properties of Polymers and Composites," vol. 1, Dekker, New York, N.Y., 1974, pp. 10–11.
(22) L. E. Nielsen, *Compos. Mater.*, **2**, 120 (1968).
(23) T. B. Lewis and L. E. Nielsen, *J. Appl. Polym. Sci.*, **14**, 1449 (1970).
(24) E. H. Kerner, *Proc. Phys. Soc. (London)*, **B69**, 808 (1956).
(25) "United States Pharmacopeia," 20th Rev., U.S. Pharmacopeial Convention, Rockville, Md., 1980.
(26) L. I. Conrad, *Am. Perfum. Essent. Oil Rev.*, **6**, 177 (1954).
(27) G. Barnett, *Drug Cosmet. Ind.*, **80**, 610 (1957).
(28) C. W. Macosko and J. Starita, *SPE Journal*, **27**, 38 (1971).
(29) G. Kraus, *Adv. Polym. Sci.*, **8**, 155 (1971).
(30) F. R. Schwarzl, H. W. Bree, C. J. Nederveen, G. A. Schwippert, C. E. Struik, and C. W. van der Waal, *Rheol. Acta*, **5**(4), 270 (1966).
(31) R. W. Gray and N. G. McCrum, *J. Polym. Sci.*, Part A-2, **7**(8), 1329 (1969).
(32) L. E. Nielsen, *Trans. Soc. Rheol.*, **13**(1), 141 (1969).

ACKNOWLEDGMENTS

Adapted in part from a dissertation submitted by Galen W. Radebaugh to the University of Connecticut in partial fulfillment of the Doctor of Philosophy degree requirements. Partially supported with funds from the Connecticut Research Foundation.

Urinary Excretion of Chlorpheniramine and Its Metabolites in Children

KEITH J. SIMONS *x, F. ESTELLE R. SIMONS ‡, GEORGE H. LUCIUK ‡, and EVELYN M. FRITH‡

Received January 27, 1983, from the *Faculty of Pharmacy, and the ‡Department of Pediatrics, Faculty of Medicine, University of Manitoba, Winnipeg, Manitoba R3T 2N2, Canada. Accepted for publication March 27, 1983.

Abstract □ The pharmacokinetics and urinary excretion of chlorpheniramine were studied in 11 patients, aged 6–16 years, with allergic rhinitis. In these children, chlorpheniramine had a mean elimination half-life of 13.1 ± 6.6 h, a mean clearance rate of 7.23 ± 3.16 mL/min/kg, and a mean apparent volume of distribution of 7.0 ± 2.8 L/kg. Over 48 h, the recovery in urine was as follows: chlorpheniramine, 11.3 ± 6.7%; demethylchlorpheniramine, 23.3 ± 11.1%; and didemethylchlorpheniramine, 9.6 ± 9.4%. Urine flow rate and urine pH were uncontrolled and ranged from 2.2 to 113.3 mL/h and 5.1–7.9, respectively, over the 48-h period. In some children urine flow rate and pH were constant, while in others there was great variability. When drug and metabolite excretion rates *versus* both urine flow rates and pH values were analyzed by multiple linear regression, the results were significantly better ($p \leq 0.05$) than when each factor was analyzed independently. The excretion rate of chlorpheniramine and its two demethylated metabolites decreased as urine pH increased and urine flow rate decreased. This information must be considered in future pharmacokinetic studies of this drug.

Keyphrases □ Chlorpheniramine—demethylated metabolites, urinary excretion in children, pharmacokinetics □ Excretion, urinary—chlorpheniramine and its demethylated metabolites, children, pharmacokinetics □ Pharmacokinetics—urinary excretion of chlorpheniramine and its demethylated metabolites, children

Chlorpheniramine, a histamine H_1 receptor antagonist, has been used for over 30 years in the treatment of allergic rhinitis (1). Recently, the development of sensitive, specific HPLC (2) and GLC-MS (3) assays have facilitated bioavailability (4–6) and pharmacokinetic (7–9) studies with chlorpheniramine. The metabolism of chlorpheniramine has been investigated in dogs (10) and humans (11), and the effect of induced, constant urine pH and flow rate on the rate of excretion of the unchanged drug has been evaluated (12). In recent single- and multiple-dose urinary studies (9, 13, 14), no correlation was determined between uncontrolled urine pH and flow rate and chlorpheniramine excretion. We have recently modified an HPLC assay (2) for chlorpheniramine (I), demethylchlorpheniramine (II), and didemethylchlorpheniramine (III) and have studied the pharmacokinetics and efficacy of chlorpheniramine in children with severe perennial allergic rhinitis (15). In this single-dose study (15), timed urine samples were also collected and the effect of uncontrolled urine pH and flow rate on the excretion of chlorpheniramine and two of its metabolites was evaluated.

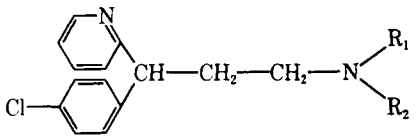

I: $R_1 = R_2 = CH_3$
II: $R_1 = CH_3$, $R_2 = H$
III: $R_1 = R_2 = H$

EXPERIMENTAL

Patients—Chlorpheniramine was given to 11 patients with allergic rhinitis, mean age 11.0 ± 3.0 years and mean weight 39.6 ± 9.2 kg. All patients had received regular chlorpheniramine treatment for at least 6 months during the course of their rhinitis, but no patient had received it within 1 month of study. The protocol for this investigation was approved by the Faculty Committee of the University of Manitoba on the Use of Human Subjects in Research, and signed informed consent was obtained from the parents and the child before the study.

Protocol—Children reported to the Children's Hospital Clinical Investigation Unit at 0800 hours after an overnight fast. They had not received any medications in the preceding 72 h and were examined for nasal symptoms. After placement of an indwelling intravenous needle and withdrawal of 2 mL of blood, each patient received a single 0.12-mg/kg dose of a commercially available chlorpheniramine maleate syrup[1] with 120 mL of water. Uniform meals and snacks were served throughout the study, beginning 2 h after drug ingestion, and standardized activities were provided. Additional blood samples were obtained from the indwelling needle 1, 3, 6, 9, 12, 15, 18, 24, and 30 h after chlorpheniramine ingestion. The serum was separated and frozen at −20°C until the samples were analyzed. Urine samples were collected and pooled every 6 h for up to 48 h. The pooled samples were mixed well and measured; an aliquot was removed and frozen at −20°C until the samples were analyzed. The pH was determined on each aliquot prior to drug analysis.

Liquid Chromatographic Analysis of Chlorpheniramine (I), Demethylchlorpheniramine (II), and Didemethylchlorpheniramine (III)—One milliliter of test serum, urine, or control serum or urine containing standards was transferred into a 16 × 100-mm test tube, and 100 μL of internal standard solution (brompheniramine maleate, 1 μg/mL) was added. To this, 250 μL of 5% KOH and 5 mL of ether were added; the sample was mixed in a vortex mixer for 20 s and centrifuged for 1 min to separate the layers. The ether layer was transferred to a new 16 × 100-mm test tube containing 0.5 mL of 0.5% phosphoric acid, mixed, and centrifuged as before. With the aid of a methanol–dry ice bath, the aqueous layer was frozen and the ether layer discarded. When the aqueous layer was completely thawed the sample was made alkaline with 250 μL of 5% KOH and extracted with 5 mL of ether again as before. The ether layer was transferred to a dry 13 × 100-mm test tube and evaporated at 25°C with the aid of dry nitrogen. The sample was redissolved in 100 μL of mobile phase, and 25–100 μL were injected directly into the HPLC.

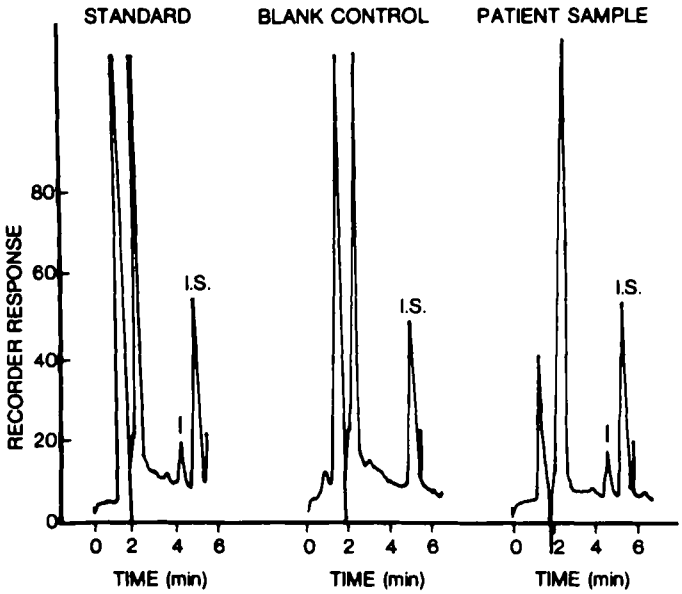

Figure 1—*Chromatograms of chlorpheniramine (I) and the internal standard (IS) in serum.*

[1] Chlortripolon Syrup; Schering Canada, Inc.

0022-3549/84/0500-0595$01.00/0
© 1984, American Pharmaceutical Association

Table I—Serum Chlorpheniramine Levels in Children Following a 0.12-mg/kg Oral Dose of Chlorpheniramine Maleate

Patient	Chlorpheniramine Level, ng/mL									
	0 h	1 h	3 h	6 h	9 h	12 h	15 h	18 h	24 h	30 h
11	5.1	17.7	15.8	13.1	11.9	11.8	9.0	7.4	7.4	—[a]
5	0	8.4	18.5	12.8	9.4	10.0	7.9	9.3	8.9	5.7
1	0.8	5.6	13.5	8.0	5.3	5.5	5.3	3.2	1.9	0
4	0	8.7	10.5	8.1	5.2	4.5	3.1	1.5	1.1	0
7	0	17.1	11.7	8.8	7.4	6.7	3.4	2.4	2.3	1.2
8	0	12.0	12.0	9.6	6.3	—	4.4	—	2.7	1.8
2	0	5.6	14.1	8.2	6.1	5.1	3.5	2.7	1.7	0
9	0	14.5	12.0	13.5	12.1	8.6	6.0	—	7.6	4.5
3	0	8.4	7.8	7.4	5.5	5.9	3.1	2.5	2.3	1.2
10	0	6.1	8.0	6.5	5.9	4.2	4.0	3.5	3.4	2.4
6	0	2.5	9.2	13.9	9.8	10.1	9.8	6.9	6.2	5.6
Mean		9.7	12.1	10.0	7.8	7.2	5.4	4.4	4.1	2.3
±SD		5.0	3.3	2.8	2.7	2.7	2.5	2.8	2.8	2.3

[a] — Sample not collected.

A component HPLC system was used, consisting of an injector, a high-pressure pump, an absorbance detector with a fixed wavelength of 254 nm, and a data module[2]. A 30 × 0.39-cm reverse-phase C_{18} stainless steel column[3] was used. The mobile phase was 25% acetonitrile in 0.075 M phosphate buffer (NaH_2PO_4), pH 2.5 (with H_3PO_4). At a flow rate of 2 mL/min, retention times were: didemethylchlorpheniramine, 2.7 min; demethylchlorpheniramine, 3.2 min; chlorpheniramine, 4.3 min; and internal standard, 5.0 min. With this procedure, drug concentrations as low as 1 ng/mL were measured.

Pharmacokinetic Data—After the initial absorption peak there was a second lower peak on all the serum chlorpheniramine concentration *versus* time plots. There were a limited number of data points, so most of the pharmacokinetic values were determined by model-independent methods (16). It was possible to determine a serum half-life by fitting the terminal linear portion of each curve to

$$C_p = C_p^0 e^{-k_e t} \qquad \text{(Eq. 1)}$$

using the BMDP[4] computer program where C_p is the serum concentration at any time t, C_p^0 is the serum concentration extrapolated to time zero (t^0), and k_e is the first-order elimination rate constant. The elimination half-life ($t_{1/2}$) was then calculated from:

$$t_{1/2} = \frac{\ln 2}{k_e} \qquad \text{(Eq. 2)}$$

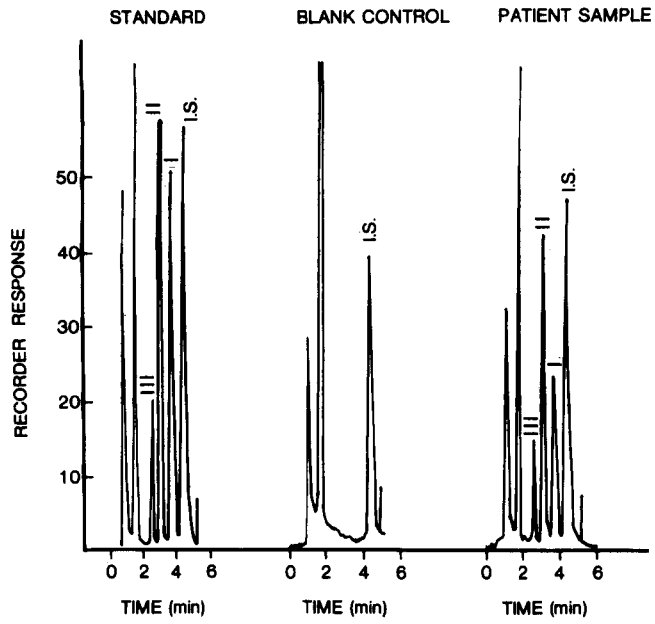

Figure 2—*Chromatograms of chlorpheniramine (I), demethylchlorpheniramine (II), didemethylchlorpheniramine (III), and the internal standard (IS) in urine.*

Total body clearance (CL) was calculated using:

$$CL = \frac{f \cdot \text{Dose}}{\text{AUC}} \qquad \text{(Eq. 3)}$$

where f is the fraction of the dose adsorbed and AUC is the area under the serum chlorpheniramine concentration *versus* time curve, calculated using the trapezoidal rule to time t_n, to which the value C_{p_n}/k was added to extrapolate to infinite time. The apparent volume of distribution (Vd) was calculated using:

$$Vd = \frac{CL}{k_e} \qquad \text{(Eq. 4)}$$

The excretion rate (ER) of chlorpheniramine and its two demethylated metabolites was calculated using:

$$\text{ER} = \frac{dX_u}{dt} \qquad \text{(Eq. 5)}$$

where dX_u was approximated by ΔX_u or the average hourly amount excreted, calculated from each 6-h urine aliquot, and dt or Δt was 1 h. The urine flow rate (UFR) was calculated using:

$$\text{UFR} = \frac{dV_u}{dt} \qquad \text{(Eq. 6)}$$

where V_u was the volume of urine voided in the 6-h period averaged to an hourly rate.

Statistical Analysis—Correlations between urine pH, flow rate, and excretion rate of chlorpheniramine or its two demethylated metabolites were determined using multiple linear regression analyses (17). Results were evaluated using the Student's paired and unpaired t tests (17). All calculations were performed on a programmable calculator[5].

RESULTS AND DISCUSSION

Typical chromatograms of chlorpheniramine (I) in serum are shown in Fig. 1. Chromatograms of I, II, and III in urine are shown in Fig. 2. Calibration curves constructed by plotting the peak height ratio of I from serum to internal standard *versus* I concentration were linear ($r = 1.00$) over the concentration range of 0–30 ng/mL. Compounds I, II, and III extracted from urine also yielded linear calibration curves when the peak height ratio of compound to internal standard was plotted *versus* concentration. The slopes and intercepts of the calibration curves did not vary significantly throughout the period of analysis of all samples from this study. Serum chlorpheniramine concentrations are shown in Table I.

The results of pharmacokinetic studies for each subject are shown in Table II. The mean elimination half-life for I of 13.1 ± 6.6 h obtained in the study (15) was not significantly different ($p = 0.05$) from the mean value of 9.6 ± 3.6 h found in seven children given an intravenous dose of this drug (8). In adults, a wide range of elimination half-life values have been reported following oral (4–6) and intravenous (7, 9) administration. The half-life values in four studies, 20.96 ± 4.94 h (4), 25.1 ± 8.4 h (5), 24.4 ± 6.6 h (7), and 27.9 ± 8.7 h (9), were significantly longer ($p \leq 0.05$) than the values in children. However, half-life values of 17.3 ± 4.4 and 14.6 ± 3.4 h in another study in adults (6) were not significantly different ($p = 0.05$). Since some of the subjects in this latter study were <20 years of age, it is probable that elimination rates for I are age dependent.

[2] U6K injector, 6000A pump, 440 absorbance detector, and a 7000 data module; Waters Associates, Milford, Mass.
[3] μBondapak; Waters Associates, Milford, Mass.
[4] BMDP-77, University of California Press, Berkeley, 1977.
[5] HP-67; Hewlett-Packard, Corvalis, Ore.

Table II—Pharmacokinetic Parameters Calculated for Children Following a 0.12-mg/kg Oral Dose of Chlorpheniramine Maleate

Patient	Sex	Age, year	Weight, kg	k_e, h^{-1}	$t_{1/2}$, h	AUC, ng/mL/h	CL, mL/min/kg	Vd, L/kg	C_{max}, ng/mL	t_{max}, h
11	F	6	29.0	0.04	17.3	432.56	3.62	4.9	17.7	1
5	M	8	40.5	0.04	17.3	430.37	3.26	4.9	18.5	3
1	M	8.5	28.3	0.11	6.3	149.48	10.68	5.8	13.5	3
4	M	9.5	32.9	0.11	6.3	117.15	12.02	6.6	10.5	3
7	F	10	49.5	0.06	11.6	173.34	8.06	8.1	17.1	1
8	M	10	29.5	0.06	11.6	187.94	7.51	7.5	12.0	1
2	M	12.5	39.3	0.09	7.7	145.37	9.63	6.4	14.1	3
9	M	13	38.0	0.09	7.7	303.38	4.64	3.1	14.5	1
3	M	13	54.6	0.06	11.6	141.85	10.07	10.1	8.4	1
10	F	14	44.3	0.03	23.1	211.58	6.63	13.3	8.0	3
6	F	16	50.0	0.03	23.1	414.75	3.39	6.8	13.9	6
Mean		11.0	39.6	0.07	13.1	246.16	7.23	7.0	13.5	2.5
±*SD*		3.0	9.2	0.03	6.6	125.42	3.16	2.8	3.5	1.5

Chlorpheniramine was only administered orally to the children in this study, so it was not possible to calculate the absolute bioavailability. The uncorrected values for clearance and volume of distribution were 7.23 ± 3.16 mL/min/kg and 7.0 ± 2.8 L/kg, respectively. When clearance values were calculated using a fraction of the dose absorbed of 0.6 (9), the mean value (4.32 ± 1.92 mL/min/kg) was not significantly different ($p = 0.05$) from the value of 5.39 ± 1.45 mL/min/kg obtained from a previous study in children (8) in which the dose was given intravenously. It was significantly different ($p \leq 0.05$) from the clearance rate of 7.92 ± 1.81 mL/min/kg found in one other study in adults (7), in which there was wide scatter in the serum chlorpheniramine concentrations *versus* time plots.

Using the same 0.6 fraction of dose absorbed (9), the mean apparent volume of distribution was 4.2 ± 1.6 L/kg. This value was not significantly different ($p = 0.05$) from those of 4.30 ± 1.26 (8) and 3.4 ± 0.3 L/kg (9) obtained in children and adults, respectively, given an intravenous dose of I. The uncorrected volume of distribution value of 7.0 ± 2.8 L/kg obtained in these 11 children was also not significantly different ($p = 0.05$) from uncorrected values of 7.6 ± 2.1 L/kg reported previously in adults (4).

The urinary excretion of I and its metabolism to II and III has been reported (13) and confirmed (11). The recovery of unchanged drug and metabolites in 48-h urine samples is shown in Table III. The urine flow rate, pH, and excretion rate values for I, II, and III for each subject are shown in Table IV. Representative plots of urine flow rate, pH, and excretion rates of chlorpheniramine and its two demethylated metabolites *versus* time are shown in Fig. 3. Urine flow rates and pH were not controlled in this study and ranged from 2.2 to 113.3 mL/h and 5.1–7.9, respectively, over the 48-h study period. In some of the children, urine flow rate and pH were constant (Fig. 3a), while in others they were quite variable (Fig. 3b).

Since urine collection intervals varied from study to study (12–14) it was difficult to compare drug recoveries. In adults, recoveries of unchanged drug in 24-h pooled urine samples were 4.5–11% (12), 5.2% (13), and 5.5–15% (14) as compared with 11.29 ± 6.68% (4.13–25.62%) in 48 h in these children. In adults 10.4% (14) and 13.2% (13) was recovered as demethylchlorpheniramine in 24 h compared with 23.30 ± 11.06% (8.40–45.51%) in 48 h in this study. The didemethylchlorpheniramine accounted for only 3.6% (14) and 5.8% (13) of the dose in adults in 24 h, while 9.60 ± 9.44% (1.20–29.20%) of the dose was recovered in the young patients in 48 h. The results were similar despite the differences in the collection intervals. In the present study, 44.19 ± 19.10% (18.60–73.45%) of the dose was recovered in 48 h. However, since only four subjects had half-life values <8 h and some had half-life values as long as 23 h, it is not valid to assume that the 48-h recovery accounts for all drug and metabolites in urine following this single oral dose. In the four subjects with half-life values <8 h, 48-h urinary recovery ranged from 35.18 to 66.29%. The missing 34–65% of the dose was assumed to be eliminated as unextractable metabolites (14). In the dog, oxidative deamination accounted for a fraction of these metabolites, as 11% was identified as 3-(*p*-chlorobenzyl)-3-(2-pyridyl)propanol and 18% as the corresponding propionic acid (10). These metabolites have not been identified in humans (11).

Table III—Percentage of a 0.12-mg/kg Oral Dose of Chlorpheniramine Maleate Recovered in Urine at 48 h

Patient	Dose,[a] mg	III[b], %	II[c], %	I, %	Dose Recovered in 48 h, %
11	2.45	2.32[d]	45.51[d]	25.62[d]	73.45[d]
5	3.41	1.90	13.16	12.90	28.20
1	2.71	23.29	33.20	9.81	66.29
4	2.78	8.80	22.25	4.13	35.18
7	4.15	29.20	34.13	5.50	68.86
8	2.50	15.20	29.80	14.90	59.84
2	3.30	11.48	20.07	4.63	36.15
9	3.21	1.62	15.82	19.74	37.17
3	4.68	6.05	16.29	7.12	29.46
10	3.73	4.57	17.42	10.88	32.87
6	4.22	1.20	8.40	9.00	18.60
Mean	3.38	9.60	23.30	11.29	44.19
±*SD*	0.75	9.44	11.06	6.68	19.10

[a] As chlorpheniramine (I) free base. [b] Percent of dose recovered as didemethylchlorpheniramine (III), expressed as chlorpheniramine equivalents. [c] Percent of dose recovered as demethylchlorpheniramine (II), expressed as chlorpheniramine equivalents. [d] Control urine from this patient showed traces of chlorpheniramine and metabolites by HPLC and TLC.

The effect of urine pH and flow rate on the excretion of chlorpheniramine and its metabolites has been reported following single- and multiple-dose studies (12–14). When the urine was acidic, significantly more chlorpheniramine was excreted as unchanged drug than when the urine was alkaline (12–14). In addition, although the demethyl metabolite was similarly affected,

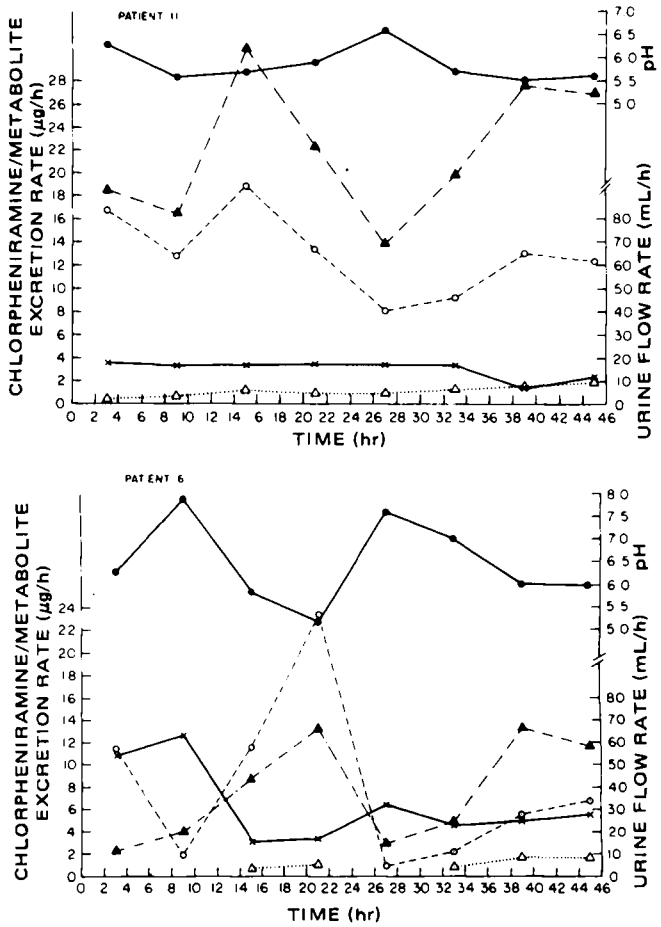

Figure 3—*Urinary excretion rates (μg/h) of chlorpheniramine (⊙), demethylchlorpheniramine (▲), and didemethylchlorpheniramine (△), urine flow rates (mL/h) (×), and urine pH (●) plotted* versus *time in young subjects given 0.12 mg/kg of drug orally.*

Table IV—Urine Flow Rates, pH, and Excretion Rates of Chlorpheniramine (I), Demethylchlorpheniramine (II), and Didemethylchlorpheniramine (III) in 11 Patients Given a 0.12-mg/kg Oral Dose of Chlorpheniramine Maleate

Patient		Time, h							
		6	12	18	24	30	36	42	48
1	Urine flow rate, mL/h	45.0	20.0	8.3	9.2	17.5	13.3	16.7	8.3
	pH	6.5	5.3	5.3	5.5	5.9	5.5	5.5	5.2
	Excretion rate, μg/h								
	I	4.8	15.1	10.0	6.4	1.9	2.5	2.0	1.7
	II	6.9	29.2	21.5	17.8	15.3	17.6	20.9	13.1
	III	4.0	15.5	11.7	10.6	9.1	12.8	18.9	11.5
2	Urine flow rate, mL/h	103.3	50.0	45.8	24.2	57.5	21.3	63.3	40.0
	pH	6.8	6.5	6.5	5.6	6.9	6.7	6.1	5.2
	Excretion rate, μg/h								
	I	10.7	4.0	3.4	3.6	1.1	0.4	1.4	1.0
	II	10.8	18.8	21.2	28.0	8.7	4.4	13.0	18.8
	III	2.8	6.0	8.3	13.5	5.3	4.2	13.6	19.2
3	Urine flow rate, mL/h	113.3	34.2	35.0	33.3	69.2	48.3	60.8	42.5
	pH	5.6	5.3	5.3	5.6	7.3	7.0	6.6	6.0
	Excretion rate, μg/h								
	I	10.6	22.5	12.0	4.8	1.3	1.3	1.2	1.9
	II	8.5	23.5	26.2	22.5	7.6	6.8	12.8	12.9
	III	2.8	3.9	5.9	5.7	3.1	3.8	8.3	8.7
4	Urine flow rate, mL/h	83.3	53.3	35.8	25.0	38.3	35.0	18.3	37.5
	pH	7.2	6.6	6.0	5.7	7.0	6.5	5.8	5.5
	Excretion rate, μg/h								
	I	4.6	3.3	4.8	3.9	—	0.77	0.55	1.3
	II	6.2	12.9	21.9	22.6	6.2	9.2	6.6	12.4
	III	0.0	3.3	5.2	7.3	2.5	4.5	4.1	9.5
5	Urine flow rate, mL/h	52.5	21.6	18.3	22.5	17.5	19.2	14.2	34.2
	pH	6.3	5.6	5.7	6.1	5.7	5.9	5.9	6.0
	Excretion rate, μg/h								
	I	10.2	16.7	13.6	9.3	6.8	5.7	4.1	7.3
	II	2.6	5.7	11.7	9.3	8.2	5.7	7.1	19.8
	III	0.4	0.5	1.0	1.0	1.0	1.3	1.1	3.2
6	Urine flow rate, mL/h	54.2	63.3	15.0	16.7	31.7	23.3	25.0	26.7
	pH	6.3	7.9	5.8	5.2	7.6	7.0	6.0	6.0
	Excretion rate, μg/h								
	I	11.4	1.9	11.5	23.3	0.9	2.2	5.5	6.7
	II	2.3	3.9	8.7	13.2	3.0	4.9	13.3	11.7
	III	0.0	1.6	0.7	1.0	0.2	0.8	1.7	1.7
7	Urine flow rate, mL/h	97.5	35.8	18.3	13.3	113.3	105.3	22.5	42.5
	pH	6.6	7.6	6.2	5.4	7.3	7.0	6.7	6.8
	Excretion rate, μg/h								
	I	7.0	1.7	7.6	8.2	2.7	3.5	2.0	5.7
	II	12.1	11.8	37.2	36.4	22.4	32.0	23.4	48.8
	III	12.2	9.5	31.5	30.1	8.6	22.0	7.8	61.4
8	Urine flow rate, mL/h	71.7	30.8	23.0	29.2	20.0	68.3	18.3	18.3
	pH	6.2	5.2	5.6	5.0	5.2	6.3	5.6	5.1
	Excretion rate, μg/h								
	I	16.3	15.7	5.4	9.8	8.1	3.3	0.9	2.5
	II	13.7	18.0	18.2	21.5	15.0	10.3	12.1	15.4
	III	7.0	7.5	8.2	10.4	6.5	5.5	7.5	10.7
9	Urine flow rate, mL/h	91.7	30.0	14.7	15.0	8.3	35.0	2.2	16.7
	pH	7.3	6.2	5.6	6.0	5.9	7.2	6.6	5.9
	Excretion rate, μg/h								
	I	7.2	21.2	28.6	18.0	4.5	3.9	10.3	11.9
	II	6.3	9.5	14.1	12.0	3.9	6.1	14.5	14.1
	III	2.4	1.1	0.9	0.6	0.3	0.7	0.9	0.8
10	Urine flow rate, mL/h	58.3	29.2	25.0	25.0	33.3	33.3	16.7	18.3
	pH	6.2	6.6	6.0	5.7	6.1	6.6	6.1	5.7
	Excretion rate, μg/h								
	I	17.6	25.1	6.9	7.5	2.6	1.7	2.8	3.4
	II	9.8	8.1	16.4	21.7	11.0	8.8	13.9	13.1
	III	1.2	1.2	2.9	4.8	3.1	3.1	5.4	3.8
11	Urine flow rate, mL/h	18.3	16.7	16.7	17.5	16.7	16.7	6.7	11.7
	pH	6.3	5.6	5.7	5.9	6.6	5.7	5.5	5.6
	Excretion rate, μg/h								
	I	16.8	12.8	18.9	13.4	8.1	9.2	13.0	12.3
	II	18.5	16.5	30.9	22.3	13.9	19.8	27.5	26.9
	III	0.4	0.5	1.2	0.9	0.9	1.3	1.6	1.9

the excretion of the didemethyl metabolite appeared to be minimally affected by pH (14). When urinary pH was maintained in the acidic range, the urinary excretion of unchanged chlorpheniramine was dependent on urine flow rate. This effect can be explained by the theory that the epithelium of the distal convoluted kidney tubules is selectively permeable to the unionized base (12). The effect of urine flow rate on the two demethylated metabolites has not been evaluated to date.

To evaluate the effect of urine flow rate and pH on the excretion rate of I, II, and III, a comparison was made between linear regression analyses of excretion rate *versus* urine flow rate and excretion rate *versus* urine pH and multiple linear regression analysis of excretion rate *versus* both urine flow rate and pH. These calculations were performed on all experimental values and on results obtained after 12 h only. It was assumed that chlorpheniramine absorption would be complete by this time and that a better correlation might be obtained in the postabsorption phase. The correlation coefficients (r) calculated for the single and multiple regression analyses are shown in Table V.

For chlorpheniramine, the mean results obtained from the postabsorption data were virtually identical to the mean results obtained from the total data. The mean correlation coefficient obtained from the multiple linear regression analysis, $r = 0.66 \pm 0.15$, was significantly better ($p \leq 0.05$) than the values obtained from the urine flow rate data, $r = 0.32 \pm 0.21$, and from the urine

Table V—Correlation Coefficients Calculated from Single and Multiple Linear Regression Analysis of Excretion Rate *versus* Urine Flow Rate and Urine pH in 11 Patients Given a 0.12-mg/kg Oral Dose of Chlorpheniramine Maleate

	Chlorpheniramine (I)						Demethylchlorpheniramine (II)						Didemethylchlorpheniramine (III)					
	Multiple Regressions[a]		Urine Flow Rate		Urine pH		Multiple Regressions[a]		Urine Flow Rate		Urine pH		Multiple Regressions[a]		Urine Flow Rate		Urine pH	
Patient	All[b]	>12 h[c]	All	>12 h	All	>12 h	All	>12 h	All	>12 h	All	>12 h	All	>12 h	All	>12 h	All	>12 h
1	0.60	0.66	0.02	0.61	0.27	0.33	0.75	0.24	0.48	0.06	0.11	0.09	0.75	0.89	0.54	0.33	0.73	0.22
2	0.75	0.23	0.75	0.12	0.29	0.22	0.65	0.67	0.05	0.19	0.64	0.19	0.95	1.00	0.37	0.07	0.88	0.96
3	0.75	0.79	0.20	0.65	0.75	0.79	0.93	0.95	0.66	0.76	0.78	0.94	0.43	0.58	0.42	0.26	0.09	0.47
4	0.54	0.26	0.52	0.18	0.36	0.14	0.57	0.53	0.32	0.00	0.56	0.48	0.90	0.94	0.63	0.06	0.90	0.82
5	0.68	0.39	0.43	0.11	0.35	0.07	0.11	0.96	0.11	0.92	0.10	0.08	0.10	0.92	0.06	0.91	0.10	0.38
6	0.85	0.87	0.36	0.77	0.83	0.85	0.80	0.98	0.66	0.43	0.77	0.90	0.11	0.81	0.06	0.06	0.11	0.58
7	0.85	0.83	0.26	0.60	0.83	0.82	0.48	0.39	0.34	0.38	0.47	0.34	0.38	0.32	0.31	0.32	0.34	0.23
8	0.69	0.71	0.38	0.78	0.00	0.49	0.77	0.75	0.44	0.45	0.72	0.73	0.70	0.77	0.53	0.54	0.70	0.77
9	0.70	0.86	0.30	0.35	0.63	0.28	0.46	0.59	0.37	0.13	0.46	0.32	0.98	0.69	0.94	—	0.59	0.06
10	0.53	0.66	0.45	0.20	0.41	0.63	0.81	0.74	0.44	0.39	0.79	0.73	0.79	0.68	0.72	0.68	0.58	0.37
11	0.34	0.58	0.11	0.45	0.21	0.51	0.68	0.82	0.51	0.43	0.24	0.82	0.74	0.82	0.73	0.73	0.52	0.70
Mean	0.66	0.62	0.32	0.34	0.45	0.46	0.64	0.62	0.40	0.48	0.51	0.50	0.69	0.77	0.38	0.39	0.51	0.51
±*SD*	0.15	0.23	0.21	0.27	0.27	0.27	0.23	0.32	0.19	0.28	0.26	0.30	0.24	0.19	0.28	0.29	0.33	0.28

[a] Excretion rate to both urine flow rate and pH. [b] Analysis on all data points. [c] Analysis on data points after 12 h only (assuming oral absorption was complete).

pH data, $r = 0.45 \pm 0.27$. The dependence of chlorpheniramine excretion rate on both urine flow rate and urine pH, even in patients where these parameters were not controlled, was clearly demonstrated.

The results obtained from the regression analysis of the demethylchlorpheniramine data were similar. There was no difference between results obtained from the postabsorption data and the total data. The mean correlation coefficient from the multiple linear regression analysis, $r = 0.64 \pm 0.23$, was significantly better ($p \leq 0.05$) than the value from the urine flow rate data, $r = 0.40 \pm 0.19$, but not significantly improved ($p = 0.05$) from the urine pH data, $r = 0.51 \pm 0.26$. Demethylchlorpheniramine appeared to be more dependent on urine pH than on urine flow rate.

For didemethylchlorpheniramine, the mean correlation coefficient for multiple linear regression analysis from the total data, $r = 0.69 \pm 0.24$, was not significantly improved ($p = 0.05$) from the results obtained for urine flow rate, $r = 0.38 \pm 0.28$, or urine pH, $r = 0.51 \pm 0.33$. However, for the postabsorption phase data, the mean multiple linear regression analysis correlation coefficient, $r = 0.77 \pm 0.19$ was significantly better ($p \leq 0.05$) than that obtained from the urine flow rate data, $r = 0.39 \pm 0.29$, or from the urine pH data, $r = 0.51 \pm 0.28$. Didemethylation is probably a sequential metabolic pathway so this metabolite would be formed from demethylchlorpheniramine and would be dependent on the rate of formation of demethylchlorpheniramine from chlorpheniramine. For this reason, the results from the data after 12 h were more consistent ($r = 0.77 \pm 0.19$) than those obtained from the total data ($r = 0.69 \pm 0.24$). From that time, absorption of chlorpheniramine would probably be complete, and the rate of demethylchlorpheniramine formation would be constant or steadily decreasing as the amount of chlorpheniramine decreased.

These results confirm that the chlorpheniramine excretion rate is dependent on urine flow rate and pH (12–14). Demethylchlorpheniramine appears to be more dependent on urine pH than on urine flow rate, and didemethylchlorpheniramine may also be dependent on both urine flow rate and pH. Since urine pH has been reported to have a minimal effect on didemethylchlorpheniramine excretion (14), further studies are required to confirm these findings.

Currently recommended doses for chlorpheniramine are 4–8 mg four times daily. The results of this study, the long chlorpheniramine half-life values (4–9, 15), and the prolonged biological effects (15) of chlorpheniramine suggest that in current dosage regimens chlorpheniramine may be prescribed more frequently than required to produce beneficial effects while minimizing adverse effects. In patients where urine pH may be chronically elevated and urine flow rate reduced, elimination of both the unchanged chlorpheniramine and its metabolites may be further decreased.

REFERENCES

(1) I. W. Schiller, F. C. Lowell, and W. Franklin, *J. Maine Med. Assoc.*, **42**, 89 (1951).

(2) N. K. Athanikar, G. W. Peng, R. L. Nation, S.-M. Huang, and W. L. Chiou, *J. Chromatogr.*, **162**, 367 (1979).

(3) J. A. Thompson and F. H. Leffert, *J. Pharm. Sci.*, **69**, 707 (1980).

(4) A. Yacobi, R. G. Stoll, G. C. Chao, J. E. Carter, D. M. Baaske, B. L. Kamath, A. H. Amann, and C.-M. Lai, *J. Pharm. Sci.*, **69**, 1077 (1980).

(5) J. J. Vallner, J. A. Kotzan, J. T. Stewart, W. J. Brown, I. L. Honigberg, T. E. Needham, and S. V. Dighe, *Biopharm. Drug Dispos.*, **3**, 95 (1982).

(6) J. A. Kotzan, J. J. Vallner, J. T. Stewart, W. J. Brown, C. T. Viswanathan, T. E. Needham, S. V. Dighe, and R. Malinowski, *J. Pharm. Sci.*, **71**, 919 (1982).

(7) J. J. Vallner, T. E. Needham, W. Chan, and C. T. Viswanathan, *Curr. Ther. Res.*, **26**, 449 (1979).

(8) J. A. Thompson, D. C. Bloedow, and F. H. Leffert, *J. Pharm. Sci.*, **70**, 1284 (1981).

(9) S. M. Huang, N. K. Athanikar, K. Sridhar, Y. C. Huang, and W. L. Chiou, *Eur. J. Clin. Pharmacol.*, **22**, 359 (1982).

(10) J. D. Osterloh, A. Karakaya, and D. E. Carter, *Drug Metab. Dispos.*, **8**, 12 (1980).

(11) E. A. Peets, M. Jackson, and S. Symchowicz, *J. Pharmacol. Exp. Ther.*, **180**, 464 (1972).

(12) A. H. Beckett and G. R. Wilkinson, *J. Pharm. Pharmacol.*, **17**, 256 (1965).

(13) P. Kabasakalian, M. Taggart, and E. Townley, *J. Pharm. Sci.*, **57**, 856 (1968).

(14) C. M. Lai, R. G. Stoll, Z. M. Look, and A. Yacobi, *J. Pharm. Sci.*, **68**, 1243 (1979).

(15) F. E. R. Simons, G. H. Luciuk, and K. J. Simons, *J. Allergy Clin. Immunol.*, **69**, 376 (1982).

(16) M. Gibaldi and D. Perrier, "Pharmacokinetics," Dekker, New York, N.Y., 1975, pp. 2–6, 11–17, 175–176, 243–250.

(17) W. Medenhall, "Introduction to Probability and Statistics," 5th ed., Duxbury Press, N. Scituate, Mass., 1979, pp. 277–300, 326–370.

ACKNOWLEDGMENTS

This project was supported by the Medical Research Council of Canada and Schering Canada, Inc. Dr. F. E. R. Simons is a Queen Elizabeth II Scientist.

The chlorpheniramine maleate, demethylchlorpheniramine, and didemethylchlorpheniramine standards were a gift from Dr. Margaret H. Sherlock, Schering Corporation, Bloomfield, N.J., and the brompheniramine maleate internal standard was a gift from A. H. Robins, Canada Ltd.

Physical Model Approach to Taste Studies of Drugs and Pharmaceutical Formulations

N. F. H. HO

Received January 21, 1982, from the *College of Pharmacy, The University of Michigan, Ann Arbor, MI 48109.* Accepted for publication March 21, 1983. Present address: Pharmacy Research, The Upjohn Co., Kalamazoo, MI 49001.

Abstract □ This paper explores the physical model approach in studying the taste of drugs and assessing physical formulation factors for improving the undesirable taste of drugs. Various aspects of physiology relevant to the taste phenomenon have been reviewed to provide the biophysical basis for mathematical modeling. The model involves non-steady-state mass transport across the aqueous boundary layer and buildup of solute concentration at the essentially impermeable tongue surface. The theoretical predictions are consistent with experimental studies on the lag time to taste perception by the electrophysiological method and also with "instantaneous" psychophysical taste perception when solute concentrations much greater than the taste threshold are applied on the tongue. Within the framework of the non-steady-state model, novel experimental studies involving the use of a porous half-diffusion cell placed on the surface of an extended human tongue and the recording of the times for psychophysical taste response are proposed to quantify and provide mechanistic understanding of the taste of drugs and also physical formulation factors in overcoming undesirable taste properties.

Keyphrases □ Taste perception—drugs and pharmaceutical formulations, physical model approach, non-steady-state mass transport □ Physical model—taste perception, drugs and pharmaceutical formulations, non-steady-state mass transport □ Mass transport—non-steady-state, physical model for taste perception, drugs and pharmaceutical formulations

The taste of drugs and the physical and chemical means to overcome or modify undesirable (usually bitter) taste are continuing and nagging problems for the pharmaceutical scientist. Understanding of structure–taste relationships (*i.e.*, taste quality and intensity) remains qualitative as pointed out by Sinkula (1), who reviewed the state of the science in improving taste properties through structural modification. The physicochemical approaches to masking undesirable taste properties remain largely empirical. The purpose of this paper is (*a*) to review the various aspects of physiology relevant to taste stimulation and (*b*) to explore the physical model approach, both theoretically and experimentally, in studying the taste of drugs and formulation factors affecting taste.

BACKGROUND

A rational approach to the understanding of taste and taste stimulation by drugs, among other important considerations relating to the physicochemical properties of the drug molecule and pharmaceutical formulation, requires some degree of knowledge of the tongue: morphology, ultrastructure, organization and functions of the cells, absorption characteristics, and taste reception.

Loci of Taste Quality—Salty, sour, bitter, and sweet sensations are recognized as the four fundamental qualities of taste. Responses to taste are found everywhere in the mouth, which includes the palate, epiglottis, tongue, and buccal area. It is generally stated in textbooks [*e.g.*, Best and Taylor (2)] that the lowest threshold for bitter is located in the back of the tongue; for salty, at the front; for sweet, on the sides near the front; and for sour, on the sides near the back of the tongue. However, it should not be construed that taste quality is confined to these loci of the tongue. Taste buds are not rigidly specific to any one taste quality, but show multiple sensitivity to taste stimulants. Taste buds appear to be differentially sensitive and may be uniquely distributed (3). A recent systematic study (4) using sodium chloride, sucrose, quinine hydrochloride, urea, and citric acid has improved the understanding of taste recognition and psychophysical intensity responses in humans as a function of locus of stimulation on the tongue and soft palate. Collings (4) found the threshold for bitter to be lower for the front of the tongue and soft palate than for the back of the tongue. The combination of the greater intensity of bitter sensation in the back of the tongue and the low threshold of the soft palate for bitter gave the subjective observation of a strong bitter taste in the back of the mouth. Differential responses to a variety of taste stimulants at specific loci were also reported.

Taste Buds and Cells—Associated with the various loci of taste stimulation on the tongue are four kinds of papillary structures (5): vallate papillae in the back of the tongue; foliate papillae on the sides and near the back; fungiform papillae at the front dorsal surface, tips, and sides; and filiform papillae, which are the prevalent type dispersed throughout the tongue surface. A keratin layer covers the surfaces of the papillae and is interrupted by the pores of the taste buds.

Taste buds are most abundant in the vallate and folliate papillae, served by the IX cranial nerve, and the fungiform papillae, served by the chorda tympani of the VII cranial nerve. The filiform papillae, whose keratinized epithelium ends in tapered points, are devoid of taste buds. With respect to the vallate papillae, which is surrounded by a moat, taste buds are dispersed about the sides of the papillae in the depths of the moat. Taste buds of the foliate (leaf-like) papillae are located on the sides, whereas the buds of the fungiform papillae are found on the flat surface portion.

Taste buds are intermingled with stratified squamous epithelial cells, and both structures rest on a thick layer of connective tissue called the basement membrane (5, 6). The bud reaches from the basement membrane to the epithelial surface and is 70 μm in length and 50 μm in its widest dimension. The pore of the taste bud, from which "taste hairs" of taste cells are extended, is found at the epithelial surface. The pore diameter is ~5 μm and, therefore, would not be a factor in excluding large molecules from penetrating the pore. The bud contains a single pore and a collection of cells. It has been assumed that the bud contains 4–20 taste cells intermingled with the more numerous supporting cells. A study by Murray (7, 8) however, states that the number of cells within a taste bud varies from 30 to 80. The cells are morphologically characterized as types I (60–80%), II (15–30%), III (3–14%), and IV (basal cells, varying from 3 to 5%). With the exception of basal cells, the others (types I, II, and III) are oblong cells which often extend from the basement membrane to the pit of the pore. The so-called "taste hairs" are microvillous structures which are extensions of the plasma membrane of cells. The membrane is thought to be a typical membrane complex, ~80 Å thick in the microvillous region and ~160 Å in the crypts, consisting of proteins, phospholipids, and lipids. The microvilli are 2-μm long and 0.1–0.2-μm wide. All cells in the vicinity of the pore are joined by tight junctions.

The cells in the taste bud are constantly being replaced. The renewal process is modulated by the activity of taste nerves. The interrelationships between cell types are not yet well understood. It is believed that cell types I, II, and III originate from the basal cells and develop into independent cell lines carrying out unique functions in the bud. On the other hand, there is evidence that the different cells may represent various stages in the metamorphosis of a single cell line. The pit of the pore is filled with a dense substance identified as mucopolysaccharides. Histochemical studies have shown the presence of ATPase, nonspecific esterases, and phosphatases in taste buds (7, 9).

Taste Reception—Taste reception appears to be mechanistically a substrate–receptor reaction, nonenzymic in nature, at the microvillous membrane level, whereby local perturbations of the membrane lead to a cascade of electrophysiological and psychophysical events known as taste perception (10–13). It does not depend on the direct interaction of taste stimulants with free nerve endings in the taste bud for the following reasons. First, the numerous nerve fibers in the underlying connective tissue enter the taste bud and continue upward to a level only a few micrometers from, but never in direct contact with, the microvillous membrane and the pit of the pore. Second, nerve fibers are found between cells, but the intercellular spaces are believed to be inaccessible to the molecular diffusion from the outside due to the presence of tight junctions. The nonpenetrability of the epithelium by sodium cyanide and colchicine is claimed to be supportive evidence of the occlusive properties of the tight junctions. Third, many taste stimulants are highly hydrophilic and yet taste is perceived instantaneously.

The sour taste of inorganic and organic acids is due to the dissociated hydrogen ions, the salty taste to the cations and anions of the dissociated salt. Bitter and sweet are found in a variety of chemicals and are not generally at-

0022-3549/84/0500-0600$01.00/0
© 1984, American Pharmaceutical Association

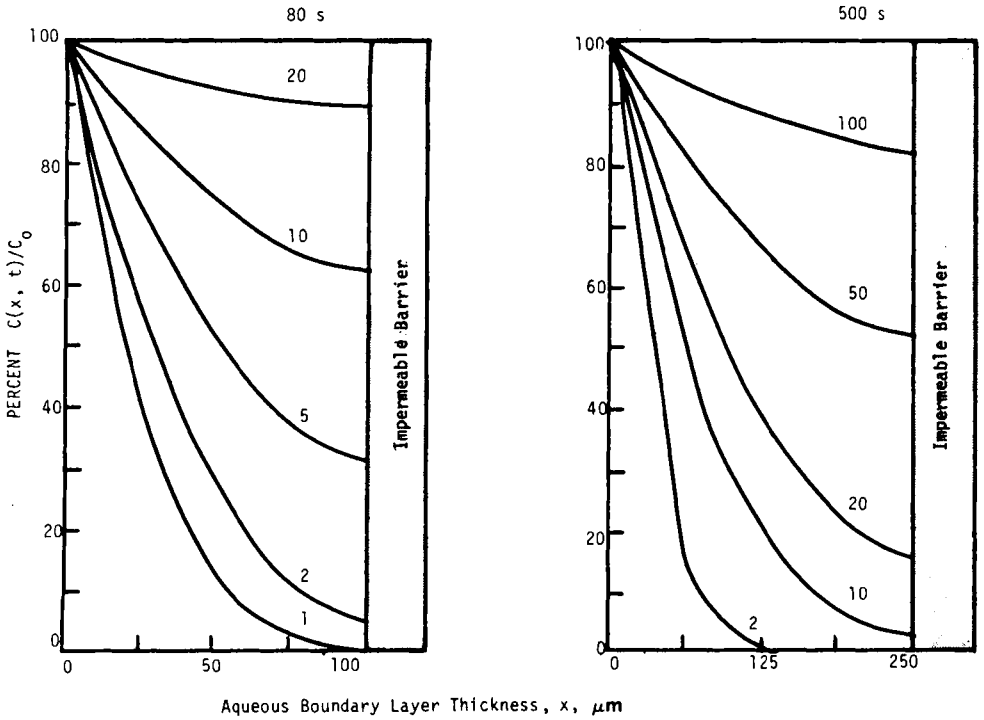

Figure 1—*Percent concentration-distance profile as a function of time for two aqueous boundary thicknesses. Aqueous diffusion coefficient is* 5×10^{-6} *cm²/s.*

tributed to ionic species. Hydrogen bonding is involved at proper geometric sites; often, a small change in configuration will change the sweet taste to bitter and *vice versa*. Beidler and Gross (14) have concluded that each taste cell has many different types of receptor sites and that the number of sites of the same type varies from cell to cell. The Beidler's taste response equation has been applied to all types of taste stimulants with reasonable success:

$$R = \frac{R_m KC}{1 + KC} \qquad \text{(Eq. 1)}$$

where R is the response, R_m is the maximum response, C is the concentration of the stimulus, and K is the binding constant. The binding energy is generally found to be weak, usually a few kilocalories per mole, which supports the reversible nature of taste and the ready removal of stimulants with water and saliva. The taste buds are physiologically rugged to chemical insults, and their sensitivity recovers readily after repeated and long exposures to stimulants.

Permeability of the Tongue—The human tongue appears to be relatively impermeable if the permeability of the rat tongue is a good indicator of the human situation. Mistretta (15) studied the permeability of the rat tongue epithelium in a two-compartment diffusion cell. The surface comprising of fungiform and filiform papillae was highly keratinized. It was estimated that the taste pores (5-μm wide and 1 pore per fungiform papilla) were only 0.0004% of the total surface area. The permeability coefficients of various permeating species are shown in Table I and range from 1.8×10^{-7} to 4.4×10^{-6} cm/s. The progression of the permeability values corresponded roughly with the ether–water partition coefficients. It is conceivable that the tongue, particularly the microvillous membrane of the taste cells, is permeable to more highly lipophilic solutes.

Methods in Studying Taste—Human taste studies are carried out by the psychophysical method. Although the method involves subjective responses on the part of test subjects within well-controlled procedures, it is sensitive and is built around a statistical design to minimize bias and variable responses within and between subjects (3, 16). The electrophysiological method is employed on anesthesized animals, since it involves the surgical implantation of electrodes in the chorda tympani nerve bundle. The response of taste buds is followed by recording neural activity with time (17, 18). The first attempts to record the electrical response in humans undergoing otological surgery under deep anesthesia were made by Diamant *et al.* (19). The electrical taste thresholds of different solutions correlated with subjective values collected from psychophysical experiments.

THEORETICAL

The tongue is a relatively impermeable surface. This important fact provides the rationale for the non-steady-state model for the transport of taste-provoking drugs across the aqueous boundary layer in front of the impermeable tongue surface. In turn, this model lays the foundation for the physical model approach in studying the taste of drugs, and the chemical and physical formulation factors affecting taste, on a quantitative and mechanistically interpretive basis.

Mass transport across the aqueous boundary layer in front of the impermeable tongue surface and the buildup with time of the concentration at the tongue surface are essentially non-steady-state diffusional kinetic situations. The model is consistent with the observation that when taste-provoking molecules in solution are applied to the tongue at concentrations much greater than the taste threshold concentration, taste is detected "instantaneously." Moreover, the model will provide the physicochemical framework in designing novel and remarkably simple experiments in studying (*a*) the taste of drugs and molecular modification effects and (*b*) physical formulation factors on a quantitative mechanistic level.

The non-steady-state change in drug concentration in the aqueous boundary layer with distance x and time t is given by Fick's second law:

$$\frac{\partial C(x,t)}{\partial t} = D\frac{\partial^2 C(x,t)}{\partial x^2} \qquad \text{(Eq. 2)}$$

$$(x > 0 \text{ and } t > 0)$$

The boundary conditions are:

$$C(0,t) = C_0$$

$$C(x,0) = 0$$

$$\left.\frac{\partial C(x,t)}{\partial x}\right|_{x=h} = 0$$

Table I—Permeability Coefficients for Rat Tongue Epithelium [a]

Permeating Species	Permeability Coefficient cm/s × 10^6	Log Partition Coefficient (Ether–Water)
Methanol	4.38	−0.85
Ethyl carbamate	4.15	−0.19
Butanol	3.53	−0.58
Ethanol	3.03	−0.57
Ethylene glycol	2.73	−2.27
Propionamide	2.60	−1.89
Thiourea	1.32	−2.15
Acetamide	1.00	−2.60
Glycerol	0.45	−3.07
Fructose	0.40	—
Sodium butyrate	0.27	—
Glucose	0.18	−5.00
Mannitol	0.18	−5.00

[a] From Ref. 15.

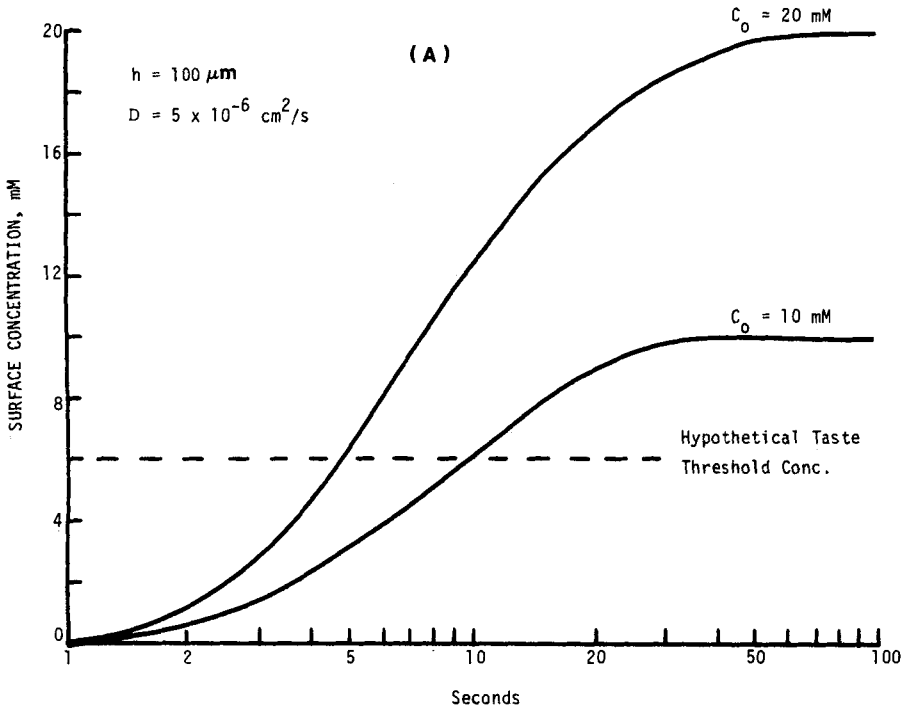

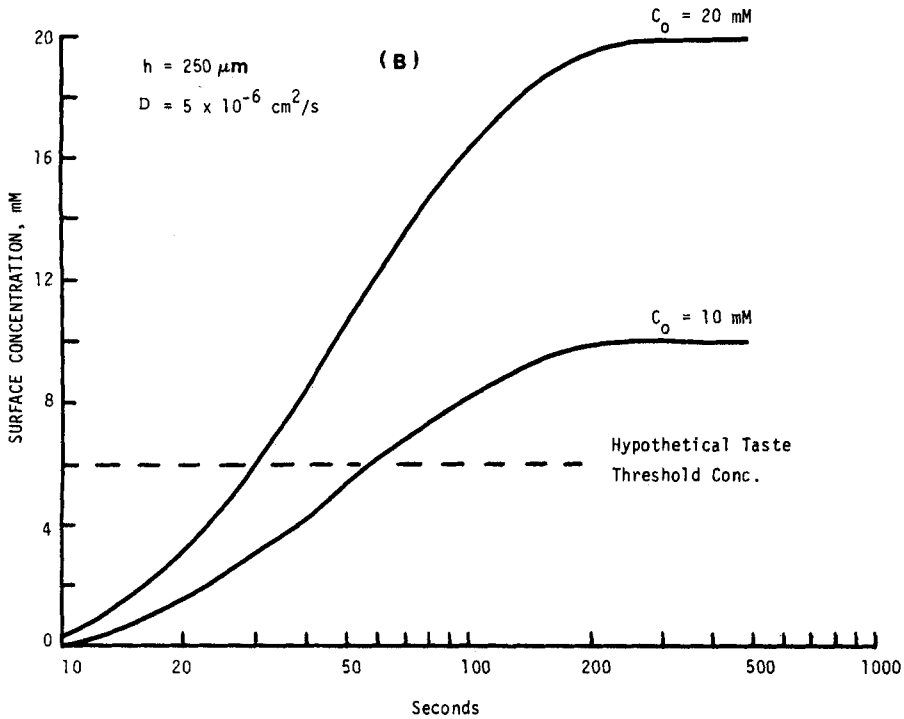

Figure 2—*Surface concentration–distance profiles as a function of time for aqueous boundary layer thicknesses of 100 (A) and 250 μm (B), diffusion coefficient of 5 × 10^{-6} cm^2/s, and bulk aqueous concentrations of 10 and 20 mM.*

The first condition states that the bulk concentration applied on the tongue does not change with time. At time zero, no drug molecules are found within the aqueous layer as described by the second conditions. Because the surface of the tongue is essentially an impermeable barrier, the flux of drug at the membrane surface is effectively zero.

Although the differential equation with its boundary conditions can be readily solved numerically with a computer, one can seek a solution by the Laplace transformation method. It follows that:

$$U(x,s) = C_0 \left[\frac{\cosh (x\sqrt{s/D})}{s} - \frac{\tanh (h\sqrt{s/D}) \cdot \sinh (x\sqrt{s/D})}{s} \right] \quad \text{(Eq. 3)}$$

where $U(x,s)$ is the Laplace transform of $C(x,t)$ and s is a variable of time t. The inverse of the above Laplacian equation is quite complicated. Since one needs only to know the drug concentration at the membrane surface at any time, *i.e.*, $C(h,t)$, with respect to taste response, then Eq. 3 simplifies to:

$$U(h,s) = C_0 \cdot \frac{\operatorname{sech} (h\sqrt{s/D})}{s} \quad \text{(Eq. 4)}$$

In series form:

$$U(h,s) = C_0 \left[2 \sum_{n=0}^{\infty} (-1)^n \cdot \frac{e^{-(2n+1)h\sqrt{s/D}}}{s} \right] \quad \text{(Eq. 5)}$$

whereupon the inverse is:

$$\frac{C(h,t)}{C_0} = 2 \sum_{n=0}^{\infty} (-1)^n \cdot \operatorname{erfc} \left[\frac{(2n+1)h}{2\sqrt{Dt}} \right] \quad \text{(Eq. 6)}$$

As can be seen, the magnitude of the surface concentration at any time t is a fraction of the bulk concentration. After sufficient time, the complementary error function converges to unity so that the surface concentration will finally be equal to the bulk concentration. It is anticipated that whenever

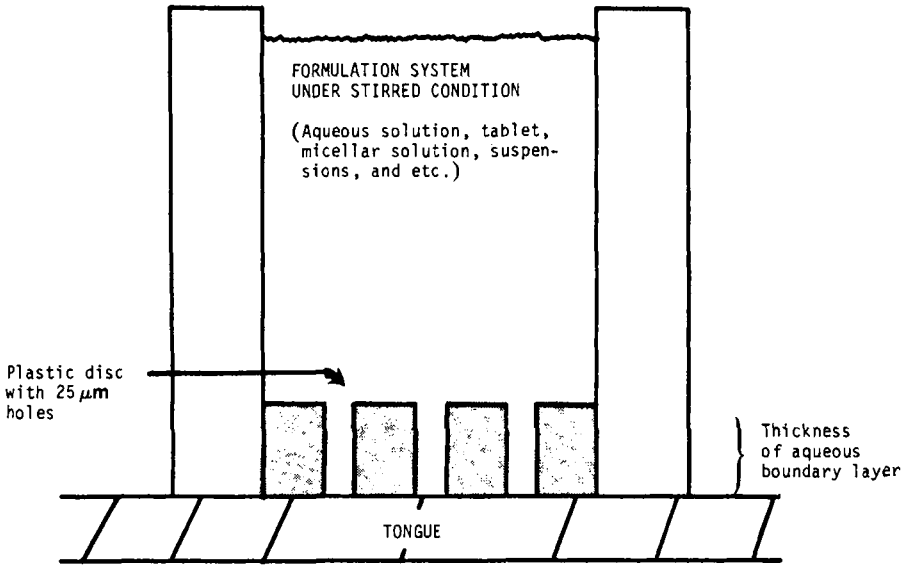

Figure 3—*Schematic diagram of a half-diffusion cell placed over an extended human tongue for psychophysical measurements under non-steady-state transport conditions.*

the concentration buildup at the membrane surface with time equals or exceeds the taste threshold concentration, response to taste occurs. Furthermore, initial taste perception is predicted to occur with high bulk concentrations, C_0, in contrast with lower bulk concentrations, all other factors (diffusion coefficients and aqueous boundary layer thickness) being constant.

DISCUSSION

Figure 1 shows the dimensionless concentration-distance profiles as a function of time for two aqueous boundary layer thicknesses, 100 and 250 μm, as generated from the numerical solution of Eq. 2 and the accompanying boundary conditions. The aqueous diffusion coefficient (D) used was 5×10^{-6} cm^2/s. The influence of the aqueous boundary layer is pronounced. For example, when $h = 100$ μm, the surface concentration is ~0.55% of the bulk concentration within 1 s; in contrast, when $h = 250$ μm, it is only $\sim 4 \times 10^{-6}$% of the bulk concentration. For the 100- and 250-μm boundary layer cases, the surface and bulk concentrations become equal in 80 and 500 s, respectively.

When the non-steady-state surface concentration is plotted against time for various bulk concentrations applied to the tongue, one obtains a family of sigmoidal curves (Fig. 2). Using a hypothetical taste threshold concentration as a point of reference one readily finds interesting relationships between the time at which taste is detected with bulk concentration and aqueous boundary thickness. The higher the bulk concentration, the quicker the detection time for a given diffusion layer thickness. Also, the thinner the diffusion layer, the quicker the detection time for a given bulk concentration. The pattern of the predictions is supportive of the everyday observation that taste is perceived within a fraction of a second after application of taste-provoking solutions at concentrations of at least an order of magnitude larger than the apparent threshold concentration.

In summary, the non-steady-state model provides the basis for the development of a novel experimental design in studying taste problems and for the understanding of the physicochemical factors in overcoming the undesirable taste of drugs *via* pharmaceutical formulations. Figure 3 shows a half-diffusion cell placed over the surface of an extended tongue. The principal feature of the cell is the bottom section which consists of straight cylindrical pores, 50 μm in diameter and of variable length. The pore length fixes the aqueous boundary thickness and may be used to experimentally increase the sensitivity of psychophysical measurements, recorded as the time at which taste is perceived after placing the drug formulation in the previously water-filled pores of the cell. Filling the pores with water before the formulation is placed in the cell fulfills the initial boundary condition for the non-steady-state transport psychophysical taste experiments. It is conceivable that molecular modification and physical formulation factors can be studied within the framework of the proposed experimental design and put on a quantitative and mechanistically interpretive plane. Studies along these lines are being planned.

REFERENCES

(1) A. A. Sinkula, in "Design of Biopharmaceutical Properties Through Prodrugs and Analogs," APhA/APS, Washington, DC, 1977, chap. 15.

(2) C. H. Best and N. B. Taylor, "The Physiological Basis of Medical Practice," Williams and Wilkins, Baltimore, Md., 1973, p. 8.

(3) C. Pfaffmann, L. M. Bartoshuk, and D. H. McBurney, in "Handbook of Sensory Physiology, Vol. IV, Chemical Senses, Part 2, Springer-Verlag, New York, N.Y., 1971, chap 5.

(4) V. B. Collings, *Percept. Psychophys.*, **16,** 169 (1974).

(5) F. H. Netter, "Digestive System, Part I: Upper Digestive Tract," Ciba-Geigy Pharmaceutical Co., Summit, N.J., 1959, p. 10.

(6) A. J. D. deLorenzo, "Olfaction and Taste," MacMillan, New York, N.Y., 1963, p. 5.

(7) R. G. Murray, "Ultrastructure of Sensory Organs," North Holland, Elsiver, N.Y., 1971a, chap. 1.

(8) R. G. Murray, in "Handbook of Sensory Physiology," Vol. IV, Chemical Senses," Part 2, Springer-Verlag, New York, N.Y., 1971, chap. 2.

(9) C. K. L. Lum and R. T. Henkin, *Biochim. Biophys. Acta*, **421,** 362 (1976).

(10) L. M. Beidler, *J. Gen. Physiol.*, **38,** 133 (1954).

(11) L. M. Beidler, "Progress in Biophysics and Biophysical Chemistry," vol. 12, Pergamon, New York, N.Y., 1961, chap. 4.

(12) L. M. Beidler, "Olfaction and Taste II," Pergamon, New York, N.Y., 1967, p. 509.

(13) L. M. Beidler, "Second Symposium on Oral Sensation and Perception," Charles C Thomas, Springfield, Ill., 1970, p. 100.

(14) L. M. Beidler and G. W. Gross, "Contributions to Sensory Physiology," vol. 5, Academic, New York, N.Y., 1971, p. 97.

(15) C. M. Mistretta, *Am. J. Physiol.*, **220,** 1162 (1971).

(16) R. Fischer, "Gustation and Olfaction," Academic, New York, N.Y., 1971, p. 187.

(17) L. M. Beidler, in "Olfaction and Taste," MacMillan, New York, N.Y., 1963, p. 133.

(18) H. T. Andersen, M. Funakoshi, and Y. Zotterman, in "Olfaction and Taste," MacMillan, New York, N.Y., 1963, p. 177.

(19) H. Diamant, M. Funakoshi, L. Strom, and Y. Zotterman, in "Olfaction and Taste," MacMillan, New York, N.Y., 1963, p. 193.

ACKNOWLEDGMENTS

The contribution of Dr. Jeffrey L. Fox, former research scientist at The University of Michigan, College of Pharmacy, for the numerical computation of the non-steady-state transport kinetic equations is gratefully acknowledged. The discussions with Drs. Walter Morozowich and Bradley Anderson of Pharmacy Research, The Upjohn Company were fruitful.

Carboxyl Group Catalysis of Acyl Transfer Reactions in Corticosteroid 17- and 21-Monoesters

B. D. ANDERSON *[x], R. A. CONRADI, and W. J. LAMBERT *

Received August 6, 1982, from *The Upjohn Company, Kalamazoo, MI 49001.* Accepted for publication March 27, 1983. *Present address: College of Pharmacy, University of Utah, Salt Lake City, UT 84112.

Abstract □ Succinate esters, although frequently employed as water-soluble prodrugs of poorly soluble parent drugs, are not sufficiently stable to allow long-term storage in solution. Intramolecular catalysis of ester hydrolysis by the terminal succinate carboxyl group is a contributing factor to this instability. Methylprednisolone 21-succinate has recently been reported to undergo both hydrolysis and 21 ⇄ 17 acyl migration in aqueous solutions. Intramolecular catalysis by the terminal carboxyl group is seen in both reactions, but the catalytic mechanisms are not well understood. While acyl migration can only be catalyzed *via* the carboxyl group acting as a general acid or general base, hydrolysis may undergo either nucleophilic or general acid–base catalysis. To gain further insight into the catalytic mechanism, hydrolysis of methylprednisolone 21-succinate was carried out in aniline buffers to trap any succinic anhydride (as the anilide) that would form if the catalysis were nucleophilic. The nucleophilic mechanism was shown to account for only 15–20% of the overall catalysis. Comparisons of the rates of the intramolecularly catalyzed reactions of methylprednisolone 21- and 17-succinate were made with the same reactions of methylprednisolone 21- and 17-acetate catalyzed intermolecularly by acetate ion. Interestingly, intramolecular catalysis appears to favor acyl migration over hydrolysis. Hence, the hydrolysis of methylprednisolone 21-succinate is faster in basic solutions (pH > 7.4), while acyl migration becomes the dominant reaction in the catalyzed region of the pH profile between pH 3.6 and 7.4. Arguments are presented to account for these differences in catalytic efficiency in terms of the transition-state structures for the two reactions.

Keyphrases □ Acyl transfer reactions—methylprednisolone 17- and 21-monoesters, carboxyl group catalysis □ Methylprednisolone 17- and 21-monoesters—acyl transfer reactions, carboxyl group catalysis □ Carboxyl group catalysis—methylprednisolone 17- and 21-monoesters, acyl transfer reactions

Carboxyl group catalysis of acyl transfer reactions is an important phenomenon in a host of chemical and biological processes involving esters or amides. Many examples of carboxyl groups acting as nucleophilic, general acid, or general base catalysts either inter- or intramolecularly have been cited (for general reviews on the subject: 1–3). Yet, more work is needed since it is still not possible to predict with certainty the extent to which carboxyl groups in the immediate environment will accelerate a given acyl transfer reaction or *via* what mechanism this will occur.

The role of carboxyl catalysis in the degradation of hemiesters of dicarboxylic acids has been of particular interest from a pharmaceutical perspective because hydroxyl-containing drugs having low water solubility are frequently solubilized for parenteral administration by forming their succinate esters. A classic example of the clinical utility of this approach was the development of soluble 21-succinate esters of corticosteroids for parenteral use. A serious drawback of such derivatives is the limited shelf life of their solutions, which is due in part to intramolecular catalysis by the terminal succinate carboxyl group.

In aqueous solution, 21-esters of corticosteroids undergo ester hydrolysis and 21 ⇆ acyl migration as depicted in Scheme I for esters of methylprednisolone (4–6). Garrett recognized in the early 1960's that the solvolysis of the 21-succinate ester of hydrocortisone is catalyzed by the terminal carboxyl group and suggested that intramolecular nucleophilic catalysis is involved (4, 5). Recently, studies of the degradation of methylprednisolone 21-succinate confirmed that hydrolysis is catalyzed intramolecularly and also revealed that 21 ⇄ 17 acyl migration which was found to occur at an initial rate comparable to the hydrolysis rate is also subject to intramolecular catalysis (6).

Shown in Fig. 1 are the pH–rate profiles for the hydrolysis and 21 → 17 acyl migration of methylprednisolone 21-succinate, reported in an earlier study (6). Intramolecular catalysis of hydrolysis is clearly seen as a deviation of the hydrolysis curve from the simple V-shaped profile (dashed line) typically observed for the hydrolysis of esters. Between pH 4.1 and 6.5, the dominant hydrolytic reaction is hydroxide-ion attack on

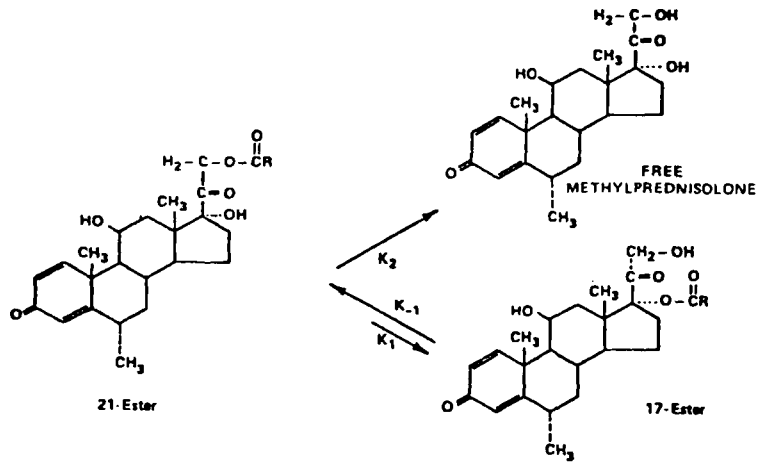

Scheme I—Degradation pathways of 21-esters of methylprednisolone in aqueous solution.

0022-3549/84/0500-0604$01.00/0
© 1984, American Pharmaceutical Association

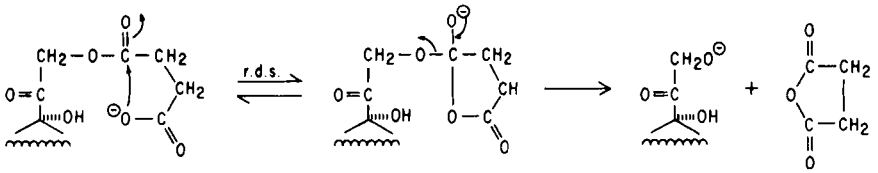

Scheme II—Intramolecular nucleophilic catalysis of 21-ester hydrolysis.

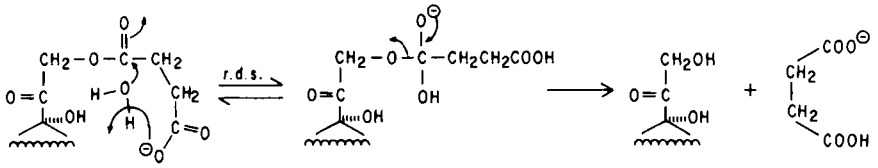

Scheme III—Intramolecular general base catalysis of 21-ester hydrolysis by water.

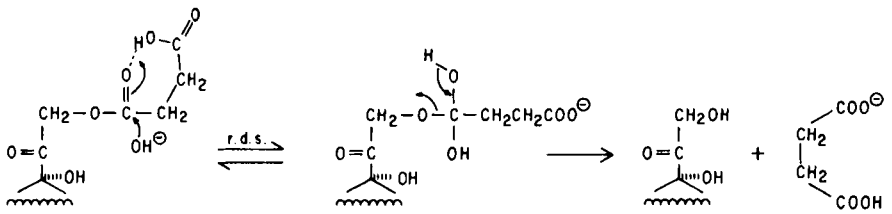

Scheme IV—Intramolecular general acid catalysis of attack by hydroxide ion on the 21-ester.

the ionized ester or the kinetically equivalent water attack on the anion. Mechanistically, the increase in rate over that expected from hydrolysis in more basic solutions can be interpreted as being due to one or more of the following kinetically equivalent reactions: (*a*) intramolecular nucleophilic attack by the terminal carboxylate anion; (*b*) intramolecular general base catalysis of attack by water; (*c*) intramolecular general acid catalysis of attack by hydroxide ion, or (*d*) repulsion of hydroxide ion by the negatively charged carboxylate. Mechanisms *a*–*c* are depicted in Schemes II–IV, respectively.

Intramolecular nucleophilic attack by carboxylate anion (Scheme II) results in the formation of succinic anhydride, which in a subsequent step then hydrolyzes in water to give succinic acid. The other possible mechanisms yield succinic acid directly.

Acyl migration is also catalyzed intramolecularly by the terminal succinate carboxyl group of methylprednisolone 21-succinate (or 17-succinate), as evident in Fig. 1, from the acceleration of the migration rate below pH ~ 7.4 compared with that expected based on the rate in more basic solutions. Two possible mechanisms may account for this acceleration: intramolecular general acid-specific base catalysis, or general base catalysis. Two plausible representations of these catalytic mechanisms are shown in Schemes V and VI, respectively, for the 21 → 17 migration. (These diagrams assume that breakdown of the tetrahedral intermediate is rate determining in going from 21 → 17 and, therefore, formation of the tetrahedral intermediate would be rate determining in going from 17 → 21.)

Since catalysis of acyl migration must occur *via* a general acid–base mechanism, it appeared likely that a general catalytic mechanism may also be operative in the hydrolysis. To ascertain the importance of the intramolecular nucleophilic mechanism in hydrolysis, an attempt was made to trap the succinic anhydride (as succinanilic acid) that would form from the intramolecular nucleophilic attack of carboxylate anion on the ester, by carrying out the hydrolysis in aniline buffers.

Of further interest was the observation that intramolecular catalysis brings about a reversal in the relative rates of the 21 → 17 migration and 21-ester hydrolysis. In solutions of pH > 7.4, hydrolysis is slightly faster than 21 → 17 acyl migration, while acyl migration is dominant in the intramolecularly catalyzed region between pH 3.6–7.4. To understand better the

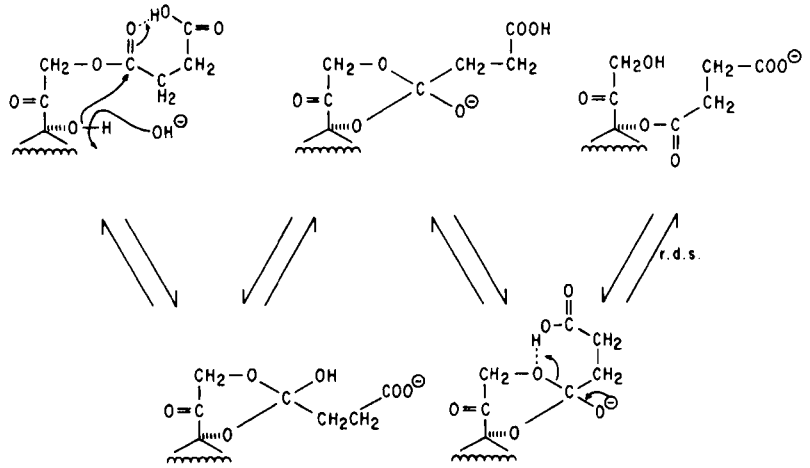

Scheme V—General acid-specific base catalysis of 21 → 17 acyl migration. (Reverse reaction reflects general base catalysis of 17 → 21 acyl migration.)

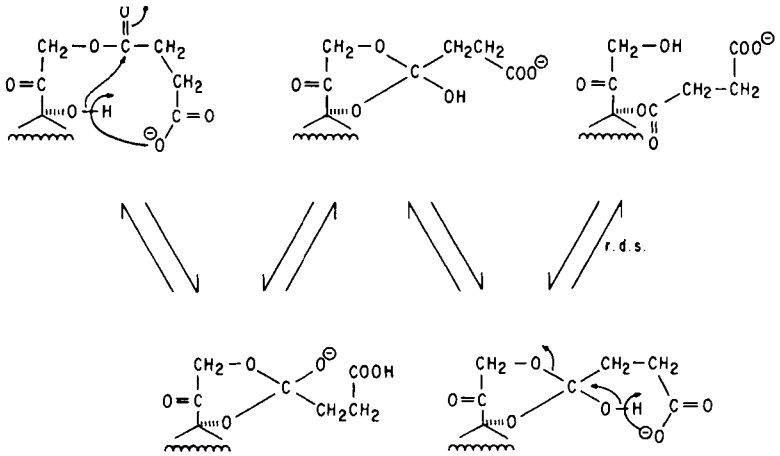

Scheme VI-- General base catalysis of 21 → 17 acyl migration. (Reverse reaction reflects general acid-specific base catalysis of 17 → 21 acyl migration.)

differences in catalysis of these two similar reactions and to generate additional background information on O → O acyl migration in corticosteroid esters, studies of the degradation of methylprednisolone 21- and 17-acetate in water and in acetate buffers were also conducted.

EXPERIMENTAL

Reagents—Methylprednisolone[1], methylprednisolone 21-hemisuccinate[2], and methylprednisolone 21-acetate[3] were commercially available and used without further purification. Methylprednisolone 17-hemisuccinate was reported previously (6).

Methylprednisolone 17-acetate was prepared as described previously (7); UV: λ_{max} 242 nm (ϵ = 14,900); ^{1}H-NMR ($CDCl_3$-DMSO-d_6, 4:1)[4] δ 7.2-7.35 (d, 1, C_1— H), 6.35-6.5 (d, 1, C_2—H), 5.9 (s, 1, C_4—H), 4.4 (br, 1, C_{11}—H), and 4.15 ppm (s, 2, C_{21}—H_2).

Anal.- Calc. for $C_{24}H_{32}O_6$: C, 69.21; H, 7.75. Found: C, 68.84; H, 7.66.

Succinanilic acid was prepared from succinic anhydride and aniline, mp 145.8-146.8°C [lit. (8) mp 150°C].

Anal.—Calc. for $C_{10}H_{11}NO_3$: C, 62.16; H, 5.74; N, 7.25. Found: C, 62.18; H, 5.82; N, 7.27.

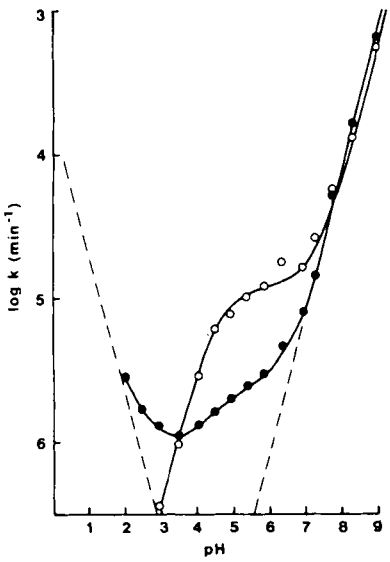

Figure 1—*pH-Log rate profiles for hydrolysis (●) and 21 → 17 acyl migration (○) of the 21-succinate ester of methylprednisolone in aqueous solutions at 25°C.*

All other reagents were of analytical or reagent grade and were used without further purification, except for aniline which was redistilled before use.

Procedure for the Anilide Trapping Experiment—Solutions of methylprednisolone 21-succinate were prepared at a concentration of 5×10^{-4} M in aqueous aniline buffers varying from 4×10^{-4} to 0.04 M aniline with pH values of 5.0, 5.5, and 6.0. At these pH values the intramolecularly catalyzed reaction dominates in the hydrolysis.

The initial rates of formation of methylprednisolone and succinanilic acid were determined at 25°C by measuring the solution concentrations of these reaction products at various times by HPLC. The solutions were monitored until ~1% of the ester had hydrolyzed to methylprednisolone. For the HPLC analysis a 25 cm × 4.6 mm i.d. reverse-phase column[5] packed with 10-μm Lichrosorb RP-8[6] was utilized with a mobile phase consisting of methanol-water-dimethyloctylamine (50:50:0.3) and 0.02 M MES buffer adjusted to pH 5.8. The solvent was pumped[7] at a flow rate of 1.3 mL/min, with sample detection at 254 nm[8].

Methylprednisolone 21- and 17-Acetate Hydrolysis, Acyl Migration Kinetics, and Acetate Buffer Catalysis Studies—Stock solutions of methylprednisolone 17- and 21-acetate in dimethylformamide were diluted 100-fold into aqueous buffers to a concentration of 2.5×10^{-5} M. These solutions were reacted at 25°C during the study. The initial rates of formation of decomposition products were determined by HPLC analysis using one of the following systems.

1. For the degradation of the 21-acetate, a reverse-phase column packed with 5-μm Spheri-5 RP-18[9] was used with a methanol-water (57:43) mobile phase. The flow rate was 1.6 mL/min[10], detection was at 243 nm[11], and the injection size was 500 μL[12].

2. The 17-acetate decomposition kinetics were monitored using conditions similar to those above, but with a mobile phase consisting of methanol-acetonitrile-water (10:32:58).

For comparison with data reported previously for the 21-succinate, the hydrolysis of methylprednisolone 21-acetate was carried out in 0.01 M ionic strength buffers. The studies of catalysis by acetate buffer were carried out

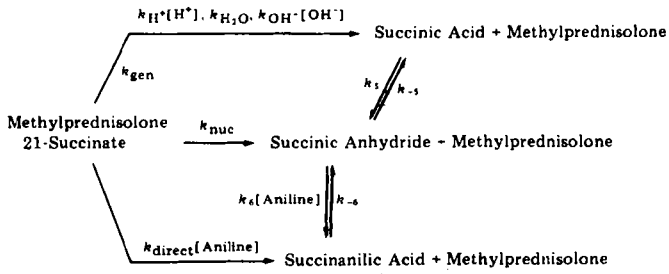

Scheme VII—Possible reactions of methylprednisolone 21-succinate in aniline buffers.

[1] Medrol; The Upjohn Co., Kalamazoo, Mich.
[2] Solu-Medrol (methylprednisolone sodium succinate); The Upjohn Co.
[3] Depo-Medrol, The Upjohn Co.
[4] Unisol-*d*; Norell, Inc., Landisville, N.J.
[5] Altex Scientific, Berkeley, Calif.
[6] E. Merck, Dermstadt, West Germany.
[7] Milton Roy Mini-Pump; Laboratory Data Control, Riviera Beach, Fla.
[8] Model 840000-901; DuPont.
[9] MPLC 10-cm column + 3-cm guard column; Brownlee Laboratories, Berkeley, Calif.
[10] Model 110A pump; Altex Scientific, Berkeley, Calif.
[11] Altex/Hitachi model 153-00; Altex Scientific, Berkeley, Calif.
[12] Wisp model 710A; Waters Associates, Milford, Mass.

Table I—Values of Rate Constants for Methylprednisolone 21-Succinate Hydrolysis and Succinanilic Acid Formation in Aniline Buffers at 25°C

Parameter	Value	95% Confidence Limit
k_{H^+}[a]	0.012 L/mol	±60%
k_{H_2O}[a]	6×10^{-5} h^{-1}	±34%
k_{cat}[a]	1.5×10^{-4} h^{-1}	±24%
k_{OH^-}[a]	4.4×10^3 L/mol-h	±19%
k_{direct}	Indeterminate[c]	—
k_{nuc}	2.28×10^{-5} h^{-1}	±13%
k_{gen}	1.3×10^{-4} h^{-1}	±30%
k_6[b]	3.6×10^4 L/mol-h	—
k_{-5}[b]	9 h^{-1}	—

[a] From Ref. 6. [b] From Ref. 9. [c] Not significantly different from zero.

in buffers containing 0.05–0.5 M total acetate adjusted to 0.5 ionic strength with NaCl.

RESULTS

Hydrolysis of Methylprednisolone 21-Succinate in Aniline Buffers— In water, methylprednisolone 21-succinate hydrolyzes *via* several kinetically distinguishable routes (6) as expressed by the following equation for the overall hydrolysis rate constant, k_{hyd}:

$$k_{hyd} = k_{H^+}[H^+]f_u + k_{H_2O} \cdot f_u + k_{cat} \cdot f_i + k_{OH^-}[OH^-]f_i \quad \text{(Eq. 1)}$$

where k_{H^+} and k_{H_2O} represent hydrogen ion and water catalysis of the degradation of the un-ionized fraction, f_u, and k_{cat} and k_{OH^-} represent water- and hydroxide-ion catalyzed breakdown of the ionized fraction, f_i.

The catalyzed region clearly evident in the plot of the logarithm of the hydrolysis rate constant for methylprednisolone 21-succinate *versus* pH in Fig. 1 between pH 4.1–6.5 is the region in which the k_{cat} term in Eq. 1 dominates. This term may represent (*a*) intramolecular nucleophilic attack by the terminal carboxylate anion on the ester linkage, as proposed by Garrett (4) (Scheme II); (*b*) intramolecular general base catalysis of attack by water (Scheme III) or its kinetic equivalent, intramolecular general acid catalysis of hydroxide ion attack (Scheme IV); or (*c*) a composite of all possibilities as expressed by:

$$k_{cat} = k_{nuc} + k_{gen} \quad \text{(Eq. 2)}$$

While they are kinetically indistinguishable, k_{nuc} (representing nucleophilic catalysis) can be differentiated from k_{gen} (representing general acid–base catalysis) since succinic anhydride would be formed as an intermediate in the nucleophilic mechanism and should be detectable by trapping with aniline as demonstrated by Higuchi *et al.* (9). In aniline buffer systems, the reactions shown in Scheme VII are envisioned.

In addition to hydrolysis by water as expressed by k_{hyd} (see Eq. 1), methylprednisolone 21-succinate may also undergo nucleophilic attack by aniline in aniline buffers, so the rate of methylprednisolone (MP) formation is expressed by:

$$\frac{d(MP)}{dt} = k_{hyd}[Ester] + k_{direct}[Free\ Aniline][Ester] \quad \text{(Eq. 3)}$$

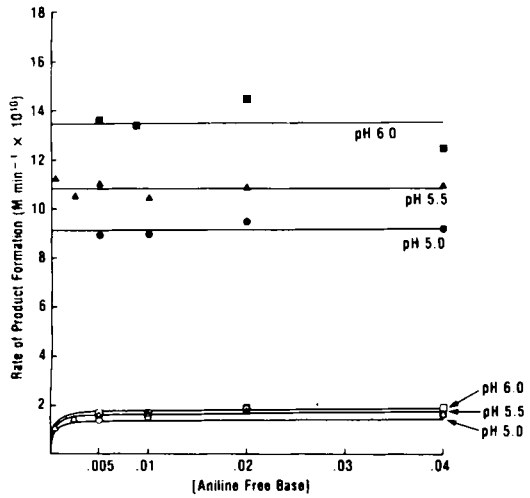

Figure 2—*Plots of the initial rates of methylprednisolone (closed symbols) and succinanilic acid (open symbols) formation* versus *aniline concentration at pH 5.0, 5.5, and 6.0: ester concentration = 5×10^{-4} M; temperature = 25°C.*

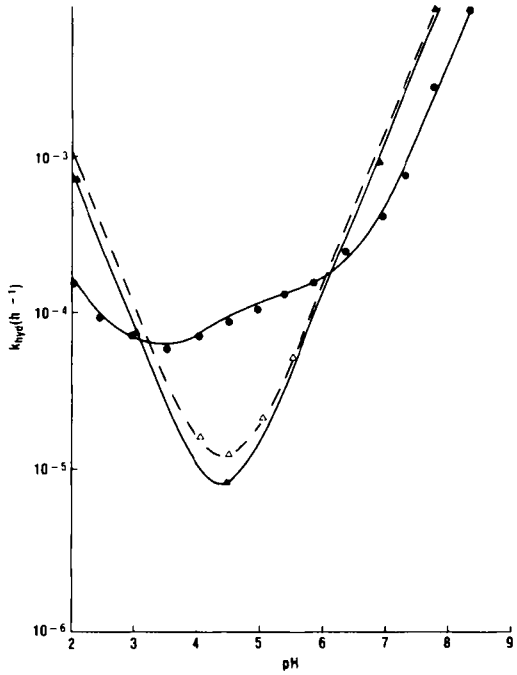

Figure 3—*pH- Hydrolysis rate profiles for methyprednisolone 21-succinate and 21-acetate at 25°C. Key: (●) 21-succinate, μ = 0.01; (▲) 21-acetate, μ = 0.01; (△) 21-acetate, μ = 0.5.*

Succinanilic acid, the product of the reaction of aniline with any succinic anhydride formed as a result of the intramolecular attack by the succinate carboxyl group on the ester linkage, could also be formed from direct attack of aniline on the ester. The rate of formation of succinanilic acid is therefore given by:

$$\frac{d[Anilide]}{dt} = k_{direct}[Free\ Aniline][Ester] + k_6[Free\ Aniline][Anhydride] - k_{-6}[Anhydride] \quad \text{(Eq. 4)}$$

The formation of succinic anhydride, the intermediate of interest, can be expressed by:

$$\frac{d[Anhydride]}{dt} = k_{nuc} \cdot f_i[Ester] - k_6[Free\ Aniline][Anhydride] - k_{-5}[Anhydride] + k_{-6}[Anilide] \quad \text{(Eq. 5)}$$

The rate of direct formation of succinic anhydride from succinic acid was calculated from literature data (9) to be very small relative to the other terms in Eq. 5 and was therefore disregarded. This was also verified experimentally by monitoring anilide formation in a solution containing 5×10^{-6} M succinic acid (equivalent to the amount formed from 1% hydrolysis of a 5×10^{-4} M solution of methylprednisolone 21-succinate) in 0.01 M aniline buffer at pH 5.5. No succinanilic acid could be detected over a 47-h period.

Assuming that the concentration of succinic anhydride would rapidly reach a low steady-state level, i.e., $d[Anhydride]/dt = 0$, this concentration can be expressed as follows:

$$[Anhydride] = \frac{k_{nuc} \cdot f_i \cdot [Ester] + k_{-6}[Anilide]}{k_6[Free\ Aniline] + k_{-5}} \quad \text{(Eq. 6)}$$

Table II—Methylprednisolone 21-Acetate Hydrolysis Rate Constants[a]

Rate Constant	Ionic Strength	Value	95% Confidence Limit
k_{H^+}	0.5 M	0.114 L/mol·h	±38%
k_{H_2O}	0.5 M	4.8×10^{-6} h^{-1}	±66%
k_{OH^-}	0.5 M	1.65×10^4 L/mol·h	±16%
k_{ga} (Acetate)	0.5 M	2.7×10^{-5} L/mol·h	±13%
k_{gb} (Acetate)	0.5 M	1.17×10^{-4} L/mol·h	±8%
k_{H^+}	0.01 M	8.5×10^{-2} L/mol·h	±82%
k_{H_2O}	0.01 M	1.9×10^{-6} h^{-1}	± >100%
k_{OH^-}	0.01 M	1.45×10^4 L/mol·h	±80%

[a] See Eq. 8.

Table III—Migration Rate Constants for Methylprednisolone Esters at 25°C [a]

Ester	Reaction	Rate Constant	Value	95% Confidence Limit
Succinate	21 → 17	k_{OH^-}	3.5×10^3 L/mol·h	±27%
		k_{cat}	7.3×10^{-4} h^{-1}	±26%
	17 → 21	k_{OH^-}	1.74×10^4 L/mol·h	±34%
		k_{cat}	3.0×10^{-3} h^{-1}	±17%
Acetate	21 → 17	k_{H^+}	–	–
		k_{H_2O}	3.9×10^{-6} h^{-1}	±22%
		k_{OH^-}	2.5×10^4 L/mol·h	±10%
		k_{ga}	1.1×10^{-5} L/mol·h	±33%
		k_{gb}	1.0×10^{-4} L/mol·h	±10%
	17 → 21	k_{H^+}	5.8×10^{-3} L/mol·h	±19%
		k_{H_2O}	3.1×10^{-5} L/h	±12%
		k_{OH^-}	3.1×10^5 L/mol·h	±13%
		k_{ga}	9.7×10^{-5} L/mol·h	±78%
		k_{gb}	1.4×10^{-3} L/mol·h	±15%

[a] See Eqs. 10 and 11.

Substituting the anhydride concentration from Eq. 6 into Eq. 4 gives, for the rate of anilide formation:

$$\frac{d[\text{Anilide}]}{dt} = k_{\text{direct}}[\text{Free Aniline}][\text{Ester}] + \frac{k_6[\text{Free Aniline}](k_{\text{nuc}}f_i[\text{Ester}] + k_{-6}[\text{Anilide}])}{k_6[\text{Free Aniline}] + k_{-5}} - k_{-6}[\text{Anilide}] \quad \text{(Eq. 7)}$$

Note in Eq. 7 that when k_6 [Free Aniline] is large relative to k_{-5}, the succinic anhydride hydrolysis rate constant, a plot of the initial rate of anilide formation *versus* free aniline concentration at constant ester concentration should be linear, with a slope equal to k_{direct} [Ester] and intercept of $k_{\text{nuc}}f_i$ [Ester]. Higuchi *et al.* (9) give rate constants for k_6 and k_{-5} of 10 L/mol·s and 2.5×10^{-3} s^{-1}, respectively. Therefore, k_6 [Free Aniline] $\gg k_{-5}$ (by 20-fold) when the free aniline concentration is ≥0.005 M. Similarly, plots of the initial rate of methylprednisolone formation *versus* free aniline (Eq. 3) should be linear with the same slope (in the absence of general catalysis by aniline), but with an intercept equal to the total hydrolysis rate in pure water, k_{hyd} [Ester].

Plots of the initial rates of methylprednisolone and succinanilic acid formation *versus* aniline concentration are shown in Fig. 2 at three pH values. The solid lines in Fig. 2 are the theoretical plots representing the rate constants in Eqs. 3 and 7 as reported in Table I.

The data clearly show that nucleophilic catalysis of the hydrolysis does occur as indicated by the level of significance of k_{nuc} in Table I and the positive intercept for the rate of anilide formation in Fig. 2. From the ratio of intercepts (anilide formation/methylprednisolone formation rates) one can obtain the percentage of the overall reaction which is catalyzed *via* the nucleophilic mechanism. These ratios are 0.12, 0.16, and 0.14 at pH 5.0, 5.5, and 6.0, respectively. Since k_{cat} accounts for 85, 88, and 76% of the total hydrolysis at these pH values, based on Eq. 1 and the rate constants in Table I, general catalysis must account for 62–73% of the total. Therefore, both general catalysis and nucleophilic catalysis occur, but the nucleophilic mechanism is a minor component accounting for only 15–20% of the overall catalysis.

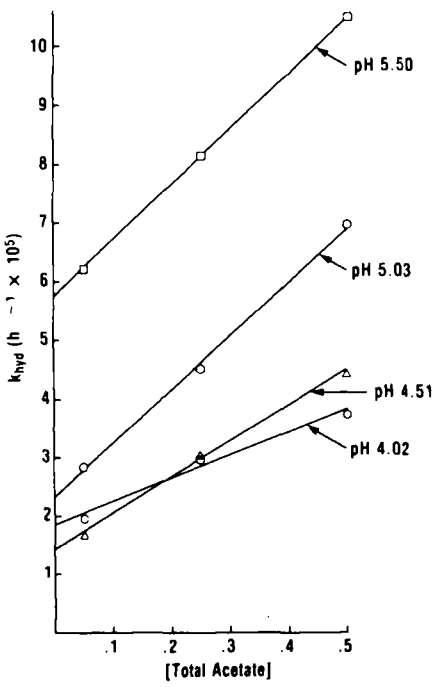

Figure 4—*Hydrolysis rate constant for methylprednisolone 21-acetate* versus *acetate buffer concentration at varying pH.*

Hydrolysis and Acyl Migration of Methylprednisolone 21-Acetate in Water and in Acetate Buffers—*Hydrolysis*—The changeover from nucleophilic to general acid-base catalysis of ester hydrolysis by a catalyst acting intermolecularly occurs when the pK_a of the leaving group is greater than that of the catalyst by ~2.5 units (10). Since the pK_a of the steroid side chain leaving group is ~11 due to possible enolization (11), while that of acetic acid is 4.8, it is assumed that acetate buffer is a general acid-base catalyst in the degradation of methylprednisolone 21-acetate.

The hydrolysis of methylprednisolone 21-acetate can be described by the following rate equation:

$$k_{hyd} = k_{H^+}[H^+] + k_{H_2O} + k_{OH^-}[OH^-] + (f_{A^-}k_{gb} + f_{HA}k_{ga})[Ac_T] \quad \text{(Eq. 8)}$$

where the final term represents the expected influence of the total acetate buffer [Ac_T] acting as either a general base catalyst ($k_{gb} \cdot f_{A^-}$) or general acid catalyst ($k_{ga} \cdot f_{HA}$). The k_{hyd} is plotted *versus* pH in Fig. 3 for systems at ionic strengths of 0.01 and 0.5 and buffer concentrations approaching infinite dilution. Superimposed on these plots is the logarithm of the hydrolysis rate constant *versus* pH for methylprednisolone 21-succinate for comparative purposes.

Figure 4 shows the acetate ester hydrolysis rate constant, k_{hyd}, at various pH values and total acetate buffer concentrations. The rate constants k_{ga} and k_{gb} were determined by rearranging Eq. 8 and plotting the left-hand side of Eq. 9 *versus* the fraction of acetate ion, f_{A^-}:

$$\frac{k_{hyd} - (k_{H^+}[H^+] + k_{H_2O} + k_{OH^-}[OH^-])}{Ac_T} = k_{ga} + (k_{gb} - k_{ga})f_{A^-} \quad \text{(Eq. 9)}$$

This plot is shown in Fig. 5. Values of the rate constants for the hydrolysis of methylprednisolone 21-acetate are shown in Table II. Kinetically, acetate buffer acts primarily as a general base catalyst in this reaction, with $k_{gb} > k_{ga}$ by about fivefold. Whether or not this is true general base catalysis or its kinetic equivalent, general acid-specific base catalysis, cannot be ascertained from the kinetic data.

21 ⇄ 17 Acyl Migration—A previous study of acyl migration in methylprednisolone succinate fit the kinetic data to an equation of the following form (6):

$$k_{mig}^{su} = k_{OH^-}^{mig}[OH^-]f_i + k_{cat}^{mig} \cdot f_i \quad \text{(Eq. 10)}$$

The 21 ⇄ 17 migration of acetate in methylprednisolone acetate esters subjected to acetate buffer can be described by the following rate equation:

$$k_{mig}^{ace} = k_{H^+}^{mig}[H^+] + k_{H_2O}^{mig} + k_{OH^-}^{mig}[OH^-] + (k_{ga}^{mig} \cdot f_u + k_{gb}^{mig} \cdot f_i)[Ac_T] \quad \text{(Eq. 11)}$$

The last term in Eq. 11 again expresses the possible role of acetate [Ac_T] acting as an intermolecular general acid, $k_{ga}^{mig} \cdot f_u$ or general base catalyst, $k_{gb}^{mig} \cdot f_i$. Plots of the logarithm of the forward and reverse migration rate constants *versus*

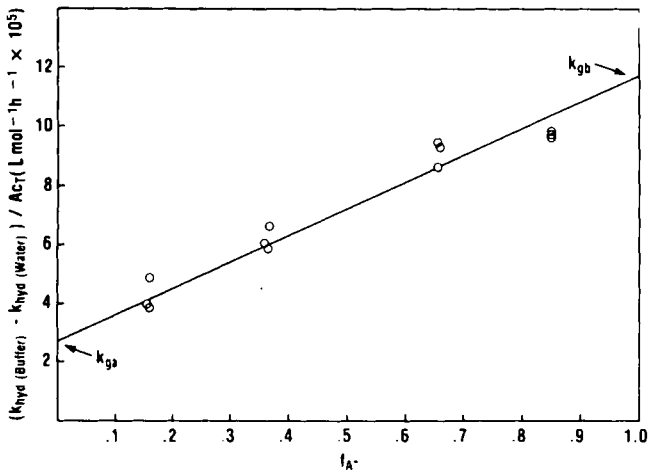

Figure 5—*Plot of* $(k_{hyd\ (buffer)} - k_{hyd\ (water)})/Ac_T$ versus *the fraction of acetate ionized for methylprednisolone 21-acetate (see Eq. 9).*

pH are shown in Fig. 6 for both methylprednisolone succinate and acetate esters in buffers approaching infinite dilution.

The influence of acetate buffer acting intermolecularly as a general acid-base catalyst in the migration (21 ⇄ 17) of acetate in methylprednisolone acetate was assessed by plotting the quantity: $[k_{mig}^{acc}$ (in buffer) − k_{acc} (no buffer)]/Ac_T *versus* the fraction of acetate buffer, Ac_T, in ionized form (f_{A^-}) as done previously for hydrolysis according to Eq. 9. These plots were linear for both the 21 → 17 and 17 → 21 reactions. Values for k_{ga}^{mig} and k_{gb}^{mig} obtained from these plots and all other migration rate constants for both the acetate and succinate esters are listed in Table III.

As observed in the hydrolysis, intermolecular catalysis of migration by acetate buffer appears to involve the acetate acting primarily as a general base in both directions. Mechanistically, however, this is most unlikely.

Calculation of the "Effective Molarity" of the Succinate Carboxyl Group Acting as a General Acid-Base Catalyst— It is a common practice to assess the effect of intramolecularity by comparing the catalytic rate constant in an intramolecular reaction with that of an analogous intermolecular one (12). While the hydrolysis and acyl migration reactions in methylprednisolone acetate are similar to those in the succinate, a correction should be made for the differences in intrinsic reactivity of the two esters. This can be done by dividing the catalytic constants k_{gen} and k_{gb} by k_{OH^-}. (Refer to Tables I and II for the values of these constants.) Thus, for the 21-succinate hydrolysis k_{gen}/k_{OH^-} is 3.0×10^{-8} M and for the 21-acetate hydrolysis k_{gb}/k_{OH^-} is 7.1×10^{-9}M. The ratio of these quantities is the effective concentration of the carboxylate anion in the hydrolysis of the hemisuccinate ester, 4.2 M.

The k_{H_2O} of 6×10^{-5} h^{-1} for the un-ionized succinate ester hydrolysis (Table I) is an order of magnitude greater than that of the acetate ester hydrolysis of 4.8×10^{-6} h^{-1} (Table II). This is evidence for intramolecular catalysis in k_{H_2O} by the terminal carboxyl group, but an effective molarity of the terminal carboxylic acid was not calculated for this reaction.

Following a procedure identical to that described above, the effective molarity of the terminal carboxylate anion of the hemisuccinate ester in catalyzing acyl migration can also be calculated. For the 21 → 17 ester migration (see Table III) k_{gb}/k_{OH^-} for the acetate ester is 4×10^{-9} M and k_{cat}/k_{OH^-} for the succinate ester is 2.1×10^{-7} M, for an effective molarity of ~50 M. In the 17 → 21 ester migration k_{gb}/k_{OH^-} for the acetate ester is 4.7×10^{-9} M and k_{cat}/k_{OH^-} for the succinate ester is 1.7×10^{-7} M, for an effective molarity of ~40 M. These numbers are the same without experimental error, but are significantly greater than the effective concentration of the terminal carboxylate anion of the succinate ester in catalyzing hydrolysis.

DISCUSSION

Comparison of the pH-Rate Profiles of Methylprednisolone Acetate and Succinate Esters—The primary evidence that hydrolysis and acyl migration in methylprednisolone succinate esters are catalyzed intramolecularly by the terminal succinate carboxyl group comes from the observation that the pH rate profiles for these reactions deviate from classical behavior. This is best illustrated by comparisons of the pH-hydrolysis rate and pH-acyl migration profiles of methylprednisolone succinate esters with those of methylprednisolone acetate esters, which exhibit the expected classical behavior (Figs. 3 and 6).

The pH-rate profile obtained for hydrolysis of the acetate ester in Fig. 3 has the typical U-shape generally observed for aliphatic ester hydrolysis in the absence of catalysis (2) and can be described by Eq. 8 (neglecting the acetate buffer term). In basic solution, the hydrolysis rate of methylprednisolone 21-succinate *versus* pH is parallel to that of methylprednisolone 21-acetate. This region represents hydroxide ion attack on the ionized succinate ester or on the neutral acetate ester. In acidic solutions (pH <2) it appears that the two curves again become parallel. This region represents H^+-catalyzed attack of water on the neutral esters. From a comparison of k_{H^+} and k_{OH^-} values in Tables I and II, it is estimated that methylprednisolone 21-succinate is more stable than the 21-acetate in acid by nearly an order of magnitude and in base by roughly fourfold. The lower reactivity of the 21-succinate is assumed to be due largely to a steric effect. Electrostatic repulsion of OH^- attack by the negatively charged succinate carboxylate anion does not appear to be a significant factor in the basic hydrolysis of methylprednisolone 21-succinate, since steric effects alone can account for its decreased reactivity. Steric effects are assumed to be equal in acidic and basic ester hydrolysis, as originally proposed by Ingold (13).

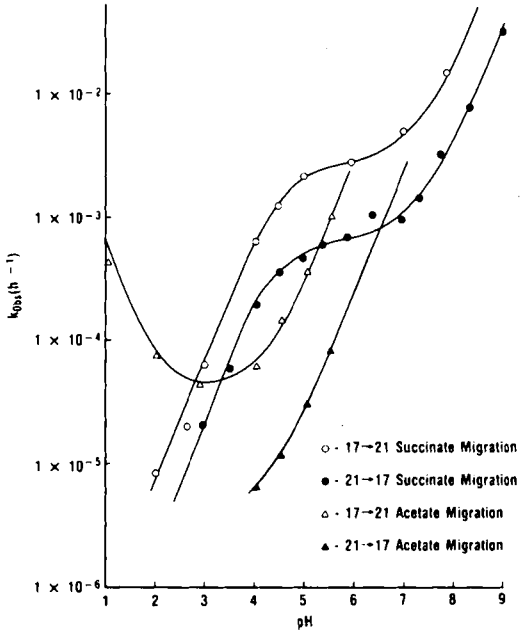

Figure 6—*pH-17 → 21 and pH-21 → 17 migration rate profiles for methyprednisolone acetate and succinate esters at 25°C.*

Between pH ~3-7 the pH-methylprednisolone 21-succinate hydrolysis rate profile deviates from the classical U-shape exhibited by the acetate ester profile. This behavior suggests intramolecular catalysis by the terminal succinate carboxyl group, as discussed previously.

From an examination of the pH-21 ⇄ 17 acyl migration rate profiles in Fig. 6 or from a comparison of k_{OH^-} values in Table III, it is evident that ester migration occurs faster in basic solution in methylprednisolone acetate esters than in the succinate esters. This decreased reactivity at high pH is again attributed to the greater steric bulk of the succinate esters. The pH-rate profiles for acetate ester migration are linear down to a pH of ~4-5, while the succinate ester pH-migration rate profiles deviate from linearity at ~pH 7. Again this behavior is rationalized as intramolecular catalysis of migration by the terminal succinate carboxyl group.

Mechanism of Intramolecular Catalysis of the Hydrolysis of the 21-Succinate— Studies on the solvolysis of 21-hemiesters of hydrocortisone (4, 5) led Garrett to conclude that intramolecular catalysis by the terminal succinate carboxyl group was nucleophilic. This mechanism has been observed in other systems and was further supported by the fact that general acid-base catalysis by acetate buffer was not observed in the reaction. However, in light of the recent observation that 21 ⇄ 17 acyl migration in methylprednisolone 21-succinate is also catalyzed intramolecularly, coupled with the realization that nucleophilic catalysis is not a plausible mechanism for catalysis of acyl migration, it seemed appropriate to reexamine the evidence for the nucleophilic mechanism in the hydrolysis and attempt to establish or refute its existence by trapping any succinic anhydride formed as a result of nucleophilic attack of the terminal carboxylate anion on the ester.

The anilide trapping experiment clearly demonstrates that, while nucleophilic catalysis does occur, the predominant mechanism is general acid-base catalysis. It is reasonable that the mechanism of intramolecular catalysis of methylprednisolone succinate should lie on the borderline between general acid base and nucleophilic but favoring general acid-base catalysis from a

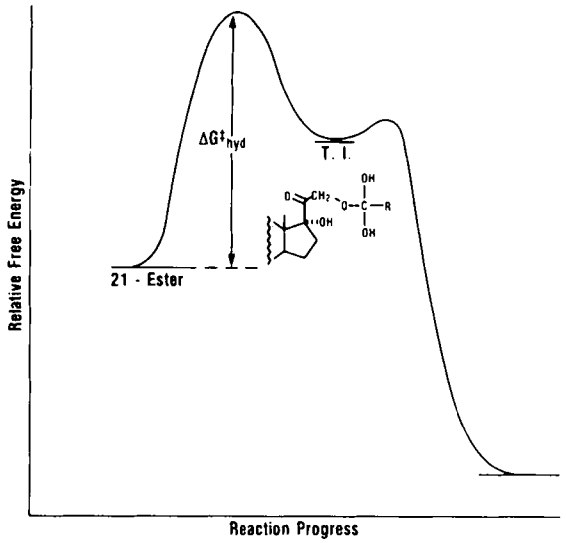

Figure 7—*Relative free energy* versus *reaction progress diagram for methylprednisolone 21-ester hydrolysis.*

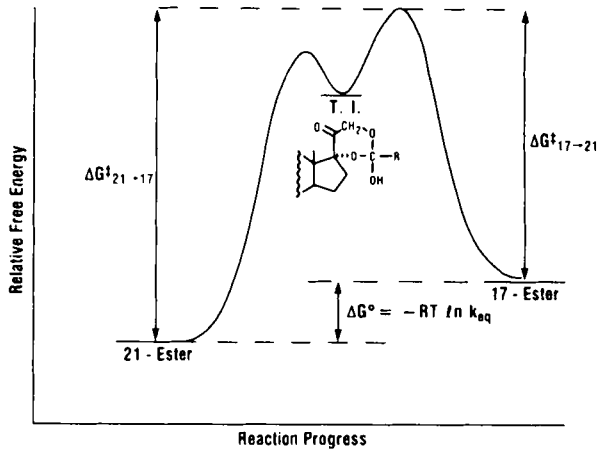

Figure 8—*Relative free energy* versus *reaction progress diagram for 21 → 17 acyl migration in methylprednisolone esters.*

consideration of the catalyst and leaving group pK_a values. Fersht and Kirby (10) have shown that in an exocyclic displacement (that is, when the leaving group does not stay attached to the intermediate anhydride formed on nucleophilic attack by a catalyst), the borderline between intramolecular general base and nucleophilic catalysis lies in the region where the pK_a of the leaving group is 5.5–6.5 units more basic than the attacking nucleophile. Due to possible enolization, the pK_a of the C-17 side chain of methylprednisolone is near 11 (11), while the terminal succinate carboxylic acid is ~4.5, for a pK_a difference of 6.5.

If the *intramolecular* catalytic mechanism is largely general acid-base, then one would expect the reaction to also be catalyzed *intermolecularly* by general acids or bases. Yet, general acid base catalysis by acetate was not seen by Garrett in his studies of the hydrolysis of hydrocortisone succinate (4,5). This is of general importance, since such information is often the primary support for or against the intramolecular nucleophilic mechanism.

General catalysis was not observed in Garrett's studies, since the reaction is already catalyzed intramolecularly. If the magnitude of intramolecular catalysis (as determined by the effective molarity of the carboxylate anion) in hydrocortisone succinate is equivalent to that which would result intermolecularly from a 4 M acetate buffer, then the increase in rate brought about by a 0.3 M solution of acetate (the highest concentration used in Garrett's study) would be only ~7% and may well be overlooked. Thus, the apparent absence of intermolecular general acid-base catalysis in a reaction that is already intramolecularly catalyzed may not be sufficient evidence to rule out a general acid-base mechanism in the intramolecular reaction.

It is more appropriate to test the presence or absence of intermolecular general acid base catalysis in a reaction that is similar to the intramolecularly catalyzed reaction but is not already catalyzed intramolecularly. The results of this study showing that acetate buffer catalyzes the hydrolysis of methylprednisolone 21-acetate make more plausible the conclusion that intramolecular general acid-base catalysis occurs in the hydrolysis of methylprednisolone 21-succinate.

Intramolecular Catalysis Favors Acyl Migration Over Hydrolysis—As shown in Fig. 1 and pointed out earlier, hydrolysis of methylprednisolone 21-succinate is slightly faster than 21 → 17 acyl migration above pH 7.4, while acyl migration dominates between pH 3.6 and 7.4. This dramatic reversal in relative reaction rates is due to the fact that intramolecular catalysis of acyl migration is 4–6 times greater than that of hydrolysis. These differences in catalytic efficiency can be rationalized from a consideration of differences in the transition states of the two reactions.

Referring to the hypothetical diagrams in Figs. 7 and 8 of relative free energy *versus* reaction progress, it is assumed that the transition state for 21-ester hydrolysis (Fig. 7) is a very early transition state, occurring prior to the formation of the tetrahedral intermediate, since OH^- is a much poorer leaving group than the 21-alcoholate. However, the transition state for the 21 → 17 migration (Fig. 8) is quite likely the breakdown of the tetrahedral intermediate. The 17-ester is thermodynamically less favored and, applying Hammond's postulate (14), the transition state should more closely resemble the less stable 17-ester than the 21-ester. In further support of the conclusion that the transition state in the migration occurs between the tetrahedral intermediate and the 17-ester are data showing that the 17,21-hemiorthoester of betamethasone benzoate, which has been isolated, breaks down in acid to the 21-ester (15). Differences in the magnitude of intramolecular catalysis of hydrolysis and 21 → 17 acyl migration are not surprising in view of the fact that the transition states are probably quite different.

Whereas *intramolecular* catalysis by the terminal succinate carboxyl group of 21 → 17 acyl migration is 4–6 times greater than intramolecular catalysis of hydrolysis, this does not appear to be the case in the analogous *intermolecularly* acetate buffer catalyzed reactions occurring in methylprednisolone 21-acetate. Comparing the ratios k_{gb}/k_{OH^-} (see Tables II and III), the magnitude of intermolecular catalysis by acetate buffer of the hydrolysis of methylprednisolone 21-acetate is nearly equal to that of 21 → 17 migration.

It is suggested that intermolecular catalysis of migration by acetate is rendered less effective due to steric (entropic) factors that come into play in the intermolecular reaction but not in the intramolecular mechanism. Using molecular models, it appears that the conformational freedom of the succinate moiety in the transition state is about the same for both hydrolysis and migration. An intermolecular general acid or base appears, however, to be conformationally more restricted in the transition state during migration as compared to hydrolysis.

Ambiguity in the Assignment of the Site of Catalysis—The acetate buffer-catalyzed 21 ⇄ 17 acyl migration reaction in methylprednisolone 21-acetate provides an excellent demonstration of what Jencks refers to as the ambiguity of the assignment of the site of catalysis (16). Applying the principle of microscopic reversibility (17), it is clear that the same transition state is involved in both the 21 → 17 and 17 → 21 migrations. This means mechanistically that if the reaction is general base catalyzed in one direction, it must be general acid-specific base catalyzed in the other. Yet, *kinetically*, both directions appear to be primarily general base catalyzed (Table III). By convention, both reactions are referred to as general base catalyzed even though mechanistically this cannot be. None of the data generated by this study specifically support one general catalytic mechanism over its kinetic equivalent. Indeed, the same ambiguity exists in much of the published literature wherein general base or general acid catalytic mechanisms have been postulated.

REFERENCES

(1) W. P. Jencks, "Catalysis in Chemistry and Enzymology," McGraw-Hill, New York, N.Y., 1969.

(2) T. C. Bruice and S. J. Benkovic, "Bioorganic Mechanisms," W. A. Benjamin, Inc., New York, N.Y., 1966.

(3) A. J. Kirby and A. R. Fersht, in "Progress in Bioorganic Chemistry," E. J. Kaiser and F. S. Kezdy, Eds., vol. 1, Wiley, New York, N.Y., 1971.

(4) E. R. Garrett, *J. Med. Pharm. Chem.*, **5**, 112 (1962).

(5) E. R. Garrett, *J. Pharm. Sci.*, **51**, 445 (1962).

(6) B. D. Anderson and V. Taphouse, *J. Pharm. Sci.*, **70**, 181 (1981).

(7) R. Gardi, R. Vitali, and A. Ercoli, *Gazz. Chim. Ital.*, **93**, 431 (1963).

(8) "The Merck Index," 9th ed., M. Windholz, Ed., Merck & Co., Rahway, N.J., 1976.

(9) T. Higuchi, T. Miki, A. C. Shah, and A. Herd, *J. Am. Chem. Soc.*, **85**, 3655 (1963).

(10) A. R. Fersht and A. J. Kirby, *J. Am. Chem. Soc.*, **90**, 5818 (1968).

(11) J. Hansen and H. Bundgaard, *Arch. Pharm. Chem., Sci. Ed.*, **7**, 135 (1979).
(12) M. I. Page, *Chem. Soc. Rev.*, **2**, 195 (1973).
(13) C. K. Ingold, "Structure and Mechanism in Organic Chemistry," 2nd ed., Cornell University Press, Ithaca, N.Y., 1969, Chap. XV.
(14) G. S. Hammond, *J. Am. Chem. Soc.*, **77**, 334 (1955).
(15) E. J. Merrill and G. G. Vernice, *J. Org. Chem.*, **36**, 2903 (1971).
(16) W. P. Jencks, "Catalysis in Chemistry and Enzymology," McGraw-Hill, New York, N.Y., 1969, p. 182.
(17) W. P. Jencks, "Catalysis in Chemistry and Enzymology," McGraw-Hill, New York, N.Y., 1969, p. 208.

ACKNOWLEDGMENTS

The authors wish to thank D. E. Ayer of The Upjohn Co., Kalamazoo, Mich. for kindly providing a sample of methylprednisolone 17-acetate. W. J. Lambert's contribution to this study was made possible by his participation in the Pharmacy Research Summer Scholar Program of The Upjohn Company.

Degradation Kinetics in Aqueous Solution of Cefotaxime Sodium, a Third-Generation Cephalosporin

H. FABRE *x, N. HUSSAM EDDINE *, and G. BERGE ‡

Received November 18, 1982, from the * *Laboratoire de Chimie Analytique* and the ‡ *Laboratoire de Pharmacie Chimique, Faculté de Pharmacie, Université de Montpellier, 34060 Montpellier Cedex, France.* Accepted for publication March 27, 1983.

Abstract □ The degradation kinetics of a 3-acetoxymethylcephalosporin, cefotaxime sodium salt, in aqueous solution investigated by HPLC under different conditions (pH, ionic strength, temperature) and using different buffers. The scheme of degradation involves a cleavage of the β-lactam nucleus and the deacetylation of the side chain. In highly acidic medium, the deacetylated derivative is easily converted to the lactone. The degradation rate constants were calculated at three pH values (1.9, 4.0, and 9.0) by measuring the residual cephalosporin and the main decomposition products. The degradation pathway is both supported by the results of a primary salt effect and by the agreement between the theoretical pH-rate profile and the experimental values. In the pH range from 3.0 to 7.0, the main process is a slow water-catalyzed or spontaneous cleavage of the β-lactam nucleus with intramolecular participation of the side chain amido fraction in the 7-position. In alkaline or strongly acidic medium, the hydrolysis is a base- or acid-catalyzed reaction. Of the buffer systems investigated, carbonate buffer (pH 8.5) and borate buffers (pH 9.5 and 10.0) are found to increase the degradation rates, while acetate buffer decreases the degradation rates. The apparent activation energies determined at different pH values are compatible with a solvolysis mechanism and similar to those previously given in the literature for other cephalosporins. Cefotaxime in aqueous solution is slightly less stable than the main cephalosporin derivatives, despite its high resistance to the β-lactamases and its remarkable biological activity.

Keyphrases □ 3-Acetoxymethylcephalosporins—stability in aqueous solutions, HPLC, pH effect, primary salt effect, buffer effect, temperature effect □ Cefotaxime—kinetics and mechanism of degradation, pH-rate profile □ Antibiotics—cefotaxime, stability, degradation profile, kinetics

Systematic studies on the degradation of cephalosporin derivatives are of interest for several reasons: (*a*) a correlation between degradation and antibiotic activity has been shown in first- and second-generation cephalosporins (1), (*b*) some degradation products may be involved in allergic reaction (2), and (*c*) the stability of the compounds has to be known for the synthesis of derivatives (3) and the formulation of drugs. The kinetics of first- and second-generation cephalosporins have been reported in a few instances (1, 3–6). These studies concern a quantitative analysis of the antibiotic itself and sometimes the kinetics of the major degradation product (1, 3). In this report, a systematic kinetic study of a recently commercially available third-generation cephalosporin, cefotaxime sodium salt[1], has been carried out. The quantitation of this cephalosporin and its major decomposition products allowed the proposal of a degradation pathway.

BACKGROUND

Cefotaxime sodium (I) is sodium [6(*R*)-[6α,7β(*Z*)]]-3-[(acetyloxy)-methyl]-7-[[(2-amino-4-thiazolyl)(methoxyimino)acetyl]-8-oxo-5-thia-1-azabicyclo[4.2.0]oct-2-ene-2-carboxylate]. The possible *in vitro* degradation products are deacetylcefotaxime (II), deacetoxycefotaxime (III), deacetylcefotaxime lactone (IV), thiazoximic acid (V), and 7-aminocephalosporanic acid (VI). The *anti* isomer which could be expected as a potential degradation product of I has been shown to be formed only in nonaqueous medium (7) and has not been taken into consideration in this study.

Cefotaxime sodium (I) is an original cephalosporin derivative with a 2-amino-4-thiazolyl side chain and an α-methoximino group in the *syn* position. The former is probably responsible for the very great affinity for transpeptidase, involved in the construction of the bacterial wall, and of the great activity against Gram-negative bacilli. The latter is probably responsible for the stability of the drug against most β-lactamases (8, 9). An exhaustive review of the bacteriological and clinical properties of I has been presented (10).

EXPERIMENTAL

Materials—Compounds I–VI were used as received[2]. UV, IR, and NMR spectra were used to confirm the structure of these compounds. All other chemicals were analytical reagent grade.

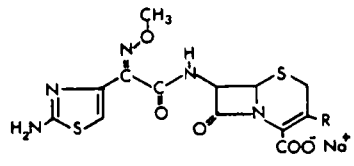

R

I: R=CH_2-O-CO-CH_3
II: R=CH_2-OH
III: R=CH_3

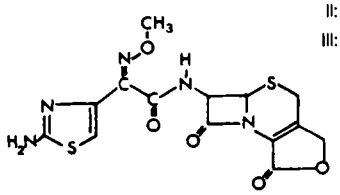

IV

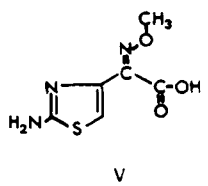

V

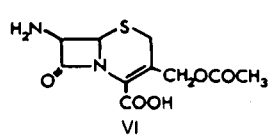

VI

[1] Trade names: Claforan, Tarivid, Zariviz, and Primafen.

[2] Gifts from Roussel UCLAF Laboratories.

0022-3549/84/0500-0611$01.00/0
© 1984, American Pharmaceutical Association

(11) J. Hansen and H. Bundgaard, *Arch. Pharm. Chem., Sci. Ed.*, **7**, 135 (1979).
(12) M. I. Page, *Chem. Soc. Rev.*, **2**, 195 (1973).
(13) C. K. Ingold, "Structure and Mechanism in Organic Chemistry," 2nd ed., Cornell University Press, Ithaca, N.Y., 1969, Chap. XV.
(14) G. S. Hammond, *J. Am. Chem. Soc.*, **77**, 334 (1955).
(15) E. J. Merrill and G. G. Vernice, *J. Org. Chem.*, **36**, 2903 (1971).
(16) W. P. Jencks, "Catalysis in Chemistry and Enzymology," McGraw-Hill, New York, N.Y., 1969, p. 182.
(17) W. P. Jencks, "Catalysis in Chemistry and Enzymology," McGraw-Hill, New York, N.Y., 1969, p. 208.

ACKNOWLEDGMENTS

The authors wish to thank D. E. Ayer of The Upjohn Co., Kalamazoo, Mich. for kindly providing a sample of methylprednisolone 17-acetate. W. J. Lambert's contribution to this study was made possible by his participation in the Pharmacy Research Summer Scholar Program of The Upjohn Company.

Degradation Kinetics in Aqueous Solution of Cefotaxime Sodium, a Third-Generation Cephalosporin

H. FABRE *x, N. HUSSAM EDDINE *, and G. BERGE ‡

Received November 18, 1982, from the * *Laboratoire de Chimie Analytique* and the ‡ *Laboratoire de Pharmacie Chimique, Faculté de Pharmacie, Université de Montpellier, 34060 Montpellier Cedex, France.* Accepted for publication March 27, 1983.

Abstract □ The degradation kinetics of a 3-acetoxymethylcephalosporin, cefotaxime sodium salt, in aqueous solution investigated by HPLC under different conditions (pH, ionic strength, temperature) and using different buffers. The scheme of degradation involves a cleavage of the β-lactam nucleus and the deacetylation of the side chain. In highly acidic medium, the deacetylated derivative is easily converted to the lactone. The degradation rate constants were calculated at three pH values (1.9, 4.0, and 9.0) by measuring the residual cephalosporin and the main decomposition products. The degradation pathway is both supported by the results of a primary salt effect and by the agreement between the theoretical pH-rate profile and the experimental values. In the pH range from 3.0 to 7.0, the main process is a slow water-catalyzed or spontaneous cleavage of the β-lactam nucleus with intramolecular participation of the side chain amido fraction in the 7-position. In alkaline or strongly acidic medium, the hydrolysis is a base- or acid-catalyzed reaction. Of the buffer systems investigated, carbonate buffer (pH 8.5) and borate buffers (pH 9.5 and 10.0) are found to increase the degradation rates, while acetate buffer decreases the degradation rates. The apparent activation energies determined at different pH values are compatible with a solvolysis mechanism and similar to those previously given in the literature for other cephalosporins. Cefotaxime in aqueous solution is slightly less stable than the main cephalosporin derivatives, despite its high resistance to the β-lactamases and its remarkable biological activity.

Keyphrases □ 3-Acetoxymethylcephalosporins—stability in aqueous solutions, HPLC, pH effect, primary salt effect, buffer effect, temperature effect □ Cefotaxime—kinetics and mechanism of degradation, pH-rate profile □ Antibiotics—cefotaxime, stability, degradation profile, kinetics

Systematic studies on the degradation of cephalosporin derivatives are of interest for several reasons: (*a*) a correlation between degradation and antibiotic activity has been shown in first- and second-generation cephalosporins (1), (*b*) some degradation products may be involved in allergic reaction (2), and (*c*) the stability of the compounds has to be known for the synthesis of derivatives (3) and the formulation of drugs. The kinetics of first- and second-generation cephalosporins have been reported in a few instances (1, 3–6). These studies concern a quantitative analysis of the antibiotic itself and sometimes the kinetics of the major degradation product (1, 3). In this report, a systematic kinetic study of a recently commercially available third-generation cephalosporin, cefotaxime sodium salt[1], has been carried out. The quantitation of this cephalosporin and its major decomposition products allowed the proposal of a degradation pathway.

BACKGROUND

Cefotaxime sodium (I) is sodium [6(*R*)-[6α,7β(*Z*)]]-3-[(acetyloxy)-methyl]-7-[[(2-amino-4-thiazolyl)(methoxyimino)acetyl]-8-oxo-5-thia-1-azabicyclo[4.2.0]oct-2-ene-2-carboxylate]. The possible *in vitro* degradation products are deacetylcefotaxime (II), deacetoxycefotaxime (III), deacetylcefotaxime lactone (IV), thiazoximic acid (V), and 7-aminocephalosporanic acid (VI). The *anti* isomer which could be expected as a potential degradation product of I has been shown to be formed only in nonaqueous medium (7) and has not been taken into consideration in this study.

Cefotaxime sodium (I) is an original cephalosporin derivative with a 2-amino-4-thiazolyl side chain and an α-methoximino group in the *syn* position. The former is probably responsible for the very great affinity for transpeptidase, involved in the construction of the bacterial wall, and of the great activity against Gram-negative bacilli. The latter is probably responsible for the stability of the drug against most β-lactamases (8, 9). An exhaustive review of the bacteriological and clinical properties of I has been presented (10).

EXPERIMENTAL

Materials—Compounds I–VI were used as received[2]. UV, IR, and NMR spectra were used to confirm the structure of these compounds. All other chemicals were analytical reagent grade.

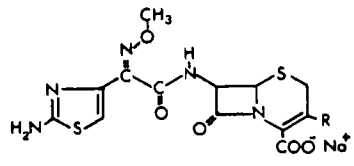

R

I: R=CH_2-O-CO-CH_3
II: R=CH_2-OH
III: R=CH_3

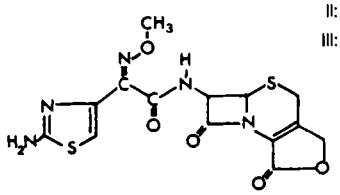

IV

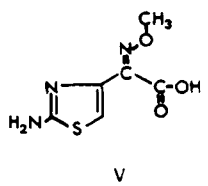

V

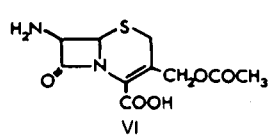

VI

[1] Trade names: Claforan, Tarivid, Zariviz, and Primafen.

[2] Gifts from Roussel UCLAF Laboratories.

0022-3549/84/0500-0611$01.00/0
© 1984, American Pharmaceutical Association

Table I—Pseudo-First-Order Rate Constants for I Degradation at Different Buffer Concentrations and Different pH

Buffer	pH	k_{obs}, $h^{-1} \times 10^3$					k_{pH}, $h^{-1} \times 10^3$
		0.05 M	0.10 M	0.15 M	0.20 M	0.30 M	
HCl–KCl	1.6	—	—	—	60.987	—	60.987
	1.9	—	—	—	38.129	—	38.129
Citrate	2.2	—	25.868	—	26.087	26.093	25.790
	3.0	—	14.290	—	14.720	15.056	13.930
Acetate	4.0	—	—	—	13.056	—	—
	5.0	—	13.020	—	12.106	10.921	14.125
Phosphate	6.0	—	14.460	—	15.019	16.528	13.267
	7.5	16.445	17.046	17.316	—	—	16.065
Carbonate	8.5	—	53.153	—	60.840	68.684	45.362
Borate	9.0	—	—	—	117.046	—	—
	9.5	—	341.016	—	359.424	383.465	318.840
	10.0	—	858.726	—	876.720	894.720	840.720

Buffer Solutions—The buffers used in the kinetic studies were hydrochloric acid–potassium chloride (pH 1.6 and 1.9), citrate (pH 2.2 and 3.0), acetate (pH 4.0 and 5.0), phosphate (pH 6.0 and 7.5), carbonate (pH 8.5), and borate (pH 9.0, 9.5, and 10.0). The buffer concentrations were 0.1, 0.2, and 0.3 M (except at pH 7.5, where concentrations were 0.05, 0.10, and 0.15 M, and at pH 4.0 and 9.0, where buffer concentrations were 0.2 M) and the ionic strength was adjusted to 0.5 with potassium chloride. Primary salt effects were investigated at 0.2 M buffer concentration at pH 2.2, 6.0, and 9.5 with ionic strengths of 0.3, 0.5, and 0.7. The pH of buffer solutions was controlled with a pH meter[3] standardized with pH 2.0, 7.0, and 9.0 solutions.

Kinetic Procedures—Experiments were performed in volumetric flasks. Compound I was dissolved in the buffer solution previously equilibrated at 4°C, 23°C, or 37°C. For the kinetics followed by HPLC, the concentrations used were $\sim 2 \times 10^{-3}$ or $\sim 1 \times 10^{-3}$ M according to the solubility. The samples were assayed immediately after a suitable dilution. For the kinetics followed by UV, the concentrations used were $\sim 2 \times 10^{-5}$ M. All experiments were conducted in the dark in a constant-temperature water bath with a thermoregulator at ±0.2°C or in a refrigerator for the trials at 4°C. pH Values were controlled at the end of each experiment; no significant change was observed.

Analytical Procedures—*Liquid Chromatography*—The liquid chromatograph[4] was equipped with a variable-wavelength UV detector[5] set at 235 nm, an RP 18 column[6], and a 10-μl injection loop. The mobile phase was phosphate buffer (pH 7.6)–methanol (83:17); the flow was 1.5 mL/min.

A mixed stock standard solution was prepared in the mobile phase using I–VI (75 μg of each/mL). This solution was suitably diluted with the mobile phase to give a concentration range from 7.5 to 37.5 μg of each compound/mL.

Ultraviolet—UV spectral changes as a function of time were followed at pH 1.9, 4.0, and 9.0 with a spectrophotometer[7].

pK_a Determinations—The pK_a values of I were determined by the potentiometric titration of a 2.8×10^{-3} M cefotaxime aqueous solution with 0.1 M NaOH, at 20°C, under nitrogen. The two functional groups corresponding to the terminal amino group of the side chain at C-7 and the carboxylic group at C-3 of the cephem ring were acidified with a stoichiometric amount of 0.1 M HCl before titration.

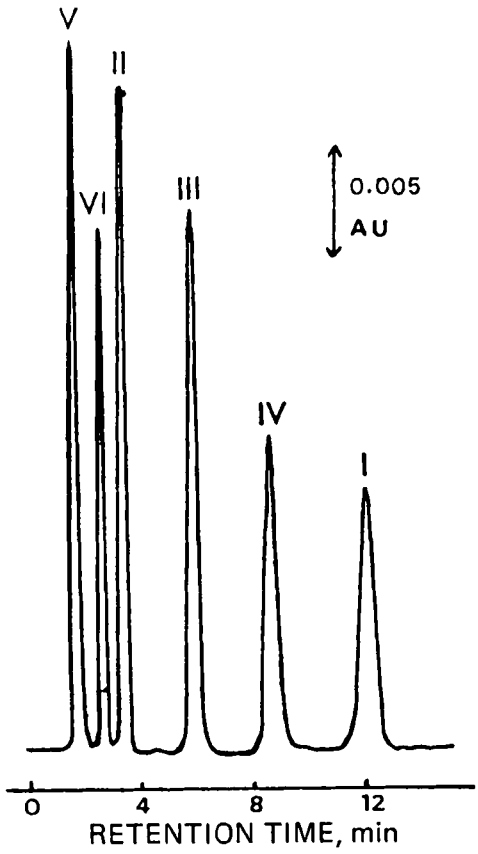

Figure 1—*Chromatogram of a standard solution of I (24.90 μg/mL), II (21.90 μg/mL), III (22.20 μg/mL), IV (23.25 μg/mL), V (14.00 μg/mL), and (26.40 μg/mL). The mobile phase was phosphate buffer (pH 7.6)–methanol (83:17); the flow was 1.5 mL/min and pressure was 175 bars. Detector sensitivity was 0.005 AUFS, chart recorder speed was 0.5 cm/min, and λ = 235 nm.*

[3] Potentiograph Metrohm E 436.

RESULTS AND DISCUSSION

Validity Tests of the Liquid Chromatographic Procedure—A chromatogram of a standard solution recorded at 235 nm (suitable wavelength for a simultaneous determination of I and its degradation products) is shown in Fig. 1. A calibration graph was plotted of the peak areas (or the height measure-

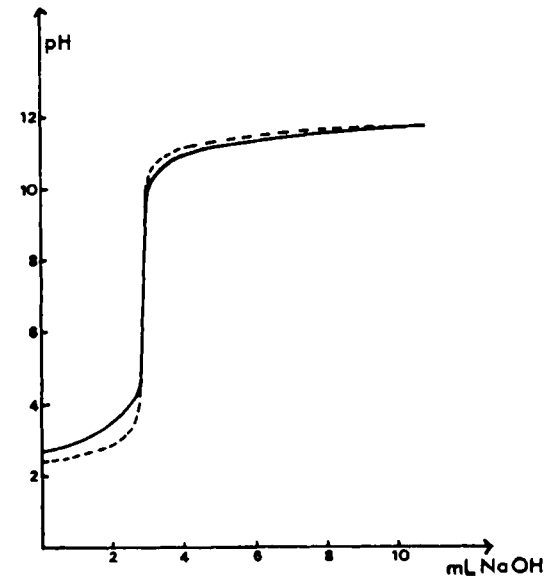

Figure 2—*Titration curve for 2.8×10^{-3} M cefotaxime sodium salt solution at 20°C. Dashed lines represent the blank determination. Two equivalents of acid have been added before titration.*

[4] Spectra-Physics SP 8000.
[5] Schoeffel, model SF 770.
[6] Merck, 7 μm, 25 cm × 0.4 cm.
[7] Beckman, model 25.

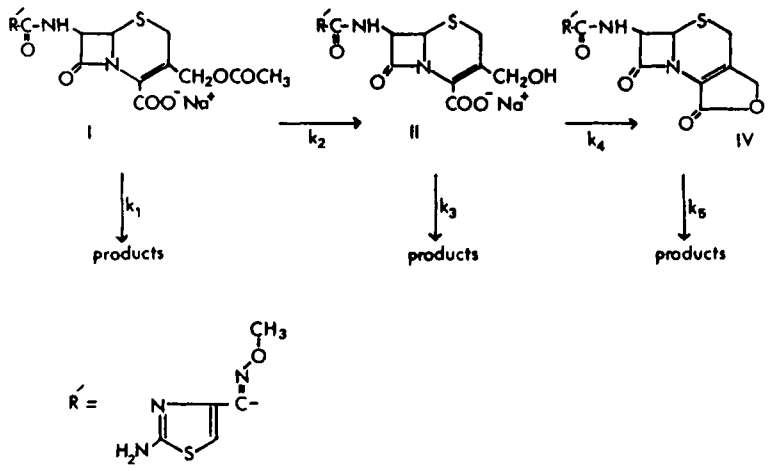

Scheme I

ments) of each solute against solute concentration. The correlation coefficients of the linear regression analysis were always >0.999 by peak areas (as well as height measurements). The repeatability, tested by six replicates and evaluated by the coefficient of variation, was 0.22% (I), 1.15% (II), 0.47% (III), 1.89% (IV), 0.60% (V), and 2.49% (VI). The recovery studies were carried out with a solution of cefotaxime with 1.0% and 3.0% (with respect to I) of II–VI added. The percentage recovered (average of two determinations) was found to be 98.17% for II, 98.64% for III, 107.52% for IV, 99.46% for V, and 98.86% for VI in the former case and 97.10% for II, 98.03% for III, 99.21% for IV, 105.66% for V, and 99.33% for VI in the latter case. Applying the same procedure to the determination of I using a suitable dilution, the recovery was 102.01 and 99.76%, respectively. The minimum amounts detectable were found to be 3.5×10^{-3} μg (I), 1.8×10^{-3} μg (II), 2.0×10^{-3} μg (III), 4.0×10^{-3} μg (IV), 0.8×10^{-3} μg (V), and 2.5×10^{-3} μg (VI). The proposed HPLC procedure therefore allows a satisfactory determination of I–VI. It is a more convenient procedure than TLC (11) for the kinetic studies.

Ionization Constants—The titration curve and the blank determination carried out under the same conditions are shown in Fig. 2. Apparent pK_a values were calculated (12) with a computer. Potentiometric comparative determination with III permitted us to attribute $pK_{a_1} = 2.1$ to the dissociation of the carboxylic group and $pK_{a_2} = 3.4$ to the terminal amino group of the side chain in the 7-position. The pK_{a_3} value of 10.9 may be referred to as the dissociation of the amino group in the α-carbonyl position on the same side chain. It must be noted that the pK_a values in acidic media are approximate values, because these pK_a values are very close to the logarithm of dilution (12).

Kinetic Results—The scheme proposed (Scheme I) for cephalosporin derivatives with an acetoxymethyl group should be valid for I in the entire pH range. The first step in the degradation involves deacetylation. The second step, in acidic medium is the conversion of the deacetylated compound (II) in its lactone form. In addition, I, II, and IV give products resulting from cleavage of the β-lactam ring. To check this postulated pathway, the kinetics of I, II, and IV between pH 1.6 and 10.0 were simultaneously followed by HPLC. Typical chromatograms of acidic, neutral, and basic solutions, withdrawn at ~30–40% cefotaxime degradation (0.2 M buffer concentration, 37°C, and $\mu = 0.5$ ionic strength) are shown in Fig. 3.

Reaction Order and HPLC Observed Constants—The example of the semilogarithmic plots of the data at various pH values (37°C, $\mu = 0.5$, and 0.2 M buffer concentration) illustrated in Fig. 4 show that the degradation of I follows a pseudo-first-order reaction. The results obtained at all the other pH, temperatures, ionic strengths, and buffer concentrations investigated gave the same order reaction. The observed constants, k_{obs}, for I calculated from the slopes are given in Table I.

According to Scheme I, in the alkaline and neutral pH media where lactone is not formed, the degradation of I may be illustrated by:

$$[I] = C_0 e^{-(k_1+k_2)t} \qquad \text{(Eq. 1)}$$

$$[II] = C_0 \frac{k_2}{(k_1+k_2)-k_3}[e^{-k_3 t} - e^{-(k_1+k_2)t}] \qquad \text{(Eq. 2)}$$

where [I] is the concentration of I at times t, C_0 is the initial concentration of I, and [II] is the concentration of II at time t. In a highly acidic medium, where the deacetylated derivative is very easily converted to lactone, the simplified degradation pathway (Scheme II[8]) was used:

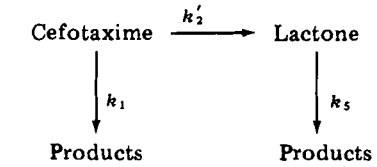

Scheme II

with corresponding equations similar to Eqs. 1 and 2.

In the entire pH range, the kinetics of I, II, and IV were followed for one half-life, but to determine the rate constants k_1–k_5, the kinetics were followed at three different pH values (1.9, 4.0, and 9.0) at 37°C, 0.2 M buffer concentration, and $\mu = 0.5$, for 4–5 half-lives (Fig. 5). The rate constants obtained at these three pH values, analyzed using Eqs. 1 and 2 and B.M.D.P. program P_3R, are listed in Table II.

Reaction Order and UV Observed Constants—Spectral changes for the degradation of I as a function of time at pH 1.9, 4.0, and 9.0 (37°C, 0.2 M buffer concentration, and $\mu = 0.5$) were recorded for 4–5 half-lives (Fig. 6). Absorbance at 260 nm is characteristic of the β-lactam linkage (13). Applying Eq. 3:

$$\ln \frac{A_t - A_\infty}{A_0 - A_\infty} = -k_1' \cdot t \qquad \text{(Eq. 3)}$$

where A_t is the absorbance at time t measured at $\lambda = 260$ nm; A_∞ is the absorbance at infinite time at $\lambda = 260$ nm; A_0 is the absorbance at time zero at $\lambda = 260$ nm; and k_1' is the rate constant determined by UV measurements. Semilogarithmic plots of $(A_t - A_\infty)/(A_0 - A_\infty)$ *versus* time were obtained with a linear correlation of $r > 0.98$. The UV data ascertain for I the first-order reaction determined from HPLC results. The UV values of the pseudo-first-order constants k_1' are listed in Table II.

Table II—Rate Constants Calculated from HPLC Results and UV Measurements [a]

pH	k, $h^{-1} \times 10^3$					
	k_1 [b]	k_1' [c]	k_2 [b]	k_3 [b]	k_2' [b]	k_5 [b]
1.9	24	36	—	—	15	39
4.0	10	13	3	6	—	—
9.0	75	83	43	29	—	—

[a] At 0.2 M buffer concentration, $\mu = 0.5$, and 37°C. [b] From HPLC results. [c] From UV measurements.

Table III—Effect of Ionic Strength on the Pseudo-First-Order Rate Constant of I Degradation [a]

Buffer	pH	k_{obs}, $h^{-1} \times 10^3$		
		$\mu = 0.3$	$\mu = 0.5$	$\mu = 0.7$
Citrate	2.2	25.395	26.087	26.381
Phosphate	6.0	14.669	15.019	15.606
Borate	9.5	321.684	359.424	383.016

[a] At 0.2 M buffer concentration and 37°C.

[8] k_2' is the approximate value of the deacetylation constant k_2.

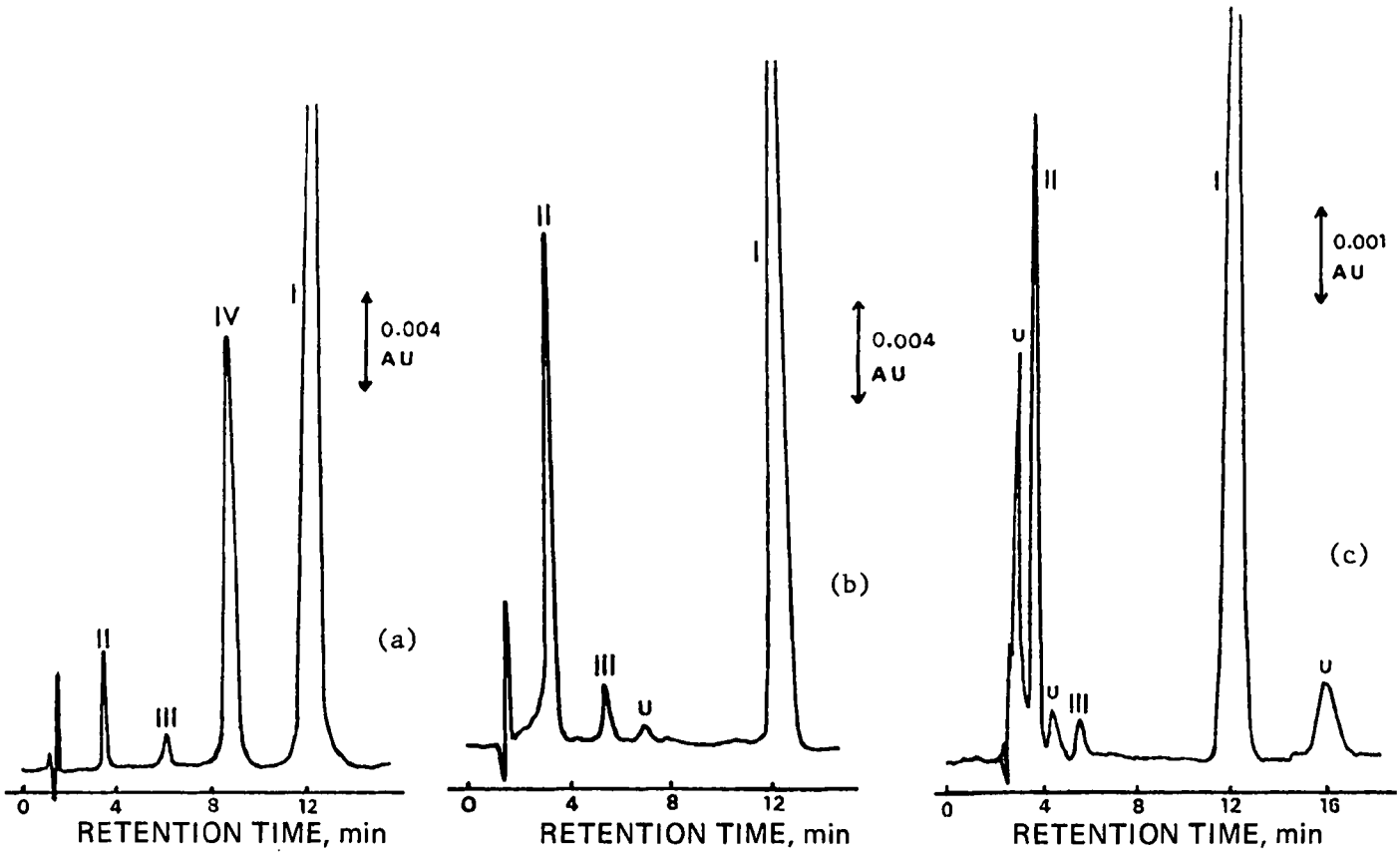

Figure 3—*Chromatogram of a 2 × 10^{-3} M degraded cefotaxime sodium salt solution withdrawn at ~30–40% degradation (0.2 M buffer concentration, 37°C, μ = 0.5) at pH 1.6 (a), pH 6.0 (b), and pH 10.0 (c). Key: (U) unknown peak.*

The UV rate constants may be considered as an estimation of the β-lactam opening rate of the cephalosporins (1, 3, 14) and may be compared with the k_1 values obtained using HPLC. Since the specific extinction coefficients at 260 nm of II ($E^{1\%}_{1cm}$ = 406 at pH 1.9, $E^{1\%}_{1cm}$ = 349 at pH 4.0, and $E^{1\%}_{1cm}$ = 340 at pH 9.0) and IV ($E^{1\%}_{1cm}$ = 418 at pH 1.9, $E^{1\%}_{1cm}$ = 361 at pH 4.0, and $E^{1\%}_{1cm}$ = 353 at pH 9.0) are very similar to those of I ($E^{1\%}_{1cm}$ = 445 at pH 1.9, $E^{1\%}_{1cm}$ = 390 at pH 4.0, and $E^{1\%}_{1cm}$ = 382 at pH 9.0), an approximate estimation of the destruction of the nucleus should be obtained with UV measurements, except if an appreciable production of an absorbing compound is noted. The k'_1 values obtained from UV determination and the k_1 values obtained from HPLC present a rather good concordance, as noted in Table II, in spite of the presence of small amounts of absorbing UV products, probably resulting from the β-lactam cleavage.

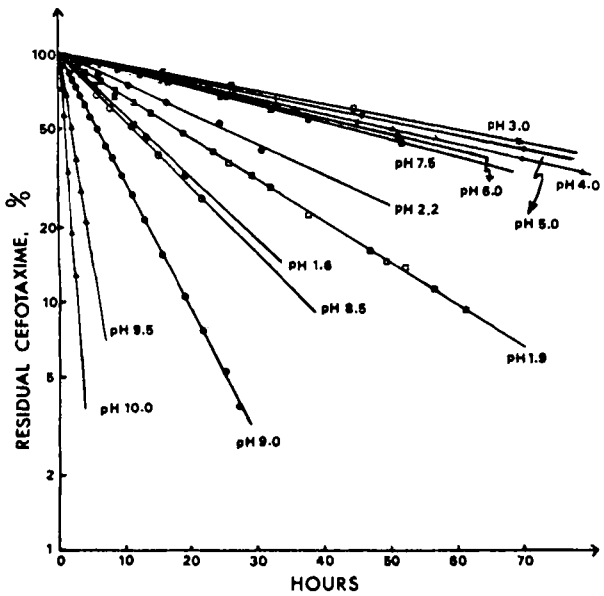

Figure 4—*Apparent first-order reaction of cefotaxime sodium salt solution at various pH values, 37°C, μ = 0.5, and 0.2 M buffer concentration (except at pH 7.5 where the buffer concentration was 0.15 M).*

Buffer Effect and General Acid–Base Catalysis—The values of k_{obs} obtained at constant pH, constant ionic strength (μ = 0.5), constant concentration of I, and constant temperature (37°C), varying only the buffer concentration, are given in Table I. The Student's *t* test was used to determine the significance of differences between the k_{obs} obtained for each buffer concentration. The catalytic effects of the buffers were estimated with a probability p = 95%.

Citrate buffer at pH 2.2 and 3.0 and phosphate buffer at pH 6.0 and 7.5 do not have a catalytic effect. At pH 2.2 and 3.0, the predominant species are H_3A and H_2A^- for citrate buffer (5); at pH 6.0 and 7.5, the predominant species are $H_2PO_4^-$ and HPO_4^{2-}. These species are not general acid–base catalysts.

Carbonate buffer at pH 8.5 and borate buffer at pH 9.5 and 10.0 give a significant catalytic effect on the degradation of cefotaxime. At these pH values, the dominant species, HCO_3^- and $H_2BO_3^-$ are general acid–base catalysts which increase the rate constants. The rate constant k_{obs} is given by:

$$k_{obs} = k_{pH} + k' \cdot [B] \qquad \text{(Eq. 4)}$$

where [B] is the buffer concentration, $k' = k_{HCO_3^-} \cdot f_{HCO_3^-}$ or $k_{H_2BO_3^-} \cdot f_{H_2BO_3^-}$, and $k_{HCO_3^-}$ and $k_{H_2BO_3^-}$ are second-order rate constants of HCO_3^- ions and $H_2BO_3^-$ ions, respectively. $f_{HCO_3^-}$ is the buffer HCO_3^- fraction (#1) at pH

Table IV—Values of Rate Constants at Different Temperatures and the Arrhenius Activation Parameter for I at Different pH [a]

Buffer	pH	Temp., °C	k_{pH}, $h^{-1} \times 10^3$	E_a, kcal·M^{-1}
Citrate	3.0	23	1.938	25.687
		37	13.930	
Acetate	5.0	23	1.607	28.307
		37	14.125	
Phosphate	7.0	4	0.194	
		23	1.679	21.755
		37	13.810	
Borate	10.0	4	3.034	
		23	31.825	28.732
		37	840.720	

[a] At 0.2 M buffer concentration, μ = 0.5.

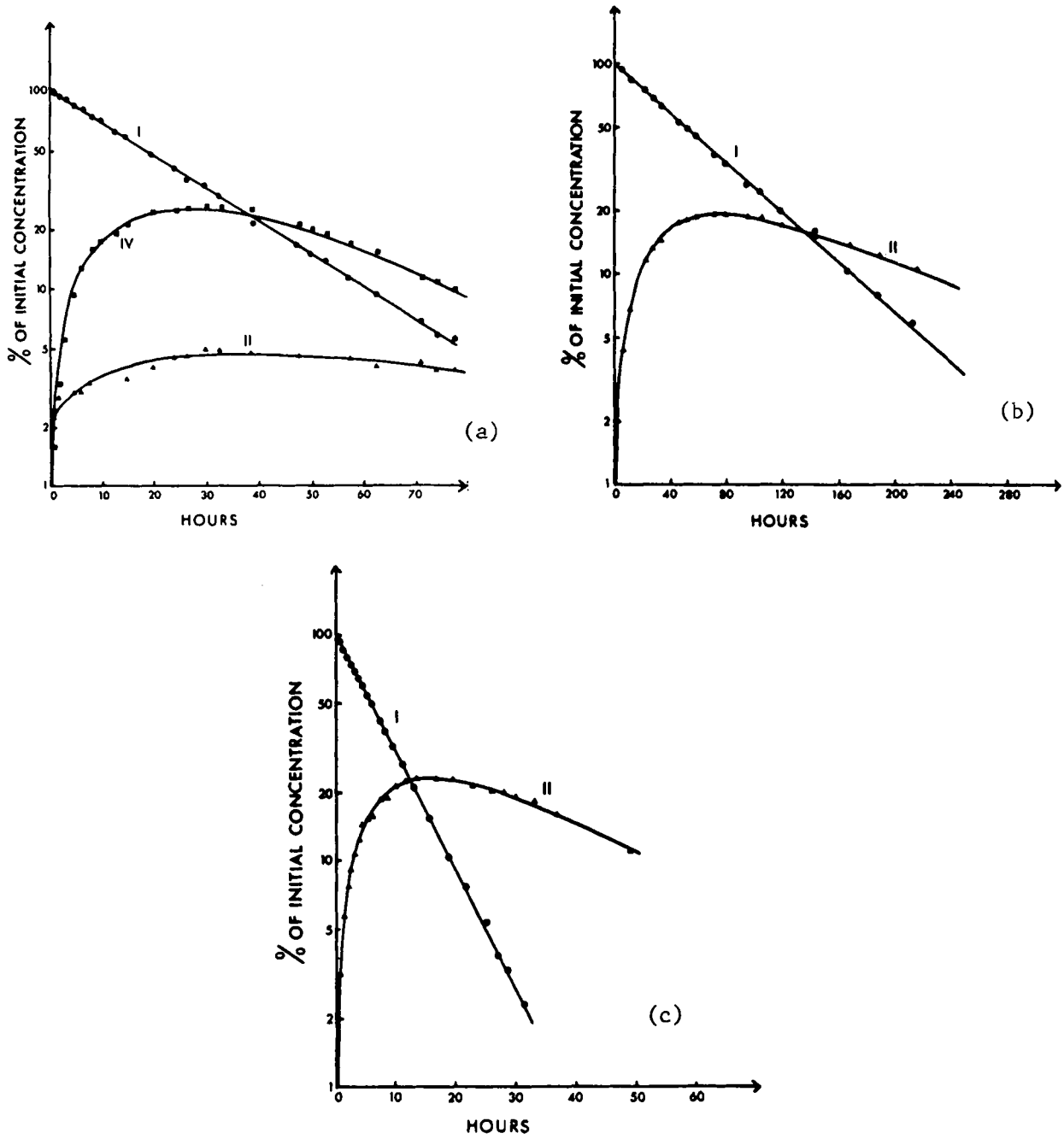

Figure 5—*Kinetics for cefotaxime (●), deacetylcefotaxime (▲), and deacetylcefotaxime lactone (■) during the degradation of a cefotaxime sodium salt solution at 37°C (μ = 0.5 and 0.2 M buffer concentration) at pH 1.9 (a), pH 4.0 (b), and pH 9.0 (c).*

8.5, $f_{H_2BO_3^-}$ is the buffer $H_2BO_3^-$ fraction (# I) at pH 9.5 and 10.0, and k_{pH} is the rate constant at zero buffer concentration.

An estimation of the catalytic effect was made from the plots of k_{obs} against the buffer concentration. The second-order rate constants were determined as $k'_{HCO_3^-} = 77.6 \times 10^{-3}$ $h^{-1}\cdot M^{-1}$ at pH 8.5; $k'_{H_2BO_3^-} = 212.28 \times 10^{-3}$ $h^{-1}\cdot M^{-1}$ at pH 9.5; and $k'_{H_2BO_3^-} = 187.25 \times 10^{-3}$ $h^{-1}\cdot M^{-1}$ at pH 10.0. k' in all cases is increasingly dependent on the buffer concentration. The rate constant, k_{pH} at zero buffer concentration, obtained by the intercept with the y-axis, gives the value of the rate constant independently of the buffer effect (Table I).

With acetate buffer, at pH 5.0 where CH_3COOH and CH_3COO^- species are present, k_{obs} decreases with the buffer concentration. At this pH, the observed rate constant is given by:

$$k_{obs} = k_{pH} + [B]\frac{k_{CH_3COOH}\cdot a_H + k_{CH_3COO^-}K_a}{a_H + K_a} \qquad \text{(Eq. 5)}$$

where K_a is the dissociation constant of acetic acid at 37°C, a_H is the hydrogen ion activity potentiometrically measured, and k_{CH_3COOH} and $k_{CH_3COO^-}$ are the second-order rate constants of CH_3COOH and CH_3COO^- ion, respectively. The catalytic negative effect of acetate buffer at this pH may be estimated by the value of the slope obtained when k_{obs} is plotted against buffer concentration (-10.5×10^{-3} $h^{-1}\cdot M^{-1}$); k_{obs} is decreasingly dependent on the buffer concentration. The protective effect against degradation observed with acetate buffer may be related to the presence of a 3-acetoxymethyl group in the molecular structure of I.

Primary Salt and Ionic Strength Effects—The primary salt effect was investigated at 37°C and pH 2.2, 6.0, and 9.5 for 0.2 M buffer concentration. Ionic strength was varied with potassium chloride solution. The data of k_{obs} for ionic strengths μ = 0.3, 0.5, and 0.7 are given in Table III. The influence of ionic strength on rate constants was demonstrated (15) by Bronsted and Bjerrum. Debye-Hückel theory applied to the kinetics shows that for ionic strengths <0.05, a linear relationship can be obtained between log k_{obs} and $\mu^{1/2}$ according to:

$$\log k_{obs} = \log k_{0,\mu_0} + 2QZ_AZ_B\sqrt{\mu} \qquad \text{(Eq. 6)}$$

where Q is a constant depending on the temperature and the dielectric constant

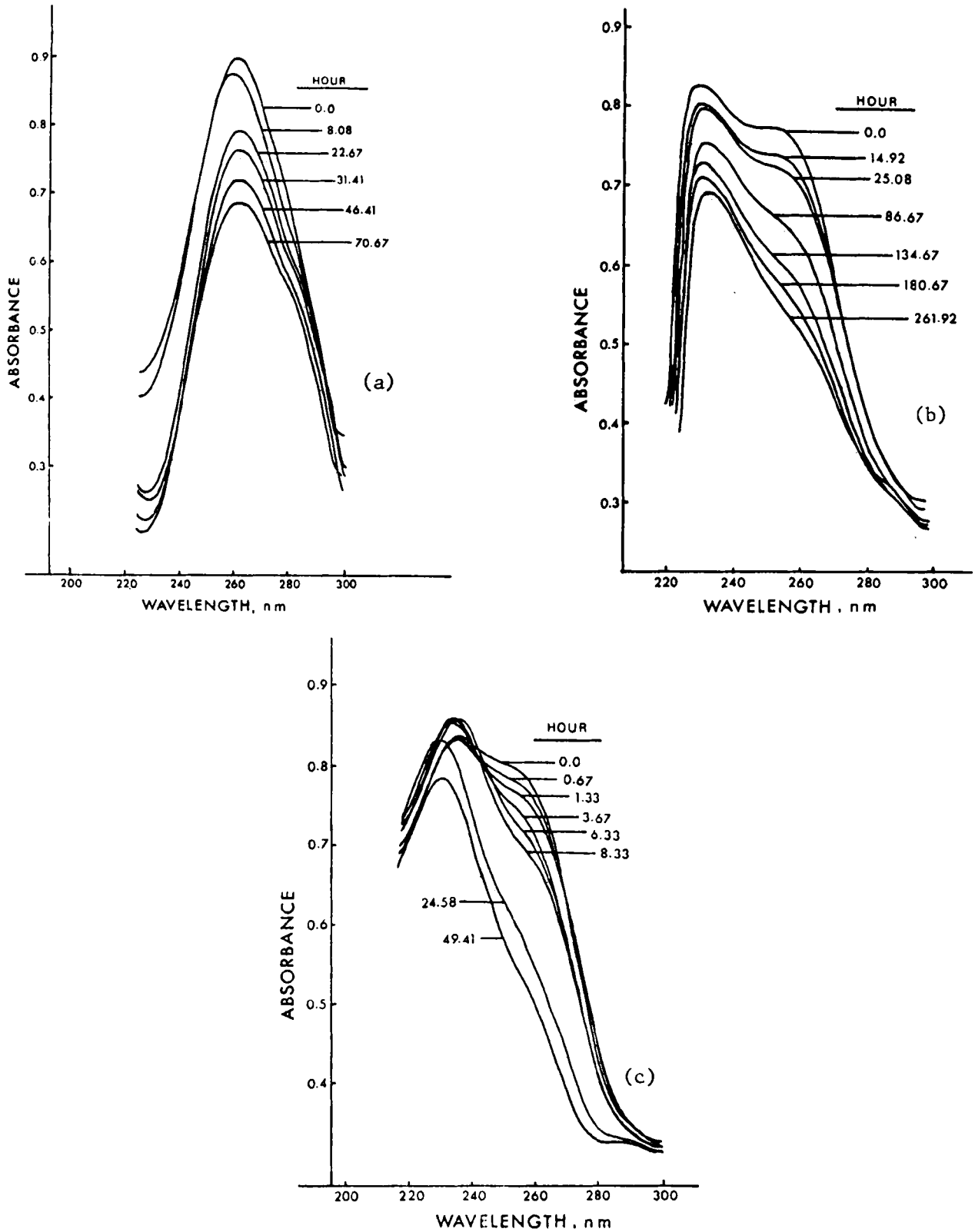

Figure 6—*Spectral changes during the degradation of a 2.0 × 10^{-5} M cefotaxime sodium salt solution (0.2 M buffer concentration, 37°C, μ = 0.5) at pH 1.9 (a), pH 4.0 (b), and pH 9.0 (c).*

of the solvent, Z_A and Z_B are the electric charges of the reactants conducting to the activated complex, and k_{0,μ_0} is the rate constant at zero ionic strength. At higher ionic strength, the second Debye-Hückle (16) relationship gives:

$$\log k_{obs} = \log k_{0,\mu_0} + \frac{2QZ_AZ_B\sqrt{\mu}}{1+\sqrt{\mu}} \qquad \text{(Eq. 7)}$$

The two ways of representation are given in Fig. 7.

A linear representation is obtained when log k_{obs} is plotted against $\mu^{1/2}$ and $\mu^{1/2}/1+\mu^{1/2}$. At pH 2.2 and 6.0 kinetic primary salt effects were negligible, in contrast to pH 9.5 where a kinetic primary salt effect was observed. At pH 2.2 and 6.0, the rate constants are almost independent of the ionic strength because one of the reactants is noncharged. At pH 9.5, the positive slope observed shows that the two reactant species have the same charge.

pH-Rate Profile—The pH-rate profile for the degradation of I was ob-

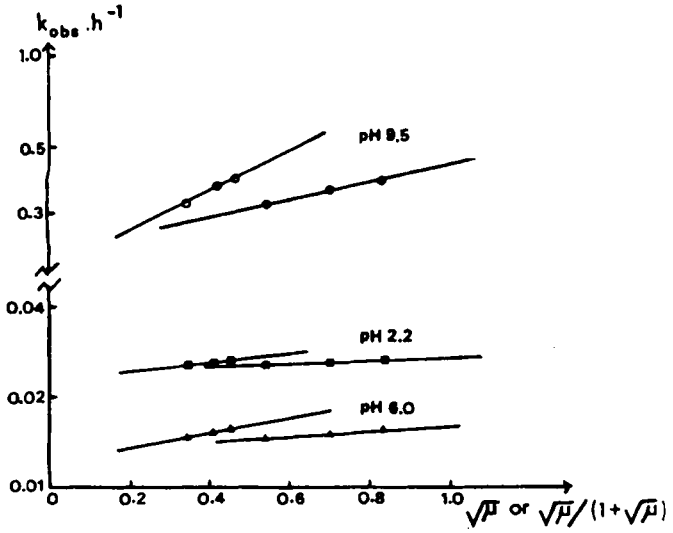

Figure 7—*Plots of log* k_{obs} versus $\sqrt{\mu}$ (●, ■, ▲) *or* $\sqrt{\mu}/1+\sqrt{\mu}$ (○, □, △) *at different pH values (0.2 M buffer concentration, 37°C) for a cefotaxime sodium salt solution.*

tained by plotting the values of log k_{pH} against pH, independently of any buffer effects (except for pH 4.0 and 9.0), at 37°C and $\mu = 0.5$ (Fig. 8). Three distinct regions can be seen: (*a*) a region where the reaction is hydrogen ion catalyzed, between pH 1.6 and 3.0, (*b*) a plateau where the reaction is not pH dependent, between pH 3.0 and 7.0, and (*c*) a region where the reaction is hydroxide ion catalyzed, above pH 7.0. The U-shape of the experimental curve, without inflexion in the pK_a zones (2.1 and 3.4), is characteristic of a reaction both hydrogen ion catalyzed and hydroxide ion catalyzed. The log k_{pH}–pH profile for I was fitted with:

$$k_{pH} = k_H \cdot a_H + k_0 + k_{OH}\frac{K_w}{a_H} \qquad \text{(Eq. 8)}$$

where k_H is the second-order rate constant for the hydrogen ion-catalyzed degradation, identical for the ionized and un-ionized cefotaxime species; a_H is the activity of hydrogen ions potentiometrically determined; k_0 is the first-order rate constant for the spontaneous or water-catalyzed reaction; k_{OH} is the second-order rate constant for the hydroxide ion-catalyzed degradation; and K_w is the autoprotolysis constant of water, $\sim 2.09 \times 10^{-14}$ at 35°C.

From the experimental values at pH 1.60, 6.00, and 9.50, k_H, k_0, and k_{OH} were calculated from Eq. 8 to be $k_H = 1.90\ h^{-1}\cdot M^{-1}$, $k_0 = 0.013\ h^{-1}$, and $k_{OH} = 4626.5\ h^{-1}\cdot M^{-1}$. These constants were used to generate the theoretical pH-rate profile given in Fig. 8, using a computer. A satisfactory fit of the data was obtained.

The good agreement between the experimental data, the theoretical profile, and the results of primary salt effects suggest the following reactions (Scheme III) to occur in the pH region investigated:

$$\text{Cef} + H^+ \xrightarrow{k_H} \text{products}$$

$$\text{Cef} \xrightarrow{k_0} \text{products}$$

$$\text{Cef} + OH^- \xrightarrow{k_{OH}} \text{products}$$

Scheme III

At pH 2.2, due to the overall average charge of the species in solution, the salt effect is not visible. At pH 6.0, I is ionized, the main process is a water attack, and no salt effect is observed. At pH 9.5, where a general base-catalytic effect has been shown with borate ions, a positive salt effect is obtained because I is negatively charged and reacts with hydroxide and borate ions.

Temperature Effect—The effect of temperature was studied with an ionic strength of 0.5 in 0.2 M buffer solutions, at pH 7.0 and 10.0, by measuring the degradation rates at 4°C, 23°C, and 37°C. Other determinations (pH 3.0 and 5.0) were conducted at only two temperatures (23°C and 37°C). The values of rate constants at different temperatures and the Arrhenius activation parameter are given in Table IV. These values are very similar to those obtained for other cephalosporins (1, 5, 6) and correspond to the values generally observed for solvolysis.

Comparative Stability and Reaction Mechanism—In Fig. 8, a stability comparison of I and other cephalosporins is plotted. This graph lists cephalosporins with an acetoxymethyl group in the C-3 position (cephalothin and

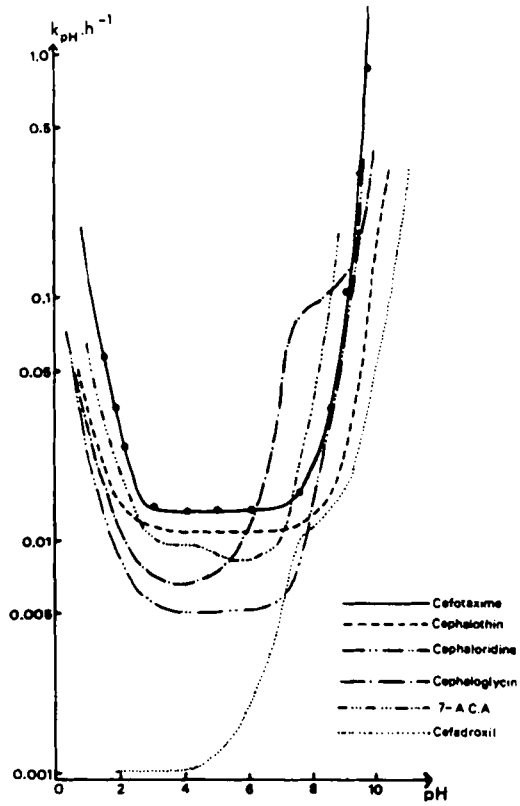

Figure 8—*log* k_{pH}*–pH profile for cefotaxime sodium salt solution at 37°C,* $\mu = 0.5$*. The points are experimental values. The solid lines were generated from Eq. 8 with an analog computer. Comparative stability study with other cephalosporins [cephalothin, cephaloridine, cephaloglycin, and 7-amino-cephalosporanic acid (7-A.C.A). from Ref. 1, cefadroxil from Ref. 6].*

cephaloglycin), cephalosporins without an acetoxymethyl group (cephaloridin and cefadroxil), and 7-aminocephalosporanic acid (7-A.C.A).

In the pH 3.0–7.0 range, where the degradation rates are not pH dependent, the rate constant $k_0 = 13 \times 10^{-3}\ h^{-1}$ calculated for I is similar to the k_0 values obtained from cephalothin and cephaloglycin. As suggested (1) for these two acetoxymethyl cephalosporins, the plateau in this pH range may correspond both to a hydrolytic cleavage of the β-lactam moiety and to an intramolecular attack with a side chain amino group participation. This intramolecular attack should be facilitated by the electron-donating effect of the *O*-methyloxime substituent on the side chain.

In acidic and alkaline media, the rate constants observed are higher than the rate constants given for cephalothin and cephaloglycin. This enhanced reactivity of I should imply a side-chain participation in the degradation, in contrast with cephalothin and cephaloglycin.

From the present results, the scheme of degradation of I in the entire pH range has been found similar to the other acetoxymethyl cephalosporins of the first generation (cephalothin and cephaloglycin). The chemical stability of I under alkaline conditions has not been proven to be reliable for β-lactamase hydrolysis and consequently for the activity against Gram-negative bacteria, as suggested for the cephalosporins of the first and second generations (1). Cefotaxime sodium (I) has a remarkable resistance to hydrolysis of these enzymes (17), in contrast to a fair stability under alkaline conditions. The enhanced resistance to the β-lactamase deactivation has been attributed to the presence of a rigid *syn O*-methyloxime group (17). The biological activity of I has also been related to the original structure of the 7-substituent aminothiazole ring, which plays an important role in the affinity of the molecule against transpeptidase activity in the synthesis of the bacterial wall.

REFERENCES

(1) T. Yamana and A. Tsuji, *J. Pharm. Sci.*, **65**, 1563 (1976).

(2) A. L. de Weck and C. H. Schneider, *J. Antimicrob. Chemother.*, **6**, Suppl. A, 161 (1980).

(3) J. Konecny, E. Felber, and J. Gruner, *J. Antibiot.*, **26**, 135 (1973).

(4) E. S. Rattie, D. E. Guttman, and L. J. Ravin, *Arzneim.-Forsch., Drug Res.*, **28**, 6, 944 (1978).

(5) E. S. Rattie, J. J. Zimmerman, and L. J. Ravin, *J. Pharm. Sci.*, **68**, 1369 (1979).
(6) A. Tsuji, E. Nakashima, Y. Deguchi, K. Nishide, T. Shimizu, S. Horiuchi, K. Ishikawa, and T. Yamana, *J. Pharm. Sci.*, **70**, 1120 (1981).
(7) R. Bucourt, D. Bormann, R. Heymes, and M. Perronnet, *J. Antimicrob. Chemother.*, **6**, Suppl. A, 63 (1980).
(8) E. Bergogne-Berezin, *Les Actualités Pharmaceutiques*, No. 185, 44 (1982).
(9) F. Kees, E. Strehl, K. Seeger, G. Seidel, P. Dominiak, and H. Grobecker, *Arzneim.-Forsch. Drug Res.*, **31**, 362 (1981).
(10) *J Antimicrob. Chemother.* **6**, suppl. A, (1980).
(11) H. Fabre and N. Hussam-Eddine. *J. Pharm. Pharmacol.*, **34**, 425 (1982).
(12) A. Albert and E. P. Serjeant "The Determination of Ionization Constants," Chapman and Hall, London, England, 1971, pp. 22, 41.
(13) L. D. Sabath, M. Jago, and E. P. Abraham, *Biochem. J.*, **96**, 739 (1965).
(14) J. M. Indelicato, T. T. Norvilas, R. R. Pfeiffer, W. J. Wheeler, and W. L. Wilham, *J. Med. Chem.*, **17**, 523 (1974).
(15) K. J. Laidler, "Reaction Kinetics, Vol. 2, Reactions in Solution," Pergamon, New York, N.Y., 1963, p. 18.
(16) A. N. Martin, J. Swarbrick, and A. Cammarata, "Physical Pharmacy," Lea and Febiger, Philadelphia, Pa., 1970, pp. 184–185.
(17) M. H. Richmond, in *J. Antimicrob. Chemother.*, Suppl. A **6**, 13 (1980).

ACKNOWLEDGMENTS

The authors thank Roussel UCLAF laboratories for supplying cefotaxime and its degradation products, and Mr. Sezerat for his helpful comments and suggestions.

Ocular Delivery of Pilocarpine from Erodible Matrices

GEORGE M. GRASS *ˣ, JOHN COBBY ‡, and MICHAEL C. MAKOID §

Received January 13, 1983, from the *College of Pharmacy, University of Nebraska Medical Center, Omaha, NE 68105.* Accepted for publication March 21, 1983. Present addresses: *School of Pharmacy, University of Wisconsin, Madison, WI 53706; ‡ICI Pharma, 16 Falconer Drive, Mississauga, Ontario, L5N 3M1 Canada; §School of Pharmacy, Creighton University, Omaha, NE 68178.

Abstract □ The present study examined the feasibility of sustaining the release of a water-soluble drug, pilocarpine, to the tear film. Both gels and dried films were utilized as drug delivery systems. *In vitro* studies demonstrated significant prolongation of drug release from these systems as compared with simple aqueous or viscous solutions. The *in vitro* results were supported by *in vivo* miosis studies in albino rabbits.

Keyphrases □ Pilocarpine—sustained release, polymeric delivery systems, *in vitro* release studies, *in vivo* miosis in rabbits □ Drug delivery systems—polymeric gels and films, pilocarpine, sustained release to the cornea, rabbits □ Polymeric matrices—sustained release of pilocarpine to the cornea, *in vivo* miosis in rabbits, *in vitro* release studies

It is well established that ocular drug bioavailability from topical dosing is dependent on several factors, one of the most prominent being the contact time of drug with tissues in the precorneal area of the eye (1). Several investigators (2, 3) have reported that the relatively low-viscosity ophthalmic solutions, while able to somewhat improve the amount of drug that penetrates the cornea to the anterior chamber, generally do not provide a sustaining effect. Conversely, Schoenwald *et al.* (4) and Patton and Robinson (2) have demonstrated that moderately viscous systems, such as gels, can sustain drug delivery to the cornea and anterior segment of the eye. Furthermore, it is known that slowly dissolving lamellae remain in the eye for extended periods of time. Therefore, it is of interest to examine and assess these systems for their potential in ocular drug delivery.

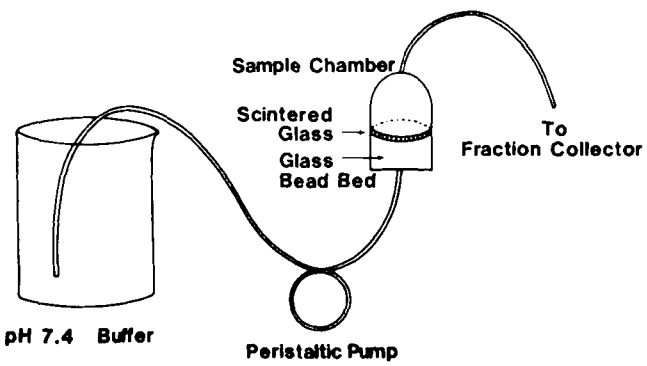

Figure 1—In vitro *dissolution apparatus used to measure appearance of pilocarpine from solutions and lamellae.*

A chronic problem with dissolving hydrogels is their usual high water content, which allows low molecular weight substances to diffuse quickly out of the gel, leaving a "ghost" without active ingredients. Extensive cross-linking of polymers, or dehydration of the gel to a dry film state, could measurably improve the release characteristics of the system.

Due to the need for frequent dosing of pilocarpine from commercial solution preparations, the expense of currently marketed controlled-release devices, and because extensive work has been published regarding ocular absorption of pilocarpine from both solutions and various gel systems, this drug was selected as a model compound for release from several types of ocular polymeric systems.

EXPERIMENTAL

Materials—Reagent-grade polyvinyl alcohol (PVA)[1], with an average mol. wt. of 16,000, and carboxyvinyl copolymer (carbomer 934)[2] were used as received. Tritiated pilocarpine[3], with a specific activity of 20 mCi/mg, was purified by vacuum evaporation immediately prior to use (5). All other chemicals were reagent or analytical grade.

Male albino rabbits[4], weighing 2.5–3.5 kg, were used throughout the study. No special dietary restrictions were used for the animals, and they were maintained in a normal lighting and auditory environment.

Methods—*Preparation of Solutions and Films*—A 4% w/v solution of pilocarpine nitrate, made isotonic with sodium chloride, was prepared in pH 7.4 Sorensen's phosphate buffer. To 10 mL of this solution, tritiated pilocarpine (10 μL) was added to yield a specific activity of ~1.5 μCi/mL. A negligible change in pilocarpine solution concentration occurred through this spiking procedure.

Pilocarpine, 2% in 10% PVA in phosphate buffer, was prepared with a specific activity of ~0.9 μCi/mL. Solutions were refrigerated between uses and were discarded within 7 d.

Erodible polymer films containing drug were prepared in the following manner. The 10% PVA solution in distilled water (40 mL) was poured into

[1] Aldrich Chemical Co., Milwaukee, Wis.
[2] Carbopol 934; B. F. Goodrich, Cleveland, Ohio.
[3] New England Nuclear, Boston, Mass.
[4] Sasko, Omaha Neb.

0022-3549/84/0500-0618$01.00/0
© 1984, American Pharmaceutical Association

(5) E. S. Rattie, J. J. Zimmerman, and L. J. Ravin, *J. Pharm. Sci.*, **68**, 1369 (1979).
(6) A. Tsuji, E. Nakashima, Y. Deguchi, K. Nishide, T. Shimizu, S. Horiuchi, K. Ishikawa, and T. Yamana, *J. Pharm. Sci.*, **70**, 1120 (1981).
(7) R. Bucourt, D. Bormann, R. Heymes, and M. Perronnet, *J. Antimicrob. Chemother.*, **6**, Suppl. A, 63 (1980).
(8) E. Bergogne-Berezin, *Les Actualités Pharmaceutiques*, No. 185, 44 (1982).
(9) F. Kees, E. Strehl, K. Seeger, G. Seidel, P. Dominiak, and H. Grobecker, *Arzneim.-Forsch. Drug Res.*, **31**, 362 (1981).
(10) *J Antimicrob. Chemother.* **6**, suppl. A, (1980).
(11) H. Fabre and N. Hussam-Eddine. *J. Pharm. Pharmacol.*, **34**, 425 (1982).
(12) A. Albert and E. P. Serjeant "The Determination of Ionization Constants," Chapman and Hall, London, England, 1971, pp. 22, 41.
(13) L. D. Sabath, M. Jago, and E. P. Abraham, *Biochem. J.*, **96**, 739 (1965).
(14) J. M. Indelicato, T. T. Norvilas, R. R. Pfeiffer, W. J. Wheeler, and W. L. Wilham, *J. Med. Chem.*, **17**, 523 (1974).
(15) K. J. Laidler, "Reaction Kinetics, Vol. 2, Reactions in Solution," Pergamon, New York, N.Y., 1963, p. 18.
(16) A. N. Martin, J. Swarbrick, and A. Cammarata, "Physical Pharmacy," Lea and Febiger, Philadelphia, Pa., 1970, pp. 184–185.
(17) M. H. Richmond, in *J. Antimicrob. Chemother.*, Suppl. A **6**, 13 (1980).

ACKNOWLEDGMENTS

The authors thank Roussel UCLAF laboratories for supplying cefotaxime and its degradation products, and Mr. Sezerat for his helpful comments and suggestions.

Ocular Delivery of Pilocarpine from Erodible Matrices

GEORGE M. GRASS *ˣ, JOHN COBBY ‡, and MICHAEL C. MAKOID §

Received January 13, 1983, from the *College of Pharmacy, University of Nebraska Medical Center, Omaha, NE 68105.* Accepted for publication March 21, 1983. Present addresses: *School of Pharmacy, University of Wisconsin, Madison, WI 53706; ‡ICI Pharma, 16 Falconer Drive, Mississauga, Ontario, L5N 3M1 Canada; §School of Pharmacy, Creighton University, Omaha, NE 68178.

Abstract □ The present study examined the feasibility of sustaining the release of a water-soluble drug, pilocarpine, to the tear film. Both gels and dried films were utilized as drug delivery systems. *In vitro* studies demonstrated significant prolongation of drug release from these systems as compared with simple aqueous or viscous solutions. The *in vitro* results were supported by *in vivo* miosis studies in albino rabbits.

Keyphrases □ Pilocarpine—sustained release, polymeric delivery systems, *in vitro* release studies, *in vivo* miosis in rabbits □ Drug delivery systems—polymeric gels and films, pilocarpine, sustained release to the cornea, rabbits □ Polymeric matrices—sustained release of pilocarpine to the cornea, *in vivo* miosis in rabbits, *in vitro* release studies

It is well established that ocular drug bioavailability from topical dosing is dependent on several factors, one of the most prominent being the contact time of drug with tissues in the precorneal area of the eye (1). Several investigators (2, 3) have reported that the relatively low-viscosity ophthalmic solutions, while able to somewhat improve the amount of drug that penetrates the cornea to the anterior chamber, generally do not provide a sustaining effect. Conversely, Schoenwald *et al.* (4) and Patton and Robinson (2) have demonstrated that moderately viscous systems, such as gels, can sustain drug delivery to the cornea and anterior segment of the eye. Furthermore, it is known that slowly dissolving lamellae remain in the eye for extended periods of time. Therefore, it is of interest to examine and assess these systems for their potential in ocular drug delivery.

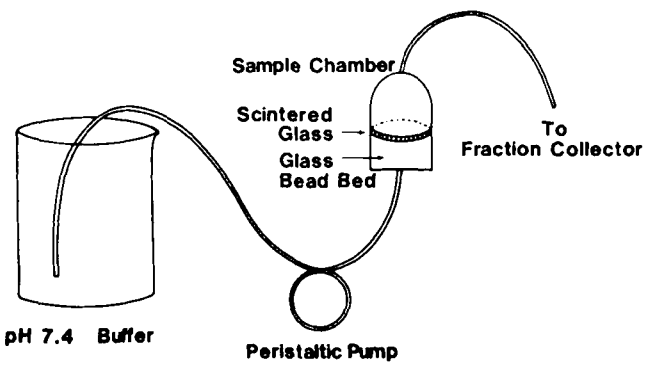

Figure 1—In vitro *dissolution apparatus used to measure appearance of pilocarpine from solutions and lamellae.*

A chronic problem with dissolving hydrogels is their usual high water content, which allows low molecular weight substances to diffuse quickly out of the gel, leaving a "ghost" without active ingredients. Extensive cross-linking of polymers, or dehydration of the gel to a dry film state, could measurably improve the release characteristics of the system.

Due to the need for frequent dosing of pilocarpine from commercial solution preparations, the expense of currently marketed controlled-release devices, and because extensive work has been published regarding ocular absorption of pilocarpine from both solutions and various gel systems, this drug was selected as a model compound for release from several types of ocular polymeric systems.

EXPERIMENTAL

Materials—Reagent-grade polyvinyl alcohol (PVA)[1], with an average mol. wt. of 16,000, and carboxyvinyl copolymer (carbomer 934)[2] were used as received. Tritiated pilocarpine[3], with a specific activity of 20 mCi/mg, was purified by vacuum evaporation immediately prior to use (5). All other chemicals were reagent or analytical grade.

Male albino rabbits[4], weighing 2.5–3.5 kg, were used throughout the study. No special dietary restrictions were used for the animals, and they were maintained in a normal lighting and auditory environment.

Methods—*Preparation of Solutions and Films*—A 4% w/v solution of pilocarpine nitrate, made isotonic with sodium chloride, was prepared in pH 7.4 Sorensen's phosphate buffer. To 10 mL of this solution, tritiated pilocarpine (10 μL) was added to yield a specific activity of ~1.5 μCi/mL. A negligible change in pilocarpine solution concentration occurred through this spiking procedure.

Pilocarpine, 2% in 10% PVA in phosphate buffer, was prepared with a specific activity of ~0.9 μCi/mL. Solutions were refrigerated between uses and were discarded within 7 d.

Erodible polymer films containing drug were prepared in the following manner. The 10% PVA solution in distilled water (40 mL) was poured into

[1] Aldrich Chemical Co., Milwaukee, Wis.
[2] Carbopol 934; B. F. Goodrich, Cleveland, Ohio.
[3] New England Nuclear, Boston, Mass.
[4] Sasko, Omaha Neb.

0022-3549/84/0500-0618$01.00/0
© 1984, American Pharmaceutical Association

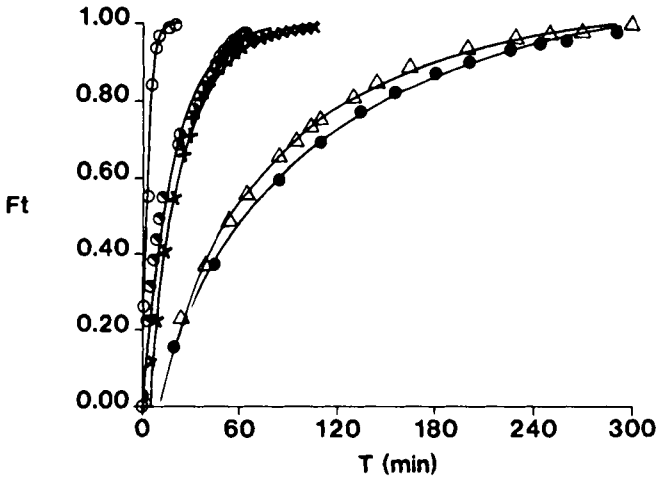

Figure 2—*Plots representing appearance of pilocarpine from solutions and lamellae. Points represent data from* in vitro *experiments. Curves were fit by nonlinear regression, r >0.99 for all formulations. Standard error of the mean is less than point size for all formulations. Key: Ft is fraction of drug released at t; (○) 25-μL solution (1.0 cps); (◑) 25-μL solution (60 cps); (×) erodible lamellae (both); (△) nonerodible lamella (no carbomer 934); (●) nonerodible lamella (with carbomer 934).*

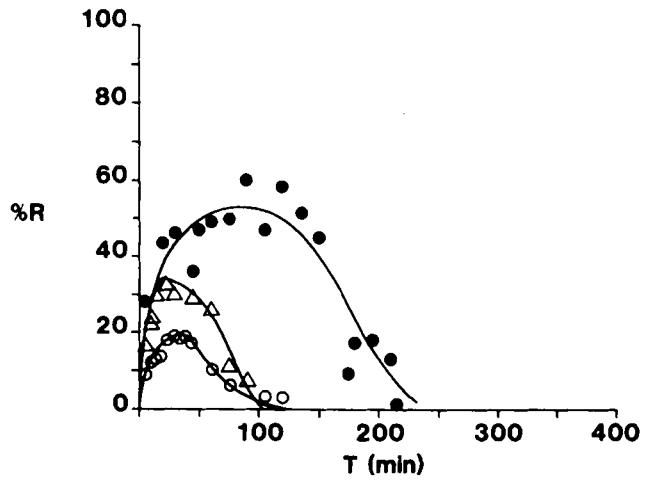

Figure 3—In vivo *comparison of miotic response to a 70-μg dose of pilocarpine nitrate administered as solutions and erodible lamellae. Key: (○) 25-μL solution (1.0 cps); (△) 25-μL solution (60 cps); (●) erodible lamellae (both).*

a glass petri dish and allowed to gel for 1 h at 4°C. A 40-mL volume of 2% pilocarpine (specific activity of ~2.75 μCi/mL) in 4% boric acid solution was layered on the PVA gel, covered[5], and allowed to remain at room temperature for 2 h before being refrigerated for an additional 24 h. At this point the excess fluid was drained away, and the dish was covered and stored in the refrigerator (4°C) until use.

Samples were punched from the gel film using a No. 4 cork borer and were weighed on an analytical balance. The gel buttons were employed in dissolution tests within 15 min of punching.

Nonerodible dried films were prepared by adding 1.125 g of glycerol to 40 mL of 0.875% pilocarpine solution (specific activity of ~1.0 μCi/mL) and 40 mL of 20% PVA solution. This solution was poured into a 100 × 50-mm glass petri dish and allowed to air dry for 7 d at ambient conditions. It was assumed that any remaining labile tritium would exchange with water and evaporate with the solvent. Stability of the tritium label was determined after 10 d by dissolving film samples in water and flash evaporating the solvent. Analysis of this solvent by scintillation counting revealed <7% loss of tritium. Samples were punched out as described for the gel matrix.

Carboxyvinyl copolymer (carbomer 934) films were also prepared. Films were prepared as described above (erodible and nonerodible films) with the exception that 100 mg of carbomer 934, neutralized with 2.4 mL of 20% NaOH, was added to the PVA (10% or 20%) solution prior to the addition of other ingredients. Preparation of the sample lamellae and storage was as previously described.

In Vitro *Dissolution*—A pictorial representation of the dissolution apparatus is shown in Fig. 1. The apparatus utilized a peristaltic pump which delivered phosphate buffer (Sorensen's pH 7.4, isotonic) from a reservoir through a flow cell containing the sample lamella and emptied into a fraction collector at a rate of 15 mL/h. The dissolution cell chamber (1 mL) was separated into two compartments by a scintered glass disk. A glass bead bed was placed below the disk to prevent a "tunnel current" through the center of the cell.

The lamella was placed on the scintered glass disk and buffer was pumped through the chamber exiting at a central opening above. Buffer effluent was collected[6] at either 2- or 5-min intervals, depending on the duration of the experiment. The collected samples were assayed by liquid scintillation[7] using liquid scintillation cocktail[8]. Based on standards, counts were converted to concentration of drug. A minimum of six runs was conducted for each experiment.

In Vivo *Studies*—Rabbits, previously acclimated to the testing procedure, were positioned in restraining cages and placed in a room with controlled lighting. A television camera with a macrolens was focused on the rabbit's eye. A television monitor and an observer were physically outside the room containing the rabbit during the experiment to minimize observer interference. To measure pupillary diameter, the observer used a transparent grid placed on the television monitor.

[5] Parafilm M.
[6] Fraction Collector; ISCO, Lincoln, Neb.
[7] Beckman model 230; Fullerton, Calif.
[8] Aquasol II; New England Nuclear, Boston, Mass.

In an attempt to assess the biological performance of these drug delivery systems, the miotic response in albino rabbits was determined. The percent miotic response in the rabbit (%R) was calculated with reference to the diameter of the pupil after prolonged exposure to a high-intensity light source (D_{min}). The appropriate equation is given as:

$$\%R = 100\,[(D_0 - D_t)/(D_0 - D_{min})] \qquad \text{(Eq. 1)}$$

where D_t is the observed pupillary diameter at time t and D_0 is the initial pupillary diameter. D_{min} was measured before dosing, and drug treatment was not initiated until pupil diameter had returned to preexposure values.

Pilocarpine concentration in the solution was selected to be identical to the amount of drug in the gel/film, *i.e.*, 70 μg/25-μL dose as compared with 70 μg/25-mg dose of lamella. In the dried film cases, the dose of drug was 700 μg and, thus, an appropriate level of drug in the solution dosage form was prepared. This method gave reproducible results such that pupillary diameter changes of 0.1 mm (~2%) could be observed easily.

The lamella or solution was then instilled into the eye by pulling the lower eyelid away from the globe and placing the dose in the lower portion of the conjunctival sac. The eyelid was immediately returned to its normal position. During each experimental run, only one eye of each animal was dosed with drug. After instillation of the dose, the observer left the testing room.

Measurements of pupillary diameter were made at 5-min intervals for the first 15 min and every 15 min thereafter. A minimum of three runs was conducted for each experiment. Significance of results was determined by comparison of response values by t test.

RESULTS

***In Vitro* Dissolution**—Pilocarpine solution data fit by nonlinear regression (NONLIN) were found to be cleared by first-order kinetics as given by the following expression:

$$W_r = W_f e^{-k_d t} \qquad \text{(Eq. 2)}$$

where W_r is the weight of drug remaining to be cleared at time t, W_f is the final weight of drug cleared from the chamber, and k_d is the rate constant for clearance. Typical release profiles are shown in Fig. 2. It was found that the half-life ($t_{1/2}$) for clearance of a pilocarpine solution with a viscosity of 1.0 cps was 2.0 min and for a 60-cps PVA solution it was 12.7 min. To account for the delay in appearance of drug from the dissolution chamber to the sample collection (physical distance), a lag time ($t = t_0 - t_{lag}$) was required for all solutions and gel/films.

Pilocarpine release from gel/films is also shown in Fig. 2. Release from these systems, as compared with simple aqueous solutions, is sustained for a significantly longer time.

Release of drug from the gel/films could be either by a dissolution- or diffusion-controlled process or, in some cases, by a combination of both mechanisms. The data were fit by nonlinear regression (NONLIN) to both the Hixon–Crowell dissolution cube root equation (6, 7) and to a diffusion-controlled dissolution equation (8, 9):

$$F_t = 3k_r t^{1/2} - 3(k_r t^{1/2})^2 + (k_r t^{1/2})^3 \qquad \text{(Eq. 3)}$$

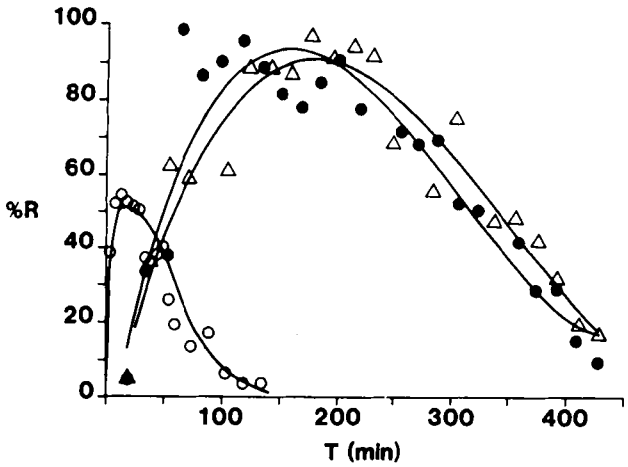

Figure 4—In vivo *comparison of miotic response to a 700-μg dose of pilocarpine nitrate administered as solutions and nonerodible lamellae. Key: (○) 25-μL solution (1.0 cps); (●) nonerodible lamella (no carbomer 934); (△) nonerodible lamella (with carbomer 934).*

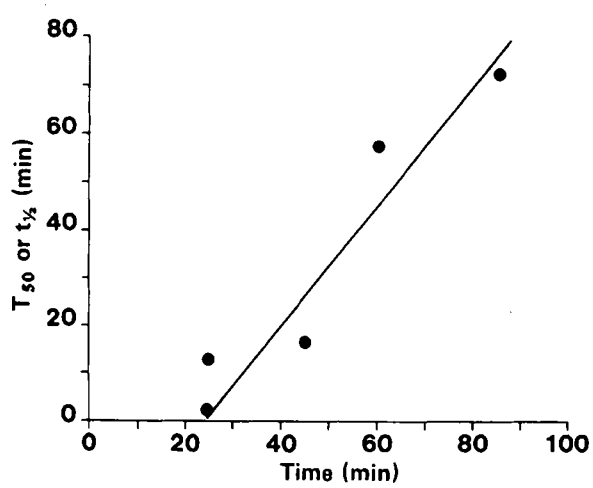

Figure 5—In vivo–in vitro *correlation utilizing* $t_{1/2}$ *for solutions and* T_{50} *for lamellae. Key: (●)* T_{50} *or* $t_{1/2}$. *The time indicated on the* x-*axis is the time at which 90% of the observed maximum response is first obtained.*

where F_t is the fraction of drug released to time t and k_r is the release rate constant.

Both erodible cross-linked lamella types (with and without carbomer 934) displayed identical release characteristics which were best fit by the diffusion equation (Eq. 3). The time to half dissolution (T_{50}) from these cross-linked systems was 16.2 min, calculated from the following equation:

$$T_{50} = (T_0^{1/2} + 0.206/k_r)^2 \qquad \text{(Eq. 4)}$$

where $T_0^{1/2}$ is the root lag time (9).

The cross-linked lamella samples dissolved during the testing procedure, and no visible swelling of the sample was noted during the test period. Although it was anticipated that an ionic-exchange release could retard the release of the cationic pilocarpine, the presence or absence of anionic copolymer in these preparations made no difference in the release rate of pilocarpine from the samples.

Nonerodible dried films were also tested, and the release of drug was best described by the diffusion expression (Eq. 3). Dried films without carbomer 934 did not appear to swell during the time course of testing. These films gave a T_{50} of appearance of 57.5 min. Conversely, the copolymer-containing films swelled to two or three times their original size, but did not undergo appreciable dissolution. These films gave a T_{50} of pilocarpine appearance of 72.4 min.

***In Vivo* Miotic Response**—The low-dose case results are shown in Fig. 3. Note that the peak response times and the 25–30-min postdosing intervals for the 1.0- and 60-cps solutions appear identical. However, the slowly eroding lamellae show a longer time to reach a maximum. The 60-cps solution shows approximately a 1.7 times greater response than the 1.0-cps solution. These results are in agreement with published data on the bioavailability of low- and medium-viscosity ocular pilocarpine solutions (5). The erodible lamellae also show a statistically greater response ($p < 0.001$) as compared with the solution dosage forms. The most significant aspect is the extended duration of effect of the erodible lamellae as compared with the solutions. Bearing in mind that although measurement of miosis allows continuous monitoring of pharmacological response, it is not as sensitive an indicator of drug bioavailability as direct sampling of ocular tissues or aqueous humor for drug concentration (5, 10). Therefore, this extended duration is significant.

The high-dose dried film systems (Fig. 4) show a number of significant differences between the nonerodible systems and the solution dosage form. These lamellae show a greater miotic response ($p < 0.001$) and a longer period of response, as compared with the solutions. There is no statistically significant difference between the lamellae with carbomer 934 as compared with the system without this copolymer.

It has been established previously that there is a linear relationship between dose and bioavailability for pilocarpine over six orders of magnitude of dose (6). The effect of different doses with the solution is clearly different: 20 and 50% of maximum to the 70- and 700-μg doses, respectively. This differential effect is expected on the basis of published drug bioavailability data (11).

***In Vivo–In Vitro* Correlation**—Since a strictly definable peak from miotic response is not discernable, especially for the lamellae formulations, the time at which 90% of the observed maximum response was first obtained was selected. This value correlates reasonably well with the time for 50% release ($t_{1/2}$ or T_{50}) of drug in the *in vitro* studies (Fig. 5). Note that for both drug solutions, the half-life of drug clearance corresponds to the time for removal of drug from the chamber, whereas in the case of lamellae, the dissolution–diffusion process is assumed to be rate limiting. It is recognized that other parameters such as duration of effect or area under the response curve may allow correlation with *in vitro* performance, but these were not examined.

DISCUSSION

To assess the merits of the gel/film pilocarpine systems, it is first necessary to comment on the performance of aqueous and viscous pilocarpine solutions. These systems, therefore, serve as a baseline.

The nonviscous (1.0 cps) solutions provide drug to the absorbing tissue, *i.e.*, the cornea, readily so that the amount of drug absorbed is proportional to the concentration instilled (5). However, the system is not very efficient and ~98% of the applied dose is lost. Significant dilution with tears occurs within 5 min of instillation, thus effectively stopping the flux of drug across the cornea (1). This effect coupled with nonproductive absorption of drug accounts for most of the drug loss.

Conversely, viscous solutions (60 cps) increase the amount of drug absorbed by a factor of 2 or 3 and exhibit a correspondingly greater biological response. This positive influence of viscosity on drug bioavailability can be due to several factors. The better wetting of the cornea by the polymer solution would allow more intimate contact of drug with the absorbing tissue. The increased viscosity of the solution would decrease drainage loss of the drug solution and thereby promote a greater ocular drug bioavailability. Finally, some adsorption of the polymer to the corneal tissue would favor greater absorption of the drug.

The gel/film system would have several of the positive attributes of the viscous solution and should be more dramatic in influence on drug bioavailability. The most obvious expectation is a decreased drainage loss of drug and slow availability of drug from the gel/film to the corneal surface. Both the *in vitro* and *in vivo* results support these postulates.

In an attempt to decrease appearance of drug from the films, the carbomer 934 salt of pilocarpine was prepared and used. No noticeable improvement in the system was evident. This may be explained on the basis that dissolution of the gel itself in the cross-linked systems was prompt and, thus, there was insufficient time for dissolution and subsequent diffusion of the drug from the film. In the dried film case, substantial swelling was noted which would increase both water content and channels for diffusion.

It is evident from this preliminary study that gels/films can sustain the release of water-soluble drugs to the precorneal area. Moreover, it appears that the *in vitro* assessment of drug release provides at least a qualitative yardstick on *in vivo* performance.

REFERENCES

(1) S. S. Chrai, M. C. Makoid, S. P. Ericksen, and J. R. Robinson, *J. Pharm. Sci.*, **63**, 337 (1974).

(2) T. F. Patton and J. R. Robinson, *J. Pharm. Sci.*, **64**, 1312 (1975).

(3) S. S. Chrai and J. R. Robinson, *J. Pharm. Sci.*, **63**, 1218 (1974).

(4) R. D. Schoenwald, R. L. Ward, L. M. DeSantis, and R. E. Roehrs, *J. Pharm. Sci.*, **67**, 1280 (1978).

(5) S. S. Chrai and J. R. Robinson, *Am. J. Ophthamol.*, **77**, 735 (1975).

(6) A. W. Hixon and J. H. Crowell, *Ind. Eng. Chem.*, **23**, 923 (1931).
(7) A. W. Hixon and J. H. Crowell, *Ind. Eng. Chem.*, **23**, 1002 (1931).
(8) J. Cobby, M. Mayersohn, and G. C. Walker, *J. Pharm. Sci.*, **63**, 725 (1974).
(9) J. Cobby, M. Mayersohn, and G. C. Walker, *J. Pharm. Sci.*, **63**, 732 (1974).
(10) S. Mishima and S. Nagataki, *Contact Intraocular Lens Med. J.*, **4**(3), (Conrad Berens Memorial Lecture; Pharmacology of Ophthalmic Solutions), 23 (1978).
(11) S. S. Chrai, T. F. Patton, A. Mehte, and J. R. Robinson, *J. Pharm. Sci.*, **62**, 1112 (1973).

Electrochemical Chromatographic Determinations of Morphine Antagonists in Biological Fluids, with Applications

HARTMUT DERENDORF, ALAA EL-DIN A. EL-KOUSSI, and EDWARD R. GARRETT ˣ

Received December 17, 1982, from *The Beehive, College of Pharmacy, J. Hillis Miller Health Center, University of Florida, Gainesville, FL 32610.* Accepted for publication January 27, 1983.

Abstract □ The morphine antagonists naltrexone and naloxone were extracted from plasma and urine, separated on a chromatographic column, and assayed by electrochemical detection. Optimum oxidation potentials were 0.65 V for morphine and 0.75 V for naloxone and naltrexone. Assay sensitivities were 2–5 ng/mL for plasma and 10 ng/mL for urine. The assays were applied to determine red blood cell partition coefficients of 1.83 ± 0.15 (*SD*) for naltrexone and 1.49 ± 0.27 (*SD*) for naloxone in a concentration range of 10–3500 ng/mL. No significant time dependence for the partitioning could be observed. Plasma protein binding in the same concentration range, determined by ultracentrifugation, was 27.7% ± 2.5% (*SD*) for naltrexone and 30.1% ± 5.1% (*SD*) for naloxone. The degree of protein binding did not change in the presence of morphine for morphine–antagonist ratios between 1:10 and 10:1. No concentration dependencies of red blood cell partitioning or protein binding were observed.

Keyphrases □ Naltrexone—HPLC with electrochemical detection, plasma and urine, applications to protein binding and red blood cell partitioning □ Naloxone—HPLC with electrochemical detection, plasma and urine, applications to protein binding and red blood cell partitioning □ Protein binding—naltrexone and naloxone in the presence of morphine, HPLC with electrochemical detection, red blood cell partitioning □ Red blood cell partitioning—naltrexone and naloxone in the presence of morphine, HPLC with electrochemical detection, protein binding

The classical detection methods for high-performance liquid chromatography (HPLC) by spectrophotometric and fluorescence detection are not useful for some drugs with low absorptivities or low fluorescence. Electrochemical detection has been a method of recent choice in selected instances. It combines amperometric titration and liquid chromatography (1) and has been applied to the assays of catecholamines (2), phenolic compounds (3), phenothiazines (4, 5), and morphine (I) (6–8).

The present study describes sensitive and accurate HPLC assays for the antagonists of morphine, naloxone (II) and naltrexone (III) in biological fluids with electrochemical detection. Studies on possible pharmacokinetic interactions between morphine and its antagonists are needed since naltrexone or naloxone are given to morphine-overdosed subjects. Prerequisites for such studies are specific and sensitive assays that allow simultaneous determinations of agonist and antagonist as well as their metabolites.

A facile procedure for the simultaneous determination of I and III or II is described using HPLC with electrochemical detection. The assay was applied to the determination of the protein binding of II and III and the influence of I on their protein binding. The red blood cell partition properties of both antagonists were also investigated.

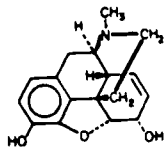

I

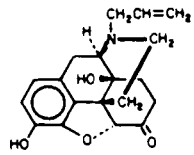

II

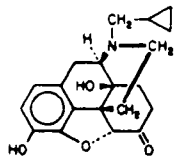

III

EXPERIMENTAL

Materials—The following analytical-grade materials were used: sodium bicarbonate[1], monobasic potassium phosphate[1], volumetric concentrates of hydrochloric acid and sodium hydroxide[2], 1-butanol[3], and benzene[4]. Acetonitrile[4] was HPLC grade. Morphine (I)[5], naloxone (II)[5], and naltrexone (III)[5] were used as received. Sodium chloride injection USP[6], sodium heparin injection[7], and disposable syringes[8] were used in the preparation of red blood cell suspensions.

Apparatus—For the HPLC assay the following instruments were used: high-pressure pump[9], a six-port injector[10], an electrochemical detector[11] with a working electrode of glassy carbon[12], a strip-chart recorder[13], and an octadecylsilane column[14] with a guard column of the same material.

Plasma protein binding was determined with an ultracentrifuge[15]. A laboratory centrifuge[16] was used in the separation of organic extracts from aqueous phases.

Chromatographic Conditions—The mobile phase was a mixture of 0.04 M monobasic potassium phosphate and acetonitrile (90:10). The flow rate was

[1] Mallinckrodt, Paris, Ky.
[2] Ricca Chemical Co., Arlington, Tex.
[3] Burdick & Jackson Laboratories, Muskegon, Mich.
[4] Fisher Scientific Co., Fair Lawn, N.J.
[5] National Institute on Drug Abuse, Research Technology Branch, Rockville, Md.
[6] McGaw Laboratories, Irvine, Calif.
[7] The Upjohn Co., Kalamazoo, Mich.
[8] Monoject, Division of Sherwood Medical, A. Brunswick Co., St. Louis, Mo.
[9] Series 3B Microcomputer controlled pump module; Perkin-Elmer, Norwalk, Conn.
[10] Model 7105; Rheodyne, Cotati, Calif.
[11] LC 4A; Bioanalytical Systems, West Lafayette, Ind.
[12] TLS; Bioanalytical Systems, West Lafayette, Ind.
[13] Series 5000, Fisher Recordall; Fisher Scientific Co., Fair Lawn, N.J.
[14] C_{18} μBondapak column; Waters Associates, Milford, Mass.
[15] Ultracentrifuge Model LS-50 with rotor Ti 50; Beckman Instruments, Norcross, Ga.
[16] Lab centrifuge; International Centrifuge Equipment Co., Needham, Mass.

0022-3549/84/0500-0621$01.00/0
© 1984, American Pharmaceutical Association

(6) A. W. Hixon and J. H. Crowell, *Ind. Eng. Chem.*, **23**, 923 (1931).
(7) A. W. Hixon and J. H. Crowell, *Ind. Eng. Chem.*, **23**, 1002 (1931).
(8) J. Cobby, M. Mayersohn, and G. C. Walker, *J. Pharm. Sci.*, **63**, 725 (1974).
(9) J. Cobby, M. Mayersohn, and G. C. Walker, *J. Pharm. Sci.*, **63**, 732 (1974).
(10) S. Mishima and S. Nagataki, *Contact Intraocular Lens Med. J.*, **4**(3), (Conrad Berens Memorial Lecture; Pharmacology of Ophthalmic Solutions), 23 (1978).
(11) S. S. Chrai, T. F. Patton, A. Mehte, and J. R. Robinson, *J. Pharm. Sci.*, **62**, 1112 (1973).

Electrochemical Chromatographic Determinations of Morphine Antagonists in Biological Fluids, with Applications

HARTMUT DERENDORF, ALAA EL-DIN A. EL-KOUSSI, and EDWARD R. GARRETT ˣ

Received December 17, 1982, from *The Beehive, College of Pharmacy, J. Hillis Miller Health Center, University of Florida, Gainesville, FL 32610.* Accepted for publication January 27, 1983.

Abstract □ The morphine antagonists naltrexone and naloxone were extracted from plasma and urine, separated on a chromatographic column, and assayed by electrochemical detection. Optimum oxidation potentials were 0.65 V for morphine and 0.75 V for naloxone and naltrexone. Assay sensitivities were 2–5 ng/mL for plasma and 10 ng/mL for urine. The assays were applied to determine red blood cell partition coefficients of 1.83 ± 0.15 (*SD*) for naltrexone and 1.49 ± 0.27 (*SD*) for naloxone in a concentration range of 10–3500 ng/mL. No significant time dependence for the partitioning could be observed. Plasma protein binding in the same concentration range, determined by ultracentrifugation, was 27.7% ± 2.5% (*SD*) for naltrexone and 30.1% ± 5.1% (*SD*) for naloxone. The degree of protein binding did not change in the presence of morphine for morphine–antagonist ratios between 1:10 and 10:1. No concentration dependencies of red blood cell partitioning or protein binding were observed.

Keyphrases □ Naltrexone—HPLC with electrochemical detection, plasma and urine, applications to protein binding and red blood cell partitioning □ Naloxone—HPLC with electrochemical detection, plasma and urine, applications to protein binding and red blood cell partitioning □ Protein binding—naltrexone and naloxone in the presence of morphine, HPLC with electrochemical detection, red blood cell partitioning □ Red blood cell partitioning—naltrexone and naloxone in the presence of morphine, HPLC with electrochemical detection, protein binding

The classical detection methods for high-performance liquid chromatography (HPLC) by spectrophotometric and fluorescence detection are not useful for some drugs with low absorptivities or low fluorescence. Electrochemical detection has been a method of recent choice in selected instances. It combines amperometric titration and liquid chromatography (1) and has been applied to the assays of catecholamines (2), phenolic compounds (3), phenothiazines (4, 5), and morphine (I) (6–8).

The present study describes sensitive and accurate HPLC assays for the antagonists of morphine, naloxone (II) and naltrexone (III) in biological fluids with electrochemical detection. Studies on possible pharmacokinetic interactions between morphine and its antagonists are needed since naltrexone or naloxone are given to morphine-overdosed subjects. Prerequisites for such studies are specific and sensitive assays that allow simultaneous determinations of agonist and antagonist as well as their metabolites.

A facile procedure for the simultaneous determination of I and III or II is described using HPLC with electrochemical detection. The assay was applied to the determination of the protein binding of II and III and the influence of I on their protein binding. The red blood cell partition properties of both antagonists were also investigated.

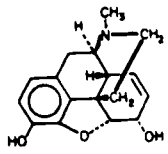

I

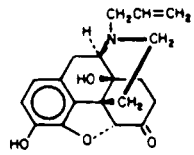

II

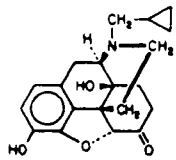

III

EXPERIMENTAL

Materials—The following analytical-grade materials were used: sodium bicarbonate[1], monobasic potassium phosphate[1], volumetric concentrates of hydrochloric acid and sodium hydroxide[2], 1-butanol[3], and benzene[4]. Acetonitrile[4] was HPLC grade. Morphine (I)[5], naloxone (II)[5], and naltrexone (III)[5] were used as received. Sodium chloride injection USP[6], sodium heparin injection[7], and disposable syringes[8] were used in the preparation of red blood cell suspensions.

Apparatus—For the HPLC assay the following instruments were used: high-pressure pump[9], a six-port injector[10], an electrochemical detector[11] with a working electrode of glassy carbon[12], a strip-chart recorder[13], and an octadecylsilane column[14] with a guard column of the same material.

Plasma protein binding was determined with an ultracentrifuge[15]. A laboratory centrifuge[16] was used in the separation of organic extracts from aqueous phases.

Chromatographic Conditions—The mobile phase was a mixture of 0.04 M monobasic potassium phosphate and acetonitrile (90:10). The flow rate was

[1] Mallinckrodt, Paris, Ky.
[2] Ricca Chemical Co., Arlington, Tex.
[3] Burdick & Jackson Laboratories, Muskegon, Mich.
[4] Fisher Scientific Co., Fair Lawn, N.J.
[5] National Institute on Drug Abuse, Research Technology Branch, Rockville, Md.
[6] McGaw Laboratories, Irvine, Calif.
[7] The Upjohn Co., Kalamazoo, Mich.
[8] Monoject, Division of Sherwood Medical, A. Brunswick Co., St. Louis, Mo.
[9] Series 3B Microcomputer controlled pump module; Perkin-Elmer, Norwalk, Conn.
[10] Model 7105; Rheodyne, Cotati, Calif.
[11] LC 4A; Bioanalytical Systems, West Lafayette, Ind.
[12] TLS; Bioanalytical Systems, West Lafayette, Ind.
[13] Series 5000, Fisher Recordall; Fisher Scientific Co., Fair Lawn, N.J.
[14] C_{18} μBondapak column; Waters Associates, Milford, Mass.
[15] Ultracentrifuge Model LS-50 with rotor Ti 50; Beckman Instruments, Norcross, Ga.
[16] Lab centrifuge; International Centrifuge Equipment Co., Needham, Mass.

0022-3549/84/0500-0621$01.00/0
© 1984, American Pharmaceutical Association

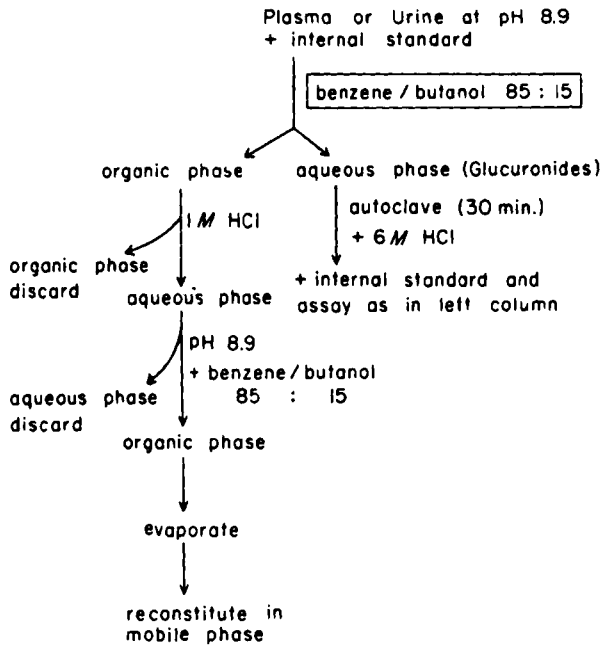

Scheme I—Extraction procedure for plasma and urine.

1.2 mL/min, with a back pressure of 6 MPa. Electrochemical detection was performed with an applied potential of 0.75 V.

Extraction Procedure from Plasma and Urine—Plasma or urine (1.0 mL) was placed in a tube containing 0.25 mL of 1 M sodium bicarbonate adjusted to pH 8.9 with 1 M NaOH. An appropriate amount of internal standard (II, I, or III depending on the compound assayed) was added to give peak height ratios between 0.2 and 4. A 2-mL volume of benzene–1-butanol (85:15) was added, and the mixture was vortexed for 30 s. The phases were separated by centrifugation for 10 min at 3000 rpm, and the organic phase was transferred with a silylated Pasteur pipet into another tube. The extraction was repeated with 2 mL of fresh solvent.

The aqueous phase can be saved for the analysis of the glucuronides. The combined organic phases were extracted with 0.5 mL of 1 M HCl and discarded. The acidic aqueous phase was washed with 2 mL of fresh organic solvent and then neutralized with 0.5 mL of 1 M NaOH. The pH was adjusted to 8.9 with 1 M sodium bicarbonate buffer, and the solution was twice reextracted with 2 mL of benzene–1-butanol (85:15). The organic phases were combined in a vial and evaporated under a nitrogen stream at 55°C. The dried residue was dissolved in 75 μL of mobile phase, and 10–25 μL was injected into the HPLC system. The extraction procedure is given in Scheme I.

The aqueous phase saved after the first extraction can be assayed for glucuronides of the compounds by the method given for morphine after hydrolysis of the conjugate (9).

Determination of Plasma Protein Binding by Ultracentrifugation—Fresh heparinized dog blood was centrifuged for 15 min at 3000 rpm. Plasma aliquots (5 mL) were spiked with different amounts of III or II to give concentrations between 10 and 3500 ng/mL of plasma. Plasma (1 mL) was taken for analysis before ultracentrifugation. After ultracentrifugation at 35,000

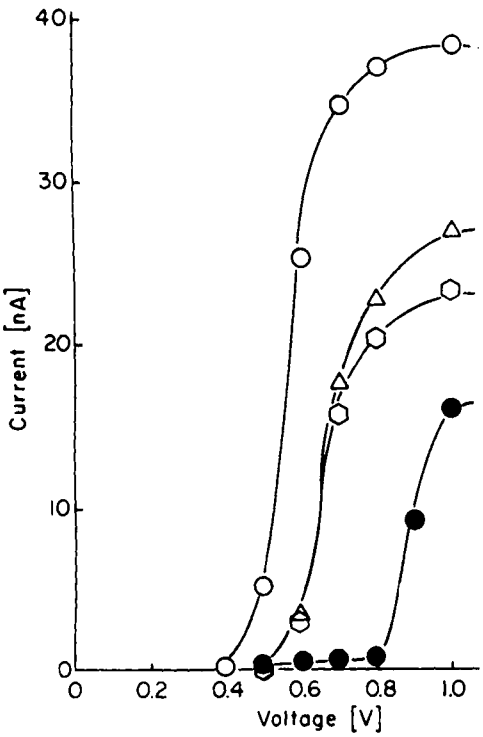

Figure 1—*Chromatographic amperogram for I (○), II (△), III (○), and the background (●) determined by application of different oxidation potentials. The background arises from oxidation of electroactive impurities in the mobile phase.*

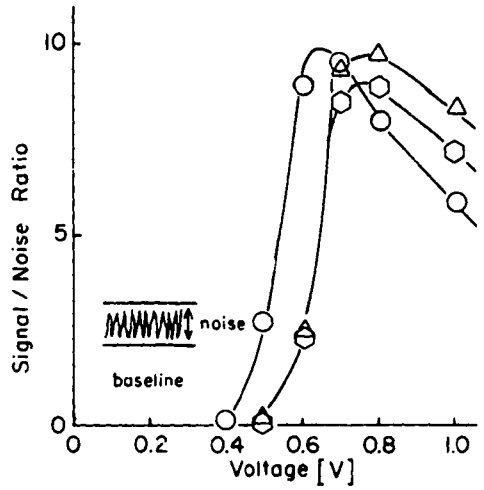

Figure 2—*Determination of optimum oxidation potential by maximization of the signal/noise ratio. Noise was measured as the amplitude of the baseline. The optimum potentials to be applied for detection are 0.65 V for I (○) and 0.75 V for III (○) and II (△).*

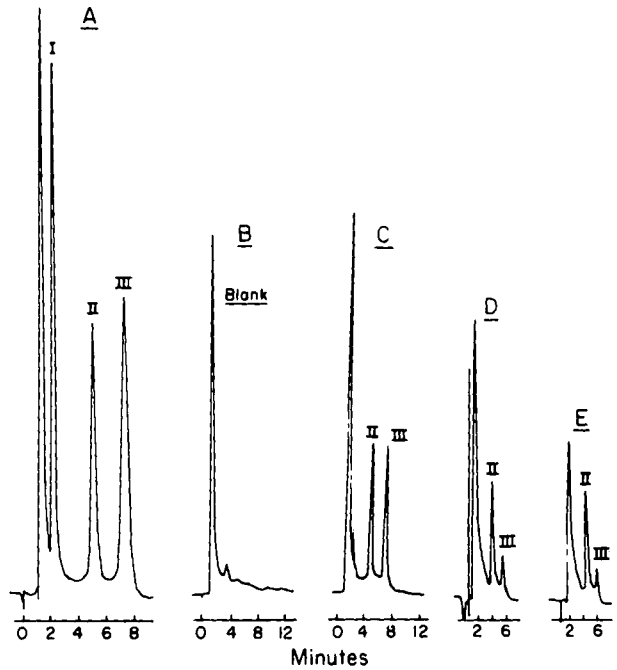

Figure 3—*Chromatograms of I, II, and III. Key: (A) 500 ng/mL in water, injection volume 20 μL; (B) 1 mL of plasma extracted, evaporated to dryness under nitrogen, and reconstituted in 75 μL of mobile phase. Injection volume 20 μL; (C) 1 mL of plasma containing 100 ng/mL of II and III, extracted and treated as in B; (D) 1 mL of plasma containing 10 ng/mL of III extracted with 50 ng/mL of II as internal standard; (E) plasma sample of D after ultracentrifugation for the determination of protein binding.*

Table I—Statistics of Calibration Curves [a]

Compound	Extracted Medium	Internal Standard	C_{IS}, ng/mL	$m \pm s_m$	$b \pm s_b$	$s_{x,y}$ [b]
Naloxone (II)	Plasma	III	30.0	10.73 ± 0.81	2.11 ± 2.34	2.35
Naltrexone (III)	Aqueous Solution	I	100.0	147.95 ± 1.66	2.35 ± 1.36	1.61
	Plasma	II	30.0	71.85 ± 5.24	1.84 ± 2.29	2.29
	Urine	II	100.0	256.47 ± 4.24	3.57 ± 4.96	6.44

[a] Concentrations (C) in ng/mL *versus* peak height ratios (PHR) relative to the internal standard, $C \pm s_{x,y} = (m \pm s_m)\text{PHR} + (b \pm s_b)$ (15). [b] Standard error of estimate y on x, concentration in ng/mL, on peak height ratio.

Table II—Protein Binding of II by Ultracentrifugation

C_{pre}, ng/mL [a]	C_{post}, ng/mL [b]	R [c]	V_{dil}, mL [d]	m [e]	$f_b \cdot 100$, % [f]
10.0	7.5	0.750	0.050	1.010	25.2
35.0	22.1	0.631	0.175	1.035	37.7
100.0	66.4	0.664	0.050	1.010	33.8
350.0	259.0	0.740	0.175	1.035	26.7
1000.0	743.6	0.744	0.050	1.010	25.8
3500.0	2418.5	0.691	0.175	1.035	31.6
Mean ± *SD*					30.1 ± 5.1

[a] Before ultracentrifugation. [b] In plasma water after ultracentrifugation. [c] Ratio between the concentrations after and before ultracentrifugation. [d] Volume of spiked solution added to 5 mL of plasma. [e] Dilution factor $(5 + V_{dil})/5$. [f] Percentage bound to plasma proteins.

Table III—Protein Binding of III by Ultracentrifugation

C_{pre}, ng/mL [a]	C_{post}, ng/mL [b]	$f_b \cdot 100$, % [c]
10.0	7.6	24.2
35.0	25.3	28.4
100.0	73.5	26.7
350.0	253.3	28.3
1000.0	684.2	31.8
3500.0	2592.6	26.6
Mean ± *SD*		27.7 ± 2.5

[a] Before ultracentrifugation. [b] In plasma water after ultracentrifugation. V_{dil} was 0.050–0.175 mL; the dilution factor was $(5 + V_{dil})/5$. [c] Percentage bound to plasma proteins.

rpm for 18 h, 1 mL of the supernatant plasma water was analyzed for III or II. The influence of I on the protein binding of both antagonists was studied in ratios 1:10, 1:2, 2:1, and 10:1.

Red Blood Cell Partition Studies—Fresh heparinized dog blood was centrifuged for 15 min at 2000 rpm. The plasma was removed and isoosmotic phosphate buffer (pH 7.4) was added to the erythrocytes. The red blood cells were gently suspended and centrifuged for 10 min at 2000 rpm; this washing procedure was repeated three times. Red blood cell suspensions in plasma water were spiked with III or II to yield total drug concentrations of 10–3500 ng/mL. The hematocrit was determined routinely using a microcentrifuge with capillary tubes. The spiked suspensions were allowed to equilibrate for 60 min and then centrifuged for 10 min at 2000 rpm. An aliquot of the supernatant solution was analyzed, and the red blood cell partition coefficient was calculated.

For the investigation of a time dependency of the red blood cell partitioning, the procedure was repeated and samples were taken after 4, 6, 8, 10, and 15 min after spiking. A minimum of 4 min of centrifugation is necessary to get a clear supernatant.

To reconfirm the observed red blood cell partition coefficients, the ratio between the drug concentrations in whole blood and plasma were determined. Whole blood (5 mL) was spiked with different amounts of drug to give whole blood concentrations between 10 and 3500 ng/mL. The blood was allowed to equilibrate for 60 min and then centrifuged for 10 min at 3000 rpm. An aliquot of the supernatant plasma was analyzed.

RESULTS AND DISCUSSION

Determination of the Optimum Detection Conditions—Signals for the three compounds were measured after application of voltages between 0.4 and 1.0 V to determine the optimum conditions for the electrochemical detection (Fig. 1). Background is defined as the Faradaic current arising from the oxidation of electroactive impurities in the mobile phase, analogous to the background absorbance in UV detectors. The detection conditions were optimized to find the maximal signal/noise ratio for each of the investigated compounds. Usually measured from peak to peak, the noise is due to pump pulsation, flow hydrodynamics, cell surface reactions, power line noise, and electronic amplification (10). The noise with an electrochemical detector is dependent on the magnitude of the background signal; the greater the background, the greater the noise. The signal/noise ratios for the three compounds are shown in Fig. 2. The maxima of these plots are the optimum potentials to be applied for detection: 0.65 V for I and 0.75 V for II and III.

Chromatographic Separation—With a mobile phase of 0.04 M monobasic potassium phosphate–acetonitrile (90:10) I–III are well separated and can be assayed simultaneously (Fig. 3A). The chromatographic background after extracting blank plasma is clean, so that low concentrations of the compounds can be detected (Fig. 3B, C). Statistics for calibration curves of II and III after extraction from plasma and urine are given in Table I. The limit of assay sensitivity for all compounds was 2–5 ng/mL for plasma and 10 ng/mL for urine. A chromatogram of a plasma sample containing 10 ng/mL of III is shown in Fig. 3D.

Protein Binding of II and III by Ultracentrifugation—The protein binding was determined by the ultracentrifugation method (11) and can be calculated from:

$$f_b = \frac{m(1 - R)}{R + m(1 - R)} \qquad \text{(Eq. 1)}$$

where f_b is the fraction bound to the plasma proteins, R is the ratio of the drug concentration (C_{post}) in plasma water after ultracentrifugation to the concentration (C_{pre}) in plasma before ultracentrifugation, and m is a dilution factor to compensate for the slight dilution of plasma on spiking. A chromatogram of a plasma sample containing 7.6 ng/mL of plasma water after ultracentrifugation is shown in Fig. 3E. The results are summarized in Tables

Table IV—Protein Binding of II and III in the Presence of I at Different Morphine–Morphine Antagonist Ratios

Antagonist	R [a]	C_{pre}, ng/mL [b]	C_{post}, ng/mL [c]	R [d]	V_{dil}, ml [e]	m [f]	$f_b \cdot 100$, % [g]
Naloxone (II)	0.1	98.0	66.1	0.674	0.100	1.020	33.0
	0.5	98.5	72.0	0.731	0.075	1.015	27.2
	2.0	97.1	72.7	0.749	0.150	1.030	25.6
	10.0	98.0	70.3	0.717	0.100	1.020	28.7
Naltrexone (III)	0.1	98.0	71.3	0.727	0.100	1.020	27.7
	0.5	98.5	69.1	0.702	0.075	1.015	30.1
	2.0	97.1	72.0	0.741	0.150	1.030	26.5
	10.0	98.0	70.8	0.722	0.100	1.020	28.2

[a] Ratio of I-antagonist for 100 ng of antagonist/mL of plasma. [b] Before ultracentrifugation. [c] In plasma water after ultracentrifugation. [d] Ratios between the concentration after and before ultracentrifugation. [e] Volume of spike solution added to 5 mL of plasma. [f] Dilution factor $(5 + V_{dil}/5)$. [g] Percentage bound to plasma proteins.

Table V—Red Blood Cell Partition Coefficients for III at Different Concentrations

A_{tot}, μg[a]	C_{PW}, ng/mL[b]	V_{PW}, mL[b]	Hematocrit	D[c]
0.050	7.7	3.15	0.370	1.82
0.050	7.6	3.08	0.385	1.84
0.175	26.3	3.15	0.370	1.89
0.175	24.3	3.05	0.390	2.14
0.500	73.1	3.18	0.365	2.00
0.500	78.0	3.00	0.400	1.70
1.750	284.7	3.70	0.260	1.88
1.750	261.0	3.00	0.400	1.85
5.000	783.0	3.03	0.395	1.70
5.000	821.6	3.05	0.390	1.56
17.500	2724.8	3.15	0.370	1.76
17.500	2651.5	2.95	0.410	1.78
Mean ± *SD*				1.83 ± 0.15

[a] Total amount of drug added to a 5.0-mL red blood cell suspension. [b] PW = plasma water. [c] Red blood cell-plasma water partition coefficient.

II and III. Protein binding of both compounds is low, averaging 30.1 ± 5.1% (*SD*) for II and 27.7 ± 2.5% (*SD*) for III, with no observable concentration dependence. The results are in excellent agreement with a study by Ludden *et al.* (12), who reported a concentration-independent protein binding of tritiated III in dog plasma of 26% over a concentration range of 1–500 ng/mL, determined by equilibrium dialysis. The protein binding of I had been determined to be concentration independent at 36% (13). The presence of I in up to 10-fold higher concentrations than its antagonists does not change the degree of plasma protein binding of II or III (Table IV).

Determination of the Red Blood Cell Partition Coefficient—The red blood cell partition coefficient (D) of a drug can be defined (11) as:

$$D = \frac{C_{RBC}}{C_{PW}} = \frac{A_{tot} - C_{PW}V_{PW}}{C_{PW}(V_B - V_{PW})} \quad \text{(Eq. 2)}$$

where C_{RBC} is the concentration of the drug in the erythrocyte, C_{PW} is the drug concentration in plasma water, A_{tot} is the total amount of drug added to the red blood cell suspension, and V_{PW} is the volume of plasma water (calculated from the hematocrit of the erythrocyte suspension).

The red blood cell partition coefficients of III were determined for six different concentrations (Table V), averaging 1.83 ± 0.15 (*SD*). There was no concentration dependence for the partitioning in the studied concentration range up to 3.5 μg/mL. This relatively high partition coefficient was confirmed by comparing the concentration of III in blood, C_B, and plasma, C_P, after spiking whole blood. The ratio of these two concentrations is related to the degree of protein binding in plasma, expressed as fraction bound (f_b), to the red blood cell partition coefficient D and the hematocrit (H) (14):

$$\frac{C_B}{C_P} = DH(1 - f_b) + 1 - H \quad \text{(Eq. 3)}$$

Substitution of the values previously obtained for D and f_b gives a blood/plasma ratio of 1.16 for blood with a hematocrit of 0.49. This calculated ratio agrees with that obtained experimentally (1.21 ± 0.08) in blood in the investigated concentration range.

The red blood cell partition coefficients of II in the same concentration range are given in Table VI, averaging 1.49 ± 0.25 (*SD*), also with no concentration dependence. Both partition coefficients for III and II were significantly higher than the D = 1.11 previously reported for I (13), in agreement with the hypothesis that erythrocyte partitioning is related to the lipophilicity, which is mirrored by the HPLC retention times on a reverse-phase column. This theory

Table VI—Red Blood Cell Partition Coefficients for II at Different Concentrations

A_{tot}, μg[a]	C_{PW}, ng/mL	D[b]
0.050	9.3	1.30
0.175	28.8	1.79
0.500	87.9	1.47
1.750	278.1	1.83
5.000	955.9	1.16
17.500	3166.7	1.41
Mean ± *SD*		1.49 ± 0.27

[a] Total amount of drug added to a 5.0-mL red blood cell suspension when the volume of plasma water (PW) was 3.45–3.70 mL and the hematocrits were 0.260–0.310. [b] Red blood cell-plasma water partition coefficient.

is further confirmed by the fact that the more lipophilic derivative of I, buprenorphine, has an extremely high red blood cell partition coefficient[17] of ~10.

No time dependence in the red blood cell partitioning could be observed for either compound. Samples assayed 4–5 min after spiking were not significantly different from the samples that were allowed to equilibrate for 60 min, indicating that the partitioning was relatively fast. The lack of correlation between the protein binding and red blood cell partitioning for the investigated compounds suggests that these two properties should be studied separately.

REFERENCES

(1) P. T. Kissinger, *Anal. Chem.*, **46,** 15R (1974).

(2) D. D. Koch and P. T. Kissinger, *J. Chromatogr.* **164,** 441 (1979).

(3) D. A. Roston and P. T. Kissinger, *Anal. Chem.*, **53,** 1695 (1981).

(4) J. E. Wallace, E. L. Shimek, S. Stavchansky, and S. C. Harris, *Anal. Chem.*, **53,** 960 (1981).

(5) S. H. Curry, E. A. Brown, O. Y.-P. Hu, and J. H. Perrin, *J. Chromatogr.*, **231,** 361 (1982).

(6) J. E. Wallace, S. G. Harris, and M. W. Peek, *Anal. Chem.*, **52,** 1328 (1980).

(7) M. W. White, *J. Chromatogr.*, **178,** 229 (1979).

(8) K. Ishikawa, J. L. Martinez, and J. L. McCaugh, *J. Chromatogr.*, **231,** 255 (1982).

(9) E. R. Garrett and T. Gürkan, *J. Pharm. Sci.*, **69,** 1116 (1980).

(10) "BAS 4A Manual," Bioanalytical Systems Inc., West Lafayette, Ind., 1981.

(11) H. Derendorf and E. R. Garrett, *J. Pharm. Sci.*, **72,** 630 (1983).

(12) T. M. Ludden, L. Malspeis, J. D. Baggot, T. D. Sokolski, S. G. Frank, and R. H. Reuning, *J. Pharm. Sci.*, **65,** 712 (1976).

(13) E. R. Garrett and A. J. Jackson, *J. Pharm. Sci.*, **68,** 753 (1979).

(14) E. R. Garrett and H. T. Lambert, *J. Pharm. Sci.*, **62,** 550 (1973).

(15) Stat 1-22A "Linear Regression" HP-65 Stat-Pac 1, Hewlett-Packard, Cupertino, Calif., pp. 49–51.

ACKNOWLEDGMENTS

Supported in part by Grant 2-RO1-DA-00743 from the National Institute of Drug Abuse, Rockville, MD 20852. Dr. A. A. El-Koussi was supported by Peace Fellowship Program for Egypt, administered by American Mid-East Educational and Training Services Inc., Washington, D.C.

[17] E. R. Garrett, V. Ravichandran, and H. Derendorf, unpublished results.

Liquid Chromatographic Determination of Lipophilicity with Application to a Homologous Series of Barbiturates

STEPHEN TOON *, JOACHIM MAYER, and MALCOLM ROWLAND ˣ

Received June 17, 1982, from the *Department of Pharmacy, University of Manchester, Manchester M13 9PL, England.* Accepted for publication May 9, 1983. *Present address: School of Pharmacy, University of Washington, Seattle, WA 98105.

Abstract □ A graphical method for determining the lipophilicity of the members of a homologous series of barbituric acids, from a consideration of their reverse-phase HPLC retention data, is described. The HPLC parameter used as the index of lipophilicity, R_Q, is shown not only to form excellent correlations with the more commonly employed indices of lipophilicity, R_m and log P, but also to have a predictive capability for those log P values that had not previously been determined experimentally.

Keyphrases □ Lipophilicity—homologous series of barbiturates, determination by the HPLC parameter R_Q □ Barbiturates—lipophilicity, determination by the HPLC parameter R_Q □ HPLC—use of the parameter R_Q to determine lipophilicity, homologous series of barbiturates

Since Meyer (1) and Overton (2) first postulated a relationship between the biological response elicited by a drug substance and its lipophilic character, medicinal chemists have sought rapid and reliable methods of determining molecular lipophilicity. The octanol-water partition coefficient (P), classically being determined using the "shake-flask" method (3), has been the index of lipophilicity most commonly employed in correlations between molecular structure and biological response (4, 5). The "shake-flask" approach to the determination of lipophilic character has been shown, however, to have many inherent practical difficulties associated with it (6–8), and as a consequence alternative methods of determining P or other indices of lipophilicity have been sought.

Many of the alternatives have been derived from TLC (9–12) and high-performance liquid chromatography (HPLC) (13–16), but in nearly all instances problems arise when characterizing highly lipophilic or hydrophilic molecules. The potential of the HPLC-based term R_Q (17) as an index of molecular lipophilicity was explored using a homologous series of barbituric acids. Special reference was paid to the correlation of R_Q with the more commonly accepted indices of lipophilicity, log P and R_m, the latter being experimentally determined from reverse-phase TLC studies within the series.

EXPERIMENTAL

The barbituric acids comprising the series (Table I) were obtained either from commercial sources or synthetically by condensing the respective diethyl 2-alkyl-2-ethylmalonate with urea in the presence of sodium ethoxide. The synthetic barbituric acids were characterized by ^{1}H-NMR, elemental analyses, and melting point determinations. All were calculated to be >99% pure.

Liquid Chromatographic Analysis and the Determination of R_Q Values—The analytical system has been previously outlined (17). The basis of the HPLC assay is that the un-ionized barbiturates are separated using a reverse-phase column[1], and then by the postcolumn infusion of pH 10 buffer, the barbiturates are converted to the more strongly UV-absorbing monoanionic species, facilitating detection at 254 nm.

The acetonitrile[2] and acetic acid[3] used in the preparation of the mobile phases were HPLC and analytical grade, respectively. All water used was freshly glass-distilled. The mobile phases were deaerated prior to use by filtration under vacuum through a 0.22-μm microbial filter[4].

The barbiturates were studied individually as solutions in acetonitrile (50 μg/mL), 10 μL of which was used in the analysis, thereby facilitating the measurement of retention times of the various barbiturates (R_T) relative to the unretained solute peak (10 μL of methanol, R_0) at varying concentrations of acetonitrile in the mobile phase. To improve the retention characteristics of 5-ethylbarbituric acid, 0.05% (v/v) acetic acid was added to the mobile phase; the retention of the other members of the series was unaffected by this addition.

R_Q values were calculated at the various acetonitrile concentrations according to:

$$R_Q = \log\left(\frac{R_T - R_0}{R_T}\right) \qquad \text{(Eq. 1)}$$

where R_T is the retention time of the solute and R_0 is the retention time of the unretained solvent. Values of R_Q at 0% v/v acetonitrile (100% v/v water; R_{Q0}) and at 40% v/v acetonitrile (R_{Q40}) were derived for all of the compounds either by direct measurement or by extrapolation/interpolation of the plots of the R_Q *versus* concentration (% v/v) of acetonitrile in the mobile phase.

Thin-Layer Chromatography and Calculation of R_m Values—Silica gel[5] was spread as a water slurry onto 20 × 20-cm glass plates to a thickness of 0.25 mm. After air drying, the plates were activated by heating overnight in an oven at 110°C. The plates were predeveloped in an 1-octanol–acetone (1:9) mixture, after which the acetone was evaporated from the plates by the use of an air blower. The silica gel plates were thus coated with a layer of 1-octanol.

Solutions of the individual barbiturates in acetone (2 mg/mL) were prepared, and 30 μl of each were applied as discrete spots along the baseline, positioned 1 cm from the bottom edge of the TLC plate. The prepared plates were developed in one of seven possible solvent systems composed of differing concentrations of acetone in water (5, 15, 25, 30, 35, 37, and 40% v/v acetone in water).

The ratio of the distance traveled by a given solute (barbiturate), relative to that traveled by the solvent front, was calculated in each instance yielding R_f values, which in turn allowed the calculation of R_m values for the individual barbiturates at varying acetone concentrations according to (18, 19):

$$R_m = \log\left(\frac{1}{R_f} - 1\right) \qquad \text{(Eq. 2)}$$

Assessment of log P—A solution (5×10^{-4} M) of the compound to be investigated (compounds 1, 2, and 3; Table I) was prepared in Sörensen's buffer (pH 5.1, 0.07 M) saturated with 1-octanol. This solution was then shaken gently for 1 h with 1-octanol that had been previously washed successively with 1 M NaOH, 1 M HCl, and the Sörensen's buffer. A period of 1 h to ensure that equilibrium had been achieved is more than adequate; only a few minutes are generally needed (3). The ratio of the volumes of the two phases was chosen so that 20–60% of the solute remains in the aqueous phase after extraction. The concentration of compound in the aqueous phase, adjusted to pH 10 by addition of dilute NaOH, was determined spectrometrically (240 nm) before and after extraction. The partition coefficient (P) of the acid was calculated from the relationship:

$$P = \frac{V_a}{V_o}\left[\frac{Ca(0)}{Ca} - 1\right] \qquad \text{(Eq. 3)}$$

where $Ca(0)$ and Ca are the respective concentrations of the compound in the aqueous phase before and after extraction and V_a and V_o are the volumes of the aqueous and organic phases, respectively.

[1] Hypersil ODS 5μm; Shandon Southern Products, U.K.
[2] Acetonitrile; Rathburn Chemicals, U.K.
[3] Acetic acid; May & Baker Ltd., U.K.
[4] Millipore Corp.
[5] Kieselgel, G type 60 and Kieselgel 60 GF_{254} in a 1:1 ratio; E. Merck, West Germany.

0022-3549/84/0500-0625$01.00/0
© 1984, American Pharmaceutical Association

Table I—Chromatographic and Literature Indices [a] of Lipophilicity for the Barbiturates

Key	Compound	R_m (25% v/v Acetone)	log P (Octanol–Water)	R_{Q0}	R_{Q40}
1	5-Ethylbarbituric acid	—	−1.52	−0.083	−1.215
2	5-Ethyl-5-methylbarbituric acid	−0.31	0.02	−0.002	−0.562
3	Barbital	−0.02	0.68[b]	0.051	−0.469
4	5-Ethyl-5-*n*-propylbarbituric acid	0.38	0.87[c]	0.114	−0.314
5	Butethal	0.83	1.70[c]	0.187	−0.221
6	5-Ethyl-5-*n*-hexylbarbituric acid	—	3.08[c]	0.292	−0.084
7	5-Ethyl-5-*n*-heptylbarbituric acid	—	3.64[c]	0.304	−0.040
8	5-Ethyl-5-*n*-octylbarbituric acid	—	3.85[c]	0.361	0.017
9	5-Ethyl-5-*n*-nonylbarbituric acid	—	4.13[c]	0.384	0.052
10	Pentobarbital	1.06	2.13[c]	0.190	−0.166
11	Amobarbital	1.12	2.11[c]	0.235	−0.157
12	Phenobarbital	0.48	1.42[b]	0.140	−0.244

[a] Leo *et al.* (3) reported $R_{Q40} = 0.121 \cdot \log P - 0.447$ ($n = 10, r^2 = 0.9470$); $R_{Q0} = 0.086 \cdot \log P + 0.021$ ($n = 10, r^2 = 0.9740$); $R_{Q40} = 0.280 \cdot R_m - 0.446$ ($n = 7, r^2 = 0.9470$); and $\log P = 1.465 \cdot R_m + 0.520$ ($n = 6, r^2 = 0.9619$). [b] Taken from Hansch and Leo (30). [c] Taken from Yih (31).

RESULTS AND DISCUSSION

The barbituric acid series under investigation varies widely in lipophilic character (Table I) and problems were encountered in determining TLC R_m values for the more lipophilic members of the series. Although a TLC solvent containing <40% acetone yielded a suitable migration from the baseline of the more hydrophilic homologues, hence facilitating the calculation of R_m values, elution from the baseline of the lipophilic *n*-hexyl through *n*-nonyl homologues was not afforded under such conditions. Furthermore, a solvent containing ≥40% acetone was found to strip the 1-octanol layer from the precoated plates, rendering them useless for the purpose in hand.

For those members of the series that did lend themselves to TLC analysis, a linear relationship was shown to exist between R_m and the acetone concentration (% v/v) in the developing solvent (Fig. 1). Similar relationships have previously been demonstrated for other molecular series, including the benzodiazepines and penicillins (9, 11).

Our results highlight the problem in quantitating lipophilic character of highly nonpolar compounds by TLC. Hulshoff and Perrin (20) have proposed a TLC-based method for the determination of the relative partition coefficients of very lipophilic basic compounds, based on the manipulation of developing solvent pH. While promising, this method has received only limited application (21).

Most HPLC approaches to the determination of lipophilicity are based on attempts made at formulating relationships between the capacity factor k' [$k' = (R_T - R_0)/R_0$; R_T and R_0 as previously defined] and P. The capacity factor (k') of a solute is only constant under any given set of chromatographic conditions. If k' values are to serve as the index of lipophilicity for the members of a homologous series, therefore, they should be obtained, for each homologue, under identical chromatographic conditions, an almost impossible constraint when dealing with a series of widely ranging lipophilicities.

Initial attempts at obtaining k' values for the barbituric acid series using a single isocratic HPLC system proved fruitless. The maximum possible concentration of organic solvent in the mobile phase that allowed a suitable retention time for the most hydrophilic homologue, 5-ethylbarbituric acid, was 10% v/v acetonitrile in 0.05% v/v aqueous acetic acid. Elution of the more hydrophobic homologues was not afforded under these conditions, with predicted retention times for these compounds being in excess of 10 h.

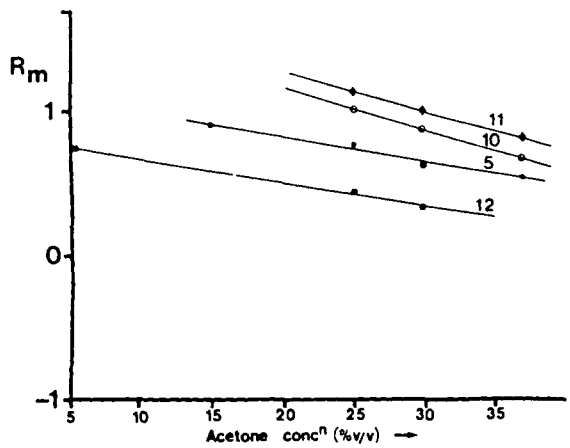

Figure 1—*Plot of* R_m *against acetone concentration in the mobile phase for various barbiturates. See Table I for key to the numbers.*

Yamana *et al.* (22) noted a linear relationship between log k' and the concentration of methanol in the HPLC mobile phase for a series of penicillins and cephalosporins. Such a relationship facilitates the calculation of k' values for the individual homologues at two or more mobile phase compositions, those which yield adequate retention times of the solute in question. These empirically determined k' values may then be extrapolated to give k' values at any desired mobile phase composition. Yamana *et al.* extrapolated their plots of log k' *versus* mobile phase composition to obtain log k' values for all members of their series at 0% v/v methanol (100% v/v water), these values in turn being shown to be highly correlated with the respective log P and R_m values.

The values of k' and log k' do not always vary linearly with mobile phase composition (17); thus, extrapolation of k' *versus* mobile phase plots is not always possible. As seen in Fig. 2, log k' for the barbiturate series is proportional to the concentration of acetonitrile in the mobile phase for many, but not all, of the homologues.

In contrast to k', we have found R_Q to vary linearly with mobile phase composition in all the cases we have examined, even when marked nonlinearity has been shown to exist between log k' and mobile phase composition (17). Plots of R_Q *versus* the concentration of acetonitrile in the mobile phase (Fig. 3) were back-extrapolated to yield R_Q values at 0% v/v acetonitrile (R_{Q0}) for all of the homologues. R_{Q0} values obtained in this manner were found to form good correlations with both TLC R_m values as well as with literature log P values (Fig. 4). The choice of a reference state of 0% v/v acetonitrile in water in relating R_Q values to other measures of lipophilicity is arbitrary. A better reference point would be one at which R_Q could be empirically determined for the maximum number of homologues, thereby reducing the number of R_Q values obtained by extrapolation, giving increased confidence in the R_Q data. A mobile phase of 40% v/v aqueous acetonitrile provides such a reference point.

Using the regression equation of R_{Q0} against log P, octanol–water partition coefficients were predicted for the two lowest homologues as being (log P) −1.52 for 5-ethylbarbituric acid and 0.02 for 5-methylbarbituric acid. As no literature values for log P were available for these two homologues, empirical determination was necessary to check the predicted values. The experimentally determined values for 5-ethylbarbituric acid and 5-ethyl-5-methylbarbituric

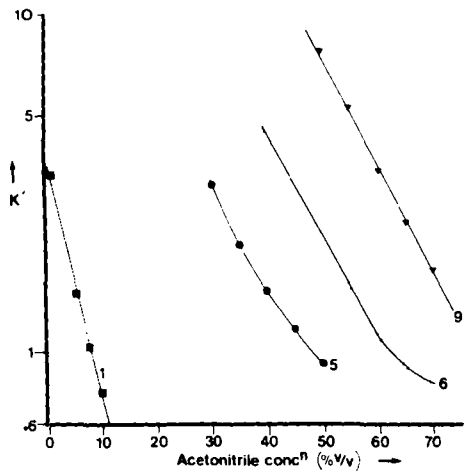

Figure 2—*Semilogarithmic plot of log* k' *against the organic modifier, acetonitrile, in the mobile phase for various barbiturates. See Table I for key to the numbers.*

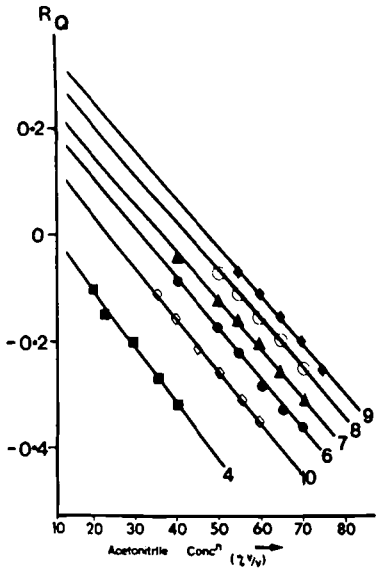

Figure 3—*Plot of* R_Q *against the organic modifier, acetonitrile, in the mobile phase for various barbiturates. See Table I for key to the numbers.*

acid were −1.26 and 0.2, respectively, illustrating the good predictive capabilities of R_Q.

Pretreatment of column packings prior to the determination of lipophilicity using an HPLC based method has been the cause of considerable debate. Several workers have capped the reverse-phase column prior to use (23), while others have coated the column with 1-octanol (24–26). Baker *et al.* (27), proposed that the ordered side chains and residual silanol groups of untreated octadecylsilane packing material best reflects a biolayer, and partition data obtained from such systems are more suitable for use in biological correlations. A commercially available untreated reverse-phase packing material was used throughout our experimental procedure. In view of the excellent correlations obtained between R_Q values and other indices of molecular lipophilicity, we feel that pretreatment of the column packing prior to use may be unnecessary.

The thermodynamic basis of HPLC-derived lipophilicity data has been the subject of several investigations (28, 29). The thermodynamic basis of R_Q, if there is one, is unclear. From a theoretical standpoint, however, we should point out that the ratio $(R_T - R_0)/R_T$ cannot exceed 1 and R_Q cannot therefore exceed 0. Several of the extrapolated R_{Q0} values (Table I) are numerically greater than zero. Even so, these R_Q values form excellent correlations with the more commonly accepted indices of lipophilicity.

HPLC offers several advantages in the determination of lipophilicity over more conventional approaches, the main ones being speed and analytical sensitivity; these advantages are inherent in the proposed parameter R_Q. Unlike k' (the HPLC term most commonly used to quantiate molecular lipophilicity), R_Q has been found to vary linearly with mobile phase composition

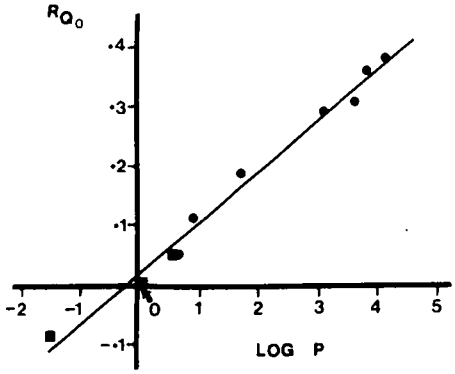

Figure 4—*Plot of* R_{Q0} *against log P for various barbiturates taken from the literature (●) or determined experimentally (■). Straight line is the line of best fit using the 10 literature log P values. See Table I for key to the numbers.*

in all cases examined. This linear correlation allows interpolation and some extrapolation from empirically determined R_Q values to values at any selected mobile phase composition. At a minimum, R_Q values need only be empirically determined at two differing mobile phase compositions to obtain any desired value of R_Q. From a practical viewpoint, we feel that as many empirically determined R_Q values as possible should be used, from solute retention data where R_T falls within the range of $1.5\text{–}15 \times R_0$. R_Q thus provides a rapidly determined index of lipophilicity which can be applied to compounds of widely ranging lipophilic character.

REFERENCES

(1) K. H. Meyer, *Arch. Exp. Pathol. Pharmacol.*, **42,** 109 (1899).

(2) E. Overton, "Studien über die Narkose," Jena, Germany, 1901.

(3) A. Leo, C. Hansch, and D. Elkins, *Chem. Rev.*, **71,** 525 (1971).

(4) C. Hansch, "Drug Design," Vol. 1, E. J. Ariens, Ed., Academic, New York, N.Y., 1971.

(5) C. Hansch, R. T. Muir, T. Fujita, P. P. Maloney, F. Geiger, and M. Streich, *J. Am. Chem. Soc.*, **85,** 2817 (1963).

(6) C. B. C. Boyce and B. V. Milborrow, *Nature (London)*, **208,** 537 (1965).

(7) T. Braumann and L. H. Grimme, *J. Chromatogr.*, **206,** 7 (1981).

(8) S. H. Unger, J. R. Crook, and J. S. Hollenberg, *J. Pharm. Sci.*, **67,** 1364 (1978).

(9) G. L. Biagi, A. M. Barbaro, M. C. Gverra, M. Babbini, M. Gaiardi, and M. Bartoletti, *J. Med. Chem.*, **23,** 193 (1980).

(10) M. Bachrata, M. Blesova, A. Schultrova, L. Grohchova, Z. Bezakova, and A. Lukas, *J. Chromatogr.*, **171,** 29 (1979).

(11) G. L. Biagi, A. M. Barbaro, M. F. Gamba, and M. C. Gverra, *J. Chromatogr.*, **41,** 371 (1969).

(12) M. Kuchar, V. Rejholec, B. Brunova, and M. Jelinkova, *J. Chromatogr.*, **195,** 329 (1980).

(13) A. Nahum and C. Horvath, *J. Chromatogr.*, **192,** 315 (1980).

(14) B. Riftich, M. Polster, and O. Kralik, *J. Chromatogr.* **197,** 43 (1980).

(15) J. F. K. Huber, C. A. M. Meyers, and J. A. R. J. Hulsman, *Anal. Chem.*, **44,** 111 (1972).

(16) S. H. Unger and C. H. Chiang, *J. Med. Chem.*, **24,** 262 (1981).

(17) S. Toon and M. Rowland, *J. Chromatogr.*, **208,** 391 (1981).

(18) E. C. Bate-Smith and R. G. Westall, *Biochim. Biophys. Acta*, **4,** 427 (1950).

(19) S. Marcinkiewicz, J. Green, and S. McHale, *J. Chromatogr.*, **10,** 42 (1963).

(20) A. Hulshoff and J. H. Perrin, *J. Chromatogr.*, **120,** 65 (1976).

(21) G. Maksay, Z. Teggery, and L. Otuos, *J. Chromatogr.*, **174,** 447 (1979).

(22) T. Yamana, A. Tsuji, E. Mizamoto, and O. Kubo, *J. Pharm. Sci.*, **66,** 747 (1977).

(23) J. M. McCall, *J. Med. Chem.*, **18,** 549 (1975).

(24) M. S. Mirlees, S. J. Moutlon, C. T. Murphy, and P. J. Taylor, *J. Med. Chem.*, **19,** 615 (1976).

(25) D. Henry, J. H. Block, J. L. Anderson, and G. R. Carlson, *J. Med. Chem.*, **19,** 619 (1976).

(26) S. H. Unger and T. F. Feverman, *J. Chromatogr.*, **176,** 426 (1979).

(27) J. K. Baker, D. O. Rauls, and R. F. Borne, *J. Med. Chem.*, **22,** 1301 (1979).

(28) E. Tomlinson, H. Poppe, and J. C. Kraak, *Int. J. Pharmaceut.*, **7,** 225 (1981).

(29) C. M. Riley, E. Tomlinson, and T. M. Jefferies, *J. Chromatogr.*, **185,** 197 (1979).

(30) C. Hansch and A. Leo, "Substituent Constants for Correlation Analysis in Chemistry and Biology," Interscience, New York, N.Y., 1979.

(31) T. D. Yih, Ph.D. Thesis, University of Nijmegen, The Netherlands (1976).

ACKNOWLEDGMENTS

We gratefully acknowledge grants from the British Science and Engineering Research Council (for S.T.) and Swiss National Science Foundation/Royal Society (for J.M.M.) and a grant-in-aid from Merck Sharp & Dohme Research Laboratories.

Agglutination Kinetics of Enzymatically Treated Normal and Diabetic Rat Hepatocytes

ANWAR B. BIKHAZI *x and LUTFIYYEH H. TURYAKI

Received April 6, 1982, from the *Department of Physiology, Faculty of Medicine, American University of Beirut, Beirut, Lebanon.* Accepted for publication January 13, 1983. *Present address: Department of Physiology, Faculty of Medicine, c/o Office of the American University of Beirut, 850 Third Ave., New York, NY 10022.

Abstract □ The effect of trypsin and neuraminidase treatments on concanavalin A-induced agglutination of viable hepatocytes from normal and diabetic rats are reported. Trypsin (1.0 μg/mL) treatment resulted in an increased rate of hepatocyte agglutination in both normal and diabetic cells in the presence of 100 μg/mL of concanavalin A. However, neuraminidase treatment resulted in a decrease in the rate of cytoagglutination in the normal cells and an increase in the rate in the diabetic counterpart. The results suggest that trypsin may have caused the removal of a surface protein and/or split a peptide bond on the agglutinin receptors resulting in identical receptor exposure and clustering in normal and diabetic cells. The neuraminidase data suggest that the arrangements of the neuraminic acid moieties on the receptors in normal cell membranes were different from those in the diabetic cells, eliminating the possible effect of changes in the surface charge density. In conclusion, normal cells carry numerous clustered (possibly some in the "cryptic" state) agglutinin receptors in the cell membrane as compared with cells from diabetic rats.

Keyphrases □ Agglutination—kinetics of enzymatically treated normal and diabetic rat hepatocytes, trypsin, neuraminidase □ Trypsin—agglutination kinetics of enzymatically treated normal and diabetic rat hepatocytes, neuraminidase □ Kinetics—agglutination of enzymatically treated normal and diabetic rat hepatocytes, trypsin, neuraminidase □ Neuraminidase—agglutination kinetics of enzymatically treated normal and diabetic rat hepatocytes, trypsin

The cell surface is considered to be an attractive target for the binding of proteins like lectins. The carbohydrate-binding specificity of the lectin concanavalin A has been useful in the detection, characterization, and study of membrane alterations and cytodifferentiations in cell surface membranes (1–5). Studies on the pretreatment of normal and transformed cells with proteolytic enzymes, neuraminidase, β-galactosidase, phospholipases, and other enzymes prior to agglutination have elucidated the mode and extent of cell membrane transformations (6–9).

Recently, it was reported (10) that rat hepatocytes dispersed by collagenase perfusion were highly agglutinable by concanavalin A. Furthermore, agglutination was twice as fast in normal cells as compared with cells obtained from streptozocin-treated diabetic rats. This manuscript reports cytoagglutination studies with concanavalin A after pretreating the normal and diabetic hepatocytes with trypsin and neuraminidase.

EXPERIMENTAL

Preparation of Rat Hepatocytes—Dispersed liver parenchymal cells were isolated and tested for viability by the procedure of Bikhazi *et al.* (10, 11). The trypan blue exclusion test for cellular viability was routinely performed before and after the experiments, and preparations showing ≥90% viable cells were used.

The metabolic state of the hepatocytes during the incubation period was examined by following the respiration rate of cell suspensions in several separate experiments. Oxygen tension was recorded continuously with the aid of a biological oxygen monitor. Rates were determined from the slopes of the oxygen tension curves and were calculated in terms of microliters of O_2 per milligram of cell protein. Protein was determined by the biuret reaction, with bovine serum albumin as a standard, using centrifuged cell pellets dissolved in 1 M NaOH to minimize possible interference from medium components.

Preparation of Diabetic Rats—Rats were rendered diabetic by injection with 65 mg/kg iv of streptozocin[1]. The procedure and blood glucose level tests were reported previously by Bikhazi *et al.* (10, 11).

Agglutination of Hepatocytes from Normal and Diabetic Rats—For the control experiments ~9×10^6 hepatocytes were suspended in 225 mL of Ca^{2+}- and Mg^{2+}-free phophate-buffered saline (pH 7.4). Cell counts were recorded kinetically by an automated counter[2] at 0, 5, 10, 20, and 30 min (10, 11).

Treatment with Concanavalin A—Two milliliters of Ca^{2+}- and Mg^{2+}-free phosphate solution containing concanavalin A was added to 225 mL of buffer to obtain a 100-μg/mL solution of the lectin. The hepatocytes were then dispersed in this solution, and cell counts were obtained as described above.

Treatment with Trypsin and/or Neuraminidase—The experiments included treatment of normal or diabetic cells with trypsin or neuraminidase and measuring agglutination in the absence of the lectin. The cells were dispersed in Ca^{2+}- and Mg^{2+}-free buffer solutions containing 0.22, 0.74, or 1.0 μg/mL of trypsin[3]. Treatment was allowed to proceed for 5 min, then cell counts were recorded at 0, 5, 10, 20, and 30 min. For neuraminidase[3] (88 ng/mL), the hepatocytes were treated with the enzyme for 15 min before cell counts were recorded. In another experiment, concanavalin A (100 μg/mL in the suspension) was added after the above treatments to induce agglutination.

Treatment with Neuraminidase, Trypsin, and Concanavalin A—After treating the hepatocytes for 15 min with 88 ng/mL of neuraminidase, trypsin (1.0 μg/mL) was added and the suspension was allowed to mix for 5 min. Concanavalin A was then added and the cytoagglutination was recorded as above.

Treatment with Trypsin, Trypsin Inhibitor, Neuraminidase, and Concanavalin A—Trypsin (1.0 μg/mL) was added to the cell suspension after cell counts were recorded. After 5 min, trypsin inhibitor (1.3 μg/mL) was added to quench the trypsin activity. Neuraminidase (88 ng/mL) was then added, the suspension was stirred for 15 min, and a second cell count recording was obtained. Afterward, concanavalin A (100 μg/mL) was added, and cell counts were recorded at 5, 10, and 20 min.

Data Analysis—The physical model on irreversible agglutination (10, 12) was used in the data analysis and interpretation. The general second-order rate relationship derived by Higuchi *et al.* (13) and further supported by Bikhazi *et al.* (10, 12) was used to describe the agglutination rate. The following equations were used:

$$\frac{1}{H_S} = \frac{1}{H_S^0} + Kt \qquad \text{(Eq. 1)}$$

where:

$$K = \frac{16\gamma K_0 r_S T}{3\eta} \qquad \text{(Eq. 2)}$$

and H_S is the number of hepatocyte singlets at any time t, H_S^0 is the number of singlets at $t = 0$, γ is the sticking probability constant (which measures the stickiness of the cells), K_0 is the Boltzmann constant, r_S is the hepatocyte radius, T is the temperature in degrees Kelvin, and η is the viscosity of the medium (10, 12).

RESULTS

Average Number, Mean Diameter, and Viability of Rat Hepatocytes—The average number of isolated cells per liver was ~1.2×10^8 hepatocytes. The mean hepatocyte diameter was taken as 20 μm (10), and cellular viability was routinely tested using the trypan blue exclusion test. The rate of oxygen production was estimated to be 1.0 μL/mg dry weight/h, which is within the normal range for mammalian cells (11). The protein content of hepatocytes was ~16% of the wet weight, near the value reported for whole liver (11).

[1] U-9889, lot number 60,273-9; courtesy of The Upjohn Co., Kalamazoo, Mich.
[2] Coulter Counter model A; Coulter Electronics, Hialeah, Fla.
[3] Sigma Chemical Co., St. Louis, Mo.

0022-3549/84/0500-0628$01.00/0
© 1984, American Pharmaceutical Association

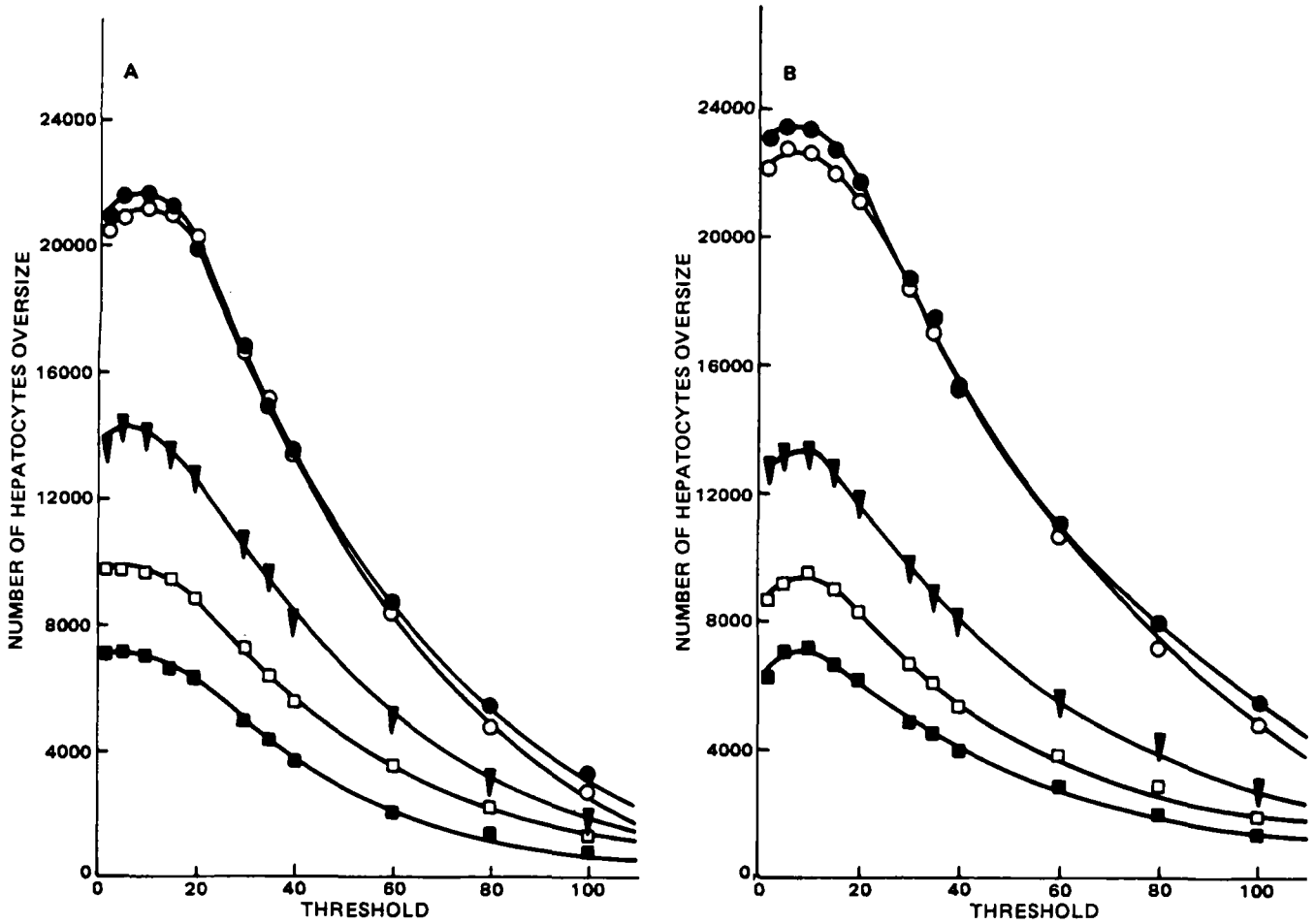

Figure 1—*Representative cumulative size distribution curves for normal (A) and diabetic (B) rat hepatocytes with respect to time in the presence of 1 μg/mL of trypsin and 100 μg/mL of concanavalin A. Key: (●) 0 min, trypsin-treated cells without concanavalin A; (○) 0 min, concanavalin A added after trypsin treatment; (▼) 5 min; (□) 10 min; (■) 20 min.*

Second-Order Rate Plots for Agglutination—The value of H_S (Eq. 1) was estimated from the cumulative size distribution curves as exemplified in Fig. 1. The cell counts (H_S) at threshold 30 (volume 4.2×10^3 μm^3) and at 0, 5, 10, and 20 min were used to draw the linear curves of $1/H_S$ *versus* time (t). All data were treated similarly to Fig. 2, which represents the least-squares line fitted to the experimental data. The slopes of the least-squares lines were estimated, and γ values (Eq. 2) were calculated (10, 12) (Table I).

Hepatocyte Agglutination—Bikhazi *et al.* (10) observed that the agglutination rate of normal cells was double that of diabetic cells in the presence of 100 μg/mL of the lectin. Hepatocytes were not agglutinable after trypsin treatment. Figure 1 represents typical time-dependent cumulative size distribution plots of normal and diabetic cells after treatment with trypsin followed by concanavalin A. The effect of trypsin treatment was obvious when compared with the non-trypsin-treated cells (Table I).

Curves similar to those of Fig. 1 were observed after treatment with trypsin and trypsin inhibitor followed by concanavalin A, except that the rate of agglutination was less than when the inhibitor was absent. These findings suggest that trypsin has no proteolytic action on concanavalin A.

Table I—Sticking Probability Constants for Hepatocyte Agglutination with Concanavalin A after Various Treatments

Treatment[a]	Sticking Probability Constants[b], $\gamma \times 10^7$ cm^{-1}/hepatocyte	
	Normal Cells	Diabetic Cells
Concanavalin A	8.78 ± 0.92 (A)	3.23 ± 0.46 (G)
Trypsin	3.23 ± 0.02 (B)	4.16 ± 0.92 (H)
Neuraminidase	0	0
Trypsin plus concanavalin A	36.05 ± 3.23 (C)	34.20 ± 4.16 (I)
Neuraminidase plus concanavalin A	4.53 ± 0.69 (D)	8.78 ± 0.92 (J)
Trypsin plus trypsin inhibitor plus concanavalin A	13.86 ± 3.70 (E)	9.70 ± 1.84 (K)
Trypsin plus trypsin inhibitor plus neuraminidase plus concanavalin A	7.85 ± 1.85 (F)	13.86 ± 0.46 (L)

[a] Concentrations: concanavalin A, 100 μg/mL; trypsin, 1.0 μg/mL; neuraminidase, 88 ng/mL; trypsin inhibitor, 1.3 μg/mL. [b] Mean ± *SEM*; $n = 6$. Letters in parentheses are codes for statistical analysis. Significant differences: $p < 0.001$ (A,C), (A,G), (B,C), (B,E), (C,E), (G,I), (G,K), (H,I), (K,L), (G,J); $0.001 < p < 0.01$ (E,F), (J,L); $0.01 < p < 0.02$ (F,L), (H,K); $0.02 < p < 0.05$ (A,E), (E,K); $0.05 < p < 0.1$ (B,H); $0.1 < p < 0.2$ (A,D), (D,J). No other combinations showed statistical differences.

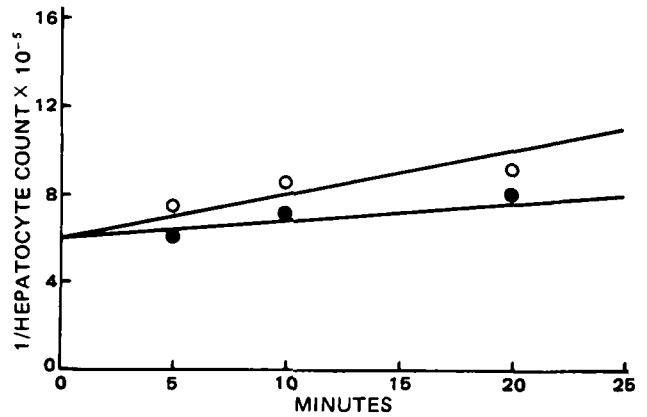

Figure 2—*Representative second-order plot of diabetic rat hepatocyte agglutination, 1/hepatocyte count* versus *time. Straight lines are least-squares fit to the experimental data in the presence of 88 ng/mL of neuraminidase and 100 μg/mL of concanavalin A. Key: (●) 100 μg/mL of concanavalin A; (○) 88 ng/mL of neuraminidase plus 100 μg/mL of concanavalin A.*

No agglutination was seen after neuraminidase treatment. Table I shows that there was no effect of neuraminidase treatment on concanavalin A-induced agglutination in normal cells, but a drastic increase in cytoagglutination was observed in diabetic cells.

Neuraminidase treatment after trypsin treatment caused a marked decrease of γ in normal cells, while the reverse was true for diabetic cells (Table I). After treatment with both enzymes, the agglutination rate of normal cells remained the same as those of the untreated cells. However, diabetic hepatocytes showed an increase in the agglutination rate after trypsin treatment followed by the neuraminidase effect. This was also observed for the neuraminidase *versus* the trypsin-neuraminidase results.

DISCUSSION

A number of postulations have been reported in the literature on the effect of proteolytic enzymes on normal and transformed cell agglutination induced by lectins. These include the exposure of cryptic receptors (14, 15), clustering of receptors (16–18), and changes in surface morphology characterized by a reduction (19) or increase in surface microvilli (20, 21).

In the absence of trypsin inhibitor, the proteolytic effect of trypsin continued throughout the course of the experiments, suggesting that the 5-min enzymatic treatment was not sufficient for complete receptor exposure and/or rearrangement. The agglutination rates of both cell types with concanavalin A after trypsin treatment (with and without inhibitor) were almost the same. Therefore, the proteolytic action of trypsin may have caused the removal of a surface protein and/or split a peptide bond on the agglutinin receptors, which could result in identical exposure and clustering (rearrangements) of the receptors in normal and diabetic cells.

Neuraminidase is an enzyme which normally hydrolyzes peripheral *n*-acetylneuraminic (sialic) acids. After hydrolysis, the removal of the surface sialic acid could cause a reduction in the net negative surface charge of the cells thus reducing the forces of repulsion between adjacent cells, favoring cytoagglutination (22). The results presented in Table I indicated cytodispersion and repulsion rather than agglutination after normal cells were treated with neuraminidase. It is, therefore, possible that the hydrolysis of the neuraminic acid moieties (the target moieties for concanavalin A-induced agglutination) on the glycoprotein receptors actually took place. However, in the case of diabetic cells, the opposite effect was observed. Therefore, in normal hepatocytes, the arrangements of the neuraminic acid moieties on the glycoprotein receptors seemed to be different from those in the diabetic cell membranes. The surface charge density may not be a factor since after neuraminidase treatment and in the absence of concanavalin A, agglutination was not observed (Table I).

The pretreatment of normal cells first with trypsin and then neuraminidase had no effect on the rate of concanavalin A-induced hepatocyte agglutination (Table I). This was contrary to diabetic cells, where the rate of agglutination drastically increased after consecutive treatment with both enzymes. The data suggest that normal cells (as compared with diabetic cells) carry clustered agglutinin receptors, some of which may be in the "cryptic" state. Trypsin normally causes increased receptor mobility and further exposure of the "cryptic" receptors. In the presence of both trypsin and neuraminidase, agglutination of the diabetic cells was maximal.

REFERENCES

(1) I. J. Goldstein, C. E. Hollerman, and E. E. Smith, *Biochemistry*, **4,** 876 (1965).

(2) A. Martinez-Palomo, R. Wicker, and W. Bernhard, *Int. J. Cancer*, **9,** 676 (1972).

(3) G. Poste and P. Reeve, *Nature (London), New Biol.*, **237,** 113 (1972).

(4) I. J. Goldstein, C. M. Reichert, and A. Misaki, *Ann. N.Y. Acad. Sci.*, **234,** 283 (1974).

(5) E. M. Davis, J. J. Starling, and E. F. Walborg, Jr., *Exp. Cell Res.*, **99,** 37 (1976).

(6) P. Cuatrecasas, *J. Biol. Chem.*, **246,** 6522 (1971).

(7) P. Cuatrecasas and G. Illiano, *J. Biol. Chem.*, **246,** 4938 (1971).

(8) J. W. Rosenthal and J. N. Fain, *J. Biol. Chem.*, **246,** 5888 (1971).

(9) S. Clark, M. De Luise, R. G. Larkins, R. A. Melick, and L. C. Harrison, *Biochem. J.*, **174,** 37 (1978).

(10) A. B. Bikhazi, E. H. Abboud, S. K. Agulian, and C. F. Nassar, *Pflugers Arch.*, **386,** 245 (1980).

(11) A. B. Bikhazi, H. M. Nubani, and E. L. Coe, *J. Pharm. Sci.*, **72,** 116 (1983).

(12) A. B. Bikhazi and G. E. Ayyub, *J. Pharm. Sci.*, **67,** 939 (1978).

(13) W. I. Higuchi, R. Okada, G. A. Stelter, and A. P. Lemberger, *J. Pharm. Sci.*, **52,** 49 (1963).

(14) M. Inbar and L. Sachs, *Proc. Natl. Acad. Sci. USA*, **63,** 1418 (1969).

(15) G. Poste and P. Reeve, *Nature (London), New Biol.*, **247,** 469 (1974).

(16) G. L. Nicolson, *Nature (London) New Biol.*, **233,** 244 (1971).

(17) J. Z. Rosenblith, T. E. Ukena, H. H. Yin, R. D. Berlin, and M. J. Karnovsky, *Proc. Natl. Acad. Sci. USA*, **70,** 1625 (1973).

(18) J. Roth, *Int. J. Cancer*, **14,** 762 (1974).

(19) J. J. Starling, D. C. Hixon, E. M. Davis, and E. F. Walborg, Jr., *Exp. Cell Res.*, **104,** 165 (1977).

(20) K. Porter, D. Prescott, and J. Frye, *J. Cell Biol.*, **57,** 815 (1973).

(21) J. K. Reddy, M. S. Rao, J. R. Warren, and O. T. Minnick, *Exp. Cell Res.*, **120,** 55 (1979).

(22) Y. Marikovsky, M. Inbar, D. Donan, and L. Sachs, *Exp. Cell Res.*, **89,** 359 (1974).

ACKNOWLEDGMENTS

This work was supported, in part, by Grant 38-5829, from the Lebanese Council for Scientific Research.

Effect of Sulfaphenazole on Tolbutamide Distribution in Rabbits: Analysis of Interspecies Differences in Tissue Distribution of Tolbutamide

OSAMU SUGITA, YASUFUMI SAWADA, YUICHI SUGIYAMA, TATSUJI IGA[x], and MANABU HANANO

Received October 4, 1982 from the *University of Tokyo, Faculty of Pharmaceutical Sciences, Department of Pharmaceutics, 3-1, 7-Chome, Hongo, Bunkyo-ku, Tokyo 113, Japan.* Accepted for publication April 5, 1983.

Abstract □ The effect of sulfaphenazole on the distribution of tolbutamide was examined by comparing the change in the steady-state volume of distribution (Vd_{ss}) determined from *in vivo* plasma elimination with the tissue-to-plasma concentration ratio of various tissues (K_p) in rabbits; this effect was compared with that previously reported in rats. In rabbits, the K_p values of six tissues studied (*i.e.*, brain, heart, spleen, small intestine, muscle, and skin) increased in the presence of sulfaphenazole; except for brain, lung, and adipose tissue, the tissue-to-plasma unbound concentration ratio ($K_{p,f}$) of other tissues did show a significant decrease. This suggested that both the tissue and plasma protein binding of tolbutamide were affected by sulfaphenazole and that the increase in K_p was due mainly to the displacement of plasma protein binding of tolbutamide by sulfaphenazole, which was greater than that of tissue binding, while no change in K_p was due to a parallel change in both the plasma protein binding and tissue binding of tolbutamide. In both rabbits and rats, the Vd_{ss} calculated from plasma concentration *versus* time curve was very close to that calculated from the K_p values and volumes of various tissues in the presence and absence of sulfaphenazole, respectively. The interspecies difference of the effect of sulfaphenazole on the tissue distribution of tolbutamide between rabbits and rats was elucidated from both *in vivo* tissue distribution and *in vitro* plasma protein binding studies.

Keyphrases: □ Sulfaphenazole—effect on tissue distribution of tolbutamide, rabbits, interspecies comparison □ Tolbutamide—tissue distribution in rabbits, effect of sulfaphenazole, interspecies comparison □ Tissue distribution—tolbutamide in rabbits, effect of sulfaphenazole, interspecies comparison

In previous papers (1, 2) a blood flow rate-limited pharmacokinetic model was developed to study the effect of sulfonamide on the plasma elimination and tissue distribution of tolbutamide in rats. The tissue-to-plasma concentration ratio (K_p) of all tissues studied increased in the presence of sulfaphenazole, but the tissue-to-plasma unbound concentration ratio ($K_{p,f}$) did not show a significant alteration. This suggested that the tissue binding of tolbutamide is not affected by sulfaphenazole and that the increase of K_p is due mainly to the displacement of plasma protein binding of tolbutamide by sulfaphenazole. The purpose of this study was to investigate an interspecies difference in the effect of sulfaphenazole on the tissue distribution of tolbutamide in rabbits and rats, and to determine whether this finding would encompass other species.

EXPERIMENTAL

Sodium tolbutamide[1] and sulfaphenazole[2] were used. [^{14}C-carbonyl]tolbutamide[3] (48.09 mCi/mmol), which was found to be ≥98–99% pure by TLC, was used as the radioactive compound. All other reagents were commercially available and analytical grade.

Animal Experiments—Adult male albino rabbits[4], weighing 2.6–2.9 kg, were used. Under light ether anesthesia, the femoral vein and artery were cannulated with polyethylene tubing[5]. Cannulated rabbits were kept in a supine position on restraining plates. After a loading dose of 53.6 mg of sulfaphenazole/kg, 57.1 mg/kg/h was infused through the femoral vein cannula for 8 h with a constant-rate infusion pump[6]; with this dosage, steady-state concentrations of sulfaphenazole (153.3 ± 3.5 μg/mL, n = 4) and N^4-acetyl sulfaphenazole (201.7 ± 9.6 μg/mL, n = 3) were obtained at 2 h after the initiation of infusion, as reported previously (3). The rabbits were then given 80 mg/kg of tolbutamide containing 3.33 μCi/kg of [^{14}C]tolbutamide in physiological saline through the other femoral vein cannula. The control rabbits were given physiological saline instead of sulfaphenazole. The body temperature was kept at 37°C by a heat lamp.

After removal of arterial blood samples, the animals were sacrificed 6 h after tolbutamide administration by an injection of saturated potassium chloride solution into the carotid artery. The brain, heart, lung, liver, kidney, spleen, pancreas, small intestine, adipose tissue (around the kidneys and bladder), muscle (abdominal), and skin (dorsal) were quickly excised, rinsed well with cold saline, blotted, and weighed. The wet weights of these tissues were not altered in the presence of sulfaphenazole. All tissues and plasma were stored at −20°C until assayed.

The separation of the metabolites from tolbutamide was carried out according to Shibasaki *et al.* (4) as described in a previous paper (2). With this method, unchanged tolbutamide could be separated from its metabolites, *i.e.*, hydroxy- and carboxytolbutamides (4). Briefly, tissue samples except for skin were homogenized[7] with a threefold excess volume of 0.5 M phosphate buffer (pH 5.0). Four milliliters of each homogenate or 50 μL of the plasma was shaken for 30 min and then extracted twice with 6 mL of *n*-heptane–chloroform (4:1 v/v). The extracts were combined and shaken with 1 mL of 0.5 M NaOH for 15 min, and the aqueous phase was used for the determination of tolbutamide. The concentration of ^{14}C-labeled tolbutamide was determined[8] after addition of a 0.5 mL of 0.5 M HCl and 10 mL of scintillation fluid[9].

The skin was oxidized to $^{14}CO_2$ in a sample oxidizer[10], and then the radioactivity was determined as described before. The value of the plasma free fraction of rats was obtained from a previous paper (2), but that of rabbits was determined by an ultrafiltration method at 37°C as reported previously (1, 3).

Statistical Analysis—All means are presented with their standard error (mean ± SE). Statistical analysis was performed using the Student's t test, with p = 0.05 as the minimal level of significance.

RESULTS

The tissue-to-plasma concentration ratios (K_p) in rabbits 6 h after intravenous bolus administration of tolbutamide in the presence and absence of sulfaphenazole are listed in Table I. In the presence of sulfaphenazole, the K_p values of six tissues, *i.e.*, brain, heart, spleen, small intestine, muscle, and skin, increased significantly. The relationships between the K_p values in the presence and those in the absence of sulfaphenazole are shown in Fig. 1a and are compared with that of rats (Fig. 1b), which were reported previously (2). The plasma free fractions (f_p) of tolbutamide in the absence and presence of sulfaphenazole are listed in Table II. The f_p increased significantly in the presence of sulfaphenazole. The tissue-to-plasma unbound concentration ratios ($K_{p,f}$) were calculated by the following equation and are also listed in Table II:

$$K_{p,f} = \frac{K_p}{f_p} \qquad \text{(Eq. 1)}$$

Significant decreases in $K_{p,f}$ were shown in the heart, liver, kidney, spleen,

[1] Japan Hext, Tokyo, Japan.
[2] Dainippon Pharm. Co., Tokyo, Japan.
[3] New England Nuclear Co., Boston, Mass.
[4] Ichikawaya, Tokyo, Japan.
[5] Type PE-50, Clay Adams; Becton, Dickinson Co., Parsippany, N.J.
[6] Model KN, Type 12H; Natsume Seisakusho Co., Tokyo, Japan.
[7] Teflon glass homogenizer.
[8] Aloka Tri-Carb counter; Aloka Instruments Co., Tokyo, Japan.
[9] 0.1 g of 1,4-bis[2-(4 methyl-5-phenyloxazo-lyl)]-benzene, 4.0 g of 2,5 diphenyloxazole, and 500 mL of Triton X-100/L of toluene.
[10] Model 306; Packard Instruments Corp., Downers Grove, Ill.

0022-3549/84/0500-0631$01.00/0
© 1984, American Pharmaceutical Association

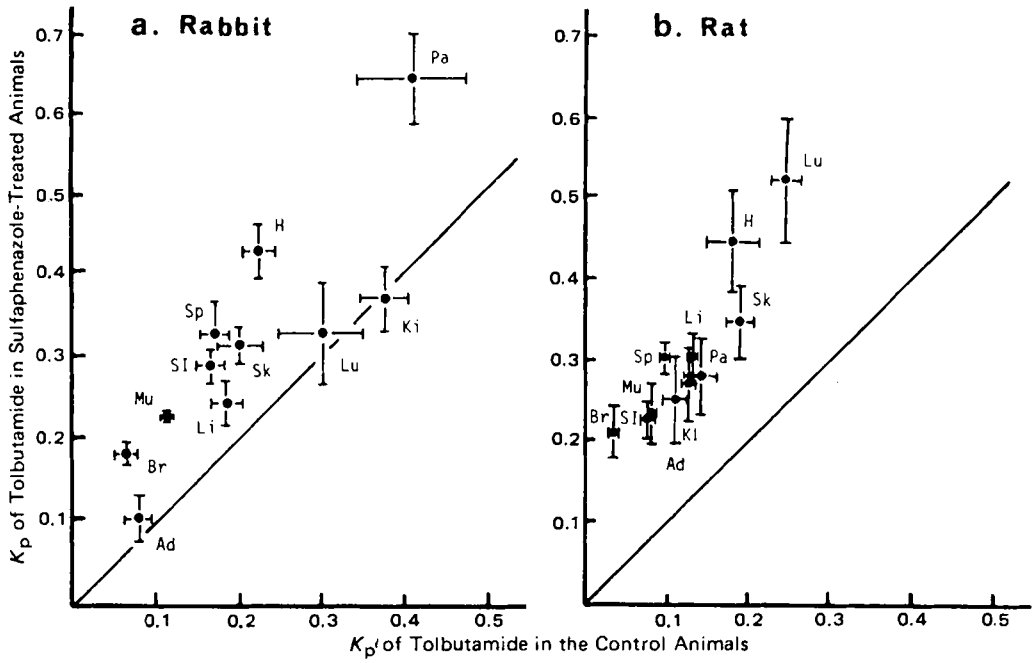

Figure 1—*Relationship between the tissue-to-plasma concentration ratios* (K_p) *of tolbutamide in the presence and absence of sulfaphenazole in rabbits* (*a*) *and rats* (*b*). *The abbreviations, Li, Ki, SI, Lu, H, Mu, Br, Pa, Sp, Ad, and Sk denote liver, kidney, small intestine, lung, heart, muscle, brain, pancreas, spleen, adipose tissue, and skin, respectively. The data for rats were obtained from a previous paper* (*2*). *The line shows that of unity* (*slope = 1*).

pancreas, small intestine, muscle, and skin of the sulfaphenazole-treated rabbits, but there did not appear to be significant changes in the brain, lung, and adipose tissues. The relationships between the $K_{p,f}$ values in the presence and those in the absence of sulfaphenazole are shown in Fig. 2a, and are compared with those of rats (Fig. 2b) as reported previously (2).

The volume of distribution at steady state (Vd_{ss}) calculated by Eq. 5 in the *Appendix* and that based on the unbound drug except for the blood space ($Vd_{T,f}$) calculated by Eq. 7 in the *Appendix I* are listed in Table III along with those for rats, which were calculated from the data reported previously (2). In both the sulfaphenazole-treated rabbits and rats, a significant increase was observed in $\overline{Vd}_{ss}$, whereas in $\overline{Vd}_{T,f}$ a significant decrease was observed only in rabbits. The extent of decrease in $Vd_{T,f}$ for rabbits in the presence of sulfaphenazole was smaller than that of the bound fraction ($1 - f_p$) calculated by f_p in Table II. Using the values of K_p, $K_{p,f}$, and volumes of various tissues listed in Tables I, II, and IV, the Vd_{ss} and $Vd_{T,f}$ were calculated by Eqs. 8 and 10 from the *Appendix I*, respectively, and are listed in Table III with those of rats, which were calculated from the data reported previously (2). The Vd_{ss} significantly increased in the presence of sulfaphenazole in rabbits as well as in rats. A significant decrease in $Vd_{T,f}$ was shown in rabbits in the presence of sulfaphenazole, but in rats no alteration was shown. The extent of changes in $\overline{Vd}_{ss}$ and $\overline{Vd}_{T,f}$ calculated by Eqs. 5 and 7 in the *Appendix I* was comparable with that of those parameters (Vd_{ss} and $Vd_{T,f}$) calculated by Eqs. 8 and 10 in the *Appendix I*, respectively.

DISCUSSION

When metabolism is the rate-determining step of plasma drug elimination (1, 3), the Vd_{ss} can be expressed as follows (10) (see *Appendix I*):

$$Vd_{ss} = \frac{V_B}{s} + \sum_j K_{p_j} \cdot V_j = \frac{V_B}{s} + \sum_j f_p \cdot K_{p,f_j} \cdot V_j \qquad \text{(Eq. 2)}$$

Previously, the effects of sulfaphenazole on the plasma free fraction and intrinsic clearance of tolbutamide in rats (2) and rabbits (3) have been reported. The plasma protein binding showed a nonlinearity and was decreased in the presence of sulfaphenazole in both animals. But little has been reported for the effect of sulfaphenazole on the tissue distribution of tolbutamide (1).

Although the K_p values for many tissues studied in the presence of sulfaphenazole significantly increased in rabbits, the $K_{p,f}$ values calculated by Eq. 1 showed a significant decrease. From these findings, it was suggested that the tissue binding of tolbutamide in rabbits may depend on the plasma tolbutamide concentration or may be decreased in the presence of sulfaphenazole or N^4-acetylsulfaphenazole. The increase in Vd_{ss} (1.2-fold of that for the control rabbits) might be explained by a simultaneous decrease in the plasma protein binding of tolbutamide (0.45-fold of that for the control; Table II) and in the tissue binding (0.53-fold of that for the control; Table III). The decrease in the tissue binding of tolbutamide can be seen in the decrease in $Vd_{T,f}$ (Table III).

In sheep, Thiessen and Rowland (5) reported that although the plasma free fraction of tolbutamide increased, the distribution volume did not show an alteration in the presence of sulfadimethoxine. Accordingly, in sheep a parallel change in both the plasma protein binding and the tissue binding of tolbutamide might minimize any change in Vd as a function of the plasma free fraction. However, in rats, although the K_p values for most of the tissues

Table I—Tissue-to-Plasma Concentration Ratios (K_p) of Tolbutamide in Rabbits [a]

Tissue	Control, $n = 4$	Sulfaphenazole, $n = 3$
Brain	0.062 ± 0.011	0.186 ± 0.008[b]
Heart	0.230 ± 0.014	0.420 ± 0.033[b]
Lung	0.297 ± 0.054	0.325 ± 0.064
Liver	0.184 ± 0.009	0.240 ± 0.033
Kidney	0.382 ± 0.028	0.368 ± 0.028
Spleen	0.171 ± 0.009	0.329 ± 0.025[b]
Pancreas	0.405 ± 0.074[c]	0.629 ± 0.047
Small intestine	0.169 ± 0.016	0.287 ± 0.022[b]
Adipose tissue	0.080 ± 0.015	0.107 ± 0.021
Muscle	0.111 ± 0.004	0.229 ± 0.007[b]
Skin	0.200 ± 0.026	0.316 ± 0.014[b]

[a] Results are given as the mean ± *SE*; at 6 h after bolus injection of tolbutamide. [b] Significantly different ($p < 0.05$) from the control. [c] $n = 2$.

Table II—Tissue-to-Plasma Unbound Concentration Ratios ($K_{p,f}$) of Tolbutamide in Rabbits [a]

Tissue	Control, $n = 4$	Sulfaphenazole, $n = 3$
C_p, g/mL[b]	118.6 ± 11.3	94.8 ± 1.5[d]
f_p[c]	0.094 ± 0.003	0.273 ± 0.001[d]
Brain	0.706 ± 0.135	0.682 ± 0.030
Heart	2.474 ± 0.229	1.543 ± 0.124[d]
Lung	3.210 ± 0.663	1.195 ± 0.236
Liver	1.971 ± 0.158	0.880 ± 0.150[d]
Kidney	4.117 ± 0.439	1.353 ± 0.104[d]
Spleen	1.821 ± 0.079	1.212 ± 0.091[d]
Pancreas	4.369 ± 1.020[e]	2.310 ± 0.174[d]
Small intestine	1.812 ± 0.205	1.055 ± 0.081[d]
Adipose tissue	0.868 ± 0.184	0.393 ± 0.078
Muscle	1.188 ± 0.072	0.841 ± 0.031[d]
Skin	2.139 ± 0.278	1.160 ± 0.050[d]

[a] Results are given as the mean ± *SE*; at 6 h after bolus injection of tolbutamide. [b] Plasma concentration of tolbutamide. [c] Plasma free fraction of tolbutamide. [d] Significantly different ($p < 0.05$) from the control. [e] $n = 2$.

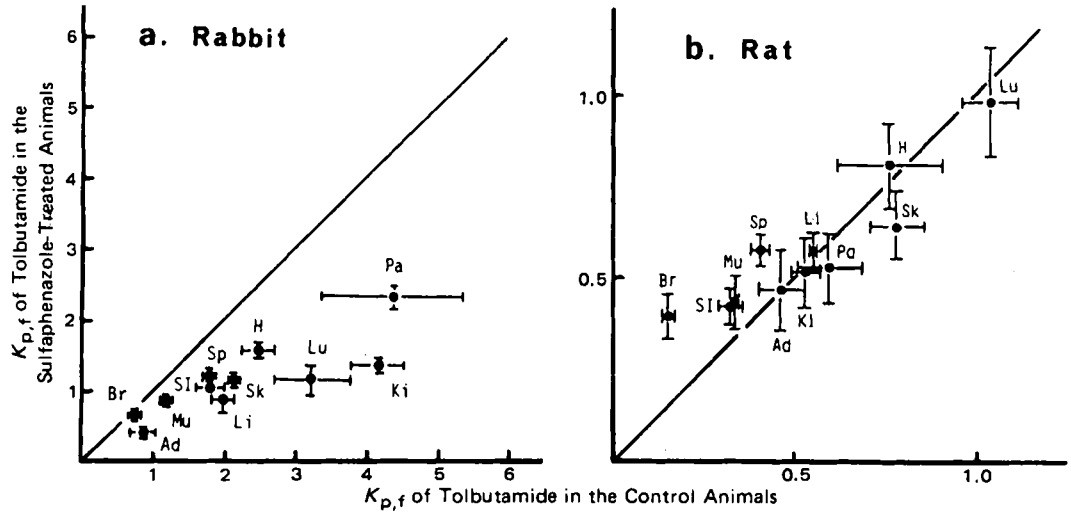

Figure 2—*Relationship between the tissue-to-plasma unbound concentration ratios ($K_{p,f}$) of tolbutamide in the presence and absence of sulfaphenazole in rabbits (a) and rats (b). Abbreviations are the same as those in Fig. 1. The data for rats were obtained from a previous paper (2). The line shows that of unity (slope = 1).*

studied in the presence of sulfaphenazole and at a higher steady-state concentration of tolbutamide than that of the control, significantly increased, the $K_{p,f}$ values calculated by Eq. 1 did not show an alteration (Figs. 1b and 2b). Consequently, the tissue binding of tolbutamide may not depend on the plasma tolbutamide concentration and may not be decreased in the presence of sulfaphenazole, whereas the plasma protein binding of tolbutamide showed a nonlinearity and was decreased in the presence of sulfaphenazole (2). From these findings, it was suggested that in rats the increase in K_p might be explained mainly by an alteration of the plasma protein binding of tolbutamide.

The difference in the effect of sulfaphenazole on the tissue distribution of tolbutamide between rats and rabbits may be due to the presence of a higher concentration of N^4-acetylsulfaphenazole in rabbits than in rats. As previously reported, the displacement of thiopental by sulfadimethoxine was not revealed in the tissue binding using rat muscle, liver, and adipose tissue homogenates (6). Moreover, the tissue binding of tolbutamide was not significantly influenced by phenylbutazone using rabbit muscle homogenates (7). Wardell (8) also reported that phenylbutazone did not affect significantly the tissue binding of sulfadimethoxine using rat muscle, liver, and kidney homogenates. Consequently, the increase in Vd_{ss} of tolbutamide in rats in the presence of sulfaphenazole might be explained by the unchanged tissue binding of tolbutamide and the increase in the plasma free fraction of tolbutamide, caused by the displacement of the plasma tolbutamide binding by sulfaphenazole. As shown in Table IV, the difference between $\overline{Vd}_{ss}$ and Vd_{ss}, calculated by Eqs. 5 and 8, respectively, in both the control rabbits and rats may result from the nonlinearity of the plasma protein binding (2, 3), since the plasma concentration of tolbutamide 6 h after intravenous bolus administration was lower than the *in vivo* mean plasma concentration for 6 h (see footnote in Table III). On the other hand, the close agreement between $\overline{Vd}_{ss}$ and Vd_{ss} in the presence of sulfaphenazole may be due to the linearity of the plasma protein binding of tolbutamide, which was observed only in the presence of sulfaphenazole (2, 3).

In rabbits, the $K_{p,f}$ values were greater than unity in most of the tissues studied (Fig. 2 and Table II) and were different from those of rats, which were not greater than unity in all tissues (1). The comparison of $Vd_{T,f}$ and f_p among rabbits, rats, sheep, and humans is summarized in Table V. It was shown that the distribution of tolbutamide to the tissues was approximately two times higher in rabbits and sheep than that in humans and rats. A remarkable interspecies difference was also shown in f_p between humans and rats, whereas only a small difference was shown in the tissue distribution of tolbutamide between the two species. This suggests the possibility of the animal scale-up from rats to humans for the prediction of Vd of humans using the data of the tissue distribution of tolbutamide obtained in the rat study.

In the present study, the interspecies difference of the tissue distribution of tolbutamide between rabbits and rats was demonstrated from both the *in vivo* tissue distribution and *in vitro* plasma protein binding.

APPENDIX I: Calculation of the Volume of Distribution

The volume of distribution at steady state (Vd_{ss}) is given by:

$$Vd_{ss} = Vd_B + Vd_T \qquad \text{(Eq. 3)}$$

The volume of distribution for the blood space (Vd_B) can be expressed by:

$$Vd_B = \frac{V_B \cdot C_B}{C_p} = \frac{V_B}{s} \qquad \text{(Eq. 4)}$$

The Vd_{ss} is calculated by two methods as follows:

Method 1—The Vd_{ss} calculated by plasma concentration *versus* time curve ($\overline{Vd}_{ss}$) is given by (9):

$$\overline{Vd}_{ss} = \frac{\text{Dose} \cdot \text{AUMC}}{(\text{AUC})^2} \qquad \text{(Eq. 5)}$$

From Eq. 3 (10), the following equation is obtained:

$$\overline{Vd}_T = \overline{Vd}_{ss} - Vd_B = f_p \cdot \overline{Vd}_{T,f} \qquad \text{(Eq. 6)}$$

Table III—Effect of Sulfaphenazole on Volume of Distribution of Tolbutamide [a]

Animal	Volume of Distribution, mL/kg	Control, $n = 4$	Sulfaphenazole, $n = 3$
Rabbit	$\overline{Vd}_{ss}$ [b]	222.84 ± 1.89	268.90 ± 13.97[f]
	$Vd_{T,f}$ [c]	1336.54 ± 14.88	703.42 ± 46.72[f]
	Vd_{ss} [d]	152.19 ± 4.91	237.41 ± 3.82[f]
	$Vd_{T,f}$ [e]	1061.01 ± 74.68	656.00 ± 13.23[f]
Rat	$\overline{Vd}_{ss}$ [b]	216.76 ± 2.13	297.79 ± 6.46[f]
	$\overline{Vd}_{T,f}$ [c]	597.39 ± 7.95	436.73 ± 11.83
	Vd_{ss} [d]	146.79 ± 3.50	273.89 ± 26.82[f]
	$Vd_{T,f}$ [e]	381.90 ± 13.99	405.59 ± 53.82

[a] Results are given as the mean ± *SE*. [b] Calculated by Eq. 5 in *Appendix I*: Dose·AUMC/(AUC)^2 (9). [c] Calculated by Eq. 7 in *Appendix I*: $(\overline{Vd}_{ss} - V_B/s)/f_p$. The f_p values calculated from the C_f of the *in vivo* mean plasma concentration (C_t) for 360 min were used. The C_t was calculated mathematically by: $C_t = \text{AUC}_{0\ 360\ min}/360$ min. In rabbits, the mean f_p values were 0.127 in the absence and 0.299 in the presence of sulfaphenazole, respectively, while in rats the mean f_p values were 0.286 in the absence and 0.546 in the presence of sulfaphenazole, respectively. [d] Calculated by Eq. 8 of *Appendix I*: $Vd_B + \Sigma K_{p,j} \cdot V_j$ (10). [e] Calculated by Eq. 10 of *Appendix I*: $\Sigma_j K_{p,j} \cdot V_j / f_p$. The f_p values at 360 min after intravenous bolus administration of tolbutamide were used (see Table II). [f] Significantly different ($p < 0.05$) from the control.

Table IV—Volumes of Blood and Tissues in Rabbits and Rats [a]

Tissue	Rabbits, mL/kg	Rats, mL/kg
Blood	73.8[b]	75.4[b]
Gastrointestinal tract[c]	51.5	44.3
Lung	7.3	4.6
Brain	2.6	4.6
Heart	2.6	4.3
Liver	42.8	44.3
Kidney	6.4	7.9
Muscle	500.0[d]	500.0[d]
Skin	100.0	175.0
Adipose tissue	51.5	40.0
Pancreas	0.4	3.6
Spleen	0.4	3.6

[a] Determined experimentally from the wet tissue weight by assuming a density of 1.0, except for muscle and blood volume. [b] The blood volume was calculated according to Bischoff *et al.* (11) as: $V_{plasma} = 44 \times (\text{body weight, kg})^{0.99}$ and $V_{blood} = V_{plasma}/(1 - H_t)$, where H_t is the hematocrit value and was determined to be 0.41 in this study. Body weights used were 2.8 kg for rabbits and 280 g for rats. [c] Includes the stomach, small intestine, and large intestine; the K_p of the small intestine was used to calculate the distribution volume (Vd) of tolbutamide for this tissue. [d] The muscle volume was assumed to be half of the body weight (12).

The volume of distribution based on the measurement of the unbound drug in plasma except for the blood space ($\overline{Vd}_{T,f}$) is given by:

$$\overline{Vd}_{T,f} = \frac{\overline{Vd}_{ss} - V_B/s}{f_p} \quad \text{(Eq. 7)}$$

In this paper, the $\overline{Vd}_{T,f}$ of humans and sheep were calculated by using the data reported previously (4, 12), respectively. The mean value of 1.36 (1.33 for rats and 1.39 for rabbits) was used as the value of s. The V_B was calculated by the equation in footnote b of Table IV.

Method 2—The Vd_{ss} calculated by tissue-to-plasma concentration ratios at 6 h after intravenous administration of tolbutamide is given by the following (10):

$$Vd_{ss} \simeq Vd_B + \sum_j K_{pj} \cdot V_j \quad \text{(Eq. 8)}$$

The subscript j represents all tissues studied. From Eqs. 3 and 8, the following equation is obtained:

$$Vd_T = \sum_j K_{pj} \cdot V_j \quad \text{(Eq. 9)}$$

The volume of distribution based on the measurement of the unbound drug in plasma except for the blood space ($Vd_{T,f}$) is given by:

$$Vd_{T,f} = \sum_j K_{p,f_j} \cdot V_j = \sum_j K_{pj} \cdot V_j/f_p \quad \text{(Eq. 10)}$$

Appendix II: Glossary

Vd_{ss} = volume of distribution at steady state (mL)
Vd_B = total amount of the drug in the blood compartment divided by the concentration of the drug in plasma (mL)
Vd_T = total amount of the drug in all tissue compartments divided by the concentration of the drug in plasma (mL)
$Vd_{T,f}$ = total amount of the drug in all tissue compartments divided by the concentration of the unbound drug in plasma (mL)
K_p = tissue-to-plasma concentration ratio
$K_{p,f}$ = tissue-to-plasma unbound concentration ratio
V_B = blood volume (mL)
V = volume of the tissue (mL)
s = plasma-to-blood concentration ratio
C_p = plasma concentration (μg/mL)
C_B = blood concentration (μg/mL)
AUC = area under the plasma concentration *versus* time curve [μg/(ml·min)]
AUMC = area under the moment curve (μg/[mL·(min)^2])
f_p = plasma free fraction

Table V—Interspecies Difference in the Total Amount of Drug in All Tissue Compartments Divided by the Concentration of the Unbound Drug in Plasma ($Vd_{T,f}$) and the Plasma Free Fraction (f_p)

Species	$Vd_{T,f}$, mL/kg	f_p
Rabbit	1336.5	0.127
Rat	597.4	0.286
Sheep	1341.2[a]	0.146
Human	639.2[b]	0.093

[a] Calculated by Eq. 7 of *Appendix I* using the reported value (5). [b] Calculated by Eq. 7 of *Appendix I* using the reported value (13).

REFERENCES

(1) O. Sugita, Y. Sawada, Y. Sugiyama, T. Iga, and M. Hanano, *Biochem. Pharmacol.*, **30,** 3347 (1981).

(2) O. Sugita, Y. Sawada, Y. Sugiyama, T. Iga, and M. Hanano, *J. Pharmacokinet. Biopharm.*, **10,** 297 (1982).

(3) O. Sugita, Y. Sawada, Y. Sugiyama, T. Iga, and M. Hanano, *Drug Metab. Dispos.*, **12,** 131 (1984).

(4) *J. Shibasaki, R. Konishi, and K. Yamasaki, J. Pharmacokinet. Biopharm.* **5,** 277 (1977).

(5) J. J. Thiessen and M. Rowland, *J. Pharm. Sci.*, **66,** 1063 (1977).

(6) H. Y. Yu, Y. Sawada, Y. Sugiyama, T. Iga, and M. Hanano, *J. Pharm. Sci.*, **70,** 323 (1981).

(7) B. Fichtl, H. Kurz, I. Wachter, and A. Ziegler, *Naunyn-Schmiedeberg's Arch. Pharmacol.*, **302,** R2 (1978).

(8) W. M. Wardell, *Br. J. Pharmacol.*, **43,** 325 (1971).

(9) L. Z. Benet and R. L. Galeazzi, *J. Pharm. Sci.*, **68,** 1071 (1979).

(10) J. R. Gillette and J. R. Mitchell, "Concepts in Biochemical Pharmacology, Other Aspects of Pharmacokinetics," Springer-Verlag Berlin, Heidelberg, New York, 1975, p. 35-85.

(11) R. L. Dedrick, *J. Pharmacokinet. Biopharm.*, **1,** 435 (1973).

(12) K. B. Bishoff, R. L. Dedrick, D. S. Zaharko, and J. A. Longstreth, *J. Pharm. Sci.*, **60,** 1128 (1971).

(13) S. B. Matin, *Clin. Pharmacol. Ther.*, **16,** 1052 (1974).

Bioanalyses and Pharmacokinetics of Nafronyl in the Dog

EDWARD R. GARRETT

Received November 24, 1982, from *The Beehive, College of Pharmacy, J. Hillis Miller Health Center, University of Florida, Gainesville, FL 32610.* Accepted for publication January 10, 1983.

Abstract □ Improved specific and sensitive reverse-phase HPLC assays of nafronyl (I) and its acidic metabolite and hydrolysis product (II) in biological fluids were developed with sensitivities of 3–6 ng/mL using fluorometric detection with 225 nm excitation and 330 nm emission wavelengths. There were no significant differences in the stabilities and assays of I and II in plasma obtained using heparin, citrate phosphate dextrose solution, EDTA, citrate, or oxalate as anticoagulant. Inordinately high membrane binding did not permit the quantification of the high plasma protein binding of I by ultrafiltration; its instability precluded the use of equilibrium dialysis. Plasma protein binding of II by ultrafiltration was 76.4% and was not concentration dependent. The apparent red blood cell–plasma partition coefficients for I and II were 2.00 and 0.49, respectively, with almost all anticoagulants; the red blood cell–plasma water partition coefficient for II was 2.08 when corrected for plasma protein binding. Thus, both I and II had erythrocyte binding sites in addition to simple volume partitioning. Only heparin-treated blood gave anomalously low erythrocyte–plasma partition coefficients, indicating that heparin inhibited the partitioning of I and II into red blood cells from plasma water. The total body clearance of nafronyl (I) referenced to total plasma concentration [1295 ± 65(*SEM*) mL/min] was dose independent (35–70-mg range) and showed biphasic plasma half-lives (intravenous) of 12 and 100 min. Only 34% of the nafronyl appears as systemically circulating II in the plasma. Apparent volumes of distribution similarly referenced were 39.8 and 163 L for the central compartment and total body, respectively. Renal clearances referenced to total plasma concentration were 8.3 and 0.18 mL/min for I and II, respectively. The respective total urinary excretions of I, II, and the glucuronide of II (III) were 0.48, 0.021, and 0.32% of the administered intravenous doses. The respective total urinary excretions of I, II, and III for a bile-cannulated dog were 0.005, 0.16, and 0.40%. The total body clearance of intravenously administered II was 225 mL/min, with a renal clearance of 0.057 mL/min referenced to total plasma concentration. The respective total urinary excretions of II and III were 0.027 and 0.44% of the intravenous dose of II. Respective plasma half-lives of II (intravenous) were 2.5, 10.9, and 225 min. The apparent volume of distribution referenced to total plasma concentration was 2.2 L (9.1 L referenced to plasma water concentration). The apparent overall volume of distribution referenced to plasma concentration was 73 L. The bioavailability of nafronyl (I) was 0.3–2.7% of the oral 250-mg dose of I. The bioavailability of II was 10–17% of the oral 250-mg dose of I, indicating high presystemic and/or first-pass metabolism of I and II. Additional metabolites of nafronyl, probably the major ones, could be chromatographically identified and quantified. Their extraction and fluorescent properties indicated that they were hydroxylated naphthalenic compounds containing carboxylic acid groups and their glucuronides. Only one major unconjugated metabolite (IV) was found in significant quantities in plasma. In addition to IV, other organic extractable nonconjugated compounds (V, VI, and VII) appeared in urine and bile. Conjugates of VII were also present in urine and bile.

Keyphrases □ Nafronyl—pharmacokinetics in the dog, HPLC, red blood cell partitioning, plasma protein binding, effect of different anticoagulants, bioavailability □ Pharmacokinetics—nafronyl in the dog, HPLC, red blood cell partitioning, plasma protein binding, effect of different anticoagulants, bioavailability □ Bioavailability—nafronyl in the dog, HPLC, red blood cell partitioning, plasma protein binding, effect of different anticoagulants, pharmacokinetics

The vasodilator and metabolic activator nafronyl [2-diethylamino)ethyl tetrahydro-α-(1-naphthylmethyl)-2-furnpropionate (I) (1, 2) is prepared as the oxalate. Its smooth ıuscle relaxation properties, along with its ability to increase ɔripheral and cerebral blood flow, cerebral ATP concentraɔns, and glucose utilization may have value in the treatment senile brain disease (1–3). Tetrahydro-α-(1-naphthyl-ɔthyl)-2-furanpropionic acid (II), a hydrolysis product of ı (Scheme I), was observed by TLC in the plasma and urine of dogs, humans, and rats (4, 5) administered I, but was not

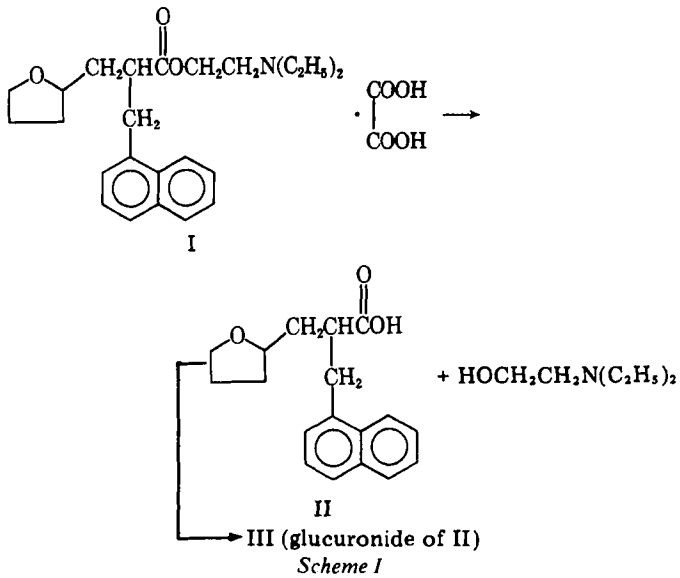

Scheme I

quantified. The glucuronide of II (III) was also observed in the bile and urine of dogs administered I intramuscularly (4).

Fontaine *et al.* (4) showed prolonged (at least through 5 h, but low, plasma levels of I (3.4–5.1 μg/mL of plasma) after administration of 40 mg/kg im of I to dogs. Detection of I in plasma was 80 ng/mL for three of six dogs at 24 h after intramuscular administration, with maxima of ~5 μg/mL at 1 h by the use of a nonspecific fluorometric assay (6). Minor amounts of the intramuscularly administered dose (0–0.4%) were excreted unchanged into dog urine, half within 6 h. As much as 20% of the dose was still present at the site of intramuscular injection at that time (4).

Bile collected over 12 h from bile-cannulated dogs contained 0.013% of the intramuscular dose of I and contained 0.42% of the injected dose as total I (free and liberated by β-glucuronidase), presumably fluorometrically analyzed; this agreed with the estimates of nafronyl equivalents obtained from measured spectrophotometric absorbance at 224 nm of acid extracts of ether-extracted alkalinized bile (4). The remaining aqueous phase after this extraction was acidified and extracted with ether. These ether extracts, back-extracted into 0.1 M NaOH and assayed spectrophotometrically at 224 nm, accounted for 33% of the dose in nafronyl absorbance equivalents, of which 22% was II, measured by quantifying TLC-separated amounts. After β-glucuronidase hydrolysis, the similarly treated bile accounted for 40% of the dose in nafronyl absorbance equivalents, of which 29% was II (free and liberated by β-glucuronidase). These ether extracts showed at least three identifiable TLC spots in addition to the one assignable to II. The IR chromatograms indicated the presence of both the naphthalenic and carboxyl groups in these metabolites, and two of the three contained phenolic hydroxyls. Since there was an increase in their presence after β-glucuronidase treatment, the glucuronide conjugates of these naphthols must also be metabolites of nafronyl (4).

0022-3549/84/0500-0635$01.00/0
© 1984, American Pharmaceutical Association

After oral administration of 150 mg of nafronyl to a human, plasma levels of I of 720 ng/mL at 1 h and 110 ng/mL at 6 h were claimed (4), and 0.6% of unchanged I was recovered in the urine within 2 d. After administration of 80 mg im of nafronyl to a human, plasma levels of I of 290 ng/mL at 1 h and 550 ng/mL at 3 h were noted, and 1.6% of unchanged I was recovered in the urine within 2 d (4). An apparent terminal plasma half-life of 90 min was observed for I when 100 mg of nafronyl was administered orally to two human subjects (7).

Since the above is the sum total of published studies on nafronyl pharmacokinetics, there is a need for systemically determined pharmacokinetics, disposition, and bioavailabilities. The purpose of this study was to determine the pharmacokinetic parameters of nafronyl after intravenous administration by quantitatively monitoring the time courses of both I and II and their possible conjugates in plasma, urine, and bile as a function of dose in the dog. Selected studies were conducted to estimate the oral bioavailability of nafronyl and to identify possible quantitative methods of monitoring the time courses of as yet unidentified metabolites.

The recent developments of HPLC methods for the bioanalyses of nafronyl (7) and nafronyl plus its derived metabolite, II (8), using UV detection at 224 nm after selective extractions from biological fluids, have provided specific and sensitive assays. These methods have been applied recently to the complete delineation of the solution stability of nafronyl as a function of pH and the optimization of analytical methods (8) in plasma. In this present report, further assay modifications and increased sensitivities with the use of fluorometric detection are given. Since questions had been raised as to the possible effects of different anticoagulants on the stability and assay of nafronyl in plasma, these factors were studied when various anticoagulants were used in blood procurement.

EXPERIMENTAL

Materials—Acetic acid[1], sodium acetate[1], potassium and ammonium oxalate[1], dibasic and monobasic potassium phosphate[1], and volumetric concentrations of sodium hydroxide[2] and hydrochloric acid[2] were all analytical grade. Dichloromethane[3] and acetonitrile[3] were HPLC and UV grade. β-Glucuronidase, purified from *Escherichia coli*[4], (1,344,100 Fishman U/g, 1,816,490 U/g with $CHCl_3$) and beef liver[5] (50 Fishman U/g) were used as received. EDTA was a 2% solution of the disodium salt[6]. Citrate phosphate dextrose solution USP[6] contained 1.61 g of hydrous dextrose USP, 1.66 g of sodium citrate dihydrate USP, 0.19 g of anhydrous citric acid USP, and 0.14 g of sodium biphosphate USP dissolved to 63 mL with water for injection USP. The oxalate anticoagulant solution was 1.2 g of ammonium oxalate and 0.89 g of potassium oxalate in 100 mL of water for injection USP.

The pharmacokinetic studies used sodium chloride injection USP[6], sodium heparin injection USP[7], intravenous delivery system sets[6], evacuated blood collection tubes[8], disposable syringes[9], 5-French urethral catheters[9], three-way stopcocks[10], 16-gauge vein catheters, 14-gauge needles[11], and carbocaine hydrochloride[12]. Pure I and II were used as received[13].

Crystalline butacaine hemisulfate[4] was the internal standard for red blood cell partitioning, protein binding, plasma stability studies, the pharmacokinetic studies of bile-cannulated dog E, and most of the oral studies. Procaine hydrochloride[4] was the internal standard in all other pharmacokinetic studies.

Apparatus—The HPLC system[14] used for plasma stability, red blood cell partitioning, and protein binding studies contained a single pump, an alkyl phenyl column, and a manual injector. The variable-wavelength detector[15] was set at 225 nm, with a strip-chart recorder[16]. The system was modified for analyses in the intravenous pharmacokinetic studies to use a radial-compression module[17], an automatic injector[17], a fluorescence detector[18] with excitation at 225 nm and emission at 330 nm, and an integrator[19]. In the bile-cannulated dog E pharmacokinetic study, a different detector[20] and injector[20] were used.

Liquid Chromatography—*With Haloalkane Extraction (Method A)*—This method was used in the pharmacokinetic studies. Plasma (2 mL) was adjusted to pH 3.5 with 0.35 mL of 0.2 M HCl, vortexed, and extracted with 5.0 mL of dichloromethane with mild shaking. The samples were centrifuged at 3000 rpm for 10 min and 3 mL of the organic phase was evaporated to dryness under a stream of nitrogen. The residue was reconstituted with 0.5 mL of acetonitrile–0.1 M acetate buffer pH 4.0 (80:20) containing 9.8 μg of procaine hydrochloride and 50 μL was injected into the HPLC (for method A1) or the residue was reconstituted with 0.5 mL of acetonitrile–0.1 M acetate buffer, pH 4.2, (10:90) containing 46 μg of butacaine hemisulfate, and 30 μL was injected into the HPLC (for method A2). Undiluted urine (1 mL) was adjusted to pH 3.5 with 0.175 mL of 0.2 M HCl, vortexed, extracted, evaporated, and reconstituted as above.

Method A1—This method was used for all intravenous pharmacokinetic studies except with the bile-cannulated dog study. Assay of I (retention time 5.4 min) used a mobile phase of acetonitrile–0.1 M acetate buffer pH 4.0 (80:20) through a radial cyano cartridge[21], with a flow rate of 3.0 mL/min. The assay of II (retention time 4.8 min) used a mobile phase of acetonitrile–acetate buffer pH 4.5 (50:50) through a radial C_8 cartridge[21], with a flow rate of 2.0 mL/min.

Method A2—In the oral and bile-cannulated dog studies only one system was used for the assay of I and II. A 5-μm C_8 column[22] (12 cm) maintained at 45°C was used, with a mobile phase of acetonitrile–0.05 M acetate buffer pH 4.0, (53:47) with a flow rate of 1.1 mL/min. A 25-μL aliquot of the 0.5-mL reconstituted residue was injected onto the HPLC. Peak area ratios to internal standard were used in all these pharmacokinetic studies for the assays.

Acetonitrile Deproteinization (Method B)—This method was used in the plasma stability, red blood cell partitioning, and protein binding studies. Acetonitrile (1.5 mL) containing 5.0 μg/mL of the internal standard butacaine sulfate was added to a 0.5-mL plasma sample, vortexed at high speed for 20 s, and centrifuged at 3000 rpm for 5 min; 50 μL of the supernatant was injected into the HPLC. The mobile phase of acetonitrile–0.1 M acetate buffer pH 4.5 (50:50) was passed through an alkyl phenyl column at a flow rate of 1.5 mL/min. Peak height ratios to internal standard were used in these *in vitro* studies.

Glucuronide Assay in Urine (Method C)—After extraction of the pH 3.5-adjusted urine with dichloromethane for assay of I and II as in method A1 and checking, in several instances, a second extraction to ascertain complete extraction, the urine samples were hydrolyzed with freshly prepared (100 Sigma or Fishman U/mL) β-glucuronidase (*E. coli*). Phosphate buffer at pH 7.0 (1 mL) and β-glucuronidase solution (0.2 mL) were added to 1 mL of the previously extracted urine. The mixture was incubated at 37.5°C for 30–40 min. An aliquot (1 mL) was adjusted to pH 2.5–3.0 with 0.5 mL of 0.2 M HCl, extracted with dichloromethane, and assayed for the aglycone using method A1. In one study, plasma was treated similarly to determine the presence of a generated aglycone, II. No significant II was found in plasma after β-glucuronidase treatment.

Glucuronide Assay in Urine and Bile in Bile-Cannulated Dog E (Method D)—Plasma and nonhydrolyzed urine and bile were extracted at pH 3.5, and the extracts were assayed by the single-injection HPLC method (method A2) in the bile-cannulated dog E study for the simultaneous determination I and II, using butacaine as the internal standard. The bile and urine were hydrolyzed by β-glucuronidase (*E. coli*) as in method C, except that the samples

[1] Mallinckrodt, Paris, Ky.
[2] Ricca Chemical Co., Arlington, Tex.
[3] Burdick and Jackson Laboratories, Muskegon, Mich.
[4] Sigma Chemical Co., St. Louis, Mo., β-glucuronidase (*E. coli*) was Type VII.
[5] Lot 042967; Aldrich Chemical Co., Milwaukee, Wis.
[6] McGaw Laboratories, Irvine, Calif.
[7] The Upjohn Co., Kalamazoo, Mich.
[8] Vacutainer blood collection tube with sodium heparin; Becton, Dickinson and Co., Rutherford, N.J.
[9] Monoject; Sherwood Medical, St. Louis, Mo.
[10] Pharmaseal, Inc., Toa Alta, P.R.
[11] Intracath; The Deseret Co., Sandy, Utah.
[12] Winthrop Laboratories, New York, N.Y.
[13] Nafronyl (I) LS 121, Lot 1956, IND 9571 and Lot 6260, analysis 23569; LS 74 (II) IND 9575, Lot 2357, Lipha Chemicals Inc., New York, N.Y.
[14] Model M 6000A solvent delivery system and Model U6k universal liquid chromatograph injector with a μBondapak column; Water Associates, Milford, Mass.
[15] LC 75 spectrophotometer detector for liquid chromatography; Perkin-Elmer Norwalk, Conn.
[16] Fisher recordall series 5000; Fisher Scientific Co., Pittsburgh, Pa.
[17] Wisp 710A automatic sampling device and RCM 100 module; Waters Associate Milford, Mass.
[18] Varian Fluorichrom fluorescence detector; Varian Instruments, Walnut Cree Calif.
[19] Model 3380A; Hewlett Packard, Avondale, Pa.
[20] PE models 420B and 630-10S; Perkin-Elmer, Norwalk, Conn.
[21] Waters Associates, Milford, Mass.
[22] Perkin Elmer HS 5-μm C_8 column; Perkin-Elmer, Norwalk, Conn.

were adjusted to pH 2.0 before extraction and the dried extracts were reconstituted in acetonitrile–0.1 M acetate buffer pH 4.2 (10:90) for injection because interfering impurities resulted from the plastic tips of the automatic injector[20] when the acetonitrile concentration was as high as that in the mobile phase (53% acetonitrile). The preextracted bile was also hydrolyzed with 0.2 M NaOH for 30 min at room temperature and adjusted to pH 2 with HCl before extraction and assay by method A2.

Pharmacokinetic Studies in Dogs—The dogs were healthy mongrels weighing 22–26 kg; dog E was female. All were negative for microfilaria. Initial hematocrits ranged between 0.43 and 0.38, with white blood counts of 11,500–15,000 (normal range).

The dogs were fasted for 24 h before each study, and a jugular vein catheter[12] was inserted *via* venipuncture using carbocaine as an anesthetic. The end of the catheter was fitted with the three-way stopcock[10]. The dead volume of the catheter was filled with 0.5 mL of heparinized sodium chloride solution (100 U/mL) to prevent clotting. The dog was placed in a clean metabolism cage overnight. On the day of the study the dog was placed in a dog sling[23] and an intravenous drip of 0.9% NaCl was started to keep the catheter open and to water-load the dog. A 5-French urethral catheter[9] was placed and the dog voided of urine prior to drug administration.

The drug was prepared by dissolving the appropriately weighed amount in 10 mL of isotonic saline. In the metabolite study, the appropriate amount of II was dissolved in 0.1 mL of propylene glycol before adding isotonic sodium bicarbonate to 10 mL. The percentage of propylene glycol was 0.67%.

Blood (60 mL) was drawn before drug injection for use in the plasma calibration curves. The drug solution (10 mL) was injected *via* the jugular catheter, and the stopcock and the catheter were flushed with 10 mL of isotonic saline; the time was measured from the end of the flush. For the oral studies, 250 mg of I was dissolved in 20 mL of deionized water. The solution was injected through a plastic feeding tube[9], which had been inserted orally to reach the stomach. It was followed by a 30-mL rinse of deionized water.

The normal time course for sampling in the intravenous pharmacokinetic studies was 2, 4, 6, 9, 12, 15, 20, 25, 30, 40, 50, 60, 70, 80, 90, 110, 150, 180, 240, and 300 min. The catheter and stopcock were filled with 1.0 mL of fresh blood before sampling, which was then discarded. Blood (5 mL) was taken in a syringe and transferred to a heparinized tube. The sample was centrifuged at 3000 rpm for 5 min, and the plasma was extracted immediately for assay of I and II. The red blood cells were handled under sterile conditions, resuspended in isotonic saline, and infused back into the dog after the last urine sample was obtained. The dog was then treated with antibiotics to lower the risk of infection.

Urine samples were collected through the urethral catheter at the following times: 15, 30, 45, 60, 75, 90, 105, 120, 140, 160, 180, 210, 240, 300, and 360 min. The volume and pH were recorded, and the samples were placed in an ice bath. All samples were extracted after the last plasma sample had been obtained and were assayed for I, II, and glucuronide by the methods described previously.

The sampling times were modified for the oral studies. Blood samples were obtained at 10-min intervals up to 200 min and then at 30-min intervals up to 480 min. Urine was collected at 20-min intervals up to 240 min and thereafter at 30-min intervals up to 540 min. Bile was collected at 20-min intervals up to 220 min in the bile-cannulated dog study.

Evaluation of β-Glucuronidase, Acid, and Alkaline Release of Conjugates of the Derived Acid—Biological fluids to be assayed for conjugates of II (*i.e.*, III) were obtained from the nondosed animal and were used to establish calibration curves, with graded amounts of II added to dichloromethane-preextracted fluids prior to the solvolytic and analytical processes. A 1-mL aliquot of urine, plasma, or bile was extracted at pH 3.5 with 5 mL of dichloromethane for 10 min with shaking, the normal process in the assay of nonconjugated I or II. The aspirated aqueous phase was then hydrolyzed at 37.5°C with *E. coli* β-glucuronidase (40 Fishman U/mL) after adjustment to pH 7.0 with phosphate buffer or with beef liver β-glucuronidase (0.016 Fishman U/mL) after adjustment to pH 4.5 with acetate buffer. Finally, the solutions were adjusted to pH 3.5 and extracted with 10 mL of dichloromethane. The organic extract was evaporated under nitrogen and reconstituted in 500 μL of mobile phase, with 50 μL injected for assay by method A1.

Urine samples, taken at different times from dog A (dosed with 70 mg of *nafronyl*), were assayed several times to determine when complete release of the conjugates of II was obtained. Dichloromethane-preextracted urine (1.0 mL) from dog A was mixed 1:1 with 0.1 M NaOH, 0.2 M NaOH, 1 M HCl, and 6 M HCl. After 15 and 30 min at room temperature, the alkaline samples were adjusted to pH 2. The urine samples were extracted with 10 mL of dichloromethane and assayed by method A1 for II.

Nafronyl Stability in Plasma Containing Various Anticoagulants—The stability of nafronyl (I) was investigated in fresh dog plasma prepared with different anticoagulants. The amounts per milliliter of blood were: heparin, 0.5 U; citrate phosphate dextrose solution USP, 0.14 mL; 0.2% EDTA, 0.125 mL; 3.78% sodium citrate, 0.111 mL; and ammonium–potassium oxalate solution, 0.1 mL. Blood (50–80 mL) was withdrawn from the jugular vein using a 16-gauge needle and syringe containing the necessary amount of anticoagulant. The blood was centrifuged for 15 min at 3000 rpm; no hemolysis was observed. Clear plasma (5–17 mL) was transferred into a clean stoppered tube and equilibrated. Nafronyl (I) (0.075–0.27 mg) was added, and the mixture was vortexed 1 min to give final concentrations between 15 and 19 μg/mL. After the addition of plasma to I, a timer was started. Aliquots (0.5 mL) of the mixture were assayed with time by the acetonitrile deproteinization procedure (method B).

Table I—Nafronyl Stabilities in Fresh Dog Plasma Prepared Using Various Anticoagulants [a]

Anticoagulant	$10^3 k$ [b], min^{-1}	$t_{1/2}$, h	Amount Transformed at t_∞, %
Heparin	1.99	5.77	49.3
Citrate phosphate dextrose solution	4.40	2.63	40.7
EDTA	3.68	3.19	38.5
Sodium citrate	3.49	3.31	36.1
Oxalate	3.41	3.33	40.4

[a] All studies, except for heparin at 22°C, were performed at 37.5°C. The concentration of nafronyl was 16 μg/mL. [b] Obtained from the slopes of data plotted in accordance with Eq. 5.

Calibration curves were prepared (0.4–4 μg/mL of injected solution) from stock solutions of I, II, and butacaine dissolved in acetonitrile. In the EDTA, sodium citrate, and oxalate studies, the calibration curves were prepared from the same blank plasma that was used for the stability study, and the injected solutions had the same composition as those injections made in the studies. The plasma used for the calibration curves in the heparin study had been refrigerated overnight. The calibration curve for the citrate phosphate dextrose solution study was prepared from compounds in the mobile phase.

Protein Binding—The protein binding of I and II in the heparinized dog plasma was investigated using a cone[24] filtration technique (9). Fresh whole dog plasma was filtered to obtain the plasma water. Plasma water (1.5 mL) and plasma (1.5 mL) were spiked with 2–16-μg/mL concentrations of I and II. A 0.5-mL aliquot of each was assayed using acetonitrile deproteinization (method B) to determine the initial concentrations. The plasma water was then filtered at 3000 rpm for 20 min, and 0.5 mL of filtrate was assayed. The spiked plasma was then filtered through the same cone used to filter the plasma water, which contained substances at the same concentration.

Red Blood Cell Partitioning—Calibration curves for the assay of I, II, and mixtures of I and II were prepared at 0.2–16 μg/mL in whole blood and plasma obtained by centrifugation from the same blood. Calibration curves were established for mobile phases at 25% of these concentrations, since they were injected without the dilution by acetonitrile needed for deproteinization. The blood samples were obtained with different anticoagulants: heparin, oxalate, citrate phosphate dextrose solution, and 0.2% EDTA in concentrations given previously. The hematocrits (H) of the blood samples were measured and portions centrifuged to recover the plasma. The spiked blood samples were carefully mixed and centrifuged at 3000 rpm for 5 min, and the separated plasma samples were assayed by method B using acetonitrile denaturation. The final hematocrits of the spiked blood samples were corrected for the dilutions made by the addition of the compounds. The corrected hematocrits (H') were 0.83 of those experimentally determined in the blood samples.

The spiked plasma and mobile phase were also assayed by this method. The concentrations per milliliter (C_p) in the separated plasma of spiked blood were ascertained from the calibration curve established for spiked plasma. The amount of drug in the plasma obtained from 1 mL of spiked blood is $A_{P-B} = (1 - H')C_p$. The amount of drug in the red blood cells obtained from 1 mL of spiked blood is $A_{RBC-B} = C_0 - A_{P-B}$, where C_0 is the concentration of spiked drug per milliliter of blood. The concentration of drug in the red blood cells of spiked blood is $C_{RBC} = A_{RBC-B}/H'$. Thus, the apparent red blood cell–plasma partition coefficient is:

$$D' = C_{RBC}/C_p = A_{RBC-B}/H'C_p = \frac{(C_0 - A_{P-B})/H'}{C_p} = \frac{C_0 - (1 - H')C_p}{H'C_p} = \frac{C_0}{H'C_p} - \frac{1 - H'}{H'} \quad \text{(Eq. 1)}$$

An alternate method to calculate the apparent red blood cell–plasma par-

[23] Dog Sling; Alice King Chatham, Medical Arts, Los Angeles, Calif.

[24] Centriflo Ultrafiltration Membrane Cones CF 50A; Amicon Corp., Lexington, Mass.

Table II—Parameters[a] for Calculation of the Apparent Red Blood Cell–Plasma Partition Coefficients, $D' = (1 - R + RH')/RH'$, of I and II

Anti-coagulant	I			II	
	H'	R	D'	R	D'
Citrate phosphate dextrose solution	0.327[b]	0.70	2.29	1.14	0.62
	0.275[c]	0.83	1.75	1.13	0.58
	0.275[c]	0.79	1.94	1.16	0.50
	Mean ± *SEM*		2.00 ± 0.15		0.57 ± 0.04
Oxalate	0.346[b]	0.60	2.93	1.23	0.47
EDTA	0.300[c]	0.89	1.41	1.19	0.46
	0.300[c]	0.78	1.92	0.96	1.15
	0.330[c]	0.65	2.67	1.30	0.30
	Mean ± *SEM*		2.00 ± 0.37		0.64 ± 0.26
Heparin	0.252[c]	1.00	1.00	1.51	−0.3
	0.252[b]	1.00	1.00	1.56	−0.1
	0.281[c]	1.00	1.00	1.32	0.14
	0.281[b]	0.81	1.85	1.28	0.23
	Mean ± *SEM*		1.2 ± 0.2		0.0 ± 0.1

[a] $D' = C_{RBC}/C_p = R = m/m'$, where m is $\Delta PHR_p/\Delta C_p$ in the plasma concentration curve, $m' = \Delta PHR/\Delta C_0$ in the blood concentration curve, PHR is the peak height ratio of I and II, and H' is the corrected hematocrit of the spiked blood samples. [b] Effected on mixtures of I and II, each 0.4–4.0 μg/mL of blood. [c] Separate studies for I and II.

tition coefficient, D', is based on the HPLC calibration curves, established in spiked plasma or mobile phase, that pass through the origin and conform to:

$$PHR_p = mC_p \qquad \text{(Eq. 2)}$$

where C_p is the spiked concentration in plasma or mobile phase that gives the peak height ratio, PHR_p. Calibration curves for drugs spiked in plasma and mobile phase were superimposable.

Apparent calibration curves were also prepared for the assay of drug in the plasma samples separated from spiked blood of different concentrations, C_0, obtained with different anticoagulants. This conformed to:

$$PHR_p = m'C_0 = m[(1 - H')C_p + H'C_{RBC}] = mC_p \qquad \text{(Eq. 3)}$$

Since $D' = C_{RBC}/C_p$ and $R = m'/m$, this equation can be rearranged to:

$$D' = \frac{1 - R + RH'}{RH'} \qquad \text{(Eq. 4)}$$

for the estimations of D'.

RESULTS AND DISCUSSION

Unless specified all concentrations of I, II, and III are given as equivalent to nafronyl (as the oxalate).

Improvements in Chromatographic Assays—The HPLC assay methods developed herein substantially improved analytical sensitivity for nafronyl (I) and its derived acid metabolite (II) over those published previously (8) for a haloalkane extraction method using 224-nm spectrometric detection, where the standard errors of regression of concentration on peak area or peak height or their ratios to that of a butacaine internal standard were 100–200 ng/mL of plasma. The columns and conditions for these new studies with fluorometric detection (225-nm excitation, 335-nm emission) using method A1 and dichloromethane extraction gave calibration curves in the 0–300-ng/mL range, which indicated analytical sensitivities of 2–15 ng/mL in urine and plasma.

Some examples of linear regression equations with standard errors of the estimates for nafronyl (I) concentrations in plasma (ng/mL) as the oxalate in plasma are: $C \pm 4.0$ ng/mL = (522.6 ± 10.0)PHR − 11.9 ± 3.3, r = 0.99960; $C \pm 6.2$ = (347.0 ± 2.5)PAR + 10.9 ± 3.1, r = 0.99983; $C \pm 5.1$ = (10.27 ± 0.06) PH + 0.60 ± 2.60, r = 0.9991. Some examples of linear regression equations with standard errors of the estimates of II concentrations in plasma (ng/mL) are: $C \pm 3.6$ = (8.56 ± 0.60)PH − 5.8 ± 5.2, r = 0.9952; $C \pm 2.15$ = (4.744 ± 0.072)PA + 8.3 ± 1.6, r = 0.99965. In urine for I: $C \pm 5.6$ = (3.78 ± 0.17)PH − 7.11 ± 5.10, r = 0.9993; $C \pm 6.1$ = (894.0 ± 5.6) PHR − 6.4 ± 2.8, r = 0.99986; $C \pm 7.1$ = (828.9 ± 20.6)PAR − 5.4 ± 9.8, r = 0.9993. In urine for II: $C \pm 0.59$ = (2.363 ± 0.016)PH − 4.6 ± 0.6, r = 0.9979; $C \pm 5.6$ = (3.78 ± 1.71)PH − 7.1 ± 5.1, r = 0.996. Similar values were obtained for II in urine treated with β-glucuronidase for the assay of III.

The different mobile phases and columns selected for the respective assays of I and II in method A1 permitted the assay of I with a respectable retention time of 5.4 min. The faster moving II in this system eluted with large peaks for urine (0–2 min) and plasma components (0–1.5 min). The system for II increased its retention time to 4.74 min, well separated from interferences from plasma. It was difficult to observe any metabolite that had smaller retention times to I and II and would fall within the retention time intervals of interfering plasma and urine components.

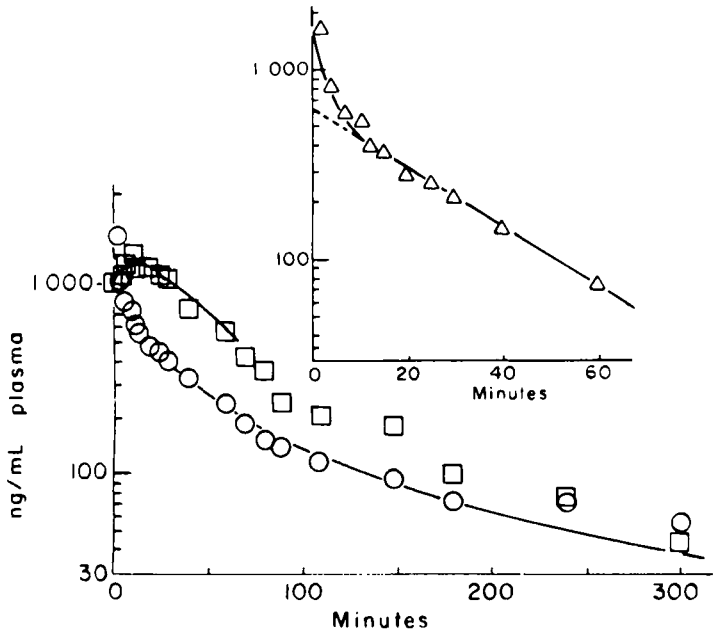

Figure 1—*Plasma concentrations of I (○) and II (□) in equivalents of nafronyl oxalate against time for dog A given a 70-mg iv bolus dose of I. The curve through I was calculated from the sum of exponentials (Eq. 10) using the parameters in Table III. The inset (△) is the feathered data for I with the curve calculated from the first two exponentials. The curve through II was calculated from Eq. 15 using the parameters in Table III.*

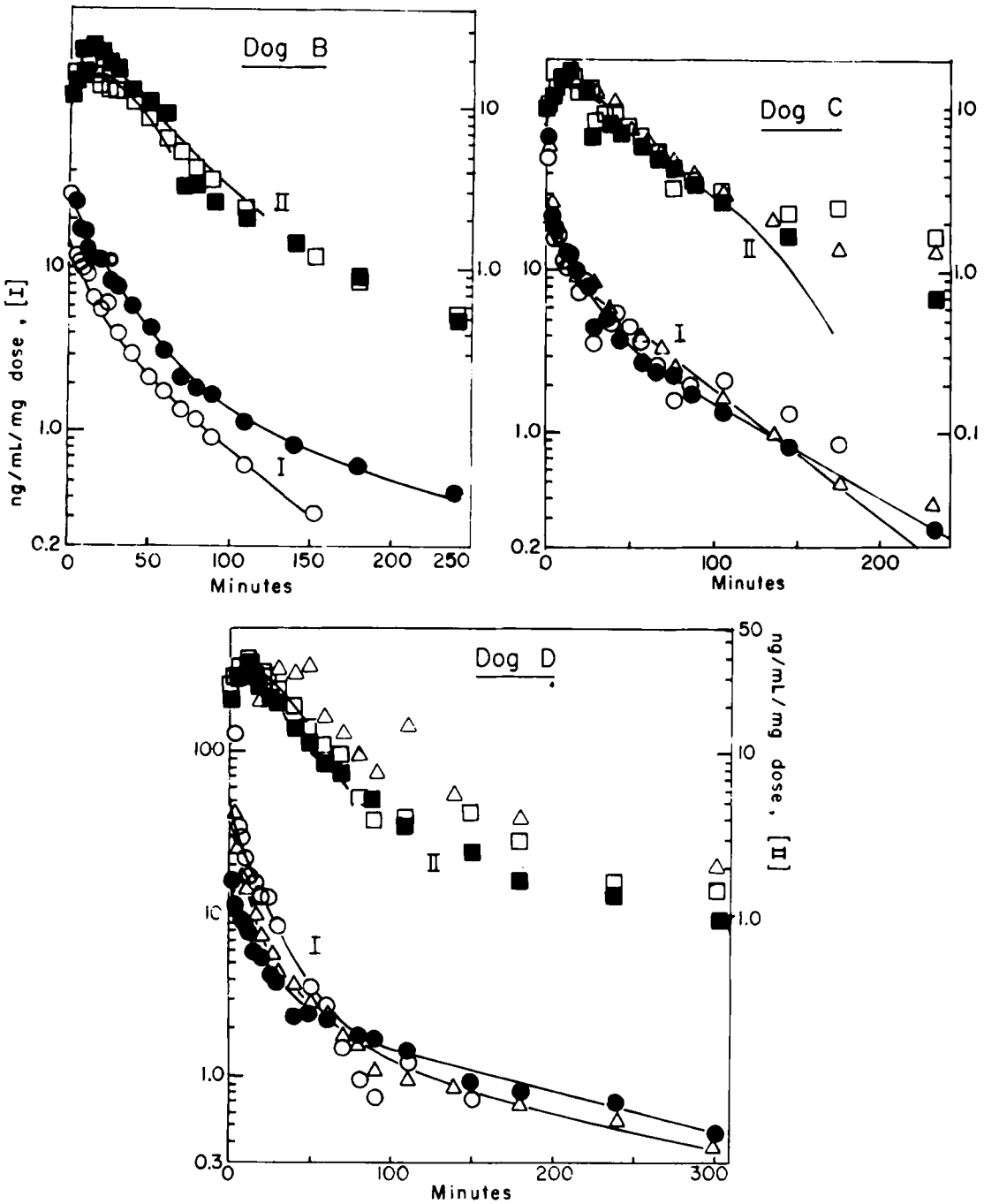

Figure 2 *Plasma concentrations of I and II in equivalents of nafronyl oxalate per milligram of an intravenous dose of I against time for dogs B, C, and D. The curves through I were calculated from the sum of exponentials (Eq. 10) using the parameters in Table III. The curves through II were calculated from Eq. 15 using the parameters in Table III. Key: (○, □) 35 mg; (△) 53 mg; (●, ■) 70 mg.*

Examples of linear regression equations from HPLC method A2 for simultaneous assay of I (10.9 min) and II (3.9 min) with butacaine internal standard (6.1 min) (2.25-nm excitation, 330-nm emission) for plasma are $C_I \pm 21.4$ ng/mL = (51.8 ± 1.4)PA + 4.1 ± 14.7, $r = 0.9940$; $C_I \pm 21.8$ ng/mL = (537.4 ± 14.7)PAR + 4.7 ± 15, $r = 0.9992$; $C_{II} \pm 23$ = (37.6 ± 4.2)PA − 17.9 ± 24, $r = 0.9937$. For urine, they are: $C_{II} \pm 12.5$ ng/mL = (732 ± 40)PAR − 25 ± 10.6; $C_I \pm 8.4$ ng/mL = (70.9 ± 2.6)PA − 23 ± 7. For bile examples are: $C_{II} \pm 18$ ng/mL = (547 ± 44)PAR − 8.5 ± 14.4; $C_{II} \pm 29$ ng/mL = (58.4 ± 7.7)PA − 11.7 ± 23.5. The symbols PH and PA represent peak height and peak area, respectively, whereas PHR and PAR are the respective ratios to the internal standard.

Release of Conjugates of Derived Acid from the Urine of a Nafronyl-Dosed Dog—Preliminary studies of urine samples obtained from dog A treated with *E. coli* β-glucuronidase showed no significant change at 15, 30, and 60 min in the HPLC assay of generated II from dichloromethane-preextracted urine containing III. A similar study with β-glucuronidase (beef liver) showed no significant change in the HPLC assay of generated II at 3, 5.5, and 9 h.

Dichloromethane-preextracted urine (1.0 ml) from a nafronyl-dosed dog was hydrolyzed with 0.1 M NaOH, 0.2 M NaOH, 1 M HCl, and 6 M HCl. Significant peaks for II were observed from the alkaline hydrolyses, but none for the acid hydrolyses. There was a decided NaOH concentration effect. Peak heights of generated II were 19 and 11 mm after 15 and 30 min of hydrolysis, respectively, for 0.1 M NaOH and 40 and 49.5 mm after 15 and 30 min of hydrolysis, respectively, for 0.2 M NaOH. The latter peak height corresponds to 200 ng of II/mL of urine and compared well with the 251 and 192 ng/mL assayed after glucuronidase hydrolyses from bovine and *E. coli* (30 min at 37.5°C) sources, respectively.

Effect of the Use of Different Anticoagulants on the Plasma Stability Studies of Nafronyl—Previous studies of nafronyl stability at 1.25 μg/mL of fresh dog plasma at 24.5°C showed an apparent half-life of 3.2 h for the loss of 50% of nafronyl to II. The remaining 50% of nafronyl appeared to maintain its stability thereafter (see Figs. 10 and 11 in Ref. 8).

Table III—Pharmacokinetics of Intravenously Administered Nafronyl (I), Derived Acid (II), and Derived Acid Glucuronide (III)

Parameter											
Dose (D)[a], mg	70.0	70.2	35.07	71.52	53.6	35.4	70.0	53.0	35.6	70.46	Mean ± *SEM*
Dog (Weight, kg)	A (22.7)	B (26.6)	B (27.0)	C (22.5)	C (23.0)	C (23.0)	D (25.0)	D (24.3)	D (23.0)	E (22.5)[p]	
Parameters[b] from plasma data											
A ($+A'$)[c], ng/mL	630 (+1000)	1670	325	1460	1320	440	940	590 (+1200)	1035 (+825)	1920	1425 ± 168[r]
B	222	107	220	467	600	182	182	90	35[m]	950	245 ± 78[r]
$10^2\,\alpha$, min^{-1} ($t_{1/2}$, min)	3.57 (19)	4.06 (17)	9.40 (7.4)	7.41 (9.4)	18.6 (3.7)	4.13 (17)	7.15 (9.7)	3.87 (18)	4.27 (16)	29.0 (2.4)	9.2 ± 2.6 (12 ± 2)
$10^3\,\beta$	5.77 (120)	5.30 (131)	21.3 (33)	13.4 (52)	17.6 (39)	9.35 (74)	5.79 (120)	5.05 (137)	5.1[m]	26.0 (27)	8.82 ± 2.2 (100 ± 18)[s]
Clearances, mL/min											
Total (CL^{I}_{tot})[d]	1190	1145	2546	1311	1302	1175	1570	1296	1031	1634	1295 ± 65[t]
Renal (CL^{I}_{ren})[e]	3.47	5.71	2.59	12.1	26.8	3.0	1.46	11.0	—[n]	—[q]	8.3 ± 3.0
$10^{-4}\,AUC^{I}_{0}$[f]	0	−1.26	1.16	3.1	−4.25	1.8	1.65	−5.01	—[n]	—[q]	
CL^{II}_{ren}[e]	0.48	0.14	0.11	0.13	0.21	0.21	0.093	0.03	0.22	—[q]	0.18 ± 0.04
$10^{-4}\,AUC^{II}_{0}$[f]	5.8	3.4	2.1	0	2.8	2.1	3.0	−3.0	2.7	—[q]	
$CL^{I\to II}/V_{II}$[g]	0.200	0.192	0.221	0.260	0.175	0.093	0.616	0.280	0.233	0.192	0.246 ± 0.044
$CL^{II\to X}/V_{II}$ ($t_{1/2}$, min)[g]	0.098 (7.1)	0.125 (5.7)	0.080 (8.7)	0.131 (5.3)	0.144 (6.1)	0.071 (9.7)	0.168 (4.1)	0.116 (6.0)	0.129 (5.7)	0.135 (5.2)	0.120 ± 0.009 (6.4 ± 0.5)
Recoveries, %											
$100\cdot\Sigma U^{I}_{330\,min}/D$	0.291	0.547	0.016	0.529	4.2	0.172	0.041	1.81	—[n]	—[q]	0.49 ± 0.24[u]
$100\cdot\Sigma U^{I}_{\infty}/D$[h]	0.292	0.601	0.016	0.399[o]	4.2	0.103[o]	0.059	1.89	—[n]	—[q]	0.48 ± 0.25[u]
$100\cdot\Sigma U^{II}_{330\,min}/D$	0.0313	0.0126	0.0049	0.0146	0.0085	0.0134	0.0137	0.0056	0.0331	—[q]	0.015 ± 0.003
$100\cdot\Sigma U^{II}_{\infty}/D$[h]	0.0363	0.0128	0.0084	0.0162	0.0202	0.0234	0.0168	0.0131	0.0445	—[q]	0.021 ± 0.004
$100\cdot\Sigma U^{III}_{330\,min}/D$	0.65	0.61	—[n]	0.025	0.039	0.025	0.090	0.151	0.441	—[q]	0.25 ± 0.09
$100\cdot\Sigma U^{III}_{\infty}/D$[i]	0.86	0.68	—[n]	0.024	0.050	0.037	0.114	0.189	0.562	—[q]	0.32 ± 0.12
Other Parameters											
$10^3\,k^{i}_{III}$, min^{-1} ($t_{1/2}$, min)	4.52 (153)	9.21 (75)	—[n]	7.94 (87)	5.16 (134)	4.03 (172)	2.91 (239)	4.43 (156)	4.73 (147)	—[q]	5.37 ± 0.75 (145 ± 18)
ΣU^{III}_{∞}, μg ($\Sigma U'_{\infty}{}^{III}$)[i]	600 (497)	480 (480)	—[n]	17 (15)	24 (28)	13 (13)	80 (55.5)	600 (497)	200 (200)	—[q]	
$10^{-4}\,AUC^{II}_{240\,min}$, ng·min/mL	9.57	8.75	4.01	7.86	6.05	4.0	12.0	16.8	8.21	6.80	8.11 ± 0.33[v]
$10^{-4}\,AUC^{II}_{\infty}$[j]	11.10	9.82	4.79	8.91	7.90	6.04	15.1	20.2	9.90	7.37	9.83 ± 0.57[v]
Apparent Volumes of Distribution											
V^{I}_{c}, L[k]	37.8	39.5	64.4	37.1	27.9	56.9	62.4	28.2	18.8	24.6	39.8 ± 5.1
Vd^{I}[l]	206	216	119	98	74	126	271	256	202	63	163 ± 24

[a] As oxalate salt (I). [b] Estimated from best fit of experimental plasma levels, $[I] = A'e^{-\alpha' t} + Ae^{-\alpha t} + Be^{-\beta t}$ in ng/mL *versus* time t. [c] For most studies only the latter two exponentials were needed, *i.e.*, $A' = 0$. However a third exponential was needed in three cases; estimated values of α' in min^{-1} ($t_{1/2}^{\alpha}$ in min) were: dog A 0.371 (1.87); dog D 0.153 (4.52); dog D 0.243 (2.85). [d] Ratio of dose to total area under plasma level of I–time curve, where the calculated $AUC_{\infty}^{I} = A'/\alpha' + A/\alpha + B/\beta$ and that calculated from the trapezoidal rule plus the quotient of the last observed plasma level, p_n, and β were within 2% of each other in all cases. [e] Estimates from slopes of ng excreted renally/min against plasma level in ng/mL at the midtime of the interval of excretion agreed with estimates from the slope of cumulative amounts renally excreted at time t plotted against the area under the plasma level–time curve (AUC_t) at that time in accordance with $\Sigma U = CL_{ren}^{I}$ ($AUC_t - AUC_0$) (see Figs. 3 and 4). [f] Value of AUC at $\Sigma U = 0$ from the best linear plot of prior data in Figs. 3 and 4. [g] Estimated from appropriate plots (Fig. 7) in accordance with $[II]/AUC_I = CL^{I \to II}/V_{II} - (CL^{II \to X}/V_{II})(AUC_{II}/AUC_I)$. [h] Calculated from $\Sigma U_{\infty} = CL_{ren}^{I}$ ($AUC_{\infty} - AUC_0$). [i] Determined by best fit of terminal urine data to $\Sigma U^{III} = \Sigma U_{\infty}^{III} - \Sigma U_{\infty} e^{-kIII t}$. [j] Estimated from the AUC^{II} calculated from the trapezoidal rule plus the quotient of the terminal plasma level of II and the estimated terminal rate constant of 3.08×10^{-3} min^{-1}. $kV_C^I = D/(A' + A + B)$. [k] CL_{tot}^{II}/β. [m] Data were widely scattered at the low level of assay detection; this value is only a crude estimate. [n] Due to equipment failure, urinary amounts could not be assayed. [o] Final urinary amounts excreted were higher than predicted from the best linear fit of $\Sigma U = CL_{ren}^{I}$ ($AUC - AUC_0$). [p] Bile-cannulated female dog. [q] Renal catheter improperly placed in female dog so that urine could not be obtained at timed intervals. [r] Average only for the 70-mg doses of all normal dogs; bile-cannulated dog E excluded. [s] Average excluded 35-mg doses and bile-cannulated dog E. [t] Average excluded outlier value for dog B at 35-mg dose. [u] Average excluded outlier dog C at 53.6-mg dose. [v] Average is 10^{-4} AUC^{II} adjusted for 70-mg dose, *i.e.*, 10^{-4} AUC/70-mg dose; excludes the studies of dog D, which gave values significantly higher with average 10^{-4} AUC adjusted for 70-mg doses at 240 min and at infinity of 16.8 ± 3.0 and 20.4 ± 3.4, respectively. The overall averages, including dog D studies were 10.7 ± 1.5 and 13.0 ± 1.8 at 240 min and at infinity, respectively.

Plots in accordance with:

$$\ln (P_{\infty} - P) = -kt + \ln P_{\infty} \qquad \text{(Eq. 5)}$$

were linear for both I and II and of the same slope, where P_{∞} is the asymptotic peak height or area ratio of nafronyl or II to internal standard with time, P is the peak height or area ratio of I or II at time t, and $t_{1/2} = 0.693/k$. The curves for nafronyl concentration *versus* time in fresh dog plasma were similar in the present studies when different anticoagulants were used. They decreased with decelerating rates to an asymptote, and changes in both I and II concentrations could be characterized by Eq. 5. The data are given in Table I. The use of different anticoagulants has no significant effect on the stability estimates of nafronyl in fresh dog plasma.

There were no interferences in the chromatograms of I and II by any of the anticoagulants used in these studies in the assay range of 0.4–4.0 μg/mL of injected solutions. Calibration curves constructed in plasma obtained from blood samples using the different anticoagulants did not show any significantly different regression statistics. A typical calibration curve by method B in the range of 0.4–4.0 μg/mL using a 50-μl sample of the supernatant from acetonitrile-denatured plasma showed a standard error of estimate for the assay from linear regression of ±43 and ±30 ng/mL for I and II, respectively. Correlation coefficients for six values were >0.9996.

There was no significant difference in the calibration curve statistics of I when materials were injected in the mobile phase or in the supernatant of acetonitrile-denatured plasma. However, II gave a 10% decrease in peak height ratio when injected in the supernatant of acetonitrile-denatured plasma than in mobile phase.

Protein Binding—Filtration (33%) of 2.0–16.0 μg/mL of I in spiked plasma water and plasma subsequently filtered through cones prefiltered with plasma containing the same concentration showed no detectable I in the respective filtrates. This inordinately high cone binding did not permit protein binding estimates of I by this method. Filtration (30%) of 2.0–16.0 μg/mL of II in plasma water gave the same concentrations of II in the filtrate as was in the plasma water, indicating insignificant cone binding of II. When the plasma containing II was filtered through the cone previously used to filter the plasma water, with the same concentration of the fraction bound, f_b, could be calculated from:

$$f_b = \frac{PHR_p - PHR_f}{PHR_p} \qquad \text{(Eq. 6)}$$

where PHR_p and PHR_f were the peak height ratios for the assay of the same volumes of each by method B in the plasma and filtrate, respectively. The respective plasma concentrations (C_p in μg/mL) and fractions bound, f_b, were (C_p, f_b): 16.0, 0.762; 12.0, 0.777; 8.0, 0.751; 4.0, 0.767; and 2.0, and 0.815. If the last datum is excluded, since assay sensitivity was less at this lowest concentration, the average fraction of II bound to plasma protein is 0.764, and no concentration dependence is indicated.

Red Blood Cell–Plasma Partition Coefficients—The red blood cell-plasma partition coefficient D' (Table II) of I was 2.00 when the anticoagulants citrate phosphate dextrose solution, oxalate, and EDTA were used. This indicated a specific binding to erythrocytes in addition to volume partitioning. When the blood samples were heparinized, there was a significant decrease in the partition coefficient to 1.2, indicating a possible competition between I and heparin for these erythrocyte binding sites.

The red blood cell–plasma partition coefficient of II (Table II) averaged 0.49 (excluding one outlier of 1.15) when the anticoagulants citrate phosphate dextrose solution, oxalate, and EDTA were used. If the fraction of II bound to protein, f_b, was taken as 0.764, the true partition coefficient, D, between the concentration in red blood cells, C_{RBC}, and plasma water, C_{PW}, would be 2.08, indicating an erythrocyte binding in addition to volume partitioning. Since:

$$D' = C_{RBC}/C_p = \frac{C_{RBC}}{C_{PB} + C_{PW}} \qquad \text{(Eq. 7)}$$

where C_{PB} is the concentration of II bound to plasma protein, and:

$$1 - f_B = \frac{C_{PW}}{C_{PB} + C_{PW}} \qquad \text{(Eq. 8)}$$

thus:

$$D = \frac{C_{RBC}}{C_{PW}} = D'/(1 - f_b) = 0.49/0.236 = 2.08 \qquad \text{(Eq. 9)}$$

When the blood samples were heparinized, there was an apparent inhibition of the partitioning of II into the red blood cells from plasma.

Plasma Pharmacokinetics and Possible Dose Dependencies— Plasma level–time data for nafronyl (I) were fitted to a sum of exponentials. A typical

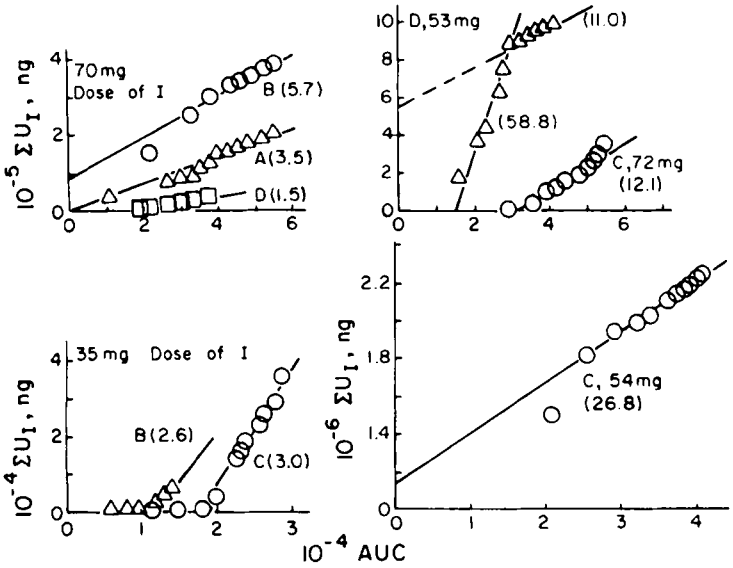

Figure 3—*Renal clearance plots for I in accordance with Eq. 11, where AUC_0^I (ng·min/mL) is the area under the plasma level–time curve from the intercept of the linear plots. The plots are labeled with the dog identification, nafronyl dose, and the estimated CL^I_{ren} values in mL/min (in parentheses).*

example is given in Fig. 1, and the parameters of best fit in accordance with:

$$C(\text{ng/mL}) = A'e^{-\alpha' t} + Ae^{-\alpha t} + Be^{-\beta t} \qquad \text{(Eq. 10)}$$

are listed in Table III for the various studies. In most cases, only two exponentials were needed.

The plasma level–time data for I and its derived acid (II) as ng/mL/mg of the dose of I are plotted semilogarithmically against time for the studies at various doses in dogs B, C, and D (Fig. 2). Such plots of I and II for three different doses were superimposable for dog C, indicating no dose dependency of nafronyl pharmacokinetics. Whereas nafronyl (I) and the acid (II) plasma levels/mg of dose were higher at the 70-mg dose than at the 35-mg dose in dog B, the reverse was observed in dog D. Thus, dose-dependent pharmacokinetics of nafronyl (I) and its derived acid (II) cannot be concluded.

The apparent parallelism, in general, of these semilogarithmic plots of plasma levels against time for the various doses (Fig. 2) indicates that there are insignificant differences in the fitted rate constants (α and β) within a dog, notwithstanding the apparent differences in the best-fit parameters (Table III). The terminal plasma levels at the lower doses have the expected higher errors in their estimation since their levels approach the limits of valid detection. The half-lives of the biphasic curve for nafronyl averaged 12 ± 12 (*SEM*) min for α and 100 ± 18 min for β.

The apparent volumes of distribution references to total plasma concentration of nafronyl averaged 39.8 ± 5.1 (*SEM*) and 163 ± 24 (*SEM*) L for the central compartment and total body, respectively (Table III). These values are in high excess of extracellular and total body water, respectively, indicating a high degree of sequestration in body tissues.

Clearances—Total body clearances of nafronyl (CL^I_{tot} = Dose/AUC_∞) averaged (excluding outlier dog B at the 35-mg dose) 1295 ± 65 (*SEM*) mL/min. The renal clearances of nafronyl (CL^I_{ren}), estimated from both the slopes of plots of the rates of urinary excretion ($\Delta U^I/\Delta t$) against plasma levels at the midpoint of the urinary collection interval ($p_{t\,mid}$) and the slopes of plots of cumulative amounts excreted (ΣU^I) against area under plasma level–time curves (AUC^I), were not significantly different and averaged 8.3 ± 3.0 mL/min, which would indicate a high protein binding if unbound drug was excreted solely by glomerular filtration. These latter plots (Fig. 3) frequently did not go through the origin and could be best characterized by a straight line conforming to the equation:

$$\Sigma U = CL_{ren}(\text{AUC} - \text{AUC}_0) \qquad \text{(Eq. 11)}$$

where AUC_0 is the area under the plasma level–time curve at $\Sigma U = 0$ as estimated from the extrapolation of the best linear plot of ΣU *versus* AUC. The plots for $\Delta U/\Delta t$ *versus* $p_{t\,mid}$ which gave the same estimates of renal clearance, were linear for the lower plasma concentrations and did go through the origin. There were no significant urinary pH changes within a study and no statistical dependence of apparent renal clearance $(\Delta U/\Delta t)/p_{t\,mid}$ on urine flow rate.

A rational explanation for the non-zero intercepts of the linear plots in

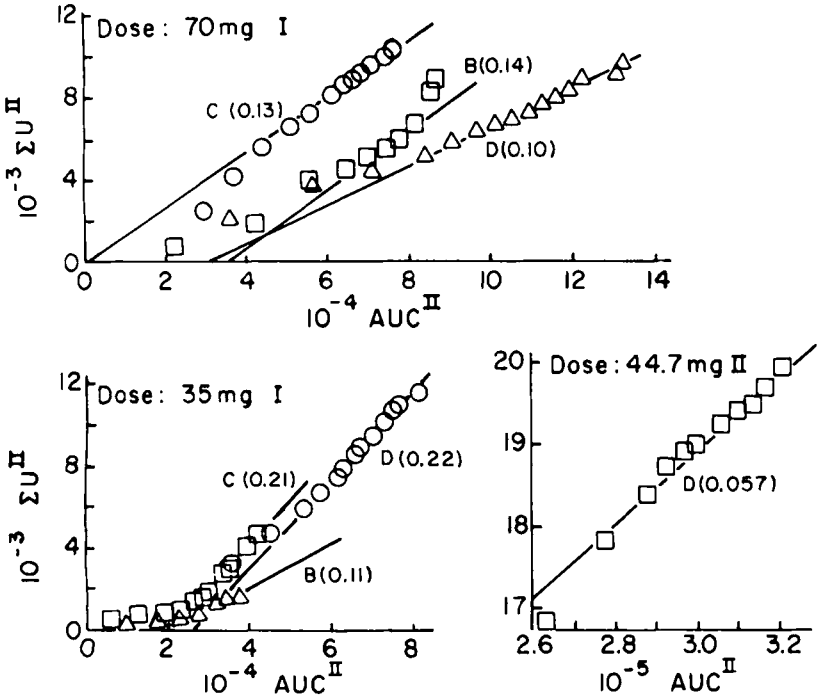

Figure 4—*Renal clearance plots for II (dose equivalent to 74.8 mg of nafronyl oxalate) in accordance with Eq. 11, where AUC_0^{II} is as defined in Fig. 3. The plots are labeled with the dog identification, dose, and the estimated CL^{II}_{ren} values in mL/min (in parentheses).*

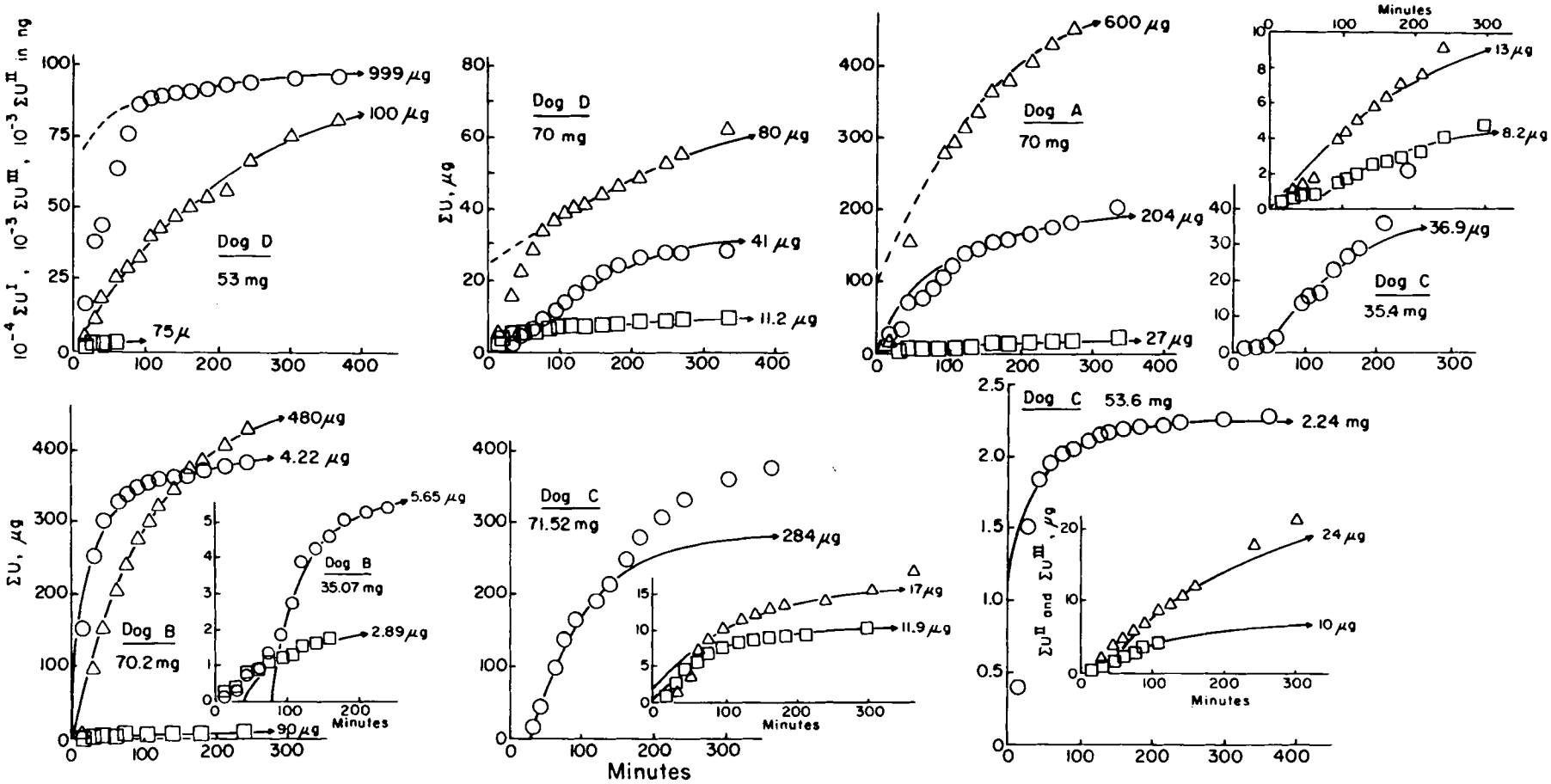

Figure 5—*Cumulative amounts of I (○), II (□) and the glucuronide III (△) excreted into the urine after intravenous administration of a labeled dose of I. The curves through the data for I and II were calculated from* $\Sigma U = CL_{ren}(AUC - AUC_0)$ *for the parameters in Table III. The curves through III were calculated from* $\Sigma U^{III} = \Sigma U_\infty - \Sigma U'^{III}_\infty e^{-k_{III}t}$ *using the parameters in Table III.*

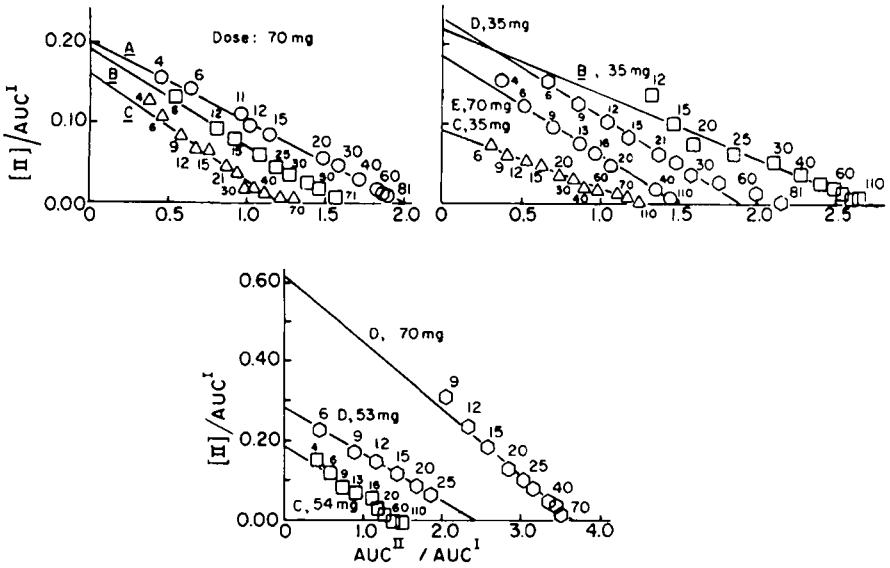

Figure 6—*Plots of the quotients of II plasma levels and the area under the plasma level-time curve of I against the ratios of the areas of II and I until that time in accordance with* $[II]/AUC^{I} = CL^{I\rightarrow II}/V_{II} - (CL^{II\rightarrow X}/V_{II})(AUC^{II}/AUC^{I})$ *where* $CL^{I\rightarrow II}$ *and* $CL^{II\rightarrow X}$ *are the clearances of I to II and of II, respectively, and where* V_{II} *is the apparent volume of distribution of II. The curves are labeled with the intravenous dose of I and the dog identification; each datum point is labeled with the time after administration.*

accordance with Eq. 11 is that monitored plasma levels did not reflect those at the sites of renal clearance at early time periods when pseudo-steady-state conditions had not been achieved for the drug. The hypothesis of decreasing concentration gradient from the plasma monitoring site to the glomerulus is a reasonable explanation for this renal lag. This is also consistent with the possible extrahepatic clearance of nafronyl, supported by its 3.2-h half-life in plasma *in vitro* (1). In one dog study (dog D, 53.0-mg dose) the assays of initial plasma levels of I from the femoral vein were consistently less than those taken simultaneously from the jugular [time(min), femoral, jugular (ng/mL)]: 4, 595, 1318; 6, 477, 950; and 15, 185, 536. This has been observed previously with other highly metabolized and quickly cleared drugs. An example is sulmazole (10) where the initial early plasma levels from the femoral and jugular veins did not agree. Drugs that are not highly metabolized and are more slowly cleared do not show significant differences between levels from jugular and femoral plasma. An example is the immunomodulatory 1,2-*O*-isopropylidene-3-*O*-3′-(*N*′,*N*′-dimethylamino-*n*-propyl)-D-glucofuranose hydrochloride (11).

The hepatic flow in the dog is in the range of 30–45 mL/min/kg [750–1125 mL/min for a 25-kg dog (12)]. If there is no biliary excretion of unchanged nafronyl, its metabolic clearance, $CL^{I}_{tot} - CL^{I}_{ren}$, referenced to total plasma

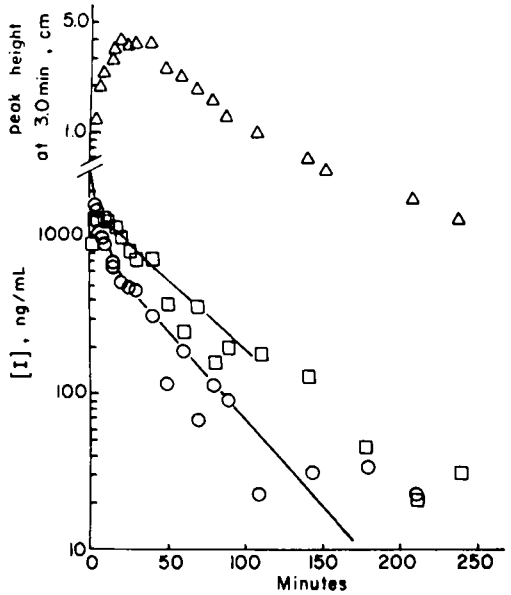

Figure 7—*Plasma concentrations of I (○) and II (□) in equivalents of nafronyl oxalate against time for bile-cannulated dog E after a 70.5-mg iv bolus dose of I. The curve through I was calculated from the sum of exponentials (Eq. 10); the curve through II was calculated from Eq. 15. The peak height at retention time 3.00 min of IV, which differed from I (10.9 min), II (3.90 min), and the internal standard (6.15 min), is also plotted against time (△).*

concentration is 1287 mL/min. Since this value exceeds even the highest expected extreme of maximal hepatic flow rate, which is the maximal hepatic clearnace possible, extrahepatic metabolism of nafronyl is indicated.

The renal clearances of the derived acid (CL^{II}_{ren}) were obtained by the methods described for nafronyl and averaged even lower, 0.18 ± 0.04 mL/min. This would imply a renal clearance of unbound II of 0.8 mL/min (0.18/fraction unbound), indicative of a high excess of tubular reabsorption. Generally, an AUC_0 was observed in accordance with Eq. 11 (Fig. 4). The assay of initial plasma levels of II from the femoral vein were consistently less than those taken simultaneously from the jugular [time(min), femoral, jugular (ng/mL in nafronyl equivalents)]: 4, 807, 1930; 6, 1116, 1930; and 15, 1324, 1789.

Urinary Excretions—The percentage of the dose renally eliminated at 330 min and the estimated total eliminated at infinite time are given in Table III. The latter values for I and II were estimated from Eq. 11 for $AUC = AUC_\infty$ using the estimates of CL_{ren} and AUC_0 given in Table III. Extremely small percentages of the dose are eliminated by this route; averaging 0.48 ± 0.25% for nafronyl (I) and 0.021 ± 0.004% for the derived acid (II). Plots of the cumulative urinary excretion of I and II with time are given in Fig. 5 for the various studies. The curves through the data were drawn in accordance with Eq. 11 for the particular AUC_0 and CL_{ren} values given in Table III.

Semilogarithmic plots of amount not-yet-excreted of the conjugate of II, (*i.e.*, III), assayed as II for solvolysis, against time ($\Sigma U^{III}_\infty - \Sigma U^{III}$) were linear after the first 10–70 min, for a chosen ΣU^{III}_∞ in accordance with:

$$\ln (\Sigma U^{III}_\infty - \Sigma U^{III}) = \ln \Sigma U^{III}_\infty - k_{III}t \qquad \text{(Eq. 12)}$$

where ΣU^{III}_∞ is obtained from the intercept of the extrapolated linear terminal data. The estimated ΣU^{III}_∞, $\Sigma U'^{III}_\infty$, and k_{III} values of urinary excretion of the III are given in Table III. The cumulative amounts of renally excreted conjugates are plotted against time in Fig. 5. The curve through the data is plotted in accordance with the nonlogarithmic transformation of Eq. 12:

$$\Sigma U^{III} = \Sigma U_\infty - \Sigma U'_\infty e^{-k_{III}t} \qquad \text{(Eq. 13)}$$

for the specific parameters listed in Table III and, as expected, gave excellent fits. The terminal half-lives of urinary excretion of III derived from k_{III} averaged 145 ± 18 min. The percentage of the dose renally eliminated as III (the conjugates of II) were the ΣU^{III}_∞ values and averaged 0.32 ± 0.12%.

Since the total amounts of these three compounds (I, II, and III) were only 0.82% of the total administered nafronyl dose, it is apparent that >99% of the administered dose is eliminated by processes other than renal and/or as other metabolites in the dog.

Relationships Between Metabolic Clearances of Nafronyl (I) and the Total Clearance of Its Acid Metabolite (II), and the Fitting of II Plasma Levels with Time—If there are no dose-dependent pharmacokinetics of I and its produced acid metabolite, a relation can be constructed (13, 14) from the constant metabolic clearance of nafronyl to the metabolite, $CL^{I\rightarrow II}$, and for the constant total clearance of the metabolite, $CL^{II\rightarrow X}$, as:

$$II = CL^{I\rightarrow II}AUC^{I} - CL^{II\rightarrow X}AUC^{II} \qquad \text{(Eq. 14)}$$

to calculate the amount of metabolite II in the body at any time, where AUC^{I} and AUC^{II} are the areas under the plasma level-time curves of I and II at that time. The amount of II can be formulated as $V_{II}[II]$ on the presumption that

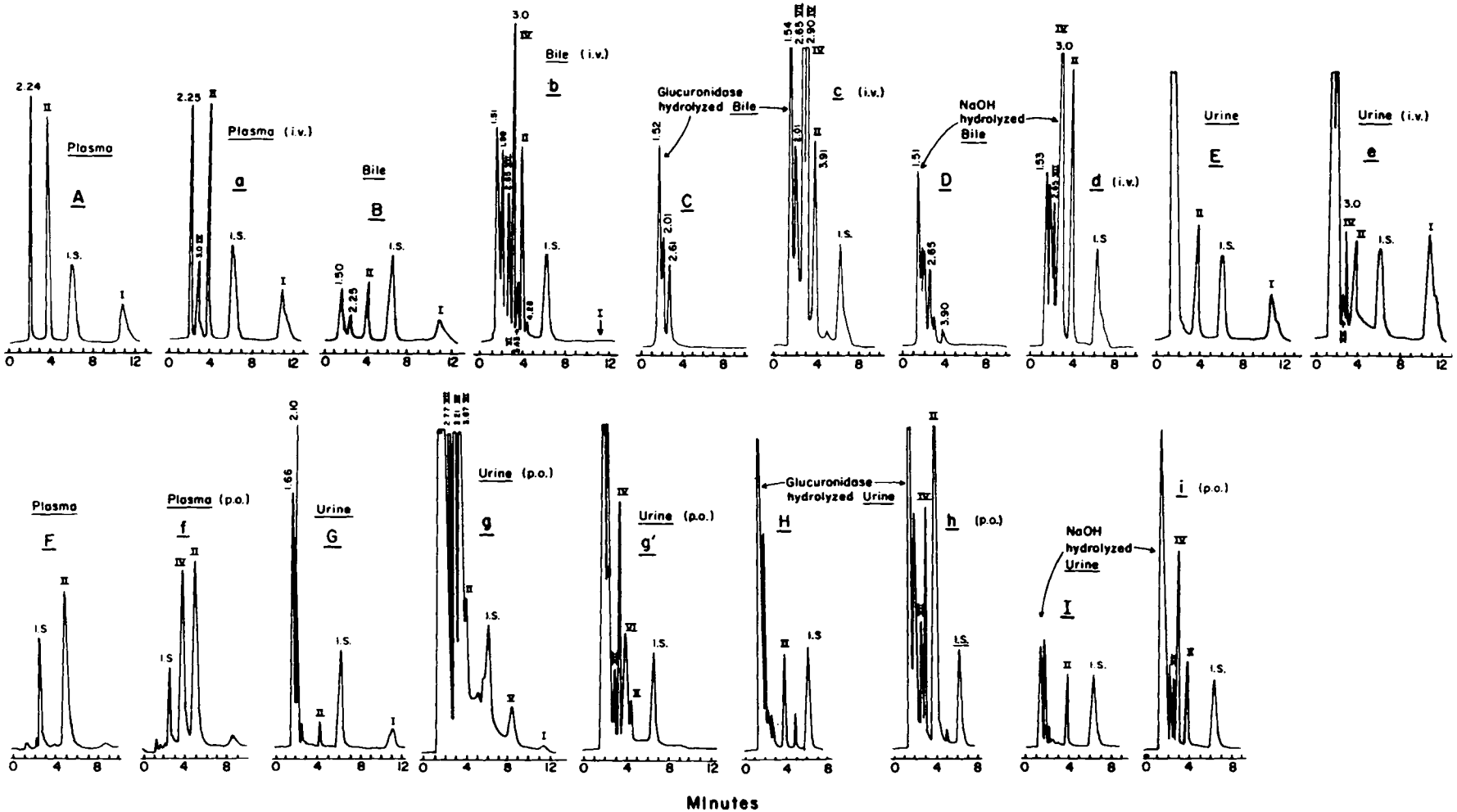

Figure 8—*Chromatograms (method A2) of organic extracts of plasma, urine, and bile, alone or spiked with I and II, from normal dogs (A–E) and from bile-cannulated dog E (a–e) after a 70.46-mg iv bolus dose of I. The internal standard (I.S.) was butacaine. Numbers at peaks represent retention times. Key: (A) plasma spiked with 325 ng/mL of I and 328 ng/mL of II; (a) plasma sample at 40 min; (B) nonhydrolyzed bile spiked with 250 ng/mL of I and 101 ng/mL of II; (b) nonhydrolyzed bile sample at 200 min; (C) blank bile treated with β-glucuronidase; (c) β-glucuronidase-treated bile sample at 214 min; (D) Blank bile treated with 0.2 M NaOH; (d) 0.2 M NaOH-treated bile sample at 214 min; (E) urine spiked with 752 ng/mL of I and 303 ng/mL of II; (e) urine sample at 190 min. Comparisons of chromatograms of organic extracts of plasma and urine spiked with I and II (identified (F–I) with samples taken from a dog orally administered 250 mg of I (f–i) are also presented. Key: (F) plasma spiked with procaine (internal standard) and 530 ng/mL of II using method A1; (f) plasma sample of dog C at 140 min; (G) urine spiked with butacaine (internal standard), 103 ng/mL of I, and 84 ng/mL of II using method A2; (g) urine sample of dog D at 201 min; (g') urine sample at 482 min; (H) urine spiked with butacaine and 303 ng/mL of II, treated with β-glucuronidase using method A2; (h) β-Glucuronidase-treated 160-min urine samples from dog D; (I) urine spiked with butacaine and 788 ng/mL of II, treated with 0.2 M NaOH using method A2; (i) 0.2 M NaOH-treated 270-min urine sample from dog D.*

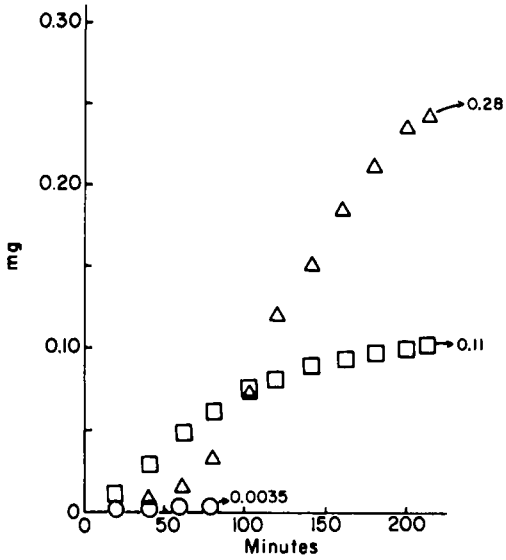

Figure 9—*Plots of cumulative amounts of I (○), II (□), and III (△) excreted into bile with time in the study of bile-cannulated dog E. The curves are labeled with the estimated total amounts eliminated in bile.*

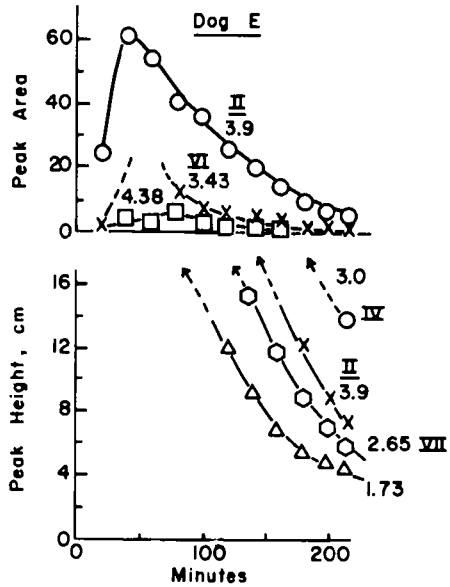

Figure 10—*Time course of peak heights and areas of peaks, labeled with retention times, appearing in chromatograms (method A2) of nonhydrolyzed bile taken from dog E (administered 70.46 mg iv of I) that did not appear in bile from the control dog. The dashed lines indicate higher values that could not be estimated. Values for II (3.9-min retention time) are given for comparison.*

the formed II is rapidly equilibrated in a one-compartment body model of volume V_{II} and plasma concentration [II]. Thus, Eq. 14 can be rearranged to:

$$[II] = \frac{CL^{I\to II}}{V_{II}} \cdot AUC^{I} - \frac{CL^{II\to X}}{V_{II}} \cdot AUC^{II} \qquad \text{(Eq. 15)}$$

or:

$$\frac{[II]}{AUC^{I}} = \frac{CL^{I\to II}}{V_{II}} - \frac{CL^{II\to X}}{V_{II}} \cdot \frac{AUC^{II}}{AUC^{I}} \qquad \text{(Eq. 16)}$$

Thus, if the premises are valid, plots of the quotient of acid metabolite plasma concentrations and the area under the plasma level–time curve of nafronyl ($[II]/AUC^{I}$) against the ratios of the respective areas of II and I (AUC^{II}/AUC^{I}) should give a straight line where $CL^{I\to II}/V_{II}$ and $CL^{II\to X}/V_{II}$ can be obtained from the intercept and slope, respectively.

Such plots for the various studies in the dogs are given in Fig. 6, and their linearities are consistent with the premises. The derived clearance/volume ratios are listed in Table III. The $CL^{II\to X}/V_{II}$ ($= 0.693/t_{1/2}$) ratio also has the significance of an elimination rate constant for II. The average of the half-lives (Table III) for this II elimination was 6.4 ± 0.5 min.

The total areas under the curves for II (obtained by the trapezoidal rule plus terminal plasma divided by terminal rate constant for II) per 70-mg dose were consistent for dogs A, B, and C at all doses and averaged 9.83 ± 0.57 × 10^4 ng·min/mL for a 70-mg dose of I. Dog D showed a significantly higher total area under the curve for II, which averaged 26.4 ± 3.4 × 10^4 ng·min/mL for a 70-mg dose of I. This implies that dog D has a greater metabolic formation of II from I and/or a smaller apparent volume of distribution, V_{II}, for the acid metabolite.

The validity of this development was challenged by calculating plasma levels of II from Eq. 15 using the obtained parameters given in Table III. The curves drawn through the plasma level [II] against time in Figs. 1, 2, and 7 are based on these calculations and are consistent with the actual data for a significant portion of their time course (*i.e.*, up to 110 min), but not for all. This can be reconciled by postulating that V_{II} is the volume of the central compartment for the acid metabolite, II, and V_{II} is not representative of the apparent overall volume of distribution of II when the slow equilibration of II among other tissues becomes significant.

Pharmacokinetic Study in Bile-Cannulated Dog E—In the pharmacokinetic study of bile-cannulated dog E, a single injection method (method A2) was used for the simultaneous assay of both II (retention time, 3.90 min) and I (10.9 min) with butacaine as internal standard (6.15 min). Plasma (Fig. 7) and bile were assayed for both I and II. An additional peak (IV) at 3.00-min retention time was observed in plasma samples (compare Fig. 8 A and a). The maximum concentration of IV (Fig. 7) in the plasma was observed at 25 min, in comparison with the 9-min maximum of II in plasma, with a peak height equivalent to IV to that of 350 ng/mL of II at retention time 3.90 min in the plasma. It is apparent that an unknown metabolite (IV) can be observed in plasma that lags after II. This could be a metabolite derived from II.

The cumulative amount of II excreted in the bile can be estimated as 0.16% of the dose (0.14% at 214 min). The low amount of I was 0.005% (0.0043% at 80 min) (Fig. 9). Additional HPLC peaks were observed on bile assay after drug administration (Fig. 8b). These peaks did not appear in the bile assay when drugs were not administered (Fig. 8B). The chromatograms of the extracts (before hydrolysis) gave peaks at 1.5, 1.73, 1.99, 2.65 (VII), 3.0 (IV), 3.43 (VI), and 4.38 min, as well as the very small amounts of I (10.9 min) and II (3.9 min). The time courses of the concentrations of these compounds of different retention times, in terms of peak height or peak area, are shown in Fig. 10 at the times they could be evaluated. Since bile at each time interval was very constant (3.4 ± 0.2 mL/20 min), these peak heights and areas are good estimates of the relative rates of elimination. The dashed lines in Fig. 10 indicate peak heights or areas that were so out of scale that they could not be estimated. For purposes of comparison, the peak heights and areas of II from the bile samples are also given. It is apparent that there were large amounts of the same 3.0-min retention time material (IV) that could be detected in plasma (Figs. 7 and 8a). It must be concluded that multiple organic-extractable metabolites derived from nafronyl are excreted into the bile in significant quantities and have the potential of being quantified by HPLC.

The extracted bile samples were subjected to alkaline (0.2 M NaOH) and β-glucuronidase (*E. coli*) hydrolysis and again extracted with methylene chloride. These extracts were assayed and showed significant peaks at 3.0 (IV), 3.6 (VI), and 3.9 (II) min for β-glucuronidase hydrolysis (Fig. 8, C and c) and at 3.0 (IV) and 3.9 (II) min for alkaline hydrolysis. There may be others, but the background from similarly treated bile samples from the nondosed animal makes it difficult to determine conclusively if the metabolites were present in the extracts of hydrolyzed bile. The presence of II in these hydrolyzed bile extracts is conclusive proof of conjugates of II, *i.e.*, III, excreted into bile; this can be estimated as 0.40% (0.34% at 214 min) of the administered nafronyl dose (Fig. 9). This estimated yield of III was based on the assay of the extract of alkaline-hydrolyzed bile, preextracted for II since the HPLC base line at 3.90 min (Fig. 8d) was so much better than that of the extract of β-glucuronidase-treated bile (Fig. 8c). The question is yet unanswered as to whether the presence of IV is due to its release from a conjugate or due to its incomplete extraction from the bile prior to the hydrolysis. The total areas under the respective peaks up to 214 min after drug administration were 215 (IV, 3.0 min) as compared with 149 (II, 3.9 min) after β-glucuronidase treatment. The 3.6-min (VI) peak total area was 36.5. The total areas up to 214 min were 248 (IV, 3.0 min) as compared with 278 (II, 3.9 min) after alkaline hydrolysis of the bile. The 2.65-min (VII) peak total area was 118.

In general,the dichloromethane extracts of β-glucuronidase-treated samples showed large backgrounds; the 3.0-, 3.4-, and 3.9-min peaks did not arise from a constant baseline, so peak area quantification of these peaks may not be accurate. This may possibly explain, in part, the difference in the estimates of these peak areas from the two methods of hydrolysis (Fig. 11).

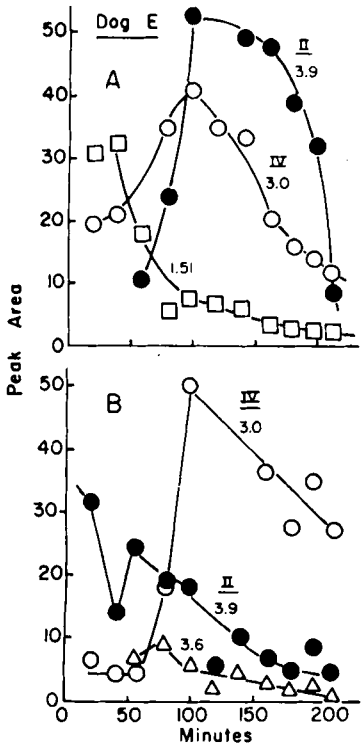

Figure 11—*Time course of peak areas, labeled with retention time, appearing in chromatograms (method A2) of hydrolyzed bile taken from dog E (administered 70.46 mg iv of I) that did not appear in hydrolyzed bile from the control dog. Values for II are given for comparison. Key: (A) β-glucuronidase-treated bile; (B) 0.2 M NaOH-treated bile.*

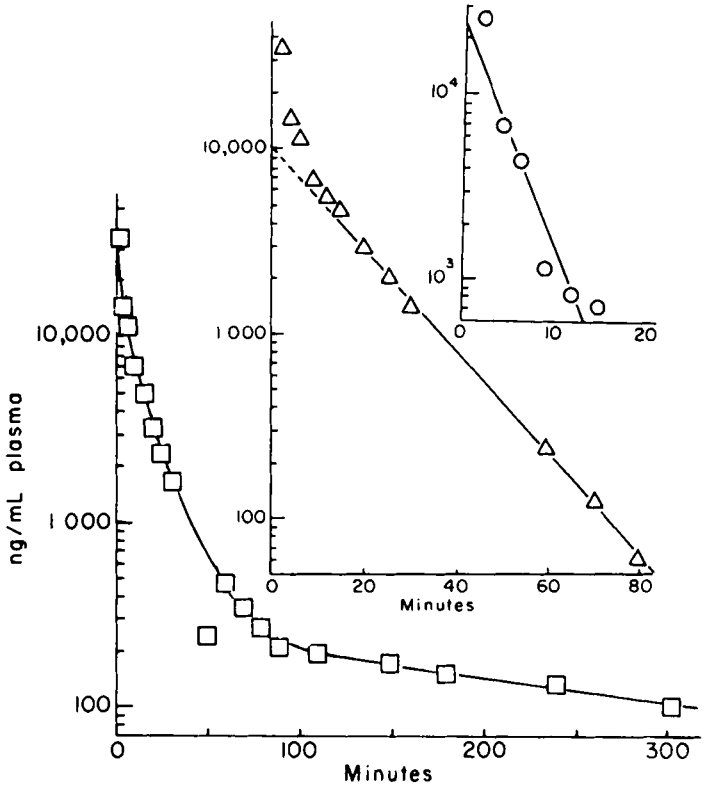

Figure 12—*Plasma levels of II, in equivalents of nafronyl oxalate, against time for a 44.7-mg iv (74.8-mg equivalent) bolus dose of II given to dog D. The curve through the data points was calculated from the sum of exponentials (see text). The insets show the successive feathering necessary to obtain the parameters of the three exponentials.*

Unfortunately the urinary catheterization of female dog E did not permit the collection of urine at different intervals of time. Nevertheless, assay of the organic extracts of the few urine samples obtained show a compound (IV) at a retention time of 3.0 in addition to those peaks assignable to I (10.9 min) and II (3.9 min); this peak did not exist in spiked urine from the same dog (compare E and e, Fig. 8). The 2.66-min peak (VII) observed in extract of nonhydrolyzed and alkaline-hydrolyzed bile was also observed.

Pharmacokinetics of an Intravenously Administered Bolus of II—The plasma levels of II on administration of 44.7 mg iv (74.8 mg as equivalents of nafronyl oxalate, I) of II are plotted against time in Fig. 12. The data were fitted to the sum of three exponentials for time t, in min, to calculate plasma levels in ng/mL as equivalents of nafronyl oxalate by:

$$[\mathrm{II}],\ \mathrm{ng/mL} = 24{,}500e^{-0.280t} + 10{,}000e^{-6.34\times10^{-2}t} + 270e^{-3.08\times10^{-3}t} \qquad \text{(Eq. 17)}$$

to demonstrate half-lives of the three respective phases as 2.47, 10.91, and 225 min. The total clearance of II is 225 mL/min. The area under the curve per milligram of nafronyl equivalent dose is 4451 ng·min/mL per milligram.

The renal clearance of II from a plot (Fig. 4) in accordance with Eq. 11 was 0.057 mL/min, the same value obtained from the slope of the linear plot with zero intercept of the rate of urinary excretion against the plasma level at the midpoint of the urine collection interval. The estimated total urinary excretions were 0.027 and 0.441% of the dose, unchanged and as the glucuronide, respectively. The terminal rate constant of renal elimination of the glucuronide, k_{III}, was 9.59×10^{-3} min^{-1} for a half-life of 72 min. In addition to [II] in the urine (retention time, 4.0 min), extremely large peaks due to other compounds were observed at ~1- and 2-min retention times.

The apparent volumes of distribution of the central and pseudo-steady-state volumes of distribution referenced to total plasma concentration are 2.15 and 73.0 L, respectively. The respective values for a 0.236 fraction unbound to plasma proteins are 9.1 and 310 L, respectively. The former value implies relatively instantaneous distribution in the total body water; the latter implies a high degree of sequestration in the relatively slowly equilibrated total body tissues.

Estimation of the Extent of Nafronyl Metabolic Transformation through Its Acid Metabolite—There are several methods to estimate the fraction of nafronyl generating its acid metabolite (II). The relative area under the plasma level-time curve of II for administered nafronyl (I) to administered acid (II) can estimate the fraction being metabolized by this route:

$$f_{\mathrm{I}\to\mathrm{II}} = \mathrm{AUC}^{\mathrm{II}}_{\mathrm{II\ admin}}/\mathrm{AUC}^{\mathrm{II}}_{\mathrm{I\ admin}} = 1404/4451 = 0.32 \qquad \text{(Eq. 18)}$$

where both the numerator and denominator are given per milligram of the administered dose of I and the latter is based on the $\mathrm{AUC}^{\mathrm{II}}_{\infty}$ average per 70-mg dose given in Table III.

The average of the ratio of total clearance of II to its apparent volume of distribution ($CL^{\mathrm{II}\to\mathrm{X}}/V_{\mathrm{II}}$), as based on application of Eq. 16 to the plasma concentration data obtained from the pharmacokinetic studies of intravenously administered I (Fig. 6), was 0.120 ± 0.009 min^{-1}. This value can also represent the apparent rate constant ($t_{1/2} = 6.4 \pm 0.5$ min) for the elimination of II and is of the same magnitude as the 10.9 min half-life observed for intravenously administered II (Fig. 12) during the significant portion of the time courses of I and II (Figs. 1, 2, 7) on which the estimations of $CL^{\mathrm{II}\to\mathrm{X}}/V_{\mathrm{II}}$ were based (Eq. 16). If $CL^{\mathrm{II}\to\mathrm{X}}$ is equated to the 225 mL/min observed in the pharmacokinetic study of II (Fig. 12), the apparent volume of distribution, V_{II}, is estimated as $(0.120 \pm 0.009) \times 225 = 1875 \pm 245$ mL, which is not significantly different from the estimated apparent volume of distribution of the central compartment of II (Fig. 12) of 2151 mL. These considerations support the premise that the greater time course of II formation from I, with its concomitant elimination, occurs largely in the central compartment before significant equilibration of II among the tissues has been effected. The average of the ratio of the clearance of I *via* II to the apparent volume of distribution, V_{II}, is $CL^{\mathrm{I}\to\mathrm{II}}/V_{\mathrm{II}} = 0.246 \pm 0.044$ min^{-1} (Table III, Eq. 16, Fig. 6). Thus, if V_{II} is 1875 ± 245 mL, the estimated clearance ($CL^{\mathrm{I}\to\mathrm{II}}$) is $0.246 \times 1875 = 461$ mL/min. Since the average total clearance of I less its renal clearance is $CL^{\mathrm{I}}_{\mathrm{met}} = 1287$ mL/min, the fraction of I cleared to II is:

$$f_{\mathrm{I}\to\mathrm{II}} = CL^{\mathrm{I}\to\mathrm{II}}/CL^{\mathrm{I}}_{\mathrm{met}} = 461/1287 = 0.36 \qquad \text{(Eq. 19)}$$

This latter value is in reasonable agreement with the 0.32 value estimated from Eq. 18, implying that not all of the I is metabolized through systemically appearing II, that 60–70% of nafronyl has primary metabolites other than II, and/or that I and its derived metabolites are excreted in bile so as not to appear in the systemic circulation. The high metabolic clearance of I, in excess of the hepatic flow, could permit sequential metabolism within the first pass through the liver.

Pharmacokinetics and Bioavailabilities of Orally Administered Nafronyl—Extremely small concentrations of orally administered nafronyl (I) were observed in the plasma of dogs (Fig. 13). The apparent terminal half-lives

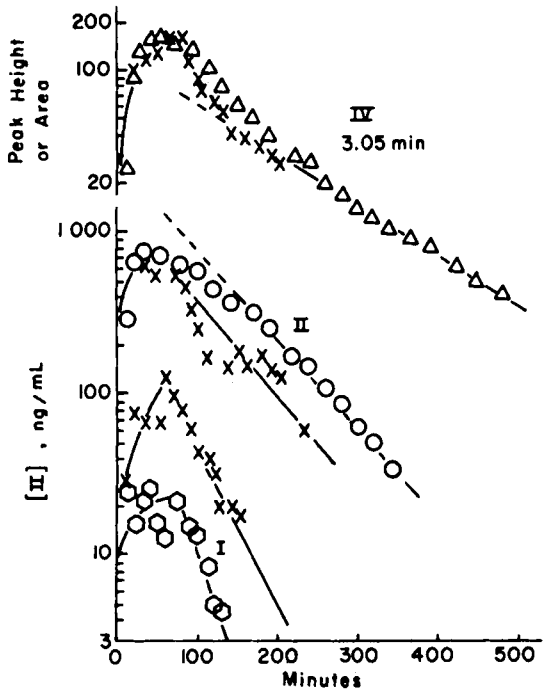

Figure 13—*Time courses of I, II (plotted as I equivalents), and IV in plasma after oral administration of 250 mg of I to dogs D (○, △, ○) and C (×), as assayed by the single-injection method A2 or its modification. The peak heights of IV at 3.05 min are plotted for dog D; the peak areas of IV at 2.48 min are plotted for dog C.*

(20–30 min) of I on oral administration were between those of the α (9 min) and β (100 min) phases obtained on intravenous administration. The estimated bioavailabilities of I, determined from the ratios of the AUC^{I}/mg values (oral to intravenous), were 0.3–2.7% of the 250-mg oral dose in three studies (Table IV). When dog D was administered 502 mg, the dog regurgitated the material 25 min after administration.

The apparent terminal plasma half-lives of II after oral administration of 250 mg of I were 55–110 min (Figs. 13 and 14). The estimated bioavailabilities of II, determined from the ratios of the AUC^{II}/mg values obtained after oral administration of I to those obtained after intravenous administration of II, were 9.7–16.7%. It is apparent that there is a definite presystemic and/or first-pass metabolism of both I and II on oral administration. In one of the 250-mg po studies of dog C, a time lag of 100 min was observed before significant appearance of II in the plasma (Fig. 14).

In all dogs, a peak assignable to a compound other than I or II was observed in the plasma, but was not present in control plasma. This peak, IV, was observed with all HPLC methods. The chromatograms of extracted plasma for dog D, 250 mg po, were similar to those given in Fig. 8a. Chromatograms for dog D in the second study are given in Fig. 8F,f. The retention times of I, II, and IV from plasma extracts in other mobile phases and HPLC systems are listed in Table IV. The time course of IV in the plasma generally paralleled that of II (Figs. 13 and 14). Peak heights and areas of IV and II were very similar at a given time (Fig. 14). For purposes of comparison, the maximum peak height of IV for dog D, 250 mg (Fig. 13) at 3.05-min retention time, corresponded to a concentration of II (retention time, 4.03 min) of 678 ng/mL equivalents of I.

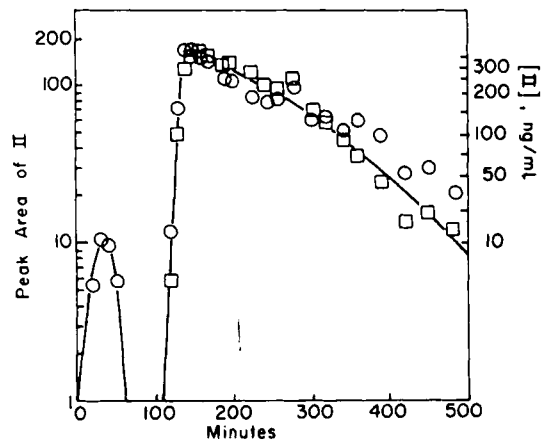

Figure 14—*Time course of peak areas of II (○) and IV (□) in extracts of plasma after oral administration of 250 mg of I to dog C. In this system the retention times of II and IV were 4.97 and 3.74 min, respectively. A 100-min lag period existed before significant absorption of I and II was observed.*

Table IV—Parameters and Bioavailabilities of Orally Administered Nafronyl (I)

Dog (Weight, kg)	D(26.0)	C(23.8)	C(21.8)	D(25.0)
Dose, mg	250	251	251	502
AUC^{I}_{∞}/mg dose[a]	8.39	35.1	3.54	—[f]
AUC^{II}_{∞}/mg dose[a]	744	470	430	440
Bioavailability, %				
I[b]	0.65	2.71	0.27	—[f]
II[c]	16.7	10.6	9.7	9.9
Dose recovery in urine, %[d]				
I	0.003	0.061	—[g]	—[g]
II	0.030	0.42	—[g]	—[g]
Glucuronidase III	0.28	0.07	—[g]	—[g]
NaOH	0.22	0.13	—[g]	—[g]
Plasma terminal half-lives, min				
I	20	30	—[h]	—[g]
II	55	58	110	74
IV	105	105	78	47
Assay Method	A2	Modified A2[e]	A1	A1
Plasma retention times, min				
I	10.33	7.69	—[i]	—[i]
II	4.03	2.78	4.97	4.80
IV	3.05	2.48	3.74	3.57
Urine retention times, min				
I	11.6	9.26	—[i]	—[i]
V	8.6 (small)	7.81	—	—
II	4.26	2.96	4.92	—[g]
VI	3.7	—	3.76	—[g]
IV	3.20	2.51	5.20	—[g]
VII	2.78	<2.08	<2.8	—[g]
Hydrolyzed urine retention times, min				
II	3.95	3.92	—[j]	—[j]
IV	3.00	2.98	—[j]	—[j]
VII	2.62	2.62	—[j]	—[j]

[a] Estimated total area in nafronyl equivalents under plasma level-time curve per mg of oral dose calculated from trapezoidal rule plus the quotient of terminal plasma level and the rate constant for the terminal loss of plasma concentration. [b] Calculated from 100-AUC^{I}_{∞}/mg dose po ÷ AUC^{I}_{∞}/mg dose iv, where the latter denominator is the total clearance, 1295 mL/min. [c] Bioavailability of II from the administered oral dose of I, calculated from 1.666-AUC^{II}_{∞}/mg dose po ÷ AUC^{II}_{∞}/mg dose iv, where the latter value is 4451/mg dose of II (as I equivalents) taken from the intravenous study. [d] Based on total amounts excreted in urine at 430 min in nafronyl equivalents; III was assayed as organic-extractable II after hydrolysis of previously extracted urine by either β glucuronidase or 0.2 M NaOH. [e] Mobile phase composition and column differed, but single-injection method was used. [f] Peak for I merged with the peak for the internal standard and could not be readily quantified as to peak height or area. Also, dog regurgitated at 23 min after oral administration. [g] Too many interferences with the peaks for I and II to permit their quantification and/or identification in urine. [h] Plasma level data for I were too scattered to estimate. [i] The assay for I used a different mobile phase than the assay for II where IV was observed. Retention times for I were 4.2 min for dog C and 6.62 min for dog D. The urine studies for these dogs showed peaks in addition to those in blank urine for the mobile phase used to assay I, with decreasing peak height magnitudes at 1.85 > 3.86 > 2.63 > 3.55 > 4.20 (I) min for dog C and at 4.15 and 3.00 min for dog D. [j] Not studied.

The cumulative amounts of I and II excreted unchanged in the urine after oral administration of 250 mg of I were in the ranges of 0.003–0.061 and 0.030–0.42%, respectively. In addition to these compounds, extractable from nonhydrolyzed urine, IV, V, VI, and VII were identifiable at separate retention times in the urine extracts (Fig. 8G, g, and g′). Retention times in various mobile phases and systems are given in Table IV. The time courses of peak heights in sampled urine at these various retention times are given in Fig. 15 and can be compared with that for II. Some of these peaks were well out of the recording range for many of the collection intervals. Corresponding peaks for IV and VII had been observed previously in organic extracts of nonhydrolyzed urine samples obtained from a dog administered I intravenously (Fig. 8e). Corresponding peaks for IV, VI, and VII have been observed previously in organic extracts of bile from this dog (Figs. 8b, c, d).

β-Glucuronidase and NaOH treatment, after prior extraction of the urine, gave chromatograms of subsequent organic extracts (compare H and h and I and i in Fig. 8) that indicated significant amounts of II (3.95 min) derived from its glucuronide (*i.e.*, III) and additional higher peaks with retention times

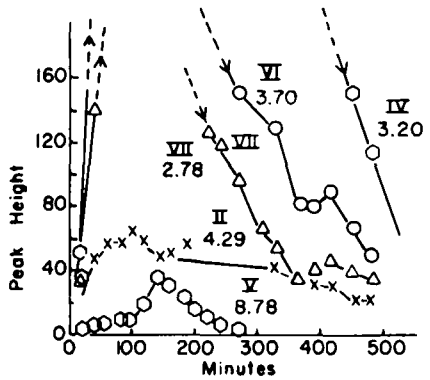

Figure 15—*Plots of peak heights against time of various chromatographic peaks obtained on assay (method A2) of urine extracts of dog D after oral administration of 250 mg of I.*

of 3.00 min (IV) and 2.62 min (VII). It is not possible to state if IV or VII were derived from glucuronides or if they were just not as completely removed as II in the extraction prior to hydrolysis. The cumulative amount of III in the urine (estimated as II after treatment) was 0.07–0.28% of the dose (Table IV).

Summary of Pharmacokinetics of Nafronyl in the Dog—Intravenously administered nafronyl (I) is rapidly cleared, with a total body clearance referenced to total plasma concentration of 1295 mL/min. Dose-dependent plasma pharmacokinetics of I and derived II could not be concluded in the 35–70-mg dose range. The plasma level–time data of I were usually well characterized by a sum of two exponentials with respective half-lives of 12 and 100 min. The latter was similar to the 90 min suggested for humans (7). The initial phase accounted for the major fraction (0.85) of the loss of I in plasma. The time course of derived II from I in the plasma could be quantified by a systemic metabolic clearance of I to II of 461 mL/min in an apparent volume of distribution, V_{II}, of the central compartment of II of 1.88 L, with a simultaneous total body clearance of II of 225 mL/min.

The estimated renal clearance of nafronyl was 8.3 mL/min with a renal elimination of only 0.5% of unchanged drug. This indicated a net metabolic clearance of I in excess of hepatic blood flow, favoring extrahepatic metabolism. Although the derived acid (II) was a major plasma metabolite of nafronyl, it could only account for 30–40% of the intravenously administered drug in the plasma and 0.02% in the urine, with a renal clearance of II of 0.18 mL/min. Thus, other metabolic transformations of nafronyl must exist that do not give direct formation of systemically appearing II.

The glucuronide (III) of II in the urine, liberated by β-glucuronidase or alkali, only accounted for 0.32% of the intravenous dose of I. The bile accounted for 0.005% of the dose as I, 0.16% of the dose as II, and 0.40% of the dose as III. Thus, >98.5% of the intravenously administered nafronyl dose is not eliminated as I, II, or III in bile and urine, and these compounds do not account for the principal fates for nafronyl disposition in the dog.

Considerable amounts of a chromatographically identifiable compound (IV) also extractable into dichloromethane, appeared in plasma after intravenous and oral nafronyl administration. It also appeared in normal and hydrolyzed preextracted bile and urine in considerable quantities and was consistent with the naphthol-containing carboxylic acid suggested previously to be a metabolite (4). Chromatographically identifiable, but as yet uncharacterized, compounds other than IV that were also extractable into dichloromethane appeared in normal (V, VI, and VII) and hydrolyzed preextracted (VII) urine and in normal (VI and VII) and hydrolyzed preextracted (VII) bile in apparently large quantities. Undoubtedly, these compounds can account for the major fates of nafronyl (I) and II in the dog. Other possible unextractable compounds could exist.

A study of the pharmacokinetics of intravenously administered II demonstrated a triphasic plasma level–time curve with respective half-lives of 2.5, 10.9, and 225 min. The initial two phases accounted for 99.2% of the loss of II in plasma. The total body and renal clearances were 225 and 0.057 mL/min, respectively. The percentages of the dose renally excreted and as glucuronide were 0.027 and 0.44%, respectively. Thus, II is also metabolized by routes other than glucuronidation.

The bioavailability of I after oral administration of 250 mg of nafronyl to the dog is only 0.3–2.7%. The percentage of potentially systemically available II was only 10–17%. These facts clearly demonstrate presystemic and/or first-pass metabolisms of both I and II.

REFERENCES

(1) L. Fontaine, M. Grand, J. Chabert, E. Szarvasi, and M. Bayssat, *Chim. Ther.*, **3**, 463 (1968).

(2) L. Fontaine, M. Grand, E. Szarvasi, and M. Bayssat, *Chim. Ther.*, **4**, 39 (1969).

(3) A. Meynaud, M. Grand, and L. Fontaine, *Arzneim.-Forsch.*, **23**, 1431 (1973).

(4) L. Fontaine, M. Belleville, J. C. Lechevin, M. Silie, J. Delahaye, and M. Boucherat, *Chim. Ther.*, **4**, 44 (1969).

(5) H. Kitagawa, R. Nakata, and H. Yano, *Oyo Yakuri*, **7**, 1231 (1973); through *Chem. Abstr.*, **81**, 99189a (1974).

(6) M. Belleville and J. C. Lechevin, *Ann. Pharm. Fr.*, **26**, 641 (1968).

(7) R. R. Brodie, L. F. Chasseaud, T. Taylor, J. O. Hunter, and P. J. Ciclitira, *J. Chromatogr.*, **164**, 534 (1979).

(8) E. R. Garrett and R. Barbhaiya, *J. Pharm. Sci.*, **70**, 39 (1981).

(9) P. H. Hinderling, J. Brès, and E. R. Garrett, *J. Pharm. Sci.*, **63**, 1684 (1974).

(10) E. R. Garrett and W. Roth, *J. Pharm. Sci.*, **72**, 105 (1983).

(11) E. R. Garrett and A. Van Peer, *J. Pharm. Sci.*, **72**, 1045 (1983).

(12) P. L. Altman and D. S. Dittmer "Respiration and Circulation," Biological Handbooks, Federation of American Societies for Experimental Biology, Bethesda, Md. 1971, p. 429.

(13) E. R. Garrett and A. Jackson, *J. Pharm. Sci.*, **68**, 753 (1979).

(14) E. R. Garrett, R. S. Süverkrup, K. Eberst, R. L. Yost, and J. P. O'Leary, *Biopharm. Drug Dispos.*, **2**, 329 (1981).

ACKNOWLEDGMENTS

Supported in part by an unrestricted grant from Lipha Chemicals Inc., New York, N.Y.

The technological assistance of Scott McClung, the clerical assistance of V. Ravichandran, the animal surgery of Dr. Paul Altmayer, and the animal care of Kathy Eberst are gratefully acknowledged.

Quantitative Microradiography for Studying Dental Enamel Demineralization and Remineralization

DAVID H. BERGSTROM *, JEFFREY L. FOX *, and WILLIAM I. HIGUCHI *x

Received May 17, 1982, from *The Dental Research Institute* and the *College of Pharmacy, The University of Michigan, Ann Arbor, MI 48109.* Accepted for publication March 7, 1983. * Present address: Department of Pharmaceutics, College of Pharmacy, The University of Utah, Salt Lake City, UT 84112.

Abstract □ A method for quantitative determination of mineral density changes in dental enamel has been developed. It utilizes the quantitative microscopy capabilities of image analysis or photometer systems. Characteristic demineralization of bovine enamel in acetate buffers containing calcium and phosphate has been used to demonstrate the results. The method together with chemical kinetic data obtained from spectrophotometric and ion-selective electrode measurements of the bulk solution for calcium, phosphate, and fluoride permit important basic studies to be conducted on demineralization and remineralization of dental enamel.

Keyphrases □ Microradiography—quantitative study of dental enamel demineralization/remineralization □ Dental enamel—demineralization/remineralization, quantitative study using microradiography □ Demineralization—dental enamel, simultaneous remineralization, quantitative study using microradiography

Although the literature contains many references (1-5) utilizing microradiographic techniques to observe mineral changes that occur in enamel, the vast majority of these are largely qualitative in nature and are thereby limited in their usefulness. Until recent years, technology has limited the ability of researchers to obtain quantitative information from microradiographic images. The purpose of this present study was to develop and critically examine such a quantitative method and its limitations. The application of an image analysis system[1] to this quantitative determination of mineral density changes has been successful. Close examination of the density profiles obtained after incorporation of the internal standard data yields information not readily apparent from visual examination. The method is demonstrated here using demineralization of bovine tooth enamel, but it has also found application in synthetic hydroxyapatite compacts as well as examining the mineral density changes occurring in solutions containing fluoride.

EXPERIMENTAL

Dissolution Medium - A buffered solution ~32% saturated (on a molar basis) with respect to the thermodynamic solubility of hydroxyapatite was used for the demineralization procedure. The solution was a 0.1 M acetate buffer containing 7.05 mM each of total calcium and phosphate in the form of calcium chloride and dibasic sodium phosphate. The pH was adjusted to 4.5 with concentrated sodium hydroxide and the ionic strength to 0.5 M by the addition of sodium chloride.

Bovine Teeth Preparation—Incisors from 8-week old strictly Kosher calves were obtained from packing houses in the Chicago area. These are crate-fed calves whose diets are uniformly controlled and thus provide an excellent experimental system. From these, only reasonably flat teeth without any obvious surface defects were used experimentally. The pellicle was removed from the labial surface using 400-, and 600-grit silicon carbide[2] abrasive disks.

Dissolution Procedure—A bovine tooth was selected and covered with nail enamel, except for a 0.25 cm^2 square window on the labial surface. The tooth was then placed in 10 mL of 0.1 M acetate buffer containing 7.05 mM each of calcium and phosphate for varying lengths of time. It has been calculated that the dissolution medium is not saturated with respect to hydroxyapatite after these periods of dissolution. During demeneralization the solution and sample were gently agitated with a wrist-action shaker[3]. The temperature was maintained at 30°C throughout the procedure.

Sample Preparation for X-ray Analysis—The demineralized sample was mounted in a circular saw[4] with a high concentration diamond wafering blade.[5] Sections were cut through the exposed window perpendicular to the enamel surface as thin as possible. Each thin section was then ground with 600-grit silicon carbide paper plane-parallel to a thickness of 100 μm as determined by a micrometer. Final polishing using diamond paste[6] on a rayon cloth was done to remove any small aberrations resulting from the initial grinding procedure.

X-ray Method—The thin section of enamel was placed in direct contact with the emulsion of a 5 × 5 cm high-resolution glass plate[7]. A wedge made of bovine enamel was cut from the block enamel using the circular saw. The wedge was placed on the plate directly opposite the enamel surface to be analyzed. The internal standard is essential because it allows comparison of the negatives of different samples by factoring out any deviations due to variations in the time and temperature during the film development process. The sample was positioned in the center of the X-ray beam[8] for 25 min, with the instrument settings at 40 kVp and 3 mA. The exposed negative was developed in developer solution[9] according to the manufacturer's instructions. Quantitation of the mineral density *versus* position was accomplished using the image analysis system (Fig. 1). Scans were made through the demineralized region as well as the adjacent wedge (Fig. 2). The data were recorded on magnetic tape; a program[10] utilizing the wedge and sample data was employed to calculate the mineral density *versus* position.

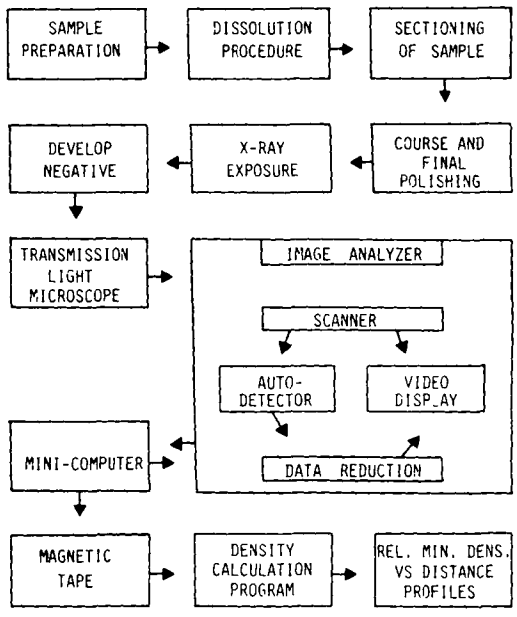

Figure 1—*Schematic representation of the methodology for obtaining relative mineral density* versus *position in enamel.*

[1] Quantimet-720, Cambridge Instruments, Inc., Monsey, N.Y.
[2] 3-M Co., St. Paul, Minn.
[3] Burrel Co., Pittsburgh, Pa.
[4] South Bay Technology, Temple City, Calif.
[5] Norton, Worcester, Mass.
[6] Mager Scientific, Inc., Ann Arbor, Mich.
[7] Type 1A; Eastman Kodak, Rochester, N.Y.
[8] Hewlett-Packard, McMinnville, Ore.
[9] D-19 Developer; Eastman Kodak, Rochester, N.Y.
[10] Developed by J. L. Fox, unpublished results.

0022-3549/84/0500-0650$01.00/0
© 1984, American Pharmaceutical Association

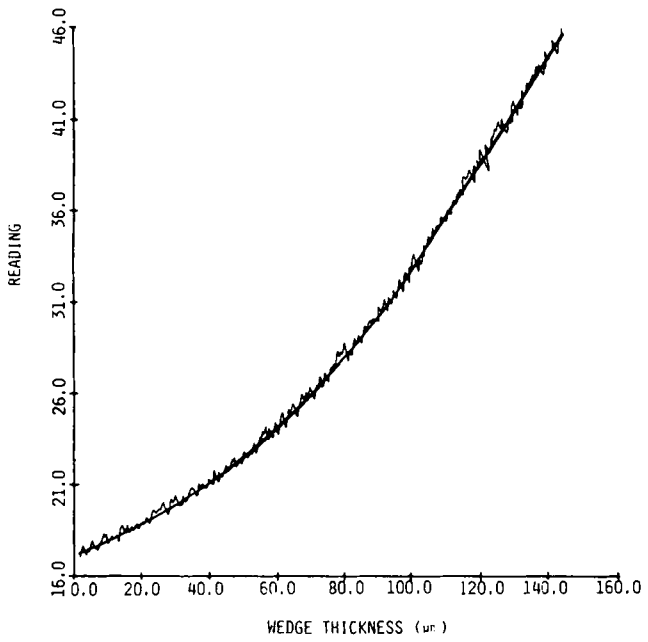

Figure 2—*Calibration plot using a wedge of enamel, providing the crucial link in allowing quantitative comparisons to be drawn between different microradiographs.*

RESULTS AND DISCUSSION

Contact Microradiography Technique—Contact microradiography, an extension of the conventional macroradiography, allows a rapid and convenient means of studying the density changes that occur within a block of enamel or a synthetic pellet (1) during the demineralization and/or remineralization process. This method possesses a very great depth of field and has the same resolution limit as transmitted light microscopy (~0.25 μm) (6). Several factors limit the resolution: (*a*) a lack of geometric sharpness results from the finite apparent source of the X-rays in relation to the source film distance; under the experimental procedure followed here this blurring of the image would be insignificant at ~0.02 μm as calculated by a previously described method (7); (*b*) high resolution glass plates have a photographic graininess limit of 0.15 μm; and (*c*) the lack of sharpness in the image at the edge of a sample resulting from the diffraction of the X-ray beam at the edge of a sharp electron-dense boundary. Again this effect was calculated to be ~0.2 μm and comparable to the film graininess (6). Considering all these contributions it can be assumed that structural detail down to ~0.5 μm can be observed. To test the resolution limit of the entire quantitative procedure, a scan was made over the sharp edge of a nondemineralized bovine tooth sample (Fig. 3), and the resolution limit was ~4 μm.

The system used to generate X-rays was operated at an accelerating voltage of 40 kVp and a current of 3 mA. The exposure time was 25 min, and the source-to-sample distance was 25 cm. A continuous spectrum of X-rays was produced, the wavelength of the most energetic being 0.05 nm. In an enamel sample the principal X-ray absorber at this wavelength is the calcium atom. The mass absorption coefficients of the inorganic *versus* organic components of enamel differ by a factor of 20. Absorption of X-rays of this wavelength by the organic material can be considered negligible.

The use of a wedge of bovine enamel exposed and further processed under the exact same conditions as the sample permits comparisons to be made between different negatives. Corrections can be thus made for any differences between negatives which may arise due to variations in time and temperature during the film development process. The angle of the wedge was determined by the trigonometric tangent function examining a negative on which the wedge resting on its side, had been exposed to X-rays.

Data Handling and Generation of Density Profiles—Using a computer program[10] the image data on the magnetic tape was transformed using the bovine wedge data as an internal standard to allow calculation and plotting of relative mineral density *versus* position.

In preparing a scan across the sample, the overall light level of the total image produced must be adjusted to allow maximum sensitivity of all the pixels (picture elements). The level of grayness can vary greatly between samples, so this adjustment must be made before each scan. When adjusting what is called white level sensitivity, the gray level values or scanner reading for the baseline value obtained from the exposed negative was not identical for two scans from the same negative (Fig. 3B *versus* Fig. 4B).

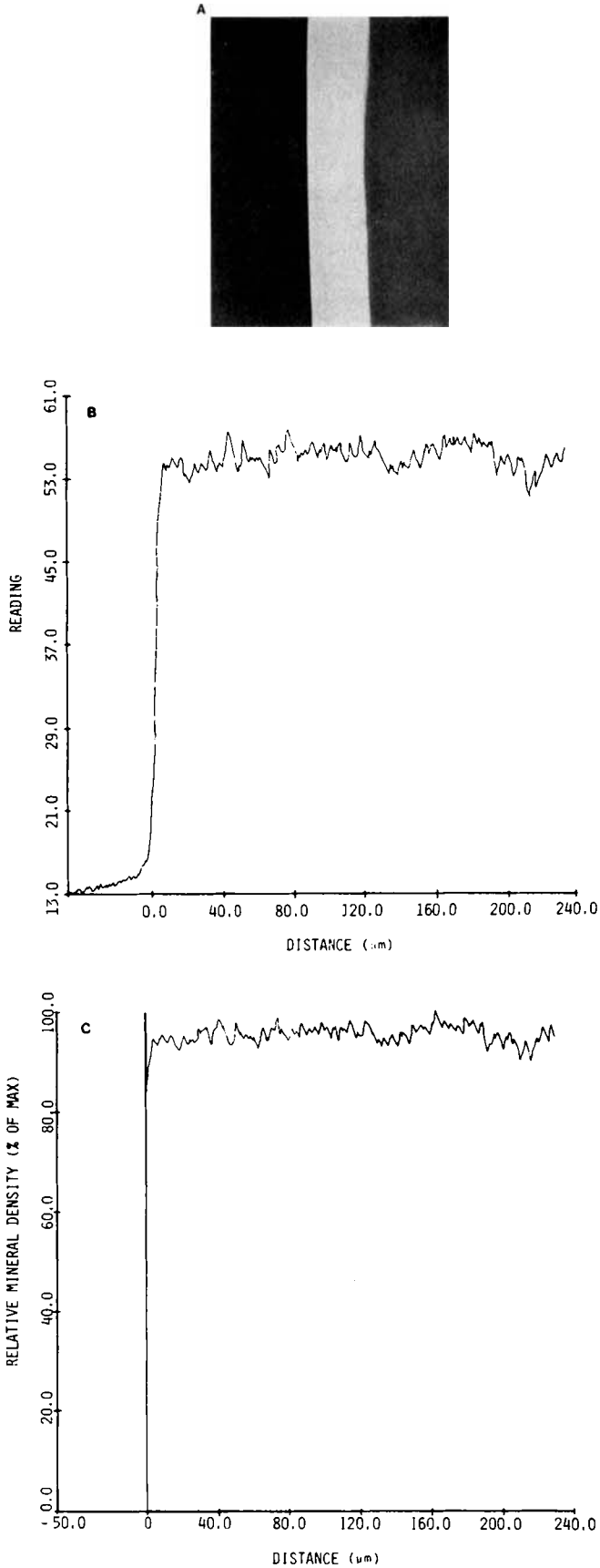

Figure 3—*(A) Photograph of a control sample of bovine enamel. Note the sharp edge between the exposed negative and the enamel. (B) Data obtained directly from the image analyzer after scanning from the negative onto the enamel to a depth of 230 μm. (C) Profile of relative mineral density* versus *position in enamel obtained after including the information obtained from the wedge data.*

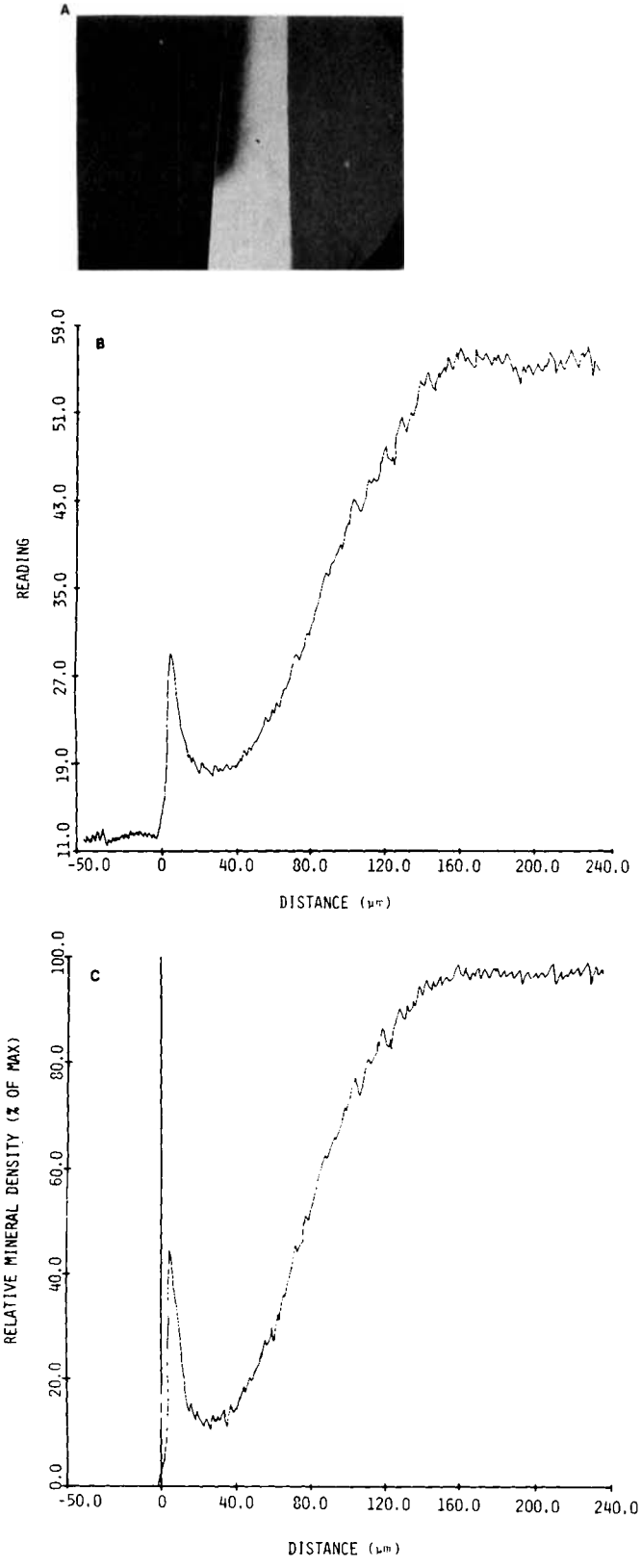

Figure 4—*(A) Photomicrograph of bovine enamel after 24 h demineralization at pH 4.5 in solution containing [calcium] = [phosphate] = 7.05 mM. (B) Image analyzer scanning of the microradiograph indicates mineralization of surface enamel is greater than that at depths further into the enamel. (C) Profile of mineral density* versus *position for (A) relative to the enamel at a depth of 230 μm.*

Initially it was thought that either the X-ray beam intensity or the photographic emulsion was not uniform, but scans made across different regions of blank negatives were essentially flat, indicating uniform exposure. To test

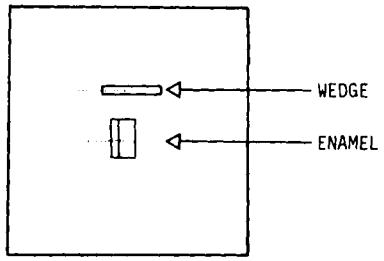

Figure 5—*Pictorial representation of microradiograph depicting relative positions of wedge and sample. The dotted lines show direction of image analysis scan.*

whether this variable baseline reading was due to this need to change the light intensity between samples, several scans across the same wedge in the exact same spot on the same negative were made. Results indicated that although the absolute values were changing they were changing at both ends of the curve so that the shape of the calibration curve remained constant. The placement of the wedge and sample (not to scale for clarification) is depicted in Fig. 5. The dotted line indicates the path each scan followed. These data allow normalizing the raw image analysis data obtained from the sample to that of the wedge and calculating from this the relative mineral density *versus* distance (see Figs. 2, 4B, and 4C).

The relative mineral density is defined as the normalized scanner reading at a point divided by the maximum reading in the sample × 100. The maximum scanner reading in the sample is taken as the average of the last 20 data points. In this it is assumed that there has been no acid demineralization in this deep recess of the enamel.

Application of the Method as Shown by Results of Experiments on Bovine Tooth Dissolution—In the development of this quantitative technique, samples of bovine enamel were exposed to a demineralizing solution for varying lengths of time (0, 1, 2, 3, 4, 5, 6, 12, and 24 h) and the resultant changes in mineral density were observed. For samples in which dissolution occurred for short periods of time, the mineral density was very low at the surface and increased monotonically until it reached the density of sound enamel. With increasing dissolution time, the mineral density at the original surface tended to increase, while the mineral beneath it remained less dense. The density again reached the maximum of sound enamel at sufficient depth (Fig. 4C). The longer dissolution times give rise to what has been termed a "subsurface lesion" or "white spot" phenomenon. This quantitative X-ray microradiographic technique has been shown to be an excellent method to study the demineralization and/or remineralization of enamel as well as synthetic hydroxyapatite compacts.

APPENDIX: Image Analysis

Image Analysis—Quantitative determination of the mineral density *versus* position in the tooth was obtained from the microradiograph using the image analysis system. This system is composed of three major components. The first is a transmission light microscope with high-quality optics, fitted with a 16× objective and 10× eye piece. The image analyzer itself is of modular design capable of a variety of image analysis functions, one of which is the image digitization used here. The third component of the system is a minicomputer system with a peripheral terminal and tape drive. The minicomputer functions here to collect and store the digitized image as it comes from the image analyzer and later to transfer this information to magnetic tape for further processing. A second function of the minicomputer is to instruct the system in its operations according to a user-defined protocol (average gray level determination) to be discussed later.

Image Production—The image analyzer uses a television camera to convert an optical image into an electronic signal. The first step then is to produce a high-quality image of the sample. The image analyzer cannot improve the quality of the projected image; in fact, its usefulness is severely limited by the quality of the image. Inherent in any image of good quality is lack of shading or uneven illumination in the image plane. Although an excellent grade microscope is used to produce the image, the optics are limited and image analysis off the optical axis of the microscope can result in incorrect measurements. In object plane scanning systems, *i.e.*, conventional microdensitometers, this problem is overcome by restricting the measurement area to a very small region in the center of the field on the optical axis of the microscope. In image plane scanners, *i.e.*, the system used herein, the measurement area is over a broad range, not limited to the optical axis of the microscope, so the resultant potential for error in off-axis operation must be corrected for. Fortunately, a unique comprehensive shading device has been developed which automatically corrects for illumination errors.

Glare or stray light arising from multiple reflections within the microscope

is another major source of error in microdensitometry, not unique to the image analysis method used here. Some of this stray light can affect the apparent optical density of the measured object. Glare tends to be specimen dependent, so its effect varies from field to field. In this system a dynamic glare correction is automatically applied. The transmission light microscope is the device utilized to produce an optical image which is then projected onto the photosensitive face of the vidicon tube scanner[11].

Image Scanning—The face of the vidicon tube is made of material that produces a local potential difference proportional to the intensity of light striking it. The sampling method of the scanner then converts the optical image to an electronic signal consisting of continuously varying analog voltage. High voltage corresponds to bright (white) portions of the image, while low voltage corresponds to the darker regions.

Image Digitization—The total image is composed of ~500,000 picture points or pixels, each of which is sensitive to the light intensity incident on it and contributes to the total analog video signal. It is within the auto detector module (see Fig. 1) that the analog video signal of each pixel is assigned a "gray level" value between 0 and 63. The 63 value corresponds to the brightest area over the total image, the 0 value set to some internal standard for black. The result of this digitization procedure is a digital image consisting of a matrix of numbers each with a value between 0 and 63. This is the basic data set produced by the image analysis system.

Data Reduction Module—To allow selectivity as to what portion of the total field is to be scanned, a variable frame size option is employed. This allows restricting the measurement to some quadrilaterally defined portion of the field. A frame size measuring 600 pixels horizontally by 10 pixels vertically is used to scan each sample. The 600 horizontal pixels under the 160× magnification of the microradiograph allows a sufficiently wide scan to be made across the sample and adjacent negative.

The minicomputer interface allows further processing of the 600 × 10 matrix of pixels, each with a value between 0 and 63. In this case, it is the 10 vertical pixels that are acted upon. To minimize any error due to variable sensitivity of a particular pixel, some defect in the microradiograph itself (dust or a scratch), a single value is obtained from the 10 vertical numbers by simply taking the average. This produces what is called an "average gray level" for 600 horizontal sampling points. Using appropriate calibration methods it was determined that under these conditions each pixel has a width of 0.46 μm. The data are then transferred to magnetic tape as a pair of numbers corresponding to position in scan and the average gray level or "reading" at that position.

[11] E.M.I., London, England.

REFERENCES

(1) T. Aoba, M. Okazaki, J. Takahashi, and Y. Moriwaki, *Caries Res.*, **12**, 223 (1978).

(2) A. I. Darling, *Intl. Dent.*, **17**, 684 (1967).

(3) D. J. Langdon, J. C. Elliott, and R. W. Fernhead, *Caries Res.*, **14**, 359 (1980).

(4) A. N. Sharpe, *Arch. Oral Biol.*, **12**, 583 (1967).

(5) H. M. Theuns and A. Groeneveld, *Caries Res.*, **11**, 293 (1977).

(6) J. B. Nelson, *Microscope*, **19**, 347 (1971).

(7) A. Engstrom, "Elsevier Monographs, Biophysics Section," Elsevier, New York, N.Y., 1962.

ACKNOWLEDGMENTS

This project was supported by NIDR Grants DE-01830 and DE-04600.

Quantitative Microradiographic Study of Simultaneous Demineralization/Remineralization of Dental Enamel in Weak Acid Buffers

DAVID H. BERGSTROM *, JEFFREY L. FOX *, and WILLIAM I. HIGUCHI *x

Received May 17, 1982, from *the Dental Research Institute and the College of Pharmacy, The University of Michigan, Ann Arbor, MI 48109.* Accepted for publication March 7, 1983.

*Present address: Department of Pharmaceutics, College of Pharmacy, The University of Utah, Salt Lake City, UT 84112.

Abstract □ The remineralization behavior of weak acid-treated bovine tooth enamel has been investigated using a recently developed quantitative microradiographic method. Acetate buffer solutions at pH 4.5 containing calcium, phosphate, and 10 ppm fluoride were used in this study. When the solution ion activity product ($K_{FAP} = a_{Ca}^{10} a_{PO_4}^{6} a_F^2$) was 1×10^{-108}, the remineralization of the demineralized region was relatively uniform and complete. On the other hand, when the K_{FAP} was $\sim \leq 1 \times 10^{-112}$, remineralization of the outer 10–20 μm was incomplete. In addition, for the smaller K_{FAP} solutions there was significant demineralization in the deeper recesses of the originally demineralized region. These results agree with a recent chemical kinetics study in which it was proposed that $K_{FAP} = 1 \times 10^{-112}$ demarcated the region of solution conditions in which remineralization only occurs from that in which simultaneous demineralization/remineralization takes place. A model consistent with all of the data is proposed.

Keyphrases □ Microradiography—quantitative study of dental enamel demineralization/remineralization, solution ion activity product □ Dental enamel—demineralization/remineralization, solution ion activity product, quantitative microradiography □ Demineralization—dental enamel, simultaneous remineralization, solution ion activity product, quantitative microradiography

Recently, Fox *et al.* (1) investigated the influence of the solution ion activity product ($K_{FAP} = a_{Ca}^{10} a_{PO_4}^{6} a_F^2$) on the remineralization of weak acid-treated bovine tooth enamel and hydroxyapatite pellets. Solutions containing calcium-45, phosphate, and fluoride in acetate buffers were used. The calcium-45/fluoride molar ratios determined for the remineralized enamel by perchloric acid etch biopsy indicated the predominant formation of fluorapatite [$Ca_{10}(PO_4)_6F_2$; FAP] or fluoridated hydroxyapatite [$Ca_{10}(PO_4)_6(OH)_{2-x}F_x$], where $0 \leq x \leq 2$ when $pK_{FAP} \simeq 108$. When the pK_{FAP} of the solutions were ≥112, the calcium-45/fluoride ratios were found to be considerably <5. From these results, the authors proposed that a pK_{FAP} value of ~112 marked the demarcation between remineralization only and simultaneous demineralization/remineralization for these acidic remineralizing solutions.

The purpose of the present investigation was to study the remineralization of bovine tooth enamel under the same conditions as those of Fox *et al.* (1), employing a recently developed (2) quantitative microradiographic technique. A special point of interest was to examine the hypothesis that simultaneous demineralization/remineralization sets in when the pK_{FAP} value is ~ ≥112 for these solutions.

0022-3549/84/0500-0653$01.00/0

© 1984, American Pharmaceutical Association

is another major source of error in microdensitometry, not unique to the image analysis method used here. Some of this stray light can affect the apparent optical density of the measured object. Glare tends to be specimen dependent, so its effect varies from field to field. In this system a dynamic glare correction is automatically applied. The transmission light microscope is the device utilized to produce an optical image which is then projected onto the photosensitive face of the vidicon tube scanner[11].

Image Scanning—The face of the vidicon tube is made of material that produces a local potential difference proportional to the intensity of light striking it. The sampling method of the scanner then converts the optical image to an electronic signal consisting of continuously varying analog voltage. High voltage corresponds to bright (white) portions of the image, while low voltage corresponds to the darker regions.

Image Digitization—The total image is composed of ~500,000 picture points or pixels, each of which is sensitive to the light intensity incident on it and contributes to the total analog video signal. It is within the auto detector module (see Fig. 1) that the analog video signal of each pixel is assigned a "gray level" value between 0 and 63. The 63 value corresponds to the brightest area over the total image, the 0 value set to some internal standard for black. The result of this digitization procedure is a digital image consisting of a matrix of numbers each with a value between 0 and 63. This is the basic data set produced by the image analysis system.

Data Reduction Module—To allow selectivity as to what portion of the total field is to be scanned, a variable frame size option is employed. This allows restricting the measurement to some quadrilaterally defined portion of the field. A frame size measuring 600 pixels horizontally by 10 pixels vertically is used to scan each sample. The 600 horizontal pixels under the 160× magnification of the microradiograph allows a sufficiently wide scan to be made across the sample and adjacent negative.

The minicomputer interface allows further processing of the 600 × 10 matrix of pixels, each with a value between 0 and 63. In this case, it is the 10 vertical pixels that are acted upon. To minimize any error due to variable sensitivity of a particular pixel, some defect in the microradiograph itself (dust or a scratch), a single value is obtained from the 10 vertical numbers by simply taking the average. This produces what is called an "average gray level" for 600 horizontal sampling points. Using appropriate calibration methods it was determined that under these conditions each pixel has a width of 0.46 μm. The data are then transferred to magnetic tape as a pair of numbers corresponding to position in scan and the average gray level or "reading" at that position.

[11] E.M.I., London, England.

REFERENCES

(1) T. Aoba, M. Okazaki, J. Takahashi, and Y. Moriwaki, *Caries Res.*, **12**, 223 (1978).

(2) A. I. Darling, *Intl. Dent.*, **17**, 684 (1967).

(3) D. J. Langdon, J. C. Elliott, and R. W. Fernhead, *Caries Res.*, **14**, 359 (1980).

(4) A. N. Sharpe, *Arch. Oral Biol.*, **12**, 583 (1967).

(5) H. M. Theuns and A. Groeneveld, *Caries Res.*, **11**, 293 (1977).

(6) J. B. Nelson, *Microscope*, **19**, 347 (1971).

(7) A. Engstrom, "Elsevier Monographs, Biophysics Section," Elsevier, New York, N.Y., 1962.

ACKNOWLEDGMENTS

This project was supported by NIDR Grants DE-01830 and DE-04600.

Quantitative Microradiographic Study of Simultaneous Demineralization/Remineralization of Dental Enamel in Weak Acid Buffers

DAVID H. BERGSTROM *, JEFFREY L. FOX *, and WILLIAM I. HIGUCHI *x

Received May 17, 1982, from *the Dental Research Institute and the College of Pharmacy, The University of Michigan, Ann Arbor, MI 48109.* Accepted for publication March 7, 1983.

*Present address: Department of Pharmaceutics, College of Pharmacy, The University of Utah, Salt Lake City, UT 84112.

Abstract □ The remineralization behavior of weak acid-treated bovine tooth enamel has been investigated using a recently developed quantitative microradiographic method. Acetate buffer solutions at pH 4.5 containing calcium, phosphate, and 10 ppm fluoride were used in this study. When the solution ion activity product ($K_{FAP} = a_{Ca}^{10} a_{PO_4}^{6} a_F^2$) was 1×10^{-108}, the remineralization of the demineralized region was relatively uniform and complete. On the other hand, when the K_{FAP} was $\sim \leq 1 \times 10^{-112}$, remineralization of the outer 10–20 μm was incomplete. In addition, for the smaller K_{FAP} solutions there was significant demineralization in the deeper recesses of the originally demineralized region. These results agree with a recent chemical kinetics study in which it was proposed that $K_{FAP} = 1 \times 10^{-112}$ demarcated the region of solution conditions in which remineralization only occurs from that in which simultaneous demineralization/remineralization takes place. A model consistent with all of the data is proposed.

Keyphrases □ Microradiography—quantitative study of dental enamel demineralization/remineralization, solution ion activity product □ Dental enamel—demineralization/remineralization, solution ion activity product, quantitative microradiography □ Demineralization—dental enamel, simultaneous remineralization, solution ion activity product, quantitative microradiography

Recently, Fox *et al.* (1) investigated the influence of the solution ion activity product ($K_{FAP} = a_{Ca}^{10} a_{PO_4}^{6} a_F^2$) on the remineralization of weak acid-treated bovine tooth enamel and hydroxyapatite pellets. Solutions containing calcium-45, phosphate, and fluoride in acetate buffers were used. The calcium-45/fluoride molar ratios determined for the remineralized enamel by perchloric acid etch biopsy indicated the predominant formation of fluorapatite [$Ca_{10}(PO_4)_6F_2$; FAP] or fluoridated hydroxyapatite [$Ca_{10}(PO_4)_6(OH)_{2-x}F_x$], where $0 \leq x \leq 2$ when $pK_{FAP} \simeq 108$. When the pK_{FAP} of the solutions were ≥112, the calcium-45/fluoride ratios were found to be considerably <5. From these results, the authors proposed that a pK_{FAP} value of ~112 marked the demarcation between remineralization only and simultaneous demineralization/remineralization for these acidic remineralizing solutions.

The purpose of the present investigation was to study the remineralization of bovine tooth enamel under the same conditions as those of Fox *et al.* (1), employing a recently developed (2) quantitative microradiographic technique. A special point of interest was to examine the hypothesis that simultaneous demineralization/remineralization sets in when the pK_{FAP} value is ~ ≥112 for these solutions.

0022-3549/84/0500-0653$01.00/0

© 1984, American Pharmaceutical Association

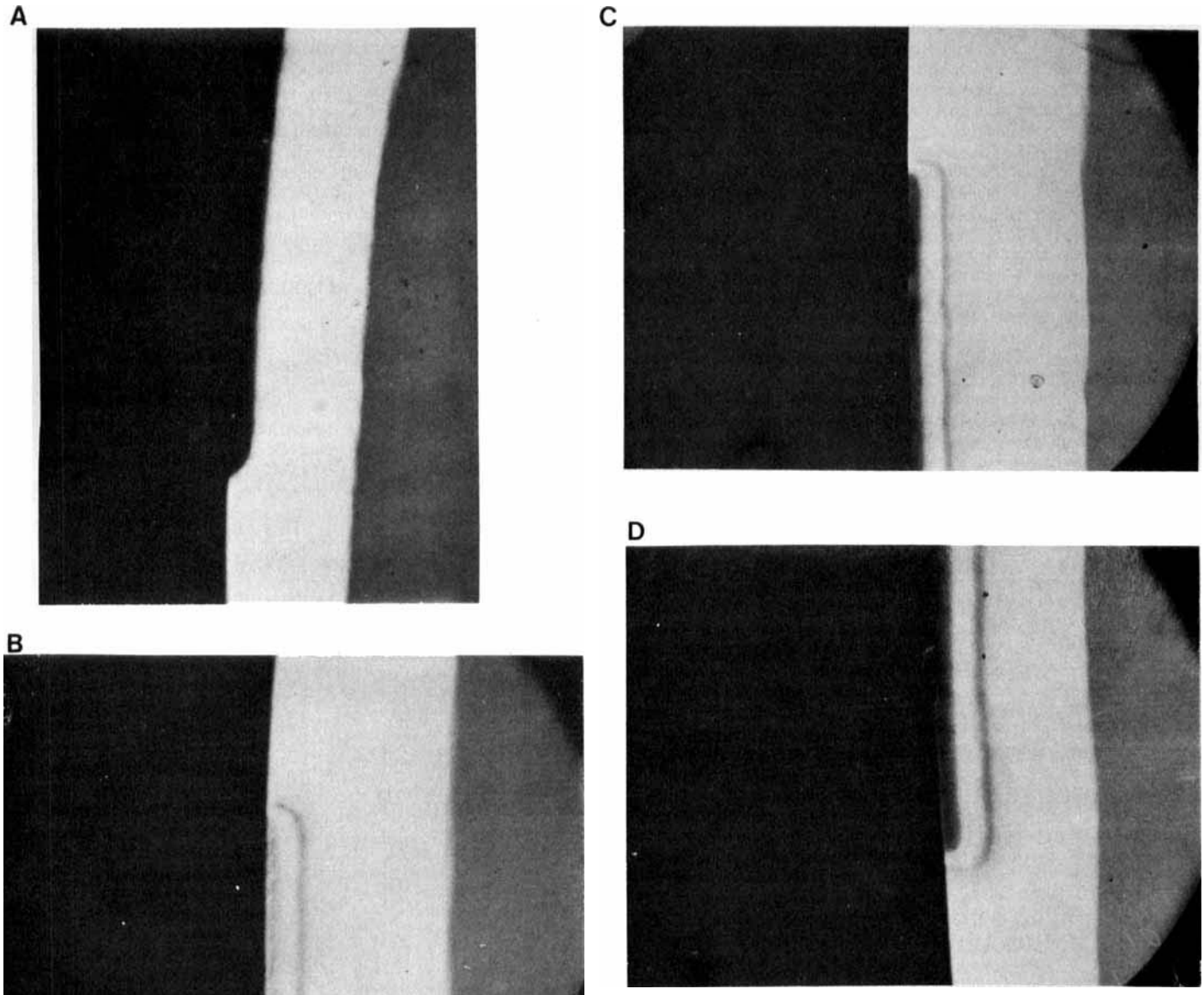

Figure 1—*Bovine tooth enamel demineralized for 6 h in 10 mL of 0.10 M acetate buffer (μ = 0.5, pH 4.5) with calcium = phosphate = 3.5 mM. Remineralization was done in different solutions (see Table I) for 24 h. Key: (A) no remineralization; (B) solution 1, pK_{FAP} = 108; (C) solution 2, pK_{FAP} = 112; (D) solution 3, pK_{FAP} = 118.*

EXPERIMENTAL

Buffer Dissolutions—*Dissolution*—A solution ~16% saturated (on a molar basis) with respect to the thermodynamic solubility of hydroxyapatite was used for demineralization. The solution was 0.1 M acetate buffer containing 3.5 mM each of total calcium and phosphate. The pH was adjusted to 4.5 with sodium hydroxide and the ionic strength to 0.5 M by the addition of sodium chloride.

Remineralization—For remineralization, 0.1 M acetate buffers (pH 4.5) containing different amounts of total calcium and phosphate depending on the desired bulk solution activity product ($K_{FAP} = a_{Ca}^{10} a_{PO_4}^{6} a_F^2$) as shown in Table I were employed. These solutions also contained 10 ppm fluoride (in the form of sodium fluoride) with sodium chloride added to adjust the ionic strength to 0.5 M. All chemicals used were of analytical grade.

Bovine Teeth—Teeth from 8-week old strictly Kosher calves were obtained from packing houses in the Chicago area. From these, only reasonably flat incisors without any visible surface defects were used experimentally. The pellicle was removed from the labial surface using 400- and 600-grit silicon carbide abrasive disks.

Demineralization and Remineralization Procedures—A selected bovine tooth was covered with nail enamel except for a 0.25-cm^2 window on the labial surface. The tooth was then placed in 10 mL of the 16% partially saturated buffer solution for 6 h. From experimental results obtained by Yonese *et al.* (3) the demineralizing solution was not saturated with respect to hydroxyapatite after 6 h of demineralization. During demineralization the solution was gently agitated with a wrist-action shaker. The temperature was maintained at 30°C.

Table I—Ion Activity Products of Solutions [a] Used in this Study

Solution	Calcium, mM	Phosphate, mM	Fluoride, ppm	pK_{FAP}	pK_{HAP}
1	12.00	12.00	10	108	120
2	6.87	6.87	10	112	124
3	2.86	2.86	10	118	130

[a] pH 4.5; μ = 0.5; 0.1 M acetate buffer.

The previously demineralized sample was immediately placed in 50 mL of the desired remineralization solution. During the remineralization the solution was again gently agitated and maintained at 30°C.

Sample Preparation—The demineralized/remineralized tooth was mounted on a circular saw fitted with a high concentration diamond wafering blade. Sections as thin as possible were cut through the exposed window perpendicular to the enamel surface. Each section was then ground plane-parallel to a thickness of exactly 100 μm as determined by a micrometer. Final polishing, using diamond paste on a rayon cloth, was done to remove any small aberra-

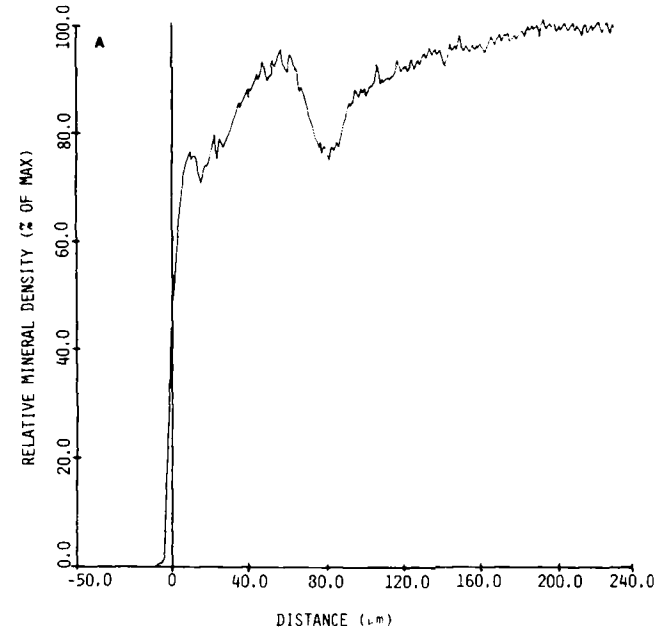

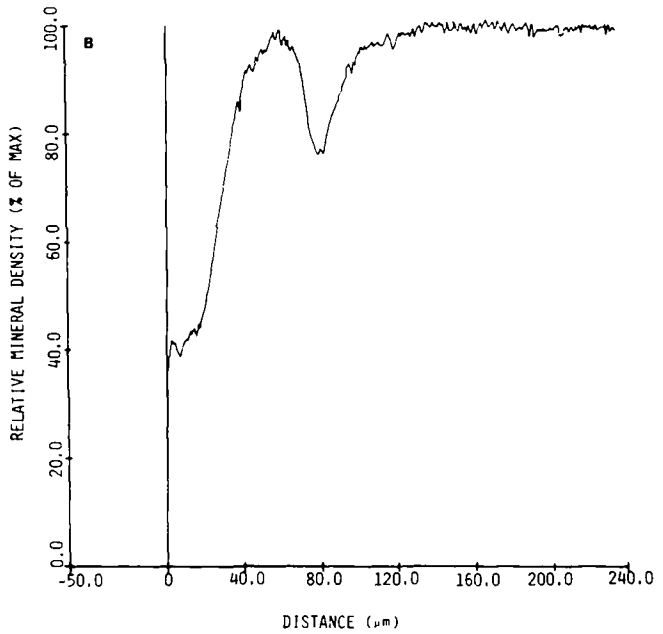

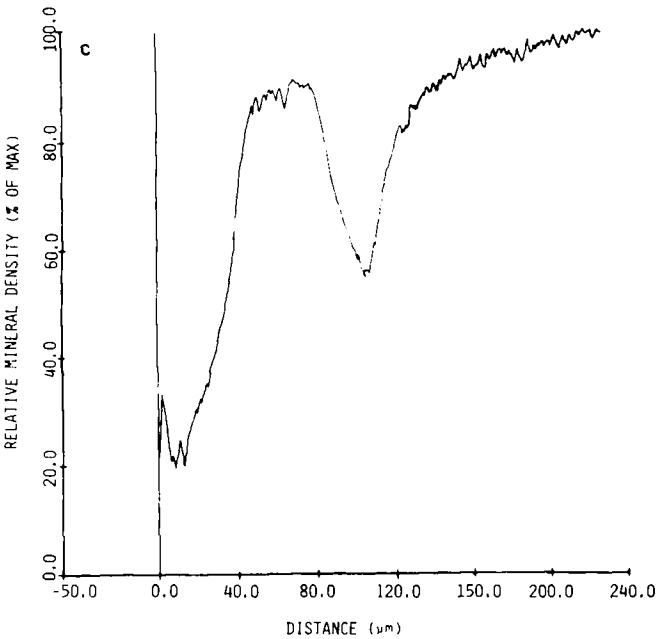

Figure 2—*Relative mineral density* versus *distance for remineralization experiments described in Fig. 1. Key: (A) $pK_{FAP} = 108$; (B) $pK_{FAP} = 112$; (C) $pK_{FAP} = 118$.*

tions resulting from the initial grinding using 600-grit silicon carbide paper.

X-Ray—A section was placed in direct contact with the emulsion on a 5 × 5 cm high-resolution glass plate[1]. Directly opposite the enamel surface to be analyzed, a wedge made of bovine enamel was placed. The wedge allowed comparison of the negatives of different samples by factoring out any deviations in the time- and temperature-dependent film development process.

The sample was placed in the center of the X-ray beam[2] for 25 min. The instrument settings were 40 kVp and 3 mA. The negative was developed in developer solution[3] according to the manufacturer's instructions.

Density Profiles—Quantitation of the demineralization/remineralization process was accomplished using the image analysis system[4]. By the procedure outlined in the previous article (2), scans were made across the sample as well as on the adjacent step wedge. The data recorded on magnetic tape were analyzed by a computer program in which the wedge data and sample data were used to calculate the mineral density *versus* position in the tooth.

[1] Eastman Kodak, Rochester, N.Y.
[2] Hewlett-Packard, McMinnville, Ore.
[3] D-19 *Developer*; Eastman Kodak, Rochester, N.Y.
[4] Cambridge Instruments, Inc., Monsey, N.Y.

RESULTS AND DISCUSSION

As shown by the photomicroradiographs (Fig. 1) and the mineral density *versus* position profiles (Fig. 2), the influence of the solution activity product on the remineralization of bovine tooth enamel is profound. Remineralization under conditions in which the solution activity product equals 10^{-108} gives a relatively uniform and essentially complete recovery of mineral density to the original surface of the previously demineralized sample (Figs. 1B and 2A). Under conditions where the pK_{FAP} of the remineralization solution is high (*i.e.*, 112) the recovery appears less complete, particularly in the outer 20 μm (Figs. 1C and 2B). There is also the appearance of a less dense band at a depth slightly greater than that produced by the demineralization treatment alone. The experimental results for conditions in which the solution activity product was varied from 10^{-114} to 10^{-118} also indicated this less dense outer 20 μm in the enamel sample. The band below the original "lesion" (Fig. 1A) depth was now significantly deeper and more diffuse (Figs. 1D and 2C).

Mineral density profiles of this type indicate that the situation is more complex than that of simple mineral deposition in the form of fluorapatite (1). Indeed, simultaneous dissolution must also be occurring in order to explain the loss of mineral deeper than the original "lesion." The presence of a more highly remineralized region under the less dense outer 20 μm found when remineralization was done in solutions with $pK_{FAP} \geq 110$ indicates that the

bulk solution activity product is not the sole determinant of the remineralization process.

The following discussion attempts to present a mechanism that is consistent with the present observations and with the chemical kinetic data obtained by Ludwig *et al.* (4), Fox *et al.* (1), and Katdare *et al.* (5). Thermodynamic calculations show (Table I) that a bulk solution with $pK_{FAP} = 108$ is supersaturated with respect to fluorapatite and saturated or supersaturated with respect to the ion activity products, K_{HAP} values, governing the relatively rapid rate of hydroxyapatite dissolution [*i.e.*, $pK_{HAP} = 120$ for site 1 and $pK_{HAP} = 128$ for site 2 described by Fox *et al.* (6)]. Ludwig *et al.* (4) have shown, however, that for apatite powder containing ~5% carbonate, the corresponding apparent solubilities may be greater by approximately four orders of magnitude in the K_{HAP} values. The carbonate level in the bovine enamel used in these experiments is ~4%. The modest band of demineralization (at ~80 μm depth) observed with the $pK_{FAP} = 108$ case is consistent with this consideration. With increasing pK_{FAP} the solutions become increasingly unsaturated with respect to hydroxyapatite (and carbonate apatite), and the deeper and wider band of demineralization observed at ~110 μm for $pK_{FAP} = 118$ would be consistent with this thinking.

The remineralization behavior in the region 0–20 μm is in agreement with the results of experiments with hydroxyapatite and carbonate containing apatite crystal suspensions reported by Katdare *et al.* (5). At $pK_{FAP} = 108$, fluorapatite suspension crystal growth rates were found to be relatively rapid but decreased significantly (*i.e.*, by a factor of ~10) at $pK_{FAP} = 112$, and the rates were negligibly slow at $pK_{FAP} = 116$. These findings by Katdare *et al.* (5) may easily explain the rather complete and uniform remineralization observed at $pK_{FAP} = 108$ in the region 0–20 μm and the much poorer extent of remineralization in this region at $pK_{FAP} = 112$ and 118. It may be concluded, therefore, that the remineralization behavior in the outer 10–20 μm may be primarily controlled by the bulk solution activity product.

The most interesting aspect of the results in Figs. 1 and 2 is that related to the highly mineralized region at intermediate depths (*e.g.*, at ~50 μm in the $pK_{FAP} = 112$ experiment). The following process is proposed to explain why remineralization occurs at intermediate depths but not at or near the surface (for the $pK_{FAP} = 112$ and 118 experiments). Ludwig *et al.* (4) have shown that, even for apatites containing ~5% carbonate, dissolution rates should be negligible when $pK_{FAP} \leq 115$. Therefore, for lesions to form at 80–90 μm in the $pK_{FAP} = 108$ and 112 experiments, it is reasonable to postulate that the microenvironment (aqueous pores) pK_{FAP} values in the deep recesses of the lesion must be >115 as a result of aqueous fluoride depletion caused by fluorapatite (or fluorhydroxyapatite) formation or fluoride adsorption in the outer layer and at intermediate depths. Fluorapatite deposition and fluoride depletion at the intermediate depths (40–50 μms) would be enhanced because mineral dissolution at 80–90 μm and the resultant outward flow of calcium and phosphate ions may significantly elevate the K_{FAP} values to far above the bulk K_{FAP} value. This simultaneous dissolution (at 80–90 μm) and remineralization (at 40–80 μm) process continues until sufficient aqueous fluoride concentrations (corresponding to $pK_{FAP} \simeq 115$) can build up in the deeper regions of the lesion.

To test the hypothesis that continued dissolution beneath the level of the original lesion is a transient phenomenon, additional studies have been conducted at different pK_{FAP} values for 3, 6, 12, 24, 48, and 96 h. At $pK_{FAP} = 116$, for example, the simultaneous dissolution and remineralization did not proceed beyond 12 h, and the lesion pattern remained essentially unchanged beyond that time period. Interestingly, Fox *et al.* (1) found that ^{45}Ca-labeled hydroxyapatite pellets dissolved only for 12–16 h in $pK_{FAP} = 116$ solutions. These are bulk-solution conditions for which simultaneous dissolution and remineralization will occur. The simultaneous demineralization/remineralization then appears to be a transient phenomenon indicating that once sufficient remineralization has occurred at the intermediate depths, dissolution no longer continues under the control of the microenvironmental K_{HAP} in the deeper regions of the enamel.

These results support the hypothesis by Fox *et al.* (1) that $pK_{FAP} \simeq 112$ marks the demarcation between mainly remineralization only and simultaneous demineralization/remineralization. For high pK_{FAP} solutions (*e.g.*, 118), fluoride deposition *via* fluorapatite or fluorhydroxyapatite formation occurs mainly at intermediate depths and involves, to a large extent, the reaction between bulk solution fluoride and the calcium and phosphate ions dissolved from the deeper regions of the lesion. For $pK_{FAP} = 108$, the remineralization is mainly controlled by the bulk solution, and the contribution to fluorapatite or fluorhydroxyapatite formation from the mineral dissolved in the lesion is minimal.

REFERENCES

(1) J. L. Fox, B. V. Iyer, W. I. Higuchi, and J. J. Hefferren, *J. Pharm. Sci.*, **72,** 1252 (1983).

(2) D. H. Bergstrom, J. L. Fox, and W. I. Higuchi, *J. Pharm. Sci.*, **73,** 650 (1984).

(3) M. Yonese, J. L. Fox, N. Nambu, J. J. Hefferren, and W. I. Higuchi, *J. Pharm. Sci.*, **70,** 904 (1981).

(4) A. M. Ludwig, S. C. Dave, W. I. Higuchi, J. L. Fox, and A. V. Katdare, *J. Dent. Res.*, (Abstracts) **61,** 196 (1982).

(5) A. V. Katdare, J. L. Fox, D. J. A. Crommelin, and W. I. Higuchi, *J. Dent. Res., Spec. Issue A*, **59,** 926a (1980).

(6) J. L. Fox, W. I. Higuchi, M. B. Fawzi, and M. S. Wu, *J. Colloid Inter. Sci.*, **67,** 312 (1978).

ACKNOWLEDGMENTS

The project was supported by NIDR Grants DE-02731 and DE-04600.

Statistical Prediction of Drug Stability Based on Nonlinear Parameter Estimation

SHANG-YING P. KING *, MIN-SHYA KUNG ‡, and HO-LEUNG FUNG *x

Received November 15, 1982, from the *Department of Pharmaceutics and ‡Department of Statistics, State University of New York at Buffalo, Amherst, NY 14260. Accepted for publication April 28, 1983.

Abstract □ The classical approach in Arrhenius prediction of drug stability uses two sequential steps of linear regression involving (*a*) a function of drug content *versus* time to obtain the rate constants (*k*) at several elevated temperatures and (*b*) the relationship of logarithm of mean *k versus* reciprocal temperature to predict the room temperature rate constant and hence the shelf-life of the drug. Uncertainties in drug content determinations are often neglected in the second regression. The classical approach also provides a wide and unsymmetrical 95% confidence interval for the predicted shelf-life. We have developed equations which allow for direct statistical prediction of shelf-life using observed values of drug content, time, and temperature. Nonlinear regression analysis was employed to provide parameter estimates of drug shelf-life and the energy of activation. The developed approach was shown to provide good estimates of shelf-life with meaningful statistics of reactions over a wide range of stability and energetics, with various kinetic orders, with different levels of noise in the data, and with different types of data structure. Comparison between the nonlinear approach and the classical approach showed that the nonlinear approach provided better mean estimates of shelf-life with much smaller and more symmetrical 95% confidence intervals than the classical approach. The method appears sufficiently robust and wide-ranging as to be potentially applicable for the prediction of the drug stability of pharmaceutical products.

Keyphrases □ Drug stability—statistical prediction of shelf-life, nonlinear parameter estimation, comparison with classical Arrhenius prediction □ Nonlinear parameter estimation—drug stability, statistical prediction of shelf-life, comparison with classical Arrhenius prediction □ Shelf-life—statistical prediction of drug stability, nonlinear parameter estimation, comparison with classical Arrhenius prediction

The establishment of the projected expiration date (or shelf-life) of a pharmaceutical product is of importance to the pharmaceutical industry. Accelerated stability testing using the Arrhenius equation is often employed to treat stability data obtained under elevated temperature storage conditions for the prediction of the shelf-life of drug products. The classical approach consists of two sequential steps which include (*a*) the choice of a proper order for the degradation reactions to describe the drug content (amount or concentration) *versus* time relationship for determining rate constants at each elevated temperature and (*b*) the application of the Arrhenius equation to predict (or extrapolate) the room temperature rate constant, and hence the shelf-life of the drug, through the use of the mean rate constants obtained at several elevated temperatures. Linear regression analysis (1) is the statistical method employed in each of these two steps.

Although this classical linear approach has been used quite frequently, the method of data treatment appears to suffer from two statistical problems. First, since Arrhenius treatment often employs only the mean rate constants obtained at elevated temperatures to predict drug shelf-life, errors associated with the determination of drug content are not included (and thus they are often ignored) in the analysis of accelerated stability data. Second, the 95% confidence interval of the predicted room temperature rate constant derived from the confidence band of the best-fitted straight line may be so wide as to make the predicted shelf-life of little value (2). Because of these inherent problems in the classical approach, it seems desirable to develop an alternate approach for the treatment of accelerated stability data so as to provide an improved prediction of drug shelf-life.

This study was initiated to develop and test mathematical relationships among drug content, time, and temperature, which take into account the errors in the drug content data for the prediction of shelf-life of drug products. A one-step nonlinear approach is proposed for the treatment of accelerated stability data. Comparison of this approach with the classical method is reported.

BACKGROUND

The shelf-life or expiration date of a drug product is defined as the time period required for a drug to decompose to a specified fraction of the labeled drug content, usually 90%. This shelf-life may be determined by directly monitoring the drug content in the drug product as a function of time at some ambient storage conditions, *e.g.*, 25°C and certain humidity and light levels. The proper order for the degradation reactions was determined usually by examining the best fit of plots of drug content *versus* time (for a zero-order reaction) or of the logarithm of drug content *versus* time (for a first-order reaction). Linear regression analysis may then be used to estimate the rate constant at the specified storage conditions. The time for the lower 95% confidence limit curve about the fitted straight line to reach 90% of the labeled drug content is assigned as the shelf-life of the pharmaceutical product (3, 4).

Although the shelf-life of the drug product can be accurately determined by the previously described method, it is usually a time-consuming process. To obtain a predicted shelf-life in a shorter period of time, accelerated stability testing is employed. Most frequently, accelerated stability testing is coupled with the use of the Arrhenius equation for the prediction of drug stability (5, 6). This approach involves two steps. First, a correct order of degradation reaction is determined to describe the functional relationship between drug content and time at several elevated temperatures. The equations for zero-, first-, and second-order degradation reactions are respectively:

$$C = C_0 - kt \qquad \text{(Eq. 1)}$$

$$C = C_0 \exp(-kt) \qquad \text{(Eq. 2)}$$

$$\frac{1}{C} - \frac{1}{C_0} = kt \qquad \text{(Eq. 3)}$$

where k is the rate constant. C_0 and C are the drug contents at time zero and time t, respectively. Both reactants are assumed to have the same initial contents for the second-order reaction. The equation for the first-order reaction can also be expressed in a linearized form:

$$\ln C = \ln C_0 - kt \qquad \text{(Eq. 4)}$$

The linear regression method may then be used to obtain the rate constant at each elevated temperature by using Eq. 1, 4, or 3 for each order of reaction.

In the second step, the Arrhenius equation (Eq. 5 or 6) is employed to relate the logarithm of mean k linearly to the reciprocal of the elevated temperature, T.

$$k = A \exp\left(\frac{-E_a}{RT}\right) \qquad \text{(Eq. 5)}$$

$$\ln k = \ln A - \frac{E_a}{RT} \qquad \text{(Eq. 6)}$$

where R is the gas constant.

In employing the Arrhenius approach, several assumptions are implicit:

0022-3549/84/0500-0657$01.00/0
© 1984, American Pharmaceutical Association

(*a*) that the kinetic model is valid, (*b*) that analytical accuracy is not compromised over the time of the stability study, and (*c*) that the Arrhenius equation is valid, *i.e.*, linear extrapolation beyond the observed data is feasible. In practice, after obtaining the estimates of the energy of activation (E_a) and frequency factor (A) through the use of Eq. 6 *via* the least-squares technique, the rate constant at room temperature and, subsequently, the shelf-life can then be predicted. The 95% confidence interval of the predicted room temperature rate constant can be derived from the confidence band of the regressed straight line (2, 7). The linearity of the Arrhenius plot can be checked statistically using the F ratio test (8, 9).

Besides the classical linear approach described, other methods using the Arrhenius relationship were also reported for stability prediction. Lordi and Scott (10) designed stability charts to facilitate the analysis of accelerated stability data. Kirkwood (11) suggested a maximum likelihood nonlinear approach for the prediction of the shelf-life of biological products using all the available drug potency *versus* time data. Nonisothermal kinetic methods (12–18) have also been developed for stability prediction.

Carstensen and Su (7) suggested a nonlinear approach for estimating the parameters of E_a and A in the Arrhenius equation (Eq. 5). The equations were derived by substituting the Arrhenius equation (Eq. 5) into either the equation of a zero-order reaction (Eq. 1) or that of a first-order reaction (Eq. 2). The form of the zero-order equation (Eq. 7) and first-order equation (Eq. 8) were, respectively:

$$C = C_0 - tA \exp\left(\frac{-E_a}{RT}\right) \quad \text{(Eq. 7)}$$

$$C = C_0 \exp\left[-tA \exp\left(\frac{-E_a}{RT}\right)\right] \quad \text{(Eq. 8)}$$

The Gauss-Newton iterative technique was used to obtain the parameter estimates of E_a and A. However, a digital computer was not used and the computational steps associated with the estimation of A and E_a may be too tedious.

Recently, Scher (19) proposed a method of kinetic ratio parameter for product stability calculation. Both Eqs. 7 and 8 were used to derive equations for the calculation of the shelf-life (t_{90}) of the drug. Equations 9 and 10 were employed for the zero-order and first-order reactions, respectively:

$$t_{90} = (C_0 - C) \Big/ \left[A \exp\left(\frac{-E_a}{RT}\right)\right] \quad \text{(Eq. 9)}$$

$$t_{90} = \ln (C_0/C) \Big/ \left[A \exp\left(\frac{-E_a}{RT}\right)\right] \quad \text{(Eq. 10)}$$

Davies et al. (20, 21) suggested the use of the logarithmic forms of Eqs. 8 and 10 to calculate drug shelf-life. The statistical properties of the parameter estimates of E_a and A in the equation for the first-order reaction (Eq. 8) were evaluated through the use of the Monte Carlo method of computer simulations (22). The simulation results showed that estimates of E_a and A were robust, and meaningful statistics of these two parameter estimates could be obtained. The relative standard deviation of the frequency factor (A) was large in comparison with the prescribed standard deviation of normal distribution for generating random errors in the data. After obtaining estimates of A and E_a, the shelf-life (t_{90}) may then be estimated using Eq. 10. The "approximate" standard deviation of the shelf-life (t_{90}) may be calculated by using the standard Taylor expansion (23) expressed as:

$$(SD_{t_{90}})^2 = (t_{90,A} SD_A)^2 + (t_{90,E_a} SD_{E_a})^2 + 2(t_{90,A} t_{90,E_a} \mathrm{COV}_{E_a,A}) \quad \text{(Eq. 11)}$$

where $t_{90,A}$ and t_{90,E_a} are, respectively, the partial derivatives of t_{90} with respect to A and E_a; SD_A and SD_{E_a} are the standard deviations of A and E_a, respectively; and $\mathrm{COV}_{E_a,A}$ is the covariance of E_a and A. No simulation was attempted to evaluate the statistical properties of the predicted shelf-life (t_{90}) as estimated by this nonlinear approach.

In this report, the nonlinear approach was further modified to facilitate a direct prediction of drug stability using observed values of drug content, time, and temperature. Extensive computer simulations were made to evaluate the statistical properties of the parameter estimates of E_a and t_{90}. The applicability and versatility of this nonlinear approach were evaluated as well.

THEORETICAL

The assumptions made in the subsequent mathematical derivations are that (*a*) the energy of activation (E_a) is not a function of temperature and (*b*) normal storage condition at room temperature is set at 25°C. Since a direct prediction of the shelf-life of the drug at 25°C is desired, modification of the Arrhenius equation appears necessary. The degradation rate constant at 25°C (k_{298}) can be obtained from the Arrhenius equation:

$$k_{298} = A \exp\left(-\frac{E_a}{R298}\right) \quad \text{(Eq. 12)}$$

Rearrangement of Eq. 12 yields:

$$A = k_{298} \exp\left(\frac{E_a}{R298}\right) \quad \text{(Eq. 13)}$$

Substituting Eq. 13 for A into the Arrhenius equation (Eq. 5) yields:

$$k = k_{298} \exp\left(\frac{E_a}{R298}\right) \exp\left(-\frac{E_a}{RT}\right) \quad \text{(Eq. 14)}$$

If drug degradation follows a first-order reaction, Eq. 2 can be used to describe the functional relationship between content and time. Substitution of Eq. 14 for k into Eq. 2 and rearrangement yields:

$$C = C_0 \exp\{-k_{298} t \exp[(E_a/R)(1/298 - 1/T)]\} \quad \text{(Eq. 15)}$$

For a first-order reaction, t_{90} can be determined by using the following relationship:

$$t_{90} = 0.1054/k_{298} \quad \text{(Eq. 16)}$$

Substituting Eq. 16 for k_{298} into Eq. 15 yields:

$$C = C_0 \exp\{-t(0.1054/t_{90}) \exp[(E_a/R)(1/298 - 1/T)]\} \quad \text{(Eq. 17)}$$

Equation 17 can be used now to provide direct estimates of t_{90} and E_a *via* nonlinear regression analysis. Time (t) and temperature (T) are the two independent variables. Similarly, equations for either zero- (Eq. 18) or second-order (Eq. 19) degradation can be derived as follows:

$$C = C_0\{1 - t(0.1/t_{90}) \exp[(E_a/R)(1/298 - 1/T)]\} \quad \text{(Eq. 18)}$$

$$C = \frac{C_0}{1 + t(0.11/t_{90}) \exp[(E_a/R)(1/298 - 1/T)]} \quad \text{(Eq. 19)}$$

EXPERIMENTAL

Generation of Data With or Without Error—Data were generated by using Eqs. 17–19 for first-, zero-, and second-order reactions, respectively. Different sets of input theoretical values of E_a and t_{90} were assigned to each case. A single temperature sequence [323 K, 333 K, 343 K, and 353 K (50–80°C)] and a specified time scale for each temperature were employed to generate, at first, errorless drug content data. Drug content data were expressed as percent of content at time zero. Random numbers, which were also expressed as percent, were selected from a normal distribution with a mean of zero and a prescribed standard deviation (24, 25). These selected random numbers (used as noise) were added to the errorless drug content data to obtain simulated experimental "raw data." The normality of the generated error distribution was tested by using the chi-square goodness-of-fit test (26). The mean and standard deviation of the error distribution were also computed to ascertain that the mean was close to zero and that the standard deviation was close to that prescribed.

Calculation of Initial Estimates for Nonlinear Regression Analysis—Since the nonlinear regression method uses the iterative technique, the proper initial estimates of the parameters should be provided to initiate the iteration (27). The initial estimates of E_a and t_{90} were calculated in the following manner: (*a*) the functional relationships between drug content and time (Eqs. 1, 4, and 3) were employed to estimate the rate constants at these temperatures; (*b*) the linearized form of the Arrhenius relationship (Eq. 6) was used to obtain the values of E_a and A; and (*c*) the shelf-lives (t_{90}) can be calculated using Eqs. 20–22 for zero-, first-, and second-order reactions, respectively:

$$t_{90} = (0.1C_0/A) \exp\left(\frac{E_a}{R298}\right) \quad \text{(Eq. 20)}$$

$$t_{90} = (0.1054/A) \exp\left(\frac{E_a}{R298}\right) \quad \text{(Eq. 21)}$$

Table I—Specification of Computer Simulation Using a Random Error Structure

Order of Reaction	Parameter E_a	Parameter t_{90}	n^a	N^b
First	25.00	124.0	32	30
	25.00	260.0	32	30
	10.00	124.0	32	30
	10.00	260.0	32	30
Zero	25.00	124.0	32	30
Second	25.00	124.0	32	30

[a] Number of data points in each set of data. [b] Number of data sets.

Table II—Influence of Data Noise on Final Parameter Estimates of a First-Order Reaction with Standard Deviations of 2.5, 5.0, and 7.5% [a]

	Standard Deviation					
	2.5%		5.0%		7.5%	
	E_a	t_{90}	E_a	t_{90}	E_a	t_{90}
Estimate[b]	25.02 ± 0.28 (1.1%)	124.6 ± 7.6 (6.1%)	25.06 ± 0.57 (2.3%)	126.4 ± 15.5 (12.3%)	25.09 ± 0.88 (3.5%)	128.1 ± 24.8 (19.3%)
Range of Estimate	24.61-25.57	113.0-139.6	24.14-26.19	101.9-159.7	23.70-26.91	91.9-185.8
SD of Estimate	0.29 ± 0.04	7.50 ± 1.12	0.60 ± 0.07	15.6 ± 2.9	0.88 ± 0.11	23.4 ± 5.7
Range of *SD* of Estimate	0.23-0.39	5.57-10.8	0.48-0.76	11.0-20.6	0.70-1.12	14.5-39.5
Bias[c]	0.23 (0.9%) ± 0.16	6.03 (4.9%) ± 4.53	0.44 (1.8%) ± 0.34	12.1 (9.8%) ± 9.8	0.68 (2.7%) ± 0.55	18.7 (15.1%) ± 16.4
Range of Bias	0.020-0.57	0.343-15.6	0.040-1.19	0.689-35.7	0.030-1.9	1.10-61.8

[a] Theoretical values: E_a = 25.00 kcal/mol; t_{90} = 124 weeks. [b] Mean ± *SEM*; *CV* in parentheses. [c] Percent error from the theoretical values in parentheses.

$$t_{90} = \left(\frac{0.11}{C_0 A}\right) \exp\left(\frac{E_a}{R298}\right) \qquad \text{(Eq. 22)}$$

Statistical Methods—The Monte Carlo method of computer simulations (28) was used to evaluate the reliability of the statistics for the estimates of E_a and t_{90}. The NONLIN computer program (29) was employed to obtain values of final estimates of E_a and t_{90} in the nonlinear approach. After obtaining the final estimates of E_a and t_{90} for each set of data, a certain sampling distribution for either E_a or t_{90} was formed. The mean, standard deviation, and bias of the sampling distribution of the parameter estimates were determined. The bias, in absolute values, is defined as the difference between the parameter estimate and the theoretical value. The statistics of the parameter estimates were evaluated by the closeness of the mean of the sampling distribution of each parameter estimate to its theoretical value, and the relative magnitudes of the standard deviation and the bias.

For comparison, the classical linear approach was also used to obtain the predicted shelf-life of the drug. The shelf-life was estimated through steps involving (*a*) the use of the linearized form of drug content-time relationship to obtain the rate constants at elevated temperatures, (*b*) the application of the Arrhenius equation (Eq. 6) to estimate E_a and A, (*c*) the extrapolation from straight line with the best fit in the Arrhenius plot to obtain the room temperature rate constant and its 95% confidence interval, and (*d*) the transformation of the room temperature rate constant and its 95% confidence interval to the corresponding value of shelf-life and its 95% confidence interval. Three computer programs written in FORTRAN IV were employed to generate the simulated experimental data, to calculate the initial estimates for nonlinear regression analysis, and to obtain values of the shelf-life and its 95% confidence interval through the use of the classical linear approach.

RESULTS

Before performing the computer simulations, Eqs. 17–19 were fitted to errorless data. In every case, NONLIN gave final estimates of E_a and t_{90} exactly identical to the input theoretical values. Standard deviations of these two estimates were close to zero. However, they were found to be highly correlated, with a correlation coefficient of 0.97 in all cases. Estimates of E_a and t_{90} obtained from the simulated "raw data" with prescribed errors also had the same high correlation coefficient. The high dependence between parameter estimates might complicate the separate estimation of each parameter (30). Metzler and Tong (31) indicated that this high correlation between parameters may imply meaningless statistics of the final estimates.

To examine this high correlation problem between the computer estimates of E_a and t_{90} and to evaluate the applicability of this "one-step" nonlinear approach, the Monte Carlo method of computer simulations was employed to probe into the statistical properties of these two final estimates. The simulations were divided into four parts which examined (*a*) the influence of data noise on the final estimates of E_a and t_{90}, (*b*) the influence of different theoretical values on the estimates of E_a and t_{90}, (*c*) the influence of various orders of reaction on the final estimates of E_a and t_{90}, and (*d*) the influence of the "extensiveness" of stability data on the estimates of E_a and t_{90}. It was reasoned that if estimates of these two parameters with meaningful statistical properties could be obtained under a wide range of conditions and different distributions of random errors in the data set, this high correlation between them may be assumed to be attributed to the nature of the mathematical function employed for estimating these parameters.

The simulated experimental "raw data" employed for examining the influence of data noise, different theoretical values, and various orders of reaction on these two final parameter estimates were generated using a single temperature sequence of 50–80°C and a variable time scale for each temperature. The time scales were selected to achieve ≥60% degradation of drug content at the lowest temperature and ≥80% degradation of content for three higher temperatures. The specifications of the computer simulations is shown in Table I. A wide range of stability and energetics values were chosen to test this nonlinear mathematical relationship. Thirty sets of data with 32 data points per set were generated for each case.

Table III—Influence of Initial Estimates on Final Parameter Estimates of a First-Order Reaction [a]

	Initial Estimate		Final Estimate	
SD	E_a	t_{90}	E_a	t_{90}
2.5%	17.50	219.0	25.17 ± 0.27	127.4 ± 7.0
	27.11	185.1	25.17 ± 0.27	127.5 ± 7.0
	32.50	40.00	25.17 ± 0.27	127.5 ± 7.0
5.0%	32.50	40.00	24.85 ± 0.60	120.5 ± 14.9
	24.19	108.6	24.85 ± 0.60	120.5 ± 14.9
	17.50	210.0	24.85 ± 0.60	120.5 ± 14.9
7.5%	17.50	210.0	25.07 ± 0.77	125.5 ± 19.9
	24.75	118.1	25.07 ± 0.77	125.6 ± 19.9
	32.50	40.00	25.07 ± 0.77	125.6 ± 19.9

[a] Theoretical values: E_a = 25.00 kcal/mol; t_{90} = 124 week.

The results for simulations which examined the influence of data noise on final estimates of E_a and t_{90} are shown in Tables II–IV. At all three noise levels, mean estimates for E_a and t_{90}, obtained as the average from 30 individual estimates given by NONLIN, were very close (within 3.3%) to the assigned theoretical values. The standard deviations of the estimates given by NONLIN, on the average, were found to be acceptable estimates of the standard errors of mean estimates for both E_a and t_{90} in all cases. Both standard errors of mean estimates and average biases of the estimates were small and responded well to the change of the noise level in the constructed data. Estimates of E_a and t_{90} also did not vary excessively among these 30 sets of data.

The effect of initial estimates on the computed estimates of E_a and t_{90} was also tested for each set of data. The data, shown in Table III, represented simulation trials from one representative run for each noise level. One of these three sets of initial estimates was calculated using the linear approach, as described in the experimental section. The other two sets of initial estimates were arbitrarily chosen to provide different starting points to initiate the iteration step. The results clearly indicated that the locations of the initial estimates had no apparent effect on final estimates of E_a and t_{90}.

The examination of the residuals in the regression analysis revealed that the standard deviations of residuals obtained were also consistent with the prescribed standard deviations (Table IV). The r^2 values, which can be used as measures of good fit (27), were close to 1.0 in all cases. The randomness of the residuals in a representative set of data is shown in Fig. 1. The composite results showed, therefore, that estimates of E_a and t_{90} with meaningful statistics can be obtained with Eq. 17 using simulated data with different levels of data noise.

Results for studies which examined the influence of different theoretical values and of various orders of reaction on the parameter estimates of E_a and t_{90} are shown in Tables V and VI, respectively. The statistics of the parameter estimates for E_a and t_{90} were shown to be satisfactory for these conditions.

The influence of the "extensiveness" of stability data on the final parameter estimates of E_a and t_{90} was also tested. Specification of different types of data

Table IV—Goodness of Fit of Data from a First-Order Reaction with Standard Deviations of 2.5, 5.0, and 7.5% [a]

	Standard Deviation		
	2.5%	5.0%	7.5%
SD of Residuals	2.4 ± 0.3	5.0 ± 0.6	7.4 ± 1.0
r^2	0.989 ± 0.0003	0.954 ± 0.013	0.900 ± 0.031

[a] Theoretical values: E_a = 25.00 kcal/mol; t_{90} = 124 weeks.

Table V—Influence of Different Theoretical Values on Final Parameter Estimates of a First-Order Reaction using Data with a Standard Deviation of 5.0% [a]

	Set 1		Set 2		Set 3	
	E_a	t_{90}	E_a	t_{90}	E_a	t_{90}
Estimate[b]	24.99 ± 0.57 (2.3%)	259.9 ± 32.8 (12.6%)	9.99 ± 0.59 (5.9%)	124.0 ± 16.2 (13.1%)	9.99 ± 0.60 (6.1%)	260.0 ± 34.7 (13.4%)
Range of Estimate	24.09-26.30	215.7-343.4	8.98-11.38	101.8-166.0	8.96-11.42	212.5-351.1
SD of Estimate	0.61 ± 0.09	32.9 ± 6.6	0.61 ± 0.09	15.8 ± 3.2	0.62 ± 0.09	33.8 ± 7.0
Range of *SD* of Estimate	0.49-0.78	22.6-51.7	0.46-0.79	10.8-25.0	0.47-0.80	22.9-53.4
Bias	0.44 (1.8%) ± 0.35	25.0 (9.6%) ± 20.5	0.46 (4.6%) ± 0.37	12.5 (10.1%) ± 10.1	0.47 (4.7%) ± 0.38	26.7 (10.3%) ± 21.7
Range of Bias	0.010-1.3	0.291-83.4	0.020-1.4	0.340±42.0	0.030-1.4	1.20-91.1

[a] Theoretical values: (set 1) E_a = 25.00 kcal/mol, t_{90} = 260 weeks; (set 2) E_a = 10.00 kcal/mol, t_{90} = 124 weeks; (set 3) E_a = 10.00 kcal/mol, t_{90} = 260 weeks. [b] Mean ± *SEM; CV* in parentheses. [c] Percent error from the theoretical value in parentheses.

Table VI—Influence of Different Orders of Reaction on Final Parameter Estimates using Data with a Standard Deviation of 5.0% [a]

	Zero Order		Second Order	
	E_a	t_{90}	E_a	t_{90}
Estimate[b]	25.00 ± 0.16 (0.6%)	124.0 ± 10.8 (8.7%)	24.96 ± 0.77 (3.1%)	124.0 ± 21.1 (17.0%)
Range of Estimate	24.15-26.06	105.8-153.7	23.72-26.75	94.6-177.2
SD of Estimate	0.40 ± 0.06	10.2 ± 1.9	0.86 ± 0.13	21.3 ± 4.9
Range of *SD* of Estimate	0.30-0.53	7.06-13.0	0.69-1.1	14.7-37.3
Bias[c]	0.32 (1.3%) ± 0.26	8.22 (6.6%) ± 6.77	0.62 (2.5%) ± 0.45	16.5 (13.3%) ± 12.8
Range of Bias	0.0010-1.1	0.785-29.7	0.0020-1.8	0.138-53.2

[a] Theoretical values: E_a = 25.00 kcal/mol; t_{90} = 124 weeks. [b] Mean ± *SEM; CV* in parentheses. [c] Percent error from the theoretical value in parentheses.

Table VII—Specification of Different Types of Data Structure

Structure	Temp. K	Time Scale, week Sampling Time	Last Sample	Percent Remaining of Drug Content[a]
Type I	323	10.0	80.0	16.8
	333	3.0	24.0	17.8
	343	1.0	8.0	17.7
	353	0.4	3.2	14.1
Type II	323	2.0	16.0	70.0
	333	0.7	5.6	66.9
	343	0.2	1.6	70.7
	353	0.07	0.56	71.0
Type III	323	0.4	3.2	93.1
	333	0.4	3.2	79.5
	343	0.4	3.2	50.1
	353	0.4	3.2	14.1

[a] At the last sampling time, using errorless data for estimation.

structure is shown in Table VII. The same temperature sequence (50-80°C) was used for all three types of data structure. "Raw data" with type I structure, representing an example of extensive data gathering, were generated employing a variable time scale to achieve ≥80% degradation in drug content at each temperature. Simulated "raw data" with type II structure were generated using a variable time scale for each temperature as well. However, these time scales were set to account for degradation of the drug content to only ~30% completion. Data with type III data structure were generated by employing a fixed sampling time and frequency for all four temperatures studied. Thus, data structures shown as type II and III represented situations in which only limited kinetic data were available, as often the case in real accelerated stability trials. Simulations using these types of data structures are shown in Table VIII. Despite considerable differences in the degree of "extensiveness" in the data base, it was shown that good estimates of E_a and t_{90} with satisfactory statistical properties could be obtained for each type of data structure.

Sometimes the initial drug content, C_0, is not known and should be estimated together with the estimation of E_a and t_{90}. Simulations for estimating these three parameters are shown in Table IX. The nonlinear approach is shown to be capable of providing good mean estimates and meaningful statistics for C_0, E_a, and t_{90}. Based on kinetic principles, Eqs. 17-19 can be easily modified to determine the shelf-life at any chosen content, *i.e.*, either as percent of initial or of labeled strength.

Comparison between the classical linear approach and the nonlinear approach for the prediction of drug stability was made by using a first-order degradation reaction as an example. The "raw data" generated for the study that examined the influence of data noise on the final estimates of E_a and t_{90} were employed for this comparison between the two methods. The shelf-lives (t_{90}) and their 95% confidence intervals as estimated by using either the classical linear approach or the present nonlinear approach for three representative sets of data (each at three noise levels) are shown in Fig. 2. The nonlinear approach appeared to provide better mean estimates of drug shelf-life with much smaller and more symmetrical 95% confidence intervals than did the classical approach in all cases examined.

It is desirable to compare the nonlinear approach with the classical linear approach using real stability data. Accelerated stability data of vitamin A in multivitamin tablets (2) and of NAD (32) were employed for this purpose; results of this comparison are shown in Table X. The linear and nonlinear methods provided identical mean estimates of shelf-life in both cases. Moreover, the nonlinear method also provided a more symmetrical and smaller 95% confidence interval in the prediction of vitamin A stability than did the classical linear approach. However, both linear and nonlinear methods predicted somewhat longer shelf-lives of these two compounds than that experimentally determined at room temperature. It is possible that both systems possess some degree of non-Arrhenius behavior, a problem that neither the linear nor the nonlinear approach can correct.

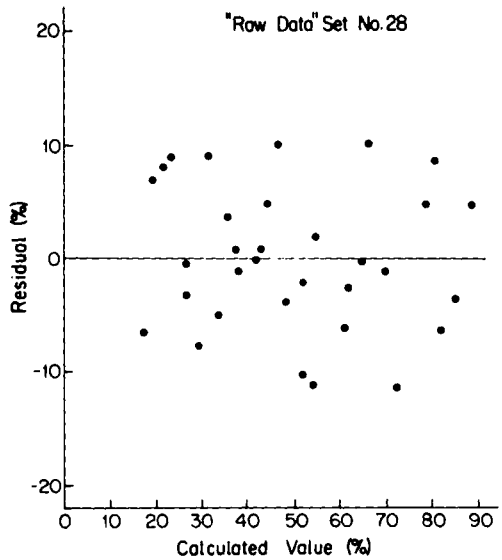

Figure 1—*Representative plot of residuals. Calculated values are expressed as percent of drug content at time zero. Residual is the difference between the observed value and calculated value of drug content for each data point.*

Table VIII—Influence of Different Types of Data Structure on Final Parameter Estimates of a First-Order Reaction using Data with a Standard Deviation of 2.5% [a]

	Data Structure					
	Type I		Type II		Type III	
	E_a	t_{90}	E_a	t_{90}	E_a	t_{90}
Estimate[b]	25.12 ± 0.32[c] (1.3%)	127.7 ± 8.6 (6.7%)	25.19 ± 0.73 (2.9%)	130.5 ± 18.6 (14.2%)	25.23 ± 0.84 (3.3%)	133.4 ± 26.7 (20.0%)
Range of Estimate	24.61-25.59	115.1-136.9	24.53-26.31	101.6-161.5	24.15-26.77	100.3-187.0
SD of Estimate	0.26 ± 0.03	6.90 ± 0.90	0.50 ± 0.05	13.2 ± 2.7	0.68 ± 0.07	22.1 ± 6.0
Range of *SD* of Estimate	0.23-0.30	5.55-8.22	0.43-0.59	8.96-17.8	0.56-0.80	14.0-34.0
Bias[d]	0.29 (1.1%) ± 0.17	7.76 (6.3%) ± 4.63	0.61 (2.4%) ± 0.41	15.5 (12.5%) ± 11.1	0.67 (2.7%) ± 0.51	21.2 (17.1%) ± 17.6
Range of Bias	0.10-0.48	0.490-16.2	0.029-1.3	0.0900-37.5	0.068-1.7	2.60-63.0

[a] Theoretical values: E_a = 25.00 kcal/mol; t_{90} = 124 weeks. [b] Mean ± *SEM*; *CV* in parentheses. [c] N = 10. [d] Percent error from the theoretical value in parentheses.

Table IX—Values of Parameter Estimates for a First-Order Reaction, Including the Initial Drug Content, C_0, as a Parameter, using Data with a Standard Deviation of 2.5% [a]

	Parameter		
	E_a	t_{90}	C_0
Estimate[b]	24.97 ± 0.22 (0.9%)	122.3 ± 6.0 (4.9%)	100.2 ± 1.9 (1.9%)
Range of estimate	24.76-25.45	113.3-131.1	97.19-102.6
SD of estimate	0.33 ± 0.05	9.34 ± 1.51	1.66 ± 0.25
Range of *SD* of Estimate	0.26-0.41	7.94-11.8	1.30±1.99
Bias[c]	0.17 (0.7%) ± 0.13	5.26 (4.2%) ± 2.85	1.55 (1.6%) ± 0.89
Range of Bias	0.030-0.450	0.740-10.7	0.270-2.81

[a] Theoretical values: E_a = 25.00 kcal/mol; t_{90} = 124 weeks; C_0 = 100%. [b] Mean ± *SEM*; *CV* in parentheses. [c] Percent error from the theoretical value in parentheses.

DISCUSSION

The nonlinear approach shown in this report appears to be capable of predicting the shelf-life (t_{90}) directly and reproducibly. The uncertainties in the estimated t_{90} are the reflection of the errors inherent in the observed drug content data. The nonlinear approach can be applied to various orders of degradation reaction and a wide range of different theoretical values of E_a and t_{90}. It was shown that although some experimental "raw data" may not be very extensive, good estimation of shelf-life with meaningful statistical properties can still be obtained. Furthermore, this approach provides better mean estimates of t_{90} with much smaller 95% confidence intervals than the classical approach. Obviously, this method of drug stability prediction will be of little value without the aid of appropriate computer programs to carry out the nonlinear parameter estimation procedure. Fortunately, several computer programs including NONLIN (29), BMDP-P3R (33), SAAM (34), *etc.* are available for nonlinear regression analysis. The 1974 version of the NONLIN program was selected in this study because this particular computer program, which can be used to fit various models (27), is a widely used program in the area of pharmacokinetics and related pharmaceutical sciences.

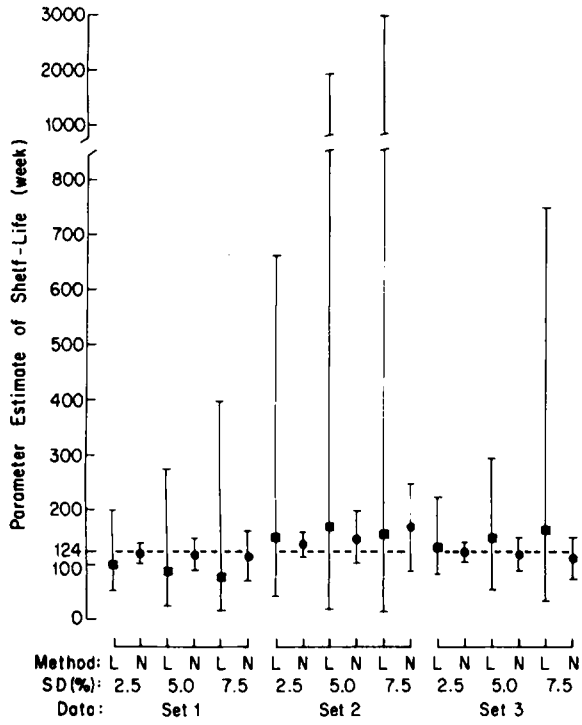

Figure 2—*Plot of the parameter estimate of the shelf-life (t_{90}) for each of the two methods of estimation in three sets of data with three different levels of noise. Data represent mean estimate and its 95% confidence interval after using the nonlinear approach (N, ●) and the classical linear approach (L, ■); (- - - -) represents the theoretical value of shelf-life of 124 weeks.*

A high correlation between E_a and t_{90} was found during the study of computer simulations. This high dependency between the parameter estimates was suggested by Metzler and Tong as a possible indication of meaningless statistics of these estimates (31). The Monte Carlo method of computer simulations was used to examine this high correlation problem and to evaluate the statistical properties of the final estimates of E_a and t_{90} in this report. During the regression analysis for each set of data by NONLIN, the final parameter estimates of E_a and t_{90} converged on the mathematical minimum after only 3-5 iteration steps without any computational difficulty.

The statistics of the parameter estimates can be evaluated by examining the sampling distributions of both E_a and t_{90}. The sampling distributions of both E_a and t_{90} were symmetrical about the mean estimates and had small standard deviations and biases. A large standard deviation is usually reflective of a poor determination of a parameter estimate (35, 36). Examination of the residuals (36) and of the correlation of the observations (r^2 value) can also be used to evaluate the statistics of the parameter estimates in a model. Our results indicated that (*a*) the standard deviations of the residuals were consistent with the prescribed standard deviations and (*b*) the plots of the residuals *versus* the calculated values for each set of data showed the random nature of the residuals. The r^2 values found were close to perfection (*i.e.*, 1.0) in all the data sets examined. Furthermore, it has been stated (37) that if the nonlinear regression method is correct, different sets of initial estimates for each set of data should converge on the same final estimates. Our simulation trials (Table III) showed this to be the case here. Therefore, it appears that good mean estimates of E_a and t_{90} with meaningful statistical properties are obtained using the nonlinear method, even though these two parameters are highly correlated.

Our observation of a correlation between the final estimates of E_a and t_{90} is not unique. Metzler and Tong (31) showed the high correlation between V_{max} and K_m in the parameter estimations of the Michaelis-Menten equation to be accompanied by meaningless statistics. They attributed this result to the peculiar nature of the mathematical function that relates these two variables, in that a change in the estimate of V_{max} may be compensated by a simultaneous change in K_m. However, Bard (22) had shown that meaningful statistical properties of the parameter estimates of A and E_a (Eq. 8) could be obtained despite the high correlation (*i.e.*, r = 0.98) between them. Thus,

Table X—Comparison Between the Classical Linear Approach and Nonlinear Method for the Prediction of Drug Stability using Literature Data

Literature Study	Shelf-Life, week			
	Linear Method		Nonlinear Method	
	Mean	95% CI[a]	Mean	95% CI[a]
I[b]	113.3[d]	49.25-262.2[d]	109.0	61.73-156.2
II[c]	6.49	5.67-7.44	6.63	5.54-7.71

[a] Confidence interval. [b] Prediction of vitamin A stability in multivitamin tablets. The accelerated stability data were obtained from Fig. 1 in the Ref. 2. [c] Prediction of the stability of NAD, taken from Ref. 32. [d] These values were calculated by using the reported rate constants.

it seems that the presence of a high correlation between parameter estimates may not necessarily indicate that the statistical properties of these final estimates are meaningless.

In conclusion, meaningful statistics of the final parameter estimates of E_a and t_{90} can be obtained by the nonlinear approach described in this paper. This approach is applicable over a wide range of different theoretical values of E_a and t_{90}, different orders of reaction, different levels of noise in data, and different types of data structure. The advantage of this nonlinear approach is that it uses data of drug content, time, and temperature to provide a direct estimation of shelf-life with relevant statistics. This method may be potentially useful for the realistic prediction of drug stability of pharmaceutical products.

REFERENCES

(1) N. R. Draper and H. Smith, "Applied Regression Analysis," Wiley, New York, N.Y., 1966, chap. 1.

(2) J. G. Slater, H. A. Stone, B. T. Palermo, and R. N. Duvall, *J. Pharm. Sci.*, **68**, 49 (1979).

(3) J. T. Carstensen and E. Nelson, *J. Pharm. Sci.*, **65**, 311 (1976).

(4) W.-H. Yang, *Drug Dev. Ind. Pharm.*, **7**, 63 (1981).

(5) E. R. Garrett, *J. Pharm. Sci.*, **51**, 811 (1962).

(6) S.-L. Lin, *Bull. Parent. Drug Assoc.*, **23**, 269 (1969).

(7) J. T. Cartensen and K. S. E. Su, *Bull. Parent. Drug Assoc.*, **25**, 287 (1971).

(8) C. J. Clark and H. F. Hudson, *Manuf. Chem. Aeros. News*, **39**, 25 (1968).

(9) D. J. Bentley, *J. Pharm. Sci.*, **59**, 464 (1970).

(10) N. G. Lordi and M. W. Scott, *J. Pharm. Sci.*, **54**, 531 (1965).

(11) T. B. L. Kirkwood, *Biometrics*, **33**, 736 (1977).

(12) S. P. Eriksen and H. Stelmach, *J. Pharm. Sci.*, **54**, 1029 (1965).

(13) M. A. Zoglio, J. J. Windheuser, R. Vatti, H. V. Maulding, S. S. Kornblum, A. Jacobs, and H. Hamot, *J. Pharm. Sci.*, **57**, 2080 (1968).

(14) H. V. Maulding and M. A. Zoglio, *J. Pharm. Sci.*, **59**, 333 (1970).

(15) M. A. Zoglio, H. V. Maulding, W. H. Streng, and W. C. Vincek, *J. Pharm. Sci.*, **64**, 1381 (1975).

(16) B. Edel and M. O. Baltzer, *J. Pharm. Sci.*, **69**, 287 (1980).

(17) J.-O. Waltersson and P. Lundgren, *Acta Pharm. Suec.*, **19**, 127 (1982).

(18) W.-H. Yang, *Drug Dev. Ind. Pharm.*, **8**, 189 (1982).

(19) M. Scher, *J. Pharm. Sci.*, **69**, 325 (1980).

(20) O. L. Davies and D. A. Budgett, *J. Pharm. Pharmacol.*, **32**, 155 (1980).

(21) O. L. Davies and H. E. Hudson, in "Statistics in the Pharmaceutical Industry," C. R. Buncher and J.-Y. Tsay, Eds., Dekker, New York, N.Y., 1981, chap. 15.

(22) Y. Bard, "Nonlinear Parameter Estimation," Academic, New York, N.Y., 1974, pp. 206–212.

(23) H. G. Boxenbaum, S. Riegelman, and R. M. Elashoff, *J. Pharmacokinet. Biopharm.*, **2**, 123 (1974).

(24) D. H. Lehmer, *Ann. Comp. Lab. Harvard Univ.*, **26**, 141 (1951).

(25) P. A. W. Lewis, A. S. Goodman, and J. M. Miller, *IBM Systems J.*, **8**, 136 (1969).

(26) G. W. Snedecor and W. G. Cochran, "Statistical Methods," 6th ed., The Iowa State University Press, Ames, Iowa, 1967, pp. 84–85.

(27) C. M. Metzler, *Pharmacol. Ther.*, **13**, 543 (1981).

(28) Y. Bard, "Nonlinear Parameter Estimation," Academic, New York, N.Y., 1974, chap. 3.

(29) C. M. Metzler, G. L. Elfring, and A. J. McEwen, "A Users Manual for NONLIN and Associated Programs," The Upjohn Co., Kalamazoo, Mich., 1974.

(30) G. P. Box and W. G. Hunter, *Technometrics*, **4**, 301 (1962).

(31) C. M. Metzler and D. D. M. Tong, *J. Pharm. Sci.*, **70**, 733 (1981).

(32) B. M. Colombo, P. Causa, P. Primavera, and V. Villano, *Il Farmaco, Ed. Pr.*, **27**, 327 (1972).

(33) J. Garcia-Pena and S. P. Azen, *Comput. Prog. Biomed.*, **10**, 185 (1979).

(34) M. Berman and M. F. Weiss, "Users Manual for SAAM," National Institutes of Health, Bethesda, Md., 1974.

(35) H. P. Wijnand and C. J. Timmer, *J. Pharmacokinet. Biopharm.*, **7**, 681 (1979).

(36) Y. Bard, "Nonlinear Parameter Estimation," Academic, New York, N.Y., 1974, chap. 7.

(37) K. T. Muir, *Comput. Biomed. Res.*, **13**, 307 (1980).

ACKNOWLEDGMENTS

Supported in part by NIH Grants GM 20852 and HL 22273.

Behavior of ATP Toward Phenothiazine Drugs

M. R. GASCO ˣ, M. E. CARLOTTI, and M. TROTTA

Received January 4, 1982, from the *Istituto di Chimica Farmaceutica e Tossicologica, Università di Torino, Corso Raffaello 31, 10125 Torino, Italy.* Accepted for publication February 21, 1983.

Abstract □ The tricyclic amines promazine, promethazine, chlorpromazine, triflupromazine, and trifluperazine form solid ion pairs with ATP in a 1:2 molar ratio. There is a good correlation between the measured K_{sp} and the apparent diffusion constants of the ion pairs with the critical micelle concentration (CMC) of the corresponding phenothiazines. Solid ion pairs are solubilized by phenothiazine micelles; the binding constants of ATP to drug micelles are calculated from solubility data at 25°C and can be related to the CMC of the phenothiazines.

Keyphrases □ ATP—behavior toward phenothiazine drugs, binding, micellar solubilization □ Binding—behavior of ATP toward phenothiazine drugs, micellar solubilization □ Phenothiazine drugs—behavior of ATP, binding, micellar solubilization □ Micellar solubilization—behavior of ATP toward phenothiazine drugs, binding

The mechanism of action of phenothiazine drugs is difficult to explain because of their great variety of biochemical and physiological effects. Membrane interactions seem to be important particularly in the case of chlorpromazine (1–4). Phenothiazines, like many tricyclic amines, have amphiphatic properties and are surface-active drugs (4–7). Their micelles are able to solubilize *in vitro* various high molecular weight drugs such as pteridine and porphyrin derivatives (8, 9); the binding constants of solubilized compounds with micelles are rather high. Previously, Blei (10) studied the decrease of chlorpromazine surface tension in the presence of ATP, while Moriguchi *et al.* (11) observed the formation of a 1:1 complex between the neuroleptic agent and ATP.

The aim of the present work is to investigate the behavior of five phenothiazines with different pharmacological activity

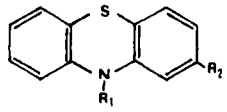

Promethazine	$R_1 = CH_2CH(CH_3)N(CH_3)_2$	$R_2 = H$
Promazine	$R_1 = CH_2CH_2CH_2N(CH_3)_2$	$R_2 = H$
Chlorpromazine	$R_1 = CH_2CH_2CH_2N(CH_3)_2$	$R_2 = Cl$
Triflupromazine	$R_1 = CH_2CH_2CH_2N(CH_3)_2$	$R_2 = CF_3$
Trifluperazine	$R_1 = CH_2CH_2CH_2$—N N—CH_3	$R_2 = CF_3$

0022-3549/84/0500-0662$01.00/0

© 1984, American Pharmaceutical Association

it seems that the presence of a high correlation between parameter estimates may not necessarily indicate that the statistical properties of these final estimates are meaningless.

In conclusion, meaningful statistics of the final parameter estimates of E_a and t_{90} can be obtained by the nonlinear approach described in this paper. This approach is applicable over a wide range of different theoretical values of E_a and t_{90}, different orders of reaction, different levels of noise in data, and different types of data structure. The advantage of this nonlinear approach is that it uses data of drug content, time, and temperature to provide a direct estimation of shelf-life with relevant statistics. This method may be potentially useful for the realistic prediction of drug stability of pharmaceutical products.

REFERENCES

(1) N. R. Draper and H. Smith, "Applied Regression Analysis," Wiley, New York, N.Y., 1966, chap. 1.

(2) J. G. Slater, H. A. Stone, B. T. Palermo, and R. N. Duvall, *J. Pharm. Sci.*, **68**, 49 (1979).

(3) J. T. Carstensen and E. Nelson, *J. Pharm. Sci.*, **65**, 311 (1976).

(4) W.-H. Yang, *Drug Dev. Ind. Pharm.*, **7**, 63 (1981).

(5) E. R. Garrett, *J. Pharm. Sci.*, **51**, 811 (1962).

(6) S.-L. Lin, *Bull. Parent. Drug Assoc.*, **23**, 269 (1969).

(7) J. T. Cartensen and K. S. E. Su, *Bull. Parent. Drug Assoc.*, **25**, 287 (1971).

(8) C. J. Clark and H. F. Hudson, *Manuf. Chem. Aeros. News*, **39**, 25 (1968).

(9) D. J. Bentley, *J. Pharm. Sci.*, **59**, 464 (1970).

(10) N. G. Lordi and M. W. Scott, *J. Pharm. Sci.*, **54**, 531 (1965).

(11) T. B. L. Kirkwood, *Biometrics*, **33**, 736 (1977).

(12) S. P. Eriksen and H. Stelmach, *J. Pharm. Sci.*, **54**, 1029 (1965).

(13) M. A. Zoglio, J. J. Windheuser, R. Vatti, H. V. Maulding, S. S. Kornblum, A. Jacobs, and H. Hamot, *J. Pharm. Sci.*, **57**, 2080 (1968).

(14) H. V. Maulding and M. A. Zoglio, *J. Pharm. Sci.*, **59**, 333 (1970).

(15) M. A. Zoglio, H. V. Maulding, W. H. Streng, and W. C. Vincek, *J. Pharm. Sci.*, **64**, 1381 (1975).

(16) B. Edel and M. O. Baltzer, *J. Pharm. Sci.*, **69**, 287 (1980).

(17) J.-O. Waltersson and P. Lundgren, *Acta Pharm. Suec.*, **19**, 127 (1982).

(18) W.-H. Yang, *Drug Dev. Ind. Pharm.*, **8**, 189 (1982).

(19) M. Scher, *J. Pharm. Sci.*, **69**, 325 (1980).

(20) O. L. Davies and D. A. Budgett, *J. Pharm. Pharmacol.*, **32**, 155 (1980).

(21) O. L. Davies and H. E. Hudson, in "Statistics in the Pharmaceutical Industry," C. R. Buncher and J.-Y. Tsay, Eds., Dekker, New York, N.Y., 1981, chap. 15.

(22) Y. Bard, "Nonlinear Parameter Estimation," Academic, New York, N.Y., 1974, pp. 206–212.

(23) H. G. Boxenbaum, S. Riegelman, and R. M. Elashoff, *J. Pharmacokinet. Biopharm.*, **2**, 123 (1974).

(24) D. H. Lehmer, *Ann. Comp. Lab. Harvard Univ.*, **26**, 141 (1951).

(25) P. A. W. Lewis, A. S. Goodman, and J. M. Miller, *IBM Systems J.*, **8**, 136 (1969).

(26) G. W. Snedecor and W. G. Cochran, "Statistical Methods," 6th ed., The Iowa State University Press, Ames, Iowa, 1967, pp. 84–85.

(27) C. M. Metzler, *Pharmacol. Ther.*, **13**, 543 (1981).

(28) Y. Bard, "Nonlinear Parameter Estimation," Academic, New York, N.Y., 1974, chap. 3.

(29) C. M. Metzler, G. L. Elfring, and A. J. McEwen, "A Users Manual for NONLIN and Associated Programs," The Upjohn Co., Kalamazoo, Mich., 1974.

(30) G. P. Box and W. G. Hunter, *Technometrics*, **4**, 301 (1962).

(31) C. M. Metzler and D. D. M. Tong, *J. Pharm. Sci.*, **70**, 733 (1981).

(32) B. M. Colombo, P. Causa, P. Primavera, and V. Villano, *Il Farmaco, Ed. Pr.*, **27**, 327 (1972).

(33) J. Garcia-Pena and S. P. Azen, *Comput. Prog. Biomed.*, **10**, 185 (1979).

(34) M. Berman and M. F. Weiss, "Users Manual for SAAM," National Institutes of Health, Bethesda, Md., 1974.

(35) H. P. Wijnand and C. J. Timmer, *J. Pharmacokinet. Biopharm.*, **7**, 681 (1979).

(36) Y. Bard, "Nonlinear Parameter Estimation," Academic, New York, N.Y., 1974, chap. 7.

(37) K. T. Muir, *Comput. Biomed. Res.*, **13**, 307 (1980).

ACKNOWLEDGMENTS

Supported in part by NIH Grants GM 20852 and HL 22273.

Behavior of ATP Toward Phenothiazine Drugs

M. R. GASCO ˣ, M. E. CARLOTTI, and M. TROTTA

Received January 4, 1982, from the *Istituto di Chimica Farmaceutica e Tossicologica, Università di Torino, Corso Raffaello 31, 10125 Torino, Italy.* Accepted for publication February 21, 1983.

Abstract □ The tricyclic amines promazine, promethazine, chlorpromazine, triflupromazine, and trifluperazine form solid ion pairs with ATP in a 1:2 molar ratio. There is a good correlation between the measured K_{sp} and the apparent diffusion constants of the ion pairs with the critical micelle concentration (CMC) of the corresponding phenothiazines. Solid ion pairs are solubilized by phenothiazine micelles; the binding constants of ATP to drug micelles are calculated from solubility data at 25°C and can be related to the CMC of the phenothiazines.

Keyphrases □ ATP—behavior toward phenothiazine drugs, binding, micellar solubilization □ Binding—behavior of ATP toward phenothiazine drugs, micellar solubilization □ Phenothiazine drugs—behavior of ATP, binding, micellar solubilization □ Micellar solubilization—behavior of ATP toward phenothiazine drugs, binding

The mechanism of action of phenothiazine drugs is difficult to explain because of their great variety of biochemical and physiological effects. Membrane interactions seem to be important particularly in the case of chlorpromazine (1–4). Phenothiazines, like many tricyclic amines, have amphiphatic properties and are surface-active drugs (4–7). Their micelles are able to solubilize *in vitro* various high molecular weight drugs such as pteridine and porphyrin derivatives (8, 9); the binding constants of solubilized compounds with micelles are rather high. Previously, Blei (10) studied the decrease of chlorpromazine surface tension in the presence of ATP, while Moriguchi *et al.* (11) observed the formation of a 1:1 complex between the neuroleptic agent and ATP.

The aim of the present work is to investigate the behavior of five phenothiazines with different pharmacological activity

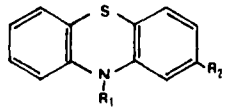

Promethazine	$R_1 = CH_2CH(CH_3)N(CH_3)_2$	$R_2 = H$
Promazine	$R_1 = CH_2CH_2CH_2N(CH_3)_2$	$R_2 = H$
Chlorpromazine	$R_1 = CH_2CH_2CH_2N(CH_3)_2$	$R_2 = Cl$
Triflupromazine	$R_1 = CH_2CH_2CH_2N(CH_3)_2$	$R_2 = CF_3$
Trifluperazine	$R_1 = CH_2CH_2CH_2$—N N—CH_3	$R_2 = CF_3$

0022-3549/84/0500-0662$01.00/0

© 1984, American Pharmaceutical Association

toward ATP, paying attention particularly to variations in the lipophilicity of ATP in the presence of the drugs and to its possible solubilization by phenothiazine micelles.

EXPERIMENTAL

Materials—Promethazine hydrochloride[1], promazine hydrochloride[1], chlorpromazine hydrochloride[1], trifluperazine hydrochloride[1], and triflupromazine hydrochloride[1], ATP[2], non-reinforced dimethylpolysiloxane[3] sheeting in a labeled thickness of 5 mil [12.5×10^{-3} cm, thoroughly rinsed and treated as previously described (12)]; 0.25-μm filter disks[4], Sephadex G-25 medium[5], and glass microfiber papers[6] were commercial samples. A pH meter[7], a spectrophotometer[8], a plate tensiometer[9], a conductimeter[10], and an automatic fraction collector[11] were also used.

Preparation of Solid Complexes—The solid complexes were obtained in aqueous media by mixing 50 mL of ATP (8.0×10^{-3} M) with 50 mL of tricyclic amine ($16.0\text{-}32 \times 10^{-3}$ M). The suspensions were pH 3.5-4.0. All the phenothiazines formed a precipitate, which was separated and analyzed. The same molar ratios of ATP-phenothiazine were employed throughout. The pH was fixed at 5.5 and 6.0 by adding 0.1 M NaOH and 0.1 M 2-morpholineethansulfonate buffer, respectively. This buffer was selected because permeability measurements have shown (12) that it does not form ion pairs with phenothiazines.

Solutions at fixed concentrations of ATP (4.0×10^{-3} M) and chlorpromazine (8.0×10^{-3} M) and increasing concentrations of calcium chloride (2.0×10^{-3}, 4.0×10^{-3}, and 8.0×10^{-3} M) were prepared. No solid complex was obtained from the solution with 8.0×10^{-3} M calcium chloride.

Analysis of Solid Complexes—Solid ion pairs (8-15 mg) were treated with 10 mL of 2 M HCl, and the solution was heated for 15 min in a water bath to promote ATP hydrolysis, then diluted to 25 mL with 2 M HCl. ATP was determined by the malachite green method (13) to evaluate the phosphate obtained by hydrolysis.

The concentration of phenothiazine was determined spectrophotometrically at 310 nm (chlorpromazine, log ϵ = 3.62; promazine, log ϵ = 3.56; promethazine, log ϵ = 3.56; triflupromazine, log ϵ = 3.43; and trifluperazine, log ϵ = 3.60). ATP does not interfere at this wavelength.

The analysis data are reported in Table I. Each molar ratio is the average of three determinations. All the phenothiazines studied form a 1:2 solid complex with ATP. A 1:2 molar ratio was also obtained for the solid ATP-chlorpromazine complex formed at different molar ratios of reactants and in the presence of calcium chloride. In Table II the yields of the solid complex obtained in different media are listed.

Determination of Solubility Products—*Spectrophotometry at 25°C*—Glass-stoppered cylinders containing an excess of solid complex in 6 mL of water were shaken in a water bath kept at 25 ± 0.5°C for 24 h. The samples were then filtered through 0.25-μm filter disks. The ATP and phenothiazine concentrations were determined by the malachite green method and absorbance measurements, respectively, on the filtrate as previously described. The results reported in Table III confirm an ATP-tricyclic amine molar ratio of 1:2.

Conductimetry—Twenty-five milliliters of the drug solution was placed in the titrimeter cell kept at 25 ± 0.5°C. A concentrated solution of ATP was then added; the rate of addition was generally between 0.1 and 1 mL/min, with titration usually complete within 5-10 min. Complexation between the two ions was taken to be the point on the conductimetric titration trace where a marked change in the gradient is observed (Fig. 1a).

Several titration curves were determined using different concentrations of phenothiazines. Double-logarithmic plots were then constructed, reporting ATP concentrations at the break point against drug concentrations. All the studied systems exhibited a straight-line relationship between cation and anion concentration (Fig. 1b), showing that, over the concentration ranges studied, the areas of ion self-association have been avoided (14, 15). Analysis of these double-logarithmic plots gave slopes of ~0.5; the intercept was at log $K_{sp}/2$. By substituting the values:

$$\log [\text{drug}] = \frac{\log K_{sp}}{2} - \frac{\log [\text{ATP}]}{2} \qquad \text{(Eq. 1)}$$

[1] Rhône-Poulenc.
[2] Merck.
[3] Silastic.
[4] Millipore.
[5] Pharmacia.
[6] Whatman.
[7] Orion-701/A.
[8] Perkin-Elmer EPS-3T.
[9] Dognon-Abribat.
[10] Amel Model 123.
[11] LKB-Redirec 2112.

Table I—Experimental Molar Ratios [a] for ATP-Phenothiazine Complexes

Complex	Amount, g	ATP, mol $\times 10^{-5}$ [b]	Phenothiazine, mol $\times 10^{-5}$ [b]
ATP-chlorpromazine	0.0150	1.2	2.5
ATP-promazine	0.0080	0.65	1.4
ATP-promethazine	0.0100	1.0	2.1
ATP-triflupromazine	0.0150	1.0	2.2
ATP-trifluperazine	0.0130	1.0	1.9

[a] Determined spectrophotometrically. [b] Standard deviation of each value is within 5-10%; *e.g.*, for the ATP-chlorpromazine complex, the molar ratio, averaged over three separate measurements, is 2.08 ± 0.11. If the molar ratio is averaged over all the measurements concerning all the complexes (assuming that the ratio is the same for all the phenothiazines) a value of 2.09 ± 0.08 is obtained.

Table II—Solid ATP-Phenothiazine Complexes (1:2) Formed in Solutions of ATP [a] and Phenothiazine Drugs [b] in Water and in the Presence of Increasing Concentrations of $CaCl_2$

	Yield, %					
				In the Presence of $CaCl_2$		
				2.0×10^{-3}	4.0×10^{-3}	8.0×10^{-3}
Drug	H_2O [c]	pH 5.5	pH 6.0	M	M	M
Promethazine	4.2	1.8	7.5	—	—	—
Promazine	19.1	7.4	31.9	—	—	—
Chlorpromazine	26.8	35.0	44.2	18.1	13.8	0
Triflupromazine	30.0	25.5	42.3	—	—	—
Trifluperazine	30.0	42.5	44.9	—	—	—

[a] 4.0×10^{-3} M. [b] 8.0×10^{-3} M. [c] pH 3.5-4.0.

Table III—Solubility Products of Phenothiazine-ATP Ion Pairs

	K_{sp}, $(\text{mol/L})^3$		
	25°C		37°C
Drug	Spectrophotometry	Conductimetry	Conductimetry
Promethazine	6.1×10^{-8}	8.3×10^{-8}	9.3×10^{-8}
Promazine	4.6×10^{-8}	4.7×10^{-8}	5.3×10^{-8}
Chlorpromazine	1.4×10^{-8}	1.6×10^{-8}	1.5×10^{-8}
Triflupromazine	9.2×10^{-9}	9.2×10^{-9}	1.2×10^{-8}
Trifluperazine	1.0×10^{-8}	8.7×10^{-9}	1.1×10^{-8}

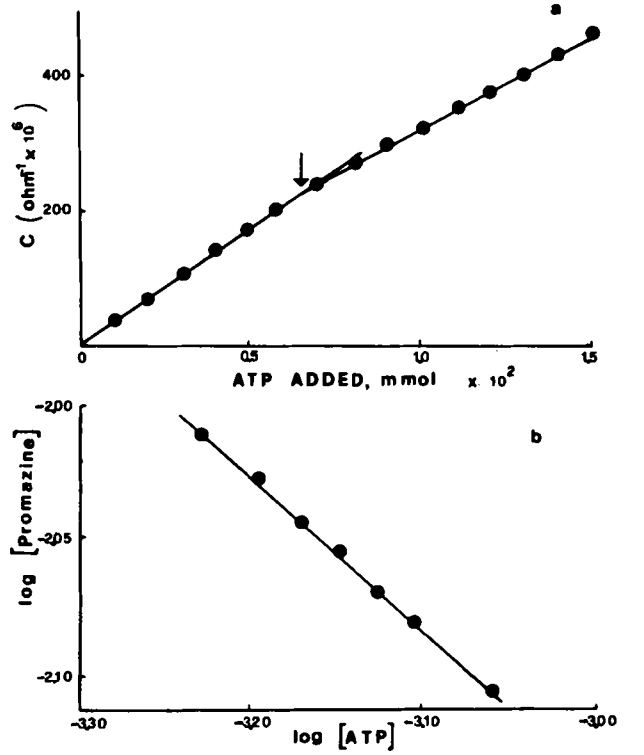

Figure 1—*(a) Conductimetric titration for ATP* versus *promazine at 25°C, original promazine concentration: 9.0×10^{-3} M. (b) Double logarithm plot for the promazine-ATP system of the concentration of each interacting ion at the K_{sp} point: slope 0.47.*

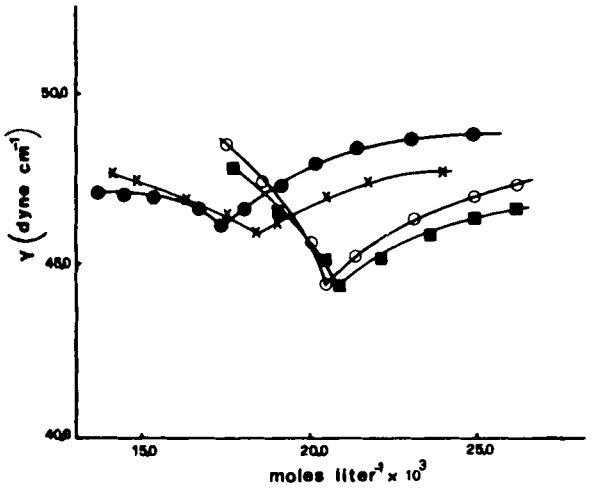

Figure 2—*Surface tension* versus *the molar concentration of chlorpromazine at 25°C. Key: (○) chlorpromazine alone; (●) chlorpromazine in the presence of 0.8 × 10⁻⁴ M ATP; (×) chlorpromazine in the presence of 0.8 × 10⁻⁴ M ATP and 0.6 × 10⁻⁴ M $CaCl_2$; (■) chlorpromazine in the presence of 0.8 × 10⁻⁴ M ATP and 0.8 × 10⁻⁴ M $CaCl_2$.*

a 1:2 interaction between the ATP and the drug was inferred.

Determination of the Critical Micelle Concentration—The critical micelle concentrations (CMC) of phenothiazines were determined by measurements of surface tension using a plate tensiometer at 25 ± 0.5°C in 0.9% NaCl at pH 6.0. The CMC of chlorpromazine was also determined in the presence of ATP and of calcium ions ([ATP] = 0.8 × 10⁻⁴ M; [Ca^{2+}] = 0.6 × 10⁻⁴ M ÷ 0.8 × 10⁻⁴ M) (Fig. 2).

Determination of the Apparent Diffusion Constant—The diffusion cell was of the type used by Nakano and co-workers (16, 17). The glass cell consists of donor and receptor compartments (volume of each, 20 mL) and a membrane (available area, 3.80 cm^2). Twenty milliliters of 0.01 M HCl were added to one arm, and an equal volume of the test solution was placed in the other arm. The concentration of the diffusible phenothiazine drug in the desorbing hydrochloric acid solution was kept at zero, maintaining diffusing phenothiazine in a dissociated form. All solutions were brought to 37°C before being placed in the cell, which was kept at 37°C. The contents of each compartment were stirred by a magnet attached to an electric motor turning at 300 rpm. At scheduled times an aliquot (0.5 mL) of the receptor solution was removed for the absorbance measurements, and the same volume of 0.01 M HCl was added.

The equation derived by Garrett and Chemburkar (18) for steady-state diffusion was used to obtain the apparent diffusion constants, $D = C_1XV/tC_2S$ where C_1 is the concentration of diffusate in the desorbing solution, X is the thickness of the membrane, S is the available area of membrane, V is the volume of the desorbing solution, and C_2 is the concentration of the diffusate. The diffusing solution in 0.9% NaCl at pH 6.0 at 37°C contained 0.8–1.0 × 10⁻³ M tricyclic amine and an ATP concentration eight times the molarity of the drug. D values are reported in Table IV.

Determination of the Binding Constants of ATP to Phenothiazine Micelles by a Solubility Method—Increasing concentrations of tricyclic amines (0.5–40.0 × 10⁻³ M) were added to the solutions of ATP (1.0 × 10⁻³ M) in glass-stoppered cylinders at pH 6.0 in 0.9% NaCl. The cylinders were placed in a water bath and rotated at 25 ± 0.5°C until equilibrium was reached. Agitation for 24 h was sufficient. The ionic strength of the solutions was brought to 0.155 with 0.9% NaCl; therefore, the small amounts of sodium hydroxide used for pH adjustment did not appreciably influence the ionic strength. After 24 h an appropriate volume (4 mL) was filtered through a 0.25-μm filter disk. The concentration of ATP was determined by the malachite green method; each value is an average of three determinations. Comparable results were obtained using glass microfiber papers instead of filter disks. The same procedure was employed to study the solubility of the ATP–chlorpromazine complex at increasing concentrations of chlorpromazine in the presence of a fixed concentration of calcium chloride (7.5 × 10⁻³ M).

The solubility measurements for all the studied phenothiazines were also performed in 0.1 M 2-morpholineethansulfonate buffer (pH 6.0). The results are in agreement with previous data. Variation in the solubility of the ATP–phenothiazine complex was quite similar to the variation of the solubilization of slightly soluble hydrophobic solutes by aggregating micelle-forming surfactants (19, 20). At first, ATP concentration decreases because of solid complex formation; at higher concentrations of the drug, ATP concentration increases since the solid ion pair is solubilized by surfactant micelles. From the solubilization curves the apparent binding constants of ATP with phenothiazine micelles were calculated using (21):

$$\frac{S_{M,W}}{S_W} = 1 + K_bC \qquad \text{(Eq. 2)}$$

where S_W is the concentration of ATP at the CMC, $S_{M,W}$ is the concentration in the presence of micelles of the drug, and C is the surfactant concentration (molarity), which exceeds the CMC value (Table V).

Determination of the Binding Constant of ATP with Chlorpromazine Micelles by Gel Filtration—The binding constant (K_b) of ATP with chlorpromazine micelles was determined by gel filtration according to Herries *et al.* and Yatsimirskii *et al.* (21, 22). The chromatography of Sephadex G-25 was carried out on a 2-cm diameter column with a total volume of 72 mL. Using blue dextran 2000, the void volume V_0 of the packed column was determined to be 29.5 mL. The imbibed volume of the gel V_i, calculated from the water regain and wet density data, was 34.0. Prior to each run the column was first equilibrated with 0.9% NaCl at pH 6.0 and then with the appropriate concentration of chlorpromazine (in 0.9% NaCl at pH 6.0). The run was initiated by addition of 0.5 mL of ATP solution (2 mg/mL) to the column. All runs were done at 25°C. The elution volume V_e was calculated by ATP determined according to the method previously described. The K_b value was determined using (22, 23):

$$\frac{V_i}{V_e - V_0} = \frac{\overline{V}(K_p - 1)}{k'K_d}C + \frac{1}{k'K_d} \qquad \text{(Eq. 3)}$$

where V_i, V_e, and V_0 are the imbibed (stationary), elution, and void volumes, $\overline{V}$ is the molar volume of chlorpromazine in the micelle, K_d is the molecular sieving constant, k' is the proportionality constant between the solute absorbed per unit volume of gel matrix and the equilibrium concentration of monomer solute in liquid, C is the concentration of chlorpromazine, and K_p is the micelle–water partition coefficient of ATP. A plot of the left-hand side of Eq. 3 ($V_i/V_e - V_0$) *versus* chlorpromazine concentration (C) is shown in Fig. 3. At low drug concentrations the values of $V_i/V_e - V_0$ are independent of the concentration of the surfactant. Above the CMC, the values of $V_i/V_e - V_0$ increase linearly with the micelle concentrations.

The product $\overline{V}(K_p - 1)$ can be determined from the slope of the straight line according to Yatsimirskii *et al.* (21). The binding constant is then calculated as $K_b = \overline{V}(K_p - 1)$. Intersection of the lines in Fig. 3 define the CMC of chlorpromazine hydrochloride in the presence of the solute and of Sephadex G-25. The CMC is about twice as great as that determined by the surface tension method. According to other authors (23, 24), such a discrepancy is probably due to strong interaction between the Sephadex dextran and chlorpromazine. In Table V the K_b value obtained by gel filtration is reported.

Table IV—Apparent Constants of Diffusion Through Dimethylpolysiloxane Membrane at 37°C of Phenothiazines[a] Alone and in the Presence of ATP

Drug	D, L/s·cm: Alone	D, L/s·cm: In the Presence of ATP[b]
Promethazine	1.3 × 10⁻¹⁰	4.6 × 10⁻¹⁰
Promazine	1.4 × 10⁻¹⁰	5.3 × 10⁻¹⁰
Chlorpromazine	1.7 × 10⁻¹⁰	16.1 × 10⁻¹⁰
Triflupromazine	4.7 × 10⁻¹⁰	14.8 × 10⁻¹⁰
Trifluperazine	2.7 × 10⁻¹⁰	21.4 × 10⁻¹⁰

[a] In 0.9% NaCl, pH 6.0. [b] Eight times the concentration of the tricyclic amines.

Table V—Binding Constants of ATP to Phenothiazine Micelles[a]

Drug	K_b: Solubility Method, In the Absence of $CaCl_2$, micelles/L	K_b: Solubility Method, In the Absence of $CaCl_2$, mol/L	K_b: Solubility Method, In the Presence of $CaCl_2$, micelles/L	K_b: Solubility Method, In the Presence of $CaCl_2$, mol/L	K_b: Gel Filtration Method, mol/L
Promethazine	1215	45	—	—	—
Promazine	1665	45	—	—	—
Chlorpromazine	3360	80	1974	47	79
Triflupromazine	8000	200	—	—	—
Trifluperazine	6000	120	—	—	—

[a] In 0.9% NaCl, pH 6.0, at 25°C.

RESULTS

ATP interacts with phenothiazine drugs to form water-insoluble complexes. A 1:2 ATP–drug complex was obtained (Table I) in the presence and absence

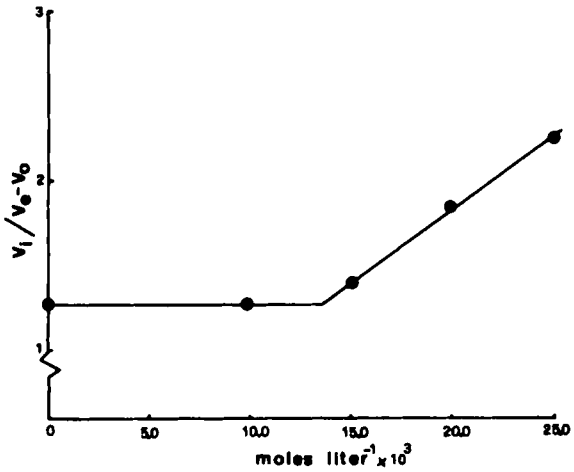

Figure 3—*Plots of* $V_i/V_e - V_0$ versus *chlorpromazine molar concentration.*

of calcium ions. Trifluperazine with two basic sites on the piperazine ring shows a similar behavior. The yields change with the different drugs examined and are pH dependent; all the phenothiazines show a maximum at pH 6.0, where ATP dissociation is highest (Table II). The formation of the ion pairs at pH > 6.0 was not studied because of the partial coprecipitation of some phenothiazine bases.

The CMC of chlorpromazine (Fig. 2) varies in the presence of ATP and calcium ions; by adding only ATP at low concentration, the CMC decreases, probably due to the greater hydrophobicity of the ion pairs. If calcium ions are then also added to the solution, the CMC rises and when the molarity of calcium and ATP are equal, the initial CMC is obtained. This behavior could indicate that a high calcium ion concentration interferes with ion pair formation.

The permeation rate of different phenothiazines through a dimethylpolysiloxane membrane increases in the presence of ATP (Table V). The effect of ATP on the apparent diffusion constant (D) was studied examining solutions containing ATP at concentrations only eight times the molarity of the drug, to avoid the precipitation of the solid complex. Phenothiazine micelles solubilize ATP, giving high apparent binding constants (K_b). The concentration of the drug was indicated in two ways: as molar concentration (C) and as micellar concentration (C_m), where $C_m = (C - \text{CMC})/N$ (N is the aggregation number obtained from the literature (6, 25) assuming that the solubilized compound does not change the size of the micelles). The binding constant of ATP with chlorpromazine micelles decreases in the presence of calcium ions in aqueous solution. The K_b of ATP with chlorpromazine was verified by two methods, obtaining comparable values within the limits of experimental error.

DISCUSSION

The solubility products of the 1:2 solid complexes, obtained by two methods (Table IV), are in good agreement with the yields obtained at pH 6.0. The sequence of solubility products is consistent with that of the surface tensions of the phenothiazine drugs in Ringer's solution at pH 6.0 (26).

A good correlation was also established between the logarithm of the solubility product and the logarithm of the CMC of the phenothiazine involved in the interaction (Fig. 4a, b). A similar dependence was previously observed (15). These results suggest that the increased hydrophobic nature of the interacting amines raises the ion pair stability. Further support to this hypothesis can be noted from Fig. 5, where log D *versus* CMC of phenothiazine is reported. The CMC describes the lipophilicity of the amphiphilic substances; the relation between log D and log CMC shows a linear trend and could be an indirect measure of the lipophilicity of the ion pair. As a consequence, in the presence of phenothiazines at concentrations lower than the CMC, the lipophilicity of ATP greatly increases.

Baur (27) noted that for tricyclic amines the tranquilizing potency rises exponentially with increasing lysis index, a measure of the relative hemolytic potency. Using the lysis index of chlorpromazine (*i.e.*, 1) (27) for comparison, we note a relationship between log (lysis index) and log D of the phenothiazines in the presence of ATP (Fig. 6); permeability data, in this case, can be related to data obtained *in vivo*. On the contrary, no relationship can be found between permeability constants of the ion pairs and partition coefficients (27, 28) or pK_a values (29) of the phenothiazines.

It was shown that certain drugs can be absorbed in their undissociated state,

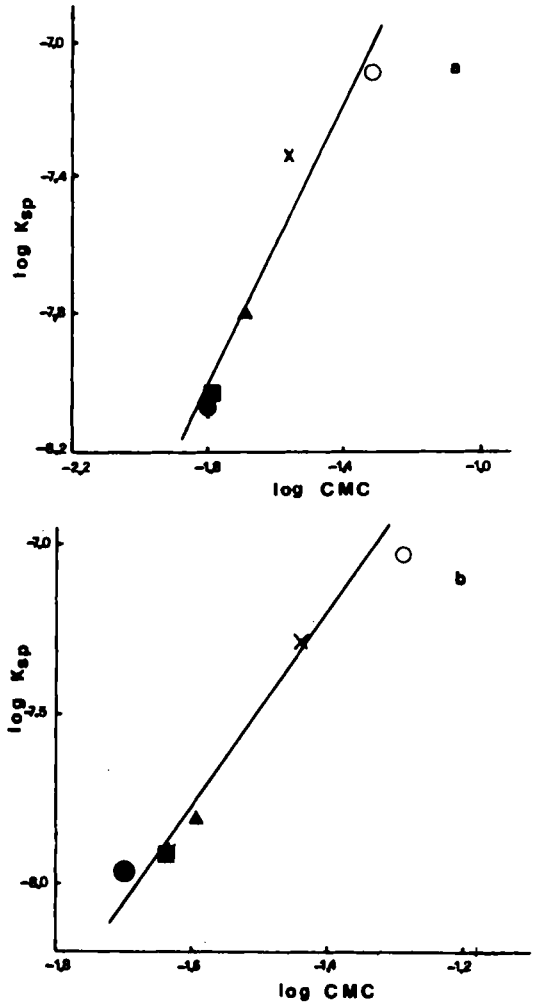

Figure 4—*Relationship between solubility products (log* K_{sp}*) of the ion pairs determined by conductimetry and log CMC of the phenothiazines at 25°C (a) and at 37°C (b). Key: (○) promethazine; (×) promazine; (▲) chlorpromazine; (■) triflupromazine; (●) trifluperazine.*

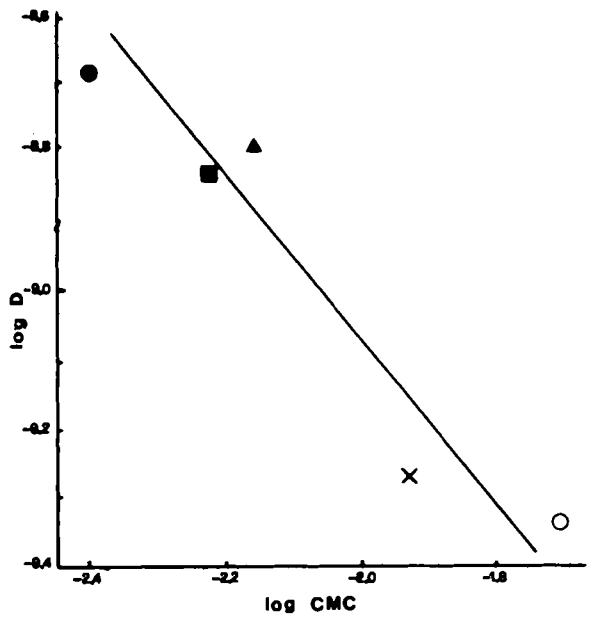

Figure 5—*Relationship between apparent diffusion constants* D *of phenothiazines in the presence of ATP and log CMC (0.9% NaCl, pH 6.0, at 37°C). Key: (○) promethazine; (×) promazine; (▲) chlorpromazine; (■) triflupromazine; (●) trifluperazine.*

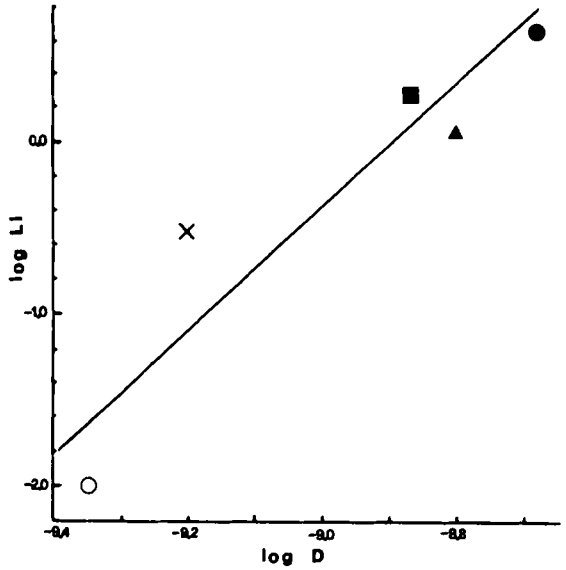

Figure 6—*Relationship between lysis index (LI) and apparent diffusion constants* D *of phenothiazines in the presence of ATP (0.9% NaCl, pH 6.0, at 37°C). Key: (○) promethazine; (×) promazine; (▲) chlorpromazine; (■) triflupromazine; (●) trifluperazine.*

either directly or by ion pair or complex formation[12]; but ion pairs can also be formed in biological fluids, *e.g.*, between basic drugs and biogenic acids. The role of ATP in the uptake and in the release of biogenic amines is complex and not clearly understood. The behavior of chlorpromazine in the release and uptake of serotonin and biogenic amines from storage sites has not yet been explained (30). In particular, the existence of serotonin–ATP aggregates (up to 12,000–15,000 mol. wt.) was shown by Berneis *et al.* (31) in the storage organelles of blood platelets. Chlorpromazine may interfere with ATP–serotonin aggregates in storage organelles. It is possible that the hydrophobicity of the depressant at first promotes its transport through biological membranes. Subsequently, chlorpromazine might form an ion pair with ATP, partially removing the nucleotide from its aggregates with serotonin. The consequence might be an interference in the uptake mechanism of the monoamine.

Basically, we can regard the micelles as dispersed oil droplets in water (32); the peculiar solvent property of micelle-forming surfactants is closely related to the peculiar nature of the self-association responsible for the formation of the micelles themselves. Micellar solubilization can provide considerable insight into the nature of the interaction of molecules with other lipid assemblies, such as biological membranes, which are responsible for the binding or uptake of molecules and their transport (33).

Figure 7 shows clear trends that suggest a linear correlation, between log CMC and log K_b; probably, lipophilicity of phenothiazines could determine the binding stability between ATP and the micelles. Further support for this

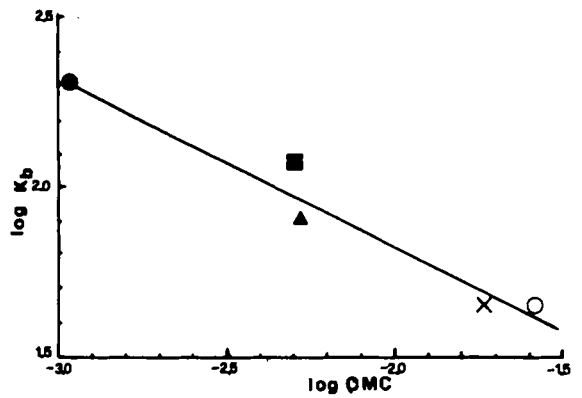

Figure 7—*Relationship between binding constants of ATP to phenothiazine micelles and log CMC of the drugs (0.9% NaCl, pH 6.0, at 25°C). Key: (○) promethazine; (×) promazine; (▲) chlorpromazine; (■) triflupromazine; (●) trifluperazine.*

[12] Unpublished results.

hypothesis arises from the increase of the binding constants (Table V) going from promethazine, an antihistaminic drug, to neuroleptics. The location and distribution of ATP inside micelles could be of interest in elucidating the role of its molecular structure in the solubilization process and in understanding the solubilization capacity of micelles. Phenothiazines are ionic surfactants and their micelles (34) have a core formed from their tricyclic moiety with their cationic head-group outside.

Previously (8, 9), we noted that phenothiazine micelles can solubilize polar molecules; their solubilization occurs, in all cases examined, only when the formation of an ion pair is noted. The solubilization of ATP by phenothiazine micelles can be explained in several ways. Solubilization of ATP might occur as the poorly dissociated ion pair; the lipophilicity of the ion pair is greater than that of ATP, as permeability constants show, for the presence of two phenothiazine hydrophobic molecules. Furthermore, solubilization of the ion pair could be facilitated because the phenothiazine molecules forming the complex are the same as those forming the micelles.

It is possible that *in vivo* bioactive molecules can be solubilized into micelles formed by a drug alone, into mixed micelles of drug and phospholipid, or into membranes, by an ion pair mechanism. Such an interaction might be responsible in part for the activity of drugs and endogenous substances.

REFERENCES

(1) P. S. Guth, G. Amaro, O. Z. Sellinger, and L. Elmer, *Biochem. Pharmacol.*, **14,** 769 (1965).

(2) C. H. Popov, *Compt. Rend. Acad. Bulg. Sci.*, **25,** 829 (1972).

(3) H. A. Spirtes, A. S. Morgan, and E. S. Cohen, *Biochem. Pharmacol.*, **14,** 295 (1965).

(4) D. Attwood, A. T. Florence, and J. M. N. Gillan, *J. Pharm. Sci.*, **63,** 988 (1974).

(5) S. Keipert, J. Becker, and R. Voigt, *Pharmazie*, **31,** 296 (1976).

(6) K. Thoma and M. Arning, *Arch. Pharm.*, **309,** 851 (1976).

(7) K. Thoma and M. Arning, *Arch. Pharm.*, **309,** 837 (1976).

(8) M. R. Gasco, M. Trotta, and M. E. Carlotti, *Pharm. Acta Helv.*, **56,** 276 (1981).

(9) M. R. Gasco, M. E. Carlotti, and M. Trotta, *Pharm. Acta Helv.*, **56,** 82 (1981).

(10) L. Bei, *Arch. Biochem. Biophys.* **109,** 321 (1965).

(11) L. Moriguchi, S. Fushimi, R. Umehara, and R. Kaneniwa, *Chem. Pharm. Bull.*, **20,** 834 (1972).

(12) M. R. Gasco, M. Trotta, and M. E. Carlotti, *J. Pharm. Sci.*, **71,** 240 (1982).

(13) W. Hohenwaller and E. Wimmer, *Clin. Chim. Acta*, **45,** 169 (1973).

(14) G. I. Mukayer and S. S. Davis, *J. Colloid Interface Sci.*, **59,** 350 (1977).

(15) E. Tomlinson and S. S. Davis, *J. Colloid Interface Sci.*, **66,** 355 (1978).

(16) K. Juni, M. Nakano, and T. Arita, *Chem. Pharm. Bull.*, **25,** 2807 (1977).

(17) M. Nakano and N. K. Patel, *J. Pharm. Sci.*, **59,** 77 (1970).

(18) E. R. Garrett and P. B. Chemburkar, *J. Pharm. Sci.*, **57,** 949 (1968).

(19) A. G. Mitchell, *J. Pharm. Pharmacol.*, **14,** 172 (1962); **15,** 761 (1963); **16,** 43 (1964); A. G. Mitchell and J. F. Broadhead, *J. Pharm. Sci.*, **56,** 1261 (1967).

(20) P. Mukerjie and J. R. Cardinal, *J. Pharm. Sci.*, **65,** 882 (1976).

(21) A. K. Yatsimirskii, K. Martinek, and I. V. Berezin, *Tetrahedron*, **27,** 2855 (1971).

(22) D. G. Herries, W. Bishop, and F. M. Richards, *J. Phys. Chem.*, **68,** 1842 (1964).

(23) D. W. Armstrong, R. Seguin, and J. H. Fendler, *J. Mol. Evol.*, **10,** 241 (1977).

(24) J. Nagyvary, J. A. Harvey, F. Nome, D. Armstrong, and J. H. Fendler, *Precambian Res.*, **3,** 509 (1976).

(25) W. Scholtan, *Kolloid-Z.*, **142,** 84 (1955).

(26) P. Seeman and H. S. Bialy, *Biochem. Pharmacol.*, **12,** 1181 (1963).

(27) E. W. Baur, *J. Pharmacol. Exp. Ther.*, **177,** 219 (1971).

(28) A. Leo, C. Hansch, and D. Elkins, *Chem. Rev.*, **71,** 525 (1971).

(29) A. L. Green, *J. Pharm. Pharmacol.*, **22,** 705 (1971).

(30) T. N. Chase, *J. Neurochem.*, **16,** 607 (1969).

(31) K. H. Berneis, M. Da Prada, and A. Pletscher, *Science*, **165,** 913 (1969).

(32) M. Almgren, F. Grieser, and J. K. Thomas, *J. Am. Chem. Soc.*, **101,** 279 (1979).

(33) P. Mukerjie, *Pure Appl. Chem.*, **52**, 1317 (1980).
(34) A. T. Florence and R. T. Parfitt, *J. Pharm. Pharmacol.*, **22**, 121 (1970).

ACKNOWLEDGMENTS

This study was supported by a "Progetto Finalizzato Chimica Fine e Secondaria" CNR grant.

High-Performance Liquid Chromatographic Determination of Tracazolate and Its Major Metabolite in Plasma

M. HERMES ˣ and J. O. MALBICA

Received December 1, 1982, from the *Biomedical Research Department, Stuart Pharmaceutical Div. of ICI Americas Inc., Wilmington, DE 19897.* Accepted for publication April 12, 1983.

Abstract □ A high-performance liquid chromatographic (HPLC) method is reported that provides for either separate or simultaneous plasma determination of tracazolate and its major metabolite, the free carboxylic acid. Tracazolate is extracted from plasma with hexane and is quantitated by reverse-phase HPLC using an internal standard. The metabolite is extracted in an additional step, methylated, and either quantitated using the same HPLC conditions in a separate determination or combined with the hexane extract for the simultaneous HPLC determination of drug and metabolite. The plasma concentrations of metabolite were as much as 60 times greater than free drug in some animal species, therefore requiring the use of separate determinations for the two compounds. The analyses have limits of reproducible quantitation of 20 ng/mL for tracazolate and 50 ng/mL for the metabolite in plasma. The simultaneous analysis for tracazolate and the metabolite was used to evaluate plasma levels of both compounds *versus* time and dose. Data generated in conjunction with a toxicology study are reported to demonstrate the applicability of the procedure.

Keyphrases □ Tracazolate—free carboxylic acid metabolite, individual and simultaneous assay in plasma, HPLC □ HPLC—tracazolate and its free carboxylic acid metabolite, individual and simultaneous assay in plasma

Tracazolate (I) (ICI 136,753; 4-(butylamino)-1-ethyl-6-methyl-1*H*-pyrazolo[3,4-*b*]pyridine-5-carboxylic acid ethyl ester), a nonbenzodiazepine agent with potential clinical utility as a nonsedative anxiolytic drug (1, 2), is extensively metabolized by a first-pass effect in the rat and dog. The major metabolite (II) is the acid resulting from deesterification of I (3). Although II is inactive in pharmacological screening tests, it is of interest since the circulating levels can be 3- to 60-fold greater than I depending on the species and dosage. Metabolite (II) may be the only drug-related compound in sufficient concentration to measure in plasma, therefore, the quantitation of II may provide an indication of absorption of I at low dosages should plasma levels of I fall below the limits of detection.

The analytical procedures described herein allow for either the separate determination of I and II or for the simultaneous determination of both in plasma. The internal standard used was the 1-butyl analogue of tracazolate (III). Compound IV is the methyl ester of II.

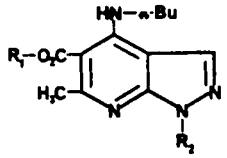

I: $R_1 = R_2 = -CH_2CH_3$ (mol. wt. 304)
II: $R_1 = H$; $R_2 = -CH_2CH_3$ (mol. wt. 276)
III: $R_1 = -CH_2CH_3$; $R_2 = -(CH_2)_3CH_3$ (mol. wt. 332)
IV: $R_1 = -CH_3$; $R_2 = -CH_2CH_3$ (mol. wt. 290)

EXPERIMENTAL

Chemicals and Reagents—All organic solvents used were HPLC grade[1]. The water was purified by ion exchange, activated charcoal filtration, and distillation. Ammonium hydroxide was high purity[2], and 10% aqueous trichloroacetic acid was made from reagent-grade trichloroacetic acid[3]. The methylation of II was carried out with diazomethane[4] (4).

Instrumentation—A liquid chromatograph fitted with an automatic sampler[5] was used with a variable-wavelength UV detector[6] set at 240 nm. The columns used were: a 30 cm × 3.9 mm i.d. stainless steel precolumn (prior to the injector) hand packed with 30–38-μm pellicular packing[7], a 3-cm guard cartridge (between the injector and the analytical column) packed with 5-μm octadecylsilane-bonded packing (ODS)[8], and a 25 cm × 4.6-mm i.d. stainless-steel analytical column packed with 7-μm spherical ODS packing[9]. The mobile phase of methanol–water–20% NH_3OH (90:10:0.05 v/v/v) was pumped at ~2 mL/min and produced ~3000 psi back-pressure. A strip-chart recorder[10] provided a real time record of the chromatography; however, the quantitation was done by computer[11]. The detector signal for the computer was tapped prior to attenuation and had an output of 1 V/AU.

Standard Solutions—Stock solutions of I, II, IV, and the internal standard (III) (1.0 mg/mL) were prepared in methanol. Aliquots of the above stock solutions were further diluted in methanol as spiking solutions. Standard solutions of I, III, and IV were brought to volume with mobile phase solution and were chromatographed directly. Ester IV was previously synthesized in bulk and was used directly to make a stock solution. Matrix standards were prepared with control plasma, 200 μL in a 15-mL centrifuge tube, and spiked with methanol solutions of I and III, for the analysis of I only; II only for the separate analysis of II; or I, II, and III for the dual analysis of I and II. Matrix blanks were not spiked. The internal standard (III) was added to samples obtained from dosed animals for either the single or dual analysis where I was being determined. A 20-μL aliquot of a 1.0-μg/mL internal standard solution in methanol was added to the 200-μL plasma aliquots. The resulting concentration of internal standard was 110 ng/mL.

Sample Preparation—For the extraction of I, 2.5 mL of *n*-hexane was added to each plasma sample in a 15-mL centrifuge tube, vortexed for 30 s, and centrifuged. The hexane layer containing I and III was removed with a Pasteur pipet, and if I was to be measured it was transferred into a labeled test tube. If II was to be extracted, a 10% trichloroacetic acid solution (0.04 mL) and 2.5 mL of methyl *tert*-butyl ether were added to the aqueous residues, which were then vortexed and centrifuged. The methyl *tert*-butyl ether layer containing II was removed with a Pasteur pipet and transferred into a test tube. If both I and II were to be determined simultaneously the methyl *tert*-butyl ether layer was added to the *n*-hexane layer from the previous extraction. The

[1] Burdick and Jackson; methanol, *n*-hexane, methyl *tert*-butyl ether, and ether; USI Chemicals: 200 proof ethanol.
[2] Baker Chemicals; "Ultrex" grade 20% ammonium hydroxide.
[3] Baker Chemicals; trichloroacetic acid.
[4] Aldrich Chemical Co., diazald (*N*-methyl-*N*-nitroso-*p*-toluene); Baker Chemical Co., glacial acetic acid (diluted 25% in water); Fisher Chemical Co., potassium hydroxide (0.7 M in 10% v/v water–ethanol).
[5] Model 1081B HPLC; Hewlett-Packard, Palo Alto, Calif.
[6] Spectromonitor III (model 1204); Laboratory Data Control, Riviera Beach, Fla.
[7] 30–38-μm HC Pellosil; Whatman, Clifton N.J.
[8] Guard Holder and 5 μm C18 cartridges; Brownlee, Santa Clara, Calif.
[9] Zorbax ODS packing and columns; DuPont, Wilmington, Del.
[10] Model 391 recorder; Linear Instruments, Irvine, Calif.
[11] Model 3356 Laboratory Automation System; Hewlett-Packard, Palo Alto, Calif.

0022-3549/84/0500-0667$01.00/0
© 1984, American Pharmaceutical Association

(33) P. Mukerjie, *Pure Appl. Chem.*, **52**, 1317 (1980).
(34) A. T. Florence and R. T. Parfitt, *J. Pharm. Pharmacol.*, **22**, 121 (1970).

ACKNOWLEDGMENTS

This study was supported by a "Progetto Finalizzato Chimica Fine e Secondaria" CNR grant.

High-Performance Liquid Chromatographic Determination of Tracazolate and Its Major Metabolite in Plasma

M. HERMES ˣ and J. O. MALBICA

Received December 1, 1982, from the *Biomedical Research Department, Stuart Pharmaceutical Div. of ICI Americas Inc., Wilmington, DE 19897.* Accepted for publication April 12, 1983.

Abstract □ A high-performance liquid chromatographic (HPLC) method is reported that provides for either separate or simultaneous plasma determination of tracazolate and its major metabolite, the free carboxylic acid. Tracazolate is extracted from plasma with hexane and is quantitated by reverse-phase HPLC using an internal standard. The metabolite is extracted in an additional step, methylated, and either quantitated using the same HPLC conditions in a separate determination or combined with the hexane extract for the simultaneous HPLC determination of drug and metabolite. The plasma concentrations of metabolite were as much as 60 times greater than free drug in some animal species, therefore requiring the use of separate determinations for the two compounds. The analyses have limits of reproducible quantitation of 20 ng/mL for tracazolate and 50 ng/mL for the metabolite in plasma. The simultaneous analysis for tracazolate and the metabolite was used to evaluate plasma levels of both compounds *versus* time and dose. Data generated in conjunction with a toxicology study are reported to demonstrate the applicability of the procedure.

Keyphrases □ Tracazolate—free carboxylic acid metabolite, individual and simultaneous assay in plasma, HPLC □ HPLC—tracazolate and its free carboxylic acid metabolite, individual and simultaneous assay in plasma

Tracazolate (I) (ICI 136,753; 4-(butylamino)-1-ethyl-6-methyl-1*H*-pyrazolo[3,4-*b*]pyridine-5-carboxylic acid ethyl ester), a nonbenzodiazepine agent with potential clinical utility as a nonsedative anxiolytic drug (1, 2), is extensively metabolized by a first-pass effect in the rat and dog. The major metabolite (II) is the acid resulting from deesterification of I (3). Although II is inactive in pharmacological screening tests, it is of interest since the circulating levels can be 3- to 60-fold greater than I depending on the species and dosage. Metabolite (II) may be the only drug-related compound in sufficient concentration to measure in plasma, therefore, the quantitation of II may provide an indication of absorption of I at low dosages should plasma levels of I fall below the limits of detection.

The analytical procedures described herein allow for either the separate determination of I and II or for the simultaneous determination of both in plasma. The internal standard used was the 1-butyl analogue of tracazolate (III). Compound IV is the methyl ester of II.

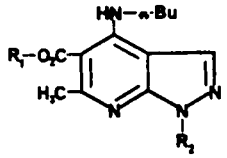

I: $R_1 = R_2 = -CH_2CH_3$ (mol. wt. 304)
II: $R_1 = H$; $R_2 = -CH_2CH_3$ (mol. wt. 276)
III: $R_1 = -CH_2CH_3$; $R_2 = -(CH_2)_3CH_3$ (mol. wt. 332)
IV: $R_1 = -CH_3$; $R_2 = -CH_2CH_3$ (mol. wt. 290)

EXPERIMENTAL

Chemicals and Reagents—All organic solvents used were HPLC grade[1]. The water was purified by ion exchange, activated charcoal filtration, and distillation. Ammonium hydroxide was high purity[2], and 10% aqueous trichloroacetic acid was made from reagent-grade trichloroacetic acid[3]. The methylation of II was carried out with diazomethane[4] (4).

Instrumentation—A liquid chromatograph fitted with an automatic sampler[5] was used with a variable-wavelength UV detector[6] set at 240 nm. The columns used were: a 30 cm × 3.9 mm i.d. stainless steel precolumn (prior to the injector) hand packed with 30–38-μm pellicular packing[7], a 3-cm guard cartridge (between the injector and the analytical column) packed with 5-μm octadecylsilane-bonded packing (ODS)[8], and a 25 cm × 4.6-mm i.d. stainless-steel analytical column packed with 7-μm spherical ODS packing[9]. The mobile phase of methanol–water–20% NH_3OH (90:10:0.05 v/v/v) was pumped at ~2 mL/min and produced ~3000 psi back-pressure. A strip-chart recorder[10] provided a real time record of the chromatography; however, the quantitation was done by computer[11]. The detector signal for the computer was tapped prior to attenuation and had an output of 1 V/AU.

Standard Solutions—Stock solutions of I, II, IV, and the internal standard (III) (1.0 mg/mL) were prepared in methanol. Aliquots of the above stock solutions were further diluted in methanol as spiking solutions. Standard solutions of I, III, and IV were brought to volume with mobile phase solution and were chromatographed directly. Ester IV was previously synthesized in bulk and was used directly to make a stock solution. Matrix standards were prepared with control plasma, 200 μL in a 15-mL centrifuge tube, and spiked with methanol solutions of I and III, for the analysis of I only; II only for the separate analysis of II; or I, II, and III for the dual analysis of I and II. Matrix blanks were not spiked. The internal standard (III) was added to samples obtained from dosed animals for either the single or dual analysis where I was being determined. A 20-μL aliquot of a 1.0-μg/mL internal standard solution in methanol was added to the 200-μL plasma aliquots. The resulting concentration of internal standard was 110 ng/mL.

Sample Preparation—For the extraction of I, 2.5 mL of *n*-hexane was added to each plasma sample in a 15-mL centrifuge tube, vortexed for 30 s, and centrifuged. The hexane layer containing I and III was removed with a Pasteur pipet, and if I was to be measured it was transferred into a labeled test tube. If II was to be extracted, a 10% trichloroacetic acid solution (0.04 mL) and 2.5 mL of methyl *tert*-butyl ether were added to the aqueous residues, which were then vortexed and centrifuged. The methyl *tert*-butyl ether layer containing II was removed with a Pasteur pipet and transferred into a test tube. If both I and II were to be determined simultaneously the methyl *tert*-butyl ether layer was added to the *n*-hexane layer from the previous extraction. The

[1] Burdick and Jackson; methanol, *n*-hexane, methyl *tert*-butyl ether, and ether; USI Chemicals: 200 proof ethanol.
[2] Baker Chemicals; "Ultrex" grade 20% ammonium hydroxide.
[3] Baker Chemicals; trichloroacetic acid.
[4] Aldrich Chemical Co., diazald (*N*-methyl-*N*-nitroso-*p*-toluene); Baker Chemical Co., glacial acetic acid (diluted 25% in water); Fisher Chemical Co., potassium hydroxide (0.7 M in 10% v/v water–ethanol).
[5] Model 1081B HPLC; Hewlett-Packard, Palo Alto, Calif.
[6] Spectromonitor III (model 1204); Laboratory Data Control, Riviera Beach, Fla.
[7] 30–38-μm HC Pellosil; Whatman, Clifton N.J.
[8] Guard Holder and 5 μm C18 cartridges; Brownlee, Santa Clara, Calif.
[9] Zorbax ODS packing and columns; DuPont, Wilmington, Del.
[10] Model 391 recorder; Linear Instruments, Irvine, Calif.
[11] Model 3356 Laboratory Automation System; Hewlett-Packard, Palo Alto, Calif.

0022-3549/84/0500-0667$01.00/0
© 1984, American Pharmaceutical Association

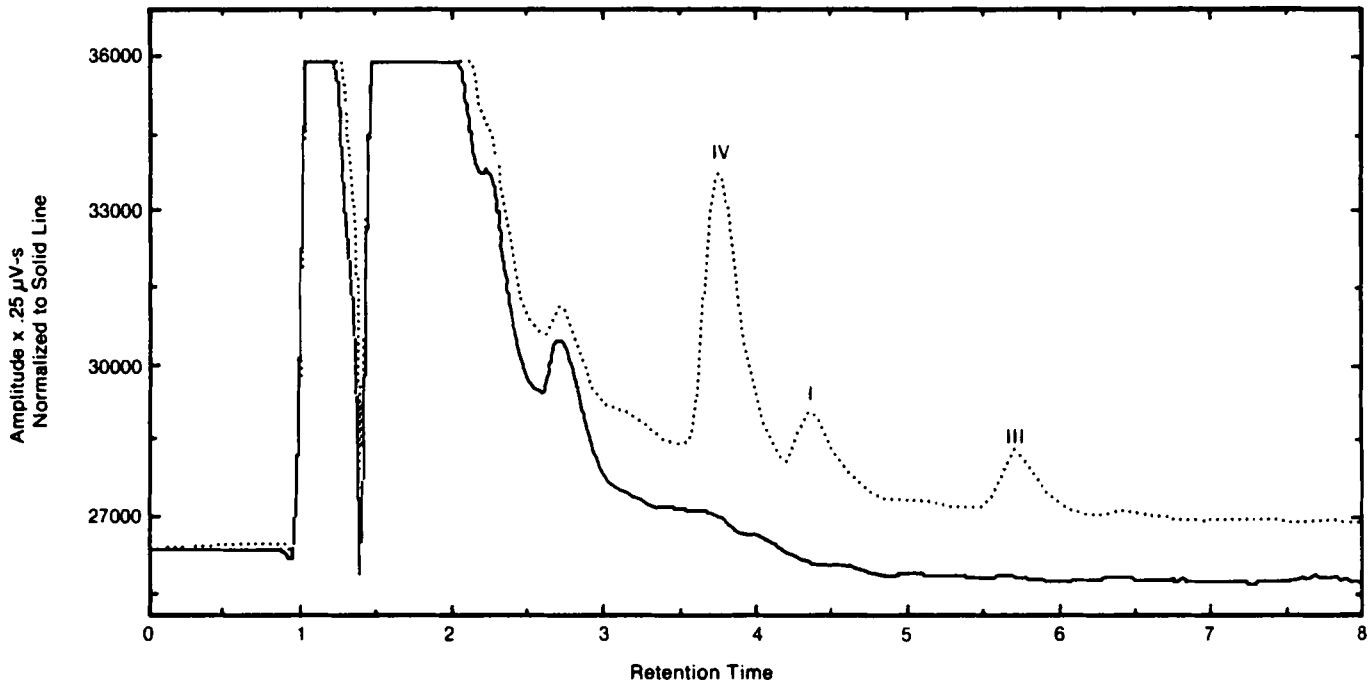

Figure 1—*Tracing of a computer reconstructed chromatogram of a 50-μL injection of a matrix standard (. . .) with 500 ng/mL of IV, 100 ng/mL of I, and 100 ng/mL of III from canine plasma superimposed on the chromatogram of a matrix blank (—). Compound II is not retained on the column, so its methyl ester IV is the species chromatographed and quantitated.*

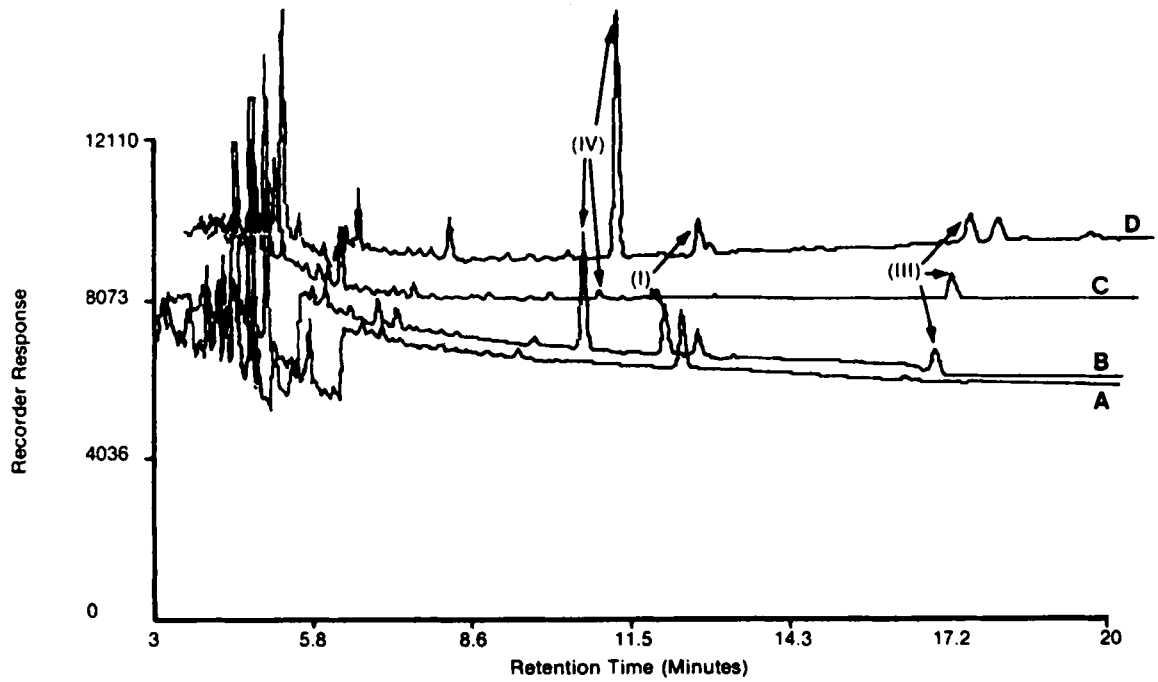

Figure 2—*Tracing of the computer reconstruction of capillary gas chromatograms of a plasma blank (A), a spiked plasma standard (B), and samples at 1 (C) and 6 h (D) postdose from a dog dosed with 80 mg/kg of I.*

organic extracts containing II were evaporated under a gentle stream of dry nitrogen at room temperature to ~0.1 mL. The diazomethane-ether solution (~0.2 mL) was added to each tube, and the tubes were carefully agitated, loosely covered, and let stand for 30 min at room temperature[12]. The extracts were evaporated under an efficient hood with a gentle stream of dry nitrogen at room temperature and removed as soon as they were dry. The dried residues were either tightly capped and stored at −10°C for up to 72 h or diluted with mobile phase solution which remained stable overnight at room temperature.

[12] Mild conditions were required for derivatization because of the potential for the decarboxylation of II at elevated temperatures.

Liquid Chromatographic Procedure—At least four matrix standards were prepared for each sequence of samples. The matrix standard solutions were positioned between the standard solutions and the samples and again after the samples as a reproducibility check. Compound concentration ranges were the same for the standard solutions and matrix standards (see Table I). Peak heights (PH) of I, IV, and III were used as the measure of detector response. Results for the dual determination of I and II or the separate determination of I were calculated by the internal standard method using the average of matrix standard response factors in a multipoint calibration. The concentration of II in the separate determination was calculated using the external standard method, since the internal standard (III) was removed in the initial *n*-hexane extraction.

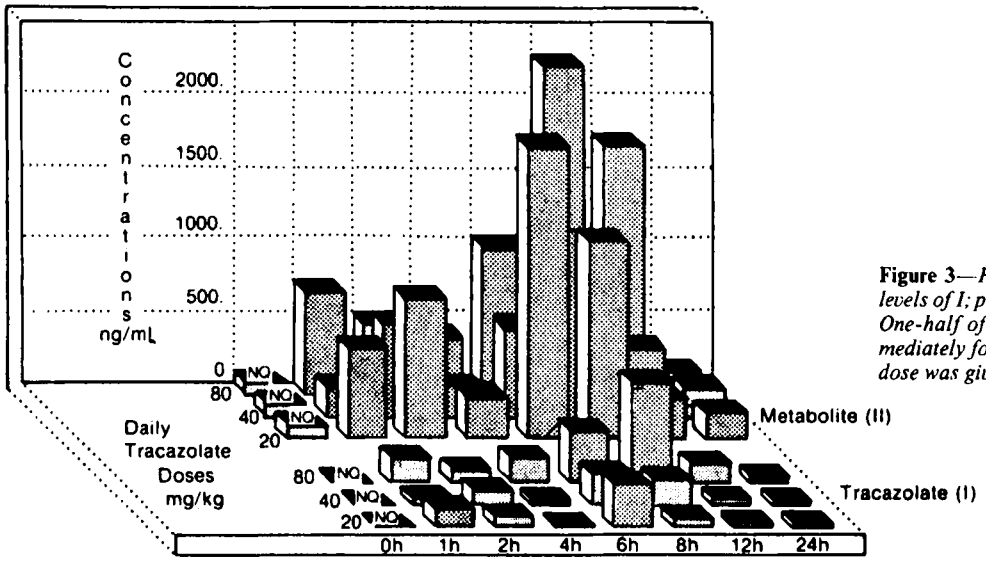

Figure 3—*Pharmacokinetic data from dogs at 3 dosing levels of I; plasma levels of I and II are reported in ng/mL. One-half of the daily dose of I was given by gavage immediately following the predose sample, and the remaining dose was given after the 4-h sample.*

RESULTS

A representative chromatogram, shown in Fig. 1, was from a study for which the dual analysis of I and II was used.

Recovery—Control of plasma pH was found not to be critical for the efficient extraction of I or III. However both pH control and efficient protein precipitation were found to be critical for the extraction of II from plasma. The plasma sample was buffered to pH 1.6 and protein was precipitated (5) when 10% trichloroacetic acid was added at a 1:5 volume ratio to the samples. Methanol spiking solutions were not found to affect the recoveries of I and II when added to plasma at levels of <1% up to 20% (v/v). External standard response factors were calculated and averaged for the matrix standards and the standard solutions. The ratio of the average standard solution response factor and the average matrix standard response factor was used to evaluate the percent recovery of desired compound[13]. Average recoveries of I and II, when extracted from spiked plasma, were 102 and 96%, respectively, during the production of the data listed in Table II. The coefficients of variation for recoveries across the concentration ranges listed in Table II were 4.3% for I and 6.8% for II. The diazomethane methylation of II had an efficiency of 94% *versus* standard solutions of IV. Hexane extracts of plasma resulted in a recovery of 86% of ^{14}C-labeled I added at the 1.0-μg/mL level measured by radiochemical techniques. Methyl *tert*-butyl ether extracts of plasma recovered 85% of ^{14}C-labeled II added at the 2 μg/mL level. Recoveries of [^{14}C]I and [^{14}C]IV were complete when injected directly into the HPLC as solutions in mobile phase.

UV detection was done at the maximum absorbance of I, which occurred at 240 nm with $\epsilon > 30{,}000$ and provided high sensitivity. From Table I, the peak height ratios for the matrix standards were reproducible and linear from 20 to 2000 ng/mL for I and from 100 to 5000 ng/mL for II measured as IV. Correlation coefficients were >0.99 for both curves, and y-intercepts were 0.0478 and 0.5834, respectively. Accuracy and precision were measured from routine calibration data which reflected the accuracy and precision expected in practice. The coefficients of variation were <10% and relatively constant over a wide analytical range for both compounds. The limits of quantification, represented in Table II, were selected to ensure reproducibility of the determination of the low standards on a daily basis.

Specificity—Capillary GC of sample extracts from animals dosed with I was used in the evaluation of specificity. The samples were carried through the sample preparation procedure for the dual determination of I and II described above. The dry residue of the sample extractions containing I, IV, and III was reconstituted in isooctane. This mixture was injected onto a 15-m fused silica capillary column coated with SE52 methyl silicone gum[14]. The column was temperature programmed from 80°C to 230°C in a gas chromatograph equipped with an alkali bead nitrogen detector[15]. As demonstrated in Fig. 2, the elution order of IV, I, and III was the same order as in the HPLC method.

Table I—Peak Height Ratios from Matrix Standards: Dual Determination of I and II [a]

Spiked Conc. in Plasma, ng/mL	Peak Height Ratios[b]	
	I	II (Measured as IV)
20	0.296	
	0.292	
50	0.710	
	0.691	
100	1.280	1.534
	1.276	1.384
250		2.850
		2.732
500	6.360	4.682
	6.504	4.572
2000	26.607	
	26.773	
2500		19.715
		20.036
5000		40.438
		41.135

[a] Procedure used for canine plasma samples. [b] Peak height ratios: a sample peak height/III peak height.

No interfering peaks with I or IV were seen under these GC conditions. Specificity was also evaluated by a GC–MS analysis of samples prepared according to the dual procedure from animals dosed with I. Isolated fractions of HPLC eluant of these samples corresponding to the HPLC peaks of I and IV were dried under nitrogen and the residue analyzed by GC–MS[16]. The pure compounds displayed molecular ions of m/z 304 and 290 for I and IV, respectively, a base peak of m/z 215, and several fragments including m/z 99. The mass spectra as well as the GC retention times of the HPLC eluants corresponded to the respective data of the pure compounds.

Stability of Prepared Samples—Plasma samples from animals dosed with I were analyzed several times for both I and II over a period of 5 months and were found to be stable. These plasma samples were stored frozen with intermittant thawing and maintenance at room temperature for several hours during preparation for analysis. Stock and standard solutions of I, II, III, and IV were stable, without measurable alteration, for at least 1 month if refrigerated between uses.

DISCUSSION

The quantitative HPLC procedures for tracazolate and its major metabolite described herein have been used to evaluate circulating levels of these com-

[13] The molecular weight ratio of II and IV was used to properly adjust the percent recovery to a molar basis.

[14] *Fused silica capillary column*; J & W Scientific, Rancho Cordova, Calif.

[15] Hewlett-Packard Model 5730 GC fitted for capillary columns.

[16] Model 4000 GC/MS; Finnigan Instruments, Sunnyvale, Calif., utilizing the same GC capillary conditions described above with the quadrupole MS operating under EI conditions at 70 eV and scanning from m/z 60–350.

Table II—Accuracy and Precision from Matrix Standards: Individual Determinations of I and II [a]

Compound	Value Expected, ng/mL	Mean Found[b], ng/mL	CV[c], %
I	20	23	4.7
	50	50	3.3
	100	100	6.3
	500	503	1.5
	2000	1852	4.5
II	100	100	7.9
	250	250	1.0
	500	515	4.3
	2500	2405	2.0
	5000	5146	3.6
	10,000	9835	3.5

[a] Procedure used for mouse plasma samples. [b] Found calculated from peak height ratio and peak height ratio response factors for I and II, respectively, from four standard curves each run on a different day for each compound. [c] For four determinations.

pounds in pharmacological, pharmacokinetic, and toxicological studies in rats, dogs, mice, monkeys, and rabbits. These procedures had reproducible quantifiable limits of 20 ng/mL for I and 50 ng/mL for II. Separate determinations of I and II were required for animal samples in which ratios of the concentration of II to the concentration of I were large enough to significantly degrade the resolution between the HPLC peaks. These high ratios occurred in plasma samples from dosed rats, mice, and rabbits. The separate determinations were used in these cases; otherwise, the selectivity, sensitivity, and other analytical indicators were the same for the plasma of all species tested.

Results from the dual determination of I and II in plasma from dogs are shown in Fig. 3. Part of these results were generated using the standardization curve data reported in Table I. The animals were dosed orally with one-half of the daily dose of I just after the time zero samples were taken and with the remainder of the daily dose after the 4-h samples. The data were evaluated for peak plasma level times (6–8 h) as well as for relationships between dose and plasma levels (no consistent dose response). The low detection limits for both I and II and the low plasma volume requirements for analysis have made this procedure very useful in multisampling and small animal studies. These points and the versatility of this procedure are amply demonstrated in Fig. 3.

REFERENCES

(1) J. B. Patel and J. B. Malick, *Eur. J. Pharmacol.*, **78**, 323 (1982).

(2) B. A. Meiners and A. I. Salama, *Eur. J. Pharmacol.*, **78**, 315 (1982).

(3) M. Melgar, F. Zuleski, and J. O. Malbica, *Fed. Proc.* **40**(3), 633 (1981).

(4) A. Darbre, in "Handbook of Derivatives for Chromatography," K. Blau and G. S. King, Eds, Hayden and Sons; 1977, p. 92–95 and 212.

(5) J. Blanchard, *J. Chromatogr.*, **226**, 455 (1981).

ACKNOWLEDGMENTS

We thank C. A. Hughes, D. Santarelli, J. P. Pollock Jr., K. R. Monson, and K. L. Nielson for their expert technical assistance, and R. Dedinas for the preparation of labeled compounds.

Collaborative Study of the USP Dissolution Test for Prednisone Tablets with Apparatus 2

DON C. COX ˣ **and WILLIAM B. FURMAN**

Received April, 19, 1982 from the *National Center for Drug Analysis, Food and Drug Administration, St. Louis, MO 63101.* Accepted for publication April 7, 1983.

Abstract □ Five lots of prednisone tablets that disintegrate within 5 min were collaboratively studied by 11 laboratories using USP Apparatus 2 under carefully controlled conditions. One lot gave complete dissolution. The reproducibility and repeatability of Apparatus 2 for the four lots still dissolving at the end of the test were 2.6 and 1.6% of label claim, respectively, for the 11 laboratories.

Keyphrases □ USP dissolution test—collaborative study of Apparatus 2, five lots of prednisone tablets, 11 laboratories □ USP Apparatus 2—collaborative study of dissolution of five lots of prednisone tablets, 11 laboratories □ Prednisone tablets—dissolution of five lots with USP Apparatus 2, collaborative study by 11 laboratories

The USP dissolution test for prednisone tablets (1) requires that when 12 tablets are tested, an average of ≥80% of the labeled amount of prednisone must dissolve in 30 min. The tablets are individually tested under experimental conditions which must be carefully controlled if reproducible results are to be obtained.

Four common sources of error associated with Apparatus 2 have been identified: misalignment of equipment (2), nonuniformity of the bottom curvature of vessels (3), excess gases in the dissolution medium (4), and the interaction of the test with slowly disintegrating tablets (4). Equipment, tools, and technique were developed and improved between 1978 and 1980 to control the first three sources of error. Certain products consist of slowly disintegrating tablets that do not always settle at the center of the bottom of the vessels; such variability of tablet position before disintegration can give imprecise results (4). However, rapidly disintegrating tablets gave results of sufficient precision to warrant a collaborative study.

The purpose of this collaborative study, conducted by 11 laboratories in the second half of 1980, was to measure the reproducibility and repeatability of Apparatus 2 under state-of-the-art conditions for prednisone tablets that disintegrate within 5 min. The secondary objectives were to determine whether personnel in many laboratories could correctly adjust Apparatus 2 by following a set of detailed instructions and whether the apparatus would hold the adjustment over an ~2-week test period.

EXPERIMENTAL

Dissolution Test—The instructions[1] to collaborators conformed to the USP conditions for testing prednisone tablets (1) with two exceptions. The collaborators were instructed to drop a tablet down the side of the vessel with the paddle rotating rather than to drop a tablet into the vessel and then start paddle rotation. The collaborators were instructed to position each vessel so that its vertical axis was not more than 1 mm at any point from the axis of the paddle shaft. A 2-mm tolerance is allowed in the USP specifications. If this second

[1] The complete instructions are available from the authors on request.

0022-3549/84/0500-0670$01.00/0

© 1984, American Pharmaceutical Association

Table II—Accuracy and Precision from Matrix Standards: Individual Determinations of I and II [a]

Compound	Value Expected, ng/mL	Mean Found[b], ng/mL	CV[c], %
I	20	23	4.7
	50	50	3.3
	100	100	6.3
	500	503	1.5
	2000	1852	4.5
II	100	100	7.9
	250	250	1.0
	500	515	4.3
	2500	2405	2.0
	5000	5146	3.6
	10,000	9835	3.5

[a] Procedure used for mouse plasma samples. [b] Found calculated from peak height ratio and peak height ratio response factors for I and II, respectively, from four standard curves each run on a different day for each compound. [c] For four determinations.

pounds in pharmacological, pharmacokinetic, and toxicological studies in rats, dogs, mice, monkeys, and rabbits. These procedures had reproducible quantifiable limits of 20 ng/mL for I and 50 ng/mL for II. Separate determinations of I and II were required for animal samples in which ratios of the concentration of II to the concentration of I were large enough to significantly degrade the resolution between the HPLC peaks. These high ratios occurred in plasma samples from dosed rats, mice, and rabbits. The separate determinations were used in these cases; otherwise, the selectivity, sensitivity, and other analytical indicators were the same for the plasma of all species tested.

Results from the dual determination of I and II in plasma from dogs are shown in Fig. 3. Part of these results were generated using the standardization curve data reported in Table I. The animals were dosed orally with one-half of the daily dose of I just after the time zero samples were taken and with the remainder of the daily dose after the 4-h samples. The data were evaluated for peak plasma level times (6–8 h) as well as for relationships between dose and plasma levels (no consistent dose response). The low detection limits for both I and II and the low plasma volume requirements for analysis have made this procedure very useful in multisampling and small animal studies. These points and the versatility of this procedure are amply demonstrated in Fig. 3.

REFERENCES

(1) J. B. Patel and J. B. Malick, *Eur. J. Pharmacol.*, **78**, 323 (1982).

(2) B. A. Meiners and A. I. Salama, *Eur. J. Pharmacol.*, **78**, 315 (1982).

(3) M. Melgar, F. Zuleski, and J. O. Malbica, *Fed. Proc.* **40**(3), 633 (1981).

(4) A. Darbre, in "Handbook of Derivatives for Chromatography," K. Blau and G. S. King, Eds, Hayden and Sons; 1977, p. 92–95 and 212.

(5) J. Blanchard, *J. Chromatogr.*, **226**, 455 (1981).

ACKNOWLEDGMENTS

We thank C. A. Hughes, D. Santarelli, J. P. Pollock Jr., K. R. Monson, and K. L. Nielson for their expert technical assistance, and R. Dedinas for the preparation of labeled compounds.

Collaborative Study of the USP Dissolution Test for Prednisone Tablets with Apparatus 2

DON C. COX ˣ **and WILLIAM B. FURMAN**

Received April, 19, 1982 from the *National Center for Drug Analysis, Food and Drug Administration, St. Louis, MO 63101.* Accepted for publication April 7, 1983.

Abstract □ Five lots of prednisone tablets that disintegrate within 5 min were collaboratively studied by 11 laboratories using USP Apparatus 2 under carefully controlled conditions. One lot gave complete dissolution. The reproducibility and repeatability of Apparatus 2 for the four lots still dissolving at the end of the test were 2.6 and 1.6% of label claim, respectively, for the 11 laboratories.

Keyphrases □ USP dissolution test—collaborative study of Apparatus 2, five lots of prednisone tablets, 11 laboratories □ USP Apparatus 2—collaborative study of dissolution of five lots of prednisone tablets, 11 laboratories □ Prednisone tablets—dissolution of five lots with USP Apparatus 2, collaborative study by 11 laboratories

The USP dissolution test for prednisone tablets (1) requires that when 12 tablets are tested, an average of ≥80% of the labeled amount of prednisone must dissolve in 30 min. The tablets are individually tested under experimental conditions which must be carefully controlled if reproducible results are to be obtained.

Four common sources of error associated with Apparatus 2 have been identified: misalignment of equipment (2), nonuniformity of the bottom curvature of vessels (3), excess gases in the dissolution medium (4), and the interaction of the test with slowly disintegrating tablets (4). Equipment, tools, and technique were developed and improved between 1978 and 1980 to control the first three sources of error. Certain products consist of slowly disintegrating tablets that do not always settle at the center of the bottom of the vessels; such variability of tablet position before disintegration can give imprecise results (4). However, rapidly disintegrating tablets gave results of sufficient precision to warrant a collaborative study.

The purpose of this collaborative study, conducted by 11 laboratories in the second half of 1980, was to measure the reproducibility and repeatability of Apparatus 2 under state-of-the-art conditions for prednisone tablets that disintegrate within 5 min. The secondary objectives were to determine whether personnel in many laboratories could correctly adjust Apparatus 2 by following a set of detailed instructions and whether the apparatus would hold the adjustment over an ~2-week test period.

EXPERIMENTAL

Dissolution Test—The instructions[1] to collaborators conformed to the USP conditions for testing prednisone tablets (1) with two exceptions. The collaborators were instructed to drop a tablet down the side of the vessel with the paddle rotating rather than to drop a tablet into the vessel and then start paddle rotation. The collaborators were instructed to position each vessel so that its vertical axis was not more than 1 mm at any point from the axis of the paddle shaft. A 2-mm tolerance is allowed in the USP specifications. If this second

[1] The complete instructions are available from the authors on request.

0022-3549/84/0500-0670$01.00/0

© 1984, American Pharmaceutical Association

Table I—Collaborative Dissolution Results [a] for Tablet 2, 10-mg Prednisone Tablets

Laboratory	Individual Tablet Results, % of label claim						Mean ± *SD*
	1	2	3	4	5	6	
1	41.7	44.1	42.9	37.0	43.7	44.1	42.3 ± 2.7
	43.8	43.3	39.6	40.2	43.8	42.6	42.2 ± 1.9
2	40.2	36.9	37.4	36.9	36.9	39.1	37.9 ± 1.4
	42.0	43.8	38.0	33.4	36.9	38.0	38.7 ± 3.7
3	41.9	36.0	37.6	37.8	44.2	43.1	40.1 ± 3.4
	34.8	33.0	34.2	34.5	32.7	34.7	34.0 ± 0.9
4	33.5	31.7	33.8	35.4	35.0	34.2	33.9 ± 1.3
	41.2	37.8	42.4	41.1	32.0	40.7	39.2 ± 3.8
5	33.7	35.9	41.1	33.3	40.4	37.6	37.0 ± 3.3
	35.1	33.2	39.0	34.6	34.6	37.6	35.7 ± 2.2
6	33.1	35.4	40.8	32.8	36.8	37.3	36.0 ± 3.0
	36.9	33.9	33.8	39.9	32.6	39.7	36.1 ± 3.2
7	32.1	36.4	34.8	38.9	37.6	33.7	35.6 ± 2.5
	33.9	43.2	45.6	34.6	43.9	42.8	40.7 ± 5.1
8	36.7	42.3	31.3	39.4	35.4	39.5	37.4 ± 3.8
	32.0	42.3	36.1	37.4	37.4	41.9	37.8 ± 3.8
9	46.2	44.5	41.5	41.8	39.4	42.1	42.6 ± 2.4
	45.7	49.1	46.4	46.7	44.4	45.8	46.3 ± 1.6
10	42.3	40.2	42.2	44.6	42.9	43.6	42.6 ± 1.5
	39.9	37.8	37.8	41.5	38.0	39.8	39.1 ± 1.5
11	38.8	43.8	31.2	41.1	41.0	39.2	39.2 ± 4.3
	45.6	47.5	39.6	37.0	41.8	39.4	41.8 ± 4.0

[a] Duplicate subsamples of six tablets.

Table II—Collaborative Dissolution Results [a] for Lot A, 5-mg Prednisone Tablets

Laboratory	Individual Tablet Results, % of label claim						Mean ± *SD*
	1	2	3	4	5	6	
1	99.2	102.7	98.6	96.2	103.1	100.7	100.1 ± 2.6
	102.5	98.9	97.3	101.3	101.2	98.1	99.9 ± 2.1
2	96.6	93.3	93.3	94.4	94.4	94.4	94.4 ± 1.2
	99.1	99.1	100.2	99.1	99.1	101.3	99.6 ± 0.9
3	96.2	98.7	96.6	98.4	98.2	97.8	97.6 ± 1.0
	100.0	98.4	95.6	100.7	100.7	98.4	99.0 ± 2.0
4	95.8	96.4	97.7	100.3	94.7	97.1	97.0 ± 1.9
	100.0	98.7	98.4	98.4	97.3	100.2	98.8 ± 1.1
5	98.2	100.2	101.2	100.7	100.2	98.8	99.9 ± 1.2
	100.0	102.1	97.7	101.0	102.3	99.6	100.4 ± 1.7
6	96.5	102.0	101.1	97.2	98.6	103.4	99.8 ± 2.8
	104.9	99.4	98.3	96.4	101.0	101.0	100.2 ± 2.9
7	98.0	96.6	100.8	96.9	96.7	98.6	97.9 ± 1.6
	99.3	100.6	99.2	101.0	96.0	101.7	99.6 ± 2.0
8	98.1	103.8	97.9	102.0	100.6	102.2	100.8 ± 2.4
	99.5	99.2	99.5	97.6	99.5	99.5	99.1 ± 0.8
9	95.9	97.0	93.5	94.1	97.4	96.1	95.7 ± 1.6
	96.0	103.5	97.8	110.6	100.5	103.1	101.9 ± 5.2
10	97.7	102.0	97.3	101.4	102.7	100.6	100.3 ± 2.3
	97.1	96.8	97.4	98.2	99.2	100.2	98.1 ± 1.3
11	103.0	98.9	102.3	98.4	101.4	97.9	100.3 ± 2.2
	95.3	96.4	93.7	94.6	99.1	95.9	95.8 ± 1.9

[a] Duplicate subsamples of six tablets.

requirement could not be met, the dissolution drive was deemed unsuitable for the study.

All laboratories used similar six-spindle dissolution drives[2], paddles[3], vessels[4], and slotted vessel covers[3] without guide bushings. A transparent water bath was specified. The collaborators were required to use a specially designed centering tool (5), a 2.5-cm depth gauge, and a torpedo level with two bubble indicators at right angles to each other. Step-by-step instructions for the setup of equipment were supplied. The volumes of deaerated dissolution medium were measured[5] in volumetric flasks or calibrated graduated cylinders. The medium was preheated to 37°C before it was added to the vessels[6]. After the medium was placed in the vessels, paddle rotation was started and the system was allowed to equilibrate for 15 min.

Each vessel, vessel position, and corrresponding tablet result were assigned the same number. Thus, for each subsample of six tablets tested simultaneously, every individual tablet result was identified with a particular vessel and position.

The tablets were immersed at 1-min intervals to permit the collaborator to draw and filter an aliquot of dissolution medium after each tablet had been subjected to the test for precisely 30 min. A 50-ml aliquot was taken from the same point in each vessel with a syringe equipped with a glass tube. The aliquot was then forced through a 0.8-μm porosity membrane filter[7], and the first 25 mL was discarded to wash the filter free of material that might interfere with the determinative step and to saturate the filter with drug. The filtered aliquots were diluted, if required, and the absorbances of the solutions were measured manually at 242 nm in a 1-cm cell. Portions of the same batch of dissolution medium used for a subsample were also used as the reference solution in the spectrophotometer and as the diluent for the standard.

Collaborative Study—An intralaboratory study was first conducted in this laboratory. Two analysts, one inexperienced with the dissolution test and the other experienced with the test, were able to follow the instructions and obtain similar results from different equipment. Portions of each lot of tablets, the instructions, and standard prednisone powder were then sent to 10 other FDA laboratories. Seven of the eleven laboratories have been conducting dissolution tests for several years and are considered experienced with the test. The others (laboratories 1, 5, 7 and 10) had received their dissolution equipment within 12 months of participating in the study and were considered relatively inexperienced.

Lots Studied—Four of the lots were commercially manufactured for use as drugs and were received under a certification program conducted in this laboratory. The fifth lot subjected to collaborative study was the USP disintegrating calibrator. All five lots were selected because they disintegrated within 5 min, gave means of six-tablet dissolution results that fell within a range of ~4% of label claim when tested in this laboratory, and responded to minor variations in the test to different extents.

One of the lots subjected to study will be referred to as Tablet 2, the name used to designate this lot in previous papers. Tablet 2, a lot labeled to contain 10 mg of prednisone per tablet, has been extensively studied (3, 4) and was provided for practice and to allow a collaborator to test the apparatus after it had been aligned. The collaborators were required to obtain results from six tablets that fell within 30–50% of label claim and whose mean fell within 35–43%. If the results were outside of these ranges, the collaborator was instructed to discuss the results with this laboratory before continuing the study. The disintegrated tablet particles stay on the bottom of the vessel throughout the test and are somewhat affected by misalignment of equipment and nonuniformity of vessel curvature. If excess gases are present in the dissolution medium, the tablet particles are lifted from the bottom of the vessel during the test, and dissolution results range from 50 to 90% of label claim.

Lot A, tablets labeled to contain 5 mg of prednisone, gives complete dissolution of drug content within 15 min. Lot A was used to assess the technique of each laboratory in the determinative steps: aliquoting, filtering, and measuring absorbance. The dissolution results should agree closely with the content uniformity results. When tested for content uniformity in this laboratory (6), 60 tablets gave a mean of 98.7% of label claim with an *SD* of 1.7%.

Lot B, tablets labeled to contain 5 mg of prednisone, gives dissolution results close to 80% of label claim at 30 min[8]. The disintegrated tablet particles stay on the bottom of the vessel throughout the test; lot B is similar to Tablet 2 in this respect. Lot B, though not extensively studied, is sensitive to misalignment of equipment. When tested for content uniformity (6), 60 tablets gave a mean of 95.1% of label claim with an *SD* of 1.5%.

Lot C, tablets labeled to contain 50 mg of prednisone, was selected because it also gives dissolution results of ~80% of label claim at 30 min[8]. The disintegrated tablet particles rise and circulate in the dissolution medium during the test. The tablets, though not studied extensively, appear insensitive to misalignment of equipment. When tested for content uniformity (6), 60 tablets gave a mean of 105.1% of label claim with an *SD* of 2.3%.

Lot D is the USP disintegrating calibrator[9], labeled to contain 50 mg of prednisone/tablet. This lot has been studied extensively in this laboratory (4) and was included in two collaborative studies (7, 8) conducted by the Pharmaceutical Manufacturers Association. The latter studies revealed large differences in results among laboratories. Although the tablets do not respond to the common systematic errors associated with the test (4), they were included as a blind sample for further study. Lot D is similar to lot C in physical

[2] Nine laboratories used the Model 72RL and two laboratories used the Model 72SI.; Hanson Research Corp., Northridge, Calif.

[3] Hanson Research Corp.

[4] Eli Lilly and Co., Indianapolis, Ind.

[5] Five laboratories used 500- and 900-mL flasks marked T.D./T.C.; Kimble Products, Vineland, N.J. Three laboratories used 500-ml. flasks marked T.C. and 1000-mL graduated cylinders. Three laboratories used 500- and 1000-mL graduated cylinders.

[6] One laboratory deviated from these instructions. Deaerated medium was added to the vessels from graduated cylinders at room temperature. The medium was then brought to 37°C.

[7] No. AAWP, 2.5-cm diameter; Millipore Corp., Bedford, Mass., or equivalent.

[8] This is not a "limiting value." If the paddle speed is increased and the test continued, complete drug dissolution is eventually achieved.

[9] USP lot F.

Table III—Collaborative Dissolution Results [a] for Lot B, 5-mg Prednisone Tablets

Laboratory	Individual Tablet Results, % of label claim 1	2	3	4	5	6	Mean ± *SD*
1	72.1	75.0	75.7	74.2	73.0	73.2	73.9 ± 1.4
	76.1	73.7	73.3	70.8	72.3	73.6	73.3 ± 1.8
2	78.1	73.8	82.5	73.8	80.3	76.0	77.4 ± 3.5
	85.2	73.7	71.4	78.4	76.0	76.0	76.8 ± 4.8
3	84.2	86.7	75.1	92.6	92.4	90.6	86.9 ± 6.7
	77.2	79.9	72.8	79.2	83.8	79.7	78.8 ± 3.6
4	70.8	78.0	73.6	71.2	67.0	73.4	72.3 ± 3.7
	68.4	70.7	80.8	78.8	71.2	74.5	74.1 ± 4.9
5	81.4	75.6	81.4	75.4	87.0	82.6	80.6 ± 4.4
	71.4	74.0	76.1	74.7	81.6	83.9	76.9 ± 4.8
6	73.6	78.3	74.0	73.3	73.1	76.5	74.8 ± 2.1
	70.7	72.7	71.4	67.7	69.8	72.5	70.8 ± 1.9
7	71.8	73.5	80.2	72.0	79.5	71.5	74.8 ± 4.0
	71.8	75.2	80.8	72.4	81.8	70.6	75.4 ± 4.8
8	71.4	78.0	70.5	77.4	68.2	74.6	73.4 ± 4.0
	73.5	80.0	68.2	76.4	67.5	76.9	73.8 ± 5.0
9	103.3	75.0	82.9	71.9	71.9	79.3	80.7 ± 11.9
	81.0	78.3	77.4	73.7	69.1	80.1	76.6 ± 4.5
10	80.3	74.5	72.3	79.6	76.4	77.0	76.7 ± 3.0
	80.4	75.0	75.0	74.7	75.9	73.1	75.7 ± 2.5
11	77.6	86.4	73.2	79.5	76.0	71.8	77.4 ± 5.2
	73.0	81.5	79.0	83.5	80.8	70.8	78.1 ± 5.1

[a] Duplicate subsamples of six tablets.

behavior; the tablet particles rise and circulate in the dissolution medium during the test.

Tablet 2 was packaged and labeled in 100-tablet bottles. The tablets from each of lots A, B, and C were tumbled in beakers until each lot was thoroughly mixed. Ten newly purchased bottles of the USP disintegrating calibrator were used as lot D in this study. Lots A, B, C, and D were repackaged in this laboratory by nesting 24 tablets from each lot in cotton in glass bottles possessing metal screw caps. The glass bottles were identified with the appropriate letter designation. Each collaborator was sent one unopened 100-tablet bottle of Tablet 2 and one repacked 24-tablet bottle of each of lots A–D.

Test Sequence—The collaborators were instructed to test a total of 12 tablets from each lot in the following sequence, six tablets being tested at a time: Tablet 2, lots A, B, C, D, A, B, C, and D, and Tablet 2. The study was planned to cover two 5-d work weeks. The first 4 d of the first week were devoted to setting up equipment and testing Tablet 2. The collaborators were then instructed to test six tablets from each of two lots as follows: day 5, lots A and B; day 6, lots C and D; day 7, lots A and B; day 8, lots C and D; and day 9, six tablets of Tablet 2. Laboratories 1, 3, 5, 6, 10, and 11 conformed to this schedule. All laboratories conformed to the sequence in which the tablets were tested. Often, several six-tablet subsamples of Tablet 2 were tested at the beginning of the study; however, only the last six results taken by each laboratory before progressing to lots A–D were used in the statistical analysis.

Table IV—Collaborative Dissolution Results [a] for Lot C, 50-mg Prednisone Tablets

Laboratory	Individual Tablet Results, % of label claim 1	2	3	4	5	6	Mean ± *SD*
1	79.0	78.7	75.8	77.0	77.1	78.9	77.8 ± 1.3
	78.4	79.6	77.7	77.4	77.1	75.4	77.6 ± 1.4
2	69.2	69.2	68.2	67.2	71.2	69.7	69.1 ± 1.4
	75.8	74.7	75.2	74.7	73.7	74.7	74.8 ± 0.7
3	77.5	77.0	75.1	76.4	76.7	75.4	76.4 ± 0.9
	77.2	77.6	77.2	76.3	77.4	75.2	76.8 ± 0.9
4	76.4	76.0	76.2	72.4	75.7	76.6	75.6 ± 1.6
	74.7	72.8	76.1	71.7	73.9	73.6	73.8 ± 1.5
5	78.6	75.9	76.9	76.3	77.9	75.6	76.9 ± 1.2
	77.0	77.8	77.9	77.6	76.4	77.8	77.4 ± 0.6
6	74.1	74.2	75.9	77.0	77.8	77.6	76.1 ± 1.6
	76.3	76.7	74.8	78.5	76.1	77.2	76.6 ± 1.2
7	77.7	77.6	75.8	77.8	78.4	77.5	77.5 ± 0.9
	76.3	75.5	79.5	77.8	77.4	77.0	77.3 ± 1.4
8	81.3	78.6	81.5	80.3	81.5	79.5	80.4 ± 1.2
	78.9	79.2	77.4	77.9	77.2	78.1	78.1 ± 0.8
9	70.1	69.0	72.3	71.9	67.1	70.5	70.1 ± 1.9
	73.3	76.4	75.0	75.7	78.4	78.2	76.2 ± 2.0
10	78.2	79.9	78.2	77.6	79.0	79.1	78.7 ± 0.8
	78.6	79.4	80.1	81.7	80.5	78.8	79.9 ± 1.2
11	77.9	76.4	78.1	76.3	78.8	77.4	77.5 ± 1.0
	79.3	76.5	78.9	79.3	77.7	76.6	78.1 ± 1.3

[a] Duplicate subsamples of six tablets.

Table V—Collaborative Dissolution Results [a] for Lot D, the USP Disintegrating Calibrator Tablets

Laboratory	Individual Tablet Results, % of label claim 1	2	3	4	5	6	Mean ± *SD*
1	67.6	65.3	64.8	66.0	67.2	66.5	66.2 ± 1.1
	64.6	67.8	66.3	65.7	67.7	66.7	66.5 ± 1.2
2	66.6	65.0	64.0	65.5	63.5	65.5	65.0 ± 1.1
	65.5	64.4	64.4	65.0	65.0	63.9	64.7 ± 0.6
3	66.5	63.8	59.8	63.5	64.2	65.6	63.9 ± 2.3
	68.5	66.6	59.2	66.3	65.0	62.2	64.6 ± 3.4
4	65.0	67.3	65.8	65.4	67.2	68.5	66.5 ± 1.4
	62.2	63.6	64.8	62.5	62.7	64.3	63.3 ± 1.0
5	68.2	70.6	69.5	63.2	69.2	68.2	68.1 ± 2.6
	69.2	65.3	66.1	64.1	65.3	68.7	66.4 ± 2.0
6	60.1	65.4	66.5	65.3	67.6	67.8	65.4 ± 2.8
	65.6	66.5	67.9	71.9	68.8	67.7	68.1 ± 2.2
7	64.1	68.5	66.6	68.3	67.8	66.7	67.0 ± 1.6
	68.1	68.2	68.1	68.5	66.4	67.4	67.8 ± 0.8
8	70.2	68.1	64.5	67.6	66.1	70.0	67.8 ± 2.2
	66.0	69.4	66.3	64.8	63.9	70.9	66.9 ± 2.7
9	64.4	61.3	63.6	64.6	57.0	60.4	61.9 ± 2.9
	62.9	65.5	65.6	61.0	63.1	65.3	63.9 ± 1.9
10	70.3	69.7	68.6	69.3	67.3	67.3	68.8 ± 1.2
	68.1	67.1	70.3	68.3	65.2	64.8	67.3 ± 2.1
11	61.0	66.7	66.5	69.7	67.6	65.8	66.2 ± 2.9
	69.7	65.8	68.1	68.1	72.1	68.2	68.7 ± 2.1

[a] Duplicate subsamples of six tablets.

Reported Difficulties—When laboratory 3 first tested Tablet 2, high results traced to excess gases in the medium were obtained; subsequent tests of Tablet 2 were satisfactory. At the beginning of the study, laboratory 4 reported that the mean of six tablet results from Tablet 2 fell slightly below the acceptance range. Since the individual tablet results fell within the specified range, laboratory 4 was instructed to continue the study. Midway through the study, laboratory 6 observed background interference in the UV spectra of the tablets and repeated the second six-tablet tests for lots A and B. The background interference was attributed to dirty spectrophotometer cells. Laboratory 9 obtained high results from Tablet 2 at the beginning of the study. A loose drive belt was found on the apparatus. After the belt was adjusted, satisfactory results were obtained.

Laboratory 11 obtained high results from Tablet 2 at the end of the study. Inspection of the dissolution drive revealed that the base of the unit was warped. After the base had been mounted on a plastic plate to provide additional support, laboratory 11 repeated the study and obtained 12-tablet means that were lower by 3.0, 0.8, 7.0, 1.9, and 1.4% of label claim, respectively, for Tablet 2 and lots A, B, C, and D; these means were significantly ($p < 0.001$) lower for lots B and C. The results from the repeated study were used in the statistical analysis.

The results obtained by laboratory 2 for lots C and D were ~20% of label claim below those reported by the other laboratories. Although an adequate explanation could not be found, the cause of the discrepancy was shown to be related to the laboratory and not to the stability of the tablets. Laboratory 2 was asked to repeat the test for lots C and D, and the results of the repeated tests were used in the statistical analysis.

RESULTS AND DISCUSSION

The individual tablet results for each lot and laboratory are given in Tables I–V. The results of the six-tablet subsamples are grouped in rows of six across the tables and correspond to the tablets tested simultaneously. The first subsample tested by each laboratory appears above the second subsample. The results correspond by number to position and vessel number: the results in the "tablet 1" column were obtained from position and vessel 1, *etc.*

To achieve the purpose of the study, it was necessary that the laboratories conduct the dissolution tests under similar conditions and that the laboratories be able to maintain these conditions with respect to time. Because each lot responds differently to changes in the test conditions, such changes within a laboratory could only be monitored by staggering the times at which the lots were tested. Only Tablet 2 and lot B responded to known systematic errors associated with the test. Thus, Tablet 2 was purposely tested at the beginning and end of the sequence, and tests of lot B were spaced within the sequence.

The possibility of a "settling in" effect was noted in a previous collaborative study of Apparatus 2 (9); *i.e.*, differences among dissolution results with re-

Table VI—Analysis of Variance for 11 Laboratories and Group 1 [a]

Source	Sum of Squares	*DF*	Mean Square	*F* Ratio	*F* (0.95)
Laboratories	115.44	10	11.54	0.89	2.2
Grouped lots	20,694.52	3	—	—	—
Interaction	388.39	30	12.95	3.16	1.7
Means of six	180.20	44	4.10	—	—
Total	21,378.55	87			—
Reproducibility *SD*[b]			2.89		
Repeatability *SD*[b]			2.02		

[a] Six-tablet subsamples; Group 1 is Tablet 2 and lots B, C, and D. [b] In percent of label claim.

spect to time were present in the early days of the study but not later on. In the present study the time between tests and the test sequence were both specified so that all laboratories would be subjected to the same time effects, if present. Several laboratories stated that they could not participate in the study if they were required to observe the exact daily schedule, and these laboratories were instructed to ignore it. However, all laboratories were required to follow the same test sequence.

Reproducibility and Repeatability—The statistical techniques of Steiner, presented in Youden and Steiner (10) were used to assess the reproducibility and repeatability standard deviations of the tablets tested with Apparatus 2. The reproducibility standard deviation measures the agreement of individual results obtained by different laboratories with the same method on identical test material. It may be expressed by:

$$R = (L + I + W)^{1/2} \qquad \text{(Eq. 1)}$$

where L is the error variance among laboratories, I is the error variance of the interaction among laboratories and test material, and W is the error variance within laboratories.

The repeatability standard deviation measures the agreement of successive results obtained by a single laboratory with the same method on identical test materials and conditions. It may be expressed by:

$$S = (W)^{1/2} \qquad \text{(Eq. 2)}$$

The variances necessary to calculate these two standard deviations are obtained from the mean squares derived from an analysis of variance of two crossed classifications, laboratories and test materials, with replication.

The means of the two six-tablet subsamples reported by each laboratory for each lot were treated as duplicate determinations in the step-by-step procedure suggested by Steiner (10) to obtain the reproducibility and repeatability standard deviations. If the subsamples from each lot could be considered identical, the differences among the mean values within and among the laboratories could be attributed to method error. In reality, associated with these subsample means is an inherent variance that is one-sixth the variance of the tablets. The within-laboratory variance contains this source of variance in addition to the within-laboratory error variance. A reduction of this inherent variance would have required a substantial increase in the workload of each collaborator, an impractical approach. Thus, it was important to select lots that gave reasonably uniform dissolution results. The inherent tablet variance is dealt with later in this paper.

Examination of the Reported Means—The six-tablet means reported by each laboratory (Tables I–V) were averaged into 12-tablet means that were then ranked from low to high for each lot. These rank values were summed across the five lots for each laboratory. The rank totals were then tested at the 5% significance level to determine if a laboratory consistently reported high or low results; none did. The ranked 12-tablet means within each lot were then tested at the 5% significance level to determine if any mean within the lot was abnormally high or low [Dixon's test (10)]; none were.

When an analysis of variance is performed on data that can be broken down into classifications of laboratories and lots, the assumption is made that the within-lot variance is constant for the lots. When data are obtained from lots that respond to minor variations in the method to different extents, the within-lot variance can be different from lot to lot. Steiner (10) suggests a statistical test, based on comparison of ranges of laboratory means, to determine groups of lots that have similar variances. The test indicated, at the 5% significance level, that the data from all five lots could not be grouped together. The data from Tablet 2 and lots B, C, and D could be grouped if the data from lot A were removed. Tablet 2 and lots B, C, and D have a common characteristic—they do not give complete dissolution of prednisone at 30 min. Thus, it is logical to treat these lots together in an analysis of variance and to treat lot A separately. When grouped for statistical analysis, Tablet 2 and lots B, C, and D were designated Group 1.

The variances of the six-tablet means reported by each laboratory for each lot in Group 1 were calculated. The ratio of the largest variance to the smallest variance was tested at the 5% significance level and showed that the within-lot variance could be considered constant for the group. An analysis of variance was then performed on this group.

Reproducibility and Repeatability of Group 1—The analysis of variance is shown in Table VI. The *F* ratios indicate that there are no significant differences among the laboratories at the 5% level, but that there is a significant interaction among the laboratories and lots. The significant interaction mean square implies that the lots in this group responded differently to Apparatus 2 from one laboratory to the next. For example, laboratories 2, 3, and 9 reported among the highest results for lot B and the lowest results for lot D; laboratories 6 and 8 reported among the lowest results for lot B and among the highest results for lot D. This interaction was great enough overall to be significant.

The among-laboratory variance, the interaction variance, and the within-laboratory variance were obtained from the mean squares given in Table VI. The reproducibility and repeatability standard deviations were then calculated and are also shown in the table.

Physical Dissolution Characteristics—A tablet whose disintegrated particles stay on the bottom of the dissolution vessel will usually react more to minor differences in Apparatus 2 than tablets whose disintegrated particles are lifted and circulated by the dissolution medium. In this study the former type of product was represented by Tablet 2 and lot B, termed Group 2, and the latter type of product by lots C and D, termed Group 3.

Reproducibility and Repeatability of Groups 2 and 3—Because of their distinctly different physical behavior in the dissolution test, it was of interest to perform an analysis of variance for groups 2 and 3 and to calculate the reproducibility and repeatability standard deviations for each group. Analyses of variance for these groups are shown in Table VII. Group 2 did not show significant differences among laboratories, but did show significant interaction among the laboratories and lots. Group 3 showed significant differences among laboratories, but no significant interaction among laboratories and lots. Thus, lots C and D responded in the same manner to Apparatus 2 in a given laboratory; Tablet 2 and lot B did not. The reproducibility and repeatability standard deviations of each group are given in Table VII. As expected, these terms are somewhat higher for group 2.

Examination of the Individual Tablet Results—A total of 132 results were reported by the 11 laboratories for each lot. Steiner provides a statistical test for rejection of outlying results at the 5% significance level, based on the distance, in standard deviations, that an individual result lies away from the mean Youden and Steiner (10). When one examines a total of 100–200 results, a single result must lie from 3.4 to 3.6 *SD* away from the mean before it can be considered an outlier. The mean and standard deviation for the 132 results for each lot are given in Table VIII. For each of lots A, B, and D, laboratory 9 reported one individual tablet result that was, respectively, 4.4, 4.9, and 3.5 *SD* from the mean of the lot. No cause for these outlying results could be found. The outlier from lot D was borderline and was not far removed from

Table VII—Analysis of Variance for 11 Laboratories and Two Groups [a]

Source	*DF*	Group 2 Mean Square	Group 2 *F* Ratio	Group 3 Mean Square	Group 3 *F* Ratio	*F* (0.95)
Laboratories	10	18.75	1.24	14.46	7.23	3.0
Grouped lots	1	15,393.84		1178.35	—	—
Interaction	10	15.17	2.73	2.00	0.76	2.3
Means of six	22	5.56	—	2.63		
Total	43	368.73	—	32.58	—	
Reproducibility *SD*[b]		3.29		2.33		
Repeatability *SD*[b]		2.36		1.62		

[a] Six-tablet subsamples. Group 2 is Tablet 2 and lot B; group 3 is lots C and D. [b] In percent of label claim.

Table VIII—Statistical Summary of Collaborative Dissolution Results (Percent of Label Claim) for Individual Results from Prednisone Tablets by USP Apparatus 2

Statistics	Tablet 2	Lot A	Lot B	Lot C	Lot D
Mean[a]	38.9	98.9	76.3	76.5	66.1
Total SD[a]	4.2	2.7	5.5	2.9	2.6
S_t[b]	3.0	2.1	4.7	1.3	2.1
S_m[c]	3.2	1.8	3.5	2.7	1.9

[a] $n = 132$. [b] Standard deviation of six tablet results (see text). [c] Standard deviation of means of six tablet results (see text).

results reported by other laboratories. Though the outliers from lots A and B are far removed from the rest of the results for these lots, it is doubtful that including them in an analysis of variance would alter conclusions drawn from the analysis.

Analysis of Variance of Each Lot—Usually, the dissolution test is performed on six tablets at one time, each in its own dissolution environment. Differences in the individual tablet results can be attributed to differences in the tablets only if the dissolution environments affect the tablets similarly. Nonuniform environments, such as differences in liquid velocities generated by misaligned paddle shafts or irregular vessels, may cause individual tablets to disintegrate and dissolve at different rates. With the type of six-spindle dissolution apparatus used in this study, each combination of paddle and vessel may produce a different environment; however, each environment can be reproduced. Thus, if the assumptions are made that there is no interaction between subsamples and positions of an apparatus within a laboratory and that the variance obtained from the positions of the apparatus can be pooled, a two-way analysis of variance can be performed on the data reported by each laboratory for each lot. These sources of variances can then be pooled for all the laboratories.

The analyses for all the lots are shown in Table IX. The sources of variance from subsamples, positions, and the interaction between them are vested with the laboratories (11). The F ratios of the laboratories (the laboratories' mean square divided by the between-subsample mean square) indicate differences among laboratories for lots B, C, and D. The between-subsamples' F ratios (the between-subsamples' mean square divided by the interaction mean square) indicate highly significant differences between subsamples within laboratories for all the lots. The among-positions' F ratios (the among-position mean square divided by the interaction mean square) indicate marginal differences among positions for Tablet 2 and lot D, but the F ratio for lot B is highly significant.

Intepretation of the Mean Squares—The interaction mean squares (Table IX) are residual variances that contain the inherent tablet variance and the within-laboratory error variance of the analytical procedure used to determine the quantity of dissolved drug. The design of the study does not permit these variances to be separated. It is reasonable to assume, however, that the variance of the analytical procedure is constant within a laboratory for all the lots. Because lot A dissolves completely, one would expect its dissolution results to be similar to its content uniformity results. If the standard deviation of the content uniformity results for lot A from this laboratory is converted to a variance, a value of 2.89 is obtained. This variance also contains the inherent tablet variance and the within-laboratory error variance (0.77, as percent of label claim) obtained by a different procedure that was used to determine the quantity of the dissolved drug (6). If it is assumed that this laboratory is typical of those in that collaborative study (6), the within-laboratory error variance obtained from that study (0.77) may be subtracted from the variance of the content uniformity results (2.89) to obtain an independent estimate of 2.12 for the tablet variance of lot A. This value for lot A may then be subtracted from the interaction mean square in Table IX (4.79) to obtain an estimate of 2.67 for the within-laboratory error variance of the analytical procedure used in this study. The latter value indicates that the inherent tablet variance is a relatively small part of the interaction mean square of lot C, whereas it contributes a large portion of the interaction variance of lot B.

The among-position mean square contains the interaction mean square and possibly a mean square associated with the influence exerted by different apparatus positions on the tablet results. The magnitude of the latter mean square depends on the dissolution characteristics of the lot under test and on the extent that the positions differ with respect to the alignment of the paddles in the vessels and the uniformity of the vessels. It has been shown that the results obtained for lots A and C are affected very little by the differences in apparatus positions, but that the results for Tablet 2, lot B, and lot D are influenced to various extents by such differences.

The within-subsample mean square is a pooled variance that measures the dispersion of the results of six tablets tested simultaneously. It is obtained by pooling the interaction mean square with the among-position mean square for each lot and is 9.05, 4.58, 22.50, 1.61, and 4.26, respectively, for Tablet 2 and lots A, B, C, and D. It may be expressed by:

$$MS_w = A \qquad \text{(Eq. 3)}$$

The collaborators verified that the apparatuses met or exceeded USP specifications before they started the study. From a practical viewpoint, therefore, the within-subsample mean square represents the residual variance obtainable for each lot at the current state of the art and was taken to represent the tablet variance.

The between-subsample mean square is a pooled variance that measures the dispersion of six-tablet means within a laboratory. It may be expressed by:

$$MS_b = A + 6B \qquad \text{(Eq. 4)}$$

where B is a variance that measures a dispersion that cannot be attributed to A. The B term may be considered as a pooled within-laboratory error variance.

The laboratories mean square is a variance that measures the dispersion of 12-tablet means. It may be expressed by:

$$MS_l = MS_b + 12C \qquad \text{(Eq. 5)}$$

where C is a variance that measures a dispersion that cannot be attributed to A and B. The C term may be considered as a pooled among-laboratory error variance.

If no error existed within or among laboratories, the three mean squares would, in theory, be the same and the corresponding F ratios would be unity. In practice, the mean squares will almost always be different. If they are the same, the F ratios will fluctuate around unity. To measure the probability that the mean squares are the same, the F ratios are compared with tabulated values that would not be exceeded at that probability level. Equations 3–5 can be used to calculate algebraically the within-laboratory error variance (B) and the between-laboratory error variance (C) for each lot. Since the F ratio may fluctuate around unity if two mean squares are equal, the values calculated for B and C may be negative or positive. The significance of B or C should be judged against the probability of the corresponding F ratios.

Acceptance Ranges—If laboratories that exemplified the 11 laboratories in the study obtained mean results from six tablets tested simultaneously, those means would have a dispersion about the overall mean of a lot that can be expressed by:

$$S_m = [(A/6) + B + C]^{1/2} \qquad \text{(Eq. 6)}$$

where S_m is a standard deviation that may be considered as the standard error about the overall mean result. It is the standard deviation for means of six tablets. If B or C is negative, the value may still be summed algebraically as long as the sum of B and C is positive. If the sum of B and C is negative, the sum is assumed to be zero (10) and

$$S_m = (A/6)^{1/2} \qquad \text{(Eq. 7)}$$

The standard deviation of the six tablets in a subsample is expressed as

$$S_t = A^{1/2} \qquad \text{(Eq. 8)}$$

S_m and S_t for each lot are given in Table VIII.

Table IX—Analysis of Variance for 11 Laboratories and All Lots

Source	DF	Tablet 2 Mean Square	Tablet 2 F Ratio	Lot A Mean Square	Lot A F Ratio	Lot B Mean Square	Lot B F Ratio	Lot C Mean Square	Lot C F Ratio	Lot D Mean Square	Lot D F Ratio	F (0.95)
Laboratories	10	89.42	2.58	12.86	0.46	114.66	3.56	65.56	3.02	32.53	3.50	2.85
Between subsamples	11	34.61	5.00	27.98	5.84	32.33	2.94	21.70	12.19	9.30	2.96	1.95
Among positions	55	11.19	1.62	4.38	0.91	33.99	3.09	1.44	0.81	5.39	1.72	1.54
Interaction	55	6.91	—	4.79	—	11.01	—	1.78	—	3.14	—	—
Total	131	17.33	—	7.18	—	30.36	—	8.18	—	6.84	—	—

Acceptance ranges for each of the lots may be established in a manner similar to that used in the PMA studies (7, 8) to establish the acceptance range for the USP calibrators. An acceptance range of six-tablet means could be defined as mean $\pm 2S_m$ for 132 tablets. The standard deviation of six individual tablets should not exceed $1.97S_t$ (12). Thus, from the data in this study, the acceptance range of means of six tablet results for Tablet 2 would be from 32.5 to 45.3% of label claim; the standard deviation of six tablet results should not exceed 5.9%. The acceptance range of means of six tablet results for lot D, the USP disintegrating calibrator, would be from 62.4 to 69.8% of label claim; the standard deviation of six tablet results should not exceed 4.1%.

Reproducibility and Repeatability of Apparatus 2—The repeatability standard deviations of groups 1, 2, and 3 contain two sources of variance: the inherent variance of the tablets and a within-laboratory error variance. The following relationship exists for the mean square of the means of six given in Tables VI and VII and the between-subsample mean squares for the lots reported in Table IX:

$$MS_m = \Sigma(MS_{bj})/mq = \Sigma(A_j)/mq + \Sigma(B_j)/q \qquad \text{(Eq. 9)}$$

where MS_m is the mean square of means of six results for q lots in the group, MS_{bj} is the between-subsample mean square for the jth lot in the group, m is the number of tablets in a subsample, A_j is the within-subsample mean square for the jth lot in the group, and B_j is the within-laboratory error variance attributed to the jth lot. The term $\Sigma(B_j)/q$ can be considered as the within-laboratory mean-square error for the group.

For group 1 (Tablet 2 and lots B, C, and D) this term is 2.52. The repeatability standard deviation of Apparatus 2 for this group is the square root of 2.52, or 1.59% of label claim. The error from the interaction of the laboratories with the samples and the error among the laboratories remain unchanged. The corresponding reproducibility standard deviation of Apparatus 2 for this group is then 2.60% of label claim. The reproducibility and repeatability standard deviations of Apparatus 2 are, respectively, in percent of label claim: for group 2 (Tablet 2 and lot B), 2.86 and 1.71; for group 3 (lots C and D), 2.22 and 1.46.

Effect of Time and Test Sequence—Table IX shows significant differences between subsamples within laboratories. A difference between subsamples within laboratories might indicate an effect that could be associated with time or the sequence in which the lots were tested. Therefore, the data from the six laboratories that followed the daily schedule were tested. For each lot the six-tablet means reported for the first subsample were grouped and compared with a similar group from the second subsample. A one-way analysis of variance showed no significance difference ($p > 0.25$) between the first and second subsample for any of the lots. The test was then repeated for the data from all laboratories. Again, no significant difference was found ($p > 0.1$). Thus, neither the time of testing nor the order of testing contributed significantly to the results.

Effect of Experience—For each lot, the 12-tablet means of the four laboratories that had the least experience were grouped together for comparison to the 12-tablet means of the seven experienced laboratories. A one-way analysis of variance showed no significant difference ($p > 0.05$) between these groups for any of the five lots. Thus, if a laboratory carefully follows the instructions used in this study, the level of previous experience with the test is not significant.

CONCLUSIONS

The laboratories satisfactorily controlled the critical parameters of Apparatus 2. Of a total of 660 tablet results reported by 11 laboratories, only two were considered outliers. The reproducibility standard deviation of Apparatus 2 for means of six tablet results was found to be 2.60% of label claim for a group of four lots of tablets that disintegrate rapidly, are undergoing dissolution at the time the aliquots are taken, and exhibit different dissolution characteristics. The corresponding repeatability standard deviation was 1.59%. Statistical analysis indicated that the lots in this group responded somewhat differently from one laboratory to the next.

Tablet 2 was useful in several laboratories for identification and correction of problems with technique and equipment. The requirement that each laboratory obtain acceptable results from this difficult lot at the beginning of the study was integral to the success of the study. The results indicate that Tablet 2 was marginally affected by the internal paddle-vessel combinations of the dissolution apparatuses used in the laboratories. The mean of 132 tablet results (38.9%) of label claim, and the standard deviation from the within-subsample (38.9% of label claim), results (3.0%) compare favorably with the mean of 72 tablet results (39.7% of label claim) and the standard deviation from the within-position results (2.7%) reported previously by this laboratory (3).

For lot A, the mean (98.9% of label claim) and the within-subsample standard deviation (2.1%) obtained from this dissolution study, compare favorably with the respective values (98.7 and 1.7%) obtained from the content uniformity results in this laboratory. Thus, the laboratories exercised good control over the analytical procedures associated with the measurement of dissolved prednisone. The standard deviation for means of six tablet results (1.8%) is similar to that expected if several laboratories were to test these tablets for content uniformity.

For lot B, the mean of 132 tablets (76.3% of label claim) indicates that this lot comes within 4% of label claim of passing the USP dissolution requirement. This is precisely the type of tablet product that often leads to disagreement in "pass-fail" decisions in different laboratories. The results indicate that lot B was affected by the internal paddle-vessel combinations of the dissolution apparatuses used in the laboratories. Even though lot B possesses this degree of sensitivity to minor variations in the test, 10 of the 11 laboratories obtained results that showed that lot B failed the USP requirement.

Lot C also comes within 4% of label claim of passing the USP requirement. All of the laboratories obtained results that showed that this lot fails the requirement. Since this lot is not affected by the paddle-vessel combinations of the dissolution apparatus, better agreement among laboratories is to be expected.

For lot D, the USP disintegrating calibrator, the mean of 66.1% of label claim obtained in this study compares favorably with the mean of 66.8% obtained in the Pharmaceutical Manufacturers Association study of 1980 (7). The within-subsample standard deviation (2.1%) compares well with that of the PMA study (2.3%). The standard deviation of means of six tablet results found in this study (1.9%) is considerably smaller than that reported previously (7) (5.1%). Both studies indicate significant differences among laboratories. In addition, this study indicates significant differences within laboratories. However, the magnitude of the differences associated with the laboratories is smaller in this study than in the Pharmaceutical Manufacturers Association study. The results indicate that lot D was marginally affected by the internal paddle-vessel combinations of the dissolution apparatuses. This laboratory, however, has not been able to show a correlation between results obtained with this lot and misaligned paddles or irregular vessels (4).

The analysis of variance for group 3 (lots C and D) indicates that the lots respond to Apparatus 2 similarly within a laboratory and that there is a significant bias among laboratories. Thus, a laboratory that obtains a high or low result for lot C is likely to obtain a correspondly high or low result for lot D. The reproducibility and repeatability standard deviations for this group were found to be 2.22 and 1.46% of label claim, respectively, for Apparatus 2.

The analysis of variance for group 2 (Tablet 2 and lot B) indicates that each lot responds differently to perturbations in Apparatus 2 from one laboratory to the next, but that there are no significant differences among laboratories for the group. That the lots respond differently from one laboratory to the next may be explained by the differing degrees of sensitivity these lots show toward dissolved air in the dissolution medium and internal misalignment of the dissolution apparatuses. The reproducibility and repeatability standard deviations for this group were found to be 2.86 and 1.71% of label claim, respectively, for Apparatus 2. These standard deviations indicate that, at present, tablets whose disintegrated particles stay on the bottom of the vessel cannot be tested with the same precision as tablets whose disintegrated particles are lifted and swirled by the dissolution medium. It is encouraging to note that the differences between the precisions are fairly small.

REFERENCES

(1) "The United States Pharmacopeia," 20th rev., U.S. Pharmacopeial Convention, Inc., Rockville, Md., 1980, p. 655.

(2) D. C. Cox and W. B. Furman, *J. Pharm. Sci.*, **71**, 451 (1982).

(3) D. C. Cox, C. E. Wells, W. B. Furman, T. S. Savage, and A. C. King, *J. Pharm. Sci.*, **71**, 395 (1982).

(4) D. C. Cox, W. B. Furman, L. K. Thornton, T. W. Moore, and E. H. Jefferson, *J. Pharm. Sci.*, **72**, 910 (1983).

(5) A. A. Serino, *J. Pharm. Sci.*, **71**, 725 (1982).

(6) J. F. Brower, *J. Assoc. Off. Anal. Chem.*, **60**, 27 (1977).

(7) A. C. Sarapu, A. R. Lewis, and M. F. Grostic, *Pharmacopeial Forum*, **6**, 172 (1980).

(8) S. Fusari, M. F. Grostic, A. R. Lewis, J. Poole, and A. C. Sarapu, *Pharm. Technol.*, **5**(9), 135 (1981).

(9) D. J. Schuirmann, *Pharmacopeial Forum*, **6**, 75 (1980).

(10) W. J. Youden and E. H. Steiner, "Statistical Manual of the Association of Official Analytical Chemists," Association of Official Analytical Chemists, Washington, D.C., 1975, pp. 72–82.

(11) C. A. Bennett and N. L. Franklin, "Statistical Analysis in Chemistry and the Chemical Industry," Wiley, New York, N.Y., 1954, pp. 350–368.

(12) "ASTM Manual on Presentation of Data and Control Chart Analysis," ASTM Special Technical Publication 15D, American Society for Testing and Materials, Philadelphia, Pa., 1976, p. 83.

ACKNOWLEDGMENTS

The authors acknowledge J. F. Brower for participating in the intralaboratory study and for helping to clarify the instructions to collaborators; D. J. Schuirmann, Division of Biometrics, National Center for Drugs and Biologics, for suggesting the time schedule used in the study; and S. M. Marchese, Winchester Engineering and Analytical Center, for his contribution toward the success of the study. The authors thank the following FDA collaborators who participated in this study: M. M. Shepherd, Atlanta Regional Laboratory, P. Knight and V. P. Shah, Biopharmaceutics Laboratory, Washington, D.C., J. S. Elkins, Dallas District, R. L. Ballbach, Detroit District, D. E. Ready, Kansas City District, T. S. Savage, Los Angeles District, T. Hoffmann, Minneapolis District, E. S. Moore, New York Regional Laboratory, R. H. Johnson, Seattle District, and L. Gelber, Winchester Engineering and Analytical Center. The authors also thank Dr. S. Bolton, St. John's University, Jamaica, N.Y., for his constructive reviews of this paper.

Physicopharmaceutical Characteristics of an Oil-in-Water Emulsion-Type Ointment Containing Diclofenac Sodium

AKIRA TAKAMURA *x, FUMIYOSHI ISHII *, SHUN'ICHI NORO *, and MASUMI KOISHI ‡

Received July 26, 1982, from the **Meiji College of Pharmacy, 1-22-1, Yato-cho, Tanashi-shi, Tokyo, Japan*, and the ‡*Faculty of Pharmaceutical Science, Science University of Tokyo, 12, Ichigaya Funagawara-machi, Shinjuku-ku, Tokyo, Japan.* Accepted for publication April 5, 1983.

Abstract □ The oil-in-water (o/w) emulsion-type ointment was prepared with food additives containing diclofenac sodium. The oil phase and the emulsifier used were 1,2,3-propanetriyl trioctanoate (caprylic acid glyceryl ester) and sugar wax, and sugar ester, respectively. The emulsion stability of the o/w emulsion-type ointment as well as the diclofenac sodium release profile were investigated and compared with those from conventional ointments. The emulsion stability was evaluated in terms of the viscosity of the emulsion product, the particle size distribution of oil droplets, and the zeta potential of the droplets. It was found that sugar esters have excellent properties as emulsifiers, based on the results of viscosity and zeta potential measurements. The *in vitro* release test revealed that the amount of diclofenac sodium released from o/w emulsion-type ointment was greater than from the hydrophilic and absorptive ointments. Accordingly, it was concluded that o/w emulsion-type bases are suitable for pharmaceutical use in ointment products.

Keyphrases □ Diclofenac sodium—release from various topical ointment bases, oil-in-water emulsions, physicopharmaceutical characteristics □ Oil-in-water emulsions—use as a topical ointment base for diclofenac sodium, release rate, physicopharmaceutical characteristics □ Ointment bases—oil-in-water emulsions, topical release of diclofenac sodium, physicopharmaceutical characteristics

In developing procedures for the design of pharmaceutical products, it is necessary to consider the bioavailability and safety of both the drugs and bases. Potent steroidal agents, which have substantial anti-inflammatory properties, have been used for external application for a long time. However, these steroidal agents have side effects (1), which were found to be directly dependent on the amount of drug applied to the skin. Therefore, various nonsteroidal agents (2, 3) have been developed recently to replace the steroidal agents.

Diclofenac sodium is a potent nonsteroidal anti-inflammatory agent, which has been limited to oral (4) and rectal administrations (5). In this investigation, diclofenac sodium was selected for topical application because no toxicity or topical irritation has been reported.

Although reports on ointment application have been published (6–8), few have dealt with the selection of optimum conditions for the preparation of the ointment. Oil-in-water (o/w) emulsion-type ointment bases offer many advantages over other preparations (9): they permit incorporation of aqueous and oleaginous ingredients, they allow a greater release of many incorporated medicaments, and their rheological properties can be controlled easily. Therefore, the selection of oil base and emulsifier is one of the most important factors in the preparation of o/w emulsion-type bases.

1,2,3-Propanetriyl trioctanoate (caprylic acid glyceryl ester, I) a medium-chain triglyceride, and sugar wax were chosen as the oil phase, since the combination is very stable, solubilizes various drugs, is nontoxic, and does not irritate the human skin (10). Sugar ester is a nontoxic, tasteless, odorless, and nonirritative sucrose fatty acid ester (11). Because it is widely and safely used in food (12), cosmetic (13), and pharmaceutical fields (14), it was selected as an emulsifier in this investigation. It is available in a wide range of hydrophilic–lipophilic balances (HLB) from oil to water soluble and has excellent emulsifying and dispersing abilities. Furthermore, Nobile *et al.* conducted standard tests with the sugar ester, and they reported no irritation to the human skin (11).

Various methods have been reported for the examination of drug release from ointment (15–17); however, no unified and simplified method has yet been established. In view of the

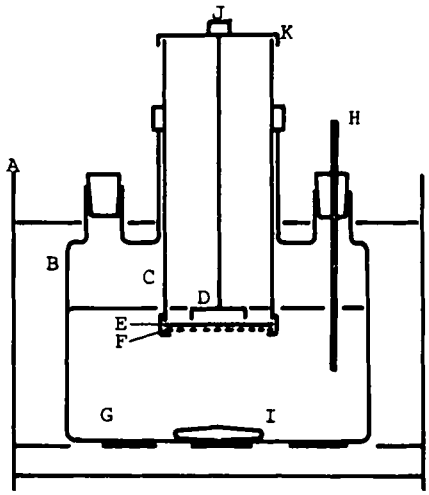

Figure 1—*Cross-sectional diagram of the drug release apparatus. Key: (A) thermostat equipment; (B) releasing fluid glass vessel; (C) inner cylindrical cell; (D) metal dish; (E) membrane; (F) metallic net; (G) releasing fluid; (H) thermometer; (I) stirring bar; (J) stopper; (K) cover.*

0022-3549/84/0500-0676$01.00/0
© 1984, American Pharmaceutical Association

ACKNOWLEDGMENTS

The authors acknowledge J. F. Brower for participating in the intralaboratory study and for helping to clarify the instructions to collaborators; D. J. Schuirmann, Division of Biometrics, National Center for Drugs and Biologics, for suggesting the time schedule used in the study; and S. M. Marchese, Winchester Engineering and Analytical Center, for his contribution toward the success of the study. The authors thank the following FDA collaborators who participated in this study: M. M. Shepherd, Atlanta Regional Laboratory, P. Knight and V. P. Shah, Biopharmaceutics Laboratory, Washington, D.C., J. S. Elkins, Dallas District, R. L. Ballbach, Detroit District, D. E. Ready, Kansas City District, T. S. Savage, Los Angeles District, T. Hoffmann, Minneapolis District, E. S. Moore, New York Regional Laboratory, R. H. Johnson, Seattle District, and L. Gelber, Winchester Engineering and Analytical Center. The authors also thank Dr. S. Bolton, St. John's University, Jamaica, N.Y., for his constructive reviews of this paper.

Physicopharmaceutical Characteristics of an Oil-in-Water Emulsion-Type Ointment Containing Diclofenac Sodium

AKIRA TAKAMURA *x, FUMIYOSHI ISHII *, SHUN'ICHI NORO *, and MASUMI KOISHI ‡

Received July 26, 1982, from the **Meiji College of Pharmacy, 1-22-1, Yato-cho, Tanashi-shi, Tokyo, Japan*, and the ‡*Faculty of Pharmaceutical Science, Science University of Tokyo, 12, Ichigaya Funagawara-machi, Shinjuku-ku, Tokyo, Japan.* Accepted for publication April 5, 1983.

Abstract □ The oil-in-water (o/w) emulsion-type ointment was prepared with food additives containing diclofenac sodium. The oil phase and the emulsifier used were 1,2,3-propanetriyl trioctanoate (caprylic acid glyceryl ester) and sugar wax, and sugar ester, respectively. The emulsion stability of the o/w emulsion-type ointment as well as the diclofenac sodium release profile were investigated and compared with those from conventional ointments. The emulsion stability was evaluated in terms of the viscosity of the emulsion product, the particle size distribution of oil droplets, and the zeta potential of the droplets. It was found that sugar esters have excellent properties as emulsifiers, based on the results of viscosity and zeta potential measurements. The *in vitro* release test revealed that the amount of diclofenac sodium released from o/w emulsion-type ointment was greater than from the hydrophilic and absorptive ointments. Accordingly, it was concluded that o/w emulsion-type bases are suitable for pharmaceutical use in ointment products.

Keyphrases □ Diclofenac sodium—release from various topical ointment bases, oil-in-water emulsions, physicopharmaceutical characteristics □ Oil-in-water emulsions—use as a topical ointment base for diclofenac sodium, release rate, physicopharmaceutical characteristics □ Ointment bases—oil-in-water emulsions, topical release of diclofenac sodium, physicopharmaceutical characteristics

In developing procedures for the design of pharmaceutical products, it is necessary to consider the bioavailability and safety of both the drugs and bases. Potent steroidal agents, which have substantial anti-inflammatory properties, have been used for external application for a long time. However, these steroidal agents have side effects (1), which were found to be directly dependent on the amount of drug applied to the skin. Therefore, various nonsteroidal agents (2, 3) have been developed recently to replace the steroidal agents.

Diclofenac sodium is a potent nonsteroidal anti-inflammatory agent, which has been limited to oral (4) and rectal administrations (5). In this investigation, diclofenac sodium was selected for topical application because no toxicity or topical irritation has been reported.

Although reports on ointment application have been published (6–8), few have dealt with the selection of optimum conditions for the preparation of the ointment. Oil-in-water (o/w) emulsion-type ointment bases offer many advantages over other preparations (9): they permit incorporation of aqueous and oleaginous ingredients, they allow a greater release of many incorporated medicaments, and their rheological properties can be controlled easily. Therefore, the selection of oil base and emulsifier is one of the most important factors in the preparation of o/w emulsion-type bases.

1,2,3-Propanetriyl trioctanoate (caprylic acid glyceryl ester, I) a medium-chain triglyceride, and sugar wax were chosen as the oil phase, since the combination is very stable, solubilizes various drugs, is nontoxic, and does not irritate the human skin (10). Sugar ester is a nontoxic, tasteless, odorless, and nonirritative sucrose fatty acid ester (11). Because it is widely and safely used in food (12), cosmetic (13), and pharmaceutical fields (14), it was selected as an emulsifier in this investigation. It is available in a wide range of hydrophilic–lipophilic balances (HLB) from oil to water soluble and has excellent emulsifying and dispersing abilities. Furthermore, Nobile *et al.* conducted standard tests with the sugar ester, and they reported no irritation to the human skin (11).

Various methods have been reported for the examination of drug release from ointment (15–17); however, no unified and simplified method has yet been established. In view of the

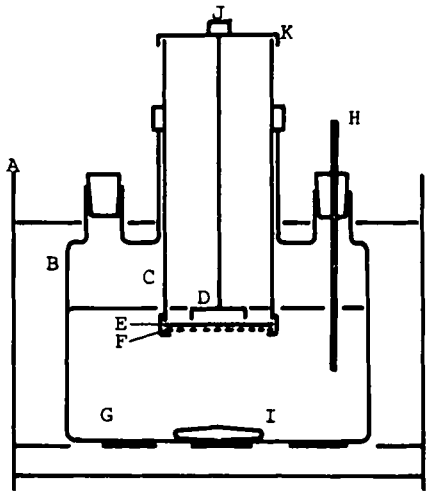

Figure 1—*Cross-sectional diagram of the drug release apparatus. Key: (A) thermostat equipment; (B) releasing fluid glass vessel; (C) inner cylindrical cell; (D) metal dish; (E) membrane; (F) metallic net; (G) releasing fluid; (H) thermometer; (I) stirring bar; (J) stopper; (K) cover.*

0022-3549/84/0500-0676$01.00/0
© 1984, American Pharmaceutical Association

Table I—The Constituents of the Hydrophilic and Absorptive Ointments

Hydrophilic Ointment		Absorptive Ointment	
White petrolatum	250.00 g	White petrolatum	400 g
Stearyl alcohol	220.00 g	Cetyl alcohol	180 g
Propylene glycol	120.00 g	Sorbitan sesquioleate	50 g
Sodium lauryl sulfate	15.00 g	Polyoxyethylene lauryl alcohol ether	5 g
Methylparaben	0.25 g	Methylparaben	1 g
Propylparaben	0.15 g	Propylparaben	1 g
Purified water	395.00 g	Purified water	363 g
Volume	1000 g	Volume	1000 g

aforementioned considerations, the o/w-type emulsion, which is a dispersion of microscopic oil droplets in a water phase, seems to be one of the most promising as an ointment base. The purpose of this work was to investigate the effects of surfactant and oil base on the physicochemical properties of ointment bases. In addition, the emulsion stability of the ointment base was evaluated in terms of (*a*) the viscosity of the emulsion product, (*b*) the particle diameter and distribution of oil droplets, and (*c*) the zeta potential of the droplets. The diclofenac sodium release profile from an o/w emulsion-type ointment was investigated and compared with those from conventional ointments.

EXPERIMENTAL

Materials—Diclofenac sodium[1] was recrystallized twice from water, with a melting range of 283–285°C. Sugar wax[2] and 1,2,3-propanetriyl trioctanoate (I, caprylic acid glyceryl ester)[3] were the dispersed phases.

Sugar wax is a sugar ester compound prepared from sucrose and palmitic acid or stearic acid. The average number of fatty acid molecules incorporated is 6.0, and its hydroxyl value and melting point are in the ranges of 80–130 and 60–66°C, respectively. Compound I is the triglyceride of caprylic acid and has the following properties: a saponification value of ~340–360, an acid value of <0.1, an iodine number of <1.0, and a hydroxyl value of <0.5.

The emulsifier used was sugar ester[4] of commercial grade, which is a nonionic surface-active agent synthesized from sucrose and palmitic acid or stearic acid. The average number of fatty acid molecules incorporated is 1.7. The content of dimethylformamide, arsenic, and heavy metals in sugar ester are very low as compared with those allowed by the Japanese Standard of Food Additives. Therefore, sugar ester is absolutely safe as a food, cosmetic, and/or pharmaceutical additive.

Preparation of o/w Emulsion-Type Ointment—The agitator used was a homomixer[5] which has two different blades: a homomixer and a paddle-mixer.

Diclofenac sodium was dissolved in the oil phase, the solution was kept at 80°C in the tank, and water preheated to 80°C was added. The concentration of diclofenac sodium in the ointment was always kept constant at 3.0% in all experiments.

The oil and water were vigorously stirred by both the homomixer and the paddlemixer at 80°C for 10 min. The speed of the homomixer was kept constant throughout the emulsification. The water-in-oil emulsion at 80°C was cooled quickly with ice water and then inverted to an o/w-type emulsion at 55°C. After this temperature was attained, the emulsion was stirred with the paddlemixer alone and gradually cooled to 20°C. The air bubbles trapped in the ointment were removed completely with a vacuum pump during the cooling process.

The conventional ointment bases used were commercial-grade hydrophilic ointment[6] and absorptive ointment[6]. The compositions of these ointments are shown in Table I.

Measurement of the Physicochemical Properties of Ointment Bases—The stability of an emulsion as an ointment base was evaluated by measuring such physicochemical properties as viscosity, particle size, and zeta potential (18). The rheological properties were measured with a rheometer[7] under a shear rate of 7.5–75 s^{-1} at 20 ± 0.1°C. The particle size distribution and the mean diameter of oil droplets were measured with a particle counter[8]. The zeta potential of oil droplets was obtained with the laser system[9]. A 0.1-g volume of o/w emulsion-type ointment was diluted with 50 mL of distilled water, and the zeta potential was measured at 20.0°C.

In addition, the o/w emulsion-type ointment was sealed in a calibrated glass tube and stored in a constant-temperature water bath at 40 ± 0.1°C. The flocculate depth and viscosity of the ointment were measured periodically to evaluate its emulsion stability. A short description of these procedures for evaluation of emulsion stability were given in a previous paper (19).

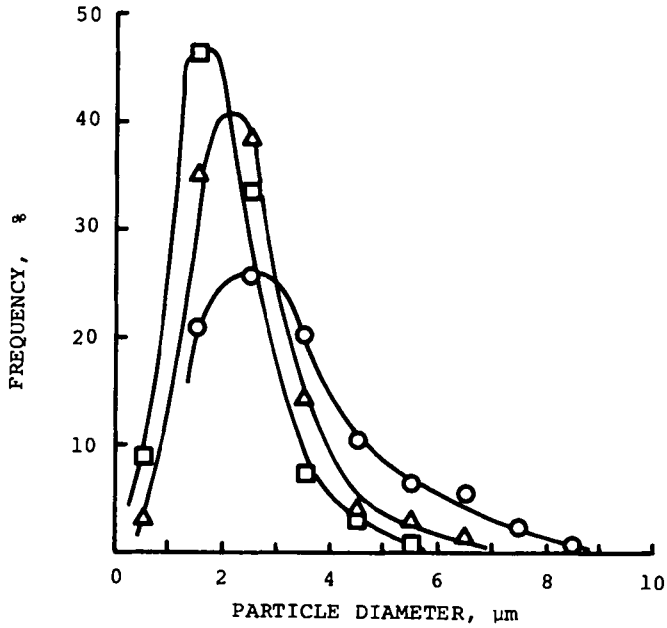

Figure 2—*Effect of rpm of the homomixer on particle diameter distribution of the o/w emulsion-type ointment. Key: (○) 3000 rpm; (△) 6000 rpm; (□) 10,000 rpm.*

Release of Diclofenac Sodium from the Ointment—The apparatus used for studying the drug released from the ointment is a modification of a common dissolution test instrument[10] (20) and is shown in Fig. 1. It consists of a metal dish (25 mm o.d., depth 6 mm), which floats on the surface of distilled water in an inner cylindrical cell. The bottom end of the inner cylindrical cell is covered with a membrane[11]. The distilled water (300 mL) was stirred at 100 rpm with a polytef-coated magnetic stirring bar placed at the bottom of the sink. The external chamber was immersed in a constant-temperature water bath maintained at 37 ± 0.1°C.

The release of the drug from various o/w emulsion-type ointment bases was examined. After reaching the required equilibrium temperature, 2.5 g of the ointment was placed on the bottom surface of the metal dish. This allowed direct contact of the donor ointment with the releasing liquid. Three-milliliter samples were withdrawn from the sink nine times over a 120-min period. The receptor phase volume was kept constant through the release run by replacing the removed sample with an equal volume of distilled water. The drug concentration was determined with a UV spectrometer[12] at a wavelength of 267 nm (21).

In the cases of the hydrophilic and absorptive ointments, diclofenac sodium powder that had been sieved through 150–200-mesh screens was mixed with molten base. The whole base was agitated at 50°C for 10 min until the solid diclofenac sodium melted completely in the base, then the ointment was cooled to 20°C. The drug release from the bases was examined in the same manner as in the case of the o/w emulsion-type ointment. The measurements were repeated five times, and the mean value of drug release concentration was calculated in all experiments.

RESULTS AND DISCUSSION

Selection of Optimum Conditions for Preparation of the o/w Emulsion-Type Ointment—The effect of impeller speed of the homomixer on the particle size distribution of the o/w emulsion-type ointment is shown in Fig. 2. In this case,

[1] Hamari Pharmaceutical Inds., Ltd., Osaka, Japan.
[2] S-10E; Dai-ichi Kogyo Seiyaku Co., Ltd., Kyoto, Japan.
[3] Panacete 800; Nippon Oil and Fats Co., Ltd., Tokoyo, Japan.
[4] S-50; Dai-ichi Kogyo Seiyaku Co., Ltd., Kyoto, Japan.
[5] Model M; Tokushu Kika Kogyo Co., Ltd., Osaka, Japan.
[6] JP X; Toho Yakuhin Co., Ltd., Tokyo, Japan.
[7] Model RM-1; Shimadzu Seisakusho Ltd., Kyoto, Japan.
[8] Model ZB; Coulter Electronics Inc, Hialeah, Fla.
[9] Lasu-Zee, Model 500; Pen Kem Inc., New York.
[10] Model TMS-103; Toyama Sangyo Co., Ltd., Osaka, Japan.
[11] SSWP 04700; Millipore Co., Milford, Mass.
[12] Model 200-20; Hitachi Ltd., Tokyo, Japan.

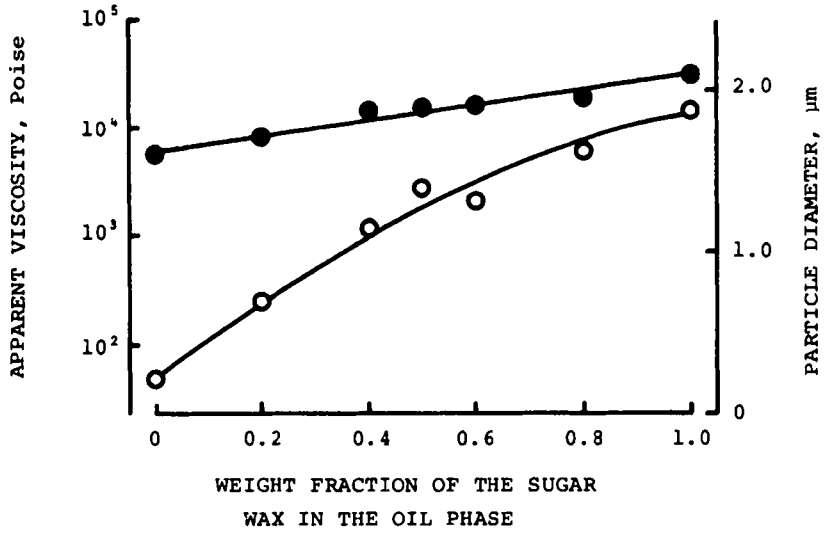

Figure 3—*Plot of viscosity and particle diameter* versus *weight fraction of sugar wax in the oil phase. Key: (○) viscosity; (●) particle diameter. Concentration of oil phase, 42%; concentration of emulsifier, 15%; revolution rate of homomixer, 10,000 rpm. The rate of shear and temperature in the measurement of viscosity were 7.5 s^{-1} and 20.0°C; the time of shear application was 30 s.*

the revolution rate of the paddlemixer was kept constant at 70 rpm. A significant effect of the difference in impeller speed was found on the size distribution curve. A narrower size distribution and a smaller standard deviation were observed with increase of the revolution rate of the homomixer. The mean diameters were 3.51 ± 1.91, 2.31 ± 1.18, and 1.93 ± 0.89 μm at 3000, 6000, and 10,000 rpm, respectively. As is evident in Fig. 2, the revolution rate of the homomixer is a very important dynamic factor in the preparation of a stable emulsion. Hence, it was kept constant at 10,000 rpm in all subsequent experiments.

Figure 3 shows the effect of the weight fraction of sugar wax in the oil phase on the viscosity and the particle size of the o/w emulsion-type ointment. The shear rate in the measurement of viscosity was 7.5 s^{-1}. It is obvious in this curve that the viscosity is remarkably increased with the increase of the weight fraction of sugar wax. This is also associated with a slight increase in the mean diameter of the droplet. This phenomenon would probably be due to complex formation between the crystallized sugar wax molecule and the emulsifier molecule on the surface of droplets during the cooling process of emulsification. Therefore, the o/w emulsion-type ointment would be sufficiently stable due to its high viscosity, which prevents flocculation and coalescence.

The zeta potential is a controlling parameter in the emulsion stability. Changes in the zeta potential with the weight fraction of sugar wax in the oil phase of the emulsion are shown in Fig. 4. The zeta potential of emulsion droplets was −38 mV when the oil phase of emulsion consisted of I alone. The value of the zeta potential gradually decreased with increase of the weight fraction of sugar wax in the oil phase of the emulsion. The minimum in this curve appears at a weight fraction of ~0.5. After the minimum, the curve increases rather rapidly with the increase in the sugar wax concentration. If the oil phase consists of equal parts of sugar wax and I, there probably exists a stable electric double layer on the surface of each droplet in the emulsion. These emulsions are semisolid at room temperature, however, and it seems that the high viscosity is a more important factor in preventing coalescence than the high zeta potential. Based on the results shown in Figs. 3 and 4, a weight fraction of 0.5 of sugar wax in the oil phase was used in all subsequent experiments.

Figure 5 shows the effect of emulsifier concentration on the viscosity of the o/w emulsion-type ointment. The shear rate in the measurement of viscosity was 7.5 s^{-1}. As the emulsifier concentration increased, the viscosity of the ointment increased linearly on a semilogarithmic plot at all concentrations of the oil phase studied. The viscosity of the ointment base was strongly affected by the concentration of sugar ester as an emulsifier. The emulsion prepared with sugar ester presumably has a stable gel structure around each droplet surface, because the globule surfaces of the oil may adsorb and consequently be stabilized by many sugar ester molecules. The viscosity of the emulsion increased remarkably with the increase of the oil concentration at all emulsifier concentrations. The reason for this result could be that as the concentration of the dispersed phase increases, the interaction between oil droplets also increases due to their closer approach in the continuous phase. This will lead to the eventual overlapping of the stream lines surrounding the individual droplets. At this stage, the overall viscosity is no longer the sum of the effects of the individual droplets. In highly concentrated emulsions, small increments in oil concentration produce large increases in relative viscosity.

When comparing the flow behavior of emulsions prepared using two or more different concentrations of emulsifier and/or oil phase, their viscosity should be measured over a wide range of shear rates. Rheograms of the ointment base prepared with four different concentrations of the emulsifier are shown in Fig.

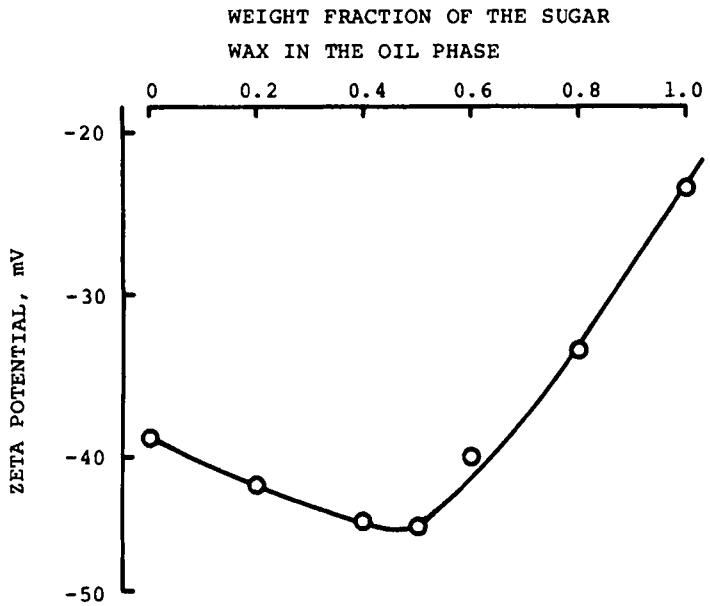

Figure 4—*Plot of zeta potential* versus *weight fraction of sugar wax in the oil phase. The temperature in the measurement of zeta potential was 20.0°C.*

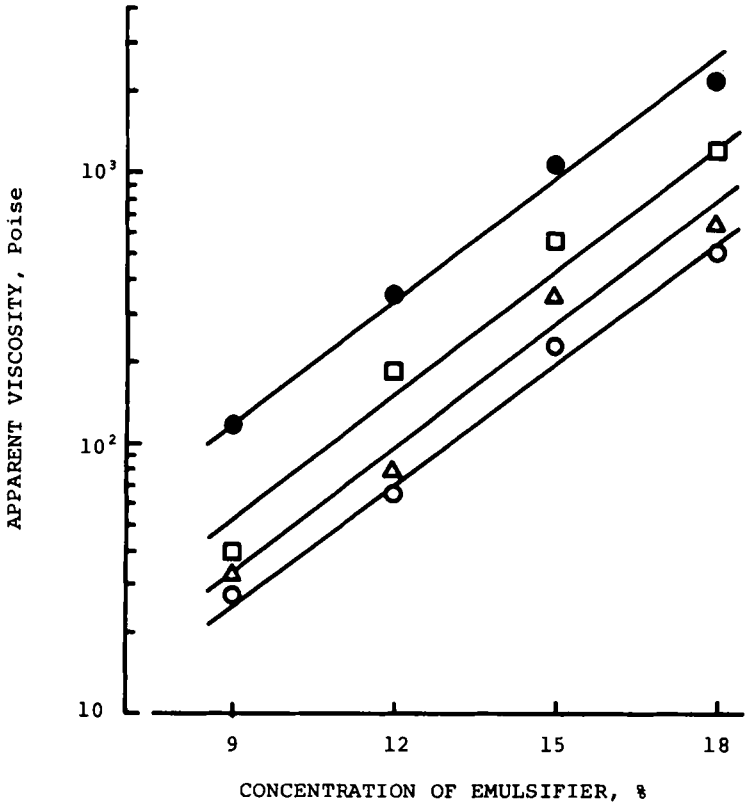

Figure 5—*Semilogarithmic plot of viscosity* versus *concentration of emulsifier. Key: concentration of oil phase (○) 30%; (△) 34%; (□) 38%; and (●) 42%. The rate of shear and temperature in the measurement of viscosity were 7.5 s^{-1} and 20.0°C; the time of shear application was 30 s.*

6. The curves show the relationship between viscosity and shear rate. As is evident in Fig. 6, it is not a horizontal relationship: the viscosity decreased markedly at first and then monotonically with an increase in shear rate. When a low steady shear was applied to the concentrated emulsion, it was often found that a steady stress did not develop instantly. This phenomenon is known as trixotropy. A hysteresis effect appears in all thixotropic ointment bases, as shown in Fig. 6.

The thixotropic behavior of an emulsion-type ointment base is of primary importance in pharmaceutical systems. Thus, it plays an important role in the mixing and flow of materials, their packaging into containers, physical stability, and even patient acceptability. Furthermore, the thixotropic property of a semisolid ointment base may affect the absorption rate of drugs through the skin as well as their biological availability. On the basis of the results shown in Figs. 5 and 6, it is possible to prepare ointments which have desirable rheological properties by controlling the amount of additives such as sugar wax, I, and sugar ester.

***In Vitro* Drug Release Profiles from the Emulsion-Type Ointment**—The equation for the release rate of drugs from an ointment base was derived by T. Higuchi (22), and subsequently, W. Higuchi (23) simplified the equation to:

$$Q = 2C_0(Dt/\pi)^{1/2} \qquad \text{(Eq. 1)}$$

where Q is the amount of drug released to the skin at time t per unit area of contact (mg/m^2), C_0 is the initial concentration of drug in the vehicle (mg/m^3), and D is the diffusion coefficient of drug in the vehicle (m^2/s), respectively. The release characteristic of diclofenac sodium from various o/w emulsion-type ointment bases over a 120-min period is illustrated in Fig. 7. The curve does not start at the origin, but has a short lag time. The experimental data were fairly well approximated by a straight line within 120 min when the amount of diclofenac sodium released was plotted against the square root of time. As shown in Fig. 7, the amount of drug released is indirectly related to the amount of oil phase in the ointment.

In general, the drug release from an emulsion base occurs in two steps: (*a*) transport of the drug dissolved in droplets of oil to the aqueous medium and (*b*) transport of the drug in the continuous aqueous phase across the membrane. In this o/w emulsion-type ointment, the amount of drug released could be controlled and the release prolonged by increasing the concentration of dispersed phase which, in turn, may affect the rate of transfer of the drug molecule from the oil droplets to the aqueous medium, the rate-limiting step for the release.

Figure 8 shows the release profiles of diclofenac sodium from o/w emulsion-type, hydrophilic, and absorptive ointments. The release rate was found to decrease in the order o/w emulsion-type ointment > absorptive ointment > hydrophilic ointment. Comparison of Fig. 7 with Fig. 8 reveals that the amounts of drug released from all o/w emulsion-type ointments are larger than from the hydrophilic ointment. This indicates that the o/w emulsion-type base prepared in this experiment has excellent properties as compared with the commercial grade hydrophilic ointment, and it appears to be very suitable

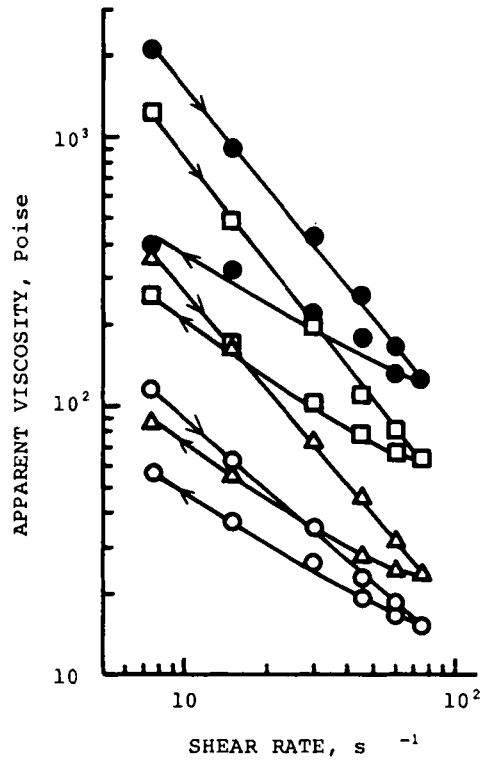

Figure 6—*Plot of viscosity against rate of shear. Key: concentration of emulsifier (○) 9%; (△) 12%; (□) 15%; and (●) 18%. Concentration of oil phase was 42%. The temperature in the measurement of viscosity was 20.0°C; the total time of shear application was 330 s.*

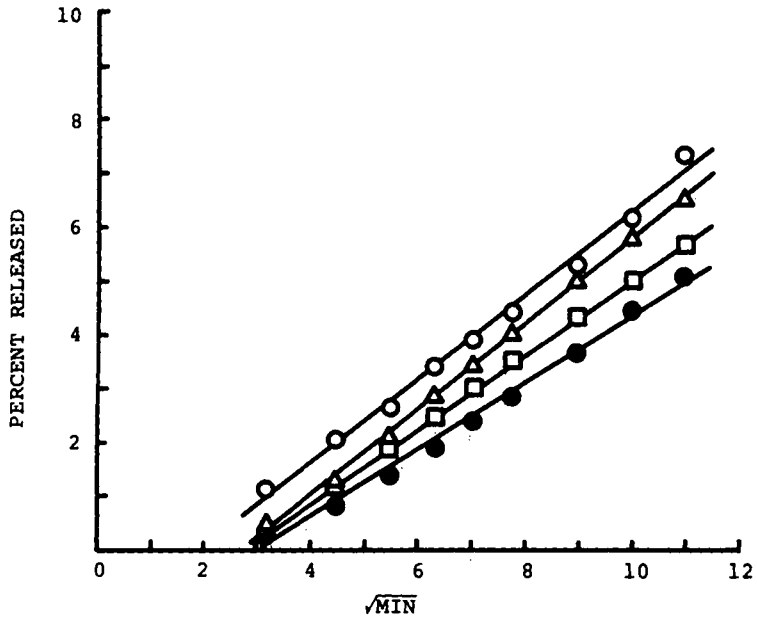

Figure 7—*Diclofenac sodium release from various o/w emulsion-type ointments. Key: concentration of oil phase (○) 30%; (△) 34%; (□) 38%; and (●) 42%.*

for use as an ointment base. In this release exeriment, dissolution of the base itself into the aqueous phase is not a serious problem within 120 min from initiation.

Evaluation of Emulsion Stability in Three Different Ointment Bases—The emulsion stability of the ointment base was evaluated in terms of visual observation and the rheology of the emulsion product. Here, 3% diclofenac sodium was admixed with each of the three different bases: hydrophilic, absorptive, and o/w emulsion-type ointments. Gross visual analysis was used to observe flocculation and creaming of the emulsions stored at a constant temperature of 40 ± 0.1°C after preparation. This analysis utilized three 15-mL calibrated glass tubes to observe each of the emulsions over a 30-d period.

In the hydrophilic ointment, a separated water phase was observed after 10 d. A flocculated oil layer appeared on the top of emulsion of absorptive ointment after 3 d only. However, no significant change was detected at all in the o/w emulsion-type ointment over a 50-d period. Accordingly, the o/w emulsion-type ointment including 3% diclofenac sodium is considered to be more stable than the other ointments, even if it is stored at room temperature for a long period.

The viscosity of each ointment stored at 40 ± 0.1°C was measured periodically with a rheometer over a 14-d period. Figure 9 illustrates the change in relative viscosity of ointment with storage time. Here, the relative viscosity, η_{rel}, was determined according to the equation:

$$\eta_{rel} = \eta/\eta_0 \qquad \text{(Eq. 2)}$$

where η is the viscosity at each storage time and η_0 at the initiation, respectively.

In the cases of the hydrophilic and absorptive ointments, the relative viscosity decreased markedly with the increase in time. The viscosity of the absorptive ointment could not be determined by this rheological method after 7 d because of the appearance of separated oil phase on the surface of the emulsion. On the other hand, no significant change was found in the viscosity of o/w emulsion-type ointment over a 50-d period. Furthermore, it was confirmed that the other physicochemical properties such as melting range, blooming, and deposition of drug crystals were almost unchanged with this base after 50 d at 40°C.

CONCLUSIONS

On the basis of physicochemical tests, it seems that the oil phase in the emulsion base consisting of 50 parts each of sugar wax and I shows excellent stability. From the results of viscosity and zeta potential measurements, sugar ester in the region of 9–18% was found to have excellent properties as an emulsifier, and it appears to be very suitable for use as an ingredient in emulsion-type ointment bases. The *in vitro* release test reveals that the amount of diclofenac sodium released from the o/w emulsion-type ointment was greater than that from the hydrophilic and absorptive ointments. The o/w emulsion-type ointment containing 3% diclofenac sodium appears to be better than conventional ointments, as indicated by visual observations and viscosity

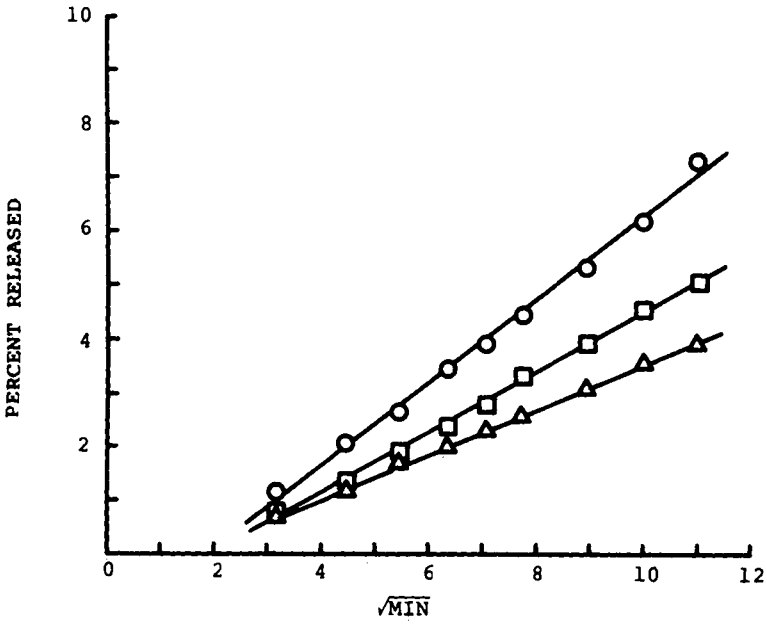

Figure 8—*Plot of diclofenac sodium released* versus *the square root of time. Key: (○) o/w emulsion-type ointment (concentration of oil phase was 30%); (△) hydrophilic ointment; (□) absorptive ointment.*

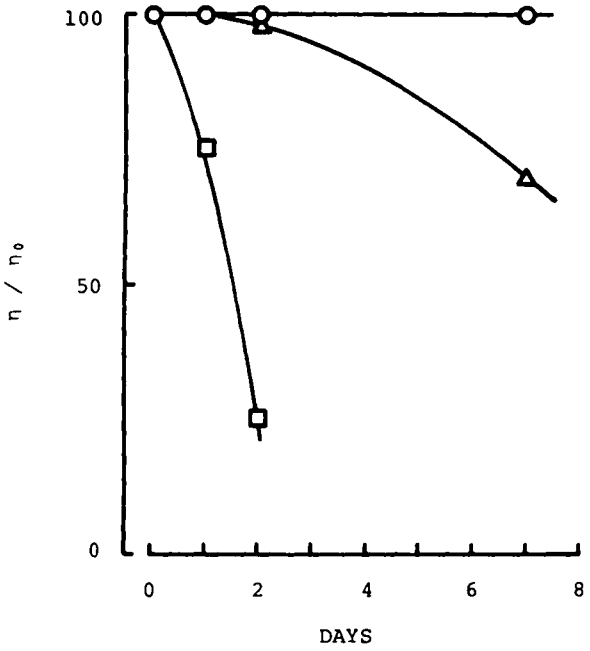

Figure 9—*Change of the viscosity of the ointment with storage time. Key: (○) o/w emulsion-type ointment; (△) hydrophilic ointment; (□) absorptive ointment. The ointments were stored at 40°C. The temperature in the measurement of viscosity was 20.0°C; the time of shear application was 30 s.*

measurements of the base over a 50-d experimental period at 40°C. Finally, the aforementioned properties suggest that these o/w-type emulsions prepared with sugar ester, I, sugar wax, and distilled water are suitable for the pharmaceutical preparation of ointments for clinical use. Future investigations will evaluate the effect of physicochemical properties of the o/w emulsion-type ointment on the indices of bioavailability through *in vivo* percutaneous absorption.

REFERENCES

(1) G. Weber, *Br. J. Dermatol.*, **86,** 253 (1972).

(2) K. Shima, C. Matsusaka, M. Hirose, T. Noguchi, T. Noguchi, and Y. Yamahira, *Chem. Pharm. Bull.*, **29,** 2238 (1981).

(3) Y. Oketani, N. Kobayashi, K. Ichikawa, and T. Uesugi, *Ōyō Yakuri*, **19,** 399 (1980).

(4) K. Tsurumi, Y. Hiramatsu, M. Nozaki, M. Hayashi, T. Shibuya, and H. Fujimura, *Folia. Pharmacol. (Japan)*, **69,** 299 (1973).

(5) H. Yaginuma, T. Nakata, H. Toya, T. Murakami, M. Yamazaki, A. Kamada, H. Shimazu, and I. Makita, *Chem. Pharm. Bull.*, **29,** 3326 (1981).

(6) S. Sved, W. M. McLean, and I. J. McGilveray, *J. Pharm. Sci.*, **70,** 1368 (1981).

(7) N. A. Orr, E. A. Hill, and J. F. Smith, *J. Pharm. Pharmacol.*, **32,** 766 (1980).

(8) P. A. Cossum and M. S. Roberts, *J. Pharm. Sci.*, **70,** 832 (1981).

(9) M. E. Stolar, G. V. Rossi, and M. Barr, *J. Am. Pharm. Assoc., Sci. Ed.*, **49,** 144 (1960).

(10) R. W. Harkins and H. P. Sarett, *J. Am. Oil Chem. Soc.*, **45,** 26 (1968).

(11) L. Nobile, P. Rovesti, and M. B. Svampa, *Am. Perfum. Cosmet.*, **79,** 19 (1964).

(12) K. Yamauchi, M. Shimizu, and T. Kamiya, *J. Food Sci.*, **45,** 1237 (1980).

(13) G. J. Brooks, *Cosmet. Toilet.*, **95,** 73 (1980).

(14) H. Hopkins and L. D. Small, *J. Am. Pharm. Assoc., Sci. Ed.*, **49,** 220 (1960).

(15) A. L. Weiss and B. J. Sciarrone, *J. Pharm. Sci.*, **58,** 980 (1969).

(16) F. Bottari, G. D. Colo, E. Nannipieri, M. F. Saettone, and M. F. Serafini, *J. Pharm. Sci.*, **63,** 1779 (1974).

(17) Z. T. Chowhan and R. Pritchard, *J. Pharm. Sci.*, **64,** 754 (1975).

(18) P. Sennet and J. P. Oliver, *Ind. Eng. Chem.*, **57,** 33 (1965).

(19) S. Noro, A. Takamura, and M. Koishi, *Chem. Pharm. Bull.*, **27,** 309 (1979).

(20) S. Muranishi, Y. Okubo, and H. Sezaki, *Yakazaigaku*, **39,** 1 (1979).

(21) M. Takasugi, K. Minakuchi, and K. Miyata, *Rinsho Yakuri*, **10,** 335 (1979).

(22) T. Higuchi, *J. Soc. Cosmet. Chem.*, **11,** 85 (1960).

(23) W. I. Higuchi, *J. Pharm. Sci.*, **51,** 802 (1962).

NOTES

Determination of Calcium Gluconate by Selective Oxidation with Periodate

CHEN KUANG-PAIO

Received July 19, 1982, from the *Second Pharmaceutical Factory of Wenchow, Chekiang, People's Republic of China.* Accepted for publication March 7, 1983.

Abstract □ A modified analytical method was developed which can accurately quantitate calcium gluconate and its pharmaceutical preparations in the presence of other calcium compounds or other cations able to complex with EDTA. The proposed method was based on the principle of the Malaprade reaction, according to which gluconic acid is selectively and quantitatively oxidized by sodium periodate. The content of calcium gluconate was calculated from the amount of gluconic acid found. The selective oxidation proceeded at 50°C for 10 min, yielding ~100% recovery of calcium gluconate. The proposed method was accurate, precise, and superior to the compendia EDTA-complexometric method in terms of specificity.

Keyphrases □ Calcium gluconate—determination by selective oxidation with periodate, quantitation, Malaprade reaction □ Periodate—selective oxidation, determination of calcium gluconate, quantitation, Malaprade reaction □ Malaprade reaction—determination of calcium gluconate with selective oxidation by periodate, quantitation

The EDTA-complexometric titration for the determination of calcium gluconate (I) and its pharmaceutical formulations is most commonly adopted by many current national pharmacopoeias (1–6). However, it is known that the official compendia method is only suitable for determining a sample of I which does not contain other calcium compounds or other

0022-3549/84/0500-0681$01.00/0
© 1984, American Pharmaceutical Association

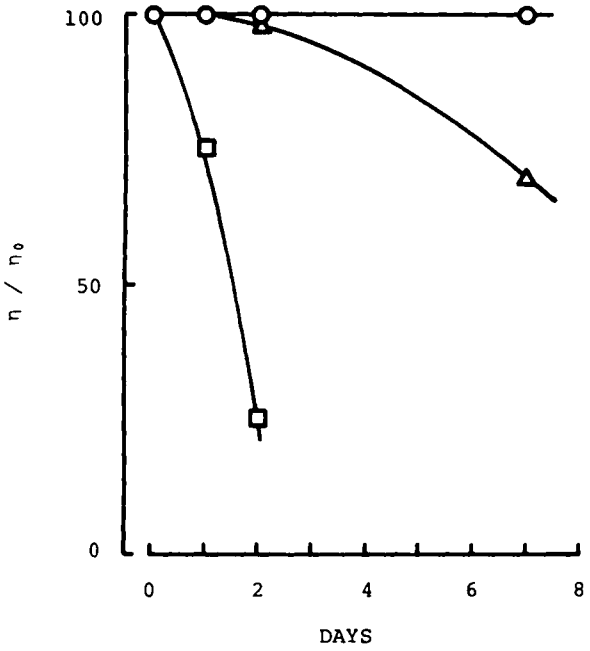

Figure 9—*Change of the viscosity of the ointment with storage time. Key: (○) o/w emulsion-type ointment; (△) hydrophilic ointment; (□) absorptive ointment. The ointments were stored at 40°C. The temperature in the measurement of viscosity was 20.0°C; the time of shear application was 30 s.*

measurements of the base over a 50-d experimental period at 40°C. Finally, the aforementioned properties suggest that these o/w-type emulsions prepared with sugar ester, I, sugar wax, and distilled water are suitable for the pharmaceutical preparation of ointments for clinical use. Future investigations will evaluate the effect of physicochemical properties of the o/w emulsion-type ointment on the indices of bioavailability through *in vivo* percutaneous absorption.

REFERENCES

(1) G. Weber, *Br. J. Dermatol.*, **86,** 253 (1972).

(2) K. Shima, C. Matsusaka, M. Hirose, T. Noguchi, T. Noguchi, and Y. Yamahira, *Chem. Pharm. Bull.*, **29,** 2238 (1981).

(3) Y. Oketani, N. Kobayashi, K. Ichikawa, and T. Uesugi, *Ōyō Yakuri*, **19,** 399 (1980).

(4) K. Tsurumi, Y. Hiramatsu, M. Nozaki, M. Hayashi, T. Shibuya, and H. Fujimura, *Folia. Pharmacol. (Japan)*, **69,** 299 (1973).

(5) H. Yaginuma, T. Nakata, H. Toya, T. Murakami, M. Yamazaki, A. Kamada, H. Shimazu, and I. Makita, *Chem. Pharm. Bull.*, **29,** 3326 (1981).

(6) S. Sved, W. M. McLean, and I. J. McGilveray, *J. Pharm. Sci.*, **70,** 1368 (1981).

(7) N. A. Orr, E. A. Hill, and J. F. Smith, *J. Pharm. Pharmacol.*, **32,** 766 (1980).

(8) P. A. Cossum and M. S. Roberts, *J. Pharm. Sci.*, **70,** 832 (1981).

(9) M. E. Stolar, G. V. Rossi, and M. Barr, *J. Am. Pharm. Assoc., Sci. Ed.*, **49,** 144 (1960).

(10) R. W. Harkins and H. P. Sarett, *J. Am. Oil Chem. Soc.*, **45,** 26 (1968).

(11) L. Nobile, P. Rovesti, and M. B. Svampa, *Am. Perfum. Cosmet.*, **79,** 19 (1964).

(12) K. Yamauchi, M. Shimizu, and T. Kamiya, *J. Food Sci.*, **45,** 1237 (1980).

(13) G. J. Brooks, *Cosmet. Toilet.*, **95,** 73 (1980).

(14) H. Hopkins and L. D. Small, *J. Am. Pharm. Assoc., Sci. Ed.*, **49,** 220 (1960).

(15) A. L. Weiss and B. J. Sciarrone, *J. Pharm. Sci.*, **58,** 980 (1969).

(16) F. Bottari, G. D. Colo, E. Nannipieri, M. F. Saettone, and M. F. Serafini, *J. Pharm. Sci.*, **63,** 1779 (1974).

(17) Z. T. Chowhan and R. Pritchard, *J. Pharm. Sci.*, **64,** 754 (1975).

(18) P. Sennet and J. P. Oliver, *Ind. Eng. Chem.*, **57,** 33 (1965).

(19) S. Noro, A. Takamura, and M. Koishi, *Chem. Pharm. Bull.*, **27,** 309 (1979).

(20) S. Muranishi, Y. Okubo, and H. Sezaki, *Yakazaigaku*, **39,** 1 (1979).

(21) M. Takasugi, K. Minakuchi, and K. Miyata, *Rinsho Yakuri*, **10,** 335 (1979).

(22) T. Higuchi, *J. Soc. Cosmet. Chem.*, **11,** 85 (1960).

(23) W. I. Higuchi, *J. Pharm. Sci.*, **51,** 802 (1962).

NOTES

Determination of Calcium Gluconate by Selective Oxidation with Periodate

CHEN KUANG-PAIO

Received July 19, 1982, from the *Second Pharmaceutical Factory of Wenchow, Chekiang, People's Republic of China.* Accepted for publication March 7, 1983.

Abstract □ A modified analytical method was developed which can accurately quantitate calcium gluconate and its pharmaceutical preparations in the presence of other calcium compounds or other cations able to complex with EDTA. The proposed method was based on the principle of the Malaprade reaction, according to which gluconic acid is selectively and quantitatively oxidized by sodium periodate. The content of calcium gluconate was calculated from the amount of gluconic acid found. The selective oxidation proceeded at 50°C for 10 min, yielding ~100% recovery of calcium gluconate. The proposed method was accurate, precise, and superior to the compendia EDTA-complexometric method in terms of specificity.

Keyphrases □ Calcium gluconate—determination by selective oxidation with periodate, quantitation, Malaprade reaction □ Periodate—selective oxidation, determination of calcium gluconate, quantitation, Malaprade reaction □ Malaprade reaction—determination of calcium gluconate with selective oxidation by periodate, quantitation

The EDTA-complexometric titration for the determination of calcium gluconate (I) and its pharmaceutical formulations is most commonly adopted by many current national pharmacopoeias (1–6). However, it is known that the official compendia method is only suitable for determining a sample of I which does not contain other calcium compounds or other

0022-3549/84/0500-0681$01.00/0
© 1984, American Pharmaceutical Association

Table I—Molar Ratio of I to Periodate in the Selective Oxidation

I Reference Standard		Amounts of 0.05 M I_2 Subtracted by the blank, mL	Moles of $NaIO_4$ Reacted, $\times 10^{-3}$	Molar Ratio of I to $NaIO_4$	Equivalents of I for 1 mL of 0.05 M I_2, g
Added, mg	mol $\times 10^{-3}$				
55.64	0.1241	24.81	1.241	1:10.0	0.002242
50.23	0.1120	22.42	1.121	1:10.01	0.002241
51.32	0.1145	22.89	1.145	1:10.0	0.002241
48.32	0.1074	21.56	1.078	1:10.0	0.002243
53.53	0.1194	23.85	1.193	1:9.992	0.002242
Mean				1:10	0.002242

Table II—Recovery of I

I Added[a], mg	I Found[b], mg	Recovery of I, %
51.32	51.30	99.96
55.64	55.62	99.96
50.23	50.24	100.0
48.32	48.35	100.1
53.53	53.50	99.94
Mean		99.99
SD		0.0161

[a] According to Table I. [b] Calculated as 1 mL of 0.05 M I_2 equivalent to 2.242 mg of I.

cations capable of complexing with EDTA. However, I as prepared by some domestic manufacturers usually contains a certain amount of calcium oxalate, which is a byproduct produced in the fermentation of glucose with *Aspergillus niger*. Commercially available injections of I usually contain a small amount of solubilizing agent, such as calcium lactate (7). Therefore, it is impossible to accurately estimate I with the compendia methods. Because gluconic acid is considered to be a vicinal polyhydroxy alcohol and since some earlier investigators have applied the Malaprade reaction to determine vicinal polyhydroxy alcohols and aldoses (8–11), we were interested in studying the reaction of I with periodate to develop an assay method for I. The proposed method is based on the selective oxidation of gluconic acid with periodate, calculating the amount of I from the amount of gluconic acid found.

EXPERIMENTAL

Drugs and Chemicals—ChP-grade powder[1], tablets[1], and injections[1] of I, starch, talc, magnesium stearate, lactic acid, and analytical- or base-reagent-grade iodine, potassium iodide, arsenic(III) oxide, sodium oxalate, magnesium chloride, sodium bicarbonate, disodium EDTA, and sodium periodate were used.

Volumetric Solutions—Solutions of 0.05 M iodine, 0.025 M sodium arsenite, 0.05 M disodium EDTA, and 0.05 M sodium periodate were prepared and standardized by compendia methods.

Preparation of I Reference Standard—Parenteral grade I (1) was dissolved, recrystallized from redistilled water three times, and dried at 70°C. The content of I was determined by the ChP method (1), containing 100 ± 0.01% of $C_{12}H_{22}O_{14}Ca{\cdot}H_2O$. The oxalate content was <15 ppm, determined by the ferric perchlorate method (12, 13).

Stoichiometric Relation in the Selective Oxidation of I with Sodium Periodate—About 50 mg of I reference standard, accurately weighed, was placed in a glass-stoppered 500-mL flask, 20 mL of water was added, and the mixture was stirred until the sample was completely dissolved. Forty milliliters of 0.05 M sodium periodate was added and mixed. The solution was heated on a 50°C water bath for 10 min. After cooling, 1 g of potassium iodide, 1.5 g of sodium bicarbonate, and 50 mL of 0.025 M sodium arsenite were added. The flask was stoppered, thoroughly mixed, and allowed to stand in the dark for 5 min. The inner walls of the flask and the stopper were rinsed, and the residual sodium arsenite was titrated with 0.05 M I_2, using the starch test system as the indicator. A blank determination was performed simultaneously. The titration reading of 0.05 M I_2 for I reference standard, corrected for the blank, was equivalent to the amount of 0.05 M sodium periodate that reacted with I.

Selection of Optimum Condition for the Selective Oxidation of I with Sodium Periodate—To 5 mL of I reference standard solution (1.00%), were added 20 mL of water and 40 mL of 0.05 M sodium periodate. The solution was mixed as described above, except when the selective oxidation was carried out at different temperatures and time periods.

Recovery of I in the Presence of Other Substances in Accordance with the Sodium Periodate Method—Twenty milliliters of water was added to three 5-mL portions of I reference standard solution (1.00%), respectively. To the first portion, 20 mg of starch, 12.5 mg of talc, and 2.5 mg of magnesium stearate were added. To the second portion, 25 mg of sodium oxalate and 2 mg of magnesium chloride were added. Then, to each portion, 40 mL of 0.05 M sodium periodate was added, and the solution was mixed and heated on a 50°C water bath for 10 min. The procedure was continued as described above.

Comparison of the Sodium Periodate Method with the ChP Method (1) in the Determination of I and its Pharmaceutical Preparations—An aliquot of the sample, equivalent to ~50 or 500 mg of I, was accurately weighed or transferred and analyzed as described above or under the ChP method, respectively.

RESULTS AND DISCUSSION

In 1928, Malaprade (14) described that vicinal hydroxy groups in a C—C bond might be selectively oxidized by a reagent such as periodic acid to produce two aldehyde fragments. Kolthoff and Belcher (15) have reviewed this oxidation, known as the Malaprade reaction, at length and assured that all of the polyatomic alcohols, including vicinal hydroxyl groups, could be oxidized by periodate according to the following general formula (Scheme I):

$$HOCH_2(CHOH)_nCH_2OH + (n+1)IO_4^- \rightarrow 2CH_2O + nHCOOH + (n+1)IO_3^- + H_2O$$

Scheme I

The hydroxyl group at the terminal carbon atom was oxidized to yield formaldehyde, but the hydroxyl group at the intermediate carbon atom was alternatively oxidized to yield formic acid. If a carbonyl and a hydroxyl group were vicinal, the periodate oxidation would yield a carboxyl and a carbonyl function, respectively. Because gluconic acid belongs to a vicinal polyhydroxy alcohol having a terminal carboxyl group, it is possible that gluconic acid may be oxidized by periodate as in Scheme II:

$$HOCH_2(CHOH)_4COOH + 5IO_4^- \rightarrow CH_2O + 3HCOOH + (CO_2H)_2 + 5IO_3^- + H_2O$$

Scheme II

In the bicarbonate alkaline condition, the excess periodate can oxidize the added iodide to iodine quantitatively, but the iodate does not. The liberated iodine subsequently oxidizes the added arsenite and the residual arsenite is then back-titrated by 0.05 M I_2 (Scheme III):

$$IO_4^- + 2I^- + H_2O \rightarrow IO_3^- + I_2 + 2OH^-$$

$$I_2 + AsO_3^{3-} + 2OH^- \rightarrow 2I^- + AsO_4^{3-} + H_2O$$

Scheme III

As a consequence, it is obvious that 1 mol of gluconic acid is equivalent to

Table III—Recovery of I as a Function of Time and Temperature During Selective Oxidation

Temperatures, °C	Recovery of I, %[a]		
	5 min	10 min	30 min
15	89.2	90.9	91.3
40	99.2	99.9	100.2
50	100.0	100.0	100.3
60	100.0	100.2	100.6
80	100.2	100.9	102.1
100	100.9	102.6	104.2

[a] Average of triplicate analyses.

[1] Prepared by the Second Pharmaceutical Factory of Wenchow, China.

Table IV—Recovery of I in the Presence of Other Substances

I Added, mg	Other Substances Added, mg	I Found, mg[a]	Recovery of I, %[a]
50.00	Starch, 20; talc, 12.5 Magnesium stearate, 2.5	50.45	100.9 (*SD* 0.02)
50.00	Lactic acid, 25; calcium hydroxide, 2.5	50.37	100.7 (*SD* 0.08)
50.00	Magnesium chloride, 2; sodium oxalate, 0.5	49.98	99.96 (*SD* 0.05)

[a] Average of triplicate analyses.

5 mol of periodate or to 10 g equivalents of iodine. Hence, 1 mol of I is equivalent to 10 mol of sodium periodate or 20 g equivalents of iodine, *i.e.*, the molar ratio of I to periodate in the selective oxidation is 1:10, and each milliliter of 0.05 M I_2 is equivalent to 0.002242 g of I ($C_{12}H_{22}O_{14}Ca{\cdot}H_2O$, Table I). The average recovery of I is 99.99% (*SD* 0.0161, Table II).

When I reacts with periodate at 100°C over 10 min or at 80°C over 30 min, the formaldehyde would be oxidized successively so that the recovery of I may exceed 100%. On the other hand, if the reaction temperature is low and the period of reaction is short, the selective oxidation of I may be incomplete, resulting in a lowering of recovery. As a rule, it is favorable to keep the selective oxidation at 50°C for as long as 10 min, resulting ~100% recovery (Table III).

Table IV gives the results of recovery of I by the sodium periodate method in the presence of other substances. Some excipients such as starch, talc, magnesium stearate, lactic acid, calcium hydroxide, magnesium ions, and oxalate, *etc.*, occurring in amounts as much as 10-fold of formulation weight in tablets or injections of I, or far more than the compendia prescribed limits, do not interfere with the determination of I using the periodate method. Although lactic acid is an α-hydroxycarboxylic acid, it is not oxidized by periodate under the conditions described previously (16).

Table V—Results of the Determination by use of the Sodium Periodate Method and the ChP Method (1)

Sample of I	Content of Oxalate, ppm[a]	Content of I, %[b] $NaIO_4$ Method	Content of I, %[b] ChP Method
Oral			
Lot 820131	585.4	99.87	100.7
Lot 820303	909.6	99.50	101.0
Lot 820207	1527.1	99.24	101.7
Parenteral			
Lot 820314	<15	99.98	99.96
Lot 820310	<15	99.99	99.99
Tablets			
Lot 820405		98.92[c]	101.7[c]
Lot 820406		97.45[c]	99.83[c]
Injection			
Lot 801222		101.4[c]	103.2[c]
Lot 801226		100.6[c]	102.4[c]

[a] From Refs. 12 and 13. [b] Average of triplicate analyses. [c] Percent of labeled amount.

Because the amounts of oxalate present in oral grade I (1) commonly reach 500 ppm (sometimes >1000 ppm) and additive amounts of calcium lactate in I injections are approximated to 1.5% (7), results of analysis in oral grade I or its preparations with the EDTA-complexometric method are usually higher than with the sodium periodate method. Alternatively, owing to the low oxalate content in parenteral grade I (in general, the amounts of oxalate are controlled to <150 ppm in parenteral grade I; if the injections are prepared by I containing oxalate >150 ppm, microcrystalline calcium oxalate would precipitate after standing for several weeks), results of determination obtained by the two methods are almost identical (Table V).

In conclusion, it is apparent that the sodium periodate method is superior to the official EDTA-complexometric method with high specificity, no interference by any excipients or oxalate, *etc.* The proposed method is accurate and precise, not requiring any special apparatus or costly reagents.

REFERENCES

(1) "The People's Republic of China Pharmacopoeia," 1977 ed, vol. II., Pharmacopoeial Committee, Ministry of Public-Health, PRC, People-Health Publishing House, China, pp. 592, 593, 594.

(2) "The United States Pharmacopeia," 20th rev., United States Pharmacopoeial Convention, Rockville, Md., 1980, p. 108.

(3) "The British Pharmacopeia 1980," HM Stationery Office, London, 1980, p. 72.

(4) "Commentary of the Japanese Pharmacopoeia," 9th ed., Hirokawa Publishing Co, Tokyo, Japan, 1976, C-600.

(5) "USSR State Pharmacopoeia X," Ministry of Health of the USSR, Moscow, p. 131.

(6) H. Böhme and K. Hartke, "Deutsches Arzneibuch 7. Ausgabe 1968 Kommentar" 2, Neubearbeitete Auflage, Wissenschftliche Verlagsgesellschaft MBH Stuttgart, 1973, S. 587.

(7) G. Xue-Qiu, "Commentary of Drug Preparations," 2nd ed., People-Health Publishing House, China, 1981, p. 79.

(8) L. Hough, T. J. Tayler, and G. H. Thomas, *J. Chem. Soc.*, **3**, 1212 (1958).

(9) R. D. Corlett, W. G. Breck, and G. W. Hay, *Can. J. Chem.*, **48**, 2474 (1970).

(10) T. Higuchi and E. Brochmann-Hanssen, "Pharmaceutical Analysis," Interscience, New York, N.Y., 1961, p. 33-34.

(11) V. Ya. Zaharans and V. V. Elkin, *Chem. Pharm. J. (USSR)*, **15**(5), 97 (1981).

(12) T. Nazaki, F. Hori, and H. Kurihara, *J. Chem. Soc. Jpn.*, **82**, 713 (1961).

(13) H. Men-Ru, G. Gui-fen, and Z. Ru-Bao, "Summary of Monograph for Qualitative Study of Calcium Gluconate," Unpublished data (1966).

(14) L. Malaprade, *Bull. Chim. France*, **43**, 683 (1928).

(15) I. M. Kolthoff and R. Belcher, "Volumetric Analysis," Vol. III, Interscience, New York, N.Y., 1957, p. 475.

(16) D. B. Sprinson and E. Chargaff, *J. Biol. Chem.*, **164**, 433 (1946).

ACKNOWLEDGMENTS

The author thanks Ms. Chen Mei-Yu for her assistance with these experiments.

Nasal Absorption of Nafarelin Acetate, the Decapeptide [D-Nal(2)^6]LHRH, in Rhesus Monkeys I

SHABBIR T. ANIK ˣ, GEORGIA McRAE, CLINTON NERENBERG, ANN WORDEN, JOANN FOREMAN, JIIN-YU HWANG, STANLEY KUSHINSKY, RICHARD E. JONES, and BRIAN VICKERY

Received January 11, 1983, from the *Institutes of Pharmaceutical Sciences, Biological Sciences, and Pharmacology and Metabolism, Syntex Research, Palo Alto, CA 94304.* Accepted for publication March 1, 1983.

Abstract □ Nafarelin acetate, [D-Nal(2)^6]LHRH, a highly potent superagonist of luteinizing hormone-releasing hormone, was given intranasally to six female rhesus monkeys. Absorption was rapid and very reproducible, with peak levels occurring at 15–30 min and a bioavailability of ~2% relative to a subcutaneous dose. The nasal dose response was highly nonlinear. The nonlinearity was apparently associated with the absorption phase, since elimination profiles at all doses were similar.

Keyphrases □ Nafarelin acetate—nasal absorption, [D-Nal(2)^6]LHRH, rhesus monkeys □ Absorption, nasal—nafarelin acetate, [D-Nal(2)^6]LHRH, rhesus monkeys □ Luteinizing hormone-releasing hormone—analogue, nafarelin acetate, nasal absorption, rhesus monkeys

The delivery of drugs by the nasal route is receiving increased attention as a convenient and efficient method of drug delivery (1–7). In addition to offering advantages such as rapid absorption and avoiding the first-pass effect, it provides for delivery of drugs such as peptides and proteins which are degraded in the GI tract and cannot be given orally. The efficiency of absorption, however, varies considerably between drugs. Whereas a bioavailability of 100% (relative to intravenous) has been reported for nasally administered propranolol in humans (3), the bioavailability was only 1–1.5% for luteinizing hormone-releasing hormone (LHRH) (8). Nevertheless, the high potency of LHRH and its analogues, their large therapeutic ratio, and the need for daily administration in both men and women makes the nasal route extremely attractive for systemic delivery of these compounds.

Nafarelin acetate, a highly potent agonist of LHRH activity, has recently been described (9). In this compound, [D-Nal(2)^6]LHRH, the sixth amino acid in the LHRH decapeptide has been replaced by 3-(2-naphthyl)-D-alanine. This analogue has ~200 times the potency of the native hormone.

The objective of this work was to study the nasal absorption of nafarelin acetate in monkeys, with the purpose of studying the effects of dose and concentration on the systemic availability of this compound *via* nasal administration and establishing a nasal dose equivalent to a therapeutic subcutaneous dose.

EXPERIMENTAL

Study Design—Six adult female rhesus monkeys were used for each dose. The monkeys were sedated before dosing with a 5-mg/kg im injection of ketamine hydrochloride[1]. Approximately 100 μL of a buffered aqueous drug solution was sprayed into each nostril while the animal was held with the head in a vertical position. Immediately after dosing, the animals were placed in a supine position for 5 min.

A heparinized blood sample of ~3 mL was collected from the saphenous vein of each animal at 0 (predose), 5, 15, and 30 min, and 1, 2, 4, and 8 h after administration of the drug. Additional injections of lower doses of ketamine hydrochloride were administered at ~30 min after dosing and immediately prior to the 2-, 4-, and 8-h blood sampling. Blood samples were cooled on ice, and the plasma was separated within 2 h by centrifugation, after which it was stored at −20°C until analyzed by RIA. The monkeys were rested for a minimum of 1 week between doses. In the case of the subcutaneous injection, 0.5 mL of a 10-μg/mL solution of the drug in aqueous buffer was injected in the interscapular area of the monkey, and blood sampling was done as described above.

Radioimmunoassay (10)—A slightly modified nafarelin acetate was conjugated to keyhole limpet hemocyanin (*Megathura crenulta*, mol. wt. 3–7.5 million) using a water-soluble carbodiimide. To provide a suitable functional group for conjugation to the protein, the pyroglutamyl residue in nafarelin acetate was replaced by glutaric acid. Immunization with the protein conjugate was carried out in New Zealand White rabbits using Freund's complete and incomplete adjuvant. The resulting antiserum at a dilution of 1:30,000 yielded a total binding of 45–55%. The radioactive isotope used for labeling was iodine-125. Separation of bound from free radioactivity was carried out with charcoal. The RIA buffer was 0.1 M Tris-HCl, pH 7.2, with 0.5% bovine serum albumin.

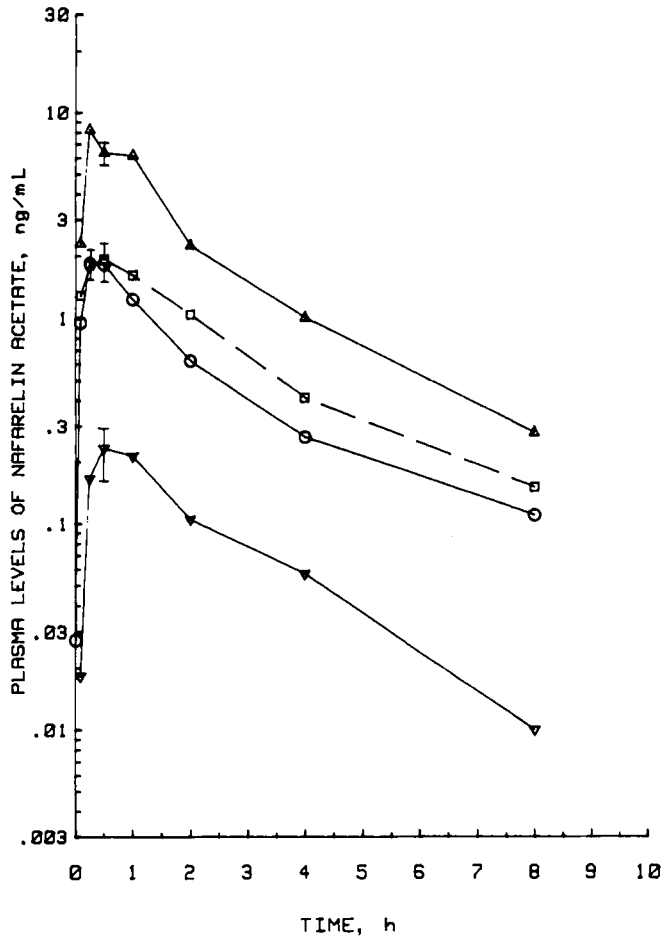

Figure 1—*Mean concentrations (±SEM) of nafarelin acetate in the plasma of monkeys after a single subcutaneous or intranasal dose. Key: (△) 431 μg, nasal; (○) 272 μg, nasal; (▽) 133 μg, nasal; (□) 5 μg, subcutaneous.*

[1] Vetalar; Parke-Davis.

0022-3549/84/0500-0684$01.00/0
© 1984, American Pharmaceutical Association

Table I—Plasma Level Parameters of Nafarelin Acetate Following Nasal and Subcutaneous Administration in Rhesus Monkeys [a]

Conc. of Solution, mg/mL	Average Volume Administered, μL	Average Dose, μg	Peak Height, ng/mL	AUC, ng·h/mL
Nasal				
0.625	213	133(1.8)	0.23(0.07)	0.63(0.3)
1.25[b]	217	272(4.1)	1.84(0.35)	4.56(1.1)
2.5[b]	173	431(15.7)	8.24(0.7)	15.9(2.1)
1.2	121	140(10.3)	0.82(0.28)	2.31(0.76)
Subcutaneous				
0.01	500	5	1.93(0.35)	5.57(0.97)

[a] Six animals per group except where noted; numbers in parentheses are standard errors. [b] Four animals per group due to inadequate dosing of two animals.

The method was validated by adding known quantities of nafarelin acetate to blank plasma and determining the ratios of measured to added compound. Linear regression analysis for the concentration range of 50–500 pg/mL yielded a slope of 0.96 with a correlation coefficient of 0.999. At 50 pg/mL, the *CV* was 11.3%. Additional validation was obtained from an *in vivo* study in which [^{3}H]nafarelin acetate was administered to monkeys, and plasma profiles were determined by RIA and an HPLC–radiochemical method. Excellent agreement was obtained between the two sets of results.

RESULTS AND DISCUSSION

The plasma level profiles of nafarelin acetate for the three nasal doses and the subcutaneous injection are shown in Fig. 1. As with other drugs, nasal absorption is quite rapid, with peak levels being achieved within 15 min. Reproducibility between animals is excellent, particularly at the higher doses, and suggests that at least in a controlled situation, the nasal route has considerable potential for delivery of this LHRH analogue.

The peak heights and areas under the curve (AUC)[2] are listed in Table I. It is immediately evident that there is a pronounced nonlinearity between the dose administered and the resulting levels of drug in the plasma. For example, a roughly twofold increase in dose from 125 to 270 μg results in an approximate 8-fold increase in peak height and a 6.5-fold increase in AUC. Increasing the dose to 430 μg results in a further fourfold increase in peak height and AUC. Since the elimination profiles are similar for all three doses, this suggests that the nonlinearity is associated with changes in the absorption phase. To determine whether the nonlinearity is a function of the concentration of drug in the solution, or of the total dose administered, an additional experiment was conducted where the drug concentration was 1.2 mg/mL (similar to the previous experiment), but the dose was halved by reducing the volume administered. The results shown in Table I suggest that the nonlinearity in peak levels and AUC observed with the increase in dose appears to be associated with the concomitant increase in the concentration of drug in solution. At a concentration of 1.25 mg/mL, a twofold increase in dose results in a slightly greater than twofold increase in peak height. On the other hand, a twofold increase in concentration (from 0.625 to 1.2 mg/mL) results in a 3.5-fold increase in peak height, even though the dose administered is the same (130–140 μg). An increase in flux across the nasal membrane due to the higher concentration or saturable binding and/or metabolism with membrane or enzyme systems are plausible explanations for these observations. Enzymes such as leucine amino peptidase are known to be present in the nasal membrane (11).

In comparing the plasma level profiles for nasal delivery with that found for subcutaneous injection, it is apparent that the plasma levels for the 270-μg nasal dose are almost superimposable on those for the 5-μg sc dose. This gives a bioavailability of ~2% relative to the subcutaneous dose. These data also agree well with bioassay results, where the minimum effective dose for inhibition of ovulation in female rhesus monkeys was 250 and 5 μg administered daily *via* nasal spray and subcutaneous injection, respectively (12). The reason for the relatively low bioavailability of this compound is presently unknown. Enzymatic degradation in the nasal membrane could be a factor, and there may have been some loss of solution *via* postnasal drip. In any case, these studies show that the monkey can serve as a useful animal for studying nasal delivery of drugs.

[2] AUC values were determined for the 0–8-h time period, since plasma blood levels were below detectable limits at 24 h.

REFERENCES

(1) T. Yokosuka, Y. Omuri, Y. Hirata, and S. Hirai, *J. Jpn. Diabetes Soc.*, **20,** 146 (1977).

(2) A. A. Hussain, S. Hirai, and R. Bawarshi, *J. Pharm. Sci.*, **68,** 1196 (1979).

(3) A. A. Hussain, T. Foster, S. Hirai, T. Kashihara, R. Batenhorst, and M. Jones, *J. Pharm. Sci.*, **69,** 1240 (1980).

(4) A. A. Hussain, S. Hirai, and R. Bawarshi, *J. Pharm. Sci.*, **69,** 1411 (1980).

(5) A. Grossman, A. Fabbri, P. L. Goldberg, and G. M. Besser, *Br. Med. J.*, **17,** 1215 (1980).

(6) A. A. Hussain, S. Hirai, and R. Bawarshi, *J. Pharm. Sci.*, **70,** 466 (1981).

(7) A. E. Pontiroli, M. Alberetto, A. Secchi, G. Dossi, I. Bosi, and G. Pozza, *Br. Med. J.*, **284,** 303 (1982).

(8) G. Fink, G. Gennser, P. Liedholm, J. Thorell, and J. Mulder, *J. Endocrinol.*, 63, 351 (1974).

(9) J. J. Nestor, Jr., T. L. Ho, R. R. Simpson, B. L. Horner, G. H. Jones, G. I. McRae, and B. H. Vickery, *J. Med. Chem.*, **25,** 795 (1982).

(10) C. Nerenberg and S. Kushinsky, *Analy. Biochem.*, in press.

(11) S. Hirai, T. Yashiki, and H. Mima, *Int. J. Pharm.*, **9,** 173 (1981).

(12) B. H. Vickery, in "LHRH Peptides as Female and Male Contraceptives," G. I. Zatuchni, J. D. Shelton, and J. J. Sciarra, Eds., Harper and Row, Philadelphia, Pa., 1981, p. 109.

ACKNOWLEDGMENTS

The authors thank Bryan Robert and David Donahue for assistance with some of the animal experiments.

Analysis of Captopril and Hydrochlorothiazide Combination Tablet Formulations by Liquid Chromatography

JOEL KIRSCHBAUM ˣ **and SOLOMON PERLMAN**

Received January 10, 1983, from *The Squibb Institute for Medical Research, New Brunswick, NJ 08903.* Accepted for publication March 17, 1983.

Abstract □ A reverse-phase, high-performance liquid chromatographic (HPLC) procedure was developed for the simultaneous assay of captopril and hydrochlorothiazide in a combination tablet formulation. Gradient elution was used to quantify these two drugs, as well as the oxidized form of captopril, the disulfide. Tablets were extracted with methanol and, after centrifugation, were chromatographed. Initially, a methanol–0.05% aqueous phosphoric acid (25:75, v/v) solution was pumped at 2 mL/min into a phenyl column. After 8 min, the flow rate was increased to 4.5 mL/min and the methanol content of the mobile phase was increased to 45% to elute the disulfide. Detection was at 210 nm. Linearity and repeatability of all constituents were satisfactory. The hydrolytic degradation product of hydrochlorothiazide, 4-amino-6-chloro-1,3-benzene disulfonamide (also called the disulfonamide), could be resolved in test solutions but was not visible in chromatograms of tablets carried through the gradient procedure even after storage at elevated temperatures for prolonged time periods prior to assay. The method can be automated.

Keyphrases □ Captopril—analysis by HPLC, combination with hydrochlorothiazide, tablet formulations □ Hydrochlorothiazide—analysis by HPLC, combination with captopril, tablet formulations

Captopril (I), an antihypertensive agent (1), has been formulated with the diuretic hydrochlorothiazide (II). An assay was needed to quantify these two drugs in a combination tablet formulation (2) together with two degradation products, the disulfide (IV) of captopril and the disulfonamide of hydrochlorothiazide [4-amino-6-chloro-1,3-benzene disulfonamide (III)]. High-performance liquid chromatography (HPLC) has the potential for assaying all four compounds simultaneously. Such an assay should elute the isomeric forms of captopril (3) as one peak, as described in a previously developed assay for captopril bulk material (4). HPLC assays were previously developed for hydrochlorothiazide in tablets (5, 6) and in body tissues (7, 8). The method described below is stability indicating and amenable to automation.

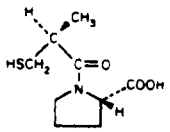

I

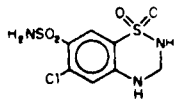

II

EXPERIMENTAL

Materials—Captopril[1], the disulfide[1] of captopril, and hydrochlorothiazide[1] were used as received. Water was double-distilled and stored in glass. The disulfonamide[2], HPLC-grade methanol[3], and ACS reagent-grade phosphoric acid[4] were obtained commercially.

Apparatus—A gradient system[5] capable of both flow-rate and mobile-phase composition adjustments was connected to a 50 × 0.2-cm saturator column packed with 37-μm silica. Next in sequence were an inlet filter[6] (2-μm pore size) and a precision loop injector[7] (nominal volume 20 μL), attached to a reverse-phase (medium polarity) phenyl column[8], 5 or 10 μm, 250–300 mm × 4.6 mm i.d., with >7000 theoretical plates per column. The column temperature was maintained slightly above ambient (30°C) by a thermostatically controlled heater[9], to avoid variation in retention time. A variable-wavelength detector[10] set to 210 nm was used. The 20- or 25-cm two-channel strip-chart recorder[11] had input compatible with the detector output. One recorder channel was adjusted to trace the captopril and hydrochlorothiazide peaks on scale. The other channel was set to be ~40 times more sensitive to detect possible impurities. For automated unattended analysis, an autosampler[12] was used in conjunction with a laboratory computer system[13]. Calculations are based on peak area or peak height, which appear to be interchangeable.

Mobile Phase and Gradient Program—At time zero, a mobile phase consisting of methanol–0.05% phosphoric acid in water (25:75, v/v) was pumped at 2 mL/min. After 8 min, the flow rate was increased to 4.5 mL/min and the methanol content to 45%. After 15 min, the methanol content was returned to 25%, and after 20 min, the flow rate was also returned to the original 2 mL/min.

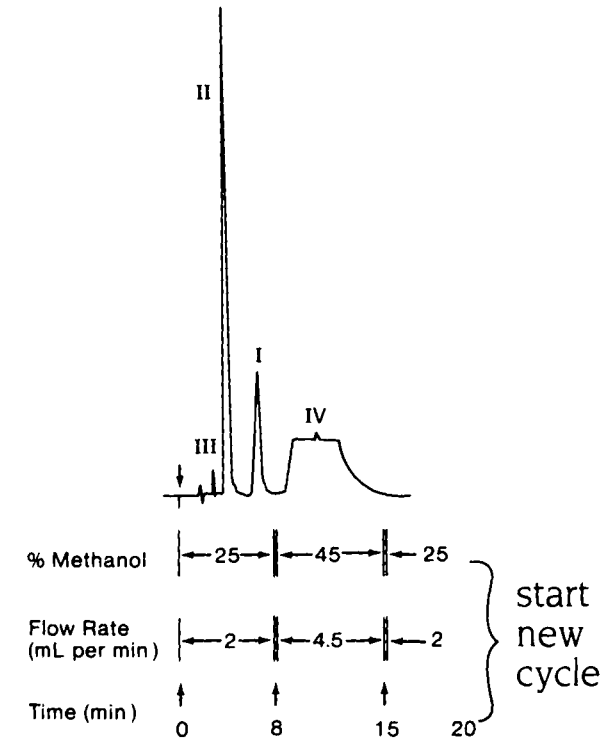

Figure 1—*HPLC of mixed standards for analyzing captopril (I) and hydrochlorothiazide (II) combination tablets, also including the disulfonamide (III) and disulfide (IV). Gradient conditions are appropriately noted, using methanol and 0.05% aqueous phosphoric acid. Detection was at 210 nm (0.16 AUFS) using a phenyl column. For captopril, typical asymmetry factor is 1.25, and number of theoretical plates is 470 (manufacturers' specifications are for >7000 theoretical plates/column using their test systems). Tailing of both standards and samples gradually appears with prolonged use of the column.*

[1] E. R. Squibb House Standard.
[2] Aldrich.
[3] Baker.
[4] Fisher.
[5] Beckman.
[6] Rheodyne Model 7362.
[7] Rheodyne Model 7010.
[8] Waters Associates or E.S. Industries or Waters columns repacked by Analytical Sciences, Inc.
[9] Bioanalytical Systems LC-22 and LC-23.
[10] Schoeffel 770 or 773 or Perkin-Elmer LC-75 or LC-85.
[11] Kipp and Zonen or Linear Instruments.
[12] Perkin-Elmer Model 420B or ISS-100.
[13] Hewlett-Packard 3356.

0022-3549/84/0500-0686$01.00/0
© 1984, American Pharmaceutical Association

Table I—Gradient and Isocratic Systems for Captopril and Hydrochlorothiazide

Captopril (Theory: 50 mg/tablet)			Hydrochlorothiazide (Theory: 25 mg/tablet)		
Gradient	Isocratic	Δ	Gradient	Isocratic	Δ
52.8	50.8	+2.0	24.9	25.1	−0.2
50.8	51.6	−0.8	25.1	24.8	+0.3
49.5	50.1	−0.6	24.6	24.8	−0.2
49.5	50.9	−1.4	24.6	24.3	+0.3
50.8	50.5	+0.3	24.3	24.3	—
50.1	51.6	−1.5	24.6	24.8	−0.2
51.3	50.1	+1.2	24.7	24.0	+0.7
49.6	49.3	+0.3	23.9	23.8	+0.1
52.0	51.9	+0.1	24.3	24.5	−0.2
50.0	50.3	−0.3	24.4	24.6	−0.2
Mean 50.6	50.7	−0.7	24.5	24.5	+0.4
RSD 2.2%	1.6%		1.5%	1.6%	

Tablet Analyses—Ten formulations were assayed: 12.5, 25, 37.5, 50, and 100 mg of captopril with either 15 or 25 mg of hydrochlorothiazide. For content uniformity, the intact, weighed tablet was extracted with methanol; Twenty-five milliliters of methanol was added to a 12.5-mg captopril/15-mg hydrochlorothiazide combination tablet, and 40 mL of methanol was used to extract all other potencies. For the assay of the drug content of a tablet, 10–20 tablets were ground and the weight of powder equivalent to one tablet was extracted with methanol. After 20 min of ultrasonication, the suspensions were shaken vigorously and then centrifuged at 1500 rpm (1200×*g*).

A mixed standard was prepared consisting of captopril and hydrochlorothiazide equivalent in concentration to the potency of the tablets being analyzed and 0.1% disulfonamide. A second standard containing 0.6% disulfide is necessary since captopril normally contains traces of this reversible oxidation product.

Assay—The column was initially equilibrated by passing 100 mL of methanol 0.5% aqueous phosphoric acid (1:3) through it. Prior to the first injection, the gradient program was activated. After the first cycle, the mixed captopril—hydrochlorothiazide disulfonamide standard was injected twice. All subsequent samples and standards (including the disulfide) were then injected into the column. No daily column cleaning was necessary.

System Suitability Test—The resolution of the mixed standard constituents was as follows: disulfonamide from void volume, ≫1.4; disulfonamide from hydrochlorothiazide, ≫1.4; hydrochlorothiazide from captopril, >2; and captopril from disulfide, >2. Resolution was calculated using $R_S = 2(t_2 - t_1)/(W_1 + W_2)$, where R_S is resolution, t_1 and t_2 are the retention times or distances, and W_1 and W_2 are the respective peak widths of tangents drawn to the baseline. Responses from the initial injections of standard are usually within 1.5% of each other, indicating continuation of the assay.

RESULTS AND DISCUSSION

The gradient HPLC system was developed to quantify captopril, its reversible oxidized form, hydrochlorothiazide, and its possible hydrolytic product, the disulfonamide. Figure 1 illustrates the separation of all four constituents. The baseline aberration occurring after the captopril peak is due to a change in the refractive index of the mobile phase as its composition varies. The disulfide peak is clearly visible above the plateau. (Detectors are available with autozero capability which can electronically correct for such shifts. Alternatively, we successfully used a laboratory data acquisition system[13] to make such a baseline correction.) Separation of all four constituents indicates selectivity of the HPLC system and is the basis of a system suitability test.

Precision of the system (9) was determined by means of six injections of mixed standards to give the following relative standard deviations: disulfonamide, 1.2%; hydrochlorothiazide, 0.5%; captopril, 1.9%; and disulfide, 3.5%. The disulfide value is high due to a combination of long retention time and low (0.6%) concentration. The precision of the method was determined by pooling 10 tablets and then analyzing six tablet weights carried through the recommended procedure. The relative standard deviations are as follows: hydrochlorothiazide, 0.86%; captopril, 1.1%; and disulfide, 4.8%.

The response *versus* concentration curves from 10 to 200% of the concentrations of the standards were found to be linear for all four substances, with calculated correlation coefficients of ≥0.99 for all substances except the disulfide, which was 0.98. Recoveries of captopril and hydrochlorothiazide added to placebo formulation were 100.5% ($n = 5$, $RSD = 0.8$) and 98.7% ($n = 5$, $RSD = 0.8\%$) respectively. No interfering peaks were noted after extracting and injecting placebo tablets. At least six phenyl columns from two vendors[8] have been used, indicating ruggedness.

The gradient assay was verified by using an isocratic HPLC system which could quantitate captopril, hydrochlorothiazide, and the disulfide. This assay used methanol–0.05% aqueous phosphoric acid (55:45, v/v) and a 15%-loaded octadecylsilane column. This system failed to resolve the disulfonamide from the void volume; however, since no disulfonamide appears to be present in any sample studied, it is suitable for verifying the gradient system. Individual tablets of 50 mg of captopril and 25 mg of hydrochlorothiazide were extracted with methanol and simultaneously injected onto the recommended gradient and alternative isocratic systems. The results (Table I) show that the gradient and isocratic systems give similar results for captopril and hydrochlorothiazide, indicating the statistical reliability of the gradient system. The disulfide contents of 0.3% are identical using both systems. No change in strength was observed after storage for 52 weeks at temperatures between ambient and 40°C for these or any other formulations. No other extraneous peaks were detected.

Verification of the absence of disulfonamide was by TLC[14]. The disulfonamide limit of detection by TLC is ~0.01%. However, the compendial (10) colorimetric assay gave values of 0.2–0.4%. Kinetic studies (11) showed these values to be an artifact of the colorimetric method and indicate that this HPLC method has additional utility by replacing an erroneous assay.

For routine assays of the disulfonamide, hydrochlorothiazide, and captopril (but omitting the disulfide), the mobile phase used in the first 8 min of the gradient assay can be used. In this second isocratic system, the disulfide slowly elutes from the column as a broad peak that is unnoticeable because disulfide contents are very low. The first and last chromatograms from a series of repetitive injections are superimposable, indicating that the slow elution of disulfide does not affect the system. The remainder of the chromatogram is similar to Fig. 1, except for the lack of the disulfide plateau region.

In summary, an assay using gradient HPLC has been developed for the active constituents and possible impurities in captopril–hydrochlorothiazide combination tablets. This multiconstituent assay is selective, amenable to automation, and stability indicating.

REFERENCES

(1) M. A. Ondetti, B. Rubin, and D. W. Cushman, *Science*, **196,** 441 (1977).

(2) M. H. Weinberger, *Br. J. Clin. Pharmacol.*, **14,** 127s (1982).

(3) D. L. Rabenstein and A. A. Isab, *Anal. Chem.*, **54,** 526 (1982).

(4) S. Perlman and J. Kirschbaum, *J. Chromatogr.*, **206,** 311 (1981).

(5) S. L. Daniels and A. J. Vanderwielen, *J. Pharm. Sci.*, **70,** 211 (1981).

(6) A. G. Butterfield, E. G. Lovering, and R. W. Sears, *J. Pharm. Sci.*, **67,** 651 (1978).

(7) E. Redalieu, V. V. Tipnis, and W. E. Wagner, Jr., *J. Pharm. Sci.*, **67,** 726 (1978).

(8) M. J. Cooper, A. R. Sinaiko, M. W. Anders, and B. L. Mirkin, *Anal. Chem.*, **48,** 1110 (1976).

(9) E. Debesis, J. P. Boehlert, T. E. Giuand, and J. C. Sheridan, *Pharm. Tech.*, **6,** 120 (1982).

(10) "United States Pharmacopeia," 20th rev., U.S. Pharmacopeial Convention, Rockville, Md., p. 378, 1980.

(11) D. Sich and S. Perlman, *J. Pharm. Sci.*, in press.

ACKNOWLEDGMENTS

The authors thank Harry Sambucini for performing many of the assays and Dr. Glenn Brewer, Dr. Klaus Florey, Mr. Raymond Poet, and Dr. G. Reier for their help and critical reading of this manuscript. The talents of S. Meloni in illustrating, Mr. D. Wisdon in photography, and Mrs. Connie Saloom in typing this paper are all gratefully appreciated.

[14] Henry Roberts, personal communication.

Quantitation of Diltiazem and Desacetyldiltiazem in Dog Plasma by High-Performance Liquid Chromatography

ROBERT E. WIENS *, DENNIS J. RUNSER ‡, JOSEPH P. LACZ ‡, and DAN C. DIMMITT‡x

Received May 17, 1982, from **Harris Laboratories, Inc., P.O. Box 80837, Lincoln, NE 68501* and ‡*Marion Laboratories, Inc., Kansas City, MO 64137.* Accepted for publication March 24, 1983.

Abstract □ A high-performance liquid chromatographic procedure was developed for the determination of diltiazem and desacetyldiltiazem in dog plasma. Two milliliters of plasma is extracted with a hexane–2-propanol mixture. The assay uses a reverse-phase column maintained at 55°C with a silica saturation column and a pellicular precolumn. The mobile phase is acetonitrile–water (50:50) at pH 6.6 with 1.5-g/L heptanesulfonic acid added as the ion-pair reagent. The procedure is sensitive to 5 ng/mL for both compounds in dog plasma and is linear up to 2000 ng/mL for diltiazem and 1000 ng/mL for desacetyldiltiazem. Preliminary dog mean plasma profiles of diltiazem and desacetyldiltiazem are presented.

Keyphrases □ Diltiazem—quantitation with desacetyldiltiazem, dog plasma, HPLC □ Desacetyldiltiazem—quantitation with diltiazem, dog plasma, HPLC □ HPLC—quantitation of diltiazem and desacetyldiltiazem, dog plasma

Diltiazem hydrochloride, a new antianginal drug being used in Japan for the treatment of angina pectoris, is classified as a calcium antagonist. It affects vascular smooth muscle and dilates coronary vessels, making the drug clinically useful in the treatment of ischemic heart disease (1, 2).

Methods have been published for the determination of diltiazem and/or desacetyldiltiazem, the principal blood metabolite of diltiazem in plasma. A GC method of Rovei *et al* (3), which uses a hexane plasma extract at pH 7 with a nitrogen–phosphorus detector after a complex derivatization procedure, and a TLC–spectrophotometric procedure (4) have been presented. These methods either lack sensitivity (TLC) or are time consuming (GC).

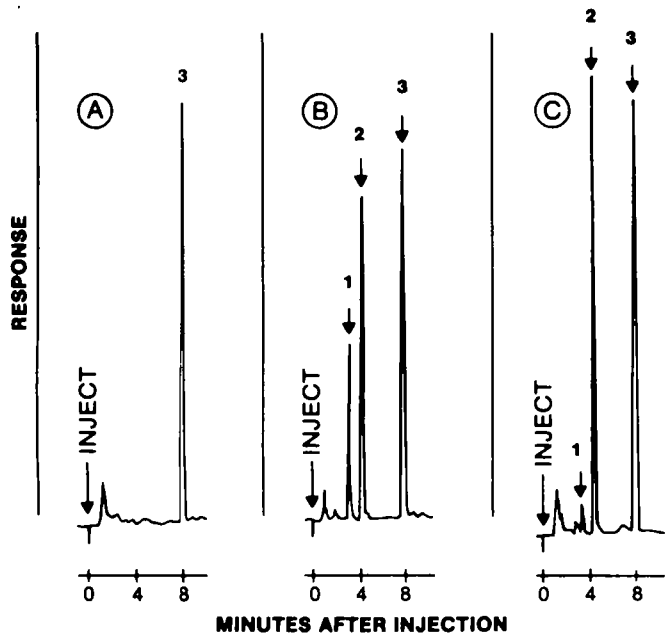

Figure 1—*Chromatograms from (A) blank dog plasma containing 400 ng of prazepam (3), (B) plasma spiked with 100 ng/mL of desacetyldiltiazem (1) and 200 ng/mL of diltiazem (2), and (C) dog plasma following the intravenous administration of diltiazem (2 mg/kg, 1-h postdose).*

Many clinical trials and pharmacology studies have been conducted with this compound; however, few studies have reported the pharmacokinetic parameters in humans or other animal species. The objective of this study was to develop a rapid and sensitive diltiazem and desacetyldiltiazem plasma assay to assess the pharmacokinetics of diltiazem and to present preliminary plasma level data for the beagle dog.

EXPERIMENTAL

Protocol—Six beagle dogs were administered diltiazem hydrochloride in solution at an oral dose of 5 mg/kg and as a bolus dose of 2 mg/kg iv in a crossover design. The dogs were fasted overnight before drug administration and until the 6-h blood collection. Blood samples were collected immediately before dosing and up to 10 h postdose, using sodium heparin as the anticoagulant. The plasma was immediately frozen at −20°C until analysis.

Reagents—Chromatography-grade acetonitrile[1], 2-propanol[1], methanol[1], and hexane[1] were used. Sodium acetate[1] and sodium borate[1] were ACS analytical reagents. Heptanesulfonic acid sodium salt[2] was used as received.

Apparatus—A high-performance liquid chromatograph[3] with an automatic sampler[4] and a reverse-phase C_{18} column[5] was used. A silica saturation column[6] was installed in the oven in front of the injector and a precolumn of pellicular C_{18} packing[7] was inserted after the injector. The column effluent was monitored with a variable-wavelength UV absorbance detector[8] using a dual-pen recorder[9].

Standards—Primary standard solutions of diltiazem hydrochloride [10] (500 μg of free base/mL) and desacetyldiltiazem[10] (500 μg of free base/mL) were prepared in distilled water. A secondary standard solution containing both diltiazem (100 μg/mL) and desacetyldiltiazem (50 μg/mL) was prepared in water. Eight dilutions were made such that 0.1 mL of each dilution would be used to spike 2 mL of blank dog plasma to the concentrations used for the standard curve. The resulting plasma standard curve concentrations were 50, 100, 200, 400, 800, 1600, and 2000 ng/mL of diltiazem and 25, 50, 100, 200, 400, 800, and 1000 ng/mL for desacetyldiltiazem. The internal standard, prazepam[11] (200 μg/mL), was prepared in methanol and then diluted 1:500 in 0.1 M sodium borate buffer (pH 9).

Extraction—A 2.0-mL plasma aliquot from a control dog (standard curve) or unknown sample was placed in a 16 × 150-mm glass culture tube and 1.0 mL of internal standard buffer and 7 mL of hexane–2-propanol (98:2) was added. The tube was closed with a polyef-lined screw-cap and shaken 30 min on a horizonal shaker[12].

Each sample was centrifuged 10 min at room temperature, and 6 mL of the upper hexane layer was transferred to a clean 13 × 100-mm culture tube. The tube was placed in a 40–50°C water bath and evaporated to dryness under a nitrogen stream. The residue was reconstituted by adding 200 μL of mobile phase. The tube was vortexed[13] 30 s to ensure dissolution and centrifuged 2 min to collect the solution. The resulting concentrate was transferred to a microcentrifuge tube[14] and injected onto the HPLC column by the automatic sampler.

Chromatographic Conditions—The mobile phase consisted of acetoni-

[1] Chrom AR; Mallinckrodt, Paris.
[2] Eastman Kodak Co., Rochester, N.Y.
[3] Series 3 with Model LC65T Oven-detector; Perkin-Elmer, Norwalk, Conn.
[4] WISP 710B; Waters Associates, Milford, Mass.
[5] μBondapack C_{18} (300 × 3.9 mm. i.d.); Waters Associates, Milford, Mass.
[6] Pre-SAT Kit; Applied Science, State College, Pa.
[7] 60 × 2 mm Perisorb RP18, 30–40 μm; EM Reagents, Darmstadt, W. Germany.
[8] LC-75; Perkin-Elmer, Norwalk, Conn.
[9] Omniscribe B5217-SI; Houston Instruments, Austin, Tex.
[10] Marion Laboratories, Kansas City, Mo.
[11] Warner-Lambert, Ann Arbor, Mich.
[12] Model 6010; Eberbach Corporation, Ann Arbor, Mich.
[13] Multi-Tube Vortexer, Model 2600; SMI Industries, Emeryville, Calif.
[14] 250-μL polyethylene; Brinkman Instruments.

0022-3549/84/0500-0688$01.00/0
© 1984, American Pharmaceutical Association

Table I—Standard Curve Summary for Diltiazem and Desacetyldiltiazem in Dog Plasma

Standard Curve	Diltiazem			Desacetyldiltiazem		
	r	Slope $\times 10^2$	Intercept	r	Slope $\times 10^2$	Intercept
1	0.9999	0.4464	0.0001	0.9999	0.5003	−0.020
2	0.9999	0.4328	0.003	0.9999	0.4864	−0.003
3	0.9999	0.4460	−0.003	0.9999	0.5100	−0.006
n	3	3	3	3	3	3
Mean	0.9999	0.4417	0.0003	0.9999	0.4989	−0.010
SD	0	0.008	0.003	0	0.012	0.009
CV	0	1.8%	917%	0	2.4%	94.9%

trile–water (50:50) containing 1.5 g of heptanesulfonic acid sodium salt/L and 8 g of sodium acetate/L. The final solution was adjusted to pH 6.6 with glacial acetic acid and filtered[15]. The flow rate was 1.5 mL/min, the column temperature 55°C, the detector wavelength 240 nm, and the injection volume 100 μL.

Quantitation—All determinations were performed by hand measuring the peak heights and computing the peak height ratios of each compound as compared with the internal standard. This ratio was calculated and compared with the slope of the standard curve. Replicate and quality control samples (Table II) were processed from blank dog plasma with each set of samples, and a computer program was developed to calculate the ratios, slopes, and intercepts of the standard curves. The quality control samples were spiked and frozen before study initiation, and the replicate samples were spiked at the time of extraction.

RESULTS AND DISCUSSION

A method has been developed to determine diltiazem and desacetyldiltiazem plasma levels utilizing a 10-min HPLC separation. Typical chromatograms obtained from blank plasma spiked with the internal standard, a standard curve sample, and an actual dog plasma sample are presented in Fig. 1. Blank dog plasma without internal standard indicated no interfering peaks.

Sample extraction is pH, solvent, and time dependent. A pH value of 7 has been shown to be successful for the extraction of diltiazem into hexane (3). However, adjustment to pH 9 and the addition of 2% 2-propanol to the hexane increased recovery from 55 to 77% for desacetyldiltiazem and from 70 to 85% for diltiazem, as compared with the pH 7 extraction. Recovery of diltiazem decreased when the two phases were mixed <30 min on the shaker. No diltiazem degradation has been observed under the pH 9 extraction conditions.

Several drugs were tested for use as internal standards and for possible interference with diltiazem and desacetyldiltiazem. Prazepam, diazepam, oxazepam, clonazepam, chlordiazepoxide, medazepam, and propranolol did not interfere with the HPLC separation. Prazepam was chosen as the internal

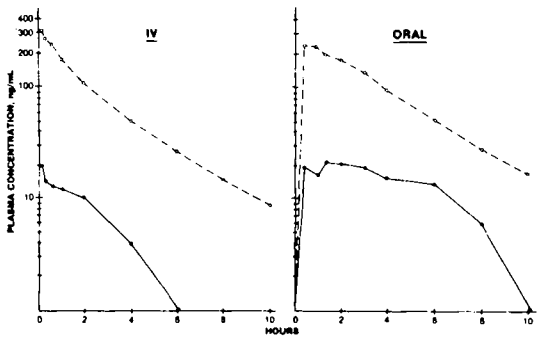

Figure 2—*Mean plasma levels of six beagle dogs administered 2 mg/kg iv of diltiazem or 5 mg/kg of diltiazem orally. Key: (○) diltiazem; (●) desacetyldiltiazem.*

[15] 0.45-μm pore, Nylon 66; Rainin Instruments, Emeryville, Calif.

Table II—Reproducibility for Diltiazem and Desacetyldiltiazem in Dog Plasma

Conc. in Plasma, ng/mL	*n*	Mean, ng/mL	*SD*	*CV*, %
		Diltiazem		
5[a]	5	4.9	0.3	6.5
10[a]	11	12.0	1.4	11.9
25[a]	6	28.0	1.2	4.2
100[b]	4	100.9	2.4	2.4
800[b]	4	801.1	2.1	0.3
		Desacetyldiltiazem		
5[a]	6	5.4	0.5	8.6
10[a]	10	10.8	1.3	12.1
12.5[a]	6	14.6	1.4	9.7
50[b]	4	50.6	2.0	4.0
400[b]	4	395.2	6.6	1.7

[a] Within-day replicate samples. [b] Quality control samples.

standard because of its symmetrical peak shape, extraction recovery properties (90%), and appropriate retention time.

Three standard curves were run on successive days (Table I). The accuracy and precision of the method are shown in Table II by the coefficient of variation and mean values for the two quality control samples and two replicate samples. The lower limit of quantitation was calculated after completion of the study by the method of Gabriels (5). The method uses the mean baseline value of the blank plasma samples, a corresponding F value, and the standard deviation. The lower limit of quantitation was 5 ng/mL for diltiazem and desacetydiltiazem.

Stability test samples of diltiazem and desacetyldiltiazem in plasma stored for up to 13 weeks at −20°C indicated no significant breakdown. The tests concentrations of diltiazem ranged from 50 to 500 ng/mL and those of desacetyldiltiazem from 25 to 250 ng/mL.

The mean of the individual plasma diltiazem and desacetyldiltiazem profiles of the six beagle dogs are presented in Fig. 2 for the 2-mg/kg iv and 5-mg/kg oral doses. Both the intravenous and oral data indicate a terminal diltiazem half-life of ~2.2 h and an absolute bioavailability of 55% when the mean of the individual diltiazem areas under the curve from zero to infinity ($AUC_{0\to\infty}$) of the intravenous and oral results are normalized and compared (6). The half-lives were calculated from the elimination rate constant (k) by the equation $t_{1/2} = 0.693/k$. The elimination rate constant (k) was obtained by an intravenous two-compartment model with bolus administration and an oral two-compartment model with first-order absorption and elimination from the central compartment. The data were fitted by the NONLIN (7) regression analysis using subroutines for both sets of data. The $AUC_{0\to\infty}$ values were calculated by the trapezoidal method and normalized for dose assuming linear kinetics.

REFERENCES

(1) R. F. Zelis, *Hospital Practice*, **16(8)**, 49 (1981).

(2) J. S. Schroeder and R. F. Zelis, *Chest*, **78(1)**, Suppl., July, (1980).

(3) V. Rovei, M. Mitchard, and P. L. Morselli, *J. Chromatogr.*, **138**, 391 (1977).

(4) K. Kohno, Y. Takeuchi, A. Ethoh, and K. Noda, *Arzneim.-Forsch. Drug Res.*, **27**, 1424 (1977).

(5) R. Gabriels, *Anal. Chem.*, **42**, 1439 (1970).

(6) R. W. Piepho, D. C. Bloedow, J. P. Lacz, D. J. Runser, D. C. Dimmitt, and R. K. Browne, *Am. J. Cardiol.* **49**, 525 (1982).

(7) C. M. Metzler, G. L. Elfring, and A. J. McEwen, "A Users Manual for NONLIN and Associated Programs," The Upjohn Company, Kalamazoo, Mich., 1974.

ACKNOWLEDGMENTS

The authors thank Dr. E. Heath for technical advice, D. Bell for programming assistance, and D. Schenaman for technical assistance. All are from Harris Laboratories, Inc., Lincoln, Neb.

Analysis of 4-Methylpyrazole in Plasma and Urine by Gas Chromatography with Nitrogen-Selective Detection

RAMANUJ ACHARI* and MICHAEL MAYERSOHN ˣ

Received January 25, 1983, from the *Department of Pharmaceutical Sciences, College of Pharmacy, The University of Arizona, Tucson, AZ 85721.* Accepted for publication March 31, 1983. * Present address: American Critical Care, McGaw Park, IL 60085.

Abstract □ A simple, sensitive, and specific gas chromatographic method for the quantitation of 4-methylpyrazole in plasma and urine is described. Samples containing 4-methylpyrazole, with 3-methylpyrazole as the internal standard, are extracted into ether and the concentrated ethereal extracts are chromatographed on a Carbowax 20M column using nitrogen-selective detection. Standard curves are linear and reproducible over the range of 25–1000 ng/mL for plasma and 0.5–5 μg/mL for urine. Recovery of 4-methylpyrazole is complete from plasma and urine, and the overall between-day coefficient of variation is within 6.0%. No interference is observed from the extractive constituents of plasma and urine. The assay method is suitable for an examination of 4-methylpyrazole disposition in animals and humans.

Keyphrases □ 4-Methylpyrazole—analysis in urine and plasma, gas chromatography with nitrogen-selective detection □ Gas chromatography—analysis of 4-methylpyrazole in plasma and urine, nitrogen-selective detection.

Pyrazole and several of its derivatives have been shown to be inhibitors of the alcohol dehydrogenase enzyme system (1). Because of its apparent low systemic toxicity, 4-methylpyrazole (I) is of particular interest. This compound inhibits the *in vitro* metabolism of alcohols in various animal species (1–3), and it reduces the rate of ethanol elimination in animals (4, 5) and humans (6–8). Several studies have also indicated its effectiveness in reducing the rate of metabolism of methanol (9, 10) and ethylene glycol (11, 12). As a result, 4-methylpyrazole may be a promising alternative to ethanol in treatment of poisoning with alcohols whose toxicity is associated with metabolites formed *via* alcohol dehydrogenase. There have been relatively few studies, however, where plasma concentrations of the compound have been determined (9, 10, 13, 14).

The methods currently available for the determination of I in biological fluids are quite limited. Rydberg and Buijten (15) described potential gas chromatographic (GC) conditions for I which simply involved injecting aqueous solutions of the compound into the column and identifying the chromatographic peak by mass spectrometry. Furthermore, a flame-ionization detector (FID) was employed. With FID, we found that the broad solvent front severely limits the lower measurable concentrations. The GC–MS method (16) of determining I in plasma, although specific, is time consuming and lacking in sensitivity. To examine the disposition of I in animals there is need for a simple, sensitive, and reproducible analytical method for plasma and urine. The present report describes such an assay method, utilizing GC and nitrogen-selective detection, for 4-methylpyrazole (I) using 3-methylpyrazole (II) as an internal standard.

EXPERIMENTAL

Chemicals—4-Methylpyrazole[1] and 3-methylpyrazole[1], the internal standard, were used as supplied. All organic solvents were HPLC grade[2]. Sodium carbonate, sodium chloride, and hydrochloric acid were reagent grade[3].

I II

Gas Chromatography—Samples were analyzed using a gas chromatograph[4] equipped with a nitrogen–phosphorus detector. A 122.0 cm × 2 mm i.d. glass column packed with 5% Carbowax 20M + 2% KOH on 80–100 mesh Chromosorb G (HP)[5] was used. Hydrogen and air flow rates were 3 and 50 mL/min, respectively. Helium was used as a carrier gas at a flow rate of 30 mL/min. The collector voltage was adjusted for adequate sensitivity. The column oven was operated isothermally at 135°C, injection port and detector temperatures were 250°C and 300°C, respectively.

Stock Solutions—A stock solution of I was prepared by dissolving 20 mg in 100 mL of methanol. Working standards were prepared by serial dilution of the stock solution with methanol to encompass the appropriate concentration ranges for plasma and urine. Concentrations of the standards were such that 50 μL added to 1 mL of biological fluid would produce the desired concentration. Solutions of the internal standard were prepared in methanol at a concentration of 4 μg/mL for plasma and 20 μg/mL for urine. All solutions were stored in the refrigerator (0–4°C).

Extraction of Plasma—One milliliter of plasma (containing I) was transferred into a glass culture tube with a polytef-lined screw cap. Fifty microliters (200 ng) of the internal standard solution, 1 g of NaCl, and 0.5 mL of 2 M HCl were added. After addition of 6 mL of ether, the tube was shaken gently for 5 min in a mechanical shaker, centrifuged at 3000 rpm (1000×*g*) for 5 min, and the upper organic layer was withdrawn and discarded. Five hundred microliters of 1 M sodium carbonate was added to the aqueous phase, mixed, and extracted as above with 6 mL of ether. After centrifugation, the clear ether layer was transferred into a 13 × 100-mm disposable glass culture tube containing 30 μL of *n*-butyl alcohol. A boiling chip was added to the tube which was placed in a water bath (45°C). The tube was removed from the water bath after most of the ether had evaporated. If necessary, the extract can be concentrated further by leaving the tube in the water bath for a few minutes after the boiling has ceased. Three microliters of the concentrated ethereal extract was injected into the column. The peak height ratio of I to the internal standard was calculated and the concentration of I was determined with reference to a standard curve.

Extraction of Urine—To 1.0 mL of urine in a glass culture tube (with a screw cap) were added 50 μL (1 μg) of internal standard solution, 1 g of NaCl, and 6 mL of ether. The tube was shaken gently for 5 min in a mechanical shaker and centrifuged for 5 min. The clear organic layer was transferred into a 13 × 100-mm glass culture tube containing 30 μL of *n*-butyl alcohol and treated as described above for the extraction of plasma.

Hydrolytic Treatment of Urine—A 1.0-mL sample of urine was placed into a glass culture tube, 0.5 mL of 2 M HCl was added, and the contents were mixed. The tube was capped tightly and placed in an oven at 115°C. After 1 h the tube was removed from the oven and cooled. One gram of sodium chloride, 50 μL (1 μg) of internal standard solution, and 0.5 mL of 1 M sodium carbonate were added. After addition of 6 mL of ether, the sample was carried through the procedure outlined above.

Standard Curves—Duplicate standards were prepared by transferring 50 μL of the working standards of I and 1.0 mL of blank plasma or urine to glass culture tubes to give final concentrations in the ranges of 25–1000 ng/mL and 0.5–5 μg/mL for plasma and urine, respectively. After addition of 50 μL of internal standard solution, the samples were treated as described above. Standard curves were prepared by plotting peak height ratios of I to the internal standard *versus* concentrations of I.

Extraction Efficiency (Analytical Recovery)—Analytical recoveries of I

[1] Aldrich Chemical Co., Milwaukee, Wis.
[2] Burdick and Jackson, Muskegon, Mich.
[3] Fisher Scientific Co., Fair Lawn, N.J.
[4] Model 5710A; Hewlett-Packard, Palto Alto, Calif.
[5] Supelco Inc., Bellefonte, Pa.

0022-3549/84/0500-0690$01.00/0
© 1984, American Pharmaceutical Association

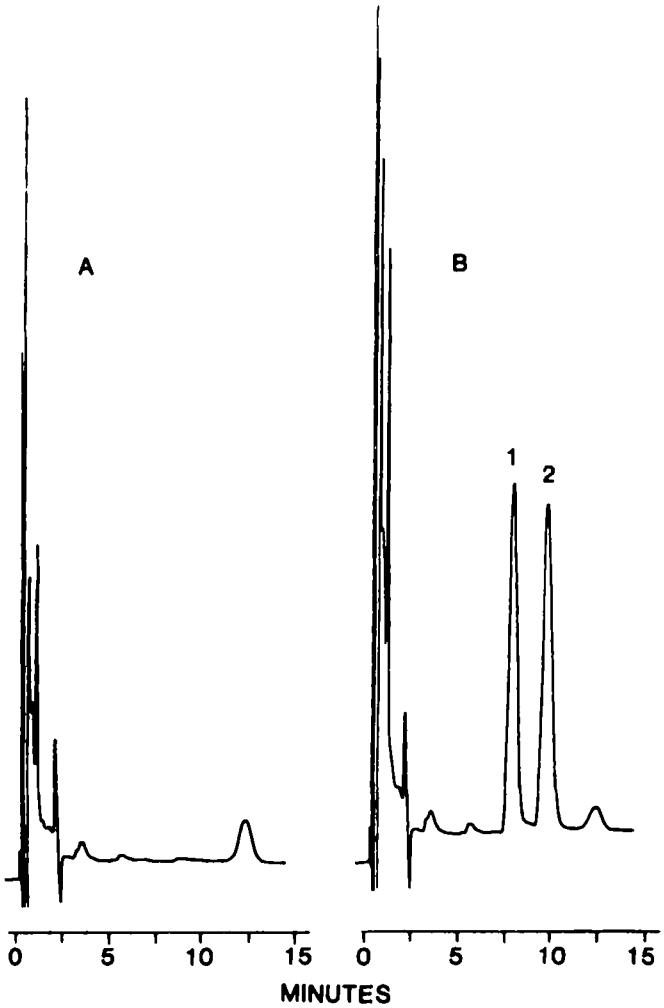

Figure 1—*Chromatograms of ethereal extracts of human plasma. Key: (A) plasma blank; (B) plasma spiked with 200 ng each of 3-methylpyrazole (1) and 4-methylpyrazole (2) (attenuation: 1 × 32).*

and the internal standard from plasma and urine were determined by comparing, respectively, the peak heights of I and internal standard obtained from the extracted spiked plasma and urine samples to those obtained from direct injection of methanolic standards containing equivalent amounts of the compounds. Recoveries of I were also calculated by comparing the peak height ratios of I to the internal standard in the extracted standards to those in the methanolic standards. Three different concentrations of I were used.

RESULTS AND DISCUSSION

A number of different solvents were used for the extraction of I and II from plasma and urine. Hexane and *n*-pentane did not extract either compound. Chlorinated solvents were not suitable for the nitrogen–phosphorus detector. Ethyl acetate gave good extraction of I, but the plasma extracts were not clean and, furthermore, ethyl acetate has a high boiling point. Ether gave the best extraction of I and II; both compounds were completely recovered with a single ether extraction. However, to obtain cleaner extracts an acid-wash step was used for the plasma samples.

Bjorkhem *et al.* (16) also used ether for extraction of I from plasma. However, recovery and reproducibility data were not presented. The ethereal extract was concentrated to ~50-μL under nitrogen. This method of concentrating the ethereal extract would require constant attention since, if the solvent was allowed to evaporate to dryness, almost complete (>90%) loss of I would occur. In our procedure we added 30 μL of *n*-butyl alcohol to the ethereal extract, and the ether was allowed to boil-off in a water bath (45°C). The main advantage of this technique is that the tubes can be left unattended in the water bath without the risk of losing the compound. When ether is evaporated, the compound is retained in *n*-butyl alcohol. However, nitrogen cannot be used to aid solvent evaporation as this will cause the tube to dry and result in almost complete loss of both I and the internal standard (II).

Although I extracts well in the pH range of 4.5–11.5, at higher pH values a small interfering peak was present in the extracts of dog plasma but not in the extracts of human plasma. In the present procedure, plasma was extracted at pH 6–7, which was achieved by adding 1 M sodium carbonate to the acidified plasma.

Table I—Within-Day and Between-Day Reproducibility of the Plasma Assay [a]

Amount Added, ng/mL	Within-Day Found, ng/mL	Within-Day *CV*, %	Between-Day Found, ng/mL	Between-Day *CV*, %
40	41.1 ± 0.45	1.1	40.8 ±0.77	1.9
160	158.5 ± 2.6	1.6	158.7 ± 4.8	3.0
800	805.1 ± 14.4	1.8	790.5 ± 24.3	3.0

[a] Mean ± *SD*; $n = 5$.

Typical chromatograms obtained from the ethereal extracts of human blank plasma and plasma spiked with 200 ng each of I and II are shown in Fig. 1. The column used gave sharp and symmetrical peaks for both compounds. The internal standard (II) eluted close to I, but was well resolved. Under the conditions employed, the retention times for I and II were 10 and 8 min, respectively. Extracts of both dog and human blank plasma showed a small and broad peak at 24 min at high sensitivity (attenuation <1 × 64). By carefully spacing the sample injections this peak can be eluted in the region between the solvent front and sample peaks.

Analytical recoveries (mean ± *SD*) of I and internal standard using peak height comparison were 102.6 ± 2.6, and 101.6 ± 1.9%, respectively. Peak heights from the extracted standards were consistently greater than those from the methanolic standards. This would result from the smaller volume of the concentrated extracts in the extracted standards compared with the volume (0.1 mL) of the methanolic standards. This discrepancy could be obviated if the sample extracts could be evaporated to dryness and reconstituted to the

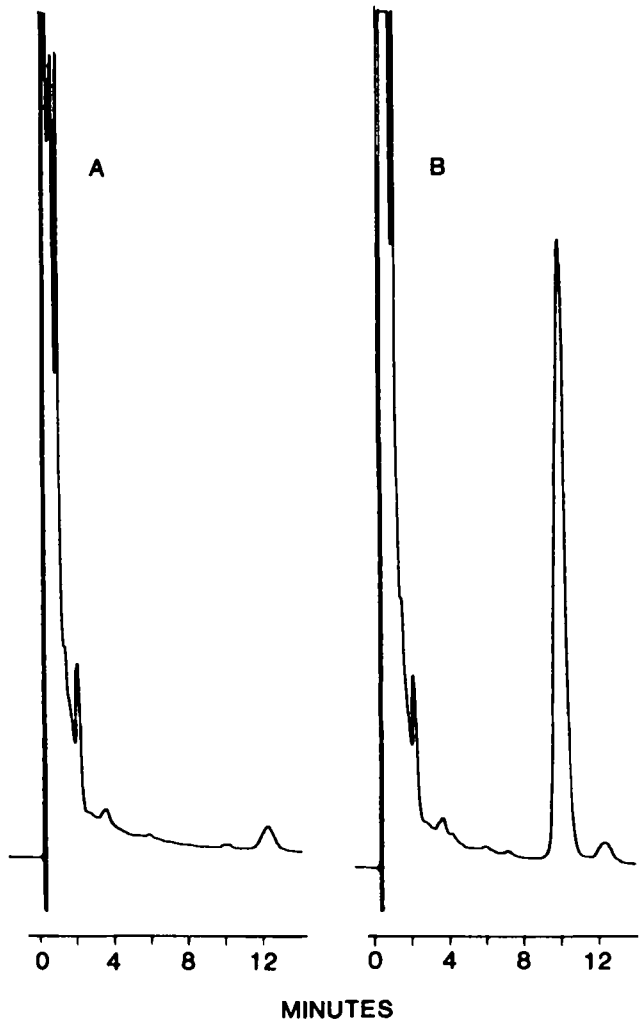

Figure 2—*Chromatograms of ethereal extracts of dog plasma before (A) and 16 h after (B) a 10-mg/kg iv dose of 4-methylpyrazole. The peak corresponds to a concentration of 640 ng/mL (attenuation: 1 × 64).*

Table II—Within-Day and Between-Day Reproducibility of the Urine Assay [a]

Added, μg/mL	Within-Day Found, μg/mL	Within-Day CV, %	Between-Day Found, μg/mL	Between-Day CV, %
1.6	1.62 ± 0.03	1.8	1.62 ± 0.066	4.0
2.7	2.75 ± 0.04	1.5	2.78 ± 0.114	4.1
3.9	4.15 ± 0.14	3.4	4.18 ± 0.194	4.6

[a] Mean ± *SD*; $n = 4$.

same volume as the methanolic standards. Peak height ratio, however, would not be affected by volume difference. Since the extraction efficiencies of I and of the internal standard were independent of each other and the internal standard was completely recovered, recovery of I calculated from peak height ratio measurement would provide a more meaningful value. Using peak height ratio measurement, mean (±*SD*) recoveries of I (six samples) at 100, 500, and 1000 ng/mL were 99.0 ± 1.0, 98.5 ± 1.8, and 99.0 ± 1.5%, respectively.

Standard curves were linear and reproducible over the concentration range of 25–1000 ng/mL. Linear regression statistics for five standard curves prepared on different days over a period of 2 weeks produced a slope of 0.0044 (±0.0001), an intercept of −0.024 (±0.032), and a mean coefficient of determination (r^2) of 0.999.

Assay reproducibility was determined by repeated analysis of plasma samples containing I. Three different concentrations other than those used in the preparation of the standard curves were used. The mean concentrations, standard deviations, and coefficients of variation for within-day and between-day analysis are presented in Table I. These data indicate excellent assay reproducibility, which is further supported by the reproducible nature of the standard curves as shown above.

Plasma spiked with I (1 μg/mL) was stored in the refrigerator (0–4°C), and 1-mL aliquots were analyzed once a week for 6 weeks. Recoveries of I were similar over the 6-week period indicating good stability of I in plasma.

Recovery of I from urine was similar to that from plasma. Standard curves were linear and reproducible over the concentration range of 0.5 to 5 μg/mL with $r^2 > 0.999$. No interference was observed from the extractive constituents of blank urine. Both within-day and between-day assay reproducibility was excellent (Table II). The procedure can be used for concentrations down to 0.1 μg/mL with good reproducibility (coefficient of variation, 4.5%).

The lower sensitivity limit of the GC–MS method (16) was only ~100 ng/mL when 2 mL of plasma was used. Our GC method is simple, rapid, able to quantitate I down to 25 ng/mL with good precision (coefficient of variation, 6.0%), and requires only 1 mL of plasma. This is advantageous, since with greater assay sensitivity plasma concentrations can be monitored for a longer period of time and a smaller dose can be used. The versatile nature of the present method makes it particularly suitable for pharmacokinetic studies of I.

To further evaluate the usefulness of the assay procedure, a 14.5-kg dog was given a 10-mg/kg iv dose of I, and blood and urine samples were obtained. Figure 2 shows the chromatograms of ethereal extracts of dog plasma before and after the administration of I. After hydrolytic treatment of urine samples, the total recovery of I was 2.3% over a period of 96 h. Disposition studies in the dog are currently in progress.

REFERENCES

(1) R. Pietruszko, *Biochem. Pharmacol.*, **24**, 1603 (1975).

(2) H. Theorell, T. Yonetani, and B. Sjoberg, *Acta Chem. Scand.*, **23**, 255 (1969).

(3) A. B. Makar and T. R. Tephly, *Biochem. Med.*, **13**, 334 (1975).

(4) D. Lester, W. Z. Keokosky, and F. Felzenberg, *Q. J. Stud. Alcohol*, **29**, 449 (1968).

(5) U. Rydberg and A. Neri, *Acta Pharmacol. Toxicol.*, **31**, 421 (1972).

(6) R. Blomstrand and H. Theorell, *Life Sci.*, **9**, 631 (1970).

(7) M. P. Salaspuro, P. Pikkarainen, and K. Lindros, *Eur. J. Clin. Invest.*, **7**, 487 (1977).

(8) M. P. Salaspuro, K. O. Lindros, and P. H. Pikkarainen, *Metabolism*, **27**, 631 (1978).

(9) K. E. McMartin, K-G. Hedstrom, B-R. Tolf, H. Ostling-Wintzell, and R. Blomstrand, *Arch. Biochem. Biophys.*, **199**, 606 (1980).

(10) R. Blomstrand, H. Ostling-Wintzell, A. Lof, K. McMartin, B-R. Tolf, and K-G. Hedstrom, *Proc. Natl. Acad. Sci.*, **76**, 3499 (1979).

(11) J. Y. Chou and K. E. Richardson, *Toxicol. Appl. Pharmacol.*, **43**, 33 (1978).

(12) K. L Clay and R. C. Murphy, *Toxicol. Appl. Pharmacol.*, **39**, 39 (1977).

(13) R. Blomstrand, A. Ellin, A. Lof, and H. Ostling-Wintzell, *Arch. Biochem. Biophys.*, **199**, 591 (1980).

(14) U. Rydberg, J. Buijten, and A. Neri, *J. Pharm. Pharmacol.*, **24**, 651 (1972).

(15) U. Rydberg and J. C. Buijten, *J. Chromatogr.*, **64**, 170 (1972).

(16) J. Bjorkhem, R. Blomstrand, O. Lantto, and L. Svensson, *Biochem. Med.*, **12**, 205 (1975).

[^{14}C]Normacromerine Fate in the Rat

P. W. FERGUSON ˣ, W. J. KELLER, and F. O. RISINGER

Received August 19, 1982, from the *School of Pharmacy, Northeast Louisiana University, Monroe, LA 71209.* Accepted for publication March 17, 1983.

Abstract □ The biological fate of [^{14}C]normacromerine, a dimethoxylated phenethylamine derivative with putative hallucinogenic properties, was evaluated in male Sprague–Dawley rats at 100 mg/kg po. Urine was the primary elimination route accounting for 50% of administered carbon-14 after 24 h. Of this urine radioactivity, normacromerine comprised 30% at 8 h decreasing to nondetectable levels at 24 h. Carbon-14 in feces represented <10% of the administered dose at 24 h, and $^{14}CO_2$ expiration was not detected. Studies of normacromerine fate in comparison with previously studied phenethylamines may enhance evaluation of hallucinogenic potential of normacromerine.

Keyphrases □ Normacromerine—biological fate in the rat, hallucinogenic potential □ Biological fate—[^{14}C]normacromerine, rat, hallucinogenic potential □ Hallucinogens—normacromerine, biological fate in the rat

Normacromerine (*N*-methyl-3,4-dimethoxy-β-hydroxyphenethylamine), the major alkaloid in extracts of the Dona Ana cactus [*Coryphantha macromeris* (Engelm.) Br. and R.], has been implicated as the chemical responsible for hallucinogenic effects experienced by humans ingesting the cactus (1, 2). The potency of the Dona Ana cactus has been estimated to be one-fifth that of the peyote cactus [*Lophophora williamsii* (Lem.) Coult.] which contains mescaline, another natural hallucinogen (2, 3).

Laboratory studies of the behavioral effects of normacromerine in rats have provided both positive (4) and negative (5) results in support of the hallucinogenic properties of the drug. Absent from these studies has been a thorough evaluation of the mammalian disposition of normacromerine after ingestion. Studies of biological fate of the compound are unavailable in the literature.

Patterns of absorption, distribution, metabolism, and excretion of chemicals determine their extent and duration of action within biological systems (6). Such studies of norma-

0022-3549/84/0500-0692$01.00/0

© 1984, American Pharmaceutical Association

Table II—Within-Day and Between-Day Reproducibility of the Urine Assay [a]

Added, μg/mL	Within-Day Found, μg/mL	Within-Day CV, %	Between-Day Found, μg/mL	Between-Day CV, %
1.6	1.62 ± 0.03	1.8	1.62 ± 0.066	4.0
2.7	2.75 ± 0.04	1.5	2.78 ± 0.114	4.1
3.9	4.15 ± 0.14	3.4	4.18 ± 0.194	4.6

[a] Mean ± *SD*; $n = 4$.

same volume as the methanolic standards. Peak height ratio, however, would not be affected by volume difference. Since the extraction efficiencies of I and of the internal standard were independent of each other and the internal standard was completely recovered, recovery of I calculated from peak height ratio measurement would provide a more meaningful value. Using peak height ratio measurement, mean (±*SD*) recoveries of I (six samples) at 100, 500, and 1000 ng/mL were 99.0 ± 1.0, 98.5 ± 1.8, and 99.0 ± 1.5%, respectively.

Standard curves were linear and reproducible over the concentration range of 25–1000 ng/mL. Linear regression statistics for five standard curves prepared on different days over a period of 2 weeks produced a slope of 0.0044 (±0.0001), an intercept of −0.024 (±0.032), and a mean coefficient of determination (r^2) of 0.999.

Assay reproducibility was determined by repeated analysis of plasma samples containing I. Three different concentrations other than those used in the preparation of the standard curves were used. The mean concentrations, standard deviations, and coefficients of variation for within-day and between-day analysis are presented in Table I. These data indicate excellent assay reproducibility, which is further supported by the reproducible nature of the standard curves as shown above.

Plasma spiked with I (1 μg/mL) was stored in the refrigerator (0–4°C), and 1-mL aliquots were analyzed once a week for 6 weeks. Recoveries of I were similar over the 6-week period indicating good stability of I in plasma.

Recovery of I from urine was similar to that from plasma. Standard curves were linear and reproducible over the concentration range of 0.5 to 5 μg/mL with $r^2 > 0.999$. No interference was observed from the extractive constituents of blank urine. Both within-day and between-day assay reproducibility was excellent (Table II). The procedure can be used for concentrations down to 0.1 μg/mL with good reproducibility (coefficient of variation, 4.5%).

The lower sensitivity limit of the GC–MS method (16) was only ~100 ng/mL when 2 mL of plasma was used. Our GC method is simple, rapid, able to quantitate I down to 25 ng/mL with good precision (coefficient of variation, 6.0%), and requires only 1 mL of plasma. This is advantageous, since with greater assay sensitivity plasma concentrations can be monitored for a longer period of time and a smaller dose can be used. The versatile nature of the present method makes it particularly suitable for pharmacokinetic studies of I.

To further evaluate the usefulness of the assay procedure, a 14.5-kg dog was given a 10-mg/kg iv dose of I, and blood and urine samples were obtained. Figure 2 shows the chromatograms of ethereal extracts of dog plasma before and after the administration of I. After hydrolytic treatment of urine samples, the total recovery of I was 2.3% over a period of 96 h. Disposition studies in the dog are currently in progress.

REFERENCES

(1) R. Pietruszko, *Biochem. Pharmacol.*, **24**, 1603 (1975).

(2) H. Theorell, T. Yonetani, and B. Sjoberg, *Acta Chem. Scand.*, **23**, 255 (1969).

(3) A. B. Makar and T. R. Tephly, *Biochem. Med.*, **13**, 334 (1975).

(4) D. Lester, W. Z. Keokosky, and F. Felzenberg, *Q. J. Stud. Alcohol*, **29**, 449 (1968).

(5) U. Rydberg and A. Neri, *Acta Pharmacol. Toxicol.*, **31**, 421 (1972).

(6) R. Blomstrand and H. Theorell, *Life Sci.*, **9**, 631 (1970).

(7) M. P. Salaspuro, P. Pikkarainen, and K. Lindros, *Eur. J. Clin. Invest.*, **7**, 487 (1977).

(8) M. P. Salaspuro, K. O. Lindros, and P. H. Pikkarainen, *Metabolism*, **27**, 631 (1978).

(9) K. E. McMartin, K-G. Hedstrom, B-R. Tolf, H. Ostling-Wintzell, and R. Blomstrand, *Arch. Biochem. Biophys.*, **199**, 606 (1980).

(10) R. Blomstrand, H. Ostling-Wintzell, A. Lof, K. McMartin, B-R. Tolf, and K-G. Hedstrom, *Proc. Natl. Acad. Sci.*, **76**, 3499 (1979).

(11) J. Y. Chou and K. E. Richardson, *Toxicol. Appl. Pharmacol.*, **43**, 33 (1978).

(12) K. L Clay and R. C. Murphy, *Toxicol. Appl. Pharmacol.*, **39**, 39 (1977).

(13) R. Blomstrand, A. Ellin, A. Lof, and H. Ostling-Wintzell, *Arch. Biochem. Biophys.*, **199**, 591 (1980).

(14) U. Rydberg, J. Buijten, and A. Neri, *J. Pharm. Pharmacol.*, **24**, 651 (1972).

(15) U. Rydberg and J. C. Buijten, *J. Chromatogr.*, **64**, 170 (1972).

(16) J. Bjorkhem, R. Blomstrand, O. Lantto, and L. Svensson, *Biochem. Med.*, **12**, 205 (1975).

[^{14}C]Normacromerine Fate in the Rat

P. W. FERGUSON ˣ, W. J. KELLER, and F. O. RISINGER

Received August 19, 1982, from the *School of Pharmacy, Northeast Louisiana University, Monroe, LA 71209.* Accepted for publication March 17, 1983.

Abstract □ The biological fate of [^{14}C]normacromerine, a dimethoxylated phenethylamine derivative with putative hallucinogenic properties, was evaluated in male Sprague–Dawley rats at 100 mg/kg po. Urine was the primary elimination route accounting for 50% of administered carbon-14 after 24 h. Of this urine radioactivity, normacromerine comprised 30% at 8 h decreasing to nondetectable levels at 24 h. Carbon-14 in feces represented <10% of the administered dose at 24 h, and $^{14}CO_2$ expiration was not detected. Studies of normacromerine fate in comparison with previously studied phenethylamines may enhance evaluation of hallucinogenic potential of normacromerine.

Keyphrases □ Normacromerine—biological fate in the rat, hallucinogenic potential □ Biological fate—[^{14}C]normacromerine, rat, hallucinogenic potential □ Hallucinogens—normacromerine, biological fate in the rat

Normacromerine (*N*-methyl-3,4-dimethoxy-β-hydroxyphenethylamine), the major alkaloid in extracts of the Dona Ana cactus [*Coryphantha macromeris* (Engelm.) Br. and R.], has been implicated as the chemical responsible for hallucinogenic effects experienced by humans ingesting the cactus (1, 2). The potency of the Dona Ana cactus has been estimated to be one-fifth that of the peyote cactus [*Lophophora williamsii* (Lem.) Coult.] which contains mescaline, another natural hallucinogen (2, 3).

Laboratory studies of the behavioral effects of normacromerine in rats have provided both positive (4) and negative (5) results in support of the hallucinogenic properties of the drug. Absent from these studies has been a thorough evaluation of the mammalian disposition of normacromerine after ingestion. Studies of biological fate of the compound are unavailable in the literature.

Patterns of absorption, distribution, metabolism, and excretion of chemicals determine their extent and duration of action within biological systems (6). Such studies of norma-

0022-3549/84/0500-0692$01.00/0

© 1984, American Pharmaceutical Association

Table I—Fate of Carbon-14 8, 16, and 24 h after Exposure to [^{14}C]-Normacromerine, 100 mg/kg po

Time, h	Percent of Administered Carbon-14[a]	
	Urine	Feces
8 (n = 6)	41.0 ± 2.6	0
16 (n = 4)	8.3 ± 1.85	8.0 ± 3
24 (n = 4)	1.4 ± 0.23	1.8 ± 0.32

[a] Total carbon-14 recovered (urine + feces + carcass + carbon dioxide) was 80 ± 3% of the administered dose. Each sample analysis was performed in duplicate. Values are the mean of the sample average ±SE; n is the number of animals evaluated.

cromerine may therefore provide a foundation for more enlightened evaluation of its hallucinogenic activity. Our initial objective in the evaluation of normacromerine was to characterize its previously unknown fate in a mammalian system, thereby establishing a framework for future metabolite studies.

EXPERIMENTAL

[^{14}C]Normacromerine—[^{14}C]Normacromerine (1 μCi/mmol, labeled in the β position) and nonlabeled normacromerine were synthesized *in vivo* from *Coryphantha macromeris* var. *runyonii*, as described by Keller (7, 8). Radiopurity (>99%) was evaluated using silica gel GF 254 TLC plates[1] developed in benzene–chloroform–methanol–58% ammonium hydroxide (8:6:5:1). All normacromerine analyses were performed using this chromatographic system.

Animal Exposures—Male Sprague-Dawley rats (300–400 g) were fasted 16–18 h prior to exposure; however, water was provided *ad libitum*. Each animal received 100 mg/kg of [^{14}C]normacromerine hydrochloride (in water) by oral gavage. This replicated dosage levels used in previous behavioral studies (5). After dosing, the animals were placed into metabolism chambers[2] for collection of expired CO_2, urine, and feces. Chamber air was drawn by vacuum (1 L/min) through 1 N KOH to collect the $^{14}CO_2$. One milliliter of KOH was sampled periodically throughout the initial 8-h postexposure. Each sample was placed into 15 ml of scintillation cocktail[3] for ^{14}C-radioassay using a liquid scintillation counter[4]. Urine and feces were collected and analyzed at 8, 16, and 24 h postexposure. At each time period collected urine was sampled into scintillation cocktail for total ^{14}C-radioassay and the remainder frozen until normacromerine analysis. Feces were collected, freeze-dried, ground to a fine powder, and combusted in a sample oxidizer[5] for total ^{14}C-radioassay. At 8 and 24 h, carcasses were also analyzed for total carbon-14. Following homogenization (1:1 with H_2O), samples of the carcass were combusted and radioassayed to provide a complete carbon-14 animal mass balance (carbon dioxide + urine + feces + carcass).

Urine Analysis—[^{14}C]Normacromerine was extracted (75% efficiency) from alkalinized urine with toluene. The toluene extract was then concentrated under nitrogen in a 40°C water bath[6]. [^{14}C]Normacromerine concentrates were spotted on TLC plates and developed by the standard solvent system. Co-chromatography with nonradioactive normacromerine standards allowed identification and isolation of [^{14}C]normacromerine. Silica gel spots containing [^{14}C]normacromerine were transferred (>90% recovery) into 15 mL of scintillation cocktail for subsequent radioassay.

RESULTS AND DISCUSSION

The 24-h carbon-14 elimination pattern is given in Table I. Urine was the major elimination route; feces accounted for minor excretion of the radiolabel. Elimination as $^{14}CO_2$ was not detected. Total carbon-14 recovery (urine + feces + carbon dioxide + carcass) was 80 ± 3% of the administered dose. This less than optimum recovery reflects an inability to accurately assay the total carbon-14 remaining in the animal at 8 and 24 h postexposure. Levels (<100 cpm/g of tissue) at two to three times the background radioactivity were measured in triplicate 500-mg tissue samples for each of 10 animals. The significant dilution of carbon-14 remaining in the animal (354 ± 72 dpm/g of tissue) was an unavoidable limitation due to the low normacromerine specific activity available from the *in vivo* synthesis.

[1] Fisher Scientific Co., Pittsburgh, Pa.
[2] Crown Scientific Glass Co., Orland Park, Ill.
[3] Packard Instruments Co., Downers Grove, Ill.
[4] Model LS-230 Liquid Scintillation System; Beckman, Fullerton, Calif.
[5] Model B306 Tri Carb Sample Oxidizer; Packard, Downers Grove, Ill.
[6] Organomation Associates, Inc., Northborough, Mass.

Table II—Percentage of Urinary Carbon-14 Analyzed as Normacromerine 8, 16, and 24 h after Exposure to [^{14}C]Normacromerine, 100 mg/kg po

Time, h	Percent Normacromerine[a]
8 (n = 4)	30.0 ± 3.8
16 (n = 4)	2.8 ± 1.5
24 (n = 4)	not detected

[a] Values are the mean of sample average ±SE; n is the number of animals evaluated. Each sample was analyzed in duplicate.

Since urine served as the primary elimination route, urine samples were further characterized to quantify [^{14}C]normacromerine. Table II indicates significant *in vivo* mammalian biotransformation of normacromerine. Thirty percent of urine radioactivity at 8 h was normacromerine, decreasing to 0% by 24 h. The remainder was accountable as water-soluble ^{14}C-labeled metabolites.

Our study in rats described normacromerine elimination primarily in urine, minimally in feces, and none as CO_2. Urine and feces analyses indicated normacromerine was significantly absorbed and metabolized to water-soluble metabolites.

Normacromerine is an *O*-methylated analogue of the endogenous neurotransmitter epinephrine and its singly *O*-methylated derivative, metanephrine. In fact, the biosynthesis of normacromerine in *Coryphantha macromeris* involves these catecholamines as precursors (7, 8). Consequently, the mammalian fate of normacromerine could be similar to the mammalian biotransformation of epinephrine and metanephrine. Previous studies of intravenously administered [^{3}H]epinephrine and [^{14}C]metanephrine in rats (9) demonstrated a similar biological fate as observed in these normacromerine studies. Urine was the significant elimination route (65–70% of administered dose after 48 h) and feces a secondary route (15 and 0.3% for epinephrine and metanephrine, respectively). Carbon dioxide was not analyzed. Since [^{14}C]-normacromerine was radiolabeled at the side-chain β position, loss of this carbon as $^{14}CO_2$ was not expected (10) and was not observed in our study. Cumulative carbon-14 recovery in urine and feces at 48 and 24 h postexposure was similar for metanephrine (65–68%) and normacromerine (61%), respectively. Free epinephrine and metanephrine accounted for <10% of urine radioactivity at 48 h. In comparison, no normacromerine was detected at 24 h postexposure. This may reflect enhanced oxidation of normacromerine by liver monoamine oxidases following the oral route of exposure (10). Metabolites of epinephrine and metanephrine in urine were products of monoamine oxidase reactions (3-methoxy-4-hydroxymandelic acid and 3-methoxy-4-hydroxyphenylglycol).

In vitro studies of methoxylated β-hydroxyphenethylamines, such as normacromerine, indicate significant interactions with mammalian monoamine oxidases (11–13). Therefore, the structural similarities between normacromerine, epinephrine, and metanephrine, as well as similar elimination patterns in the rat, suggest that normacromerine elimination products may be similar to monoamine oxidase products of its catecholamine analogues. The synthesis of these novel normacromerine metabolites and their *in vivo* identification, underway in our laboratory, are necessary for complete evaluation of normacromerine fate in the rat.

Understanding of normacromerine disposition will not only enhance evaluation of its hallucinogenic potential, but will provide further insight into comparative metabolism of xenobiotics by plant and animal systems.

REFERENCES

(1) W. J. Keller, *Clin. Toxicol.*, **16,** 233 (1980).
(2) M. J. Superweed, "Herbal Highs," Stone Kingdom Syndicate, San Francisco, Calif., 1972, p. 5.
(3) W. J. Keller, *J. Pharm. Sci.*, **68,** 85 (1979).
(4) W. M. Bourn, W. J. Keller, and J. F. Bonfiglio, *Life Sci.*, **23,** 1175 (1978).
(5) W. H. Vogel, B. D. Evans, E. M. Bonnem, J. F. Fischer, and J. L. McLaughlin, *Psychopharmacologia*, **30,** 145 (1973).
(6) B. N. LaDu, H. G. Mandel, and E. L. Way, "Fundamentals of Drug Metabolism and Disposition," Williams and Wilkins, Baltimore, Md., 1971, pp. 1–181.
(7) W. J. Keller, *Lloydia*, **41,** 37 (1978).
(8) W. J. Keller, *Phytochemistry*, **20,** 2165 (1981).
(9) I. J. Kopin, J. Axelrod, and E. Gordon, *J. Biol. Chem.*, **236,** 2109 (1961).
(10) H. Blaschko, *Pharmacol. Rev.*, **4,** 415 (1952).
(11) G. G. Ferguson and W. J. Keller, *J. Pharm. Sci.*, **64,** 1431 (1975).
(12) W. J. Keller and G. G. Ferguson, *J. Pharm. Sci.*, **65,** 1539 (1976).
(13) W. J. Keller and G. G. Ferguson, *J. Pharm. Sci.*, **66,** 1048 (1977).

Investigation of the Antitumor Activity of Podocarpic Acid Derivatives

EDWARD J. PARISH *x **and D. HOWARD MILES** ‡

Received August 16, 1982 from the *Department of Chemistry, Auburn University, Auburn University, AL 36849 and the ‡Department of Chemistry, Mississippi State University, Mississippi State, MS 37962. Accepted for publication March 23, 1983.

Abstract □ As a class, octahydrophenanthrene lactones, podolactones, and related podocarpic acid derivatives have been reported to possess a wide variety of biological activities, including antileukemic activity, inhibition of plant cell growth, and hormonal and anti-inflammatory properties. In the present study, a series of synthetic intermediates derived from podocarpic acid have been prepared and evaluated with respect to their ability to inhibit human epidermoid carcinoma of the nasopharynx *in vitro*. The significant cytotoxicity demonstrated by methyl 6α-bromo-7-oxo-*O*-methylpodocarpate (50% inhibition of cells at 8.85×10^{-9} M) was markedly higher than that of the other derivatives examined. Further evaluation against L1210 and P388 lymphoid leukemias in mice failed to demonstrate significant antitumor activity.

Keyphrases □ Podocarpic acid derivatives—synthesis, antitumor activity, *in vitro* human epidermoid carcinoma (nasopharynx) screen, L1210 and P388 screens in mice □ Antineoplastic agents—potential, podocarpic acid derivatives, synthesis, *in vitro* human epidermoid carcinoma (nasopharynx) screen, L1210 and P388 screens in mice

Octahydrophenanthrene lactones (I) and related podocarpic acid derivatives (II) have been reported to possess hormonal and anti-inflammatory properties (1). Other similar podolactones have been shown to inhibit the expansion and division of plant cells (III) (2–4) and to have antileukemic activity (IV) (5). In view of their documented biological properties it appeared worthwhile to test a series of synthetic intermediates derived from podocarpic acid for antitumor activity. This report describes the preparation of these derivatives and the results obtained in biological tests against tumors.

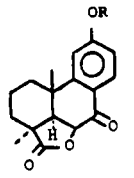

Ia, R=H
Ib, R=CH_3
Ic, R=CH_2CH_3

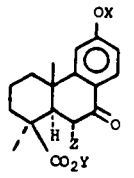

II a, X=Y=CH_3, Z=H
II b, X=Y=CH_3, Z=Br
II c, X=CH_3, Y=Z=H
II d, X=CH_2CH_3, Y=CH_3, Z=H

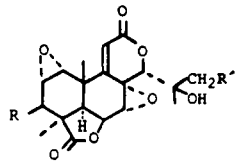

III a, R=H, R'=OH
III b, R=CH_3, R'=OH
III c, R=H, R'=$SOCH_3$

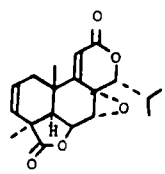

IV

RESULTS AND DISCUSSION

Preparation of all derivatives shown in Scheme I proceeded *via* methyl *O*-methyl-7-ketopodocarpate (VI), which was synthesized from podocarpic acid by methylation with dimethyl sulfate and subsequent oxidation using the approach described by Bible and Grove (1) in the synthesis of bromoketone (IIb).

Compound VII was prepared from VI by reduction of the 7-keto group to the corresponding alcohol with sodium borohydride. The resulting epimeric alcohol mixture (the 7α-hydroxyl derivative would be expected to be present in greater abundance) was efficiently dehydrated by *p*-toluenesulfonic acid in refluxing dihydropyran. The synthesis of epoxide VIII was completed by treatment of VII with *m*-chloroperbenzoic acid in ether. The α-configuration of the epoxide in VIII is inferred from X-ray crystallographic studies (6) of IIb and related 6α-bromo-7-oxo-diterpenoids (7). These studies indicate significant intramolecular steric hindrance in that region of the molecule resulting from 1,3-diaxial interactions of the angular methyl group at C-10 and the axial carbomethoxy group at C-4. Both of these groups reside on the β face of the molecule and would mediate an α-approach of the peracid.

Bromoketone IIb was prepared by an adapted procedure derived from the work of Bible and Grove (1). Compounds IX and X were prepared from bromoketone IIb by treatment with *N*-phenylbenzamidine and 1,5-diazabicyclo[5.4.0]undec-5-ene (DBU), respectively, utilizing procedures reported previously (8, 9).

The activity of the freshly prepared synthetic intermediates (Scheme I) against human epidermoid carcinoma of the nasopharynx is shown in Table I. The *in vitro* activity of bromoketone IIb in the 9KB test system was markedly higher than that of VII–X. Since the cytotoxicity demonstrated by IIb was sufficient for confirmation as an active compound at the National Cancer Institute, these compounds were tested in the LE and PS tumor systems (Table II). All derivatives were inactive in both the L1210 and PS tumor systems.

EXPERIMENTAL[1]

Methyl *O*-Methyl-7-ketopodocarpate (VI)—To crude podocarpic acid (V, 500 g) was added ice (500 g), methanol (500 mL), and sodium hydroxide (240 g). This mixture was stirred for 2 h until a dark-brown color persisted, indicative of the formation of the phenoxy anion. The solution was cooled to 15°C and dimethyl sulfate (425 mL, 566.5 g, 4.5 mol) was added dropwise, with stirring, over a period of 1.5 h. The reaction was completed, as evidenced by solidification of the solution. A light-brown solid was obtained by filtration after the addition of 1 L of water. This solid was stirred with 1 L of water and removed by filtration. Recrystallization from acetone yielded 460.1 g of methyl *O*-methylpodocarpate as white crystals, mp 127.0–128.5°C [lit. (10) mp 128°C]. IR(KBr): 1725, 1500, and 1450 cm^{-1}; ^{1}H-NMR ($CDCl_3$): δ 1.10 (s, 3, C—CH_3), 1.32 (s, 3, C—CH_3), 3.70 (s, 3, O—CH_3), 3.80 (s, 3, O—CH_3), 6.71 (m, 2, ArH), and 7.72 ppm (d, 1, J = 7.5 Hz, ArH).

Methyl *O*-methylpodocarpate (100 g, 0.331 mol) was dissolved in 1 L of acetic acid. Chromium trioxide (94 g, 0.93 mol) was dissolved in an 800-mL acetic acid–200-mL water solution, which was then added to the ester solution at room temperature with stirring. After allowing the mixture to stand overnight at room temperature, it was poured into 6 L of saturated aqueous sodium chloride solution. After allowing this solution to stand overnight, the precipitate was removed by filtration and washed with water to yield 74 g (71%) of ketone VI as yellow crystals, mp 121–123°C [lit. mp 121–123°C (11) and 122–124°C (1)]. IR (KBr): 1725 and 1600 cm^{-1}; ^{1}H-NMR ($CDCl_3$): δ 0.98 (s, 3, C—CH_3), 1.20 (s, 3, C—CH_3), 3.68 (s, 3, O—CH_3), 3.86 (s, 3, O—CH_3), 6.66 (m, 2, ArH), and 7.83 ppm (d, 1, J = 8 Hz, ArH).

Compound VII—Methyl *O*-methyl-7-ketopodocarpate (VI, 10 g, 31.6 mmol) was dissolved in tetrahydrofuran (14 mL) and 95% ethanol (20 mL). After dissolving sodium borohydride (2 g) in water (8 mL) and 95% ethanol (3 mL), this solution was added slowly to the ketoester solution. The resulting solution was stirred for 24 h at room temperature, after which the precipitate

[1] IR spectra were obtained using a Perkin-Elmer Model 137 G or a Perkin-Elmer Model 580 spectrophotometer. NMR were obtained on a Jeolco Minimar or a Varian EM-390 spectrometer using $CDCl_3$ as the solvent; tetramethylsilane was used as an internal standard. Mass spectra were obtained using a Perkin-Elmer model 270 mass spectrometer. GC was performed using a Hewlett-Packard Model 402 gas chromatograph with a hydrogen flame detector. A glass column packed with 3% SE-30 on 100–120 mesh GCQ at a column temperature at 270°C with a nitrogen flow rate of 35 mL/min was used for all GC analyses unless otherwise stated. Melting points were obtained on a Fisher-Jones apparatus and are uncorrected. Elemental analyses were performed by Galbraith Laboratories, Inc., Knoxville, Tenn.

0022-3549/84/0500-0694$01.00/0
© 1984, American Pharmaceutical Association

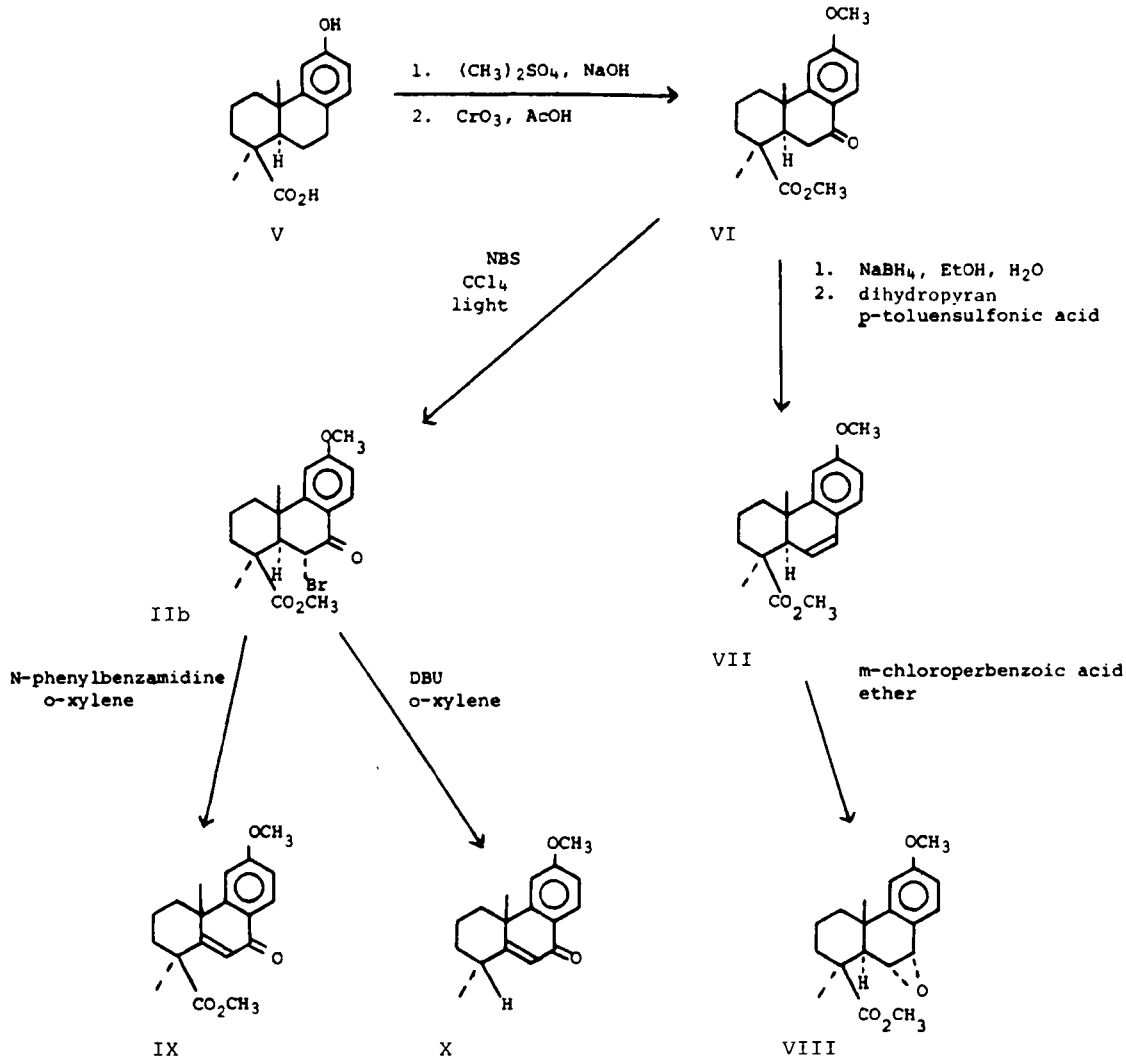

Scheme I

was removed by filtration. Evaporation of the solution *in vacuo* gave a pink syrup. The syrup was dissolved in ether (25 mL), followed by addition of 5% aqueous sodium chloride solution (10 mL). The aqueous layer was extracted several times with 50-mL portions of ether. The ether extracts were combined, washed twice with 5% aqueous sodium chloride (20 mL), dried over anhydrous magnesium sulfate, and evaporated *in vacuo*. Crystallization from ether solution gave 8.8 g (88%) of the alcohol methyl *O*-methyl-7-hydroxypodocarpate as white crystals, mp 100–106°C. IR (KBr): 3500, 1715, 1610, and 1575 cm^{-1}; ^{1}H-NMR ($CDCl_3$): δ 0.88 (s, 3, C—CH_3), 1.32 (s, 3, C—CH_3), 3.70 (s, 3, O—CH_3), 3.82 (s, 3, O—CH_3), 4.51 (m, 1, C*H*OH), and 6.83 ppm (m, 3, ArH). MS: *m/z* 318 (M^+); Calcd. for $C_{19}H_{26}O_4$: *m/z* 318 (M^+).

Anal.—Calc. for $C_{19}H_{26}O_4$: C, 71.76; H, 8.24. Found: C, 71.88; H, 8.35.

The aforementioned alcohol (8 g, 25.2 mmol), dihydropyran (5 mL), and 0.5 g of *p*-toluenesulfonic acid were heated at reflux for 8 h. The mixture was extracted with 200 mL of ether. The organic phase was washed with water, 5% aqueous sodium carbonate, and then water, and dried over anhydrous magnesium sulfate. Evaporation *in vacuo* yielded a yellow syrup, which was chromatographed (dry silica gel, 50:1). Elution with petroleum ether–methylene chloride gave excess dihydropyran in the early fractions and the unsaturated ester VII as a solid in the later fractions (monitored by GC). Compound VII was recrystallized from CCl_4–hexane (slow evaporation) to give light-brown crystals (6.4 g, 85%), mp 84–85°C. IR(KBr): 2950, 1720, and 1600 cm^{-1}; ^{1}H-NMR ($CDCl_3$): δ 0.86 (s, 3, C—CH_3), 1.35 (s, 3, C—CH_3), 3.75 (s, 3, O—CH_3), 3.88 (s, 3, O—CH_3), 6.51 (s, 2, vinylic), and 6.90 ppm (m, 3, ArH).

Anal.—Calc. for $C_{19}H_{24}O_3$: C. 75.96; H, 8.07. Found: C, 75.82; H, 8.14.

Epoxide VIII—To a solution of the unsaturated ester VII (5 g, 16.6 mmol) in 100 mL of dry ether was added slowly a solution of 3 g of *m*-chloroperbenzoic acid in 15 mL of dry ether with stirring. The solution was stirred for 6 h and then was allowed to stand overnight. After the addition of 10% $NaHCO_3$ (15 mL), the mixture was extracted with ether. The organic phase was washed (H_2O), dried ($MgSO_4$), and the solvent was removed to give a light-yellow syrup, which solidified on standing. Recrystallization from chloroform yielded 4.6 g (87%) of white crystals of VIII, mp 158–159°C. IR(KBr): 2950, 1725, and 1500 cm^{-1}; ^{1}H-NMR ($CDCl_3$): δ 1.12 (s, 3, C—CH_3), 1.28 (s, 3, C—CH_3), 3.69 (s, 3, O—CH_3), 3.78 (s, 3, O—CH_3), and 6.88 ppm (m, 3, ArH).

Anal.—Calc. for $C_{19}H_{24}O_4$: C, 72.13; H, 7.65. Found: C, 72.16; H. 7.72.

Methyl *O*-Methyl-6-α-bromo-7-ketopodocarpate (IIb)—To ester VI (46 g, 0.2226 mol) was added 550 mL of carbon tetrachloride. After heating to dissolve the ketone, 28 g (0.157 mol) of *N*-bromosuccinimide was added, and the solution was allowed to stand (catalyzed by sunlight) for 96 h with occasional stirring. The solution was filtered and evaporated *in vacuo*. The residue (mp 123–124°C) was recrystallized five times from aqueous methanol to give

Table I—Activity of Podocarpic Acid Derivatives Against Human Epidermoid Carcinoma of the Nasopharynx *In Vitro* [a]

Compound	ED_{50} [b]	Slope [c]
IIb	3.1	−1.14
	3.4	−1.59
	4.0	−1.62
VII	7.9	−0.51
VIII	23.0	−0.95
IX	100.0	−0.21
X	21.0	−0.90

[a] Cell culture assay with a vehicle of dimethylformamide. [b] Expressed in micrograms per milliliter that inhibited 50% of the control dose. [c] The change of response from each one-log change of dose.

Table II—Activity of Podocarpic Acid Derivatives Against L1210 Lymphoid Leukemia

Compound	Host Mice[a]	Weight Difference,[b] g	Dose, mg/kg	T/C[c]
IIb	BDF_1	−0.8	400	101
		−0.2	200	101
		0.5	100	97
	CDF_1[d]	−0.8	200	112
		−0.2	100	100
		0.9	50	103
VII	BDF_1	0.7	400	87
		0.7	200	90
		−0.3	100	90
	CDF_1	−0.5	400	103
		−1.0	200	106
		−1.1	100	104
VIII	BDF_1	−0.2	400	101
		0.0	200	100
		−0.1	100	103
IX	BDF_1	1.1	400	87
		−0.3	200	89
		−0.3	100	92
X	BDF_1[e]	−0.4	400	90
		−0.4	200	88
		−0.4	100	97
		−0.2	50	100
		−0.1	25	100

[a] Intraperitoneal injections with saline with Tween 80 as a vehicle unless otherwise indicated. [b] Average weight change of test group minus average weight change of control animals. [c] Ratio of the mean survival time of the test animals to the control animals. [d] P388 lymphocytic leukemia screen. [e] Tested using another screen.

49 g (81%) of bromoketone IIb as a white crystalline solid, mp 142–144°C [lit. mp 142–144.5°C (1), 141–142°C (12), 135–137°C (13), and 123–126°C (14)]. IR (KBr): 2950, 1725, 1684, and 1604 cm^{-1}; ^1H-NMR ($CDCl_3$): δ 0.85 (s, 3, C_{10}-CH_3) [lit. (7, 13) 0.85], 1.54 (s, 3, C_4-CH_3) [lit. (7, 13) 1.53], 3.70 (s, 3, OCH_3, ester), 3.84 (s, 3, OCH_3, ether), 5.80 (d, 1, J = 7 cps, CBrH) [lit. (7, 13) J = 7 cps], 6.85 (m, 2, ArH), and 7.80 ppm (d, 1, J = 9 cps, ArH).

Biological Procedures All biological tests were performed at the Cancer Chemotherapy National Service Center, Bethesda, Md. The general procedure, protocols, and data interpretation used at the National Cancer Institute have been published previously (15, 16).

REFERENCES

(1) R. H. Bible and M. Grove (to G. D. Searle and Co.) U.S. Pat. No. 2,753,357, July 3, 1956; *Chem. Abstr.*, **51**, 2869d (1957).

(2) M. N. Galbraith, D. H. S. Horn, J. M. Sasse, and D. Adamson, *Chem. Commun.*, **1970**, 170.

(3) J. M. Sasse, M. N. Galbraith, D. H. S. Horn, and D. A. Adamson, in "Plant Growth Substances, 1970," D. J. Carr, Ed., Springer Verlag, 1972, p. 430.

(4) M. N. Galbraith, D. H. S. Horn, and J. M. Sasse, *Chem. Commun.*, **1971**, 1362.

(5) R. F. Bryan and P. M. Smith, *J. Chem. Soc.* (Perkin II), **1975**, 148.

(6) G. R. Clark and T. N. Waters, *J. Chem. Soc.* (C) **1970**, 887.

(7) J. F. Cutfield, T. N. Waters, and G. R. Clark, *J. Chem. Soc.* (Perkin II), **1974**, 150.

(8) E. J. Parish and D. H. Miles, *J. Org. Chem.*, **38**, 3800 (1973).

(9) E. J. Parish and D. H. Miles, *J. Org. Chem.*, **38**, 1223 (1973).

(10) I. R. Sherwood and W. F. Short, *J. Chem. Soc.* **1938**, 1010.

(11) E. Wenkert, A. Fuchs, and J. D. McChesney, *J. Org. Chem.*, **30**, 2931 (1965).

(12) A. K. Bose, M. S. Manhas, and R. C. Cambie, *J. Org. Chem.*, **30**, 501 (1965).

(13) A. E. Lickei, A. C. Rieke, and D. M. S. Wheeler, *J. Org. Chem.*, **32**, 1647 (1967).

(14) E. Wenkert, *et al.*, *Can. J. Chem.*, **41**, 1924 (1963).

(15) R. I. Geren, N. H. Greenberg, M. M. MacDonald, A. M. Schumacker and B. J. Abbott, *Cancer Chemother. Rep., Part 3*, **3**(2), 1 (1972).

(16) "Screening Date Summary Interpretation and Outline of Current Screen," Drug Evaluation Branch Instruction Booklet 14, Division of Cancer Treatment, National Cancer Institute, Bethesda, 1978.

ACKNOWLEDGEMENTS

We thank the graduate school and the Biological and Physical Sciences Institute for partial financial support. We express our sincere appreciation to Dr. Ian K. Walker, Department of Scientific and Industrial Research, Wellington, New Zealand, for generous supplies of podocarpic acid.

Isocratic Liquid Chromatographic Method for the Determination of Amoxapine and its Metabolites

SCOTT M. JOHNSON, GLORIA NYGARD, and S. K. WAHBA KHALIL ˣ

Received October 1, 1982; from *The Pharmacokinetic Drug Analysis Laboratory, Pharmaceutical Science Dept., College of Pharmacy, North Dakota State University*, and *Veterans Administration Medical Center, Fargo, ND 58105.* Accepted for publication March 23, 1983.

Abstract □ An isocratic reverse-phase liquid chromatographic method for the determination of amoxapine and its major metabolites in human plasma utilizing UV detection is described. Plasma samples were extracted with ethyl acetate after pH adjustement. The reconstituted extracts were injected onto a cyanopropylsilane column and eluted with a mobile phase consisting of 65% acetonitrile and 35% sodium acetate buffer 0.03 M and pH 6. The minimum detectable limit was <10 ng/mL of plasma. Possible interferences from other drugs which might be administered concurrently were studied. The reproducibility and precision of the method are demonstrated by the analysis of samples containing 25–600 ng/mL of plasma. The method is being applied successfully in our laboratory for the analysis of plasma from patients receiving amoxapine.

Keyphrases □ Amoxapine—isocratic HPLC method, determination of metabolites □ Metabolites—isocratic HPLC method, determination of amoxapine

Amoxapine[1], 2-chloro-11-(1-piperazinyl)dibenz[*b,f*]-[1,4]oxazepine, a relatively new antidepressant of the dibenzoxazepine class, has been shown to be a potent antidepressant (1–3). The relationship between tricyclic antidepressant plasma concentrations and therapeutic response has been studied extensively, with inconclusive results (4, 5). The side effects of tricyclic antidepressants have also been correlated to plasma concentrations with mixed results (6). Since the major metabolic pathway of amoxapine is hydroxylation (7), monitoring therapeutic levels of the parent drug and its active

[1] Lederle Laboratories, Pearl River, N.Y.

0022-3549/84/0500-0696$01.00/0

© 1984, American Pharmaceutical Association

Table II—Activity of Podocarpic Acid Derivatives Against L1210 Lymphoid Leukemia

Compound	Host Mice[a]	Weight Difference,[b] g	Dose, mg/kg	T/C[c]
IIb	BDF_1	−0.8	400	101
		−0.2	200	101
		0.5	100	97
	CDF_1[d]	−0.8	200	112
		−0.2	100	100
		0.9	50	103
VII	BDF_1	0.7	400	87
		0.7	200	90
		−0.3	100	90
	CDF_1	−0.5	400	103
		−1.0	200	106
		−1.1	100	104
VIII	BDF_1	−0.2	400	101
		0.0	200	100
		−0.1	100	103
IX	BDF_1	1.1	400	87
		−0.3	200	89
		−0.3	100	92
X	BDF_1[e]	−0.4	400	90
		−0.4	200	88
		−0.4	100	97
		−0.2	50	100
		−0.1	25	100

[a] Intraperitoneal injections with saline with Tween 80 as a vehicle unless otherwise indicated. [b] Average weight change of test group minus average weight change of control animals. [c] Ratio of the mean survival time of the test animals to the control animals. [d] P388 lymphocytic leukemia screen. [e] Tested using another screen.

49 g (81%) of bromoketone IIb as a white crystalline solid, mp 142–144°C [lit. mp 142–144.5°C (1), 141–142°C (12), 135–137°C (13), and 123–126°C (14)]. IR (KBr): 2950, 1725, 1684, and 1604 cm^{-1}; ^1H-NMR ($CDCl_3$): δ 0.85 (s, 3, C_{10}-CH_3) [lit. (7, 13) 0.85], 1.54 (s, 3, C_4-CH_3) [lit. (7, 13) 1.53], 3.70 (s, 3, OCH_3, ester), 3.84 (s, 3, OCH_3, ether), 5.80 (d, 1, J = 7 cps, CBrH) [lit. (7, 13) J = 7 cps], 6.85 (m, 2, ArH), and 7.80 ppm (d, 1, J = 9 cps, ArH).

Biological Procedures All biological tests were performed at the Cancer Chemotherapy National Service Center, Bethesda, Md. The general procedure, protocols, and data interpretation used at the National Cancer Institute have been published previously (15, 16).

REFERENCES

(1) R. H. Bible and M. Grove (to G. D. Searle and Co.) U.S. Pat. No. 2,753,357, July 3, 1956; *Chem. Abstr.*, **51**, 2869d (1957).

(2) M. N. Galbraith, D. H. S. Horn, J. M. Sasse, and D. Adamson, *Chem. Commun.*, **1970**, 170.

(3) J. M. Sasse, M. N. Galbraith, D. H. S. Horn, and D. A. Adamson, in "Plant Growth Substances, 1970," D. J. Carr, Ed., Springer Verlag, 1972, p. 430.

(4) M. N. Galbraith, D. H. S. Horn, and J. M. Sasse, *Chem. Commun.*, **1971**, 1362.

(5) R. F. Bryan and P. M. Smith, *J. Chem. Soc.* (Perkin II), **1975**, 148.

(6) G. R. Clark and T. N. Waters, *J. Chem. Soc.* (C) **1970**, 887.

(7) J. F. Cutfield, T. N. Waters, and G. R. Clark, *J. Chem. Soc.* (Perkin II), **1974**, 150.

(8) E. J. Parish and D. H. Miles, *J. Org. Chem.*, **38**, 3800 (1973).

(9) E. J. Parish and D. H. Miles, *J. Org. Chem.*, **38**, 1223 (1973).

(10) I. R. Sherwood and W. F. Short, *J. Chem. Soc.* **1938**, 1010.

(11) E. Wenkert, A. Fuchs, and J. D. McChesney, *J. Org. Chem.*, **30**, 2931 (1965).

(12) A. K. Bose, M. S. Manhas, and R. C. Cambie, *J. Org. Chem.*, **30**, 501 (1965).

(13) A. E. Lickei, A. C. Rieke, and D. M. S. Wheeler, *J. Org. Chem.*, **32**, 1647 (1967).

(14) E. Wenkert, *et al.*, *Can. J. Chem.*, **41**, 1924 (1963).

(15) R. I. Geren, N. H. Greenberg, M. M. MacDonald, A. M. Schumacker and B. J. Abbott, *Cancer Chemother. Rep., Part 3*, **3**(2), 1 (1972).

(16) "Screening Date Summary Interpretation and Outline of Current Screen," Drug Evaluation Branch Instruction Booklet 14, Division of Cancer Treatment, National Cancer Institute, Bethesda, 1978.

ACKNOWLEDGEMENTS

We thank the graduate school and the Biological and Physical Sciences Institute for partial financial support. We express our sincere appreciation to Dr. Ian K. Walker, Department of Scientific and Industrial Research, Wellington, New Zealand, for generous supplies of podocarpic acid.

Isocratic Liquid Chromatographic Method for the Determination of Amoxapine and its Metabolites

SCOTT M. JOHNSON, GLORIA NYGARD, and S. K. WAHBA KHALIL ˣ

Received October 1, 1982; from *The Pharmacokinetic Drug Analysis Laboratory, Pharmaceutical Science Dept., College of Pharmacy, North Dakota State University*, and *Veterans Administration Medical Center, Fargo, ND 58105.* Accepted for publication March 23, 1983.

Abstract □ An isocratic reverse-phase liquid chromatographic method for the determination of amoxapine and its major metabolites in human plasma utilizing UV detection is described. Plasma samples were extracted with ethyl acetate after pH adjustement. The reconstituted extracts were injected onto a cyanopropylsilane column and eluted with a mobile phase consisting of 65% acetonitrile and 35% sodium acetate buffer 0.03 M and pH 6. The minimum detectable limit was <10 ng/mL of plasma. Possible interferences from other drugs which might be administered concurrently were studied. The reproducibility and precision of the method are demonstrated by the analysis of samples containing 25–600 ng/mL of plasma. The method is being applied successfully in our laboratory for the analysis of plasma from patients receiving amoxapine.

Keyphrases □ Amoxapine—isocratic HPLC method, determination of metabolites □ Metabolites—isocratic HPLC method, determination of amoxapine

Amoxapine[1], 2-chloro-11-(1-piperazinyl)dibenz[*b,f*]-[1,4]oxazepine, a relatively new antidepressant of the dibenzoxazepine class, has been shown to be a potent antidepressant (1–3). The relationship between tricyclic antidepressant plasma concentrations and therapeutic response has been studied extensively, with inconclusive results (4, 5). The side effects of tricyclic antidepressants have also been correlated to plasma concentrations with mixed results (6). Since the major metabolic pathway of amoxapine is hydroxylation (7), monitoring therapeutic levels of the parent drug and its active

[1] Lederle Laboratories, Pearl River, N.Y.

0022-3549/84/0500-0696$01.00/0

© 1984, American Pharmaceutical Association

Table I—Precision and Accuracy of the Determination of Amoxapine and Its Metabolites in Human Plasma [a]

Amount Added, ng/mL	Amount Found, ng/mL					
	Day 1			Day 2		
	I	II	III	I	II	III
25	29.3 ± 4.7	30.9 ± 2.4	26.6 ± 0.9	30.5 ± 5.7	33.4 ± 7.3	27.5 ± 6.9
50	49.2 ± 4.7	52.7 ± 5.1	48.1 ± 4.2	—	—	—
100	99.5 ± 4.0	99.9 ± 6.4	96.4 ± 4.9	99.1 ± 6.4	92.6 ± 2.4	97.2 ± 7.1
200	202.5 ± 7.5	202.2 ± 2.6	197.4 ± 55.7	—	—	—
300	305.9 ± 14.9	305.9 ± 13.0	309.6 ± 13.6	308.8 ± 18.6	308.4 ± 20.0	303.3 ± 13.4
400	413.9 ± 17.6	396.6 ± 7.3	404.2 ± 15.8	—	—	—
600	600.9 ± 16.2	593.1 ± 20.2	590.5 ± 14.9	607.4 ± 27.3	594.1 ± 24.8	593.5 ± 21.6
Correlation coefficient (r)	0.996	0.995	0.995	0.997	0.997	0.998
n	35	35	35	20	20	20
r^2	0.993	0.991	0.990	0.994	0.993	0.996

[a] Mean ± *SD*.

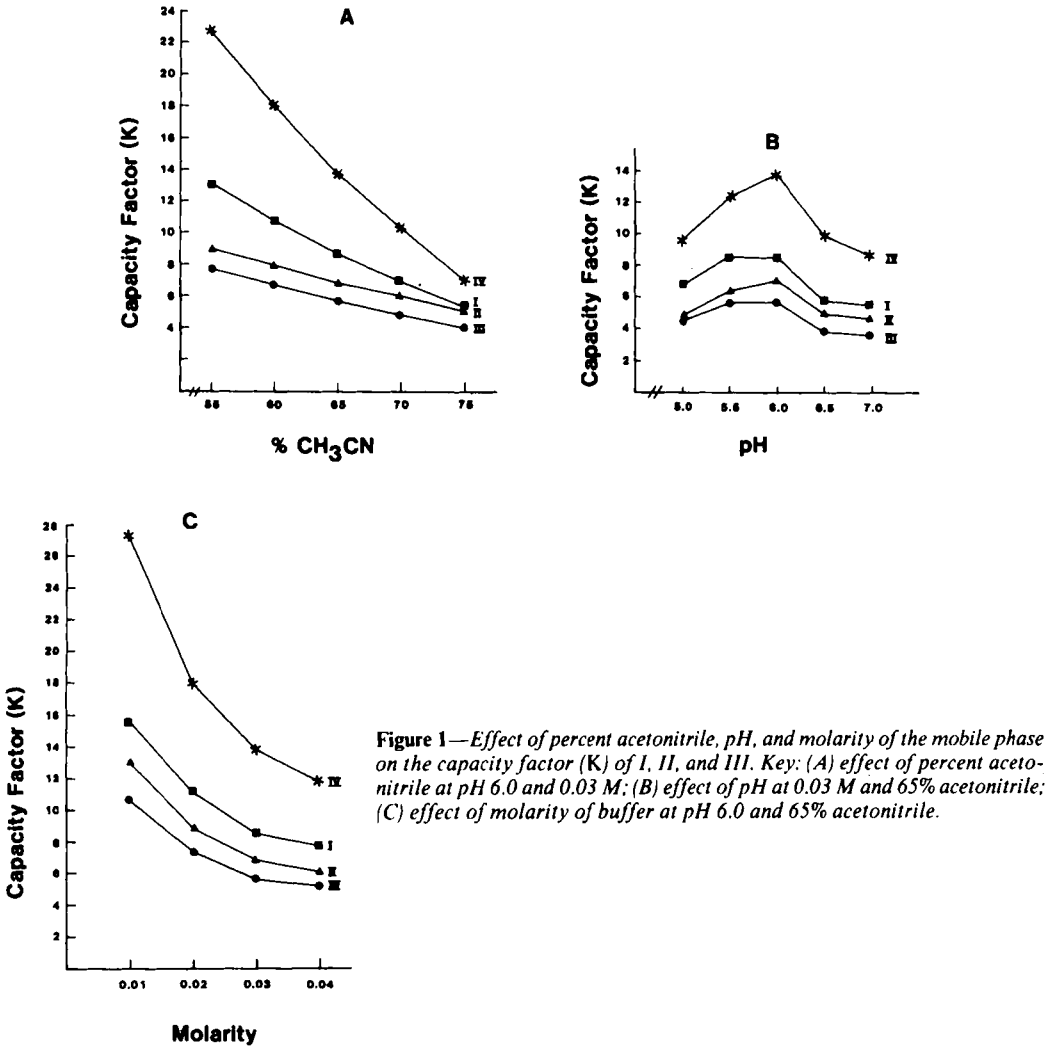

Figure 1—*Effect of percent acetonitrile, pH, and molarity of the mobile phase on the capacity factor (K) of I, II, and III. Key: (A) effect of percent acetonitrile at pH 6.0 and 0.03 M; (B) effect of pH at 0.03 M and 65% acetonitrile; (C) effect of molarity of buffer at pH 6.0 and 65% acetonitrile.*

hydroxylated metabolites is important for studying the kinetics and correlating the plasma concentrations with therapeutic response and side effects.

Methodology to determine amoxapine and its metabolites in serum has been limited to GC using derivatization and electron-capture detection (8, 9). However, recently a high-performance liquid chromatographic (HPLC) method (10) was developed using an ODS reverse-phase column and an elaborate three-step extraction procedure. The structurally related compound loxapine (*N*-methylamoxapine) has been analyzed by GC using derivatization and electron-capture detection (8, 9), nitrogen–phosphorus detection (11), or MS (9, 11).

This paper describes the separation and quantitation of amoxapine and its 7- and 8-hydroxylated metabolites from human plasma using HPLC with a reverse-phase cyanopropylsilane column and UV detection. The method has the advantages of involving only one extraction step and no derivatization. The method is sensitive and applicable to the direct determination of plasma levels in the presence of one or more

Table II—Drugs Tested for Possible Interference

Compound	Retention time, min
Diazepam	1.25
Trazodone	1.43
Lidocaine	1.43
8-Hydroxyloxapine	2.42
7-Hydroxyloxapine	2.83
8-Methoxyloxapine	3.09
Loxapine	3.23
Fluphenazine	3.20
Procaine	4.02
Perphenazine	4.65
8-Hydroxyamoxapine (III)	4.65
7-Hydroxyamoxapine (II)	5.57
Haloperidol	5.59
N-Acetylprocainamide	6.22
Amoxapine (I)	6.61
Procainamide	7.27
10-Hydroxyamitriptyline	8.27
Quinidine	8.38
Trimipramine (IV)	8.42
Thiothixene	8.72
10-Hydroxynortriptyline	9.17
p-Chlorodisopyramide	9.82
Disopyramide	10.08
Doxepin	10.44
Chlorprothixene	10.74
Trifluoperazine	11.35
Amitriptyline	11.39
Demethyldoxepin	11.65
Clomipramine	11.97
Protriptyline	12.15
Imipramine	12.33
Nortriptyline	12.35
Maprotiline	12.36
Desipramine	12.66
Chlorpromazine	13.09
Thioridazine	14.96

of several drugs which might be prescribed concurrently. The applicability of the method has been demonstrated by the analysis of plasma from patients receiving amoxapine.

EXPERIMENTAL

Instrumentation—A high-performance liquid chromatograph[2] was equipped with a cyanopropylsilane column[3], 250 mm × 4.6 mm i.d. The deaerated mobile phase was pumped through the column at 3.0 mL/min (13–15 mPa). The column compartment was maintained at 45°C, with UV monitoring at 250 nm.

Chemicals and Reagents—Sodium hydroxide, acetic acid, and sodium acetate were reagent grade. HPLC-grade ethyl acetate, acetonitrile, and methanol were used. Amoxapine (I)[1], 7-hydroxyamoxapine (II)[1], 8-hydroxyamoxapine (III)[1], and trimipramine hydrochloride (IV)[4] were supplied by the manufacturers.

Solutions—Sodium acetate solution, 0.03 M, was prepared in deionized distilled water, and the pH was adjusted to 6 by the gradual addition of acetic acid. The mobile phase consisted of 65% acetonitrile and 35% buffer.

Separate solutions of the drug, each metabolite, and the internal standard were made containing 5 mg/10 mL of methanol. A dilution to a working concentration (5 ng/μL for each) was made in methanol for the drug-metabolite group (I, II, and III). The internal standard stock solution (IV) was diluted with ethyl acetate to a concentration of 20 ng/mL.

Sample Preparation—To 1.0 mL of heparinized plasma in a 15-mL screw-capped centrifuge tube was added an aliquot (5–120 μL) of the drug and metabolite working solution containing 25–600 ng, 0.5 mL of 0.1 M NaOH, and 10 mL of extraction solution. The tubes were vortexed for 10 s and centrifuged for 5 min at 900×*g*. A 9-mL volume of the organic phase was transferred to special concentration tubes[5] and evaporated to dryness at 50°C under a gentle stream of nitrogen.

Separation and Quantitation—The residue was dissolved in 100 μL of methanol and transferred to a polypropylene microvial[6] before injection of 30 μL into the chromatograph. A standard curve was constructed utilizing a minimum of four replicate plasma extractions simulating concentrations of drug and metabolites from 25 to 600 ng/mL. The chromatograms were recorded at a chart speed of 5 mm/min. The peak heights were measured, and the ratios (drug/internal standard and metabolite/internal standard) were calculated and plotted *versus* concentration expressed as nanograms per milliliter of plasma.

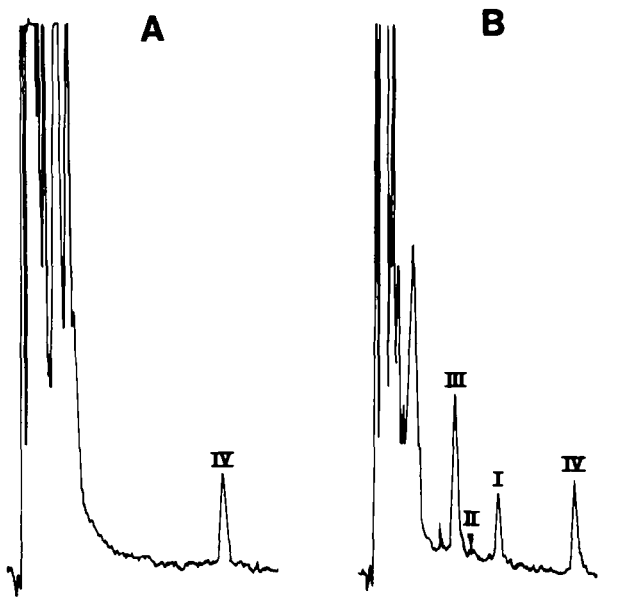

Figure 2—*Typical chromatograms of ethyl acetate extracts of 1.0 mL of plasma. The extracts were reconstituted with 100 μL of methanol, injection volume 30 μL, absorbance at 250 nm. Key: (A) drug free; (B) patient receiving I orally, concentrations of compounds expressed as ng/mL of plasma are I = 72, II = <10, and III = 227.*

Patient Samples—Heparinized plasma samples from patients receiving oral amoxapine were extracted in duplicate using the same procedure. The amounts of drug and metabolites in patient samples were calculated by comparison with a standard curve prepared daily. Possible interferences from normal plasma constituents, as well as other drugs and metabolites, were also studied.

RESULTS AND DISCUSSION

Amoxapine can be extracted readily from basified plasma using a solvent mixture (hexane containing 0.5% diethylamine) reported for the extraction of several tricyclic antidepressants and their metabolites (12). The active hydroxylated metabolites of amoxapine cannot, however, be extracted with that system and, therefore, the polar solvent ethyl acetate was selected.

The use of a cyanopropylsilane column in a reverse-phase mode with a mobile phase of acetonitrile–0.03 M acetate buffer at pH 6 (65:35, v/v) produced excellent separation of the drug from its metabolites and the internal standard. The separation depends on the pH and molarity of the buffer as well as the percentage of acetonitrile in the mobile phase. The mobile phase composition selected for this assay was based on the capacity factor (K) data plotted in Fig. 1. Detection at 250 nm was optimum for the drug, its metabolites, and the internal standard. Monitoring at 254 nm resulted in only a slight loss of sensitivity.

The ratios of peak heights of the drug and metabolites to the peak height of the internal standard were calculated. Linear regression analysis of the data on two separate days (Table I) indicated linearity and reproducibility in the range of 25–600 ng/mL of plasma. Extension of the standard curve beyond 600 ng/mL exhibited nonlinearity. A normal therapeutic range has not been established for amoxapine or its metabolites, but the linear portion of the standard curve encompasses the plasma concentrations which are expected based on normal dosages of amoxapine. Absolute recovery of the drug and its 7- and 8-hydroxy metabolites from plasma were 63, 69, and 68%, respectively, of the theoretical amounts. These values correlate well with data published recently (10). This low recovery may be responsible for the variation in the amount found at low concentrations (Table I). The minimum detectable limits of the assay are 6.5, 9.4, and 8.5 ng/mL of plasma for I, II, and III.

[2] Model 1084B chromatograph with variable-wavelength UV detector and autoinjector; Hewlett-Packard Co., Avondale, Pa.
[3] Zorbax-CN; Dupont Co., Wilmington, Del.
[4] Ives Laboratories, Inc., New York, N.Y.
[5] Concentratubes; Laboratory Research Co., Los Angeles, Calif.
[6] Micro-volume sample flask; P. Weidmann & Co., Romanshorn, Switzerland.

No interference with the drug or its metabolites from normal plasma constitutes was observed (Fig. 2A). The retention times of several drugs that might be prescribed simultaneously with amoxapine were determined (Table II). Little interference would be expected under the experimental conditions.

The method has been applied to the analysis of many samples obtained from patients receiving amoxapine orally. The drug and its 8-hydroxy metabolite are present in relatively high concentrations (Fig. 2B). However, the 7-hydroxy metabolite is found in low concentration. This may be due to its short half-life (8).

Major advantages of the method are the small sample volume required, the simplicity and high recovery using a single extraction step with no derivatization, and the use of an isocratic mobile phase. The sensitivity is sufficient for routine analysis of patient samples and for pharmacokinetic studies.

REFERENCES

(1) G. L. Sathananthan, R. Matz, H. Thompson, and S. Gershon, *Curr. Ther. Res.*, **15**, 919 (1973).

(2) R. C. Smith, *Curr. Ther. Res.*, **18**, 346 (1975).

(3) L. J. Hekimian, A. J. Friedhoff, and E. Deever, *J. Clin. Psychiatry*, **39**, 633 (1978).

(4) G. D. Burrows, B. A. Scoggins, L. R. Pureck, and B. Davis, *Clin. Pharmacol. Ther.*, **16**, 637 (1974).

(5) A. H. Glassman, J. M. Perel, M. Shostak, S. J. Kantor, and J. L. Fleiss, *Arch. J. Psychiatry*, **34**, 197 (1977).

(6) V. E. Ziegler, J. R. Taylor, R. D. Wedzel, and J. T. Biggs, *Br. J. Psychiatry*, **132**, 55 (1978).

(7) J. Coupet, C. E. Rauh, V. A. Szues-Myers, and L. M. Yunger, *Biochem. Pharmacol.*, **28**, 2514 (1979).

(8) T. B. Cooper and R. G. Kelly, *J. Pharm. Sci.*, **68**, 216 (1979).

(9) S. F. Cooper, R. Dugal, and M. J. Bertrand, *Xenobiotica*, **9**, 405 (1979).

(10) J. J. Tasset and F. M. Hassan, *Clin. Chem.*, **28**, 2154 (1982).

(11) J. Vasiliades, T. M. Sahawneh, and C. Owens, *J. Chromatogr.*, **164**, 457 (1979).

(12) S. M. Johnson, C. Chan, S. Cheng, J. L. Shimek, G. Nygard, and S. K. W. Khalil, *J. Pharm. Sci.*, **71**, 1027 (1982).

ACKNOWLEDGMENTS

The authors thank Robert I. Biberdorf for his valuable help. Also, the authors acknowledge Lederle Laboratories and Ives Laboratories for providing free authentic samples of the drugs and metabolites.

Isosorbide Dinitrate Plasma Concentrations and Bioavailability in Human Subjects after Administration of Standard Oral and Sublingual Formulations

L. F. CHASSEAUD ˣ, A. DARRAGH, E. DOYLE, R. F. LAMBE, and T. TAYLOR

Received September 13, 1982, from the *Department of Metabolism and Pharmacokinetics, Huntingdon Research Centre, Huntingdon, PE18 6ES England and the Institute of Clinical Pharmacology, Dublin, Ireland.* Accepted for publication December 23, 1982.

Abstract □ The bioavailability of isosorbide dinitrate from formulations containing 5, 10, and 20 mg in tablets and 10 mg in solution for oral use and 5 mg in tablets for sublingual use, has been compared. When adjusted for dose, the peak mean plasma drug concentrations after oral administration were similar (*e.g.*, 9.2 ng/mL after a 10-mg tablet) and about one-half that obtained after sublingual administration. Drug concentrations declined monoexponentially with mean half-lives ranging from 25–36 min. The relative bioavailability of isosorbide dinitrate from the oral formulations was not significantly different ($p > 0.05$) over the dose range studied, whereas the relative bioavailability after sublingual administration was about twice as great ($p < 0.01$) as that after oral administration. The plasma drug concentration–time profile after administering the 5-mg sublingual tablet was similar to that obtained after administering orally a solution containing 10 mg, indicating that the latter should be as clinically effective as the former.

Keyphrases □ Isosorbide dinitrate—rate and extent of bioavailability from various oral formulations compared, oral and sublingual formulations compared, humans □ Bioavailability—isosorbide dinitrate, oral and sublingual formulations compared, human □ Vasodilators—isosorbide dinitrate, oral and sublingual formulations compared, humans

Isosorbide dinitrate is an anti-anginal organic nitrate vasodilator that is in extensive clinical use. Following the development of suitably sensitive GC assays (1–3) for the measurement of isosorbide dinitrate in plasma, there have been several reports of the plasma levels of isosorbide dinitrate after the administration of different formulations of the drug (4–9). Sustained-release formulations have proven to be of particular interest. However, none of these reports have compared the relative bioavailability of isosorbide dinitrate from increasing doses of standard oral formulations. Such studies are described in this paper.

EXPERIMENTAL

Drug Administration—Two studies were conducted: the first compared a 5-mg sublingual tablet formulation with a 10-mg oral solution and 10- and 20-mg standard oral tablet formulations of isosorbide dinitrate[1]. The second study compared a 5-mg standard oral tablet formulation[1] with its 10-mg counterpart investigated in the first study. In each study, separate groups of 12 male volunteers each were involved, and the experimental conditions were the same. All subjects (18–40 years old and 58–85 kg) gave their written consent. Within 7 d before and after either study, each subject was given a complete physical examination including routine laboratory screening tests. During the study, the subjects remained under medical supervision. No adverse reactions, apart from headache (4 subjects), were reported by any subject. The studies were approved by the Institutional Review Board. Each of the oral dosage formulations was administered with 100 mL of water according to a complete crossover repeated Latin-square design with an interval of 1 week between doses. The sublingual formulation was retained under the tongue until it completely disintegrated; the subjects were instructed to avoid swallowing during this period. For at least 12 h predosing and for 4 h postdose the subjects fasted, and activity and subsequent diet were standardized.

At predose and after dosing, blood samples were collected into heparinized tubes by venipuncture, immediately cooled, and centrifuged. The resultant plasma was removed and stored at −20°C under conditions in which the drug was stable throughout the assay period.

Drug Assay—Isosorbide dinitrate in plasma was measured by an electron

[1] Formulations (Risordan) were provided by Theraplix, Paris, France. The respective batch numbers were 416, 430, 6659, 6665, 6747 for Risordan 5 mg (sublingual), 5 mg (oral), 10 mg (tablet), 20 mg and 10 mg (solution), respectively.

0022-3549/84/0500-0699$01.00/0

© 1984, American Pharmaceutical Association

No interference with the drug or its metabolites from normal plasma constitutes was observed (Fig. 2A). The retention times of several drugs that might be prescribed simultaneously with amoxapine were determined (Table II). Little interference would be expected under the experimental conditions.

The method has been applied to the analysis of many samples obtained from patients receiving amoxapine orally. The drug and its 8-hydroxy metabolite are present in relatively high concentrations (Fig. 2B). However, the 7-hydroxy metabolite is found in low concentration. This may be due to its short half-life (8).

Major advantages of the method are the small sample volume required, the simplicity and high recovery using a single extraction step with no derivatization, and the use of an isocratic mobile phase. The sensitivity is sufficient for routine analysis of patient samples and for pharmacokinetic studies.

REFERENCES

(1) G. L. Sathananthan, R. Matz, H. Thompson, and S. Gershon, *Curr. Ther. Res.*, **15**, 919 (1973).

(2) R. C. Smith, *Curr. Ther. Res.*, **18**, 346 (1975).

(3) L. J. Hekimian, A. J. Friedhoff, and E. Deever, *J. Clin. Psychiatry*, **39**, 633 (1978).

(4) G. D. Burrows, B. A. Scoggins, L. R. Pureck, and B. Davis, *Clin. Pharmacol. Ther.*, **16**, 637 (1974).

(5) A. H. Glassman, J. M. Perel, M. Shostak, S. J. Kantor, and J. L. Fleiss, *Arch. J. Psychiatry*, **34**, 197 (1977).

(6) V. E. Ziegler, J. R. Taylor, R. D. Wedzel, and J. T. Biggs, *Br. J. Psychiatry*, **132**, 55 (1978).

(7) J. Coupet, C. E. Rauh, V. A. Szues-Myers, and L. M. Yunger, *Biochem. Pharmacol.*, **28**, 2514 (1979).

(8) T. B. Cooper and R. G. Kelly, *J. Pharm. Sci.*, **68**, 216 (1979).

(9) S. F. Cooper, R. Dugal, and M. J. Bertrand, *Xenobiotica*, **9**, 405 (1979).

(10) J. J. Tasset and F. M. Hassan, *Clin. Chem.*, **28**, 2154 (1982).

(11) J. Vasiliades, T. M. Sahawneh, and C. Owens, *J. Chromatogr.*, **164**, 457 (1979).

(12) S. M. Johnson, C. Chan, S. Cheng, J. L. Shimek, G. Nygard, and S. K. W. Khalil, *J. Pharm. Sci.*, **71**, 1027 (1982).

ACKNOWLEDGMENTS

The authors thank Robert I. Biberdorf for his valuable help. Also, the authors acknowledge Lederle Laboratories and Ives Laboratories for providing free authentic samples of the drugs and metabolites.

Isosorbide Dinitrate Plasma Concentrations and Bioavailability in Human Subjects after Administration of Standard Oral and Sublingual Formulations

L. F. CHASSEAUD ˣ, A. DARRAGH, E. DOYLE, R. F. LAMBE, and T. TAYLOR

Received September 13, 1982, from the *Department of Metabolism and Pharmacokinetics, Huntingdon Research Centre, Huntingdon, PE18 6ES England and the Institute of Clinical Pharmacology, Dublin, Ireland.* Accepted for publication December 23, 1982.

Abstract □ The bioavailability of isosorbide dinitrate from formulations containing 5, 10, and 20 mg in tablets and 10 mg in solution for oral use and 5 mg in tablets for sublingual use, has been compared. When adjusted for dose, the peak mean plasma drug concentrations after oral administration were similar (*e.g.*, 9.2 ng/mL after a 10-mg tablet) and about one-half that obtained after sublingual administration. Drug concentrations declined monoexponentially with mean half-lives ranging from 25–36 min. The relative bioavailability of isosorbide dinitrate from the oral formulations was not significantly different ($p > 0.05$) over the dose range studied, whereas the relative bioavailability after sublingual administration was about twice as great ($p < 0.01$) as that after oral administration. The plasma drug concentration–time profile after administering the 5-mg sublingual tablet was similar to that obtained after administering orally a solution containing 10 mg, indicating that the latter should be as clinically effective as the former.

Keyphrases □ Isosorbide dinitrate—rate and extent of bioavailability from various oral formulations compared, oral and sublingual formulations compared, humans □ Bioavailability—isosorbide dinitrate, oral and sublingual formulations compared, human □ Vasodilators—isosorbide dinitrate, oral and sublingual formulations compared, humans

Isosorbide dinitrate is an anti-anginal organic nitrate vasodilator that is in extensive clinical use. Following the development of suitably sensitive GC assays (1–3) for the measurement of isosorbide dinitrate in plasma, there have been several reports of the plasma levels of isosorbide dinitrate after the administration of different formulations of the drug (4–9). Sustained-release formulations have proven to be of particular interest. However, none of these reports have compared the relative bioavailability of isosorbide dinitrate from increasing doses of standard oral formulations. Such studies are described in this paper.

EXPERIMENTAL

Drug Administration—Two studies were conducted: the first compared a 5-mg sublingual tablet formulation with a 10-mg oral solution and 10- and 20-mg standard oral tablet formulations of isosorbide dinitrate[1]. The second study compared a 5-mg standard oral tablet formulation[1] with its 10-mg counterpart investigated in the first study. In each study, separate groups of 12 male volunteers each were involved, and the experimental conditions were the same. All subjects (18–40 years old and 58–85 kg) gave their written consent. Within 7 d before and after either study, each subject was given a complete physical examination including routine laboratory screening tests. During the study, the subjects remained under medical supervision. No adverse reactions, apart from headache (4 subjects), were reported by any subject. The studies were approved by the Institutional Review Board. Each of the oral dosage formulations was administered with 100 mL of water according to a complete crossover repeated Latin-square design with an interval of 1 week between doses. The sublingual formulation was retained under the tongue until it completely disintegrated; the subjects were instructed to avoid swallowing during this period. For at least 12 h predosing and for 4 h postdose the subjects fasted, and activity and subsequent diet were standardized.

At predose and after dosing, blood samples were collected into heparinized tubes by venipuncture, immediately cooled, and centrifuged. The resultant plasma was removed and stored at −20°C under conditions in which the drug was stable throughout the assay period.

Drug Assay—Isosorbide dinitrate in plasma was measured by an electron

[1] Formulations (Risordan) were provided by Theraplix, Paris, France. The respective batch numbers were 416, 430, 6659, 6665, 6747 for Risordan 5 mg (sublingual), 5 mg (oral), 10 mg (tablet), 20 mg and 10 mg (solution), respectively.

0022-3549/84/0500-0699$01.00/0

© 1984, American Pharmaceutical Association

Table I—Mean Plasma Drug Concentrations [a] after Administration of Oral and Sublingual Formulations of Isosorbide Dinitrate

Time, Min	Oral 10-mg Solution	Oral 10-mg Tablet	Oral 20-mg Tablet	Sublingual 5 mg Tablet
10	8.2 ± 6.6	3.2 ± 3.3	3.2 ± 4.0	7.7 ± 6.7
20	9.4 ± 3.9	7.6 ± 3.7	14.0 ± 11.6	8.6 ± 4.4
30	9.2 ± 3.4	9.2 ± 2.9	17.5 ± 10.6	7.6 ± 2.8
40	7.3 ± 2.6	9.1 ± 2.6	16.9 ± 7.7	6.4 ± 2.7
50	5.6 ± 1.9	7.1 ± 2.7	13.6 ± 4.7	4.2 ± 1.7
60	4.3 ± 1.6	5.3 ± 2.1	12.0 ± 4.2	3.2 ± 1.0
75	2.7 ± 1.1	3.6 ± 1.9	9.2 ± 3.6	2.0 ± 0.7
90	1.7 ± 0.7	2.4 ± 1.8	7.2 ± 3.5	1.5 ± 0.9
120	0.8 ± 0.5	1.2 ± 1.1	3.9 ± 1.9	0.7 ± 0.5
150	ND[b]	ND[b]	2.2 ± 1.2	ND[b]

[a] Nanograms per milliliter ± *SD*. [b] ND = not detected (<0.5 ng/mL).

Table II—Mean Plasma Drug Concentrations [a] after Administration of Two Oral Formulations of Isosorbide Dinitrate

Time, Min	5-mg Tablet[b]	10-mg Tablet
10	1.8 ± 1.7	5.7 ± 3.7
20	10.4 ± 6.3	12.6 ± 3.5
30	11.2 ± 4.5	10.9 ± 2.9
40	10.3 ± 5.5	9.0 ± 3.7
50	7.8 ± 3.2	6.6 ± 2.3
60	6.5 ± 3.0	5.1 ± 2.4
75	4.5 ± 2.2	3.4 ± 1.1
90	3.0 ± 1.4	2.2 ± 0.7
120	1.5 ± 0.9	1.2 ± 0.4
150	0.7 ± 0.7	ND[c]

[a] Nanograms per milliliter ± *SD*. [b] Two tablets (10 mg) administered. [c] ND = not detected (<0.5 ng/mL).

capture GC assay (3) with glyceryl trinitrate as the internal standard. Plasma isosorbide dinitrate levels were calculated by reference to standard curves constructed by adding known amounts of the drug to control human plasma. During this procedure and the subsequent assay, isosorbide dinitrate was completely stable at 4° or 20°C. The recovery of isosorbide dinitrate from plasma over the concentration range 1–15 ng/mL was 91 ± 10% *SD*. The precision of the method for the measurement of isosorbide dinitrate in plasma (n = 5) was 18, 9, and 11% at 1, 5, and 10 ng/mL, respectively.

Data Processing—Apparent half-lives for the decline of plasma drug concentrations were calculated by least-squares regression analysis of log concentration against time from measurements during the terminal linear phase of the plasma drug concentration–time curves. As isosorbide dinitrate kinetics appear to follow a "flip-flop" model (10), these half-lives relate to drug absorption, not to elimination. Areas under the plasma concentration–time curves, scaled to equal doses, were calculated by the trapezoidal rule or by using spline functions, and adjusted to infinite time. Whether the infinite time adjustment was carried out at a concentration of ~2 ng/mL (where assay precision was ~≤10%) or at a lower concentration (where assay precision was poorer), the difference in the resultant calculated mean areas was <~3% (mean 1.4% range 0.3–3.3%).

Areas, peak plasma concentrations and their times of occurrence, and apparent "absorption" half-lives were subjected to an ANOVA for crossover designs (11). Formulation means were compared with the reference mean by Dunnett's test (12, 13) and compared pairwise by the Newman-Keuls procedure (14, 15). The total variance was separated into that due to subjects, day of administration, formulations, and residual.

RESULTS AND DISCUSSION

Plasma Drug Concentrations—Mean concentrations of isosorbide dinitrate in plasma after administration of the various formulations are shown in Tables I and II. Drug levels were detected in the plasma of at least eight subjects at the first sampling time after administration of the tablet formulations and in all subjects after administration of the solution. Drug was not detected (<0.5 ng/mL) in at least five subjects at 150 min after administration of all formulations except the 20-mg dose. Drug was even undetected in the plasma of some subjects at 120 min after administration. Mean plasma drug levels obtained after equivalent oral doses as a solution and as a tablet were generally similar, but as expected, peak mean levels were reached sooner after administration of the solution.

Inspection of the data shows that the peak mean plasma drug levels obtained after administration of 5-, 10-, and 20-mg tablet formulations were linearly related to dose.

The mean plasma drug levels obtained after administration of the 10-mg tablet to two separate groups of subjects in different studies were remarkably similar (*cf.* Tables I and II).

Mean plasma drug levels obtained after the 5-mg sublingual dose were similar to those after a 10-mg oral dose and in the same range as previously reported (4, 9, 16).

With respect to the type of isosorbide dinitrate formulation administered, the plasma drug levels shown in Tables I and II are similar to those reported in the literature (4–7).

Bioavailability Parameters—Peak plasma levels of isosorbide dinitrate and the times of occurrence are shown in Table III. Although the peak levels of the 10-mg tablet and 10-mg solution were similar, the times at which they were reached were significantly different. With due allowance for dose, mean peak levels from the 20-, 10-, and 5-mg tablets (the latter given as 2 × 5 mg) were similar as were their times of occurrence. The former result suggests that over this dose range, at least, a similar proportion of isosorbide dinitrate was probably absorbed unchanged into the peripheral circulation. It should be noted that an oral dose of [^{14}C]isosorbide dinitrate was almost completely absorbed with respect to radioactivity (17), whereas the systemic availability of isosorbide dinitrate orally is ~25% (18) due to considerable first-pass metabolism in the liver and perhaps even during absorption from the GI tract. It has also been reported that a similar proportion of isosorbide dinitrate was absorbed from a 20-mg sustained-release formulation over the 20–100-mg dose range in healthy subjects (19), and from an apparently standard formulation over the 15–120-mg dose range in patients (20).

Although relatively greater with respect to the administered dose, the mean peak level of isosorbide dinitrate following a sublingual dose was reached hardly any sooner than from a 10-mg solution. This result, and the similarity between the respective plasma drug concentration–time curves, implies that a dose of 10 mg of isosorbide dinitrate as an oral solution should produce about the same onset and duration of clinical effect as a 5-mg sublingual dose.

Measured areas under the plasma drug concentration–time curves are shown in Table III. The mean AUC ratios, when adjusted for dose/body weight, after administration of 5-, 10-, and 20-mg tablet formulations were

Table III—Mean (± *SD*) Bioavailability Parameters of Isosorbide Dinitrate for the Various Formulations [a]

Parameter	Oral 5-mg Tablet[b]	Oral 10-mg Tablet	Oral 20-mg Tablet	Oral 10-mg Solution	Sublingual 5-mg Tablet
Peak concentration in individuals (ng/mL)	(14.0 ± 6.1)	10.6 ± 2.3 (14.0 ± 2.8)	22.4 ± 9.9[c,f,g]	11.7 ± 6.2[d]	10.9 ± 5.3
Time of peak concentration (min)	(34.2 ± 13.8)	35.0 ± 9.0[e] (22.5 ± 8.7)	39.1 ± 13.1[c]	24.4 ± 9.0	21.7 ± 11.1[d,f]
Area (ng min/ml)	(711 ± 229)	600 ± 185 (668 ± 152)	1370 ± 361[c,f,g]	583 ± 158	497 ± 168[h]
Half-life (min)	(30.2 ± 5.5)	26.9 ± 9.4 (28.2 ± 5.2)	36.3 ± 8.2[c,f,g]	25.3 ± 9.4	28.7 ± 7.4

[a] Data in parentheses have been obtained from a different group of subjects. [b] This formulation (given as 2 × 5 mg) was compared statistically ($p > 0.05$) with the 10-mg tablet only. [c] Significantly different ($p < 0.01$) from 10-mg solution (Dunnett's test). [d] Significantly different ($p < 0.01$) from 20-mg tablet (Newman-Keuls pairwise comparison). [e] Significantly different ($p < 0.05$) from 10-mg solution (Dunnett's test). [f] Significantly different ($p < 0.01$) from 10-mg tablet (Newman-Keuls pairwise comparison). [g] Significantly different ($p < 0.01$ or <0.05) from 5-mg sublingual tablet (Newman-Keuls pairwise comparison). [h] Significant differences occur (*c,d,f*) with this parameter when data were adjusted for dose/body weight.

similar to that after a 10-mg solution indicating that there were no dosage form or dose level effects on the extent of bioavailability of isosorbide dinitrate over the 5–20 mg dose range (*i.e.*, a similar relative fraction of the dose of isosorbide dinitrate reached the peripheral circulation unchanged after administration of each formulation). The mean adjusted AUC after administration of the sublingual 5-mg dose was significantly different from those after the oral tablet formulations, as might be expected. Indeed, previous studies have shown that the extent of bioavailability of isosorbide dinitrate from a sublingual formulation was at least twice that from the same formulation given orally (4), since some but not all of a sublingual dose avoids first-pass elimination. A large proportion of a sublingual dose is usually swallowed (18).

The conventional 95% confidence limits (21, 22) of mean areas expressed as a percent of the mean from the 10-mg solution formulation taken as a reference were −19 to +29%, −6 to +50%, and +32 to +109% from the 10-mg oral tablet, 20-mg oral tablet, and 5-mg sublingual tablet, respectively. These limits were −11 to +24% for the 5-mg oral tablet when the 10-mg oral tablet was taken as the reference (Table III). These confidence limits are fairly narrow even though plasma concentrations of isosorbide dinitrate can vary by several-fold between subjects, and the group of subjects studied was not particularly large.

Drug Half-Life—Isosorbide dinitrate kinetics appear to follow a "flip-flop" model (10, 18) and, therefore, the monoexponential decline of the concentrations in plasma can be regarded as reflecting the rate of drug absorption.

Among the orally administered formulations, the drug absorption half-life was shortest after the 10-mg solution dose, but only the drug half-life observed after the 20-mg tablet was significantly longer ($p < 0.01$) than that after the 10-mg solution. A shorter half-life after the sublingual dose would not be expected because the 5-mg tablet was retained in the mouth during disintegration before a notable proportion was swallowed. The half-lives measured in these studies are in close agreement with those reported in the literature (4, 9, 10, 18).

REFERENCES

(1) M. T. Rosseel and M. G. Bogaert, *J. Pharm. Sci.*, **62**, 754 (1973).

(2) E. Doyle, L. F. Chasseaud, and T. Taylor, *Biopharm. Drug Dispos.*, **1**, 141 (1980).

(3) J. O. Malbica, K. Monson, K. Neilson, and R. Sprissler, *J. Pharm. Sci.*, **66**, 384 (1977).

(4) D. F. Assinder, L. F. Chasseaud, and T. Taylor, *J. Pharm. Sci.*, **66**, 775 (1977).

(5) D. F. Assinder, L. F. Chasseaud, J. O. Hunter, R. J. Jung, and T. Taylor, *Arzneim.-Forsch.*, **27**, 156 (1977).

(6) J. M. Orr, G. P. Klein, and S. F. Shaar, *Can. J. Pharm. Sci.*, **13**, 45 (1978).

(7) L. F. Chasseaud and T. Taylor, in "Nitrate II," W. Rudolph and A. Schrey, Eds., Urban and Schwarzenberg, Munich, West Germany, 1980, p. 22.

(8) U. Thadani, D. Manyari, J. O. Parker, and H. L. Fung, *Circulation*, **61**, 526 (1980).

(9) S. Sporl-Radun, G. Betzien, B. Kaufmann, V. Liede, and U. Abshagen, *Eur. J. Clin. Pharmacol.*, **18**, 237 (1980).

(10) T. Taylor, L. F. Chasseaud, E. Doyle, A. Darragh, D. A. O'Kelly, and D. Fitzgerald, *Biopharm. Drug Dispos.*, **1**, 149 (1980).

(11) W. G. Cochran and G. M. Cox, "Experimental Designs," Wiley, New York, N.Y., 1957, p. 117.

(12) C. W. Dunnett, *J. Am. Stat. Assoc.*, **50**, 1096 (1955).

(13) C. W. Dunnett, *Biometrics*, **20**, 483 (1964).

(14) D. Newman, *Biometrika*, **31**, 20 (1939).

(15) M. Keuls, *Euphytica*, **1**, 112 (1952).

(16) D. Mansel-Jones, T. Taylor, E. Doyle, L. F. Chasseaud, A. Darragh, D. A. O'Kelly, and H. Over, *J. Clin. Pharmacol.*, **18**, 544 (1978).

(17) W. H. Down, L. F. Chasseaud, and R. K. Grundy, *J. Pharm. Sci.*, **63**, 1147 (1974).

(18) T. Taylor, L. F. Chasseaud, E. Doyle, R. Bonn, A. Darragh, and R. F. Lambe, *Arzneim.-Forsch.*, **32**, 1329 (1982).

(19) T. Taylor, D. A. O'Kelly, R. M. Major, A. Darragh, and L. F. Chasseaud, *Arzneim.-Forsch.*, **28**, 1426 (1978).

(20) H. L. Fung, E. F. McNiff, D. Ruggirello, A. Darke, U. Thadani, and J. O. Parker, *Br. J. Clin. Pharmacol.*, **11**, 579 (1981).

(21) C. Metzler, *Biometrics*, **30**, 109 (1974).

(22) E. Shirley, *J. Pharm. Pharmacol.*, **28**, 312 (1976).

ACKNOWLEDGMENTS

The authors are grateful to Theraplix, Paris, for financial support.

Disintegrating Force as a New Formulation Parameter

PAOLO COLOMBO *, UBALDO CONTE *, CARLA CARAMELLA *, MARIO GEDDO ‡, and ALDO LA MANNA *x

Received November 17, 1982, from the **Dipartimento di Chimica Farmaceutica* and ‡*Istituto di Fisica Generale, Unità G.N.S.M., Università di Pavia, Viale Taramelli 12, 27100, Pavia, Italy.* Accepted for publication March 24, 1983.

Abstract □ Some coated aspirin tablet formulations were evaluated by relating their properties to disintegrating force development patterns. The treatment of disintegrating force–time curves was effected using the Weibull distribution as proposed for dissolution. Such parameters as the maximum disintegrating force developed, the time needed to reach 63.2% maximum disintegrating force (τ_d) the shape parameter, the lag time, and the input value were used for evaluating the formulas examined. It was concluded that the input values, the integrating force development rate at time τ_d, can be employed as a new formulation parameter since, when correlated with the crushing strength, it allows an overall evaluation of the formula examined.

Keyphrases □ Disintegrating force—new formulation parameter, Weibull distribution, coated aspirin tablets □ Formulations—disintegrating force as a new parameter, Weibull distribution, coated aspirin tablets □ Weibull distribution—disintegrating force as a new formulation parameter, coated aspirin tablets

In a previous paper (1), the disintegrating force of tablets was defined as the force developed inside a tablet depending on the liquid–solid contact. It was shown that curves obtained by plotting disintegrating force *versus* liquid contact time had patterns following saturation kinetics dependent on the liquid penetration into voids. Since compact structure (defined by voids distribution and interparticle bonding) and disintegration–dissolution performance are strictly related, the investigations of the disintegration behavior of a tablet should provide a means for the evaluation of the structure obtained.

It is well known that disintegration time as measured by official apparatuses does not satisfactorily describe the disintegration properties of tablets, as demonstrated by the methods proposed to evaluate disintegration (2–5). Because disintegrating force–time curves could be related to the structure of tablets (6), these deserved a deeper investigation in view of their employment not only for studying the bioavailability-related properties of tablets, but also to assess the structure–technological parameter relationships.

The aim of the present work was to employ the disintegrating force parameters for studying coated aspirin tablet

0022-3549/84/0500-0701$01.00/0

© 1984, American Pharmaceutical Association

similar to that after a 10-mg solution indicating that there were no dosage form or dose level effects on the extent of bioavailability of isosorbide dinitrate over the 5–20 mg dose range (*i.e.*, a similar relative fraction of the dose of isosorbide dinitrate reached the peripheral circulation unchanged after administration of each formulation). The mean adjusted AUC after administration of the sublingual 5-mg dose was significantly different from those after the oral tablet formulations, as might be expected. Indeed, previous studies have shown that the extent of bioavailability of isosorbide dinitrate from a sublingual formulation was at least twice that from the same formulation given orally (4), since some but not all of a sublingual dose avoids first-pass elimination. A large proportion of a sublingual dose is usually swallowed (18).

The conventional 95% confidence limits (21, 22) of mean areas expressed as a percent of the mean from the 10-mg solution formulation taken as a reference were −19 to +29%, −6 to +50%, and +32 to +109% from the 10-mg oral tablet, 20-mg oral tablet, and 5-mg sublingual tablet, respectively. These limits were −11 to +24% for the 5-mg oral tablet when the 10-mg oral tablet was taken as the reference (Table III). These confidence limits are fairly narrow even though plasma concentrations of isosorbide dinitrate can vary by several-fold between subjects, and the group of subjects studied was not particularly large.

Drug Half-Life—Isosorbide dinitrate kinetics appear to follow a "flip-flop" model (10, 18) and, therefore, the monoexponential decline of the concentrations in plasma can be regarded as reflecting the rate of drug absorption.

Among the orally administered formulations, the drug absorption half-life was shortest after the 10-mg solution dose, but only the drug half-life observed after the 20-mg tablet was significantly longer ($p < 0.01$) than that after the 10-mg solution. A shorter half-life after the sublingual dose would not be expected because the 5-mg tablet was retained in the mouth during disintegration before a notable proportion was swallowed. The half-lives measured in these studies are in close agreement with those reported in the literature (4, 9, 10, 18).

REFERENCES

(1) M. T. Rosseel and M. G. Bogaert, *J. Pharm. Sci.*, **62**, 754 (1973).

(2) E. Doyle, L. F. Chasseaud, and T. Taylor, *Biopharm. Drug Dispos.*, **1**, 141 (1980).

(3) J. O. Malbica, K. Monson, K. Neilson, and R. Sprissler, *J. Pharm. Sci.*, **66**, 384 (1977).

(4) D. F. Assinder, L. F. Chasseaud, and T. Taylor, *J. Pharm. Sci.*, **66**, 775 (1977).

(5) D. F. Assinder, L. F. Chasseaud, J. O. Hunter, R. J. Jung, and T. Taylor, *Arzneim.-Forsch.*, **27**, 156 (1977).

(6) J. M. Orr, G. P. Klein, and S. F. Shaar, *Can. J. Pharm. Sci.*, **13**, 45 (1978).

(7) L. F. Chasseaud and T. Taylor, in "Nitrate II," W. Rudolph and A. Schrey, Eds., Urban and Schwarzenberg, Munich, West Germany, 1980, p. 22.

(8) U. Thadani, D. Manyari, J. O. Parker, and H. L. Fung, *Circulation*, **61**, 526 (1980).

(9) S. Sporl-Radun, G. Betzien, B. Kaufmann, V. Liede, and U. Abshagen, *Eur. J. Clin. Pharmacol.*, **18**, 237 (1980).

(10) T. Taylor, L. F. Chasseaud, E. Doyle, A. Darragh, D. A. O'Kelly, and D. Fitzgerald, *Biopharm. Drug Dispos.*, **1**, 149 (1980).

(11) W. G. Cochran and G. M. Cox, "Experimental Designs," Wiley, New York, N.Y., 1957, p. 117.

(12) C. W. Dunnett, *J. Am. Stat. Assoc.*, **50**, 1096 (1955).

(13) C. W. Dunnett, *Biometrics*, **20**, 483 (1964).

(14) D. Newman, *Biometrika*, **31**, 20 (1939).

(15) M. Keuls, *Euphytica*, **1**, 112 (1952).

(16) D. Mansel-Jones, T. Taylor, E. Doyle, L. F. Chasseaud, A. Darragh, D. A. O'Kelly, and H. Over, *J. Clin. Pharmacol.*, **18**, 544 (1978).

(17) W. H. Down, L. F. Chasseaud, and R. K. Grundy, *J. Pharm. Sci.*, **63**, 1147 (1974).

(18) T. Taylor, L. F. Chasseaud, E. Doyle, R. Bonn, A. Darragh, and R. F. Lambe, *Arzneim.-Forsch.*, **32**, 1329 (1982).

(19) T. Taylor, D. A. O'Kelly, R. M. Major, A. Darragh, and L. F. Chasseaud, *Arzneim.-Forsch.*, **28**, 1426 (1978).

(20) H. L. Fung, E. F. McNiff, D. Ruggirello, A. Darke, U. Thadani, and J. O. Parker, *Br. J. Clin. Pharmacol.*, **11**, 579 (1981).

(21) C. Metzler, *Biometrics*, **30**, 109 (1974).

(22) E. Shirley, *J. Pharm. Pharmacol.*, **28**, 312 (1976).

ACKNOWLEDGMENTS

The authors are grateful to Theraplix, Paris, for financial support.

Disintegrating Force as a New Formulation Parameter

PAOLO COLOMBO *, UBALDO CONTE *, CARLA CARAMELLA *, MARIO GEDDO ‡, and ALDO LA MANNA *x

Received November 17, 1982, from the **Dipartimento di Chimica Farmaceutica* and ‡*Istituto di Fisica Generale, Unità G.N.S.M., Università di Pavia, Viale Taramelli 12, 27100, Pavia, Italy.* Accepted for publication March 24, 1983.

Abstract □ Some coated aspirin tablet formulations were evaluated by relating their properties to disintegrating force development patterns. The treatment of disintegrating force–time curves was effected using the Weibull distribution as proposed for dissolution. Such parameters as the maximum disintegrating force developed, the time needed to reach 63.2% maximum disintegrating force (τ_d) the shape parameter, the lag time, and the input value were used for evaluating the formulas examined. It was concluded that the input values, the integrating force development rate at time τ_d, can be employed as a new formulation parameter since, when correlated with the crushing strength, it allows an overall evaluation of the formula examined.

Keyphrases □ Disintegrating force—new formulation parameter, Weibull distribution, coated aspirin tablets □ Formulations—disintegrating force as a new parameter, Weibull distribution, coated aspirin tablets □ Weibull distribution—disintegrating force as a new formulation parameter, coated aspirin tablets

In a previous paper (1), the disintegrating force of tablets was defined as the force developed inside a tablet depending on the liquid–solid contact. It was shown that curves obtained by plotting disintegrating force *versus* liquid contact time had patterns following saturation kinetics dependent on the liquid penetration into voids. Since compact structure (defined by voids distribution and interparticle bonding) and disintegration–dissolution performance are strictly related, the investigations of the disintegration behavior of a tablet should provide a means for the evaluation of the structure obtained.

It is well known that disintegration time as measured by official apparatuses does not satisfactorily describe the disintegration properties of tablets, as demonstrated by the methods proposed to evaluate disintegration (2–5). Because disintegrating force–time curves could be related to the structure of tablets (6), these deserved a deeper investigation in view of their employment not only for studying the bioavailability-related properties of tablets, but also to assess the structure–technological parameter relationships.

The aim of the present work was to employ the disintegrating force parameters for studying coated aspirin tablet

0022-3549/84/0500-0701$01.00/0

© 1984, American Pharmaceutical Association

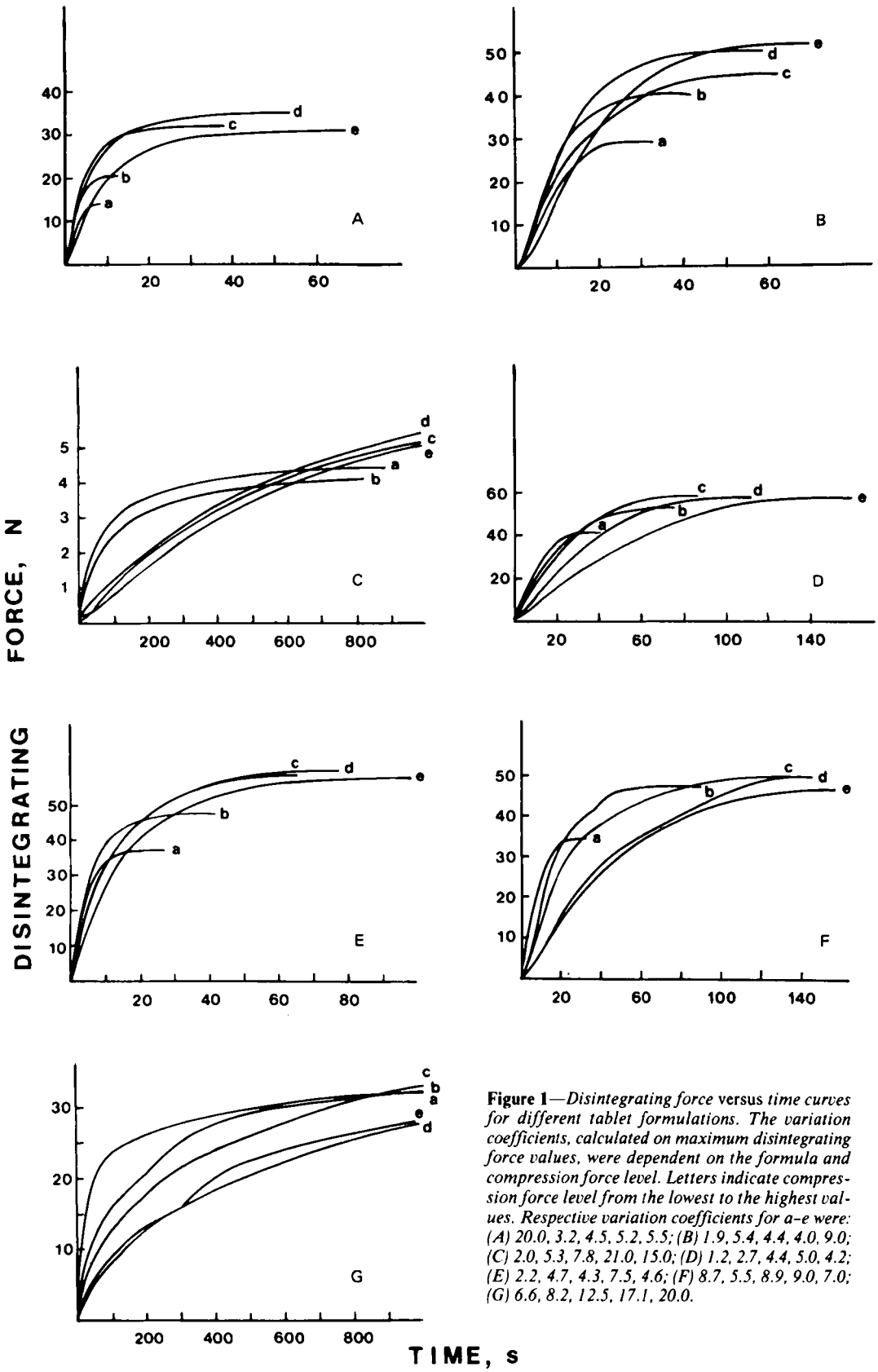

Figure 1—*Disintegrating force* versus *time curves for different tablet formulations. The variation coefficients, calculated on maximum disintegrating force values, were dependent on the formula and compression force level. Letters indicate compression force level from the lowest to the highest values. Respective variation coefficients for a–e were: (A) 20.0, 3.2, 4.5, 5.2, 5.5; (B) 1.9, 5.4, 4.4, 4.0, 9.0; (C) 2.0, 5.3, 7.8, 21.0, 15.0; (D) 1.2, 2.7, 4.4, 5.0, 4.2; (E) 2.2, 4.7, 4.3, 7.5, 4.6; (F) 8.7, 5.5, 8.9, 9.0, 7.0; (G) 6.6, 8.2, 12.5, 17.1, 20.0.*

formulations for the purpose of giving a new tool for a rational tablet formulation. The choice of coated aspirin as base material was justified by the results previously obtained when studying the influence of the disintegrating agent on the tablets' mechanical and release characteristics (7).

EXPERIMENTAL

Mixtures of coated aspirin as reported in Table I were prepared under controlled conditions with a compression apparatus[1]. The tablets were com-

[1] Turbula T2A.

Table I—Composition of the Coated Aspirin Mixtures (g/Tablet)

Mixture[a]	Coated Aspirin[b]	Cornstarch[c]	Mycrocrystalline Cellulose[d]	Crospovidone[e]	Modified Starch[f]	Cation-Exchange Resin[g]	Sodium Carboxymethylcellulose[h]
A	0.515	0.075	—	—	—	—	—
B	0.515	0.025	0.050	—	—	—	—
C	0.515	—	—		0.075	—	—
D	0.515	—	0.075	—	—	—	—
E	0.515	—	0.060	—	—	0.015	—
F	0.515	—	0.060	0.015	—	—	—
G	0.515	—	0.060	—	—	—	0.015

[a] All mixtures contained 2% (w/w) talc, F.U. grade. [b] Bayer Italy, Milan. [c] F.U. VIII Ed. grade. [d] Elcema G 250; Eigenmann-Veronelli, Milan. [e] Polyplasdone XL; GAF Italy, Milan. [f] STA-RX 1500; Eigenmann-Veronelli, Milan. [g] Amberlite IRP 88; C. Erba, Milan. [h] Nymcel ZSB 16; Nyma, Holland.

pressed at five different force levels and checked 24 h after compression for porosity, crushing strength, disintegration time (USP XX), and disintegrating force development using the apparatus previously described (1). The results are the mean of at least six determinations.

RESULTS AND DISCUSSION

The disintegrating force–time curves obtained for different formulations are given in Fig. 1. Some show a sigmoidal pattern (*e.g.*, mixture B), some are simple first-order exponential (*e.g.*, mixture E), and some present a steeper initial slope followed by a flattened "tail" in the final part (*e.g.*, mixture G). The analogy existing between these curves and dissolution curves from tablets suggested linearizing them in the way proposed (8) for dissolution, using the Weibull distribution rearranged into the form:

$$\log [-\ln (1 - F/F_\infty)] = b \log (t - t_0) - \log a \qquad \text{(Eq. 1)}$$

where F is the disintegrating force developed at time t and F_∞ is the maximum disintegrating force.

A plot of $[-\ln (1 - F/F_\infty)]$ *versus* t on log–log paper will give a straight line defined by the slope b, the ordinate intercept a, and the lag time t_0. The slope b characterizes the shape of the curve and is dependent on whether a sigmoidal, a simple first-order exponential, or an initially steeper exponential curve is considered. The parameter a can be replaced by the more informative disintegrating force time τ_d defined by:

$$a = (\tau_d)^b \qquad \text{(Eq. 2)}$$

where τ_d represents the time needed to obtain 63.2% of maximum disintegrating force, taken from the end of lag time t_0.

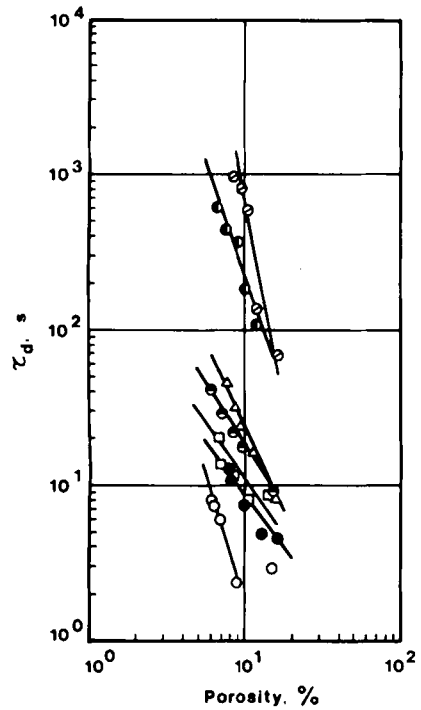

Figure 2—*Log–log plot of τ_d values* versus *porosity. Key: (○) A; (□) B; (⊘) C; (⊖) D; (●) E; (△) F; (◐) G.*

The evaluation of Weibull distribution parameters was performed by means of a program run on a computer[2]. Linear regression analysis, performed on the Weibull distribution rearranged into the form of Eq. 1, allowed the evaluation of b and a parameters. Experimental data were then fitted with a least-squares technique on the original $F(t)$ form of Weibull distribution. Numerical values of t_0, b, and a were estimated from the best fit of the experimental data. Uncertainty of a and b values was <1% ($p = 0.95$).

The results obtained for various mixtures examined are given in Table II. The maximum disintegrating force expresses the ability of the disintegrator, when contacting water, to push apart the bound particles. For the mixtures examined, the higher values of disintegrating force were obtained for E, F, and D, whereas smaller values were measured for C. The maximum disintegrating force increases as compression force increases, until an almost constant value is reached. This confirms that the swelling or repulsion energy of disintegrators can best work when particles are closer to one another (9). For mixture G, the disintegrating force-increasing pattern is not so evident. The disintegrating force development time (expressed by τ_d) always increases as compression force increases, and porosity decreases as shown in Fig. 2. Mixtures G and C have τ_d values markedly higher than the remaining mixtures at the same levels of compression force or porosity.

The comparison between maximum disintegrating force (F_∞) and disintegration time shows that a high value of maximum disintegrating force does not always correspond to a fast disintegration. For example, although mixtures G and A show comparable maximum disintegrating force values (at the highest compression force levels), their disintegration times are markedly different. In this case, τ_d seems to be the decisive factor. In other cases, the opposite situation is seen. The comparison between A (third compression force level) and G (fifth compression force level) mixtures shows that comparable

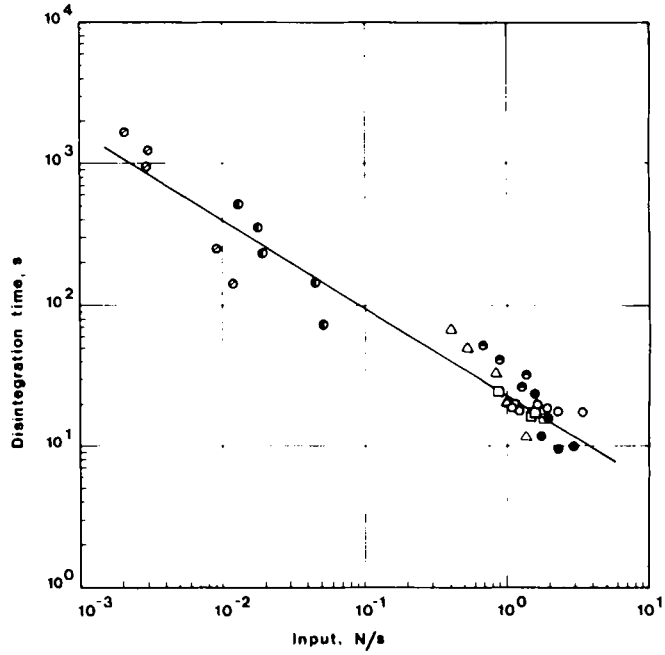

Figure 3—*Log–log plot of disintegration time* versus *input values. The linear regression equation is log* y = −0.6076·*log* x + 1.3925 (*r* = 0.968). *Key: (○) A; (□) B; (⊘) C; (⊖) D; (●) E; (△) F; (◐) G.*

[2] Minc-11 Digital.

Table II—Disintegration Time and Disintegrating Force Parameters of Different Tablets

Mixture	Compression Force, hN	Disintegration Time, s	Disintegrating Force (F_∞), N	τ_d, s	Shape Parameter (b)
A	43	18	14	3	1.3
	79	18	18	2	1.0
	154	19	31	6	1.0
	186	18	34	7	0.7
	280	19	34	8	0.7
B	56	18	26	8	1.3
	93	16	33	8	1.2
	145	17	40	11	1.1
	196	20	42	14	1.0
	251	25	43	20	1.1
C	53	146	4	70	0.6
	72	256	5	140	0.7
	135	964	5	610	1.0
	164	1223	6	840	1.3
	287	1695	5	990	1.2
D	50	20	37	9	1.1
	102	27	51	18	1.2
	135	32	56	21	1.4
	193	41	58	29	1.2
	274	53	52	42	1.5
E	66	9	34	5	0.9
	89	10	42	5	0.9
	130	12	47	8	0.8
	170	16	53	11	1.1
	242	24	50	13	1.1
F	44	12	34	9	1.0
	92	21	44	16	1.0
	144	34	53	24	1.0
	188	49	50	33	0.9
	252	66	48	48	1.1
G	62	72	28	110	0.5
	104	143	32	185	0.7
	127	237	32	380	0.6
	177	359	32	450	0.7
	223	505	27	630	0.8

τ_d values correspond to disintegration time values 50% of the other due to differences in disintegrating force values. The above examples clearly indicate that disintegration time depends on both parameters. As previously indicated (6), the joint consideration of F_∞ and τ_d allows an evaluation of the kinetic aspect of the disintegrating force development, which, as recently outlined (10), seems to be the factor governing the disintegration process. The derivative of the Weibull equation at time $t = t_0 + \tau_d$, termed "input," was calculated and employed for the quantitative evaluation of disintegration kinetics.

The good correlation found between input and disintegration time, as expressed in Fig. 3, indicates that it is the disintegrating force development rate that determines the disintegration of the compact. Input depends on compression force (Fig. 4), and a complete characterization of the compact can

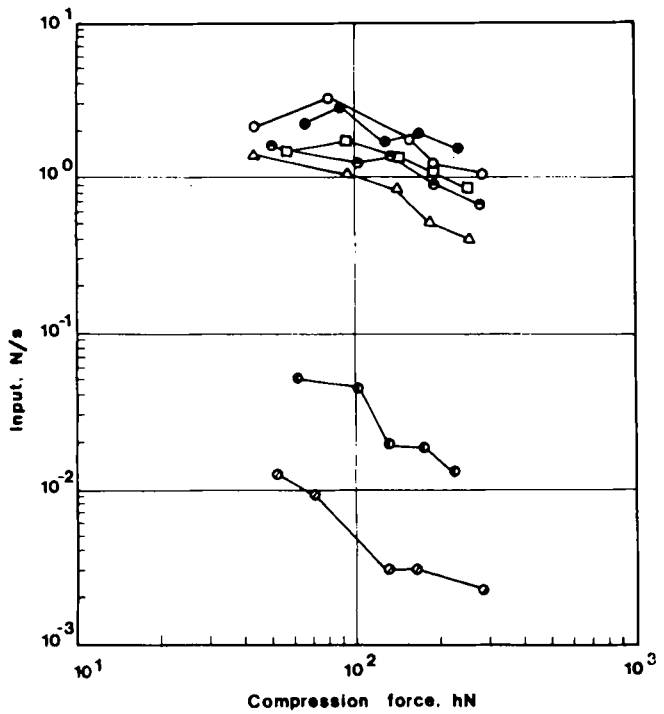

Figure 4—*Log-log plot of input values* versus *compression force. Key: (○) A; (□) B; (⊘) C; (⊖) D; (●) E; (△) F; (◐) G.*

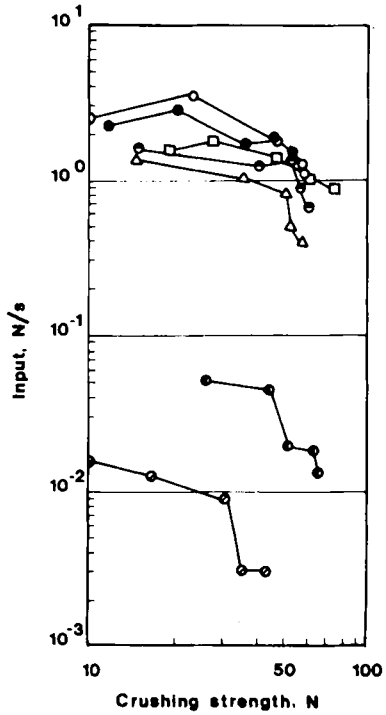

Figure 5—*Log-log plot of input* versus *crushing strength. Key: (○) A; (□) B; (⊘) C; (⊖) D; (●) E; (△) F; (◐) G.*

be obtained by plotting crushing strength *versus* input values (Fig. 5). The graphs allow a visual determination of mixtures for which the crushing strength can be increased without significantly reducing the input value. Mixtures A, E, and B, for which an increase in crushing strength does not correspond to a marked decrease in input values, are easy to handle. For mixtures C and G, the increase of crushing strength corresponds to a concomitant marked reduction of input values, as evidenced by curve slopes. Mixtures F and D show a limiting value of crushing strength above which a little increase causes a large decrease of the input value.

The shape parameter b (Eq. 1) seems to be linked to the disintegration process in the following way:

1. An S-shaped disintegrating force development curve ($b > 1$) indicates the presence of an initial obstacle to water penetration linked to the surface conditions of the tablet.
2. A steeper initial slope in the disintegrating force development curve ($b < 1$) can indicate the presence of an obstacle to water penetration arising inside the tablet.
3. An exponential disintegrating force development curve ($b = 1$) indicates a regular fluid penetration.

The situation relative to $b < 1$ is more critical, since resistence to fluid penetration arising inside the tablet may lead to considerable delay in disintegration, whereas for $b > 1$, the small values of time lag found in the cases examined indicate that the tablet surface conditions do not influence disintegration time too much.

For the mixtures examined, b values depend on compression force and reflect the changes in compact structure. Mixture G shows b values constantly <1, thus enabling the presumption that disintegrator gelatinization enhances the resistance to fluid penetration. Mixtures D, F, B, and E show b values of ~ 1, thus indicating a regular disintegrating force development. Mixtures A and C show the opposite behavior. For the former, b values decrease as compression force increases. This is consistent with the product compression behavior, *i.e.*, starch granules deformed by compression readily absorb water forming a viscosity-increasing gel[3]. For the latter, the poor absorption is likely to be influenced by porosity conditions, thus enhancing the initial hindrance to water penetration. The results obtained indicate that, of the various mixtures examined, A, B, and E show the best overall performances.

CONCLUSIONS

The measurement of disintegrating force provides a deeper insight into the tablet structure obtained by processing a given formula. Whereas a "static" structure evaluation can be obtained through porosity, pore size distribution, *etc.*, disintegrating force measurements allow a "dynamic" evaluation of the structure itself, linked to the disintegration process and consequent active ingredient liberation. The input value, *i.e.*, the disintegrating force development rate at time $t = t_0 + \tau_d$, can be employed as a new parameter for tablet formulation. It is very sensitive to formulation and tablet structure changes and, if correlated with the crushing strength, allows an overall evaluation of the formula examined. The measure of the shape parameter b is a good reflection of the conditions of the compact and completes the structural information on tablet structure. On the basis of the results obtained, it seems justified to propose the measure of the disintegrating force as a very useful and decisive means for formulation evaluation.

[3] C. Fuhrer, personal communication.

REFERENCES

(1) P. Colombo, U. Conte, C. Caramella, A. La Manna, A. M. Guyot-Hermann, and J. Ringard, *Farmaco Ed. Prat.*, **35**, 391 (1980).

(2) M. H. Rubinstein and D. M. Bodey, *J. Pharm. Sci.*, **65**, 1749 (1976).

(3) J. Ringard, A. M. Guyot-Hermann, and H. Robert, *Labo-Pharma-Probl. Tech.*, **265**, 409 (1977).

(4) C. F. Lerk, G. K. Bolhuis, and A. H. de Boer, *J. Pharm. Sci.*, **68**, 205 (1979).

(5) E. Fukuoka, S. Kimura, and M. Yamzaki, *Chem. Pharm. Bull.*, **29**, 205 (1981).

(6) P. Colombo, C. Caramella, U. Conte, A. La Manna, A. M. Guyot-Hermann, and J. Ringard, *Drug Dev. Ind. Pharm.*, **7**, 135 (1981).

(7) C. Caramella, P. Colombo, U. Conte, and A. La Manna, *Farmaco Ed. Prat.*, **33**, 498 (1978).

(8) F. Langenbucher, *J. Pharm. Pharmacol.*, **24**, 979 (1972).

(9) P. M. Hill, *J. Pharm. Sci.*, **65**, 1694 (1976).

(10) E. M. Rudnic, C. T. Rhodes, S. Welch, and P. Bernardo, *Drug. Dev. Ind. Pharm.*, **8**(1), 87 (1982).

ACKNOWLEDGMENTS

This work was partially supported by a grant of Ministero Pubblica Istruzione.

The authors gratefully thank Prof. P. DeLuca, College of Pharmacy, University of Kentucky, for helpful comments and review of the manuscript. In addition, the authors wish to acknowledge Mrs. M. C. Sacchi for assistance in text and figure preparation.

Disposition of Ibuprofen in Nephrectomized Dogs

D. S.-L. AU *x, T. H. KUO *, B. MEDERSKI-SAMORAJ ‡, and C. S. LEE *

Received August 26, 1982, from the **Department of Pharmaceutics, College of Pharmacy, University of Houston*, and ‡*Infectious Disease and Clinical Microbiology Program, University of Texas Medical School, Houston, TX 77030.* Accepted for publication March 17, 1983.

Abstract □ The pharmacokinetics of ibuprofen were studied in four nephrectomized and three normal dogs after administration of 214.3–227.6 mg iv of ibuprofen. Blood samples were collected at various time intervals for up to 10 h and serum concentrations of ibuprofen were assayed by an HPLC method. The elimination of serum ibuprofen followed first-order kinetics, with mean half-lives of 2.51 ± 1.10 and 2.81 ± 0.72 h in normal and nephrectomized dogs, respectively. Mean serum clearance of ibuprofen in nephrectomized dogs, 31.0 ± 5.2 mL/h/kg, was higher than that in normal dogs, 12.2 ± 8.6 mL/h/kg, ($p < 0.02$). The difference may be attributed to the greater volume of distribution for ibuprofen in nephrectomized dogs, 125.2 ± 39.0 (88.8–160.4) mL/kg as compared with 53.4 ± 57.8 (26.0–119.9) mL/kg in the normal group ($p < 0.2$).

Keyphrases □ Ibuprofen—disposition in nephrectomized dogs, pharmacokinetics □ Disposition—ibuprofen, nephrectomized dogs, pharmacokinetics □ Pharmacokinetics—disposition of ibuprofen in nephrectomized dogs

Ibuprofen, (±)-2-(*p*-isobutylphenyl)propionic acid (I), is a nonsteroidal anti-inflammatory agent indicated primarily for rheumatic diseases (1). The pharmacokinetics of I have been studied in normal volunteers. The drug is readily absorbed orally, and plasma peak levels are reached within 2 h of administration. The elimination of I from plasma is first order with apparent half-lives of 1.4–2.5 h (2–6). Similar half-lives are observed in arthritic patients, suggestive of no tissue accumulation of I in rheumatic patients (2). Patients with chronic circulatory insufficiency exhibit pharmacokinetic parameter values comparable with those of healthy subjects (7).

The metabolism of I has been studied in humans and several

© 1984, American Pharmaceutical Association

be obtained by plotting crushing strength *versus* input values (Fig. 5). The graphs allow a visual determination of mixtures for which the crushing strength can be increased without significantly reducing the input value. Mixtures A, E, and B, for which an increase in crushing strength does not correspond to a marked decrease in input values, are easy to handle. For mixtures C and G, the increase of crushing strength corresponds to a concomitant marked reduction of input values, as evidenced by curve slopes. Mixtures F and D show a limiting value of crushing strength above which a little increase causes a large decrease of the input value.

The shape parameter b (Eq. 1) seems to be linked to the disintegration process in the following way:

1. An S-shaped disintegrating force development curve ($b > 1$) indicates the presence of an initial obstacle to water penetration linked to the surface conditions of the tablet.
2. A steeper initial slope in the disintegrating force development curve ($b < 1$) can indicate the presence of an obstacle to water penetration arising inside the tablet.
3. An exponential disintegrating force development curve ($b = 1$) indicates a regular fluid penetration.

The situation relative to $b < 1$ is more critical, since resistence to fluid penetration arising inside the tablet may lead to considerable delay in disintegration, whereas for $b > 1$, the small values of time lag found in the cases examined indicate that the tablet surface conditions do not influence disintegration time too much.

For the mixtures examined, b values depend on compression force and reflect the changes in compact structure. Mixture G shows b values constantly <1, thus enabling the presumption that disintegrator gelatinization enhances the resistance to fluid penetration. Mixtures D, F, B, and E show b values of ~ 1, thus indicating a regular disintegrating force development. Mixtures A and C show the opposite behavior. For the former, b values decrease as compression force increases. This is consistent with the product compression behavior, *i.e.*, starch granules deformed by compression readily absorb water forming a viscosity-increasing gel[3]. For the latter, the poor absorption is likely to be influenced by porosity conditions, thus enhancing the initial hindrance to water penetration. The results obtained indicate that, of the various mixtures examined, A, B, and E show the best overall performances.

CONCLUSIONS

The measurement of disintegrating force provides a deeper insight into the tablet structure obtained by processing a given formula. Whereas a "static" structure evaluation can be obtained through porosity, pore size distribution, *etc.*, disintegrating force measurements allow a "dynamic" evaluation of the structure itself, linked to the disintegration process and consequent active ingredient liberation. The input value, *i.e.*, the disintegrating force development rate at time $t = t_0 + \tau_d$, can be employed as a new parameter for tablet formulation. It is very sensitive to formulation and tablet structure changes and, if correlated with the crushing strength, allows an overall evaluation of the formula examined. The measure of the shape parameter b is a good reflection of the conditions of the compact and completes the structural information on tablet structure. On the basis of the results obtained, it seems justified to propose the measure of the disintegrating force as a very useful and decisive means for formulation evaluation.

[3] C. Fuhrer, personal communication.

REFERENCES

(1) P. Colombo, U. Conte, C. Caramella, A. La Manna, A. M. Guyot-Hermann, and J. Ringard, *Farmaco Ed. Prat.*, **35**, 391 (1980).

(2) M. H. Rubinstein and D. M. Bodey, *J. Pharm. Sci.*, **65**, 1749 (1976).

(3) J. Ringard, A. M. Guyot-Hermann, and H. Robert, *Labo-Pharma-Probl. Tech.*, **265**, 409 (1977).

(4) C. F. Lerk, G. K. Bolhuis, and A. H. de Boer, *J. Pharm. Sci.*, **68**, 205 (1979).

(5) E. Fukuoka, S. Kimura, and M. Yamzaki, *Chem. Pharm. Bull.*, **29**, 205 (1981).

(6) P. Colombo, C. Caramella, U. Conte, A. La Manna, A. M. Guyot-Hermann, and J. Ringard, *Drug Dev. Ind. Pharm.*, **7**, 135 (1981).

(7) C. Caramella, P. Colombo, U. Conte, and A. La Manna, *Farmaco Ed. Prat.*, **33**, 498 (1978).

(8) F. Langenbucher, *J. Pharm. Pharmacol.*, **24**, 979 (1972).

(9) P. M. Hill, *J. Pharm. Sci.*, **65**, 1694 (1976).

(10) E. M. Rudnic, C. T. Rhodes, S. Welch, and P. Bernardo, *Drug. Dev. Ind. Pharm.*, **8**(1), 87 (1982).

ACKNOWLEDGMENTS

This work was partially supported by a grant of Ministero Pubblica Istruzione.

The authors gratefully thank Prof. P. DeLuca, College of Pharmacy, University of Kentucky, for helpful comments and review of the manuscript. In addition, the authors wish to acknowledge Mrs. M. C. Sacchi for assistance in text and figure preparation.

Disposition of Ibuprofen in Nephrectomized Dogs

D. S.-L. AU *x, T. H. KUO *, B. MEDERSKI-SAMORAJ ‡, and C. S. LEE *

Received August 26, 1982, from the **Department of Pharmaceutics, College of Pharmacy, University of Houston*, and ‡*Infectious Disease and Clinical Microbiology Program, University of Texas Medical School, Houston, TX 77030.* Accepted for publication March 17, 1983.

Abstract □ The pharmacokinetics of ibuprofen were studied in four nephrectomized and three normal dogs after administration of 214.3–227.6 mg iv of ibuprofen. Blood samples were collected at various time intervals for up to 10 h and serum concentrations of ibuprofen were assayed by an HPLC method. The elimination of serum ibuprofen followed first-order kinetics, with mean half-lives of 2.51 ± 1.10 and 2.81 ± 0.72 h in normal and nephrectomized dogs, respectively. Mean serum clearance of ibuprofen in nephrectomized dogs, 31.0 ± 5.2 mL/h/kg, was higher than that in normal dogs, 12.2 ± 8.6 mL/h/kg, ($p < 0.02$). The difference may be attributed to the greater volume of distribution for ibuprofen in nephrectomized dogs, 125.2 ± 39.0 (88.8–160.4) mL/kg as compared with 53.4 ± 57.8 (26.0–119.9) mL/kg in the normal group ($p < 0.2$).

Keyphrases □ Ibuprofen—disposition in nephrectomized dogs, pharmacokinetics □ Disposition—ibuprofen, nephrectomized dogs, pharmacokinetics □ Pharmacokinetics—disposition of ibuprofen in nephrectomized dogs

Ibuprofen, (±)-2-(*p*-isobutylphenyl)propionic acid (I), is a nonsteroidal anti-inflammatory agent indicated primarily for rheumatic diseases (1). The pharmacokinetics of I have been studied in normal volunteers. The drug is readily absorbed orally, and plasma peak levels are reached within 2 h of administration. The elimination of I from plasma is first order with apparent half-lives of 1.4–2.5 h (2–6). Similar half-lives are observed in arthritic patients, suggestive of no tissue accumulation of I in rheumatic patients (2). Patients with chronic circulatory insufficiency exhibit pharmacokinetic parameter values comparable with those of healthy subjects (7).

The metabolism of I has been studied in humans and several

© 1984, American Pharmaceutical Association

Table I—Description of Normal and Nephrectomized Dogs

Dog	Sex	Weight, kg	Physiological Status[a]	Dose, mg iv
1	M	20.0	N	223.5
2	M	18.6	N	227.6
3	F	20.5	N	223.0
4	M	16.0	SN	214.3
5	M	16.8	SN	216.0
6	M	20.6	SN	216.0
7	M	17.4	SN	214.3

[a] Key: (N) normal; (SN) surgically nephrectomized.

animal species, including rats, baboons, and dogs (8, 9). Two major metabolites, the hydroxylated and the carboxylated derivatives of I, were identified in the plasma of the rat, baboon, and human, but not in dog plasma (9, 10). Both metabolites were found in the urine of all four species (9). All species, except the baboon, excreted >50% of the single oral dose in the urine. Of particular interest is the observation in dogs that 46% of the ibuprofen dose appeared in the urine as conjugated and unconjugated metabolites, while no metabolites were detected in plasma, indicating a slow formation but rapid excretion of the metabolites (9). In humans, urinary excretion of I was complete within 24 h following a single oral 200-mg dose (11). In dogs, measurements of total radioactivity in urine and feces accounted for 60% of dose eliminated in 24 h, 80–100% in 3–5 d. The ratio of excreted ibuprofen in urine and feces was on the order of 2:1 (10, 11). In addition, biliary excretion in dogs within 3 h of administration accounted for 25% of a single intravenous dose (9, 10). Ibuprofen (I) is highly bound (~99%) to serum albumin in humans and experimental animals (9). Because of the extensive protein binding, I is characterized by a small volume of distribution, 0.12–0.13 L/kg and 0.18 L/kg in humans (12, 13) and in normal dogs (14), respectively. Half-lives of I ranged from 3 to 3.81 h (14, 15), serum clearance was ~0.5 mL/kg/min (14) in normal dogs.

The pharmacokinetics of I in subjects with renal insufficiency has not yet been reported. Brogard *et al.* (16) recently investigated the pharmacokinetics of benoxaprofen, an analogue of I with a normal half-life of 28 h, and reported a prolonged half-life of up to 69 h in patients with end-stage renal failure. Dosage reduction of benoxaprofen in patients with renal impairment was thus recommended. It is not clear whether I is similarly affected in the renal disease state.

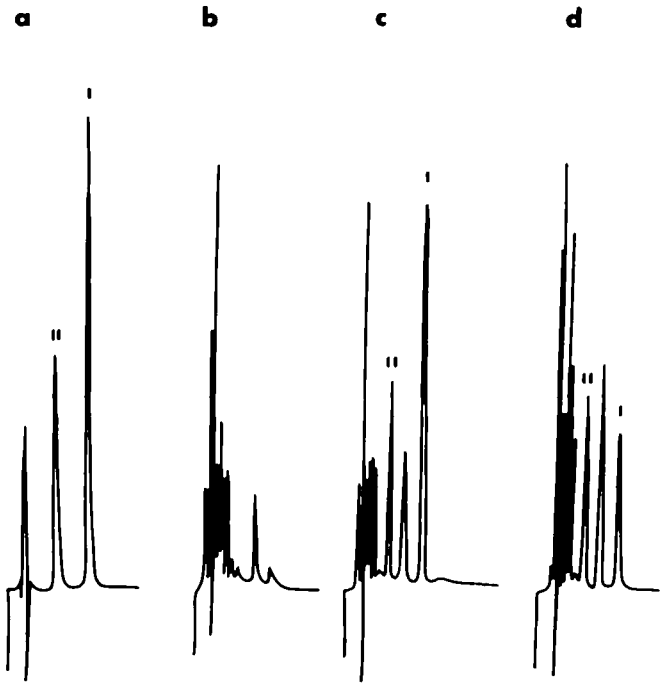

Figure 1 *Typical chromatograms of I and II. Key: (a) standard solution; (b) dog serum blank; (c) spiked sample; (d) dog serum sample.*

Table II—Pharmacokinetic Parameters of I in Normal Dogs Administered a Single Intravenous Dose

Dog	β, h^{-1}	$t_{1/2,\beta}$, h	CL_T, mL/h/kg	Vd_β, mL/kg
1	0.184	3.76	22.1	119.9
2	0.336	2.06	8.7	26.0
3	0.408	1.70	5.9	14.5
Mean	0.309	2.51	12.2	53.4
SD	0.114	1.10	8.6	57.8

Pharmacokinetic information of I in renal failure is of clinical importance, since a majority of patients with rheumatic arthritis are often the elderly who may be renally insufficient. This study was undertaken to investigate the effect of renal failure in pharmacokinetics of I using a nephrectomized dog model.

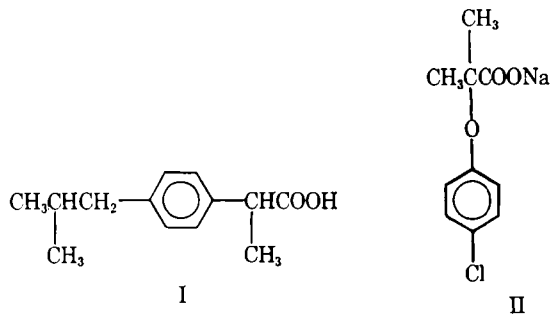

EXPERIMENTAL

Materials—Ibuprofen(I) was supplied as free acid[1]. Sodium clofibrate[2] (II) was used as an internal standard for the assay of I. HPLC-grade methanol[3] and acetonitrile[3] were glass-distilled and filtered before use.

Seven beagle dogs, 6 male and 1 female (weighing 16.0–20.6 kg), were used in the study. Specific dog data are shown in Table I. Four dogs were bilaterally nephrectomized, while three normal dogs served as the control. All dogs were catheterized at the radial and jugular veins to facilitate drug administration and blood collection, respectively.

Drug Administration and Sampling Schedule—Doses of I were administered as 5-mL aliquots of a 50% ethanolic solution in normal saline *via* the catheterized radial vein of the forearm. Blood samples, 3–5 mL each, were drawn from a cannula in the jugular vein at 0 (blank), 30, 45, 60, 90, 120, 180, 240, 300, 360, 420, 480, 540, and 600 min following the intravenous administration. Samples were allowed to clot in the evacuated tubes, and sera were collected and stored at −20°C until assayed.

Assay—Serum samples of appropriate size, to which 2 μg of II was added, were acidified with 400 μL of 1 M HCl followed by extraction with 8 mL of ether. The ether extract was separated after centrifugation and evaporated to dryness under a nitrogen stream. The residue was reconstituted in 200 μL of methanol and subjected to HPLC analysis.

A chromatograph[4] equipped with a 100-μL sample loop[5], a variable-wavelength UV detector[6], and a microparticulate reverse-phase octyl column[7] (250 mm × 4.6 mm i.d.) was used for the HPLC analysis. The system was operated at ambient temperature with acetonitrile–water as the mobile phase (50:50, v/v, pH 2.5 as adjusted with phosphoric acid[8]). The flow rate was

[1] U-18,573, Lot No. R-51316; kindly supplied by The Upjohn Co., Kalamzoo, Mich.
[2] ICI, Great Britain.
[3] Omnisolv solvents; MCB Mfg. Chemicals Inc., Gibbstown, N.J.
[4] Consta Metric II; Laboratory Data Control, Riviera Beach, Fla.
[5] Model SV-7; Glenco Scientific Inc., Houston, Tex.
[6] Spectro Monitor III; Laboratory Data Control, Riviera Beach, Fla.
[7] Spherisorb; Custom LC Inc., Houston, Tex.
[8] ACS reagent; MCB Mfg. Chemicals Inc., Gibbstown, N.J.

Table III—Pharmacokinetic Parameters of I in Nephrectomized Dogs Administered a Single Intravenous Dose

Dog	β, h^{-1}	$t_{1/2,\beta}$, h	CL_T, mL/h/kg	Vd_β, mL/kg
4	0.336	1.89	34.5	94.3
5	0.217	3.20	34.7	160.4
6	0.266	2.61	23.6	88.8
7	0.197	3.52	31.0	157.5
Mean	0.262	2.81	31.0	125.2
SD	0.075	0.72	5.2	39.0

maintained at 2.0 mL/min, and the effluent was measured at 225 nm for absorbance.

Protein Binding Study—Protein binding of I was determined by the equilibrium dialysis method. Serum samples were spiked with known amounts of I to yield concentrations of 5, 10, and 20 μg/mL and incubated at 37°C for 16 h. The spiked samples were dialyzed against isotonic phosphate-saline buffer, consisting of 154 mM NaCl, 0.44 mM KH_2PO_4, and 2.20 mM K_2HPO_4 (pH 7.4) at 37°C for 6 h. After the equilibrium dialysis, the concentrations of I in the serum and the dialysate were measured by the HPLC assay. Dialysate samples were concentrated by lyophilization to raise the concentrations above the detection limit of the assay procedure.

Data Treatment—Serum concentration–time data were fitted to a two-compartment model using the NONLIN program (17). A series of pharmacokinetic parameters were obtained, of which β, the overall elimination rate constant, was further used for area calculation. The area under the concentration–time curve (AUC) was calculated by $AUC_{0\to\infty} = AUC_{0\to t} + C_t/\beta$, where C_t is the last measured serum concentration and $AUC_{0\to t}$ is the area covering the time interval 0 to t, which was calculated by the trapezoidal method. Half-life ($t_{1/2,\beta}$), total clearance (CL_T), and volume of distribution (Vd_β) were subsequently calculated as: $t_{1/2,\beta} = 0.693/\beta$, CL_T = Dose/$AUC_{0\to\infty}$, and $Vd_\beta = CL_T/\beta$. The significance of difference in mean parameter values between normal and nephrectomized groups, including $t_{1/2,\beta}$, CL_T, and Vd_β, were tested by a nonpaired Student's t test.

RESULTS AND DISCUSSION

The HPLC procedures described herein provided adequate sensitivity and good reproducibility for the analysis of I. Figure 1 depicts typical chromatograms, in which I and II exhibited retention times of 7.0 and 4.0 min, respectively. Baseline resolution was achieved without interference of endogenous substances from the blank dog serum. The typical calibration curve, constructed at a concentration range of 0.5–10 μg/mL, yielded a linearity of $y = 0.311x - 0.045$, $r^2 = 0.999$. The mean coefficient of variation was 3.7 ± 1.4% (n = 5), indicating a satisfactory reproducibility of the assay procedure.

Table IV—Unbound Fractions of I in the Sera of Dogs and Humans

Conc. of I, μg/mL	Percent Unbound to Serum Protein			
	Dog		Human	
	Nephrectomized[a]	Normal[b]	Uremic[c]	Normal[c]
5	7.2	0.9	11.0 ± 2.8	4.5 ± 0.3
10	7.5	1.5	10.9 ± 2.4	5.5 ± 0.1
20	5.6	1.4	10.0 ± 2.3	4.6 ± 1.3
Mean	6.8	1.3	10.6	4.9
SD	1.0	0.3	4.4	1.3

[a] Dog 7. [b] Dog 3. [c] n = 3.

Serum concentration profiles for I are shown in Figs. 2 and 3 for normal and nephrectomized dogs, respectively. First-order elimination of I was apparent in all dogs following the single-dose intravenous drug administration. The pharmacokinetic parameters of I in normal and nephrectomized dogs are reported in Tables II and III, respectively. The mean half-life was 2.51 ± 1.10 h for the normal group and 2.81 ± 0.72 h for the nephrectomized group; the difference was not significant ($p > 0.6$). The total clearance of I in nephrectomized dogs ranged from 23.6 to 34.5 mL/h/kg (mean, 31.0 ± 5.2 mL/h/kg), and that in normal dogs averaged 12.2 ± 8.6 mL/h/kg (range, 5.9–22.1 mL/h/kg). Nephrectomized dogs exhibited significantly higher total clearance than normal dogs ($p < 0.02$). The volume of distribution in nephrectomized dogs, 125.2 ± 39.0 mL/kg, was slightly greater than that in normal dogs, 53.4 ± 57.8 mL/kg; the difference was marginally significant ($p < 0.2$). Wide within-group variations were observed for total clearance and volume of distribution in dogs, indicating intersubject variability in the disposition of I.

Half-lives of I in normal dogs, 2.51 ± 1.10 h, as obtained in this study, were comparable with those reported by Kearns and Wilson, 3.81 h (14), and by Fujise, 3 h (15). The total clearance (12.2 ± 8.6 mL/h/kg) and the volume of distribution (53.4 ± 57.8 mL/kg), however, were smaller than the corresponding literature values, 30.1 mL/h/kg and 180 mL/kg (14). It should be

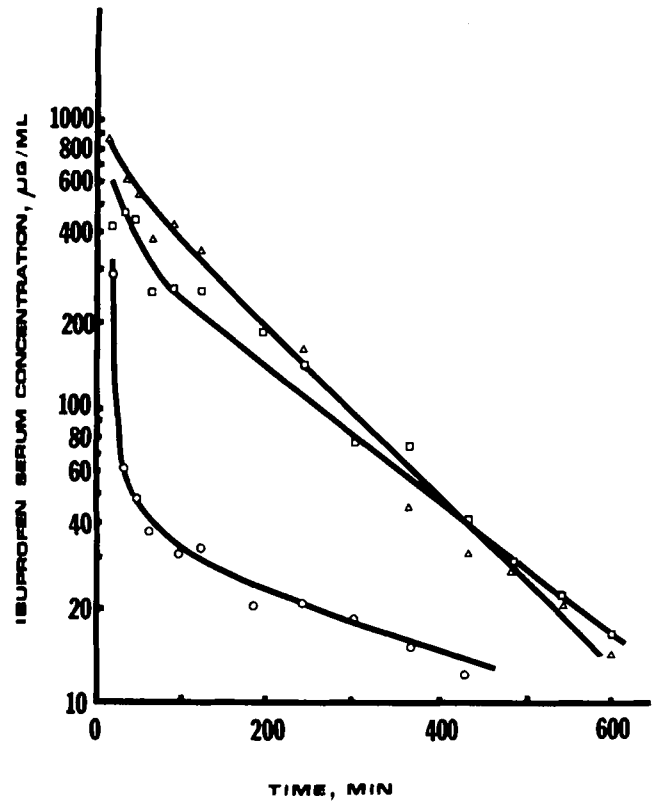

Figure 2—*Time profile of serum concentrations of I in normal dogs. Key: (○) dog 1; (□) dog 2; (△) dog 3.*

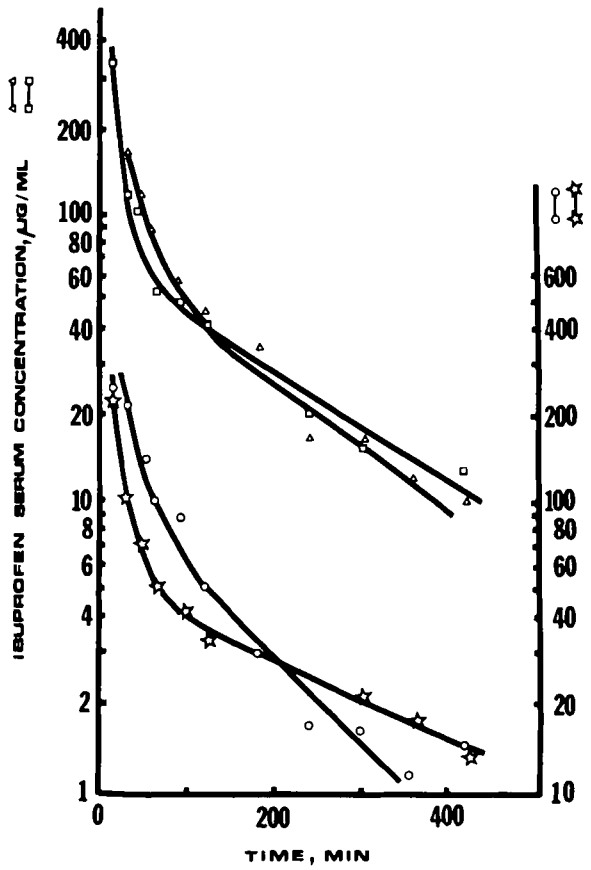

Figure 3—*Time profile of serum concentrations of I in nephrectomized dogs. Key: (○) dog 4; (△) dog 5; (□) dog 6; (☆) dog 7.*

noted that the parameter values reported by Kearns and Wilson were derived from a one-dog study.

No literature information regarding the pharmacokinetics of I in nephrectomized dogs is available. In this study, serum concentrations of I in nephrectomized dogs were lower than the corresponding concentrations in the normal ones. This observation suggests a greater volume of distribution for the nephrectomized dogs, which could be attributable to a reduced protein binding of I in the nephrectomized state. Reduced binding of highly bound organic acid to uremic plasma protein has been demonstrated for phenytoin, resulting in an increased volume of distribution (18). A similar mechanism may be suggested for I, which is also an organic acid with extensive protein binding (9). The reduction in binding of I to serum protein on nephrectomy is shown in Table IV for two dogs, one normal and the other nephrectomized. The protein binding was independent of concentration in the range of 5–20 μg/mL. The percentage of I unbound to serum protein in the nephrectomized dog, 6.8 ± 1.0%, was significantly greater than that in the normal dog, 1.3 ± 0.3% ($p < 0.001$). In a separate binding study of I in uremic patients (19), the fraction of free I in uremic plasma was also found to be higher than that in normal plasma (Table IV). The dogs used for this investigation were nephrectomized 3 d prior to the study and presumably were approaching the chronic uremic state.

Nephrectomy did not significantly alter the half-life of I in dogs; however, increases in both the volume of distribution and total clearance were apparent. Since <8% of the dose is excreted intact in the urine (9, 20), the lack of effect of nephrectomy on the half-life of I was anticipated. Nephrectomy induced increases in the total clearance and volume of distribution. The increased volume of distribution could result from a decreased protein binding of I in the nephrectomized state (Table IV), leaving more free drug available for distribution into the body tissue. The increase in total clearance is secondary to the increase in volume of distribution.

The effects of renal failure on the disposition of I in dogs and those of benoxaprofen in humans (16) are disparate. In dogs, the half-life of I remained unchanged, whereas the volume of distribution and total clearance increased. In humans the half-life of benoxaprofen was significantly prolonged with no distinct changes in other pharmacokinetic parameters. The disparity cautions against the extrapolation of conclusions from one drug analogue to another and from animal model to human subject.

REFERENCES

(1) T. G. Kantor, *Ann. Intern. Med.*, **91**, 877 (1979).

(2) P. S. Collier, P. F. D'Arcy, D. W. G. Harron, and N. Morrow, *Br. J. Clin. Pharmacol.*, **5**, 528 (1978).

(3) D. G. Kaiser and R. S. Martin, *J. Pharm. Sci.*, **67**, 627 (1978).

(4) D. G. Kaiser and G. J. Vengiessen, *J. Pharm. Sci.*, **63**, 219 (1974).

(5) K. A. DeSante and R. E. Monovich, "Technical Report, Clinical Service No. 063," The Upjohn Co., Kalamazoo, Mich., 1979.

(6) K. S. Alberts and S. W. Brown, "Technical Report, Clinical Service No. 034," The Upjohn Co., Kalamazoo, Mich., 1980.

(7) W. Tkaczewski, H. Adamska-Dyniewska, H. Gelo, A. Gebauer, and B. Gajemska, *Pol. Tyg. Lek.*, **35**, 627 (1980).

(8) S. S. Adam, E. E. Cliff, B. Lesel, and J. S. Nicholson, *J. Pharm. Sci.*, **56**, 1686 (1967).

(9) R. F. N. Mills, S. S. Adam, E. E. Cliff, W. Dickinson, and J. S. Nicholson, *Xenobiotica*, **3**, 589 (1973).

(10) S. S. Adam, R. G. Bough, E. E. Cliff, B. Lesel, and R. F. N. Mills, *Toxicol. Appl. Pharmacol.*, **15**, 310 (1969).

(11) E. F. Davies and G. S. Avey, *Drugs*, **4**, 416 (1971).

(12) K. A. DeSante and R. E. Monovich, "Technical Report, Clinical Service No. 033," The Upjohn Co., Kalamazoo, Mich., 1975.

(13) E. Corzi and R. J. Townsend, "Technical Report, Medical Bioavailability Unit," The Upjohn Co., Kalamazoo, Mich., 1981.

(14) G. L. Kearns and J. T. Wilson, *J. Chromatogr.*, **226**, 183 (1981).

(15) H. Fujise, *Jpn. J. Vet. Sci.*, **39**, 671 (1977).

(16) J. M. Brogard, F. Comte, M. Madon, B. Audhuy, and M. O. Spach, *Curr. Ther. Res.*, **30**, 161 (1981).

(17) C. M. Metzler, G. L. Elfring, and A. J. McEwen, Biometrics., **30**, 562 (1974).

(18) I. Odar-Cederlof and O. Borga, *Eur J. Clin. Pharmacol.*, **7**, 31 (1974).

(19) H. O. Senekjian, C. S. Lee, T. H. Kuo, D. S-L. Au, and R. Krothapalli, *Eur. J. Rheumatol. Inflamm.*, **6**, 155 (1983).

(20) C. J. W. Brooks and M. T. Gilbert, *J. Chromatogr.*, **99**, 541 (1974).

ACKOWLEDGMENTS

Presented in part at the 129th APhA Annual Meeting, Las Vegas, Nevada, April 1982. The authors gratefully acknowledge the assistance of the Word Processing Center of the University of Houston in preparing the manuscript.

COMMUNICATIONS

Dynamic Method for Estimating the Extent of Plasma Protein Binding in a Dialysis Experiment

Keyphrases □ Plasma protein binding—dialysis, experimental time □ Dialysis—plasma protein binding, experimental time

To the Editor:

In a protein binding experiment one has a choice between two initial conditions: to place the drug in the plasma or in the buffer. Recent analyses (1, 2) of a linear system with a constant extent of plasma protein have revealed that it takes less time for the buffer drug concentration to reach a given limit of the equilibrium value when the drug is initially placed in the plasma rather than the buffer. This conclusion is also valid for a nonlinear system in which the number of binding sites is finite (3).

Despite the advantage of placing the drug initially in the plasma, a long experimental time may still be needed if permeation of the drug through the dialysis membrane is slow. This may cause some difficulties particularly in maintaining a constant volume in both compartments. In this report, a simple strategy is proposed to shorten the experimental time. The strategy requires two experiments: one with the drug initially placed in the buffer and the other with the drug initially placed in the plasma. The equilibrium value is derived from buffer drug concentrations measured at any given time during these two experiments. Experimental error notwithstanding, the estimate is exact provided the extent of protein binding is constant over the concentration range studied. The errors in applying the proposed method to a nonlinear situation are also considered. This is demonstrated by applying the method to a set of data simulated according to a model with saturable protein binding.

In the following discussion, we consider a dialysis experiment using a membrane with a mass transfer coefficient, M. The mass transfer coefficient is the product of the membrane permeability and the surface area. It has a dimension of volume per unit time. The volumes of the buffer in compartment 1 and the plasma in compartment 2 are V_1 and V_2, respectively. It is assumed that there is no material loss from the solution system and that there are no volume changes in either com-

0022-3549/84/0500-0708$01.00/0

© 1984, American Pharmaceutical Association

noted that the parameter values reported by Kearns and Wilson were derived from a one-dog study.

No literature information regarding the pharmacokinetics of I in nephrectomized dogs is available. In this study, serum concentrations of I in nephrectomized dogs were lower than the corresponding concentrations in the normal ones. This observation suggests a greater volume of distribution for the nephrectomized dogs, which could be attributable to a reduced protein binding of I in the nephrectomized state. Reduced binding of highly bound organic acid to uremic plasma protein has been demonstrated for phenytoin, resulting in an increased volume of distribution (18). A similar mechanism may be suggested for I, which is also an organic acid with extensive protein binding (9). The reduction in binding of I to serum protein on nephrectomy is shown in Table IV for two dogs, one normal and the other nephrectomized. The protein binding was independent of concentration in the range of 5–20 μg/mL. The percentage of I unbound to serum protein in the nephrectomized dog, 6.8 ± 1.0%, was significantly greater than that in the normal dog, 1.3 ± 0.3% ($p < 0.001$). In a separate binding study of I in uremic patients (19), the fraction of free I in uremic plasma was also found to be higher than that in normal plasma (Table IV). The dogs used for this investigation were nephrectomized 3 d prior to the study and presumably were approaching the chronic uremic state.

Nephrectomy did not significantly alter the half-life of I in dogs; however, increases in both the volume of distribution and total clearance were apparent. Since <8% of the dose is excreted intact in the urine (9, 20), the lack of effect of nephrectomy on the half-life of I was anticipated. Nephrectomy induced increases in the total clearance and volume of distribution. The increased volume of distribution could result from a decreased protein binding of I in the nephrectomized state (Table IV), leaving more free drug available for distribution into the body tissue. The increase in total clearance is secondary to the increase in volume of distribution.

The effects of renal failure on the disposition of I in dogs and those of benoxaprofen in humans (16) are disparate. In dogs, the half-life of I remained unchanged, whereas the volume of distribution and total clearance increased. In humans the half-life of benoxaprofen was significantly prolonged with no distinct changes in other pharmacokinetic parameters. The disparity cautions against the extrapolation of conclusions from one drug analogue to another and from animal model to human subject.

REFERENCES

(1) T. G. Kantor, *Ann. Intern. Med.*, **91**, 877 (1979).

(2) P. S. Collier, P. F. D'Arcy, D. W. G. Harron, and N. Morrow, *Br. J. Clin. Pharmacol.*, **5**, 528 (1978).

(3) D. G. Kaiser and R. S. Martin, *J. Pharm. Sci.*, **67**, 627 (1978).

(4) D. G. Kaiser and G. J. Vengiessen, *J. Pharm. Sci.*, **63**, 219 (1974).

(5) K. A. DeSante and R. E. Monovich, "Technical Report, Clinical Service No. 063," The Upjohn Co., Kalamazoo, Mich., 1979.

(6) K. S. Alberts and S. W. Brown, "Technical Report, Clinical Service No. 034," The Upjohn Co., Kalamazoo, Mich., 1980.

(7) W. Tkaczewski, H. Adamska-Dyniewska, H. Gelo, A. Gebauer, and B. Gajemska, *Pol. Tyg. Lek.*, **35**, 627 (1980).

(8) S. S. Adam, E. E. Cliff, B. Lesel, and J. S. Nicholson, *J. Pharm. Sci.*, **56**, 1686 (1967).

(9) R. F. N. Mills, S. S. Adam, E. E. Cliff, W. Dickinson, and J. S. Nicholson, *Xenobiotica*, **3**, 589 (1973).

(10) S. S. Adam, R. G. Bough, E. E. Cliff, B. Lesel, and R. F. N. Mills, *Toxicol. Appl. Pharmacol.*, **15**, 310 (1969).

(11) E. F. Davies and G. S. Avey, *Drugs*, **4**, 416 (1971).

(12) K. A. DeSante and R. E. Monovich, "Technical Report, Clinical Service No. 033," The Upjohn Co., Kalamazoo, Mich., 1975.

(13) E. Corzi and R. J. Townsend, "Technical Report, Medical Bioavailability Unit," The Upjohn Co., Kalamazoo, Mich., 1981.

(14) G. L. Kearns and J. T. Wilson, *J. Chromatogr.*, **226**, 183 (1981).

(15) H. Fujise, *Jpn. J. Vet. Sci.*, **39**, 671 (1977).

(16) J. M. Brogard, F. Comte, M. Madon, B. Audhuy, and M. O. Spach, *Curr. Ther. Res.*, **30**, 161 (1981).

(17) C. M. Metzler, G. L. Elfring, and A. J. McEwen, Biometrics., **30**, 562 (1974).

(18) I. Odar-Cederlof and O. Borga, *Eur J. Clin. Pharmacol.*, **7**, 31 (1974).

(19) H. O. Senekjian, C. S. Lee, T. H. Kuo, D. S-L. Au, and R. Krothapalli, *Eur. J. Rheumatol. Inflamm.*, **6**, 155 (1983).

(20) C. J. W. Brooks and M. T. Gilbert, *J. Chromatogr.*, **99**, 541 (1974).

ACKOWLEDGMENTS

Presented in part at the 129th APhA Annual Meeting, Las Vegas, Nevada, April 1982. The authors gratefully acknowledge the assistance of the Word Processing Center of the University of Houston in preparing the manuscript.

COMMUNICATIONS

Dynamic Method for Estimating the Extent of Plasma Protein Binding in a Dialysis Experiment

Keyphrases □ Plasma protein binding—dialysis, experimental time □ Dialysis—plasma protein binding, experimental time

To the Editor:

In a protein binding experiment one has a choice between two initial conditions: to place the drug in the plasma or in the buffer. Recent analyses (1, 2) of a linear system with a constant extent of plasma protein have revealed that it takes less time for the buffer drug concentration to reach a given limit of the equilibrium value when the drug is initially placed in the plasma rather than the buffer. This conclusion is also valid for a nonlinear system in which the number of binding sites is finite (3).

Despite the advantage of placing the drug initially in the plasma, a long experimental time may still be needed if permeation of the drug through the dialysis membrane is slow. This may cause some difficulties particularly in maintaining a constant volume in both compartments. In this report, a simple strategy is proposed to shorten the experimental time. The strategy requires two experiments: one with the drug initially placed in the buffer and the other with the drug initially placed in the plasma. The equilibrium value is derived from buffer drug concentrations measured at any given time during these two experiments. Experimental error notwithstanding, the estimate is exact provided the extent of protein binding is constant over the concentration range studied. The errors in applying the proposed method to a nonlinear situation are also considered. This is demonstrated by applying the method to a set of data simulated according to a model with saturable protein binding.

In the following discussion, we consider a dialysis experiment using a membrane with a mass transfer coefficient, M. The mass transfer coefficient is the product of the membrane permeability and the surface area. It has a dimension of volume per unit time. The volumes of the buffer in compartment 1 and the plasma in compartment 2 are V_1 and V_2, respectively. It is assumed that there is no material loss from the solution system and that there are no volume changes in either com-

0022-3549/84/0500-0708$01.00/0

© 1984, American Pharmaceutical Association

partment. Furthermore, it is assumed that the free and bound drug are in equilibrium at all times and the binding is linear such that the free fraction of the drug in the plasma is a constant, α.

The proposed approach consists of two experiments: (*a*) a given amount of drug, A_0, is initially added to the plasma compartment; (*b*) the same amount is added to the buffer compartment. When the drug is initially added to the plasma, the total plasma drug concentration is A_0/V_2, and the buffer drug concentration is zero at time zero. The buffer drug concentration at any time, t, is given as:

$$C_P(t) = C_E[1 - e^{-(1/V_1+\alpha/V_2)Mt}] \qquad \text{(Eq. 1)}$$

where subscript P is used to indicate that drug is initially added to the plasma. C_E is the buffer concentration at equilibrium and is given as:

$$C_E = \frac{A_0}{V_1 + V_2/\alpha} \qquad \text{(Eq. 2)}$$

When drug is initially added to the buffer, its concentration is $C_0 = A_0/V_1$ and the plasma concentration is zero at $t = 0$. The drug concentration in the buffer at any time t is given as:

$$C_B(t) = C_E + (C_0 - C_E)e^{-(1/V_1+\alpha/V_2)Mt} \qquad \text{(Eq. 3)}$$

where subscript B is used to indicate that all the drug is initially placed in the buffer and C_E is defined by Eq. 2.

If both C_B and C_P are measured at time t (>0), one can calculate the expected equilibrium concentration by the following expression:

$$C_E = \frac{C_0 \cdot C_P(t)}{C_0 + C_P(t) - C_B(t)} \qquad \text{(Eq. 4)}$$

Equation 4 is derived by simply combining Eqs. 1 and 3.

When the amounts of drug used for these two experiments are not identical, Eq. 4 can still be used with proper correction, because of the linearity of the system. For example, if the initial amount placed in the plasma is A'_0 instead of A_0, and the measured buffer concentration at time t is $C'_P(t)$, the corresponding buffer concentration $C_P(t)$ for an initial amount A_0 in the plasma is:

$$C_P(t) = C'_P(t) \cdot A_0/A'_0 \qquad \text{(Eq. 5)}$$

The adjusted concentration $C_P(t)$ can then be used in Eq. 4 to obtain the equilibrium concentration. Thus, Eq. 4 is a useful expression for calculating the equilibrium concentration in protein binding experiments when the free fraction remains constant over the drug concentration range studied. The basic assumptions of mass conservation and no volume shift within the time frame of the experiment should be independently verified before the application of this expression.

In the following discussion, we will consider the application of this method to situations of nonlinear binding. As an example, we consider a dialysis experiment with unit volume of plasma and buffer. The mass transfer coefficient of the dialysis membrane is 1 volume unit/unit time. There is protein in compartment 2 only. The amount of binding sites, B, in compartment 2 is 100. The dissociation constant, K, is 0.01. The differential equations governing this system are given below:

$$V_1 \frac{dC_1}{dt} = -M(C_1 - C_2) \qquad \text{(Eq. 6)}$$

$$V_2\left[1 + \frac{B \cdot K/V_2}{(K + C_2)^2}\right]\frac{dC_2}{dt} = M(C_1 - C_2) \qquad \text{(Eq. 7)}$$

where C_1 and C_2 are free drug concentrations in compartments 1 and 2, respectively. These equations are numerically solved (4) to generate C_P and C_B at $t = 0.693$ and 1.386 for different initial concentrations. The equilibrium value is then estimated from C_P and C_B using Eq. 4. The percent error of this estimate is defined as the absolute value of the difference between the estimation by Eq. 4 and the theoretical value divided by the theoretical value and multiplied by 100. The theoretical equilibrium concentration for a given initial amount of drug A_0 is:

$$C_E = \frac{-[(V_1 + V_2)K + B - A_0] + \{[(V_1 + V_2)K + B - A_0]^2 + 4A_0K(V_1 + V_2)\}^{1/2}}{2(V_1 + V_2)} \qquad \text{(Eq. 8)}$$

The error is graphically presented as a function of initial amount in Fig. 1. The errors are very small when the initial amount is small. The error starts to increase precipitously when the initial amount exceeds 90. The error peaks between 100 and 110 and eventually drops back to zero when the initial amount becomes very large. The data also indicate a significant decrease in error as the experiment is prolonged.

In addition to the errors in the equilibrium concentrations obtained using Eq. 4, the errors obtained by assuming that the buffer concentrations $C_P(t)$ (drug initially added to plasma) are estimates of the equilibrium concentrations are also presented in Fig. 1. It can be seen that a better estimate of C_E is obtained by $C_P(t)$ alone rather than by application of Eq. 4 in a region (initial amount 100–140) where nonlinear kinetics is expected to prevail. The example serves to point the dangers of the indiscriminate use of Eq. 4 in the nonlinear region.

The errors which result at both low and high initial amounts (relative to $B = 100$) can be appreciated by reference to Eq. 1. Since α, the free fraction in plasma, will vary from $\sim K/B$

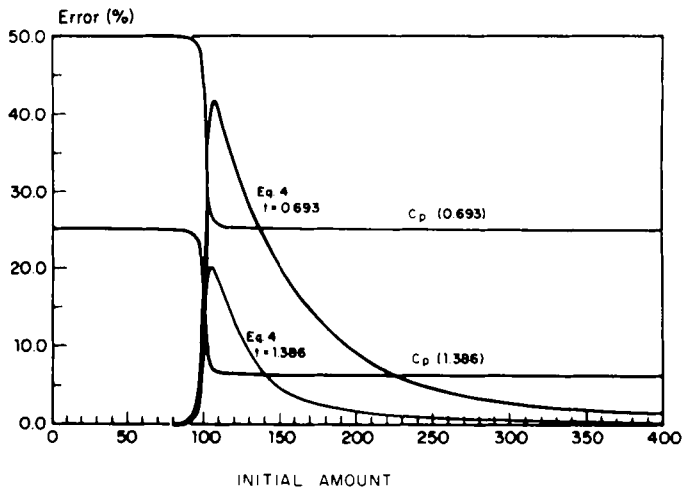

Figure 1—*Errors of estimating the equilibrium value by C_P and Eq. 4 at indicated sampling time plotted as a function of the initial amounts.*

($K \ll B$) at low initial amounts to 1 at high initial amounts, the exponent in Eq. 1 (the reciprocal of the time constant) will vary from M/V to $M/2V$ in those cases where $V_1 = V_2$. For the example considered, where the volumes are unity, the respective time constants are 1 and 0.05, and the respective half-lives are 0.693 and 0.693/2. At low initial amounts, C_P is ~0.5 C_E and 0.75 C_E at the times 0.693 and 0.693 × 2, respectively. The corresponding errors as previously defined would be 50 and 25%. At high initial amounts, C_P is ~0.75 C_E and 0.9375 C_E ($1 - 0.5^4$) C_E at the times 0.693 and 0.693 × 2, respectively. The corresponding errors are 25 and 6.25%.

A criterion for deciding whether Eq. 4 is applicable is easily established by using the equation with a few concentrations paired in time from the two experiments. Since the equilibrium concentration is time independent, the values calculated by concentrations obtained at different times should be in agreement within experimental error. Having established linearity, the free fraction α can be evaluated using Eq. 2.

Nonlinear kinetics should be suspected when a lack of consistency in the estimated equilibrium concentrations is manifested. In principle, the estimated equilibrium values calculated using Eq. 4 converge to the true equilibrium value when evaluated with concentrations obtained at later times (note how relative error changes as function of time in the nonlinear region in Fig. 1). Under such circumstances, Eq. 4 should not be employed.

(1) S. Øie and T. W. Guentert, *J. Pharm. Sci.*, **71**, 127 (1982).
(2) P. J. McNamara and J. B. Bogardus, *J. Pharm. Sci.*, **71**, 1066 (1982).
(3) W. F. Bayne and S. S. Hwang, unpublished results.
(4) IMSL Library, Reference Manual, Subroutine DGEAR, 9th ed., June 1982.

S. S. Hwang[x]
W. F. Bayne
Merck Sharp & Dohme Research Laboratories
West Point, PA 19486

Received November 21, 1983.
Accepted for publication March 1, 1984.

Influence of Protein Binding on the Accumulation and Depletion of Drug from the Skin

Keyphrases □ Protein binding--accumulation and depletion of drug from skin

To the Editor:

Recently the drug scopolamine has been shown to exhibit a nonlinear sorption isotherm with skin (1). The binding was deduced to be associated with the proteinaceous phase since the sorption isotherm was not significantly changed by removal of lipids (1). For drugs that bind in a saturable fashion to skin, the binding can have dramatic effects on the transport process as manifested by an increase in the diffusional lag time with a decrease in the upstream concentration (2). To elucidate the effect of reversible binding, describable by the law of mass action, on the accumulation and depletion of drug from the skin, a simple model will be considered. A fixed volume of skin will be considered to be well-stirred such that within the skin there are no gradients of free drug normal to the surface. The clearance per unit surface area of free drug from this volume is equivalent to the permeability of the drug through the skin. Sink conditions are assumed to exist, and the product of the free concentration and clearance represents the mass rate input into the body. Analysis of the simple model rather than the transport model characterized by a nonlinear diffusion equation suffices to bring forth the influence of the saturable, reversible binding on the accumulation and depletion of drug in the skin.

The dynamics of the accumulation and depletion of drug will individually be investigated as a function of the steady-state concentration in the skin. The dynamics will then be compared between the two modes at given steady-state concentrations. During the accumulation mode, steady-state concentrations will be envisioned to be established by constant fluxes applied to the skin. Upon removal of the input, the steady-state concentrations become the initial concentrations for the depletion mode. The use of the nonlinear binding to achieved prolonged delivery to the body in the depletion mode and methods to shorten accumulation rates relative to depletion rates are then discussed.

The nonlinear system will exhibit linear behavior when the binding isotherm is in the linear region or the fraction of bound drug becomes very small. Thus, a linear system serves as an extrapolative extreme for the nonlinear system. In the linear system the accumulation of drug within the skin is given by the following equation:

$$C = C_{ss}(1 - e^{-k_{el}t}) \qquad \text{(Eq. 1)}$$

$$C_{ss} = \frac{J \cdot A}{CL}$$

where C is the concentration in the skin during accumulation, C_{ss} is the steady-state concentration, J is the flux applied to the skin, A is the area to which the flux is applied, k_{el} is the elimination rate constant from the skin, CL is the clearance from the skin, and t is time. The depletion of drug from the skin once steady state has been achieved and the input removed is given by:

$$C = C_{ss}e^{-k_{el}t} \qquad \text{(Eq. 2)}$$

where C is the concentration during depletion. In Eq. 2 t is relative to the time depletion commences. The accumulation and depletion curves are symmetrical around $C = 0.5\ C_{ss}$. The symmetry of the curves is maintained regardless of the magnitude of the elimination rate constant. The time to reach 50% of the steady-state concentration in the accumulation mode and the time to fall to 50% of the steady-state concentration in the depletion mode are equal. The equality becomes apparent when the equations are rearranged to express time explicitly as a function of the ratio of the concentration at time t to the steady-state concentration. Equations 3 and 4 correspond to Eqs. 1 and 2, respectively.

$$t = (1/k_{el}) \ln \frac{1}{1 - C/C_{ss}} \qquad \text{(Eq. 3)}$$

and

$$t = (1/k_{el}) \ln \frac{C_{ss}}{C} \qquad \text{(Eq. 4)}$$

Thus, from either Eq. 3 or 4, the time at which $C/C_{ss} = 0.5$ (hereafter called t_{50}), is $(1/k_{el}) \ln 2$.

0022-3549/84/0500-0710$01.00/0
© 1984, American Pharmaceutical Association

($K \ll B$) at low initial amounts to 1 at high initial amounts, the exponent in Eq. 1 (the reciprocal of the time constant) will vary from M/V to $M/2V$ in those cases where $V_1 = V_2$. For the example considered, where the volumes are unity, the respective time constants are 1 and 0.05, and the respective half-lives are 0.693 and 0.693/2. At low initial amounts, C_P is ~0.5 C_E and 0.75 C_E at the times 0.693 and 0.693 × 2, respectively. The corresponding errors as previously defined would be 50 and 25%. At high initial amounts, C_P is ~0.75 C_E and 0.9375 C_E ($1 - 0.5^4$) C_E at the times 0.693 and 0.693 × 2, respectively. The corresponding errors are 25 and 6.25%.

A criterion for deciding whether Eq. 4 is applicable is easily established by using the equation with a few concentrations paired in time from the two experiments. Since the equilibrium concentration is time independent, the values calculated by concentrations obtained at different times should be in agreement within experimental error. Having established linearity, the free fraction α can be evaluated using Eq. 2.

Nonlinear kinetics should be suspected when a lack of consistency in the estimated equilibrium concentrations is manifested. In principle, the estimated equilibrium values calculated using Eq. 4 converge to the true equilibrium value when evaluated with concentrations obtained at later times (note how relative error changes as function of time in the nonlinear region in Fig. 1). Under such circumstances, Eq. 4 should not be employed.

(1) S. Øie and T. W. Guentert, *J. Pharm. Sci.*, **71**, 127 (1982).
(2) P. J. McNamara and J. B. Bogardus, *J. Pharm. Sci.*, **71**, 1066 (1982).
(3) W. F. Bayne and S. S. Hwang, unpublished results.
(4) IMSL Library, Reference Manual, Subroutine DGEAR, 9th ed., June 1982.

S. S. Hwang[x]
W. F. Bayne
Merck Sharp & Dohme Research Laboratories
West Point, PA 19486

Received November 21, 1983.
Accepted for publication March 1, 1984.

Influence of Protein Binding on the Accumulation and Depletion of Drug from the Skin

Keyphrases □ Protein binding--accumulation and depletion of drug from skin

To the Editor:

Recently the drug scopolamine has been shown to exhibit a nonlinear sorption isotherm with skin (1). The binding was deduced to be associated with the proteinaceous phase since the sorption isotherm was not significantly changed by removal of lipids (1). For drugs that bind in a saturable fashion to skin, the binding can have dramatic effects on the transport process as manifested by an increase in the diffusional lag time with a decrease in the upstream concentration (2). To elucidate the effect of reversible binding, describable by the law of mass action, on the accumulation and depletion of drug from the skin, a simple model will be considered. A fixed volume of skin will be considered to be well-stirred such that within the skin there are no gradients of free drug normal to the surface. The clearance per unit surface area of free drug from this volume is equivalent to the permeability of the drug through the skin. Sink conditions are assumed to exist, and the product of the free concentration and clearance represents the mass rate input into the body. Analysis of the simple model rather than the transport model characterized by a nonlinear diffusion equation suffices to bring forth the influence of the saturable, reversible binding on the accumulation and depletion of drug in the skin.

The dynamics of the accumulation and depletion of drug will individually be investigated as a function of the steady-state concentration in the skin. The dynamics will then be compared between the two modes at given steady-state concentrations. During the accumulation mode, steady-state concentrations will be envisioned to be established by constant fluxes applied to the skin. Upon removal of the input, the steady-state concentrations become the initial concentrations for the depletion mode. The use of the nonlinear binding to achieved prolonged delivery to the body in the depletion mode and methods to shorten accumulation rates relative to depletion rates are then discussed.

The nonlinear system will exhibit linear behavior when the binding isotherm is in the linear region or the fraction of bound drug becomes very small. Thus, a linear system serves as an extrapolative extreme for the nonlinear system. In the linear system the accumulation of drug within the skin is given by the following equation:

$$C = C_{ss}(1 - e^{-k_{el}t}) \qquad \text{(Eq. 1)}$$

$$C_{ss} = \frac{J \cdot A}{CL}$$

where C is the concentration in the skin during accumulation, C_{ss} is the steady-state concentration, J is the flux applied to the skin, A is the area to which the flux is applied, k_{el} is the elimination rate constant from the skin, CL is the clearance from the skin, and t is time. The depletion of drug from the skin once steady state has been achieved and the input removed is given by:

$$C = C_{ss}e^{-k_{el}t} \qquad \text{(Eq. 2)}$$

where C is the concentration during depletion. In Eq. 2 t is relative to the time depletion commences. The accumulation and depletion curves are symmetrical around $C = 0.5\ C_{ss}$. The symmetry of the curves is maintained regardless of the magnitude of the elimination rate constant. The time to reach 50% of the steady-state concentration in the accumulation mode and the time to fall to 50% of the steady-state concentration in the depletion mode are equal. The equality becomes apparent when the equations are rearranged to express time explicitly as a function of the ratio of the concentration at time t to the steady-state concentration. Equations 3 and 4 correspond to Eqs. 1 and 2, respectively.

$$t = (1/k_{el}) \ln \frac{1}{1 - C/C_{ss}} \qquad \text{(Eq. 3)}$$

and

$$t = (1/k_{el}) \ln \frac{C_{ss}}{C} \qquad \text{(Eq. 4)}$$

Thus, from either Eq. 3 or 4, the time at which $C/C_{ss} = 0.5$ (hereafter called t_{50}), is $(1/k_{el}) \ln 2$.

0022-3549/84/0500-0710$01.00/0
© 1984, American Pharmaceutical Association

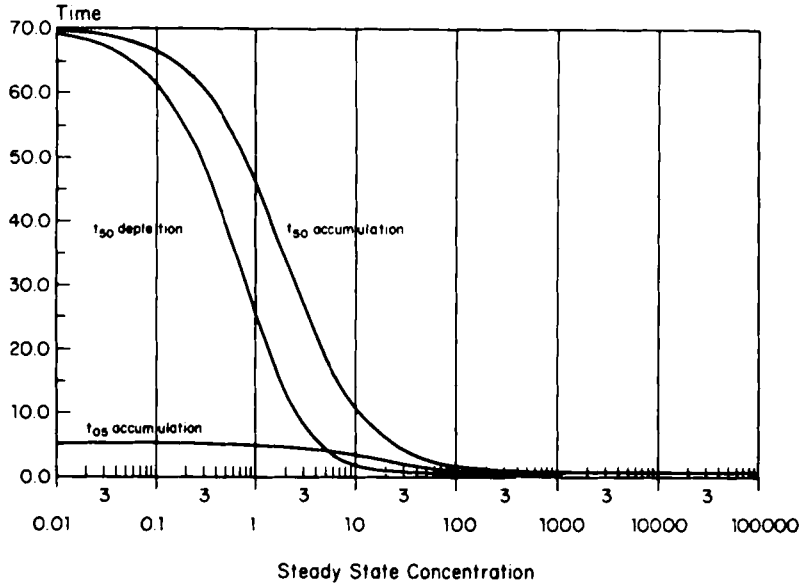

Figure 1—t_{50} *for accumulation and depletion, and* t_{05} *for accumulation,* versus, *the steady-state concentration or normalized flux* (k_{el} = *1*, B = *100*, K = *1*).

The equations representing the accumulation and depletion in the nonlinear system have been solved in closed form (3). The nonlinear differential equations for both modes are integrable and yield implicit solutions of the concentration as a function of time. The equation for the accumulation mode is:

$$\left[\frac{BK}{(K+C_{ss})^2}+1\right]\ln\frac{1}{1-C/C_{ss}} + \frac{BK}{(K+C_{ss})^2}\ln\frac{K+C}{K}+\frac{B}{K+C_{ss}}\cdot\frac{C}{K+C}=k_{el}t \quad \text{(Eq. 5)}$$

where C is the concentration of free drug in the skin at time t, C_{ss} is the steady-state concentration, K is the dissociation constant of the drug protein complex, B is the equivalent concentration of binding sites, and k_{el} is the elimination rate constant.

The equation for the depletion mode is:

$$\left(\frac{B}{K}+1\right)\ln\frac{C_{ss}}{C}+\frac{B}{K}\ln\frac{K+C}{K+C_{ss}}+\frac{B(C-C_{ss})}{(K+C_{ss})(K+C)}=k_{el}t \quad \text{(Eq. 6)}$$

The t_{50} of the steady-state concentration in both the accumulation and depletion modes was evaluated as a function of the steady-state concentration for a nonlinear system where $B = 100$, $K = 1$, and $k_{el} = 1$. The steady-state concentration can be achieved through a constant mass delivery to a defined area of skin. The results of the analysis are presented in Fig. 1. Since the elimination rate constant from the skin is unity, the abscissa for Fig. 1 can be viewed as the flux per unit thickness of skin. Considering the abscissa to represent a flux-like term will be particularly useful when discussing the accumulation mode.

Examination of Fig. 1 reveals that t_{50} for the accumulation mode is always greater than that for the depletion mode except at the extremes in steady-state concentration. At either extreme (high- or low-steady-state concentration) t_{50} for both the accumulation and depletion modes converge, and the common values become independent of the steady-state concentration. At low-steady-state concentrations the binding remains in the linear region throughout the accumulation to and depletion from these upper bounds (steady-state concentrations). At high steady-state concentrations the bound fraction becomes small relative to these steady-state concentrations and the system assumes a linear character. When the free concentrations are in the nonlinear region of protein binding for a significant period of time in either mode relative to the time used to characterize the system, *e.g.*, t_{50}, an asymmetry will be manifested in these times.

The independence of t_{50} from the steady-state concentration, exhibited at the extremes in Fig. 1, is a manifestation of linearity. Note that the time in either Eq. 3 or 4 is a function of C/C_{ss}. In contrast the nonlinear equations (Eqs. 5 and 6) cannot be rearranged to eliminate an explicit dependence of t_{50} on C_{ss}.

The larger value of t_{50} at the low concentration, linear limit compared with the high concentration, linear limit is a manifestation of an apparent volume increase due to the protein binding. Since the clearance from a fixed area of skin is constant, t_{50} will increase as the volume increases. The apparent volume of distribution at the low concentration linear limit relative to the volume at the high concentration linear limit is $(1 + B/K)$. Thus, the apparent 100-fold expansion in volume at the low concentration, linear limit becomes reflected in a corresponding increase in t_{50} at this limit relative to the high concentration, linear limit.

In the nonlinear region between the linear extremes, t_{50} increases monotonically as the steady-state concentration decreases for both the accumulation and depletion modes. The lower the initial concentration, the longer the free concentrations will remain above 50% of the initial concentration (steady-state concentration) in the depletion mode. The depletion of the drug in the skin as measured by the decline in the free concentrations is buffered by the drug–protein interaction. The buffering effect is greater with low concentrations, since under these conditions a larger fraction of the drug will be bound.

Since the steady-state free concentration is proportional to the flux, low initial concentrations can be achieved with low fluxes. To achieve the same mass rate input into the body at steady state, and the same amount of free drug in the skin at the initiation of the depletion mode, a reduction in the flux must be compensated for by an increase in the area. Thus, after removal of the input to the skin, the mass rate input to the body declines from a common value but more slowly with the lower

initial concentration. The extra mass required to prolong delivery to the body is provided for by the larger amount of bound drug in the skin in cases where low initial concentrations and appropriately adjusted areas are used to obtain the same initial amount of free drug.

On the other hand, t_{50} for the accumulation mode is always greater than or equal to that for the depletion mode. Thus, in achieving prolongation to the body by reducing the steady-state concentration a price is paid in terms of an increase in t_{50} for accumulation. The protraction in time required to reach steady state with the reduced flux can be circumvented by first delivering drug to the skin at a high flux for a short duration. After application of the pulse to promote the rapid attainment of the desired free concentration, the mass delivery rate to the body can easily be maintained. For the simple model, the system will be in steady-state instantly if the second flux (maintenance flux) is initiated at a concentration that is its steady-state concentration.

The effect of a pulse, which has a flux 10-fold higher than the maintenance flux, can be elucidated by comparing t_{05}, the time to reach 5% of the steady-state value for the pulse, with t_{50} for the maintenance flux. Since the higher flux establishes a proportionally higher steady state concentration, 50% of the steady-state concentration generated with a given flux and 5% of the steady-state concentration generated with a flux 10-fold higher are the same concentration. The curve representing the relationship between the t_{05} values and the steady-state concentration is presented in Fig. 1. In comparing the difference between t_{50} and t_{05} in Fig. 1, the comparison should be made with t_{05} values at steady-state concentrations 10-fold higher than those for corresponding t_{50} values. The difference increases as the steady-state concentration decreases, reaching the maximum value at the low flux, linear limit. Both t_{05} and t_{50} will become independent of the flux at the limit. The large apparent volume of distribution at this limit causes a magnification of the time constant, t_{50}, t_{05}, and the time differences.

A comparison of the t_{05} values for accumulation with the t_{50} values for depletion, where the flux is 10-fold higher for the former compared with the latter values, indicates the effect of the pulse on the dynamics of accumulation relative to depletion. The t_{05} values are generally less than the t_{50} values for depletion. The pulse reduces the accumulation time such that it is now less than the depletion time; without the pulse the accumulation time is always greater than or equal to the depletion time. Thus, with the use of a pulse followed by a reduced flux, the rapid attainment of steady state, low free concentrations, and prolonged delivery to the body after removal of the input are all achievable.

In principle there is maximum flux on the upper limit of the flux which the skin can accept, hereafter called the maximum flux. The maximum flux is achieved when the penetrant is at unit thermodynamic activity on the skin surface. Conceivably there are circumstances under which the maximum flux should be employed; for instance, if the minimum area of coverage and/or the most rapid termination is desired. The bend (region of nonlinearity) in the free concentration *versus* time curve for the simple nonlinear model occurs at concentrations in the vicinity of dissociation constant and is independent of the initial concentration (4). Therefore, a larger fraction of the drug can be removed from the skin in a given period of time the larger the initial concentration. In a linear system, the same fraction would be removed in a given period of time regardless of the initial concentration.

Using the maximum flux to achieve the highest steady-state concentration in the skin fixes the accumulation time t_{50}. The use of a two-pulse sequence where the flux of the first pulse exceeds the maximum flux is not possible. Although the accumulation time could be shortened by applying the maximum flux to a larger area of skin for a defined period and then reducing the flux, considerations of minimum coverage and/or rapid termination would be compromised.

In conclusion, transdermal input should be designed with a consideration of the influence of protein binding on the transport process. Because of the protein binding, the accumulation and depletion times, defined on the basis of the times to reach or decline to a given fraction of the steady-state concentration, respectively, are not independent of the steady-state concentration. Thus, the dynamics will vary for cases where different fluxes and corresponding changes in area are used to obtain the same total mass input rate. In addition, protein binding creates an inherent assymmetry in the dynamics of the accumulation and depletion modes.

(1) S. K. Chandrasekaran, A. S. Michaels, P. Campbell, and J. E. Shaw, *AICH&J*, **22**, 828 (1976).

(2) S. K. Chandrasekaran and W. F. Bayne, *J. Pharm. Sci.*, **67**, 713 (1978).

(3) J. G. Wagner, "Fundamentals of Clinical Pharmacokinetics," Drug Intelligence Publications, Hamilton, Ill., 1975, pp. 272–274.

(4) J. R. Gillette, in "Handbuch der Experimentellen Pharmakologie, Vol. XXVIII: Concepts in Biochemical Pharmacology," part 3, J. R. Gillette and J. R. Mitchell, Eds., Springer-Verlag, Berlin, West Germany, 1975, p. 78.

S. S. Hwang[x]
W. F. Bayne

Merck Sharp & Dohme Research Laboratories
West Point, PA 19486

Received November 21, 1983.
Accepted for publication March 1, 1984.

A publication of the
American Pharmaceutical Association—
the National Professional Society
of Pharmacists

JOURNAL OF PHARMACEUTICAL SCIENCES

Volume 73, 1984

JPMSAE 73(1-12) 1-1910 (1984)
ISSN 0022-3549

Sharon G. Boots
Editor

Sue A. Kruger
Production Editor

Margaret M. Madeleine
Assistant Production Editor

Karen A. Blakney
Copy Editor

Edward G. Feldmann
Contributing Editor

Samuel W. Goldstein
Contributing Editor

Patricia A. Evich
Editorial Secretary

Editorial Advisory Board

Jordan L. Cohen
Kenneth A. Connors
Louis Diamond
Ho-Leung Fung
Milo Gibaldi
Everett N. Hiestand
W. Homer Lawrence
Ian W. Mathison
Carl M. Metzler
Robert E. Notari
Paul L. Schiff, Jr.
Jane E. Shaw

Published monthly under the supervision of the Board of Trustees

"Coming of Age" for Device Technology

Medically related hoaxes and quackery have been with us for many, many years. The American Medical Association's principal activity during the late 19th century and early 20th century was to expose and debunk such phoney remedies and their fraudulent promoters. Subsequently, after the predecessor to the present-day U.S. Food and Drug Administration was established in 1906, that federal agency assumed national leadership for monitoring the promotion of devices and gadgets claimed to have therapeutic properties or diagnostic value. Other groups—including the American Pharmaceutical Association in particular—provided strong support to these efforts, as well as conducting their own educational programs and professional projects.

Copper bracelets for arthritis sufferers probably have been the most common and well-known hoax, but there have been hundreds and perhaps even thousands of others. The FDA had a museum—a so-called "Chamber of Horrors"—in which its collection of the more unusual and ingenious such items had been exhibited. The agency made wide use of that exhibit in conjunction with its educational campaigns to warn the general public about the uselessness—and, in some cases, even the potential hazard—of such devices.

Those of us educated in the sciences, and especially in the medical and pharmaceutical sciences, recognize the lack of any plausible scientific basis for expecting these devices to have any curative value. But to the average lay person, who is at best only casually schooled in the sciences, the claims appear to be within the realm of possibility. And when one is desperate for a cure—due to the absence of other proven remedies, coupled with pain or a fatal prognosis—that person is quite receptive to the pitch of a medical charlatan.

For years, the FDA has so relentlessly pursued this activity, so dramatically exposed the devices as fraudulent, so widely publicized their worthlessness, and so vigorously prosecuted those people who promoted them, that one might reasonably question whether the agency has been able to adequately retain its objectivity in the matter. In other words, if some seemingly exotic device or treatment came along that did indeed do what was claimed for it, would the FDA be able to recognize its worth, and publicly acknowledge its usefulness? The krebiozen and laetrile episodes were fueled by just such doubts on the part of the public and some of the medical community.

Well, in our view, any such question can now be put to rest.

We recently saw the April issue of the *FDA Consumer*—which is the Agency's magazine for lay readers.

The lead article was entitled "Sealing Teeth to Prevent Cavities." And rather than expose the procedure as a hoax, or even as a well-intended but worthless effort by dentists to protect against the ravages of caries, the article gave a ringing endorsement to the procedure! The FDA staff writer explained in easy-to-understand language the susceptibility of tooth fissures to dental decay, the theory behind the sealants, how they are applied, their relative safety, and the clinical test results recorded for them. The general message of the article can best be conveyed by the writer's own abstract-summary: "*A group of experts recently agreed that sealants can be effective in protecting teeth of youngsters, particularly those teeth that are pitted and have fissures.*" The article itself stated that "*the occurrence of pit and fissure cavities was reduced by approximately 95 percent at the end of one year and at least 50 percent at the end of five years.*"

Then, later on in that same April issue of *FDA Consumer*, was an article discussing a heat-generating device that has been promoted as a treatment of cancer. Our initial reaction was: "*Old hat! FDA has been debunking such devices, and hounding their promoters for as long as we can remember!*"

But, again, this was another case of "man bites dog!"

The FDA staff author described how a new medical device that uses controlled microwave energy to treat certain kinds of cancer has won FDA approval for marketing. The microwave energy produces hyperthermia and is now approved specifically for treatment of four types of malignant tumors: melanoma, squamous carcinoma, adenocarcinoma, and sarcoma.

The article points out that hyperthermia has certain limitations and is a palliative treatment rather than a true cure. But just to suppress and halt the growth of a malignant cancer is a great achievement with respect to this terrible disease. Also described are the clinical test results (with full to partial regression of 83 percent of tumors in one major study), the theoretical basis of the device's principle of activity, the technique employed in utilizing the device, the specialists who will initially employ the device and where it will be available, and the technique that manufacturers will use in testing and standardizing the machines they produce without needing to use human subjects in the testing process.

This FDA author's own abstract-summary also conveys very well the general message of the article: "*A recently approved device offers a new way to treat four types of cancer. In a process called hyperthermia, cancer cells are destroyed by microwave-type heat.*"

And less than a week earlier, we had read that, effective March 30, FDA had granted approval for the general marketing of nuclear magnetic resonance (NMR) imaging equipment for medical diagnostic purposes. NMR is expected to be very useful for *in vivo* pathological analyses as well as more effective three-dimensional visualization than can be achieved by currently available CAT scanning. Other exotic diagnostic applications are anticipated in the near future, and there is a good possibility that certain therapeutic or treatment applications will be approved eventually.

All of this is welcome news in the overall health care picture. New drug discoveries will continue to be important, but there is a growing recognition that pharmaceuticals alone are not sufficient to provide the most efficient and effective treatment for many diseases.

What we are seeing is the emerging era of applied technology. Although, as in the case of drugs, we have long enjoyed some benefits of device technology, they have been very limited and elementary when compared to the new gadgetry, electronics, and computer systems now becoming available.

And even in the pharmaceutical field, the present research and development emphasis is shifting more and more toward sophisticated drug delivery systems and away from exclusive interest in new drug entities. Again, this is applied technology.

In conclusion, what we are witnessing is truly a medical revolution. A field that just a few years ago had been full of phoniness and quackery has now been transformed by modern technology into one of hope and promise. For all of us who are involved, or even just witnessing these events, these indeed are exciting times!

—EDWARD G. FELDMANN
American Pharmaceutical Association
Washington, DC 20037

0022-3549/84/0600-0713$01.00/0
© 1984, American Pharmaceutical Association

JOURNAL OF PHARMACEUTICAL SCIENCES

JUNE 1984
VOLUME 73 NUMBER 6

RESEARCH ARTICLES

New Insights in the Clastic Binding Hypothesis for Opiate–Receptor Interactions I: Electron-Transfer Mechanism

VERA M. KOLB

Received August 9, 1982, from the *Department of Chemistry and Biochemistry, Southern Illinois University, Carbondale, IL 62901.* Accepted for publication January 19, 1983.

Abstract □ A clastic binding hypothesis for opiate–receptor interactions, in which the key step in eliciting the opiate response is an electron transfer from the opiate nitrogen to the receptor, is analyzed from a chemical point of view and is found to be chemically feasible. An extended form of this hypothesis is proposed in order to accommodate recent observations about the N-demethylation of morphines in the brain. An *in vitro* model system for studying the electron-transfer reactions of morphines is proposed, and the initial experiments in this system are reported.

Keyphrases □ Clastic binding hypothesis—electron-transfer mechanism, opiate receptor interactions, *in vitro* model system □ Opiate-receptor interactions—electron-transfer mechanism, extended clastic binding hypothesis, *in vitro* model system □ Electron transfer—mechanism, extended clastic binding hypothesis, opiate-receptor interactions, *in vitro* model system

Belleau *et al.* (1, 2) presented experimental evidence that the directionality of the lone electron pair on nitrogen (N lone pair) of morphine-type opiates is directly related to their opiate activity. On this basis Belleau and Morgan (3) proposed the clastic binding hypothesis for opiate–receptor interactions. According to this hypothesis, morphine-type opiates achieve productive binding with the opiate receptor *via* a clastic binding process that includes a stereospecific electron transfer from the lone electron pair of opiates to some electrophilic site at the receptor. Such clastic binding is tantamount to injecting electrons at the receptor level. The electron transfer from nitrogen to the receptor was proposed to lead to the oxidation of the *N*-methyl substituent. Such oxidation may lead to a subsequent *N*-demethylation. Contrary to the *N*-demethylation hypothesis of Beckett *et al.* (4) in which the *N*-demethylation is an extrinsic preliminary step in the mechanism of opiate action, in the clastic binding the *N*-demethylation process participates *in conjunction with the opiate receptor* in eliciting the opiate response. According to Belleau and Morgan "the opiate receptor complex would possess an intrinsic and specific oxidative *N*-demethylase activity."

The aforementioned concept obviously requires that the location of the sites of *N*-demethylation within the CNS is proximal to or coincident with that of the opiate receptors. This was indeed found to be the case by Fishman *et al.* (5–7). They have demonstrated that the *N*-demethylation of morphine in rat brain is localized in sites with high opiate-receptor content. Moreover, the *N*-demethylation in the brain was found to proceed only when pharmacological concentrations of the substrate were present: the fact which indicated the biological significance of the reaction. This brain dealkylase was found to be different from that responsible for the same transformation in the liver (6). The brain demethylation of morphine was decreased by tolerance and by opiate antagonists such as naloxone, which itself was not dealkylated in the brain (7). These results provided strong support for the concept that *N*-dealkylation of narcotics in their CNS target sites is intimately involved in the expression of their action.

The *N*-dealkylation reaction occurring in the enzymatic process described above may follow the same mechanistic path as the same reaction occurring in the "test-tube" with the "regular" chemical reagents, or it may follow a different path. We were interested in exploring the former possibility. Specifically, we wanted to find out if the currently available chemical data on electron transfers from the N lone pair of morphines or model compounds, such as tertiary aliphatic amines, to electron acceptors are compatible with the hypothesis of Belleau and Morgan (3) and the findings of Fishman *et al.* (5–7).

THEORETICAL

Electron-Transfer Reactions and *N*-Dealkylations of Morphines—A possible mechanism by which the electron transfer from the N lone pair of the tertiary aliphatic amines to various electron acceptors leads to the *N*-dealkylation is presented in Scheme I. This mechanism has been found to be valid

0022-3549/84/0600-0715$01.00/0
© 1984, American Pharmaceutical Association

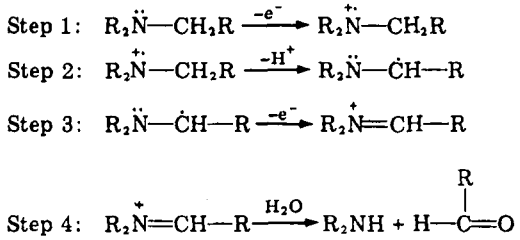

Scheme I—Possible mechanism of the oxidative N*-dealkylation of tertiary aliphatic amines.*

for the electrochemical (anodic) oxidations and dealkylations of tertiary aliphatic amines (8, 9) as well as for their reactions with various chemical agents, such as chlorine dioxide, *N*-bromosuccinimide, manganese dioxide, and ozone (10). Such a mechanism has been recently proposed also for the mitochondrial monoamine oxidase-catalyzed amine oxidation (11).

The first step of the mechanism shown in Scheme I is a one-electron transfer from the nitrogen of a tertiary amine to a suitable (redox-matched) electron acceptor (not shown). This slow step was found to be rate determining in the chemical and electrochemical reactions (8–10). The radical cation produced in the first step undergoes a loss of proton from an α-position yielding, after the rearrangement of electrons, an α-amino radical; this is shown in the second step. The α-amino radical species undergoes a one-electron transfer from nitrogen to give an immonium species, as shown in the third step. The immonium ion is readily hydrolyzed into a secondary (*N*-dealkylated) amine and an aldehyde, as shown in the fourth step.

The mechanism presented in Scheme I may be proposed to operate in the cases when the *N*-demethylation of morphine occurs in the brain, namely when the concentration of morphine is at its pharmacological level (5). From this mechanism, however, it is not obvious why the *N*-demethylation does not occur at concentrations of morphine lower than the pharmacological concentration (5). The latter observation may be accommodated, however, by the following hypothesis. The electron transfer from the N lone pair of the morphine nitrogen to the electron acceptor (E) at the receptor may result in the formation of a stable caged radical-anion–radical-cation (RARC[1]) pair (Scheme II) between morphine and a hypothetical electron acceptor at the receptor. No bonds are made or broken in this process[2].

The formation of a RARC (charge-transfer) complex may be the most frequently occurring mode by which the morphine nitrogen interacts with the electron acceptor at the receptor. This mode of interaction, however, would not elicit the biological response according to the clastic binding hypothesis, since the electron transferred from the N lone pair is *not free* to be injected into the receptor, but is confined within the RARC cage. The formation of the RARC complex may be responsible for the affinity of nitrogen to the "amine-binding site" of the receptor (14), which would contribute to the overall affinity of morphine to the receptor, while the injection of the electron from the morphine nitrogen to the receptor would be responsible for the intrinsic activity (efficacy) (15) of morphine.

Only as a rare event would the electron from the N lone pair be injected to the receptor and, thus, be lost from nitrogen. The latter species would become a *free* radical cation which then could further react, as shown in Scheme I, to ultimately lead to *N*-dealkylation. Thus, according to this concept, the pharmacological concentration of morphine would be some critical concentration at which these rare events of the injecting the N lone pair electrons to the receptor cumulate and become "visible." A necessary condition for

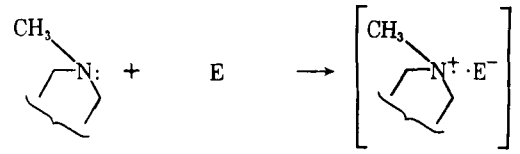

Scheme II

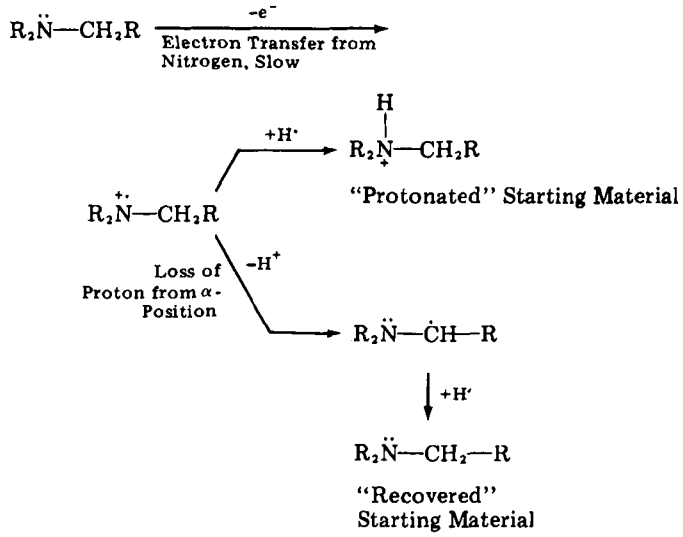

Scheme III

inducing analgesia would be the injection of the N lone pair electrons to the receptor, and the *N*-dealkylation would normally accompany this reaction.

From the chemical point of view, however, one would predict that the injection of the N lone pair electron to the receptor does not necessarily have to be accompanied by *N*-dealkylation, since the nitrogen radical cation may react by a pathway different than that shown in Scheme I. Two such possible pathways are shown in Scheme III. According to this Scheme the nitrogen radical cation, formed by the loss of one electron from the N lone pair, may give either "protonated" or "recovered" starting material. The upper arrow in Scheme III shows that the nitrogen radical cation may pick up a hydrogen atom from the receptor (probably in a random fashion), giving material that is the same as the protonated starting material, but is obviously not obtained by protonation of the starting material. (Hence the word protonated in Scheme III is in quotations.) The lower arrow in Scheme III shows a pathway where the nitrogen radical cation loses an α-proton (the same as the step 2 in Scheme I) and the resulting α-amino radical picks up a hydrogen atom from the receptor, giving material that is the same as the starting material, but is not the recovered starting material since the α-hydrogen was exchanged. (Hence the word recovered in Scheme III is in quotations.) This pathway has been observed to occur during photooxidations of tertiary amines[3].

If the morphine radical cation at the receptor follows the pathway(s) shown in Scheme III, even as a rare event, it is conceivable that the abstraction of H· from the receptor would be random and, thus, may cause damage of the receptor site normally involved in the *N*-demethylation, as well as to the electron acceptor at the receptor. The damage of the receptor may become permanent and irreversible in the cases of prolonged use or abuse of morphines. The extent of the damage to the electron-acceptor site does not have to be the same as that to the *N*-dealkylation site. The opiate response still may be achieved if the latter site is damaged. The observed decrease of the brain *N*-demethylation of morphine by tolerance (7) may be caused by the damage of the *N*-dealkylation sites.

In summary, our view of the clastic binding process is the following. The attraction of morphine to its amine-binding site at the receptor is proposed to be achieved *via* formation of a RARC (charge-transfer) complex (Scheme II), an event which is *not* accompanied by the opiate response. Only occasionally a true electron transfer, *i.e.*, the electron injection, to the receptor occurs, leading to the opiate response. Normally, this electron injection is accompanied by *N*-demethylation (Scheme I), but it does not have to be, since other chemically feasible pathways are available, leading to "recovered" or "protonated" morphine, for example (Scheme III). These pathways may normally operate for various *N*-alkyl opiates which may not be dealkylated in the brain and, in the case of tolerance, when the *N*-demethylation is decreased.

Chemical considerations presented above in conjunction with the pharmacological observations on the *N*-demethylation of morphine in the brain suggest that the extended version of the clastic binding hypothesis is feasible both chemically and pharmacologically. Therefore, a detailed study of the electron-transfer reactions of morphines seems worthwhile.

Study of Electron-Transfer Reactions of Morphines in an *In Vitro* Model System—Despite a very extensive research in the field of opiate receptors, relatively little is known about these receptors because they are quite labile

[1] We are suggesting the term RARC pair for the caged radical-anion–radical-cation pair in accordance with the nomenclature introduced by Meyers *et al.* (12) who named the caged radical-anion–radical pair RARP.

[2] The RARC pair is an outer-sphere electron-transfer complex (13). In the latter complexes no bonds are made or broken during the course of the reaction (13). The immediate effect of the outer-sphere electron transfer is the change in the charge on the reactants (13). In the example shown in Scheme II the electron donor (nitrogen) which was neutral became positive, and the electron acceptor (E) which was neutral became negative. These complexes are also called charge-transfer complexes.

[3] Private communication by Prof. Fred D. Lewis, to whom thanks are expressed.

and easily denatured (16). The true nature of these receptors has not as yet being elucidated; after years of careful research by independent investigators, there still exists appreciable controversy over whether the receptor is a protein, a lipid, or both (16, 17).

The question if the protein or the protein part of the opiate receptor can function as an electron-transfer protein, as required by the clastic binding hypothesis, cannot be answered at this time since so little is known about the opiate receptor. If the opiate receptor protein can indeed function as an electron-transfer protein, one may visualize it, in general terms, as shown in Scheme IV (18):

Source of Electron ⟶

Way In ⟶ Trap ⟶ Way Out ⟶ Sink

Scheme IV

Scheme IV represents a directed electron transfer from a source of electron, morphine in this case, to the electron-transfer protein, in this case the opiate receptor (the enclosed block). In this model, the electron-transfer protein has the capability of controlling the electron transfer by a mechanism which "gates" either the "entering" or "leaving" channel. The movement of an electron through the protein may be realized, as suggested previously (18), *via* a localized hop mechanism and electron tunnelling.

We shall concentration only on the "way in" channel of the opiate receptor protein (Scheme IV), since the clastic binding hypothesis deals thus far only with this part of the opiate receptor. It is our desire to model this "way in" channel in such a way as to fulfill the chemical requirements of the proposed extended form of the clastic binding hypothesis, and then to study the chemistry of the electron transfer from morphines in such a model.

The "way in" channel in Scheme IV is actually the point of injection of the morphine N lone pair to the receptor, and it already has been discussed as "the electron acceptor at the receptor" (E) (Scheme II; see previous section). The chemical requirement for E was that morphine nitrogen can form a persistent RARC or charge-transfer complex with E (Scheme II), which only rarely leads to the actual loss of the N lone pair electron to the electron acceptor, *i.e.*, to the full electron transfer (Schemes I and III).

We decided to explore a possibility that perhalomethanes (CX_4, X = Cl or Br) may represent such models, since we were familiar with their exceptionally good electron-accepting ability (12, 19). In this paper we explore the behavior of carbon tetrachloride (CCl_4) in its reactions with amines in general and with a series of morphines. Work with CCl_3Br, which is a better electron acceptor than CCl_4, is in progress.

The reaction of amines with CCl_4 has been studied extensively (20-30). It is a well-established fact that amines—primary, secondary, and tertiary aliphatic, as well as aromatic—form charge-transfer complexes with CCl_4 (20, 25-27, 30). For example, amines such as triethylamine, di-*n*-propylamine, and tri-*n*-propylamine have been found spectrometrically to form 1:1 charge-transfer complexes with halomethanes (25). The K_f value for the *n*-butylamine-CCl_4 complex of 0.032 M^{-1} indicates a weak bond between the two species, as expected in a charge-transfer complex (27). Since these charge-transfer complexes are outer-sphere electron-transfer complexes in which no bonds are made or broken, their persistency shows as a lack of the actual chemical reaction.

When the N lone pair electron is fully transferred to CCl_4, a series of chemical reactions are initiated which ultimately lead to amine hydrochloride and other products (Scheme V). Such reactions in the case of morphines must be very slow if CCl_4 is to be used as a model for the electron acceptor at the opiate receptor, since the actual loss (injection) of the N lone pair electron to the receptor is proposed to be a rare event. Since the ultimate product of the reaction of an amine with CCl_4 is the amine hydrochloride, as shown in Scheme V and amply demonstrated in other examples (20-29), the speed and the extent of this reaction can be determined by measuring, respectively, the rate of appearance and the amount of amine hydrochloride, or just the halide ion.

The literature data on the rates of the reactions of amines with CCl_4 could not be extrapolated with confidence to the case of morphines, since they are somewhat contradictory. Thus, reports exist stating that amine hydrochloride precipitates were formed rather rapidly after dissolving the amines in CCl_4 (25, 27) and also that the formation of such precipitates is extremely slow (21). These discrepancies may be due to the uncontrolled presence of catalysts, such as UV light, oxygen, Cu^+, Cu^{2+}, Fe^{2+}, brass, and even traces of metal impurities from a stirring bar, all of which have been found to influence the reaction rate. However, the influence of these catalysts is not clear in all the cases. Thus, one report states that the reaction is prevented if light or other catalysts are excluded (26), but another report describes that the reaction proceeds in dark without a catalyst (28).

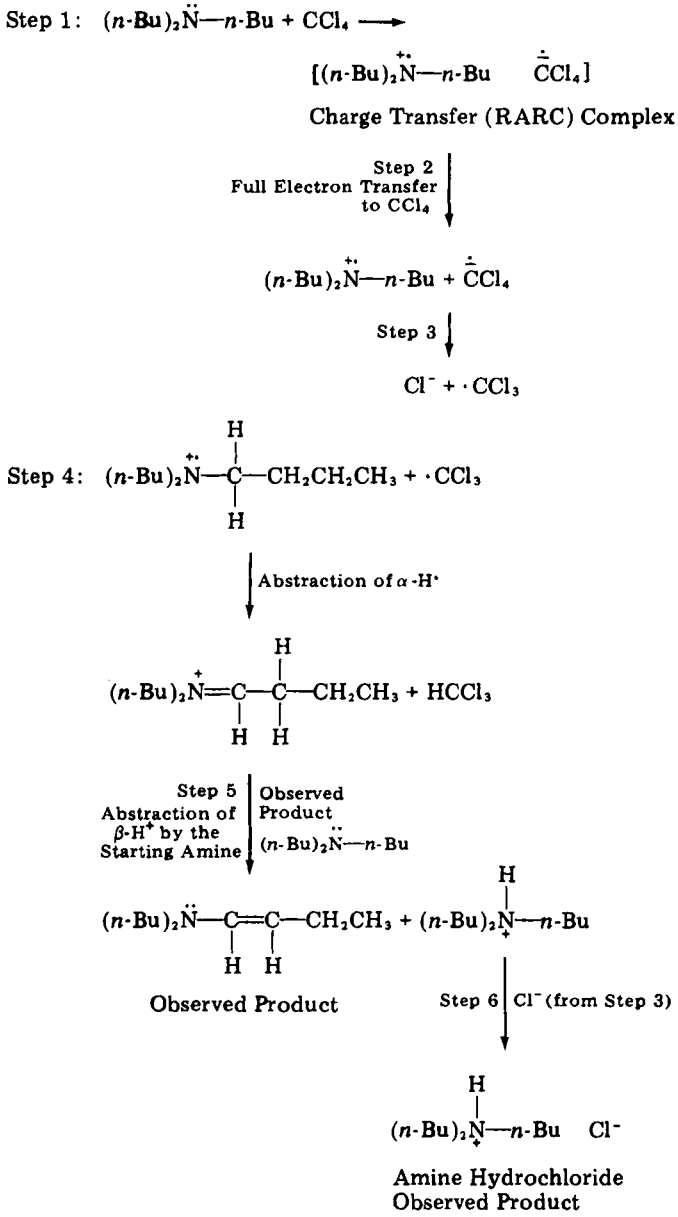

Scheme V—Chemical reactions leading to the amine hydrochloride (based on Ref. 28).

Therefore, since there were no satisfactory literature data that we could extrapolate to the case of morphines, we undertook the study of the reactions of morphine, oxymorphone, and naloxone with CCl_4.

EXPERIMENTAL

Melting points were determined on a capillary melting-point apparatus[4] and were not corrected. The NMR spectra were taken on a 90-MHz spectrometer[5], and the IR spectra were recorded on a spectrophotometer[6]. TLC was done on aluminum sheets precoated with 0.2 mm of silica gel[7]; the eluant was chloroform–methanol–concentrated ammonium hydroxide (132:12:0.9 by volume). The spots were observed in a UV chamber at the wavelength of 254 nm. The carbon tetrachloride used was an ACS-analyzed reagent[8], containing only 0.5 ppm of chloride ion and 0.02 ppm of heavy metals. Oxymorphone hydrochloride[9], naloxone hydrochloride[9], and morphine[10] were from outside sources.

Conversion of Naloxone Hydrochloride to Naloxone—A solution of nal-

[4] Thomas-Hoover.
[5] Perkin-Elmer R 32.
[6] Beckman IR-10 and Perkin-Elmer 297 spectrophotometers.
[7] Silica gel 60, F_{254}; EM Reagents.
[8] MCB.
[9] ENDO Laboratories.
[10] Scripps Clinic and Research Foundation.

Table I—Reaction of Selected Morphines and Other Amines with Carbon Tetrachloride

Amine	Reaction Time, h	Isolated Product(s)	Yield, %	Reference
Naloxone	3	Trace of amine hydrochloride was presumably formed[a]	trace of Cl^- was observed	this work
Morphine	20	—	—	this work
Oxymorphone	30	Trace of amine hydrochloride was presumably formed[a]	trace of Cl^- was observed	this work
Triethylamine	72	Amine hydrochloride	2.2	21
2-Diethylaminoethanol	72	Amine hydrochloride	24.4	21
Piperidine	24	—	—	22
	72	Amine hydrochloride	2.6	22

[a] See *Experimental*.

oxone hydrochloride (0.70 g, 0.0019 mol) in ethanol and water was poured into an aqueous solution of borax[11] (sodium tetraborate, $Na_2B_4O_7 \cdot 10H_2O$; certified ACS). The resulting solution was extracted three times with chloroform (ACS quality, distilled). The combined chloroform extracts were washed with borax and water, dried (anhydrous magnesium sulfate), and evaporated leaving naloxone as 0.56 g of a white solid (90% yield), mp (chloroform–petroleum ether) 177–178.5°C, (ethyl acetate) 177–178.5°C [lit. (31) mp (ethyl acetate) 177–178°C, 184°C]. The crude as well as the recrystallized material was TLC pure, R_f 0.65.

Treatment of Naloxone with Carbon Tetrachloride—Naloxone (0.35 g, 1.1×10^{-3} mol) was mixed with carbon tetrachloride (30 mL, ~300 times molar excess over naloxone) and the mixture was refluxed to achieve dissolution. After the dissolution was complete, the reflux was continued for 1.5 h under the laboratory fluorescent lights. Air was not excluded, as the reflux was performed in a reflux apparatus equipped with a $CaCl_2$ drying tube on top of the reflux condenser. The solution was then stirred at room temperature for the 1.5-h period. After that time, the solvent was evaporated on a rotary evaporator, and the white solid residue was dried in a vacuum oven, giving 0.34 g of the material (97% recovery).

The IR spectrum of this material was essentially identical with that of the starting material. The C=O stretch was at 1728 cm^{-1} (nujol) as in the starting material, and no peak was observed at 1713 cm^{-1}, which corresponds to the C=O stretch of naloxone hydrochloride (nujol). The NMR spectrum ($CDCl_3$) of the recovered material was essentially identical with that of the starting material. TLC showed only one spot at R_f 0.65, corresponding to naloxone (the eluant would convert any naloxone hydrochloride to naloxone), indicating that no oxidative-degradation products were present.

A test for the presence of trace amounts of naloxone hydrochloride was performed as follows. The recovered material was dissolved in ether (ACS quality, distilled). The ethereal solution was washed three times with distilled water, the combined aqueous layers were acidified with 6 M HNO_3, and an aqueous solution of $AgNO_3$ was added. At first no cloudiness appeared, and only after ~5 min of standing a barely visible cloudiness developed, but no visible precipitate was formed. The theoretical yield of AgCl is 0.154 g. We have found that the AgCl test described above gave an immediate precipitate when applied to only a few milligrams of oxymorphone hydrochloride. This AgCl test gave us >99% accuracy when applied to the determination of chloride ion in a small (0.4×10^{-3} mol) sample of pure thymoxyethyl diethylamine hydrochloride (theoretical yield of AgCl, 0.058 g).

The ether which was used for the extraction, when treated as above (washed with water, the aqueous layer acidified with 6 M HNO_3, and aqueous $AgNO_3$ added), gave a completely clear solution which remained clear even after prolonged standing, thus indicating the absence of chloride ion as determined by the AgCl test. An experiment (blank) was also performed, in which 50 mL of CCl_4 was refluxed under laboratory lights for 13 h and stirred at room temperature in the dark for 17 h, and then worked up in the identical manner as the sample containing naloxone. No trace of chloride ion was observed in the AgCl test.

Conversion of Oxymorphone Hydrochloride to Oxymorphone—Oxymorphone hydrochloride (0.86 g, 0.025 mol) dissolved in water was converted into oxymorphone in the same fashion as the naloxone hydrochloride conversion into naloxone, yielding 0.48 g of oxymorphone (62%), mp (chloroform–petroleum ether) 249–250°C (dec.) [lit. (31) mp. (boiling ethanol, ethyl acetate, or benzene) 248–249°C (dec.)]. The crude as well as the recrystallized material were TLC pure, R_f 0.55.

Treatment of Oxymorphone with Carbon Tetrachloride—Oxymorphone (0.14 g, 0.47×10^{-3} mol) was treated with carbon tetrachloride (50 mL; ~1100 molar excess over oxymorphone) in the same manner as naloxone (*vide supra*), except that the reaction time was 10 times longer in the oxymorphone case. Thus, oxymorphone and CCl_4 were refluxed for 15 h under the laboratory fluorescent lights and stirred at room temperature for 15 h in the dark. The same work-up as for naloxone provided a white fine solid, which represented essentially quantitatively recovered starting material. The IR and NMR spectra of this material did not reveal the presence of oxymorphone hydrochloride and were identical to the corresponding spectra of the starting material. The AgCl test did not provide a visible precipitate, but the cloudiness observed was much more pronounced than in the case of the naloxone reaction; the theoretical yield of AgCl is 0.068 g. TLC showed the presence of only one spot, R_f 0.55, corresponding to oxymorphone, which indicated that no other compounds, such as degradation or oxidation products, were present.

Treatment of Morphine with Carbon Tetrachloride—Morphine (0.0965 g, 0.318×10^{-3} mol), mp 248–250°C (dec.) [lit. (31) mp for the monohydrate 254–256°C (dec.)], was treated with carbon tetrachloride (55 mL; ~1800 molar excess over morphine) under reflux and laboratory fluorescent lights for 5 h and at room temperature in the dark for 15 h. Again, as in the previous experiments, air was not excluded. After the above period, the solvent was removed by evaporation and the residual white solid was dried in a vacuum oven. The IR of this solid was identical, peak by peak, to the IR of the starting material.

This solid was suspended in water in a separatory funnel and shaken with ether, and the precipitate was removed by filtration. The white solid thus obtained showed only one spot on TLC (R_f 0.16) at the same place as morphine, thus indicating that no oxidative-degradation products were present. The aqueous and ether layers were separated. No material was recovered from the ether layer. The aqueous layer was acidified with 6 M HNO_3, and an aqueous solution of $AgNO_3$ was added. No precipitate or cloudiness was observed even after several hours. Only when the solution was looked at against a black background was a slight bluish-gray opaqueness, characteristic of AgCl, observed. After 10 d, a trace of precipitate (AgCl) was observed on the bottom of the flask.

RESULTS AND DISCUSSION

Morphine, oxymorphone, and naloxone, as freshly prepared free bases, were treated with CCl_4 open to air, under the laboratory fluorescent lights, and under reflux. A new polytef-coated stirring bar was used each time to avoid metal contamination, which is possible with used stirring bars. The carbon tetrachloride used was of analyzed-reagent quality and contained only 0.02 ppm of heavy metals. We used the above morphines, with an unprotected phenol moiety, so that the free phenol group could act as a built-in inhibitor (19) for free radicals: this narrowed the number of possible products. The extent of the reaction was followed by measuring the amount of chloride ion, which is formed by the decomposition of $CCl_4^{\cdot-}$ (step 3 in Scheme V). The recovered morphines were inspected by NMR and IR to see if there were any CCl_3-adducts in the phenol ring, since the latter ring would act as scavenger for the CCl_3 radicals formed simultaneously with the chloride ion (step 3).

We have found that the morphines studied react extremely slowly with CCl_4 (Table I and *Experimental Section*). For example, oxymorphone after 30 h of treatment with CCl_4 was completely recovered, with no spectrometric evidence of CCl_3- or other adducts, and only traces of chloride ion were detected.

Table I illustrates, for comparison, the literature results for some other amines of interest: triethylamine, as an example of tertiary amine; 2-diethylaminoethanol, as an example of a hydroxy amine in which, like in oxymorphone and naloxone, the hydroxyl group is in a close proximity to the amino group; and piperidine, a cyclic amine which is found as part of all the morphines. While the results for triethylamine and piperidine show slow reactions similar to our results for the morphines, the reaction of 2-diethylaminoethanol seems to be much faster. This point deserves further investigation. Further studies and evaluations of CCl_4 as an *in vitro* model for an electron acceptor at the receptor are in progress.

REFERENCES

(1) B. Belleau, T. Conway, F. R. Ahmed, and A. D. Hardy, *J. Med. Chem.*, **17**, 907 (1974).

[11] Fisher Scientific Co.

(2) J. Dimaio, F. R. Ahmed, P. Schiller, and B. Belleau, in "Recent Advances in Receptor Chemistry," F. Gualtieri, M. Giannella, and C. Melchiorre, Eds., Elsevier/North-Holland Biomedical, 1979, pp. 221-234.
(3) B. Belleau and P. Morgan, *J. Med. Chem.*, **17**, 908 (1974).
(4) A. H. Beckett, A. F. Casy, and N. J. Harper, *J. Pharm. Pharmacol.*, **6**, 874 (1956).
(5) J. Fishman, E. F. Hahn, and B. I. Norton, *Nature (London)*, **261**, 64 (1976).
(6) E. F. Hahn, B. I. Norton, and J. Fishman, *Biochem. Biophys. Res. Comm.*, **89**, 233 (1979).
(7) E. F. Hahn, B. I. Norton, and J. Fishman, in "Endogenous and Exogenous Opiate Agonists and Antagonists," E. L. Way, Ed., Pergamon, New York, N.Y., 1980, pp. 529-532.
(8) P. J. Smith and C. K. Mann, *J. Org. Chem.*, **34**, 1821 (1969), and references therein.
(9) L. C. Portis, V. V. Bhat, and C. K. Mann, *J. Org. Chem.*, **35**, 2175 (1970).
(10) F. D. Lewis and T.-I. Ho, *J. Am. Chem. Soc.*, **102**, 1751 (1980), and references therein.
(11) R. B. Silverman, S. J. Hofman, and W. B. Catus III, *J. Am. Chem. Soc.*, **102**, 7126 (1980).
(12) C. Y. Meyers, W. S. Matthews, L. L. Ho, V. M. Kolb, and T. E. Parady, in "Catalysis in Organic Synthesis," G. V. Smith, Ed., Academic, New York, N.Y., 1977, pp. 217, 260-278.
(13) N. Sutin in "Oxidases and Related Redox Systems," Vol. I, T. E. King, H. S. Mason, and M. Morrison, Eds., Wiley, New York, N.Y., 1965, pp. 37-50.
(14) V. M. Kolb, *J. Pharm. Sci.*, **67**, 999 (1978).
(15) A. Korolkovas, in "Essentials of Molecular Pharmacology," Wiley-Interscience, New York, N.Y., 1970, pp. 265-288, and references therein.
(16) N. M. Lee and A. P. Smith, *Life Sci.*, **26**, 1459 (1980), and references therein.
(17) T. M. Cho, P. Y. Law, and H. H. Loh, in "Neurochemical Mechanisms of Opiates and Endorphins, Advance Biochemical Phychopharmacology," Vol. 20, H. H. Loh, and D. H. Ross, Eds., Raven, New York, N.Y., 1979, pp. 69-101, and references therein.
(18) G. R. Moore and R. J. P. Williams, *Coordination Chem. Rev.*, **18**, 125 (1976), and references therein.
(19) C. Y. Meyers and V. M. Kolb, *J. Org. Chem.*, **43**, 1985 (1978).
(20) R. Foster, "Organic Charge-Transfer Complexes," Academic, New York, N.Y., 1969, pp. 278-280, 300, and references cited therein.
(21) R. F. Collins, *Chem. Ind. (London)*, **1957**, 704.
(22) N. H. Cromwell, P. W. Foster, and M. M. Wheeler, *Chem. Ind. (London)*, **1959**, 228.
(23) R. Foster, *Chem. Ind. (London)*, (**1960**) 1354.
(24) G. J. Beichl, J. E. Colwell, and J. G. Miller, *Chem. Ind. (London)*, **1960**, 203.
(25) D. P. Stevenson and G. M. Coppinger, *J. Am. Chem. Soc.*, **84**, 149 (1962).
(26) W. J. Lautenberger, E. N. Jones, and J. G. Miller, *J. Am. Chem. Soc.*, **90**, 1100 (1968).
(27) C. J. Biaselle and J. G. Miller, *J. Am. Chem. Soc.*, **96**, 3813 (1974).
(28) D. N. Kender, *Diss. Abstr. Int. B*, **37**, 1689 (1976).
(29) S. A. Markarian and H. Fisher, *J. Chem. Soc. Chem. Commun.*, **1979**, 1055.
(30) K. M. C. Davis and M. F. Farmer, *J. Chem. Soc. B*, **1967**, 28.
(31) The Merck Index, 9th ed., Merck and Co., Rahway, N.J., 1976.

ACKNOWLEDGMENTS

Presented at the National Meeting of the American Chemical Society, Seattle, Washington, March 1983, in the Medicinal Chemistry Section, Abstract 22 (Electron-Transfer Mechanism).

This work was supported in part by the University Research Foundation, La Jolla, Calif. Discussions of the electron-transfer reactions of amines with carbon tetrachloride with Prof. Cal Y. Meyers are gratefully acknowledged.

New Insights in the Clastic Binding Hypothesis for Opiate–Receptor Interactions II: Proton-Transfer Mechanism

VERA M. KOLB ˣ and STEVE SCHEINER

Received June 22, 1983, from the *Department of Chemistry and Biochemistry, Southern Illinois University, Carbondale, IL 62901.* Accepted for publication August 12, 1983.

Abstract □ *Ab initio* (4-31G) molecular orbital calculations were performed on model systems to investigate the proton-transfer version of the clastic binding hypothesis for opiate-receptor interactions. Ammonia was chosen as the model for the nitrogen-containing portion of the opiate molecule, while ammonia and water were chosen as models for the proton acceptor at the receptor. The equilibrium position of a proton situated between the two molecules is found to be determined primarily by the orientation of the proton-donor molecule with some influence also from the other molecule. Misalignments of the lone pairs can significantly alter equilibrium populations when the proton affinities of the two molecules are similar.

Keyphrases □ Clastic binding hypothesis—proton-transfer mechanism, opiate-receptor interactions, *ab initio* molecular orbital calculations □ Opiate-receptor interactions—proton-transfer mechanism, clastic binding hypothesis, *ab initio* molecular orbital calculations □ Proton transfer—mechanism, clastic binding hypothesis, opiate-receptor interactions, *ab initio* molecular orbital calculations

Belleau *et al.* (1, 2) have presented concrete evidence that the relative spatial orientation of the lone electron pair on nitrogen (N lone pair) or morphine-type opiates is crucial for their opiate activity. On this basis they proposed the clastic binding hypothesis for opiate-receptor interactions (3). According to this hypothesis, morphine-type opiates achieve productive binding with the opiate receptor through a clastic binding process involving a stereospecific electron transfer from the nitrogen lone electron pair of the opiate to some electrophilic site at the opiate receptor. This hypothesis was recently analyzed from a chemical point of view and was found to be chemically feasible (4). An extended form of this hypothesis was proposed (4) to accommodate recent observations by Fishman *et al.* concerning the *N*-demethylation of morphines in the brain (5-7).

Belleau and co-worker (2) later proposed another version of the clastic binding hypothesis according to which the N lone pair of opiates is involved in a stereospecific proton transfer to the receptor leading to strong analgesia. For optimal analgesia, a morphine should have the N lone pair oriented properly for a facile proton transfer. This version of the clastic binding

© 1984, American Pharmaceutical Association

(2) J. Dimaio, F. R. Ahmed, P. Schiller, and B. Belleau, in "Recent Advances in Receptor Chemistry," F. Gualtieri, M. Giannella, and C. Melchiorre, Eds., Elsevier/North-Holland Biomedical, 1979, pp. 221-234.
(3) B. Belleau and P. Morgan, *J. Med. Chem.*, **17**, 908 (1974).
(4) A. H. Beckett, A. F. Casy, and N. J. Harper, *J. Pharm. Pharmacol.*, **6**, 874 (1956).
(5) J. Fishman, E. F. Hahn, and B. I. Norton, *Nature (London)*, **261**, 64 (1976).
(6) E. F. Hahn, B. I. Norton, and J. Fishman, *Biochem. Biophys. Res. Comm.*, **89**, 233 (1979).
(7) E. F. Hahn, B. I. Norton, and J. Fishman, in "Endogenous and Exogenous Opiate Agonists and Antagonists," E. L. Way, Ed., Pergamon, New York, N.Y., 1980, pp. 529-532.
(8) P. J. Smith and C. K. Mann, *J. Org. Chem.*, **34**, 1821 (1969), and references therein.
(9) L. C. Portis, V. V. Bhat, and C. K. Mann, *J. Org. Chem.*, **35**, 2175 (1970).
(10) F. D. Lewis and T.-I. Ho, *J. Am. Chem. Soc.*, **102**, 1751 (1980), and references therein.
(11) R. B. Silverman, S. J. Hofman, and W. B. Catus III, *J. Am. Chem. Soc.*, **102**, 7126 (1980).
(12) C. Y. Meyers, W. S. Matthews, L. L. Ho, V. M. Kolb, and T. E. Parady, in "Catalysis in Organic Synthesis," G. V. Smith, Ed., Academic, New York, N.Y., 1977, pp. 217, 260-278.
(13) N. Sutin in "Oxidases and Related Redox Systems," Vol. I, T. E. King, H. S. Mason, and M. Morrison, Eds., Wiley, New York, N.Y., 1965, pp. 37-50.
(14) V. M. Kolb, *J. Pharm. Sci.*, **67**, 999 (1978).
(15) A. Korolkovas, in "Essentials of Molecular Pharmacology," Wiley-Interscience, New York, N.Y., 1970, pp. 265-288, and references therein.
(16) N. M. Lee and A. P. Smith, *Life Sci.*, **26**, 1459 (1980), and references therein.
(17) T. M. Cho, P. Y. Law, and H. H. Loh, in "Neurochemical Mechanisms of Opiates and Endorphins, Advance Biochemical Phychopharmacology," Vol. 20, H. H. Loh, and D. H. Ross, Eds., Raven, New York, N.Y., 1979, pp. 69-101, and references therein.
(18) G. R. Moore and R. J. P. Williams, *Coordination Chem. Rev.*, **18**, 125 (1976), and references therein.
(19) C. Y. Meyers and V. M. Kolb, *J. Org. Chem.*, **43**, 1985 (1978).
(20) R. Foster, "Organic Charge-Transfer Complexes," Academic, New York, N.Y., 1969, pp. 278-280, 300, and references cited therein.
(21) R. F. Collins, *Chem. Ind. (London)*, **1957**, 704.
(22) N. H. Cromwell, P. W. Foster, and M. M. Wheeler, *Chem. Ind. (London)*, **1959**, 228.
(23) R. Foster, *Chem. Ind. (London)*, (**1960**) 1354.
(24) G. J. Beichl, J. E. Colwell, and J. G. Miller, *Chem. Ind. (London)*, **1960**, 203.
(25) D. P. Stevenson and G. M. Coppinger, *J. Am. Chem. Soc.*, **84**, 149 (1962).
(26) W. J. Lautenberger, E. N. Jones, and J. G. Miller, *J. Am. Chem. Soc.*, **90**, 1100 (1968).
(27) C. J. Biaselle and J. G. Miller, *J. Am. Chem. Soc.*, **96**, 3813 (1974).
(28) D. N. Kender, *Diss. Abstr. Int. B*, **37**, 1689 (1976).
(29) S. A. Markarian and H. Fisher, *J. Chem. Soc. Chem. Commun.*, **1979**, 1055.
(30) K. M. C. Davis and M. F. Farmer, *J. Chem. Soc. B*, **1967**, 28.
(31) The Merck Index, 9th ed., Merck and Co., Rahway, N.J., 1976.

ACKNOWLEDGMENTS

Presented at the National Meeting of the American Chemical Society, Seattle, Washington, March 1983, in the Medicinal Chemistry Section, Abstract 22 (Electron-Transfer Mechanism).

This work was supported in part by the University Research Foundation, La Jolla, Calif. Discussions of the electron-transfer reactions of amines with carbon tetrachloride with Prof. Cal Y. Meyers are gratefully acknowledged.

New Insights in the Clastic Binding Hypothesis for Opiate–Receptor Interactions II: Proton-Transfer Mechanism

VERA M. KOLB ˣ and STEVE SCHEINER

Received June 22, 1983, from the *Department of Chemistry and Biochemistry, Southern Illinois University, Carbondale, IL 62901.* Accepted for publication August 12, 1983.

Abstract □ *Ab initio* (4-31G) molecular orbital calculations were performed on model systems to investigate the proton-transfer version of the clastic binding hypothesis for opiate-receptor interactions. Ammonia was chosen as the model for the nitrogen-containing portion of the opiate molecule, while ammonia and water were chosen as models for the proton acceptor at the receptor. The equilibrium position of a proton situated between the two molecules is found to be determined primarily by the orientation of the proton-donor molecule with some influence also from the other molecule. Misalignments of the lone pairs can significantly alter equilibrium populations when the proton affinities of the two molecules are similar.

Keyphrases □ Clastic binding hypothesis—proton-transfer mechanism, opiate-receptor interactions, *ab initio* molecular orbital calculations □ Opiate-receptor interactions—proton-transfer mechanism, clastic binding hypothesis, *ab initio* molecular orbital calculations □ Proton transfer—mechanism, clastic binding hypothesis, opiate-receptor interactions, *ab initio* molecular orbital calculations

Belleau *et al.* (1, 2) have presented concrete evidence that the relative spatial orientation of the lone electron pair on nitrogen (N lone pair) or morphine-type opiates is crucial for their opiate activity. On this basis they proposed the clastic binding hypothesis for opiate-receptor interactions (3). According to this hypothesis, morphine-type opiates achieve productive binding with the opiate receptor through a clastic binding process involving a stereospecific electron transfer from the nitrogen lone electron pair of the opiate to some electrophilic site at the opiate receptor. This hypothesis was recently analyzed from a chemical point of view and was found to be chemically feasible (4). An extended form of this hypothesis was proposed (4) to accommodate recent observations by Fishman *et al.* concerning the *N*-demethylation of morphines in the brain (5-7).

Belleau and co-worker (2) later proposed another version of the clastic binding hypothesis according to which the N lone pair of opiates is involved in a stereospecific proton transfer to the receptor leading to strong analgesia. For optimal analgesia, a morphine should have the N lone pair oriented properly for a facile proton transfer. This version of the clastic binding

© 1984, American Pharmaceutical Association

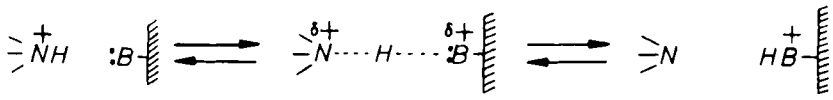

Figure 1—*Schematic representation of the proton transfer between a protonated morphine-type opiate (only nitrogen is shown) and an acceptor base (B) of the opiate receptor (shaded area) (adapted from Ref. 2).*

hypothesis shall be referred to as the proton-transfer version, as opposed to the electron-transfer version which was discussed in the previous paper (4).

We believe that the clastic binding hypothesis shows promise of explaining the mechanism of opiate-receptor interactions and, therefore, deserves further examination. The objective of this paper is to provide new insights into this hypothesis. This paper deals with the proton-transfer version of this hypothesis, while the previous paper (4) concerns the electron-transfer version. (An extensive discussion of the proton-transfer version of the clastic binding hypothesis can be found in Ref. 2.) We summarize here some crucial points with emphasis on those which we are going to investigate (*vide infra*).

BACKGROUND

Belleau and coworkers (2) visualized the proton transfer between a morphine-type opiate and the opiate receptor as shown in Fig. 1. The potency of an analgesic, according to these authors, depends on the position of the equilibrium of the proton, which is affected by the basicity of nitrogen of morphines. To account for the observed influence of the directionality of the N lone pair of morphine-type compounds on their opiate activity, it was proposed that:

1. Only the orientation of the N lone pair which allows a facile, *i.e.*, energetically favorable, proton transfer is favorable for induction of analgesia. There are other orientations of the N lone pair from which the proton transfer is energetically unfavorable.

2. The position of equilibrium of the proton will depend on the N lone pair orientation (in addition to basicity of nitrogen).

We decided to investigate the above two statements in a quantitative manner using *ab initio* quantum chemical methods. These methods are suitable for this type of study since the relative orientations of species to be studied (amine, proton, and the base at the receptor) may be precisely specified and easily varied. SCF calculations were carried out with the 4-31G basis set since this procedure furnishes proton-transfer energy barriers in excellent agreement with much more sophisticated theoretical treatments using large basis sets and configuration interactions (8–11).

To perform *ab initio* calculations it was necessary to model the large morphine molecules by smaller representative systems. Ammonia was chosen as the simplest model of the amine-type nitrogen-containing portion of a biologically active morphine-type opiate. Two different models were chosen to represent the base at the opiate receptor, the nature of which has not as yet been elucidated. We examine the possibility that such a base contains nitrogen or oxygen, as is frequently the case for bases encountered in biological systems (12). The first model is the nitrogen base ammonia which contains a single lone electron pair (Fig. 2). Water was used as the simplest model of an oxygen base and contains two lone pairs (Fig. 3). These two models for the base provide a wide range of basicity, which is expected to include the pK of the receptor within it.

EXPERIMENTAL

All molecular orbital calculations were performed using the *ab initio* Gaussian-70 system of programs (13). The 4-31G basis set (14) was used within the restricted Hartree-Fock formalism.

Before we present our calculations on the simple model systems (Figs. 2 and 3) it is important to define clearly all the parameters of these models in conjunction with the actual case of a morphine undergoing a proton transfer at the opiate receptor (Fig. 4). Both the morphine molecule and the hypothetical base at the receptor have been shown to be sterically fixed at the receptor: morphine by virtue of the noncovalent "lock-and-key" fit (15) and the base at the receptor by virtue of a covalent bond (Fig. 4). The example of a morphine shown in Fig. 4 is oxymorphone, a potent opiate agonist. The example of a base B at the receptor shown in Fig. 4 is a neutral base having one lone electron pair. The N lone pairs of oxymorphone and the base B are shown to be in a less than perfect alignment along the N···B internuclear axis, which is a more likely case than perfect alignment, since morphines may not be the ideal substrates for the opiate-receptor cavity [etorphine, for example, may be a better candidate (16)].

The N···B distance R is unknown. In our calculations on the model systems this distance varied from 2.75 to 3.15 Å, which is a typical range between proton donors and acceptors encountered in biologically important hydrogen-bonded systems (12). The N···B distance R shown in Fig. 4 is likely to be longer than the equilibrium N···B distance (in the absence of steric constraints), due to the postulated less-than-perfect fit between morphine and the receptor. In Figs. 2–4, r refers to the distance between the proton-donating nitrogen atom and the central proton in its equilibrium position. This parameter, r, will depend to some extent on the internitrogen distance R, as will be demonstrated below.

To study the dependence of the properties of the proton transfer on the directionality of the lone pairs, the NH_3 and base molecules (NH_3 or OH_2) were twisted, as illustrated in Figs. 2 and 3. α_1 and α_2 are angles describing the rotation of the nitrogen proton donor and the proton-acceptor B, respectively, from their optimal orientation. Both conrotatory and disrotatory misalignments were studied. For each configuration (defined by R, α_1, and α_2), the equilibrium position of the central proton was located. Scheme I conveniently summarizes the relevant features of the energetics of the proton-transfer process. The left well corresponds to the NH···B state and the right well to N···HB. Between the two is an energy barrier $E^\dagger$ over which the proton must pass. A high value of $E^\dagger$ may prevent proton transfer. ΔE refers to the energy difference between the states ($N^+H\cdots B$) and ($N\cdots H^+B$), and its value will determine the equilibrium population of the proton between the two states (assuming equilibrium is achieved).

RESULTS

$(H_3N\cdots H\cdots NH_3)^+$ System—We begin our discussion with the system in which a proton may be transferred between two ammonia molecules, one of which models the morphine base and the other represents the base at the opiate receptor (Fig. 2). We shall refer to this model as the $(H_3N\cdots H\cdots NH_3)^+$ system.

A study of the energetics of proton transfer in the $(H_3N\cdots H\cdots NH_3)^+$ system has recently been published by Scheiner (17). We summarize briefly here some conclusions of the latter work which are relevant to the objectives of this study. Calculated potential energy curves of the type shown in Scheme I are illustrated in Fig. 5. For internitrogen distances R <2.5 Å, the potential may be seen to contain a single centrally located minimum. At this distance, the preferred position of the proton is midway between the two nitrogens. However, for larger values of R, the potential acquires a symmetric double-well character. The two equivalent energy minima each correspond to a configuration in which the central proton is associated with one ammonia molecule or the other. The magnitudes of the energy barriers to proton transfer increase rather quickly as R is increased. In all configurations, for values of R ranging from 2.45 to 3.15 Å, the hydrogen bond is linear.

If one assumes that there is a meaningful parallel between the model system $(H_3N\cdots H\cdots NH_3)^+$ and the morphine-receptor complex shown in Fig. 4, an important feature emerges: there may be a significant energy barrier for the proton transfer between the morphine and the receptor which may be enlarged or reduced by increasing or decreasing, respectively, the distance R. This feature could provide a simple regulatory mechanism in case the re-

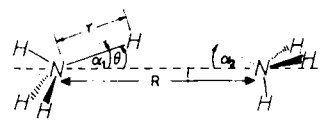

Figure 2—*Model representing a proton transfer from the protonated nitrogen of a morphine-type opiate (NH_3 on the left) and a base B at the receptor (NH_3 on the right). Both NH_3 units belong to the C_{3v} point group with r(NH) = 1.008 Å, θ(HNH) = 109.3°. The equilibrium position of the central proton is defined by the N—H distance r and the angle θ between the N—H and N···N axes. Angles α_1 and α_2 describe the rotations of the proton-donating amine and proton-accepting base, respectively, from their optimal orientations, $\alpha_1 = \alpha_2 = 0°$. Dotted lines represent the C-3 rotation axis of each molecule.*

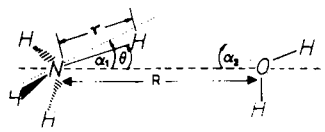

Figure 3—*Analogous to Fig. 2, except that the proton-accepting base at the receptor is modeled by OH_2 with r(OH) = 0.95 Å, θ(HOH) = 111.3°. The corresponding dotted line indicates the C-2 symmetry axis of OH_2.*

ceptor has a point of flexibility (dashed line on the boundary of the receptor in Fig. 4).

Belleau's claim that only certain orientations of the N lone pair in the system shown in Fig. 1 allow a facile (*i.e.*, energetically favorable) proton transfer is supported to some extent by the study of the energetics in the $(H_3N\cdots H\cdots NH_3)^+$ system in terms of α_1 and α_2 for a range of R values (17). Thus, Scheiner has found that for each R studied (2.73, 2.95, and 3.15 Å) the activation barriers of the systems having $\alpha \neq 0$, *i.e.*, the N lone pair(s) misaligned relative to their optimal orientation, are larger than those of the systems in which the N lone pair(s) are optimally oriented, *i.e.*, $\alpha = 0$. The magnitude of the energy barrier depends on the type of misalignment between the two N lone pairs, and is largest for disrotatory misalignments (*e.g.*, 42.0 kcal/mol for $\alpha_1 = -40°$, $\alpha_2 = 40°$, and $R = 3.15$ Å). Misalignments of 20° produce barrier increases in the range of 1–2 kcal/mol, while much more drastic increases are observed for greater misalignments of the N lone pairs.

In this paper we focus on the influence of the relative spatial orientation of the N lone pairs on the equilibrium position of the central proton and the relative equilibrium populations of the $(H_3NH\cdots NH_3)^+$ and $(H_3N\cdots HNH_3)^+$ states.

Table I contains a summary of the equilibrium position of the central proton in the $(H_3NH\cdots NH_3)^+$ state for a range of intermolecular configurations specified by R, α_1, and α_2. We note that the equilibrium NH distance r remains virtually the same, ~1 Å (1.002–1.087), for all α values and R values studied. As R increases the proton is slightly closer to the NH_3, the proton donor, which is expected since the influence of the other NH_3, the proton acceptor (ammonia on right in Fig. 2), becomes weaker as the distance R increases. The only exception to this trend is found in the last entry of Table I, namely for the largest misalignment studied ($\alpha_1 = 40°$ and $\alpha_2 = -40°$), in which the distance r actually increases very slightly with the increased R. With changing α values the proton is rotated at approximately constant r so that it partially follows the N lone pair of the NH_3, the proton donor. This is seen, for example, in entries 4 and 5 of Table I, which show that when the NH_3 proton donor is rotated by 20° and 40°, the proton is rotated off the N···N axis by 11.9° and 30.3°, respectively, for $R = 2.75$ Å. If we consider the N lone pair as lying along the C-3 symmetry axis of NH_3, α may be thought of as a measure of the "directionality" of the lone pair. [However, this correspondence is only true near the nucleus, as the N lone pair may undergo "bending" toward the proton as illustrated in similar examples (18, 19).]

The calculated values of Θ are a compromise between the left NH_3 which attempts to pull the proton along the lone pair direction (α_1) and the right NH_3 which pulls the proton toward the N···N axis (0°). The difference between α_1 and θ, listed in Table I, provides a measure of the strength of the latter attraction. As the distance R increases, θ becomes closer to α_1, *i.e.*, the proton follows the N lone pair of the proton-donating NH_3 more closely, since the influence of the proton-accepting ammonia diminishes for greater R. The only exception, again, is the case of the largest misalignment, presented in entry 9. In conclusion, the equilibrium position of the proton depends primarily on the direction of the donor lone pair and to a lesser extent on the relative position of the acceptor lone pair. The equilibrium N···H distance, r, generally remains within a narrow range, ~1.05 Å.

As mentioned above, the clastic binding hypothesis requires a proton transfer from the nitrogen of the morphine to the base in order to initiate analgesia. The calculated energetics are able to provide information about the rate of this proton transfer *via* the barrier to transfer $E^\dagger$. In addition, it

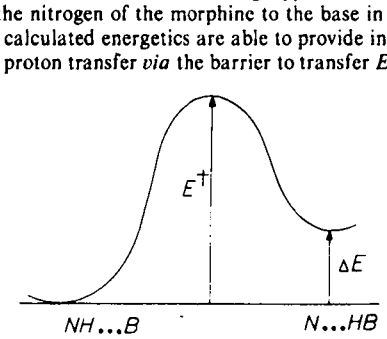

Scheme I

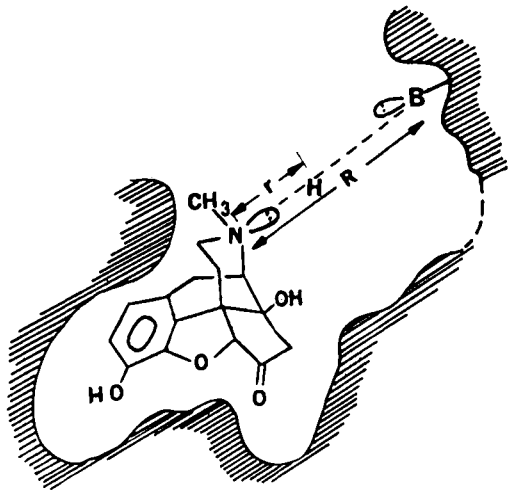

Figure 4—*Schematic representation of a proton transfer from the nitrogen of a morphine-type opiate (oxymorphone) to a hypothetical base B at the opiate receptor. The latter is shown as a shaded area whose shape should not be taken literally. The broken boundary of the receptor indicates a point of possible receptor flexibility and leads to uncertainty in distance R. The lone pairs of oxymorphone and the base B are shown to be in a less-than-perfect alignment along the N···B internuclear axis for reasons discussed in the text.*

would be useful to know something about the relative populations of the NH···B and N···HB states as it is only the latter that leads to analgesia. Information of this type is available from the difference in energy between these two states, corresponding to ΔE in Scheme I. At thermodynamic equilibrium the ratio of relative populations is given by:

$$K = \frac{n(\text{N}\cdots\text{HB})}{n(\text{NH}\cdots\text{B})} = \exp(-\Delta G°/RT)$$

where $\Delta G°$ refers to the difference in Gibbs free energy between the two states. By equating our calculated values of ΔE to $\Delta G°$ we make the following assumptions: (*a*) the difference in entropy between the two states is negligible and (*b*) the zero-point vibrational energies of the two states are about the same. The lack of any major changes in bonding structure, with the exception of the proton motion, would lead one to expect these assumptions to be reasonable.

For the angularly undistorted system ($\alpha_1 = \alpha_2 = 0°$), the symmetry of the potential energy curve leads to a value of $\Delta E = 0$ and therefore to $K = 1$. The same is true for both conrotatory and disrotatory distortions where $\alpha_1 = \pm\alpha_2$. In all of these cases, we would expect equal populations of NH···B and N···HB. However, when one molecule is rotated and the other is not, the symmetry is destroyed and $\Delta E \neq 0$. The calculated values of ΔE in cases where the proton-donor molecule is rotated by α and the acceptor molecule is left undistorted are provided in Table II. Along with these calculated energy differences are included the associated equilibrium constants K. For distortions of only 20°, the ΔE values are quite small and K is thus nearly equal to 1. However, for greater distortions of 40°, the energy differences are greater than 1 kcal/mol and K is of the order of 0.1. We thus see that for such distortions, the population of state NH···B is an order of magnitude greater than that of N···HB. In other words, the equilibrium of the two states is shifted toward that configuration in which the proton is associated with the lone pair with the misalignment.

$(H_3N\cdots H\cdots OH_2)^+$ System—The second system we studied is $(H_3N\cdots H\cdots OH_2)^+$ in which the morphine base is represented by H_3N and the proton acceptor at the receptor is modeled by H_2O (Fig. 3). The latter base has two lone electron pairs, thus providing an electronically different environment than that of the aforementioned NH_3 system. In addition, H_2O has a different basicity than NH_3.

A study of the energetics of proton transfer in the $(H_3N\cdots H\cdots OH_2)^+$ system as a function of R, α_1, and α_2 has recently been published (10, 20). The results of these studies are qualitatively parallel to that of the $(H_3N\cdots H\cdots NH_3)^+$ system, except that the asymmetry of the former system leads to two activation barriers. one for the proton transfer from NH_4^+ to H_2O ($E^\dagger_{NH\to O}$) and one for the proton transfer from H_3O^+ to NH_3 ($E^\dagger_{OH\to N}$). The latter barrier is smaller than the former. The values of activation barriers for proton transfers from NH_4^+ to H_2O vary from 29.1 kcal/mol for the optimally aligned system ($\alpha_1 = \alpha_2 = 0°$) to 52.2 kcal/mol for the system with the greatest misalignment studied ($\alpha_1 = 40°$ and $\alpha_2 = -40°$). The corre-

Table I—Equilibrium Position of Proton as Function of α in the $(H_3N\cdots H\cdots NH_3)^+$ System for R Values of 2.75, 2.95, and 3.15 Å

Entry	α_1	α_2	R = 2.75 Å			R = 2.95 Å			R = 3.15 Å		
			r, Å	θ, °	$\alpha_1 - \theta$ °	r, Å	θ, °	$\alpha_1 - \theta$, °	r Å	θ, °	$\alpha_1 - \theta$, °
1	0	0	1.087	0	0	1.062	0	0	1.048	0	0
2	0	20	1.076	3.0	−3.0	1.057	2.2	−2.2	1.045	1.7	−1.7
3	0	40	1.059	5.6	−5.6	1.046	4.1	−4.1	1.037	3.1	−3.1
4	20	0	1.068	11.9	8.1	1.051	13.5	6.5	1.039	14.8	5.2
5	40	0	1.028	30.3	9.7	1.024	32.2	7.8	1.021	33.8	6.2
6	20	20	1.069	14.7	5.3	1.051	15.6	4.4	1.041	16.4	3.6
7	40	40	1.036	33.4	6.6	1.030	34.5	5.5	1.025	35.5	4.5
8	20	−20	1.055	10.0	10.0	1.041	12.2	7.8	1.033	13.9	6.1
9	40	−40	1.002	35.3	4.7	1.007	35.3	4.7	1.010	35.8	4.2

Table II—Energy Differences and Relative Populations [a] for $(H_3N\cdots H\cdots NH_3)^+$

α	R = 2.75 Å		R = 2.95 Å		R = 3.15 Å	
	ΔE, kcal/mol	K	ΔE, kcal/mol	K	ΔE, kcal/mol	K
20°	−0.126	1.23	−0.107	1.19	−0.032	1.052
40°	1.192	0.145	1.161	0.152	1.321	0.119

[a] For t = 27° C.

sponding values for the barriers for proton transfer from H_3O^+ to NH_3 are much smaller: 2.7 and 16.9 kcal/mol.

The comparison between the values for the energy barriers for the proton transfer from NH_4^+ to H_2O and to NH_3 reveals that the latter are much smaller than the former. This difference is undoubtedly due chiefly to the difference in the electronegativities of nitrogen and oxygen atoms (10, 20). The activation barriers for the proton transfer in the $(H_3N\cdots H\cdots OH_2)^+$ system depend on the misalignments between the proton donor and acceptor in a manner very similar to that observed for the $(H_3N\cdots H\cdots NH_3)^+$ system (10, 20).

We report here the effect of the relative spatial orientation of the lone electron pairs in the $(H_3N\cdots H\cdots OH_2)^+$ system on the equilibrium position of the proton (Table III). The analysis of data presented in Table III reveals a picture analogous to that of the $(H_3N\cdots H\cdots NH_3)^+$ system. The r distance, again, is essentially constant and is ~1 Å (1.000–1.046 Å). This distance again decreases slightly with increased R, except for the case of the largest misalignment (entry 9 of Table III), in which r increases slightly. θ Follows α_1 again (*cf.* entries 4 and 5) and to a smaller extent α_2 (*cf.* entries 2 and 3). The $\alpha_1 - \theta$ difference here is as large as 7.3°.

DISCUSSION

While it would be presumptuous to generalize our data on the $(H_3N\cdots H\cdots NH_3)^+$ and $(H_3N\cdots H\cdots OH_2)^+$ systems and claim that they are directly applicable to the situations where the proton is being transferred between the morphine-type opiates and the opiate receptor, we believe that our findings should be considered qualitatively when picturing morphine–receptor interactions in conjunction with the clastic binding hypothesis of Belleau. The previously published calculations of the energetics of proton transfer in the $(H_3N\cdots H\cdots NH_3)^+$ and $(H_3N\cdots H\cdots OH_2)^+$ systems as a function of the distance and the relative spatial orientation of the species between which the proton is being transferred (10, 17, 20) support the claim by Belleau and co-workers (2) that the ease of proton transfer depends on the directionality of the N lone pair (2).

We have presented calculations which show that the equilibrium position of the proton depends on both the N lone pair direction and the orientation of the proton-acceptor molecule. We have shown in both model systems—$(H_3N\cdots H\cdots NH_3)^+$ and $(H_3N\cdots H\cdots OH_2)^+$—that the proton "follows" the N lone pair of the proton donor, and to a lesser extent that of the acceptor. The result is that if the "directionality" of the N lone pair is changed by a certain angle α_1, the proton will change its position by an angle θ, which may differ from α_1 by up to 10° in our model systems. The distance r between the proton and the proton-donating NH_3 stays pretty much constant at ~1 Å. However, the equilibrium populations of the proton on the two molecules may depend significantly on the N lone pair directions. This dependence is maximized in a system such as $(H_3N\cdots H\cdots NH_3)^+$ where the proton-donor and -acceptor molecules have identical proton affinities. When the proton affinities are significantly different there is little dependence on angular characteristics for the following reasons. Even in the angularly undistorted case, ΔE is quite different from 0. In the case of $(H_3N\cdots H\cdots OH_2)^+$, this quantity is about 38 kcal/mol. The equilibrium population of $N\cdots HO$ relative to $NH\cdots O$ is negligible (10^{-28}). Angular distortions of the two groups may increase or decrease ΔE by only a small amount relative to the original 38 kcal/mol. For example, a reduction of ΔE by 2 kcal/mol would only change K from 10^{-28} to 10^{-26}, an increase of 100-fold, but still a negligible amount of $N\cdots HO$. Therefore, for the angular orientations of the lone pairs to have a major effect on the relative populations of the two states, it would be necessary for the morphine and receptor base to have very similar proton affinities.

With regard to the accuracy of the particular quantum chemical method used here, we do not expect our results to be changed in any major way by use of larger basis sets or inclusion of electron correlation. While the specific r(NH) distances in Tables I and III may be somewhat altered, our finding of very small changes in this distance with variations of the hydrogen-bond configuration is expected to be verified. The energetics calculated with the 4-31G basis set at the Hartree–Fock level are also expected to be little changed with more sophisticated procedures, as has been demonstrated previously (8–11, 17, 20).

We may use our results to draw some inferences about the effects of modifications of the relative orientation of the morphine and receptor in Fig. 4. A rotation of the morphine molecule as a whole, with the nitrogen atom as a stationary "pivot" would correspond to twisting of the proton-donor molecule (α_1) in Figs. 2 and 3. α_2,Rotation of the proton acceptor, would be effected by a translatory motion of the entire morphine molecule to bring the nitrogen atom more out of line with the base lone pair. Our results provide evidence that small rotations of these types, *i.e.*, $\leq$20°, would not significantly alter the populations of the "untransferred" state $NH\cdots B$ and the "transferred" state $N\cdots HB$. On the other hand, a large rotation was shown above to lead to a preferential population of the proton on the group with the misaligned lone pair. We therefore infer that a rotation of the morphine about its nitrogen atom (α_1) will inhibit transfer of its proton to the base. This transfer would, however, be enhanced by a translation of the morphine off the base lone pair direction (α_2).

The reader is cautioned that these conclusions are based only on equilibrium populations. Equilibrium might not be achieved in these systems. Secondly, while the equilibrium population of the $N\cdots HB$ state might be increased by the second motion described above, the angular distortion also produces an enlargement of the energy barrier to proton transfer which would act to inhibit

Table III—Equilibrium Position of Proton as Function of α in the $(H_3N\cdots H\cdots OH_2)^+$ System for R Values of 2.75, 2.95, and 3.15 Å

Entry	α_1	α_2	R = 2.75 Å			R = 2.95 Å			R = 3.15 Å		
			r, Å	θ, °	$\alpha_1 - \theta$ °	r, Å	θ, °	$\alpha_1 - \theta$, °	r Å	θ, °	$\alpha_1 - \theta$, °
1	0	0	1.046	0	0	1.039	0	0	1.033	0	0
2	0	20	1.042	2.3	−2.3	1.037	1.7	−1.7	1.031	1.3	−1.3
3	0	40	1.032	4.6	−4.6	1.030	3.4	−3.4	1.026	2.6	−2.6
4	20	0	1.037	14.2	5.8	1.032	15.3	4.7	1.027	16.2	3.8
5	40	0	1.017	33.3	6.7	1.017	34.5	5.5	1.016	35.6	4.4
6	20	20	1.039	16.1	3.9	1.033	16.7	3.3	1.028	17.4	2.6
7	40	40	1.025	35.1	4.9	1.022	36.0	4.0	1.020	36.8	3.2
8	20	−20	1.030	12.7	7.3	1.026	14.2	5.8	1.023	15.5	4.5
9	40	−40	1.000	36.1	3.9	1.005	36.3	3.7	1.008	36.8	3.2

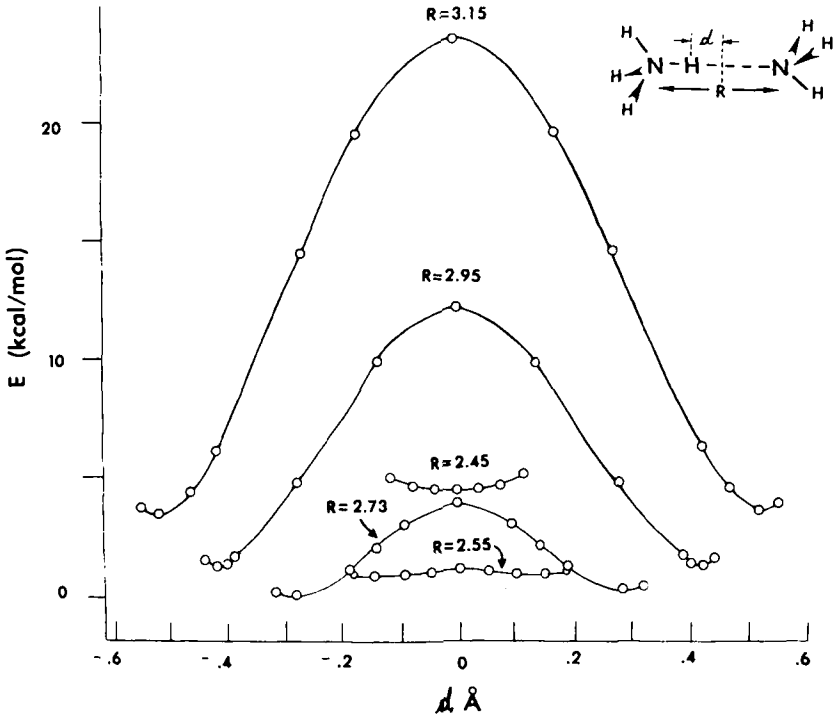

Figure 5—*Energetics of proton transfer in the* $(H_3N\cdots H\cdots NH_3)^+$ *system for various internitrogen distances* R. *Energies are all shown relative to that of the fully optimized structure* (R = 2.73 Å, r = 1.087 Å, E = −112.6132 a.u.).

this transfer. Finally, the changes in relative populations would be greatly reduced if the basicities of the morphine and receptor are different. It remains, of course, to elucidate the biological details, such as how the opiate response is elicited by the proton transfer and how the equilibrium population of the proton mediates the opiate activity.

REFERENCES

(1) B. Belleau, T. Conway, F. R. Ahmed, and A. D. Hardy, *J. Med. Chem.*, **17**, 907 (1974).

(2) J. Dimaio, F. R. Ahmed, P. Shiller, and B. Belleau, in "Recent Advances in Receptor Chemistry," F. Gualtieri, M. Giannella, and C. Melchiorre, Eds., Elsevier/North Holland Biomedical Press, 1979, pp. 221–234.

(3) B. Belleau and P. Morgan, *J. Med. Chem.*, **17**, 908 (1974).

(4) V. M. Kolb, *J. Pharm. Sci.*, **73**, 715 (1984).

(5) J. Fishman, E. F. Hahn, and B. I. Norton, *Nature (London)*, **261**, 64 (1976).

(6) E. F. Hahn, B. I. Norton, and J. Fishman, *Biochem. Biophys. Res. Commun.*, **89**, 233 (1979).

(7) E. F. Hahn, B. I. Norton, and J. Fishman, in "Endogenous and Exogenous Opiate Agonists and Antagonists," E. L. Way, Ed., Pergamon, New York, N.Y., 1980, pp. 529–532.

(8) S. Scheiner, *J. Am. Chem. Soc.*, **103**, 315 (1981).

(9) S. Scheiner and L. B. Harding, *J. Am. Chem. Soc.*, **103**, 2169 (1981).

(10) S. Scheiner and L. B. Harding, *J. Phys. Chem.*, **87**, 1145 (1983).

(11) S. Scheiner, M. M. Szcześniak, and L. D. Bigham, *Int. J. Quant. Chem.*, **23**, 739 (1983).

(12) S. N. Vinogradov, in "Molecular Interactions," Vol. 2, H. Ratajczak and W. J. Orville-Thomas, Eds., Wiley, New York, N.Y., 1980, pp. 179–229 (see pp. 181–185 for a summary of information on lengths of hydrogen bonds in peptides and related molecules).

(13) W. J. Hehre, W. A. Lathan, R. Ditchfield, M. D. Newton, and J. A. Pople, *Quantum Chemistry Program Exchange*, **11**, 236 (1973).

(14) R. Ditchfield, W. J. Hehre, and J. A. Pople, *J. Chem. Phys.*, **54**, 724 (1971).

(15) S. H. Snyder and S. Matthysse, "Opiate Receptor Mechanisms," The MIT Press, Cambridge, Mass., 1975, pp. 63–65, 78, 137.

(16) S. H. Snyder and S. Matthysse, "Opiate Receptor Mechanisms," The MIT Press, Cambridge, Mass., 1975, p. 77.

(17) S. Scheiner, *J. Phys. Chem.*, **86**, 376 (1982).

(18) V. M. Kolb and S. Scheiner, *J. Pharm. Sci.*, **73**, 389 (1984).

(19) S. Scheiner and V. M. Kolb, *Proc. Natl. Acad. Sci. USA*, **77**, 5602 (1980).

(20) S. Scheiner, *J. Chem. Phys.*, **77**, 4039 (1982).

ACKNOWLEDGMENTS

This work was supported in part by grants from the University Research Foundation (La Jolla, California) to V. M. K. and from the National Institutes of Health (GM 29391), the Research Corporation, and NIH (Research Career Development Award, 1982–1987) to S. S.

Presented at the National Meeting of the American Chemical Society, Seattle, Washington, March 1983, in the Medicinal Chemistry Section: Abstract 22 (Electron-Transfer Mechanism) and Abstract 27 (Proton-Transfer Mechanism).

A generous allocation of computer time from the Computing Center of Southern Illinois University is gratefully acknowledged.

Theoretical Basis for the Detection of General-Base Catalysis in the Presence of Predominating Hydroxide Catalysis

LEE E. KIRSCH * **and ROBERT E. NOTARI** ˣ

Received November 22, 1982, from the *Lloyd M. Parks Hall, College of Pharmacy, The Ohio State University, Columbus, OH 43210.* Accepted for publication April 19, 1983. *Present address: Product Development Division, Eli Lilly and Company, Indianapolis, IN 46206.

Abstract □ The detection of general-base catalysis in the presence of predominating specific-base catalysis in aqueous buffer solutions is examined for various relationships between k^0_{cat} and k^0_{OH}, the bimolecular rate constants for general-base and hydroxide-ion attack. The three experimental variables that affect the detection of buffer-base catalysis are the type of buffer, conjugate-acid concentration, and ionic strength. Various buffers used in pharmaceutical kinetic studies are considered, and it is concluded that buffers with high K_a values favor detection. Additionally, high conjugate-acid concentrations and ionic strengths appear to optimize the detection of general-base catalysis.

Keyphrases □ Catalysis, general base—detection in the presence of specific-base catalysis, theoretical basis, effect of buffer composition, acid concentration, and ionic strength □ Hydroxide catalysis—detection of coexisting general-base catalysis, theoretical basis, effect of buffer composition, acid concentration, and ionic strength

Aqueous stability studies often attempt to quantitate the dependence of an observed first-order rate constant on the concentrations of potential reactants such as hydroxide ions, hydronium ions, and buffer components (1). Failure to accurately define the rate expression or the reaction pathway can preclude the establishment of a reaction mechanism and limit the accuracy of stability predictions.

The quantitative assessment of buffer catalysis in the presence of predominating hydroxide- or hydronium-ion attack is difficult. The reasons are twofold. First, the pH region of greatest instability is also the region where the efficiency of specific catalysts (*i.e.*, hydroxide or hydronium ions) overshadows that of the buffer catalysts. If one attempts to make use of these faster rates to establish the reaction pathways, then buffer catalysis would probably be overlooked. Subsequent stability predictions would then underestimate the long-term rate of drug loss in buffer solutions in the pH region where buffer catalysis can compete with specific catalysis. The second reason is that in the presence of relatively high ionic strength and buffer concentrations, which are needed to quantitatively determine buffer catalysis in the presence of predominating specific-ion catalysis, secondary-type ionic atmosphere effects can occur even at constant ionic strength. These effects cause small pH changes, which tend to obscure buffer catalysis.

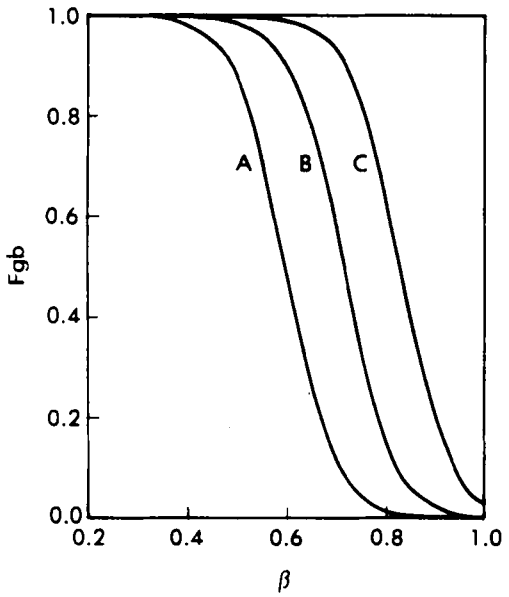

Figure 1—*Fraction of observed general-base catalysis, F_{gb}, as a function of the Brönsted coefficient for a typical buffer (phosphate, pK_a (25°C) = 7.21, p = q = 2). Curves A, B, and C were generated using Eq. 6 and [HB] = 0.01, 0.1, and 1.0, respectively. Ionic atmosphere effects were not included.*

The purpose of this study is to examine the effect of the design of stability studies on the detection of catalysis. A simple rate law was used involving general-base and a related specific-hydroxide degradation pathway. Equations were derived which quantitate the effect of the experimental design on the ability to measure buffer catalysis. Recommendations for detecting buffer-base catalysis in the presence of predominating hydroxide-ion attack are made, and potential problems are examined.

THEORETICAL

Rate Law—When drug degradation is accelerated by general- and specific-base catalysis, the observed first-order rate constant for drug loss, k_{obs}, may be defined:

$$k_{obs} = k^0_{OH}[OH]\frac{\gamma_d\gamma_{OH}}{\gamma_\ddagger} + k^0_{cat}[B]\frac{\gamma_d\gamma_B}{\gamma_{\ddagger'}} \qquad \text{(Eq. 1)}$$

where k^0_{OH} is the bimolecular rate constant for specific-base attack at ionic strength zero, k^0_{cat} is the bimolecular rate constant for general-base attack, [OH] and [B] are specific- and general-base concentrations, γ_d is the activity coefficient of the drug, γ_{OH} and γ_B are the specific- and general-base activity coefficients, and $\gamma_\ddagger$ and $\gamma_{\ddagger'}$ are the transition-state activity coefficients for the specific- and general-base pathways (2). Specific-base attack can involve either nucleophilic hydroxide addition or rate-limiting hydroxide-ion proton abstraction.

General-base catalysis is kinetically indistinguishable from specific-hydroxide and general-acid catalyses (3, 4), which may be defined as:

$$k_{obs(gb)} = \frac{k^0_{cat}K_a}{K_w}[HB][OH^-]\frac{\gamma_{HB}\gamma_{OH}\gamma_d}{\gamma_{\ddagger'}} \qquad \text{(Eq. 2)}$$

where K_a and K_w are the dissociation constants of the buffer and water, and [HB] and γ_{HB} represent the concentration and activity coefficient of the conjugate acid of the base. Division of $k_{obs(gb)}$ by k_{obs} (Eq. 1) yields the fraction due to the general-base pathway, F_{gb}:

$$F_{gb} = \frac{k^0_{cat}[HB]}{\left(\frac{K_w k^0_{OH}\gamma_\ddagger'}{K_a\gamma_{HB}\gamma_\ddagger}\right) + k^0_{cat}[HB]} \qquad \text{(Eq. 3)}$$

The Brönsted relationship may be given by:

$$\log(k/q) = \log GB + \beta(pK_a + \log p/q) \qquad \text{(Eq. 4)}$$

where k is the bimolecular rate constant for the reaction pathway (k^0_{OH} or k^0_{cat}), GB is a constant, β is the Brönsted coefficient, pK_a is the negative logarithm of the dissociation constant for the conjugate acid (and is equal to $pK_w + \log a_{H_2O}$ for hydroxide attack), p is the number of nonequivalent dissociable protons on the conjugate acid base, and q is the number of sites on

0022-3549/84/0600-0724$01.00/0
© 1984, American Pharmaceutical Association

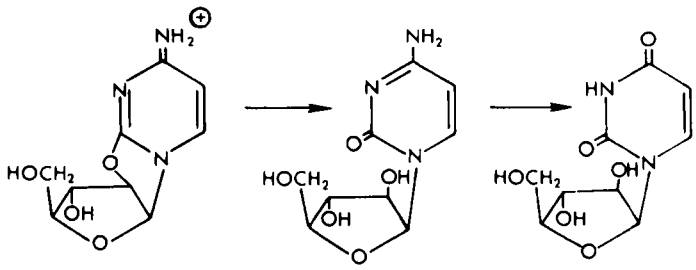

Scheme I

the general base able to accept a proton (3). In practice the Brönsted correlation line may or may not include k^0_{OH}; frequently, specific hydroxide-ion catalysis exhibits negative deviation (3, 4). Assuming that k^0_{OH} is on the Brönsted line made up of k^0_{cat} values allows Eq. 4 to be used to define k^0_{cat} as:

$$k^0_{cat} = k^0_{OH} q \left\{\frac{(p)K_w}{K_a(q)a_{H_2O}}\right\}^{\beta} \qquad \text{(Eq. 5)}$$

and substitution of Eq. 5 into Eq. 3 yields:

$$F_{gb} = \frac{\left\{\frac{(p)K_w}{K_a(q)a_{H_2O}}\right\}^{\beta} K_a[HB]_q}{K_w\left(\frac{\gamma_{t'}}{\gamma_t\gamma_{HB}}\right) + q\left\{\frac{K_w(p)}{K_a(q)a_{H_2O}}\right\}^{\beta} K_a[HB]} \qquad \text{(Eq. 6)}$$

This approach was used to develop the present theory. Where k^0_{OH} values show negative deviation, general-base catalysis will be more readily observed than indicated by this treatment.

DISCUSSION

In Eq. 6, the fraction of general-base attack, F_{gb}, is dependent on the Brönsted coefficient, the activity coefficients for conjugate acid and transition states, the conjugate acid concentration, and the identity of the buffer (*i.e.*, its K_a, q, and p). Initially, for simplicity, it will be assumed that $(\gamma_{t'}/\gamma_t\gamma_{HB}) \cong 1$.

Specific-base attack predominates as the Brönsted coefficient approaches 1. In Fig. 1, F_{gb} is shown as a function of the Brönsted coefficient for a typical general base, dibasic phosphate [$p = q = 2$, pK_a (25°C) = 7.21 (5)], and conjugate acid concentrations equal to 0.01, 0.1, and 1.0 M. The value of F_{gb} decreases sharply when the Brönsted coefficient is between 0.6 and 0.8. A β value of 1.0 is the limiting case, which implies that proton transfer is complete in the transition state (3). Equation 6 then becomes:

$$F_{gb} = \frac{p[HB]}{a_{H_2O} + p[HB]} \qquad \text{(Eq. 7)}$$

Here, except for different p values, all general bases are capable of the same F_{gb} at equal conjugate acid concentrations. Additionally, Eq. 7 shows that for a buffer with $p = 2$, a conjugate acid concentration greater than 9 M is required for 25% buffer-base attack. Clearly this is not experimentally realistic. In contrast, if k^0_{OH} exhibits negative deviation from the Brönsted plot, buffer catalysis may be observed in this limiting case ($\beta = 1.0$). For instance, the log k^0_{OH} value for the conversion of ancitabine to the antileukemic drug cytarabine (Scheme I) was observed to deviate from the Brönsted plot ($\beta \cong 1.0$) by −log 55.

In this case Eq. 6 simplifies to:

$$F_{gb} \cong \frac{p[HB]}{1 + p[HB]} \qquad \text{(Eq. 8)}$$

The prodrug conversion constant in a buffer containing 0.250 M sodium bicarbonate and 0.025 M disodium carbonate ($p = 1$) was observed to be ~24% general-base catalysis (Table I), whereas Eq. 8 predicts 20%.

The value of the Brönsted coefficient will determine whether experimental design is critical in detecting buffer-base attack. The two most important design features are the choice of buffer and concentration of the conjugate acid.

The ability of a buffer to act as a general base is related to the pK_a of its conjugate acid. The larger the pK_a, the better the general base. Therefore, one might expect that general-base attack would be most apparent with an efficient general base such as dibasic carbonate or tribasic phosphate. However, the presence of predominating hydroxide attack, *i.e.*, a Brönsted coefficient of 0.8–1.0, in the high pH range required for the existence of these bases negates the possibility of observing general-base attack. In Fig. 2 the relative amount of general-base attack is shown as a function of the pK_a of the buffer system at three conjugate acid concentrations. Figure 2, generated from Eq. 6 by assuming $p = q = 1$ and $\beta = 0.8$, shows that at a conjugate acid concentration of 0.1 M, general-base catalysis by buffers of p$K_a \geq 7$ cannot be detected. If the conjugate acid concentration is below 0.01 M, it is likely that general-base catalysis will not be detected at $\beta = 0.8$ regardless of the buffer used. In general the lower the pK_a, the more useful the buffer in observing general-base catalysis. By viewing the x-axis in Fig. 2 as a pH scale, the pH region of competitive general-base catalysis can be seen. At lower pH, hydroxide catalysis becomes less effective and, thus, general-base catalysis can become significant.

Figure 3 shows the relationship between F_{gb} and the conjugate acid concentrations for a series of common buffers at $\beta = 0.8$. As the conjugate-acid concentration increases, F_{gb} increases. Thus, doubling the concentration of the general base while maintaining constant conjugate acid concentration will not increase the relative amount of general-base attack. This is due to the fact that such an increase in general-base concentration will also increase the hydroxide-ion concentration.

The kinetics of ancitabine conversion to cytarabine provide an example of the effect of changing conjugate-acid concentrations on F_{gb}. The Brönsted slope for this reaction is approximately one; however, the hydroxide rate constant deviated negatively from the Brönsted plot, allowing general-base catalysis to be observed. The value of k_{obs} is described by Eq. 1 where $k_{OH} = k^0_{OH}\gamma_{OH}\gamma_d/\gamma_t$. The fraction of general-base catalysis, F_{gb}, was determined by estimating k_{OH} from high pH studies and using the following relationship:

$$F_{gb} = (k_{obs} - k_{OH}[OH])/k_{obs} \qquad \text{(Eq. 9)}$$

where [OH] was calculated from measured pH. These values were also approximated using Eq. 8, which allows negative hydroxide rate constant deviation from the Brönsted plot. The agreement between the results (Table I) tends to support the experimental approximations ($\beta \cong 1.0$ and deviation ≅ −log 55) and theoretical considerations (Eq. 6) that were used to derive Eq.

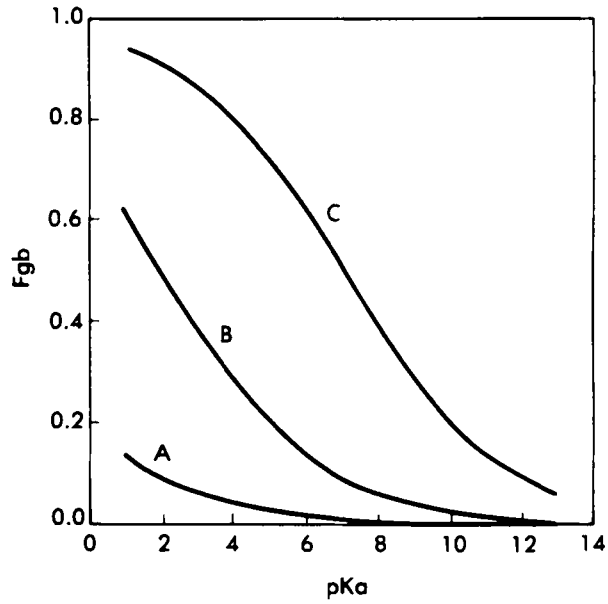

Figure 2—*Fraction of observed general-base catalysis, F_{gb}, as a function of the pK_a of a series of buffer systems. Curves were generated using Eq. 6; p and q were assigned unity and curves A, B, and C correspond to [HB] = 0.01, 0.1, and 1.0, respectively. Ionic atmosphere effects were ignored.*

Table I—Observed First-Order Rate Constants and Fraction of General-Base Catalysis For Ancitabine Prodrug Conversion in Carbonate Buffers at 60°C and μ = 1.0 [a]

Concentration, M				F_{gb}	
HCO_3^-	CO_3^{2-}	pH	k_{obs}, h^{-1}	Obs.[b]	Calc.[c]
0.200	0.025	8.46	13.0	0.20	0.17
0.250	0.025	8.38	11.4	0.24	0.20
0.300	0.025	8.32	10.1	0.25	0.23
0.400	0.025	8.25	9.39	0.31	0.29
0.800	0.025	8.13	9.84	0.50	0.44

[a] Ionic strength adjusted with sodium chloride. [b] Calculated from $k_{OH}(60°C, \mu = 1) = 2.0 \times 10^5\ h^{-1}\ M^{-1}$ and the k_{obs} values using Eq. 9. [c] Calculated from Eq. 8.

8. It is interesting to note that in all of the carbonate buffers used, the concentration of the catalytic buffer base (CO_3^{2-}) was kept constant while the conjugate acid and pH changed (see Table I).

The popular technique of increasing the total buffer concentration while maintaining a constant pH and base-to-acid ratio may or may not allow detection of general-base catalysis. Suppose the Brönsted coefficient is 0.8, and one is attempting to detect base attack using Tris buffers. If constant pH is maintained while the total buffer concentration is increased 10-fold, the conjugate-acid concentration might increase from 0.01 to 0.1 M. The percentage increase in the relative amount of observed general-base catalysis will be only 6% (Fig. 3). Therefore, general-base catalysis would be overlooked. The same technique applied to the monobasic/dibasic phosphate system would result in a 15% increase in k_{obs}, while the formate/formic acid buffer would result in an ~30% increase in k_{obs}.

If one objective in a series of stability studies is to determine buffer-base catalysis, then the approach should be to employ buffers with pK_a values as low as possible using conjugate-acid concentrations as high as is experimentally feasible. Experimental designs which seek to otherwise optimize either the general-base or total buffer concentrations are misdirected.

Activity coefficients are used in Eq. 1 to describe ionic atmosphere effects. Direct extrakinetic measurements of activity coefficients are rare in the pharmaceutical literature. Instead, approximations based on the empirical effect of ionic strength on the logarithm of the activity coefficient of an ion are commonly used (6). Although there are problems associated with these approximations, particularly (as will be discussed later) in solutions of moderately high ionic strength, they conveniently allow the charge of the ion to affect the reaction rate but not its specific chemical identity. By employing ionic strength approximations, salt effects on the two reaction pathways can be evaluated for various combinations of charged and uncharged substrates and buffer components.

As can be seen in Eq. 6, ionic atmosphere effects will influence the relative amount of general-base attack (F_{gb}) to the extent that $\gamma_{\dagger'}/\gamma_{\dagger}\gamma_{HB}$ is affected. Under the ionic strength assumption, ionic atmosphere effects will depend on the charges of the various ions. Since the transition-state charges are equal to the sum of the charges on the reactants (7), the charges on the specific-base ($Z_{\dagger}$) and general-base ($Z_{\dagger'}$) transition states are given by:

$$Z_{\dagger'} = Z_d - 1 \qquad \text{(Eq. 10)}$$

$$Z_{\dagger'} = Z_d + Z_B \qquad \text{(Eq. 11)}$$

where Z_d and Z_B are the charges on the drug and general base and $Z_{OH} = -1$. For a buffer system in which the general base is a monovalent anion and the conjugate acid is neutral (*e.g.*, acetate–acetic acid), $\gamma_{\dagger'}/\gamma_{\dagger}\gamma_{HB} \cong 1$ because $Z_{\dagger'} = Z_{\dagger}$ and $\gamma_{HB} \cong 1$. The value of $\gamma_{\dagger'}/\gamma_{\dagger}\gamma_{HB}$ is also ~1 if the substrate is a monovalent cation, regardless of the charge type of the buffer system. This is because $\gamma_{\dagger'} \cong \gamma_{HB}$ and $\gamma_{\dagger} \cong 1$. In these two situations F_{gb} is unaffected by ionic strength. However, for other combinations of neutral and charged substrates and buffers, the effect of ionic strength can be approximated by using the Güntelberg equation:

$$\log \gamma_i = -Z_i^2 A\sqrt{\mu}/(1 + \sqrt{\mu}) \qquad \text{(Eq. 12)}$$

in which i denotes a central ion, Z_i is the charge on i, A is a function of temperature and solution dielectric constant, and μ is the ionic strength (6).

Table II summarizes the approximated values of $\gamma_{\dagger'}/\gamma_{HB}\gamma_{\dagger}$ for monovalent or neutral substrates and various buffer systems. For neutral or anionic drugs, the effect of increasing ionic strength is to increase F_{gb} if the conjugate buffer acid is anionic and to decrease F_{gb} if the conjugate acid is a cation.

Ionic strength is often maintained constant in pharmaceutical kinetic studies (6). Charged drugs are subject to significant primary and secondary kinetic salt effects which should be quantitated at various fixed ionic strengths or should be normalized by conducting all studies at a constant ionic strength. Uncharged drugs can also be subject to secondary-type salt effects in buffered solutions, and the logarithm of their activity coefficients may display a linear dependence on ionic strength (8).

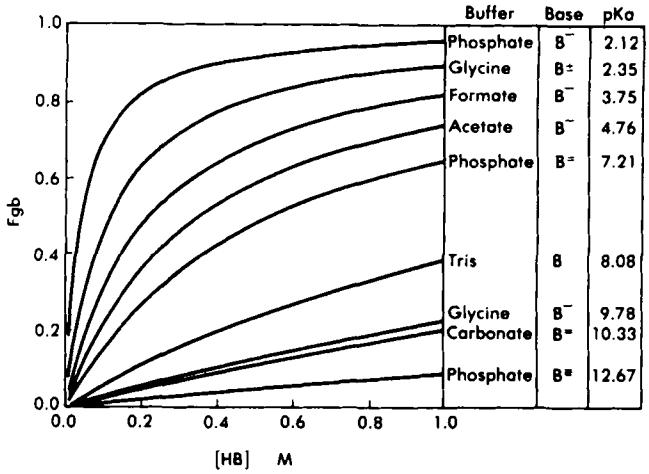

Figure 3—*Fraction of observed general-base catalysis, F_{gb}, as a function of the conjugate-buffer acid concentration for a series of buffers used in pharmaceutical stability studies. Curves were generated using Eq. 6; pK_a (25°C) values were taken from the literature (5). Ionic atmosphere effects were ignored.*

The condition of constant ionic strength sets mathematical limits on the maximum concentration of any given buffer and, thus, sets limits on the maximum F_{gb} value. The maximum concentrations occur in solutions with no added neutral salts. For instance, for a buffer with dibasic and monobasic components such as carbonate or phosphate, the maximum conjugate acid concentration, $[HB]_{max}$, for a fixed ionic strength of μ is given by:

$$[HB]_{max} = \mu - 3[B]_{min} \qquad \text{(Eq. 13)}$$

where $[B]_{min}$ is the minimum concentration of the general base and Eq. 13 was derived using the definition of ionic strength.

To maintain first-order conditions, the attacking species concentrations must be sufficiently higher than the initial substrate concentration to prevent significant loss of buffer catalysts or hydroxide ions. A 5% loss of the attacking species is well within first-order conditions (9). Thus, the minimum general-base concentration should be 20 times that of the initial substrate concentration. Equation 13 can then be written:

$$[HB]_{max} = \mu - 60[D_0] \qquad \text{(Eq. 14)}$$

where $[D_0]$ is the initial drug concentration and is usually selected on the basis of stability-indicating assay detection limits. Since $[HB]_{max}$ can be used in Eq. 6 to calculate the maximum F_{gb} for any given buffer system, a high constant ionic strength chosen by the experimenter will allow for a high maximum F_{gb} value.

CONCLUSIONS

The detection of buffer-base catalysis in the presence of predominating specific-base catalysis is directly influenced by the choice of buffer, conjugate acid concentration, and ionic strength. Two characteristics favor one buffer over another: lower pK_a and, to a lesser extent, the charge types of the buffer base and acid. Despite the fact that buffers with high pK_a values are more efficient general bases, they are unable to compete with hydroxide ions in the pH range where they exist. As can be seen in Fig. 2, it is possible to observe significant buffer-base catalysis in relatively low pK_a buffers.

The ionic charges of the buffer components affect F_{gb} in two ways. First, the maximum conjugate-acid concentration is dependent on the buffer charges, as can be seen in the following equation:

$$[HB]_{max} = \frac{2\mu - \{20(Z_B^2 + |Z_B|)[D_0]\}}{Z_{HB}^2 + |Z_{HB}|} \qquad \text{(Eq. 15)}$$

which is a generalized form of Eq. 14 and was derived from the definitions of ionic strength and first-order conditions. Second, the buffer component charges affect the activity coefficient ratio $\gamma_{\dagger'}/\gamma_{\dagger}\gamma_{HB}$.

The maximum conjugate-acid concentration allows observation of the maximum F_{gb} for any given buffer, and kinetic studies should be conducted near this maximum in order to obtain accurate estimates of k^0_{cat}. Maximum conjugate-acid concentrations are generally ionic strength limited. The higher the ionic strength, the larger the allowable maximum conjugate-acid concentration and, thus, the larger the relative amount of buffer-base catalysis.

Table II—Values for x in the Approximate Equation, $(\gamma_{t^+}/\gamma_t\gamma_{HB}) \cong 10^{x[A\sqrt{\mu}/(1+\sqrt{\mu})]}$, for Monovalent and Neutral Drug in Buffers

Buffer Charges			Values for x Drug Charges		
Base	Acid	Examples (pK_a)	Neutral	Anion	Cation
Monovalent anion	Neutral	Acetate (4.76)	0	0	0
Divalent anion	Monovalent anion	Carbonate (10.33)	−2	−4	0
Trivalent anion	Divalent anion	Phosphate (12.67)	−4	−8	0
Monovalent anion	Zwitterion	Glycine (9.78)	0	0	0
Neutral	Monovalent cation	Tris (8.08)	2	4	0

But, choosing relatively high ionic strength has drawbacks. In particular the ionic atmosphere assumptions used in deriving Eq. 6 tend to fail. In solutions of high ionic strength, the logarithm of an activity coefficient of an ion is not only affected by the ionic strength of the solution, but also by the chemical identities and concentrations of all ions of charges opposite to that of the central ion. This relationship has been empirically described by:

$$\log \gamma_i = \frac{-AZ_i^2\sqrt{\mu}}{1+\sqrt{\mu}} + \sum_j \beta_{ij}C_j \qquad \text{(Eq. 16)}$$

where γ_i is the activity coefficient of an ion i, Z_i is the charge on i, A is a function of the temperature and solution dielectric constant, C_j is the concentration of the jth ion of charge opposite to that of ion i, and β_{ij} is the specific ionic interaction coefficient for ions i and j (7, 10).

The magnitude of the extra-ionic strength salt effects depends on the concentrations of ions and the values of the specific ionic interaction coefficients. One of the major effects of specific ionic interactions in buffer solutions is to cause pH changes at constant ionic strengths. The pH of a buffer solution, such as sodium hydrogen phosphate, sodium dihydrogen phosphate, and sodium chloride, is given by the following equation:

$$pH = pK_a + \log [B]/[HB] + \log (\gamma_B/\gamma_{HB}) \qquad \text{(Eq. 17)}$$

and substitution of Eq. 16 for $\log (\gamma_B/\gamma_{HB})$ yields:

$$pH = pK_a + \log \frac{[B]}{[HB]} - \frac{3A\sqrt{\mu}}{1+\sqrt{\mu}} + \Delta\beta_{Na}[Na^+] \qquad \text{(Eq. 18)}$$

where $[Na^+]$ is the molar concentration of sodium ion and $\Delta\beta_{Na}$ is the difference between the specific interaction coefficient for sodium ion and dibasic and monobasic phosphate ions. For example, the percent change in the hydroxide-ion activity based on measured pH in phosphate buffers at 60°C, wherein the base-acid concentration ratio was kept constant and the ionic strength was kept constant at 1.0, was as much as 80%. The problem of quantitating buffer-base attack in the presence of predominating hydroxide attack is compounded if the hydroxide-ion activity is changing due to specific ionic interactions.

One method of correcting the observed first-order rate constant for the type of secondary ionic atmosphere effect described above has been used in ancitabine hydrolysis studies. It is a general method for cationic substrates that only partly eliminates ionic atmosphere effects at constant ionic strength. It does not correct k_{obs} for specific ionic interactions between the substrate and anions. The approach is to calculate the activity coefficient ratio of the buffer base-acid from experimentally measured pH using:

$$(\gamma_B/\gamma_{HB}) = K_a[HB]/[B]10^{-pH} \qquad \text{(Eq. 19)}$$

Division of k_{obs} as defined in Eq. 1 by Eq. 19 eliminates all activity coefficients except that of the substrate. In the case of ancitabine, it was shown by kinetic measurements in buffers of various ionic strengths that the activity coefficient of the substrate could be approximated by Eq. 12. Similar experimental approaches to the problem of ionic atmosphere effects in solutions of high ionic strength may be necessary to detect buffer catalysis in the presence of predominant specific-acid attack.

REFERENCES

(1) E. R. Garrett, *Adv. Pharm. Sci.*, **2**, 2 (1967).

(2) A. W. Moore and R. G. Pearson, "Kinetics and Mechanisms," 3rd ed., Wiley, New York, N.Y., 1981, pp. 347–353.

(3) W. P. Jencks, "Catalysis in Chemistry and Enzymology," McGraw-Hill, New York, N.Y., 1969, pp. 163–242.

(4) T. C. Bruice and S. Benkovic, "Bioorganic Mechanisms," vol. 1, W. A. Benjamin, New York, N.Y., 1966, pp. 4–46.

(5) H. S. Harned and B. B. Owen, "The Physical Chemistry of Electrolytic Solutions," Reinhold, New York, N.Y., 1958, chap. 15.

(6) J. T. Carstensen, *J. Pharm. Sci.*, **59**, 1140 (1970).

(7) B. Perlmutter-Hayman, *Prog. React. Kinet.*, **6**, 239, (1972).

(8) E. S. Amis and J. F. Hinton, "Solvent Effects on Chemical Phenomena," Academic, New York, N.Y., 1973, chap. 5.

(9) E. R. Garrett, *J. Pharm. Sci.*, **51**, 841 (1962).

(10) A. D. Pethybridge and J. E. Prue, *Prog. Inorg. Chem.*, **17**, 327 (1972).

ACKNOWLEDGMENTS

The authors gratefully acknowledge the Elsa U. Purdee Foundation, The National Institutes of Health (Predoctoral Training Grant T32GM07622-05), The Upjohn Company and its Medical Sciences Liaison, David F. Lichtenauer, for partial support of this work.

Pharmacokinetic Prodrug Modeling: *In Vitro* and *In Vivo* Kinetics and Mechanisms of Ancitabine Bioconversion to Cytarabine

LEE E. KIRSCH * **and ROBERT E. NOTARI** ˣ

Received November 22, 1982, from the *Lloyd M. Parks Hall, College of Pharmacy, The Ohio State University, Columbus, OH 43210.* Accepted for publication April 18, 1983. *Present address: Product Development Division, Eli Lilly and Company, Indianapolis, IN 46206.

Abstract □ Conversion rates of the prodrug ancitabine to the antileukemic cytarabine have been measured *in vivo* (rabbits) and *in vitro* (in the presence of rabbit blood and human red blood cells, blood, and plasma) using HPLC analyses for the prodrug, drug, and its inactive metabolite, 1-β-D-arabinosyluracil. These observed pH-dependent *in vitro* rate constants were consistent with those for chemical hydrolysis determined from controls using Tris buffers. Hydrolysis of ancitabine to cytarabine is chemically, not enzymatically, mediated. The blood concentration–time course for administered compound was described by a two-compartment open model following a rapid intravenous injection of prodrug, drug, or metabolite in each of three rabbits. The *in vivo* conversion rate constant (k_c) following a rapid intravenous prodrug injection was estimated by simultaneous nonlinear regression of ancitabine and cytarabine blood concentration–time courses using equations for two-compartment prodrug and drug with all possible models describing potential conversion sites. The best fit was obtained for the case allowing simultaneous conversion of the prodrug in both central and peripheral compartments to the drug in the central compartment with a common value for k_c. The resulting k_c value (0.09 h^{-1}, three rabbits) is similar to that for chemical hydrolysis (0.07 h^{-1}) at 38.8°C. Reasons why this agreement is regarded as fortuitous are discussed.

Keyphrases □ Ancitabine—bioconversion to cytarabine, mechanism, *in vivo* and *in vitro* pharmacokinetics □ Prodrug modeling—pharmacokinetics of ancitabine bioconversion to cytarabine *in vivo* and *in vitro*, mechanism □ Pharmacokinetics—prodrug modeling, ancitabine bioconversion to cytarabine *in vivo* and *in vitro*, mechanism

Ancitabine (I) has shown promise as a prodrug of the antileukemic agent, cytarabine (II) in Phase 1 (1, 2) and limited Phase 2 (2) clinical trials in the treatment of human neoplasms which respond to treatment with II. It is resistant to cytidine deaminase which rapidly inactivates II (3–5) to 1-β-D-arabinosyluracil (III) (Scheme I). In theory, the advantage of this prodrug would be to extend the biological duration of cytarabine through rate-limiting conversion (6). However, the acceptability of I is limited by acute vascular instability and parotid pain which have occurred at therapeutic doses (2).

The bioconversion mechanism of I was reported to be chemically rather than enzymatically mediated (7, 8). However, these studies report some striking dissimilarities in observed reversal rates. Wang *et al.* (7) reported 50% conversion of I to II within 6 h in mouse plasma while Ho (8) reported 45–93%, 40–55%, and 43% conversion within 1 h in human, dog, and mouse plasma. Thus, the first-order rates for hydrolysis of I based on the data reported by Ho were ~5–20 times faster than that based on data of Wang *et al.* (7). Despite this, both reports concluded that prodrug reversal was chemically mediated based on the observation that preboiling the plasma resulted in little or no decrease in hydrolysis rates.

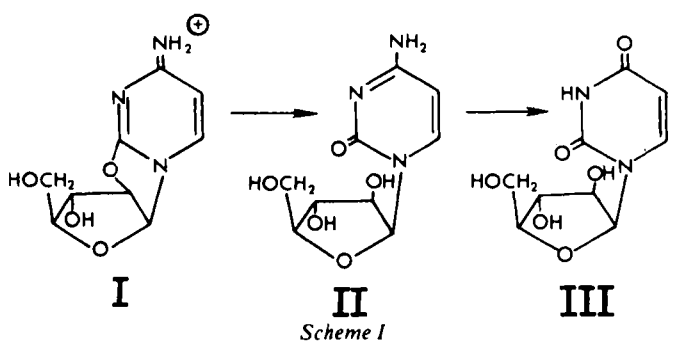

Scheme I

An *in vitro* first-order hydrolysis rate constant derived from the data of Ho was employed in a physiological pharmacokinetic model (9). The first-order hydrolysis rate constant value of 0.3 h^{-1}, which may be calculated from data presented by Ho in Fig. 6 (8) for *in vitro* hydrolysis in human plasma, did not describe the human blood concentration–time course for I and II as well as did the value 0.6 h^{-1}. This was taken as evidence that *in vivo* hydrolysis is somewhat faster than that seen *in vitro* (9).

The goals of the present study were: (*a*) to compare the conversion rates of I in blood and plasma with those predicted from aqueous hydrolysis kinetics, (*b*) to estimate the value of the *in vivo* conversion constant using classical pharmacokinetic modeling, and (*c*) to compare the observed and predicted conversion rates with those previously reported.

EXPERIMENTAL

Analytical Methods -A previously reported UV differential assay was used to measure the conversion of I to II in aqueous Tris buffers (10). Biological samples were assayed using reverse-phase HPLC. A fixed-wavelength UV detector and 20-μL sample injector loop were used in conjunction with a 3-cm precolumn and 15-cm analytical column[1]. Sodium heptanesulfonate was used as an ion-pairing agent, and *p*-hydroxybenzoic acid was the internal standard.

Cells were separated from plasma by centrifugation[2]. Plasma proteins were precipitated with 40 μL of 20% trichloroacetic acid/0.25 mL of plasma. The precipitate was removed by centrifugation, and the supernatant was filtered using a microfilter with a 0.2-μm cellulose filter membrane[3]. The filtered samples were assayed using one of three mobile phases at a flow rate of 1.2 mL/min. System A was 0.01 M acetic acid, 0.001 M sodium acetate, 0.005 M sodium heptanesulfonate, and 6% v/v methanol; the detection wavelength was 254 nm. System B was the same except that sodium acetate was 0.01 M. System C was identical to B except that 1% v/v methanol was used, and the detection wavelength was 280 nm.

The HPLC columns were preequilibrated with mobile phase for 12–24 h. Calibration curves were prepared daily from biological fluids spiked with known concentrations of I, II, III, and the internal standard. Two linear plots of peak height ratios *versus* the known concentrations were prepared for each compound in the ranges of 10^{-6}–10^{-4} and 10^{-4}–5×10^{-3} M.

***In Vitro* Kinetic Studies**—Tris buffers were prepared by weighing the free base and hydrochloride salt into double-distilled deionized water to give solutions of the following molar concentrations (base/acid): 0.016/0.084, 0.061/0.0388, and 0.085/0.0156. Sodium chloride was added to adjust the ionic strength to 0.15, which is the approximate value for plasma (11). Reaction solutions were maintained in closed water-jacketed beakers at 38°C, which is between the normal body temperature of humans (37°C) and rabbits (38.8°C) (12). Reactions were initiated by introducing an aliquot of a stock

[1] Model 332 Beckman Gradient Liquid Chromatograph with Model 153 Analytical Detector and Altex Ultrasphere-octyl 5-μm column (15 cm × 4.6 mm i.d.); Beckman Instruments, Inc., Irvine, Calif.
[2] Eppendorf Centrifuge, Model 5412; Brinkman Instruments, Westbury, N.Y.
[3] Microfilter (MF-1); Bioanalytical Systems, West Lafayette, Ind.

0022-3549/84/0600-0728$01.00/0
© 1984, American Pharmaceutical Association

Table I—Concentrations of I, II, and III in Blood Resulting from an Intravenous Bolus Dose of I (3.8×10^{-4} mol/kg) in Rabbits [a]

Rabbit	Time, h	Concentration, 10^5 M I	II	III
1	0.06	117.33	(3.43)[b]	—
	0.36	36.15	1.05	0.52
	0.57	23.66	1.13	1.02
	0.99	5.12	0.86	1.34
	1.50	2.26	0.67	1.41
	2.27	1.07	0.45	1.01
	2.78	0.84	0.58	1.37
	3.17	1.03	0.47	1.50
	4.23	0.69	0.38	1.67
	5.15	0.61	0.26	1.07
	6.00	0.38	0.24	1.07
	6.93	0.34	0.24	1.09
2	0.05	159.75	(3.72)[b]	—
	0.23	63.17	1.76	—
	0.39	42.54	1.64	—
	0.73	22.43	1.48	—
	0.92	17.12	1.52	0.65
	1.49	5.54	1.23	1.15
	2.00	—	0.74	1.20
	3.40	1.11	0.58	1.68
	4.30	0.80	0.37	1.35
	5.20	0.61	0.25	1.31
	6.10	—	0.12	0.78
3	0.08	116.26	(2.54)[b]	—
	0.27	40.13	1.74	—
	0.62	15.75	1.47	0.66
	1.00	7.11	1.56	0.93
	1.49	1.95	1.26	1.20
	2.00	0.99	1.06	1.16
	3.42	0.46	0.90	1.32
	4.13	—	0.88	2.46
	5.02	0.36	0.72	2.07
	5.85	—	0.70	1.69
	6.57	0.22	0.70	1.32

[a] Concentrations are in M and dose is mol/kg because these units, unlike mass per volume or body weight, are meaningful in considering prodrug → drug stoichiometry. [b] Data points were not used in estimating k_c as explained in the *Results*.

solution of I to give a reaction concentration of 8×10^{-4} M. Samples were removed as a function of time and quenched with 0.1 M HCl. The reaction pH was measured before and after each kinetic run.

Blood was obtained from heparinized rabbits[4] *via* venipuncture of the marginal ear vein. Human venous blood was obtained from healthy volunteers and was heparinized. Heparin solutions were freshly prepared from the sodium salt because commercially available heparin injection USP contains methyl- and ethylparabens as preservatives; the parabens were observed to degrade to the internal standard, *p*-hydroxybenzoic acid. Blood which was not immediately used was refrigerated.

Biological fluids were prepared from heparinized whole human blood which was diluted to 10, 20, and 37% v/v in isotonic phosphate buffer. Human plasma and red blood cells were obtained from heparinized blood by centrifugation. Plasma was similarly diluted in isotonic phosphate buffer to 10, 20, or 37% v/v, while cells were diluted in isotonic saline to 5, 10, and 18% v/v. Although deamination of II has not been reported in human plasma, all dilutions of biological fluids were spiked with the deaminase inhibitor tetrahydrouridine to a final concentration of 1×10^{-4} M as a precaution. Rabbit plasma and heparinized whole blood were diluted to 67% v/v with isotonic saline. One reaction rate, measured in tetrahydrouridine-spiked rabbit blood and in unspiked diluted rabbit blood, showed no apparent change.

These dilutions were maintained at 38°C in water-jacketed beakers, which were stirred and closed. Reactions were initiated by addition of a solution of I to a final concentration of $\sim 1 \times 10^{-3}$ M. Aliquots were withdrawn at appropriate time intervals. Samples of whole blood and resuspended cells were immediately chilled on ice to quench the reaction, whereas plasma was quenched with trichloroacetic acid. Samples were prepared and assayed using the aforementioned HPLC procedures. The pH values of the solutions were determined at frequent intervals.

***In Vivo* Kinetic Studies**—Rabbits[4] were weighed and placed in a restraining cage[5]. Animals were heparinized (1000 U/kg of body weight) with freshly prepared heparin in sterile normal saline. A catheter attached to a sampling port[6] filled with 0.3 mL of 0.1% (w/v) heparin in normal saline was inserted into a peripheral ear artery. A sample of blood (3–5 mL) was withdrawn *via* the catheter after first removing and discarding the heparin solution and five volumes of blood totalling 1.5 mL. This preinjection blood sample was assayed as a blank and also used to prepare the standard curves with known amounts of internal standard and I, II, and/or III. After the blank was withdrawn, 0.5 mL of 0.1% heparin was placed into the port.

For each experiment, solutions of I, II, or III in sterile normal saline were injected *via* the peripheral vein in the ear opposite to that of the arterial catheter. Samples of 0.5 mL were taken at appropriate intervals *via* the arterial catheter using the procedure outlined above for the preinjection blood samples. The samples were placed in microcentrifuge tubes[7] containing 20 μL of the internal standard solution (0.25 mg/mL) and 5 μL of 0.2 M tetrahydrouridine and kept on ice until sample preparation was initiated.

Three animals were used, each of which was given an intravenous bolus dose of I, II, and III (Tables I, II, and III) with sufficient time between experiments to prevent residual blood levels from the previous study. Samples were assayed as described above for I, II, and III.

Table II—Concentrations of II in Blood as a Function of Time from an Intravenous Bolus Dose in Rabbits

Rabbit 1[a] Time, h	Conc., 10^5 M	Rabbit 2[b] Time, h	Conc., 10^5 M	Rabbit 3[c] Time, h	Conc., 10^5 M
0.06	5.96	0.06	33.88	0.39	3.85
0.25	3.74	0.10	30.59	0.60	2.69
0.51	2.10	0.23	17.85	1.08	1.80
1.06	0.99	0.63	10.24	2.00	1.05
1.55	0.82	0.85	8.84	3.12	0.57
2.60	0.41	1.16	6.91	4.36	0.34
3.65	0.29	1.48	5.39	5.20	0.21
4.50	0.23	1.90	4.11		
5.40	0.19	2.25	3.33		
		2.48	3.37		
		2.88	3.41		
		3.35	1.68		
		4.20	1.12		
		5.00	0.72		

[a] Dose = 3.39×10^{-5} mol/kg. [b] Dose = 2.06×10^{-4} mol/kg. [c] Dose = 3.80×10^{-5} mol/kg.

RESULTS

Analytical Methods—The chromatographic characteristics of I, II, and III in the HPLC systems are summarized in Table IV. Mobile phases were varied for each compound to optimize their distance from background inter-

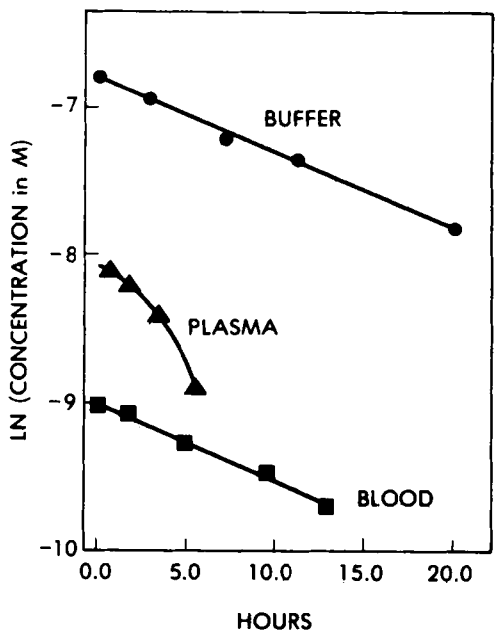

Figure 1—*First-order plots for* in vitro *conversion of I in Tris buffer (pH 7.0), diluted human blood (20% v/v), and plasma (20% v/v) at 38°C.*

[4] New Zealand White male rabbits; King's Wheel Rabbitry, Mount Vernon, Ohio.
[5] Plas-Labs, Lansing, Mich.
[6] Angiocath 22-gauge, 1 in., and PRN Adapter; the Deseret Co., Sandy, Utah.
[7] Micro test tubes, 1.5-mL polyethylene; Brinkman Instruments, Westbury, N.Y.

Table III—Concentrations of III in Blood as a Function of Time from an Intravenous Bolus Dose in Rabbits

Rabbit 1[a]		Rabbit 2[b]		Rabbit 3[c]	
Time, h	Conc., 10^4 M	Time, h	Conc., 10^4 M	Time, h	Conc., 10^4 M
0.04	2.64	0.05	3.76	0.07	3.01
0.59	1.05	0.24	2.31	0.40	1.32
1.03	0.77	0.58	1.66	0.80	1.06
1.58	0.57	1.00	1.47	1.50	0.75
2.01	0.49	1.80	1.25	2.00	0.66
3.15	0.34	3.10	1.00	3.20	0.59
4.02	0.24	4.00	0.85	4.40	0.57
5.30	0.15	5.00	0.70	5.60	0.47
6.02	0.10				

[a] Dose = 1.02×10^{-4} mol/kg. [b] Dose = 1.38×10^{-4} mol/kg. [c] Dose = 1.02×10^{-4} mol/kg.

ference, and two wavelengths (254 and 280 nm) were used to increase sensitivity. The detection ranges are given in Table IV. The lower limit of III was somewhat higher than for I or II because of background interference near the solvent front where III eluted (see capacity factors, Table IV).

During sample preparation, the treatment of plasma with trichloroacetic acid, in addition to precipitating plasma proteins, effectively quenched the conversion of I to II because I is relatively acid stable (10). This was confirmed by quantitative recovery of I from spiked plasma. Trichloroacetic acid was not added directly to blood samples because the resultant cell lysis caused unacceptable background. Instead, blood samples were kept on ice until plasma was separated by centrifugation. To test the effectiveness of the ice-bath quench, synthetic mixtures of I and II were spiked into fresh rabbit blood in concentrations similar to those observed for the first three samples of the intravenous prodrug studies (Table I) and were maintained in an ice bath for periods of time which simulated actual experimental conditions. Controls containing equivalent concentrations of I in blood and in Tris buffer (pH 7.4 at 38°C) were similarly stored. All samples were then prepared and assayed as described under *Experimental*. The mixture (1.1×10^{-3} M I, 2.5×10^{-5} M II) representing the first time point, which was stored for the longest period of 1 h, allowed <2% conversion of I to II. However, this produced a peak height for II which was 70% of those observed for the controls. Therefore, the initial assays for II (labeled as footnote b in Table I) were not used. For the remaining mixtures and storage periods, the peak heights for II in the controls were <15% of that observed in the samples. The rest of the data for II in Table I were therefore used without correction.

***In Vitro* Conversion Kinetics**—Mass balance was confirmed by the sum of the time-dependent concentrations of I and II; III was not detected in any of the reactions. Good first-order plots were obtained for reactions in Tris buffers and diluted whole blood according to:

$$\ln [I] = \ln [I_0] - k_{obs}t \qquad \text{(Eq. 1)}$$

where [I] and $[I_0]$ are the concentrations of I at time t and zero and k_{obs} is the apparent first-order conversion rate constant (Fig. 1).

First-order plots using plasma data showed significant negative deviation (Fig. 1). This was due to an increase in pH with time, thus increasing the hydroxide-ion activity (a_{OH}) which is the dominant catalytic species in aqueous solutions (10). To show that the rate in plasma was consistent with that for chemical hydrolysis, a_{OH} was calculated from measured pH and incorporated into:

$$\frac{-d[I]}{dt} = k_{OH}a_{OH}[I] \qquad \text{(Eq. 2)}$$

The resulting value for the bimolecular rate constant, k_{OH}, agreed with that observed in aqueous solutions (10).

Pharmacokinetics of II and III—The blood concentrations of II (Table II) and III (Table III) arising from rapid intravenous doses (D) of II and III were fitted using NONLIN (13) and Eq. 3:

$$C_1 = \frac{D}{V_1}\left\{\frac{(k_{21}-\alpha)}{(\beta-\alpha)}e^{-\alpha t} + \frac{(k_{21}-\beta)}{(\alpha-\beta)}e^{-\beta t}\right\} \qquad \text{(Eq. 3)}$$

which describes the time-dependent central compartment concentration (C_1) according to a two-compartment open model (Scheme II) where A1 and A2 are the amounts of drug in the central and peripheral compartments and:

$$\alpha,\beta = 0.5\{(k_{12}+k_{10}+k_{21}) \pm \sqrt{(k_{12}+k_{10}+k_{21})^2 - 4k_{21}k_{10}}\} \qquad \text{(Eq. 4)}$$

The estimated parameters are given in Table V.

Table IV—HPLC Analyses for I, II, and III in Biological Fluids

Compound	λ_{max}[a], nm	HPLC System	Capacity Factors	Detection Ranges, 10^4 M	*CV*, %[b]
I	264	A	6.8	1.0-30.0	4.0
		B	7.3	0.019-19.0	2.0
II	280	A	9.7	1.0-30.0	6.4
		C	13.7	0.010-4.0	3.9
III	260	C	4.3	0.050-4.0	6.1

[a] UV wavelength of maximum absorptivity in 0.1 M HCl. [b] Coefficient of variation is based on peak height ratios from five analyses of rabbit blood samples containing 10 μg/mL of the compound.

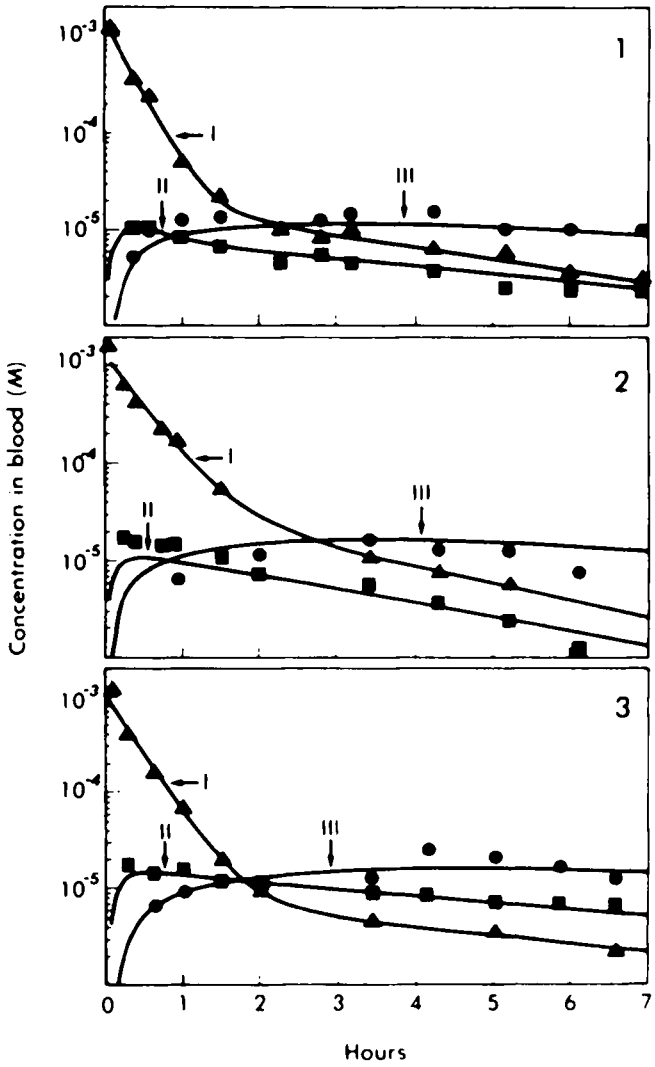

Figure 2—*Time courses for concentrations of I (▲), II (■), and III (●) following administration of 3.8 × 10^{-4}-mol/kg iv doses of I to rabbits 1, 2, and 3. Curves are based on NONLIN (13) fits using Eqs. 5, 6, and 7 for I, II, and III, as described in Scheme III.*

Prodrug Pharmacokinetics—Attempts were made to describe the blood concentrations of I and II arising from doses of I (Table I) using four different models. The elimination (k_{10}) and distribution (k_{12} and k_{21}) parameters of II were fixed at the values obtained from the NONLIN estimates using Eq. 3 following an intravenous dose of II. The elimination and distribution parameters of I (k_c, k'_{10}, k'_{12}, k'_{21}, and V'_1) were adjusted by NONLIN. The four models differed in their routes for prodrug conversion. The simplest model

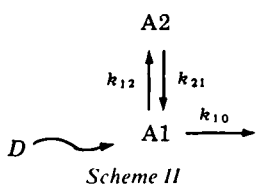

Scheme II

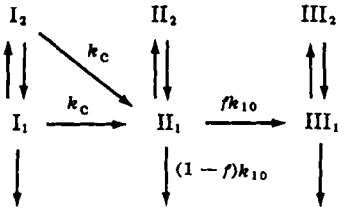

Scheme III

allowed conversion from I_1 to II_1 only. In the other models conversion was set at $I_1 \rightarrow II_1$ and $II_2 \rightarrow II_1$ (see Scheme III); $I_1 \rightarrow II_1$, $I_2 \rightarrow II_1$, and $I_2 \rightarrow II_2$; or $I_1 \rightarrow II_1$ and $I_2 \rightarrow II_2$. NONLIN fits limiting conversion to $I_1 \rightarrow II_1$ with or without $I_2 \rightarrow II_2$ consistently underestimated the concentration of II, while those using all three routes ($I_1 \rightarrow II_1$, $I_2 \rightarrow II_1$, and $I_2 \rightarrow II_2$) significantly underestimated data for the terminal phase of I_1. However, Eqs. 5–7, based on Scheme III, yielded excellent fits to the blood concentration data for I and good fits for II (Fig. 2):

$$[I] = \frac{D}{V'_1}\left\{\left[\frac{(k_c + k'_{21} - \alpha')}{(\beta' - \alpha')}\right] e^{-\alpha' t} + \left[\frac{(k_c + k'_{21} - \beta')}{(\alpha' - \beta')}\right] e^{-\beta' t}\right\} \quad \text{(Eq. 5)}$$

$$[II] = \frac{Dk_c}{V_1}\left\{\left[\frac{(k_{21} - \alpha)(k_c + k'_{21} + k'_{12} - \alpha)}{(\beta' - \alpha)(\alpha' - \alpha)(\beta - \alpha)}\right] e^{-\alpha t} + \left[\frac{(k_{21} - \beta)(k_c + k'_{21} + k'_{12} - \beta)}{(\beta' - \beta)(\alpha' - \beta)(\alpha - \beta)}\right] e^{-\beta t} + \left[\frac{(k_{21} - \beta')(k_c + k'_{21} + k'_{12} - \beta')}{(\alpha' - \beta')(\alpha - \beta')(\beta - \beta')}\right] e^{-\beta' t} + \left[\frac{(k_{21} - \alpha')(k_c + k'_{21} + k'_{12} - \alpha')}{(\beta' - \alpha')(\alpha - \alpha')(\beta - \alpha')}\right] e^{-\alpha' t}\right\} \quad \text{(Eq. 6)}$$

where α' and β' refer to I and are defined as:

$$\alpha', \beta' = 0.5\{(k'_{21} + k'_{12} + k'_{10} + 2k_c) \pm \sqrt{(k'_{21} + k'_{12} + k'_{10} + 2k_c)^2 - 4[k_c^2 + k_c(k'_{10} + k'_{12} + k'_{21}) + k'_{21}k'_{10}]}\} \quad \text{(Eq. 7)}$$

and α and β are defined in Eq. 4. Allowing unequal k_c values for conversion of $I_2 \rightarrow II_1$ and $I_1 \rightarrow II_1$ did not improve these fits.

The common method for calculating f, the fraction of II that is metabolized to III, is to determine the area under the concentration–time curve for III following an intravenous dose of II (14). Since the duration of III was long relative to I and II and the research goals did not require an accurate assessment of f, the terminal data for III were obtained only after intravenous doses of III. The observed concentration–time course for III, following an intravenous dose of I, was then described by reiterating f values in:

$$[III] = \frac{Dk'_c f k_{10}}{V_1^*}\left\{\left[\frac{(k_{21} - \alpha')(k^*_{21} - \alpha')(k_c + k'_{21} + k'_{12} - \alpha')}{(\beta' - \alpha')(\alpha - \alpha')(\beta - \alpha')(\alpha'' - \alpha')(\beta'' - \alpha')}\right] e^{-\alpha' t} + \left[\frac{(k_{21} - \alpha)(k^*_{21} - \alpha)(k_c + k'_{21} + k'_{12} - \alpha)}{(\alpha' - \alpha)(\beta' - \alpha)(\beta - \alpha)(\alpha'' - \alpha)(\beta'' - \alpha)}\right] e^{-\alpha t} + \left[\frac{(k_{21} - \alpha'')(k^*_{21} - \alpha'')(k_c + k'_{21} + k'_{12} - \alpha'')}{(\alpha' - \alpha'')(\beta' - \alpha'')(\alpha - \alpha'')(\beta - \alpha'')(\beta'' - \alpha'')}\right] e^{-\alpha'' t} + \left[\frac{(k_{21} - \beta')(k^*_{21} - \beta')(k_c + k'_{21} + k'_{12} - \beta')}{(\alpha' - \beta')(\alpha - \beta')(\beta - \beta')(\alpha'' - \beta')(\beta'' - \beta')}\right] e^{-\beta' t} + \left[\frac{(k_{21} - \beta)(k^*_{21} - \beta)(k_c + k'_{21} + k'_{12} - \beta)}{(\alpha' - \beta)(\beta' - \beta)(\alpha - \beta)(\alpha'' - \beta)(\beta'' - \beta)}\right] e^{-\beta t} + \left[\frac{(k_{21} - \beta'')(k^*_{21} - \beta'')(k_c + k'_{21} + k'_{12} - \beta'')}{(\alpha' - \beta'')(\beta' - \beta'')(\alpha - \beta'')(\beta - \beta'')(\alpha'' - \beta'')}\right] e^{-\beta'' t}\right\} \quad \text{(Eq. 8)}$$

which is based on Scheme III wherein α'' and β'' refer to III as evaluated in Eq. 3. All pharmacokinetic values were those previously obtained, while the value for f was manually adjusted between its limits, $0 \le f \le 1$. The best fits (Fig. 2), assessed by visual inspection, were obtained as f approached 1 (Table V).

DISCUSSION

***In Vitro* Conversion**—The pH–rate profile for the hydrolytic conversion of I in the temperature range of 19–80°C, at ionic strengths (μ) of 0.01–1.5 and pH values from 1 to 12 can be constructed by plotting the logarithm of the apparent first-order rate constant (k_{app}) calculated from Eq. 9 *versus* pH:

$$k_{app}\,(\text{in h}^{-1}) = 1.74 \times 10^{17}\, a_{OH} \times \exp\left\{\frac{-1.15\sqrt{\mu}}{1 + \sqrt{\mu}} - \frac{8662}{T}\right\} + 1.12 \times 10^{11} \exp\{-10121/T\} \quad \text{(Eq. 9)}$$

where T is absolute temperature. The accuracy of Eq. 9 is generally good (10). The average deviation between calculated and observed rate constants in aqueous solutions is <20%. The line in Fig. 3 represents the calculated pH–rate profile for chemical conversion at 38°C, $\mu = 0.15$, using Eq. 9. Agreement with the observed constants from studies in Tris buffers (Fig. 3) substantiates the accuracy of the predictive equation.

Each bimolecular rate constant from the three human plasma dilutions was multiplied by a_{OH} for the median pH value of the run. The logarithm of these pseudo first-order constants, together with the k_{obs} values obtained in diluted human blood, red blood cells, and rabbit blood are shown in Fig. 3 as a function of pH. These data agree with those for chemical conversion. The slight positive deviations were independent of the concentration of biological fluid and solids in the dilutions. Therefore, it is concluded that the mechanism of prodrug conversion in human and rabbit blood is chemical hydrolysis.

The results of this study were compared with those in the literature by approximating first-order conversion rate constants from reported data using:

$$k_{app} = \ln(F_r)/t_i \quad \text{(Eq. 10)}$$

where F_r is the reported fraction of $[I_0]$ remaining at the end of the incubation period, t_i. This assumes first-order kinetics and constant pH and mass balance based on [I] and [II]. Based on this study, the first and last assumptions are probably valid. The logarithms of the calculated k_{app} values are plotted in Fig. 3 at the reported pH. The data of Wang *et al.* (7) agree with the results obtained in this study, as do the Tris buffer studies of Ho (8). However the k_{app} values calculated from the biological fluid data of Ho show a large positive deviation.

An unequivocal explanation of the large positive deviation is not possible. However it is likely that chemical conversion continued after the incubation period, which would result in erroneously high rate constants. Ho employed ethanol to quench the reactions. The rate constants for conversion at room temperature in cleaned plasma (the supernatant of plasma treated with ethanol) were determined for comparison. These rate constants, shown in Fig. 3, are similar to those based on data reported by Ho, but much larger than those predicted for hydrolysis at 38°C. The methods of quenching used in this paper (acidification or chilling) were shown to be 100 and 98% effective, respectively.

***In Vivo* Conversion**—The kinetics of simultaneous hydrolysis and distribution in an isobutyl alcohol–aqueous acid two-phase transfer cell behave like the two-compartment open model shown in Scheme II (15). The time-de-

Table V—Pharmacokinetic Parameters of I, II, and III

Compound	Rabbit 1	Rabbit 2	Rabbit 3
I[a]			
k_c (h^{-1})	0.066(0.005)	0.091(0.017)	0.108(0.008)
k_{12} (h^{-1})	0.619(0.042)	0.402(0.070)	0.497(0.051)
k_{21} (h^{-1})	0.259(0.025)	0.421(0.113)	0.137(0.028)
k_{10} (h^{-1})	2.785(0.148)	1.938(0.142)	2.356(0.189)
V_1 (L/kg)	0.288(0.027)	0.301(0.031)	0.351(0.054)
CL (L/kg·h)	0.86	0.63	0.95
II[b]			
k_{12} (h^{-1})	1.063(0.212)	3.551(1.427)	1.459(0.719)
k_{21} (h^{-1})	0.633(0.122)	2.096(0.297)	1.434(0.261)
k_{10} (h^{-1})	1.433(0.167)	2.025(0.620)	1.243(0.601)
V_1 (L/kg)	0.420(0.058)	0.343(0.123)	0.413(0.218)
CL (L/kg·h)	0.60	0.69	0.51
f_c	0.06[c]	0.08[c]	0.12[c]
III[d]			
k_{12} (h^{-1})	1.675(0.361)	4.074(0.157)	2.619(0.547)
k_{21} (h^{-1})	1.635(0.219)	1.500(0.045)	0.492(0.124)
k_{10} (h^{-1})	0.780[e] (0.110)	0.746(0.027)	0.823(0.167)
V_1 (L/kg)	0.290[e] (0.050)	0.175(0.007)	0.123(0.025)
CL (L/kg·h)	0.23	0.13	0.10
f	1.0	0.9	0.9

[a] From simultaneous NONLIN fits of concentration time courses for [I] and [III] arising from an intravenous bolus dose of I (Table I). [b] From NONLIN fit of [II] time course following an intravenous bolus dose of II (Table II). [c] Based on dose-adjusted (3.8×10^{-4} mol/kg) AUC values for drug after intravenous administration of prodrug (AUC_{pd}) and drug (AUC_d) where f_c, the fraction of prodrug converted to drug, is $(AUC_{pd})/(AUC_d)$ and values (in 10^5 mol·h/kg) are: (4.1/64), (4.2/55), and (9.0/74). [d] From NONLIN fit of [III] time course arising from an intravenous bolus dose of III (Table III) except for f, which was estimated as described in the *Results*. [e] Value of NONLIN estimate after adjustment to accommodate [III] time course arising from an intravenous bolus dose of I. Reported value is within the 95% confidence interval of the original NONLIN estimate.

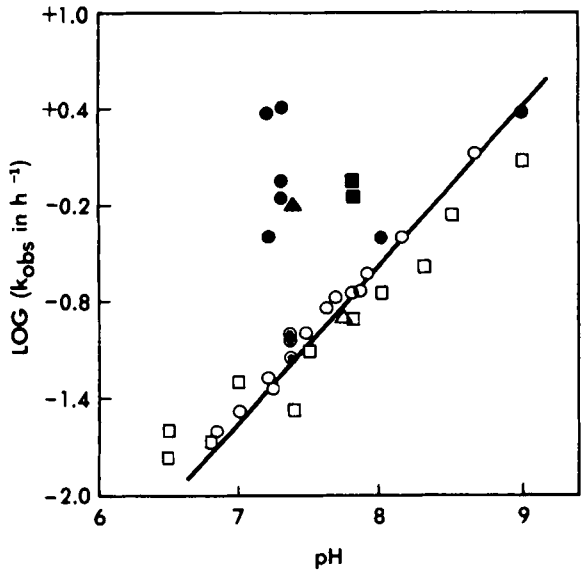

Figure 3—*The pH-rate profile for the conversion of I in rabbits (◎) and* in vitro. *The line represents chemical conversion in aqueous solution at 38°C, μ = 0.15, calculated by Eq. 9. The* in vitro *rate constants are: (○) Tris buffers, diluted human red blood cells, blood, and plasma; (△) diluted rabbit blood; (■) human plasma treated with ethanol; calculated by applying Eq. 10 to the data of (□) Wang* et al. *(7) and (●) Ho (8); (▲) applied to a physiological pharmacokinetic model by Himmelstein and Gross (9).*

pendent concentrations in the aqueous phase were described by Eq. 3, which employed the first-order rate constants for distribution (k_{12} and k_{21}) and hydrolysis (k_{10}). Hydrolysis rate constants (k_h) measured independently in aqueous acid controls agreed with the k_{10} values, which were dependent on acid concentration but independent of stirring rate, which increased k_{12} and k_{21}. Thus, the hydrolysis rate constant can be calculated from the biexponential aqueous phase data using Eq. 3 without any knowledge of the volumes in the transfer cell. The application of an *in vitro* hydrolysis rate constant to an *in vivo* classical pharmacokinetic model would require the achievement of a constant homogeneous apparent volume of distribution in a manner kinetically analogous to the transfer-cell experiments. Thus, if a chemically reversing prodrug were uniformly distributed in a fixed aqueous volume (such as extracellular fluid) with little tissue or plasma protein binding, one would expect its *in vitro* conversion constant to agree with the mechanistically related *in vivo* pharmacokinetic microconstant. *A priori*, ancitabine (I) appeared to possess the pharmacodynamic properties required to demonstrate such a correlation. It does not readily enter cells or deposit into fat (16–18) and its *in vivo* conversion is chemical hydrolysis.

It was not possible to achieve this result with data from rabbits. Although the *in vivo* conversion constants (k_c) agree with those for chemical hydrolysis (Fig. 3), the model of best fit required conversion of both I_1 and I_2 to II_1. A physiological interpretation of the resulting model (Scheme III) is not possible. The average model-independent *Vd* value for I (calculated from CL/β) is 2.9 L/kg, which is larger than that for II (1.4 L/kg) and much greater than the total body water (0.7 L/kg) for rabbits (19). Thus, one (or more) of the requirements for a meaningful correlation is absent, and the observed agreement between the *in vivo* and *in vitro* hydrolysis rate constants must be regarded as fortuitous.

In Fig. 3, the rate constant successfully used by Himmelstein and Gross (9) shows a large positive deviation from the rate constants for chemical, *in vitro* (blood), and *in vivo* (rabbit) conversion. An increased value for the *in vivo* rate constant over the initial *in vitro* estimate based on the results of Ho caused the authors to conclude that hydrolysis occurs somewhat faster *in vivo*. Another explanation for the successful prediction of concentration–time profiles of I and II in humans using high k_c estimates in the physiologically based model might be that the distribution volume for I was underestimated. Since the apparent first-order rate constant is always multiplied by the volume of the specific tissue to obtain a corresponding clearance value, an underestimate in the total volume of distribution would require an overestimate in the conversion constant in order to describe the data. The volume of distribution for I, which was unknown in humans, was assigned a value equal to that for II. The average *Vd* for I in rabbits is twice the value for II. This could explain the successful fit obtained with the high hydrolysis rate constant if the same trend holds in humans. Thus, the conclusion that *in vivo* hydrolysis is somewhat faster than hydrolysis *in vitro* was speculative. No conformatory evidence of facilitated *in vivo* conversion was found in the present study. While both the physiologically based model and the classical model described the *in vivo* data, neither was based on physiological actuality.

The hypothesis that prolonged duration of I is due to the slow hydrolytic conversion of I to II, as proposed by Ho (8) and supported by Himmelstein and Gross (9), is corroborated by the present study. The terminal half-life of II from an intravenous dose of I (Fig. 2, average $t_{0.5} \cong 5$ h) is three times that observed following an intravenous dose of II.

REFERENCES

(1) P. L. Chawla, J. J. Lokich, N. Jaffe, and E. Frei, *Proc. Am. Assoc. Cancer Res.*, **15**, 188 (1974).

(2) J. H. Burchenal, K. Kalaher, B. Clarkson, N. Kememey, C. Young, J. Fox, and I. Krakoff, *Curr. Chemother., Proc. Int. Congr. Ther., 10th*, **2**, 1206 (1978).

(3) D. H. W. Ho, C. J. K. Carter, T. L. Loo, R. L. Abbott, and C. M. McBride, *Drug Metab. Dispos.*, **3**, 309 (1975).

(4) A. Hoshi, M. Iigo, M. Saneyoshi, and L. Kurentani, *Chem. Pharm. Bull.*, **21**, 1235 (1973).

(5) W. Kreis, T. M. Woodcock, M. B. Meyers, L. A. Carlevarini, and I. H. Krakoff, *Cancer Chemother. Res.*, **61**, 723 (1977).

(6) R. E. Notari, *Pharmacol. Ther.*, **14**, 25 (1981).

(7) M. C. Wang, R. A. Sharma, and A. Bloch, *Cancer Res.*, **33**, 1265 (1973).

(8) D. H. W. Ho, *Biochem. Pharmacol.*, **23**, 1235 (1974).

(9) K. J. Himmelstein and J. F. Gross, *J. Pharm. Sci.*, **66**, 1441 (1977).

(10) L. E. Kirsch, Ph.D. Thesis, College of Pharmacy, The Ohio State University, Columbus, Ohio, 1982.

(11) E. J. Masoro, "Acid-Base Regulation: Its Physiology and Pathophysiology," W. B. Sanders, Philadelphia, Pa., 1971, pp. 3, and 30.

(12) B. M. Mitruka and H. M. Rawnsley, "Clinical Biochemical Hematological Reference Values in Normal Experimental Animals," Masson, New York, N.Y., 1977, p. 6.

(13) C. M. Metzler, G. L. Elfring, and A. J. McEwen, *Biometrics*, **30**, 3 (1974).

(14) R. E. Notari, "Biopharmaceutics and Clinical Pharmacokinetics," 3rd ed., Dekker, New York, N.Y., 1980, pp. 55, 231, and 267.

(15) E. Tomlinson, R. E. Notari, and P. R. Byron, *J. Pharm. Sci.*, **69**, 655 (1980).

(16) M. C. Wang, R. A. Sharma, and A. Bloch, *Cancer Res.*, **33**, 1265 (1973).

(17) H. Hirayama, T. Sugihara, F. Hamada, T. Kanai, J. Hikita, Y. Araki, K. Kuretani, and A. Hoshi, *Gann*, **65**, 153 (1974).

(18) S. M. ElDareer, V. M. White, K. Tillery, F. P. Chen, L. B. Mellett, and D. L. Hill, *Cancer Treat. Rep.*, **61**, 805 (1977).

(19) P. L. Altemann and D. S. Dittmer, "Biology Data Book," Federation of Americas Societies for Experimental Biology, Bethesda, Md., 1974, p. 1990.

ACKNOWLEDGMENTS

The authors gratefully acknowledge the Elsa U. Purdee Foundation, The National Institutes of Health (Predoctoral Training Grant T32GM07622-05), The Upjohn Company and its Medical Sciences Liaison, David F. Lichtenauer, for partial support of this work.

Evaluation of the Bioavailability of a Solid Dispersion of Phenytoin in Polyethylene Glycol 6000 and a Commercial Phenytoin Sodium Capsule in the Dog

S. STAVCHANSKY ˣ and WALTER G. GOWAN

Received November 29, 1982, from the *College of Pharmacy, Drug Dynamics Institute, The University of Texas, Austin, TX 78712.* Accepted for publication April 6, 1983.

Abstract □ In this study a solid dispersion of phenytoin in polyethylene glycol 6000 was prepared by the melt method. The content uniformity of the dispersion indicated a range of 98.7–102.0%. X-ray crystallographic data showed no changes in the crystalline structure of the phenytoin in the dispersion when compared with that in the bulk reagent. Scanning electron micrographs of the dispersion show a reduction in the size of the crystals when compared with the bulk reagent. The commercial product and the dispersion were compared using the USP criteria for the prompt phenytoin sodium dissolution test. The salt dissolved at a rate four times greater than the dispersion. Bioequivalency comparisons between the dispersion containing phenytoin and the commercial prompt phenytoin sodium were studied in six mixed-breed dogs. All samples were analyzed using a commercial enzyme immunoassay system. Statistical analysis of the plasma levels obtained from the animal studies indicate no significant differences ($p > 0.05$) between area under the curve, maximum plasma concentration, and time to peak for the commercial salt and the acid formulation.

Keyphrases □ Phenytoin—bioavailability of the acid and sodium salt in dogs, comparison with *in vitro* dissolution data □ Dissolution—phenytoin and phenytoin sodium *in vitro*, comparison to the *in vivo* bioavailability in dogs

The use of finely subdivided or micronized particles as a means of increasing the rate of dissolution has been considered (1–4). Theoretically, if the dissolution rate is enhanced, the oral absorption rate should be increased if the absorption process is dissolution rate limited. Sekiguchi *et al.* proposed using an inert water-soluble material as a vehicle for a poorly water-soluble drug to enhance the rate and extent of the absorption of the drug (5, 6). Several carriers have been employed to prepare solid dispersions. The most successful include polyethylene glycols (7–11), urea (12), dextrose (12), citric acid (12), succinic acid (13), and polyvinylpyrrolidone (14, 15). Polyethylene glycols have been used to increase the dissolution rate of griseofulvin (7), coumarin (8), dicumarol (9), indomethacin (10), and glyburide (11).

Phenytoin is practically insoluble in water (≅14 μg/mL) at room temperature (16), whereas the solubility of phenytoin sodium is ~66 g/dL in water (17). This difference in solubility results in higher bioavailability for the salt (18–20). If the poor solubility of phenytoin in GI fluids is partially responsible for the great variability observed in phenytoin dosing, then enhancing the dissolution step may result in a more uniform absorption and improved bioavailability.

The purpose of this study is to evaluate the bioavailability in dogs of a phenytoin solid dispersion in polyethylene glycol 6000 using a commercial prompt phenytoin sodium capsule as the reference formulation. Data are presented which indicate that the phenytoin dispersion is bioequivalent to the commercial prompt phenytoin sodium, which is contrary to what one would expect based on the *in vitro* data obtained from the USP dissolution test for phenytoin sodium. The designation "prompt" refers to the fast dissolution category of phenytoin sodium set forth in the USP XX.

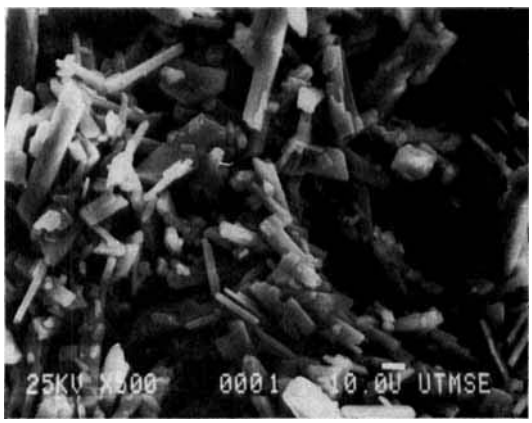

Figure 1—*Photomicrograph of the reagent-grade phenytoin (5,5-diphenylhydantoin). The 10-μm calibration bar is located in the lower right corner.*

EXPERIMENTAL

Preparation of Formulation—A 40% (w/w) solid dispersion of phenytoin[1] in polyethylene glycol 6000[2] was prepared using a melt method. The polymer was melted in a beaker on a thermostatically controlled hot plate at ~65–70°C. The reagent phenytoin was added with constant stirring until a clear liquid was observed. This liquid was poured into a glass mortar which was encased in ice. Solidification of the melt occurred on contact. The mass was dried in an oven at ~40°C for at least 1 h to remove excess moisture. The melt was triturated and then dried for at least 6 h. The powder was sieved through a 60-mesh sieve, and the batch was divided into 750-mg units.

Content Uniformity—Five of the 750-mg units of the phenytoin–polyethylene glycol 6000 dispersion were each dissolved in 1000 mL of 0.1 M NaOH, pH 12.5, in volumetric flasks. Duplicate samples were assayed using a commercial enzyme immunoassay[3]. The five determinations resulted in 98.7–102.0% of the theoretical amount.

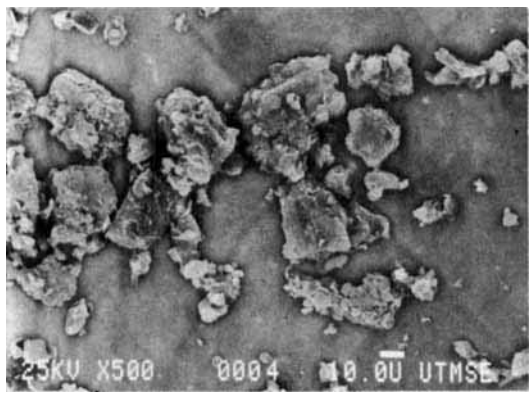

Figure 2—*Photomicrograph of the 40% phenytoin solid dispersion. The 10-μm calibration bar is located in the lower right corner.*

[1] 5,5-Diphenylhydantoin, 99+%, Gold Label; Aldrich Chemical Co., Milwaukee, Wis.
[2] Lot B-586; Alcon Laboratories, Fort Worth, Tex.
[3] EMIT Systems; Syva Co., Palo Alto, Calif.

0022-3549/84/0600-0733$01.00/0
© 1984, American Pharmaceutical Association

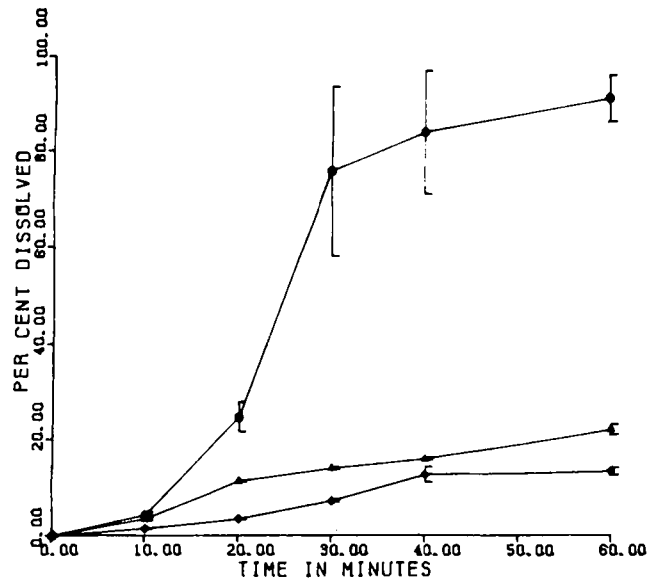

Figure 3—*Dissolution of the test preparations. Each point represents six capsules sampled and assayed in duplicate. All doses are equivalent to 92 mg of phenytoin. Key: (●) 100 mg of prompt phenytoin sodium; (▲) 230 mg of 40% solid dispersion of phenytoin in polyethylene glycol 6000; (◆) 92 mg of the reagent phenytoin. Bars represent 1 SD.*

Assay Procedure—A commercial enzyme immunoassay technique was utilized to assay all samples. This technique has been shown to be comparable in specificity and reproducibility (21, 22) to RIA (21, 23) and GC (21–24), and superior to spectrophotometry (21, 23). The range recommended was expanded by adding or deleting one dilution. Calibrated solutions provided by the manufacturers were used to check the effect of dilutions of samples on accuracy. A coefficient of variation of <10% was observed in each procedure.

Electron Microscopy—The sizes of the various particles were estimated by observation under a scanning electron microscope. Figure 1 shows a sample from the reagent phenytoin. A great variability in dimensions is observed. Figure 2 is a micrograph of the dispersion particles. The large particles are ~10 × 40 μm with several smaller fragments.

Dissolution Studies—Six 100-mg capsules of the commercial prompt phenytoin sodium were compared with six 92-mg samples of the reagent phenytoin and six 230-mg samples of the 40% (w/w) solid dispersion. All

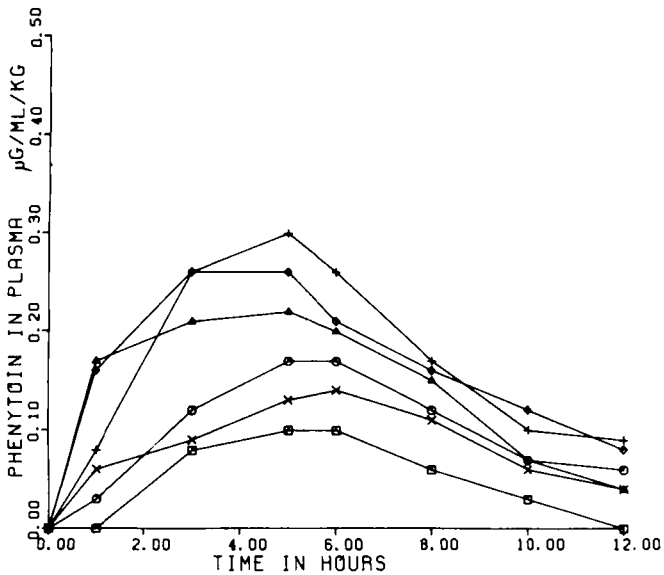

Figure 4—*Observed plasma concentrations of phenytoin obtained from six dogs (13–24 kg). Each animal received 300 mg of the prompt phenytoin sodium.*

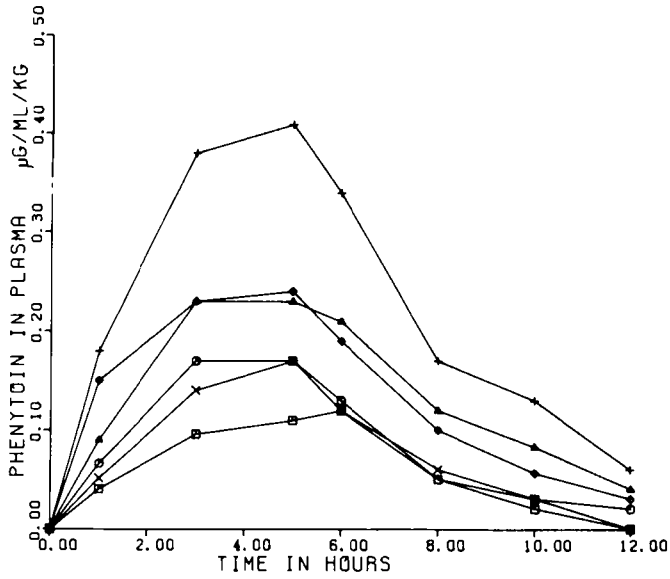

Figure 5—*Observed plasma concentrations of phenytoin obtained from six dogs (13–24 kg). Each animal received 750 mg of the 40% phenytoin solid dispersion.*

samples, equivalent to 92 mg of the phenytoin, were placed in size 1 gelatin capsules. The dissolution criteria were those stipulated for the oral phenytoin sodium in the USP XX. Duplicate samples were drawn and filtered through 0.45-μm filters[4], and were assayed at least twice. An additional study of six intact commercial prompt phenytoin sodium capsules using the same criteria was also performed.

X-ray Diffraction—Spectra were obtained from the reagent phenytoin, polyethylene glycol 6000, and the dispersion. A scanning rate of 3°/min was made from 6° to 70°. The minimum peak height was 2% of the reference peak. Spectra indicate that the phenytoin in the dispersion is the same crystalline form as that in the reagent. Also, no change was noted in the polyethylene glycol 6000 spectra.

Bioequivalence Studies—Six mixed-breed dogs (three of each sex), ~13–24 kg in weight, were used in this study. The animals were housed at the Animal Resources Center, The University of Texas. The dogs were fasted overnight prior to drug administration; water was allowed *ad libitum*. Each animal received 30 mL of water prior to and immediately after oral administration. The dogs were observed for 30 min and then returned to their cages for blood sampling.

The experimental design in the study is a balance of preparations over weeks and each animal received each preparation. The design was repeated twice for a total of two Latin squares. Two dogs received either 300 mg of the commercial prompt phenytoin sodium, 300 mg of phenytoin in the 40% dispersion, or 300 mg of a commercial intravenous phenytoin sodium on each study day. Studies were separated by 1-week wash-out periods to allow for drug elimination as well as to allow for stabilization of the animals' blood volume.

Blood samples were drawn by serial venipuncture. Sampling times after oral administration were at 0, 1, 3, 5, 6, 8, 10, 12, 24, 72, and 96 h. Samples were drawn at 0, 10, 20, 30, 45, and 60 min, and 2, 4, 12, 24, 48, 72, and 96 h after intravenous infusion at 50 mg/min. All blood samples were collected in heparinized evacuated tubes[5] which were gently inverted to allow for complete mixing. The samples were centrifuged at 2500 rpm for 15 min. The plasma was transferred into polyethylene tubes and frozen until assayed.

Statistical Analysis—A three-way ANOVA was performed on the *in vivo* data. The F ratio, as expected, was significant ($\alpha = 0.05$) for the intravenous data for $AUC_{0\rightarrow12}$ when compared with either of the oral preparations. The F ratio was not significant ($\alpha = 0.05$) when the two oral formulations were compared. Paired t tests compared the 40% phenytoin solid dispersion and the commercial prompt phenytoin sodium; this resulted in $p > 0.2$ for C_{max}, t_{peak}, and $AUC_{0\rightarrow12}$.

RESULTS AND DISCUSSION

***In Vitro* Studies**—Figure 1 is the electron micrograph of the reagent phenytoin. It shows a great variation in crystal size; many of the crystals exceed 40 μm in length and 10 μm in width. The micrograph of the dispersion par-

[4] Millipore Corp., Bedford, Mass.

[5] Vacutainer; B. D. Dickenson & Co.

Table I—Pharmacokinetic Parameters Obtained in Plasma after Oral Administration of Phenytoin

Parameter	Treatment A[a] Observed Mean (*SD*)	Treatment A[a] Calculated Mean[c]	Treatment B[b] Observed Mean (*SD*)	Treatment B[b] Calculated Mean[c]
C_{max} (μg/mL/kg)				
All subjects	0.20 (0.076)	0.20	0.22 (0.10)	0.24
Excluding dog 3	0.18 (0.063)	0.18	0.19 (0.049)	0.19
T_{peak} (h)				
All subjects	5.1 (0.41)	3.8	4.5 (1.2)	3.6
Excluding dog 3	5.2 (0.45)	4.0	4.4 (1.3)	3.6
$AUC_{0\rightarrow12}$ (μg/mL/h)				
All subjects	1.49 (0.602)	1.48	1.60 (0.808)	1.52
Excluding dog 3	1.37 (0.585)	1.33	1.22 (0.470)	1.22

[a] 300 mg of commercial prompt phenytoin sodium. [b] 750 mg of the 40% phenytoin solid dispersion. [c] Calculated values were obtained using Eq. 2.

ticles (Fig. 2) shows no large, discrete crystals in the formulation. The majority of the dispersion particles were ≤30 μm. A very small percentage exceeded 50 μm. An accurate estimate of the size of the phenytoin crystals in the dispersion could not be made, although some crystalline shapes could be discerned in the particles. Since none of the large rectangular crystals (>40 μm) observed in the reagent were noted in the dispersion or the residue, the formulation method used in this study must have reduced the particle size of the crystals. This probably occurred during the rapid solidification of the melt and during the trituration steps.

There is no compendial dissolution medium recommended for the comparison of the phenytoin and its sodium salt. Dissolution criteria do exist for the prompt and extended phenytoin sodium. These criteria were utilized to compare the dissolution rates of the phenytoin solid dispersion and the commercial prompt phenytoin sodium. Use of this dissolution test would indicate whether the commercial prompt phenytoin sodium samples would meet compendial standards. It would also serve to indicate whether one could use these dissolution criteria to compare two chemically different commercially available phenytoin products: the salt and the acid. The USP dissolution test for phenytoin sodium stipulates the use of 900 mL of water at 37 ± 0.5°C in Apparatus 1[6] (basket assembly) rotating at 50 rpm.

Prior to the dissolution test, all samples were placed in size 1 gelatin capsule. This was done to compare the rates of dissolution from a uniform capsule size. The percent dissolved of the commercial prompt phenytoin sodium at 30 min was 75.9%, which is much greater than the value obtained at 30 min for the solid dispersion (14.1%), or the reagent phenytoin (7.3%). At 60 min, 22.2 and 13.4% of the solid dispersion and the reagent phenytoin, respectively, were dissolved. After 180 min the percent dissolved in both preparations was almost equal: 29.4% for the reagent and 29.2% for the dispersion. The commercial prompt phenytoin sodium was 91.5% dissolved at 60 min.

The faster dissolution rate of the dispersion, when compared with the reagent phenytoin, may be due to the particle size reduction as previously noted in the electron micrographs. The X-ray diffraction data indicate that any change in the solubility of the two phenytoin samples cannot be due to a more-soluble polymorph existing in the dispersion. Comparison of the rate of dissolution of each preparation is presented in Fig. 3. Each point represents six capsules sampled and assayed in duplicate.

The USP states that at least 85% of a commercial prompt phenytoin sodium capsule should be dissolved in 30 min. Two of the size 1 capsules containing the transferred commercial prompt phenytoin sodium did not meet this specification. Thus, an additional study was undertaken. Six intact 100-mg capsules from the same lot were tested using the USP basket dissolution method as specified for phenytoin sodium capsules. At 30 min duplicate samples were taken and filtered through a 0.45-μm filter. Samples were kept in a water bath at ~37°C and assayed within 1 h after sampling. Each sample was assayed in duplicate. The six intact capsules showed an average dissolution of 81.5%, with SD = 14.5 and CV = 17.8%. The large variation noted in the six capsules may be due to two samples that had capsule-shaped masses which remained in the rotating basket apparatus after 30 min. The presence of these masses after a dissolution test has been noted in a previous study done with commercial phenytoin sodium products (25). A Student's t test was done to compare the data obtained from the transferred capsules *versus* the intact capsules. No significant difference was found (α = 0.05).

***In Vivo* Studies**—Each animal received 750 mg of the 40% solid dispersion, 300 mg of the commercial prompt phenytoin sodium, or 300 mg of the commercial intravenous phenytoin sodium. The oral doses were administered in three hard gelatin capsules. The 300-mg dose of each oral formulation was used to represent actual dosage strengths commercially available and dosing practices. The individual plasma levels obtained from these treatments are represented in Figs. 4 and 5. The plasma levels of the phenytoin sodium were normalized according to the phenytoin. It should be noted that dog 3 exhibits the highest blood levels in both Figs. 4 and 5. The difference in the curves demonstrates the effect of dog 3 on the data. Therefore, the t tests on C_{max}, t_{peak}, and $AUC_{0\rightarrow12}$ were done with and without the data obtained from dog 3. These data are presented in Table I. All areas were calculated using the trapezoidal rule. The probability values in the t_{peak}, C_{max}, and AUC were the same regardless of whether or not dog 3 was included. In all cases, $p > 0.2$.

Speculation on the cause of the large difference in the C_{max} found in dog 3 should include the observation that phenytoin exhibits nonlinear kinetics in dogs (26). Dog 3 was also the smallest dog and, therefore, received the largest mg/kg dose since all subjects received the same amount. It is possible that the small increase in the amount of phenytoin in the dispersion, when

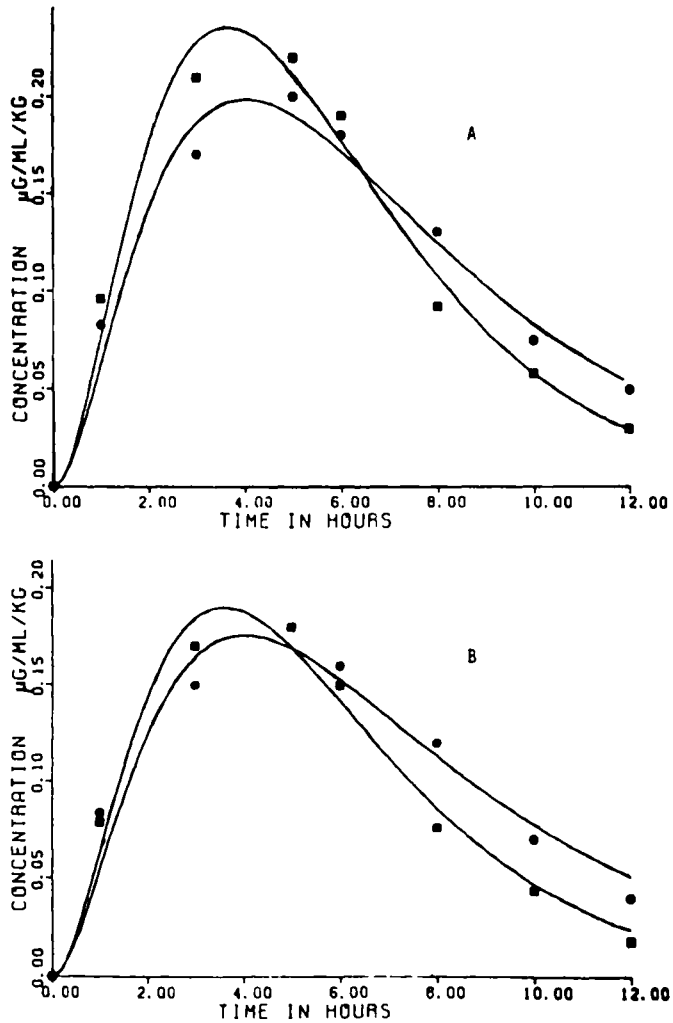

Figure 6— *Plots obtained from fitting averaged data to Eq. 2. Plot A represents the fit of all six animals, plot B represents the fit without the data from dog 3. Key: (■) 40% phenytoin dispersion; (●) commercial prompt phenytoin sodium.*

[6] Easi-Lift Dissolution Test Station; Hanson Research Corp., Nothridge, Calif.

Table II—Estimates of the Parameters Obtained from the Averaged Phenytoin Plasma Concentrations Utilizing Eq. 2

Parameter	Treatment[a] A	B	C	D
k_1 (h^{-1})	0.557	0.434	0.419	0.447
k_2 (h^{-1})	0.721	0.820	1.20	1.19
k_e (h^{-1})	0.414	0.482	0.268	0.241
C_0 ($\mu g/mL/kg$)	0.673	0.632	0.460	0.379

[a] Key: (A) 750 mg of 40% phenytoin solid dispersion, $n = 6$; (B) 750 mg of 40% phenytoin solid dispersion, $n = 5$ (without dog 3); (C) 300 mg of commercial prompt phenytoin sodium, $n = 6$; (D) 300 mg of commercial prompt phenytoin sodium, $n = 5$ (without dog 3).

compared with the same milligram dose of the salt, may have been enough to cause this animal to enter the nonlinear kinetics range.

The averaged data were fitted to a model with two first-order input steps:

$$A \xrightarrow{k_1} B \xrightarrow{k_2} C \xrightarrow{k_e} \quad \text{(Eq. 1)}$$

where k_1 and k_2 are the apparent first-order rate constants for the overall absorption process and k_e is the apparent elimination rate constant. The equation used to calculate the theoretical line is:

$$C_t = k_1 k_2 C_0 \left[\frac{e^{-k_1 t}}{(k_2 - k_1)(k_e - k_1)} + \frac{e^{-k_2 t}}{(k_1 - k_2)(k_e - k_2)} + \frac{e^{-k_e t}}{(k_1 - k_e)(k_2 - k_e)}\right] \quad \text{(Eq. 2)}$$

where C_0 is the fraction of the dose absorbed divided by the volume of distribution.

The estimates for k_1, k_2, k_e, and C_0 were obtained using a nonlinear digital computer program (27) and are presented in Table II. The plots of the average data and the lines generated from Eq. 2 are represented in Fig. 6. Other equations representing biexponential or triexponential oral absorption models, including those that utilized a lag time, were attempted; however, this fit resulted in a smaller sum of squared deviations and larger r and r^2 values. Weights of 1 were used. The parameters obtained were used to calculate the $AUC_{0\to12}$, C_{max}, and t_{peak}. Good agreement is observed between the estimates obtained from the computer fits and the observed data, as seen in Table I. The relative bioavailability of the observed data is 1.01 for all subjects and 0.90 when excluding dog 3.

The data indicate that the dispersion is bioequivalent to the commercial prompt phenytoin sodium whether or not the data from dog 3 are included in the statistical analysis. Since the solubility of the salt and the acid are very different, the formulation method must be partially responsible for the increased acid solubility. The particle size reduction, as verified by the micrographs, of the phenytoin has been shown to increase plasma levels in dogs (18). The polyethylene glycol 6000 may have also affected the solubility of the dispersion. Previous studies have stated possible vehicle effects: a solubilizing effect by the vehicle (13), increased wettability (5), and a decrease in aggregation and agglomeration in hydrophobic drugs (28).

In this study, the combined effects of phenytoin crystal size reduction and any vehicle effects demonstrated bioequivalency with the much more water-soluble salt. This contradicts the *in vitro* dissolution study, which demonstrated a fivefold difference in the percent dissolved at 30 min, and a fourfold difference at 60 min. If the absorption of phenytoin is dissolution rate limited, then a significant difference should exist in the blood levels obtained from these two products. But according to the C_{max}, t_{peak}, and AUC data obtained from the animal studies, no statistical difference exists. This implies that the dispersion method must have increased the bioavailability of phenytoin.

It is possible that the particle size reduction and any vehicle effects on the *in vivo* microenvironment may be responsible for the increased dissolution rate of phenytoin. It is also possible that in an aqueous acidic environment, the relatively high concentration of free phenytoin provided by the dissolution of the salt may result in some precipitation of the free acid, as has been previously postulated (29). If this occurred, then the rate of absorption of the precipitated crystals may be comparable to the rate of absorption of the reduced crystals found in the 40% solid dispersion, and thus, demonstrate bioequivalency. If, indeed, this is a valid consideration, then any conclusions based on the greater dissolution rate of the salt implying better bioavailability must be reexamined.

The results of this study indicate that the phenytoin solid dispersion dissolution profile does not meet the criteria used by the USP XX to define a "prompt" phenytoin sodium, yet the dispersion was found to be bioequivalent to the prompt phenytoin sodium. Unless the vehicle played a very significant part in the phenytoin-microenvironment interaction *in vivo*, the use of a more representative dissolution medium to simulate the gastric fluid should be considered to improve the *in vitro–in vivo* correlation of the different phenytoin products. This study demonstrates once again the difficulties that may be encountered when selecting appropriate dissolution criteria to predict bioavailability.

REFERENCES

(1) J. H. Fincher, J. G. Adams, and H. M. Beal, *J. Pharm. Sci.*, **54**, 704 (1965).

(2) R. M. Atkinson, C. B. Bedford, K. J. Child, and E. J. Tomich, *Nature (London)*, **193**, 588 (1962).

(3) A. H. Goldberg, M. Gibaldi, and J. L. Kanig, *J. Pharm. Sci.*, **54**, 1145 (1965).

(4) A. H. Goldberg, M. Gibaldi, and J. L. Kanig, *J. Pharm. Sci.*, **55**, 482 (1966).

(5) K. Sekiguchi and N. Obi, *Chem. Pharm. Bull.*, **9**, 866 (1961).

(6) K. Sekiguchi, N. Obi, and Y. Useda, *Chem. Pharm. Bull.*, **12**, 134 (1964).

(7) W. Chiou and S. Riegelman, *J. Pharm. Sci.*, **59**, 941 (1970).

(8) A. S. Geneidi, A. A. Ali, and R. B. Salama, *J. Pharm. Sci.*, **67**, 114 (1978).

(9) W. R. Ravis and C. Chen, *J. Pharm. Sci.*, **70**, 1353 (1981).

(10) J. Ford and M. Rubenstein, *Pharm. Acta. Helv.*, **55**, 1 (1980).

(11) A. S. Geneidi, M. S. Adel, and E. Shehata, *Can. J. Pharm. Sci.*, **15**, 70 (1980).

(12) J. W. McGinity, D. D. Maness, and G. J. Yakatan, *Drug Dev. Commun.*, **1**, 369 (1975).

(13) A. H. Goldberg, M. Gibaldi, and J. Kanig, *J. Pharm. Sci.*, **55**, 482 (1966).

(14) E. I. Stupak and T. R. Bates, *J. Pharm. Sci.*, **61**, 400 (1972).

(15) R. G. Stoll, T. R. Bates, K. A. Nieforth, and J. Swarbrick, *J. Pharm. Sci.*, **58**, 1457 (1969).

(16) W. A. Dill, A. Kazenko, L. M. Wolf, and A. J. Glazko, *J. Pharmacol. Exp. Ther.*, **118**, 270 (1956).

(17) "Merck Index," 9th ed., Merck and Co., Rahway, N.J., 1976.

(18) A. J. Glazko, W. A. Dill, J. C. Drach, and T. Chang, Sympos. Papers, 5th Nat'l Meeting, APhA APS, Washington, D.C., 1970, p. 326.

(19) K. S. Albert, E. Sakmar, M. R. Hallmark, D. J. Weidler, and J. G. Wagner, *Clin. Pharmacol. Ther.*, **16**, 727 (1974).

(20) L. Lund, *Eur. J. Clin. Pharmacol.*, **7**, 119 (1974).

(21) S. Stavchansky, T. Ludden, J. P. Allen, and P. Wu, *Anal. Chim. Acta*, **92**, 213 (1977).

(22) M. Legaz and V. Raisys, *Clin. Biochem.*, **9**, 35 (1976).

(23) V. Spiehler, L. Sun, D. S. Miyada, S. G. Sarandis, E. R. Walwick, M. W. Klein, D. B. Jordan, and B. Jessen, *Clin. Chem.*, **22**, 749 (1976).

(24) H. Booker and B. Darcey, *Clin. Chem.*, **21**, 1766 (1975).

(25) K. Arnold, N. Gerber, and G. Levy, *Can. J. Pharm. Sci.*, **5**, 89 (1970).

(26) P. G. Dayton, S. A. Cucinell, M. Weiss, and J. M. Perel, *J. Pharm. Exp. Ther.*, **158**, 305 (1967).

(27) C. M. Metzler, G. L. Elfring, and A. J. McEwen, *Biometrics*, **30**, 562 (1974).

(28) W. Chiou and S. Riegelman, *J. Pharm. Sci.*, **60**, 1281 (1971).

(29) A. J. Glazko and T. Chang, *Antiepileptic Drugs*, **127**, (1972).

ACKNOWLEDGMENTS

The authors wish to thank Ms. Sally Boyd of the Syva Company for providing some of the reagents and equipment.

Discriminative Structural Analysis Using Pattern Recognition Techniques in the Structure–Taste Problem of Perillartines

YOSHIMASA TAKAHASHI ‡, YOSHIKATSU MIYASHITA *, YUICHIRO TANAKA *, HIROSHI HAYASAKA *, HIDETSUGU ABE ‡, and SHIN-ICHI SASAKI *x

Received July 19, 1982, from the *School of Materials Science and the ‡Research Center for Chemometrics, Toyohashi University of Technology, Tempaku-cho, Toyohashi 440, Japan. Accepted for publication April 15, 1983.

Abstract □ Pattern recognition techniques have been applied to the study of structure–taste correlations for perillartine derivatives. The structure of each compound was described by hydrophobicity (log P), logarithm of water solubility (log S), and topological descriptors relating to some positions which were assigned by superposing each compound on a "template" structure. The fragment molecular connectivities were calculated as the topological descriptors. The discriminant functions between the sweet and bitter taste classes were computed by the use of the simplex optimization technique, which correctly recognized most of the compounds under investigation. It was found that the hydrophobicity and one or two topological descriptors concerned with a specific part of the molecules contributed significantly to the discrimination. The discriminant function obtained correctly classified seven of nine compounds (which were not involved in the data set for developing the function) into the taste class to which they belonged.

Keyphrases □ Structure–taste relationships—discriminative structural analyses using pattern recognition techniques, perillartine derivatives □ Perillartine derivatives—taste, discriminative structural analyses using pattern recognition techniques □ Topology—structure–taste relationships, perillartine derivatives, pattern recognition techniques

Inspection of various classes of sweet-tasting substances shows a very diverse group of chemical compounds having common activity. To establish a structure–taste relationship, a large number of compounds have been tested, and several hypotheses for the sweet taste impression have been proposed by different groups (1). Shallenberger and Acree (2) postulated the first glucophore for sweet-tasting compounds. Their model is referred to as AH—B theory, where A and B are electronegative atoms and H is a hydrogen atom. This AH—B system was extended by Kier (3), who pointed out that the third feature was a nonpolar region, X, which was capable of interacting with a corresponding site on a receptor by dispersion forces. Although there are many exceptions, it seems that the extended theory, the AH—B—X system, is the most sophisticated model among the various theories. However, there remain many problems to be solved for developing new synthetic sweeteners, including that sweet-tasting compounds are often accompanied by bitter and/or other unpreferable tastes. This fact has puzzled chemists interested in searching for new sweeteners. Relating to this taste dichotomy, Belitz and his co-workers (4) suggested the presence of a sweet–bitter receptor, which could be given by formal representation as a hydrophobic pocket with a bipolar system.

Recently, Acton and Stone (5) synthesized 51 perillartine derivatives to develop new potent sweeteners. In their article, taste potencies and taste qualities (sweetness, bitterness, and other tastes) for the perillartines are represented by relative potencies to sucrose and percentages for total taste potencies, respectively. Using this data set, Iwamura (6) implemented the regression analysis with physicochemical and the STERIMOL parameters (7) of the compounds. From the results, he suggested that sweet and bitter receptors have common features. Furthermore, we (8) have shown that the sweet taste receptor might be more restricted (from the viewpoint of spatial shape) than the bitter receptor, by means of class discrimination using the STERIMOL parameters. On the other hand, Kier tried to discriminate between these sweet- and bitter-tasting compounds using discriminant analysis with molecular connectivities (9). He pointed out that unsaturation or heteroatoms are not critical to the structures that influence the sweet and bitter tastes.

In this article, we discuss the results of a discriminative structural analysis of perillartines using pattern recognition techniques; to describe the topological features of these molecules, molecular connectivity indices are also used. However, they are not calculated for whole molecules, but for the fragments related to some specific positions based on a template structure. The use of the indices may give some local topological information on a molecule.

In view of the class discrimination between the sweet and bitter tastes of perillartines, these indices are used in developing the best discriminant function together with two other descriptors. In such classification problems, statistical discriminant analysis (9–11) is frequently used. But the results of such statistical analysis is less reliable when the size of the data set available is not large enough. In contrast, nonparametric pattern recognition is applicable for such small data sets with proper reliability. Therefore, we employed the simplex pattern recognition method for the present study.

EXPERIMENTAL

Data Selection—In the present study, 22 compounds (11 sweet and 11 bitter) were selected as representative compounds from those previously reported by Acton (5). Each possesses >50% of the total taste potency with respect to only the most potent taste quality (Fig. 1). Nine compounds were used as a prediction set for discriminating the taste classes of unknowns by the use of the discriminant function, which was obtained by the former set of compounds. All of the compounds selected are aldoximes.

Template Structure and Fragment Molecular Connectivity—For generating the structural descriptors, a template structure was considered based on the chemical structure of perillartine and related compounds (Fig. 2). Ten positions of interest were considered. Assignments of the positions on the structure for the topological descriptors were made as shown in Fig. 2. For each compound to be analyzed, the positions a–j were assigned by superposing the structure in the manner of planar representation on the template structure. The α,β-unsaturated bonds of skeletons always correspond to the edge between a and b on the template structure. Three positions (h, i, and j) were designated in the descending order of the bulkiness or size of the side chains on each position. As topological descriptors, 20 fragment molecular connectivity (FMC) indices (${}^1\chi_a$–${}^1\chi_j$, ${}^1\chi^v_a$–${}^1\chi^v_j$) related to the 10 positions were adopted for use in this study. These indices are those for path 1 fragments with respect to the given position, which were calculated as the sum of the first-order terms for each edge joining the position of interest (12). Thus, for this study, the path 1 FMC value ${}^1\chi$ (or ${}^1\chi^v$) for the vertex k is given by:

$$\mathrm{FMC}_k = \sum_l (\delta_k \cdot \delta_l)^{-1/2} \qquad \text{(Eq. 1)}$$

0022-3549/84/0600-0737$01.00/0
© 1984, American Pharmaceutical Association

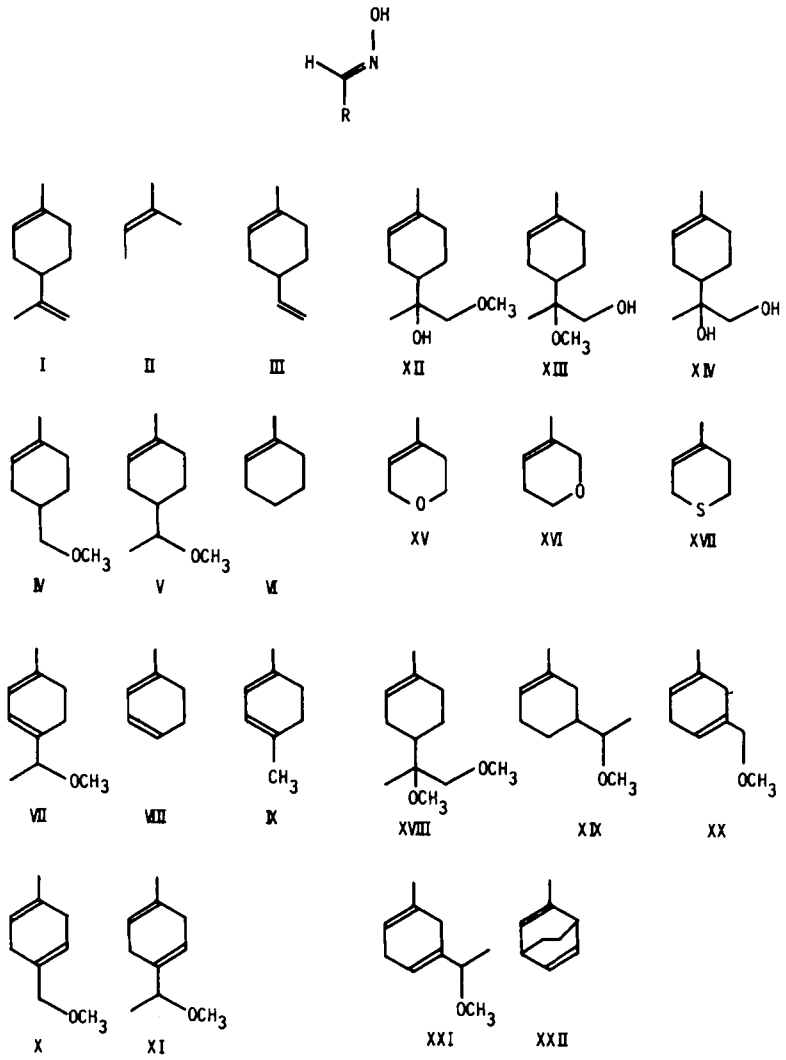

Figure 1—*Perillartine analogues.*

where δ is the valence of a vertex which corresponds to an atom and l is a vertex adjacent to k on the template structure. As a convention, positions were coded with zero for FMC if there were no substituents at the given positions. These structural descriptors were used to describe local topological features of the molecules.

In addition, two other descriptors were used in this study, hydrophobicity (log P) and the logarithm of water solubility (log S) of the compounds. These values were taken from the literature (5, 6). The values of ${}^{1}\chi_a - {}^{1}\chi_j$, log P, and log S for the compounds are shown in Table I.

In the present study, each value of the descriptors employed was normalized in such manner that the mean value was zero and the standard deviation was one for each of 22 descriptors. This process, which is sometimes called autoscaling, will not alter any of the classification results since no change of the relative positions of the pattern points occurs.

Feature Selection—Descriptors not relevant to the classification problem should be eliminated because they may disturb the correct classification or enlarge the computational work. An exhaustive search for the best subset of features is only possible for a small number of descriptors. In this study, the number of original features is too large, and it was necessary to reduce the dimensionality due to the reason mentioned above.

Feature (descriptor) selection was performed with the Fisher ratio (13). The Fisher ratio is a quantitative estimate of the significance of a given parameter for separating two classes. The Fisher ratio of the descriptor k (F_k)

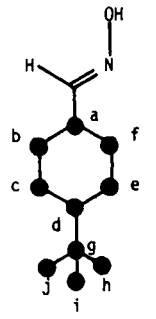

Figure 2—*Template structure for perillartines.*

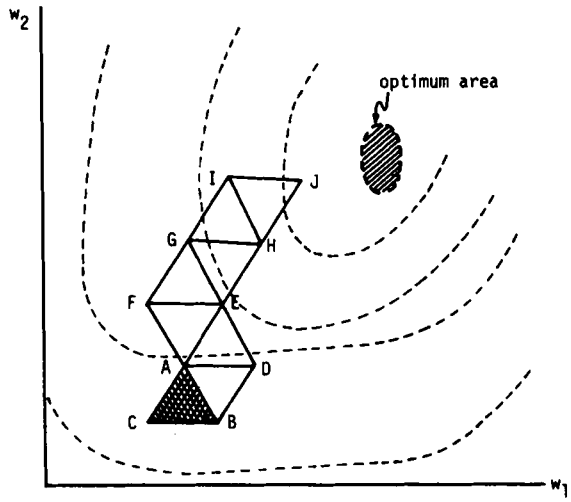

Figure 3—*Progress of the two-dimensional simplex toward the optimum area.*

Table I—Percentages of Taste Qualities and Descriptor Values

Compound	S/B[a]	log P[b]	log S[c]	$^1\chi_a$	$^1\chi_b$	$^1\chi_c$	$^1\chi_d$	$^1\chi_e$	$^1\chi_f$	$^1\chi_g$	$^1\chi_h$	$^1\chi_i$	$^1\chi_j$
I	60/25	2.58	−3.301	1.224	0.908	0.908	1.149	0.908	0.908	1.488	0.577	0.577	0.000
II	55/8	0.87	−0.824	1.393	1.115	0.707	0.000	0.000	0.577	0.000	0.000	0.000	0.000
III	50/10	2.28	−3.699	1.224	0.908	0.908	1.224	0.908	0.908	1.115	0.707	0.000	0.000
IV	53/22	1.10	−1.523	1.224	0.908	0.908	1.224	0.908	0.908	0.908	1.207	0.000	0.000
V	50/20	1.40	−2.523	1.224	0.908	0.908	1.129	0.908	0.908	1.318	1.115	0.577	0.000
VI	50/15	1.48	−1.745	1.224	0.908	1.000	1.000	1.000	0.908	0.000	0.000	0.000	0.000
VII	65/7	1.10	−2.398	1.224	0.908	0.908	1.149	0.908	0.908	1.318	1.115	0.577	0.000
VIII	70/3	1.48	−1.824	1.224	0.908	1.000	1.000	1.000	0.908	0.000	0.000	0.000	0.000
IX	78/3	0.78	−3.222	1.224	0.908	0.908	1.393	0.908	0.908	0.577	0.000	0.000	0.000
X	90/2	0.80	−1.699	1.224	0.908	0.908	1.224	0.908	0.908	0.908	1.204	0.000	0.000
XI	92/1	1.10	−2.398	1.224	0.908	0.908	1.149	0.908	0.908	1.318	1.115	0.577	0.000
XII	6/70	−0.10	−1.921	1.224	0.908	0.908	1.105	0.908	0.908	1.644	0.853	0.500	0.500
XIII	4/93	−0.10	−1.796	1.224	0.908	0.908	1.105	0.908	0.908	1.495	1.060	0.500	1.060
XIV	5/73	−0.92	0.301	1.224	0.908	0.908	1.105	0.908	0.908	1.642	1.060	0.500	0.500
XV	0/50	−0.72	−0.155	1.224	0.908	1.000	1.000	1.000	0.908	0.000	0.000	0.000	0.000
XVI	2/65	−0.72	−1.097	1.224	0.908	1.000	1.000	1.000	0.908	0.000	0.000	0.000	0.000
XVII	0/70	0.34	−1.260	1.224	0.908	1.000	1.000	1.000	0.908	0.000	0.000	0.000	0.000
XVIII	0/78	0.72	−2.046	1.224	0.908	0.908	1.105	0.908	0.908	1.495	0.853	0.500	1.060
XIX	2/52	1.40	−2.523	1.224	0.908	1.000	0.908	1.149	0.816	0.000	0.000	0.000	0.000
XX	0/75	0.80	−1.699	1.224	0.908	1.000	0.908	1.224	0.816	0.000	0.000	0.000	0.000
XXI	0/67	1.10	−2.398	1.224	0.908	1.000	0.908	1.149	0.816	0.000	0.000	0.000	0.000
XXII	0/50	1.90	−1.921	1.149	0.816	1.224	0.908	0.908	1.149	0.000	0.000	0.000	0.000

[a] Compounds with (sweet/total taste) ≥0.5 are taken as sweet and those with (bitter/total taste) ≥0.5 as bitter. [b] Taken from Ref. 6. [c] Taken from Ref. 5.

is calculated from Eq. 2; it is the ratio between the square of the difference in interclass means and the sum of squared intraclass standard deviations:

$$F_k = \frac{(\bar{x}_k^{(1)} - \bar{x}_k^{(2)})^2}{\sigma_k^{(1)2} + \sigma_k^{(2)2}} \qquad \text{(Eq. 2)}$$

where $\bar{x}_k^{(1)}$ and $\bar{x}_k^{(2)}$ are the mean values of the descriptor k in classes 1 and 2, respectively, and $\sigma_k^{(1)}$ and $\sigma_k^{(2)}$ are the standard deviations of those classes. The features are ranked according to their importance, and less important features are discarded.

Development of the Discriminant Function—The simplex pattern recognition method was applied to develop a near optimum discriminant function for discrimination between the sweet- and bitter-tasting compounds. The simplex method is an approach to optimize an objective function (*e.g.*, discriminant function). This optimization technique was previously applied to the optimization of linear discriminant functions for chemical applications by Ritter *et al.* (14). In the present work, the simplex pattern recognition program(SPLX), which was developed in our laboratory according to their algorithm with a small modification, was used.

In the case of two classes, if pattern points on one side of a discriminant surface always belong to class 1 and those on the other side belong to class 2, the data are linearly separable by a linear discriminant function of the following form:

$$g(\mathbf{X}) = w_1x_1 + w_2x_2 + \ldots + w_dx_d = |\mathbf{W}||\mathbf{X}|\cos\theta \qquad \text{(Eq. 3)}$$

where x_i is the ith component of a pattern $\mathbf{X}$ and w_i is the weight assigned to that component. Hence, the classification into two categories can be implemented with the sign of $g(\mathbf{X})$ given by the dot product of a pattern vector $\mathbf{X}$ and a weight vector $\mathbf{W}$. The optimization problem of that function, in this case, can be placed in that of the corresponding weight vector in the weight space.

A simplex is a geometric figure in d-dimensional space, which consists of $d + 1$ vertices. For example, a two-dimensional simplex is a triangle, a three-dimensional simplex is a tetrahedron, *etc.* Figure 3 shows a two-dimensional simplex superimposed on a contour map, which represents the various equiresponse lines of a function of two variables. In this case, the search variables are the components of the weight vector. On the other hand, two criterion functions are evaluated in terms of the response. These are given by:

$$R = N_c/N_t \qquad \text{(Eq. 4)}$$

$$P = \sum_{\mathbf{X}_i \in S_E} |\mathbf{W} \cdot \mathbf{X}_i| \qquad \text{(Eq. 5)}$$

In Eq. 4, N_t is the total number of compounds tested and N_c is that of compounds correctly classified, so R is a recognition rate. On the other hand, in Eq. 5, S_E is the set of all patterns misclassified by $\mathbf{W}$. Thus, P is the sum of the absolute values of the dot products of all misclassified patterns by the use of the weight vector $\mathbf{W}$. In general, the value of P will become small if few compounds are misclassified or if those misclassified lie close to the discriminant surface. This criterion is used only as a smoothing function, so that the ultimate solution will be given by the minimum P value for a weight vector giving maximum recognition rate.

The optimization procedure begins by locating initial simplex (initial weight vectors) on the d-dimensional weight vector space. These were generated as follows:

$$\begin{aligned}
\mathbf{W}_1 &= (w_1, w_2, w_3, \ldots, w_d, w_{d+1}) \\
\mathbf{W}_2 &= (w_1 + \delta_1, w_2, w_3, \ldots, w_d, w_{d+1}) \\
\mathbf{W}_3 &= (w_1, w_2 + \delta_2, w_3, \ldots, w_d, w_{d+1}) \\
&\vdots \\
\mathbf{W}_{d+1} &= (w_1, w_2, w_3, \ldots, w_d + \delta_d, w_{d+1})
\end{aligned} \qquad \text{(Eq. 6)}$$

where $w_{d+1} = -1$ and δ_j was defined as:

$$\delta_j = \alpha w_j \qquad \text{(Eq. 7)}$$

The constraint of $w_{d+1} = -1$ describes a unique weight vector for a given decision surface (14). In Eq. 7, α is an arbitrary constant parameter concerned

Table II—Fisher Ratios of Descriptors

Descriptor	Fisher Ratio	Rank
log P	7.84×10^{-2}	1
$^1\chi_c$	4.21×10^{-2}	2
$^1\chi_j$	3.93×10^{-2}	3
log S	3.63×10^{-2}	4
$^1\chi_e$	2.61×10^{-2}	5
$^1\chi_h$	1.45×10^{-2}	6
$^1\chi_a$	1.44×10^{-2}	7
$^1\chi_b$	1.44×10^{-2}	8
$^1\chi_g$	5.58×10^{-3}	9
$^1\chi_f$	3.63×10^{-3}	10
$^1\chi_d$	1.97×10^{-3}	11
$^1\chi_i$	4.85×10^{-4}	12

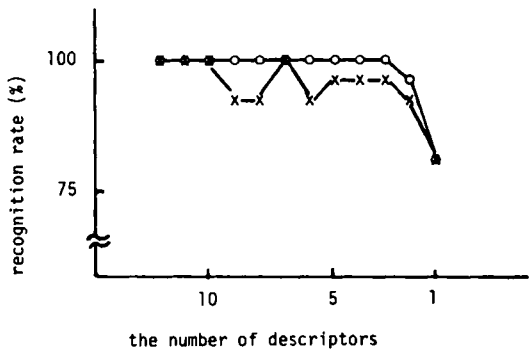

Figure 4—*Recognition rates obtained by the use of various descriptor set contained with $^1\chi$ FMC indices. Key: (○) simplex method; (X) discriminant analysis.*

Table III—Cross-Correlation Table of Five Descriptors

	log P	log S	$^1\chi_c$	$^1\chi_e$	$^1\chi_j$
log P	1.00				
log S	−0.76	1.00			
$^1\chi_c$	0.10	0.00	1.00		
$^1\chi_e$	−0.01	−0.19	0.65	1.00	
$^1\chi_j$	−0.39	0.16	−0.19	−0.03	1.00

with a kind of size on the initial simplex. In the present study, α was selected to be 0.5.

A prototype weight vector (initial weight vector) $\mathbf{W}_1$, in generating the initial simplex, was determined by the use of the bisecting approach in which the linear discriminant surface might be approximate as the hyperplane bisecting two class centers (14). Once the initial simplex was located in the objective space, optimization of the simplex (or weight vectors) by a certain moving algorithm was attempted. Moving the simplex in the optimization process was performed according to the algorithm suggested by Nelder and Mead (15), which is a logical algorithm consisting of reflection, expansion, and contraction rules. Since this procedure has been described in detail elsewhere (14–16), it will not be repeated here.

In addition, another approach was also employed for the development of discriminant functions. Ordinary statistical discriminant analysis was implemented to the same data set for comparison with the above method.

RESULTS AND DISCUSSION

The correlations between the descriptors under investigation were examined. The results of the correlation analysis showed that the values of descriptors $^1\chi$ and $^1\chi^v$ were highly correlated (correlation coefficients = 0.78–1.00) with each other on the same position of the molecule. In such classification problems, the use of highly correlated pairs among descriptors may lead to the reduction of reliability of discriminant functions, decreasing the intrinsic dimensionality in the pattern space and increasing the probability of chance classification. Thus, in the present work $^1\chi$ values were taken as the topological variables relating to each position on the template structure. Furthermore, for the purpose of reducing the number of descriptors, preselection of the descriptors was implemented by the use of the Fisher ratio, which is a measure of the significance of a given parameter for differentiating between the taste classes. Each descriptor was ranked in decreasing order of the Fisher ratio (Table II). According to the ranking, the descriptors were eliminated one at a time and then a linear discriminant function was developed with the descriptor set using the simplex method or statistical discriminant analysis. The plots of recognition rate R *versus* the number of descriptors are illustrated in Fig. 4.

As shown in Fig. 4, in most cases the results for discriminant analysis were not as good as those for the simplex method. This would be anticipated because the $^1\chi$ FMC indices show noticeably non-normal distributions (Table I). It seemed that the simplex pattern recognition was more suitable for the discriminative analysis for the present data set, rather than the other method.

It was shown, in this case, that only two or three descriptors were enough to discriminate between the two taste classes from the result of the simplex method: log P, $^1\chi_c$, and $^1\chi_j$. During the analysis described above, only the Fisher ratios were used for the feature selection. However, because the Fisher ratio is based on the global class separation information of the data structure, it is not always true that the obtained result is the best. Thus, further examinations would be required for the descriptors. Five of the best descriptors were selected on the basis of the Fisher ratio, log P, log S, $^1\chi_c$, $^1\chi_h$, and $^1\chi_j$. The cross-correlation table among the descriptors is shown in Table III. These descriptors were used in the following studies.

To develop a discriminant function with the best set of variables among the combinations of the above descriptors, implementations were performed. The best linear discriminant function with three or two descriptors is shown as follows:

$$g_3(\mathbf{X}) = 0.595 \cdot \log P - 0.773 \cdot {}^1\chi_c - 0.220 \cdot {}^1\chi_j - 0.882 \times 10^{-5} \quad \text{(Eq. 8)}$$

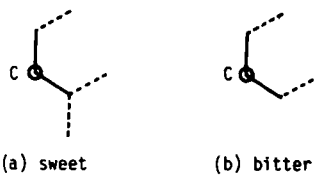

Figure 5—*Characteristic topological fragments for the sweet or bitter compounds.*

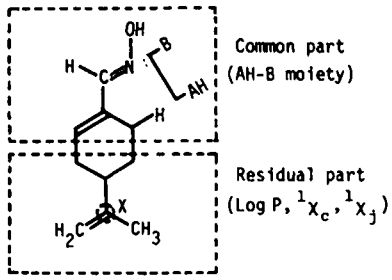

Figure 6—*AH—B—X postulation for perillaldehyde oxime (3).*

$$g_2(\mathbf{X}) = 0.696 \cdot \log P - 0.718 \cdot {}^1\chi_c - 0.220 \times 10^{-5} \quad \text{(Eq. 9)}$$

$$g(\mathbf{X}) \begin{cases} \geq 0 \text{ implies sweet class} \\ < 0 \text{ implies bitter class} \end{cases}$$

Equation 8 correctly classified all compounds into the observed classes. On the other hand, Equation 9 correctly discriminated all of the 11 sweet-tasting compounds and 10 of the 11 bitter-tasting compounds. The average recognition rate was 95%; only XVIII was misclassified.

Equations 8 and 9 suggest that the log P and fragment molecular connectivity index, $^1\chi_c$, are significant characteristics that influence whether a compound is sweet or bitter. In the two equations, as the hydrophobicity of a compound increases, the $g(\mathbf{X})$ values are larger due to the positive value of that coefficient. The compound then tends to be classified as sweet.

The negative coefficient for the $^1\chi_c$ term suggests that a smaller value of $^1\chi_c$ enhances the sweet-taste impression. For the data set employed in the present work, however, the values of $^1\chi_c$ do not vary much. In this case, it is helpful to consider the contribution of $^1\chi_c$ in terms of topological features. The $^1\chi_c$ index describes the branching information or the topological form concerned with the path 1 fragment at position c. Although each value does not always correspond to a unique fragment, it is meaningful to examine the topological fragment. The topological fragments concerned with those positions are illustrated in Fig. 5. Most compounds in the sweet class involve a fragment such as a in Fig. 5; the compounds in another class involve fragment b, excepting some compounds. It should be noted that fragment b is embedded in another fragment.

Furthermore, the third term (which was weighted by a negative coefficient in Eq. 8) suggests that bulky side chains on the j position may prevent the impression of sweetness. Alternatively, because $^1\chi_j$ is zero except for four compounds in the bitter class, this variable could be replaced by an indicator variable related to the presence of a quaternary carbon at the g position. Thus, it is postulated that the occupancy by a substituent at the position j may influence the taste quality of these compounds.

In the present data set, since the aldoxime moiety is a common part of all molecules, the variation of log P is due to the residual part. Thus, the observations are consistent with Kier's postulation of perillartine in his AH—B—X

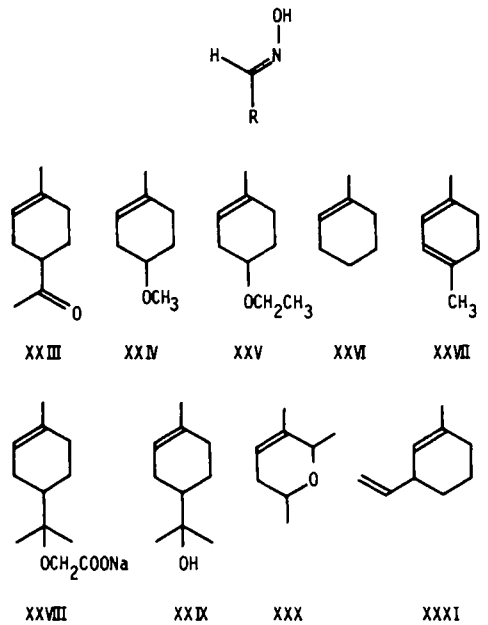

Figure 7—*A set of compounds for the taste predictions.*

Table IV—Descriptor Values and Percentages of Taste Qualities in Prediction Set

Compound	S/B	log P	log S	$^1\chi_a$	$^1\chi_b$	$^1\chi_c$	$^1\chi_d$	$^1\chi_e$	$^1\chi_f$	$^1\chi_g$	$^1\chi_h$	$^1\chi_i$	$^1\chi_j$
XXIII	23/14	0.32	−1.96	1.224	0.908	0.908	1.149	0.908	0.908	1.488	0.577	0.577	0.000
XXIV	42/26	0.60	−1.30	1.224	0.908	0.908	1.224	0.908	0.908	1.115	0.707	0.000	0.000
XXV	45/26	1.10	−1.96	1.224	0.908	0.908	1.224	0.908	0.908	0.908	1.207	0.000	0.000
XXVI	40/16	1.78	−1.77	1.224	0.908	1.000	1.000	1.000	0.908	0.000	0.000	0.000	0.000
XXVII	22/13	0.78	−3.22	1.224	0.908	0.908	1.393	0.908	0.908	0.577	0.000	0.000	0.000
XXVIII	0/38	−4.08	−2.30	1.224	0.908	0.908	1.105	0.908	0.908	1.642	0.500	0.500	0.853
XXIX	4/18	0.88	−1.57	1.224	0.908	0.908	1.105	0.908	0.908	0.788	0.500	0.500	0.500
XXX	0/36	−0.16	−1.64	1.149	0.908	0.908	1.393	0.908	1.318	0.577	0.000	0.000	0.000
XXXI	14/34	2.28	−3.70	1.224	0.816	1.224	0.908	1.000	0.908	0.000	0.000	0.000	0.000

theory (3). The AH—B—X system of perillartine is illustrated in Fig. 6. Furthermore, the aforementioned results suggest that the shape of the moiety concerned with the third site (X) plays an important role in the taste impression (especially, sweetness). This insight would be clear in the following predictive analysis.

The discriminant ability of the linear discriminant function obtained in the present study can be tested by predicting the taste classes of compounds not used in the development of the function. For this test, as shown in Fig. 7, nine compounds were selected from a previous study (5). These compounds are not dominant in one taste class, as seen by the total taste potency (Table IV). However, on the basis of the sweet-bitter taste ratios, each compound could be assigned to either the sweet or bitter taste class. The first five compounds (XXIII-XXVII) are categorized as sweet, and the other compounds (XXVIII-XXXI) are categorized as bitter. The prediction results of their taste classes are shown in Table V. Both discriminant functions, $g_2(X)$ and $g_3(X)$, correctly predicted the class of seven of the tested compounds.

Compounds XXIII and XXIX were misclassified (Fig. 7). They are the smallest in terms of the difference between the sweet and bitter taste ratios (Table IV). Considering that the compounds tested were not so typically sweet or bitter, this result may be more favorable.

The results of this prediction encouraged us to apply the methodology of this study to the structure-taste problem for the series of perillartines. In such a discrimination, the influence of hetero atoms or unsaturated bonds on a structure was examined in the same manner by the use of FMC indices ($^1\chi^v_{a-j}$) with the weighted valences. The values of the weighted valences were obtained from a previous paper (12). But, the result was not as favorable, as shown in Fig. 8. Furthermore, an additional analysis in which $^1\chi$ and $^1\chi^v$ FMC indices were used together in developing the best discriminant function had the same results as using only $^1\chi$ FMC indices. These examinations suggest that the hetero atoms and unsaturated bonds are not so critical in the aforementioned residual part.

CONCLUSION

The structural discriminative analysis of the sweet and bitter perillartines using a template structure was successfully performed by pattern recognition techniques. It was shown that the fragment molecular connectivity indices are useful in describing the local features of molecules in terms of topological structure.

The results for the series of perillartines offer some explanations of the structure-taste correlation. The hydrophobicity of the residual part except for the AH—B moiety in the analogues influenced the taste quality, and furthermore the topological shape of the residual part is also predominantly concerned with the sweet or the bitter taste impression. The information obtained from the best discriminant functions was used to examine additional molecules, and it improved predictions of their taste classes. This study confirms Kier's original postulation (3) of the sweet pharmacophore for perillartine.

Table V—Prediction Results from Simplex Pattern Recognition

Compound	(S/B)	Prediction $g_2(X)$	Prediction $g_3(X)$
XXIII	(S)	X	X
XXIV	(S)	O	O
XXV	(S)	O	O
XXVI	(S)	O	O
XXVII	(S)	O	O
XXVIII	(B)	O	O
XXIX	(B)	X	X
XXX	(B)	O	O
XXXI	(B)	O	O

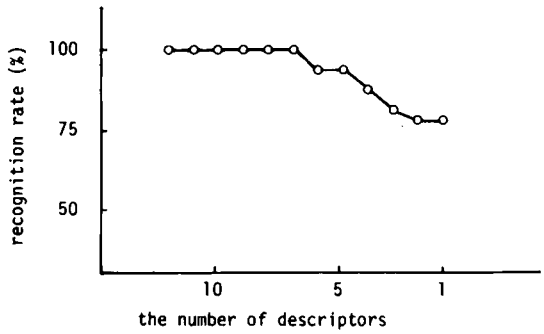

Figure 8—*Recognition rates obtained by the use of various descriptor sets with $^1\chi^v$ FMC indices using the simplex method.*

REFERENCES

(1) J. C. Boudreau (Ed.), "Food Taste Chemistry," ACS Symposium Series, No. 115, American Chemical Society, Washington, D.C., 1979.

(2) R. S. Shallenberger and T. E. Acree, *Nature (London)*, **216**, 480 (1967).

(3) L. B. Kier, *J. Pharm. Sci.*, **61**, 1394 (1972).

(4) H. D. Belitz, W. Chen, H. Jugei, R. Treleanco, H. Wieser, J. Gasteiger, and M. Marsili, in "Food Taste Chemistry," J. C. Boudreau, Ed., p. 93.

(5) E. M. Acton and H. Stone, *Science*, **193**, 584 (1976).

(6) H. Iwamura, *J. Med. Chem.*, **23**, 308 (1980).

(7) A. Verloop, W. Hoogenstraaten, and J. Tipker, in "Drug Design," vol. 7, E. J. Ariens, Ed., Academic, New York, N.Y., 1976, p. 165.

(8) Y. Takahashi, Y. Miyashita, Y. Tanaka, H. Abe, and S. Sasaki, *J. Med. Chem.*, **25**, 1245 (1982).

(9) L. B. Kier, *J. Pharm. Sci.*, **69**, 416 (1980).

(10) Y. C. Martin, J. B. Holland, C. H. Jarboe, and N. Plotnikoff, *J. Med. Chem.*, **17**, 409 (1974).

(11) D. R. Henry and J. H. Block, *J. Med. Chem.*, **22**, 465 (1979).

(12) L. B. Kier and L. H. Hall, "Molecular Connectivity in Chemistry and Drug Research," Academic, New York, N.Y., 1976.

(13) B. R. Kowalski, "Chemometrics, Theory and Application," ACS Symposium Series, No. 52, American Chemical Society, Washington, D.C., 1977.

(14) G. L. Ritter, S. R. Lowry, C. L. Wilkins, and T. L. Isenhour, *Anal. Chem.*, **47**, 1951 (1975).

(15) J. A. Nelder and G. Mead, *Comput. J.*, **7**, 308 (1965).

(16) S. N. Deming and S. L. Morgan, *Anal. Chem.*, **45**, 278A (1973).

ACKNOWLEDGMENTS

The authors thank the Computer Center, Institute for Molecular Science for affording facilities for computation. The authors also thank Dr. C. Takayama for his invaluable discussion.

Membrane Solubility Parameter and *In Situ* Release of Theophylline

A. ADJEI *, J. NEWBURGER, S. STAVCHANSKY, and A. MARTIN ˣ

Received December 6, 1982, from the *University of Texas, College of Pharmacy, Drug Dynamics Institute, Austin, TX 78712.* Accepted for publication February 2, 1983. * Present address: Pharmaceutical Products Division, Abbott Laboratories, North Chicago, IL 60064.

Abstract □ The solubility of theophylline in polyethylene glycol 400–water binary mixtures was analyzed in terms of solute-solvent interaction using the solubility parameter principle of Hildebrand. Preliminary *in situ* (rat gut permeation) studies with the solvent mixtures having varying polarity as expressed by the solubility parameter showed that (*a*) the more alike the solubility parameter of theophylline (δ_2 = 14, as obtained from solubility studies) and the solubility parameter of the solvent mixture, the greater was the attraction of solvent for the drug (*b*) sufficient similarity must exist between the solubility parameter of theophylline and that of the intestinal mucosa to promote bioabsorption, and (*c*) from the above, it follows that there exists a competition between solvent and rat gut membrane for the drug. The solubility parameter of the solvent vehicle must be such that it does not impede absorption of the molecules into the intestinal mucosa.

Keyphrases □ Solubility parameter—theophylline in propylene glycol 400–water, *in situ* release in the rat gut, membrane solublity parameter □ Release rate—theophylline in propylene glycol 400–water, *in situ* rat gut model, membrane solubility parameter □ Solute-solvent interactions—effect on the solubility of theophylline in propylene glycol 400–water, *in situ* release in the rat gut, membrane solubility parameter

The principle of solute–solvent interaction and its influence on drug solubility and solubilization has been studied extensively (1–10). Recent works (11–13) have extended the Hildebrand–Scatchard model (1, 2) to handle solubility predictions of drugs in polar solvents.

This report examines the influence of solvent polarity, solvent attraction for the solute (theophylline), and the effect of this interaction on theophylline release. The method of Doluisio *et al.* (14), in which drug absorption is followed using an *in situ* rat gut preparation, was employed to monitor theophylline disappearance from various polyethylene glycol 400–water mixtures into the rat intestinal membrane. The results of this study are analyzed according to the postulates of previous work (3–5, 15–17).

EXPERIMENTAL

***In Situ* Rat Gut Method**—Male Sprague–Dawley rats, 220–250 g, were fasted for 16 h with free access to water and housed in mesh screen cages to prevent coprophagy. The rats were anesthetized with 75 mg/kg ip injections of sodium pentobarbital. After the onset of anesthesia, a midline incision was made to expose the intestines. Two L-shaped glass cannulae were inserted into the intestine and ligated. The proximal cannula, which was placed just below the bile duct, and the distal cannula were spaced ~61 cm apart. Four-centimeter lengths of Tygon tubing were attached to each cannula, and a 30-mL hypodermic syringe was connected to each Tygon tube using a three-way stopcock as a connector. The proximal syringe was filled with a pH 7 phosphate buffer, previously warmed to 37°C, and the intestine was flushed until the perfusate was observed to be clear as it left the distal cannula. Nine milliliters of various polyethylene glycol 400–water mixtures, having a range of solubility parameters and resulting in varing solubility for the drug, were formulated with each containing 2 mg/mL of theophylline and 1200 cpm of ^{14}C-labeled polyethylene glycol 4000, which was used as a nonabsorbable marker to monitor water flux. These solutions were placed in the prepared gut *via* the distal cannula and flushed back and forth through the intestines several times to effect uniform mixing. Two time zero samples (0.1 mL each) of the solution were then removed. After sampling, the solution was returned to the intestine and the stopcocks were closed to maintain the solution in place. A stop watch was activated, and serial time samples were removed thereafter. The stop watch was stopped during sampling time and restarted when the solution was returned to the gut. Samples were removed from alternate syringes at each time period. One of the two samples removed was placed in a 20-mL vial, 15 mL of scintillation cocktail was added, and the sample was counted in a liquid scintillation counter utilizing single-channel counting to monitor water flux. The second sample was added to a 10-mL volumetric flask, brought to volume with the same solvent that the drug was dissolved in, and the absorbance measured in a spectrophotometer[1] at 272 nm.

Solubility Studies—Data from an earlier investigation (11) on the solubility of theophylline in dioxane–water mixtures were utilized in the study to obtain the solubility parameter of theophylline and to assess its solubility in solvent mixtures of varying solubility parameters (δ values).

RESULTS

Rate Constants for Absorption—The disappearance of theophylline from the solvent provided semilogarithmic plots, as observed in Fig. 1, which when analyzed, suggested the following model:

$$D_G \underset{k_2}{\overset{k_1}{\rightleftharpoons}} D_M \xrightarrow{k_3} D_B \qquad \text{(Eq. 1)}$$

The quantity D_G represents the concentration of drug in the intestine, D_M is the drug concentration in the membrane, k_1, k_2, and k_3 are the rate constants for transfer of drug between the compartments, and D_B is the drug concentration in the blood.

Differential equations for the process represented by the above model were written from which the following solutions were obtained:

$$D_G = D\frac{(k_2 + k_3 - \alpha)e^{-\alpha t}}{(\beta - \alpha)} + D\frac{(k_2 + k_3 - \beta)e^{-\beta t}}{(\alpha - \beta)} \qquad \text{(Eq. 2)}$$

where D represents the concentration of drug in the solution that was perfused into the intestine. The general form of Eq. 2 may be written as:

$$D_G = X_1 e^{-\alpha t} + X_2 e^{-\beta t} \qquad \text{(Eq. 3)}$$

where α is the slope of the residual line feathered from the nonlinear initial phase of the curve in Fig. 1, and β is the slope of the terminal log-linear phase. The respective intercepts of these two straight lines are X_1 and X_2, and are written as:

$$X_1 = D\frac{(k_2 + k_3 - \alpha)}{\beta - \alpha} \qquad \text{(Eq. 4)}$$

$$X_2 = D\frac{(k_2 + k_3 - \beta)}{\alpha - \beta} \qquad \text{(Eq. 5)}$$

where D_G is defined at time zero, *i.e.*, D_{G0}, by the expression:

$$D_{G0} = X_1 + X_2 \qquad \text{(Eq. 6)}$$

k_1, k_2, and k_3 are obtained from the identities:

$$\alpha + \beta = k_1 + k_2 + k_3 \qquad \text{(Eq. 7)}$$

and:

$$\alpha\beta = k_1 k_3 \qquad \text{(Eq. 8)}$$

Substituting Eqs. 6 and 7 into Eq. 4 and rearranging yields:

$$k_1 = \frac{X_2\beta + X_1\alpha}{X_1 + X_2} \qquad \text{(Eq. 9)}$$

which enables one to calculate k_3 from Eq. 8 and k_2 from Eq. 7.

Biological Partition Parameter and a Membrane Solubility Parameter—From the shape of the experiemental curve of Fig. 1, it is assumed that equilibrium of theophylline exists between compartments G and M due to a par-

[1] Beckman.

0022-3549/84/0600-0742$01.00/0
© 1984, American Pharmaceutical Association

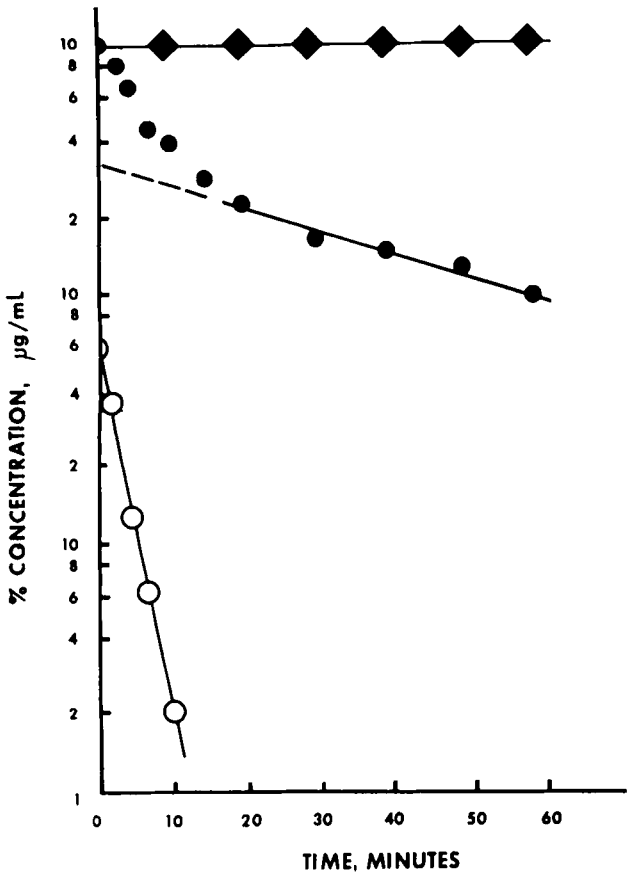

Figure 1—*Semilogarithmic plot showing first-order biexponential absorption of theophylline from the rat small intestine. Key: (◆) water flux as monitored using the nonabsorbable marker [^{14}C]polyethylene glycol 4000; the straight line shows concentration of the pure binary solvent in the rat intestine after correction for water flux; (●) theophylline concentrations in the rat intestine, $\beta = 0.021$; (○) residual feathered line representing the equilibrium phase of drug between contents of the gut and the rat intestinal membrane, $\alpha = 0.348$.*

titioning of the drug. The partition parameter, K_p, for this process (absorption and desorption of theophylline in the intestinal membrane) is written as:

$$K_p = \frac{k_1}{k_2} \qquad \text{(Eq. 10)}$$

The parameter K_p of Eq. 10, obtained from *in situ* rat gut data, should be related to the physicochemical properties of the drug–solvent carrier system. An equation, written in different forms by Davis (15), Cammarata and Rogers (18), Weimer and Prausnitz (19), Yeh and Higuchi (20), and Srebrenik and Cohen (21), and introducing δ_0 as the solubility parameter representing the rat gut membrane, is shown below:

$$\log K_p = \frac{V_2 \phi_1^2}{2.303RT}[(\delta_1 - \delta_2)^2 - (\delta_0 - \delta_2)^2] \qquad \text{(Eq. 11)}$$

This equation may be used to analyze the data of the current study. The quantity R is the gas constant, T is the absolute temperature, and V_2 is the liquid molar volume of the solute, which for theophylline is 124 mL/mol. The terms ϕ_1 and δ_1 are, respectively, the volume fraction and the solubility parameter of the solvent, and δ_2 is the solubility parameter of the solute. Mullins (16) has reviewed various methods by which δ_0 for biological membranes may be obtained. He estimated from thermodynamic considerations that the δ_0 value of the frog sciatic nerve ranges from ~10.0 to 13.0. Mullins also noted for the frog nonsynaptic membrane that a value of 11.5 was in agreement with experimental results, whereas a value of 10.0 seemed more favorable for the δ value of synaptic nerve membranes. Cammarata *et al.* (17), using the erythrocyte membrane as a model for drug partitioning in biological systems, obtained a value of 8.05 as the apparent solubility parameter for the erythrocyte membrane.

Equation 11 does not account for entropic effects such as molecular size differences between solvent, solute, and membrane. Flory (22, 23) and Huggins (24, 25) introduced such size differences, *i.e.*, the molar volumes of solute and solvent, to account for deviations of solution phenomena from ideality. The inclusion of these factors together with corrections for possible membrane metabolism and changes in solute molar volume across the biomembrane would seem warranted. Nevertheless, the present simplified approach was attempted as a first approach to the calculation of solute–solvent attractions and the estimation of δ_0 values in biological systems.

Table I—Solubility of Theophylline, $\delta_2 = 14.0$ (cal/mL)$^{1/2}$, $V_2 = 124$ mL/mol, in Selected Polyethylene Glycol 400–Water Mixtures at 25°C

Perecentage of Polyethylene Glycol 400	δ_1	ϕ_1	$(\delta_1 - \delta_2)^a$	Solubility, mg/mL	*SD*
100	10.5	0.9893	−3.5	15.539	±0.174
90	11.8	0.9879	−2.2	17.594	±0.102
80	13.1	0.9876	−0.9	17.937	±0.257
75	13.7	0.9885	−0.3	16.728	±0.096
70	14.4	0.9908	0.4	13.294	±0.231
65	15.0	0.9920	1.0	11.660	±0.058
60	15.7	0.9928	1.7	10.445	±0.034

[a] δ_1 is the solubility parameter of the mixed solvent; δ_2 is the solubility parameter of the solute, theophylline.

Solubility Parameters, Drug Release, and Bioabsorption—The terms of Eq. 11describe solute–solvent and solute–membrane interaction forces due to polar interactions, in addition to dispersion or van der Waals forces as expressed by the classical Hildebrand equation (1). Analysis of the data using Eqs. 1, 3, and 7–10 provided pharmcokinetic parameters, which were correlated with solubility of theophylline and its release from the respective polyethylene glycol 400–water mixtures. A listing of these parameters is found in Tables I and II. Figure 2 shows that the closer the solubility parameter of theophylline (14.0)[2] and the solubility parameter of the particular solvent mixture (polyethylene glycol 400–water), the greater the attraction of solvent vehicle for the drug. A solvent whose solubility parameter is identical to that of theophylline would, according to regular solution theory, lead to the greatest solubility of the drug, barring solute–solvent interactions.

One would also expect an interplay of multiple physicochemical attractive forces in the drug release process due to differences between the membrane solubility parameter and that of the solvent and solute (Eq. 11). In this case,

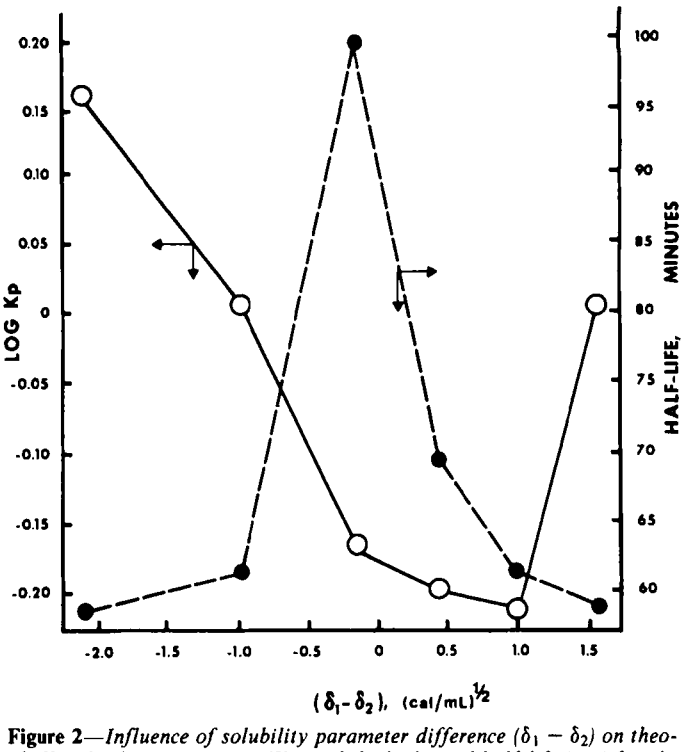

Figure 2—*Influence of solubility parameter difference ($\delta_1 - \delta_2$) on theophylline* in situ *partitioning (K_p) and the biological half-life ($t_{1/2}$) for absorption across the rat gut membrane. δ_1 is the solubility parameter of the mixed solvent; δ_2 is the solubility parameter of the drug, theophylline. Key: (●) half-life for theophylline absorption; (○) partition coefficient for theophylline absorption from solvent mixtures of varying solubility parameters.*

[2] The solubility parameter of theophylline was taken from Ref. 12.

Table II—Pharmacokinetic Parameters Obtained for Theophylline $\delta_2 = 14.0$ (cal/mL)$^{1/2}$, $V_2 = 124.0$ mL/mol, from *In Situ* Rat Gut Absorption Studies

Percentage of Polyethylene Glycol 400	$t_{1/2,\beta}$, min	β, min^{-1}	α, min^{-1}	X_1, mg/mL	X_2 mg/mL	k_1, min^{-1}	k_2, min^{-1}	k_3, min^{-1}	K_p[a]	log K_p	δ_0 high[b] / low
90	58	0.012	0.080	0.490	0.672	0.041	0.028	0.023	1.464	0.166	15.72 12.28
80	63	0.011	0.094	0.396	0.752	0.040	0.039	0.026	1.026	0.011	14,83 13.17
75	99	0.007	0.149	0.382	0.768	0.054	0.083	0.019	0,651	−0.186	14.53 13.47
70	69	0.010	0.143	0.302	0.750	0.048	0.075	0.030	0.640	−0.194	15.53 12.47
65	63	0.011	0.128	0.226	0.838	0.036	0.064	0.039	0.563	−0.250	15.98 12.02
60	58	0.012	0.090	0.340	0.740	0.037	0.036	0.029	1.028	0.012	15.66 12.34

[a] $K_p = k_1 \div k_2$. [b] Membrane solubility parameters were calculated from the quadratic Eq. 11, and the two roots designated high and low are reported here.

Eq. 11 seems to suggest that δ_0, the membrane solubility parameter, would be important in evaluating the effects of solvent solubility parameters on drug absorption. Figure 2 shows that as the solubility parameter of the solvent gets closer to that of the solute, there is a rapid fall in the *in situ* partition parameter and a significant increase in the half-life for absorption (disappearance from the intestine) of theophylline. This is considered to be due to stronger interactions of solute and solvent. Conversely, when the solubility parameter of the solvent and solute are significantly different, the extent to which the drug and solvent molecules interact would be expected to be small. In such case, drug solubility would be reduced, resulting in greater release from the vehicle and a larger absorption rate constant.

Inspection of the lines in Fig. 2 and the parameters of Eq. 11 reveals a dependence of K_p (drug partitioning parameter) on δ_2 and δ_0, the membrane solubility parameter. A solvent mixture for optimum theophylline release and bioabsorption would have a solubility parameter that operates in conjunction with δ_2 and δ_0 so that solubility and partitioning effects were simultaneously changed. That is to say, the solubility parameter of drug and solvent (vehicle) must be sufficiently different to allow ready release of theophylline from the solvent, yet be similar enough to provide a reasonable concentration of the drug. And δ_2 and δ_0 must be sufficiently alike to favor drug absorption into the membrane.

To obtain quantitative measurements for the solubility parameter δ_0 of the rat gut membrane, the data summarized in Tables I and II were substituted into Eq. 11 for each polyethylene glycol 400–water solvent mixture, assuming $\phi_1^2 \cong 1.00$. Average values for the two roots of the resulting quadratic equations were found to be 15.4 and 12.6. A δ_0 value of 12.6 for the rat gut membrane would seem to be more reasonable, since it is generally accepted that the intestinal membrane has low polarity. It is in fair agreement with the value of 11.6 suggested by Mullins (16) for synaptic nerve tissue. A value of 15.4 would suggest a polar membrane in conflict with the relatively lipophilic character of the intestinal mucosa (26).

Membrane solubility parameters may play a critical role in drug permeation and partitioning studies. The values may differ depending on the part of the intestines under consideration, such as for some antibiotics (27–29) for which "windows" or regions exist in the upper intestines where the drug is more readily absorbed.

DISCUSSION

Attempts have been made by some workers (30–32) to analyze the movement of drugs across cell membranes. These authors studied the kinetics of absorption of sulfonamides and barbiturates in the intestinal, gastric, and rectal regions of the GI tract. Utilizing theoretical models and introducing physical dimensions, some of which are associated with various membranes and others determined by *in vitro* experiments, these authors attempted to calculate physical constants consistent with the experimental data.

Khalil and Martin (5) studied the kinetics of [^{14}C]carboxyl salicylic acid through model membranes and observed that the closer the δ value of the drug molecule to that of the lipoidal barrier, the faster the disappearance of the drug from an aqueous buffer layer of pH 2 (representing stomach contents) and the slower its appearance in an aqueous buffer of pH 7.4 (representing plasma). Khalil *et al.* (33, 34) employed the solubility parameter as an index of drug activity of several barbiturates. In their investigation, these authors observed that there was a linear relationship between the solubility parameter and logarithm of the partition coefficient reported in the literature for the various barbituric acid derivatives studied. They also observed a good correlation between solubility parameters of the barbiturates and their reported activities, and suggested that the solubility parameter concept might be a possible substitute for the partition coefficient in structure-activity relationships. Pagay *et al.* (35) studied the influence of acetaminophen bioavailability and the dielectric properties of the vehicle. These studies, like those presented here, are attempts to understand the many factors that affect the solubility of drugs and their absorption properties.

Some workers (3–5, 33–38) have suggested that solubility parameters and dielectric requirements affect the bioavailability of drugs *in vivo*. Others (18, 19, 39–44) have concluded that permeability and the partition coefficient are useful parameters to be employed in monitoring drug absorption. Hansch *et al.* (45) have reported on a optimum log P for drug partitioning or penetration into the central nervous system which appears to be remarkably constant at a value of 2.0. The work reported in this paper suggests that not only the solubility parameter of the drug and solvent (drug carrier) but also the δ_0 of biological membranes should be considered by formulators in drug design work. However, the solubility parameter for the membrane as well as for the solute and solvent will probably have to be redefined to reflect the polar and hydrogen-bonding interactive forces involved in solute-solvent attraction and the permeation of the membrane by the solute. This problem has been studied (11–13) and is the subject of continuing work.

CONCLUSIONS

A method has been developed to optimize *in vivo* release characteristics of drug molecules based on solute-solvent interactive forces and use of the Hildebrand solubility parameter. A solubility parameter of 12.6 for the rat gut membrane has been estimated and is used to demonstrate the role of solute-solvent interactive forces in drug release studies. This method for obtaining the solubility parameter of a membrane uses an *in situ* drug absorption approach and a living membrane (rat gut) as the permeation barrier. The results obtained from this preliminary work are encouraging. However, further work must be done with various pharmaceutical drug-solvent systems before definitive conclusions can be made. Extended testing may provide improved solubility and penetration parameters characteristic of various living membranes and tissues which would prove useful in physical medicinal chemistry and quantitative drug design. It is suggested that theophylline, and possibly other poorly soluble drugs whose solubility and biological activity require careful control for optimum therapeutic effects, may be formulated using a generalized solubility parameter approach. Relative interaction of drug molecules with the vehicles in which they are formulated and the biological membranes they penetrate must be assessed in a number of systems before fundamental principles can be established.

REFERENCES

(1) J. H. Hildebrand, J. M. Prausnitz, and R. L. Scott, "Regular and Related Solutions," Van Nostrand Reinhold, New York, N.Y., 1970.

(2) J. H. Hildebrand and R. L. Scott, "The Solubility of Nonelectrolytes," 3rd ed., Reinhold, New York, N.Y., 1950.

(3) M. S. Chertkoff and A. Martin, *J. Am. Pharm. Assoc., Sci. Ed.*, **49**, 444 (1960).

(4) F. A. Restaino and A. Martin, *J. Pharm. Sci.*, **53**, 636 (1964).

(5) S. A. Khalil and A. Martin, *J. Pharm. Sci.*, **56**, 1225 (1967).

(6) A. N. Paruta and S. A. Irani, *J. Pharm. Sci.*, **54**, 838 (1965).

(7) S. H. Yalkowsky, G. L. Amidon, and G. L. Flynn, *J. Pharm. Sci.*, **61**, 1983 (1972).

(8) S. H. Yalkowsky, G. L. Amidon, and G. L. Flynn, *J. Pharm. Sci.*, **64**, 48 (1975).

(9) A. R. Gianquinto, R. E. Lindstrom, J. Swarbrick, and A. LoSurdo, *J. Soln. Chem.*, **6**, 687 (1977).

(10) A. Cesaro, E. Russo, and V. Crescenzi, *J. Phys. Chem.*, **80**, 335 (1979).
(11) A. Martin, J. Newburger, and A. Adjei, *J. Pharm. Sci.*, **68**(10), iv (1979).
(12) A. Martin, J. Newburger, and A. Adjei, *J. Pharm. Sci.*, **69**, 487 (1980).
(13) A. Adjei, J. Newburger, and A. Martin, *J. Pharm. Sci.*, **69**, 659 (1980).
(14) J. T. Doluisio, M. F. Billups, L. N. Dittert, E. T. Sugita, and J. V. Swintosky, *J. Pharm. Sci.*, **58**, 1196 (1969).
(15) S. S. Davis, *Experientia*, **26**, 671 (1970).
(16) L. J. Mullins, *Chem. Rev.*, **54**, 289 (1954).
(17) A. Cammarata, S. J. Yau, and K. S. Rogers, *Pure Appl. Chem.*, **35**, 495 (1973).
(18) A. Cammarata and K. S. Rogers, *J. Med. Chem.*, **14**, 1211 (1971).
(19) R. F. Weimer and J. M. Prausnitz, *Hydrocarbon Process*, **44**, 237 (1965).
(20) K. C. Yeh and W. I. Higuchi, *J. Pharm. Sci.*, **65**, 743 (1976).
(21) S. Srebrenik and S. Cohen, *J. Phys. Chem.*, **80**, 996 (1976).
(22) P. J. Flory, *J. Chem. Phys.*, **9**, 660 (1941).
(23) P. J. Flory, *J. Chem. Phys.*, **10**, 51 (1942).
(24) M. L. Huggins, *J. Chem. Phys.*, **9**, 440 (1941).
(25) M. L. Huggins, *Ann. N.Y. Acad. Sci.*, **43**, 1 (1942).
(26) C. Hansch, in "Drug Design," E. J. Ariens, Ed., Academic, New York, N.Y., 1971, p. 271.
(27) E. Nelson, *Chem. Pharm. Bull.*, **11**, 1099 (1962).
(28) T. H. Lin, J. R. Guarini, S. P. Eriksen, and J. V. Swintosky, *J. Pharm. Sci.*, **53**, 1357 (1964).
(29) A. Swahn, *Eur. J. Clin. Pharmacol.*, **9**, 117 (1965).
(30) K. Kakemi, T. Arita, and T. Koizumi, *Chem. Pharm. Bull.*, **12**, 413 (1964).
(31) T. Koizumi, T. Arita, and K. Kakemi, *Chem. Pharm. Bull.*, **12**, 421 (1964).
(32) B. Stehle and W. I. Higuchi, *J. Pharm. Sci.*, **56**, 1367 (1967).
(33) S. A. Khalil, Y. Ossama, and M. A. Moustafa, *Can. J. Pharm. Sci.*, **11**, 121 (1976).
(34) S. A. Khalil, Y. Ossama, and M. A. Moustafa, *Can. J. Pharm. Sci.*, **11**, 26 (1976).
(35) S. N. Pagay, R. I. Poust, and J. L. Colaizzi, *J. Pharm. Sci.*, **63**, 44 (1974).
(36) A. N. Paruta and B. B. Sheith, *J. Pharm. Sci.*, **55**, 896 (1966).
(37) A. N. Paruta and S. A. Irani, *J. Pharm. Sci.*, **55**, 1055 (1966).
(38) A. N. Paruta and S. A. Irani, *J. Pharm. Sci.*, **55**, 1060 (1966).
(39) A. Suziki, W. I. Higuchi, and N. F. Ho., *J. Pharm. Sci.*, **59**, 644 (1970).
(40) A. Suziki, W. I. Higuchi, and N. F. Ho, *J. Pharm. Sci.*, **59**, 651 (1970).
(41) A. Suziki, W. I. Higuchi, and N. F. Ho., *J. Pharm. Sci.*, **59**, 537 (1970).
(42) J. S. Turi, W. I. Higuchi, N. F. Ho, and C. Shipman, Jr., *J. Pharm. Sci.*, **64**, 622 (1975).
(43) J. S. Turi, W. I. Higuchi, N. F. Ho, and C. Shipman, Jr., *J. Pharm. Sci.*, **64**, 627 (1975).
(44) N. F. Ho, W. I. Higuchi, and J. Turi, *J. Pharm. Sci.*, **61**, 193 (1972).
(45) C. Hansch, R. Steward, S. M. Anderson, and D. Bentley, *J. Med. Chem.*, **11**, 1 (1968).

ACKNOWLEDGMENTS

The authors wish to thank James T. Doluisio and Robert Pearlman for helpful suggestions in the preparation of this manuscript.

Supported in part by the endowed professorship provided to A. Martin by Coulter R. Sublett.

Synthesis and Properties of Some 13-*cis*- and All-*trans*-retinamides

Y. FULMER SHEALY *x, JERRY L. FRYE *, C. ALLEN O'DELL *, MARTHA C. THORPE *, MARION C. KIRK *, W. C. COBURN, JR. *, and MICHAEL B. SPORN ‡

Received March 15, 1982, from the **Southern Research Institute, P.O. Box 55305, Birmingham, AL 35255-5305* and the ‡*Laboratory of Chemoprevention, National Cancer Institute, Bethesda, MD 20205.* Accepted for publication March 1, 1983.

Abstract □ Several 13-*cis*-retinamides were synthesized from 13-*cis*-retinoic acid *via* either 13-*cis*-retinoyl chloride or 13-*cis*-1-retinoylimidazole. All-*trans*-retinoylglycine was prepared from all-*trans*-retinoyl chloride and ethyl glycinate. Detailed procedures were developed for the preparation of other all-*trans*-retinamides on a large scale for studies of the chemoprevention of cancer.

Keyphrases □ 13-*cis*-Retinamides—synthesis and chemical properties □ All-*trans*-retinamides—synthesis and chemical properties □ Synthesis—13-*cis*- and all-*trans*-retinamides, chemical properties

Compounds of the vitamin A group (retinoids) are essential for normal cellular differentiation and for the growth of epithelial tissues (1–4). During recent years, many studies, reviewed by Sporn and co-workers (3–9) and Bollag and co-workers (10–12), have shown that retinoid deficiency in animals enhances susceptibility to chemical carcinogenesis, that epithelia in certain organ cultures develop preneoplastic lesions in the absence of retinoids, and that administration of certain retinoids may prevent or reduce carcinogen-induced neoplasia in epithelial tissues of animals, as well as preneoplasia (6, 13–16) in organs in culture. In particular, certain derivatives and analogues of all-*trans*-retinoic acid (tretinoin, also known as vitamin A acid; Ia) exert a prophylactic (and, in some cases, a therapeutic) effect on the development of preneoplastic and malignant epithelial lesions (*e.g.*, 11, 16–25). Among the more interesting derivatives of retinoic acid and its analogues are the amides (retinamides and retinamide analogues). The purpose of this report is to describe the preparation of several all-*trans*-retinamides (II) and 13-*cis*-retinamides (IV) for long-term studies of chemoprevention in animals. Only one 13-*cis*-retinamide, the primary amide (IV, R = H), had been previously described (without a synthesis procedure) in the literature (26).

RESULTS AND DISCUSSION

The preparation of all-*trans*-retinamides IIa–d (27) and IIe (28) has been briefly outlined in the patent literature, but the characterization data (mp, UV) were sparse. The 4-hydroxyphenyl amide (all-*trans*-*N*-(4-hydroxyphenyl)retinamide; IIm) was synthesized originally by Gander and co-workers (24, 28). The preparation of IIf–l has not been described previously, but IIf–i

© 1984, American Pharmaceutical Association

(10) A. Cesaro, E. Russo, and V. Crescenzi, *J. Phys. Chem.*, **80**, 335 (1979).
(11) A. Martin, J. Newburger, and A. Adjei, *J. Pharm. Sci.*, **68**(10), iv (1979).
(12) A. Martin, J. Newburger, and A. Adjei, *J. Pharm. Sci.*, **69**, 487 (1980).
(13) A. Adjei, J. Newburger, and A. Martin, *J. Pharm. Sci.*, **69**, 659 (1980).
(14) J. T. Doluisio, M. F. Billups, L. N. Dittert, E. T. Sugita, and J. V. Swintosky, *J. Pharm. Sci.*, **58**, 1196 (1969).
(15) S. S. Davis, *Experientia*, **26**, 671 (1970).
(16) L. J. Mullins, *Chem. Rev.*, **54**, 289 (1954).
(17) A. Cammarata, S. J. Yau, and K. S. Rogers, *Pure Appl. Chem.*, **35**, 495 (1973).
(18) A. Cammarata and K. S. Rogers, *J. Med. Chem.*, **14**, 1211 (1971).
(19) R. F. Weimer and J. M. Prausnitz, *Hydrocarbon Process*, **44**, 237 (1965).
(20) K. C. Yeh and W. I. Higuchi, *J. Pharm. Sci.*, **65**, 743 (1976).
(21) S. Srebrenik and S. Cohen, *J. Phys. Chem.*, **80**, 996 (1976).
(22) P. J. Flory, *J. Chem. Phys.*, **9**, 660 (1941).
(23) P. J. Flory, *J. Chem. Phys.*, **10**, 51 (1942).
(24) M. L. Huggins, *J. Chem. Phys.*, **9**, 440 (1941).
(25) M. L. Huggins, *Ann. N.Y. Acad. Sci.*, **43**, 1 (1942).
(26) C. Hansch, in "Drug Design," E. J. Ariens, Ed., Academic, New York, N.Y., 1971, p. 271.
(27) E. Nelson, *Chem. Pharm. Bull.*, **11**, 1099 (1962).
(28) T. H. Lin, J. R. Guarini, S. P. Eriksen, and J. V. Swintosky, *J. Pharm. Sci.*, **53**, 1357 (1964).
(29) A. Swahn, *Eur. J. Clin. Pharmacol.*, **9**, 117 (1965).
(30) K. Kakemi, T. Arita, and T. Koizumi, *Chem. Pharm. Bull.*, **12**, 413 (1964).
(31) T. Koizumi, T. Arita, and K. Kakemi, *Chem. Pharm. Bull.*, **12**, 421 (1964).
(32) B. Stehle and W. I. Higuchi, *J. Pharm. Sci.*, **56**, 1367 (1967).
(33) S. A. Khalil, Y. Ossama, and M. A. Moustafa, *Can. J. Pharm. Sci.*, **11**, 121 (1976).
(34) S. A. Khalil, Y. Ossama, and M. A. Moustafa, *Can. J. Pharm. Sci.*, **11**, 26 (1976).
(35) S. N. Pagay, R. I. Poust, and J. L. Colaizzi, *J. Pharm. Sci.*, **63**, 44 (1974).
(36) A. N. Paruta and B. B. Sheith, *J. Pharm. Sci.*, **55**, 896 (1966).
(37) A. N. Paruta and S. A. Irani, *J. Pharm. Sci.*, **55**, 1055 (1966).
(38) A. N. Paruta and S. A. Irani, *J. Pharm. Sci.*, **55**, 1060 (1966).
(39) A. Suziki, W. I. Higuchi, and N. F. Ho., *J. Pharm. Sci.*, **59**, 644 (1970).
(40) A. Suziki, W. I. Higuchi, and N. F. Ho, *J. Pharm. Sci.*, **59**, 651 (1970).
(41) A. Suziki, W. I. Higuchi, and N. F. Ho., *J. Pharm. Sci.*, **59**, 537 (1970).
(42) J. S. Turi, W. I. Higuchi, N. F. Ho, and C. Shipman, Jr., *J. Pharm. Sci.*, **64**, 622 (1975).
(43) J. S. Turi, W. I. Higuchi, N. F. Ho, and C. Shipman, Jr., *J. Pharm. Sci.*, **64**, 627 (1975).
(44) N. F. Ho, W. I. Higuchi, and J. Turi, *J. Pharm. Sci.*, **61**, 193 (1972).
(45) C. Hansch, R. Steward, S. M. Anderson, and D. Bentley, *J. Med. Chem.*, **11**, 1 (1968).

ACKNOWLEDGMENTS

The authors wish to thank James T. Doluisio and Robert Pearlman for helpful suggestions in the preparation of this manuscript.

Supported in part by the endowed professorship provided to A. Martin by Coulter R. Sublett.

Synthesis and Properties of Some 13-*cis*- and All-*trans*-retinamides

Y. FULMER SHEALY *x, JERRY L. FRYE *, C. ALLEN O'DELL *, MARTHA C. THORPE *, MARION C. KIRK *, W. C. COBURN, JR. *, and MICHAEL B. SPORN ‡

Received March 15, 1982, from the **Southern Research Institute, P.O. Box 55305, Birmingham, AL 35255-5305* and the ‡*Laboratory of Chemoprevention, National Cancer Institute, Bethesda, MD 20205.* Accepted for publication March 1, 1983.

Abstract □ Several 13-*cis*-retinamides were synthesized from 13-*cis*-retinoic acid *via* either 13-*cis*-retinoyl chloride or 13-*cis*-1-retinoylimidazole. All-*trans*-retinoylglycine was prepared from all-*trans*-retinoyl chloride and ethyl glycinate. Detailed procedures were developed for the preparation of other all-*trans*-retinamides on a large scale for studies of the chemoprevention of cancer.

Keyphrases □ 13-*cis*-Retinamides—synthesis and chemical properties □ All-*trans*-retinamides—synthesis and chemical properties □ Synthesis—13-*cis*- and all-*trans*-retinamides, chemical properties

Compounds of the vitamin A group (retinoids) are essential for normal cellular differentiation and for the growth of epithelial tissues (1–4). During recent years, many studies, reviewed by Sporn and co-workers (3–9) and Bollag and co-workers (10–12), have shown that retinoid deficiency in animals enhances susceptibility to chemical carcinogenesis, that epithelia in certain organ cultures develop preneoplastic lesions in the absence of retinoids, and that administration of certain retinoids may prevent or reduce carcinogen-induced neoplasia in epithelial tissues of animals, as well as preneoplasia (6, 13–16) in organs in culture. In particular, certain derivatives and analogues of all-*trans*-retinoic acid (tretinoin, also known as vitamin A acid; Ia) exert a prophylactic (and, in some cases, a therapeutic) effect on the development of preneoplastic and malignant epithelial lesions (*e.g.*, 11, 16–25). Among the more interesting derivatives of retinoic acid and its analogues are the amides (retinamides and retinamide analogues). The purpose of this report is to describe the preparation of several all-*trans*-retinamides (II) and 13-*cis*-retinamides (IV) for long-term studies of chemoprevention in animals. Only one 13-*cis*-retinamide, the primary amide (IV, R = H), had been previously described (without a synthesis procedure) in the literature (26).

RESULTS AND DISCUSSION

The preparation of all-*trans*-retinamides IIa–d (27) and IIe (28) has been briefly outlined in the patent literature, but the characterization data (mp, UV) were sparse. The 4-hydroxyphenyl amide (all-*trans*-*N*-(4-hydroxyphenyl)retinamide; IIm) was synthesized originally by Gander and co-workers (24, 28). The preparation of IIf–l has not been described previously, but IIf–i

© 1984, American Pharmaceutical Association

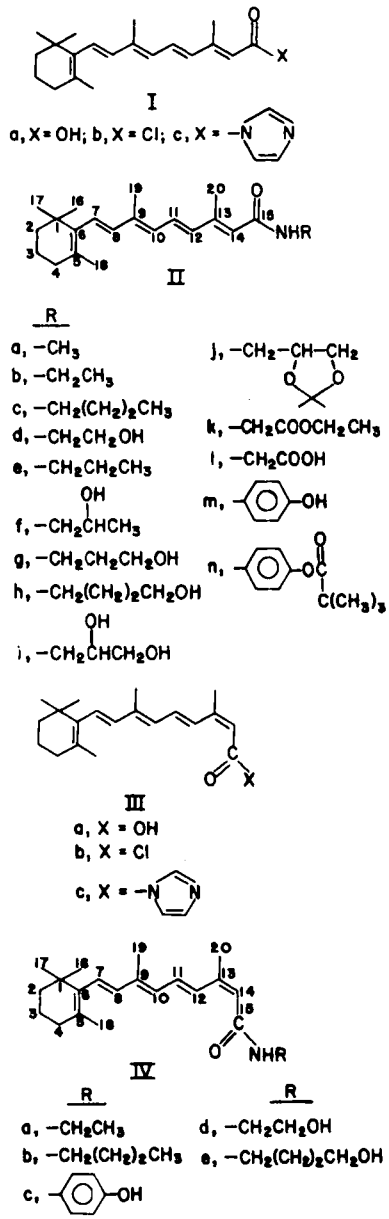

and II l were among the retinoids evaluated in organ culture by Newton *et al.* (16) and were synthesized, originally, elsewhere[1].

All-*trans*-retinamides have been prepared (24–31) from retinoic acid (Ia) *via* all-*trans*-retinoyl chloride (Ib) in benzene (29), benzene–dimethylformamide (24, 28), or ether (27). The acid chloride (Ib) was prepared initially from Ia and phosphorus trichloride in benzene (29) and subsequently from Ia and thionyl chloride in pyridine–ether (30). Most of the retinamides described here were obtained by modifying the phosphorus trichloride method and adapting it to large-scale syntheses. The volume of benzene may be reduced considerably below that used in the original procedure (29) for the preparation of a retinamide. Although IIa–i and IIk have the same general structure, the isolation procedures used to obtain good yields of the various retinamides differ in detail. Compound IIh could also be obtained *via* Ib, but it was more conveniently prepared from 1-(all-*trans*-retinoyl)imidazole (Ic), which was prepared from Ia and 1,1′-carbonyldiimidazole (32). The dihydroxypropyl amide (IIi) was prepared by both methods; the isopropylidene derivative (IIj) was prepared from IIi by a procedure adapted from nucleoside chemistry (33). All-*trans*-*N*-retinoylglycine (II l) was prepared by treating IIb with an excess of ethyl glycinate free base and saponifying the resulting ester (IIk).

Differences among some of the all-*trans*-retinamides in their sensitivity to atmospheric oxygen were observed. Since all have the same basic retinoid structure, these differences are probably due principally to differences in crystal structure and particle size (*Experimental*). The 2,3-dihydroxypropyl amide (IIi) appeared to be the most sensitive of the all-*trans*-retinamides to deliberate exposure to air, whereas the ethyl amide (IIb) and 4-hydroxyphenyl amide (IIm) appeared to be among the least susceptible to atmospheric oxygen.

The 13-*cis*-retinamides (IV) were prepared from 13-*cis*-retinoic acid (IIIa) by way of either 13-*cis*-retinoyl chloride (IIIb) or 1-(13-*cis*-retinoyl)imidazole (IIIc). In initial runs, it was shown by NMR and HPLC that 13-*cis*-retinoic acid (IIIa) could be converted to 13-*cis*-retinoyl chloride (IIIb) and thence to 13-*cis*-*N*-ethylretinamide (IVa) without causing isomerization of the 13-*cis* structure to the all-*trans* isomer. Compounds IVa–c could be prepared *via* IIIb in yields of 74–82% from IIIa. 1-(13-*cis*-Retinoyl)imidazole (IIIc) was prepared from IIIa and 1,1′-carbonyldiimidazole by a procedure similar to that employed for the preparation of the all-*trans* isomer. A specimen of IIIc was purified, but less pure specimens, which might have contained varying amounts of imidazole, were satisfactory for the formation of 13-*cis*-retinamides. The conversion *via* IIIc was quite satisfactory, and superior to the acid chloride method, for the preparation of the hydroxyalkyl amides (IVd,e). In later, large-scale runs, IIIc was prepared and used *in situ;* consequently, the use of IIIc for the preparation of 13-*cis*-retinamides is comparable in simplicity to the acid chloride method. Yields of IVd,e were 60–70%.

Although amides are simple derivatives and IVa–e are all representatives of the same general structure, the preparation of these 13-*cis*-retinamides was not without difficulties. The most serious problem was the occasional formation during the preparation or isolation of IVa and IVb of considerable amounts (10–25%) of the all-*trans* isomer. The reasons for these occasional lapses were not apparent, but it is evident that the synthesis of a 13-*cis*-retinamide should be carefully monitored by HPLC and NMR to ensure the absence of significant amounts of the corresponding all-*trans* isomers. Other operational difficulties were caused by idiosyncracies of individual structures. The 4-hydroxybutyl derivative (IVe) could be crystallized initially only from cyclohexane; it then retained cyclohexane (~1:1) tenaciously (*Experimental*). Once a crystalline specimen was obtained free of cyclohexane, IVe could be readily recrystallized from acetonitrile–water. The 2-hydroxyethyl amide (IVd), which is isolated as a syrup, dissolves in hexane at room temperature and crystallizes. The crystalline solid is then only sparingly soluble in boiling hexane, but it is soluble in cyclohexane and can be recrystallized from the latter solvent. Compound IVc showed a tendency to retain benzene, the reaction solvent. The butyl amide (IVb) resisted crystallization and appeared to undergo considerable degradation during attempts to purify and crystallize it until seed crystals were finally obtained.

Other than differences owing to absorptions of the R groups, there is little, or no, variation in the NMR spectra[2] of the all-*trans*-retinamides (II) or of the 13-*cis*-retinamides (IV). The major differences between the 100-MHz ^{1}H-NMR spectra of the all-*trans* (IIa–l) and the 13-*cis* amides (IVa, b, d, and e) are the pronounced downfield shift of the C-12 proton signal and the upfield shifts of the C-14 and C-20 proton signals in the spectra of the 13-*cis* amides. For example, the C-12 proton signal in the spectrum of all-*trans*-*N*-ethylretinamide (IIb) is part of a multiplet (CH of C-7, C-8, C-10, and C-12 + NH) at δ 6.0–6.4 ppm, and the C-20 and C-14 proton signals are approximate singlets at δ 2.37 and δ 5.71 ppm, respectively; whereas the corresponding proton signals in the spectrum of the 13-*cis* isomer (IVa) are δ 7.84 (d, C-12), 2.01 (s, C-20), and 5.57 ppm (s, C-14). The ^{13}C-NMR spectra of the all-*trans*-retinamides are in excellent agreement with one another and with data from spectra of other all-*trans*-retinoids determined by Englert (35) and assigned with the use of lanthanide shift reagents. The greatest differences in the ^{13}C-NMR spectra (obtained in $CDCl_3$) of the 13-*cis*-retinamides (IVa, b, d, and e) relative to the spectra of the all-*trans* amides (IIa–l) are the downfield shift of C-20 (~7.2 ppm) and the upfield shift of C-12 (5–6 ppm). Significant upfield shifts were also observed in the C-13 (1.8–2.1 ppm), C-14 (1.7–1.8 ppm), and C-15 (0.4–0.5 ppm) peaks in the 13-*cis*-retinamide spectra. These differences are exemplified by chemical shifts in the ^{13}C-NMR spectra of the all-*trans*- and 13-*cis*-*N*-ethyl amides: C-20, δ 13.54 (IIb) and 20.73 ppm (IVa); C-12, δ 135.79 (IIb) and 129.7–130.6 ppm [one of four closely spaced peaks (C-5, C-10, C-11, and C-12) in the spectrum of IVa]; C-13, δ 147.89 (IIb) and 145.98 ppm (IVa); C-14, δ 121.95 (IIb) and 120.23 ppm (IVa); C-15, δ 167.12 (IIb) and 166.66 ppm (IVa).

The UV spectra[2] of the aliphatic all-*trans*-retinamides have an absorption maximum at 347–348 nm with a molar absorptivity (ϵ) of ~50,000–51,000. This maximum is shifted slightly (2–4 nm) to longer wavelengths in the spectra of the 13-*cis*-retinamides, and the molar absorptivity is lower (range: 42,200–47,700). Both the absorption maxima and the absorptivity are greater in the *N*-aryl amides. The IR spectra[2] of all of these retinamides (II and IV)

[1] Compounds IIf–i were first supplied for biological evaluation (16) by BASF Aktiengesellschaft, Ludwigshafen am Rhein, West Germany, and compounds IIm,n, by Johnson and Johnson, New Brunswick, N.J.

[2] Detailed spectrometric data for the individual retinamides (IIa–n and IVa–e) are listed in a complementary publication (34).

show at least one strong band in the region of 965–985 cm^{-1}. This band is due to the C—H out-of-plane vibrations of the *trans*-disubstituted ethylene groups (36). The molecular ion (M) is one of the most intense peaks observed above *m/z* 200 in the mass spectra of the retinamides (II and IV) when the spectra[2] are measured in the electron-impact mode at a direct-probe temperature of ~20°C. Additional characteristic, though less intense, peaks observed are M − 15, loss of a methyl group; M − 123, loss of the 2,6,6-trimethyl-1-cyclohexenyl group; and M − R, *m/z* 298, loss of the R group, when R is not an aryl group. In all of the spectra in the region above *m/z* 200, other characteristic peaks that are usually more intense than the peak at M − 15 or at *m/z* 298 are *m/z* 282 (M − NHR − H), 267 (282 − CH_3), 255 (M − CONHR), 241 (M − CH_3 − CONHR + H), 240, 239, 225 (240 − CH_3), 213, 211, and 201. Other prominent peaks, as well as less intense peaks, also appear in the region above *m/z* 200, and numerous strong peaks are present in all of the spectra in the region below *m/z* 200.

Most of these retinamides have been evaluated in the hamster trachael organ assay and are highly active (16). Several have been shown to have chemopreventive activity (24, 25) *in vivo* and to be significantly less toxic than is all-*trans*-retinoic acid (37). All-*trans*-retinoylglycine, (II l) like all-*trans*- and 13-*cis*-retinoic acids, is a strong inducer of retinoic acid metabolism (38) and is more active against hyperplasia in mouse prostate organ cultures than is all-*trans*-retinoic acid (39).

EXPERIMENTAL

All operations involved in the preparation, isolation, purification, and transfer of retinoids were performed in an atmosphere, or under a current, of dry nitrogen or argon. All such operations were also performed in dim light or photographic darkroom light and, insofar as possible, with containers wrapped with aluminum foil or with black cloths. All retinoids were stored in an atmosphere of argon or nitrogen in hermetically sealed containers at −20°C or −80°C.

Melting temperatures were determined in capillary tubes[3]. UV spectra[4] were determined with ethanol solutions (except for IIm, where methanol was employed). IR spectra[5,6] were determined from specimens in pressed potassium bromide disks. Mass spectral data were taken from low-resolution, electron-impact spectra determined at 70 eV[7]; the direct-probe temperature was 20°C. ^{1}H-NMR spectra were determined at 100 MHz[8]. ^{13}C-NMR spectra were determined at 25.2 MHz[8] or 100.6 MHz[9]. Both the ^{1}H- and ^{13}C-NMR spectra were recorded from $CDCl_3$ solutions except for the spectra of IIm and IVc, which were recorded from Me_2SO-d_6 solutions. The more salient spectroscopic data are summarized in the discussion.

TLC was performed on plates of fluorescing silica gel[10], and developed plates were examined with UV lamps (254 and 365 nm) unless otherwise indicated in parentheses. Other pertinent information (amount applied, developing solvent, other methods of detection) is given parenthetically at the appropriate places in the experimental procedures.

HPLC was performed with a components system[11] and an integrator[12] or with a complete system[13] and was monitored by UV at 340 nm, unless otherwise indicated. Reverse-phase HPLC was performed on columns of octadecylsilane (ODS) chemically bonded to silica: column A, μBondapak[11] C_{18}, 10-μm particle size; column B, Spherisorb[14] ODS, 5-μm particle size; column C, Partisil[15] ODS-2, 10-μm particle size. HPLC eluting solvents were: solvent A, gradient 60:40 acetonitrile–water (solution *a*) → 98:2 acetonitrile–water (solution *b*), 0% solution *b* → 100% solution *b*; solvent B, 85:15 acetonitrile–1% aqueous ammonium acetate, isocratic; solvent C, 80:20 acetonitrile–1% aqueous ammonium acetate, isocratic.

All-*trans*-retinoyl Chloride (Ib)—All-*trans* retinoic acid (Ia, 400 g, 1.33 mol) was suspended in 4 L of dry, reagent-grade benzene in a dry 12-L, 3-necked, round-bottom flask fitted with a motor-driven stirrer, thermometer, addition funnel, and inlet and exit tubes for nitrogen. A solution of 129.3 g (0.94 mol) of phosphorus trichloride in 1.6 L of dry benzene was added in a fast, continuous stream to the vigorously stirred mixture at ~25°C. No increase in temperature was observed during the addition; stirring was continued under a brisk current of nitrogen and with occasional warming to maintain the temperature at 25–30°C. The retinoic acid slowly dissolved, and the mixture changed from a suspension to an orange solution plus a gummy precipitate (phosphorus compounds) that generally collected on the walls of the flask. On this scale, all of the retinoic acid dissolved within ~3 h. The solution was stirred for an additional 1 h, stirring was discontinued, and the gummy precipitate was allowed to settle.

While the retinoyl chloride solution was being prepared, a dry benzene or benzene–dimethylformamide solution of the amine required for the desired retinamide was prepared under nitrogen and cooled. The retinoyl chloride solution was decanted under nitrogen into an addition funnel for introduction into the appropriate amine solution.

All-*trans*-*N*-methylretinamide (IIa)—By the procedure described for the preparation of IIb (below), methylretinamide IIa was prepared from Ib and methylamine, recrystallized from methanol, and dried *in vacuo* at room temperature to yield 11.3 g from 15 g of Ia (72%), mp 175–176°C. Since TLC revealed a trace impurity and NMR showed the presence of a small amount of methanol, the product was recrystallized from ethanol (300 mL) to yield 8.6 g (55%), mp 175–176°C [lit. (27) mp 174–175°C]; TLC: 1 spot (99:1 chloroform–methanol); HPLC: 100% (column A, solvent A, monitored at 345 and 254 nm).

Anal.—Calc. for $C_{21}H_{31}NO$: C, 80.47; H, 9.97; N, 4.47. Found: C, 80.42; H, 10.03; N, 4.40.

All-*trans*-*N*-ethylretinamide (IIb)—The general procedure (25) for the preparation of IIb and similar all-*trans*-retinamides is illustrated by the following procedure. A solution of all-*trans*-retinoyl chloride (Ib) prepared, as described above, from 400 g (1.33 mol) of Ia was added during 0.5 h to a stirred solution of 595 g (13.2 mol) of ethylamine in 1100 mL of dry, reagent-grade benzene at 10°C. The temperature was maintained at 10–15°C with an ice–salt bath, and the reaction mixture was stirred an additional 0.5 h at 10°C. Cold water (4 L) was added during ~10 min, stirring was continued for 15 min, and the mixture was concentrated *in vacuo* with a large rotating evaporator to remove the benzene and excess ethylamine. The yellow, crystalline solid suspended in the aqueous mixture was collected by filtration, pressed by suction with a rubber sheet to remove a yellow, oily material, washed thoroughly on the filter with water, pressed again with a rubber sheet to remove as much water as possible, and dried further *in vacuo*. The solid was dissolved in hot methanol (~5 L), the solution was filtered, and the hot filtrate was diluted with warm water to the cloud point. The mixture was allowed to cool to room temperature and was then stored in a refrigerator overnight. The yellow, crystalline product was collected by filtration, washed with cold methanol–water (4:1), and dried *in vacuo* to constant weight to yield 356 g (82%), mp 138–140°C [lit. (27) mp 137–138°]; TLC: 1 spot (99:1 chloroform–methanol); HPLC: 99.7–100% (column B with solvent B or column A or C with solvent C, monitored at 350 and 254 nm).

All-*trans*-*N*-butylretinamide (IIc)—Compound IIc was prepared by the procedure described for IIb from butylamine (580 mL in 1 L of dry benzene) and a solution of Ib (prepared from 400 g of Ia, 81.3 mL of phosphorus trichloride, and 5 L of dry benzene). The mixture was stirred for 45 min and then washed thoroughly with cold water (1.5 L). The organic layer was washed again with cold water (1 L), concentrated to ~1 L, filtered to collect a yellow precipitate, and concentrated further to obtain a second crop[16]. The crude product (450 g) obtained by combining the two crops was recrystallized from methanol–water (9:1, 2.7 L). The yellow, crystalline solid was collected by filtration, washed with cold methanol–water, and dried *in vacuo* at room temperature to yield 376 g (79%) of IIc, mp 92–94°C [lit. (27) mp 92–93°C]; TLC: 1 spot (99:1 chloroform–methanol); HPLC: >99.9% (column B, solvent B).

Anal.—Calc. for $C_{24}H_{37}NO$: C, 81.07; H, 10.49; N, 3.94. Found: C, 81.03; H, 10.68; N, 3.75.

All-*trans*-*N*-(2-hydroxyethyl)retinamide (IId)—Compound IId was prepared by the procedure described for IIb from ethanolamine (dried over molecular sieves, 600 mL in 1 L of dry benzene) and a solution of Ib (prepared from 350 g of Ia in 4.8 L of dry benzene). After a reaction period of 45 min at 10°C, the product (pasty solid) was isolated (difficult filtrations) as was IIb, washed with cold methanol–water (1:1), triturated with cold methanol–water (2:1, 400 mL), and recrystallized (*cf.*, IIb) twice from methanol–water (3:1). The yellow crystals were dried *in vacuo* at room temperature to yield 335 g (84%) of IId, mp 139–141°C [lit. (27) mp 138–139°C]; TLC: 1 spot with tailing (95:5 chloroform–methanol); HPLC: 99.8–100% (column B and solvent B or column C and solvent D).

Anal.—Calc. for $C_{22}H_{33}NO_2$: C, 76.93; H, 9.68; N, 4.08. Found: C, 76.63; H, 9.88; N, 3.98.

[3] Mel-Temp apparatus.
[4] Cary Model 17 UV spectrophotometer.
[5] Perkin-Elmer Model 621 spectrometer.
[6] Nicolet Model MX-1 Fourier Transform spectrometer.
[7] Varian/MAT Model 113 A mass spectrometer.
[8] Varian XL-100-15 NMR spectrometer.
[9] Bruker WH-400 NMR spectrometer.
[10] Silica Gel GF precoated TLC plates (fluorescent), 250 μm thickness; Analtech Inc., Newark, Del.
[11] Waters Associates, Milford, Mass.
[12] Model 3380 S; Hewlett-Packard.
[13] Model 1084 B; Hewlett-Packard.
[14] Spectra-Physics, Houston, Tex. or Universal Scientific Inc., Atlanta, Ga.
[15] Whatman Inc., Clifton, N.J.

[16] Compound IIc could also be isolated by evaporating benzene and butylamine from the water-organic mixture (*cf.*, IIb) after addition of the second portion of water and then including the yellow, oily layer to crystallize.

All-*trans*-*N*-propylretinamide (IIe)—Compound IIe was prepared from Ia (50 g) and *n*-propylamine (59 g) by the procedure described for IIb. The crude product (51 g) was recrystallized from ethanol-water (5:1, 600 mL) to yield 45.8 g (81%), mp 113–114°C [lit. (28) mp 113–115°C]; HPLC: 99.4% (column B, solvent B).

Anal.—Calc. for $C_{23}H_{35}NO$: C, 80.88, H, 10.33; N, 4.10. Found: C, 81.18; H, 10.69; N, 3.89.

(±)-All-*trans*-*N*-(2-hydroxypropyl)retinamide (IIf)—Compound IIf was prepared by the procedure described for IIb from (±)-1-amino-2-propanol (420 mL in 1.8 L of dry benzene) and a solution of Ib (prepared from 300 g of Ia, 60.8 mL of phosphorus trichloride, and 3.8 L of dry benzene). After a reaction time of 1 h at 10–15°C and concentration of the reaction mixture to ~50% of the original volume, the addition of cold water (1.5 L) to the stirring mixture caused precipitation of the product. The mixture was allowed to stand in an ice bath, and the precipitate was then collected by filtration, pressed with a rubber sheet by suction on the filter, washed with water, and dried. The benzene layer was separated from the filtrate, concentrated, and diluted with cold water (500 mL). A second portion of IIf was separated by filtration as above. The two portions were combined (279 g) and recrystallized from 2:1 acetonitrile-water (3 L). The pale yellow, crystalline product was collected by filtration and dried at room temperature to yield 237 g (67%) of IIf, mp 116–117°C; TLC: 1 spot (95:5 chloroform-methanol); HPLC: 99.4–99.9% (column B, solvent B).

Anal.—Calc. for $C_{23}H_{35}NO_2$: C, 77.27; H, 9.87; N, 3.92. Found: C, 77.58; H, 10.11; N, 4.08.

All-*trans*-*N*-(3-hydroxypropyl)retinamide (IIg)—A mixture of Ia (200 g, 0.67 mol), 1,1′-carbonyldiimidazole (124 g, 0.79 mol), and anhydrous benzene (2 L) was stirred at room temperature for 2 h. The resulting solution was warmed at 50°C in a water bath for 15 min, cooled to room temperature, and slowly added to a cold (10°C), stirred solution of 3-amino-1-propanol (260 mL, 3.6 mol) in anhydrous benzene (1 L). The reaction mixture was stirred at 10°C for 2 h, allowed to stand at room temperature overnight, and diluted with ether (~1 L) to minimize emulsification. The resulting solution was washed with water (2 × 1 L), and the organic layer was dried over sodium sulfate and concentrated to a low volume. The yellow, finely divided precipitate was collected by filtration, washed with small amounts of benzene and ether, and dried *in vacuo* to yield 195 g. A second crop (18 g) was obtained from the filtrate (total yield of crude IIg = 89.4%). The two portions were combined and dissolved in hot ethyl acetate (1 L). The pale yellow precipitate was filtered from the cool mixture and dried *in vacuo* to yield 154 g (65%) of IIg, mp 110–111°C (cap., inserted at 95°C); TLC: 1 spot (95:5 chloroform-methanol); HPLC: 99.7–100% (column B, solvent B).

Anal.—Calc. for $C_{23}H_{35}NO_2$: C, 77.27; H, 9.87; N, 3.92. Found: C, 77.30; H, 10.05; N, 4.14.

All-*trans*-*N*-(4-hydroxybutyl)retinamide (IIh)—The procedure was similar to that described for the preparation of IIg except that the ratio of the amine (4-aminobutanol, 0.97 mol) to Ia (0.33 mol, 100 g) was lower. After the benzene-ether solution had been washed with cold water (3×), it was concentrated to a viscous oil that crystallized after seed crystals were added. The yellow, crystalline solid was triturated with cyclohexane-hexane (1:2, 100 mL), collected by filtration, dried *in vacuo* (weight, 96 g), and recrystallized from acetonitrile (hot). The pale yellow crystals were filtered from the cold mixture and dried *in vacuo* at room temperature to yield 93 g (73%) of IIh, mp 111–113°C (cap., inserted at 80°C); TLC: 1 spot (95:5 chloroform-methanol); HPLC: 99.8% (column B, solvent B).

Anal.—Calc. for $C_{24}H_{37}NO_2$: C, 77.58; H, 10.04; N, 3.77. Found: C, 77.76; H, 10.30; N, 3.65.

A polymorphic form of IIh was also obtained (from cyclohexane or acetonitrile), mp 95–96°C. The solid-state IR spectrum differed from, but was similar to, that of the higher-melting form. The two forms were shown to be identical by TLC, HPLC, ^{1}H-NMR, and ^{13}C-NMR.

(±)-All-*trans*-*N*-(2,3-dihydroxypropyl)retinamide (IIi)—A solution of all-*trans*-retinoyl chloride (prepared from 100 g of Ia, 21 mL of phosphorus trichloride, and 1300 mL of dry benzene) was added to a solution of 200 g of (±)-3-amino-1,2-propanediol in 1200 mL of dry benzene and 300 mL of dimethylformamide at a rate that did not cause the mixture temperature to exceed 20°C. The orange, two-phase mixture was stirred overnight at room temperature. The supernatent solution was decanted from the gummy amine hydrochloride and divided into approximately equal amounts in two 5-L separatory funnels, each containing 1 L of water and 1.5 L of ethyl acetate. The emulsions separated during standing, and the aqueous layers were removed. The organic layers were extracted repeatedly (5–8 times) with 600-mL portions of water. Additional amounts of ethyl acetate and small portions of sodium chloride were added, as needed, during these extractions to cause separation of the emulsions. The two organic layers were combined, and the solution was chilled in an ice bath, dried over anhydrous magnesium sulfate, and concentrated *in vacuo* to ~1 L. (Much magnesium sulfate was required to dry the solution and considerable heat was evolved.) Finely divided, yellow crystals formed, and 1 L of cyclohexane was added. After the mixture had been stored in a freezer overnight, IIi was collected by filtration, washed with 1:1 ethyl acetate-cyclohexane, and dried *in vacuo* at room temperature to constant weight to yield 103 g (83%), mp 101–104°C. Polymorphic forms of IIi were obtained: mp 83–85°C from acetonitrile; mp 101–104°C from ethyl acetate. The specimen described above (103 g) was recrystallized from acetonitrile to yield 98 g (79%) of IIi, mp 83–85°C; HPLC: 98–100% (column B, solvent B).

Anal.—Calc. for $C_{23}H_{35}NO_3$: C, 73.96; H, 9.44; N, 3.75. Found: C, 73.21; H, 9.64; N, 3.63.

Preparation of Derivative IIj—A solution prepared by carefully adding 16.74 mL of 60% perchloric acid to a stirred solution of 11.16 mL of 2,2-dimethoxypropane and 415 mL of anhydrous acetone was stirred for 5 min, (±)-all-*trans*-*N*-(2,3-dihydroxypropyl)retinamide (12.5 g) was added in one portion, and the resulting solution was stirred for 50 min. Pyridine (16.75 mL) was added, and the solution was concentrated *in vacuo* to a gummy residue that was partitioned between chloroform (500 mL) and saturated aqueous sodium bicarbonate (500 mL). The aqueous layer was reextracted twice with 250-mL portions of chloroform, and the chloroform solution (3 portions combined) was dried over magnesium sulfate and concentrated *in vacuo* to an orange syrup. A solution of the residual syrup in petroleum ether (125 mL, bp 30–60°C) was filtered and then refrigerated. A yellow precipitate was collected by filtration, washed with cold petroleum ether, and dried *in vacuo* at room temperature to give 11.8 g. Since TLC showed that this material still contained some of the starting material, it was chromatographed on a column of silica gel. The column was eluted with 95:5 chloroform-methanol, and the fractions containing IIj were located by TLC. Concentration of these fractions *in vacuo* left a yellow syrup (8.2 g) that was crystallized from petroleum ether (150 mL). Yellow crystals were filtered from the cold mixture, washed with petroleum ether, and dried *in vacuo* at room temperature to yield 6.02 g (43.5%) of IIj, mp 106–110°C; HPLC: 97.2% (column B, solvent B); UV_{max} (ethanol): 348 nm (ϵ 47,500).

All-*trans*-*N*-retinoylglycine Ethyl Ester (IIk)—A solution of 196 g (1.40 mol) of glycine ethyl ester hydrochloride in 200 mL of water was covered with 400 mL of ether. The mixture was cooled to 0°C in an ice bath, and 160 mL of 33% aqueous NaOH was added at such a rate that the temperature of the reaction mixture did not exceed 4°C. Immediately after the sodium hydroxide had been added, anhydrous potassium carbonate was added until the water layer was a pasty mass. The ether layer was decanted, and the residual mass was extracted twice with 250-mL portions of ether. The combined, cold, ether extracts were dried over a 9:1 mixture of anhydrous potassium carbonate and barium hydroxide and filtered through a pad of anhydrous magnesium sulfate. The total volume of the combined filtrate and ether washings was 900 mL. The solution was cooled to 5°C and used in the coupling reaction with Ib. (In an earlier, small-scale reaction, concentration of the dried, ether extracts afforded a fluid, colorless oil; examination of this product by MS and by ^{1}H-NMR indicated that little or no diketopiperazine was present.)

A solution of Ib in 450 mL of dry benzene (prepared from 45 g of Ia) was added to the vigorously stirred ethyl glycinate solution (described above) at a rate that did not cause the temperature to exceed 10°C. The mixture was then stirred at 10°C for 1 h. Ice-cold water (450 mL) was added in a dropwise manner, the two-phase mixture was concentrated *in vacuo* at ~35°C to remove the ether and benzene, and the fluid yellow syrup that remained in suspension was extracted into a minimum amount of ether. The ether layer was stirred vigorously with water (400 mL) to ensure thorough mixing, the mixture was concentrated *in vacuo* to remove the ether, and the water was decanted from the viscous syrup. This process was repeated, but the water-syrup mixture was refrigerated overnight before the water was decanted. An ether solution of the residual syrup was dried ($MgSO_4$) and concentrated *in vacuo* at 35°C to constant weight to yield 55 g (95%) of a yellow glassy material. Crystalline IIk was obtained by dissolving the glassy material in warm ethanol and storing the filtered solution at −15°C; mp 91–93°C; TLC: 1 spot (10:1 chloroform-acetone); HPLC: 99% (column A, solvent A).

Anal.—Calc. for $C_{24}H_{35}NO_3$: C, 74.76; H, 9.15; N, 3.63. Found: C, 74.39; H, 8.95; N, 3.36.

All-*trans*-*N*-retinoylglycine (II l)—A stirred solution of 15.0 g (38.9 mmol) of crude *N*-retinoylglycine ethyl ester in 265 mL of ethanol that contained 15.0 g of 85% KOH was heated at 60°C for 1 h. The reaction mixture was poured into 600 mL of water at 0°C, and the solution was extracted with ether (3 × 250 mL) to remove neutral and basic impurities. When the aqueous layer was acidified to pH 3 with 1.5 M sulfuric acid, a fluid oil separated. The mixture was extracted with 250 mL of ether, and the extract was washed twice with water and dried over anhydrous magnesium sulfate. Concentration of the dried extract afforded 13.5 g (97%) of a viscous orange syrup. Crystallization of the crude product twice from acetonitrile (about 10 ml/g) gave yellow microcrystals, mp 94–97°C; TLC: 1 spot (8:2:1 butanol-acetic acid-

water); HPLC: >98% (column A, solvent 1:1 acetonitrile–1% ammonium acetate).

Anal.—Calc. for $C_{22}H_{31}NO_3$: C, 73.91; H, 8.74; N, 3.92. Found: C, 73.68; H, 8.21; N, 3.78.

All-*trans*-*N*-(4-hydroxyphenyl)retinamide (IIm)—The preparation of IIm was based on the procedure of Gander and co-workers (24, 28) and is similar to the preparation of other all-*trans*-retinamides from IIb. The literature procedure (24, 28) was modified to adapt it to large-scale synthesis as follows. The precipitate of 4-aminophenol hydrochloride was filtered from the reaction mixture; the filtrate was washed with water, concentrated, and chilled; and the crude, crystalline product was collected (1–3 crops). These modifications obviate the need for the large quantities of ether used in the original procedure and permit the preparation of 300–400 g of IIm per run. (Some ether was added during the workup of some of the preparations of IIm in order to minimize emulsification.) The crude product was recrystallized from methanol–water and then from ethanol–water, mp 173–175°C; TLC: 1 spot (95:5 chloroform–methanol); HPLC: 99.9% (column B, solvent B).

Anal.—Calc. for $C_{26}H_{33}NO_2$: C, 79.77; H, 8.50; N, 3.58. Found: C, 79.55; H, 8.75; N, 3.54.

This compound evidently crystallizes in several polymorphic or solvated forms. Among many specimens prepared by the procedure outlined above, the mp of 173–175°C was typical, and the IR spectra of most of these specimens were identical; however, the solid-state IR spectra of a few specimens that melted over a 1–2°C range between 171°C and 176°C differed in fine structure from the typical spectrum. Therefore, there may be more than one form with a melting point in this range. Also, a form obtained by slow crystallization of IIm from methanol melted at 178–181°C and retained methanol. The form reported by Gander and co-workers (24) melted at 162–163°C and apparently is more soluble in chloroform than the typical form described above. All of these forms, including a specimen with mp 162–163°C (24), were shown by UV, ^{1}H-NMR, ^{13}C-NMR, MS, TLC, and HPLC to be identical with one another and to be IIm of high purity.

All-*trans*-*N*-[4-(pivaloyloxy)phenyl]retinamide (IIn)—This compound was prepared by acylating IIm with pivaloyl chloride in benzene–pyridine, pouring the reaction mixture into water, and recrystallizing the yellow precipitate from methanol–water and then from ethanol–water, mp 158–160°C; TLC: 1 spot (99:1 chloroform–methanol); HPLC: 99.9–100% (column B, solvent B).

Anal.—Calc. for $C_{31}H_{41}NO_3$: C, 78.28; H, 8.69; N, 2.94. Found: C, 78.23; H, 8.72; N, 2.71.

1-(13-*cis*-Retinoyl)imidazole (IIIc)—A mixture of 13-*cis*-retinoic acid (20 g, 66 mmol) and 1,1′-carbonyldiimidazole (12.4 g, 76 mmol) in benzene (300 mL) was stirred at room temperature for 3 h; gas evolution had ended by this time. The solution was warmed to 50°C for 15 min and then concentrated *in vacuo* to an orange syrup. A mixture of the residue and cyclohexane (250 mL) was stirred at room temperature, filtered to remove a beige solid, and concentrated to dryness under reduced pressure. A solution of the residue in cyclohexane (150 mL) was diluted with hexane (50 mL) and cooled with stirring in an acetone–dry ice bath at −10°C. A yellow precipitate was collected by filtration and dried to yield 18 g (77% yield of crude product). Recrystallization of a 13-g portion of this material from cyclohexane and refrigeration of the mixture afforded 7 g of a yellow solid, mp 70–85°C; HPLC: 98%. A second crop of 2.4 g (mp 75–80°C; HPLC: 96.6%) was obtained after the filtrate was diluted with hexane and refrigerated. A cyclohexane (150 mL) solution of 6.9 g of this material (crop 2 plus part of crop 1) was washed with water (2 × 50 mL), dried ($MgSO_4$), concentrated to ~30 mL, and stored at −15°C. A yellow crystalline solid was collected by filtration and dried *in vacuo* to yield 5.0 g of IIIc, mp 85–86°C (cap., inserted at 65°C); HPLC (column B, solvent B): 98.2% IIIc (retention time, 20.2 min) and 1.2% of an impurity (retention time, 17.6 min). A spike at δ 1.42 ppm on the upfield side of a multiplet in the ^{1}H-NMR spectrum indicated the presence of a small amount of cyclohexane in this specimen. A portion was crushed to a powder and dried thoroughly *in vacuo* prior to microanalysis.

Anal.—Calc. for $C_{23}H_{30}N_2O$: C, 78.82; H, 8.63; N, 7.99. Found: C, 78.94; H, 8.79; N, 8.26.

From another run beginning with 40 g of 13-*cis*-retinoic acid, compound IIIc was obtained in three crops of crystals from cyclohexane–hexane: 2.4 g, mp 77–80°C; 22.6 g, mp 73–83°C; and 13.3 g, mp 82–84°C. The total yield of IIIc satisfactory for use as an intermediate was 82%.

13-*cis*-*N*-Ethylretinamide (IVa)—13-*cis*-Retinoic acid (IIIa, 75 g, 0.25 mol, dried *in vacuo* over P_2O_5) was suspended in 700 mL of dry, reagent-grade benzene, and a solution of 15.2 mL of phosphorus trichloride in 200 mL of dry benzene was added rapidly to the vigorously stirred mixture. The reaction mixture was then stirred at 25°C for 3 h. During this time, 13-*cis*-retinoic acid slowly dissolved and a gummy precipitate formed. Stirring was discontinued, the precipitate was allowed to settle, and the supernatant solution was decanted into an addition funnel.

The acid chloride (IIIb) solution was added slowly to a stirring solution of 130 mL of ethylamine in 300 mL of dry benzene at 10°C, and stirring was continued for 0.5 h. Cold water (250 mL) was added with stirring, the layers were separated, and the aqueous layer was discarded. The benzene layer was washed with two more 250-mL portions of water and concentrated *in vacuo* to a viscous, yellow syrup. The syrup was dissolved in methanol (175 mL), and the solution was diluted slowly with water just short of the cloud point and then seeded with previously obtained crystals of IVa. After some crystallization had occurred, more water was added slowly with stirring (50–75 mL), and the mixture was refrigerated overnight. The precipitate (68 g) was collected by filtration, dried, and recrystallized by dissolving it in refluxing acetonitrile and adding water (~6:1 acetonitrile–water) to yield 64 g (78%), mp 114–115°C (cap., inserted at 95°C); TLC: 1 spot (99:1 chloroform–methanol); HPLC (column B, solvent B): >99.9%.

Anal.—Calc. for $C_{22}H_{33}NO$: C, 80.68; H, 10.16; N, 4.28. Found: C, 80.75; H, 10.44; N, 4.41.

13-*cis*-*N*-Butylretinamide (IVb)—A solution of 13-*cis*-retinoyl chloride (IIIb) [prepared as described above (IVa) from 40 g (133 mmol) of 13-*cis*-retinoic acid in 400 mL of dry benzene and 8.1 mL (93 mmol) of phosphorus trichloride in 155 mL of dry benzene] was added slowly to a vigorously stirred, cold (10°C) solution of 64 mL (650 mmol) of *n*-butylamine in 300 mL of dry benzene. Stirring was continued for 1 h, the mixture was extracted with cold water (2 × 500 mL), and the benzene layer was dried with anhydrous sodium sulfate and concentrated *in vacuo* to give a viscous, orange syrup. A solution of the syrup in 95% acetonitrile at room temperature was seeded with previously obtained crystals of IVb and refrigerated. The pale yellow, crystalline solid was collected by filtration, washed sparingly with cold 95% acetonitrile, and dried *in vacuo* to yield 35 g (74%), mp 77–78°C (cap., inserted at 50°C); TLC: 1 spot (98:2 chloroform–methanol); HPLC (column B, solvent B): >99.9%.

Anal.—Calc. for $C_{24}H_{37}NO$: C, 81.07; H, 10.49; N, 3.94. Found: C, 81.11; H, 10.69; N, 4.03.

13-*cis*-*N*-(4-Hydroxyphenyl)retinamide (IVc)—A solution of 13-*cis*-retinoyl chloride in benzene was prepared by the procedure described above for IVa from 65 g of 13-*cis*-retinoic acid (dried *in vacuo* overnight over P_2O_5), 13.2 mL of phosphorus trichloride, and 750 mL of dry benzene. The benzene solution of IIIa was added slowly to a cold (10°C), stirring solution of 100 g of 4-aminophenol in 400 mL of dimethylformamide (spectral grade), and the reaction mixture was allowed to warm to room temperature and stirred overnight. The mixture, containing precipitated 4-aminophenol hydrochloride, was stirred in an ice bath for 1 h before it was filtered to remove the precipitate. Water (400 mL) was added to the stirring filtrate, and the aqueous layer was separated and discarded. (Much of the product sometimes precipitated during the water extraction or during a second water washing.) The benzene layer was concentrated under reduced pressure to ~300 mL, cooled in an ice bath, and filtered to remove the yellow precipitate, which was washed with benzene and dried. This material (66 g) was combined with a second crop (14 g), obtained similarly from the filtrate and washings, and the total product was recrystallized from methanol–water. A refluxing ethanol solution of the recrystallized material (72 g) was diluted with water well past the point at which crystallization began, and the mixture was cooled to room temperature and then refrigerated. The yellow, crystalline precipitate was collected and dried to yield 70 g (82%) of IVc; mp 186–188°C (cap., inserted at 165°C); TLC: 1 spot (95:5 chloroform–methanol); HPLC (column B, solvent B): >99.7%.

Anal.—Calc. for $C_{26}H_{33}NO_2$: C, 79.77; H, 8.50; N, 3.58. Found: C, 79.99; H, 8.86; N, 3.66.

13-*cis*-*N*-(2-Hydroxyethyl)retinamide (IVd)—*From Isolated IIIc*—A solution of 5 g (14.3 mmol) of 1-(13-*cis*-retinoyl)imidazole (IIIc) in 50 mL of dry benzene was added slowly to a stirring mixture of 6.4 mL (105 mmol) of ethanolamine and 50 mL of benzene at 5–10°C. The mixture was stirred vigorously at 5°C for 2 h and then diluted with cold water (50 mL). Ether (100 mL) was added to cause separation of the emulsion. The benzene–ether layer was separated, washed with saturated aqueous sodium chloride, dried (Na_2SO_4), and concentrated under reduced pressure to a viscous syrup. The syrup was dissolved in hexane (50 mL) at room temperature, and the solution was filtered and stored at 5°C. A yellow, crystalline precipitate was collected by filtration and dried to give 3.5 g (71%). The crystalline product was only sparingly soluble in hexane, but it could be recrystallized by dissolving it in hot cyclohexane and cooling: yield 2.8 g (57%) of IVd; mp 107–109°C (cap., inserted at 95°C); HPLC (column B, solvent B): 98.8%.

From IIIc In Situ—A mixture of 13-*cis*-retinoic acid (50 g), 1,1′-carbonyldiimidazole (31 g), and dry benzene (500 mL) was stirred for 3 h at 20–25°C and then heated to 50°C for 15 min. The dark orange solution was slowly added to a stirring mixture of ethanolamine (62 mL) in benzene (500 mL) at ~10°C. This mixture was stirred for 2 h at 10–20°C; at this time TLC showed the absence of starting material. Cold, saturated, aqueous sodium chloride solution (500 mL) and then ether (500 mL) were added to the stirring

reaction mixture. The organic layer was separated and washed again with saturated aqueous NaCl. The benzene–ether solution was dried (Na_2SO_4) and concentrated *in vacuo* to a viscous syrup that was dissolved in hexane (450 mL) and refrigerated overnight. A yellow, crystalline precipitate was separated by filtration, slurried with hot hexane (400 mL) in which it was only slightly soluble, and recrystallized from cyclohexane to yield 38 g (66%) of IVd, mp 107–109°C (cap., inserted at 80°C); TLC: major spot and two slower, trace impurities (95:9 chloroform–methanol); HPLC (column B, solvent B): 99% IVd, retention time 6.6 min; 0.5% impurity, retention time 5.1 min; and 0.5% impurity, retention time 8 min.

Anal.—Calc. for $C_{22}H_{33}NO_2$: C, 76.93; H, 9.68; N, 4.08. Found: C, 76.82; H, 9.65; N, 3.94.

13-cis-*N*-(4-Hydroxybutyl)retinamide (IVe)—Compound IVe was prepared from 35 g (117 mmol) of IIIa, 21.7 g (134 mmol) of 1,1′-carbonyldiimidazole, and 350 mL of benzene by the second procedure described for the preparation of IVd, but the reaction mixture was concentrated under reduced pressure to a viscous syrup without first adding water. An ether (500 mL) solution of the syrup was extracted with water (2 × 250 mL), dried (Na_2SO_4), and evaporated to a viscous, orange syrup. A solution of the syrup in warm acetonitrile (200 mL) was filtered, diluted with warm water (~50 mL), seeded with IVe previously induced to crystallize from acetonitrile–water, cooled (with scratching) to room temperature, and stored in a refrigerator overnight. The pale yellow, crystalline precipitate was collected by filtration, washed sparingly with acetonitrile–water (2:1), and dried *in vacuo* to yield 26 g (60%) of IVe; mp 53–57°C (cap., inserted at 45°C); TLC: 1 spot with streaking (95:5 chloroform–methanol); HPLC (column B, solvent B): 99.3% IVe (retention time 6.8 min); 0.2% impurity, retention time 5.3 min; and 0.3% impurity, retention time 8.4 min.

Anal.—Calc. for $C_{24}H_{37}NO_2 \cdot 0.5H_2O$: C, 75.76; H, 10.07; N, 3.68. Found: C, 75.82; H, 10.08; N, 3.56.

Compound IVe was first obtained as a solvate with cyclohexane. The syrup obtained by the procedure described above from the ether solution was dissolved in warm cyclohexane. The solution was cooled to room temperature, refrigerated, and filtered to remove a yellow, crystalline product, mp 71–76°C (63% yield calculated as a 1:1 solvate). The solvate was recrystallized from cyclohexane (92% recovery) mp 73–76°C (cap., inserted at 65°C); TLC: IVe as a strong spot and a trace impurity (95:5 chloroform–methanol); HPLC: 99%. ^{1}H-NMR (δ 1.42, s, $CDCl_3$) and mass spectra (*m/z* 284) revealed the presence of cyclohexane; elemental analysis, UV, and ^{1}H-NMR indicated that the molar ratio of cyclohexane to IVe was ~1:1.

Anal.—Calc. for $C_{24}H_{37}NO_2 \cdot C_6H_{12}$: C, 79.08; H, 10.83; N, 3.08. Found: C, 78.87; H, 10.86; N, 3.00.

A specimen (43 g) kept in a high vacuum (continuous pumping, oil pump) at room temperature for 5 d did not lose weight. A specimen recrystallized from 90% acetonitrile appeared to retain at least some of the cyclohexane (mp 54–75°C; MS, *m/z* 84). A solution of the solvate in ethanol was evaorated to dryness *in vacuo*, and this process was repeated four times. The residual syrup was crystallized from acetonitrile–water, mp 53–57°C; HPLC: 98%. ^{1}H-NMR, UV, and MS indicated that the cyclohexane had been removed.

Stability and Storage—Observations of the sensitivity of several all-*trans*-retinamides in the crystalline state to atmospheric oxygen indicated that there are differences among compounds with this structure. The 2,3-dihydroxypropyl amide (IIi, polymorph with mp 83–85°C) appeared to be the most susceptible to deterioration during deliberate exposure to air. The crystalline material became amorphous, and the UV maximum decreased markedly. Eventually, the UV spectrum became a broad plateau with very low absorbance from 220–360 nm and slight elevations centered near 340 and 240 nm. HPLC analyses monitored by UV and based on relative areas may give grossly inaccurate (and high) assays of retinoids that have deteriorated in this manner. However, IIi could be stored for long periods in a liquid-nitrogen freezer, at low temperatures in flame-sealed ampules containing an inert atmosphere, or at low temperatures in heat-sealed, impervious plastic bags (below) containing an inert atmosphere. Crystalline specimens of the 2-hydroxyethyl (IId), 2-hydroxypropyl (IIf), and 4-hydroxybutyl (IIh) all-*trans* amides were also susceptible, but less so, to absorption of atmospheric oxygen; the ethyl (IIb) and 4-hydroxyphenyl (IIm) amides appeared to be more stable. These differences probably arise from differences in crystal form and particle size. For example, as expected, a finely crushed specimen of IIi (lower-melting polymorph) absorbed oxygen more rapidly than did an uncrushed specimen; also, the lower-melting polymorph of IIi absorbed oxygen more rapidly than did the higher-melting polymorph. Storage of retinoids at very low temperatures does not necessarily prevent deterioration unless the retinoids are continuously in an inert atmosphere such as that provided by a liquid-nitrogen freezer, flame-sealed ampules containing nitrogen or argon, or heat-sealed plastic bags containing argon or nitrogen. If a retinoid is placed in a container sealed at room temperature with a screw cap and if the container contracts more than the cap, crevices may develop at low temperatures that would permit the exchange of outside air with the container atmosphere.

Crystalline specimens of the retinamides (II and IV) were stored in an argon atmosphere in flame-sealed, all-glass ampules or in a liquid-nitrogen freezer. The ampules were the freeze-drying type, so they could withstand evacuation with a vacuum pump. The retinamide were put into ampules in a nitrogen atmosphere in a controlled-atmosphere box. After the ampules were loaded with the retinoids, the ampule necks were cleared of adhering crystals to prevent decomposition of small amounts of the retinoids during flame-sealing. The ampules were then attached to a system that included a manometer and a vacuum pump and evacuated; argon was then admitted into the ampules to atmospheric pressure. This process was repeated five times. After the final admission of argon, the neck of the ampule (still attached to the closed system) was sealed with a torch while the body of the ampule containing the retinoid was kept cool. The seals of the ampules were examined with a stereoscope (magnification 30×). The ampules were then placed in dry ice or in a freezer at −80°C at least overnight. The seals were then reexamined with the stereoscope to see if cracks had developed because of stresses during storage at low temperatures. If the retinoid was to be stored for extended periods, the ampules were kept either at −20°C or at −80°C. Retinoids stored for short periods of time were put in brown, screw-cap bottles. Argon or nitrogen was admitted into these bottles in an evacuated desiccator. Each sealed bottle, with tape around the cap, was then placed in an impervious plastic bag. The bag was heat-sealed except for a hole in a corner, flushed with nitrogen or argon with a tube through the corner, and then sealed completely. The sealing was done with a heat-pressure device.

REFERENCES

(1) S. B. Wolbach and P. R. Howe, *J. Exp. Med.*, **42**, 753 (1925).

(2) T. Moore in "The Vitamins," vol. 1, 2nd ed., W. H. Sebrell, Jr. and R. S. Harris, Eds., Academic, New York, N.Y., 1967, pp. 245–266.

(3) M. B. Sporn, N. M. Dunlop, D. L. Newton, and J. M. Smith, *Fed. Proc. Fed. Am. Soc. Exp. Biol.*, **35**, 1332 (1976).

(4) M. B. Sporn, *Curr. Concepts Nutr.*, **6** (*Nutr. Cancer*), 119 (1977).

(5) M. B. Sporn, *Cancer Res.*, **36**, 2699 (1976).

(6) M. B. Sporn, N. M. Dunlop, D. L. Newton, and W. R. Henderson, *Nature* (*London*), **263**, 110 (1976).

(7) M. B. Sporn, *Nutr. Rev.*, **35**, 65 (1977).

(8) M. B. Sporn in "Carcinogenesis—A Comprehensive Survey," vol. 5, T.J. Slaga, Ed., Raven, New York, N.Y., 1980, pp. 99–109.

(9) M. B. Sporn and D. L. Newton, *Fed. Proc. Fed. Am. Soc. Exp. Biol.*, **38**, 2528 (1979).

(10) W. Bollag, *Int. J. Vit. Res.*, **40**, 299 (1970).

(11) H. Mayer, W. Bollag, R. Hanni, and R. Rüegg, *Experientia*, **34**, 1105 (1978).

(12) W. Bollag, *Cancer Chemother. Pharmacol.*, **3**, 207 (1979).

(13) M. B. Sporn, G. H. Clamon, N. M. Dunlop, D. L. Newton, J. M. Smith, and U. Saffiotti, *Nature* (*London*), **253**, 47 (1975).

(14) L. J. Wilkoff, J. C. Peckham, E. A. Dulmadge, R. W. Mowry, and D. P. Chopra, *Cancer Res.*, **36**, 964 (1976).

(15) D. P. Chopra and L. J. Wilkoff, *J. Natl. Cancer Inst.*, **58**, 923 (1977).

(16) D. L. Newton, W. R. Henderson, and M. B. Sporn, *Cancer Res.*, **40**, 3413 (1980).

(17) W. Bollag, *Eur. J. Cancer*, **8**, 689 (1972).

(18) W. Bollag, *Eur. J. Cancer*, **10**, 731 (1974).

(19) W. Bollag, *Chemotherapy, Basel*, **21**, 236 (1975).

(20) M. B. Sporn, R. A. Squire, C. C. Brown, J. M. Smith, M. L. Wenk, and S. Springer, *Science*, **195**, 487 (1977).

(21) C. J. Grubbs, R. C. Moon, R. A. Squire, G. M. Farrow, S. F. Stinson, D. G. Goodman, C. C. Brown, and M. B. Sporn, *Science*, **198**, 743 (1977).

(22) C. J. Grubbs, R. C. Moon, M. B. Sporn, and D. L. Newton, *Cancer Res.*, **37**, 599 (1977).

(23) P. J. Becci, H. J. Thompson, C. J. Grubbs, R. A. Squire, C. C. Brown, M. B. Sporn, and R. C. Moon, *Cancer Res.*, **38**, 4463 (1978).

(24) R. C. Moon, H. J. Thompson, P. J. Becci, C. J. Grubbs, R. J. Gander, D. L. Newton, J. M. Smith, S. L. Phillips, W. R. Henderson, L. T. Mullen, C. C. Brown, and M. B. Sporn, *Cancer Res.*, **39**, 1339 (1979).

(25) H. J. Thompson, P. J. Becci, C. J. Grubbs, Y. F. Shealy, E. J. Stanek, C. C. Brown, M. B. Sporn, and R. C. Moon, *Cancer Res.*, **41**, 933 (1981).

(26) P. H. van Leeuwen, J. R. Roborgh, and P. G. J. Wesselman, *Int. Z. Vit. Forsch.*, **38**, 138 (1968).

(27) W. Bollag, R. Rüegg, and G. Ryser, German Pat. 2,102,586, August 12, 1971 [*Chem. Abstr.*, **75**, 98697 (1971)]; U.S. Pat. 3,950,418, April 13, 1976.

(28) R. J. Gander and J. A. Gurney, U.S. Pat. 4,108,880, August 22, 1978.
(29) H. O. Huisman, A. Smit, and J. Meltzer, *Rec. Trav. Chim.*, **77**, 97 (1958).
(30) H. König, J. Peh, H. Scholz, and J. Paust, German Pat. 2,300,107, July 11, 1974.
(31) R. Miller, *Eur. J. Med. Chem. Chim. Ther.*, **9**, 298 (1974).
(32) H. A. Staab and H. Bräunling, *Ann. Chemie.*, **654**, 119 (1962).
(33) J. Smrt, J. Beránek, and F. Sorm, *Collect. Czech. Chem. Commun.*, **25**, 130 (1960).
(34) W. C. Coburn, Jr., M. C. Thorpe, Y. F. Shealy, M. C. Kirk, J. L. Frye, and C. A. O'Dell, *J. Chem. Eng. Data*, **28**, 442 (1983).
(35) G. Englert, *Helv. Chim. Acta*, **58**, 2367 (1975).
(36) B. C. L. Weedon in "Carotenoids," O. Isler, Ed., Birkhauser Verlag, Basel, Switzerland, 1971, p. 275.
(37) E. J. Hixson and E. P. Denine, *J. Natl. Cancer Inst.*, **63**, 1359 (1979).
(38) A. B. Roberts, C. A. Frolik, M. D. Nichols, and M. B. Sporn, *J. Biol. Chem.*, **254**, 6303 (1979).
(39) D. P. Chopra and L. J. Wilkoff, *Eur. J. Cancer*, **15**, 1417 (1979).

ACKNOWLEDGMENTS

The work was supported by Contract No. N01-CP-85616 with the Division of Cancer Cause and Prevention, National Cancer Institute. UV and IR spectra and microelemental analyses were determined by Christine Richards, and HPLC was performed by Anita T. Shortnacy and Sheila R. Campbell. Some of the NMR spectra were determined with a Bruker WH-400 spectrometer, through the courtesy of Dr. Jerry D. Glickson, at the NMR Core Facility, Comprehensive Cancer Center, University of Alabama in Birmingham. 13-*cis*-Retinoic acid (synthesized by BASF Aktiengesellschaft, Ludwigshafen am Rhein, West Germany) was supplied by the Laboratory of Chemoprevention, National Cancer Institute.

Analysis of Oxprenolol in Formulations by High-Performance Liquid Chromatography

ADNAN EL-YAZIGI

Received December 6, 1982, from the *Department of Cancer and Radiation Biology Research, King Faisal Specialist Hospital and Research Centre, Riyadh 11211, Saudi Arabia.* Accepted for publication May 10, 1983.

Abstract □ A simple, accurate, and rapid high-performance liquid chromatographic method for the analysis of oxprenolol in commercial formulations is described. The analysis was performed on a cyano radial compression cartridge, with 0.0539 M, pH 3 phosphate buffer–acetonitrile–methanol (76:15.6:8.4) as the mobile phase. The flow rate was 5 mL/min, with detection at 272 nm; the mobile phase was employed for extraction. The assay was applied to the content uniformity test of three oxprenolol hydrochloride tablet formulations of different strengths and the contents of a 2-mg dry ampule for intravenous/intramuscular injection. The percent of label claim for each formulation tested was within 91.7–110%. The applicability of this assay to the analysis of some other β-blocking drugs was investigated. It was found that under the above conditions, atenolol, metoprolol, oxprenolol, and propranolol can be fully resolved in <3 min.

Keyphrases □ Oxprenolol—tablet and dry ampule formulations, assay alone or simultaneously with other β-adrenergic drugs, HPLC □ β-Adrenergic drugs—oxprenolol, propranolol, atenolol, and metoprolol, individual and simultaneous assay in formulations, HPLC

Oxprenolol, (±)-1-[*o*-(allyloxy)phenoxy]-3-(isopropylamino)-2-propanol (I), is a β-adrenergic drug frequently used in the treatment of hypertension (1), cardiac arrhythmias (2), and angina pectoris (3). The low dosage of I, particularly when administered intravenously, and its susceptibility to light and other storage conditions require assurance of potency and content uniformity of its dosage forms.

Several methods have been reported for the analysis of I in biological fluids including GC (4–8), TLC with fluorescence detection (9), and high-performance liquid chromatography (HPLC) (10, 11). While the GC assays involve prechromatography derivatization and multiple-step extraction, the TLC method includes derivatization of I to a fluorescing compound. The utilization of HPLC for the analysis of I provides a real advantage, since it does not involve lengthy derivatization steps and the compound is detected directly. However, the previously reported HPLC methods, in addition to lacking a high chromatographic efficiency, have not been applied to the analysis of I in formulations. No pharmacopeial assay of I is available.

The present report describes an expedient, accurate, and specific HPLC method for the analysis of I in formulations. The procedure can be applied for the chromatography of some other β-blocking drugs (atenolol, metoprolol, nadolol, and propranolol) under the same conditions employed for I.

EXPERIMENTAL

Materials—Methanol[1], acetonitrile[1], hexane[2], monobasic sodium phosphate[2], and 85% phosphoric acid[2] were either analytical or HPLC grade. Purified water[3] was used as obtained. The oxprenolol hydrochloride formulations[4] tested (20-, 40-, and 80-mg tablets and 2-mg dry ampules) were obtained in-house. Propranolol hydrochloride[5], nadolol[6], atenolol[5], and metoprolol tartrate[7] were used as received. Oxprenolol (I) was first extracted from a saturated solution of oxprenolol hydrochloride in 5 M NaOH with boiling hexane and was recrystallized several times (mp 77.1°C) from hexane.

Apparatus—The chromatograph used consisted of dual solvent delivery systems[8] with a mixing chamber, automatic sample injection processor[9], printer-plotter integrator data module[10], variable-wavelength UV detector[11], and radial compression module[12]. The analysis was performed on a 10-μm, 8-mm × 10-cm cartridge[13].

Chromatography Conditions—The mobile phase was methanol–acetonitrile–0.0539 M sodium phosphate buffer solution at pH 3 (8.4:15.6:76) filtered twice and deaerated before use. A flow rate of 5 mL/min was used throughout (pressure = 1100 psi). The UV detector was set at 272 nm, and the volume injected into the cyano cartridge was 40–60 μL.

[1] Burdick and Jackson Laboratories Inc., Muskegon, Mich.
[2] Fisher Scientific Company, Fair Lawn, N.J.
[3] Du Pont, Wilmington, Del.
[4] Ciba Laboratories, Horsham, Switzerland.
[5] ICI Limited, Macclesfield, Cheshire, U.K.
[6] E. R. Squibb & Sons, New Brunswick, N.J.
[7] Ciba-Geigy Co., Basle, Switzerland.
[8] Model M45; Waters Associates, Milford, Mass.
[9] Model 710B WISP; Waters Associates, Milford, Mass.
[10] Model 730 Data Module; Waters Associates, Milford, Mass.
[11] Model 480 Lambda; Waters Associates, Milford, Mass.
[12] Model RCM-100; Waters Associates, Milford, Mass.
[13] Radial Pak μ Bondapak CN; Waters Associates, Milford, Mass.

0022-3549/84/0600-0751$01.00/0
© 1984, American Pharmaceutical Association

(28) R. J. Gander and J. A. Gurney, U.S. Pat. 4,108,880, August 22, 1978.
(29) H. O. Huisman, A. Smit, and J. Meltzer, *Rec. Trav. Chim.*, **77**, 97 (1958).
(30) H. König, J. Peh, H. Scholz, and J. Paust, German Pat. 2,300,107, July 11, 1974.
(31) R. Miller, *Eur. J. Med. Chem. Chim. Ther.*, **9**, 298 (1974).
(32) H. A. Staab and H. Bräunling, *Ann. Chemie.*, **654**, 119 (1962).
(33) J. Smrt, J. Beránek, and F. Sorm, *Collect. Czech. Chem. Commun.*, **25**, 130 (1960).
(34) W. C. Coburn, Jr., M. C. Thorpe, Y. F. Shealy, M. C. Kirk, J. L. Frye, and C. A. O'Dell, *J. Chem. Eng. Data*, **28**, 442 (1983).
(35) G. Englert, *Helv. Chim. Acta*, **58**, 2367 (1975).
(36) B. C. L. Weedon in "Carotenoids," O. Isler, Ed., Birkhauser Verlag, Basel, Switzerland, 1971, p. 275.
(37) E. J. Hixson and E. P. Denine, *J. Natl. Cancer Inst.*, **63**, 1359 (1979).
(38) A. B. Roberts, C. A. Frolik, M. D. Nichols, and M. B. Sporn, *J. Biol. Chem.*, **254**, 6303 (1979).
(39) D. P. Chopra and L. J. Wilkoff, *Eur. J. Cancer*, **15**, 1417 (1979).

ACKNOWLEDGMENTS

The work was supported by Contract No. N01-CP-85616 with the Division of Cancer Cause and Prevention, National Cancer Institute. UV and IR spectra and microelemental analyses were determined by Christine Richards, and HPLC was performed by Anita T. Shortnacy and Sheila R. Campbell. Some of the NMR spectra were determined with a Bruker WH-400 spectrometer, through the courtesy of Dr. Jerry D. Glickson, at the NMR Core Facility, Comprehensive Cancer Center, University of Alabama in Birmingham. 13-*cis*-Retinoic acid (synthesized by BASF Aktiengesellschaft, Ludwigshafen am Rhein, West Germany) was supplied by the Laboratory of Chemoprevention, National Cancer Institute.

Analysis of Oxprenolol in Formulations by High-Performance Liquid Chromatography

ADNAN EL-YAZIGI

Received December 6, 1982, from the *Department of Cancer and Radiation Biology Research, King Faisal Specialist Hospital and Research Centre, Riyadh 11211, Saudi Arabia.* Accepted for publication May 10, 1983.

Abstract □ A simple, accurate, and rapid high-performance liquid chromatographic method for the analysis of oxprenolol in commercial formulations is described. The analysis was performed on a cyano radial compression cartridge, with 0.0539 M, pH 3 phosphate buffer–acetonitrile–methanol (76:15.6:8.4) as the mobile phase. The flow rate was 5 mL/min, with detection at 272 nm; the mobile phase was employed for extraction. The assay was applied to the content uniformity test of three oxprenolol hydrochloride tablet formulations of different strengths and the contents of a 2-mg dry ampule for intravenous/intramuscular injection. The percent of label claim for each formulation tested was within 91.7–110%. The applicability of this assay to the analysis of some other β-blocking drugs was investigated. It was found that under the above conditions, atenolol, metoprolol, oxprenolol, and propranolol can be fully resolved in <3 min.

Keyphrases □ Oxprenolol—tablet and dry ampule formulations, assay alone or simultaneously with other β-adrenergic drugs, HPLC □ β-Adrenergic drugs—oxprenolol, propranolol, atenolol, and metoprolol, individual and simultaneous assay in formulations, HPLC

Oxprenolol, (±)-1-[*o*-(allyloxy)phenoxy]-3-(isopropylamino)-2-propanol (I), is a β-adrenergic drug frequently used in the treatment of hypertension (1), cardiac arrhythmias (2), and angina pectoris (3). The low dosage of I, particularly when administered intravenously, and its susceptibility to light and other storage conditions require assurance of potency and content uniformity of its dosage forms.

Several methods have been reported for the analysis of I in biological fluids including GC (4–8), TLC with fluorescence detection (9), and high-performance liquid chromatography (HPLC) (10, 11). While the GC assays involve prechromatography derivatization and multiple-step extraction, the TLC method includes derivatization of I to a fluorescing compound. The utilization of HPLC for the analysis of I provides a real advantage, since it does not involve lengthy derivatization steps and the compound is detected directly. However, the previously reported HPLC methods, in addition to lacking a high chromatographic efficiency, have not been applied to the analysis of I in formulations. No pharmacopeial assay of I is available.

The present report describes an expedient, accurate, and specific HPLC method for the analysis of I in formulations. The procedure can be applied for the chromatography of some other β-blocking drugs (atenolol, metoprolol, nadolol, and propranolol) under the same conditions employed for I.

EXPERIMENTAL

Materials—Methanol[1], acetonitrile[1], hexane[2], monobasic sodium phosphate[2], and 85% phosphoric acid[2] were either analytical or HPLC grade. Purified water[3] was used as obtained. The oxprenolol hydrochloride formulations[4] tested (20-, 40-, and 80-mg tablets and 2-mg dry ampules) were obtained in-house. Propranolol hydrochloride[5], nadolol[6], atenolol[5], and metoprolol tartrate[7] were used as received. Oxprenolol (I) was first extracted from a saturated solution of oxprenolol hydrochloride in 5 M NaOH with boiling hexane and was recrystallized several times (mp 77.1°C) from hexane.

Apparatus—The chromatograph used consisted of dual solvent delivery systems[8] with a mixing chamber, automatic sample injection processor[9], printer-plotter integrator data module[10], variable-wavelength UV detector[11], and radial compression module[12]. The analysis was performed on a 10-μm, 8-mm × 10-cm cartridge[13].

Chromatography Conditions—The mobile phase was methanol–acetonitrile–0.0539 M sodium phosphate buffer solution at pH 3 (8.4:15.6:76) filtered twice and deaerated before use. A flow rate of 5 mL/min was used throughout (pressure = 1100 psi). The UV detector was set at 272 nm, and the volume injected into the cyano cartridge was 40–60 μL.

[1] Burdick and Jackson Laboratories Inc., Muskegon, Mich.
[2] Fisher Scientific Company, Fair Lawn, N.J.
[3] Du Pont, Wilmington, Del.
[4] Ciba Laboratories, Horsham, Switzerland.
[5] ICI Limited, Macclesfield, Cheshire, U.K.
[6] E. R. Squibb & Sons, New Brunswick, N.J.
[7] Ciba-Geigy Co., Basle, Switzerland.
[8] Model M45; Waters Associates, Milford, Mass.
[9] Model 710B WISP; Waters Associates, Milford, Mass.
[10] Model 730 Data Module; Waters Associates, Milford, Mass.
[11] Model 480 Lambda; Waters Associates, Milford, Mass.
[12] Model RCM-100; Waters Associates, Milford, Mass.
[13] Radial Pak μ Bondapak CN; Waters Associates, Milford, Mass.

0022-3549/84/0600-0751$01.00/0
© 1984, American Pharmaceutical Association

Table I—Calibration Curve Data [a] Obtained on Different Days

Day	Intercept	Slope	Correlation Coefficient
1	0.0193	3.031	0.99995
2	0.00945	3.043	0.99999
3	0.0138	3.031	0.99999
4	0.0159	3.027	0.99999
5	0.0139	3.033	0.99999

[a] Peak area ratio *versus* concentration plots obtained by linear regression analysis; mean of four determinations (two samples in duplicate injections).

Preparation of the Buffer and Standard Solutions—The buffer solution was prepared by adding dropwise (≅0.45 mL/drop) 85% phosphoric acid to 1 L of 0.05 M monobasic sodium phosphate to adjust the pH to 3. The final buffer concentration was ≅0.0539 M.

Fifty milligrams of I or propranolol hydrochloride (internal standard) was weighed and carefully transferred into a 50-mL volumetric flask with fresh mobile phase. The solution was shaken until a complete dissolution was obtained, then brought to volume with a fresh mobile phase.

Calibration Curves—Calibration curves were constructed by transferring 1, 3, 5, 10, and 20 mL of the I standard solution into 25-mL volumetric flasks, and 5 mL of the internal standard solution was added to each flask. The solutions were brought to volume with fresh mobile phase and thoroughly mixed. An aliquot (~3 mL) of each solution was transferred into an autosampler vial and placed on the tray. The automatic sample injection processor was programmed to inject 50 μL of each vial in duplicate. Standard curves were prepared on different days, to establish linearity, and prior to each assay, for the calculation of I in the samples analyzed.

Combined Tablet Sample Assay—Fifteen tablets of each strength, *i.e.*, 80, 40, and 20 mg, were weighed and pulverized into a fine powder. An aliquot equivalent to 20 mg of oxprenolol hydrochloride (17.58 mg of I) was accurately weighed and carefully transferred to a 100-mL volumetric flask with fresh mobile phase. The flask was then shaken for 2 min, and the fluid was brought to volume with fresh mobile phase. The suspension was filtered through a filtration unit[14], and ~20 mL of the filtrate was transferred to a 25-mL volumetric flask containing 5 mL of the internal standard solution. The solution was then shaken and brought to volume with an adequate aliquot of the above filtrate. An aliquot (~3 mL) of this solution (theoretical final concentration is 0.14 mg/mL of I) was transferred to an autosampler vial and analyzed as described earlier. This assay was performed on eight replicate samples in duplicate injections.

Combined 2-mg Dry Ampule Samples Assay—The contents of five dry ampules were carefully transferred to a 50-mL volumetric flask with a syringe after reconstitution with fresh mobile phase. The ampules and syringe were thoroughly rinsed with mobile phase, and the rinse was added to the flask.

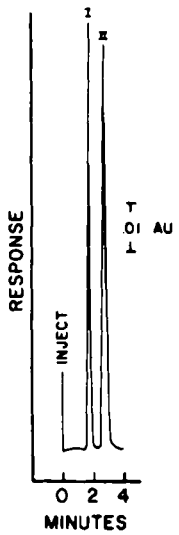

Figure 1—*Representative chromatogram of a calibration curve sample containing oxprenolol (I) with propranolol (II) as internal standard at a concentration of 0.2 mg/mL each. The mobile phase was pH 3 phosphate buffer–acetonitrile–methanol (76:15.6:8.4) at a flow rate of 5 mL/min; the stationary phase was a cyano cartridge.*

[14] Millipore.

Table II—Analyses of the Combined Dosage Unit Samples Showing the Reproducibility of the Assay

Sample	Percent of Label Claim[a] 80-mg Tablet	40-mg Tablet	20-mg Tablet	2-mg Dry Ampule
1	104.8	102.3	99.5	104.0
2	106.1	98.3	99.6	105.5
3	107.8	101.4	103.0	107.0
4	107.6	99.4	103.0	109.5
5	99.9	102.5	101.4	110.0
6	101.7	103.4	101.0	—
7	106.8	99.7	101.2	—
8	105.9	99.9	104.3	—
Mean	105.1	100.9	101.6	107.2
SD	2.85	1.79	1.70	2.56
CV	2.71	1.78	1.67	2.39

[a] Mean value of two injections.

After the volume was brought to the mark with mobile phase, 8 mL of the solution was transferred to a 10-mL volumetric flask containing 2 mL of the internal standard solution. The flask was then shaken, and an aliquot (~3 mL) of this solution (theoretical final concentration 0.14 mg/mL of I) was transferred to an autosampler vial and analyzed as described earlier. This assay was performed on five replicate samples in duplicate injections.

Content Uniformity Test—*Tablet Formulations*—The tablet was pulverized into a fine powder and carefully transferred to a 100-mL volumetric flask with fresh mobile phase, and 20 mL of the internal standard solution was added. The suspension was then brought to volume with fresh mobile phase and shaken vigorously for 2 min. A sufficient aliquot of the suspension was filtered through a filtration unit[14], and the filtrate was transferred to an autosampler vial and analyzed in duplicate as described earlier.

Dry Ampule for Intravenous/Intramuscular Injection—The content of the dry ampule was reconstituted with 2-mL aliquots of fresh mobile phase and transferred with a syringe to a 10-mL volumetric flask containing 2 mL of the internal standard solution. The ampule and syringe were rinsed with small aliquots of the mobile phase, and the rinse was added to the 10-mL volumetric flask. The solution was then shaken and brought to volume with

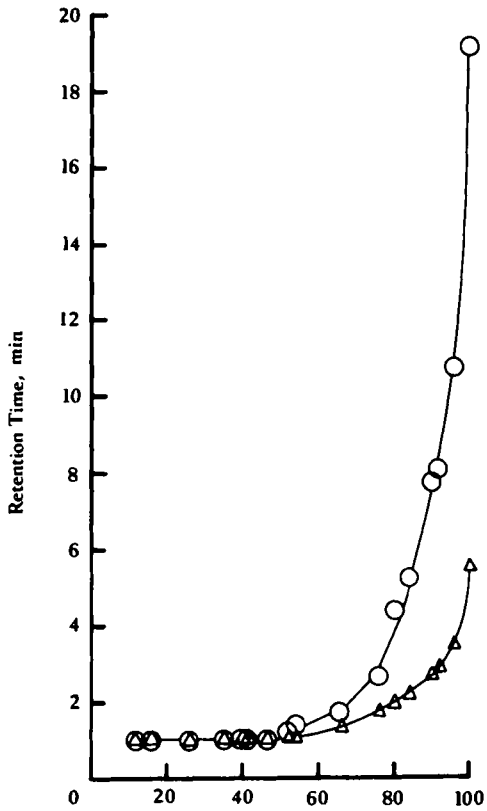

Figure 2—*Effect of the 0.0539 M phosphate buffer (pH 3) concentration in the mobile phase on the retention times of oxprenolol (Δ) and propranolol (○).*

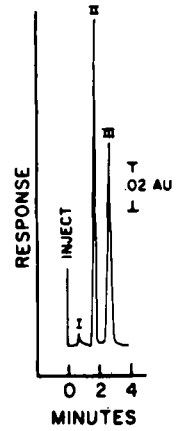

Figure 3—*Typical chromatogram obtained from the analysis of powdered 80-mg tablets. Key: (I) impurity; (II) oxprenolol; (III) propranolol.*

fresh mobile phase. An aliquot of this solution was transferred to an autosampler vial and analyzed in duplicate as described earlier.

Recovery of I from Tablets—Six accurately weighed 50-mg aliquots of a combined tablet powder (80-mg tablets) were transferred to 100-mL volumetric flasks. To five of these flasks, 5 mg of I was added; the remaining flask received no I. These samples were analyzed according to the procedure described under combined tablet sample assay using the sample which did not receive the additional 5 mg of I as a blank.

Chromatograph of Other β-Blockers—Dilute solutions of nadolol, atenolol, and metoprolol tartrate in fresh mobile phase were prepared and transferred to autosampler vials. The retention time of each drug was then determined under the same chromatographic conditions employed for I. A combined solution of atenolol, metoprolol tartrate, I, and propranolol hydrochloride in mobile phase was also prepared and chromatographed.

RESULTS AND DISCUSSION

A typical chromatogram of I and propranolol under the conditions employed is depicted in Fig. 1. As can be seen in this figure, a high efficiency (sharp, symmetrical peaks) and full resolution between I and propranolol are obtained in <3 min. Using C_{18} packing, the retention times under the conditions used were excessive, and although at high concentrations of methanol–acetonitrile in mobile phase the elution was quite rapid, tailing prevailed, suggesting strong binding of both compounds to silanol groups of the C_{18} packing. With the 0.0539 M phosphate buffer (pH 3)–acetonitrile–methanol mixture as the mobile phase, these compounds seemingly favor cyano packing, where both the normal- and reverse-phase modes of chromatography operate.

In an attempt to optimize the chromatography conditions of I and propranolol, the effect of the composition of the mobile phase on the retention times of these compounds was studied (Fig. 2). At zero concentration of the organic mixture (acetonitrile–methanol; 65:35) in the mobile phase the retention times of I and propranolol were 5.58 and 19.15 min, respectively, but the peaks were broad. As the concentration of the organic phase was increased, shorter retention times and sharper peaks were obtained; however, at an inorganic phase concentration of ≤46% (v/v), both compounds were eluted concomitantly without an appreciable change in retention times.

Based on these findings, it was concluded that the 76% phosphate buffer concentration in the mobile phase is an ideal composition for performing the chromatography, since it yields a high chromatographic efficiency and full resolution between I and propranolol in the shortest possible time; this was therefore selected for the analysis.

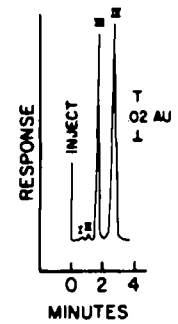

Figure 4—*Typical chromatogram obtained from the analysis of the contents of a 2-mg dry ampule. Key: (I, II) impurities; (III) oxprenolol; (IV) propranolol.*

Table III—Content Uniformity Test of Oxprenolol Hydrochloride Formulations According to the Described Assay

Sample	Percent of Label Claim[a] 20-mg Tablet	40-mg Tablet	80-mg Tablet	2-mg Dry Ampule
1	102.5	94.8	103.5	101.7
2	103.2	105.8	104.3	105.0
3	94.8	105.7	102.3	100.4
4	107.8	104.5	103.3	97.0
5	91.6	104.3	99.5	100.0
6	103.0	104.1	102.1	104.0
7	108.7	107.3	101.7	109.4
8	98.6	104.0	103.8	105.4
9	106.3	106.0	105.2	107.0
10	103.3	101.5	103.5	110.0
Mean	102.0	104.0	102.9	104.0
SD	5.50	3.60	1.60	4.22
Range	91.6–108.7	94.8–107.3	99.5–105.2	97.0–110.0

[a] Mean of four determinations (two samples in duplicate injections).

The peak area ratio (I/internal standard) *versus* concentration calibration curves were linear ($r > 0.9999$) in the concentration range employed in this study (0.04–0.8 mg/mL) and were utilized to calculate I concentrations in the samples analyzed. The day-to-day variations in the slope and intercept were very small (Table I), indicating excellent concentration–response reproducibility.

The chromatogram presented in Fig. 3 is representative of a combined 80-mg tablet sample assay. The small front peak (retention time = 0.7 min) is an impurity or tablet excipient peak and does not interfere with the assay, since it is fully resolved from the peaks in question. The two minor peaks (retention times 0.86 and 1.15 min) which appear in the chromatogram of a single dry ampule analysis (Fig. 4) were also fully resolved.

The recovery of I from tablets was determined by adding 5 mg of I to 50 mg of powdered 80-mg oxprenolol hydrochloride tablets, equivalent to ~14 mg of I. The analysis of five such samples yielded the following recoveries: 100.8, 98.5, 98.3, 99.2, and 99.1% with a mean of 99.2% and a coefficient of variation of 0.991%. These data indicate that the assay precision is excellent and that the extraction procedure (using mobile phase and 2 min of shaking) employed is adequate, yielding a full recovery of I from tablets.

The reproducibility of the assay to analyze I in commercial formulations is clearly evident from the results of the combined tablets or dry ampule assay (Table II) where eight replicate analyses of each tablet lot and five replicate analyses of the combined dry ampule were performed. At no instance did the coefficient of variation exceed 2.7%, which indicates excellent assay reproducibility.

The results of the content uniformity test of commercial oxprenolol hydrochloride formulations are provided in Table III. The data were obtained from the application of the assay to three different-strength tablet formulations and a dry ampule for injection. Ten samples of each lot were analyzed individually, and the percent of label claim for each was calculated using an oxprenolol hydrochloride to I conversion factor of 0.879. As demonstrated in

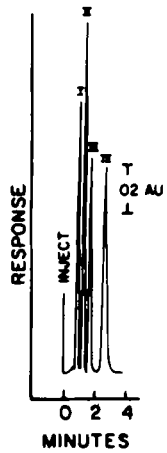

Figure 5—*Chromatogram obtained for a solution containing atenolol (I), metoprolol (II), oxprenolol (III), and propranolol (IV) in mobile phase.*

Table IV—Relative Retention Times[a] of Various β-Adrenergic Blocking Drugs

β-Blocking Drug	Relative Retention Time
Atenolol	0.340
Metoprolol	0.479
Nadolol	0.394
Oxprenolol	0.641
Propranolol	1.000

[a] Retention time of the β-blocking drug/retention time of propranolol.

Table III, the percent of label claim for all formulations tested were within the range of 91.6–110%. Unfortunately, no official USP or BP assay for I is available and, therefore, a comparison between the content uniformity test results obtained according to this method and those of an official assay was not possible. However, if this assay is to be used for such a test, it is clear that all the formulations investigated meet the USP content uniformity requirements (100 ± 15%).

The applicability of this assay for the analysis of some other β-blocking drugs was investigated, and the relative retention times (retention time of drug/retention time of propranolol) of these agents are listed in Table IV. It is clear that, with the exception of nadolol–atenolol (due to poor resolution), it is possible to analyze these drugs under the described chromatography conditions using one drug as the internal standard and the other as the unknown. Indeed, without changing a single chromatography condition, this assay can be utilized for the chromatography of atenolol, metoprolol, I, and propranolol simultaneously with a high efficiency and good resolution (Fig. 5) in <3.0 min.

REFERENCES

(1) W. A. Forrest, *Br. J. Clin. Pract.*, **27**, 331 (1973).

(2) G. Sandler and A. C. Pistevos, *Br. Med. J.*, **1**, 254 (1971).

(3) W. A. Forrest, *Br. J. Clin. Pract.*, **26**, 217 (1972).

(4) D. DeBrucyne, H. Kinsun, M. A. Moulin, and M. C. Bigot, *J. Pharm. Sci.*, **68**, 511 (1979).

(5) D. B. Jack and W. Riess, *J. Chromatogr.*, **88**, 173 (1974).

(6) P. H. Dezen and W. Riess, *J. Chromatogr.*, **121**, 72 (1976).

(7) T. Walle, *J. Pharm. Sci.*, **63**, 1885 (1974).

(8) C. P. Quarterman, M. J. Kendall, and D. B. Jack, *J. Chromatogr.*, **183**, 92 (1980).

(9) M. Schafer and E. Mutschler, *J. Chromatogr.*, **164**, 247 (1979).

(10) S. E. Tsuei, J. Thomas, and R. G. Moore, *J. Chromatogr.*, **181**, 135 (1980).

(11) M. A. Lefebvre, J. Girault, and J. B. Fountillan, *J. Liq. Chromatogr.*, **4**, 483 (1981).

ACKNOWLEDGMENTS

The author thanks Dr. Nizar Feteih, the Executive/Medical Director of the King Faisal Specialist Hospital and Research Centre, Dr. K. Alvin Merendino, the Director of the Research Center, and Dr. Farouk Al-Watban, the Deputy Director of the Research Center, for their encouragement and support for the establishment of the excellent analytical chemistry facilities in the Institute, without which this work could not have been possible.

Improved Liquid Chromatographic Assay for the Analysis of Pirmenol in Plasma and Urine

E. L. JOHNSON and L. A. PACHLA ˣ

Received September 7, 1982, from the *Department of Pharmacokinetics/Drug Metabolism, Warner-Lambert/Parke-Davis Pharmaceutical Research, Ann Arbor, MI 48105.* Accepted for publication April 22, 1983.

Abstract □ A sensitive, specific, and rapid high-performance liquid chromatographic procedure was developed for the determination of pirmenol in human biological fluids. Plasma or urine samples were alkalinized and extracted with cyclohexane. The organic extract was evaporated to dryness, reconstituted with the mobile phase, and then chromatographed on a microparticulate spherical trimethylsilane stationary phase with UV detection at 254 nm. The procedure for the assay of pirmenol in plasma was linear from 0.125 to 5.0 μg/mL. The reproducibility of the peak area ratios of the standard curves had relative standard deviations between 7.7 and 1.8% and a relative error of 0–4.6% over the linear range. The accuracy for the determination of pirmenol in human plasma containing 0.5, 2.5, and 4.0 μg/mL had relative errors of 9.0, 3.8, and 3.6%, respectively. Thirty compounds were tested and found not to interfere in the assay of the drug in plasma, and the method was found to be suitable for clinical samples. The urine procedure was linear between 1.0 and 30.0 μg/mL. The reproducibility of the peak areas of the standard curves had relative standard deviations that ranged from 1.9 to 6.2% over the linear range. The accuracy for the determination of pirmenol in human urine containing 5.0, 17.5, and 25.0 μg/mL had relative errors of 1.4, 0.5, and 2.8%, respectively.

Keyphrases □ Pirmenol—improved HPLC assay, plasma and urine, cyclohexane extraction □ HPLC—improved assay for pirmenol, plasma and urine, cyclohexane extraction

Pirmenol hydrochloride, (±)-*cis*-α-[3-(2,6-dimethyl-1-piperidinyl)propyl]-α-phenyl-2-pyridinemethanol monohydrochloride (I), a new antiarrhythmic drug currently being tested in Phase 1 clinical trials, is a promising agent because of its therapeutic response, lack of toxicity, and relatively long half-life (1). This report describes an improved procedure for the analysis of pirmenol when compared to a recently reported procedure (2). The present method is more accurate and precise due to the choice of extraction solvent and internal standard. The method has been validated for human biological samples, and various potential interfering compounds have been evaluated to demonstrate method specificity.

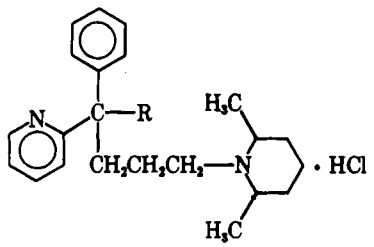

I: R = OH
II: R = H

EXPERIMENTAL

Reagents—Pirmenol hydrochloride[1] and the internal standard[1] (±)-*cis*-2-[4-(2,6-dimethyl-1-piperidinyl)-1-phenylbutyl]pyridine monohydrochloride (II) were used as received. Distilled water was further purified using an ion-exchange charcoal filtration system[2]. Cyclohexane[3] and acetonitrile[3] were

[1] Warner-Lambert/Parke-Davis, Ann Arbor, Mich.
[2] Water-I; Gelman Filtration Products, Ann Arbor, Mich.
[3] Omni-solv grade; MCB, Cincinnati, Ohio.

0022-3549/84/0600-0754$01.00/0

© 1984, American Pharmaceutical Association

Table IV—Relative Retention Times[a] of Various β-Adrenergic Blocking Drugs

β-Blocking Drug	Relative Retention Time
Atenolol	0.340
Metoprolol	0.479
Nadolol	0.394
Oxprenolol	0.641
Propranolol	1.000

[a] Retention time of the β-blocking drug/retention time of propranolol.

Table III, the percent of label claim for all formulations tested were within the range of 91.6–110%. Unfortunately, no official USP or BP assay for I is available and, therefore, a comparison between the content uniformity test results obtained according to this method and those of an official assay was not possible. However, if this assay is to be used for such a test, it is clear that all the formulations investigated meet the USP content uniformity requirements (100 ± 15%).

The applicability of this assay for the analysis of some other β-blocking drugs was investigated, and the relative retention times (retention time of drug/retention time of propranolol) of these agents are listed in Table IV. It is clear that, with the exception of nadolol–atenolol (due to poor resolution), it is possible to analyze these drugs under the described chromatography conditions using one drug as the internal standard and the other as the unknown. Indeed, without changing a single chromatography condition, this assay can be utilized for the chromatography of atenolol, metoprolol, I, and propranolol simultaneously with a high efficiency and good resolution (Fig. 5) in <3.0 min.

REFERENCES

(1) W. A. Forrest, *Br. J. Clin. Pract.*, **27**, 331 (1973).

(2) G. Sandler and A. C. Pistevos, *Br. Med. J.*, **1**, 254 (1971).

(3) W. A. Forrest, *Br. J. Clin. Pract.*, **26**, 217 (1972).

(4) D. DeBrucyne, H. Kinsun, M. A. Moulin, and M. C. Bigot, *J. Pharm. Sci.*, **68**, 511 (1979).

(5) D. B. Jack and W. Riess, *J. Chromatogr.*, **88**, 173 (1974).

(6) P. H. Dezen and W. Riess, *J. Chromatogr.*, **121**, 72 (1976).

(7) T. Walle, *J. Pharm. Sci.*, **63**, 1885 (1974).

(8) C. P. Quarterman, M. J. Kendall, and D. B. Jack, *J. Chromatogr.*, **183**, 92 (1980).

(9) M. Schafer and E. Mutschler, *J. Chromatogr.*, **164**, 247 (1979).

(10) S. E. Tsuei, J. Thomas, and R. G. Moore, *J. Chromatogr.*, **181**, 135 (1980).

(11) M. A. Lefebvre, J. Girault, and J. B. Fountillan, *J. Liq. Chromatogr.*, **4**, 483 (1981).

ACKNOWLEDGMENTS

The author thanks Dr. Nizar Feteih, the Executive/Medical Director of the King Faisal Specialist Hospital and Research Centre, Dr. K. Alvin Merendino, the Director of the Research Center, and Dr. Farouk Al-Watban, the Deputy Director of the Research Center, for their encouragement and support for the establishment of the excellent analytical chemistry facilities in the Institute, without which this work could not have been possible.

Improved Liquid Chromatographic Assay for the Analysis of Pirmenol in Plasma and Urine

E. L. JOHNSON and L. A. PACHLA ˣ

Received September 7, 1982, from the *Department of Pharmacokinetics/Drug Metabolism, Warner-Lambert/Parke-Davis Pharmaceutical Research, Ann Arbor, MI 48105.* Accepted for publication April 22, 1983.

Abstract □ A sensitive, specific, and rapid high-performance liquid chromatographic procedure was developed for the determination of pirmenol in human biological fluids. Plasma or urine samples were alkalinized and extracted with cyclohexane. The organic extract was evaporated to dryness, reconstituted with the mobile phase, and then chromatographed on a microparticulate spherical trimethylsilane stationary phase with UV detection at 254 nm. The procedure for the assay of pirmenol in plasma was linear from 0.125 to 5.0 μg/mL. The reproducibility of the peak area ratios of the standard curves had relative standard deviations between 7.7 and 1.8% and a relative error of 0–4.6% over the linear range. The accuracy for the determination of pirmenol in human plasma containing 0.5, 2.5, and 4.0 μg/mL had relative errors of 9.0, 3.8, and 3.6%, respectively. Thirty compounds were tested and found not to interfere in the assay of the drug in plasma, and the method was found to be suitable for clinical samples. The urine procedure was linear between 1.0 and 30.0 μg/mL. The reproducibility of the peak areas of the standard curves had relative standard deviations that ranged from 1.9 to 6.2% over the linear range. The accuracy for the determination of pirmenol in human urine containing 5.0, 17.5, and 25.0 μg/mL had relative errors of 1.4, 0.5, and 2.8%, respectively.

Keyphrases □ Pirmenol—improved HPLC assay, plasma and urine, cyclohexane extraction □ HPLC—improved assay for pirmenol, plasma and urine, cyclohexane extraction

Pirmenol hydrochloride, (±)-*cis*-α-[3-(2,6-dimethyl-1-piperidinyl)propyl]-α-phenyl-2-pyridinemethanol monohydrochloride (I), a new antiarrhythmic drug currently being tested in Phase 1 clinical trials, is a promising agent because of its therapeutic response, lack of toxicity, and relatively long half-life (1). This report describes an improved procedure for the analysis of pirmenol when compared to a recently reported procedure (2). The present method is more accurate and precise due to the choice of extraction solvent and internal standard. The method has been validated for human biological samples, and various potential interfering compounds have been evaluated to demonstrate method specificity.

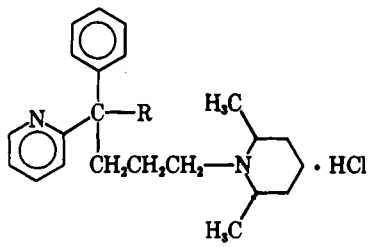

I: R = OH
II: R = H

EXPERIMENTAL

Reagents—Pirmenol hydrochloride[1] and the internal standard[1] (±)-*cis*-2-[4-(2,6-dimethyl-1-piperidinyl)-1-phenylbutyl]pyridine monohydrochloride (II) were used as received. Distilled water was further purified using an ion-exchange charcoal filtration system[2]. Cyclohexane[3] and acetonitrile[3] were

[1] Warner-Lambert/Parke-Davis, Ann Arbor, Mich.
[2] Water-I; Gelman Filtration Products, Ann Arbor, Mich.
[3] Omni-solv grade; MCB, Cincinnati, Ohio.

0022-3549/84/0600-0754$01.00/0

© 1984, American Pharmaceutical Association

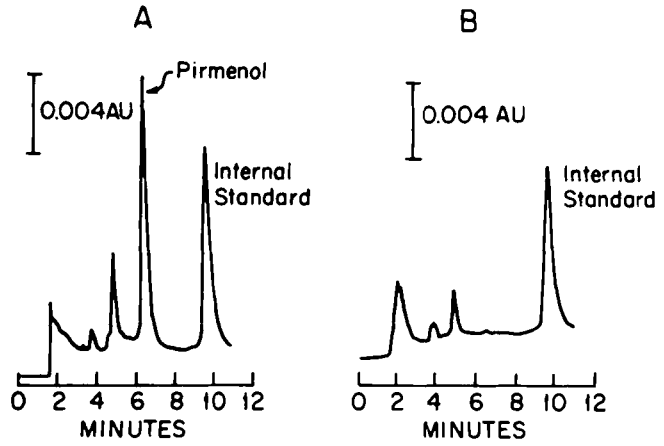

Figure 1—*Typical chromatograms for pirmenol and the internal standard in plasma. Key: (A) pirmenol in a 40-min plasma sample following infusion (150 mg iv at 5 mg/min) was estimated to be 1.7 μg/mL); (B) preinfusion plasma sample.*

chromatographic grade. Monobasic sodium phosphate[4], triethylamine[4], phosphoric acid[4], hydrochloric acid[5], and sodium hydroxide[5] were analytical reagent grade and were used as received.

Apparatus—The liquid chromatographic system was equipped with a constant-volume pump[6], valve-type injector[7], 254-nm fixed-wavelength detector[8], and a data acquisition system[9]. Separations were performed on a 25 cm × 4.6 mm i.d. stainless steel column containing 6-μm spherical trimethylsilane stationary phase[10].

Mobile Phase—The mobile phase was prepared by diluting 150 mL of acetonitrile to 1 L with phosphate buffer containing 0.5% triethylamine. The phosphate-triethylamine buffer was prepared by adding 6.9 g of monobasic sodium phosphate monohydrate and 5.0 mL of triethylamine to water, adjusting the pH to 2.6 with phosphoric acid, and then diluting to 1 L with water. The mobile phase was filtered through a 0.2-μm filter and deaerated by vacuum. The flow rate of the mobile phase was 1.5 mL/min, which produced a pressure of ~2700 psi. All separations were performed at ambient temperature. A 50-μL aliquot of extracted sample was injected into the chromatographic system.

Standard and Stock Solutions—Stock solutions of pirmenol (110.7 mg of pirmenol hydrochloride/10 mL of 0.05 M HCl) and the internal standard (II) (11.1 mg of II/100 mL of 0.05 HCl) were prepared. Standard solutions for plasma containing 0.25, 1.0, 2.0, 4.0, 6.0, 8.0, and 10 μg/mL and standard solutions for urine containing 4, 20, 40, 60, 80, 100, and 120 μg/mL were prepared by serial dilution of the stock pirmenol solution with 0.05 M HCl. The internal standard solution was further diluted 3:100.

Pirmenol Plasma and Urine Seeded Control Pools—One milliliter of 50-, 250-, or 400-μg/mL solutions of pirmenol (in 0.05 M HCl) was added to a 100-mL volumetric flask and brought to volume with control plasma to yield seeded control samples of 0.5, 2.5, and 4.0 μg/mL of pirmenol. Urine seeded controls were prepared by adding 0.5, 1.75, and 2.5 mL of a 1.0 mg/mL standard solution and diluting to 100 mL with control urine to yield 5.0-, 17.5-, and 25.0-μg/mL samples. The plasma and urine samples were then divided into 2.5-mL portions and frozen.

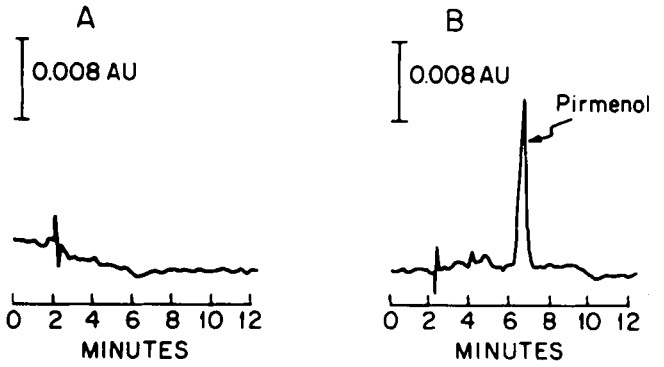

Figure 2—*Typical chromatograms for pirmenol in human urine. Key: (A) predrug urine sample; (B) pirmenol in an 18-h postdose urine sample of a patient administered 150 mg of pirmenol was estimated to be 4.0 μg/mL.*

[4] J. T. Baker, Phillipsburg, N.J.
[5] Acculute; Anachemia Chemical, Champlain, N.Y.
[6] Model-M-45; Waters Associates, Milford, Mass.
[7] Model U6K; Waters Associates, Milford, Mass.
[8] Model 440; Waters Associates, Milford, Mass.
[9] Sigma 10; Perkin Elmer, Norwalk, Conn.
[10] Zorbax TMS; DuPont, Wilmington, Del.

Table I—Precision and Accuracy of the Pirmenol Calibration Curves During a 3-d Period

Pirmenol Conc. Added, μg/mL	N	Peak Area Ratio[a]	RSD, %	Relative Error, %
Plasma				
0.125	9	0.037	7.7%	−0.8
0.500	8	0.254	4.7%	4.6
1.00	9	0.491	5.7%	−4.3
2.00	9	1.02	4.2%	−3.5
3.00	8	1.61	3.0%	0
4.00	9	2.15	5.1%	0.5
5.00	8	2.78	1.8%	2.8
Urine				
1.0	6	0.376	3.1%	0
5.0	8	1.62	6.0%	−8
10.0	8	3.53	3.8%	−2
15.0	9	5.48	6.2%	0
20.0	8	7.51	1.90%	2
25.0	8	9.54	2.0%	3.2
30.0	9	11.5	2.2%	4.3

[a] Peak area used for urine samples.

Assay for Pirmenol in Plasma and Urine—To a 1-mL sample in a 10-mL screw-top test tube were added 0.5 mL (0.25 mL for urine samples) of either 0.05 M HCl or pirmenol standard solution, 0.5 mL of internal standard solution (no internal standard is used for urine samples), 4 mL of cyclohexane, and 0.15 mL (0.2 mL for urine samples) of 1 M NaOH. After shaking for 10 min on a horizontal shaker and centrifuging[11] at 206×*g* for 5 min, 3 mL of the organic phase was transferred to a clean tube and evaporated to dryness. The residue was reconstituted in 0.2 mL (1 mL for urine samples) of the mobile phase by vortexing, and 50 μL (100 μL for urine samples) was injected into the chromatograph.

Interference Study—The specificity of the plasma procedure was assessed by direct injection of a number of potentially interfering compounds. If a compound eluted in the void volume or had a retention time >12 min, then the compound was deemed not to interfere in the assay. Those compounds having a retention time similar to either pirmenol or the internal standard were further tested in the following manner. Plasma containing 1 μg/mL of pirmenol was spiked with 100 μg/mL of the potentially interfering compounds. These samples were then assayed for pirmenol. If the pirmenol concentration deviated >±5% of the established value, than the compound was considered to interfere in the assay.

Method Application—To test the suitability of the procedure, samples from a clinical trial were assayed. In this trial, patients received a 150-mg dose of pirmenol intravenously or orally. For the intravenous dosing, patients were infused over a 30-min period with the drug dissolved in 5% dextrose. Blood samples were drawn at 15, 30, 32, 35, 40, 50, 60, 75, 90 min, and 2, 3, 5, 7, 9,

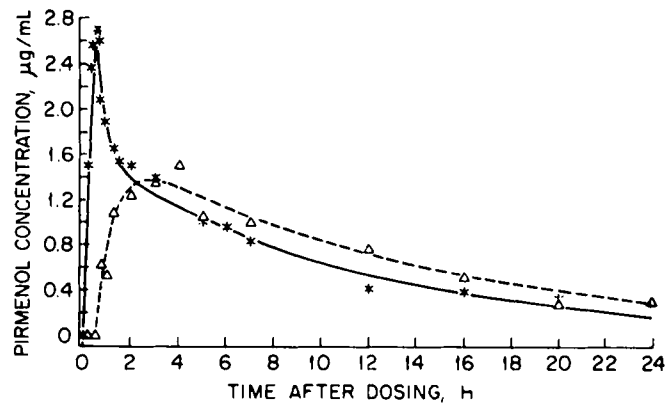

Figure 3—*Plasma concentration-time curve in a patient given 150 mg of pirmenol. Key: (*) intravenous; (Δ) oral.*

[11] Centra 7R, International Equipment Company, Needham Hts, Mass.

Table II—Extraction Efficiency of Tritiated Pirmenol in Plasma and Urine Determined by Liquid Scintillation Counting

	Plasma			Urine		
[^{3}H]Pirmenol Added, (μg/mL)	0.1	1.0	5.0	1.0	10.0	25.0
N	3	4	3	4	4	4
Mean Recovery (%)	84.8	85.2	87.4	82.5	89.4	90.3
RSD (%)	7.6	8.8	1.6	4.4	1.1	1.2

Table III—Determination of Pirmenol Concentrations in Seeded Plasma and Urine Control Pooled Samples Assayed During a 3-d Period

	Plasma			Urine		
Pirmenol Conc. Added, (μg/mL)	0.500	2.500	4.000	5.0	17.5	25.0
N]9	9	8	9	9	9	9
Mean Conc. Found, (μg/mL)	0.545	2.594	4.144	4.9	17.6	25.7
RSD (%)	5.0	3.4	3.6	5.2	1.5	1.8
Relative Error (%)	9.0	3.8	3.6	−1.4	0.5	2.8

12, 16, 20, and 24 h into heparinized tubes, and the plasma was harvested following centrifugation. For the oral study, the same patients were administered 150-mg capsules 48 h after the intravenous dose. Blood samples were taken at 0, 0.25, 0.50, 0.75, 1, 1.25, 1.5, 2, 3, 4, 5, 7, 12, 16, 20, and 24 h following drug administration. The plasma was harvested following centrifugation. Timed urine collections of 2 h were collected for the first 6-h period followed by 6-h collections for 48 h postdose.

RESULTS AND DISCUSSION

The present procedure for the analysis of pirmenol in human plasma and urine involves a single-step alkaline extraction with cyclohexane. The supernatant is evaporated to dryness and reconstituted with the mobile phase. Cyclohexane was found to give improved extraction recoveries and cleaner sample extracts compared with ether (2). An internal standard was found not to be necessary in the urine procedure due to the high pirmenol concentration and simple sample preparation (3). The validity of the assay was established through a careful study of linearity of response, reproducibility of standard curve, extraction recovery, accuracy, precision, and potential interference studies.

The retention times for pirmenol and the internal standard were 6.4 and 9.5 min, respectively. Figure 1 illustrates typical chromatograms for control human plasma and that from the plasma of a patient who received an intravenous dose of pirmenol. Figure 2 illustrates typical chromatograms for blank urine and an 18-h postdose urine sample. The total time required for the plasma and urine assays was 12 and 7 min, respectively.

The linearity of response of the amount of pirmenol added to control human plasma and urine was found to be linear over a range of 0.125–5.00 μg/mL for plasma and 1–30 μg/mL for urine. These ranges cover the projected therapeutic plasma and urine concentration ranges. The best-fit line was obtained using linear regression analysis with weighting factors of 1/concentration squared (4). The results of a typical regression analysis were: peak area ratio = 0.563 × plasma concentration + 0.0357 (r = 0.9987) and peak area = 0.367 × urine concentration + 0.0067 (r = 0.9948).

The reproducibility of the calibration curves was assessed by assaying triplicates of each plasma and urine standard over a 3-d period. The relative standard deviations of the peak area ratios for plasma and peak areas for urine between the lowest and highest concentrations were found to range from 7.7 to 1.8% and from 1.9 to 6.2%, respectively. The accuracy for these standards had relative errors of 0–4.6% and 0–4.3% for plasma and urine, respectively. These data are summarized in Table I.

The extraction efficiency for tritium-labeled pirmenol was determined using liquid scintillation counting[12] and is given in Table II. These data show that the extraction efficiency of pirmenol from plasma and urine ranges from 85 to 87% and 82 to 90%, respectively.

The relative error of the plasma procedure was determined by assaying seeded control plasma pooled samples containing 0.5, 2.5, and 4.0 μg of pirmenol/mL over a 3-d interval and was found to be 9.0, 3.8, and 3.6%, respectively. The relative error of the urine procedure was assessed by assaying seeded control urine pooled samples containing 5.0, 17.5, and 25.0 μg/mL and was found to be 1.4, 0.5, and 2.8%, respectively (Table III).

The specificity of the plasma assay was assessed by determining the chromatographic behavior of a number of potentially interfering compounds. The following compounds were found not to interfere with the quantification of pirmenol based on retention time: acetaminophen, clonidine hydrochloride, diazepam, disopyramide, ethacrynic acid, fenoprofen sodium, furosemide, hydralazine hydrochloride, hydrochlorothiazide, ibuprofen, methotrimeprazine, methyldopa, prazepam, prazosin hydrochloride, procainamide, propranolol hydrochloride, propoxyphene hydrochloride, reserpine, and tolmetin sodium. Compounds that had a similar retention time as primenol, but were found not to interfere were: aspirin, bretylium tosylate, chlorthalidone, naproxen, oxazepam, quinidine, salicylate, triamterene, and zomepirac sodium. To date, over 650 human plasma samples and 200 urine samples have been assayed for pirmenol using this methodology, and no apparent interfering compounds have been detected. Figure 3 illustrates typical plasma time courses for pirmenol after intravenous and oral dosing.

The method provides several improvements over a previous procedure (2). The improvements include cleaner sample extracts, improvement in chromatographic baseline due to choice of reconstitution solvent, an internal standard for plasma that is structurally similar to pirmenol, and increased sample throughput and ability to reinject samples if required. The data for the procedure are in agreement with the predicted precision expected for the internal or external calibration technique (3).

REFERENCES

(1) S. C. Hammill, D. G. Shand, P. A. Rutledge, M. C. Hindman, J. T. Baker, and E. L. C. Pritchett, *Circulation*, **65**, 369 (1982).

(2) D. G. Shand, C. Verghese, A. Banchowsky, S. C. Hammill, and E. L. C. Pritchett, *J. Chromatogr.*, **224**, 343 (1981).

(3) P. Haefelfinger, *J. Chromatogr.*, **218**, 73 (1981).

(4) P. R. Bevington, "Data Reduction and Error Analysis for the Physical Sciences," McGraw-Hill, New York, N.Y., 1969, p. 105.

[12] Tricarb Model No. 3375; Packard Instruments, Downers Grove, Ill.

Characteristics of Drug–Phospholipid Coprecipitates I: Physical Properties and Dissolution Behavior of Griseofulvin–Dimyristoylphosphatidylcholine Systems

S. VENKATARAM and J. A. ROGERS ˣ

Received February 24, 1983, from the *Faculty of Pharmacy and Pharmaceutical Sciences, University of Alberta, Edmonton, Alberta, Canada.* Accepted for publication May 11, 1983.

Abstract □ Solid dispersions of griseofulvin and dimyristoylphosphatidylcholine (lecithin) have been prepared as both coprecipitates and physical mixtures, and their physical characteristics and dissolution behavior compared with pure griseofulvin. The dissolution of the physical mixtures was similar to pure drug, but the coprecipitates yielded a 3.5-fold greater initial dissolution rate and a limiting concentration after 60 min which was 72% greater at a griseofulvin–lecithin weight ratio of 19:1. Increasing the lecithin content to 1.5:1 compositions resulted in only a further 50% increase in the initial dissolution rate and a further 12% increase in the limiting concentration. The effect of the pH of the medium on dissolution was slight, but varied with the composition of the system. The phase diagram indicated that these systems have no significant eutectic or solid solution formation. X-ray diffraction spectra further showed that freshly prepared or aged coprecipitates contained griseofulvin crystals, and photomicrographs showed that the crystals essentially retained their characteristic shapes and sizes in all systems. Differential thermal analysis yielded heats of fusion that gave a good linear correlation with the percent of griseofulvin dissolved from coprecipitates at all time intervals, but not with physical mixtures. Furthermore, aged coprecipitates underwent a slower rate of dissolution compared with fresh samples. The results are interpreted to suggest that griseofulvin undergoes improved dissolution from coprecipitates due to the formation of crystals of lower stability. In addition, the rapid dispersion of lecithin in the aqueous medium (as seen microscopically) entraps griseofulvin in myelinic structures and liposomes and effectively increases the saturation concentration of drug in the diffusion layer during the dissolution process.

Keyphrases □ Drug–phospholipid coprecipitates—griseofulvin–dimyristoylphosphatidylcholine system, dissolution behavior, physical properties □ Dissolution—griseofulvin–dimyristoylphosphatidylcholine coprecipitates, comparison with physical mixtures, physical properties □ Griseofulvin—coprecipitates with dimyristoylphosphatidylcholine, physical properties, dissolution behavior

The dissolution of solid drugs having low water solubility is often a rate-limiting step in obtaining bioavailability. Thus, several formulation approaches have been explored to improve bioavailability of such drugs, including the use of lipid vehicles and the preparation of solid dispersions. In those cases where lipids have been used, the dissolution and bioavailability of drugs have been found to be dependent on the nature of the lipids used in the formulation, being either increased (1–4), decreased (1, 3–5), or unaffected (1). In most instances, the dosage form contains a large proportion of lipid. Likewise, solid dispersions involving water-soluble carriers require a large proportion of carrier to be effective. On the other hand, it would be advantageous to incorporate a minimal amount of carrier to produce either rapid dissolution or sustained release of a drug from a solid dosage form.

Phospholipids spontaneously disperse in aqueous media to form bilayer structures which have the capacity to entrap or sequester solutes. This dual behavior could prove beneficial for improving bioavailability of drugs in a number of ways. According to the Nernst film theory of dissolution, an increased saturation concentration of drug in the stationary layer leads to an increase in the dissolution rate. It is not important that the concentration achieved is due to the intrinsic solubility of the drug in the medium of the stationary layer or due to a partitioning process. Encapsulated or entrapped drug within the bilayer structures (myelinic or liposomal) during the dissolution process may be transported, first to the stationary or diffusion layer, then to the bulk solution, then to the site of absorption to yield rapid delivery of a drug to the general circulation. Furthermore, for drugs which may be susceptible to degradation or solubility changes within the GI fluids, entrapment may afford a degree of protection (6, 7).

The system of griseofulvin–dimyristoylphosphatidylcholine has been chosen to test these hypotheses and to evaluate the performance of a phospholipid in a solid dispersion formulation. The purpose of the present report is to present some preliminary data for this system and to evaluate its potential in controlled-release dosage form design.

EXPERIMENTAL

Materials—Micronized griseofulvin[1] (I) was pretreated by dissolving it in chloroform then removing the solvent by warming slightly over a water bath and applying a gentle stream of air. Drying of the crystals was carried out under vacuum over desiccants. The melting points of untreated and treated I were identical. Pure I and all binary mixtures were passed through an 80-mesh sieve[2] prior to testing.

L-α-Dimyristoylphosphatidylcholine[3] (II), claimed to be 98% pure, was used as received. All solvents and chemicals were reagent grade, and distilled water was used to prepare the dissolution media.

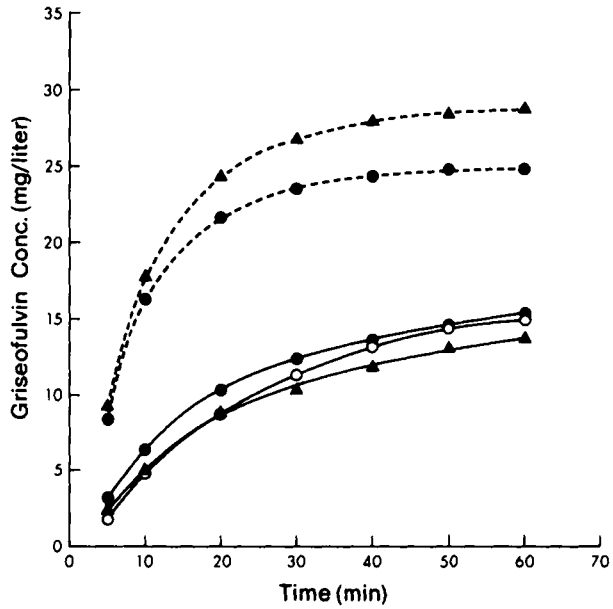

Figure 1—*Dissolution behavior of I and I–II solid dispersion systems at pH 2.0 and 37°C. Key: (- - -) coprecipitates; and (—) physical mixtures or pure I; (○) chloroform-treated I; (●) 9:1 composition of I–II; (▲) 1.5:1 composition of I–II.*

[1] Glaxo Canada Ltd., Toronto, Ontario.
[2] Standard (U.S. Series) sieve.
[3] Sigma Chemical Co., St. Louis, Mo.

0022-3549/84/0600-0757$01.00/0
© 1984, American Pharmaceutical Association

Table I—Dissolution of Griseofulvin–Dimyristoylphosphatidylcholine Compositions at pH 2.0 and 37°C

Composition (Weight Ratio)	Initial Dissolution Rate, mg/L/min		Limiting Conc. After 60 min, mg/L	
	Coprecipitates	Physical Mixtures	Coprecipitates	Physical Mixtures
1:0	0.36	0.36	15.0	15.0
19:1	1.26	—	25.8	—
9:1	1.68	0.60	24.9	15.3
4:1	1.67	—	35.3	—
1.5:1	1.86	0.48	28.8	13.7

Preparation of Coprecipitates and Physical Mixtures—Solid dispersions of I–II compositions were prepared by the solvent method from chloroform, yielding coprecipitates which were subsequently dried under vacuum over desiccants as before. Coprecipitates were usually examined within 48 h after preparation. Physical mixtures were prepared by triturating appropriate quantities of I and II using a mortar and pestle, then transferring to a vacuum desiccator until ready for use.

Thermalmicroscopic Method—The thaw and melt temperatures of all samples were determined by the hot-stage microscopic technique[4]. The heating rate was set at 2°C/min. just below the predetermined thaw temperature.

Differential Thermal Analysis—The differential thermal analyzer[5] was calibrated with indium[6], tin[6], and lead[6] using a 15-mg sample against an empty pan as reference. The heating rate was set at 10°C/min, the differential temperature sensitivity was 0.3°C/2.54 cm, and the reference temperature sensitivity was 13.7°C/2.54 cm. Heats of fusion were determined from the areas under the endothermic peaks (planimeter method), and the corresponding calibration coefficients were obtained from the fusion temperatures (taken at the peak of the endothermic event) and the calibration curve (8).

X-ray Diffraction Studies—Samples for low-angle powder X-ray diffraction studies (~50 mg) were uniformly dispersed on a glass slide. A piece of transparent cellulose tape was then used to secure the powder in position. X-ray diffraction spectra[7] were obtained employing CuK_α radiation and run at 2°/min and a 2θ angle.

Dissolution Studies—The spin-filter dissolution test apparatus[8] employing a 1-μm porosity filter screen was used (9). Filter rotation speed was maintained at 600 rpm in 900 mL of dissolution medium, which was either HCl–KCl buffer at pH 2.0 or phosphate buffer at pH 5.0, at 37°C. Measurement of concentrations of I in the dissolution medium was carried out employing automated UV spectrometry at $\lambda = 293$ nm (10). A 50-mg sample was dispersed in the dissolution medium in each instance. The presence of II in the dissolution medium did not interfere with the analysis of I. Experiments were run in duplicate and the results averaged, although at no time was a significant difference found between duplicates.

Photomicrographic Analysis—Representative samples of powders were examined microscopically[9], 320× magnification, in either light mineral oil or water. Photomicrographs[10] were obtained for comparison of crystal shape and size and to record the various stages of dissolution.

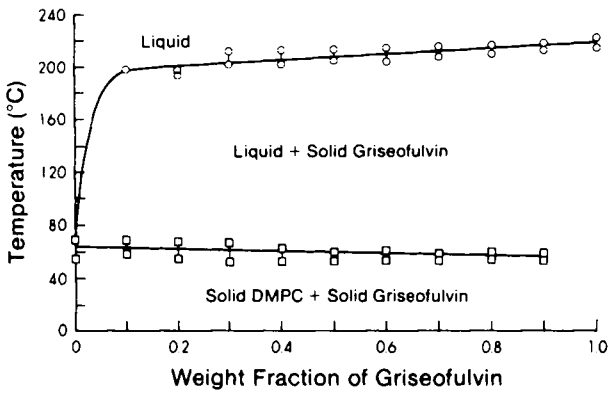

Figure 2—*Phase diagram of binary systems of I and II determined from differential thermal analysis and hot-stage microscopy. Key: (□) thaw and melt temperatures of the lower-melting component (II); (○) thaw and melt temperatures of the higher-melting component (I).*

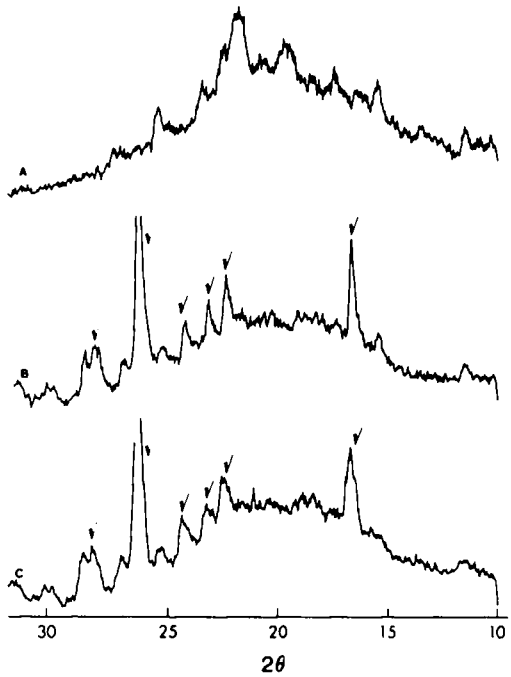

Figure 3—*Low angle powder X-ray diffraction spectra of II (A), chloroform-treated I (B), and 19:1, I–II coprecipitate (C).*

RESULTS

Dissolution Studies—The dissolution of I from a multiparticulate I–II coprecipitate was found to be considerably greater than from physical mixtures or pure I. Typical dissolution profiles are given in Fig. 1, where it is apparent that the initial dissolution rates and the amount of I dissolved after 60 min from the coprecipitates exceeded those of pure I or the corresponding physical mixtures. Furthermore, the dissolution of 1.5:1 coprecipitates was greater than that of the 9:1 composition, whereas the dissolution behavior of the corresponding physical mixtures was in the reverse order. The initial dissolution rates (IDR) (computed over the first 5 min of dissolution) and concentrations of I achieved after 60 min, which were essentially limiting after this period (LDC), are compared in Table I. The IDR of the I–II coprecipitate exhibits an increase of 3.5-fold with as little as 5% of II in the total sample (19:1 weight ratio) and an increase of 5-fold for samples containing 40% of II (1.5:1 weight ratio). In contrast, the IDR of I from physical mixtures increased only slightly with a higher content of II. Values of LDC obtained from coprecipitates clearly indicate a substantial increase in the apparent solubility of I in the dissolution medium. On the other hand, an increased fraction of II in the physical mixture compositions does not increase the apparent solubility of I and, indeed, at 40% II the LDC is somewhat lower than that for pure I. The superior dissolution of I–II coprecipitates is further exemplified by the data in Table II. Percent dissolved of I from coprecipitates is more than twice that dissolved from physical mixtures at corresponding times.

The dissolution of I appears to have a slight dependency on the pH of the dissolution medium. This is more pronounced after the first 10 min of dissolution and is reflected in the LDC as shown in Table III. In all cases, except the 9:1 coprecipitate, the LDC is less at pH 5.0 than pH 2.0 which is consistent with other reports of the dissolution of griseofulvin coprecipitates at various pH values (4). However, the 9:1 coprecipitate displayed a reverse and significant pH dependency in its dissolution profile which is not readily explained. This result, together with the unusually greater LDC of the 4:1 coprecipitates, suggest that the physical characteristics of the crystals formed in the coprecipitates differ from sample to sample and are dependent on the proportions of I and II.

Solid-State Analysis—Differential thermal analysis (DTA) of I pretreated with chloroform yielded a sharp major endothermic peak at 221°C [lit. (4) mp 220–222°C]. However, a distinct, broad peak also occurred at 120–126°C.

[4] Mettler FP52, hot-stage microscope; Mettler Instrument Corp., Princeton, N.J.
[5] Fisher Thermalyzer, Model 370; Fisher Scientific Co., N.J.
[6] Calorimetric Standards; Fisher Scientific Co., N.J.
[7] Philips X-Ray Diffractometer, Model 1380, with a Norelco focusing monochromator.
[8] Magne-Drive Dissolution Test Apparatus; Clow-Coffman Industries, Kansas City, Kan.
[9] Zeiss standard microscope with integral 6-V 10-W halogen illuminator equipped with an MC63 photomicrographic camera; Carl Zeiss, Oberkochen, West Germany.
[10] Kodak Plus-X Pan Film, ASA 125, 1/15-s exposure.

Table II—Comparison of Percent Dissolved from Griseofulvin–Dimyristoylphosphatidylcholine Coprecipitates, Physical Mixtures, and Pure Griseofulvin

Composition (Weight Ratio)	Coprecipitates				Physical Mixtures			
	5 min	20 min	40 min	60 min	5 min	20 min	40 min	60 min
1:0	3.2	15.8	23.8	27.0	3.2	15.8	23.8	27.0
9:1	16.8	43.1	48.7	49.8	5.6	18.5	24.5	17.5
1.5:1	27.9	72.8	83.9	86.4	7.0	25.1	35.7	41.1

It also appeared in the thermograms of coprecipitates and physical mixtures, but its height varied in proportion to the I content of the sample. This peak did not appear in thermograms of I pretreated with methanol or acetone or untreated I. Chloroform solvates of I have been reported (11, 12) and, therefore, it is concluded that the unexpected peak was due to chloroform, in spite of fairly rigorous drying of each treated sample.

Thermograms of the binary systems contained two peaks: a peak corresponding to the melting of I and a peak corresponding to the melting of II. Determination of the thaw and melt temperatures from each peak enabled construction of the phase diagram (Fig. 2). The line for the solid indicates a slight depression of the melting point of II as the composition increases with respect to I. Likewise, the line for the liquid displays a slight decrease in the melting point of I as the composition decreases with respect to I. Hot-stage microscopy permitted visualization of the melting of each component and confirmed the thaw and melt temperatures. Above 70% II, the I peak on the DTA thermogram was too small to accurately measure, so hot-stage microscopy results are recorded only. The phase diagram is typical of a monotectic system (13), which indicates the absence of eutectic or solid solution formation. Thus, no strong interaction between I and II exists.

The relevant fusion temperatures and heats of fusion (ΔH_f) for systems examined for their dissolution behavior are given in Table IV. It can be seen that the fusion temperatures are similar for coprecipitates and physical mixtures, but the heats of fusion differ. There is a gradual and uniform decrease in ΔH_f with coprecipitate compositions, whereas an abrupt decrease in ΔH_f occurs with the 19:1 physical mixture; it remains essentially constant for all other compositions.

The dissolution studies demonstrated that the dissolution of I from the 19:1 coprecipitate was nearly as dramatic as from other coprecipitates containing a larger fraction of II (Table I). Thus, the physical state of the 19:1 composition was studied in detail in order to gain an insight into the mechanisms of dissolution of these systems. Several possibilities exist which may account for the increased dissolution of I–II coprecipitates. Therefore, X-ray diffraction spectra were prepared to attempt to resolve some of these issues. Typical X-ray diffraction patterns of powdered samples of II, chloroform-treated I, and the 19:1 coprecipitate are shown in Fig. 3. The crystalline properties of I are characterized by two major and four minor peaks in the spectrum, whereas the II spectrum displays the properties of an amorphous material. The identifiable peaks of I are also visible in the spectrum of the 19:1 coprecipitate even though there appears that some broadening and loss of detail of the peaks has occurred. The positions of the diffraction peaks of I were not altered compared with that of the pure compound. Physical mixtures and 19:1 coprecipitates all exhibited the identifiable peaks of I in their spectra 2 h, 1 week, and 2 weeks after preparation although there were variations in the shapes and intensities of the peaks. These clearly indicate that I does not exhibit polymorphism, complex formation, eutectic, or solid solution formation with II in the coprecipitate.

DISCUSSION

When the solid dispersion system has been employed to formulate drugs having low water solubility, invariably the inert carrier is one which either undergoes rapid dissolution (*e.g.*, urea, polyethylene glycol, or polyvinylpyrrolidone) to increase the dissolution of the drug (14) or it is one which undergoes slow dispersion in aqueous media to provide sustained release [*e.g.*, tristearin, cholesterol, or cholesteryl ester (3, 7)]. If the lipid has significant surface activity [*e.g.*, cholesteryl stearate (3) or polyoxyl 40 stearate (4)] usually an increase in dissolution of drug due to wetting is observed. Solubilization of the drug during dissolution may also play a role (4). Phospholipids have not previously been employed to prepare solid dispersions of drugs. Yet these nontoxic agents have the ability to both increase the wetting of hydrophobic drug particles and to spontaneously disperse into colloidal aggregates, with the capacity to sequester substantial quantities of drug in lipidic or aqueous compartments.

The best solid dispersion systems from the point of view of rapid release of drug have been those containing large ratios of carrier to drug (15), although compositions high in drug content have been chosen in some instances as

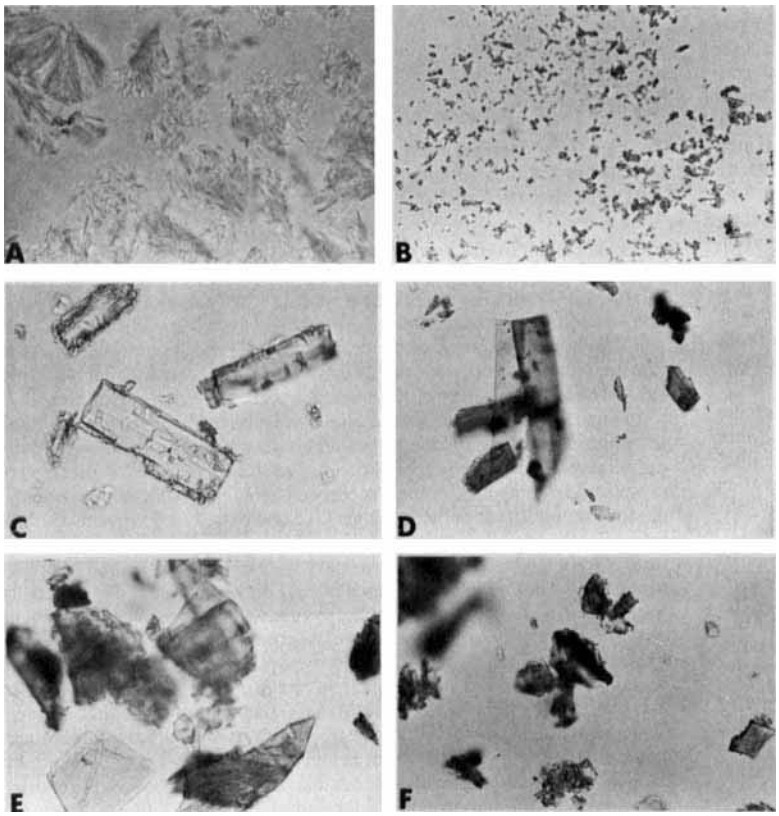

Figure 4—*Photomicrographs of various test samples dispersed in light mineral oil (320× magnification). Key: (A) untreated II; (B) untreated, micronized I; (C) chloroform-treated I; (D) 9:1 I–II coprecipitate; (E) 4:1 I–II coprecipitate; (F) 1.5:1 I–II coprecipitate.*

Table III—Effet of pH on the Dissolution of Coprecipitates of Griseofulvin and Dimyristoylphosphatidylcholine

Composition (Weight Ratio)	Initial Dissolution Rate, mg/L/min		Limiting Conc. After 60 min, mg/L	
	pH 2.0	pH 5.0	pH 2.0	pH 5.0
1:0	0.36	0.40	15.0	12.4
19:1	1.26	1.21	25.8	25.4
9:1	1.68	1.53	25.9	28.8
4:1	1.67	1.63	35.3	34.0
1.5:1	1.86	1.56	28.8	26.2

representing eutectic mixtures (16-18). However, it has now been demonstrated that high rates of dissolution are possible from coprecipitates with drug content as high as 95% using a phospholipid carrier. Furthermore, as the carrier content of the coprecipitate is increased, the IDR of I increases by a further 50%, while the apparent solubility of I at pH 2.0 (LDC) increases by a further 12%, following an 8-fold increase in the percentage of phospholipid in the sample (see Table I). Thus, unlike the griseofulvin-succinic acid solid dispersion (19), decreasing the carrier content, when it is phospholipid, does not necessarily result in the formation of larger crystals of I.

The X-ray diffraction spectra and the phase diagram for the I-II system clearly indicate the lack of any specific I-II interaction. This is substantiated by the observation that under the microscope crystals of I and I-II coprecipitates have approximately the same shape and size (Fig. 4C-F).

In view of the above discussion, there are two possible mechanisms which may be responsible for the greater dissolution behavior of coprecipitates than for pure drug or physical mixtures. In the first instance, it is reasonable to assume that on coprecipitation of I and II from chloroform, crystals are formed having mainly characteristics of chloroform-treated I, at least with medium to high I compositions. The chloroform solvate of I is an important factor in its physical state, as described earlier in the DTA results and previously by others (11, 12, 20). However, it would appear that the packing arrangement of the molecules in the coprecipitate crystal is different than in the absence of II, leading to a major change in the stabilization energy of the crystals. This packing arrangement would appear to be ideal for rapid release of I and its transfer from the solid state to the solution state. A good linear correlation was found between the percent of I dissolved and ΔH_f for coprecipitates ($r > 0.97$) at all dissolution times, but not with physical mixtures after 5 min. Furthermore, aging of the coprecipitates resulted in reduced dissolution rates, although X-ray diffraction patterns of aged samples were essentially unchanged. The dissolution behaviors of untreated micronized I, treated I, and aged treated I were essentially identical.

According to the film theory of dissolution (21) factors influencing the rate of dissolution include the diffusion coefficient, the stationary or diffusion layer thickness, the surface area, and the difference between the saturation concentration in the diffusion layer and the bulk solution concentration. Under identical conditions of dissolution testing for the same compositions of I-II, differences in dissolution behavior between coprecipitates and physical mixtures or pure drug are likely to originate from changes in the total surface area during the dissolution process and the diffusion layer concentration-bulk solution concentration difference at any given time. In the case of the coprecipitate, very fine crystallites of I may become available as the original crystals fracture and break up in the dissolution medium, thereby increasing the total surface area of I. The situation is obviously different with regard to the physical mixtures, where the phospholipid, which may not undergo rapid dispersion, provides very little wetting of the crystals of I and only a minor increase in the effective surface area. The result is a slight increase in the IDR as seen in Table I.

The solubilization effect in the diffusion layer surrounding the particles may be exerting the most substantial effect in the dissolution process. More specifically, it is the rapid, spontaneous dispersion of II into colloidal aggregates of phospholipid bilayers (liposomes) and the simultaneous incorporation

Table IV—Fusion Temperatures and Heats of Fusion of Griseofulvin and Griseofulvin-Dimyristoylphosphatidylcholine Compositions

Composition (Weight Ratio)	Fusion Temp., °C		ΔH_f, cal/g	
	Coprecipitates	Physical Mixtures	Coprecipitates	Physical Mixtures
1:0	221.8	221.8	28.4	28.4
19:1	219.0	219.3	25.7	19.7
9:1	217.0	218.8	24.0	19.6
4:1	217.4	216.0	20.8	19.3
1.5:1	215.3	214.5	18.2	20.5
0:1	67.9	67.9	17.1	17.1

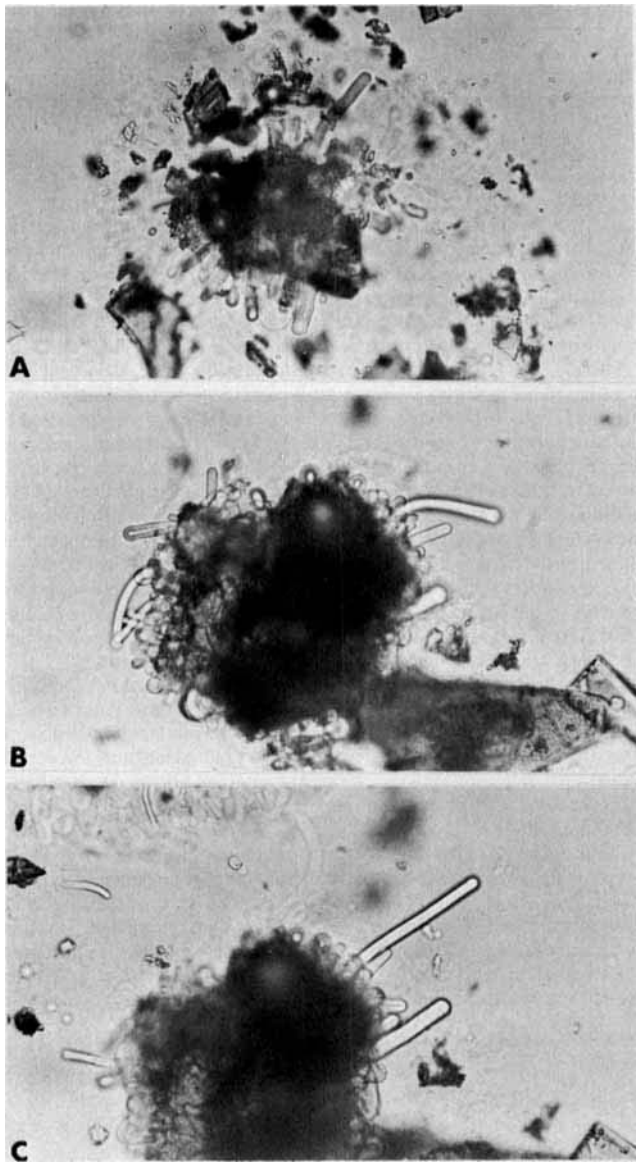

Figure 5—*Photomicrographs of 1.5:1 I-II coprecipitate crystals dispersed in water at various time periods after preparation (320× magnification) Key: (A) 2 min; (B) 3 min; (C) 5 min.*

of I molecules into this partitioning system that is analogous to an increase in the saturation concentration in the diffusion layer. In the case of physical mixtures, II is not in as desirable a physical state for spontaneous dispersion and, in addition, I molecules must be dissociated from the solid state by solvent and then become sequestered by the liposomes. The vigorous agitation of the dissolution medium coupled with its large volume decrease the chances of any substantial sequestering of I molecules adjacent to the particle surfaces.

In an attempt to determine the validity of this reasoning, microscopic observation of coprecipitate crystals undergoing dissolution in water was carried out. Figure 5 shows a sequence of photomicrographs of a 1.5:1 coprecipitate sample undergoing dissolution. As early as 2 min following mixing, it is apparent that multitudes of long, finger-like bodies (myelinic structures) had formed at the crystal surfaces. These could be seen as growing and extending further outward into the medium as part of a rapid, dynamic process of dispersion and what may be considered as part of the process of dissolution. It was interesting to note that a similar picture was observed when a physical mixture was examined, but the formation and dispersal of the myelinic structures was much slower. Although these observations are based on what must be considered as a static system, in relative terms, it demonstrates that phospholipids can play a role in solid dispersion formulations that is much different than that observed with other lipids or surfactants. Studies are continuing along these lines to determine the potential of phospholipids in developing formulations which have the dual roles of controlled release of drug and bioavailability improvement following oral administration.

REFERENCES

(1) D. C. Bloedow and W. L. Hayton, *J. Pharm. Sci.*, **65**, 328 (1976).
(2) K. Taniguchi, S. Muranishi, and H. Sezaki, *Int. J. Pharm.*, **4**, 219 (1980).
(3) K. H. Kim and C. I. Jarowski, *J. Pharm. Sci.*, **66**, 1536 (1977).
(4) R. Kaur, D. J. W. Grant, and T. Eaves, *J. Pharm. Sci.*, **69**, 1321 (1980).
(5) J. A. Grisafe and W. L. Hayton, *J. Pharm. Sci.*, **67**, 895 (1978).
(6) S. P. Patel and C. I. Jarowski, *J. Pharm. Sci.*, **64**, 869 (1975).
(7) K. S. Chang and C. I. Jarowski, *J. Pharm. Sci.*, **69**, 466 (1980).
(8) H. J. Borchart and F. Daniels, *J. Am. Chem. Soc.*, **79**, 41 (1957).
(9) A. C. Shah, C. B. Peot, and J. F. Ochs, *J. Pharm. Sci.*, **62**, 671 (1973).
(10) J. C. Wallach, *Pharm. Tech. Int.*, **3**, 34 (1980).
(11) M. Mayersohn and M. Gilbaldi, *J. Pharm. Sci.*, **55**, 1323 (1966).
(12) K. C. Cheng, E. Shefter, and T. Srikrishnan, *Int. J. Pharm.*, **2**, 81 (1979).
(13) R. Kaur, D. J. W. Grant, and T. Eaves, *J. Pharm. Sci.*, **69**, 1317 (1980).
(14) W. L. Chiou and S. Riegelman, *J. Pharm. Sci.*, **60**, 1281 (1971).
(15) A. P. Simonelli, S. C. Mehta, and W. I. Higuchi, *J. Pharm. Sci.*, **58**, 538 (1969).
(16) K. Sekiguchi, N. Obi, and Y. Ueda, *Chem. Pharm. Bull.*, **12**, 134 (1964).
(17) W. L. Chiou, *J. Pharm. Sci.*, **60**, 1406 (1971).
(18) J. A. Rogers and A. J. Anderson, *Pharm. Acta. Helv.*, **10–11**, 276 (1982).
(19) W. L. Chiou, *J. Pharm. Sci.*, **66**, 989 (1977).
(20) K. Sekiguchi, I. Horikoshi, and I. Himuro, *Chem. Pharm. Bull.*, **16**, 2495 (1968).
(21) J. T. Carstensen, in "Dissolution Technology," L. G. Leeson and J. T. Carstensen, Eds., Academy of Pharmaceutical Sciences, Washington, D.C., 1974, pp 1–28.

ACKNOWLEDGMENTS

Presented to the Basic Pharmaceutics Section at the 33rd National Meeting of the APhA Academy of Pharmaceutical Sciences, San Diego, Calif., November 1982.

The award of an Alberta Heritage Foundation for Medical Research Studentship to S.V. is greatly appreciated. A gift of griseofulvin from Glaxo Canada Ltd. is kindly acknowledged. The X-ray diffraction spectra were carried out in the Department of Mineral Engineering, University of Alberta, with the generous cooperation of Dr. S. Bradford and the expert technical assistance of Mrs. T. Parker.

Model-Independent Steady-State Plasma Level Predictions in Autonomic Nonlinear Pharmacokinetics I: Derivation and Theoretical Analysis

PETER VENG-PEDERSEN

Received January 17, 1983, from the *Divison of Pharmacokinetics, School of Pharmacy and Pharmacal Sciences, Purdue University, West Lafayette, IN 47907.* Accepted for publication May 21, 1983.

Abstract □ Current drug level predictions in nonlinear pharmacokinetics are based on specific pharmacokinetic models in contrast to the model-independent (structureless), dose-linearity, and superposition principles used in linear pharmacokinetics. Such model-dependent methods may not provide reliable predictions due to their inherent nonuniqueness, computational complexity, and often unrealistic kinetic assumptions. Some novel model-independent methods for predicting the steady-state drug levels of extravascular, intravenous bolus, and intravenous infusion administrations are presented that should overcome such disadvantages. The methods only assume an autonomic nonlinear kinetic behavior, which implies that following an intravenous bolus administration the derivatives of the drug concentration–time profile at arbitrary drug levels are independent of the dose given. Such a kinetic behavior is found for any nonlinear pharmacokinetic system when the rate of change of the drug level following an intravenous bolus administrations depends only on the drug level, *i.e.*, $dC/dt = -q(C)$, where q can be any function dependent only on C and time-invariant kinetic parameters. The basic approach presented represents a novel alternative which avoids the very difficult and often impractical task of identifying and incorporating the numerous kinetic parameters and processes responsible for the observed drug concentration data into a useful pharmacokinetic model. The focus in the kinetic analysis is instead on two much simpler processes: (*a*) fitting empirical functions to estimate the mean drug disposition behavior of the subject or population and (*b*) testing the validity of the assumptions involved.

Keyphrases □ Pharmacokinetics—nonlinear, model independent, steady-state plasma drug-level predictions, theory and mathematical models □ Plasma drug levels—prediction at steady state, model-independent nonlinear pharmacokinetics, theory and mathematical models

Steady-state plasma level predictions in linear pharmacokinetics are done by extrapolations using the dose-linearity and superposition principles or by using the convolution property of linear pharmacokinetics. The plasma level profiles used for the predictions are most commonly determined by fitting suitable model-independent[1] equations, typically of an exponential type, to available plasma level data. Such model-independent methods cannot be used for drugs showing nonlinear pharmacokinetics because the superposition and dose-linearity principles do not apply. Consequently, drug level predictions in nonlinear pharmacokinetics have been based on model-dependent methods, which may not provide reliable predictions due to their inherent nonuniqueness, computational complexity, and often unrealistic model assumptions. A model-independent approach is presented which overcomes some of these disadvantages.

THEORETICAL

The proposed methodology applies to drugs showing what will be called *autonomic nonlinear pharmacokinetics; i.e.*, the drug-concentration profile resulting from an intravenous bolus dose adheres to the autonomic differential equation:

$$\frac{dC}{dt} = -q(C) \qquad \text{(Eq. 1)}$$

where q stands for any function only dependent on the drug concentration C and time-invariant kinetic parameters. It is assumed that q is such that the solution of Eq. 1, $C(t)$, is monotonically decreasing with time. Autonomic nonlinear pharmacokinetics is readily identified in a model-independent manner from "the horizontal superposition property" (Fig. 1). Different intravenous bolus doses result in drug-concentration profiles with identical slopes

[1] The terminology "model-independent" is used here to denote a general approach not based on a specific structured (model-dependent) kinetic analysis of the individual kinetic components of the pharmacokinetics.

0022-3549/84/0600-0761$01.00/0

© 1984, American Pharmaceutical Association

REFERENCES

(1) D. C. Bloedow and W. L. Hayton, *J. Pharm. Sci.*, **65**, 328 (1976).
(2) K. Taniguchi, S. Muranishi, and H. Sezaki, *Int. J. Pharm.*, **4**, 219 (1980).
(3) K. H. Kim and C. I. Jarowski, *J. Pharm. Sci.*, **66**, 1536 (1977).
(4) R. Kaur, D. J. W. Grant, and T. Eaves, *J. Pharm. Sci.*, **69**, 1321 (1980).
(5) J. A. Grisafe and W. L. Hayton, *J. Pharm. Sci.*, **67**, 895 (1978).
(6) S. P. Patel and C. I. Jarowski, *J. Pharm. Sci.*, **64**, 869 (1975).
(7) K. S. Chang and C. I. Jarowski, *J. Pharm. Sci.*, **69**, 466 (1980).
(8) H. J. Borchart and F. Daniels, *J. Am. Chem. Soc.*, **79**, 41 (1957).
(9) A. C. Shah, C. B. Peot, and J. F. Ochs, *J. Pharm. Sci.*, **62**, 671 (1973).
(10) J. C. Wallach, *Pharm. Tech. Int.*, **3**, 34 (1980).
(11) M. Mayersohn and M. Gilbaldi, *J. Pharm. Sci.*, **55**, 1323 (1966).
(12) K. C. Cheng, E. Shefter, and T. Srikrishnan, *Int. J. Pharm.*, **2**, 81 (1979).
(13) R. Kaur, D. J. W. Grant, and T. Eaves, *J. Pharm. Sci.*, **69**, 1317 (1980).
(14) W. L. Chiou and S. Riegelman, *J. Pharm. Sci.*, **60**, 1281 (1971).
(15) A. P. Simonelli, S. C. Mehta, and W. I. Higuchi, *J. Pharm. Sci.*, **58**, 538 (1969).
(16) K. Sekiguchi, N. Obi, and Y. Ueda, *Chem. Pharm. Bull.*, **12**, 134 (1964).
(17) W. L. Chiou, *J. Pharm. Sci.*, **60**, 1406 (1971).
(18) J. A. Rogers and A. J. Anderson, *Pharm. Acta. Helv.*, **10–11**, 276 (1982).
(19) W. L. Chiou, *J. Pharm. Sci.*, **66**, 989 (1977).
(20) K. Sekiguchi, I. Horikoshi, and I. Himuro, *Chem. Pharm. Bull.*, **16**, 2495 (1968).
(21) J. T. Carstensen, in "Dissolution Technology," L. G. Leeson and J. T. Carstensen, Eds., Academy of Pharmaceutical Sciences, Washington, D.C., 1974, pp 1–28.

ACKNOWLEDGMENTS

Presented to the Basic Pharmaceutics Section at the 33rd National Meeting of the APhA Academy of Pharmaceutical Sciences, San Diego, Calif., November 1982.

The award of an Alberta Heritage Foundation for Medical Research Studentship to S.V. is greatly appreciated. A gift of griseofulvin from Glaxo Canada Ltd. is kindly acknowledged. The X-ray diffraction spectra were carried out in the Department of Mineral Engineering, University of Alberta, with the generous cooperation of Dr. S. Bradford and the expert technical assistance of Mrs. T. Parker.

Model-Independent Steady-State Plasma Level Predictions in Autonomic Nonlinear Pharmacokinetics I: Derivation and Theoretical Analysis

PETER VENG-PEDERSEN

Received January 17, 1983, from the *Divison of Pharmacokinetics, School of Pharmacy and Pharmacal Sciences, Purdue University, West Lafayette, IN 47907.* Accepted for publication May 21, 1983.

Abstract □ Current drug level predictions in nonlinear pharmacokinetics are based on specific pharmacokinetic models in contrast to the model-independent (structureless), dose-linearity, and superposition principles used in linear pharmacokinetics. Such model-dependent methods may not provide reliable predictions due to their inherent nonuniqueness, computational complexity, and often unrealistic kinetic assumptions. Some novel model-independent methods for predicting the steady-state drug levels of extravascular, intravenous bolus, and intravenous infusion administrations are presented that should overcome such disadvantages. The methods only assume an autonomic nonlinear kinetic behavior, which implies that following an intravenous bolus administration the derivatives of the drug concentration–time profile at arbitrary drug levels are independent of the dose given. Such a kinetic behavior is found for any nonlinear pharmacokinetic system when the rate of change of the drug level following an intravenous bolus administrations depends only on the drug level, *i.e.*, $dC/dt = -q(C)$, where q can be any function dependent only on C and time-invariant kinetic parameters. The basic approach presented represents a novel alternative which avoids the very difficult and often impractical task of identifying and incorporating the numerous kinetic parameters and processes responsible for the observed drug concentration data into a useful pharmacokinetic model. The focus in the kinetic analysis is instead on two much simpler processes: (*a*) fitting empirical functions to estimate the mean drug disposition behavior of the subject or population and (*b*) testing the validity of the assumptions involved.

Keyphrases □ Pharmacokinetics—nonlinear, model independent, steady-state plasma drug-level predictions, theory and mathematical models □ Plasma drug levels—prediction at steady state, model-independent nonlinear pharmacokinetics, theory and mathematical models

Steady-state plasma level predictions in linear pharmacokinetics are done by extrapolations using the dose-linearity and superposition principles or by using the convolution property of linear pharmacokinetics. The plasma level profiles used for the predictions are most commonly determined by fitting suitable model-independent[1] equations, typically of an exponential type, to available plasma level data. Such model-independent methods cannot be used for drugs showing nonlinear pharmacokinetics because the superposition and dose-linearity principles do not apply. Consequently, drug level predictions in nonlinear pharmacokinetics have been based on model-dependent methods, which may not provide reliable predictions due to their inherent nonuniqueness, computational complexity, and often unrealistic model assumptions. A model-independent approach is presented which overcomes some of these disadvantages.

THEORETICAL

The proposed methodology applies to drugs showing what will be called *autonomic nonlinear pharmacokinetics; i.e.*, the drug-concentration profile resulting from an intravenous bolus dose adheres to the autonomic differential equation:

$$\frac{dC}{dt} = -q(C) \qquad \text{(Eq. 1)}$$

where q stands for any function only dependent on the drug concentration C and time-invariant kinetic parameters. It is assumed that q is such that the solution of Eq. 1, $C(t)$, is monotonically decreasing with time. Autonomic nonlinear pharmacokinetics is readily identified in a model-independent manner from "the horizontal superposition property" (Fig. 1). Different intravenous bolus doses result in drug-concentration profiles with identical slopes

[1] The terminology "model-independent" is used here to denote a general approach not based on a specific structured (model-dependent) kinetic analysis of the individual kinetic components of the pharmacokinetics.

0022-3549/84/0600-0761$01.00/0

© 1984, American Pharmaceutical Association

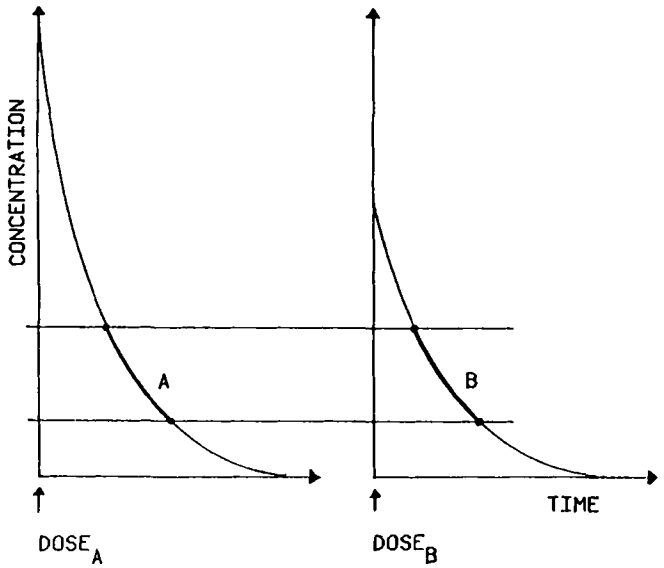

Figure 1—*Illustration of the horizontal superposition property of autonomic nonlinear pharmacokinetics (A = B), which is characterized by an intravenous bolus disposition behavior that follows to the general autonomic differential equation (Eq. 1).*

at the same concentration levels. Thus, a horizontal shift of the curves will result in their exact superposition (Fig. 1). For example, a parallel first-order and Michaelis–Menten elimination:

$$\frac{dC}{dt} = -KC - \frac{V_m C}{K_m + C} \qquad \text{(Eq. 2)}$$

will result in this behavior; so will any pharmacokinetic system incorporating nonlinear binding, excretion, metabolism, *etc.*, as long as the kinetics can be described in the general form of Eq. 1. However, due to the model-independent nature of the method proposed, there is no need to postulate a specific kinetic relationship.

The most studied nonlinear drug, phenytoin, appears quite consistent to show autonomic disposition kinetics (1). The fall-off curves studied for 10 subjects for a period of 4 consecutive days after different daily doses of phenytoin were discontinued seem to agree well with Eq. 1 (1). Other examples of the horizontal shift and the superposition concept include the pharmacokinetics of alcohol (2).

Steady-State Prediction of Extravascular Dosing—In linear pharmacokinetics, steady-state predictions can be made solely from a single dose, without using the information about the basic disposition of the drug provided by an intravenous drug administration. For example, if data from a single extravascular dose is well approximated by a sum of exponentials:

$$C(t) = \sum_{i=1}^{m} A_i e^{-\alpha_i t} \qquad \text{(Eq. 3)}$$

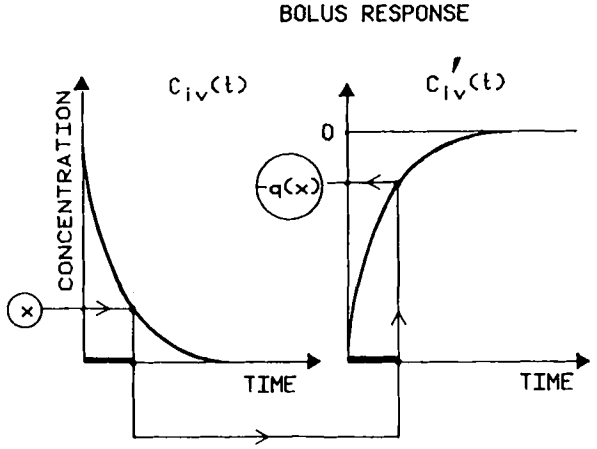

Figure 2—*Empirical evaluation of the disposition function* q *(Eq. 1) according to Eq. 9. The function* $C_{iv}(t)$ *denotes a suitable, monotonically decreasing function fitted to data from an intravenous bolus injection;* $C'_{iv} = dC_{iv}(t)/dt$.

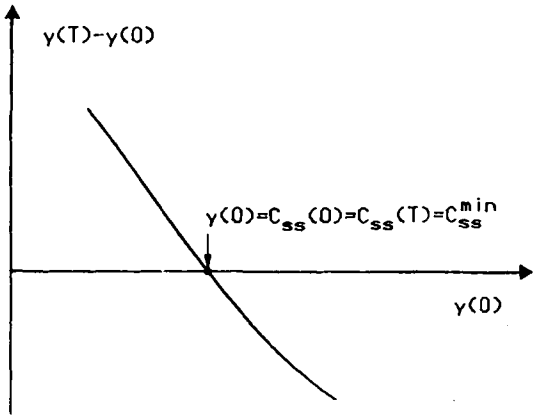

Figure 3—*Boundary value behavior of Eq. 14 (Eq. 13 simplified). An initial value for* y(0) *is chosen and improved by an iterative procedure until the corresponding* y(T) *value, obtained by numerical integration of Eq. 14, is the same as* y(0), *in which case the steady-state solution* $C_{ss}(t) = y(t)$ *is obtained.*

where $\Sigma A_i = 0$, then the steady state can be predicted by:

$$C_{ss}(t) = \sum_{i=1}^{n} \frac{A_i e^{-\alpha_i t}}{1 - e^{-\alpha_i T}} \qquad \text{(Eq. 4)}$$

where T is the dosing interval.

To make predictions in nonlinear pharmacokinetics in a model-independent way, it is, contrary to the linear case above, always necessary to have data available from a known intravenous administration to evaluate and properly account for the basic disposition behavior[2]. In the present case, data from an intravenous administration are used to empirically determine the functional behavior of the disposition function q (Eq. 1) without knowing its functional (algebraic) form. This is done as follows. Let $C_{iv}(t)$ denote a suitable monotonically decreasing equation that fits the intravenous bolus data well (*e.g.*, by least-squares regression):

$$C = C_{iv}(t) \qquad \text{(Eq. 5)}$$

then:

$$\frac{dC}{dt} = dC_{iv}(t)/dt = C'_{iv}(t) \qquad \text{(Eq. 6)}$$

Since $C_{iv}(t)$ is monotonically decreasing its inverse $C_{iv}^{-1}(C)$ exists, and can be found algebraically or numerically:

$$t = C_{iv}^{-1}(C) \qquad \text{(Eq. 7)}$$

Substituting Eq. 7 into Eq. 6 gives:

$$\frac{dC}{dt} = C'_{iv}[C_{iv}^{-1}(C)] \qquad \text{(Eq. 8)}$$

Comparing Eqs. 8 and 1, it is seen that the disposition function q can be evaluated empirically from the function $C_{iv}(t)$ fitted to the intravenous bolus data:

$$q(x) = -C'_{iv}[C_{iv}^{-1}(x)] \qquad \text{(Eq. 9)}$$

The simple evaluation of $q(x)$ is illustrated graphically in Fig. 2.

Consider now a single extravascular dosing, which results in some arbitrary systemic drug input $f(t)$ (mass/time). The differential equation relating to this input is:

$$\frac{dC}{dt} = -q(C) + \frac{f(t)}{v} \qquad \text{(Eq. 10)}$$

where v is a constant of dimension volume. Let $C_f(t)$ denote a suitable arbitrary equation that fits the data from the extravascular dosing well, then $C_f(t)$ should satisfy Eq. 10 to give:

$$f(t) = v[q(C_f(t)) + C'_f(t)] \qquad \text{(Eq. 11)}$$

[2] This may seem as a disadvantage in comparison with the model-dependent methods, where such predictions can be made without this additional information. However, such predictions will be highly inaccurate and unreliable because the disposition parameters in such models are allowed to "float" in an unconstrained way in the curve fitting. There is only hope for reasonable predictions if additional data from an intravenous administration are available, so the disposition parameters can be estimated without the confounding interference from the absorption process.

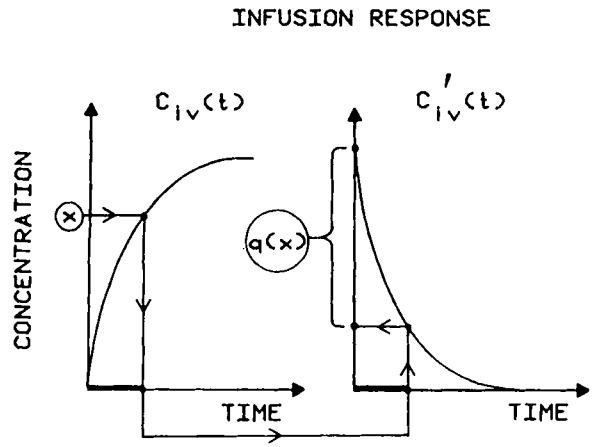

Figure 4—*Empirical evaluation of the disposition function* q *(Eq. 1) according to Eq. 17. The function* $C_{iv}(t)$ *denotes a suitable monotonically increasing function fitted to data from a constant-rate intravenous infusion;* $C'_{iv}(t) = dC_{iv}(t)/dt$.

Consider next the same extravascular dose given to the same subject at regular dosing intervals, T. Let the following assumptions be made:

1. The drug disposition kinetics do not change (kinetic parameters of q are time invariant).
2. The drug absorption $f(t)$ from each dose is reproducible.
3. The drug is absorbed quickly enough in comparison with the dosing interval T, so that the absorption is completed before a new dose is given.

The steady-state drug level profile will, under these assumptions, follow Eq. 10:

$$\frac{dC_{ss}}{dt} = -q(C_{ss}) + \frac{f(t)}{v} \qquad \text{(Eq. 12)}$$

The drug absorption is assumed reproducible; thus, $f(t)$ in Eq. 12 can be substituted with the expression in Eq. 11 to give:

$$\frac{dC_{ss}}{dt} = -q(C_{ss}) + q[C_f(t)] + C'_f(t) \qquad \text{(Eq. 13)}$$

Equation 13 is the final differential equation from which the steady-state drug level profile $C_{ss}(t)$ can be calculated, when data from a single extravascular dose are available in addition to data from an intravenous bolus administration. Mathematically $C_{ss}(t)$ is the solution, $y(t)$, to a boundary value problem, which can be stated in its most simplified form as follows. Find the particular solution $y(t)$ of the differential equation:

$$\frac{dy}{dt} = -q(y) + g(t) \qquad \text{(Eq. 14)}$$

which satisfies the boundary condition:

$$y(0) = y(T) \qquad \text{(Eq. 15)}$$

Equation 14, which is a simplified restatement of Eq. 13, is recognized as a simple first-order differential equation which can be integrated numerically using a suitable algorithm[3]. The initial value $y(0)$ of Eq. 14 is unknown. An initial estimate for $y(0)$ is therefore required as a tentative solution which can be improved in an iterative manner as follows. Integration of Eq. 14 (from $t = 0$ to tT) produces a $y(T)$ corresponding to the current $y(0)$. If $y(T) > y(0)$, then $y(0)$ is too small and must be increased in the next iteration. Similarly if $y(T) < y(0)$, then $y(0)$ should be decreased in the next iteration. The $y(0) - y(T)$ *versus* $y(0)$ relationship is sketched in Fig. 3. The above so-called "shooting method" is a standard approach to solve nonlinear boundary value problems and is easily implemented on a computer. When the process converges, *i.e.*, $y(0) = y(T)$, then the steady-state profile $C_{ss}(t) = y(t)$ is given by the integration of Eq. 14 in the last iteration. The steady-state minimum and maximum levels are simple "by-products" of the process; *i.e.*, $C_{ss}^{min} = y(0) = y(T)$ and C_{ss}^{max} is the maximum value of $y(t)$ reached in the last integration. The mean steady-state level can readily be calculated by integrating the $y(t)$ points (*e.g.*, using a trapezoidal or log-trapezoidal rule) and dividing the area by the dosing interval (4):

$$\bar{C}_{ss} = \int_0^T y(t)dt/T \qquad \text{(Eq. 16)}$$

[3] A Runge-Kutta method (3) appears to be a suitable first choice because of its simplicity and economical evaluation. However, it must be expected that in some cases Eq. 14 may be numerically unstable in the integration region (which varies during the boundary value iterations), in which case the Runge-Kutta method is inaccurate. This inaccuracy can readily be detected by comparing the integration results to those obtained using a substantially smaller (*e.g.*, 1/10) step size. In such cases, it is necessary to switch to a more elaborate and accurate multistep predictor-corrector type algorithm (3).

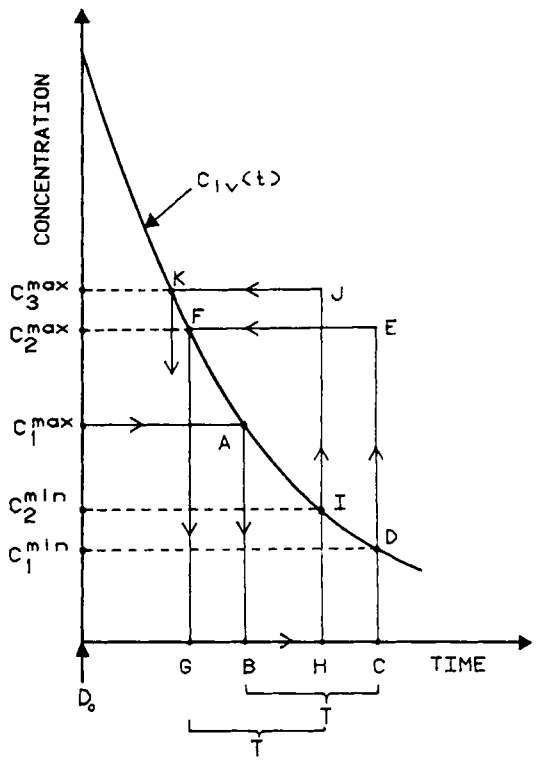

Figure 5—*Hysteresis iteration method (Eqs. 19–24) to predict peak and trough plasma levels in multiple intravenous bolus dosing. The steady-state drug level is reached at convergence when* $C_{n+1}^{max} \simeq C_n^{max}$ *and* $C_{n+1}^{min} \simeq C_n^{min}$. *The function* $C_{iv}(t)$ *denotes a suitable monotonically decreasing function fitted to data from an intravenous bolus administration, and* T *is the dosing period.*

In summary, the steps required to predict the steady-state plasma levels are:

1. Suitable arbitrary equations $C_{iv}(t)$ and $C_f(t)$ are fitted to data from a single intravenous bolus and extravascular (*e.g.*, oral) administration, respectively.
2. The intravenous bolus response approximation, $C_{iv}(t)$, and the absorption response approximation, $C_f(t)$, are differentiated algebraically to define $C'_{iv}(t)$ and $C'_f(t)$.
3. An initial estimate for $y(0)$ is chosen (*e.g.*, zero) and Eq. 14 (*i.e.*, Eq. 13) is integrated repeatedly in an iterative manner that improves the $y(0)$ value until it closely agrees with its corresponding $y(T)$ value. When converged the steady-state drug level is given by the integrated equation, $C_{ss}(t) = y(t)$.

Not all drugs can be given by an intravenous bolus administration due to excessive side effects resulting from a too rapid systemic input. However, Eq. 13 can still be applied if the drug in question can be administered by a constant-rate intravenous infusion. In this case it can be shown (Appendix I) that the disposition function q in Eq. 13 can be evaluated empirically according to:

$$q(x) = C'_{iv}(0) - C'_{iv}[C_{iv}^{-1}(x)] \qquad \text{(Eq. 17)}$$

where C_{iv} (contrary to C_{iv} in Eq. 8) is an arbitrary monotonically increasing function which provides a good fit to the data from the constant-rate drug infusion. The evaluation of $q(x)$ in this case is illustrated graphically in Fig. 4.

A simple precaution must be taken in the initial ($t = 0$) evaluation of q during the numerical integration of Eq. 14 (Eq. 13). An evaluation of $q(0)$ according to Eq. 9 may cause floating point overflow. For example, if a monotonically decreasing function $C_{iv}(t)$ which asymptotically approaches zero for $t \to \infty$ has been chosen for the intravenous bolus approximation, then $C_{iv}^{-1}(x) \to \infty$ for $x \to 0$ and $C_{iv}^{-1}(0)$ is not defined. Thus, $q(0)$ cannot be evaluated according to Eq. 9 in this case. However, by setting $q(0) = 0$ (see Appendix I) the problem is readily solved. Subsequent evaluations of $q(x)$ for $x > 0$ should not cause any numerical problems.

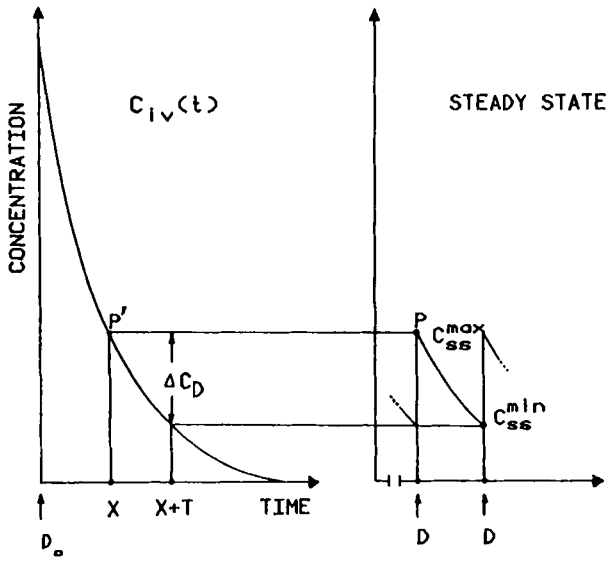

Figure 6—*Solution configuration of the root-solving method (Eq. 30) to determine the steady-state peak and trough drug levels in intravenous bolus administration. The function $C_{iv}(t)$ denotes a suitable, monotonically decreasing function fitted to data from an intravenous bolus administration, and T is the dosing period.*

The evaluation of the inverse $C_{iv}(t)$ function (Eq. 7) is done in a straightforward manner by numerically finding the root, t, of the expression:

$$C - C_{iv}(t) = 0 \qquad \text{(Eq. 18)}$$

for given values of C, where $C_{iv}(t)$ is the function previously fitted to the data from the intravenous drug administration. Most scientific computer program libraries (5-7) and many books dealing with numerical analysis (3, 8) have general programs for finding the root of an arbitrary nonlinear equation, suitable for solving Eq. 18 in a routine manner. The same root-finding algorithm used to solve Eq. 18 can also be used in the "shooting method" to find the root of the boundary value function (Fig. 3).

It is evident from Eq. 13 that in order to calculate the steady-state drug levels, the single-dose response function $C_f(t)$ only needs to be evaluated in the time interval $t = 0$ to $t = T$. This is a definite advantage, since the difficult problem of evaluating or extrapolating $C_f(t)$ beyond $t = T$ is avoided. This would not be the case for a method that makes use of area under the curve (AUC) or total clearance.

Steady-State Prediction of Intravenous Bolus Dosing—The following derivation shows how the plasma level profile in any drug interval in multiple dosing can be predicted from data from a single intravenous bolus dosing. Let $C_{iv}(t)$ denote an arbitrary monotonically decreasing function that provides a good fit to data from an intravenous bolus dose D_0. If after the drug is eliminated the same subject is given an intravenous bolus dose D every T hours,

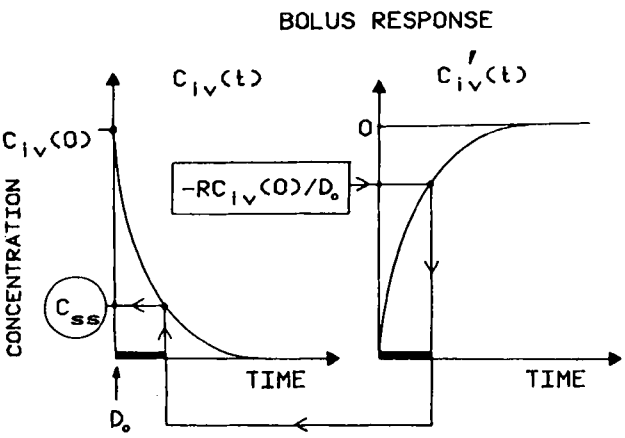

Figure 7—*Method to predict the steady-state drug level, C_{ss}, resulting from a constant rate, R, drug infusion. The prediction is done according to Eq. 36 on the basis of data from an intravenous bolus (D_0) administration. The function $C_{iv}(t)$ denotes a suitable monotonically decreasing function fitted to the intravenous bolus data; $C'_{iv}(t) = dC_{iv}(t)/dt$.*

then the predicted initial concentration C^{max} will be $DC_{iv}(0)/D_0$ if it is assumed that the autonomic nonlinear pharmacokinetics show a dose-linear initial behavior. This appears a reasonable assumption, since the nonlinearity is more likely to be due to secretion and metabolic processes than to the initial distribution.

The decline in the drug level from C_1^{max} will, due to the horizontal superposition property (Fig. 1), follow the $C_{iv}(t)$ curve. Thus, if point A in Fig. 5 is the point on the $C_{iv}(t)$ curve at the C_1^{max} level, then the first dosing profile is predicted by the curve segment AD which stretches over T hours (BC, Fig. 5). When the second dose is given at point D, then the drug level rises to point E where ED = AB = C_1^{max} (Fig. 5). Point E (C_2^{max}) is projected to point F on the $C_{iv}(t)$ curve. Point F now becomes the new point replacing the original point A and the same procedure is iterated, *i.e.*, GH = T hours, I = C_2^{min}, J = C_3^{max}, *etc.*

The peak and trough levels C_n^{max} and C_n^{min} ($n = 1, 2, \ldots$) can quickly be predicted graphically according to this hysteresis iteration method. However, it is more accurate to evaluate these quantities on a computer according to the corresponding algorithm, specified by Eqs. 19-24:

$$C_1^{max} = DC_{iv}(0)/D_0 \qquad \text{(Eq. 19)}$$

$$n = 1 \qquad \text{(Eq. 20)}$$

$$t = C_{iv}^{-1}(C_n^{max}) + T \qquad \text{(Eq. 21)}$$

$$C_n^{min} = C_{iv}(t) \qquad \text{(Eq. 22)}$$

$$n = n + 1 \qquad \text{(Eq. 23)}$$

$$C_n^{max} = C_{n-1}^{min} + C_1^{max} \qquad \text{(Eq. 24)}$$

The peak and trough levels are obtained sequentially when iterating Eqs. 21-24 as indicated. The iterations will eventually converge such that $C_{n+1}^{max} \simeq C_n^{max}$ and $C_{n+1}^{min} \simeq C_n^{min}$, in which case, by definition, the steady-state drug level profile has been reached. The mean steady-state drug level can subsequently be calculated from:

$$\bar{C}_{ss} = \int_{t-T}^{t} C_{iv}(u)du/T \qquad \text{(Eq. 25)}$$

where t in Eq. 25 is the t value calculated in Eq. 21 at convergence.

The steady-state drug levels can be calculated more directly without having to evaluate the inverse $C_{iv}(t)$ function (Eq. 21) according to the following alternative method. The peak level at steady state is equal to the trough level plus the concentration increment ΔC_D resulting from the dose injected at the end of the dosing interval:

$$C_{ss}^{max} = C_{ss}^{min} + \Delta C_D \qquad \text{(Eq. 26)}$$

As previously discussed, it is assumed that the pharmacokinetics show a dose-linear initial value behavior, so that ΔC_D is proportional to the dose:

$$\Delta C_D = D/V \qquad \text{(Eq. 27)}$$

Equation 26 can, as illustrated in Fig. 6, be transformed into an equivalent expression involving C_{iv}:

$$C_{iv}(X) = C_{iv}(X + T) + \Delta C_D \qquad \text{(Eq. 28)}$$

The proportionality term V in Eq. 27 is given by:

$$V = D_0/C_{iv}(0) \qquad \text{(Eq. 29)}$$

Combining Eqs. 27-29 yields the expression:

$$C_{iv}(X + T) + \frac{D}{D_0} C_{iv}(0) - C_{iv}(X) = 0 \qquad \text{(Eq. 30)}$$

Solving Eq. 30 for X numerically using any suitable general purpose root-finding program will subsequently give the steady-state peak, trough, and mean drug levels:

$$C_{ss}^{max} = C_{iv}(X) \qquad \text{(Eq. 31)}$$

$$C_{ss}^{min} = C_{iv}(X + T) \qquad \text{(Eq. 32)}$$

$$\bar{C}_{ss} = \int_{X}^{X+T} C_{iv}(u)du/T \qquad \text{(Eq. 33)}$$

The root-solving method (Eq. 30) is the most suitable because of its simplicity when the primary interest is to predict the steady-state quantities $\bar{C}_{ss}$, C_{ss}^{max}, and C_{ss}^{min}. However, if additionally it is desirable to evaluate how long (nT) it will take to reach 90% of steady state, then the hysteresis iteration method (Eqs. 19-24) must be used.

Steady-State Prediction of Constant-Rate Infusion—The differential

equation describing the drug level profile resulting from a constant-rate (R) intravenous infusion is given by Eq. 1A (see Appendix I). At steady state, $dC/dt = 0$, in which case Eqs. 1A and 29 give:

$$q(C_{ss}) = RC_{iv}(0)/D_0 \qquad \text{(Eq. 34)}$$

Let $q^{-1}(x)$ denote the inverse of the disposition function; then, the steady-state level is obtained by inversion of Eq. 34:

$$C_{ss} = q^{-1}(RC_{iv}(0)/D_0) \qquad \text{(Eq. 35)}$$

The problem is now to evaluate the $q^{-1}(x)$ function, which is best illustrated graphically as "q evaluated in reverse." If $-q(x)$ in Fig. 2 is set equal to $-RC_{iv}(0)/D_0$, then x will be $q^{-1}(RC_{iv}(0)/D_0)$, *i.e.*, x will be C_{ss} (Eq. 35). From this it is seen (Fig. 2) that:

$$C_{ss} = C_{iv}\,[C_{iv}^{-1}(-RC_{iv}(0)/D_0)] \qquad \text{(Eq. 36)}$$

where $C_{iv}^{-1}(\ )$ denotes the inverse of the $C_{iv}'(\ )$ function. Equation 36 enables the steady-state drug level resulting from a constant-rate (R) drug infusion to be predicted in a model-independent manner when data from an intravenous bolus dose (D_0) are available. The procedure is simply:

1. A suitable monotonically decreasing function $C_{iv}(t)$ is fitted (*e.g.*, by least-squares technique) to the intravenous bolus data to appropriately approximate the bolus response.
2. The function is differentiated to give $C_{iv}'(t)$.
3. The predicted steady-state drug level is calculated according to Eq. 36.

The evaluation procedure is graphically illustrated in Fig. 7. The evaluation of the inverse of $C_{iv}'(t)$ (Fig. 7) can be done readily in the same way as the inverse of $C_{iv}(t)$, as previously discussed (Eq. 18).

DISCUSSION

The above derivations and theoretical analysis have shown how steady-state predictions can be made for extravascular, intravenous bolus, and intravenous infusion administrations for drugs showing autonomic nonlinear pharmacokinetics. The methodology is certainly not a general solution to the very difficult prediction problems in nonlinear pharmacokinetics. However, the methodology does seem appealing because it is model independent and requires few assumptions, which can be tested readily (*e.g.*, the horizontal superposition property, Fig. 1). It represents a novel alternative that appears less academic and more practical than the model-dependent methods with their often unrealistic kinetic assumptions and computational complexity. The methodology avoids the very difficult and often impractical task of identifying and incorporating the numerous kinetic parameters and processes responsible for the observed drug concentration data into a useful mathematical model. The focus in the kinetic analysis is instead on two much simpler processes: (*a*) fitting empirical functions to drug concentration data to estimate the mean drug disposition behavior of the subject or population (*i.e.*, the disposition function q) and (*b*) testing the validity of the assumptions involved.

The empirical sum of exponentials, which are fitted quite successfully in linear pharmacokinetics, apparently do not fit nonlinear pharmacokinetic data properly. Preliminary investigations were therefore carried out to identify a suitable type of function that could be used. It was found that the following function:

$$C_{iv}(t) = \frac{p_1 e^{-p_2 t}}{1 + e^{(p_3 - p_4 t)}} \qquad p_i > 0 \qquad \text{(Eq. 37)}$$

produced very excellent fits to all typical Michaelis-Menten type intravenous bolus data investigated. Extensions of the numerator and denominator in Eq. 37 to include more exponential terms seem to hold some promise for other types of administrations and other types of nonlinearities. Alternatively, the use of least-squares splines may provide a more general and flexible approximation approach (9). Work is in progress to experimentally investigate the methodology proposed.

APPENDIX I

The differential equation describing the drug level profile resulting from a constant-rate (R) intravenous infusion is:

$$\frac{dC}{dt} = -q(C) + \frac{R}{V} \qquad \text{(Eq. 1A)}$$

Let $C_{iv}(t)$ denote an arbitrary monotonically increasing function which fit the data from a constant-rate infusion well; then, dC/dt can be determined according to Eq. 8 as previously described. By comparing Eqs. 1A and 8, it is seen that the disposition function q can be estimated empirically from the function $C_{iv}(t)$ fitted to the intravenous infusion data according to:

$$q(x) = \frac{R}{V} - C_{iv}'(C_{iv}^{-1}(x)) \qquad \text{(Eq. 2a)}$$

It is evident from Eq. 1 that $q(0) = 0$ since $dC/dt = 0$ for $C = 0$ following an intravenous bolus administration. Thus, the volume term in Eq. 2A can be evaluated from the initial condition of Eq. 1A to give:

$$V = R/C_{iv}'(0) \qquad \text{(Eq. 3A)}$$

Inserting this expression for V into Eq. 2A gives Eq. 17.

APPENDIX II: GLOSSARY

A_i, α_i = Constants (parameters) of an empirical equation (Eq. 3)
C = Drug concentration
$C_f(t)$ = Drug concentration-time profile resulting from an arbitrary rate of systemic input $f(t)$
$C_f'(t)$ = $dC_f(t)/dt$
$C_{iv}(t)$ = Drug concentration-time profile resulting from an intravenous bolus dose or a constant-rate drug infusion (as indicated)
$C_{iv}^{-1}(\ )$ = Inverse function of $C_{iv}(t)$
$C_{iv}'(t)$ = $dC_{iv}(t)/dt$
$C_{iv}^{-1}(\ )$ = Inverse function of $C_{iv}'(t)$
C_n^{max}, C_n^{min} ($n = 1, 2, \ldots$) = Peak and trough drug concentrations, respectively, in the nth dosing period in an intravenous bolus dosing regimen
C_{ss} = Steady-state drug concentration
$\bar{C}_{ss}$ = Mean steady-state drug concentration
D = Intravenous bolus dose in multiple administration
D_0 = Intravenous bolus dose in a single administration
$f(t)$ = Arbitrary rate of systemic drug input (mass/time) resulting from an extravascular dose
$g(t)$ = $q[C_f(t)] + C_f'(t)$ (Eq. 14)
K = Constant kinetic parameter (Eq. 2)
K_m = Michaelis-Menten parameter (Eq. 2)
p_i = Constants (parameters) of an empirical equation (Eq. 37)
$q(\ )$ = Disposition function (Eq. 1)
$q^{-1}(\ )$ = Inverse of the disposition function q
R = Constant rate of intravenous drug infusion
t = Time
T = Dosing interval
v = Constant of dimension volume
V_m = Michaelis-Menten parameter (Eq. 2)
y = Variable defined by Eqs. 13 and 14

REFERENCES

(1) K. Arnold and N. Gerber, *Clin Pharmacol. Ther.*, **11**, 121 (1969).

(2) A. J. Sedman, P. K. Wilkinson, E. Sakmar, D. J. Weidler, and J. G. Wagner, *J. Studies Alcohol*, **37**, 1197 (1976).

(3) S. D. Conte and C. de Boor, "Elementary Numerical Analysis," McGraw-Hill, New York, N.Y., 1972, chaps. 6 and 7.

(4) J. G. Wagner, J. I. Northam, C. D. Alway, and O. S. Carpenter, *Nature (London)*, **207**, 201 (1965).

(5) SUBROUTINE *ZBRENT*, IMSL, GNP Building, Houston, Texas.

(6) SUBROUTINE *RTMI*, System 360 Scientific Subroutine Package (360A-CM-03X). Programmer's Manual. IBM, Technical Publications Department, White Plains, N.Y. 1968.

(7) SUBROUTINE *NB01A*, Harwell Subroutine Library, Computer Science and Systems Division, AERE Harwell, Oxfordshire, England.

(8) G. Dahlquist and Å. Björk, "Numerical Methods," Prentice Hall, Englewood Cliffs, N.J., 1974, chap. 6.

(9) C. de Boor, "A Practical Guide to Splines," Springer-Verlag, New York, N.Y., 1978, chap. 14.

Self-Association of Doxorubicin and Related Compounds in Aqueous Solution

MILENA MENOZZI ˣ, LUIGI VALENTINI, ELISABETTA VANNINI, and FEDERICO ARCAMONE

Received January 24, 1983, from *Farmitalia Carlo Erba, Ricerca e Sviluppo Chimico, Via dei Gracchi 35, 20146 Milano, Italy.* Accepted for publication May 11, 1983.

Abstract □ The dimerization of doxorubicin, daunorubicin, and their 4-demethoxy, 4′-epi, and 4′-deoxy analogues was studied spectrophotometrically. Self-association was found to be influenced by buffer composition and ionic strength. K_d values were 1.3×10^4 and 2.3×10^4 M^{-1} for doxorubicin and daunorubicin, respectively, and ranged from 3.8×10^3 to 6.1×10^3 M^{-1} for the 4-demethoxy analogues. For 4′-epi- and 4′-deoxydoxorubicin, tetramerization has also been considered. On this basis, values of 2.0×10^4 and 2.2×10^4 M^{-1} were found, respectively, for the formation constant of the dimerization process. Stability of the dimeric species appears to be strongly influenced by substitution of the chromophore moiety.

Keyphrases □ Doxorubicin—self-association, 4-demethoxy, 4′-epi, 4′-deoxy, 4-demethoxy-4′-epi, analogues, effect of buffer concentration and ionic strength □ Daunorubicin—self-association, 4-demethoxy analogues, effect of buffer concentration and ionic strength □ Dimerization—doxorubicin, daunorubicin, and their 4-demethoxy, 4′-epi, and 4′-deoxy analogues, effect of buffer concentration and ionic strength

During investigations carried out in this laboratory on doxorubicin–biopolymer interactions, knowledge of the drug dimerization process under the conditions used was necessary. The self-association of doxorubicin (I) and daunorubicin (II) in aqueous solutions has been the subject of several studies; such self-association was generally considered to be of the same type as that shown by actinomycin (1), acridine dyes (2, 3), and purine derivatives (4). The cooperative-type phenomena related to the effect of ligand dimerization on the manifestation of the binding process have been well documented (3, 5, 6).

For this reason, and also because the available literature data (7–15) exhibited large variations apparently related to the different experimental conditions used, we have determined the dimerization constants of these clinically important anthracyclines in three aqueous buffer systems, employing a spectrophotometric technique with the elimination of interference due to fluorescence. Figure 1 shows the differences among specific absorption spectra of doxorubicin at various concentrations in Tris buffer plus NaCl. These differences are considered to be due to dimerization (8, 10, 12). New second generation antitumor anthracyclines, showing more favorable pharmacological properties, have also been included in the study.

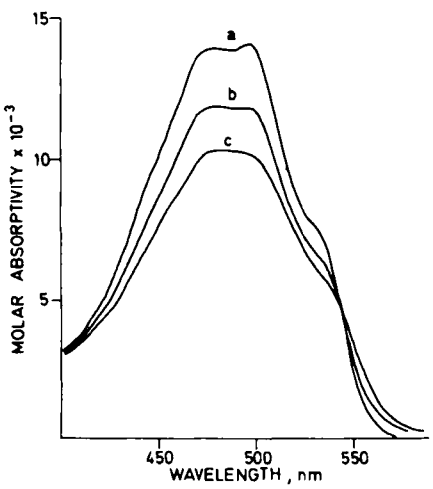

Figure 1—*Visible absorption spectra of I at different concentrations in pH = 7.0 Tris buffer + NaCl. Key: (a) 1.7×10^{-6} M; (b) 1.7×10^{-5} M; (c) 1.7×10^{-4} M.*

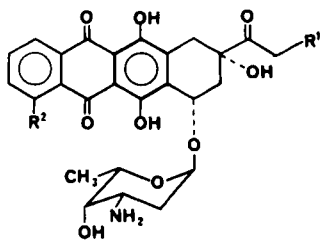

I : R^1 = OH ; R^2 = OCH_3
II : R^1 = H ; R^2 = OCH_3
III : R^1 = OH ; R^2 = H
IV : R^1 = R^2 = H

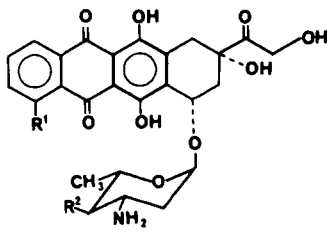

V : R^1 = OCH_3 ; R^2 = OH
VI : R^1 = OCH_3 ; R^2 = H
VII : R^1 = H ; R^2 = OH

EXPERIMENTAL

Chemicals—Doxorubicin (I), daunorubicin (II), 4-demethoxydoxorubicin (III), 4-demethoxydaunorubicin (IV), 4′-epidoxorubicin (V), 4′-deoxydoxorubicin (VI), and 4-demethoxy-4′-epidoxorubicin (VII) were used as hydrochlorides. All the drugs were isolated or synthesized in our laboratories and purified by crystallization as hydrochloride salts. The chemical titers of I–VII were ≥97% as determined by an HPLC procedure (16). Phosphate and Tris buffer solutions at pH 7.0 were prepared at the same ionic strength (μ = 0.05). Tris buffer plus NaCl was prepared by adding NaCl (final concentration: 0.15 M) to pH 7.0, 0.05 M Tris-HCl in order to make the ionic strength 0.196 M.

Apparatus—Spectrophotometric measurements[1] were carried out at 477 nm (22°C), and interferential filters were placed beyond the cells to cut off the emitted fluorescence. The concentration range of the drugs was 1×10^{-6}–5×10^{-4} M, and 5-, 2-, and 1-cm path length cells were used. The wall adsorption effect, as already described by others (11), prevents the use of cells of small volume (such as 0.1-cm path length) for which the surface to volume ratio is very unfavorable.

[1] Coleman, Perkin-Elmer model 575.

0022-3549/84/0600-0766$01.00/0
© 1984, American Pharmaceutical Association

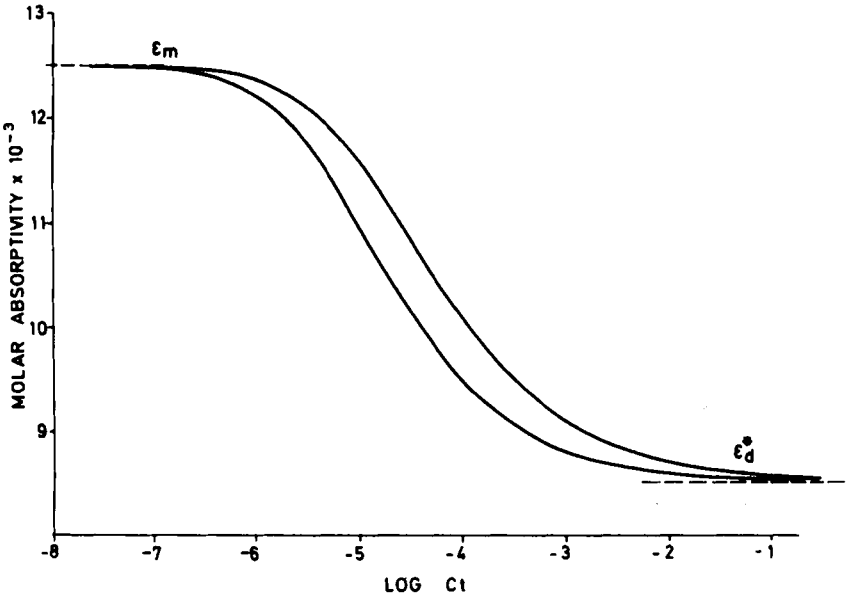

Figure 2—*Theoretical behavior of* $A/[C_t] = f([C_t])$ *(upper) and* $dA/d[C_t] = f([C_t])$ *(lower), described by Eqs. 5 and 6, respectively.*

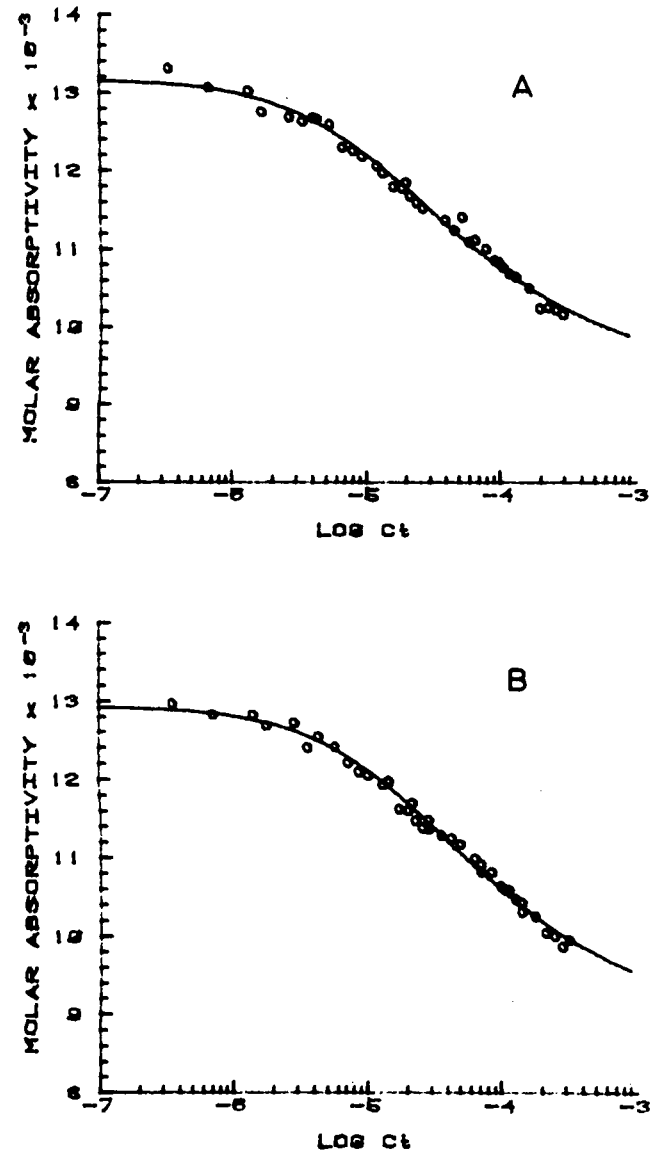

Figure 3—*Molar absorptivity* versus *log* C_t *for I (A) and II (B) in pH 7.0 Tris buffer + NaCl, according to the direct procedure. The solid lines represent the best fit of experimental points according to Eq. 5.*

Direct Procedure—Different amounts of a stock drug aqueous solution were diluted with the buffer up to the desired concentrations. The absorbance of each sample was measured without delay in 5- and 1-cm path length cells according to the concentration used. Each sample was prepared at least in triplicate.

Incremental Procedure—Increasing amounts of buffered stock drug solution were pipetted into the cell containing a predetermined volume of the same buffer. For concentration values ranging from 8×10^{-7} to 3×10^{-5} M, 15-mL cells of 2-cm path length were employed, with a starting volume of 10 mL of buffer solution, to which from 200 to 900 μL of buffered stock drug solution was added. For concentration values ranging from 6×10^{-6} to 2×10^{-4} M, 1-cm path length cells containing 2 mL of buffer were used. Absorbance was measured after the addition of increasing amounts (from 50 to 200 μL) of the drug solution.

True Spectra of Monomer and Dimer—The true spectra of monomer and dimer were obtained by differential measurements, using two cuvettes of different path length (5 and 1 cm) in order to allow subtraction of the absorption contribution due to the other species.

THEORETICAL

The absorbance of a monomeric species in equilibrium with its dimeric form is defined by:

$$A = \epsilon_m[C_m] + 2\epsilon_d^*[C_d] \qquad \text{(Eq. 1)}$$

where A is the experimental absorbance divided by the cell path length (in centimeters) at a stated wavelength; ϵ_m and ϵ_d^* are the molar absorptivities of monomer and dimer, respectively, calculated using the monomer molecular weight; and $[C_m]$ and $[C_d]$ are the molar concentrations of the monomer and dimer, respectively. For the mass balance, the total concentration is:

$$[C_t] = [C_m] + 2[C_d] \qquad \text{(Eq. 2)}$$

where $[C_t]$ is the total molar concentration expressed as monomeric units. The dimerization constant is defined by:

$$K_d = \frac{[C_d]}{[C_m]^2} \qquad \text{(Eq. 3)}$$

Table I—Dimerization Constants and Molar Absorptivities

Compound	$K_d \pm SE$, $10^3 \times M^{-1}$	$\epsilon_m \pm SE$, $10^3 \times M^{-1} \times cm^{-1}$	$\epsilon_d^* \pm SE$, $10^3 \times M^{-1} \times cm^{-1}$
I	16.64 ± 2.16[a]	13.10 ± 0.05	9.26 ± 0.14
	12.99 ± 1.19[b]	13.15 ± 0.03	9.27 ± 0.09
	22.79 ± 2.68[c]	13.16 ± 0.05	9.33 ± 0.09
	17.18 ± 2.34[c,d]	13.08 ± 0.08	8.15 ± 0.15
II	12.98 ± 1.74[a]	12.96 ± 0.06	8.84 ± 0.14
	13.44 ± 1.91[b]	12.93 ± 0.05	8.85 ± 0.15
	16.07 ± 1.53[c]	12.93 ± 0.04	8.88 ± 0.09

[a] pH 7.0, μ = 0.05, phosphate buffer. [b] pH 7.0, μ = 0.05, Tris buffer. [c] pH 7.0, μ = 0.196, Tris buffer + NaCl. [d] Value obtained without interferential filters.

Table II—Dimerization and Tetramerization Constants

Compound	$K_d \pm SE$, $10^3 \times M^{-1}$	$\epsilon_m \pm SE$, $10^3 \times M^{-1} \times cm^{-1}$	$\epsilon_d^* \pm SE$, $10^3 \times M^{-1} \times cm^{-1}$	$K_t \pm SE$, $10^3 \times M^{-1}$	$\epsilon_t^* \pm SE$, $10^3 \times M^{-1} \times cm^{-1}$
V[a]	11.10 ± 0.76	13.05 ± 0.03	8.18 ± 0.09		
	19.84 ± 12.28[c]	13.10 ± 0.05	9.57 ± 1.59	9.61 ± 3.01	8.43 ± 0.49
VI[a]	12.54 ± 0.94	13.07 ± 0.04	7.72 ± 0.10		
	22.13 ± 11.94[c]	13.14 ± 0.05	9.11 ± 1.44	6.84 ± 3.64	7.68 ± 0.97
III[a]	6.11 ± 1.01	10.79 ± 0.01	7.64 ± 0.33		
IV[a]	4.25 ± 0.57	10.79 ± 0.03	6.79 ± 0.20		
VII[b]	3.79 ± 1.40	10.46 ± 0.07	6.66 ± 0.60		

[a] pH 7.0, μ = 0.196, Tris buffer + NaCl. [b] pH 7.0, μ = 0.05, Tris buffer. [c] The large value of SE is due to the high correlation coefficients found between the parameters of the model.

Equations 1–3 can provide the evaluation of the dimerization constant (5, 11). Solving the system of Eqs. 1–3 for the absorbance in terms of the total concentration, one obtains:

$$A = \epsilon_d^*[C_t] + \frac{\Delta\epsilon}{4K_d}\sqrt{1 + 8K_d[C_t]} - \frac{\Delta\epsilon}{4K_d} \qquad \text{(Eq. 4)}$$

where $\Delta\epsilon = \epsilon_m - \epsilon_d^*$. Dividing Eq. 4 by $[C_t]$ the result is:

$$\frac{A}{[C_t]} = \epsilon_d^* + \frac{\Delta\epsilon}{4K_d[C_t]}(\sqrt{1 + 8K_d[C_t]} - 1) \qquad \text{(Eq. 5)}$$

and by derivation of Eq. 4 with respect to $[C_t]$ we obtain:

$$\frac{dA}{d[C_t]} = \frac{\Delta\epsilon}{\sqrt{1 + 8K_d[C_t]}} + \epsilon_d^* \qquad \text{(Eq. 6)}$$

The unknown parameters of Eqs. 4–6 are K_d, ϵ_m, and ϵ_d^*. They can be simultaneously estimated by a nonlinear least-squares fitting procedure from each of the three preceeding equations. Theoretical behavior of functions 5 and 6 is shown in Fig. 2. Data obtained following the direct procedure were treated by Eq. 5, applying a modified version of the Fletcher and Shrager program (17). The incremental procedure was employed for I and II in phosphate buffer. The data obtained, together with those from the direct procedure, were simultaneously treated by a nonlinear fitting, taking into account both Eqs. 5 and 6. The parameters describing the tetramerization process were obtained by the same fitting procedure, employing a suitable extension of Eqs. 1–3 to obtain the solving equation corresponding to Eq. 5.

RESULTS

Doxorubicin and Daunorubicin—Figure 3 shows the molar absorptivities of I and II as a function of the total concentration in pH 7.0 Tris buffer plus NaCl, μ = 0.196, following the direct procedure. Estimates of K_d, ϵ_m, and ϵ_d^*, obtained from the best fitting of Eq. 5 for the three buffers employed, are reported in Table I. Different K_d values were found for the three conditions.

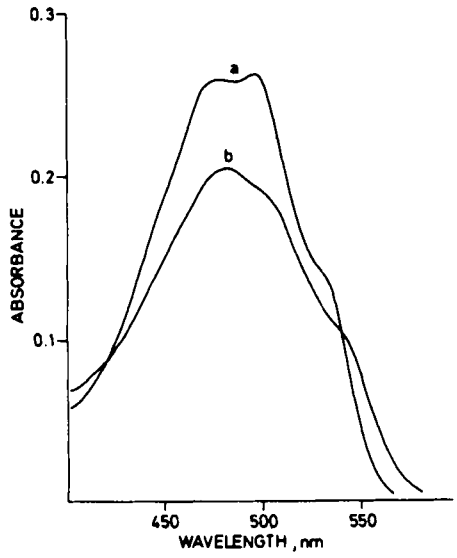

Figure 4—*True spectra of I monomer (a) and dimer (b), obtained by differential measurements, at 2.14 × 10⁻⁵ M × cm in pH 7.0 Tris buffer + NaCl. Key: (a) 1.05 × 10⁻⁵ M solution in a 5-cm cuvette against 3.10 × 10⁻⁵ M solution in a 1-cm cuvette; (b) 5.10 × 10⁻⁵ M solution in a 1-cm cuvette against 5.92 × 10⁻⁶ M solution in a 5-cm cuvette.*

Figure 4 shows the differential spectra, in Tris buffer plus NaCl, of the monomeric and dimeric species of I. The concentrations were calculated using the corresponding parameters reported in Table I.

Figure 5 reports the molar absorptivities obtained from the direct and incremental procedure for I and II in phosphate buffer. The two sets of experimental data were treated simultaneously as described above. The values of the parameters K_d, ϵ_m, and ϵ_d^* so obtained were found to be in close agreement with those presented in Table I. To evaluate the influence of the ionic strength on K_d values, measurements were performed in pH 7.0 phosphate buffer, with concentrations ranging from ~1.8×10^{-3} to 1.8×10^{-1} M. K_d values were

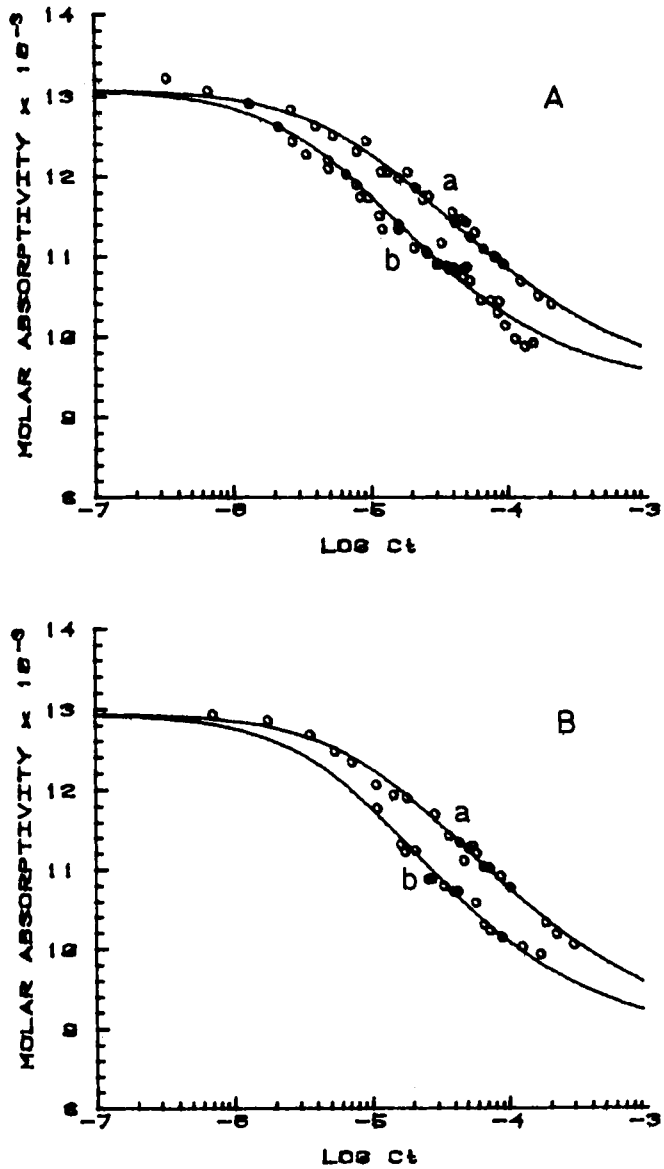

Figure 5—*Molar absorptivity (a) and incremental molar absorptivity (b) versus log C_t for I (A) and II (B), in pH 7.0 phosphate buffer, according to the direct and incremental procedures.*

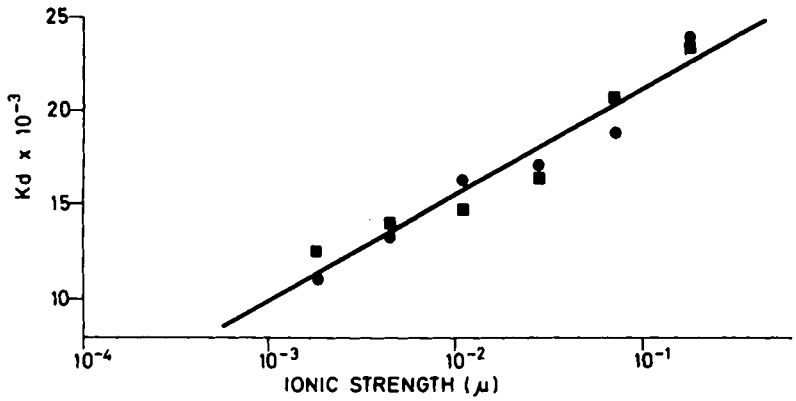

Figure 6—*Variation of the* K_d *as a function of the ionic strength.*

obtained from the absorbance measurements applying Eqs. 1-3 and using the ϵ_m and ϵ_d^* values previously determined. The dependence of K_d on the ionic strength is reported in Fig. 6.

4'-Epi, 4'-Deoxy, and 4-Demethoxy Analogues—As shown in Table II, V and VI exhibit apparent ϵ_d^* and K_d values significantly lower than those of the parent drug. The corresponding dimerization curves are presented in Fig. 7. Table II also shows the results obtained for V and VI when a tetramerization process is taken into account. The occurrence of such a process is strongly suggested by the behavior of the curves of Fig. 7 and by the low value of ϵ_d^* calculated on the basis of a simple dimerization.

A clearly lower dimerization constant is also shown by the analogues carrying a modification in the chromophore portion of the molecule, namely the 4-demethoxy derivatives (III, IV, and VII). Figure 8 shows the dimerization curves of the latter compounds.

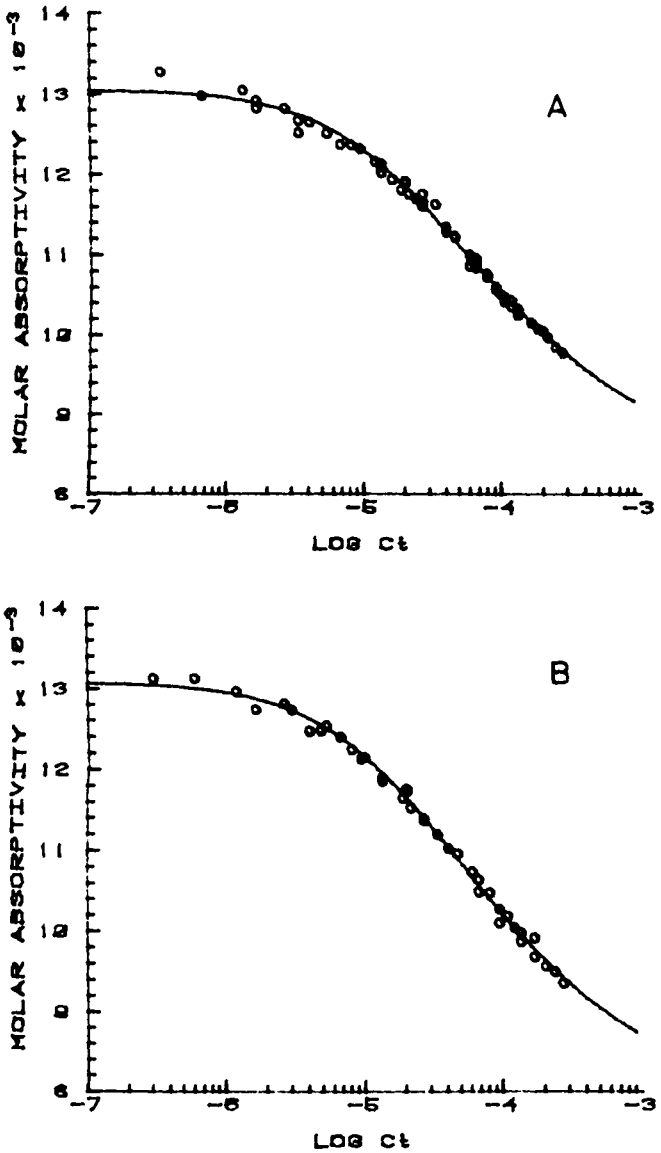

Figure 7—*Molar absorptivity* versus *log* C_t *for V (A) and VI (B). The conditions were the same as those in Fig. 3.*

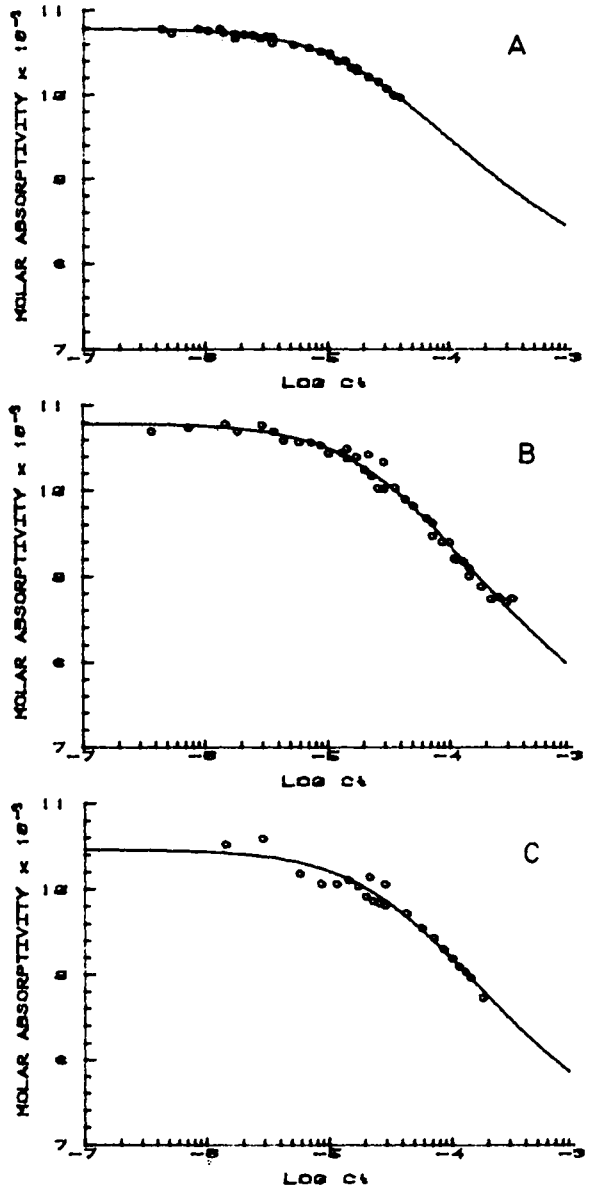

Figure 8—*Molar absorptivity* versus *log* C_t *for III (A), IV (B), and VII (C). Compound VII was in 0.05 M Tris buffer; all other conditions were the same as those in Fig. 3.*

DISCUSSION

The spectrophotometric behavior of I and II, as shown by the curves of Figs. 3 and 5, is near to that theoretically expected for a simple dimerization process. The values of the parameters obtained in different conditions (Table I) indicate that the dimerization constant is dependent on both the buffer composition and ionic strength. The K_d values observed for I seem to experience, on increase of the ionic strength, a larger variation than the corresponding K_d values of II, strongly suggesting an involvement of the 14-hydroxyl group in the dimerization process, either directly (*e.g.*, by formation of hydrogen bonds) or indirectly (*e.g.*, dipole effects). The dimerization constant values of I and II, as found in this study, are generally larger than those reported by others. Indeed the K_d values we found are twice as large as those reported by Stutter *et al.* (14) and Martin (12) for I and II, respectively, although the latter author worked with a lower buffer ionic strength. The results we obtained are practically identical to those reported by Eksborg (9), but markedly differ from those of Schütz *et al.* (11) and Chaires *et al.* (15) for II. No explanation can be given at this point for these differences, and it may be noted that the values of the molar extinction coefficients of both monomer and dimer given by these authors are not in agreement with the values reported in the present study.

Among the hundreds of doxorubicin analogues, V and VI have been selected for further development toward clinical evaluation because of their favorable pharmacological properties (18, 19). In this connection, a comparison of their properties at the molecular level with those of I is of particular interest. As regard to self-aggregation in solution, the two analogues either give rise to a somewhat less stable dimeric species or show a higher tendency toward the formation of tetramers. In both cases the latter interpretation of the results would give a slightly better fitting of the experimental data (RMS[2] = 70.2 for V and 75.8 for VI) than does the former (RMS = 75 and 81 for V and VI, respectively). The greater ability to form tetrameric species can be tentatively related to the lower hydrophilicity of V and VI as compared with I, favoring hydrophobic stacking aggregation. Accepting the tetramerization hypothesis, the dimerization constants for V and VI are very near to that found for I, in agreement with the identical electronic structure of the chromophoric moiety.

A clearly different situation exists in the case of the 4-demethoxy analogues. Compounds III, IV, and VII show a distinctly lower tendency toward dimerization when compared with the parent drugs. The reduced dimer stability appears to be a consequence of the substitution of the C-4 methoxyl group with a hydrogen atom, a modification that strongly influences the electronic structure of the chromophore. The demethoxy analogues are up to 10 times more potent than the corresponding methoxylated derivatives in different biological systems (20, 21); this property is not based on a higher affinity for the DNA receptor (22). Whether the lower tendency to self-aggregation mirrors a diminished tendency to other aspecific interactions and therefore increases, for instance, the rate of accumulation within the cells and correspondingly the availability at the receptor site, remains to be established.

[2] Root mean square.

REFERENCES

(1) N. S. Angerman, T. A. Victor, C. L. Bell, and S. S. Danyluk, *Biochemistry*, **11**, 2402 (1972).

(2) H. H. Li and D. M. Crothers, *Biopolymers*, **8**, 217 (1969).

(3) W. Müller and D. M. Crothers, *Eur. J. Biochem.*, **54**, 267 (1975).

(4) J. L. Dimicoli and C. Hélène, *J. Am. Chem. Soc.*, **95**, 1036 (1973).

(5) G. Schwarz, S. Klose, and W. Balthasar, *Eur. J. Biochem.*, **12**, 454 (1970).

(6) G. Schwarz and W. Balthasar, *Eur. J. Biochem.*, **12**, 461 (1970).

(7) V. Barthelemy-Clavey, J. L. Maurizot, J. L. Dimicoli, and P. Sicard, *FEBS Lett.*, **46**, 5 (1974).

(8) V. Crescenzi and F. Quadrifoglio, in "Polyelectrolytes and Their Applications," A. Rembaum and E. Sélégny, Eds., D. Reidel Publishing Dordrecht, Holland, 1975, p. 217.

(9) S. Eksborg, *J. Pharm. Sci.*, **67**, 782 (1978).

(10) H. Porumb, *Prog. Biophys. Mol. Biol.*, **34**, 175 (1978).

(11) H. Schütz, F. A. Gollmick, and E. Stutter, *Stud. Biophys.*, **75**, 147 (1979).

(12) S. R. Martin, *Biopolymers*, **19**, 713 (1980).

(13) E. Goormaghtigh, P. Chatelain, J. Caspers, and J. M. Ruysschaert, *Biochim. Biophys. Acta*, **597**, 1 (1980).

(14) E. Stutter, F. A. Gollmick, and H. Schütz, *Stud. Biophys.*, **88**, 131 (1982).

(15) J. B. Chaires, N. Dattagupta, and D. M. Crothers, *Biochemistry*, **21**, 3927 (1982).

(16) "Code of Federal Regulations," Food and Drug Administration, Washington, D.C., April 1, 1982, § 436.322.

(17) J. E. Fletcher and R. I. Shrager, "A User's Guide to Least-Squares Model Fitting," DCRT Technical Report No. 1, 1968.

(18) A. M. Casazza, A. Di Marco, C. Bertazzoli, F. Formelli, F. Giuliani, and G. Pratesi, in "Current Chemotherapy," vol. 2, W. Siegenthaler and R. Luthy, Eds., American Society for Microbiology, Washington, D.C., 1978, p. 1257.

(19) F. Arcamone, S. Penco, S. Redaelli, and S. Hanessian, *J. Med. Chem.*, **19**, 1424 (1976).

(20) A. M. Casazza, G. Pratesi, F. Giuliani, and A. Di Marco, *Tumori*, **66**, 549 (1980).

(21) A. Di Marco, A. M. Casazza, F. Giuliani, G. Pratesi, F. Arcamone, L. Bernardi, P. Giardino, and B. Patelli, *Cancer Treat. Rep.*, **62**, 375 (1978).

(22) F. Arcamone, "Doxorubicin Anticancer Antibiotics: Medicinal Chemistry," vol. 17, Academic, New York, N.Y., 1981, p. 265.

ACKNOWLEDGMENTS

The authors are very indebted to Prof. A. Vacca, University of Florence, for his helpful contribution in data handling.

High-Performance Liquid Chromatographic Determination of Diltiazem and Six of Its Metabolites in Human Urine

J. P. CLOZEL, G. CAILLÉ ˣ, Y. TAEYMANS, P. THÉROUX, P. BIRON, and F. TRUDEL

Received February 24, 1982, from the *Département de pharmacologie, Faculté de médecine, Université de Montréal, Case postale 6128, Succursale "A", Montréal, Québec H3C 3J7, Canada.* Accepted for publication May 5, 1983.

Abstract □ The use of the calcium antagonist diltiazem (I) is increasing, particularly in treating unstable angina. This study describes a simple and specific high-performance liquid chromatographic method for the determination of I and six of its metabolites in urine. Diltiazem and its conjugated and unconjugated metabolites were assayed in the urine of patients treated with a dose of 120 mg po of diltiazem tid. Sensitivity of the method was 100 ng/mL for I and the metabolites desacetyldiltiazem (II), *N*-desmethyldesacetyldiltiazem (IV), *O*-desmethyldesacetyldiltiazem (V), *O*-desmethyl-*N*-desmethyldesacetyldiltiazem (VII), *N*-oxide desacetyldiltiazem (III), and *O*-desmethyl-*N*-oxide desacetyldiltiazem (VI). In the urine of patients, the extent of conjugation of six metabolites was >80%.

Keyphrases □ Diltiazem—HPLC determination, six metabolites, human urine □ HPLC—diltiazem and six metabolites, human urine

Diltiazem, (+)-*cis*-3-(acetyloxy)-5-[2-(dimethylamino)-ethyl]-2,3-dihydro-2-(4-methoxyphenyl)-1,5-benzothiazepin-4(5*H*)one monohydrochloride, is a new calcium antagonist which has been shown to be useful in the treatment of unstable angina (1, 2). Limited data are available on the metabolism and pharmacokinetics of this new drug, but the recent development of sensitive and specific analytical methods will advance understanding in these areas. A GC method (3, 4) has been published, but it did not separate diltiazem (I) from its six metabolites and required a derivatization of the principal metabolite, desacetyldiltiazem (II). A spectrophotometric method has also been published (5), but it has limited specificity and sensitivity.

The present article describes a simple method for the determination of I and its six metabolites in urine using high-performance liquid chromatography (HPLC). This method has been applied to the measurement of urine metabolites (conjugated and unconjugated) of I in two patients receiving 120 mg po of I tid.

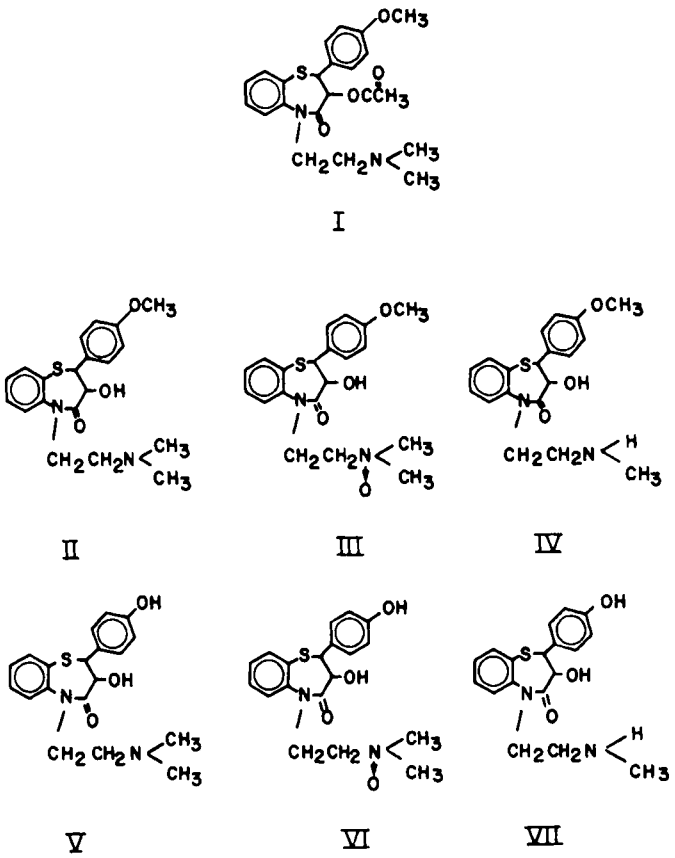

EXPERIMENTAL

Materials—Diltiazem[1] (I), the six metabolites (II–VII)[1], and loxapine[2] (the internal standard) were used as hydrochloride salts. All solvents and reagents were of analytical grade except acetonitrile and water, which were HPLC grade.

Apparatus—The assays were performed on a liquid chromatograph[3] equipped with a variable-wavelength UV detector set at 210 nm with attenuation at 128 AU × 10^{-4} cm. The 25 × 0.46 cm i.d. C_{18} column[4] packed with 5-μm Spherisorb ODS was eluted with acetonitrile–0.01 M phosphate buffer, pH 3 (72:28). The mobile phase had a flow rate of 2.5 mL/min from 0 to 5.5 min, increasing to 3 mL/min from 5.5 to 13 min.

Extraction—*Unconjugated Metabolites*—To 1 mL of urine, contained in a culture tube, were added 1 mL of 0.1 M acetate buffer adjusted to pH 5 and 100 μL of internal standard solution (100 μg/mL). The solution was vortexed for 30 s and extracted with 10 mL of chloroform containing 1% isoamyl alcohol. The mixture was agitated for 10 min on a reciprocating shaker and then centrifuged at 2500 rpm. The organic phase was transferred to a second culture tube and evaporated to dryness on a hot plate at 60°C under a nitrogen stream. The aqueous phase was then passed over a C_{18} cartridge[5] (previously prepared with 2.5 mL of H_2O, 2.0 mL of methanol, and another 2.5 mL of H_2O, fol-

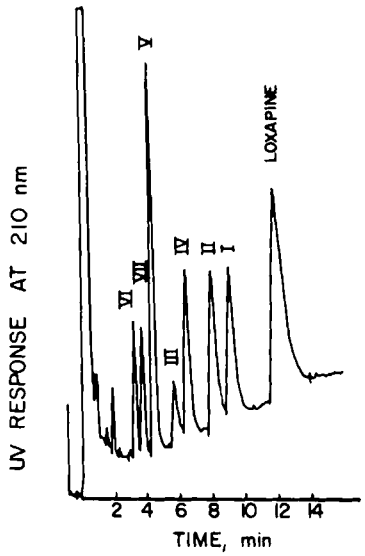

Figure 1—*Typical chromatogram of a urine extract.*

[1] Tanage Seigaku Ltd. Japan.
[2] Lederle.
[3] Hewlett-Packard 1080B.
[4] Cosyns and Spain.
[5] SEP-PAK; Waters Associates.

0022-3549/84/0600-0771$01.00/0
© 1984, American Pharmaceutical Association

Table I—Retention Time, Lower Limit of Detection, and Calibration Curve of Diltiazem and Its Six Metabolites in Urine

Compound	Retention Time, min	Limit of Sensitivity[a], μg/mL	Calibration Curve	r^2
Diltiazem (I)	10.09	0.100	$y = 0.2004x - 0.0046$	0.9999
II	8.94	0.100	$y = 0.2259x - 0.0029$	0.9999
IV	7.37	0.100	$y = 0.2210x - 0.0028$	0.9991
V	6.59	0.100	$y = 0.2134x - 0.0027$	0.9996
VII	5.25	0.100	$y = 0.2205x - 0.0031$	0.9964
III	4.63	0.100	$y = 0.2199x - 0.0038$	0.9885
VI	4.13	0.10	$y = 0.2105x - 0.0026$	0.9905

[a] Limit of detection 0.050 μg/mL.

Table II—Recovery of Diltiazem and Its Metabolites at Different Urine Concentrations

Urine conc., μg/mL	Recovery, %[a]						
	Diltiazem (I)	II	IV	V	VII	III	VI
0.1	99.6 ± 3.4	100.0 ± 2.5	91.5 ± 4.68	74.3 ± 10.1	73.8 ± 4.9	91.4 ± 3.0	85.0 ± 3.3
0.2	100.0 ± 2.7	100.0 ± 2.7	93.8 ± 5.2	78.5 ± 9.4	74.0 ± 5.3	92.4 ± 3.9	84.5 ± 3.1
0.4	101.4 ± 3.3	99.8 ± 2.8	90.9 ± 5.0	77.8 ± 8.5	73.8 ± 6.0	90.9 ± 4.0	82.3 ± 2.4
0.8	98.5 ± 2.9	99.5 ± 2.5	92.1 ± 4.9	75.2 ± 7.8	75.5 ± 5.5	94.5 ± 3.8	85.0 ± 3.0
1.6	100.0 ± 3.1	100.0 ± 3.1	91.6 ± 4.5	77.4 ± 8.5	76.0 ± 4.8	95.0 ± 3.7	84.8 ± 3.0
4.0	100.0 ± 2.9	98.2 ± 3.5	93.8 ± 6.0	76.5 ± 7.4	74.9 ± 4.8	92.9 ± 4.5	86.2 ± 3.4
4.8	99.5 ± 3.2	95.8 ± 4.0	94.5 ± 5.4	76.9 ± 7.0	78.5 ± 5.6	94.5 ± 3.0	85.0 ± 2.0

[a] Percent recovery ± *SE* (mean of three assays).

lowed by 2 mL of 0.1 M phosphate buffer at pH 3.0 and finally 3 mL of acetonitrile). The filtrate (acetonitrile) was transferred to the tube containing the residue of the organic phase. The solution was vortexed for 30 s and the solution was evaporated to dryness. The residue was dissolved in 0.3 mL of 0.01 M HCl, and a 150-μL aliquot was analyzed by HPLC.

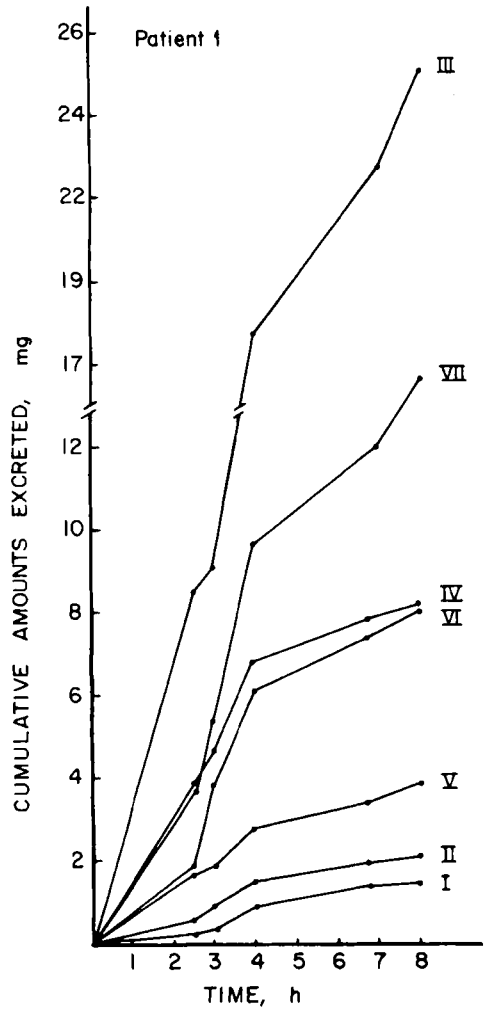

Figure 2—*Cumulative amounts of I and its metabolites excreted in urine after a single oral 120-mg dose.*

Conjugated Metabolites—To determine the total amount of I and metabolites excreted in urine, the conjugated products were hydrolyzed. The optimum conditions necessary for complete hydrolysis were evaluated. The conditions chosen consisted of incubation of 1 mL of urine containing 100 μg of loxapine with 0.1 mL of β-glucuronidase-sulfatase solution[6] at 37°C for 16 h. After incubation, the extraction was done as described above for unconjugated metabolites.

Calibration Curves—Standard samples were prepared by spiking human urine samples with increasing concentrations (0.1, 0.2, 0.4, 0.8, 1.6, 4.0, and 4.8 μg/mL) of I and the six metabolites. Calibration curves were constructed by plotting the ratios of the peak areas of I–VII to that of the internal standard

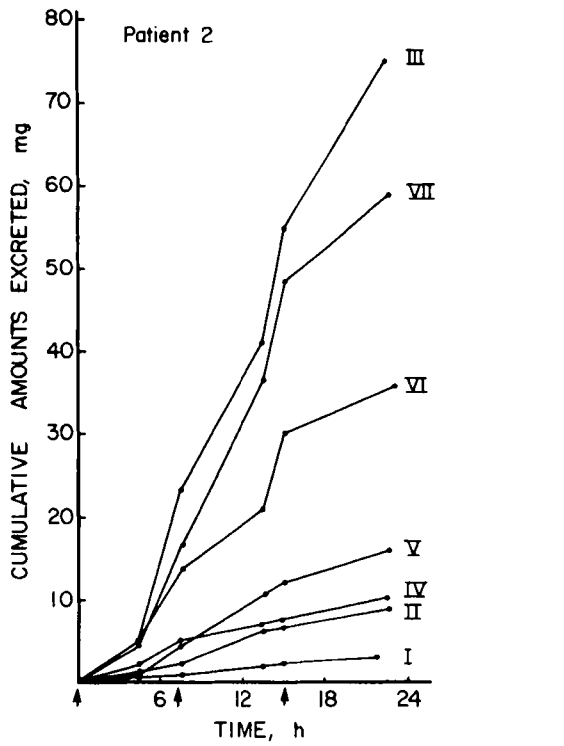

Figure 3—*Cumulative amounts of I and its metabolites excreted in urine after administration of the first three doses (120 mg tid). Arrows indicate the times of dosing.*

[6] Glusulase (5000 U of arylsulfatase and β-glucuronidase in 0.14 M sodium acetate buffer pH 5); Sigma.

Table III—Reproducibility of the Assay of Diltiazem and Metabolites

Compound	Urine Conc., μg/mL	N	CV, %
Diltiazem (I)	0.8	12	3.0
	4.8	12	3.2
II	0.8	9	4.1
	4.8	9	3.9
IV	0.8	9	4.7
	4.8	9	4.5
V	0.8	9	5.1
	4.8	9	2.8
VII	0.8	9	6.1
	4.8	9	3.7
III	1.6	9	6.2
	4.8	9	4.7
VI	1.6	9	7.4
	4.8	9	3.3

against the respective concentrations I–VII. Five samples were run for each of the seven concentrations.

Analytical recoveries of I and metabolites were determined by comparing the peak areas obtained by direct injection of standard aqueous solution with those obtained after the extraction procedure. This procedure was done for each concentration of I and metabolites used in the calibration curves.

Clinical Study—Urine samples were taken from two patients treated for unstable angina with 120 mg po tid of diltiazem. In patient 1, the urine samples were taken at 2.5, 3, 4, 7, and 8 h after the first dose. In patient 2, the urine samples were taken over a period of 24 h, during and after the first three doses, at 5, 6, 14, 15, and 24 h following the first dose.

RESULTS AND DISCUSSION

A typical chromatogram showing the separation of I and the metabolites is presented in Fig. 1. Table I gives the retention time, sensitivity of the method, and results obtained for the calibration curve of I and its metabolites. The standard curves were linear throughout the range studied, and the limit of sensitivity of I and its metabolites was 100 ng/mL. Analytical recovery of I and its metabolites is presented in Table II. The day-to-day reproducibility of replicate analyses of standard urine samples containing different concentrations of I and metabolites is presented in Table III and shows a very good precision, with a coefficient of variation of 3–7.4%. Standard solutions of I and metabolites were freshly prepared and stored in darkness at low temperature (refrigerator) for short periods of time. New standard solutions were made every week, and particular attention was given to stock solutions of metabolites IV, V, and VII, which showed degradation products after a few hours at room temperature.

Cardiovascular drugs that may be given to patients without producing interferences in the assay of I and metabolites are: digoxin, propranolol, procainamide, nitroglycerin, isosorbide dinitrate, and furosemide. On the other hand, benzodiazepines (flurazepam and diazepam) interfere with the metabolites of I, but not with I itself.

Table IV—Percent of Conjugated Diltiazem and Metabolites in the Urine of Two Patients

	Patient 1	Patient 2
Diltiazem (I)	0%	0%
II	70%	77%
IV	80%	75%
V	90%	96%
VII	95%	96%
III	98%	95%
VI	97%	98%

In Figs. 2 and 3 the cumulative amounts of I and metabolites excreted in urine are presented, and Table IV gives the ratio of conjugated to free products in the urine of two patients. In fact, >80% of each metabolite excreted in urine is conjugated, and only a small amount of I was found unchanged in the urine (Table II). More than 50% of the dose was excreted in the first 8 h.

After a single oral 120-mg dose, metabolites III and VII appeared to be the main metabolites in urine, followed by successively smaller amounts of IV, VI, V, and II. The same metabolic pattern is observed during chronic administration (120 mg tid) with the exception of IV, which did not show a significant increase (Fig. 3). In fact, the cumulative amounts of IV excreted were 8 mg after a single dose and 10 mg after chronic administration. For I and other metabolites, there is a three- or fourfold difference in concentrations between single and chronic dosing.

This method was applied to the measurement of plasma concentrations of I and metabolites, but the lack of sensitivity does not permit adequate pharmacokinetic studies when concentrations are as low as 20 ng/mL.

REFERENCES

(1) D. D. Waters, P. Theroux, J. Szlachcic, and M. Mizgala, *Clin. Invest. Med.*, **3**, 129 (1980).

(2) P. Theroux, D. D. Waters, G. S. Affaki, J. Crittin, R. Bonan, and M. Mizgala, *Circulation*, **60**, 504 (1979).

(3) V. Rovei, M. Mitchard, and P. Morselli, *J. Chromatogr.*, **138**, 391 (1977).

(4) J. P. Clozel, G. Caille, Y. Taeymans, P. Theroux, P. Biron, and J. G. Besner, *J. Pharm. Sci.*, **73**, 207 (1984).

(5) K. Kohno, Y. Takeuchi, A. Etom, and K. Noda, *Arzneim.-Forsch.*, **27**, 1424 (1977).

ACKNOWLEDGMENTS

The authors thank Dr. Léo Gosselin and Dr. David Bensemana of Laboratories Nordic Inc. and the Tanabe Seigaku Ltd., Company, Japan, for providing diltiazem and the six metabolites.

Fluid Shifts and Other Factors Affecting Plasma Protein Binding of Prednisolone by Equilibrium Dialysis

F. DOUGLAS BOUDINOT and WILLIAM J. JUSKO ˣ

Received February 9, 1983, from the *Department of Pharmaceutics, School of Pharmacy, State University of New York at Buffalo, Buffalo, NY 14260.* Accepted for publication April 22, 1983.

Abstract □ The effects of drug stability, radioactive tracer purity, buffer composition, protein concentration, and fluid shifts on the nonlinear plasma protein binding of prednisolone were examined by equilibrium dialysis. Prednisolone exhibits a concentration-dependent degradation; however, the limited extent of this does not affect protein binding. Impure tritiated prednisolone used as a tracer produces incorrect, low fractional binding values with the binding parameters generated for transcortin affected more than those for albumin. Isotonic sodium phosphate and Krebs original Ringer phosphate buffers yield similar fractional binding of prednisolone and identical protein binding parameters. Fractional binding of the steroid decreases with total plasma protein concentration, but the association constants remain constant over a twofold dilution of plasma proteins. Further dilution increases these parameters. A time-dependent colloidal osmotic fluid shift during dialysis causes dilution of plasma protein concentrations and diminished drug binding. Theoretical simulations show that the osmotic fluid shifts produce the largest changes in fractional binding for compounds that are bound by low-capacity proteins with low association constants ($K < 10^6$ M^{-1}). A mathematical equation was developed to correct bound drug concentrations and fraction bound for protein dilution caused by this effect. The fluid shifts can be prevented by the addition of dextran (mol. wt. 70,000) to the dialysis buffer in a concentration of 55% of the total protein concentration. Multiple factors can diminish the nonlinear prednisolone binding as artifacts during equilibrium dialysis, but the changes are relatively modest.

Keyphrases □ Plasma protein binding—prednisolone, equilibrium dialysis, effects of drug stability, radiotracer purity, buffer composition, and fluid shifts □ Prednisolone—plasma protein binding, equilibrium dialysis, effects of drug stability, radiotracer purity, buffer composition, and fluid shifts □ Equilibrium dialysis—plasma protein binding of prednisolone, effects of drug stability, radiotracer purity, buffer composition, and fluid shifts

Determinants of the plasma protein binding of ligands can be separated into two categories: authentic and experimental. Authentic factors include drug concentrations, plasma protein concentrations, competitors or inhibitors of binding that may be present in plasma, and other natural physiological factors such as pH. Experimental determinants are due to the manipulations that are necessary to obtain *in vitro* measurements. These factors are often characteristic of the experimental method employed. The most widely used method of determining the extent of drug plasma protein binding is equilibrium dialysis. Protein binding by this method can be affected by drug stability, radioactive tracer purity, time of equilibration, dilution, temperature, pH, buffer composition, and colloidal osmotic fluid shifts caused by plasma proteins.

The interaction of glucocorticoids with proteins and the examination of factors affecting binding have been the subject of numerous publications over the past 25 years. These steroids are bound in plasma principally by transcortin, albumin, and α_1-acid glycoprotein. Hydrocortisone, corticosterone (1), and prednisolone (2) are bound strongly to transcortin, but this protein is easily saturated due to its low binding capacity (2, 3). Albumin has a large capacity, but low affinity for binding these steroids. α_1-Acid glycoprotein exhibits both weak affinity for binding hydrocortisone (4) and prednisolone (5), as well as low binding capacity. Its contribution to overall steroid binding in plasma can be neglected (5).

Saturation of transcortin binding sites results in a nonlinear relationship between the fraction bound and the plasma prednisolone concentration. There is a decrease in the fraction of prednisolone bound at higher drug concentrations. Thus, one concern in measuring prednisolone binding by equilibrium dialysis has been the effects of dilution of the original plasma drug concentration, which shifts binding to a greater fraction bound than exists at the original *in vivo* concentration (6, 7). In addition, lower plasma albumin concentrations produce less drug binding, but increase the number of binding sites or affinity constants (*i.e.*, $N{\cdot}K$), of several drugs (8) including hydrocortisone (9, 10). The net movement of fluid from buffer to plasma that occurs during equilibrium dialysis results in a dilution of the plasma proteins. Thus, fluid shifts that occur during equilibrium dialysis may yield unpredictable changes in prednisolone binding. Equations for correcting for such dilution effects on thyroxine binding were originally proposed by Oppenheimer and Surks (11).

The composition of the buffer used in equilibrium dialysis can have a marked influence on drug binding. For example, the fractional binding of quinidine to albumin is higher when isotonic phosphate rather than Krebs–Ringer phosphate buffer is used (12, 13).

Impure radioactive tracer or degradation of ligand during dialysis may lead to inaccurate results (14). Impurities in a radioactive tracer, more likely than not, bind differently than the ligand being examined. Degradation products of an unstable ligand may also either interfere with the protein binding of the ligand itself or decrease the amount of ligand in the dialysis system. The latter also occurs if the drug binds nonspecifically to the membrane or cell.

The purpose of the present study was to assess the effects of drug stability, radioactive tracer purity, time of equilibration, buffer composition, protein concentration, and volume shifts on prednisolone binding by equilibrium dialysis. A mathematical approach to correct for protein dilution caused by fluid shifts was developed. Physically preventing fluid shifts from occurring by adding dextran to the buffer was examined. Simulations were performed to assess the expected degree of perturbation in binding caused by fluid shifts for drugs and proteins with diverse association constants.

EXPERIMENTAL

Equilibrium Dialysis—Prednisolone[1] was added to pooled human plasma, treated with charcoal to remove endogenous steroids, to yield concentrations ranging from 0 to 1000 ng/mL (2.8 μM). Total plasma protein and albumin concentrations were measured chemically[2]. Acrylic[3] dialysis cells, checked to ensure that no leakage occurred, and dialysis membrane[4] with a 12,000–14,000 molecular weight cutoff were used. Tritiated prednisolone[5] (41 Ci/mmol) was purified by HPLC (15). Plasma (0.8 mL) with trace amounts

[1] Sigma Chemical Co., St. Louis, Mo.
[2] Technicon Auto Analyzer, Tarrytown, N.Y.
[3] Plexiglas.
[4] Spectrapor II; Spectrum Medical Industries, Inc., Los Angeles, Calif.
[5] Amersham Corp., Arlington Heights, Ill.

0022-3549/84/0600-0774$01.00/0
© 1984, American Pharmaceutical Association

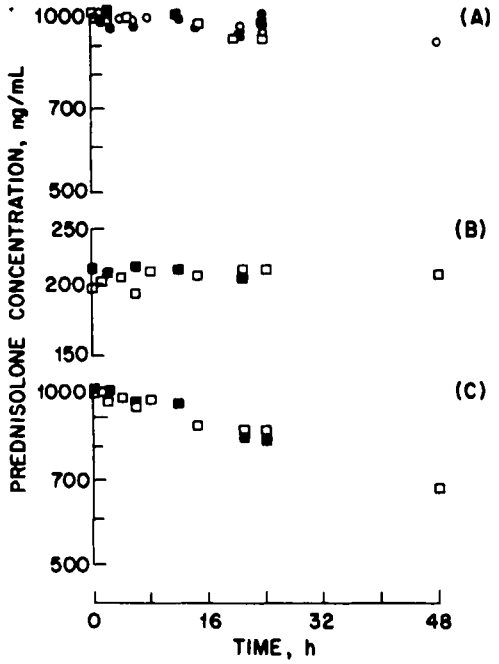

Figure 1—*Stability of prednisolone as a function of time at 37°C. Key: (A) Stability profiles for prednisolone in normal (○) and nephrotic (□) serum contained in glass tubes and normal (●) and nephrotic serum (■) in the dialysis cells. The initial concentration of each set of samples was 1000 ng/mL. (B) Stability profiles for prednisolone in normal serum contained in glass tubes (□) and normal serum in the dialysis cells (■). The initial concentration of each set of samples was 200 ng/mL. (C) Stability profiles for prednisolone in isotonic phosphate buffer, pH 7.4, contained in glass tubes (□) and in the dialysis apparatus (■) at an initial concentration of 1000 ng/mL.*

(10,000 cpm) of tritiated prednisolone was dialyzed against isotonic sodium phosphate buffer, pH 7.4, (0.8 mL) at 37°C for 16 h. Postdialysis plasma and buffer volumes were measured using a syringe[6]. Aliquots (0.5 mL) of plasma and buffer were added to water (2.5 mL) and scintillation cocktail[7] (10 mL) and counted with a scintillation counter[8]. Counts per minute were converted to disintegrations per minute using the external standard ratio method (16). Experiments were done in duplicate or triplicate.

Stability and Membrane Binding—The stability of prednisolone was assessed in normal and pooled nephrotic patient serum and in isotonic phosphate buffer, pH 7.4. Prednisolone was dissolved in each of these fluids to produce concentrations of 200 or 1000 ng/mL. Serum and buffer samples were gently shaken in glass tubes maintained at 37°C with samples of each solution taken at 0, 1, 2, 4, 6, 8, 14.5, 21, 24, and 48 h after placement into a water bath.

To determine the stability and extent of adsorption of prednisolone in the presence of dialysis membranes and dialysis cells, aliquots of the above solutions were added to the dialysis apparatus. The cells were gently shaken in a water bath at 37°C, with removal of samples at 0, 2, 6, 12, 21, and 24 h after initiation of the study.

All samples were frozen (−20°C) immediately on removal from the water bath. Prednisolone concentrations were determined in all samples using the HPLC technique of Rose and Jusko (15).

Radioactive Tracer Purity—Equilibrium dialysis experiments were carried out using tritiated prednisolone, which had been maintained in a freezer (−20°C) in benzene-ethanol (9:1) for 6 months. The material was purified by HPLC, and the dialysis experiments were repeated. The same plasma was used for both experiments.

Equilibrium Rate—The time required to obtain equilibration of free prednisolone concentrations between the plasma and buffer compartments of dialysis cells was evaluated at both low (50-ng/mL) and high (1000-ng/mL) plasma prednisolone concentrations. Plasma, with prednisolone added, was dialyzed against either isotonic sodium phosphate buffer or isotonic buffer with dextran added. At various times after the initiation of dialysis, plasma and buffer samples were removed from the cells. The volumes of the samples were measured and aliquots placed in scintillation vials for counting of the radioactive tracer. Samples were obtained over a 24-h period. Fractional binding of prednisolone was calculated at each sampling time.

[6] Unimetrics Corp., Anaheim, Calif.
[7] Aquasol; New England Nuclear, Boston, Mass.
[8] Packard.

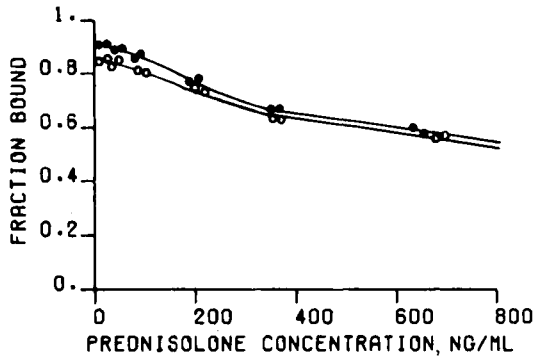

Figure 2—*Fraction bound* versus *postdialysis plasma prednisolone concentration before (○) and after (●) purification of the tritiated prednisolone tracer by HPLC.*

Influence of Buffer Composition—Krebs original Ringer phosphate, pH 7.4 (0.14 M), was prepared according to Dawson *et al.* (17). Isotonic sodium phosphate buffer, pH 7.4 (0.14 M), was composed of 0.054 M Na_2HPO_4, 0.013 M KH_2PO_4 and 0.075 M NaCl. Both buffers were prepared in distilled deionized water. Plasma, with prednisolone added, was dialyzed against the Krebs and phosphate buffers.

Effect of Protein Concentration—The total protein concentration of pooled human plasma (total protein = 5.5 g/dL, albumin = 3.7 g/dL) was defined as 100%. This plasma was diluted with various volumes of isotonic sodium phosphate buffer, pH 7.4, to yield total protein concentrations of 87.5% (4.8 g/dL), 75% (4.1 g/dL), 50% (2.8 g/dL), and 25% (1.4 g/dL). Prednisolone was added to each protein dilution (0–1000 ng/mL) and dialyzed as described previously.

Fluid Shifts—*Mathematical Correction*—The concentration of drug bound was corrected for protein dilution due to fluid shifts by:

$$D_B = (D_{Te} - D_F) \cdot \frac{V_{pe}}{V_{pi}} \qquad \text{(Eq. 1)}$$

where D_F and D_B are the free and protein-bound plasma prednisolone concentrations, D_{Te} is the total plasma prednisolone concentration at equilibrium, and V_{pi} and V_{pe} are the initial and equilibrium plasma volumes. The fraction of prednisolone bound to plasma proteins (F_B) can be calculated by:

$$F_B = \frac{(D_{Te} - D_F) \cdot \frac{V_{pe}}{V_{pi}}}{\left[(D_{Te} - D_F) \cdot \frac{V_{pe}}{V_{pi}}\right] + D_F} \qquad \text{(Eq. 2)}$$

The derivation of these equations is provided in the *Appendix*.

Dextran—Dextran[9] with an average mol. wt. of 70,000 was added to the isotonic sodium phosphate buffer to offset osmotic fluid shifts caused by plasma proteins. Various concentrations of dextran (0–5 g/dL) in buffer with prednisolone (0–2000 ng/mL) added were dialyzed against buffer to assess whether binding of prednisolone to dextran occurs. To develop an equation to predict the concentration of dextran needed to prevent fluid shifts, dextran (0–5 g/dL) in buffer was dialyzed against plasma (total protein = 5.5 g/dL),

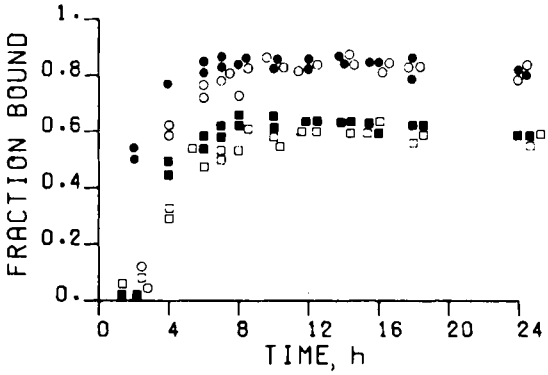

Figure 3—*Apparent fraction bound* versus *equilibration time for prednisolone plasma concentrations of 50 ng/mL (○,●) and 1000 ng/mL (□,■), dialyzed against isotonic sodium phosphate buffer (closed symbols) and phosphate buffer with dextran added (open symbols).*

[9] Pharmacia Fine Chemicals AB, Uppsala, Sweden.

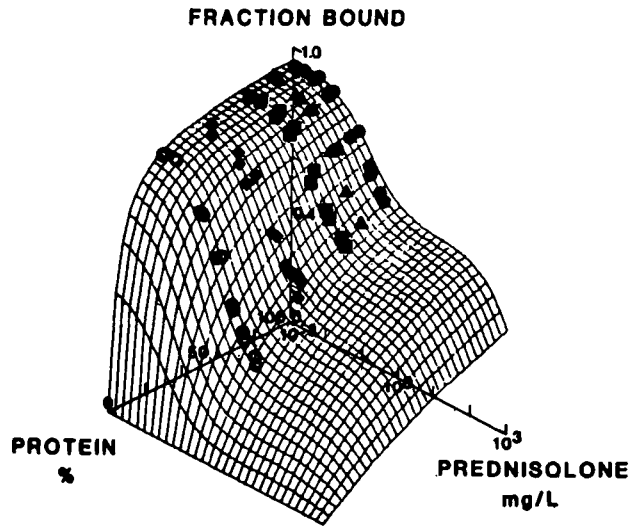

Figure 4—*Relationship between the plasma protein binding of prednisolone, unbound drug concentrations, and protein concentrations of 100% (●), 87.5% (▲), 75% (■), 50% (◆), and 25% (○).*

and postdialysis plasma and buffer volumes were measured. Mean postdialysis plasma and buffer volumes were plotted as a function of dextran concentration. The intersect of ordinary least-squares regression lines drawn through the postdialysis plasma and buffer volumes *versus* dextran concentration points occurs at the dextran concentration (3.0 g/dL) needed to offset perfectly fluid shifts caused by a total protein concentration of 5.5 g/dL. Rearrangement of the direct proportionality:

$$\frac{[\text{Dextran}]}{[\text{Total Plasma Protein}]} = \frac{3.0\ \text{g/dL}}{5.5\ \text{g/dL}} \qquad \text{(Eq. 3)}$$

yields

$$[\text{Dextran}] = [\text{Total Plasma Protein}] \times 0.5455 \qquad \text{(Eq. 4)}$$

which can be used to predict the dextran concentration required to prevent fluid shifts based on total plasma protein concentration. The predictive value of Eq. 4 was examined over a wide range of total plasma protein concentrations by employing plasma from 10 normal volunteers and 9 patients with nephrotic syndrome, a condition that results in hypoproteinemia. Total plasma protein concentrations were measured, and the appropriate dextran concentrations were determined using Eq. 4. Samples were dialyzed against buffer containing the calculated dextran concentrations, and postdialysis plasma and buffer volumes were measured. To examine the effect of dextran on prednisolone binding, plasma containing prednisolone was dialyzed against buffer in the absence and presence of dextran.

Data Analysis—When radioactive tracer methods are employed to determine the fractional binding, Eq. 2 can be written as:

$$F_B = \frac{(\text{DPM}_p - \text{DPM}_B) \cdot \frac{V_{pe}}{V_{pi}}}{(\text{DPM}_P - \text{DPM}_B) \cdot \frac{V_{pe}}{V_{pi}} + \text{DPM}_B} \qquad \text{(Eq. 5)}$$

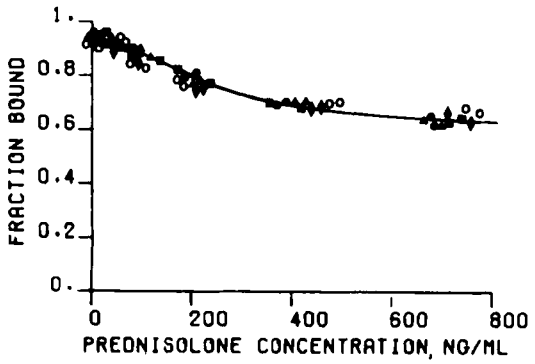

Figure 5—*Fraction of prednisolone bound* versus *postdialysis plasma prednisolone concentrations showing results of correction for protein dilutions. Symbols represent experimental data at protein concentrations of 100% (●), 87.5% (▲), 75% (■), 50% (◆), and 25% (○).*

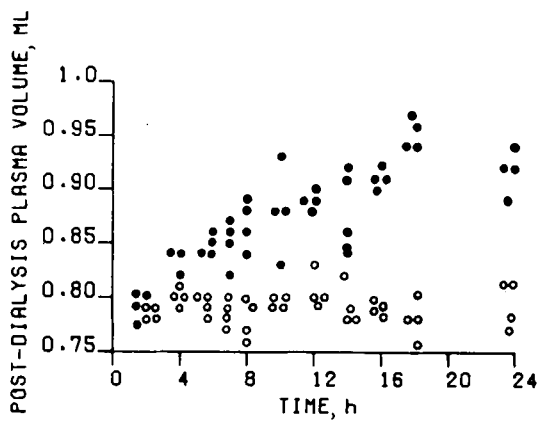

Figure 6—*Postdialysis plasma volume* versus *time where plasma was dialyzed against isotonic sodium phosphate buffer (●) and buffer with dextran (○).*

where DPM_P and DPM_B are disintegrations per minute in the plasma and buffer after background counts have been subtracted. When fluid shifts were observed, Eq. 5 was used to calculate the fraction of prednisolone bound. In the absence of fluid shifts (*i.e.*, when dextran was added to the dialysis buffer), the fraction bound was calculated by:

$$F_B = \frac{\text{DPM}_P - \text{DPM}_B}{\text{DPM}_P} \qquad \text{(Eq. 6)}$$

The plasma protein binding of prednisolone can be described by the relationship:

$$D_B = \frac{N_T K_T P_T D_F}{1 + K_T D_F} + \frac{N_A K_A P_A D_F}{1 + K_A D_F} \qquad \text{(Eq. 7)}$$

where N_T and N_A are the number of binding sites on transcortin and albumin, K_T and K_A are the association constants for transcortin and albumin, P_T and P_A are the plasma concentrations of transcortin and albumin, and D_B and D_F are the plasma concentrations of bound and free prednisolone. Least-squares estimates of $N_T K_T P_T$, K_T, and $N_A K_A P_A$ were obtained by the method of Priore and Rosenthal (18). Since P_A was measured chemically, $N_A K_A$ could be calculated. P_T was calculated assuming an N_T value of one. The total prednisolone concentration at equilibrium was generated using a variation of the methods of Behm and Wagner (6) and Rose *et al.* (7).

Statistics—The paired *t* test was used to determine whether there were any differences in the binding parameters obtained with phosphate and Krebs buffers. Regression lines for protein concentration *versus* postdialysis volumes were fitted by the weighted perpendicular least-squares method assuming error in both variables (19).

RESULTS AND DISCUSSION

Stability—The results from the stability study are presented in Fig. 1. At initial prednisolone concentrations of 1000 ng/mL, degradation in normal serum, nephrotic serum, and buffer at the end of 24 h was 6.7, 14.2, and 16.5% as determined by log-linear regression of concentration–time data. This degradation appears to be concentration dependent since no significant loss occurred in normal serum at initial drug concentrations of 200 ng/mL (Fig. 1B). The extent of this degradation does not appear to present any problem in analyzing prednisolone binding data. While the protein binding of the steroid was examined at concentrations as high as 1000 ng/mL, most samples have concentrations that were much lower and, therefore, may be subject to less degradation. There was no significant difference between the loss of prednisolone as a function of time from solutions contained in glass tubes *versus* solutions studied in the dialysis cells. This suggests that adsorption of prednisolone onto dialysis membranes and cell walls does not occur.

Radioactive Tracer Purity—The effects on binding of using aged *versus* freshly purified tritiated prednisolone tracer are shown in Fig. 2. The use of pure radioactive tracer resulted in fractional binding data higher than the data obtained using impure tracer. The binding parameters $N_T K_T P_T$, K_T, and $N_A K_A P_A$ were 5.33, $1.21 \times 10^7\ M^{-1}$, and 0.84 when impure radioactive tracer was used and 8.56, $2.16 \times 10^7\ M^{-1}$, and 0.85 when purified tracer was employed. Thus, the products of both radiolysis and of chemical degradation bind less readily, if at all, to transcortin and albumin, resulting in an increased apparent free drug concentration and incorrect, low fractional binding data. We have found that purification of tritiated prednisolone approximately every 3 months is required to obtain valid binding results.

Table I—Plasma Protein Binding Parameters for Prednisolone Related to Protein Concentration Without and With Correction for Dilution

Protein Conc., g/dL	$N_TK_TP_T$ Without Correction	$N_TK_TP_T$ With Correction	K_T, $M^{-1} \times 10^{-7}$ Without Correction	K_T, $M^{-1} \times 10^{-7}$ With Correction	$N_AK_AP_A$ Without Correction	$N_AK_AP_A$ With Correction	N_AK_A, $M^{-1} \times 10^{-3}$ Without Correction	N_AK_A, $M^{-1} \times 10^{-3}$ With Correction
5.5	11.4	13.2	2.87	3.26	0.917	1.12	1.94	2.06
4.8	11.6	14.4	3.16	3.35	0.793	1.03	1.88	1.89
4.1	8.91	12.6	2.62	3.28	0.704	1.11	1.88	2.04
2.8	6.98	13.8	3.10	4.86	0.566	1.36	2.18	2.50
1.4	4.93	15.8	4.37	7.40	0.359	1.61	2.64	2.96

Equilibration Rate—The results of the equilibration study are presented in Fig. 3. When isotonic sodium phosphate buffer is used as the dialysate, equilibration of free prednisolone occurs within 8 h and is independent of the prednisolone concentration. The inclusion of dextran in the buffer results in a slower equilibration rate (10–14 h), with the higher prednisolone concentrations requiring a longer time to attain equilibrium. This may be due to obstruction of pores in the dialysis membrane by dextran. Fractional binding values remain constant from the minimum time required to reach equilibrium of free prednisolone to at least 18 h, reinforcing our conclusion that prednisolone degradation during dialysis is minimal.

Buffer Composition—Isotonic sodium phosphate buffer and Krebs original Ringer phosphate yield similar binding of prednisolone. The mean (*SD*) $N_TK_TP_T$, K_T, and $N_AK_AP_A$ obtained were 8.59 (2.53), 1.71×10^7 (0.35×10^7) M^{-1}, and 0.92 (0.15) when isotonic phosphate buffer was used and 8.17 (3.02), 1.73×10^7 (0.48×10^7) M^{-1}, and 0.91 (0.15) when Krebs buffer was employed. There were no statistically significant differences between the binding parameters obtained using the two buffers.

These protein binding parameters agree well with previously reported values for prednisolone (2, 20–22). Chan and Slaunwhite (23) noted small decreases in the binding of hydrocortisone and progesterone to transcortin as dialysate NaCl concentrations decreased below 0.15 M. However, lower NaCl concentrations in the isotonic sodium phosphate buffer than in Krebs original Ringer phosphate (0.075 *versus* 0.118 M) did not produce this effect with prednisolone.

Protein Concentration—Figure 4 illustrates the fraction of prednisolone bound as a function of unbound prednisolone concentration and plasma protein concentration. The surface was calculated using binding parameters obtained by fitting fractional binding data from the 75–100% protein concentration range, where no differences were found in the binding parameters (see below). The data from the 25% protein concentration deviates slightly from the predicted values. Nonlinear binding is seen at all protein concentrations examined, with less fractional binding of prednisolone at lower plasma protein concentrations. The fractional binding of prednisolone diminished as the total protein concentration decreased as a result of lower plasma transcortin and albumin concentrations. At higher prednisolone concentrations, the drug is predominantly bound to albumin. Because the affinity of albumin for prednisolone is low (10^3 M^{-1}), the diminished fractional binding is proportional to the reduced protein concentration (24). At low prednisolone concentrations, where transcortin is the major protein responsible for binding prednisolone, the change in the fractional binding is less marked owing to the high affinity of transcortin for prednisolone (24). At the middle range (100–300 ng/mL) of prednisolone concentrations, the fractional binding changes are also appreciable because of the saturation of transcortin binding. Figure 5 presents the fractional binding data shown in Fig. 4 after corrections for the protein dilutions have been made. All the corrected data, except that from the 25% protein concentration, cluster together.

Decreases in albumin concentrations in albumin solutions (9, 10) and in serum (10) have resulted in increases in the binding parameter $N{\cdot}K$. Increases in α_1-acid glycoprotein concentrations, on the other hand, result in increases in the binding affinity for hydrocortisone and corticosterone (4), but not for prednisolone (5). The computer-fitted binding parameters obtained at each protein concentration, before and after correcting for plasma dilution, are listed in Table I. Without any correction, K_T remains constant over the protein concentration range of 100–50%, but increases at the 25% protein concentration. The N_AK_A values remain constant between 100 and 75% protein concentrations, but increase at lower protein concentrations. After correcting the binding data for the plasma protein dilutions, the K_T and N_AK_A values remain constant above the 75% protein concentration, but increase at lower total protein concentrations. Inspection of Table I shows that the correction for protein dilution in the protein concentration range of 75–100% does not appreciably affect K_T and N_AK_A values.

The magnitude of the increases in K_T and N_AK_A at low protein concentration is not particularly great, yet helps explain the deviations noted at the 25% protein concentration (Figs. 4 and 5). The N_AK_A for prednisolone, which does not increase until the albumin concentration has decreased to 50% ($P_A = 2.7 \times 10^{-4}$ M), appears to be more resistant to changes in albumin concentration than hydrocortisone, which shows increases in N_AK_A at albumin concentrations $<9 \times 10^{-4}$ M (10). No change occurs in K_T until protein concentrations are reduced to 25% ($P_T = 1.1 \times 10^{-7}$ M). When diluting plasma, the possibility arises that the increases seen in the binding parameters

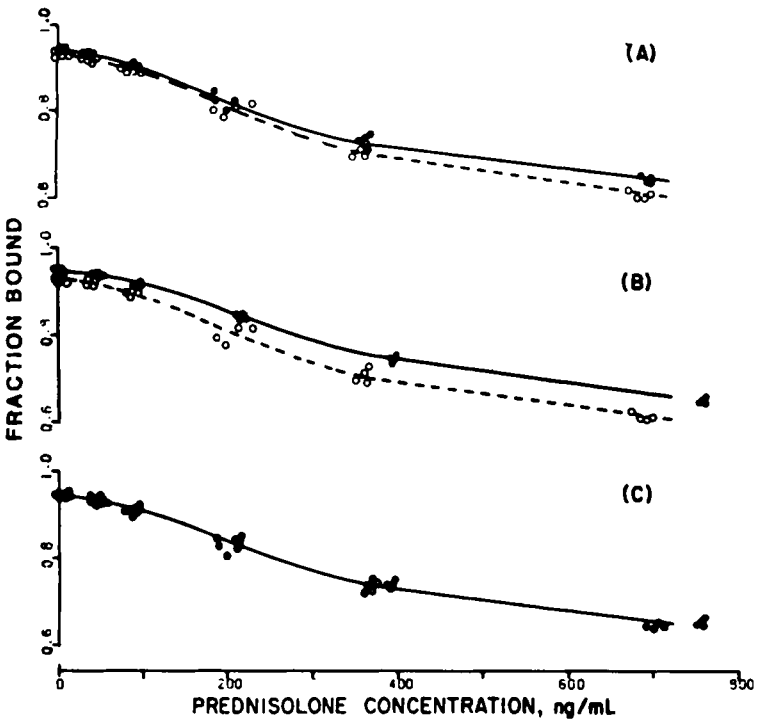

Figure 7—*Plasma protein binding of prednisolone in relation to free drug concentrations under the following conditions: (A) without (○) and with (●) mathematical correction for fluid shifts using Eq. 5, maximum difference 6%; (B) without (○) and with (●) dextran added to prevent fluid shifts; (C) with dextran added to buffer (●) and after mathematical correction (Eq. 5) for the fluid shifts that occur with buffer alone (○).*

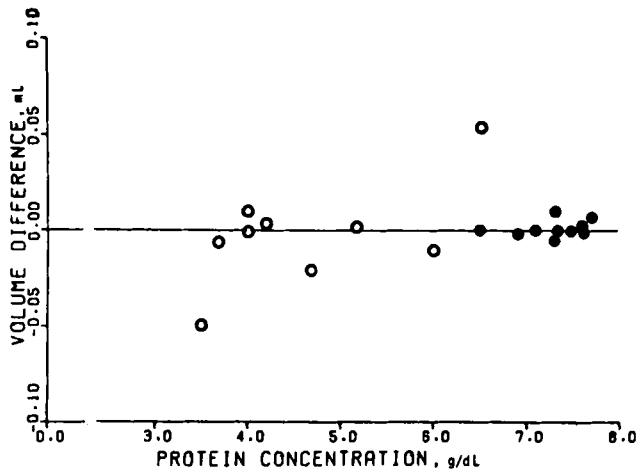

Figure 8—*Postdialysis volume differences (plasma side minus buffer side) observed when plasma containing various total protein concentrations were dialyzed against buffer, with dextran content calculated by Eq. 4. Key: (●) normal subjects; (○) patients with nephrotic syndrome; (—) no fluid shift.*

are due to lower concentrations of binding inhibitors, although these were probably removed by the charcoal. Another explanation might be that conformational changes in the albumin molecule may make available binding sites that were previously inaccessible (25). This may explain the increases in N_AK_A, but no increase occurs in the number of binding sites on the transcortin molecule. The trimer-polymer form of albumin has been shown to have a lower binding affinity for progesterone than the monomer or dimer forms (26). The binding affinity of transcortin in the rat (27) and rabbit (28) has also been shown to decrease owing to polymer formation. Whether or not human transcortin forms polymers is still being debated (29–31). A decrease in polymer formation at low protein concentrations may explain the increases seen in K_T and N_AK_A. It is important to note that K_T and N_AK_A remain constant up to a twofold dilution of the plasma proteins.

The colloidal osmotic pressure of plasma proteins tends to pull fluid into the plasma compartment of a dialysis cell, resulting in lower postdialysis protein concentrations. A decrease in the fractional binding of ligand to protein may also occur. Linear relationships were observed between postdialysis plasma ($r = 0.994, p < 0.005$) and buffer ($r = 0.966, p < 0.01$) volumes and plasma protein concentration. Fluid shifts were greatest with undiluted plasma and decreased as plasma protein concentration decreased. The decreases in protein concentration caused by these fluid shifts resulted in decreases in the fractional binding of prednisolone. As the protein binding parameters for prednisolone are constant over the range of dilutions that result from fluid shifts, this low fractional binding of prednisolone can be corrected mathematically.

Volume Shifts—*Mathematical Correction*—Equal volumes (0.8 mL) of plasma and isotonic sodium phosphate buffer were placed in each equilibrium dialysis cell. Figure 6 presents measured postdialysis plasma volumes as a function of time, showing progressive increases in the plasma volume between 2 and 14 h. Plasma volumes were static after 14 h. Mean (*SD*) plasma and buffer volumes typically found at 16 h are 0.91 (0.04) mL and 0.67 (0.04) mL, respectively. Volume shifts of similar magnitude were noted when plasma was dialyzed against Krebs original Ringer phosphate and with both hypotonic and hypertonic sodium phosphate buffers. This produces postdialysis protein concentrations that are ~86% of the initial concentrations. Equation 5 was employed to correct for this fluid shift, and Fig. 7A presents the binding results with (Eq. 5) and without (Eq. 6) this adjustment. The dilution of plasma proteins caused by fluid shifts results in lower values for the fractional binding of prednisolone. The K_T and N_AK_A were $2.83 \times 10^7\ M^{-1}$ and $2.06 \times 10^3\ M^{-1}$ without correction and $3.55 \times 10^7\ M^{-1}$ and $2.28 \times 10^3\ M^{-1}$ with correction.

Oppenheimer and Surks (11), in the first attempts to correct protein binding data for dilution of plasma proteins, corrected the free drug concentration for dilution in terms of the total volume of the dialysis system. Our method differs in that we correct the bound drug concentration for dilution of proteins using pre- and postdialysis volumes of the plasma compartment only. The bound drug concentration was corrected since this is the variable that is dependent on drug and protein concentrations (Eq. 7). Correction of the free drug concentration would appear to introduce an artifact into the system, particularly when binding is nonlinear.

Volume shifts that occur in our equilibrium dialysis system yield postdialysis protein concentrations that are ~86% of their initial value. As shown previously, protein dilutions of this magnitude have no effect on $N_TK_TP_T$, K_T, or N_AK_A. If D_F is held constant, the only changing variables in Eq. 7 are P_T and P_A. These can be corrected for by use of a dilution factor and D_B can then be calculated. This dilution factor can be expressed as the ratio of the equilibrium plasma volume (V_{pe}) to the initial plasma volume (V_{pi}). The higher D_B and F_B obtained after correction are then functions of the initial protein concentration. A dilution factor could also be calculated from directly assayed pre- and postdialysis protein concentrations. Mathematical correction for fluid shifts cannot be used if the binding parameters are highly dependent on protein concentration.

Dextran—Dextran, when added to dialysis buffer, alters the magnitude and direction of fluid shifts. Equation 4 was found to be useful for calculating the dextran concentration required to prevent fluid shifts, based on total plasma protein concentration. As shown in Fig. 8, 19 samples dialyzed against buffer containing dextran resulted in fluid shifts of <0.05 mL, while 16 resulted in shifts of <0.01 mL. No binding of prednisolone to dextran occurred.

The results of dialyzing plasma containing prednisolone against buffer alone and buffer with dextran added are shown in Fig. 7B. The fractional binding of prednisolone determined by dialyzing plasma against plain buffer is lower as a result of the dilution of plasma proteins. When dextran was added to the buffer, no fluid shifts occurred. The K_T and N_AK_A values were $2.38 \times 10^7\ M^{-1}$ and $2.06 \times 10^3\ M^{-1}$ for plain buffer and $3.54 \times 10^7\ M^{-1}$ and 2.25×10^3

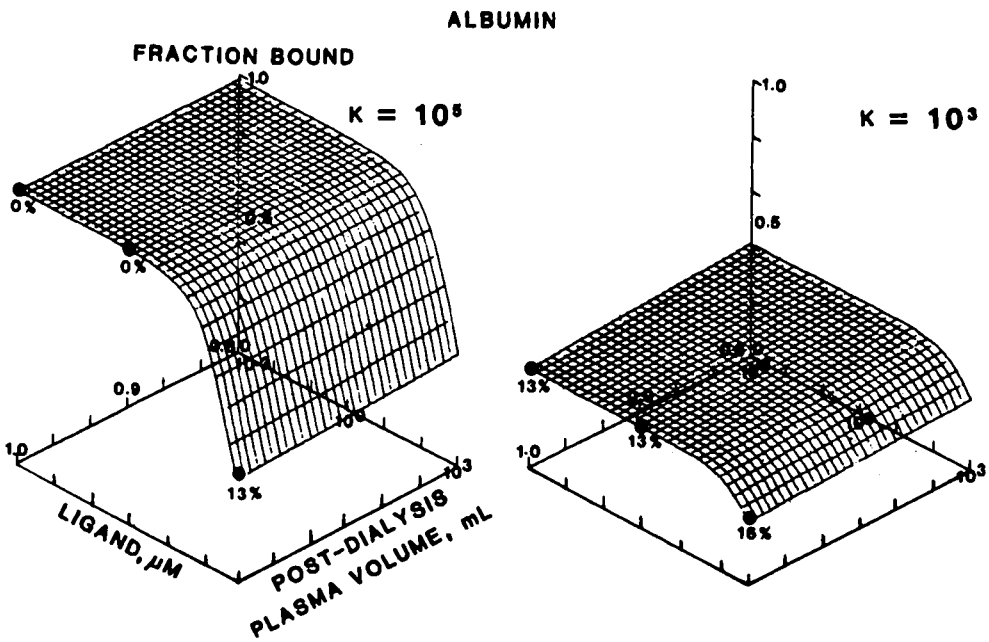

Figure 9—*Relationship between the fraction of ligand bound to albumin, free ligand concentration, and postdialysis plasma volume. Dots indicate the percent decrease in fractional binding due to volume shifts at ligand concentrations of 10^{-3}, 10^0, and 10^3 μM.*

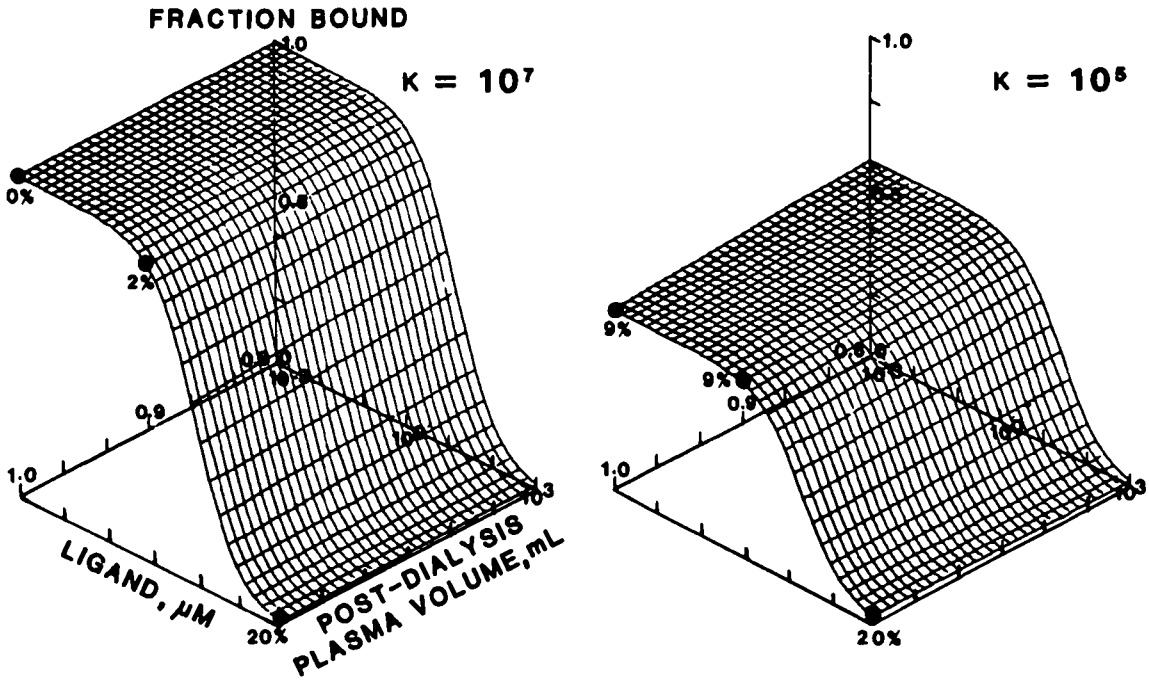

Figure 10—*Relationship between the fraction of ligand bound to α_1-acid glycoprotein, free ligand concentration, and post-dialysis plasma volume. Dots indicate the percent decrease in fractional binding due to volume shifts at ligand concentrations of 10^{-3}, 10^{0}, and 10^{3} μM.*

M^{-1} for buffer with dextran. Figure 7C shows the same data with correction for the typical volume shifts. The results with dextran and those obtained with the mathematical correction coincide on the same binding curve, although the latter are shifted slightly to the left as a result of the increased plasma volume (6, 7). The computer-fitted K_T and $N_A K_A$ were 3.54×10^7 M^{-1} and 2.25×10^3 M^{-1} for results obtained with dextran and 3.55×10^7 M^{-1} and 2.28×10^3 M^{-1} for the mathematically corrected binding data.

Dextran, when added to buffer in appropriate amounts, prevents the occurrence of any fluid shift, so that the binding results obtained are then directly related to the initial protein concentration. Inhibitors of binding also remain undiluted. The concentration of dextran (mol. wt. 70,000) required to prevent volume shifts is 55% of the total plasma protein concentration.

The use of other dialysis membranes or systems may also prevent volume shifts. Lima *et al.* (32) found that a thicker membrane with a molecular weight cutoff of 6000–8000 will diminish the fluid shift. We also examined equilibrium dialysis of prednisolone with cells that have a larger membrane-to-volume surface area[10]. Equilibration was obtained by 2 h, and no volume shifts were observed. Prednisolone binding data in these cells were identical with results obtained by mathematical correction or addition of dextran in the present system.

Calculated Effects of Volume Shifts—Simulations were employed to illustrate the effects of volume shifts on the protein binding (D_B) of ligands at various protein concentrations (P), association constants (K), and free ligand concentrations (D_F). Normal values of albumin (4.8 g/dL) and α_1-acid glycoprotein (70 mg/dL) concentrations were used to depict high and low protein concentrations. Association constants employed were 10^3 M^{-1} and 10^5 M^{-1} for albumin and 10^5 M^{-1} and 10^7 M^{-1} for α_1-acid glycoprotein. The number of binding sites per protein molecule (N) was assigned as 1 for both proteins. It was assumed that neither N nor K changed as a result of increases in the postdialysis plasma volume. The equation used for these simulations is:

$$D_B = \frac{N \cdot K \cdot P \cdot D_F \cdot \frac{V_{pi}}{V_{pe}}}{1 + K \cdot D_F} \qquad \text{(Eq. 8)}$$

where ligand concentration ranged from 10^{-9} to 10^{-3} M. Postdialysis plasma volumes (V_{pe}) ranged from 0.8 mL (no volume shift, V_{pi}) to 1.0 mL.

Simulations depicting drug binding to albumin in relation to volume changes are shown in Fig. 9. The fractional binding calculated with both association constants is linear over a wide range of ligand concentrations due to the high binding capacity of albumin. The higher association constant ($K = 10^5$ M^{-1}) yields higher fractional binding at all ligand concentrations. When $K = 10^5$ M^{-1}, an increase in the plasma volume from 0.8 mL to 1.0 mL produces <1% decrease in the fraction bound over a ligand concentration range of 10^{-3}–10^1 μM. At higher ligand concentrations, volume shifts produce progressively larger decreases in fractional binding. At a ligand concentration of 10^3 μM, a shift in plasma volume from 0.8 to 1.0 mL results in a 13% decrease (from 0.41 to 0.36) in fraction bound. When $K = 10^3$ M^{-1}, the same volume shift produces a 13% (0.05 absolute F_B) decrease in fractional binding up to a ligand concentration of 10^2 μM. A similar 16% decrease (from 0.26 to 0.22) in fractional binding occurs at a ligand concentration of 10^3 μM.

Simulations illustrating binding of ligand to α_1-acid glycoprotein are presented in Fig. 10. Saturation of this low-capacity protein at $D_F > 10^{-2}$ μM produces marked nonlinearity in the fractional binding. As expected, the higher association constant yields greater fractional binding of the drug. When $K = 10^7$ M^{-1}, volume shifts produce no change in fractional binding when ligand concentrations range from 10^{-3} to 10^{-1} μM. At a ligand concentration of 10^0 μM, the 20% increase in plasma volume results in a 2% decrease (0.94 to 0.92) in fractional binding. As the ligand concentration increases further, the percent decrease in fractional binding caused by volume shifts progressively increases. The largest absolute change in fractional binding (0.05) as a result of fluid shifts occurs at a ligand concentration of 10^1 μM. When $K = 10^5$ M^{-1}, volume shifts produce a 9% (0.05 absolute) decrease in fractional binding over a ligand concentration range of 10^3–10^1 μM. At higher ligand concentrations the absolute changes in fractional binding are extremely small.

These theoretical simulations show that changes in protein binding of a ligand are dependent on the protein concentration, the association constant, the free ligand concentration, and the magnitude of the volume shift. In general, the decrease in fractional binding is greatest with lower initial protein concentrations, lower association constants, higher free drug concentrations, and larger fluid shifts. The fluid shifts can be either corrected for mathematically or prevented with dextran.

With prednisolone, the binding results obtained by correction or dextran addition agree well. The mathematical approach requires that binding parameters remain constant and also that possible competitors or inhibitors of binding are not influenced by fluid shifts. The equations used can easily be written into a computer program. The dextran approach requires an accurate measurement of the total plasma protein concentration for each compound. For prednisolone, the fluid shifts produce a slight decrease in the fractional binding and do not present any major errors in binding results.

APPENDIX: Correction for Volume Shifts in Protein Binding

The amount of protein (AP_i) initially placed in the dialysis cell is:

$$AP_i = P_i \cdot V_{pi} \qquad \text{(Eq. A1)}$$

[10] Spectrum Medical Industries Inc., Los Angeles, Calif.

where P_i is the initial protein concentration and V_{pi} is the initial dialysate volume. After equilibration of free drug, the amount of protein (AP_e) in the plasma compartment is:

$$AP_e = P_e \cdot V_{pe} \qquad \text{(Eq. A2)}$$

where P_e is the postdialysis protein concentration and V_{pe} is the postdialysis dialysate volume. Assuming there is no loss of protein from the protein compartment:

$$AP_i = AP_e \qquad \text{(Eq. A3)}$$

and therefore:

$$P_i \cdot V_{pi} = P_e \cdot V_{pe} \qquad \text{(Eq. A4)}$$

Rearranging:

$$P_e = P_i \cdot \frac{V_{pi}}{V_{pe}} \qquad \text{(Eq. A5)}$$

In the absence of volume shifts, the concentration of bound drug (D_{Bi}) for m classes of binding sites can be predicted by:

$$D_{Bi} = \sum_{i=1}^{m} \frac{N \cdot K \cdot P_i \cdot D_F}{1 + K \cdot D_F} \qquad \text{(Eq. A6)}$$

given the number of binding sites per protein molecule (N), the association constant (K), the free drug concentration (D_F), and P_i. When volume shifts occur, the same equation applies, except for the change in protein concentration. Thus, the bound drug concentration (D_{Be}) is given by:

$$D_{Be} = \sum_{i=1}^{m} \frac{N \cdot K \cdot P_e \cdot D_F}{1 + K \cdot D_F} \qquad \text{(Eq. A7)}$$

Substituting for P_e:

$$D_{Be} = \sum_{i=1}^{m} \frac{N \cdot K\left(P_i \cdot \frac{V_{pi}}{V_{pe}}\right) D_F}{1 + K \cdot D_F} \qquad \text{(Eq. A8)}$$

If it is assumed that N and K do not vary with changes in P, then:

$$D_{Be} \cdot \frac{V_{pe}}{V_{pi}} = \sum_{i=1}^{m} \frac{N \cdot K \cdot P_i \cdot D_F}{1 + K \cdot D_F} = D_{Bi} \qquad \text{(Eq. A9)}$$

Note that the same value for the independent variable, D_F, is used with and without volume shifts. However, the measured D_F would differ from the D_F obtained had no fluid change occurred. This causes the corrected binding curve to shift up and to the right when plotting fraction bound *versus* equilibrium total drug concentration (see Fig. 7).

The fraction of drug bound at the initial protein concentration is calculated by:

$$F_{Bi} = \frac{D_{Bi}}{D_{Bi} + D_F} \qquad \text{(Eq. A10)}$$

From Eq. A9:

$$D_{Bi} = D_{Be} \cdot \frac{V_{pe}}{V_{pi}} \qquad \text{(Eq. A11)}$$

Substituting for D_{Bi}:

$$F_{Bi} = \frac{D_{Be} \cdot \frac{V_{pe}}{V_{pi}}}{D_{Be} \cdot \frac{V_{pe}}{V_{pi}} + D_F} \qquad \text{(Eq. A12)}$$

The values of D_{Te} and D_F are obtained experimentally. Since:

$$D_{Te} = D_{Be} + D_F \qquad \text{(Eq. A13)}$$

then:

$$D_{Be} = D_{Te} - D_F \qquad \text{(Eq. A14)}$$

thus:

$$F_{Bi} = \frac{(D_{Te} - D_F) \cdot \frac{V_{pe}}{V_{pi}}}{(D_{Te} - D_F) \cdot \frac{V_{pe}}{V_{pi}} + D_F} \qquad \text{(Eq. 2)}$$

as presented in the text.

REFERENCES

(1) W. R. Slaunwhite, Jr., and A. A. Sandberg, *J. Clin. Invest.*, **38,** 384 (1959).

(2) M. L. Rocci, Jr., N. F. Johnson, and W. J. Jusko, *J. Pharm. Sci.*, **69,** 977 (1980).

(3) A. A. Sandberg, W. R. Slaunwhite, Jr., and H. N. Antoniades, *Rec. Prog. Horm. Res.*, **13,** 209 (1957).

(4) J. Kerkay and U. Westphal, *Biochim. Biophys. Acta*, **170,** 324 (1968).

(5) R. L. Milsap and W. J. Jusko, *J. Steroid Biochem.*, **18,** 191 (1983).

(6) H. L. Behm and J. G. Wagner, *Res. Commun. Chem. Pathol. Pharmacol.*, **26,** 145 (1979).

(7) J. Q. Rose, A. M. Yurchak, and W. J. Jusko, *J. Pharmacokinet. Biopharm.*, **9,** 389 (1981).

(8) J. Judis, *J. Pharm. Sci.*, **69,** 71 (1980).

(9) W. K. Brunkhorst and E. L. Hess, *Arch. Biochem. Biophys.*, **111,** 54 (1965).

(10) U. W. Mueller and J. M. Potter, *Biochem. Pharmacol.*, **30,** 727 (1981).

(11) J. H. Oppenheimer and M. I. Surks, *J. Clin. Endocrinol. Metab.*, **24,** 785 (1964).

(12) O. G. Nilsen and S. Jacobsen, *Biochem. Pharmacol.*, **25,** 1261 (1976).

(13) T. W. Guentert and S. Øie, *J. Pharm. Sci.*, **71,** 325 (1982).

(14) A. Yacobi and G. Levy, *J. Pharmacokinet. Biopharm.*, **3,** 439 (1975).

(15) J. Q. Rose and W. J. Jusko, *J. Chromatogr.* **162,** 273 (1979).

(16) Packard Instrument Co., Instrument Manual 2136, Downers Grove, Ill. (1977).

(17) R. M. C. Dawson, D. C. Elliott, W. H. Elliott, and K. M. Jones, "Data for Biochemical Research," Oxford University Press, New York, N.Y., 1969, p. 507.

(18) R. L. Priore and H. E. Rosenthal, *Anal. Biochem.*, **70,** 231 (1976).

(19) D. S. Riggs, J. A. Guarnieri, and S. Addelman, *Life Sci.*, **22,** 1305 (1978).

(20) M. L. Rocci, Jr., R. D'Ambrosio, N. F. Johnson, and W. J. Jusko, *Biochem. Pharmacol.*, **31,** 289 (1982).

(21) I. T. Ağabeyoğlu, R. F. Bergstrom, W. R. Gillespie, J. G. Wagner, and D. R. Kay, *Eur. J. Clin. Pharmacol.*, **16,** 399 (1979).

(22) G. P. Lewis, W. J. Jusko, C. W. Burke, and L. Graves, *Lancet*, **ii,** 778 (1971).

(23) D. W. Chan and W. R. Slaunwhite, Jr., *Arch. Biochem. Biophys.*, **182,** 437 (1977).

(24) W. J. Jusko and M. Gretch, *Drug Metab. Rev.*, **5,** 43 (1976).

(25) F. Karush, *J. Am. Chem. Soc.*, **72,** 2705 (1950).

(26) U. Westphal and G. B. Harding, *Biochim. Biophys. Acta.*, **310,** 518 (1973).

(27) G. J. Chader and U. Westphal, *Biochemistry*, **7,** 4272 (1968).

(28) G. J. Chader and U. Westphal, *J. Biol. Chem.*, **243,** 928 (1968).

(29) W. Rosner, *J. Ster. Biochem.*, **3,** 531 (1972).

(30) T. G. Muldoon and U. Westphal, *J. Biol. Chem.*, **242,** 5636 (1967).

(31) S. Schneider and W. R. Slaunwhite, Jr., *Biochemistry*, **10,** 2086 (1971).

(32) J. J. Lima, N. Libertin, J. Sabino, and J. J. MacKichan, *J. Pharmacokinet. Biopharm.*, **11,** 483 (1983).

ACKNOWLEDGMENTS

Supported in part by Grant 24211 from the National Institute of General Medical Sciences, National Institutes of Health. Stability of prednisolone (Fig. 1) was determined by Mario L. Rocci, Jr. The authors appreciate discussion of the topic with Drs. Samuel F. Sisenwine, John J. Lima, and Mario L. Rocci, Jr.

Effect of Compressional Force on Tablets Containing Cellulosic Disintegrators I: Dimensionless Disintegration Values

E. B. VADAS ˣ, G. R. B. DOWN, and R. A. MILLER

Received July 22, 1982, from *Merck Frosst Canada Inc., Pharmacy Research & Development, P.O. Box 1005, Pointe Claire-Dorval, Quebec, H9R 4P8, Canada.* Accepted for publication May 11, 1983.

Abstract □ Spray-dried lactose tablets containing cellulosic disintegrators or microcrystalline cellulose were compressed at different compressional forces. USP disintegration times were measured as a function of pH and compressional force. Two dimensionless quantities were derived from the experimentally determined disintegration times, and their utility in the study of tablet formulations was demonstrated. These dimensionless quantities were used to assess the effect of compressional force and pH on distintegration behavior as well as to compare disintegrator efficiency. Two internally cross-linked sodium carboxymethylcellulose disintegrators were found to be the most efficient; their efficiency increased with increasing compressional force at all pH values.

Keyphrases □ Compressional force—effect on tablets containing cellulosic disintegrators, dimensionless disintegration values □ Disintegrators, cellulosic—effect of compressional force on tablets, dimensionless disintegration values □ Disintegration—dimensionless values, effect of compressional forces on tablets containing cellulosic disintegrators

Considerable knowledge has been accumulated in the past concerning the behavior and mechanism of action of disintegrators, particularly those belonging to the starch family (1, 2). With the introduction of several new disintegrators in recent years, interest has become focused on methods of evaluation of disintegrator function and on the elucidation of their mechanism of action (3–7). The one basic measurement generally used in evaluating disintegrators in a tablet formulation, regardless of all other aspects of the study, is the measurement of disintegration time.

It is the aim of this paper to define two dimensionless quantities which can be derived from the experimentally determined disintegration times and, furthermore, to illustrate by the use of a simple tablet formulation that their application gives access to a wealth of information concerning the performance of disintegrators under a variety of processing and testing conditions. Also, our aim is to demonstrate that information inherent, but not immediately evident, in disintegration times can be extracted by a simple and considerably underutilized technique of data analysis. Compressional force was chosen as the processing variable and pH as the testing variable to demonstrate the utility of dimensionless disintegration values. The importance of pH in the evaluation of disintegrator behavior has been demonstrated by Shangraw *et al.* (4).

EXPERIMENTAL

Materials—The tablet matrix consisted of spray-dried lactose[1] containing 0.25% magnesium stearate[2] as the lubricant. The disintegrators used were two sodium carboxymethylcellulose derivatives (croscarmellose sodium type A[3] and type B[4]) and low-substituted hydroxypropyl cellulose[5]. Microcrystalline cellulose[6] was included for comparison in an additional series of tablets. All excipients were used at a fixed concentration of 3%.

Methods—A portion of the spray-dried lactose (~90%) was mixed with the disintegrator in a laboratory-scale twin-shell blender[7] for 7 min. The remaining spray-dried lactose was mixed with the magnesium stearate, the mix passed through a 60-mesh screen, and added to the bulk material. The entire mixture was then blended for 7 min.

Tablets were compressed on an instrumented rotary tablet machine (8) tooled with 12.7-mm round flat-faced punches. The tablet weight of each formulation was 725 mg. Samples of each tablet formulation were compressed at four different compressional forces. Although the forces were not identical in each series, their values were comparable (Table I). Values for tablet hardness were determined using a Schleuniger hardness tester[8] and are reported in kiloponds (kp, 1 kilogram-force) as the average of 10 measurements.

Disintegration times were measured according to USP XX method. Besides distilled water (pH 6.0), USP simulated gastric fluid (pH 1.5) and intestinal fluid (pH 7.5) without enzymes were also used to assess the effect of pH. All measurements were carried out using 1-day-old tablets.

RESULTS AND DISCUSSION

Physical Properties and USP Disintegration Times—The compressional forces used and the resulting physical properties of the control matrix and tablets containing the disintegrators are listed in Table I. Tablet hardness showed typical compressional force-dependent behavior as expected; *i.e.*, tablet breaking strength increased with increasing compressional force within each tablet formulation. Tablets containing low-substituted hydroxypropyl cellulose or microcrystalline cellulose had breaking strengths considerably higher than the control matrix. The increase was found to be approximately the same with these two excipients.

Since spray-dried lactose is soluble in aqueous media, its behavior in the absence of disintegrators should be properly described as slow dissolution rather than disintegration. However, for sake of uniformity and for purposes of comparison, the term disintegration will be used throughout the paper to describe the behavior of the control matrix.

Disintegration times of the control tablets were found to be both compressional force and pH dependent, as indicated by the values listed in Table II. Regardless of the pH of the test fluid, disintegration times increased with increasing compressional force and at each compressional force, the shortest disintegration time was measured at pH 1.5.

Tablets containing croscarmellose sodium, type A or B, had disintegration times apparently independent of both the processing and testing variable, *i.e.*, within both series, disintegration times were approximately the same at all compressional forces and at all pH values. A somewhat similar insensitivity of disintegration times to compressional force was found by Miller *et al.* (9) when studying the behavior of acetaminophen tablets containing these disintegrators. The disintegration times of tablets containing low-substituted hydroxypropyl cellulose were relatively insensitive to pH, but varied with compressional force exhibiting a minimum at 92.9 MN/m^2 (sample 2) and then increasing with increasing compressional force. The presence of 3% microcrystalline cellulose resulted in a decrease in disintegration times for the lower compressional forces (samples 1 and 2), followed by a considerable increase at higher compressional forces (samples 3 and 4) at all pH values.

Except for the control matrix, disintegration times did not correlate with tablet hardness in any of the tablet formulations. Such a lack of correlation has been reported recently (10) for theobromine tablets containing cornstarch, microcrystalline cellulose, or crospovidone as disintegrators.

Dimensionless Disintegration Value, T_N—To facilitate comparison among

[1] Foremost Foods, agent Charles Tennant & Co. Canada Ltd., Dorval, Quebec.
[2] Witco Chemicals, Montreal, Quebec.
[3] AcDiSol; FMC Corp, Dorval, Quebec.
[4] CLD-2; Buckeye Cellulose, Memphis, Tenn.
[5] L-HPC Type LH-11; Shinetsu, agent Biddle Sawyer, New York, N.Y.
[6] Avicel PH 101; FMC Corp., Dorval, Quebec.
[7] The Patterson-Kelley Co. Inc., East Stroudsburg, Pa.
[8] Vector Corp., Marion, Iowa.

0022-3549/84/0600-0781$01.00/0
© 1984, American Pharmaceutical Association

Table I—Physical Properties of Tablets

Disintegrator	Sample No.	Average Compressional Force, MN/m^2	Average Tablet Thickness ± *SD*, mm	Average Breaking Strength ± *SD*, kp
Control	1	52.9	4.81 ± 0.02	4.1 ± 0.1
	2	86.1	4.60 ± 0.01	6.4 ± 0.2
	3	120.3	4.38 ± 0.01	9.3 ± 0.2
	4	155.9	4.24 ± 0.01	13.9 ± 0.5
Croscarmellose sodium Type A	1	64.9	4.82 ± 0.02	3.2 ± 0.2
	2	93.2	4.60 ± 0.01	5.9 ± 0.3
	3	128.8	4.40 ± 0.01	9.3 ± 0.4
	4	161.8	4.28 ± 0.01	12.7 ± 0.5
Type B	1	63.0	4.88 ± 0.02	4.5 ± 0.2
	2	90.1	4.62 ± 0.01	6.7 ± 0.3
	3	129.1	4.36 ± 0.01	11.2 ± 0.3
	4	166.2	4.23 ± 0.01	15.1 ± 0.5
Low-substituted hydroxypropyl cellulose	1	55.0	4.74 ± 0.01	5.2 ± 0.5
	2	92.0	4.45 ± 0.01	8.0 ± 0.2
	3	125.4	4.29 ± 0.01	13.0 ± 0.2
	4	167.2	4.14 ± 0.01	17.2 ± 0.9
Microcrystalline cellulose	1	61.9	4.74 ± 0.02	5.7 ± 0.3
	2	92.9	4.47 ± 0.02	9.3 ± 0.3
	3	123.8	4.29 ± 0.02	13.1 ± 0.6
	4	159.4	4.18 ± 0.02	17.5 ± 0.6

tablets of different compositions, the disintegration times were normalized to that of tablets compressed at the lowest compressional force (sample 1) in each series according to the definition given by Eq. 1A (see *APPENDIX*). Values of T_N are plotted in Fig. 1.

The use of a dimensionless quantity such as T_N allows direct comparison of trends in tablet behavior with compressional force or with any other variable affecting disintegration times, *e.g.*, concentration of disintegrator, concentration of other excipients such as materials to improve the powder flow and lubricants, and the length of time of mixing of tablet ingredients prior to compression. In such a comparison the disintegration time of the first tablet of the series (in this case the tablet compressed at the lowest compressional force) becomes unity. Values of $T_N < 1$ are indicative of a beneficial effect of the variable on disintegration, whereas values of $T_N > 1$ indicate a detrimental effect.

In addition to overall trends, small differences in disintegration properties due to the presence of different disintegrators in the tablet matrix become immediately apparent, as illustrated in Fig. 1. Admixing of croscarmellose sodium type A is shown to result in a complete insensitivity of disintegration behavior to both pH and compressional force, at least within the limits used in this study. The addition of croscarmellose sodium type B results in complete pH insensitivity and an apparent slight compressional force dependence. This behavior was found to be reproducible.

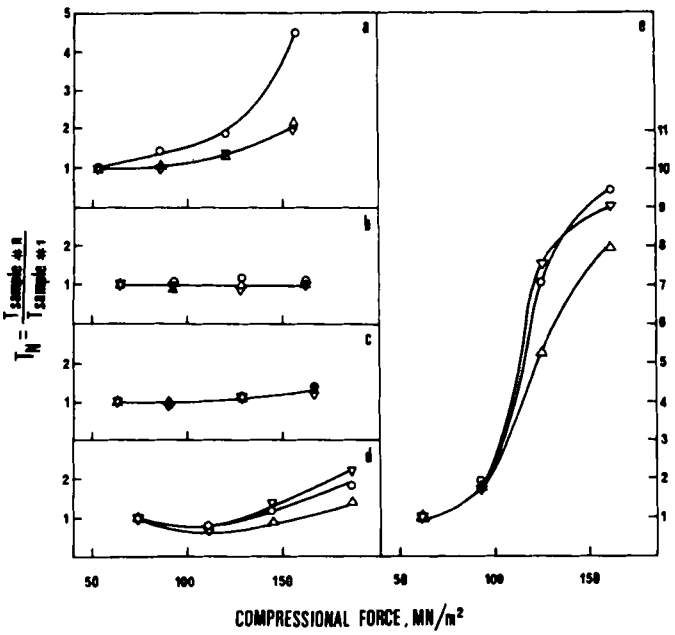

Figure 1—*Plots of the dimensionless disintegration quantity (Eq. 1A) as a function of compressional force and pH of test fluid. Values of* T_N *were calculated from the experimentally determined USP disintegration times for spray-dried lactose tablets containing (a) no disintegrant, (b) croscarmellose sodium, type A, (c) croscarmellose sodium, type B, (d) low-substituted hydroxypropyl cellulose, and (e) microcrystalline cellulose. Key: (○) pH 1.5; (△) pH 6.0; (▽) pH 7.5.*

Dimensionless Disintegration Value, T_C—A second dimensionless quantity may be derived from the experimentally determined disintegration times according to Eq. 2A (see *Appendix*). Here, the disintegration times of tablets containing a variety of disintegrators are normalized to the disintegration times of a common matrix. The quantity so obtained allows one to quantitatively assess and compare disintegrator efficiency.

Values of T_C are plotted in Fig. 2. While the previously discussed dimensionless quantity T_N allows direct comparison of the disintegration behavior of tablets of widely different disintegration times, T_C gives clear indications of disintegrator performance with respect to pH, *i.e.*, whether the tablet is effectively designed to disintegrate in a particular medium.

To illustrate this point one may compare the behavior of tablets compressed at ~90 MN/m^2 (sample 2) and containing either croscarmellose sodium (type

Table II—Disintegration Times [a] as a Function of Compressional Force and pH of Test Fluid

Disintegrator	Sample No.	Disintegration Time, s pH 1.5	pH 6.0	pH 7.5
Control	1	115	312	340
	2	168	345	370
	3	218	392	500
	4	525	680	720
Croscarmellose sodium Type A	1	90	95	115
	2	100	83	110
	3	105	88	100
	4	100	100	120
Type B	1	73	78	95
	2	70	78	90
	3	85	83	102
	4	98	98	110
Low-substituted hydroxypropyl cellulose	1	125	180	138
	2	100	145	88
	3	150	160	188
	4	225	250	283
Microcrystalline cellulose	1	64	95	105
	2	125	165	180
	3	460	500	790
	4	615	755	945

[a] The average of the longest disintegration times measured on two sets of six tablets is given.

A or B) or low-substituted hydroxypropyl cellulose. In simulated gastric fluid, the tablet containing croscarmellose sodium type A has a T_C value of 0.6; *i.e.*, due to the presence of the disintegrator, the disintegration time of the tablet is 60% of that of the control matrix in a highly acidic medium. The tablet containing croscarmellose sodium type B has a T_C value of 0.42, and that containing low-substituted hydroxypropyl cellulose has $T_C = 0.60$. Clearly, the most efficient disintegrator in this case is croscarmellose sodium type B, since its presence in the tablet formulation results in a larger reduction of disintegration time than the inclusion of either of the other two cellulosic disintegrators.

In simulated intestinal fluid, however, the behavior of all three tablet formulations is very nearly identical, as indicated by the values of T_C. For the tablet containing croscarmellose sodium type A, $T_C = 0.30$ (*i.e.*, a 70% reduction in disintegration time in a near neutral medium), and for those containing croscarmellose sodium type B or low-substituted hydroxypropyl cellulose, $T_C = 0.24$. Here, then, any of the three disintegrators would be similarly efficient.

In addition to allowing the formulator to assess disintegrator efficiency, the dimensionless disintegration quantity, T_C, has further utility. It was noted earlier that the absolute values of disintegration times were independent of compressional force when either croscarmellose sodium type A or B were used as the disintegrator. When describing the behavior of these tablet formulations in terms of T_C, the effect of compressional force becomes evident. In fact, values of T_C indicate that all tablet formulations used in this study exhibited compressional force as well as pH-dependent behavior from the point of view of disintegrator efficiency. In all tablet formulations the disintegrators were found to be the least efficient at pH 1.5, where the spray-dried lactose matrix disintegrated most readily, and were about equally efficient at pH 6.0 and 7.5, except low-substituted hydroxypropyl cellulose, which seemed to be most efficient at pH 7.5 in tablets processed at low compressional forces.

Examining the trends shown by tablets containing the sodium carboxymethylcellulose derivatives, the effect of compressional force on these two disintegrators is highlighted quite dramatically. The higher the compressional force applied to the tablets, the more efficient these two disintegrators become, *i.e.*, the reduction in disintegration times from that of control increases with increasing compressional force. This effect is most pronounced at pH 1.5, as illustrated by Fig. 2a and b. It is felt that this type of behavior is a strong indication of the importance of deformation due to compression in the mechanism of action of croscarmellose sodium.

Tablets containing microcrystalline cellulose show a biphasic trend, as already mentioned when discussing disintegration times (Table II). It is interesting to note here that in terms of disintegrator efficiency, microcrystalline cellulose (used at the unusually low concentration of 3%) did indeed act as a true disintegrator at the two lower compressional forces, where the reduction of disintegration time with respect to the control was found to be comparable with that obtained with the other disintegrators. The two samples made at higher compressional force, however, showed increased disintegration times at all pH values when compared with the appropriate controls. Here, the excipient caused retardation of disintegration rather than facilitating it. The extent to which microcrystalline cellulose facilitated or hindered disintegration is numerically expressed by values of T_C.

CONCLUSIONS

Two dimensionless quantities were defined and calculated from the experimentally determined USP disintegration times, and their use was demonstrated with a simple tablet formulation. Although the practice of using dimensionless quantities is not widespread in physical pharmacy, their utility may be considerable when comparisons must be made among systems of widely differing properties, such as those encountered during the development of pharmaceutical dosage forms.

APPENDIX—DEFINITION OF DIMENSIONLESS DISINTEGRATION VALUES

The first dimensionless quantity, T_N, facilitates comparison within a given tablet formulation and is defined as:

$$T_N = \frac{T_{\text{sample } n}}{T_{\text{sample 1}}} \qquad \text{(Eq. 1A)}$$

where $T_{\text{sample } n}$ is the disintegration time of the nth member of a series of tablets all containing the same disintegrator and compressed at different compressional forces, and $T_{\text{sample 1}}$ is the disintegration time of the tablet processed at the lowest compressional force within the series. Both disintegration times must be determined at the same pH.

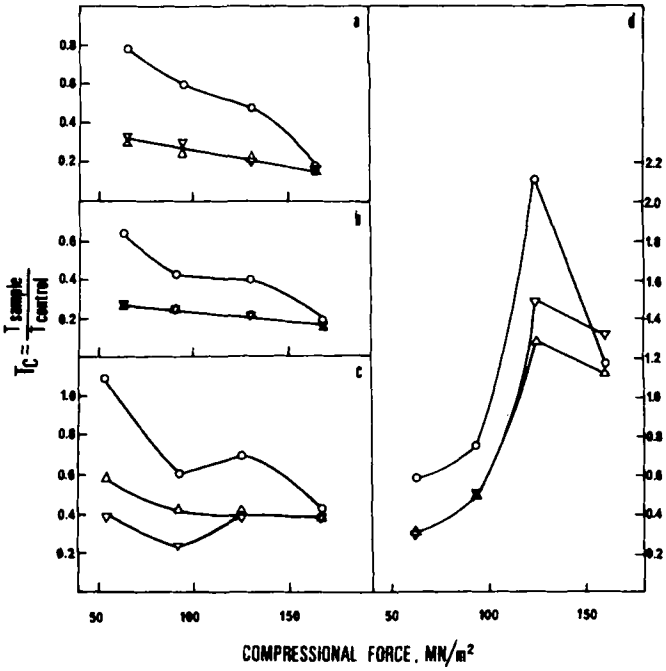

Figure 2—*Plots of the dimensionless disintegration quantity (Eq. 2A) as a function of compressional force and pH of test fluid obtained for spray-dried lactose tablets containing (a) croscarmellose sodium, type A, (b) croscarmellose sodium, type B, (c) low-substituted hydroxypropyl cellulose, and (d) microcrystalline cellulose. Key: (○) pH 1.5; (△) pH 6.0; (▽) pH 7.5.*

The second dimensionless quantity, T_C, is used to evaluate disintegrator efficiency and is given by:

$$T_C = \frac{T_{\text{sample}}}{T_{\text{control}}} \qquad \text{(Eq. 2A)}$$

where T_{sample} is the disintegration time of a tablet containing a specific disintegrator and compressed at a given compressional force, and T_{control} is the disintegration time of a tablet which contains no disintegrator and is compressed at the same compressional force. Both T_{sample} and T_{control} must be determined at the same pH.

REFERENCES

(1) W. Lowenthal, *Pharm. Acta Helv.*, **42**, 589 (1972).

(2) W. Lowenthal, *J.* Pharm. Sci., **61**, 1695 (1972).

(3) H. Hess, *Pharm. Tech.*, **2**(9), 36 (1978).

(4) R. Shangraw, A. Mitrevej, and M. Shah, *Pharm. Tech.*, **4**(10), 49 (1980).

(5) E. M. Rudnic, C. T. Rhodes, S. Welch, and P. Bernardo, *Drug Dev. Ind. Pharm.*, **8**, 87 (1982).

(6) S. R. Kalidindi and R. F. Shangraw, *Drug Dev. Ind. Pharm.*, **8**, 215 (1982).

(7) M. H. Alkan and M. J. Groves, *Pharm. Tech.*, **6**(4), 56 (1982).

(8) G. R. B. Down, R. A. Miller, S. K. Chopra, and J. F. Millar, *Drug Dev. Ind. Pharm.*, **6**, 311 (1980).

(9) R. A. Miller, G. R. B. Down, C. H. Yates, and J. F. Millar, *Can. J. Pharm. Sci.*, **15**, 55 (1980).

(10) B. Selmeci, A. Keresztes, P. R. Szabone, and K. H. Pintyene, *Acta. Pharm. Hung.*, **51**, 20 (1981).

ACKNOWLEDGMENTS

Presented in part at the IPT Section, APhA Academy of Pharmaceutical Sciences, Las Vegas Meeting, April 1982.

Freeze-Drying of Oxyhemoglobin: Protection Against Oxidation in the Presence of EDTA Salts, Sulfonic Acid Buffers, and Pantothenic Acid Derivatives

A. FAUVEL *, P. LABRUDE ‡x, and C. VIGNERON *

Received February 17, 1983, from the *Laboratoire d'Hématologie et Physiologie, Faculté des Sciences, Pharmaceutiques et Biologiques, B.P. 403, 54001 NANCY Cédex and ‡Laboratoire de Chimie Hématologique, Centre Régional de Transfusion Sanguine et d'Hématologie, 54500 Vandoeuvre les Nancy, France. Accepted for publication May 4, 1983.

Abstract □ Hemoglobin was freeze-dried in the presence of salts of EDTA, sulfonic acids used as buffers, or derivatives of pantothenic acid. At 0.25 M most of the compounds effectively inhibited the formation of methemoglobin. The various model compounds used (sodium zinc EDTA, tris(hydroxymethyl)methylaminopropanesulfonic acid, and DL-pantothenol) produced similar decreases in methemoglobin formation as a function of the concentration of protective agent between 0.01 and 0.20 M. Experiments on the storage of the freeze-dried materials revealed substantial denaturation of oxyhemoglobin after 12 months at 4°C. On the whole, these compounds were less effective than amino acid salts, during both desiccation and storage. The multiplicity of compounds that inhibit the denaturation of hemoglobin during freeze-drying indicates that their mode of action is nonspecific.

Keyphrases □ Oxyhemoglobin—oxidation to methemoglobin during freeze-drying, protection by EDTA salts, sulfonic acid buffers, and pantothenic acid derivatives □ EDTA salts—protection of oxyhemoglobin during freeze-drying, prevention of methemoglobin formation □ Sulfonic acid buffers—protection of oxyhemoglobin during freeze-drying, prevention of methemoglobin formation □ Pantothenic acid derivatives—protection of oxyhemoglobin during freeze-drying, prevention of methemoglobin formation

Oxyhemoglobin has been freeze-dried under various conditions, and it has been definitely established that desiccation leads to oxidation of the heme iron and to the formation of methemoglobin (metHb) representing up to 60% of the original hemoglobin (1-3). Until now, the only way of obtaining nondenatured freeze-dried hemoglobin has been to add a sufficient concentration of a protective agent before freezing the solution. The demonstration by Smith and Pennell in 1952 (4) of a protective effect of glucose has been followed more recently by exploration of a series of chemical compounds such as amine buffers (5), carbohydrates (6), and macromolecules (7), for which dose-response relationships have been established. Better understanding of protective agents would be useful in stabilizing solutions of hemoglobin for eventual use as a blood substitute and in other biotechnologies.

We describe here experiments with representatives of three series of chemical compounds not previously studied as protective agents in freeze-drying, chosen for the following reasons: EDTA salts, because of their effects on the process of oxidation of hemoglobin (8, 9); buffer compounds, to follow up our earlier studies of Tris derivatives (5); and derivatives of pantothenic acid, because their parent molecule is structurally related to some protective compounds already known—β-alanine and quaternary carbon polyols (2, 5).

Table I—Physiological Properties of Hemoglobin after Freeze-Drying in the Presence of 250 mM of Different EDTA Salts

EDTA Salt	*n*	Oxyhemoglobin, %	Methemoglobin, %	pH	Hill coefficient
Dipotassium	3	85.3	14.0	5.31	1.96
Sodium zinc	3	91.9	6.5	7.07	2.18
Dipotassium magnesium	3	89.7	3.5	7.30	2.36
Disodium magnesium	3	92.8	2.9	7.26	2.52
Tetrasodium	3	84.4	1.5	8.56	2.88
Tripotassium	3	86.9	2.8	7.70	2.52

EXPERIMENTAL

Reagents—A solution of human hemoglobin was prepared from citrated blood samples taken 3 weeks earlier. The red blood cells were separated and washed in 0.15 M NaCl, and then hemolyzed in deionized water. The stromata were separated by centrifugation twice at 25,000×*g* for 30 min and decantation of the hemoglobin solution. This solution was dialyzed against deionized water at 4°C for 15 h, then centrifuged once again to remove the remaining stromata and adjusted to a hemoglobin concentration of 100 g/L. The EDTA salts used were: dipotassium·2 $_2O$[1], sodium zinc·4H_2O[2], dipotassium magnesium[1], disodium magnesium·H_2O[2], tetrasodium[1], and tripotassium[3]. The pantothenic acid (vitamin B_5) derivatives were: calcium D-pantothenate[4], DL-pantothenic alcohol[4], D-pantothenic alcohol[4], (−)-D-pantoyllactone[4], and sodium DL-pantoyltaurinate[4]. The buffers were 3-(*N*-morpholino)propanesulfonic acid (I)[4], *N*-(2-hydroxyethyl)-1-piperazinepropanesulfonic acid (II)[4], 2[(2-amino 2-oxoethyl)amino]ethanesulfonic acid (III)[2], *N*,*N*-bis(2-hydroxyethyl)-2-aminoethanesulfonic acid (IV)[2], *N*-tris(hydroxymethyl) methyl-2-aminoethanesulfonic acid (V)[2], and tris(hydroxymethyl)methylaminopropanesulfonic acid (VI)[2].

Procedures—In the initial series of experiments, the samples to be freeze-dried were made up of a homogeneous mixture of 5 mL of an aqueous 100-g/L solution of hemoglobin and 5 mL of an aqueous 0.5 M solution of the protective agent being studied. This made it possible to verify that these materials were indeed soluble. Next, for one agent from each of the three chemical series we looked at the dose-response relationship, plotting the percentage of methemoglobin formed *versus* the molar concentration of the protective agent, from 0.01 to 0.2 M, at a constant hemoglobin concentration as before and with a volume of 10 mL before freeze-drying. Each sample was studied in triplicate.

More detailed studies were carried out with EDTA. First, a series of excellent freeze-dried materials, obtained from 10 mL of solutions containing 100 g/L of hemoglobin and 0.25 M of each of its salts, were stored in darkness for 12 months in air at 4°C. Next, samples freeze-dried in the presence of 0.01-0.20 M sodium zinc EDTA were stored in the same conditions for 12 months. Finally, we wished to find out (as has not yet to our knowledge been systematically studied) whether the concentration of hemoglobin influenced the proportion of methemoglobin formed, at a constant concentration of protective agent chosen to give a level of oxidation that was neither zero nor too high. The experiments were carried out on 10 mL of freeze-dried material, with 0.05 M sodium zinc EDTA and 250-1000 mg of hemoglobin.

The freeze-drying was carried out in a freeze-drying apparatus[5] under the following conditions. Samples (10 mL) were frozen at −40°C in the bottom of 100-mL flasks in the apparatus, followed by desiccation with the control set at 70% (heating of shelf 70% of time) and final temperature displayed as 4°C. The vacuum was broken and the freeze-dried materials were immediately stoppered in air. The samples were macroscopically examined (for appearance and color) and dissolved in 10 mL of Sörensen's 0.066 M phosphate buffer of pH 6.4, 7.4, or 7.8, depending on the pH before freeze-drying. The other examinations carried out were:

1. Estimation of methemoglobin by the method of Evelyn and Malloy (10).

[1] Prolabo.
[2] Fluka.
[3] Touzart-Matignon.
[4] Sigma.
[5] USIFROID SMH 15; Maurepas, France.

0022-3549/84/0600-0784$01.00/0
© 1984, American Pharmaceutical Association

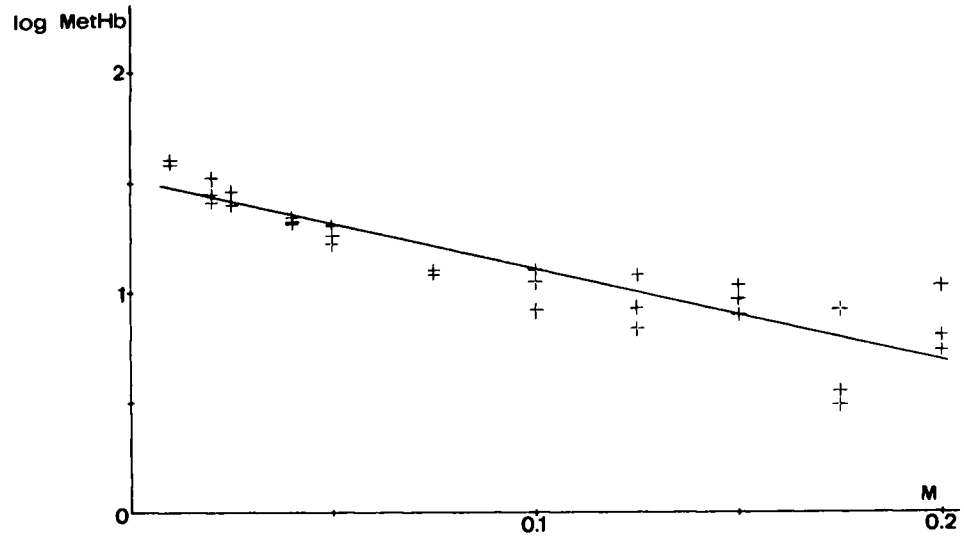

Figure 1—*Linear regression between the log methemoglobin (%) and molar concentration (0.01 to 0.20 M) of Na-Zn EDTA.*

2. Measurement of oxyhemoglobin in the aqueous solution with an oximeter[6], without correction for the concentrations of methemoglobin.

3. Determination of the pH[7] of the reconstituted hemoglobin solution.

4. Plotting of the dissociation curve[8] of the hemoglobin at 37°C and $P\,CO_2$ of 40 Torr, and calculation of the Hill coefficient.

5. Plotting of the spectrum[9] of the hemoglobin from 500 to 700 nm.

6. Calculation of the concentration-protection relationships using a programmable calculator[10] linked to a plotter.

RESULTS AND DISCUSSION

In all our previous experiments on freeze-drying carried out under similar conditions, unprotected hemoglobin contained 49 ± 8% of methemoglobin (metHb) after freeze-drying (n = 45). Its oxygen saturation was 56 ± 5% (n = 29), and its cooperativity was lost (Hill coefficient = 1.76 ± 0.07, compared with a normal value of >2.6).

Protection Due to EDTA Salts—On coming out of the freeze-drier, the samples were red and powdery; they dissolved rapidly and totally. All the EDTA salts studied here, except for dipotassium EDTA, seemed to be protective agents that inhibited the formation of methemoglobin, giving <10% methemoglobin (Table I). The tetrasodium salt was the most effective, but it led to the lowest saturation values and a pH very different from physiologic values. Least-squares best estimates were calculated for straight lines on Hill plots; the Hill coefficients obtained demonstrated that the physiological properties of the hemoglobin were well preserved, except with the dipotassium salt.

We arbitrarily chose the sodium zinc salt for the other studies. The color of the dry freeze-dried materials, ranging from brown to red, indicated decreasing proportions of methemoglobin as the concentration of protective agent increased. The samples showed no turbidity when reconstituted with a pH 7.4 buffer, but the more altered the hemoglobin, the slower they were to dissolve. The relationship between the percentage of methemoglobin (y-axis) and the percentage of oxyhemoglobin (x-axis) fitted the equation $y = -x + 97.1$ (n = 33, $r = -0.97$, $p < 0.001$). There was a linear relationship between the logarithm of the proportion of methemoglobin and the molar concentration of protective agent: $y = -4.12x + 1.51$ (n = 33, $r = -0.903$, $p < 0.001$) (Fig. 1). After 12 months, the freeze-dried materials obtained with the EDTA salts showed methemoglobin levels between 8.8% (with the tetrasodium salt) and 64.7% (with the dipotassium salt). The order of effectiveness of the various salts was the same as at time zero. The saturations were low (56–70%), especially in the presence of tetrasodium EDTA, although the spectrum of the hemoglobin of this sample was altered very little.

The samples containing various concentrations of sodium zinc EDTA displayed proportions of methemoglobin between 50.9 and 26.8%, yielding the correlation line $y = -185.6x + 58.9$ (n = 10, $r = -0.918$, $p < 0.001$); this line cuts the x-axis at 0.32 M, which is the hypothetical concentration of EDTA in a hemoglobin solution that will prevent any oxidation to methemoglobin during both desiccation and storage. This concentration is much higher than those we found with other protective agents under similar conditions (11), which indicates that EDTA salts are much less effective. The proportion of methemoglobin varied greatly with the concentration of hemoglobin, as seen in Fig. 2 ($y = 0.026x + 2.89$; n = 14, $r = 0.98$, $p < 0.001$). This relationship between hemoglobin and protective agent is in accordance with the previous relationship (Fig. 1): both show that hemoglobin was correctly protected only in certain narrowly defined conditions of concentration. This sensitivity of hemoglobin to small changes in concentration was found also for the other classic protective agents (such as glucose or sucrose) for which we have established equations of the same type[11].

Table II—Physiological Properties of Hemoglobin after Freeze-Drying in the Presence of 250 mM of Buffer Compounds

Buffer	n	Oxyhemoglobin, %	Methemoglobin, %	pH	Hill coefficient
I	3	93.6	2.2	6.15	2.90
II	3	99.0	1.9	6.65	2.40
III	3	65.5	47.1	6.35	—
IV	3	94.6	4.6	6.23	2.01
V	3	96.0	2.2	6.33	2.07
VI	3	97.6	3.5	7.13	3.00

Protection Due to Buffer Compounds—Buffer III is poorly soluble in aqueous media and had no protective effect, whereas the five other buffers gave satisfactory protection (Table II). The structure of these compounds (sulfonic acids) and their concentrations produced acid solutions despite their being dissolved in an alkaline buffer solution. At these pH values, the Barcroft curve was displaced towards low affinities and the $p50$ values were high (21–45 Torr).

The dose-response relationship was studied with VI. At concentrations of ≥0.075 M it gave satisfactory levels of methemoglobin, *i.e.* <10%. The relationship between the logarithm of the percentage of methemoglobin and the concentration of VI took the form $y = -5.76x + 1.52$ (n = 33, $r = -0.867$, $p < 0.001$) (Fig. 3). Here too, the correlation between methemoglobin and oxyhemoglobin was very significant: $y = -0.75x + 75.62$ (n = 33, $r = -0.975$, $p < 0.001$). Two samples of hemoglobin freeze-dried in the presence of VI or V were stored for 12 months at 4°C; the levels of oxyhemoglobin and methemoglobin were then found to be 76% and 22%, respectively, and their respective Hill coefficients were 2.13 and 1.66. As with the EDTA salts, these protective agents seemed to be greatly inferior to the amino acid salts and sucrose studied previously (11).

Protection Due to Derivatives of Pantothenic Acid—These derivatives were quite difficult to study, because D-pantothenol is very viscous and dissolves poorly in water, while (−)-D-pantoyllactone yielded a poorly soluble freeze-dried material, whose solution was slightly turbid, brown, and in need of centrifugation. Calcium pantothenate yielded even greater turbidity, which prevented any precise estimation of methemoglobin in the centrifugation supernatant. Nevertheless these compounds were effective protective agents, as seen in Table III. The correlations established above were again found for log (methemoglobin percentage) *versus* molarity of the protective agent

[6] Radiometer OSM 2 Hemoximeter.
[7] Corning 161 Blood-gas analyzer.
[8] Hem-O-Scan analyzer Aminco.
[9] Shimadzu spectrophotometer.
[10] Hewlett-Packard Calculor 9810 A.
[11] Unpublished results.

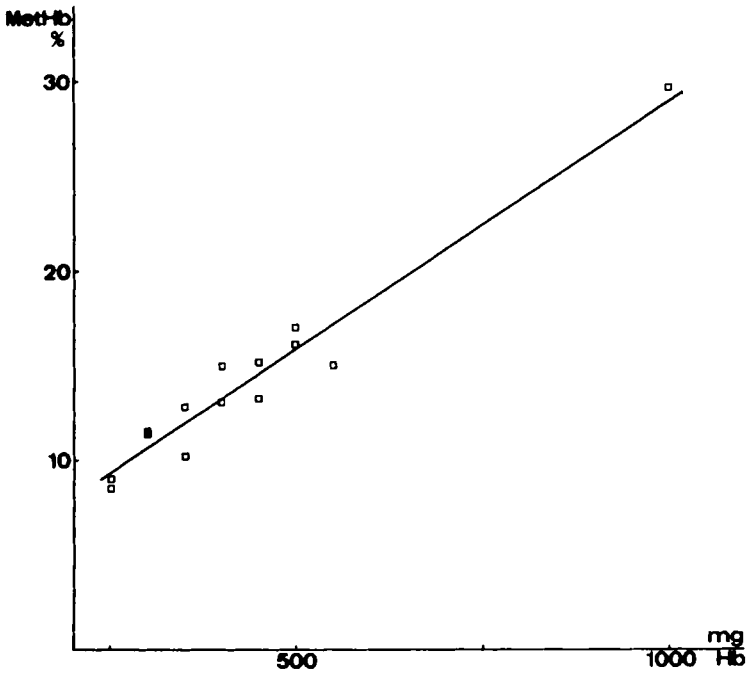

Figure 2—*Linear regression between methemoglobin (%) and the amount (or concentration) of hemoglobin during freeze-drying with 50 mM Na-Zn EDTA.*

DL-pantothenol [$y = -7.19x + 1.64$ (Fig. 4) ($n = 33, r = -0.95, p < 0.001$)] and for methemoglobin *versus* oxyhemoglobin [$y = -0.86x + 84.6$ ($n = 33$, $r = -0.98, p < 0.001$)].

CONCLUSIONS

This study has demonstrated the protective effect during the freeze-drying of hemoglobin of representatives of three different chemical series, adding to those already known (5–7). With EDTA salts, where only the cation and the pH differed, the proportion of oxyhemoglobin was generally low, and pH seemed to be involved, since the extreme pH values gave both the best and the worst results. With one exception, the sulfonic acids used as biological buffers were effective protective agents. The same was true for the pantothenate family that we have investigated, since they derive from both β-alanine and a quaternary carbon alcohol. This remark suggests that there may be possible structure-activity relationships in this series.

On the other hand, three reasons lead us instead to conclude that a nonspecific antioxidant action is present: (*a*) the multiplicity and the variety of chemical families in which protective agents for hemoglobin have already been found—carbohydrates, amine buffers, macromolecules, amino acids, *etc.*, (*b*) the observation by ESR that glucose, β-alanine, or Tris, taken as models, do not interact with heme iron and its environment (12), and (*c*) the result with the same models using circular dichroism (CD) that the absence of protector only weakly influences the conformation in the vicinity of the heme and alters the secondary structure by slightly increasing the helicity. The CD spectra also suggest that the protector may not enter into the heme pocket, since one would then observe much greater spectral changes in the visible region and the Soret band (13).

Table III—Physiological Properties of Hemoglobin after Freeze-Drying in the Presence of 250 mM of Pantothenic Acid Derivatives[a]

Derivative	*n*	Oxyhemoglobin, %	Methemoglobin, %	pH	Hill's Number
D-Pantothenic acid, hemicalcium salt	3	97.4	—	5.61	—
DL-Panthenol	3	99.3	2.3	7.29	2.51
D-panthenol	3	98.3	3.4	7.35	2.49
(−)-D-Pantoyllactone	3	75.3	23.3	7.28	2.11
DL-Pantoyltaurine sodium salt	3	100.0	2.0	8.28	2.53

[a] Derivatives were dissolved in buffer, pH 6.38.

Taking in account the preceding remarks, it appears that the oxidation of ferrous iron remains the main denaturer of hemoglobin and that the estimation of methemoglobin is the first and one of the best tests to evaluate the effects of freeze-drying on hemoglobin. The mechanism of action of the protectors is still poorly understood, but our current experiments link this action with concomitant effects of vacuum and removal of water. It is not impossible that

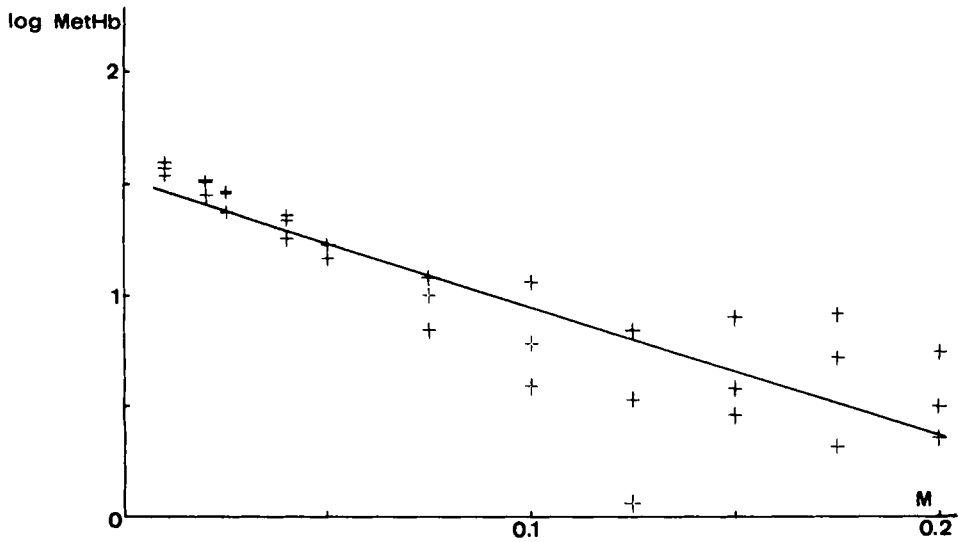

Figure 3—*Linear regression between the log of methemoglobin (%) and molar concentration (0.01 to 0.20 M) of VI.*

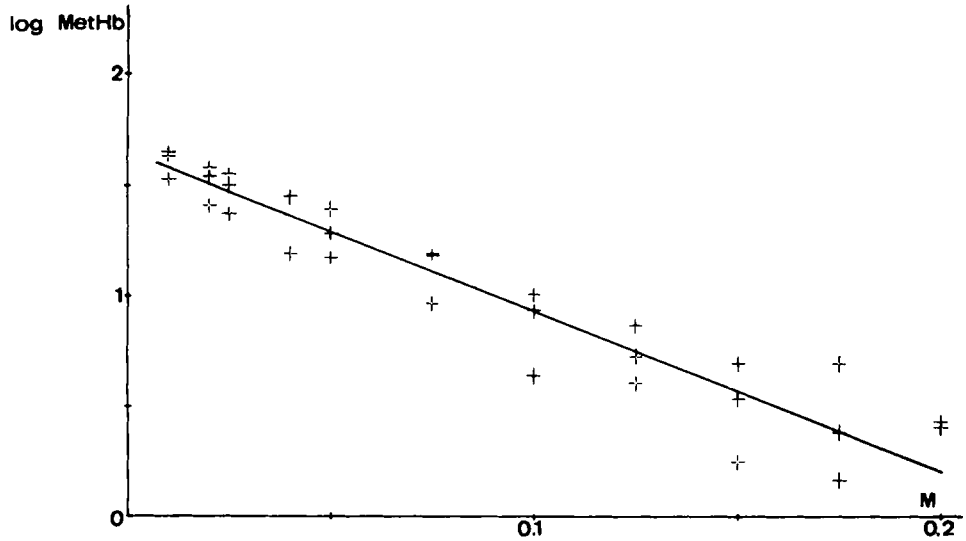

Figure 4—*Linear regression between the log of methemoglobin (%) and molar concentration (0.01 to 0.20 M) of* DL-*panthenol.*

such protectors "modify" the structure of globin as has been described for some proteins and glycerol by Gekko and Timasheff (14).

The changes in the proportion of methemoglobin as a function of concentration of the protective agent always fitted a hyperbola that could be linearized by a logarithmic transformation, giving a straight line with a negative slope. The three correlation lines thus obtained had slopes of the same order of magnitude, which indicates that these three model compounds are fairly similar in effectiveness. However, they are much less effective, during both freeze-drying and storage, than the amino acid salts that we have studied previously. This difference in behavior, which undoubtedly derives from quite specific physicochemical properties of the protective agents, remains unexplained.

REFERENCES

(1) L. E. Farr, A. Hiller, and D. D. Van Slyke, *J. Exp. Med.*, **86**, 465 (1947).

(2) P. Labrude, V. Loppinet, and C. Vigneron, *Ann. Pharm. Fr.*, **34**, 143 (1976).

(3) T. I. Pristoupil, M. Kramlova, and S. Ulrych, *Cesk. Farm.*, **27**, 311 (1978).

(4) W. E. Smith and R. B. Pennell, *Blood*, **7**, 368 (1952).

(5) P. Labrude and C. Vigneron, *J. Pharm. Pharmacol.*, **32**, 305 (1980).

(6) P. Labrude, B. Chaillot, F. Bonneaux, and C. Vigneron, *J. Pharm. Pharmacol.*, **32**, 588 (1980).

(7) P. Labrude, F. Bonneaux, and C. Vigneron, *J. Pharm. Pharmacol.*, **33**, 115 (1981).

(8) L. J. Sannes and D. E. Hultquist, *Biochem. Biophys. Res. Commun.*, **91**, 1309 (1979).

(9) K. Kikugawa, T. Sasahara, T. Sasaki, and T. Kurechi, *Chem. Pharm. Bull.*, **29**, 1382 (1981).

(10) K. A. Evelyn and H. I. Malloy, *J. Biol. Chem.*, **126**, 655 (1938).

(11) P. Labrude and C. Vigneron, *J. Pharm. Pharmacol.*, **35**, 23 (1983).

(12) B. Chaillot, P. Labrude, C. Vigneron, and D. Simatos, *Am. J. Hematol.*, **10**, 319 (1981).

(13) C. Thirion, D. Larcher, B. Chaillot, P. Labrude, and C. Vigneron, *Biopolymers*, **22**, 2367 (1983).

(14) K. Gekko and S. N. Timasheff, *Biochemistry*, **20**, 4667 (1981).

Disposition Kinetics of Ethambutol in Nephrectomized Dogs

CHING-SAN C. LEE ˣ **and ABRAHAM VARUGHESE**

Received March 14, 1983, from the *Department of Pharmaceutics, College of Pharmacy, University of Houston, Houston, TX 77030.* Accepted for publication May 9, 1983.

Abstract □ The effect of nephrectomy on the disposition of ethambutol was investigated in seven adult mongrel dogs: five were nephrectomized and two served as the control. Each dog was intravenously administerd 500 mg ethambutol, followed by blood sample collection for 12 h. Total urine was collected over 24 h from the normal control dogs. Ethambutol contents in plasma and urine were assayed by a GC method. The nephrectomized group and the control group exhibited differences in the following pharmacokinetic parameters: half-life, 5.0 *versus* 4.1 h (significant at $p < 0.1$); total body clearance, 8.4 *versus* 13.2 mL/min/kg (significant at $p < 0.1$); and volume of distribution, 2.7 *versus* 3.8 L/kg (significant at $p < 0.1$). Comparison of pharamacokinetic parameters among rabbits, dogs, and humans revealed distinct interspecies differences with regard to total body clearance, renal clearance, volume of distribution, and fractional renal excretion. One comparable parameter shared by all species is the β-phase half-life.

Keyphrases □ Ethambutol—disposition, pharmacokinetics in the dog, effect of nephrectomy, interspecies comparison □ Pharmacokinetics—ethambutol disposition in the dog, effect of nephrectomy, interspecies comparison □ Distribution—ethambutol in the dog, effect of nephrectomy, pharmacokinetics, interspecies comparison

Ethambutol (I), an antitubercular agent, is used alone or in combination with other drugs for the treatment of tuberculosis. The absorption and excretion of I has been studied in rats and mice (1), dogs (2, 3), and human subjects (4–6). In mice receiving single oral doses of I, peak serum concentrations were reached within 1 h of administration, and the compound

0022-3549/84/0600-0787$01.00/0
© 1984, American Pharmaceutical Association

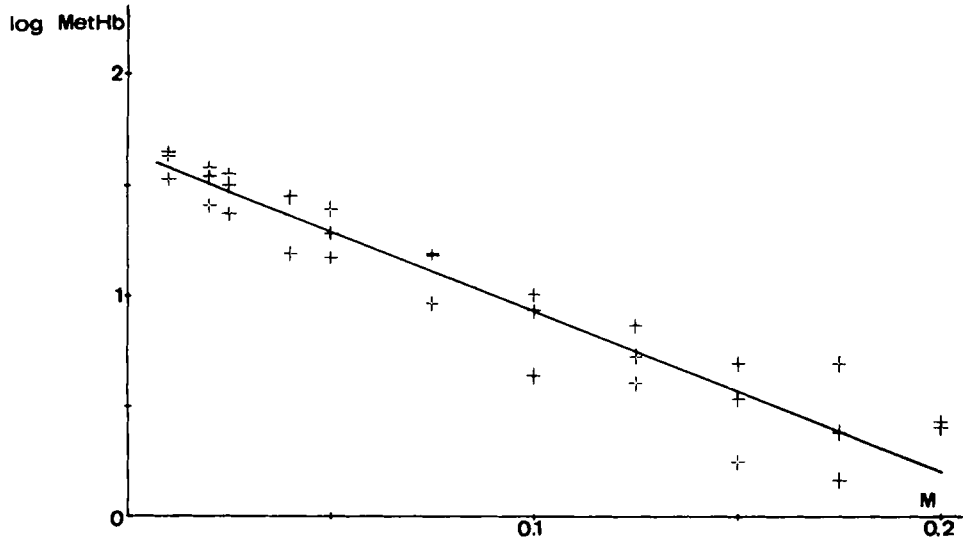

Figure 4—*Linear regression between the log of methemoglobin (%) and molar concentration (0.01 to 0.20 M) of* DL-*panthenol.*

such protectors "modify" the structure of globin as has been described for some proteins and glycerol by Gekko and Timasheff (14).

The changes in the proportion of methemoglobin as a function of concentration of the protective agent always fitted a hyperbola that could be linearized by a logarithmic transformation, giving a straight line with a negative slope. The three correlation lines thus obtained had slopes of the same order of magnitude, which indicates that these three model compounds are fairly similar in effectiveness. However, they are much less effective, during both freeze-drying and storage, than the amino acid salts that we have studied previously. This difference in behavior, which undoubtedly derives from quite specific physicochemical properties of the protective agents, remains unexplained.

REFERENCES

(1) L. E. Farr, A. Hiller, and D. D. Van Slyke, *J. Exp. Med.*, **86**, 465 (1947).

(2) P. Labrude, V. Loppinet, and C. Vigneron, *Ann. Pharm. Fr.*, **34**, 143 (1976).

(3) T. I. Pristoupil, M. Kramlova, and S. Ulrych, *Cesk. Farm.*, **27**, 311 (1978).

(4) W. E. Smith and R. B. Pennell, *Blood*, **7**, 368 (1952).

(5) P. Labrude and C. Vigneron, *J. Pharm. Pharmacol.*, **32**, 305 (1980).

(6) P. Labrude, B. Chaillot, F. Bonneaux, and C. Vigneron, *J. Pharm. Pharmacol.*, **32**, 588 (1980).

(7) P. Labrude, F. Bonneaux, and C. Vigneron, *J. Pharm. Pharmacol.*, **33**, 115 (1981).

(8) L. J. Sannes and D. E. Hultquist, *Biochem. Biophys. Res. Commun.*, **91**, 1309 (1979).

(9) K. Kikugawa, T. Sasahara, T. Sasaki, and T. Kurechi, *Chem. Pharm. Bull.*, **29**, 1382 (1981).

(10) K. A. Evelyn and H. I. Malloy, *J. Biol. Chem.*, **126**, 655 (1938).

(11) P. Labrude and C. Vigneron, *J. Pharm. Pharmacol.*, **35**, 23 (1983).

(12) B. Chaillot, P. Labrude, C. Vigneron, and D. Simatos, *Am. J. Hematol.*, **10**, 319 (1981).

(13) C. Thirion, D. Larcher, B. Chaillot, P. Labrude, and C. Vigneron, *Biopolymers*, **22**, 2367 (1983).

(14) K. Gekko and S. N. Timasheff, *Biochemistry*, **20**, 4667 (1981).

Disposition Kinetics of Ethambutol in Nephrectomized Dogs

CHING-SAN C. LEE ˣ **and ABRAHAM VARUGHESE**

Received March 14, 1983, from the *Department of Pharmaceutics, College of Pharmacy, University of Houston, Houston, TX 77030.* Accepted for publication May 9, 1983.

Abstract □ The effect of nephrectomy on the disposition of ethambutol was investigated in seven adult mongrel dogs: five were nephrectomized and two served as the control. Each dog was intravenously administerd 500 mg ethambutol, followed by blood sample collection for 12 h. Total urine was collected over 24 h from the normal control dogs. Ethambutol contents in plasma and urine were assayed by a GC method. The nephrectomized group and the control group exhibited differences in the following pharmacokinetic parameters: half-life, 5.0 *versus* 4.1 h (significant at $p < 0.1$); total body clearance, 8.4 *versus* 13.2 mL/min/kg (significant at $p < 0.1$); and volume of distribution, 2.7 *versus* 3.8 L/kg (significant at $p < 0.1$). Comparison of pharamacokinetic parameters among rabbits, dogs, and humans revealed distinct interspecies differences with regard to total body clearance, renal clearance, volume of distribution, and fractional renal excretion. One comparable parameter shared by all species is the β-phase half-life.

Keyphrases □ Ethambutol—disposition, pharmacokinetics in the dog, effect of nephrectomy, interspecies comparison □ Pharmacokinetics—ethambutol disposition in the dog, effect of nephrectomy, interspecies comparison □ Distribution—ethambutol in the dog, effect of nephrectomy, pharmacokinetics, interspecies comparison

Ethambutol (I), an antitubercular agent, is used alone or in combination with other drugs for the treatment of tuberculosis. The absorption and excretion of I has been studied in rats and mice (1), dogs (2, 3), and human subjects (4–6). In mice receiving single oral doses of I, peak serum concentrations were reached within 1 h of administration, and the compound

0022-3549/84/0600-0787$01.00/0
© 1984, American Pharmaceutical Association

Table I—Mean Plasma Ethambutol Concentrations in Five Nephrectomized Dogs and Two Normal Control Dogs [a]

		Plasma Concentrations (μg/mL) at Time (min)														
		5	30	60	90	120	150	180	210	240	300	360	420	480	600	720
Nephrectomized dogs (n = 5)	Mean	33.18	13.93	10.43	9.14	7.91	6.35	5.91	5.30	4.27	3.75	3.26	2.26	1.88	1.55	1.21
	SD	6.26	5.79	4.44	3.62	2.95	2.75	3.43	2.33	2.64	2.51	2.49	1.34	1.18	0.92	0.81
Normal dogs (n = 2)	Mean	--	18.84	12.41	3.35	2.73	1.57	1.45	1.01	1.07	0.91	0.79	0.76	0.63	0.42	0.33
	SD	—	13.67	13.85	2.23	1.40	0.57	0.21	0.28	0.54	0.18	0.17	0.25	0.36	0.24	0.18

[a] Ethambutol was administered to each dog at a dose of 500 mg iv.

was rapidly excreted (1). The medium lethal dose of I varied considerably for the different routes of drug administration to mice (1), suggesting a first-pass metabolism of the drug when administered nonparenterally. The first-pass effect was demonstrated for I using a rabbit model in which a low bioavailability of 28% was observed[1], in comparison with the nearly 80% oral bioavailability in humans (5).

After a single oral 100-mg/kg dose of I to dogs, absorption was rapid and the drug was cleared from the blood with a half-life of 1.5 h (2). Within 8 h of an intravenous injection of [^{14}C]I, 57% of the radioactivity appeared in the urine as the unchanged drug, determined after separation of metabolites by counter-current distribution (3). Arnaud *et al.* (7) reported a substantial urinary excretion of the unchanged I in two dogs, up to 50% of the dose within 2 h of a rapid intravenous injection. Limited studies of I in dogs make it difficult to relate the pharmacokinetic similarities between dogs and humans, especially with respect to renal excretion. This study was intended to investigate the effect of nephrectomy on the disposition of I in dogs and to compare the pharmacokinetics of I in rabbits, dogs, and humans.

$$HOCH_2CH(R)NH(CH_2)_2NHCH(R)CH_2OH$$

I R = C_2H_5
II R = CH_3

EXPERIMENTAL

Materials—Ethambutol[2] and the methyl analogue of ethambutol (II)[2] were supplied as the dihydrochloride salts. Trifluoroacetic anhydride[3] and pyridine[3] were used as derivatizing agents. Chromatographic-grade chloroform[4] and benzene[4] were used as supplied.

Animal Experiments—Seven adult mongrel dogs weighing 13.6–24.5 kg were used in the study. Five dogs were bilaterally nephrectomized, while two normal dogs served as the control. Dogs were surgically prepared after being anesthetized with 50 mg/kg of pentobarbital. The jugular and anticubital veins were cannulated for blood drawing and drug infusion, respectively. Normal dogs were allowed sufficient time to recover from anesthesia before drug administration. In the nephrectomized group, the drug study was not initiated until 2 d after the nephrectomization. During the waiting period, dogs were allowed limited access to food and water. Sham operations were not performed on the normal control dogs; otherwise, both groups of dogs were similarly treated prior to and during the experiment. Each dog was intravenously administered 500 mg of I *via* the anticubital vein of the forelimb over a 3-min period. Blood samples were collected at various times for 12 h. In the control dog study, total urine was collected by natural voiding over a 24-h period and aliquots were pooled. Plasma and urine samples were frozen at −20°C until analysis.

Analytical Procedure—Plasma and urine samples, to which a specific quantity of II (the internal standard) was added, were extracted with chloroform, derivatized with trifluoroacetic anhydride, and subjected to a GC analysis (8). A gas chromatograph[5] equipped with a ^{63}Ni electron-capture detector, a 61-cm × 32-mm i.d. glass column, and a 5% liquid[6] on solid support[6] stationary phase was used. The carrier gas was nitrogen at 20 mL/min; temperatures for the oven, injector, and detector were 155°C, 210°C, and 240°C, respectively.

Pharmacokinetic Analysis—Plasma data were fitted to a two-compartment open body model using the NONLIN program (9). The β-phase half-life ($t_{1/2,\beta}$) and the total body clearance (CL_t) were determined as:

$$t_{1/2,\beta} = \ln 2/\beta \quad \text{(Eq. 1)}$$

$$CL_t = D_0/AUC_\infty \quad \text{(Eq. 2)}$$

where β is the slope of the log-linear phase of the plasma decay curve, D_0 is the dose, and AUC_∞ is the area under the plasma concentration (C_p) *versus* time curve, calculated by the trapezoidal rule in conjunction with an area extrapolation method. The steady-state volume of distribution (Vd_{ss}) was determined using the model-independent expression of Benet and Galeazzi (10):

$$Vd_{ss} = D_0 \cdot (AUMC_\infty)/(AUC_\infty)^2 \quad \text{(Eq. 3)}$$

where AUMC is the area under the first moment of the plasma curve.

The fraction of renal excretion (f_e) in normal dogs was calculated as

$$f_e = (A_{e,24} + CL_r \int_t^\infty C_p dt)/D_0 \quad \text{(Eq. 4)}$$

where $A_{e,24}$ is the amount of I excreted in the 24-h urine sample and CL_r is the renal clearance determined by A_e/AUC using parameter values of up to 12 h. The integration term actually represents the extrapolated urinary recovery of the drug from the last plasma sampling point to infinite time. In this study, the last plasma datum at 24 h was extrapolated since the assay sensitivity could not allow accurate detection of plasma concentration <0.25 μg/mL.

Difference in mean pharmacokinetic parameters of the control and nephrectomized dogs was tested for significance by nonpaired Student's t statistics.

RESULTS AND DISCUSSION

Table I records the mean plasma data obtained for the five nephrectomized and two normal dogs. The normal group appeared to maintain higher plasma levels of I during the first hour of intravenous drug injection, whereas the nephrectomized group retained substantially greater plasma concentrations after 1.5 h. At the end of the blood sampling period of 12 h, the mean plasma concentrations observed were 1.21 μg/mL for the nephrectomized group and 0.33 μg/mL for the control group. Figure 1 depicts the time profiles for mean plasma levels in the normal and nephrectomized dogs. A distinct distribution phase was noted in the normal control dogs, and the distribution equilibrium was not reached until 2.5 h after the drug injection. In the nephrectomized

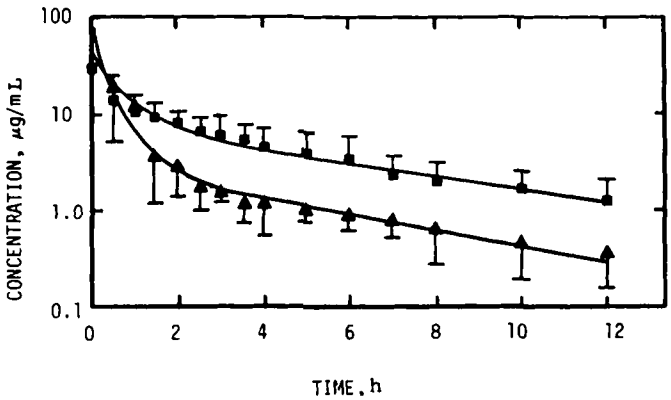

Figure 1—*Mean plasma concentration* versus *time plots for nephrectomized* (■) *and normal dogs* (▲) *over a 12-h period following single 500-mg iv doses of ethambutol.*

[1] C. S. Lee *et al.*, unpublished results.
[2] Lederle Laboratories, Pearl River, N.Y.
[3] Pierce Chemical, Rockford, Ill.
[4] MCB, Norwood, Ohio.
[5] Hewlett-Packard, Model 5730 A.
[6] OV-101 on Gas Chrom Q 100/120 mesh; Applied Science, State College, Pa.

Table II—Half-life, Total Body Clearance, and Volume of Distribution of Ethambutol in Five Nephrectomized and Two Normal Dogs

Dog	Weight, kg	$t_{1/2,\beta}$, h	CL_t, mL/min/kg	Vd_{ss}, L/kg
Nephrectomized				
1	17.0	4.29	11.7	3.2
2	20.0	5.18	12.4	3.6
3	13.6	4.73	6.2	2.3
4	16.3	4.79	5.0	1.8
5	20.2	5.93	6.7	2.4
Mean	17.4	4.98	8.4	2.7
SD	2.8	0.62	3.4	0.7
Normal				
6	24.5	3.52	16.5	4.4
7	19.8	4.72	10.0	3.2
Mean	22.2	4.12	13.2	3.8
SD	3.3	0.85	4.6	0.9

group, the distribution phase was apparent, but less extensive. The rapid and extensive distribution phenomena of I have also been noted in rabbits[1] and in human subjects (5).

Since a distinct distribution phase was noted after drug injection, plasma concentrations of I were subjected to computer analysis using a two-compartment open body model. Table II lists the pharmacokinetic parameters, and Table III compares the mean parameter values. Half-lives in the nephrectomized group varied from 4.29 to 5.93 h and those of the normal dogs were 3.52 and 4.72 h. The difference in the mean half-life of the two groups represented a 20.9% prolongation of half-life, presumably caused by nephrectomization, and was statistically significant ($p < 0.1$). Mean total body clearances of the nephrectomized (8.4 ± 3.4 mL/min/kg) and the normal dogs (13.2 ± 4.6 mL/min/kg) showed a significant difference of 36.33% ($p < 0.1$). In the limited number of dogs studied, nephrectomy induced a general trend for the increased half-life and reduced total body clearance of I, reflecting the renal excretory feature of the drug. The effect of nephrectomy on the elimination of I has not been reported in dogs, perhaps because such an effect is generally regarded as obvious. In humans, chronic renal failure caused a reduction of total body clearance from 500 mL/min to <10 mL/min (4). A prolongation of the half-life of I to ~10 h was also reported in renal failure (11).

Nephrectomized dogs were found to have a smaller volume of distribution (mean, 2.7 L/kg) than normal dogs (mean, 3.8 L/kg); the difference was statistically significant ($p < 0.1$). Nephrectomy would presumably cause a decreased volume of distribution due, in part, to the organ removal and the ligation of the vascular system. Chronic renal failure has been reported to alter the apparent volume of distribution for a number of drugs, notably digoxin (12) and phenytoin (13). It should be noted, however, that the nephrectomized dogs used in this study could only be deemed as approaching the chronic uremic state, since the drug investigation was initiated 2 d after the surgical preparation. Had the study been carried out at the steady state of chronic uremia, the change of pharmacokinetic parameters would have been more pronounced. Nevertheless, one can generally conclude that nephrectomy increased the half-life, decreased the total body clearance, and decreased the volume of distribution of I in dogs.

In a recent study of the effect of aluminum hydroxide on the absorption of I in rabbits[1], a substantially lower bioavailability of 28% was observed in comparison with the 80% bioavailability in humans, suggesting a first-pass metabolism of I in rabbits. With respect to renal excretion, rabbits excreted <5% of the intravenous dose as the unchanged compound in 24 h; the equivalent values were 30% for normal dogs and 70% in healthy human volunteers (Table IV). The observations of renal excretion of I in rabbits and dogs are contradictory to the general belief that I is predominantly excreted unchanged in all animal species. Arnaud *et al.* (7) reported a substantial urinary excretion of up to 50% for I; however, the urine assay was performed by a relatively

Table III—Comparison of Mean Pharmacokinetic Parameter Values for Half-Life, Total Body Clearance, and Volume of Distribution Between the Nephrectomized and Normal Dogs

Dog	$t_{1/2,\beta}$, h	CL_t, mL/min/kg	Vd_{ss}, L/kg
Nephrectomized	4.98	8.4	2.7
Normal	4.12	13.2	3.8
Percent change[a]	20.9	36.3	28.9
t value	1.54	1.51	1.81

[a] All differences are significant at $p < 0.1$.

Table IV—Comparison of Half-life, Total Body Clearance, Renal Clearance, Volume of Distribution, and Fractional Renal Excretion among Rabbits, Dogs, and Humans

Parameter	Rabbit[a]	Dog[b]	Human
$t_{1/2,\beta}$ (h)	3.87	4.12	4.21[c]
CL_t (mL/min/kg)	43.7	13.2	8.6[c]
CL_r (mL/min/kg)[d]	2.2	4.0	6.0
Vd_{ss} (L/kg)	8.5	3.8	3.9[c]
f_e (%)	5	30	70[c,e]

[a] C. S. Lee *et al.*, unpublished results. [b] Present study with normal dogs. [c] From Ref. 5. [d] Calculated as f_e-CL_t based on the f_e values listed. [e] From Ref. 3.

nonspecific and less sensitive colorimetric method (14). With regard to volume of distribution, rabbits exhibited the highest value (13.6 L/kg), followed by dogs (4.6 L/kg), and humans had the smallest distribution volume (2.3 L/kg) of the three species. In all cases, the volume of distribution exceeded total body weight, suggesting a localized distribution of I in the dogs. Pujet and Pujet (15) have noted a preferential distribution of I in the deep layers of the lung. In addition, I has been demonstrated, both *in vivo* and *in vitro*, to have a preference for partition into red blood cells (3, 16).

Total body clearance followed the same rank order as that of distribution volume: 43.7 mL/min/kg in rabbits, 13.2 mL/min/kg in dogs, and 8.6 mL/min/kg in humans, respectively. Since all clearance values listed in Table IV were calculated independent of a pharmacokinetic model ($CL = D_0/AUC$), compartmentalization would not have contributed to the difference in clearances observed among the three species. Assuming a renal excretion of 5% in rabbits, 30% in dogs, and 70% in humans, the respective renal clearances can be calculated as $CL_r = f_e \cdot CL_t$ and values of 2.2, 4.0, and 6.0 mL/min/kg would be obtained. In all cases, the renal clearance would exceed the glomerular filtration rate normalized to the body weight, indicating a net renal tubule secretion of the drug in all species. The active secretory mechanism of I has been demonstrated in humans, whose renal clearance was ~400 mL/min (4, 16). Since half-life is a function of both clearance and volume of distribution ($t_{1/2} = 0.693V/CL$), the three species actually shared similar half-lives—3.87 h in rabbits, 4.12 h in dogs, and 4.21 h in humans. However, there were distinct differences in other pharmacokinetic parameters, including total body clearance, renal clearance, volume of distribution, and fractional renal excretion.

REFERENCES

(1) J. P. Thomas, C. O. Baughn, R. G. Wilkinson, and R. G. Shepherd, *Am. Rev. Respir. Dis.*, **83,** 891 (1961).

(2) D. A. Buyske, W. Sterling, and E. Peets, *Ann N.Y. Acad. Sci.*, **135,** 711 (1966).

(3) E. A. Peets and D. A. Buyske, *Biochem. Pharmacol.*, **13,** 1403 (1964).

(4) T. G. Christopher, A. Blair, A. Forrey, and E. Cutler, *Proc. Dialysis Transplant Forum*, **3,** 96 (1973).

(5) C. S. Lee, D. C. Brater, J. G. Gambertoglio, and L. Z. Benet, *J. Pharmacokinet. Biopharm*, **8,** 335 (1980).

(6) E. A. Peets, W. M. Sweeney, V. A. Place, and D. A. Buyske, *Am. Rev. Respir. Dis.*, **91,** 51 (1965).

(7) G. M. Arnaud, M. Gavend, A. Roulet, B. Paramelle, and G. Bessard, *Med. J. France*, **79** (suppl), 7321 (1972).

(8) C. S. Lee and L. Z. Benet, *J. Pharm. Sci.*, **67,** 470 (1978).

(9) C. M. Metzler, G. L. Elfring, and A. J. McEwen, *Biometrics*, **30,** 562 (1974).

(10) L. Z. Benet and R. L. Galeazzi, *J. Pharm. Sci.*, **68,** 1071 (1979).

(11) C. S. Lee and L. Z. Benet, in "Analytical Profiles of Drug Substances," Academic, New York, N.Y., 1978, p. 231.

(12) R. H. Reuning, R. A. Sams, and R. E. Notari, *J. Clin. Pharmacol.*, **13,** 127 (1973).

(13) I. Odar-Cederlof and O. Borga, *Eur. J. Clin. Pharmacol.*, **7,** 31 (1974).

(14) B. Froseth, *Scand. J. Respir. Dis.*, **69,** 81 (1969).

(15) J. C. Pujet and C. Pujet, *Med. J. France*, **79** (suppl.), 7312 (1972).

(16) C. S. Lee, J. G. Gambertoglio, D. C. Brater, and L. Z. Benet, *Clin. Pharmacol. Ther.*, **22,** 615 (1970).

ACKNOWLEDGMENTS

This work was presented in part at the 129th APhA Annual Meeting, Las Vegas, Nevada, April 1982. The authors gratefully acknowledge the surgical assistance of Dr. Otto Ramos in preparing the nephrectomized dogs.

Solubility Parameter and Hydrophilic–Lipophilic Balance of Nonionic Surfactants

HANS SCHOTT

Received January 24, 1983, from the *School of Pharmacy, Temple University, Philadelphia, PA 19140.* Accepted for publication May 4, 1983.

Abstract □ The solubility parameters of various polyoxyethylated nonionic surfactants were compared with their hydrophilic–lipophilic balance (HLB) numbers. The compounds included three homologous surfactant series based on dodecanol, octylphenol, and fatty acid esters of sorbitan, respectively, a polyoxyethylated sorbitol ester, and a polyethylene glycol. Solubility parameters were calculated from measured heats of vaporization for the polyoxyethylated dodecanol series and from molar attraction constants for all three surfactant series. The values remained nearly constant and independent of the degree of polyoxyethylation, increasing at most by 1 $(cal/cm^3)^{1/2}$ while the HLB increased from 0 to 10. This discrepancy arose because HLB values are based on emulsification experiments, in which the polyoxyethylene or polyol moiety of the surfactants is hydrated, while the solubility parameter was calculated for anhydrous conditions. When the solubility parameter was corrected for hydration by including a hydrogen-bonding component, plots of HLB *versus* this new solubility parameter were nearly linear and parallel for the three series of surfactants, with slopes of 5.0 ± 0.2. The three lines were spaced apart only ~1.2 $(cal/cm^3)^{1/2}$ despite structural differences among the surfactants, indicating that the chemical nature of the hydrocarbon moiety exerts only a limited effect on the solubility parameter. The HLB, which considers only the weight percent of the hydrocarbon moieties of nonionic surfactants and completely disregards differences in structural features, is, therefore, not as bad an approximation as had previously been thought.

Keyphrases □ Solubility parameter—polyoxyethylated nonionic surfactants, comparison with hydrophilic-lipophilic balance □ Hydrophilic-lipophilic balance—polyoxyethylated nonionic surfactants, comparison with solubility parameter □ Surfactants, nonionic—polyoxyethylated, solubility parameters compared with hydrophilic-lipophilic balance values

The hydrophilic–lipophilic balance (HLB) system was developed by Griffin to characterize the emulsifying efficiency of nonionic surfactants (1). Because the experimental determination of HLB values through emulsification experiments is laborious and not very accurate, the following equation was developed (2, 3):

$$HLB = \frac{E + P}{5} \qquad \text{(Eq. 1)}$$

where E is the percent (w/w) of polyoxyethylene and P the percent (w/w) of polyhydric alcohols in the surfactant molecule.

A criticism leveled against the HLB concept, as embodied in Eq. 1, was that it disregards the effect of the chemical nature of the hydrocarbon moiety of the surfactants (4). The purpose of this work is to investigate the application of the solubility parameter concept (5–7) to nonionic surfactants, because it takes into consideration the nature of their hydrophilic as well as their hydrophobic moieties. Even though the solubility parameter is the subject of much current pharmaceutically oriented research (8, 9), it has been investigated only briefly in connection with nonionic surfactants (10, 11).

Table I—Values of Hydrophilic–Lipophilic Balance and Solubility Parameters for Polyoxyethylated Dodecanols

p^a	HLB[b]	δ^c	δ^d	δ^e	$\delta_O{}^f$
0	0	8.04	—	8.39	9.63
1	3.83	8.04	—	8.38	10.39
2	6.42	7.97	—	8.47	11.02
3	8.30	8.51	—	8.47	11.42
4	9.72	8.92	—	8.45	11.70
6	11.73	—	9.49	8.41	12.09
8	13.08	—	9.86	8.39	12.37
10	14.05			8.37	12.57
12	14.79			8.37	12.73

[a] Average number of oxyethylene units per molecule. [b] Calculated by Eq. 1. [c] Calculated by Eq. 2 from experimental ΔH values (12). [d] Calculated by Eq. 2 from ΔH values extrapolated with Eq. 3. [e] Calculated from molar attraction constants in Table II and Eq. 7. [f] Calculated by Eq. 8.

BACKGROUND

The solubility parameter, δ, is the square root of the cohesive energy density, *i.e.*, the molar internal energy of vaporization ΔE per unit volume:

$$\delta = \sqrt{\frac{\Delta E}{V_l}} = \sqrt{\frac{(\Delta H - RT)d}{M_r}} \qquad \text{(Eq. 2)}$$

where $V_l = M_r/d$ is the molar volume in the liquid state, d is the density, and M_r is the molecular weight. The molar heat of vaporization ΔH refers to constant pressure P. Therefore, it exceeds the molar energy of vaporization, which refers to constant volume, by the expansion term during vaporization $P(V_g - V_l) \cong PV_g = RT$; V_g is the molar volume in the gaseous state, R is the gas constant, and T is the absolute temperature (5–7).

RESULTS

Solubility Parameters from Heats of Vaporization—Vapor pressure measurements from which heats of vaporization can be calculated require such high temperatures that all but homologues with the lowest degrees of oxyethylation undergo decomposition. For polyoxyethylated dodecanol surfactants, $C_{12}H_{25}O(CH_2CH_2O)_pH$, heats of vaporization were measured for p values up to 4 (12). A plot of the ΔH values for surfactants with $p = 2$, 3, and 4 fall on a straight line represented by the equation:

$$\Delta H = 8.4 + 5.65p \qquad \text{(Eq. 3)}$$

where the units of ΔH are kcal/mol.

The densities, d, of polyoxyethylated dodecanols at 25°C are related to the logarithm of the average number, p, of oxyethylene units per molecule by the equation:

$$\log p = -6.64 + 7.63d \qquad \text{(Eq. 4)}$$

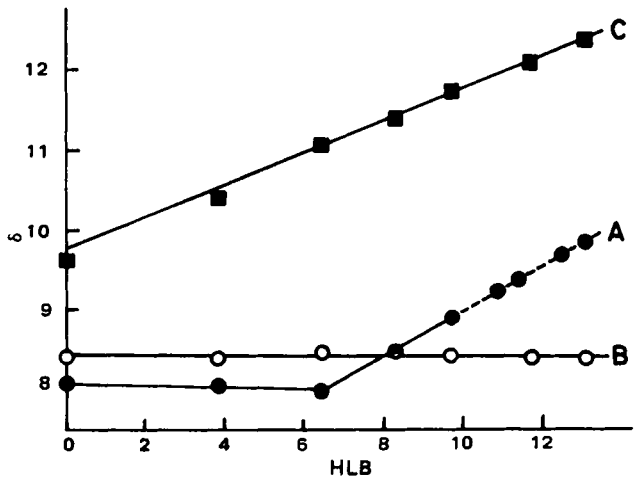

Figure 1—*Solubility parameters of polyoxyethylated dodecanols obtained by three methods* versus *HLB. Key: (●) curve A, δ based on measured (—) and extrapolated (- - -) heats of vaporization calculated by Eq. 2; (○) curve B, δ calculated from molar attraction constants with Eq. 7; (■) curve C, δ_O corrected for hydration, based on Eqs. 8 and 9.*

0022-3549/84/0600-0790$01.00/0
© 1984, American Pharmaceutical Association

For polyoxyethylated *p-tert*-octylphenols, the following linear relation holds for p values <20:

$$\log p = -12.53 + 12.72d \qquad \text{(Eq. 5)}$$

Applying Eq. 2 to the measured heats of vaporization (12) of dodecanol-based surfactants with p values of 0–4 and to the heats of vaporization extrapolated by Eq. 3 for surfactants with p values of 6 and 8 results in the δ values in the third and fourth columns of Table I, respectively, and curve A of Fig. 1. The curve consists of two segments. The first is nearly horizontal. The second, for HLB values >5 ($p \geq 2$), is linear and represented by the equation:

$$\delta = 6.16 + 0.283 \cdot \text{HLB} \qquad \text{(Eq. 6)}$$

The slopes of both segments are unrealistically small. For the second segment, a change of 1 HLB unit produces a change of only 0.3 $(\text{cal/cm}^3)^{1/2}$. The two parameters actually span similar ranges of values: the HLB scale extends from 0 to 20 (Eq. 1) and the δ scale from 5 to 23 (13).

The HLB values of the surfactants in Table I range from 0 to 15, *i.e.*, from surfactants primarily soluble in liquids of low polarity such as vegetable or mineral oils ($\delta \cong 8$) to surfactants primarily soluble in polar liquids like ethyl alcohol ($\delta = 12.8$), propylene glycol ($\delta = 15.0$), and water ($\delta = 23.6$) (1–3). Compounds are most soluble in solvents whose δ values match their own most closely. Since the δ values of the best solvents for the surfactants in Table I cover the range from 8 to at least 15, the δ values of the surfactants should cover a similar range, rather than the more limited range of 8–10 obtained from heats of vaporization. The 8–10 range would indicate highest solubility in liquids of intermediate polarity, such as esters, amines, and ketones (13), for all surfactants. One possible explanation for this discrepancy is that the linear extrapolation by Eq. 3 is unwarranted.

Solubility Parameters from Molar Attraction Constants—Small (14) treated the solubility parameter as an additive-constitutive property. He noted that the so-called molar attraction constants, $F = (\Delta e \cdot v_1)^{1/2}$, were additive; Δe and v_1 are the contributions of the organic functional groups to the molar energy of vaporization and to the molar volume in the liquid state at 25°C, respectively. Therefore, the solubility parameter of a compound can be calculated from the F values of its functional groups according to the following equation (14):

$$\delta = \frac{d\Sigma F}{M_r} \qquad \text{(Eq. 7)}$$

The F values used here, selected from the various published sets (14, 15), are listed in Table II.

The structures for the three classes of surfactants investigated are $CH_3(CH_2)_{11}(OCH_2CH_2)_pOH$, and I and II (shown below). In addition to the lauric acid ester of sorbitan shown (II), the stearic and oleic acid esters are also included. The total number of ethylene oxide molecules added during oxyethylation of the sorbitan monoesters are $a + b + c = p$. As long as the value of p remains constant, the value of ΣF is not changed if a polyoxyethylene chain is inserted by transesterification between the ester group of the fatty acid and the hexitan ring during the oxyethylation reaction (16). Sorbitan is a mixture of 5- and 6-membered rings. These two ring structures make the same contribution to ΣF.

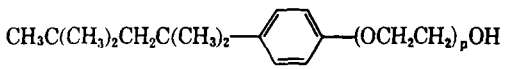

I

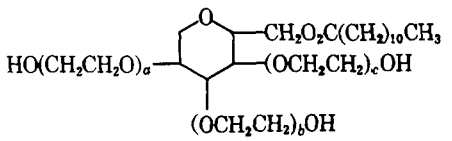

II

For dodecanol derivatives, the δ values are represented by curve B in Fig. 1 and the fifth column of Table I. For octylphenol and polyol derivatives, the results are listed in the third columns of Tables III and IV, respectively.

The δ values of the dodecanol derivatives based on heats of vaporization are in good agreement with those calculated from molar attraction constants for derivatives with HLB ≤ 10 ($p \leq 4$) (compare the solid portion of curve A with curve B in Fig. 1). As the number, p, of oxyethylene units increases, the calculated δ values remain constant for the dodecanol derivatives: curve B of Fig. 1 is horizontal. The δ values actually decrease slightly for the octylphenol and sorbitan derivatives. Similar observations have been published (10, 11).

Table II—Molar Attraction Constants F for Functional Groups of Nonionic Surfactants

Group	F, $(\text{cal/cm}^3)^{1/2}$/mol
$-CH_3$	179
$-CH_2-$	133
$CH\lessgtr$	67
$>C<$	0
$-CH=CH-$	231
$-C_6H_4-$ (o-, m-, or p-phenylene)	658
Saturated 5- or 6-membered ring	105
—OH aliphatic hydroxyl	240
—C(=O)O— ester	303
—O— ether	70

An empirical parameter, the product of the contribution of the hydrocarbon moiety to ΣF times the weight fraction of that moiety, was developed as a consequence. It was inversely proportional to the HLB (11) and offers, therefore, no advantage over that parameter.

The reason that the solubility parameters obtained from these two approaches are nearly independent of the percentage of oxyethylene in the surfactant molecule or its HLB is that they were computed for anhydrous systems. In the absence of water, the molar attraction constant for the ether oxygen is only 70, *i.e.*, not much larger than that of a hydrogen atom. Consequently, the polyoxyethylene moiety increases the polarity of the nonionic surfactant molecule little or not at all above that of its hydrophobic moiety. It is only in the presence of water, where the ether groups are extensively hydrated, that the polyoxyethylene moiety becomes polar and raises the effective δ of the surfactant.

Emulsification experiments measure the HLB values of hydrated surfactants. Even surfactants dissolved in oil have their polyoxyethylene or polyol moieties immersed in water when they are concentrated at the oil–water interface during emulsification. Hydrogen bonding between water and the ether oxygens and/or hydroxyl groups of nonionic surfactants is responsible for their water solubility or, in the case of oil-soluble surfactants, for their surface activity. The two treatments underestimate the solubility parameters because they do not take into account these intermolecular hydrogen bonds.

Solubility Parameters Corrected for Hydrogen Bonding—Intermolecular forces affecting the cohesive energy density of surfactants in the presence of water include not only the dispersion forces (subscript D), which constitute the major components of the F values of Table II, but also the dipole–dipole forces (subscript P) and the hydrogen-bonding forces (subscript H). The overall solubility parameter δ_O is calculated from these three components according to (7, 15, 17, 18):

$$\delta_O = \sqrt{\delta_D^2 + \delta_P^2 + \delta_H^2} \qquad \text{(Eq. 8)}$$

The contribution of the polar forces, δ_P, can be neglected because it is small in relation to the hydrogen-bonding forces (18, 19). Furthermore, the p oxygen–carbon dipoles in a randomly coiled polyoxyethylene moiety weaken each other to the point of annihilation (15).

On the assumptions that each hydrogen bond contributes 5000 cal/mol to the energy of vaporization and that each of the p ether groups and each hydroxyl group forms one hydrogen bond with water, the hydrogen-bonding component of the solubility parameter is calculated (20) as:

$$\delta_H = \sqrt{\frac{5000(p+1)d}{M_r}} \qquad \text{(Eq. 9)}$$

Table III—Values of Hydrophilic–Lipophilic Balance and Solubility Parameters for Polyoxyethylated Octylphenols

p[a]	HLB[b]	δ[c]	δ_O[d]
0	0	8.85	10.06
1	3.52	8.90	10.89
2	5.98	8.90	11.43
3	7.81	8.87	11.80
4	9.21	8.83	12.06
6	11.23	8.77	12.44
8	12.61	8.73	12.70
10	13.62	8.70	12.89
13	14.70	8.67	13.10

[a] Average number of oxyethylene units per molecule. [b] Calculated by Eq. 1. [c] Calculated from molar attraction constants in Table II and Eq. 7. [d] Calculated by Eq. 8.

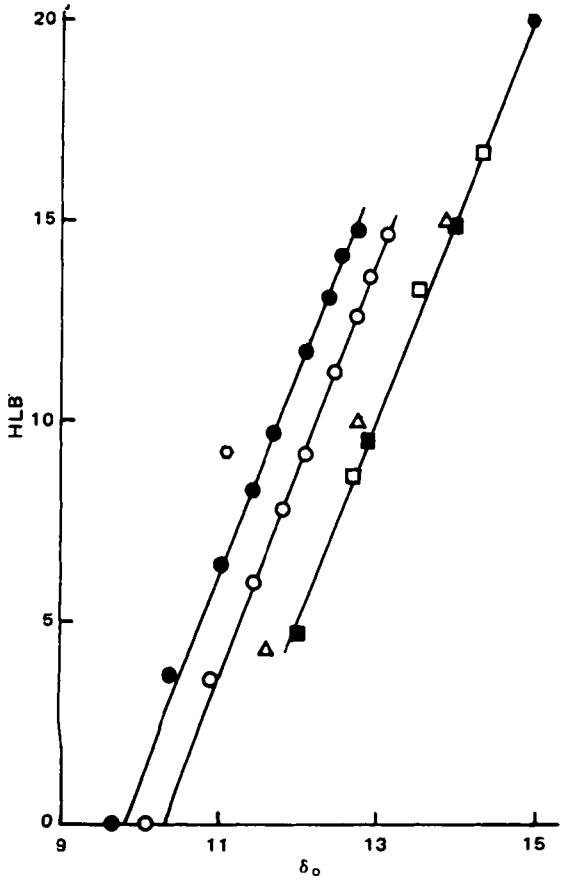

Figure 2—*Relationship between HLB and δ_O for three classes of polyoxyethylated surfactants. Key: (●) dodecanol derivatives; (○) octylphenol derivatives; (△) sorbitan monooleate derivatives; (■) sorbitan monostearate derivatives; (□) sorbitan monolaurate derivatives; (○) polyoxyl 40 sorbitol septaoleate; (●) polyethylene glycol 3350.*

for the dodecanol and octylphenol derivatives, which have one hydroxyl group per molecule. For sorbitan derivatives containing p oxyethylene units, the coefficient is $p + 4$ to account for the ether linkage in the ring and the three hydroxyl groups. For a polyethylene glycol formed by adding p ethylene oxide molecules to one water molecule, it is $p + 1$ since the compound contains $p - 1$ ether linkages and two hydroxyl groups.

Because hydrogen bonding is an unsymmetrical interaction, two δ_H parameters are sometimes employed, one for proton donation or acid character, the other for acceptor or base effects (18). In the present study, almost all donors are water molecules and all acceptor groups are ether linkages. Therefore, the acid nature of the donor groups and the basic nature of the acceptor groups were constant in all surfactant systems, justifying the use of a single δ_H parameter and the assumption of a constant contribution of 5000 cal/mol for all hydrogen bonds to the molar energies of vaporization (20).

The overall solubility parameter δ_O was calculated according to Eq. 8 as follows. The δ values based on the molar attraction constants and Eq. 7 were used as the dispersion component δ_D; δ_P was neglected, and δ_H was calculated by Eq. 9. The δ_O values for the three classes of surfactants are listed in the last columns of Tables I, III, and IV. For the dodecanol derivatives, they are plotted in Fig. 1 on curve C. They include the effect of hydration on the polarity of the nonionic surfactants, *i.e.*, they are corrected for intermolecular hydrogen bonds.

For polyethylene glycol 3350[1], δ or δ_D is 9.28 and δ_O is 14.96. These two values are in good agreement with the experimental δ values determined for this compound, namely, 8.9 as the lower end of the range in poorly hydrogen-bonded solvents and 14.5 as the upper end of the range in strongly hydrogen-bonded solvents, especially, water (18). The former value corresponds to δ_D and the latter to δ_O. This agreement validates the methods for computing δ_O, δ_D, and δ_H.

[1] Carbowax 4000; Union Carbide Corp.

Table IV—Values of Hydrophilic-Lipophilic Balance and Solubility Parameters for Polyoxyethylated Polyols

Polyol	p[a]	HLB[b]	δ[c]	δ_O[d]
Sorbitan monolaurate	0	8.6	10.02	12.73
	4	13.3	9.83	13.51
	20	16.7	9.50	14.31
Sorbitan monostearate	0	4.7	9.77	11.99
	4	9.6	9.68	12.87
	20	14.9	9.44	13.94
Sorbitan monooleate	0	4.3	9.36	11.59
	5	10.0	9.38	12.74
	20	15.0	9.34	13.85
Sorbitol septaoleate[e]	40	9.2	8.41	11.10

[a] Average number of oxyethylene units per molecule. [b] Taken from "General Characteristics of Surfactants," ICI Americas, Inc., Wilmington, Del., 1979. [c] Calculated from molar attraction constants in Table II and Eq. 7. [d] Calculated by Eq. 8. [e] Atlox 1087; ICI Americas, Inc., Wilmington, Del.

CONCLUSIONS

The δ_O values for the nonionic surfactants based on dodecanol, octylphenol, and sorbitan are plotted against their HLB values in Fig. 2. The points for the three classes of sorbitan esters based on lauric, stearic, and oleic acid, respectively, nearly fall on a single straight line which also includes polyethylene glycol 3350. The curves for the dodecanol and octylphenol derivatives are linear down to HLB values of 6. The three straight lines are parallel with slopes, $d\text{HLB}/d\delta_O$, of 5.0 ± 0.2; the ± sign precedes the range of values.

The surprising fact is that the three curves belonging to three different categories of surfactants are spaced only ~1.2 $(\text{cal/cm}^3)^{1/2}$ apart despite the structural differences. This observation indicates that the nature of the hydrocarbon moiety of nonionic surfactants affects their solubility parameter only to a limited extent. The objection that the HLB calculated by Eq. 1 does not take into account the nature of the hydrocarbon moiety but only its weight percentage (or the weight percentage of the polyoxyethylene or polyol moiety, E or P) (4) has only limited validity. The solubility parameter takes the nature of the hydrocarbon moiety into account. Yet, at comparable HLB values, solubility parameters for different classes of surfactants based on different types of hydrocarbons are identical within limits that are narrower than ±1 $(\text{cal/cm}^3)^{1/2}$.

REFERENCES

(1) W. C. Griffin, *J. Soc. Cosmet. Chem.*, **1**, 311 (1949).

(2) W. C. Griffin, *J. Soc. Cosmet. Chem.*, **5**, 249 (1954).

(3) W. C. Griffin, H. J. Ranauto, and A. D. Adams, *Am. Perfum. Cosmet.*, **81**(9), 1 (1966).

(4) H. Schott, *J. Pharm. Sci.*, **58**, 1443 (1969).

(5) J. H. Hildebrand and R. L. Scott, "The Solubility of Nonelectrolytes," 3rd ed., Dover, New York, N.Y., 1964, chap. 23 and Appendix I.

(6) J. H. Hildebrand, J. M. Prausnitz, and R. L. Scott, "Regular and Related Solutions," Van Nostrand Reinhold, New York, N.Y., 1970, chap. 6 and Appendix 5.

(7) K. Shinoda, "Principles of Solution and Solubility," Dekker, New York, N.Y., 1978, chap. 4.

(8) A. Martin, J. Newburger, and A. Adjei, *J. Pharm. Sci.*, **69**, 487 (1980).

(9) A. Martin, P. L. Wu, A. Adjei, M. Mehdizadeh, K. C. James, and C. Metzler, *J. Pharm. Sci.*, **71**, 1334 (1982).

(10) R. C. Little, *J. Colloid Interface Sci.*, **65**, 587 (1978).

(11) C. McDonald, *Can. J. Pharm. Sci.*, **5**, 81 (1970).

(12) M. Nakamura, K. Eda, and K. Kosiyama, *Bull. Chem. Soc. Jpn*, **47**, 2877 (1974).

(13) K. L. Hoy, *J. Paint Technol.*, **42**, 76 (1970).

(14) P. A. Small, *J. Appl. Chem.*, **3**, 71 (1953).

(15) D. W. van Krevelen, "Properties of Polymers, their Estimation and Correlation with Chemical Structure," 2nd ed., Elsevier, Amsterdam, Netherlands, 1976, chap. 7.

(16) F. R. Benson, in "Nonionic Surfactants," M. J. Schick, Ed., Dekker, New York, N.Y., 1967, chap. 9.

(17) C. M. Hansen, *Ind. Eng. Chem., Prod. Res. Dev.*, **8**, 2 (1969).

(18) A. F. M. Barton, *Acc. Chem. Res.*, **75**, 731 (1975).

(19) H. Burrell, *J. Paint Technol.*, **40**, 197 (1968).

(20) C. M. Hansen and K. Skaarup, *J. Paint Technol.*, **39**, 511 (1967).

Effect of Inorganic Additives on Solutions of Nonionic Surfactants VI: Further Cloud Point Relations

HANS SCHOTT ˣ and ALAN E. ROYCE

Received September 4, 1982, from the *School of Pharmacy, Temple University, Philadelphia, PA 19140.* Accepted for publication May 4, 1983.

Abstract □ Disperse dosage forms stabilized with nonionic surfactants frequently contain electrolytes as active ingredients or adjuvants. Salting out of the surfactants by these electrolytes may cause breakdown of the dosage forms. The cloud point of an aqueous solution of octoxynol 9 was used to measure the salt effects. Electrolytes which salt octoxynol 9 out lower its cloud point, while salting-in electrolytes raise it. The observed cloud point effects are discussed according to the mechanisms involved. Salting out by dehydration in competition with octoxynol 9 for the available water was observed with sulfate and phosphate anions, sodium, potassium, and ammonium tribasic cations, and the nonelectrolyte sorbitol. The extensive self-association of water by hydrogen bonds at and below room temperature weakens its solvent power. Ions which reduce this self-association, breaking the structure of water, increased the cloud point of octoxynol 9. Among them were the iodide, thiocyanate, and nitroprusside anions. Ions which tighten the structure of water and enhance its self-association salted the surfactant out, lowering its cloud point. Among these were the fluoride and hydroxide anions. Complex formation between the ether linkages of octoxynol 9 and the following cations increased its cloud point: hydrogen (from strong acids), silver, magnesium, and zinc. Including published data, the only cations which do not form complexes with polyoxyethylated surfactants (and are, therefore, unable to salt them in) were the alkali metal ions sodium, potassium, and cesium and the ammonium ion. The cloud point increases produced by a weak organic base and acids are ascribed to the formation of mixed solvents with water. The hydrotropes sodium salicylate, phenobarbital sodium, and sodium benzoate raised the cloud point appreciably even at low concentrations. The most efficient cloud point boosters were the three surfactants studied, namely, two ionic and a nonionic surfactant with an elevated cloud point. They formed mixed micelles with octoxynol 9. The changes in cloud point caused by electrolytes having a common ion were compared at equal values of a concentration parameter chosen to produce cloud point additivity. By using the nitrate ion as a reference and arbitrarily equating its change in cloud point to zero, cloud point shift values could be assigned to other individual ions. For the anions, these cloud point shift values were related by a smooth function to the lyotropic numbers in the Hofmeister series. There was no correlation between the cloud point shift values and the lyotropic numbers of cations, presumably because of complexation between the ether groups of octoxynol 9 and many of the cations.

Keyphrases □ Surfactants, nonionic—octoxynol 9, effect of inorganic additives, cloud point relations □ Octoxynol 9—effect of inorganic additives on nonionic surfactants, cloud point relations □ Cloud point relations—effect of inorganic additives on nonionic surfactants, octoxynol 9

The influence of electrolytes on the solubility of nonionic polyoxyethylated surfactants can be assessed by their effect on the cloud point (1–5). The present work extends cloud point measurements of a representative nonionic surfactant to solutions containing electrolytes with anions and/or cations used in dosage forms. It also presents a numerical system for rating the capacity of various ions to salt the polyoxyethylated surfactant in or out.

BACKGROUND

Dosage forms consisting of micellar solutions and of disperse systems—suspensions, emulsions, ointments, and aerosols—are commonly stabilized with surfactants. Electrolytes may be present as active ingredients, adjuvants, or impurities. They frequently have an adverse effect on stability. Salting out of the surfactants by the electrolytes may cause breakdown of the dosage form.

The method generally used to study the effect of electrolytes on the solubility of nonelectrolytes is to determine that solubility in water (S_n^o) and in aqueous solutions containing C_e mol/L of electrolyte (S_n). These parameters are related by the Setschenow equation (6):

$$\log (S_n^o/S_n) = K \cdot C_e \qquad \text{(Eq. 1)}$$

where the magnitude and sign of the salt parameter, K, indicate the extent of salting in or out.

Solubility measurements of nonionic surfactants in water or aqueous salt solutions are difficult to perform because of the high values and the appearance, in concentrated systems, of viscous mesomorphic phases (7). The cloud point of these surfactants is sensitive to electrolytes (1–5), but insensitive to surfactant concentration within rather wide limits (8, 9). It can be measured readily and reproducibly and serves, therefore, as a convenient parameter for salt effects.

Electrolytes that raise the cloud point expand the region in the surfactant–water phase diagram between the upper consolute temperature, represented by the cloud point curve, and either the Krafft point curve or the freezing point curve. In this region (Region II of Fig. 1 in Ref. 10), which contains a single phase, the surfactant exists in an undersaturated isotropic solution. Such electrolytes increase the solubility of the surfactant, salting it in ($K < 0$). Electrolytes that depress the cloud point reduce the region in which the surfactant is soluble, *i.e.*, they salt it out ($K > 0$).

Information on the effect of electrolytes on the cloud point of nonionic surfactants also has practical uses. Dosage forms stabilized with nonionic surfactants frequently break down when heated above the cloud point, *e.g.*, during thermal sterilization.

EXPERIMENTAL

Materials—The surfactant, octoxynol 9 NF[1], was an anhydrous, viscous liquid. The following reagents were USP/NF grade: boric acid, citric acid, light magnesium carbonate, phenobarbital sodium, sodium benzoate, sodium fluoride, sorbitol, and trolamine (2,2′,2″-nitrilotriethanol). Sodium bromide was purified[2], tribasic sodium phosphate was technical grade[2], and sodium salicylate was certified[3]. Sodium dodecyl sulfate, triethanolamine hydrochloride, hexadecane, and xylenes were research chemical grade[4]. Another nonionic surfactant, polyoxyl 20 oleyl ether[5] (oleyl alcohol with 20 ethylene oxide units), was solid at room temperature. All other chemicals were ACS reagent grade.

A stock solution of dibasic magnesium citrate, $MgH(C_6H_5O_7)$, was made by dissolving light magnesium carbonate in a citric acid solution. Stock solutions of the sodium citrates were made by neutralizing citric acid solutions

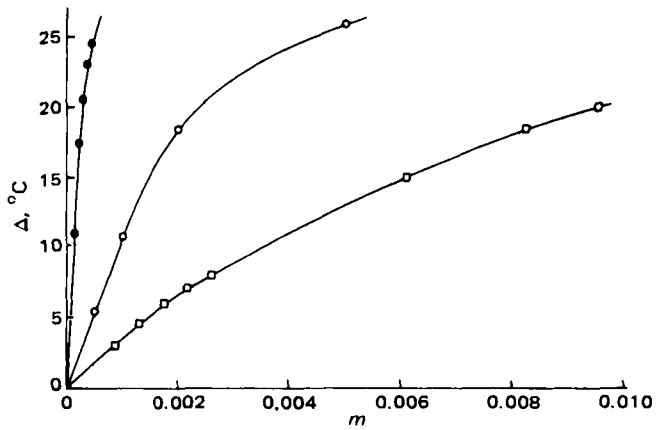

Figure 1—*Cloud point increases by surfactants as a function of their molal concentrations. Key: (●) sodium lauryl sulfate; (○) decylammonium chloride; (□) polyoxyl 20 oleyl ether.*

[1] Supplied by Rohm & Haas Co. as Triton X-100.
[2] Amend Drug & Chemical Co.
[3] Fisher Scientific Co.
[4] Eastman Organic Chemicals.
[5] Supplied by ICI Americas Inc. as Brij 98.

0022-3549/84/0600-0793$01.00/0
© 1984, American Pharmaceutical Association

Table I—Effect of Surfactants and Hydrotropes on the Cloud Point of Octoxynol 9

Rank No.	Additive	Concentration to Produce Δ = 10°C, *m*	Δ at Molality, °C 0.0005	0.001	0.005	0.010	0.050	0.100	0.500
1	Sodium lauryl sulfate	0.00013	26						
2	Decylammonium chloride	0.00093	5.5	11	26				
3	Polyoxyl 20 oleyl ether	0.0035	2	3.5	13	20.5			
4	Sodium salicylate	0.023			3.5	6	13.5	20	
5	Phenobarbital sodium	0.065				2	8	14	
6	Sodium benzoate	0.128				2	5.5	8.5	24.5

Table II—Effect of Acids on the Cloud Point of Octoxynol 9

Rank No.	Additive	Concentration to Produce Δ = 10°C, *m*	Δ at Molality, °C 0.10	0.50	1.0	3.0
7	Citric acid	0.45	2.5[b]	11	23	
13	Acetic acid	1.13	0.5	4	9	27.5
15	Hydrochloric acid[a]	1.46	−1	2	5	28.5
16	Phosphoric acid	1.50		2	6	22.5
18	Sulfuric acid[a]	1.70	−2	0.2	3	28
—	Boric acid	—		2		

[a] Taken from Refs. 4 and 5 plus present data. [b] Taken from Ref. 1.

Table III—Effect of Various Salting-In Electrolytes on the Cloud Point of Octoxynol 9

Rank No.	Additive	Concentration to Produce Δ = 10°C, *m*	Δ at Molality, °C 0.50	1.0	2.0
7	NaSCN	0.32	14.5	21	
9	$Na_2[Fe(CN)_5NO]$	0.55	9.5	15	
11	NaI	0.87	6.5	11	16
10	$AgNO_3$	0.87	6.5	11	18
14	$Zn(NO_3)_2$	1.43	4.5	7.5	
17	$Mg(NO_3)_2$[a]	1.56	4.5	7.5	12.5
19	$Al(NO_3)_3$[a]	1.89	5	7.5	10

[a] Taken from Ref. 4.

with sodium hydroxide solutions to varying degrees. The water used was double distilled.

Methods—Concentrated stock solutions of the electrolytes were analyzed as reported (4, 5) or by the official USP methods. Octoxynol 9 solutions were aged for at least 48 h before mixing with the electrolyte solutions to permit complete hydration and breakdown of mesomorphic phases and large micelles.

Cloud points were determined at the 2.00% octoxynol 9 level (4, 5). All concentrations in the ternary mixtures are based on the weight of water.

An analysis of the errors incurred in weighing out stock solutions and water and in measuring cloud points indicates that the reported electrolyte molalities are accurate to three significant figures, resulting in an accuracy for the cloud points of ±0.5°C or better.

RESULTS AND DISCUSSION

Five lots of octoxynol 9 were used. Their cloud points ranged from 64.5°C to 67°C. Therefore, the changes in the cloud point of 2.00% octoxynol 9 solutions, Δ, were calculated as the difference between the cloud point of the solutions containing octoxynol 9 plus the additive and the cloud point of the corresponding blank octoxynol 9 solution. A positive Δ indicates salting in, and a negative Δ indicates salting out. The data are listed in Tables I–VI and plotted in Figs. 1–8.

Cloud points usually varied monotonically with increasing additive concentrations. The main exceptions were magnesium chloride and sulfuric acid. The plot of Δ *versus* molality for the former (Fig. 6) went through a minimum of −16°C at 2 *m*. However, at 3.4 *m*, Δ was only −11°C, the same value as at 0.7 *m*. The chloride ion probably acts as a ligand for magnesium in competition with the ether groups of octoxynol 9. The upturn in the curve is ascribed to increasing complexation with the latter at higher salt concentrations, either as a result of the law of mass action or because the coordination number of magnesium is increased to 6. Sulfuric acid depressed the cloud point of octoxynol 9 by 2°C at 0.10 *m*, but raised it considerably more at higher concentrations (4). The Δ values of ammonia cover the narrow interval from 2°C to −6°C in the broad concentration range extending to 10 *m* (Table IV, Fig. 5).

Some of the plots of Δ *versus* concentration were curved, indicating that the tendency towards salting octoxynol 9 in or out increased less than proportionally with the additive concentration. Linear plots of Δ *versus* concentration were observed for the following additives in the entire concentration range investigated: trolamine, acetic acid, dibasic sodium citrate, and tribasic sodium phosphate. Linearity for most of the plots was observed for citric acid (Fig. 3) and sodium nitrate (4). Sodium, ammonium, and magnesium sulfates had linear plots over 50–67% of the concentration ranges investigated (Fig. 7).

The numbers in the first columns of Tables I–VI rank the salting-in or salting-out efficiency of the additives. Increasing numbers from 1 to 19 indicate that progressively higher additive molalities were required to boost the cloud point of octoxynol 9 by 10°C. These numbers thus rank the additives in order of decreasing salting-in capacity. Increasing numbers from 20 to 40 indicate that progressively lower additive concentrations were required to reduce the cloud point of octoxynol 9 by 10°C. These numbers rank the additives in order of increasing salting-out capacity. Thus, additive no. 1 is the most efficient salting-in agent, and additive no. 40 is the most efficient salting-out agent on a molal basis. Boric acid was not assigned a number because its solubility was too low to produce a Δ value of 10°C. The tabulated Δ values at the listed additive molalities were either measured directly or interpolated. No extrapolated values were used.

Mechanisms of Electrolyte–Octoxynol 9 Interaction— Polyoxyethylated surfactants are soluble in water because of the hydration of their ether linkages. Studies with model ethers have shown that a maximum of two water molecules are bound directly to each oxygen by hydrogen bonding (11). The hydration

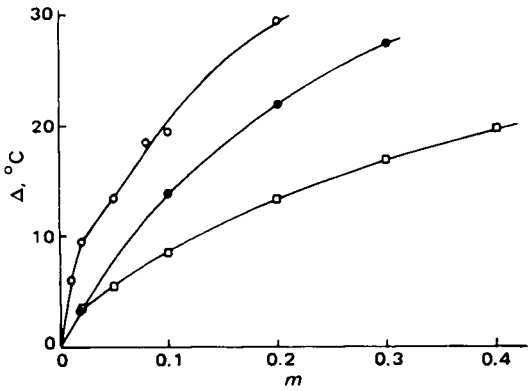

Figure 2—*Cloud point increases by hydrotropes as a function of their molal concentrations. Key: (○) sodium salicylate; (●) phenobarbital sodium; (□) sodium benzoate.*

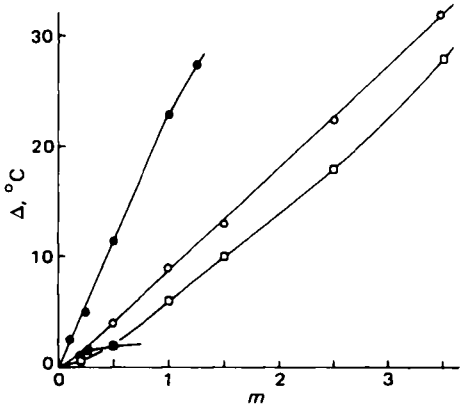

Figure 3—*Cloud point increases by acids as a function of their molal concentrations. Key: (●) citric; (○) acetic; (□) phosphoric; (■) boric.*

Table IV—Effect of Various Additives on the Cloud Point of Octoxynol 9

Rank No.	Additive	Concentration to Produce Δ = ±10°C, *m*	Δ at Molality, °C 0.50	1.0	3.0	6.0	10.0
20	NH_3	~12		1	2	−0.5	−6
21	NH_4NO_3	3.0	−1	−1	−10		
24	NH_4Cl	0.96	−6	−10.5	−20.5		
35	$(NH_4)_2SO_4$	0.16	−28	−52			
12	Trolamine	0.98[a]	6	10			
26	Trolamine hydrochloride	0.80	−7.5	−12			
30	Tetramethylammonium chloride[b]	0.45	−11	−19			
25	Sorbitol	0.93	−4.5	−11	−38.5		

[a] Δ = 10°C. For the other additives, Δ = −10°C. [b] Taken from Ref. 18.

Table V—Effect of Various Salting-Out Electrolytes on the Cloud Point of Octoxynol 9

Rank No.	Additive	Concentration to Produce Δ = −10°C, *m*	Δ at Molality, °C 0.10	0.50	1.0	2.5	5.0
22	NaBr	1.90		−3.5	−6	−12.5	
23	$NaNO_3$[a]	1.59	−1	−2	−6	−13	
29	NaCl	0.50	−2	−10	−16.5	−33	−50
32	NaOH	0.28	−4	−16.5	−30.5		
33	NaF	0.24	−4.5	−19			
27	$MgCl_2$	0.59		−9	−13	−15	
36	$MgSO_4$	0.16	−6.5	−29.5	−68		
37	Na_2SO_4	0.12	−8.5	−37			
39	Na_3PO_4	0.093	−11				
40	$Al_2(SO_4)_3$	0.063	−16				

[a] Taken from Ref. 4.

of small and nearly spherical nonionic micelles varies between 0.4 and 6.3 water molecules per micellar ether linkage (12). Water solubility and cloud point increase with the number of ether groups and the hydrophilic–lipophilic balance (HLB) of the surfactants. The various mechanisms by which electrolytes affect hydration, cloud point, and solubility of octoxynol 9 are discussed below and used to interpret present and previously published data.

Salting Out by Dehydration—Many cloud point-depressing electrolytes act through water binding or dehydration, reducing the amount of water available for the hydration of the polyoxyethylene moiety of the surfactant by tying up water through their own hydration. The sulfate and phosphate anions are examples of ions that salt out octoxynol 9 by competing with the surfactant for water of hydration (see Table V, Figs. 4 and 7) (1–4).

Dehydration is probably the most important salting-out mechanism for nonelectrolytes. Additional mechanisms include dielectric effects and electrostriction. Their application to nonionic surfactants has been discussed (5).

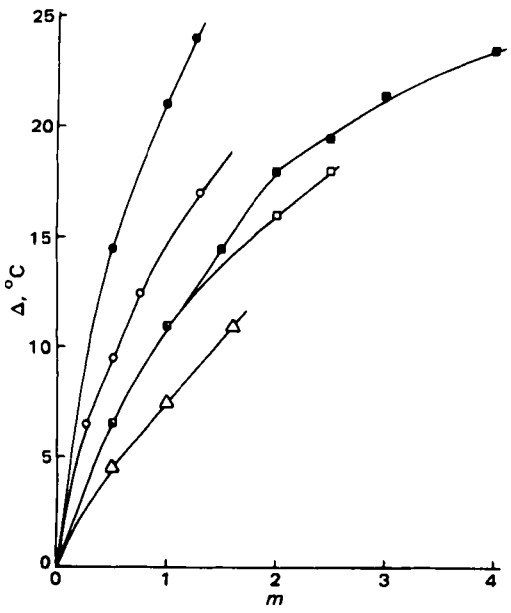

Figure 4—*Cloud point increases by salting-in electrolytes as a function of their molal concentrations. Key: (●) NaSCN; (○) $Na_2[Fe(CCN)_5NO]$; (■) $AgNO_3$; (□) NaI; (△) $Zn(NO_3)_2$.*

Sorbitol also depresses the cloud point through water binding or dehydration (Table IV, Fig. 6). Although not an electrolyte, it was included among the additives because it is so hygroscopic that it is used as a humectant.

Modification of Water Structure—At and below room temperature, water molecules are extensively self-associated by hydrogen bonding into "icebergs" or "flickering clusters" (13). Ions that reduce the self-association among water molecules, depolymerizing water and reducing its viscosity, are designated as structure breakers (13, 14). Only monomeric or nonassociated water molecules can hydrate the ether linkages of octoxynol 9 effectively. Therefore, structure-breaking ions increase the solubility of octoxynol 9 (raising its cloud point) by increasing the hydrogen bonding between ether groups and nonassociated water molecules at the expense of the hydrogen bonding among water molecules.

Examples of structure breakers are the large and polarizable iodide, thiocyanate, and nitroprusside anions (13). These anions were also efficient cloud point boosters (Table III, Fig. 4). The nonelectrolyte urea has also been found effective in breaking the structure of water and in raising the cloud point of nonionic surfactants (5).

The mucolytic action of potassium iodide and sodium thiocyanate (15, 16) is probably due to the same mechanism as their salting-in of octoxynol 9. By breaking the structure of water and making the aqueous environment a better solvent, the gel structure and viscoelasticity of mucus are reduced.

Ions that tighten the structure of water and increase its viscosity are designated as structure promoters. They include the fluoride and hydroxide ions (13). These anions salt octoxynol 9 out by enhancing the self-association of water molecules, thereby reducing the association of water molecules with the ether linkages of the surfactant (Table V, Figs. 6 and 7). The tetramethylammonium cation, which enhances the hydrogen bonding among water

Table VI—Effect of Various Citrates on the Cloud Point of Octoxynol 9

Rank No.	Additive	Concentration to Produce Δ = −10°C, *m*	Δ at Molality, °C 0.10	0.50	1.0
31	Dibasic magnesium citrate	0.37	−3		
28	Monobasic sodium citrate	0.53	−2	−9.5	−17.5
34	Dibasic sodium citrate	0.17	−6	−29.5	−61
38	Trisodium citrate	0.10	−10	−45.5	

Table VII—Effect of Octoxynol 9 on the pH of Solutions of Weak Acids

Acid	Concentration, *m*	pH[a] In Water	pH[a] In 2.00% Octoxynol 9	Percent Ionized in Water
Citric	1.00	1.50	1.53	2
	0.216	1.95	1.95	6
	0.0515	2.28	2.30	12
Acetic	2.50	2.19	2.19	0.3
	0.554	2.55	2.58	0.6
	0.132	2.90	2.91	1.4

[a] At 26°C; pH of 2.00% (0.032 *m*) octoxynol 9 solution was 5.32.

molecules and the structure of water by hydrophobic bonding (17) also salts the surfactant out (18).

Complex Formation—The ether oxygen atoms of model ethers like dioxane, ethyl ether, and eucalyptol act as ligands for most cations, forming adducts similar to hydrates. Nonionic polyoxyethylated surfactants, with their multiplicity of ether groups, act as polydentate ligands and may, therefore, even displace water of hydration from these cations (4). Solid, water-soluble complexes with calcium chloride were isolated (19).

When octoxynol 9 solutions and silver nitrate solutions were combined to produce mixtures containing 2.00% octoxynol 9, a white precipitate formed when the silver nitrate concentration exceeded 1.50 *m*. Higher silver nitrate concentrations produced larger amounts of precipitate. This precipitate, which is probably a complex between the two compounds, dissolved when the mixture was heated for the cloud point determination. Mixtures containing 2.5 and 3.0 *m* $AgNO_3$ turned clear at ~38°C and 43°C, respectively. The precipitate reappeared on cooling.

Complex formation between octoxynol 9 and metal ions salts the octoxynol 9 in, raising its cloud point. The only cations unable to form complexes with model ethers and to raise the cloud point of nonionic surfactants were sodium, potassium, cesium, ammonium (Tables IV and V, Figs. 5 and 7) (4), and presumably rubidium. Among other monovalent cations, lithium, silver, and especially the hydrogen ion, which forms oxonium ions with ether linkages, as well as all di- and trivalent cations raised the cloud point of nonionic surfactants (Tables II and III, Fig. 3) (4, 5). Zinc and magnesium ions are in this category. Their nitrates raised the cloud point of octoxynol 9, while magnesium sulfate and citrate lowered it (Tables V and VI, Figs. 7 and 8). The nitrate anion has an intermediate lyotropic number (20); it has a slight tendency towards salting in. Unlike the chloride ion, it does not tend to act as a ligand for metal ions in competition with ether linkages. The cloud point-depressing effect of the citrate and sulfate anions, which have low lyotropic numbers, overcame the cloud point-raising effect of the magnesium cation.

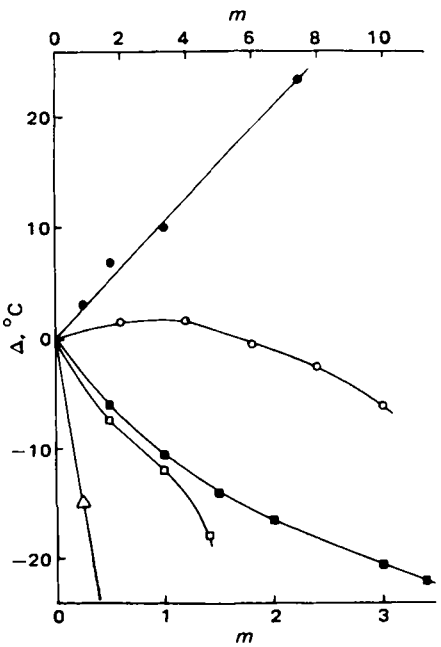

Figure 5—*Cloud point changes by weak bases and their salts as a function of their molal concentrations. Upper abscissa scale refers to molality of ammonia (○), lower abscissa scale refers to molality of trolamine (●), trolamine hydrochloride (□), ammonium chloride (■), and ammonium sulfate (△).*

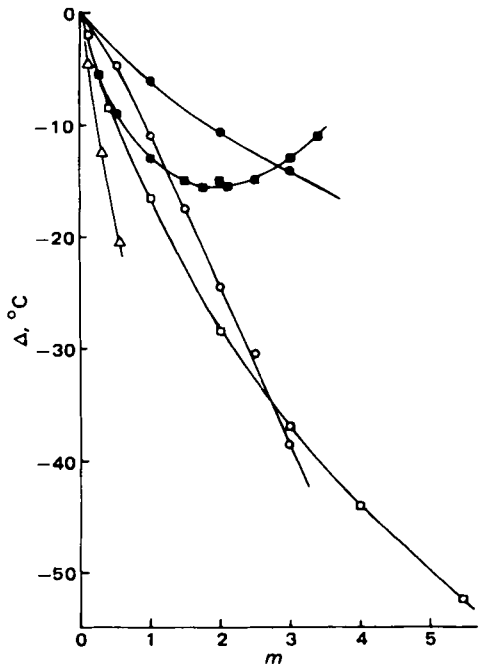

Figure 6—*Cloud point decreases by salting-out additives as a function of their molal concentrations. Key: (●) NaBr; (○) sorbitol; (□) NaCl; (■) $MgCl_2$; (△) NaF.*

On the other hand, in sulfuric acid, the cloud point-boosting effect of the two hydrogen ions overcame the cloud point-depressing effect of the sulfate ion. The cloud point-depressing action of the chloride anion when combined with the cloud point-raising lithium (1, 2), calcium (1-3), magnesium (2), or aluminum cation (1) is ascribed to its tendency to act as a ligand, displacing the ether group. This mechanism may also apply to the fluoride ion, which forms more stable complexes with some of these cations than the chloride ion.

Mixed Micelles and Micellar Solubilization—The two ionic and the nonionic surfactants listed in Table I were the most effective cloud point boosters (Fig. 1). Ionic surfactants exhibit no cloud points; their solubilities increase with temperature. The nonionic surfactant, polyoxyl 20 oleyl ether,

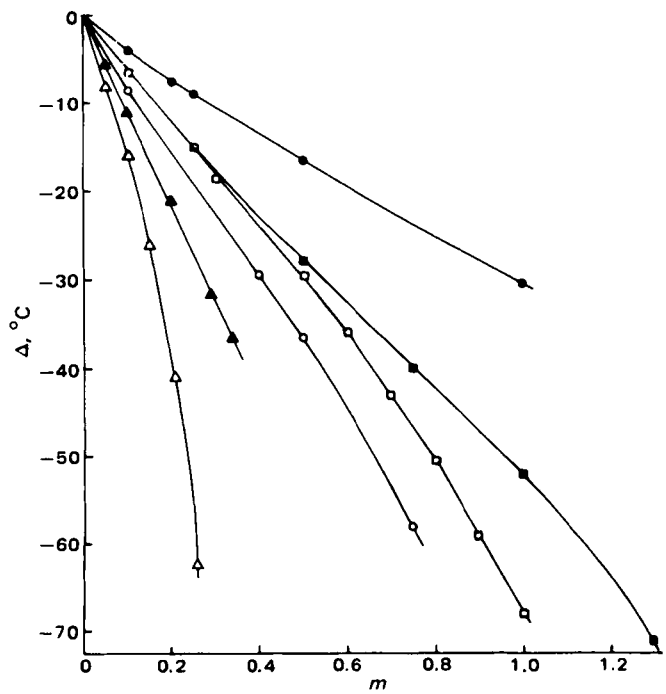

Figure 7—*Cloud point decreases by salting-out electrolytes as a function of their molal concentrations. Key: (●) NaOH; (■) $(NH_4)_2SO_4$; (□) $MgSO_4$; (○) Na_2SO_4; (▲) Na_3PO_4; (△) $Al_2(SO_4)_3$.*

Table VIII—Additivity of Cloud Point Effects Caused by Electrolytes and Solubilized Hydrocarbons

Hydrocarbon	Electrolyte	Conc., *m*	Δ_{obs}[a], °C	Δ_{calc}[b], °C
Hexadecane	None	—	14.5	—
	HCl	2.00	29.5	29.5
	$Mg(NO_3)_2$	2.00	25	27
	NaSCN	1.50	~33	41.5
	Na_2SO_4	0.40	−18	−15
	NaCl	2.00	−18	−14
Xylene	None	—	−42.5	—
	HCl	2.00	−17.5	−26
	$Mg(NO_3)_2$	2.00	−20	−30
	NaSCN	1.50	−9.5	−15.5
	Na_2SO_4	0.40	−60.5	−72
	NaCl	2.00	−58.5	−71

[a] In systems containing 2.00% octoxynol 9 + 0.50% hydrocarbon + electrolyte. [b] Calculated as the sum of the Δ values of the systems containing 2.00% octoxynol 9 + 0.50% hydrocarbon and 2.00% octoxynol 9 + electrolyte, respectively.

has an HLB of 15.3 and a cloud point above 100°C. The great salting-in effectiveness of surfactants has been ascribed to mixed micelles (1). The formation of mixed micelles between anionic and nonionic surfactants has been substantiated by various techniques (21, 22).

An alternate mechanism for the increase in cloud point of octoxynol 9 by other surfactants is the following. At temperatures well above its cloud point, the nonionic surfactant precipitates from its aqueous solution due to insufficient hydration. The precipitated octoxynol 9 is then solubilized by micelles of the more soluble surfactants. The two mechanisms are related because micelles of the soluble surfactant containing solubilized octoxynol 9 molecules are, in effect, mixed micelles.

A third mechanism, compatible with the previous two, to explain the increase in cloud point of octoxynol 9 by the other surfactants is complex formation. Anionic surfactants are bound far more extensively to polyethylene oxide and to its low molecular weight analogue, polyethylene glycol, than cationic surfactants (23–25). The strong interaction of sodium lauryl sulfate with polyethylene oxide has been investigated by various techniques (26–28). Presumably, the binding or complexation of one nonionic surfactant by another is the weakest of the three classes of surfactants. Accordingly, sodium lauryl sulfate was 5–7 times more efficient in raising the cloud point of octoxynol 9 than decylammonium chloride and 13–27 times more efficient than polyoxyl 20 oleyl ether.

Hydrotropy—The pronounced increases in cloud point produced by sodium salicylate, sodium benzoate, and phenobarbital sodium (Table I, Fig. 2) are ascribed to hydrotropy (18). The first two of these compounds are recognized as typical hydrotropes (29).

Mixed Solvents—As the temperature of nonionic surfactant solutions is increased, the critical micelle concentrations decrease and the micellar molecular weights increase. The cloud point can be regarded as the temperature at which the micelles have become infinitely large, resulting in macroscopic phase separation. The addition of increasing amounts of ethanol, dioxane, methanol, or propanol to aqueous solutions of nonionic surfactants at constant temperature progressively increased the critical micelle concentration and decreased the micellar size (30–34), thereby lowering the cloud point (30, 33, 34). For instance, 5% (v/v) or 0.90 *m* ethanol decreased the micellar molecular weight of nonoxynol 10 by 18% and increased its cloud point by 12°C (33). These reductions in cloud point are analogous to the effect of several water-miscible solvents, whose addition to water increases the solubility of compounds poorly soluble in water but appreciably soluble in the solvent. Mixed solvents act through reductions in the dielectric constant, solubility parameter, or structure of water. The cloud point-boosting action of acetic acid, trolamine, and possibly also of citric acid (Table II, Fig. 3) is attributed to the formation of such mixed solvent systems with water. At the pH values prevailing in their solutions, these compounds exist mainly in the un-ionized form (see Table VII for the two acids).

Alternate salting-in mechanisms for the two acids are discussed below. Less soluble carboxylic acids, such as benzoic, *p*-hydroxybenzoic, and salicylic acids, formed complexes with polyethylene glycol (35) and were solubilized in micelles of nonionic surfactants (36). The extent to which citric and acetic acids are distributed between the polyoxyethylene shell of octoxynol 9 micelles and water will be the subject of future investigations. Table VII shows only insignificant increases in the pH of citric and acetic acid solutions on the addition of 2.00% or 0.032 *m* octoxynol 9. Since the bulk of the two acids exists in the un-ionized form, the hydrogen ion activity is not a sensitive indicator for their binding to micellar octoxynol 9.

Increasing ionization of citric acid converted it progressively from an effective cloud point booster to an effective cloud point depressant (Table VI, Fig. 8). The tribasic citrate ion was the third most powerful salting-out additive. Tribasic magnesium citrate was not investigated because of its low solubility. In the dibasic magnesium citrate, the salting-out capacity of the $C_6H_6O_7^{2-}$ anion outweighed the salting-in capacity of the magnesium cation, making the salt a cloud point depressant.

Whereas ammonia exerted only a weak action on the cloud point of octoxynol 9, trolamine boosted it substantially. This observation is in keeping with the pronounced salting-in capacity of ethanol for polyoxyethylated surfactants and the similarity in structure between trolamine and ethanol. The hydrochlorides of both bases reduced the cloud point of octoxynol 9 substantially (Table IV, Fig. 5).

Additivity of Cloud Point Effects of Electrolytes and Hydrocarbons—Organic liquids of low water solubility either lowered or raised the cloud points of nonionic surfactants (1, 9). The additivity of these effects with the cloud point-lowering or -boosting effects of electrolytes is examined below.

The effect of solubilized hexadecane and xylene on the cloud point of octoxynol 9 is shown in Fig. 9. The onset of turbidity on heating and the disappearance of turbidity on cooling were more gradual in the presence of the two hydrocarbons, especially at higher levels. The recorded cloud points, corresponding to the temperatures at which the solutions turned substantially cloudy on heating or cleared appreciably on cooling, were as much as 3–4°C above the temperatures at which the first cloudiness appeared or at which the last cloudiness disappeared. The arrow in Fig. 9 indicates the solubility limit of hexadecane in 2.00% octoxynol 9 solution at room temperature. Systems with higher hexadecane concentration separated visible oil droplets at room temperature. On heating, these droplets largely dissolved before the systems became cloudy due to octoxynol 9 separation. The solubility limit of xylene in 2.00% octoxynol 9 was over twice as large as that of hexadecane.

The solvent systems in Table VIII contained either 0.5 g of hexadecane/100 g of octoxynol 9 solution (0.023 *m*) or 0.5 g of xylene/100 g of octoxynol 9 solution (0.048 *m*). The table compares the Δ values produced by the joint addition of hydrocarbon plus electrolyte (Δ_{obs}) with the sum of the Δ values

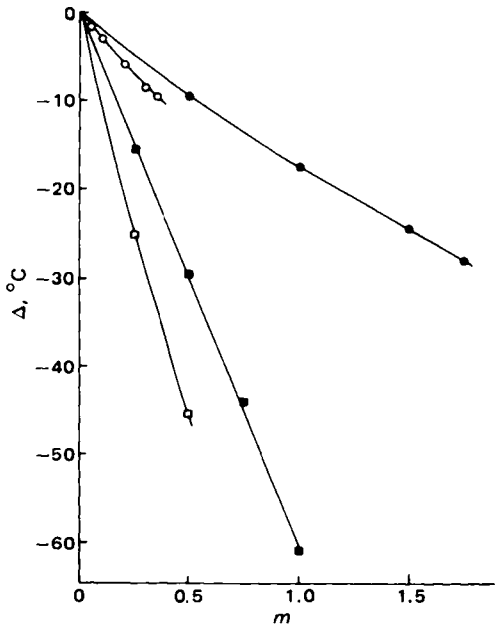

Figure 8—*Cloud point decreases by various citrates as a function of their molal concentrations. Key: (●) NaH_2; (○) MgH; (■) Na_2H; (□) Na_3.*

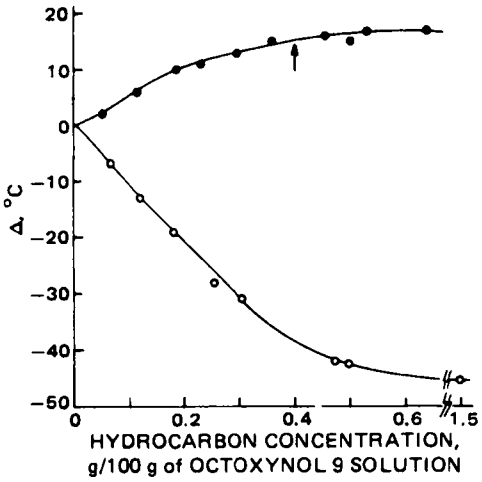

Figure 9—*Cloud point changes by two solubilized hydrocarbons as a function of their concentrations. Arrow indicates solubilization limit of hexadecane at 25°C. Key: (●) hexadecane; (○) xylene.*

produced when the hydrocarbon and the electrolyte were added to separate octoxynol 9 solutions (Δ_{calc}). All systems contained 2.00% (w/w) octoxynol 9 based on the weight of water.

Table VIII indicates that the cloud point-raising effect of hexadecane was approximately additive with the cloud point-raising or -lowering effects of salting-in and salting-out electrolytes. However, the cloud point lowering by xylene was between 6°C and 12.5°C smaller in the presence of salting-in as well as salting-out electrolytes than in their absence.

Additivity of Cloud Point Effects of Electrolyte Mixtures and Ionic Cloud Point Shifts—The effects of mixtures of electrolytes on the cloud point of octoxynol 9 were approximately additive. For instance, $\Delta MgSO_4$ at 0.25 *m* was −15°C, ΔNa_2SO_4 at 0.25 *m* was −19°C. A solution containing both 0.25 *m* $MgSO_4$ and 0.25 *m* Na_2SO_4 had $\Delta = -33$°C compared with the additive value of −34°C. Similarly, a mixture containing 0.5 *m* NaCl and 0.5 *m* NH_4Cl has a Δ value of −16°C, identical to the sum of the Δ values of the two salts at 0.5 *m* concentrations. The Δ value of a mixture of 1.0 *m* NaCl and 1.0 *m* NaBr was −21°C compared with an additive Δ value of −22.5°C.

The only discrepancies arose when one component was hydrochloric or sulfuric acid, presumably because they had slightly negative Δ values at low concentrations which became large and positive at higher concentrations. A solution containing 1.0 *m* NaCl and 1.0 *m* HCl had a Δ value of −8°C compared with an additive value of −11°C. A solution containing 0.25 *m* $MgSO_4$ and 0.25 *m* H_2SO_4 had a Δ value of −11°C compared with an additive Δ of −16°C.

Since the effects of individual ions on the cloud point are approximately additive, it is possible to assign a "cloud point shift" or Δ value to each ion.

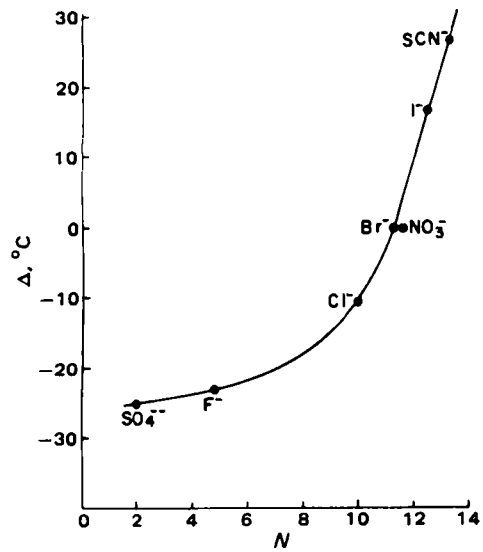

Figure 10—*Ionic cloud point shift values, Δ, of various anions at* W = 2 *as a function of their lyotropic numbers,* N.

Table IX—Effect of Various Ions on the Cloud Point of Octoxynol 9 at W = 2

Ion	Cloud Point Shift Δ, °C: From Sodium Salt	From Ammonium Salt	From Magnesium Salt
PO_4^{3-}	−18		
Cl^-	−10.5	−9.5	−7[a]
SO_4^{2-}	−25	−26	−34
OH^-	−24.5		
F^-	−23		
Br^-	0		
I^-	17	17.5	
SCN^-	27	26	
	From Nitrate	From Chloride	From Bromide
Na^+	−6		
NH_4^+	−1	1	−2
Al^{3+}	4		
Mg^{2+}	4.5		
Zn^{2+}	4.5		
Ag^+	11		
	From H_2SO_4	From HCl	From HNO_3
H^+	13	15	15

[a] Probably low due to complexation, see text.

To do this, the Δ values of different electrolytes must be compared at identical values of some concentration parameter. Various parameters, including ionic strength, were investigated by trial and error. The following two criteria must be satisfied when comparisons of Δ values are made at equal values of a concentration parameter that is suitable:

1. The cloud point shift values calculated for various individual ions must add up to the changes in cloud point observed for the electrolytes containing these ions.
2. Different electrolytes containing a common ion must furnish the same cloud point shift value for that ion. A self-consistent set of ionic cloud point shift values can then be calculated.

The simplest concentration parameter that satisfied these conditions, designated molal strength (*W*), is defined by:

$$W = \Sigma mz \qquad \text{(Eq. 2)}$$

where *m* is the molality and *z* is the valence of the ions that constitute the electrolyte. According to this equation, a molal strength value of $W = 2$ corresponds to the following molalities: for sodium chloride (a 1:1 electrolyte), 1.0; for sodium sulfate (a 1:2 electrolyte) and magnesium nitrate (a 2:1 electrolyte), 0.50; for magnesium sulfate (a 2:2 electrolyte), 0.50; and for tribasic sodium phosphate (a 1:3 electrolyte) and aluminum nitrate (a 3:1 electrolyte), 0.33. It is necessary to assign an arbitrary Δ value to one given ion to serve as reference. Accordingly, the cloud point shift value for the nitrate anion, ΔNO_3^-, was set equal to zero.

The following calculations illustrate how the data in Table IX were obtained. At $W = 2$, sodium nitrate (no. 23, Table V) has a molality of 1.0. A solution containing 1.0 *m* $NaNO_3$ and 2.00% octoxynol 9 had a cloud point of 59°C, while a 2.00% solution of octoxynol 9 from the same batch had a cloud point of 65°C. Hence, $\Delta NaNO_3 = 59 - 65 = -6$°C. Since $\Delta NaNO_3 = \Delta Na^+ + \Delta NO_3^-$ and ΔNO_3^- was arbitrarily set equal to zero, $\Delta Na^+ = -6$°C. The molality for sodium sulfate at $W = 2$ is 0.50 according to Eq. 2. The Δ value of 0.50 *m* Na_2SO_4 was −37°C (no. 37, Table V). Therefore, $\Delta SO_4^{2-} = \Delta Na_2SO_4 - 2\Delta Na^+ = -37 - (2)(-6) = -25$°C. Since the Δ value of 0.50 *m* H_2SO_4 was 1°C, $\Delta H^+ = \frac{1}{2}(\Delta H_2SO_4 - \Delta SO_4^{2-}) = \frac{1}{2}[1 - (-25)] = 13$°C.

Data at $W = 1$ and 4 were also calculated. To conserve space, they were not included in Table IX, but they showed trends comparable with the data at $W = 2$. As expected from the shape of the Δ *versus m* plots and Eq. 2, as the *W* values increase, the absolute values of the ionic cloud point shifts increase commensurately.

The ΔCl^- values obtained from magnesium chloride were consistently lower than those obtained from sodium chloride or ammonium chloride. This discrepancy is ascribed to the fact that the chloride ion acts as a ligand for magnesium, in competition with the ether groups of octoxynol 9, whereas the nitrate and sulfate ions do not.

The ionic cloud point shift values of the anions are related by a smooth function to their lyotropic numbers in the Hofmeister series (20), shown in Fig. 10. As the lyotropic numbers of the anions decrease, the negative values of the standard free energies of formation of the aqueous anions at 25°C increase (37). A plot of the ionic cloud point shift values *versus* the standard free energies of formation of the anions in water has a shape similar to Fig. 10 and can almost be superimposed on it.

For cations, the points of ionic cloud point shift values *versus* either lyotropic numbers or standard free energies of formation in water are scattered and do not fall on a single curve. This lack of correlation is ascribed to the fact that all cations except sodium, potassium, ammonium, rubidium, and cesium form complexes with the ether groups of octoxynol 9. The cloud points of polyoxyethylated surfactants are thus affected by cations in two ways. First, all cations tend to become hydrated, binding water and altering its structure. Second, there is a specific interaction by complexation between the ether groups of the surfactants and most cations, which predominates over their dehydrating effect to various degrees, resulting in net salting in or positive Δ values (4, 5). The ionic cloud point shift values for the complexing cations are probably related to the stability constants of the complexes they form with the ether linkages of the polyoxyethylated surfactants and the standard free energy changes of complexation.

Anions do not form complexes with the ether groups. Therefore, their effect on the cloud points of nonionic surfactants depends entirely on their interaction with water, which is also the dominant factor in ranking the anions in the Hofmeister series.

The ionic cloud point shift values of Table IX refer to octoxynol 9. They are higher than the corresponding absolute Δ values for polyoxyethylated surfactants having practically the same average number of ethylene oxide units per molecule and the same HLB but lacking an aromatic ring. Calculating the ionic cloud point shift values with the aid of Eq. 2 from the data of Ref. 5, it was found that polyoxyl 10 cetyl ether and polyoxyl 10 stearyl ether had the lowest absolute Δ values. Those of polyoxyl 10 oleyl ether were somewhat higher, but still well below the corresponding values for octoxynol 9. As the polarity of the hydrocarbon moiety of the surfactants decreased, the ionic cloud point shift values at a given W also decreased. Since the HLB values of the four surfactants were the same within one unit, this observation points up the major shortcoming of the HLB system, namely, that it does not take into account the nature of the hydrophobic moiety of the surfactants (8, 38).

REFERENCES

(1) W. N. Maclay, *J. Colloid Sci.*, **11**, 272 (1956).
(2) M. J. Schick, *J. Colloid Sci.*, **17**, 801 (1962).
(3) H. Saito and K. Shinoda, *J. Colloid Interface Sci.*, **24**, 10 (1967).
(4) H. Schott, *J. Colloid Interface Sci.*, **43**, 150 (1973).
(5) H. Schott and S. K. Han, *J. Pharm. Sci.*, **64**, 658 (1975).
(6) F. A. Long and W. F. McDevit, *Chem. Rev.*, **52**, 119 (1952).
(7) J. M. Corkill and J. F. Goodman, *Adv. Colloid Interface Sci.*, **2**, 297 (1969).
(8) H. Schott, *J. Pharm. Sci.*, **58**, 1443 (1969).
(9) K. Shinoda, in "Solvent Properties of Surfactant Solutions," K. Shinoda, Ed., Dekker, New York, N.Y., 1967, chap. 2.
(10) H. Schott and S. K. Han, *J. Pharm. Sci.*, **65**, 979 (1976).
(11) H. Schott, *J. Chem. Eng. Data*, **11**, 417 (1966).
(12) H. Schott, *J. Colloid Interface Sci.*, **24**, 193 (1967).
(13) J. L. Kavanau, "Water and Solute-Water Interactions," Holden-Day, San Francisco, Calif., 1964.
(14) G. E. Walrafen, *J. Chem. Phys.*, **55**, 768 (1971).
(15) M. A. Khan, D. P. Wolf, and M. Litt, *Biochim. Biophys. Acta*, **444**, 369 (1976).
(16) P. S. Richardson, *Eur. J. Respir. Dis.*, **61**, (suppl 110), 67 (1980).
(17) W.-Y. Wen, in "Water and Aqueous Solutions," R. A. Horne, Ed., Wiley-Interscience, New York, N.Y., 1972, chap. 15.
(18) H. Schott and S. K. Han, *J. Pharm. Sci.*, **66**, 165 (1977).
(19) T. M. Doscher, G. E. Myers, and D. C. Atkins, *J. Colloid Sci.*, **6**, 223 (1951).
(20) A. Voet, *Chem. Rev.*, **20**, 169 (1937).
(21) J. M. Corkill, J. F. Goodman, and J. R. Tate, *Trans. Faraday Soc.*, **60**, 986 (1964).
(22) F. Tokiwa and K. Tsujii, *J. Phys. Chem.*, **75**, 3560 (1971).
(23) S. Saito and H. Hirata, *Kolloid-Z.*, **165**, 162 (1959).
(24) S. Saito, *J. Colloid Interface Sci.*, **24**, 227 (1967).
(25) S. Saito, *Kolloid-Z. u. Z. Polymere*, **215**, 16 (1967).
(26) M. N. Jones, *J. Colloid Interface Sci.*, **23**, 36 (1967).
(27) B. Cabane, *J. Phys. Chem.*, **81**, 1639 (1977).
(28) T. Sasaki, K. Kushima, K. Matsuda, and H. Suzuki, *Bull. Chem. Soc. Jpn.*, **53**, 1864 (1980).
(29) P. H. Elworthy, A. T. Florence, and C. B. Macfarlane, "Solubilization by Surface-Active Agents," Chapman and Hall, London, England, 1968, chaps. 2 and 3.
(30) M. Aoki and Y. Iwayama, *Yakugaku Zasshi*, **79**, 516 (1959).
(31) H. Sasaki and N. Sata, *Kolloid-Z. u. Z. Polymere*, **199**, 49 (1964).
(32) P. Becher, *J. Colloid Sci.*, **20**, 728 (1965).
(33) H. Arai, *J. Colloid Interface Sci.*, **23**, 348 (1967).
(34) L. Marszall, *J. Colloid Interface Sci.*, **60**, 570 (1977).
(35) T. Higuchi and J. L. Lach, *J. Am. Pharm. Assoc., Sci. Ed.*, **43**, 465 (1954).
(36) W. P. Evans, *J. Pharm. Pharmacol.*, **16**, 323 (1964).
(37) L. H. N. Cooper, *Nature*, **139**, 284 (1937).
(38) H. Schott, *J. Pharm. Sci.*, **60**, 649 (1971).

ACKNOWLEDGMENTS

Support by the National Institutes of Health under Grant GM 27802 is gratefully acknowledged.

Dissolution Profile Determination of a Multicomponent Product Using a Rapid Liquid Chromatographic Analysis

RICHARD SOLTERO *x, JOHN ROBINSON ‡, and DENNIS ADAIR §

Received June 9, 1982, from the *Research and Development Department, Pharmaceuticals Division, Ciba-Geigy Corporation, Summit, NJ 07901.* Accepted for publication May 9, 1983.

Present address: *Berlex Labs., 110 E. Hanover Ave., Cedar Knolls, NJ 07927; ‡Varian Corp., Florham Park, NJ; §Schering Corp., Bloomfield, NJ 07003.

Abstract □ A system was developed which is capable of monitoring the dissolution profiles of each of the active components in a two-component combination product. The UV spectra of the two drugs (metoprolol and hydrochlorothiazide) overlap considerably, making conventional UV analysis of either component unrealistic. By resolving the two drugs on a high-performance liquid chromatographic (HPLC) system both can be quantitated after separation. The analysis is sufficiently short to allow for the use of a six-station dissolution tester in tandem with an HPLC for determination of dissolution profiles. The HPLC system and equipment, can monitor six samples of this product at 5-min intervals in real analysis time.

Keyphrases □ Dissolution—multicomponent product, rapid HPLC, metoprolol, hydrochlorothiazide □ Metoprolol—dissolution profile, multicomponent product with hydrochlorothiazide, rapid HPLC □ Hydrochlorothiazide—dissolution profile, multicomponent product with metoprolol rapid HPLC.

The determination of the release rate of an active drug from pharmaceutical dosage forms has become a standard technique in pharmaceutical development, research, and quality control testing laboratories. This information is valuable to formulators in selecting an optimum solid dosage formulation. *In vivo–in vitro* correlations can often be established which are

0022-3549/84/0600-0799$01.00/0

© 1984, American Pharmaceutical Association

For cations, the points of ionic cloud point shift values *versus* either lyotropic numbers or standard free energies of formation in water are scattered and do not fall on a single curve. This lack of correlation is ascribed to the fact that all cations except sodium, potassium, ammonium, rubidium, and cesium form complexes with the ether groups of octoxynol 9. The cloud points of polyoxyethylated surfactants are thus affected by cations in two ways. First, all cations tend to become hydrated, binding water and altering its structure. Second, there is a specific interaction by complexation between the ether groups of the surfactants and most cations, which predominates over their dehydrating effect to various degrees, resulting in net salting in or positive Δ values (4, 5). The ionic cloud point shift values for the complexing cations are probably related to the stability constants of the complexes they form with the ether linkages of the polyoxyethylated surfactants and the standard free energy changes of complexation.

Anions do not form complexes with the ether groups. Therefore, their effect on the cloud points of nonionic surfactants depends entirely on their interaction with water, which is also the dominant factor in ranking the anions in the Hofmeister series.

The ionic cloud point shift values of Table IX refer to octoxynol 9. They are higher than the corresponding absolute Δ values for polyoxyethylated surfactants having practically the same average number of ethylene oxide units per molecule and the same HLB but lacking an aromatic ring. Calculating the ionic cloud point shift values with the aid of Eq. 2 from the data of Ref. 5, it was found that polyoxyl 10 cetyl ether and polyoxyl 10 stearyl ether had the lowest absolute Δ values. Those of polyoxyl 10 oleyl ether were somewhat higher, but still well below the corresponding values for octoxynol 9. As the polarity of the hydrocarbon moiety of the surfactants decreased, the ionic cloud point shift values at a given W also decreased. Since the HLB values of the four surfactants were the same within one unit, this observation points up the major shortcoming of the HLB system, namely, that it does not take into account the nature of the hydrophobic moiety of the surfactants (8, 38).

REFERENCES

(1) W. N. Maclay, *J. Colloid Sci.*, **11**, 272 (1956).
(2) M. J. Schick, *J. Colloid Sci.*, **17**, 801 (1962).
(3) H. Saito and K. Shinoda, *J. Colloid Interface Sci.*, **24**, 10 (1967).
(4) H. Schott, *J. Colloid Interface Sci.*, **43**, 150 (1973).
(5) H. Schott and S. K. Han, *J. Pharm. Sci.*, **64**, 658 (1975).
(6) F. A. Long and W. F. McDevit, *Chem. Rev.*, **52**, 119 (1952).
(7) J. M. Corkill and J. F. Goodman, *Adv. Colloid Interface Sci.*, **2**, 297 (1969).
(8) H. Schott, *J. Pharm. Sci.*, **58**, 1443 (1969).
(9) K. Shinoda, in "Solvent Properties of Surfactant Solutions," K. Shinoda, Ed., Dekker, New York, N.Y., 1967, chap. 2.
(10) H. Schott and S. K. Han, *J. Pharm. Sci.*, **65**, 979 (1976).
(11) H. Schott, *J. Chem. Eng. Data*, **11**, 417 (1966).
(12) H. Schott, *J. Colloid Interface Sci.*, **24**, 193 (1967).
(13) J. L. Kavanau, "Water and Solute-Water Interactions," Holden-Day, San Francisco, Calif., 1964.
(14) G. E. Walrafen, *J. Chem. Phys.*, **55**, 768 (1971).
(15) M. A. Khan, D. P. Wolf, and M. Litt, *Biochim. Biophys. Acta*, **444**, 369 (1976).
(16) P. S. Richardson, *Eur. J. Respir. Dis.*, **61**, (suppl 110), 67 (1980).
(17) W.-Y. Wen, in "Water and Aqueous Solutions," R. A. Horne, Ed., Wiley-Interscience, New York, N.Y., 1972, chap. 15.
(18) H. Schott and S. K. Han, *J. Pharm. Sci.*, **66**, 165 (1977).
(19) T. M. Doscher, G. E. Myers, and D. C. Atkins, *J. Colloid Sci.*, **6**, 223 (1951).
(20) A. Voet, *Chem. Rev.*, **20**, 169 (1937).
(21) J. M. Corkill, J. F. Goodman, and J. R. Tate, *Trans. Faraday Soc.*, **60**, 986 (1964).
(22) F. Tokiwa and K. Tsujii, *J. Phys. Chem.*, **75**, 3560 (1971).
(23) S. Saito and H. Hirata, *Kolloid-Z.*, **165**, 162 (1959).
(24) S. Saito, *J. Colloid Interface Sci.*, **24**, 227 (1967).
(25) S. Saito, *Kolloid-Z. u. Z. Polymere*, **215**, 16 (1967).
(26) M. N. Jones, *J. Colloid Interface Sci.*, **23**, 36 (1967).
(27) B. Cabane, *J. Phys. Chem.*, **81**, 1639 (1977).
(28) T. Sasaki, K. Kushima, K. Matsuda, and H. Suzuki, *Bull. Chem. Soc. Jpn.*, **53**, 1864 (1980).
(29) P. H. Elworthy, A. T. Florence, and C. B. Macfarlane, "Solubilization by Surface-Active Agents," Chapman and Hall, London, England, 1968, chaps. 2 and 3.
(30) M. Aoki and Y. Iwayama, *Yakugaku Zasshi*, **79**, 516 (1959).
(31) H. Sasaki and N. Sata, *Kolloid-Z. u. Z. Polymere*, **199**, 49 (1964).
(32) P. Becher, *J. Colloid Sci.*, **20**, 728 (1965).
(33) H. Arai, *J. Colloid Interface Sci.*, **23**, 348 (1967).
(34) L. Marszall, *J. Colloid Interface Sci.*, **60**, 570 (1977).
(35) T. Higuchi and J. L. Lach, *J. Am. Pharm. Assoc., Sci. Ed.*, **43**, 465 (1954).
(36) W. P. Evans, *J. Pharm. Pharmacol.*, **16**, 323 (1964).
(37) L. H. N. Cooper, *Nature*, **139**, 284 (1937).
(38) H. Schott, *J. Pharm. Sci.*, **60**, 649 (1971).

ACKNOWLEDGMENTS

Support by the National Institutes of Health under Grant GM 27802 is gratefully acknowledged.

Dissolution Profile Determination of a Multicomponent Product Using a Rapid Liquid Chromatographic Analysis

RICHARD SOLTERO *x, JOHN ROBINSON ‡, and DENNIS ADAIR §

Received June 9, 1982, from the *Research and Development Department, Pharmaceuticals Division, Ciba-Geigy Corporation, Summit, NJ 07901.* Accepted for publication May 9, 1983.

Present address: *Berlex Labs., 110 E. Hanover Ave., Cedar Knolls, NJ 07927; ‡Varian Corp., Florham Park, NJ; §Schering Corp., Bloomfield, NJ 07003.

Abstract □ A system was developed which is capable of monitoring the dissolution profiles of each of the active components in a two-component combination product. The UV spectra of the two drugs (metoprolol and hydrochlorothiazide) overlap considerably, making conventional UV analysis of either component unrealistic. By resolving the two drugs on a high-performance liquid chromatographic (HPLC) system both can be quantitated after separation. The analysis is sufficiently short to allow for the use of a six-station dissolution tester in tandem with an HPLC for determination of dissolution profiles. The HPLC system and equipment, can monitor six samples of this product at 5-min intervals in real analysis time.

Keyphrases □ Dissolution—multicomponent product, rapid HPLC, metoprolol, hydrochlorothiazide □ Metoprolol—dissolution profile, multicomponent product with hydrochlorothiazide, rapid HPLC □ Hydrochlorothiazide—dissolution profile, multicomponent product with metoprolol rapid HPLC.

The determination of the release rate of an active drug from pharmaceutical dosage forms has become a standard technique in pharmaceutical development, research, and quality control testing laboratories. This information is valuable to formulators in selecting an optimum solid dosage formulation. *In vivo–in vitro* correlations can often be established which are

0022-3549/84/0600-0799$01.00/0

© 1984, American Pharmaceutical Association

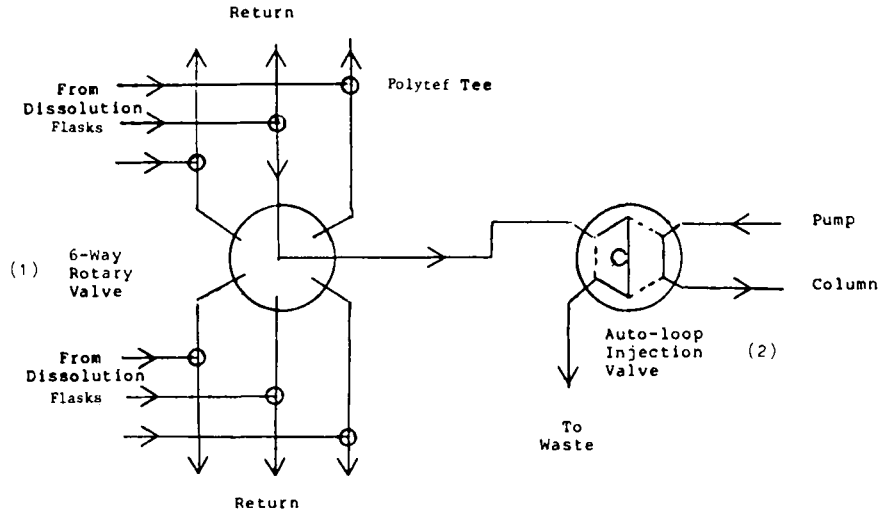

Figure 1—*Schematic diagram of the sampling and injection hardware. Key: (1) six-way rotary valve driven by a 60° stepping actuator; (2) loop injector of the liquid chromatograph.*

useful for predicting bioavailability, and at times it is possible to employ dissolution to satisfy the FDA requirements concerning the bioavailability of a product.

Many dissolution techniques have been proposed, and several are in general usage. The most frequently used techniques are the USP rotating basket and USP rotating paddle methods (1). Other methods that have been employed are the spin filter (2, 3), the rotating flask (4), and the USP disintegration basket (5). Typically, samples of the test solution are taken at one or more time points, and the concentrations of the active component(s) are determined. Various analytical techniques are employed for evaluation concentrations. Wet chemistry techniques can be used to prepare the sample for analysis, or the samples can be analyzed directly without preparation depending on the particular drug excipients and the relative concentration ranges. Several automated dissolution methods have been proposed (6–8). In addition, several commercial instruments are available which will sample, store, and prepare samples for UV analysis[1]. The development of high-performance liquid chromatographic (HPLC) techniques and equipment has simplified the analysis of aqueous samples. This method can be employed for analyzing samples taken from the dissolution medium using a fraction collector, or the solution can be sampled automatically (9).

This paper presents HPLC techniques and equipment which can be used in conjunction with most dissolution test methods. The system is capable of sequentially sampling six streams from the dissolution apparatus and subjecting these samples to chromatographic analysis in <5 min. In operation, all six streams from a dissolution test unit[2] are continuously pumped, through in-line filters, into a six-way rotary valve[3], which selects one stream to be diverted to the injection loop of a chromatograph, while the other streams are returned to the dissolution flasks. Kent *et al.* (10) used a similar valve to monitor the UV absorbance of six dissolution streams. This system has the advantage of performing an HPLC separation and analysis of several components of a multicomponent product during the dissolution experiment.

EXPERIMENTAL

Equipment—An HPLC[4] with programmable external events and a pneumatic loop valve injector was used. The position of the injection valve was controlled by a program in the chromatograph that used solenoids to control the pneumatic pressure to the valve. "Tee" fittings were placed in the pneumatic lines to control the action of a 60° stepping actuator. This actuator was used to rotate a six-way rotary valve[5]. As shown in Fig. 1, each of six streams of dissolution medium from a dissolution unit is pumped to the six-way valve, where one stream is selected to go to the injection valve and the rest are returned through polytef tee fittings to the dissolution unit. The stream going to the injection valve flows through the injection loop and then to waste (~2–3 mL of medium is lost in a 30-min analysis).

On program command (external event), the injection valve switches from the load position to the inject position, and the sample is washed onto the analytical column. At the same time, the pneumatic pressure switches the 60° stepping actuator to the return position. The next external events command causes the injector valve to return to the load position, and the stepping actuator is advanced simultaneously to select the next stream from the dissolution unit and send it through the injection loop. The injection loop is thus continuously flushed with new sample throughout the time required for the chromatographic separation.

Chromatographic Conditions—Since rapid turnaround is required for this application, the chromatography was optimized with a short (5-cm) column and a high flow rate. An analysis time of 30–45 s/sample was the targeted range.

The rapid HPLC method used a 50 × 2.5-mm column packed with nucleosil 5 SA. At ambient temperature, an isocratic mobile phase composed of 0.015 M $KMeSO_3$, 0.025 M tetramethylammonium chloride, and 50% acetonitrile was employed at a flow rate of 2.7 mL/min (~150 atm) with a 10-μL injection loop. The detection was at 212 nm, with 0.2 AUFS attenuation; resolution of the two components was achieved within 0.8 min. The samples in the dissolution experiment were started at 0.8-min intervals so that the timing of the analysis would be synchronized with the dissolution time. This process allowed six samples to be analyzed in sequence within 5 min.

Additionally, as an alternate system, a microprocessor[6] was used to control the sequence of steps and provide the timing in an automated HPLC system. All of the instrument conditions were kept constant, except for the pneumatic actuation and the HPLC pumping system. In this case, two solenoid valves[7] were used under the control of the microprocessor. The microprocessor has 16 I/O ports, which are extensions of a resident versatile interface adapter. Two of these ports were used to control the solenoid valves. The pneumatic pressure released by the solenoid valves was used to simultaneously power an automatic injector and 60° stepping actuator[8]. The timing and the sequence

[1] SASDRA; Technician Industrial Systems, Tarrytown, N.Y.; DISOGRAPH; Hanson Research Corp. Northridge, Calif.

[2] Hanson, multiple, six-station, variable-speed model 72R-QC; Hanson Research Corp. Northridge, Calif.

[3] Altex model 50-11, six-way Teflon rotary valves.

[4] Model 5020LC with external events and pneumatic loop valve injector; Varian Instrument Co.

[5] Rheodyne model K 50-03 60° stepping actuator with two model 50-11 six-way Teflon rotary valves.

[6] AIM 65; Rockwell International, Anaheim, Calif.

[7] Rheodyne Model 7163 solenoid valve.

[8] Rheodyne Model 7010 sample injector valve with Rheodyne Model 7001 RV pneumatic actuator.

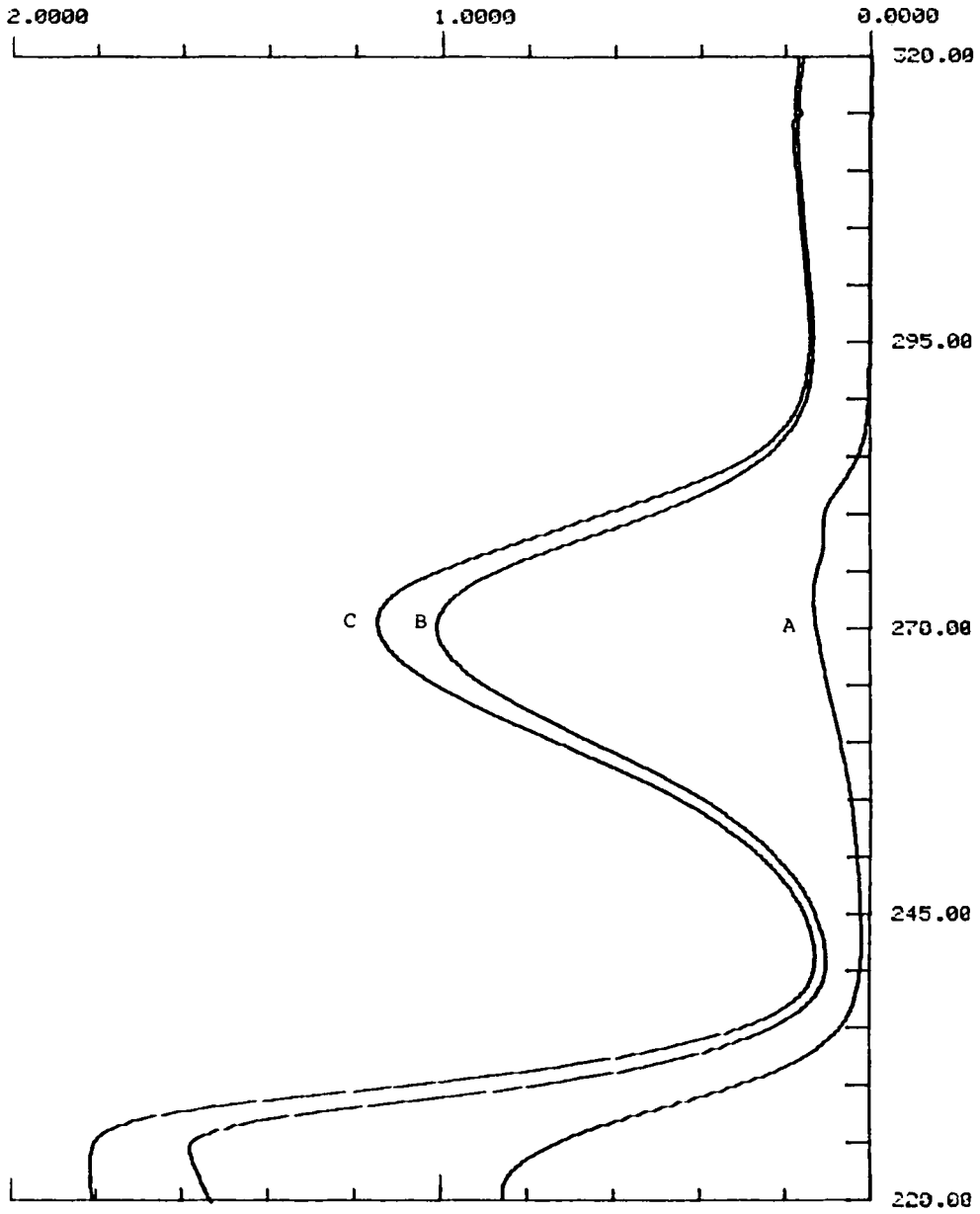

Figure 2—*UV spectra of metoprolol and hydrochorothiazide. Key: (A) metoprolol, 0.1 mg/mL; (B) hydrochlorothiazide, 0.025 mg/mL; (C) metoprolol-hydrochlorothiazide 0.1–0.025 mg/mL.*

of steps were programmed in BASIC. Driving the injector to the load or inject positions was done by sending the appropriate signals through the I/O port to the appropriate solenoid (one for inject position, one for load position). System delays were easily accomplished by sending the BASIC program into a loop for the appropriate period of time.

The advantages of the microprocessor-based system are that (*a*) it can be retrofitted to an existing HPLC pump and detector, (*b*) all of the hardware is commercially available and is relatively inexpensive, and (*c*) the programming on the microprocessor can be tailored to specific applications and is independent of another operating system (such as the timed event functions necessary on the chromatograph for this procedure).

Dissolution Apparatus and UV Analyses—The USP paddle method was used at 50 rpm employing 1 L of distilled water as the dissolution medium. The dissolution profiles were determined by continuously monitoring the absorbance of the media through a series of flow cells in a UV-visible spectrophotometer[9]. The media were circulated through polytef tubing with an in-line filter holder[10] using a thick prefilter[11]. A wavelength of 252 nm was selected, where the sum of the absorbance is due to the hydrochorothiazide and the absorbance due to the metoprolol will be in a convenient range for analysis.

[9] Zeiss Model DM-4, with multiple cell attachment; Karl Zeiss, New York, N.Y.
[10] Swinex, 47 mm; Millipore Corp., Bedford, Mass.
[11] Cat. No. AP25 040 00; Millipore Corp., Bedford, Mass.

RESULTS AND DISCUSSION

This system is applicable for either single-component products (which have low extinction coefficients or some inactive material in the formulation that interferes with normal analysis) or multicomponent products. The obvious advantage is that the release rate profiles of the individual components in multicomponent products can be determined. The system proposed here can analyze six separate dissolution samples within a 5-min turnaround time. This allows for the dissolution experiment and the HPLC analysis of the active components to be conducted simultaneously.

In developing an HPLC method for use in conjunction with a standard six-sample dissolution apparatus, analysis time is the prime consideration. For example, if the required dissolution profile allows for 5-min time intervals between groups of six samples for this apparatus, ~0.8 min is available for each chromatogram. For separations which cannot be performed this quickly, longer sampling intervals such as 10 or 15 min would be required.

The product, metoprolol-hydrochorothiazide, was prepared in three strengths: 50:25, 100:25, and 100:50 mg. Each of the strengths was analyzed for dissolution profiles and each compared using the two different analytical methods. All results are the mean of six tests.

The UV spectra of metoprolol and hydrochorothiazide are shown in Fig. 2. The spectra are seen to overlap at all points of the UV spectrum. It would nearly be impossible to develop an accurate multiple-wavelength analysis for this combination product. HPLC analysis would be an obvious method of choice in this case.

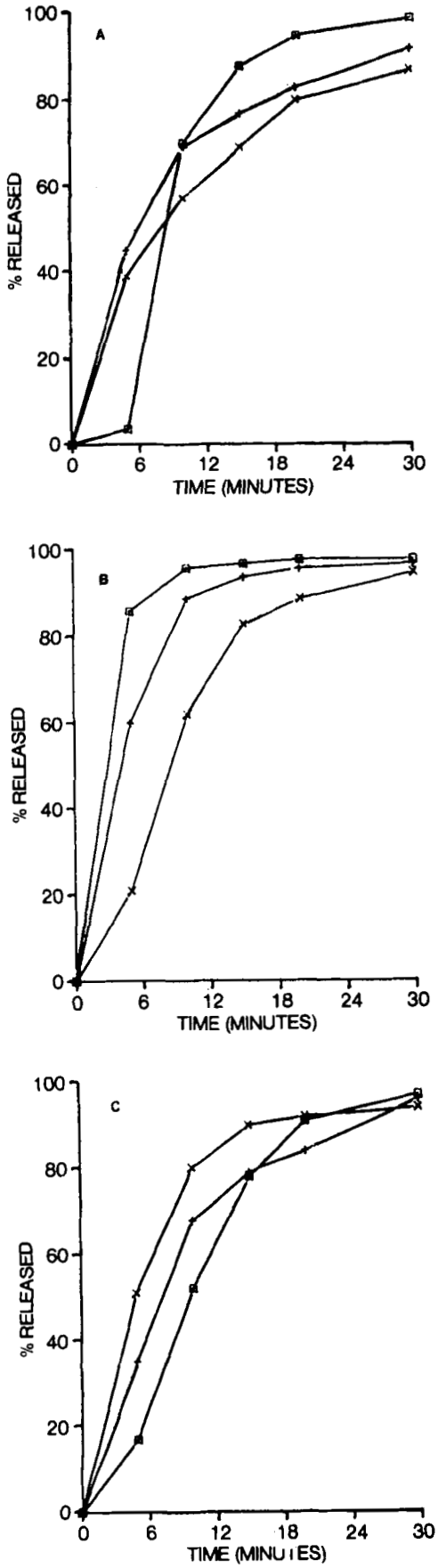

Figure 3—*Comparison of the dissolution rates of (A) 50:25-, (B) 100:25-, and (C) 100:50-mg combinations of metoprolol-hydrochlorothiazide. Key: (+) UV analysis (combination); (x) HPLC analysis of metoprolol; (□) HPLC analysis of hydrochlorothiazide.*

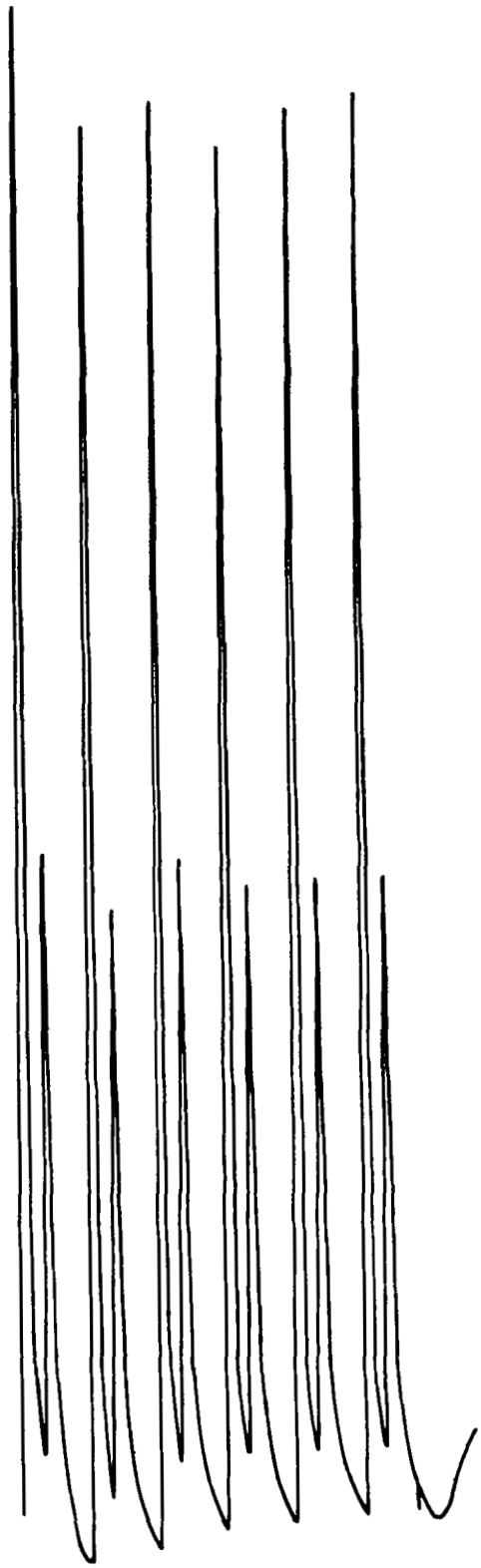

Figure 4—*Chromatogram showing six injections made in a 5-min period.*

The three strengths of metoprolol-hydrochlorothiazide were tested using this rapid HPLC method, and comparison data were generated using the UV analysis method (Fig. 3). It can be seen that the UV analysis yields a dissolution profile which is a composite of the individual release rates measured by the rapid HPLC method. For these sets of experiments, the analysis time for each batch of tablets required ~1.5 h using the rapid HPLC technique. For a conventional HPLC analysis technique, the time required to pull manual aliquots and analyze each sample is much greater. Before this technique was introduced into our laboratory, it required ~5 h to analyze a similar dissolution.

Table I—Peak Heights of Metoprolol–Hydrochlorothiazide Standard Solutions

	Concentration in Simulated Gastric Fluid, mg/L									
	10:5		20:10		60:30		80:40		100:50	
	MET[a]	HCT[b]	MET	HCT	MET	HCT	MET	HCT	MET	HCT
	6.3	4.2	17.1	8.4	58.7	24.8	75.0	32.0	98.0	41.0
	6.3	4.1	17.2	9.1	58.1	32.5	75.0	32.0	98.0	42.0
	6.3	4.2	17.0	8.6	56.5	23.7	74.2	31.2	98.0	41.0
	6.1	4.0	17.0	8.2	56.5	24.3	75.7	31.6	96.5	40.5
Mean	6.3	4.1	17.1	8.6	57.5	24.1	75.0	31.7	97.6	41.1
SD	0.1	0.1	0.1	0.4	1.1	0.6	0.6	0.4	0.8	0.6

[a] MET, metoprolol. [b] HCT, hydrochlorothiazide.

The advantage of a rapid screening technique for monitoring individual release rates of the active components of a multicomponent product is shown in Fig. 3. The composite release from the 100:25- and 100:50-mg formulations appear similar; however, the hydrochlorothiazide is the faster component in Fig. 3B (100:25 mg) and the slower component in Fig. 3C (100:50 mg).

A typical chromatogram is shown in Fig. 4, where six analyses were completed. Peak height measurements for a series of standards are listed in Table I. Linear regression analysis on the mean peak height values of metoprolol and hydrochlorothiazide *versus* concentration yielded correlation coefficients of 0.9996 and 0.9994, respectively.

The intent of these experiments was to demonstrate the utility of a novel approach to analyzing the dissolution rate profile of combination products. For this article, we selected an example of a dual-entity product which was manufactured in several strengths. The ease of operation and facility of this technique is demonstrated in the reduced time required for quantitative analysis of each of the two components of this combination product. The progress being made in HPLC techniques and equipment should allow this technique to be developed for other combination products and for single-entity products which have excipients that interfere in normal UV analyses.

REFERENCES

(1) "U.S. Pharmacopeia," 20th rev., U.S. Pharmacopeial Convention, Inc., Rockville, Md. 1970, p. 959.

(2) A. C. Shah, C. B. Peot, and T. F. Ochs, *J. Pharm. Sci.*, **62**, 671 (1973).

(3) J. W. Manager, S. A. Howard, and A. Khwangsopha, *J. Pharm. Sci.*, **68**, 1084 (1979).

(4) M. Gibaldi and H. Weintraub, *J. Pharm. Sci.*, **59**, 725 (1970).

(5) L. C. Schroeter and J. G. Wagner, *J. Pharm. Sci.*, **51**, 957 (1962).

(6) R. A. Castello, G. Jellinek, J. M. Konieczny, K. C. Kwan, and R. O. Toberman, *J. Pharm. Sci.*, **57**, 485 (1968).

(7) F. J. Cioffi, H. M. Abdou, and A. J. Warren, *J. Pharm. Sci.*, **65**, 1234 (1976).

(8) F. J. Cioffi, S. Martynovych, and H. Bendrot, *J. Pharm. Sci.*, **68**, 1280 (1979).

(9) D. Wurster, W. Wargin, and M. DeBaradinis, Jr., *J. Pharm. Sci.*, **70**, 764 (1981).

(10) J. Kent, P. Wong, and G. Hedge, *J. Pharm. Sci.*, **66**, 1665 (1977).

Some Effects of 1-(2,4-Dichlorophenyl)-4-dimethylaminomethyl-1-nonen-3-one Hydrochloride on *Escherichia coli* GK-19

G. G. KHACHATOURIANS *‡ˣ, P. K. HOLMLUND ‡, and J. R. DIMMOCK §

Received December 27, 1982, from the **Department of Applied Microbiology and Food Science, College of Agriculture*, ‡*Department of Microbiology, College of Medicine*, and §*College of Pharmacy, University of Saskatchewan, Saskatoon, Saskatchewan S7N 0W0, Canada.* Accepted for publication April 26, 1983.

Abstract □ 1-(2,4-Dichlorophenyl)-4-dimethylaminomethyl-1-nonen-3-one hydrochloride (Id) was shown to inhibit the growth of *Escherichia coli* GK-19 at a concentration of 50 μg/mL in a medium of pH 6.5. Maximal antibacterial activity was found during the logarithmic growth phases rather than at the early stationary phase. Electron microscopy revealed that Id caused lysis, and inhibition of respiration and retardation of RNA and protein syntheses occurred in the bacteria with this compound at 50 μg/mL.

Keyphrases □ 1-(2,4-Dichlorophenyl)-4-dimethylaminomethyl-1-nonen-3-one hydrochloride—antibacterial activity in *Escherichia coli*, effects of concentration, temperature, and medium pH □ Antibacterial activity—1-(2,4-dichlorophenyl)-4-dimethylaminomethyl-1-nonen-3-one hydrochloride against *Escherichia coli*, effects of concentration, temperature, and medium pH

Previous work from these laboratories showed that a number of Mannich bases derived from conjugated styryl ketones had antibacterial properties (1–3). The aim of the present investigation was twofold. First, it was hoped to unravel some of the factors affecting the action of a representative Mannich base on bacterial growth, and second, to discern the site or sites of action of the compound toward the bacteria.

EXPERIMENTAL

Synthesis of Compounds—Compound Ia was prepared by the literature method (4); Ib, d–f were synthesized by a previously described procedure (5), as was Ic (6).

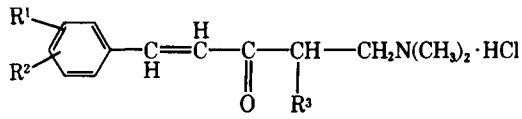

Ia: $R^1 = R^2 = R^3 = H$
Ib: $R^1 = R^2 = H$; $R^3 = (CH_2)_4CH_3$
Ic: R^1 = 3-OH; $R^2 = H$; $R^3 = (CH_2)_4CH_3$
Id: R^1 = 2-Cl; R^2 = 4-Cl; $R^3 = (CH_2)_4CH_3$
Ie: R^1 = 2-Cl; R^2 = 6-Cl; $R^3 = (CH_2)_4CH_3$
If: R^1 = 3-Cl; R^2 = 4-Cl; $R^3 = (CH_2)_4CH_3$

Measurement of Bacterial Growth—In this study, an isolate of *Escherichia coli* K-12 strain designated GK-19 (7) was employed. The bacteria were grown in a minimal salts medium (8) to which casamino acids (0.5% w/v) and thiamine (7.5 μg/mL) had been added. Adjustment of the pH was made using Sörensen's buffer solutions (9). The cultures were grown in Erlenmeyer flasks

© 1984, American Pharmaceutical Association

Table I—Peak Heights of Metoprolol–Hydrochlorothiazide Standard Solutions

	Concentration in Simulated Gastric Fluid, mg/L									
	10:5		20:10		60:30		80:40		100:50	
	MET[a]	HCT[b]	MET	HCT	MET	HCT	MET	HCT	MET	HCT
	6.3	4.2	17.1	8.4	58.7	24.8	75.0	32.0	98.0	41.0
	6.3	4.1	17.2	9.1	58.1	32.5	75.0	32.0	98.0	42.0
	6.3	4.2	17.0	8.6	56.5	23.7	74.2	31.2	98.0	41.0
	6.1	4.0	17.0	8.2	56.5	24.3	75.7	31.6	96.5	40.5
Mean	6.3	4.1	17.1	8.6	57.5	24.1	75.0	31.7	97.6	41.1
SD	0.1	0.1	0.1	0.4	1.1	0.6	0.6	0.4	0.8	0.6

[a] MET, metoprolol. [b] HCT, hydrochlorothiazide.

The advantage of a rapid screening technique for monitoring individual release rates of the active components of a multicomponent product is shown in Fig. 3. The composite release from the 100:25- and 100:50-mg formulations appear similar; however, the hydrochlorothiazide is the faster component in Fig. 3B (100:25 mg) and the slower component in Fig. 3C (100:50 mg).

A typical chromatogram is shown in Fig. 4, where six analyses were completed. Peak height measurements for a series of standards are listed in Table I. Linear regression analysis on the mean peak height values of metoprolol and hydrochlorothiazide *versus* concentration yielded correlation coefficients of 0.9996 and 0.9994, respectively.

The intent of these experiments was to demonstrate the utility of a novel approach to analyzing the dissolution rate profile of combination products. For this article, we selected an example of a dual-entity product which was manufactured in several strengths. The ease of operation and facility of this technique is demonstrated in the reduced time required for quantitative analysis of each of the two components of this combination product. The progress being made in HPLC techniques and equipment should allow this technique to be developed for other combination products and for single-entity products which have excipients that interfere in normal UV analyses.

REFERENCES

(1) "U.S. Pharmacopeia," 20th rev., U.S. Pharmacopeial Convention, Inc., Rockville, Md. 1970, p. 959.

(2) A. C. Shah, C. B. Peot, and T. F. Ochs, *J. Pharm. Sci.*, **62**, 671 (1973).

(3) J. W. Manager, S. A. Howard, and A. Khwangsopha, *J. Pharm. Sci.*, **68**, 1084 (1979).

(4) M. Gibaldi and H. Weintraub, *J. Pharm. Sci.*, **59**, 725 (1970).

(5) L. C. Schroeter and J. G. Wagner, *J. Pharm. Sci.*, **51**, 957 (1962).

(6) R. A. Castello, G. Jellinek, J. M. Konieczny, K. C. Kwan, and R. O. Toberman, *J. Pharm. Sci.*, **57**, 485 (1968).

(7) F. J. Cioffi, H. M. Abdou, and A. J. Warren, *J. Pharm. Sci.*, **65**, 1234 (1976).

(8) F. J. Cioffi, S. Martynovych, and H. Bendrot, *J. Pharm. Sci.*, **68**, 1280 (1979).

(9) D. Wurster, W. Wargin, and M. DeBaradinis, Jr., *J. Pharm. Sci.*, **70**, 764 (1981).

(10) J. Kent, P. Wong, and G. Hedge, *J. Pharm. Sci.*, **66**, 1665 (1977).

Some Effects of 1-(2,4-Dichlorophenyl)-4-dimethylaminomethyl-1-nonen-3-one Hydrochloride on *Escherichia coli* GK-19

G. G. KHACHATOURIANS *‡ˣ, P. K. HOLMLUND ‡, and J. R. DIMMOCK §

Received December 27, 1982, from the **Department of Applied Microbiology and Food Science, College of Agriculture*, ‡*Department of Microbiology, College of Medicine*, and §*College of Pharmacy, University of Saskatchewan, Saskatoon, Saskatchewan S7N 0W0, Canada.* Accepted for publication April 26, 1983.

Abstract □ 1-(2,4-Dichlorophenyl)-4-dimethylaminomethyl-1-nonen-3-one hydrochloride (Id) was shown to inhibit the growth of *Escherichia coli* GK-19 at a concentration of 50 μg/mL in a medium of pH 6.5. Maximal antibacterial activity was found during the logarithmic growth phases rather than at the early stationary phase. Electron microscopy revealed that Id caused lysis, and inhibition of respiration and retardation of RNA and protein syntheses occurred in the bacteria with this compound at 50 μg/mL.

Keyphrases □ 1-(2,4-Dichlorophenyl)-4-dimethylaminomethyl-1-nonen-3-one hydrochloride—antibacterial activity in *Escherichia coli*, effects of concentration, temperature, and medium pH □ Antibacterial activity—1-(2,4-dichlorophenyl)-4-dimethylaminomethyl-1-nonen-3-one hydrochloride against *Escherichia coli*, effects of concentration, temperature, and medium pH

Previous work from these laboratories showed that a number of Mannich bases derived from conjugated styryl ketones had antibacterial properties (1–3). The aim of the present investigation was twofold. First, it was hoped to unravel some of the factors affecting the action of a representative Mannich base on bacterial growth, and second, to discern the site or sites of action of the compound toward the bacteria.

EXPERIMENTAL

Synthesis of Compounds—Compound Ia was prepared by the literature method (4); Ib, d–f were synthesized by a previously described procedure (5), as was Ic (6).

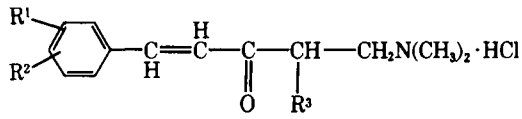

Ia: $R^1 = R^2 = R^3 = H$
Ib: $R^1 = R^2 = H$; $R^3 = (CH_2)_4CH_3$
Ic: R^1 = 3-OH; $R^2 = H$; $R^3 = (CH_2)_4CH_3$
Id: R^1 = 2-Cl; R^2 = 4-Cl; $R^3 = (CH_2)_4CH_3$
Ie: R^1 = 2-Cl; R^2 = 6-Cl; $R^3 = (CH_2)_4CH_3$
If: R^1 = 3-Cl; R^2 = 4-Cl; $R^3 = (CH_2)_4CH_3$

Measurement of Bacterial Growth—In this study, an isolate of *Escherichia coli* K-12 strain designated GK-19 (7) was employed. The bacteria were grown in a minimal salts medium (8) to which casamino acids (0.5% w/v) and thiamine (7.5 μg/mL) had been added. Adjustment of the pH was made using Sörensen's buffer solutions (9). The cultures were grown in Erlenmeyer flasks

© 1984, American Pharmaceutical Association

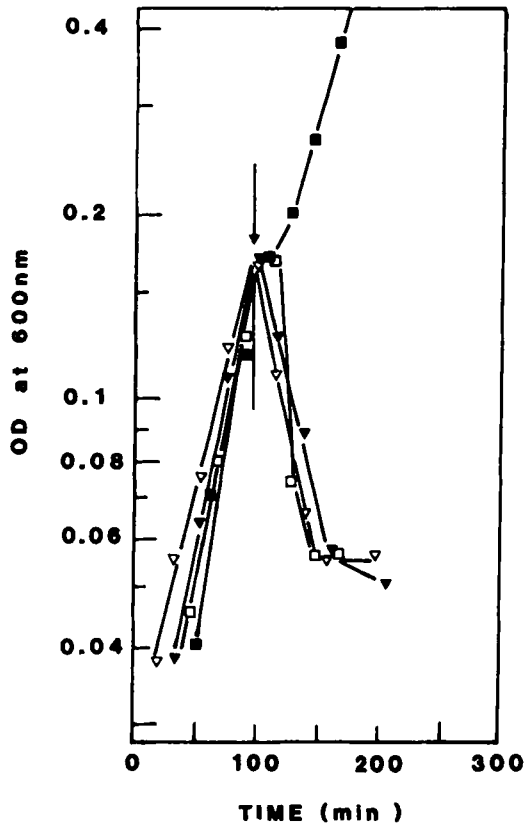

Figure 1—*Effect of Id (50 μg/mL) on the growth of* E. coli *GK-19 at pH 7.0 (■), 6.5 (□), 6.0 (▼), and 5.0 (▽). Compound Id was added (arrow) after exponential growth of the bacteria had commenced.*

at 37°C (unless otherwise stated) with a culture-to-flask volume of 1:5 or 1:10, using a gyratory shaker incubator[1]. The growth of the cultures was monitored by determining the absorbancy at 600[2] and 610[3] nm. The determination of cell viability was made by the appropriate dilutions of the culture being placed onto nutrient agar[4] and incubated at 37°C for 24–36 h. Colony-forming units were determined by plating. The compounds were dissolved in water prior to the addition of the medium unless otherwise indicated.

Electron Microscopy—A pellet of bacterial cells was prepared[5] by centrifugation (9650×*g* for 3 min), and the cells were fixed in a solution of glutaraldehyde (2.5% w/v) in 0.1 M cacodylate buffer, pH 7.4. After this process (105 min), the cells were embedded in a resin[6], and ultrathin sections were prepared[7] and stained with uranyl acetate solution in methanol (1% w/v) followed by lead citrate solution (2.66% w/v). Negative staining was accomplished by placing the cells prior to the fixation process, on 200-mesh grids followed by treatment with phosphotungstic acid solution (3% w/v). The samples obtained by these procedures were examined by electron microscopy[8].

Measurement of Respiration—Compound Id was added to *E. coli* GK-19 at log phase in standard biological oxidation-demand bottles attached to a polarographic dissolved-oxygen electrode[9]. The addition and mixing process was complete within 30 s and oxygen consumption was measured[10] every 2 min at 22–23°C.

Effect of Id on DNA and RNA Syntheses—Compound Id (50 μg/mL) was added to a culture of *E. coli* GK-19 at an optical density of 0.44, and the extent of incorporation of [^{3}H]thymidine (1 μCi/mL of culture) and [^{3}H]uracil (0.1 μCi/mL of culture) into DNA and RNA, respectively, was made by the batch method described previously (8) using a scintillation counter[11]. The experiments examining the rates of DNA and RNA syntheses were undertaken once and in triplicate (±5%), respectively.

[1] New Brunswick Scientific Co., Edison, N.J.
[2] Spectronic 20 spectrophotometer; Bausch and Lomb, Rochester, N.Y.
[3] Horizon 5965-50 spectrophotometer; Horizon Ecology Co., Chicago, Ill.
[4] Difco, Detroit, Mich.
[5] Microfuge B; Beckman, Palo Alto, Calif.
[6] Araldite epon mixture.
[7] LKB III ultratome; Stockholm, Sweden.
[8] Hitachi H412 electron microscope.
[9] Model 97-08; Orion Research Inc., Cambridge, Mass.
[10] Model 301; Orion Research Inc., Cambridge, Mass.
[11] Model LS-9000 scintillation counter; Beckman, Palo Alto, Calif.

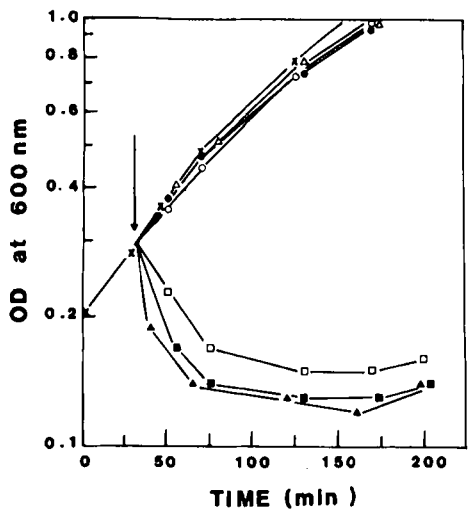

Figure 2—*Effect of Ia–f (100 μg/mL) on the growth of* E. coli *GK-19. The arrow indicates the time of addition of Ia (○), Ib (●), Ic (△), Id (▲), Ie (□), and If (■); (X) untreated controls.*

RESULTS AND DISCUSSION

Six candidate antibacterial agents I were considered in which the substitution pattern of the aromatic ring varied, while the *n*-pentyl group present in Ib–f was absent in Ia. A laboratory strain of *E. coli* K-12, designated as strain GK-19, was used as the test organism.

The initial experiments were designed to examine some of the factors affecting the bacterial growth by a representative Mannich base. Since Mannich bases are known to be unstable under alkaline conditions (5, 10), one of the derivatives (Id) was evaluated against *E. coli* GK-19 at neutral pH and in media which was mildly acidic (Fig. 1). At pH 7.0, a transient reduction of the growth rate of the bacteria was observed after the addition of Id, but afterward virtually normal growth resumed. Under acidic conditions (pH values of 6.5, 6.0, and 5.0) minimum absorbancy was noted after 1 h. Changes in pH can affect the ratio of un-ionized and ionized molecules (11), and it is conceivable that lowering the pH increases the percentage of Id existing in the ionic form, which may be the bioactive species.

The six Mannich bases were also examined at pH 6.5 for their effect on bacterial growth (Fig. 2). Compounds Ia–c were virtually bereft of antibacterial activity, while the dichlorinated derivatives (Id–f) caused a marked decrease in culture turbidity. Mannich base Id was selected for further studies. Reduction of the concentration of Id showed that the antibacterial effect was detectable at the lowest concentration examined, *i.e.*, 5 μg/mL (Fig. 3), while at 35 μg/mL substantial antibacterial activity was observed. However, this effect reversed after ~1 h, and colony-forming ability returned. At 35 μg/mL, Id was bacteriostatic (Fig. 3A) and at 50 μg/mL it was bactericidal (Fig. 3A and B). Figure 3B shows that at 50 μg/mL, the bactericidal activity is >99.9%.

Compound Id was dissolved in three different solvents to observe the effect of solvent on the antibacterial activity of Id (Fig. 4). When Id was dissolved in water and ethanol, minimal absorbancy was attained more rapidly than when a solution of Id in dimethyl sulfoxide was administered to a culture of the microorganisms. Gradual recovery occurred with solutions of Id in dimethyl sulfoxide and ethanol, but not when water was used.

The effect of the antibacterial effect of Id on *E. coli* GK-19 at different temperatures is seen in Fig. 5. At 6°C, little bacterial growth is observed, in contrast to that seen at 23°C, 37°C, and 40°C. At 23°C, addition of Id virtually abolished growth, but it was only after 1 h that the lytic effect was noted. At 37°C and 40°C, lysis began on addition of Id. This observation is of interest insofar that a reduction in the respiration-inhibitory properties of some related Mannich bases on mitochondrial function was noted at 20°C compared with 37°C (12) and, hence, the present study is germane to recent reports in changes of biochemical function with variation in temperature (13–15). In addition, the fatty acid composition of a yeast membrane varied with temperature (16). In summary, unless otherwise indicated subsequent experimentation utilized compound Id at a concentration of 50 μg/mL in a medium of pH 6.5 and a temperature of 37°C.

A further question posed was the effect of Id on the age of the culture of

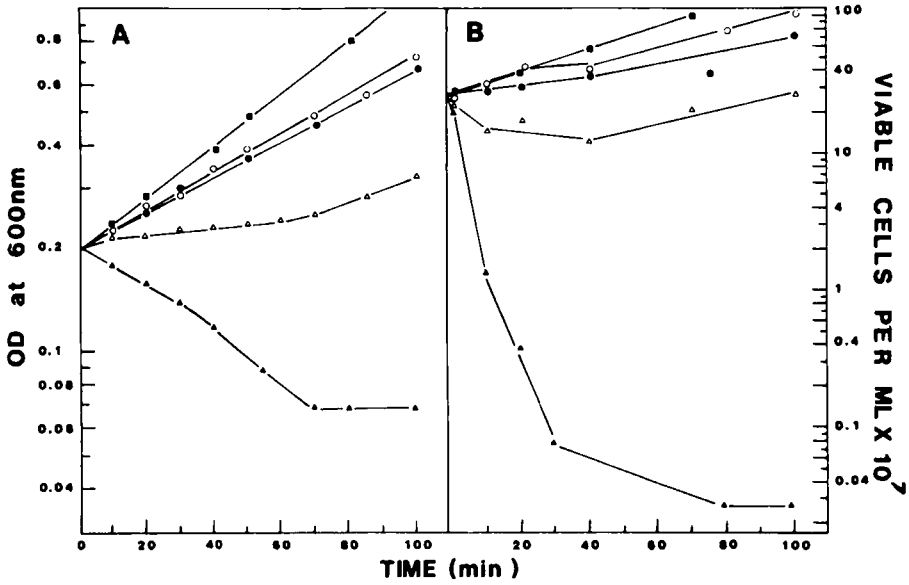

Figure 3—*Effect of Id at concentrations of 5 (○), 20 (●), 35 (△), and 50 (▲) μg/mL on the growth of* E. coli *GK-19, (■) untreated controls. Optical density (A) and colony-forming ability (B) were measured at different intervals.*

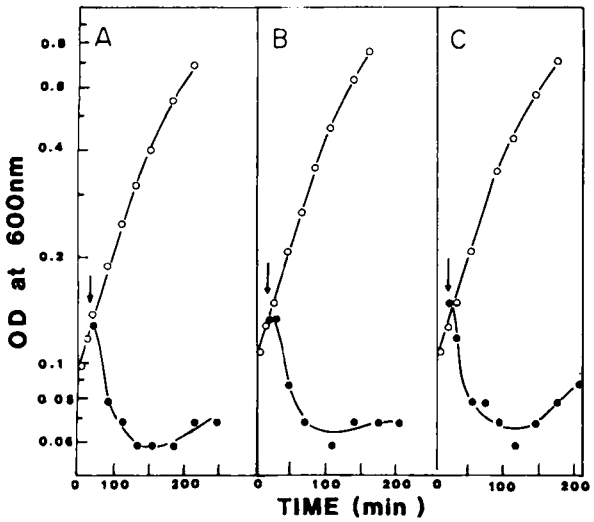

Figure 4—*Effect of the addition (arrow) of Id (50 μg/mL) dissolved in dimethyl sulfoxide (A), water (B), and ethanol (C) on the growth of treated (●) and untreated (○) cultures of* E. coli *GK-19.*

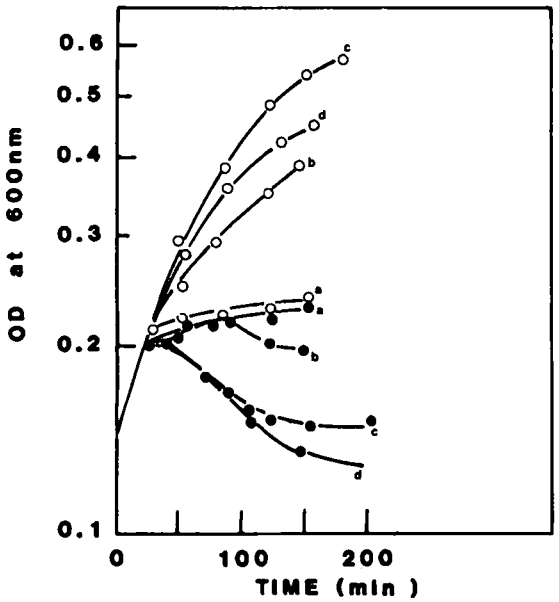

Figure 5—*Effect of the addition of Id (50 μg/mL) on treated (●) and untreated (○) cultures of* E. coli *GK-19 at 6°C (a), 23°C (b), 37°C (c), and 40°C (d).*

E. coli GK-19. Figure 6 shows that after a short lag phase of ~0.5 h, the bacteria entered their logarithmic (log) growth phase, which continued for 5 h. Compound Id was added to culture aliquots at times corresponding to early log, mid log, late log, and early stationary phases; antibacterial activity was demonstrated on all four occasions, although greater activity was seen during the logarithmic growth phases. However, the larger number of cells present in the early stationary phase could be an explanation for the reduced antimicrobial activity of Id at this point in time. To examine such a possibility, a culture of *E. coli* GK-19 was grown to early-mid log phase and concentrated fivefold by centrifugation; two quantities of Id (50 μg/mL) were added, separated by a 40-min period, and then the turbidity of the culture was followed for a further 90 min. No different effect was observed to that found for the early stationary phase shown in Fig. 6. In addition, the difference in the culture growth phase sensitivity to Id could be due to changes in the growth media, *i.e.*, the concentration of certain nutrients could have diminished by the time the bacteria had entered the stationary phase or, alternatively, new compounds could have formed and be present in the media. To test this possibility, cells at the mid log phase were harvested by centrifugation and resuspended in both freshly prepared media and also in media from which bacteria at the early stationary phase had been removed. The bacteria in both media responded to Id in an identical manner and, hence, the differential

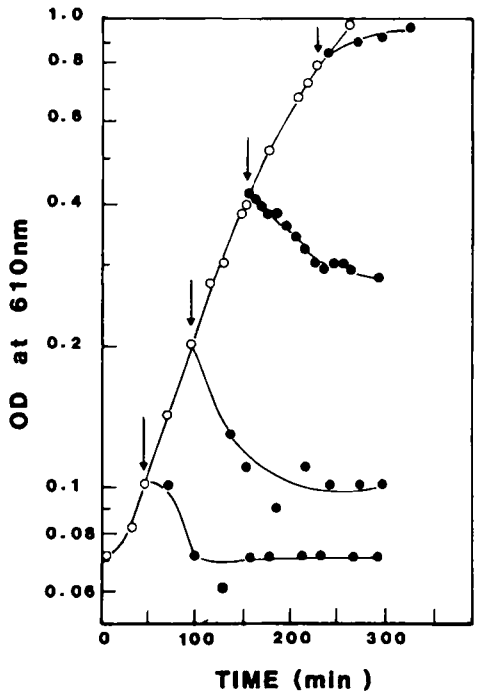

Figure 6—*Effect of multiple additions (arrows) of Id (50 μg/mL) on treated (●) and untreated (○) cultures of* E. coli *GK-19.*

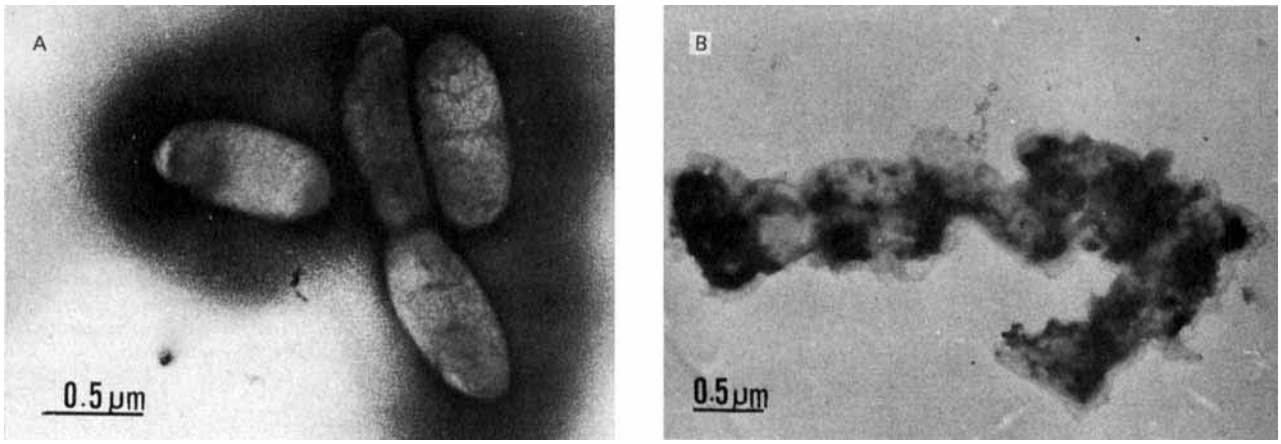

Figure 7—*Electron micrographs of negatively stained cells of* E. coli *GK-19 before (A) and after (B) treatment with Id (50 μg/mL).*

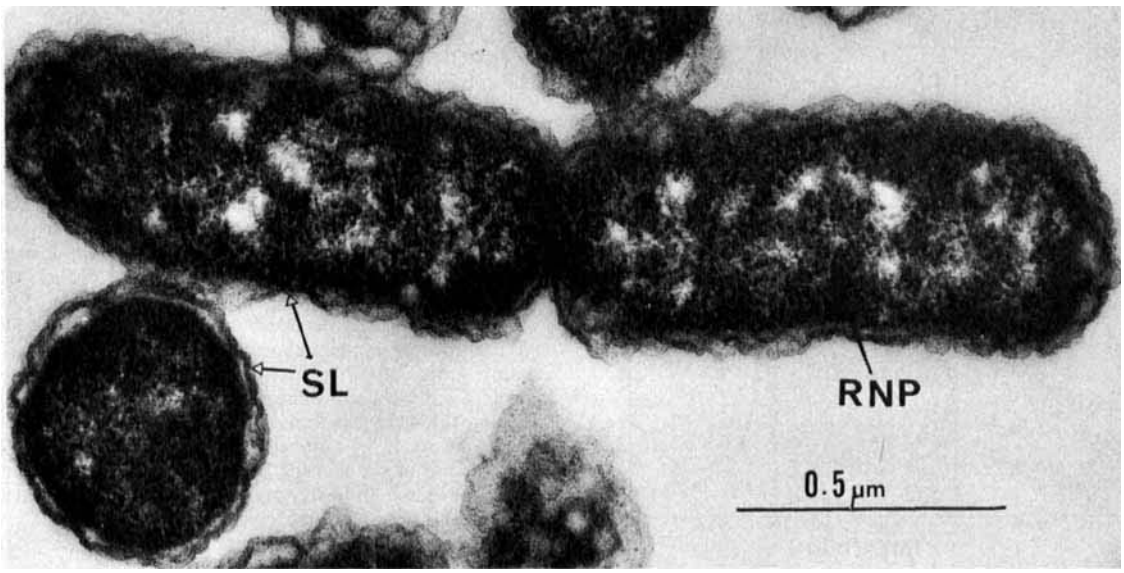

Figure 8—*Electron micrograph of thin sections of* E. coli *GK-19 displaying surface layers (SL) and ribonucleoprotein (RNP).*

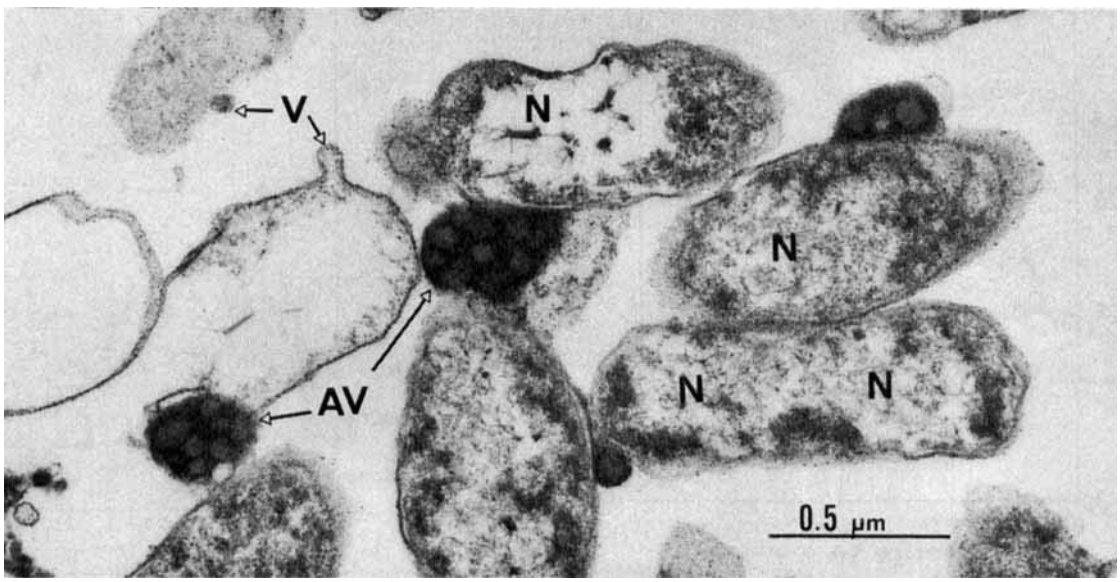

Figure 9—*Electron micrograph of thin sections of* E. coli *GK-19 after treatment with Id (50 μg/mL) displaying nuclear condensation (N), vesicle formation (V), and aggregated vesicles (AV).*

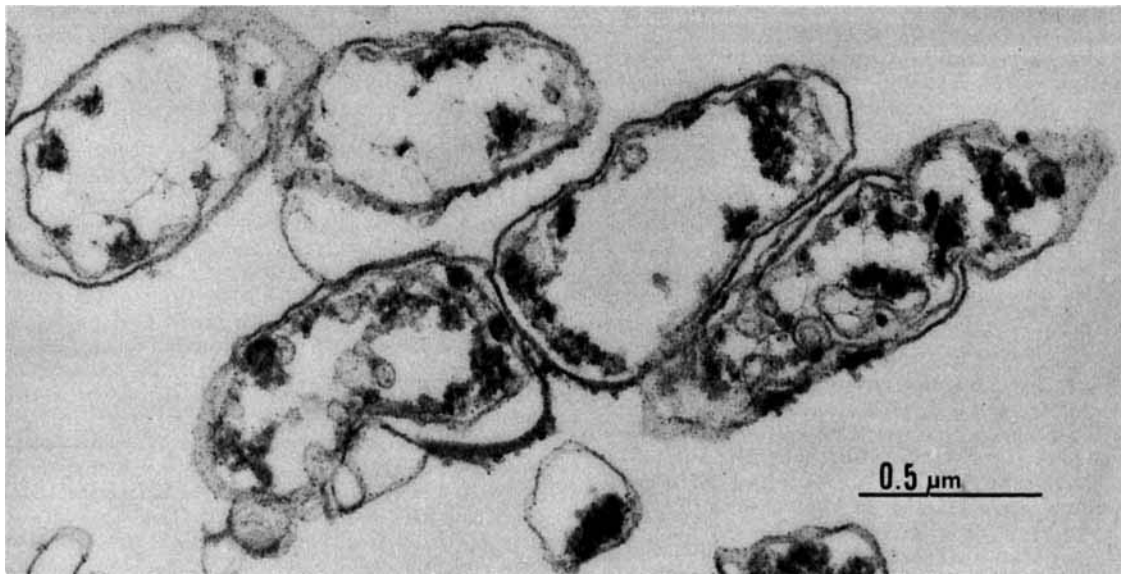

Figure 10—*Electron micrograph of thin sections of lysed cells of* E. coli *GK-19 caused by treatment of Id (50 μg/mL).*

sensitivity of Id at various growth stages was not due to changes in content of the media occurring during the growth of the bacteria.

The second phase of the investigation consisted of attempts to delineate the site(s) of action of Id on *E. coli* GK-19. An initial question posed was whether there was retention of the integrity of the cell membrane and cellular constituents after treatment with Id or whether a lytic process occurred, in which case rupture of the cell membrane and leakage of intracellular material would take place. Figure 7A is an electron micrograph of *E. coli* GK-19 cells taken from a culture of cells in the mid log growth phase, while Fig. 7B shows the effect of Id on these cells. After addition of Id, there are distortions of the cell shapes, loss of surface layer, and altered stainability compared with the untreated cells as noted in Fig. 7. Thin sections of some of the untreated cells revealed the cell membrane and the cytoplasmic regions containing ribonucleoprotein complexes (Fig. 8); regions of nuclear material are shown as lighter areas. After treatment with Id, there is the appearance of condensation of nuclear material, disorganization of the cell membrane, disappearance of the ribonucleoprotein structures, and appearance of pockets of small rounded vesicles inside cells, as well as in aggregate forms outside the cells (Fig. 9). Lysed cells of *E. coli* GK-19 after treatment with Id showed an increased loss of cellular constituents (Fig. 10). Hence, the Mannich base Id exerts a lytic effect on these bacteria at 50 μg/mL.

It is conceivable that Id could exert antibacterial activity in addition to lysis. In other words, while the lysis was in progress, Id could also act, for example, on the respiration apparatus and the macromolecular synthetic pathways of the bacteria. Figure 11 shows the effect of the addition of various concentrations of Id on oxygen consumption; at 50 μg/mL, there is complete inhibition of respiration. A plot of the rate of oxygen consumption at the end of 20 min *versus* concentration of Id (on linear paper) is shown as an inset in Fig. 11.

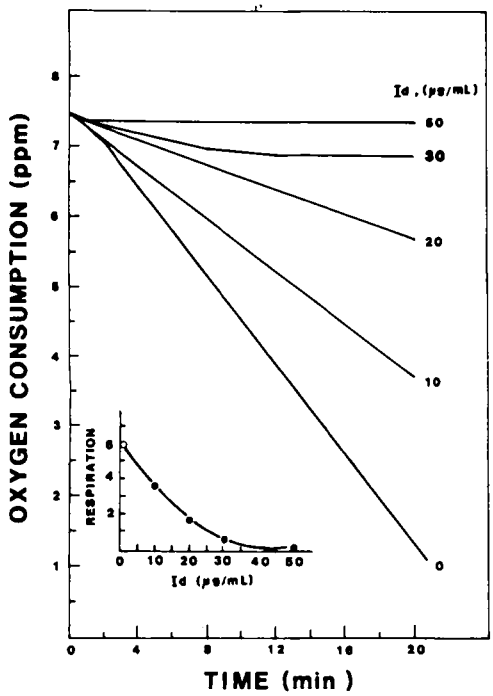

Figure 11—*Effect of Id on oxygen consumption in* E. coli *GK-19.*

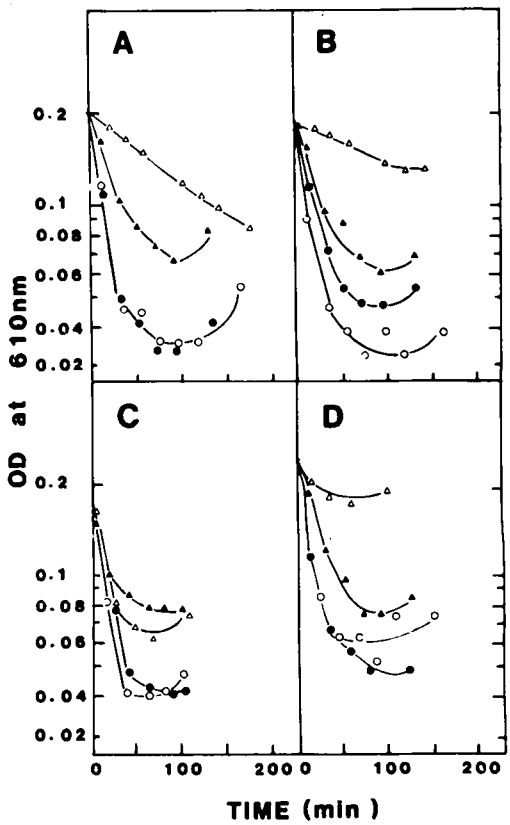

Figure 12—*Effect of the sensitivity of* E. coli *GK-19 to Id (50 μg/mL) by treatment with metabolic inhibitors. Key: (A) potassium cyanide (1950 μg/mL); (B) sodium azide (1950 μg/mL); (C) 2,4-dinitrophenol (18.4 mg/mL); (D) chloramphenicol (150 μg/mL). Compound Id was added simultaneously (●), 5 (○), 30 (△), or 120 (▲) min after the addition of the metabolic inhibitor.*

Table I—Effect of Id (50 μg/mL) on the Incorporation of [^{3}H]Thymidine and [^{3}H]Uracil into the DNA and RNA of *E. coli* GK-19.

Time, min	Counts per Minute of [^{3}H]-Thymidine[a]		Counts per Minute of [^{3}H]-Uracil[a]	
	Control	Treated	Control	Treated
5	100	100	100	100
10	102	100	294	193
20	106	99	650	224
30	108	97	650	237
40	112	96	650	255

[a] Figures in the table are relative to the counts per minute of labeled precursor in control experiments at the end of 5 min.

In addition, treatment of *E. coli* GK-19 with potassium cyanide, sodium azide, and 2,4-dinitrophenol, which are known inhibitors of respiration and energy production, was undertaken; Id was added simultaneously or at varying times after the addition of the inhibitors. The results are portrayed in Fig. 12A-C. With pretreatment times of 30 and 120 min, the antibacterial effect of Id is markedly reduced, which further indicates that cellular respiration or energy, in part at least, is likely required for the lytic effect of Id on *E. coli* to be manifested.

A similar study with chloramphenicol, which is an inhibitor of protein synthesis, showed that protein synthesis is required for the lysis of cells (Fig. 12D). It is concluded that in order for Id to exert its maximum lytic effect, normal respiration, energy production, and protein synthesis are required. Because of the cellular physiological functions that were affected by Id, it was suspected that macromolecular synthesis, in general, could also be affected. The conviction that protein synthesis was a site of action of this Mannich base was strengthened by its inhibition of the biosynthesis of the enzyme β-galactosidase. In *E. coli* GK-19, it is possible to induce the synthesis of this enzyme within 2-3 min with isopropylthiogalactoside (17), but addition of Id to a culture of this microorganism abolished the ability of the cells to synthesize this enzyme.

The effect of Id on the synthesis of DNA and RNA was measured using radioactively labeled thymidine and uracil, respectively, and the results are shown in Table I. The data indicate that while the synthesis of DNA is virtually unaffected, the inhibition of RNA synthesis commences after 5 min and is reduced by 66% after 20 min.

In conclusion, this study has unearthed some of the factors which affect the antibacterial activity of 1-(2,4-dichlorophenyl)-4-dimethylaminomethyl-1-nonen-3-one hydrochloride (Id) against *E. coli* GK-19. In addition, the bioactivity of this compound is due, at least in part, to its causation of lysis, and adverse effects on respiration, as well as protein and RNA biosynthesis, take place.

REFERENCES

(1) J. R. Dimmock and W. G. Taylor, *J. Pharm. Sci.*, **64**, 241 (1975).

(2) J. R. Dimmock, C. B. Nyathi, and P. J. Smith, *J. Pharm. Sci.*, **67**, 1543 (1978).

(3) J. R. Dimmock and L. M. Smith, *J. Pharm. Sci.*, **69**, 575 (1980).

(4) J. R. Dimmock, N. W. Hamon, K. W. Hindmarsh, D. G. Mills, L. E. Negrave, G. H. Rank, and A. J. Robertson, *J. Pharm. Sci.*, **65**, 482 (1976).

(5) J. R. Dimmock and W. G. Taylor, *J. Pharm. Sci.*, **63**, 69 (1974).

(6) J. R. Dimmock, C. B. Nyathi and P. J. Smith, *J. Pharm. Sci.*, **68**, 1216 (1979).

(7) G. G. Khachatourians and D. J. Tipper, *Antimicrob. Agents Chemother.*, **6**, 304 (1974).

(8) G. G. Khachatourians, R. J. Sheehy, and R. Curtiss III, *Mol. Gen. Genet.*, **128**, 23 (1974).

(9) D. L. Deardoff in "Remington's Pharmaceutical Sciences," 14th ed., Mack Publishing, Easton, Pa., 1970, p. 1554.

(10) F. F. Blicke in "Organic Reactions," Vol. 1, R. Adams, Ed., Wiley, New York, N.Y., 1942, p. 303.

(11) A. Albert, "Selective Toxicity," 5th ed., Chapman and Hall, London, 1973, pp. 287, 500, and 501.

(12) J. R. Dimmock, K. Shyam, N. W. Hamon, B. M. Logan, S. K. Raghavan, D. J. Harwood, and P. J. Smith, *J. Pharm. Sci.*, **72**, 887 (1983).

(13) T. Psenakova and J. Kolek, *Biologia*, **36**, 1109 (1981).

(14) I. A. Goroshinskay, A. A. Krichevskaya, and Z. G. Bronovitskaya, *Bull. Exp. Biol. Med.*, **91**, 464 (1981).

(15) E. I. Grodums, *Cell Tissue Res.*, **185**, 231 (1977).

(16) P. C. Patel and M. J. Lewis, *J. Am. Soc. Brew. Chem.*, **40**, 26 (1982).

(17) G. G. Khachatourians and D. J. Tipper, *J. Bacteriol.*, **119**, 795 (1974).

ACKNOWLEDGMENTS

Financial support for this project was provided by the students' funds of the Dean of Medicine, University of Saskatchewan to P. K. Holmlund and the Medical Research Council of Canada to J. R. Dimmock. Technical assistance was also given by Miss B. M. Logan and Mr. M. Diocee.

Determination of Amphetamine, Norephedrine, and Their Phenolic Metabolites in Rat Brain by Gas Chromatography

RONALD T. COUTTS ˣ, DANIEL B. PRELUSKY, and GLEN B. BAKER

Received March 29, 1982, from the *Neurochemical Research Unit, Faculty of Pharmacy and Pharmaceutical Sciences* and *Department of Psychiatry, University of Alberta, Edmonton, Alberta T6G 2N8, Canada.* Accepted for publication April 25, 1983.

Abstract □ A specific analytical procedure for the quantitation of amphetamine (I), norephedrine (III), and their amphoteric metabolites, *p*-hydroxyamphetamine (II) and *p*-hydroxynorephedrine (IV), in biological samples using electron-capture gas chromatography (GC-EC) is described. The procedure utilizes the ion-pairing reagent, bis(2-ethylhexyl)phosphoric acid, which frees the amines from most contaminants and permits the efficient extraction of the amphoteric compounds (as acetates) from the aqueous solution. Amines I and III and acetylated amines II and IV were perfluoroacetylated prior to GC-EC analysis. Metabolism of I, II, and III in the rat brain was studied. Results indicate that both *in vivo* and *in vitro* amines I and III are *p*-hydroxylated to II and IV, respectively, and II is β-hydroxylated to give IV. Norephedrine (III) was not detected as a rat brain metabolite of amphetamine (I).

Keyphrases □ Amphetamine—rat brain metabolism, norephedrine, phenolic metabolites, gas chromatography □ Norephedrine—rat brain metabolites, amphetamine, phenolic metabolites, gas chromatography □ Metabolites, phenolic—amphetamine and norephedrine, rat brain metabolism, gas chromatography

When amphetamine (I) is administered systemically to rats, appreciable amounts of I and trace quantities of *p*-hydroxyamphetamine (II) and *p*-hydroxynorephedrine (IV) are detected in the brain tissue. In attempts to associate these metabolites with some of the pharmacological actions of I, their presence in various brain regions and other tissues have been

0022-3549/84/0600-0808$01.00/0

© 1984, American Pharmaceutical Association

Table I—Effect of Id (50 μg/mL) on the Incorporation of [^{3}H]Thymidine and [^{3}H]Uracil into the DNA and RNA of *E. coli* GK-19.

Time, min	Counts per Minute of [^{3}H]-Thymidine[a]		Counts per Minute of [^{3}H]-Uracil[a]	
	Control	Treated	Control	Treated
5	100	100	100	100
10	102	100	294	193
20	106	99	650	224
30	108	97	650	237
40	112	96	650	255

[a] Figures in the table are relative to the counts per minute of labeled precursor in control experiments at the end of 5 min.

In addition, treatment of *E. coli* GK-19 with potassium cyanide, sodium azide, and 2,4-dinitrophenol, which are known inhibitors of respiration and energy production, was undertaken; Id was added simultaneously or at varying times after the addition of the inhibitors. The results are portrayed in Fig. 12A-C. With pretreatment times of 30 and 120 min, the antibacterial effect of Id is markedly reduced, which further indicates that cellular respiration or energy, in part at least, is likely required for the lytic effect of Id on *E. coli* to be manifested.

A similar study with chloramphenicol, which is an inhibitor of protein synthesis, showed that protein synthesis is required for the lysis of cells (Fig. 12D). It is concluded that in order for Id to exert its maximum lytic effect, normal respiration, energy production, and protein synthesis are required. Because of the cellular physiological functions that were affected by Id, it was suspected that macromolecular synthesis, in general, could also be affected. The conviction that protein synthesis was a site of action of this Mannich base was strengthened by its inhibition of the biosynthesis of the enzyme β-galactosidase. In *E. coli* GK-19, it is possible to induce the synthesis of this enzyme within 2-3 min with isopropylthiogalactoside (17), but addition of Id to a culture of this microorganism abolished the ability of the cells to synthesize this enzyme.

The effect of Id on the synthesis of DNA and RNA was measured using radioactively labeled thymidine and uracil, respectively, and the results are shown in Table I. The data indicate that while the synthesis of DNA is virtually unaffected, the inhibition of RNA synthesis commences after 5 min and is reduced by 66% after 20 min.

In conclusion, this study has unearthed some of the factors which affect the antibacterial activity of 1-(2,4-dichlorophenyl)-4-dimethylaminomethyl-1-nonen-3-one hydrochloride (Id) against *E. coli* GK-19. In addition, the bioactivity of this compound is due, at least in part, to its causation of lysis, and adverse effects on respiration, as well as protein and RNA biosynthesis, take place.

REFERENCES

(1) J. R. Dimmock and W. G. Taylor, *J. Pharm. Sci.*, **64**, 241 (1975).

(2) J. R. Dimmock, C. B. Nyathi, and P. J. Smith, *J. Pharm. Sci.*, **67**, 1543 (1978).

(3) J. R. Dimmock and L. M. Smith, *J. Pharm. Sci.*, **69**, 575 (1980).

(4) J. R. Dimmock, N. W. Hamon, K. W. Hindmarsh, D. G. Mills, L. E. Negrave, G. H. Rank, and A. J. Robertson, *J. Pharm. Sci.*, **65**, 482 (1976).

(5) J. R. Dimmock and W. G. Taylor, *J. Pharm. Sci.*, **63**, 69 (1974).

(6) J. R. Dimmock, C. B. Nyathi and P. J. Smith, *J. Pharm. Sci.*, **68**, 1216 (1979).

(7) G. G. Khachatourians and D. J. Tipper, *Antimicrob. Agents Chemother.*, **6**, 304 (1974).

(8) G. G. Khachatourians, R. J. Sheehy, and R. Curtiss III, *Mol. Gen. Genet.*, **128**, 23 (1974).

(9) D. L. Deardoff in "Remington's Pharmaceutical Sciences," 14th ed., Mack Publishing, Easton, Pa., 1970, p. 1554.

(10) F. F. Blicke in "Organic Reactions," Vol. 1, R. Adams, Ed., Wiley, New York, N.Y., 1942, p. 303.

(11) A. Albert, "Selective Toxicity," 5th ed., Chapman and Hall, London, 1973, pp. 287, 500, and 501.

(12) J. R. Dimmock, K. Shyam, N. W. Hamon, B. M. Logan, S. K. Raghavan, D. J. Harwood, and P. J. Smith, *J. Pharm. Sci.*, **72**, 887 (1983).

(13) T. Psenakova and J. Kolek, *Biologia*, **36**, 1109 (1981).

(14) I. A. Goroshinskay, A. A. Krichevskaya, and Z. G. Bronovitskaya, *Bull. Exp. Biol. Med.*, **91**, 464 (1981).

(15) E. I. Grodums, *Cell Tissue Res.*, **185**, 231 (1977).

(16) P. C. Patel and M. J. Lewis, *J. Am. Soc. Brew. Chem.*, **40**, 26 (1982).

(17) G. G. Khachatourians and D. J. Tipper, *J. Bacteriol.*, **119**, 795 (1974).

ACKNOWLEDGMENTS

Financial support for this project was provided by the students' funds of the Dean of Medicine, University of Saskatchewan to P. K. Holmlund and the Medical Research Council of Canada to J. R. Dimmock. Technical assistance was also given by Miss B. M. Logan and Mr. M. Diocee.

Determination of Amphetamine, Norephedrine, and Their Phenolic Metabolites in Rat Brain by Gas Chromatography

RONALD T. COUTTS ˣ, DANIEL B. PRELUSKY, and GLEN B. BAKER

Received March 29, 1982, from the *Neurochemical Research Unit, Faculty of Pharmacy and Pharmaceutical Sciences* and *Department of Psychiatry, University of Alberta, Edmonton, Alberta T6G 2N8, Canada.* Accepted for publication April 25, 1983.

Abstract □ A specific analytical procedure for the quantitation of amphetamine (I), norephedrine (III), and their amphoteric metabolites, *p*-hydroxyamphetamine (II) and *p*-hydroxynorephedrine (IV), in biological samples using electron-capture gas chromatography (GC-EC) is described. The procedure utilizes the ion-pairing reagent, bis(2-ethylhexyl)phosphoric acid, which frees the amines from most contaminants and permits the efficient extraction of the amphoteric compounds (as acetates) from the aqueous solution. Amines I and III and acetylated amines II and IV were perfluoroacetylated prior to GC-EC analysis. Metabolism of I, II, and III in the rat brain was studied. Results indicate that both *in vivo* and *in vitro* amines I and III are *p*-hydroxylated to II and IV, respectively, and II is β-hydroxylated to give IV. Norephedrine (III) was not detected as a rat brain metabolite of amphetamine (I).

Keyphrases □ Amphetamine—rat brain metabolism, norephedrine, phenolic metabolites, gas chromatography □ Norephedrine—rat brain metabolites, amphetamine, phenolic metabolites, gas chromatography □ Metabolites, phenolic—amphetamine and norephedrine, rat brain metabolism, gas chromatography

When amphetamine (I) is administered systemically to rats, appreciable amounts of I and trace quantities of *p*-hydroxyamphetamine (II) and *p*-hydroxynorephedrine (IV) are detected in the brain tissue. In attempts to associate these metabolites with some of the pharmacological actions of I, their presence in various brain regions and other tissues have been

0022-3549/84/0600-0808$01.00/0

© 1984, American Pharmaceutical Association

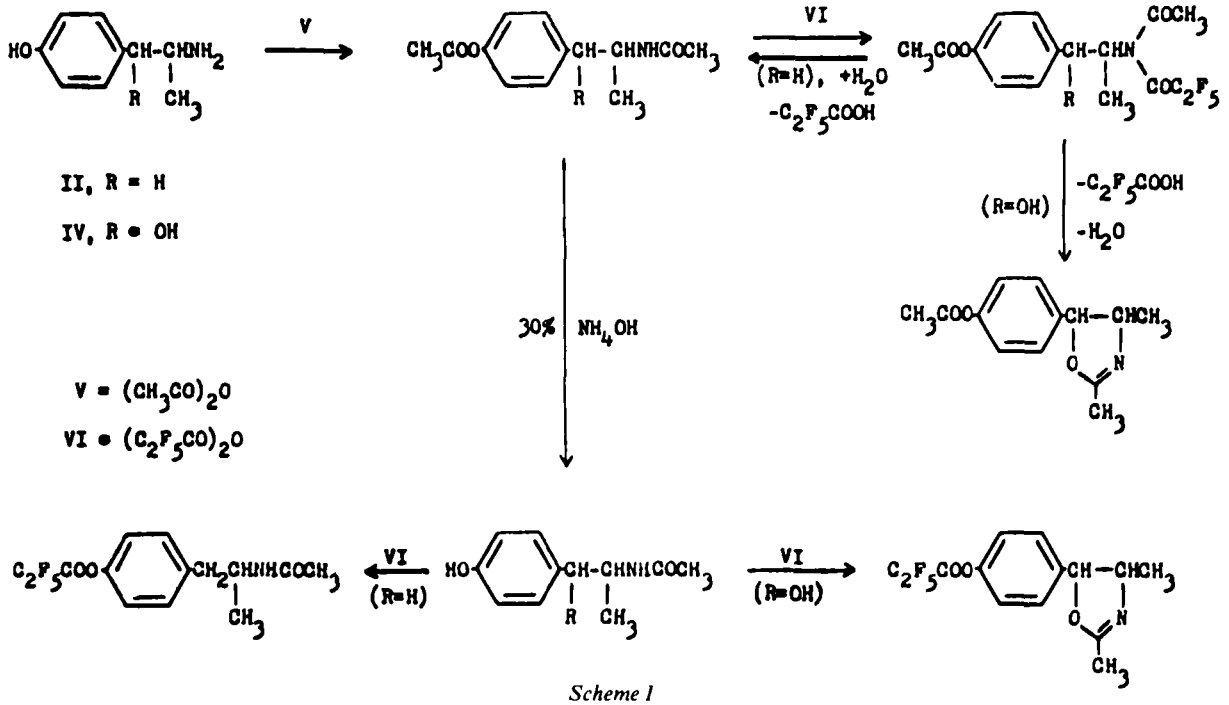

Scheme I

determined (1–11). It has been suggested (2, 5, 12, 13) that amphetamine (I) is first *p*-hydroxylated in the liver, and trace amounts of the resulting *p*-hydroxyamphetamine (II) penetrate the blood–brain barrier and accumulate in brain tissue where β-hydroxylation of II to *p*-hydroxynorephedrine (IV) occurs (14, 15). However, there is alternative evidence from *in vitro* studies to suggest that *p*-hydroxylation of I can also occur in the brain (9).

In a continuation of our studies on trace amines in the brain, we wished to determine whether analytical techniques previously developed (16–18) could be applied to the measurement of amphetamine (I), *p*-hydroxyamphetamine (II), norephedrine (III), and *p*-hydroxynorephedrine (IV) and provide information on the extent to which *p*- and β-hydroxylation occur in the brain tissue.

Current analytical procedures rely on the extraction of the amines into an organic solvent followed by derivatization with a reagent sensitive to electron-capture detection (EC) (2, 11, 19) or utilize technically more complex procedures involving tritiated compounds (1, 6, 8, 9, 11, 13, 14, 20) or mass fragmentography (3, 7). The simple extraction procedure is adequate for the analysis of many amines but usually demonstrates a poor gas chromatographic (GC) detection linearity over wide concentration ranges, as well as a poor sensitivity for phenolic amines, which are normally inefficiently extracted from aqueous solution.

We now report a rapid analytical method that permits the identification and efficient quantitation of amphoteric compounds (II and IV) in tissues and that can be employed to improve the GC sensitivity limits of simple amines (I and III). By utilizing this analytical procedure the levels of I–IV in rat brain tissues were determined after intraperitoneal administration of each amine. The results of an *in vitro* study on the metabolism of I–III with rat brain homogenate is also reported.

EXPERIMENTAL

Animal Studies—Male Sprague-Dawley rats (150 ± 20 g) were used. For the *in vivo* studies, rats were injected intraperitoneally with equimolar quantities (74 μmol/kg) of amphetamine hydrochloride[1], *p*-hydroxyamphetamine hydrobromide[1], norephedrine hydrochloride[2], and *p*-hydroxynorephedrine hydrobromide[2], (*i.e.*, 10.0, 11.19, 11.19, and 12.37 mg/kg, respectively, calculated as the free bases). Physiological saline was used as the vehicle, and injection volumes of ~0.3 mL were employed. Control rats received the same volume of vehicle without drug. All animals were sacrificed exactly 60 min after injection. The complete brain was rapidly removed, homogenized in three volumes of cold 0.4 M perchloric acid, and centrifuged at 10,000×*g* for 15 min. Supernatant equal to 1.0 g of whole brain tissue was used in the analyses.

For the *in vitro* studies, the whole brains from untreated rats were removed, homogenized in three volumes of ice-cold 1.15% KCl solution, and centrifuged at 10,000×*g* for 20 min. Supernatant corresponding to 0.5 g of the original tissue was incubated at 37°C with shaking in open 15-mL Erlenmeyer flasks containing an NADPH-generating system (20 μmol of glucose 6-phosphate[3], 20 μmol of magnesium chloride, and 4.4 μmol of NADP[4]) in Tris-HCl buffer (pH 7.4) and 1.0 μmol of the appropriate substrate (total volume 3.8 mL). Incubations were terminated after 60 min by the addition of 0.2 mL of 2.0 M perchloric acid. *In vitro* experiments were performed in triplicate.

Extraction and Derivatization—The samples [*in vivo* brain supernatant (4 mL) or *in vitro* incubation mixture (4 mL)], to which 1.0 μg of 2-(*p*-chlorophenyl)ethylamine[5] was added as internal standard, were adjusted to pH 7.8 by the addition of solid potassium bicarbonate and centrifuged (2000×*g*) to remove any precipitate formed. The supernatant was then extracted with 5.0 mL of a 2.5% solution of bis(2-ethylhexyl)phosphoric acid[6] in chloroform. After separation of the two phases, the aqueous layer was discarded and the chloroform layer was back-extracted with 3.0 mL of 0.5 M HCl.

Method a—For the analysis of I and III, the acid layer was adjusted to a pH value of >10.5 and extracted with 4.0 mL of ethyl acetate. The organic layer was evaporated to dryness under a stream of nitrogen, and the residue was pentafluoroacylated and treated further as described below.

Method b—For the analysis of II and IV, the acid layer was made slightly basic by addition of solid sodium bicarbonate, 300 μL of acetic anhydride (V) was added to the basified solution followed by small additional quantities of sodium bicarbonate with shaking until all effervescence ceased, and the so-

[1] Smith Kline and French Laboratories, Philadelphia, Pa.; lot no. 365-A for amphetamine sulfate, converted to hydrochloride, lot no. 988-64E for *p*-hydroxyamphetamine hydrobromide.

[2] Aldrich Chemical Co., Milwaukee, Wis.; lot no. 1414 TD for norephedrine hydrochloride, lot no. 122627PC for β-hydroxynorephedrine hydrobromide.

[3] Sigma grade, disodium salt; Sigma Chemical Co., St. Louis, Mo.

[4] Oxidized form, Sigma grade, monosodium salt; Sigma Chemical Co., St. Louis, Mo.

[5] Purchased as the free base (Sigma Chemical Co., St. Louis, Mo.) and converted to its hydrochloride in the usual way.

[6] Sigma Chemical Co., St. Louis, Mo.

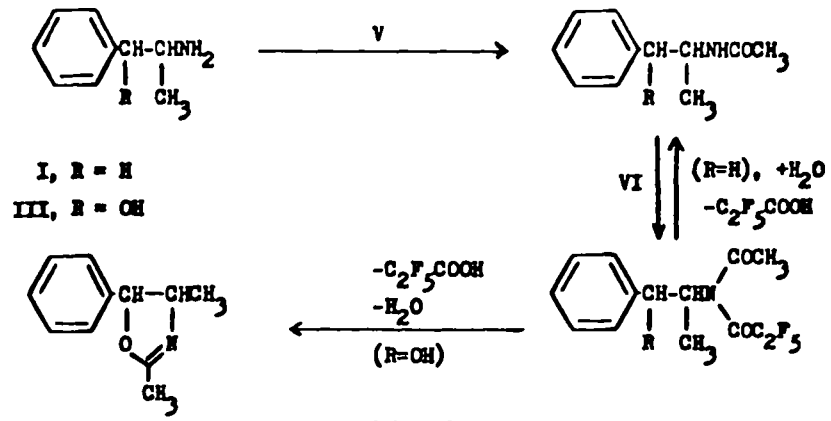

Scheme II

lution was extracted with 4.0 mL of ethyl acetate. To the separated organic layer, 300 μL of a 30% NH_4OH solution was added and the mixture was vortexed for 40 min. After neutralization of the NH_4OH solution, the layers were separated by centrifugation. The ethyl acetate layer was then evaporated to dryness in a stream of nitrogen.

The residues obtained from each of the methods were separately dissolved in a mixture of 35 μL of ethyl acetate and 75 μL of pentafluoropropionic anhydride (VI)[7], and the ensuing reaction was allowed to proceed at 85°C for 1 h. Each mixture was reduced in volume under a stream of nitrogen and partitioned between toluene (200 μL) and 0.1 M sodium phosphate buffer (200 μL; pH 7.4). Each organic layer was retained for GC analysis.

Instrumentation—Analyses were performed with a gas chromatograph[8] equipped with a 15-mCi ^{63}Ni-source linear EC detector. A fused silica capillary column (Carbowax 20M, 12 m) was used with temperature programming, 80–220°C at 20°C/min, and injection port and detector temperatures of 250°C. The carrier gas was helium at 7 psi; argon–methane (95:5) at a flow rate of 36 mL/min was used as the make-up gas at the detector. The mass spectrometer[9] separator and ionization source temperatures were 180°C with an ionization energy of 70 eV. The gas chromatographic column and operating conditions were as described above. All spectra were consistent with the structures assigned; the mass spectra are described elsewhere[10].

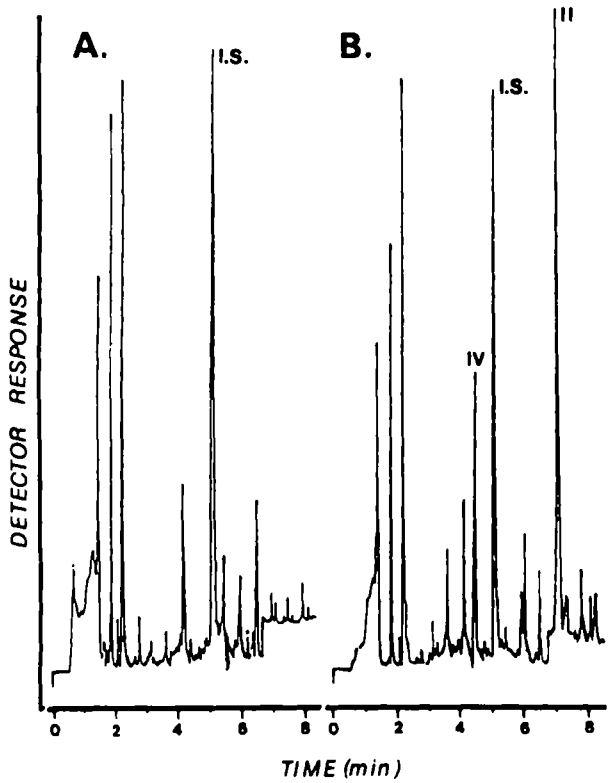

Figure 1—*Typical chromatograms of rat brain extracts which have been derivatized by method b. Key: (A) from rats injected with physiological saline; (B) from rats injected with norephedrine; (II) derivatized norephedrine; (IV) derivatized p-hydroxynorephedrine; (I.S.) derivatized internal standard.*

RESULTS AND DISCUSSION

Amphetamine (I), norephedrine (III), and their metabolites, *p*-hydroxyamphetamine (II) and *p*-hydroxynorephedrine (IV), were present in brain samples in trace concentrations. An analytical technique was required which would not only permit the adequate extraction of I–IV from aqueous solution, but also eliminate the interference created by the simultaneous extraction of endogenous contaminants. Such interference was found to be a particularly troublesome problem when utilizing GC–EC detection methods following the perfluoroacylation of sample extracts.

The described method proved to be a suitable analytical procedure. The four amines were efficiently extracted from brain supernatant or *in vitro* incubation mixtures with chloroform containing the ion-pairing reagent, bis(2-ethylhexyl)phosphoric acid (21) and were recovered from the organic solution by extracting the latter with dilute hydrochloric acid. The amine-containing aqueous solution was now free of most contaminants. The reextraction of the amphoteric metabolites II and IV into an organic solvent was made possible by their prior acetylation in the basified aqueous medium with acetic anhydride (V) to lipophillic *N,O*-diacetates (Scheme I). This acetylation procedure also converted amphetamine (I) and norephedrine (III) to their *N*-acetates (Scheme II). The β-hydroxyl group of either III or IV did not undergo acetylation.

Attempts were made to pentafluoroacylate the extracted acetates to increase their sensitivities to GC–EC. However, the *N*-pentafluoropropionyl derivatives of all four *N*-acetylated derivatives proved to be unstable. The derivatives of I and III rapidly lost the pentafluoroacetate moiety by hydrolysis, and the derivatives of III and IV cyclized to GC–EC-insensitive oxazoline products (Schemes I and II). The problem of insufficient sensitivity was overcome for II and IV by the preferential hydrolysis of the *O*-acetate moiety of their *N,O*-diacetates using ammonium hydroxide. This treatment freed the phenolic hydroxyl group for reaction with VI and resulted in the formation of the final derivatives identified in Scheme I. These *O*-pentafluoroacetyl derivatives were stable for at least 2 weeks if refrigerated. Typical GC traces are shown in Fig. 1.

Since neither amphetamine (I) nor norephedrine (III) contains a phenolic group, the analytical procedure just described for the analysis of II and IV was not applicable to the quantification of I and III; a separate analytical procedure was necessary for the latter two amines. They were directly removed from the aforementioned dilute hydrochloric acid solution containing I–IV by basifying the solution and extracting it with ethyl acetate. The extracts were treated with VI and the resulting *N*-pentafluoropropionyl derivatives (Scheme III) proved to be both stable to hydrolysis and GC–EC sensitive. This procedure permitted effective recovery and detection of both I and III without interference from the amphoteric metabolites.

Overall recoveries for the compounds (based on 100-ng amounts), using the methods described above, were as follows: I (87.7 ± 0.6%), II (65.0 ± 2.7%), III (80.3 ± 1.2%), IV (52.7 ± 2.5%), and internal standard (80.1 ± 1.7%); values represent mean ± *SD* ($n = 3$). The structures of all final de-

[7] Pierce Chemical Co., Rockford, Ill.
[8] Hewlett-Packard model 5830A.
[9] Hewlett-Packard model 5710 coupled to a Hewlett-Packard quadrupole mass spectrometer (model 5981A) and a model 5934A data system.
[10] Coutts, Baker, Pasutto, Liu, LeGatt, and Prelusky, Biomed. Mass Spectrum, in press.

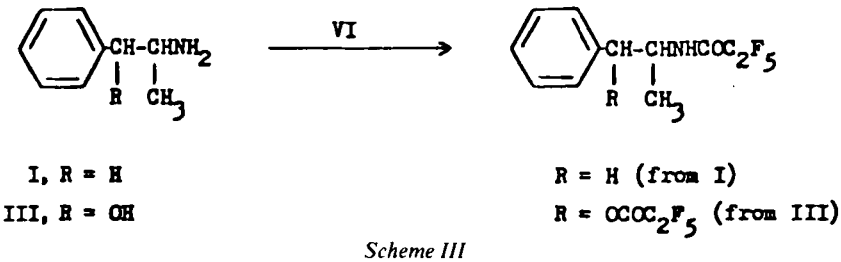

Scheme III

rivatized products were confirmed by mass spectrometric analysis. Calibration plots of the derivatized form of all four amines were constructed using varying quantities of each amine and 2-(*p*-chlorophenyl)ethylamine as internal standard. All plots were linear over a 10–10,000-ng range. The minimal detection level of each amine was 10 ng/g of tissue sample.

The levels of substrates and metabolites found in whole brain tissue after intraperitoneal injection of rats with equimolar quantities of each amine are given in Table I. Levels of I, II, and IV after administration of amphetamine (I) are comparable to values obtained in other studies (2, 4, 5, 19, 20). Rat whole brain levels of III and IV after intraperitoneal injection of norephedrine (III), of *p*-hydroxynorephedrine (IV) after its intraperitoneal injection, and of II and IV after intraperitoneal injection of *p*-hydroxyamphetamine (II) have apparently not been determined previously.

Rat whole brain levels of *p*-hydroxyamphetamine (II) (114.1 ng/g), resulting from the administration of amphetamine (I) were significantly higher ($p < 0.025$; Student's t test) than those obtained (74.9 ng/g) when II was injected directly. Thus, even if all the intraperitoneally injected I had been metabolized to II in the liver (and this had not occurred—see Table I), this would not account for the levels of II observed. One possible explanation of these is that *p*-hydroxylation of I to II occurs in the rat brain to an appreciable extent. Similar results were observed when norephedrine (III) was the substrate. Although 80.9 ng/g of *p*-hydroxynorephedrine (IV) was measured in brain tissue after injection of IV, this does not fully account for the significantly higher ($p < 0.01$) brain levels (131.7 ng/g) of IV detected after injection of III.

Attempts to show that norephedrine (III) was an *in vivo* rat brain metabolite of amphetamine (I) were unsuccessful. If any III was so formed, it was in an amount which was below the detection limit of the assay (10 ng/g). This failure to detect III in rat tissues after intraperitoneal injection of I agrees with previous reports (6, 9, 15). In contrast, Lewander (2) detected [^{14}C]III in rat brain after injection of [^{14}C]I, although the levels measured (<10 ng/g of tissue) were below the detection limits of most other analytical procedures. Kuhn *et al.* (9) found appreciable amounts of III in brain following the intracisternal injection of amphetamine (I).

In vitro studies using rat brain 10,000×*g* homogenate supernatant confirmed that both *p*- and β-hydroxylating enzymes are present in brain tissue (Table II). Metabolism of amphetamine (I) (1.0 μmol) produced trace amounts of II (0.744 nmol) and IV (0.498 nmol), but no norephedrine (III). The incubation of III (1.0 μmol) similarly produced IV (0.789 nmol); conversion of II (1.0 μmol) to IV (1.117 nmol) was also demonstrated. These metabolic conversions were not observed *in vitro* in the absence of brain homogenate supernatant.

CONCLUSIONS

A sensitive analytical procedure has been developed that permits extraction and analysis of amphetamine, norephedrine, and their *p*-hydroxylated metabolites from rat brain. The phenolic metabolites are derivatized by a combination of aqueous acetylation, specific basic hydrolysis of phenolic acetyl groups, and perfluoroacylation under anhydrous conditions. The procedure permits the analysis of *p*-hydroxyamphetamine and *p*-hydroxynorephedrine without interference from amphetamine or norephedrine; this is particularly important in the study reported here, since in the *in vitro* investigation concentrations of the parent compounds were many times higher than those of the metabolites. The results obtained with this procedure suggest that (*a*) both amphetamine (I) and norephedrine (III) are *p*-hydroxylated to some extent in rat brain, both *in vivo* and *in vitro*, (*b*) *p*-hydroxyamphetamine (II) undergoes intracerebral conversion to *p*-hydroxynorephedrine (IV), and (*c*) norephedrine (III) could not be detected as either an *in vivo* or an *in vitro* brain metabolite. Thus, the results of this preliminary study suggest that a β-hydroxylation of *p*-hydroxyamphetamine, but not of amphetamine, occurs in rat brain. Factors such as differential metabolism and elimination rates in brain and liver must be considered, and future comprehensive time studies in these two organs may yield additional information on the formation of amphetamine metabolites.

Table I—Rat Whole Brain Levels of Amphetamine (I), Norephedrine (III), *p*-Hydroxyamphetamine (II), and *p*-Hydroxynorephedrine (IV)

Substrate[a]	Metabolite, nmol/g of Brain Tissue[b] I	II	III	IV
I	67.05 ± 4.50 (3)	0.756 ± 0.093 (15)	ND[c] (3)	0.498 ± 0.076 (12)
II	—	0.496 ± 0.074 (13)	—	0.318 ± 0.097 (13)
III	—	—	41.17 ± 4.05 (3)	0.789 ± 0.097 (11)
IV	—	—	—	0.484 ± 0.056 (9)

[a] 74.0 μmol/kg (free base) ip. [b] Mean ± *SD*; number of experiments in parentheses. [c] ND—not detected.

Table II—*In Vitro* Rat Brain Metabolism of Amphetamine (I), *p*-Hydroxyamphetamine (II), and Norephedrine (III)

Substrate[a]	Metabolite, nmol/g of Brain Incubation[b] I	II	III	IV
I	*[c]	0.744 ± 0.121 (10)	ND[d] (5)	0.211 ± 0.050 (10)
II	—	*[c]	—	1.117 ± 0.121 (6)
III	—	—	*[c]	0.533 ± 0.091 (6)

[a] Substrate (1.0 μmol) added as free base. [b] Mean ± *SD*; number of experiments in parentheses. [c] Recovery of substrate not determined. [d] ND—not detected.

REFERENCES

(1) A. Groppetti and E. Costa, *Life Sci.*, **8** (Part I), 653 (1969).

(2) T. Lewander, *Acta Pharmacol. Toxicol.*, **29**, 33 (1971).

(3) F. Cattabeni, G. Racagni, and A. Groppetti, in "Advances in Biochemical Psychopharmacology," Vol. 7, E. Costa and B. Holmstedt, Eds., Raven, New York, N.Y., 1973, p. 45.

(4) A. Jori, and S. Caccia, *J. Pharm. Pharmacol.*, **26**, 746 (1974).

(5) T. J. Danielson and A. A. Boulton, *Eur. J. Pharmacol.*, **37**, 257 (1976).

(6) B. B. Brodie, A. K. Cho, and G. L. Gessa, in "Amphetamines and Related Compounds," E. Costa and S. Garattini, Eds., Raven, New York, N.Y., 1970, p. 217.

(7) E. Costa and A. Groppetti, in "Amphetamines and Related Compounds," E. Costa and S. Garattini, Eds., Raven, New York, N.Y., 1970, p. 231.

(8) T. J. Danielson, E. H. Petrali, and T. B. Wishart, *Life Sci.*, **19**, 1265 (1976).

(9) C. M. Kuhn, S. M. Schanberg, and G. R. Breese, *Biochem. Pharmacol.*, **27**, 343 (1978).

(10) C. M. Kuhn and S. M. Schanberg, *J. Pharmacol. Exp. Ther.*, **207**, 544 (1978).

(11) A. Jori, S. Caccia, A. Guiso, M. Ballabio, and S. Garattini, *Biochem. Pharmacol.*, **28**, 1205 (1979).

(12) J. J. Freeman and F. Sulser, *Neuropharmacol.*, **13**, 1187 (1974).

(13) J. A. Jonsson, *Acta Pharmacol. Toxicol.*, **40**, 517 (1977).

(14) M. Goldstein and J. J. Contrera, *Biochem. Pharmacol.*, **7**, 277 (1961).

(15) M. Goldstein and B. Anagnoste, *Biochim. Biophys. Acta*, **107**, 166 (1965).

(16) R. T. Coutts, G. B. Baker, and D. G. Calverley, *Res. Commun. Chem. Path. Pharmacol.*, **28**, 177 (1980).

(17) G. B. Baker, R. T. Coutts, and D. F. LeGatt, *Biochem. Soc. Trans.*, **8**, 622 (1980).
(18) D. F. LeGatt, G. B. Baker, and R. T. Coutts, *J. Chromatogr.*, **225**, 301 (1981).
(19) G. Belvedere, S. Caccia, A. Frigerio, and A. Jori, *J. Chromatogr.*, **84**, 355 (1973).
(20) G. A. Clay, A. K. Cho, and M. Roberfroid, *Biochem. Pharmacol.*, **20**, 1821 (1971).
(21) R. Modin and M. Johansson, *Acta Pharm. Suec.*, **8**, 561 (1971).

ACKNOWLEDGMENTS

Funds were provided by the Medical Research Council of Canada and the Alberta Heritage Foundation for Medical Research.

Hypolipidemic Activity of 4-Phenyl-5,5-dicarbethoxy-2-pyrrolidinone in Rodents

I. H. HALL ˣ, G. H. COCOLAS, and P. J. VOORSTAD

Received March 11, 1983, from the *School of Pharmacy, University of North Carolina at Chapel Hill, Chapel Hill, NC 27514.* Accepted for publication May 12, 1983.

Abstract □ A series of pyrrolidinones have been reported to possess hypolipidemic activity in mice. The most active agent, 4-phenyl-5-5-dicarbethoxy-2-pyrrolidinone, effectively lowered both serum cholesterol and triglyceride levels at 20–30 mg/kg/d. The agent suppressed liver mitochondrial citrate exchange, phosphatidate phosphohydrolase, and *sn*-glycerol-3-phosphate acyl transferase activities. Lipid content of the liver, small intestine, and serum lipoprotein fractions was reduced by drug treatment, but lipid levels increased in the bile and fecal samples, suggesting the drug accelerated lipid excretion. The mode of action of the pyrrolidinone appears similar to that of the cyclic imides.

Keyphrases □ 4-Phenyl -5,5- dicarbethoxy -2- pyrrolidinone—hypolipidemic activity, rodents □ Hypolipidemic agents—potential, 4-phenyl-5,5-dicarbethoxy-2-pyrrolidinone, rodent screen

A series of substituted 2-pyrrolidinones have previously been examined for hypolipidemic activity in mice and have been observed to be active between 20–30 mg/kg/d. Similarly, types of moieties such as succinimide (1) also have hypolipidemic activity in the dosage range. One particular compound, 4-phenyl-5,5-dicarbethoxy-2-pyrrolidinone (2), demonstrated potent activity and lowered serum cholesterol and triglycerides >40% at 30 mg/kg/d after 16 d. The current study involves the mode of action of 4-phenyl-5,5-dicarbethoxy-2-pyrrolidinone in lowering lipid levels of the body.

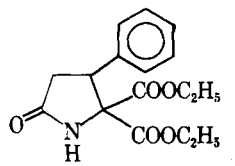

4-Phenyl-5,5-dicarbethoxy-2-pyrrolidinone

EXPERIMENTAL

Antihyperlipidemic Screens in Normal Rodents—4-Phenyl-5,5-dicarbethoxy-2-pyrrolidinone was suspended in 1% aqueous carboxymethylcellulose and administered to male CF_1 mice (~25 g) intraperitoneally for 16 d or male Holtzman rats (~350 g) orally by an intubation needle for 14 d. On days 9 and 14 or 16, blood was obtained by tail vein bleeding, and the serum was separated by centrifugation for 3 min. The serum cholesterol levels were determined by a modification of the Liebermann–Burchard reaction (3). Serum was also collected on day 14 or 16, and the triglyceride content was determined using a commercial kit[1].

Testing in Atherogenic Mice—Male CF_1 mice (~25 g) were placed on a commercial diet[2] which contained butterfat (400 g), cellulose[3] (60 g), cholesterol (53 g), choline dihydrogen citrate (4 g), salt mixture oil[4] (40 g), sodium cholate (20 g), sucrose (223 g), vitamin-free casein (200 g), and total vitamin supplement for 10 d. After the cholesterol and triglyceride levels were assayed and observed to be elevated, the mice were administered the test drug at 20 mg/kg/d ip for an additional 12-d period. Serum cholesterol and triglyceride levels were measured after 12 d of drug administration.

Animal Weights and Food Intake—Periodic animal weights were obtained during the experiments and expressed as a percentage of the animals' weights on day 0. After dosing for 14 d with the test drug, selected organs were excised, trimmed of fat, and weighed.

Toxicity Studies—The acute toxicity (LD_{50} value) (4) was determined in male CF_1 mice by administering the test drug intraperitoneally from 100 mg to 2 g/kg as a single dose. The number of deaths were recorded over a 7-d period for each group.

Enzymatic Studies—*In vitro* enzymatic studies were determined using 10% homogenates of male CF_1 mouse liver with 50–200 μmol of the test drug. *In vivo* enzymatic studies were determined using 10% homogenates of liver obtained from male CF_1 mice after administering the agents for 16 d at a dose ranging from 10 to 60 mg/kg/d ip. The liver homogenates for both *in vitro* and *in vivo* studies were prepared in 0.25 M sucrose plus 0.001 M EDTA.

Acetyl CoA synthetase (5) and ATP-dependent citrate lyase (6) activities were determined spectrophotometrically at 540 nm as the hydroxamate of acetyl CoA formed after 30 min at 37°C. Mitochondrial citrate exchange was determined by the procedure of Robinson *et al.* (7, 8) using sodium [^{14}C]-bicarbonate (41 mCi/mmol) incorporated into mitochondrial [^{14}C]citrate after isolating rat mitochondria (9000×*g* for 10 min) from the homogenates. The exchanges of the [^{14}C]citrate were determined after incubating the mitochondrial fraction, which was loaded with labeled citrate and test drug for 10 min. The radioactivity was then measured in the mitochondrial and supernatant fractions in scintillation fluid[5] and expressed as a percentage. Cholesterol side-chain oxidation was determined by the method of Kritchevsky and Tepper (9) using [26-^{14}C]cholesterol (50 mCi/mmol) and mitochondria isolated from rat liver homogenates. After 18 h of incubation at 37°C with the test drug, the generated $^{14}CO_2$ was trapped in the center well in {2-[2-(*p* - 1,1,3,3-tetramethylbutylcresoxy)ethoxy]ethyl}dimethylbenzylammonium hydroxide[6] and counted[5]. 3-Hydroxy-3-methylglutaryl CoA reductase (HMG CoA reductase) activity was measured using [1-^{14}C]acetate (56 mCi/mmol) and a postmitochondrial supernatant (9000×*g* for 20 min) incubated for 60 min at 37°C (10). The digitonide derivative of cholesterol was isolated and counted (11). Acetyl CoA carboxylase activity was measured by the method of Greenspan and Lowenstein (12). Initially, the enzyme had to be polymerized for 30 min at 37°C and then the assay mixture containing sodium [^{14}C]bicarbonate (41.0 mCi/mmol) was added and incubated for 30 min at 37°C with the test drug. Fatty acid synthetase activity was determined by the method of Brady *et al.* (13) using [2-^{14}C]malonyl CoA (37.5 mCi/mmol), which was incorporated into newly synthesized fatty acids that were extracted

[1] Hycel Triglyceride Test Kit; Fisher.

[2] Basal atherogenic test diet; U.S. Biochemical Corp.
[3] Celufil.
[4] Wesson.
[5] Fisher Scintiverse in a Packard scintillation counter.
[6] Hyamine Hydroxide; New England Nuclear, Boston, Mass.

0022-3549/84/0600-0812$01.00/0
© 1984, American Pharmaceutical Association

(17) G. B. Baker, R. T. Coutts, and D. F. LeGatt, *Biochem. Soc. Trans.*, **8**, 622 (1980).
(18) D. F. LeGatt, G. B. Baker, and R. T. Coutts, *J. Chromatogr.*, **225**, 301 (1981).
(19) G. Belvedere, S. Caccia, A. Frigerio, and A. Jori, *J. Chromatogr.*, **84**, 355 (1973).
(20) G. A. Clay, A. K. Cho, and M. Roberfroid, *Biochem. Pharmacol.*, **20**, 1821 (1971).
(21) R. Modin and M. Johansson, *Acta Pharm. Suec.*, **8**, 561 (1971).

ACKNOWLEDGMENTS

Funds were provided by the Medical Research Council of Canada and the Alberta Heritage Foundation for Medical Research.

Hypolipidemic Activity of 4-Phenyl-5,5-dicarbethoxy-2-pyrrolidinone in Rodents

I. H. HALL ˣ, G. H. COCOLAS, and P. J. VOORSTAD

Received March 11, 1983, from the *School of Pharmacy, University of North Carolina at Chapel Hill, Chapel Hill, NC 27514.* Accepted for publication May 12, 1983.

Abstract □ A series of pyrrolidinones have been reported to possess hypolipidemic activity in mice. The most active agent, 4-phenyl-5-5-dicarbethoxy-2-pyrrolidinone, effectively lowered both serum cholesterol and triglyceride levels at 20–30 mg/kg/d. The agent suppressed liver mitochondrial citrate exchange, phosphatidate phosphohydrolase, and *sn*-glycerol-3-phosphate acyl transferase activities. Lipid content of the liver, small intestine, and serum lipoprotein fractions was reduced by drug treatment, but lipid levels increased in the bile and fecal samples, suggesting the drug accelerated lipid excretion. The mode of action of the pyrrolidinone appears similar to that of the cyclic imides.

Keyphrases □ 4-Phenyl -5,5- dicarbethoxy -2- pyrrolidinone—hypolipidemic activity, rodents □ Hypolipidemic agents—potential, 4-phenyl-5,5-dicarbethoxy-2-pyrrolidinone, rodent screen

A series of substituted 2-pyrrolidinones have previously been examined for hypolipidemic activity in mice and have been observed to be active between 20–30 mg/kg/d. Similarly, types of moieties such as succinimide (1) also have hypolipidemic activity in the dosage range. One particular compound, 4-phenyl-5,5-dicarbethoxy-2-pyrrolidinone (2), demonstrated potent activity and lowered serum cholesterol and triglycerides >40% at 30 mg/kg/d after 16 d. The current study involves the mode of action of 4-phenyl-5,5-dicarbethoxy-2-pyrrolidinone in lowering lipid levels of the body.

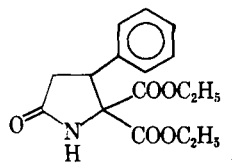

4-Phenyl-5,5-dicarbethoxy-2-pyrrolidinone

EXPERIMENTAL

Antihyperlipidemic Screens in Normal Rodents—4-Phenyl-5,5-dicarbethoxy-2-pyrrolidinone was suspended in 1% aqueous carboxymethylcellulose and administered to male CF_1 mice (~25 g) intraperitoneally for 16 d or male Holtzman rats (~350 g) orally by an intubation needle for 14 d. On days 9 and 14 or 16, blood was obtained by tail vein bleeding, and the serum was separated by centrifugation for 3 min. The serum cholesterol levels were determined by a modification of the Liebermann–Burchard reaction (3). Serum was also collected on day 14 or 16, and the triglyceride content was determined using a commercial kit[1].

Testing in Atherogenic Mice—Male CF_1 mice (~25 g) were placed on a commercial diet[2] which contained butterfat (400 g), cellulose[3] (60 g), cholesterol (53 g), choline dihydrogen citrate (4 g), salt mixture oil[4] (40 g), sodium cholate (20 g), sucrose (223 g), vitamin-free casein (200 g), and total vitamin supplement for 10 d. After the cholesterol and triglyceride levels were assayed and observed to be elevated, the mice were administered the test drug at 20 mg/kg/d ip for an additional 12-d period. Serum cholesterol and triglyceride levels were measured after 12 d of drug administration.

Animal Weights and Food Intake—Periodic animal weights were obtained during the experiments and expressed as a percentage of the animals' weights on day 0. After dosing for 14 d with the test drug, selected organs were excised, trimmed of fat, and weighed.

Toxicity Studies—The acute toxicity (LD_{50} value) (4) was determined in male CF_1 mice by administering the test drug intraperitoneally from 100 mg to 2 g/kg as a single dose. The number of deaths were recorded over a 7-d period for each group.

Enzymatic Studies—*In vitro* enzymatic studies were determined using 10% homogenates of male CF_1 mouse liver with 50–200 μmol of the test drug. *In vivo* enzymatic studies were determined using 10% homogenates of liver obtained from male CF_1 mice after administering the agents for 16 d at a dose ranging from 10 to 60 mg/kg/d ip. The liver homogenates for both *in vitro* and *in vivo* studies were prepared in 0.25 M sucrose plus 0.001 M EDTA.

Acetyl CoA synthetase (5) and ATP-dependent citrate lyase (6) activities were determined spectrophotometrically at 540 nm as the hydroxamate of acetyl CoA formed after 30 min at 37°C. Mitochondrial citrate exchange was determined by the procedure of Robinson *et al.* (7, 8) using sodium [^{14}C]-bicarbonate (41 mCi/mmol) incorporated into mitochondrial [^{14}C]citrate after isolating rat mitochondria (9000×*g* for 10 min) from the homogenates. The exchanges of the [^{14}C]citrate were determined after incubating the mitochondrial fraction, which was loaded with labeled citrate and test drug for 10 min. The radioactivity was then measured in the mitochondrial and supernatant fractions in scintillation fluid[5] and expressed as a percentage. Cholesterol side-chain oxidation was determined by the method of Kritchevsky and Tepper (9) using [26-^{14}C]cholesterol (50 mCi/mmol) and mitochondria isolated from rat liver homogenates. After 18 h of incubation at 37°C with the test drug, the generated $^{14}CO_2$ was trapped in the center well in {2-[2-(*p* - 1,1,3,3-tetramethylbutylcresoxy)ethoxy]ethyl}dimethylbenzylammonium hydroxide[6] and counted[5]. 3-Hydroxy-3-methylglutaryl CoA reductase (HMG CoA reductase) activity was measured using [1-^{14}C]acetate (56 mCi/mmol) and a postmitochondrial supernatant (9000×*g* for 20 min) incubated for 60 min at 37°C (10). The digitonide derivative of cholesterol was isolated and counted (11). Acetyl CoA carboxylase activity was measured by the method of Greenspan and Lowenstein (12). Initially, the enzyme had to be polymerized for 30 min at 37°C and then the assay mixture containing sodium [^{14}C]bicarbonate (41.0 mCi/mmol) was added and incubated for 30 min at 37°C with the test drug. Fatty acid synthetase activity was determined by the method of Brady *et al.* (13) using [2-^{14}C]malonyl CoA (37.5 mCi/mmol), which was incorporated into newly synthesized fatty acids that were extracted

[1] Hycel Triglyceride Test Kit; Fisher.

[2] Basal atherogenic test diet; U.S. Biochemical Corp.
[3] Celufil.
[4] Wesson.
[5] Fisher Scintiverse in a Packard scintillation counter.
[6] Hyamine Hydroxide; New England Nuclear, Boston, Mass.

0022-3549/84/0600-0812$01.00/0
© 1984, American Pharmaceutical Association

Table I—Effects of 4-Phenyl-5,5-dicarbethoxy-2-pyrrolidinone on Serum Lipid Levels in Rodents[a]

Dose, mg/kg/d	Mice			Rats		
	Serum Cholesterol		Serum Triglyceride,	Serum Cholesterol		Serum Triglyceride,
	Day 9	Day 16	Day 16	Day 9	Day 14	Day 14
Control						
(1% carboxymethylcellulose)	100 ± 5[c]	100 ± 6[d]	100 ± 6[e]	100 ± 9[f]	100 ± 7[g]	100 ± 8[h]
10	96 ± 6	50 ± 5[b]	63 ± 5[b]			
20	94 ± 5	58 ± 5[b]	58 ± 4[b]	90 ± 8	60 ± 6[b]	59 ± 5[b]
30	55 ± 6[b]	52 ± 5[b]	48 ± 5[b]			
40	65 ± 6[b]	62 ± 6[b]	65 ± 5[b]			
60	61 ± 4[b]	53 ± 4[b]	68 ± 6[b]			

[a] Expressed as percentage of control (mean ± *SD*); $n = 6$. [b] $p \leq 0.001$. [c] 118 mg%. [d] 122 mg%. [e] 137 mg%. [f] 73 mg%. [g] 78 mg%. [h] 110 mg%.

Table II—Effects of 4-Phenyl-5,5-dicarbethoxy-2-pyrrolidinone on CF_1 Mouse Liver Enzyme Activities *In Vitro*[a]

	Mitochondrial Citrate Exchange	ATP-Dependent Citrate Lyase	Acetyl CoA Synthetase	HMG CoA Reductase	Cholesterol Side-Chain Oxidation
Control					
(1% carboxymethylcellulose)	100 ± 7[c]	100 ± 5[d]	100 ± 7[e]	100 ± 7[f]	100 ± 9[g]
Treated					
0.050 mM	80 ± 6[b]	100 ± 6	95 ± 8	94 ± 7	—
0.100 mM	76 ± 7[b]	98 ± 5	96 ± 7	87 ± 6	56 ± 7[b]
0.200 mM	69 ± 7[b]	97 ± 6	98 ± 7	109 ± 8	—

	Acetyl CoA Carboxylase	Fatty Acid Synthetase	Phosphatidate Phosphohydrolase	*sn*-Glycerol-3-Phosphate Acyl Transferase
Control				
(1% carboxymethylcellulose)	100 ± 7[h]	100 ± 5[i]	100 ± 6[j]	100 ± 6[k]
Treated				
0.050 mM	107 ± 8	100 ± 6	45 ± 4[b]	100 ± 5
0.100 mM	91 ± 7	100 ± 7	43 ± 3[b]	91 ± 6
0.200 mM	111 ± 5	82 ± 5[b]	26 ± 3[b]	69 ± 6[b]

[a] Expressed as percentage of control (mean ± *SD*); $n = 6$. [b] $p \leq 0.001$. [c] 30.8% exchange of mitochondrial citrate. [d] 30.5 mg of citrate hydrolyzed/g wet tissue/20 min. [e] 28.5 mg of acetyl CoA formed/g wet tissue/20 min. [f] 384,900 dpm of cholesterol formed/g wet tissue/60 min. [g] 6080 dpm of CO_2 formed/g wet tissue/18 h. [h] 32,010 dpm/g wet tissue/30 min. [i] 37,656 dpm/g wet tissue/20 min. [j] 16.7 μg Pi/g wet tissue/15 min. [k] 537,800 dpm/g wet tissue/20 min.

with ether and counted[5]. *sn*-Glycerol-3-phosphate acyl transferase activity was determined with L-[2-^{3}H]glycerol-3-phosphate (7.1 Ci/mmol) and the microsomal fraction of the liver homogenates (14). The reaction was terminated after 20 min, and the lipids were extracted with chloroform–methanol (1:2) containing 1% concentrated HCl and counted. Phosphatidate phosphohydrolase activity was measured as the inorganic phosphate released after 15 min by the method of Mavis *et al.* (15). The released inorganic phosphate after development with ascorbic acid and ammonium molybdate was determined at 820 nm.

Liver, Small Intestine, and Fecal Lipid Extraction—In male CF_1 mice that had been administered the test drug for 16 d, the liver, small intestine, and fecal materials (24-h collection) were removed and a 10% homogenate in 0.25 M sucrose–0.001 M EDTA was prepared. A 2-mL aliquot of the homogenate was extracted by the methods of Folch *et al.* (16) and Bligh and Dyer (17), and the number of milligrams of lipid was determined. The lipid was taken up in dichloromethane and cholesterol level (3), triglyceride levels[7], neutral lipid (18), and phospholipid content (19) were determined.

[^{3}H]Cholesterol Distribution in Rats—Male Holtzman rats (~350 g) were administered the test agent orally for 14 d. On day 13, 10 μCi of [^{3}H]cholesterol was administered intraperitoneally in mice and orally in rats, and feces were collected after 24 h. Twenty-four hours after cholesterol administration, the major organs were excised and samples of blood, chyme, and urine were obtained. Homogenates (10%) were prepared of the tissues, which were combusted[8] and counted[5]. Some tissue samples were plated on filter paper[9], dried, and digested for 24 h in base[6] at 40°C and counted[5]. Results were expressed as dpm per total organ.

Cholesterol Absorption Study—Male Holtzman rats (~400 g) were administered the test drug intraperitoneally for 14 d at 20 mg/kg/d. On day 13, 10 μCi of [1,2-^{3}H]cholesterol (40.7 mCi/mmol) was administered to the rat orally. Twenty-four hours later, the blood was collected and the serum separated by centrifugation (20). Both the serum and the precipitate were counted[5].

Bile Cannulation Study—Male Holtzman rats (~400 g) were treated with the test drug at 20 mg/kg/d orally for 14 d. The rats were anesthetized with chlorpromazine[10] (25 mg/kg ip) followed after 30 min by pentobarbital[11] (22 mg/kg ip). The duodenal section of the small intestine was isolated, and ligatures were placed around the pyloric sphincter and distally to a site approximately one-third down the duodenum. Sterile isotonic saline was injected into the sectioned-off duodenal segment. The saline expanded the duodenum and the common bile duct. Once the bile duct was identified, a loose ligature was placed around it, an incision was made, and plastic tubing[12] was introduced into the duct. Once past the ligature, the tubing was tied in place, and the ligatures around the duodenum were removed. Once bile was freely moving down the cannulated tube, [1,2-^{3}H]cholesterol (40.7 mCi/mmol) was injected subcutaneously into the rats. The bile was collected over the next 6 h and the volume was measured. Aliquots were counted[5] as well as analyzed for cholesterol (3), neutral lipid (18), and phospholipid (19) content[13].

Plasma Lipoprotein Fractions—Male Holtzman rats (~400 g) were administered the test drug at 20 mg/kg/d for 14 d. On day 14, blood was collected from the abdominal aorta. The serum was separated from whole blood by centrifugation at 3500 rpm. Aliquots (3 mL) were separated by density gradient ultracentrifugation according to the method of Hatch and Lees (21) and Havel *et al.* (22) into the chylomicrons and very low-density, high-density, and low-density lipoproteins. Each fraction was analyzed for cholesterol (3), triglycerides[7], neutral lipids (18), phospholipids (19), and protein levels (23).

RESULTS

Data are expressed in the tables as mean percent of control ± *SD*. The probable significant level (p) between each test group and the control group was determined by the Student's t test.

[7] Bio-Dynamics/bmc Triglyceride Kit.
[8] Packard Tissue Oxidizer.
[9] Whatman No. 1.

[10] Thorazine, chlorpromazine hydrochloride; Smith, Kline & French Laboratories.
[11] Nembutal, sodium pentobarbital; Abbott Laboratories.
[12] PE-10 Intramedic Polyethylene Tubing.
[13] In the first hour chlorpromazine decreases bile flow, while pentobarbital increases the flow. Neither agent interferes with lipid assay methods.

Table III—Effects of 4-Phenyl-5,5-dicarbethoxy-2-pyrrolidinone on CF_1 Mouse Liver Enzyme Activities *In Vivo*[a]

	ATP-Dependent Citrate Lyase	Acetyl CoA Synthetase	HMG CoA Reductase
Control (1% carboxymethylcellulose)	100 ± 8	100 ± 6	100 ± 7
Treated			
10 mg/kg/d	96 ± 7	78 ± 7	100 ± 8
20 mg/kg/d	94 ± 8	114 ± 8	94 ± 7
40 mg/kg/d	90 ± 7	94 ± 6	84 ± 6[c]
60 mg/kg/d	87 ± 7	68 ± 5[b]	83 ± 6[c]

	Acetyl CoA Carboxylase	Fatty Acid Synthetase	Phosphatidate Phosphohydrolase	*sn*-Glycerol-3-Phosphate Acyl Transferase
Control (1% carboxymethylcellulose)	100 ± 8	100 ± 6	100 ± 6	100 ± 7
Treated				
10 mg/kg/d	109 ± 7	105 ± 7	100 ± 6	81 ± 6[b]
20 mg/kg/d	76 ± 6[b]	115 ± 7[c]	98 ± 6	79 ± 5[b]
40 mg/kg/d	84 ± 6[c]	92 ± 6	43 ± 4[b]	77 ± 4[b]
60 mg/kg/d	93 ± 7	100 ± 6	59 ± 5[b]	52 ± 6[b]

[a] Expressed as percentage of control (mean ± *SD*); $n = 6$. [b] $p \leq 0.001$. [c] $p \leq 0.010$.

Table IV—Effects of 4-Phenyl-5,5-dicarbethoxy-2-pyrrolidinone on Holtzman Rat Organ Lipid Levels[a]

	Lipid Extracted, mg	Cholesterol	Triglycerides	Neutral Lipids	Phospholipids	Protein
Liver						
Control	100 ± 7	100 ± 8[d]	100 ± 5[e]	100 ± 8[f]	100 ± 7[g]	100 ± 6[h]
Treated	76 ± 6[b]	73 ± 7[b]	71 ± 5[b]	45 ± 5[b]	76 ± 6[b]	97 ± 6
Small Intestine						
Control	100 ± 5	100 ± 7[i]	100 ± 6[j]	100 ± 7[k]	100 ± 8[l]	100 ± 8[m]
Treated	71 ± 6[b]	88 ± 7	20 ± 3[b]	63 ± 6[b]	98 ± 9	102 ± 7
Feces						
Control	100 ± 8	100 ± 6[n]	100 ± 7[o]	100 ± 6[p]	100 ± 7[q]	100 ± 5[r]
Treated	111 ± 7	117 ± 7[c]	137 ± 6[b]	109 ± 7	79 ± 6[b]	88 ± 6
Bile						
Control	—	100 ± 8[s]	100 ± 7[t]	100 ± 7[u]	100 ± 8[v]	—
Treated	—	112 ± 9	80 ± 6[b]	133 ± 8[b]	121 ± 5[b]	—
Lipoproteins						
Chylomicrons						
Control	—	100 ± 6[w]	100 ± 7[x]	100 ± 6[y]	100 ± 8[z]	100 ± 8[aa]
Treated	—	57 ± 4[b]	75 ± 5[b]	60 ± 5[b]	143 ± 5[b]	93 ± 7
Very-low density lipoproteins						
Control	—	100 ± 7[bb]	100 ± 6[cc]	100 ± 7[dd]	100 ± 8[ee]	100 ± 8[ff]
Treated	—	71 ± 6[b]	65 ± 5[b]	53 ± 4[b]	118 ± 7[c]	105 ± 6
Low-density lipoproteins						
Control	—	100 ± 8[gg]	100 ± 7[hh]	100 ± 7[ii]	100 ± 6[jj]	100 ± 9[kk]
Treated	—	63 ± 5[b]	86 ± 6[c]	41 ± 3[b]	128 ± 7	87 ± 7
High-density lipoproteins						
Control	—	100 ± 6[ll]	100 ± 7[mm]	100 ± 6[nn]	100 ± 8[oo]	100 ± 6[pp]
Treated	—	66 ± 7[b]	100 ± 8	93 ■ 7	103 ± 6	92 ± 7

[a] Expressed as percentage of control (mean ± *SD*); $n = 6$. [b] $p \leq 0.001$. [c] $p \leq 0.010$. [d] 24.03 mg of cholesterol/g tissue. [e] 44.11 mg of neutral lipid/g tissue. [f] 6.37 mg of triglyceride/g tissue. [g] 7.19 mg. [h] 4.5 mg of protein/g wet tissue. [i] 7.82 mg/g. [j] 6.98 mg/g. [k] 1.12 mg/g. [l] 2.06 mg/g. [m] 42 mg/g. [n] 28.47 mg/g. [o] 33.94 mg/g. [p] 1.86 mg/g. [q] 1.39 kg/g. [r] 6.99 mg/g. [s] 118 mg%. [t] 5 mg/dL. [u] 170 mg/mL. [v] 1.75 mg/mL. [w] 337 μg/ml. [x] 67 mg/mL. [y] 420 μg/mL. [z] 149 μg/mL. [aa] 3 μg/mL. [bb] 190 μg/mL. [cc] 98 μg/mL. [dd] 22 μg/mL. [ee] 26 μg/mL. [ff] 50 μg/mL. [gg] 210 μg/mL. [hh] 10 μg/mL. [ii] 45 μg/mL. [jj] 41 μg/mL. [kk] 0.681 μg/mL. [ll] 544 μg/mL. [mm] 620 μg/mL. [nn] 27 μg/mL. [oo] 153 μg/mL. [pp] 5.677 μg/mL.

4-Phenyl-5,5-dicarbethoxy-2-pyrrolidinone proved to be a potent hypolipidemic agent in both mice and rats by the oral route as well as intraperitoneally (Table I). A dose-response curve showed that cholesterol levels were lowered approximately the same, 47–50%, at 10, 30, and 60 mg/kg/d. Serum triglyceride levels were reduced 52% maximally at 30 mg/kg/d in mice. In rats the serum cholesterol and triglyceride levels were approximately the same at 20 mg/kg/d as those observed in mice. After inducing a hyperlipidemic state in mice, in which case serum cholesterol levels were elevated 183% (354 mg%) above control values (125 mg%), drug treatment at 20 mg/kg reduced serum cholesterol to 184 mg%, 47% above normal. Serum triglyceride levels in the hyperlipidemic mice were elevated 168% (367 mg/dL) above control values. Drug administration lowered triglycerides to 176 mg/dL, which was 28% above normal triglyceride values (138 mg/dL).

In vitro enzyme assays (Table II) showed that the presence of the drug caused a decrease in mitochondrial citrate exchange to the cytoplasm, with 200 μM resulting in a 31% reduction. Cholesterol side-chain oxidation was reduced 44% at 100 μM. Phosphatidate phosphohydrolase activity was suppressed in a dose-dependent manner, with 200 μM resulting in 74% inhibition. *sn*-Glycerol-3-phosphate activity was lowered 31% at 200 μM.

In the *in vivo* enzymatic studies (Table III), marginal inhibition was observed in ATP-dependent citrate lyase at 60 mg/kg (13%) and in acetyl CoA synthetase at 10 (22%) and 60 mg/kg (32%). HMG CoA reductase activity was slightly inhibited at 40 and 60 mg/kg by 16–17%. Acetyl CoA carboxylase activity was suppressed 16% at 40 mg/kg/d. The maximum effect of the drug appeared to be on phosphatidate phosphohydrolase and *sn*-glycerol-3-phosphate acyl transferase activities. 4-Phenyl-5,5-dicarbethoxy-2-pyrrolidinone reduced phosphatidate phosphohydrolase activity 57% at 40 mg/kg/d and 41% at 60 mg/kg/d. *sn*-Glycerol-3-phosphate acyl transferase activity was reduced in a dose-dependent manner, with 60 mg/kg/d causing 48% reduction.

In an attempt to determine if the lipids were being removed from the blood compartment and being deposited in the tissues, the liver and small intestine were examined for lipid content after drug treatment (Table IV). In the liver, cholesterol was lowered 27%, triglycerides 29%, neutral lipids 45%, and phospholipids 24%. In the small intestine, cholesterol levels were reduced 12%; however, marked reduction of triglyceride levels was evident (80%). The drug treatment did not affect [^{3}H]cholesterol absorption from the intestine over a 24-h period after oral administration. Nevertheless, biliary excretion of lipids

Table V—Effects of 4-Phenyl-5,5-dicarbethoxy-2-pyrrolidinone on Rat [^{3}H]Cholesterol Distribution 24-h After Administration and Organ Weights After 14 d of Administration Orally

	Organ Weight, g		[^{3}H]Cholesterol/Total Organ, dpm	
	Control	Treated	Control	Treated
Brain	1.97	1.97	5877	1232
Lung	2.60	1.70	7069	3632
Heart	1.33	1.20	4004	1280
Liver	14.47	12.67	47429	25328
Kidney	3.37	3.13	8170	2592
Spleen	0.67	0.77	2315	2633
Adrenal	0.0504	0.050	—	—
Stomach	2.97	2.43	11375	1440
Small intestine	10.17	6.33	41656	73152
Large intestine	4.10	3.57	14104	10832
Chyme	2.57	7.58	9226	30048
Feces	2.63	5.03	8349	9664

was altered by drug treatment. Cholesterol excretion was elevated 12%, neutral lipids 37%, and phospholipids 21%. The fecal sample also demonstrated increases in lipid content, *i.e.*, 17% and 37% increases in cholesterol and triglycerides, respectively, and a 21% reduction in phospholipids.

Examination of the lipoprotein fractions of the blood showed reduction of cholesterol content in all four fractions. Triglycerides were lowered in chylomicrons and in the very low-density fraction, which contain most of the triglyceride content of the lipoprotein fractions. Neutral lipids were also lowered in the chylomicron, very low-, and low-density lipoprotein fractions. Phospholipid content was elevated in these three fractions. Examination of the effects of drug treatment on [^{3}H]cholesterol distribution in the body shows that there is a reduction of cholesterol in the brain, lung, heart, liver, kidney, and stomach (Table V). However, high concentrations of labeled material were found in the small intestine (76%), chyme (226%), and feces (16%). The organ weights of the treated animals were lower than those of the control animals. The LD_{50} in mice was >2 g/kg ip.

DISCUSSION

4-Phenyl-5,5-dicarbethoxy-2-pyrrolidinone proved to be a potent hypolipidemic agent, lowering serum cholesterol and triglyceride levels >45%. The agent was more active than clofibrate, which is inactive at 10–60 mg/kg/d. Clofibrate requires dosages of 150–200 mg/kg/d to reduce cholesterol ~15% and triglyceride levels 25%. The pyrrolidinone was active in the dosage range where succinimide (1) had proven to be active as well as the cyclic imide, phthalimide, saccharin, and 1,8-naphthalimide (24). In fact, its mode of action of lowering serum lipids seems to be similar to the cyclic imides. For example, inhibition of mitochondrial citrate exchange would lower the cytoplasmic levels of acetyl CoA, a key intermediate precursor in the *de novo* synthesis of cholesterol and fatty acids. Two regulatory enzymes of the triglyceride pathway, phosphatidate phosphohydrolase and *sn*-glycerol-3-phosphate acyl transferase activities, were inhibited by the pyrrolidinones as well as the cyclic imides. Positive correlations between the inhibition of the activities of these enzymes with the lowering of serum triglyceride levels have been made previously (14).

Removal of lipids from the blood was not related to an increase in organ lipids. Three observations support this thesis: (*a*) the lipid content of liver and small intestine was actually reduced; (*b*) there was no increase in organ weights over the control values; (*c*) the [^{3}H]cholesterol content was lower in the major organs of the treated animals compared with the control animals.

The lipids appeared to be excreted in the bile at an accelerated rate after drug treatment. This excretion of [^{3}H]cholesterol was also reflected in the higher radioactive content observed in the small intestine, chyme, and feces. Similar observations have been made with phthalimide and saccharin (25).

Cholesterol, triglycerides, and neutral lipid content of rat serum lipoprotein fractions were also lowered by treatment with the pyrrolidinones. Cholesterol content probably did not change when examining the high-density to low-density ratio. High cholesterol in the high-density lipoprotein fraction and low content in the low-density lipoprotein supposedly protects against myocardial infarction. Nevertheless, lowering the cholesterol content of the low-density lipoprotein fraction is probably beneficial since this is the lipoprotein fraction which deposits lipids in the atherosclerotic plaque. These preliminary studies do suggest that pyrrolidinones may have potential as hypolipidemic agents and are worthy of further study.

REFERENCES

(1) I. H. Hall, J. M. Chapman, Jr., and G. H. Cocolas, *J. Pharm. Sci.*, **70**, 326 (1981).

(2) G. H. Cocolas, J. M. Chapman, Jr., P. J. Voorstad, and I. H. Hall, *J. Pharm. Sci.*, **72**, 812 (1983).

(3) A. T. Ness, J. V. Pastewka, and A. C. Peacock, *Clin. Chim. Acta*, **10**, 229 (1964).

(4) J. T. Litchfield, Jr. and F. Wilcoxon, *J. Pharmacol. Exp. Ther.*, **96**, 99 (1949).

(5) A. G. Goodridge, *J. Biol. Chem.*, **248**, 4218 (1973).

(6) M. Hoffman, L. Weiss, and O. H. Wieland, *Anal. Biochem.*, **84**, 441 (1978).

(7) B. H. Robinson, G. R. Williams, M. L. Halperin, and C. C. Leznoff, *Eur. J. Biochem.*, **15**, 263 (1970).

(8) B. H. Robinson and G. R. Williams, *Biochim. Biophys. Acta*, **216**, 63 (1970).

(9) D. Kritchevsky and S. A. Tepper, *Atherosclerosis*, **18**, 93 (1973).

(10) G. T. Haven, J. R. Krzemien, and T. T. Nguyen, *Res. Commun. Chem. Pathol. Pharmacol.*, **6**, 253 (1973).

(11) F. Wada, K. Hirata and Y. Sakameto, *J. Biochem. (Tokyo)*, **65**, 71 (1969).

(12) M. D. Greenspan and J. M. Lowenstein, *J. Biol. Chem.*, **243**, 6273 (1968).

(13) R. O. Brady, R. M. Bradley, and E. G. Trams, *J. Biol. Chem.*, **235**, 3093 (1960).

(14) R. G. Lamb, S. D. Wyrick, and C. Piantadosi, *Atherosclerosis*, **27**, 147 (1977).

(15) R. D. Mavis, J. N. Finkelstein, and B. P. Hall, *J. Lipid. Res.*, **19**, 467 (1978).

(16) J. Folch, M. Lees, and G. H. C. Stanley, *J. Biol. Chem.*, **266**, 497 (1957).

(17) E. G. Bligh and W. J. Dyer, *Can. J. Biochem. Physiol.*, **37**, 911 (1957).

(18) J. H. Bragdon, *J. Biol. Chem.*, **190**, 513 (1951).

(19) C. P. Stewart and E. B. Henday, *Biochem. J.*, **29**, 1683 (1935).

(20) A. Adam, J. van Cantfort, and J. Gielen, *Lipids*, **11**, 610 (1976).

(21) F. T. Hatch and R. S. Lees, *Adv. Lipid Res.*, **6**, 33 (1968).

(22) R. J. Havel, H. A. Eder, and J. H. Bragdon, *J. Clin. Invest.*, **34**, 1395 (1955).

(23) O. H. Lowry, N. J. Rosebrough, A. L. Farr, and R. J. Randall, *J. Biol. Chem.*, **193**, 265 (1951).

(24) I. H. Hall, J. M. Chapman, Jr., P. J. Voorstad, and G. H. Cocolas, *J. Pharm. Sci.*, **72**, 845 (1983).

(25) I. H. Hall, P. J. Voorstad, J. M. Chapman, Jr., and G. H. Cocolas, *J. Pharm. Sci.*, **72**, 1192 (1983).

ACKNOWLEDGMENTS

Financially supported by National Heart, Lung, and Blood Institute Grant 2 R01 HL25680.

We thank Michelle Tousignant, Martha Pullium, and Macdonald Bowden for their technical assistance.

Novel Device for Quantitatively Collecting Small Volumes of Urine from Laboratory Rats

ANDRE J. JACKSON *x and JOHN C. SUTHERLAND‡

Received November 5, 1982, from the *Department of Pharmaceutics, School of Pharmacy and the ‡ University of Maryland Cancer Center, University of Maryland, Baltimore, MD 21201. Accepted for publication May 26, 1983.

Abstract □ A reusable urinary collection device suitable for quantitative collection of uncontaminated urinary samples from rats without using a metabolism cage has been designed. The device can be attached to the pelvic skin within 5 min with minimum handling and discomfort to the unanesthetized rat using an adhesive. The suitability of this device was investigated by collecting and analyzing urine over a 48-h period following the intraperitoneal injection of [^{14}C]inulin. A two-way crossover study was done with samples from one of the two experiments being collected while the animal was housed in a commercially available metabolism cage equipped to separate urine and feces. The percent of the dose excreted, food and water consumption, and the urinary output were not statistically different for rats housed in the metabolism cages or with the collection device attached. Histopathological examination of the rats revealed no pathology after a 24-h period except minor skin inflammation which occurred both in controls and animals to which the device was attached. These studies demonstrate the comparability of the new urine collection device to a commercially available metabolism cage in the quantitative collection of small (0–7 mL) urine samples with less contamination of the samples from the environment.

Keyphrases □ Urine collection—quantitative, rats, reusable device, comparison with metabolism cages

The preclinical evaluation of a drug requires that the acute and chronic toxicity, metabolic pattern, and bioavailability be evaluated in animal species. Two of the primary species utilized in preclinical screening are rats and mice. These species have proven useful because of their low cost, minimal holding space, relatively short life span, and defined genetic lineage. Several recent reports have presented data related to the bioavailability of drugs in rats and mice comparing gavage with administration in the diet (1, 2).

Despite the reported results, a major concern in these and other studies that require analysis of urinary and fecal data is the possible contact and resultant contamination of these excreta by each other or by the environment. A new commercially available cage[1] has made progress in this area, but it still cannot completely eliminate contamination of urine by either animal fur-containing food particles or contact between urine and feces, especially if the animal has diarrhea.

There are currently several modified metabolism units which have been presented in the literature (3, 4). The general approach to the construction of these units has been to place the animal in a cage with a stainless steel floor and then, utilizing either another screen of smaller mesh or a funnel with various designs, to effect the separation and collection of urine and feces. However, flat-bottom and polycarbonate metabolism cages have proven unsatisfactory because of food contamination of urine and contamination of samples for GC analysis by leached plastics following repeated washes of the polycarbonate cage with benzene (3). The modified unit, which is quite similar to those commercially available, still utilizes the same basic principles and in addition has metal in direct contact with the urine prior to collection (3).

A urine-collecting device (patent pending) has been developed in our laboratory that (*a*) prevents contact and assures 100% separation of urine and feces, (*b*) gives a quantitative collection of small (0–7 mL) urine samples comparable with those obtained with a commercially available metabolism cage, (*c*) is devoid of metal in its design, and (*d*) is resistant to organic solvents. The application of this device to the quantitative collection of urine from rats is described in this report.

EXPERIMENTAL

Materials—[Carboxy-^{14}C]inulin[2] had a specific activity of 2.02 μCi/mg. Phosphate-buffered saline contained 92 mM sodium chloride, 23 mM dibasic sodium phosphate, and 11 mM monobasic sodium phosphate. A commercially available metabolism cage[3] was used for comparison to the urine collection device[4].

Urine-Collecting Device Design—A perspective side photograph of a rat with the collection device attached to the pelvic region is presented in Fig. 1. The collection device apparatus is shown schematically in Fig. 2, with portions represented in phantom.

The mounting plate has a projecting funnel which receives the penis of the rat (or urethral region for female animals), with the plate being adhered to the pelvic skin by a quick-drying methylcyanoacrylate adhesive[5]. The mounting plate is made from either acetal resin[6] or acetal resin coated with polymethyl methacrylate[7] with the container being constructed of either material. The urine collector and funnel are separate units joined by screw threads disposed around a cylindrical projection or annulus at the mouth of the funnel. Screw threads couple with screw threads in an opening through the top wall of the container, with the container being essentially a chamber that is vented in the top wall.

To empty the container, a drain is positioned in the end wall. The drain is threaded and plugged with a nylon screw. Urine can be sampled with a syringe or by merely removing the container from the funnel. A metal set screw, which is not in contact with the collecting chamber, is utilized as a detent to keep the longitudinal axes of the container and mounting plate aligned. The set screw is advanced to set in an indentation formed in the bottom surface of the funnel mounting plate. When the screw is advanced to set tightly in the indentation, the container rotates with difficulty about the axis of the funnel. Consequently, the container remains in place and thus eliminates urine loss and the amount of gnawing which the rat can do to the mounting plate.

Attachment of the Urine Collecting Device—The hair was removed from the region around the penis using small animal clippers[8] fitted with a size 40 blade, without the use of soap since surfactants interfere with subsequent bonding of the funnel to the skin. In addition, the abdomen of female animals was shaven using a disposal razor (again without soap). The skin was then cleaned with isopropyl alcohol, and the methyl cyanoacrylate glue was applied as a thin film to the mounting plate to effectively bond it to the skin. Attachment was accomplished by having the rat restrained by hand while the mounting plate was positioned. (During the attachment the animal can be restrained by hand with careful alignment of the penis or urethral opening (female rats) with the funnel opening; contact between the respective urethral opening and the adhesive should be avoided.) Bonding was rapid (1–5 min). Curing occurs best at a relative humidity of 58–68%. Once the plate was firmly attached, the container was screwed onto the funnel.

Although still in place at 24 h, the edges of the mounting plate may not be as securely bonded to the skin due to normal turnover of epidermal cells and the animals tendency to gnaw at this surface, but the device can be rebonded

[1] Nalgene Co., Rochester, N.Y.

[2] Amersham Corp., Arlington Heights, Ill.
[3] Econo; Maryland Plastics Co., Federalsburg, Md.
[4] Jackson and Weems, Assoc., P.O. Box 4407, Alexandria, VA 22303.
[5] Permabond.
[6] Delrin; E. I. DuPont de Nemours & Co.
[7] Plexiglas;
[8] Oster; Scientific Products, Columbia, Md.

0022-3549/84/0600-0816$01.00/0
© 1984, American Pharmaceutical Association

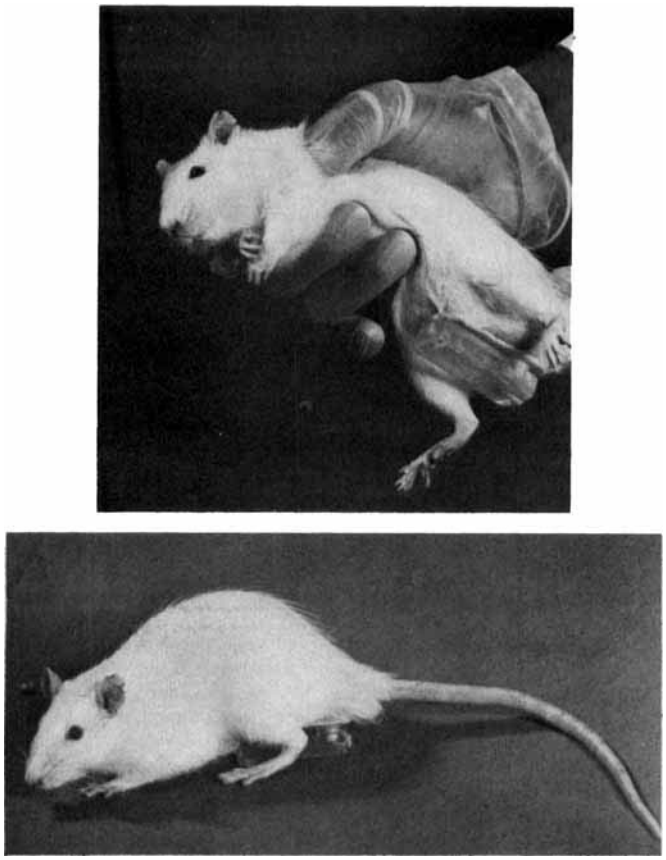

Figure 1—*Photographs (lateral and ventral views) of a rat which has had the urine-collection device attached to the pelvic skin for a 48-h period.*

readily by application of the adhesive to the mounting plate in any exposed area. Although not done in these studies, the animal can be lightly anesthetized with ether and the funnel sutured around the edges after attachment with the glue[9]. Either acetone or nail polish remover can be applied to the skin to remove the device at the termination of the study if only glue is used for attachment. The collection device can also be gently pulled from the abdomen with some minor discomfort to the animal.

Experimental Design—The comparison of the urinary excretion of [^{14}C]inulin administered in phosphate-buffered saline (pH 7.4) to 12 male Dub (SDD) rats[10] was investigated using the metabolism cage and the urine collection device. The animals were divided into three groups (50–200 g; 200–400 g; >400 g) with four animals in each group. A comparative excretion study was also done in eight female rats (four/group) with weights ranging between 50–200 g and 200–400 g. One microcurie of [^{14}C]inulin was administered intraperitoneally (0.5 mL) using a 1-mL plastic syringe fitted with a 27-gauge needle. Animals were housed in a metabolism cage (after being prepared similar to device-carrying rats) or in a regular stainless steel cage while the urinary collection device was attached. Food pellets[11] and distilled water were provided *ad libitum*. Urine was sampled by restraining the rat by hand, removing the drain screw, and collecting the samples using a syringe.

All samples were analyzed by liquid scintillation counting. The collection period for all studies was 48 h with animals randomly receiving either treatment. Following a 7-d washout period, the rats received the other treatment, *i.e.*, those animals that had been housed in metabolism cages had the urine collection device attached while animals that had urine collected with the urine device were housed in metabolism cages for urine collection. Food and water consumption, urinary output, and percent inulin recovered in urine were determined for each collection method at 48 h.

Histopathology—In a separate study using nine male rats (150–550 g) and nine female rats (100–400 g), the attachment area was examined for evidence of pathology. The rats were equally divided into three groups, with the rats in control groups I and II having their pelvic region shaven or shaven with glue (identical lot) applied, respectively. Animals in treatment group III were

[9] Unpublished results.
[10] Flow Laboratories, Dublin, Va.
[11] Lab Chow; Ralston Purina, Richmond, Ind.

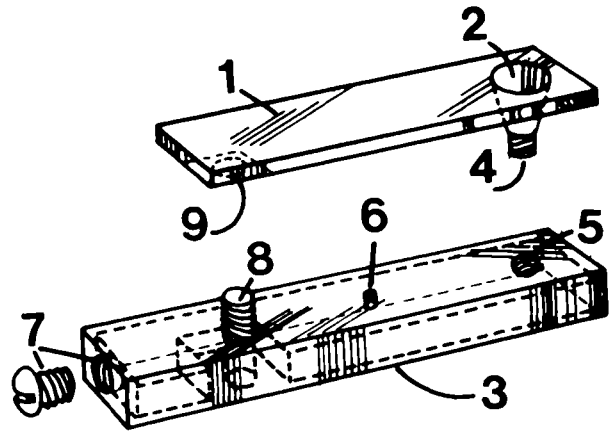

Figure 2—*Representation of the urine-collection device showing the major components. Key: (1) mounting plate; (2) removable funnel; (3) urine container; (4, 5) screwthreads; (6) vent; (7) drain; (8) set screw; (9) indentation.*

shaven with the urine collection device attached for a 24-h period. After 24 h the animals in groups I and II were anesthetized with ether and necropsied. Sections were taken of the skin of the lower abdomen adjacent to the penis, the urinary bladder, and one testicle for male animals. For female animals, the skin adjacent to the urethral opening, vagina, uterus, ovaries, and urinary bladder were evaluated.

Rats from treatment group III were similarly examined following removal of the urine in the urine collection device. Sections of the aforementioned tissues were fixed in 10% formaldehyde, embedded, sectioned, and stained with hematoxylin and eosin for histopathological examination.

RESULTS

Urinary Excretion of Inulin—Data for the urinary collection of [^{14}C]inulin over the 48-h period is presented in Table I. Food and water consumption, urinary volume, and percent inulin recovered were not significantly different for the two methods of urine collection. Urine samples collected with the device were free from contamination, while those collected while the animal was housed in the cage contained elements from the environment such as food, hair, and feces.

Histopathology—*Male Rats*—Intradermal abscesses were observed in the skin from six rats. Four of these animals were controls: one was from control group II, shaven plus adhesive, while the other three were from control group I, in which the animals were only shaven. The abscesses were usually superficial, although a rat from control group II exhibited more extensive abscesses extending into the superficial dermis with a mild infiltration of polymorphonuclear leucocytes into the superficial fat. Such infiltration was also seen in one of the rats carrying the collection device and in one control animal from group II. Inflammation was always localized, never extending beyond the boundaries of the shaved area of skin.

A slight infiltrate of eosinophilic leucocytes was seen in the subcutaneous tissue of the penis for two rats in control group II and one animal in treatment group III. The urinary bladders all appeared normal, except in two of the animals in control group I where there was a small amount of blood in each bladder. The testicles in all animals were unremarkable. Two of the animals that had the collection device attached showed dilated preputial glands, and in one of these animals a plug was found that appeared to be desquamated squamous cells from a preputial gland. These results are summarized in Table II.

Female Rats—No pathological findings were noted in the ovaries or the urinary bladder. The chief findings were those in the skin. Like the male rats, there were epidermal abscesses noted in one rat which was only shaven and in all of those shaven with glue applied and the cup-bearing rats. Inflammation increased, extending into the dermis, for both rats to which glue had been applied and the cup-bearing rats. Also two rats from each of these groups showed abscesses in the dermis. Inflammation continued into the fat for these two groups. Sections of the vaginas showed a few polymorphonuclear leucocytes in the mucosa of all rats. Two rats, both shaven with glue applied, appeared to have long-standing vaginal infections with pus. In the second and third groups (shaven with glue and cup-bearing), there were a few more polymorphonuclear leucocytes in the wall of the vagina as compared with those only shaven.

Eosinophils were found in the wall of all vaginas, with two rats having more

Table I—Food and Water Consumption, Urine Output, and Percent [^{14}C]Inulin Recovered Following Collection of Urine from Rats using the Urine-Collection Device (UCD) or Metabolism Cages [a]

	50–200 g				200–400 g				>400 g [d]	
	Male [b]		Female [c]		Male [c]		Female [c]		Male [c]	
	Cage	UCD	Cage	UCD	Cage	UCD	Cage	UCD	Cage	UCD
Food consumption (g)	40.8 ± 1.1	40.9 ± 1.3	38.7 ± 5.1	36.7 ± 5.3	26.0 ± 8.7	22.7 ± 7.2	35.1 ± 3.2	31.9 ± 8.0	30.6 ± 9.4	27.6 ± 5.1
Water consumption (mL) [e]	79.0 ± 12.7	73.5 ± 9.2	72.7 ± 7.8	70.0 ± 1.09	35.7 ± 9.8	46.7 ± 3.1	71.0 ± 9.2	67.2 ± 12.7	79.0 ± 2.7	90.2 ± 18.4
Urine output (mL)	27.5 ± 3.5	16.0 ± 5.6	25.5 ± 3.8	21.2 ± 2.1	20.5 ± 7.8	15.3 ± 3.2	23.4 ± 1.8	20.0 ± 2.0	29.3 ± 17.5	21.5 ± 7.9
[^{14}C]Inulin recovered, % of dose	89.1 ± 5.9	81.0 ± 1.4	89.3 ± 4.1	91.7 ± 2.14	89.6 ± 9.1	91.2 ± 3.9	87.3 ± 3.7	90.3 ± 2.8	78.8 ± 5.0	85.9 ± 3.4

[a] 48-h collection; all values are mean ± *SD*, $n = 4$. [b] Not statistically different, paired *t* test ($p > 0.20$) for all parameters except urine output and inulin recovery, which were not different at the ($p > 0.10$) level. [c] Not statistically different, paired *t* test ($p > 0.20$). [d] Dub (SDD) female rats do not weigh >400 g. [e] Some of the *SD* values are unusually large because of water loss from the inverted bottle.

eosinophils than the others. One of these was a rat which had been shaven with glue applied and another was a cup-bearing rat. Otherwise, the eosinophilic distribution seemed about equal. Examination of uteri showed eosinophils in the submucosa and muscularis of the uteri of all rats with very little difference between the three groups. A summary of these pathological findings is presented in Table II.

DISCUSSION

The accurate collection and evaluation of data from experimental animals utilized in toxicity feeding, pharmacokinetic, and metabolic studies is essential in the preclinical screening of biologically active drug products. Current methods of collecting urinary samples are somewhat compromised because of the tendency of these samples to become contaminated by the environment. The method presented in this report provides a means of accomplishing this objective with overall rat response similar to that of those housed in a standard metabolism cage. Based on the results of the study, it would appear that the device is well tolerated by laboratory rodents and did not appear to alter their food and water consumption nor their excretion of inulin. The urinary collection device is suitable for male and female rats as evidenced by the results from the current study.

Table II—Number of Rats in which Pathological Abnormalities were Found *versus* the number of Rats Examined

Pathological Observation	Treatment: Shaven Only	Treatment: Shaven Plus Adhesive	Urine Collecting Device Attached
Intraepidermal abscess(es), cup site	4/6	4/6	5/6
Abscess(es) in superficial dermis, cup site	2/6	2/6	5/6
Acute inflammation of dermis, diffuse	4/6	4/6	4/6
Acute inflammation of penile skin	1/3	1/3	2/3
Acute vaginitis	3/3	3/3	3/3
Eosinophilia in skin, cup site	0/6	2/6	1/6

Preparing the abdominal region for device attachment appears to be a limitation, since hair removal of this area with clippers resulted in intradermal abscesses of the abdominal and, in some cases, penile skin. The presence of abcesses in both control and treated groups (male and female) indicates that the preparation of the area was the primary cause, not device attachment. The presence of the mild infiltrate of eosinophilic leucocytes suggested a slight hypersensitivity to the adhesive, which is consistent with the manufacturer's report of a mild irritant effect to the skin from the adhesive. Dilation of the preputial glands (male and female rats) was the only histological observation that was exclusive to device-carrying animals. Therefore, one would conclude that the acute pathology associated with the device is indeed minor.

Because of the limited capacity of this self-contained unit, it will not allow quantitative collection over 24 h without intermittent collections. Nevertheless, judicious utilization of the urine collection device in conjunction with other established methods of rodent urine collection could prove a valuable tool. It would be especially applicable in validating urinary excretion data obtained from rodents by conventional methods during toxicological feeding, pharmacokinetic, or metabolic studies without removing the animals from their normal environment.

REFERENCES

(1) S. M. Singhvi, K. J. Kripalani, A. V. Dean, G. R. Keim, J. S. Kulesza, F. S. Meeker, Jr., J. J. Ross, Jr., J. M. Shaw, and B. H. Migdalof, *J. Pharm. Sci.*, **70**, 885 (1981).

(2) D. R. Van Harken and G. H. Hottendorf, *Toxicol. Appl. Pharmacol.*, **43**, 407 (1978).

(3) J. Bazare, Jr., M. L. Leamons, and J. F. Young, *J. Pharmacol. Meth.*, **5**, 99 (1981).

(4) S. Toon and M. Rowland, *J. Pharmacol. Meth.*, **5**, 321 (1981).

Long-Term Stability of Aqueous Solutions of Luteinizing Hormone-Releasing Hormone Assessed by an *In Vitro* Bioassay and Liquid Chromatography

YI-FAN SHI *, RICHARD J. SHERINS *, DAVID BRIGHTWELL *, JOSEPH F. GALLELLI ‡, and DULAL C. CHATTERJI ‡§x

Received December 13, 1982, from the *Developmental Endocrinology Branch, National Institute of Child Health and Human Development, and the ‡Pharmaceutical Development Service Section, Pharmacy Department, The Clinical Center, National Institutes of Health, Bethesda, MD 20205. Accepted for publication May 20, 1983. §Present address: Research and Development, Lypho-Med Inc., Melrose Park, IL 60160.

Abstract □ The stability of aqueous solutions of luteinizing hormone-releasing hormone (LHRH) after extended storage at various temperatures was investigated using a newly developed HPLC assay and an *in vitro* dispersed pituitary cell culture bioassay. Good correlations were obtained between the potency obtained by HPLC and bioassay in samples stored at 37°C or subjected to different stress conditions. No significant decrease in activity of LHRH was observed in aqueous solutions stored at 37°C for up to 10 weeks, at 4°C for 2 years, or subjected to repeated freezing and thawing for 5 d. Heating to 60°C in sterile pH 9.0 buffer up to 11 d and storage at ambient temperature in nonsterile solution for 4 months produced well-distinguished degradation products and a decrease in potency. It is concluded that sterile aqueous solutions of LHRH are stable for at least 10 weeks at 37°C and, thus, could be reliably used for chronic administration when long-term stability at body temperature is important.

Keyphrases □ Luteinizing hormone-releasing hormone—stability, aqueous solutions, *in vitro* bioassay, HPLC □ Stability—LHRH, aqueous solutions, *in vitro* bioassay, HPLC □ Degradation—LHRH aqueous solutions, *in vitro* bioassay, HPLC

Luteinizing hormone-releasing hormone (LHRH), isolated from porcine hypothalami by Schally *et al.* (1), was found to release both luteinizing hormone and follicle-stimulating hormone from the pituitary of several species, including humans (1, 2). LHRH has recently been found to be clinically useful in stimulating gonadotropin release, testicular development (3–5), and follicular maturation and ovulation (6, 7) in hypogonadotropia in humans, especially when small doses of LHRH are administered chronically by intermittent intravenous injection (8–10) or by a portable infusion pump (11–13).

We have evaluated the stability of LHRH solutions under commonly used storage conditions and after long-term exposure to body temperature (37°C) to determine how long and under what conditions LHRH solutions might be utilized for chronic hormone administration. LHRH activity was assayed by *in vitro* pituicyte bioassay as well as a newly developed HPLC technique.

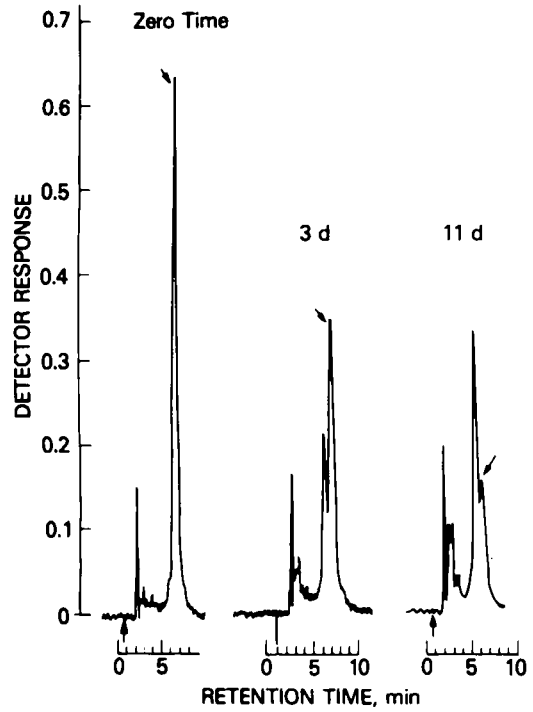

Figure 1—*HPLC profile of LHRH solutions prepared in 0.01 M borate buffer (pH 9.0) kept at 60°C for 0, 3, and 11 d. The arrows indicate intact LHRH peaks.*

EXPERIMENTAL

General Experimental Protocol—Sterile stock solutions of synthetic LHRH[1] were prepared at a concentration of 1 mg/mL in distilled water or 0.01 M borate buffer (pH 9.0). Aliquots (1 mL) of the stock solution were dispensed into 2-mL glass vials and sealed with polytef-lined stoppers. The samples were stored at various temperatures as specified below. At selected time intervals, two individual vials were removed and stored at −20°C for

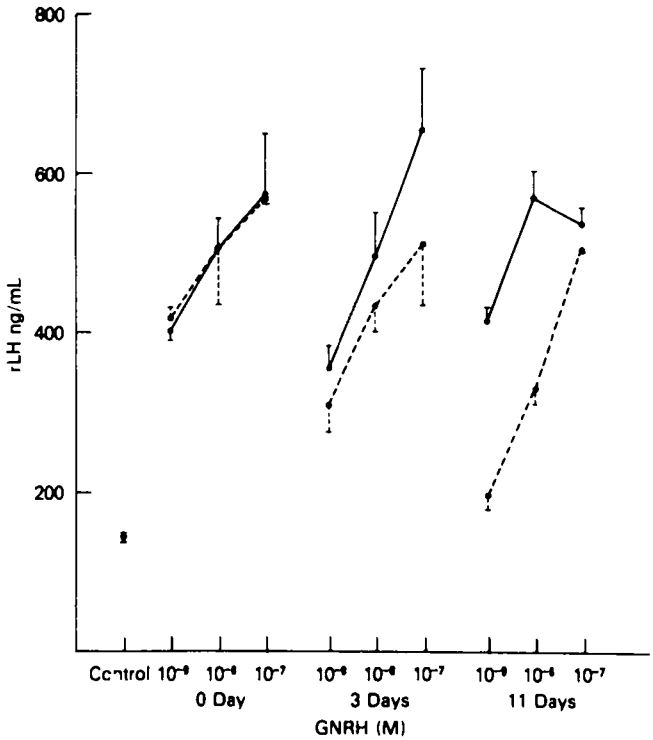

Figure 2—*Luteinizing hormone release from dispersed rat pituitary cells in culture following incubation with LHRH solutions kept at 60°C for 0, 3, and 11 d. Key: (—) in distilled water; (- - -) in buffer (pH 9.0).*

[1] Synthesized by Dr. Erhard Gross at NIH; lot CCD 332 78-135.

0022-3549/84/0600-0819$01.00/0
© 1984, American Pharmaceutical Association

Table I—Stability of LHRH at 60°C

	Day	Potency, % HPLC	Potency, % Bioassay	
	0	100	100	
Distilled water	3	96	118	($p > 0.25$)
	11	96	142	($p > 0.25$)
Buffer pH 9.0	3	40	15	($p < 0.02$)
	11	5	7	($p < 0.01$)

subsequent analysis: one was analyzed by HPLC and the other by an *in vitro* bioassay using dispersed rat anterior pituitary cells in culture. The potency of all treated samples was compared with freshly prepared LHRH solutions.

Experiment 1—To check the specificity of the HPLC analysis, stock solutions of LHRH in distilled water and in borate buffer pH 9.0 were heated to 60 ± 2°C in a constant-temperature oven for 0, 3, and 11 d. The potency of the samples was anlayzed by both HPLC and bioassay.

Experiment 2—To provide a different set of degradation products to test the specificity of HPLC assay, a degraded LHRH solution was prepared by leaving a nonsterile solution of LHRH at ambient temperature for 4 months. Three mixtures of LHRH solutions were then prepared: (A) 90% fresh LHRH + 10% degraded LHRH, (B) 90% fresh LHRH + 10% normal saline, and (C) 100% degraded LHRH solution. Solution B was used as the control sample.

Experiment 3—To determine the long-term stability at body temperature, stock LHRH solutions in distilled water were kept at 37 ± 0.1°C in a constant-temperature water bath, and the activity of LHRH was assayed by HPLC and pituitary cell culture. Samples were incubated for 0, 4, 6, and 10 weeks in the first experiment and for 0, 10, and 27 weeks in a second study.

Experiment 4—To obtain the long-term shelf life, sterile solutions of LHRH were stored for 2 years at 4°C. The LHRH potency was determined by the HPLC method alone.

Experiment 5—To evaluate the effect of accidental freezing and thawing, one set of samples was stored at −20°C in a freezer but subjected to a 1-h thaw at room temperature every day for 5 d. The potency of the frozen and thawed samples was compared with the original control vials, which remained frozen until HPLC assay.

Liquid Chromatographic Assay of the LHRH Solution— HPLC was performed on a 25 cm × 4-6 mm i.d. reverse-phase column[2] using a liquid chromatograph[3] equipped with a variable-wavelength detector[4] and a fixed-volume injector[5]. A mobile phase of acetonitrile–acetic acid–sodium hexylsulfonate–water (35:0.1:0.2:64.7) at a flow rate of 1.6 mL/min was used as the eluant. Retention time of LHRH was 6.0 min under these conditions.

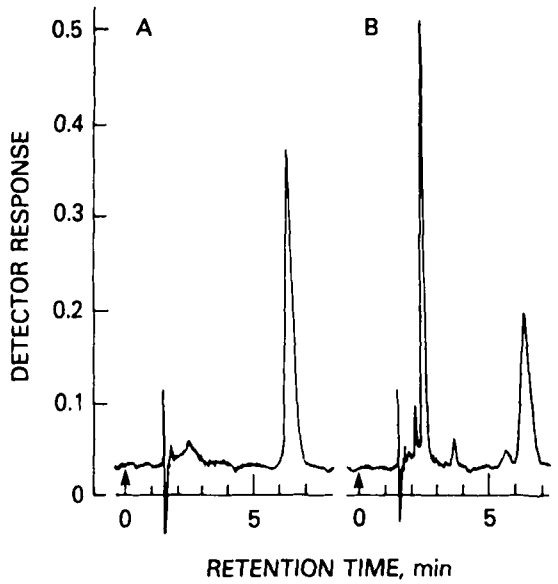

Figure 3—*HPLC profile of nonsterile LHRH solutions stored at ambient temperature. Key: (A) time zero; (B) 4 months.*

[2] Zorbax-C8; DuPont Instruments, Wilmington, Del.
[3] Model 3500 B; Spectra-Physics, Santa Clara, Calif.
[4] S.F. 770; Schoeffel Instruments, Western, N.J.
[5] Velco, Houston, Tex.

Table II—Specificity of the HPLC Assay

Solution	Potency, % HPLC	Potency, % Bioassay	
A	106	106	($p > 0.25$)
B	100	100	($p < 0.001$)
C	55	31	

Testosterone, which was used as internal standard in a few runs to check the quantitation accuracy, had a retention time of 11.5 min. The wavelength for quantitation was 220 nm.

Solutions of LHRH were diluted quantitatively to 20 μg/mL, and 50 μL of this solution was injected using the fixed-loop injector. Testosterone, when added to check the accuracy, was added at a concentration of 10 μg/mL in the mobile phase used for dilution of stock LHRH solutions. Either the peak height of LHRH or peak height ratio of LHRH to testosterone was used for quantitation. The potency of the treated samples was compared with the freshly prepared samples.

Bioassay of the LHRH Solutions—The bioactivity of LHRH was assessed by quantitating the release of luteinizing hormone into the media of dispersed rat anterior pituitary cells placed into short-term monolayer culture according to the method of Vale *et al.* (14). The control and experimental LHRH samples were added to the cell culture in the dose range of 10^{-7}–10^{-10} M for 3 h, and the medium was then aspirated, centrifuged to remove any suspended cells, and the luteinizing hormone concentration was measured by double-antibody RIA using LHRH-1 as standard (15). Reagents were provided by the NIAMDDK National Hormone and Pituitary Program. All samples from one experiment were measured individually in duplicate in a single assay to eliminate between-assay variation. The assay detection limit was 2 ng/mL.

Statistical Analysis—All bioassay results are presented as the mean ± *SEM*. Potency estimates were determined within each cell culture experiment relative to the LHRH stock solution prepared on day 0. Each LHRH dose-response curve was first tested for linearity (*t* test) and then for parallelism (*F* test) to the control curve prior to the estimation of potency. The relative precision (x) for symmetrical experimental designs was determined according to the method of Finney (16).

RESULTS AND DISCUSSION

Specificity of the Liquid Chromatographic Method and Its Correlation with the Bioassay—The HPLC method gave sharp and reproducible peaks for LHRH, and the height of the LHRH peak was directly proportional to the concentration of LHRH in a series of freshly prepared solutions. The HPLC profile of LHRH in borate buffer pH 9.0 heated to 60°C showed a degradation product peak which was well separated from the intact LHRH peak (arrow, Fig. 1). The small shoulder (corresponding to the retention time of the degradation product) in the time-zero sample in Fig. 1 is, however, attributible to a chromatographic artifact. Purity of the LHRH peak was verified by comparison of the retention times and peak height ratios at 210, 220, and 230 nm of the sample peaks to those from a freshly prepared solution of LHRH. Solutions of LHRH in distilled water were stable after being heated to 60°C for up to 11 d. By contrast, significant loss of integrity was observed at pH 9.0 during the same time interval. The results of the HPLC assay correlated well with those obtained by bioassay (Fig. 2, Table I). The potency of the mild

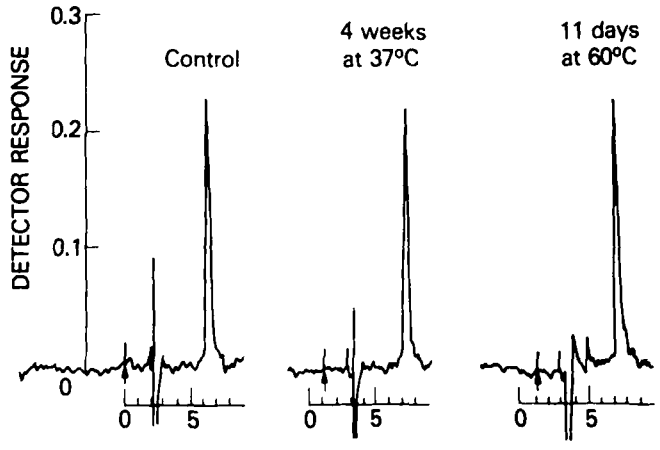

Figure 4—*HPLC profile of LHRH solutions prepared in distilled water kept at 60°C for 11 d or at 37°C for 4 weeks.*

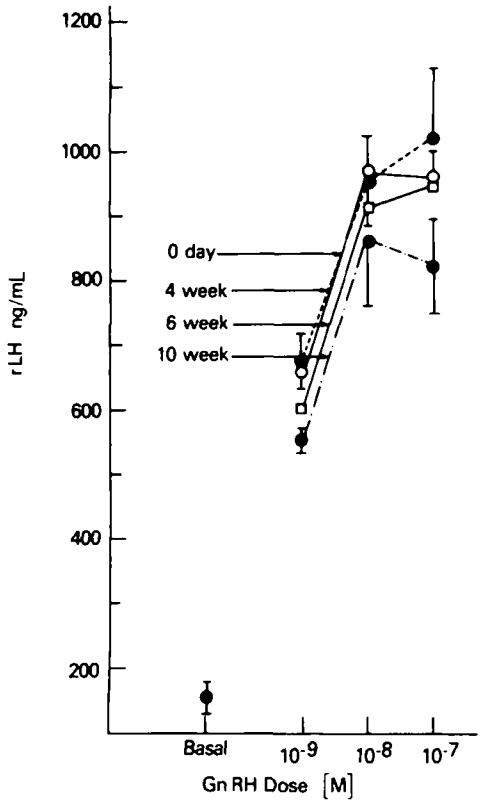

Figure 5—*Luteinizing hormone release from dispersed rat pituitary cells in culture following incubation with LHRH solutions prepared in distilled water (pH 6) and kept at 37°C for 0, 4, 6, and 10 weeks.*

alkaline solution of LHRH stored at 60°C for 11 d was 5% by the HPLC assay and 7% by bioassay.

The HPLC profile of the degradation product of the nonsterile LHRH solution stored at ambient temperature for 4 months was different from that obtained from LHRH solution stored at 60°C in borate buffer (Fig. 3). The potencies of this degraded LHRH product were 55 and 31% when assayed by HPLC and pituitary cell culture, respectively (Table II). There was no significant difference in the potency between LHRH solutions mixed with normal saline or the degradation product at a final concentration of 10% (Table II).

Analysis of the HPLC assay shows that under the conditions tested in this study (*a*) it gives reproducible LHRH peaks both in terms of retention time and peak height ratio at three different wavelengths, (*b*) the intact LHRH peak can be distinguished from the degradation peak(s) produced from two separate stress conditions, and (*c*) the chemical integrity of LHRH obtained by HPLC assay correlates well with the biological potency obtained by pituitary cell culture. It is concluded, therefore, that the reported HPLC method can be used as a rapid and reliable assay.

Stability of the LHRH Solution—The HPLC chromatograms and the LHRH response curves of pituitary cultures of some representative solutions of LHRH in distilled water kept at 37°C are shown in Figs. 4 and 5 and Table III. The potency of LHRH in samples stored at 37°C for 27 weeks was reduced 10% as measured by HPLC, but showed a 40–50% decrease by bioassay between 10–27 weeks. The significant difference between the HPLC and bioassay results for the 27-week sample is real, as confirmed by reassaying samples from the same vial by both HPLC and bioassay (experiment 2, Table III). Bacterial contamination cannot be completely ruled out as a possible cause of this difference.

LHRH stored at 4°C for up to 2 years and that subjected to repeated freezing and thawing for 5 d retained 94 ± 2% and 95 ± 2%, respectively, of their chemical integrity by HPLC. These results indicate that LHRH survived for at least 10 weeks at 37°C and for at least 2 years when refrigerated. Accidental freezing and thawing causes no change in the HPLC profile, and short-term exposure to 60°C does not induce significant deterioration of the peptide hormone in distilled water as assayed by either HPLC or the biological response of pituitary cell culture. It appears that a sterile LHRH solution is adequately stable for formulation and storage either frozen or refrigerated and could be reliably used in pumps for at least 10 weeks.

Our results also demonstrate that a nonsterile solution of LHRH at ambient temperature was chemically degraded 45% in 4 months. Based on HPLC assay

Table III—Stability of LHRH in Distilled Water at 37°C

Experiment	Weeks	Potency, % HPLC	Potency, % Bioassay	
1	0	100	100	
	4	98	100	$p > 0.25$
	6	96	65	$p < 0.2$
	10	90	47	$p < 0.02$
2	0	10	100	
	10	92	66	$p < 0.2$
	27	89	60	$p < 0.05$

values of sterile LHRH solutions at 4°C or 37°C, storage for 4 months at ambient temperature of LHRH should produce little degradation. The increased degradation is probably attributable to bacterial contamination, which causes a dramatic loss of activity of polypeptides[6]. This might also explain the shorter stability of LHRH solutions observed by Dermody *et al.* (17) at 4°C (stable for 14 weeks at 4°C compared with 2 years in our experiments). They observed bacterial contamination in their solutions stored at 4°C, and the rather abrupt loss of activity reported by them between 14 and 23 weeks suggests that LHRH degradation was catalyzed by bacteria. One should, therefore, be careful in extrapolating the stability data presented in this paper to nonsterile solutions of LHRH.

Identification and isolation of degradation products was not attempted in this investigation. However, it is known that minor changes in amino acid composition of LHRH impart marked changes in agonist or antagonist bioactivity[7]. Significant differences in the bioassay and HPLC results obtained in our experiments may be due to an altered biological activity of the degradation products.

REFERENCES

(1) A. V. Schally, A. Arimura, A. J. Kastin, H. Matsuo, Y. Baba, T. W. Redding, M. G. Nair, L. Debelizuk, and W. F. White, *Science*, **173**, 1036 (1971).

(2) A. V. Schally, A. J. Kastin, and D. H. Coy, *Int. J. Fertil.*, **21**, 1 (1976).

(3) C. H. Mortimer, A. S. McNeilly, R. A. Fisher, M. A. F. Murry, and G. M. Besser *Br. Med. J.*, **4**, 617 (1974).

(4) C. H. Mortimer, G. N. Besser, and A. S. McNeilly in "Hypothalamic Hormones," M. Motta, P. G. Crosignani, and L. Martini, Eds., Academic, London, 1975, p. 325.

(5) C. H. Mortimer and G. M. Besser, in "Endocrinology, I," V. H. T. James, Ed., Excerpta Medica, Amsterdam, 1977, p. 237.

(6) S. J. Nillius and L. Wide, *Br. Med. J.*, **3**, 405 (1975).

(7) S. J. Nillius, H. Fries, and L. Wide, *Am. J. Obstet. Gynecol.*, **122**, 921 (1975).

(8) T. W. Valk, K. P. Corley, R. P. Kelch, and J. C. Marshall, *J. Clin. Endocrinol. Metab.*, **51**, 730, (1980).

(9) W. F. Crowley, Jr. and J. W. McArthur, *J. Clin. Endocrinol. Metab.*, **51**, 173 (1980).

(10) J. C. Marshall and R. P. Kelch, *J. Clin. Endocrinol. Metab.*, **49**, 712 (1979).

(11) R. I. Jacobson, L. E. Seyler, Jr., W. H. Tamborlane, Jr., J. M. Gertner, and M. Genol, *J. Clin. Endocrinol. Metab.*, **49**, 652, (1979).

(12) G. Leyenderker, L. Wildt, and M. Hansmann, *J. Clin Endocrinol. Metab.*, **51**, 1214 (1980).

(13) A. R. Hoffman and W. F. Crowley, *N. Engl. J. Med.*, **307**, 1237, (1982).

(14) W. Vale, G. Grant, M. Amoss, R. Blackwell, and R. Guillemin, *Endocrinology*, **91**, 562 (1972).

(15) P. M. Krueger, G. D. Hodgen, and R. J. Sherins, *Endocrinology*, **95**, 955 (1974).

(16) D. J. Finney, "Statistical Methods in Biological Assay," 1st ed., Griffin, London, 1952, p. 179.

(17) W. C. Dermody, C. A. Patstushok, R. Sakowki, J. W. Vaitkus, and J. R. Reel, *N. Engl. J. Med.*, **295**, 173 (1976).

ACKNOWLEDGMENTS

The authors thank Dr. David Rodbard for his valuable assistance in statistical analysis of the biological potency of the LHRH and Mrs. Penny Colbert for her preparation of the manuscript.

[6] Dilute solutions (0.1–1.0 mg/mL in water) of β-endorphin (32 amino acid peptide) and corticotropine-releasing hormone (41 amino acid peptide) could lose their activity completely in 2 d at 37°C if kept nonsterile, whereas sterile solutions show little degradation (unpublished results from this laboratory).

[7] Substituting D-trypophan as the 6th amino acid of LHRH increases *in vivo* response ~100-fold.

Liquid Chromatographic Analysis of Dichlorophen and Its Major Impurity

KIRIT A. SHAH ˣ, SUSAN A. SAMUELS, MICHAEL K. MICHAELS, and JAMES W. WARREN

Received October 27, 1982, from the *Product Development Department, R. P. Scherer North America, Clearwater, FL 33518.* Accepted for publication May 12, 1983.

Abstract □ A rapid and simple high-performance liquid chromatographic (HPLC) method for the analysis of dichlorophen in raw material and in dichlorophen-toluene soft gelatin capsules for veterinary use was developed using a reverse-phase technique. This HPLC system was shown to isolate dichlorophen from its major impurity (the trimer). Three formulations were assayed and were found to contain 7.14, 7.90, and 8.4% of the trimer. A C-18 column was used with a mobile phase of methanol–water (75:25). The flow rate was 1.5 mL/min, and the effluent was monitored at 290 nm for both dichlorophen and the trimer. Dichlorophen and the trimer had retention times of 6.5 and 9.0 min, respectively.

Keyphrases □ Dichlorophen—HPLC, major impurity □ HPLC—analysis of dichlorophen and its major impurity

Dichlorophen (I), 2,2′-methylenebis(4-chlorophenol), is an anthelmintic which is used mainly for the removal of ascarids and hookworms and as an aid in the removal of tapeworms from dogs and cats. Dichlorophen is used in combination with toluene and is available in a soft gelatin capsule formulation for veterinary use. The USP XX (1) does not contain an official monograph for dichlorophen or dichlorophen capsule formulations; however, the British Pharmacopoeia (2) does for dichlorophen tablets. Dichlorophen is often contaminated with a trimer (II), 4-chloro-2,6-bis(5-chloro-2-hydroxybenzyl)-phenol, which is a result of the synthesis process. The trimer constitutes 5–10% by weight of dichlorophen.

The BP (2) method for dichlorophen assay involves a nonaqueous titration. Various analytical methods have appeared in the literature (3–7) for the determination of dichlorophen. Unfortunately, these methods cannot detect the presence of the trimer impurity. The present method offers a rapid and simple high-performance liquid chromatographic (HPLC) procedure for the simultaneous determination of dichlorophen and the trimer in raw material and capsule formulations.

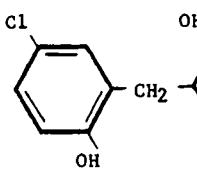

I

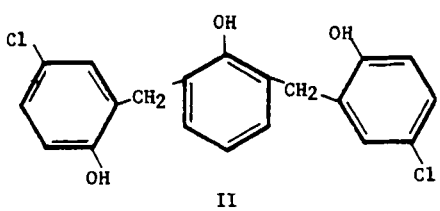

II

Table I—Analysis of Raw Material Samples of Dichlorophen [a]

Sample	HPLC Assay		Methoxide Titration Method
	Dichlorophen	Trimer	Dichlorophen
1	93.6	7.5	97.0
2	93.7	9.9	96.8
3	95.2	7.6	96.9
4	94.9	3.3	98.4
5	93.9	7.5	97.7
6	95.1	6.1	97.3
Mean	94.40	6.98	97.35
SD [b]	0.74	2.18	0.61

[a] Reported as a percentage. [b] Standard deviation.

EXPERIMENTAL

Materials—Dichlorophen[1] and the trimer[1], were used as received. Methanol and water were HPLC quality[2]. A gradient liquid chromatograph[3] equipped with two single-piston pumps[4] was operated in the isocratic mode. A 20-μL loop injector[5], variable-wavelength detector[6], electronic data printer-plotter[7], and nonpolar column (3.9 mm × 30 cm[8]) were used throughout. The mobile phase consisted of methanol–water (75:25) and was pumped at 1.5 mL/min. The detector was set at 290 nm and sensitivity was 0.018 AUFS.

Sample Preparation—Stock solutions of dichlorophen (60 mg/dL) and the trimer (30 mg/dL) were prepared in methanol. Solutions of dichlorophen containing 5, 9, 12, 15, and 18 μg/mL were prepared in methanol. Solutions of the trimer containing 6, 9, 12, 18, and 24 μg/mL were also prepared in methanol.

One capsule was cut, the fill material was squeezed into a 500-mL graduated cylinder, and the volume was adjusted with methanol. This was allowed to stand for 4 h, and then 8 mL of solution was diluted to 100 mL with methanol. Five milliliters of this diluted solution was further diluted to 50 mL with methanol to produce a solution having approximate concentration of 16 μg/mL. Twenty microliters of the resulting solution was used for analysis.

Calculations—Since linearity experiments indicated that the peak areas (and also peak heights) were related directly to the concentrations of dichlorophen (range 6–18 μg/mL) as well as the trimer (range 6–24 μg/mL), the results were calculated using:

$$\frac{Ph_a}{Ph_s} \times \frac{C}{L} \times D \times 100 = \text{Percent of label claim}$$

Where Ph_a is the peak area for the unknown solution, pH_s is the peak area for standard solution, C is the concentration of standard solution (g/mL), L is label claim (g), and D is the dilution factor (mL)

RESULTS AND DISCUSSION

Dichlorophen contains two phenolic groups. Use of the phenolic properties is made in several methods for the assay of dichlorophen (8); the results ob-

[1] Generously supplied by Givaudan, Clifton, N.J.
[2] Fisher Scientific Co., Fair Lawn, N.J.
[3] Model 344; Beckman Instruments, Berkeley, Calif.
[4] Model 112; Beckman Instruments, Berkeley, Calif.
[5] Model 210; Beckman Instruments, Berkeley, Calif.
[6] Model 165; Beckman Instruments, Berkeley, Calif.
[7] Model 3353; Hewlett-Packard, Palo Alto, Calif.
[8] μ-Bondapak C_{18}; Waters Associates, Milford, Mass.

0022-3549/84/0600-0822$01.00/0
© 1984, American Pharmaceutical Association

Table II—Analysis of Dichlorophen-Toluene Capsule Formulations by the HPLC Method[a]

Number	Formulation A		Formulation B		Formulation C	
	Dichlorophen	Trimer	Dichlorophen	Trimer	Dichlorophen	Trimer
1	93.2	7.8	99.8	7.5	97.8	9.1
2	92.8	7.4	102.1	7.2	96.4	8.8
3	95.1	7.8	98.6	6.7	97.2	8.6
4	89.9	8.4	100.7	7.3	96.3	7.9
5	93.9	8.1	99.3	7.0	95.4	7.6
Mean	92.98	7.90	100.10	7.14	96.62	8.4
SD^b	1.93	0.37	1.35	0.30	0.92	0.63

[a] Reported as a percentage of the theoretical label claim of 1 g. [b] Standard deviation.

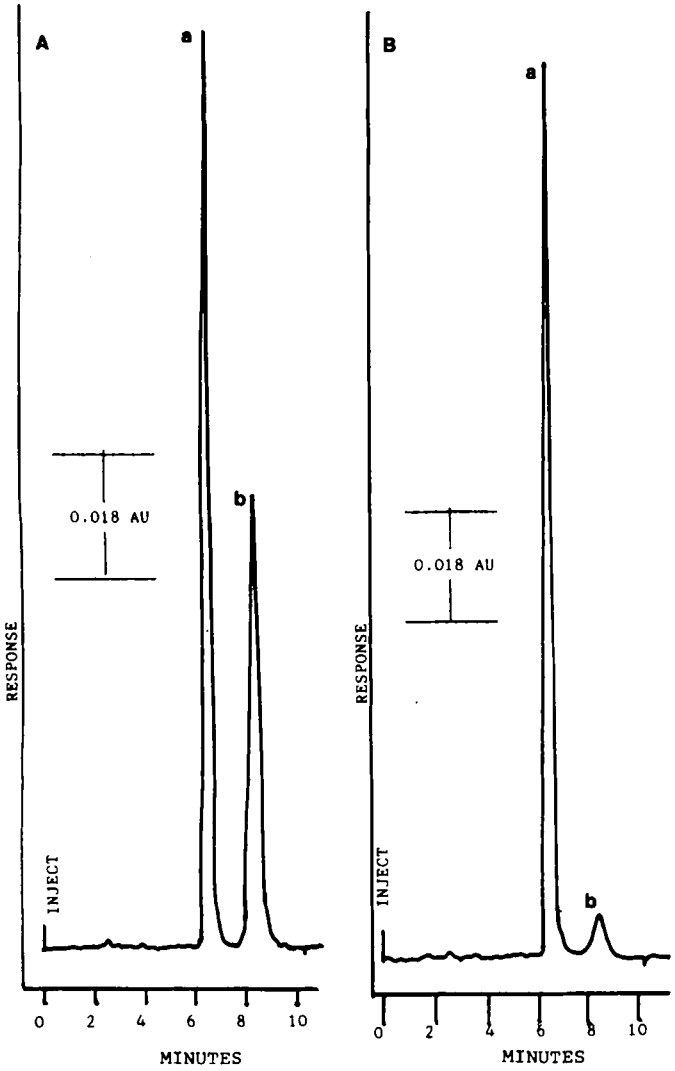

Figure 1—*Typical chromatograms of a standard solution of dichlorophen (19 μg/mL) and trimer (19 μg/mL) (A) and dichlorophen-toluene soft gelatin capsules containing 1 g of dichlorophen. Key: (a) dichlorophen; and (b) trimer.*

tained using these methods included the presence of the trimer. The chromatogram shown in Fig. 1A was obtained for a standard mixture of dichlorophen and the trimer. Figure 1B represents a chromatogram from a dichlorophen-toluene soft gelatin veterinary capsule formulation.

The calibration curve for dichlorophen was linear (r^2 = 0.99) over the concentration range of 6–18 μg/mL. The trimer calibration curve was also linear (r^2 = 0.99) over a concentration range of 6–24 μg/mL. The precision of this method was determined using 20 μL of each of a series of 10 standard solutions containing 12 μg/mL of dichlorophen and 12 μg/mL of the trimer. The coefficient of variation averaged 1.76% for dichlorophen and 2.02% for the trimer.

The recovery data for dichlorophen were determined by adding different amounts of the reference standard equivalent to one-third of the amount of dichlorophen contained in the dichlorophen-toluene veterinary capsules. The analysis of five such samples resulted in recovery values of 99.3, 100.0, 99.7, 101.0, and 99.8% of the total quantity expected. The mean and standard deviation were 99.96 and 0.64, respectively. The recovery data for the trimer were also determined by adding different amounts of the trimer equivalent to one-third of the amount of the trimer contained in the dichlorophen-toluene capsules. The analysis of five such samples resulted in recovery values of 98.2, 98.9, 98.9, 96.5, and 100.5% of the total quantity expected. The mean and standard deviation were 98.60 and 1.46, respectively. Therefore, it was determined from the above data that the assay provides satisfactory accuracy and precision.

Application of the HPLC assay to commercial source dichlorophen raw material provided the results given in Table I. The methoxide titration produced a higher percentage of dichlorophen because this value represents a summation of dichlorophen and the trimer. However, the HPLC procedure differentiated dichlorophen from the trimer, producing lower percentages.

Application of the HPLC procedure to three commercial dichlorophen-toluene soft gelatin veterinary capsules produced the results given in Table II. All formulations were labeled as having 1 g of dichlorophen. Mean dichlorophen potencies were 92.98, 100.10, and 96.62%, with respective standard deviations of 1.93, 1.35, and 0.92. The trimer means were 7.90, 7.14, and 8.40, with respective standard deviations of 0.37, 0.30, and 0.63.

The dichlorophen content for formulations A, B, and C were also determined using the methoxide titration method. This method provided mean dichlorophen potencies of 99.9, 105.0, and 103.0% for formulations A, B, and C, respectively. Again, the methoxide titration provided higher percentages of dichlorophen. The method presented here is rapid, precise, accurate, and simpler than the methoxide titration method. The trimer content in dichlorophen raw material can be easily determined.

REFERENCES

(1) "The United States Pharmacopeia XX," U.S. Pharmacopeial Convention, Rockville, Md., 1980.

(2) "The British Pharmacopoeia, Vol. I," Her Majesty's Stationary Office, London, England, 1980, p. 149.

(3) J. E. Clemens and S. H. Newburger, *JAOAC*, **37**, 190 (1954).

(4) P. D. Derry, M. Holden, and S. H. Newburger, *Proc. Sci. Sect. Toilet Goods Assoc.*, **36**, 25 (1961).

(5) Q. R. Bravo and A. F. Hernandez, *J. Chromatogr.*, **7**, 60 (1962).

(6) F. C. Ashton, *Analyst*, **85**, 685 (1960).

(7) P. J. Porcaro, *Anal. Chem.*, **36**, 1664 (1964).

(8) R. J. Collins and B. E. Porkiss, *Text. Manuf. J.*, **1960**, 241.

Binding of Disopyramide to α_1-Acid Glycoprotein in Plasma Measured by Competitive Equilibrium Dialysis

R. L. G. NORRIS *x, J. T. AHOKAS ‡, P. J. RAVENSCROFT *, and M. HENRY §

Received September 7, 1982, from the *Department of Clinical Pharmacology, Princess Alexandra Hospital, ‡Department of Medicine, University of Queensland, Princess Alexandra Hospital, and the §Department of Chemistry, Queensland Institute of Technology, Brisbane, Qld 4102, Australia. Accepted for publication May 3, 1983.

Abstract □ A modification of equilibrium dialysis in which α_1-acid glycoprotein and plasma compete directly for disopyramide has been used in conjunction with binding curves to measure the extent of the α_1-acid glycoprotein–disopyramide interaction. At concentrations in the therapeutic range, 80–90% of disopyramide was bound to α_1-acid glycoprotein for plasma from each of six healthy adults. Also, equilibrium dialysis data are presented, indicating that pH does not influence the binding of disopyramide within the therapeutic range.

Keyphrases □ Disopyramide—binding to α_1-acid glycoprotein, competitive equilibrium dialysis □ Equilibrium dialysis, competitive—binding of disopyramide to α_1-acid glycoprotein □ α_1-Acid glycoprotein—binding of disopyramide, competitive equilibrium dialysis

The antiarrhythmic drug disopyramide has concentration-dependent plasma protein binding (1) and variability in therapeutic response which may be due, at least in part, to variability in protein binding. An increased number of reports have associated the binding of basic drugs with α_1-acid glycoprotein (2–10). Interindividual variability in the free concentration of the drug and its effect could conceivably be produced by differing concentrations of this protein, as even the reference range for α_1-acid glycoprotein is wide (55–140 mg/dL). As α_1-acid glycoprotein is an acute phase reactant that can approximately double in concentration following acute myocardial infarction (11, 12), its involvement in disopyramide binding may be of even greater significance in this situation.

In previous studies, parameters obtained either from Scatchard plots or the bound fraction of the drug in buffered solution of protein alone were compared with data obtained in plasma (5, 8–10). This approach was also used to implicate α_1-acid glycoprotein in the binding of disopyramide by David *et al*[1]. Others have implied the relationship from correlations of plasma protein concentration with the extent of protein binding (2–4, 6).

To assess the contribution of a specific protein to the total binding occurring in plasma, a more direct evaluation of the interaction would be desirable. The work presented here utilizes a procedure in which the moles of drug bound to protein and to macromolecules in plasma are determined while both protein and plasma compete for the drug. As this procedure is essentially a variation of equilibrium dialysis, we have called the method competitive equilibrium dialysis. The effect of pH on the binding has also been investigated because of its potential importance in binding results.

EXPERIMENTAL

Reagents—The buffer used was 0.1 M Na_2HPO_4 (0.3% NaCl) unless otherwise stated; it was prepared from analytical-grade reagents and distilled water[2]. Disopyramide and the ^{14}C-radiolabeled disopyramide were supplied[3]. The [^{14}C]disopyramide was further purified by HPLC and stored at 4°C in 0.1 M pH 7.4 Na_2HPO_4 buffer containing 0.3% NaCl. The radiochemical purity of the purified disopyramide was >98%. Human α_1-acid glycoprotein purified from Cohn's fraction VI was obtained commercially[4] and used without further treatment. A stock solution of α_1-acid glycoprotein was prepared in buffer, and the concentration was determined from the molar absorbance at 278 nm. Appropriate dilutions were then used to provide all α_1-acid glycoprotein solutions including standards for assays by radial immunodiffusion. Comparison of these standards with commercially available standard human serum[5] indicates the glycoprotein to be >90% pure.

Scintillation Counting—Sufficient [^{14}C]disopyramide was used in all samples to ensure more than 1000 cpm/vial. For all samples, 200-μL duplicates were placed in respective polyethylene vials followed by 2 mL of tissue solubilizer[6]. After mixing and standing for 30 min, 12 mL of scintilation fluid[7] containing 100 μL of glacial acetic acid was added before capping and further mixing. Scintillation counting was carried out until at least 10,000 counts were accumulated using a scintillation counter[8] with external standardization. Means of duplicate counts were used for all calculations. Samples were counted before dialysis to determine specific activities as well as sampling contents of each dialysis compartment at equilibrium.

α_1-Acid Glycoprotein Determinations—Quantitation of α_1-acid glycoprotein employed the method of Mancini *et al.* (13) using radial immunodiffusion plates[9]. Four standards were run per plate. Interassay variability was evaluated by repeated analysis of a single sample, and accuracy was estimated by duplicate analysis of standard human serum containing 92 mg/dL of the glycoprotein[8].

Dialysis—Blood from six healthy volunteers was obtained by venipuncture in plain glass syringes and immediately transferred to EDTA tubes from which the stoppers had been discarded. Plasma was obtained ~30 min later after centrifugation, and the samples assayed for α_1-acid glycoprotein before being stored at −18°C in glass tubes with polytef-lined screw caps.

Each of 20 polymethyl methacrylate dialysis cells having two 1-mL compartments were prepared using dialysis membrane[10] that had been soaked in distilled water for 30–60 min. The experiment consisted of three sections: First, plasma from each of the subjects was dialyzed against six different concentrations of disopyramide in pH 6.7 buffer (pH 7.2 at equilibrium). These results were used to prepare a binding curve for each subject. The second section involved competitive equilibrium dialysis. This was experimentally identical to the first section except sufficient glycoprotein was added to the buffer to produce approximately equal concentrations in opposing compartments of each cell at equilibrium. In the third section, the effect of pH on the binding was evaluated. Three of the disopyramide concentrations used in the binding curve were prepared in pH 6.4 buffer (equilibrium pH 6.9) and pH 7.2 buffer (equilibrium pH 7.6). These solutions were then also dialyzed against plasma. By also utilizing the data from the binding curve, three disopyramide concentrations at three pH values were investigated.

Dialysis was carried out for 5 h at 37°C. These dialysis conditions have been shown to produce equilibrium for disopyramide concentrations (at equilibrium in the plasma) across the range of 1.0–18 mg/L for equilibrium dialysis and across the range of 2.5–10 mg/L during competitive equilibrium dialysis. On conclusion of dialysis in all three sections of the experiment, the contents of each compartment were transferred to glass vials using a 500-μL syringe[11].

[1] B. M. David, E. G. Whitford and K. F. Ilett, Presentation at the 15th annual meeting of the Australasian Society of Clinical and Experimental Pharmacologists, Adelaide, Australia, December 1981.

[2] Milli-Q System; Millipore Pty. Ltd., North Ryde, NSW, Australia.
[3] Hoechst-Roussel Pharmaceuticals Pty. Ltd., Sydney, Australia.
[4] Sigma Chemical Co., St. Louis, Mo.
[5] Behring Institute, Marburg, W. Germany.
[6] NCS; Amersham Aust. Pty. Ltd., Surrey Hills, NSW, Australia.
[7] PCS II; Amersham Aust. Pty. Ltd., Surrey Hills, NSW, Australia.
[8] Model 2660; Packard Instrument Co., Downers Grove, Ill.
[9] Calbiochem Behring Aust. Pty. Ltd., Carlingford, NSW, Australia.
[10] Spectrapor II; Spectrum Medical Industries, Los Angeles, Calif.
[11] Hamilton Co., Reno, Nev.

0022-3549/84/0600-0824$01.00/0
© 1984, American Pharmaceutical Association

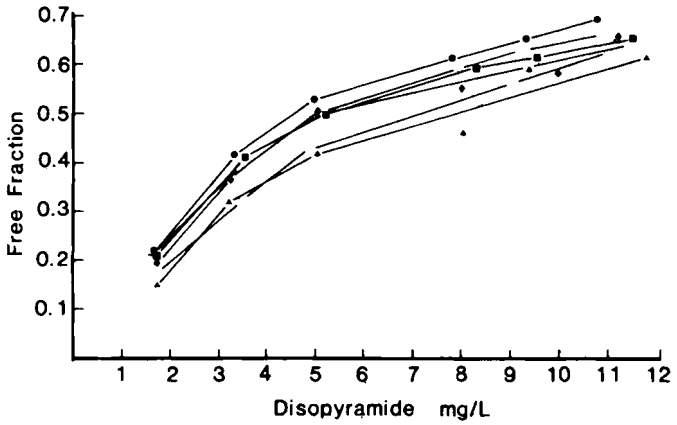

Figure 1—*Relationship of free fraction of disopyramide in plasma to total disopyramide concentration curves for disopyramide. No mathematical curve fitting procedures were used. Key: (■) subject 1; (▲) subject 2; (●) subject 3; (◆) subject 4; (□) subject 5; (○) subject 6.*

The contents of each compartment were then sampled for scintillation counting and α_1-acid glycoprotein assay.

To provide sufficient volume to determine pH, samples were combined in the following manner: For samples from sections 1 and 2, the contents of the plasma side of the dialysis unit from the three lowest disopyramide concentrations were combined; the four highest concentrations were also combined. A similar combination regimen was used for the samples from the buffer side. For samples from section 3, all three concentrations were combined, again keeping plasma side and buffer side samples separate.

RESULTS AND DISCUSSION

Interassay coefficient of variation for α_1-acid glycoprotein assays was 2.2% (n = 17; mean = 84 mg/dL). The results of duplicate analyses of standard human serum (92 mg/dL) were 97 and 100 mg/dL, indicating the accuracy of this method. Ratios of volumes of buffer compartment to plasma compartment at equilibrium were determined for all cells. The mean values ($\pm SD$) of this ratio for all cells dialyzed was 0.92 ± 0.05, illustrating the osmotic effect of the macromolecular components of plasma, as isotonic solutions were used. Total disopyramide concentrations at equilibrium and free fractions were calculated from equilibrium radiolabel concentrations and initial specific activities as per Norris *et al.* (14).

The curves of free fraction of disopyramide against total disopyramide concentration are shown as Fig. 1. These were then used as standard curves to determine the free fraction of disopyramide present after competitive dialysis in respective plasma samples at their equilibrium concentrations. From the free fraction and total drug concentration, the free and bound concentrations in the plasma were calculated. As the free concentration is the same in both compartments at equilibrium, the bound concentrations in the buffer side were also readily calculated. The contribution of α_1-acid glycoprotein to the binding in the plasma was calculated by Eq. 1. This equation assumes equal glycoprotein concentrations in both compartments at equilibrium and, under such conditions, provides direct quantitation of the relative importance of α_1-acid glycoprotein in the plasma protein binding of disopyramide:

$$\text{Fraction of binding attributable to } \alpha_1\text{-acid glycoprotein} = \frac{DISO_\beta^b}{DISO_\beta^p} \qquad \text{(Eq. 1)}$$

where $DISO_\beta^b$ and $DISO_\beta^p$ are the concentrations of disopyramide bound at equilibrium in the buffer and plasma compartments, respectively.

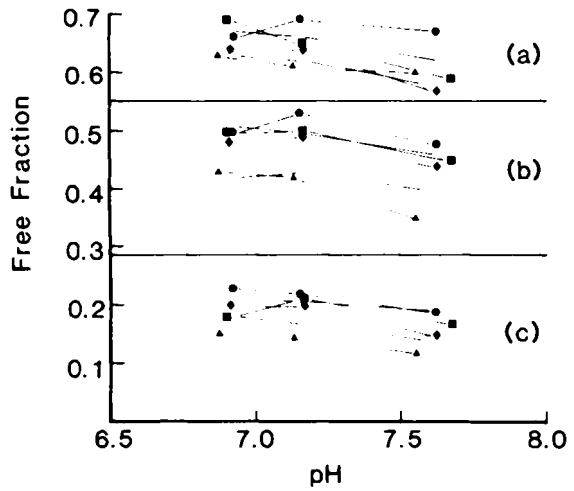

Figure 2—*Effect of pH on the binding of disopyramide to plasma. Symbols as for Fig. 1. Mean (and range) of disopyramide concentrations in plasma equilibrium: (a) 11.2 (10.5–11.8) mg/L; (b) 5.06 (4.74–5.27) mg/L; (c) 1.63 (1.3–1.75) mg/L.*

Table I—Binding Curves and Competitive Equilibrium Dialyses of α_1-Acid Glycoprotein at Equilibrium[a]

Subject	Binding Curve, Plasma	Competitive Equilibrium Dialysis Buffer	Competitive Equilibrium Dialysis Plasma
1	79.8 ± 2.2	77.3 ± 4.3	77.1 ± 3.2
2	80.6 ± 2.5	85.1 ± 2.7	75.9 ± 3.2
3	57.0 ± 1.1	64.4 ± 1.9	59.5 ± 1.2
4	67.6 ± 0.6	75.1 ± 1.0	67.0 ± 2.3
5	84.6 ± 1.6	85.9 ± 2.3	84.4 ± 1.5
6	72.3 ± 2.1	75.7 ± 3.1	73.0 ± 2.5

[a] Mean ± SD (mg/dL); n = 6 for binding curve studies and n = 5 for the competitive equilibrium dialyses.

Table II—Ratios of Disopyramide Bound to α_1-Acid Glycoprotein/ Disopyramide Bound to Plasma, Determined by Competitive Equilibrium Dialysis

Subject	Plasma Disopyramide at Equilibrium, mg/L 2.6	4.2	6.7	8.1	9.9
1	0.85	—[a]	—[a]	0.78	0.86
2	0.85	0.75	0.83	0.74	0.80
3	0.77	0.71	0.80	0.67	0.73
4	0.82	0.78	0.84	0.77	0.83
5	0.96	0.88	0.93	0.86	0.81
6	1.05	0.90	0.88	0.84	0.88

[a] —Missing value.

Table I reports the mean values of α_1-acid glycoprotein concentrations of compartments at equilibrium for each of the subjects. As these results do not show exact agreement in the glycoprotein concentration between compartments, some comment regarding subsequent errors in data obtained from Eq. 1 is necessary. With the relatively narrow range of α_1-acid glycoprotein concentrations being considered for plasma from each subject, it is reasonable to assume that the moles of drug bound varies linearly with the protein concentration. The percent error in data obtained using Eq. 1 is therefore given by:

$$\%\ \text{error} = 1 - \frac{[\alpha_1 AG]^b}{[\alpha_1 AG]^p} \times 100 \qquad \text{(Eq. 2)}$$

where $[\alpha_1 AG]^b$ and $[\alpha_1 AG]^p$ are the concentrations of α_1-acid glycoprotein in the buffer and plasma compartments at equilibrium, respectively.

Application of Eq. 2 to the data in Table I indicates the errors associated with the calculations from Eq. 1 to be 0.3, 12, 8, 12, 2, and 4%, respectively, for subjects 1–6. Data obtained using Eq. 1 is presented as Table II, showing that α_1-acid glycoprotein is responsible for ~80–90% of the binding of disopyramide at concentrations from 2.6 to 9.9 mg/L. Therefore, this glycoprotein is the major binding protein in plasma for disopyramide at therapeutic concentrations.

The free fraction of drug at each of three pH values for three different concentrations is presented as Fig. 2. Variations in pH within the physiological range have no important effect on the protein binding of disopyramide.

REFERENCES

(1) P. J. Meffin, E. W. Robert, R. A. Winkel, S. Harapat, F. A. Peters, and D. G. Harrison, *J. Pharmacokinet. Biopharm.*, **7**, 29 (1979).

(2) K. M. Piafsky, O. Borga, I. Odar-Cederlof, C. Johnansson, and J. Sjoqvist, *N. Engl. J. Med.*, **299**, 1435 (1978).

(3) R. L. Nation, *Clin. Pharmacol. Ther.*, **29**(4), 472 (1981).

(4) M. Wood and A. J. J. Wood, *Clin. Pharmacol. Ther.*, **29**(4), 522 (1981).

(5) M. Brinkschulte and V. Breyer Pfaff, *Arch Pharmacol.*, **314**, 61 (1980).

(6) M. K. Romach, K. M. Piafsky, J. G. Abel, V. Khouw, and E. M. Sellars, *Clin. Pharmacol. Ther.*, **29**(2), 211 (1981).

(7) K. M. Piafsky, *Clin. Pharmacokinet.*, **5**, 246 (1980).
(8) E. Pike, B. Skuterud, P. Kierulf, D. Fremstad, S. M. Abdel Sayed, and P. K. M. Lunde, *Clin. Pharmacokinet.*, **6**, 367 (1981).
(9) P. J. McNamara, R. L. Slaughter, J. A. Pieper, M. G. Wyman, and D. Lalka, *An. Analg.*, **60**, 295 (1981).
(10) D. Fremstad, K. Bergerud, J. F. W. Haffner, and P. K. M. Lunde, *Eur. J. Clin. Pharmacol.*, **10**, 411 (1976).
(11) B. G. Johansson, C. O. Kindmark, E. Y. Trell, and F. A. Wollheim, *Scand. J. Clin. Lab. Invest.*, **291** (suppl) 124, 117 (1972).
(12) S. J. Smith, G. Bos, M. R. Esseveld, H. G. Van Eijk, and J. Gerbrandy, *Clin. Chim. Acta.*, **81**, 75 (1977).
(13) G. Mancini, A. O. Carbonara, and J. F. Hereman, *Immunochemistry*, **2**, 235 (1965).
(14) R. L. G. Norris, J. T. Ahokas, and P. J. Ravenscroft, *J. Pharmacol. Meth.* **7**, 143 (1982).

ACKNOWLEDGMENTS

Financial support from the Lions Kidney and Medical Research Foundation is gratefully acknowledged. This work has been undertaken in partial fulfillment of the requirements of a Master of Applied Science Degree at the Queensland Institute of Technology by R.L.G.N.

The authors thank Dr. J. Cameron of Hoechst-Roussel Pty. Ltd., Castle Hill, New South Wales, Australia, for assistance with equipment and provision of disopyramide, both ^{14}C-labeled and unlabeled.

In Vitro and *In Vivo* Assessment of Hepatic and Extrahepatic Metabolism of Diazepam in the Rat

YASUTAKA IGARI, YUICHI SUGIYAMA, YASUFUMI SAWADA, TATSUJI IGA ˣ, and MANABU HANANO

Received December 30, 1982, from the *Faculty of Pharmaceutical Sciences, University of Tokyo, Bunkyo-ku, Tokyo 113, Japan.* Accepted for publication April 27, 1983.

Abstract □ Since diazepam is metabolized by many organs in the rat, the microsomal fractions of the liver, kidney, and lung from male Wistar rats were assayed for NADPH-dependent metabolism of diazepam and enzymatic parameters. The predicted extraction ratios were obtained from this *in vitro* experimental system. The organ clearances of the liver, kidney, and lung were then calculated for the determination of the relative contribution of each eliminating organ to the total body clearance (CL_{tot}) of diazepam in the rat. The liver was the most effective eliminating organ, followed by the kidney and the lung, in that order. The hepatic extraction ratio of diazepam was determined *in vivo* after portal and femoral vein administrations of diazepam. The validity of the *in vitro* experimental system for the liver was demonstrated by a good agreement between the calculated hepatic extraction ratio of diazepam from *in vitro* enzymatic parameters (0.616) and that derived *in vivo* (0.648). However, the sum of organ clearances of the liver, kidney, and lung did not account for CL_{tot} of diazepam in the rat, suggesting the possible contribution of the metabolism in the other organs or tissues, or an underestimation of the pulmonary and renal metabolism.

Keyphrases □ Diazepam -metabolism, hepatic and extrahepatic, *in vitro* assessment, comparison with *in vivo* parameters in the rat □ Metabolism—diazepam in the rat, hepatic and extrahepatic, *in vitro* assessment compared with *in vivo* parameters

Diazepam is a clinically important minor tranquilizer which is extensively metabolized by all species studied. However, there are pronounced interspecies differences in the total plasma clearance (CL_{tot}) per unit of body weight that presumably reflect differences in organ intrinsic clearances, blood flow, plasma binding, and the relative contributions of eliminating organs (1). In humans the total clearance is small [26.6 ± 4.1 mL/min (mean ± *SD*; $n = 5$)] (2) and it is assumed to reflect only hepatic metabolism. In contrast, in the rat the total clearance exceeds the liver blood flow, suggesting the involvement of extrahepatic elimination. The relative contribution of different organs to the overall metabolism of a drug may be assessed *in vivo*, but this is often difficult. Instead, comparison is often made between the *in vitro* enzymatic characteristics of an organ. This approach has recently received new impetus, since it has been shown to be readily extrapolated to the whole organ.

In the present study, the *in vitro* experimental system using microsomal fractions was employed to evaluate enzymatic parameters of the hepatic and extrahepatic diazepam elimination systems in the rat. The kidney and the lung were selected as the representative extrahepatic eliminating organs, since these two organs are reported to contain considerable amounts of cytochrome P_{450} (3). Enzymatic parameters of the liver, kidney, and lung were extrapolated to those of the whole organs. Using these parameters, the relative contributions of individual disposing organs were evaluated and, in the case of the liver, compared with an *in vivo* assessment.

EXPERIMENTAL

Materials—Male Wistar rats[1], weighing 250–270 g, on a normal laboratory diet were used throughout. [2-^{14}C]Diazepam (40–60 mCi/mmoL)[2] was used. Unlabeled diazepam[3], demethyldiazepam[4], oxazepam[4], and 3-hydroxydiazepam[4] were gifts from commerical sources. NADP, glucose-6-phosphate and glucose-6-phosphate dehydrogenase were obtained commercially[5]. All other chemicals were reagent grade.

Assay of Radioactivity—[2-^{14}C]Diazepam was diluted with unlabeled drug prior to the studies. The determination of carbon-14 and the assay of labeled drug and its metabolites were described elsewhere (4). The radiochemical purity was >98–99% for [2-^{14}C]diazepam by TLC.

Tissue Preparation and Drug Metabolism Study—Each of the 3–5 separate determinations were conducted on a separate pool of organs, each pool containing organs from 2–10 individual animals. After overnight fasting, the rats were exsanguinated *via* a carotid artery and perfused *in situ* with cold physiological saline *via* the venous trunk just inferior to the renal veins and *via* the portal vein until the effusate became colorless. The liver, kidney, and lung were excised, blotted, weighed, and pooled to obtain 10–11 g of each organ. The preparation of microsomal fractions was described elsewhere (5).

Incubation mixtures for the mixed function oxidation consisted of microsomal protein, 50 mM Tris-HCl buffer (pH 7.4), the NADPH-generating system (1 mM NADP, 10 mM glucose-6-phosphate, 2 U of glucose-6-phosphate dehydrogenase, and 5 mM magnesium chloride), and various amounts of [^{14}C]diazepam diluted with unlabeled diazepam to a final volume of 1.0 mL. The NADPH-generating system, microsomal protein solution, and [^{14}C]diazepam solution were preincubated separately for 2 min at 37°C. The

[1] Nihon Seibutsu Zairyo, Tokyo, Japan.
[2] Radiochemical Center, Amersham, England.
[3] Yamanouchi Pharm. Co., Tokyo, Japan.
[4] Banyu Pharm. Co., Tokyo, Japan.
[5] Boehringer Mannheim Yamanouchi Co., Tokyo, Japan.

0022-3549/84/0600-0826$01.00/
© 1984, American Pharmaceutical Associatic

(7) K. M. Piafsky, *Clin. Pharmacokinet.*, **5**, 246 (1980).
(8) E. Pike, B. Skuterud, P. Kierulf, D. Fremstad, S. M. Abdel Sayed, and P. K. M. Lunde, *Clin. Pharmacokinet.*, **6**, 367 (1981).
(9) P. J. McNamara, R. L. Slaughter, J. A. Pieper, M. G. Wyman, and D. Lalka, *An. Analg.*, **60**, 295 (1981).
(10) D. Fremstad, K. Bergerud, J. F. W. Haffner, and P. K. M. Lunde, *Eur. J. Clin. Pharmacol.*, **10**, 411 (1976).
(11) B. G. Johansson, C. O. Kindmark, E. Y. Trell, and F. A. Wollheim, *Scand. J. Clin. Lab. Invest.*, **291** (suppl) 124, 117 (1972).
(12) S. J. Smith, G. Bos, M. R. Esseveld, H. G. Van Eijk, and J. Gerbrandy, *Clin. Chim. Acta.*, **81**, 75 (1977).
(13) G. Mancini, A. O. Carbonara, and J. F. Hereman, *Immunochemistry*, **2**, 235 (1965).
(14) R. L. G. Norris, J. T. Ahokas, and P. J. Ravenscroft, *J. Pharmacol. Meth.* **7**, 143 (1982).

ACKNOWLEDGMENTS

Financial support from the Lions Kidney and Medical Research Foundation is gratefully acknowledged. This work has been undertaken in partial fulfillment of the requirements of a Master of Applied Science Degree at the Queensland Institute of Technology by R.L.G.N.

The authors thank Dr. J. Cameron of Hoechst-Roussel Pty. Ltd., Castle Hill, New South Wales, Australia, for assistance with equipment and provision of disopyramide, both ^{14}C-labeled and unlabeled.

In Vitro and *In Vivo* Assessment of Hepatic and Extrahepatic Metabolism of Diazepam in the Rat

YASUTAKA IGARI, YUICHI SUGIYAMA, YASUFUMI SAWADA, TATSUJI IGA ˣ, and MANABU HANANO

Received December 30, 1982, from the *Faculty of Pharmaceutical Sciences, University of Tokyo, Bunkyo-ku, Tokyo 113, Japan.* Accepted for publication April 27, 1983.

Abstract □ Since diazepam is metabolized by many organs in the rat, the microsomal fractions of the liver, kidney, and lung from male Wistar rats were assayed for NADPH-dependent metabolism of diazepam and enzymatic parameters. The predicted extraction ratios were obtained from this *in vitro* experimental system. The organ clearances of the liver, kidney, and lung were then calculated for the determination of the relative contribution of each eliminating organ to the total body clearance (CL_{tot}) of diazepam in the rat. The liver was the most effective eliminating organ, followed by the kidney and the lung, in that order. The hepatic extraction ratio of diazepam was determined *in vivo* after portal and femoral vein administrations of diazepam. The validity of the *in vitro* experimental system for the liver was demonstrated by a good agreement between the calculated hepatic extraction ratio of diazepam from *in vitro* enzymatic parameters (0.616) and that derived *in vivo* (0.648). However, the sum of organ clearances of the liver, kidney, and lung did not account for CL_{tot} of diazepam in the rat, suggesting the possible contribution of the metabolism in the other organs or tissues, or an underestimation of the pulmonary and renal metabolism.

Keyphrases □ Diazepam -metabolism, hepatic and extrahepatic, *in vitro* assessment, comparison with *in vivo* parameters in the rat □ Metabolism—diazepam in the rat, hepatic and extrahepatic, *in vitro* assessment compared with *in vivo* parameters

Diazepam is a clinically important minor tranquilizer which is extensively metabolized by all species studied. However, there are pronounced interspecies differences in the total plasma clearance (CL_{tot}) per unit of body weight that presumably reflect differences in organ intrinsic clearances, blood flow, plasma binding, and the relative contributions of eliminating organs (1). In humans the total clearance is small [26.6 ± 4.1 mL/min (mean ± *SD*; $n = 5$)] (2) and it is assumed to reflect only hepatic metabolism. In contrast, in the rat the total clearance exceeds the liver blood flow, suggesting the involvement of extrahepatic elimination. The relative contribution of different organs to the overall metabolism of a drug may be assessed *in vivo*, but this is often difficult. Instead, comparison is often made between the *in vitro* enzymatic characteristics of an organ. This approach has recently received new impetus, since it has been shown to be readily extrapolated to the whole organ.

In the present study, the *in vitro* experimental system using microsomal fractions was employed to evaluate enzymatic parameters of the hepatic and extrahepatic diazepam elimination systems in the rat. The kidney and the lung were selected as the representative extrahepatic eliminating organs, since these two organs are reported to contain considerable amounts of cytochrome P_{450} (3). Enzymatic parameters of the liver, kidney, and lung were extrapolated to those of the whole organs. Using these parameters, the relative contributions of individual disposing organs were evaluated and, in the case of the liver, compared with an *in vivo* assessment.

EXPERIMENTAL

Materials—Male Wistar rats[1], weighing 250–270 g, on a normal laboratory diet were used throughout. [2-^{14}C]Diazepam (40–60 mCi/mmoL)[2] was used. Unlabeled diazepam[3], demethyldiazepam[4], oxazepam[4], and 3-hydroxydiazepam[4] were gifts from commerical sources. NADP, glucose-6-phosphate and glucose-6-phosphate dehydrogenase were obtained commercially[5]. All other chemicals were reagent grade.

Assay of Radioactivity—[2-^{14}C]Diazepam was diluted with unlabeled drug prior to the studies. The determination of carbon-14 and the assay of labeled drug and its metabolites were described elsewhere (4). The radiochemical purity was >98–99% for [2-^{14}C]diazepam by TLC.

Tissue Preparation and Drug Metabolism Study—Each of the 3–5 separate determinations were conducted on a separate pool of organs, each pool containing organs from 2–10 individual animals. After overnight fasting, the rats were exsanguinated *via* a carotid artery and perfused *in situ* with cold physiological saline *via* the venous trunk just inferior to the renal veins and *via* the portal vein until the effusate became colorless. The liver, kidney, and lung were excised, blotted, weighed, and pooled to obtain 10–11 g of each organ. The preparation of microsomal fractions was described elsewhere (5).

Incubation mixtures for the mixed function oxidation consisted of microsomal protein, 50 mM Tris-HCl buffer (pH 7.4), the NADPH-generating system (1 mM NADP, 10 mM glucose-6-phosphate, 2 U of glucose-6-phosphate dehydrogenase, and 5 mM magnesium chloride), and various amounts of [^{14}C]diazepam diluted with unlabeled diazepam to a final volume of 1.0 mL. The NADPH-generating system, microsomal protein solution, and [^{14}C]diazepam solution were preincubated separately for 2 min at 37°C. The

[1] Nihon Seibutsu Zairyo, Tokyo, Japan.
[2] Radiochemical Center, Amersham, England.
[3] Yamanouchi Pharm. Co., Tokyo, Japan.
[4] Banyu Pharm. Co., Tokyo, Japan.
[5] Boehringer Mannheim Yamanouchi Co., Tokyo, Japan.

0022-3549/84/0600-0826$01.00/
© 1984, American Pharmaceutical Associatic

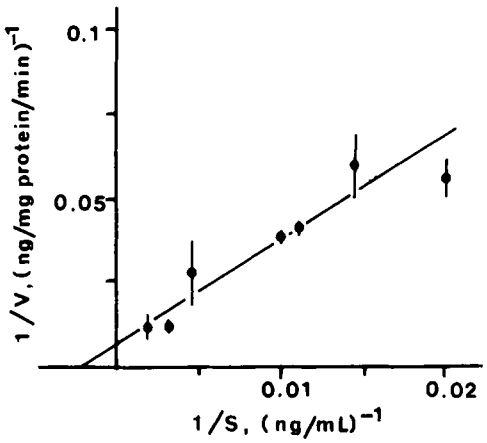

Figure 1—*Lineweaver-Burk plot of metabolism of diazepam by liver microsomes. Each point represents the mean of 3–5 separate determinations with standard error. The solid line represents the best fit to these data by a least-squares method (10).*

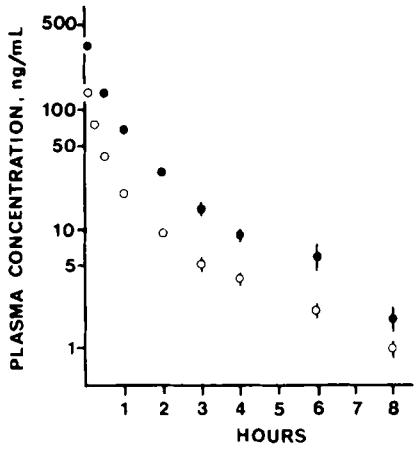

Figure 2—*Concentration-time profiles of diazepam after an injection of diazepam (1.2 mg/kg) intravenously (●) or intraportally (○) in rats (250–270 g). Each datum point represents the mean of 3–5 separate determinations ± SE. The data points without the vertical bars include the* SE *within the symbol mark.*

reaction was initiated by mixing these three solutions. The final concentration of diazepam ranged between 0.05–0.5 μg/mL. The reaction for 2 min at 37°C was stopped by transferring 0.5 mL of the incubation mixture into a stoppered glass tube containing 6 mL of cold benzene and subsequent mixing on an automatic mixer. After extraction and evaporation in boiling water (6), the amount of diazepam metabolized during 2 min was determined as previously described (4).

There are two pathways for diazepam metabolism, and the metabolites are further metabolized (7–9). Therefore, the rate of diazepam metabolized instead of the product formed was used for the enzyme assays. The spontaneous degradation of diazepam in the incubation mixture without the NADPH-generating system during incubation at 37°C did not occur. The recoveries from the extraction were determined and used for the correction. The enzymatic parameters (K_m and V_{max}) of the rat liver, kidney, and lung for diazepam metabolism were determined by Lineweaver-Burk analysis of the data of microsomal metabolism by a least-squares method (data were weighted with reciprocals of their variance) (10) using a digital computer[6].

Animal Experiments—Under light ether anesthesia, the femoral vein and artery were cannulated with polyethylene tubing[7] for intravenous drug administration and blood sampling, respectively. For intraportal venous administration, the portal vein was cannulated with polyethylene tubing[7] attached to a 27-gauge injection needle for drug administration, and the femoral artery was cannulated with polyethylene tubing[7] for blood sampling. Rats were then restrained in a Bollman cage. After 2 h of recovery from anesthesia, [^{14}C]diazepam diluted with unlabeled diazepam (1.2 mg/kg) in 0.25 mL of polyethylene glycol 300 (11) was injected, followed by 0.5 mL of physiological saline. At various times postinjection, a blood sample (0.3 mL) was withdrawn *via* a femoral artery using the cannula into a heparinized polyethylene tube followed by subsequent centrifugation[8]. Plasma samples were treated as described above.

Calculation of the Metabolic Capacity of each Disposing Organ—The enzymatic parameters (K_m and V_{max}) determined in the *in vitro* experimental system using microsomal fractions were extrapolated to those of whole organs as described previously (11–13), and the following calculations were performed. The intrinsic clearance (CL_{int}), related to the enzymatic parameters, is given as follows, assuming a single-enzyme system:

$$CL_{int} = V_{max}/(K_m + C_u) \quad \text{(Eq. 1)}$$

where C_u is the concentration of unbound drug in the water surrounding the enzyme. The CL_{int} is reduced to the following under nonsaturable conditions, *i.e.*, $K_m \gg C_u$:

$$CL_{int} \simeq V_{max}/K_m \quad \text{(Eq. 2)}$$

Assuming rapid equilibrium between organs and the effluent venous blood, the whole organ clearance (CL) of the liver or kidney is given as follows (14, 15):

$$CL = \frac{Qf_BCL_{int}}{Q + f_BCL_{int}} \quad \text{(Eq. 3)}$$

where f_B is the fraction of the drug in blood that is unbound, the Q is the blood flow supplied to the organ. The whole organ clearance of lung (CL_{Lu}) is given as follows, assuming rapid equilibrium (16):

$$CL_{Lu} \simeq f_BCL_{int(Lu)} \quad \text{(Eq. 4)}$$

The capacity of an eliminating organ to metabolize the drug can also be expressed as the extraction ratio (E). The extraction ratio of liver (E_H) derived from *in vitro* or *in vivo* experiments (17) is as follows:

$$E_H = \frac{f_BCL_{int(H)}}{Q_H + f_BCL_{int(H)}} \quad \text{(Eq. 5)}$$

$$E_H = 1 - \frac{AUC_{ip}/Dose}{AUC_{iv}/Dose} \quad \text{(Eq. 6)}$$

where AUC_{ip} and AUC_{iv} are the area under concentration-time curves of diazepam from zero to the infinity after portal venous and intravenous administration, respectively.

RESULTS

Drug Metabolism Study—The Lineweaver-Burk plot of the disappearance rates of diazepam *versus* the initial diazepam concentrations using liver microsome is shown in Fig. 1. The enzymatic parameters (K_m and V_{max}) derived from *in vitro* experiments and those extrapolated to the whole organs for the liver, kidney, and lung are listed in Table I. Since the unbound diazepam concentration in plasma was sufficiently small compared with the values of K_m of the three disposing organs (see footnote to Table I), Eq. 2 was used to

Table I—Enzymatic Parameters for Metabolism of Diazepam by Microsomes of Rat Liver, Kidney, and Lung

Organ	K_m[a], μg/mL	V_{max}, μg/min/g of Microsomal Protein	V_{max}[b], μg/min/g of Organ	CL_{int}[c], mL/min/g of Organ	CL_{org}[d], mL/min/0.25-kg rat
Liver	0.409	125.0	6.08	14.87	8.95
Kidney	0.198	18.5	0.33	1.68	0.22
Lung	0.343	27.8	0.26	0.76	0.10

[a] Michaelis–Menten constant for the unbound drug. Nonspecific binding of the drug to each microsomal suspension was low, determined by an equilibrium dialysis technique at 37°C in the absence of an NADPH-generating system (5), and was used for the correction. [b] Grams of microsomal protein per gram of liver was calculated as reported by Igari *et al.* (5) according to the methods of Lin *et al.* (12) and Smith and Bend (13), and that of kidney or lung was calculated according to the methods of Lin *et al.* (12) and Smith and Bend (13) by using the data rreported by Litterst *et al.* (3). [c] The fraction of unbound drug in plasma and the blood-to-plasma concentration ratio were 0.14 and 1.04, respectively, taken from the report by Igari *et al.* (4). The free diazepam concentrations in the systemic blood postinjection of 1.2 mg/kg iv of diazepam into the rat were below ~60 ng/mL and adequately smaller than K_m values over time, since diazepam concentration in the systemic blood declined very rapidly with time. Therefore, since the nonsaturable condition approximately holds, CL_{int} can be described by Eq. 2. [d] The values of CL_{org} of liver and kidney were calculated by Eq. 3, and that of the lung was calculated by Eq. 4. The blood flow rates of the liver and kidney were 14.7 mL/min/0.25-kg rat and 11.4 mL/min/0.25-kg rat, respectively, taken from the reports of Sasaki and Wagner (32), Dedrick *et al.* (33), and Lutz *et al.* (34).

[6] HITACHI M200-H; Hitachi, Tokyo, Japan.
[7] PE-50; Clay Adams, N.J.
[8] Beckman Instruments, Fullerton, Calif.

calculate CL_{int}. The calculated CL_{int} and CL are also listed in Table I. The liver is, as expected, the most potent contributor to total clearance, followed by the kidney and the lung in that order.

Evaluation of the Hepatic Extraction Ratio of Diazepam—After intravenous or intraportal administration of 1.2 mg/kg of [^{14}C]diazepam into the rat, the concentrations of diazepam in plasma declined biexponentially, as shown in Fig. 2, and could be fitted using a digital computer program (10). The AUC values are 15.4 ± 0.6 μg/mL·min (mean ± *SE*) following intravenous administration and 5.4 ± 0.7 μg/mL·min (mean ± *SE*) following intraportal administration, respectively. The extraction ratio of the liver, calculated according to Eq. 6 using the mean AUC values of postintravenous and intraportal injection, was 0.648, while that calculated according to Eq. 5 using enzymatic parameters derived from the *in vitro* experiments was 0.616 (for the hepatic blood flow rate and the blood free fraction, refer to the footnote to Table I).

The observed total clearance, calculated using CL_{tot} = Dose/AUC_{iv}, was 19.6 mL/min/0.25-kg rat.

DISCUSSION

Drug metabolism systems exist not only in the liver, but also in the kidney, intestine, lung, skin, brain, testes, placenta, adrenals, spleen, and plasma (11, 16–22); each enzyme system may have different enzymatic parameters. Since total clearance cannot be ascribed to only the liver for drugs which are metabolized by multiple organs, an accurate assessment of metabolic capacities of individual disposing organs would be indispensable in describing the drug kinetics in plasma and various tissues or organs using the physiologically based pharmacokinetic model developed by Dedrick *et al.* (23, 24). Some authors have dealt with the drug metabolism study using experimental systems prepared from the liver and the other organs. For example, Lake *et al.* (25) and Litterst *et al.* (3) reported the hepatic and extrahepatic *in vitro* metabolism of some drugs using subcellular fractions. Hayes and Brendel (26) and Devereux *et al.* (27) reported the metabolism of drugs using isolated liver and lung cell preparations, respectively. However, to incorporate the *in vitro* data into a physiologically based pharmacokinetic model, an appropriate scaling is needed to extrapolate the *in vitro* data to the *in vivo* situation, and comparison should be made between the capacity of the whole organ predicted from the *in vitro* data and observed to validate the scaling. On this point, Rane *et al.* (11) have successfully predicted intrinsic clearance and hence the extraction ratio of the liver of a wide spectrum of compounds using the values of V_{max} and K_m determined from liver homogenates, compared with those observed in the isolated liver perfusion study. Furthermore, Collins *et al.* (28) and Lin *et al.* (29) also reported the *in vitro* and *in vivo* correlation of the drug metabolism using isolated liver preparations.

In the present study, the enzymatic parameters K_m and V_{max} for the microsomal oxidation of diazepam in the liver, kidney, and lung were estimated using *in vitro* enzyme assays. It was demonstrated that the kidney and lung in addition to the liver contributed to the total clearance of diazepam in the rat. As expected, the liver was the most efficient organ for diazepam metabolism, followed by the kidney and the lung in that order. This is because there were differences in the values of V_{max} among three organs, as shown in Table I. The sum of the predicted organ clearances of the liver, kidney, and lung (9.3 mL/min/0.25-kg rat; Table I), however, was still below the observed total clearance (19.6 mL/min/0.25-kg rat). Since the predicted liver organ clearance (CL_{li}) in the present study was probably an estimate, the microsomes of the kidney and lung might not be prepared with enzymatic activity matching those of the intact kidney and lung.

Recently, the extrapolation of the *in vitro* enzymatic parameters to those *in vivo* has been demonstrated also in the lung. For example, Smith and Bend (13) and Law (30) succeeded in the extrapolation using benzo[*a*]pyrene 4,5-oxide and phencyclidine as substrates, respectively, both of which are metabolized mainly by microsomal enzymes. In the case of 5-hydroxytryptamide, which is mainly metabolized by mitochondrial monoamine oxidase, the prediction of its clearance from the *in vitro* enzymatic parameters was successful for the liver, but underestimated the observed clearance in the lung (31). Our present study using diazepam showed results similar to those for 5-hydroxytryptamine (31), although the intracellular localization of the enzymes is different.

Thus, the estimation of the enzymatic parameters of the metabolism from the *in vitro* assay systems of the liver and an appropriate scaling to the whole organ V_{max} value proved to be a useful tool for the estimation of the metabolic occurrences of diazepam *in vivo*. Since diazepam is metabolized by the kidney and lung in addition to the liver, the preparation of microsomes of the kidney and lung or experimental conditions such as components and concentrations of cofactors to yield appropriate enzymatic degradation rates should be further studied to assess the extrahepatic metabolism of diazepam.

REFERENCES

(1) U. Klotz, K. H. Antonin, and P. R. Bieck, *J. Pharmacol. Exp. Ther.*, **199,** 67 (1976).

(2) U. Klotz, G. R. Avant, A. Hoyumpa, S. Schenker, and G. R. Wilkinson, *J. Clin. Invest.*, **55,** 347 (1975).

(3) C. L. Litterst, E. G. Mimnaugh, R. L. Reagan, and T. E. Gram, *Drug Metab. Dispos.*, **3,** 259 (1975).

(4) Y. Igari, Y. Sugiyama, Y. Sawada, T. Iga, and M. Hanano, *Drug Metab. Dispos.*, **10,** 676 (1982).

(5) Y. Igari, Y. Sugiyama, S. Awazu, and M. Hanano, *J. Pharmacokinet. Biopharm.*, **10,** 53 (1982).

(6) I. A. Zingales, *J. Chromatogr.*, **75,** 55 (1973).

(7) M. A. Schwartz, R. A. Koechlin, E. Postman, S. Palmer, and G. Krol, *J. Pharmacol. Exp. Ther.*, **149,** 423 (1965).

(8) J. A. F. de Silva, R. A. Koechlin, and G. Bader, *J. Pharm. Sci.*, **55,** 692 (1966).

(9) J. A. F. de Silva and G. Bader, *Fed. Proc.*, **25** (part 1), 532 (1966).

(10) T. Nakagawa, Y. Koyanagi, and H. Togawa, "SALS, a Computer Program for Statistical Analysis with Least-Squares Fitting," Library Program of the University of Tokyo Computer Center, Tokyo, Japan, 1978.

(11) A. Rane, G. R. Wilkinson, and D. G. Shand, *J. Pharmacol. Exp. Ther.*, **200,** 420 (1977).

(12) J. H. Lin, Y. Sugiyama, S. Awazu, and M. Hanano, *Biochem. Pharmacol.*, **29,** 2825 (1980).

(13) B. R. Smith and J. R. Bend, *J. Pharmacol. Exp. Ther.*, **214,** 478 (1980).

(14) M. Rowland, L. Z. Benet, and G. G. Graham, *J. Pharmacokinet. Biopharm.*, **1,** 123 (1973).

(15) G. R. Wilkinson and D. G. Shand, *Clin. Pharmacol. Ther.*, **18,** 377 (1975).

(16) L. W. Wattenberg and J. L. Leong, *J. Histochem. Cytochem.*, **10,** 412 (1962).

(17) J. R. Gillette and K. S. Pang, *Clin. Pharmacol. Ther.*, **22,** 623 (1977).

(18) L. W. Wattenberg, J. L. Leong, and P. J. Strand, *Cancer Res.*, **22,** 1120 (1962).

(19) E. Schlede and A. H. Conney, *Life. Sci.*, **9,** 1295 (1970).

(20) G. Feuer, J. C. Sosa-Lucero, G. Lumb, and G. Moddel, *Toxicol Appl. Pharmacol.*, **19,** 579 (1971).

(21) M. R. Jeuchau, *Fed. Proc.*, **31,** 48 (1972).

(22) M. Rowland, S. Riegelman, P. A. Harris, and S. D. Sholkoff, *J. Pharm. Sci.*, **61,** 379 (1972).

(23) R. L. Dedrick and K. B. Bischoff, *Chem. Eng. Prog. Symp. Ser.*, **64,** 32 (1968).

(24) R. L. Dedrick, D. D. Forrester, and D. H. W. Ho, *Biochem. Pharmacol.*, **21,** 1 (1972).

(25) B. G. Lake, R. Hopkins, J. Chakraborty, J. W. Bridges, and D. V. W. Parke, *Drug Metab. Dispos.*, **1,** 342 (1973).

(26) J. S. Hayes and K. Brendel, *Biochem. Pharmacol.*, **25,** 1495 (1976).

(27) T. R. Devereux, G. E. R. Hook, and J. R. Fouts, *Drug Metab. Dispos.*, **7,** 70 (1979).

(28) J. M. Collins, D. A. Blake, and P. G. Egner, *Drug Metab. Dispos.*, **6,** 251 (1978).

(29) J. H. Lin, M. Hayashi, S. Awazu, and M. Hanano, *J. Pharmacokinet. Biopharm.*, **6,** 327 (1978).

(30) F. C. P. Law, *Drug Metab. Dispos.*, **10,** 361 (1982).

(31) D. A. Wiersma and R. A. Roth, *J. Pharm. Exp. Ther.*, **212,** 97 (1980).

(32) Y. Sasaki and N. Wagner, *J. Appl. Physiol.*, **30,** 879 (1968).

(33) R. L. Dedrick, D. S. Zaharko, and R. J. Lutz, *J. Pharm. Sci.*, **62,** 882 (1973).

(34) R. J. Lutz, R. L. Dedrick, H. B. Mathews, T. E. Eling, and M. W. Anderson, *Drug Metab. Dispos.*, **5,** 386 (1977).

ACKNOWLEDGMENTS

Portions of the paper appeared in a dissertation submitted by Y. Igari to the Graduate Division, University of Tokyo, Tokyo, Japan, in partial fulfillment of the requirements for the Ph.D. degree.

This study was supported by a grant-in-aid for Scientific Research provided by the Ministry of Education, Science and Culture of Japan. The authors thank Dr. G. R. Wilkinson for his review of this manuscript.

Physicochemical and Analytical Characteristics of Amiodarone

M. BONATI ˣ, F. GASPARI, V. D'ARANNO, E. BENFENATI, P. NEYROZ, F. GALLETTI, and G. TOGNONI

Received July 14, 1982, from the *Laboratory of Clinical Pharmacology, Istituto di Ricerche Farmacologiche "Mario Negri," Via Eritrea 62, 20157 Milan, Italy.* Accepted for publication May 10, 1983.

Abstract □ Data are reported on the analytical and physicochemical characteristics of amiodarone, for use in identifying and/or assaying this antiarrhythmic agent. The drug is highly soluble in chloroform and poorly soluble in water. Its acid-base constant (pK_a) is 6.56, and its maximal lipid solubility range is from pH 3.5 to 5.5.

Keyphrases □ Amiodarone—physicochemical and analytical characteristics, HPLC and IR, UV, and mass spectrometries □ Antiarrhythmic agents—amiodarone, physicochemical and analytical characteristics, HPLC and IR, UV, and mass spectrometries

In addition to electrophysiological (1, 2) and clinical findings (3, 4), the disposition of amiodarone[1] has been extensively investigated in animals and humans (5–7). Its metabolic pathway and tissue distribution are still largely unknown, but they do offer some clues to understanding the therapeutic and toxic effects during chronic treatment (8, 9). Despite all the work done, little is known to date of the basic physical and physicochemical properties of the drug.

EXPERIMENTAL

Equipment—Amiodarone hydrochloride was synthesized, purified by recrystallization from acetone (10), and supplied by Labaz[2]. All other chemicals were reagent or UV grade.

A double-beam spectrophotometer[3] equipped with a constant-temperature control block was used for UV analysis. A high-pressure liquid chromatograph[4] was equipped with a UV-absorption detector[5] (254 nm, fixed wavelength) and a reverse-phase column[6] (7-μm particle size, 250 nm × 4 mm length). The mobile phase was acetonitrile–water–acetic acid (80:19:1, adjusted to pH 5.8 with ammonium hydroxide) at a flow rate of 2 mL/min. Melting points were determined on a hot-stage[7] and were not corrected. A mass spectrometer[8] equipped with a computer[9] was used for MS analysis. Analyses were made by the direct inlet system, scanning repetitively throughout the sample evaporation period and heating the probe to 180°C. Electron energy ranged from 20 to 60 eV. IR spectra were obtained on a spectrophotometer using potassium bromide pellets (1%, w/v).

UV Spectrometry—To obtain a spectrum and determine its molar extinction coefficient (ϵ), methanolic solutions of amiodarone were prepared in triplicate at a concentration of 10 μg/mL (14.7×10^{-6} M). UV analyses were carried out at 208, 241, 270, and 280 nm at 25°C. The molar extinction coefficient was calculated by Lambert and Beer's law:

$$\log I_0/I = \epsilon \times 1 \times C \qquad \text{(Eq. 1)}$$

where $\log I_0/I$ is the absorption intensity of the sample, 1 is the cuvette path beam length (in cm), and C is the molar concentration; hence, ϵ = Absorbance × cm^{-1} × M^{-1}.

Solubility—The percentage (w/v) of amiodarone soluble in different solvents was determined by adding an excess of drug to obtain saturation of 20 mL of each solvent tested, calculating the amount of dissolved amiodarone. The tubes were rotated end-over-end for 1 h (longer than needed to dissolve the drug in all solvents employed) at 25 ± 0.1°C in a water bath and then centrifuged at the same temperature. The supernatant was diluted and spectrophotometrically assayed for amiodarone. Three determinations were made for each solvent.

Determination of pK_a—According to a long-used method (11) the pK_a values were determined by UV titration (at λ_{max}) of aqueous solutions containing known amounts of amiodarone. A range of pH 1–5 was achieved by addition of hydrochloric acid, pH 5.8–9.2, by 0.05 M borate phosphate (adjustment being made with hydrochloric acid), while higher values were obtained by addition of sodium hydroxide solutions. Sodium chloride was used to adjust the ionic strength. All solutions were prepared immediately before use and all pH values were checked at 25°C using a standard pH-meter. In the temperature range of 20–30°C there was no substantial effect on the true pH of the solutions, but only 3–4 h after preparation we found a 10% decrease in amiodarone concentration at pH values >7.0.

The extinction coefficient was related to different hydrogen ion concentrations to check the λ_{max} shift. The dissociation constant (K_a) was determined according to the equation

$$\epsilon = \frac{A_H \times [H^+] + A_B \times K_a}{[H^+] + K_a} \qquad \text{(Eq. 2)}$$

where A_H and A_B are the extinction coefficients when amiodarone exists under acidic and basic conditions, respectively. Experimental values of ϵ *versus* pH were then fitted by a nonlinear regression iterative program on a desk computer[10]. Determinations were done in triplicate.

Partition Coefficients—According to the suggestions of Leo *et al.* (12), amiodarone was partitioned between buffer solutions saturated with 1-octanol and 1-octanol saturated with buffer solutions (as reported for the determination of pK_a). Known amounts of amiodarone were dissolved in 20 mL of buffer solution and gently shaken for 2 h (long enough to achieve equilibrium) at 25 ± 0.1°C in a shaking incubator with 5 mL of organic solvent. The two phases were separated by centrifugation, and the amount of amiodarone in the aqueous layer was determined spectrophotometrically. The apparent partition coefficient was calculated as:

$$P_{app} = \frac{C_{octanol}}{C_{buffer}} = \frac{(C_1 - C_2) \cdot a}{C_2 \cdot b} \qquad \text{(Eq. 3)}$$

where C_1 and C_2 are the amiodarone concentrations (w/v) in the buffer before and after equilibration, and a and b are the volumes of the buffer and 1-octanol layers, respectively. Each determination was made three times for each pH value checked. The true or corrected partition coefficient, knowing the pK_a value of the drug, was calculated as:

$$P_{corr} = \frac{C_{octanol}}{C_{buffer}\,(1 - \alpha)} = \frac{P_{app}}{1 - \alpha} \qquad \text{(Eq. 4)}$$

where α is the degree of ionization at a given pH and can be calculated as:

$$\alpha = \frac{1}{[1 + \text{antilog}\,(pK_a - pH)]} \qquad \text{(Eq. 5)}$$

RESULTS AND DISCUSSION

Solubility—Table I sets out the findings as percentages (w/v). The coefficient of variation was always <5% for each solvent employed. The two extremes of solubility are represented by chloroform and petroleum ether, in which the ratio of amiodarone solubility is around 30,000:1. The pH of water was 6.5, and solubility was not substantially affected by a pH range of 1.5–7.5 in aqueous solutions (physiological fluids).

UV Spectrometry—The spectrum of amiodarone in methanolic solution using 1-cm quartz cells showed λ_{max} at 208 and 241 nm. Two shoulders were resolved near 270 and 280 nm; mean ϵ values were 4.7×10^4 at 208 nm, 4.4×10^4 at 241 nm, 1.8×10^4 at 270 nm, and 1.6×10^4 at 280 nm, respectively.

[1] Cordarone; Labaz Laboratories, Ambares, France.
[2] Labaz, Centre de Recherche, Brussels, Belgium.
[3] Model UV-300; Shimadzu, Kyoto, Japan.
[4] Series 1; Perkin-Elmer, Norwalk, Conn.
[5] Model LC 15; Perkin-Elmer, Norwalk, Conn.
[6] Hibar LiChrosorb RP-8; Merck, Darmstadt, Federal Republic of Germany.
[7] Kofler, C. Reichert AG, Vienna, Austria.
[8] Model 3091; LKB, Bromma, Sweden.
[9] Model 2130; LKB, Bromma, Sweden.
[10] Model HP-85; Hewlett-Packard, USA.

0022-3549/84/0600-0829$01.00/0
© 1984, American Pharmaceutical Association

Table I—Percentage Solubility (w/v) of Amiodarone in Various Solvents at 25°C [a]

Solvent	Solubility, g/100 mL
Chloroform	44.51282
Methylene chloride	19.20000
Methanol	9.98400
Ethanol	1.28000
Benzene	0.64657
Tetrahydrofuran	0.60377
Acetonitrile	0.31889
1-Octanol	0.29500
Ether	0.17436
1-Propanol	0.13435
Water	0.07164
Hexane	0.02559
Petroleum ether	0.00137

[a] Values are the average of determinations done in triplicate.

High-Performance Liquid Chromatography—The procedures described by Lesko *et al.* (13) for the preparation of biological samples were followed first. Because of the longer column life (efficiency) and greater simplicity using an aqueous mobile phase, we subsequently relied on a reverse-phase system. Values for sensitivity (0.05 μg/mL), within-day coefficients of variation (1.9% at 0.50 μg/mL and 6.5% at 5.00 μg/mL), and day-to-day coefficients of variation (7.5% at 0.50 μg/mL and 7.0% at 5.00 μg/mL) confirm the reliability of the method. The calibration curves were linear over the concentration range studied.

Melting Point—Amiodarone occurs as a white crystalline powder, with a melting point of 159 ± 2°C after recrystallization from acetone (10).

IR Spectrometry—The IR spectrum (KBr pellets) revealed characteristic bands that agreed with the suggested structure: 3000–3070 (ArCH), 2860–2960 (aliphatic CH), 2200–2700 (*tert*-amine NH^+), 1635 (diAr C=O), 1560 and 1015 (benzofuran C=C), 1380 (aliphatic CH_3), 1285 (ketonic C—C), 1250 and 1075 (ether C—O—C), and 1225 and 1025 cm^{-1} (*tert*-amine C—N).

Mass Spectrometry—The molecular peak of amiodarone was observed at *m/z* 645, corresponding to the molecular mass. The most characteristic fragments of amiodarone gave peaks at *m/z* 630 ($M^+ - CH_3$), 546, 517 ($M^+ - HI$), 420, 391, 373, 201, and 159. The peak at *m/z* 546 corresponds to cleavage of the aromatic ether with elimination of the aliphatic aminic chain. The other ions at *m/z* 420, 391, 373, 201, and 159 are all fragments of this aromatic part of the molecule.

Determination of pK_a—The UV absorption curves of amiodarone at different hydrogen ion concentrations (Fig. 1a) showed a characteristic bathochromic shift (toward the red) of λ_{max} (241 nm) from pH 6.0 to higher values. The apparent dissociation constant, calculated for amiodarone using Eq. 2, (Fig. 1b) was 6.56 ± 0.06 (*SD*). By appropriate substitution into the Henderson–Hasselbach equation of the pK_a value for amiodarone (weak acid) and considering the pH range (1.0–8.0), which encompasses the pH in all body sites, it can be affirmed that amiodarone is essentially un-ionized at acidic pH sites.

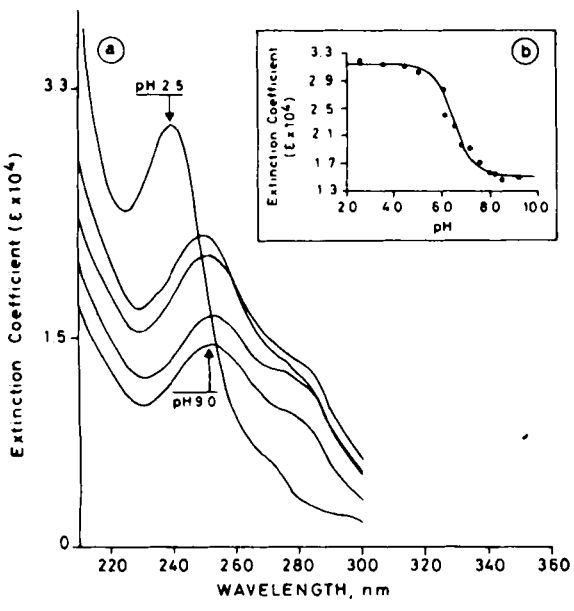

Figure 1—*Representative changes with pH in the absorption spectrum of amiodarone (a), and curve plotted to calculate the* pK_a *value for amiodarone (b).*

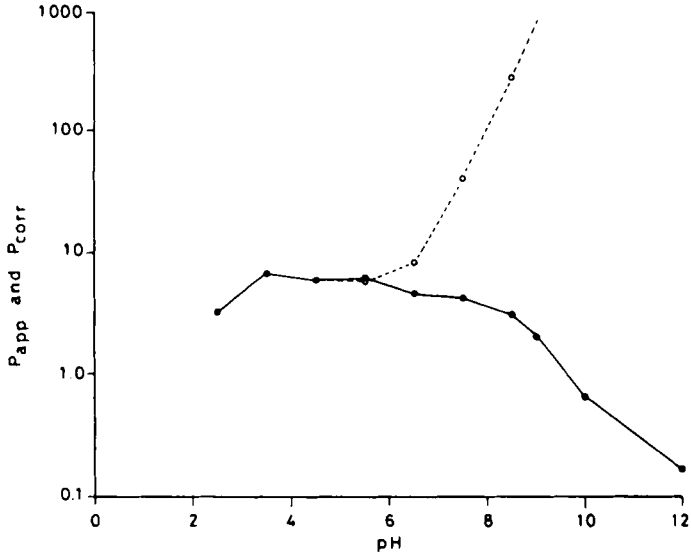

Figure 2—*Changes with pH in the apparent (●) and corrected (○) partition coefficients of amiodarone.*

Partition Coefficients—Apparent and corrected partition coefficients are plotted in Fig. 2. A typical dependence of coefficients on pH was found, with maximum lipid solubility of amiodarone between pH 3.5 and 5.5. The same behavior is described for other compounds [such as tetracycline and sulfa drugs (14, 15)].

The present findings confirm that an acidic pH (~4.5) is optimal for the extraction of amiodarone from biological specimens (7, 13). Furthermore, considering the dissociation characteristics and taking into account the "pH-partition hypothesis" (16) and Schanker's statement (17) that ". . .lipid solubility is most likely the dominant characteristic, since the relevance of the degree of ionization is probably a consequence of the poor lipid-solubility of organic ions," the absorption of amiodarone, whose extent and specific mechanism are at present unknown, should be far greater in the duodenum and jejunum than in the stomach and lower alimentary canal. Thus, gastric emptying time and changes of pH are likely to be critical in the absorption of amiodarone.

Wide variability can be expected in absorption rates and bioavailability of the drug. This is specifically relevant in protocols to investigate the correlations between amiodarone blood levels after acute and repeated oral administration and electrophysiological effects.

REFERENCES

(1) A. W. Hamer, W. B. Finerman Jr., T. Peter, and W. J. Mandel, *Am. Heart J.*, **102**, 992 (1981).

(2) F. I. Marcus, G. H. Fontaine, R. Frank, and Y. Grosgogeat, *Am. Heart J.*, **101**, 480 (1981).

(3) P. J. Podrid and B. Lown, *Am. Heart J.* **101**, 374 (1981).

(4) J. J. Heger, E. N. Prystowsky, W. M. Jackman, G. V. Naccarelli, K. A. Warfel, R. L. Rinkenberger, and D. P. Zipes, *N. Engl. J. Med.*, **305**, 539 (1981).

(5) E. Riva, M. Gerna, P. Neyroz, R. Urso, I. Bartosek, and A. Guaitani, *J. Cardiovasc. Pharmacol.*, **4**, 270 (1982).

(6) F. Andreasen, H. Agerbaek, P. Bjerregaard, and H. Gøtzsche, *Eur. J. Clin. Pharmacol.*, **19**, 293 (1981).

(7) E. Riva, M. Gerna, R. Latini, P. Giani, A. Volpi, and A. Maggioni, *J. Cardiovasc. Pharmacol.*, **4**, 264 (1982).

(8) K. Nademanee and B. N. Singh, *J. Am. Med. Assoc.*, **247**, 217 (1982).

(9) J. C. Kaski, L. A. Girotti, H. Messuti, B. Rutitzky, and M. B. Rosenbaum, *Circulation*, **64**, 273 (1981).

(10) J. Broekhuysen, R. Laruel, and R. Sion, *Arch. Int. Pharmacodyn.*, **177**, 340 (1969).

(11) W. Stenström and N. Goldsmith, *J. Phys. Chem.*, **30**, 1683 (1926).

(12) A. Leo, C. Hansch, and D. Elkins, *Chem. Rev.*, **71**, 525 (1971).

(13) L. J. Lesko, A. Marion, A. T. Canada, and C. Haffajee, *J. Pharm. Sci.*, **70**, 1366 (1981).
(14) J. L. Colaizzi and P. R. Klink, *J. Pharm. Sci.*, **58**, 1184 (1969).
(15) W. Scholtan, *Arzneim.-Forsch.*, **18**, 505 (1968).
(16) P. A. Shore, B. B. Brodie, and C. A. M. Hogben, *J. Pharmacol. Exp. Ther.*, **119**, 361 (1957).
(17) L. S. Schanker, *Pharmacol. Rev.*, **14**, 501 (1962).

ACKNOWLEDGMENTS

This work was partially funded by the CNR (National Research Council, Rome, Italy) program on Clinical Pharmacology and Rare Diseases. The authors would like to thank Dr. C. Peck, Uniformed Services University, Bethesda, Md. for making available his iterative program, Dr. D. Castelli, Dr. E. Fabbri, and Mr. L. Sansotera for their technical help.

Liquid Chromatographic Analysis of Triamterene and Its Major Metabolite, Hydroxytriamterene Sulfate, in Blood, Plasma, and Urine

FRITZ SÖRGEL *, EMIL T. LIN, JIRO HASEGAWA ‡, and LESLIE Z. BENET ˣ

Received November 1, 1982, from the *Department of Pharmacy, School of Pharmacy, University of California, San Francisco, CA 94143.* Accepted for publication April 7, 1983. Present Addresses: *Carl-Korth Institute for Cardiovascular Research, Division of Clinical Pharmacology, 852 Erlangen, West Germany and ‡Eisai Co. Ltd., 6-10 Koishikawa 4-Chome, Bunkyo-ku, Tokyo 112, Japan.

Abstract □ The first rapid and highly sensitive high-performance liquid chromatographic (HPLC) assay for triamterene, hydroxytriamterene, and hydroxytriamterene sulfate is reported. Plasma samples were processed by protein precipitation, while urine was used untreated. Three different solvent systems were used to analyze (*a*) triamterene in plasma (30% acetonitrile, pH 4.0; internal standard: furosemide; sensitivity limit: 1 ng/mL); (*b*) hydroxytriamterene and hydroxytriamterene sulfate in plasma (12% acetonitrile, pH 5.5; internal standard: cefamandole; sensitivity limits: 20 and 2 ng/mL, respectively) and (*c*) triamterene, hydroxytriamterene, and hydroxytriamterene sulfate in urine (13% acetonitrile, pH 5.3; internal standard: hydroflumethiazide; sensitivity limits: 0.04 μg/mL, 0.5 μg/mL, and 0.1 μg/mL, respectively). Fluorescence detection of compounds was performed at 365-nm excitation and 440-nm emission wavelengths. Recovery of triamterene and its metabolites from plasma was complete, and calibration curves were linear. Intraday variation was <6% except for the lowest plasma concentration. The assay procedure has already been used in several pharmacokinetic studies.

Keyphrases □ Triamterene—HPLC analysis, major metabolites, hydroxytriamterene sulfate, blood, plasma, and urine □ Hydroxytriamterene sulfate—HPLC analysis, major metabolite of triamterene, blood, plasma, and urine

Although triamterene has been clinically available since the 1960's, the metabolic pathways for this drug have been a matter of controversy, with conflicting reports appearing up through 1982. Early work by Lehmann (1) indicated that triamterene undergoes hydroxylation and subsequent sulfation to hydroxytriamterene sulfate, which he found in urine. Pruitt *et al.* (2), using TLC separation, could only detect hydroxytriamterene, whereas Grebian *et al.* (3) and our group (4, 5) did find the sulfate ester of hydroxytriamterene using TLC techniques.

More recently, three HPLC techniques for triamterene analysis have been published (6-8). One of these research groups (6) assumed, on the basis of the work of Pruitt *et al.* (2), that hydroxytriamterene was the major metabolite of triamterene and did not develop a method to specifically measure the sulfate conjugate. The other two groups did not measure any metabolites. The first HPLC assay by which the specific measurement of hydroxytriamterene sulfate can be obtained and by which very low concentrations of unchanged triamterene and hydroxytriamterene sulfate can be quantitated is reported herein. The method is simple, fast, and accurate.

EXPERIMENTAL

Reagents—Triamterene[1], hydroxytriamterene[2], hydroxytriamterene sulfate[2], and the internal standards hydroflumethiazide[3], furosemide[4], and cefamandole[5] were used as received. Acetonitrile[6] for the HPLC measurements was glass-distilled; water was redistilled and stored in glass.

Apparatus—A high-performance liquid chromatograph[7] equipped with a sample processor[8], a fluorescence spectrophotometer[9], and a UV detector[10] was used. The assay was carried out on a 10-μm particle size, 4 × 300-mm reverse-phase column[11] at a solvent flow rate of 2 mL/min.

Mobile Phase and Retention Times—Three different solvent systems were used for the measurement of triamterene, hydroxytriamterene, and hydroxytriamterene sulfate. Each solvent system (A-C, as indicated in Table I) was used for a particular quantitation problem.

Detection Wavelengths—Triamterene, hydroxytriamterene, and hydroxytriamterene sulfate as well as the internal standards furosemide and hydroflumethiazide were analyzed using their native fluorescence at an excitation wavelength of 365 nm and an emission wavelength of 440 nm. Cefamandole, which was used as an internal standard in mobile phase B, was measured by UV detection at 254 nm. For that purpose the HPLC system was equipped with two detector systems, one for fluorescence and another for UV detection.

Methods—Each plasma or total blood sample (0.1 mL) was deproteinated by adding 0.4 mL of acetonitrile containing both furosemide (3.5 μg/mL) and cefamandole (60 μg/mL) internal standards. After mixing[12] for 1 min, the sample was centrifuged[13] for 10 min at 3200 rpm. The supernatant was transferred to a clean test tube and, if necessary, evaporated at room temperature to 0.2 mL under nitrogen when very low concentrations had to be measured. However, most of the samples could be analyzed by injection of a volume as little as 5 μL.

Urine samples ranging from 0.02 to 0.1 mL were added to 1 mL of an acetonitrile solution containing hydroflumethiazide as an internal standard (500 μg/mL). After mixing[12] and centrifugation[13], 2 μL was injected onto the HPLC system.

Human plasma, blood, and urine were stored at −20°C. Blank plasma and blood for assay development was obtained from healthy volunteers using 143 IU/10 mL of lithium heparin as anticoagulant. To test the stability of tri-

[1] Mylan Pharmaceuticals Inc., Morgantown, W.Va.
[2] Röhm-Pharma, Darmstadt, West Germany.
[3] Le Pharmaceutical Products, 2750 Ballerup, Denmark.
[4] Hoechst Pharmaceuticals Inc., Somerville, N.J.
[5] Eli Lilly & Co., Indianapolis, Ind.
[6] J. T. Baker Chemical Co., Phillipsburg, N.J.
[7] Perkin-Elmer Series 3, Norwalk, Conn.
[8] WISP Model 710A; Waters Associates, Milford, Mass.
[9] 204 S; Perkin-Elmer, Norwalk, Conn.
[10] LC 65 T; Perkin-Elmer, Norwalk, Conn.
[11] Micro Pak MCH; Varian, Los Altos, Calif.
[12] Vortex-Genie Mixer; Scientific Industries Inc., Bohemia, N.J.
[13] IEC HN-SII Centrifuge, Damon IEC Div.; Needham Heights, Mass.

0022-3549/84/0600-0831$01.00/0
© 1984, American Pharmaceutical Association

(13) L. J. Lesko, A. Marion, A. T. Canada, and C. Haffajee, *J. Pharm. Sci.*, **70**, 1366 (1981).
(14) J. L. Colaizzi and P. R. Klink, *J. Pharm. Sci.*, **58**, 1184 (1969).
(15) W. Scholtan, *Arzneim.-Forsch.*, **18**, 505 (1968).
(16) P. A. Shore, B. B. Brodie, and C. A. M. Hogben, *J. Pharmacol. Exp. Ther.*, **119**, 361 (1957).
(17) L. S. Schanker, *Pharmacol. Rev.*, **14**, 501 (1962).

ACKNOWLEDGMENTS

This work was partially funded by the CNR (National Research Council, Rome, Italy) program on Clinical Pharmacology and Rare Diseases. The authors would like to thank Dr. C. Peck, Uniformed Services University, Bethesda, Md. for making available his iterative program, Dr. D. Castelli, Dr. E. Fabbri, and Mr. L. Sansotera for their technical help.

Liquid Chromatographic Analysis of Triamterene and Its Major Metabolite, Hydroxytriamterene Sulfate, in Blood, Plasma, and Urine

FRITZ SÖRGEL *, EMIL T. LIN, JIRO HASEGAWA ‡, and LESLIE Z. BENET ˣ

Received November 1, 1982, from the *Department of Pharmacy, School of Pharmacy, University of California, San Francisco, CA 94143.* Accepted for publication April 7, 1983. Present Addresses: *Carl-Korth Institute for Cardiovascular Research, Division of Clinical Pharmacology, 852 Erlangen, West Germany and ‡Eisai Co. Ltd., 6-10 Koishikawa 4-Chome, Bunkyo-ku, Tokyo 112, Japan.

Abstract □ The first rapid and highly sensitive high-performance liquid chromatographic (HPLC) assay for triamterene, hydroxytriamterene, and hydroxytriamterene sulfate is reported. Plasma samples were processed by protein precipitation, while urine was used untreated. Three different solvent systems were used to analyze (*a*) triamterene in plasma (30% acetonitrile, pH 4.0; internal standard: furosemide; sensitivity limit: 1 ng/mL); (*b*) hydroxytriamterene and hydroxytriamterene sulfate in plasma (12% acetonitrile, pH 5.5; internal standard: cefamandole; sensitivity limits: 20 and 2 ng/mL, respectively) and (*c*) triamterene, hydroxytriamterene, and hydroxytriamterene sulfate in urine (13% acetonitrile, pH 5.3; internal standard: hydroflumethiazide; sensitivity limits: 0.04 μg/mL, 0.5 μg/mL, and 0.1 μg/mL, respectively). Fluorescence detection of compounds was performed at 365-nm excitation and 440-nm emission wavelengths. Recovery of triamterene and its metabolites from plasma was complete, and calibration curves were linear. Intraday variation was <6% except for the lowest plasma concentration. The assay procedure has already been used in several pharmacokinetic studies.

Keyphrases □ Triamterene—HPLC analysis, major metabolites, hydroxytriamterene sulfate, blood, plasma, and urine □ Hydroxytriamterene sulfate—HPLC analysis, major metabolite of triamterene, blood, plasma, and urine

Although triamterene has been clinically available since the 1960's, the metabolic pathways for this drug have been a matter of controversy, with conflicting reports appearing up through 1982. Early work by Lehmann (1) indicated that triamterene undergoes hydroxylation and subsequent sulfation to hydroxytriamterene sulfate, which he found in urine. Pruitt *et al.* (2), using TLC separation, could only detect hydroxytriamterene, whereas Grebian *et al.* (3) and our group (4, 5) did find the sulfate ester of hydroxytriamterene using TLC techniques.

More recently, three HPLC techniques for triamterene analysis have been published (6-8). One of these research groups (6) assumed, on the basis of the work of Pruitt *et al.* (2), that hydroxytriamterene was the major metabolite of triamterene and did not develop a method to specifically measure the sulfate conjugate. The other two groups did not measure any metabolites. The first HPLC assay by which the specific measurement of hydroxytriamterene sulfate can be obtained and by which very low concentrations of unchanged triamterene and hydroxytriamterene sulfate can be quantitated is reported herein. The method is simple, fast, and accurate.

EXPERIMENTAL

Reagents—Triamterene[1], hydroxytriamterene[2], hydroxytriamterene sulfate[2], and the internal standards hydroflumethiazide[3], furosemide[4], and cefamandole[5] were used as received. Acetonitrile[6] for the HPLC measurements was glass-distilled; water was redistilled and stored in glass.

Apparatus—A high-performance liquid chromatograph[7] equipped with a sample processor[8], a fluorescence spectrophotometer[9], and a UV detector[10] was used. The assay was carried out on a 10-μm particle size, 4 × 300-mm reverse-phase column[11] at a solvent flow rate of 2 mL/min.

Mobile Phase and Retention Times—Three different solvent systems were used for the measurement of triamterene, hydroxytriamterene, and hydroxytriamterene sulfate. Each solvent system (A-C, as indicated in Table I) was used for a particular quantitation problem.

Detection Wavelengths—Triamterene, hydroxytriamterene, and hydroxytriamterene sulfate as well as the internal standards furosemide and hydroflumethiazide were analyzed using their native fluorescence at an excitation wavelength of 365 nm and an emission wavelength of 440 nm. Cefamandole, which was used as an internal standard in mobile phase B, was measured by UV detection at 254 nm. For that purpose the HPLC system was equipped with two detector systems, one for fluorescence and another for UV detection.

Methods—Each plasma or total blood sample (0.1 mL) was deproteinated by adding 0.4 mL of acetonitrile containing both furosemide (3.5 μg/mL) and cefamandole (60 μg/mL) internal standards. After mixing[12] for 1 min, the sample was centrifuged[13] for 10 min at 3200 rpm. The supernatant was transferred to a clean test tube and, if necessary, evaporated at room temperature to 0.2 mL under nitrogen when very low concentrations had to be measured. However, most of the samples could be analyzed by injection of a volume as little as 5 μL.

Urine samples ranging from 0.02 to 0.1 mL were added to 1 mL of an acetonitrile solution containing hydroflumethiazide as an internal standard (500 μg/mL). After mixing[12] and centrifugation[13], 2 μL was injected onto the HPLC system.

Human plasma, blood, and urine were stored at −20°C. Blank plasma and blood for assay development was obtained from healthy volunteers using 143 IU/10 mL of lithium heparin as anticoagulant. To test the stability of tri-

[1] Mylan Pharmaceuticals Inc., Morgantown, W.Va.
[2] Röhm-Pharma, Darmstadt, West Germany.
[3] Le Pharmaceutical Products, 2750 Ballerup, Denmark.
[4] Hoechst Pharmaceuticals Inc., Somerville, N.J.
[5] Eli Lilly & Co., Indianapolis, Ind.
[6] J. T. Baker Chemical Co., Phillipsburg, N.J.
[7] Perkin-Elmer Series 3, Norwalk, Conn.
[8] WISP Model 710A; Waters Associates, Milford, Mass.
[9] 204 S; Perkin-Elmer, Norwalk, Conn.
[10] LC 65 T; Perkin-Elmer, Norwalk, Conn.
[11] Micro Pak MCH; Varian, Los Altos, Calif.
[12] Vortex-Genie Mixer; Scientific Industries Inc., Bohemia, N.J.
[13] IEC HN-SII Centrifuge, Damon IEC Div.; Needham Heights, Mass.

0022-3549/84/0600-0831$01.00/0
© 1984, American Pharmaceutical Association

Table I—Retention Times (min) for Triamterene, Its Metabolites, and the Internal Standards in Three Different Solvent Systems

Compound	Mobile Phase A[a]	Mobile Phase B[b]	Mobile Phase C[c]
Triamterene	5.7	—	8.6
Hydroxytriamterene	—[d]	9.0	4.8
Hydroxytriamterene sulfate	—	5.7	3.2
Furosemide (I.S.)[e]	8.1	—	—
Cefamandole (I.S.)	—	8.7	—
Hydroflumethiazide (I.S.)	—	—	7.0

[a] 30% Acetonitrile in 0.02% H_3PO_4, adjusted to pH 4 with NaOH (for plasma or blood). [b] 12% Acetonitrile in 0.02% H_3PO_4, adjusted to pH 5.5 with NaOH (for plasma or blood). [c] 13% Acetonitrile in 0.02% H_3PO_4, adjusted to pH 5.3 with NaOH (for urine). [d] — = Not measured. [e] I.S. = internal standard.

amterene and its primary metabolite over time, biological samples (over the concentrations measured) were analyzed after 6 and 12 months storage at −20°C. They did not show any degradation. On the basis of our work it appears that samples can be stored for more than 1 year at −20°C without significant degradation.

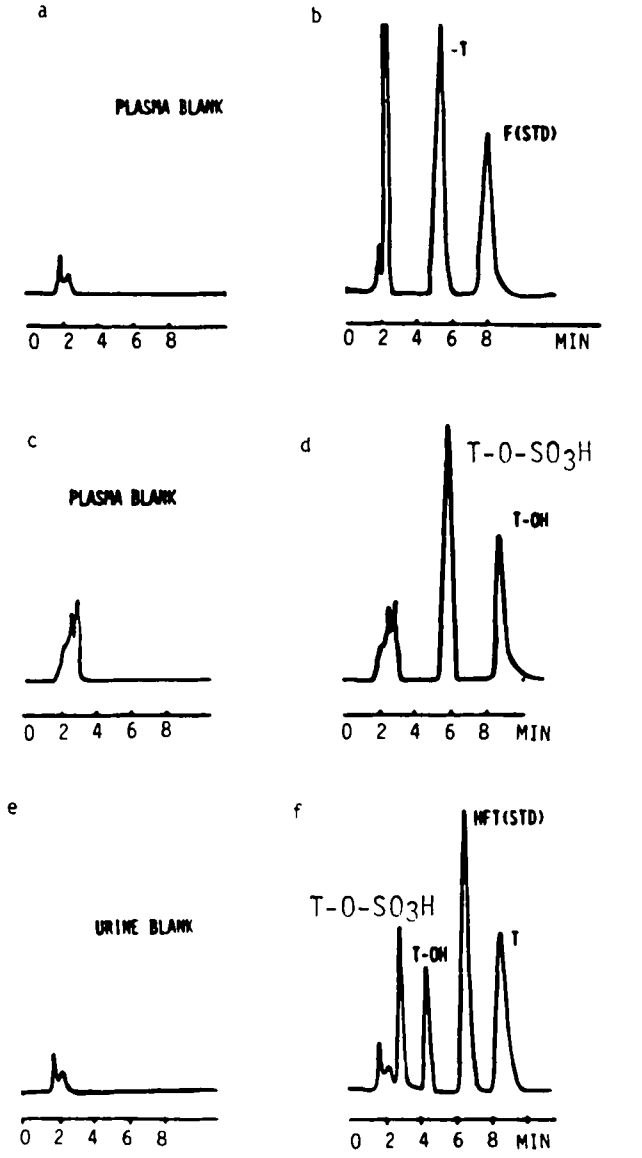

Figure 1– *Chromatograms developed using methods A–C. (Cefamandole was measured by UV and is not shown here.) Key: (a) blank plasma (method A); (b) actual plasma sample (method A); (c) blank plasma sample (method B); (d) actual plasma sample (method B); (e) blank urine (method C); (f) actual urine sample (method C); (STD) internal standard; (T) triamterene; (T-OH) hydroxytriamterene; (T-O-SO$_3$H) hydroxytriamterene sulfate; (F) furosemide; (HFT) hydroflumethiazide.*

Table II—Recovery of Triamterene and Hydroxytriamterene Sulfate from Human Plasma

Compound	Plasma Conc., ng/mL	Recovery, %
Triamterene	1.21	118.1
	3.27	100.0
	5.24	103.4
	9.83	97.6
	19.7	101.9
	32.8	98.6
	49.2	99.3
Hydroxytriamterene sulfate	10.8	96.6
	21.6	101.8
	32.4	100.7
	54.0	103.4
	86.4	103.3
	108.0	100.0
	215.0	97.4

RESULTS

Three different solvent systems were used to analyze triamterene, hydroxytriamterene, and hydroxytriamterene sulfate in plasma and urine (Table I).

Triamterene (Mobile Phase A)—Triamterene was analyzed using a 30% acetonitrile in 0.02% H_3PO_4 solvent system, adjusted to pH 4.0 with 0.5 M NaOH. As can be seen in Fig. 1a and b these conditions allowed excellent separation of triamterene (retention time 5.7 min) from endogenous materials. The internal standard, furosemide, has a retention time of 8.1 min, which means that the total run time for one sample is <10 min, allowing a large number of samples to be measured each day. Standard curves for triamterene obtained using mobile phase A exhibited linearity over the concentration range of 1–50 ng/mL. The limit of quantitation was 1 ng/mL.

Hydroxytriamterene (Mobile Phases B and C)—Hydroxytriamterene, had it been present in actual plasma or urine samples, could have been detected with solvent systems B and C. Since the retention times for hydroxytriamterene and the internal standard, cefamandole, were so close with mobile phase B (Table I), plasma samples with and without the internal standard were injected onto the column. Hydroxytriamterene peaks were not detected in either plasma or urine from healthy volunteers even when the instruments were set to the highest sensitivity. Therefore, no further attempts were made to fully establish a method of quantitation. The lower limit of quantitation was 20 ng/mL in plasma and 0.5 μg/mL in urine.

Hydroxytriamterene Sulfate (Mobile Phase B)—Hydroxytriamterene sulfate was separated from hydroxytriamterene and from endogenous compounds in solvents B and C with retention times of 5.7 and 3.2 min, respectively, in each solvent. Cefamandole used as an internal standard for mobile phase B had a retention time of 8.7 min, maintaining the total run time for hydroxytriamterene sulfate below 10 min (see representative chromatograms, Fig. 1c and d). Standard curves for hydroxytriamterene sulfate were shown to be linear over a 10–215-ng/mL concentration range. The lower limit of quantitation was 2 ng/mL.

Urine Assay (Mobile Phase C)—In urine, all three triamterene compounds can be measured simultaneously with the internal standard hydroflumethi-

Table III—Within-Day Assay Precision for Triamterene and Hydroxytriamterene Sulfate in Plasma

Plasma Conc., ng/mL	Peak Height Ratio[a]	*CV*, %
	Triamterine	
1.21	0.080 ± 0.010	12.6
3.27	0.180 ± 0.003	1.4
5.24	0.279 ± 0.013	4.7
9.83	0.537 ± 0.018	3.4
19.7	1.087 ± 0.044	4.0
32.8	1.800 ± 0.050	2.8
49.2	2.745 ± 0.094	3.4
	Hydroxytriamterene Sulfate	
10.8	0.295 ± 0.019	6.4
21.6	0.615 ± 0.011	1.9
32.4	0.861 ± 0.024	2.8
54.0	1.62 ± 0.10	5.9
86.4	2.52 ± 0.13	5.0
108.0	3.07 ± 0.12	4.0
215.0	6.17 ± 0.04	0.6

[a] Mean ± *SD*; *n* = 4.

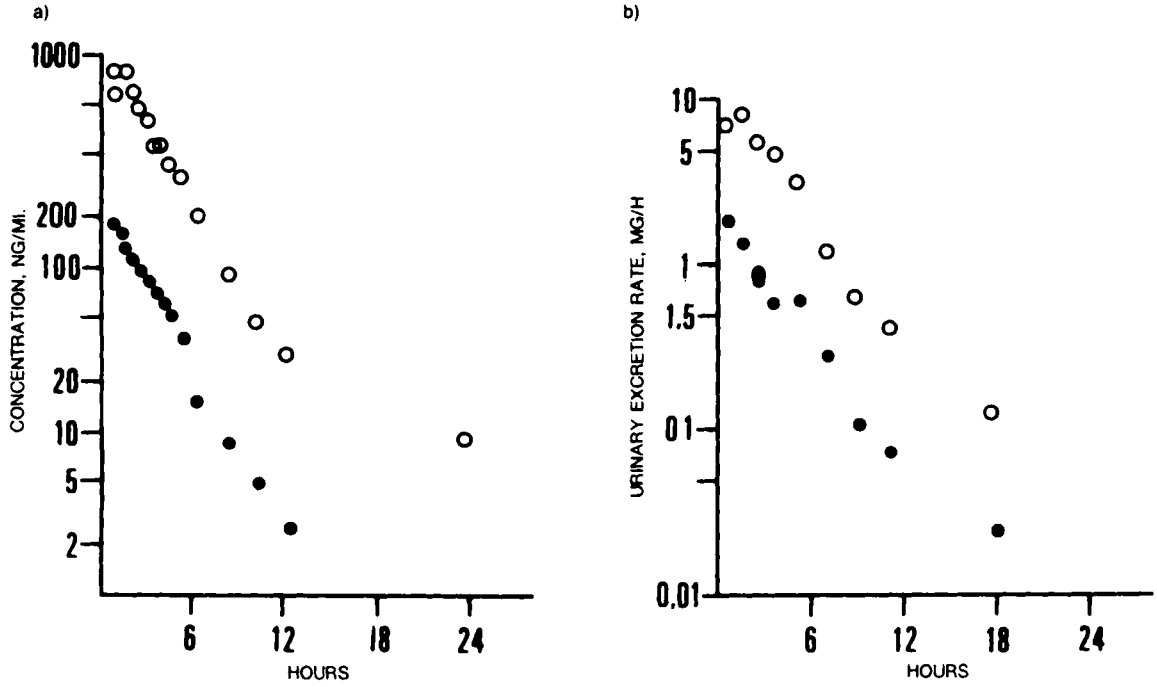

Figure 2—*Semilogarithmic plasma concentration* versus *time plot (a) and urinary excretion rate* versus *midpoint time (b) following a 100-mg oral suspension dose of triamterene to a healthy volunteer. Key: (●) triamterine; (○) hydroxytriamterine sulfate.*

azide (Fig. 1e,f); the limits of quantitation of triamterene and hydroxytriamterene sulfate were 0.04 μg/mL and 0.1 μg/mL, respectively. Standard curves for these two compounds were prepared over the following concentration ranges: triamterene, 0.15–2.35 μg/mL; hydroxytriamterene sulfate, 0.75–57.0 μg/mL.

Recovery—The recoveries of triamterene and hydroxytriamterene sulfate from plasma were determined by acetonitrile precipitation. The peak height ratios of samples prepared with plasma and water were compared. As shown in Table II, the recovery of triamterene and hydroxytriamterene sulfate was complete.

Within-Day Precision—The within-day precision was assessed by conducting replicate analyses. As shown in Table III, the coefficients of variation ranged from 0.5–6.4 for all concentrations except the lowest plasma concentration (12.6% *CV*), indicating good precision for the assay.

Blood Sample Assays—Analysis of triamterene and hydroxytriamterene sulfate were undertaken so as to determine the blood-to-plasma ratios of these compounds. The blood–plasma ratios were examined in two subjects and found to be constant over the concentration range measured following a 100-mg oral dose of triamterene (9). The ratio was 1.03 ± 0.14 for triamterene and 0.60 ± 0.07 for hydroxytriamterene sulfate.

DISCUSSION

There have been several reports in the literature regarding the quantitation of triamterene and its metabolites in humans. On the basis of a probably inappropriate TLC procedure, Pruitt *et al* (2) concluded that the major metabolite of triamterene was hydroxytriamterene rather than the sulfate conjugate (1, 3, 4).

Following the detection of hydroxytriamterene sulfate, but not hydroxytriamterene, in actual biological specimens and by using synthetic hydroxytriamterene sulfate as a reference compound, it was possible to develop a procedure to quantitatively measure hydroxytriamterene sulfate in urine and plasma. Hydroxytriamterene, the intermediate metabolite of triamterene, was not detected in any study. Had it been present, it could have been detected with our HPLC method. The most recent report on the measurement of triamterene and metabolites of Yakatan *et al.* (6) only provides information about hydroxytriamterene measurements, not mentioning the sulfate conjugate. The techniques described here have been used successfully in several pharmacokinetic studies in both humans and dogs (4, 5, 9) and are suitable to quantify triamterene and its metabolite, hydroxytriamterene sulfate.

The results of a representative experiment in a healthy volunteer receiving a 100-mg oral suspension dose of triamterene are shown in Fig. 2a and b. As indicated earlier no hydroxytriamterene could be detected in either plasma or urine. The concentration of hydroxytriamterene sulfate exceeded that of unchanged triameterene ~10-fold in plasma and ~5-fold in urine, indicating that hydroxytriamterene sulfate is the major metabolite of triamterene. Further analysis of the pharmacokinetic data in humans using the analytical techniques described here has been recently reported (9).

REFERENCES

(1) K. Lehmann, *Arzneim.-Forsch.* (Drug Res.), **15,** 812 (1965).

(2) A. W. Pruitt, J. S. Winkel, and P. G. Dayton, *Clin. Pharmacol. Ther.*, **21,** 610 (1977).

(3) B. Grebian, H. E. Geissler, and E. Mutschler, *Arzneim.-Forsch.* (Drug Res.), **26,** 2125 (1976).

(4) F. Sörgel, E. T. Lin, E. Mutschler, B. Ettinger, M. Hropot, W. Fabian, and L. Z. Benet, Abstract No. 542, 1st World Conference on Clinical Pharmacology and Therapeutics, London, 1980.

(5) F. Sörgel, H. Kiefl, J. Hasegawa, M. Geldmacher-v. Mallinckrodt, E. Mutschler, and L. Z. Benet, *Clin. Pharmacol. Ther.*, **31,** 271 (1982).

(6) G. J. Yakatan and J. E. Cruz, *J. Pharm. Sci.*, **70,** 949 (1981).

(7) S. Sved, J. A. A. Sertie, and I. J. McGilveray, *J. Chromatogr.*, **162,** 474 (1979).

(8) R. R. Brodie, L. F. Chasseaud, T. Taylor, and L. M. Walmsley, *J. Chromatogr.*, **164,** 527 (1979).

(9) J. Hasegawa, E. T. Lin, R. L. Williams, F. Sörgel, and L. Z. Benet, *J. Pharmacokinet. Biopharm.*, **10,** 507 (1982).

ACKNOWLEDGMENTS

Presented in part at the APhA Academy of Pharmaceutical Sciences, San Antonio, Texas, meeting in November 1980. During this work Dr. F. Sörgel was supported by the German Research Foundation (Deutsche Forschungsgemeinschaft). Supported in part by NIH grant AM 20884.

The authors express their gratitude to Dr. Bruce Ettinger, Kaiser Foundation, San Francisco, for donating hydroxytriamterene and hydroxytriamterene sulfate, which he had received from Röhm Pharma, Darmstadt, West Germany. They also thank Dr. P. Magnusson, Leo Pharmaceutical Products for donating hydroflumethiazide. The technical assistance of Mrs. Regina Sörgel is greatly appreciated.

Chemical Modification of Triamcinolone Acetonide to Improve Liposomal Encapsulation

ASHOK GOUNDALKAR and MICHAEL MEZEI ˣ

Received February 7, 1983, from the *College of Pharmacy, Dalhousie University, Halifax, N.S. B3H 3J5, Canada.* Accepted for publication April 18, 1983.

Abstract □ The 21-palmitate of triamcinolone acetonide was synthesized to aid in the liposomal encapsulation of the drug. Encapsulation efficiency of triamcinolone acetonide-21-palmitate was 85%, compared with 5% for the parent drug.

Keyphrases □ Triamcinolone acetonide—synthesis of the 21-palmitate ester, liposomal encapsulation □ Liposomes—encapsulation of triamcinolone acetonide-21-palmitate, synthesis

Liposomes are microscopic vesicles composed of phospholipid bilayers separated by aqueous compartments. Their potential as temporal and spatiotemporal drug delivery systems is being widely investigated (1–3). The applicability of liposomes as selective drug delivery systems for cutaneous administration of drugs has been studied (4, 5) in this laboratory using triamcinolone acetonide as the model drug. Attempts to test various types of liposomes with the same drug revealed a low level of encapsulation of the drug in the multilamellar liposomes.

A relationship between liposomal encapsulation and the structure of the derivatives of another corticosteroid, hydrocortisone, has been reported by Shaw *et al.* (6). The observation that among a variety of derivatives, hydrocortisone-21-palmitate had the maximum encapsulation in the liposomes led us to study a similar approach for enhancing encapsulation of triamcinolone acetonide. The synthesis and purification of triamcinolone acetonide-21-palmitate, based on the principles of the methods reported by Shaw *et al.* (6) and Diamanti and Bianchi (7), is described in this report.

EXPERIMENTAL

9-Fluoro-21-(1-oxohexadecoxy)-11-hydroxy-16,17-[(1-methylethylidene)-bis(oxy)]-pregna-1,4-diene-3,20-dione—Triamcinolone acetonide (435 mg, 1 mmol) was dissolved in 4 mL of *N,N*-dimethylformamide. Pyridine (160 mg, 2 mmol) and palmitoyl chloride (550 mg, 2 mmol) were added, the mixture was stirred magnetically at room temperature for 22 h, and then was poured into 0.5 M sulfuric acid (1600 mL) and stirred vigorously. The product was removed by filtration and was purified by column chromatography on silica gel (toluene–ethyl acetate–acetic acid, 90:10:1). Recrystallization from methanol, gave 471 mg (70% yield) of triamcinolone acetonide-21-palmitate, mp 143–147°C; IR (Nujol): 1760 (ester C=O), 1740 (ketone C=O), 1670 (α,β; $\alpha'\beta'$-unsaturated ketone C=O), 1620 (C=C conjugated with ketone), and 890 cm^{-1} (*cis*-CH of Δ-1,4 system); ^{1}H-NMR ($CDCl_3$): δ 0.88 (t, 3, terminal CH_3), 0.94 (s, 3, 18-CH_3), 1.25 (narrow m, 27, acetonide β-CH_3 and CH_2 chain), 1.42 (s, 3, acetonide α-CH_3), 1.55 (s, 3, 19-CH_3), 1.6–2.5 (m, 4, $CH_2CH_2CO_2$), 4.90 (s, 2, 21-CH_2O), 4.97 (br, 1, 16-CHO), 6.12 (d, 1, $J_{2,4}$ = 0.6 Hz, 4-CH), 6.44 (dd, 1, $J_{2,4}$ = 0.6 Hz, $J_{1,2}$ = 9.5 Hz, 2-CH), and 7.22 ppm (d, 1, $J_{1,2}$ = 9.5 Hz, 1-CH).

Anal.—Calc. for $C_{24}H_{61}FO_7$: C, 71.39; H, 9.44; F, 2.82. Found: C, 71.26; H, 9.25; F, 2.80.

Table I—Comparative Data for Liposomal Encapsulation of Triamcinolone Acetonide and Triamcinolone Acetonide-21-Palmitate.

Procedure	Fraction	Concentration, mg/22 mL: Triamcinolone Acetonide	Concentration, mg/22 mL: Triamcinolone Acetonide-21-Palmitate
Preparation	Crude product	20	20
Filtration	Filtrate	7	19
Centrifugation	Supernatant	6	2
	Pellet (liposomes)	1	17

Preparation of Liposomes—To reliably determine encapsulation efficiency, radioactive triamcinolone acetonide-21-palmitate was prepared as above from [6,7-^{3}H]triamcinolone acetonide. Multilamellar liposomes were prepared as described by Mezei and Gulasekharam (4). Dipalmitoyl phosphatidyl choline (160 mg) and triamcinolone acetonide-21-palmitate (22 mg, 350 μCi) in chloroform–methanol (2:1) were evaporated using a rotary evaporator. The film was then dispersed with 22 mL of aqueous 8 mM $CaCl_2$ solution at 60°C. The preparation was evaluated microscopically and then filtered through a 12-μm polycarbonate filter. The filtrate was then centrifuged at 22,000×*g* for 25 min. Radioactivity in each fraction was measured after each treatment. Triamcinolone acetonide liposomes were prepared in a similar manner.

RESULTS AND DISCUSSION

Results presented in Table I indicate considerable improvement in liposomal encapsulation of triamcinolone acetonide as a result of palmitoylation. In the case of the triamcinolone acetonide liposomal preparation the first major loss occurred after filtration through a 12-μm polycarbonate filter. This filtration step is necessary with the liposomal encapsulation of a lipophilic drug. Since the drug is insoluble or very slightly soluble in the aqueous medium, only that portion is encapsulated that is in solution and intimately associated with the lipid bilayers; the remaining portion is in solid form which, although it is unencapsulated, would be present in the liposomal fraction after centrifugation. The loss of 13 mg (*i.e.*, 65%) of triamcinolone acetonide by the filtration process was due mainly to unencapsulated crystals observed in the crude preparation. Such crystals were absent in the filtrate. No crystals were seen even in the unfiltered triamcinolone acetonide-21-palmitate liposomal fraction; consequently, only 1 mg (*i.e.*, 5%) was lost by the filtration. This suggests that the palmitate form has a stronger association with the lipid layers and that almost complete encapsulation is achieved.

The second major loss in the case of triamcinolone acetonide liposomes was in the supernatant after centrifugation of the filtrate. This is due mainly to the drug in solution but not associated with liposomes. Evidence for this was demonstrated by gel filtration chromatography. Thus, the overall encapsulation of triamcinolone acetonide, determined in the final purified liposomal fraction, was only 5% while that of its palmitate derivative was found to be 85%. The encapsulation of the palmitate derivative could be close to 100%, if one considers the unavoidable loss due to the filtration and centrifugation procedures, *i.e.*, by adsorption to the filter and glassware. Another minor but inherent loss of liposomes could be due to the presence of small (<0.5-μm) liposomes, which are not completely sedimented by centrifugation. However, for comparison purposes, both preparations were analyzed by the same procedures, and consequently, the same considerations should be applied.

A possible reason for increased encapsulation of the palmitate derivative could be the change in the partition coefficient. For lipid-soluble compounds a logarithmic partition coefficient (log P) between 1.7 and 4 is unfavorable for liposomal encapsulation (8). Triamcinolone acetonide has a log P of 2.53 (9). Palmitoylation would increase this to ~11 as calculated using substituent constants (9).

The mechanism for increased encapsulation could be predicted to be analogous to that of hydrocortisone-21-palmitate (10). The palmitoyl chain may act as "hydrophobic anchor" holding the steroid head group on the surface of the lipid bilayer.

One of the drawbacks in liposomal drug delivery systems is the poor encapsulation of the drug in the liposomes. Chemical modification is likely to be a powerful approach to overcome such an obstacle, as evidenced here and elsewhere (6). Although only a small amount of the drug was associated with the liposomes, the drug disposition was altered favorably on dermal application of a triamcinolone acetonide liposomal preparation (4, 5). In light of this, the potential usefulness of this highly concentrated liposomal triamcinolone

0022-3549/84/0600-0834$01.00/0
© 1984, American Pharmaceutical Association

acetonide-21-palmitate preparation as a selective drug delivery system for cutaneous administration may be optimal.

REFERENCES

(1) G. Gregoriadis, in "Liposomes in Biological Systems," G. Gregoriadis and A. C. Alison, Eds., Wiley, New York, N.Y., 1980 p. 377.

(2) R. L. Juliano and D. Layton, in "Drug Delivery Systems," R. L. Juliano, Ed., Oxford University Press, New York, N.Y., 1980, p. 189.

(3) M. B. Yatvin and P. I. Lelkes, *Med. Phys.*, **9**, 149 (1982).

(4) M. Mezei and V. Gulasekharam, *Life Sci.*, **26**, 1473 (1980).

(5) M. Mezei and V. Gulasekharam, *J. Pharm. Pharmacol.*, **34**, 473 (1982).

(6) J. H. Shaw, C. G. Knight, and J. T. Dingle, *Biochem. J.*, **158**, 473 (1976).

(7) E. Diamanti and G. E. Bianchi, *Arzneim.-Forsch.*, **21**, 251 (1971).

(8) F. Defrise-Quertain, P. Chetalain, J. M. Rnysschaert, and M. Delmelle, *Biochim. Biophys. Acta*, **628**, 57 (1980).

(9) C. Hansch and A. Leo, "Substituent Constants For Correlation Analysis in Chemistry and Biology," Wiley, New York, N.Y., 1979 pp. 19, 315.

(10) F. J. T. Fildes and J. E. Oliver, *J. Pharm. Pharmacol.*, **30**, 337 (1978).

ACKNOWLEDGMENTS

This study was supported by the Medical Research Council of Canada (MA 6664). The authors thank Dr. P. S. Farmer, College of Pharmacy, Dalhousie University, Halifax, Nova Scotia, for his advice and assistance during the course of this project.

Quantitation of Amphotericins by Reverse-Phase High-Performance Liquid Chromatography

MICHEL MARGOSIS ˣ and ADORJAN ASZALOS

Received February 26, 1982, from the *Food and Drug Administration, Division of Drug Biology, Washington, DC 20204.* Accepted for publication April 26, 1983.

Abstract □ A reverse-phase high-performance liquid chromatographic (HPLC) method was developed for simultaneous potency determination of amphotericin A and amphotericin B in bulk amphotericin B preparations. This single, rapid, specific, and simple method can be used for qualitative and quantitative analyses and is proposed to replace a combination of cumbersome official tests presently in use. This new HPLC method employs an isocratic acidic phosphate buffer–methanol mixture in a reverse mode on an octadecylsilane-bonded silica column at ambient temperature, using UV detection at 313 nm. Results obtained by HPLC compare favorably with the official assay results. During these studies, an apparent heptaenic component, not previously described, was detected in commercial amphotericin B preparations at concentrations ranging from ~6 to 14%.

Keyphrases □ Quantitation—amphotericin B, amphotericin A, reverse-phase HPLC □ Amphotericin B—quantitation with amphotericin A, reverse-phase HPLC

Amphotericin B (1) (CAS registry 1397-89-3), produced by a strain of *Streptomycetes nodusus*, is an amphoteric macrocyclic polyene antibiotic that has become a valuable therapeutic agent in the treatment of fungal and monilial infections in humans (1). Polyene antibiotics are characterized chemically by strong absorption in the UV and visible regions of the spectrum, ascribed mainly to conjugated unsaturation with four (tetraenes) to seven (heptaenes) double bonds (1, 2). These substances are relatively unstable, and the heptaenes, in particular, are insoluble in most solvents.

Bulk amphotericin B is commercially available in two forms—one is purified for use in parenteral products (type I) and the other is a cruder grade for topical applications (type II). According to the official monograph (3), the potency of each form must be ≥750 μg/mg on the anhydrous basis. Both types may also contain amphotericin A, a cofermented tetraene very similar to nystatin; however, type I may contain ≤5% amphotericin A, whereas type II may contain ≤15% amphotericin A. Characteristics of amphotericin B are extensively discussed and reviewed with respect to physicochemical and analytical properties by Asher *et al.* (1) and Thomas (2).

Official requirements for the premarketing certification of amphotericin B (3) include a microbiological agar diffusion assay, a quantitative differential UV spectrophotometric procedure for the determination of the amphotericin A content, and a qualitative UV spectrophotometric identity test for amphotericin B. The microbiological assay measures the total activity of substances responding to a particular organism in comparison with an established standard of defined activity. Selectivity, precision, and reliability of this microbiological assay are inadequate, especially because of the deleterious effect of the high pH (4, 5) needed to solubilize the substance during this assay.

Reverse-phase high-performance liquid chromatography (HPLC) was demonstrated by Mechlinski and Schaffner (6) to be well suited to the qualitative analysis of such intractable

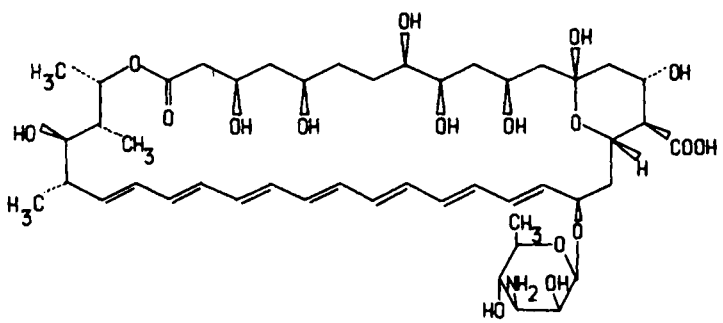

© 1984, American Pharmaceutical Association

acetonide-21-palmitate preparation as a selective drug delivery system for cutaneous administration may be optimal.

REFERENCES

(1) G. Gregoriadis, in "Liposomes in Biological Systems," G. Gregoriadis and A. C. Alison, Eds., Wiley, New York, N.Y., 1980 p. 377.

(2) R. L. Juliano and D. Layton, in "Drug Delivery Systems," R. L. Juliano, Ed., Oxford University Press, New York, N.Y., 1980, p. 189.

(3) M. B. Yatvin and P. I. Lelkes, *Med. Phys.*, **9**, 149 (1982).

(4) M. Mezei and V. Gulasekharam, *Life Sci.*, **26**, 1473 (1980).

(5) M. Mezei and V. Gulasekharam, *J. Pharm. Pharmacol.*, **34**, 473 (1982).

(6) J. H. Shaw, C. G. Knight, and J. T. Dingle, *Biochem. J.*, **158**, 473 (1976).

(7) E. Diamanti and G. E. Bianchi, *Arzneim.-Forsch.*, **21**, 251 (1971).

(8) F. Defrise-Quertain, P. Chetalain, J. M. Rnysschaert, and M. Delmelle, *Biochim. Biophys. Acta*, **628**, 57 (1980).

(9) C. Hansch and A. Leo, "Substituent Constants For Correlation Analysis in Chemistry and Biology," Wiley, New York, N.Y., 1979 pp. 19, 315.

(10) F. J. T. Fildes and J. E. Oliver, *J. Pharm. Pharmacol.*, **30**, 337 (1978).

ACKNOWLEDGMENTS

This study was supported by the Medical Research Council of Canada (MA 6664). The authors thank Dr. P. S. Farmer, College of Pharmacy, Dalhousie University, Halifax, Nova Scotia, for his advice and assistance during the course of this project.

Quantitation of Amphotericins by Reverse-Phase High-Performance Liquid Chromatography

MICHEL MARGOSIS ˣ and ADORJAN ASZALOS

Received February 26, 1982, from the *Food and Drug Administration, Division of Drug Biology, Washington, DC 20204.* Accepted for publication April 26, 1983.

Abstract □ A reverse-phase high-performance liquid chromatographic (HPLC) method was developed for simultaneous potency determination of amphotericin A and amphotericin B in bulk amphotericin B preparations. This single, rapid, specific, and simple method can be used for qualitative and quantitative analyses and is proposed to replace a combination of cumbersome official tests presently in use. This new HPLC method employs an isocratic acidic phosphate buffer–methanol mixture in a reverse mode on an octadecylsilane-bonded silica column at ambient temperature, using UV detection at 313 nm. Results obtained by HPLC compare favorably with the official assay results. During these studies, an apparent heptaenic component, not previously described, was detected in commercial amphotericin B preparations at concentrations ranging from ~6 to 14%.

Keyphrases □ Quantitation—amphotericin B, amphotericin A, reverse-phase HPLC □ Amphotericin B—quantitation with amphotericin A, reverse-phase HPLC

Amphotericin B (1) (CAS registry 1397-89-3), produced by a strain of *Streptomycetes nodusus*, is an amphoteric macrocyclic polyene antibiotic that has become a valuable therapeutic agent in the treatment of fungal and monilial infections in humans (1). Polyene antibiotics are characterized chemically by strong absorption in the UV and visible regions of the spectrum, ascribed mainly to conjugated unsaturation with four (tetraenes) to seven (heptaenes) double bonds (1, 2). These substances are relatively unstable, and the heptaenes, in particular, are insoluble in most solvents.

Bulk amphotericin B is commercially available in two forms—one is purified for use in parenteral products (type I) and the other is a cruder grade for topical applications (type II). According to the official monograph (3), the potency of each form must be ≥750 μg/mg on the anhydrous basis. Both types may also contain amphotericin A, a cofermented tetraene very similar to nystatin; however, type I may contain ≤5% amphotericin A, whereas type II may contain ≤15% amphotericin A. Characteristics of amphotericin B are extensively discussed and reviewed with respect to physicochemical and analytical properties by Asher *et al.* (1) and Thomas (2).

Official requirements for the premarketing certification of amphotericin B (3) include a microbiological agar diffusion assay, a quantitative differential UV spectrophotometric procedure for the determination of the amphotericin A content, and a qualitative UV spectrophotometric identity test for amphotericin B. The microbiological assay measures the total activity of substances responding to a particular organism in comparison with an established standard of defined activity. Selectivity, precision, and reliability of this microbiological assay are inadequate, especially because of the deleterious effect of the high pH (4, 5) needed to solubilize the substance during this assay.

Reverse-phase high-performance liquid chromatography (HPLC) was demonstrated by Mechlinski and Schaffner (6) to be well suited to the qualitative analysis of such intractable

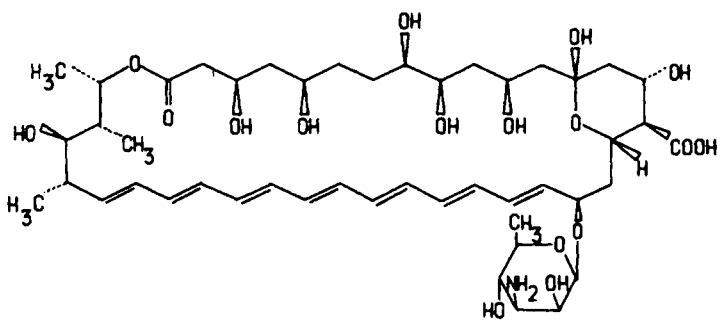

© 1984, American Pharmaceutical Association

Table I—Comparison of the Code of Federal Regulation (CFR) and Liquid Chromatographic Methods for the Quantitation of Amphotericin B

Sample[a]	Potency, μg/mg[b] Mfg. Cert.	CFR Method	HPLC Method
Standard[c]	954	954	954
1[c]	952	924 ± 23 (4)	936 ± 33 (9)
2[d]	784	720 ± 63 (24)	784 ± 33 (9)
3[d]	807	755 ± 46 (6)	819 ± 42 (5)
4[d]	798	749 ± 53 (8)	754 ± 68 (15)
5[c]	939	840 ± 65 (7)	886 ± 37 (6)

[a] Batch numbers for samples 1–5 obtained from E. R. Squibb & Sons, Inc. are 58022-002, 58334-404, 58334-406, 53834-405, and 58366-003, respectively. [b] Mean ± *SD;* multiply by 0.1 to convert to percent potency. The number of analyses is given in parentheses. [c] Type I. Standard labeled at 954 μg of amphotericin B/mg. [d] Type II.

Table II—Comparison of the Code of Federal Regulations (CFR) and Liquid Chromatographic Methods for the Quantitation of Amphotericin A

Sample[a]	Amphotericin A Content, % Mfg. Cert.	CFR Method	HPLC Method
Standard[b]	0.24	0.24	0.24
1[b]	0.4	NT[c]	0.52
2[d]	0.27	0.32	0.26

[a] Batch numbers for samples 1–5 obtained from E. R. Squibb & Sons, Inc. are 58022-002, 58334-404, 58334-406, 53834-405, and 58366-003, respectively. [b] Type I. Standard amphotericin B containing 0.24% amphotericin A. [c] NT = Not tested. [d] Type II.

substances as the polyene antibiotics. Subsequently, Nillson-Ehle *et al.* (7) used this technique to quantitate amphotericin B in biological fluids. An HPLC system showing a partial separation of amphotericin A and amphotericin B was also described by Asher *et al.* (1). However, none of these methods provide the separation needed for a reliable assay of the components present in the bulk material. The method described and discussed here is proposed to replace the three methods (3) that are currently used for the certification of amphotericin B bulk preparations.

Instrument—A liquid chromatograph[1] equipped with a septumless valve injector[2] and a fixed-wavelength UV detector[3] with a 313-nm filter was used for all quantitative analysis. This was connected to a recording device[4] and an electronic integrator[5]. A special system[6] described by DiCesare *et al.* (8) was used for the qualitative analysis.

Column—A stainless steel column (4.6 × 150 mm) commercially packed with fully porous 7- to 8-μm silica particles to which a monomolecular layer of octadecylsilane was chemically bonded[7] was used in the quantitative phase of this study. The inlet of this analytical column was connected to a guard precolumn (4.6 × 100 mm) gravity-packed with an octadecylsilane-bonded silica of ~40-μm particle size[8]. The column system was equilibrated and conditioned with passage of ~10–15 void volumes of mobile phase, and tested for initial performance and suitability as described previously (7). A stainless steel column (4.6 × 100 mm) commercially packed with 3-μm octadecylsilane-bonded silica especially designed for high-speed analysis[9] was used in the qualitative study.

Chemicals and Reagents—Amphotericin B[10], labeled to contain 954 μg of amphotericin B/mg of powdered standard (containing 0.24% amphotericin A), was used as the external standard. Standards of amphotericin A[11] of unknown purity and nystatin[12] were also used. The dimethyl sulfoxide was spectro grade, phosphoric acid and sodium dihydrogen phosphate were reagent grade, and methanol was distilled-in-glass quality[13]. All the water used was deionized[14].

Stock Solutions—Approximately 6.3 g of sodium dihydrogen phosphate was dissolved in 950 mL of deionized water in a 1-L volumetric flask. The pH was adjusted to 2.6 with concentrated phosphoric acid, and the solution was diluted to volume with water.

Mobile Phase—A 300-mL aliquot of the phosphate solution was diluted to 1.00 L with methanol. This solution was mixed and deaerated by passing it through a 0.5-μm filter and ultrasonicating it for 2 min before use. As an added precaution, helium was allowed to sparge perceptibly through a 2-μm metal filter into this mobile phase during analysis to ensure maximum elimination of dissolved air. If necessary, the ratio of methanol to aqueous buffer can be adjusted to obtain adequate retention and peak separation.

Standard Solution and Sample—Approximately 25 mg of the amphotericin B standard was accurately weighed into a 25-mL volumetric flask, which was then filled to volume with dimethyl sulfoxide. The solution was mixed, shaken, and ultrasonicated until totally clear. The amphotericin B samples were prepared in a manner identical with that of the standard with ~25 mg of amphotericin B type I and ~30 mg of amphotericin B type II. All solutions of amphotericin B should be prepared fresh just before use.

Conditions for Quantitation—A constant operating temperature (ambient) was maintained, and the mobile phase flow rate of 2.0–2.5 mL/min was adjusted to give peaks of satisfactory configuration. The detector sensitivity was controlled to produce peak heights >50% full scale deflection with a chart speed of 2.5 mm/min. Chromatograms used for calculating performance parameters were obtained at a chart speed of at least 25 mm/min to allow better visual measurement of peak geometry for greater accuracy. The column was rinsed with methanol for 1 min and equilibrium was reestablished with the mobile phase before each injection.

Assay and Calculations—Carefully measured 15.0-μL aliquots of standard and sample solutions were injected sequentially into the chromatograph. Quantitation was achieved by comparing peak heights (and/or areas) of samples to that of the standard according to the following equations:

tericin B sample, C_A is the concentration of amphotericin A in the amphotericin B sample solution, P_B is the height (or area) of the amphotericin B peak in the amphotericin B sample, C_B is the concentration of amphotericin B in the amphotericin B sample solution, P_S is the height (or area) of the corresponding component peak in the amphotericin B standard reference material, and C_S is the concentration of the corresponding component in the solution of amphotericin B standard reference material. An APL time-sharing computer system[15] was used to plot all graphs and to perform all calculations and data reduction.

Amphotericin B is quite insoluble in most organic solvents; for this analysis it was dissolved in neat dimethyl sulfoxide. Initial attempts to dilute the dimethyl sulfoxide solutions with methanol frequently caused gelatinous precipitates, particularly with methanol–dimethyl sulfoxide ratios >9:1. One beneficial effect of neat dimethyl sulfoxide injections was slightly better peak resolution. On the other hand, the inactivating effect of dimethyl sulfoxide and residual sample (retained solutes) in the column diminished retention time with each subsequent injection. However, the original retention time was restored rapidly with a 1-min methanol rinse. One may alternate injections of samples and methanol rinses to maximize replication of retention; however, the actual frequency of column rinsings will depend on the total amount of solute injected. For samples analyzed within 1 d, peak heights for seven injections of standard interspersed with samples and rinses showed a coefficient of variation of 1.46%.

The stability of amphotericin B is greatest at a neutral pH where it exists as a zwitterion; however, better separation was achieved with ion suppression of the acid function. The use of acidic media in the HPLC procedure tends

[1] Model 6000A solvent delivery system; Waters Associates, Milford, Mass.
[2] Model U6K; Waters Associates.
[3] Model 440; Waters Associates.
[4]
[5]
[6] Model 3B solvent delivery system, Sigma 15 chromatography data station, model LC-85 spectrophotometric detector, and autocontrol; Perkin-Elmer Corp., Norwalk, Conn.
[7] Zorbax ODS; DuPont Instruments, Wilmington, Del.
[8] Bondapak (C_{18}/Corasil); Waters Associates.
[9] HS-3-C18; Perkin-Elmer Corp.
[10] USP reference standard.
[11] USP reference standard, lot no. HV-718.
[12] USP reference standard, lot F.
[13] Burdick & Jackson Laboratories, Inc., Muskegon, Mich.
[14] Milli-Q Reagent-Grade water system; Millipore Corp., Bedford, Mass.

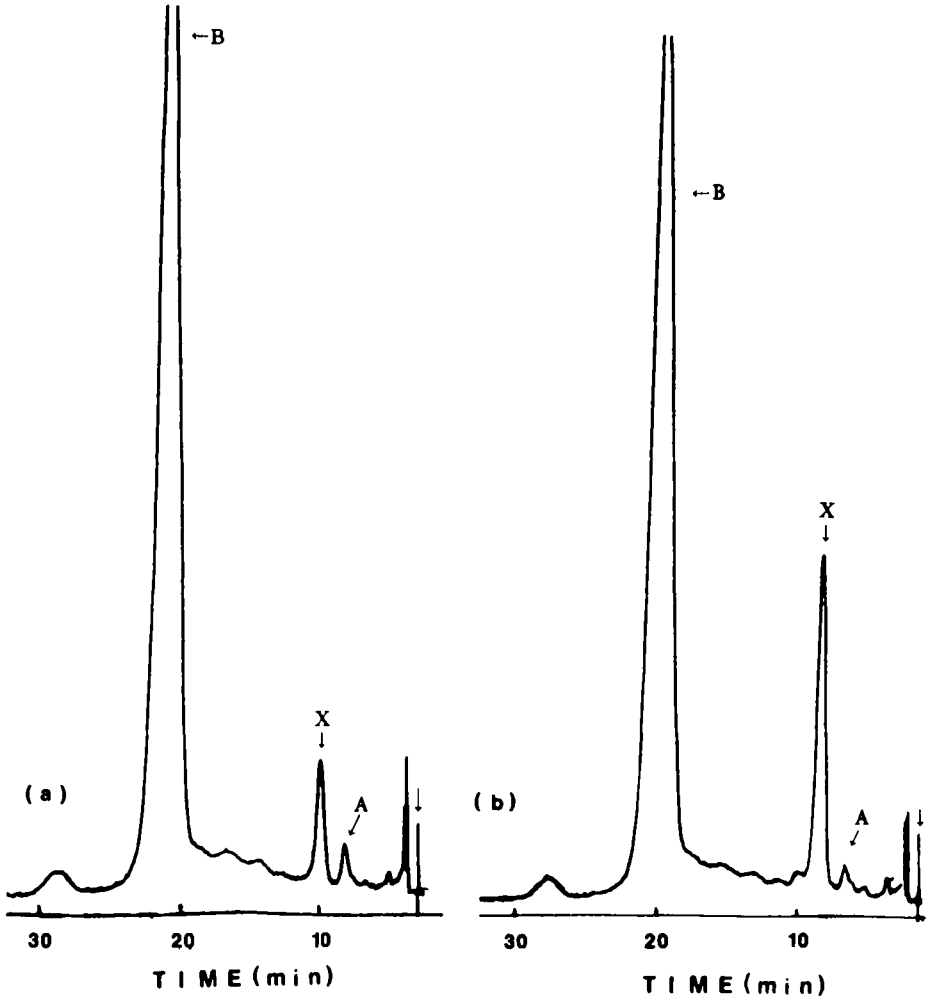

Figure 1—*Chromatograms of bulk amphotericin B from E. R. Squibb & Sons, Inc., type I (a) (batch #58022-002) and type II (b) (batch #58334-404). Key: (A) amphotericin A; (B) amphotericin B; and (X) amphotericin X.*

to approximate the method of isolation of the antibiotic from the broth in commercial production. The adverse effect of the acidity of the buffer is diminished by the high concentration of methanol in the mobile phase.

The capacity factor for amphotericin B is 25, but in spite of its magnitude, the column efficiency calculated as the reduced plate height is ~32. The separation factors for amphotericin A and amphotericin X (unidentified heptaene component) compared with amphotericin B are 4.3 and 2.7, respectively, with resolution factors of 4.4 and 3.4 between the same pairs of peaks. It is noted that although the column of 3-μm particles yielded substantially more plates, it provided about the same absolute efficiency as the column of larger particles (7–8 μm).

Qualitative Analysis—Samples of type I and type II amphotericin B yielded the chromatographic profiles shown in Fig. 1a and b, respectively, showing peaks attributed to amphotericin A and one labeled amphotericin X. These chromatograms are meant merely to provide a visual example of a separation previously unavailable from a qualitative standpoint and to indicate the relatively large quantitative difference between the two types (I and II) of commercial amphotericins. However, note that these chromatograms were not necessarily obtained the same day.

To the authors' knowledge, the presence of this newly discovered component in amphotericin B has never been described in the literature. Although the chromatograms of the type I and type II samples appear to be very similar from a qualitative standpoint, the type I sample is purer because it has a higher potency and contains less than half the amount of amphotericin X.

Amphotericin A and nystatin were believed for a long time to be identical. Consequently, because the spectral characteristics of both of these substances are so similar and because nystatin is more readily available than amphotericin A, the former is used as a standard to assay for the latter. Although these two substances had been separated under different conditions[16], they were not resolved by the method described here, demonstrating again their close similarity[17].

Chromatographic peaks were examined on-line by UV spectrophotometry (6) with the system[6] previously described. This system allows rapid elution (4 *versus* 30 min) with good resolution of peaks because of the short column packed with smaller particles (3 μm) and because of the accessory spectrophotometer especially designed with a 2.4-μL cell. This system also provides fast response time and a very low dead volume. Several peaks were subjected to UV scanning in an attempt to confirm or identify them. The resultant spectra indicated correctly that the peak attributed to amphotericin A is that of a tetraene; four other peaks including those labeled amphotericin B and amphotericin X were characterized as heptaene peaks on the basis of UV characteristics identical to those of known heptaenes.

Polyene antibiotics exhibit multiplet absorption peaks in the UV region; absorption maxima for the tetraene amphotericin A occur with decreasing intensity at 305, 318, 290, and 280 nm and at 406, 382, 363, and 356 nm for heptaenes (*e.g.*, amphotericin B) with this system[6]. The 313-nm filter of a photometer with a band spread of 10 ± 2 nm allows good sensitivity for minor tetraene peaks while simultaneously enabling adequate detection of heptaenes. Spectra of the amphotericins have also been published (1, 2).

Quantitative Analysis—Table I lists the calculated potency of several lots of commercial amphotericins; Table II gives the content of amphotericin A in the same samples.

A calibration curve for amphotericin B was obtained by plotting amounts ranging from ~5 to 26 μg of the injected drug against peak height and peak area. A rectilinear relationship was observed with corresponding correlation coefficients of 0.9999 and 0.9991 and corresponding relative percentage errors of 0.58 and 1.50. Optimum quantitation is obtained when injections of both standard and sample solutions are of approximately the same concentration and volume because errors due to nonlinearity of the detector[3] and the injector[2] are minimized (9). The addition of an internal standard to improve precision is advisable, if possible, but the complexity of the chromatogram precluded its use here.

Because the standard addition method did not prove satisfactory, the content of amphotericin A in commercial samples was calculated from peak heights by direct comparison to the content of amphotericin A in the amphotericin B standard. This standard had been established to contain 0.24% of amphotericin A by the official procedure, which is based on differential spectrophotometry of a standard solution of amphotericin B and a standard solution

of nystatin. The latter has been shown to possess spectral characteristics nearly identical to that of amphotericin A[16,17].

The paired t test was used to compare bioassay results from the manufacturer with those from the HPLC method. No significant statistical difference was found at the 95% confidence level. It would be difficult and impractical at this juncture to make further comparisons among sample results because of the poor precision of microbiological assays for antifungal substances.

It can, therefore, be concluded that the commercial bulk material is predominantly amphotericin B containing a limited amount of the A congener and several heptaenes. The potency of type I amphotericin B may measure >900 μg/mg with ~6% amphotericin X, whereas type II shows a potency of ~800 μg/mg with ~11-14% amphotericin X.

REFERENCES

(1) I. M. Asher, G. Schwartzman, and the USASRG (U.S. Antibiotics Standards Research Group), "Analytical Profiles of Drug Substances," vol. 6, Klaus Florey, Ed., Academic, New York, N.Y., 1977, pp. 1-42.

(2) A. H. Thomas, *Analyst (London)*, **101**, 321 (1976).

(3) "Code of Federal Regulations," Food and Drugs, Title 21, part 449.4, U.S. Government Printing Office, Washington, D.C., 1981.

(4) J. M. T. Hamilton-Miller, *J. Pharm. Pharmacol.*, **25**, 401 (1973).

(5) S. C. Cheung, G. Medoff, D. Schlessinger, and G. S. Kobayashi, *Antimicrob. Agents Chemother.*, **8**, 426 (1975).

(6) W. Mechlinski and C. P. Schaffner, *J. Chromatogr.*, **99**, 619 (1974).

(7) I. Nillson-Ehle, T. T. Yoshikawa, J. E. Edwards, M. Schotz, and L. B. Guze, *J. Infect. Dis.*, **135**, 414 (1977).

(8) J. L. DiCesare, M. W. Dong, and L. S. Ettre, *Chromatographia*, **14**(5), 257 (1981).

(9) M. Margosis, *J. Chromatogr.*, **236**, 469 (1982).

[16] V. Walton, Food and Drug Administration, 1979, unpublished results. FDA semiannual report available from M. Margosis, Pharmaceutical Research and Testing, FDA, HFN-178, 200 C St., S.W., Washington, DC 20204.

[17] A. Aszalos, J. D. Weber, E. P. Mazzola, M. J. Hayden, and T. Alexander, Food and Drug Administration, 1981, unpublished results. FDA semiannual report available from M. Margosis, Pharmaceutical Research and Testing, FDA, HFN-178, 200 C St., S.W., Washington, DC 20204.

ACKNOWLEDGMENTS

Presented at the American Pharmaceutical Association, Academy of Pharmaceutical Sciences annual meeting, Orlando, Fla., November 1981.

The authors express their gratitude to David G. Skiados of the Perkin-Elmer Corporation for graciously providing the use of the scanning system in the Rockville, Md., laboratories and to Alice Marcotte of the Technical Editing Section, Food and Drug Administration, for editorial assistance.

In Vitro Stability of Sodium Nitroprusside Solutions for Intravenous Administration

CHERYL MAHONY *x, JAMES E. BROWN, W. WAYNE STARGEL, CHACKO P. VERGHESE, and THORIR D. BJORNSSON

Received August 27, 1982, from the *Divisions of Clinical Pharmacology and Cardiology, Departments of Pharmacology and Medicine, Duke University Medical Center, Durham, NC 27710.* Accepted for publication March 21, 1983.

*Present address: Division of Cardiology, College of Medicine, University of Kentucky Medical Center, Lexington, KY 40536.

Abstract □ A sensitive high-performance liquid chromatographic assay for nitroprusside using an ion-exchange column and UV detection was developed to evaluate the stability of aqueous solutions of sodium nitroprusside in light-protected glass and plastic containers and during simulated infusions. The results showed that sodium nitroprusside is stable in 5% dextrose, normal saline, and lactated Ringer's solutions in light-protected glass or plastic containers. In addition, there was no decrease in the delivered potency of sodium nitroprusside solutions during simulated infusions lasting up to 24 h.

Keyphrases □ Sodium nitroprusside—*in vitro* stability, solutions, intravenous administration, HPLC □ Stability—*in vitro*, sodium nitroprusside solutions, intravenous administration, HPLC

Sodium nitroprusside [$Na_2Fe(CN)_5NO{\cdot}2H_2O$] is a valuable agent in the treatment of congestive heart failure (1), cardiogenic shock complicating acute myocardial infarction (2), and hypertensive crisis (3). This drug is also used for the production of intraoperative hypotension (4). However, there are several problems associated with the clinical use of sodium nitroprusside, including tolerance (5), tachyphylaxis (6), and the toxicity of its metabolites, cyanide and thiocyanate (7). Some of these problems might be alleviated by an understanding of the pharmacokinetics of nitroprusside in humans. To derive pharmacokinetic parameters from data collected during a constant infusion, the amount of sodium nitroprusside delivered must be known. The purpose of this study was to investigate the stability of sodium nitroprusside in various intravenous solutions and during simulated infusions.

EXPERIMENTAL

Reagents and Chemicals—Sodium nitroprusside[1] was used as received. Analytical-grade KH_2PO_4 and H_3PO_4 and deionized water were used to prepare the mobile phase. All glassware used for sampling or storage of stock solutions was silanized[2].

Instruments and Chromatographic Conditions—An anion-exchange column[3] and a 0.5 M KH_2PO_4 buffer (pH 3.0) with H_3PO_4, were used to achieve the chromatographic separation. The high-performance liquid chromatography (HPLC) was performed with a solvent pumping system[4], a variable-wavelength UV detector[5], and an injector equipped with a 50-μL sample loop[6]. The absorbance was measured at 230 nm with a 0.1 AUFS deflection and was recorded on a three-pen recorder[7]. The flow rate was 1.4 mL/min, and the mobile phase was filtered and deaerated prior to use.

Stability Studies—Sodium nitroprusside (50 mg) was dissolved in 5 mL of water and then added to 500 or 1000 mL of a test solution, resulting in a final concentration of 100 and 50 μg/mL, respectively. The stability of sodium nitroprusside was tested in 5% dextrose, normal saline (0.9% NaCl), and lactated Ringer's solutions[8] in both glass[8] and plastic[8] containers. After the addition of the sodium nitroprusside concentrate, the test solution was mixed and a sample was withdrawn for use in the construction of a standard curve. The bottle or plastic bag was wrapped in aluminum foil and left exposed to laboratory (fluorescent) light for 48 h. Sodium nitroprusside standards were protected from light and stored at 4°C. The stability of the standard solutions was verified by comparing their concentrations with freshly prepared 100-

[1] Roche Laboratories, Nutley, N.J.
[2] Prosil-28; PCR Research Chemicals, Gainesville, Fla.
[3] Partisil 10-SAX; Whatman Inc., Clifton, N.J.
[4] Constametric I; Laboratory Data Control, Riviera Beach, Fla.
[5] Spectromonitor III; Laboratory Data Control, Riviera Beach, Fla.
[6] Model 7120; Rheodyne Inc., Berkeley, Calif.
[7] Linear Instruments, Irvine, Calif.
[8] Abbott Laboratories, North Chicago, Ill.

0022-3549/84/0600-0838$01.00/0

© 1984, American Pharmaceutical Association

of nystatin. The latter has been shown to possess spectral characteristics nearly identical to that of amphotericin A[16,17].

The paired t test was used to compare bioassay results from the manufacturer with those from the HPLC method. No significant statistical difference was found at the 95% confidence level. It would be difficult and impractical at this juncture to make further comparisons among sample results because of the poor precision of microbiological assays for antifungal substances.

It can, therefore, be concluded that the commercial bulk material is predominantly amphotericin B containing a limited amount of the A congener and several heptaenes. The potency of type I amphotericin B may measure >900 μg/mg with ~6% amphotericin X, whereas type II shows a potency of ~800 μg/mg with ~11-14% amphotericin X.

REFERENCES

(1) I. M. Asher, G. Schwartzman, and the USASRG (U.S. Antibiotics Standards Research Group), "Analytical Profiles of Drug Substances," vol. 6, Klaus Florey, Ed., Academic, New York, N.Y., 1977, pp. 1-42.

(2) A. H. Thomas, *Analyst (London)*, **101**, 321 (1976).

(3) "Code of Federal Regulations," Food and Drugs, Title 21, part 449.4, U.S. Government Printing Office, Washington, D.C., 1981.

(4) J. M. T. Hamilton-Miller, *J. Pharm. Pharmacol.*, **25**, 401 (1973).

(5) S. C. Cheung, G. Medoff, D. Schlessinger, and G. S. Kobayashi, *Antimicrob. Agents Chemother.*, **8**, 426 (1975).

(6) W. Mechlinski and C. P. Schaffner, *J. Chromatogr.*, **99**, 619 (1974).

(7) I. Nillson-Ehle, T. T. Yoshikawa, J. E. Edwards, M. Schotz, and L. B. Guze, *J. Infect. Dis.*, **135**, 414 (1977).

(8) J. L. DiCesare, M. W. Dong, and L. S. Ettre, *Chromatographia*, **14**(5), 257 (1981).

(9) M. Margosis, *J. Chromatogr.*, **236**, 469 (1982).

[16] V. Walton, Food and Drug Administration, 1979, unpublished results. FDA semiannual report available from M. Margosis, Pharmaceutical Research and Testing, FDA, HFN-178, 200 C St., S.W., Washington, DC 20204.

[17] A. Aszalos, J. D. Weber, E. P. Mazzola, M. J. Hayden, and T. Alexander, Food and Drug Administration, 1981, unpublished results. FDA semiannual report available from M. Margosis, Pharmaceutical Research and Testing, FDA, HFN-178, 200 C St., S.W., Washington, DC 20204.

ACKNOWLEDGMENTS

Presented at the American Pharmaceutical Association, Academy of Pharmaceutical Sciences annual meeting, Orlando, Fla., November 1981.

The authors express their gratitude to David G. Skiados of the Perkin-Elmer Corporation for graciously providing the use of the scanning system in the Rockville, Md., laboratories and to Alice Marcotte of the Technical Editing Section, Food and Drug Administration, for editorial assistance.

In Vitro Stability of Sodium Nitroprusside Solutions for Intravenous Administration

CHERYL MAHONY *x, JAMES E. BROWN, W. WAYNE STARGEL, CHACKO P. VERGHESE, and THORIR D. BJORNSSON

Received August 27, 1982, from the *Divisions of Clinical Pharmacology and Cardiology, Departments of Pharmacology and Medicine, Duke University Medical Center, Durham, NC 27710.* Accepted for publication March 21, 1983. *Present address: Division of Cardiology, College of Medicine, University of Kentucky Medical Center, Lexington, KY 40536.

Abstract □ A sensitive high-performance liquid chromatographic assay for nitroprusside using an ion-exchange column and UV detection was developed to evaluate the stability of aqueous solutions of sodium nitroprusside in light-protected glass and plastic containers and during simulated infusions. The results showed that sodium nitroprusside is stable in 5% dextrose, normal saline, and lactated Ringer's solutions in light-protected glass or plastic containers. In addition, there was no decrease in the delivered potency of sodium nitroprusside solutions during simulated infusions lasting up to 24 h.

Keyphrases □ Sodium nitroprusside—*in vitro* stability, solutions, intravenous administration, HPLC □ Stability—*in vitro*, sodium nitroprusside solutions, intravenous administration, HPLC

Sodium nitroprusside [$Na_2Fe(CN)_5NO{\cdot}2H_2O$] is a valuable agent in the treatment of congestive heart failure (1), cardiogenic shock complicating acute myocardial infarction (2), and hypertensive crisis (3). This drug is also used for the production of intraoperative hypotension (4). However, there are several problems associated with the clinical use of sodium nitroprusside, including tolerance (5), tachyphylaxis (6), and the toxicity of its metabolites, cyanide and thiocyanate (7). Some of these problems might be alleviated by an understanding of the pharmacokinetics of nitroprusside in humans. To derive pharmacokinetic parameters from data collected during a constant infusion, the amount of sodium nitroprusside delivered must be known. The purpose of this study was to investigate the stability of sodium nitroprusside in various intravenous solutions and during simulated infusions.

EXPERIMENTAL

Reagents and Chemicals—Sodium nitroprusside[1] was used as received. Analytical-grade KH_2PO_4 and H_3PO_4 and deionized water were used to prepare the mobile phase. All glassware used for sampling or storage of stock solutions was silanized[2].

Instruments and Chromatographic Conditions—An anion-exchange column[3] and a 0.5 M KH_2PO_4 buffer (pH 3.0) with H_3PO_4, were used to achieve the chromatographic separation. The high-performance liquid chromatography (HPLC) was performed with a solvent pumping system[4], a variable-wavelength UV detector[5], and an injector equipped with a 50-μL sample loop[6]. The absorbance was measured at 230 nm with a 0.1 AUFS deflection and was recorded on a three-pen recorder[7]. The flow rate was 1.4 mL/min, and the mobile phase was filtered and deaerated prior to use.

Stability Studies—Sodium nitroprusside (50 mg) was dissolved in 5 mL of water and then added to 500 or 1000 mL of a test solution, resulting in a final concentration of 100 and 50 μg/mL, respectively. The stability of sodium nitroprusside was tested in 5% dextrose, normal saline (0.9% NaCl), and lactated Ringer's solutions[8] in both glass[8] and plastic[8] containers. After the addition of the sodium nitroprusside concentrate, the test solution was mixed and a sample was withdrawn for use in the construction of a standard curve. The bottle or plastic bag was wrapped in aluminum foil and left exposed to laboratory (fluorescent) light for 48 h. Sodium nitroprusside standards were protected from light and stored at 4°C. The stability of the standard solutions was verified by comparing their concentrations with freshly prepared 100-

[1] Roche Laboratories, Nutley, N.J.
[2] Prosil-28; PCR Research Chemicals, Gainesville, Fla.
[3] Partisil 10-SAX; Whatman Inc., Clifton, N.J.
[4] Constametric I; Laboratory Data Control, Riviera Beach, Fla.
[5] Spectromonitor III; Laboratory Data Control, Riviera Beach, Fla.
[6] Model 7120; Rheodyne Inc., Berkeley, Calif.
[7] Linear Instruments, Irvine, Calif.
[8] Abbott Laboratories, North Chicago, Ill.

0022-3549/84/0600-0838$01.00/0

© 1984, American Pharmaceutical Association

Table I—Sodium Nitroprusside Stability in Lactated Ringer's, Normal Saline, and 5% Dextrose over 48 h in Glass and Plastic Containers [a]

Concentration, μg/mL	Lactated Ringer's		Normal Saline		5% Dextrose	
	Glass 50	Plastic 100	Glass 100	Plastic 50	Glass 50	Plastic 100
Time, h						
2	104.0	100.7	100.4	100.4	101.0	100
4	103.7	100.7	100.6	100.4	103.4	101.0
8	101.7	99.4	100.2	100.9	98.7	100.9
24	98.2	99.4	104.0	101.0	100.7	101.7
32	102.7	101.9	98.2	100.4	98.8	101.8
48	103.1	100.3	101.3	100.7	100.0	104.2

[a] Each value represents the mean of two experiments and is expressed as percent of control.

or 50-μg/mL sodium nitroprusside standard solutions; no deterioration in the refrigerated and light-protected stock solutions was noted over a 48-h period.

Infusion Studies—A volumetric pump[9] and infusion set[8] were employed. The plastic tubing made of polyvinyl chloride was left exposed to light. The infusion set tubing was 3 m long and held a volume of 20 mL. Flow rates of 10 and 50 mL/h for 24 and 8 h, respectively, were studied. Samples were taken from both the bottle and directly from the end of the tubing at each sampling interval.

Standard Curves—The standard solution of sodium nitroprusside, serially diluted with water to yield concentrations of 6.25, 12.5, 25, and 50 μg/mL, was injected directly onto the column with measurement of peak heights to generate a calibration curve. Each sample was injected in duplicate. The coefficients of variation for the standard curves ranged from 1 to 3%. The unknown samples were analyzed immediately after withdrawal from the container or infusion set at 0, 2, 4, 8, 24, 32, and 48 h after preparation. All experiments were performed in duplicate.

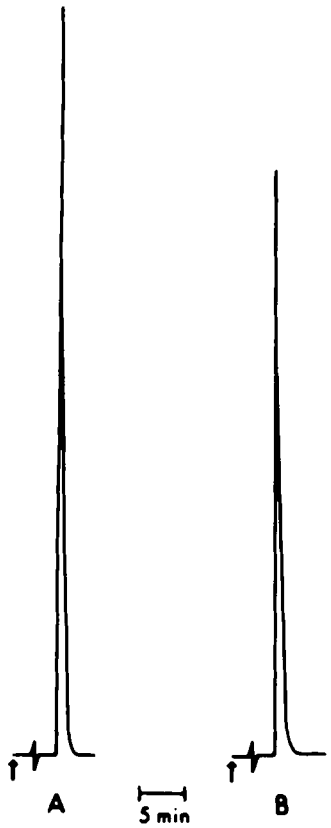

Figure 1—*Chromatogram of 5 μg of sodium nitroprusside in 5% dextrose before (A) and after exposure to light for 4 h (B). The arrow denotes the time of injection.*

[9] Life Care Pump; Abbott Laboratories, North Chicago, Ill.

Table II—Sodium Nitroprusside Stability in Intravenous Infusion Sets at Flow Rates of 10 and 50 mL/h [a]

Time, h	10 mL/h	50 mL/h
2	99.6	101.8
4	100.9	101.8
8	100.9	103.2
24	100.3	—

[a] Values represent the mean of two experiments and are expressed as percent of control.

RESULTS AND DISCUSSION

A chromatogram of sodium nitroprusside, 100 μg/mL in 5% dextrose, is shown in Fig. 1. Using the previously described chromatographic conditions, the retention time is ~5 min. Also shown in Fig. 1 is a chromatogram of the same solution of sodium nitroprusside after exposure to light for 4 h. At 230 nm, the degradation of sodium nitroprusside is manifested as a decrease in the peak height; none of the breakdown products are visible on the chromatogram. Beer's law is obeyed over the sodium nitroprusside concentration range of 1–200 μg/mL. The precision of the assay was evaluated by injecting four replicate samples of 12.5, 25, 50, and 100 μg/mL of sodium nitroprusside; the coefficient of variation was <1%.

The results of the stability studies of sodium nitroprusside in 5% dextrose, lactated Ringer's, and normal saline are shown in Table I. When a glass or plastic container is wrapped in aluminum foil and then left exposed to light for 48 h, there is no appreciable breakdown of sodium nitroprusside at a concentration of either 50 or 100 μg/mL. Other studies have found that sodium nitroprusside is stable in 5% dextrose in glass (8, 9) and plastic (10) containers when protected from light, and this study extends those observations to include normal saline and lactated Ringer's solution. There appears to be no factual basis for the current recommendation that sodium nitroprusside be administered solely in 5% dextrose.

Table II shows the effect of light exposure on sodium nitroprusside solutions while traversing plastic intravenous infusion sets. Duplicate determinations in either 5% dextrose, normal saline, or lactated Ringer's solution at flow rates of 10 or 50 mL/h showed no deterioration in the delivered concentration of the sodium nitroprusside solution over 24 and 8 h, respectively. This finding contrasts with that of Baaske *et al.* (8) who noted a small (3.5%), but consistent, decrease in the potency of a nitroprusside solution delivered from an intravenous infusion set exposed to light for 5 h. This discrepancy may possibly be explained by differences in the composition, and therefore the light diffusion characteristics, of the infusion sets.

REFERENCES

(1) N. H. Guiha, J. N. Cohn, E. Mikulic, J. A. Franciosa, and C. J. Limas, *N. Engl. J. Med.*, **291**, 587 (1974).

(2) K. Chatterjee, W. W. Parmley, W. Ganz, J. Forrester, P. Walinsky, C. Crexells, and H. J. C. Swan, *Circulation*, **48**, 1183 (1973).

(3) I. Tuzel, R. Limjuco, and B. Kahn, *Curr. Ther. Res. Clin. Exp.*, **17**, 95 (1975).

(4) T. H. Taylor, M. Styles, and A. J. Lamming, *Br. J. Anaesth.*, **42**, 859 (1970).

(5) P. P. Moraca, E. M. Bitte, D. E. Hale, C. E. Wasmuth, and E. F. Poutasse, *Anesthesiology*, **23**, 193 (1962).

(6) L. Amaranath and W. F. Kellermeyer, Jr., *Anesthesiology*, **44**, 345 (1976).

(7) J. E. Cottrell, P. Casthely, J. D. Brodie, K. Patel, A. Klein, and H. Turndorf, *N. Engl. J. Med.*, **298**, 809 (1978).

(8) D. M. Baaske, M. D. Smith, N. Karnatz, and J. E. Carter, *J. Chromatogr.*, **212**, 339 (1981).

(9) M. J. Frank, J. B. Johnson, and S. H. Rubin, *J. Pharm. Sci.*, **65**, 44 (1976).

(10) R. A. Anderson and W. Rae, *Aust. J. Pharm. Sci.*, **NS1**(2), 45 (1972).

ACKNOWLEDGMENTS

Cheryl Mahony is the recipient of a Pharmaceutical Manufacturers Association Foundation Award for Cancers in Clinical Pharmacology. Thorir D. Bjornsson is the recipient of a Pharmaceutical Manufacturers Association Foundation Faculty Development Award in Clinical Pharmacology.

Influence of Isotonic Agents on the Stability of Thimerosal in Ophthalmic Formulations

M. J. READER

Received September 9, 1982, from the *Central Analytical Laboratories (Chemical), The Wellcome Foundation Limited, Temple Hill, Dartford, Kent DA1 5AH, U.K.* Accepted for publication April 5, 1983.

Abstract □ Storage tests on the stability of thimerosal in trimethoprim-polymyxin B eyedrop formulations containing isotonic agents other than sodium chloride have been carried out. The HPLC assay of thimerosal in stored formulations containing boric acid and EDTA decreased with time and temperature, while formulations containing propylene glycol, glycerol, and mannitol showed no significant decrease in thimerosal assay compared with a formulation containing no isotonic agent. The latter group provide suitable alternatives to sodium chloride, which has been shown to have a seriously detrimental effect on thimerosal stability.

Keyphrases □ Thimerosal—stability in ophthalmic formulations, influence of isotonic agents, boric acid, EDTA, propylene glycol, glycerol, mannitol □ Isotonic agents—boric acid, EDTA, propylene glycol, glycerol, mannitol, effect on the stability of thimerosal, ophthalmic formulations □ Ophthalmic solutions—thimerosal stability with isotonic agents, boric acid, EDTA, propylene glycol, glycerol, mannitol

Thimerosal, ethyl (sodium *o*-mercaptobenzoato)mercury (I), is an effective antibacterial and antifungal agent widely used as a preservative in pharmaceutical formulations, particularly liquid formulations such as ophthalmic solutions. Ophthalmic solutions also frequently contain agents to ensure that the formulation is isotonic with lachrymal secretions. While such formulations may be presented in a nonisotonic form, it is generally preferred to render them isotonic in order to avoid patient discomfort, biological damage to the patient, or ineffective treatment. The most commonly employed isotonic agents are ionic, in particular sodium chloride. However, it has been reported (1-3) that the presence of halides in solutions of thimerosal can have an adverse influence on the stability of I.

This study was undertaken to examine the effects of several isotonic agent alternatives to sodium chloride on the stability of thimerosal in aqueous formulations when stored under realistic and moderately accelerated conditions.

EXPERIMENTAL

Compounds and Reagents—Thimerosal was obtained commercially[1], and the isotonic agents listed in Table I were "AnalaR" grade[1], with the exception of boric acid which was "Aristar" [1] and propylene glycol which was "GPR" [1]. Methanol used for chromatography was HPLC grade[2], and all water used was freshly distilled.

High-Performance Liquid Chromatography—A constant-flow pump[3] was used to deliver the eluant to two stainless steel columns (each 250 mm × 4 mm i.d.) connected in series and packed with 10-μm silica particles bonded with octadecylsilane[4]. Injections were made with a rotary valve injector[5] equipped with a 50-μL loop. No attempt was made to control the column temperature. A variable-wavelength detector[6] set at 222 nm was employed at an attenuation of 0.04 AUFS.

The chromatographic mobile phase consisted of a mixture of methanol–water–phosphoric acid in a ratio of 60:50:1. The pressure, at a flow rate of 4.0 mL/min was, 4800 psig. Separations were effected isocratically at ambient temperature, and quantification was carried out by comparison of the height of the peak obtained from test solutions with the height of the peak obtained from the control solution.

Preparation of Test Formulations and Analytical Procedure—A series of eyedrop formulations containing thimerosal (0.001% w/v) in water, trimethoprim sulfate, polymyxin B sulfate (as active ingredients), and an isotonic agent (as shown in Table I) were prepared and stored at 5°C overnight. Aliquots (5 mL) of each test formulation were transferred to 10-mL glass ampules, which were then sealed and placed in storage at 5°C, 25°C, 37°C, and 50°C for periods up to 6 weeks. Solutions in ampules were allowed to warm or cool to ambient temperature for 1 h prior to analysis. These solutions were sampled directly for assay. The mean of duplicate determinations was taken, the two results generally showing an agreement of better than 2%. The formulation containing no excipient was used as a control for the initial assay (the results being normalized to 100% in Table II), and the same formulation, stored at 5°C, was used as a control in the subsequent assays.

RESULTS AND DISCUSSION

The results shown in Table II indicate that thimerosal manifested a significantly better stability using all five alternative isotonic agents when compared with its stability in saline. Previous published work (4) has shown only 36% thimerosal to remain after storage at 25°C for 3 d in normal saline.

The five formulations readily fell into two groups. The first group containing the ionic excipients (boric acid and EDTA) showed a decreased level of I throughout the study, dependent on time and temperature. Quite early in the trial a decrease in the assay of I was observed with eventually only 35-45% I remaining after 6 weeks at 50°C. In contrast, the second group of formulations containing the nonionic polyhydroxy alcohols (propylene glycol, glycerol, and mannitol) showed the thimerosal to have good stability compared with the control formulation with no excipient. Here 80-84% of I remained after 6 weeks at 50°C compared with 85% for the control, reflecting an essentially insignificant difference. At a more realistic temperature of 25°C, the first group showed a loss of 10-20% of I after 6 weeks, while the second group showed no decomposition after the same period.

The exact reasons for the marked effect of sodium chloride on the decomposition of thimerosal are not clear at present. It is well known that chloride and other halides have a marked affinity to coordinate with mercury(II) compounds, and this could be a contributory factor in the detrimental effect of sodium chloride on the stability of thimerosal in solution. There is some evidence (5) to show that the decomposition of thimerosal in water to thiosalicylic acid and ethylmercuric hydroxide is a reversible reaction. The effect of chloride anions could be to disturb this equilibrium by reaction with the ethylmercuric hydroxide to give ethylmercuric chloride, which does not combine nearly as readily with thiosalicylic acid in neutral solution to give thimerosal by the back-reaction. A possible reason for the improved stability of thimerosal in the case of the first group of isotonic agents (boric acid and EDTA) is that their respective anions may not have such a marked affinity to coordinate with mercury(II), and so the back-reaction to thimerosal is not so readily suppressed.

In contrast, the second group of isotonic agents (propylene glycol, glycerol, and mannitol) are nonionic, and the equilibrium of thimerosal with its hydrolysis products is not affected by their presence, hence the observed insignificant differences in thimerosal assay between the formulations containing these polyhydroxy alcohols and the control formulation containing no isotonic

Table I—Concentrations of Isotonic Agents

Isotonic Agent	Concentration, % w/v
EDTA	4.10
Boric acid	1.75
Propylene glycol	1.84
Glycerol	2.40
Mannitol	4.68

[1] BDH Chemicals Ltd., Poole, England.
[2] Rathburn Chemicals Ltd., Walkerburn, Peeblesshire, Scotland.
[3] Model 740B; Spectra-Physics, Santa Clara, Calif.
[4] Spherisorb 10 ODS; Phase Separations Ltd., Clwyd, Wales.
[5] Rheodyne Inc., Cotati, Calif.
[6] Model LC3; Pye Unicam Ltd., Cambridge, England.

0022-3549/84/0600-0840$01.00/0
© 1984, American Pharmaceutical Association

Table II—Thimerosal Assay by HPLC after Storage in Trimethoprim–Polymyxin B Eyedrops with Alternatives to Sodium Chloride as Isotonic Agent [a]

Storage Temp.	Control [b] Week 1	Control [b] Week 3	Control [b] Week 6	Boric Acid Week 1	Boric Acid Week 3	Boric Acid Week 6	EDTA Week 1	EDTA Week 3	EDTA Week 6	Propylene Glycol Week 1	Propylene Glycol Week 3	Propylene Glycol Week 6	Glycerol Week 1	Glycerol Week 3	Glycerol Week 6	Mannitol Week 1	Mannitol Week 3	Mannitol Week 6
5°C	NA	NA	100	NA	NA	94	NA	NA	98	NA	NA	103	NA	NA	107	NA	NA	100
25°C	100	103	98	93	91	89	96	86	83	98	97	99	103	100	102	98	100	102
37°C	101	98	94	90	84	72	93	80	64	101	95	91	103	88	84	101	95	94
50°C	98.5	91	85	81	57	35	70	56	43	92	87	81	100	91	82	96	95	84

[a] Initial values at 5°C for each additive were 100%. NA = not assayed. [b] No isotonic agent.

agent. Nonionic compounds, such as these polyhydroxy alcohols, provide suitable alternatives to sodium chloride as isotonic agents in ophthalmic formulations containing thimerosal.

REFERENCES

(1) K. Horworka, B. Horworka, and R. Meyer, *Pharmazie*, **28**, 136 (1973).

(2) E. Lüdtke and R. Pohloudek-Fabini, *Pharmazie*, **32**, 625 (1977).

(3) E. Lüdtke, H. Darsow, and R. Pohloudek-Fabini, *Pharmazie*, **32**, 99 (1977).

(4) Great Britain Patent, 2072015A (1981).

(5) F. Tanaka and M. Mitsuno, *Ann. Rept. Takeda Research Lab.*, **10**, 65 (1951).

ACKNOWLEDGMENTS

The author wishes to thank Mr. C. B. Lines for helpful discussions during the preparation of this paper.

Comparative Effects of Selected Phenothiazine Tranquilizers and Antihistaminics on Bacterial Cells and Possible Interactions with Antibiotics

A. M. SHIBL ˣ, Y. HAMMOUDA, and I. AL-SOWAYGH

Received January 13, 1983, from the *College of Pharmacy, King Saud University, Riyadh, Saudi Arabia.* Accepted for publication April 21, 1983.

Abstract □ Evaluation of the antibacterial effect of phenothiazine antihistaminics (trimeprazine, promethazine, and fonazine) and phenothiazine tranquilizers (promazine, chlorpromazine, triflupromazine, and propiomazine) on *Staphylococcus aureus* showed that tranquilizers were more active [minimum inhibitory concentration (MIC) 0.5–1.6 μg/mL] than antihistaminics (MIC > 1.6 μg/mL). The antibacterial activity was found to correlate with both the rate of adsorption of these drugs on the bacterial cells and the surface tension of their solutions. Phenothiazine tranquilizers caused rapid and extensive leakage of potassium ions from bacterial cells, while phenothiazine antihistaminics produced relatively slower leakage of these ions. A study of the effect of the phenothiazines on the antibacterial activity of some antibiotics showed that all phenothiazines produced a synergistic effect with erythromycin and an antagonistic effect with tobramycin. Variable effects were observed with chloramphenicol, and no effect was observed with penicillin. Results were explained on the basis of structural characteristics of the phenothiazines.

Keyphrases □ Phenothiazine tranquilizers—effects on bacterial cells, interaction with antibiotics, *Staphylococcus aureus* □ Phenothiazine antihistaminics—effects on bacterial cells, interaction with antibiotics, *Staphylococcus aureus* □ Antibiotics—interaction with phenothiazine tranquilizers and antihistaminics, *Staphylococcus aureus*

The phenothiazine group encompasses drugs of different therapeutic uses, most important of which are the antihistaminics and the tranquilizers. Most patients receiving these drugs are potential recipients of antibiotic therapy because of their increased susceptibility to infections (1). Synergism and antagonism between antibiotic combinations have been documented. Little attention, however, has been paid to possible interaction between antibiotics and phenothiazines. Some phenothiazines have measurable antibacterial activity *in vitro* (2–4), but are not used clinically for this purpose because of the high doses which would be required. The present work was undertaken to investigate the effect of a variety of combinations of antibiotics and phenothiazines against microorganisms, using *Staphylococcus aureus* as a model.

EXPERIMENTAL

Organism, Drugs, and Antibiotics—*Staphylococcus aureus* NCTC 6571 was used throughout this study. Cultures were maintained on blood agar slants. The drugs used were trimeprazine tartrate[1], fonazine mesylate[1], chlorpromazine hydrochloride[1], promazine hydrochloride[2], propiomazine hydrochloride[2], promethazine[3], and triflupromazine[3]. The antibiotics used were chloramphenicol[4], erythromycin[5], tobramycin[6], and penicillin[6]. Stock solutions of the phenothiazines and the antibiotics were prepared in sterilized distilled water to obtain concentrations of 1.0 mg/mL and 100 μg/mL, respectively.

Determination of Minimum Inhibitory Concentration (MIC)—The MIC values were determined by a standard twofold serial dilution method in brain-heart infusion (BHI) broth[7]. Tubes were inoculated with 10^5 colony forming units (CFU)/mL of *S. aureus*. The lowest concentration showing no visible growth after 18 h of incubation at 37°C was considered as the MIC.

Measurement of Surface Tension—Surface tension was measured by the ring method using a torsion balance[8]. All experiments were carried out in duplicate at 25°C. Distilled water was used as the reference ($\gamma_{25} = 72.4$).

Determination of Potassium Ion Efflux—The test organism was grown at 37°C for 18 h in BHI broth, and the cells were washed with saline to remove extracellular potassium ions before they were suspended in saline. Five milliliters of the suspension was boiled for 30 min, and the amount of potassium

[1] May & Baker, Dagenham, England.
[2] Wyeth, Andover, Mass.
[3] Squibb & Sons, Princeton, N.J.
[4] Parke-Davis & Co., Detroit, Mich.
[5] Abbott Laboratories, North Chicago, Ill.
[6] Eli Lilly & Co., Indianapolis, Ind.
[7] Oxoid Limited, England.
[8] Type OS; White Electronic Instrument Co., Worcestershire, England.

0022-3549/84/0600-0841$01.00/0

© 1984, American Pharmaceutical Association

Table II—Thimerosal Assay by HPLC after Storage in Trimethoprim–Polymyxin B Eyedrops with Alternatives to Sodium Chloride as Isotonic Agent [a]

Storage Temp.	Control [b] Week 1	Control [b] Week 3	Control [b] Week 6	Boric Acid Week 1	Boric Acid Week 3	Boric Acid Week 6	EDTA Week 1	EDTA Week 3	EDTA Week 6	Propylene Glycol Week 1	Propylene Glycol Week 3	Propylene Glycol Week 6	Glycerol Week 1	Glycerol Week 3	Glycerol Week 6	Mannitol Week 1	Mannitol Week 3	Mannitol Week 6
5°C	NA	NA	100	NA	NA	94	NA	NA	98	NA	NA	103	NA	NA	107	NA	NA	100
25°C	100	103	98	93	91	89	96	86	83	98	97	99	103	100	102	98	100	102
37°C	101	98	94	90	84	72	93	80	64	101	95	91	103	88	84	101	95	94
50°C	98.5	91	85	81	57	35	70	56	43	92	87	81	100	91	82	96	95	84

[a] Initial values at 5°C for each additive were 100%. NA = not assayed. [b] No isotonic agent.

agent. Nonionic compounds, such as these polyhydroxy alcohols, provide suitable alternatives to sodium chloride as isotonic agents in ophthalmic formulations containing thimerosal.

REFERENCES

(1) K. Horworka, B. Horworka, and R. Meyer, *Pharmazie*, **28**, 136 (1973).

(2) E. Lüdtke and R. Pohloudek-Fabini, *Pharmazie*, **32**, 625 (1977).

(3) E. Lüdtke, H. Darsow, and R. Pohloudek-Fabini, *Pharmazie*, **32**, 99 (1977).

(4) Great Britain Patent, 2072015A (1981).

(5) F. Tanaka and M. Mitsuno, *Ann. Rept. Takeda Research Lab.*, **10**, 65 (1951).

ACKNOWLEDGMENTS

The author wishes to thank Mr. C. B. Lines for helpful discussions during the preparation of this paper.

Comparative Effects of Selected Phenothiazine Tranquilizers and Antihistaminics on Bacterial Cells and Possible Interactions with Antibiotics

A. M. SHIBL ˣ, Y. HAMMOUDA, and I. AL-SOWAYGH

Received January 13, 1983, from the *College of Pharmacy, King Saud University, Riyadh, Saudi Arabia.* Accepted for publication April 21, 1983.

Abstract □ Evaluation of the antibacterial effect of phenothiazine antihistaminics (trimeprazine, promethazine, and fonazine) and phenothiazine tranquilizers (promazine, chlorpromazine, triflupromazine, and propiomazine) on *Staphylococcus aureus* showed that tranquilizers were more active [minimum inhibitory concentration (MIC) 0.5–1.6 μg/mL] than antihistaminics (MIC > 1.6 μg/mL). The antibacterial activity was found to correlate with both the rate of adsorption of these drugs on the bacterial cells and the surface tension of their solutions. Phenothiazine tranquilizers caused rapid and extensive leakage of potassium ions from bacterial cells, while phenothiazine antihistaminics produced relatively slower leakage of these ions. A study of the effect of the phenothiazines on the antibacterial activity of some antibiotics showed that all phenothiazines produced a synergistic effect with erythromycin and an antagonistic effect with tobramycin. Variable effects were observed with chloramphenicol, and no effect was observed with penicillin. Results were explained on the basis of structural characteristics of the phenothiazines.

Keyphrases □ Phenothiazine tranquilizers—effects on bacterial cells, interaction with antibiotics, *Staphylococcus aureus* □ Phenothiazine antihistaminics—effects on bacterial cells, interaction with antibiotics, *Staphylococcus aureus* □ Antibiotics—interaction with phenothiazine tranquilizers and antihistaminics, *Staphylococcus aureus*

The phenothiazine group encompasses drugs of different therapeutic uses, most important of which are the antihistaminics and the tranquilizers. Most patients receiving these drugs are potential recipients of antibiotic therapy because of their increased susceptibility to infections (1). Synergism and antagonism between antibiotic combinations have been documented. Little attention, however, has been paid to possible interaction between antibiotics and phenothiazines. Some phenothiazines have measurable antibacterial activity *in vitro* (2–4), but are not used clinically for this purpose because of the high doses which would be required. The present work was undertaken to investigate the effect of a variety of combinations of antibiotics and phenothiazines against microorganisms, using *Staphylococcus aureus* as a model.

EXPERIMENTAL

Organism, Drugs, and Antibiotics—*Staphylococcus aureus* NCTC 6571 was used throughout this study. Cultures were maintained on blood agar slants. The drugs used were trimeprazine tartrate[1], fonazine mesylate[1], chlorpromazine hydrochloride[1], promazine hydrochloride[2], propiomazine hydrochloride[2], promethazine[3], and triflupromazine[3]. The antibiotics used were chloramphenicol[4], erythromycin[5], tobramycin[6], and penicillin[6]. Stock solutions of the phenothiazines and the antibiotics were prepared in sterilized distilled water to obtain concentrations of 1.0 mg/mL and 100 μg/mL, respectively.

Determination of Minimum Inhibitory Concentration (MIC)—The MIC values were determined by a standard twofold serial dilution method in brain-heart infusion (BHI) broth[7]. Tubes were inoculated with 10^5 colony forming units (CFU)/mL of *S. aureus*. The lowest concentration showing no visible growth after 18 h of incubation at 37°C was considered as the MIC.

Measurement of Surface Tension—Surface tension was measured by the ring method using a torsion balance[8]. All experiments were carried out in duplicate at 25°C. Distilled water was used as the reference ($\gamma_{25} = 72.4$).

Determination of Potassium Ion Efflux—The test organism was grown at 37°C for 18 h in BHI broth, and the cells were washed with saline to remove extracellular potassium ions before they were suspended in saline. Five milliliters of the suspension was boiled for 30 min, and the amount of potassium

[1] May & Baker, Dagenham, England.
[2] Wyeth, Andover, Mass.
[3] Squibb & Sons, Princeton, N.J.
[4] Parke-Davis & Co., Detroit, Mich.
[5] Abbott Laboratories, North Chicago, Ill.
[6] Eli Lilly & Co., Indianapolis, Ind.
[7] Oxoid Limited, England.
[8] Type OS; White Electronic Instrument Co., Worcestershire, England.

0022-3549/84/0600-0841$01.00/0

© 1984, American Pharmaceutical Association

Table I—Comparative Effects of Phenothiazine on *S. aureus*

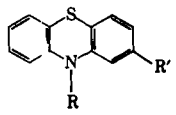

Phenothiazine	Substituent R	Substituent R′	MIC[a], μg/mL	γ, D/cm	K^+, % Released	Adsorption, % of Control
Tranquilizers						
Chlorpromazine	$(CH_2)_3N(CH_3)_2$	Cl	0.5	56	72	94
Promazine	$(CH_2)_3N(CH_3)_2$	H	0.8	66	62	80
Propiomazine	$CH_2CH(CH_3)N(CH_3)_2$	$COCH_2CH_3$	1.6	61	72	82
Triflupromazine	$(CH_2)_3N(CH_3)_2$	CF_3	0.1	56	74	93
Antihistaminics						
Fonazine	$CH_2CH(CH_3)N(CH_3)_2$	$SO_2N(CH_3)_2$	6.2	63	30	75
Promethazine	$CH_2CH(CH_3)N(CH_3)_2$	H	6.2	65	58	74
Trimeprazine	$CH_2CH(CH_3)CH_2N(CH_3)_2$	H	1.6	61	64	80

[a] Minimum inhibitory concentration.

Table II—Effect of Phenothiazine Drugs on the Antimicrobial Activity of Antibiotic Against *S. aureus*

Phenothiazine (MIC[a], μg/mL)	Antibiotic (MIC[a], μg/mL): Erythromycin (0.12) MIC[a] in Combination	FIC[b]	Tobramycin (0.5) MIC[a] in Combination	FIC[b]	Chloramphenicol (0.12) MIC[a] in Combination	FIC[b]	Penicillin (0.02) MIC[a] in Combination	FIC[b]
Chlorpromazine (0.5)	0.03 + 0.02	0.3	0.5 + 0.1	1.2	0.06 + 0.25	1	0.01 + 0.25	1
Promazine (0.8)	0.05 + 0.1	0.53	0.5 + 0.8	2	0.06 + 0.4	1	0.01 + 0.4	1
Propiomazine (1.6)	0.03 + 0.24	0.4	0.25 + 3.2	2.5	0.06 + 0.8	1	0.01 + 0.8	1
Triflupromazine (0.1)	0.04 + 0.02	0.53	0.25 + 0.1	1.5	0.06 + 0.05	1	0.01 + 0.05	1
Fonazine (6.2)	0.05 + 0.8	0.54	0.5 + 6.2	2	0.03 + 1.5	0.5	0.01 + 3.1	1
Promethazine (6.2)	0.05 + 1.0	0.43	0.5 + 6.2	2	0.03 + 1.5	0.5	0.01 + 3.1	1
Trimeprazine	0.03 + 0.26	0.41	0.25 + 1.6	1.5	0.12 + 0.8	1.5	0.01 + 0.8	1

[a] Minimum inhibitory concentration. [b] Fractional inhibitory concentration.

ions released was determined using a flame photometer[9]. The result was calculated as a percentage of the result obtained for untreated control cells. All experiments were performed in duplicate.

Adsorption and Interaction Experiments—Adsorption was carried out as previously described (5). MIC determinations were performed on BHI broth with an inoculum of 10^5 CFU. Antibiotics and drugs were mixed in checkerboard fashion. Incubation took place at 37°C for 18 h. Synergism was defined as a fractional inhibitory concentration (FIC) index as follows:

$$\text{FIC} = \frac{(A)}{(\text{MIC}_A)} + \frac{(B)}{(\text{MIC}_B)}$$

Where (A) is the MIC of drug A in the presence of drug B, and (MIC_A) is the MIC of drug A alone. (B) and (MIC_B) are defined in the same fashion for drug B. Synergism is present if the FIC index is <1, and antagonism is present if the FIC index is >1. An index value of 1 shows addition (6).

Spectrophotometric Assay—When solutions of the phenothiazines and the antibiotics, separately and in combination at different molecular ratios, were scanned in the UV region[10], no evidence of interaction could be observed in the resulting spectra.

RESULTS AND DISCUSSION

The results (Table I) suggest that there is some relationship between the antibacterial activity of the phenothiazines studied and their surface activity, rate of adsorption, and potassium ion release. Chlorpromazine and triflupromazine, which possess the highest antibacterial activity also showed the highest values for potassium ion release and adsorption and the lowest surface tension. It is possible that by virtue of their high surface activity, these compounds adsorb to the bacterial surfaces, thereby changing the permeability characteristics of the cell membrane. Both drugs have a halogen substitution at R (Cl or CF_3), which increases their lipophilic character and thereby their surface activity. On the other hand, fonazine, which contains the relatively polar *N*-dimethylsulfonyl functional group at R [$SO_2N(CH_3)_2$], causes only a slight potassium ion release and exhibits the least antibacterial activity. The lower antibacterial activity of promethazine and trimeprazine as compared with promazine, all of which have a hydrogen atom at R′, could be attributed to the length of the carbon chain between the two nitrogen atoms in their substituents and also to the branching of their side chain. The relatively higher activity of trimeprazine when compared with promethazine could be due to the additional methylene group at R′ in trimeprazine, which could confer a lipophilic property to the drug.

The antibacterial activity of the phenothiazines and antibiotics, separately and in combination, is shown in Table II. The phenothiazines did not enhance the antibacterial activity of penicillin, and they had an antagonistic effect on the action of tobramycin. The antibacterial activity of erythromycin, on the other hand, was enhanced in the presence of the phenothiazines. Fonazine and promethiazine potentiated the activity of chloramphenicol, while trimeprazine had an antagonistic effect. The remaining phenothiazines did not affect the antibacterial activity of chloramphenicol. The variable results obtained in these experiments are in agreement with previously published reports (7).

The potassium ion efflux from bacterial cells after exposure to the phenothiazines could be due to the effect of these drugs on the bacterial cell membrane. The same type of effect could facilitate the entry of an antibiotic into the bacterial cell and thus potentiate the activity of that antibiotic. The antagonistic effects observed with some phenothiazine-antibiotic combinations might be explained on the basis that these drugs could unselectively block certain receptor sites essential to the action of the antibiotics.

The present results suggest that the action of phenothiazines on the bacterial membrane cannot be the sole factor that determines the type and degree of interaction with antibiotics. Since spectrophotometric measurements of mixtures of antibiotics and phenothiazines excluded chemical interaction, there must be another site of activity of the phenothiazines in the bacterial cell. This type of interaction may have clinical implications in psychotic patients who have to take antibiotics while on phenothiazine tranquilizers. Further work, using different antibiotics in combination with these drugs against different organisms, as well as *in vivo* studies are needed to investigate such interactions.

[9] EEL Flame Photometer, Model 150.

[10] Pye Unicam SP 8100 recording spectrophotometer.

REFERENCES

(1) R. B. Scott, "Price's Textbook of the Practice of Medicine," 12th ed., Oxford University Press, Oxford, New York, Delhi, 1978.

(2) M. W. Brown, *J. Pharm. Sci.*, **64**, 700 (1975).

(3) J. Molnar, Y. Mandi, and Y. Kiraly, *Acta Microbial. Acad. Sci. Hung.*, **23**, 45 (1976).

(4) E. L. Hewlett, G. A. Myers, and R. D. Pearson, *Antimicrob. Agents Chemother.*, **23**, 201 (1983).
(5) I. A. Al-Sowaygh, A. M. Shibl, and Y. Hammouda, *Curr. Chemother.*, **1**, 683 (1980).
(6) M. C. Berenhaum, *J. Infect. Dis.*, **137**, 122 (1978).
(7) H. Nisimura, H. Shimohira, and K. Nakajima, *Ann Rep. Schionogi Research Lab.*, **6**, 257 (1956).

ACKNOWLEDGMENTS

Presented at the 21st Interscience Conference on Antimicrobial Agents and Chemotherapy, Chicago, 1981.

The authors are grateful to the companies for the courtesy of supplying drugs and antibiotics. Thanks are also given to Mr. H. El-Sammani for his technical assistance and to Mr. K. Abbas for typing this manuscript.

Structural Determination of Nootkatol, a New Sesquiterpene Isolated from *Alpinia oxyphylla* Miquel Possessing Calcium-Antagonistic Activity

N. SHOJI *, A. UMEYAMA *, Y. ASAKAWA *, T. TAKEMOTO *, K. NOMOTO ‡, and Y. OHIZUMI §x

Received February 24, 1983, from the **Faculty of Pharmacy, Tokushima-Bunri University, Tokushima-shi, Tokushima 770*, the ‡*Suntory Institute for Bioorganic Research, Wakayamadai, Shimamoto-cho, Mishima-gun, Osaka 618*, and the §*Mitsubishi-Kasei Institute of Life Sciences, Machida-shi, Tokyo 194, Japan.* Accepted for publication April 28, 1983.

Abstract □ Nootkatol, a new sesquiterpene possessing calcium-antagonistic activity, was isolated from *Alpinia oxyphylla* Miquel and characterized as (2*R*,4*R*,5*S*,7*R*)-eremophil-1(10),11-dien-2-ol.

Keyphrases □ Nootkatol—isolation from *Alpinia oxyphylla* Miquel, calcium-antagonistic activity □ Calcium antagonists—isolation of nootkatol from *Alpinia oxyphylla* Miquel

In the course of our survey of various crude drugs prepared from plant materials for pharmacologically active metabolites, we have found that a methanolic extract of the fruit of *Alpinia oxyphylla* Miquel (Zingiberaceae) has calcium-antagonistic activity in the rabbit aorta. Other work (1–3) on calcium antagonists, such as verapamil and gallopamil, have revealed that such drugs selectively inhibit the potassium chloride-induced contraction of vascular smooth muscle. In this paper, we have isolated for the first time a substance possessing calcium-antagonistic activity from a plant source.

EXPERIMENTAL[1]

Method of the Bioassay—Rabbits (2–3 kg) were killed by cervical dislocation. The aortas (60 × 4 mm) were removed and cut into helical strips. The strips were mounted vertically in a 20-mL organ bath containing Krebs-Ringer bicarbonate solution of the following composition (mM concentration): NaCl, 120; KCl, 4.8; $CaCl_2$, 1.2; $MgSO_4 \cdot 7H_2O$, 1.3; KH_2PO_4, 1.2; $NaHCO_3$, 25.2; and glucose, 5.8, pH 7.4. This was bubbled with a gas mixture of oxygen-carbon dioxide (95:5) and maintained at 37°C. A resting tension of 1 g was applied to the strips and tension changes were isometrically recorded with a force-displacement transducer.

Isolation—The dried, powdered fruit[2] (10 kg) of *A. oxyphylla* Miquel were extracted three times with cold methanol (20 L). The methanolic extract was concentrated *in vacuo*, and the residue (1 kg) was partitioned between ethyl acetate and water. The aqueous layer was extracted with 1-butanol. The pharmacologically active ethyl acetate fraction (605 g) was chromatographed on silica gel[3] (benzene–ethyl acetate). The fractions containing the bioactive material [benzene–ethyl acetate (9:1)] were combined and further purified on a silica gel column with *n*-hexane–acetone (97:3) to afford 3.0 g of an active substance (Ia, 0.03% yield), named nootkatol, as colorless needles, mp 78–80°C (recrystallized from *n*-hexane), $[\alpha]_D$ + 208° (*c* 1.1 $CHCl_3$); IR (KBr): 3250 cm^{-1} (OH); MS: *m/z* 220 (M^+, 53%) and 177 (100); ^{1}H-NMR ($CDCl_3$): δ 0.89 (s, 3, C(5)—CH_3), 0.89 (d, 3, *J* = 6 Hz, C(4)—CH_3), 1.01 (t, 1, *J* = 13 Hz, C(6)—βH), 1.24 (dq, 1, *J* = 12 Hz and *J* = 4 Hz, C(8)—βH), 1.55 (m, 1, C(3)—βH), 1.63 (dt, 1, *J* = 13 Hz and *J* = 4 Hz, C(3)—αH), 1.71 (m, 3, C(11)—CH_3), 1.71 (m, 1, C(4)—βH), 1.79 (m, 1, C(8)—αH), 1.89 (dt, 1, *J* = 13 Hz and *J* = 3 Hz, C(6)—αH), 2.13 (m, 1, C(9)—βH), 2.23 (tt, 1, *J* = 13 Hz and *J* = 3 Hz, C(7)—H), 2.32 (m, 1, C(9)—αH), 4.06 (m, 1, C(2)—H), 4.68 (m, 2, C(12)—H_2), and 5.49 ppm (bd, 1, *J* = 5 Hz, C(1)—H); ^{13}C-NMR ($CDCl_3$): δ 15.21 (q, C-14), 16.83 (q, C-15), 20.79 (d, C-4), 32.54 (t, C-6*), 32.62 (t, C-8*), 34.98 (q, C-13), 36.21 (t, C-3), 38.32 (s, C-5), 40.72 (d, C-7), 44.60 (t, C-9), 64.37 (d, C-2), 108.71 (t, C-12), 121.73 (d, C-1), 148.55 (s, C-11), and 150.13 ppm (s, C-10). Assignments are interchangeable between carbon atoms with asterisks.

Anal.—Calc. for $C_{15}H_{24}O$: C, 81.76; H, 10.98. Found: C, 81.53; H, 11.28.

Reduction of Nootkatone (II)—To the ether solution (50 mL) of nootkatone[4] (1.9 g), 200 mg of $LiAlH_4$ was added and stirred overnight at room temperature. The suspension was treated as usual and extracted with ether. The organic phase was dried over Na_2SO_4 and the solvent was removed under reduced pressure. The residue was chromatographed on silica gel [*n*-hexane–acetone (97:3)]. Nootkatol (Ia) (40 mg) was eluted, followed by epinootkatol (Ib) (oily, 1980 mg). The aforementioned synthetic nootkatol was identical by IR, optical rotation, and melting point comparison with the material isolated from *A. oxyphylla*.

RESULTS AND DISCUSSION

From the fruit of *A. oxyphylla* Miquel, a calcium-antagonistic substance, named nootkatol, was isolated. In the mass spectrum the molecular ion (*m/z* 220) indicates a molecular formula of $C_{15}H_{24}O$. The single oxygen func-

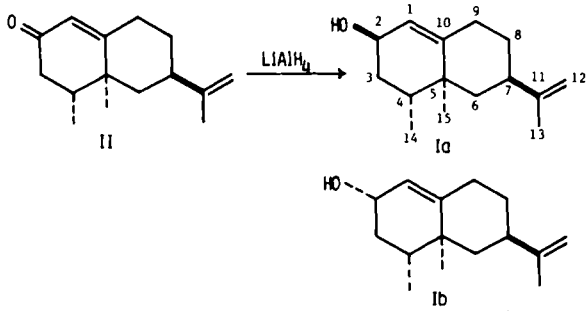

Scheme I—Reduction of nootkatone (II) to nootkatol (Ia).

[1] Melting points were obtained on a Yanagimoto micro melting point apparatus and are uncorrected. Optical rotation was recorded on a Jasco DIP-180 digital polarimeter. IR spectra were obtained on a Shimadzu IR-27G photometer. ^{1}H-NMR spectra were recorded on a Nicolet NT-360 spectrometer. ^{13}C-NMR spectra were recorded on a Hitachi R-22 spectrometer. Mass spectra were obtained on a Shimadzu LKB-9000B.

[2] Purchased from Nippon Hunmatsu Yakuhin, Ltd., Osaka, Japan.

[3] Silica gel 60 (230–400 mesh); Merck.

[4] Supplied by Shiono Kohryo Co., Ltd., Osaka, Japan.

0022-3549/84/0600-0843$01.00/0
© 1984, American Pharmaceutical Association

(4) E. L. Hewlett, G. A. Myers, and R. D. Pearson, *Antimicrob. Agents Chemother.*, **23**, 201 (1983).
(5) I. A. Al-Sowaygh, A. M. Shibl, and Y. Hammouda, *Curr. Chemother.*, **1**, 683 (1980).
(6) M. C. Berenhaum, *J. Infect. Dis.*, **137**, 122 (1978).
(7) H. Nisimura, H. Shimohira, and K. Nakajima, *Ann Rep. Schionogi Research Lab.*, **6**, 257 (1956).

ACKNOWLEDGMENTS

Presented at the 21st Interscience Conference on Antimicrobial Agents and Chemotherapy, Chicago, 1981.

The authors are grateful to the companies for the courtesy of supplying drugs and antibiotics. Thanks are also given to Mr. H. El-Sammani for his technical assistance and to Mr. K. Abbas for typing this manuscript.

Structural Determination of Nootkatol, a New Sesquiterpene Isolated from *Alpinia oxyphylla* Miquel Possessing Calcium-Antagonistic Activity

N. SHOJI *, A. UMEYAMA *, Y. ASAKAWA *, T. TAKEMOTO *, K. NOMOTO ‡, and Y. OHIZUMI §x

Received February 24, 1983, from the **Faculty of Pharmacy, Tokushima-Bunri University, Tokushima-shi, Tokushima 770*, the ‡*Suntory Institute for Bioorganic Research, Wakayamadai, Shimamoto-cho, Mishima-gun, Osaka 618*, and the §*Mitsubishi-Kasei Institute of Life Sciences, Machida-shi, Tokyo 194, Japan.* Accepted for publication April 28, 1983.

Abstract □ Nootkatol, a new sesquiterpene possessing calcium-antagonistic activity, was isolated from *Alpinia oxyphylla* Miquel and characterized as (2*R*,4*R*,5*S*,7*R*)-eremophil-1(10),11-dien-2-ol.

Keyphrases □ Nootkatol—isolation from *Alpinia oxyphylla* Miquel, calcium-antagonistic activity □ Calcium antagonists—isolation of nootkatol from *Alpinia oxyphylla* Miquel

In the course of our survey of various crude drugs prepared from plant materials for pharmacologically active metabolites, we have found that a methanolic extract of the fruit of *Alpinia oxyphylla* Miquel (Zingiberaceae) has calcium-antagonistic activity in the rabbit aorta. Other work (1–3) on calcium antagonists, such as verapamil and gallopamil, have revealed that such drugs selectively inhibit the potassium chloride-induced contraction of vascular smooth muscle. In this paper, we have isolated for the first time a substance possessing calcium-antagonistic activity from a plant source.

EXPERIMENTAL[1]

Method of the Bioassay—Rabbits (2–3 kg) were killed by cervical dislocation. The aortas (60 × 4 mm) were removed and cut into helical strips. The strips were mounted vertically in a 20-mL organ bath containing Krebs-Ringer bicarbonate solution of the following composition (mM concentration): NaCl, 120; KCl, 4.8; $CaCl_2$, 1.2; $MgSO_4 \cdot 7H_2O$, 1.3; KH_2PO_4, 1.2; $NaHCO_3$, 25.2; and glucose, 5.8, pH 7.4. This was bubbled with a gas mixture of oxygen-carbon dioxide (95:5) and maintained at 37°C. A resting tension of 1 g was applied to the strips and tension changes were isometrically recorded with a force-displacement transducer.

Isolation—The dried, powdered fruit[2] (10 kg) of *A. oxyphylla* Miquel were extracted three times with cold methanol (20 L). The methanolic extract was concentrated *in vacuo*, and the residue (1 kg) was partitioned between ethyl acetate and water. The aqueous layer was extracted with 1-butanol. The pharmacologically active ethyl acetate fraction (605 g) was chromatographed on silica gel[3] (benzene–ethyl acetate). The fractions containing the bioactive material [benzene–ethyl acetate (9:1)] were combined and further purified on a silica gel column with *n*-hexane–acetone (97:3) to afford 3.0 g of an active substance (Ia, 0.03% yield), named nootkatol, as colorless needles, mp 78–80°C (recrystallized from *n*-hexane), $[\alpha]_D$ + 208° (*c* 1.1 $CHCl_3$); IR (KBr): 3250 cm^{-1} (OH); MS: *m/z* 220 (M^+, 53%) and 177 (100); ^{1}H-NMR ($CDCl_3$): δ 0.89 (s, 3, C(5)—CH_3), 0.89 (d, 3, *J* = 6 Hz, C(4)—CH_3), 1.01 (t, 1, *J* = 13 Hz, C(6)—βH), 1.24 (dq, 1, *J* = 12 Hz and *J* = 4 Hz, C(8)—βH), 1.55 (m, 1, C(3)—βH), 1.63 (dt, 1, *J* = 13 Hz and *J* = 4 Hz, C(3)—αH), 1.71 (m, 3, C(11)—CH_3), 1.71 (m, 1, C(4)—βH), 1.79 (m, 1, C(8)—αH), 1.89 (dt, 1, *J* = 13 Hz and *J* = 3 Hz, C(6)—αH), 2.13 (m, 1, C(9)—βH), 2.23 (tt, 1, *J* = 13 Hz and *J* = 3 Hz, C(7)—H), 2.32 (m, 1, C(9)—αH), 4.06 (m, 1, C(2)—H), 4.68 (m, 2, C(12)—H_2), and 5.49 ppm (bd, 1, *J* = 5 Hz, C(1)—H); ^{13}C-NMR ($CDCl_3$): δ 15.21 (q, C-14), 16.83 (q, C-15), 20.79 (d, C-4), 32.54 (t, C-6*), 32.62 (t, C-8*), 34.98 (q, C-13), 36.21 (t, C-3), 38.32 (s, C-5), 40.72 (d, C-7), 44.60 (t, C-9), 64.37 (d, C-2), 108.71 (t, C-12), 121.73 (d, C-1), 148.55 (s, C-11), and 150.13 ppm (s, C-10). Assignments are interchangeable between carbon atoms with asterisks.

Anal.—Calc. for $C_{15}H_{24}O$: C, 81.76; H, 10.98. Found: C, 81.53; H, 11.28.

Reduction of Nootkatone (II)—To the ether solution (50 mL) of nootkatone[4] (1.9 g), 200 mg of $LiAlH_4$ was added and stirred overnight at room temperature. The suspension was treated as usual and extracted with ether. The organic phase was dried over Na_2SO_4 and the solvent was removed under reduced pressure. The residue was chromatographed on silica gel [*n*-hexane–acetone (97:3)]. Nootkatol (Ia) (40 mg) was eluted, followed by epinootkatol (Ib) (oily, 1980 mg). The aforementioned synthetic nootkatol was identical by IR, optical rotation, and melting point comparison with the material isolated from *A. oxyphylla*.

RESULTS AND DISCUSSION

From the fruit of *A. oxyphylla* Miquel, a calcium-antagonistic substance, named nootkatol, was isolated. In the mass spectrum the molecular ion (*m/z* 220) indicates a molecular formula of $C_{15}H_{24}O$. The single oxygen func-

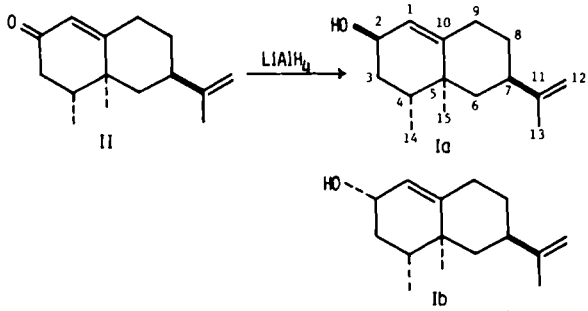

Scheme I—Reduction of nootkatone (II) to nootkatol (Ia).

[1] Melting points were obtained on a Yanagimoto micro melting point apparatus and are uncorrected. Optical rotation was recorded on a Jasco DIP-180 digital polarimeter. IR spectra were obtained on a Shimadzu IR-27G photometer. ^{1}H-NMR spectra were recorded on a Nicolet NT-360 spectrometer. ^{13}C-NMR spectra were recorded on a Hitachi R-22 spectrometer. Mass spectra were obtained on a Shimadzu LKB-9000B.

[2] Purchased from Nippon Hunmatsu Yakuhin, Ltd., Osaka, Japan.

[3] Silica gel 60 (230–400 mesh); Merck.

[4] Supplied by Shiono Kohryo Co., Ltd., Osaka, Japan.

0022-3549/84/0600-0843$01.00/0
© 1984, American Pharmaceutical Association

tionality is ascribable to a hydroxyl group based on the absorption band at 3250 cm^{-1} in the IR spectrum. The ^{13}C-NMR signals at 108.71 (t), 121.73 (d), 148.55 (s), and 150.13 (s) ppm suggest that the molecule has two double bonds and, therefore, it appears to be bicyclic. Furthermore, the ^1H-NMR spectrum shows the presence of a tertiary methyl group at 0.89 (s, 3), a secondary methyl group at 0.89 (d, 3, J = 6 Hz), and isopropenyl groups at 1.71 (m, 3) and 4.68 ppm (m, 2). From the above data the structure of Ia appears to be similar to that of nootkatone (II), which has been isolated from *Chamaecyparis nootkatensis* (Lamb.)sprach and *Citrus paradisi* Macfad. (4–6). The main difference appears to be the presence of a hydroxyl group in the newly isolated material. The proton attached to the hydroxyl-bearing carbon is observed as a multiplet at 4.06 ppm in the ^1H-NMR spectrum, suggesting the hydroxyl group was β-oriented. To verify the proposed structure, II was reduced with $LiAlH_4$ in ether to yield two products (Scheme I). As expected, the minor one was identical with Ia on the basis of its melting point, IR spectrum, and optical rotation. Thus, Ia is characterized as (2*R*,4*R*,5*S*,7*R*)-eremophil-1(10),11-dien-2-ol.

It has been reported that in vascular smooth muscle, contractile response to potassium chloride is caused for the most part by increasing membrane permeability to Ca^{2+}, while the response to norepinephrine is caused mainly by releasing an intracellular pool of Ca^{2+} (7). Calcium antagonists such as verapamil and gallopamil have been shown to selectively inhibit the contractile activity produced by potassium chloride without having any effect on that induced by norepinephrine (8). In the present experiment, purified Ia (3×10^{-5} M) markedly inhibited the potassium chloride (40 mM)-induced contraction of the aorta, but did not have any effect on that produced by norepinephrine (10^{-6} M). The 50% inhibitory doses of Ia and verapamil for the potassium chloride (40 mM)-induced contraction were $\sim 10^{-5}$ and $\sim 10^{-7}$ M, respectively, indicating that the potency of Ia was approximately 100 times less than that of verapamil[5]. Furthermore, Ia (3×10^{-5} M) profoundly inhibited the increase in the $^{45}Ca^{2+}$ uptake of the aorta induced by potassium chloride[5]. These observations suggest that Ia specifically blocks the Ca^{2+}-influx into the muscle cell of the aorta.

REFERENCES

(1) U. Peiper, L. Griebl, and W. Wende, *Pfluegers Arch.*, **330**, 74 (1971).

(2) R. Massingham, *Eur. J. Pharmacol.*, **22**, 75 (1973).

(3) A. Fleckenstein, *Ann. Rev. Pharmacol. Toxicol.*, **17**, 149 (1977).

(4) H. Erdman and Y. Hirose, *Acta Chem. Scand.*, **16**, 1311 (1962).

(5) W. D. McLeod, Jr. and N. Buiges, *J. Food Science*, **29**, 565 (1964).

(6) W. D. McLeod, Jr., *Tetrahedron Lett.*, **1965**, 4779.

(7) C. van Breemen, P. Aaronson, and R. Loutzenhiser, *Pharmacol. Rev.*, **30**, 167 (1979).

(8) G. B. Weiss, "New Perspectives on Calcium Antagonists," American Physiological Society, Bethesda, Md., 1980, p. 83.

[5] Unpublished results.

Reverse-Phase Liquid Chromatography and Pharmacokinetic Study of Two Hydroxylated Analogues of Quinidine in Dogs

R. LEROYER *, C. JARREAU ‡, M. PAYS ‡x, O. VAROQUAUX §, and C. ADVENIER §

Received August 12, 1982, from the **Department of Analytical Chemistry, Faculty of Pharmaceutical and Biological Sciences, CAEN University, 14032 CAEN Cedex,* ‡*Department of Clinical Biochemistry,* and the §*Department of Pharmacology, Centre Hospitalier, 78000 Versailles, France.* Accepted for publication April 20, 1983.

Abstract □ Two hydroxylated analogues of quinidine with antiarrhythmic properties, 3*S*-hydroxyquinidine and 3*R*-hydroxydihydroquinidine were assayed by reverse-phase high-performance liquid chromatography. The analytical technique uses plasma protein precipitation and direct injection on a C_{18} column, with an isocratic mobile phase and spectrofluorometric detection. 3*R*-Hydroxyquinidine is employed as the internal standard. Linearity is verified up to 5 mg/L for the two drugs; concentrations between 0.5 and 2.5 mg/L were measured with a *CV* of 0.5–2.07% for a given day and a sensitivity limit of 50 μg/L. Plasma concentration–time profiles and pharmacokinetic parameters in three dogs are presented after intravenous or oral administration. A significant difference is observed in terminal half-life, terminal rate constant, and total clearance of the two polar analogues of quinidine.

Keyphrases □ Quinidine analogues—hydroxylated, HPLC, pharmacokinetics in the dog □ Pharmacokinetics—hydroxylated analogues of quinidine in the dog, HPLC

Some of the metabolites of quinidine, especially 3*S*-hydroxyquinidine (I), 2′-oxoquinidine, and *O*-demethylquinidine, possess antiarrhythmic activity in mice and rabbits (1) and possibly in humans (2). Other analogues of quinidine, derived from *O*-demethylquinidine (3–6) or 7′-trifluoromethyldihydrocinchonidine (7), have recently been tested. Preliminary studies of I and 3*R*-hydroxydihydroquinidine (II) (8) indicate pharmacological activity of these two compounds when tested against chloroform-induced ventricular fibrillation and aconitine-induced arrhythmia in mice and rats or against coronary ligature in dogs.

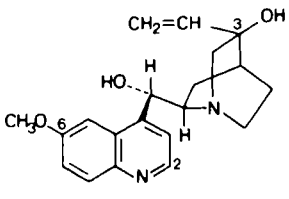

(I)

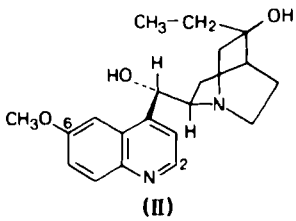

(II)

This report describes a rapid, specific, accurate, and sensitive high-performance liquid chromatographic (HPLC) method for the determination of I and II in plasma. The procedure involves a modification of a recently published reverse-phase HPLC method for quinidine (9) using 3*R*-hydroxyquinidine as internal standard, with an isocratic mobile phase of acetonitrile–acetic acid–water and sensitive spectrofluorometric detection. Preliminary pharmacokinetic parameters of these two hydroxylated analogues of quinidine in the dog are reported.

EXPERIMENTAL

Reagents and Standards—All solvents used were analytical reagent grade[1]: acetonitrile for spectrometry, methanol, and 100% acetic acid. A phosphate buffer (0.05 M, pH 7.4) was prepared in distilled water. Pure standards of

[1] E. Merck, Darmstadt, West Germany.

0022-3549/84/0600-0844$01.00/0

© 1984, American Pharmaceutical Association

tionality is ascribable to a hydroxyl group based on the absorption band at 3250 cm^{-1} in the IR spectrum. The ^{13}C-NMR signals at 108.71 (t), 121.73 (d), 148.55 (s), and 150.13 (s) ppm suggest that the molecule has two double bonds and, therefore, it appears to be bicyclic. Furthermore, the ^1H-NMR spectrum shows the presence of a tertiary methyl group at 0.89 (s, 3), a secondary methyl group at 0.89 (d, 3, J = 6 Hz), and isopropenyl groups at 1.71 (m, 3) and 4.68 ppm (m, 2). From the above data the structure of Ia appears to be similar to that of nootkatone (II), which has been isolated from *Chamaecyparis nootkatensis* (Lamb.)sprach and *Citrus paradisi* Macfad. (4–6). The main difference appears to be the presence of a hydroxyl group in the newly isolated material. The proton attached to the hydroxyl-bearing carbon is observed as a multiplet at 4.06 ppm in the ^1H-NMR spectrum, suggesting the hydroxyl group was β-oriented. To verify the proposed structure, II was reduced with $LiAlH_4$ in ether to yield two products (Scheme I). As expected, the minor one was identical with Ia on the basis of its melting point, IR spectrum, and optical rotation. Thus, Ia is characterized as (2*R*,4*R*,5*S*,7*R*)-eremophil-1(10),11-dien-2-ol.

It has been reported that in vascular smooth muscle, contractile response to potassium chloride is caused for the most part by increasing membrane permeability to Ca^{2+}, while the response to norepinephrine is caused mainly by releasing an intracellular pool of Ca^{2+} (7). Calcium antagonists such as verapamil and gallopamil have been shown to selectively inhibit the contractile activity produced by potassium chloride without having any effect on that induced by norepinephrine (8). In the present experiment, purified Ia (3×10^{-5} M) markedly inhibited the potassium chloride (40 mM)-induced contraction of the aorta, but did not have any effect on that produced by norepinephrine (10^{-6} M). The 50% inhibitory doses of Ia and verapamil for the potassium chloride (40 mM)-induced contraction were $\sim 10^{-5}$ and $\sim 10^{-7}$ M, respectively, indicating that the potency of Ia was approximately 100 times less than that of verapamil[5]. Furthermore, Ia (3×10^{-5} M) profoundly inhibited the increase in the $^{45}Ca^{2+}$ uptake of the aorta induced by potassium chloride[5]. These observations suggest that Ia specifically blocks the Ca^{2+}-influx into the muscle cell of the aorta.

REFERENCES

(1) U. Peiper, L. Griebl, and W. Wende, *Pfluegers Arch.*, **330**, 74 (1971).

(2) R. Massingham, *Eur. J. Pharmacol.*, **22**, 75 (1973).

(3) A. Fleckenstein, *Ann. Rev. Pharmacol. Toxicol.*, **17**, 149 (1977).

(4) H. Erdman and Y. Hirose, *Acta Chem. Scand.*, **16**, 1311 (1962).

(5) W. D. McLeod, Jr. and N. Buiges, *J. Food Science*, **29**, 565 (1964).

(6) W. D. McLeod, Jr., *Tetrahedron Lett.*, **1965**, 4779.

(7) C. van Breemen, P. Aaronson, and R. Loutzenhiser, *Pharmacol. Rev.*, **30**, 167 (1979).

(8) G. B. Weiss, "New Perspectives on Calcium Antagonists," American Physiological Society, Bethesda, Md., 1980, p. 83.

[5] Unpublished results.

Reverse-Phase Liquid Chromatography and Pharmacokinetic Study of Two Hydroxylated Analogues of Quinidine in Dogs

R. LEROYER *, C. JARREAU ‡, M. PAYS ‡x, O. VAROQUAUX §, and C. ADVENIER §

Received August 12, 1982, from the **Department of Analytical Chemistry, Faculty of Pharmaceutical and Biological Sciences, CAEN University, 14032 CAEN Cedex,* ‡*Department of Clinical Biochemistry,* and the §*Department of Pharmacology, Centre Hospitalier, 78000 Versailles, France.* Accepted for publication April 20, 1983.

Abstract □ Two hydroxylated analogues of quinidine with antiarrhythmic properties, 3*S*-hydroxyquinidine and 3*R*-hydroxydihydroquinidine were assayed by reverse-phase high-performance liquid chromatography. The analytical technique uses plasma protein precipitation and direct injection on a C_{18} column, with an isocratic mobile phase and spectrofluorometric detection. 3*R*-Hydroxyquinidine is employed as the internal standard. Linearity is verified up to 5 mg/L for the two drugs; concentrations between 0.5 and 2.5 mg/L were measured with a *CV* of 0.5–2.07% for a given day and a sensitivity limit of 50 μg/L. Plasma concentration–time profiles and pharmacokinetic parameters in three dogs are presented after intravenous or oral administration. A significant difference is observed in terminal half-life, terminal rate constant, and total clearance of the two polar analogues of quinidine.

Keyphrases □ Quinidine analogues—hydroxylated, HPLC, pharmacokinetics in the dog □ Pharmacokinetics—hydroxylated analogues of quinidine in the dog, HPLC

Some of the metabolites of quinidine, especially 3*S*-hydroxyquinidine (I), 2′-oxoquinidine, and *O*-demethylquinidine, possess antiarrhythmic activity in mice and rabbits (1) and possibly in humans (2). Other analogues of quinidine, derived from *O*-demethylquinidine (3–6) or 7′-trifluoromethyldihydrocinchonidine (7), have recently been tested. Preliminary studies of I and 3*R*-hydroxydihydroquinidine (II) (8) indicate pharmacological activity of these two compounds when tested against chloroform-induced ventricular fibrillation and aconitine-induced arrhythmia in mice and rats or against coronary ligature in dogs.

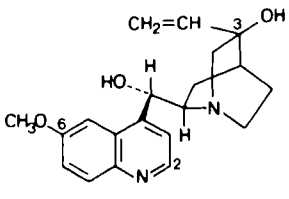

(I)

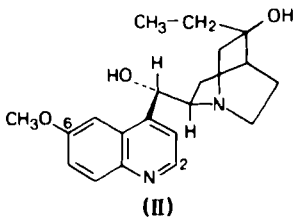

(II)

This report describes a rapid, specific, accurate, and sensitive high-performance liquid chromatographic (HPLC) method for the determination of I and II in plasma. The procedure involves a modification of a recently published reverse-phase HPLC method for quinidine (9) using 3*R*-hydroxyquinidine as internal standard, with an isocratic mobile phase of acetonitrile–acetic acid–water and sensitive spectrofluorometric detection. Preliminary pharmacokinetic parameters of these two hydroxylated analogues of quinidine in the dog are reported.

EXPERIMENTAL

Reagents and Standards—All solvents used were analytical reagent grade[1]: acetonitrile for spectrometry, methanol, and 100% acetic acid. A phosphate buffer (0.05 M, pH 7.4) was prepared in distilled water. Pure standards of

[1] E. Merck, Darmstadt, West Germany.

0022-3549/84/0600-0844$01.00/0

© 1984, American Pharmaceutical Association

Table I—Variations in Replicate Standards from Spiked Plasma [a]

Compound	Within-Run Concentrations, mg/L				Day-to-Day Concentrations, mg/L			
	0.5	1	2	2.5	0.5	1	2	2.5
I								
SD	0.14	0.12	—	0.12	0.36	0.7	—	2.3
CV (%)	1.5	0.6	—	0.5	4.1	4	—	5.2
II								
SD	0.05	0.09	0.20	0.18	0.07	0.15	0.21	0.34
CV (%)	2.07	1.66	1.89	1.33	2.51	2.71	1.86	2.46

[a] $n = 6$.

Table II—Pharmacokinetic Parameters for I and II after Bolus Injection in Dogs (10 mg/kg iv) [a]

Parameter	I	II	Significance Level
α (h^{-1})	2.25 ± 0.52	2.93 ± 1.27	NS
$T_{1/2\alpha}$ (h)	0.285 ± 0.155	0.27 ± 0.13	NS
β (h^{-1})	0.0875 ± 0.0075	0.1593 ± 0.0096	$p < 0.001$
$t_{1/2\beta}$ (h)	7.95 ± 0.68	4.36 ± 0.27	$p < 0.01$
AUC_∞ (mg/L·h)	55.82 ± 2.36	30.05 ± 5.08	$p < 0.01$
CL_T (L/h·kg)	0.189 ± 0.002	0.325 ± 0.037	$p < 0.01$
V_c (L/kg)	1.04 ± 0.48	0.95 ± 0.18	NS
Vd_β (L/kg)	2.11 ± 0.28	1.96 ± 0.26	NS

[a] Mean ± *SD*; $n = 3$. NS = not significant.

quinidine, dihydroquinidine, I, the internal standard, II, and quinidine *N*-oxide (as bases) were used as supplied[2]. Quinine was used in the sulfate form. Purity of these compounds was verified by HPLC as described here or by TLC on precoated silica gel plates (20 × 20 cm × 0.25 mm)[3], developed in methanol–acetone (4:1) and visualized under UV light (366 nm).

Stock solutions were prepared in methanol at a concentration of 1 g/L (stable for 2 months at 4°C), and working solutions at concentrations of 0.5–5 mg/L were prepared by diluting the stock solutions in acetonitrile–phosphate buffer 0.05 M (1:1). The stock solution of 3*R*-hydroxyquinidine was used to prepare a standard solution at 2.5 mg/L in pure acetonitrile.

Apparatus and Operating Conditions—The analysis was performed using a high-performance liquid chromatograph[4] equipped with an injection system[4] with a 10-μL loop, a stainless steel column[5], 30 cm × 3.9 mm i.d. (particle size 10 μm)[5], a spectrofluorometer[6] (λ_{ex} = 340 nm, λ_{em} = cut-off filter 418 nm) set at 0.5 μAUFS sensitivity with a time constant of 6 s. The mobile phase was a deaerated mixture of acetonitrile–acetic acid–water (8:4:88) with a flow rate of 1.8 mL/min (2200 psi).

Experimental Protocol in Dogs—Fasting mongrel dogs, 10–20 kg, received 10 mg/kg of I or II orally (capsules) or as an intravenous bolus dose (parenteral solutions in acidified saline, pH 4). Sixteen blood samples were collected from the saphenous vein in heparinized tubes and centrifuged at 1200×*g*; the plasma was stored at −18°C until assayed.

After intravenous administration of I or II, plasma concentrations declined biexponentially; pharmacokinetic parameters corresponding to a two-compartment open model were determined with a nonlinear least-squares Graphakin program, according to:

$$C_p = Ae^{-\alpha t} + Be^{-\beta t} \quad \text{(Eq. 1)}$$

where C_p is the plasma concentration at time t, A and B are ordinate intercept constants, and α and β are first-order rate constants. For oral administration of II, a one-compartment open model was used with the following:

$$C_p = X(e^{-k_e t} - e^{-k_a t}) \quad \text{(Eq. 2)}$$

where X is a hybrid intercept term, and k_a and k_e are respective apparent first-order absorption and elimination rate constants. Area under the plasma concentration curve from zero to infinity (AUC_∞), total plasma drug clearance (CL_T), central compartment volume (V_c), apparent volume of distribution (Vd) were calculated by the following equations:

$$AUC_\infty = \int_0^{C_{24\,h}} C_p dt + \frac{C_{24\,h}}{\beta} \quad \text{(Eq. 3)}$$

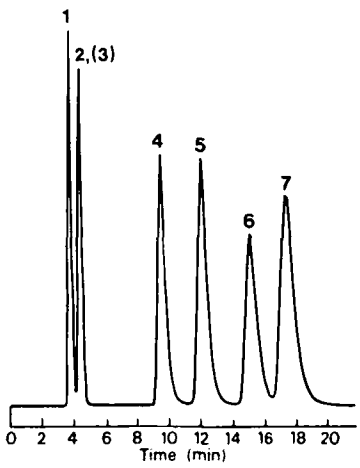

Figure 1—*Chromatogram of pure standards. Key: (1) 3R-hydroxyquinidine (retention time 3.8 min); [2, (3)] I (4.4 min); (4) quinidine N-oxide (9.5 min); (5) quinidine (12.2 min); (6) quinine (15.1 min); (7) dihydroquinidine (17.3 min).*

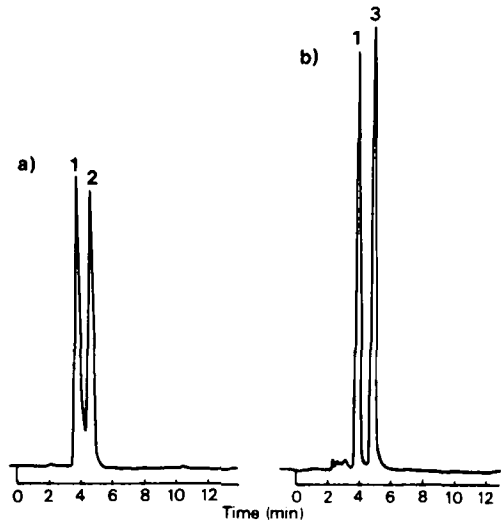

Figure 2—*Chromatogram of a 0.1-mL dog plasma sample after a dose of 10 mg/kg. Key: (1) 3R-hydroxyquinidine, internal standard, 2.5 mg/L; (2) I, (2.78 mg/L, 4.4 min); (3) II (2.95 mg/L, 4.8 min).*

[2] Nativelle Laboratories SA, Paris, France.
[3] Precoated TLC plates ref 5715; E. Merck, Darmstadt, West Germany.
[4] Model 5000 Varian; Varian Instrument, Palo Alto, Calif.
[5] Bondapak C_{18}; Waters Associates, Milford, Mass.
[6] Model FS 970; Schoeffel Instrument Corp., Westwood, N.J.

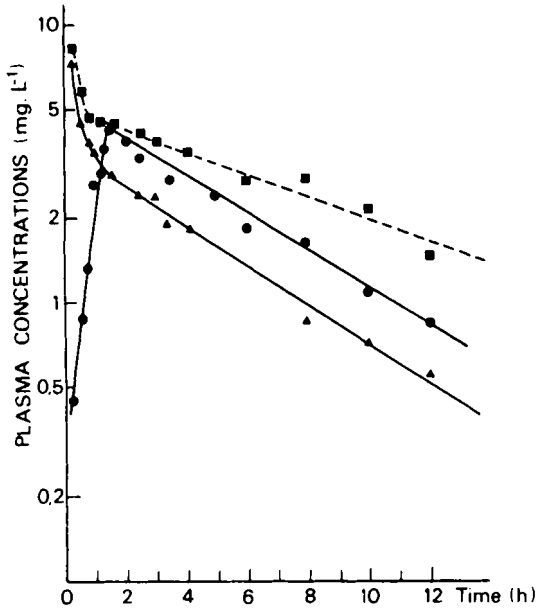

Figure 3—*Plasma concentration in a dog following oral administration of II (●) and intravenous administration of I (■), and II (▲) (10 mg/kg).*

$$CL_T = \frac{\text{Dose}}{AUC_\infty} \quad \text{(Eq. 4)}$$

$$V_c = \frac{\text{Dose}}{A + B} \quad \text{(Eq. 5)}$$

$$Vd_\beta = \frac{CL_T}{\beta} \quad \text{(Eq. 6)}$$

The Student's t test was used to evaluate statistical significance of observed differences between pharmacokinetic parameters of I and II.

Procedure—To precipitate proteins, 100 μL of plasma or diluted plasma was added to 100 μL of a 2.5-mg/L solution of the internal standard in acetonitrile. After closing with laboratory film[7], the mixture was shaken gently on a vortex mixer, centrifuged at 1200×g for 10 min, and 10 μL of the resultant clear supernatant was injected directly into the column. Peak height ratios were measured and reported on standard curves established with loaded plasma sample concentrations.

RESULTS AND DISCUSSION

Figures 1 and 2 show typical chromatograms of pure standards with the retention times observed in these conditions (Fig. 1) and dog plasma samples (Fig. 2). Because of their excessively long retention times, quinidine, quinine, and dihydroquinidine were not used as the internal standard. Quinidine *N*-oxide, a new metabolite described by Guentert *et al.* (10), has the same retention times as an unidentified metabolite in a previous assay for quinidine (9); because of its limited availability, it was not used. 3*R*-Hydroxyquinidine seems to be the most convenient internal standard, because of its same fluorescence characteristics with I and II. As shown in Fig. 2a and b, it is possible to resolve the internal standard from that of I (resolution factor = 1) or II (resolution factor = 1.66); incomplete resolution between I and II (resolution factor = 0.66) is never observed in the determination of plasma levels of either of these two drugs (no simultaneous administration).

The reproducibility assay gave small coefficients of variation (Table I) and recovery was 100 ± 3% when the concentrations of plasma loaded with different compounds were compared with standards solutions in a mixture (1:1) of acetonitrile and 0.05 M phosphate buffer. Linearity of the standard curves was verified by measuring the peak height ratio for concentrations up to 5 mg/L for I and II. An external standardization, by measuring peak height, may be used (no internal standard added to plasma) to detect the possible presence of a peak with retention time identical to that of the internal standard and corresponding to an eventual polar metabolite of I or II. The same results (linearity and plasma levels) are obtained in this procedure. When setting the detector at 0.2 μAUFS, the limit sensitivity, corresponding to a 2:1 signal-noise ratio, is 50 μg/L for the two compounds.

[7] Parafilm; American Com. Company, Dixie Marathon, Greenwich.

Table III—Pharmacokinetic Parameters for II after Oral Administration (10 mg/kg) in Dogs [a]

Parameter	II
k_a (h^{-1})	1.73 ± 1.18
$t_{1/2a}$ (h)	0.56 ± 0.38
k_e (h^{-1})	0.134 ± 0.0073
$t_{1/2e}$ (h)	5.15 ± 0.24
Vd (L/kg)	2.238 ± 0.176
CL_T (L/h·kg)	0.302 ± 0.036
AUC (mg/L·h)	33.42 ± 4.06
C_{max} (mg/L)	4.53 ± 0.34
t_{max} (h)	1.83 ± 0.61

[a] n = 3.

As shown in Fig. 3 for a representative animal, the plasma concentration-times curves for I and II decline biexponentially after intravenous administration (10 mg/kg). Corresponding pharmacokinetic parameters (Table II) indicate a significant difference between the two tested drugs for β, $t_{1/2\,\beta}$, AUC_∞, and CL_T, but not for V_c and Vd_β. The terminal half-life value for I (7.95 ± 0.68 h) is in good agreement with the observed values reported by Jaillon and Kates (11) in dogs (7.27 ± 2.79 h) after oral administration of quinidine, but II is eliminated more rapidly ($t_{1/2\,\beta}$ = 4.36 ± 0.27 h, CL_T = 0.325 ± 0.037 L/h·kg). Similar values for α indicate that I and II are initially distributed in the same order in the body.

For oral administration of II (10 mg/kg), the peak plasma level (4.53 ± 0.34 mg/L) was obtained 1.83 ± 0.61 h after the dose. A higher value for elimination half-life (5.15 ± 0.24 h) was observed than for the intravenous route, but AUC_∞ and CL_T were of the same magnitude, as shown in Table III.

REFERENCES

(1) D. E. Drayer, D. T. Lowenthal, K. M. Restivo, A. Schwartz, C. E. Cook, and M. M. Reidenberg, *Clin. Pharmacol. Ther.*, **24**, 31 (1978).

(2) N. H. G. Holford, P. E. Coates, T. W. Guentert, S. Riegelman, and L. B. Sheiner, *Br. J. Clin. Pharmacol.*, **11**, 187 (1981).

(3) C. T. Ueda and J. G. Nickols, *J. Pharm. Sci.*, **69**, 1400 (1980).

(4) P. U. Nwangwu, T. L. Holsclaw, H. Rosenberg, L. D. Small, and S. J. Stohs, *J. Pharm. Pharmacol.*, **31**, 488 (1979).

(5) P. U. Nwangwu, S. J. Stohs, K. Mereish, T. L. Holsclaw, H. Rosenberg, and L. D. Small, *Toxicology*, **16**, 73 (1980).

(6) P. U. Nwangwu, S. J. Stohs, H. Rosenberg, L. D. Small, and T. L. Holsclaw, *Curr. Ther. Res.*, **29**, 416 (1981).

(7) J. Pao and J. A. F. De Silva, *J. Chromatogr.*, **221**, 97 (1980).

(8) F. X. Jarreau and J. J. Koenig, (Ets Nativelle) *Brevet France*, 81.100.24 (20 May 1981).

(9) R. Leroyer, C. Jarreau, and M. Pays, *J. Chromatogr.*, **228**, 366 (1982).

(10) T. W. Guentert, J. J. Daly, and S. R. Riegelman, *Eur. J. Drug Metab. Pharmacokinet.*, **7**, 31 (1982).

(11) P. Jaillon and R. E. Kates, *J. Pharmacol. Exp. Ther.*, **213**, 33 (1980).

Nuclear Magnetic Resonance Spectrometry and Liquid Chromatography of Two Bile Acid Epimers: Ursodeoxycholic and Chenodeoxycholic Acid

A. BAILLET-GUFFROY, D. BAYLOCQ ˣ, A. RABARON, and F. PELLERIN

Received February 5, 1981 from the *U.E.R. de Chimie Therapeutique, Centre d'Études Pharmaceutiques, 92290 Chatenay-Malabry, France.* Accepted for publication October 14, 1982.

Abstract □ A specific reverse-phase high-performance liquid chromatographic (HPLC) technique is described for the analysis of bile acids and their conjugates in human serum. Precise quantitation is obtained using UV detection. ^{13}C-NMR spectrometry suggests a structural explanation for the different HPLC retention times of chenodeoxycholic acid, its epimer (ursodeoxycholic acid), and their methyl esters.

Keyphrases □ Ursodeoxycholic acid—HPLC in human serum, ^{13}C-NMR elucidation of structure, methyl ester □ Chenodeoxycholic acid—HPLC in human serum, ^{13}C-NMR elucidation of structure, methyl ester

Determination of individual bile acids in biological fluids by TLC, fluorometry, and GC has been reported (1–3). The glycine and taurine conjugates were determined by TLC; however, the resolution was unsatisfactory. Fluorometry (4) using 3α-hydroxy steroid dehydrogenase allows one to quantitate total bile acids only, while the GC method is tedious. High-performance liquid chromatography (HPLC) offers the possibility of separation and quantitation of individual bile acids without sample derivatization. This method is rapid and sensitive and can be used for many routine applications.

EXPERIMENTAL

Apparatus—A high-performance liquid chromatograph[1] equipped with a 20-μL loop injector[2] and a variable-wavelength absorbance detector[3] set at 201 nm was used. The chromatograms were plotted on a strip-chart recorder[4]. The stainless-steel column (3.9 × 15 mm) was packed with C_{18}-bonded microparticles[5].

Reagents and Solvents—The free bile acids and the taurine and glycine conjugates were obtained commercially[6]. Methyl esters of chenodeoxycholic acid and ursodeoxycholic acid were prepared by treatment of the acids with diazomethane. Further purification was carried out by TLC on silica gel (benzene–acetone–methanol, 85:5:10). UV-grade methanol[7] and double-distilled water were filtered[8] (pore size, 0.5 μm), stored in glass apparatus, and deaerated before use. Perchloric acid[9], analytical reagent grade, was used to adjust the pH of the mobile phase.

Samples—Serum (1 mL) was passed through a C_{18} microparticulate microcolumn[10] fixed onto a syringe. The column was washed with double-distilled water (2 × 4 mL), then by four methanol–water mixtures with increasing concentration of methanol (0–50%) (2 × 2 mL). Bile acids were eluted with pure methanol (3 mL). The filtrate was evaporated under nitrogen at 80°C. The residue was dissolved in 50 μL of double-distilled water, and a 20-μL aliquot was injected onto the column using the injector loop.

No internal standard was used. A 20-μL portion of external standard was also analyzed under the same chromatographic conditions. The standard solution was prepared daily by dissolving weighed amounts of each bile acid in water. The extraction ratio depended on each bile acid, ranging from 95 to 100%.

Chromatographic Conditions—Methanol (76%) in aqueous potassium dihydrogen phosphate (30 mmol/L) was used as the mobile phase. The pH of the mobile phase was adjusted after addition of methanol using perchloric acid (0.02%). The flow rate was 1.2 mL/min. The absorbance was measured at 201 nm (0.02 AUFS). The limit of sensitivity was 1 ng/μL of injected solution.

pK_a Determination—The apparent ionization constants (pK'_a) for ursodeoxycholic and chenodeoxycholic acid and their methyl esters were determinted by potentiometry[11] with a hydrogen electrode at 25°C in methanol–water (70:30, w/w). The pK_a values were calculated by the usual method (5).

^{13}C-NMR Spectra—A Fourier transform ^{13}C-NMR spectrometer[12] was used at probe temperature. Samples were dissolved in methanol-d_4 giving final concentration of 1 mol/L. Shifts from the methanol reference were measured on a 2000-Hz sweep width with 8192 data points (0.488 Hz/resolution point). The spectral parameters were: flip angle 45° (10-μs pulse width); repetition rate, 2.05 s; weighting function for sensitivity enhancement, 0.4 s; decoupling power, 4500 Hz; decoupling frequency, offset 52 (CFT 20 program); noise bandwith, 1000 Hz; and total experiment time, 160 nm (4700 scans). For S.F.O.R.D., the experimental decoupler frequency offset was 42 (cft 20 program) and the noise bandwith was off.

These typical experimental conditions were specially adapted to noise decoupling spectra of steroid molecules. They were determinated empirically for this spectrometer to obtain different signal heights for CH_3, CH_2, CH, and quaternary C. The association of information provided by this method with single frequency off-resonance spectra has improved the assignment of carbon signals in steroids.

RESULTS AND DISCUSSION

Bile acids have a 5β-cholanic acid skeleton and possess one, two, or three hydroxyl groups; they are found in serum as free acids (pK_a 5.5–7.0) and the glycine and taurine conjugates (pK_a 3.5–4.5 and ~2, respectively).

Separation and quantitative analysis of bile acids can be used in the diagnosis and study of hepatic and biliary diseases. Using reverse-phase HPLC, the taurine conjugates are eluted first, followed by the glycine conjugates, and then the free bile acids (6). Ursodeoxycholic acid (I) is eluted earlier than the epimeric chenodeoxycholic acid (II). Figure 1 shows a chromatogram under the described conditions; the retention times of ursodeoxycholic and chenodeoxycholic acids, the calculated capacity factors k', were very different: $k' = 3.4$ for ursodeoxycholic acid (I) and $k' = 11.4$ for chenodeoxycholic acid (II).

This surprising observation led to a study of the physical properties and

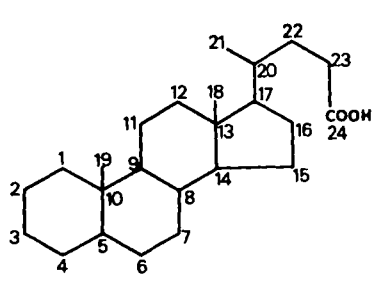

Cholanic Acid
(I) Ursodeoxycholic Acid: 3α,7β - dihydroxy 5β - cholanic acid
(II) Chenodeoxycholic Acid: 3α,7α - dihydroxy 5β - cholanic acid

[1] Pump Chromatem M380; Touzart et Matignon, France.
[2] Model 210 sample injection valve; Altex Scientific, Palo Alto, Calif.
[3] Model 450 variable-wavelength detector; Waters Associates.
[4] Servotrace PE 1521; Sefram, Paris.
[5] Lichrosorb RP 18, 5 μm; Merck, Darmstadt, W. Germany.
[6] Calbiochem-Behring Corp.
[7] SDS.
[8] Millipore Corp., Mass.
[9] RP Normapur, Prolabo, France.
[10] Waters Associates.
[11] pH-meter E 516; Titriskop Metrohm, Switzerland.
[12] Varian CFT 20 spectrometer.

0022-3549/84/0600-0847$01.00/0
© 1984, American Pharmaceutical Association

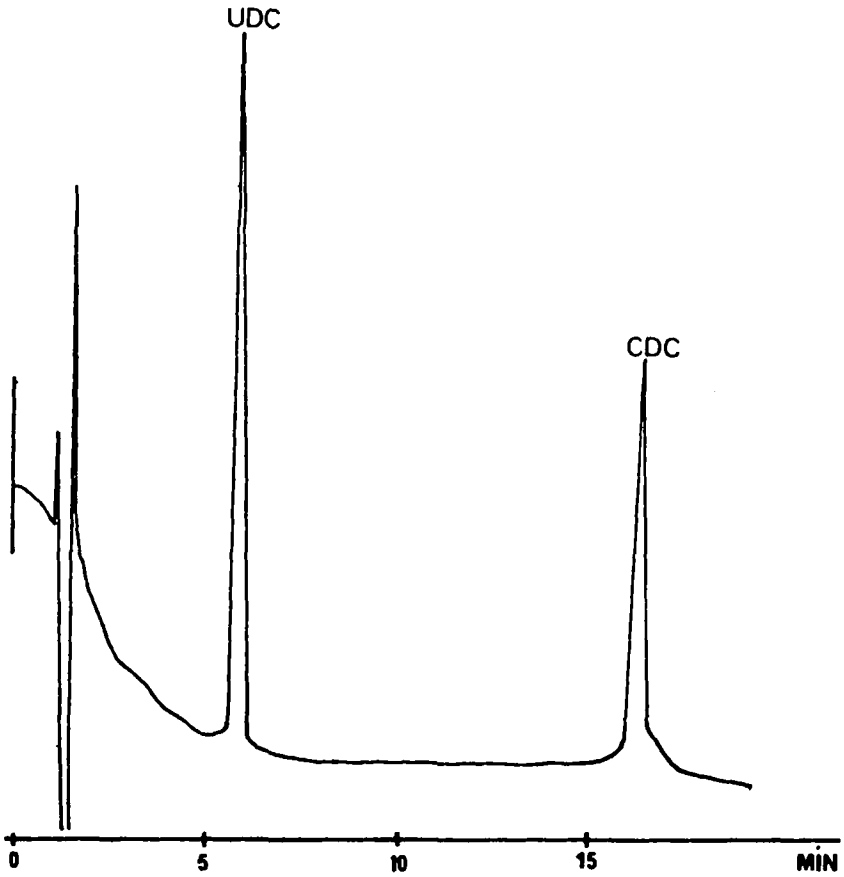

Figure 1—*Chromatogram of ursodeoxycholic acid (UDC) and chenodeoxycholic acid (CDC). Operating conditions were: flow rate, 1.2 mL/min; detector, 201 nm; scale, 0.2 AUFS; sample size, 70 μg/20 μL.*

structural characteristics of these compounds. The melting points and rotations $[\alpha_D]$ of each compound were quite different: ursodeoxycholic acid, mp 203°C, $[\alpha]_D$ +11.5°; chenodeoxycholic acid, mp 143°C, $[\alpha]_D$ +57° (7).

This report describes the pK_a values and the ^{13}C-NMR spectra of these compounds. The pK_a values of ursodeoxycholic acid, chenodeoxycholic acid, and their methyl esters were determined by potentiometry using a hydrogen electrode. The results (Table I) are inconsistent with the physical and chromatographic data in the case of the methyl esters, with the carbonyl function masked; only the hydroxyl group are weakly acidic and the pK_a values are similar. However, the variation of pK_a values in the free acids should be more significant than the observed values obtained by electrochemical methods.

Our hypothesis was that these differences could be explained by a hydrogen bond involving the 7-hydroxyl group of chenodeoxycholic acid. This hydrogen-bonded internal complex could react with the nonpolar stationary phase in liquid chromatography and increase its elution time.

We attempted to show the existence of the hydrogen bond by ^{13}C-NMR spectrometry. The ^{13}C-NMR spectra of common bile acids and their methyl esters have been described and attributions discussed (8, 9) (Table II). Blunt and Stothers (10) describe substitution increments in the steroid carbon skeleton of 5α- and 5β-androstane. With these increments, it is possible to predict the effect of hydroxyl inversion of C-7 on the chemical shifts of neighboring carbon atoms. The corresponding increments were calculated from the published values and are presented in Table III.

The ^{13}C-NMR spectra of ursodeoxycholic acid and its methyl ester have not been described. We assigned carbon signals and compared these with observed chemical shifts using the inversion increment from ursodeoxycholic acid, to obtain the chemical shifts on chenodeoxycholic carbon atoms. Table II compares the values of the observed chemical shifts of ursodeoxycholic acid, chenodeoxycholic acid, and their methyl esters with the calculated chemical shifts of chenodeoxycholic acid and its methyl ester (Fig. 2). Observed and calculated chemical shifts of chenodeoxycholic acid carbons are very similar (deviations, 1 ppm) for all carbons except C-7 (bearing a hydroxyl group) and

Table I—$pK_{a'}$ Values in Methanol–Water (70:30, w/w) at 25°C

Compound	$pK_{a'}$
Ursodeoxycholic acid	6.70
Chenodeoxycholic acid	6.78
Methyl ursodeoxycholate	11.00
Methyl chenodeoxycholate	11.10

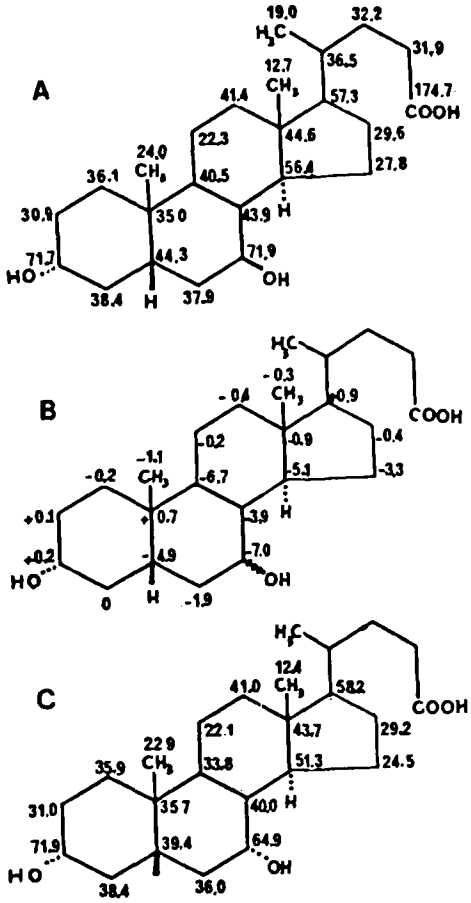

Figure 2—*(A) Observed chemical shifts of ursodeoxycholic acid; (B) increments for 7β → 7α inversion; (C) calculated chemical shifts of chenodeoxycholic acid.*

Table II—Carbon-13 Chemical Shifts of Ursodeoxycholic Acid and Chenodeoxycholic Acid in CH_3OH-d_4 Using Tetramethylsilane as an Internal Standard [a]

	UDC Acid	CDC Acid		Methyl Ester	Methyl Ester CDC	
	7β Obs.	7α Calc.	7α Obs.	UDC 7β Obs.	7α Calc.	7α Obs.
C-1	36.1	35.9	36.5	34.8	34.6	35.1
C-2	30.9	31.0	31.2	30.4	30.5	30.7
C-3	71.7	71.9	72.7	70.9	71.1	71.6
C-4	38.4	38.4	40.3	40.0	40.0	39.2
C-5	44.3	39.4	43.1	43.4	38.5	41.3
C-6	37.9	36.0	36.1	36.9	35.0	34.4
C-7	71.9	64.9	68.9	70.9	63.9	68.2
C-8	43.9	40.0	40.7	42.3	38.4	39.2
C-9	40.5	33.8	33.9	36.9	30.2	32.6
C-10	35.0	35.7	35.8	33.3	34.0	34.9
C-11	22.3	22.1	21.7	21.0	20.8	20.3
C-12	41.4	41.0	41.0	39.1	38.7	39.2
C-13	44.6	43.7	43.6	43.5	42.6	42.4
C-14	56.4	51.3	51.4	54.8	49.7	50.1
C-15	27.8	24.5	24.6	26.7	23.4	23.4
C-16	39.6	29.2	29.1	28.4	28.0	27.9
C-17	57.3	58.2	57.2	55.6	56.5	55.6
C-18	12.7	12.4	12.2	11.9	11.6	11.5
C-19	24.0	22.9	23.4	23.2	22.1	22.6
C-20	36.5		36.6	35.1		35.1
C-21	19.0		18.8	18.2		18.0
C-22	32.2		32.2	30.4		30.7
C-23	31.9		31.9	29.9		30.3
C-24	174.7		175.1	174.7		174.7

[a] UDC = ursodeoxycholic acid; CDC = chenodeoxycholic acid.

C-5 and C-9, which support an important γ-effect from the axial hydroxyl group.

The carbon chemical shifts of the methyl esters also agree closely. Nevertheless, the increments used involve the isolated variation of C-7 configuration and do not take into account the hypothetical intramolecular hydrogen bond between the C-7 hydroxyl and neighboring protons.

Thus, the observed deviations in the chemical shifts of C-4, C-5, C-7, and C-9 as compared with shifts calculated by the increment method may be explained by the existence of a hydrogen bond involving the axial C-7 hydroxyl group of chenodeoxycholic acid and C-4 protons. The values of these deviations agree with a delocalization of σ-bond on a hydrogen bond and an improvement of the γ-axial effect of the C-7 hydroxyl group taking part in a hydrogen bond with C-5 and C-9.

The existence of a hydrogen bond and steric congestion around the C-7 hydroxyl group appears to explain the polarity of these bile acids. Chenodeoxycholic acid appears to be less polar than ursodeoxycholic acid, in agreement with the experimental results obtained by HPLC.

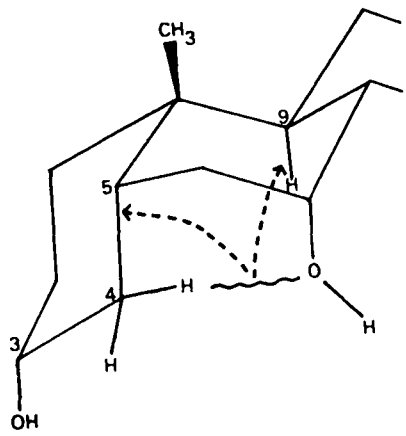

Table III—Substitution Increments in the Steroid Carbon Skeleton: Effect of Hydroxyl Inversion on C-7

Carbon of Steroid Skeleton	Effect of 7αOH [a]	Effect of 7βOH [a]	Effect of 7β → 7α Inversion
C-1	−0.3	−0.1	−0.2
C-2	−0.1	−0.2	+0.1
C-3	−0.1	−0.3	+0.2
C-4	−0.5	−0.5	0
C-5	−7.9	−3.0	−4.9
C-6	+7.6	+9.5	−1.9
C-7	+36.0	+43.0	−7.0
C-8	+4.1	+8.0	−3.9
C-9	−8.5	−1.8	−6.7
C-10	+0.1	−0.6	+0.7
C-11	−0.2	0	−0.2
C-12	−0.5	−0.1	−0.4
C-13	−1.0	+0.1	−0.9
C-14	−5.9	−0.8	−5.1
C-15	−0.5	+2.8	−3.3
C-16	0	+0.4	−0.4
C-17	−0.2	−1.1	+0.9
C-18	−0.3	0	−0.3
C-19	−1.0	+0.1	−1.1

[a] On the chemical shift of neighboring carbon atoms.

REFERENCES

(1) E. Rocchi, E. Gibertini, V. Santunione, M. L. Zeneroli, and E. Ventura, *Med. Chir. Dig.*, **6**, 7445 (1977).

(2) O. Fausa, *Scand. J. Gastroenterol*, **10**, 747 (1975).

(3) J. Roovers, E. Evrard, and H. Vanderhaeghe, *Clin. Chim. Acta*, **19**, 449 (1968).

(4) J. C. Nicolas, J. Chaintreuil, B. Descomps, and A. Crastes De Paulet, *Ann. Biol. Clin. (Paris)*, **103**, 170 (1980).

(5) R. G. Bates, "Determination of pH," 2nd ed., Interscience, New York, N.Y., 1973, chap. 8.

(6) A. Baillet-Guffroy, D. Baylocq, P. Rafidisson, and F. Pellerin, *Talanta*, **28**, 675 (1981).

(7) D. M. Small, "The Bile Acids—Chemistry, Physiology and Metabolism," P. P. Nair and D. Kritchevsky, Eds., Plenum, New York, N.Y., 1971, p. 249.

(8) H. J. Reich, M. Jautelat, M. T. Messe, F. J. Weigert, and J. D. Roberts, *J. Am. Chem. Soc.*, **91**, 7445 (1969).

(9) D. Leibfritz and J. D. Roberts, *J. Am. Chem. Soc.*, **95**, 15 (1973).

(10) J. W. Blunt and J. B. Stothers, *Org. Mag. Res.*, **9**, 8, 439 (1977).

Triazolines XIII: Δ^2-1,2,3-Triazolines, a New Class of Anticonvulsants

PANKAJA K. KADABA

Received June 15, 1981, from the *Division of Medicinal Chemistry and Pharmacognosy, College of Pharmacy, University of Kentucky, Lexington, KY 40506.* Accepted for publication March 23, 1983.

Abstract □ A series of 1,5-diaryl-Δ^2-1,2,3-triazolines has been synthesized and evaluated for the first time as potential anticonvulsant agents using the standard subcutaneous pentylenetetrazol seizure threshold and maximal electroshock seizure tests. Out of the 31 triazolines that were screened, 11 exhibited moderate anticonvulsant activity; 9 of the compounds afforded protection against pentylenetetrazol-induced seizures, while two antagonized electrically induced convulsions.

Keyphrases □ 1,5-Diaryl-Δ^2-1,2,3-triazolines—synthesis, anticonvulsant activity in mice □ Anticonvulsants—potential, 1,5-diaryl-Δ^2-1,2,3-triazolines, synthesis, screening in mice

Although several five-membered heterocyclic ring systems containing up to four nitrogen atoms have been synthesized and screened for anticonvulsant activity (1, 2), no studies have appeared describing the Δ^2-1,2,3-triazolines(4,5-dihydro-1*H*-1,2,3-triazoles; II). Since better anticonvulsants are needed in the treatment of epilepsy (2, 3) and since the triazolines are a new class of heterocyclic compounds (4), we decided to investigate these compounds as potential anticonvulsants.

Although triazolines are formed when Schiff bases (I) react with diazomethane (5, 6) (Scheme I), earlier synthetic procedures have either failed to give a triazoline adduct or have yielded insignificant amounts of the products (5).

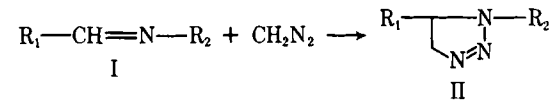

I II

Studies in our laboratories on the role of protic and dipolar aprotic solvents in 1,3-cycloaddition reactions (7–10) have led to a versatile method for the synthesis of the rarely encountered triazolines (11). By utilizing the accelerating effect of protic solvents, such as water, on the addition of diazomethane to Schiff bases, a variety of previously unknown triazolines bearing aryl (11) or heteroaryl (12) substituent groups has become readily available in sufficient quantities to permit, for the first time, a detailed screening of these compounds for biological activity. Two earlier papers reported the results of screening for herbicidal activity (13) and pesticidal properties (14). The present paper investigates the potential of the triazoline heterocycles as anticonvulsant compounds.

RESULTS AND DISCUSSION

The triazoline ring system is different from those of the conventional anticonvulsant drugs, the majority of which have a dicarboximide (ureylene) —CO—NH—CO—, function as in barbiturates, hydantoins, succinimides, and oxazolidinediones or a closely related structure as in primidones. The absence of the dicarboximide function, which contributes to the inherent hypnotic and sedative activity of the barbiturates and related compounds, may be expected to reduce the toxic side effects in potential triazoline anticonvulsants.

The triazolines may be considered to be derived from the succinimides (III) by the loss of one C=O moiety (IV) and the replacement of the other by an N=N group (II). Several azetidinones have been reported to have varying degrees of anticonvulsant activity (15) as well as some 2-azetidinthiones (16).

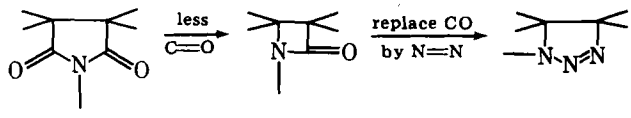

III IV II

Pharmacology—The compounds were evaluated for anticonvulsant activity in two seizure models in the mouse, the maximal electroshock seizure (MES) test and the subcutaneous pentylenetetrazol seizure threshold (scMet) test. These two methods of seizure provocation are known to reliably elicit well-characterized seizure phenomena (17) and are the standard screens of choice for identification of anticonvulsant activity in a compound (18). CNS toxicity is determined in the rotorod ataxia test (19). This test has a clear end-point, is quantifiable, and correlates well with the clinical assessment of minimal toxicity. Testing is done in the dose range of 30–600 mg/kg (with a few exceptions) at both 30-min and 4-h intervals. This provides a profile of the anticonvulsant activity, toxicity, potency, and pharmacokinetics of each compound and minimizes the likelihood of failing to identify slowly absorbed compounds or those with possible anticonvulsant activity in a metabolite.

Structure–Activity Relationships—The results of screening 31 1,5-diaryl-substituted Δ^2-1,2,3-triazolines are reported in Table I. Eleven compounds exhibited moderate anticonvulsant activity; while nine of these afforded protection against scMet-induced seizures, only two (IX and XVI) were active in the MES test. The parent compound (V) is the most potent and is active at the 100-mg/kg dose level. Six other compounds (XVI, XX, XXI, XXIV, XXIX, and XXXIV) afforded protection in the scMet test at 300 mg/kg and three more (VI, VII, and XIX) at the 600-mg/kg dose level. Compounds IX and XXI show delayed activity after 4 h: IX in the MES test at 600 mg/kg and XXI in the scMet test at 300 mg/kg. Compound XVI, in addition to its activity in the scMet test, shows activity in the MES test at the 600-mg/kg level at both 0.5 and 4 h. With the exception of XVI and XXIV, the triazoline compounds are relatively nontoxic.

Certain structure–activity relationships have emerged from the varying substitution patterns on the phenyl rings of the parent compound. Introduction of a 2-chloro substituent on the 5-phenyl ring gives VI, which affords 75% protection at 0.5 h and 50% at 4 h with no symptoms of neurological deficit. When the chloro group is in the 4-position of either phenyl ring, activity disappears in the scMet test, although the 5-(4-chlorophenyl) compound, IX, evinces delayed activity in the MES test.

Compounds XV–XXIII illustrate the effect of different substituents on the 1-phenyl of VI. A 3-CF_3 group increases activity as well as toxicity, while a 4-CF_3 or 4-C_2H_5 affords protection at the same dose level without signs of neurotoxicity. The almost parallel activities of VI and XIX are interesting, since the 4-F analogue XIX provides minimal change in π and σ effects (20) compared with the unsubstituted VI. The presence of 4-Cl, 4-Br, 4-OCH_3, or 3,4-Cl_2 yields inactive compounds XVIII, XVII, XXII, and XXIII, respectively. However, with the introduction of a second chloro group in the 6-position of the 5-phenyl ring of XVII, activity reappears, as in XXXIV; similar substitution in XIX leads to a loss of activity in XXXV. A more meaningful analysis of the structure–activity pattern to obtain information on parameter dependency using the Topliss manual approach (20) to Hansch analysis in this compound group, XV–XXIII, has not been possible, since the activity spread between the members is not large enough (20). However, the structure–activity relationships do indicate the anticonvulsant potential of appropriately substituted 1,2,3-triazolines.

Finally, the effect of a nitro substituent is noteworthy. While a 4-NO_2 on either phenyl ring does not contribute to activity, a 3-NO_2 by itself, as in VII, or in combination with 2,4-Cl_2, as in XXIX, yields an active compound.

EXPERIMENTAL

Chemistry—The 1,5-diaryl-Δ^2-1,2,3-triazolines were prepared as described previously (7–12). All compounds except XIII–XVI, XVIII–XXII, XXIV, XXVIII, XXX, and XXXII–XXXV have been reported previously (11). Data on the newly synthesized compounds are presented in Table II.

0022-3549/84/0600-0850$01.00/0
© 1984, American Pharmaceutical Association

Table I—Results of Screening 1,5-Diaryl-Δ^2-1,2,3-triazolines for Anticonvulsant Activity in the Mouse after Intraperitoneal Administration

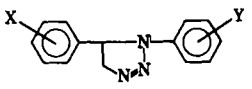

Compound	X	Y	Anticonvulsant Activity (scMet) Effective Dose, mg/kg	Animals Protected, % 0.5 h	4 h	Neurotoxicity Animals Toxic at 0.5 h, %
V	H	H	100	25	0	0
VI	2-Cl	H	600	75	50	0
VII	3-NO_2	H	600	75	0	0
VIII	4-NO_2	H	600	0	0	0
IX	4-Cl	H	600[a,b,c]	0	0	0
X	H	4-NO_2	600	0	0	0
XI	H	4-Cl	600	0	0	0
XII	H	4-CH_3	600	0	0	0
XIII	4-Cl	4-Br	600	0	0	0
XIV	3-Cl	4-Br	600	0	0	0
XV	2-Cl	3-Cl	600	0	0	0
XVI	2-Cl	3-CF_3	300[c,d]	100[c]	0	100
XVII	2-Cl	4-Br	600	0	0	0
XVIII	2-Cl	4-Cl	600	0	0	0
XIX	2-Cl	4-F	600	100	0	25
XX	2-Cl	4-CF_3	300	25	0	0
XXI	2-Cl	4-C_2H_5	300	0	100[b,c]	0
XXII	2-Cl	4-OCH_3	600	0	0	0
XXIII	2-Cl	3,4-Cl_2	600	0	0	0
XXIV	2-NO_2	3-Cl	300	25	0	25
XXV	2-NO_2	3-NO_2	300	0	0	0
XXVI	2,4-Cl_2	H	300	0	0	0
XXVII	2,4-Cl_2	3-Cl	600	0	0	0
XXVIII	2,4-Cl_2	3-CF_3	600	0	0	0
XXIX	2,4-Cl_2	3-NO_2	300	100[c]	0	0
XXX	2,4-Cl_2	4-Cl	600	0	0	0
XXXI	2,4-Cl_2	4-COOEt	600	0	0	0
XXXII	2,6-Cl_2	H	300	0	0	0
XXXIII	2,6-Cl_2	3-Cl	600	0	0	0
XXXIV	2,6-Cl_2	4-Br	300	25	0	0
XXXV	2,6-Cl_2	4-F	600	0	0	0

[a] At the same dose level, the compound afforded 100% protection in the MES test after 4 h. [b] The delayed effect could be because it is slowly absorbed or it has anticonvulsant activity in a metabolite. [c] Only one animal was tested. [d] At 600 mg/kg, this compound protected 100% animals in the MES test at 0.5 and 4 h, but it also showed 100% toxicity at both time periods.

Pharmacology—The 31 triazolines were screened by the Anticonvulsant Screening Project (ASP) under the Antiepileptic Drug Development (ADD) program of the Epilepsy Branch of the National Institute of Neurological and Communicative Disorders and Stroke (NINCDS).

The compounds were solubilized in 30% polyethylene glycol 400. The solvent was tested for anticonvulsant and toxic effects and was found to introduce no significant bias into the testing of anticonvulsant activity. The compounds were administered intraperitoneally in a volume of 0.01 mL/g to male Carworth Farms #1 mice weighing ~20 g (21). Testing was done at dose levels of 30, 100, 300, and 600 mg/kg, and a total of 16 animals were used, four for each dose. After 30 min, each animal was examined for toxicity in the rotorod test (19). Immediately thereafter, anticonvulsant activity was evaluated by subjecting one mouse to the MES test and another to the scMet test. The same tests were repeated 4 h later on the two remaining mice at each dose level. When compounds were found to afford protection, the test was repeated at that dose level and time using four animals, and the results were expressed as number of animals protected/number of animals tested or as percent of animals protected (Table I).

The maximal electroshock seizure test (MES) was performed according to the method of Swinyard *et al.* (22), and abolition of the hind limb tonic extension component of the seizure was defined as protection. In the subcutaneous pentylenetetrazol seizure threshold test (scMet), 85 mg/kg of pen-

Table II—Newly Synthesized 1,5-Diaryl-Δ^2-1,2,3-triazolines

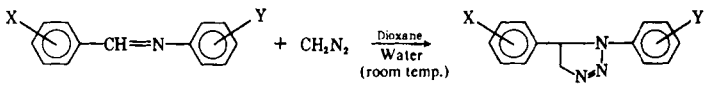

Compound	Substituent X	Substituent Y	Schiff base mp, °C[a]	Schiff base Yield, %	Schiff base Formula[b]	Triazoline Reaction time, h	Triazoline mp, °C[a]	Triazoline Yield, %	Triazoline Formula[b]
XIII	4-Cl	4-Br	118-121	72	$C_{13}H_9BrClN$	240	147-149	88	$C_{14}H_{11}BrClN_3$
XIV	3-Cl	4-Br	60-61	77	$C_{13}H_9BrClN$	120	134-135	90	$C_{14}H_{11}BrClN_3$
XV	2-Cl	3-Cl	41-43	81	$C_{13}H_9Cl_2N$	96	72-74	69	$C_{14}H_{11}Cl_2N_3$
XVI	2-Cl	3-CF_3	Oil	Q[c]	$C_{14}H_9ClF_3N$	144	49-51	77	$C_{15}H_{11}ClF_3N_3$
XVIII	2-Cl	4-Cl	68-70	75	$C_{13}H_9Cl_2N$	88	126-127	92	$C_{14}H_{11}Cl_2N_3$
XIX	2-Cl	4-F	56-58	74	$C_{13}H_9ClFN$	113	71-72	78	$C_{14}H_{11}ClFN_3$
XX	2-Cl	4-CF_3	48-50	40	$C_{14}H_9ClF_3N$	96	83-86	80	$C_{15}H_{11}ClF_3N_3$
XXI	2-Cl	4-C_2H_5	33-34	93	$C_{15}H_{14}ClN$	336	44-46	48	$C_{16}H_{16}ClN_3$
XXII	2-Cl	4-OCH_3	63	Q[c]	$C_{14}H_{12}ClNO$	144	95-97	61	$C_{15}H_{14}ClN_3O$
XXIV	2-NO_2	3-Cl	76-78	89	$C_{13}H_9ClN_2O_2$	120	90-92	60	$C_{14}H_{11}ClN_4O_2$
XXVIII	2,4-Cl_2	3-CF_3	78-80	85	$C_{14}H_8Cl_2F_3N$	96	68-69	82	$C_{15}H_{10}Cl_2F_3N_3$
XXX	2,4-Cl_2	4-Cl	129-130	96	$C_{13}H_8Cl_3N$	192	106-108	90	$C_{14}H_{10}Cl_3N_3$
XXXII	2,6-Cl_2	H	62-63	82	$C_{13}H_9Cl_2N$	116	182-184	70	$C_{14}H_{11}Cl_2N_3$
XXXIII	2,6-Cl_2	3-Cl	114-115	90	$C_{13}H_8Cl_3N$	48	148-148.5	88	$C_{14}H_{10}Cl_3N_3$
XXXIV	2,6-Cl_2	4-Br	80-81	81	$C_{13}H_8BrCl_2N$	51	156-157	75	$C_{14}H_{10}BrCl_2N_3$
XXXV	2,6-Cl_2	4-F	128-130	93	$C_{13}H_8Cl_2FN$	70	132-133	70	$C_{14}H_{10}Cl_2FN_3$

[a] Melting points were determined in a Thomas-Hoover apparatus and are uncorrected. [b] The elemental analyses (C, H, and N) for all new compounds were within ±0.4% of the theoretical values. [c] Quantitative.

tylenetetrazol was administered as a 0.5% solution subcutaneously in the posterior midline, and failure to observe even a threshold seizure (a single episode of clonic spasms of at least 5-s duration) was defined as protection (22).

Neurotoxicity was evaluated by the rotorod ataxia test (19). The animal was placed on a wooden rod of 2.8-cm diameter rotating at 6 rpm. Normal mice can remain on a rod rotating at this speed indefinitely. Neurologic toxicity was defined as the failure of the animal to remain on the rod for 1 min and was expressed as number of animals exhibiting toxicity/number of animals tested or as percent of animals showing toxicity.

REFERENCES

(1) P. K. Kadaba, *J. Prakt. Chem.*, **324,** 857 (1982).

(2) F. D. Popp, in "Anticonvulsants," J. A. Vida, Ed., Academic, New York, N.Y., 1977, p. 333.

(3) D. A. Woodbury, J. K. Penry, and R. P. Schmidt, "Antiepileptic Drugs," Raven, New York, N.Y., 1972.

(4) P. Scheiner, in "Selective Organic Transformations," Vol. 1, B. S. Thyagarajan Ed., Wiley-Interscience, New York, N.Y., 1970; P. K. Kadaba, B. Stanovnik, and M. Tisler, *Adv. Heterocycl. Chem.*, **37,** 1984 (in press).

(5) A. Mustafa, *J. Chem. Soc.*, **1949,** 234.

(6) G. D. Buckley, *J. Chem. Soc.*, **1954,** 1850.

(7) P. K. Kadaba and J. O. Edwards, *J. Org. Chem.*, **26,** 2331 (1961).

(8) P. K. Kadaba, *Tetrahedron*, **25,** 3053 (1969).

(9) P. K. Kadaba and T. F. Colturi, *J. Heterocycl. Chem.*, **6,** 829 (1969).

(10) P. K. Kadaba, *Synthesis* **1973,** 71.

(11) P. K. Kadaba, *Tetrahedron*, **22,** 2453 (1966); P. K. Kadaba and N. F. Fannin, *J. Heterocycl. Chem.*, **4,** 301 (1967).

(12) P. K. Kadaba, *J. Heterocycl. Chem.*, **12,** 143 (1975).

(13) P. K. Kadaba, *J. Pharm. Sci.*, **59,** 1190 (1970).

(14) P. K. Kadaba, *Pestic. Sci.*, **5,** 255 (1974).

(15) G. Maffii, *Farmaco. Ed. Sci.*, **14,** 176 (1959); Calanda-Stiftung, British Pat. 924, 589, (1963); *Chem. Abstr.*, **59,** 11424 (1963); E. Testa and L. Fontanella, British Pat. 829, 663 (1957), *Chem. Abstr.*, **56,** 1429 (1962).

(16) E. Testa, L. Fontanella, and G. Maffii, South African Pat. 6707, 088 (1968); *Chem. Abstr.*, **70,** 57602 (1969).

(17) G. Chen, B. Bohner, and C. Ensor, *Proc. Soc. Exp. Biol. Med.*, **87,** 334 (1954).

(18) D. A. Woodbury, in "Experimental Models of Epilepsy," Raven, New York, N.Y., 1972, p. 557.

(19) N. W. Dunham and T. S. Miya, *J. Am. Pharm. Assoc., Sci. Ed.*, **46,** 208 (1957).

(20) J. G. Topliss, *J. Med. Chem.*, **20,** 463 (1977).

(21) M. L. Torchiana and C. A. Stone, *Proc. Soc. Exp. Biol. Med.*, **100,** 290 (1959).

(22) E. A. Swinyard, W. C. Brown, and L. S. Goodman, *J. Pharmacol. Exp. Ther.*, **106,** 319 (1952).

ACKNOWLEDGMENTS

The author wishes to acknowledge and thank the ASP of NINCDS for conducting the screening studies under the liaison of Dr. Gill D. Gladding, Pharmacy Consultant, Epilepsy Branch. The author is grateful to the National Institute of Neurological and Communicative Disorders and Stroke for the award of research grant 1RO1 NS16843-01A1, which made this work possible. All the anticonvulsant compounds reported in this paper are protected by patents.

Depletion of Endogenous Inorganic Sulfate in the Mammalian Central Nervous System by Acetaminophen

Keyphrases □ Acetaminophen—cerebrospinal fluid, sulfate depletion in rats □ Endogenous inorganic sulfate—depletion in cerebrospinal fluid of rats by acetaminophen

To the Editor:

Acetaminophen is metabolized in part by conjugation with sulfate (1, 2), a process that causes transient depletion of endogenous inorganic sulfate in plasma of rats and humans (3, 4). Sulfate activation (5) and conjugation (6) occur in the mammalian brain and may have a significant role in regulating the levels of biogenic amine neurotransmitters (7). Sulfate is also needed for the synthesis of certain brain tissue constituents such as mucopolysaccharides and sulfatides (5). It is of interest, therefore, to determine if the widely used analgesic and antipyretic agent acetaminophen can deplete inorganic sulfate in the central nervous system.

Female Lewis rats, 170–195 g, were cannulated (right jugular vein) under light ether anesthesia 1 d before the experiment. On the next day, the animals were placed in individual plastic metabolism cages, and food and water were withdrawn. Acetaminophen (10 mg/mL in normal saline solution) was infused at a rate of ~12 mg/h/rat for 6 h; control rats received an infusion of drug-free saline solution. At the end of the infusion, the animals were anesthetized with ether, ~0.1 mL cerebrospinal fluid (CSF) was obtained from the cisterna magna, and blood was collected from the abdominal aorta into heparinized tubes. The concentrations of inorganic sulfate in CSF and plasma were determined by single-column ion chromatography, using a mobile phase of 4 mM potassium hydrogen phthalate adjusted to pH 4.5 with potassium hydroxide, a Wescan anion exchange column, and conductivity detection (8). Potassium nitrate was added to the plasma samples as an internal standard; CSF samples were assayed without internal standard because of the presence of interfering peaks. Heparin did not affect the assay.

The results of the study are summarized in Table I. The normal concentration ratio of endogenous sulfate, CSF-plasma, was on average 0.224. This is similar to the reported concentration ratio of 0.24 in cats (9), 0.17 in rabbits (9), and 0.30 in humans (10). The 6-h infusion of acetaminophen caused a pronounced reduction of inorganic sulfate concentrations in plasma, as already reported (3), and also reduced the concentration of inorganic sulfate in CSF. However, the CSF-plasma concentration ratio increased to 0.530 on the average. There was a significant negative correlation between the CSF-plasma concentration ratio and the plasma concentration of inorganic sulfate ($r = -0.926$, $p < 0.01$).

Table I—Effect of Acetaminophen Administration on Endogenous Inorganic Sulfate Concentrations in the Cerebrospinal Fluid and Plasma of Rats [a]

	Controls ($n = 5$)	Acetaminophen Treated ($n = 8$)
Cerebrospinal fluid	0.164 ± 0.023	0.067 ± 0.022[b]
Plasma	0.731 ± 0.020	0.132 ± 0.055[b]
CSF-plasma concentration ratio	0.224 ± 0.028	0.530 ± 0.141[b]

[a] Results are expressed as mean ± *SD*. Concentrations are millimolar. [b] Significantly different from corresponding control value, $p < 0.01$ by two-sample rank test.

These observations demonstrate that treatment with acetaminophen can cause depletion of endogenous inorganic sulfate not only in plasma but also in the central nervous system. Since plasma protein binding of inorganic sulfate is negligible (10, 11), the substantially lower concentration of the anion in CSF than in plasma suggests that sulfate is transported by a specialized process from CSF to plasma, as already suggested by others (12). Moreover, the increased CSF-plasma concentration ratio in the sulfate-depleted acetaminophen-treated rats (Table I), and the decreased ratio when plasma sulfate concentrations are increased by intravenous injection of sodium sulfate (9), indicate that the transport process is saturable. In this respect, sulfate homeostasis in CSF is facilitated as is plasma sulfate homeostasis, the latter by a specialized renal transport process (4, 13). While the specialized transport processes dampen fluctuations of endogenous sulfate concentrations, they do not prevent substantial concentration changes due to depletion of endogenous sulfate resulting from its utilization for sulfate conjugation of phenolic drugs such as acetaminophen. It is desirable, therefore, to determine the effect of acetaminophen on endogenous sulfate concentrations in the CSF of human subjects and such studies are now in progress.

(1) G. Levy and H. Yamada, *J. Pharm. Sci.*, **60**, 784 (1971).
(2) R. E. Galinsky and G. Levy, *J. Pharmacol. Exp. Ther.*, **219**, 14 (1981).
(3) J. H. Lin and G. Levy, *Biochem. Pharmacol.*, **30**, 2723 (1981).
(4) M. E. Morris and G. Levy, *Clin. Pharmacol. Ther.*, **33**, 529 (1983).
(5) A. S. Balasubramanian and B. K. Bachhawat, *Brain Res.*, **20**, 341 (1970).
(6) J. L. Meek and N. H. Neff, *J. Neurochem.*, **21**, 1 (1973).
(7) J. A. Roth and A. J. Rivett, *Biochem. Pharmacol.*, **31**, 3017 (1982).
(8) M. E. Morris, Ph.D. Dissertation, State University of New York at Buffalo, 1984.
(9) A. Van Harreveld, N. Ahmed, and D. J. Tanner, *Am. J. Physiol.*, **210**, 777 (1966).
(10) E. Watchorn and R. A. McCance, *Biochem. J.*, **29**, 2291 (1935).
(11) M. Walser, D. W. Seldin, and A. Grollman, *J. Clin. Invest.*, **32**, 299 (1953).
(12) J. E. Richmond and A. B. Hastings, *Am. J. Physiol.*, **199**, 814 (1960).
(13) J. H. Lin and G. Levy, *J. Pharm. Sci.*, **72**, 213 (1983).

Marilyn E. Morris
Raymond E. Galinsky
Gerhard Levy[x]

Department of Pharmaceutics
School of Pharmacy
State University of NY at Buffalo
Amherst, NY 14260

Received January 30, 1984.
Accepted for publication March 8, 1984.
Supported in part by Grant 19568 from the National Institute of General Medical Sciences of the National Institutes of Health. Mr. David M. Soda provided competent technical assistance.

0022-3549/84/0600-0853$01.00/0
© 1984, American Pharmaceutical Association

Organ Perfusion Studies: A Rebuttal

Keyphrases □ Organ perfusion—pharmacokinetics, sampling □ Pharmacokinetics—organ perfusion, effect of sampling

To the Editor:

Colburn *et al.* (1) discussed the influence of sampling in organ perfusion studies. In this respect we want to make the following critical remarks. These authors defined the elimination rate constant K as Q/V_R, in which Q represents the perfusion flow rate and V_R represents the reservoir volume. According to this equation, however, K is *not* the elimination rate constant.

It is explicitly stated by Rowland *et al.* in their Table I (2), that the rate constant k_{12} of the compartmental model corresponds to $\dot{V}_B/V_R$ of the perfusion model. In Colburn's terminology $\dot{V}_B = Q$. Since Colburn states that $K = Q/V_R$, it is erroneous to call K an elimination rate constant; it simply is the transport rate constant from the reservoir to the eliminating perfused organ in terms of the perfusion model. Similarly, the rate constant k_{12} of the compartmental model represents the transport rate constant from the central to the peripheral compartment in the compartmental model. The elimination rate constant itself, k_e, contrary to the opinion of Colburn *et al.*, is independent of the perfusion flow rate, since it reflects the intrinsic ability of the organ to eliminate drug. As we have pointed out (3), the drug decrease in the reservoir will be more rapid under the influence of sampling than without sampling. Consequently, a pharmacokinetic analysis based on the uncorrected time course of drug concentration in the reservoir will result in overestimation of the parameter k_e.

Colburn *et al.* stated that clearance will be unaffected by sampling from the reservoir. We do not agree with their statement. They define clearance as:

$$CL_o = Q\left(\frac{C_{in} - C_o}{C_{in}}\right) \qquad \text{(Eq. 1)}$$

where C_{in} and C_o represent the inflow and outflow concentrations of the eliminating organ. This expression, however, defines *instantaneous* clearance (2), which is time- and concentration-dependent. A more relevant measure of clearance is the *mean* clearance, which essentially is a steady-state concept. The mean clearance equals:

$$CL = \frac{Q \cdot k_e}{Q/(K_p \cdot V_o) + k_e} \qquad \text{(Eq. 2)}$$

where V_o is the physical organ volume and K_p is the apparent partition coefficient of drug between the eliminating organ and the emergent perfusion fluid (2). This leaves K_p and k_e as two independent parameters to be estimated from the concentration *versus* time curve as measured in the reservoir.

As discussed above, the parameter k_e will be overestimated due to sampling. Similarly, the estimate of the parameter K_p is biased, in a complicated way, by sampling (3). It follows that sampling from the reservoir definitely influences the estimate of clearance. The extent to which clearance is biased by neglecting corrections for sampling is dependent on the numerical values of Q, K_p, k_e, and of course the sample volumes.

In conclusion it can be stated that the instantaneous clearance is the wrong parameter to look at and that the mean clearance estimated from concentration *versus* time curves in the reservoir will certainly depend on sampling from this reservoir.

(1) W. A. Colburn, R. K. Brazzell, and I. Bekersky, *J. Pharm. Sci.*, **72**, 970 (1983).

(2) M. Rowland, L. Z. Benet, and G. G. Graham, *J. Pharmacokinet. Biopharm.*, **1**, 123 (1973).

(3) C. J. Timmer and H. P. Wijnand, *J. Pharmacokinet. Biopharm.*, **5**, 335 (1977).

Cornelis J. Timmer[x]
Herman P. Wijnand
Organon Scientific Development Group
P.O. Box 20
5340 BH Oss
The Netherlands

Received October 31, 1983.
Accepted for publication February 17, 1984.

Estimation of Mean Residence Time from Data Obtained when Multiple-Dosing Steady State Has Been Reached

Keyphrases □ Pharmacokinetics—multiple dosing, mean residence time

To the Editor:

When the plasma concentration (C) *versus* time (t) profile of a drug, on single dosing, can be described, irrespective of dosing route, as an exponential series:

$$C = \sum_{i=1}^{n} A_i \cdot \exp(-k_i t) \qquad \text{(Eq. 1)}$$

then the concentration *versus* time profile on multiple dosing to steady state, at a constant interval, Υ, can be described (1) as:

$$C_{ss} = \sum_{i=1}^{n} \frac{A_i}{1 - \exp(-k_i \Upsilon)} \cdot \exp(-k_i t) \qquad \text{(Eq. 2)}$$

where C_{ss} represents the plasma concentration at multiple-dosing steady state and, in this case, t is time after the last dose administered. Equation 2 is valid on the assumptions that the dose remains constant, the dosing interval is constant, and clearance is constant. It has been demonstrated (see Ref. 1) that under these conditions:

$$\int_0^\infty C dt = \int_0^\Upsilon C_{ss} dt \qquad \text{(Eq. 3)}$$

When the time course of drug concentration is regarded as a statistical distribution curve (2) the mean residence time (MRT) of the drug, on single dosing, can be defined (3) as:

$$\text{MRT} = \int_0^\infty tCdt \Big/ \int_0^\infty Cdt = \left(\sum_{i=1}^{n} A_i/k_i^2\right) \Big/ \left(\sum_{i=1}^{n} A_i/k_i\right) \qquad \text{(Eq. 4)}$$

In addition to using the analytical integrals of Eq. 1, as shown in Eq. 4, the MRT has been calculated using integrals estimated by the trapezoidal rule (4).

On the basis of Eq. 2, the first moment curve at steady state would be:

0022-3549/84/0600-0854$01.00/0
© 1984, American Pharmaceutical Association

Organ Perfusion Studies: A Rebuttal

Keyphrases □ Organ perfusion—pharmacokinetics, sampling □ Pharmacokinetics—organ perfusion, effect of sampling

To the Editor:

Colburn *et al.* (1) discussed the influence of sampling in organ perfusion studies. In this respect we want to make the following critical remarks. These authors defined the elimination rate constant K as Q/V_R, in which Q represents the perfusion flow rate and V_R represents the reservoir volume. According to this equation, however, K is *not* the elimination rate constant.

It is explicitly stated by Rowland *et al.* in their Table I (2), that the rate constant k_{12} of the compartmental model corresponds to $\dot{V}_B/V_R$ of the perfusion model. In Colburn's terminology $\dot{V}_B = Q$. Since Colburn states that $K = Q/V_R$, it is erroneous to call K an elimination rate constant; it simply is the transport rate constant from the reservoir to the eliminating perfused organ in terms of the perfusion model. Similarly, the rate constant k_{12} of the compartmental model represents the transport rate constant from the central to the peripheral compartment in the compartmental model. The elimination rate constant itself, k_e, contrary to the opinion of Colburn *et al.*, is independent of the perfusion flow rate, since it reflects the intrinsic ability of the organ to eliminate drug. As we have pointed out (3), the drug decrease in the reservoir will be more rapid under the influence of sampling than without sampling. Consequently, a pharmacokinetic analysis based on the uncorrected time course of drug concentration in the reservoir will result in overestimation of the parameter k_e.

Colburn *et al.* stated that clearance will be unaffected by sampling from the reservoir. We do not agree with their statement. They define clearance as:

$$CL_o = Q\left(\frac{C_{in} - C_o}{C_{in}}\right) \qquad \text{(Eq. 1)}$$

where C_{in} and C_o represent the inflow and outflow concentrations of the eliminating organ. This expression, however, defines *instantaneous* clearance (2), which is time- and concentration-dependent. A more relevant measure of clearance is the *mean* clearance, which essentially is a steady-state concept. The mean clearance equals:

$$CL = \frac{Q \cdot k_e}{Q/(K_p \cdot V_o) + k_e} \qquad \text{(Eq. 2)}$$

where V_o is the physical organ volume and K_p is the apparent partition coefficient of drug between the eliminating organ and the emergent perfusion fluid (2). This leaves K_p and k_e as two independent parameters to be estimated from the concentration *versus* time curve as measured in the reservoir.

As discussed above, the parameter k_e will be overestimated due to sampling. Similarly, the estimate of the parameter K_p is biased, in a complicated way, by sampling (3). It follows that sampling from the reservoir definitely influences the estimate of clearance. The extent to which clearance is biased by neglecting corrections for sampling is dependent on the numerical values of Q, K_p, k_e, and of course the sample volumes.

In conclusion it can be stated that the instantaneous clearance is the wrong parameter to look at and that the mean clearance estimated from concentration *versus* time curves in the reservoir will certainly depend on sampling from this reservoir.

(1) W. A. Colburn, R. K. Brazzell, and I. Bekersky, *J. Pharm. Sci.*, **72**, 970 (1983).

(2) M. Rowland, L. Z. Benet, and G. G. Graham, *J. Pharmacokinet. Biopharm.*, **1**, 123 (1973).

(3) C. J. Timmer and H. P. Wijnand, *J. Pharmacokinet. Biopharm.*, **5**, 335 (1977).

Cornelis J. Timmer[x]
Herman P. Wijnand
Organon Scientific Development Group
P.O. Box 20
5340 BH Oss
The Netherlands

Received October 31, 1983.
Accepted for publication February 17, 1984.

Estimation of Mean Residence Time from Data Obtained when Multiple-Dosing Steady State Has Been Reached

Keyphrases □ Pharmacokinetics—multiple dosing, mean residence time

To the Editor:

When the plasma concentration (C) *versus* time (t) profile of a drug, on single dosing, can be described, irrespective of dosing route, as an exponential series:

$$C = \sum_{i=1}^{n} A_i \cdot \exp(-k_i t) \qquad \text{(Eq. 1)}$$

then the concentration *versus* time profile on multiple dosing to steady state, at a constant interval, Υ, can be described (1) as:

$$C_{ss} = \sum_{i=1}^{n} \frac{A_i}{1 - \exp(-k_i \Upsilon)} \cdot \exp(-k_i t) \qquad \text{(Eq. 2)}$$

where C_{ss} represents the plasma concentration at multiple-dosing steady state and, in this case, t is time after the last dose administered. Equation 2 is valid on the assumptions that the dose remains constant, the dosing interval is constant, and clearance is constant. It has been demonstrated (see Ref. 1) that under these conditions:

$$\int_0^\infty C dt = \int_0^\Upsilon C_{ss} dt \qquad \text{(Eq. 3)}$$

When the time course of drug concentration is regarded as a statistical distribution curve (2) the mean residence time (MRT) of the drug, on single dosing, can be defined (3) as:

$$\text{MRT} = \int_0^\infty tCdt \Big/ \int_0^\infty Cdt = \left(\sum_{i=1}^{n} A_i/k_i^2\right) \Big/ \left(\sum_{i=1}^{n} A_i/k_i\right) \qquad \text{(Eq. 4)}$$

In addition to using the analytical integrals of Eq. 1, as shown in Eq. 4, the MRT has been calculated using integrals estimated by the trapezoidal rule (4).

On the basis of Eq. 2, the first moment curve at steady state would be:

0022-3549/84/0600-0854$01.00/0
© 1984, American Pharmaceutical Association

$$tC_{ss} = \sum_{i=1}^{n} \frac{tA_i}{1 - \exp(-k_i\Upsilon)} \cdot \exp(-k_i t) \quad \text{(Eq. 5)}$$

The integral of Eq. 5 is:

$$\int_0^t tC_{ss}dt = \sum_{i=1}^{n} \frac{A_i}{1 - \exp(-k_i\Upsilon)} \left[\frac{1}{k_i^2}(1 - \exp(-k_i t)) - \frac{t}{k_i} \cdot \exp(-k_i t)\right] \quad \text{(Eq. 6)}$$

$\int_0^\Upsilon tC_{ss}dt$ is, therefore:

$$\int_0^\Upsilon tC_{ss}dt = \sum_{i=1}^{n} \frac{A_i}{k_i^2} - \sum_{i=1}^{n} \frac{A_i\Upsilon \cdot \exp(-k_i\Upsilon)}{k_i[1 - \exp(-k_i\Upsilon)]} = \int_0^\infty tCdt - \Upsilon \sum_{i=1}^{n} \frac{A_i \exp(-k_i\Upsilon)}{k_i[1 - \exp(-k_i\Upsilon)]} \quad \text{(Eq. 7)}$$

Rearranging Eq. 7:

$$\int_0^\infty tCdt = \int_0^\Upsilon tC_{ss}dt + \Upsilon \sum_{i=1}^{n} \frac{A_i \cdot \exp(-k_i\Upsilon)}{A_i[1 - \exp(-k_i\Upsilon)]} \quad \text{(Eq. 8)}$$

Equation 8 indicates that MRT cannot be estimated by using the area under the multiple-dosing first moment curve from time zero to time Υ as a numerator in an equation analogous to Eq. 4. However, since $\int_0^\Upsilon C_{ss}dt = \Sigma_{i=1}^{n} A_i/k_i$ and:

$$\int_0^\infty C_{ss}dt = \sum_{i=1}^{n} \frac{A_i}{k_i[1 - \exp(-k_i\Upsilon)]} \quad \text{(Eq. 9)}$$

then:

$$\sum_{i=1}^{n} \frac{A_i \cdot \exp(-k_i\Upsilon)}{k_i[1 - \exp(-k_i\Upsilon)]} = \int_0^\infty C_{ss}dt - \int_0^\Upsilon C_{ss}dt = \int_\Upsilon^\infty C_{ss}dt \quad \text{(Eq. 10)}$$

Equation 8 is equivalent to:

$$\int_0^\infty tCdt = \int_0^\Upsilon tC_{ss}dt + \Upsilon \int_\Upsilon^\infty C_{ss}dt \quad \text{(Eq. 11)}$$

Table I—MRT Calculation [a]

Time, h	C_{ss}, μg/mL	tC_{ss}, μg·h/mL	$\int_0^t C_{ss}dt$, μg·h/mL	$\int_0^t tC_{ss}dt$, μg·h²/mL
0	124.68	0	0[a]	0[a]
0.0833	103.51	8.62	9.5	0.4
0.1667	89.53	14.93	17.6	1.3
0.25	80.31	20.08	24.6	2.8
0.5	67.34	33.67	43.1	9.5
0.75	63.23	47.43	59.4	19.6
1.0	61.65	61.65	75.0	33.3
1.5	60.09	90.14	105.4	71.2
2.0	58.89	117.78	135.2	123.2
3.0	56.60	169.82	192.9	267.0
5.0	52.30	261.52	301.8	698.3
7.0	48.33	338.30	402.5	1298.1
9.0	44.66	401.90	495.5	2038.4
12.0	39.66	475.96	621.9	3355.2
18.0	31.29	563.22	834.8	6472.6
24.0	24.68	592.43	1002.7	9399.2
36.0	15.36	553.06	1242.9	16810.9
48.0	9.56	458.93	1392.5	22881.9
72.0	3.70	266.64	1551.6	31585.3
96.0	1.43	154.44	1613.1	36429.4
120.0	0.56	66.67	1637.0	38883.2
∞	0	0	1651.2	40942.2

[a] All integrals approximated by using the linear trapezoidal rule.

MRT may be estimated from multiple dosing data by:

$$\text{MRT} = \frac{\int_0^\Upsilon tC_{ss}dt + \Upsilon \int_\Upsilon^\infty C_{ss}dt}{\int_0^\Upsilon C_{ss}dt} \quad \text{(Eq. 12)}$$

The data necessary to compute MRT, using the trapezoidal rule, on multiple dosing to steady state may be obtained by continued sampling of the declining plasma concentrations until, perhaps, 4–7 drug half-lives have elapsed or the limit of detection of the assay is reached, rather than redosing at time Υ. The purpose is to ensure that the postabsorption and postdistribution phase has been reached and the area under the curve from the last sampling time can be properly extrapolated by $(C_m)_{ss}/k_n$ where $(C_m)_{ss}$ is the last sampled concentration and k_n the terminal rate constant. If the dosing interval has been such that the terminal data point, at Υ, were known to be well into the postabsorption and postdistribution phase, then Eq. 12 could be simplified to:

$$\text{MRT} = \frac{\int_0^\Upsilon tC_{ss}dt + \Upsilon(C_m)_{ss}/k_n}{\int_0^\Upsilon C_{ss}dt} \quad \text{(Eq. 13)}$$

In such a case it would be unnecessary to interrupt the dosing schedule.

Wagner (5) and Benet and Galeazzi (6) have used the equation:

$$C = 60.9545 \cdot \exp(-5.060t) + 39.0459 \cdot \exp(-0.03952t) \quad \text{(Eq. 14)}$$

to demonstrate methods of calculating steady-state volume of distribution. Substituting values from Eq. 14 into Eq. 4 to obtain analytical integrals yields MRT = 25.00 h. Values calculated for $\int_0^\infty tCdt$ and $\int_0^\infty Cdt$ by Benet and Galeazzi (6) using the linear trapezoidal rule yield MRT = 24.88 h.

If multiple dosing with Υ = 24 h is assumed:

$$C_{ss} = 60.9545 \cdot \exp(-5.0605t) + 63.7306 \cdot \exp(-0.03952t) \quad \text{(Eq. 15)}$$

Using Eq. 15, plasma concentrations were calculated over a 120-h period (Table I). The first moment curve and cumulative values of $\int_0^t tC_{ss}dt$ and $\int_0^t c_{ss}dt$, calculated using the linear trapezoidal rule, are also given. Using these trapezoidal rule values, according to Eq. 12:

$$\text{MRT} = \frac{9399.2 + 24(648.5)}{1002.7} = 24.90 \quad \text{(Eq. 16)}$$

The analytical integrals, derived from Eq. 15 and substituted into Eq. 12, yield MRT = 25.00 h.

Using analytical integrals, Eq. 4, for single dose data, and Eq. 12, for multiple dosing steady-state data, yield equivalent values for MRT. Using the trapezoidal rule approximations gave MRT 0.4% less than the actual MRT value. The difference is inherent in rounding the calculated plasma concentrations and in the trapezoidal rule approximations. It is, therefore, possible to obtain at least as accurate an estimate of MRT from multiple-dosing steady-state data as from single-dose data providing the plasma sampling schedule is adequate. It might, however, be necessary to interrupt the multi-

ple-dosing regime which might limit the application of the method in patient studies.

Bauer and Gibaldi (7) have proposed an alternative method for performing moment-analysis calculations on multiple-dosing data. It should be noted that their Eq. 7 is equivalent to Eq. 6 in this presentation. The Bauer and Gibaldi method requires the use of calculated concentrations to calculate area under the curve, while this presently proposed method employs only the data observed at multiple-dosing steady state. This raises the possibility of being able to determine whether pharmacokinetic changes, as observed in mean retention times or, perhaps, steady-state volumes of distribution, could have been induced during multiple dosing.

(1) M. Gibaldi and D. Perrier, "Pharmacokinetics," 2nd ed, Dekker, New York, N.Y., 1982, chap. 3.
(2) D. M. Himmelbau and K. B. Bischoff, "Deterministic Systems," Wiley, New York, N.Y., 1968.
(3) W. Perl and P. Samuels, *Circ. Res.*, **25**, 191 (1969).
(4) S. Riegelman and P. Collier, *J. Pharmacokinet. Biopharm.*, **8**, 509 (1980).
(5) J. G. Wagner, *J. Pharmacokinet. Biopharm.*, **4**, 443 (1976).
(6) L. Z. Benet and R. L. Galeazzi, *J. Pharm. Sci.*, **68**, 1071 (1979).
(7) L. A. Bauer and M. Gibaldi, *J. Pharm. Sci.*, **72**, 978 (1983).

M. Pfeffer
Bristol-Myers Company
Pharmaceutical Research and Development Division
Syracuse, NY 13221-4755

Received October 4, 1983.
Accepted for publication March 30, 1984.

Alterations of α-Lactose During Differential Scanning Calorimetry

Keyphrases □ α-Lactose—alterations, differential scanning calorimetry

To the Editor:

Lactose is a natural disaccharide widely used as a diluent in tablet formations. As a solid it is known to occur either in one of four crystalline forms or in an amorphous state. α-Lactose monohydrate is obtained by crystallization from a super-saturated solution at temperatures <93.5°C, whereas β-lactose crystals are obtained at temperatures >93.5°C (1). During crystallization of β-lactose, no water is incorporated in the crystal lattice. The crystals of β-lactose exist in a nonhygroscopic anhydrous form only, in contrast with α-lactose, which occurs both as monohydrate and as anhydrous α-lactose. Thermal dehydration, or desiccation of the hydrate crystals with suitable liquids, converts α-lactose monohydrate into its anhydrous form. A very hygroscopic product, generally called unstable anhydrous α-lactose, is formed when α-lactose hydrate crystals are heated, mostly *in vacuo*, at temperatures of 100–130°C (2–4). Thermal treatment in a moist atmosphere at temperatures over ~110°C, or desiccation with suitable liquids, such as dry methanol, may result in a nonhygroscopic product, generally called stable anhydrous α-lactose (2, 4).

The different types of lactose are increasingly studied by thermal analysis. Berlin *et al.* (5) determined the heat of desorption of water from α-lactose monohydrate by differential scanning calorimetry. Itoh *et al.* (3, 6) used differential thermal analysis in studying the characteristics of α-lactose hydrate and of β-lactose, next to IR absorption and X-ray powder diffraction techniques. Differential scanning calorimetry has been applied by Ross (7) for the direct measurement of the amount of α- and β-lactose in whey powders.

This communication reports the occurrence of changes in the solid state during differential scanning calorimetry of α-lactoses. Figure 1 illustrates the DSC-curves of α-lactose monohydrate and of stable and unstable anhydrous α-lactose, respectively, as recorded by means of a thermal analyzer[1]. The DSC-curve of α-lactose monohydrate shows an endothermic

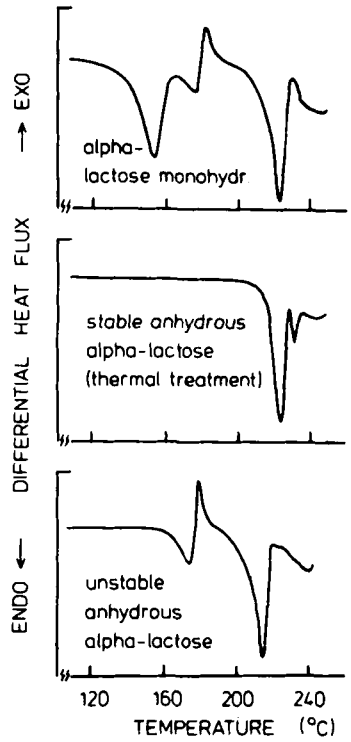

Figure 1—*DSC-curves of α-lactose monohydrate, stable anhydrous α-lactose, and unstable anhydrous α-lactose, respectively, recorded at a heating rate of 10°C/min.*

Table I—Change in β-Content (GLC Determination) and the Solid State (X-ray Diffraction Analysis) of α-Lactose During Thermal Treatment (DSC-cell 910; Heating Rate 10°C/min)[a]

	Temperature, °C						
	20	120	160	180	200	210	220
β-content (%)							
α-Lactose monohydrate	4	5	19	21	23	—	44
Stable anhydrous α-lactose	20	20	—	20	22	34	56
Unstable anhydrous α-lactose	18	—	18	42	—	54	—
Solid State							
α-Lactose monohydrate	AM	SA+(UA)		—	SA+(BA)		
Stable anhydrous α-lactose	SA			SA			
Unstable anhydrous α-lactose	UA				BA		

[a] AM = α-lactose monohydrate; SA = stable anhydrous α-lactose; UA = unstable anhydrous α-lactose; BA = β/α-lactose compound crystal; (UA) and (BA) refer to a heating rate of 2°C/min.

[1] Dupont Model 990 with DSC-cell 910.

0022-3549/84/0600-0856$01.00/0
© 1984, American Pharmaceutical Association

ple-dosing regime which might limit the application of the method in patient studies.

Bauer and Gibaldi (7) have proposed an alternative method for performing moment-analysis calculations on multiple-dosing data. It should be noted that their Eq. 7 is equivalent to Eq. 6 in this presentation. The Bauer and Gibaldi method requires the use of calculated concentrations to calculate area under the curve, while this presently proposed method employs only the data observed at multiple-dosing steady state. This raises the possibility of being able to determine whether pharmacokinetic changes, as observed in mean retention times or, perhaps, steady-state volumes of distribution, could have been induced during multiple dosing.

(1) M. Gibaldi and D. Perrier, "Pharmacokinetics," 2nd ed, Dekker, New York, N.Y., 1982, chap. 3.
(2) D. M. Himmelbau and K. B. Bischoff, "Deterministic Systems," Wiley, New York, N.Y., 1968.
(3) W. Perl and P. Samuels, *Circ. Res.*, **25**, 191 (1969).
(4) S. Riegelman and P. Collier, *J. Pharmacokinet. Biopharm.*, **8**, 509 (1980).
(5) J. G. Wagner, *J. Pharmacokinet. Biopharm.*, **4**, 443 (1976).
(6) L. Z. Benet and R. L. Galeazzi, *J. Pharm. Sci.*, **68**, 1071 (1979).
(7) L. A. Bauer and M. Gibaldi, *J. Pharm. Sci.*, **72**, 978 (1983).

M. Pfeffer
Bristol-Myers Company
Pharmaceutical Research and Development Division
Syracuse, NY 13221-4755

Received October 4, 1983.
Accepted for publication March 30, 1984.

Alterations of α-Lactose During Differential Scanning Calorimetry

Keyphrases □ α-Lactose—alterations, differential scanning calorimetry

To the Editor:

Lactose is a natural disaccharide widely used as a diluent in tablet formations. As a solid it is known to occur either in one of four crystalline forms or in an amorphous state. α-Lactose monohydrate is obtained by crystallization from a super-saturated solution at temperatures <93.5°C, whereas β-lactose crystals are obtained at temperatures >93.5°C (1). During crystallization of β-lactose, no water is incorporated in the crystal lattice. The crystals of β-lactose exist in a nonhygroscopic anhydrous form only, in contrast with α-lactose, which occurs both as monohydrate and as anhydrous α-lactose. Thermal dehydration, or desiccation of the hydrate crystals with suitable liquids, converts α-lactose monohydrate into its anhydrous form. A very hygroscopic product, generally called unstable anhydrous α-lactose, is formed when α-lactose hydrate crystals are heated, mostly *in vacuo*, at temperatures of 100–130°C (2–4). Thermal treatment in a moist atmosphere at temperatures over ~110°C, or desiccation with suitable liquids, such as dry methanol, may result in a nonhygroscopic product, generally called stable anhydrous α-lactose (2, 4).

The different types of lactose are increasingly studied by thermal analysis. Berlin *et al.* (5) determined the heat of desorption of water from α-lactose monohydrate by differential scanning calorimetry. Itoh *et al.* (3, 6) used differential thermal analysis in studying the characteristics of α-lactose hydrate and of β-lactose, next to IR absorption and X-ray powder diffraction techniques. Differential scanning calorimetry has been applied by Ross (7) for the direct measurement of the amount of α- and β-lactose in whey powders.

This communication reports the occurrence of changes in the solid state during differential scanning calorimetry of α-lactoses. Figure 1 illustrates the DSC-curves of α-lactose monohydrate and of stable and unstable anhydrous α-lactose, respectively, as recorded by means of a thermal analyzer[1]. The DSC-curve of α-lactose monohydrate shows an endothermic

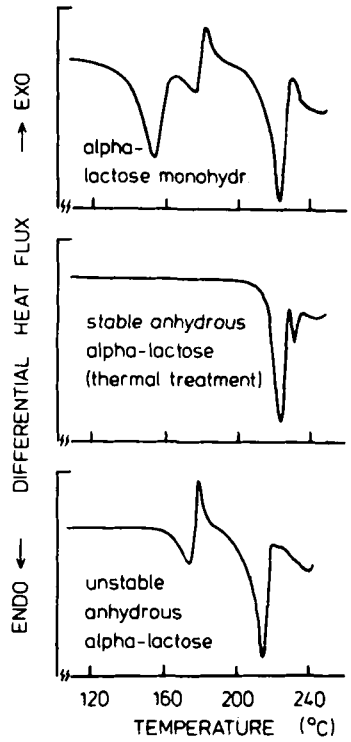

Figure 1—*DSC-curves of α-lactose monohydrate, stable anhydrous α-lactose, and unstable anhydrous α-lactose, respectively, recorded at a heating rate of 10°C/min.*

Table I—Change in β-Content (GLC Determination) and the Solid State (X-ray Diffraction Analysis) of α-Lactose During Thermal Treatment (DSC-cell 910; Heating Rate 10°C/min)[a]

	Temperature, °C						
	20	120	160	180	200	210	220
β-content (%)							
α-Lactose monohydrate	4	5	19	21	23	—	44
Stable anhydrous α-lactose	20	20	—	20	22	34	56
Unstable anhydrous α-lactose	18	—	18	42	—	54	—
Solid State							
α-Lactose monohydrate	AM	SA+(UA)		—	SA+(BA)		
Stable anhydrous α-lactose	SA			SA			
Unstable anhydrous α-lactose	UA				BA		

[a] AM = α-lactose monohydrate; SA = stable anhydrous α-lactose; UA = unstable anhydrous α-lactose; BA = β/α-lactose compound crystal; (UA) and (BA) refer to a heating rate of 2°C/min.

[1] Dupont Model 990 with DSC-cell 910.

0022-3549/84/0600-0856$01.00/0
© 1984, American Pharmaceutical Association

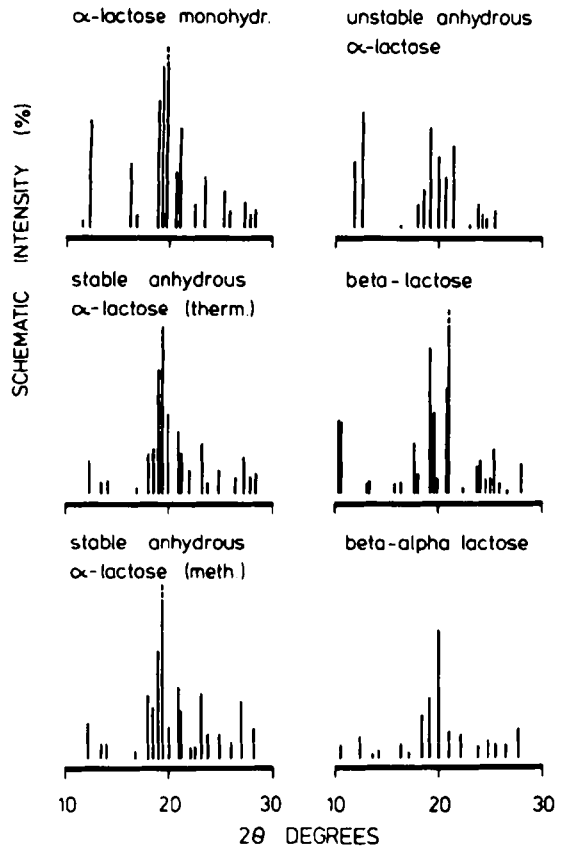

Figure 2—*Representation of the X-ray diffraction patterns of the different forms of lactose*[2].

transition starting at ~140°C, when scanned with a heating rate of 10°C/min, corresponding to dehydration of the product. All three α-lactoses exhibit a melting endotherm beginning at ~210°C. The melting endotherm of unstable α-lactose is, however, preceded, as reported earlier by Itoh *et al.* (3), by an endo- and exothermic peak at ~170°C and 180°C, respectively. This indication of thermal alteration was elucidated in our study by X-ray diffraction analysis and by determination of the β-content performed on samples which were heated to different temperatures as mentioned in Table I. The results show a conversion at ~180°C of unstable α-lactose into a product with a crystallographic structure different from both hydrous and anhydrous α-lactose and from β-lactose.

X-ray diffraction analysis showed the conversion product to agree with lactose crystals, which were prepared by Buma (8) by crystallization from methanol. Buma concluded from specific gravity measurements and sedimentation analysis that the "crystalline lactose obtained from methanol did not consist of α-lactose crystals and β-lactose crystals, as was reported by [Lim and Nickerson (9)], but of crystals consisting of α- and β-lactose." Analysis of the X-ray diffraction patterns (Fig 2) of α-lactose monohydrate, stable anhydrous α-lactose produced by thermal dehydration, stable anhydrous α-lactose obtained by methanol desiccation, unstable anhydrous α-lactose, β-lactose, and the conversion product mentioned before, indicate in our opinion that the last product can best be characterized as a crystalline β/α-lactose compound, having a β:α ratio of ~1:1. From these results it may be concluded, that the first endotherm at ~170°C as shown by the DSC-curves of unstable anhydrous α-lactose (Fig. 1), is the result of the melting of the unstable anhydrous α-lactose, whereas the second endotherm at ~210°C corresponds with the melting point of the crystalline β/α-lactose compound, which crystallized at ~180°C.

These results and the observation of endo- and exothermic transitions at ~160°C and 180°C, respectively, in the DSC-curves of α-lactose monohydrate gave rise to a detailed examination of the thermal treatment of this product. X-ray diffraction analysis performed on samples that were heated at a rate of 2°C/min (instead of the usual 10°C/min) showed at 160°C the occurrence of unstable next to stable anhydrous α-lactose (see Table I). As expected, the crystalline β/α-compound was consequently detected at 200°C. This implies that α-lactose monohydrate loses its water upon heating and changes into both stable and unstable anhydrous α-lactose, the latter being converted into the crystalline β/α-lactose compound at temperatures >180°C. Besides, it is interesting to note that the α-lactoses show a significant conversion into β-lactose upon melting at a temperature of ~220°C.

In conclusion, thermal treatment of α-lactoses involves changes in β-content and in crystal structure.

(1) T. A. Nickerson, "Fundamentals of Dairy Chemistry," 2nd ed. AVI-Publishing Co. Inc., Westport, Conn., p. 300.
(2) T. J. Buma and G. A. Wiegers, *Neth. Milk Dairy J.*, **21**, 208 (1967).
(3) T. Itoh, M. Satoh, and S. Adachi, *J. Dairy Sci.*, **60**, 1230 (1977).
(4) P. F. Sharp, U.S. Patent 2,319,562 (1943).
(5) E. Berlin, P. G. Kliman, B. A. Anderson, and M. J. Pallansch, *Thermochim. Acta*, **2**, 143 (1971).
(6) T. Itoh, M. Katoh, and S. Adachi, *J. Dairy Res.*, **45**, 363 (1978).
(7) K. D. Ross, *J. Dairy Sci.*, **61**, 255 (1978).
(8) T. J. Buma, *Neth. Milk Dairy J.*, **32**, 258 (1978).
(9) S. G. Lim and T. A. Nickerson, *J. Dairy Sci.*, **56**, 843 (1973).

C. F. Lerk[x]
A. C. Andreae
A. H. de Boer
Laboratory for Pharmaceutical Technology and Dispensing
State University of Groningen
Ant. Deusinglaan 2, 9713 AW Groningen
The Netherlands
P. de Hoog
K. Kussendrager
J. van Leverink
D.M.V.
P.O. Box 13, 5460 BA Veghel
The Netherlands

Received July 11, 1983.
Accepted for publication March 21, 1984.

Transitions of Lactoses by Mechanical and Thermal Treatment

Keyphrases □ α-Lactose—mechanical and thermal treatment, transition

To the Editor:

Comminution techniques, such as crushing and grinding, are frequently used to prepare samples for the determination

[2] Philips Defractometer CuK radiation was used.

0022-3549/84/0600-0857$01.00/0
© 1984, American Pharmaceutical Association

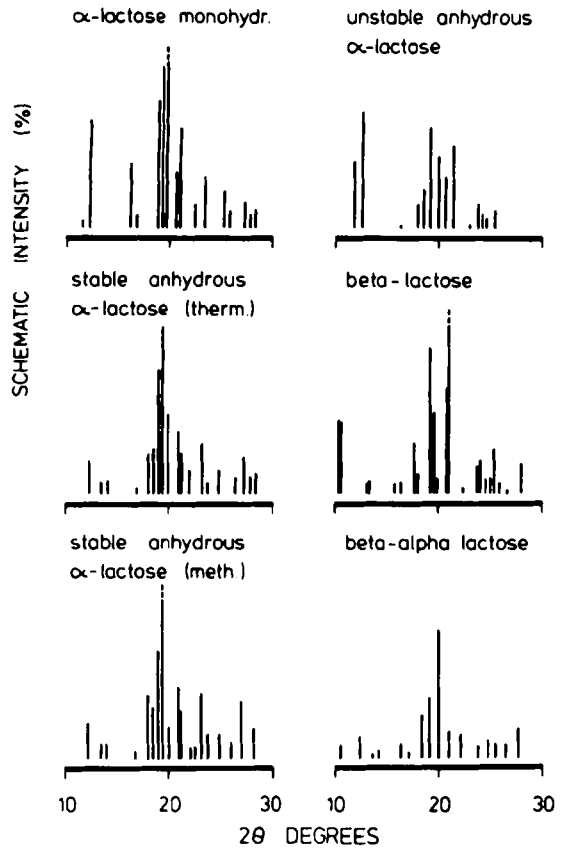

Figure 2—*Representation of the X-ray diffraction patterns of the different forms of lactose*[2].

transition starting at ~140°C, when scanned with a heating rate of 10°C/min, corresponding to dehydration of the product. All three α-lactoses exhibit a melting endotherm beginning at ~210°C. The melting endotherm of unstable α-lactose is, however, preceded, as reported earlier by Itoh *et al.* (3), by an endo- and exothermic peak at ~170°C and 180°C, respectively. This indication of thermal alteration was elucidated in our study by X-ray diffraction analysis and by determination of the β-content performed on samples which were heated to different temperatures as mentioned in Table I. The results show a conversion at ~180°C of unstable α-lactose into a product with a crystallographic structure different from both hydrous and anhydrous α-lactose and from β-lactose.

X-ray diffraction analysis showed the conversion product to agree with lactose crystals, which were prepared by Buma (8) by crystallization from methanol. Buma concluded from specific gravity measurements and sedimentation analysis that the "crystalline lactose obtained from methanol did not consist of α-lactose crystals and β-lactose crystals, as was reported by [Lim and Nickerson (9)], but of crystals consisting of α- and β-lactose." Analysis of the X-ray diffraction patterns (Fig 2) of α-lactose monohydrate, stable anhydrous α-lactose produced by thermal dehydration, stable anhydrous α-lactose obtained by methanol desiccation, unstable anhydrous α-lactose, β-lactose, and the conversion product mentioned before, indicate in our opinion that the last product can best be characterized as a crystalline β/α-lactose compound, having a β:α ratio of ~1:1. From these results it may be concluded, that the first endotherm at ~170°C as shown by the DSC-curves of unstable anhydrous α-lactose (Fig. 1), is the result of the melting of the unstable anhydrous α-lactose, whereas the second endotherm at ~210°C corresponds with the melting point of the crystalline β/α-lactose compound, which crystallized at ~180°C.

These results and the observation of endo- and exothermic transitions at ~160°C and 180°C, respectively, in the DSC-curves of α-lactose monohydrate gave rise to a detailed examination of the thermal treatment of this product. X-ray diffraction analysis performed on samples that were heated at a rate of 2°C/min (instead of the usual 10°C/min) showed at 160°C the occurrence of unstable next to stable anhydrous α-lactose (see Table I). As expected, the crystalline β/α-compound was consequently detected at 200°C. This implies that α-lactose monohydrate loses its water upon heating and changes into both stable and unstable anhydrous α-lactose, the latter being converted into the crystalline β/α-lactose compound at temperatures >180°C. Besides, it is interesting to note that the α-lactoses show a significant conversion into β-lactose upon melting at a temperature of ~220°C.

In conclusion, thermal treatment of α-lactoses involves changes in β-content and in crystal structure.

(1) T. A. Nickerson, "Fundamentals of Dairy Chemistry," 2nd ed. AVI-Publishing Co. Inc., Westport, Conn., p. 300.
(2) T. J. Buma and G. A. Wiegers, *Neth. Milk Dairy J.*, **21**, 208 (1967).
(3) T. Itoh, M. Satoh, and S. Adachi, *J. Dairy Sci.*, **60**, 1230 (1977).
(4) P. F. Sharp, U.S. Patent 2,319,562 (1943).
(5) E. Berlin, P. G. Kliman, B. A. Anderson, and M. J. Pallansch, *Thermochim. Acta*, **2**, 143 (1971).
(6) T. Itoh, M. Katoh, and S. Adachi, *J. Dairy Res.*, **45**, 363 (1978).
(7) K. D. Ross, *J. Dairy Sci.*, **61**, 255 (1978).
(8) T. J. Buma, *Neth. Milk Dairy J.*, **32**, 258 (1978).
(9) S. G. Lim and T. A. Nickerson, *J. Dairy Sci.*, **56**, 843 (1973).

C. F. Lerk[x]
A. C. Andreae
A. H. de Boer
Laboratory for Pharmaceutical Technology and Dispensing
State University of Groningen
Ant. Deusinglaan 2, 9713 AW Groningen
The Netherlands
P. de Hoog
K. Kussendrager
J. van Leverink
D.M.V.
P.O. Box 13, 5460 BA Veghel
The Netherlands

Received July 11, 1983.
Accepted for publication March 21, 1984.

Transitions of Lactoses by Mechanical and Thermal Treatment

Keyphrases □ α-Lactose—mechanical and thermal treatment, transition

To the Editor:

Comminution techniques, such as crushing and grinding, are frequently used to prepare samples for the determination

[2] Philips Defractometer CuK radiation was used.

0022-3549/84/0600-0857$01.00/0
© 1984, American Pharmaceutical Association

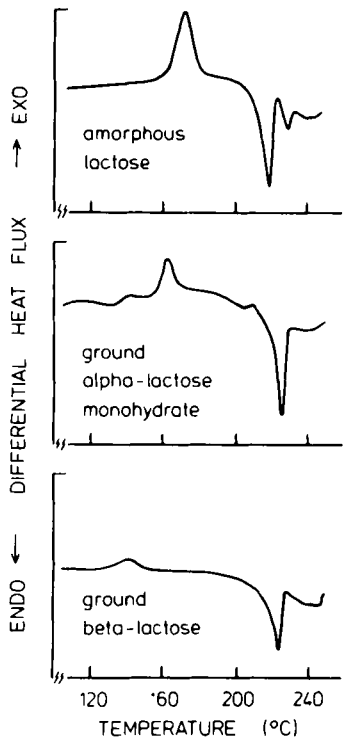

Figure 1—*DSC-curves of amorphous lactose, intensively ground α-lactose monohydrate, and intensively ground β-lactose, respectively, recorded at a heating rate of 10°C/min.*

Table I—Changes in β-Content (GLC-Determination) and in the Solid State (X-ray Diffraction Analysis). During Thermal Treatment (DSC-cell 910; Heating Rate 10°C/min)[a]

	Temperature, °C	
	20	180
β-content (%)		
Amorphous lactose	54	50
Ground α-lactose monohydrate	2	42
Ground β-lactose	82	79
Solid State		
Amorphous lactose	(—)	BA
Ground α-lactose monohydrate	(—)	BA
Ground β-lactose	(—)	B

[a] B = β-lactose; BA = β/α-lactose compound crystal; (—) = amorphous lactose (no or only a few very weak diffraction lines could be detected.

of the physicochemical properties of solid materials. Size reduction is, however, a very active process, supplying energy to a particle during fragmentation. It is well known that mechanical treatment of minerals can result in activation and changes in surface properties, in polymorphic transitions and alterations in physical properties of the bulk phase, in uncrystallization, as well as in mechanochemical solid-state reactions (1).

Hüttenrauch, in his series on molecular pharmaceutics, studied the mechanical activation of drugs and excipients and showed uncrystallization of α-lactose monohydrate during milling (2). We reported earlier (3) changes in the β-content and in the solid state of α-lactose monohydrate, stable anhydrous α-lactose, and unstable anhydrous α-lactose, respectively, by thermal treatment. Continuing this study, amorphous lactose and intensively ground samples of α-lactose monohydrate and β-lactose, respectively, were examined for their thermal characteristics. Figure 1 illustrates the Differential Scanning Calorimetry (DSC)-curves of these preparations, obtained at a heating rate of 10°C/min, using a thermal analyzer[1].

The DSC-curve of the amorphous lactose, prepared by spray-drying, shows an exothermic transition at ~160°C and an endotherm at ~210°C. An analogous pattern was recorded for intensively ground α-lactose monohydrate. Its DSC-curve shows, in contrast to that of nonground α-lactose monohydrate, hardly a dehydration endotherm, but an exotherm at ~160°C. Intensively ground β-lactose exhibited an exotherm as well, but at a slightly lower temperature (≃140°C).

To elucidate the indication of thermal transition during the dynamic process of DSC, X-ray diffraction patterns were made of samples, both prior to and after thermal treatment by heating to ~180°C followed by immediate cooling to room temperature. As expected, the nonthermally treated but intensively ground samples showed no, or at least very weak, diffraction lines (Table I). This indicates that comminution had resulted in uncrystallization of both α-lactose monohydrate and β-lactose. The uncrystallized products crystallized on heating. X-ray diffraction analyses of samples of amorphous lactose and of intensively ground α-lactose hydrate, respectively, both proved to correspond with a crystalline β/α-lactose compound, when heated to 180°C with subsequent cooling to room temperatures.

Uncrystallized β-lactose was, however, found to crystallize into β-lactose on thermal treatment. This difference in thermal behavior between samples of intensively ground α-lactose monohydrate and β-lactose, respectively, is supported by the observation of an increase in β-content for ground α-lactose monohydrate from 2 to 42% and hardly any change in β-content for uncrystallized β-lactose on thermal treatment (Table I).

To investigate more thoroughly the formation of the crystalline β/α-lactose compound from amorphous lactose, six batches of amorphous lactose, differing in ratio from ~3:7 to ~8:2 and prepared by freeze- or spray-drying, were heated to different temperatures and subsequently cooled to room

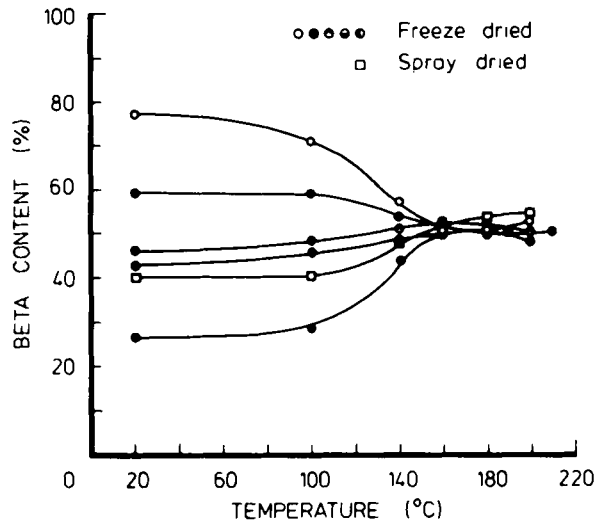

Figure 2—*Change in β-content of different amorphous lactose products with temperature[2] heating rate 10°C/min.*

[1] DuPont Model 990 with DSC-cell 910.
[2] Mettler TA 2000.

temperature. Determination of the β-content of the products showed that all preparations had a final β:α ratio of ~1:1 (see Fig. 2). X-ray diffractograms of the samples that were heated to ~200°C proved to correspond to a crystalline β/α-lactose compound.

In conclusion, α-lactose monohydrate is found to lose its water of crystallization and like β-lactose, changes into an amorphous state on intensive grinding. Thermal treatment of both amorphous lactose and uncrystallized α-lactose monohydrate results in crystallization of a crystalline β/α-lactose compound. This is in contrast to uncrystallized β-lactose, which crystallizes into β-lactose.

(1) I. J. Lim, S. Nadiv, and D. J. M. Grodzian, *Miner. Sci. Eng.*, **7**, 313 (1975).

(2) R. Hüttenrauch, *Acta Pharm. Technol.*, suppl. **6**, 55 (1978).

(3) C. F. Lerk, A. C. Andreae, A. H. de Boer, P. de Hoog, K. Kussendrager, and J. van Leverink, *J. Pharm. Sci.*, in press.

C. F. Lerk ˣ
A. C. Andreae
A. H. de Boer
Laboratory for Pharmaceutical Technology and Dispensing
State University of Groningen
Ant. Deusinglaan 2
9713 AW Groningen
The Netherlands
P. de Hoog
K. Kussendrager
J. van Leverink

D.M.V.
P.O. Box 13
5460 BA Veghel
The Netherlands

Received July 11, 1983.
Accepted for publication March 21, 1984.

Concentration Ratio Method to Determine the Rate Constant for the Special Case when $k_a = k_e$

Keyphrases □ Pharmacokinetics—one-compartment open model, concentration ratio method to determine rate constant

To the Editor:

In a one-compartment open model with first-order absorption and elimination processes, the plasma concentrations (C_p) of a drug at any time, t, after its extravascular administration are generally described by:

$$C_p = \frac{FDk_a(e^{-k_e t} - e^{-k_a t})}{Vd(k_a - k_e)} \qquad \text{(Eq. 1)}$$

where F is the fraction of dose (D) absorbed, k_a and k_e are absorption and elimination rate constants, respectively, and Vd is the apparent volume of distribution. In the special case where k_a is equal to k_e, Eq. 1 becomes mathematically indeterminable, and the general equation (Eq. 2) describing the $C_p t$ profile can be explicitly obtained by setting $k_a = k_e = k$ and using the standard integration technique:

$$C_p = \frac{FDkte^{-kt}}{Vd} \qquad \text{(Eq. 2)}$$

It was proposed recently by Chan and Miller (1) that the $C_p t$ data of this special case could be described by Eq. 1 using the nonlinear regression program NONLIN (2) provided there was at least a small difference between k_a and k_e. This analysis will yield similar values for k_a and k_e which will, in essence, identify equality between k_a and k_e. This approach, applied successfully by the authors to one data set containing 5% random noise, seemed superior to the one proposed by Bialer (3). The shortcomings of the latter were recently discussed by Barzegar-Jalali and Toomanian (4).

In this study, a simple plasma concentration ratio method is proposed to determine the rate constant k using plasma concentrations at any two consecutive times, t_{n-1} and t_n (as defined by Eq. 2):

$$C_p^{n-1} = \frac{FDkt_{n-1}e^{-kt_{n-1}}}{Vd} \qquad \text{(Eq. 3)}$$

and

$$C_p^{n} = \frac{FDkt_{n}e^{-kt_{n}}}{Vd} \qquad \text{(Eq. 4)}$$

Dividing Eq. 4 by Eq. 3, taking the natural logarithm of the resulting expression, and solving for k yields the following relationship:

$$k = \frac{\ln(t_n/t_{n-1}) - \ln(C_p^n/C_p^{n-1})}{(t_n - t_{n-1})} \qquad \text{(Eq. 5)}$$

Where k represents the estimated rate constant between the time interval t_{n-1} to t_n. Since a datum set will usually contain several plasma concentrations, k can be estimated for each time interval and averaged to obtain an overall estimate of k:

$$k = \frac{1}{n-1}\sum_{i=2}^{n}\frac{\ln(t_n/t_{n-1}) - \ln(C_p^n/C_p^{n-1})}{(t_n - t_{n-1})} \qquad \text{(Eq. 6)}$$

It is apparent from Eq. 5 that the proposed method does not require blood sampling at close intervals. Also, the proposed method is applicable to the entire time course of a drug and even to those cases where sampling schedule is limited and regression analysis of the $C_p t$ data according to Eq. 1 is not practical.

The concentration ratio method was compared against the approach of Chan and Miller (1) as well as the theoretical method (Eq. 2). Plasma concentrations with only rounding error were calculated at 0.25, 0.5, 1, 1.5, 2, 2.5, 3, 4, 5, 6, 8, 10, 12, 14, and 16 h using Eq. 2 with $FD/Vd = 10.0$ and $k = 0.5$. Twelve additional datum sets were generated by adding normally distributed random error with an RSD of ±10%. Each set was analyzed by curve-fitting the data to Eqs. 1 and 2 using the NONLIN program as well as by the present concentration ratio method. The curve-fitting of the data to Eqs. 1 and 2 was performed using the reciprocal of plasma concentration as a weighting function. The results are compared in Table I.

The nonlinear regression analysis of the $C_p t$ data according to Eq. 1 identified equality[1] of k_a and k_e in several cases (cases 1, 6–12, Table I). The estimated k_e values by Eq. 1 were smaller (>10%) than that estimated by Eq. 2 in 4 of 14 cases. The mean k_e value estimated by Eq. 1, 0.458, was 8% smaller

[1] Equality was identified when $k_a \pm SD$ overlapped $k_e \pm SD$.

0022-3549/84/0600-0859$01.00/0
© 1984, American Pharmaceutical Association

temperature. Determination of the β-content of the products showed that all preparations had a final β:α ratio of ~1:1 (see Fig. 2). X-ray diffractograms of the samples that were heated to ~200°C proved to correspond to a crystalline β/α-lactose compound.

In conclusion, α-lactose monohydrate is found to lose its water of crystallization and like β-lactose, changes into an amorphous state on intensive grinding. Thermal treatment of both amorphous lactose and uncrystallized α-lactose monohydrate results in crystallization of a crystalline β/α-lactose compound. This is in contrast to uncrystallized β-lactose, which crystallizes into β-lactose.

(1) I. J. Lim, S. Nadiv, and D. J. M. Grodzian, *Miner. Sci. Eng.*, **7**, 313 (1975).

(2) R. Hüttenrauch, *Acta Pharm. Technol.*, suppl. **6**, 55 (1978).

(3) C. F. Lerk, A. C. Andreae, A. H. de Boer, P. de Hoog, K. Kussendrager, and J. van Leverink, *J. Pharm. Sci.*, in press.

C. F. Lerk ˣ
A. C. Andreae
A. H. de Boer
Laboratory for Pharmaceutical Technology and Dispensing
State University of Groningen
Ant. Deusinglaan 2
9713 AW Groningen
The Netherlands
P. de Hoog
K. Kussendrager
J. van Leverink

D.M.V.
P.O. Box 13
5460 BA Veghel
The Netherlands

Received July 11, 1983.
Accepted for publication March 21, 1984.

Concentration Ratio Method to Determine the Rate Constant for the Special Case when $k_a = k_e$

Keyphrases □ Pharmacokinetics—one-compartment open model, concentration ratio method to determine rate constant

To the Editor:

In a one-compartment open model with first-order absorption and elimination processes, the plasma concentrations (C_p) of a drug at any time, t, after its extravascular administration are generally described by:

$$C_p = \frac{FDk_a(e^{-k_e t} - e^{-k_a t})}{Vd(k_a - k_e)} \qquad \text{(Eq. 1)}$$

where F is the fraction of dose (D) absorbed, k_a and k_e are absorption and elimination rate constants, respectively, and Vd is the apparent volume of distribution. In the special case where k_a is equal to k_e, Eq. 1 becomes mathematically indeterminable, and the general equation (Eq. 2) describing the $C_p t$ profile can be explicitly obtained by setting $k_a = k_e = k$ and using the standard integration technique:

$$C_p = \frac{FDkte^{-kt}}{Vd} \qquad \text{(Eq. 2)}$$

It was proposed recently by Chan and Miller (1) that the $C_p t$ data of this special case could be described by Eq. 1 using the nonlinear regression program NONLIN (2) provided there was at least a small difference between k_a and k_e. This analysis will yield similar values for k_a and k_e which will, in essence, identify equality between k_a and k_e. This approach, applied successfully by the authors to one data set containing 5% random noise, seemed superior to the one proposed by Bialer (3). The shortcomings of the latter were recently discussed by Barzegar-Jalali and Toomanian (4).

In this study, a simple plasma concentration ratio method is proposed to determine the rate constant k using plasma concentrations at any two consecutive times, t_{n-1} and t_n (as defined by Eq. 2):

$$C_p^{n-1} = \frac{FDkt_{n-1}e^{-kt_{n-1}}}{Vd} \qquad \text{(Eq. 3)}$$

and

$$C_p^{n} = \frac{FDkt_{n}e^{-kt_{n}}}{Vd} \qquad \text{(Eq. 4)}$$

Dividing Eq. 4 by Eq. 3, taking the natural logarithm of the resulting expression, and solving for k yields the following relationship:

$$k = \frac{\ln(t_n/t_{n-1}) - \ln(C_p^n/C_p^{n-1})}{(t_n - t_{n-1})} \qquad \text{(Eq. 5)}$$

Where k represents the estimated rate constant between the time interval t_{n-1} to t_n. Since a datum set will usually contain several plasma concentrations, k can be estimated for each time interval and averaged to obtain an overall estimate of k:

$$k = \frac{1}{n-1}\sum_{i=2}^{n}\frac{\ln(t_n/t_{n-1}) - \ln(C_p^n/C_p^{n-1})}{(t_n - t_{n-1})} \qquad \text{(Eq. 6)}$$

It is apparent from Eq. 5 that the proposed method does not require blood sampling at close intervals. Also, the proposed method is applicable to the entire time course of a drug and even to those cases where sampling schedule is limited and regression analysis of the $C_p t$ data according to Eq. 1 is not practical.

The concentration ratio method was compared against the approach of Chan and Miller (1) as well as the theoretical method (Eq. 2). Plasma concentrations with only rounding error were calculated at 0.25, 0.5, 1, 1.5, 2, 2.5, 3, 4, 5, 6, 8, 10, 12, 14, and 16 h using Eq. 2 with $FD/Vd = 10.0$ and $k = 0.5$. Twelve additional datum sets were generated by adding normally distributed random error with an RSD of ±10%. Each set was analyzed by curve-fitting the data to Eqs. 1 and 2 using the NONLIN program as well as by the present concentration ratio method. The curve-fitting of the data to Eqs. 1 and 2 was performed using the reciprocal of plasma concentration as a weighting function. The results are compared in Table I.

The nonlinear regression analysis of the $C_p t$ data according to Eq. 1 identified equality[1] of k_a and k_e in several cases (cases 1, 6–12, Table I). The estimated k_e values by Eq. 1 were smaller (>10%) than that estimated by Eq. 2 in 4 of 14 cases. The mean k_e value estimated by Eq. 1, 0.458, was 8% smaller

[1] Equality was identified when $k_a \pm SD$ overlapped $k_e \pm SD$.

0022-3549/84/0600-0859$01.00/0
© 1984, American Pharmaceutical Association

Table I—Comparison of Concentration Ratio (Eq. 6) and Nonlinear Regression (NONLIN) Methods for Estimation of Rate Constant for the Special Case of One-Compartment Open Model where $k_a = k_e = k$

Data Set	NONLIN Analysis According to Equation 1 k_a		NONLIN Analysis According to Equation 1 k_e		NONLIN Analysis According to Equation 2 k		Concentration Ratio Method k[a]	
Errorless	0.515	(0.01)[c]	0.485	(0.01)	0.500	(0.0002)	0.499	(0.006)
Errant[b]								
1	0.499	(3.15)	0.495	(3.11)	0.500	(0.009)	0.463	(0.27)
2	0.593	(0.12)	0.430	(0.07)	0.501	(0.01)	0.545	(0.26)
3	0.710	(0.01)	0.387	(0.04)	0.510	(0.01)	0.473	(0.20)
4	0.853	(0.12)	0.349	(0.03)	0.513	(0.02)	0.534	(0.19)
5	0.721	(0.14)	0.377	(0.05)	0.502	(0.02)	0.490	(0.25)
6	0.518	(0.57)	0.474	(0.49)	0.495	(0.02)	0.541	(0.27)
7	0.492	(9.65)	0.489	(9.56)	0.493	(0.02)	0.501	(0.23)
8	0.499	(2.06)	0.485	(1.97)	0.497	(0.02)	0.513	(0.27)
9	0.500	(134)	0.500	(134)	0.501	(0.02)	0.517	(0.29)
10	0.496	(1.38)	0.481	(1.31)	0.498	(0.01)	0.479	(0.27)
11	0.496	(0.96)	0.479	(0.91)	0.479	(0.01)	0.416	(0.39)
12	0.507	(2.68)	0.502	(2.64)	0.504	(0.01)	0.507	(0.21)
Mean	0.570		0.458		0.500		0.498	
SD	0.124		0.057		0.007		0.040	
Mean profile	0.534	(0.01)	0.469	(0.008)	0.500	(0.0004)	0.498	(0.009)

[a] Mean k value (n = 14 time intervals). [b] ±10% Random error as explained in text. [c] Standard deviation (*SD*) in parentheses. The standard deviations reported for parameters estimated by Eqs. 1 and 2 are the standard deviation estimated by NONLIN program whereas the standard deviation obtained from concentration ratio method is the standard deviation of the calculated k values for each interval.

Table II—Comparison of Concentration Ratio and Nonlinear Regression Methods to Data Sets Containing Limited C_p,t Data [a]

Data Set	NONLIN Analysis According to Equation 1 k_a		NONLIN Analysis According to Equation 1 k_e		NONLIN Analysis According to Equation 2 k		Concentration Ratio Method k[b]	
Errorless	0.517	(0.02)[d]	0.484	(0.02)	0.500	(0.0004)	0.500	(0.003)
Errant[c]								
1	0.642	(0.19)	0.412	(0.10)	0.507	(0.02)	0.573	(0.19)
2	0.621	(0.30)	0.416	(0.17)	0.504	(0.02)	0.446	(0.13)
3	0.875	(0.12)	0.355	(0.03)	0.531	(0.02)	0.697	(0.40)
4	1.020	(0.30)	0.319	(0.06)	0.533	(0.04)	0.479	(0.20)
5	0.514	(34.4)	0.513	(34.3)	0.514	(0.02)	0.582	(0.14)
6	0.644	(0.28)	0.398	(0.13)	0.497	(0.02)	0.534	(0.11)
7	0.500	(633)	0.500	(634)	0.500	(0.04)	0.535	(0.17)
8	0.499	(8.05)	0.493	(7.89)	0.500	(0.02)	0.515	(0.20)
9	0.470	(70.7)	0.469	(70.5)	0.468	(0.02)	0.471	(0.15)
10	0.490	(3.20)	0.471	(3.02)	0.484	(0.03)	0.355	(0.29)
11	0.484	(1.72)	0.466	(1.62)	0.478	(0.02)	0.521	(0.10)
12	0.594	(0.24)	0.442	(0.16)	0.509	(0.01)	0.448	(0.17)
Mean	0.613		0.438		0.502		0.513	
SD	0.172		0.060		0.019		0.085	
Mean profile	0.544	(0.02)	0.461	(0.02)	0.500	(0.001)	0.499	(0.005)

[a] Plasma concentration at 0.5, 1, 2, 4, 8, and 12 h only. [b] Mean k value (n = 5 time intervals). [c] ±10% Random error. [d] Standard deviation (*SD*) in parentheses. The standard deviations reported for parameters estimated by Eqs. 1 and 2 are the standard deviation estimated by NONLIN program whereas the standard deviation obtained from concentration ratio method is the standard deviation of the calculated k values for each interval.

Table III—Comparison of Concentration Ratio and Nonlinear Regression (NONLIN) Methods to Data Sets where $k_a > k_e$ by 10% (FD/V_p = 10; k_a = 0.55 and k_e = 0.5)

Data Set	NONLIN Analysis According to Equation 1 k_a		NONLIN Analysis According to Equation 1 k_e		Concentration Ratio Method k[a]	
Errorless	0.525	(3.22)[c]	0.524	(3.22)	0.525	(0.004)
Errant[b]						
1	0.599	(0.17)	0.475	(0.12)	0.527	(0.15)
2	0.599	(0.16)	0.475	(0.11)	0.518	(0.15)
3	0.558	(0.30)	0.500	(0.25)	0.509	(0.15)
4	0.523	(2.31)	0.517	(2.26)	0.521	(0.14)
5	0.517	(4.58)	0.514	(4.54)	0.509	(0.09)
6	0.520	(1.56)	0.510	(1.51)	0.554	(0.20)
7	0.521	(73.1)	0.520	(73.0)	0.530	(0.12)
8	0.525	(4.18)	0.521	(4.13)	0.513	(0.12)
9	0.579	(0.17)	0.478	(0.12)	0.512	(0.12)
10	0.545	(0.35)	0.502	(0.31)	0.494	(0.16)
11	0.591	(0.15)	0.466	(0.10)	0.570	(0.25)
12	0.603	(0.15)	0.465	(0.10)	0.545	(0.15)
Mean	0.557		0.495		0.525	
SD	0.036		0.022		0.022	
Mean profile	0.527	(0.11)	0.522	(0.11)	0.526	(0.007)

[a] Mean k value (n = 14 time intervals). [b] ±10% random error. [c] Standard deviation (*SD*) in parentheses. The standard deviations reported for parameters estimated by Eqs. 1 and 2 are the standard deviation estimated by NONLIN program whereas the standard deviation obtained from concentration ratio method is the standard deviation of the calculated k values for each interval.

than the input value of k_e (0.5) or that estimated by Eq. 2. In contrast, the k values estimated by the concentration ratio method correspond well with those estimated by Eq. 2 (0.5). The concentration ratio method performed adequately when the $C_p t$ data were limited (Table II) and even when k_a was larger than k_e by 10% (Table III).

It must be noted that the nonlinear regression analysis of the $C_p t$ data in terms of Eq. 2 represents the most appropriate method to calculate the rate constant for the special case of the one compartment open model where $k_a = k_e$ (Tables I and II). The pharmacokinetic analysis of the data using Eq. 1 with the NONLIN program is, as suggested by Chan and Miller, the only method known to date to identify the equality between k_a and k_e. The proposed concentration ratio method represents a simple, complimental method which can be applied even in those cases with limited, $C_p t$ data when the model is identified *a priori*.

(1) K. K. H. Chan and K. W. Miller, *J. Pharm. Sci.*, **72,** 574 (1983).
(2) C. M. Metzler, G. L. Elfring, and A. J. McEwen, *Biometrics*, **30,** 562 (1974).
(3) M. Bialer, *J. Pharmacokinet. Biopharm.*, **8,** 111 (1980).
(4) M. Barzegar-Jalali and M. Toomanian, *Int. J. Pharm.*, **12,** 351 (1982).

Indravadan H. Patel

Department of Pharmacokinetics, Biopharmaceutics and Drug Metabolism
Hoffmann-La Roche Inc.
Nutley, NJ 07110

Received September 6, 1983.
Accepted for publication April 4, 1984.

OPEN FORUM

Problems Involved with Developing a Suitable Model for Evaluating Exposure to Bis(2-ethylhexyl) Phthalate from Medical Devices

In a recent article, "Effect of Renal Failure and Bis(2-ethylhexyl) Phthalate Pretreatment on the Disposition and Metabolism of Antipyrine in the Rat" [1], Pollack and Shen presented an experimental model for studying chronic exposure of hemodialysis patients to bis(2-ethylhexyl) phthalate (I) [also known as di-2-ethylhexyl phthalate or DEHP]. Their model, however, utilized oral administration (intragastric intubation) of I rather than a parenteral route. Since the authors did not demonstrate that the effects of I upon antipyrine metabolism and disposition were the same when I was administered orally as when it is given parenterally, one must question acceptance of this as a suitable model for evaluating I exposures from hemodialyzers or other medical devices.

A number of reports, including those of Albro and Thomas[2], Rowland[3], and Lake *et al.*[4], indicate that orally administered I leads to absorption primarily of its hydrolytic product, mono-2-ethylhexyl phthalate or MEHP (II). Therefore, the proposed model[1] should be suitable for evaluating exposure to I from food packagings or other oral exposure, but in order for it to be accepted as a suitable model for clinical exposure to I from medical devices it will be necessary to demonstrate that the parameters evaluated are not affected by the route of administration of I.

There is no dispute that I is metabolized *in vivo* to produce II along with other metabolic products. However, the unanswered question in this case is whether or not the diester (I), to which the patient would initially be exposed intravenously during hemodialysis, *etc.*, would produce qualitatively and quantitatively similar effects on antipyrine metabolism and disposition prior to its metabolic conversion, as would the monoester (II) and other metabolic products. A number of reports have indicated differences in biological activity between I and II, or oral *versus* parenteral administration of I. Some of these reported differences include acute LD_{50}[5], *mutagenicity in bacterial systems*[6], *pentobarbital sleeping time* and effects on aminopyrine-*N*-demethylase and aniline hydroxylase[7], and mitochondrial (state 3) respiration[8].

The authors[1] commented on the findings of Agarwal *et al.*[7], that effects on enzyme activities were associated with the route of I administration, but then they dismiss these findings by attributing the differences to doses administered, not route of administration. However, an examination of the data[7] reveal that when an enzyme or biochemical system was affected by oral or parenteral administration of I (*a*) there was generally a dose-related response, and (*b*) comparisons of similar doses (5.2 and 13.0 po *versus* 5.0 and 10.0 ip) often produced markedly different responses.

Thus, because of the various literature reports (a few of which were cited) showing or suggesting a difference in biological activity between I and II or II plus other metabolites, the model proposed to study the effects of I, from artificial kidneys or other medical device exposure, on antipyrine metabolism and disposition cannot be accepted until it is demonstrated that I produces the same effects on these parameters when administered parenterally as when given by gastric intubation.

[1] G. M. Pollack and D. D. Shen, *J. Pharm. Sci.*, **73,** 29 (1984).
[2] P. W. Albro and R. O. Thomas, *Biochem. Biophys. Acta*, **306**(L23), 380 (1973).
[3] I. R. Rowland, *Food Cosmet. Toxicol.*, **12,** 293 (1974).
[4] B. G. Lake, J. C. Phillips, J. C. Linnell, and S. D. Gangolli, *Toxicol. Appl. Pharmacol.*, **39,** 239 (1977).
[5] J. A. Thomas, T. D. Darby, R. F. Wallin, P. J. Garvin, and L. Martis, *Toxicol. Appl. Pharmacol.*, **45,** 1 (1978).
[6] I. Tomita, Y. Nakamura, N. Aoki, and N. Inui, *Environ. Health Perspect.*, **45,** 119 (1982).
[7] D. K. Agarwal, S. Agarwal, and P. K. Seth, *Drug Metab. Dispos.*, **10,** 77 (1982).
[8] T. Takahashi, *Biochem. Pharmacol.*, **26,** 19 (1977).

W. H. Lawrence[x]
John Autian
Materials Science Toxicology Laboratories and Department of Medicinal Chemistry
Colleges of Pharmacy and Dentistry
University of Tennessee Center for the Health Sciences
Memphis, TN 38163

Received February 28, 1984.

0022-3549/84/0600-0861$01.00/0
© 1984, American Pharmaceutical Association

than the input value of k_e (0.5) or that estimated by Eq. 2. In contrast, the k values estimated by the concentration ratio method correspond well with those estimated by Eq. 2 (0.5). The concentration ratio method performed adequately when the $C_p t$ data were limited (Table II) and even when k_a was larger than k_e by 10% (Table III).

It must be noted that the nonlinear regression analysis of the $C_p t$ data in terms of Eq. 2 represents the most appropriate method to calculate the rate constant for the special case of the one compartment open model where $k_a = k_e$ (Tables I and II). The pharmacokinetic analysis of the data using Eq. 1 with the NONLIN program is, as suggested by Chan and Miller, the only method known to date to identify the equality between k_a and k_e. The proposed concentration ratio method represents a simple, complimental method which can be applied even in those cases with limited, $C_p t$ data when the model is identified *a priori*.

(1) K. K. H. Chan and K. W. Miller, *J. Pharm. Sci.*, **72,** 574 (1983).
(2) C. M. Metzler, G. L. Elfring, and A. J. McEwen, *Biometrics*, **30,** 562 (1974).
(3) M. Bialer, *J. Pharmacokinet. Biopharm.*, **8,** 111 (1980).
(4) M. Barzegar-Jalali and M. Toomanian, *Int. J. Pharm.*, **12,** 351 (1982).

Indravadan H. Patel

Department of Pharmacokinetics, Biopharmaceutics and Drug Metabolism
Hoffmann-La Roche Inc.
Nutley, NJ 07110

Received September 6, 1983.
Accepted for publication April 4, 1984.

OPEN FORUM

Problems Involved with Developing a Suitable Model for Evaluating Exposure to Bis(2-ethylhexyl) Phthalate from Medical Devices

In a recent article, "Effect of Renal Failure and Bis(2-ethylhexyl) Phthalate Pretreatment on the Disposition and Metabolism of Antipyrine in the Rat" [1], Pollack and Shen presented an experimental model for studying chronic exposure of hemodialysis patients to bis(2-ethylhexyl) phthalate (I) [also known as di-2-ethylhexyl phthalate or DEHP]. Their model, however, utilized oral administration (intragastric intubation) of I rather than a parenteral route. Since the authors did not demonstrate that the effects of I upon antipyrine metabolism and disposition were the same when I was administered orally as when it is given parenterally, one must question acceptance of this as a suitable model for evaluating I exposures from hemodialyzers or other medical devices.

A number of reports, including those of Albro and Thomas[2], Rowland[3], and Lake *et al.*[4], indicate that orally administered I leads to absorption primarily of its hydrolytic product, mono-2-ethylhexyl phthalate or MEHP (II). Therefore, the proposed model[1] should be suitable for evaluating exposure to I from food packagings or other oral exposure, but in order for it to be accepted as a suitable model for clinical exposure to I from medical devices it will be necessary to demonstrate that the parameters evaluated are not affected by the route of administration of I.

There is no dispute that I is metabolized *in vivo* to produce II along with other metabolic products. However, the unanswered question in this case is whether or not the diester (I), to which the patient would initially be exposed intravenously during hemodialysis, *etc.*, would produce qualitatively and quantitatively similar effects on antipyrine metabolism and disposition prior to its metabolic conversion, as would the monoester (II) and other metabolic products. A number of reports have indicated differences in biological activity between I and II, or oral *versus* parenteral administration of I. Some of these reported differences include acute LD_{50}[5], *mutagenicity in bacterial systems*[6], *pentobarbital sleeping time* and effects on aminopyrine-*N*-demethylase and aniline hydroxylase[7], and mitochondrial (state 3) respiration[8].

The authors[1] commented on the findings of Agarwal *et al.*[7], that effects on enzyme activities were associated with the route of I administration, but then they dismiss these findings by attributing the differences to doses administered, not route of administration. However, an examination of the data[7] reveal that when an enzyme or biochemical system was affected by oral or parenteral administration of I (*a*) there was generally a dose-related response, and (*b*) comparisons of similar doses (5.2 and 13.0 po *versus* 5.0 and 10.0 ip) often produced markedly different responses.

Thus, because of the various literature reports (a few of which were cited) showing or suggesting a difference in biological activity between I and II or II plus other metabolites, the model proposed to study the effects of I, from artificial kidneys or other medical device exposure, on antipyrine metabolism and disposition cannot be accepted until it is demonstrated that I produces the same effects on these parameters when administered parenterally as when given by gastric intubation.

[1] G. M. Pollack and D. D. Shen, *J. Pharm. Sci.*, **73,** 29 (1984).
[2] P. W. Albro and R. O. Thomas, *Biochem. Biophys. Acta*, **306**(L23), 380 (1973).
[3] I. R. Rowland, *Food Cosmet. Toxicol.*, **12,** 293 (1974).
[4] B. G. Lake, J. C. Phillips, J. C. Linnell, and S. D. Gangolli, *Toxicol. Appl. Pharmacol.*, **39,** 239 (1977).
[5] J. A. Thomas, T. D. Darby, R. F. Wallin, P. J. Garvin, and L. Martis, *Toxicol. Appl. Pharmacol.*, **45,** 1 (1978).
[6] I. Tomita, Y. Nakamura, N. Aoki, and N. Inui, *Environ. Health Perspect.*, **45,** 119 (1982).
[7] D. K. Agarwal, S. Agarwal, and P. K. Seth, *Drug Metab. Dispos.*, **10,** 77 (1982).
[8] T. Takahashi, *Biochem. Pharmacol.*, **26,** 19 (1977).

W. H. Lawrence[x]
John Autian
Materials Science Toxicology Laboratories and Department of Medicinal Chemistry
Colleges of Pharmacy and Dentistry
University of Tennessee Center for the Health Sciences
Memphis, TN 38163

Received February 28, 1984.

0022-3549/84/0600-0861$01.00/0
© 1984, American Pharmaceutical Association

REVIEWS

USAN and the USP Dictionary of Drug Names, 1984 Ed. Edited by MARY C. GRIFFITHS. United States Pharmacopeial Convention, Inc., 12061 Twinbrook Parkway, Rockville, MD 20852. 1983. 640 pp. 21 × 28 cm. Price $45.00 (discounts for 11+ copies).

The 1984 cumulative edition of *USAN* contains over 18,500 nonproprietary (USAN and INN) and proprietary drug names in one compact volume. Most entries include current CAS names, graphic formulas, and manufacturers. Combined with the cross-index by pharmacologic-therapeutic category, list of CAS registry numbers, and appendix of molecular formulas, this volume constitutes a definitive source of information on drug substances used in the United States. A must for all researchers in the pharmaceutical field.

—Staff Review

The Merck Index, 10th Ed. Edited by MARTHA WINDHOLZ. Merck & Co., P.O. Box 2000, Rahway, NJ 07065. 1983. 2052 pp. 18 × 25.5 cm. Price $28.50.

This encyclopedia of chemicals, drugs, and biological substances, now in its 94th year of publication, is internationally recognized as an authoritative reference work. Written and edited by the chemists of Merck & Co., the 10th edition continues in the tradition, incorporating the considerable new knowledge in the field that has accumulated in the 7 years since the 9th edition was published. This reasonably priced single volume of precise up-to-date data is an essential laboratory and library resource.

—Staff Review

Cologne Atherosclerosis Conference No. I: Inflammatory Aspects. Edited by MICHAEL J. PARNHAM and JOHANNES WINKELMAN. Birkhäuser Boston, Inc., 380 Green Street, Cambridge, MA 02139. 1982. 265 pp. 16 × 24 cm. Price $31.95.

If one were to judge a book by its title, this one would be a disappointment. The title suggests an exposition of the role of inflammation in the siting and development of atherosclerosis. Instead, this is a monograph on inflammation, particularly as it relates to arthritis. Hopefully, the right audience will find the book.

The material is divided into three sections: six chapters on the role of the microvasculature in inflammation, five chapters on the role of various cell types in inflammation, and six chapters on the mediators of inflammation. The "Microvasculature in Inflammation" section is very well covered. The four presentations of Hensen, Williams, Bray, and Bjork form a cogent and provocative overview of the field. The second section, "Cells in Inflammation," is largely limited to a discussion of the monocyte/macrophage. With that constraint, the inflammatory panoply had to be selectively unfolded. This is not a serious problem since the role of the neutrophil was well covered in the first section and the lymphocyte, although in the background, is ever present as a regulator of macrophage activity. For an integrated account of the role of helper and suppressor lymphocytes in the maintenance of chronic inflammation, one would need to look elsewhere. The third section, "Mediators of Inflammation," is a potpourri of topics ranging from complement to oxygen radicals to antigen-induced arthritis. The contribution of Bitter-Sauermann on the role of complement in inflammation is outstanding as a succinct essay on complement C3a and C5a anaphylatoxin activation and regulation. The difficult task of integrating all of this material is attempted in a summary overview. It is noteworthy principally for reminding us of the plurality of cells, products, and processes involved in inflammation.

In addition, a number of narrow contributions are scattered throughout the three sections. They may appeal to the specialist, but for most they will add to the cost rather than the value of the volume. Overall, this multicontributor book has ample good articles to recommend it to those seeking an up-to-date, albeit selective, overview of inflammation as related to the arthritides. It cannot be recommended to those whose primary interest is atherosclerosis.

Reviewed by Ivan Otterness
Central Research Division
Pfizer, Inc.
Groton, CT 06340

MARTINDALE: The Extra Pharmacopeia, 28th Ed. Edited by JAMES E. F. REYNOLDS and ANNE B. PRASAD. The Pharmaceopeial Press, 1 Lamberth High Street, London, SE1 7JN. Distributed in the U.S. by Rittenhouse Book Distributors, Inc., King of Prussia, PA 19406. 1982. 2025 pp. 21 × 25 cm. Price $130.00.

A 25% increase in information, extensive revisions, and 900 new monographs have been incorporated in the 28th edition of *Martindale*. This longstanding reference for pharmacists, which has evolved over a 100-year period, contains monographs of current, new, and investigational drugs grouped by class. Each monograph contains the chemical name, molecular weight and formula, proprietary names, literature documentation, and other information.

Although *Martindale* continues to place emphasis on drugs used in the U.K., it is international in scope, listing proprietary names from many different countries. With an index of drug names containing over 50,000 entries to provide easy access, this volume is an essential reference tool for all pharmaceutical scientists and libraries.

—Staff Review

Drug Fate and Metabolism: Methods and Techniques, Vol. 4. Edited by EDWARD R. GARRETT and JEAN L. HIRTZ. Marcel Dekker, Inc., 270 Madison Avenue, New York, NY 10016. 1983. 504 pp. 15 × 23 cm. Price $75.00 (20% higher outside the U.S. and Canada).

This book is the fourth in a series, each volume of which represents a compilation of individually authored chapters. The topics treated are concerned with various aspects of drug disposition and analytical methods that are useful for quantitating and characterizing drugs and metabolites in biological fluids. The present volume contains a cumulative subject index for this and the previous volumes.

This volume contains six chapters covering a wide range of interests. The first chapter, "Computer Use in Pharmacokinetics," will be useful to those individuals currently employing or contemplating the use of computer programs for the pharmacokinetic analysis of data. There is a good basic discussion of the statistical foundation for curve-fitting routines and practical concerns that arise from such analyses. A particularly attractive aspect of this chapter is a series of appendices (18, 68 pages) that discuss analog computation (Appendix 1) along with a brief summary of many currently available digital computer programs. Each summary includes a description, subroutines, input requirements, output, limitations, and practical considerations. To this re-

REVIEWS

USAN and the USP Dictionary of Drug Names, 1984 Ed. Edited by MARY C. GRIFFITHS. United States Pharmacopeial Convention, Inc., 12061 Twinbrook Parkway, Rockville, MD 20852. 1983. 640 pp. 21 × 28 cm. Price $45.00 (discounts for 11+ copies).

The 1984 cumulative edition of *USAN* contains over 18,500 nonproprietary (USAN and INN) and proprietary drug names in one compact volume. Most entries include current CAS names, graphic formulas, and manufacturers. Combined with the cross-index by pharmacologic-therapeutic category, list of CAS registry numbers, and appendix of molecular formulas, this volume constitutes a definitive source of information on drug substances used in the United States. A must for all researchers in the pharmaceutical field.

—Staff Review

The Merck Index, 10th Ed. Edited by MARTHA WINDHOLZ. Merck & Co., P.O. Box 2000, Rahway, NJ 07065. 1983. 2052 pp. 18 × 25.5 cm. Price $28.50.

This encyclopedia of chemicals, drugs, and biological substances, now in its 94th year of publication, is internationally recognized as an authoritative reference work. Written and edited by the chemists of Merck & Co., the 10th edition continues in the tradition, incorporating the considerable new knowledge in the field that has accumulated in the 7 years since the 9th edition was published. This reasonably priced single volume of precise up-to-date data is an essential laboratory and library resource.

—Staff Review

Cologne Atherosclerosis Conference No. I: Inflammatory Aspects. Edited by MICHAEL J. PARNHAM and JOHANNES WINKELMAN. Birkhäuser Boston, Inc., 380 Green Street, Cambridge, MA 02139. 1982. 265 pp. 16 × 24 cm. Price $31.95.

If one were to judge a book by its title, this one would be a disappointment. The title suggests an exposition of the role of inflammation in the siting and development of atherosclerosis. Instead, this is a monograph on inflammation, particularly as it relates to arthritis. Hopefully, the right audience will find the book.

The material is divided into three sections: six chapters on the role of the microvasculature in inflammation, five chapters on the role of various cell types in inflammation, and six chapters on the mediators of inflammation. The "Microvasculature in Inflammation" section is very well covered. The four presentations of Hensen, Williams, Bray, and Bjork form a cogent and provocative overview of the field. The second section, "Cells in Inflammation," is largely limited to a discussion of the monocyte/macrophage. With that constraint, the inflammatory panoply had to be selectively unfolded. This is not a serious problem since the role of the neutrophil was well covered in the first section and the lymphocyte, although in the background, is ever present as a regulator of macrophage activity. For an integrated account of the role of helper and suppressor lymphocytes in the maintenance of chronic inflammation, one would need to look elsewhere. The third section, "Mediators of Inflammation," is a potpourri of topics ranging from complement to oxygen radicals to antigen-induced arthritis. The contribution of Bitter-Sauermann on the role of complement in inflammation is outstanding as a succinct essay on complement C3a and C5a anaphylatoxin activation and regulation. The difficult task of integrating all of this material is attempted in a summary overview. It is noteworthy principally for reminding us of the plurality of cells, products, and processes involved in inflammation.

In addition, a number of narrow contributions are scattered throughout the three sections. They may appeal to the specialist, but for most they will add to the cost rather than the value of the volume. Overall, this multicontributor book has ample good articles to recommend it to those seeking an up-to-date, albeit selective, overview of inflammation as related to the arthritides. It cannot be recommended to those whose primary interest is atherosclerosis.

Reviewed by Ivan Otterness
Central Research Division
Pfizer, Inc.
Groton, CT 06340

MARTINDALE: The Extra Pharmacopeia, 28th Ed. Edited by JAMES E. F. REYNOLDS and ANNE B. PRASAD. The Pharmaceopeial Press, 1 Lamberth High Street, London, SE1 7JN. Distributed in the U.S. by Rittenhouse Book Distributors, Inc., King of Prussia, PA 19406. 1982. 2025 pp. 21 × 25 cm. Price $130.00.

A 25% increase in information, extensive revisions, and 900 new monographs have been incorporated in the 28th edition of *Martindale*. This longstanding reference for pharmacists, which has evolved over a 100-year period, contains monographs of current, new, and investigational drugs grouped by class. Each monograph contains the chemical name, molecular weight and formula, proprietary names, literature documentation, and other information.

Although *Martindale* continues to place emphasis on drugs used in the U.K., it is international in scope, listing proprietary names from many different countries. With an index of drug names containing over 50,000 entries to provide easy access, this volume is an essential reference tool for all pharmaceutical scientists and libraries.

—Staff Review

Drug Fate and Metabolism: Methods and Techniques, Vol. 4. Edited by EDWARD R. GARRETT and JEAN L. HIRTZ. Marcel Dekker, Inc., 270 Madison Avenue, New York, NY 10016. 1983. 504 pp. 15 × 23 cm. Price $75.00 (20% higher outside the U.S. and Canada).

This book is the fourth in a series, each volume of which represents a compilation of individually authored chapters. The topics treated are concerned with various aspects of drug disposition and analytical methods that are useful for quantitating and characterizing drugs and metabolites in biological fluids. The present volume contains a cumulative subject index for this and the previous volumes.

This volume contains six chapters covering a wide range of interests. The first chapter, "Computer Use in Pharmacokinetics," will be useful to those individuals currently employing or contemplating the use of computer programs for the pharmacokinetic analysis of data. There is a good basic discussion of the statistical foundation for curve-fitting routines and practical concerns that arise from such analyses. A particularly attractive aspect of this chapter is a series of appendices (18, 68 pages) that discuss analog computation (Appendix 1) along with a brief summary of many currently available digital computer programs. Each summary includes a description, subroutines, input requirements, output, limitations, and practical considerations. To this re-

REVIEWS

USAN and the USP Dictionary of Drug Names, 1984 Ed. Edited by MARY C. GRIFFITHS. United States Pharmacopeial Convention, Inc., 12061 Twinbrook Parkway, Rockville, MD 20852. 1983. 640 pp. 21 × 28 cm. Price $45.00 (discounts for 11+ copies).

The 1984 cumulative edition of *USAN* contains over 18,500 nonproprietary (USAN and INN) and proprietary drug names in one compact volume. Most entries include current CAS names, graphic formulas, and manufacturers. Combined with the cross-index by pharmacologic-therapeutic category, list of CAS registry numbers, and appendix of molecular formulas, this volume constitutes a definitive source of information on drug substances used in the United States. A must for all researchers in the pharmaceutical field.

—Staff Review

The Merck Index, 10th Ed. Edited by MARTHA WINDHOLZ. Merck & Co., P.O. Box 2000, Rahway, NJ 07065. 1983. 2052 pp. 18 × 25.5 cm. Price $28.50.

This encyclopedia of chemicals, drugs, and biological substances, now in its 94th year of publication, is internationally recognized as an authoritative reference work. Written and edited by the chemists of Merck & Co., the 10th edition continues in the tradition, incorporating the considerable new knowledge in the field that has accumulated in the 7 years since the 9th edition was published. This reasonably priced single volume of precise up-to-date data is an essential laboratory and library resource.

—Staff Review

Cologne Atherosclerosis Conference No. I: Inflammatory Aspects. Edited by MICHAEL J. PARNHAM and JOHANNES WINKELMAN. Birkhäuser Boston, Inc., 380 Green Street, Cambridge, MA 02139. 1982. 265 pp. 16 × 24 cm. Price $31.95.

If one were to judge a book by its title, this one would be a disappointment. The title suggests an exposition of the role of inflammation in the siting and development of atherosclerosis. Instead, this is a monograph on inflammation, particularly as it relates to arthritis. Hopefully, the right audience will find the book.

The material is divided into three sections: six chapters on the role of the microvasculature in inflammation, five chapters on the role of various cell types in inflammation, and six chapters on the mediators of inflammation. The "Microvasculature in Inflammation" section is very well covered. The four presentations of Hensen, Williams, Bray, and Bjork form a cogent and provocative overview of the field. The second section, "Cells in Inflammation," is largely limited to a discussion of the monocyte/macrophage. With that constraint, the inflammatory panoply had to be selectively unfolded. This is not a serious problem since the role of the neutrophil was well covered in the first section and the lymphocyte, although in the background, is ever present as a regulator of macrophage activity. For an integrated account of the role of helper and suppressor lymphocytes in the maintenance of chronic inflammation, one would need to look elsewhere. The third section, "Mediators of Inflammation," is a potpourri of topics ranging from complement to oxygen radicals to antigen-induced arthritis. The contribution of Bitter-Sauermann on the role of complement in inflammation is outstanding as a succinct essay on complement C3a and C5a anaphylatoxin activation and regulation. The difficult task of integrating all of this material is attempted in a summary overview. It is noteworthy principally for reminding us of the plurality of cells, products, and processes involved in inflammation.

In addition, a number of narrow contributions are scattered throughout the three sections. They may appeal to the specialist, but for most they will add to the cost rather than the value of the volume. Overall, this multicontributor book has ample good articles to recommend it to those seeking an up-to-date, albeit selective, overview of inflammation as related to the arthritides. It cannot be recommended to those whose primary interest is atherosclerosis.

Reviewed by Ivan Otterness
Central Research Division
Pfizer, Inc.
Groton, CT 06340

MARTINDALE: The Extra Pharmacopeia, 28th Ed. Edited by JAMES E. F. REYNOLDS and ANNE B. PRASAD. The Pharmaceopeial Press, 1 Lamberth High Street, London, SE1 7JN. Distributed in the U.S. by Rittenhouse Book Distributors, Inc., King of Prussia, PA 19406. 1982. 2025 pp. 21 × 25 cm. Price $130.00.

A 25% increase in information, extensive revisions, and 900 new monographs have been incorporated in the 28th edition of *Martindale*. This longstanding reference for pharmacists, which has evolved over a 100-year period, contains monographs of current, new, and investigational drugs grouped by class. Each monograph contains the chemical name, molecular weight and formula, proprietary names, literature documentation, and other information.

Although *Martindale* continues to place emphasis on drugs used in the U.K., it is international in scope, listing proprietary names from many different countries. With an index of drug names containing over 50,000 entries to provide easy access, this volume is an essential reference tool for all pharmaceutical scientists and libraries.

—Staff Review

Drug Fate and Metabolism: Methods and Techniques, Vol. 4. Edited by EDWARD R. GARRETT and JEAN L. HIRTZ. Marcel Dekker, Inc., 270 Madison Avenue, New York, NY 10016. 1983. 504 pp. 15 × 23 cm. Price $75.00 (20% higher outside the U.S. and Canada).

This book is the fourth in a series, each volume of which represents a compilation of individually authored chapters. The topics treated are concerned with various aspects of drug disposition and analytical methods that are useful for quantitating and characterizing drugs and metabolites in biological fluids. The present volume contains a cumulative subject index for this and the previous volumes.

This volume contains six chapters covering a wide range of interests. The first chapter, "Computer Use in Pharmacokinetics," will be useful to those individuals currently employing or contemplating the use of computer programs for the pharmacokinetic analysis of data. There is a good basic discussion of the statistical foundation for curve-fitting routines and practical concerns that arise from such analyses. A particularly attractive aspect of this chapter is a series of appendices (18, 68 pages) that discuss analog computation (Appendix 1) along with a brief summary of many currently available digital computer programs. Each summary includes a description, subroutines, input requirements, output, limitations, and practical considerations. To this re-

REVIEWS

USAN and the USP Dictionary of Drug Names, 1984 Ed. Edited by MARY C. GRIFFITHS. United States Pharmacopeial Convention, Inc., 12061 Twinbrook Parkway, Rockville, MD 20852. 1983. 640 pp. 21 × 28 cm. Price $45.00 (discounts for 11+ copies).

The 1984 cumulative edition of *USAN* contains over 18,500 nonproprietary (USAN and INN) and proprietary drug names in one compact volume. Most entries include current CAS names, graphic formulas, and manufacturers. Combined with the cross-index by pharmacologic-therapeutic category, list of CAS registry numbers, and appendix of molecular formulas, this volume constitutes a definitive source of information on drug substances used in the United States. A must for all researchers in the pharmaceutical field.

—Staff Review

The Merck Index, 10th Ed. Edited by MARTHA WINDHOLZ. Merck & Co., P.O. Box 2000, Rahway, NJ 07065. 1983. 2052 pp. 18 × 25.5 cm. Price $28.50.

This encyclopedia of chemicals, drugs, and biological substances, now in its 94th year of publication, is internationally recognized as an authoritative reference work. Written and edited by the chemists of Merck & Co., the 10th edition continues in the tradition, incorporating the considerable new knowledge in the field that has accumulated in the 7 years since the 9th edition was published. This reasonably priced single volume of precise up-to-date data is an essential laboratory and library resource.

—Staff Review

Cologne Atherosclerosis Conference No. I: Inflammatory Aspects. Edited by MICHAEL J. PARNHAM and JOHANNES WINKELMAN. Birkhäuser Boston, Inc., 380 Green Street, Cambridge, MA 02139. 1982. 265 pp. 16 × 24 cm. Price $31.95.

If one were to judge a book by its title, this one would be a disappointment. The title suggests an exposition of the role of inflammation in the siting and development of atherosclerosis. Instead, this is a monograph on inflammation, particularly as it relates to arthritis. Hopefully, the right audience will find the book.

The material is divided into three sections: six chapters on the role of the microvasculature in inflammation, five chapters on the role of various cell types in inflammation, and six chapters on the mediators of inflammation. The "Microvasculature in Inflammation" section is very well covered. The four presentations of Hensen, Williams, Bray, and Bjork form a cogent and provocative overview of the field. The second section, "Cells in Inflammation," is largely limited to a discussion of the monocyte/macrophage. With that constraint, the inflammatory panoply had to be selectively unfolded. This is not a serious problem since the role of the neutrophil was well covered in the first section and the lymphocyte, although in the background, is ever present as a regulator of macrophage activity. For an integrated account of the role of helper and suppressor lymphocytes in the maintenance of chronic inflammation, one would need to look elsewhere. The third section, "Mediators of Inflammation," is a potpourri of topics ranging from complement to oxygen radicals to antigen-induced arthritis. The contribution of Bitter-Sauermann on the role of complement in inflammation is outstanding as a succinct essay on complement C3a and C5a anaphylatoxin activation and regulation. The difficult task of integrating all of this material is attempted in a summary overview. It is noteworthy principally for reminding us of the plurality of cells, products, and processes involved in inflammation.

In addition, a number of narrow contributions are scattered throughout the three sections. They may appeal to the specialist, but for most they will add to the cost rather than the value of the volume. Overall, this multicontributor book has ample good articles to recommend it to those seeking an up-to-date, albeit selective, overview of inflammation as related to the arthritides. It cannot be recommended to those whose primary interest is atherosclerosis.

Reviewed by Ivan Otterness
Central Research Division
Pfizer, Inc.
Groton, CT 06340

MARTINDALE: The Extra Pharmacopeia, 28th Ed. Edited by JAMES E. F. REYNOLDS and ANNE B. PRASAD. The Pharmaceopeial Press, 1 Lamberth High Street, London, SE1 7JN. Distributed in the U.S. by Rittenhouse Book Distributors, Inc., King of Prussia, PA 19406. 1982. 2025 pp. 21 × 25 cm. Price $130.00.

A 25% increase in information, extensive revisions, and 900 new monographs have been incorporated in the 28th edition of *Martindale*. This longstanding reference for pharmacists, which has evolved over a 100-year period, contains monographs of current, new, and investigational drugs grouped by class. Each monograph contains the chemical name, molecular weight and formula, proprietary names, literature documentation, and other information.

Although *Martindale* continues to place emphasis on drugs used in the U.K., it is international in scope, listing proprietary names from many different countries. With an index of drug names containing over 50,000 entries to provide easy access, this volume is an essential reference tool for all pharmaceutical scientists and libraries.

—Staff Review

Drug Fate and Metabolism: Methods and Techniques, Vol. 4. Edited by EDWARD R. GARRETT and JEAN L. HIRTZ. Marcel Dekker, Inc., 270 Madison Avenue, New York, NY 10016. 1983. 504 pp. 15 × 23 cm. Price $75.00 (20% higher outside the U.S. and Canada).

This book is the fourth in a series, each volume of which represents a compilation of individually authored chapters. The topics treated are concerned with various aspects of drug disposition and analytical methods that are useful for quantitating and characterizing drugs and metabolites in biological fluids. The present volume contains a cumulative subject index for this and the previous volumes.

This volume contains six chapters covering a wide range of interests. The first chapter, "Computer Use in Pharmacokinetics," will be useful to those individuals currently employing or contemplating the use of computer programs for the pharmacokinetic analysis of data. There is a good basic discussion of the statistical foundation for curve-fitting routines and practical concerns that arise from such analyses. A particularly attractive aspect of this chapter is a series of appendices (18, 68 pages) that discuss analog computation (Appendix 1) along with a brief summary of many currently available digital computer programs. Each summary includes a description, subroutines, input requirements, output, limitations, and practical considerations. To this re-

REVIEWS

USAN and the USP Dictionary of Drug Names, 1984 Ed. Edited by MARY C. GRIFFITHS. United States Pharmacopeial Convention, Inc., 12061 Twinbrook Parkway, Rockville, MD 20852. 1983. 640 pp. 21 × 28 cm. Price $45.00 (discounts for 11+ copies).

The 1984 cumulative edition of *USAN* contains over 18,500 nonproprietary (USAN and INN) and proprietary drug names in one compact volume. Most entries include current CAS names, graphic formulas, and manufacturers. Combined with the cross-index by pharmacologic-therapeutic category, list of CAS registry numbers, and appendix of molecular formulas, this volume constitutes a definitive source of information on drug substances used in the United States. A must for all researchers in the pharmaceutical field.

—Staff Review

The Merck Index, 10th Ed. Edited by MARTHA WINDHOLZ. Merck & Co., P.O. Box 2000, Rahway, NJ 07065. 1983. 2052 pp. 18 × 25.5 cm. Price $28.50.

This encyclopedia of chemicals, drugs, and biological substances, now in its 94th year of publication, is internationally recognized as an authoritative reference work. Written and edited by the chemists of Merck & Co., the 10th edition continues in the tradition, incorporating the considerable new knowledge in the field that has accumulated in the 7 years since the 9th edition was published. This reasonably priced single volume of precise up-to-date data is an essential laboratory and library resource.

—Staff Review

Cologne Atherosclerosis Conference No. I: Inflammatory Aspects. Edited by MICHAEL J. PARNHAM and JOHANNES WINKELMAN. Birkhäuser Boston, Inc., 380 Green Street, Cambridge, MA 02139. 1982. 265 pp. 16 × 24 cm. Price $31.95.

If one were to judge a book by its title, this one would be a disappointment. The title suggests an exposition of the role of inflammation in the siting and development of atherosclerosis. Instead, this is a monograph on inflammation, particularly as it relates to arthritis. Hopefully, the right audience will find the book.

The material is divided into three sections: six chapters on the role of the microvasculature in inflammation, five chapters on the role of various cell types in inflammation, and six chapters on the mediators of inflammation. The "Microvasculature in Inflammation" section is very well covered. The four presentations of Hensen, Williams, Bray, and Bjork form a cogent and provocative overview of the field. The second section, "Cells in Inflammation," is largely limited to a discussion of the monocyte/macrophage. With that constraint, the inflammatory panoply had to be selectively unfolded. This is not a serious problem since the role of the neutrophil was well covered in the first section and the lymphocyte, although in the background, is ever present as a regulator of macrophage activity. For an integrated account of the role of helper and suppressor lymphocytes in the maintenance of chronic inflammation, one would need to look elsewhere. The third section, "Mediators of Inflammation," is a potpourri of topics ranging from complement to oxygen radicals to antigen-induced arthritis. The contribution of Bitter-Sauermann on the role of complement in inflammation is outstanding as a succinct essay on complement C3a and C5a anaphylatoxin activation and regulation. The difficult task of integrating all of this material is attempted in a summary overview. It is noteworthy principally for reminding us of the plurality of cells, products, and processes involved in inflammation.

In addition, a number of narrow contributions are scattered throughout the three sections. They may appeal to the specialist, but for most they will add to the cost rather than the value of the volume. Overall, this multicontributor book has ample good articles to recommend it to those seeking an up-to-date, albeit selective, overview of inflammation as related to the arthritides. It cannot be recommended to those whose primary interest is atherosclerosis.

Reviewed by Ivan Otterness
Central Research Division
Pfizer, Inc.
Groton, CT 06340

MARTINDALE: The Extra Pharmacopeia, 28th Ed. Edited by JAMES E. F. REYNOLDS and ANNE B. PRASAD. The Pharmaceopeial Press, 1 Lamberth High Street, London, SE1 7JN. Distributed in the U.S. by Rittenhouse Book Distributors, Inc., King of Prussia, PA 19406. 1982. 2025 pp. 21 × 25 cm. Price $130.00.

A 25% increase in information, extensive revisions, and 900 new monographs have been incorporated in the 28th edition of *Martindale*. This longstanding reference for pharmacists, which has evolved over a 100-year period, contains monographs of current, new, and investigational drugs grouped by class. Each monograph contains the chemical name, molecular weight and formula, proprietary names, literature documentation, and other information.

Although *Martindale* continues to place emphasis on drugs used in the U.K., it is international in scope, listing proprietary names from many different countries. With an index of drug names containing over 50,000 entries to provide easy access, this volume is an essential reference tool for all pharmaceutical scientists and libraries.

—Staff Review

Drug Fate and Metabolism: Methods and Techniques, Vol. 4. Edited by EDWARD R. GARRETT and JEAN L. HIRTZ. Marcel Dekker, Inc., 270 Madison Avenue, New York, NY 10016. 1983. 504 pp. 15 × 23 cm. Price $75.00 (20% higher outside the U.S. and Canada).

This book is the fourth in a series, each volume of which represents a compilation of individually authored chapters. The topics treated are concerned with various aspects of drug disposition and analytical methods that are useful for quantitating and characterizing drugs and metabolites in biological fluids. The present volume contains a cumulative subject index for this and the previous volumes.

This volume contains six chapters covering a wide range of interests. The first chapter, "Computer Use in Pharmacokinetics," will be useful to those individuals currently employing or contemplating the use of computer programs for the pharmacokinetic analysis of data. There is a good basic discussion of the statistical foundation for curve-fitting routines and practical concerns that arise from such analyses. A particularly attractive aspect of this chapter is a series of appendices (18, 68 pages) that discuss analog computation (Appendix 1) along with a brief summary of many currently available digital computer programs. Each summary includes a description, subroutines, input requirements, output, limitations, and practical considerations. To this re-

viewer's knowledge, this is the first time that such information appears in one publication.

"Preanalytical Methodology for Drug Analysis in Biological Fluids" discusses a variety of factors that need to be considered prior to performing an assay (subject selection; collection, handling, and storage of specimens; storage, processing, and treatment of sample). Each type of biological fluid is discussed in turn, with consideration for each of the preceding factors (blood, saliva, bile, urine, and feces). The chapter has many useful practical suggestions, and several drug examples are used as illustrations. Over 300 references are provided.

"Isotope Derivatization Analysis" describes the principles of this analytical technique and how it may be applied to the determination of drugs and metabolites, with emphasis given to the double-isotope method. The advantages and limitations of the technique are discussed with respect to sensitivity and specificity. There is also a discussion of the development of this method for a needed application. Numerous examples are provided throughout the chapter.

"Electron Capture Gas-Liquid Chromatography in Drug Analysis" presents a thorough discussion of the operation of the electron-capture detector and its utility in the analysis of drugs and metabolites. There is an extensive compilation of information from the drug assay literature with over 250 references. Numerous practical considerations are presented, along with a comparison of this detector with electron-capture-negative chemical-ionization GC MS analysis.

The chapter on "Animal Species" addresses the question of which animal species is the best metabolic model for the human for a particular type of chemical structure. This chapter is based on a survey of the literature between 1970 and 1979 and is divided according to metabolic pathways under phase I and phase II reactions. There is an extensive compilation of data using the above classification in numerous tables which present compound, species, and the presence or absence of the metabolic product discussed.

The final chapter is entitled "Quantitative Pharmaco-EEG in Determining Bioavailability and Bioequivalency of Psychotropic Drugs." This chapter addresses a specific pharmacodynamic technique, electroencephalography, for the quantitative measurement of response to psychotropic drugs. The authors present a thorough discussion of this technique with numerous drug examples. This is a relatively new area which has promise for a variety of investigations.

The chapters of this book are well written, current, and thorough. The book is recommended to those readers who have a specific interest in or who require an overview of any of the individual topics covered. Certainly it is worthwhile library purchase.

Reviewed by Michael Mayersohn
College of Pharmacy
Department of Pharmaceutical Sciences
The University of Arizona
Tuscon, AZ 85721

Nutrition and Drugs. (Current Concepts in Nutrition, Vol. 12.) Edited by MYRON WINICK. Wiley-Interscience, 605 Third Avenue, New York, NY 10016. 1983. 206 pp. 16 × 23.5 cm. Price $40.00.

For various reasons most pharmacy schools provide little education in nutrition. But just as nutrition is important in maintaining proper health, it is also important in ensuring the proper response to drugs and in limiting their side effects. This volume provides a diverse group of topics on the subject of nutrition and drugs. The following list provides for each chapter the title, the first three authors, the chapter length in pages, and the number, average date, and percentage of reference citations published in 1978 and subsequent years:

1. "Drug-Vitamin B_6 Interaction," H. Bhagavan and M. Brin, 12, 22, 1972, 35%.
2. "Effects of Drugs on Cellular Transport of Nutrients," R. Branda, 16, 61, 1976, 50%.
3. "Vitamin D Metabolism and Metabolic Bone Disease," Z. Gaut, 20, 80, 1977, 58%.
4. "Alcohol, Protein Nutrition, and Liver Injury," C. Lieber, 24, 105, 1972, 25%.
5. "Drugs and Vitamin B_{12} and Folate Metabolism," J. Lindenbaum, 16, 79, 1975, 40%.
6. "Drugs in the Food Supply," S. Miller and J. Harris, 12, 0, none.
7. "Lipid-Lowering Drugs and Low Fat Diets," R. Palmer, 10, 0, none.
8. "Effect of Diet and Sulfonylurea Drugs on Insulin Resistance and Insulin-Receptor Function," F. Pi-Sunyer, 18, 99, 1974, 30%.
9. "Drugs and Nutrient Absorption," D. Roe, 10, 40, 1973, 22%.
10. "Appetite Regulation by Drugs and Endogenous Substances," A. Sullivan, J. Triscari, and L. Cheng, 30, 235, 1978, 65%.
11. "Drugs and Diet Therapy," A. Stunkard, 6, 0, none.
12. "Diuretics and Salt Restriction in Blood Pressure Control," S. Wassertheil-Smoller, H. Langford, M. Blaufox *et al.*, 16, 20, 1966, 38%.
13. "Vitamin A Analogs in Skin Disease," D. Windhorst, 12, 34, 1978, 62%.

Statistical results obtained for the entire volume and each chapter indicate some shortcomings of this volume. This book provides 765 published and 10 in-press citations with an average reference date of 1975; although 50% of the references cited were published in 1978 or later years, some 30% were published prior to 1975, a fact which questions use of the word "current" in the series title.

Overall quality control was poor. Some chapters were good; others were far less so. Aside from being well done, chapters 2, 3, 10, and 13 had 50–65% of the cited references published in 1978 and subsequent years. Chapters 1, 4, 5, 8, 9, and 12 are satisfactory, in general, but have reduced utility because of dated references; only 22–40% of the cited references were published in 1978 and later years. Chapter 12, with some of the most recent references in this group, also had some of the most dated references.

Although the content was interesting, a few chapters seem to detract from this work more than they support it. Chapters 6, 7, and 11 have no reference citations at all. Moreover, many of the missing references would seem critical to the point being made; their absence is astonishing.

There are a few instances where anticipated topics and citations were not mentioned. This diminished the breadth of the article. Specifically, chapter 5 makes no mention of the depletion of vitamin B_{12} by chronic cyanide ingestion, a fact based on substantial research. Furthermore, it was also surprising that no mention was made of food additives and the possible link to hyperactivity in certain children in the discussion of chapter 6.

The volume contained a satisfactory index and although most chapters were easily read, chapter 11 warrants mention because of its complex and lengthy sentence structure. One example is both sufficient and classic:

> "We recommend this because they act, I believe, by lowering the body weight set point, they do not rapidly lose their efficacy, at least in humans, tolerance does not develop, and therefore, when they are withdrawn, the body weight set point that had been artifically suppressed by the drug is elevated to the pretreatment level, resulting in very severe pressures upon people to regain the weight they lost with the aid of these drugs."

In summary, the highly variable quality and topical approach makes this volume more valuable to established libraries than to a general home library. While scientists actively engaged in research involving nutrition and drugs or pharmacology–toxicology will find this work useful, interest in this volume by many scientists will probably depend instead on the topic discussed. Because of limited prior exposure to this subject, pharmacists may find many of the topics to be refreshing and relevant both to their continuing education and to their dealings with a public increasingly fascinated by "nutrition" and dieting. Clearly, however, individuals interested in this subject should examine the work before purchase.

Reviewed by John E. Garst
Department of Animal Science
College of Agriculture
University of Illinois at Urbana-Champaign
Urbana, IL 61801

Progress in Drug Metabolism, Vol. 7. Edited by J. W. BRIDGES and L. F. CHASSEAUD. John Wiley and Sons, One Wiley Drive, Somerset, NJ 08873. 1983. 440 pp. 24 × 15 cm. Price $90.00.

Within this volume are six independent, authorative reviews consisting of a monograph on the renal excretion of drugs; the absorption, distribution, and excretion of two therapeutic classes of compounds; the metabolism and toxicity of two environmentally important compounds; and the relationship between metabolism and toxicity in the avian species. Each chapter is concise, well written, and includes pertinent structures and graphic illustrations. As in the

viewer's knowledge, this is the first time that such information appears in one publication.

"Preanalytical Methodology for Drug Analysis in Biological Fluids" discusses a variety of factors that need to be considered prior to performing an assay (subject selection; collection, handling, and storage of specimens; storage, processing, and treatment of sample). Each type of biological fluid is discussed in turn, with consideration for each of the preceding factors (blood, saliva, bile, urine, and feces). The chapter has many useful practical suggestions, and several drug examples are used as illustrations. Over 300 references are provided.

"Isotope Derivatization Analysis" describes the principles of this analytical technique and how it may be applied to the determination of drugs and metabolites, with emphasis given to the double-isotope method. The advantages and limitations of the technique are discussed with respect to sensitivity and specificity. There is also a discussion of the development of this method for a needed application. Numerous examples are provided throughout the chapter.

"Electron Capture Gas-Liquid Chromatography in Drug Analysis" presents a thorough discussion of the operation of the electron-capture detector and its utility in the analysis of drugs and metabolites. There is an extensive compilation of information from the drug assay literature with over 250 references. Numerous practical considerations are presented, along with a comparison of this detector with electron-capture-negative chemical-ionization GC MS analysis.

The chapter on "Animal Species" addresses the question of which animal species is the best metabolic model for the human for a particular type of chemical structure. This chapter is based on a survey of the literature between 1970 and 1979 and is divided according to metabolic pathways under phase I and phase II reactions. There is an extensive compilation of data using the above classification in numerous tables which present compound, species, and the presence or absence of the metabolic product discussed.

The final chapter is entitled "Quantitative Pharmaco-EEG in Determining Bioavailability and Bioequivalency of Psychotropic Drugs." This chapter addresses a specific pharmacodynamic technique, electroencephalography, for the quantitative measurement of response to psychotropic drugs. The authors present a thorough discussion of this technique with numerous drug examples. This is a relatively new area which has promise for a variety of investigations.

The chapters of this book are well written, current, and thorough. The book is recommended to those readers who have a specific interest in or who require an overview of any of the individual topics covered. Certainly it is worthwhile library purchase.

Reviewed by Michael Mayersohn
College of Pharmacy
Department of Pharmaceutical Sciences
The University of Arizona
Tuscon, AZ 85721

Nutrition and Drugs. (Current Concepts in Nutrition, Vol. 12.) Edited by MYRON WINICK. Wiley-Interscience, 605 Third Avenue, New York, NY 10016. 1983. 206 pp. 16 × 23.5 cm. Price $40.00.

For various reasons most pharmacy schools provide little education in nutrition. But just as nutrition is important in maintaining proper health, it is also important in ensuring the proper response to drugs and in limiting their side effects. This volume provides a diverse group of topics on the subject of nutrition and drugs. The following list provides for each chapter the title, the first three authors, the chapter length in pages, and the number, average date, and percentage of reference citations published in 1978 and subsequent years:

1. "Drug-Vitamin B_6 Interaction," H. Bhagavan and M. Brin, 12, 22, 1972, 35%.
2. "Effects of Drugs on Cellular Transport of Nutrients," R. Branda, 16, 61, 1976, 50%.
3. "Vitamin D Metabolism and Metabolic Bone Disease," Z. Gaut, 20, 80, 1977, 58%.
4. "Alcohol, Protein Nutrition, and Liver Injury," C. Lieber, 24, 105, 1972, 25%.
5. "Drugs and Vitamin B_{12} and Folate Metabolism," J. Lindenbaum, 16, 79, 1975, 40%.
6. "Drugs in the Food Supply," S. Miller and J. Harris, 12, 0, none.
7. "Lipid-Lowering Drugs and Low Fat Diets," R. Palmer, 10, 0, none.
8. "Effect of Diet and Sulfonylurea Drugs on Insulin Resistance and Insulin-Receptor Function," F. Pi-Sunyer, 18, 99, 1974, 30%.
9. "Drugs and Nutrient Absorption," D. Roe, 10, 40, 1973, 22%.
10. "Appetite Regulation by Drugs and Endogenous Substances," A. Sullivan, J. Triscari, and L. Cheng, 30, 235, 1978, 65%.
11. "Drugs and Diet Therapy," A. Stunkard, 6, 0, none.
12. "Diuretics and Salt Restriction in Blood Pressure Control," S. Wassertheil-Smoller, H. Langford, M. Blaufox *et al.*, 16, 20, 1966, 38%.
13. "Vitamin A Analogs in Skin Disease," D. Windhorst, 12, 34, 1978, 62%.

Statistical results obtained for the entire volume and each chapter indicate some shortcomings of this volume. This book provides 765 published and 10 in-press citations with an average reference date of 1975; although 50% of the references cited were published in 1978 or later years, some 30% were published prior to 1975, a fact which questions use of the word "current" in the series title.

Overall quality control was poor. Some chapters were good; others were far less so. Aside from being well done, chapters 2, 3, 10, and 13 had 50–65% of the cited references published in 1978 and subsequent years. Chapters 1, 4, 5, 8, 9, and 12 are satisfactory, in general, but have reduced utility because of dated references; only 22–40% of the cited references were published in 1978 and later years. Chapter 12, with some of the most recent references in this group, also had some of the most dated references.

Although the content was interesting, a few chapters seem to detract from this work more than they support it. Chapters 6, 7, and 11 have no reference citations at all. Moreover, many of the missing references would seem critical to the point being made; their absence is astonishing.

There are a few instances where anticipated topics and citations were not mentioned. This diminished the breadth of the article. Specifically, chapter 5 makes no mention of the depletion of vitamin B_{12} by chronic cyanide ingestion, a fact based on substantial research. Furthermore, it was also surprising that no mention was made of food additives and the possible link to hyperactivity in certain children in the discussion of chapter 6.

The volume contained a satisfactory index and although most chapters were easily read, chapter 11 warrants mention because of its complex and lengthy sentence structure. One example is both sufficient and classic:

> "We recommend this because they act, I believe, by lowering the body weight set point, they do not rapidly lose their efficacy, at least in humans, tolerance does not develop, and therefore, when they are withdrawn, the body weight set point that had been artifically suppressed by the drug is elevated to the pretreatment level, resulting in very severe pressures upon people to regain the weight they lost with the aid of these drugs."

In summary, the highly variable quality and topical approach makes this volume more valuable to established libraries than to a general home library. While scientists actively engaged in research involving nutrition and drugs or pharmacology–toxicology will find this work useful, interest in this volume by many scientists will probably depend instead on the topic discussed. Because of limited prior exposure to this subject, pharmacists may find many of the topics to be refreshing and relevant both to their continuing education and to their dealings with a public increasingly fascinated by "nutrition" and dieting. Clearly, however, individuals interested in this subject should examine the work before purchase.

Reviewed by John E. Garst
Department of Animal Science
College of Agriculture
University of Illinois at Urbana-Champaign
Urbana, IL 61801

Progress in Drug Metabolism, Vol. 7. Edited by J. W. BRIDGES and L. F. CHASSEAUD. John Wiley and Sons, One Wiley Drive, Somerset, NJ 08873. 1983. 440 pp. 24 × 15 cm. Price $90.00.

Within this volume are six independent, authorative reviews consisting of a monograph on the renal excretion of drugs; the absorption, distribution, and excretion of two therapeutic classes of compounds; the metabolism and toxicity of two environmentally important compounds; and the relationship between metabolism and toxicity in the avian species. Each chapter is concise, well written, and includes pertinent structures and graphic illustrations. As in the

viewer's knowledge, this is the first time that such information appears in one publication.

"Preanalytical Methodology for Drug Analysis in Biological Fluids" discusses a variety of factors that need to be considered prior to performing an assay (subject selection; collection, handling, and storage of specimens; storage, processing, and treatment of sample). Each type of biological fluid is discussed in turn, with consideration for each of the preceding factors (blood, saliva, bile, urine, and feces). The chapter has many useful practical suggestions, and several drug examples are used as illustrations. Over 300 references are provided.

"Isotope Derivatization Analysis" describes the principles of this analytical technique and how it may be applied to the determination of drugs and metabolites, with emphasis given to the double-isotope method. The advantages and limitations of the technique are discussed with respect to sensitivity and specificity. There is also a discussion of the development of this method for a needed application. Numerous examples are provided throughout the chapter.

"Electron Capture Gas-Liquid Chromatography in Drug Analysis" presents a thorough discussion of the operation of the electron-capture detector and its utility in the analysis of drugs and metabolites. There is an extensive compilation of information from the drug assay literature with over 250 references. Numerous practical considerations are presented, along with a comparison of this detector with electron-capture-negative chemical-ionization GC MS analysis.

The chapter on "Animal Species" addresses the question of which animal species is the best metabolic model for the human for a particular type of chemical structure. This chapter is based on a survey of the literature between 1970 and 1979 and is divided according to metabolic pathways under phase I and phase II reactions. There is an extensive compilation of data using the above classification in numerous tables which present compound, species, and the presence or absence of the metabolic product discussed.

The final chapter is entitled "Quantitative Pharmaco-EEG in Determining Bioavailability and Bioequivalency of Psychotropic Drugs." This chapter addresses a specific pharmacodynamic technique, electroencephalography, for the quantitative measurement of response to psychotropic drugs. The authors present a thorough discussion of this technique with numerous drug examples. This is a relatively new area which has promise for a variety of investigations.

The chapters of this book are well written, current, and thorough. The book is recommended to those readers who have a specific interest in or who require an overview of any of the individual topics covered. Certainly it is worthwhile library purchase.

Reviewed by Michael Mayersohn
College of Pharmacy
Department of Pharmaceutical Sciences
The University of Arizona
Tuscon, AZ 85721

Nutrition and Drugs. (Current Concepts in Nutrition, Vol. 12.) Edited by MYRON WINICK. Wiley-Interscience, 605 Third Avenue, New York, NY 10016. 1983. 206 pp. 16 × 23.5 cm. Price $40.00.

For various reasons most pharmacy schools provide little education in nutrition. But just as nutrition is important in maintaining proper health, it is also important in ensuring the proper response to drugs and in limiting their side effects. This volume provides a diverse group of topics on the subject of nutrition and drugs. The following list provides for each chapter the title, the first three authors, the chapter length in pages, and the number, average date, and percentage of reference citations published in 1978 and subsequent years:

1. "Drug-Vitamin B_6 Interaction," H. Bhagavan and M. Brin, 12, 22, 1972, 35%.
2. "Effects of Drugs on Cellular Transport of Nutrients," R. Branda, 16, 61, 1976, 50%.
3. "Vitamin D Metabolism and Metabolic Bone Disease," Z. Gaut, 20, 80, 1977, 58%.
4. "Alcohol, Protein Nutrition, and Liver Injury," C. Lieber, 24, 105, 1972, 25%.
5. "Drugs and Vitamin B_{12} and Folate Metabolism," J. Lindenbaum, 16, 79, 1975, 40%.
6. "Drugs in the Food Supply," S. Miller and J. Harris, 12, 0, none.
7. "Lipid-Lowering Drugs and Low Fat Diets," R. Palmer, 10, 0, none.
8. "Effect of Diet and Sulfonylurea Drugs on Insulin Resistance and Insulin-Receptor Function," F. Pi-Sunyer, 18, 99, 1974, 30%.
9. "Drugs and Nutrient Absorption," D. Roe, 10, 40, 1973, 22%.
10. "Appetite Regulation by Drugs and Endogenous Substances," A. Sullivan, J. Triscari, and L. Cheng, 30, 235, 1978, 65%.
11. "Drugs and Diet Therapy," A. Stunkard, 6, 0, none.
12. "Diuretics and Salt Restriction in Blood Pressure Control," S. Wassertheil-Smoller, H. Langford, M. Blaufox *et al.*, 16, 20, 1966, 38%.
13. "Vitamin A Analogs in Skin Disease," D. Windhorst, 12, 34, 1978, 62%.

Statistical results obtained for the entire volume and each chapter indicate some shortcomings of this volume. This book provides 765 published and 10 in-press citations with an average reference date of 1975; although 50% of the references cited were published in 1978 or later years, some 30% were published prior to 1975, a fact which questions use of the word "current" in the series title.

Overall quality control was poor. Some chapters were good; others were far less so. Aside from being well done, chapters 2, 3, 10, and 13 had 50–65% of the cited references published in 1978 and subsequent years. Chapters 1, 4, 5, 8, 9, and 12 are satisfactory, in general, but have reduced utility because of dated references; only 22–40% of the cited references were published in 1978 and later years. Chapter 12, with some of the most recent references in this group, also had some of the most dated references.

Although the content was interesting, a few chapters seem to detract from this work more than they support it. Chapters 6, 7, and 11 have no reference citations at all. Moreover, many of the missing references would seem critical to the point being made; their absence is astonishing.

There are a few instances where anticipated topics and citations were not mentioned. This diminished the breadth of the article. Specifically, chapter 5 makes no mention of the depletion of vitamin B_{12} by chronic cyanide ingestion, a fact based on substantial research. Furthermore, it was also surprising that no mention was made of food additives and the possible link to hyperactivity in certain children in the discussion of chapter 6.

The volume contained a satisfactory index and although most chapters were easily read, chapter 11 warrants mention because of its complex and lengthy sentence structure. One example is both sufficient and classic:

> "We recommend this because they act, I believe, by lowering the body weight set point, they do not rapidly lose their efficacy, at least in humans, tolerance does not develop, and therefore, when they are withdrawn, the body weight set point that had been artifically suppressed by the drug is elevated to the pretreatment level, resulting in very severe pressures upon people to regain the weight they lost with the aid of these drugs."

In summary, the highly variable quality and topical approach makes this volume more valuable to established libraries than to a general home library. While scientists actively engaged in research involving nutrition and drugs or pharmacology–toxicology will find this work useful, interest in this volume by many scientists will probably depend instead on the topic discussed. Because of limited prior exposure to this subject, pharmacists may find many of the topics to be refreshing and relevant both to their continuing education and to their dealings with a public increasingly fascinated by "nutrition" and dieting. Clearly, however, individuals interested in this subject should examine the work before purchase.

Reviewed by John E. Garst
Department of Animal Science
College of Agriculture
University of Illinois at Urbana-Champaign
Urbana, IL 61801

Progress in Drug Metabolism, Vol. 7. Edited by J. W. BRIDGES and L. F. CHASSEAUD. John Wiley and Sons, One Wiley Drive, Somerset, NJ 08873. 1983. 440 pp. 24 × 15 cm. Price $90.00.

Within this volume are six independent, authorative reviews consisting of a monograph on the renal excretion of drugs; the absorption, distribution, and excretion of two therapeutic classes of compounds; the metabolism and toxicity of two environmentally important compounds; and the relationship between metabolism and toxicity in the avian species. Each chapter is concise, well written, and includes pertinent structures and graphic illustrations. As in the

previous volumes, the relationships between drug levels, therapeutic response, and special disease states are discussed.

The following monographs are contained in this volume:

Chapter I, "The Renal Excretion of Drugs" (W. R. Hewitt and J. B. Hook), provides a comprehensive review of the important physiological processes whereby drugs are processed by the kidney. This excellent review contains 202 references.

Chapter II, "Pharmacokinetics and Metabolism of Diuretics" (R. M. J. Ings and L. A. Stevens), containing 436 references, has been devoted to the following classes of diuretics: carbonic anhydrase inhibitors, thiazides, loop and uricosuric agents, potassium-sparing agents, mercurials, and osmotic diuretics.

Chapter III, "Metabolism and Pharmacokinetics of Antihyperlipidaemic Agents" (M. N. Cayen), describes the absorption, distribution, metabolism, and excretion of the following therapeutic agents: clofibrate and congeners, nicotinic acid, and absorbable and nonabsorbable lipid-lowering agents. The review also contains discussions concerning drug interaction and the effects of this class of compounds on the liver. A total of 314 references have been cited.

Chapter IV, "Aliphatic Nitriles: Metabolism and Toxicity" (A. E. Ahmed and N. M. Trieff), contains 257 references. This chapter summarizes the metabolism, toxicity, and environmental impact of aliphatic saturated, unsaturated, and substituted nitriles.

Chapter V, "The Metabolism and Activation of Benzo[*a*]pyrene" (C. S. Cooper, P. L. Grover, and P. Sims), is an outstanding monograph in which the authors have compiled and reviewed the information in 447 references concerning the metabolism and activation of benzo[*a*]pyrene. The reaction of its metabolites with DNA and their involvement with mutagenesis are discussed.

Chapter VI, "Relationship Between Metabolism and Toxicity of Xenobiotics in Avian Species" (A. R. Buckpitt and M. R. Boyd), provides valuable insights into the use of the avian species to predict specific metabolites of a toxicant and its relationship to target tissue toxicity (82 references).

Reviewed by Lawrence A. Pachla
Warner-Lambert/Parke-Davis
Pharmaceutical Research Division
Pharmacokinetics/Drug Metabolism
Ann Arbor, MI 48105

Pharmaceutical Quality Control. By Dr. WILLIAM F. HEAD, JR. Exposition Press, Inc., 325 Rabro Drive, Smithtown, NY 11787-0817. 1983. 90 pp. 15.5 × 23.5 cm. Price $8.00.

In 90 pages Dr. Head covers an enormous amount of information about the manufacture and control of pharmaceutical products. When you start to read such a short book on such a vast subject, there is considerable doubt that it is possible to do the subject justice.

In order to cover the subject of pharmaceutical quality control, which Dr. Head does reasonably well, he is forced to use a great many generalizations. The style in which the book is written could have the uninformed reader believing that the approach stated in the multitude of situations discussed is the only accepted way to perform the task being discussed. This is certainly far from the actual situation in the pharmaceutical industry. For example, there are several references to the use of stickers to identify the status of incoming, in-process, and finished products. The use of stickers is just one of several ways pharmaceutical companies identify the status of materials. Today more and more companies use computerized systems for inventory control and find these systems equally effective as the sticker system at a considerably reduced cost. This is not to say that the sticker system is no longer used or acceptable; there are probably many companies still using this system effectively.

This brings us to the critical issue of the audience for whom the book is written. The author singles out students of analytical and pharmaceutical chemistry, who have relatively little idea of the objectives of how to manage or work within a quality control organization. This is a limited audience. But, on careful examination it represents the initial work experience of many of the people who manage the quality control organizations of a large number of pharmaceutical companies. By reading this book, you will not learn what a quality control manager in the pharmaceutical industry does, you will not learn quality control statistics, nor will you learn the various skills of the quality engineer as they apply to the pharmaceutical industry. However, you will get a good view of many of the basic situations the quality control professional in the pharmaceutical industry frequently faces and how some companies handle these tasks.

Reviewed by L. Pasteelnick
Director of Quality Assurance
Parke-Davis div.
Warner-Lambert Company
Morris Plains, NJ 07950

previous volumes, the relationships between drug levels, therapeutic response, and special disease states are discussed.

The following monographs are contained in this volume:

Chapter I, "The Renal Excretion of Drugs" (W. R. Hewitt and J. B. Hook), provides a comprehensive review of the important physiological processes whereby drugs are processed by the kidney. This excellent review contains 202 references.

Chapter II, "Pharmacokinetics and Metabolism of Diuretics" (R. M. J. Ings and L. A. Stevens), containing 436 references, has been devoted to the following classes of diuretics: carbonic anhydrase inhibitors, thiazides, loop and uricosuric agents, potassium-sparing agents, mercurials, and osmotic diuretics.

Chapter III, "Metabolism and Pharmacokinetics of Antihyperlipidaemic Agents" (M. N. Cayen), describes the absorption, distribution, metabolism, and excretion of the following therapeutic agents: clofibrate and congeners, nicotinic acid, and absorbable and nonabsorbable lipid-lowering agents. The review also contains discussions concerning drug interaction and the effects of this class of compounds on the liver. A total of 314 references have been cited.

Chapter IV, "Aliphatic Nitriles: Metabolism and Toxicity" (A. E. Ahmed and N. M. Trieff), contains 257 references. This chapter summarizes the metabolism, toxicity, and environmental impact of aliphatic saturated, unsaturated, and substituted nitriles.

Chapter V, "The Metabolism and Activation of Benzo[*a*]pyrene" (C. S. Cooper, P. L. Grover, and P. Sims), is an outstanding monograph in which the authors have compiled and reviewed the information in 447 references concerning the metabolism and activation of benzo[*a*]pyrene. The reaction of its metabolites with DNA and their involvement with mutagenesis are discussed.

Chapter VI, "Relationship Between Metabolism and Toxicity of Xenobiotics in Avian Species" (A. R. Buckpitt and M. R. Boyd), provides valuable insights into the use of the avian species to predict specific metabolites of a toxicant and its relationship to target tissue toxicity (82 references).

Reviewed by Lawrence A. Pachla
Warner-Lambert/Parke-Davis
Pharmaceutical Research Division
Pharmacokinetics/Drug Metabolism
Ann Arbor, MI 48105

Pharmaceutical Quality Control. By Dr. WILLIAM F. HEAD, JR. Exposition Press, Inc., 325 Rabro Drive, Smithtown, NY 11787-0817. 1983. 90 pp. 15.5 × 23.5 cm. Price $8.00.

In 90 pages Dr. Head covers an enormous amount of information about the manufacture and control of pharmaceutical products. When you start to read such a short book on such a vast subject, there is considerable doubt that it is possible to do the subject justice.

In order to cover the subject of pharmaceutical quality control, which Dr. Head does reasonably well, he is forced to use a great many generalizations. The style in which the book is written could have the uninformed reader believing that the approach stated in the multitude of situations discussed is the only accepted way to perform the task being discussed. This is certainly far from the actual situation in the pharmaceutical industry. For example, there are several references to the use of stickers to identify the status of incoming, in-process, and finished products. The use of stickers is just one of several ways pharmaceutical companies identify the status of materials. Today more and more companies use computerized systems for inventory control and find these systems equally effective as the sticker system at a considerably reduced cost. This is not to say that the sticker system is no longer used or acceptable; there are probably many companies still using this system effectively.

This brings us to the critical issue of the audience for whom the book is written. The author singles out students of analytical and pharmaceutical chemistry, who have relatively little idea of the objectives of how to manage or work within a quality control organization. This is a limited audience. But, on careful examination it represents the initial work experience of many of the people who manage the quality control organizations of a large number of pharmaceutical companies. By reading this book, you will not learn what a quality control manager in the pharmaceutical industry does, you will not learn quality control statistics, nor will you learn the various skills of the quality engineer as they apply to the pharmaceutical industry. However, you will get a good view of many of the basic situations the quality control professional in the pharmaceutical industry frequently faces and how some companies handle these tasks.

Reviewed by L. Pasteelnick
Director of Quality Assurance
Parke-Davis div.
Warner-Lambert Company
Morris Plains, NJ 07950

A publication of the
American Pharmaceutical Association—
the National Professional Society
of Pharmacists

JOURNAL OF PHARMACEUTICAL SCIENCES

Volume 73, 1984

JPMSAE 73(1-12) 1-1910 (1984)
ISSN 0022-3549

Sharon G. Boots
Editor

Sue A. Kruger
Production Editor

Margaret M. Madeleine
Assistant Production Editor

Karen A. Blakney
Copy Editor

Edward G. Feldmann
Contributing Editor

Samuel W. Goldstein
Contributing Editor

Patricia A. Evich
Editorial Secretary

Editorial Advisory Board

Jordan L. Cohen
Kenneth A. Connors
Louis Diamond
Ho-Leung Fung
Milo Gibaldi
Everett N. Hiestand
W. Homer Lawrence
Ian W. Mathison
Carl M. Metzler
Robert E. Notari
Paul L. Schiff, Jr.
Jane E. Shaw

Published monthly under the supervision of the Board of Trustees

The Sad State of Current Research Instruments

Ever since the 1980 U.S. Presidential election, there has been a greater than usual national debate on the subject of what constitutes the most appropriate level of federal spending for national defense. In particular, those who have advocated budgetary increases have emphasized the need for committing major expenditures for new and up-to-date military "hardware." Ships, tanks, and planes all are very expensive, but they enable a smaller army to achieve military superiority over a much larger force that is inferiorly equipped. In short, more "firepower" requires less "manpower" to achieve the same military capability.

We do not pretend to have any expertise in the area of national defense; therefore, we will not venture any opinion as to the relative merits of our military establishment's need for the added funds it has been requesting for major armaments. However, we do see a striking parallel here to the hardware needed to successfully wage another type of "battle."

The "battle" in this case is research, and the "hardware" is laboratory instruments—modern, up-to-date equipment that is capable of increasing the performance and "firepower" of the laboratory scientist just as surely and as dramatically as the advanced technology weaponry will for military personnel.

Consequently, the state of usefulness of laboratory research equipment in the nation's university research and development centers is a critical factor in considering how effectively and how efficiently these centers are able to fulfill their primary mission.

The National Science Foundation (NSF) felt that this critical question was one that needed to be addressed and answered. As a result, it surveyed the state of academic research equipment during calendar year 1982 in three selected fields—computer sciences, physical sciences, and engineering. As a second stage, data are now being collected for the agricultural, biological, environmental, and medical sciences. There is little reason to expect that the pattern found for these latter areas will differ significantly from the pattern found in the original three test areas. Hence, it warrants our attention and consideration.

The NSF issued its initial report in the April 18, 1984, issue of its publication "Science Resource Studies Highlights" (NSF document 84-312). The report title bluntly and concisely summarized the bottom line of the agency's study: "One-fourth of Academic Research Equipment Classified Obsolete."

The study report describes the considerations given to methodology, purchase price, age, funding patterns, utilization, and equipment adequacy. In particular, the study was limited to "research instrument systems costing from $10,000 to $1,000,000." In this manner, very simple and expendable equipment was eliminated, as well as ultra-costly items that are not really representative and could distort the overall data.

Selected excerpts from the highlights of the report provide considerable information and insight as to the status of the subject. A number of the key points that we found of special significance are as follows:

- *University researchers classified about one-fourth of the 22,300 items in their 1982 research equipment inventories as obsolete and no longer in research use.*
- *Of all academic research equipment listed in the 1982 inventories, only 16% was characterized as "state-of-the-art."*
- *About one-half of department chairpersons reported existing equipment to be "insufficient."*
- *More than 90% of the departmental chairpersons reported that the lack of equipment inhibited the conduct of critical research.*
- *One-half of all academic research instrument systems in use in 1982 were purchased within the previous 5 years, but 31 percent were more than 10 years old.*
- *Two-thirds of all academic research instrument systems in use during 1982 were acquired partly or entirely with federal funds.*
- *Each instrument system in use in 1982 was used by a median of seven researchers.*

Undoubtedly, many of our readers—and especially those in academic research centers—will find little, if any, of this surprising. It simply confirms what they have felt all along.

But the important point is that it *does confirm* what previously had been only claims and conjecture. Solid data is in hand to support those past critical assessments.

Now given this situation, what, if anything, can or should be done about it?

We have read other recent reports released by pertinent government agencies that have been at least equally critical—or more so—of the condition of the nation's interstate highway system, of its major bridges, of its dams, and even the national air traffic control system. Considering that hundreds and even thousands of lives may be at substantial risk due to those faulty, antiquated, or overtaxed systems, many citizens would argue that they require federal funding priority over new research instruments.

Furthermore, as noted above, one of the NSF survey findings is that two-thirds of instrument systems currently in use were already partially or totally funded by the federal government.

It would seem, therefore, that universities should look, and will need to look, to the private sector for increased support in this area. But the philanthropy of industry also has limits, and fairness to the consuming public as well as to company stockholders dictates that only so much money can be given away no matter how worthy the cause.

But what about "quid pro quo" arrangements? For example, the company that needs a nuclear magnetic resonance study conducted might donate such an instrument to a university with the explicit understanding that the university will conduct the study without additional funding support, except perhaps for incidentals. The equipment could then be used at spare time during the period of the study, and full-time thereafter, for whatever other research applications the university staff might find it appropriate.

The point is that the quality of our academic research laboratories is deteriorating badly, and the situation will continue to grow worse unless some concerted efforts and innovative actions are soon initiated.

—EDWARD G. FELDMANN
American Pharmaceutical Association
2215 Constitution Avenue, N.W.
Washington, DC 20037

0022-3549/84/0700-0865$01.00/0
© 1984, American Pharmaceutical Association

JOURNAL OF PHARMACEUTICAL SCIENCES

JULY 1984
VOLUME 73 NUMBER 7

RESEARCH ARTICLES

Pharmacokinetics of Capacity-Limited Tissue Distribution of Methicillin in Rabbits

FRANCIS M. GENGO *‡x, JEROME J. SCHENTAG‡, and WILLIAM J. JUSKO

Received December 8, 1982, from the *Departments of Pharmaceutics and Pharmacy, School of Pharmacy, State University of New York at Buffalo and ‡The Clinical Pharmacokinetics Laboratory, Millard Fillmore Hospital, Buffalo, NY 14209. Accepted for publication April 21, 1983.

Abstract □ Single-dose and steady-state studies were carried out in rabbits to characterize the pharmacokinetics of methicillin elimination and tissue distribution. Serum methicillin concentrations after single doses exhibited a biexponential decline with a mean terminal half-life of 27 ± 5 min. Steady-state volume of distribution (Vd_{ss}) decreased twofold as doses increased from 5 to 125 mg/kg, while total clearance was consistent over this dosage range. During steady-state infusions of 8.7–87.2 mg/kg/h, the serum and extravascular fluid concentrations increased in proportion to dose, while clearance remained constant. Methicillin tissue concentrations did not increase in proportion to dose and serum concentration, and the Vd_{ss} measured from tissue recovery decreased as dosage and serum concentrations increased. Central compartment volume and serum protein binding did not change. The cause of the dose-dependent change in Vd_{ss} was a capacity-limited uptake of methicillin into essentially all nonexcretory tissues. This process was described by a partial physiological pharmacokinetic model based on the actual weights or volumes of the rabbit tissues. Distribution into extracellular fluids was assumed to be complete, while entry into cellular, nonexcretory tissue became capacity limited as the K_m (17.2 μg/mL) was exceeded. The result was a decline in Vd_{ss} with increasing serum concentrations to a limiting value which approached the volume of the central space (V_c) and was similar to the extracellular water volume of the rabbit (0.17 L/kg). In the dosage range where total clearance was independent of serum concentration, the distribution of methicillin was concentration dependent and could be predicted by equations derived from the Michaelis–Menten equation.

Keyphrases □ Methicillin—pharmacokinetics in the rabbit, capacity-limited tissue distribution, single-dose and steady-state conditions □ Pharmacokinetics—methicillin in the rabbit, capacity-limited tissue distribution, single-dose and steady-state conditions □ Tissue distribution—capacity limited, methicillin, rabbits, pharmacokinetics, single-dose and steady-state conditions

Nonlinear disposition of drugs commonly occurs as a result of saturation in transformation, transport, or binding with or by biological substrates. Processes that are most frequently nonlinear are the enzyme-mediated active biotransformations of compounds, such as the metabolism of salicylates, ethanol, and phenytoin (1). Renal tubular secretory mechanisms of compounds such as *p*-aminohippuric acid are capacity limited (2), while tubular reabsorption of at least two cephalosporins is also a nonlinear process (3). Some radiocontrast agents such as iodipamide undergo apparent Michaelis–Menten-type biliary excretion in dogs (4). The GI absorption of some penicillins appear to be zero-order or capacity limited (5). Transport between CSF and blood is often active, as demonstrated for benzylpenicillin (6), but a generalized nonlinear tissue distribution pattern has not been reported for penicillins or any other drugs. If protein binding sites can be saturated to produce nonlinear kinetics, there is no reason why the same process cannot occur in the tissues (7). As an example of capacity-limited tissue binding, DiSanto and Wagner (8) have proposed a nonlinear tissue binding model to account for methylene blue distribution. Saturable or nonlinear plasma protein binding can have diverse effects on both drug distribution and clearance as evidenced with prednisolone (9).

The purpose of this report is to provide a pharmacokinetic description of methicillin serum and tissue concentrations in rabbits. The model incorporates capacity-limited transfer between extravascular fluid and tissues, and utilizes and tests transit time concepts to convert between single-dose and steady-state conditions.

THEORETICAL SECTION

Saturable tissue uptake and linear plasma clearance are the fundamental mechanisms proposed to describe the pharmacokinetics of methicillin over most of the dosage range of interest. A minimal model which describes the experimental data is shown in Fig. 1. The plasma and interstitial fluid comprise the central compartment (V_c), while remaining body tissues were considered as V_T. Total clearance, or the systemic plasma clearance of the drug (CL), occurs from the central compartment. Methicillin uptake into cellular spaces (CL_{12}) was nonlinear and Michaelis–Menten kinetics (T_{max}, K_m) were used to describe the rate-limiting mechanism. Return of drug from tissue to plasma (CL_{21}) was assumed to be linear.

0022-3549/84/0700-0867$01.00/0
© 1984, American Pharmaceutical Association

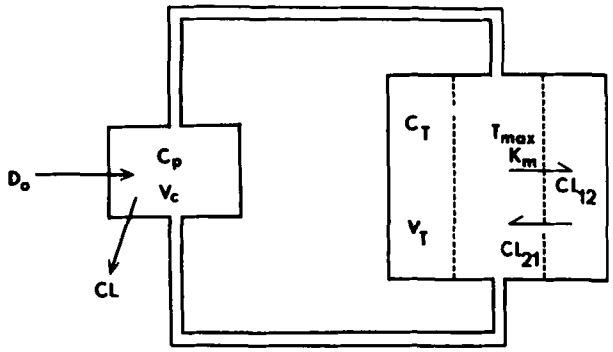

Figure 1—*Partial physiological model for methicillin distribution and clearance in the rabbit. The central volume (V_c) is assumed to comprise plasma and interstitial fluid, from which systemic clearance (CL) occurs. Remaining body tissues (V_T) attain drug concentrations (C_T) by nonlinear transport clearance [$CL_{12} = f(T_{max}, K_m)$] and linear distribution clearance (CL_{21}).*

The differential equations which describe serum (C) and overall tissue (C_T) concentrations are:

$$V_c \frac{dC}{dt} = -CL \cdot C - C \cdot CL_{12} + CL_{21} \cdot C_T \qquad \text{(Eq. 1)}$$

$$V_T \frac{dC_T}{dt} = CL_{12} \cdot C - CL_{21} \cdot C_T \qquad \text{(Eq. 2)}$$

where:

$$CL_{12} = \frac{T_{max}}{K_m + C} \qquad \text{(Eq. 3)}$$

reflects the nonlinear nature of tissue uptake of the drug. Unlike a perfusion model, where the concentration of drug in venous blood should be used in Eq. 2, V_T and C_T are employed here as the actual tissue (cellular) volumes and concentrations (excluding plasma and interstitial fluid). Equilibration between plasma and interstitial fluid was assumed to be very rapid in comparison with the rates of tissue uptake, and cellular transport or binding was considered to be the only mechanism for tissue uptake and retention. The nonlinearity of Eq. 3 prevents direct integration of these equations, but some of the model parameters can be estimated under initial, time-average, low-dose, and steady-state conditions.

Single-Dose Conditions—Serum concentrations following single intravenous bolus injections declined in a biexponential manner and were initially described by their SHAM (slope, height, area, moment) characteristics (10) with:

$$C = C_1^{-\lambda_1 t} + C_2^{-\lambda_2 t} \qquad \text{(Eq. 4)}$$

where C_i are intercepts and λ_i are slope values. These coefficients yield the total area (AUC) and first moment (AUMC) of each curve from:

$$\text{AUC} = \sum C_i/\lambda_i \qquad \text{(Eq. 5)}$$

$$\text{AUMC} = \sum \frac{C_i}{\lambda_i^2} \qquad \text{(Eq. 6)}$$

This permits calculation of mean transit time ($\bar{t}$) for each dose as:

$$\bar{t} = \text{AUMC}/\text{AUC} \qquad \text{(Eq. 7)}$$

The total plasma clearance of a drug is independent of distribution parameters (except for blood flow to the eliminating organ) and can be calculated from:

$$CL = \frac{D_0}{\text{AUC}} \qquad \text{(Eq. 8)}$$

where D_0 is the intravenous bolus dose. The volume of distribution at steady state (Vd_{ss}) can be obtained (11) as:

$$Vd_{ss} = CL \cdot \bar{t} \qquad \text{(Eq. 9)}$$

This parameter is generated initially as a time-average parameter, and its meaning and limitations will be described in more detail below. The volume of the central compartment is calculated from:

$$V_c = D_0/\sum C_i \qquad \text{(Eq. 10)}$$

If very small intravenous doses are used, the system operates under linear conditions, thus collapsing to the conventional two-compartment model within the context of this treatment. This permits the slope/intercept values to be defined as (7):

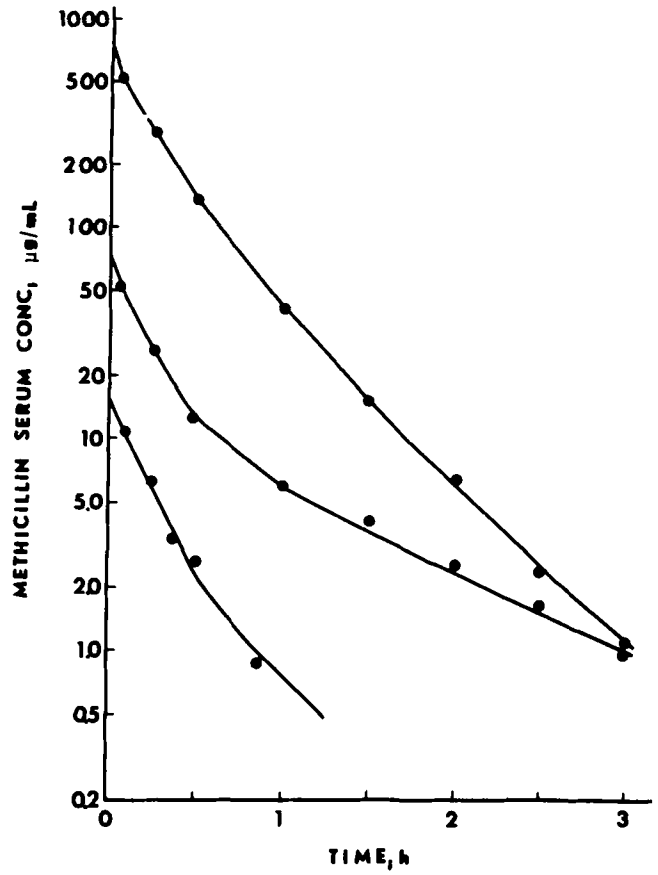

Figure 2—*Concentration-time course of 15-, 50-, and 500-mg/kg iv doses of methicillin in three different rabbits.*

$$\lambda_1 + \lambda_2 = CL/V_c + CL_{12}/V_c + CL_{21}/V_T = -b \qquad \text{(Eq. 11a)}$$

$$\lambda_1\lambda_2 = \frac{CL_{21} \cdot CL}{V_c \cdot V_T} = c \qquad \text{(Eq. 11b)}$$

$$\lambda_1,\lambda_2 = \frac{(-b \pm \sqrt{b^2 - 4c})}{2} \qquad \text{(Eq. 12)}$$

$$C_1 = \frac{D_0\left(\frac{CL_{21}}{V_T} - \lambda_1\right)}{V_c(\lambda_2 - \lambda_1)} \qquad \text{(Eq. 13)}$$

$$C_2 = \frac{D_0\left(\frac{CL_{21}}{V_T} - \lambda_2\right)}{V_c(\lambda_1 - \lambda_2)} \qquad \text{(Eq. 14)}$$

Estimates of the primary model parameters can be obtained, since CL, V_c, and Vd_{ss} are already solved. It is initially assumed (and will be demonstrated) that V_c and V_T have physiological meaning and represent the extracellular water and remaining body spaces of the animal. Thus:

$$V_T = \text{TBW}_t - V_c \qquad \text{(Eq. 15)}$$

where TBW_t is the total body weight of the animal. For convenience, these equations assume a body density of one, and thus body weight and volume are considered equivalent. From Eq. 11b we obtain:

$$CL_{21} = \frac{\lambda_1\lambda_2 \cdot V_c \cdot V_T}{CL} \qquad \text{(Eq. 16)}$$

thus providing CL_{12} from rearrangement of Eq. 11a:

$$CL_{12} = V_c(\lambda_1 + \lambda_2 - CL/V_c - CL_{21}/V_T \qquad \text{(Eq. 17)}$$

Alternatively, since (see below):

$$Vd_{ss} = V_c + \frac{CL_{12} \cdot V_T}{CL_{21}} \qquad \text{(Eq. 18)}$$

Table I—Time-Average Pharmacokinetic Parameters of Methicillin in Rabbits Following Single Intravenous Bolus Doses

Rabbit	Dose, mg/kg	CL, L/h/kg[a]	$\bar{t}$, h[b]	C_{av}, μg/mL[c]	Vd_{ss}, L/kg[d]	V_c, L/kg[e]	CL_{12}, L/h/kg[f]	CL_{21}, L/h/kg[g]
1	5.0	0.91	0.53	10.3	0.48	0.28	0.363	1.09
2	10.9	0.87	0.36	34.7	0.33	0.25	0.250	2.39
3	13.5	0.50	0.80	34.3	0.40	0.18	0.238	1.27
4	13.5	0.55	0.41	47.5	0.32	0.20	0.356	1.35
5	15.0	0.58	0.62	39.5	0.35	0.24	0.218	2.17
6	15.0	0.43	0.67	51.5	0.30	0.18	0.248	1.79
7	18.0	0.40	0.83	57.8	0.31	0.18	0.266	1.68
8	22.5	0.82	0.36	76.9	0.30	0.18	0.305	2.08
9	30.0	0.56	0.40	134.2	0.22	0.17	0.139	2.28
10	36.0	0.57	0.40	154.4	0.23	0.17	0.052	2.43
11	82.5	0.50	0.45	368.7	0.22	0.17	0.100	2.08
12	83.3	0.67	0.38	321.0	0.25	0.24	0.022	1.53
13	113.5	0.60	0.38	491.0	0.23	0.19	0.130	2.62
14	120.0	0.55	0.44	495.4	0.24	0.19	0.083	2.37
15	125.0	0.54	0.40	577.5	0.21	0.17	0.100	2.39

[a] Eq. 8. [b] Eq. 7. [c] Eq. 31. [d] Eq. 9. [e] Eq. 10. [f] Eq. 17. [g] Eq. 16.

a more direct solution is:

$$CL_{12} = \frac{CL_{21} \cdot (Vd_{ss} - V_c)}{V_T} \quad \text{(Eq. 19)}$$

Both Vd_{ss} and CL_{12} are time-average parameters when calculated in this manner and must be used cautiously when nonlinear conditions exist.

Steady-State Conditions—Ordinarily, the only pharmacokinetic parameter that can be obtained at steady state is the total clearance (CL). This value is usually calculated from the infusion rate (k_0) and the steady-state serum concentration (C^{ss}) as:

$$CL = k_0/C^{ss} \quad \text{(Eq. 20)}$$

However, the analysis and recovery of total body drug content (X_B^{ss}) also yields a direct value of Vd_{ss} from:

$$Vd_{ss} = X_B^{ss}/C^{ss} \quad \text{(Eq. 21)}$$

The conventional definition of Vd_{ss} is:

$$Vd_{ss} = V_c + \sum K_{pi} \cdot V_{ti} \quad \text{(Eq. 22)}$$

where K_{pi} and V_{ti} represent the partition coefficients and actual tissue weights or volumes for either the nonplasma or noncentral spaces of the body. In whole body terms, this can be written as:

$$Vd_{ss} = V_c + K_d \cdot \sum V_{ti} = V_c + (K_d \cdot V_T) \quad \text{(Eq. 23)}$$

where K_d is the overall tissue–serum distribution ratio. For the present model, K_d can be solved by considering steady-state conditions with Eq. 2 set to zero, yielding:

$$K_d = C_T^{ss}/C^{ss} = CL_{12}/CL_{21} \quad \text{(Eq. 24)}$$

or:

$$K_d = \frac{T_{max}}{CL_{21}(K_m + C^{ss})} \quad \text{(Eq. 25)}$$

or:

$$Vd_{ss} = V_c + \frac{T_{max} \cdot V_T}{(K_m + C^{ss})CL_{21}} \quad \text{(Eq. 26)}$$

With appropriate data, the unknown parameters of Eq. 26 can be solved by nonlinear least-squares iteration. To assist in resolution of such parameters, consider that as C^{ss} becomes very large ($C^{ss} \gg K_m$), the limiting value of Vd_{ss} is:

$$\lim_{C^{ss} \to \infty} Vd_{ss} = V_c \quad \text{(Eq. 27)}$$

At very low serum concentrations where linear distribution applies ($C^{ss} < K_m$):

$$\lim_{C^{ss} \to 0} Vd_{ss} = V_c + \frac{T_{max}V_T}{K_m \cdot CL_{21}} \quad \text{(Eq. 28)}$$

A typical Michaelis-Menten function usually has sufficient degrees of freedom to solve only two parameters. Equation 26 contains five parameters. In the present study, the single-dose experiments and large-dose infusions yield values of V_c (Eqs. 10 and 27). Retaining physiological equivalence for V_T permits its calculation from Eq. 15. The upper limit of CL_{12} (the quotient of T_{max}/K_m) and CL_{21} can be generated from single low-dose data (Eqs. 16 and 19). This leaves one unknown parameter. If Eq. 26 is rearranged to:

$$G = CL_{21} \cdot \frac{Vd_{ss} - V_c}{V_T} = \frac{T_{max}}{K_m + C^{ss}} \quad \text{(Eq. 29)}$$

then, the function G *versus* C^{ss} can be cast into linear form:

$$1/G = K_m/T_{max} + C^{ss}/T_{max} \quad \text{(Eq. 30)}$$

where a graph of $1/G$ *versus* C^{ss} yields a slope of $1/T_{max}$ and the ordinate intercept is K_m/T_{max}. However, by this stage the function G contains several inserted parameters and may be inaccurate. Thus, Eq. 30 is most useful for obtaining initial estimates. This allows the least-squares values of CL_{21}, T_{max}, and K_m to be generated by NONLIN curve-fitting of Eq. 26, using individual values of V_c and V_T from each animal and Vd_{ss} and C^{ss} as the dependent and independent variables. Because an array of T_{max} and CL_{21} values would yield an identical Vd_{ss} in Eq. 26, it is important to obtain reasonable parameter estimates to initiate computer fitting and to restrict the upper limit of T_{max}/K_m to CL_{12} as generated from the low-dose data (Eq. 3).

Single-Dose to Steady-State Conversion—For drugs with linear pharmacokinetic properties, any single-dose parameters apply directly to the steady-state situation. For drugs with nonlinear CL or Vd_{ss}, the parameters generated using Eqs. 8 and 9 were obtained as time-average values and must be considered valid only for the corresponding time-average serum concentration C_{av}. This is easily calculated as:

$$C_{av} = \text{AUC}/\bar{t} \quad \text{(Eq. 31)}$$

Thus, the equivalence between single-dose and steady-state conditions can be described as:

$$CL = \frac{k_0}{C_{av} \text{ or } C^{ss}} \quad \text{(Eq. 32)}$$

and:

$$Vd_{ss} = \frac{X_B^{ss}}{C^{ss}} = \frac{D_0}{C_{av}} \quad \text{(Eq. 33)}$$

These concepts are experimentally tested in this report.

EXPERIMENTAL SECTION

Protocol—A total of 31 male New Zealand White rabbits ranging in weight from 2.5 to 5.5 kg were studied. Fifteen animals were given single, rapid intravenous bolus doses of methicillin ranging from 5.0 to 125.0 mg/kg. Blood samples were collected from the marginal ear vein over the following 7 h.

Another group of 11 rabbits were given methicillin by constant infusion through a jugular vein catheter. Dosages ranged from 8.6 to 87.2 mg/kg/h, and infusion times ranged from 6.5 to 10 h. Cumulative total urine was collected from all of the animals over the next 24-h period, or until sacrifice. Five additional rabbits (2.5–2.7 kg) were each given a 15-, 50-, and 500-mg/kg bolus dose on different days in random sequence. Blood samples were collected from the marginal ear vein.

For collection of extravascular fluid, 5 of the 31 rabbits had perforated plastic balls (17-mL capacity) placed subcutaneously at 10–14 d prior to the methicillin infusion. In the other rabbits, peritoneal fluid was collected at sacrifice in a capillary tube or onto filter disks. The preweighed filter disks were placed in the abdominal cavity immediately after the animals were

Table II—Steady-State Pharmacokinetic Parameters of Methicillin in Rabbits Following Constant-Infusion Dosing

Rabbit	Weight, kg	Infusion Rate, mg/kg/h	CL, L/h/kg[a]	C^{ss}, μg/mL	Vd_{ss}, L/kg[b]	X_B^{ss}, mg
16	3.3	8.7	0.67	13.0	0.43	18.9
17	3.1	17.8	1.30	15.0	0.49	25.0
18	4.0	16.8	0.96	17.4	0.53	36.2
19	3.3	19.8	0.88	22.5	0.48	36.4
20	3.1	33.3	1.08	30.7	0.36	37.8
21	3.5	22.1	0.64	34.5	0.40	46.3
22	3.1	30.9	0.81	38.5	0.29	35.7
23	2.5	58.5	0.99	58.9	0.17	25.2
24	3.5	50.6	0.84	60.0	0.26	53.4
25	3.3	53.8	0.75	71.0	0.27	64.6
26	3.2	87.2	0.69	125.0	0.25	100.0

[a] Eq. 20. [b] Eq. 21.

sacrificed. Fluid in the abdominal cavity was tested for occult blood[1]; only negative samples were used for analysis.

At the end of the sampling procedures, all rabbits given continuous infusion were sacrificed, and samples of essentially all organs and tissues were obtained for methicillin assay. Urine was collected from the intact bladder. All organs and the remaining carcass were weighed for use in determining the organ content of methicillin.

Assays—Methicillin concentrations in serum, peritoneal fluid, and urine were determined by an agar well diffusion microbiological assay as outlined by Kavanaugh (12) using *Bacillus subtilis* as the test organism. The range of concentrations assayed without dilution was 0.5–25.0 μg/mL, and the day-to-day coefficient of variation was <10%. Samples were assayed in triplicate on two or more occasions and quantitated in reference to appropriate standards prepared in blank tissue homogenate, urine, or pooled rabbit serum. Plasma protein binding was measured by equilibrium dialysis at 37°C.

Tissue concentrations were determined by methods similar to those used previously (13). Necropsy samples were blotted on gauze and two 100–200-mg samples were weighed to be within 10 mg of each other. Each sample was individually homogenized following the addition of 1–2 mL of phosphate buffer (pH 7.4). To one of the two samples, a known amount of methicillin was also added. Samples were allowed to stand for 24–48 h at 4°C and then centrifuged. The supernatant was assayed using the microbiological assay and homogenate standards. The phosphate buffer in the homogenized tissue was replaced, and the extraction procedure was repeated until no further methicillin could be measured.

Extraction recovery was calculated using the following:

$$\frac{\begin{pmatrix}\text{Methicillin recovered}\\ \text{from "spiked" sample}\end{pmatrix} - \begin{pmatrix}\text{Methicillin recovered}\\ \text{from "unspiked" sample}\end{pmatrix}}{\text{Amount of Methicillin "spiked"}} \quad \text{(Eq. 34)}$$

The fractional extraction recovery using this method ranged from 0.9 to 1.05 in all tissues.

Tissue concentrations were calculated by dividing the amount recovered from a tissue sample by the weight of the tissue sample. The total amount recovered from each animal was the product of the specific organ concentration and the individual organ weight. The sum of all tissue weights in each animal approximated the total body weight minus the total weight of any GI contents and urine.

RESULTS

Single-Dose Pharmacokinetics of Methicillin—Following single bolus doses of methicillin, serum concentrations declined in a biexponential fashion, as shown for three representative rabbits in Fig. 2. Such profiles were fitted to Eq. 4 by nonlinear least-squares regression (14). The SHAM properties were then inserted into Eqs. 7–17 to obtain the pharmacokinetic parameters describing clearance and distribution in the 15 rabbits given single doses. These data are given in rank order of dose in Table I, and show that the average serum concentration remains proportional to dose with increasing doses, while the plasma clearance remained essentially constant, averaging 0.60 ± 0.15 L/h/kg. The terminal half-life averaged 27 ± 2 min in the rabbits. The other parameters that remained constant over this dosage range were V_c, which averaged 0.20 ± 0.03 L/kg, and CL_{21}, which averaged 1.86 ± 0.60 L/h/kg. The t, Vd_{ss}, and CL_{12} values varied with dose. Vd_{ss} decreased by approximately twofold as the dose covered a 10-fold range. The change in t with dose was a direct result of the Vd_{ss}/CL ratio, as the plasma clearance remained unchanged with increasing doses. The distributional clearances (CL_{12}) listed in Table I exhibited a fourfold range (0.10–0.35 L/kg/h) with increasing doses of methicillin.

[1] A Hemoccult pad was placed in the abdominal cavity next to the collection tube or filter disk.

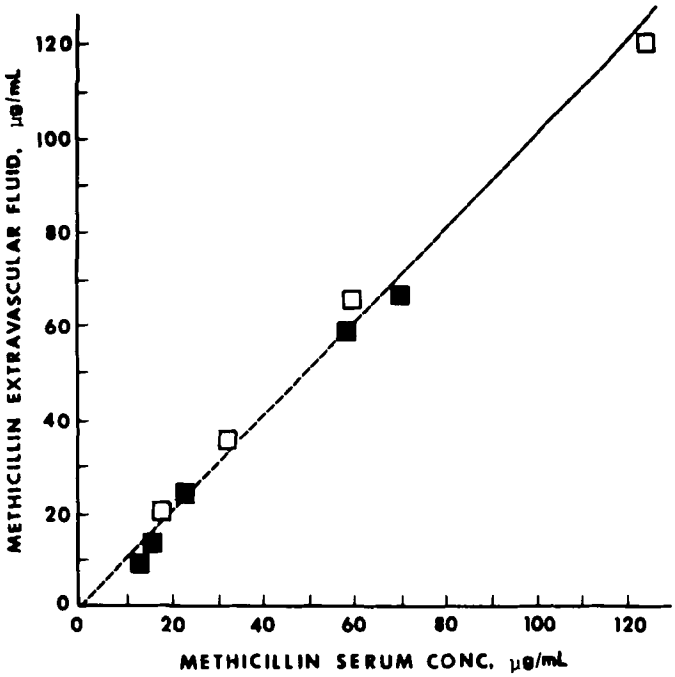

Figure 3—*Simultaneous steady-state concentrations of methicillin in serum and extravascular fluids: Key: (■) tissue chamber fluid; (□) peritoneal fluid.*

To assess the possibility of protein binding changes altering the distribution volume, we measured protein binding by equilibrium dialysis on serum samples over a 20-fold range of serum concentrations. The binding of methicillin to serum proteins averaged 17 ± 2%.

Methicillin Pharmacokinetics after Continuous Infusions—Methicillin was infused into 11 different rabbits for 6–10 h. The infused doses, clearances, volumes of distribution, total body methicillin content (X_B^{ss}), and serum concentrations measured at steady state are listed in Table II for each of these rabbits. The C^{ss} values were proportional to the infusion rate, yielding relatively constant CL values which averaged 0.86 ± 0.19 L/kg/h. These values were in good agreement with the single dose CL values of Table I. As was observed in the single-dose rabbits, Vd_{ss} steadily declined as doses and steady-state serum concentrations increased.

Steady-State Extravascular Fluid Distribution—Table III gives the steady-state serum drug concentrations for all 11 rabbits, ranging from 13.0 to 125.0 μg/mL. As serum concentrations increased as a result of the increasing dosing rates, a proportional rise was noted in the extravascular fluid concentrations, *i.e.*, both the tissue chamber and peritoneal fluid. The data indicate complete and dose-independent penetration of methicillin into extravascular fluids, as shown by the identity line in Fig. 3.

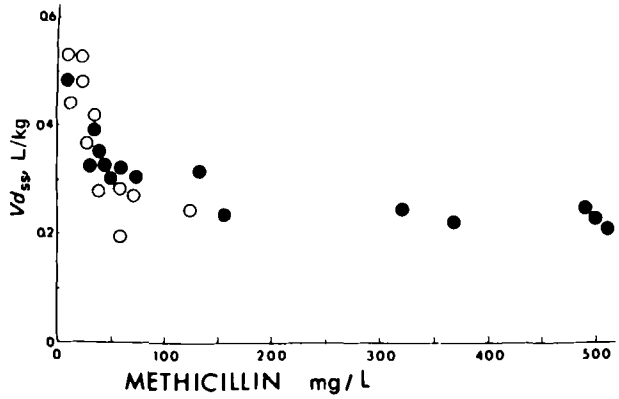

Figure 4—*Steady-state volume of distribution following a single dose (●) and constant infusion (○) of methicillin in relation to time average (C_{av}) and steady-state (C^{ss}) serum drug concentrations.*

Table III—Steady-State Serum, Extravascular Fluid, and Nonexcretory Tissue Concentrations Following Constant Infusion

Rabbit	C^{ss}, μg/mL[a]	Conc. in Tissue Chamber[b] or Peritoneal Fluid[c], μg/mL	Steady-State Tissue Conc., μg/g[c]			
			Heart	Lung	Liver	Skeletal Muscle
16	13.0 ± 1.5	11.0	5.0	4.8	5.0	4.4
17	15.0 ± 1.2	13.8	7.5	4.6	6.3	7.5
18	17.4 ± 1.8	20.0[d]	8.8	8.9	7.8	8.9
19	22.5 ± 1.3	24.0	23.0	3.9	9.7	7.1
20	30.7 ± 2.1	—[e]	8.2	6.5	8.8	11.0
21	34.5 ± 2.7	32.0[d]	10.7	10.0	16.6	11.2
22	38.5 ± 1.3	—[e]	9.0	7.7	8.2	10.2
23	58.9 ± 2.4	65.0[d]	23.0	34.6	30.4	6.7
24	60.0 ± 3.0	58.0	10.0	9.6	14.0	13.5
25	71.0 ± 2.6	67.0	10.4	8.8	11.3	15.8
26	125.0 ± 6.3	120.0[d]	31.0	35.0	35.0	24.0

[a] Steady-state methicillin serum concentration verified by measurement every 30 min over the 6-10-h infusion period (values ± *SD*). [b] Steady-state methicillin concentration measured in fluid obtained from a subcutaneously implanted perforated plastic catheter. [c] Methicillin concentrations measured at the time of sacrifice, immediately following the infusion. [d] Peritoneal fluid samples. [e] Not analyzed because sample contained occult blood.

The methicillin content of the bile was <5% of the infused dose, but represented only the bile present in the gallbladder at the time of sacrifice. The volume of bile that entered the GI tract during the infusion period was not assessed.

Urinary Excretion—Urine collected over the first 24 h from animals receiving single doses of methicillin contained 80 ± 2% of the administered dose. In animals infused to steady state and sacrificed, urine was collected from the intact bladder at the end of infusion. Greater than 85% of the administered dose could be accounted for in the serum, tissue, and urine of this group of rabbits. The percentage of the total dose that appeared in the urine at the time of sacrifice consistently increased as the cumulative dose infused increased. At the lowest infusion dose, 67% of the dose appeared in the urine, while at the highest dose, 96% of the total dose appeared in the urine. Despite this finding, the total body clearance of methicillin in these two rabbits was similar: 0.67 and 0.69 L/kg/h.

In vitro experiments revealed that methicillin was not completely stable in rabbit urine. The half-life for methicillin degradation in rabbit urine maintained at 39°C averaged 31 ± 4 h. If a degradation rate constant is incorporated into the urine recovery and the total amount of methicillin excreted in the bile estimated, essentially all of the total infused dose can be accounted for in the rabbits sacrificed at steady state.

Steady-State Tissue Penetration—The steady-state concentrations of methicillin in representative nonexcretory tissue are listed in Table III along with simultaneous C^{ss} and extravascular fluid concentrations. Unlike steady-state serum and extravascular concentrations, steady-state concentrations in nonexcretory tissue did not increase proportionally with increases in infusion rate. Steady-state tissue concentrations seemed to reach an apparent plateau as steady-state serum concentrations exceeded 25–30 μg/mL. Furthermore, the total amount in the body at the time of sacrifice (X_B^{ss}) appeared to approach a maximum value as infusion rates increased. Steady-state kidney concentrations of methicillin were generally 10-fold greater than concentrations in nonexcretory tissue, and the plateau of concentrations with increased doses was less marked. However, true renal tissue concentrations could not be discerned because we were also measuring drug in retained urine in the kidney samples.

Consistent with the individual values in tissue, the total amount of methicillin recovered from each rabbit at steady state also failed to increase proportionally to increased infusion doses, as shown in Table III. The steady-state volume of distribution of methicillin varied over twofold, but values consistently diminished as steady-state concentrations were increased with increasing dosing rates.

Nonlinear Steady-State Volume of Distribution—The nonlinear relationship between Vd_{ss} and methicillin steady-state serum concentrations can be evaluated directly from the data in Table II. The single-dose studies in Table I yield time-average Vd_{ss} values which can be assessed only at the time-average serum concentration (C_{av}). Figure 4 depicts all methicillin Vd_{ss} values in relation to either C_{av} or C^{ss}; these data are consistent with a single nonlinear curve. It should be noted that the largest C_{av} range produced Vd_{ss} values which approach a limiting value of ~0.20 L/kg, similar to the mean central compartment volume of distribution.

The decline in both Vd_{ss} and CL_{12} with increasing C^{ss} suggested that limiting tissue uptake was a common factor. Equation 26 was employed to characterize the data of Fig. 4 in the following manner. The NONLIN computer program was used to fit individual Vd_{ss} values as a function of actual C_{av} from each animal dosed by rapid intravenous bolus doses. Individual values of V_c were available, and specific values of V_T were then directly calculated for each animal using Eq. 15. This left three unknown parameters, T_{max}, K_m, and CL_{21}. These were generated using least-squares regression. Initial estimates were obtained as described in the *Theoretical Section.*

The mean (± *SD*) least-squares values which described the nonlinear extravascular penetration of methicillin in the rabbit following single intravenous bolus doses were: T_{max} = 9.79 ± 4.3 mg/kg/h; K_m = 17.2 ± 7.0 μg/mL; and CL_{21} = 1.02 ± 0.6 L/kg/h. To test the ability of this model to predict distribution at steady-state from single-dose data, the parameter estimates from the single-dose data were used to calculate the Vd_{ss} in animals infused to steady state, using Eq. 26. As shown in Fig. 5, these calculated values were in good agreement with the measured values in all rabbits infused to steady state.

Multiple Single Doses—Additional studies were performed using a wider range of single doses (15–500 mg/kg) in crossover fashion to further examine the linearity of the disposition of methicillin. The *CL* from Eq. 8 and Vd_{ss} from Eq. 9 following these doses of methicillin in each of five rabbits are shown in Table IV. The Vd_{ss} following the 15-mg/kg dose was significantly larger than the Vd_{ss} following the 50-mg/kg dose. The Vd_{ss} changes are in agreement with those predicted in previous rabbits given large doses of methicillin either by rapid bolus or continuous infusion. The Vd_{ss} following the 500-mg/kg doses approximates the total extracellular fluid volume of 0.17 L/kg in New Zealand White rabbits (15).

The 500-mg/kg methicillin dose yielded a lower clearance compared with those following the lower doses. The *CL* values from the lower doses were similar. These data indicate that the assumption of linearity in total methicillin clearance is tenable only over a limited dose and concentration range.

DISCUSSION

Disposition in Rabbits—From measurements of the drug in serum and urine, it appears that methicillin is primarily cleared by the kidney and excreted in the urine of the rabbit. This is in agreement with other reports of methicillin pharmacokinetics in rabbits (16) and is also consistent with human studies (17). The renal clearance of methicillin, like other penicillins, has been attributed to both glomerular filtration as well as active tubular secretion (18). Concomitant administration of organic acids such as *p*-aminohippuric acid and probenecid have shown to competitively inhibit the active secretion process (19, 20). At sufficiently high methicillin concentrations, renal clearance also becomes nonlinear, as was observed after single 500-mg/kg doses in these studies (Table IV). The model assumptions only apply to the region of linear clearance.

There was a consistent, near-total recovery of the infused dose of methicillin from tissue, serum, and urine in all animals dosed to steady state, regardless of the total dosage. Furthermore, the unrecovered drug can be accounted for by the instability of methicillin in rabbit urine and incomplete collection of bile. Thus, the pharmacokinetic model can be applied in a setting where mass balance is essentialy complete without uncertainties related to incomplete tissue extraction or analytical difficulties. The pharmacokinetic characterization of serum concentration *versus* time profiles yielding nonlinear tissue distribution properties was directly confirmed by analysis of actual tissue drug uptake. This diminishes the need for speculative inferences regarding the physiological relevance of the pharmacokinetic analysis of only serum concentrations.

Tissue Distribution—The distribution of methicillin into extravascular spaces can be described by two processes. Methicillin distributed freely and rapidly between serum and extravascular fluids since peritoneal fluid and tissue chamber fluid concentrations are in good agreement with serum concentra-

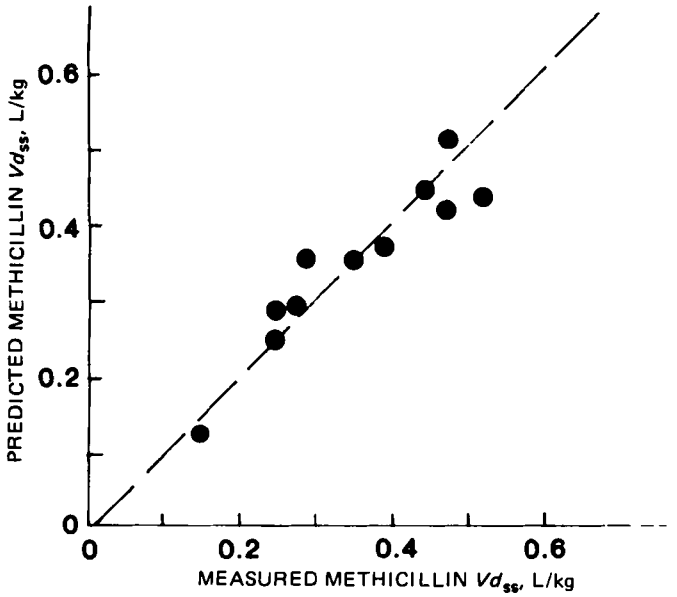

Figure 5- *Agreement between predicted* Vd_{ss} *(Eq. 26) using the* V_c, V_T, T_{max}, K_m, *and* CL_{21} *values obtained from single-dose studies and measured* Vd_{ss} *based on recovery of drug from body tissue.*

tions, even following single doses. This process is a simple linear relationship. Similar findings with other penicillins have been reported in animals (21) and in humans (22). In contrast, the intracellular distribution of methicillin appears to be governed by a different process. A plateauing of steady-state tissue concentrations occurred as C^{ss} exceeded 20–25 μg/mL. Linear uptake occurs at low serum concentrations, but saturation begins to occur as the K_m (17 μg/mL) is exceeded. Each tissue analyzed contains cells, interstitial fluid, and trapped blood. Interstitial fluids are in rapid equilibrium with drug in plasma (Fig. 3). When the conglomerate of tissue and interstitial fluid is homogenized for assay, measured concentrations of methicillin continue to rise slightly as C^{ss} increases, but not to a proportional degree. Apparently, interstitial fluid concentrations continue to parallel serum, while true tissue concentrations reach a limiting value. Similar tissue penetration data using ampicillin have recently been reported by Cars and Ogren (23). Skeletal muscle concentrations of ampicillin were substantially lower than serum concentrations, but concentrations declined at a similar rate from both tissue and serum. They, like we, suggest that ampicillin concentrations in interstitial fluid are considerably higher than whole tissue concentrations.

The capacity-limited nature of methicillin tissue distribution in rabbits was best described by a pharmacokinetic model incorporating a linear systemic clearance and a Michaelis-Menten-type, nonlinear distributional clearance. The unique pharmacokinetic manifestation of the nonlinear distributional clearance is that the Vd_{ss} changes as serum concentrations or doses change. At high serum concentrations, Vd_{ss} approaches its minimal value, which is V_c. This occurs following both rapid intravenous bolus or steady-state infusion of the drug. The volume of the central compartment was consistent for all rabbits and was independent of dose. The central volume takes on physiological significance because it is slightly larger than the value for extracellular fluid volume in New Zealand White rabbits (15). The excellent agreement between measured concentrations of methicillin in serum and extravascular fluids confirms that V_c is comprised of the plasma and interstitial volumes. The tissue volume V_T also retains physiological significance because it is simply the summation of the tissue weights excluding the weight of blood and interstitial fluids.

This is not the first observation of an apparent capacity-limited process with penicillins. Active processes for tubular secretion have been known. The active tubular secretion of penicillins can be saturated (24) and inhibited by *p*-aminohippuric acid (19). Saturable renal tubular processes have also been observed following the administration of mezlocillin (25), cephapirin (3), and cephaloridine (3) to human volunteers. This also appears to occur for methicillin at very high doses.

Regarding tissue uptake, Bergholtz *et al.* (26) reported that probenecid, an inhibitor of the active secretion of penicillin, can affect skeletal muscle concentrations of penicillin. Pappenheimer *et al.* reported an active transport process for the movement of organic acids from CSF to plasma (27) which has been shown to be operative for benzylpenicillin (6). There are numerous reports of penicillin neurotoxicity following massive dosing, presumably overwhelming the central nervous system active transport system for penicillin

Table IV—Methicillin Clearance and Vd_{ss} in Five Rabbits, Each Given Three Doses of Methicillin in Randomized Order

	Clearance, L/h/kg			Vd_{ss}, L/kg		
Rabbit	15 mg/kg	50 mg/kg	500 mg/kg	15 mg/kg	50 mg/kg	500 mg/kg
27	0.97	0.70	0.55	0.42	0.27	0.19
28	0.88	0.78	0.73	0.35	0.20	0.22
29	1.50	1.30	0.90	0.49	0.21	0.25
30	1.00	1.00	0.60	0.40	0.25	0.19
31	1.10	1.10	0.60	0.36	0.29	0.19
Mean	1.09	0.97	0.67	0.40	0.24	0.20
± *SD*	0.24	0.28	0.14	0.05	0.03	0.02
		$p < 0.05$		$p < 0.05$		

removal (28, 29). Studies by Fishman (30) suggest that probenecid may cause CNS accumulation of penicillin.

Similar active transport systems have been proposed to explain the concentration dependence of ampicillin excretion into bile (31). Recent data obtained from rats suggest that the absorption of amino penicillins is best described by Michaelis-Menten kinetics and postulate that similar saturable absorption processes govern cephalexin and cephradine absorption (5).

In addition to concentration dependence in renal and biliary secretion and GI absorption, another recently described concentration-dependent process with β-lactam antibiotics occurs with protein binding. The third generation caphalosporin, ceftriaxone, is a particularly good example of this phenomenon, as the saturation of binding occurs at plasma concentrations in the usual therapeutic range (32).

Concentration-dependent tissue distribution has not been described for β-lactam antibiotics. The data presented here for methicillin suggest that essentially all nonexcretory tissues can be involved in this process, and establish a limit to achievable "tissue" concentrations for these antibiotics. Such an observation, if confirmed for other β-lactam antibiotics, has clinical relevance to the treatment of infection. However, not only do other drugs need study for similar concentration dependence, but also it is not yet possible for the data presented to differentiate whether this phenomenon is caused by capacity limits in binding to tissue proteins or a saturable cellular uptake process. It does appear from these data that whichever the underlying mechanism, the process limits the concentrations of methicillin that can be realistically achieved in normal tissue.

Transit Times—An innovative approach was evolved to relate a single-dose disposition of methicillin to true steady-state conditions. The analysis of single-dose kinetics based on the SHAM characteristics is valid for linear conditions, but entails the generation of dose and time-average pharmacokinetic parameters in the nonlinear dosage range. In the latter case, these time-average parameters ought to directly apply to steady-state conditions only at an equivalent time-average substrate concentration. This was confirmed experimentally for Vd_{ss} (Fig. 4, Table IV) and by the dual characterization of single-dose and steady-state data with a single nonlinear function (Eq. 26). Other uses of transit-time analysis have been reviewed recently (33).

APPENDIX: GLOSSARY

Concentrations

C	Serum or plasma concentration
C_T	Mean tissue concentration
C^{ss}	Steady-state serum concentration
C_i	Intercepts of C_p *versus* time curve
C_{av}	Time-average serum concentration
K_m	Michaelis-Menten constant for transport

Time

t	Experimental time
$\bar{t}$	Mean transit time

Slopes

λ_i	Slope of C_p *versus* time curve

Integrals

AUC	Area of C_p *versus* time curves
AUMC	Area of $t \cdot C_p$ *versus* time curve (moment)

Volumes, Weights

V_c	Volume of plasma and interstitial fluid
Vd_{ss}	Steady-state volume of distribution
TBW_t	Total body weight
V_T	Cellular tissue volume
V_{Ti}	Individual tissue weights

Clearances

CL	Systemic plasma clearance

CL_{12}	Clearance from plasma to cell water = $f(T_{max},K_m)$
CL_{21}	Clearance from cell water to plasma
Amounts	
D_0	Dose
X_B^{ss}	Amount in body at steady-state
Rates	
k_0	Zero-order infusion rate
T_{max}	Maximum cellular transport rate
Ratios	
K_d	Tissue-plasma partition coefficient
K_{pi}	Individual tissue-plasma partition coefficients

REFERENCES

(1) G. Levy, in "Importance of Fundamental Principles in Drug Evaluation," D. H. Tedeschi and R. E. Tedeschi, Eds., Raven, New York, N.Y., 1968, pp. 141-171.

(2) I. M. Weiner and G. H. Mudge, *Am. J. Med.*, **36**, 743 (1964).

(3) A. Arvidson, O. Borga, and G. Alvan, *Clin. Pharmacol. Ther.*, **25**, 870 (1979).

(4) S. K. Lin, A. A. Moss, and S. Riegelman, *J. Pharm. Sci.*, **66**, 1670 (1977).

(5) A. Tsuji, E. Nakashima, I. Kagami, T. Asano, and R. Yamana, *J. Pharm. Pharmacol.*, **30**, 508 (1978).

(6) R. L. Dixson, E. S. Owens, and D. P. Rall, *J. Pharm. Sci.*, **58**, 1106 (1969).

(7) W. J. Jusko and M. Gretch, *Drug Metab. Rev.* **5**, 43 (1976).

(8) A. R. DiSanto and J. G. Wagner, *J. Pharm. Sci.*, **61**, 1040 (1972).

(9) W. J. Jusko and J. Q. Rose, in "Frontiers in Therapeutic Drug Monitoring," G. Togoni, R. Latini, and W. J. Jusko, Eds., Raven, New York, N.Y., 1980, pp. 153-161.

(10) N. A. Lassen and W. Perl, "Tracer Kinetic Methods in Medical Physiology," Raven, New York, N.Y., 1979.

(11) L. Z. Benet and R. L. Galeazzi, *J. Pharm. Sci.*, **68**, 1071 (1979).

(12) F. W. Kavanaugh, *Pharm. Technol.*, **63**, 1459 (1974).

(13) J. J. Schentag, W. J. Jusko, J. W. Vance, E. Abrutyn, M. DeLattre, and M. Gerbracht, *J. Pharmacokinet. Biopharm.*, **5**, 559 (1977).

(14) C. M. Metzler, G. L. Elfring, and A. J. McEwen, *Biometrics*, **30**, 562 (1974).

(15) P. Altman and D. Dittmer, "Biology Data Book," 2nd ed., Vol. III, Federation of American Societies for Experimental Biology, Bethesda, Md., 1974, p. 1990.

(16) J. Carrizosa, W. Kobasa, and D. Kaye, *Antimicrob. Agents Chemother.*, **15**, 735 (1979).

(17) C. Kunin, *Clin. Pharmacol. Ther.*, **7**, 166 (1966).

(18) A. G. Gilman, L. S. Goodman, and A. Gilman, "The Pharmacological Basis of Therapeutics," 6th ed., Macmillan, New York, N.Y., 1980, p. 1136.

(19) K. Beyer, F. Woodward, L. Peters, W. Verwey, and P. Mattis, *Science*, **100**, 107 (1944).

(20) H. Eagle and E. Neuman, *J. Exp. Med.*, **25**, 903 (1947).

(21) M. Barza and L. Weinstein, *J. Infect. Dis.*, **129**, 59 (1974).

(22) J. Tan, A. Trott, J. Phair, and C. Watanakunakorn, *J. Infect. Dis.*, **126**, 492 (1972).

(23) O. Cars and S. Ogren, *J. Antimicrob. Ther.*, **6**, 408 (1980).

(24) T. Bergan and B. Oydvin, *Chemotherapy*, **20**, 263 (1974).

(25) A. Mangione, F. D. Boudinot, R. W. Schultz, and W. J. Jusko, *Antimicrob. Agents Chemother.*, **21**, 428 (1982).

(26) H. Bergholtz, R. R. Erttmann, and K. Damm, *Experentia*, **36**, 333 (1980).

(27) J. Pappenheimer, S. Heisey, and E. Jordan, *Am. J. Physiol.*, **200**, 1 (1961).

(28) K. Seamans, P. Gloor, R. Dobell, and J. Wyant, *N. Engl. J. Med.*, **278**, 861 (1968).

(29) P. New and C. Wells, *Neurology*, **15**, 1053 (1965).

(30) R. Fishman. *Arch. Neurol.*, **15**, 113 (1966).

(31) J. Kampman, F. Lindahl, J. Hansen, and K. Siersbaek-Nielsen, *Br. J. Pharmacol.*, **47**, 782 (1973).

(32) K. Stoeckel, P. J. McNamara, R. Brandt, H. Plozza-Nottebrock, and W. H. Ziegler, *Clin. Pharmacol. Ther.*, **29**, 650 (1981).

(33) W. J. Jusko, in "Applied Pharmacokinetics," W. Evans, J. J. Schentag, and W. J. Jusko, Eds., Applied Therapeutics, Inc., San Francisco, Calif., 1980, p. 639-680.

Pharmacokinetics of Nitroglycerin after Parenteral and Oral Dosing in the Rat

HO-LEUNG FUNG ˣ, H. OGATA *, A. KAMIYA ‡, and G. A. MAIER §

Received May 17, 1982, from the *Department of Pharmaceutics, School of Pharmacy, State University of New York at Buffalo, Amherst, NY 14260.* Accepted for publication June 23, 1983. Present addresses: *National Institute of Hygienic Sciences, Tokyo, Japan, ‡Kyoto University Hospital, Kyoto, Japan, and § Schering Corporation, Bloomfield, NJ 07003.

Abstract □ The pharmacokinetics of nitroglycerin was characterized in detail using venous plasma after different intravenous bolus doses (0.15-2.48 mg/kg), intra-arterial infusion (8.2 μg/min over 5 h), and oral doses (7-100 mg/kg). Venous plasma clearance was found to be ~650 mL/kg and was independent of the intravenous or intra-arterial dose. This confirmed earlier reports that the venous plasma clearance of nitroglycerin in rats exceeded the value of normal cardiac output. A terminal half-life of ~15 min was observed after high intravenous bolus doses of nitroglycerin. This slow disappearance phase was likely rate limited by redistribution of drug back into the plasma. The bioavailability of oral nitroglycerin (F) showed an apparent Michaelis-Menten dependency on dose. F was <5% at doses <20 mg/kg, but increased to a plateau of ~20% from 50-100 mg/kg. First-pass metabolism of nitroglycerin is thus apparently controlled by at least two systems (sites or enzymes). Coadministration of mannitol hexanitrate, a potential competitive inhibitor of first-pass metabolism, did not increase F.

Keyphrases □ Pharmacokinetics—nitroglycerin, parenteral and oral dosing, rats □ Nitroglycerin—pharmacokinetics, parenteral and oral dosing, rats

Interest in the clinical use of intravenous nitroglycerin has intensified in recent years because of its demonstrated efficacy in treating the resultant manifestations of myocardial infarction, congestive heart failure, and unstable angina. Several reports (1-3) have shown that intravenous infusion of nitroglycerin can appreciably decrease cardiac work load and relieve the increase in left ventricular and diastolic pressure secondary to congestive heart failure or myocardial infarction (2).

Despite the increasing popularity of the use of intravenous nitroglycerin in therapy, very little is known about the pharmacokinetic behavior of this potent drug. There are indications

0022-3549/84/0700-0873$01.00/0

© 1984, American Pharmaceutical Association

CL_{12}	Clearance from plasma to cell water = $f(T_{max},K_m)$
CL_{21}	Clearance from cell water to plasma
Amounts	
D_0	Dose
X_B^{ss}	Amount in body at steady-state
Rates	
k_0	Zero-order infusion rate
T_{max}	Maximum cellular transport rate
Ratios	
K_d	Tissue-plasma partition coefficient
K_{pi}	Individual tissue-plasma partition coefficients

REFERENCES

(1) G. Levy, in "Importance of Fundamental Principles in Drug Evaluation," D. H. Tedeschi and R. E. Tedeschi, Eds., Raven, New York, N.Y., 1968, pp. 141-171.

(2) I. M. Weiner and G. H. Mudge, *Am. J. Med.*, **36**, 743 (1964).

(3) A. Arvidson, O. Borga, and G. Alvan, *Clin. Pharmacol. Ther.*, **25**, 870 (1979).

(4) S. K. Lin, A. A. Moss, and S. Riegelman, *J. Pharm. Sci.*, **66**, 1670 (1977).

(5) A. Tsuji, E. Nakashima, I. Kagami, T. Asano, and R. Yamana, *J. Pharm. Pharmacol.*, **30**, 508 (1978).

(6) R. L. Dixson, E. S. Owens, and D. P. Rall, *J. Pharm. Sci.*, **58**, 1106 (1969).

(7) W. J. Jusko and M. Gretch, *Drug Metab. Rev.* **5**, 43 (1976).

(8) A. R. DiSanto and J. G. Wagner, *J. Pharm. Sci.*, **61**, 1040 (1972).

(9) W. J. Jusko and J. Q. Rose, in "Frontiers in Therapeutic Drug Monitoring," G. Togoni, R. Latini, and W. J. Jusko, Eds., Raven, New York, N.Y., 1980, pp. 153-161.

(10) N. A. Lassen and W. Perl, "Tracer Kinetic Methods in Medical Physiology," Raven, New York, N.Y., 1979.

(11) L. Z. Benet and R. L. Galeazzi, *J. Pharm. Sci.*, **68**, 1071 (1979).

(12) F. W. Kavanaugh, *Pharm. Technol.*, **63**, 1459 (1974).

(13) J. J. Schentag, W. J. Jusko, J. W. Vance, E. Abrutyn, M. DeLattre, and M. Gerbracht, *J. Pharmacokinet. Biopharm.*, **5**, 559 (1977).

(14) C. M. Metzler, G. L. Elfring, and A. J. McEwen, *Biometrics*, **30**, 562 (1974).

(15) P. Altman and D. Dittmer, "Biology Data Book," 2nd ed., Vol. III, Federation of American Societies for Experimental Biology, Bethesda, Md., 1974, p. 1990.

(16) J. Carrizosa, W. Kobasa, and D. Kaye, *Antimicrob. Agents Chemother.*, **15**, 735 (1979).

(17) C. Kunin, *Clin. Pharmacol. Ther.*, **7**, 166 (1966).

(18) A. G. Gilman, L. S. Goodman, and A. Gilman, "The Pharmacological Basis of Therapeutics," 6th ed., Macmillan, New York, N.Y., 1980, p. 1136.

(19) K. Beyer, F. Woodward, L. Peters, W. Verwey, and P. Mattis, *Science*, **100**, 107 (1944).

(20) H. Eagle and E. Neuman, *J. Exp. Med.*, **25**, 903 (1947).

(21) M. Barza and L. Weinstein, *J. Infect. Dis.*, **129**, 59 (1974).

(22) J. Tan, A. Trott, J. Phair, and C. Watanakunakorn, *J. Infect. Dis.*, **126**, 492 (1972).

(23) O. Cars and S. Ogren, *J. Antimicrob. Ther.*, **6**, 408 (1980).

(24) T. Bergan and B. Oydvin, *Chemotherapy*, **20**, 263 (1974).

(25) A. Mangione, F. D. Boudinot, R. W. Schultz, and W. J. Jusko, *Antimicrob. Agents Chemother.*, **21**, 428 (1982).

(26) H. Bergholtz, R. R. Erttmann, and K. Damm, *Experentia*, **36**, 333 (1980).

(27) J. Pappenheimer, S. Heisey, and E. Jordan, *Am. J. Physiol.*, **200**, 1 (1961).

(28) K. Seamans, P. Gloor, R. Dobell, and J. Wyant, *N. Engl. J. Med.*, **278**, 861 (1968).

(29) P. New and C. Wells, *Neurology*, **15**, 1053 (1965).

(30) R. Fishman. *Arch. Neurol.*, **15**, 113 (1966).

(31) J. Kampman, F. Lindahl, J. Hansen, and K. Siersbaek-Nielsen, *Br. J. Pharmacol.*, **47**, 782 (1973).

(32) K. Stoeckel, P. J. McNamara, R. Brandt, H. Plozza-Nottebrock, and W. H. Ziegler, *Clin. Pharmacol. Ther.*, **29**, 650 (1981).

(33) W. J. Jusko, in "Applied Pharmacokinetics," W. Evans, J. J. Schentag, and W. J. Jusko, Eds., Applied Therapeutics, Inc., San Francisco, Calif., 1980, p. 639-680.

Pharmacokinetics of Nitroglycerin after Parenteral and Oral Dosing in the Rat

HO-LEUNG FUNG ˣ, H. OGATA *, A. KAMIYA ‡, and G. A. MAIER §

Received May 17, 1982, from the *Department of Pharmaceutics, School of Pharmacy, State University of New York at Buffalo, Amherst, NY 14260.* Accepted for publication June 23, 1983. Present addresses: *National Institute of Hygienic Sciences, Tokyo, Japan, ‡Kyoto University Hospital, Kyoto, Japan, and § Schering Corporation, Bloomfield, NJ 07003.

Abstract □ The pharmacokinetics of nitroglycerin was characterized in detail using venous plasma after different intravenous bolus doses (0.15-2.48 mg/kg), intra-arterial infusion (8.2 μg/min over 5 h), and oral doses (7-100 mg/kg). Venous plasma clearance was found to be ~650 mL/kg and was independent of the intravenous or intra-arterial dose. This confirmed earlier reports that the venous plasma clearance of nitroglycerin in rats exceeded the value of normal cardiac output. A terminal half-life of ~15 min was observed after high intravenous bolus doses of nitroglycerin. This slow disappearance phase was likely rate limited by redistribution of drug back into the plasma. The bioavailability of oral nitroglycerin (F) showed an apparent Michaelis-Menten dependency on dose. F was <5% at doses <20 mg/kg, but increased to a plateau of ~20% from 50-100 mg/kg. First-pass metabolism of nitroglycerin is thus apparently controlled by at least two systems (sites or enzymes). Coadministration of mannitol hexanitrate, a potential competitive inhibitor of first-pass metabolism, did not increase F.

Keyphrases □ Pharmacokinetics—nitroglycerin, parenteral and oral dosing, rats □ Nitroglycerin—pharmacokinetics, parenteral and oral dosing, rats

Interest in the clinical use of intravenous nitroglycerin has intensified in recent years because of its demonstrated efficacy in treating the resultant manifestations of myocardial infarction, congestive heart failure, and unstable angina. Several reports (1-3) have shown that intravenous infusion of nitroglycerin can appreciably decrease cardiac work load and relieve the increase in left ventricular and diastolic pressure secondary to congestive heart failure or myocardial infarction (2).

Despite the increasing popularity of the use of intravenous nitroglycerin in therapy, very little is known about the pharmacokinetic behavior of this potent drug. There are indications

0022-3549/84/0700-0873$01.00/0

© 1984, American Pharmaceutical Association

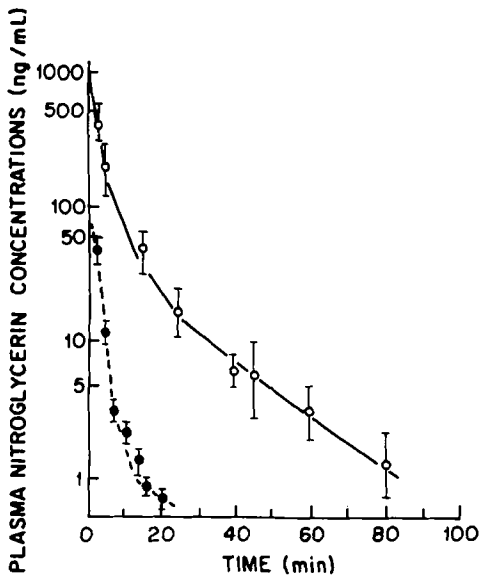

Figure 1—*Mean ± SE (bars) of plasma nitroglycerin concentrations after intravenous bolus doses of 0.15 mg/kg (●, n = 4) and 2.48 mg/kg (○, n = 6). The lines are drawn based on the pharmacokinetic parameters shown in Table I for each of the doses.*

(4–6) that circulatory changes in heart rate and blood pressure in humans may parallel those in nitroglycerin plasma concentrations. Several reports have also suggested the observed systemic clearance in humans (7–9) and in rats (10) to be greater than the normal cardiac output in the respective species. However, the underlying mechanism for this observation is still unclear, and many of the basic aspects of nitroglycerin kinetics remain unknown.

Another important issue in nitroglycerin therapy relates to the efficacy of this drug when given orally. Numerous metabolic and pharmacological studies show that nitroglycerin undergoes nearly complete first-pass metabolism when the drug is administered at <3 mg/kg in several animal species (11–14). It was argued (14) that similar first-pass metabolism of oral nitroglycerin also exists in humans, and that oral use of this drug and other organic nitrates in therapy is irrational and ineffective. This viewpoint was strongly contested and refuted by Krantz and Leake (15) based on clinical experience. Convincing clinical data have appeared (16) that also affirm the prophylactic effectiveness of oral nitroglycerin against angina attacks.

There is no literature report on the effect of an oral dose on the extent of first-pass inactivation of nitroglycerin in humans or animals. If the extent of inactivation is capacity limited, oral bioavailability of nitroglycerin may be dose dependent and, thus, extrapolation of absorption data from trace or low doses to infer lack of bioavailability at other doses may be incorrect.

In this report, we describe the effect of intravenous dose on nitroglycerin disposition kinetics and the effect of oral dose on the bioavailability of nitroglycerin in the rat. Since the aqueous solubility of nitroglycerin is limited to ~1 mg/mL (17) and doses of nitroglycerin in this study necessitated the use of an organic solvent mixture of 10% ethanol in propylene glycol, a comparison of the bioavailability of nitroglycerin from this organic vehicle and water was carried out. Finally, the possible interference of nitroglycerin bioavailability by coadministration of another organic nitrate, *viz.*, mannitol hexanitrate, was explored.

EXPERIMENTAL SECTION

Materials—All reagents were of analytical grade unless otherwise stated.

Preparation of Stock Nitroglycerin Solutions—Nitroglycerin was isolated from the lactose adsorbate[1]. The powder was dissolved in distilled water and nitroglycerin was extracted with ether in a separatory funnel. The ether was separated and evaporated under a gentle stream of dry nitrogen. Nitroglycerin was recovered as a liquid and a weighed amount was dissolved in the appropriate solvent. The precise concentration of the stock solution was determined either by the USP assay (18) or the kinetic method developed by Fung *et al.* (19).

Intravenous Bolus Dosing—Male Sprague-Dawley rats, 250–360 g, underwent right jugular vein cannulation according to the procedure developed by Weeks and Davis (20). The animals were fasted overnight and administered an intravenous bolus dose into the jugular vein cannula, followed by flushing with saline and then with circulating blood. Blood samples were collected into heparinized tubes *via* the jugular vein cannula. The dosing volume was 0.5–0.75 mL in aqueous vehicle after appropriate dilution of the stock solution; the doses administered were 0.15, 0.35, 1.75, and 2.48 mg/kg of nitroglycerin with 4, 7, 5, and 6 animals in each group, respectively. A bolus intravenous dose of 3.5 mg/kg was also attempted but was found to cause severe convulsions in the animals. Pharmacokinetic information was not obtained from this group of animals.

Intra-Arterial Infusion—Four male Sprague-Dawley rats, 250–300 g, had jugular vein and carotid artery cannulas surgically implanted. One day after surgery, nitroglycerin was infused into the carotid artery, and blood samples were withdrawn *via* the jugular vein cannula at appropriate intervals. The infusion time was 5 h and the infusion rate was 6.8 μL/min *via* an infusion pump. The infusion solution concentration was 1.2 mg/mL, and the dosing rate was 8.2 μg/min in each animal.

Crossover Study of Oral Dosing—Six male Sprague-Dawley rats, weighing ~300 g, underwent jugular vein cannulation and were given an oral dose of either 20 or 100 mg/kg of nitroglycerin in a randomized crossover fashion. The vehicle was 10% alcohol in propylene glycol. All animals were fasted overnight, and the drug was given *via* gastric intubation under light ether anesthesia. The interval between doses was 3 d. Blood was harvested from the jugular vein cannula. The separated plasma was assayed for nitroglycerin as described later.

Bioavailability of Nitroglycerin at Five Different Oral Doses—Different male Sprague-Dawley rats were each given an oral dose of nitroglycerin in 10% alcohol in propylene glycol. Each dose, 7, 20, 50, 75, and 100 mg/kg, was adminstered by oral intubation under light ether anesthesia. The oral dose of vehicle was normalized to body weight so that each animal received the same volume on a mL/kg basis (~1 mL per animal). Blood (~0.3 mL) was collected from the tail vein at appropriate intervals, and the plasma was separated immediately for determination of nitroglycerin concentrations. All animals were fasted overnight with free access to water prior to drug administration.

Organic Nitrate Interaction Study—Since mannitol hexanitrate has been shown (12) to be a better *in vitro* substrate for organic nitrate reductase (the enzyme responsible for nitroglycerin metabolism), the possibility of enhancement in nitroglycerin bioavailability with the coadministration of mannitol hexanitrate was tested. Seven rats received an oral dose of nitroglycerin or a combination dose of mannitol hexanitrate and nitroglycerin, in a randomized crossover fashion. Essentially the same procedure was used as in the oral dosing experiments described previously. The molar ratio of mannitol hexanitrate to nitroglycerin was ~1.6. Preliminary studies showed that mannitol hexanitrate did not interfere with the assay: mannitol hexanitrate did not alter the plasma recovery of nitroglycerin; after an intravenous dose of mannitol hexanitrate at 60 μg/kg, no noticeable peaks were observed in the chromatogram which would interfere with the determination of nitroglycerin.

Nitroglycerin Assay—Blood samples were centrifuged immediately, and 0.1–0.2 mL of plasma was removed. A 10–20-μL aliquot of silver nitrate was added to each plasma sample to prevent degradation of the drug. Plasma samples were stored overnight at −20°C and nitroglycerin levels were determined according to the GC assay developed by Yap *et al.* (21). Isosorbide dinitrate was added as the internal standard. In this study, the average recovery of nitroglycerin from plasma was ~92% with a coefficient of variation of 10%.

Pharmacokinetic Calculations—*Parenteral Doses (Model-Independent Parameters)*—The plasma concentration *versus* time profiles after various bolus intravenous doses exhibited biexponential characteristics. The composite data were therefore fitted (NONLIN[2]) to the biexponential equation C_t =

[1] Nitroglycerin 10% (w/w) in lactose; ICI Americas, Atlas Chemical Div., Wilmington, Del.

[2] See, *e.g.*, C. M. Metzler, G. L. Elfring, and A. J. McEwen, *Users Manual for NONLIN and Associated Programs*, 1974. The Upjohn Co., Kalamazoo, Mich.

Table I—Mean Estimated Values of Model-Independent Pharmacokinetic Parameters of Nitroglycerin at Various Intravenous Bolus Doses [a]

Parameter [b]	Dose, mg/kg			
	0.15	0.35	1.75	2.48
A_1 (ng/mL)	69.8(4.9)	160(9)	506(54)	809(49)
λ_1 (min^{-1})	0.41(0.01)	0.35(0.01)	0.24(0.02)	0.27(0.02)
A_2 (ng/mL)	1.7(0.2)	3.0(0.3)	33.1(3.9)	43.6(8.0)
λ_2 (min^{-1})	0.045[c]	0.045[c]	0.036(0.002)	0.044(0.0004)
Venous plasma clearance (mL/min/kg)	669(46)	642(40)	528(60)	654(49)
Vd_{ss} (L/kg)	3.9(0.3)	4.4(0.3)	6.1(0.6)	6.2(0.5)

[a] Expressed as mean (*SE*). [b] Typical parameters used to describe a biexponential equation, $C_t = A_1e^{-\lambda_1 t} + A_2e^{-\lambda_2 t}$. [c] Set as corresponding value obtained from curve-fitting of normalized, composite data of the two high doses.

$A_1e^{-\lambda_1 t} + A_2e^{-\lambda_2 t}$, where C_t is the plasma concentration of nitroglycerin at time t and A_1, A_2, λ_1 and λ_2 are the pharmacokinetic constants used to describe a biexponential decay curve. Initial estimates for the NONLIN computer program were either obtained graphically (method of residuals) or from CSTRIP[3]. Various weighting factors (1, $C_t^{-1/2}$, C_t^{-1}, and C_t^{-2}) were used to obtain the best fit, as determined by the residual sum of squares, parameter standard deviations, and r^2 values.

The apparent systemic plasma clearance was calculated by dividing the intravenous dose by the area under the plasma concentration *versus* time curve (AUC) from time zero to infinity. The individual concentration at time zero (C_0) for each animal in the low-dose group was estimated by extrapolation of the linearly regressed line composed of the first three plasma concentration *versus* time points. For the two high-dose groups C_0 was obtained either by linear extrapolation, as described, or from computer estimates, whichever was considered more accurate. The AUC from time zero to the last concentration-time point was calculated by the Spline Method[4]. The residual AUC was calculated from C^*/λ_2 where C^* is the last concentration-time point determined experimentally. For the two small doses, where the λ_2 phase could not be characterized fully because of assay limitations, the residual AUC was calculated using the mean λ_2 obtained from the higher doses. The volume of distribution at steady state was obtained by a model-independent approach which relied on AUC calculations (22). Thus:

$$Vd_{ss} = \frac{\text{Dose}_{iv} \cdot \text{AUMC}}{\text{AUC}^2} \qquad \text{(Eq. 1)}$$

where AUMC is the area under the moment curve, obtained *via* Eq. 2:

$$\text{AUMC} = \int_0^{t^*} tC_t dt + t^*C^*/\lambda_2 + C^*/\lambda_2^2 \qquad \text{(Eq. 2)}$$

where t^* is the time at which the last data point was collected. All other terms were defined previously.

Oral Doses—AUC from time zero to t^*, $AUC_{0\text{-}t^*}$, was estimated by the Spline Method[4]. The residual area from time t^* to ∞ was calculated by C^*/λ_t where λ_t was the terminal rate constant. In several cases, only two or three data points could be identified in the terminal phase. Nevertheless, the residual portion of the curve accounted for ≤10% of the total area and would not be expected to bias the overall analysis seriously.

The apparent bioavailability (F), defined as the fraction of the dose reaching the systemic circulation intact, was calculated from $CL \times AUC_{0\text{-}\infty}/\text{dose}$, where CL is the plasma clearance observed after intravenous dosing, set here at a value of 650 mL/min/kg. The paired t test was used to determine statistical differences in the two crossover studies, and the Kruskal-Wallis test was used in the study in which the effect of dose was examined in separate animals.

RESULTS AND DISCUSSION

Parenteral Dosing—Figure 1 shows the plasma nitroglycerin concentrations obtained after the highest and lowest intravenous bolus doses (*i.e.*, 2.48 and 0.15 mg/kg, respectively). Because of the relatively small plasma sample size that could be obtained from the rat (0.1-0.2 mL), the detection limit of nitroglycerin was ~0.5-1 ng/mL of plasma in these studies. Consequently, with the two lower doses, measurable concentrations were only recorded up to 20 min after injection. At the two higher doses, sample collection (and detectable concentrations) could be extended to 90 min after dosing. In fitting these data with the NONLIN program, a weighting factor of C_t^{-2} was found to produce the best fit in the groups given the two high doses. This weighting factor was then used in all other curve fittings.

Table I shows the pharmacokinetic parameters obtained from these fittings. The fit of data from all four doses appeared quite reasonable, since, for each dose, the AUC_∞ calculated directly from the experimental data agreed well with that estimated from the curve fit. A striking feature observed from Table I is that the apparent plasma clearance is independent of dose and is on the order of 500-700 mL/min/kg, well in excess of the normal cardiac output of ~300 mL/min/kg in this species (23). This large plasma clearance, which is now documented for several doses and from more detailed sampling, is consistent with the preliminary observation in the rat reported by Yap and Fung (10) and also with all the available human data (7-9, 24). The apparent volume of distribution at steady state, Vd_{ss}, was 4-6 L/kg. This large volume is consistent with the moderate binding (~60%) of nitroglycerin to rat plasma protein (25), and the location of rather high radioactivity in the carcass and other soft tissues after oral administration of [^{14}C]nitroglycerin (26).

After intravenous doses of 1.75 and 2.48 mg/kg, nitroglycerin disappearance from plasma was clearly biphasic. At lower doses, this biexponential decay was less evident because assay limitations did not permit characterization of the second disappearance phase. The λ_1 half-life observed here, at 2-3 min, is consistent with values reported previously in rats (10) and in humans (7-9). The second disappearance phase, with a half-life of 15-20 min, has not been reported previously in the literature.

Recent experiments by Kamiya *et al.*[5] showed that when nitroglycerin was incubated in whole blood, the *in vitro* degradation half-life was ~11 min. This half-life could be assumed to represent the slowest possible elimination half-life of nitroglycerin in the systemic circulation. Interestingly, however, this half-life is somewhat shorter than the observed *in vivo* plasma λ_2 half-life of 15-20 min. This would seem to indicate that tissue redistribution rather than elimination is an important factor in describing the second disappearance phase.

Although there was no apparent dose dependency in the venous plasma clearance of nitroglycerin, examination of the data presented in Table I suggested that there are possibly minor differences in the λ_1 and Vd_{ss} terms between the two lower doses (0.15 and 0.35 mg/kg) and the two higher ones (1.75 and 2.48 mg/kg). There are some theoretical reasons to anticipate possible dose dependency in nitroglycerin disposition kinetics. The venous plasma clearance is so large that flow limitation may be expected to play an important role. The higher bolus doses administered were close enough to an observed toxic dose of 3.5 mg/kg that dose-dependent changes in blood perfusion to various tissues are likely. Recently, Wu *et al.* (27) suggested that the rate constant for the loss of nitroglycerin from human blood decreases as the initial concentration of nitroglycerin increases. The implication of this finding to the present situation is unclear.

A possible contribution to the large plasma clearance observed for nitroglycerin is the existence of pharmacokinetic phases that were undetected because of the methodological difficulties involved. Johnson *et al.* (28) and recently Stein *et al.* (29) suggested the presence of a rapid disappearance phase of nitroglycerin in blood that exhibited a half-life of ~15 s. In both of these studies, however, the drug ([^{14}C]nitroglycerin) was introduced into the jugular

Table II—Normalized AUC of Nitroglycerin in Rats Given Both 20-mg/kg and 100-mg/kg Oral Doses

Animal	AUC/Dose × 10^4 min·kg·mL^{-1}	
	20 mg/kg	100 mg/kg
1	1.11[a]	3.35
2	1.16	2.10[a]
3	1.53	2.07[a]
4	1.76[a]	2.09
5	1.76[a]	2.77
6	0.91	3.37[a]
Mean	1.37	2.63[b]
SE	0.15	0.26

[a] Animal given this dose first. [b] $p < 0.01$ compared with AUC/Dose at 20 mg/kg.

[3] "CSTRIP—A Fortran IV computer program for obtaining initial polyexponential parameter estimates," J. G. Wagner, College of Pharmacy, University of Michigan, Ann Arbor, Mich.

[4] Desktop computer, general utility program tape #9825; Hewlett-Packard, Fort Collins, Colo.

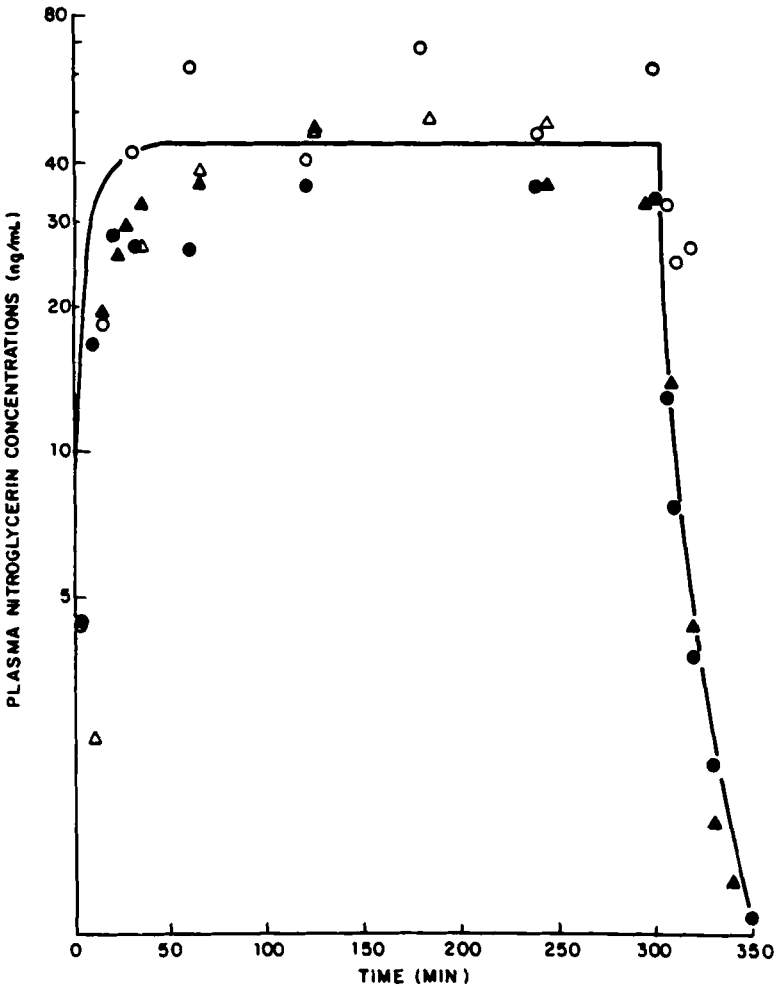

Figure 2—*Venous plasma nitroglycerin concentrations obtained after intra-arterial infusion at 8.2 μg/min. Symbols represent different animals (250–300 g). The line was drawn using the pharmacokinetic parameters generated compositely from the two high intravenous bolus doses.*

vein and blood was collected from the carotid artery. Thus, the early blood samples might have been collected before the dose was distributed throughout the systemic circulation, and the existence of a true pharmacokinetic phase with such a short half-life is uncertain. On the other hand, if such a fast "distributional" phase does exist and the sampling protocol adopted here was incapable of detecting it, an erroneously large plasma clearance could have resulted because a significant portion of the AUC was not included in the calculation. This problem also can exist if a slow terminal-phase λ_3 is present, but it, too, could not be detected because of assay limitations.

Figure 2 shows the venous plasma concentrations of nitroglycerin in four rats infused intra-arterially for 5 h at 28.5 μg/min/kg. Since the drug was infused *via* the carotid artery and blood was collected from the jugular vein [reverse of Johnson *et al.* (28) and Stein *et al.* (29)], drug mixing in the systemic circulation was unlikely to be a complicating factor. Under these conditions an apparent steady-state in nitroglycerin concentration was observed. The plasma concentrations observed from this infusion were generally consistent with those predicted using the pharmacokinetic parameters generated from the composite data of the two high-dose groups (Table I). It would thus appear unlikely that a rapid disappearance phase had been missed in the bolus injection study. The data also suggested that if a hidden λ_3 phase existed, its half-life would be considerably longer than 1–2 h, since infusion for 5 h failed to detect its presence. Since the pharmacokinetic parameters obtained are similar after bolus injection and after slow infusion, it would appear that the errors incurred in assuming instantaneous input after bolus injection (30, 31) are not large for nitroglycerin.

Table III—Effect of Solvent on the Area Under the Plasma Nitroglycerin Concentration *versus* Time Curve after a 7-mg/kg Oral Dose

Animal	$AUC_{0-\infty} \times 10^{-2}$, ng·min·mL^{-1}		AUC Ratio (Alcohol Co-solvent/Water)
	Water	Alcohol Cosolvent[a]	
7	5.2[b]	7.8	1.5
8	6.4	7.2[b]	1.1
9	3.2	3.7[b]	1.1
10	1.5[b]	2.8	1.9
11	2.0[b]	2.2	1.1
12	1.3	2.2[b]	1.8
Mean	3.3	4.3[c]	1.4
SE	0.9	1.0	0.2

[a] 10% Ethanol in propylene glycol. [b] Animal given this vehicle first. [c] $p < 0.05$ compared with animals dosed with aqueous vehicle.

Another consideration in the interpretation of the observed plasma clearance is how it may be related to the blood degradation clearance of nitroglycerin. Our group, in a separate study[5], has examined the *in vitro* partitioning of nitroglycerin between red blood cells and plasma and the rate of *in vitro* degradation of nitroglycerin in these components of rat blood. It was found that the partitioning of nitroglycerin into red blood cells was nearly instantaneous; the ratio of nitroglycerin concentration in red blood cells *versus* that in plasma was a constant, $\simeq 2.6$, over an incubation period of 30 s to 30 min at 37°C. The rate of degradation of nitroglycerin in red blood cells was approximately the same as that found in plasma. If a hematocrit value of 0.45 for the rat (23) is used, blood nitroglycerin concentrations could be estimated to be 1.72 times the corresponding plasma concentrations. Thus, *in vivo* venous blood nitroglycerin clearance could be estimated by dividing the venous plasma clearance by 1.72; *i.e.*, $650/1.72 \simeq 378$ mL/min/kg. This value is near that of cardiac output.

The extent of contribution of blood degradation *per se* to the total *in vivo* venous blood clearance of nitroglycerin could also be estimated. Assuming a blood volume of 65 mL/kg in the rat and a degradation half-life of 11 min, the clearance due to blood degradation is $65 \times 0.693/11 \simeq 4.1$ mL/min/kg, which accounts for <1% of the total *in vivo* venous blood clearance.

A further complication in interpreting nitroglycerin pharmacokinetics is the existence of concentration differences in the systemic circulation depending on the sampling site. Thus, Hill *et al.* (32) showed that after intranasal administration of nitroglycerin in humans, the apparent clearance was about twice as large in peripheral venous blood (~37 L/min) than in the arterial circulation (~19 L/min). Armstrong *et al.* (24) recently showed that arterial plasma clearance of nitroglycerin in 20 patients with heart failure was ~12

[5] A. Kamiya, T. Schmitt, and H.-L. Fung, unpublished results.

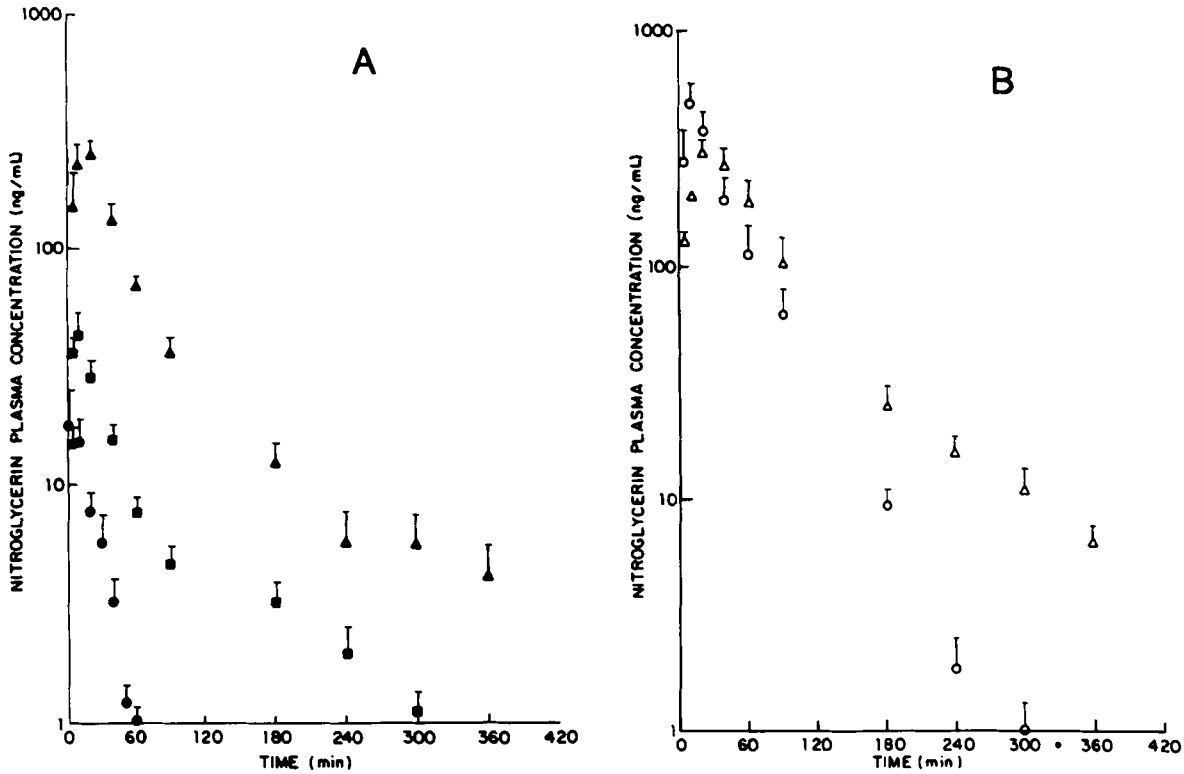

Figure 3 *Plasma nitroglycerin concentrations (mean ± SE) at various times after oral dosing at 7 (●), 20 (■), 50 (▲), 75 (○), and 100 (△) mg/kg.*

L/min compared with a venous clearance of 39 L/min. These authors calculated an extraction ratio of 61% for nitroglycerin across the arterial-venous bed. The existence of arterial-venous differences in blood concentrations have been shown for several drugs by Chiou and co-workers (31, 33). In these examples, however, the arterial drug clearance was always found to be similar to its venous clearance, suggesting that distributional factors were primarily responsible for the observed arterial-venous difference in concentration. In contrast, metabolic factors may be involved in the case for nitroglycerin, because an arterial-venous difference in systemic clearance has been demonstrated and *in vitro* metabolic activity toward nitroglycerin by isolated blood vessels has also been shown (34).

Oral Dosing—Table II shows the results of the randomized crossover study in which six rats were given both 20 and 100-mg/kg oral doses. The normalized AUC was statistically different between the two doses, at $p < 0.01$, using the paired t test. Since the apparent venous plasma clearance of nitroglycerin was not concentration dependent, the increase in normalized AUC after the 100-mg/kg dose is probably due to an increase in bioavailability at this dose. Using an average value of 650 mL/min/kg for the apparent plasma clearance of nitroglycerin, the mean apparent bioavailability at 20 and 100 mg/kg could be estimated as 10.3 and 19.4%, respectively.

These apparent bioavailability values were considerably higher than those suggested by Needleman *et al.* (14) and by Yap and Fung (10) at lower doses. The former group of authors estimated the bioavailability of nitroglycerin to be ≃2% at a dose of 0.5 mg/kg while the latter workers, in a preliminary study, reported a bioavailability estimate of ~2% after an oral dose of nitroglycerin at 7 mg/kg. It must be pointed out that in the second study (10), an aqueous vehicle was used, while in the present work a vehicle containing 10% ethanol in propylene glycol was administered. The possible effect of solvent was examined in a randomized crossover study in which six rats were dosed alternately with nitroglycerin dissolved in water or in 10% ethanol in propylene glycol. The AUC data can be found in Table III. It is apparent that there is a substantial degree of variability in each of the treatment groups, but this observation was quite typical of other kinetic studies of this high-clearance drug (7-10). Nevertheless, there is a modest, but significant ($p < 0.05$), increase in AUC when nitroglycerin administration was changed from the aqueous to the alcoholic vehicle (Table III). It is not known, at present, how much of this increase was influenced by the effect of the vehicle on the systemic clearance and how much was due to a change in presystemic metabolism. Oguma and Levy showed recently that ethanol infusion into the portal vein, from −3 to +3 h of propoxyphene dosing, increased both the systemic clearance and the systemic availability of this analgesic (35). Since the alcohol mixture was administered with the drug, it might be speculated that the apparent plasma clearance of nitroglycerin, which is well in excess of liver blood flow (23), might not be greatly affected by the organic solvents. Regardless of the mechanism involved, the effect of solvent on the apparent systemic availability of nitroglycerin at 7 mg/kg appeared to be relatively small.

An expanded study was carried out to examine, in further detail, the relationship between oral nitroglycerin dosage and bioavailability. Since five to six different doses were involved, a crossover design was not practical and, therefore, was not attempted.

Figure 3A and B shows the mean plasma concentrations of nitroglycerin obtained in different rats after oral doses of 7, 20, 50, 75, and 100 mg/kg administered in the alcohol solvent mixture. Peak plasma drug concentrations were observed generally between 2-20 min after dosing for all doses; however, the values of peak concentrations were not proportional to dose. The profiles of these curves were generally biphasic, except in the case of the lowest dose, 7 mg/kg, where characterization of plasma nitroglycerin concentrations beyond 60 min was impossible due to assay limitations. The apparent terminal half-life observed after oral dosing at 20, 50, and 100 mg/kg ranged from 60-140 min, considerably longer than the λ_2 half-life of 15-18 min observed after intravenous administration. The data suggested, therefore, that absorption "flip-flop" kinetics (36) is operative here and that the apparent terminal half-life observed reflected more of absorption than of elimination. After a dose of 75 mg/kg, the apparent terminal half-life was shorter ($t_{1/2}$ at ~30 min) than those observed for doses >20 mg/kg. Interestingly, after this dose, peak concentration was higher and the time to peak was shorter than found with the highest dose, 100 mg/kg. These observations suggest that the absorption rate might be faster at 75 mg/kg than at other doses; however, the reasons for these observations are unknown at present.

The relationship between dose and dose-normalized AUC is shown in Table

Table IV—Effect of Dose on the Normalized AUC and Apparent Bioavailability (F)

Dose	n	AUC/Dose × 10^4	F, %[e,f]
3.5[a]	5	0.25 ± 0.05[d]	1.6 ± 0.3
7[a]	6	0.47 ± 0.12	3.2 ± 0.8
7[b]	11	0.64 ± 0.05	4.2 ± 0.3
14[b,c]	7	0.51 ± 0.19	3.3 ± 1.2
20[b]	13	1.59 ± 0.20	10.3 ± 1.3
50[b]	9	3.05 ± 0.50	19.8 ± 3.2
75[b]	4	2.86 ± 0.07	18.6 ± 0.4
100[b]	22	2.98 ± 0.45	19.4 ± 2.9

[a] Aqueous vehicle. [b] Vehicle of 10% ethanol in propylene glycol. [c] From interaction study with mannitol hexanitrate. [d] Mean ± SE, unit of min·kg·mL^{-1}. [e] Mean ± SE; $F = (AUC_{0-\infty}/Dose) \times CL$; CL = 650 mL · min^{-1} · kg^{-1}. [f] F is found to be dose dependent (Kruskal-Wallis test, $p < 0.001$).

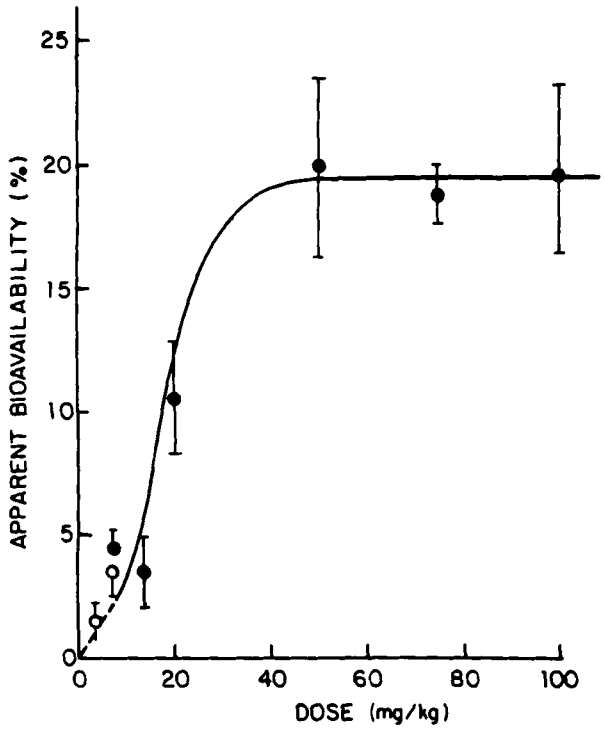

Figure 4—*Apparent oral bioavailability of nitroglycerin (mean ± SE) as a function of dose. The drug was administered either in water (○) or alcohol cosolvent (●).*

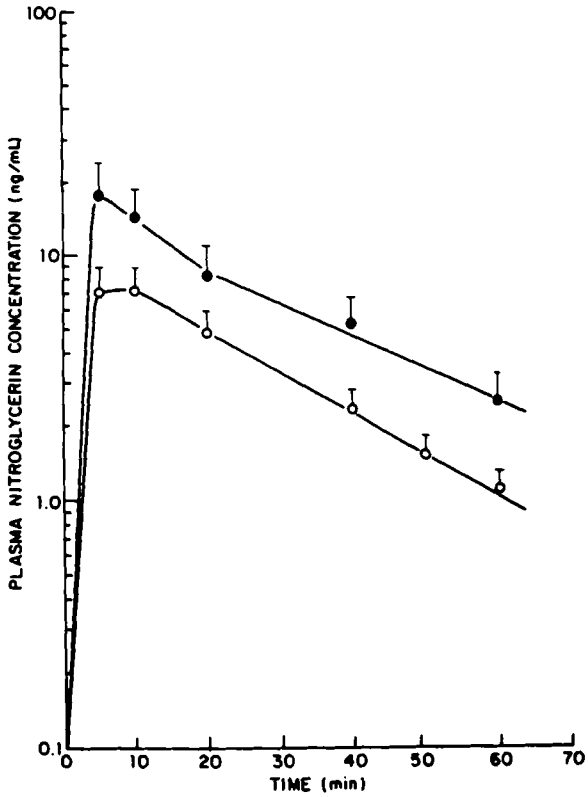

Figure 5— *Plasma nitroglycerin concentrations (mean ± SE) after a 14-mg/kg oral dose of nitroglycerin by itself (●) or in combination with 47 mg/kg of mannitol hexanitrate (○).*

IV. Similar data obtained with the aqueous vehicle at 3.5 mg/kg (37) and 7 mg/kg (10) are included for comparison. It is evident that, as the dose increased, the normalized AUC increased and then plateaued. If the systemic clearance obtained after intravenous administration of nitroglycerin in aqueous solution is assumed to be applicable under these experimental conditions, then the apparent bioavailability obtained after these oral doses may be estimated (Table IV). Thus, the apparent bioavailability appeared to increase with dose between 0–50 mg/kg. Between doses of 50–100 mg/kg, however, the apparent bioavailability remained constant at ~19%.

The interesting relationship between oral dose and apparent bioavailability, as observed here, supports the following conclusions. First, consistent with previous reports (14, 17, 21, 38), the oral bioavailability of nitroglycerin in the rat is indeed very small (< 3%) at doses <5 mg/kg. This poor bioavailability is probably a result of extensive first-pass metabolism (10, 14) rather than of lack of absorption *per se*, since radioactivity studies (39) showed absorption of the dose to be essentially complete. Second, the oral bioavailability of nitroglycerin is a rather complex function of dose. A possible model consistent with the data is that nitroglycerin is metabolized during absorption by at least two enzyme systems (or sites) which have different affinities and/or capacities for the drug substrate. This model is consistent with the observation by Jacoby (40) who suggested that organic nitrate reductase may, in fact, be one of several activities inherent to the glutathione-*S*-transferase system, which may consist of several "enzyme units." One could speculate that these different "enzyme units" may possess different substrate affinities and maximal velocities. Third, the bioavailability of oral nitroglycerin is highly variable at any dose. We have examined the source of this inter-animal variability and have shown (41) that it was due, in part, to the variability of the intrinsic hepatic organic nitrate reductase activity in individual rats. In view of the observed dose-dependent increase in bioavailability and the high inter-animal variability, some animals could have substantial or near complete bioavailability when given high doses of oral nitroglycerin. Thus, the general statement that nitroglycerin is poorly bioavailable has to be qualified by consideration of the dose administered and the individual animal being examined.

The dependency of F on dose (and thus also on hepatic drug concentration) points out a possibly important consideration in designing oral controlled-release dosage forms of nitroglycerin. If a similar relationship exists in humans, the dependency of F on drug release rate will have the same temporal pattern as is shown for dose (Fig. 4).

Figure 5 shows the plasma concentration of nitroglycerin after coadministration with mannitol hexanitrate. Surprisingly, the mean plasma concentration profile and AUC were actually smaller in the presence of the hexanitrate. However, despite a threefold difference in the mean AUC, statistical significance was not achieved due to the large coefficients of variation (100 and 50%, respectively, for nitroglycerin alone and combined administration). The effect of mannitol hexanitrate (if any) on bioavailability was extremely variable. For example, one rat exhibited almost a 10-fold decrease in AUC, whereas another showed a 1.6-fold increase in AUC in the presence of mannitol hexanitrate. In any event, mannitol hexanitrate did not apparently improve the bioavailability of nitroglycerin under the conditions tested.

There are several possible explanations for the apparent lack of effect. One possibility may be that an insufficient amount of mannitol hexanitrate was absorbed due to its poor aqueous solubility. Consequently, the organ concentration of mannitol hexanitrate would be too small to exert an inhibitory effect on nitroglycerin metabolism by organic nitrate reductase. Second, because of permeability and flow considerations, the relative affinity of mannitol hexanitrate *versus* nitroglycerin for the enzyme site *in vivo* may not be as favorable as *in vitro* determinations have suggested. Third, it is possible that mannitol hexanitrate coadministration may have altered the systemic clearance of nitroglycerin. Because of the very poor aqueous solubility of mannitol hexanitrate, a rigorous experiment involving intravenous administration of mannitol hexanitrate at the same dose was not carried out. Whatever the mechanism(s), however, oral coadministration of mannitol hexanitrate with nitroglycerin, under the conditions described, did not lead to any apparent increase in nitroglycerin bioavailability.

REFERENCES

(1) W. Ganz and H. S. Marcus, *Circulation*, **46**, 88 (1972).

(2) S. E. Epstein, R. E. Goldstein, D. R. Redwood, K. M. Kent, and E. R. Smith, *Ann. Intern. Med.*, **78**, 918 (1973).

(3) N. S. Hill, E. M. Antman, L. H. Green, and J. S. Alpert, *Chest*, **79**, 69 (1981).

(4) P. R. Imhof, O. P. Frankhauser, L.-C. Chu, and J. Hodler, *Eur. J. Clin. Pharmacol.*, **18**, 455 (1980).

(5) H. P. Blumenthal, H.-L. Fung, E. F. McNiff, and S. K. Yap, *Br. J. Clin. Pharmacol.*, **4**, 241 (1977).

(6) V. M. S. Oh and P. R. Reid, *Pharmacologist*, **21**, 308 (1979).

(7) J. T. Wei and P. R. Reid, *Circulation*, **59**, 588 (1979).

(8) P. W. Armstrong, J. A. Armstrong, and G. S. Marks, *Circulation*, **62**, 160 (1980).

(9) E. F. McNiff, A. Yacobi, F. M. Young-Chang, L. H. Golden, A. Goldfarb, and H.-L. Fung, *J. Pharm. Sci.*, **70**, 1054 (1981).

(10) P. S. K. Yap and H.-L. Fung, *J. Pharm. Sci.*, **67**, 584 (1978).
(11) L. A. Heppel and R. S. Hilmoe, *J. Biol. Chem.*, **183**, 129 (1950).
(12) P. Needleman and E. F. Hunter, *Mol. Pharmacol.*, **1**, 77 (1965).
(13) W. Modell, *Clin. Pharmacol. Ther.*, **3**, 97 (1962).
(14) P. Needleman, S. Lang, and E. M. Johnson, *J. Pharmacol. Exp. Ther.*, **181**, 489 (1972).
(15) J. C. Krantz and C. D. Leake, *Am. J. Cardiol.*, **36**, 407 (1976).
(16) T. Winsor and H. Berger, *Am. Heart J.*, **90**, 611 (1975).
(17) P. Needleman, in "Organic Nitrates," Springer-Verlag, Berlin, New York, 1975.
(18) "The United States Pharmacopeia," 19th rev., U.S. Pharmacopeial Convention, Inc., Rockville, Md., 1975.
(19) H.-L. Fung, P. Dalecki, E. Tse, and C. T. Rhodes, *J. Pharm. Sci.*, **62**, 696 (1973).
(20) J. R. Weeks and J. D. Davis, *J. Appl. Physiol.*, **19**, 540 (1964).
(21) P. S. K. Yap, E. F. McNiff, and H.-L. Fung, *J. Pharm. Sci.*, **67**, 582 (1978).
(22) W. J. Jusko, in "Applied Pharmacokinetics: Principles of Therapeutic Drug Monitoring," W. E. Evans, J. J. Schentag, and W. J. Jusko, Eds., Applied Therapeutics, Inc., San Francisco, Calif., 1980.
(23) L. Jansky and J. S. Hart, *Can. J. Physiol. Pharmacol.*, **46**, 653 (1968).
(24) P. M. Armstrong, J. A. Moffat, and G. S. Marks, *Circulation*, **66**, 1273 (1982).
(25) F. J. DiCarlo and M. D. Melgar, *Proc. Soc. Exp. Biol.*, **131**, 406 (1969).
(26) F. J. DiCarlo, M. C. Crew, L. J. Haynes, M. D. Melgar, R. L. Gala, *Biochem. Pharmacol.*, **17**, 3179 (1968).
(27) C.-C. Wu, T. Sokoloski, M. F. Blanford, and A. M. Burkman, *Int. J. Pharmaceut.*, **8**, 323 (1981).
(28) E. M. Johnson, A. B. Harkey, D. J. Blehm, and P. Needleman, *J. Pharmacol. Exp. Ther.*, **182**, 56 (1972).
(29) R. L. Stein, J. K. O'Brien, C. Irwin, J. K. Townsend-Parchman, F. E. Hunter, *Biochem. Pharmacol.*, **29**, 1807 (1980).
(30) W. L. Chiou, G. Lam, M.-L. Chen, and M. G. Lee, *J. Pharm. Sci.*, **70**, 1037 (1981).
(31) M.-L. Chen, G. Lam, M. G. Lee, and W. L. Chiou, *J. Pharm. Sci.*, **71**, 1386 (1982).
(32) A. B. Hill, C. J. Bowley, M. L. Nahrwold, P. R. Knight, M. M. Kirsch, and J. K. Denlinger, *Anesthesiology*, **54**, 346 (1981).
(33) W. L. Chiou, G. Lam, M. L. Chen and M. G. Lee, *Res. Commun. Chem. Pathol. Pharmacol.*, **32**, 27 (1981).
(34) S. C. Sutton, Ph.D. Thesis, State University of New York at Buffalo (1983).
(35) T. Oguma and G. Levy, *J. Pharmacol. Exp. Ther.*, **219**, 7 (1981).
(36) M. Gibaldi and D. Perrier, "Pharmacokinetics," Dekker, New York, N.Y., 1975.
(37) A. Kamiya, H. Ogata, and H.-L. Fung, *J. Pharm. Sci.*, **71**, 621 (1982).
(38) M. A. Commarato, M. W. Winbury, and H. R. Kaplan, *J. Pharmacol. Exp. Ther.*, **187**, 300 (1973).
(39) J. R. Hodgson and C. C. Lee, *Toxicol. Appl. Pharmacol.*, **34**, 449 (1975).
(40) W. B. Jacoby, *Adv. Enzymol.*, **46**, 383 (1978).
(41) G. A. Maier, C. Arena, and H.-L. Fung, *Biochem. Pharmacol.*, **29**, 646 (1980).

ACKNOWLEDGMENTS

Supported in part by NIH grant HL 22273. G. A. Maier was a graduate trainee supported by 5T53 GM 07145.

Phase Separation Induced in Gelatin–Base Coacervation Systems by Addition of Water-Soluble Nonionic Polymers I: Microencapsulation

HIROAKI JIZOMOTO

Received January 17, 1983, from the *Shionogi Research Laboratories, Shionogi & Co., Ltd., Fukushima-ku, Osaka 553, Japan.* Accepted for publication June 13, 1983.

Abstract □ A microencapsulation procedure in which water-soluble nonionic polymers (especially, polyethylene oxide or polyethylene glycol) were added to gelatin–base coacervation systems is described. The advantages of this method are: (*a*) The addition of a small amount of polyethylene glycol (PEG) or polyethylene oxide (PEO) to a complex coacervation system (*e.g.*, gelatin–acacia) allows microencapsulation to occur over an expanded pH region (pH 2–9 in gelatin–acacia). (*b*) These polymers induce phase separation in an aqueous solution of gelatin alone and enable the preparation of gelatin-coated microcapsules not only in the vicinity of the isoelectric point (pH 9.0), but over a wide pH range (pH 5.5–9.5). (*c*) Spherical single-seeded microcapsules can be obtained.

Keyphrases □ Microencapsulation—gelatin–base coacervation systems, water-soluble nonionic polymer □ Phase separation—coacervation induced by the addition of water-soluble nonionic polymer □ Coacervation—gelatin–acacia, polyethylene glycol, polyethylene oxide, phase separation, microencapsulation

Microencapsulation using coacervation of gelatin or gelatin–acacia is the most popular of the aqueous media procedures. The practicality of the gelatin–acacia complex coacervation method (1–3) is evidenced by products such as no-carbon paper and liquid crystal thermometers. Complex coacervation is the phase separation caused in a mixture of anionic and cationic polymers (*e.g.*, acacia and gelatin) under restricted pH conditions and colloid concentration. This limitation is the disadvantage of the conventional microencapsulation procedure by complex coacervation.

On the other hand, under certain conditions the addition of a water-miscible organic solvent (*e.g.*, ethanol) or salt (*e.g.*, sodium sulfate) to the aqueous solution of a polymer (*e.g.*, gelatin) causes phase separation. This phenomenon has been used in microencapsulation as a simple coacervation method (4–8). The disadvantages of the simple coacervation method are the requirement of a large quantity of the organic solvent, the necessity of desalting, and the difficulty of setting the optimum conditions to obtain satisfactory microcapsules. Therefore, in this work, improvement of the conventional coacervating techniques was attempted.

EXPERIMENTAL SECTION

Materials—The gelatin used has the following specifications as provided by the manufacturer[1]: bloom, 300; viscosity, 60.9 millipoises; pH 4.2; moisture, 9.9%; and isoelectric point, 9.0. The anionic polymers were acacia[2], carboxymethylcellulose (CMC)[3], and ethylene–maleic anhydride copolymer

[1] Miyagi Kagaku Kogyo.
[2] Spray-dried powder; Gokyo Sangyo.
[3] Serogen PR; Daiichi Kogyo Seiyaku.

0022-3549/84/0700-0879$01.00/0
© 1984, American Pharmaceutical Association

(10) P. S. K. Yap and H.-L. Fung, *J. Pharm. Sci.*, **67**, 584 (1978).
(11) L. A. Heppel and R. S. Hilmoe, *J. Biol. Chem.*, **183**, 129 (1950).
(12) P. Needleman and E. F. Hunter, *Mol. Pharmacol.*, **1**, 77 (1965).
(13) W. Modell, *Clin. Pharmacol. Ther.*, **3**, 97 (1962).
(14) P. Needleman, S. Lang, and E. M. Johnson, *J. Pharmacol. Exp. Ther.*, **181**, 489 (1972).
(15) J. C. Krantz and C. D. Leake, *Am. J. Cardiol.*, **36**, 407 (1976).
(16) T. Winsor and H. Berger, *Am. Heart J.*, **90**, 611 (1975).
(17) P. Needleman, in "Organic Nitrates," Springer-Verlag, Berlin, New York, 1975.
(18) "The United States Pharmacopeia," 19th rev., U.S. Pharmacopeial Convention, Inc., Rockville, Md., 1975.
(19) H.-L. Fung, P. Dalecki, E. Tse, and C. T. Rhodes, *J. Pharm. Sci.*, **62**, 696 (1973).
(20) J. R. Weeks and J. D. Davis, *J. Appl. Physiol.*, **19**, 540 (1964).
(21) P. S. K. Yap, E. F. McNiff, and H.-L. Fung, *J. Pharm. Sci.*, **67**, 582 (1978).
(22) W. J. Jusko, in "Applied Pharmacokinetics: Principles of Therapeutic Drug Monitoring," W. E. Evans, J. J. Schentag, and W. J. Jusko, Eds., Applied Therapeutics, Inc., San Francisco, Calif., 1980.
(23) L. Jansky and J. S. Hart, *Can. J. Physiol. Pharmacol.*, **46**, 653 (1968).
(24) P. M. Armstrong, J. A. Moffat, and G. S. Marks, *Circulation*, **66**, 1273 (1982).
(25) F. J. DiCarlo and M. D. Melgar, *Proc. Soc. Exp. Biol.*, **131**, 406 (1969).
(26) F. J. DiCarlo, M. C. Crew, L. J. Haynes, M. D. Melgar, R. L. Gala, *Biochem. Pharmacol.*, **17**, 3179 (1968).
(27) C.-C. Wu, T. Sokoloski, M. F. Blanford, and A. M. Burkman, *Int. J. Pharmaceut.*, **8**, 323 (1981).
(28) E. M. Johnson, A. B. Harkey, D. J. Blehm, and P. Needleman, *J. Pharmacol. Exp. Ther.*, **182**, 56 (1972).
(29) R. L. Stein, J. K. O'Brien, C. Irwin, J. K. Townsend-Parchman, F. E. Hunter, *Biochem. Pharmacol.*, **29**, 1807 (1980).
(30) W. L. Chiou, G. Lam, M.-L. Chen, and M. G. Lee, *J. Pharm. Sci.*, **70**, 1037 (1981).
(31) M.-L. Chen, G. Lam, M. G. Lee, and W. L. Chiou, *J. Pharm. Sci.*, **71**, 1386 (1982).
(32) A. B. Hill, C. J. Bowley, M. L. Nahrwold, P. R. Knight, M. M. Kirsch, and J. K. Denlinger, *Anesthesiology*, **54**, 346 (1981).
(33) W. L. Chiou, G. Lam, M. L. Chen and M. G. Lee, *Res. Commun. Chem. Pathol. Pharmacol.*, **32**, 27 (1981).
(34) S. C. Sutton, Ph.D. Thesis, State University of New York at Buffalo (1983).
(35) T. Oguma and G. Levy, *J. Pharmacol. Exp. Ther.*, **219**, 7 (1981).
(36) M. Gibaldi and D. Perrier, "Pharmacokinetics," Dekker, New York, N.Y., 1975.
(37) A. Kamiya, H. Ogata, and H.-L. Fung, *J. Pharm. Sci.*, **71**, 621 (1982).
(38) M. A. Commarato, M. W. Winbury, and H. R. Kaplan, *J. Pharmacol. Exp. Ther.*, **187**, 300 (1973).
(39) J. R. Hodgson and C. C. Lee, *Toxicol. Appl. Pharmacol.*, **34**, 449 (1975).
(40) W. B. Jacoby, *Adv. Enzymol.*, **46**, 383 (1978).
(41) G. A. Maier, C. Arena, and H.-L. Fung, *Biochem. Pharmacol.*, **29**, 646 (1980).

ACKNOWLEDGMENTS

Supported in part by NIH grant HL 22273. G. A. Maier was a graduate trainee supported by 5T53 GM 07145.

Phase Separation Induced in Gelatin–Base Coacervation Systems by Addition of Water-Soluble Nonionic Polymers I: Microencapsulation

HIROAKI JIZOMOTO

Received January 17, 1983, from the *Shionogi Research Laboratories, Shionogi & Co., Ltd., Fukushima-ku, Osaka 553, Japan.* Accepted for publication June 13, 1983.

Abstract □ A microencapsulation procedure in which water-soluble nonionic polymers (especially, polyethylene oxide or polyethylene glycol) were added to gelatin–base coacervation systems is described. The advantages of this method are: (*a*) The addition of a small amount of polyethylene glycol (PEG) or polyethylene oxide (PEO) to a complex coacervation system (*e.g.*, gelatin–acacia) allows microencapsulation to occur over an expanded pH region (pH 2–9 in gelatin–acacia). (*b*) These polymers induce phase separation in an aqueous solution of gelatin alone and enable the preparation of gelatin-coated microcapsules not only in the vicinity of the isoelectric point (pH 9.0), but over a wide pH range (pH 5.5–9.5). (*c*) Spherical single-seeded microcapsules can be obtained.

Keyphrases □ Microencapsulation—gelatin–base coacervation systems, water-soluble nonionic polymer □ Phase separation—coacervation induced by the addition of water-soluble nonionic polymer □ Coacervation—gelatin–acacia, polyethylene glycol, polyethylene oxide, phase separation, microencapsulation

Microencapsulation using coacervation of gelatin or gelatin–acacia is the most popular of the aqueous media procedures. The practicality of the gelatin–acacia complex coacervation method (1–3) is evidenced by products such as no-carbon paper and liquid crystal thermometers. Complex coacervation is the phase separation caused in a mixture of anionic and cationic polymers (*e.g.*, acacia and gelatin) under restricted pH conditions and colloid concentration. This limitation is the disadvantage of the conventional microencapsulation procedure by complex coacervation.

On the other hand, under certain conditions the addition of a water-miscible organic solvent (*e.g.*, ethanol) or salt (*e.g.*, sodium sulfate) to the aqueous solution of a polymer (*e.g.*, gelatin) causes phase separation. This phenomenon has been used in microencapsulation as a simple coacervation method (4–8). The disadvantages of the simple coacervation method are the requirement of a large quantity of the organic solvent, the necessity of desalting, and the difficulty of setting the optimum conditions to obtain satisfactory microcapsules. Therefore, in this work, improvement of the conventional coacervating techniques was attempted.

EXPERIMENTAL SECTION

Materials—The gelatin used has the following specifications as provided by the manufacturer[1]: bloom, 300; viscosity, 60.9 millipoises; pH 4.2; moisture, 9.9%; and isoelectric point, 9.0. The anionic polymers were acacia[2], carboxymethylcellulose (CMC)[3], and ethylene–maleic anhydride copolymer

[1] Miyagi Kagaku Kogyo.
[2] Spray-dried powder; Gokyo Sangyo.
[3] Serogen PR; Daiichi Kogyo Seiyaku.

0022-3549/84/0700-0879$01.00/0
© 1984, American Pharmaceutical Association

Table I—Microencapsulation Procedure with the Addition of Water-Soluble Nonionic Polymers to Complex Coacervation Systems

Example	Core Substance: Species	Core Substance: Final Conc., % w/w	Anionic Polymer: Species	Anionic Polymer: Final Conc., % w/w	Cationic Polymer: Species	Cationic Polymer: Final Conc., % w/w	Nonionic Polymer: Species	Nonionic Polymer: Final Conc., % w/w	pH	Shape of Microcapsule[a]
1	Fluid paraffin	5.7	Acacia	2.0	Gelatin	2.0	PEO-1	0.85	7.7	H.S.
2	2,6-Dinitro-*N*,*N*-dipropyl-4-trifluoroaniline[b]	4.3	Acacia	2.0	Gelatin	2.0	PEG-6000	2.3	7.6	I.S.
3	Fluid paraffin	10.6	CMC	0.5	Gelatin	3.9	PEO-1	0.88	8.3	I.S.
4	Fluid paraffin	10.0	Acacia	2.2	Gelatin	2.2	PVA	1.0	7.6	R.S.
5	Fluid paraffin	10.0	Acacia	2.2	Gelatin	2.2	Dextran	1.5	7.5	R.S.
6	Fluid paraffin	10.0	Acacia	2.2	Gelatin	2.2	PVP	3.0	6.2	R.S.
7	Fluid paraffin	10.0	Acacia	2.2	Gelatin	2.2	Polysaccharide	2.0	7.3	R.S.
8	Fluid paraffin	6.7	EMA	0.23	Gelatin	2.5	PEG-6000	2.0	7.5	I.S.

[a] H.S. = spherical, single seed; I.S. = spindle, single seed; R.S. = irregular shape, single seed. [b] Trifluralin.

Table II—Microencapsulation Procedure with the Addition of Nonionic Surfactants to Aqueous Solution Containing Gelatin and Core Substances

Example	Core Substance: Species	Core Substance: Final Conc., % w/w	Final Conc. of Gelatin, % w/w	Nonionic Polymer: Species	Nonionic Polymer: Final Conc., % w/w	pH	Shape of Microcapsule[a]
9	2,6-Dinitro-*N*,*N*-dipropyl-4-trifluoroaniline[b]	4.8	2.8	PEG-6000	3.0	9.0	I.S.
10	Fluid paraffin with pigment	12.0	2.8	PEO-1	1.2	8.6	H.S.
11	Fluid paraffin with pigment	5.7	2.0	PEO-18	0.39	9.0	H.S.
12	Chlorpromazine (dissolved in sesame oil)	0.5 (5.2)	2.0	PEO-1	1.5	9.0	I.S. H.S.

[a] H.S. = spherical, single seed; I.S. = spindle, single seed. [b] Trifluralin.

(EMA)[4]. Nonionic polymers used were polyethylene glycol (PEG)[5], polyethylene oxide (PEO)[6], polysaccharide[7], polyvinylpyrrolidone[8], dextran[9], and polyvinyl alcohol[10]. All the polymers were used as supplied by the manufacturers.

Both PEG and PEO have the same general structural formula: HO—$(CH_2CH_2O)_nH$. The former is usually used for polymers having molecular weights $< \sim 20{,}000$ and the latter for those with molecular weights greater than tens of thousands.

Microencapsulation Procedures—The microencapsulation methods are illustrated in Fig. 1. Examples a and b demonstrate the procedure for the complex coacervation system using PEO-18 and for the aqueous solution of gelatin using PEG-6000, respectively. In these example, high concentrations (11%) of acacia and gelatin were used as starting concentrations according to the method of Green and Schleicher (9, 10), although low concentrations [*e.g.*, 3% (11)] can also be used. First, the core substances were emulsified above 40°C with a homogenizer[11] in aqueous solutions containing acacia (Example a) or gelatin (Example b) in 100-mL beakers. After emulsification, the colloidal dispersions were added to 500-mL beakers in which three-blade metal propellers with 2.5-cm blades were fixed 1.5 cm from the bottom, and water, and aqueous solution of gelatin (Example a), and nonionic polymers were successively added with stirring until the final concentrations of gelatin and acacia were adjusted to 1.5–3.0%. In this step, the nonionic polymers may be added in a neat state (powder or flakes) instead of as an aqueous solution.

After adjusting the pH with 20 and 1% NaOH solutions at 40°C, the mixtures were cooled gradually to 20°C with continuous stirring at 400–900 rpm and then cooled abruptly to ≤10°C. The mixtures were subjected to hardening treatment for 14 h after a dropwise addition of diluted glutaraldehyde (8%, 10 mL) and/or formaldehyde (7.4%, 10 mL)[12]. The products

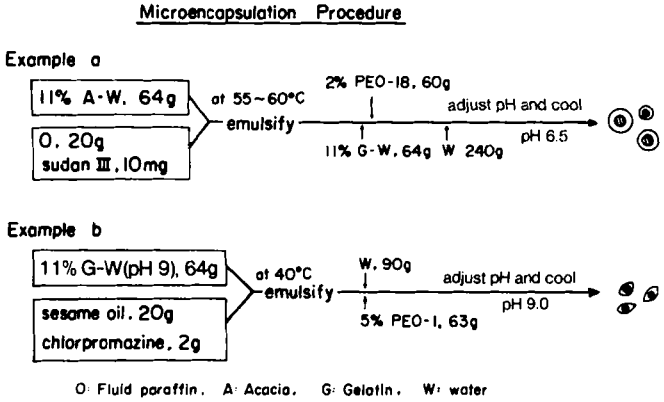

Figure 1—*Microencapsulation procedures by the addition of water-soluble nonionic polymers to a complex coacervation system (Example a) and the simple aqueous system of gelatin (Example b).*

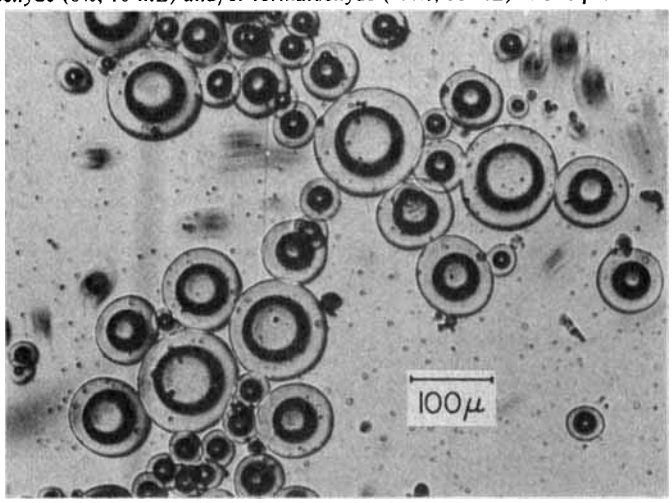

Figure 2—*Photomicrograph of spherical single-seed microcapsules obtained from the dispersion system of gelatin–acacia and liquid paraffin by the addition of PEO-18 at pH 6.5.*

[4] EMA-31; Monsanto Chemical Co.
[5] PEG-6000, PEG-20000; Nippon Oils & Fats Co., Ltd.
[6] PEO-1, PEO-18; Seitetsu Kagaku Kogyo.
[7] Pullulan PF-10, mol. wt. 100,000–300,000; Sumitomo Chemical Co., Ltd.
[8] Luviscol K-30 (mol. wt. 40,000); Badische Anilin and Soda Fabrik A.G.
[9] Mol. wt. 100,000–200,000; Wako Pure Chemical Industries, Ltd.
[10] Gohsenol GM; Nippon Gosei Kagaku Kogyo.

[11] Silverson Machines Ltd.
[12] It is described in the patent (Japan 52-38097) that the combined use of glutaraldehyde and formaldehyde prevents yellowing. Formaldehyde is preferable to glutaraldehyde for hardening of microcapsules in a neutral pH region, because the latter has some tendency to cause aggregation of microcapsules in this pH region.

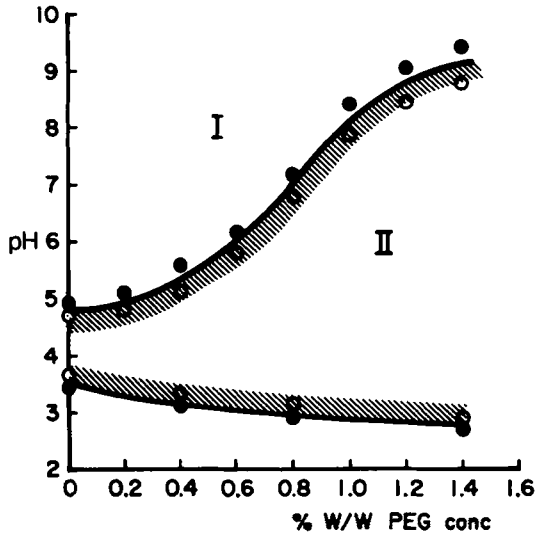

Figure 3—*Phase diagram of the acacia-gelatin (2.2% w/w each) complex coacervation system containing PEG-20,000. The coacervating region is represented by the shaded area (II); I represents a region of one-phase colloidal solution. Key: (●) no coacervation; (○) formation of coacervate.*

were then removed by filtration and washed. Microcapsules in the form of a free-flowing powder can be obtained according to the method of Madan *et al.* (6) or Palmieri (12) by the use of colloidal silica. The unhardened microcapsules can also be recovered as discrete free-flowing particles according to the aforementioned methods.

Phase Diagram—The nonionic polymers were added to the aqueous gelatin-acacia (2.2% each) solution or the aqueous gelatin (2.2%) solution without core materials under stirring at 40°C, and the formation of coacervates at various pH values was observed with a microscope at room temperature (~23°C). The dependence of the phase diagram on the concentrations of gelatin and acacia was also observed for PEO-1 and PEG-20,000.

RESULTS AND DISCUSSION

Microencapsulation—The various types of microcapsules formed in gelatin-base systems using water-soluble nonionic polymers are listed in Tables I and II. Examples of complex coacervation systems are shown in Table I, while examples of simple gelatin coacervation systems are shown in Table II.

In Examples 3 and 8, carboxymethylcellulose (CMC) and ethylene-maleic anhydride copolymer (EMA) were used instead of acacia as the anionic polymer, respectively. Examples 4–7 are of microencapsulation using polyvinyl

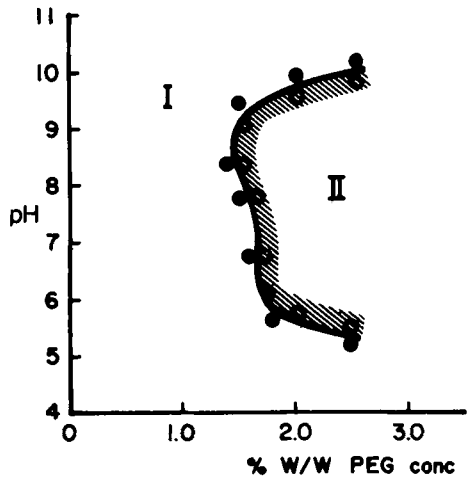

Figure 4—*Phase diagram of a simple coacervation of gelatin (2.2% w/w) with PEG-20,000. The coacervation region is represented by the shaded area (II); I represents a region of one-phase colloidal solution. Key: (●) no coacervation; (○) formation of coacervate.*

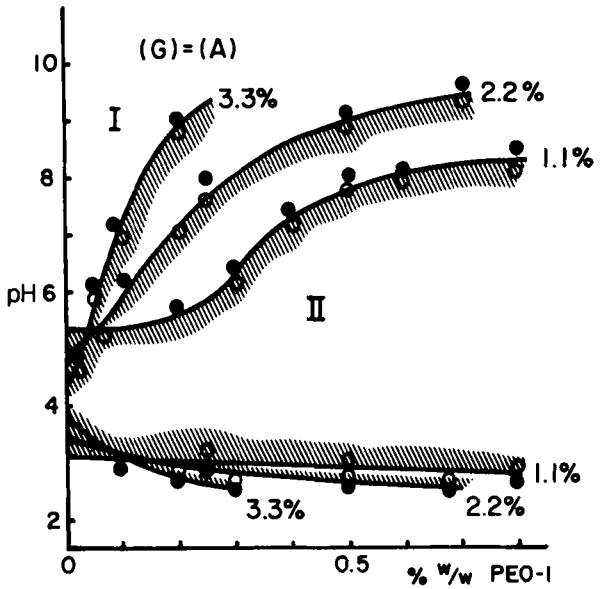

Figure 5—*Phase diagrams of acacia-gelatin complex coacervation systems containing PEO-1. The effect of colloidal concentrations of acacia and gelatin (1.1, 2.2, and 3.3% w/w) on the phase diagram was observed. The coacervating regions are represented by shaded areas (II); I represents the regions of one-phase colloidal solution. Key: (●) no coacervation; (○) formation of coacervate.*

alcohol (PVA) dextran, polyvinylpyrrolidone (PVP), and polysaccharide as the nonionic polymers, respectively. PEO and PEG were better than these nonionic polymers, which gave coacervation systems of high viscosity in the cooling process and made it difficult to prepare good microcapsules. On the other hand, the results of experiments on the homologous series of PEO and PEG indicated that the minimum concentrations of the molecules required to obtain microcapsules became lower with increasing molecular weight, although the system containing the larger molecule was more viscous. In the conventional method, spindle-shaped microcapsules are usually formed under the conditions used for obtaining single-seed microcapsules; in the present method, however, spherical shapes were obtained in many cases using PEO with a higher molecular weight than PEO-1. Although the viscosities were not measured, the systems in which the spherical shapes were obtained were, in general, more viscous in appearance. Therefore, the viscosity of the medium is considered an important factor in forming spherical shapes, but extended polymer chains with high molecular weight included in the medium might prevent the deformation (from sphere to spindle) of the microcapsule induced by the stress of distortion. On the other hand, stirring speed is also an important factor, and a speed of 400–900 rpm was necessary to overcome the retardation or to stop the flow of the dispersion in the vicinity of gelation temperature.

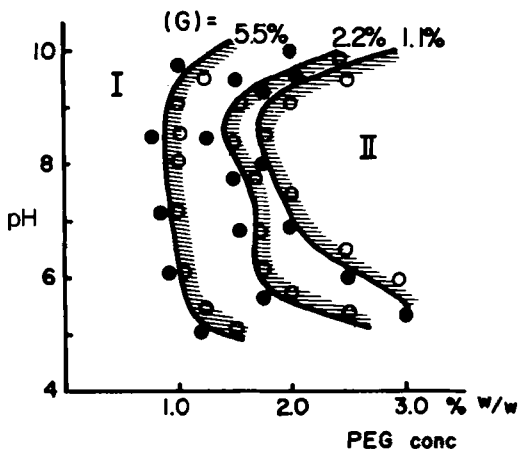

Figure 6—*Phase separations induced in the simple coacervation systems containing different amounts of gelatin (1.1, 2.2, and 5.5% w/w) by the addition of PEG-20,000. The coacervating regions are represented by shaded areas (II); I represents the regions of one-phase colloidal solution. Key: (●) no coacervation; (○) formation of coacervate.*

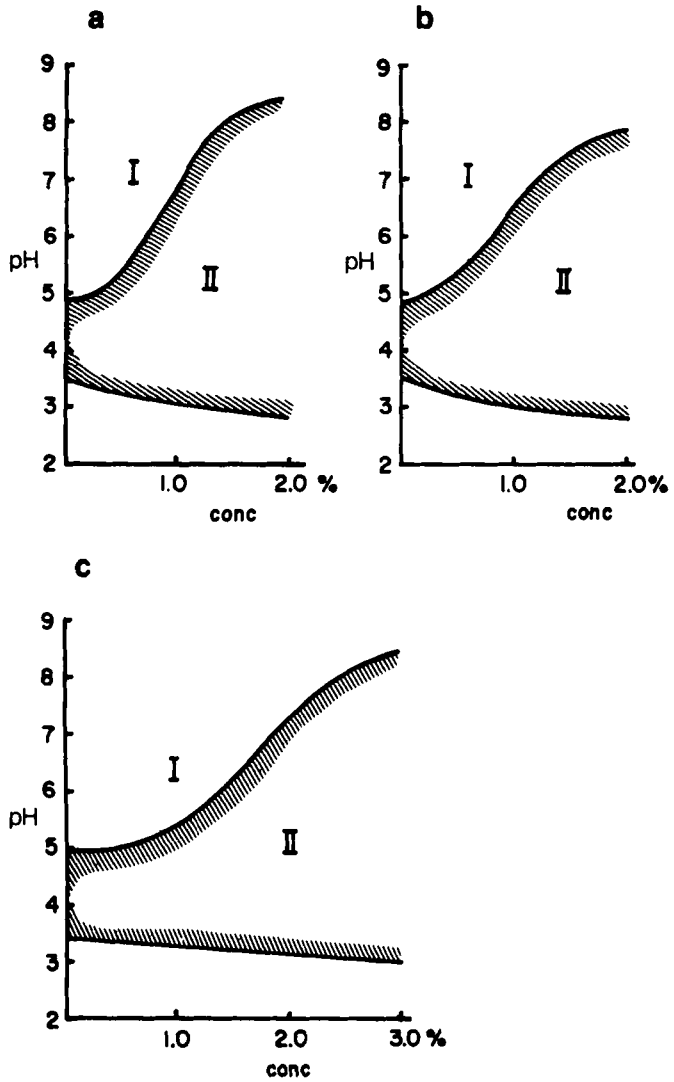

Figure 7—*Phase diagrams of acacia-gelatin (2.2% w/w each) complex coacervation systems with various water-soluble nonionic polymers. The coacervation regions are represented by the shaded areas (II); I represents the regions of one-phase colloidal solution. Key: (a) dextran; (b) polysaccharide; (c) PVP.*

Figure 2 shows a photomicrograph of spherical single-seed microcapsules obtained from the dispersion systems of gelatin-acacia (1.6% each) and liquid paraffin (4.7%) by the addition of PEO-18 (0.3%) at pH 6.5. The product was recovered as free-flowing powder (diameter, 30–100 μm) after filtration without hardening treatment, according to the method of Madan *et al.* (6).

Phase Diagram—The coacervation areas are represented by shading (indicated by the symbol II) in the phase diagrams. The areas represented by the symbol I indicate one-phase colloidal dispersions.

Figure 3 shows the result of the gelatin-acacia complex coacervation systems and Fig. 4 the results of the aqueous solution of gelatin alone. Figure 3 indicates that the intercept of the shaded area to the ordinate is in the pH range of conventional complex coacervation and that the addition of a small amount of PEG-20,000 to the gelatin-acacia coacervation system causes phase separation in a remarkably expanded pH range. Figure 4 shows that in the aqueous solution containing gelatin alone, phase separation does not take place at every pH value without the addition of foreign molecules, but with the addition of PEG-20,000, the pH range is expanded.

Figure 5 shows that the pH range of complex coacervation without the addition of foreign molecules (conventional method) decreases with increasing colloidal concentration, but that the addition of PEO-1 expands the effective pH range of phase separation with increasing colloidal concentrations of gelatin and acacia. The minimum concentration of PEG-20,000 required to cause the phase separation in the aqueous solutions of gelatin alone becomes lower with increasing gelatin concentration, as shown in Fig. 6.

The results of other water-soluble nonionic polymers (polysaccharide, dextran, and PVP) can be seen in Fig. 7. Although all of these nonionic polymers have molecular weights greater than that of PEG-20,000, they are not more effective.

Coacervation from ethylcellulose-cyclohexane solution is widely used in the microencapsulation of water-soluble drugs, using a combination of coacervation-inducing agents (*e.g.*, polyethylene and polyisobutylene) (13, 14). However, the role and effect of the coacervation-inducing agents in the organic solvent systems differ from those of the water-soluble nonionic polymers in the aqueous coacervation systems described in the present paper.

In the coacervation system of ethylcellulose-cyclohexane, the coacervation-inducing agents effectively cause phase separation and prevent aggregation of microcapsules, but the microcapsules can also be prepared without these agents. In the aqueous solution of gelatin, on the other hand, phase separation does not occur without the addition of the water-soluble nonionic polymers. In the acacia-gelatin complex coacervation system, the nonionic polymers can cause phase separation even at pH values at which separation does not occur using the conventional method. The phenomenon of inducing coacervation in these two solvent systems might be caused (possibly common to both systems) by the contributions of the added polymers to the thermodynamic properties of mixing (ΔH_{mix} and ΔS_{mix}).

CONCLUSIONS

The addition of a small amount of high molecular weight PEO or PEG to a gelatin-acacia coacervation system enables coacervation over an expanded pH range (pH 2–9). These polymers also induce phase separation in the aqueous solution of gelatin alone over a wide range (pH 5.5–9.5). The microencapsulation procedure using this phenomenon is useful for the microencapsulation of materials which are labile or water-soluble in the acidic pH region but stable and insoluble in the neutral pH region.

REFERENCES

(1) H. G. B. de Jong, in "Colloid Science," vol. 2, H. R. Kruyt, Ed., Elsevier, New York, N.Y., 1949, p. 335.

(2) A. B. Dhruv, T. E. Needham, J. R. Luzzi, and L. A. Luzzi, *Can. J. Pharm. Sci.*, **10**, 33 (1975).

(3) J. R. Nixon and G. A. Agyilirah, *Int. J. Pharm.*, **6**, 277 (1980).

(4) R. E. Phares, Jr. and G. J. Sperandio, *J. Pharm. Sci.*, **53**, 515 (1964).

(5) R. E. Phares, Jr. and G. J. Sperandio, *J. Pharm. Sci.*, **53**, 518 (1964).

(6) P. L. Madan, D. K. Madan, and J. C. Price, *J. Pharm. Sci.*, **65**, 1476 (1976).

(7) J. R. Nixon, S. A. H. Khalil, and J. E. Carless, *J. Pharm. Pharmacol.*, **20**, 528 (1967).

(8) J. R. Nixon and S. E. Walker, *J. Pharm. Pharmacol.*, Suppl., **23**, 147S (1971).

(9) B. K. Green and L. Schleicher, U.S. Pat. 2,730,456 (1956).

(10) B. K. Green and L. Schleicher, U.S. Pat. 2,800,457 (1957).

(11) L. A. Luzzi and R. J. Gerraughty, *J. Pharm. Sci.*, **53**, 429 (1964).

(12) A. Palmieri, *J. Pharm. Sci.*, **68**, 1561 (1979).

(13) M. Samejima, G. Hirata, and Y. Koida, *Chem. Pharm. Bull.*, **30**, 2894 (1982).

(14) M. Donbrow and S. Benita, *J. Pharm. Pharmacol.*, **29**, 4p (1977).

ACKNOWLEDGMENTS

Grateful acknowledgment is made to Dr. O. Ohodaira for his many helpful suggestions.

Prediction of Drug Disposition Kinetics in Skin and Plasma Following Topical Administration

RICHARD H. GUY *x and JONATHAN HADGRAFT ‡

Received February 28, 1983, from the **Departments of Pharmacy and Pharmaceutical Chemistry, School of Pharmacy, University of California-San Francisco, San Francisco, CA 94143* and the ‡*Department of Pharmacy, University of Nottingham, University Park, Nottingham, NG7 2RD, U.K.* Accepted for publication May 23, 1983.

Abstract □ The development of a physically based pharmacokinetic model for percutaneous absorption is described. The simulation includes four first-order rate constants assigned the following significance: (*a*) absorption across the stratum corneum; (*b*) diffusion through the viable tissue; (*c*) a retardation process which retains penetrant in the stratum corneum (and hence provides a means to mathematically produce a "reservoir" effect, for example); and (*d*) uptake from the skin into the systemic circulation and subsequent elimination from the body. The kinetic equations of the model are solved and expressions are obtained for the concentration of penetrant within the stratum corneum (and available to subsequently partition into the viable epidermis) and the plasma concentration of the administered substance, as a function of time. Using example values for the four rate parameters, disposition profiles for the penetrant in skin and plasma were derived. The cases considered cover slow and fast stratum corneum penetrants, substances which are excreted rapidly or slowly from the body, and absorbing molecules with a variety of relative stratum corneum-viable tissue affinities. The results suggest a framework for the prediction of pharmaceutically and clinically relevant information following the topical administration of therapeutic agents for local or systemic effect.

Keyphrases □ Percutaneous absorption—pharmacokinetics of skin penetration, plasma concentration prediction □ Plasma concentration prediction—pharmacokinetics, percutaneous absorption, topical administration □ Pharmacokinetics—percutaneous absorption, plasma concentration prediction, topical administration

Percutaneous absorption is a complex phenomenon which is currently attracting an increasing level of study. In addition to the fundamental goal of more completely understanding skin penetration, an important reason for this expanded effort is the somewhat recently realized potential for effective systemic drug delivery using the transdermal route (1-3). Equally pertinent, and now subject to some reexamination, is consideration of the efficaciousness of existing drugs and dosage regimens for the treatment of local dermatological disease.

The heightened interest in percutaneous absorption encompasses many aspects: (*a*) the development of new delivery systems (4-6), (*b*) the search for agents capable of enhancing penetration (7-11), and (*c*) the continuing effort to understand skin absorption rate and extent in terms of accepted biological facts and penetrant physicochemical properties (12-20). In the first group, one may cite the appearance of transdermal therapeutic systems containing nitroglycerin for the treatment of angina pectoris (21) and the surprising suggestion that topically applied liposomes are able to exert an influence on the local and systemic distribution of an encapsulated drug (22, 23). Of the agents offered as penetration enhancers, pyrrolidone, formamide, and sulfoxide derivatives are recent examples (7-11, 24). Another new compound, dodecylazacycloheptan-2-one (25, 26), appears to have enhancement potential, although its mechanism of promotion remains unclear.

It is the third category, however, to which this paper is directed. Specifically, the objectives are to present a physically based pharmacokinetic model for percutaneous absorption and to demonstrate its application to the prediction of drug disposition kinetics in skin and plasma following topical administration. The simulation is that recently described by Guy *et al.* (27). The approach is simplistic in concept, but sensitive to physicochemical changes in penetrant properties and to the manner in which the absorbing molecule may be expected to interact with the various strata of the skin. Four rate constants are specified in the model and are assigned specific physical significance. The previous work (27) showed that the urinary excretion rate data of three compounds (testosterone, benzoic acid, and hydrocortisone), obtained following topical application, can be successfully explained by the simulation and that rate constants, which are physicochemically consistent, can be derived. In this paper, the rate equations of the model are solved for (*a*) the concentration of penetrant within the stratum corneum and (*b*) the concentration of drug in plasma. Reasonable, representative values are assigned to the four kinetic parameters and drug disposition profiles are generated for a variety of example cases. The predictive capacity of the approach in clinically relevant situations is indicated and discussed.

THEORETICAL SECTION

Schematic and compartmental representations of the pharmacokinetic model are shown in Fig. 1 and are designed to indicate the putative physical significance on which this work is based. The simulation is linear and includes four first-order rate constants. The first (k_1) describes drug input across the stratum corneum and is a parameter that might be estimated, for example,

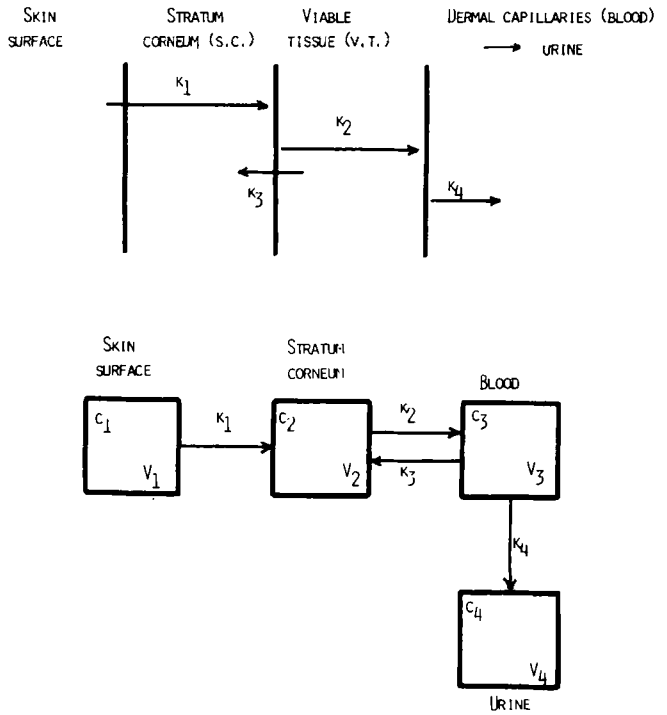

Figure 1—*Schematic and compartmental representations of the percutaneous absorption pharmacokinetic model.*

0022-3549/84/0700-0883$01.00/0
© 1984, American Pharmaceutical Association

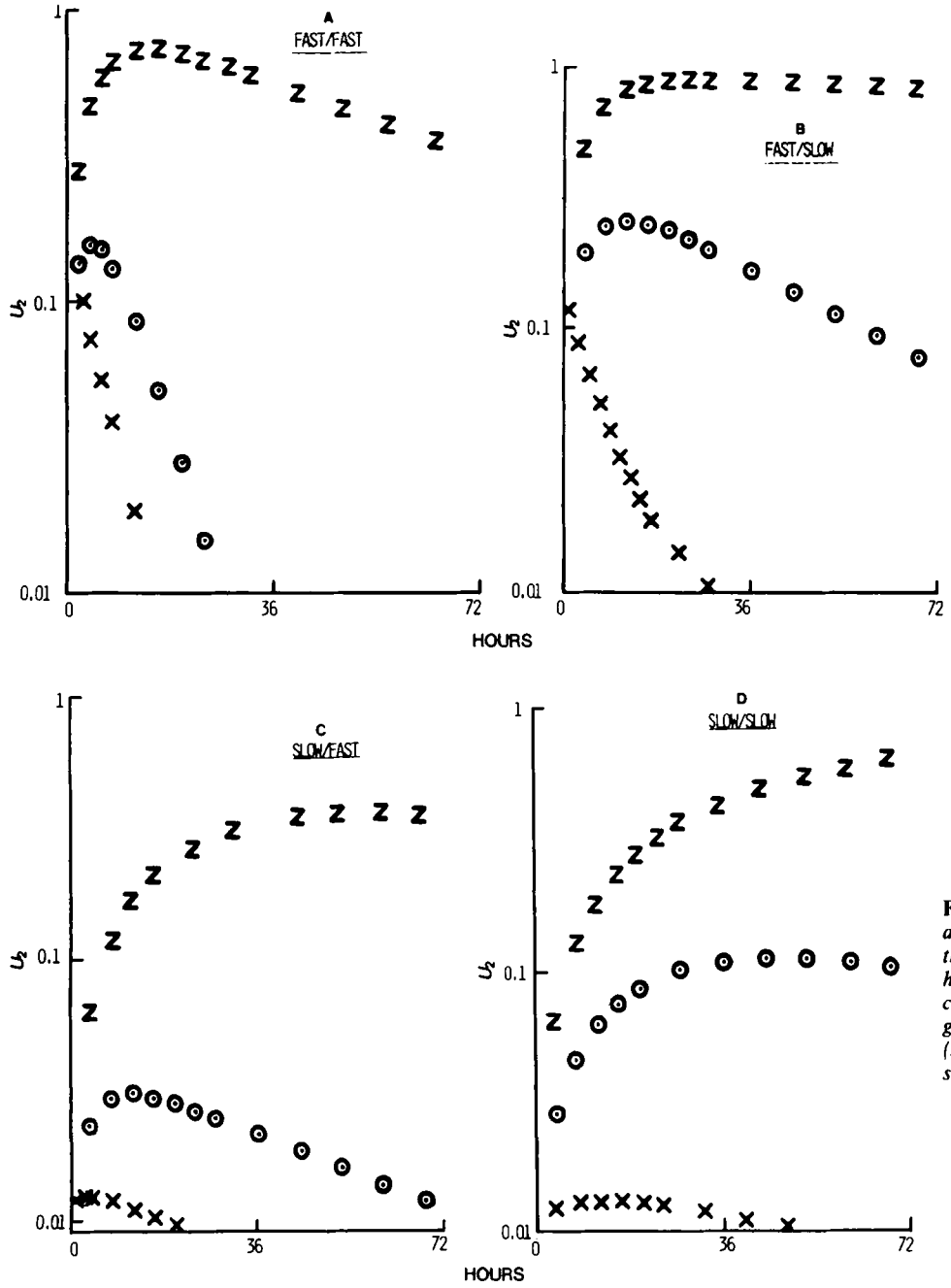

Figure 2—*Prediction of skin disposition kinetics as a plot of normalized concentration* u_2 versus *time. The curves correspond to penetrants with high (Z), medium (⊙), and low (X) stratum corneum affinities. Rate constants* k_1-k_4 *are given in Tables I and II. Key: (A) case fast/fast; (B) case fast/slow; (C) case slow/fast; (D) case slow/slow.*

by the disappearance of radioactivity from the skin surface following topical application of labeled compound (28, 29). The second, k_2, relates to drug penetration further into the skin, specifically movement across the aqueous viable tissue. The kinetic constant k_3 reflects the relative affinity of the penetrant for the stratum corneum compared with the viable tissue; in other words, k_3 will be large (relative to k_2) for substances that bind tightly to the stratum corneum or that exhibit a marked "reservoir" effect (30–33). Finally, k_4 describes drug elimination from the systemic circulation into the urine. The assignment of a first-order process for this step may, of course, be inadequate, in which case a more complex formulation will be necessary. In this instance, the theoretical treatment becomes more complicated but far from intractable. The previous description of this model indicates that it is particularly useful if the elimination of drug following parenteral administration is known (27, 29). Thus, ideally, application of the simulation includes independent assessment of the elimination process described by k_4 or a more sophisticated alternative.

Four concentrations are identified by the compartmentalization of the model. Surface concentration is C_1 and, in the following mathematical development, $C_1 = C_0$, the initial applied concentration, at time $t = 0$, *i.e.*, at the beginning of the experiment. Because of the assigned significance of k_2 and k_3, C_2 may be equated with the concentration of drug in the stratum corneum and available for subsequent partitioning into the viable tissue. Estimation of this parameter is useful, therefore, in terms of the dermatological application of the model. The concentration of drug in blood is represented by C_3. No attempt is made to differentiate between drug in the local cutaneous

Table I—Input (k_1) and Output (k_4) Rate Constants Selected for Application of the Model

Case	k_1, h^{-1}	k_4, h^{-1}
Fast/Fast	0.180	0.360
Fast/Slow	0.180	0.036
Slow/Fast	0.018	0.360
Slow/Slow	0.018	0.036

Table II—Rate Constants (k_2 and k_3) Chosen for Application of the Model

k_2, h^{-1}	k_3, h^{-1}	k_3/k_2	Relative Stratum Corneum Affinity
1.440	28.800	20.00	"High"
1.440	0.720	0.50	"Medium"
1.440	0.029	0.02	"Low"

Table III—Rate Constants (k_1–k_4), Previously Determined for Testosterone, Benzoic Acid, and Hydrocortisone, Used to Generate the Disposition Profiles[a]

Compound	k_1, h^{-1}	k_2, h^{-1}	k_3, h^{-1}	k_4, h^{-1}
Testosterone	0.058	1.44	2.70	0.104
Benzoic acid	0.184	2.88	0.014	0.592
Hydrocortisone	0.022	1.44	0.180	0.158

[a] See Figs. 3 and 5; the values were taken from Ref. 27.

microvasculature and drug systemically available. Because it is not possible to sample the dermal capillaries, such a refinement is not presently justified by experimental capabilities. Lastly, C_4 is the concentration of drug in the urine; it follows that attention is focused on the renal excretion of the drug and this may or may not be an appropriate decision. However, because of the stipulation suggested above that drug excretion following intravenous dosing be assessed as a matter of course, then suitable corrections can be applied to take into account the elimination of the drug by other routes (29).

Four rate equations describe the kinetics of the model in Fig. 1:

$$\frac{dC_1}{dt} = -k_1 C_1 \qquad \text{(Eq. 1)}$$

$$\frac{dC_2}{dt} = \frac{V_1}{V_2} k_1 C_1 - k_2 C_2 + \frac{V_3}{V_2} k_3 C_3 \qquad \text{(Eq. 2)}$$

$$\frac{dC_3}{dt} = \frac{V_2}{V_3} k_2 C_2 - (k_3 + k_4) C_3 \qquad \text{(Eq. 3)}$$

$$\frac{dC_4}{dt} = \frac{V_3}{V_4} k_4 C_3 \qquad \text{(Eq. 4)}$$

where V_1–V_4 correspond to the volumes of compartments 1–4, respectively. Manipulation of the equations to obtain an expression for the amount of drug appearing in the urine as a function of time has been presented previously (27). The reduction to achieve relationships pertaining to drug levels in skin (C_2) and plasma (C_3) follow parallel steps (see *Appendix*). The drug concentration in the stratum corneum available for partitioning into the viable epidermis is:

$$u_2 = \frac{V_1}{V_2} k_1 \left[\frac{(k_3 + k_4 - k_1) \cdot \exp(-k_1 t)}{(k_1 - \alpha)(k_1 - \beta)} + \frac{(k_3 + k_4 - \alpha) \cdot \exp(-\alpha t)}{(\alpha - \beta)(\alpha - k_1)} + \frac{(k_3 + k_4 - \beta) \cdot \exp(-\beta t)}{(\beta - k_1)(\beta - \alpha)} \right] \qquad \text{(Eq. 5)}$$

The drug concentration in blood is given by:

$$u_3 = \frac{V_1}{V_3} k_1 k_2 \left[\frac{\exp(-k_1 t)}{(k_1 - \alpha)(k_1 - \beta)} + \frac{\exp(-\alpha t)}{(\alpha - \beta)(\alpha - k_1)} + \frac{\exp(-\beta t)}{(\beta - k_1)(\beta - \alpha)} \right] \qquad \text{(Eq. 6)}$$

In Eqs. 5 and 6, u_2 and u_3 are normalized concentrations (with respect to the initial applied concentration, C_0), *i.e.*:

$$u_2 = C_2/C_0 \qquad \text{(Eq. 7)}$$

$$u_3 = C_3/C_0 \qquad \text{(Eq. 8)}$$

and α and β are the roots of a quadratic (see *Appendix*) such that:

$$\alpha\beta = k_2 k_4 \qquad \text{(Eq. 9)}$$

$$\alpha + \beta = k_2 + k_3 + k_4 \qquad \text{(Eq. 10)}$$

As discussed previously for drug in urine (27), Eqs. 5 and 6 may be multiplied by a factor F, which is the fraction of the applied topical dose and metabolites recovered (and corrected for nonrenal excretion) in compartment 4.

EXPERIMENTAL SECTION

Using Eqs. 5 and 6, it is now possible to predict drug disposition kinetics in skin and plasma for various combinations of the four rate constants k_1–k_4. To illustrate this ability, the following approach is adopted. The input (k_1) and output (k_4) processes are arbitrarily defined as "fast" and "slow," thereby allowing four possible combinations (fast/fast, fast/slow, slow/fast, and slow/slow). Then, for each of these combinations, u_2 and u_3 are calculated for "high," "medium," and "low" ratios of k_3/k_2, *i.e.*, for different relative stratum corneum–viable tissue affinities. The numerical values selected for the rate constants are given in Tables I and II. The choice of the k_1 and k_4 ranges reflects the span observed previously between benzoic acid, testosterone, and hydrocortisone (27, 29). The k_3/k_2 ratios are designed to illustrate the ramifications of varying the effective stratum corneum–viable tissue partition coefficient[1] of the penetrant over a range of three orders of magnitude. A value of $40 \times 10^{-5}\ s^{-1}$ ($1.44\ h^{-1}$) was assigned to k_2 throughout. Such a figure has been shown to correspond to an effective solute diffusion coefficient through the viable tissue of $\sim 10^{-7}\ cm^2/s$; this is in reasonable agreement with earlier independent assessments (34). The k_3 values employed again span, but also extend, the range identified for the three penetrants given above (27). Because it is unlikely that a penetrant with less reservoir-forming ability than benzoic acid will be identified, the k_3 range has been extended in the direction of increasing stratum corneum affinity. Finally, to evaluate u_2 and u_3, V_1 and V_2 have been estimated as essentially equal for typical topical applications (*i.e.*, $V_1/V_2 \simeq 1$) and V_1/V_3 has been set equal to 2×10^{-5}, based on an applied volume of 100 μL and a plasma volume of 5 L. Hence, with four combinations of k_1 and k_4 and three k_3/k_2 values, twelve assessments each of u_2 and u_3 can be made.

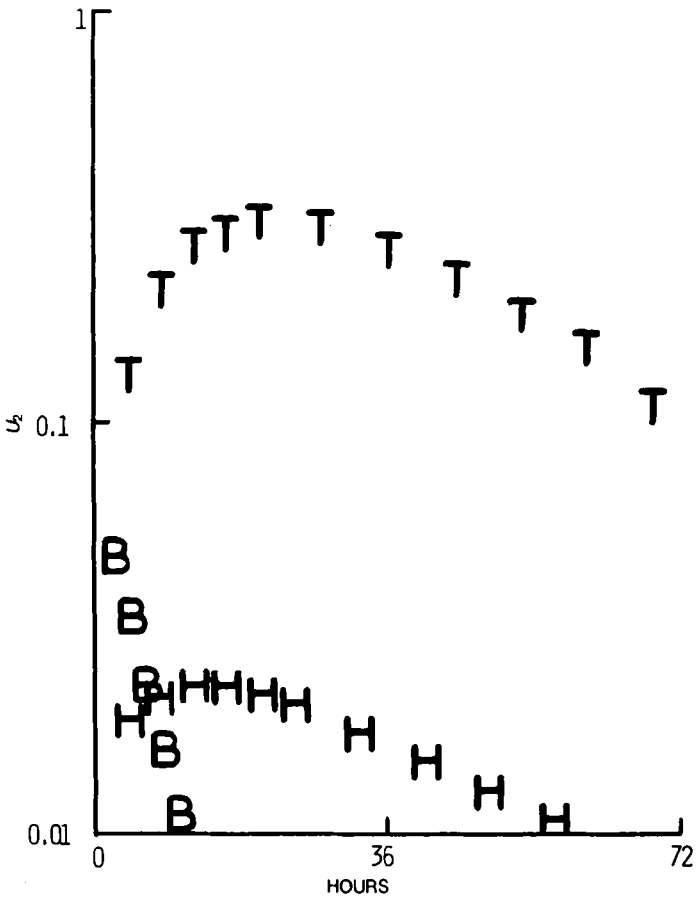

Figure 3—*Skin disposition profiles (u_2) as a function of time for testosterone (T), benzoic acid (B), and hydrocortisone (H). The curves were evaluated using the rate constants in Table III and Eq. 5.*

RESULTS AND DISCUSSION

Disposition Profiles in Skin—The graphs in Fig. 2 show a wide variety of behavior for the concentration–time course of a penetrant within the skin. There are marked differences between the curves in a quantitative sense of how much material can be found in the skin and for how long the substance is maintained within the cutaneous region. The curves clearly indicate combinations of rate constants which may not prove efficacious for the treatment of local (nonsurface) dermatological disease. For example, penetrants with low k_3/k_2 ratios fall into this category: either the drug is very rapidly eliminated from the skin (Fig. 2A–C) or it is present in relatively insignificant amounts (Fig. 2D). On the other hand, penetrants which are expected to ex-

[1] It is important to point out that the ratio of k_3/k_2 is not a true partition coefficient in the classical sense. However, because of the assigned significance of the rate processes which k_2 and k_3 describe, their ratio (a "pseudo-partition coefficient") will be related to the conventional, though not easily measurable, distribution constant of the drug between the stratum corneum and the viable tissue.

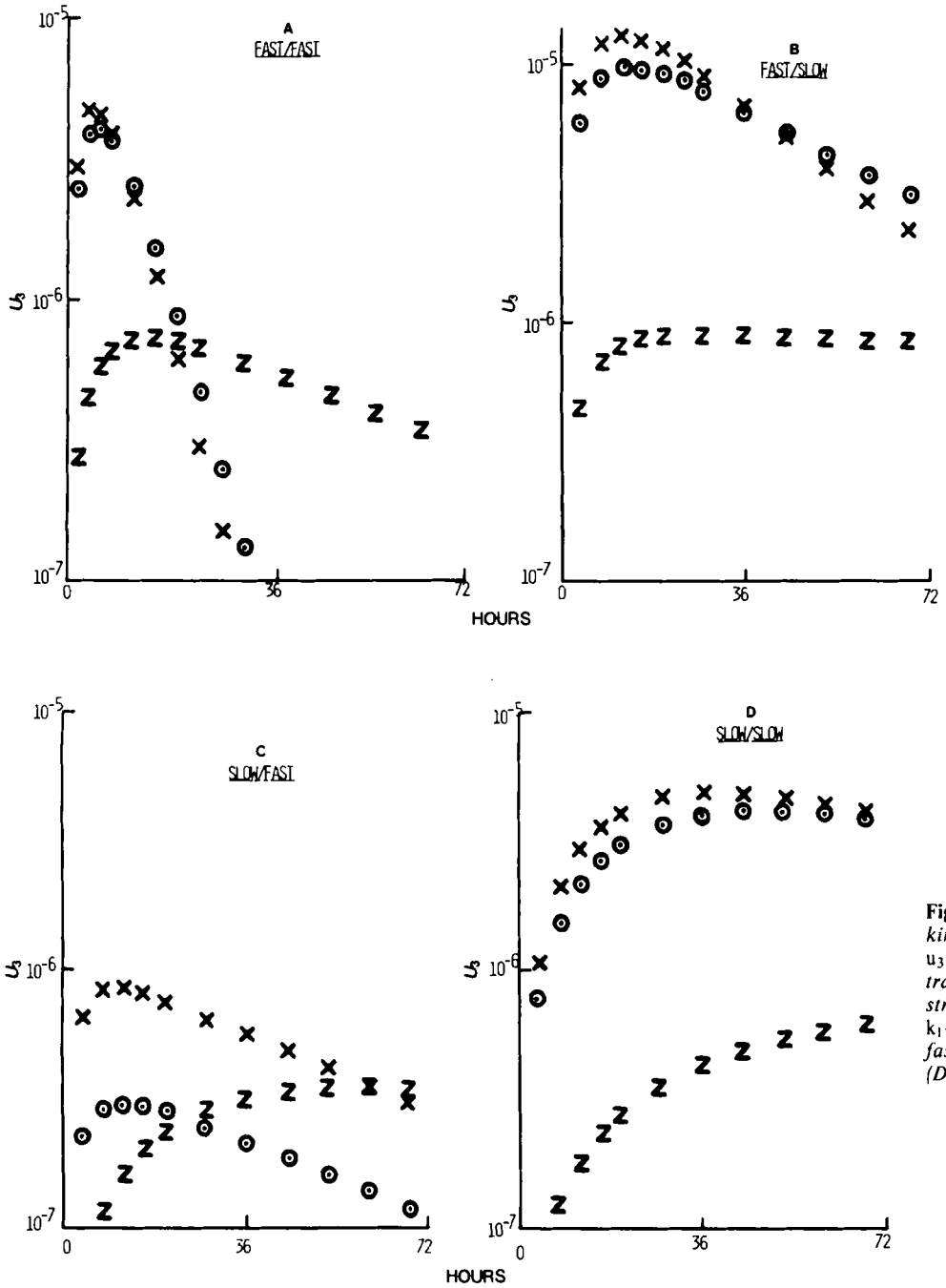

Figure 4—*Prediction of plasma disposition kinetics as a plot of normalized concentration* u_3 versus *time. The curves correspond to penetrants with high (Z), medium (⊙), and low (X) stratum corneum affinities. Rate constants* k_1-k_4 *are given in Tables I and II. Key: (A) case fast/fast; (B) case fast/slow, (C) case slow/fast; (D) case slow/slow.*

hibit substantial reservoir effects (30-33), *i.e.*, those with high k_3/k_2 values, achieve substantial and prolonged levels within the tissue. It may be noted that a fast/slow penetrant with $k_3/k_2 = 20$ (Fig. 2B, curve Z) produces potentially ideal local sustained-release characteristics over an extended time period. Of course, certain combinations of kinetic parameters may prove unlikely, *e.g.*, fast/fast with high k_3/k_2 and slow/slow with a low ratio. Furthermore, the model may not be able to distinguish between certain alternatives [the high k_3/k_2 curves in Fig. 2C (slow/fast) and D (slow/slow) provide such a case]. However, on the whole, the delineation between different permutations is good and the profiles, and their relative juxtaposition to one another, are consistent with the assigned physicochemical significance of the model.

In Figure 3, skin disposition curves are shown for testosterone, benzoic acid, and hydrocortisone. The profiles have been calculated using the rate constants quoted in the previous publication (27) of this kinetic model (see Table III). The distinction between the three compounds is striking—benzoic acid shows virtually no residence within the skin, merely a transient presence. The time course for the steroids is similar yet, quantitatively, testosterone achieves levels an order of magnitude greater than those of hydrocortisone. This observation is consistent with larger k_1 and k_3 values of testosterone and its consequently higher potential for stratum corneum reservoir formation.

Disposition Profiles in Plasma—Figure 4 shows the relative plasma disposition profiles for the various k_1-k_4 combinations considered. The curves provide a preliminary insight into the desirable transcutaneous properties required by a penetrant to be a candidate for systemic delivery *via* the topical route. Indication of sensible dosing intervals for such an objective is also available. Interestingly, the medium and low stratum corneum affinity penetrants are not distinguishable in terms of plasma level except for the slow/fast situation (Fig. 4C). Even then, the time course is identical; only the amounts are different. These observations are apparent despite a 25-fold difference between the k_3 values used in the medium and low cases. The reason for the apparent anomaly is straightforward. Only for slow/fast is the input (k_1) process substantially slower than the output (k_4) such that the differences in k_3 (medium *versus* low) can be reflected in the values of u_3.

In Figure 5, u_3 profiles for testosterone, benzoic acid, and hydrocortisone are plotted. The rate constants used for the calculations are given in Table III (27). Benzoic acid clearly falls into the fast/fast, low k_3/k_2 ratio, category. Testosterone and hydrocortisone climb to their maximum plasma levels more gradually and maintain appreciable concentrations over a prolonged period. The potential for sustained transdermal delivery of endogeneous corticosteroid hormones to treat clinical deficiencies would, therefore, appear attractive.

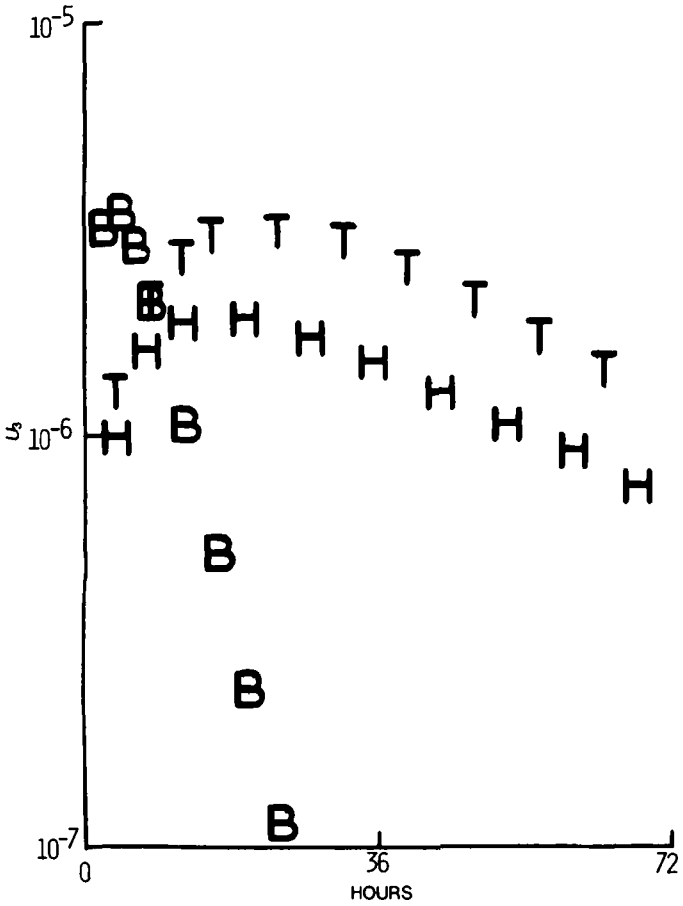

Figure 5—*Plasma disposition profiles (u_3) as a function of time for testosterone (T), benzoic acid (B), and hydrocortisone (H). The curves were evaluated using the rate constants in Table III and Eq. 6.*

APPENDIX

In this appendix, the derivation of Eqs. 5 and 6 is outlined. First, all concentrations are normalized with respect to C_0, the concentration in compartment 1 at $t = 0$:

$$u_i = C_i/C_0 \; (i = 1, 2, 3, 4) \qquad \text{(Eq. A1)}$$

Solutions for u_2 and u_3 are obtained using the technique of Laplace transformation. Substituting Eq. A1 into Eqs. 1-4 and transforming gives:

$$s\bar{u}_1 = 1 - k_1\bar{u}_1 \qquad \text{(Eq. A2)}$$

$$s\bar{u}_2 = \frac{V_1}{V_2}k_1\bar{u}_1 - k_2u_2 + \frac{V_3}{V_2}k_3\bar{u}_3 \qquad \text{(Eq. 3A)}$$

$$s\bar{u}_3 = \frac{V_2}{V_3}k_2\bar{u}_2 - (k_3 + k_4)\bar{u}_3 \qquad \text{(Eq. A4)}$$

$$s\bar{u}_4 = \frac{V_3}{V_4}k_4\bar{u}_3 \qquad \text{(Eq. A5)}$$

Equation A2 gives an expression for u_1, which may be substituted into Eq. A3. This latter equation and Eq. A4 then provide a pair of simultaneous equations which may be solved for u_2 and u_3. The algebra is trivial and the following results are obtained:

$$\bar{u}_2 = \frac{V_1}{V_2}\left[\frac{k_1(s + k_3 + k_4)}{(s + k_1)(s + \alpha)(s + \beta)}\right] \qquad \text{(Eq. A6)}$$

$$\bar{u}_3 = \frac{V_1}{V_3}\left[\frac{k_1k_2}{(s + k_1)(s + \alpha)(s + \beta)}\right] \qquad \text{(Eq. A7)}$$

where α and β are the roots of the quadratic:

$$s^2 + (k_2 + k_3 + k_4)s + k_2k_4 = 0 \qquad \text{(Eq. A8)}$$

Simple inversion of Eqs. A6 and A7 results in the expressions for u_2 and u_3 quoted in the text as Eqs. 5 and 6, respectively.

REFERENCES

(1) Y. W. Chien, "Novel Drug Delivery Systems," Dekker, New York, N.Y., 1982, pp. 149-217.

(2) S. K. Chandrasekaran and J. E. Shaw, in "Controlled Release of Bioactive Materials," R. Baker, Ed., Academic, New York, N.Y., 1980, pp 99-106.

(3) S. K. Chandrasekaran, H. Benson, and J. Urquhart, in "Sustained and Controlled Release Drug Delivery Systems," J. R. Robinson, Ed., Dekker, New York, N.Y., 1978, pp. 557-593.

(4) S. K. Chandrasekaran, A. S. Michaels, P. Campbell, and J. E. Shaw, *A.I.Ch.E.J.*, **22,** 828 (1976).

(5) J. E. Shaw, S. K. Chandrasekaran, A. S. Michaels, and L. Taskovich, in "Animal Models in Dermatology," H. I. Maibach, Ed., Churchill Livingstone, Edinburgh, U.K., 1975, pp. 138-146.

(6) S. K. Chandrasekaran, W. Bayne, and J. E. Shaw, *J. Pharm. Sci.*, **67,** 1370 (1978).

(7) S. A. Akhter, B. W. Barry, and M. C. Meyer, *J. Pharm. Pharmacol.*, **34,** 34P (1982).

(8) D. Southwell and B. W. Barry, *J. Pharm. Pharmacol.*, **33,** 1P (1981).

(9) D. Southwell and B. W. Barry, *J. Pharm. Pharmacol.*, **33,** 3P (1981).

(10) D. Southwell and B. W. Barry, "Abstracts," vol. 12(2), APhA Academy of Pharmaceutical Sciences, 1982, p. 129.

(11) S. A. Akhter, B. W. Barry, and M. C. Meyer, "Abstracts," vol. 12(2), APhA Academy of Pharmaceutical Sciences, 1982, p. 129.

(12) C. D. Yu, J. L. Fox, N. F. H. Ho, and W. I. Higuchi, *J. Pharm. Sci.*, **68,** 1341 (1979).

(13) C. D. Yu, J. L. Fox, N. F. H. Ho, and W. I. Higuchi, *J. Pharm. Sci.*, **68,** 1397 (1979).

(14) J. L. Fox, C. D. Yu, W. I. Higuchi, and N. F. H. Ho, *Int. J. Pharm.*, **2,** 41 (1979).

(15) W. J. Albery and J. Hadgraft, *J. Pharm. Pharmacol.*, **31,** 129 (1979).

(16) W. J. Albery and J. Hadgraft, *J. Pharm. Pharmacol.*, **31,** 140 (1979).

(17) J. Hadgraft, *Int. J. Pharm.*, **4,** 229 (1980).

(18) R. H. Guy and J. Hadgraft, *Int. J. Pharm.*, **11,** 187 (1982).

(19) J. Hadgraft, *Int. J. Pharm.*, **2,** 265 (1979).

(20) R. H. Guy and J. Hadgraft, *Int. J. Pharm.*, **6,** 321 (1980).

(21) P. Muller, P. R. Imhof, F. Burkart, L-C. Chu, and A. Gerardin, *Eur. J. Clin. Pharmacol.*, **22,** 473 (1982).

(22) M. Mezei and V. Gulasekharan, *Life Sci.*, **26,** 1473 (1980).

(23) M. Mezei and V. Gulasekharan, *J. Pharm. Pharmacol.*, **34,** 473 (1982).

(24) E. R. Copper, "Abstracts," vol. 12(2), APhA Academy of Pharmaceutical Sciences, 1982, p. 129.

(25) R. B. Stoughton, *Arch. Dermatol.*, **118,** 474 (1982).

(26) R. Vaidyanathan, G. L. Flynn, and W. I. Higuchi, "Abstracts," vol. 12(2), APhA Academy of Pharmaceutical Sciences, 1982, p. 126.

(27) R. H. Guy, J. Hadgraft, and H. I. Maibach, *Int. J. Pharm.*, **11,** 119 (1982).

(28) F. D. Malkinson, *J. Invest. Dermatol.*, **31,** 19 (1958).

(29) D. M. Anjo, R. J. Feldman, and H. I. Maibach, in "Percutaneous Penetration of Steroids," P. Mauvais-Jarvais, J. Wepierre, and C. F. H. Vickers, Eds., Academic, New York, N.Y., 1980, pp. 31-51.

(30) A. W. McKenzie and R. B. Stoughton, *Arch. Dermatol.*, **86,** 608 (1962).

(31) C. F. H. Vickers, *Arch. Dermatol.*, **88,** 20 (1963).

(32) R. B. Stoughton, *Arch. Dermatol.*, **91,** 657 (1965).

(33) R. K. Winkelman, *Br. J. Dermatol.*, **81** (Suppl. 4), 11 (1969).

(34) R. J. Scheuplein, *J. Invest. Dermatol.*, **48,** 79 (1967).

ACKNOWLEDGMENTS

This research was supported in part by the Wellcome Trust and the Burroughs Wellcome Fund.

Effect of Film Irregularities on Sunscreen Efficacy

JOHN J. O'NEILL

Received March 28, 1983, from *Avon Products, Inc., Suffern, NY 10901.* Accepted for publication June 24, 1983.

Abstract □ The effect of distortion of a uniform film on its opacity has been calculated for a simple step film model. Nonuniform distribution of sunscreen films on skin and of the absorber within the film would account for large discrepancies between naively predicted efficacy and that observed clinically.

Keyphrases □ Film irregularities—effect on sunscreen efficacy, opacity □ Sunscreens—effect of film irregularities, opacity

Cosmetic sunscreen products are effective in protecting the user from sunburn by absorbing injurious UV radiation, but it is well known that their performance is not nearly as good as would be predicted from the absorption spectra of their active ingredients. Spectra of strongly absorbing materials are usually measured at weight concentrations of ~0.001% in transparent solvents like water or ethanol in a cuvette with an optical path length of 1 cm. A sunscreen on the skin contains several percent of the absorber in a film with an average thickness of ~0.002 cm. The fact that such lengthy extrapolation of spectrophotometric data leads to predictions of efficacy far greater than those obtained in clinical measurements is occasionally ascribed to misapplication or even to a failure of the physical laws underlying spectrophotometry. More often it is ascribed to vehicle effects and to skin topography.

In this paper the average opacity of a simple model film is calculated as a function of its departure from uniform thickness and chemical homogeneity. It is suggested that plausible irregularities can account for discrepancies of many orders of magnitude between naively predicted and observed sunscreen efficacy.

BACKGROUND

The pharmacological measure of sunscreen efficacy, the sun protection factor (SPF), is the factor by which the product allows the time of exposure to sunlight to be increased before a given degree of sunburn occurs. For example, someone who suffers a slight sunburn after 20-min exposure could remain in sunlight of the same intensity for 40 min wearing an ointment with an SPF of 2 before suffering the same slight burn.

The equivalent physical definition is:

$$\mathrm{SPF} = \frac{\int (S \times A) \cdot d\lambda}{\int (S \times A \times T) \cdot d\lambda} \qquad \text{(Eq. 1)}$$

where $S(\lambda)$ is the intensity of sunlight under standardized conditions of altitude, latitude, time of day, *etc.* (usually replaced in clinical practice with the more accessible and intense emission spectrum of a solar simulator); $A(\lambda)$ is the skin sensitivity or action spectrum, the reciprocal of the energy per unit area of exposed skin producing a standard degree of burn (usually the minimum perceptible erythema); and $T(\lambda)$ is the fractional transmission of the sunscreen.

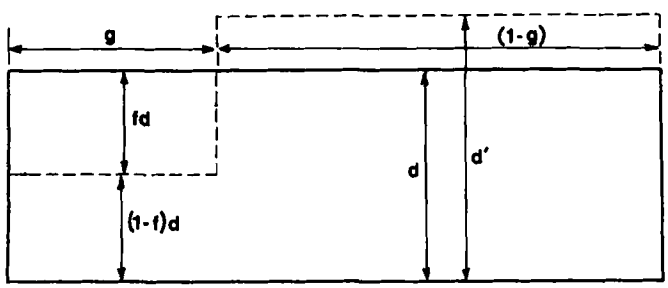

Figure 1—*Step film geometry: cross section of a rectangular slab of unit width.*

In both integrals the lower limit is ~290 nm because the function, $S(\lambda)$, is negligibly small in the standard solar spectrum at lower wavelengths. The upper limit is the wavelength above which the action spectrum, $A(\lambda)$, is so small that the product $S \times A$ is negligible. From our own experience with sunscreens, we take this limit as ~350 nm but its exact location is immaterial in the discussion that follows.

Since the dimensions of S in Eq. 1 are energy × area^{-1} × time^{-1} and those of A are erythema × energy^{-1} × area, and since T is the dimensionless ratio of transmitted to incident intensity, both the numerator and denominator have "dimensions" of erythema per unit of time. For a given degree of erythema, this reduces to the time ratio of the pharmacological definition.

For convenience, we define a protection factor for monochromatic radiation as:

$$\mathrm{MPF}(\lambda) = \frac{S(\lambda) \times A(\lambda)}{S(\lambda) \times A(\lambda) \times T(\lambda)} = 1/T(\lambda) = P(\lambda) \qquad \text{(Eq. 2)}$$

where $P(\lambda)$ is the opacity of the film. This definition is used rather than the more cumbersome Eq. 1 in the discussion that follows. For the most part, the notation of wavelength dependence is dropped, but we emphasize that MPF is a strong function of the wavelength and that it is not simply related to the SPF except in special cases (*e.g.*, where the transmission is a constant, independent of wavelength, as might be true of a dispersion of an opaque, reflective solid like aluminum powder; in this case SPF = P). The extension of conclusions regarding the effect of sunscreen film irregularities on MPF to that on SPF is discussed below where appropriate.

The opacity of a cosmetic sunscreen is given, in the first approximation, by the absorption spectrum of the active ingredient as measured in dilute solution in a transparent solvent expressed according to the Beer-Lambert law:

$$P(\lambda) = \left(\frac{I_0}{I}\right)_\lambda = 10^{k(\lambda)Cd} \qquad \text{(Eq. 3)}$$

where I_0 and I are the intensities of incident and transmitted light, $k(\lambda)$ is the absorptivity in units corresponding to those of the concentration, C, and the path length d.

Although the concentrations and path lengths in applied sunscreens differ by several orders of magnitude from those used in spectrophotometry, there are no obvious grounds for suspecting that the opacities will not be related according to Eq. 3. There are no known exceptions to Lambert's law relating opacity to path length through homogeneous bodies, and marked deviations from Beer's law (the concentration effect) are usually attributable to gross physicochemical departures from simple molecular solutions, such as ionization or complexation, which are not likely to occur with the absorbers used in sunscreens at either very high or very low concentrations. Nevertheless, sunscreen efficacy as predicted from spectrophotometry using Eq. 1, assuming a film thickness corresponding to the application level, is usually higher, sometimes by several orders of magnitude, than the SPF value measured clinically. The following calculations show that seemingly plausible deviations from uniformity of film thickness or of distribution of the absorber can account for these discrepancies.

DISCUSSION

Opacity of Step Films—Figure 1 shows the cross section of a uniform, homogeneous film of thickness d of a solution of concentration C of an absorbing solute whose absorptivity in the transparent medium is k. The broken lines show what we call a step film, produced by removing a fraction (f) of the uniform film over a fraction (g) of its area and redepositing it uniformly over the remaining area. The average intensity of light transmitted by the step film is:

$$I_s = gI_1 + (1 - g)I_2 \qquad \text{(Eq. 4)}$$

0022-3549/84/0700-0888$01.00/0
© 1984, American Pharmaceutical Association

Table I—MPF (Opacity) of Step Films Derived from a Uniform Film of Opacity 10

f^a	Fraction of Area Depleted, g					
	0.1	0.3	0.5	0.7	0.9	1.0
0.1	9.968	9.882	9.740	9.464	8.728	7.943
0.3	9.680	8.934	8.011	7.267	5.568	5.011
0.5	9.023	7.267	5.749	4.476	3.513	3.162
0.7	7.976	5.392	3.837	2.844	2.216	1.995
0.9	6.626	3.743	2.478	1.797	1.398	1.258
1.0	5.893	3.066	1.980	1.428	1.111	1.000

[a] Depth fraction.

Table II—MPF (Opacity) of Step Films Derived From a Uniform Film of Opacity 1000

f^a	Fraction of Area Depleted, g					
	0.1	0.3	0.5	0.7	0.9	1.0
0.1	968.0	893.4	801.1	686.5	556.8	501.1
0.3	662.5	374.3	247.8	179.7	139.8	125.8
0.5	264.8	103.6	63.18	45.17	35.13	31.62
0.7	76.24	26.41	15.88	11.34	8.825	7.943
0.9	19.77	6.648	3.990	2.850	2.216	1.995
1.0	9.958	3.332	1.999	1.428	1.111	1.000

[a] Depth fraction.

Table III—MPF (Opacity) of Step Films Derived From a Uniform Film of Opacity 1,000,000 [a]

f^b	Fraction of Area Depleted, g					
	0.1	0.3	0.5	0.7	0.9	1.0
0.1	845,676	632,295	472,560	357,309	279,098	251,188
0.3	145,403	52,501	31,689	22,641	17,609	15,848
0.5	9,958	3,332	2,000	1,428	1,111	1,000
0.7	630.8	210.3	126.1	90.13	70.10	63.09
0.9	39.81	13.27	7.962	5.687	4.423	3.981
1.0	10.00	3.333	2.000	1.428	1.111	1.000

[a] A 20-μm thick film of an absorber solution whose molar extinction coefficient is 30,000 L · mol^{-1} · cm^{-1} reaches this opacity at a concentration of 0.1 mol/L; for octyl dimethyl *p*-aminobenzoate (Escalol 507 brand of padimate O) this corresponds to a weight concentration ~2.8%. [b] Depth fraction.

where I_1 and I_2 are the intensities of light transmitted by the depleted and augmented areas. These are given by the Beer-Lambert law as:

$$I_1 = I_0 \cdot \exp_{10}[-kCd(1-f)] \qquad \text{(Eq. 5)}$$

$$I_2 = I_0 \cdot \exp_{10}\left[-kCd\left(\frac{fg}{1-g}+1\right)\right] \qquad \text{(Eq. 6)}$$

where I_0 is the intensity of the light normally incident on both areas. In Eqs. 5 and 6 the expressions in parentheses are the factors by which the thickness of the film is changed; the expression in Eq. 6 can be derived by equating the volumes removed, $fd \times ga$, and redeposited, $(d' - d) \times (1 - g)a$, where a is the area of the film. The average opacity of the step film, P_s, as a function of f and g, is given by combining Eqs. 3-6:

$$P_s = P_c\left[g \cdot \exp_{10}(kCdf) + (1-g) \cdot \exp_{10}\left(\frac{-kCdfg}{1-g}\right)\right]^{-1} \qquad \text{(Eq. 7)}$$

where P_c is the opacity of the uniform parent film.

Tables I-III give the calculated opacities of the step films derived from uniform films of opacities 10, 1000, and 1,000,000. The most obvious feature of these tables is that all the calculated average opacities are less than that of the uniform parent film. It might have been expected that for some range of values of the distortion factors f and g, the increase in opacity of the area on which the film thickness is increased would more than offset the loss of opacity of the depleted area. This is not so in any case: the distorted film is always less opaque.

Another disturbing feature of the behavior of the model is the dependence of the relative loss in opacity on the opacity of the parent film: for any set of values of f and g, the greater the opacity of the parent film, the greater the relative decrease in opacity. For example, at $f = g = 0.9$ (removal of 90% of the film over 90% of the area) uniform films of opacities 10, 1000, and 1,000,000 are degraded to step films with respective opacities of 14%, 0.22%, and 0.00044% of those of the parent films.

The same behavior can be viewed in terms of the absorption spectrum of the active ingredient. Note that according to Eq. 7 the ratio of step film opacity, P_s, to that of the uniform film, P_c, depends on the wavelength, because for a given film distortion (fixed values of f and g) the ratio is the reciprocal of the sum of two terms which vary exponentially with k, the absorptivity. In this view, film distortion has its greatest relative effect at the absorption maxima where the absorber is expected to be most effective; distortion blunts the spectrum of the absorber.

In Tables I-III the bottom row, where $f = 1.0$, shows the result of completely removing part of the film. Even if only 10% of the area is so depleted ($g = 0.1$), the step film opacity drops to ≤10 as would be expected from ordinary experience: if the parent film were a metallic foil of virtually infinite opacity, a few pin pricks would degrade it into an imperfect screen transmitting a fraction of incident light equal to the areal fraction of the holes, as is the case, to four significant figures in the bottom row of Table III.

The right-hand column of each table illustrates Lambert's Law relating opacity to thickness over the entire area of the film ($g = 1.0$). Removal of 90% of the film ($f = 0.9$) reduces the opacity to the tenth root of that of the parent film—from 1,000,000 to 4.0 for example, as seen in Table III.

If the geometry of sunscreens on human skin corresonds to large values of f and moderate-to-large values of g, then the values of MPF(λ) predicted according to Eq. 7, and, by inference, of SPF itself, will be very modest compared with those predicted on the assumption of a uniform film.

The dependence of step film opacity on absorber concentration as given by Eq. 7 is illustrated in Fig. 2 where the opacity of the uniform film, P_c is also shown for comparison. The opacities for a given combination of f and g are plotted on semilogarithmic graphs against the $\log_{10}$ of the opacity of the uniform parent film, which, according to Eq. 3, is proportional to the concentration C for fixed k and d. In all cases, the curve is more or less concave down, near the origin ($C = 0$, $P = 1$) and then becomes nearly log-linear at high concentration. The latter occurs when the second term in Eq. 7 becomes negligible compared with the first (when the transmittance of the augmented area is negligible compared with that of the depleted area):

$$\log P_s = \log P_c - \log g - kCdf \qquad \text{(Eq. 8)}$$

or, since $\log P_c = kCd$:

$$\log P_s = (1-f)kCd - \log g \qquad \text{(Eq. 9)}$$

which corresponds to a straight line with the slope reduced by a factor of 1 − f relative to that of $\log P_c$ against C, and with an intercept of $-\log g$ (as shown by extrapolation in a few cases).

For $f = 0.9$, P_s or MPF appears to increase linearly with absorber concentration over the range covered in Fig. 2C, as can be seen from the linear plots

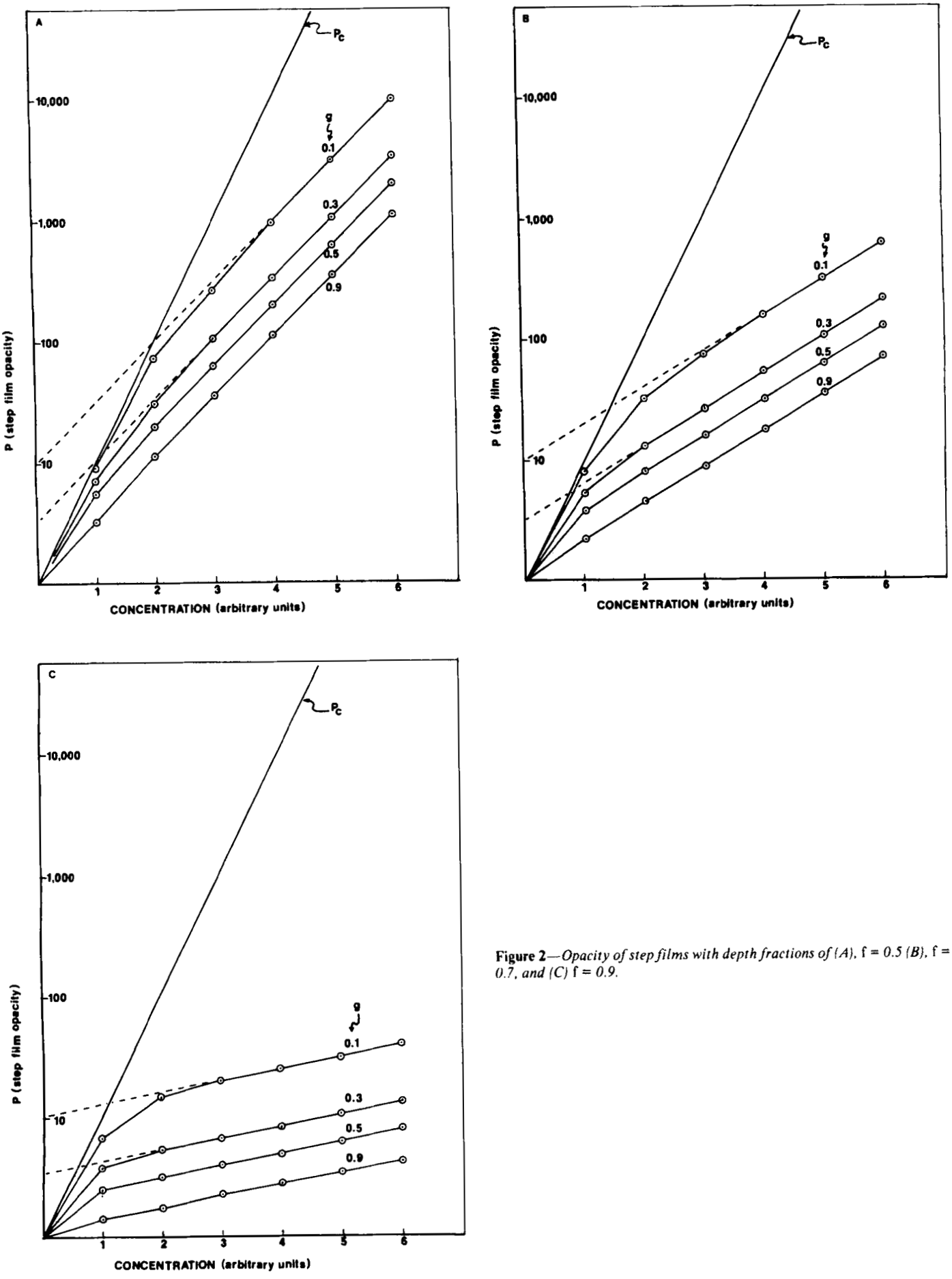

Figure 2—*Opacity of step films with depth fractions of (A), f = 0.5 (B), f = 0.7, and (C) f = 0.9.*

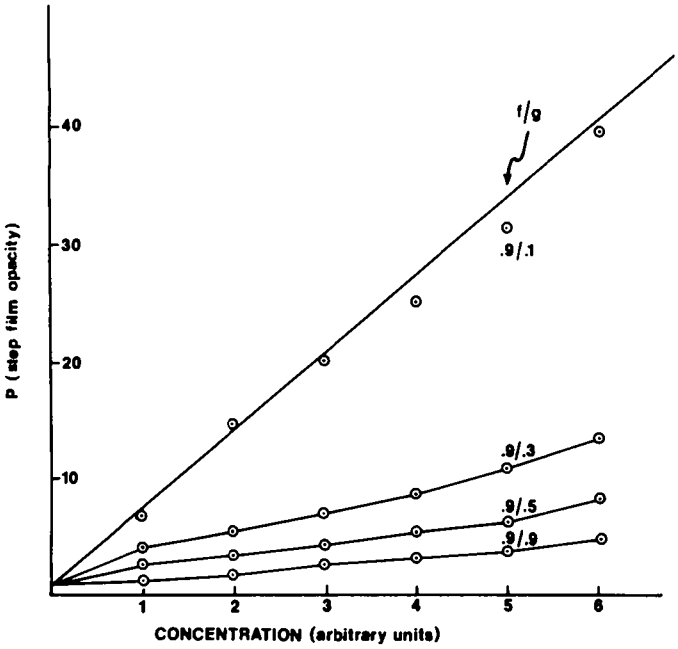

Figure 3—*Opacity of step films: linear plots against absorber concentration in arbitrary units.*

in Fig. 3. For $f = 0.7$ and 0.5, similar plots are distinctly concave up. We take this as an indication that high values of f apply to sunscreens on skin because in our clinical measurements SPF values increase roughly in proportion to absorber concentration rather than exponentially, as might be expected from Eqs. 2 and 3.

Opacity of Nonhomogeneous Films—The effect of nonuniform distribution of the absorber on the opacity of a film of uniform thickness can be treated in the same fashion as that of nonuniform thickness of a homogeneous film. The vertical dimension in Fig. 1 can be taken as a measure of absorber concentration by replacing d and d' with C and C', and deriving Eqs. 5 and 6 from conservation of the mass of absorber rather than film volume. Equation 7 follows identically; it is now immaterial whether the parameter f refers to the extent of transfer of the bulk of the film or to relocation of the absorber (except that the result of bulk transfer follows with certainty from Lambert's law while that of relocation of the absorber assumes that Beer's law applies with the same absorptivity, k, in both parts of the film; the latter is certainly not exact for some kinds of nonhomogeneity, such as recrystallization of the absorber).

Figures 2 and 3 can now be interpreted in terms of the transposed variables by labeling the abscissas as "thickness" rather than "concentration." They then show that nonhomogeneity frustrates the response of opacity to thickness (or product usage level) just as irregularities in thickness frustrates response to absorber concentration.

Origins of Irregularities—The particular geometry of the step film chosen in Fig. 1 does not enter into the derivation of average opacity. The depleted area can be broken up into any number of elements of arbitrary size and shape as seen from above (from the origin of the incident beam); only its fraction, g, enters the calculation. In fact, it is tacitly assumed in reference to sunscreens that the irregularities of thickness or concentration are distributed on a scale of distances fine enough that the resulting pattern of burned and protected skin will be averaged when subjectively scoring the degree of erythema. The only evident physical limitation is that the irregularities be large compared with the wavelength of UV light (of the order of 1 μm).

The topography of human skin is an obvious source of variation in the thickness of an applied film. Any fluid which wets the skin tends to accumulate in the sulci, the furrows which unfold to spare the inelastic epidermis from tensile stress when body movements, such as making a fist, increase the contour length along the surface. Heavily dyed mineral oil moderately applied to the skin discloses a map of the sulci; very little color is seen on the plateaus (the roughly triangular areas bounded by sulci). This pattern develops spontaneously on relaxed skin as soon as rubbing is stopped, partly because surface tension reduces the pressure of the fluid under the concave surfaces over unfilled sulci and pumps it away from the plateaus (except where it wicks up into a cone at the base of each hair). Dyed petrolatum gives somewhat more uniform coverage showing the importance of viscosity in retarding the effects of capillary action. With fluid mineral oil the plateaus are well covered only at repugnantly high levels of application.

This effect could be quantified by measurements of the cross-sectional area of the sulci and the length of sulci per unit area of skin on surface replicas (like those used in scanning electron microscopic studies of skin). The product of these two would give the sulcus volume per unit area of skin, and this would indicate the fraction of the residue of a sunscreen (or any other applied fluid) "lost" by this mechanism (which might vary from subject to subject and on different parts of the body); but, even in the absence of such data it seems evident from observation of dyed mineral oil on skin that the assumption of a uniform film thickness at tolerable application levels is a poor one.

Nonhomogeneity of the sunscreen residue on the skin is another likely cause of the disappointing performance of commercial products. When a typical sunscreen lotion is rubbed out on a microscope slide, dried at room humidity, and examined at moderate magnification, it has the irregular appearance of an ordinary emulsion residue. At least two phases are usually present: one probably derived from the water phase and another from the oil phase (as can be seen when an unrubbed, thin film is examined as it dries). Except in the very unlikely event that the UV absorber partitions between these residual phases at equal opacity, the resulting film must be optically more or less similar to a slice of Swiss cheese. If two or more absorbers are present, the array of possible distortions becomes more complex, especially if the absorbers were selected to be complementary on the basis of their dilute solution spectra, but the likelihood of a near optimal distribution seems remote.

A solution of *p*-aminobenzoic acid (PABA) in alcohol is an extreme case of poor absorber distribution in the residue. On glass the residue is a crust of small well-formed crystals with a large areal fraction of voids. On skin it is a loosely held, chalky-looking deposit which can be resolved into individual crystals with a magnifier. In either case it is obvious that even if the crystals are infinitely opaque, the residue can have an opacity no greater than the reciprocal of the areal fraction of voids (as in the bottom row of Table III). This situation is probably not altered much when a glycol or an oil is added to mask the chalkiness. Since neither of these fluids is a good PABA solvent, they would be almost as transparent to harmful radiation as the voids they fill.

CONCLUSION

The ideal sunscreen leaves a chemically and physically uniform residue on the skin. The physical form of the product as applied is not important. It may be a simple solution or a coarse emulsion but the residue after casual application should be a single continuous phase in which the absorbers are in true solution. It should tend to remain well spread on the plateaus of the skin and not accumulate in the sulci.

Quantitative Investigation of Renal Handling of Drugs in Dogs with Renal Insufficiency

AKIRA KAMIYA, KATSUHIKO OKUMURA, and RYOHEI HORI ˣ

Received January 13, 1983, from the *Department of Pharmacy, Kyoto University Hospital, Faculty of Medicine, Kyoto University, Sakyo-ku, Kyoto, 606, Japan.* Accepted for publication June 15, 1983.

Abstract □ A quantitative analytical method for studying renal handling of drugs in dogs with mild renal impairment is described. Renal damage was induced experimentally by pretreatment with mercuric chloride or neomycin. Analytical results of renal handling in those animals indicated a reduction in maximum transport of secretion, while the affinity of drugs to secretion site and reabsorption showed slight or no change. These results were consistent qualitatively with other renal function test values which demonstrated the state of glomerular or proximal renal tubular function. Evidence for the applicability of the proposed analytical method for quantitative validation of functional changes in the nephron in renally impaired animals, as well as the precise determination of the site of damage, was demonstrated. This work holds considerable promise for the study of dosage adjustments in patients with renal disease.

Keyphrases □ Renal insufficiency—effect on the renal handling of drugs, dogs, sulfamethizole, cephalexin, ampicillin, quantitative analytical method □ Sulfamethizole—renal handling in dogs, quantitative analytical method, effect of renal insufficiency □ Cephalexin—renal handling in dogs, quantitative analytical method, effect of renal insufficiency □ Ampicillin—renal handling in dogs, quantitative analytical method, effect of renal insufficiency

In the pharmacokinetics of drugs, renal excretion plays an important role. Recent reviews (1–3) have shown that the pharmacokinetics of drugs change in patients with renal failure necessitating dosage adjustments. However, there have been few reports on the quantitative measurement of renal excretion alterations. In previous papers (4–6) we have introduced a new and simple analytical method for studying renal handling of drugs in rabbits, dogs, and humans under normal conditions. Quantitative analyses of glomerular filtration, renal tubular secretion, and renal tubular reabsorption were performed simultaneously.

Patients with renal failure show complicated patterns of renal functional impairment. In some cases, such as the early phase of pyelonephritis, kidney stone, and prostatic hypertrophy, the patients have selective renal tubular dysfunction. However, changes in renal handling of drugs in such patients have not been investigated.

In this paper, we focused on the application of our method to disease models in dogs. Thus, dogs with acute renal insufficiency (induced by nephrotoxic compounds) were chosen as the model for selective renal tubular damage in humans. The changes of renal functions and renal handling of drugs on each of the transport processes were followed in these dogs. On the simultaneous measurement of the processes mentioned, the analysis indicated the great potential of the method for diagnosing the site of the dysfunction and/or the degree of severity of nephron disorders affecting the rates of urinary excretion of drugs in patients with renal impairment.

Table I—Effects of Mercuric Chloride on Renal Tubular Secretion and Reabsorption of Sulfamethizole in a 7.5-kg Dog

	V_{max}[b], μmol/min	K_m[c], μM	R[d]	V'_m[e], μmol/min/kg
Control	17	100	0.10	2.3
24 h[a]	16	100	0.20	2.1
48 h[a]	11	98	0.21	1.5
72 h[a]	7	99	0.23	0.9

[a] Time after mercuric chloride injection. [b] Maximum velocity of secretion. [c] Michaelis constant. [d] Reabsorption fraction. [e] Corrected V_{max}.

EXPERIMENTAL SECTION

Materials—Sulfamethizole was of JP IX grade[1]. Cephalexin monohydrate[2], sodium ampicillin[2], and neomycin sulfate[3] were obtained commercially. All other chemicals were reagent grade.

Analytical Methods—*Sulfamethizole*—Plasma and urine samples were treated with deproteinizing reagents (7) and then analyzed by the procedure of Bratton and Marshall (8), using 2-dimethylaminoethyl-1-naphthylamine as the coupling reagent. Unbound (protein-free) sulfamethizole concentrations in plasma were determined by ultrafiltration using a membrane cone[4].

Cephalexin and Ampicillin—Drug concentrations in plasma and urine were determined fluorometrically (9, 10). Unbound drugs in plasma were assayed after ultrafiltration using cellulose tubing[5].

Inulin and Creatinine—Inulin concentrations in plasma and urine were measured by a modification of the method of Dische and Borenfreund (11). Creatinine levels in plasma and urine were analyzed by Jaffe's reaction using picric acid (12).

Other Urinalyses—Urine lysozyme activity was determined by the method of Litwack (13), and urine glutamic oxaloacetic transaminase (GOT) activity was assayed using 2,4-dinitrophenylhydrazine as the color reagent (14). Blood urea nitrogen (BUN) was measured by the modified diacetylmonoxime method (15). Urinary protein was estimated using urinalysis reagent strips[6].

Animal Model—Male mongrel dogs weighing 5–15 kg were used. The animals each received a single 15-mg/kg im injection of mercuric chloride or 45-mg/kg sc injections of neomycin sulfate daily for 7 d. These doses of nephrotoxic compounds were chosen to produce the selective renal tubular damage and the mild disease states, which changed slowly. Under these conditions, we could follow the changes in renal function and renal handling of drugs with time. These dosages did not cause diarrhea, and food intake and body weight did not change more than 10% throughout the experimental period. For the dogs with acute renal insufficiency induced by mercuric chloride, renal clearance experiments were performed before and after mercuric chloride injection. For the neomycin-treated dogs, the experiments were carried out before injection, 3 and 7 d after the first injection, and 1 and 2 weeks after the final injection.

Renal Clearance Experiment—Animals were anesthetized with pentobarbital (27 mg/kg ip). Each animal received a constant infusion of 4% (w/v) mannitol and 0.3% (w/v) inulin in saline at 3 mL/min throughout the experiment. Blood samples were taken by venipuncture. Urine samples were collected *via* a catheter. Urinary pH was measured immediately after collection.

Each drug was dissolved in saline and given intravenously. Urine was collected for 2 h beginning 5 min[1] after injection and at 10-min intervals thereafter. During this 2-h experiment, 6–10 blood samples were drawn, and total and unbound drug were determined in the plasma as described under *Analytical Methods*. Blood collection was performed at 1 min before the midpoint of the selected urine collection period in order to correct the delay time of drug appearance from blood to urine.

The glomerular filtration rate (GFR) was determined by inulin clearance. Clearance ratios were calculated for each sample using the unbound drug concentration in plasma (Pf) and expressed as the excretion ratio (ER) using the following:

$$ER = \frac{U \cdot V}{GFR \cdot Pf} \qquad \text{(Eq. 1)}$$

[1] Eizai Co. Ltd.
[2] Toyo Jozo Co. Ltd.
[3] Meiji Seika Co. Ltd.
[4] Centriflo CF-50A; Amicon Co. Ltd.
[5] 8/32; Visking Co.
[6] G. P. Pretest Wako; Wako Pure Chemicals.

0022-3549/84/0700-0892$01.00/0
© 1984, American Pharmaceutical Association

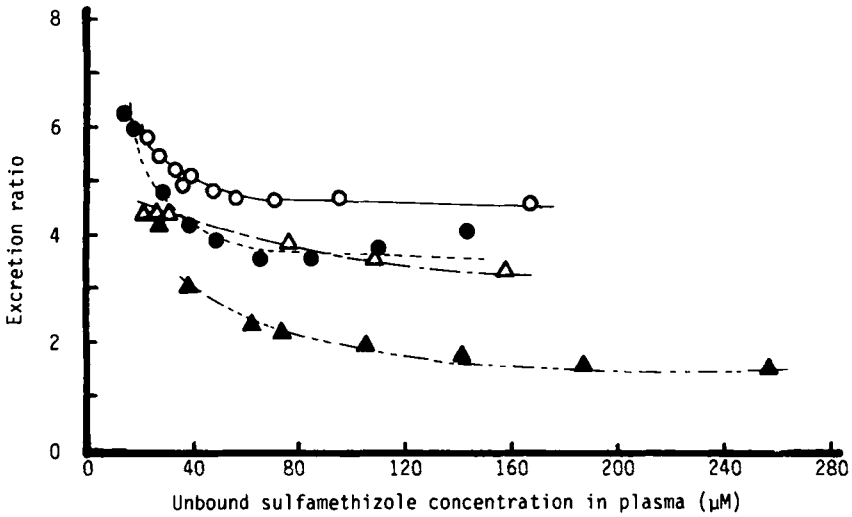

Figure 1—*Representative plot of renal clearance of sulfamethizole in a dog and computer-simulated curves before and after mercuric chloride injection. Key: (○) control (before mercuric chloride injection); (●) 24 h; (△) 48 h; (▲) 72 h.*

where U is drug concentration in urine and V is the urine flow rate. In some animals, the clearance experiments were repeated two to three times within 2–7 d under normal conditions to check the reproducibility of these experiments; the excretion ratios among the experiments were almost the same. The last clearance experiment was used as "control" in those cases.

Computer Analyses—Computer analyses were carried out using the following equation as previously described (4–6):

$$ER = \left(1 + \frac{V_{max}}{(K_m + Pf) \cdot GFR}\right) \cdot (1 - R) \qquad \text{(Eq. 2)}$$

where V_{max} is the maximum velocity of secretion, K_m is the Michaelis constant, and R is the reabsorption fraction.

RESULTS

The effects of disease on the renal clearance of various drugs injected intravenously were investigated in dogs with mild renal insufficiency induced by the administration of mercuric chloride. Figure 1 shows typical patterns of sulfamethizole secretion through the kidney and computer-simulated curves using the data listed in Table I. Excretion ratios of sulfamethizole declined as a function of time after administration of mercuric chloride. Using each curve, the maximum velocity of secretion (V_{max}), affinity constant of drug to the site of secretion (K_m), and tubular reabsorption fraction (R) were calculated. The analytical results indicated that the treatment with mercuric chloride markedly reduced the V_{max}, but K_m remained unchanged (Table I, Fig. 2). Also, administration of mercuric chloride produced an increase in renal tubular reabsorption as the urine pH decreased (Fig. 2), but glomerular filtration rate (GFR), creatinine clearance (Ccr), and BUN remained unaltered. Regarding the renal tubular functions, however, urine lysozyme activity, urine GOT activity, and urinary protein increased with time after mercuric chloride injection.

Concomitantly, the effects of disease on the renal clearance of ampicillin (Fig. 3a) and cephalexin (Fig. 3b) were also studied 48 h after the injection of mercuric chloride. Similar results as those for sulfamethizole were obtained using either drug; *i.e.*, V_{max} diminished substantially (50–60% of control), while K_m and R showed no significant change compared with the control values. Urine lysozyme activity increased markedly, while GFR decreased slightly.

Renal clearance experiments for sulfamethizole were then carried out on neomycin-treated dogs. Figure 4 shows representative results of this experi-

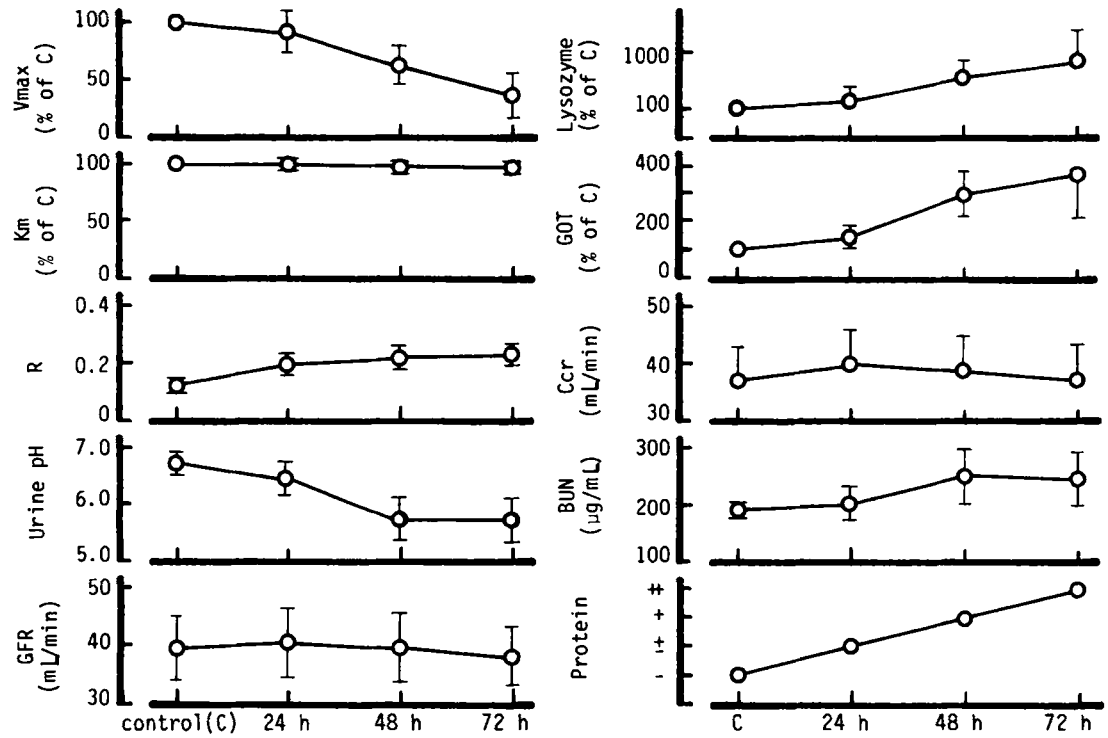

Figure 2—*Effects of mercuric chloride on various renal functions in dogs. Data represent mean ± SD of three animals. Key: (V_{max}) maximum velocity of secretion of sulfamethizole; (K_m) Michaelis constant for secretion of sulfamethizole; (R) reabsorption fraction of sulfamethizole; (GFR) glomerular filtration rate; (Lysozyme) lysozyme activity in urine; (GOT) glutamic oxaloacetic transaminase activity in urine; (Ccr) creatinine clearance; (BUN) blood urea nitrogen; (Protein) urinary protein; (C) control.*

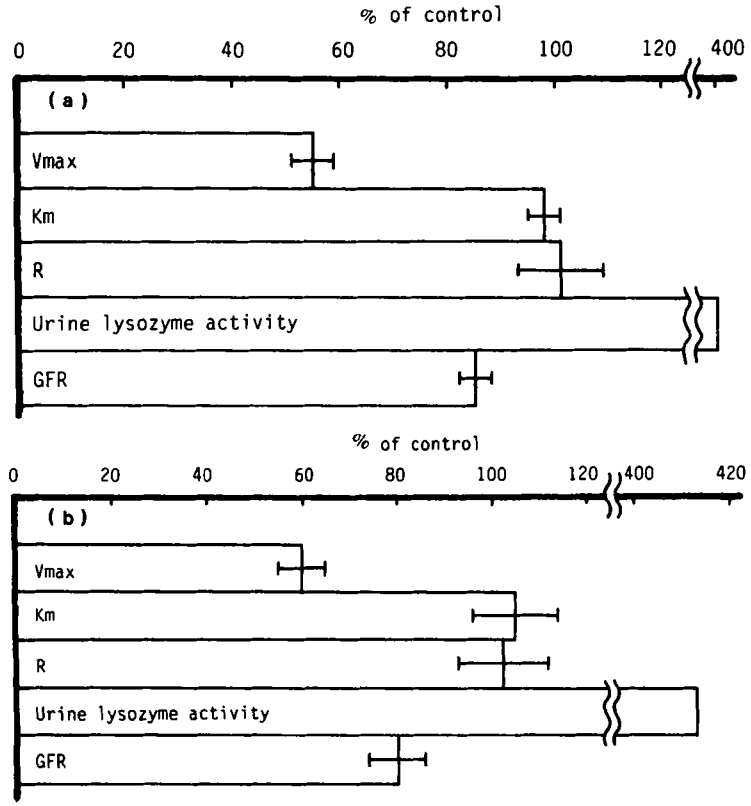

Figure 3—*Effects of mercuric chloride on the renal clearances of ampicillin (a) and cephalexin (b) and renal function of dogs 48 h after injection. Data represent mean ± SD of three animals. Abbreviations are as described in Fig. 2.*

ment with computer-simulated curves, and Table II presents the analytical data. The administration of neomycin decreased the excretion ratio for sulfamethizole, with a gradual recovery on the cessation of neomycin effect with time (Figs. 4 and 5). Our analysis clearly demonstrated the substantial reduction of V_{max} during the neomycin treatment (Table II, Fig. 5: 3 and 7 d). One and two weeks after the end of neomycin treatment, V_{max} increased and approached the values of the control, although K_m and R remained unmodified throughout the experiments (Table II, Fig. 5). Slight increases in lysozyme and GOT excretion in urine were detected (Fig. 5). GFR and Ccr were decreased ~20% as compared with the controls, but BUN showed no increase, except 7 d after the start of neomycin treatment (Fig. 5).

DISCUSSION

Some patients with renal failure show a nonparallel decrease of glomerular and tubular functions. However, the changes in renal handling of drugs in such patients are unknown. Thus, experiments were performed to clarify those quantitative changes using our proposed method. As a subclinical study, mercuric chloride- or neomycin-treated dogs were chosen as the model of selective renal tubular impairment.

Induction of renal impairment by mercuric chloride is well known. Histological studies have shown primary damage in the proximal tubular cells (16, 17). Thus, dogs treated with mercuric chloride were used as a model for the study of the effect of acute renal disease on drug clearance.

Dogs treated with mercuric chloride showed no significant change in the indices of glomerular filtration (GFR, Ccr, and BUN) as compared with the normal condition (Fig. 2). However, the urine pH decreased (Fig. 2), indicating alteration of the kidney function. The significant increases of lysozyme, GOT, and protein in the urine indicated renal tubular damage.

Lysozyme and GOT in urine have been reported to reflect the proximal tubular cell function (18, 19). As these two enzymes are actively reabsorbed by the proximal tubular cells, they are excreted into urine in minute amounts

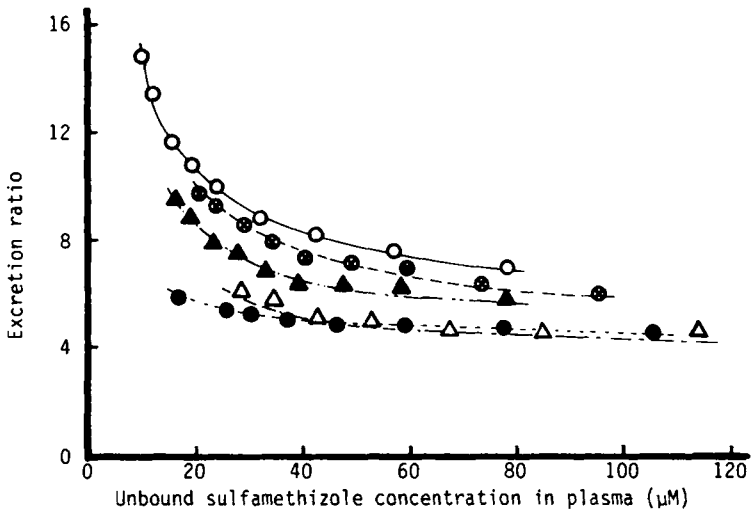

Figure 4—*Representative plot of renal clearance of sulfamethizole in a dog and computer-simulated curves before, during, and after neomycin injections. Key: (○) control (before injection); (●) 3 d and (△) 7 d after the first neomycin injection; (▲) 1 week and (⊗) 2 weeks after the final neomycin injection.*

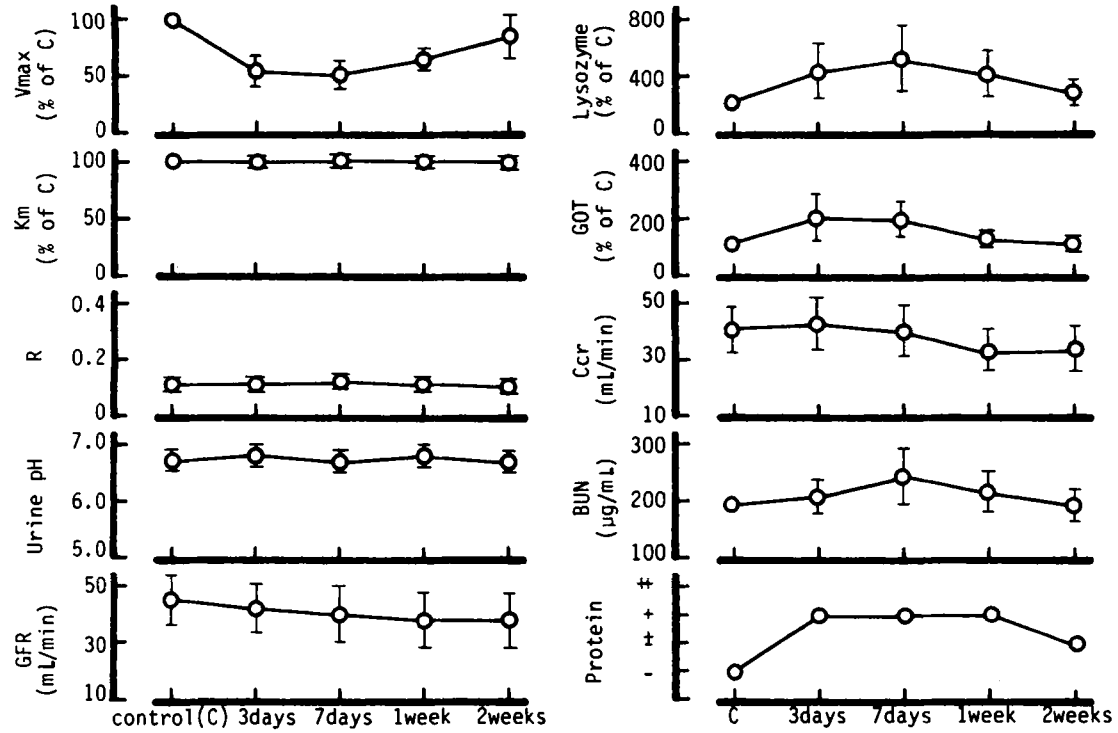

Figure 5—*Effects of neomycin on various renal functions in dogs. Data represent mean ± SD of three animals. Abbreviations are as described in Fig. 2.*

under normal conditions. The excreted amounts of these enzymes increase as the number of injured renal tubular cells increase. Increased lysozyme and GOT activities in urine, therefore, indicate damage of the proximal renal tubules (Fig. 2). Further, the increase in urinary protein has been considered due to cell debris from damaged tubular cells.

Results gathered in the study of sulfamethizole using the clearance method fitted the above findings with good qualitative compatibility, *i.e.*, a marked decrease in maximum velocity of secretion, V_{max}, and no change in the affinity constant of secretion, K_m, which suggested the reduction in the number of intact proximal tubules. Also, the absence of alteration in reabsorption for cephalexin and ampicillin, as shown in Fig. 3, and the pH-dependent changes in the reabsorption for sulfamethizole supported the finding that renal tubular reabsorptive function was intact. The analytical data clearly demonstrated that the reduction in excretion ratios were mainly due to decreases in V_{max} for secretion.

Specific proximal tubular cell damage has also been reported for neomycin (20, 21). Our results indicated only mild damage to the proximal tubules, as shown in Fig. 5. Subsequently, signs of recovery from damage caused by neomycin injections were detected. Under this slightly impaired condition (Ccr remained the same or decreased slightly), the excretion ratios were substantially diminished, and the analytical data revealed that this reduction was due to the decrease in V_{max} (Table II). These results were consistent with the early report of neomycin effects by Gol'dberg (20). He reported changes in the transport maximum of *p*-aminohippurate (Tm PAH) and Ccr under the conditions we used, with greater reduction of Tm PAH than of Ccr. Present results also showed a greater reduction of V_{max} than of Ccr.

Although body weights did not change more than 10% over the course of the experiment, since the dogs varied in weight from 5 to 15 kg, V_{max} per unit weight (V'_m) was calculated. V'_m showed small variation among dogs (Tables I and II).

Table II—Effects of Neomycin on Renal Tubular Secretion and Reabsorption of Sulfamethizole in a 15-kg Dog

	V_{max}[c], μmol/min	K_m[d], μM	R[e]	V'_m[f], μmol/min/kg
Control	33	90	0.90	2.2
3 d[a]	18	89	0.10	1.1
7 d[a]	18	98	0.12	1.2
1 week[b]	21	95	0.10	1.4
2 weeks[b]	28	93	0.09	1.9

[a] Days after the first neomycin injection. [b] Weeks after the final neomycin injection. [c] Maximum velocity of secretion. [d] Michaelis constant. [e] Reabsorption fraction. [f] Corrected V_{max}.

In conclusion, the quantitative data gathered on the renal handling of drugs in dogs with experimentally induced acute renal insufficiency provided conclusive evidence for the reliability of the clearance method for qualitatively testing renal function. Functional changes in the nephron could be also quantitatively estimated.

Recently, a kinetic model (using normal dogs) of the renal excretion of iodopyracet has been proposed (22). That method has not been useful clinically since data fitting for plasma concentrations must be done prior to the calculation of parameters for urinary excretion rates. Our equation was simple and suitable for clinical application in patients with renal failure and was found to be more appropriate than that method using the Akaike's information criterion (23, 24).

This study suggests the use of the described method in dosage adjustments for patients with renal disease. This possibility is now being tested clinically in patients with renal failure where the renal tubular functions are reduced more than their creatinine clearance.

REFERENCES

(1) E. A. Jackson and D. C. McLeod, *Am. J. Hosp. Pharm.*, **31**, 36, 137 (1974).

(2) R. Guglar and D. L. Azernoff, *Clin. Pharmacokinet.*, **1**, 25 (1976).

(3) W. M. Bennet, R. S. Muther, R. A. Parker, P. Feig, G. Morrison, T. A. Golper, and I. Singer, *Ann. Intern. Med.*, **93**, 62,286 (1980).

(4) R. Hori, K. Sunayashiki, and A. Kamiya, *J. Pharm. Sci.*, **65**, 463 (1976).

(5) R. Hori, K. Sunayashiki, and A. Kamiya, *Chem. Pharm. Bull.*, **26**, 740 (1978).

(6) A. Kamiya, K. Okumura, and R. Hori, *J. Pharm. Sci.*, **72**, 440 (1983).

(7) M. Somogyi, *J. Biol. Chem.*, **86**, 655 (1930).

(8) A. C. Bratton and E. K. Marshall, *J. Biol. Chem.*, **128**, 537 (1939).

(9) K. Miyazaki, O. Ogino, and T. Arita, *Chem. Pharm. Bull.*, **22**, 1910 (1974).

(10) K. Miyazaki, O. Ogino, and T. Arita, *Chem. Pharm. Bull.*, **27**, 2273 (1979).

(11) Z. Dische and F. Borenfreund, *J. Biol. Chem.*, **192**, 583 (1951).

(12) R. W. Bonsnes and H. H. Taussky, *J. Biol. Chem.*, **158**, 581 (1945).

(13) G. Litwack, *Proc. Soc. Exp. Biol. Med.*, **89**, 401 (1955).

(14) S. Reitman and S. Frankel, *Am. J. Clin. Pathol.*, **28**, 56 (1957).

(15) S. Natelson, M. L. Scott, and C. Belfa, *Am. J. Clin. Pathol.*, **21**, 275 (1951).
(16) H. L. Conn, Jr., L. Wilds, and J. Helwig, *J. Clin. Invest.*, **33**, 732 (1954).
(17) A. Kleinzeller and J. H. Cort, *Biochem. J.*, **67**, 15 (1954).
(18) T. Fujita and M. Itakura, *J. Lab. Clin. Med.*, **92**, 135 (1978).
(19) C. Kobayashi, *Jikeikai Med. J.*, **89**, 46 (1974).
(20) L. E. Gol'dberg, *Antibiotiki*, **12**, 588 (1967).
(21) L. E. Gol'dberg and I. P. Belova, *Antibiotiki*, **13**, 1076 (1968).
(22) P. Hekman and C. A. M. van Ginneken *J. Pharmacokinet. Biopharm.*, **10**, 77 (1982).
(23) H. Akaike, *Math. Sci.*, **14** (153), 5 (1976).
(24) K. Yamaoka, T. Nakagawa, and T. Uno, *J. Pharmacokinet. Biopharm.*, **6**, 165 (1978).

Aqueous Conversion Kinetics and Mechanisms of Ancitabine, a Prodrug of the Antileukemic Agent Cytarabine

LEE E. KIRSCH * and ROBERT E. NOTARI ˣ

Received November 22, 1982 from *Lloyd M. Parks Hall, College of Pharmacy, The Ohio State University, Columbus, OH 43210.* Accepted for publication June 1, 1983. *Present address: Product Development Division, Eli Lilly and Co., Indianapolis, IN 46206.

Abstract □ The kinetics of conversion of the prodrug ancitabine to the anticancer drug cytarabine have been studied in aqueous solutions in the pH range of 1.5–10.7, temperature range of 19.5–80.0°C, ionic strength range of 10^{-4} to 1.5, and in the presence of several general-base catalysts. Under all conditions ancitabine was quantitatively converted to cytarabine. The pH–rate profiles were linear with slope = 1 in alkaline pH, becoming pH independent in the region of maximum stability at pH ≤ 4, where buffer catalysis was found to be insignificant and $k_{obs} \cong (1.12 \times 10^{11}\ h^{-1})\exp\{-10121\ deg/T\}$. At 30°C, pH ≤ 4, it is calculated that an aqueous ancitabine solution will maintain 90% of its initial concentration for 12 d. A novel method for measuring general-base catalysis in competition with predominating specific-base catalysis and in the presence of secondary salt effects at constant ionic strength was developed. Three mechanisms of hydrolytic prodrug conversion are proposed: nucleophilic hydroxide addition, general base-assisted nucleophilic water attack, and spontaneous water attack.

Keyphrases □ Ancitabine—conversion to cytarabine, kinetics, aqueous solutions □ Cytarabine—conversion of ancitabine, aqueous solutions, kinetics □ Kinetics—ancitabine conversion to cytarabine, aqueous solutions

Ancitabine (I), a prodrug of the antileukemic agent cytarabine (II), has been shown to be more effective than II in several animal tumor systems (1, 2) (Scheme I). The pharmacological activity of I is attributed to its conversion to II rather than any direct effect on nucleic acid synthesis (3, 4). Although incubation of I with Ehrlich ascites carcinoma cells demonstrated very little uptake of I, significant intracellular concentrations of II were nonetheless observed (5).

Intravenous doses of I are primarily excreted unchanged in urine together with II and its inactive metabolite, 1-β-D-arabinosyluracil (III) (3, 6, 7). The efficacy of II is limited by its rapid deamination to III (6). It has been suggested that a depot form of II might be useful in maintaining effective levels (8).

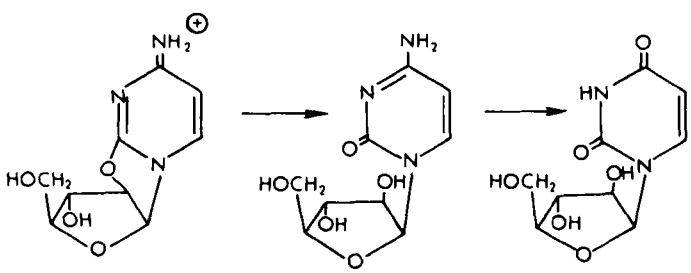

I II III

Scheme I

Unlike II, I is not phosphorylated nor deaminated (6, 9, 10). A prodrug may extend the biological duration of the drug through slow prodrug absorption or rate-limiting conversion to the drug (11). Ancitabine may act as a reservoir through hydrolytic production of II (8).

In vivo conversion of I is thought to be chemical rather than enzymatic hydrolysis (8, 12, 13). The purpose of this study was to investigate the kinetics and mechanisms of prodrug hydrolysis in aqueous solutions. Since I, like II, is not orally active (6), it is important to define its stability for preparation and storage of parenteral formulations.

EXPERIMENTAL SECTION

Stability in Sodium Hydroxide and Hydrochloric Acid Solutions Using Thin-Layer Chromatography—Samples of 0.01 M ancitabine (I)[1] in 0.1 M HCl and 0.05 M NaOH at 50°C were taken over a 4-d period, and 10-μL aliquots were spotted together with reference samples of I, II[2], III[3], and cyclouridine[4] on 20 × 20-cm TLC plates (0.25 mm silica gel GF)[5]. The plates were developed to 10 cm in water-saturated 1-butanol–propanol (3:1), air dried, and examined at 254 nm. A time zero plate was also impregnated with I_2 vapor, and 0- and 1-h plates were sprayed with sulfuric acid and heated. This procedure was also used periodically in the kinetic studies to identify the components in the reaction mixtures.

Spectrophotometric Analysis of Ancitabine and Cytarabine in Mixtures—Absorbance spectra from 220 to 330 nm were obtained for synthetic mixtures to determine which wavelengths could best be monitored for reaction time-course changes[6]. These showed an isosbestic point at 267 nm.

Beer's law plots in 0.1 M HCl provided molar absorptivities (ε) at 240 and 290 nm of 7.25×10^3 and 4.70×10^2 for I and 1.38×10^3 and 1.05×10^4 for II. Known concentrations in mixtures were successfully calculated using:

$$10^5 \cdot [I] = 13.914A_{240} - 1.828A_{290} \quad \text{(Eq. 1)}$$

$$10^5 \cdot [II] = 9.604A_{290} - 0.623A_{240} \quad \text{(Eq. 2)}$$

which were derived from simultaneous equations for total absorbance, A, at 240 and 290 nm for mixtures of I and II.

Analysis of Three-Component Mixtures—Reverse-phase HPLC with

[1] 2,2′-Anhydro-(1-β-D-arabinofuranosyl)-cytosine; Sigma Chemical Co., St. Louis, Mo.
[2] Cytarabine; The Upjohn Co., Kalamazoo, Mich. The chemical name is 1-β-D-arabinofuranosylcytosine, the IUPAC name is arabinosylcytosine, and the common name is cytosine arabinoside (ara-C).
[3] Uracil-β-D-arabinofuranoside; Sigma Chemical Co., St. Louis, Mo.
[4] β-D-O^2,2′-cyclouridine; Terra-Marine Bioresearch, La Jolla, Calif.
[5] Type TLP 109; New England Nuclear, Boston, Mass.
[6] Model 250 spectrophotometer with model 6051 recorder, model 2451A automatic cell positioner, and model 6047 thermosensor; Gilford Instruments, Oberlin, Ohio.

0022-3549/84/0700-0896$01.00/0
© 1984, American Pharmaceutical Association

(15) S. Natelson, M. L. Scott, and C. Belfa, *Am. J. Clin. Pathol.*, **21**, 275 (1951).
(16) H. L. Conn, Jr., L. Wilds, and J. Helwig, *J. Clin. Invest.*, **33**, 732 (1954).
(17) A. Kleinzeller and J. H. Cort, *Biochem. J.*, **67**, 15 (1954).
(18) T. Fujita and M. Itakura, *J. Lab. Clin. Med.*, **92**, 135 (1978).
(19) C. Kobayashi, *Jikeikai Med. J.*, **89**, 46 (1974).
(20) L. E. Gol'dberg, *Antibiotiki*, **12**, 588 (1967).
(21) L. E. Gol'dberg and I. P. Belova, *Antibiotiki*, **13**, 1076 (1968).
(22) P. Hekman and C. A. M. van Ginneken *J. Pharmacokinet. Biopharm.*, **10**, 77 (1982).
(23) H. Akaike, *Math. Sci.*, **14** (153), 5 (1976).
(24) K. Yamaoka, T. Nakagawa, and T. Uno, *J. Pharmacokinet. Biopharm.*, **6**, 165 (1978).

Aqueous Conversion Kinetics and Mechanisms of Ancitabine, a Prodrug of the Antileukemic Agent Cytarabine

LEE E. KIRSCH * and ROBERT E. NOTARI ˣ

Received November 22, 1982 from *Lloyd M. Parks Hall, College of Pharmacy, The Ohio State University, Columbus, OH 43210.* Accepted for publication June 1, 1983. *Present address: Product Development Division, Eli Lilly and Co., Indianapolis, IN 46206.

Abstract □ The kinetics of conversion of the prodrug ancitabine to the anticancer drug cytarabine have been studied in aqueous solutions in the pH range of 1.5–10.7, temperature range of 19.5–80.0°C, ionic strength range of 10^{-4} to 1.5, and in the presence of several general-base catalysts. Under all conditions ancitabine was quantitatively converted to cytarabine. The pH–rate profiles were linear with slope = 1 in alkaline pH, becoming pH independent in the region of maximum stability at pH ≤ 4, where buffer catalysis was found to be insignificant and $k_{obs} \cong (1.12 \times 10^{11}\ h^{-1})\exp\{-10121\ deg/T\}$. At 30°C, pH ≤ 4, it is calculated that an aqueous ancitabine solution will maintain 90% of its initial concentration for 12 d. A novel method for measuring general-base catalysis in competition with predominating specific-base catalysis and in the presence of secondary salt effects at constant ionic strength was developed. Three mechanisms of hydrolytic prodrug conversion are proposed: nucleophilic hydroxide addition, general base-assisted nucleophilic water attack, and spontaneous water attack.

Keyphrases □ Ancitabine—conversion to cytarabine, kinetics, aqueous solutions □ Cytarabine—conversion of ancitabine, aqueous solutions, kinetics □ Kinetics—ancitabine conversion to cytarabine, aqueous solutions

Ancitabine (I), a prodrug of the antileukemic agent cytarabine (II), has been shown to be more effective than II in several animal tumor systems (1, 2) (Scheme I). The pharmacological activity of I is attributed to its conversion to II rather than any direct effect on nucleic acid synthesis (3, 4). Although incubation of I with Ehrlich ascites carcinoma cells demonstrated very little uptake of I, significant intracellular concentrations of II were nonetheless observed (5).

Intravenous doses of I are primarily excreted unchanged in urine together with II and its inactive metabolite, 1-β-D-arabinosyluracil (III) (3, 6, 7). The efficacy of II is limited by its rapid deamination to III (6). It has been suggested that a depot form of II might be useful in maintaining effective levels (8).

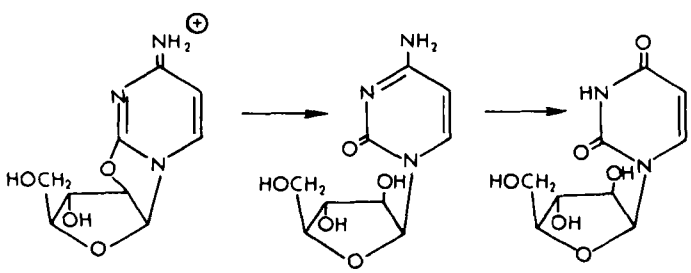

I II III

Scheme I

Unlike II, I is not phosphorylated nor deaminated (6, 9, 10). A prodrug may extend the biological duration of the drug through slow prodrug absorption or rate-limiting conversion to the drug (11). Ancitabine may act as a reservoir through hydrolytic production of II (8).

In vivo conversion of I is thought to be chemical rather than enzymatic hydrolysis (8, 12, 13). The purpose of this study was to investigate the kinetics and mechanisms of prodrug hydrolysis in aqueous solutions. Since I, like II, is not orally active (6), it is important to define its stability for preparation and storage of parenteral formulations.

EXPERIMENTAL SECTION

Stability in Sodium Hydroxide and Hydrochloric Acid Solutions Using Thin-Layer Chromatography—Samples of 0.01 M ancitabine (I)[1] in 0.1 M HCl and 0.05 M NaOH at 50°C were taken over a 4-d period, and 10-μL aliquots were spotted together with reference samples of I, II[2], III[3], and cyclouridine[4] on 20 × 20-cm TLC plates (0.25 mm silica gel GF)[5]. The plates were developed to 10 cm in water-saturated 1-butanol–propanol (3:1), air dried, and examined at 254 nm. A time zero plate was also impregnated with I_2 vapor, and 0- and 1-h plates were sprayed with sulfuric acid and heated. This procedure was also used periodically in the kinetic studies to identify the components in the reaction mixtures.

Spectrophotometric Analysis of Ancitabine and Cytarabine in Mixtures—Absorbance spectra from 220 to 330 nm were obtained for synthetic mixtures to determine which wavelengths could best be monitored for reaction time-course changes[6]. These showed an isosbestic point at 267 nm.

Beer's law plots in 0.1 M HCl provided molar absorptivities (ε) at 240 and 290 nm of 7.25×10^3 and 4.70×10^2 for I and 1.38×10^3 and 1.05×10^4 for II. Known concentrations in mixtures were successfully calculated using:

$$10^5 \cdot [I] = 13.914A_{240} - 1.828A_{290} \quad \text{(Eq. 1)}$$

$$10^5 \cdot [II] = 9.604A_{290} - 0.623A_{240} \quad \text{(Eq. 2)}$$

which were derived from simultaneous equations for total absorbance, A, at 240 and 290 nm for mixtures of I and II.

Analysis of Three-Component Mixtures—Reverse-phase HPLC with

[1] 2,2′-Anhydro-(1-β-D-arabinofuranosyl)-cytosine; Sigma Chemical Co., St. Louis, Mo.
[2] Cytarabine; The Upjohn Co., Kalamazoo, Mich. The chemical name is 1-β-D-arabinofuranosylcytosine, the IUPAC name is arabinosylcytosine, and the common name is cytosine arabinoside (ara-C).
[3] Uracil-β-D-arabinofuranoside; Sigma Chemical Co., St. Louis, Mo.
[4] β-D-O^2,2′-cyclouridine; Terra-Marine Bioresearch, La Jolla, Calif.
[5] Type TLP 109; New England Nuclear, Boston, Mass.
[6] Model 250 spectrophotometer with model 6051 recorder, model 2451A automatic cell positioner, and model 6047 thermosensor; Gilford Instruments, Oberlin, Ohio.

0022-3549/84/0700-0896$01.00/0
© 1984, American Pharmaceutical Association

Table I—Experimental Conditions for Kinetics of Ancitabine Hydrolysis

Temp., °C	Components[a]	μ[b]	pH	n[c]
19.5	NaOH	0.005-1.0	10.3[d]	7
21.1	NaOH	0.0003-0.00075	10.3-10.7[d]	5
21.2	NaOD[e]	0.0003	10.3[d]	3
26.4	NaOH	1.00	10.7[d]	2
31.4	Na_2CO_3, $NaHCO_3$	1.0	8.6-9.9	7
40.0	H_3BO_3, NaH_2BO_3	1.0	7.8-10.0	8
50.0	NaH_2PO_4, Na_2HPO_4	0.5-1.5	6.2-7.6	24
60.0	NaH_2PO_4, Na_2HPO_4	1.0	5.2-7.4	19
	H_3BO_3, NaH_2BO_3	0.5-1.0	6.4-9.4	29
	$NaHCO_3$, Na_2CO_3	1.0	8.1-8.4	5
	$(CH_2OH)_3CNH_2$, $(CH_2OH)_3CNH_3^+$	1.0	7.8-8.8	5
	$^+H_3NCH_2CO_2Na$, $H_2NCH_2CO_2Na$	1.0	8.5-9.1	6
	CH_3COOH, CH_3COONa	0.01	3.1-3.9	2
	HCl	0.002-0.02	1.6-2.6	2
70.0	NaH_2PO_4, Na_2HPO_4	1.0	6.4-7.5	5
	HCl	0.02	1.6	1
80.0	NaH_2PO_4, Na_2HPO_4	1.0	6.4-7.4	6
	HCl	0.002-1.00	1.5-2.7	4

[a] All reactions aqueous unless otherwise specified. [b] Adjusted with sodium chloride. [c] Number of rate constants determined. [d] Calculated values. [e] Solvent was D_2O.

254-nm fixed-wavelength detection[7] was used to assay I, II, and III in mixtures. The mobile phase was filtered and deaerated, double-distilled water containing 12% (v/v) methanol[8], 0.01 M acetic acid, 0.01 M sodium acetate, and 0.005 M sodium heptanesulfonate as an ion-pairing agent, at 1.0 mL/min. The capacity factors of I, II, and III were 4.4, 1.8, and 0.52, respectively. The peak height *versus* concentration plots were linear in the 1.0×10^{-5} to 10^{-4} M range for all three compounds. Some analyses were carried out using the HPLC method of Tuncel *et al.* (14), with similar results.

Kinetics in Buffers and in Dilute Hydrochloric Acid—Reaction solutions containing I were prepared at various pH values and temperatures (Table I). Those in the pH range of 5.2-10 were assayed as a function of time by diluting aliquots with an appropriate volume of 0.1 M HCl before employing the spectrophotometric analysis (Eqs. 1 and 2) or the HPLC assay (14). In the pH range of 5.2-6.2, mass balance was confirmed by HPLC analysis of [I], [II], and [III] with time (14). For reactions in the pH range of 6.2-10, mass balance was confirmed by monitoring both the isosbestic point and the percent recovery of [I] and [II] as a function of time.

Reactions in the pH range of 1.5-4 were assayed as a function of time by cooling aliquots and applying the HPLC assay reported herein. The sum of the molar concentrations of I, II, and III did not equal the initial concentration of I, $[I_0]$. Complete conversion of I to II was confirmed by fitting concentration-time profiles of II to a biexponential equation using NONLIN (15), calculating the areas under these curves (AUC), and showing them to be equal to the expected values of $[I_0]/k'$, where k' is the rate constant for loss of II.

Kinetics of hydrolysis of I at 80°C were compared with that of II in 0.01 and 0.001 M HCl and in 0.01 M HCl containing 1.0 M NaCl. Samples were assayed as a function of time using the HPLC assay described herein. The concentration of IV (Scheme II) were determined as a function of time by subtracting the sum of the time-dependent concentrations from the initial concentrations of starting material. The rate constants k_{obs}, k', and k_x were determined by simultaneously fitting a series of differential equations describing the concentration-time courses of I, II, III, and IV in Scheme II.

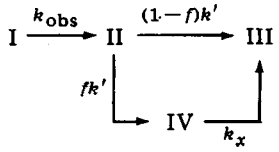

Scheme II

Both k_{obs} and k' were independent of pH and ionic strength in acid. The two pairs of values for k_x provided fractional negative slopes for plots of log k_x *versus* pH or $[\sqrt{\mu}/(1+\sqrt{\mu})]$. Although data are limited, they may indicate that loss of IV may not be a single irreversible process as shown in Scheme II. The value for k' (0.076 h^{-1}) agrees with that previously reported under similar conditions (16).

Kinetics in Dilute Sodium Hydroxide—Distilled-deionized water was refluxed, cooled under nitrogen, and used to prepare solutions containing I in the presence of sodium hydroxide and sodium chloride (Table I). These were maintained at constant temperature under a stream of nitrogen and assayed as a function of time by acidifying aliquots with HCl, measuring absorbances, and applying Eqs. 1 and 2. The influence of ionic strength was quantitated by varying the sodium concentration at 19.5°C (Table II).

***In Situ* Spectrophotometric Analysis of Alkaline Reactions**—Studies for estimating the kinetic isotope effect required the analysis of I and II in reactions carried out in the spectrophotometer using either aqueous sodium hydroxide or sodium deuteroxide in deuterium oxide. Potentiometric titrations of 0.057 M I in 0.05 M HCl with sodium hydroxide showed no evidence for a pK_a. Spectrophotometric data were consistent with this observation. Spectra were superimposable below pH ~8.4. At pH 10.4 and 11.2 absorbance changed with time. The ϵ value at 230 nm, calculated from the intercepts of $\ln(A_t - A_\infty)$ *versus* time, was the same as in acidic solutions.

This pH-independent spectrum for I was compared with that for II in carbonate-free 1×10^{-4} M NaOH. The maximum absorbance differences occurred at 258 and 280 nm. Molar absorptivities (ϵ) at 258 and 280 nm were 1.01×10^4 and 4.69×10^3 for I in double-distilled water and 6.78×10^3 and 7.88×10^3 for II in carbonate-free 1×10^{-4} M NaOH. Concentrations of I and II were calculated from the following equations, derived from simultaneous equations for the total absorbances at 258 and 280 nm:

$$10^4 \cdot [I] = 1.651A_{258} - 1.420A_{280} \quad \text{(Eq. 3)}$$

$$10^4 \cdot [II] = 2.112A_{280} - 0.986A_{258} \quad \text{(Eq. 4)}$$

The accuracy was assumed to be similar to the acid-quenched assay although its assessment using known mixtures under basic conditions was not possible due to the instability of I.

Comparison of Ancitabine Kinetics in Sodium Hydroxide to Those in Sodium Deuteroxide—A closed system with nitrogen-flushed head space was used to limit uptake of atmospheric carbon dioxide and hydrogen-deuterium exchange. Polytef-capped cuvettes were filled with solutions containing either 1.9×10^{-4} M NaOD in deuterium oxide or 1.9×10^{-4} M NaOH in carbonate-free, double-distilled water. Stock solutions of I were prepared free of carbon dioxide and maintained at ambient temperatures. Each reaction in deuterated solvent was duplicated by a corresponding aqueous reaction. An aliquot of the stock solution was quickly added to each cuvette, capped, mixed, and the time of mixing was marked on the recorder[6]. The cuvettes were placed in the thermostated chamber along with a blank. Absorbances of each reaction mixture were automatically recorded at 258 and 280 nm as a function of time using a 2-s dwell time for each cuvette, with automatic reference compensation before and after each reading[6]. Reactions were allowed to proceed until absorbances were constant with time. The temperature in the cuvette chamber was automatically recorded before and after each run. The concentrations of I and II were calculated using Eqs. 3 and 4.

RESULTS

Hydrolysis Products—Reactions monitored by TLC showed I to be stable over a 4-d period at 50°C in water and in 0.1 M HCl, while converting immediately to II in 0.05 M NaOH. At pH ≅ 1.5-6, HPLC analyses detected subsequent deamination of II to III, in accordance with Scheme II. As the pH decreases in this range, the formation of III becomes detectable during the hydrolysis of I because k' passes through a maximum value at pH 3, whereas k_{obs} decreases to a minimum and is constant below pH 4. The AUC values

[7] Model 332 Beckman gradient liquid chromatograph with model 153 analytical detector and Altex ultrasphere-octyl 5-μm column (15 cm × 4.6 mm i.d.); Beckman Instruments, Irvine, Calif.

[8] Omnisolv methanol (glass distilled); MCB Reagents, Norwood, Ohio.

Table II—Selected Experimental Conditions and Rate Constants[a]

Temp., °C	pH	Buffer Concentrations, M		k_{obs}, h^{-1}
		NaH_2PO_4	Na_2HPO_4	
60.0	7.37	0.018	0.180	1.09
	7.25	0.010	0.100	0.816
	7.15	0.005	0.050	0.640
	7.27	0.060	0.300	0.966
	7.17	0.040	0.200	0.750
	7.06	0.025	0.125	0.612
	7.01	0.010	0.050	0.408
	6.98	0.070	0.210	0.540
	6.94	0.050	0.150	0.442
	6.86	0.030	0.090	0.363
	6.80	0.015	0.045	0.294
	6.45	0.250	0.250	0.274
	6.40	0.125	0.125	0.168
	6.33	0.050	0.50	0.122
	6.29	0.025	0.025	0.0935
	5.25	0.500	0.050	0.0354
	5.22	0.250	0.025	0.0232
	5.23	0.100	0.010	0.0182
	5.23	0.050	0.005	0.0152
80.0	6.42	0.200	0.200	2.57
	7.38	0.020	0.200	13.9
	7.08	0.30	0.150	7.86
	6.56	0.100	0.150	2.86
	6.63	0.050	0.100	3.02
	6.42	0.060	0.080	1.92
		$NaHCO_3$	Na_2CO_3	
31.4	9.82	0.060	0.100	4.94
	9.94	0.80	0.160	6.27
	9.61	0.100	0.100	3.07
	9.49	0.130	0.100	2.33
	9.18	0.280	0.100	1.20
	8.89	0.200	0.040	0.661
	8.69	0.450	0.050	0.446
		HCl	μ	
80.0	1.63	0.020	0.02	0.0386
	2.68	0.002	0.002	0.0382
	1.60	0.020	0.100	0.0364
	1.52	0.020	1.000	0.0341
70.0	1.60	0.020	0.02	0.0181
60.0	1.58	0.020	0.02	0.00680
	2.60	0.002	0.002	0.00664
		NaOH		k_{OH}, $10^4(M^{-1}h^{-1})$
19.5	10.44[b]	0.000195	0.005	2.12
	10.43		0.010	2.02
	10.38		0.050	1.68
	10.35		0.100	1.51
	10.32		0.200	1.16
	10.26		0.500	1.04
	10.22		1.000	0.568

[a] The experimental conditions and results presented here are a representative sample of a much larger body of kinetic data. All buffer studies were adjusted to μ = 1.0 using NaCl. [b] Calculated values.

of the concentration–time profiles for II showed that I was quantitatively converted to II. The appearance of an additional, nonchromophoric intermediate in the chemical deamination of II to III, demonstrated previously (16), was confirmed.

Hydrolysis in Acid—In the presence of dilute hydrochloric acid, first-order rate constants $k_s a_{H_2O}$, obtained from linear plots based on:

$$\ln [I] = \ln [I_0] - k_s a_{H_2O} t \qquad \text{(Eq. 5)}$$

were found to be temperature dependent but independent of pH and ionic strength (Fig. 1, Table II).

Hydrolysis in Alkali—In the presence of dilute sodium hydroxide (or deuteroxide), the second-order rate constants, k_{OH}, were obtained from the slopes of linear plots based on:

$$\left\{\frac{1}{[I_0] - [OH_0]}\right\} \cdot \ln \left\{\frac{[I][OH_0]}{[I_0][OH]}\right\} = k_{OH} t \qquad \text{(Eq. 6)}$$

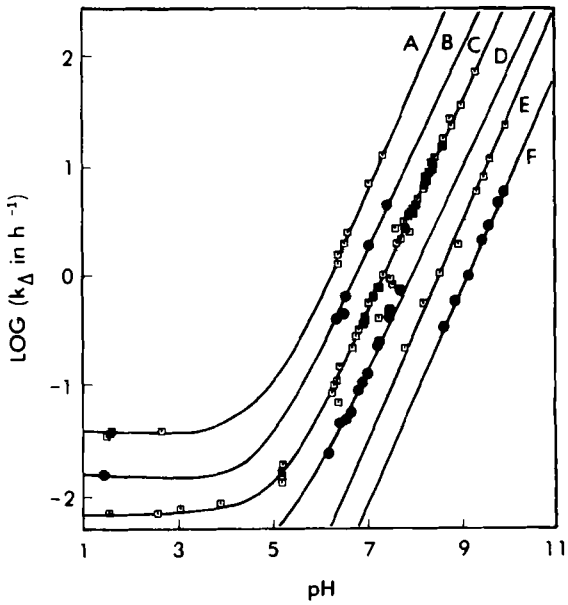

Figure 1—*The pH–rate profile for quantitative conversion of I to II. Data points (k_Δ) represent k_{obs} values corrected for buffer catalysis. Curves are calculated (Eq. 29) at 80°C (A), 70°C (B), 60°C (C), 50°C (D), 40°C (E), and 31.4°C (F). μ = 1.0.*

where [OH] is the concentration of either hydroxide or deuteroxide as determined from $[OH] = [OH_0] - [II]$.

Kinetics in Buffers—In the presence of excess buffer, first-order rate constants (k_{obs}) were obtained from linear plots based on $\ln [I] = \ln [I_0] - k_{obs} t$. Buffer participation was recognized in plots of log k_{obs} *versus* pH, which showed that hydroxide and solvent attack were not sufficient to describe the observed rate constants under all conditions (Fig. 2). General base-catalyzed water attack was hypothesized leading to the overall expression (17):

$$k_{obs} = \left(k^0_{OH}[OH]\frac{\gamma_{OH}\gamma_I}{\gamma_\dagger}\right) + \left(a_{H_2O}\sum_{i=1}^{n} k^0_{B_i}[B_i]\frac{\gamma_I\gamma_{B_i}}{\gamma_{\dagger i}}\right) + (k_s a_{H_2O}) \qquad \text{(Eq. 7)}$$

where k^0_{OH} is the rate constant for hydroxide attack at zero ionic strength, γ_{OH} is the activity coefficient for hydroxide, γ_I is the activity coefficient for I, $\gamma_\dagger$ is activity coefficient for the hydroxide-attack transition state, $[B_i]$ is the concentration of the ith general base, γ_{B_i} is the activity coefficient for the ith base, $\gamma_{\dagger i}$ is the activity coefficient for the transition state for B_i attack, $k^0_{B_i} a_{H_2O}$

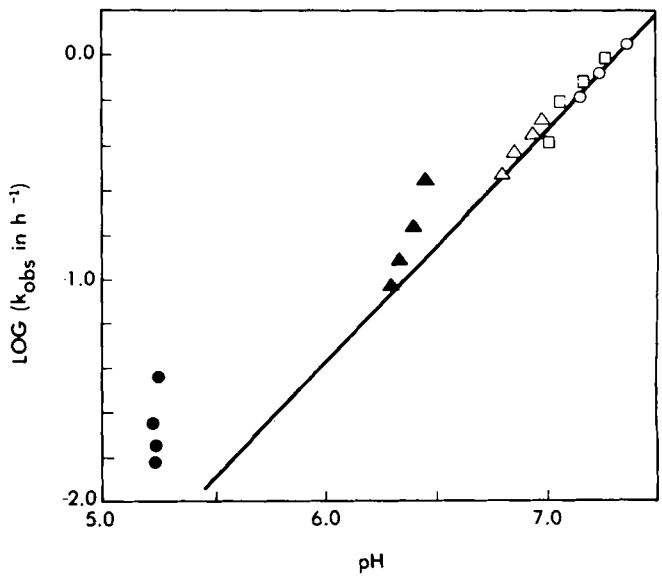

Figure 2—*Log k_{obs} versus pH for quantitative conversion of I to II in phosphate buffers at 60°C, μ = 1.0, where the ratios of $[NaH_2PO_4]/[Na_2HPO_4]$ are: 0.1 (○), 0.2 (□), 0.33 (△), 1.0 (▲), and 10 (●) (see Table II). The regression line, based on the 0.1 ratio buffers (○), has a slope of one.*

Table III—Biomolecular Rate Constants (1/M·h) as a Function of Temperature

Temp., °C	$10^{-5}k^0_{OH}$	$10^{-1}k^0_{cat}$ Phosphate	Borate	Carbonate	
80.0	43.1	5.67	—	—	
70.0	18.5	1.35	—	—	
60.0	7.59	0.444	13.7	88.3	
50.0	4.47	0.115	—	—	
40.0	1.66	—	1.12	—	
31.4	0.779	—	—	1.62	
		Temp., °C	Tris	Glycine	10^2k_s
26.4	0.531	80	—	—	3.84
21.2	0.303	70	—	—	1.81
19.0	0.220	60	0.212	14.3	0.672

equals k^0_{cat}, the bimolecular rate constant for catalysis by the ith base at zero ionic strength, and k_s is the bimolecular rate constant for solvent attack.

Reaction kinetics were studied in solutions of Tris, borate, carbonate, acetate, glycine, and phosphate buffers. Tris, acetate, and borate buffers contained only one Brönsted base species. Although carbonate, glycine, and phosphate buffer contained two general bases, their acids differed by a minimum of four orders of magnitude in K_a values. According to the Brönsted relationship, the efficiency of a general base catalyst increases with the increasing pK_a of its conjugate acid (18). Therefore, the contribution of the more acid base species to k_{obs} was not detectable. The contribution of $k_s a_{H_2O}$ was also insignificant except in buffer solutions of pH ≤5.3. Above this, the observed rate constants in buffers can be described by hydroxide attack plus catalysis by one general base component, B, so that Eq. 7 can be rewritten:

$$k_{obs} = (k^0_{OH} a_{OH} \gamma_I / \gamma_\ddagger) + (k^0_B a_{H_2O} [B] \gamma_B \gamma_I / \gamma_\ddagger') \qquad \text{(Eq. 8)}$$

where $a_{OH} = \gamma_{OH}[OH^-]$ and $k_B{}^0 a_{H_2O} = k_{cat}{}^0$. After taking ionic atmosphere effects into account (see discussion below), observed first-order rate constants were adequately described by this equation. The pH-rate profiles, constructed by subtracting the general base contributions, were linear at pH > 6 with slopes approaching unity, which is the theoretical value when a reaction is first-order in hydroxide (Fig. 1).

Ionic Atmosphere Effects—In dilute hydroxide and buffered solutions, the activity coefficients of the reactants and transition states appear in the rate law for hydrolysis of I. The influence of ionic atmosphere effects on activity coefficients is greater for reactions between ions than for reactions between polar molecules or ions and dipoles (19). Under all conditions studied, I was a cation while hydroxide ion and the general bases (except Tris) were anions.

According to absolute reaction-rate theory, the rate constant is proportional to the concentration equilibrium constant ($k_c^\ddagger$) between the activated complex and the reactants (20). This concentration equilibium constant is affected by the ionic environment and is related to a thermodynamic equilibrium constant ($K_a^\ddagger$) by the ratio of the transition state activity coefficient to the product of the activity coefficients for the reactants (20). For a bimolecular reaction such as the reaction between hydroxide and I:

$$k_{OH} = (k^0_{OH} \gamma_{OH} \gamma_I) \gamma_\ddagger \qquad \text{(Eq. 9)}$$

where k^0_{OH} is the second-order rate constant expressed in terms of the thermodynamic equilibrium constant $K^\ddagger_a$. Carstensen (21) has shown that Eq. 10 adequately describes the logarithm of an activity coefficient based on the kinetic salt effects as reported for the degradation of a number of drugs over a wide range of ionic strengths:

$$\log \gamma_i = \frac{-AZ_i^2\sqrt{\mu}}{1+\sqrt{\mu}} \qquad \text{(Eq. 10)}$$

where γ_i is the activity coefficient of the ith ion, Z_i is its charge, μ is the ionic strength, and A is a function of the temperature and dielectric constant of the solution. According to theory the charge on the transition state is the sum of the charges on the reactants (20). Substitution of Eq. 10 into the logarithmic form of Eq. 9 yields Eq. 11, which predicts a linear relationship between log k_{OH} and $\sqrt{\mu}/(1+\sqrt{\mu})$ with a slope of $-2A$:

$$\log k_{OH} = \log k^0_{OH} - \frac{2A\sqrt{\mu}}{1+\sqrt{\mu}} \qquad \text{(Eq. 11)}$$

This relationship was observed for hydroxide attack on I. Kinetic analyses are more complex in buffers, wherein both primary and secondary salt effects can depend not only on ionic strength but also on specific ionic interactions (22). Activity coefficients of buffer ions can be influenced by the concentration of ions of opposite charge, which often are added as neutral salts to maintain constant ionic strength. This is reflected in the final term of the Guggenheim equation:

$$\log \gamma_i = \frac{-AZ_i^2\sqrt{\mu}}{1+\sqrt{\mu}} + \sum_j \beta_{ij} C_j \qquad \text{(Eq 12)}$$

where β_{ij} represents the interaction coefficients between ion i and all other j ions of opposite charge (20, 22). The activity coefficients in the Henderson-Hasselbach equation:

$$pH = pK_a + \log [B]/[HB] + \log (\gamma_B/\gamma_{HB}) \qquad \text{(Eq. 13)}$$

can be described by Eq. 12 to give:

$$pH = pK_a + \log \frac{[B]}{[HB]} + \frac{(Z_{HB}^2 - Z_B^2)A\sqrt{\mu}}{1+\sqrt{\mu}} + \sum_j \Delta\beta C_j \qquad \text{(Eq. 14)}$$

where HB designates the buffer conjugate acid, $\Delta\beta = \beta_{B_j} - \beta_{HB_j}$, and the summation involves the concentration (C_j) of all the ions of charge opposite to that of buffer ions.

Equation 14 shows that the pH can change as a function of the concentration of ions of charge opposite to that of the buffer ions ($\Sigma_j \Delta\beta C_j$) at constant μ and buffer concentration ratio ([B]/[HB]). For example, the decreasing pH at each constant ($[HPO_4^{2-}]/[H_2PO_4^-]$) ratio observed in Table II is due to increasing sodium ion concentration. In the extreme case, hydroxide activity was observed to decrease from 1.79×10^{-6} to 0.98×10^{-6}, which will have a pronounced effect when hydroxide attack is significant. Therefore, the rate constants for hydrolysis of I in buffers with high concentrations of added neutral salts are not adequately described in terms of concentration.

The following method was developed to solve for the contributions of hydroxide attack and general-base catalysis to the observed first-order rate constants in buffers. Equation 8 was employed to calculate $k_{OH}{}^0$ and $k_{cat}{}^0$ using approximations for $\gamma_\ddagger$, $\gamma_\ddagger'$, and γ_I in the following manner. According to theory the charge on the transition state is the sum of the charges on the species involved in its formation, $Z_\ddagger = Z_A + Z_B + \cdots Z_N$ (20). Therefore, the transition state formed from the hydroxide anion and the I cation was assumed neutral, and its activity coefficient was taken as unity, *i.e.* $\gamma_\ddagger \cong 1$.

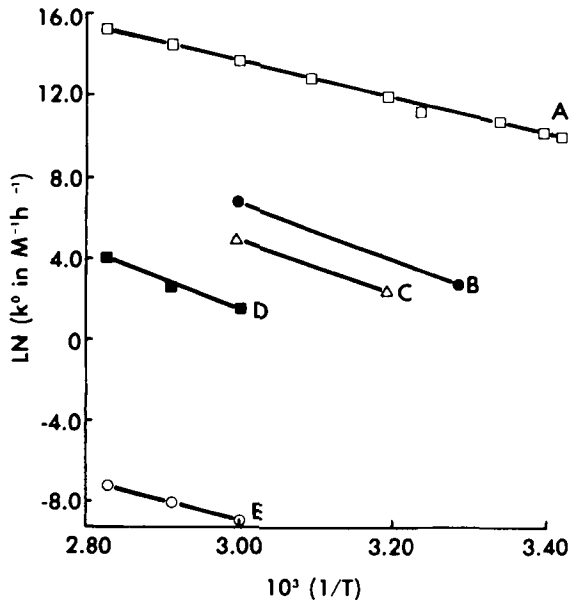

Figure 3—*Arrhenius plots for rate constants at infinite dilution where* k^0 *is* k^0_{OH} *(A),* k^0_{cat} *for carbonate (B), borate (C), and dibasic phosphate (D), and* k_s *(E).*

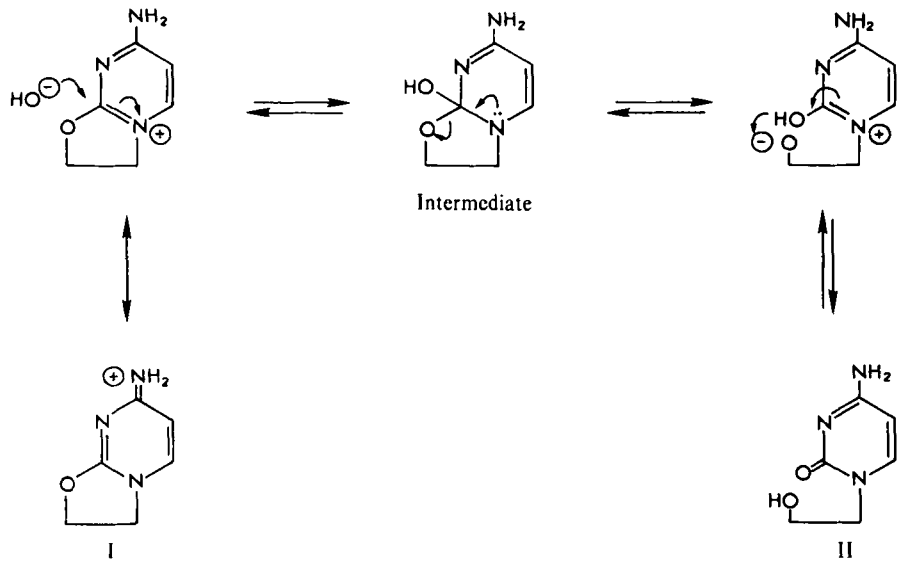

Scheme III

Table IV—Energetics of I Hydrolysis

Rate Constant $M^{-1}h^{-1}$	E_a, kcal/mol-deg	A, $M^{-1}h^{-1}$ [a]	$\Delta H^{\ddagger}$ (kcal/mol-deg) Obs.[a]	Calc.[b]	$\Delta S^{\ddagger}$, e.u.[c]
k^0_{OH}	17.21	1.74×10^{17}	16.6	—	18.0
k^0_{cat}					
Phosphate	29.84	1.45×10^{20}	29.2	29.2	23.6
Carbonate	28.26	2.96×10^{21}	27.2	26.9	28.2
Borate	26.00	1.51×10^{19}	25.4	26.7	17.7
k_s	20.11	2.02×10^{9}	19.4	—	−10.6

[a] Values were calculated at each temperature studied using Eq. 21; the mean values are tabulated. [b] Values were calculated at each temperature studied using Eq. 22 where ΔH^0_{HB} and $\Delta H^0_{H_2O}$ were calculated from literature equations (24). The mean values are tabulated. [c] Values were calculated at each temperature studied using literature equations (25); the mean values are tabulated.

General base-assisted water attack on I would produce the same net charge as protonation of the base to form its conjugate acid, $Z_{\ddagger}' = Z_{HB}$. On this basis, it was assumed that the activity coefficients of these transition states and their corresponding buffer conjugate acids were sufficiently similar to use the approximation $\gamma_{\ddagger}' \cong \gamma_{HB}$. Substitution into Eq. 8 yields:

$$k_{obs} = (k^0_{OH} a_{OH} \gamma_I) + (k^0_B a_{H_2O} [B] \gamma_B \gamma_I / \gamma_{HB}) \qquad \text{(Eq. 15)}$$

Substituting $(K_w[B]\gamma_B/K_a[HB]\gamma_{HB})$ for a_{OH} and dividing the equation by $([B]\gamma_B/\gamma_{HB})$ provides:

$$\frac{k_{obs}}{[B]\gamma_B/\gamma_{HB}} = \left\{\frac{k^0_{OH}\gamma_I K_w}{K_a}\right\} \frac{1}{[HB]} + k^0_B \gamma_I a_{H_2O} \qquad \text{(Eq. 16)}$$

The buffer activity coefficient ratio, γ_B/γ_{HB}, was calculated from pH measurements, known buffer concentrations, and literature values for K_a using:

$$(\gamma_B/\gamma_{HB}) = K_a[HB]/[B]10^{-pH} \qquad \text{(Eq. 17)}$$

which is a rearrangement of the antilogarithmic form of Eq. 13.

Plots of $k_{obs}/([B]\gamma_B/\gamma_{HB})$ *versus* $1/[HB]$ were linear ($r^2 \geq 0.994$) with intercepts of $k_B{}^0\gamma_I a_{H_2O}$ and slopes which allowed the calculation of $k_{OH}{}^0\gamma_I$ after substituting for K_w and K_a. Borate buffers gave the poorest reproducibility ($r^2 = 0.985$), which was probably due to borate polymerization (23) making the true B and HB concentrations unknown.

While Eq. 16 corrects for secondary ionic atmosphere effects, γ_I (a multiplier of both the slope and intercept) is subject to primary salt effects, which are influenced by both ionic strength and specific ionic interactions. The importance of specific ionic interactions appear minor judging from the large r^2 values for each series of buffers at constant ionic strength but varying ion concentrations. To determine the effect of ionic strength on γ_I, a series of 22 reactions were studied in phosphate buffers at 50°C and $\mu = 0.05, 0.20, 0.50$, and 1.00. All reactions were described by a single linear plot ($r^2 = 0.995$) based on:

$$\frac{k_{obs}}{[B]\gamma_B\gamma_I/\gamma_{HB}} = \left\{\frac{k^0_{OH}K_w}{K_a}\right\} \frac{1}{[HB]} + k^0_B a_{H_2O} \qquad \text{(Eq. 18)}$$

since γ_I values were estimated by Eq. 10.

Temperature Dependence—From values of $k^0_{OH}\gamma_I$ and $k^0_{cat}\gamma_I$ obtained in buffers at various temperatures (Eq. 16) and the estimates for γ_I (Eq. 10), k^0_{OH} and k^0_{cat} were calculated at each temperature. Additional k^0_{OH} values were calculated from dilute hydroxide reactions using Eq. 11. Where k_{obs} (*i.e.*, $k_s a_{H_2O}$) values were independent of pH and ionic strength in hydrochloric acid, k_s values were calculated from k_{obs}/a_{H_2O} (Table III). The Arrhenius relationship:

$$\ln k = \ln \underline{A} - E_a/RT \qquad \text{(Eq. 19)}$$

was used to determine the temperature dependence of k^0_{OH}, k^0_s, and k^0_{cat}, where E_a is the activation energy, $\underline{A}$ is the preexponential constant, R is the molar gas constant, and T is the absolute temperature (Fig. 3). The activation energies are given in Table IV.

General Base Catalysis—At 60°C and $\mu = 1.0$, a series of buffers were studied and a Brönsted linear-free energy correlation was demonstrated using:

$$\log\left(\frac{k}{q}\right) = \log G_B + \beta(pK_a + \log p/q) \qquad \text{(Eq. 20)}$$

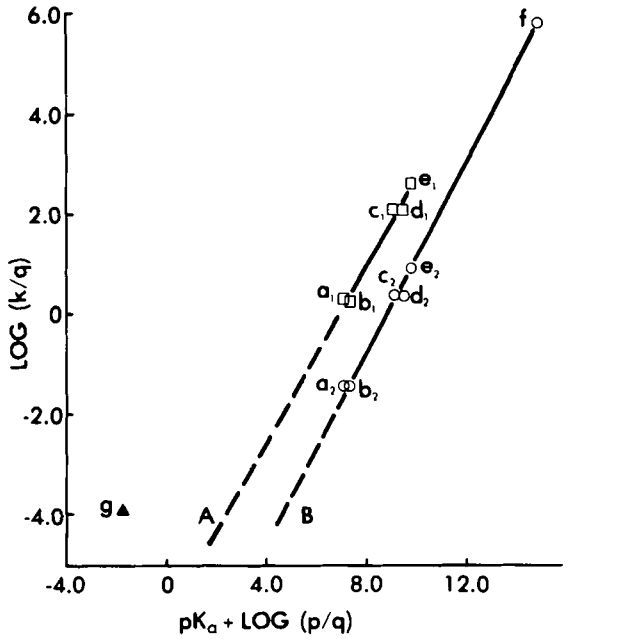

Figure 4—*Brönsted plot relating the rate constants at 60°C for general-base, specific-base, and solvent attack at infinite dilution to the dissociation constants of their conjugate acids (24). Data points represent phosphate (a), Tris (b), glycine (c), borate (d), carbonate (e), k^0_{OH} (f), and k_s (g). Buffer values with subscript 1 (A) represent k^0_{cat}, whereas those with subscript 2 (B) are the corresponding ($k^0_{cat}/55.5$) values. The slopes are 0.90 ($r^2 = 0.95$) for line A and 0.97 ($r^2 = 0.98$) for B.*

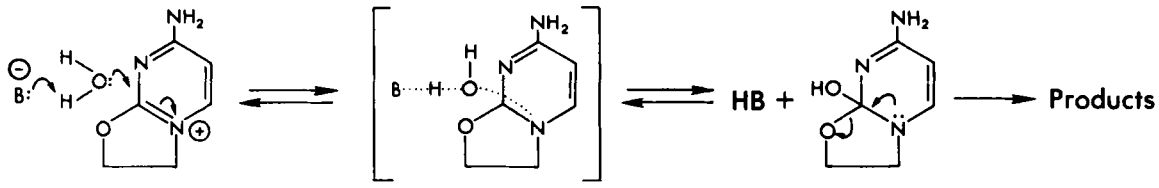

I Intermediate

Scheme IV

where k is the bimolecular rate constant (k^0_{cat}, k_s, or k^0_{OH}), G_B is a constant, β is the Brönsted coefficient, p is the number of equivalent protons which can be transferred from the conjugate acid, and q is the number of sites on the general base which can accept a proton (25). The catalytic constants for general base attack, $k^0_{cat} = k^0_B a_{H_2O}$, were calculated from plots based on Eq. 16 and comprise correlation line A in Fig. 4. As is often observed (18, 26), k^0_{OH} shows negative deviation from the plot and k_s does not fall on the line. Line B is composed of the k^0_{OH} value and those for $k^0_{cat}/55.5$. The agreement between the factor 55.5 and the molarity of pure water may be significant or fortuitous. However, this relationship (line B) will be employed to develop a predictive equation for k_{obs}.

Isotope Effect in the Hydroxide Attack of I—Studies conducted simultaneously in sodium hydroxide and sodium deuteroxide solutions yielded ratios of k^0_{OD}/k^0_{OH} which varied from 0.8 to 1.4. Thus, no significant isotope effect was observed.

DISCUSSION

Mechanism of Hydroxide Attack: Nucleophilic Addition—Scheme III illustrates nucleophilic attack of hydroxide anion at the C-2 position of I, with rate-determining formation of a C—O bond and simultaneous loss of the positive charge to form the tetrahedral intermediate. Subsequent loss of this intermediate could take place as depicted or with general-base assisted transfer of the C-2 hydroxyl proton. Rate-determining formation of the intermediate is consistent with the absence of a significant deuterium isotope effect. Simultaneous loss of the positive charge is supported by a negative ionic strength effect and a positive entropy of activation (Table IV), which is common for reactions in which charge is destroyed in polar media (25).

Mechanism of Buffer Attack: General-Base Assisted Solvent Attack—According to Scheme IV, protonation of the general base, ionization of a water, and formation of the tetrahedral intermediate occur during or prior to the rate-determining step. This is consistent with the observed linear free energy correlation, which includes both hydroxide and general-base assisted solvent attack together with a Brönsted coefficient of unity (Fig. 4). The Brönsted correlation implies that proton transfer is involved at the rate-determining step, and the coefficient value of unity implies that proton abstraction is nearly complete in the transition state (18, 26).

Confirmatory evidence for Scheme IV can be obtained from the activation energies for the rate constants (k^0_{OH} and k^0_{cat}). The enthalpies of activation can be calculated using (26):

$$\Delta H^{\dagger} = E_a - RT \qquad \text{(Eq. 21)}$$

The enthalpy of activation for general base-assisted solvent attack ($\Delta H_B^{\dagger}$), was calculated in two ways. In addition to employing the activation energy in Eq. 21, $\Delta H_B^{\dagger}$ was approximated by:

$$\Delta H_B^{\dagger} = \Delta H_{OH}^{\dagger} + \Delta H^0_{H_2O} - \Delta H^0_{HB} \qquad \text{(Eq. 22)}$$

based on Scheme IV where $\Delta H_{OH}^{\dagger}$ is enthalpy for the formation of the C—O bond calculated from the activation energy of hydroxide attack and Eq. 21, $\Delta H^0_{H_2O}$ is the enthalpy for ionization of water, and ΔH^0_{HB} is the enthalpy for ionization of the conjugate acid (therefore, it is equal to the negative enthalpy of general base-protonation process). There is excellent agreement between the values of $\Delta H_B^{\dagger}$ computed under the assumptions of Scheme IV and those values calculated directly from the experimentally observed activation energies (Table IV).

Mechanism of Solvent Attack—Scheme V depicts a mechanism for solvolysis involving intramolecular general base participation by removal of a proton during nucleophilic attack at C-2. Although there is no direct kinetic support for this anchimeric mechanism, it is consistent with the fact that solvent attack becomes prominent below the reported pK_a (4.2) of II (16) (see Fig. 1). Assuming the ability of the tetrahedral intermediate to accept a proton at N-3 is approximately the same as that of II, Eq. 20 with $pK_a = 4.2$ was used to calculate k^0_{cat}. The ratio of $k_s a_{H_2O}/k^0_{cat}$, which represents the "effective concentration" of intramolecular catalyst in the vicinity of I, was calculated to be 3 M. This value suggests that the intramolecular rate enhancement can be accounted for by local concentration effects (27).

Stability Prediction for Ancitabine Conversion—The rate constant for conversion of I to II was shown to be the sum of the rate constants for water attack (Eq. 5), hydroxide attack, and general base-catalyzed water attack (Eq. 8) and therefore can be defined:

$$k_{obs} = k^0_{OH} a_{OH} \gamma_I + k^0_{cat}[B]\left[\frac{\gamma_B \gamma_I}{\gamma_{HB}}\right] + k_s a_{H_2O} \qquad \text{(Eq. 23)}$$

It was observed that using $k^0_{cat}/55.5$ values resulted in a common Brönsted plot which included the k^0_{OH} value. The agreement between 55.5 and the molecularity of pure water may be coincidental, but the observation was used to derive a predictive equation for k_{obs}. Since $\beta \cong 1$ (line B, Fig. 4) the antilogarithmic form of Eq. 20 may be written:

$$k^0_{OH} = G_B/K'_a \qquad \text{(Eq. 24)}$$

where $p = q = 1$ and $K'_a = K_w/a_{H_2O}$ and:

$$k^0_{cat}/55.5 = G_B p/K_a \qquad \text{(Eq. 25)}$$

Therefore, k^0_{cat} can be described in terms of $k_{OH}{}^0$ as:

$$k^0_{cat} = 55.5 k^0_{OH} K'_a p/K_a \qquad \text{(Eq. 26)}$$

Arrhenius parameters were determined for k^0_{OH} and k_s (Fig. 3, Table IV) from:

$$k^0_{OH} = \underline{A} \cdot \exp(-E_a/RT) \qquad \text{(Eq. 27)}$$

$$k_s = \underline{A}' \cdot \exp(-E_a'/RT) \qquad \text{(Eq. 28)}$$

Substitution for γ_I (Eq. 10), γ_B/γ_{HB} (Eq. 17), k^0_{cat} (Eq. 26), k_s (Eq. 28), and $a_{OH} = K_w 10^{pH}$ into Eq. 23 yields:

$$k_{calc} = (1 + X)\underline{A} a_{OH} \cdot \exp\left(\frac{-2.3A\sqrt{\mu}}{1 + \sqrt{\mu}} - \frac{E_a}{RT}\right) + \underline{A}' a_{H_2O} \cdot \exp\left(-\frac{E_a}{RT}\right) \qquad \text{(Eq. 29)}$$

where a_{OH} is calculated from measured pH and K_w at temperature T. This describes the first-order rate constant for loss of I, k_{calc} in h^{-1}, as a function of pH, ionic strength, and temperature where $X = p \cdot [HB]/1$ M reflects the concentration [HB] and type (p) of the conjugate acid. Figure 5 demonstrates the agreement between rate constants calculated by Eq. 29 (k_{calc}) and those observed in this study (k_{obs}).

Substitution for the constants provides the following:

$$k_{calc}\,(h^{-1}) = (1 + X)1.74 \times 10^{17} a_{OH} \cdot \exp\left(\frac{-1.15\sqrt{\mu}}{1 + \sqrt{\mu}} - \frac{8662}{T}\right) + 1.12 \times 10^{11} \cdot \exp(-10{,}121/T) \qquad \text{(Eq. 30)}$$

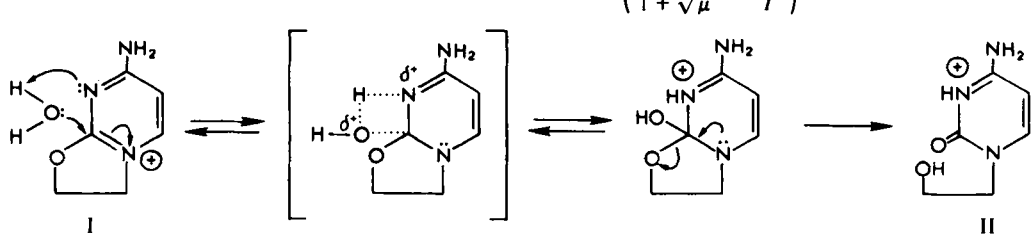

I II

Scheme V

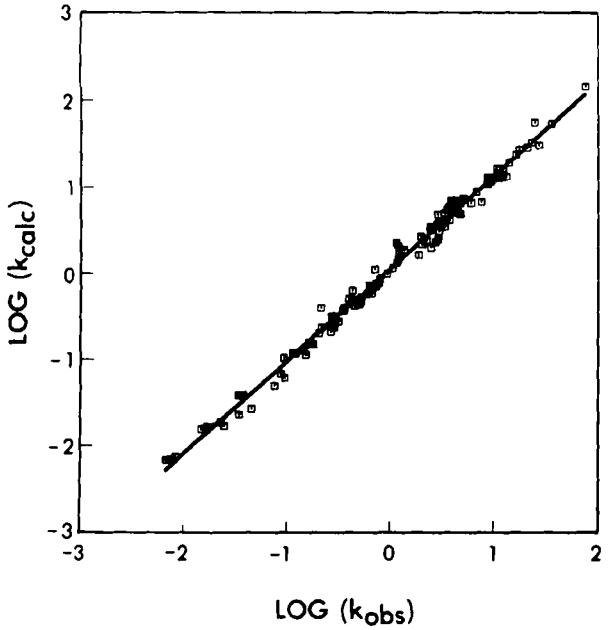

Figure 5—*Correlation between first-order rate constants for conversion of I calculated using Eq. 29 (k_{calc}) and observed (k_{obs}) in 125 reactions in the pH range 1.5–10.7, the temperature range 19.5–80°C; the ionic strength range 1×10^{-4} to 1.5; and in various concentrations of phosphate, borate, glycine, Tris, carbonate, and acetate buffers, hydrochloric acid, and sodium hydroxide solution. These rate constants were plotted* versus *the calculated rate using a log–log scale to facilitate visualization of the entire range of values. The slope of the log–log plot is 1.060 ($r^2 = 0.992$).*

which requires only the measured pH (for a_{OH}), temperature, concentration [HB], and type (p) of conjugate acid to solve for k_{calc}.

REFERENCES

(1) A. Hoshi, F. Kanzawa, and K. Kuretani, *Gann*, **63**, 353 (1972).

(2) J. M. Vanditti, M. C. Baratta, N. Greenberg, B. J. Abbott, and I. Kline, *Cancer Chemother. Rep.*, **56**, 483 (1972).

(3) F. Hamada, T. Sugihara, S. Tsuyama, H. Hirayama, T. Kani, M. Nishimure, L. Kuretani, and A. Hoshi, *Chem. Pharm. Bull.*, **23**, 586 (1975).

(4) A. Hoshi, M. Yoshida, K. Kuretani, T. Kanai, and M. Ichino, *Chem. Pharm. Bull.*, **23**, 1814 (1975).

(5) M. C. Wang, R. A. Sharma, and A. Bloch, *Cancer Res.*, **33**, 1265 (1973).

(6) D. H. W. Ho, C. J. K. Carter, T. L. Loo, R. L. Abbott, and C. M. McBride, *Drug Metab. Dispos.*, **3**, 309 (1975).

(7) D. H. W. Ho, V. Rodriguez, T. L. Loo, G. P. Bodey, and E. J. Freireich, *Clin. Pharmacol. Ther.*, **17**, 66 (1975).

(8) D. H. W. Ho, *Cancer Chemother. Rep.*, **61**, 717 (1977).

(9) A. Hoshi, M. Iigo, M. Saneyoshi, and L. Kuretani, *Chem. Pharm. Bull.*, **21**, 1535 (1973).

(10) W. Kreis, T. M. Woodcock, M. B. Meyers, L. A. Carlevarini, and I. H. Krakoff, *Cancer Chemother. Rep.*, **61**, 723 (1977).

(11) R. E. Notari, *Pharmacol. Ther.*, **14**, 25 (1981).

(12) D. H. W. Ho, *Biochem. Pharmacol.*, **23**, 1235 (1974).

(13) K. J. Himmelstein and J. F. Gross, *J. Pharm. Sci.*, **66**, 1441 (1977).

(14) M. Tuncel, R. E. Notari, and L. Malspeis, *J. Liq. Chromatogr.*, **4**, 887 (1981).

(15) C. M. Metzler, G. L. Elfring, and A. J. McEwen, *Biometrics*, **30**, 3 (1974).

(16) R. E. Notari, M. L. Chin, and R. Wittebort, *J. Pharm. Sci.*, **61**, 1189 (1972).

(17) A. W. Moore and R. G. Pearson, "Kinetics and Mechanisms," 3rd ed., Wiley, New York, N.Y., 1981, pp. 347–353.

(18) T. C. Bruice and S. Benkovic, "Bioorganic Mechanisms," vol. 1, W. A. Benjamin, New York, N.Y., 1966, pp. 27–46.

(19) E. S. Amis and J. F. Hinton, "Solvent Effects on Chemical Phenomena," Academic, New York, N.Y., 1973, chap. 5.

(20) B. Perlmutter-Hayman, *Prog. React. Kinet.*, **6**, 239 (1972).

(21) J. T. Carstensen, *J. Pharm. Sci.*, **59**, 1140 (1970).

(22) A. D. Pethybridge and J. E. Prue, *Prog. Inorg. Chem.* **17**, 327 (1972).

(23) W. P. Jencks, "Catalysis in Chemistry and Enzymology," McGraw-Hill, New York, N.Y., 1969, p. 470.

(24) H. S. Harned and B. B. Owen, "The Physical Chemistry of Electrolytic Solutions," Reinhold, New York, N.Y., 1958, chapt. 15.

(25) F. A. Carey and R. J. Sundberg, "Advanced Organic Chemistry: Part A," Plenum, New York, N.Y., 1977, pp. 137–139.

(26) W. P. Jencks, "Catalysis in Chemistry and Enzymology," McGraw-Hill, New York, N.Y., 1966, pp. 170–181.

(27) W. P. Jencks, "Catalysis in Chemistry and Enzymology," McGraw-Hill, New York, N.Y., 1966, pp. 10–18.

ACKNOWLEDGMENTS

The authors gratefully acknowledge the Elsa U. Pardee Foundation, The National Institutes of Health (Predoctoral Training Grant T32GM07622-05), and The Upjohn Company for partial support of this work.

Preformulation Method for Parenteral Preservative Efficacy Evaluation

MICHAEL J. AKERS *x, ARTHUR V. BOAND ‡, and DORIS A. BINKLEY §

Received February 24, 1983, from *Parenteral Products Development, ‡Microbiological Assay Development, and the §Statistical and Mathematical Services, Lilly Research Laboratories, Indianapolis, IN 46285. Accepted for publication May 12, 1983.

Abstract □ A method is described for rapidly and reliably evaluating parenteral preservative efficacy. Solutions containing antimicrobial preservatives were challenged with microorganisms, sampled from 0.5 to 6 h following introduction of the challenge, cultured, and counted for surviving microbial cells. Data were analyzed by computer according to two models: linear and quadratic. Decimal reduction times (D values) were calculated for each microbial challenge in each preservative solution. A D value of ≤2 h for bacteria predicts that the preservative system will pass the British Pharmacopoeia (BP) preservative efficacy test, a more rigorous test than the USP test. Fourteen preservative systems were tested in both neutral isotonic saline solutions and neutral regular insulin solutions. D values and correlation coefficients for both models were calculated. The ranking of preservative effectiveness in neutral saline solutions closely correlated with the results found using neutral regular insulin solutions. The most effective preservative systems were found to be 0.3% m-cresol and various combinations of m-cresol and phenol. The advantages and limitations of this method are discussed.

Keyphrases □ Preservatives—parenteral formulations, efficacy, preformulation determination □ Parenteral formulations—efficacy of preservatives, preformulation determination □ Antimicrobial screening—preservatives, parenteral formulations, efficacy, preformulation determination

The British Pharmacopoeial (BP) test for preservative efficacy requires that the number of bacteria recovered per milliliter in injectable preparations intended for multiple use be reduced by a factor of 10^3 within 6 h following challenge (1). This requirement imposes a far stricter criterion for antimicrobial action than the USP preservative efficacy test, which requires the bacterial concentration to be reduced by a factor of 10^3 14 d following microbial inoculation (2). A large number of preservatives at bacteriostatic concentrations will pass the USP test but will fail the BP test. Parenteral drug manufacturers who wish to market their products in countries abiding by BP requirements must reformulate their products to obtain a preservative system which, in fact, is self-sterilizing to pass the BP preservative test.

There is a need for a rapid, reliable, and inexpensive screening method to determine effective preservative systems in parenteral products. Several methods for screening and evaluating preservative efficacy have been reported (3–6); most employed the construction of time-log survivor curves during a short-time exposure period. However, previous studies have been limited in the number of preservative systems evaluated and have not attempted to correlate results from a test model to results obtained from an actual parenteral drug product. In this work, neutral isotonic sodium chloride solution was selected as the model parenteral solution, while neutral regular insulin was chosen as the actual drug product. The use of neutral isotonic saline was based on the assumption that bacteria would not be adversely affected by such an inoffensive formulation and, thus, bacterial destruction would be solely the result of preservative activity.

An additional unique feature of the work reported herein is the application of a computer statistical program generating two types of models fitted to the experimental data. The use of models to analyze the microbial survivor data facilitates the decision-making process in the selection of appropriate preservative systems in the formulation development of multidose parenteral products.

EXPERIMENTAL SECTION

Solution Preparation—The preservatives used in this study were USP grade, tested by and obtained in-house: phenol (0.2% and 0.5%), m-cresol (0.1–0.3%), benzyl alcohol (1% and 2%), methylparaben (0.1% and 0.2%), propylparaben (0.01% and 0.02%), and chlorobutanol (0.5%). Preservative combinations studied were phenol-m-cresol, methyl- and propylparabens, and methylparaben-benzyl alcohol. A total of 14 preservative systems were evaluated.

Solutions in isotonic saline were prepared using sterile glass flasks and sterile 0.9% NaCl irrigating solution[1]. The accurately weighed or measured volume of preservative was dissolved in the saline solution, and the pH was adjusted to 6.8–7.4 using sterile filtered 1.0 M NaOH or 1.0 M HCl. Solution volume was then adjusted quantitatively to the correct volume with saline.

Insulin solutions were prepared and sterile-filtered using a regular insulin formulation without a preservative. Preservatives were accurately weighed or measured and added to the insulin solution. All insulin solutions were pH 6.9–7.4.

Test Organisms—The test organisms used in this study were *Staphylococcus aureus* (ATCC 6538), *Pseudomonas aeruginosa* (ATCC 9027), *Escherichia coli* (ATCC 8739), *Candida albicans* (ATCC 10231), and *Aspergillus niger* (ATCC 16404). The bacterial cultures were grown for 18–24 h in soybean-casein digest agar[2] and the growth washed from the slants with 10 mL of sterile saline (0.85% NaCl). The stock suspensions were prepared by dilution with sterile saline to give a cell concentration of ~5×10^8 organisms/mL. Sufficient suspension was added to the test solution to obtain ~1×10^6 organisms/mL.

Yeasts and molds were grown on Sabouraud dextrose agar plates[2] at 25°C until sufficient growth appeared. Cells were washed from the plates with sterile saline, sedimented by centrifugation, and the sediment was suspended in sufficient sterile saline to yield ~5×10^8 organisms/mL. Suspensions were further diluted to give ~1×10^6 organisms/mL when added to the test solutions.

Test Procedure—A 0.1-mL amount of the test organism suspension was added to each 5-mL portion of the test solution. After mixing on a vortex mixer, an initial sample was taken for the time zero plate count. A saline control sample prepared in the same manner was also tested; this was used as the time zero count in some instances because of the very rapid bactericidal effect of some test solutions. Test samples were then retested after incubation, typically at 0.5, 1, 2, 4, and 6 h for bacteria and at 4, 8, and 24 h for yeasts and molds. All test samples were held at room temperature unless otherwise specified.

All dilutions were prepared in phosphate buffer solution, pH 7.2 ± 0.1. After shaking, 0.1- and/or 1.0-mL aliquots were transferred into duplicate petri plates. Letheen agar[3] was used as the test medium: it contains polysorbate 80 and lecithin, known to inhibit most phenolic and paraben antimicrobial agents (7, 8). Tests in our laboratories confirmed the effectiveness of this medium. Bacterial and yeast plates were incubated for 48 h at 35°C and mold plates at 25°C for 4 to 7 d. Average plate counts were calculated for each sample.

Data Analysis—The data analysis was accomplished *via* a computer program utilizing the statistical software package SAS[4]. When values of the variables "Hours" and "Counts" were entered, the program generated two types of fitted models relating log (count + 1) to hours and produced plots of the fitted equations superimposed by the original observations. The two

[1] Travenol Laboratories, Deerfield, Il.
[2] Difco, Detroit, Mich.
[3] BBL, Cockeysville, Md.
[4] Statistical Analysis System; SAS Institute, Cary, N.C.

0022-3549/84/0700-0903$01.00/0
© 1984, American Pharmaceutical Association

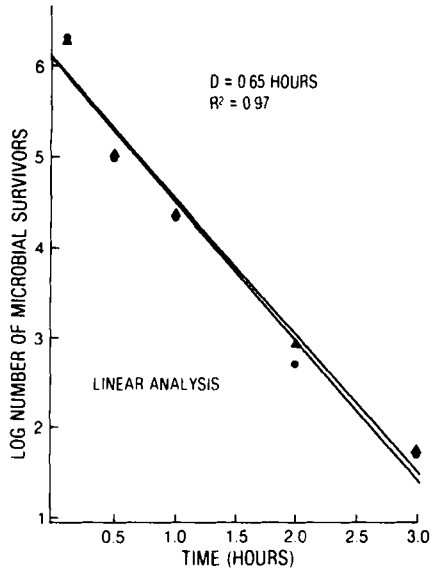

Figure 1—*Linear regression fit of the log number of microbial survivors versus time as calculated by the SAS linear analysis method. Data points represent two separate experiments;* D *and* R^2 *values are the average of two linear regression analyses.*

models used were a linear model and a quadratic model. The linear model is given by:

$$y = \alpha + \beta x + \epsilon \qquad \text{(Eq. 1)}$$

where y = log (count + 1) at hour x, α is the intercept, β is the slope of the line, and ϵ is the experimental error associated with the observation of y. The quadratic model is given by:

$$y = \alpha + \beta x + \gamma x^2 + \epsilon \qquad \text{(Eq. 2)}$$

where the additional term γx^2, represents the departure from linearity of the log (count + 1). The purpose of these model-fitting programs is to calculate estimates of the parameters α, β, and γ in the two theoretical models.

The *D* value refers to the decimal reduction time describing the death rate of the microorganisms; it represents the length of time in which a 1-log reduction in the number of survivors will be achieved. Since the term "*D* value" has heretofore been used in conjunction with a model in which the death rate is independent of the current number of survivors, it has been convenient to calculate it by the formula:

$$D = \frac{U}{\log N_0 - \log N_u} \qquad \text{(Eq. 3)}$$

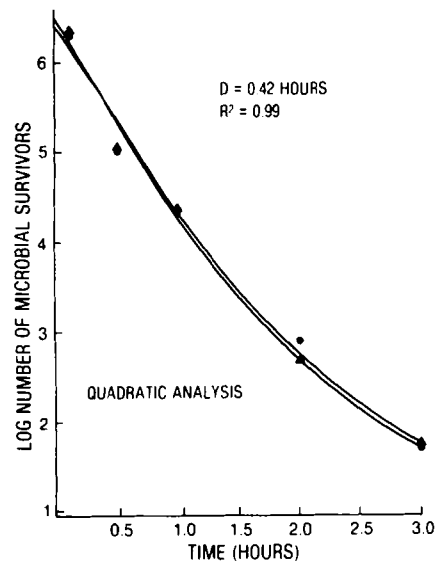

Figure 2—*Linear regression fit of the log number of microbial survivors versus time as calculated by the SAS quadratic analysis method. Data points represent two separate experiments;* D *and* R^2 *values are the average of two linear regression analyses.*

Table I—Comparison of *D* Values for the USP Challenge Organisms in Neutral Saline Solutions Containing Various Preservative Systems

Organism	Linear Method		Quadratic Method	
	D, h	R^2	*D*, h	R^2
	0.2% Phenol			
S. aureus	10.9	0.96	15.6	0.99
P. aeruginosa	7.0	0.99	4.2	1.00
E. coli	26.2	0.96	27.4	.95
A. niger	250.0	0.84	81.3	1.00
	0.3% *m*-Cresol			
S. aureus	0.7	0.98	0.4	0.99
P. aeruginosa	1.9	0.39	0.6	0.57
E. coli	1.8	0.82	0.8	0.97
A. niger	3.2	0.98	2.3	0.99
C. albicans	9.0	0.87	3.5	1.00
	0.2% Phenol + 0.3% *m*-Cresol			
S. aureus	0.5	0.78	0.2	0.95
P. aeruginosa	1.3	0.81	0.5	0.98
E. coli	2.5	0.92	3.6	0.97
A. niger	3.1	0.99	2.1	1.00
C. albicans	2.8	0.84	1.5	0.90

where U is the time exposure interval at constant temperature, N_0 is the initial number of surviving microorganisms, and N_u is the number of surviving microorganisms after exposure period U. This equation is applicable to our model, in which the log of the number of survivors is treated as a linear function of time.

A typical semilogarithmic plot of the number of living microorganisms in a preserved solution *versus* time is shown in Fig. 1. If the R^2 value was ≥0.9, the linear model shown in Fig. 1 was considered sufficient for determining the *D* value of the microorganism in the preserved parenteral system. Preservative systems especially effective in inactivating microorganisms tended to yield curvilinear plots of log count *versus* time. The rate of kill during the first 30–60 min was more rapid than the rate of kill at later times. Fitting the data according to a linear model generally resulted in a poorly fit straight line with an R^2 of ≤0.9. Also, the calculated *D* value often underestimated the actual rate of kill produced initially.

A better fit of the data was achieved by employing the quadratic equation. According to this model, a hyperbolic fit of the data is obtained, as shown in Fig. 2. The *D* value shown here corresponds to the length of time before the first log reduction in count. The fit of the data using the quadratic model improved the R^2.

RESULTS

Preliminary results comparing *D* values of USP challenge organisms in neutral saline solutions containing various preservative systems are reported in Table I. The *D* values for the mold and yeast were higher than those for bacteria. However, both USP and BP requirements for yeast and mold survival in preserved solutions are less stringent than those for bacterial survival. Of the three bacterial challenges, *E. coli* was most resistant to the antimicrobial agents tested. However, *E. coli* is not required by the BP test for injections. Either *S. aureus* or *P. aeruginosa* can be used as a prototype challenge organism to provide early predictions regarding the success or failure of a preservative system to pass the BP preservative efficacy test. *S. aureus* was selected as the model challenge organism, primarily because of the data reported in Table II. In solutions containing lower concentrations of preservatives, the *D* values for *S. aureus* were greater than those for *P. aeruginosa*.

D values for *S. aureus* in 14 different preservative systems were compared in both neutral isotonic saline and neutral regular insulin solution (Table III). The combination of 0.2% phenol + 0.3% *m*-cresol consistently produced the lowest *D* values, while 0.2% phenol consistently produced the highest *D* values. Preservative systems ranked 1–5 in Table III passed the BP requirement of reducing the bacterial population by 1 log in 2 h in both neutral saline and

Table II—Comparison of *D* Values of Three Bacterial Challenges in Phenol and *m*-Cresol Preservative Systems in Neutral Isotonic Saline Solutions

Preservative System	D_{lin}, h		
	S. aureus	*P. aeruginosa*	*E. coli*
0.2% Phenol + 0.3% *m*-Cresol	0.5	1.3	2.5
0.2% Phenol + 0.1% *m*-Cresol	3.8	1.5	7.5
0.2% Phenol	10.9	7.0	26.2
0.5% Phenol	1.1	1.3	2.5
0.2% *m*-Cresol	5.7	1.1	8.3
0.3% *m*-Cresol	0.7	1.9	1.8

Table III—D Values and Correlation Coefficients (R^2) from Linear and Quadratic Data Analyses for Saline and Insulin Solutions Containing Different Preservative Systems Ranked According to Their Effectiveness Against *S. aureus*[a]

Preservative System	Linear Analysis						Quadratic Analysis					
	Saline Solution			Insulin Solution			Saline Solution			Insulin Solution		
	Rank	D_{lin}, h	R^2	Rank	D_{lin}, h	R^2	Rank	D_{quad}, h	R^2	Rank	D_{quad}, h	R^2
0.2% Phenol + 0.3% *m*-Cresol	1	0.5	0.78	1	0.5	0.79	1	0.2	0.95	1	0.2	0.96
0.3% *m*-Cresol	2	0.7	0.98	2	0.6	0.76	2	0.4	0.99	2	0.3	0.94
0.5% Phenol	3	1.1	1.00	3	0.8	0.93	5	1.2	1.00	4	0.4	0.99
2.0% Benzyl Alcohol	4	1.6	0.68	3	0.8	0.74	3	0.6	0.94	2	0.2	0.97
0.2% Phenol + 0.2% *m*-Cresol	5	1.7	0.93	5	1.3	0.75	4	0.8	1.00	4	0.4	0.96
0.2% Methylparaben + 0.02% Propylparaben	6	1.8	0.99	10	3.0	0.92	6	1.7	1.00	8	1.6	0.99
0.1% Methylparaben + 1.0% Benzyl Alcohol	7	2.7	0.94	6	1.4	0.90	7	1.7	0.97	7	0.7	0.91
0.2% Phenol + 0.1% *m*-Cresol	8	3.8	0.99	8	2.2	1.00	8	3.6	1.00	10	2.2	1.00
0.2% *m*-Cresol	9	5.7	0.92	8	2.2	0.94	9	4.9	0.96	8	1.6	0.98
0.1% Methylparaben + 0.01% Propylparaben	10	7.4	0.97	13	12.3	0.91	10	8.3	0.98	13	12.0	0.95
0.1% Methylparaben	11	8.9	0.95	12	9.5	0.86	11	11.0	0.95	12	7.6	0.94
0.5% Chlorobutanol	12	10.1	0.81	7	1.8	0.80	—	—	—	6	0.7	0.99
1.0% Benzyl Alcohol	13	10.7	0.93	11	4.2	0.83	13	12.2	0.96	11	3.4	0.94
0.2% Phenol	14	10.9	0.96	14	16.2	0.96	14	15.6	0.99	14	12.9	0.96

[a] All data are the average of two experiments.

neutral regular insulin solutions. D values, generally, were lower in insulin solution compared with saline. Thus, the neutral isotonic saline solution conservatively estimated the preservative effectiveness against *S. aureus* observed in neutral regular insulin solutions.

Fits of the linear models of log count *versus* time were very good ($R^2 \geq 0.93$) for the majority of the saline solutions tested. Fits were not as good for the insulin solutions using the linear method, but the quadratic model improved the fits. Additionally, the quadratic model ranked the effectiveness of the various preservative systems in nearly the same order as that found using the linear model. Thus, the choice of the model did not cause any major change in the identification of best and worst systems.

DISCUSSION

The logarithmic order of death of microorganisms (9) facilitates the study of the effectiveness of destroying microorganisms within a convenient time frame. Simple techniques of microbiological assay and computer data analysis permit the generation of microbial kinetic data easily and rapidly. The methodology described in this paper can be used to evaluate preservative effectiveness in a given formulation as a function of any number of variables: type and concentration of preservatives, combination of preservatives, microbial challenge organism, solution pH, formulation differences, and temperature. The results reported in this paper show that D values can be easily obtained and used to compare the effectiveness of different preservative systems. Computers aid in the analysis of data that employ different models for an adequate fit. From the data one can select the best preservative system for the formulation being developed.

Like most experimental screens, this method has certain limitations and precautions. The initial microbial concentration cannot be determined accurately from the test sample because of the immediate action of the antimicrobial agent. Initial values must be determined using a control solution with no antimicrobial activity. At least three, preferably four, samples should be taken from the test solution for microbial analysis at various times over a maximum of 6 h. In the studies reported here, four samples were taken.

Rapid-acting preservative systems require sampling times at intervals much sooner and shorter than for long-acting preservative systems. For example, rather than taking samples at 1, 2, 4, and 6 h following the addition of the microbial challenge, rapid-acting preservative systems need to be sampled at 0.25, 0.5, 1, and 2 h after time zero. Many preservative systems caused a precipitous initial reduction in the microbial population followed by a more gradual decline. This produced curvature in the log count *versus* time graph, which necessitated the use of the quadratic model for analyzing the data. The D value calculated gave a more representative estimate of the destructive action of the preservative system than that obtained from the standard linear model.

It may not be advisable to study only a single species challenge in a screening test. Of course, the fewer the types of microorganisms used, the more expedient the test. Ideally, the most resistant microorganism in the test system is identified at the beginning of the screening study. The hazard of employing a single challenge to evaluate a large number of preservative systems is the potential for a different microbial species than that used as the challenge to be significantly more resistant in a particular preservative system. For example, *S. aureus* might be the most resistant microorganism in phenolic preservative systems, while *E. coli* might be more resistant in paraben preservative systems. It is because of these possibilities that the most effective preservative system selected as a result of its activity against one microorganism should subsequently be studied in the presence of all other compendial challenge microorganisms. This screening method is not a substitute for the USP and/or BP preservative efficacy tests, but rather serves to reduce the potential number of preservative systems to be tested by the compendial methods.

The D values reported in this study represented the average of two experiments. Preliminary investigation found that the standard deviations calculated from five replicate D value experiments of the same organism in separately prepared solutions containing the same preservative system ranged from 4.2 to 8.7%. This seemed adequate for a preformulation screening test, especially one involving a plate count microbiological test procedure.

Several of the data sets showed significant departures from linearity ($p \leq 0.01$ for the improvement in fit gained by including a quadratic term in the model). By fitting both linear and quadratic models and comparing the rankings of D values from these models, it was possible to verify that the ranking of these preservative systems was not dependent on the choice of model. Although the linear models proved to be adequate for the screening of preservatives, a quadratic model based on an adequate number of time points should be considered whenever an accurate estimate of the actual value of D is desired.

While this method provides an excellent initial estimate of preservative activity in parenteral solutions, it is not intended to evaluate other issues concerning antimicrobial preservatives, such as stability and compatibility characteristics in the final formulation and package system. The most promising systems identified by this method will be studied in greater detail for compliance to compendial standards of effectiveness, stability, and compatibility in the newly developed parenteral formulation.

REFERENCES

(1) "British Pharmacopoeia," Vol. II, Her Majesty's Stationery Office, London, 1980, A192-A194.

(2) "United States Pharmacopeia," 20th rev., U.S. Pharmacopeial Convention, Rockville, Md., 1980, pp. 873-874.

(3) W. C. Alegnani, *Develop. Biol. Standard*, **22**, 91 (1973).

(4) D. J. G. Davies, N. E. Richardson, and A. Yolande, *J. Pharm. Pharmacol.*, **28**, 49P (1976).

(5) D. S. Orth, *J. Soc. Cosmet. Chem.*, **30**, 321 (1979).

(6) M. Chan and H. N. Bruce, *Cosmet. Ind.*, **34**, 80 (1981).

(7) M. Barr and L. F. Tice, *J. Am. Pharm. Assoc., Sci. Ed.*, **46**, 445 (1957).

(8) A. M. Littell, M. J. Palmieri, and N. B. Bisciello, *J. Assoc. Off. Anal. Chem.*, **63**, 1200 (1980).

(9) O. Rahn, "Biodynamica Monograph No. 3," Biodynamica, Normandy, Mo., 1945, pp 9-41.

ACKNOWLEDGMENTS

The authors thank Irene Jones for her laboratory assistance and Sharon Amonett for preparing the manuscript.

Importance of Viscosity in the Dissolution Rate of Cholesterol in Monooctanoin Solutions

JOSEPH B. BOGARDUS

Received June 22, 1983, from the *College of Pharmacy, University of Kentucky, Lexington, KY 40506.* Accepted for publication July 14, 1983. Present address: Bristol-Myers Co., P.O. Box 4755, Syracuse, NY 13221-4755.

Abstract □ Several factors affecting the dissolution rate of cholesterol in monooctanoin were investigated. This solvent is used clinically for dissolution of residual cholesterol gallstones in the bile duct after cholecystectomy. The effect of added water on dissolution rate, measured using the static- or rotating-disk methods, was not consistent with the previously measured solubility. The discrepancy was found to be due to the decreasing viscosity of the solvent as water was added. Addition of cholesterol, however, increased the viscosity of monooctanoin. The viscosity effect on dissolution rate was investigated further by addition of polymers (povidone and poloxamer 237) which increased solvent viscosity. Dissolution rate was proportional to viscosity to the −0.4 power with these polymers. An equation was derived which predicts that dissolution rate should be proportional to viscosity to the $-\frac{2}{3}$ power. The predicted exponent was very close to reported experimental values for benzoic acid, but the dissolution rate/viscosity relationship for cholesterol in aqueous monooctanoin was nonlinear with apparent exponents of −0.65 to −2.3. Although the Arrhenius activation energies for viscosity (3.79 kcal/mol) and dissolution rate constant (3.66 kcal/mol) were almost equal for benzoic acid, a nonlinear relationship was again observed for cholesterol in aqueous monooctanoin with approximate E_a values of 5.6 10 kcal/mol. The strong influence of viscosity on dissolution rate in this system is attributed to the viscosity-increasing effect of cholesterol in the diffusion layer. The increased viscosity at higher cholesterol concentrations reduces the diffusion coefficient of cholesterol and causes the dissolution rate to be slower even though solubility may have been higher. The data suggest that it may be possible to increase cholesterol gallstone dissolution by addition of water to monooctanoin.

Keyphrases □ Cholesterol dissolution—monooctanoin, viscosity, effect of water addition □ Monooctanoin—cholesterol (gallstone) dissolution, viscosity, effect of water addition □ Viscosity—monooctanoin, cholesterol (gallstone) dissolution, effect of water addition

Monooctanoin (glyceryl monooctanoate) is being used clinically for dissolution of common bile duct cholesterol gallstones (1, 2). The solvent is infused into the bile duct through an abdominal T-tube drain inserted after cholecystectomy. Although cholesterol has high solubility in monooctanoin, most clinical studies indicate that infusion for 1–2 weeks is necessary for gallstone dissolution.

In a previous communication, the solubility of cholesterol in monooctanoin was found to be dependent on the water content of the solvent (3). With addition of water the solubility increased and then decreased with a maximum occurring at 5% water (37°C). The solubility maximum was coincident with the transition of solid cholesterol from the anhydrous to monohydrate form. Since the clinical efficacy of the solvent is primarily dependent on the dissolution rate of cholesterol, the effect of water and other factors influencing cholesterol dissolution rate in monooctanoin were investigated.

THEORETICAL SECTION

The simple Nernst diffusion layer theory is adequate for most dissolution rate studies. The dissolution rate is assumed to be proportional to the concentration gradient across an unstirred diffusion layer on the solid surface:

$$J = DA/h(C_s - C_b) \qquad \text{(Eq. 1)}$$

where J is the dissolution rate, A is the surface area of dissolving solid, D is the diffusivity of solute, C_s is the solubility of solute, C_b is the concentration of solute in bulk solution, and h is the effective diffusion layer thickness. This equation is often used with the static-pellet method for comparative dissolution rate determinations because it assumes that the dissolution rate is only affected by diffusional processes and that the factors in Eq. 1, other than solubility, are constant (4).

When diffusion and convection are both important, the Levich equation applies for a rotating dissolving disk (5):

$$J = 0.62AD^{2/3}/\nu^{1/6} \cdot \omega^{1/2}C_s \qquad \text{(Eq. 2)}$$

where ν is the kinematic viscosity and ω is the angular velocity of rotation. Since the parameters in Eq. 2 can be independently determined, the calculated dissolution rate may be compared with experimental data. Upon combination of these equations, the effective diffusion layer thickness for the rotating disk is obtained:

$$h = 1.6D^{1/2}\nu^{1/4}/\omega^{1/2} \qquad \text{(Eq. 3)}$$

EXPERIMENTAL SECTION

Dissolution Rate—Dissolution of cholesterol monohydrate from a rotating disk was measured using an apparatus similar to that reported previously (6), consisting of a synchronous motor and stirring assembly in a water-jacketed beaker. The sample was compressed in a 1.27-cm diameter die with a load of 3180 kg[1], and the die was attached to a plate on the end of the stirring shaft using cyanoacrylate glue[2] (the die was later removed by soaking the assembly in acetone). The rotation speed was changed using synchronous motors from 60–600 rpm[3]. In the static disk studies the die/disk was placed facing upward on the bottom of the beaker, and the solution was stirred at 150 rpm. To simulate the conditions of gallstone dissolution *in vivo*, 0.5-g cholesterol disks were accurately weighed and placed in screw-capped test tubes containing 40 g of solvent. The samples were left undisturbed at 37°C for 24 h and the residual cholesterol was determined gravimetrically after removing excess solvent by blotting with tissue.

Analysis—Cholesterol was analyzed by HPLC using a modification of a literature procedure (7) using an acetonitrile–methanol (5:1) mobile phase, a reverse-phase column[4], and a variable-wavelength detector at 215 nm. Dissolution samples were diluted with mobile phase and injected directly on the system. Benzoic acid was analyzed spectrophotometrically at 229 nm in 0.01 M HCl.

Water in cholesterol monohydrate and dissolution media was determined by automated Karl Fischer titrimetry[5]. Viscosity was measured using a cone-plate viscometer[6] with a circulator bath for temperature control. Cholesterol solubility was determined as previously described (3).

Fractionation of Monooctanoin—The mono- and diglyceride fractions of commercial monooctanoin were separated by column chromatography on silica gel. The diglyceride fraction was eluted with ethyl acetate–hexane (1:1) and the monoglyceride fraction was then displaced with ethyl acetate. The purity of the fractions was checked by TLC (1:1 ethyl acetate–hexane on precoated silica gel plates) and the solvent was removed by rotary evaporation. The monoglyceride melted at 36°C, and the diglyceride was an oil. The samples contained <0.5% water.

Materials—Cholesterol USP[7], monooctanoin[8], and glyceryl monolaurate[9] were obtained commercially. The ~30% diglyceride content in monooctanoin reported by the manufacturer was consistent with the column chromatography yields. Solvents were HPLC grade, and the other chemicals were reagent grade.

Cholesterol monohydrate was prepared by recrystallization from 10% aqueous acetone. The wet crystals, after filtration, were air-dried for ~1 h

[1] Fred S. Carver Inc.
[2] Krazy Glue Inc.
[3] Hurst Mfg. Co.
[4] μBondapak C_{18}, Waters Associates.
[5] Auto-aquatrator; Precision Scientific.
[6] Ferranti-Shirley, Ferranti Ltd.
[7] Sigma Chemical Co.
[8] Capmul 8210; Stokeley-Van Camp Inc.
[9] Kessco 675; Armak Industrial Chemicals.

0022-3549/84/0700-0906$01.00/0
© 1984, American Pharmaceutical Association

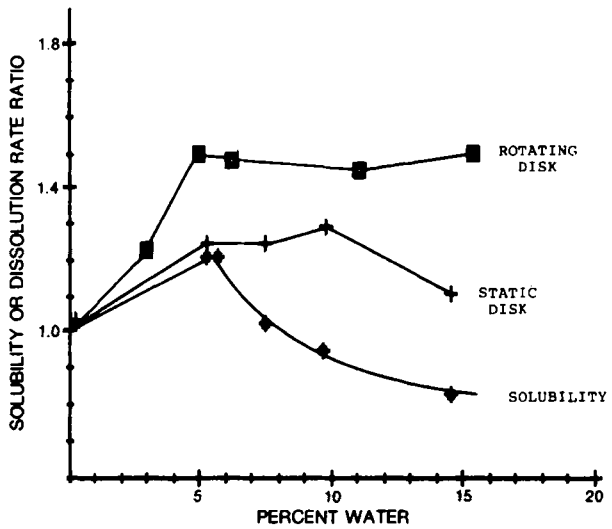

Figure 1—*Ratio of the solubilities and dissolution rates of cholesterol in aqueous monooctanoin solutions to the values in the dry solvent (37°C). Dissolution rates were measured at 150 rpm. Solubility data was taken from Ref. 3.*

and then stored in a chamber containing water. The water content of the crystals was equal to theory for a monohydrate (4.4% water). Although 95% ethanol has been widely used for preparing the monohydrate, problems were encountered in removing the residual ethanol when using this solvent. This may be due to the formation of a hemiethanol solvate (8). The vacuum drying required to remove ethanol also removed the water of hydration, so the sample was rehydrated in the water chamber. The water of hydration was quite labile. After a few hours in an open container, the water content of cholesterol monohydrate decreased to ~1%.

RESULTS AND DISCUSSION

Static-Disk Studies—Dissolution rate measurements by the static-disk method were conducted. In Fig. 1 the relative dissolution rate and solubility of cholesterol in monooctanoin solutions is plotted as a function of the water content of the solvent. At this stirring rate, there was poor agreement between the previously determined solubilities and the static-disk dissolution data. The difference was most apparent at >5% water where the dissolution rate did not decrease along with the solubility. The dissolution rate determined in the dry solvent (4.7×10^{-3} mg cm^{-2} s^{-1}) was in good agreement with the value of 4×10^{-3} reported by Thistle *et al.* (1).

Other data corroborated the poor correlation between solubility and dissolution rate. Table I shows the effect of sodium chloride on solubility and dissolution rate in 5% aqueous monooctanoin. A mixture of 0.9–2.5% aqueous NaCl with monooctanoin increased cholesterol solubility, presumably by inducing association of cholesterol with itself or the nonpolar fatty acid chains of the glycerides. As before, however, the solubility increase did not cause a corresponding change in the dissolution rate. The viscosity of the solutions was not affected by sodium chloride. Cholesterol solubility increased with addition of longer-chain glycerides. When monooctanoin was mixed with an equal amount of glyceryl monolaurate and 5% water, cholesterol solubility increased from 16.1 to 23%, whereas the dissolution rate was essentially unchanged. These data clearly show that the direct proportionality between solubility and dissolution rate expected from the Nernst equation is not being followed in this system.

Rotating-Disk Studies—Because of the uncertainty of the static-disk method with regard to hydrodynamic conditions in this system, the effect of water was redetermined using the rotating disk at 150 rpm (Fig. 1, upper

Table I—Effect of Salt on Cholesterol Solubility and Dissolution Rate (Static-Disk Method)

NaCl in Aqueous Component of 5% Monooctanoin, %	Viscosity, cP	Solubility, %	10^3 Dissolution Rate, mg cm^{-2} s^{-1}
0	37	16.1	5.7
0.9	37	18.0	5.6
1.8	38	19.1	5.5
2.5	37	18.2	5.8

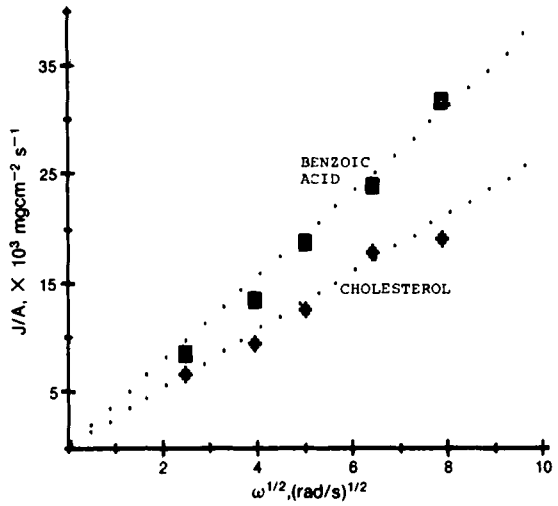

Figure 2—*Levich plots of the dissolution rate* versus *(rotation speed)*$^{1/2}$ *at 37°C for cholesterol in 10% aqueous monooctanoin and benzoic acid in 0.01 M HCl. Dotted lines were calculated using Eq. 2.*

curve). The dissolution rate and solubility data diverged still further, with an almost constant 50% increase in dissolution rate at >5% water.

The dissolution apparatus was calibrated using benzoic acid in 0.01 M HCl at 37°C. Under these conditions the dissolution rate is diffusion controlled (6). In addition, the diffusion coefficient and solubility of benzoic acid in 0.01 M HCl have been reported (4), allowing calculation of the dissolution rate according to Eq. 2. The theoretical line in Fig. 2 is in excellent agreement with the experimental data for benzoic acid.

Also shown in Fig. 2 is the dissolution rate of cholesterol in aqueous monooctanoin. The diffusion coefficient of cholesterol in the solvent was estimated to be 1.53×10^{-7} cm^2 s^{-1} using the Stokes-Einstein equation (see Eq. 4 below). With this and the other constants of Eq. 2, the theoretical line for cholesterol in Fig. 2 was calculated and found to be in good agreement with the experimental data. It may, therefore, be concluded that the dissolution rate of cholesterol under the conditions studied is a diffusion-convection-controlled process according to Eq. 2.

Effect of Water and Cholesterol on the Viscosity of Monooctanoin—During preparation of the dissolution media the viscosity of monooctanoin appeared to be reduced by the addition of water. These observations were confirmed by measuring the viscosities with a cone-plate viscometer (Fig. 3). The viscosity-lowering effect of water is generally observed with glycerol and glycols and has been attributed to the breaking of solvent-solvent hydrogen bonds by addition of water (9, 10). These data are important since viscosity changes could be an explanation for the anomalous dissolution rate results. The decreasing viscosity could be counteracting the lower cholesterol solubility, causing the dissolution rate at >5% water to be essentially constant.

Addition of cholesterol had the opposite effect on the viscosity of monooc-

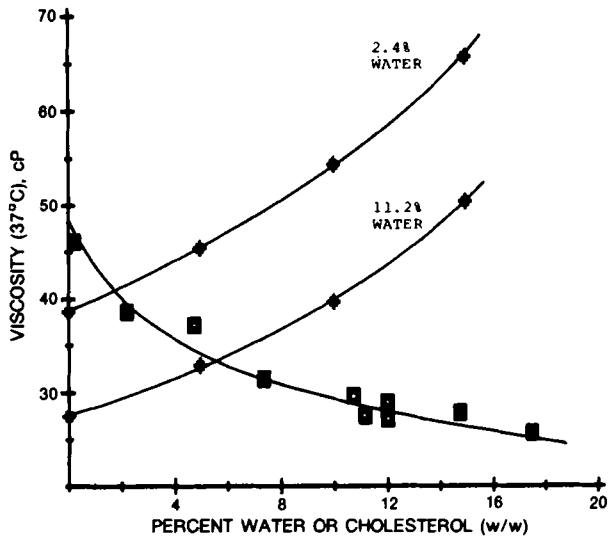

Figure 3—*Effects of water (■) and cholesterol (◆) on the viscosity of monooctanoin at 37°C.*

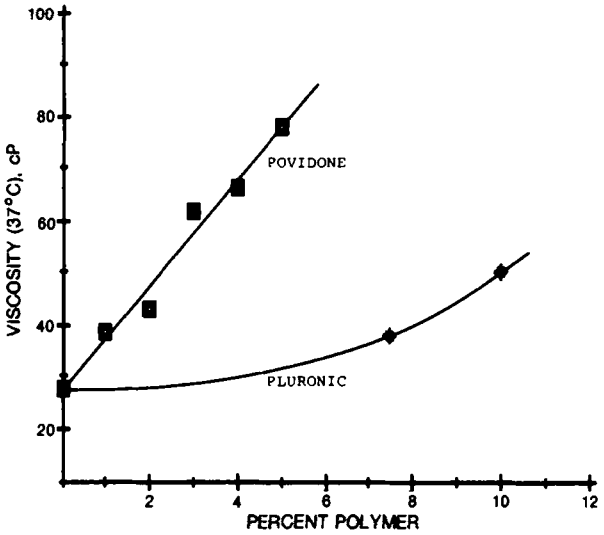

Figure 4—*Viscosity of 10% aqueous monooctanoin as a function of polymer concentration at 37°C.*

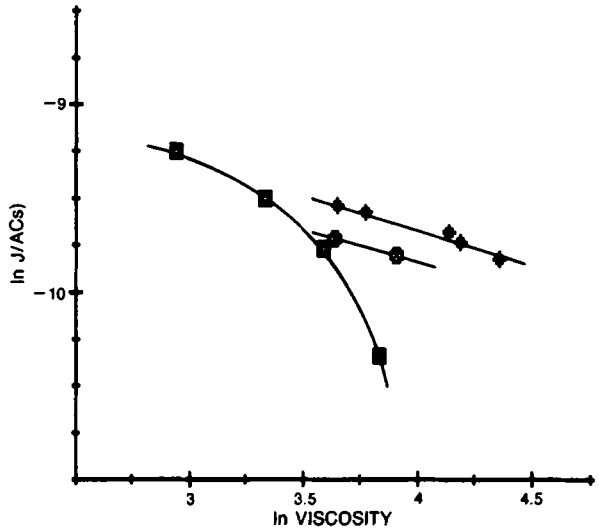

Figure 5—*Log-log plot of the dissolution rate constant* versus *the viscosity of the dissolution medium according to Eq. 5A. Key: (■) 10% aqueous monooctanoin at different temperatures; (◆) povidone in 10% aqueous monooctanoin (37°C); (◆) Poloxamer 237 in 10% aqueous monooctanoin (37°C).*

tanoin (Fig. 3). In addition, the upward curvature indicated a greater than first-order dependence on cholesterol concentration. The similarity of the two curves showed that the amount of water present had little effect on the viscosity-inducing properties of cholesterol. Since the higher concentrations in Fig. 3 are similar to the solubility of cholesterol in the dissolution experiments, the diffusion layer during dissolution must be significantly more viscous than the bulk solution. This implies also that a viscosity gradient must be present across the diffusion layer. Although it is probably not rigorously applicable to this system, the Stokes-Einstein equation predicts an inverse relationship between the diffusion coefficient and viscosity:

$$D = kT/(6\pi\eta r) \qquad \text{(Eq. 4)}$$

where k is the Boltzmann constant, T is the absolute temperature, η is the viscosity, and r is the radius of the molecule.

Viscosity Effects on Dissolution Rate—Two independent approaches were investigated for probing the effect of viscosity on dissolution rate: addition of polymers and temperature effects. The former approach has been extensively investigated in aqueous systems (11-13). In aqueous polymer solutions the exponential relationship betweeen dissolution rate and viscosity usually lies between −0.25 and −0.8 (11). The exponent was dependent on the experimental system, polymer, and dissolving solute. This specificity was proposed to be due to the difference between the measured bulk solution viscosity and the effective viscosity (resistance to solute diffusion), which controls the dissolution rate (12). In a recent study, several equations for the diffusion coefficient in polymer solutions were compared for their ability to represent benzoic acid dissolution (13). None was found to be significantly better than Eq. 4 and the average viscosity exponent was −0.62 (13).

Rearrangement of Eq. 2 gives the dissolution rate constant:

$$J/(AC_s = 0.62\nu^{-1/6}\omega^{1/2}D^{2/3} \qquad \text{(Eq. 2a)}$$

By substituting D from Eq. 4, the hypothetical effect of viscosity on dissolution rate is obtained:

$$J/(AC_s) = 0.62\nu^{-1/6}\omega^{1/2}(kT/(6\pi r))^{2/3}\eta^{-2/3} \qquad \text{(Eq. 5)}$$

$$= k'\eta^{-2/3} \qquad \text{(Eq. 5a)}$$

where $k' = 0.62\nu^{-1/6}\omega^{1/2}(kT/(6\pi r))^{2/3}$.

At constant temperature the terms of k' should be constant except for $\nu^{-1/6}$. This term, however, is almost constant over the range of viscosity usually studied. For example, a 50% increase in viscosity would change this term by only −6.5%. Equation 5 predicts that J/AC_s should be proportional to viscosity to the $-2/3$ power. This predicted value is quite similar to that experimentally determined (11-13), although previous investigators have apparently not considered this simple relationship.

In preliminary studies several polymers were screened for their effects on cholesterol solubility and monooctanoin viscosity. Povidone K-30 and poloxamer 237 were chosen because viscosity was increased without change in cholesterol solubility. In Fig. 4 the viscosity of aqueous monooctanoin is plotted as a function of polymer concentration. The povidone data are linear but the Poloxamer 237 viscosities are not, and higher concentrations were required to reach a given viscosity. Figure 5 shows the log-log relationship between dissolution rate and viscosity for these two polymers plotted according to Eq. 5a. The slopes were −0.39 for povidone and −0.36 for poloxamer 237, smaller than the $-2/3$ power predicted above.

The effect of temperature on dissolution rate has not been previously utilized for investigating viscosity effects. In Eq. 2, for the rotating disk, changing temperature affects ν, D, and C_s. Since the $\nu^{-1/6}$ term is negligible under most conditions and solubilities can be readily measured, the effect of viscosity on dissolution rate can be isolated to the changing diffusion coefficient. If Eq. 4 adequately represents the proportionality between D and η, then Eq. 5 should also be applicable for dissolution rate-temperature data. Since $T^{2/3}$ changes only 5% with the present data (20-45°C), whereas J/AC_s increases threefold, dividing J/AC_s by $T^{2/3}$ has no significant effect (Fig. 5). The slopes for this curving line are approximately −0.6 to −2.3, with the smaller value occurring at the higher temperatures (37°C and 45°C). Thus, it appears that the dissolution rate approaches theoretical behavior ($-2/3$ power of viscosity) with increasing temperature.

Activation Energies for Viscosity and Dissolution Rate—Viscosity-temperature data are commonly plotted in the Arrhenius manner to obtain the energy of activation, E_a. Figure 6 shows the temperature effect on viscosity of aqueous monooctanoin and water (14). The apparent activation energy for monooctanoin was higher than that for water. Although viscosity decreases with increasing temperature, these activation energies are reported as endothermic constants.

Previous rotating-disk dissolution rate studies reported activation energies

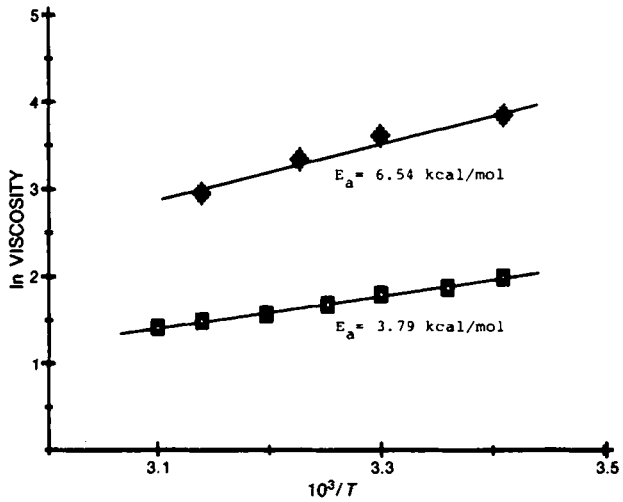

Figure 6—*Arrhenius plots of the viscosity of 10% aqueous monooctanoin (◆) and water (2 + ln η) (■) from Ref. 14.*

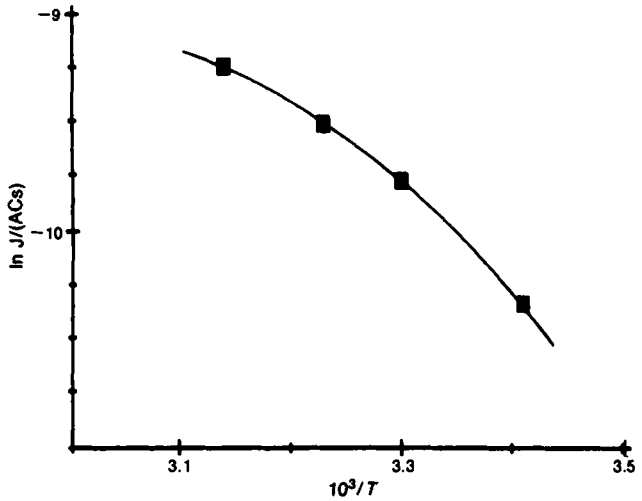

Figure 7—*Arrhenius plot for the dissolution rate constant of cholesterol in 10% aqueous monooctanoin.*

of 3.3–3.7 kcal/mol (15–17). By calculating the dissolution rate constant (J/AC_s) of benzoic acid in 0.01 M HCl from Eqs. 2 and 4, Touitou and Donbrow (17) obtained a theoretical E_a of 3.66 kcal/mol. Their experimental data showed an E_A of ~3.3 kcal/mol with some curvature in the Arrhenius plot. The difference was ascribed to the influence of interfacial kinetics at lower temperatures. The similarity between the E_a for the dissolution rate constant of benzoic acid indicates that viscosity change can almost entirely account for the change in dissolution rate.

In Fig. 7 the experimental dissolution rate constants for cholesterol are plotted against reciprocal temperature. The data again show significant curvature with an apparent range of E_a values from ~5.6 to 10 kcal/mol. As discussed previously, separation of the $T^{2/3}$ term had a negligible effect on E_a. The heat of solution for cholesterol in aqueous monooctanoin was found to be 4.1 kcal/mol (3). When ln J was plotted against T^{-1} the total heat of dissolution was ~11.5 kcal/mol. The difference in these activation energies (7.4 kcal/mol) would be the average E_a for the viscosity effect. Therefore, temperature changes exert a greater influence on dissolution rate through viscosity–diffusion coefficient effects than through solubility.

Solubility and Dissolution Rate in Mono- and Diglyceride Fractions—The monooctanoin used in these studies is a mixture containing ~30% diglyceride. The uncertainty about the individual effects of the solvent components and the previously discussed influence of viscosity prompted measurement of cholesterol solubility and dissolution rate in the mono- and diglyceride fractions of monooctanoin isolated by column chromatography. Table II compares the viscosity, solubility, and dissolution rate of the solvent and its components. The highest dissolution rates were obtained for the diglyceride fraction, even though the solubilities were the lowest. Although the data are limited, a good correlation is apparent between viscosity and dissolution rate.

A difficulty in the interpretation of Table II is that cholesterol monohydrate was used for the dissolution rate measurements, whereas the equilibrium solubility form was anhydrous (3). Curvature was not detected in the rotating-disk dissolution runs at 150 rpm, indicating that surface conversion, if occurring, was not significantly affecting the rate. This is consistent with the similar solubilities of the two forms (3). Whether conversion occurs in stirred systems depends on the hydrodynamic conditions and the potential for crystallization (supersaturation and nucleation factors).

Table II—Cholesterol Dissolution Rate in Monooctanoin and its Mono- and Diglyceride Fractions

Solvent	Water, %	Viscosity, cP	Solubility, %	10^3 Dissolution Rate, mg cm^{-2} s^{-1}
Monooctanoin	3	38	15.2	8.0
Monoglyceride fraction	3	49	15.4	7.3
Diglyceride fraction	3	18	7.3	12.1
Monooctanoin	0.4	46	13.8	6.4
Monoglyceride fraction	0.4	58	12.8	4.6
Diglyceride fraction	0.4	20	9.8	12.4

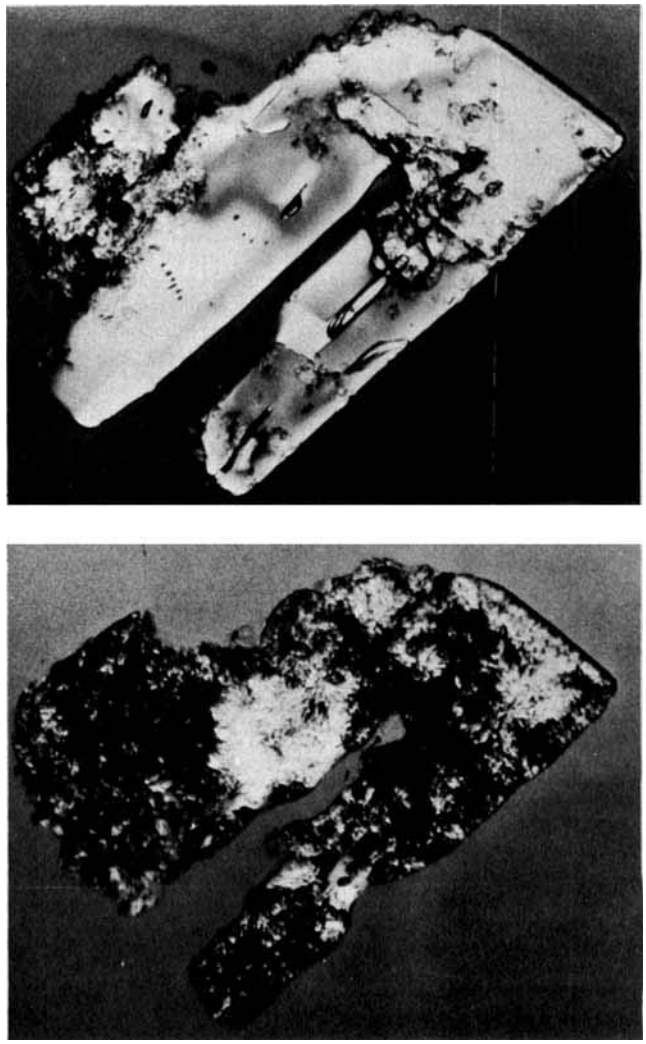

Figure 8—*Polarized light photomicrographs of a cholesterol monohydrate crystal in dry monooctanoin solution immediately upon immersion (top) and after 2 min (bottom).*

Cholesterol Dissolution in Unstirred Media—Under static (unstirred) conditions, surface transformation to the anhydrous form was observed. The photomicrographs in Fig. 8 show a cholesterol monohydrate crystal immediately and 2 min after incubation with dry monooctanoin. The darkening of the crystal is due to crystallization of the anhydrous form on the dissolving surface. In this case, the crust of anhydrous cholesterol inhibited further dissolution of the monohydrate, as shown in Table III. In the dry solvent the weight loss of tablets made from cholesterol monohydrate was less than that from the anhydrous form. The effect of water on the monohydrate in Table III parallels the results in Fig. 1, which show an essentially constant dissolution rate at >5% water. Since the conditions of these experiments are more similar to the clinical situation, which involves slow infusion into the bile duct, significant improvement in gallstone dissolution *in vivo* may be possible with monooctanoin containing water.

CONCLUSIONS

The strong effect of viscosity on dissolution rate in this system has its origin in the solute–solvent interactions which cause high solubility. These interac-

Table III—Effect of Water on Weight Loss of Unstirred Cholesterol Tablets

Water, %	Weight Loss After 24 h, %[a]	
	Monohydrate	Anhydrous[b]
0	32.5 ± 2.4	39.7 ± 1.4
5	49.8 ± 1.0	56.6 ± 3.4
10	45.8 ± 3.3	—
15	48.2 ± 4.1	—

[a] Mean ± *SD* (n = 4). [b] Dried monohydrate.

tions increase the viscosity of the diffusion layer on the dissolving cholesterol monohydrate surface. The resulting decrease in the diffusion coefficient of cholesterol in the diffusion layer causes the dissolution rate to be slower even though solubility may have been higher. For these reasons, the preferred approach for increasing the dissolution rate of cholesterol gallstones in monoglycerides would be to investigate solvents with low viscosity rather than to try to optimize solubility. The validity of this statement is supported by the data in Table II, which show that dissolution rate is greater in the diglyceride fraction of monooctanoin although cholesterol solubility is lower.

In terms of clinical applications, this study suggests that it may be possible to increase the cholesterol gallstone dissolution rate by addition of water to monooctanoin. Water may also improve local tolerance of the drug during infusion. Since the solubility of water in monooctanoin is ~15% at 37°C, the aqueous solvent would have much less potential for extraction of water from the bile duct and intestinal walls. The importance of temperature should be emphasized, since the dissolution rate of cholesterol increases 50% from 30°C to 37°C. Some of the reported variability in clinical results may be due to inadequate control of solvent temperature. Lastly, addition of water overcomes a practical problem with handling monooctanoin, *i.e.*, crystallization. By its effect on the colligative properties of the solvent, water depresses the solidification point of monooctanoin to well below room temperature.

REFERENCES

(1) J. L. Thistle, G. L. Carlson, A. F. Hofmann, N. F. LaRusso, R. L. MacCarty, G. L. Flynn, W. I. Higuchi, and V. K. Babayan, *Gastroenterology*, **78**, 1016 (1980).

(2) E. Mack, E. M. Patzer, A. B. Crummy, A. F. Hofmann, and V. K. Babayan, *Arch. Surg.*, **116**, 341 (1981).

(3) J. B. Bogardus, *J. Pharm. Sci.*, **71**, 370 (1982).

(4) W. I. Higuchi, S. Prakongpan, and F. Young, *J. Pharm. Sci.*, **62**, 945 (1973).

(5) V. G. Levich, "Physicochemical Hydrodynamics," Prentice-Hall, Englewood Cliffs, N.J., 1962.

(6) S. Prakongpan, W. I. Higuchi, K. H. Kwan, and A. M. Molokhia, *J. Pharm. Sci.*, **65**, 685 (1976).

(7) E. Hansbury and T. J. Scallen, *J. Lipid Res.*, **19**, 742 (1978).

(8) N. Garti, L. Karpuj, and S. Sarig, *J. Lipid. Res.*, **22**, 785 (1981).

(9) M. Ageno and C. Frontali, *Proc. Natl. Acad. Sci.*, USA, **57**, 856 (1967).

(10) E. Hatschek, "The Viscosity of Liquids," Van Nostrand, New York, N.Y., 1930.

(11) R. J. Braun and E. L. Parrott, *J. Pharm. Sci.*, **61**, 175 (1972).

(12) A. T. Florence, P. H. Elworthy, and A. Rahman, *J. Pharm. Pharmacol.*, **25**, 779 (1973).

(13) N. Sarisuta and E. L. Parrott, *Drug Dev. Indust. Pharm.*, **8**, 605 (1982).

(14) R. C. Weast (Ed.), "Handbook of Chemistry and Physics," 48th ed., Chemical Rubber Co., Cleveland, Ohio, 1967.

(15) H. Nogami, T. Nagai, and A. Suzuki, *Chem. Pharm. Bull.*, **14**, 329 (1966).

(16) S. Bisaillon and R. Tawashi, *J. Pharm. Sci.*, **60**, 1874 (1971).

(17) E. Touitou and M. Donbrow, *Int. J. Pharmaceut.*, **9**, 97 (1981).

ACKNOWLEDGMENTS

This work was supported by National Institutes of Health Grant No. AM31603. The technical assistance of R. Perrone is gratefully acknowledged.

Effects of Acrylic Acid Polymer and Its Arrangement on Drug Release from a Wax Matrix

HISATOSHI EMORI, TAKAFUMI ISHIZAKA ˣ, and MASUMI KOISHI

Received December 23, 1982, from the *Faculty of Pharmaceutical Sciences and Institute of Colloid and Interface Science, Science University of Tokyo, 12, Ichigaya Funagawara-machi, Shinjuku-ku, Tokyo, Japan.* Accepted for publication June 23, 1983.

Abstract □ The release of phenacetin from a wax matrix was improved by the addition of an acrylic acid polymer. Increasing the amount of polymer increased the release rate of phenacetin due to the formation of pores and channels in the matrix resulting from leaching of the polymer. The leaching was affected by the pH of the dissolution medium as well as by the methods used to prepare the granules. The polymer in ordered powder mixes behaved differently from that uniformly dispersed in a wax matrix. The drug appeared to be released by an approximate zero-order process at pH 7.5 from tablets containing the polymer.

Keyphrases □ Wax matrices, inert—release of phenacetin, effect of acrylic acid polymer □ Phenacetin release from inert wax matrices, effect of acrylic acid polymer □ Acrylic acid polymer—effect on release of phenacetin from inert wax matrices, action as a channeling agent

Recently, various methods have been developed to prolong the action of drugs by controlling their release rates. One method involves the incorporation of drugs into a wax matrix. The mechanism of drug release from a wax matrix involves the leaching of the drug by a permeating fluid that enters the drug-matrix phase through the pores, cracks, and intergranular spaces. Higuchi has treated the drug release from the matrix model in a theoretical manner (1).

Several investigators have described the incorporation of additives, such as surfactants, into the matrix (2, 3). These additives act as channeling agents and improve drug release. The drug appears to be released by a zero-order process. Others have investigated ordered powder mixes (4, 5). For example, the wettability of α-lactose powder was appreciably changed by modifying its surface with other powders (6). The purposes of this work are to evaluate an acrylic acid polymer as a channeling agent in the wax matrix and to examine the effects of powder arrangement on drug release.

EXPERIMENTAL SECTION

Materials—Carnauba wax[1] was obtained commercially, and the stearyl alcohol, sodium chloride, disodium phosphate, and hydrochloric acid were reagent grade. The phenacetin[2] was JP grade; the powder was ground with an automatic mortar[3] and then sieved to 49–105-μm particle size with stainless steel sieves. The water used in this experiment was prepared with a water purification apparatus[4]. Acrylic acid polymer[5] was cross-linked and had a viscosity of 3000 cps as a 1% aqueous solution. Molecular weight, solubility, and carboxyl group content of the acrylic acid polymer were ~2,000,000, 5% (w/w), and 60%, respectively.

Preparation of Granules—Carnauba wax (15.0 g) and stearyl alcohol (15.0 g) were mixed and melted at 90 ± 3°C. Phenacetin powder was added into the melt in small portions with constant stirring for 5 min at 90 ± 3°C, to achieve an even distribution; the mixture was then poured onto a glass plate kept at 0°C and allowed to congeal. The plate-like mass was crushed for 10

[1] Dainichi Sangyo, Ltd., Japan.
[2] Iwaki Seiyaku, Ltd., Tokyo, Japan.
[3] ANM-1000 type; Nitto Kagaku, Ltd., Nagoya, Japan.
[4] Milli-Q2; Millipore Co., Bedford, Mass.
[5] Hiviswako-104; Wako Pure Chemical Industries, Ltd., Japan.

0022-3549/84/0700-0910$01.00/0

© 1984, American Pharmaceutical Association

tions increase the viscosity of the diffusion layer on the dissolving cholesterol monohydrate surface. The resulting decrease in the diffusion coefficient of cholesterol in the diffusion layer causes the dissolution rate to be slower even though solubility may have been higher. For these reasons, the preferred approach for increasing the dissolution rate of cholesterol gallstones in monoglycerides would be to investigate solvents with low viscosity rather than to try to optimize solubility. The validity of this statement is supported by the data in Table II, which show that dissolution rate is greater in the diglyceride fraction of monooctanoin although cholesterol solubility is lower.

In terms of clinical applications, this study suggests that it may be possible to increase the cholesterol gallstone dissolution rate by addition of water to monooctanoin. Water may also improve local tolerance of the drug during infusion. Since the solubility of water in monooctanoin is ~15% at 37°C, the aqueous solvent would have much less potential for extraction of water from the bile duct and intestinal walls. The importance of temperature should be emphasized, since the dissolution rate of cholesterol increases 50% from 30°C to 37°C. Some of the reported variability in clinical results may be due to inadequate control of solvent temperature. Lastly, addition of water overcomes a practical problem with handling monooctanoin, *i.e.*, crystallization. By its effect on the colligative properties of the solvent, water depresses the solidification point of monooctanoin to well below room temperature.

REFERENCES

(1) J. L. Thistle, G. L. Carlson, A. F. Hofmann, N. F. LaRusso, R. L. MacCarty, G. L. Flynn, W. I. Higuchi, and V. K. Babayan, *Gastroenterology*, **78**, 1016 (1980).

(2) E. Mack, E. M. Patzer, A. B. Crummy, A. F. Hofmann, and V. K. Babayan, *Arch. Surg.*, **116**, 341 (1981).

(3) J. B. Bogardus, *J. Pharm. Sci.*, **71**, 370 (1982).

(4) W. I. Higuchi, S. Prakongpan, and F. Young, *J. Pharm. Sci.*, **62**, 945 (1973).

(5) V. G. Levich, "Physicochemical Hydrodynamics," Prentice-Hall, Englewood Cliffs, N.J., 1962.

(6) S. Prakongpan, W. I. Higuchi, K. H. Kwan, and A. M. Molokhia, *J. Pharm. Sci.*, **65**, 685 (1976).

(7) E. Hansbury and T. J. Scallen, *J. Lipid Res.*, **19**, 742 (1978).

(8) N. Garti, L. Karpuj, and S. Sarig, *J. Lipid. Res.*, **22**, 785 (1981).

(9) M. Ageno and C. Frontali, *Proc. Natl. Acad. Sci.*, USA, **57**, 856 (1967).

(10) E. Hatschek, "The Viscosity of Liquids," Van Nostrand, New York, N.Y., 1930.

(11) R. J. Braun and E. L. Parrott, *J. Pharm. Sci.*, **61**, 175 (1972).

(12) A. T. Florence, P. H. Elworthy, and A. Rahman, *J. Pharm. Pharmacol.*, **25**, 779 (1973).

(13) N. Sarisuta and E. L. Parrott, *Drug Dev. Indust. Pharm.*, **8**, 605 (1982).

(14) R. C. Weast (Ed.), "Handbook of Chemistry and Physics," 48th ed., Chemical Rubber Co., Cleveland, Ohio, 1967.

(15) H. Nogami, T. Nagai, and A. Suzuki, *Chem. Pharm. Bull.*, **14**, 329 (1966).

(16) S. Bisaillon and R. Tawashi, *J. Pharm. Sci.*, **60**, 1874 (1971).

(17) E. Touitou and M. Donbrow, *Int. J. Pharmaceut.*, **9**, 97 (1981).

ACKNOWLEDGMENTS

This work was supported by National Institutes of Health Grant No. AM31603. The technical assistance of R. Perrone is gratefully acknowledged.

Effects of Acrylic Acid Polymer and Its Arrangement on Drug Release from a Wax Matrix

HISATOSHI EMORI, TAKAFUMI ISHIZAKA ˣ, and MASUMI KOISHI

Received December 23, 1982, from the *Faculty of Pharmaceutical Sciences and Institute of Colloid and Interface Science, Science University of Tokyo, 12, Ichigaya Funagawara-machi, Shinjuku-ku, Tokyo, Japan.* Accepted for publication June 23, 1983.

Abstract □ The release of phenacetin from a wax matrix was improved by the addition of an acrylic acid polymer. Increasing the amount of polymer increased the release rate of phenacetin due to the formation of pores and channels in the matrix resulting from leaching of the polymer. The leaching was affected by the pH of the dissolution medium as well as by the methods used to prepare the granules. The polymer in ordered powder mixes behaved differently from that uniformly dispersed in a wax matrix. The drug appeared to be released by an approximate zero-order process at pH 7.5 from tablets containing the polymer.

Keyphrases □ Wax matrices, inert—release of phenacetin, effect of acrylic acid polymer □ Phenacetin release from inert wax matrices, effect of acrylic acid polymer □ Acrylic acid polymer—effect on release of phenacetin from inert wax matrices, action as a channeling agent

Recently, various methods have been developed to prolong the action of drugs by controlling their release rates. One method involves the incorporation of drugs into a wax matrix. The mechanism of drug release from a wax matrix involves the leaching of the drug by a permeating fluid that enters the drug-matrix phase through the pores, cracks, and intergranular spaces. Higuchi has treated the drug release from the matrix model in a theoretical manner (1).

Several investigators have described the incorporation of additives, such as surfactants, into the matrix (2, 3). These additives act as channeling agents and improve drug release. The drug appears to be released by a zero-order process. Others have investigated ordered powder mixes (4, 5). For example, the wettability of α-lactose powder was appreciably changed by modifying its surface with other powders (6). The purposes of this work are to evaluate an acrylic acid polymer as a channeling agent in the wax matrix and to examine the effects of powder arrangement on drug release.

EXPERIMENTAL SECTION

Materials—Carnauba wax[1] was obtained commercially, and the stearyl alcohol, sodium chloride, disodium phosphate, and hydrochloric acid were reagent grade. The phenacetin[2] was JP grade; the powder was ground with an automatic mortar[3] and then sieved to 49–105-μm particle size with stainless steel sieves. The water used in this experiment was prepared with a water purification apparatus[4]. Acrylic acid polymer[5] was cross-linked and had a viscosity of 3000 cps as a 1% aqueous solution. Molecular weight, solubility, and carboxyl group content of the acrylic acid polymer were ~2,000,000, 5% (w/w), and 60%, respectively.

Preparation of Granules—Carnauba wax (15.0 g) and stearyl alcohol (15.0 g) were mixed and melted at 90 ± 3°C. Phenacetin powder was added into the melt in small portions with constant stirring for 5 min at 90 ± 3°C, to achieve an even distribution; the mixture was then poured onto a glass plate kept at 0°C and allowed to congeal. The plate-like mass was crushed for 10

[1] Dainichi Sangyo, Ltd., Japan.
[2] Iwaki Seiyaku, Ltd., Tokyo, Japan.
[3] ANM-1000 type; Nitto Kagaku, Ltd., Nagoya, Japan.
[4] Milli-Q2; Millipore Co., Bedford, Mass.
[5] Hiviswako-104; Wako Pure Chemical Industries, Ltd., Japan.

0022-3549/84/0700-0910$01.00/0

© 1984, American Pharmaceutical Association

Table I—Formulations for Method 1

Acrylic Acid Polymer Conc. % (w/w)	Weight, g			
	Carnauba Wax	Stearyl Alcohol	Acrylic Acid Polymer	Phenacetin
1.0	14.775	14.775	0.45	15.0
3.0	14.325	14.325	1.35	15.0
6.0	13.650	13.650	2.70	15.0
9.0	12.975	12.975	4.05	15.0

min in a ceramic mortar and then screened to prepare a granule size of 420–590 μm.

Incorporation of Acrylic Acid Polymer into the Wax Matrix—*Method 1*—When a homogeneous melt carnauba wax and stearyl alcohol was attained at 90 ± 3°C, the polymer powder was gradually added to the melt followed by phenacetin powder, which was added in small portions at the same temperature while stirring. After pouring the mixture onto a cold glass plate, the plate-like mass was crushed and sieved to obtain the required granule size. The formulations are shown in Table I

Method 2—A 30.0-g portion of phenacetin powder and various loadings (1.0, 2.0, 3.0, and 6.0 g) of acrylic acid polymer were thoroughly blended in an automatic mortar for 5 min. Figure 1 shows scanning electron micrographs of the phenacetin and blended powders. Samples equivalent to 15.0 g of phenacetin were homogeneously incorporated into the melted mixture of carnauba wax and stearyl alcohol according to the formulations shown in Table II. The 420–590-μm granules were obtained by the same procedure described in method 1.

Preparation of Tablets—A KBr disk press[6] was used to compress the granules into tablets using a compression force of 100 kg/cm^2. The average tablet weight was ~500 mg, with a thickness and diameter of ~3.6 and 13 mm, respectively.

Dissolution Procedures—The fluids of pH 1.2 and 7.5 included in JP IX were used as the dissolution media. The former was prepared by mixing 2.0 g of sodium chloride, 24.0 mL of 10% (w/w) HCl, and a sufficient amount of water to give 1000 mL of solution; the latter was prepared by mixing 35.8 g of disodium phosphate, 6.0 mL of 10% (w/w) HCl, and water to give 1000 mL of solution.

The apparatus shown in Fig. 2 was used for the dissolution tests. The dissolution flask was covered during the experiment to prevent water evaporation. A paddle with six blades was set at 3 cm from the bottom of the flask and rotated at constant rate of 200 rpm. A stirring speed of 200 rpm was adequate to disperse the granules uniformly in the fluid. Granules (0.3 g) were added into the flask containing 500 mL of a dissolution medium maintained at 37 ± 0.1°C. After adding the granules, 3-mL aliquots of the test fluid, containing granules, were withdrawn with syringes at intervals over a 10-h period. The sample was then filtered through 0.6-μm pore membrane filter[7].

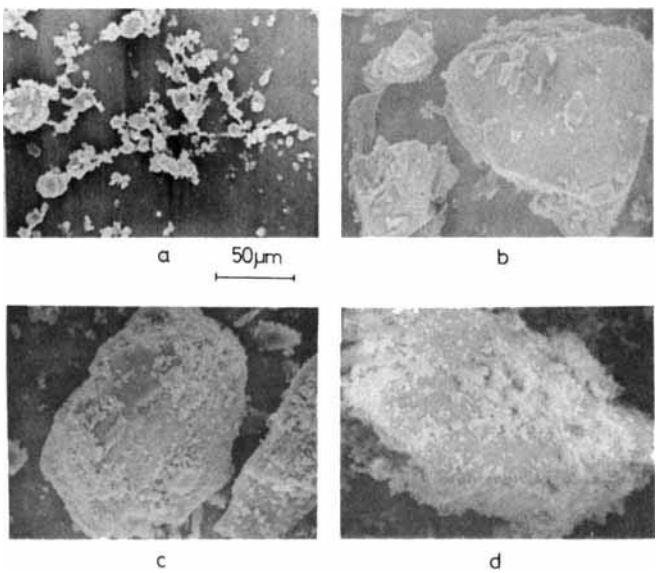

Figure 1—*Scanning electron micrographs of the powders used. Key: (a) acrylic acid polymer; (b) phenacetin; (c) polymer–phenacetin (1:10); (d) polymer–phenacetin (1:15).*

[6] Hitachi, Ltd., Tokyo, Japan.
[7] BDWP02500; Millipore Corp., Bedford, Mass.

Table II—Formulations for Method 2

Acrylic Acid Polymer Conc. % (w/w)	Acrylic Acid Polymer–Phenacetin Ratio (w/w)	Weight, g		
		Carnauba Wax	Stearyl Alcohol	Acrylic Acid Polymer–Phenacetin[a]
1.1	1:30	14.75	14.75	15.50
2.2	1:15	14.50	14.50	16.00
3.3	1:10	14.25	14.25	16.50
6.6	1:5	13.50	13.50	18.00

[a] Mixed powder.

A method similar to the USP rotating-basket method was used to investigate drug release from the tablets. A basket, in which a tablet was placed, was immersed into a flask containing 600 mL of a dissolution medium maintained at 37 ± 0.1°C. The basket was set at a height of 3 cm from the bottom of the flask and rotated at a rate of 200 rpm; this was necessary to prevent air bubbles from adhering to the basket and the tablet surface. Aliquots (3 mL) of the test fluid were then withdrawn at intervals over a 10-h period. Each sample was replaced with 3 mL of fresh dissolution medium kept at 37 ± 0.1°C to maintain the constant volume of the test fluid. The amount of phenacetin released was determined by direct measurement of the absorbance at 245 nm.

RESULTS AND DISCUSSION

Effect of Acrylic Acid Polymer Added According to Method 1 on Phenacetin Release—The release of phenacetin from the wax matrix containing acrylic acid polymer made according to method 1 was investigated. The particle sizes and concentration of phenacetin were 49–105 μm and 33.3% (w/w), respectively, the granule sizes were 420–590 μm, the compression force was 100 kg/cm^2, and acrylic acid polymer concentrations were 1.0, 3.0, 6.0, and 9.0% (w/w).

Figure 3a and b illustrates the drug release profiles at pH 1.2 from granules and tablets, respectively. The addition of acrylic acid polymer into the wax matrix affected the drug release. As is evident from Fig. 3, there was a slight increase in the release rates, in both cases, with increasing amounts of added polymer. A similar observation has been reported for a water-soluble nonelectrolytic polymer by Dakkuri *et al.* (3). The drug release from tablets for the initial 1.5 h at pH 1.2 seemed to be in accordance with the Higuchi equation, but a negative deviation was seen when the added polymer concentrations were 0, 1.0, 3.0, and 6.0% (w/w) and a positive deviation was noted when the polymer concentration was 9.0% (w/w).

The release profiles from granules and tablets at pH 7.5 are shown in Fig. 3c and d, respectively. For granules, the addition of the polymer markedly increased the drug release as compared with the polymer-free formulation. A 100% release was achieved in 10 h for the 6.0% (w/w) and in 2 h for 9.0% (w/w) polymer concentrations. Also, in the case of tablets at pH 7.5, an obvious increase in the drug release rate was associated with the amount of polymer added. The drug release appeared to follow a quasi-zero-order kinetics at high polymer concentrations (6.0 and 9.0%). Similar observations were reported by Dakkuri *et al.* (2). The deviation from a straight line after 7 h for the 9.0% (w/w) polymer concentration (Fig. 3d) could be explained by the total exhaustion of the solid drug phase.

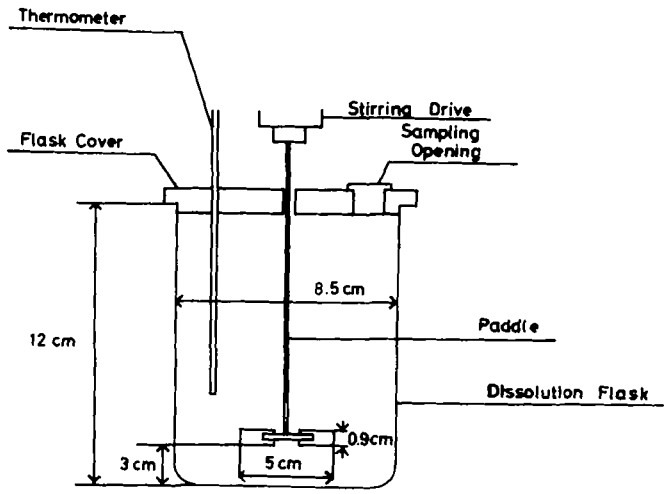

Figure 2—*Schematic diagram of apparatus for the dissolution test of granules.*

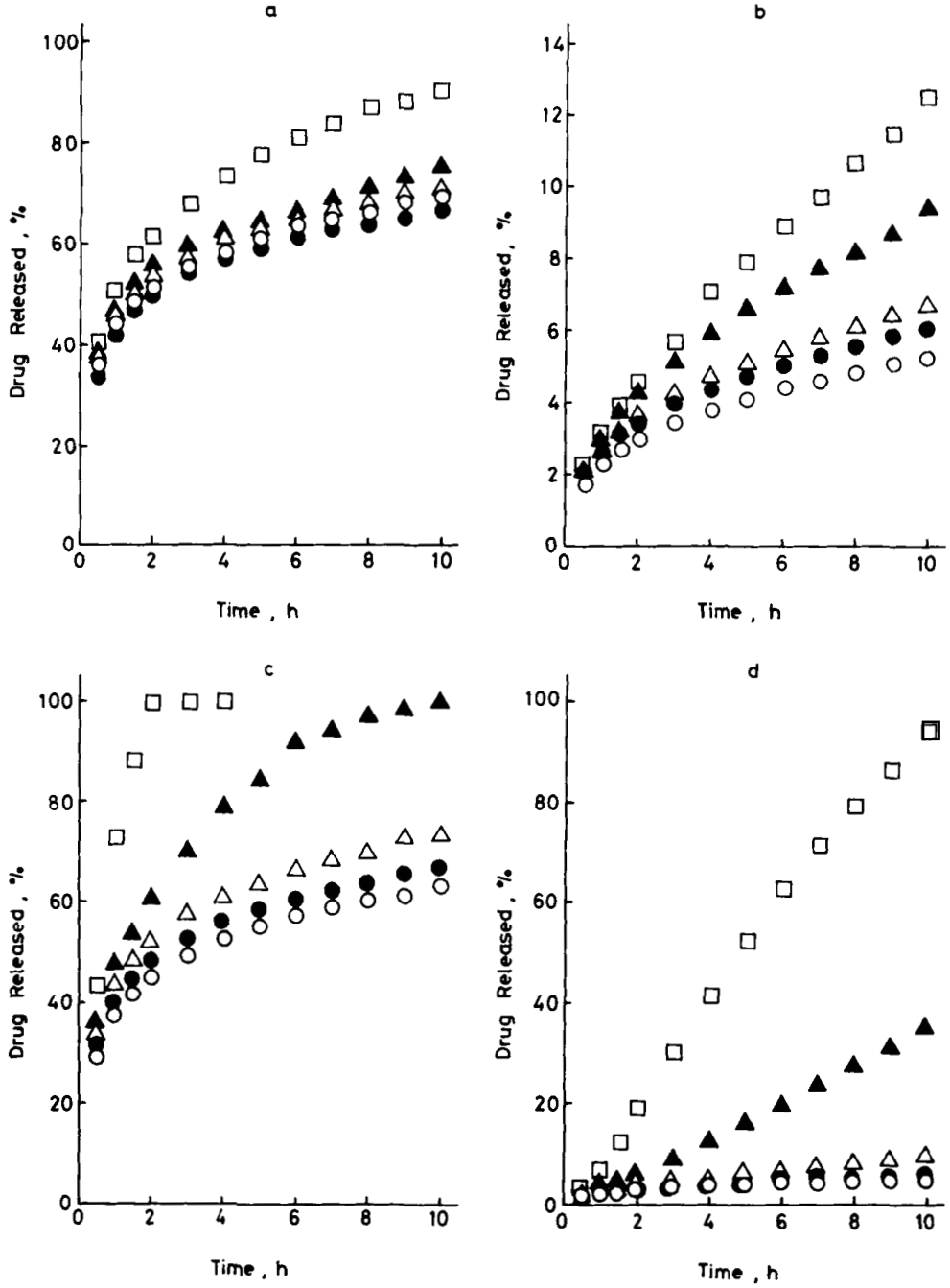

Figure 3—*Effect of acrylic acid polymer concentration on the release of phenacetin from granules at pH 1.2 (a) and pH 7.5 (c) and from tablets at pH 1.2 (b) and pH 7.5 (d), using method 1. Key: (○) 0% (w/w); (●) 1% (w/w); (△) 3% (w/w); (▲) 6% (w/w); (□) 9% (w/w).*

These distinct effects of the polymer were due to the formation of pores and channels in the matrix, which resulted from swelling and leaching of the polymer powder. The degrees of swelling and leaching of the polymer were controlled by a change in the dissolution medium pH. When the polymer in the matrix was hydrated by the dissolution medium, the degree of ionization of the carboxyl groups of the acrylic acid polymer was lower at pH 1.2 than at pH 7.5. As a result, the partially hydrated polymer molecules at pH 1.2 formed a dense jelly structure, which caused most of the polymer molecules dispersed in the matrix to be held in the pores and channels. Therefore, the drug molecules were released slowly through the pores and channels that were filled with the less-hydrated polymer molecules.

At pH 7.5, however, because the polymer chains were extended due to the repulsion of negatively charged carboxyl groups, the fully hydrated polymer became swollen. Consequently, the hydrated polymer molecules in the matrix were liberated into the dissolution medium. Leaching out of the polymer increases the internal porosity and decreases the tortuosity, as suggested by Samuelov *et al.* (7). Therefore, the drug was released rapidly at pH 7.5. The apparent quasi-zero-order kinetics of drug release from tablets at pH 7.5 and high polymer concentrations can be attributed to the increase of the diffusion rate of the drug in the channels and to the increasing number of channels after leaching of the polymer.

Effect of Acrylic Acid Polymer Added According to Method 2 on Phenacetin Release—The release of phenacetin from the wax matrix containing acrylic acid polymer made according to method 2 was studied. The particle sizes and the concentration of phenacetin were 49–105 μm and 33.3% (w/w), respectively, the granule sizes were 420–590 μm, and the compression force was 100 kg/cm^2.

The release profiles at pH 1.2 and 7.5 from granules are shown in Fig. 4a and c, respectively. These results indicated that the increase in the polymer concentration increased the release rate of phenacetin. It is also obvious that the addition of the polymer into the matrix according to method 2 significantly improved the drug release as compared with method 1. Higher release rates were also observed at pH 7.5 than at pH 1.2. Figure 4b and d illustrates the release profiles from tablets at pH 1.2 and 7.5, respectively. As described above, leaching of the polymer into the pH 1.2 dissolution medium was slight, and the effect of the addition of the polymer on the drug release at pH 1.2 was

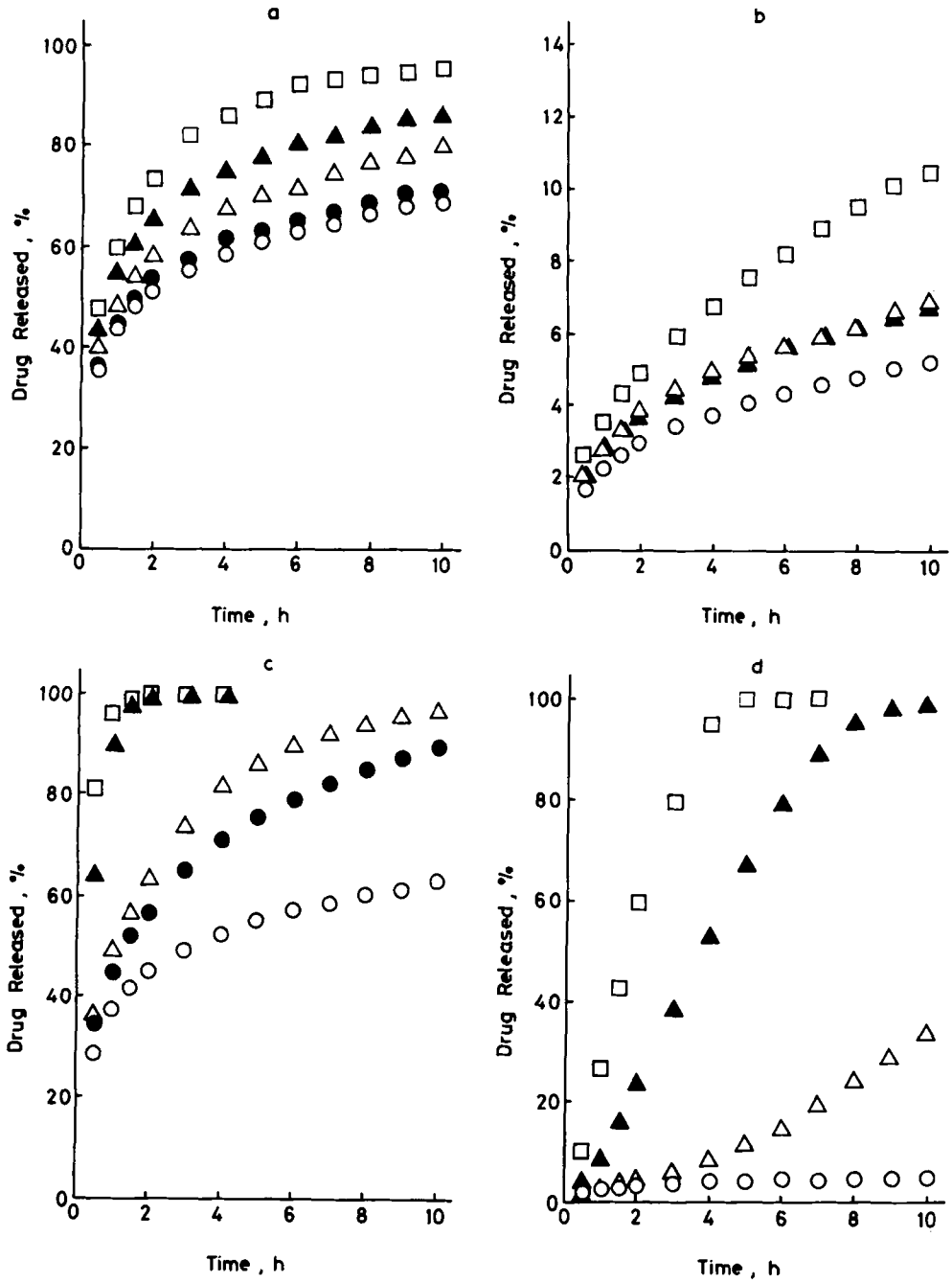

Figure 4—*Effect of acrylic acid polymer concentration on the release of phenacetin from granules at pH 1.2 (a) and pH 7.5 (b) and from tablets at pH 1.2 (b) and pH 7.5 (d), using method 2. Key: (○) 0% (w/w); (●) 1.1% (w/w); (△) 2.2% (w/w); (▲) 3.3% (w/w); (□) 6.6% (w/w).*

also negligible. At pH 1.2, the drug release from tablets in the initial period seemed to be in accordance with the Higuchi equation, and then a negative deviation was observed. However, at pH 7.5, the addition of the polymer markedly increased the drug release from tablets. The drug release followed quasi-zero-order kinetics at high polymer concentrations (3.3 and 6.6%). Moreover, tablet disintegration was observed in some cases at this pH. The drug release at a polymer concentration of 2.2% (w/w) had two zero-order rate constants, caused by slow tablet disintegration after 5 h. The tablets containing 3.3 and 6.6% (w/w) acrylic acid polymer began to disintegrate after ~1 h and 30 min, respectively. However, no burst phenomenon was observed with all the tablets. The change of the release pattern (to quasi-zero-order kinetics) at pH 7.5 and at high polymer concentrations could be caused by an increase in the diffusion rate of drug molecules through channels that resulted from leaching of the polymer and also by a shortening of this channel length due to tablet disintegration.

Differences Between the Two Methods—When the release data obtained using the two methods of polymer addition are compared (Figs. 3 and 4), it was shown that method 2 gave a more rapid release of drug than method 1

Table III—Effects of Acrylic Acid Polymer Concentration on the Zero-Order Release Rate Constant (k) for Tablets at pH 7.5

Acrylic Acid Polymer Conc., % (w/w)	k, mg/h	r
	Method 1	
1.0	0.60	0.998
3.0	1.29	0.999
6.0	6.00	0.999
9.0	18.22	0.998
	Method 2	
2.2	2.97[a]	0.998
	4.75[b]	1.000
3.3	22.89	0.999
6.6	51.63	1.000

[a] For the period up to 5 h. [b] For the period after 5 h.

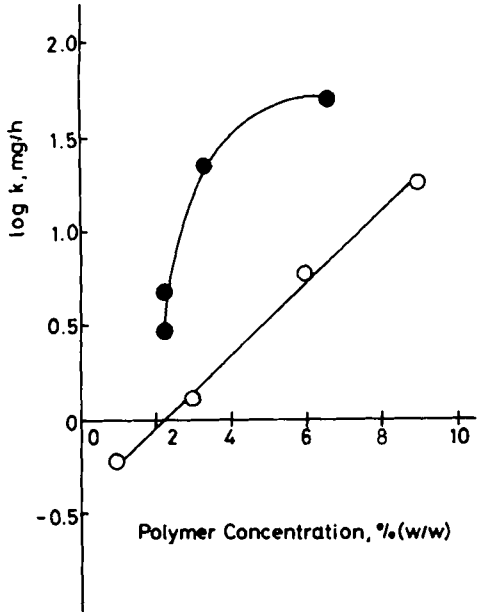

Figure 5—*Relationships of log k to the concentration of acrylic acid polymer at pH 7.5. Key: (○) method 1; (●) method 2.*

for both granules and tablets. For example, those tablets which were prepared by method 1 and contained 6.0% (w/w) polymer released only 17% of the drug in 5 h at pH 7.5, while those prepared by method 2 released 100% at pH 7.5.

The zero-order release rate constant (k) at pH 7.5 for the tablet increased with increasing polymer concentration, as shown in Table III, where k was calculated from the plots in the initial period of the test at low polymer concentrations. Attempts to relate mathematically the zero-order release rate constant, k, to the polymer concentration yielded the best results when log k was plotted against polymer concentration, giving an empirical equation similar to that suggested by Borodkin and Tucker (8). Plots of log k against polymer concentration for method 1 were linear, as shown in Fig. 5. However, log k for method 2 suddenly increased as the polymer concentration increased; there was no linear relationship between the two quantities. This difference could be explained by the formation of a polymer particle layer which adhered physically around phenacetin particles in the matrix prepared by method 2. Leaching of the polymer would, therefore, result in the formation of larger pores and channels around the phenacetin particles, increasing the surface area of the drug particle in contact with the dissolution medium. Slow disintegration of the matrix, coupled with the enhanced pore formation, would affect the drug release rate since the polymer added according to method 2 acts as a disintegrator at high concentrations (see the previous section).

Scanning electron micrographs of the tablet surface are shown in Figs. 6, 7, and 8, where the particle sizes and the concentration of phenacetin were 49–105 μm and 33.3% (w/w), respectively, the granule sizes were 420–590 μm, and the compression force was 100 kg/cm². After dissolution tests at pH 1.2 and 7.5, small pores (which had not been observed before the tests) were formed on the surface of a polymer-free tablet, as shown in Fig. 6. This was the result of phenacetin dissolution. In the case of tablets containing the polymer, larger pores were seen on the tablet surface after dissolution tests at pH 1.2 and 7.5. Figure 7 shows a tablet prepared by method 1 containing 3.0% (w/w) of the polymer. A tablet made by method 2 containing 3.3% (w/w) of the polymer is shown in Fig. 8. The pores in both tablets were formed by leaching of the polymer; the pore size was larger at pH 7.5 than at pH 1.2, and for method 2 than for method 1. The above results are in accordance with the results obtained for drug release.

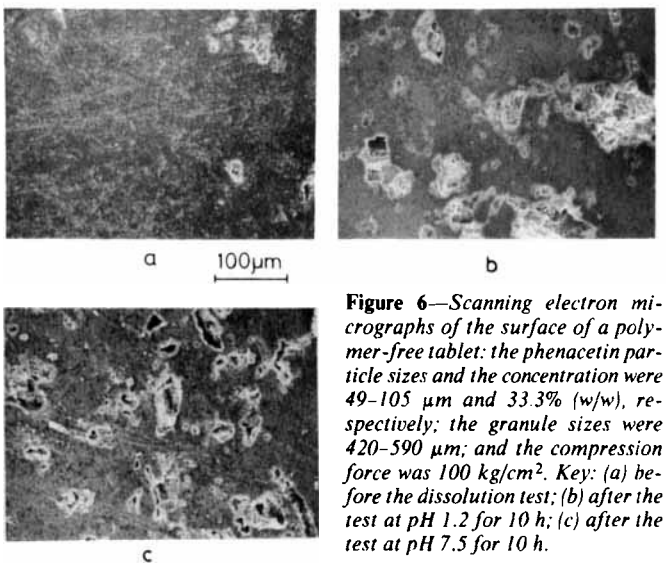

Figure 6—*Scanning electron micrographs of the surface of a polymer-free tablet: the phenacetin particle sizes and the concentration were 49–105 μm and 33.3% (w/w), respectively; the granule sizes were 420–590 μm; and the compression force was 100 kg/cm². Key: (a) before the dissolution test; (b) after the test at pH 1.2 for 10 h; (c) after the test at pH 7.5 for 10 h.*

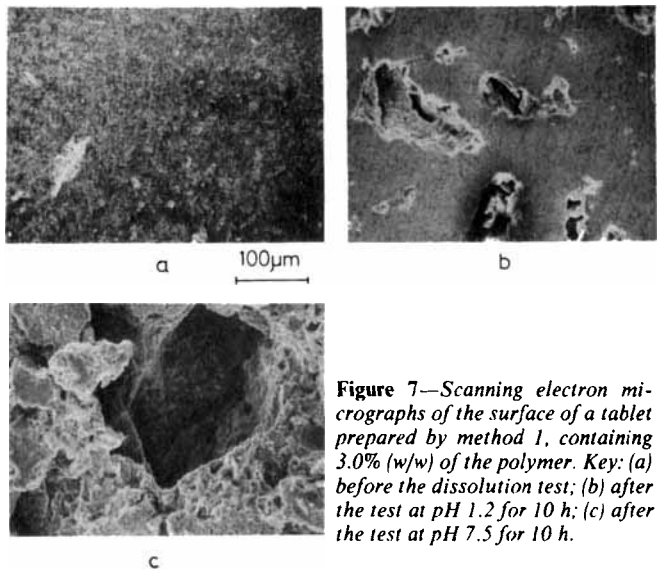

Figure 7—*Scanning electron micrographs of the surface of a tablet prepared by method 1, containing 3.0% (w/w) of the polymer. Key: (a) before the dissolution test; (b) after the test at pH 1.2 for 10 h; (c) after the test at pH 7.5 for 10 h.*

CONCLUSIONS

Acrylic acid polymer added to inert wax matrices by methods 1 and 2 acts as a channeling agent, enhancing the drug release. At high polymer concentrations, the drug release from tablets at pH 7.5 appears to follow quasi-zero-order kinetics. For both methods, the drug release rates increased with increasing polymer concentration, but method 2 was more effective than method 1. In this regard, the location of acrylic acid polymer relative to the drug particles is important, *i.e.*, leaching of the uniformly dispersed polymer in the wax matrix causes the formation of more pores and channels in addition to those formed by leaching of the drug, whereas leaching of the polymer when physically adhered around the drug particles makes the pores and channels produced by drug release larger. Therefore, the effects of powder arrangement could be one of the important factors in pharmaceutical formulation. Since addition of acrylic acid polymer to the inert wax matrix, as a channeling agent and a disintegrator, enhances the controlled release of the drug at alkaline

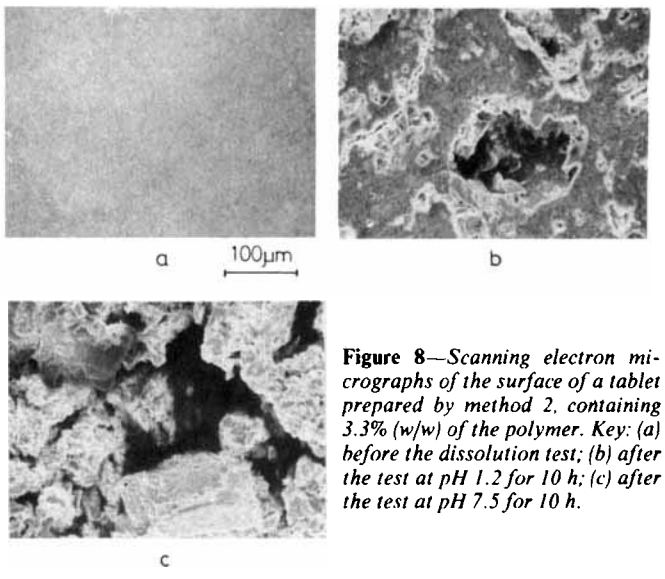

Figure 8—*Scanning electron micrographs of the surface of a tablet prepared by method 2, containing 3.3% (w/w) of the polymer. Key: (a) before the dissolution test; (b) after the test at pH 1.2 for 10 h; (c) after the test at pH 7.5 for 10 h.*

pH, the polymer could be useful in preparing an orally administered wax matrix product which releases most of its drug content in the intestinal tract.

REFERENCES

(1) T. Higuchi, *J. Pharm. Sci.*, **52**, 1145 (1963).

(2) A. Dakkuri, H. G. Schroeder, and P. P. DeLuca, *J. Pharm. Sci.*, **67**, 354 (1978).

(3) A. Dakkuri, L. D. Butler, and P. P. DeLuca, *J. Pharm. Sci.*, **67**, 357 (1978).

(4) G. K. Bolhuis, C. F. Lerk, *J. Pharm. Pharmacol.*, **33**, 790 (1981).

(5) J. N. Staniforth, J. E. Rees, F. K. Lai, and J. A. Hersey, *J. Pharm. Pharmacol.*, **34**, 141 (1982).

(6) M. Koishi, K. Yano, and T. Ishizaka, *J. Pharm. Dyn.*, **5**, s-9 (1982).

(7) Y. Samuelov, M. Donbrow, and M. Friedman, *J. Pharm. Sci.*, **68**, 325 (1979).

(8) S. Borodkin and F. E. Tucker, *J. Pharm. Sci.*, **63**, 1359 (1974).

Particle Size Analysis of Latex Suspensions and Microemulsions by Photon Correlation Spectroscopy

B. W. MÜLLER ˣ and R. H. MÜLLER

Received December 20, 1982, from the *Department of Pharmaceutics, Christian-Albrechts University of Kiel, Gutenbergstrasse 76-78, D-2300 Kiel 1, West Germany.* Accepted for publication June 7, 1983.

Abstract □ The particle size in microemulsions and other highly dispersed systems was determined by means of photon correlation spectroscopy (PCS). As PCS cannot be applied to highly concentrated dispersed phases, the measurement accuracy was tested for its dependence on the particle concentration using latex suspensions. The data obtained by clipping and scaling were compared. The particle size determination was expected to provide information about the influence of the structure of the surfactant system on microemulsions, using a homologous alcohol series as cosurfactant and potassium oleate as surfactant. In this system the region of solubilization is characteristically divided from the region of microemulsification by a zone of instability. Furthermore, there are distinct differences in mean particle sizes between microemulsions (9–30 nm) and micellar solutions (4–6 nm).

Keyphrases □ Particle size analysis—photon correlation spectroscopy, latex suspensions, microemulsions □ Photon correlation spectroscopy—particle size analysis, latex suspensions, microemulsions □ Microemulsions—particle size analysis, photon correlation spectroscopy, latex suspensions

Microemulsions appear as monophasic, more or less stable and transparent or slightly translucent, systems. They have been defined as dispersed liquid–liquid systems in which the particle size of the dispersed phase is <2000 Å. Shinoda and Friberg (1) assumed the existence of discrete micelles (oil-in-water) and reverse micelles (water-in-oil). According to the emulsion theory of Prince and co-workers (2, 3), these systems can be described as emulsions with highly dispersed internal phases. This definition includes the premise that there are essential differences between the microemulsion and the solubilization regions. The description of the structure of microemulsions as droplets is only valid for low concentrations of the internal phase. For high concentrations, Scriven (4) postulates bicontinuous microstructures. This bicoherence of microemulsions was confirmed by Lindman *et al.* (5).

These are of interest since drugs applied topically are liberated more efficiently from microemulsions than from ointments composed of the same ingredients (6). Up to now most of the known microemulsions were made with toxic surfactants or with surfactants in very high concentrations, precluding pharmaceutical use. Therefore, an attempt is made herein to determine the dependence of microemulsion formation on the structure of the emulsifier system and on other such factors, in order to find suitable excipients in suitable concentrations.

Table I—Particle Radii of Latex Suspensions (19 nm)

Particle Conc., μg/L	Radius, nm[a]	Measuring Error, %
0.05	19.3	1.6
0.1	19.2	1.1
0.25	19.4	2.1
0.5	18.9	−0.5
1	18.7	−1.6
2.5	17.8	−6.3
5	17.2	−9.5
10	16.4	−13.7
25	15.3	−19.5
50	13.8	−27.4

[a] Determined by photon correlation spectroscopy.

THEORETICAL SECTION

Light-scattering techniques are used extensively when testing microemulsions (7–12). In the following, the mean particle diameter was determined by photon correlation spectroscopy (PCS) (13, 14). A laser beam is sent through a sample and the scattered light is detected by a photomultiplier at a certain angle. The time-dependent periodical fluctuations of the scattered light are analyzed. Smaller particles diffuse faster than larger ones and, thus, cause a more rapid fluctuation of the intensity of the scattered light. The signal received by the photomultiplier is evaluated by a correlation function $C_{(\tau)} = e^{-\tau/tc}$, where τ stands for the time and tc for the correlation coefficient that describes the decay of this correlation function. The correlation coefficient is related to the diffusion coefficient D by $tc = 1/2DK^2$, where K is the absolute value of the scattering vector. As tc and K can be calculated, the diffusion constant D can be obtained; this is related to the particle radius by the Einstein relationship:

$$\bar{r} = \frac{k \cdot T}{6\pi D\eta}$$

Table II—Particle Radii of Latex Suspensions (54 nm)

Particle Conc., μg/L	Radius, nm[a]	Measuring Error, %
0.1	62	14.8
1	51	−5.6
5	50	−7.4
10	50	−7.4
20	49	−9.3
50	49	−9.3
100	50	−7.4
250	46	−14.8
500	46	−14.8
1000	44	−18.5
2500	32	−40.7

[a] Determined by photon correlation spectroscopy.

0022-3549/84/0700-0915$01.00/0

© 1984, American Pharmaceutical Association

pH, the polymer could be useful in preparing an orally administered wax matrix product which releases most of its drug content in the intestinal tract.

REFERENCES

(1) T. Higuchi, *J. Pharm. Sci.*, **52**, 1145 (1963).

(2) A. Dakkuri, H. G. Schroeder, and P. P. DeLuca, *J. Pharm. Sci.*, **67**, 354 (1978).

(3) A. Dakkuri, L. D. Butler, and P. P. DeLuca, *J. Pharm. Sci.*, **67**, 357 (1978).

(4) G. K. Bolhuis, C. F. Lerk, *J. Pharm. Pharmacol.*, **33**, 790 (1981).

(5) J. N. Staniforth, J. E. Rees, F. K. Lai, and J. A. Hersey, *J. Pharm. Pharmacol.*, **34**, 141 (1982).

(6) M. Koishi, K. Yano, and T. Ishizaka, *J. Pharm. Dyn.*, **5**, s-9 (1982).

(7) Y. Samuelov, M. Donbrow, and M. Friedman, *J. Pharm. Sci.*, **68**, 325 (1979).

(8) S. Borodkin and F. E. Tucker, *J. Pharm. Sci.*, **63**, 1359 (1974).

Particle Size Analysis of Latex Suspensions and Microemulsions by Photon Correlation Spectroscopy

B. W. MÜLLER ˣ and R. H. MÜLLER

Received December 20, 1982, from the *Department of Pharmaceutics, Christian-Albrechts University of Kiel, Gutenbergstrasse 76-78, D-2300 Kiel 1, West Germany.* Accepted for publication June 7, 1983.

Abstract □ The particle size in microemulsions and other highly dispersed systems was determined by means of photon correlation spectroscopy (PCS). As PCS cannot be applied to highly concentrated dispersed phases, the measurement accuracy was tested for its dependence on the particle concentration using latex suspensions. The data obtained by clipping and scaling were compared. The particle size determination was expected to provide information about the influence of the structure of the surfactant system on microemulsions, using a homologous alcohol series as cosurfactant and potassium oleate as surfactant. In this system the region of solubilization is characteristically divided from the region of microemulsification by a zone of instability. Furthermore, there are distinct differences in mean particle sizes between microemulsions (9–30 nm) and micellar solutions (4–6 nm).

Keyphrases □ Particle size analysis—photon correlation spectroscopy, latex suspensions, microemulsions □ Photon correlation spectroscopy—particle size analysis, latex suspensions, microemulsions □ Microemulsions—particle size analysis, photon correlation spectroscopy, latex suspensions

Microemulsions appear as monophasic, more or less stable and transparent or slightly translucent, systems. They have been defined as dispersed liquid–liquid systems in which the particle size of the dispersed phase is <2000 Å. Shinoda and Friberg (1) assumed the existence of discrete micelles (oil-in-water) and reverse micelles (water-in-oil). According to the emulsion theory of Prince and co-workers (2, 3), these systems can be described as emulsions with highly dispersed internal phases. This definition includes the premise that there are essential differences between the microemulsion and the solubilization regions. The description of the structure of microemulsions as droplets is only valid for low concentrations of the internal phase. For high concentrations, Scriven (4) postulates bicontinuous microstructures. This bicoherence of microemulsions was confirmed by Lindman *et al.* (5).

These are of interest since drugs applied topically are liberated more efficiently from microemulsions than from ointments composed of the same ingredients (6). Up to now most of the known microemulsions were made with toxic surfactants or with surfactants in very high concentrations, precluding pharmaceutical use. Therefore, an attempt is made herein to determine the dependence of microemulsion formation on the structure of the emulsifier system and on other such factors, in order to find suitable excipients in suitable concentrations.

Table I—Particle Radii of Latex Suspensions (19 nm)

Particle Conc., μg/L	Radius, nm[a]	Measuring Error, %
0.05	19.3	1.6
0.1	19.2	1.1
0.25	19.4	2.1
0.5	18.9	−0.5
1	18.7	−1.6
2.5	17.8	−6.3
5	17.2	−9.5
10	16.4	−13.7
25	15.3	−19.5
50	13.8	−27.4

[a] Determined by photon correlation spectroscopy.

THEORETICAL SECTION

Light-scattering techniques are used extensively when testing microemulsions (7–12). In the following, the mean particle diameter was determined by photon correlation spectroscopy (PCS) (13, 14). A laser beam is sent through a sample and the scattered light is detected by a photomultiplier at a certain angle. The time-dependent periodical fluctuations of the scattered light are analyzed. Smaller particles diffuse faster than larger ones and, thus, cause a more rapid fluctuation of the intensity of the scattered light. The signal received by the photomultiplier is evaluated by a correlation function $C_{(\tau)} = e^{-\tau/tc}$, where τ stands for the time and tc for the correlation coefficient that describes the decay of this correlation function. The correlation coefficient is related to the diffusion coefficient D by $tc = 1/2DK^2$, where K is the absolute value of the scattering vector. As tc and K can be calculated, the diffusion constant D can be obtained; this is related to the particle radius by the Einstein relationship:

$$\bar{r} = \frac{k \cdot T}{6\pi D\eta}$$

Table II—Particle Radii of Latex Suspensions (54 nm)

Particle Conc., μg/L	Radius, nm[a]	Measuring Error, %
0.1	62	14.8
1	51	−5.6
5	50	−7.4
10	50	−7.4
20	49	−9.3
50	49	−9.3
100	50	−7.4
250	46	−14.8
500	46	−14.8
1000	44	−18.5
2500	32	−40.7

[a] Determined by photon correlation spectroscopy.

0022-3549/84/0700-0915$01.00/0

© 1984, American Pharmaceutical Association

Table III—Particle Radii of Latex Suspensions (110 nm)

Particle Conc., μg/L	Radius, nm[a]	
	Clipping Mode	Scaling Mode
0.1	181	—
1	128	139
10	113	112
50	115	113
100	109	113
500	103	104

[a] Determined by photon correlation spectroscopy.

where k is the Boltzmann constant, T is the absolute temperature, η is the viscosity of the external medium, and $\bar{r}$ is the mean hydrodynamic radius.

EXPERIMENTAL SECTION

Materials—To determine the functional capacity of the measuring apparatus, monodispersed latex suspensions[1] (10% dry weight) were used which had particles of the following diameters (±*SD*): 0.038 (±0.0075) μm, 0.109 (±0.0027) μm, 0.220 (±0.0065) μm, 0.497 (±0.0059) μm. The quantity of particles was 1.37×10^{14}/mL for the 109-nm suspension. The stock suspensions were diluted with fresh twice-distilled water. To eliminate dust, the samples were purified using membrane filters[2] (0.22–0.8 μm), which were attached to 10-mL disposable syringes. The microemulsions were prepared using twice-distilled water, potassium oleate[3], liquid paraffin oil[4], and pentanol[5], hexanol[5], or heptanol[5]. The potassium oleate was taken from one homogeneous batch. The alcohols were used without further purification.

Apparatus—The measuring apparatus consisted of an argon laser[6], a temperature-stabilized measuring cell, and a photomultiplier[7]. This setup was fitted on an optical bank, which was stabilized against vibrations by placement on a slab of marble buffered with special shock absorbers. The sample was tempered (±0.05 K) by means of a matching fluid, regulated by a temperature controller. To eliminate the vibrations of the elastic-tube pump, the matching fluid flowed through a collecting vessel before it was returned to the measuring cell. The photomultiplier detected the scattered light to an angle of 90°.

On the basis of the photomultiplier signals the correlation function was calculated in a correlator[8]. If necessary a clipping counter[9] was added. The correlator data were analyzed in a computer[10] and simultaneously stored in a data logger. The data were transferred from the correlator to the computer using an interface constructed specifically for this purpose. This interface was connected between the punch-outlet of the correlator and the computer input terminal. This not only allowed the data transfer, but also permitted the computer to control the correlator functions.

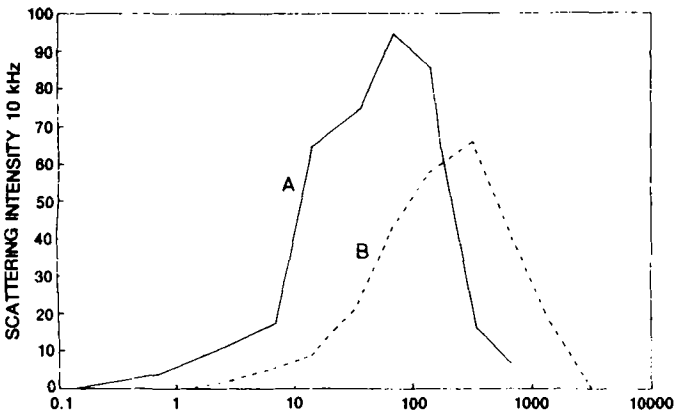

Figure 1—*Scattering intensity in dependence on the concentration of the particles. Key: (A) 55 nm; (B) 19 nm; A, units are $\times 10^{10}$/mL; B, units are $\times 10^{12}$/mL.*

[1] Dow Chemical.
[2] Millipore Corp.
[3] Depuratum grade; Roth, Karlsruhe, FRG.
[4] Pharmacopeia quality DAB 8.
[5] Merck, FRG.
[6] Model 162-03, maximum output 18 mW, air cooled; Spectra-Physics.
[7] Malvern, U.K.
[8] Model K 7023 with a connected memory; Malvern, U.K.
[9] Model R 95; Malvern, U.K.
[10] Tektronix 4052.

Table IV—Particle Radii of Latex Suspensions

Particle Conc., μg/L	Radius, nm[a]	
	Clipping Mode	Scaling Mode
1	228	259
10	229	226
50	235	244
100	222	225
500	209	213
1000	95	84

[a] Determined by photon correlation spectroscopy.

RESULTS AND DISCUSSION

The mean radii of the particles were determined by photon correlation spectroscopy (PCS) on the basis of the diffusion coefficients. This required an unhindered diffusion. Higher particle concentrations resulted in measuring faults because of an interaction between the particles on the one hand and the multiple scattering on the other. The use of a structure factor should correct for these errors (15–19). While the interactions between the particles leads to lower diffusion constants, the multiple scattering produces a higher fluctuation of scattered light intensity. The described effects result in a stronger decaying correlation function together with a higher diffusion constant and a smaller particle radius. Therefore, the determination of highly concentrated suspensions and emulsions is difficult. To determine the dependence of the measurements on the particle concentration, latex suspensions with different particle sizes were measured in a dilution series (Tables I–IV). The measuring errors obtained in the clipping and scaling modes are also compared (Tables III and IV).

In the latex suspensions of 19-nm particles (Table I) the particle radii were almost constant over a wide range of concentrations (50–1000 μg/L). In higher concentrations, the measured value was markedly low. Comparable results were obtained for the other particle sizes (Tables II–IV). In some cases, measuring errors of >60% were observed. Hence, from the standpoint of accuracy of measurement, the results of some reports (20) which neglect this effect for microemulsions are in doubt. The observed error is less in emulsions than in suspensions, but in certain concentrations, errors result whereby the data is >50% too low. If Nicholsen *et al.* (20) measure a particle radius of 2–3 nm in their microemulsions, the consideration that the micelle diameter must be at least twice the molecule length of the surfactant plus the diameter of the aqueous (oily) core reveals that their value must be too low. Moreover, the PCS determines the hydrodynamic diameter, which means that higher values are more probable.

If the scattering intensity is plotted against the particle concentration, the curves show a maximum of the scattered light (Fig. 1). When this maximum is exceeded, back-scattering predominates and the measuring error increases. The reproducibility of the experimental results is dependent on the scattering quality of the sample. It decreases when the scattering intensity, *i.e.*, the signal–noise ratio, is low. With low particle concentrations, the relative standard deviation of the results was ~1–3%. If the measuring conditions were good, a reproducibility of ±0.5% could be obtained. At a measuring angle of 90°, an optimal reproducibility within a wide concentration range of latex particles was observed.

Table V—Particle Sizes of Microemulsions Prepared with the Same Molar Concentrations of Different Alcohols[a]

Potassium Oleate, %	Alcohol, mol/L	Particle diameter, Å		
		Pentanol	Hexanol	Heptanol
1.5	0.964		225	155
2.0	0.803		205	121
	1.852	228	130	
2.5	0.482		211	110
	0.642		198	102
	0.803		128	102
	0.964		112	97
	1.124		105	108
	1.482	220	95	
	1.666	164	95	
3.0	0.642		141	92
	0.803		127	88
	0.964		108	85
	1.124		97	89
	1.296	135	101	

[a] Measured by photon correlation spectroscopy shortly after production; water content 3.6%.

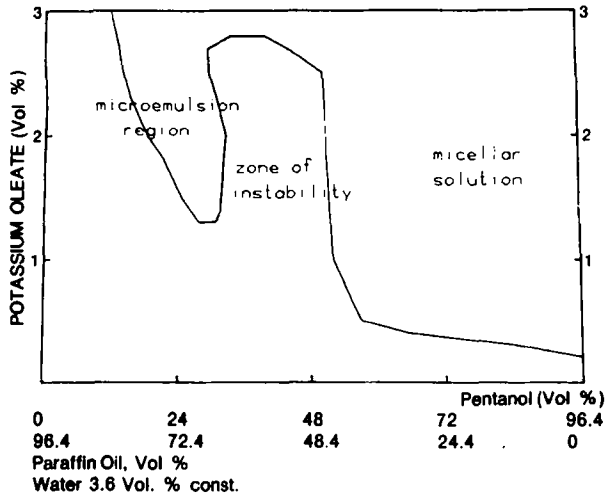

Figure 2—*Component diagram with pentanol.*

To eliminate the concentration error, microemulsions with low concentrated dispersed phases (3–6%) were measured. Microemulsion formation could already be found at a surfactant-cosurfactant concentration of 5–10% (w/w). Thus, the sample remains in a measurable concentration range for the PCS, which is also characterized by a 5–10% particle concentration in other reports (8, 19). Shinoda (21) describes microemulsions with such low surfactant-cosurfactant fractions, but he defines them as "solubilized solutions."

The tested systems consisted of a constant water fraction of 3.6%, a potassium oleate component of 0.5 3.0%, alcohol as cosurfactant, and liquid paraffin oil, added to obtain 100% volume. To determine the microemulsion region, component diagrams for each alcohol were established. They show the dependence of the microemulsion formation on the surfactant structure. The homogeneous alcohol series butanol, pentanol, hexanol, heptanol, octanol, and decanol was used. A distinct microemulsion region could only be observed for pentanol, hexanol, and heptanol at these concentrations (Figs. 2–4). Other ranges of concentration also show a distinct microemulsion formation using the remaining alcohols. Baviere *et al.* (22) describe that—in addition to the surfactant structure—factors such as salt concentration have an influence, but they are not considered here.

Figure 3 shows that hexanol is a particularly good cosurfactant. A minimum surfactant quantity (~1%) must exist before water-in-oil microemulsions are formed. Higher surfactant concentrations (2%) result in a lower particle diameter due to an optimization of the surfactant-cosurfactant ratio. The optimal surfactant-cosurfactant ratio is ~1:3 for hexanol. If the surfactant content is below the optimum, it can be compensated to a certain degree by a higher quantity of cosurfactant. With pentanol, microemulsion formation requires higher quantities of surfactant and cosurfactant. The microemulsion region is smaller than that of hexanol and shifts to higher pentanol and potassium oleate concentrations. The more hydrophilic pentanol has a larger region of solubilization than hexanol. The microemulsion region of heptanol is smaller than the other alcohols. Heptanol is more lipophilic; therefore,

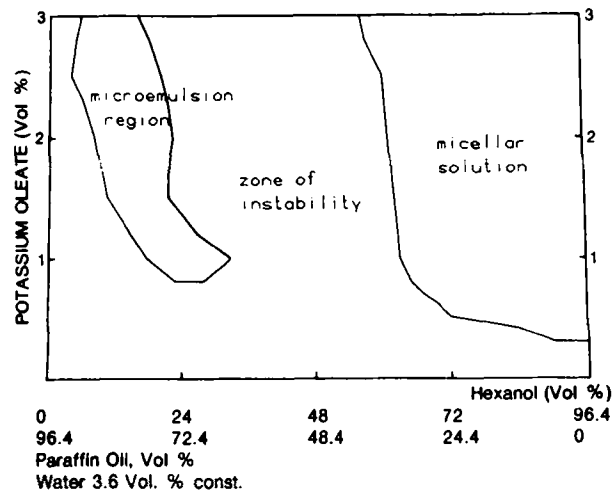

Figure 3—*Component diagram with hexanol.*

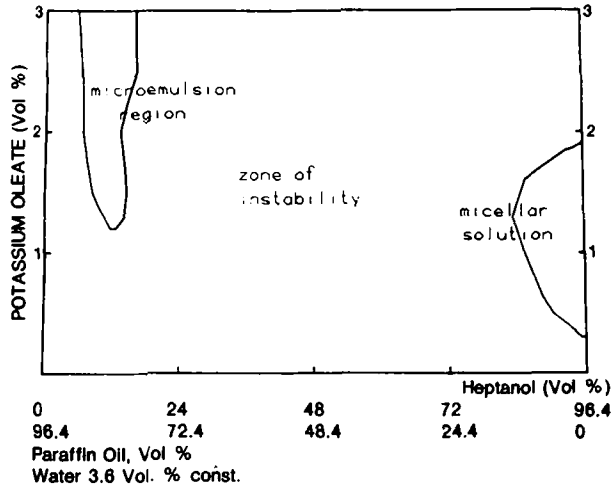

Figure 4—*Component diagram with heptanol.*

microemulsions are formed at a lower cosurfactant concentration. However, the solubilization region is narrower.

If microemulsions are considered as swollen micelles, an abrupt diminution in particle size from the macroemulsion to the microemulsion region, and after that a continuous transition to a micellar solution, should be expected. According to the emulsion theory, there should be a distinct separation between the solubilization and the microemulsion regions due to the transition of a single-phase liquid into a system with at least two phases characterized by micelles with different diameters. Between the two regions an instability zone is assumed, with big particles (in the dimension of macroemulsions) caused by coalescence. Such a zone was discovered in the component diagrams of the above systems. The storage tests showed that the microemulsions are unstable and that the dispersed phase undergoes coalescence toward the macroemulsion and also toward the solubilization regions. This fact was unexpected.

The change in particle diameter can be investigated by PCS with great accuracy and little difficulty using the specimen tubes as storage containers for the emulsions. The measured particle diameters of the microemulsions were 9–30 nm; those of the micellar solutions were 4–6 nm and smaller (Figs. 5–7). The most apparent increase in particle size before the zone of instability toward the solubilization region was observed in microemulsions prepared with hexanol. Curve B in Fig. 6 (1.5% potassium oleate) reveals a relatively big particle diameter of 225 Å at the border of the microemulsion region toward the macroemulsions. With increasing alcohol concentration, the particle diameter decreases to 160 Å. This is the smallest possible particle size at this surfactant-cosurfactant ratio, and it is constant over a wide range. Before the zone of instability, a distinct increase in particle diameter of up to 225 Å can be seen. This effect is even more obvious in the case of microemulsions with 1.0% potassium oleate (Fig. 6, curve A). After having reached 280 Å, the smallest possible particle size, a considerable increase (up to 400 Å) was found. The particle sizes measured in microemulsions with pentanol

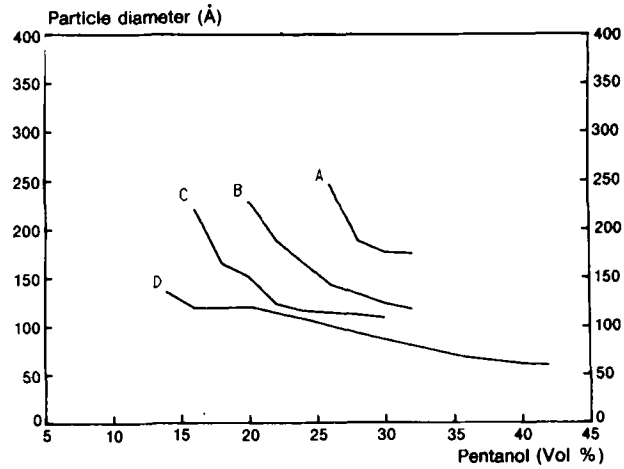

Figure 5—*Particle sizes of microemulsions with pentanol (cf. Fig. 2), measured shortly after production. Composition: 3.6% water, potassium oleate, and pentanol, q.s. to 100% with paraffin oil. Potassium oleate content: (A) 1.5%; (B) 2.0%; (C) 2.5%; (D) 3.0%.*

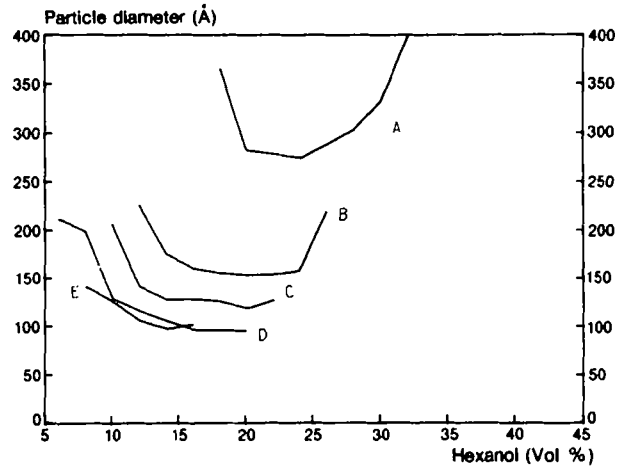

Figure 6—*Particle sizes of microemulsions with hexanol* (cf. *Fig. 3*), *measured shortly after production. Composition: 3.6% water, potassium oleate, and hexanol, q.s. to 100% with paraffin oil. Potassium oleate content: (A) 1.0%; (B) 1.5%; (C) 2.0%; (D) 2.5%; (E) 3.0%.*

(Fig. 5) show a comparable alteration. However, the increase in droplet diameter before the zone of instability appears only during the aging process and is less distinct. Constant surfactant concentration together with low cosurfactant concentrations result in big particles. If the cosurfactant concentration increases, the particle sizes decrease toward a minimal limiting value. It is remarkable that in microemulsions with hexanol, a minimal particle size of 95 Å appears (Fig. 6, curve D), which cannot be lowered by a further increase of the surfactant and cosurfactant concentrations (Fig. 6, curve E). The same limiting value can be found in microemulsions with pentanol.

The particle sizes of the emulsions formed by a minimum fraction of cosurfactant (*e.g.*, pentanol) decreased from 246 to 135 Å relative to increasing surfactant concentration (1.5 to 3.0%), due to the optimization of the surfactant-cosurfactant ratio. Figure 5 shows a continuous transition from the microemulsion to the solubilization region if the microemulsion contains ~3% potassium oleate. This seems to contradict the results described before. However, it has to be considered that the emulsions in this region break after a short storage time (23). Thus, a separation in the microemulsion and solubilization regions was obtained, and the continuous transition disappeared. With regard to the particle sizes and their alteration during the storage, the cosurfactant heptanol is comparable with pentanol. On the other hand, the formation of microemulsions is reduced to a smaller region. What is important is that the particle sizes decrease with the increasing chain length of the alcohol. Table V compares the particle sizes of microemulsions prepared with the same molar concentrations of differing alcohols.

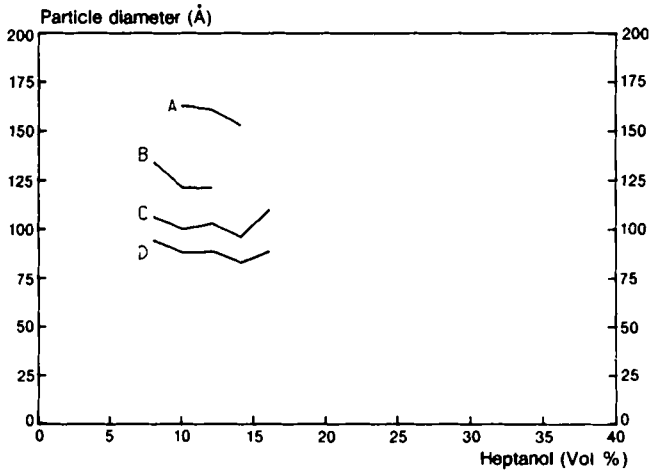

Figure 7—*Particle sizes of microemulsions with heptanol* (cf. *Fig. 4*), *measured shortly after production. Composition: 3.6% water, potassium oleate, and heptanol, q.s. to 100% with paraffin oil. Potassium oleate content: (A) 1.5%; (B) 2.0%; (C) 2.5%; (D) 3.0%.*

REFERENCES

(1) K. Shinoda and S. J. Friberg, *Colloid Interface Sci.*, **4,** 281 (1975).

(2) W. Stoeckenius, J. H. Schulman, and L. M. Prince, *Kolloid Z.*, **169,** 170 (1960).

(3) L. M. Prince, *J. Colloid Interface Sci.*, **1975,** 52.

(4) L. E. Scriven, in "Micellization, Solubilization and Microemulsions," Vol. 2, K. C. Mittal, Ed., Plenum, New York, N.Y., 1977, p. 877.

(5) B. Lindman, N. Kamenka, T. M. Kathopouois, B. Brun, and P. G. Nilsson, *J. Phys. Chem.*, **84,** 2485 (1980).

(6) J. Ziegenmeyer and C. Führer, *Acta Pharm. Technol.*, **26,** 4 (1980).

(7) A. M. Cazabat and D. Langevin, *Chem. Phys.*, **1981,** 74.

(8) P. J. Cebula, D. Y. Myers, and R. H. Ottewill, *Colloid Polymer Sci.*, **260,** 96 (1982).

(9) S. Candau and R. Zana, *J. Colloid Interface Sci.*, **1981,** 84.

(10) R. Ober and C. J. Taupin, *J. Phys. Chem.*, **84,** 2418 (1980).

(11) C. Hermansky and R. A. Mackay, *J. Colloid Interface Sci.*, **73,** 324 (1980).

(12) A. M. Cazabat, D. Langevin and A. Pouchelon, *J. Colloid Interface Sci.*, **73,** 1 (1980).

(13) H. Z. Cummins and E. R. Pike, Nato Advanced Study, Institutes Series (B), Physics, Vol. 3, Plenum, New York, N.Y., 1974.

(14) H. Z. Cummins and E. R. Pike, Nato Advanced Study Institutes Series (B), Physics, Vol. 23, Plenum, New York, N.Y., 1977.

(15) D. R. Bauer, *J. Phys. Chem.*, **1980,** 84.

(16) A. K. van Helden and A. Vrij, *J. Colloid Interface Sci.*, **1980,** 78.

(17) E. A. Nieuwenhuis and A. Vrij, *J. Colloid Interface Sci.*, **1979,** 72.

(18) M. M. Kops-Werkhoven and H. M. Fijnant, *J. Chem. Phys.*, **74,** 3 (1981).

(19) B. Alince and P. Lepoutre, *J. Colloid Interface Sci.*, **1980,** 76.

(20) J. D. Nicholson, I. V. Doherty, and I. H. R. Clarke, in "Microemulsions," J. D. Robb, Ed., Plenum, New York, N.Y. 1982, p. 33.

(21) K. Shinoda and H. Kunieda, *J. Colloid Interface Sci.*, **1973,** 42.

(22) M. Baviere, R. Schlechter, W. Wade, *J. Colloid Interface Sci.*, **1981,** 81.

(23) B. W. Müller and R. H. Müller, *J. Pharm. Sci.*, **73,** 919 (1984).

ACKNOWLEDGMENTS

This study is part of the research project "Bestimmung Molekularer Parameter von Tensiden und Tensidkomplexen mit Hilfe der Streuung von Laserlicht" which is subsidized by the Deutsche Forschungsgemeinschaft. We want to express our sincere thanks for this grant. Many thanks are also due to P. Hille (Institut für Angewandte Physik, Christian-Albrechts-Universität Kiel, W. Germany), who developed and produced parts of the hardware.

Particle Size Distributions and Particle Size Alterations in Microemulsions

B. W. MÜLLER [x] **and R. H. MÜLLER**

Received December 20, 1982, from the *Department of Pharmaceutics, Christian-Albrechts University of Kiel, Gutenbergstrasse 76-78, D-2300 Kiel 1, West Germany.* Accepted for publication June 7, 1983.

Abstract □ Several component diagrams for different alcohols as cosurfactants and potassium oleate as the surfactant were investigated. Between the regions of the water-in-oil microemulsion and the micellar solution (reverse micelles), and diagrams showed a zone of instability which was determined by particle size analysis by means of photon correlation spectroscopy (PCS). The polydispersity of the internal phase was determined at the instant of microemulsion formation and after fixed intervals of storage. At the edge of the microemulsion region, a rapid increase in particle size due to coalescence followed by breaking was observed. If a slow transition toward the region of solubilization could be seen by a slow decrease of the droplet size, coalescence was observed after storage. In the middle of the microemulsion region, the particle radius, however, was almost constant for a long interval. The velocity of the microemulsion formation depended on the alcohol used. In some cases a very fast formation (milliseconds) was observed; in others, macroemulsions were formed which became transparent within a few hours or days. PCS was used to follow the dynamic process of formation and breaking of such systems with droplet diameters of 5-200 nm by obtaining the mean hydrodynamic diameters. Distribution curves were calculated by the Laplace transform of the correlation function. The practicability of the method was demonstrated with mono- and polydispersed latex suspensions and microemulsions.

Keyphrases □ Particle size analysis--microemulsions, photon correlation spectroscopy, latex suspensions, Laplace transforms □ Emulsions--particle size analysis, photon correlation spectroscopy, Laplace transforms □ Stability--microemulsions, particle size analysis, photon correlation spectroscopy, Laplace transforms

Three types of microemulsions seem to exist: discrete micelles, microdroplets, and bicontinuous structures. To obtain an insight into the dynamics of microemulsion formation and breaking, photon correlation spectroscopy (PCS) can be used for the first two types (1). To eliminate measuring errors, interparticle effects and multiple scattering must be avoided by using low concentrations of the noncontinuous phase (5-10 %). Under these conditions, PCS might be a valid method of measuring mean particle diameters and, in combination with a Laplace transform of the data, estimating the particle size distributions. By following alterations after spontaneous emulsification, it should be possible to develop thermodynamically stable microemulsions with drugs and to find essential differences between a solubilization and a microemulsion if the system contains microdroplets or micelles.

THEORETICAL SECTION

The polydispersity of microemulsions and model suspensions was analyzed using PCS. With this method, the intensity autocorrelation function of the light, scattered by particles of the suspension, is obtained. The autocorrelation function $g(\tau)$ may be obtained from the intensity autocorrelation function $g^2(\tau)$:

$$g^2(\tau) = 1 + |g(\tau)|^2 \qquad \text{(Eq. 1)}$$

$g(\tau)$ contains information about the size distribution.

In the case of monodispersed particles, the autocorrelation function $g(\tau)$ is given by:

$$g(\tau) = g_0 \exp(-\gamma\tau) \qquad \text{(Eq. 2)}$$

where $\gamma = 2Dk^2$, D is the diffusion constant, and k is the line width constant. The decaying of the correlation function depends on the Brownian motion of the particles and may be derived from the statistics of the scattered light. In polydispersed suspensions and emulsions the autocorrelation function $g(\tau)$ can be derived from the size distribution $G(\gamma)$ by the Laplace transform:

$$g(\tau) = g_0 \int_0^\infty \exp(-\gamma\tau) \cdot G(\gamma) d\gamma \qquad \text{(Eq. 3)}$$

Ostrowsky (2) introduced a method for the inversion of this formula based on eigenvalues and eigenfunctions of the Laplace transform. The inversion problem in general has an "ill-conditioned nature" (3). This means that there is an upper limit of information about the size distribution function in the experimentally obtained correlation function. Using the method of Ostrowsky, the most complete information about the polydispersity may be obtained. Ostrowsky points out that the truncation of the correlation function due to noise leads to a band-limited Laplace transform. This is due to the fact that the maximum information about the polydispersity may be obtained by a discrete spectrum with exponentially spaced samples:

$$\gamma_{n+1} = \gamma_1 \exp(n\pi/\omega_{max})$$

$$g(\tau)_{\omega_{max}\to\infty} = \sum_{n=1}^{N} \frac{\pi}{\omega_{max}} \cdot G_D(\log \gamma_n) \cdot \exp(-\gamma_n \tau) \qquad \text{(Eq. 4)}$$

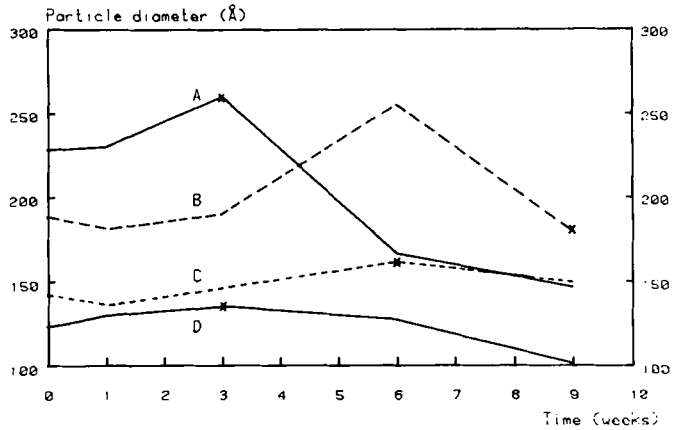

Figure 1—*Particle sizes* versus *time in microemulsions with pentanol as cosurfactant. Composition: 3.6% water, 2.0% potassium oleate, and pentanol, q.s. to 100% with paraffin oil. Pentanol content: (A) 20.0%; (B) 22.0%; (C) 26.0%; (D) 30.0%.*

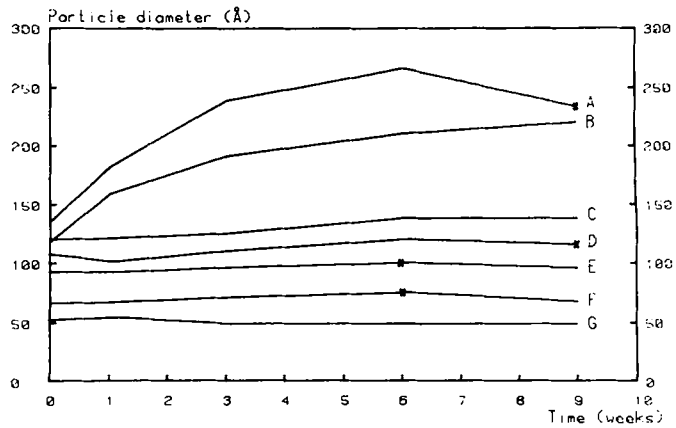

Figure 2—*Particle sizes* versus *time in microemulsions with pentanol as cosurfactant. Composition: 3.6% water, 3.0% potassium oleate, and pentanol, q.s. to 100% with paraffin oil. Pentanol content: (A) 14.0%; (B) 16.0%; (C) 20.0%; (D) 24.0%; (E) 28.0%; (F) 36.0%; (G) 40.0%.*

0022-3549/84/0700-0919$01.00/0
© 1984, American Pharmaceutical Association

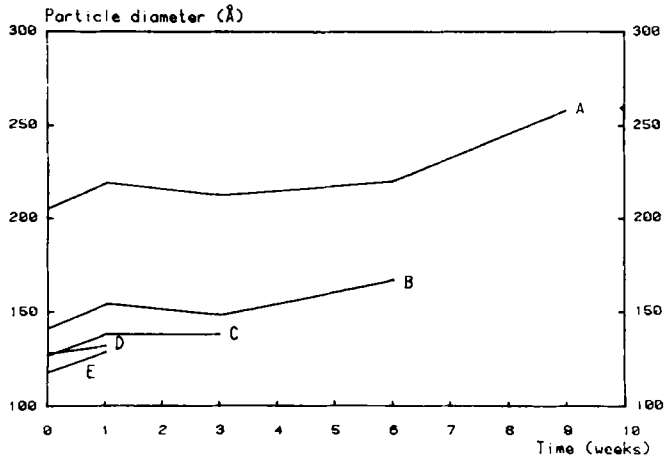

Figure 3—*Particle sizes* versus *time in microemulsions with hexanol as cosurfactant. Composition: 3.6% water, 2.0% potassium oleate, and hexanol, q.s. to 100% with paraffin oil. Hexanol content: (A) 10.0%; (B) 12.0%; (C) 14.0%; (D) 16.0%; (E) 18.0%. (Broken systems, marked by x in the Figs. 1 and 2, were not investigated.)*

where ω_{max} is the band limit. These discrete spectra points are computed from the autocorrelation function by minimizing the equation:

$$\Delta = \sum_{i=1}^{M} \left[g(\tau_i) - \sum_{n=1}^{N} \frac{\pi}{\omega_{max}} \cdot G_D(\log \gamma_n) \cdot \exp(-\gamma_n \tau_i) \right]^2 \quad \text{(Eq. 5)}$$

The continuous polydispersity spectrum can be derived from the development of the discrete spectrum:

$$\tilde{G}(\gamma) = \sum_{n=1}^{N} G_D(\log \gamma_n) \sqrt{\frac{\gamma_n}{\gamma}} \frac{\sin \omega_n \cdot \left(\log \frac{\gamma}{\gamma_n} \right)}{\omega_n \cdot \left(\log \frac{\gamma}{\gamma_n} \right)} \quad \text{(Eq. 6)}$$

This polydispersity spectrum was calculated by a computer program which includes the method of Ostrowsky (2). It must be pointed out that in addition to this method, there are other possibilities using other primary information about the polydispersity spectrum (4, 5).

EXPERIMENTAL SECTION

Materials—The microemulsions were prepared using fresh twice-distilled water, potassium oleate[1], liquid paraffin oil[2], and pentanol[3], hexanol[3], or heptanol[3]. The potassium oleate was taken from one homogeneous batch and was used without further purification. The alcohols were used as received.

To determine the accuracy of the polydispersity analysis by means of the Laplace transform of the correlation function, model suspensions were prepared by mixing latex particles of various sizes using monodispersed latex suspensions[4] (10% by weight). The stock suspensions were diluted with distilled water and mixed in different ratios. The suspensions were passed through membrane filters[5] (0.22–0.8 μm) to remove as many particle impurities as possible from the samples; the filters were attached to 10-mL disposable syringes[6].

A commercial oil-in-water emulsion was tested as an example of a pharmaceutical product; it was composed of 200 g of soybean oil, 15 g of soy oil phosphatide, and 50 g of xylitol, q.s. to 1000 mL with water. Because the concentration of the dispersed phase was too high for PCS measurements, a dilution with twice-distilled water was necessary (50 μL of the emulsion was diluted to 100 mL). To avoid contamination with dust, the samples were prepared using the laminar flow technique.

Apparatus—For the measuring apparatus used in this experiment (1), the refractive indexes were determined by a refractometer[7]. To measure the viscosity of the dispersion media, a viscometer[8] with light barriers as an automatic timing device was used. The thermostated bath had a constant temperature of ±0.05°C.

[1] Depuratum grade; Roth, Karlsruhe, FGR.
[2] Pharmacopeia quality DAB 8.
[3] "Pro synthesis" grade, >98% pure; Merck.
[4] Dow Chemical.
[5] Millipore Corp.
[6] Lipofundin S 20%, Ch. No. 117381; Braun AG, Melsungen, FGR.
[7] Carl Zeiss Abbé.
[8] Ubbelohde.

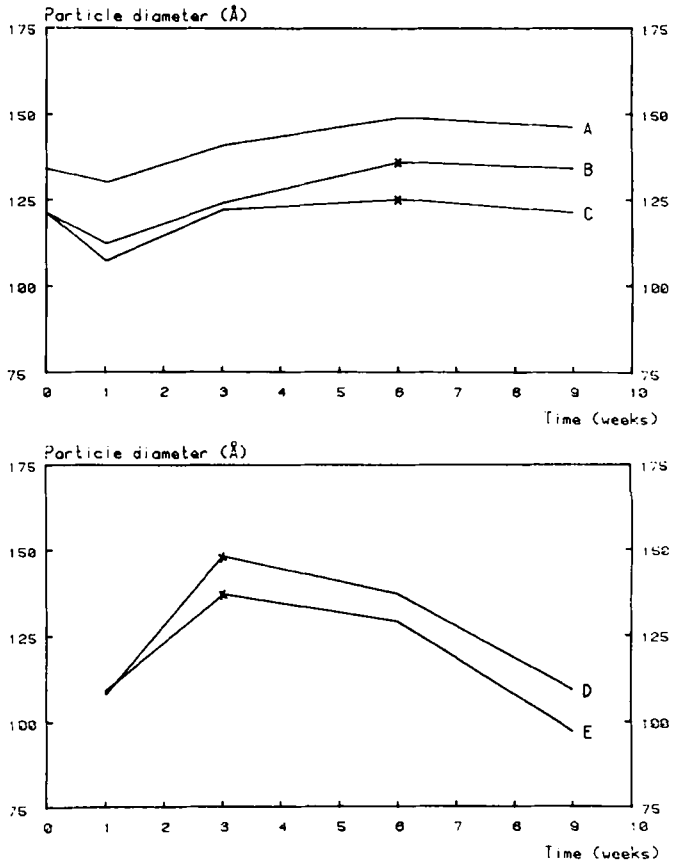

Figure 4—*Particle sizes* versus *time in microemulsions with heptanol as cosurfactant. Composition: 3.6% water, 2.0% potassium oleate, and heptanol, q.s. to 100% with paraffin oil. Heptanol content: (A) 8.0%; (B) 10.0%; (C) 12.0%; (D) 14.0%; (E) 16.0%.*

RESULTS AND DISCUSSION

A series of four-component phase diagrams was established to determine the microemulsion regions. The quaternary systems, water–paraffin oil–potassium oleate as the surfactant and various alcohols as cosurfactants, were investigated; some of the results are published in the companion paper (1). The homologous series butanol, pentanol, hexanol, heptanol, octanol, and decanol was used. A "single-phase" microemulsion region could be observed only for pentanol, hexanol, and heptanol. In this report these systems were investigated to study the variations of the particle sizes as a function of the storage time.

Most of the microemulsions stored for a period of several weeks at room temperature were found to be unstable. The particle size alterations were extreme. The instability of the tested systems was due to their composition. These systems were located at the edge of the water-in-oil microemulsion region in the tetrahedral phase diagram. A basic difficulty with PCS studies is that the concentration of the dispersed phase cannot be higher than ~10% in order to avoid concentration faults due to interparticle forces and multiple scattering (1). Only low concentrations allowed the use of the Stokes–Einstein equation without a correction factor (so called "structure factor"). The systems examined were composed of 1.0–3.0% (by volume) potassium oleate and a constant 3.6% volume of water. The following assumptions were made:

1. Some of the alcohol molecules, together with the oleate, are needed to stabilize the amphiphilic layer between the aqueous core of the microdroplets and the dispersion medium.
2. The surrounding paraffin oil contains the remainder of the alcohol.
3. All oleate molecules are in the water phase and the bilayer of the emulsifier mixture (*i.e.*, the oleate concentration in the lipophilic continuous phase is neglected). Thus, the concentration of the dispersed phase cannot be higher than ~7% (3.6% water + a maximal 3.0% potassium oleate) and the Stokes–Einstein equation is valid.

The experimental points in the compared systems were chosen to clarify the variation in particle diameter of the microemulsions for which the amount of alcohol changes at constant potassium oleate concentrations. The results are presented in the form of curves of particle size against time. All concentrations are given as volume percent.

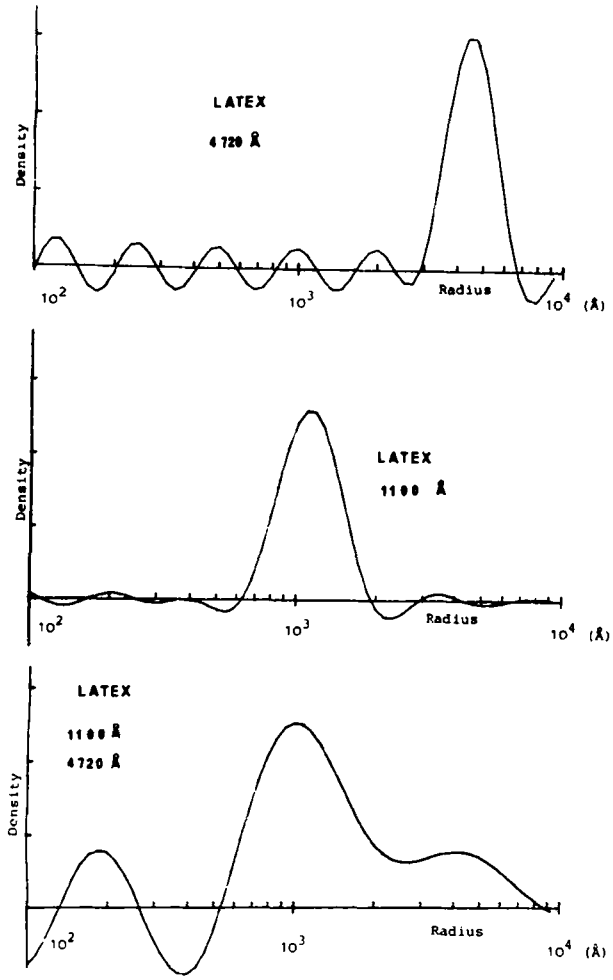

Figure 5—*Distribution curves of monodispersed latex suspensions (radii: 1100 and 4720 Å) and their mixture at the ratio of 5:1.*

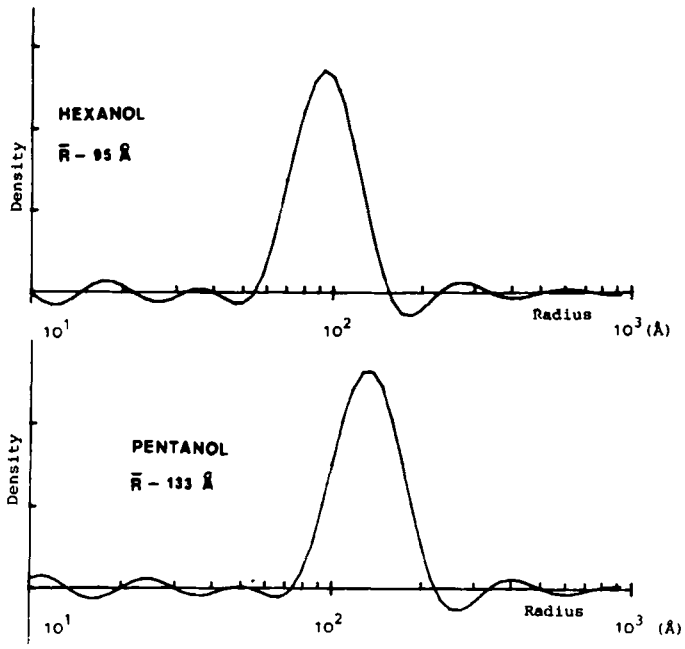

Figure 6—*Distribution curve of two microemulsions produced with equal volume fractions of hexanol and pentanol. Composition: 3.6% water, 1.5% potassium oleate, and 13.0% alcohol, q.s. to 100% with paraffin oil.*

The results obtained with pentanol are shown in Figs. 1 and 2. The phase diagram of the pseudoternary system of paraffin oil, pentanol, potassium oleate, and a constant water fraction of 3.6% showed a zone of instability between the microemulsion and the micellar solution [see Fig. 2 in the previous paper (1)]. A continuous transition from the microemulsion to the solubilization region was found only if the system contained ~3% potassium oleate. In the diagrams for the other alcohols, no continuous transition according to the swollen micelles theory was observed.

Figure 1 shows the particle sizes along a composition line with a constant concentration of 2.0% potassium oleate. Microemulsion A is formed with the smallest possible amount of alcohol, microemulsion D with a maximum amount of alcohol. Both systems are located at the edge of the microemulsion region. Microemulsion formation with a lower or higher concentration of pentanol is not possible. System A is located at the edge bordering on the macroemulsions with a low pentanol concentration. It showed a nearly constant particle size of ~230 Å for 1 week. After 3 weeks it was broken (marked by x in the curve) and an aqueous phase had formed at the bottom of the specimen cell. There was, however, still a microemulsion in the upper phase with a particle size of 260 Å, which decreased during storage. An analogous behavior was found for microemulsion D, which is located at the edge of the microemulsion region towards the solubilization region. The values obtained for compositions B and C proved that the systems in the middle of the microemulsion region were more stable.

The particle size alteration is more obvious in Fig. 2, and the reason for the alterations can easily be explained as follows. Figure 2 shows the particle sizes during the continuous transition from the microemulsion region (systems A–F) to the solubilization region (system G). After 6 weeks of storage, the "single-phase" systems in the zone of instability (systems E and F) were broken and a separation between microemulsions and micellar solutions occurred. After 3 additional weeks, systems D and A were also broken and the microemulsion field was narrowed from both sides. Microemulsion A showed a rapid increase in particle size from 135 Å to 266 Å due to the coalescence of the dispersed phase. After 9 weeks the system was broken, but a microemulsion still remained in the upper phase with a particle size of 233 Å. Relatively large unstable microdroplets had coalesced, and an aqueous subphase had formed. The remaining microdroplets in the upper phase increasingly coalesced in proportion to the length of the storage. After a period of 1 year, only a micellar solution remained, whereas the volume of the aqueous subphase had increased. Microemulsion D had a nearly constant particle size for some weeks. An increase before phase separation was not observed, as this occurred between two measurements. Systems E and F in the unstable zone at the edge of the micellar solution region showed a very slow increase in particle size. For micellar solution G, no alteration was observed. Pentanol as cosurfactant caused rapid microemulsion formation, but also rapid coalescence.

The use of hexanol as cosurfactant also results in rapid microemulsion formation, within milliseconds, but the coalescence is less distinct. Figure 3 shows that the particle size is almost constant for a long time, and the systems are more stable compared with those using pentanol. Another important difference is that only the microemulsions in the unstable zone toward the micellar solution region break at the beginning of the storage period (Fig. 3, systems D and E). The microemulsions on the opposite side (Fig. 3, system A) are, on the other hand, stable in contrast with those formed with pentanol.

Heptanol as cosurfactant causes very slow microemulsion formation. During the formation process the smallest possible particle size was not reached at

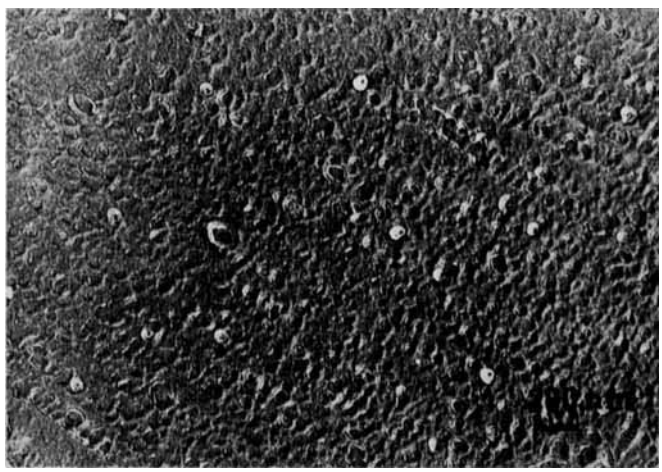

Figure 7—*Electron micrograph of an oil-in-water emulsion after 5 d of storage. The narrow distribution of the particle sizes is obvious. The determined mean radius (25 nm) is almost the same as yielded by photon correlation spectroscopy.*

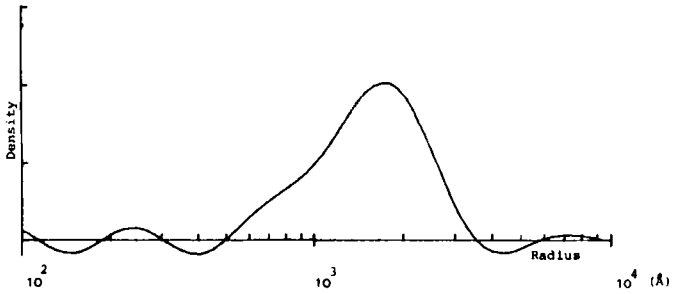

Figure 8—*Distribution curve of an oil-in-water emulsion for infusion.*

once but, rather, after 1 week of storage (Fig. 4, curves A, B, and C). In some cases, macroemulsions were first formed, becoming transparent after a few days (Fig. 4, curves D and E). These emulsions showed the same instability as those of hexanol and broke rapidly. In general, the systems with heptanol were as unstable as those with pentanol, showing a rapid increase in particle size.

In summary, pentanol and hexanol in combination with potassium oleate cause rapid microemulsion formation. The smallest possible particle size is reached at once in contrast with heptanol, where this takes some days. Pentanol and heptanol form unstable systems with a rapid increase in particle size; hexanol, however, shows more constant particle sizes during storage. Hexanol and heptanol have in common that the microemulsion systems at the edge of the solubilization region break at the beginning of the storage time, whereas those bordering the macroemulsion region only coalesce after an induction period. A simultaneous breaking on both sides of the microemulsion region occurred using pentanol. The tested microemulsions showed the same instability due to coalescence as found with macroemulsions, because they are located at the edge of the microemulsion region.

The particle size distribution can be determined with the polydispersity analysis by the Laplace transformation of the correlation function as described above. The efficiency of the method was tested using monodispersed latex suspensions and their mixtures. The two upper curves of Fig. 5 show the distributions of monodispersed latex suspensions with radii of 1100 and 4720 Å. As the particles are not exactly monodispersed and the Laplace transform inherently has some uncertainty, two relatively narrow logarithmic normal distributions are obtained. The distribution of the smaller particles is not as narrow as that of the larger ones because the signal-noise ratio is small, which results in a higher standard deviation of the values and a wider distribution. The mixing of these two types of particles in a ratio of 5:1 results in a distribution curve where the peak heights reflect the particle proportion. Most of the commercial apparatuses, however, calculate only an unsatisfactory polydispersity index.

All the tested microemulsions showed a narrow particle size distribution. Two microemulsions prepared with equal volume fractions of hexanol and pentanol are given as an example (Fig. 6). The mean diameters calculated using the Stokes-Einstein equation were 113 Å for the pentanol system and 80 Å for that with hexanol. This corresponded exactly to the peak maxima in Fig. 6. The measured distributions were confirmed by electron microscopic studies. The structure of microdroplets and the obtained particle sizes were verified (Fig. 7) using the freeze-fracture technique (6).

The described polydispersity analysis can be applied in the pharmaceutical industry. An example is process control of the liposome production, especially small unilamellar vesicles of diameters <100 nm. The liposome size can hardly be controlled during production. Up to now these analyses were made by separating the different liposome sizes into monodispersed systems using a Sephadex column and measuring each system, *e.g.*, with a particle counter. A polydispersity index of ≤2 confirmed the successful separation. A higher polydispersity index indicates a bad separation and does not allow any further statement about the distribution. Such analyses can be carried out faster with the method described herein. An illustration of the practicability is the determination of particle size distributions in oil-in-water emulsions for parenteral use. The tested emulsion[6] had a mean diameter of 446 nm. The corresponding distribution curve shows that it is a polydispersed system (Fig. 8), and the droplet distribution is not logarithmic as is generally assumed for emulsions.

REFERENCES

(1) B. W. Müller and R. H. Müller, *J. Pharm. Sci.*, **73**, 915 (1984).

(2) N. Ostrowsky, D. Sornette, P. Parker, and E. R. Pike, *Optica Acta*, **28**, 1059 (1981).

(3) J. G. McWhirter and E. R. Pike, *J. Phys. A*, **11**, 1729 (1978).

(4) E. O. Schulz-DuBois, "Photon Correlation Techniques," Springer Series in Optical Sciences, Springer-Verlag, Berlin, Heidelberg, New York 1983.

(5) S. W. Provencher, *Macromol. Chem.*, **180**, 201 (1979).

(6) J. E. Rash and C. S. Hudson, "Freeze Fracture: Methods, Artifacts, and Interpretations," Raven, New York, N.Y., 1981.

ACKNOWLEDGMENTS

This study is part of the research project "Bestimmung Molekularer Parameter von Tensiden und Tensidkomplexen mit Hilfe der Streuung von Laserlicht" which is subsidized by the Deutsche Forschungsgemeinschaft. We want to express our sincere thanks for this grant. Many thanks are also due to P. Hille and J. Merz (Institut für Angewandte Physik, Christian-Albrechts-Universität Kiel, W. Germany) for their help in the data processing and the production of the hardware.

Determination of Picogram Nitroglycerin Plasma Concentrations Using Capillary Gas Chromatography with On-Column Injection

PATRICK K. NOONAN, ISADORE KANFER *, SIDNEY RIEGELMAN †, and LESLIE Z. BENET ˣ

Received December 13, 1982, from the *Department of Pharmacy, University of California, San Francisco, CA 94143.* Accepted for publication June 8, 1983. * Present address: School of Pharmaceutical Sciences, Rhodes University, Grahamstown, 6140, South Africa. † Deceased.

Abstract □ A specific, sensitive, and precise capillary gas chromatographic (GC) assay capable of analyzing picogram concentrations of nitroglycerin in human plasma was developed. The analytical procedure involves a double extraction of 1 mL of plasma with pentane, after the addition of internal standard (1 ng of 2,6-dinitrotoluene), followed by evaporation and reconstitution in 50 μL of heptane. The extract (1 μL) was injected onto a capillary column using the on-column injection technique. The GC oven temperature was programmed from 120°C to 180°C at a rate of 5°C/min. The oven temperature was then programmed to 250°C and was maintained for 10 min. The nitroglycerin and internal standard retention times were 8.6 and 11.4 min, respectively. The position of the end of the capillary column inside the detector is a critical determinant of sensitivity: the column exit must be positioned such that nitroglycerin adsorption to the detector is minimized (*i.e.*, sensitivity maximized). The assay limit of quantitation was 25 pg/mL (CV = 7.6%) using 1 mL of plasma. This GC assay, specific for nitroglycerin in the presence of its metabolites, isosorbide dinitrate, and several other drugs, may be used to quantitate plasma levels obtained after therapeutic nitroglycerin doses.

Keyphrases □ Nitroglycerin—GC, picogram quantitation □ GC—nitroglycerin, picogram quantitation

Nitroglycerin is a potent vasodilator used in the treatment of angina pectoris and congestive heart failure associated with acute myocardial infarction (1). The pain of angina may be relieved and/or prevented by the administration of sublingual, oral, or topical nitroglycerin. Although a definitive therapeutic plasma concentration range has not yet been defined, it is still important to identify the nitroglycerin concentration–response relationship so that dose adjustments in patients may be made more effectively. Nitroglycerin administration results in venous plasma concentrations ranging from <50 pg/mL to 10 ng/mL, depending on the route of administration (2–4). Studies in the rhesus monkey (5) indicate that concentrations of ^{14}C-labeled nitroglycerin metabolites are 10- to 300-fold higher than the parent drug. Therefore, an analytical method for nitroglycerin must be both sensitive (25-pg/mL detection limit) and specific (*i.e.*, must measure nitroglycerin in the presence of metabolites).

Several different analytical methods have been developed. HPLC methods have been developed to measure nitroglycerin amounts and concentrations in dosage forms (6), waste water (7), trace level explosives (8), and blood (9). Of these HPLC methods, the last (9) used a thermal energy analyzer–detector and was the most sensitive. This method was capable of detecting 500 pg (injected on column) and required 2 mL of plasma (CV = 12% at 13 ng/mL). None of these methods are capable of detecting nitroglycerin concentrations of 50 pg/mL.

Within the past few years, four GC–MS assays for nitroglycerin have been described (10–13). These assays possess some advantages over HPLC and conventional gas chromatographic (GC) assays. GC–MS assays are selective for the parent drug and quite sensitive (typically 50 pg/mL). Several disadvantages of GC–MS methods are readily apparent. The cost and time to set up a GC–MS instrument is often prohibitive for most clinical laboratories. Several of these assays (11–13) require the use of specially synthesized internal standards labeled with stable isotopes. These internal standards often are not commercially available, which may certainly limit the utility of these assays for routine clinical monitoring.

Several GC assays utilizing conventional packed columns have been developed (14–16). These were not fully satisfactory due to lack of sensitivity (14), complicated extraction procedure and questionable precision [*i.e.*, CV = 23% at 100 pg/mL (15)], and lack of specificity (16). Wu *et al.* (16) found interfering chromatographic peaks, which varied between individuals and even varied within individuals with time. Another major obstacle to the determination of picogram concentrations of nitroglycerin with conventional packed-column GC is adsorption of nitroglycerin to the column components. Several investigators have found that preloading columns, *i.e.*, injecting large amounts of nitroglycerin immediately before analyses of plasma samples, resulted in decreased column adsorption (17–19).

Drug adsorption to GC columns may be greatly reduced, if not eliminated, with the use of inert fused-silica capillary columns (20). Douse (20) reported a fused-silica capillary GC assay capable of detecting 5 pg and quantifying 100 pg of nitroglycerin (CV = 13%). Sved *et al.* (21) recently reported nitroglycerin plasma levels after a topical dose of nitroglycerin ointment. Although a detection limit of 50 pg/mL (using a fused-silica column) was reported, details of the assay validation have not been reported to date. In the present assay, the use of an on-column injector, a syringe with a fused-silica capillary needle, and fused-silica capillary columns allows the quantitation of picogram concentrations of nitroglycerin in plasma samples.

This report describes the capillary GC determination of nitroglycerin in plasma using on-column injection and electron-capture detection (EC). The assay described possesses the precision, sensitivity, and selectivity required to analyze picogram nitroglycerin concentrations in human plasma.

EXPERIMENTAL SECTION

Chemicals and Reagents—Nitroglycerin was obtained as a 10% triturate on lactose[1] and was extracted from the lactose with ether. The internal standard was 2,6-dinitrotoluene[2]. All solvents[3] (pesticide quality) were used as supplied, with the exception of heptane. Heptane was further purified with activated charcoal. Dimethyldichlorosilane[4] was commercially obtained.

Glassware Silanization Procedure—All glassware was silanized before use. A 5% (v/v) dimethyldichlorosilane solution in toluene was prepared fresh monthly and stored at 4°C. Glassware was soaked in this solution for 20 min, rinsed in toluene, and soaked in methanol for 20 min to neutralize excess reagent. The glassware was rinsed a final time with fresh methanol, dried at 100°C for 1 h, and baked at 260°C for 6 h.

[1] Key Pharmaceuticals, Inc., Miami, Fla.
[2] K & K Laboratories, Hollywood, Calif.
[3] Glass-distilled; Burdick and Jackson, Muskegon, Mich.
[4] Aldrich Chemical Co., Milwaukee, Wis.

0022-3549/84/0700-0923$01.00/0
© 1984, American Pharmaceutical Association

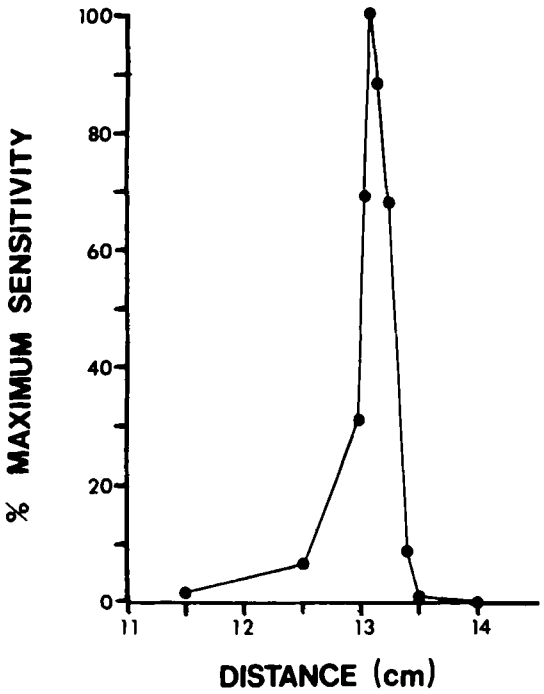

Figure 1—*Effect of capillary column alignment inside the GC detector* (i.e., *distance column is inserted through the detector insert) on nitroglycerin sensitivity.*

Instruments—The gas chromatographs[5] were equipped with ^{63}Ni electron-capture detectors (EC) and on-column injectors[6] (this assay has been validated on two separate instruments). The columns were 30 m × 0.25-mm fused silica capillary columns coated with a cross-linked methyl polysiloxane stationary phase[7]. The capillary column was wrapped in a single sheet of aluminum foil; this technique was found to eliminate peak splitting, which occurred due to uneven heat distribution within the GC oven. Helium was used as a carrier gas at a flow rate of 1.5 mL/min (inlet pressure = 40 psi). Nitrogen flow rates to the EC and column make-up were 5 and 25 mL/min, respectively. Column position inside the EC was optimized for maximum sensitivity. The detector temperature was maintained at 300°C. The oven temperature was programmed from 120°C to 180°C at 5°C/min. A second temperature ramp was used to "burn-off" the residual extract. This was accomplished by programming the oven at 50°C/min to 250°C and maintaining this final temperature for 10 min. Chromatograms were recorded and peak height ratios calculated using a recording integrator[8].

With routine use (every 100 injections) a 40-cm length of column (at the injector end) should be removed. This procedure, which results in more reproducible standard curves, removes nonvolatile extract components that accumulate and eventually cause chromatographic peaks to broaden and the sensitivity to decrease. An alternative to removing portions of the analytical column is the use of a precolumn. The precolumn is a 1-m section of column with the same liquid phase as the analytical column. The precolumn should also be wrapped in aluminum foil and connected directly to the injector. The opposite end of the precolumn is connected to the analytical column using a zero dead-volume union[9]. After ~100 injections, the precolumn may be changed and column efficiency is not lost.

Clinical Blood Sampling—Serial blood samples were drawn into chilled 7-mL evacuated tubes[10] through an indwelling venous catheter kept patent with heparin. The blood was immediately centrifuged at 12,800×*g* for 20 s. The plasma was then immediately frozen in a dry ice bath. The total amount of time required to withdraw the blood sample and centrifuge to obtain plasma prior to freezing was <2 min. This procedure minimizes the *in vitro* degradation of nitroglycerin by blood.

Sample Preparation—Nitroglycerin calibration standards were prepared as follows. Primary stock solutions (1 mg/mL each) of nitroglycerin and 2,6-dinitrotoluene were prepared in ethanol. Secondary stock solutions (10 μg/mL) were prepared fresh monthly by diluting the primary standards in ethanol (1:100, v/v). Fresh aqueous solutions of nitroglycerin (10 ng/mL) and 2,6-dinitrotoluene (20 ng/mL) in distilled water were prepared daily from the secondary stock solutions. Nitroglycerin calibration standards (0, 25, 50, 100, 200, 300, 400, 500, 750, 1000, and 2000 pg/mL) were prepared by adding the appropriate aliquot of the nitroglycerin standard and 50 μL (1 ng) of 2,6-dinitrotoluene to 1-mL samples of blank human plasma in 16 × 150-mm silanized test tubes with polytef-lined screw caps. Clinical plasma samples (1 mL) were transferred to silanized test tubes and mixed with 50 μL of the 2,6-dinitrotoluene.

Each calibration standard or clinical sample was extracted with 10 mL of pentane by vortexing for 2 min, followed by centrifugation for 10 min at 2000×*g*. The pentane layers were transferred to clean test tubes. The residual plasma layers were extracted and centrifuged a second time, as described above. The combined pentane extracts were evaporated under a stream of nitrogen (at room temperature) to a final volume of ~1 mL. The extracts were then transferred to 1-mL vials[11] and evaporated to dryness under a stream of nitrogen. Immediately after the solvent had been completely removed, 25 μL of *n*-heptane was added to each vial, and the vials were vortexed (~5 s). A 1.0-μL aliquot of each extract was injected into the gas chromatograph.

Sample application to the column was performed *via* the injector stopcock using a 10-μL gas-tight syringe which was modified to hold a 0.21 × 190-mm fused-silica capillary "needle." All extracts were stored at −20°C until chromatographed and on dry ice between GC injections.

Assay Specificity—Assay specificity was determined by injecting solutions of several drugs and some of their known metabolites on column. The oven temperature was programmed from 120°C to 200°C at a rate of 5°C/min, then ballistically to 250°C. This temperature program is only slightly different than that described earlier and will not affect the retention time of nitroglycerin, nitroglycerin metabolites, or the internal standard. This temperature program was used to show the relative retention times of a related drug, isosorbide dinitrate, and it metabolites. The analytical method described may be modified in this manner to determine plasma isosorbide dinitrate and metabolite concentrations. All of the compounds tested for possible interferences were tested using these same conditions.

Nitroglycerin Stability—Nitroglycerin stability in frozen human plasma was evaluated at −20°C. Drug-free plasma was obtained from four volunteers

Table I—Retention Times of Nitroglycerin, Nitroglycerin Metabolites, and Several Other Commonly Prescribed Drugs

Compound	GC Retention Time, min
Nitroglycerin	8.6
1,3-Dinitroglycerin	7.5
1,2-Dinitroglycerin	7.6
1-Glycerylmononitrate	4.5
2-Glycerylmononitrate	4.7
2,6-Dinitrotoluene	11.4
Isosorbide dinitrate	14.5
Isosorbide-2-mononitrate	9.8
Isosorbide-5-mononitrate	12.2
Acetaminophen	ND[a]
Acetylsalicylate	11.9
Caffeine	ND
Chloral Hydrate	1.0
Furosemide	ND
Hydrochlorothiazide	ND
Metolazone	ND
Procainamide	ND
N-Acetylprocainamide	ND
Spironolactone	ND
Triamterene	ND

[a] ND = not detected.

Table II—Within-Day Nitroglycerin Assay Precision and Accuracy

Nitroglycerin Concentrations, pg/mL			
	Calculated		
Actual	Mean ± *SD*[a]	*CV*, %	Error, %
25	21.3 ± 1.6	7.6	−16
50	49 ± 3	6.1	−2
100	104 ± 2	2.3	+4
300	288 ± 6	2.1	−4
1,000	1015 ± 39	3.8	+2
10,000[b]	9890 ± 670	6.8	−1

[a] $n = 6$. [b] Diluted 1:10 (v/v) before extraction.

[5] Varian 3700 and 6000 gas chromatographs; Varian Associates, Los Altos, Calif.
[6] On-column injector; J & W Scientific, Inc., Rancho Cordova, Calif.
[7] DB-1, 1.0-μm film thickness; J & W Scientific, Inc., Rancho Cordova, Calif.
[8] HP3390A; Hewlett Packard, Palo Alto, Calif.
[9] Zero dead volume union; J & W Scientific, Inc., Rancho Cordova, Calif.
[10] Vacutainers; Becton, Dickenson and Co., Rutherford, N.J.
[11] Reacti-vials; Pierce Chemical Co., Rockford, Ill.

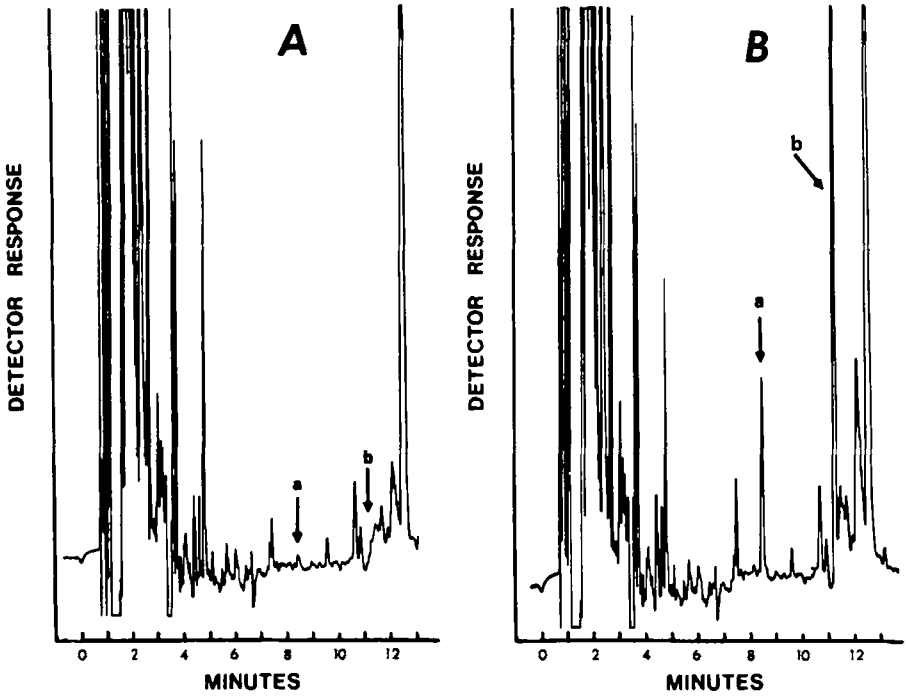

Figure 2—*Chromatograms of blank and nitroglycerin-fortified plasma extracts. Key: (A) blank plasma extract; (B) plasma extract fortified with 100 pg/mL of nitroglycerin and 1 ng/mL of 2,6-dinitrotoluene. Retention times for nitroglycerin and 2,6-dinitrotoluene are indicated in each chromatogram by* a *and* b, *respectively.*

(three male, one female) and pooled. Nitroglycerin was added to two separate 100-mL aliquots of plasma (at 0°C) to obtain final concentrations of 0.1 and 1.0 ng/mL. Each plasma solution was subdivided into multiple 1-mL aliquots, quick-frozen in dry ice, and stored at −20°C. Six aliquots of each concentration were assayed (as described above) after 0, 7, 14, 24, 40, and 60 d of storage.

Column/Electron-Capture Detector Optimization—The position of the capillary column exit inside the detector was optimized for maximum sensitivity. Sensitivity was evaluated from multiple injections of a 1.0-μL aliquot of a nitroglycerin standard solution (1.0 pg of nitroglycerin/μL and 40 pg of 2,6-dinitrotoluene/μL, in heptane). The position of the column in the detector was adjusted to increase sensitivity (maximum nitroglycerin/2,6-dinitrotoluene peak height ratio).

RESULTS AND DISCUSSION

Injector and Detector Optimization—Initial attempts to use a capillary GC system to quantitate picogram amounts of nitroglycerin were unsuccessful. Nitroglycerin may adsorb and degrade on active surfaces of capillary injectors, glass columns, and detectors. Several injection systems were evaluated. Significant nitroglycerin adsorption occurred with splitless and direct injectors[12]. Use of the split injection technique (90:1 split ratio) decreased the apparent adsorption of nitroglycerin to the injector. Lower split ratios were necessary to increase assay sensitivity, but the coefficient of variation was >20%. Finally, injector precision and assay sensitivity were evaluated using the on-column injection technique. Use of this technique allowed nitroglycerin to be applied directly onto the capillary column, thus avoiding glass and metal surfaces which may adsorb and/or degrade nitroglycerin.

Adsorption and degradation of nitroglycerin may occur not only on surfaces of conventional injectors, but also on active surfaces present in the EC. An advantage of using narrow-bore fused-silica capillary columns is that the column may be inserted entirely into the EC. Optimization of the position of the column exit inside the EC is an important determinant of assay sensitivity. The EC contains highly active surfaces which may bind or degrade labile drugs such as nitroglycerin. Therefore, the column must be positioned to both minimize nitroglycerin loss and maximize detector sensitivity.

Figure 1 shows that detector sensitivity sharply increases as the column is inserted further into the EC and peaks at 13.1 cm, *i.e.*, 13.1 cm as measured from the EC detector insert to the end of the column. Further insertion of the column into the detector results in a sharp decrease in sensitivity. Note that if the column alignment varies by as little as 1–2 mm, 50% of the maximum sensitivity is lost.

The position of the column within the EC may not be as critical in the chromatography of other compounds. For example, lindane and aldrin are easily detected even when the column outlet is placed only 0.5 cm inside the detector insert.

Extraction Precision and Recovery—Initial assay development utilized an extraction procedure in which 1.0 mL of plasma was extracted once with 10 mL of pentane. Extraction efficiencies for nitroglycerin and 2,6-dinitrotoluene (1.0 ng/mL each) were 75 ± 7% and 93 ± 2%, respectively. When biological samples (plasma) were each extracted twice, assay precision, as measured by the decrease in coefficient of variation, was increased by two- to threefold. Coefficients of variation decreased from 13.7 to 6.1%, 15.9 to 2.3%, and 9.5 to 2.9% at plasma nitroglycerin concentrations of 50, 100, and 1000 pg/mL, respectively, when single and double extractions are compared.

Nitroglycerin Chromatography and Assay Specificity—Chromatograms of blank and nitroglycerin-fortified plasma are shown in Fig. 2. Figure 2A depicts a chromatogram for a blank plasma extract. The nitroglycerin and 2,6-dinitrotoluene retention times are indicated by arrows. The small peak, indicated by arrow a, has the same retention time as nitroglycerin. This peak is due to a contaminant present in the heptane and was eliminated by purifying the heptane with activated charcoal. Figure 2B shows a representative chromatogram of plasma fortified with 100 pg/mL of nitroglycerin and 1 ng/mL of 2,6-dinitrotoluene. The retention times for nitroglycerin and 2,6-dinitrotoluene were 8.6 and 11.4 min, respectively.

Both nitroglycerin and dinitrotoluene were resolved from nitroglycerin metabolites. The retention times for the metabolites are shown in Table I. Since the capillary GC assay will be used to measure nitroglycerin plasma concentrations in patient populations, several other drugs were tested for assay interference. Table I lists the retention times, when detected, of several drugs (and metabolites) which may be prescribed to patients in a hospital cardiac care unit. None of the drugs, nor the metabolites tested, interfered with the nitroglycerin capillary GC assay. Also note that nitroglycerin may be assayed in the presence of isosorbide dinitrate, which is often concurrently administered to patients. No interference was noted for this compound and its two major metabolites, isosorbide-5-mononitrate and isosorbide-2-mononitrate.

Assay Precision, Accuracy, and Linearity—The precision and accuracy of the nitroglycerin assay procedure was assessed by analysis of six replicate

Table III—Stability of Nitroglycerin in Pooled Human Plasma at 100- and 1000-pg/mL Concentrations When Stored at −20°C

	Calculated Concentration, pg/mL			
	100 pg/mL		1000 pg/mL	
Time, d	Mean ± *SD*	*CV*, %	Mean ± *SD*	*CV*, %
0	112 ± 7	6.2	1015 ± 39	3.8
7	102 ± 5	4.9	1034 ± 31	3.0
14	109 ± 7	6.4	987 ± 31	3.1
24	102 ± 4	3.9	933 ± 33	3.5
40	113 ± 6	5.3	952 ± 31	3.4
60	106 ± 6	5.7	955 ± 41	4.2

[12] Varian Associates, Los Altos, Calif.

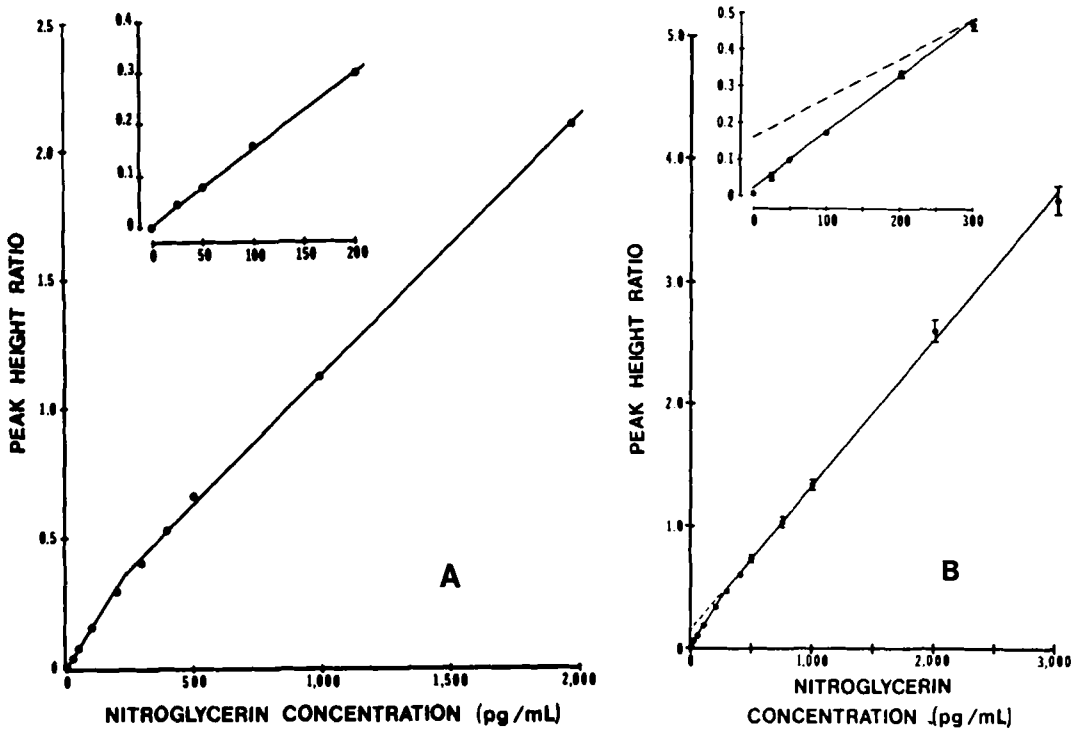

Figure 3—*Nitroglycerin standard curves. Key: (A) Representative nitroglycerin standard curve; curve is linear between 0–200 pg/mL and 200–2000 pg/mL. Inset shows the low calibration standard range. (B) Mean of six individual nitroglycerin standard curves. Standard error bars are shown except when smaller than the data symbol. Inset shows the low calibration standard range and the extrapolated line (- - -) from the high concentration range.*

plasma samples to which known amounts of nitroglycerin were added. Within-day assay precision and accuracy are summarized in Table II. Coefficients of variation over the concentration range, 25–10,000 pg/mL, were <10%. The relatively high coefficient of variation of the 10-ng/mL concentration may be due, in part, to the additional steps involved in sample analysis at higher concentrations, *i.e.*, extracting 100 μL of plasma diluted with 900 μL of blank plasma. Accuracy for all concentrations, except 25 pg/mL, was within ±5% of the actual fortified nitroglycerin concentrations. Between-day assay precision was evaluated over 2 months (40 standard curves), *i.e.*, each day for 40 d. Blank plasma samples were fortified with 0.1 and 1.0 ng/mL of nitroglycerin. These samples served as calibration controls until drug stability could be established. Coefficients of variation were 7 and 12% at 1.0 and

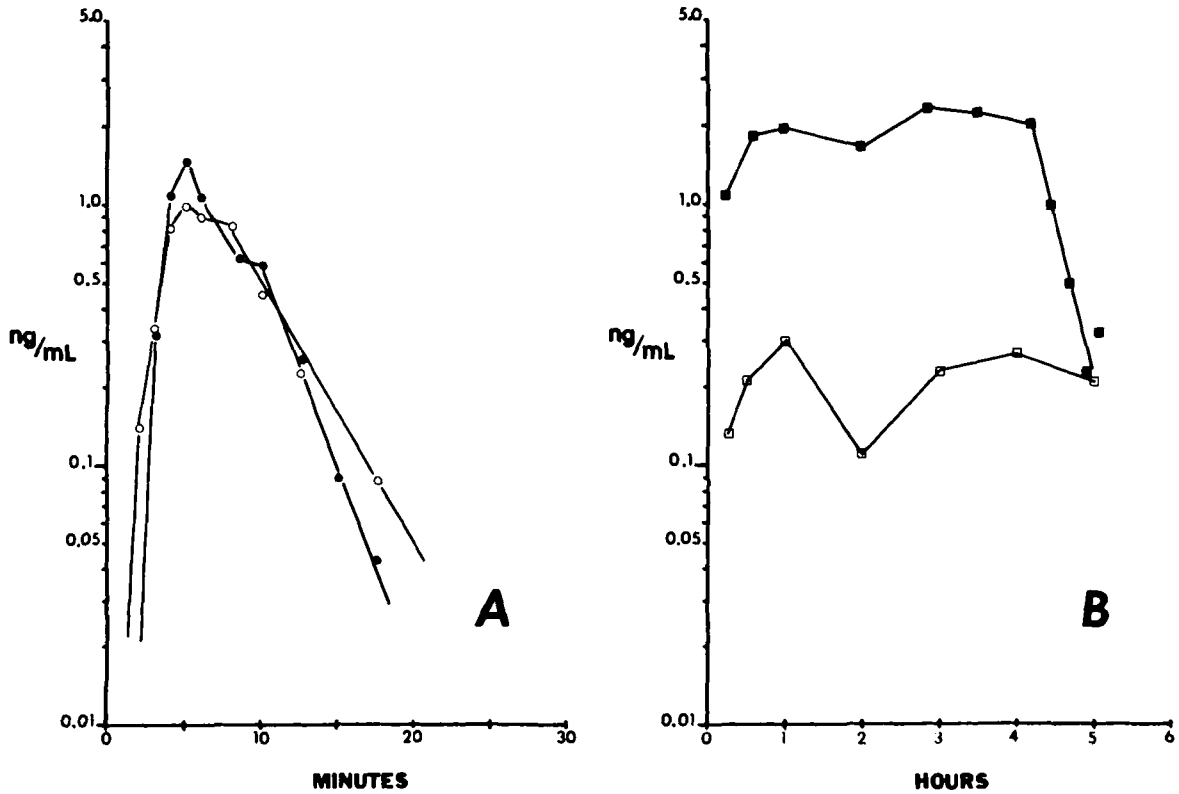

Figure 4—*Plasma nitroglycerin concentration* versus *time profiles for two subjects. Key: (A) after 0.4-mg sublingual doses to subject 1; (B) after topical doses to subject 2* via *ointment (■) and controlled-release patch (□).*

0.1 ng/mL, respectively. Accuracy (mean concentrations) were within the percent error noted for these two concentrations in Table II.

Nitroglycerin standard curves were not linear over the entire concentration range of 0–3000 pg/mL. At very low concentrations (<200–300 pg/mL) the standard curve slope was generally 50% greater than that of the high concentration range. Figure 3A shows a representative standard curve. The change in slope is not due to extraction efficiencies, since the slope change was also present when known concentrations of drug in heptane were injected. The "break-point" of the standard curve was consistent and did not change during any given day. Even when six different standard curves were averaged together (Fig. 3B), the break-point was still present. Therefore, this break-point is not due to assay variability.

The break-point may vary between different columns, instruments, or make-up gas flow rates. The standard curve in Fig. 3A was analyzed on a different instrument than the curves averaged in Fig. 3B. The break-point in Fig. 3A occurred at 200 pg/mL. In each of the six individual curves and the mean curve in Fig. 3B, the break-point occurred at 300 pg/mL. The position of the break-point may vary between instruments, but is constant within any one instrument. Although the occurrence of the break-point is quite consistent, the cause has not yet been identified.

Nitroglycerin Stability in Frozen Plasma—Nitroglycerin stability in frozen plasma has been determined in some detail by Maier *et al.* (22). Because these investigators determined nitroglycerin concentrations using a GC assay which utilized packed columns, it was necessary to validate the plasma storage conditions using the capillary GC assay reported here. The nitroglycerin stability data are shown in Table III. Nitroglycerin was stable in plasma for a minimum of 60 d when stored at −20°C.

Clinical Studies—As an illustration of the applicability of this assay procedure, nitroglycerin was administered to two healthy volunteers. Subject 1 received a 0.4-mg sublingual dose on two separate occasions (1 week apart); the plasma concentrations are shown in Fig. 4A. Nitroglycerin peak times were 5 min, and terminal half-lives were 2.0 and 3.0 min. Subject 2 received two topical doses of nitroglycerin on separate occasions. The subject received a 1-g dose of 2% nitroglycerin ointment (equivalent to 20 mg of nitroglycerin) which was spread evenly over a 200-cm^2 chest area and occluded. The second dose was a sustained-release nitroglycerin patch. Plasma concentrations are shown in Fig. 4B. The half-life (15 min) after removing the ointment was longer than that after sublingual dosing. The longer half-life is most likely due to continued absorption of nitroglycerin.

REFERENCES

(1) "Physicians Desk Reference," 36th ed., Medical Economics Co., Oradell, N.J., 1982, p. 568.

(2) M. G. Bogaert and M.-T. Rosseel, *J. Pharm. Pharmacol.*, **24,** 737 (1972).

(3) P. W. Armstrong, J. A. Armstrong, and G. S. Marks, *Circulation*, **66,** 1273 (1982).

(4) A. Bashir, M. J. Lewis, and A. H. Henderson, *Br. J. Clin. Pharmacol.*, **14,** 779 (1982).

(5) R. C. Wester, P. K. Noonan, S. Smeach, and L. Kosobud, *J. Pharm. Sci.*, **72,** 745 (1983).

(6) D. M. Baaske, J. E. Carter, and A. H. Amann, *J. Pharm. Sci.*, **68,** 481 (1979).

(7) C. D. Chandler, G. R. Gibson, and W. T. Bolleter, *J. Chromatogr.*, **100,** 185 (1974).

(8) A. L. Lafleur and B. D. Morriseau, *Anal. Chem.*, **52,** 1313 (1980).

(9) R. J. Spanggord and R. G. Keck, *J. Pharm. Sci.*, **69,** 444 (1980).

(10) P. Ottoila, J. Taskinen, and A. Sothman, *Biomed. Mass Spec.*, **9,** 108 (1982).

(11) H. Miyazaki, M. Ishibashi, Y. Hashimoto, G. Idzu, and Y. Furuta, *J. Chromatogr.*, **239,** 277 (1982).

(12) G. Idzu, M. Ishibashi, and H. Miyazaki, *J. Chromatogr.*, **229,** 327 (1982).

(13) A. Gerardin, D. Gaudry, and D. Wantiez, *Biomed. Mass Spec.*, **9,** 333 (1982).

(14) M. T. Rosseel and M. G. Bogaert, *J. Pharm. Sci.*, **62,** 754 (1973).

(15) P. S. K. Yap, E. F. McNiff, and H.-L. Fung, *J. Pharm. Sci.*, **67,** 582 (1978).

(16) C. C. Wu, T. D. Sokoloski, A. M. Burkman, M. F. Blanford, and L. S. Wu, *J. Chromatogr.*, **228,** 333 (1982).

(17) P. W. Armstrong, J. A. Armstrong, and G. S. Marks, *Circulation*, **59,** 585 (1979).

(18) I. W. Taylor, C. Ioannides, J. C. Turner, R. U. Koenigsberger, and D. V. Parke, *J. Pharm. Pharmacol.*, **33,** 244 (1981).

(19) M. A. Gonzalez, J. Hsiao, M. F. Blanford, and A. L. Golub, "Abstracts," 1982 Midwest Regional Meeting, APhA/APS, May 1982.

(20) J. M. F. Douse, *J. Chromatogr.*, **208,** 83 (1981).

(21) S. Sved, W. M. McLean, and I. J. McGilveray, *J. Pharm. Sci.*, **70,** 1368 (1981).

(22) G. A. Maier, A. Poliszczuk, and H.-L. Fung, *Int. J. Pharm.*, **4,** 75 (1979).

ACKNOWLEDGMENTS

Supported in part by NIH Grant HL 32243 and by a grant from Key Pharmaceuticals, Inc., Miami, Fla. During the course of this work, PKN received support as an AFPE James F. Hoge Memorial Fellow.

The authors thank Dr. Helga Moeller of the Zentrallabor Deutscher Apotheker, Eschborn, West Germany, for samples of isosorbide-2-mononitrate and isosorbide-5-mononitrate, Dr. Allyn Golub of Key Pharmaceuticals, Inc., for samples of isosorbide dinitrate and nitroglycerin, and both G. D. Searle and Co., Skokie, Ill., and Pohl-Boskamp, Hohenlockstedt, W. Germany, for samples of the nitroglycerin metabolites.

Dose-Dependent Pharmacokinetics and Hepatobiliary Transport of Bromophenol Blue in the Beagle

ROBERT J. WILLS *, GERALD J. YAKATAN [§x], and ROBERT S. PEARLMAN

Received September 17, 1982, from the *College of Pharmacy, University of Texas at Austin, Austin, TX 78712.* Accepted for publication May 26, 1983. Present addresses: *Hoffmann-La Roche, Department of Pharmacokinetics and Biopharmaceutics, Nutley, NJ 07110 and [§]Warner-Lambert Co., Pharmaceutical Research Division, Morris Plains, NJ 07950.

Abstract □ The pharmacokinetic profile of bromophenol blue (I) in the plasma, urine, and bile of beagle dogs was determined after intravenous administration of 5-, 20-, and 30-mg/kg doses. In addition, two competitors, probenecid and phenylbutazone, were interacted with I *in vivo* and with I and rat liver cytoplasmic protein fractions Y and Z *in vitro* as a means of elucidating the mechanism of intrahepatic transport of I. Compound I was determined spectrophotometrically at 587 nm. In plasma, I displayed apparent first-order dose-dependent kinetics. The percentage of I bound to plasma proteins was ~92.5% over the dose range studied. Consecutive injections of equal doses of I produced statistically different terminal half-lives ($p < 0.05$), suggesting the possibility of a saturable uptake process. In the presence of each competitor, the disposition of I was altered significantly ($p < 0.05$): phenylbutazone displaced I from plasma protein, while probenecid decreased the binding of I to liver proteins in the Z-fraction. The Z-fraction bound a larger amount of I than the Y-fraction, suggesting a larger binding capacity. Under no circumstances was the binding of I to the Y-fraction altered. Cumulative biliary excretion data showed that the elimination of I in bile accounted for 92–99% of the dose delivered. The biliary excretion σ^- plots displayed no dose dependency, suggesting that the dose-dependent plasma half-life is due to a dose-dependent liver uptake (as opposed to elimination) process.

Keyphrases □ Pharmacokinetics—bromophenol blue, dogs, hepatobiliary transport □ Bromophenol blue—pharmacokinetics, hepatobiliary transport, dogs □ Hepatobiliary transport—bromophenol blue, dogs, pharmacokinetics

An understanding of the complex processes involved in hepatobiliary transport will lead to a more complete understanding of the disposition of the many compounds eliminated by this route. Radiological (1–3) and pharmacological (4–7) investigations have addressed various aspects of these transport processes, but relatively few pharmacokinetic studies have been conducted. The use of blood, urine, and bile data to suggest or support a model of hepatobiliary uptake and elimination appears to be a promising research objective. Takada and coworkers (8–10) proposed the use of bromophenol blue (I) as a model compound for the study of hepatobiliary transport in rats. This was confirmed by Wills *et al.* (11), who noted that I is primarily excreted in bile, is not metabolized, elicits no pharmacological action, and is not intestinally reabsorbed. Although studies conducted in rats have been informative, the pharmacokinetics of the hepatobiliary transport of I have not been addressed in higher animals. Although a few studies using dogs have been conducted (1, 3, 12), the feasibility of obtaining a useful bile concentration profile has yet to be demonstrated.

In rat plasma, I displays a dose dependency which was related to the saturation of proteins involved in the liver uptake process (8). These proteins were separated as cytoplasmic protein fractions Y, Z, and T-binder (9, 13–15), and it was subsequently shown (10) that both Y and Z act as uptake sites, Z and T-binder act as storage sites, but only Y functions as an intracellular carrier to the bile canaliculi.

Takada and co-workers (8–10) used competitors to elucidate the hepatobiliary transport mechanism in rats. Two competitors, probenicid and phenylbutazone, were selected because of their ability to inhibit liver uptake of organic anions (13, 16, 17) and to displace drug from plasma proteins (18–20), respectively.

The nature of the hepatobiliary uptake and elimination processes in higher animals is still the subject of controversy. Shanker (21) hypothesized the existence of three different carrier systems for liver uptake of anionic, cationic, and neutral compounds. However, Schwenk (6) has recently presented conflicting data.

In this report, we discuss efforts to determine the pharmacokinetic profile (plasma and urine) of I following intravenous administration in intact beagle dogs, to determine the pharmacokinetic profile (plasma, urine, and bile) of I following intravenous administration in beagle dogs with cannulated common bile ducts and excised gallbladders, to observe the effect of probenecid and phenylbutazone on the pharmacokinetic parameters for I, and to examine the action of these two competitors by *in vitro* rat liver protein binding studies.

EXPERIMENTAL SECTION

Bromophenol blue[1] (I) was purchased from the manufacturer. Purity was established by melting point and TLC. A mixture of propylene glycol–ethanol–sterile water (4:1:5) was found to be a suitable intravenous injection vehicle[2].

One female and two male beagles, weighing 11–18 kg, were used in all studies; all three dogs were 7 years old. Hematology values were determined to be within normal limits. The dogs were fasted 18 h prior to drug administration, and at least 2 weeks were allowed between studies unless otherwise noted.

Bromophenol Blue Intravenous Bolus Studies—Compound I was administered as 5-, 20-, or 30-mg/kg doses. Sample times varied with dose, as indicated in the figures. Blood samples were transferred to stoppered evacuated tubes[3] containing sodium heparin and centrifuged. The plasma was removed and stored at −20°C until assayed. Urine was collected as produced and also stored frozen until assayed.

Competitor Studies—Probenecid[4] and phenylbutazone[5] were supplied by the manufacturers. Each competitor was administered 1 h before the I dose. The doses of probenecid, phenylbutazone, and I were 125, 75, and 20 mg/kg, respectively. The half-life of each competitor was ~8 h (17, 22).

Plasma Protein Binding Studies—The extent of binding of I was determined after dialysis using a rotary five-cell (volumes of 1.36 mL; membrane surface area of 4.52 cm^2) dialysis apparatus[6]. The dialysis apparatus was assembled with equivalent *in vivo* concentrations of I dissolved in pH 7.4 isotonic buffer on one side *versus* pooled dog plasma on the other side, placed in a water bath at 37°C, and incubated for 2 h at 10 rpm. The time required for equilibration was established by dialyzing spiked buffer against unspiked buffer.

The effect of the competitors on the plasma protein binding of I was also determined. To 4 mL of pooled dog plasma, 100 μL of a 16-mg/mL solution of competitor was added to give a final concentration equivalent to an *in vivo* concentration (17, 22) of the competitor at time zero. This solution was dialyzed against spiked buffer, which encompassed the concentrations of I found

[1] Fisher Scientific Co., Fair Lawn, N.J.
[2] Personal communication J. W. McGinity, Drug Dynamics Institute, College of Pharmacy, University of Texas, Austin, Tex.
[3] Vacutainer; Becton, Dickenson and Co., Rutherford, N.J.
[4] Merck Sharp and Dohme, West Point, Pa.
[5] Ciba-Geigy, Summit, N.J.
[6] Spectrum Medical Industries, Inc., Los Angeles, Calif.

0022-3549/84/0700-0928$01.00/0
© 1984, American Pharmaceutical Association

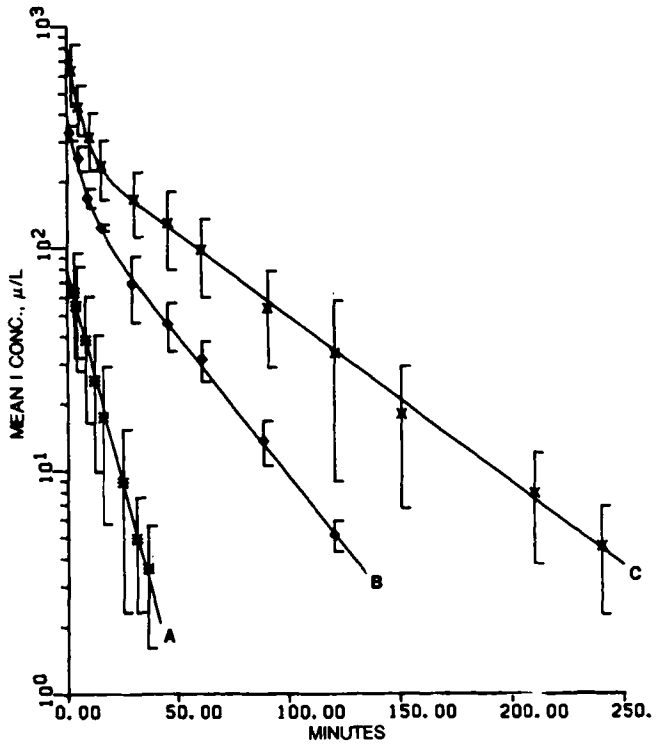

Figure 1—*Mean* ± SD (n = *3) plasma concentrations of I after an intravenous bolus injection to a dog. Key: (A) 5-mg/kg dose; (B) 20-mg/kg dose; (C) 30-mg/kg dose.*

in vivo. All solutions were collected and any cell volume changes were noted. The samples were assayed immediately after removal from the dialysis apparatus.

Bile Duct Cannulation Studies—Under pentobarbital anesthesia, a midline incision was made[7] and the common bile duct was exposed. After excising the gallbladder, a small incision in the common bile duct was made ~1 cm from its entrance to the duodenum, and a T-shaped cannula was inserted and ligated in place. A second T-shaped cannula was placed into the duodenum and both silicone rubber[8] cannulae were attached to a larger stainless steel cannula which was inserted through the abdominal wall. Although the cannula into the duodenum would have allowed the return of bile between experiments, previous experience indicated that this would subject the animals to an increased risk of hepatic infection. Thus, total bile was collected at all times. Bile salt dietary supplements[9] were given to maintain the animals' weights at constant values.

During experiments, bile was collected in pre-tared screw-capped vials[10] and frozen until assayed. In addition, blood and urine were collected. The sampling times varied with dose. Only 1 week was allowed between studies because animal viability was poor.

Liver Protein Binding Studies—Two male Sprague–Dawley rats, 400 g, were anesthetized by a 70-mg/kg ip injection of sodium pentobarbital. A midline laparotomy exposed the internal viscera. The hepatic vein was severed, followed by cannulation of the hepatic portal vein with a 22-gauge needle connected to an infusion pump[11] containing pH 7.4 isotonic phosphate buffer. The liver was perfused until the color appeared pink (after ~200 mL of buffer). The livers were then excised, dried, weighed, and stored frozen.

In preparation for extraction and purification of the liver protein fractions (9), the livers were homogenized[12] to a 25% homogenate with 0.25 M sucrose–0.01 M phosphate buffer (pH 7.4) and then ultracentrifuged[13] at 100,000 × *g* for 2 h at 20°C. After removing the surface lipids, the supernatant was collected. A 1-mL aliquot of supernatant was used for determination of the total protein concentration (23).

A total of nine mixtures containing supernatant, I, and the competitors were prepared as follows. To 5 mL of supernatant, 6.7 mg (10 μmol) of I and 0, 10, 20, 30, or 40 μmol of either probenecid or phenylbutazone were added. Each mixture was incubated for 24 h at 4°C and then eluted using 0.01 M phosphate buffer pH 7.4 on a Sephadex G-75 column (2.5 × 45 cm)[14] previously equilibrated with the phosphate buffer (24). Five-milliliter fractions were collected using a fraction collector[15]. Absorbances of I and protein for a given tube were determined at 587 and 280 nm, respectively, using a double-beam spectrophotometer[16]. The absorbances measured at 280 nm were used as a fingerprint for liver protein fraction identification.

The total amount of I bound to the void volume (X fraction), Y, and Z fractions was quantitated as follows. After determining the amount of I in each tube the amounts were then added together mathematically from tubes 0–7, 8–14, and 29–64 (representing I bound to the void volume, Y, and Z fractions, respectively). The total amount of I bound in the presence of each competitor

Table I—Pharmacokinetic Disposition Parameters Following an Intravenous Bolus Injection of I

Dog	$t_{1/2}$, min	CL_p, mL/min	Vd_{ss}, L	$AUC_{0\to\infty}$, μg/mL min
		30-mg/kg Dose		
A	40.8	22.9	1.40	22,300
B	31.5	23.1	1.01	18,300
C	31.5	32.7	1.43	10,200
Mean	34.1[a]	26.2	1.28	16,900
± *SD*		5.6	0.23	6,160
		20-mg/kg Dose		
A	25.7	51.0	1.73	6480
B	25.8	44.3	1.27	6430
C	23.0	30.1	1.02	7540
Mean	24.8[a]	42.0	1.34	6820
± *SD*		11.0	0.36	628
		5-mg/kg Dose		
A	6.7	154	2.02	570
B	6.5	159	1.81	357
C	7.7	70.8	1.01	1070
Mean	6.9[a]	128	1.61	666
± *SD*		49.4	0.53	370

[a] Harmonic mean half-life.

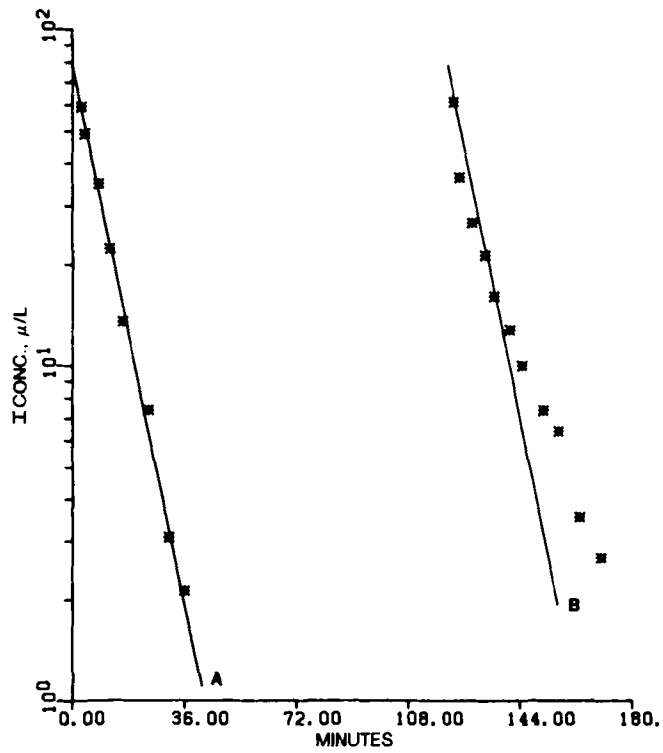

Figure 2—*Plasma concentrations of I following an intravenous bolus injection of 5 mg/kg at time zero (A) and a second injection at 2 h (B). The solid lines represent the fitted line from the first injection data.*

[7] Procedure developed by Dr. R. Shumacher and performed by Mr. J. Wiley and Ms. A. Black at Warner-Lambert, Ann Arbor, Mich.
[8] Silastic.
[9] Reheis Chemical Co., Tarrytown, N.Y.
[10] Kimble, Toledo, Ohio.
[11] Harvard Apparatus, Millis, Mass.
[12] Brinkman Instruments, Westbury, N.Y.
[13] Beckman Instruments, Inc., Palo Alto, Calif.
[14] Fisher and Porter Co., Warminster, Pa.
[15] Instrumentation Specialties Co., Lincoln, Neb.
[16] Perkin-Elmer Corp., Maywood, Ill.

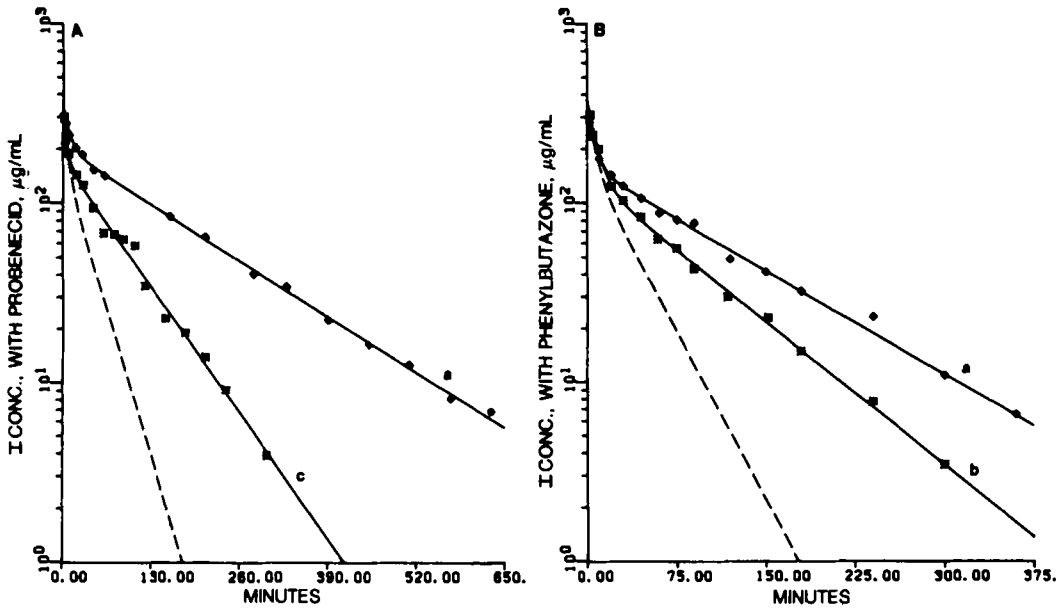

Figure 3—*Plasma concentrations of I after a 20-mg/kg dose of I with a 125-mg/kg dose of probenecid (A) or a 75-mg/kg dose of phenylbutazone (B). Key: (a) dog A; (b) dog B; (c) dog C; (- - -) 20-mg/kg dose of I without the competitor.*

at different competitor concentrations was divided by the control to give the percent reduction in I binding to either the Y or Z fraction. The amount found in the void volume was used for mass balance calculations.

Assay—In all procedures, only I was assayed. Plasma, urine, bile, and the plasma and liver protein binding samples were diluted with phosphate buffer (pH 8), and the absorbance was measured directly at 587 nm. Standards were prepared and run daily. The standard curves were linear ($r = 0.9997$); the sensitivity was 0.6 μg/mL.

RESULTS

Plasma Concentrations of Bromophenol Blue—The mean plasma concentrations of I *versus* time are shown in Fig. 1. The low dose (5 mg/kg) declined monoexponentially, while the intermediate dose (20 mg/kg) and the high dose (30 mg/kg) declined biexponentially (Fig. 1). The data were fit to a sum of exponentials using NONLIN (25). The relevant pharmacokinetic parameters are given in Table I (26, 27).

The biological half-life ($t_{1/2}$) and plasma clearance (CL_p) were not constant over the range of doses studied (Table I). These results indicate that the elimination of I from plasma is a dose-dependent process in this dose range. The area under the plasma concentration–time curve ($AUC_{0\to\infty}$) increased at a greater than linear rate with increasing dose (Table I).

The percentage of I bound to plasma proteins was 92.5 ± 1.5% at 37°C and was essentially constant over the range of I concentrations examined (100–875 μg/mL). A slight increase in the free fraction of I with increasing I concentration occurred, but was found not to be statistically significant using the Student's *t* test.

The graph in Fig. 2 indicates the plasma concentrations following two identical 5-mg/kg doses of I administered 2 h apart. The first dose was no longer detectable in the plasma just prior to the second dose, yet the second dose was eliminated at a significantly ($p < 0.005$) slower rate. The half-lives were 6.7 and 12.7 min, respectively.

Drug Competition With Bromophenol Blue—The concentration–time profiles of I following prior administration of probenecid and phenylbutazone are shown in Fig. 3a and b. The data was fit to a sum of exponentials using NONLIN (25).

In the presence of each competitor, the half-life increased, the area under the plasma concentration–time curve increased, and the clearance decreased (Table II). The volume of distribution at steady state (Vd_{ss}) was essentially unchanged, indicating that the competitors had no effect on the overall distribution of I.

Phenylbutazone produced a significant change ($p < 0.05$) in the plasma protein binding of I. The percent of I bound was 86.1 ± 2.9%, corresponding to nearly a twofold increase in the free I concentration over that found in the absence of phenylbutazone. Probenecid had no effect on the plasma protein binding of I (92.2 ± 1.2%).

Liver Protein Binding Studies—The results of the *in vitro* studies of I binding to rat liver protein fractions are presented in Table III. Figure 4a and b shows the protein and I elution profiles. From left to right the protein peaks correspond to protein in the void (unidentified protein) volume, proteins in the Y-fraction, and proteins in the Z-fraction (13–15), while the I peaks indicate binding to the respective protein peaks. Probenecid competed with I for Z-fraction binding sites, resulting in a significant decrease in the amount of I bound and a corresponding increase in the amount of free I (Table III). In Fig. 4a the profile representing I bound to Z steadily decreased with an increase in probenecid concentration. Phenylbutazone did not affect I binding to Z-fraction (Fig. 4b, Table III). Neither competitor affected the amount bound to the Y-fraction; because the amount of I bound to the Y-fraction was ~1–3% of that bound to the Z-fraction, the results were not presented.

Biliary Excretion Studies—Although all three dogs were cannulated as described above, only one animal provided complete data. Dog A developed peritonitis despite intensive postoperative maintenance, and dog B developed a colateral bile duct which bypassed the cannula 2 weeks after the surgery.

Table II—Comparison of Pharmacokinetic Disposition Parameters of I (20 mg/kg) in the Presence of a Competitor

Dog	$t_{1/2}$, min[a]	CL_p, mL/min[a]	Vd_{ss}, L	$AUC_{0\to\infty}$, μg/mL·min[a]
		Probenecid, 125 mg/kg		
A	127	9.5	1.60	37,400
C	56.0	15.1	1.08	14,300
		Phenylbutazone, 75 mg/kg		
A	77.9	18.9	1.73	18,500
B	56.3	26.3	1.27	12,200

[a] Significantly different from the no competitor case ($p < 0.005$).

Table III—Effect on the Binding of I to the Z-Fraction in the Presence of a Competitor

Competitor Conc., μmol/mL	I Conc., μmol/mL	Total Amount I Bound, μg	Reduction in I Binding, %	*t* test
		Phenylbutazone		
0.0	2.0	755	—	—
2.0	2.0	748	1.0	$p > 0.05$
4.0	2.0	754	0.1	$p > 0.05$
6.0	2.0	748	0.9	$p > 0.05$
8.0	2.0	753	0.3	$p > 0.05$
		Probenecid		
0.0	2.0	755	—	—
2.0	2.0	704	6.9	$p < 0.05$[a]
4.0	2.0	699	7.3	$p < 0.05$[a]
6.0	2.0	693	8.2	$p < 0.05$[a]
8.0	2.0	687	9.0	$p < 0.05$[a]

[a] Paired *t* test performed on duplicate data sets.

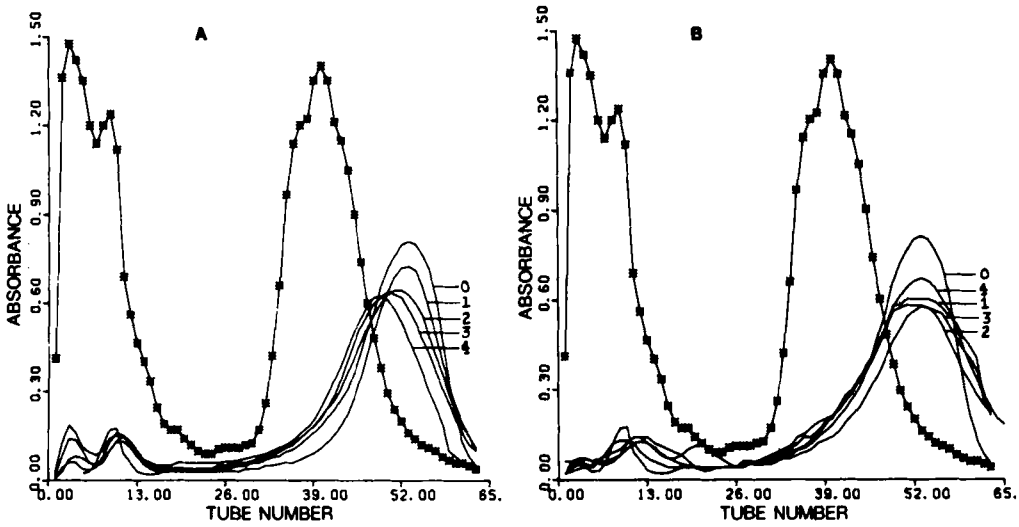

Figure 4—*Elution patterns of I, measured at 587 nm, in the presence of probenecid (A) and phenylbutazone (B) in the rat liver cytoplasmic fraction. 0, 1, 2, 3, and 4 indicate the amount of competitor added as a multiple of the amount of I present. The asterisks represent the protein fraction elution pattern measured at 280 nm. Each tube number represents a 5-mL collection.*

The pharmacokinetic parameters derived from I plasma concentrations following intravenous administration to the cannulated dogs showed an increase in half-life over the values observed in the same dogs before surgery (40.6 *versus* 24.8 min at 20 mg/kg and 11.7 *versus* 6.9 min at 5 mg/kg, respectively). Liver dysfunction did not appear to be the explanation, since hematology values were still within normal limits. The remaining parameters (clearance, volume of distribution, and area under the plasma concentration-time curve) were unchanged.

Biliary excretion σ^- is plotted in Fig. 5. The abnormalities in the curve for the 30-mg/kg dose were due to the temporary clogging of the cannula. Combined with the urine output, the amount recovered ranged from 95.7 to 101.1% of the dose. The amount recovered from the bile ranged from 92.3 to 98.9% of the dose. The σ^- plot appeared to be linear for all doses. There was no statistical difference ($p < 0.05$) between the half-lives at all doses (mean harmonic half-life = 163 min). Rate plots were also constructed, but were difficult to interpret. The biliary excretion rate data will be discussed briefly in another report (28).

Urinary Excretion Data—The amount of I recovered in urine from the intravenous and biliary excretion studies ranged from 1.5 to 7.2%. These data were considered significant in the pharmacokinetic interpretation of I and were used only for mass balance recovery purposes.

DISCUSSION

The plasma data presented in Fig. 1 and Table I clearly indicate that the rate of I elimination from plasma is dose dependent, and the rapid increase in AUC with increasing dose seems to suggest some saturable process. Since 95-101% of the dose was recovered as unchanged drug, it appears that the dose dependency is not due to I metabolism. Takada *et al.* (8) found that metabolic inhibitors did not affect the liver uptake of I in rats, suggesting that the dose dependence is not due to saturation of an active transport system. The fact that the extent of plasma protein binding of I remains essentially constant over the dose range indicates that the dose-dependent elimination kinetics are not due to changes in plasma protein binding. The data shown in Fig. 2 further suggest that, since the first dose was essentially eliminated from the plasma, the observed dose dependency may be due to the binding of I in other tissues. Accordingly, the binding of I to liver protein fractions was investigated.

The peak assignments (as discussed in the *Results*) in Fig. 4a and b are supported by earlier studies (13-15), but differ from those reported by Takada *et al.* (9). In the present study, each I peak corresponds to a protein peak while in the work of Takada *et al.* (9) the I supposedly bound to the Z-fraction did not have a corresponding protein peak; the I peak we have identified with the Z-fraction was labeled free I in their work (9). We observed free I eluting at much later times than are plotted (Fig. 4). Takada and co-workers also identified a fraction, T-binder, which elutes at a time similar to the Z-fraction. It is possible that this peak was masked by the large Z-fraction peaks in Fig. 4a and b. Since the only difference in methodology between our study and that of Takada *et al.* appeared to be the strain of rat (Sprague-Dawley in this study, Wistar in their work), further investigation may be warranted, because it is unlikely that strain differences would account for these discrepancies.

The data summarized in Table III indicate that neither competitor interfered with I binding to the Y-fraction and that probenecid competed with I for Z-fraction binding sites while phenylbutazone did not. Since both probenecid and I are anionic at physiological pH while phenylbutazone is neutral, these findings tend to support the hypothesis (21) of the existence of separate pathways for the biliary uptake and elimination of charged and neutral species.

We found that the amount of I bound to the Y-fraction is far smaller than the amount bound to the Z-fraction. This tends to support the earlier hypothesis (8, 9) that organic anions are taken up by the liver *via* two pathways (binding to the Y- and Z-fractions), one of which (Y-fraction) is of limited capacity and easily saturable. Once the Y-fraction is saturated, I is still eliminated from the plasma at a reduced, but apparently first-order, rate through uptake by the large-capacity Z-fraction.

The increased I plasma half-life following administration of probenecid appears to be due to competition for the Z-binding sites involved in the uptake process. The increased I plasma half-life following administration of phenylbutazone appears to be due to the displacement of I from plasma proteins

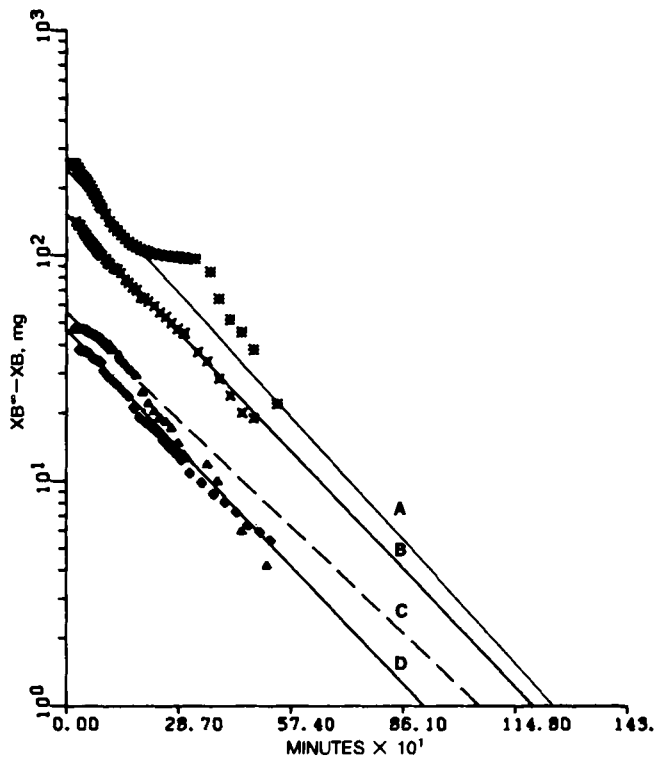

Figure 5—σ^- *Plot of I elimination in bile after doses of 30 mg/kg (A), 20 mg/kg (B), and 5 mg/kg (C) to dog C and a 5-mg/kg to dog B (D).*

and the subsequent increase in free I plasma concentrations, which saturate the uptake process in a manner similar to large doses of I.

Biliary excretion data obtained from rats (8–11) have often been of sufficient quality to enable the pharmacokinetic support of intrahepatic models such as that suggested above. Although our data was quite limited, it seems to suggest that data of sufficient quality may be difficult to obtain from dogs. The fact that the biliary excretion half-life was found not to vary with dose supports our contention that the changing plasma half-life reflects a saturable hepatic uptake rather than an elimination process.

REFERENCES

(1) F. A. Burgener, H. W. Fischer, and T. D. Kenyon, *Invest. Radiol.*, **13**, 255 (1978).

(2) A. A. Moss, S. K. Lin, E. R. Margules, R. W. Motson, and S. Ricgelman, *Invest. Radiol.*, **14**, 171 (1979).

(3) F. A. Burgener and H. W. Fischer, *Invest. Radiol.*, **14**, 502 (1979).

(4) R. Nagashima, G. Levy, and E. J. Sarcione, *J. Pharm. Sci.*, **57**, 1881 (1968).

(5) B. F. Scharschmidt, J. G. Waggoner, and P. D. Berk., *J. Clin. Invest.*, **56**, 1280 (1975).

(6) M. Schwenk, *Arch. Toxicol.*, **44**, 113 (1980).

(7) S. Agoston, M. C. Houwertjes, and P. J. Salt, *Br. J. Pharmacol.*, **68**, 637 (1980).

(8) K. Takada, Y. Mizobuchi, and S. Muranishi, *Chem. Pharm. Bull.*, **22**, 922 (1974).

(9) K. Takada, M. Ueda, M. Ohno, and S. Muranishi, *Chem. Pharm. Bull.*, **22**, 1477 (1974).

(10) K. Takada, S. Muranishi, and H. Sezaki, *J. Pharmacokinet. Biopharm.*, **2**, 495 (1974).

(11) R. J. Wills, R. B. Smith, and G. J. Yakatan, *J. Pharm. Sci.*, **72**, 1127 (1983).

(12) J. H. Kim and S. K. Hong, *Am. J. Physiol.*, **202**, 174 (1962).

(13) A. J. Levi, F. Gatmaitan, and I. M. Arias, *J. Clin. Invest.*, **48**, 2156 (1969).

(14) H. Reyes, A. J. Levi, Z. Gatmaitan, and I. M. Arias, *J. Clin. Invest.*, **50**, 2242 (1971).

(15) W. H. Habig, M. J. Pabst, G. Fleischner, Z. Gatmaitan, I. M. Arias, and W. B. Jakoby, *Proc. Natl. Acad. Sci. USA*, **71**, 3879 (1974).

(16) R. Erttman and K. H. Damn, *Arch. Int. Pharmacodyn.*, **211**, 197 (1974).

(17) R. P. G. Dayton, S. A. Cucinell, M. Weiss, and J. M. Perel, *J. Pharmacol. Exp. Ther.*, **158**, 305 (1967).

(18) P. M. Aggeles, R. A. O'Railly, L. Leong, and P. E. Kowitz, *N. Engl. J. Med.*, **276**, 496 (1967).

(19) M. H. Solovion and J. J. Schrogie, *Biochem. Pharmacol.*, **16**, 1219 (1967).

(20) B. W. Madsen and P. D. Tearne, *Life Sci.*, **26**, 173 (1967).

(21) L. D. Schanker, "Handbook of Chemistry," Vol. 5, 1st ed., American Physiological Society, Washington, D.C., p. 2433 (1968).

(22) H. Kitagawa, T. Kamataki, and S. Yoshida, *Chem. Pharm. Bull.*, **16**, 2320 (1968).

(23) O. H. Lowry, N. J. Rosebrough, A. L. Farr, and R. J. Randall, *J. Biol. Chem.*, **193**, 265 (1951).

(24) Y. Sugiyama, T. Iga, S. Awazu, and M. Hanano, *J. Pharm. Dyn.*, **2**, 193 (1979).

(25) C. M. Metzler, G. L. Elfring, and H. J. McEwen, "A Users Manual for NONLIN and Associated Programs," The Upjohn Co., Kalamazoo, Mich., 1974.

(26) M. Gibaldi and D. Perrier, in "Pharmacokinetics," Vol. 1, 1st ed., J. Swarbrick, Ed., Dekker, New York, N.Y., 1975, pp. 293–296.

(27) L. Z. Bennet and R. L. Galeazzi, *J. Pharm. Sci.*, **68**, 1071 (1979).

(28) R. S. Pearlman, G. J. Yakatan, and R. J. Wills, *J. Pharm. Sci.*, **73**, 932 (1984).

ACKNOWLEDGMENTS

Presented at the APhA meeting in St. Louis, 1981. The authors would like to thank Mr. J. Wiley and Ms. Ann Black for their assistance in the bile cannulation studies and Mrs. Judith Webster for the typing of this manuscript.

Effect of Nonuniform Bile Flow Rate on the Rate of Biliary Excretion of Bromophenol Blue in the Beagle

ROBERT S. PEARLMAN ˣ, GERALD J. YAKATAN §, and ROBERT J. WILLS *

Received September 17, 1982, from the *College of Pharmacy, The University of Texas, Austin, Texas 78712.* Accepted for publication May 26, 1983.

Present addresses: *Hoffmann-La Roche Inc., Department of Pharmacokinetics and Biopharmaceutics, Nutley, New Jersey 07110 and §Warner-Lambert Co., Pharmaceutical Research Division, Morris Plains, NJ 07950.

Abstract □ Following the intravenous administration of bromophenol blue to beagle dogs, graphs of the biliary excretion rate *versus* time displayed drastic fluctuations which render them of little value for standard pharmacokinetic modeling purposes. It was shown that these fluctuations in excretion rate are highly correlated with corresponding fluctuations in the bile flow rate. An expression was derived which accounts for the primary effect of nonuniform bile flow rate on the biliary excretion rate. This treatment would enable the use of such biliary excretion rate data for pharmacokinetic modeling. Secondary effects of nonuniform bile flow on the biliary excretion rate are also discussed. It is suggested that the modeling of other flow rate-dependent elimination processes could benefit from such a treatment.

Keyphrases □ Bromophenol blue—biliary excretion, nonuniform bile flow rate, dogs □ Biliary excretion—bromophenol blue, dogs, nonuniform bile flow rate □ Bile flow rate—nonuniform, biliary excretion of bromophenol blue, dogs

Biliary excretion has long been a subject of intensive investigation (1). Within the past decade, there has been an increase in the number of studies in which the bile duct has been cannulated to permit the determination of drugs and metabolites in the bile. These studies typically involve collecting bile samples at relatively long intervals and, usually, the cumulative amounts of drug excreted are reported as a function of time (2–5). These studies have been particularly useful in assessing the magnitude of the first-pass effect and the role of hepatobiliary elimination in the overall elimination of a wide variety of compounds (1). More recently, it has been shown that high-quality bile data can provide pharmacokinetic support for an intrahepatic model for hepatobiliary elimination in rats (6, 7). Takada *et al.* (7) obtained biliary excretion rate data (mg/h *versus* time) of sufficient quality to enable a statistically significant fit to a tetraexponential function, which they identified with a five-compartment model for hepatobiliary transport.

The possibility of obtaining similar data in higher animals is appealing, yet the problem must be viewed somewhat pessimistically due to the fact that the bile flow rate fluctuates

0022-3549/84/0700-0932$01.00/0

© 1984, American Pharmaceutical Association

and the subsequent increase in free I plasma concentrations, which saturate the uptake process in a manner similar to large doses of I.

Biliary excretion data obtained from rats (8–11) have often been of sufficient quality to enable the pharmacokinetic support of intrahepatic models such as that suggested above. Although our data was quite limited, it seems to suggest that data of sufficient quality may be difficult to obtain from dogs. The fact that the biliary excretion half-life was found not to vary with dose supports our contention that the changing plasma half-life reflects a saturable hepatic uptake rather than an elimination process.

REFERENCES

(1) F. A. Burgener, H. W. Fischer, and T. D. Kenyon, *Invest. Radiol.*, **13**, 255 (1978).

(2) A. A. Moss, S. K. Lin, E. R. Margules, R. W. Motson, and S. Ricgelman, *Invest. Radiol.*, **14**, 171 (1979).

(3) F. A. Burgener and H. W. Fischer, *Invest. Radiol.*, **14**, 502 (1979).

(4) R. Nagashima, G. Levy, and E. J. Sarcione, *J. Pharm. Sci.*, **57**, 1881 (1968).

(5) B. F. Scharschmidt, J. G. Waggoner, and P. D. Berk., *J. Clin. Invest.*, **56**, 1280 (1975).

(6) M. Schwenk, *Arch. Toxicol.*, **44**, 113 (1980).

(7) S. Agoston, M. C. Houwertjes, and P. J. Salt, *Br. J. Pharmacol.*, **68**, 637 (1980).

(8) K. Takada, Y. Mizobuchi, and S. Muranishi, *Chem. Pharm. Bull.*, **22**, 922 (1974).

(9) K. Takada, M. Ueda, M. Ohno, and S. Muranishi, *Chem. Pharm. Bull.*, **22**, 1477 (1974).

(10) K. Takada, S. Muranishi, and H. Sezaki, *J. Pharmacokinet. Biopharm.*, **2**, 495 (1974).

(11) R. J. Wills, R. B. Smith, and G. J. Yakatan, *J. Pharm. Sci.*, **72**, 1127 (1983).

(12) J. H. Kim and S. K. Hong, *Am. J. Physiol.*, **202**, 174 (1962).

(13) A. J. Levi, F. Gatmaitan, and I. M. Arias, *J. Clin. Invest.*, **48**, 2156 (1969).

(14) H. Reyes, A. J. Levi, Z. Gatmaitan, and I. M. Arias, *J. Clin. Invest.*, **50**, 2242 (1971).

(15) W. H. Habig, M. J. Pabst, G. Fleischner, Z. Gatmaitan, I. M. Arias, and W. B. Jakoby, *Proc. Natl. Acad. Sci. USA*, **71**, 3879 (1974).

(16) R. Erttman and K. H. Damn, *Arch. Int. Pharmacodyn.*, **211**, 197 (1974).

(17) R. P. G. Dayton, S. A. Cucinell, M. Weiss, and J. M. Perel, *J. Pharmacol. Exp. Ther.*, **158**, 305 (1967).

(18) P. M. Aggeles, R. A. O'Railly, L. Leong, and P. E. Kowitz, *N. Engl. J. Med.*, **276**, 496 (1967).

(19) M. H. Solovion and J. J. Schrogie, *Biochem. Pharmacol.*, **16**, 1219 (1967).

(20) B. W. Madsen and P. D. Tearne, *Life Sci.*, **26**, 173 (1967).

(21) L. D. Schanker, "Handbook of Chemistry," Vol. 5, 1st ed., American Physiological Society, Washington, D.C., p. 2433 (1968).

(22) H. Kitagawa, T. Kamataki, and S. Yoshida, *Chem. Pharm. Bull.*, **16**, 2320 (1968).

(23) O. H. Lowry, N. J. Rosebrough, A. L. Farr, and R. J. Randall, *J. Biol. Chem.*, **193**, 265 (1951).

(24) Y. Sugiyama, T. Iga, S. Awazu, and M. Hanano, *J. Pharm. Dyn.*, **2**, 193 (1979).

(25) C. M. Metzler, G. L. Elfring, and H. J. McEwen, "A Users Manual for NONLIN and Associated Programs," The Upjohn Co., Kalamazoo, Mich., 1974.

(26) M. Gibaldi and D. Perrier, in "Pharmacokinetics," Vol. 1, 1st ed., J. Swarbrick, Ed., Dekker, New York, N.Y., 1975, pp. 293–296.

(27) L. Z. Bennet and R. L. Galeazzi, *J. Pharm. Sci.*, **68**, 1071 (1979).

(28) R. S. Pearlman, G. J. Yakatan, and R. J. Wills, *J. Pharm. Sci.*, **73**, 932 (1984).

ACKNOWLEDGMENTS

Presented at the APhA meeting in St. Louis, 1981. The authors would like to thank Mr. J. Wiley and Ms. Ann Black for their assistance in the bile cannulation studies and Mrs. Judith Webster for the typing of this manuscript.

Effect of Nonuniform Bile Flow Rate on the Rate of Biliary Excretion of Bromophenol Blue in the Beagle

ROBERT S. PEARLMAN ˣ, GERALD J. YAKATAN §, and ROBERT J. WILLS *

Received September 17, 1982, from the *College of Pharmacy, The University of Texas, Austin, Texas 78712.* Accepted for publication May 26, 1983.

Present addresses: *Hoffmann-La Roche Inc., Department of Pharmacokinetics and Biopharmaceutics, Nutley, New Jersey 07110 and §Warner-Lambert Co., Pharmaceutical Research Division, Morris Plains, NJ 07950.

Abstract □ Following the intravenous administration of bromophenol blue to beagle dogs, graphs of the biliary excretion rate *versus* time displayed drastic fluctuations which render them of little value for standard pharmacokinetic modeling purposes. It was shown that these fluctuations in excretion rate are highly correlated with corresponding fluctuations in the bile flow rate. An expression was derived which accounts for the primary effect of nonuniform bile flow rate on the biliary excretion rate. This treatment would enable the use of such biliary excretion rate data for pharmacokinetic modeling. Secondary effects of nonuniform bile flow on the biliary excretion rate are also discussed. It is suggested that the modeling of other flow rate-dependent elimination processes could benefit from such a treatment.

Keyphrases □ Bromophenol blue—biliary excretion, nonuniform bile flow rate, dogs □ Biliary excretion—bromophenol blue, dogs, nonuniform bile flow rate □ Bile flow rate—nonuniform, biliary excretion of bromophenol blue, dogs

Biliary excretion has long been a subject of intensive investigation (1). Within the past decade, there has been an increase in the number of studies in which the bile duct has been cannulated to permit the determination of drugs and metabolites in the bile. These studies typically involve collecting bile samples at relatively long intervals and, usually, the cumulative amounts of drug excreted are reported as a function of time (2–5). These studies have been particularly useful in assessing the magnitude of the first-pass effect and the role of hepatobiliary elimination in the overall elimination of a wide variety of compounds (1). More recently, it has been shown that high-quality bile data can provide pharmacokinetic support for an intrahepatic model for hepatobiliary elimination in rats (6, 7). Takada *et al.* (7) obtained biliary excretion rate data (mg/h *versus* time) of sufficient quality to enable a statistically significant fit to a tetraexponential function, which they identified with a five-compartment model for hepatobiliary transport.

The possibility of obtaining similar data in higher animals is appealing, yet the problem must be viewed somewhat pessimistically due to the fact that the bile flow rate fluctuates

0022-3549/84/0700-0932$01.00/0

© 1984, American Pharmaceutical Association

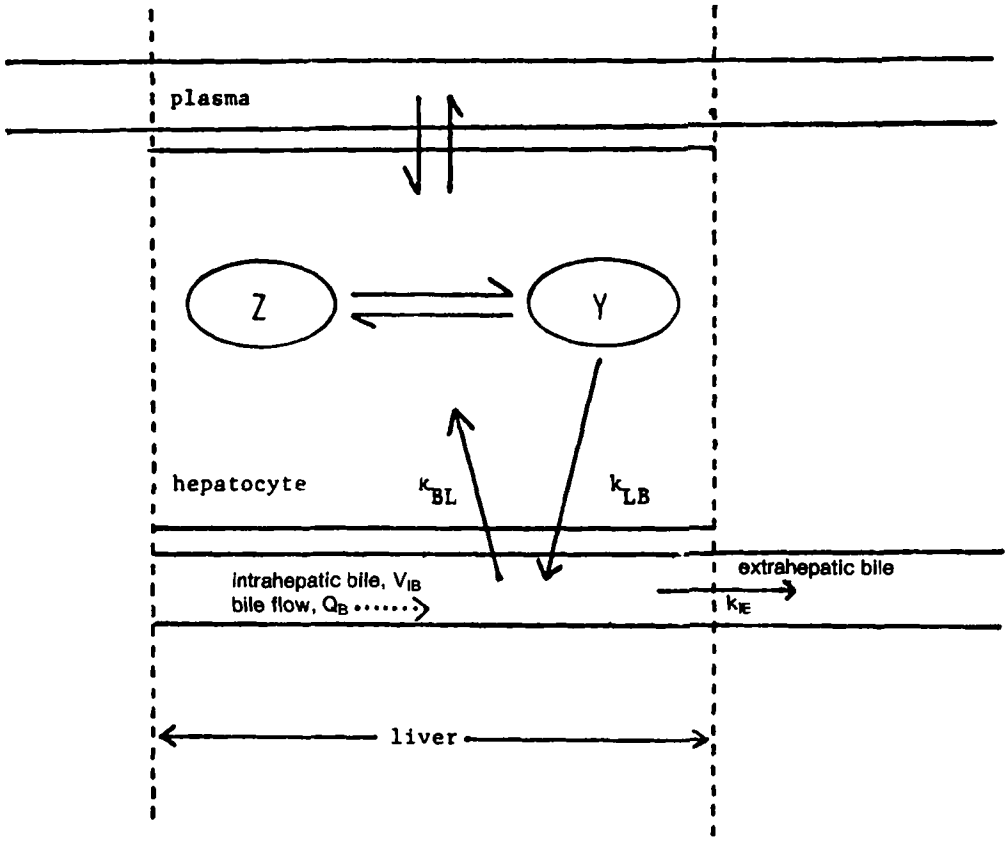

Figure 1—*Schematic representation of physiological transport and elimination via the hepatobiliary route. Y and Z represent two liver protein fractions which are involved in hepatobiliary transport (8).*

more markedly in higher animals than in the rat. The purpose of this brief communication is to present preliminary results which confirm that nonuniform bile flow rates seriously complicate the interpretation of biliary excretion rate data in the beagle dog. Possible explanations for the observed correlation between excretion rate and bile flow rate, as well as the basis for the development of a bile flow rate-dependent model for hepatobiliary transport, will be discussed.

THEORETICAL SECTION

To best treat excretion rate data, it will be necessary to develop a physical model of hepatobiliary transport which explicitly involves the biliary flow rate. Figure 1 depicts a simple model, similar to that suggested by Takada *et al.* (7) in that it distinguishes between intrahepatic and extrahepatic bile. The shaded region is intended to represent the bile canaliculus in contact with the hepatocytes. Let V_{IB} symbolize the volume of intrahepatic bile contained within the canaliculi and A_{IB} represent the amount of drug in intrahepatic bile. The transport of drug between the hepatocyte and intrahepatic bile is represented by k_{LB} and k_{BL}. If the bile production rate or flow rate, Q_B, were zero, then no drug would be excreted from the liver. The rate at which drug is actually excreted depends on the rate at which drug is eluted from the intrahepatic bile compartment, of volume V_{IB}, by newly produced bile flowing at a rate Q_B:

$$\frac{dA_{EB}}{dt} = k_{IE}A_{IB} = \frac{Q_B}{V_{IB}} \cdot A_{IB} \qquad \text{(Eq. 1)}$$

where A_{EB} is the cumulative amount of drug excreted in bile as a function of time and k_{IE} is the rate constant for transport from intrahepatic bile to extrahepatic bile[1]. In the event that Q_B is observed to vary between sample times, Eq. 1 could, as a first approximation, be assumed to hold over the individual sampling intervals. Thus, by dividing the fluctuating excretion rate by the fluctuating bile flow rate, estimation of pharmacokinetic parameters can be achieved by fitting the quotient to an expression for A_{IB}:

$$\frac{\text{excretion rate}}{\text{flow rate}} = \frac{(\Delta A_{EB})_j/\Delta t_j}{(Q_B)_j} = \frac{1}{V_{IB}} \cdot (A_{IB})_j \qquad \text{(Eq. 2)}$$

In Eq. 2, j is an index referring to the sampling interval, Δt, and V_{IB} is treated as a constant model parameter to be determined.

RESULTS

As described previously (9), bromophenol blue (I) was administered intravenously to three beagle dogs after they had each recovered from cannulation surgery. During surgery, the common bile duct was cannulated to permit collection of the total bile excreted and the gallbladder was removed to avoid bile storage and thus permit collection as the bile was produced. Bile salt dietary supplements[2] were given to maintain the body weight of each dog throughout the study.

The limited data obtained to date is shown in Figure 2a–d. The solid lines connect the biliary excretion rates of I plotted at the midpoints of the collection intervals and the dashed lines connect the corresponding bile flow rates. It is apparent that the fluctuations in the excretion rate correspond to fluctuations in the bile flow rate. It is also apparent that this excretion rate data is unsuitable for pharmacokinetic modeling in the present form.

By mathematically pooling successive samples, the rate plots can be smoothed to a considerable extent as shown in Fig. 3. In Fig. 3, the pooled collection intervals were 30 and, later, 60 min compared with actual collection intervals of 5, 10, and 15 min. Pooling the data smoothed the curve by replacing the rapidly fluctuating bile flow rate with an average flow rate. We should be somewhat critical of attempts to fit smoothed curves which are obtained by masking rather than explaining the details of the data. It should be noted that these details are analogous to excretion data when collected at longer sampling intervals.

Using Eq. 2, values for excretion rate divided by flow rate were generated and plotted, along with the excretion rate, against time (Fig. 4). It is apparent that this new treatment of bile data smoothed the curves to the extent that pharmacokinetic evaluation may be possible.

[1] Although the relationship $k_{IE} = Q_B/V_{IB}$ is discussed in any classical treatment of chromatography, the interested reader is referred to a pharmacokinetic application discussed by Gumtow *et al.* (8).

[2] Reheis Chemical Co., Tarrytown, N.Y.

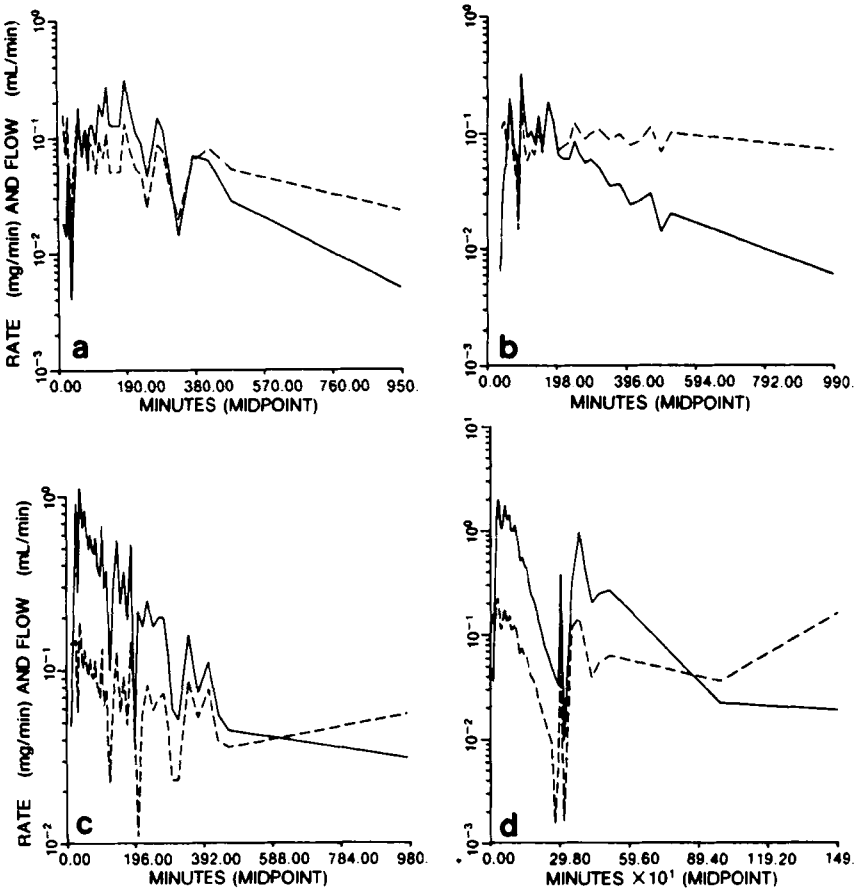

Figure 2—*Biliary excretion rate (—) and bile flow rate (- - -) of I following intravenous bolus injections of 5 mg/kg to dogs B (a) and C (b) and 20 (c) and 30 mg/kg (d) to dog C.*

DISCUSSION

Before addressing this apparent bile flow rate dependence, we note that limited information can be extracted from this data in a variety of ways. The excretion of drug in bile is somewhat analogous to the excretion of drug in urine, breast milk, sweat, saliva, and lacrimal fluid. Experimentally, we measure the accumulation (and rate of accumulation) of the amount of excreted drug in the excreted fluid, rather than the concentration, because the volume of the excreted fluid is changing. This could be contrasted with the treatment of plasma data, in which case we monitor the decreasing concentration of drug in an essentially constant volume of fluid.

In the preceding paper (9), we presented plots of the cumulative amount of bromophenol blue excreted as a function of time to indicate the extent to which various doses are eliminated through the bile, and we noted that σ^- plots of the same data seemed to suggest that the observed dose-dependent plasma elimination is due to a dose-dependent liver uptake rather than to a hepatobiliary elimination process. Both types of plots mask not only the random variability but the genuine detail (*i.e.*, fluctuations) in such excretion data (10). Excretion rate plots that provide a more precise presentation of the data are normally preferred, but as shown here, these may not be adequate for pharmacokinetic modeling.

In contrast, the data generated by Eq. 2 accounted for most of the effect of nonuniform bile flow rate and yield a graph to which one could fit a model-based expression for A_{1B}. It might be noted that the A_{1B} curve indicated in Fig. 4 is of the same shape as a corresponding curve (for X_4) that Takada *et al.* (7) simulated for a compartmental model which could be used to describe the physiological transfer processes indicated in Fig. 1. It should also be noted

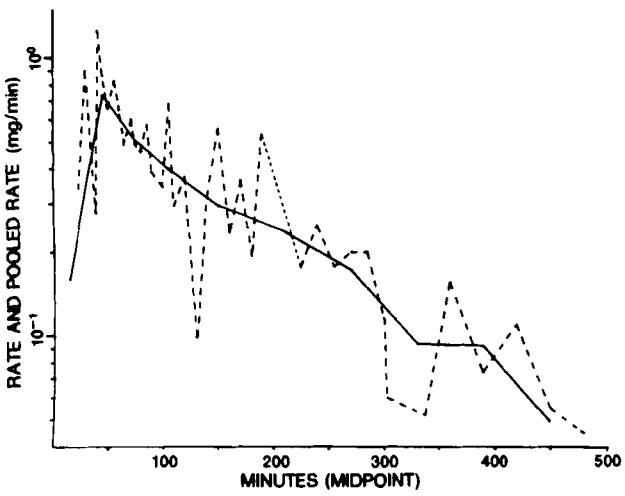

Figure 3—*Actual (- - -) and mathematically pooled (—) biliary excretion rate data for I following an intravenous bolus injection of 20 mg/kg. The small segment (· · ·) indicates missing data.*

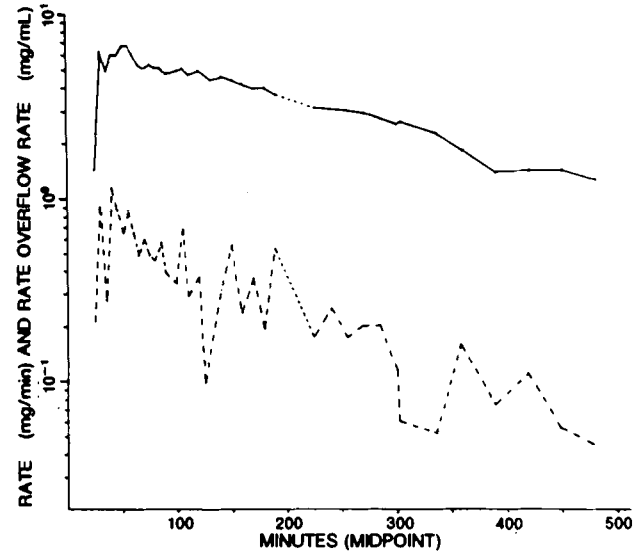

Figure 4—*Biliary excretion rate (- - -) and biliary excretion rate divided by bile flow rate (—) of I following intravenous bolus injection of 20 mg/kg. The small segments (· · ·) indicate missing data.*

that the fitting is complicated by the fact that A_{1B} is also dependent on k_{1E}, although far less markedly than A_{EB}.

We have chosen not to attempt such pharmacokinetic modeling at the present time, not only because of the incompleteness of our data but because additional analyses of the effects of nonuniform bile flow rate should be undertaken. It certainly appears that the primary effect of nonuniform bile flow rates is on k_{1E} and that our treatment of this effect describes the data. However, there are secondary effects which should also be addressed.

One example would be the effect of bile flow rate on the thickness of the diffusion layer adjacent to the bile canalicular membrane, which represents an additional barrier to the transport between the hepatocyte and intrahepatic bile. The diffusion layer thickness within a cylindrical tube is discussed by Levich (11) and it can be shown that $\delta \alpha v_0^{-1/3}$ (9), where δ is the diffusion layer thickness and v_0 is the maximum flow velocity at the axis of the tube. For a nonelastic tube of constant radius, v_0 is directly proportional to the flow rate, Q_B. Thus, passive diffusion between the hepatocyte and the canaliculi would proceed at a rate proportional to $Q_B^{1/3}$.

Nonuniform bile flow rates result in nonuniform hydrostatic pressure within the canaliculi (12), which, in turn, could affect the effective diameter of any pores existing in the canalicular membrane. If the transport between hepatocyte and intrahepatic bile involves pore filtration (12), then this secondary effect of nonuniform bile flow rates could become important. The relationship between pore size and pore filtration rate is discussed by Lakshminarayanaiah (13).

Lightfoot (14) discusses flow through elastic ducts and indirectly indicates the effect that flow rate might have on the rate of transport across the duct wall. It could also be pointed out that the elution approach discussed above is quantitatively correct only if there is perfect mixing within the intrahepatic bile compartment.

All of the secondary points mentioned above suggest that further analysis is required before biliary excretion data can be used to accurately describe a model for hepatobiliary uptake and elimination. However, if the objective is merely to use biliary excretion data to support a crude model which could be used for predictive (*i.e.*, dosing) purposes, then our treatment of nonuniform bile flow rate should be of some value.

Lastly, it should be noted that the elution approach discussed above could possibly be applied to other flow rate-dependent physiological processes. Whereas the effects of blood flow rate have received considerable attention in the pharmacokinetic literature, the effects of nonuniform flow rates on elimination *via* urine, milk, saliva, lacrimal fluid, *etc.* should account for some of the fluctuation or scatter frequently observed in that type of data.

REFERENCES

(1) W. G. Levine, *Am. Rev. Pharmacol. Toxicol.*, **18**, 81 (1978).

(2) S. K. Lin, A. A. Moss, R. Motson, and S. Riegelman, *J. Pharm. Sci.*, **67**, 930 (1978).

(3) M. J. Kreek, M. Kalisman, M. Irwin, N. F. Jaffery, and M. Scheflan, *Res. Commun. Chem. Path. Pharmacol.*, **29**, 67 (1980).

(4) D. Brewster, M. J. Humphrey, and M. A. McLeavy, *Xenobiotica*, **11**, 189 (1981).

(5) M. Yokota, T. Iga, Y. Sugiyama, A. Suyama, S. Awazu, and M. Hanano, *J. Pharm. Dyn.*, **4**, 287 (1981).

(6) W. J. O'Reilly, P. E. Coates, K. A. McMahon, E. Ting, and B. G. Priestly, *Life Sci.*, **11**, 197 (1972).

(7) K. Takada, S. Muranishi, and H. Sezaki, *J. Pharmacokinet. Biopharm.*, **2**, 495 (1974).

(8) R. Gumtow, D. Perrier, J. Heimiller, P. Blakely, and D. Nicoletti, *Am. J. Pharm. Ed.*, **38**, 560 (1974).

(9) R. J. Wills, G. J. Yakatan, and R. S. Pearlman, *J. Pharm. Sci.*, **73**, 928 (1984).

(10) H. G. Boxenbaum, S. Riegelman, and R. M. Elashoff, *J. Pharmacokinet. Biopharm.*, **2**, 123 (1974).

(11) V. G. Levich, "Physicochemical Hydrodynamics," Prentice-Hall, Englewood Cliffs, N.J., 1962, p. 115.

(12) R. L. Smith, "The Excretory Function of the Bile," Chapman and Hall, London, 1973, p. 12, 94.

(13) N. Lakshminarayanaiah, "Transport Phenomena in Membranes," Academic, New York, N.Y., 1969, p. 325.

(14) E. N. Lightfoot, "Transport Phenomena and Living Systems," Wiley, New York, N.Y., 1974, p. 80.

ACKNOWLEDGMENTS

Presented at the APhA meeting in Las Vegas, 1981. The authors thank Susan Christopher for the typing of this manuscript.

Radiotelemetric Method for Evaluating Enteric Coatings *In Vivo*

J. B. DRESSMAN *x and G. L. AMIDON *

Received April 4, 1983, from *INTERx, Merck Sharp & Dohme Research Laboratories, Lawrence, KS 66044.* Accepted for publication July 20, 1983. *Present address: College of Pharmacy, University of Michigan, Ann Arbor, MI 48109.

Abstract □ A radiotelemetric method for the *in vivo* evaluation of enteric coating performance is described, and its advantages and disadvantages are compared with those of other available methods. Hydroxypropyl methylcellulose phthalate was used as the test enteric coating. Four dogs were administered several batches of enteric-coated tablets containing buffers. Tablet disintegration was determined by radiotelemetric detection of the pH drop in the upper intestine due to release of the buffer. Premature rupture of the coating in the stomach was detected by a rise and then a fall in gastric pH prior to gastric emptying. The average gastric emptying time was 80 ± 18 min (*SEM*), while the average time for a tablet to disintegrate in the upper intestine was 14.2 ± 2 min. The average disintegration time was not affected by a change in the batch (for a given tablet core pH) or the dog used, suggesting that the method yielded readily reproducible results. Although there was little correlation with *in vitro* disintegration times, the method gave results similar to those reported in the literature for the same enteric coating in a human study. Of the formulations tested, it was concluded that buffering the core to pH 4 was most suitable for studying enteric coating performance.

Keyphrases □ Enteric coating—*in vivo* disintegration, radiotelemetry, hydroxypropyl methylcellulose phthalate □ Hydroxypropyl methylcellulose phthalate—*in vivo* disintegration, tablet coating, radiotelemetry □ Radiotelemetry—*in vivo* disintegration, hydroxypropyl methylcellulose phthalate tablet coating

Enteric coating of dosage forms has been used in several ways to improve drug delivery. For example, the bioavailability of acid-labile drugs such as erythromycin can be improved by avoiding exposure of the drug to the gastric contents (1). A second reason for using an enteric coating is to avoid gastric irritation caused by drugs such as aspirin (2). Enteric coating has also been used to delay the release of a drug taken at bedtime with the aim of ensuring therapeutic blood levels when the patient awakes (3).

Several methods are available for evaluating enteric coatings. A widely used *in vitro* test is the USP disintegration test for enteric-coated tablets (4). *In vivo* methods of following the

0022-3549/84/0700-0935$01.00/0

© 1984, American Pharmaceutical Association

that the fitting is complicated by the fact that A_{1B} is also dependent on k_{1E}, although far less markedly than A_{EB}.

We have chosen not to attempt such pharmacokinetic modeling at the present time, not only because of the incompleteness of our data but because additional analyses of the effects of nonuniform bile flow rate should be undertaken. It certainly appears that the primary effect of nonuniform bile flow rates is on k_{1E} and that our treatment of this effect describes the data. However, there are secondary effects which should also be addressed.

One example would be the effect of bile flow rate on the thickness of the diffusion layer adjacent to the bile canalicular membrane, which represents an additional barrier to the transport between the hepatocyte and intrahepatic bile. The diffusion layer thickness within a cylindrical tube is discussed by Levich (11) and it can be shown that $\delta \alpha v_0^{-1/3}$ (9), where δ is the diffusion layer thickness and v_0 is the maximum flow velocity at the axis of the tube. For a nonelastic tube of constant radius, v_0 is directly proportional to the flow rate, Q_B. Thus, passive diffusion between the hepatocyte and the canaliculi would proceed at a rate proportional to $Q_B^{1/3}$.

Nonuniform bile flow rates result in nonuniform hydrostatic pressure within the canaliculi (12), which, in turn, could affect the effective diameter of any pores existing in the canalicular membrane. If the transport between hepatocyte and intrahepatic bile involves pore filtration (12), then this secondary effect of nonuniform bile flow rates could become important. The relationship between pore size and pore filtration rate is discussed by Lakshminarayanaiah (13).

Lightfoot (14) discusses flow through elastic ducts and indirectly indicates the effect that flow rate might have on the rate of transport across the duct wall. It could also be pointed out that the elution approach discussed above is quantitatively correct only if there is perfect mixing within the intrahepatic bile compartment.

All of the secondary points mentioned above suggest that further analysis is required before biliary excretion data can be used to accurately describe a model for hepatobiliary uptake and elimination. However, if the objective is merely to use biliary excretion data to support a crude model which could be used for predictive (*i.e.*, dosing) purposes, then our treatment of nonuniform bile flow rate should be of some value.

Lastly, it should be noted that the elution approach discussed above could possibly be applied to other flow rate-dependent physiological processes. Whereas the effects of blood flow rate have received considerable attention in the pharmacokinetic literature, the effects of nonuniform flow rates on elimination *via* urine, milk, saliva, lacrimal fluid, *etc.* should account for some of the fluctuation or scatter frequently observed in that type of data.

REFERENCES

(1) W. G. Levine, *Am. Rev. Pharmacol. Toxicol.*, **18**, 81 (1978).

(2) S. K. Lin, A. A. Moss, R. Motson, and S. Riegelman, *J. Pharm. Sci.*, **67**, 930 (1978).

(3) M. J. Kreek, M. Kalisman, M. Irwin, N. F. Jaffery, and M. Scheflan, *Res. Commun. Chem. Path. Pharmacol.*, **29**, 67 (1980).

(4) D. Brewster, M. J. Humphrey, and M. A. McLeavy, *Xenobiotica*, **11**, 189 (1981).

(5) M. Yokota, T. Iga, Y. Sugiyama, A. Suyama, S. Awazu, and M. Hanano, *J. Pharm. Dyn.*, **4**, 287 (1981).

(6) W. J. O'Reilly, P. E. Coates, K. A. McMahon, E. Ting, and B. G. Priestly, *Life Sci.*, **11**, 197 (1972).

(7) K. Takada, S. Muranishi, and H. Sezaki, *J. Pharmacokinet. Biopharm.*, **2**, 495 (1974).

(8) R. Gumtow, D. Perrier, J. Heimiller, P. Blakely, and D. Nicoletti, *Am. J. Pharm. Ed.*, **38**, 560 (1974).

(9) R. J. Wills, G. J. Yakatan, and R. S. Pearlman, *J. Pharm. Sci.*, **73**, 928 (1984).

(10) H. G. Boxenbaum, S. Riegelman, and R. M. Elashoff, *J. Pharmacokinet. Biopharm.*, **2**, 123 (1974).

(11) V. G. Levich, "Physicochemical Hydrodynamics," Prentice-Hall, Englewood Cliffs, N.J., 1962, p. 115.

(12) R. L. Smith, "The Excretory Function of the Bile," Chapman and Hall, London, 1973, p. 12, 94.

(13) N. Lakshminarayanaiah, "Transport Phenomena in Membranes," Academic, New York, N.Y., 1969, p. 325.

(14) E. N. Lightfoot, "Transport Phenomena and Living Systems," Wiley, New York, N.Y., 1974, p. 80.

ACKNOWLEDGMENTS

Presented at the APhA meeting in Las Vegas, 1981. The authors thank Susan Christopher for the typing of this manuscript.

Radiotelemetric Method for Evaluating Enteric Coatings *In Vivo*

J. B. DRESSMAN *x and G. L. AMIDON *

Received April 4, 1983, from *INTERx, Merck Sharp & Dohme Research Laboratories, Lawrence, KS 66044.* Accepted for publication July 20, 1983. *Present address: College of Pharmacy, University of Michigan, Ann Arbor, MI 48109.

Abstract □ A radiotelemetric method for the *in vivo* evaluation of enteric coating performance is described, and its advantages and disadvantages are compared with those of other available methods. Hydroxypropyl methylcellulose phthalate was used as the test enteric coating. Four dogs were administered several batches of enteric-coated tablets containing buffers. Tablet disintegration was determined by radiotelemetric detection of the pH drop in the upper intestine due to release of the buffer. Premature rupture of the coating in the stomach was detected by a rise and then a fall in gastric pH prior to gastric emptying. The average gastric emptying time was 80 ± 18 min (*SEM*), while the average time for a tablet to disintegrate in the upper intestine was 14.2 ± 2 min. The average disintegration time was not affected by a change in the batch (for a given tablet core pH) or the dog used, suggesting that the method yielded readily reproducible results. Although there was little correlation with *in vitro* disintegration times, the method gave results similar to those reported in the literature for the same enteric coating in a human study. Of the formulations tested, it was concluded that buffering the core to pH 4 was most suitable for studying enteric coating performance.

Keyphrases □ Enteric coating—*in vivo* disintegration, radiotelemetry, hydroxypropyl methylcellulose phthalate □ Hydroxypropyl methylcellulose phthalate—*in vivo* disintegration, tablet coating, radiotelemetry □ Radiotelemetry—*in vivo* disintegration, hydroxypropyl methylcellulose phthalate tablet coating

Enteric coating of dosage forms has been used in several ways to improve drug delivery. For example, the bioavailability of acid-labile drugs such as erythromycin can be improved by avoiding exposure of the drug to the gastric contents (1). A second reason for using an enteric coating is to avoid gastric irritation caused by drugs such as aspirin (2). Enteric coating has also been used to delay the release of a drug taken at bedtime with the aim of ensuring therapeutic blood levels when the patient awakes (3).

Several methods are available for evaluating enteric coatings. A widely used *in vitro* test is the USP disintegration test for enteric-coated tablets (4). *In vivo* methods of following the

0022-3549/84/0700-0935$01.00/0

© 1984, American Pharmaceutical Association

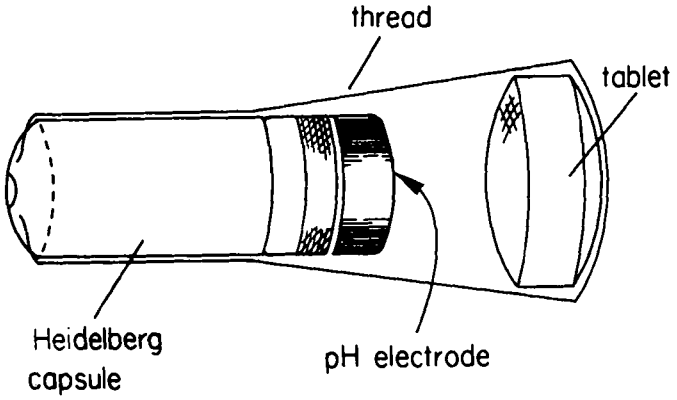

Figure 1—*Schematic for attachment of the enteric-coated tablet to the Heidelberg pH detector capsule.*

fate of dosage forms in the GI tract utilize techniques such as endoscopy (5), X-rays (3, 6), external scintigraphy (7-9), whole body scintillometry (10, 11), or a combination of these techniques (12). Pharmacokinetic data (13, 14) can also be used to estimate release times for enteric-coated products. The USP and similar *in vitro* tests have been compared with *in vivo* methods in several reports (3, 6, 15). Results indicate that *in vitro* tests tend to underestimate the disintegration time in the human GI tract. However, they provide an inexpensive and convenient way of screening the performance of the enteric coating. *In vivo* techniques have various advantages and disadvantages. The most obvious advantage is that the coating is tested under the actual conditions of use. Endoscopic, X-ray, and scintigraphic techniques have the added attraction of providing visual information. For endoscopy and X-ray techniques, data are collected at intervals rather than continuously, so exact gastric emptying and disintegration times cannot be obtained. With X-ray, scintillometry, and external scintigraphy, care must be taken to minimize exposure of the subject to radiation, although this is less of a problem in the latter cases. All the techniques for *in vivo* studies described above require either a skillful technical staff, expensive equipment, or both. Pharmacokinetic analyses of blood levels or urinary excretion data do not necessitate exposure to radiation, but there is the disadvantage of being unable to distinguish long gastric emptying times from slow enteric-coat dissolution times.

In the current report, a radiotelemetric method for the *in vivo* evaluation of enteric coatings is described, and its advantages and disadvantages are compared with those of other available methods.

EXPERIMENTAL SECTION

Tablets—Appropriate ratios of citric acid to citrate were chosen to formulate buffered tablet cores at pH 3, 4, and 5. The pH values were chosen so that disintegration/dissolution of the tablet in the upper intestine would produce an easily detectable pH drop (typically from pH ≥6 to the pH of the tablet buffers). In addition, if the coating failed, causing release of the buffers in the stomach, there would be a detectable upward shift in the gastric pH. The formula for pH 4 tablets is as follows: disodium citrate[1], 396 mg; citric acid[2], 144 mg; microcrystalline cellulose NF (PH 101)[3], 100 mg; modified cellulose gum[4], 64 mg; and lubricant[5], 14 mg.

After passing all the powders, except the lubricant, through a 40-mesh screen, they were mixed together and then wet granulated with a 50:50 mixture of ethanol–methylene chloride in a planetary blender[6]. The granules were dried at 55°C for 2 h, and the lubricant was added. Tablets weighing 720 mg were compressed using a single-punch tablet press[7]. The tablets were coated with hydroxypropyl methylcellulose phthalate[8] in a small laboratory pan coater. Other batches were prepared using the method outlined. To obtain a pH 3 buffering system, 192 mg of citric acid and 70 mg of sodium citrate[9] per tablet were used. For pH 5, the amounts were 64 mg and 290 mg, respectively. Coating weights varied from 20 to 34 mg per tablet, depending on the batch.

***In Vitro* Disintegration Test**—The USP disintegration test (4) for enteric-coated tablets was used to determine the *in vitro* disintegration time for each batch. Enzymes were omitted from the disintegration media; otherwise, the method was followed as described. Disintegration time was recorded as the time required, after transfer to simulated intestinal fluid, for all material to pass through the screen.

Animals—Four healthy male beagle dogs, ranging in weight from 10.6 to 17.3 kg, were selected for study. Before each experiment, the dogs were fasted for 24 h. Control GI pH profiles were obtained by administering a calibrated Heidelberg capsule[10] followed by 20 mL of water. The control profiles were used for comparison with profiles obtained after administering the enteric-coated tablets.

Radiotelemetric Technique—For each experiment, a Heidelberg capsule was calibrated using pH 1 and pH 7 standard buffer solutions. The enteric-coated tablet was then attached to the capsule with thread and acrylic glue (see Fig. 1). An antenna was strapped around the midriff of the dog to detect output from the Heidelberg capsule. The capsule–tablet combination was administered followed by 20 mL water, and the pH was continuously monitored using the radiotelemetric system[10] for a 6-h period. Important parameters such as baseline gastric pH, gastric emptying time, intestinal pH subsequent to gastric emptying, and time of onset of core disintegration were determined by analyzing the pH–time profile.

Statistical Analysis—The following statistical tests were applied to the data:

1. Linear regression to determine the degree of correlation between gastric emptying time and disintegration time, and between *in vivo* and *in vitro* disintegration time;
2. Analysis of variance to assess dog-to-dog, pH-to-pH, and batch-to-batch variation in the time of onset of disintegration *in vivo;*
3. Bartlett's test to analyze scatter differences between different groups of data in the *in vivo* tests.

Table I—Times for Onset of Disintegration of Enteric-Coated Buffered Tablets After Leaving the Stomach

Batch	Time for Onset, Min				
	Dog 62	Dog 72	Dog 73	Dog 74	Mean ± *SEM*
pH 3					
189/257	35	12 —[a]	—[b]	35	27.5 ± 7.5
194/080	20	10	13	11	13.5 ± 2.3
194/128	24	8	13	25	17.5 ± 4.2
pH 4					
189/096	6 18 —[a]	8 5	—[c] 5 10	40 8	12.5 ± 4.2
194/101	16	18	12	—[b]	15.3 ± 1.7
pH 5					
194/029	5	2	4	4	3.8 ± 0.6
Mean ± *SEM*	17.7 ± 3.9	9 ± 1.9	9.5 ± 1.6	20.5 ± 6.1	14.2 ± 2

Statistical Analysis		
Treatment	ANOVA	Bartlett's Test
Between dogs	NS	$p < 0.05$
Between pH values	$p < 0.05$	$p < 0.05$
Between batches at pH 3	NS	NS

[a] Failed in stomach. [b] Not tested. [c] Disintegration not observed.

RESULTS AND DISCUSSION

Performance of an enteric coating is evaluated by interpreting the pH profile generated by the radiotelemetric technique. Figure 2A shows a typical pH profile of the canine GI tract following administration of a Heidelberg capsule

[1] Fluka AG.
[2] Fisher Chemical Co.
[3] Avicel; FMC Corp.
[4] Type SD-711, Ac-Di-Sol; FMC Corp.
[5] Lubritab; Mendell.
[6] Model C100-T; Hobart Corp.
[7] Model 519-2; Stokes Equipment.
[8] HP-50; Shinetsu Chemical Co., Japan.
[9] Mallinckrodt.
[10] Telefunken, West Germany.

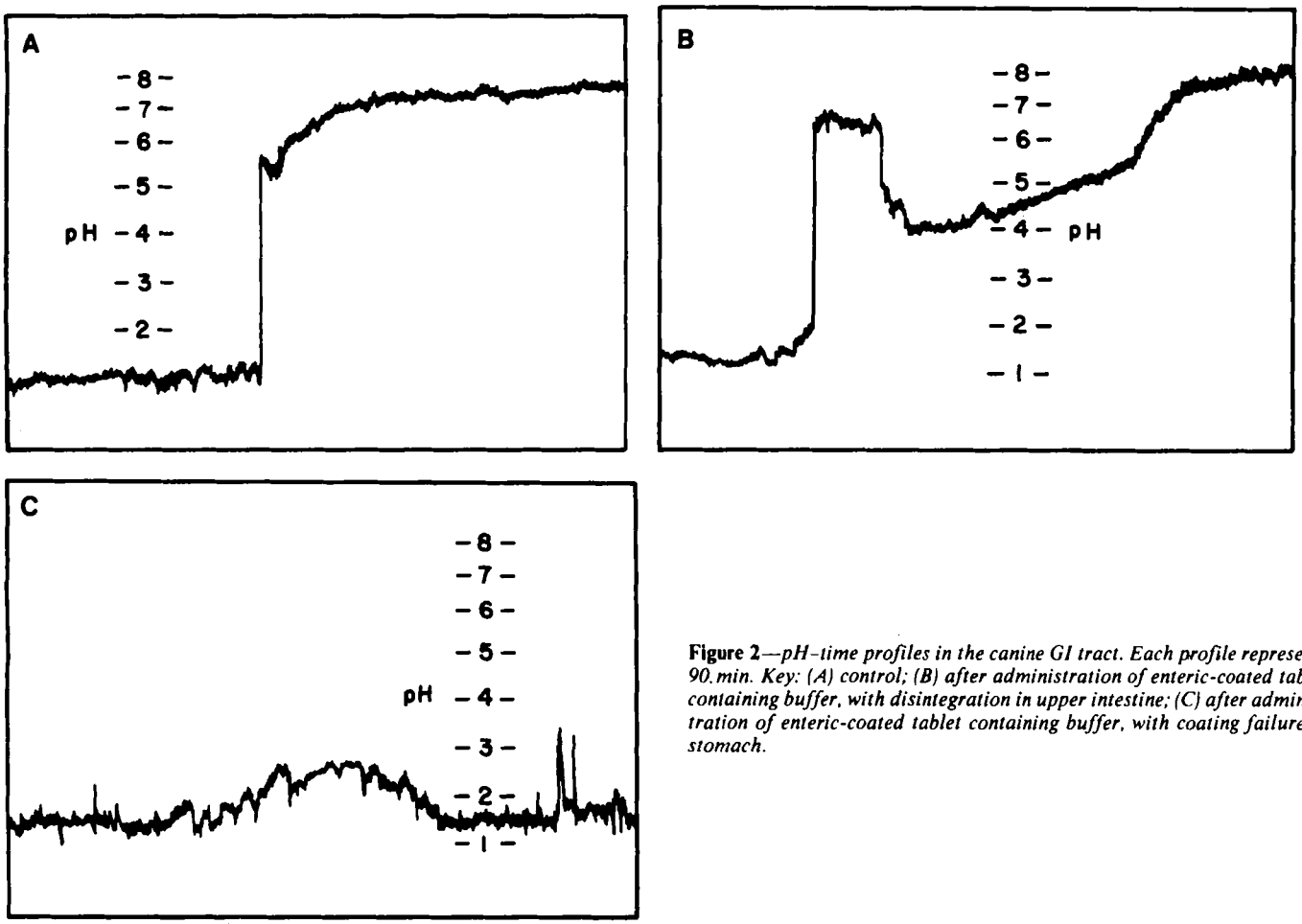

Figure 2—*pH-time profiles in the canine GI tract. Each profile represents 90 min. Key: (A) control; (B) after administration of enteric-coated tablet containing buffer, with disintegration in upper intestine; (C) after administration of enteric-coated tablet containing buffer, with coating failure in stomach.*

(control). In most cases, the gastric pH ranges from a pH slightly below pH 1 to ~2. Gastric emptying causes a sharp rise in pH to a value of 5.5–6.5, reflecting contact of the capsule with duodenal fluid. Thereafter, the pH rises gradually to ≥7.5. Note that the accurate measuring range of the Heidelberg capsule is pH 1–8, with a measuring error of ±0.5 pH units[11].

Unless the enteric coating ruptures prior to gastric emptying, the gastric pH after administration of an enteric-coated buffered tablet attached to a Heidelberg capsule is very similar to that observed in the control experiment. However, as shown in Fig. 2B, the pH profile in the upper intestine is altered distinctly when an enteric-coated buffered tablet is given. The pH rises at gastric emptying as in the control experiment, but when the coating dissolves the buffer materials are released and the pH drops rapidly. The time between gastric emptying and the start of the pH drop is designated as the time of onset of disintegration (t_{onset}). This method does not enable detection of completion of the core disintegration process. After the initial pH drop, there is a gradual rise in pH as the buffer materials are diluted and neutralized by secretion of bicarbonate ions until normal intestinal pH is recovered. Failure of the enteric coating to withstand gastric pH is detected by an increase in gastric pH from the baseline value, followed by a gradual return to the baseline value as shown in Fig. 2C.

A statistical analysis of the disintegration times for various formulations of enteric-coated buffered tablets in four dogs is presented in Table I. Twenty-nine tablets were administered: two failed in the stomach, one did not disintegrate within the observation period, and the rest disintegrated in the upper small intestine as expected. The mean disintegration time was 14.2 ± 2 min (*SEM*). Analysis of variance indicates that the mean disintegration time is not significantly different between dogs or between batches of tablets. However, there is a significant effect due to the tablet core pH ($p < 0.05$) with shorter mean disintegration time at pH 5 than at pH 3 or pH 4. Applying Bartlett's test to the results reveals that scatter in the disintegration time varies between dogs and between core pH values, but is not significantly affected (at a 95% confidence level) by the tablet batch. Overall, the statistical analysis suggests that the mean disintegration time is reproducible on both a dog-to-dog and batch-to-batch basis. Therefore, the radiotelemetric method is a reliable means of comparing enteric coating performance, provided tablet cores are formulated at the same pH. A convenient pH choice is pH 4, as in this case both gastric failure of the coat and disintegration of the coat in the upper intestine produce readily observable perturbations in pH.

The degree of correlation between *in vivo* and *in vitro* results can be judged by comparing the disintegration times presented in Table II. Linear regression analysis indicates that there is very little relationship between *in vivo* and *in vitro* disintegration test results ($r = -0.09$). The *in vivo* t_{onset} may be shorter, longer, or similar to the t_{disint} observed in the USP disintegration test for enteric-coated tablets; the times observed differed by as much as a factor of five. These results indicate that the USP test may not always be capable of predicting the *in vivo* performance of enteric coatings.

The extent of correlation between an *in vitro* test and results obtained *in vivo* depends on how closely the *in vitro* experimental conditions model the *in vivo* situation. Some specific differences between the USP test and the *in vivo* conditions encountered in this study include the following. The pH at which the hydroxypropyl methylcellulose phthalate coating used in this study begins to dissolve is pH 5.0[8]. The pH after gastric emptying in the dogs was typically between 5.5 and 6.5 (range 4.5–7.0), considerably lower than that of simulated intestinal fluid used in the *in vitro* test. This discrepancy in the *in vivo* and *in vitro* pH values, combined with the variation in the *in vivo* intestinal pH profile, may have contributed to the poor correlation in disintegration times for the coating studied. Another factor may have been the difference in the disintegration endpoints. *In vivo*, the t_{onset} was taken as the time

Table II—*In Vitro* and *In Vivo* Disintegration Times for Enteric-Coated Buffer Tablets[a]

Batch	pH	t_{disint} *in vitro*, s Mean ± *SEM*	*n*	t_{onset} *in vivo*, s Mean ± *SEM*	*n*
189/257	3	<600	3	1620 ± 456	3
194/080	3	3270 ± 118	6	810 ± 138	4
189/096	4	157 ± 10	6	750 ± 252	8
194/101	4	874 ± 102	6	918 ± 102	3
194/029	5	817 ± 71	6	225 ± 36	4

[a] Correlation coefficient = −0.09.

[11] Instruction Manual, Telefunken pH measurement system.

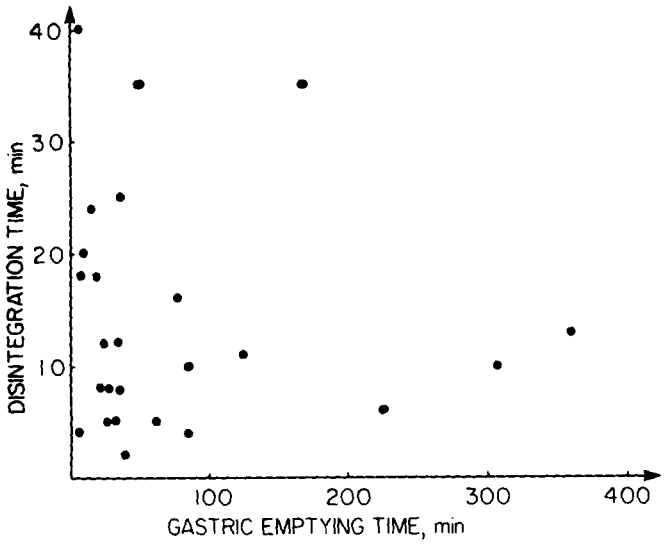

Figure 3—*Time of onset of disintegration of enteric-coated tablets in canine upper intestine* versus *gastric emptying time.*

when the pH first started to fall, whereas *in vitro* the time taken for complete disintegration was measured. Differences in other factors such as agitation and enzyme levels may also have played a role.

Two studies in the literature contain data which provide a comparison of disintegration times in humans with those observed in *in vitro* experiments (3, 14). In both cases the USP or similar test predicted shorter disintegration times than were observed *in vivo* [31 min *versus* >50 min (14), and <20 min *versus* 96 min mean disintegration time (3)]. A further study of *in vitro* and *in vivo* disintegration times of five batches of tablets in dogs (6) showed a variable ratio between *in vivo* and *in vitro* disintegration times, with up to a twofold difference in values. In that study, the batches were coated with different enteric coatings, so the variation between *in vivo* and *in vitro* results may have depended to some extent on the coating type. The value of *in vitro* disintegration tests has been further discussed by Aiache *et al.* (16).

In contrast to the poor *in vivo–in vitro* correlation, there appears to be some correlation between canine and human results. The data presented in this paper show that the average time for onset of disintegration in the canine upper intestine is 14.2 ± 2 min. This time compares closely with the time reported for disintegration in humans of tablets coated with hydroxypropyl methylcellulose phthalate. Using an endoscopic technique, Ehrhardt *et al.* (5) reported a disintegration time of 15 min after gastric emptying. This agreement suggests that use of the radiotelemetric technique in dogs gives a reasonable prediction of disintegration times in humans, at least for hydroxypropyl methylcellulose phthalate-coated tablets.

It has been proposed in the literature that the disintegration time may be dependent on the gastric emptying time. Blythe *et al.* (3) suggested that disintegration time is shorter for tablets which reside in the stomach for a long time than for those which are emptied quickly. In the current study, however, there was no significant correlation ($r = -0.08$) between gastric emptying time and disintegration time (Fig. 3).

The main advantage of the radiotelemetric method over other available methods is that the onset of disintegration of the enteric-coated tablet in the upper intestine can be accurately determined since the pH of the luminal contents is monitored continuously. It is also possible to pinpoint coating failures such as rupture in the stomach and nondisintegration in the intestine. The technique does not expose the subject or the investigators to radiation, as do other commonly used techniques. Because the dimensions of the Heidelberg capsule are fairly small (diameter, 7 mm; length, 20 mm) there is little chance of obstruction in the GI tract; no obstruction problems were encountered in the dogs studied. The Heidelberg capsule has little apparent effect on the gastric emptying of single-unit dosage forms; in the current study mean gastric-emptying time for the capsule-tablet combination was 80 ± 18 min (*SEM*) with a range of 5–360 min compared with a range of <30 min to >7 h (median 96 min) for tablets in the radiographic study by Blythe *et al.* (3).

The chief limitation of the method described in this report is that it is applicable only to monolithic dosage forms. A way of attaching more than one particle to the Heidelberg capsule must be devised, so that the method can be extended to evaluating enteric coat performance on multiparticulates. The fact that buffers must be incorporated into the test dosage form presents no more of a limitation than including barium in tablets to be evaluated by X-ray or γ-emitters in tablets studied by scintigraphic techniques. The advantages over pharmacokinetic methods lie in the greater accuracy with which the disintegration time can be determined and in avoiding blood or urine collection. The radiotelemetric technique requires less experimental expertise and less expensive equipment than other techniques and provides a facile and accurate means of evaluating enteric coating performance *in vivo.*

REFERENCES

(1) P. J. MacDonald, L. E. Mather, and M. J. Story, *J. Clin. Pharmacol.*, **17**, 601 (1977).

(2) F. L. Lanza, G. L. Royer, Jr., and R. S. Nelson, *N. Engl. J. Med.*, **303**, 136 (1980).

(3) R. H. Blythe, G. M. Grass, and D. R. MacDonell, *Am. J. Pharm.*, **131**, 206 (1959).

(4) "The United States Pharmacopeia," 20th rev., U.S. Pharmacopeial Convention, Inc., Rockville, Md., 1980, p. 958.

(5) L. Ehrhardt, V. Hartmann, and L. Patt, *Deutsche Apotheker-Zeitung*, **112**, 2005 (1972).

(6) J. G. Wagner, W. Veldkamp, and S. Long, *J. Am. Pharm. Assoc., Sci. Ed.*, **47**, 681 (1958).

(7) G. A. Digenis in "Radio-nuclide Imaging in Drug Research," C. G. Wilson, J. G. Hardy, M. Frier, and S. S. Davis, Eds., Croom Helm, London, 1982, p. 103.

(8) M. C. Theodorakis, D. R. Simpson, D. M. Leung, and M. Devous, *J. Pharm. Sci.*, **72**, 130 (1983).

(9) S. A. Müller-Lissner and A. L. Blum, *N. Engl. J. Med.*, **304**, 1365 (1981).

(10) G. Hecht, J. E. Christian, and G. S. Banker, *J. Pharm. Sci.*, **55**, 678 (1966).

(11) J. A. Clements, R. C Heading, W. S. Nimmo, and L. F. Prescott, *Clin. Pharm. Ther.*, **24**, 420 (1978).

(12) K. J. Palin, D. R. Whalley, C. G. Wilson, S. S. Davis, and A. J. Phillips, *Int. J. Pharm.*, **12**, 315 (1982).

(13) R. A. Upton, J. R. Powell, T. W. Guentart, J-P Thiercelin, L. Sansom, P. E. Coates, and S. Riegelman, *J. Pharmacokinet. Biopharm.*, **8**, 151 (1980).

(14) L. C. Lappas and W. McKechan, *J. Pharm. Sci.*, **56**, 1257 (1967).

(15) J. G. Wagner, W. Veldkamp, and S. Long, *J. Am. Pharm. Assoc., Sci. Ed.*, **49**, 128 (1960).

(16) J. M. Aiache, S. Aiache, A. Jeanneret, and F. Cornat, *Boll. Chim. Farm.*, **114**, 636 (1975).

ACKNOWLEDGMENTS

Many thanks to Karen Engle for aid in designing and conducting the *in vivo* studies and to Pam Liepitz for typing the manuscript.

Dissolution Studies of Some Sustained-Release Theophylline Dosage Forms

KEITH J. SIMONS *x, F. ESTELLE R. SIMONS ‡, KIM D. PLETT *, and CHARLES SCERBO *

Received February 8, 1983, from the **Faculty of Pharmacy, and ‡Department of Pediatrics, Faculty of Medicine, University of Manitoba, Winnipeg, Manitoba, R3T 2N2 Canada.* Accepted for publication September 19, 1983.

Abstract □ Dissolution studies were carried out with the USP rotating-basket apparatus in both simulated gastric and intestinal fluids. Four different brands of sustained-release theophylline products of different strengths (nine formulations) were studied. The percentage of the dose released in 1 h in gastric fluid ranged from (mean ± *SD*) 6.6 ± 0.9 to 50.1 ± 3.8%. By 6 h, the percentage of the dose released ranged from 10.8 ± 1.8 to 86.5 ± 5.2%. Similar formulations of different strengths released significantly different fractions of their dose at respective sampling times. In intestinal fluid, some formulations released 100% of their dose within 3–4 h, behaving more like enteric-coated preparations. One dosage form appeared to release drug by an apparent zero-order rate. From one brand of theophylline (two strengths), only 48.1 ± 5.6 and 29.9 ± 4.1% of label strength, respectively, dissolved in 25 h in intestinal fluid. Some of these *in vitro* results were rank-correlated to previously reported bioavailability and pharmacokinetic studies.

Keyphrases □ Sustained-release formulations—dissolution, USP rotating-basket apparatus, theophylline □ Theophylline—dissolution, sustained-release formulations, USP rotating-basket apparatus, □ Bioavailability—theophylline, sustained-release formulations, USP rotating-basket apparatus

The importance of using sustained-release theophylline dosage forms for the treatment of respiratory diseases in adults (1–4) and children (5–9) is well established. The absorption characteristics of many sustained-release theophylline products have been defined by several investigators (10, 11), and correlations with *in vitro* dissolution studies have been described (12, 13). However, disintegration and dissolution tests are still the compendial standards of content release and uniformity (14), and only minimal data for theophylline sustained-release products are available. Therefore, dissolution studies were performed on several sustained-release dosage forms, some of which have already been evaluated for bioavailability and pharmacokinetic characteristics (10, 15).

EXPERIMENTAL SECTION

Dosage Forms—Nine commercially available sustained-release theophylline dosage forms were evaluated. Products A[1], B[1], C[2], and D[2] were capsule forms, and products E[3], F[3], G[3], H[4], and J[4] were tablets.

Dissolution Apparatus—The USP rotating-basket dissolution apparatus (14) was used in all experiments. Studies were carried out in simulated gastric or intestinal fluids. Simulated gastric fluid was prepared by dissolving 2 g of NaCl[5] and 3.2 g of pepsin[5] in 7 mL of concentrated HCl[6] and sufficient water to make 1000 mL; the pH of this solution was 1.2. Simulated intestinal fluid was prepared by dissolving 6.8 g of KaH_2PO_4[5] in 250 mL of water. To this were added 190 mL of 0.2 M NaOH[5] and 400 mL of water. The solution was thoroughly mixed, 10 g of pancreatin[5] was added, and the pH was adjusted to 7.5 ± 0.1 with 0.2 M NaOH before the volume was made up to 1000 mL with water.

Procedure—In each study, six dosage forms were tested simultaneously, with one dosage form in each position of the dissolution apparatus. The dosage forms were not added until 900 mL of the solution had reached 37°C in a water bath. This temperature was maintained throughout the study. The baskets were rotated at 100 rpm. All dosage forms were tested in both simulated gastric and intestinal fluids under sink conditions. In simulated gastric fluid studies, 1-mL samples were removed at 0.5- or 1-h intervals for up to 6 h. In simulated intestinal fluid, the sampling times were adjusted so that the rate of release of theophylline from each different dosage form could be optimally evaluated. For dosage forms A, B, E, F, and G, 3-mL samples were removed at 1-h intervals for 12 h and at 25 h. For dosage forms C and D, 3-mL samples were removed every 15 min for a total of 3 h. For dosage forms H and J, 3-mL samples were removed at 10, 20, 30, 40, 50, 60, 75, 90, 105, 120, and 240 min. Samples were not filtered, as no particles were observed, and the volume of sample removed was replaced by fresh dissolution medium at 37°C. All samples were refrigerated until the theophylline content was determined by a spectrophotometric or HPLC procedure (15).

Theophylline Quantitation—Stock solutions of theophylline were prepared in simulated gastric or intestinal fluid at concentrations of 5, 10, 15, 20, and 25 μg/mL. The theophylline content in gastric fluid samples was determined by diluting the samples 2–20 times with gastric fluid and measuring the absorbance at 271 nm[7]. Appropriately diluted simulated gastric fluid samples were used as a reference.

In simulated intestinal fluid samples, the theophylline content had to be extracted before the absorbance could be determined spectrophotometrically. A 0.5-mL aliquot of 2.5 M acetate[5] buffer (pH 6.4) and 6 mL of chloroform–isopropyl alcohol[5] (20:1) were added to 2-mL samples of intestinal fluid.

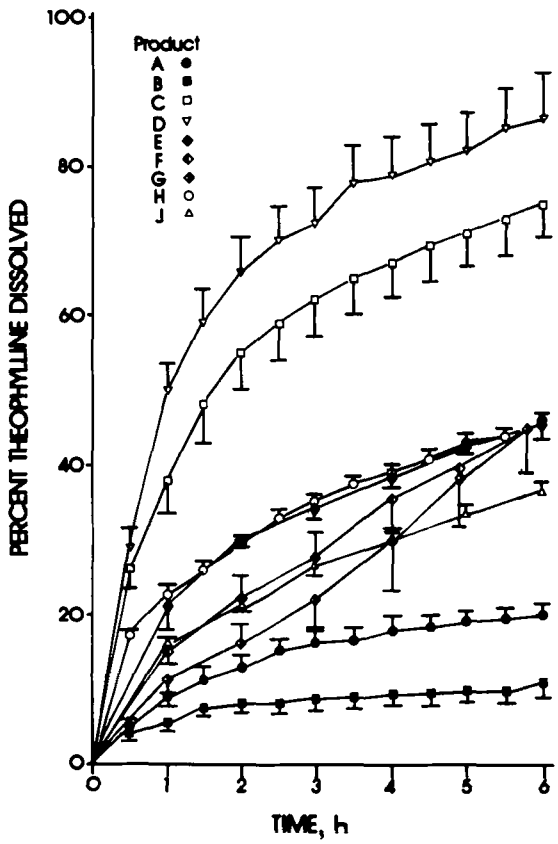

Figure 1—*Percent theophylline dissolved in simulated gastric fluid* versus *time. Results are mean + or − SD; data are from six dosage forms.*

[1] Acrolate 65- and 130-mg capsules; Fleming & Co., Fenton, Mo.
[2] Slo-phyllin 125- and 250-mg Gyrocaps; Dooner Labs, Ft. Washington, Pa.
[3] Theo-Dur 100-, 200-, and 300-mg S-A tablets; Astra Pharmaceuticals, Mississauga, Ontario, Canada L4X 1M4 (Key Pharmaceuticals, Inc., Miami, Fla.)
[4] Theo-Lair 250- and 500-mg SR tablets; Riker Labs., Northridge, Calif.
[5] Fisher Scientific Co., Fair Lawn, N.J.
[6] J. T. Baker Chemical Co., Phillipsburg, N.J.
[7] Acta III Spectrophotometer; Beckman Instruments, Inc., Palo Alto, Calif.

0022-3549/84/0700-0939$01.00/0
© 1984, American Pharmaceutical Association

Table I—Percent Theophylline Dissolved in Simulated Gastric Fluid at Various Times

Product	Theophylline Dissolved, %[a]											
	0.5 h	1.0 h	1.5 h	2.0 h	2.5 h	3.0 h	3.5 h	4.0 h	4.5 h	5.0 h	5.5 h	6.0 h
A	4.1 (0.9)	9.1 (1.7)	11.4 (1.6)	13.7 (1.8)	15.0 (1.8)	15.9 (1.8)	16.6 (1.7)	17.7 (1.9)	18.3 (1.5)	19.0 (1.6)	19.5 (1.5)	20.3 (1.5)
B	6.1 (0.8)	6.6 (0.9)	7.3 (0.8)	7.7 (1.1)	8.1 (1.3)	8.6 (1.2)	9.0 (1.3)	9.2 (1.3)	9.5 (1.6)	9.8 (1.5)	10.2 (1.7)	10.8 (1.8)
C	6.1 (2.8)	38.0 (4.6)	48.2 (5.0)	55.1 (4.9)	58.8 (5.0)	61.9 (5.2)	65.0 (4.9)	67.3 (4.8)	69.5 (4.9)	71.2 (4.7)	73.0 (5.1)	75.0 (4.5)
D	9.1 (2.4)	50.1 (3.8)	58.7 (4.8)	66.0 (4.4)	69.8 (4.8)	72.3 (4.3)	77.3 (5.6)	78.9 (5.0)	80.5 (5.2)	82.2 (4.9)	84.9 (5.4)	86.5 (5.2)
E	—[b]	21.2 (3.2)	—	29.6 (0.9)	—	34.0 (1.2)	—	39.4 (1.7)	—	43.5 (1.5)	—	46.1 (2.5)
F	—	14.8 (1.4)	—	21.8 (2.8)	—	26.8 (4.4)	—	35.3 (5.1)	—	39.4 (7.1)	—	45.6 (6.5)
G	—	11.2 (1.9)	—	15.8 (2.5)	—	22.4 (4.4)	—	30.6 (7.0)	—	38.2 (7.0)	—	45.0 (8.3)
H	7.3 (0.5)	22.8 (1.1)	26.2 (0.9)	29.4 (1.1)	33.2 (0.9)	35.3 (0.7)	37.3 (1.0)	38.9 (0.9)	41.1 (1.0)	42.8 (1.3)	44.0 (0.8)	45.9 (0.7)
J	—	15.8 (0.5)	—	21.2 (0.6)	—	26.3 (1.0)	—	30.1 (1.1)	—	33.7 (1.2)	—	36.6 (1.2)

[a] Mean values; *SD* in parentheses. [b] — Samples not collected.

Samples were extracted by shaking on a reciprocating shaker for 5 min and then centrifuging for 5 min. The upper aqueous phase was removed by aspiration, and 5 mL of the organic layer was extracted with 5 mL of 0.1 M NaOH[5] by shaking for 5 min and centrifuging for 10 min. The upper aqueous phase was transferred directly to a spectrophotometric cuvette, and the absorbance was measured at 271 nm[7]. Simulated intestinal fluid samples containing no drug and extracted by the same procedure were used as references.

Calibration curves were constructed by plotting absorbance *versus* theophylline concentration with simulated gastric and intestinal fluid stock solutions. Theophylline concentrations from studies of dosage forms E, F, and G were determined by an HPLC procedure described previously (15). Analytical procedures were compared, and results from both tests were identical.

RESULTS AND DISCUSSION

It is not usually possible to differentiate between structurally related compounds, such as decomposition products or metabolites, by spectrophotometric methods of analysis. However, for dissolution studies of a dosage form containing a single chemical entity, this spectrophotometric procedure had excellent sensitivity and specificity. Since the results from these spectrophotometric assays were identical to those obtained by HPLC analysis, it was assumed that no detectable decomposition occurred during these dissolution studies. In the gastric fluid medium, calibration curves were linear over the concentration range of 0–50 μg/mL, and through a 10-week period they had a maximum coefficient of variation of 9.6%. Nevertheless, calibration curves were determined daily for each set of analyses. Similar results were obtained for the intestinal fluid samples, with a maximum coefficient of variation of 10.6% over a 10-week period. The results from the HPLC procedure had a maximum coefficient of variation of 3.6%. In all individual curves, correlation coefficients were always >0.995.

The maximum dose of theophylline evaluated in these studies was 300 mg, and the volume of sample removed for analysis was replaced by fresh dissolution medium at 37°C, so that the 900-mL initial volume was always maintained. The solubility of theophylline at 25°C is 1 g/120 mL in distilled water (16), so that if the total 300-mg dose dissolved during the study, only 4% of the total solubility of theophylline would be achieved. Therefore, sink conditions were maintained in all studies (17).

The absolute bioavailability of orally administered theophylline in aqueous solutions was calculated to be 100%; absorption was rapid, with peak serum concentrations occurring at 1 h after dose administration (18). The rate and extent of theophylline absorption after administration of sustained-release products would, therefore, be controlled by the rate and extent of drug release from the dosage form. Also, since these dosage forms may contain larger doses of drug than conventional preparations, the rate and completeness of drug release from the matrix must be uniform and well controlled. Fluctuations in serum theophylline concentrations will then be minimal, and efficacy will be achieved without toxicity.

The efficacy and safety of most sustained-release theophylline dosage forms has been well documented (1–9). However, variability and incompleteness

Table II—Percent Theophylline Dissolved in Simulated Intestinal Fluid at Various Times

Product	Theophylline Dissolved, %[a]												
	1.0 h	2.0 h	3.0 h	4.0 h	5.0 h	6.0 h	7.0 h	8.0 h	9.0 h	10.0 h	11.0 h	12.0 h	25.0 h
A	3.0 (2.5)	6.4 (2.3)	11.5 (2.0)	14.2 (2.5)	18.4 (4.4)	19.5 (4.7)	21.6 (5.3)	24.4 (4.9)	26.2 (5.2)	28.8 (5.7)	32.1 (4.7)	37.1 (5.3)	48.1 (5.6)
B	7.1 (0.8)	11.2 (3.2)	14.7 (2.5)	17.8 (2.8)	19.9 (2.8)	22.3 (3.3)	22.3 (3.8)	23.5 (3.8)	23.3 (4.3)	24.7 (3.6)	24.5 (3.1)	24.0 (3.2)	29.5 (4.1)
E	29.1 (2.3)	37.2 (3.8)	43.1 (4.7)	47.2 (4.9)	52.3 (5.5)	56.0 (6.4)	61.0 (6.6)	64.5 (6.9)	67.7 (7.5)	72.0 (7.2)	75.2 (8.6)	78.4 (7.9)	95.1 (7.6)
F	14.0 (1.9)	21.8 (2.8)	26.8 (4.4)	35.3 (5.1)	39.4 (7.1)	45.6 (6.5)	50.1 (7.4)	54.5 (8.4)	58.9 (8.5)	61.6 (6.0)	62.2 (7.4)	66.6 (7.1)	87.6 (10.5)
G	11.2 (1.9) 0.25[b]	15.8 (2.5) 0.5[b]	22.4 (4.4) 0.75[b]	30.6 (7.0) 1.0[b]	38.2 (7.0) 1.25[b]	45.0 (8.3) 1.5[b]	53.9 (9.4) 1.75[b]	56.6 (9.6) 2.0[b]	68.0 (3.9) 2.25[b]	71.6 (2.0) 2.5[b]	75.9 (4.4) 2.75[b]	72.9 (10.9) 3.0[b]	89.4 (4.1)
C	18.4 (4.2)	39.4 (3.8)	50.7 (3.1)	60.2 (4.2)	70.1 (3.5)	79.4 (8.1)	87.7 (10.7)	94.9 (10.8)	95.5 (5.4)	95.5 (6.0)	94.9 (5.0)	93.9 (2.8)	
D	18.5 (3.4) 10[c]	40.0 (5.8) 20[c]	55.7 (5.8) 30[c]	65.7 (7.9) 40[c]	73.2 (5.6) 50[c]	78.5 (4.2) 60[c]	86.3 (3.6) 75[c]	90.5 (6.1) 90[c]	91.4 (3.3) 105[c]	96.4 (4.7) 120[c]	94.3 (1.8) 240[c]	95.7 (5.1)	
H	7.7 (1.8)	14.3 (3.9)	21.7 (4.7)	26.6 (5.6)	32.4 (7.2)	36.0 (7.2)	41.7 (9.3)	52.9 (14.3)	56.7 (12.7)	63.3 (13.7)	88.5 (18.5)		
J	3.3 (1.1)	8.4 (2.0)	13.5 (2.4)	18.4 (2.7)	22.0 (3.0)	24.9 (3.6)	30.6 (3.8)	38.8 (4.6)	43.6 (5.0)	48.8 (4.8)	77.0 (5.7)		

[a] Mean values; *SD* in parentheses. [b] Adjusted time intervals (h). [c] Adjusted time intervals (min).

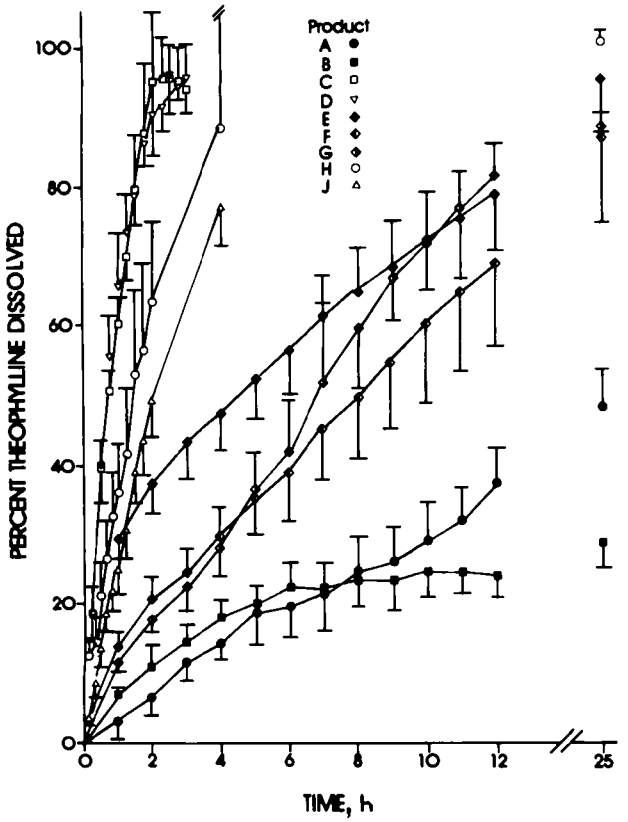

Figure 2—*Percent theophylline dissolved in simulated intestinal fluid* versus *time. Results are mean + or − SD; data are from six dosage forms.*

of theophylline release from some sustained-release preparations after single-dose administration to asthmatic patients has been demonstrated (10). Similar results have been found in the present dissolution studies with the rotating-basket dissolution apparatus (14) and by evaluating the products in both simulated gastric and intestinal fluids.

The percentages of theophylline dissolved at various times from the simulated gastric fluid studies are presented in Table I, and the percent dissolved *versus* time plot is shown in Fig. 1. The dosage forms studied released 6.6 ± 0.9 to 50.1 ± 3.8% of their drug content within 1 h in simulated gastric fluid. Although no simple correlation exists, the values obtained for the percentage of the dose released in 1 h *in vitro* from these products exhibit the same rank order as the values obtained at 1 h *in vivo* with some of these same products (10).

After the initial release of drug through the first 0.5–1.0 h, all of the products displayed some type of sustained-release characteristics (Fig. 1). However, the variability between products clearly demonstrates that these products are not readily interchangeable. Since the mean gastric residence time has been reported to be 3.61 ± 1.47 h (19), the dissolution studies in simulated gastric fluid were terminated after 6 h. At that time, the mean percentage of the dose released ranged from 10.8 ± 1.8 to 86.5 ± 5.2% (Table I).

Of greater concern is the differences in the rate of release of drug from similar preparations of different strength. Both at 3 and 6 h, products A and B, C and D, and H and J all released significantly different amounts of drug ($p \leq 0.005$). Product E released significantly more drug than F and G at 3 h ($p \leq 0.005$), but not at 6 h. Products F and G released similar amounts of drug at 3 and 6 h ($p = 0.005$). Theophylline doses are often individualized by using a combination of different strengths of the same brand of product (4). However, different strengths of the same brand cannot be arbitrarily assumed to release drug at similar rates. A more rational approach may be to adjust the dose by taking one-half of the higher strength dosage form to individualize the dosages. No significant difference was detected *in vivo* when this approach was used for product E (15). In addition, these *in vitro* studies may not reflect the *in vivo* situation. The *in vivo* results for products E and G were not significantly different (10).

Since these products were all sustained-release dosage forms, the dissolution studies in simulated intestinal fluid provide additional information. The percentage of theophylline dissolved at various times in simulated intestinal fluid is shown in Table II, and percent dissolved *versus* time plots for all dosage forms are presented in Fig. 2. The results from these studies show even greater product variability.

Almost all of the theophylline content, 93.9 ± 2.8 and 95.7 ± 5.1% from products C and D, respectively, was released in 3 h in simulated intestinal fluid. This means that the rate of release of drug from these dosage forms may be very dependent on gastric emptying time. These two products also yielded the fastest rate of drug release in simulated gastric fluid (Table I, Fig. 1) and displayed the characteristics of enteric-coated formulations rather than sustained-release dosage forms. These products also exhibited similar characteristics *in vivo* (10), as virtually 100% of the dose was absorbed in 6 h from these formulations. The results obtained from the two different strengths of this dosage form in simulated intestinal fluid were not significantly different at any time ($p = 0.005$).

Although the results from products E, F, G, and H were not significantly different in gastric fluid at 6 h ($p = 0.005$), the results obtained in intestinal fluid were different ($p \leq 0.005$). Products H and J released 88.5 ± 18.5 and 77.0 ± 5.7%, respectively, of their drug content within 4 h, whereas products E, F, and G released only 47.2 ± 4.9, 35.3 ± 5.1, and 30.6 ± 7.0%, respectively. Unfortunately, products H and J were not studied *in vivo* previously (10).

One interesting aspect of products E, F, and G is that the percent theophylline released *versus* time plots are linear after 3 h (Fig. 2). These results indicate that an approximation to zero-order release from these dosage forms was achieved. These findings have also been reported in previous studies *in vivo* (15). Despite the delayed release, virtually all of the dose was released from these products between 12 and 25 h. These results confirm the earlier *in vivo* studies (10) in which 100% of the dose appeared to be absorbed by 16 h.

Products A and B demonstrate very poor drug availability both in simulated gastric and intestinal fluids. At 25 h, only 48.1 ± 5.6 and 29.5 ± 4.1% of the dose was released, respectively, for products A and B. These results mirrored the earlier *in vivo* findings in which only 70% of the dose appeared to be absorbed by 20 h. Again, the results from the two dosage forms of different strengths were significantly different ($p \leq 0.005$).

All results were also analyzed by plotting the log percentage of the labeled dose remaining to be dissolved *versus* time. In some instances these plots were linear. However, the fact that these relationships may be simply artifacts of the systems has been thoroughly examined and discussed previously (20). Therefore, these results are not presented.

In conclusion, the *in vitro* dissolution results in this study were obtained with the rotating-basket dissolution apparatus and independent trials in both simulated gastric and intestinal fluids (14). The pattern of drug release from these sustained-release products obtained *in vitro* mirrored the *in vivo* absorption results obtained with some of these products (10, 15). These rank-order comparisons provide additional information as to the usefulness of dissolution studies as compendial methods for determining product content, uniformity, and rate and extent of drug release.

REFERENCES

(1) D. L. Spangler, D. D. Kalof, F. L. Bloom, and H. J. Wittig, *Ann. Allergy*, **40**, 6 (1978).

(2) D. Tinkelman, G. Vanderpool, M. S. Carroll, and D. L. Spangler, *Ann. Allergy*, **43**, 155 (1979).

(3) J. Dasta, J. M. Mirtallo, and M. Altman, *Am. J. Hosp. Pharm.*, **36**, 613 (1979).

(4) T. Bell and J. Bigley, *Pediatrics*, **62**, 352 (1978).

(5) D. L. Spangler, G. E. Vanderpool, M. S. Carroll, and D. G. Tinkelman, *Ann. Allergy*, **45**, 355 (1980).

(6) G. S. Rachelefsky, R. M. Katz, and S. C. Siegel, *Ann. Allergy*, **40**, 252 (1978).

(7) H. W. Kelly and S. Murphy, *Am. J. Hosp. Pharm.*, **36**, 1698 (1979).

(8) H. W. Kelly and S. Murphy, *Pediatrics*, **66**, 97 (1980).

(9) F. E. R. Simons, G. H. Luciuk, and K. J. Simons, *Am. J. Dis. Child.*, **136**, 790 (1982).

(10) M. Weinberger, L. Hendeles, and L. Bighley, *N. Engl. J. Med.*, **299**, 852 (1978).

(11) R. A. Upton, J.-F. Thiercelin, T. W. Guentert, L. Sansom, J. R. Powell, P. E. Coates, and S. Riegelman, *J. Biopharm. Pharmacokinet.*, **8**, 131 (1980).

(12) H. Moller, in "Sustained Release Theophylline," F. W. H. M. Merkus and L. Hendeles, Eds., Excerpta Medica, Princeton, N.J., 1983, pp. 57–78.

(13) J. H. G. Jonkman, W. C. Berg, and R. A. deZeeuw, in "Sustained Release Theophylline," F. W. H. M. Merkus and L. Hendeles, Eds., Excerpta Medica, Princeton, N.J., 1983, pp. 79–103.

(14) "The United States Pharmacopeia," 20th rev., U.S. Pharmacopeial Convention, Inc., Rockville, Md., 1980, pp. 959–960, 1105.

(15) K. J. Simons, E. M. Frith, and F. E. R. Simons, *J. Pharm. Sci.*, **71**, 505 (1982).
(16) E. A. Swinyard, in "Remington's Pharmaceutical Sciences," 15th ed., J. E. Hoover, Mgr. Ed., Mack Publishing Co., Easton, Pa., 1975, pp. 1069–1070.
(17) J. Swarbrick, in "Biopharmaceutics," J. Swarbrick, Ed., Lea and Febiger, Philadelphia, Pa., 1970, pp. 273–275.
(18) L. Hendeles, M. Weinberger, and L. Bighley, *Am. J. Hosp. Pharm.*, **34**, 525 (1977).
(19) J. G. Wagner, "Biopharmaceutics and Relevant Pharmacokinetics," Drug Intellegence Publications, Hamilton, Ill, 1971, pp. 98–147, 163–165.
(20) J. G. Wagner, *J. Pharm. Sci.*, **58**, 1253 (1969).

ACKNOWLEDGMENTS

Charles Scerbo and Kim Plett were the recipients of Searle Summer Research Studentship Awards provided by the G. D. Searle and Co. of Canada Ltd. The dosage forms were provided by the various pharmaceutical companies.

Dosage Form Design for Improvement of Bioavailability of Levodopa VI: Formulation of Effervescent Enteric-Coated Tablets

KENJI NISHIMURA, KUNIHIRO SASAHARA ˣ, MIKIO ARAI, TAKASHI NITANAI, YOSHIHIKO IKEGAMI, TADASHI MORIOKA, and EIICHI NAKAJIMA

Received March 4, 1983, from the *Product Development Laboratories, Sankyo Company, Ltd., 1-chome, 2-58, Hiromachi, Shinagawa, Tokyo, Japan.* Accepted for publication July 1, 1983.

Abstract □ A new dosage form of levodopa, which has the characteristics of loading high concentrations of levodopa at the upper part of the intestine, has been developed to improve its bioavailability. It is shown that an effervescent tablet formulation, coated with hydroxypropyl methylcellulose phthalate (carboxybenzoyl radical content: 20–24%) as the enteric material, is suitable for the purpose of dissolution. This was confirmed from animal experiments, which showed that tablets of this composition disintegrate instantly on reaching the upper part of the intestine. This tablet was considered appropriate for the bioavailability tests described in this paper.

Keyphrases □ Levodopa—effervescent enteric-coated tablet, intestinal absorption, dissolution □ Effervescent enteric-coated tablet—levodopa, intestinal absorption, lag time of dissolution and absorption, effect of size and shape □ Film material—hydroxypropyl methylcellulose phthalate, effervescent enteric-coated tablet, levodopa

It has been shown in previous work in this series (1, 2) that the bioavailability of levodopa could be improved by loading high concentrations of the drug at the upper part of the intestine, the optimum site of absorption, and then inducing temporary saturation of levodopa decarboxylase. The present work describes the preparation of an oral solid dosage form of levodopa with improved bioavailability. The *in vitro* dissolution and *in vivo* disintegration behavior also are reported.

EXPERIMENTAL SECTION

Preparation of Effervescent Enteric-Coated Tablets of Levodopa [I]—A granular mixture of levodopa USP and carboxymethylcellulose[1] was prepared by the wet granulation method using an aqueous solution of hydroxypropyl cellulose[2] as a binder. All other diluents, effervescent agents, lubricants, and/or coloring agents were mixed with the dried granulation, and the mixture was compressed into tablets. These tablets were coated successively with hydroxypropyl methylcellulose USP (II) (5% w/w) and then with hydroxypropyl methylcellulose phthalate (III)[3] (10% w/w) in methylene dichloride–ethanol (1:1, w/w) solution[4] to obtain enteric-coated tablets. All the coating agents that were used here are accepted for drug use by the FDA.

Dissolution Tests—A modified disintegration test apparatus was used in the dissolution tests of levodopa and/or dyes (3). The frequency rate of the basket-rack assembly was set between 5 and 20 cpm. Ten-mesh stainless steel cloth was fitted over the top of the basket-rack assembly to prevent the tablet from floating out of the tube of the assembly during dissolution.

Dissolution media (900 mL) at various pH values, prepared by mixing test solutions 1 and 2 (JP IX), were heated to 37 ± 0.5°C and placed in the dissolution apparatus. One tablet was placed in the basket. The solution was drawn from the flask through the flow cell (length 5 mm) by a pump[5] and returned to the flask at a flow rate of ~25 mL/min. The differences in absorbance between λ_1 (258.5 nm) and λ_2 (281 nm) for levodopa, λ_1 (620 nm) and λ_2 (662 nm) for methylene blue, and λ_1 (600 nm) and λ_2 (522 nm) for erythromycin were measured with a dual-wavelength spectrophotometer[6] and

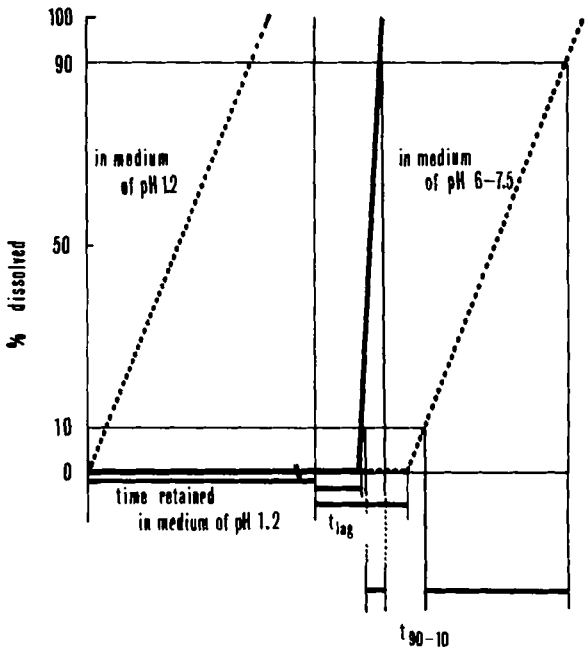

Figure 1—*Dissolution patterns of levodopa. The solid line shows the desired pattern; the dotted lines show conventional dosage forms.*

[1] Marketed as NS300, Gotoku Yakuhin, Tokyo, Japan; acid form of sodium carboxymethylcellulose USP.
[2] Nippon Soda Co., Ltd., Oiso-machi, Kanagawa, Japan; F.C.C. III P280.
[3] Shinetsu Chemicals Co., Ltd., Tokyo, Japan; Biddle Sawyer Corporation, 2, Penn-Plaza, New York, N.Y. 10121, U.S.A.; Master File No. DMF-2151.
[4] A substitute solution is acetone–ethanol solution (1:1, w/w) or acetone–isopropyl alcohol (1:1, w/w).
[5] Type MBP-100, Iwaki Co., Ltd., Japan.
[6] Hitachi-156 Spectrophotometer; Hitachi Co., Ltd., Tokyo, Japan.

0022-3549/84/0700-0942$01.00/0
© 1984, American Pharmaceutical Association

(15) K. J. Simons, E. M. Frith, and F. E. R. Simons, *J. Pharm. Sci.*, **71**, 505 (1982).
(16) E. A. Swinyard, in "Remington's Pharmaceutical Sciences," 15th ed., J. E. Hoover, Mgr. Ed., Mack Publishing Co., Easton, Pa., 1975, pp. 1069–1070.
(17) J. Swarbrick, in "Biopharmaceutics," J. Swarbrick, Ed., Lea and Febiger, Philadelphia, Pa., 1970, pp. 273–275.
(18) L. Hendeles, M. Weinberger, and L. Bighley, *Am. J. Hosp. Pharm.*, **34**, 525 (1977).
(19) J. G. Wagner, "Biopharmaceutics and Relevant Pharmacokinetics," Drug Intellegence Publications, Hamilton, Ill, 1971, pp. 98–147, 163–165.
(20) J. G. Wagner, *J. Pharm. Sci.*, **58**, 1253 (1969).

ACKNOWLEDGMENTS

Charles Scerbo and Kim Plett were the recipients of Searle Summer Research Studentship Awards provided by the G. D. Searle and Co. of Canada Ltd. The dosage forms were provided by the various pharmaceutical companies.

Dosage Form Design for Improvement of Bioavailability of Levodopa VI: Formulation of Effervescent Enteric-Coated Tablets

KENJI NISHIMURA, KUNIHIRO SASAHARA ˣ, MIKIO ARAI, TAKASHI NITANAI, YOSHIHIKO IKEGAMI, TADASHI MORIOKA, and EIICHI NAKAJIMA

Received March 4, 1983, from the *Product Development Laboratories, Sankyo Company, Ltd., 1-chome, 2-58, Hiromachi, Shinagawa, Tokyo, Japan.* Accepted for publication July 1, 1983.

Abstract □ A new dosage form of levodopa, which has the characteristics of loading high concentrations of levodopa at the upper part of the intestine, has been developed to improve its bioavailability. It is shown that an effervescent tablet formulation, coated with hydroxypropyl methylcellulose phthalate (carboxybenzoyl radical content: 20–24%) as the enteric material, is suitable for the purpose of dissolution. This was confirmed from animal experiments, which showed that tablets of this composition disintegrate instantly on reaching the upper part of the intestine. This tablet was considered appropriate for the bioavailability tests described in this paper.

Keyphrases □ Levodopa—effervescent enteric-coated tablet, intestinal absorption, dissolution □ Effervescent enteric-coated tablet—levodopa, intestinal absorption, lag time of dissolution and absorption, effect of size and shape □ Film material—hydroxypropyl methylcellulose phthalate, effervescent enteric-coated tablet, levodopa

It has been shown in previous work in this series (1, 2) that the bioavailability of levodopa could be improved by loading high concentrations of the drug at the upper part of the intestine, the optimum site of absorption, and then inducing temporary saturation of levodopa decarboxylase. The present work describes the preparation of an oral solid dosage form of levodopa with improved bioavailability. The *in vitro* dissolution and *in vivo* disintegration behavior also are reported.

EXPERIMENTAL SECTION

Preparation of Effervescent Enteric-Coated Tablets of Levodopa [I]—A granular mixture of levodopa USP and carboxymethylcellulose[1] was prepared by the wet granulation method using an aqueous solution of hydroxypropyl cellulose[2] as a binder. All other diluents, effervescent agents, lubricants, and/or coloring agents were mixed with the dried granulation, and the mixture was compressed into tablets. These tablets were coated successively with hydroxypropyl methylcellulose USP (II) (5% w/w) and then with hydroxypropyl methylcellulose phthalate (III)[3] (10% w/w) in methylene dichloride–ethanol (1:1, w/w) solution[4] to obtain enteric-coated tablets. All the coating agents that were used here are accepted for drug use by the FDA.

Dissolution Tests—A modified disintegration test apparatus was used in the dissolution tests of levodopa and/or dyes (3). The frequency rate of the basket-rack assembly was set between 5 and 20 cpm. Ten-mesh stainless steel cloth was fitted over the top of the basket-rack assembly to prevent the tablet from floating out of the tube of the assembly during dissolution.

Dissolution media (900 mL) at various pH values, prepared by mixing test solutions 1 and 2 (JP IX), were heated to 37 ± 0.5°C and placed in the dissolution apparatus. One tablet was placed in the basket. The solution was drawn from the flask through the flow cell (length 5 mm) by a pump[5] and returned to the flask at a flow rate of ~25 mL/min. The differences in absorbance between λ_1 (258.5 nm) and λ_2 (281 nm) for levodopa, λ_1 (620 nm) and λ_2 (662 nm) for methylene blue, and λ_1 (600 nm) and λ_2 (522 nm) for erythromycin were measured with a dual-wavelength spectrophotometer[6] and

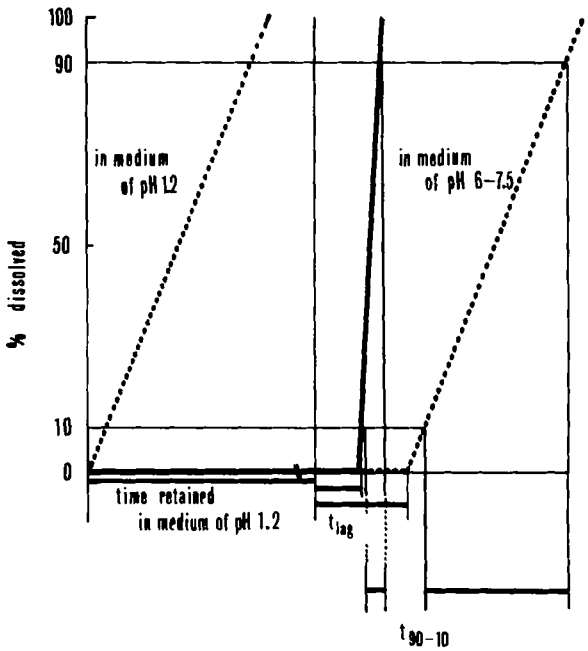

Figure 1—*Dissolution patterns of levodopa. The solid line shows the desired pattern; the dotted lines show conventional dosage forms.*

[1] Marketed as NS300, Gotoku Yakuhin, Tokyo, Japan; acid form of sodium carboxymethylcellulose USP.
[2] Nippon Soda Co., Ltd., Oiso-machi, Kanagawa, Japan; F.C.C. III P280.
[3] Shinetsu Chemicals Co., Ltd., Tokyo, Japan; Biddle Sawyer Corporation, 2, Penn-Plaza, New York, N.Y. 10121, U.S.A.; Master File No. DMF-2151.
[4] A substitute solution is acetone–ethanol solution (1:1, w/w) or acetone–isopropyl alcohol (1:1, w/w).
[5] Type MBP-100, Iwaki Co., Ltd., Japan.
[6] Hitachi-156 Spectrophotometer; Hitachi Co., Ltd., Tokyo, Japan.

0022-3549/84/0700-0942$01.00/0
© 1984, American Pharmaceutical Association

Table I—Formulations of Effervescent Enteric Tablets of Levodopa for the Tests of Dissolution Parameters

Compound	Amount per Tablet, mg				
	1	2	3	4	5
Levodopa	200	200	200	200	200
Tartaric acid	0	6.25	12.5	25	50
Sodium bicarbonate	0	7	14	28	56
Lactose	106	92.75	79.5	53	0
Carboxymethylcellulose, Magnesium aluminum silicate, Sodium bisulfate, Hydroxypropyl cellulose, Magnesium stearate	79	79	79	79	79
Hydroxypropyl methylcellulose	8	8	8	8	8
Hydroxypropyl methylcellulose phthalate-50	30	30	30	30	30
Total weight	423	423	423	423	423

recorded continuously. The following parameters were obtained from the dissolution curves in several runnings: t_{lag} (lag time of dissolution), t_{10} (time required to dissolve 10% of labeled drug), t_{90} (time required to dissolve 90% of labeled drug), and $t_{90} - t_{10}$.

Measurement of the Dissolution Time of the Enteric Coating Material—Fifty-milligram portions of 20-32-mesh fractions of each coating material were suspended in media of various pH values, as described in the dissolution test, and agitated with a magnetic stirrer (9 mm in diameter and 30 mm in length) at ~500 rpm at 37 ± 0.5°C. The dissolution time of the suspended particles was measured visually.

Lag Time Determination of Levodopa Absorption—Two samples were used for this study. Ten healthy male beagle dogs, 10.0–14.0 kg, were fasted for ~16 h and divided into two groups of five dogs each. Crossover experiments were carried out at 1-week intervals. The dogs were dosed orally, and levodopa absorption was measured by observing the time at which the dogs began vomiting, which indicated a significant release of the drug with subsequent absorption.

Measurement of the Disintegration Site of Tablets *In Vivo*—*Experiment No. 1*—Two male beagle dogs, 10.7 and 11.3 kg, were each orally dosed with two samples. Immediately after the dogs began vomiting, they were anesthetized with pentobarbital sodium[7] (0.6 mL/kg), placed on their backs, and killed by exsanguination. The abdomens were immediately opened and the entire GI tracts were excised and opened in order to observe the disintegration sites. Such observation was made possible by the dye contained in the tablets.

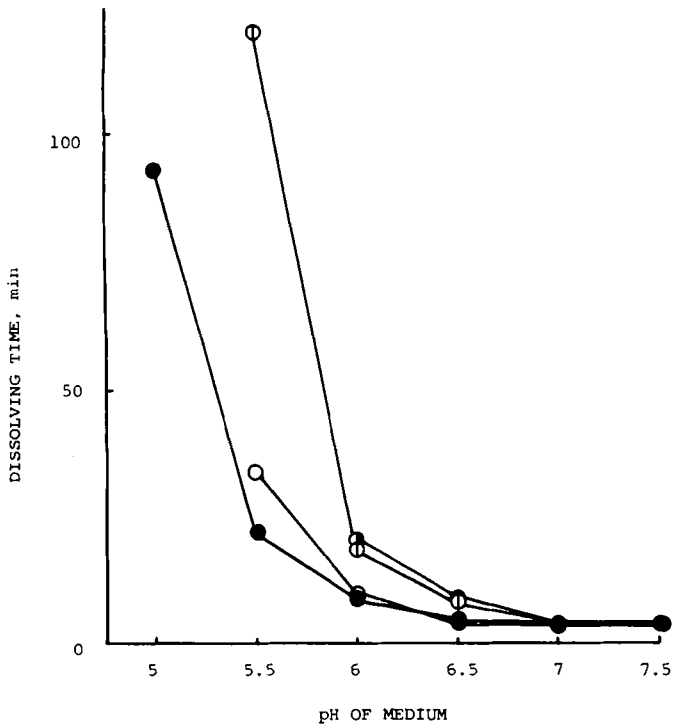

Figure 2—*pH profile of dissolution time of various enteric film materials. Key: (●) III-45; (○) III-50; (◐) III-55; (◑) IV.*

[7] Dainippon Pharmaceutical Co., Ltd.

Experiment No. 2—One male beagle dog, 13.9 kg, was orally dosed with two tablets from each sample. Fifty minutes after the dog began vomiting, it was anesthetized with pentobarbital sodium 6 and examined, as in experiment no. 1.

RESULTS AND DISCUSSION

From the results of the *in vitro* and *in situ* experiments of levodopa absorption characteristics, it was found that levodopa absorption from the solid dosage form was enhanced by:

1. Selecting the correct enteric dosage form to inhibit the levodopa decomposition in the stomach and ensure a high concentration of levodopa at the absorption site.
2. Selecting the appropriate enteric film materials to obtain rapid disintegration and dissolution characteristics in the upper part of the intestine.
3. Investigating dissolution characteristics so as to obtain a high concentration of levodopa at the onset of dissolution and to inhibit the conversion to dopamine (4) as much as possible by decarboxylase distributed in the intestine, during the absorption process.
4. Investigating product form and size to minimize variations in lag time of absorption and to shorten the lag time of absorption due to variability of individual gastric transit times.

The *in vitro* dissolution curve showing the aforementioned characteristics can be seen in Fig. 1. One of the main purposes of this report was to obtain a preparation having the dissolution characteristics shown in Fig. 1.

Selection of Enteric Film Material—The hydroxypropyl methylcellulose phthalate (III) used had different carboxybenzoyl radical contents (45[8], 50[9], 55[10]). Cellulose acetate phthalate (IV) was selected as a reference because

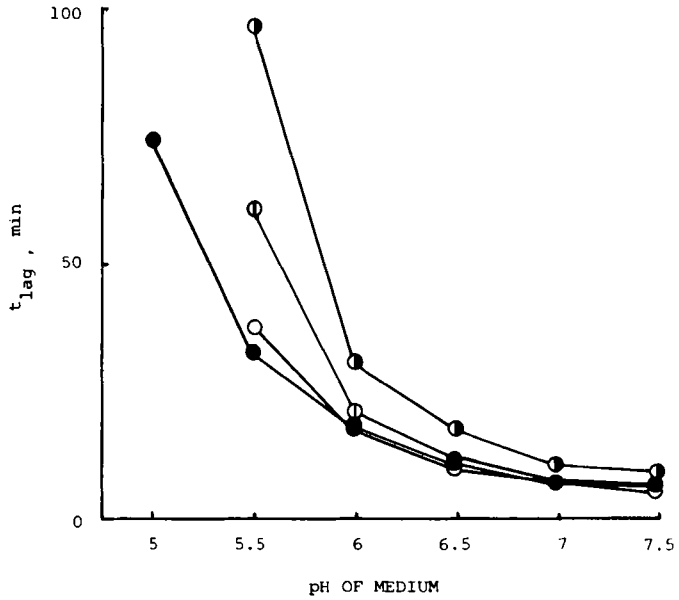

Figure 3—*pH profile of the dissolution parameter, t_{lag}, of effervescent enteric tablets of levodopa coated with various enteric film materials. Key: (●) III-45; (○) III-50; (◐) III-55; (◑) IV.*

[8] Carboxybenzoyl radical content: ~20%.
[9] Carboxybenzoyl radical content: 20–24%.
[10] Carboxybenzoyl radical content: 27–35%.

Table II—Formulations and Dissolution Parameters of Two Samples Employed for the Determination of Disintegration Sites *In Vivo*

Compound	Amount per Tablet, mg A	B
Levodopa	180	180
Methylene blue	20	0
Erythromycin	0	20
Tartaric acid	25	25
Sodium bicarbonate	28	28
Carboxymethylcellulose, Microcrystalline cellulose, Magnesium aluminum silicate, Sodium bisulfate, Hydroxypropyl cellulose, Magnesium stearate	79	79
Hydroxypropyl methylcellulose	8	8
Hydroxypropyl methylcellulose phthalate-50	30	0
Cellulose acetate phthalate	0	30
Total weight	370	370

	Dissolution Parameter, min	
Levodopa		
pH 7.5		
t_{lag}	5.3	7.0
$t_{90\text{-}10}$	1.1	1.5
pH 6.0		
t_{lag}	18.3	36.2
$t_{90\text{-}10}$	2.0	2.1
Dye		
pH 7.5		
t_{lag}	5.6	8.6
$t_{90\text{-}10}$	1.4	1.1
pH 6.0		
t_{lag}	22.7	35.1
$t_{90\text{-}10}$	1.5	1.7

it is used extensively in the marketplace. The relationship between the dissolution time of the enteric film material and the pH of the medium is shown in Fig. 2. It can be seen from Fig. 2 that there is no difference in dissolution time between materials at pH 7.0 and at pH 7.5. However, at more acidic pH levels, the dissolution time of the material was longer in the order of III-45, III-50, III-55, and IV. The relationship between dissolution lag time (t_{lag}) of tablets coated with various enteric materials and medium pH was also determined (Fig. 3), from which the same pattern as the film materials themselves can be seen.

Intestinal pH is known to be between ~6 and 7.5. It has been reported, however, that the pH of the duodenum was ~pH 7 and varied according to the pH of the stomach (5). On the other hand, it has been reported that disintegration and dissolution behavior at more acidic medium levels than the disintegration test solution (pH 7.5) should be used in evaluating bioavail-

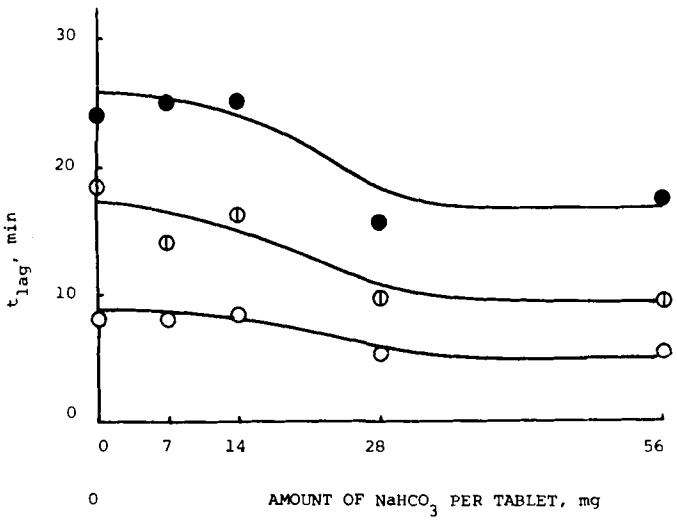

Figure 4—*Relationship between the dissolution parameter, t_{lag}, of effervescent enteric tablets of levodopa and the amount of sodium bicarbonate formulated in the tablet. Key: (●) pH 6.0, 20 strokes/min; (○) pH 7.5, 5 strokes/min; (⊖) pH 7.5, 20 strokes/min.*

Table III—*In Vivo* Disintegration of Samples A and B

	Dog 1	Dog 2	Dog 3
Body weight, kg	10.7	11.3	13.9
Length of intestine, cm	170	180	170
Length of duodenum, cm	20	25	25
Time of emesis, min postdose	120	110	130
Anesthetizing time, min postdose	120	110	180
Results from Sample A			
Dose, number of tablets	1	1	2
Appearance of tablets	d.c.[a]	d.c.	d.c.
Distance from pylorus, cm	20	23	20
Results from Sample B			
Dose, number of tablets	1	1	2
Appearance of tablets	n.d.[b]	n.d.	d.c.
Distance from pylorus, cm	50	60	40, 130

[a] Disintegrated completely. [b] Not disintegrated.

ability of enteric-coated tablets (6). Moreover, considering the prevention of disintegration in the stomach, it might be more appropriate to evaluate film dissolving time or lag time of dissolution of enteric-coated tablets at pH 6–6.5. Therefore, III-50 was selected as the most appropriate material from among the four kinds of films used.

Preparation of I—Effervescent tablets were investigated to obtain characteristics of fast disintegration and instantaneous dissolution of levodopa preparations. The compressibility of levodopa was such as to require additives. For this reason, it was difficult to obtain the characteristics mentioned above in other dosage forms. A sodium bicarbonate–tartaric acid system was selected as the effervescent component, and the five kinds of tablets shown in Table I were prepared.

For these tablets, the relationship between the amount of effervescent component and lag time of dissolution (t_{lag}) and between the amount of effervescent component and rate of dissolution ($t_{90\text{-}10}$) were studied. The results are shown in Figs. 4 and 5. In the determination of $t_{90\text{-}10}$, the frequency of the basket-rack assembly was set to 5 cpm to clarify the differences among the preparations. It can be seen from Fig. 4 that as the amount of effervescent component is increased, the dissolution lag time will decrease. However, the dissolution lag time was found to become constant, and as seen in Fig. 5, the dissolution rate became smaller with the addition of >28 mg/tablet of sodium bicarbonate. These results confirmed, therefore, that formulation 4 in Table I was the more appropriate.

It is difficult to say why the lag times are different among the preparations,

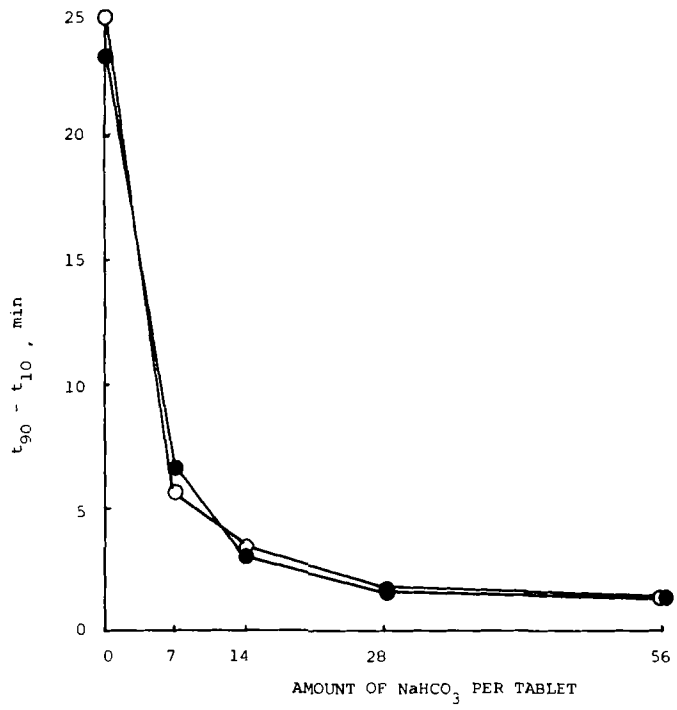

Figure 5—*Relationship between the dissolution parameter $t_{90\text{-}10}$ of effervescent enteric tablets of levodopa and the amount of sodium bicarbonate formulated in the tablet. The number of strokes was fixed at 5/min, and the pH was 7.5. Key: (●) uncoated tablet; (○) enteric tablet.*

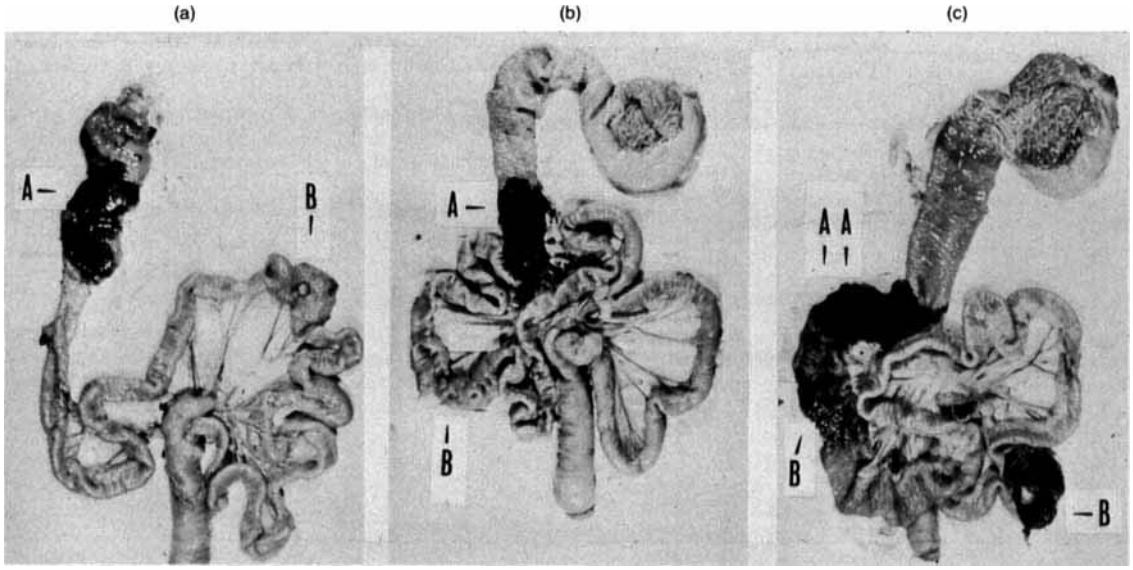

Figure 6—*Photographs of the* in vivo *disintegration site of samples A and B. Key: (a) dog 1; (b) dog 2; (c) dog 3. See Table III for experimental details.*

even with the same enteric film. One reason may be the variability in the rate of evolution of carbon dioxide due to slight differences in the rate of penetration of water into the tablet.

Disintegration Site of I—The disintegration site of I was investigated in beagle dogs to confirm *in vivo* behavior. Two samples, A and B, were used in the experiments; compositions and dissolution parameters are shown in Table II. Dyes were added to facilitate visual investigation of the site of and the rate of disintegration. Results are summarized in Table III and intestinal dissections are shown in Fig. 6.

The measured lengths of the duodenum and the small intestine are approximate. The lengths of the duodena measured were the same as that described in the literature (7) (*i.e.*, ~25 cm). As shown in Table III and Fig. 6, sample A disintegrated in the duodenum of each dog and the length of the dyeing site was short. These results suggest that disintegration of I started as soon as it reached the intestine and that the rate of disintegration or dissolution was instantaneous. In contrast, disintegration of sample B was very slow, and the sites of the disintegrations varied between the two tablets. In comparison with the dissolution parameters shown in Table III, it seems reasonable to assume that the dissolution lag time is correlated with the site of disintegration and that the rate of dissolution ($t_{90\text{-}10}$) is correlated with the length of the dyed site. Tablet I was designed for fast disintegration and high concentration in the upper intestine. From the above results, it was concluded that sample A was most suited to the purpose.

Effects of Tablet Shape and Size on the Lag Time of I—A 250-mg volume of levodopa was formulated into oval and round effervescent enteric-coated tablets. Table IV shows the characteristics of the two tablets. The tablets were compared with respect to lag time of levodopa absorption in dogs. The results (Fig. 7) indicate that the round tablet gives a shorter lag time and smaller intersubject variation in comparison with the oval one.

Three types of I, each containing 200 mg of levodopa but of different sizes, were prepared. Table IV shows the characteristics of the three sizes of tablets. Lag times of levodopa absorption were determined following oral administration of four kinds of I: the round tablet and the three types of tablets (samples 1–3) in Table IV. The results are shown in Fig. 8. The effects of size on lag time shown in Fig. 8 suggest that larger tablets have a longer levodopa absorption lag time in dogs.

Table IV—Characteristics of Effervescent Enteric Tablets of Levodopa used for the Measurement of Absorption Lag Time

	Round Tablets	Oval Tablets	Sample 1	Sample 2	Sample 3
Weight per tablet, mg	594	594	369	461	474
Diameter, mm	10.6	15.7 × 8.2	9.4	10.0	10.1
Thickness, mm	6.3	5.1	5.3	5.4	5.4
Dissolution parameter, min[a]					
t_{lag}	9.0	7.4	5.1	5.1	7.0
$t_{90\text{-}10}$	1.8	1.6	0.9	1.5	2.1

[a] Dissolution parameters were determined at pH 7.5 with 20 strokes/min.

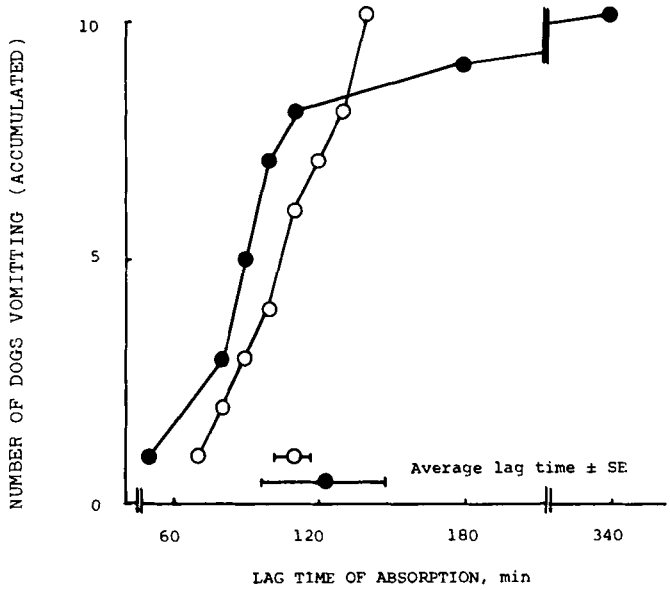

Figure 7—*Effect of tablet shape on the lag time of absorption (as indicated by emesis). Key: (○) round; (●) oval.*

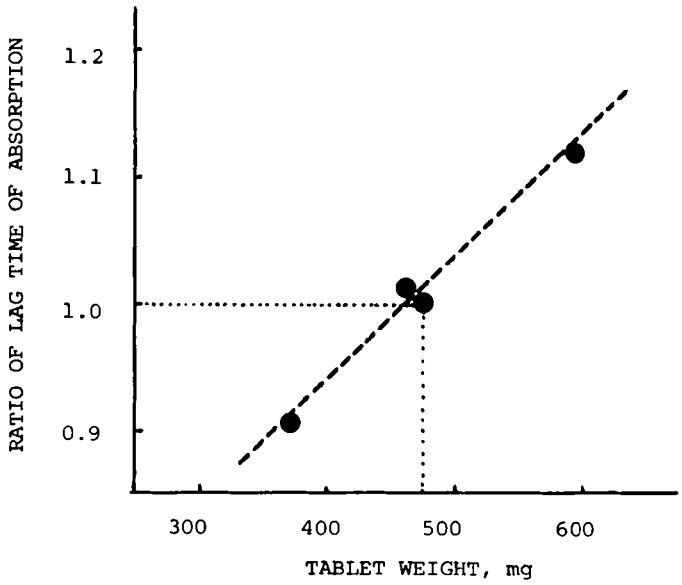

Figure 8—*Effect of tablet size on the lag time of absorption.*

CONCLUSIONS

An enteric formulation of levodopa can prevent drug absorption in the stomach and so can reduce the side effects of the drug on the stomach. Application of III-50 as an enteric coating film material resulted in an enteric tablet with rapid disintegration characteristics after passing through the stomach. Addition of an effervescent component to the tablet reduced the lag time of *in vitro* dissolution in intestinal fluid, and the rate of levodopa dissolution was accelerated. The conventional round shape was suggested as a suitable tablet shape and also a smaller size was recommended to minimize the lag time for the transit of the tablet into the intestine.

REFERENCES

(1) K. Sasahara, T. Nitanai, T. Habara, T. Kojima, Y. Kawahara, T. Morioka, and E. Nakajima, *J. Pharm. Sci.*, **70**, 730 (1981).

(2) K. Sasahara, T. Nitanai, T. Habara, T. Morioka, and E. Nakajima, *J. Pharm. Sci.*, **70**, 1157 (1981).

(3) M. Ikeda and K. Nishimura, The 91st Annual Meeting of the Pharmaceutical Society of Japan, Fukuoka, April, 1971.

(4) G. C. Cotzias, P. S. Papavasilious, and R. Gellene, *N. Engl. J. Med.*, **280**, 337 (1969).

(5) K. Matsumoto, *Jpn. J. Gastroenterol.*, **69**, 783 (1972).

(6) K. Watanabe, M. Sano, K. Motohashi, M. Mitsui, and R. Yoneda, The 96th Annual Meeting of the Pharmaceutical Society of Japan, Nagoya, April, 1976.

(7) K. Sakamoto, "Handbook of Experimental Surgery for Medical and Biological Sciences," Igaku-Shoin, Tokyo, 1967, p. 258.

ACKNOWLEDGMENTS

The authors thank Dr. T. Higuchi for valuable discussions, Drs. H. Negoro, S. Akagi, and T. Miki for encouragement and useful discussion. The authors thank Mr. S. Takamura and Mrs. E. Takayama for their assistance.

Dissolution and Ionization of Warfarin

V. J. STELLA ˣ, K. G. MOONEY *, and J. D. PIPKIN ‡

Received January 18, 1983, from the *Department of Pharmaceutical Chemistry, The University of Kansas, Lawrence, KS 66045.* Accepted for publication July 19, 1983. Present addresses: *American Cyanamid Co., Pearl River, NY 10965 and ‡Squibb Institute for Medical Research, New Brunswick, NJ 08903.

Abstract □ It has been shown in recent studies that warfarin exists in the solid state and in some nonaqueous solvents as a cyclic hemiketal. The present study was undertaken to investigate the ionization and ionization kinetics of warfarin, to confirm the probable existence of the cyclic hemiketal in aqueous solution, and to determine the possible consequences of the cyclic hemiketal to acyclic enol equilibrium and ionization kinetics on the dissolution rate of warfarin. The equilibrium aqueous solubility of un-ionized warfarin acid at 25°C and ionic strength 0.5 (with potassium chloride) was found to be 1.28×10^{-5} M, and its observed macroscopic pK_a was 5.03–5.06, depending on the method of determination. By comparing the aqueous pK_a of warfarin to phenprocoumin, a hydroxycoumarin that cannot exist in the cyclic hemiketal form, the hemiketal–acyclic enol ratio was estimated to be ~20:1. By stop-flow spectrophotometry, the ionization rate of warfarin (pH 3.5 jumped to pH 6.5) was found to have a $t_{1/2} < 1\text{–}2 \times 10^{-3}$ s. The dissolution rate of warfarin from a rotating disk (600 rpm), as a function of pH, was measured under nonbuffered but pH-stat conditions (μ = 0.5 with potassium chloride). The pH-dissolution rate profile for warfarin agreed with that calculated from an equation derived previously to describe the dissolution of instantaneous ionizing acids, *i.e.*, the profile was not perturbed from that expected from an acid of aqueous solubility 1.28×10^{-5} M (un-ionized form) and pK_a 5.06.

Keyphrases □ Dissolution—warfarin, ionization kinetics □ Warfarin—dissolution, ionization kinetics □ Ionization kinetics—warfarin, dissolution

The structure of the anticoagulant warfarin is usually depicted in the open-chain form (I) whereas it is known to exist in the solid state in the cyclic hemiketal form (II) (1, 2). Spectrometric studies (3–6) have confirmed that II is also the predominant form of warfarin in solution in various nonaqueous solvents. In water, un-ionized warfarin (I and/or II) exists in equilibrium with the enolate (III) (Scheme I).

Since warfarin exists as the hemiketal in the solid state and its ionization appears to be complex, we decided to study the dissolution rate *versus* pH (unbuffered, pH maintained by pH-stat) profile of warfarin to observe whether it behaved as an instantaneously ionizing acid (7, 8). To achieve this, the dissolution rate from a compressed rotating disk of warfarin at pH 2 and in the pH range 7–9.5 was studied along with its solubility, ionization characteristics, and ionization rate. By

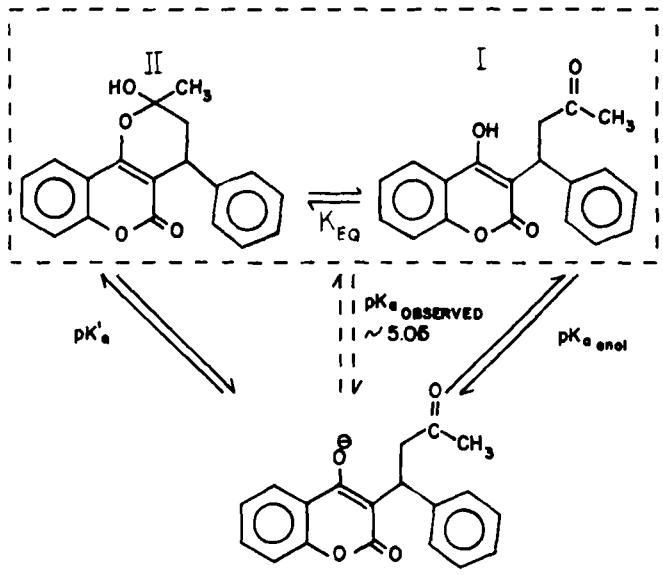

Scheme I

comparing the pK_a of warfarin with that of phenprocoumin (IV), a hydroxycoumarin which can exist only in an acyclic form, it was also possible to test for the existence of II as the predominant form of warfarin in aqueous solution.

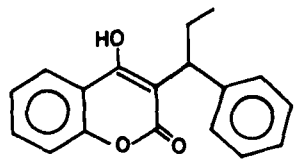

IV

0022-3549/84/0700-0946$01.00/0

© 1984, American Pharmaceutical Association

CONCLUSIONS

An enteric formulation of levodopa can prevent drug absorption in the stomach and so can reduce the side effects of the drug on the stomach. Application of III-50 as an enteric coating film material resulted in an enteric tablet with rapid disintegration characteristics after passing through the stomach. Addition of an effervescent component to the tablet reduced the lag time of *in vitro* dissolution in intestinal fluid, and the rate of levodopa dissolution was accelerated. The conventional round shape was suggested as a suitable tablet shape and also a smaller size was recommended to minimize the lag time for the transit of the tablet into the intestine.

REFERENCES

(1) K. Sasahara, T. Nitanai, T. Habara, T. Kojima, Y. Kawahara, T. Morioka, and E. Nakajima, *J. Pharm. Sci.*, **70**, 730 (1981).

(2) K. Sasahara, T. Nitanai, T. Habara, T. Morioka, and E. Nakajima, *J. Pharm. Sci.*, **70**, 1157 (1981).

(3) M. Ikeda and K. Nishimura, The 91st Annual Meeting of the Pharmaceutical Society of Japan, Fukuoka, April, 1971.

(4) G. C. Cotzias, P. S. Papavasilious, and R. Gellene, *N. Engl. J. Med.*, **280**, 337 (1969).

(5) K. Matsumoto, *Jpn. J. Gastroenterol.*, **69**, 783 (1972).

(6) K. Watanabe, M. Sano, K. Motohashi, M. Mitsui, and R. Yoneda, The 96th Annual Meeting of the Pharmaceutical Society of Japan, Nagoya, April, 1976.

(7) K. Sakamoto, "Handbook of Experimental Surgery for Medical and Biological Sciences," Igaku-Shoin, Tokyo, 1967, p. 258.

ACKNOWLEDGMENTS

The authors thank Dr. T. Higuchi for valuable discussions, Drs. H. Negoro, S. Akagi, and T. Miki for encouragement and useful discussion. The authors thank Mr. S. Takamura and Mrs. E. Takayama for their assistance.

Dissolution and Ionization of Warfarin

V. J. STELLA ˣ, K. G. MOONEY *, and J. D. PIPKIN ‡

Received January 18, 1983, from the *Department of Pharmaceutical Chemistry, The University of Kansas, Lawrence, KS 66045.* Accepted for publication July 19, 1983. Present addresses: *American Cyanamid Co., Pearl River, NY 10965 and ‡Squibb Institute for Medical Research, New Brunswick, NJ 08903.

Abstract □ It has been shown in recent studies that warfarin exists in the solid state and in some nonaqueous solvents as a cyclic hemiketal. The present study was undertaken to investigate the ionization and ionization kinetics of warfarin, to confirm the probable existence of the cyclic hemiketal in aqueous solution, and to determine the possible consequences of the cyclic hemiketal to acyclic enol equilibrium and ionization kinetics on the dissolution rate of warfarin. The equilibrium aqueous solubility of un-ionized warfarin acid at 25°C and ionic strength 0.5 (with potassium chloride) was found to be 1.28×10^{-5} M, and its observed macroscopic pK_a was 5.03–5.06, depending on the method of determination. By comparing the aqueous pK_a of warfarin to phenprocoumin, a hydroxycoumarin that cannot exist in the cyclic hemiketal form, the hemiketal–acyclic enol ratio was estimated to be ~20:1. By stop-flow spectrophotometry, the ionization rate of warfarin (pH 3.5 jumped to pH 6.5) was found to have a $t_{1/2} < 1\text{–}2 \times 10^{-3}$ s. The dissolution rate of warfarin from a rotating disk (600 rpm), as a function of pH, was measured under nonbuffered but pH-stat conditions (μ = 0.5 with potassium chloride). The pH-dissolution rate profile for warfarin agreed with that calculated from an equation derived previously to describe the dissolution of instantaneous ionizing acids, *i.e.*, the profile was not perturbed from that expected from an acid of aqueous solubility 1.28×10^{-5} M (un-ionized form) and pK_a 5.06.

Keyphrases □ Dissolution—warfarin, ionization kinetics □ Warfarin—dissolution, ionization kinetics □ Ionization kinetics—warfarin, dissolution

The structure of the anticoagulant warfarin is usually depicted in the open-chain form (I) whereas it is known to exist in the solid state in the cyclic hemiketal form (II) (1, 2). Spectrometric studies (3–6) have confirmed that II is also the predominant form of warfarin in solution in various nonaqueous solvents. In water, un-ionized warfarin (I and/or II) exists in equilibrium with the enolate (III) (Scheme I).

Since warfarin exists as the hemiketal in the solid state and its ionization appears to be complex, we decided to study the dissolution rate *versus* pH (unbuffered, pH maintained by pH-stat) profile of warfarin to observe whether it behaved as an instantaneously ionizing acid (7, 8). To achieve this, the dissolution rate from a compressed rotating disk of warfarin at pH 2 and in the pH range 7–9.5 was studied along with its solubility, ionization characteristics, and ionization rate. By

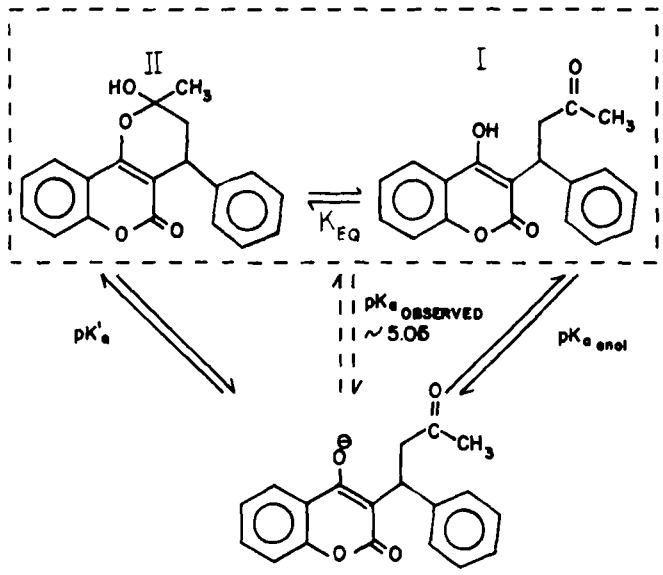

Scheme I

comparing the pK_a of warfarin with that of phenprocoumin (IV), a hydroxycoumarin which can exist only in an acyclic form, it was also possible to test for the existence of II as the predominant form of warfarin in aqueous solution.

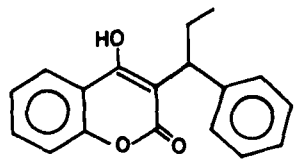

IV

0022-3549/84/0700-0946$01.00/0

© 1984, American Pharmaceutical Association

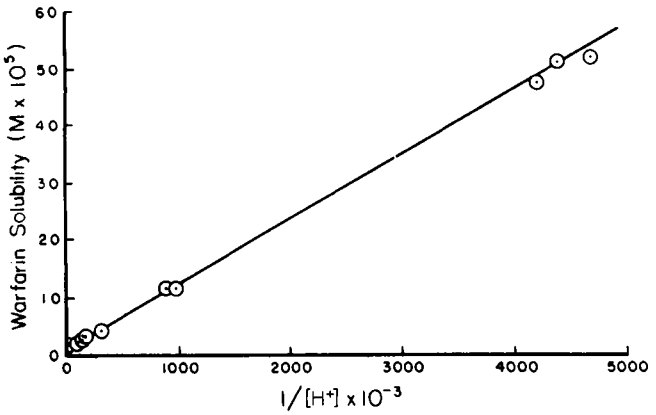

Figure 1—*Plot of the total solubility (S_T) of warfarin at 25°C* versus *$1/[H^+]$ for equilibrated 0.1 M acetate buffers, μ = 0.5 (potassium chloride): $S_T = 1.28 \times 10^{-5} + (112 \times 10^{-10}/[H^+])$ ($r = 0.999$; n = 29). $[HA]_0$ is obtained from the intercept, and K_a is obtained from slope/intercept.*

EXPERIMENTAL SECTION

Materials—Warfarin[1] and phenprocoumin[2] were used as supplied. All reactions, dissolution rates, and pK_a determinations were carried out in glass-distilled or doubly deionized carbon dioxide- and oxygen-free water. The buffer components, potassium chloride, and sodium hydroxide were of reagent or analytical reagent quality and were used without further purification.

pK_a and Solubility Determinations—*Method A*—The pK_a values of warfarin and phenprocoumin were determined spectrophotometrically[3] (9) at 282 (or 272) and 275 nm, respectively, at 25 ± 0.2°C and μ = 0.1 (with potassium chloride). The pK_a of warfarin was also determined spectrophotometrically at μ = 0.5 (with potassium chloride).

Method B—The solubility and pK_a of warfarin at 25 ± 0.5°C and μ = 0.5 (with potassium chloride) were determined by the solubility method (7, 10, 11). While determining solubility as a function of pH, care was taken to deoxygenate the solutions and to protect them from light. Analysis of the amount of dissolved warfarin was by spectrophotometry[3] of filtered samples, and the pH was adjusted to 11–12 with sodium hydroxide. A standard curve was prepared just before the measurements were taken.

Ionization Kinetics of Warfarin—The pH jump technique for studying ionization by stop-flow spectrophotometry[4] as previously described for the ionization of phenylbutazone (12), and phenindione (13, 14) was used to determine whether warfarin ionization might have a half-life measurable by this method ($t_{1/2} > 1\text{-}2 \times 10^{-3}$ s). Specifically, a 1.5×10^{-5} M (pH 3.5) solution of warfarin in 0.5 M KCl was jumped to pH 6.5 (0.1 M phosphate buffer; μ = 0.5 with potassium chloride), and transmission was recorded as a function of time (on the stop-flow spectrophotometer oscilloscope) at 272 nm[5] immediately after mixing (mixing time, $\sim 2 \times 10^{-3}$ s). Transmission changes as a function of time were observed down to 1×10^{-3} s/division on the oscilloscope.

Dissolution Study—Individual disks of 250 mg of warfarin were prepared by the method previously described for other acids (7, 8). Preslugging of the commercial warfarin and regrinding of the powder was necessary to produce disks which did not cap or crack on expulsion from the die. Dissolution rates were determined by previously described procedures (7, 8, 15). The continuous monitoring of dissolution was carried out at 285 nm for pH 2 (λ_{max} at pH 2) and at 292 nm (an isosbestic point) for all other pH values.

RESULTS AND DISCUSSION

The observed pK_a of warfarin and the macroscopic p$K_{a_{obs}}$, defined by Scheme I and Eq. 1:

$$K_{a_{obs}}{}^{warfarin} = \frac{[III][H^+]}{([I] + [II])} \qquad \text{(Eq. 1)}$$

and determined by method A at 25°C and μ = 0.1, was calculated to be 5.03 ± 0.01 (±*SD*). This was calculated from individual data points (in triplicate) for seven pH values in the range of 4.00–7.82, with the mean absorbance at pH 2.08, 2.88, and 3.02 representing the absorbancy of un-ionized warfarin and the absorbance at pH 11.77 representing the absorbancy of the enolate (9). A plotting technique described earlier (12–14) gave an identical result. The pK_a of phenprocoumin, under identical conditions, was determined to be 3.77 ± 0.01 (±*SD*). These determinations were carried out at μ = 0.1 for the purpose of comparison with earlier studies (12–14).

Inverting Eq. 1 and substituting the formulas for $K_{a_{enol}}{}^{warfarin}$ and K_a', as defined in Scheme I, gives Eq. 2 and 3, respectively:

$$\frac{1}{K_{a_{obs}}{}^{warfarin}} = \frac{[I]}{[III][H^+]} + \frac{[II]}{[III][H^+]} \qquad \text{(Eq. 2)}$$

$$= \frac{1}{K_{a_{enol}}{}^{warfarin}} + \frac{1}{K_a'} \qquad \text{(Eq. 3)}$$

The only difference in structure between warfarin enol (I) and phenprocoumin (IV) is the presence of a butanone group compared with an ethyl group at C-3, respectively. The presence of the carbonyl group in the butanone side chain of warfarin should have a negligible electron-withdrawing effect on the enol p$K_{a_{enol}}$ relative to the ethyl side chain in phenprocoumin. If it is also assumed that there is a negligible effect on p$K_{a_{enol}}$ by intramolecular hydrogen bonding and that warfarin and phenprocoumin do not exist significantly in a diketo form (12–14), then:

$$K_{a_{enol}}{}^{warfarin} \simeq K_a{}^{phenprocoumin} \qquad \text{(Eq. 4)}$$

By substituting $K_a{}^{phenprocoumin}$ for $K_{a_{enol}}{}^{warfarin}$ in Eq. 3, an estimate K_a' can be made. By using values of 9.33×10^{-6} for $K_{a_{obs}}{}^{warfarin}$ and 1.70×10^{-4} for $K_a{}^{phenprocoumin}$, Eq. 3 gives a value for K_a' of 9.87×10^{-6} or pK_a' of 5.00. Therefore, the fraction of un-ionized warfarin present in aqueous solution as II, which is defined by Eq. 5, is 0.95 or:

$$\frac{[II]}{[I] + [II]} = \frac{K_{a_{obs}}{}^{warfarin}}{K_a'} \qquad \text{(Eq. 5)}$$

The cyclic hemiketal–acyclic enol ratio is ~20:1 at 25°C and μ = 0.1. This conclusion is consistent with earlier spectrometric findings in other solvents (3–6).

Since the dissolution rate of warfarin was to be determined at μ = 0.5 for comparison with earlier studies (7, 8, 15), the pK_a of warfarin at this ionic strength was determined by both methods A and B. The observed pK_a of warfarin by method A was found to be 5.03 ± 0.02 (±*SD*).

The equilibrium solubility of a monoprotic weak acid in aqueous solution is given by:

$$S_T = [HA]_0 + [A^-] \qquad \text{(Eq. 6)}$$

where S_T is the total solubility of all the possible species, $[HA]_0$ is the saturated solubility of the un-ionized form(s) of the weak acid, *i.e.*, [I] + [II] in the case of warfarin, and $[A^-]$ is the amount of warfarin enolate, [III], present at equilibrium at the particular pH in question. Combining Eq. 6 with the K_a expression (Eq. 1) for warfarin yields:

$$S_T = [HA]_0 + \frac{K_{a_{obs}}{}^{warfarin}[HA]_0}{[H^+]} \qquad \text{(Eq. 7)}$$

A plot of S_T *versus* $1/[H^+]$ yields an intercept of $[HA]_0$ and a slope from which $K_{a_{obs}}{}^{warfarin}$ can be calculated. Figure 1 depicts this relationship for warfarin. From the intercept, the intrinsic solubility of un-ionized warfarin at 25 ± 0.5°C and μ = 0.5 was found to be 1.28×10^{-5} M, the $K_{a_{obs}}{}^{warfarin}$ was 8.75×10^{-6} ($pK_{a_{obs}}{}^{warfarin}$ = 5.06). The correlation coefficient for the plot was 0.999 (10 pH values, 2.20–6.67, and a total of 29 individual solubility determinations). The pK_a value of 5.06 correlates well with the value determined spectrophotometrically in this study and previous determinations (16, 17), and the aqueous solubility of the un-ionized warfarin acid of 1.28×10^{-5} M is similar to a recorded value in 0.1 M HCl of 1.43×10^{-5} (18).

Based on the findings that the predominant form of warfarin in the solid state and the probable predominant, un-ionized form of warfarin in solution is II, it was interesting to speculate that the conversion of II to III by whatever mechanism might not be a diffusion-controlled process. By using a stop-flow spectrophotometer and a pH jump technique, the transmission *versus* time oscilloscope tracing from mixing of an unbuffered pH 3.5 warfarin solution with a 0.1 M phosphate buffer solution of pH 6.5 (final pH on mixing, 6.5) gave a straight line (slope = 0). The absorbance calculated from the transmission tracing was consistent with a solution of 0.75×10^{-5} M warfarin of pH 6.5, *i.e.*, at all oscilloscope settings down to 1×10^{-3} s/division, the reaction (ionization) was found to be complete within the mixing time (2×10^{-3} s) of the stop-flow spectrophotometer, *i.e.*, $t_{1/2} < 1\text{-}2 \times 10^{-3}$ s. Under similar circumstances, the carbon acid phenylbutazone has a half-life of $\sim 12 \times 10^{-3}$ s (12).

[1] Sigma Chemical Co., St. Louis, Mo.
[2] Organon Pharmaceuticals, West Orange, N.J.
[3] Cary 219, Cary 118, or Zeiss PM 6 UV spectrophotometers.
[4] Durrum stopped-flow spectrophotometer, with a thermostated cell and syringes maintained at 25 ± 0.2°C.
[5] A wavelength at which there is a maximum transmission difference between un-ionized and ionized warfarin.

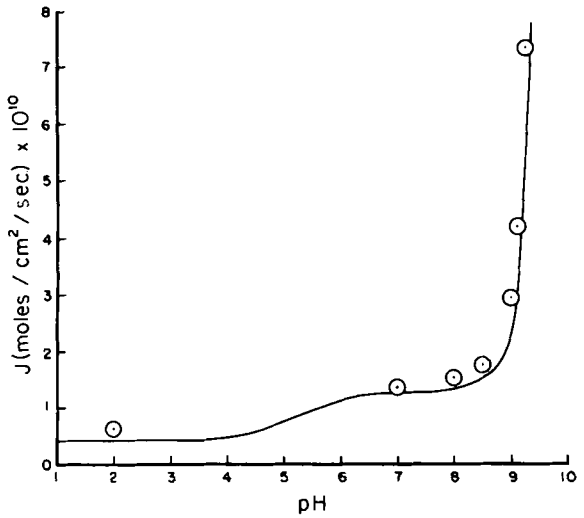

Figure 2—*Plot of the initial dissolution rate (flux) of warfarin from a rotating disk (600 rpm) as a function of pH, unbuffered but maintained by a pH-stat. Key: (⊙) experimental points (mean of 3–4 determinations at each pH); (—) predicted by Eq. 8.*

The dissolution rate of organic acids undergoing rapid ionization, dissolving from a rotating disk into nonbuffered aqueous solution under sink conditions in which the bulk solution pH has been maintained by a pH-stat, has been mathematically defined assuming a film model (7, 8) by:

$$J = \frac{D_{HA}}{h}[HA]_0 + \frac{D_H}{h}([H^+]_0 - [H^+]_h) + \frac{D_{OH}}{h}([\overline{O}H]_h - [\overline{O}H]_0) \quad \text{(Eq. 8)}$$

where J is the initial dissolution rate or flux with units of mol/cm²/s; D_{HA} is the diffusivity of the dissolving acid species in cm²/s; h is the film thickness of the diffusion resistance layer in cm; $[HA]_0$ is the molar saturated solubility of the dissolving acid under suppressed ionization conditions and is the amount of HA assumed to exist at the solid-liquid interface; D_H and D_{OH} are the diffusion coefficients (diffusivity) for hydrogen ion and hydroxide ion, respectively [2.8×10^{-5} cm²/s, (7)]; $[H^+]_0$ and $[H^+]_h$ are the hydrogen ion concentrations at the solid-liquid interface and in the bulk solution, respectively; and $[\overline{O}H]_h$ and $[\overline{O}H]_0$ are the hydroxide ion concentrations at the bulk solution and at the solid-liquid interface, respectively (calculated from the equation $[\overline{O}H] = K_w/[H^+]$). The aqueous diffusion layer thickness, h, can be calculated from (7, 8, 19):

$$h = 1.612 D_{HA}^{1/3} \nu^{1/6} \omega^{-1/2} \quad \text{(Eq. 9)}$$

where ν is the kinematic viscosity of the dissolution medium [9.77×10^{-3} stokes (7, 8)], and ω is the rotation rate of the disk in rad/s ($\omega^{1/2}$ at 600 rpm is 7.93). The value for $[H^+]_0$ can be calculated by solving Eq. 10 (7) for varying $[H^+]_h$ concentrations, as measured by the pH of the bulk medium:

$$-D_H[H^+]_0^2 + (D_H[H^+]_h - D_{OH}[\overline{O}H]_h)[H^+]_0 + K_w(D_{OH} + D_A K_1[HA]_0) = 0 \quad \text{(Eq. 10)}$$

where K_w is the dissociation constant for water at 25°C (10^{-14} M²); D_A is the diffusivity of the anionic form of HA and was assumed to be numerically equal to D_{HA} (7, 8); and K_1 is equal to K_a/K_w, where K_a is the dissociation constant of the acid. In the present case, K_a was assumed to be $K_{a_{obs}}^{warfarin}$ determined from the solubility study. Therefore, K_1 was numerically equal to 8.75×10^8.

An estimate of D_{HA} (and D_A), the diffusivity of the acid, is required to calculate J as a function of bulk solution pH (nonbuffered) with Eq. 8-10. In an earlier study, this was done by following J, the flux, as a function of $\omega^{1/2}$ under pH conditions in which ionization of the dissolving acid was suppressed and the diffusivity was calculated from the Levich equation (19). It was not possible to determine accurately the initial dissolution rate of warfarin at low pH because of its low solubility. For example, a saturated aqueous solution of warfarin at pH values < pK_a has an absorbance of only 0.16 at 285 nm, which is the absorbance maximum at pH values < pK_a. Therefore, the initial dissolution rate would require measuring very small absorbance readings[6]. The diffusivity of warfarin was, therefore, calculated from the earlier work by assuming the square root relationship to molecular weight using benzoic acid, 2-naphthoic acid, and indomethacin as standards (7). A mean value for D_{HA} for warfarin of 5.7×10^{-6} cm²/s at 25°C and $\mu = 0.5$ was therefore assumed in calculating J from Eq. 8.

Figure 2 is a plot of the initial dissolution rate of warfarin from a rotating disk (600 rpm) as a function of pH, unbuffered but maintained constant by a pH-stat (μ maintained at 0.5). The theoretical line tends to underestimate the dissolution rates by ~20%. The major differences appear to be between the estimated and calculated values for the dissolution rate at pH 2. However, as already discussed, it is very difficult to experimentally determine the initial dissolution rates at this or any acidic pH with certainty. Various parameters within Eq. 8 could be manipulated to give a better fit between the experimental and theoretical values. However, it was felt that this would serve no meaningful purpose at this stage, since the overall fit was reasonably good using parameters that were either determined experimentally or estimated from earlier studies.

If the dissolution of warfarin were to behave nonclassically due to slow ionization (15), the experimental dissolution rates would be overestimated by Eq. 8 since it is assumed in Eq. 8 that the dissolving acid dissociates at diffusion-controlled rates. If anything, Eq. 8 underestimated by ~20% the observed results in the present study. Therefore, it seems safe to conclude, based on the data in Fig. 2 and the ionization kinetics mentioned earlier, that warfarin behaves as if it were a fast-ionizing acid with a solubility in its unionized form of 1.28×10^{-5} M and a pK_a of 5.06.

REFERENCES

(1) E. Valente, W. Trager, and L. Jensen, *Acta Crystallogr., Sect. B*, **31**, 954 (1975).

(2) G. Bravic, T. Gaultier, and C. Hauw, *C. R. Hebd., Seances Acad. Sci., Ser. C*, **277**, 1215 (1973).

(3) D. Giannini, K. Chan, and J. Roberts, *Proc. Natl. Acad. USA*, **71**(10), 4221 (1974).

(4) K. Chan, D. Giannini, A. Cain, J. Roberts, W. Porter, and W. Trager, *Tetrahedron*, **33**, 899 (1977).

(5) E. J. Valente, E. C. Lingafelter, W. R. Porter, and W. F. Trager, *J. Med. Chem.*, **20**, 1489 (1977).

(6) E. J. Valente, W. R. Porter, and W. F. Trager, *J. Med. Chem.*, **21**, 231 (1978).

(7) K. G. Mooney, M. A. Mintun, K. J. Himmelstein, and V. J. Stella, *J. Pharm. Sci.*, **70**, 13 (1981).

(8) K. G. Mooney, M. A. Mintun, K. J. Himmelstein, and V. J. Stella, *J. Pharm. Sci.*, **70**, 22 (1981).

(9) A. Albert and E. P. Serjeant, "Ionization Constants of Acids and Bases," Methuen, London, England, 1962.

(10) "Physical Pharmacy," A. N. Martin, J. Swarbrick, and A. Cammarata, Eds., Lea & Febiger, Philadelphia, Pa., 1969, p. 310–312.

(11) E. R. Garrett and C. H. Won, *J. Pharm. Sci.*, **60**, 1801 (1971).

(12) V. J. Stella and J. D. Pipkin, *J. Pharm. Sci.*, **65**, 1161 (1976).

(13) V. J. Stella and R. Gish, *J. Pharm. Sci.*, **68**, 1042 (1979).

(14) V. J. Stella and R. Gish, *J. Pharm. Sci.*, **68**, 1047 (1979).

(15) K. G. Mooney, M. Rodriguez-Gaxiola, M. Mintun, K. J. Himmelstein and V. J. Stella, *J. Pharm. Sci.*, **70**, 1358 (1981).

(16) G. F. Hiskey, E. Bullock, and G. Whitman, *J. Pharm. Sci.*, **51**, 43 (1962).

(17) W. F. van der Giesen and L. H. M. Janssen, *Int. J. Pharmacol.*, **12**, 231 (1982).

(18) J. G. Wagner, P. G. Welling, K. P. Lee, and J. E. Walker, *J. Pharm. Sci.*, **60**, 666 (1971).

(19) V. G. Levich, "Physico-Chemical Hydrodynamics," Prentice-Hall, Englewood Cliffs, N.J., 1962.

ACKNOWLEDGMENTS

This work was supprted by Grant GM 22357 from the National Institutes of Health. J.D.P. acknowledges the support of the American Foundation for Pharmaceutical Education.

[6] For example, true initial dissolution rates require measuring J under conditions at which <10% of the saturated solubility has been reached. Thus, accurate absorbance measurements of <0.02 are required. Under these restraints, problems such as fines on the pellet can lead to significant overestimation of the initial fluxes.

Gastrointestinal Absorption of the Strongly Acidic Drug Proxicromil

MICHAEL G. DAVIS *, CAROL N. MANNERS ‡, DAVID W. PAYLING ‡, DENNIS A. SMITH ‡x, and CAROL A. WILSON *

Received March 16, 1983, from *The School of Natural Sciences, Biological & Environmental Sciences Division, The Hatfield Polytechnic, College Lane, Hatfield, Herts. AL10 9AB and ‡Fisons Pharmaceutical Division, Bakewell Road, Loughborough, Leics. LE11 ORH, U.K. Accepted for publication July 25, 1983.

Abstract □ Gastrointestinal absorption of the strongly acidic drug proxicromil has been studied with respect to its physical organic chemistry. The lipophilicity of the drug above pH 6 in octanol–buffer partition experiments is dependent on ion pair formation. Similar trends were demonstrated for the *in vitro* partition of the compound into GI tissue. The absorption of the compound from the perfused GI tract of rats *in vivo* was not consistent with classical un-ionized drug absorption theories and indicated the operation of other processes, especially ion pair formation, as major mechanisms of proxicromil absorption.

Keyphrases □ Proxicromil—GI absorption, lipophilicity, ion pair formation □ Absorption, GI—proxicromil, lipophilicity, ion pair formation

The transfer of acidic drugs across membranes has usually been ascribed to the un-ionized form (1). Many acidic drug substances possess only a weak acidic function which allows a significant proportion of the un-ionized drug to be present at physiological pH. The oral anti-allergy agent proxicromil (FPL 57787, I) (2) and related compounds [FPL 55365(II) and FPL 57579(III)] are of considerable interest since the strong acidity of I (pK_a 1.93) (3) causes the proportion of the drug present as the un-ionized species at physiological pH to be very small. Despite this, the compound has been demonstrated to be well absorbed in a number of animal species and in humans (>60%) (4). The compound also crosses other membrane systems, since it is transferred into the milk from the plasma when administered to lactating albino rats (5). Since the processes involved in the passage of the drug are not adequately explained by the sole passage of un-ionized drug, alternative explanations must be sought.

Several works on GI absorption refer to ion pair partitioning (for a review, see Ref. 6) as a possible mechanism of ionized drug absorption. Ion pairing forms a neutral species by electrostatic attraction between oppositely charged ions in solution. Houston and Wood (6), in their monograph on the GI absorption of drugs, state that there is no *a priori* reason why any molecular entity, regardless of ionic status, should not be absorbed if it possesses adequate partitioning characteristics. We have therefore examined the partitioning characteristics of proxicromil and related compounds from buffer systems into octanol. The partitioning of proxicromil into GI tissues has also been examined. Similarly, we have investigated the absorption of the drug in the albino rat using a perfused intestine system.

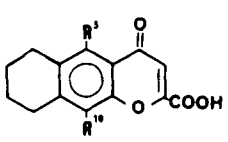

I: R^5 = OH, R^{10} = $CH_2CH_2CH_3$
II: R^5 = H, R^{10} = H
III: R^5 = H, R^{10} = $CH_2CH_2CH_3$

EXPERIMENTAL SECTION

Chemicals—[^{14}C]Proxicromil (9.67 mCi/g) and unlabeled proxicromil, prepared in-house, had a radiochemical and chemical purity of 99%. The octanol[1] used had been specially purified for the determination of partition coefficient of drugs. For physicochemical and *in vivo* studies, McIlvaine's (7) citrate–phosphate buffer (for pH 2.2–6.4) and modified Sörensen's (7) phosphate buffer (NaH_2PO_4 replaced KH_2PO_4) (for pH 7.4–8.2) had the sodium ion concentration adjusted to 0.155 M by the addition of NaCl, where necessary. Krebs–Ringer bicarbonate buffer was modified to exclude Ca^{2+} and Mg^{2+} since these ions were found to cause precipitation of proxicromil. All other reagents[2] were of analytical reagent grade.

Solubility Determination—The aqueous solubility of proxicromil was measured (single determinations) in aqueous buffers at a series of pH values covering the range 0–7. Successive aliquots (1 mg) of the compound were added to the buffer (2 mL) at 20°C until saturation was indicated by the presence of undissolved material, for up to 3 h. The pH was checked, and the sample was filtered (cellulose filter, 0.45 μm)[3] and assayed spectrophotometrically for proxicromil (360 nm)[4].

Physicochemical Measurements—All distribution coefficients were measured by the shake-flask method (8). Results are reported as the mean of at least three determinations, together with the observed spread. Compounds were partitioned between 1-octanol saturated with buffer and the same aqueous phase saturated with 1-octanol; the concentration of compound in the organic phase was analyzed (UV spectrophotometry at 360 nm)[4] before and after equilibration. Volume ratios of the two phases were selected to give a reduction of ~50% in the UV absorbance of the solution after equilibration. Equilibration was carried out by shaking at room temperature for 1 h, followed

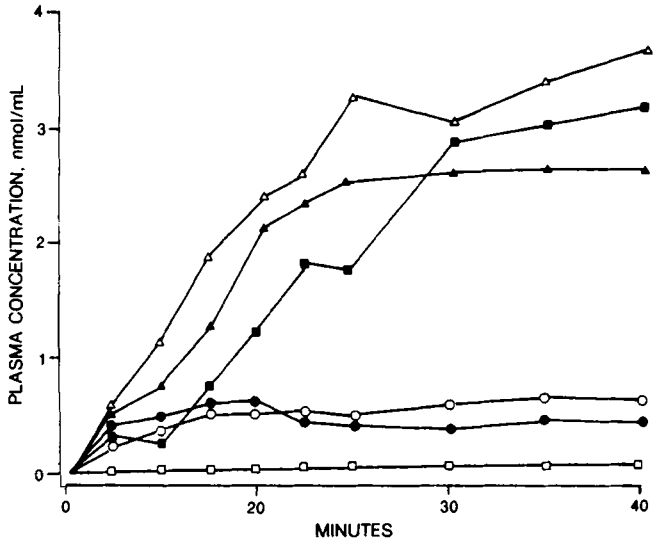

Figure 1—*Plasma concentrations of radioactivity (equivalent to proxicromil) after injection of [^{14}C]proxicromil into separate regions of the rat gut. Key: (△) duodenum; (▲) jejunum; (■) upper ileum; (○) lower ileum; (●) colon; (□) stomach and cecum. The stomach and cecum show very similar negligible absorption, and the results are represented therefore as a single point; n = 4 for each tissue.*

[1] Spectrograde; Fisons Scientific Apparatus, Loughborough, Leicestershire, U.K.
[2] BDH Ltd, Poole, Dorset, U.K.
[3] Millipore (UK) Ltd, London.
[4] Model SP1700; Pye Unicam, Cambridge, U.K.

0022-3549/84/0700-0949$01.00/0
© 1984, American Pharmaceutical Association

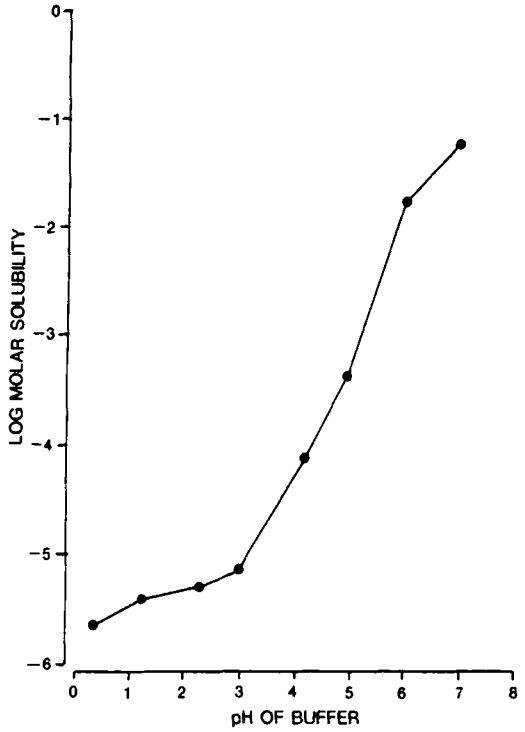

Figure 2—*Aqueous solubility of proxicromil with respect to buffer pH (see text).*

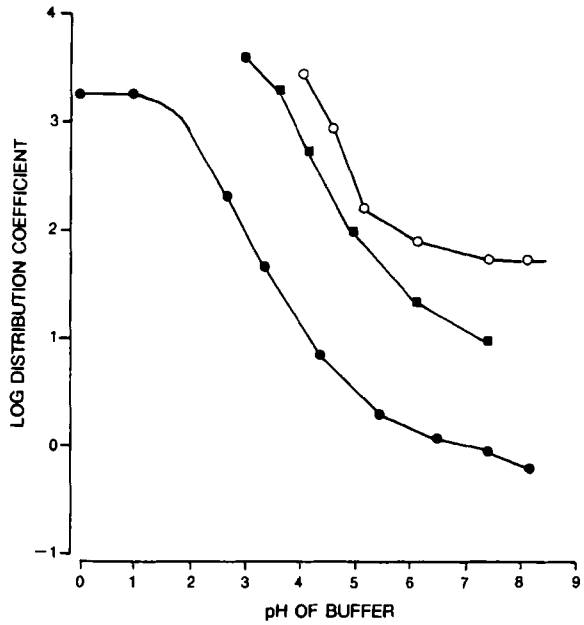

Figure 3—*Distribution coefficient (log* D*) of II (●), III (■), and proxicromil (I) (○) with respect to buffer pH. Variation of log* D *was* < ±*0.03 of the mean.*

by centrifugation[5] at 2000 rpm for 1 h. The distribution coefficient (D) was calculated from the ratio of the overall concentration of compound in the ionized and undissociated states between the two phases (9).

Measurements of distribution coefficients were made over a wide pH range for II (pH 0-8.2), III (pH 3-8.2), and I (pH 3-8.2). Control of the aqueous phase pH was achieved using the buffers described above adjusted to a sodium ion concentration of 0.155 M. Experiments at pH 0-2 employed dilute hydrochloric acid with added sodium chloride (0.155 M). Values of log $D > 4$ could not be measured to an acceptable accuracy owing to practical limitations of the spectrophotometric method.

The sodium content in the octanol phase was measured in proxicromil distribution experiments at various aqueous phase pH values between 4.0 and 8.2, by atomic emission spectrometry[6]. Sodium content results are given as the average value from two experiments at each pH value. Control experiments were carried out under the same conditions, but omitting the proxicromil (I), to estimate background sodium levels in the octanol. All test solutions contained 4 mL of octanol made up to 50 mL with methanol. Where the volume of octanol available was smaller (pH 5-8.2), additional octanol was added in order to keep the overall solvent composition constant.

The effect of cationic concentration on the octanol distribution coefficient of proxicromil was measured at a constant pH of 7.4 in a dilute phosphate buffer system (0.02 M) containing varying concentrations of either sodium chloride or potassium chloride (0.02-0.24 M).

Experiments with Everted Gut Segments—Male Wistar rats[7] were killed by a blow to the head, and the jejunal section of the small intestine removed. This section (between 3 and 18 cm from the pylorus) was everted over a glass rod and cut into 2-3-mm segments (10). Three single segments from three separate rats were incubated together in 25-mL conical flasks at 37°C in Krebs-Ringer bicarbonate buffer (2 mL) containing the appropriate concentration of [^{14}C]proxicromil. Experiments were carried out in triplicate at various pH values between 3.5 and 8.5.

The flasks were aerated for 30 s with oxygen-carbon dioxide (95:5), sealed with rubber turnover closures[8], and shaken at 37°C for the determined period of time in a shaking water bath. At the completion of the incubation the tissue was removed, rinsed twice in 0.9% NaCl solution, blotted, and weighed.

After incubation, segments were placed in aqueous sodium hydroxide (0.5 mL, 1 M) in scintillation vials. The containers were then heated in an oven to ≤80°C to speed up tissue digestion, which was continued until a uniform solution was obtained. The contents were allowed to cool to room temperature and then acidified with an equal volume of aqueous hydrochloric acid (2 M), and Bray's scintillation fluid was added (5 mL). Aliquots of incubation medium (0.2 mL) were also taken for radioactivity determination. Radioactivity was measured in a scintillation counter[9], and counting efficiency was determined using channel ratios for quench correction.

Experiments with Gut *In Situ*—Male CR/CD rats[10] (weight range, 240-280 g; fed *ad libitum*) were anesthetized with pentobarbital solution administered *via* an indwelling needle in the caudal vein. Following an incision in the throat, the carotid artery was exposed and cannulated with polyethylene tubing. For experiments to investigate the site of absorption, a midline incision was made and the GI tract was ligated in each animal with surgical thread to isolate either the stomach, duodenum, jejunum, upper ileum, lower ileum,

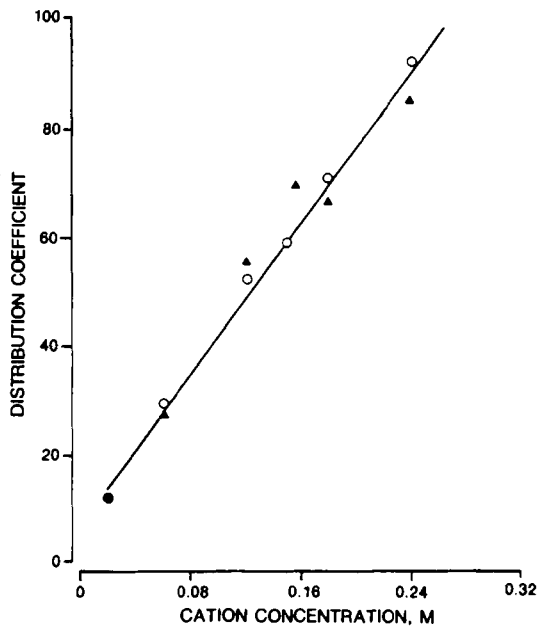

Figure 4—*Relationship between the distribution coefficient (*D*) of proxicromil and the cation concentration of Na^+ (○) or K^+ (▲). Variation in* D *was* < ±*2.5% of the mean value in all cases.*

[5] Model Mistral 4L; MSE Instruments, Crawley, U.K.
[6] Model 703; Perkin-Elmer.
[7] Hatfield Polytechnic.
[8] Suba-Seal, Barnsley, U.K.
[9] Model CM2700; Tracerlab Services Ltd., Twickenham, U.K.
[10] Charles River, Manston, Kent, U.K.

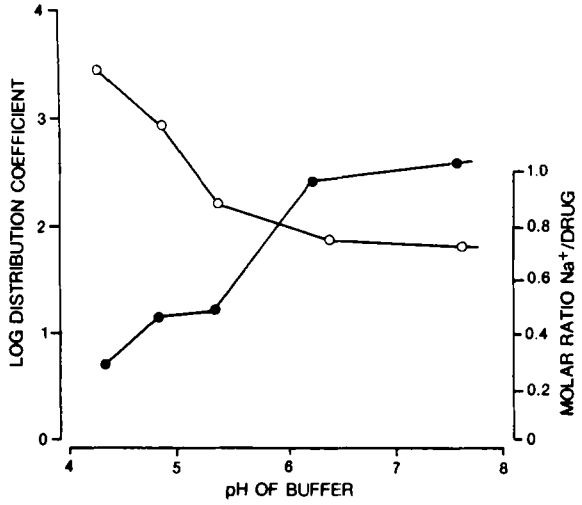

Figure 5—*Relationship between the distribution coefficient (log D) of proxicromil (○) and the ratio of Na^+ to proxicromil ions (●) present in the octanol phase with respect to pH.*

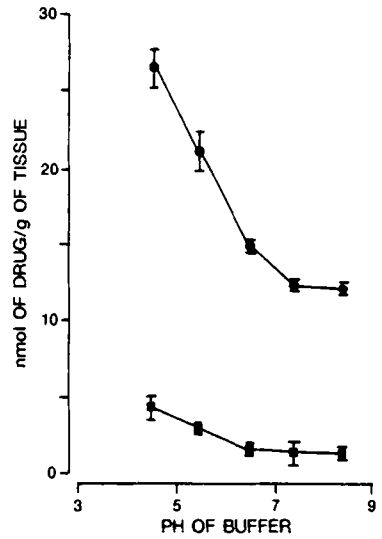

Figure 6—*Partitioning of proxicromil into everted jejunal segments with respect to pH. Incubation of the segments was conducted in proxicromil-buffer solutions for 30 min at concentrations of 1.0 mM (●) and 0.1 mM (■); n = 3 for each point.*

colon, or cecum. Proxicromil was administered as a bolus injection (0.2 mL) into the isolated segment in modified Sörensen's phosphate buffer, sodium ion concentration 0.155 M. Arterial blood samples were collected from the carotid artery at intervals for 60 min.

The absorption of the drug was investigated after single-pass perfusion at various pH values. For these experiments a midline incision was made and a 20-cm length of silicone rubber tubing (2 mm i.d.) was inserted ventrally into the duodenum 2 cm from the stomach pylorus. The end inserted into the duodenum had a number of turns of surgical thread glued to the extreme end which, in conjunction with ligation of the duodenum, secured the tubing. The other end of the tubing was adapted to take standard syringe fittings. A similar length of tubing was inserted dorsally into the jejunum and secured in an identical manner to give a 10-cm section of perfused gut. All perfusion solutions were maintained at 37°C. The gut was then flushed to remove debris by gentle perfusion of saline (5 mL) administered *via* a syringe, followed by flushing with buffer (5 mL) at the respective pH of investigation. Perfusion of the buffer was continued for a further 10 min at a steady rate of 1 mL/min. After this, a solution of [^{14}C]proxicromil (1 mM; 0.6 μCi/mL) dissolved in the same buffer was rapidly flushed through the intestine (5 mL) and then perfused at a rate of 1 mL/min for 20 min. Blood samples were collected into heparinized capillary tubes at 4-min intervals from the carotid vein cannula. The pH of the eluant buffer was monitored throughout the experiment.

In certain experiments the perfusion was performed using the segmented flow method of Winne (11). Total rate of buffer perfusion remained at 1 mL/min. Plasma was obtained by centrifugation of blood at 2500×*g* for 10 min. Radioactivity present in plasma was obtained by mixing the samples with liquid scintillation cocktail[11] followed by liquid scintillation counting. Counting efficiency was determined by the external standard channels ratio method.

RESULTS AND DISCUSSION

Site of Absorption—To determine if the absorption of proxicromil observed in animals was from the stomach or from other regions of the GI tract, a bolus of [^{14}C]proxicromil was injected into various regions of the gut, and blood samples were collected at intervals. Rapid absorption was observed from the duodenum, jejunum, and ileum, while much slower absorption occurred from the lower ileum and colon and very little absorption from the stomach and cecum (Fig. 1). Since little or no absorption occurred from the stomach, it is likely that proxicromil is absorbed in intact animals from regions of the GI tract in which the pH is approximately neutral. As little proxicromil is absorbed in the stomach *in vivo*, where the compound would be substantially in its un-ionized state, the aqueous solubility of the compound at various pH values was investigated since lack of solubility would limit absorption. Also the partitioning of the compound was determined in the octanol-aqueous buffer system over the same range of pH. Emphasis was given to the higher pH values corresponding to those of the region of the GI tract where absorption had been observed.

Solubility and Partitioning—The aqueous solubility of proxicromil is strongly pH dependent (Fig. 2). The insolubility at low pH reflects the low water solubility of the compound when its carboxyl group is undissociated (HA). At pH values above the pK_a (1.93) (3), solubility in water increases rapidly reflecting the abundant water solubility of the ionized compound (A^-). The lack of absorption of proxicromil from the stomach is paralleled by its lack of solubility and, hence, low availability at gastric pH.

The relationship between pH and partition was studied for I-III (Fig. 3). The partition coefficient (P) refers to the ratio of concentrations of the undissociated compound (HA) between the two liquid phases (Eq. 1). The distribution coefficient (D) represents the overall ratio of concentrations of proxicromil in the octanol and aqueous phases regardless of ionization (9) (Eq. 2). Equation 2 is expanded from its usual form (9) to show the possibility of the sodium salt as potentially contributing to the concentration of proxicromil in the octanol phase:

$$P = \frac{[HA]_{oct}}{[HA]_{aq}} \qquad \text{(Eq. 1)}$$

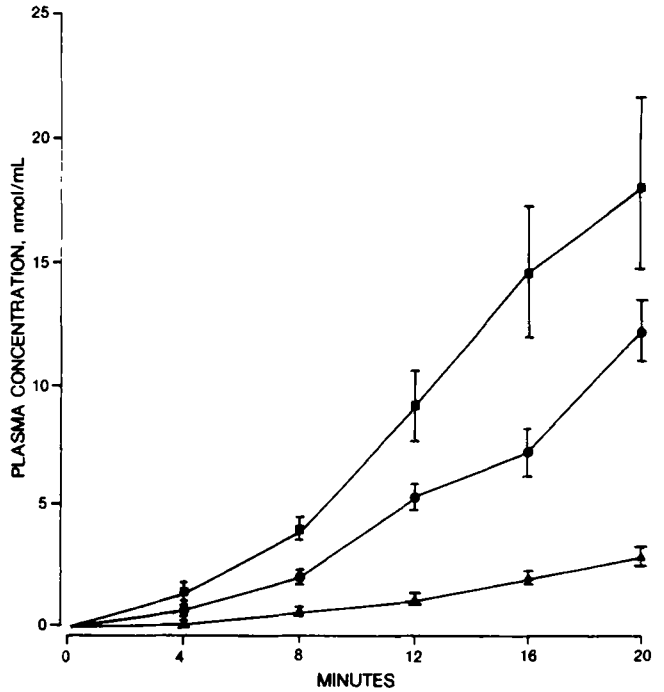

Figure 7—*Plasma concentrations of radioactivity (equivalent to proxicromil) during perfusion of the small intestine of the rat with [^{14}C]proxicromil-buffer solutions at pH 5 (■), 7 (●), and 9 (▲) (see text); n = 6 for each point.*

[11] Fisofluor mpc; Fisons Scientific Apparatus, Loughborough, Leicestershire, U.K.

Table I—Influence of pH of Perfusing Buffer on Proxicromil Absorption Expressed as Absorption Relative To pH 6.98

pH of Eluant Buffer	Absorption Ratio Calculated Using: Un-ionized Drug[a]	$AUC_{0\text{-}20\ min}$[b]	Plasma Conc. at the End of Infusion[b]
8.93 ± 0.02	0.01	0.17	0.17
6.98 ± 0.01	1.00	1.00	1.00
5.23 ± 0.01	56	1.42	1.24

[a] Expected ratio if un-ionized drug was the sole form of drug absorbed. [b] Ratio calculated from perfusion experiments. See text and Fig. 7.

$$D = \frac{[HA]_{oct} + [Na^+A^-]_{oct}}{[HA]_{aq} + [A^-]_{aq}} \quad \text{(Eq. 2)}$$

The relationship of log D to pH was measured for II over the pH range 0–8. For the other two compounds, however, log D could not be obtained below pH 3 owing to limitations of the spectrophotometric analysis. At pH values ≤5, all three compounds decrease in log D, their behavior being described by the pH-partition relationship:

$$\log\left(\frac{P}{D} - 1\right) = pH - pK_a \quad \text{(Eq. 3)}$$

Substitution of the data for II (Fig. 3) into Eq. 3 yields a pK_a value of 1.65 ± 0.1, in agreement with other reports (3).

The proportion of undissociated proxicromil in the water phase falls from 0.0676 at pH 5.1 to ~0.0001 at pH 8.0 (calculated from dissociation constant pK_a = 1.93). Using Eq. 3, it can be calculated that the observed value of log D of 2.17 at pH 5.1 should fall to −0.83 at pH 8.0. In contrast to this, however, it was found that at higher pH the distribution coefficient became progressively independent of pH. This region was examined in more detail to identify the factors which now control the distribution ratio. At pH 7.4 a linear relationship was established between observed distribution coefficient (D) and concentration of potassium or sodium ion in the aqueous phase (Fig. 4). This is parallel to the findings on the lipophilic base chlorpromazine (12), where added counterions such as chloride (Cl^-) also produced a linear relationship to distribution coefficient. This is consistent with ion pair partition, whose extent is related to the product of proxicromil ion and sodium ion concentrations in the aqueous phase. Scheme I indicates a series of equilibria which are consistent with the observed behavior. Proxicromil anion entry into the organic phase is shown as a distribution rather than a partition ratio (9), since it is a complex effect dependent in magnitude on factors including, for example, counterion concentration.

$$\begin{array}{ccc} [HA]_{oct} & & [Na^+A^-]_{oct} \\ \Big\downarrow\uparrow P_{HA} & & \Big\downarrow\uparrow \\ [HA]_{aq} & \overset{K_a}{\rightleftharpoons} & [A^-]_{aq} \end{array}$$

Scheme I

Analysis of the octanol layer for sodium ion using atomic emission analysis showed the concentrations of proxicromil (UV spectrophotometry) and sodium (atomic emission) to be in 1:1 molar agreement in distribution experiments at pH 7.4. Similar experiments at a series of lower pH values (Fig. 5) showed the penetration of sodium into the octanol to be significant only at pH > 5. Below this pH, the ratio of sodium ion to proxicromil fell as conventional pH-partition of the undissociated compound (HA) became dominant. This evidence for ion pair partition was supplemented by analysis for sodium ion in octanol equilibrated with phosphate buffer containing sodium ion (0.155 M) but no proxicromil. The penetration of sodium ions into the octanol thus was insignificant, despite its high concentration in the aqueous phase, unless proxicromil anion was available.

Effect of pH on Absorption—The experiments utilizing octanol were reproduced using gut segments *in vitro*. Uptake of [^{14}C]proxicromil into jejunal segments was studied at 0.1 and 1.0 mM concentrations of proxicromil at various pH values. The results are shown in Fig. 6 and demonstrate that at pH < 6 the lower the pH, the greater the partitioning into the tissue. At pH >6 the uptake was approximately constant. Similar trends were shown at incubation times up to 90 min. The partitioning of proxicromil into gut tissue, therefore, closely follows the characteristics observed for the partitioning of the compound into octanol with pH-dependent partitioning at low pH and a constant partitioning of the drug at pH > 6. The change in behavior for the compound takes place in both octanol and in gut tissue at pH ~6 and very far from the value of the pK_a of the drug (1.93).

The effect of buffer pH on proxicromil absorption *in vivo* was studied using *in situ* perfused gut loops. Figure 7 illustrates the plasma concentrations of radioactivity present in plasma after perfusion of the gut of anesthetized animals with [^{14}C]proxicromil dissolved in buffers of varying pH. The plasma concentrations are increased by decreasing pH. Taking either peak plasma concentration or areas under the plasma curve ($AUC_{0\ 20\ min}$ as measured by the trapezoidal method) (Table I), absorption can be shown to be increased at a nominal pH 5 and decreased at a nominal pH 9 from that at pH 7. These increases are much smaller than would be expected if un-ionized drug was the sole determinant since over the pH range evaluated (5.23–8.93), there is an ~5000-fold change in free drug concentration. The absorption at pH 5.0 is not limited by the unstirred layer (13), since in experiments in which this layer was deliberately disrupted by alternating buffer perfusion with air using the method of Winne (11), there was no significant change in proxicromil absorption.

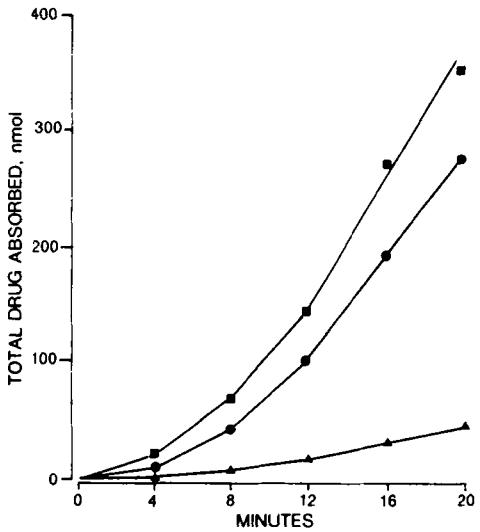

Figure 8—*Cumulative total absorption of radioactivity (equivalent to proxicromil) during perfusion of the small intestine of the rat with [^{14}C]-proxicromil–buffer solutions at pH 5 (■), 7 (●), and 9 (▲) (see text).*

The shape of the plasma curve, however, indicates that absorption is not defined by a single rate constant, since the zero-order input of drug, by perfusion, to the intestine should result in a curve resembling the classical curves following intravenous infusion. Calculation of clearance in the rat (0.3 mL/min) and volume of distribution (17 mL) from intravenous infusion experiments[12] allow calculation of the actual amount absorbed using the classical approach of Loo and Riegelman (14). Figure 8 illustrates the total amount absorbed with time during gut perfusion experiments.

The data can be interpreted by a model in which the mucosal tissue itself represents a compartment (6) in proxicromil absorption. The model is defined by Scheme II:

$$\text{proxicromil in lumen} \xrightarrow{k_0} \text{proxicromil in mucosa}$$

$$\xrightarrow{k_1} \text{proxicromil systemically absorbed}$$

Scheme II

The constant k_0 represents the zero-order absorption of the drug from the constant perfusion system and is a hybrid of the actual absorption rate constant and the perfusion rate. The constant k_1 represents the rate constant for the passage of drug from the mucosa to the circulatory system. Individual zero-order rates of absorption (k_0) were calculated by methods analogous to those used for intravenous infusion experiments (15). The linear portion of the curve for each pH value in Fig. 8 (12–20 min) represents the zero-order rate of absorption, yielding approximate values of 30, 20, and 4 nmol/min at pH 5, 7, and 9, respectively. The linear portion of the curves at each pH value can be extrapolated to give an intercept value from which k_1 can be calculated (0.14 min^{-1}).

CONCLUSIONS

The partitioning characteristics demonstrated in octanol and jejunal segments can partly be reproduced *in vivo* in the perfused intestine. While the perfusion results could be affected by a number of other factors, it is likely that at pH values > 6 ion pair formation operates to allow distribution of the

[12] Unpublished results.

compound into lipoidal phases. This process is likely to occur in the intestine as demonstrated both *in vitro* and *in vivo*. Since absorption of the compound occurs from regions of the GI tract which have pH values >6, it is suggested that ion pair formation with naturally abundant cations such as sodium plays a significant role in the absorption of proxicromil.

An alternative explanation for the GI absorption is that there is a difference between bulk and surface pH. The data of Lei *et al.* (15) suggest the real surface pH might be lower than that expected from bulk pH. To overcome surface pH effects in the intestinal perfusion experiments, we have equilibrated the gut for 10 min by perfusion of buffer at the appropriate pH at 1 mL/min. Under these conditions, surface pH and bulk pH should have tended toward an equilibrium (16), the true pH of which would be very close to that of the measured eluant buffer (see Table I). The linear rate of absorption at each pH indicated in Fig. 7 also demonstrates that an equilibrium has been achieved, since a decreasing rate of absorption would be expected at the lower pH values as the surface pH gradually increased. The significance of a surface pH of 6.5 in explaining absorption of acidic compounds is also of much greater relevance for compounds such as *n*-butyric acid (pK_a 4.9) (16) than proxicromil (pK_a 1.93).

The ion pair behavior described here is in marked contrast to the normally held concept (17). Proxicromil possesses intrinsic lipophilicity and requires only charge neutralization to partition into lipoidal phases. Endogenous ions such as sodium and potassium readily form such neutral lipophilic ion pair complexes. This can be contrasted to the facilitation of partitioning of a nonlipophilic drug by the incorporation of a lipophilic counterion, the concept of which has led Jonkman and Hunt (17) to consider ion pair absorption as more fiction than fact.

REFERENCES

(1) C. A. M. Hogben, D. J. Tocco, B. B. Brodie, and L. S. Schanker, *J. Pharmacol.*, **125**, 275 (1959).

(2) J. Augstein, H. Cairns, D. Hunter, T. B. Lee, J. Suschitzky, R. E. C. Altounyan, D. M. Jackson, J. Mann, T. S. C. Orr, and P. Sheard, *Agents Actions*, **I**, 443 (1977).

(3) J. Swarbrick, G. Lee, J. Brom, and N. P. Gensmantel, *J. Pharm. Sci.*, in press.

(4) D. A. Smith, *Br. J. Pharmacol.*, **66**, 422P (1979).

(5) A. N. Fisher, M. G. Neale, and D. A. Smith, *Xenobiotica*, **11**, 871 (1981).

(6) J. B. Houston and S. G. Wood, in "Progress in Drug Metabolism," vol. 4, J. W. Bridges and L. F. Chasseaud, Eds., Wiley, New York, N.Y., 1980, p. 100.

(7) "Documenta Geigy," K. Diem and C. Leutner, Eds., Geigy Pharmaceuticals, Macclesfield, England, 1975, p. 281.

(8) A. Leo, C. Hansch, and D. Elkins, *Chem. Rev.*, **71**, 537 (1971).

(9) R. A. Scherrer and S. M. Howard, *J. Med. Chem.*, **20**, 53 (1977).

(10) J. C. Crawhall and M. G. Davis, *Biochem. J.*, **112**, 571 (1969).

(11) D. Winne, *Experientia*, **32**, 1278 (1976).

(12) K. S. Murthy and G. Zografi, *J. Pharm. Sci.*, **59**, 1281 (1970).

(13) W. L. Hayton, *J. Pharmacokinet. Biopharm.*, **8**, 321 (1980).

(14) M. Gibaldi and D. Perrier in "Pharmacokinetics," Decker, New York, N.Y., 1975, p. 32.

(15) F-H. Lei, M. L. Lucas, and J. A. Blair, *Biochem. Soc. Trans.*, **5**, 149 (1977).

(16) W. I. Higuchi, N. F. H. Ho, J. Y. Park, and I. Komiya, in "Drug Absorption," Proceedings of the Edinburgh International Conference, L. F. Prescott and W. S. Nimmo, Eds., ADIS, 1981, p. 35.

(17) J. H. G. Jonkman and C. A. Hunt, *Pharm. Weekblad Sci. Ed.*, **5**, 41 (1983).

ACKNOWLEDGMENTS

The authors wish to thank Dr. K. Brown and Mr. S. C. Parkin for their encouragement and assistance. We would also like to thank Mr. D. Taylor for help with the atomic emission spectrometry and Dr. W. J. S. Lockley for synthesizing the radiolabeled compounds. One of us (CAW) thanks the SERC for the provision of a CASE studentship.

Relationship Between Molecular Structure and Cytochrome P_{450}–Metabolic Intermediate Complex Formation, Studied with Orphenadrine Analogues

AALT BAST ˣ, E. MARIA SAVENIJE-CHAPEL, and JAN NOORDHOEK

Received April 4, 1983, from the *Department of Pharmacology and Pharmacotherapy, Faculty of Pharmacy, State University of Utrecht, Catharijnesingel 60, 3511 GH Utrecht, The Netherlands.* Accepted for publication July 29, 1983.

Abstract □ Complexation of ferrous cytochrome P_{450} by metabolic intermediates formed during NADPH-catalyzed metabolism of compounds structurally related to orphenadrine was studied. This so-called metabolic intermediate complexation was determined in rat liver microsomes, obtained from phenobarbital-pretreated rats, at 455 nm using 33 μM of the orphenadrine derivatives. Using secondary amine derivatives with various *N*-alkyl substituents, a parabolic relationship between the logarithm of percentage of cytochrome P_{450} complexation and hydrophobic fragmental constant was observed. The derivative with a bulky tertiary butyl group, however, was devoid of metabolic intermediate-complexing activity. This indicates that steric factors besides lipid solubility may govern the complexing activity; also substitution at the phenyl group affects metabolic intermediate complex formation.

Keyphrases □ Cytochrome P_{450}—complexation with metabolic intermediates, orphenadrine analogues □ Orphenadrine—analogues, metabolic intermediate Complexation with cytochrome P_{450} □ Complexation—metabolic intermediate, orphenadrine analogues with cytochrome P_{450}

Several types of nitrogenous compounds have been shown to undergo cytochrome P_{450}-catalyzed metabolic conversions leading to metabolic intermediates that complex with cytochrome P_{450} (1–3). This complexed cytochrome P_{450} is inactive. Metabolic intermediate complex formation may therefore inhibit metabolic reactions (4). Among the nitrogenous compounds which elicit this complex formation, there are several classes of therapeutically important drugs.

Amphetamine derivatives form a metabolic intermediate complex with hepatic microsomal cytochrome P_{450} *in vitro*, but not *in vivo* (4, 5). With regard to amphetamine analogues, relationships between molecular structure and *in vitro* complexation have been described (4, 6). Recently, metabolic intermediate complex formation produced by macrolide antibiotics have gained much interest (7, 8). With a series of macrolide antibiotics, structural features which are important for the formation of metabolic intermediate complexes have been determined (9). However, with regard to compounds related to proadifen (like propoxyphene, desipramine, and orphenadrine) which produce such complexation both *in vitro* and *in vivo* (10, 11), little is known about the relationship between molecular structure and the ability to evoke complexes

0022-3549/84/0700-0953$01.00/0

© 1984, American Pharmaceutical Association

compound into lipoidal phases. This process is likely to occur in the intestine as demonstrated both *in vitro* and *in vivo*. Since absorption of the compound occurs from regions of the GI tract which have pH values >6, it is suggested that ion pair formation with naturally abundant cations such as sodium plays a significant role in the absorption of proxicromil.

An alternative explanation for the GI absorption is that there is a difference between bulk and surface pH. The data of Lei *et al.* (15) suggest the real surface pH might be lower than that expected from bulk pH. To overcome surface pH effects in the intestinal perfusion experiments, we have equilibrated the gut for 10 min by perfusion of buffer at the appropriate pH at 1 mL/min. Under these conditions, surface pH and bulk pH should have tended toward an equilibrium (16), the true pH of which would be very close to that of the measured eluant buffer (see Table I). The linear rate of absorption at each pH indicated in Fig. 7 also demonstrates that an equilibrium has been achieved, since a decreasing rate of absorption would be expected at the lower pH values as the surface pH gradually increased. The significance of a surface pH of 6.5 in explaining absorption of acidic compounds is also of much greater relevance for compounds such as *n*-butyric acid (pK_a 4.9) (16) than proxicromil (pK_a 1.93).

The ion pair behavior described here is in marked contrast to the normally held concept (17). Proxicromil possesses intrinsic lipophilicity and requires only charge neutralization to partition into lipoidal phases. Endogenous ions such as sodium and potassium readily form such neutral lipophilic ion pair complexes. This can be contrasted to the facilitation of partitioning of a nonlipophilic drug by the incorporation of a lipophilic counterion, the concept of which has led Jonkman and Hunt (17) to consider ion pair absorption as more fiction than fact.

REFERENCES

(1) C. A. M. Hogben, D. J. Tocco, B. B. Brodie, and L. S. Schanker, *J. Pharmacol.*, **125**, 275 (1959).

(2) J. Augstein, H. Cairns, D. Hunter, T. B. Lee, J. Suschitzky, R. E. C. Altounyan, D. M. Jackson, J. Mann, T. S. C. Orr, and P. Sheard, *Agents Actions*, **I**, 443 (1977).

(3) J. Swarbrick, G. Lee, J. Brom, and N. P. Gensmantel, *J. Pharm. Sci.*, in press.

(4) D. A. Smith, *Br. J. Pharmacol.*, **66**, 422P (1979).

(5) A. N. Fisher, M. G. Neale, and D. A. Smith, *Xenobiotica*, **11**, 871 (1981).

(6) J. B. Houston and S. G. Wood, in "Progress in Drug Metabolism," vol. 4, J. W. Bridges and L. F. Chasseaud, Eds., Wiley, New York, N.Y., 1980, p. 100.

(7) "Documenta Geigy," K. Diem and C. Leutner, Eds., Geigy Pharmaceuticals, Macclesfield, England, 1975, p. 281.

(8) A. Leo, C. Hansch, and D. Elkins, *Chem. Rev.*, **71**, 537 (1971).

(9) R. A. Scherrer and S. M. Howard, *J. Med. Chem.*, **20**, 53 (1977).

(10) J. C. Crawhall and M. G. Davis, *Biochem. J.*, **112**, 571 (1969).

(11) D. Winne, *Experientia*, **32**, 1278 (1976).

(12) K. S. Murthy and G. Zografi, *J. Pharm. Sci.*, **59**, 1281 (1970).

(13) W. L. Hayton, *J. Pharmacokinet. Biopharm.*, **8**, 321 (1980).

(14) M. Gibaldi and D. Perrier in "Pharmacokinetics," Decker, New York, N.Y., 1975, p. 32.

(15) F-H. Lei, M. L. Lucas, and J. A. Blair, *Biochem. Soc. Trans.*, **5**, 149 (1977).

(16) W. I. Higuchi, N. F. H. Ho, J. Y. Park, and I. Komiya, in "Drug Absorption," Proceedings of the Edinburgh International Conference, L. F. Prescott and W. S. Nimmo, Eds., ADIS, 1981, p. 35.

(17) J. H. G. Jonkman and C. A. Hunt, *Pharm. Weekblad Sci. Ed.*, **5**, 41 (1983).

ACKNOWLEDGMENTS

The authors wish to thank Dr. K. Brown and Mr. S. C. Parkin for their encouragement and assistance. We would also like to thank Mr. D. Taylor for help with the atomic emission spectrometry and Dr. W. J. S. Lockley for synthesizing the radiolabeled compounds. One of us (CAW) thanks the SERC for the provision of a CASE studentship.

Relationship Between Molecular Structure and Cytochrome P_{450}–Metabolic Intermediate Complex Formation, Studied with Orphenadrine Analogues

AALT BAST ˣ, E. MARIA SAVENIJE-CHAPEL, and JAN NOORDHOEK

Received April 4, 1983, from the *Department of Pharmacology and Pharmacotherapy, Faculty of Pharmacy, State University of Utrecht, Catharijnesingel 60, 3511 GH Utrecht, The Netherlands.* Accepted for publication July 29, 1983.

Abstract □ Complexation of ferrous cytochrome P_{450} by metabolic intermediates formed during NADPH-catalyzed metabolism of compounds structurally related to orphenadrine was studied. This so-called metabolic intermediate complexation was determined in rat liver microsomes, obtained from phenobarbital-pretreated rats, at 455 nm using 33 μM of the orphenadrine derivatives. Using secondary amine derivatives with various *N*-alkyl substituents, a parabolic relationship between the logarithm of percentage of cytochrome P_{450} complexation and hydrophobic fragmental constant was observed. The derivative with a bulky tertiary butyl group, however, was devoid of metabolic intermediate-complexing activity. This indicates that steric factors besides lipid solubility may govern the complexing activity; also substitution at the phenyl group affects metabolic intermediate complex formation.

Keyphrases □ Cytochrome P_{450}—complexation with metabolic intermediates, orphenadrine analogues □ Orphenadrine—analogues, metabolic intermediate Complexation with cytochrome P_{450} □ Complexation—metabolic intermediate, orphenadrine analogues with cytochrome P_{450}

Several types of nitrogenous compounds have been shown to undergo cytochrome P_{450}-catalyzed metabolic conversions leading to metabolic intermediates that complex with cytochrome P_{450} (1–3). This complexed cytochrome P_{450} is inactive. Metabolic intermediate complex formation may therefore inhibit metabolic reactions (4). Among the nitrogenous compounds which elicit this complex formation, there are several classes of therapeutically important drugs.

Amphetamine derivatives form a metabolic intermediate complex with hepatic microsomal cytochrome P_{450} *in vitro*, but not *in vivo* (4, 5). With regard to amphetamine analogues, relationships between molecular structure and *in vitro* complexation have been described (4, 6). Recently, metabolic intermediate complex formation produced by macrolide antibiotics have gained much interest (7, 8). With a series of macrolide antibiotics, structural features which are important for the formation of metabolic intermediate complexes have been determined (9). However, with regard to compounds related to proadifen (like propoxyphene, desipramine, and orphenadrine) which produce such complexation both *in vitro* and *in vivo* (10, 11), little is known about the relationship between molecular structure and the ability to evoke complexes

0022-3549/84/0700-0953$01.00/0

© 1984, American Pharmaceutical Association

Table I—Complexation with Cytochrome P_{450}

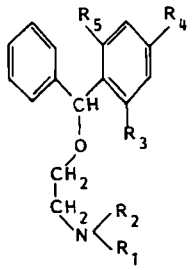

Compound	Substituents[a]					Cytochrome P_{450} Complexed[b], %
	R_1	R_2	R_3	R_4	R_5	
I	H	H	H	H	H	0.8
II	H	H	Me	H	H	—[c]
III	Me	H	H	H	H	1.8
IV (Diphenhydramine)	Me	Me	H	H	H	10.0
V (Tofenacine)	Me	H	Me	H	H	14.0
VI (Orphenadrine)	Me	Me	Me	H	H	8.8
VII (Pytamine)	Me	Me	Et	H	Et	—
VIII	Et	H	H	H	H	9.4
IX	*n*-Pr	H	H	H	H	16.7
X	*i*-Pr	H	H	H	H	10.4
XI	*i*-Pr	H	Me	H	H	6.4
XII	*i*-Pr	H	H	Me	H	—
XIII	*n*-Bu	H	H	H	H	21.0
XIV	*t*-Bu	H	H	H	H	—
XV (N—OH Tofenacine)	Me	OH	Me	H	H	50.0[d]
XVI (Proadifen)[e]						8.5

[a] Key: Me, methyl; Et, ethyl; Bu, butyl; *i*, iso-; *n*, normal; *t*, tertiary. [b] Determined using 2.5 μM cytochrome P_{450} and 33 μM of the compounds. [c] Not detectable. [d] Based on previous data. [e] Refers to the formula:

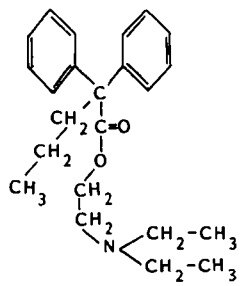

(1, 4). However, because of metabolic intermediate complex formation, peculiar kinetics (12) and adverse drug interactions may arise (4). On the other hand selective inhibition of cytochrome P_{450} subforms provides an interesting tool to manipulate these subforms. In this manner, formation of toxic metabolites might be reduced.

In the present study, therefore, we investigated the relationship between molecular structure and metabolic intermediate complex formation of several orphenadrine derivatives. In this way both structural features important in the formation of complexes as well as insight into the mechanism of complexation with this class of compounds were established.

EXPERIMENTAL SECTION

Chemicals—Orphenadrine and its derivatives were gifts[1]; NADPH was purchased[2]. All other chemicals and solvents used were of analytical-grade purity.

Preparation of Microsomes and Pretreatment of Animals—Liver microsomes were prepared from Wistar rats weighing 250–280 g, as described previously (13). The rats used were pretreated with phenobarbital, dissolved in saline, inasmuch as metabolic intermediate complex formation is specifically enhanced after induction with phenobarbital (4). The phenobarbital-pretreatment consisted of three daily injections of 80 mg/kg ip. On the fourth day the rats were killed by decapitation.

Spectral Measurements—All spectrophotometric observations were performed with the microsomal fraction (2 mg of protein/mL) suspended in 50 mM phosphate buffer (pH 7.4) containing 0.1 mM EDTA. The spectral determinations were performed with UV-visual spectrophotometer[3] at 37°C.

Metabolic intermediate complex formation was measured with the microsomal suspension containing substrate as indicated and 4.2 mM $MgCl_2$. The reaction, started with 400 μM NADPH, was followed by dual-wavelength spectrometry (455 nm *versus* 490 nm) unless stated otherwise in the text. To quantitate the percentage of cytochrome P_{450} complexed, a molar extinction coefficient (ϵ) of 65 mM^{-1} cm^{-1} was used (14, 15). The ϵ is merely a proportionality constant and not of decisive importance in this study. However, use of ϵ provides quantitation of the sequestered amount of cytochrome P_{450}.

Protein concentration (16) and cytochrome P_{450} (17) were determined according to standard procedures.

RESULTS

Scanning spectrometry (430–500 nm) with the spectrophotometer in the split-beam mode (11) was used to establish whether the compounds studied at 33 μM (Table I) exhibited a Soret absorption maximum at 455 nm due to metabolic intermediate complex formation. Inasmuch as this was the case[4], employment of dual wavelength (455–490 nm) spectrometry is valid to study this complex formation *in vitro*.

Substrate concentration dependency has been observed both for rate and extent of metabolic intermediate complex formation (11, 18). We therefore compared the extent of cytochrome P_{450} complexation with each derivative ($\Delta A_{455-490\ nm}$) at three substrate concentrations. Maximal complexation was achieved at 33 μM for each compound (Fig. 1). Moreover, using a concen-

[1] Gist-Brocades N.V., Delft, The Netherlands.
[2] Boehringer/Mannheim GmbH, Mannheim, F.R.G.
[3] Model DW2; Aminco.
[4] Unpublished results.

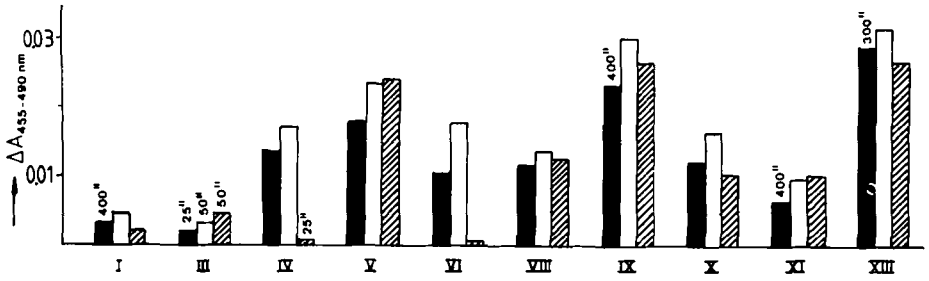

Figure 1—*Concentration dependency of extent of metabolic intermediate complexation ($\Delta A_{455\text{-}490\ nm}$) produced by various compounds (see Table I). For each compound, three concentrations were tested. Incubation has been performed for 650 s, unless stated otherwise in the figure. Key: (■) 10 μM; (□) 33 μM; (▨) 300 μM.*

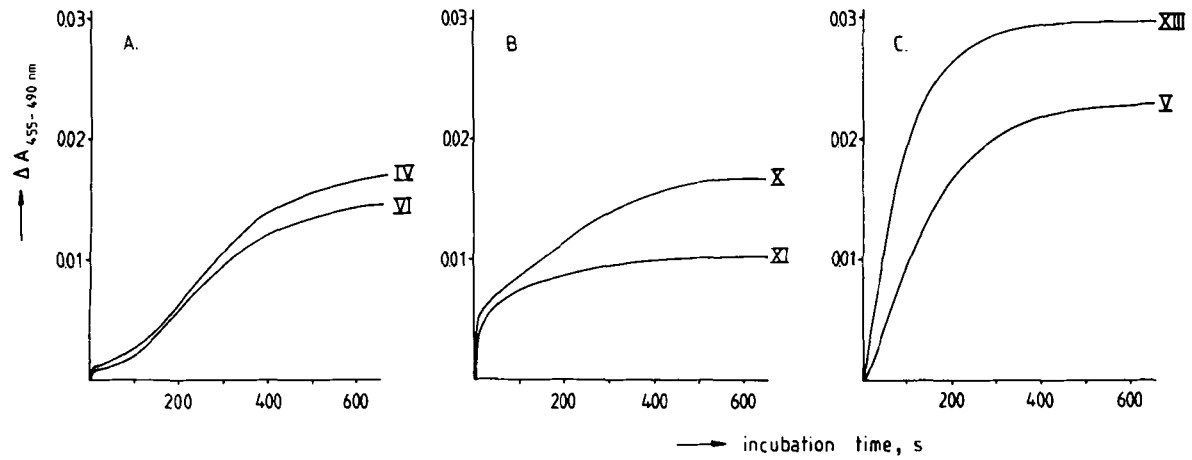

Figure 2—*Time course of metabolic intermediate complex formation, indicated by $\Delta A_{455\text{-}490\ nm}$ (see Table I). Experimental conditions as described in the* Experimental Section.

tration of 33 μM, maximal absorption at 455 nm was accomplished within an incubation time of 650 s and remained stable thereafter. The only exception, III, shows maximal absorption in 50 s, which decreased thereafter. Maximal complexation was used for further evaluation.

Within the series of compounds tested (Table I), the time course of development of absorption at 455 nm differed. Figure 2A shows that complexation produced by the tertiary amine structures (IV and VI) have a prominent initial lag phase. Compounds X and XI, containing an isopropyl substituent, display a biphasic increase in 455 nm absorption (Fig. 2B). With the secondary amines, in which an *n*-alkyl substituent is present on the nitrogen atom, (*e.g.*, V and XIII), neither a lag phase nor biphasic kinetics occur (Fig. 2C).

Using a concentration of 33 μM, the percentage of cytochrome P_{450} complexed was established for each compound (Table I). Evaluation of data of Table I reveals a possible parabolic dependence of metabolic intermediate complexation on lipophilicity. The latter was expressed by the fragmental constant (f) of the —NHR moiety of I, III, VIII, IX, X, and XIII (19) (Fig. 3). As shown in Table I, XIV, with a bulky tertiary butyl group, does not produce metabolic intermediate complexation. Substitutions on the aromatic part of the molecules give large variations in complex formation. Comparison of II with I, V with III, and XI with X shows that the effect of substitution at R_3 depends on the substituent at R_1. Moreover, XII, with a methyl substituent at R_4 and an isopropyl group at R_1, did not form a metabolic intermediate complex (Fig. 4).

DISCUSSION

The optimum concentration for metabolic intermediate complexation has often been found to be 33 μM, irrespective of whether hepatic microsomes were obtained from untreated or phenobarbital-pretreated rats (1). The same optimum concentration was established not only with different microsomal preparations, but also with different compounds (1, 11). Accordingly, the present data also suggest that 33 μM can be used for comparative purposes (Fig. 1). The concentration dependency, explained by substrate inhibition (11), hinders use of K_m values. Biphasic kinetics observed with X and XI (Fig. 2B) suggest that different forms of cytochrome P_{450} are involved in metabolic intermediate complex formation. The lag time observed with tertiary amines (Fig. 2A) is probably explained by initial *N*-demethylation, which has to occur before the complexing species can be formed (11). Because of the different time courses of metabolic intermediate complexation, we did not use the initial rate but rather the extent of such complexation.

A trend toward a parabolic relationship between percentage of cytochrome P_{450} complexed and lipophilicity was observed. The possible bilinear relationship describes transport of the substrate and, in addition, may also reflect a hydrophobic interaction (20). Dependency on the hydrophobic fragmental constant may reflect the fact that the active sites of cytochrome P_{450} are located in a hydrophobic pocket, submerged in the membrane (21). Transport between hydrophilic and hydrophobic phases as a rate-limiting step has also been suggested for *N*-oxidation of amphetamine derivatives (6). Compound X, which contains an isopropyl group, deviates (Fig. 3). This may indicate that steric factors besides lipid solubility may govern metabolic intermediate-complexing activity as well. This notion is substantiated by the fact that XIV, which has a bulky tertiary butyl group, is devoid of such complexing activity. Similar dependencies arise from literature reports, in which *N*-dealkylation of secondary amines have been described (22, 23). This suggests that the distinct correlation, which has been found between the rate of *N*-demethylation and metabolic intermediate complex formation (11, 24) can be extended to *N*-dealkylation and metabolic intermediate complexation. The differences in complex formation with secondary amines may therefore reflect *N*-dealkylation. This would correlate well with the suggestion that the actual

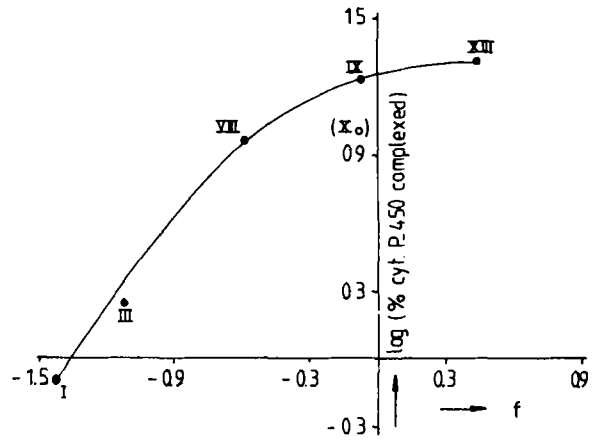

Figure 3—*Plot of the logarithm of percentage of cytochrome P_{450} complexed (obtained from Table I) against the sum of the hydrophobic fragmental constant of the substituted amine function (see text) for several compounds which vary in their amine function.*

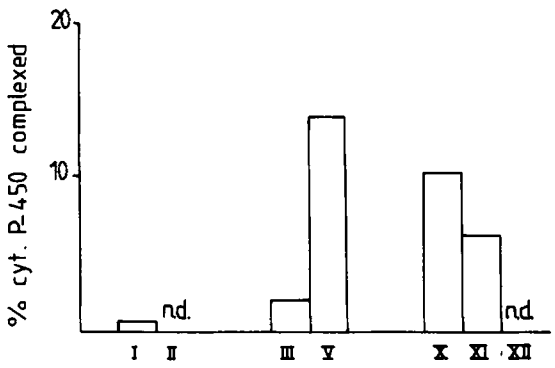

Figure 4—*Effect of substitution in the aromatic part of the substrates on metabolic intermediate-complexing activity, indicated as percentage of cytochrome* P_{450} *complexed (obtained from Table I).*

ligand responsible for such complex formation is an *N* oxidized primary amine, probably a nitroso compound or a nitroxide radical (11). Presumably the main mechanism leading to the ultimate metabolic intermediate ligand is *N*-oxidation of the secondary amines, since *N*-hydroxytofenacine (XV) leads to a large extent to complex formation. *N*-Oxidation of the *N*-hydroxy-*N*-alkylamine may lead to an unstable *N*-hydroxy-*N*-alkylamine *N*-oxide, which after rearrangement is readily *N*-dealkylated. The *N*-dealkylated *N*-hydroxylamine is rather unstable and may give the nitroxide radical. Direct *N*-oxidation of the primary amine does not have an important contribution to metabolic intermediate complex formation inasmuch as I and II do not produce a metabolic intermediate complex to any large degree.

Interpretations of data become more difficult if the effect of substitution at the aromatic portion of the molecule comes into play (Fig. 4). Substitution on one phenyl group greatly affects complexation. Moreover, the substituent on the amine function influences the effect of substitution on the aromatic part in an unpredictable manner. Clearly more compounds are needed to unravel the effect on metabolic intermediate complexation if substitution occurs in different parts of the molecule simultaneously.

In conclusion, evaluation of the relationship between structure and biological activity may be helpful in development of compounds which will show the desired pharmacological effect without metabolic intermediate complexation. One may also design compounds with prominent complexing activity with specific cytochrome P_{450} subforms, which may be used for pharmacological or toxicological purposes.

REFERENCES

(1) M. K. Buening and M. R. Franklin, *Drug Metab. Dispos.*, **2**, 386 (1974).

(2) M. R. Franklin, *Chem. Biol. Interact.*, **14**, 337 (1976).

(3) R. N. Hines and R. A. Prough, *J. Pharmacol. Exp. Ther.*, **214**, 80 (1980).

(4) M. R. Franklin, *Pharmacol. Ther. A.*, **2**, 227 (1977).

(5) M. Hirata, B. Lindeke, and S. Orrenius, *Biochem. Pharmacol.*, **28**, 479 (1979).

(6) B. Lindeke, U. Paulsen-Sörman, G. Hallström, A.-H. Khuthier, A. K. Cho, and R. C. Kammerer, *Drug Metab. Dispos.*, **10**, 700 (1982).

(7) D. Pessayre, V. Descatoire, M. Konstantinova-Mitcheva, J.-C. Wandscheer, B. Cobert, R. Level, J.-P. Benhamou, and M. Jaouen, and D. Mansuy, *Biochem. Pharmacol.*, **30**, 553 (1981).

(8) G. Danan, V. Descatoire, and D. Pessayre, *J. Pharmacol. Exp. Ther.*, **218**, 509 (1981).

(9) M. Delaforge, D. Mansuy, and M. Jaouen, "Eighth European Workshop on Drug Metabolism," Abstract 71, 1982, p. 83.

(10) S. M. Roberts and M. R. Franklin, *Life Sci.*, **25**, 845 (1979).

(11) A. Bast and J. Noordhoek, *Biochem. Pharmacol.*, **31**, 2745 (1982).

(12) J. J. M. Labout, C. T. Thijssen, G. G. J. Keijzer, and W. Hespe, *Eur. J. Clin. Pharmacol.*, **21**, 313 (1982).

(13) A. Bast and J. Noordhoek, *Biochem. Pharmacol.*, **29**, 747 (1980).

(14) M. R. Franklin, *Mol. Pharmacol.*, **10**, 975 (1974).

(15) A. Bast, F. A. A. van Kemenade, E. M. Savenije-Chapel, and J. Noordhoek, *Res. Commun. Chem. Path. Pharmacol.*, **40**, 391 (1983).

(16) O. H. Lowry, N. J. Rosebrough, A. L. Farr, and R. J. Randall, *J. Biol. Chem.*, **193**, 265 (1951).

(17) R. W. Estabrook, J. A. Peterson, J. Baron, and A. Hildebrandt, "Methods in Pharmacology," (C. F. Chignell, Ed.), vol. 2, Appleton-Century Corfts, New York, N.Y., 1972, p. 303.

(18) M. R. Franklin, *Xenobiotica*, **4**, 143 (1974).

(19) R. F. Rekker and H. M. de Korte, *Eur. J. Med. Chem.*, **14**, 479 (1979).

(20) R. F. Rekker, "The Hydrophobic Fragmental Constant," W. Th. Nauta and R. F. Rekker, Eds., Pharmacochemistry Library, vol. 1, Elsevier Scientific, Amsterdam, The Netherlands, 1977.

(21) K. A. S. Al-Gailany, J. B. Houston, and J. W. Bridges, *Biochem. Pharmacol.*, **27**, 783 (1978).

(22) B. Testa and B. Salvesen, *J. Pharm. Sci.*, **69**, 497 (1980).

(23) C. Hansch, *Drug Metab. Revs.*, **1**, 1 (1972).

(24) B. Lindeke, U. Paulsen, and E. Anderson, *Biochem. Pharmacol.*, **28**, 3629 (1979).

Hypolipidemic Activity of 3-*N*-(1′,8′-Naphthalimido)propionic Acid in Rodents

I. H. HALL ˣ, J. M. CHAPMAN, JR., P. JOSEÉ VOORSTAD, and G. H. COCOLAS

Received January 31, 1983, from the *Division of Medicinal Chemistry, School of Pharmacy, University of North Carolina at Chapel Hill, Chapel Hill, NC 27514.* Accepted for publication July 29, 1983.

Abstract □ 3-*N*-(1′,8′-Naphthalimido)propionic acid was synthesized and shown to effectively lower both serum cholesterol and triglyceride levels in rats and mice. In hyperlipidemic mice, serum lipid levels were lowered significantly, approaching normal levels of cholesterol and below normal levels of triglyceride. The serum lipid levels were reduced due to accelerated clearance of cholesterol *via* the biliary route as well as a lowering of available acetyl CoA in the cytoplasm for liver *de novo* cholesterol and triglyceride syntheses. The liver regulatory enzyme of fatty acid and triglyceride syntheses were depressed by drug treatment. Significant reduction of liver lipids as well as the lipid content of the lipoprotein fractions were observed. The agent possessed a safe therapeutic index when used as a hypolipidemic agent.

Keyphrases □ 3-*N*-(1′,8′-Naphthalimido)propionic acid—hypolipidemic activity in rodents, cholesterol and triglycerides reduction □ Antihyperlipidemic agents—3-*N*-(1′,8′-naphthalimido)propionic acid, activity in rodents, cholesterol and triglycerides reduction

N-Substituted cyclic imides have been shown to be potent hypolipidemic agents in rodents at the low dose of 20 mg/kg/d. Substitutions of four carbon atoms or an oxygen atom for one of the carbons provided the most active agent of the phthalimide, saccharin, and the 1′,8′-naphthalimide series (1). These agents effectively lowered both serum cholesterol and tri-

0022-3549/84/0700-0956$01.00/0
© 1984, American Pharmaceutical Association

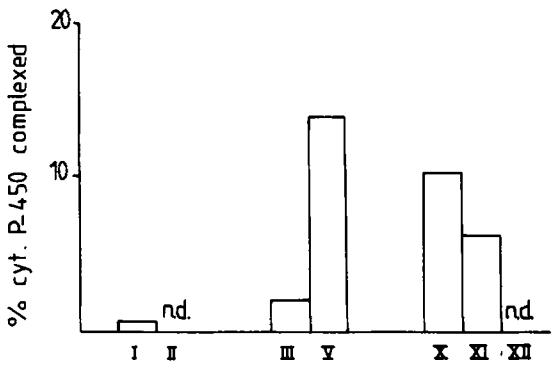

Figure 4—*Effect of substitution in the aromatic part of the substrates on metabolic intermediate-complexing activity, indicated as percentage of cytochrome* P_{450} *complexed (obtained from Table I).*

ligand responsible for such complex formation is an *N* oxidized primary amine, probably a nitroso compound or a nitroxide radical (11). Presumably the main mechanism leading to the ultimate metabolic intermediate ligand is *N*-oxidation of the secondary amines, since *N*-hydroxytofenacine (XV) leads to a large extent to complex formation. *N*-Oxidation of the *N*-hydroxy-*N*-alkylamine may lead to an unstable *N*-hydroxy-*N*-alkylamine *N*-oxide, which after rearrangement is readily *N*-dealkylated. The *N*-dealkylated *N*-hydroxylamine is rather unstable and may give the nitroxide radical. Direct *N*-oxidation of the primary amine does not have an important contribution to metabolic intermediate complex formation inasmuch as I and II do not produce a metabolic intermediate complex to any large degree.

Interpretations of data become more difficult if the effect of substitution at the aromatic portion of the molecule comes into play (Fig. 4). Substitution on one phenyl group greatly affects complexation. Moreover, the substituent on the amine function influences the effect of substitution on the aromatic part in an unpredictable manner. Clearly more compounds are needed to unravel the effect on metabolic intermediate complexation if substitution occurs in different parts of the molecule simultaneously.

In conclusion, evaluation of the relationship between structure and biological activity may be helpful in development of compounds which will show the desired pharmacological effect without metabolic intermediate complexation. One may also design compounds with prominent complexing activity with specific cytochrome P_{450} subforms, which may be used for pharmacological or toxicological purposes.

REFERENCES

(1) M. K. Buening and M. R. Franklin, *Drug Metab. Dispos.*, **2**, 386 (1974).

(2) M. R. Franklin, *Chem. Biol. Interact.*, **14**, 337 (1976).

(3) R. N. Hines and R. A. Prough, *J. Pharmacol. Exp. Ther.*, **214**, 80 (1980).

(4) M. R. Franklin, *Pharmacol. Ther. A.*, **2**, 227 (1977).

(5) M. Hirata, B. Lindeke, and S. Orrenius, *Biochem. Pharmacol.*, **28**, 479 (1979).

(6) B. Lindeke, U. Paulsen-Sörman, G. Hallström, A.-H. Khuthier, A. K. Cho, and R. C. Kammerer, *Drug Metab. Dispos.*, **10**, 700 (1982).

(7) D. Pessayre, V. Descatoire, M. Konstantinova-Mitcheva, J.-C. Wandscheer, B. Cobert, R. Level, J.-P. Benhamou, and M. Jaouen, and D. Mansuy, *Biochem. Pharmacol.*, **30**, 553 (1981).

(8) G. Danan, V. Descatoire, and D. Pessayre, *J. Pharmacol. Exp. Ther.*, **218**, 509 (1981).

(9) M. Delaforge, D. Mansuy, and M. Jaouen, "Eighth European Workshop on Drug Metabolism," Abstract 71, 1982, p. 83.

(10) S. M. Roberts and M. R. Franklin, *Life Sci.*, **25**, 845 (1979).

(11) A. Bast and J. Noordhoek, *Biochem. Pharmacol.*, **31**, 2745 (1982).

(12) J. J. M. Labout, C. T. Thijssen, G. G. J. Keijzer, and W. Hespe, *Eur. J. Clin. Pharmacol.*, **21**, 313 (1982).

(13) A. Bast and J. Noordhoek, *Biochem. Pharmacol.*, **29**, 747 (1980).

(14) M. R. Franklin, *Mol. Pharmacol.*, **10**, 975 (1974).

(15) A. Bast, F. A. A. van Kemenade, E. M. Savenije-Chapel, and J. Noordhoek, *Res. Commun. Chem. Path. Pharmacol.*, **40**, 391 (1983).

(16) O. H. Lowry, N. J. Rosebrough, A. L. Farr, and R. J. Randall, *J. Biol. Chem.*, **193**, 265 (1951).

(17) R. W. Estabrook, J. A. Peterson, J. Baron, and A. Hildebrandt, "Methods in Pharmacology," (C. F. Chignell, Ed.), vol. 2, Appleton-Century Corfts, New York, N.Y., 1972, p. 303.

(18) M. R. Franklin, *Xenobiotica*, **4**, 143 (1974).

(19) R. F. Rekker and H. M. de Korte, *Eur. J. Med. Chem.*, **14**, 479 (1979).

(20) R. F. Rekker, "The Hydrophobic Fragmental Constant," W. Th. Nauta and R. F. Rekker, Eds., Pharmacochemistry Library, vol. 1, Elsevier Scientific, Amsterdam, The Netherlands, 1977.

(21) K. A. S. Al-Gailany, J. B. Houston, and J. W. Bridges, *Biochem. Pharmacol.*, **27**, 783 (1978).

(22) B. Testa and B. Salvesen, *J. Pharm. Sci.*, **69**, 497 (1980).

(23) C. Hansch, *Drug Metab. Revs.*, **1**, 1 (1972).

(24) B. Lindeke, U. Paulsen, and E. Anderson, *Biochem. Pharmacol.*, **28**, 3629 (1979).

Hypolipidemic Activity of 3-*N*-(1′,8′-Naphthalimido)propionic Acid in Rodents

I. H. HALL ˣ, J. M. CHAPMAN, JR., P. JOSEÉ VOORSTAD, and G. H. COCOLAS

Received January 31, 1983, from the *Division of Medicinal Chemistry, School of Pharmacy, University of North Carolina at Chapel Hill, Chapel Hill, NC 27514.* Accepted for publication July 29, 1983.

Abstract □ 3-*N*-(1′,8′-Naphthalimido)propionic acid was synthesized and shown to effectively lower both serum cholesterol and triglyceride levels in rats and mice. In hyperlipidemic mice, serum lipid levels were lowered significantly, approaching normal levels of cholesterol and below normal levels of triglyceride. The serum lipid levels were reduced due to accelerated clearance of cholesterol *via* the biliary route as well as a lowering of available acetyl CoA in the cytoplasm for liver *de novo* cholesterol and triglyceride syntheses. The liver regulatory enzyme of fatty acid and triglyceride syntheses were depressed by drug treatment. Significant reduction of liver lipids as well as the lipid content of the lipoprotein fractions were observed. The agent possessed a safe therapeutic index when used as a hypolipidemic agent.

Keyphrases □ 3-*N*-(1′,8′-Naphthalimido)propionic acid—hypolipidemic activity in rodents, cholesterol and triglycerides reduction □ Antihyperlipidemic agents—3-*N*-(1′,8′-naphthalimido)propionic acid, activity in rodents, cholesterol and triglycerides reduction

N-Substituted cyclic imides have been shown to be potent hypolipidemic agents in rodents at the low dose of 20 mg/kg/d. Substitutions of four carbon atoms or an oxygen atom for one of the carbons provided the most active agent of the phthalimide, saccharin, and the 1′,8′-naphthalimide series (1). These agents effectively lowered both serum cholesterol and tri-

0022-3549/84/0700-0956$01.00/0
© 1984, American Pharmaceutical Association

Table I—Effects of 3-*N*-(1′,8′-Naphthalimido)propionic Acid on Serum Cholesterol and Triglyceride Levels of Male CF_1 Mice and Male Holtzman Rats

Compound	Rats: Dose, mg/kg/d	Rats: Serum Cholesterol Day 9	Rats: Serum Cholesterol Day 14	Rats: Serum Triglyceride Day 14	Mice: Dose, mg/kg/d	Mice: Serum Cholesterol Day 9	Mice: Serum Cholesterol Day 16	Mice: Serum Triglyceride Day 14
3-*N*-(1′,8′-Naphthalimido)propionic Acid	10	81 ± 6[b]	65 ± 7[b]	69 ± 4[b]	10	91 ± 7	78 ± 5[b]	88 ± 6
	20	78 ± 7[b]	57 ± 5[b]	66 ± 6[b]	20	92 ± 6	68 ± 6[b]	58 ± 5[b]
					40	87 ± 8	64 ± 5[b]	70 ± 4[b]
					60	81 ± 6[c]	74 ± 7[b]	72 ± 6[b]
Control (1% carboxymethylcellulose)		100 ± 5[c]	100 ± 6[d]	100 ± 6[e]		100 ± 9[f]	100 ± 7[g]	100 ± 8[h]

[a] Expressed as percent of control (mean ± *SD*); $n = 6$. [b] $p \leq 0.001$. [c] 118 mg%. [d] 122 mg%. [e] 137 mg%. [f] 73 mg%. [g] 78 mg%. [h] 110 mg%.

Table II—Effect of 3-*N*-(1′,8′-Naphthalimido)propionic Acid on Weights of Major Organs from Male Holtzman Rats after Dosing Intraperitoneally[a]

Organ	Control (1% Carboxymethylcellulose): Organ Weight, g	Control (1% Carboxymethylcellulose): Percent of Body Weight	3-*N*-(1′,8′-Naphthalimido)propionic Acid: Organ Weight, g	3-*N*-(1′,8′-Naphthalimido)propionic Acid: Percent of Body Weight
Liver	15.2	3.46	16.2	3.99
Lung	2.1	0.48	2.5	0.63
Heart	1.5	0.34	1.2	0.29
Stomach	3.0	0.68	2.3	0.58
Kidney	3.1	0.71	2.5	0.61
Spleen	1.1	0.25	1.0	0.25
Brain	1.6	0.36	1.9	0.47
Large intestine	4.8	1.09	3.6	0.89
Small intestine	10.3	2.35	10.43	2.58
Percent increase in animal weights during experiment		31		33

[a] For 14 d at 20 mg/kg/d; $n = 6$.

glyceride levels. They were active in both normal and hyperlipidemic mice. In the latter case, the agents lowered blood lipids to maintain normal ranges of cholesterol and triglycerides. The LD_{50} values of the drugs appeared to be high, *i.e.*, >2 g/kg, indicating a safe therapeutic index. No other deleterious side effects were noted, and the effects on lipid metabolism were totally reversible. The cyclic imides have been observed to reduce regulatory enzymes of lipid synthesis and to accelerate lipid excretion *via* the bile. The agents significantly lowered cholesterol and triglyceride content of the lipoprotein fractions of blood in rats. The *N*-propionic acid substitution of the cyclic ring provided one of the more active derivatives of the phthalimide (2) and saccharin (3) series in the hypolipidemic screen. Preliminary testing indicated the same findings for the propionic acid derivative of 1′,8′-naphthalimide. Thus, an in-depth study of the metabolic effects of 3-*N*-(1′,8′-naphthalimido)propionic acid was undertaken in rodents, and those results are reported.

EXPERIMENTAL SECTION

Source of Compounds—3-*N*-(1′,8′-Naphthalimido)propionic acid was prepared as follows. 1′,8′-Naphthalic anhydride (19.8 g, 0.1 mol) and 8.9 g (0.1 mol) of β-alanine were refluxed in 300 mL of dimethylformamide for 1.25 h. The resulting solution was cooled, and the solvent was removed *in vacuo* to yield a pink solid residue which was a single spot by TLC analysis. The solid was washed with ethanol to remove the pink color, yielding 24 g (89%) of an off-white solid, mp 225–243°C. Recrystallization of an analytical sample from ethyl acetate gave 3-*N*-(1′,8′-naphthalimido)propionic acid, mp 231–233°C. ^{1}H-NMR (Me_2SO-d_6): δ 7.62–8.47 (m, 6, ArH), 4.26 (t, 2, $N-CH_2$), and 2.60 ppm (t, 2, $CH_2-C=O$).

Anal.—Calc. for $C_{15}H_{11}NO_4$: C, 66.91; H, 4.12. Found: C, 66.96; H, 4.11.

Antihyperlipidemic Screens in Normal Rodents—3-*N*-(1′,8′-Naphthalimido)propionic acid was suspended in 1% aqueous carboxymethylcellulose, homogenized, and administered to male CF_1 mice (~25 g) intraperitoneally for 16 d or male Holtzman rats (~350 g) orally by an intubation needle for 14 d. Serum cholesterol (4) and triglycerides[1] were determined as described previously (2).

Testing in Atherogenic Mice—Male CF_1 mice (~25 g) were placed on a commercial diet[2] to produce a hyperlipidemic state. After the cholesterol and triglyceride levels were elevated, the mice were administered the test drug at 20 mg/kg/d ip for an additional 14-d period, and serum cholesterol (4) and triglyceride[1] levels were determined (2).

Toxicity Studies—Periodic animal weights were obtained during the experiments and expressed as a percentage of the weight of the animal on day 0 (2). The acute toxicity (LD_{50} value) (5) was determined in male CF_1 mice (~25 g) by administering the test drug intraperitoneally from 100 mg to 2 g/kg as a single dose. The number of deaths were recorded over a 7-d period for each group.

Enzymatic Studies—*In vitro* enzymatic studies were determined using 10% homogenates of male CF_1 mouse liver with 2.5–10 μmol of test drug. *In vivo* enzymatic studies were determined with 10% homogenates of liver from male CF_1 mice obtained after administering the agent for 16 d at a dose ranging from 10 to 60 mg/kg/d ip. The enzyme activities were determined by previously described techniques: acetyl CoA synthetase (6); ATP-dependent citrate lyase (7); mitochondrial citrate exchange (8, 9); cholesterol side-chain oxidation (10); 3-hydroxy-3-methylglutaryl CoA reductase (HMG CoA reductase) (11, 12); acetyl CoA carboxylase activity (13); fatty acid synthetase (14); *sn*-glycerol-3-phosphate acyl transferase (15); and phosphatidate phosphohydrolase (16). Details of the enzymatic assays have been published previously (2).

Liver, Small Intestine, and Fecal Lipid Extraction—In male CF_1 mice that had been administered test drugs for 15 d, the liver, small intestine, and fecal materials (24-h collection) were removed, extracted (17, 18) and analyzed for cholesterol (4), triglycerides[1], neutral lipids (19), and phospholipids (20).

[^{3}H]Cholesterol Distribution in Rats—Male Holtzman rats (~350 g) were administered test agents for 14 d orally. On day 13, 10 μCi of [^{3}H]cholesterol was administerted intraperitoneally in mice and orally in rats by a previously described procedure (2).

Cholesterol Absorption Study—Male Holtzman rats (~400 g) were treated with test drugs at 20 mg/kg/d orally for 14 d. [1,2-^{3}H]Cholesterol (40.7 mCi/mmol) (10 μCi) was administered orally 18 h before surgery. After the rats were anesthetized and the bile ducts were canulated by a method described previously (2), the bile was collected over the next 6 h and analyzed for tritium content (21).

Plasma Lipoprotein Fractions—Male Holtzman rats (~400 g) were administered test drugs at 20 mg/kg/d for 14 d. Blood was collected from the abdominal aorta, and lipoprotein fractions were obtained by the methods of Havel and co-workers (22, 23). Each fraction was analyzed for cholesterol (4), triglycerides[1], neutral lipids (19), phospholipids (20), and protein levels (24).

[1] Hycel Triglyceride Test Kit; Fisher Scientific Co.

[2] Basal Atherogenic Test Diet; U.S. Biochemical Corp.

Table III—*In Vitro* Effects of 3-*N*-(1′,8′-Naphthalimido)propionic Acid on Male CF_1 Mouse Liver Enzyme Activities [a]

Drug, μmol	Mitochondrial Citrate Exchange	Acetyl CoA Synthetase	Citrate Lyase	HMG CoA Reductase	Cholesterol Side-Chain Oxidation
Control (1% carboxymethylcellulose)	100 ± 10[b]	100 ± 7[c]	100 ± 9[d]	100 ± 7[c]	100 ± 8[f]
Treated					
2.5	21 ± 9[j]	82 ± 6	73 ± 3[j]	93 ± 4	68 ± 9[j]
5.0	—	83 ± 7	69 ± 7[j]	83 ± 6[k]	—
10.0	—	86 ± 6	77 ± 4[j]	79 ± 6[j]	—

Drug, μmol	Acyl CoA-Cholesterol Acyl Transferase	Acetyl CoA Carboxylase	Fatty Acid Synthetase	*sn*-Glycerol-3-phosphate Acyl Transferase	Phosphatidate Phosphohydrolase
Control (1% carboxymethylcellulose)	100 ± 9[g]	100 ± 6[h]	100 ± 7[i]	100 ± 8[l]	100 ± 7[m]
Treated					
2.5	98 ± 6	58 ± 6[j]	100 ± 5	41 ± 7[j]	55 ± 3[j]
5.0	135 ± 9[j]	51 ± 3[j]	100 ± 6	50 ± 6[j]	45 ± 6[j]
10.0	134 ± 12[j]	46 ± 4[j]	98 ± 7	24 ± 4[j]	42 ± 7[j]

	Mitochondrial Oxidative Phosphorylation			
	α-Ketoglutarate		Succinate	
	State 4	State 3	State 4	State 3
Control (1% carboxymethylcellulose)	100 ± 6[n]	100 ± 7[o]	100 ± 5[p]	100 ± 6[q]
Treated	67 ± 5[j]	50 ± 3[j]	81 ± 6[j]	65 ● 4[j]

[a] Expressed as percent control (mean ± *SD*); $n = 6$. [b] 30.8% exchange of mitochondrial citrate. [c] 28.5 mg of acetyl CoA formed/g of wet tissue/20 min. [d] 30.5 mg citrate hydrolyzed/g of wet tissue/20 min. [e] 384,900 dpm of cholesterol formed/g of wet tissue/60 min. [f] 6080 dpm of CO_2 formed/g of wet tissue/18 h. [g] 4804 dpm/mg of microsomal protein/20 min. [h] 32,010 dpm/g of wet tissue/30 min. [i] 37,656 dpm/g of wet tissue/20 min. [j] $p \leq 0.001$. [k] $p \leq 0.010$. [l] 537,800 dpm/g of wet tissue/20 min. [m] 16.7 μg inorganic phosphate/g of wet tissue/15 min. [n] 3.51 μL of oxygen consumed/h/mg of tissue. [o] 5.21 μL of oxygen consumed/h/mg of tissue. [p] 5.92 μL of oxygen consumed/h/mg of tissue. [q] 11.31 μL of oxygen consumed/h/mg of tissue.

RESULTS

3-*N*-(1′,8′-Naphthalimido)propionic acid clearly demonstrated potent hypolipidemic activity in rodents. In rats, at 20 mg/kg/d orally, serum cholesterol levels were reduced 43% and serum triglyceride levels were reduced 34% (Table I). In mice, at 20 mg/kg/d ip, serum cholesterol levels were reduced maximally at 40 mg/kg/d by 36%, whereas serum triglyceride levels were reduced 42% at 20 mg/kg/d. In hyperlipidemic mice, serum cholesterol levels were elevated 183% (354 mg%) above normal control values (125 mg%). After treatment with 3-*N*-(1′,8′-naphthalimido)propionic acid for 14 d, serum cholesterol was elevated 23% above the control values, which were reduced 160% of the diet-induced cholesterol levels. The serum triglyceride levels in the hyperlipidemic mice were elevated 168% (367 mg/dL) above the control value (137 mg/dL). Drug treatment resulted in values 13% lower than the control. The drug had no effects on the consumption of food on a daily basis in the rats. Furthermore, the weight increase of the whole animal as well as the individual weights of the major organs were not affected by drug treatment for 2 weeks (Table II).

Examination of the *in vitro* effects of 3-*N*-(1′,8′-naphthalimido)propionic acid on the activities of enzymes required for *de novo* synthesis of cholesterol and triglycerides of mice showed that mitochondrial citrate exchange was markedly inhibited by drug treatment by 79% at 2.5 μmol (Table III). Citrate lyase, acetyl CoA synthetase, and HMG CoA reductase activities were inhibited marginally (20–30%).

Enzymes involved in the clearance of free cholesterol from the liver varied in the response to drug treatment. Cholesterol side-chain oxidation was inhibited at 2.5 μmol, and acyl CoA cholesterol acyl transferase activity was enhanced at 5 and 10 μmol (~35%). Activities of regulatory enzymes involved in fatty acid and triglyceride syntheses were significantly inhibited. Acetyl CoA carboxylase, *sn*-glycerol-3-phosphate acyl transferase, and phosphatidate phosphohydrolase activities were suppressed significantly, with the highest concentration (10 μmol) affording the maximum inhibition. Fatty acid synthetase activity was not affected by drug treatment.

Evaluation of some of the same enzymes after *in vivo* administration of 3-*N*-(1′,8′-naphthalimido)propionic acid demonstrated that citrate lyase was inhibited maximally at 20 mg/kg/d by 22% (Table IV). Acetyl CoA synthetase activity was suppressed 14% at 20 and 40 mg/kg/d. HMG CoA reductase activity was not altered by *in vivo* drug administration. 7-α-Hydroxylase, the regulatory enzyme for the conversion of cholesterol to bile acids, was significantly inhibited by drug administration, with 60 mg/kg producing the maximum effect (52% reduction). Acetyl CoA carboxylase activity was suppressed maximally 45% at 20 mg/kg/d. *sn*-Glycerol-3-phosphate acyl transferase activity was likewise inhibited maximally at 20 mg/kg/d by 51%. Phosphatidate phosphohydrolase activity was inhibited 31% at 20 mg/kg/d and 48% at 40 mg/kg/d. Fatty acid synthetase activity was marginally inhibited 19–20% at 20 and 40 mg/kg/d.

Lipid analysis of the liver of mice treated for 16 d with 3-*N*-(1′,8′-naphthalimido)propionic acid intraperitoneally showed that the number of milligrams per milliliter of total lipid was reduced 47 and 52% at 20 and 40 mg/kg/d, respectively (Table V). Cholesterol levels were reduced 20–30%. Triglyceride levels were markedly reduced (92–97%), whereas neutral lipid levels were reduced 72 and 84% at the same doses. At the dosage of 60 mg/kg/d, total lipid, cholesterol, triglycerides, and neutral lipids returned to more normal levels. The phospholipid levels were reduced at 10 mg/kg/d by 34%, but were significantly elevated at 20 and 40 mg/kg/d. Fecal samples obtained on day 16 demonstrated a marked increase in total lipid excreted as well as increases in cholesterol and neutral lipid levels; however, triglyceride and phospholipid levels were not elevated in the fecal samples.

Distribution studies in rats with [^{3}H]cholesterol showed that cholesterol absorption from the GI tract over a 24-h period was reduced 7%; however, excretion in the bile was accelerated 26% (Table VI). The milligram percent of cholesterol was elevated 38%, and the bile flow rate over 6 h was accelerated

Table IV—*In Vivo* Effects of 3-*N*-(1′,8′-Naphthalimido)propionic Acid on Male CF_1 Mouse Liver Enzyme Activities [a]

Enzyme	Control (1% Carboxymethylcellulose)	Enzyme Activity, % of Control			
		10 mg/kg/d	20 mg/kg/d	40 mg/kg/d	60 mg/kg/d
Citrate lyase	100 ± 8	79 ± 7[b]	78 ± 3[b]	83 ± 8	104 ± 9
Acetyl CoA synthetase	100 ± 7	91 ± 6	86 ± 7	86 ± 6[b]	92 ± 8
HMG CoA reductase	100 ± 6	95 ± 5	110 ± 7	112 ± 8	110 ± 6
7-α-Hydroxylase	100 ± 2	65 ± 14[b]	55 ± 13[b]	49 ± 4[b]	48 ± 5[b]
Acetyl CoA carboxylase	100 ± 5	85 ± 5[b]	55 ± 4[b]	73 ± 6[b]	110 ± 5
Fatty acid synthetase	100 ± 6	83 ± 6[c]	81 ± 5[b]	80 ± 7[b]	95 ± 5
sn-Glycerol-3-phosphate acyl transferase	100 ± 8	54 ± 5[b]	49 ± 4[b]	57 ± 4[b]	67 ± 7[b]
Phosphatidate phosphohydrolase	100 ± 5	87 ± 8	69 ± 7[b]	52 ± 6[b]	70 ± 8[b]

[a] After dosing for 16 d; expressed as percent of control (mean ± *SD*), $n = 6$. [b] $p \leq 0.0001$. [c] $p \leq 0.005$.

Table V—Effects of 3-*N*-(1′,8′-Naphthalimido)propionic Acid on Lipid Distribution of Mouse Liver and Feces [a]

	Lipid Extracted, mg	Cholesterol	Neutral Lipids	Triglycerides	Phospholipids	Protein
			Liver			
Control	100 ± 9	100 ± 7[b]	100 ± 4[c]	100 ± 5[d]	100 ± 8[e]	100 ± 4[f]
Treated						
10 mg/kg	97 ± 8	96 ± 8	33 ± 3[g]	23 ± 4[g]	66 ± 7[g]	101 ± 4
20 mg/kg	53 ± 7[g]	70 ± 6[g]	28 ± 2[g]	8 ± 2[g]	131 ± 7[g]	98 ± 2
40 mg/kg	48 ± 4[g]	71 ± 6[g]	16 ± 3[g]	3 ± 2[g]	127 ± 8[g]	95 ± 2
60 mg/kg	67 ± 6[g]	84 ± 7	23 ± 3[g]	10 ± 2[g]	108 ± 8	107 ± 3
			Feces			
Control	100 ± 6	100 ± 7[h]	100 ± 8[i]	100 ± 6[j]	100 ± 6[k]	
Treated						
10 mg/kg	145 ± 7[g]	145 ± 9[g]	197 ± 9[g]	100 ± 5	95 ± 7	
20 mg/kg	138 ± 6[g]	132 ± 3[g]	133 ± 7[g]	91 ± 6	95 ± 6	
40 mg/kg	150 ± 8[g]	163 ± 7[g]	153 ± 7[g]	91 ± 6	84 ± 5[g]	
60 mg/kg	145 ± 7[g]	139 ± 5[g]	161 ± 6[g]	102 ± 6	97 ± 7[g]	

[a] At 20 mg/kg/d; expressed as percent of control (mean ± *SD*). [b] 12.24 mg of cholesterol/g of tissue. [c] 28.35 mg of neutral lipid/g of tissue. [d] 4.77 mg of triglycerides/g of tissue. [e] 4.39 mg of phospholipid/g of tissue. [f] 4.5 mg of protein/g of tissue. [g] $p \leq 0.001$. [h] 7.81 mg of cholesterol/g of tissue. [i] 7.18 mg of neutral lipid/g of tissue. [j] 1.06 mg of triglycerides/g of tissue. [k] 2.02 mg of phospholipid/g of tissue.

Table VI—Effects of 3-*N*-(1′,8′-Naphthalimido)propionic Acid on Lipid Distribution in Rat Liver, Small Intestine, Bile, and Feces [a]

	Lipid, mg	Cholesterol	Neutral Lipid	Triglycerides	Phospholipids	Protein
Liver						
Control	100 ± 6	100 ± 7	100 ± 7	100 ± 8	100 ± 5	100 ± 6
Treated	78 ± 5[b]	83 ± 6[c]	74 ± 5[b]	28 ± 3[b]	107 ± 7	99 ± 6
Small Intestine						
Control	100 ± 5	100 ± 6	100 ± 8	100 ± 9	100 ± 10	—
Treated	45 ± 5[b]	82 ± 5[b]	97 ± 9	106 ± 8	120 ± 8[c]	—
Bile						
Control	—	100 ± 10	100 ± 9	100 ± 10	100 ± 8	—
Treated	—	138 ± 12[b]	135 ± 9[b]	72 ± 5[b]	127 ± 7[b]	—
Feces						
Control	100 ± 9	100 ± 10	100 ± 9	100 ± 8	100 ± 9	—
Treated	95 ± 7	128 ± 8[b]	127 ± 8[b]	90 ± 4	123 ± 5[b]	—

[a] After 14-d administration at 20 mg/kg/d; expressed as percent of control (mean ± *SD*), $n = 6$. [b] $p \leq 0.001$. [c] $p \leq 0.010$.

18% (Table VII). Phospholipid content of the bile was also elevated 27% compared with the control. The [^{3}H]cholesterol content in the small intestine, large intestine, chyme, and feces was elevated three, two, five, and two times, respectively, after drug treatment. The urine excretion of [^{3}H]cholesterol was lowered in treated animals, and higher levels of [^{3}H]cholesterol were found in major organs, *e.g.*, brain, heart, lung, liver, and stomach (Table VIII). Adrenal weights for the treated mice were identical to the control weights, indicating that the drug did not cause hypertrophy of the adrenal cortex as a compensatory mechanism of reduced serum cholesterol levels (Table VIII).

Rat lipoprotein fractions (Table IX) were analyzed, and drug treatment reduced cholesterol and neutral lipid in the chylomicron, low-, and high-density lipoprotein fractions of rats. Neutral lipids and triglyceride levels were reduced in the very low-density fractions. Phospholipid levels were reduced in the low-density lipoproteins, but elevated significantly in the high-density lipoprotein fraction. Protein content was essentially unchanged in all of the lipoprotein fractions of the rats. The calculation of the percentage of each lipid or protein concentration of the total lipoprotein particle (Table X) demonstrated slightly different distributions of the lipids. The cholesterol content was reduced in the chylomicron, the low-, and high-density lipoprotein fractions, but not in the very low-density fraction. The cholesterol reduction by drug was most dramatic in the low-density fraction. The cholesterol ratio of high-density/low-density lipoprotein fractions for the control was 0.394 and for the treated group was 0.449. Thus, drug treatment raises the value of this ratio. Triglyceride content was lowered significantly in the chylomicrons and very low-density lipoprotein fractions. Alterations of the low- and high-density lipoprotein fractions probably are not important, since triglyceride content is low in these fractions. Neutral lipids were lowered by drug administration in all four lipoprotein fractions; however, the magnitude of reduction was not as great as for cholesterol and triglycerides. Phospholipids were lowered in the low-density fraction but raised in the other three fractions. Protein content was elevated in all four fractions, probably due to the lipid lost from the lipoprotein fraction after drug treatment.

Data in Tables I–IX are expressed as percentage of control ± *SD*. The probable significant level (p) between each test group and the control group was determined by the Student's t test.

Table VII—Effects of 3-*N*-(1′,8′-Naphthalimido)propionic Acid on Rat Bile [a]

Drug	Bile Excretion Rate, mL/6 h	Total [^{3}H]Cholesterol, dpm/h	Cholesterol Conc., mg%	Phospholipid Conc., mg/mL
Control	100 ± 8[b]	100 ± 8[c]	100 ± 7[d]	100 ± 3
Treated	118 ± 8[e]	126 ± 9[f]	138 ± 12[f]	127 ± 7[f]

[a] After dosing at 20 mg/kg/d for 14 d; expressed as percent of control (mean ± *SD*), $n = 6$. [b] 93 μL of bile eluted/min. [c] 6279 dpm/mL. [d] 111 mg%. [e] $p \leq 0.010$. [f] $p \leq 0.001$.

DISCUSSION

3-*N*-(1′,8′-Naphthalimido)propionic acid was shown to be a potent hypolipidemic agent both by oral and intraperitoneal administration in normal and hyperlipidemic rodents. The suppression of serum lipids appeared to be related to the *in vitro* and *in vivo* inhibition of *de novo* cholesterol and triglyceride

Table VIII—Effects of 3-*N*-(1′,8′-Naphthalimido)propionic Acid after 14 d of Dosing on [^{14}C]Cholesterol Distribution in Holtzman Rats 24 h after Administration

	Control		3-*N*-(1′,8′-Naphthalimido)-propionic Acid	
Organ[a]	Total Organ, dpm	Recovery, %	Total Organ, dpm	Recovery, %
Brain	8,382	0.13	11,609	0.197
Heart	7,344	0.114	10,717	0.182
Lung	22,052	0.342	47,488	0.804
Liver	46,578	0.723	70,986	1.202
Spleen	13,770	0.214	37,900	0.642
Kidney	18,920	0.294	23,114	0.392
Stomach	9,270	0.144	21,552	0.365
Small intestine	174,705	2.711	539,857	9.145
Large intestine	33,413	0.518	56,376	0.955
Chyme	33,605	0.521	163,836	2.775
Feces	193,230	2.998	340,704	5.771

[a] $n = 6$.

Table IX—Effects of 3-*N*-(1′,8′-Naphthalimido)propionic Acid on Rat Serum Lipoprotein Fractions[a]

	Chylomicrons					Very Low-Density Lipoprotein				
	Cholesterol	Neutral Lipid	Triglyceride	Phospholipid	Protein	Cholesterol	Neutral Lipid	Triglyceride	Phospholipid	Protein
Control	100 ± 9[b]	100 ± 8[c]	100 ± 6[d]	100 ± 10[e]	100 ± 7[f]	100 ± 8[g]	100 ± 9[h]	100 ± 7[i]	100 ± 7[j]	100 ± 8[k]
Treated	58 ± 5[l]	66 ± 6[l]	47 ± 5[l]	90 ± 9	90 ± 8	92 ± 8	58 ± 6[l]	46 ± 3[l]	101 ± 9	96 ± 7
	Low-Density Lipoprotein					High-Density Lipoprotein				
	Cholesterol	Neutral Lipid	Triglyceride	Phospholipid	Protein	Cholesterol	Neutral Lipid	Triglyceride	Phospholipid	Protein
Control	100 ± 9[m]	100 ± 7[n]	100 ± 8[o]	100 ± 7[p]	100 ± 8[q]	100 ± 8[r]	100 ± 9[s]	100 ± 4[t]	100 ± 6[u]	100 ± 8[v]
Treated	45 ± 5[l]	49 ± 4[l]	36 ± 4[l]	54 ± 6[l]	91 ± 7	66 ± 8[l]	76 ± 7[l]	48 ± 4[l]	185 ± 10[l]	93 ± 7

[a] After administration of 20 mg/kg/d ip for 14 d; expressed as percent of control (mean ± *SD*), $n = 6$. [b] 337 μg/mL. [c] 67 μg/mL. [d] 420 μg/mL. [e] 149 μg/mL. [f] 184 μg/mL. [g] 190 μg/mL. [h] 98 μg/mL [i] 221 μg/mL. [j] 26 μg/mL. [k] 50 μg/mL. [l] $p \leq 0.001$. [m] 210 μg/mL. [n] 10 μg/mL. [o] 45 μg/mL. [p] 41 μg/mL. [q] 122 μg/mL. [r] 544 μg/mL. [s] 620 μg/mL. [t] 27 μg/mL. [u] 153 μg/mL. [v] 657 μg/mL.

Table X—Effects of 3-*N*-(1′,8′-Naphthalimido)propionic Acid on the Percent Composition of Each Lipid and Protein Fraction of the Total Lipoprotein Particle

	Cholesterol	Triglycerides	Phospholipids	Proteins	Total, μg/mL
			Chylomicrons		
Control	30.92	38.53	13.67	16.88	1090
Treated	28.22	28.51	19.39	23.88	691
			Very Low-Density Lipoproteins		
Control	39.01	45.38	5.34	10.27	487
Treated	49.86	29.06	7.41	13.68	351
			Low-Density Lipoproteins		
Control	50.24	10.77	9.81	29.19	418
Treated	38.73	6.64	9.07	45.49	244
			High-Density Lipoproteins		
Control	39.39	1.96	11.08	47.57	1581
Treated	28.35	1.03	22.35	48.26	1266

syntheses in the liver. 3-*N*-(1′,8′-Naphthalimido)propionic acid lowered the cytoplasmic level of acetyl CoA *via* mitochondrial citrate exchange, citrate lyase, and acetyl CoA synthetase inhibition. Acetyl CoA is a key intermediate precursor required for both cholesterol and triglyceride syntheses. Reduction of its level should lower serum levels of both lipids. The regulatory enzyme of cholesterol synthesis, HMG CoA reductase activity, was not inhibited by the drug; although clofibrate inhibits this enzyme (25), phthalimide (2) and saccharin (3) have been shown to have no effect on its activity. 3-*N*-(1′,8′-Naphthalimido)propionic acid did suppress the activity of the regulatory enzymes for fatty acid synthesis (acetyl CoA synthetase) and the regulatory enzymes for triglyceride synthesis (*sn*-glycerol-3-phosphate acyl transferase and phosphatidate phosphohydrolase). These enzyme activities were also reduced by saccharin and phthalimide derivatives (2, 3). Furthermore, the magnitude of the reduction is of a level to account for the reduction of serum triglyceride levels.

The interference with liver cholesterol synthesis by 3-*N*-(1′,8′-naphthalimido)propionic acid was not significant enough to explain the lowering of serum cholesterol levels. Thus, the distribution and excretion of cholesterol after drug treatment was evaluated. First, the drug did not accelerate cholesterol conversion to bile acid; in fact, the regulatory enzyme for this conversion, 7-α-hydroxylase, was inhibited by drug treatment *in vivo*. Side-chain degradation of cholesterol also was not increased, as measured *in vitro*. Second, [^{3}H]cholesterol excretion was accelerated in the bile and feces, indicating that the drug was accelerating clearance of cholesterol from the blood *via* biliary excretion. High contents of labeled material could be observed in the small intestine and large intestine, as well as the chyme and fecal material, suggesting that the extrahepatic circulation of cholesterol was reduced by the drug. Cholesterol absorption from the intestine after oral administration was reduced 7%. Higher levels of [^{3}H]cholesterol were observed in some of the major organs; however, when the lipid content of the liver and small intestine was examined, there was a decrease in cholesterol, triglycerides, and neutral lipids. Phospholipid content was elevated in both the liver and bile. Clofibrate treatment results in an increase in phospholipid content in the liver and serum (26). Fecal lipid levels reflect the increase in bile cholesterol and neutral lipid levels, which were elevated compared with the control values.

The lipid content of the blood lipoprotein fractions was lowered. Chylomicrons, which normally contain large concentrations of triglycerides, showed lower levels of cholesterol, neutral lipid, and triglyceride. Low-density lipoproteins, which normally contain a high concentration of cholesterol had markedly reduced cholesterol, neutral lipids, triglycerides, and phospholipid levels after drug treatment. Low-density lipoproteins are responsible for lipid deposition in atherosclerotic plaque in blood vessels. Reducing lipid levels in this lipoprotein fraction should also show reduction in the quantity of lipids being deposited in these plaques. Although it is difficult to extrapolate data from lipoprotein studies in rats to lipoprotein levels in humans, since the lipoprotein fractions are different, these studies demonstrate that 3-*N*-(1′,8′-naphthalimido)propionic acid modulated the lipid levels in the lipoprotein fraction and that 3-*N*-(1′,8′-naphthalimido)propionic acid shows promise as a potential hypolipidemic agent.

REFERENCES

(1) I. H. Hall, J. M. Chapman, Jr., and G. H. Cocolas, *J. Pharm. Sci.*, **70**, 326 (1981).

(2) I. H. Hall, P. J. Voorstad, J. M. Chapman, Jr., and G. H. Cocolas, *J. Pharm. Sci.*, **72**, 845 (1983).

(3) J. M. Chapman, Jr., G. H. Cocolas, and I. H. Hall, *J. Med. Chem.*, **28**, 243 (1983).

(4) A. T. Ness, J. V. Pastewka, and A. C. Peacock, *Clin. Chim. Acta*, **10**, 229 (1964).

(5) J. T. Litchfield, Jr. and F. Wilcoxon, *J. Pharmacol. Exp. Ther.*, **96**, 99 (1949).

(6) A. G. Goodridge, *J. Biol. Chem.*, **248**, 4218 (1973).

(7) M. Hoffman, L. Weiss, and O. H. Wieland, *Anal. Biochem.*, **84**, 441 (1978).

(8) B. H. Robinson, G. R. Williams, M. L. Halperin, and C. C. Leznoff, *Eur. J. Biochem.*, **15**, 263 (1970).

(9) B. H. Robinson and G. R. Williams, *Biochem. Biophys. Acta*, **216**, 63 (1970).

(10) D. Kritchevsky and S. A. Tepper, *Atherosclerosis*, **18**, 93 (1973).

(11) G. T. Haven, J. R. Krzemien, and T. T. Nguyen, *Res. Commun. Chem. Pathol. Pharmacol.*, **6**, 253 (1973).

(12) F. Wada, K. Hirata, and Y. Sakameto, *J. Biochem. (Tokyo)* **65**, 71 (1969).

(13) M. D. Greenspan and J. M. Lowenstein, *J. Biol. Chem.*, **243**, 6273 (1968).

(14) R. O. Brady, R. M. Bradley, and E. G. Trams, *J. Biol. Chem.*, **235**, 3093 (1960).

(15) R. G. Lamb, S. D. Wyrick, and C. Piantadosi, *Atherosclerosis*, **27**, 147 (1977).

(16) R. D. Mavis, J. N. Finkelstein, and B. P. Hall, *J. Lipid Res.*, **19**, 467 (1978).

(17) J. Folch, M. Lees, and G. H. C. Stanley, *J. Biol. Chem.*, **226**, 497 (1957).

(18) E. G. Bligh and W. J. Dyer, *Can. J. Biochem. Physiol.*, **37**, 911 (1957).

(19) J. H. Bragdon, *J. Biol. Chem.*, **190**, 513 (1951).
(20) C. P. Stewart and E. B. Henday, *Biochem. J.*, **29**, 1683 (1935).
(21) A. Adam, J. van Cantfort, and J. Gielen, *Lipids*, **11**, 610 (1976).
(22) R. J. Havel and R. S. Gordan, Jr., *J. Clin. Invest.*, **39**, 1777 (1960).
(23) R. J. Havel, H. A. Eder, and J. H. Bragdon, *J. Clin. Invest.*, **34**, 1395 (1955).
(24) O. H. Lowry, N. J. Rosebrough, A. L. Farr, and R. J. Randall, *J. Biol. Chem.*, **193**, 265 (1951).
(25) J. M. Thorp and W. S. Waring, *Nature (London)*, **194**, 948 (1962).
(26) R. E. Catalán, M. P. Castillón, and J. G. Priego, *Experientia*, **35**, 859 (1979).

ACKNOWLEDGMENTS

This study was supported by Grant 2 R01 HL25680 from the National Heart, Lung and Blood Institute, National Institutes of Health. The authors thank Tim Matthews and Colleen Gilbert for technical assistance.

High-Performance Liquid Chromatographic Determination of Metoprolol and α-Hydroxymetoprolol Concentrations in Human Serum, Urine, and Cerebrospinal Fluid

F. M. GENGO ˣ, M. A. ZIEMNIAK, W. R. KINKEL, and W. B. McHUGH

Received December 27, 1982, from *The Dent Neurologic Institute, Millard Fillmore Hospital, Buffalo, NY 14209* and *The Division of Clinical Pharmacy Science, State University of New York at Buffalo, Amherst, NY 14190.* Accepted for publication July 7, 1983.

Abstract □ A sensitive and simplified high-performance liquid chromatographic procedure was developed for the simultaneous quantification of metoprolol and α-hydroxymetoprolol in human serum, as well as cerebrospinal fluid and urine. Following protein precipitation with trichloroacetic acid, the sample was alkalinized with 1 M NaOH and extracted with dichloromethane. The mobile phase consisted of acetonitrile–water (50:50) containing 0.005 M 1-heptanesulfonic acid in 0.001% acetic acid. Using pronetalol as an internal standard, compounds were quantitated using fluorescence detection at 230 nm with a 300-nm emission filter and 0.02 AUFS. Extraction recovery is ~80% for both compounds. The lower limits of detection are 5 ng/mL and 4 ng/mL for metoprolol and α-hydroxymetoprolol, respectively.

Keyphrases □ Metoprolol—HPLC, α-hydroxymetoprolol, human serum, urine, and cerebrospinal fluid □ α-Hydroxymetoprolol—HPLC, metoprolol, human serum, urine, and cerebrospinal fluid

Metoprolol, a selective β-1-receptor blocker with an active hydroxy metabolite, is widely used in the treatment of several cardiovascular and neurological disorders (1–3). Many patients treated with standard oral doses of β-blockers experience either adverse toxic effects or receive no therapeutic benefit (4). Evaluation of the serum concentration profile of metoprolol may enable optimization of therapy for some patients. Several recent reports suggest that many of the pharmacological actions of metoprolol are paralleled by serum concentrations of metoprolol and/or α-hydroxymetoprolol (5, 6). Although α-hydroxymetoprolol may have relatively weak β-adrenergic blocking potency, its contribution to the other pharmacological actions of metoprolol remain to be determined (1, 2, 7). It is known that α-hydroxymetoprolol accumulates in the serum of patients with certain disease states, such as renal failure (7).

The current assay methods for the analysis of metoprolol include GC–MS (8), GC–EC detection (9), as well as high-performance liquid chromatography (HPLC) (10, 11). Most were designed primarily for quantification of only the parent drug. The assay procedure reported here is sensitive and specific for both metoprolol and the active hydroxy metabolite. Additionally, this procedure is useful for quantification of both compounds from serum and cerebrospinal fluid (CSF).

EXPERIMENTAL SECTION

Reagents—All chemicals and reagents were analytical grade unless otherwise indicated. Metoprolol tartrate[1], α-hydroxymetoprolol[2], and pronetalol[3] were all received as powders; stock solutions were prepared in methanol. Dichloromethane, acetonitrile[4], 30% trichloroacetic acid solution, sodium hydroxide[5], and sodium-1-heptanesulfonate[6] were used as received.

The HPLC system consisted of a delivery system[7], universal injector data module[7], and a variable-wavelength fluorescence detector[8]. Separation was conducted on a reverse-phase C_{18} column, 3.9 mm × 30 cm[9]. The mobile phase consisted of 25 mL of 0.005 M sodium-1-heptanesulfonate in 1.0% acetic acid diluted to 1 L with distilled deionized water (solvent A). The same amount of heptanesulfonic acid solution (25 mL) was diluted to 1 L with acetonitrile (solvent B). The mobile phase was a mixture of solvents A and B (50:50). A flow rate of 2 mL/min was maintained. The effluent was monitored at an excitation wavelength of 230 nm with a 300-nm UV interference filter, to set the emission wavelength, with an attenuation of 0.02.

Extraction Procedure—To 1 mL of serum (in a glass tube) was added 10 μL of a 3.0-μg/mL solution of the internal standard (pronetalol) and 200 μl of 30% trichloroacetic acid solution. This mixture was vortexed and then centrifuged[10] at 5000 rpm for 10 min. The clear supernatant (750 μL) was transferred and 375 μL of 1 M NaOH and 4.0 mL of dichloromethane were added. The mixture was vortexed for 30 s, then centrifuged for 10 min at 5000 rpm. The upper aqueous phase was aspirated and discarded; the lower organic phase was transferred, evaporated to dryness under a stream of nitrogen at 30°C, and reconstituted in 100 μL of the mobile phase. The extraction procedure for urine and (CSF) is exactly the same as described for serum.

Recovery Studies—Human serum and methanol samples were each spiked with two different concentrations of metoprolol and α-hydroxymetoprolol. The methanol samples were evaporated under a stream of nitrogen at 30°C, with internal standard added just prior to injection. The serum samples were extracted as described, with the exception that internal standard was again added prior to injection. Percent recovery was determined by comparison of peak height ratios between extracted samples and methanol samples. Five replicate determinations were made at each concentration. Similar studies were conducted using blank urine and CSF. To determine the within-day

[1] Ciba Pharmaceutical Co., Summit, N.J.
[2] Hassle Subsidiary, Molndal, Sweden.
[3] Imperial Chemical Industries, Hurdsfield Indust. Estate, Macclesfield, Cheshire, U.K.
[4] Burdick and Jackson Laboratories, Muskegon, Mich.
[5] Fisher Scientific Co., Fair Lawn, N.J.
[6] Eastman Kodak Co., Rochester, N.Y.
[7] Waters Associates, Milford, Mass.
[8] Model FS970; Schoeffel Instruments, Westwood, N.J.
[9] μBondapak C_{18}; Waters Associates, Milford, Mass.
[10] GLC-1 Centrifuge; Sorvall, Newton, Conn.

0022-3549/84/0700-0961$01.00/0
© 1984, American Pharmaceutical Association

(19) J. H. Bragdon, *J. Biol. Chem.*, **190**, 513 (1951).
(20) C. P. Stewart and E. B. Henday, *Biochem. J.*, **29**, 1683 (1935).
(21) A. Adam, J. van Cantfort, and J. Gielen, *Lipids*, **11**, 610 (1976).
(22) R. J. Havel and R. S. Gordan, Jr., *J. Clin. Invest.*, **39**, 1777 (1960).
(23) R. J. Havel, H. A. Eder, and J. H. Bragdon, *J. Clin. Invest.*, **34**, 1395 (1955).
(24) O. H. Lowry, N. J. Rosebrough, A. L. Farr, and R. J. Randall, *J. Biol. Chem.*, **193**, 265 (1951).
(25) J. M. Thorp and W. S. Waring, *Nature (London)*, **194**, 948 (1962).
(26) R. E. Catalán, M. P. Castillón, and J. G. Priego, *Experientia*, **35**, 859 (1979).

ACKNOWLEDGMENTS

This study was supported by Grant 2 R01 HL25680 from the National Heart, Lung and Blood Institute, National Institutes of Health. The authors thank Tim Matthews and Colleen Gilbert for technical assistance.

High-Performance Liquid Chromatographic Determination of Metoprolol and α-Hydroxymetoprolol Concentrations in Human Serum, Urine, and Cerebrospinal Fluid

F. M. GENGO ˣ, M. A. ZIEMNIAK, W. R. KINKEL, and W. B. McHUGH

Received December 27, 1982, from *The Dent Neurologic Institute, Millard Fillmore Hospital, Buffalo, NY 14209* and *The Division of Clinical Pharmacy Science, State University of New York at Buffalo, Amherst, NY 14190.* Accepted for publication July 7, 1983.

Abstract □ A sensitive and simplified high-performance liquid chromatographic procedure was developed for the simultaneous quantification of metoprolol and α-hydroxymetoprolol in human serum, as well as cerebrospinal fluid and urine. Following protein precipitation with trichloroacetic acid, the sample was alkalinized with 1 M NaOH and extracted with dichloromethane. The mobile phase consisted of acetonitrile–water (50:50) containing 0.005 M 1-heptanesulfonic acid in 0.001% acetic acid. Using pronetalol as an internal standard, compounds were quantitated using fluorescence detection at 230 nm with a 300-nm emission filter and 0.02 AUFS. Extraction recovery is ~80% for both compounds. The lower limits of detection are 5 ng/mL and 4 ng/mL for metoprolol and α-hydroxymetoprolol, respectively.

Keyphrases □ Metoprolol—HPLC, α-hydroxymetoprolol, human serum, urine, and cerebrospinal fluid □ α-Hydroxymetoprolol—HPLC, metoprolol, human serum, urine, and cerebrospinal fluid

Metoprolol, a selective β-1-receptor blocker with an active hydroxy metabolite, is widely used in the treatment of several cardiovascular and neurological disorders (1–3). Many patients treated with standard oral doses of β-blockers experience either adverse toxic effects or receive no therapeutic benefit (4). Evaluation of the serum concentration profile of metoprolol may enable optimization of therapy for some patients. Several recent reports suggest that many of the pharmacological actions of metoprolol are paralleled by serum concentrations of metoprolol and/or α-hydroxymetoprolol (5, 6). Although α-hydroxymetoprolol may have relatively weak β-adrenergic blocking potency, its contribution to the other pharmacological actions of metoprolol remain to be determined (1, 2, 7). It is known that α-hydroxymetoprolol accumulates in the serum of patients with certain disease states, such as renal failure (7).

The current assay methods for the analysis of metoprolol include GC–MS (8), GC–EC detection (9), as well as high-performance liquid chromatography (HPLC) (10, 11). Most were designed primarily for quantification of only the parent drug. The assay procedure reported here is sensitive and specific for both metoprolol and the active hydroxy metabolite. Additionally, this procedure is useful for quantification of both compounds from serum and cerebrospinal fluid (CSF).

EXPERIMENTAL SECTION

Reagents—All chemicals and reagents were analytical grade unless otherwise indicated. Metoprolol tartrate[1], α-hydroxymetoprolol[2], and pronetalol[3] were all received as powders; stock solutions were prepared in methanol. Dichloromethane, acetonitrile[4], 30% trichloroacetic acid solution, sodium hydroxide[5], and sodium-1-heptanesulfonate[6] were used as received.

The HPLC system consisted of a delivery system[7], universal injector data module[7], and a variable-wavelength fluorescence detector[8]. Separation was conducted on a reverse-phase C_{18} column, 3.9 mm × 30 cm[9]. The mobile phase consisted of 25 mL of 0.005 M sodium-1-heptanesulfonate in 1.0% acetic acid diluted to 1 L with distilled deionized water (solvent A). The same amount of heptanesulfonic acid solution (25 mL) was diluted to 1 L with acetonitrile (solvent B). The mobile phase was a mixture of solvents A and B (50:50). A flow rate of 2 mL/min was maintained. The effluent was monitored at an excitation wavelength of 230 nm with a 300-nm UV interference filter, to set the emission wavelength, with an attenuation of 0.02.

Extraction Procedure—To 1 mL of serum (in a glass tube) was added 10 μL of a 3.0-μg/mL solution of the internal standard (pronetalol) and 200 μl of 30% trichloroacetic acid solution. This mixture was vortexed and then centrifuged[10] at 5000 rpm for 10 min. The clear supernatant (750 μL) was transferred and 375 μL of 1 M NaOH and 4.0 mL of dichloromethane were added. The mixture was vortexed for 30 s, then centrifuged for 10 min at 5000 rpm. The upper aqueous phase was aspirated and discarded; the lower organic phase was transferred, evaporated to dryness under a stream of nitrogen at 30°C, and reconstituted in 100 μL of the mobile phase. The extraction procedure for urine and (CSF) is exactly the same as described for serum.

Recovery Studies—Human serum and methanol samples were each spiked with two different concentrations of metoprolol and α-hydroxymetoprolol. The methanol samples were evaporated under a stream of nitrogen at 30°C, with internal standard added just prior to injection. The serum samples were extracted as described, with the exception that internal standard was again added prior to injection. Percent recovery was determined by comparison of peak height ratios between extracted samples and methanol samples. Five replicate determinations were made at each concentration. Similar studies were conducted using blank urine and CSF. To determine the within-day

[1] Ciba Pharmaceutical Co., Summit, N.J.
[2] Hassle Subsidiary, Molndal, Sweden.
[3] Imperial Chemical Industries, Hurdsfield Indust. Estate, Macclesfield, Cheshire, U.K.
[4] Burdick and Jackson Laboratories, Muskegon, Mich.
[5] Fisher Scientific Co., Fair Lawn, N.J.
[6] Eastman Kodak Co., Rochester, N.Y.
[7] Waters Associates, Milford, Mass.
[8] Model FS970; Schoeffel Instruments, Westwood, N.J.
[9] μBondapak C_{18}; Waters Associates, Milford, Mass.
[10] GLC-1 Centrifuge; Sorvall, Newton, Conn.

0022-3549/84/0700-0961$01.00/0
© 1984, American Pharmaceutical Association

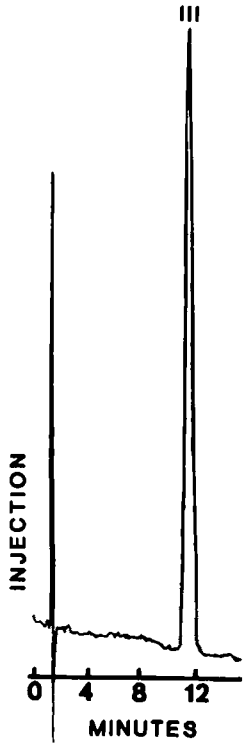

Figure 1—*Chromatogram obtained after extracting 1.0 mL of blank serum. Key: (III) internal standard.*

variation, a serum sample with known amounts of metoprolol and α-hydroxymetoprolol was assayed five times. To assess the between-day variation, another serum sample with known amounts was assayed six times over a period of 10 d.

Human Study—A patient diagnosed as having essential tremor was treated for 1 week with a regimen of 75 mg of metoprolol b.i.d. On the day 7, blood samples were collected at various times after the morning dose. The serum was stored at −30°C prior to analysis.

Stability Study—To determine the effects of temperature on the stability of metoprolol and α-hydroxymetoprolol, 1.0-mL aliquots of spiked serum were incubated at −30°C, 5°C, 25°C, and 37°C. Samples were assayed periodically over 30 d.

RESULTS

Chromatography—Figure 1 illustrates the chromatogram obtained after extracting 1.0 mL of blank serum as described. There were no additional peaks eluting that interfered with the determination of metoprolol or α-hydroxymetoprolol. A serum sample spiked with 44.4 ng/mL of metoprolol and 35.2 ng/mL of α-hydroxymetoprolol was extracted, and the resulting chromatograph is shown in Fig. 2. The retention times of metoprolol, α-hydroxymetoprolol, and the internal standard were 9.3, 5.9, and 12.0 min, respectively. A typical chromatogram of serum obtained from a patient receiving metoprolol is shown in Fig. 3.

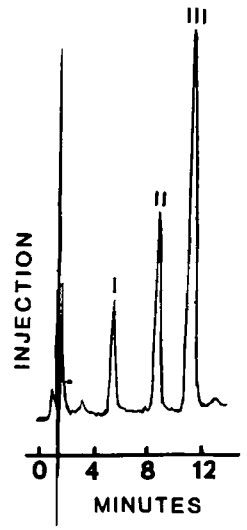

Figure 2—*Chromatogram obtained after extracting 1.0 mL of spiked serum. Key: (I) α-hydroxymetoprolol; (II) metoprolol; (III) internal standard.*

Table I—Slope of Intercept Values [a] Derived from Concentration and Peak-Height Ratio Relationship for Metoprolol and α-Hydroxymetoprolol in Various Biological Fluids

Biological Fluid	Metropolol		α-Hydroxymetoprolol	
	Slope	Intercept	Slope	Intercept
Serum	0.0025 + 0.0006	0.073 + 0.054	0.0024 + 0.0002	0.161 + 0.013
Urine	0.004 + 0.0002	0.0146 + 0.0006	0.003 + 0.0004	0.004 + 0.0004
CSF	0.005 + 0.0003	0.005 + 0.0004	0.005 + 0.0005	0.005 + 0.0002

[a] All correlation coefficients >0.99.

Table II—Recovery of Metoprolol and α-Hydroxymetoprolol from Human Serum [a]

	Drug conc., ng/mL	Mean Recovery, %	*CV*, %
Metoprolol	22.2	79.0	9.7
	266.4	78.2	7.9
α-Hydroxymetoprolol	17.6	80.0	9.1
	211.1	80.0	7.9

[a] $n = 5$.

Calibration curves, were prepared daily by plotting peak height ratios (drug or metabolite/internal standard) *versus* concentrations of spiked serum samples. These plots were linear over a 5–600-ng/mL concentration range. The mean ±*SD* slope value and intercept values are given in Table I. The lower limits of detection for metoprolol and the α-hydroxy metabolite were 4.9 and 3.8 ng/mL, respectively. Linearity was also demonstrated for metoprolol and α-hydroxymetoprolol when extracted from CSF and urine in the 15–150-ng/mL concentration range (Table I). Chromatograms of samples extracted from urine and CSF showed no additional peaks that interfere with quantification of the drug, metabolite, or internal standard (Fig. 4).

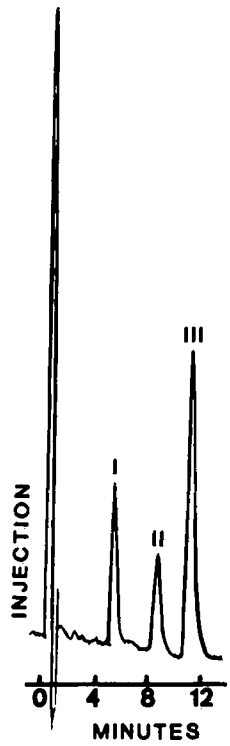

Figure 3—*Chromatogram of extracted serum from a patient receiving metoprolol. Key: (I) α-hydroxymetoprolol; (II) metoprolol; (III) internal standard.*

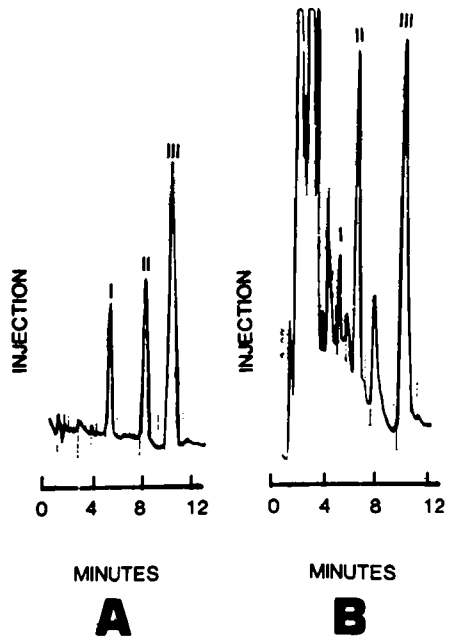

Figure 4—*Chromatograms of extracted CSF (A) and urine (B) containing α-hydroxymetoprolol (I), metoprolol (II), and internal standard (III).*

Recovery Experiments—The results of the recovery experiments are illustrated in Table II for both high and low concentrations. The overall recovery of metoprolol and α-hydroxymetoprolol ranged from 78.2 to 80.0% in serum, urine, and CSF over a 10-fold concentration range. Both metoprolol and α-hydroxymetoprolol also demonstrated similar within-day and between-day variations, as illustrated in Table III. The coefficient of variation ranged from 5.4 to 6.0% for within-day variation experiments, while the between-day studies ranged from 8.6 to 9.3%.

Human Serum Concentration Analysis—Figure 5 illustrates a serum concentration *versus* time profile for metoprolol and α-hydroxymetoprolol in the tremor patient following a 75-mg oral dose of metoprolol. After 2 h, peak concentrations were seen for the drug and its metabolite, 53.8 ng/mL and 88.1 ng/mL, respectively. After 7 h, both metoprolol and α-hydroxymetabolite decreased monoexponentially to 13.1 and 50.5 ng/mL, respectively.

Stability Study—To assess proper handling and storage conditions for

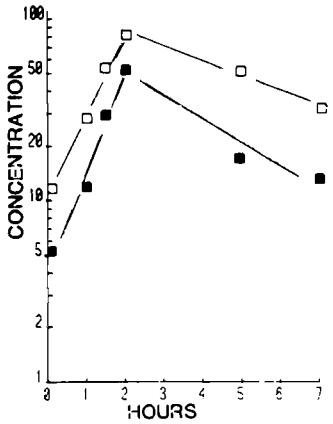

Figure 5—*Serum concentration* versus *time profiles for metoprolol (■) and α-hydroxymetoprolol (□) after a 75-mg oral dose of metoprolol.*

Table III—Within-Day and Between-Day Variation in the Determination of Metoprolol and α-Hydroxymetoprolol in Human Serum

	Mean, ng/mL	*CV*, %
Within-day,[a]		
Metoprolol	191.8	5.9
α-Hydroxymetoprolol	148.0	5.4
Between-day[b]		
Metoprolol	181.9	9.2
α-Hydroxymetoprolol	147.1	8.6

[a] $n = 5$. [b] $n = 6$.

metoprolol and α-hydroxymetoprolol, the effect of temperature on the degradation rate was monitored. Over the 30-d test period, the samples frozen at −30°C remained stable. At 37°C, 25°C, and 5°C there was degradation within 14 d.

DISCUSSION

The metoprolol assay described in this report is specific, selective, and reproducible. Both drug and active metabolite can be specifically and reproducibly quantitated in urine, serum, and CSF in concentrations that are achieved by standard doses of metoprolol.

The procedure reported here is a modification of other previously reported metoprolol assays (10, 11). Modifications in the extraction process circumvents the need to distill reagents daily. These modifications also reduce background interference peaks in blood samples and prevent emulsification of reagents during the extraction. Modification in the mobile phase enables excellent separation of the drug, metabolite, and internal standard within a 15-min time period.

This procedure quantitates drug and metabolite concentrations from urine and CSF using the same experimental procedure used for serum. This procedure has been tested in patients concomitantly taking several medications. Drugs such as thiazide, benzodiazepines, digoxin, and thyroid hormone produced no interference; however, other β-blockers such as alprenolol, atenolol, naldolol, propranolol, sotalol, and timolol did interfere. In summary, this method provides a simplified and clinically comprehensive procedure for the analysis of metoprolol and α-hydroxymetoprolol.

REFERENCES

(1) M. Peet and R. A. Yates, *J. Clin. Hosp. Pharm.* **6**, 155 (1981).

(2) D. J. Greenblatt and R. I. Shrader, *Curr. Ther. Res.* **14**, 615 (1972).

(3) G. F. Winkler and R. R. Young, *N. Engl. J. Med.*, **290**, 984 (1974).

(4) R. D. Sweet, J. Blumberg, J. E. Lee, and F. H. McDowell, *Neurology*, **1**, 64 (1974).

(5) R. G. McAllister, W. R. Markesbery, R. W. Ware, and S. M. Howel, *Ann. Neurol.*, **1**, 60 (1977).

(6) S. Calzetti, L. J. Findley, E. Perucca, and A. Richens, *J. Neurol. Neurosurg. Psych.*, **45**, 893 (1982).

(7) C. G. Regardh, K. O. Borg, R. Johansson, and L. Palmer, *J. Pharmacokinet. Biopharm.*, **2**, 347 (1972).

(8) M. Ervik, K. J. Hoffmann, and H. Kylbers-Hanssen, *Biomed. Mass Spectrom.*, **8**, 322 (1981).

(9) C. P. Quarterman, M. J. Kendall, and D. B. Jack, *J. Chromatogr.*, **183**, 92 (1980).

(10) M. T. Rosseel, F. M. Belpaire, M. Bogaert, and M. G. Bekaert, *J. Pharm. Sci.*, **71**, 114 (1982).

(11) D. P. Pautler and W. J. Jusko, *J. Chromatogr.*, **228**, 215 (1982).

ACKNOWLEDGMENTS

The authors gratefully acknowledge the secretarial assistance of Ms. Mary-Jo Jagord and Mr. William Finney.

Bioavailability of Hydrocortisone From Commercial 20-mg Tablets

RAJNI B. PATEL *§, MARK C. ROGGE *, ARZU SELEN *, THOMAS J. GOEHL ‡, VINOD P. SHAH ‡, VADLAMANI K. PRASAD ‡, and PETER G. WELLING *x¶

Received December 13, 1982, from the **School of Pharmacy, University of Wisconsin, Madison, WI 53706* and the ‡*Biopharmaceutics Laboratory Branch, Division of Biopharmaceutics, Food and Drug Administration, Washington, DC 20204.* Accepted for publication June 30, 1983. Present addresses: §Analytical R and D Subdivision, Wyeth Laboratories, P.O. Box 8299, Philadelphia, PA 19101, and ¶Department of Drug Metabolism and Pharmacokinetics, Warner Lambert Co., Ann Arbor, MI 48105.

Abstract □ The relative bioavailability of hydrocortisone was determined from four different 20-mg tablet formulations and one suspension in 15 healthy male volunteers; results were compared with *in vitro* dissolution rates. Plasma levels of hydrocortisone were determined by a liquid chromatography method developed in this laboratory. Dissolution of the tablet formulations, using the official USP test, varied from 7.8 to 93.8% in 30 min. Similar plasma profiles were obtained from all tablet products, and there were no differences among tablets in the cumulative percentage of drug absorbed. There were no clear trends in any pharmacokinetic parameter values among the tablet dosages, and the four products were considered bioequivalent. The suspension dosage yielded significantly higher plasma levels compared with some of the tablet formulations during the initial 30-min postdose, significantly higher cumulative absorption at 0.5 and 1.0 h compared with one tablet formulation, and significantly higher k_a and C_{max}, and shorter t_{max} values, compared with some of the tablets.

Keyphrases □ Hydrocortisone—bioavailability, commercial 20-mg tablets, dissolution □ Bioavailability—hydrocortisone, commercial 20-mg tablets, dissolution □ Dissolution—bioavailability of hydrocortisone, commercial 20-mg tablets

Hydrocortisone was designated by the U.S. Food and Drug Administration as a drug whose different brands and dosage forms should be examined for bioequivalence (1). Previous studies in this laboratory have described optimum conditions for hydrocortisone pharmacokinetic studies (2, 3). Circulating hydrocortisone levels have been shown to be linearly related to dose size of oral suspensions (4) and also of intravenous hydrocortisone doses that give rise to plasma levels that are within the range observed with conventional oral doses (5).

This study was designed to examine the relative *in vivo* bioavailability and pharmacokinetics of hydrocortisone from commercial 20-mg tablets that have divergent *in vitro* dissolution characteristics, and to compare these with an oral suspension.

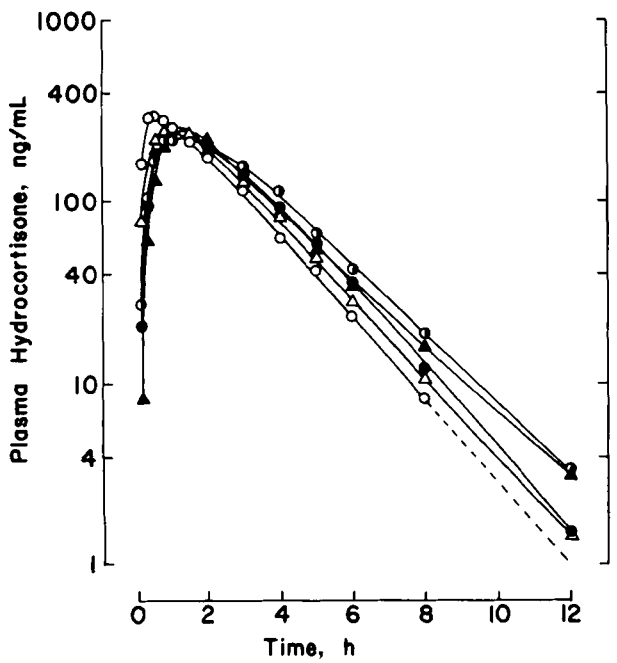

Figure 1— *Mean plasma levels of hydrocortisone in 15 healthy male volunteers following single 20-mg suspension and tablet doses. Key: (○) suspension A; (◑) tablet B; (●) tablet C; (△) tablet D; (▲) tablet E.*

EXPERIMENTAL SECTION

Products—The suspension[1] (treatment A) and the four tablet[2] formulations (treatments B–E) were purchased commercially.

Materials—Chemical standard hydrocortisone[3] and internal standard Δ^4-pregnen-17α,20β,21-triol-3,11-dione[3] were analytical grade. All other solvents and chemicals were reagent grade and were used as supplied. Plasma for construction of standard curves was obtained from healthy volunteers between 7 a.m. and 9 a.m. subsequent to administration of 2 mg of dexamethasone at 11 p.m. the previous day.

***In Vitro* Dissolution**—The *in vitro* dissolution rates of the tablets were determined in 900 mL of distilled water at 37°C using the USP rotating paddle method at 50 rpm (6).

Subjects—Fifteen male volunteers, 22–39 years old, underwent complete physical examinations, including urine and blood analyses, after giving informed consent. Vital signs and laboratory values for all subjects were normal. The subjects weighed 67–84 kg, and their heights ranged from 165 to 186 cm.

Protocol—Subjects were instructed to take no drugs for at least 1 week before, and no drugs other than the required doses of dexamethasone and hydrocortisone during the study. No caffeine-containing beverages were permitted for 1 d before or during the plasma sampling period following each dose of hydrocortisone. Each hydrocortisone dose was administered after an overnight fast, and no food was permitted until 4 h postdose.

The 15 subjects were randomly assigned to one of five groups, each consisting of three subjects. The five dosages (one suspension and four tablets) were administered to the groups according to a 5 × 5 crossover design. Dose size was 20 mg, and all dosages were separated by a 14-d interval.

At 11 p.m. on the day before hydrocortisone administration, subjects received 20 mL (2 mg) of dexamethasone elixir[4] orally together with 180 mL of water. Dexamethasone suppresses plasma levels of endogenous hydrocortisone (2). Hydrocortisone was administered the next morning at 8 a.m. The suspension was given in 20 mL of orange juice with additional water to 180 mL. Tablets were given with 180 mL of water and were swallowed whole. Heparinized blood samples (~8 mL) were taken from a forearm vein at 0, 10, 20, 30, 45 min, 1, 1.5, 2, 3, 4, 5, 6, 8, and 12 h postdose. Plasma was stored at −20°C until assayed.

Analytical Procedure—The HPLC-UV assay used to measure hydrocortisone in plasma was described previously (3, 4). The assay is linearly sensitive to plasma hydrocortisone concentrations between 5 and 700 ng/mL. The reproducibility of the assay is within 4% at the higher concentrations and within 8% at the lower concentrations. Suppressed hydrocortisone concentrations obtained immediately prior to drug administration were subtracted from all measured postdose levels.

[1] (A) Cortef intramuscular suspension, 50 mg/mL, Lot No. 027FP; The Upjohn Co.

[2] (B) Cortef, 20 mg, Lot No. 446GT; The Upjohn Co. (C) Hydrocortisone, 20 mg, Lot No. 9C483; McKesson Laboratories. (D) Hydrocortone, 20 mg, Lot No. D1048; Merck Sharp and Dohme. (E) Hydrocortisone, 20 mg, Lot No. 33993; Richlyn.

[3] Sigma Chemical Co., St. Louis, Mo.

[4] Decadron Elixir, Lot A 3240; Merck Sharp and Dohme.

0022-3549/84/0700-0964$01.00/0
© 1984, American Pharmaceutical Association

Table I—Percentage of Drug Dissolved from Tablets in 30 min in Distilled Water at 37°C Using the USP Rotating Paddle Method at 50 rpm [a]

Tablet	Percentage Dissolved in 30 min [b]
B	93.8 ± 1.9
C	40.2 ± 7.4
D	68.7 ± 7.9
E	7.8 ± 1.1

[a] See Ref. 6. [b] Mean ± *SD*, $n = 12$.

Pharmacokinetic and Statistical Analyses—Individual plasma hydrocortisone profiles were interpreted in terms of Eq. 1 (7):

$$C = \frac{FD}{V}\left(\frac{k_a}{k_a - k_{el}}\right)(e^{-k_{el}(t-t_0)} - e^{-k_a(t-t_0)}) \qquad \text{(Eq. 1)}$$

where C is the concentration of exogenous hydrocortisone in plasma at time t, t_0 is the lag time between drug administration and appearance of exogenous drug in plasma, F is the fraction of the dose (D) that is absorbed, V is the apparent distribution volume of hydrocortisone in the body, and k_a and k_{el} are first-order rate constants for drug appearance in and elimination from plasma, respectively. Cumulative drug absorption profiles were constructed from individual data sets by the method of Wagner and Nelson (8). Model-independent estimates of areas under plasma drug concentration curves from zero to infinite time (AUC) were calculated by the trapezoidal rule, with end correction where necessary (9). Concentrations of hydrocortisone in plasma at each sampling time and all pharmacokinetic values were compared with treatments by analysis of variance for crossover design (10). Differences between individual treatments were examined using Tukey's test (11).

RESULTS

***In Vitro* Dissolution**—The mean percentage dissolution of the four tablet formulations is given in Table I. Tablet B dissolved rapidly, dissolution of this product being virtually complete in 30 min. Dissolution of tablets C and D was somewhat slower than tablet B, while tablet E dissolved even more slowly, over 90% of this product being still intact at 30 min.

***In Vivo* Bioavailability**—The mean plasma levels of exogenous hydrocortisone from the suspension and tablet dosages are given, together with standard deviations, in Table II. The mean plasma profiles are summarized on a semilogarithmic scale in Fig. 1. The results of pharmacokinetic analysis are given in Table III.

Following the suspension dose, plasma hydrocortisone levels reached a mean peak concentration of 311 ng/mL at 0.5 h. Absorption was somewhat slower following the tablet dosages and mean peak levels ranging from 225 to 285 ng/mL were obtained at 1.0–1.5 h postdose. After peak levels had been achieved, plasma levels from all dosages declined monoexponentially to reach mean values of 1.5–3.5 ng/mL at 12 h following the tablet doses, and baseline values following the suspension dose. The suspension dose tended to yield higher plasma hydrocortisone levels compared with the tablets during the initial 30-min postdose period. However there were only minor differences in plasma levels between all dosage forms at times subsequent to this.

The mean cumulative percentage of doses absorbed during 4 h postdose are summarized in Fig. 2 (8). Ninety percent of systemically available drug was absorbed by 1 h following the suspension dose and by 2–3 h from the tablets. The suspension gave rise to significantly higher cumulative absorption compared with tablet E at 0.5 and 1 h, but there were no other significant treatment effects at any other sampling time.

There was considerable variation in some pharmacokinetic parameter values, both within and between treatments (Table III). For example, the mean value of k_a ranged from 0.9 ± 0.4 (*SD*) to 7.2 ± 5.4 h^{-1} for treatments E and A, respectively, with other treatments yielding intermediate values, but significant differences ($p < 0.05$) were observed only between the suspension dose and three of the tablet doses. Interpretation of the k_a values is difficult as they are influenced by the computer-generated values of t_0, which had to be arbitrarily fixed while fitting data from treatment E in order to obtain satisfactory convergence. An additional complication is that hydrocortisone has been shown to obey two-compartment kinetics following intravenous administration (5), so that the numerical value of k_a after oral doses is simultaneously influenced by both distribution and absorption phenomena. The various treatments did not significantly influence the hydrocortisone elimination rate.

Faster absorption of hydrocortisone from the suspension compared with tablets is reflected in high C_{max} and low t_{max} values from treatment A compared with some of the tablet dosages. The higher C_{max} from treatment D compared with treatment E was the only significant difference among tablets for the parameters C_{max} and t_{max}. Tablet E gave rise to somewhat slower

Table II—Mean Plasma Hydrocortisone Levels following Single 20-mg Doses of Treatment A (Suspension) and Treatments B–E (Tablets)

Treatment	Plasma Hydrocortisone, ng/mL												
	10 min	20 min	30 min	45 min	1 h	1.5 h	2 h	3 h	4 h	5 h	6 h	8 h	12 h
A													
Mean	164	291	297	281	260	216	173	113	63.6	41.2	23.2	8.4	—[a]
SD	118	77	57	52	45	42	36	37	24.5	20.3	12.8	7.7	—[a]
B													
Mean	27.3	103	170	219	219	221	210	159	114	67.7	41.9	18.7	3.5
SD	28.5	68	86	76	68	53	53	70	58	43.6	28.6	15.9	5.8
C													
Mean	20.8	96	182	244	250	221	207	144	93	57	35.4	12.2	1.5
SD	25.1	88	113	90	68	37	37	57	40	30	19.0	8.8	5.0
D													
Mean	78	165	221	248	259	233	199	132	83.2	49.6	28.7	10.5	1.5
SD	115	123	99	67	61	48	49	49	39.0	28.0	17.0	9.4	2.9
E													
Mean	8.1	60	132	204	223	230	211	148	91	56.0	34.7	15.9	3.2
SD	14.1	46	86	106	102	71	54	40	36	30.5	18.6	12.9	6.4

[a] Concentration not different from predose, baseline value.

Table III—Hydrocortisone Pharmacokinetic Parameter Values (±1 *SD*)

Parameter	Treatment					Significance[a]	HSD[b]
	A	B	C	D	E		
k_a (h^{-1})	7.2 ± 5.4	2.0 ± 1.2	2.5 ± 2.1	3.9 ± 5.6	0.9 ± 0.4	A > BCE	3.4
k_{el} (h^{-1})	0.53 ± 0.20	0.50 ± 0.13	0.62 ± 0.37	0.54 ± 0.10	0.66 ± 0.22	—[c]	0.17
$t_{1/2,el}$ (h)	1.4 ± 0.3	1.5 ± 0.4	1.3 ± 0.5	1.3 ± 0.3	1.2 ± 0.4	—	0.32
t_0 (h)	0.07 ± 0.08	0.19 ± 0.24	0.21 ± 0.15	0.13 ± 0.13	0.01 ± 0.0[d]	—	0.15
FD/V (ng/mL)	410 ± 118	445 ± 120	425 ± 103	450 ± 87	520 ± 128	E > AC	110
C_{max} (ng/mL)[e]	311 ± 41	252 ± 40	267 ± 46	285 ± 62	225 ± 43	A > BE, D > E	49
t_{max} (h)	0.7 ± 0.2	1.4 ± 0.7	1.2 ± 0.5	1.0 ± 0.6	1.4 ± 0.6	BCE > A	0.41
AUC (ng·h/mL)	800 ± 168	911 ± 234	821 ± 287	858 ± 224	897 ± 204	—	168
r^2[g]	0.98 ± 0.02	0.96 ± 0.05	0.98 ± 0.03	0.99 ± 0.01	0.92 ± 0.06	—	
SS $(ng/mL)^2 \times 10^{-3}$[h]	2.64 ± 2.41	5.82 ± 3.92	3.17 ± 1.63	3.46 ± 2.50	13.5 ± 6.1		

[a] Significant level = 95%. [b] Honestly Significant Difference detectable at $p < 0.05$ (10). [c] No significant differences. [d] The value of t_0 was fixed while fitting treatment E plasma data to Eq. 1 to obtain convergence. [e] Observed maximum concentration of hydrocortisone in plasma. [f] Time of C_{max}. [g] Coefficient of determination, $r^2 = (\Sigma obs^2 - \Sigma dev^2)/\Sigma dev^2$, obtained by fitting individual data to Eq. 1. [h] Deviation sums of squares.

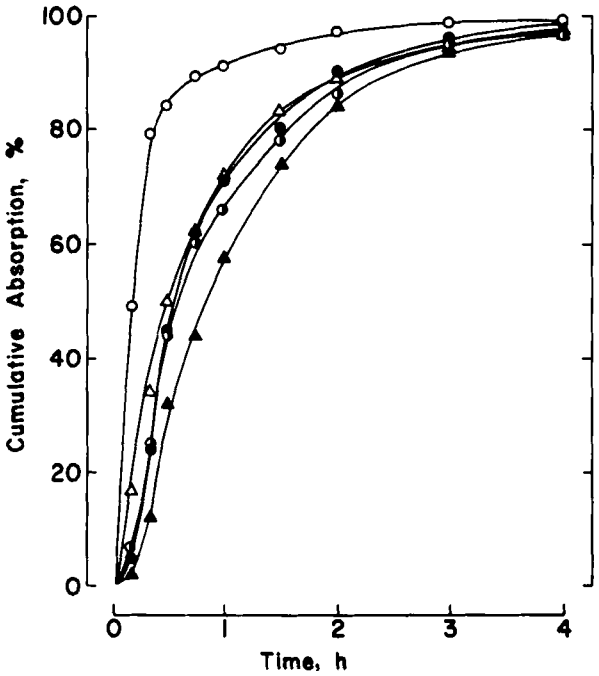

Figure 2—*Mean cumulative percentage of available hydrocortisone dose absorbed by 4 h postdose. Key: (○) suspension A; (◑) tablet B; (●) tablet C; (△) tablet D; (▲) tablet E.*

absorption compared with both the suspension and Tablet D, but the parameter *FD/V*, which is equivalent to the AUC normalized for variations in k_{el}, was significantly higher from treatment E compared with treatments A and C.

The high coefficients of determination for treatments A–D, and also similar deviation sums of squares for these treatments, indicate that individual plasma data sets were adequately described by Eq. 1. Plasma profiles tended to be somewhat more variable from tablet E, and this is reflected in the lower coefficient of determination and greater deviation sums of squares for this tablet formulation. Numerical values for pharmacokinetic values in this study are generally similar to those reported earlier (4, 5).

The HSD values in Table III indicate the difference between parameter values that this study was capable of detecting at the 95% confidence level (10). Comparison of the HSD and parameter values indicates that the study was capable of detecting a 25% difference between treatments at the 95% confidence level for all pharmacokinetic parameters except t_{max}, where a 29% difference could be detected, and k_a and t_0, for which the study was relatively insensitive.

DISCUSSION

Previous studies in this laboratory have suggested that hydrocortisone is ~50–60% available to the systemic circulation following 10–20-mg tablet or suspension doses (4, 5). The results of the present study show that incomplete absorption of hydrocortisone is probably due to intrinsic absorption effects, first-pass hepatic clearance, or both. The similar plasma profiles obtained among tablet dosages, despite a 12-fold range in their dissolution rates, and also similar overall absorption efficiency from the tablet and suspension formulations suggest that dissolution does not play a dominant role in oral hydrocortisone absorption. Our observations with hydrocortisone are similar to those reported earlier for prednisolone and prednisone (12, 13). In those studies, similar plasma profiles for prednisolone were obtained from oral tablet formulations with widely divergent dissolution characteristics in water.

Apart from the discrepancies between products C and E in the value of *FD/V*, and between products D and E in the value of C_{max}, the four tablet products examined here can be considered bioequivalent. However, two of the products (C and E) did not meet the official dissolution requirements for hydrocortisone tablets, *i.e.*, 70% dissolution in 30 min (6). Since completion of the *in vitro* dissolution studies, these products have been reformulated to meet the official requirements[5].

In conclusion, the four hydrocortisone tablet products studied here were bioequivalent. We conclude that other hydrocortisone products meeting the official dissolution test requirement will also be bioequivalent.

REFERENCES

(1) *Fed. Regist.*, **42**, 1624 (1976).

(2) T. J. Goehl, G. M. Sundaresan, J. P. Hunt, V. K. Prasad, R. D. Toothaker, and P. G. Welling, *J. Pharm. Sci.*, **69**, 1409 (1980).

(3) R. D. Toothaker, G. M. Sundaresan, J. P. Hunt, T. J. Goehl, K. S. Rotenberg, V. K. Prasad, W. A. Craig, and P. G. Welling, *J. Pharm. Sci.*, **71**, 573 (1982).

(4) R. D. Toothaker, W. A. Craig, and P. G. Welling, *J. Pharm. Sci.*, **71**, 861 (1982).

(5) R. D. Toothaker and P. G. Welling, *J. Pharmacokinet. Biopharm.*, **10**, 147 (1982).

(6) "U.S. Pharmacopeia," 20th rev., U.S. Pharmacopeial Convention, Rockville, Md., Addendum a to Supplement 1, 1980, p. 128.

(7) J. G. Wagner, "Fundamentals of Clinical Pharmacokinetics," Drug Intelligence Publications, Hamilton, Ill., 1975, p. 81.

(8) J. Wagner and E. Nelson, *J. Pharm. Sci.*, **52**, 610 (1963).

(9) M. Gibaldi and D. Perrier, "Pharmacokinetics," Dekker, New York, N.Y., 1975, p. 293.

(10) W. W. Daniel, "Biostatistics: A Foundation for Analysis in the Health Sciences," 2nd ed. Wiley, New York, N.Y., 1978, p. 203, 220.

(11) J. Netter and W. Wasserman, "Applied Linear Statistical Models," Richard D. Irwin, Homewood, Ill., 1974, p. 474.

(12) T. J. Sullivan, R. G. Stoll, E. Sakmar, D. C. Blair, and J. G. Wagner, *J. Pharmacokinet. Biopharm.*, **2**, 29 (1974).

(13) A. R. DiSanto and K. A. DeSante, *J. Pharm. Sci.*, **64**, 109 (1975).

ACKNOWLEDGMENTS

Funds for this study were provided by FDA Contract 223-78-3006.

[5] Personal communication, FDA.

Properties of Carbonate-Containing Aluminum Hydroxide Produced by Precipitation at Constant pH

EDWARD C. SCHOLTZ *, JOSEPH R. FELDKAMP ‡, JOE L. WHITE ‡, and STANLEY L. HEM *x

Received May 2, 1983, from the *Departments of *Industrial and Physical Pharmacy and ‡Agronomy, Purdue University, West Lafayette, IN 47907. Accepted for publication July 19, 1983.

Abstract □ Carbonate-containing aluminum hydroxide was precipitated at constant pH at intervals of 0.5 pH units from pH 6 to 10 by pumping 0.5 M $AlCl_3$ into the reaction vessel at a constant rate of 2 mL/min and infusing 2 M Na_2CO_3 at a rate necessary to maintain the desired pH. The pH of precipitation affected both the particle size and the composition of the precipitate. The particle size of the precipitate decreased as the pH of precipitation was increased from 6 to 10. The precipitates formed between pH 7.5 and 9.5 contained crystalline sodium aluminum hydroxycarbonate (dawsonite) in addition to amorphous carbonate-containing aluminum hydroxide.

Keyphrases □ pH—precipitation, carbonate-containing aluminum hydroxide □ Aluminum hydroxide—carbonate containing, production by precipitation at constant pH

Many processes for the preparation of aluminum hydroxide have been reported (1). Examples of these processes include (*a*) slowly cooling a concentrated sodium aluminate solution (2, 3); (*b*) bubbling CO_2 through a concentrated sodium aluminate solution (4–6); (*c*) hydrolysis of aluminum alcoholates (7, 8) or amalgamated aluminum foil (8); and (*d*) neutralization of an aluminum salt solution with a base (9–11). Aluminum hydroxide for pharmaceutical use is often prepared by the neutralization of an aluminum salt solution with a base. Some of the important variables associated with this method include temperature, pH, agitation, method of addition, reactants, reactant concentration, and addition rate (6, 12–18).

Three methods have been utilized for neutralizing an aluminum salt with a base. The first method involves the addition of the aluminum salt to the base (15, 17–20) and is limited to batch processes. The high pH of the base is decreased by the addition of the aluminum salt until a specific pH end point is reached. The second method is the opposite of the first, *i.e.*, base is added to the aluminum salt solution (12–14, 16–18, 21–23). The second method is also a batch process, as base is added until a specific pH end point is reached. In the third method, an aluminum salt solution and a base are simultaneously mixed (8, 17, 24). This method can be either a batch or a continuous process.

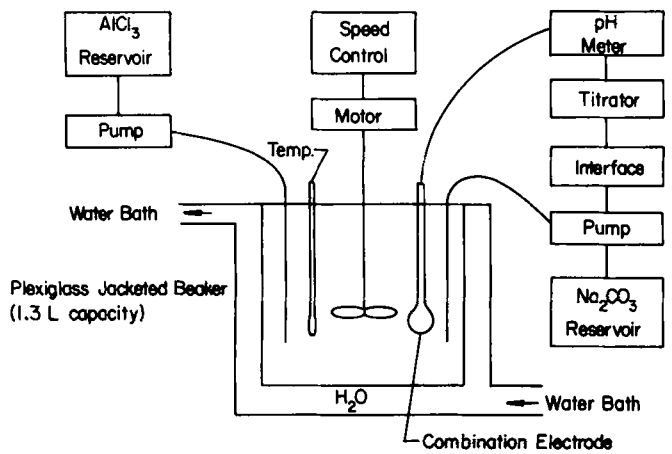

Figure 1—*Schematic of the apparatus used for constant pH precipitation of carbonate-containing aluminum hydroxide.*

Although far less common than other methods, the method of simultaneous mixing of reactants permits the precise control of pH. Since the solubility of aluminum hydroxide is very sensitive to pH, fixing this variable during the precipitation reaction should have a strong influence on the properties of the precipitate.

The objective of the present study was to examine aluminum hydroxide precipitates prepared under the constraint of constant pH. Precipitation reactions were carried out over the pH range of 6 to 10 with an automated apparatus which controls the pH within ±0.03 pH units of the desired value. Since carbonate-containing aluminum hydroxide is of considerable pharmaceutical importance (15), sodium carbonate was used as the base that was treated with aluminum chloride. After the precipitates were prepared, their physical and chemical properties were examined.

EXPERIMENTAL SECTION

Experimental laboratory gels were precipitated at 25°C from pH 6 to 10 at intervals of 0.5 pH units. The apparatus employed for the constant pH precipitations is shown in Fig. 1. The reaction vessel was a jacketed polymethyl methacrylate[1] beaker (10.2 cm i.d., 16.1 cm depth) with a capacity of 1.3 L. The vessel was fitted with four equally spaced polymethyl methacrylate baffles to provide efficient mixing.

The 0.5 M $AlCl_3$ and 2.0 M Na_2CO_3 solutions were injected into the reaction medium through submerged polytef tubes (0.1 mm i.d.). The aluminum chloride solution was pumped continuously into the reaction vessel at a constant rate of 2 mL/min. The sodium carbonate solution was infused into the system as needed to maintain the pH within 0.03 pH units of the predetermined value. The pH was constantly monitored and automatically controlled through the use of a titrator[2] linked between the pH meter and the sodium carbonate injection pump. The titrator was interfaced to the sodium carbonate pump with an opto-coupler chip.

A precipitation reaction was initiated by first placing 250 mL of 0.75 M $NaHCO_3$ into the reaction vessel. Since the pH was ~8.0, either 0.5 M $AlCl_3$ or 2.0 M Na_2CO_3 was infused until the desired pH was reached. When aluminum chloride was used, precipitation occurred during this period of pH adjustment, but the amount of precipitate formed was always insignificant when compared with the total amount of precipitate. Due to the large volume change occurring during the precipitation reaction (250 to 1300 mL), it was

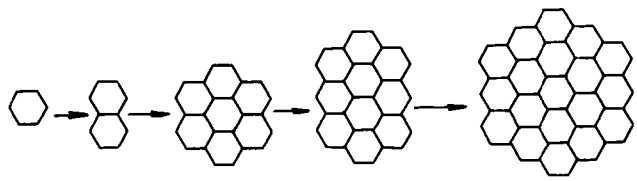

Figure 2—*Schematic of the development of crystalline aluminum hydroxide.*

[1] Plexiglas.
[2] PHM 62, TTT 60; Radiometer, Copenhagen, Denmark.

0022-3549/84/0700-0967$01.00/0
© 1984, American Pharmaceutical Association

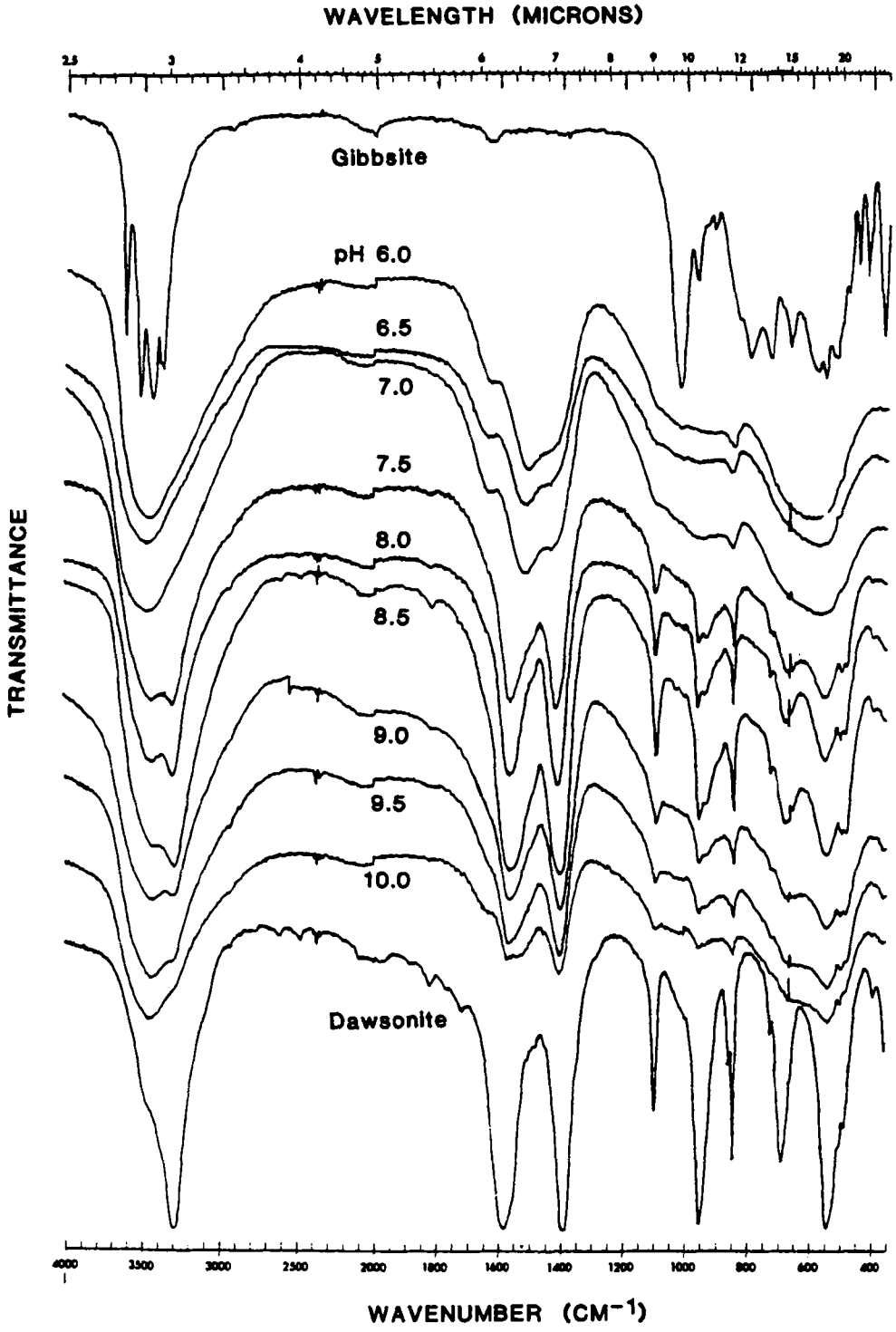

Figure 3—*IR spectra of precipitates formed at various pH_p.*

necessary to vary the stirring rate from 600 to 1200 rpm as needed. A marine propeller (diameter, 6.4 cm) was used to provide uniform mixing.

On completion of the precipitation reaction, the precipitate was washed by centrifugation with deionized water until the chloride content of the supernatant, as determined by a silver nitrate test, was $<6.2 \times 10^{-7}$ M. The washing step was always completed within 24 h of the termination of the precipitation reaction. The final suspension concentration was adjusted to fall within the range of 2–8% (w/w) equivalent Al_2O_3.

The equivalent aluminum oxide content was determined by chelatometric titration (25). IR analysis[3] was performed on air-dried samples as potassium bromide pellets (0.75 mg/300 mg of KBr). Carbonate was determined by a gasometric displacement technique (26, 27) with the Chittick apparatus[4]. The sodium ion content was measured by atomic absorption spectrometry[5]. The ability of magnesium cation to replace sodium cation in the pH 8.5 precipitate was determined by washing 600 mL of the precipitate with 600 mL of 1 M $MgCl_2$. The solids were washed four times with 1 M $MgCl_2$ by centrifugation and were then further washed with deionized water until the chloride content of the supernatant, as determined by a silver nitrate test, was $<6.2 \times 10^{-7}$ M. The point of zero charge (PZC) was determined for each sample by a continuous titration procedure (28).

To provide a qualitative measurement of particle size, the following sedimentation experiment was carried out. One hundred milliliters of sample was adjusted to the following conditions: 1% (w/v) equivalent Al_2O_3; ionic strength, 0.4; and pH = PZC. The sedimentation height in a sealed, undisturbed 100-mL graduated cylinder was monitored for 48 h. Two parameters

[3] Model 180; Perkin-Elmer Corp., Norwalk, Conn.
[4] Sargent Welch, Skokie, Ill.
[5] Model 290B; Perkin-Elmer Corp.

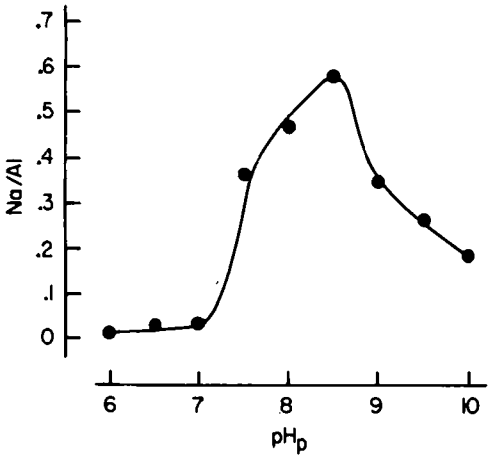

Figure 4—*Effect of pH_p on the sodium-aluminum molar ratio.*

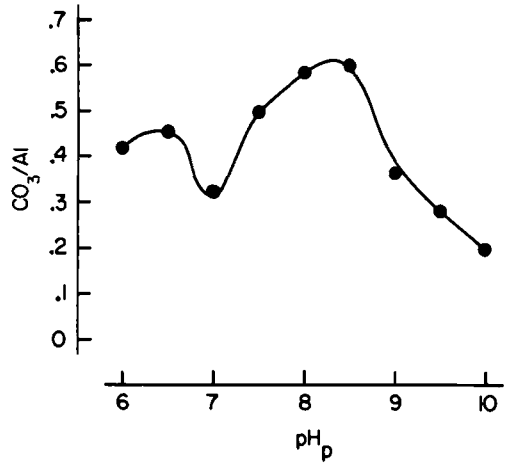

Figure 5—*Effect of pH_p on the carbonate-aluminum molar ratio.*

were used to summarize the sedimentation data: V_{48}, the sediment volume of the flocculated material at the end of the sedimentation period; and τ_{50}, the time required for the sediment volume to reach $(100 + V_{48})/2$. The values of both parameters are inversely related to particle size.

An additional qualitative measurement of particle size was the rate of acid neutralization as measured by pH-stat titration at pH 3.0 and 25°C (29). The time required to neutralize 50% of the sample, t_{50}, was used to characterize the rate of acid neutralization. A smaller value for t_{50} was assumed to infer a larger effective surface area and, hence, a smaller particle size. Particle size was directly measured for samples precipitated at pH 7.0 and 9.5 with a particle counter[6] and a fiber optic Doppler anemometer[7] (30), respectively.

RESULTS AND DISCUSSION

Chemical Structure—In a carbonate-containing system, X-ray and IR analyses have shown that aluminum hydroxide typically forms as an amorphous precipitate consisting of small, two-dimensional crystallites (primary particles) which vary widely in size (15, 31, 32). The crystallites have been identified as precursors of the various crystalline forms of aluminum hydroxide, such as gibbsite (32–34). The edges of the planar crystallites (Fig. 2) serve as sites for specific adsorption of carbonate, which likely takes place immediately after the crystallites have formed (15, 28, 31, 35).

The IR spectra of the precipitates formed at a pH of precipitation (pH_p) of 6.0, 6.5, and 7.0 (Fig. 3, Table I) are typical of amorphous aluminum hydroxide containing specifically adsorbed carbonate (15, 31) and indicate the presence of only an amorphous component. The precipitates formed between pH_p 7.5 and 9.5 exhibit a number of absorption bands in addition to the carbonate-containing aluminum hydroxide bands (Fig. 3). The new absorption bands correspond with the mineral dawsonite, a crystalline sodium aluminum hydroxycarbonate [$NaAl(OH)_2CO_3$] (Table I). The IR analysis indicates that the precipitate formed at pH_p 8.5 contained the largest fraction of dawsonite. This was confirmed by chemical analysis. The theoretical sodium-aluminum molar ratio for dawsonite is 1 and is typically near 0 for carbonate-containing aluminum hydroxide. The theoretical carbonate-aluminum molar ratio of dawsonite is 1, whereas the maximum carbonate-aluminum molar ratio of carbonate-containing aluminum hydroxide has been reported to be 0.5 (15). The maximum sodium-aluminum molar ratio (Fig. 4) and the maximum carbonate-aluminum molar ratio (Fig. 5) occurred at pH_p 8.5 and are attributed to dawsonite formation. Caution is required when interpreting the chemical analysis data since the sodium and carbonate ions do not reside exclusively in the dawsonite crystal lattice. Carbonate may be specifically adsorbed to the amorphous aluminum hydroxide component, and sodium can be bound in substantial quantities as a double-layer ion.

To more accurately determine the dawsonite content of the precipitate formed at pH_p 8.5, a portion of the precipitate was washed with 1 M $MgCl_2$ so that a magnesium-sodium cation exchange reaction might take place. Since the sodium in the dawsonite crystal lattice is not exchangeable, any nonexchangeable sodium is assumed to be associated with dawsonite. The sodium-aluminum molar ratio in carbonate-containing aluminum hydroxide-dawsonite systems can range from 0 in the absence of dawsonite to 1 in the absence of carbonate-containing aluminum hydroxide. The sodium-aluminum molar ratio of the precipitate at pH_p 8.5 decreased from 0.50 to 0.42 after magnesium exchange. The nonexchangeable sodium content indicates that dawsonite accounts for ~42% of the precipitate formed at pH_p 8.5.

The dawsonite content of the precipitate dropped sharply when the pH_p was above or below 8.5 (Figs. 3–5). For example, only trace levels of dawsonite were seen in the IR spectra at pH_p 10, and no indication of dawsonite was seen in the IR spectrum of precipitates at or below pH_p 7.0. Apparently, the requirements for the nucleation of dawsonite were best met at pH_p 8.5.

Particle Size—The rate of acid neutralization and sedimentation measurements can only be used to provide a qualitative measurement of particle size. However, since it was readily apparent from visual observation that the particle size was very sensitive to the pH_p, acid reactivity and sedimentation data were viewed as adequate for determining particle size trends as a function of pH_p. None of the three parameters was able to reflect the change in particle size over the entire pH_p range because of the substantial variation in particle size of the precipitates and the limitations of each technique. The rate of acid neutralization (Fig. 6) indicates a decrease in particle size from pH_p 6.0 to 7.5, whereas both sedimentation parameters, τ_{50} (Fig. 7) and V_{48} (Fig. 8), indicate a decrease in particle size from pH_p 7.0 to 10.0. However, when the t_{50}, τ_{50}, and V_{48} values are analyzed together, it is clear that the particle size decreases as the pH_p increases from 6 to 10.

Particle counter and fiber optic Doppler anemometer measurements were obtained for precipitates formed at pH_p 7.0 and 9.5 to confirm the conclusions drawn from the rate of acid neutralization and sedimentation studies. Particle size variation was quite large, so that measurements were made only for those samples precipitated at pH_p 7.0 and 9.5. The results indicated mean particle diameters of 12.0 and 0.20 μm at pH_p 7.0 and 9.5, respectively. Thus, over the pH_p range of 6.0 to 10.0, there is at least a 50-fold decrease in particle size.

Mechanism of Particle Size Variation—Although dawsonite was formed in significant quantities near pH_p 8.5, amorphous aluminum hydroxide formed the major component in all precipitates. Those precipitates formed at pH_p

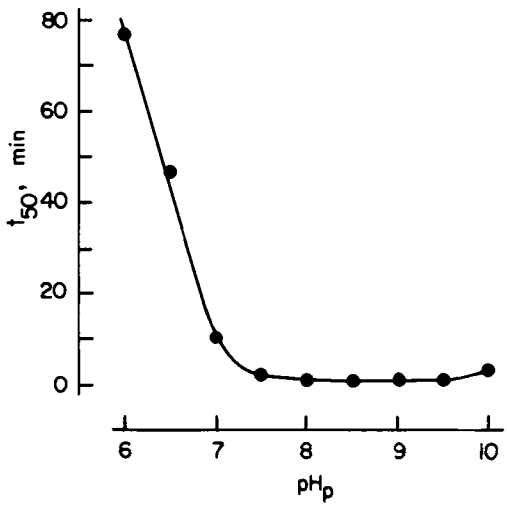

Figure 6—*Effect of the pH of precipitation on the time required to neutralize 50% of the theoretical acid (t_{50}) at pH 3 and 25°C.*

[6] Model TA II; Coulter Electronics, Inc., Hialeah, Fla.
[7] SIRA Institute, Ltd., Kent, England.

Table I—IR Absorption Bands of Precipitates Formed at Various pH_p

pH_p	Wave Number, cm^{-1}, and Assignment												
	O—H Stretching					Harmonic		Molecular H_2O	CO_3^{2-} Stretching				
Gibbsite[a]	3617	3520	3440	3390	3380			1630					
Dawsonite[b]						3285	1730		1570			1403	1100
Aluminum hydroxy-carbonate gel[c]			3440					1640		1500	1435		1090
6.0			3440					1625		1505	1435		1090
6.5			3460					1630		1505	1435		1095
7.0			3460					1630		1510	1435		1090
7.5			3430			3290			1560			1415	1093
8.0			3430			3290	1815		1560			1410	1093
8.5			3430			3290	1815		1560			1400	1093
9.0			3430			3290	1818		1560			1400	1093
9.5			3440			3290			1560			1400	1092
10.0			3440						1560			1403	1090

6.0, 6.5, 7.0, and 10.0 were found to be essentially free of dawsonite. Thus, the inverse relationship observed between pH_p and particle size is primarily related to the particle size variation of the amorphous component.

The lack of specific diffraction bands in the X-ray diffraction patterns of precipitates containing amorphous aluminum hydroxide establishes that there is no long-range atomic order in these systems (15, 31, 32, 40). The IR spectra (Fig. 3), which are much more sensitive to the presence of ordering, show broad hydroxyl-stretching bands centered at ~3440 cm^{-1}, which indicate the absence of specific proton environments. Thus, the observed large particles of amorphous carbonate-containing aluminum hydroxide (much larger than unit cell dimensions) must be composed of substantially smaller crystallites with dimensions not much larger than that of a unit cell, *i.e.*, primary particles.

The effect of the pH on the primary particle size is described by the von Weimarn law (41):

$$1/d = k(S/S_0) \qquad \text{(Eq. 1)}$$

where d is the diameter of the primary particle, k is a constant, S is the concentration of monomeric aluminum, and S_0 is the solubility, *i.e.*, the concentration of monomeric aluminum in equilibrium with infinitely large aluminum hydroxide particles, *e.g.*, highly crystalline gibbsite. The variable S is related to the concentration and infusion rate of the aluminum chloride solution. Since a 0.5 M $AlCl_3$ solution was infused into the reaction vessel at a rate of 2 mL/min for all precipitations, S is constant for all precipitates. The solubility of aluminum hydroxide (Fig. 9) is strongly influenced by pH (40, 42, 43), and therefore, S_0 varies considerably with pH_p. Since a 0.5 M $AlCl_3$ solution is infused into the reaction vessel, S/S_0 is always $\gg 1$. Therefore, precipitation is expected at all pH_p conditions.

The solubility of aluminum hydroxide is lowest at pH 5.5 to 6.0 and increases sharply as the pH is increased to 10. The ratio, S/S_0, is largest between pH 5.5 and 6.0 and decreases as the pH_p is increased. Therefore, the von Weimarn law predicts that the primary particle size is smallest near pH_p 6.0 and increases markedly as pH_p 10 is approached.

The von Weimarn law describes the size of the primary particles but does not provide any information about the subsequent formation of coagulates. However, based on the preceding conclusions concerning the primary crystallite size, DLVO theory may be used to predict the size of the coagulates. DLVO theory states that interparticle forces are a function of particle size (44, 45). In the case of electric double-layer repulsion between spherical particles of radius r, the following equation relates potential energy, V, to the separation distance, x, between two particles:

$$V = \epsilon\psi_0^2[r^2/(2r + x)]e^{-\kappa x} \qquad \text{(Eq. 2)}$$

where ϵ is the dielectric constant, ψ_0 is the surface electrical potential, and κ^{-1} is the Debye length. Clearly, the repulsive potential energy is increased for particles of larger radius. For large separation between particles, the potential energy is proportional to the square of the radius of the particles, so that the potential energy increases sharply as the particle size increases. The van der Waals attractive force, however, shows the same dependence on particle size, thereby compensating for the effect of particle size on the repulsive force (46).

Although particle size does not affect coagulation, the magnitude of the surface potential has a considerable effect which is independent of the van der Waals force. According to Eq. 2, the coulombic interaction energy varies with the square of the surface potential. For variable charge surfaces such as carbonate-containing aluminum hydroxide, ψ_0 is approximately proportional to PZC − pH (28, 47). Figure 10 shows that the difference between the PZC and the pH_p increases as the pH_p increases. The surface potential is therefore quite small for the precipitate formed at pH_p 6, but the surface potential becomes increasingly negative as the pH_p increases. Thus, the effect of surface potential on electric double-layer repulsion indicates that the probability of coagulation decreases as the pH_p increases from 6 to 10.

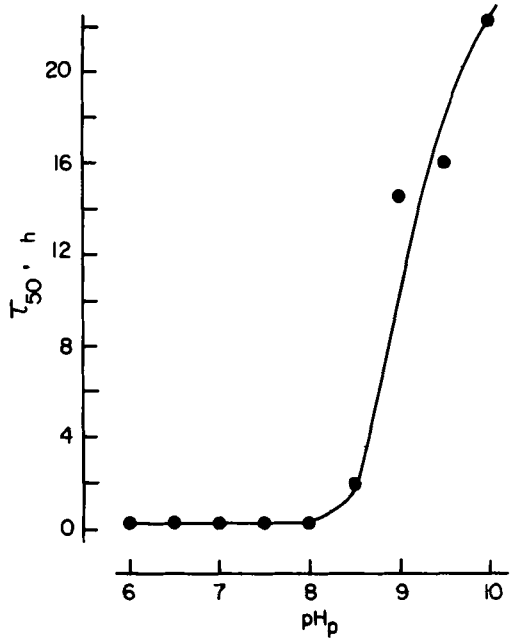

Figure 7—*Effect of pH_p on the sedimentation rate (T_{50}).*

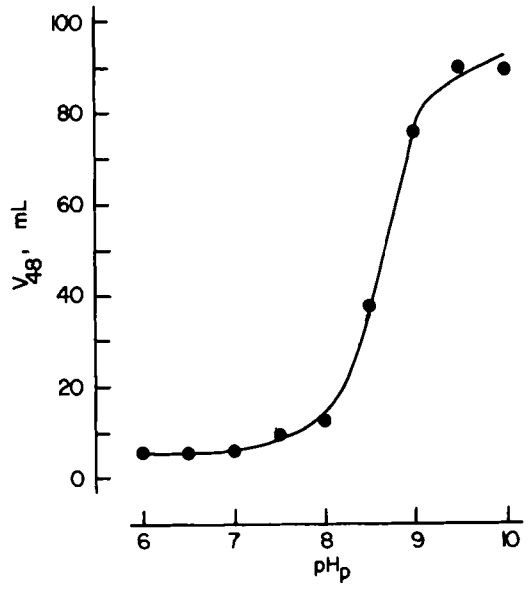

Figure 8—*Effect of pH_p on the sediment volume after 48 h (V_{48}).*

pH_p	Wave Number, cm^{-1}, and Assignment																	
	O—H Bending				CO_3^{2-} Bending		Miscellaneous[d]											
Gibbsite[a]	1025	965		910			800	740	667	585	560		515	476	450	420		
Dawsonite[b]			958	942	865	850		730	690			550	515	490				
Aluminum hydroxy-carbonate gel[c]						850				600								
6.0						848				580								
6.5						850				565								
7.0						850				565								
7.5			955	935		843		720	675			550		485				
8.0			955	935		843		727	673			550		482				
8.5			953	935		843		728	680			546		485				
9.0			952	935		842		723	670			546		480				
9.5			951			843						545						
10.0			950			843						540						

[a] References 36-38. [b] Reference 39. [c] Reference 31. [d] Including Al—O vibrations and CO_3^{2-} and O—H bending modes.

Once a coagulate has formed, its continued existence depends on its cohesive strength, which is a function of primary particle size. If only spherical particles are considered and the van der Waals attractive force is assumed to be the only interparticle force, then the following equation describes the relationship between coagulate cohesive strength, σ, the coagulate void volume fraction, ϕ, and the diameter of the primary particle, d:

$$\sigma = \frac{3(1-\phi)A}{64\phi a^2 d} \qquad \text{(Eq. 3)}$$

where A is a constant and a is the shortest interparticle separation distance (44). Equation 3 indicates that as ϕ, a, and d decrease (each decreases as the particle size decreases), the coagulate cohesive strength increases. The interparticle separation distance, a, is expected to be smaller for smaller particles due to a diminished absolute surface roughness. The coagulate void volume fraction, ϕ, decreases as the particle size, d, decreases due to packing considerations. Consequently, smaller primary particles are more likely to form survivable coagulates which are not easily destroyed when exposed to shear.

On consideration of the preceding factors, it is reasonable to conclude that the coagulate number (defined as the number of primary particles per coagulate) is largest for precipitates formed at pH_p 6 and considerably smaller for precipitates formed at pH_p 10. It is not certain, based solely on theoretical grounds, that there exists a sufficiently large variation in coagulate number to account for the greater than 50-fold variation in particle size observed by particle counter and fiber optic Doppler anemometry. However, the electric double-layer and coagulate cohesive strength considerations are of sufficient magnitude to account for the observed decrease in particle size as the pH_p is increased from 6 to 10.

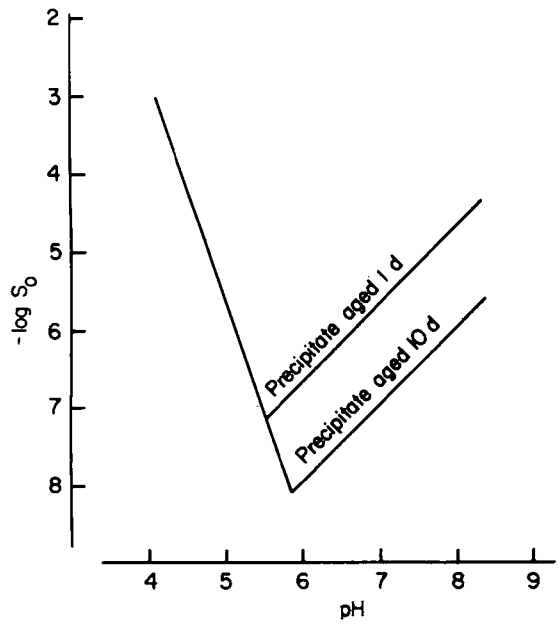

Figure 9—*Effect of pH on the solubility (S_0) of aluminum hydroxide (40).*

An excellent indication of the magnitude of the variation in coagulate number is provided by the pH-stat titrigrams for the precipitates formed at pH_p 6.0, 6.5, and 7.0 (Fig. 11). The titrigrams represent the cumulative amount of acid neutralized at pH 3 as a function of time. A very dramatic displacement of the titrigrams toward shorter reaction times is observed as the pH_p increases. If the von Weimarn law (Eq. 1) has correctly predicted that the primary particle size increases with increasing pH_p (which would tend to increase the t_{50}), then the observed increase in the rate of acid neutralization of the precipitate formed at pH_p 7.0 indicates a substantially lower coagulate number than the precipitate formed at pH_p 6.0.

Although speculative, the arrangement of primary particles within the secondary particles (coagulates) in carbonate-containing aluminum hydroxide might be comparable with the coagulate structures postulated for other materials composed of two-dimensional crystallites. The coagulate structure indicated in Fig. 12 has been proposed for carbon black (48). The edge-to-edge alignment of crystallites within the coagulates is in accord with the effects of van der Waals forces (49). The rectangular blocks represent the particles shown in Fig. 2 viewed from the edge. The results of this study suggest that such models might also describe the carbonate-containing aluminum hydroxide system.

Application to Commercial Precipitation of Carbonate-Containing Aluminum Hydroxide—The physical and chemical properties of carbonate-containing aluminum hydroxide are critically dependent on the pH_p. The property most sensitive to pH_p is particle size. The effect of pH_p on particle size is believed to be a result of variations in primary particle size as predicted by the von Weimarn law and the effects of double-layer repulsion and van der Waals attraction on coagulate formation (secondary particles). In addition to particle size effects, a crystalline phase identified as dawsonite, $NaAl(OH)_2CO_3$, was observed to form along with amorphous carbonate-containing aluminum hydroxide when the pH_p was between 7.5 and 9.5.

For most commercial aluminum hydroxide production, batch processes are utilized and, therefore, either lack pH control altogether or provide for very

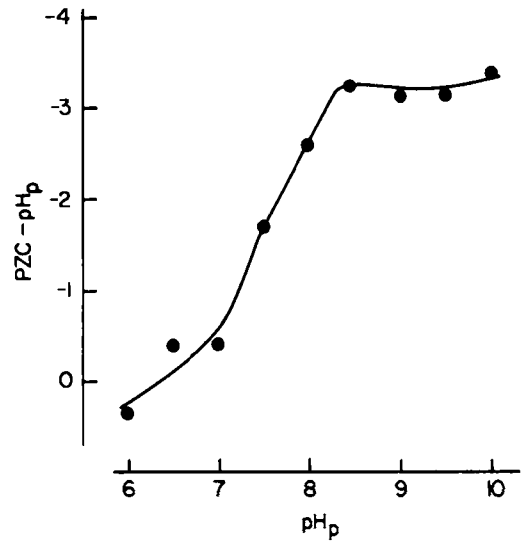

Figure 10—*Effect of pH_p on the difference between the point of zero charge (PZC) and pH_p.*

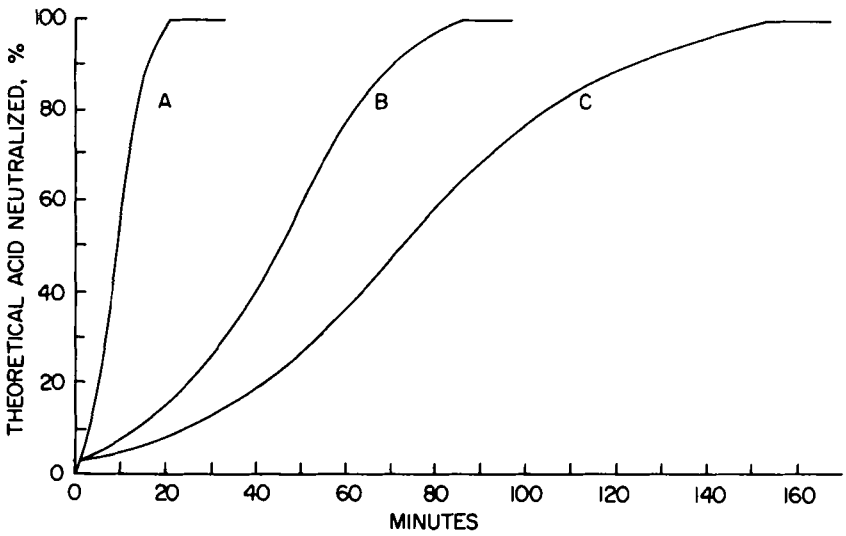

Figure 11—*Effect of pH_p on the rate of acid neutralization at pH 3.0 and 25°C. Key to pH_p: 7.0 (A); 6.5 (B); 6.0 (C).*

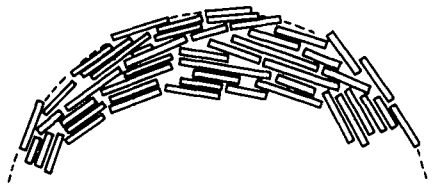

Figure 12—*Cross-sectional schematic for a coagulate (secondary particle) composed of planar primary crystallites (primary particles.)*

little control during the precipitation process. The product, therefore, is highly polydisperse and variable in composition. Consequently, considerable variation and uncertainty exist in the physical and chemical properties of carbonate-containing aluminum hydroxide precipitated by a batch process.

Certain properties may be desirable for specific applications of carbonate-containing aluminum hydroxide. The understanding gained from this study on the effect of the pH_p on the particle size and composition of the precipitate can be applied to aid in the design of precipitation processes which yield carbonate-containing aluminum hydroxides with desired properties. For example, a high surface area (small particle size) may be desired when aluminum hydroxide is used as an adsorbent. Thus, precipitation at a high pH is desired, as the smallest particle size was produced at pH_p 10.

In other situations, a low-viscosity suspension with a high solids content may be desired. To produce this property, a large particle size is necessary, and a pH_p of 6.0 is desirable. The precipitate at pH_p 6.0 formed a free-flowing suspension until a concentration of 18–20% (w/w) equivalent Al_2O_3 was reached, whereas the precipitate formed at pH_p 10 underwent gelation at only 2–3% (w/w) equivalent Al_2O_3. This behavior is readily recognized as a particle size effect since smaller particles are able to form a more extensive network or array (50).

It may also be desirable to produce carbonate-containing aluminum hydroxide which is free of sodium. The results of this study show that the precipitates formed between pH_p 7.5 and 9.5 contained appreciable amounts of dawsonite and, therefore, have a significant sodium content. The sodium in dawsonite cannot be removed through either washing or cation exchange since sodium is part of the crystal structure. Thus, batch precipitations which sweep through the pH_p range of 9.5 to 7.5 will produce precipitates which contain sodium as a permanent component.

REFERENCES

(1) B. C. Lippens and J. J. Steggerda, in "Physical and Chemical Aspects of Adsorbents and Catalysts," B. G. Linsen, Ed., Academic, New York, N.Y., 1970.

(2) V. D. Ponomarev, L. G. Romanov, and B. S. Dzhumabaev, Can. Patent No. 952,288 (1974) through *Chem. Abst.* **82,** 158321h (1975).

(3) T. Oku, K. Yamada, M. Yoshihara, and H. Kato, Japan. Kokai No. 74 04,696 (1974); through *Chem. Abst.*, **81,** 65717f (1974).

(4) J. Borska, G. Gawenda, E. Kosacka, R. Szmolke, J. Szylicki, and J. Ziembikiewicz, Pol. Patent No. 85,767 (1977); through *Chem. Abst.*, **90,** 61252p (1979).

(5) J. Matyasi, K. Nemeth, and L. Zsemberi, Fr. Demande No. 2,255,080 (1975); through *Chem. Abst.*, **84,** 184887h (1976).

(6) M. Popowicz, J. Berak, and A. Olechowska, *Przem. Chem.*, **51,** 607 (1972); through *Chem. Abst.*, **78,** 86598w (1973).

(7) C. J. Serna, J. L. White, and S. L. Hem, *Clays Clay Miner.*, **25,** 384 (1977).

(8) V. Alcvra, D. Ciomirtan, and M. Ionescu, *Rev. Roum. Chim.*, **17,** 1163 (1972).

(9) G. B. Glasscock, U.S. Patent No. 4,105,579 (1978); through *Chem. Abst.*, **90,** 76568v (1979).

(10) Barcroft Co., Neth. Appl. No. 7,806,135 (1979); through *Chem. Abst.*, **93,** 31788n (1980).

(11) Instituto de Biologia y Sueroterapia S.A., Span. Patent No. 428,760 (1977); through *Chem. Abst.*, **87,** 138017p (1977).

(12) T. Sato, *Z. Anorg. Allg. Chem.*, **391,** 69 (1972).

(13) A. C. Vermeulen, J. W. Geus, R. J. Stol, and P. L. DeBruyn, *J. Colloid Interface Sci.*, **51,** 449 (1975).

(14) C. J. Serna, J. L. White, and S. L. Hem, *J. Pharm. Sci.*, **67,** 1179 (1978).

(15) C. J. Serna, J. L. White, and S. L. Hem, *J. Pharm. Sci.*, **67,** 1144 (1978).

(16) S. L. Hem, E. J. Russo, S. M. Bahal, and R. S. Levi, *J. Pharm. Sci.*, **59,** 317 (1970).

(17) J. A. Lewis and C. A. Taylor, *J. Appl. Chem.*, **8,** 223 (1958).

(18) R. Soliman, *Pharmazie*, **29,** 62 (1974).

(19) Barcroft Co., Belg. Patent No. 867,982 (1978); through *Chem. Abst.*, **90,** 92439j (1979).

(20) C. A. Signorino and E. J. Wozinicki, Br. Patent No. 1,467,548 (1977); through *Chem. Abst.*, **87,** 69726e (1977).

(21) S. L. Nail, J. L. White, and S. L. Hem, *J. Pharm. Sci.*, **65,** 1255 (1976).

(22) S. L. Nail, J. L. White, and S. L. Hem, *J. Pharm. Sci.*, **65,** 1188 (1976).

(23) D. Papee, R. Tertian, and R. Biais, *Bull. Soc. Chim. Fr.*, **1958,** 1301.

(24) G. Drautzburg and E. Urmann, Ger. Offen. No. 1,921,999 (1970); through *Chem. Abst.*, **74,** 5113b (1971).

(25) "The United States Pharmacopeia," 20th rev., U.S. Pharmacopeial Convention, Rockville, Md., 1980, p. 25.

(26) "Official Methods of Analysis of the Association of Official Analytical Chemists," 12th ed., W. Horwitz, Ed., Assoc. of Official Analyt. Chemists, Washington, D.C., 1975, p. 147.

(27) E. C. Scholtz, Ph.D. Thesis, Purdue University, December 1981.

(28) J. R. Feldkamp, D. N. Shah, S. L. Meyer, J. L. White, and S. L. Hem, *J. Pharm. Sci.*, **70,** 638 (1981).

(29) N. J. Kerkhof, R. K. Vanderlaan, J. L. White, and S. L. Hem, *J. Pharm. Sci.*, **66,** 1528 (1977).

(30) D. A. Ross, H. S. Dhadwal, and R. B. Dyott, *J. Colloid Interface Sci.*, **64,** 533 (1978).

(31) C. J. Serna, J. L. White, and S. L. Hem, *J. Pharm. Sci.*, **67,** 324 (1978).

(32) S. L. Nail, J. L. White, and S. L. Hem, *J. Pharm. Sci.*, **64,** 1166 (1975).

(33) P. H. Hsu, in "Minerals in Soil Environments," J. B. Dixon and S. B. Weed, Eds., Soil Sci. Soc. of America, Madison, Wis., 1977, p. 120.

(34) P. H. Hsu and T. F. Bates, *Mineral. Mag.*, **33**, 749 (1964).
(35) C. J. Serna, J. L. White, and S. L. Hem, *Soil Sci. Soc. Am. J.*, **41**, 1009 (1977).
(36) L. D. Frederickson, *Anal. Chem.*, **26**, 1883 (1954).
(37) A. J. Leonard, F. Van Cauwelaert, and J. J. Fripiat, *J. Phys. Chem.*, **71**, 695 (1967).
(38) J. A. Gasden, "Infrared Spectra of Minerals and Related Inorganic Compounds," Butterworth, Reading, Mass., 1975, pp. 54, 74.
(39) A. J. Frueh and J. P. Golightly, *Can. Mineral.*, **9**, 51 (1967).
(40) J. D. Hem and C. E. Roberson, "Geological Survey Water-Supply Paper 1827-A," U.S. Government Printing Office, Washington, D.C., 1967 p. A47.
(41) A. W. Adamson, "Physical Chemistry of Surfaces," 3rd ed., Wiley, New York, N.Y., 1976, pp. 372-384.
(42) H. M. May, P. A. Helmke, and M. L. Jackson, *Geochim. Cosmochim. Acta*, **43**, 861 (1979).
(43) H. M. May, P. A. Helmke, and M. L. Jackson, *Chem. Geol.*, **24**, 259 (1979).
(44) Derjaguin, Landau, Vervey, and Overbeek (DLVO); A. Nakamura and R. Okada, *Colloid Polym., Sci.*, **254**, 497 (1976).
(45) H. van Olphen, "An Introduction to Clay Colloid Chemistry," 2nd ed., Wiley, New York, N.Y., 1977, p. 46.
(46) J. Mahanty and B. W. Ninham, "Dispersion Forces," Academic, New York, N.Y., 1976, p. 16.
(47) R. G. Gast, in "Minerals in Soil Environments," J. B. Dixon and S. B. Weed, Eds., Soil Sci. Soc. of America, Madison, Wis., 1977, pp. 36, 37.
(48) F. A. Heckman, *Rubber Chem. Technol.*, **37**, 1245 (1964).
(49) J. Mahanty and B. W. Ninham, "Dispersion Forces," Academic, New York, N.Y., 1976, pp. 21, 22.
(50) J. R. Feldkamp, J. L. White, and S. L. Hem, *J. Pharm. Sci.*, **71**, 43 (1982).

ACKNOWLEDGMENTS

This study was supported in part by William H. Rorer, Inc. This report is Journal Paper 9371, Purdue University Agricultural Experiment Station, West Lafayette, IN 47907. A preliminary report was presented at the Basic Pharmaceutics Section, Academy of Pharmaceutical Sciences, San Diego, Calif., November 1982.

Hypolipidemic Activity of Tetrakis-μ-(trimethylamine-boranecarboxylato)-*bis*(trimethylamine-carboxyborane)-dicopper(II) in Rodents and Its Effect on Lipid Metabolism

I. H. HALL *[x], W. L. WILLIAMS, Jr.*, COLLEEN J. GILBERT*, A. T. Mc PHAIL [‡], and B. F. SPIELVOGEL [‡]

Received April 25, 1983, from the **School of Pharmacy, University of North Carolina at Chapel Hill, Chapel Hill, 27514* and [‡]*Paul M. Gross Chemical Laboratory, Duke University, Durham, NC 27706.* Accepted for publication June 8, 1983.

Abstract □ A binuclear copper(II) complex was shown to have potent hypolipidemic activity in rats and mice at low doses, *i.e.*, 2.5-10 mg/kg/d. The agent moderately lowered liver ATP-dependent citrate lyase, acetyl CoA synthetase, and phosphatidate phosphohydrolase activities *in vivo*. The appetite of the animal was reduced by drug treatment, and orally administered cholesterol absorption from the intestine was markedly lowered. Higher lipid levels were found in the chyme and the feces, indicating accelerated excretion of lipids by the drug, probably *via* the biliary route. Organs, *e.g.*, liver and small intestine, as well as serum lipoprotein levels, demonstrated lower lipid content after drug administration. Thus, this chemical class of agents may have potential as a hypolipidemic agent in humans.

Keyphrases □ Binuclear copper(II) complex—antihyperlipidemic activity in rodents, effect on lipid metabolism □ Antihyperlipidemic agents—binuclear copper(II) complex, activity in rodents, effect on lipid metabolism □ Cholesterol—antihyperlipidemic effect of binuclear copper(II) complex

Recently, a series of amine-cyanoboranes and amine-carboxyboranes were observed to be hypolipidemic in mice between 5 and 20 mg/kg ip (1). From *in vitro* studies of these series, the ability to lower serum cholesterol appeared to correlate positively with the inhibition of the liver regulatory enzyme β-hydroxy-β-methyl glutaryl CoA (HMG CoA reductase) reductase activity, and the reduction of serum triglyceride was correlated with inhibition of fatty acid synthetase activity (1). Subsequently, a binuclear copper(II) complex derived from trimethylamine-carboxyborane, *viz.*, tetrakis-μ-(trimethylamine-boranecarboxylato)-*bis*(trimethylamine-carboxyborane)dicopper(II) was synthesized, and its effects on lipid metabolism is reported.

EXPERIMENTAL SECTION

Preparation of Tetrakis-μ-(trimethylamine-boranecarboxylato)-*bis*(trimethylamine-carboxyborane)dicopper(II)—Cupric chloride was purchased commercially[1]. Trimethylamine-carboxyborane was prepared as described previously (2). Trimethylamine-carboxyborane (1.8703 g, 15.9 mmol) was dissolved in 1 M NaOH (16 mL) and water (20 mL). Dropwise addition of 23 mL of a solution of $CuCl_2 \cdot 2H_2O$ (1.36 g, 8 mmol) in water (40 mL) produced a dark green solution which was allowed to stand overnight. Subsequent filtration through a fine-fritted funnel removed a greenish-brown sludge and left a dark-green filtrate, which was allowed to evaporate in the atmosphere. After 6 d, the solution evaporated, leaving many small green crystals in a clear liquor. These crystals were filtered and washed with chloroform (40°C); no $(CH_3)_3N \cdot BH_2COOH$ crystals were evident. The green crystals were then splashed with a minimal amount of cold water to ensure removal of any trace of sodium chloride and dried *in vacuo*. The yield was 0.49 g (23%), mp 165°C (dec.); IR: ν_{BH}, 2350, $\nu_{C=O}$ 1665 cm^{-1}.

Anal.—Calc. for $C_{24}H_{68}B_6Cu_2N_6O_{12}$: C, 34.95; H, 8.31; N, 10.19. Found: C, 35.00; H, 8.49; N, 10.15. The structure was determined by single-crystal X-ray analysis (3).

Antihyperlipidemic Screens in Normal Rodents—Compounds to be tested were suspended in 1% aqueous carboxymethylcellulose and administered to male CF_1 mice (~25 g) intraperitoneally for 16 d or male Holtzman rats (~350 g) orally by an intubation needle for 14 d. On days 9 and 14 or 16, blood was obtained by tail vein bleeding, and the serum was separated by centrifugation for 3 min. The serum cholesterol levels were determined by a modification of the Liebermann-Burchard reaction (4). Serum triglyceride levels were determined with a commercial kit[2] for a different group of animals bled on day 14 or 16.

Testing in Induced Hyperlipidemic Mice—Male CF_1 mice (~25 g) were

[1] Allied Chemicals, Morristown, N.J.
[2] Fisher, Hycel Triglyceride Test Kit.

0022-3549/84/0700-0973$01.00/0
© 1984, American Pharmaceutical Association

(34) P. H. Hsu and T. F. Bates, *Mineral. Mag.*, **33**, 749 (1964).
(35) C. J. Serna, J. L. White, and S. L. Hem, *Soil Sci. Soc. Am. J.*, **41**, 1009 (1977).
(36) L. D. Frederickson, *Anal. Chem.*, **26**, 1883 (1954).
(37) A. J. Leonard, F. Van Cauwelaert, and J. J. Fripiat, *J. Phys. Chem.*, **71**, 695 (1967).
(38) J. A. Gasden, "Infrared Spectra of Minerals and Related Inorganic Compounds," Butterworth, Reading, Mass., 1975, pp. 54, 74.
(39) A. J. Frueh and J. P. Golightly, *Can. Mineral.*, **9**, 51 (1967).
(40) J. D. Hem and C. E. Roberson, "Geological Survey Water-Supply Paper 1827-A," U.S. Government Printing Office, Washington, D.C., 1967 p. A47.
(41) A. W. Adamson, "Physical Chemistry of Surfaces," 3rd ed., Wiley, New York, N.Y., 1976, pp. 372-384.
(42) H. M. May, P. A. Helmke, and M. L. Jackson, *Geochim. Cosmochim. Acta*, **43**, 861 (1979).
(43) H. M. May, P. A. Helmke, and M. L. Jackson, *Chem. Geol.*, **24**, 259 (1979).
(44) Derjaguin, Landau, Vervey, and Overbeek (DLVO); A. Nakamura and R. Okada, *Colloid Polym., Sci.*, **254**, 497 (1976).
(45) H. van Olphen, "An Introduction to Clay Colloid Chemistry," 2nd ed., Wiley, New York, N.Y., 1977, p. 46.
(46) J. Mahanty and B. W. Ninham, "Dispersion Forces," Academic, New York, N.Y., 1976, p. 16.
(47) R. G. Gast, in "Minerals in Soil Environments," J. B. Dixon and S. B. Weed, Eds., Soil Sci. Soc. of America, Madison, Wis., 1977, pp. 36, 37.
(48) F. A. Heckman, *Rubber Chem. Technol.*, **37**, 1245 (1964).
(49) J. Mahanty and B. W. Ninham, "Dispersion Forces," Academic, New York, N.Y., 1976, pp. 21, 22.
(50) J. R. Feldkamp, J. L. White, and S. L. Hem, *J. Pharm. Sci.*, **71**, 43 (1982).

ACKNOWLEDGMENTS

This study was supported in part by William H. Rorer, Inc. This report is Journal Paper 9371, Purdue University Agricultural Experiment Station, West Lafayette, IN 47907. A preliminary report was presented at the Basic Pharmaceutics Section, Academy of Pharmaceutical Sciences, San Diego, Calif., November 1982.

Hypolipidemic Activity of Tetrakis-μ-(trimethylamine-boranecarboxylato)-*bis*(trimethylamine-carboxyborane)-dicopper(II) in Rodents and Its Effect on Lipid Metabolism

I. H. HALL *[x], W. L. WILLIAMS, Jr.*, COLLEEN J. GILBERT*, A. T. Mc PHAIL [‡], and B. F. SPIELVOGEL [‡]

Received April 25, 1983, from the **School of Pharmacy, University of North Carolina at Chapel Hill, Chapel Hill, 27514* and [‡]*Paul M. Gross Chemical Laboratory, Duke University, Durham, NC 27706.* Accepted for publication June 8, 1983.

Abstract □ A binuclear copper(II) complex was shown to have potent hypolipidemic activity in rats and mice at low doses, *i.e.*, 2.5-10 mg/kg/d. The agent moderately lowered liver ATP-dependent citrate lyase, acetyl CoA synthetase, and phosphatidate phosphohydrolase activities *in vivo*. The appetite of the animal was reduced by drug treatment, and orally administered cholesterol absorption from the intestine was markedly lowered. Higher lipid levels were found in the chyme and the feces, indicating accelerated excretion of lipids by the drug, probably *via* the biliary route. Organs, *e.g.*, liver and small intestine, as well as serum lipoprotein levels, demonstrated lower lipid content after drug administration. Thus, this chemical class of agents may have potential as a hypolipidemic agent in humans.

Keyphrases □ Binuclear copper(II) complex—antihyperlipidemic activity in rodents, effect on lipid metabolism □ Antihyperlipidemic agents—binuclear copper(II) complex, activity in rodents, effect on lipid metabolism □ Cholesterol—antihyperlipidemic effect of binuclear copper(II) complex

Recently, a series of amine-cyanoboranes and amine-carboxyboranes were observed to be hypolipidemic in mice between 5 and 20 mg/kg ip (1). From *in vitro* studies of these series, the ability to lower serum cholesterol appeared to correlate positively with the inhibition of the liver regulatory enzyme β-hydroxy-β-methyl glutaryl CoA (HMG CoA reductase) reductase activity, and the reduction of serum triglyceride was correlated with inhibition of fatty acid synthetase activity (1). Subsequently, a binuclear copper(II) complex derived from trimethylamine-carboxyborane, *viz.*, tetrakis-μ-(trimethylamine-boranecarboxylato)-*bis*(trimethylamine-carboxyborane)dicopper(II) was synthesized, and its effects on lipid metabolism is reported.

EXPERIMENTAL SECTION

Preparation of Tetrakis-μ-(trimethylamine-boranecarboxylato)-*bis*(trimethylamine-carboxyborane)dicopper(II)—Cupric chloride was purchased commercially[1]. Trimethylamine-carboxyborane was prepared as described previously (2). Trimethylamine-carboxyborane (1.8703 g, 15.9 mmol) was dissolved in 1 M NaOH (16 mL) and water (20 mL). Dropwise addition of 23 mL of a solution of $CuCl_2 \cdot 2H_2O$ (1.36 g, 8 mmol) in water (40 mL) produced a dark green solution which was allowed to stand overnight. Subsequent filtration through a fine-fritted funnel removed a greenish-brown sludge and left a dark-green filtrate, which was allowed to evaporate in the atmosphere. After 6 d, the solution evaporated, leaving many small green crystals in a clear liquor. These crystals were filtered and washed with chloroform (40°C); no $(CH_3)_3N \cdot BH_2COOH$ crystals were evident. The green crystals were then splashed with a minimal amount of cold water to ensure removal of any trace of sodium chloride and dried *in vacuo*. The yield was 0.49 g (23%), mp 165°C (dec.); IR: ν_{BH}, 2350, $\nu_{C=O}$ 1665 cm^{-1}.

Anal.—Calc. for $C_{24}H_{68}B_6Cu_2N_6O_{12}$: C, 34.95; H, 8.31; N, 10.19. Found: C, 35.00; H, 8.49; N, 10.15. The structure was determined by single-crystal X-ray analysis (3).

Antihyperlipidemic Screens in Normal Rodents—Compounds to be tested were suspended in 1% aqueous carboxymethylcellulose and administered to male CF_1 mice (~25 g) intraperitoneally for 16 d or male Holtzman rats (~350 g) orally by an intubation needle for 14 d. On days 9 and 14 or 16, blood was obtained by tail vein bleeding, and the serum was separated by centrifugation for 3 min. The serum cholesterol levels were determined by a modification of the Liebermann-Burchard reaction (4). Serum triglyceride levels were determined with a commercial kit[2] for a different group of animals bled on day 14 or 16.

Testing in Induced Hyperlipidemic Mice—Male CF_1 mice (~25 g) were

[1] Allied Chemicals, Morristown, N.J.
[2] Fisher, Hycel Triglyceride Test Kit.

0022-3549/84/0700-0973$01.00/0
© 1984, American Pharmaceutical Association

Table I—Effects of the Binuclear Copper(II) Complex on Serum Cholesterol and Triglyceride Levels of Male CF_1 Mice and Sprague–Dawley Rats[a]

Compound	Mice			Rats		
	Serum Cholesterol		Serum Triglycerides	Serum Cholesterol		Serum Triglycerides
	Day 9	Day 16	Day 16	Day 9	Day 16	Day 16
Control (1% carboxymethylcellulose)	100 ± 7[b]	100 ± 6[c]	100 ± 7[d]	100 ± 6[e]	100 ± 6[f]	100 ± 8[g]
Binuclear copper(II) complex						
2.5 mg/kg	61 ± 5[h]	62 ± 6[h]	50 ± 6[h]	—	—	—
5.0 mg/kg	67 ± 6[h]	63 ± 5[h]	69 ± 6[h]	—	—	—
10.0 mg/kg	71 ± 6	63 ± 5[h]	47 ± 5[h]	63 ± 5[h]	65 ± 5[h]	36 ± 4[h]
20.0 mg/kg	52 ± 5[h]	53 ± 4[h]	—	—	—	—

[a] Expressed as percent of control (mean ± *SD*); $n = 6$. Compound was administered intraperitoneally to mice and orally to rats. [b] 118 mg%. [c] 122 mg%. [d] 137 mg%. [e] 73 mg%. [f] 78 mg%. [g] 110 mg%. [h] $p \leq 0.001$.

Table II—Effects of Binuclear Copper(II) Complex on *In Vitro* CF_1 Mouse Liver Enzyme Activities[a]

Enzyme Parameter	Liver Enzyme Activity, % of Control			
	Control	50 μm	100 μm	200 μm
Mitochondrial citrate exchange	100 ± 7[b]	105 ± 6	104 ± 6	103 ± 7
ATP-dependent citrate lyase	100 ± 6[c]	110 ± 6	98 ± 5	105 ± 7
Acetyl CoA synthetase	100 ± 6[d]	104 ± 5	87 ± 4[e]	84 ± 5[f]
HMG CoA reductase	100 ± 9[g]	102 ± 8	101 ± 9	105 ± 8
Cholesterol side-chain oxidation	100 ± 5[h]	—	152 ± 7[f]	—
Acetyl CoA carboxylase	100 ± 6[i]	96 ± 6	93 ± 5	92 ± 5
Fatty acid synthetase	100 ± 8[j]	86 ± 7	96 ± 8	87 ± 7
sn-Glycerol-3-phosphate acyl transferase	100 ● 7[k]	108 ± 6	92 ± 8	89 ± 6
Phosphatidate phosphohydrolase	100 ± 7[l]	77 ± 5[f]	63 ± 6[f]	35 ± 3[f]

[a] Expressed as mean ± *SD*; $n = 6$. [b] 30.8% exchange of mitochondrial citrate. [c] 30.5 mg of citrate hydrolyzed/g of wet tissue/20 min. [d] 28.5 mg of acetyl CoA formed/g of wet tissue/20 min. [e] $p \leq 0.005$. [f] $p \leq 0.001$. [g] 384,900 dpm of cholesterol formed/g of wet tissue/60 min. [h] 6080 dpm of CO_2 formed/g of wet tissue/18 h. [i] 32,010 dpm/g of wet tissue/30 min. [j] 37,656 dpm/g of wet tissue/20 min. [k] 537,800 dpm/g of wet tissue/20 min. [l] 16.7 μg Pi/g of wet tissue/15 min.

placed on a commercial diet[3] which contained butterfat (400 g), cellulose[4] (60 g), cholesterol (53 g), choline dihydrogen citrate (4 g), salt-mixture oil[5] (40 g), sodium cholate (20 g), sucrose (223 g), vitamin-free casein (200 g), and total vitamin supplement for 10 d. After the cholesterol and triglyceride levels were assayed and observed to be elevated, the mice were administered test drugs at 10 mg/kg/d ip for an additional 12-d period. Serum cholesterol and triglyceride levels were measured after 12 d of drug administration.

Toxicity Studies—Animals weights were obtained periodically during the experiments and expressed as a percentage of the weight of the animal on day 0. After dosing for 14 d with test drugs, selected organs were excised, trimmed of fat, and weighed. The organ weights were expressed as a percentage of the total body weight of the animal. Food consumption was assessed daily[6].

The acute toxicity (LD_{50} value) (5) was determined in male CF_1 mice by administering test drugs intraperitoneally from 5 to 50 mg/kg as a single dose. The number of deaths recorded over 7 d in the group was determined for each dosage.

Enzymatic Studies—*In vitro* enzymatic studies were determined with 10% homogenates of male CF_1 mouse liver with 50–200 μM of test drugs. *In vivo* enzymatic studies were determined with 10% homogenates of liver from male CF_1 mice obtained after administering the agents for 16 d at a dose ranging from 2.5 to 20 mg/kg/d ip. The liver homogenates for both *in vitro* and *in vivo* studies were prepared in 0.25 M sucrose and 0.001 M EDTA.

Acetyl CoA synthetase (6) and ATP-dependent citrate lyase (7) activities were determined spectrophotometrically at 540 nm as the hydroxyamate of acetyl CoA formed after 30 min at 37°C. Mitochondrial citrate exchange was determined by the procedure of Robinson *et al.* (8, 9) with sodium [^{14}C]bicarbonate (41 mCi/mmol) incorporated into mitochondrial [^{14}C]citrate after isolating rat mitochondria (9000×*g* for 10 min) from the homogenates. The exchanges of the [^{14}C]citrate were determined after incubating the mitochondrial fraction, which was loaded with labeled citrate and test drugs, for 10 min. The radioactivity was then measured in the mitochondrial and supernatant fractions in scintillation fluid[7] and expressed as a percentage. Cholesterol side-chain oxidation was determined by the method of Kritchevsky and Tepper (10) using [26-^{14}C]cholesterol (50 mCi/mmol) and mitochondria isolated from rat liver homogenates. After 18 h of incubation at 37°C with test drugs, the generated $^{14}CO_2$ was trapped in the center well in [2-[2-(*p*-1,1,3,3,-tetramethylbutylcresoxy)ethoxy]ethyl]dimethylbenzylammonium hydroxide[8] and counted[7]. HMG CoA reductase activity was measured with [1-^{14}C]acetate (56 mCi/mmol) and a postmitochondrial supernatant (9000×*g* for 20 min) incubated for 60 min at 37°C (11). The digitonide derivative of cholesterol was isolated and counted (12). Acetyl CoA carboxylase activity was measured by the method of Greenspan and Lowenstein (13). Initially, the enzyme had to be polymerized for 30 min at 37°C, and then the assay mixture containing sodium [^{14}C]bicarbonate (41.0 mCi/mmol) was added and incubated for 30 min at 37°C with test drugs. Fatty acid synthetase activity was determined by the method of Brady *et al.* (14) with [2-^{14}C]malonyl CoA (37.5 mCi/mmol), which was incorporated into newly synthesized fatty acids that were extracted with ether and counted[7]. Acyl transferase activity was determined with L-[2-^{3}H]glycerol-3-phosphate (7.1 Ci/mmol) and the microsomal fraction of the liver homogenates (15). The reaction was terminated after 10 min, and the lipids were extracted with chloroform–methanol (1:2) containing 1% concentrated HCl and counted. Phosphatidate phosphohydrolase activity was measured as the inorganic phosphate released after 30 min from phosphatidic acid by the method of Mavis *et al.* (16). The inorganic phosphate released after development with ascorbic acid and ammonium molybdate was determined at 820 nm.

Liver, Small Intestine, and Fecal Lipid Extraction—In male CF_1 mice that were administered test drugs for 16 d, the liver, small intestine, and fecal materials (24-h collection) were removed, and a 10% homogenate in 0.25 M sucrose–0.001 M EDTA was prepared. An aliquot (2 mL) of the homogenate was extracted by the methods of Floch *et al.* (17) and Bligh and Dyer (18), and the number of milligrams of lipid was determined. The lipid was taken up in dichloromethane, and the cholesterol level (3), triglyceride levels[9], neutral lipid content (19), and phospholipid content (20) were determined.

[^{3}H]Cholesterol Distribution in Rats—Male Holtzman rats (350 g) were administered the test agent for 14 d orally. On day 13, 10 μCi of [^{3}H]cholesterol (40.7 mCi/mmol) was administered intraperitoneally in mice and orally in rats, and feces were collected for the next 24 h. Twenty-four hours after cholesterol administration, the major organs were excised, and samples of blood, chyme, and urine were obtained. Homogenates (10%) of the tissues were prepared, combusted[10], and counted[7]. Some tissue samples were plated on filter paper[11], dried, digested for 24 h in base[8] at 40°C, and counted[7]. Results are expressed as dpm/mg of wet tissue and dpm/total organ.

Cholesterol Absorption Study—Male Holtzman rats (~400 g) were administered the test drug orally for 14 d at 10 mg/kg/d. On day 13, 10 μCi of [1,2-^{3}H]cholesterol (40.7 Ci/mmol) was administered to the rats orally. After 24 h, the blood was collected, and the serum was separated by centrifugation (21). Both the serum and the precipitate were counted[7].

Bile Cannulation Study—Male Holtzman rats (~400 g) were treated with

[3] Basal Atherogenic Test Diet; U.S. Biochemical Corp.
[4] Celufil.
[5] Wesson.
[6] Wayne Blox Rodent Chow.
[7] Fisher Scintiverse in a Packard Scintillation Counter.
[8] Hyamine hydroxide; New England Nuclear Corp.
[9] Bio-Dynamics/bmc Triglyceride Kit.
[10] Packard Tissue Oxidizer.
[11] Whatman No. 1.

Table III—*In Vivo* Effects of the Binuclear Copper(II) Complex on CF_1 Mouse Liver Enzyme Activities After 16 d Dosing at 10 mg/kg/d i.p.[a]

Compound	ATP-Dependent Citrate Lyase	Acetyl CoA Synthetase	HMG CoA Reductase
Control (1% carboxylmethylcellulose)	100 ± 7	100 ± 8	100 ± 8
Binuclear Copper(II) Complex			
2.5 mg/kg	70 ± 6[b]	62 ± 6[b]	112 ± 8
5.0 mg/kg	79 ± 7[b]	77 ± 7[b]	108 ± 9
10.0 mg/kg	72 ± 7[b]	73 ± 7[b]	102 ± 8

	Acetyl CoA Carboxylase	Fatty Acid Synthetase	*sn*-Glycerol-3-phosphate Acyl Transferase	Phosphatidate Phosphohydrolase
Control (1% carboxymethylcellulose)	100 ± 6	100 ± 7	100 ± 6	100 ± 7
Binuclear Copper(II) Complex				
2.5 mg/kg	103 ± 6	102 ± 7	95 ± 6	55 ± 5[b]
5.0 mg/kg	95 ± 5	90 ± 6	95 ± 7	53 ± 5[b]
10.0 mg/kg	120 ± 7	94 ± 5	119 ± 7	18 ± 3[b]

[a] Expressed as percent of control (mean ± *SD*); $n = 6$. [b] $p \leq 0.001$.

test drugs at 10 mg/kg/d orally for 14 d. The rats were anesthetized with chlorpromazine[12] (25 mg/kg) followed 30 min later by pentobarbital[13] (22 mg/kg ip). The duodenum was isolated from the small intestine, and ligatures were placed around the pyloric sphincter and distally to a site approximately one-third of the way down the duodenum. Sterile isotonic saline was injected into the sectioned-off duodenal segment. The saline expanded the duodenum and the common bile duct. Once the bile duct was identified, a loose ligature was placed around it, an incision was made, and plastic tubing[14] was introduced into the duct. Once past the ligature, the tubing was tied in place, and the ligatures around the duodenum were removed. Once bile was freely moving down the cannulated tube [1,2-^{3}H]cholesterol (40.7 Ci/mmol) was injected intravenously into the rats. The bile was collected over the next 6 h and measured (in milliliters). Aliquots were counted[7] and analyzed for cholesterol content (4).

Plasma Lioprotein Fractions—Male Holtzman rats (~400 g) were administered test drugs at 20 mg/kg/d for 14 d. On day 14, blood was collected from the abdominal aorta. Serum was separated from whole blood by centrifugation at 3500 rpm. Aliquots (3 mL) were separated by density gradient ultracentrifugation by the methods of Hatch and Lees (22) and Havel *et al.* (23) into the chylomicrons, very low-density lipoproteins, high-density lipoproteins, and low-density lipoproteins. Each of the fractions was analyzed for cholesterol (4), triglycerides[9], neutral lipids (19), phospholipids (20), and protein levels (24).

RESULTS

Data are expressed in the tables as percent of control ± *SD*. The probable significant level (p) between each test group and the control group was determined by the Student's t test.

The binuclear copper(II) complex proved to be a potent hypolipidemic agent after intraperitoneal administration in mice and oral administration in rats (Table I). The reduction of serum cholesterol in normal mice was dose dependent, with 20 mg/kg/d resulting in the maximal effect of 47%. Serum triglyceride levels were reduced by >50% at 2.5 and 10 mg/kg/d. In rats administered 10 mg/kg/d, a similar reduction in serum cholesterol levels was observed as in mice, *i.e.*, 37%. However, in rats administered 10 mg/kg/d, serum triglyceride levels were reduced 64%, which was greater than the 53% reduction in mice at this dose. In hyperlipidemic-induced mice, serum cholesterol levels were elevated 183% (354 mg%) above normal values (125 mg%), which were reduced 59% to 148 mg% by drug administration over 12 d. Hyperlipidemic mice serum triglyceride levels, which were elevated 168% (367 mg/dL) above control values (137 mg/dL), were lowered 67% by drug administration to 122 mg/dL.

Examination of the *in vitro* liver enzyme studies (Table II) demonstrated that enzymes involved in the generation of the key intermediate, acetyl CoA which is required for cholesterol and fatty acid synthesis as well as cholesterol synthesis, were not affected by the presence of the drug. The degradation of cholesterol by oxidation of the side chain was accelerated significantly (52%) in the presence of drug. Fatty acid synthesis enzyme activities and *sn*-glycerol-3-phosphate acyl transferase (one of the regulatory enzymes of triglyceride synthesis) activities were not affected by the agents; however, the other regulatory enzyme of triglyceride synthesis, phosphatidate phosphohydrolase activity, was suppressed with increasing concentration of the drug.

Studies *in vivo* after dosing for 16 d in mice (Table III) showed that there was a moderate suppression of ATP-dependent citrate lyase and acetyl CoA synthetase activity at 2.5 mg/kg/d. Phosphatidate phosphohydrolase activity was reduced in a dose-dependent manner, with 10 mg/kg/d causing 82% reduction.

Lipid concentrations in the rat liver and small intestine were reduced significantly by drug treatment (Table IV). The cholesterol, triglyceride, and neutral lipid levels were reduced in both organs, and phospholipids were reduced in the small intestine. The lipid content in the livers of mice treated with the drug at 2.5–10 mg/kg/d for 16 d demonstrated similar changes (Table V); however, more dramatic effects were observed in the ability of the drug to lower triglyceride levels more than cholesterol levels. Higher lipid levels were observed in fecal samples of rats after administration of drugs for 2 weeks, particularly in the triglyceride, neutral lipid, and phospholipid levels (Table IV).

After separation of the rat serum lipoprotein fractions (Table IV), it became evident that the cholesterol, neutral lipids, and triglyceride content of each fraction was reduced. The phospholipid and protein content of the fractions were not markedly affected by drug treatment.

In rats after 14 d of treatment, the organ weights (Table VI) had not significantly altered, although in general, the treated animals had lower organ weights. In the control rats over the 2-week period, there was a 9.8% increase in body weight, and for the treated rats, there was only a 0.2% increase. The drug therapy did interfere with appetite, reducing (26%) the grams of food per day per rat from 30.35 to 22.39.

The absorption of [^{3}H]cholesterol after oral administration (Table VI) was reduced 85% over a 24-h period in rats treated for 14 d. [^{3}H]cholesterol distribution in major organs after drug therapy generally showed reductions in dpm/organ compared with the control, *e.g.*, [^{3}H]cholesterol was reduced 42% in the liver, 18% in the heart, 46% in the brain, and 91% in the kidney. There were higher contents of cholesterol in the stomach (198%), chyme (113%), large intestine (27%), small intestine (81%), and urine (336%). The LD_{50} in CF_1 mice by the intraperitoneal administration route was 39.2 mg/kg.

DISCUSSION

Tetrakis-μ-(trimethylamine-boranecarboxylato)-*bis*(trimethylamine-carboxyborane)dicopper(II) was found to be a potent hypolipidemic agent in mice and rats. However, its mode of action seemed to be somewhat different from previously reported amine-cyanoborane and amine-carboxyborane analogues in that HMG CoA reductase and fatty acid synthetase activities were essentially unaltered both in the *in vivo* and *in vitro* studies (1). The binuclear copper(II) complex was active in the dosage range previously reported for borane derivatives as hypolipidemic agents (1); nevertheless, it was more potent than commercially available clofibrate, which at doses of 150–200 mg/kg lowers serum cholesterol 6–15% and serum triglyceride levels 25% (25). Not only is the binuclear copper(II) complex active orally and intraperitoneally, it is effective in hyperlipidemic mice, lowering serum cholesterol to near normal levels and serum triglycerides below normal levels after administration for 12 d. The mode of action of this agent appeared to be by interference with cholesterol absorption from the GI tract and accelerated excretion of cholesterol *via* the fecal route. Triglyceride levels appear to be reduced due to suspension of activity of the regulatory enzyme of *de novo* triglyceride synthesis. Lamb *et al.* (15) have shown a positive correlation between lowering of serum triglyceride levels and the inhibition of hepatic and intestinal phosphatidate phosphohydrolase activity with 1-methyl-4-piperidyl-bis(*p*-chlorophenoxy)acetate and 1,3-bis(*p*-methylphenoxy)-2-propane. Similar findings

[12] Thorazine, chlorpromazine hydrochloride; Smith, Kline and French Laboratories.
[13] Nembutal, sodium pentobarbital; Abbott Laboratories.
[14] PE-10 Intramedic polyethylene tubing.

Table IV—Effects of the Binuclear Copper(II) Complex on Rat Liver, Small Intestine, and Serum Lipoprotein Fraction Lipid Content after 14-d Dosing [a]

	Lipid Extracted, mg	Cholesterol	Triglycerides	Neutral Lipids	Phospholipids	Protein
Liver						
Control	100 ± 7	100 ± 7[b]	100 ± 6[c]	100 ± 6[d]	100 ± 8[e]	100 ± 6[f]
Treated	51 ± 5[g]	65 ± 6[g]	76 ± 6[g]	76 ± 7[g]	93 ± 9	99 ± 7
Small intestine						
Control	100 ± 6	100 ± 7[h]	100 ± 5[i]	100 ± 5[j]	100 ± 7[k]	100 ± 7[l]
Treated	43 ± 5[g]	47 ± 6[g]	40 ± 4[g]	17 ± 3[g]	46 ± 5[g]	111 ± 8
Feces						
Control	100 ± 7	100 ± 6[m]	100 ± 6[n]	100 ± 8[o]	100 ± 7[p]	100 ± 5[q]
Treated	123 ± 5[g]	110 ± 6	133 ± 7[g]	131 ± 7[g]	183 ± 8[g]	68 ± 6[g]
Lipoprotein fraction						
Chylomicrons						
Control	—	100 ± 7[r]	100 ± 7[s]	100 ± 8[t]	100 ± 7[u]	100 ± 6[v]
Treated	—	88 ± 6	58 ± 5[g]	67 ± 7[g]	96 ± 6	99 ± 7
Very Low-Density						
Control	—	100 ± 6[w]	100 ± 6[x]	100 ± 7[y]	100 ± 8[z]	100 ± 7[aa]
Treated	—	32 ± 3[g]	43 ± 4[g]	62 ± 5[g]	110 ± 7	96 ± 7
Low-Density						
Control	—	100 ± 6[bb]	100 ± 7[cc]	100 ± 6[dd]	110 ± 8[ee]	100 ± 8[ff]
Treated	—	68 ± 6[g]	70 ± 6[g]	78 ± 7[g]	105 ± 6	101 ± 6
High-Density						
Control	—	100 ± 7[gg]	100 ± 6[hh]	100 ± 7[ii]	100 ± 6[jj]	100 ± 6[kk]
Treated	—	64 ± 5[g]	31 ± 5[g]	72 ± 8[g]	86 ± 7	108 ± 8

[a] At 10 mg/kg/d orally; expressed as percent of control (mean ± *SD*), $n = 6$. [b] 24.03 mg of cholesterol/g of tissue. [c] 44.11 mg of neutral lipid/g of tissue. [d] 6.37 mg of triglyceride/g of tissue. [e] 7.19 mg. [f] 4.5 g of protein/g of wet tissue. [g] $p \leq 0.001$. [h] 7.82 mg/g. [i] 6.98 mg/g. [j] 1.12 mg/g. [k] 2.06 mg/g. [l] 42 mg/g. [m] 28.47 mg/g. [n] 33.94 mg/g. [o] 1.86 mg/g. [p] 1.39 kg/g. [q] 6.99 mg/g. [r] 337 mg/mL. [s] 67 mg/mL. [t] 420 mg/mL. [u] 149 mg/mL. [v] 184 μg/mL. [w] 190 mg/mL. [x] 98 mg/mL. [y] 22 mg/mL. [z] 26 mg/mL. [aa] 50 mg/mL. [bb] 210 mg/mL. [cc] 10 mg/mL. [dd] 45 mg/mL. [ee] 41 mg/mL. [ff] 122 μg/mL. [gg] 544 mg/mL. [hh] 620 mg/mL. [ii] 27 mg/mL. [jj] 153 mg/mL. [kk] 657 μg/mL.

Table V—*In Vivo* Effects of the Binuclear Copper(II) Complex on CF_1 Mouse Liver Lipid Content after 16 d of Dosing [a]

Compound	Lipid, mg	Cholesterol	Triglycerides	Neutral Lipids	Phospholipids	Protein
Control (1% carboxymethylcellulose)	100 ± 6	100 ± 7[b]	100 ± 5[c]	100 ± 6[d]	100 ± 7[e]	100 ± 5[f]
Binuclear Copper(II) Complex						
2.5 mg/kg	82 ± 5[g]	71 ± 6[g]	40 ± 3[g]	79 ± 5[g]	67 ± 6[g]	105 ± 6
5.0 mg/kg	85 ± 6[h]	74 ± 7[g]	38 ± 4[g]	86 ± 5[h]	92 ± 7	92 ± 5
10.0 mg/kg	95 ± 6	77 ● 7[g]	36 ± 5[g]	87 ± 4[h]	152 ± 8[g]	101 ± 8

[a] Expressed as percent of control (mean ± *SD*); $n = 6$. [b] 12.24 mg of cholesterol/g of tissue. [c] 4.77 mg of triglyceride/g of tissue. [d] 28.35 mg of neutral lipid/g of tissue. [e] 4.39 mg of phospholipid/g of tissue. [f] 4.5 mg of protein/g of tissue. [g] $p \leq 0.001$. [h] $p \leq 0.010$.

have also been made with phthalamide (26), saccharin (27), and 1,8-naphthalamide (28), cyclic imide derivatives, with mouse liver. These compounds, as well as clofibrate, also suppressed *sn*-glycerol-3-phosphate acyl transferase activity, whereas the binuclear copper complex(II) did not. Clofibrate accelerates cholesterol excretion *via* the biliary route (29); however, its effects on liver metabolism include inhibition of HMG CoA reductase. Thus, the copper complex appears to be different in its mode of action than standard therapeutic agents on the market today, *e.g.*, clofibrate and the resin cholestyramine.

The serum lipoprotein fractions after 14 d of dosing at 10 mg/kg/d demonstrated consistent reductions in cholesterol, triglyceride, and neutral lipid content. Supposedly, the chylomicron and very low-density fractions contain the highest triglyceride levels, which the binuclear complex(II) reduced significantly. The low- and high-density lipoprotein fractions contain the majority of the cholesterol and its esters under normal conditions. The cholesterol content of the low-density fraction is important in controlling the amount of cholesterol being deposited in atherogenic plaques. Supposedly, the high-density fraction returns the cholesterol from peripheral tissue to the liver. The binuclear copper(II) complex reduces cholesterol approximately equally in both the low- and high-density lipoprotein fractions. Thus, the ratio of cholesterol content of low-density to high-density lipoprotein fractions probably was not altered by drug therapy; however, the absolute content of each fraction was reduced significantly.

Table VI—Effects of the Binuclear Copper(II) Complex on Rat Organ Weights and Orally Administered [^{3}H]Cholesterol after Dosing for 14 d [a]

Organ[a]	Organ Weight, g		dpm/Total Organ	
	Control	Treated	Control	Treated
Brain	1.866	1.666	29,115	15,783
Lung	1.766	1.933	15,350	17,106
Heart	1.333	1.021	24,582	20,060
Liver	12.000	10.600	47,429	27,695
Kidney	2.900	2.167	5,875	565
Spleen	0.566	0.501	19,388	13,241
Adrenal	0.036	0.031	—	—
Stomach	2.066	1.766	11,375	33,901
Small intestine	8.333	6.433	15,291	16,514
Large intestine	4.100	4.233	47,109	59,665
Chyme	5.866	5.9333	102,772	218,742
Feces	5.702	8.633	320,454	294,644

[a] At 10 mg/kg/d; $n = 6$.

Lipids removed from the serum were not deposited in the organs as demonstrated by reduced lipid content in the liver and small intestine, [^{3}H]cholesterol content in the major organs, and the weights of the organs. Adrenal weights were not altered by drug administration, indicating that there was no compensatory hyperplasia of the adrenal cortex due to stimulation of steroidogenesis because of low serum levels. The appetites of the animals were reduced by the drug; however, the magnitude of the effects of binuclear copper(II) complex on lipid metabolism and blood levels is unknown. Thus, tetrakis-μ-(trimethylamine-boranecarboxylato)-*bis*(trimethylamine-carboxyborane)dicopper(II) appears to be a potent hypolipidemic agent at low doses, lowering both cholesterol and triglyceride levels. Further chemical derivatives of this type and mechanisitic studies need to be investigated in the future.

REFERENCES

(1) I. H. Hall, M. K. Das, F. Harcheiroad, Jr., P. Wisian-Neilson, A. T. McPhail, and B. F. Spielvogel, *J. Pharm. Sci.*, **70**, 339, 1981.

(2) I. H. Hall, C. O. Starnes, Jr., B. F. Spielvogel, P. Wisian-Neilson, M. K. Das, and L. Wajnowich, *J. Pharm. Sci.*, **68**, 685 (1979).

(3) A. T. McPhail, M. Scheitlin, B. F. Spielvogel, and I. H. Hall, *J. Chem. Soc.*, in press.

(4) A. T. Ness, J. V. Pastewka, and A. C. Peacock, *Clin. Chim. Acta*, **10**, 229 (1964).

(5) J. T. Litchfield, Jr. and F. Wilcoxon, *J. Pharmacol. Exp. Ther.*, **96**, 99 (1949).

(6) A. G. Goodridge, *J. Biol. Chem.*, **248**, 4218 (1973).

(7) M. Hoffman, L. Weiss, and O. H. Wieland, *Anal. Biochem.*, **84**, 441 (1978).

(8) B. H. Robinson, G. R. Williams, M. L. Halperin, and C. C. Leznoff, *Eur. J. Biochem.*, **15**, 263 (1970).
(9) B. H. Robinson and G. R. Williams, Biochem. Biophys. Acta. **216**, 63 (1970).
(10) D. Kritchevsky and S. A. Tepper, *Atherosclerosis*, **18**, 93 (1973).
(11) G. T. Haven, J. R. Krzemien, and T. T. Nguyen, *Res. Commun. Chem. Pathol. Pharmacol.*, **6**, 253 (1973).
(12) F. Wada, K. Hirata, and Y. Sakamcto, *J. Biochem. (Tokyo)*, **65**, 71 (1969).
(13) M. D. Greenspan and J. M. Lowenstein, *J. Biol. Chem.*, **243**, 6273 (1968).
(14) R. O. Brady, R. M. Bradley, and E. G. Trams, *J. Biol. Chem.*, **235**, 3093 (1960).
(15) R. G. Lamb, S. D. Wyrick, and C. Piantadosi, *Atherosclerosis*, **27**, 147 (1977).
(16) R. D. Mavis, J. N. Finkelstein, and B. P. Hall, *J. Lipid Res.*, **19**, 467 (1978).
(17) J. Folch, M. Lees, and G. H. C. Stanley, *J. Biol. Chem.*, **226**, 497 (1957).
(18) E. G. Bligh and W. J. Dyer, *Can. J. Biochem. Physiol.*, **37**, 911 (1957).
(19) J. H. Bragdon, *J. Biol. Chem.*, **190**, 513 (1951).
(20) C. P. Stewart and E. B. Henday, *Biochem. J.*, **29**, 1683 (1935).
(21) A. Adam, J. van Cantfort, and J. Gielen, *Lipids*, **11**, 610 (1976).
(22) F. T. Hatch and R. S. Lees, *Adv. Lipid Res.*, **6**, 33 (1968).
(23) R. J. Havel, H. A. Eder, and J. H. Bragdon, *J. Clin. Invest.*, **34**, 1395 (1955).
(24) O. H. Lowry, N. J. Rosebrough, A. L. Farr, and R. J. Randall, *J. Biol. Chem.*, **193**, 265 (1951).
(25) J. M. Thorpe and W. S. Waring, *Nature (London)*, **194**, 948 (1962).
(26) I. H. Hall, J. M. Chapman, Jr., and G. H. Cocolas, *J. Pharm. Sci.*, **72**, 845 (1983).
(27) I. H. Hall, P. J. Voorstad and G. H. Cocolas, *J. Pharm. Sci.*, **72**, 1192 (1983).
(28) I. H. Hall, J. M. Chapman, Jr., P. J. Voorstad, and G. H. Cocolas, *J. Pharm. Sci.*, (in press).
(29) G. Fredj, M. Clenet, P. Cuchet, F. Rousselet, and C. Roze, *Digestion*, **19**, 228 (1979).

ACKNOWLEDGMENTS

This study was supported by grant 1 RO1 HL25680 from the National Institutes of Health and the University of North Carolina School of Pharmacy Trust Fund #72708. The authors thank Michelle Tousignant, Colleen J. Gilbert, and Timothy Matthews for technical assistance.

NOTES

Choline Magnesium Trisalicylate: Comparative Pharmacokinetic Study of Once-Daily and Twice-Daily Dosages

MONTE J. LEVITT ˣ and JULES KANN

Received December 13, 1982, from *Biodecision Laboratories, Inc., Pittsburgh, PA 15213.* Accepted for publication April 5, 1983.

Abstract □ This randomized crossover study compared the pharmacokinetics of choline magnesium trisalicylate tablets administered once daily (3000 mg of salicylate) or twice daily (1500 mg of salicylate) for six d. Serum salicylate levels were measured by HPLC. Mean "trough" concentrations fell within the therapeutic range (5–30 mg/dL) with either regimen and were relatively constant, indicating that the steady state had been reached. The 24-h area under the salicylate curve ($AUC_{0-24\ h}$) after the final 3000-mg salicylate dose averaged about twice the mean 12-h AUC after the last 1500-mg dose, indicating that the two dosing regimens were equally bioavailable. Clinical observations and results of laboratory safety studies indicate that both dosage schedules of the drug are well tolerated. The present findings support the once-daily therapeutic use of choline magnesium trisalicylate.

Keyphrases □ Choline magnesium trisalicylate—pharmacokinetic comparison of once-daily and twice-daily dosages, humans □ Bioavailability—choline magnesium trisalicylate, once-daily and twice-daily dosage schedules, humans □ Pharmacokinetics—choline magnesium trisalicylate bioavailability after once-daily and twice-daily dosages, humans

Complexity of dosage schedule may cause nonadherence to self-administered drug regimens (1, 2), particularly among ambulatory, fully active patients. Conversely, simplicity of treatment, as reflected in a single daily drug dose, is desirable from the standpoint of compliance (2, 3). In terms of this criterion, conventional salicylates, though widely regarded as first-line antiarthritic drugs, are not highly conducive to patient cooperation. These substances, notably aspirin, must often be taken at frequent intervals during the day, primarily to minimize GI irritation; daily quantities high enough to yield sustained therapeutic blood levels may be expected to cause prohibitive side effects when given as only one or two doses. Paradoxically, however, the inadequate compliance such a complex drug regimen might entail could undermine maintenance of therapeutic blood salicylate levels (4).

Published data indicate the feasibility of reducing the frequency of salicylate doses in arthritis. A recently developed nonacetylated drug of this class, choline magnesium trisalicylate (I) has been successfully used on a twice-daily basis in patients with rheumatoid arthritis or osteoarthritis (5–8). It was of interest to determine whether pharmacokinetic data would support even less frequent administration of this drug. We therefore conducted the present crossover bioavailability study in healthy volunteers to compare once-daily and twice-daily treatment schedules of I.

EXPERIMENTAL SECTION

Protocol—Twenty-four healthy males, 19–34 years old (mean, 28 years), whose weights were within 10% of ideal (58.6–96.1 kg; mean, 74.7 kg), took part in the study, which was conducted in accordance with a protocol approved by an institutional review board. The subjects had given written informed consent and were judged to be in good health on the basis of physical findings and the results of blood chemistry determinations, hematological work-up, routine urinalysis, and tests for fecal occult blood. None had a history of sensitivity to salicylates or of serious GI, hepatic, renal, or hematological

0022-3549/84/0700-0977$01.00/0
© 1984, American Pharmaceutical Association

(8) B. H. Robinson, G. R. Williams, M. L. Halperin, and C. C. Leznoff, *Eur. J. Biochem.*, **15**, 263 (1970).
(9) B. H. Robinson and G. R. Williams, Biochem. Biophys. Acta. **216**, 63 (1970).
(10) D. Kritchevsky and S. A. Tepper, *Atherosclerosis*, **18**, 93 (1973).
(11) G. T. Haven, J. R. Krzemien, and T. T. Nguyen, *Res. Commun. Chem. Pathol. Pharmacol.*, **6**, 253 (1973).
(12) F. Wada, K. Hirata, and Y. Sakamcto, *J. Biochem. (Tokyo)*, **65**, 71 (1969).
(13) M. D. Greenspan and J. M. Lowenstein, *J. Biol. Chem.*, **243**, 6273 (1968).
(14) R. O. Brady, R. M. Bradley, and E. G. Trams, *J. Biol. Chem.*, **235**, 3093 (1960).
(15) R. G. Lamb, S. D. Wyrick, and C. Piantadosi, *Atherosclerosis*, **27**, 147 (1977).
(16) R. D. Mavis, J. N. Finkelstein, and B. P. Hall, *J. Lipid Res.*, **19**, 467 (1978).
(17) J. Folch, M. Lees, and G. H. C. Stanley, *J. Biol. Chem.*, **226**, 497 (1957).
(18) E. G. Bligh and W. J. Dyer, *Can. J. Biochem. Physiol.*, **37**, 911 (1957).
(19) J. H. Bragdon, *J. Biol. Chem.*, **190**, 513 (1951).
(20) C. P. Stewart and E. B. Henday, *Biochem. J.*, **29**, 1683 (1935).
(21) A. Adam, J. van Cantfort, and J. Gielen, *Lipids*, **11**, 610 (1976).
(22) F. T. Hatch and R. S. Lees, *Adv. Lipid Res.*, **6**, 33 (1968).
(23) R. J. Havel, H. A. Eder, and J. H. Bragdon, *J. Clin. Invest.*, **34**, 1395 (1955).
(24) O. H. Lowry, N. J. Rosebrough, A. L. Farr, and R. J. Randall, *J. Biol. Chem.*, **193**, 265 (1951).
(25) J. M. Thorpe and W. S. Waring, *Nature (London)*, **194**, 948 (1962).
(26) I. H. Hall, J. M. Chapman, Jr., and G. H. Cocolas, *J. Pharm. Sci.*, **72**, 845 (1983).
(27) I. H. Hall, P. J. Voorstad and G. H. Cocolas, *J. Pharm. Sci.*, **72**, 1192 (1983).
(28) I. H. Hall, J. M. Chapman, Jr., P. J. Voorstad, and G. H. Cocolas, *J. Pharm. Sci.*, (in press).
(29) G. Fredj, M. Clenet, P. Cuchet, F. Rousselet, and C. Roze, *Digestion*, **19**, 228 (1979).

ACKNOWLEDGMENTS

This study was supported by grant 1 RO1 HL25680 from the National Institutes of Health and the University of North Carolina School of Pharmacy Trust Fund #72708. The authors thank Michelle Tousignant, Colleen J. Gilbert, and Timothy Matthews for technical assistance.

NOTES

Choline Magnesium Trisalicylate: Comparative Pharmacokinetic Study of Once-Daily and Twice-Daily Dosages

MONTE J. LEVITT ˣ and JULES KANN

Received December 13, 1982, from *Biodecision Laboratories, Inc., Pittsburgh, PA 15213.* Accepted for publication April 5, 1983.

Abstract □ This randomized crossover study compared the pharmacokinetics of choline magnesium trisalicylate tablets administered once daily (3000 mg of salicylate) or twice daily (1500 mg of salicylate) for six d. Serum salicylate levels were measured by HPLC. Mean "trough" concentrations fell within the therapeutic range (5–30 mg/dL) with either regimen and were relatively constant, indicating that the steady state had been reached. The 24-h area under the salicylate curve ($AUC_{0-24\ h}$) after the final 3000-mg salicylate dose averaged about twice the mean 12-h AUC after the last 1500-mg dose, indicating that the two dosing regimens were equally bioavailable. Clinical observations and results of laboratory safety studies indicate that both dosage schedules of the drug are well tolerated. The present findings support the once-daily therapeutic use of choline magnesium trisalicylate.

Keyphrases □ Choline magnesium trisalicylate—pharmacokinetic comparison of once-daily and twice-daily dosages, humans □ Bioavailability—choline magnesium trisalicylate, once-daily and twice-daily dosage schedules, humans □ Pharmacokinetics—choline magnesium trisalicylate bioavailability after once-daily and twice-daily dosages, humans

Complexity of dosage schedule may cause nonadherence to self-administered drug regimens (1, 2), particularly among ambulatory, fully active patients. Conversely, simplicity of treatment, as reflected in a single daily drug dose, is desirable from the standpoint of compliance (2, 3). In terms of this criterion, conventional salicylates, though widely regarded as first-line antiarthritic drugs, are not highly conducive to patient cooperation. These substances, notably aspirin, must often be taken at frequent intervals during the day, primarily to minimize GI irritation; daily quantities high enough to yield sustained therapeutic blood levels may be expected to cause prohibitive side effects when given as only one or two doses. Paradoxically, however, the inadequate compliance such a complex drug regimen might entail could undermine maintenance of therapeutic blood salicylate levels (4).

Published data indicate the feasibility of reducing the frequency of salicylate doses in arthritis. A recently developed nonacetylated drug of this class, choline magnesium trisalicylate (I) has been successfully used on a twice-daily basis in patients with rheumatoid arthritis or osteoarthritis (5–8). It was of interest to determine whether pharmacokinetic data would support even less frequent administration of this drug. We therefore conducted the present crossover bioavailability study in healthy volunteers to compare once-daily and twice-daily treatment schedules of I.

EXPERIMENTAL SECTION

Protocol—Twenty-four healthy males, 19–34 years old (mean, 28 years), whose weights were within 10% of ideal (58.6–96.1 kg; mean, 74.7 kg), took part in the study, which was conducted in accordance with a protocol approved by an institutional review board. The subjects had given written informed consent and were judged to be in good health on the basis of physical findings and the results of blood chemistry determinations, hematological work-up, routine urinalysis, and tests for fecal occult blood. None had a history of sensitivity to salicylates or of serious GI, hepatic, renal, or hematological

0022-3549/84/0700-0977$01.00/0
© 1984, American Pharmaceutical Association

Table I—Steady-State 24-h Serum Salicylate Levels in a Crossover Comparison of Once- and Twice-Daily Administration of I

Salicylate Dosage	Baseline[b]	Serum Salicylate Values, mg/dL[a] 1	2	4	8	12	18	23.5
1500 mg twice daily	13.5 ± 5.1	16.5 ± 5.7	18.9 ± 5.1	18.1 ± 4.4	14.7 ± 4.4	12.3 ± 4.6	7.0 ± 4.2	3.4 ± 3.5
3000 mg once daily	9.1 ± 4.8	17.8 ± 6.7	22.2 ± 6.4	22.9 ± 4.1	20.6 ± 3.4	17.1 ± 4.5	12.1 ± 4.4	7.0 ± 4.5

[a] Mean ± *SD*; $n = 24$. [b] "Trough" value.

Table II—Selected Steady-State Pharmacokinetic Values in a Crossover Study of Serum Salicylate Levels after Administration of I

Salicylate Regimen (6 d)	Observation Period, h	Pharmacokinetic Values After Last Dose of Regimen[a] AUC, mg·dL/h	C_{max}, mg/dL	t_{max}[b], h	$t_{1/2\ (el)}$, h	k_{el}, h^{-1}
1500 mg, twice daily	12	174.0 ± 47.7	20.0 ± 5.1	2.5 ± 1.1	7.2 ± 3.6	0.11 ± 0.04
3000 mg, once daily	24	367.3 ± 82.8	24.9 ± 4.1	4.2 ± 3.2	8.2 ± 3.5	0.10 ± 0.04

[a] Mean ± *SD*; $n = 24$. [b] Calculated assuming first-order pharmacokinetics.

disorders. The volunteers had been instructed to take no antibiotics for at least 15 d and no other drugs for at least 7 d before the start of the study; no additional medication was allowed during the trial.

Two groups, approximately comparable in terms of the body weights, were formed by random assignment; the trial proceeded in two phases, the second involving reversal of the initial dosage schedules. For phase 1, 12 subjects received four tablets of I[1] (equivalent to 3000 mg of salicylate) daily as two equal fractions, 12 h apart, for 6 consecutive days. The remaining 12 volunteers were given a single daily four-tablet dose in the evening, also for a 6-d period. The subjects reported to the research facility to receive each supervised dose, and all doses were ingested after a 1-h fast, with 180 mL of water. After a 1-week wash-out period, the treatment schedules were reversed (phase 2). Subjects treated on a twice-daily basis in phase 1 now received the single daily dose, and *vice versa*. All other experimental conditions remained unchanged.

Blood samples were obtained for the determination of "trough" serum salicylate levels just before drug administration on the evenings of study days 4–6 and 18–20. Blood specimens were also drawn at 1, 2, 4, 8, 12, 18, and 23.5 h after the final doses, *i.e.*, those doses ingested in the evenings of day 6 and day 20. The subjects were confined to the facility for sampling. The serum salicylate values obtained at these time points were used to elucidate the pharmacokinetics associated with each dosage schedule. The subjects were questioned at least once daily concerning their well-being, and the clinical and laboratory evaluations performed at the start (physical examination, blood chemistry profile, hematological work-up, urinalysis, and test for fecal occult blood) were repeated at its conclusion.

Assay Method—Serum salicylate concentrations were measured by a modification of the HPLC method described by Peng *et al* (9). After the addition of a known amount of phthalic acid as an internal standard, the serum was acidified with 85% phosphoric acid. Salicylate and internal standard were extracted into a 50:50 (by volume) mixture of benzene–ethyl acetate by vigorous mixing. After centrifugation, the organic phase was transferred to a clean tube, made alkaline by the addition of ammonium hydroxide, and evaporated to dryness at room temperature under a stream of nitrogen. The residue was dissolved in a small volume of mobile phase, acetonitrile–0.1 M phosphoric acid (40:60, v/v). An aliquot was injected onto a reverse-phase C_{18} high-pressure liquid chromatographic column. The effluent from the column was monitored continuously at a wavelength of 237 nm. Average retention times were 3.0 min for the internal standard and 7.5 min for salicylic acid when the mobile phase was pumped at a rate of 1.3 mL/min. The assay was linear over the range of salicylate concentrations from 1.5 to 50 mg/dL. As little as 1.5 mg/dL of salicylate could be measured quantitatively; lower concentrations were reported as zero. The day-to-day coefficient of variation of the assay was 10.6% at a concentration of 7.5 mg/dL.

RESULTS

There was no indication that any of the subjects violated the protocol or took drugs other than the assigned tablets. None of the volunteers left the trial before its conclusion.

Blood samples obtained just before drug ingestion on days 4–6 and 18–20 of treatment yielded consistent "trough" levels. These data indicated that the volunteers had reached steady-state concentrations by the time of the dose administered on the evening of the sixth day of each phase of the study, before sampling for the 24-h curves. Mean serum "trough" levels were within the therapeutic range of 5.0–30.0 mg/dL of salicylate.

The mean ± 1 *SD* values for the b.i.d. schedule were 13.4 ± 5.1, 12.4 ± 5.0, and 13.5 ± 5.1 mg/dL for the final 3 d of dosing in sequence. The corresponding values for the once-a-day dosage regime were 8.4 ± 4.9, 8.5 ± 4.6, and 9.1 ± 4.8 mg/dL. The 24-h serum salicylate curves showed sustained anti-inflammatory blood levels with both schedules (Table I; Fig. 1). Seventeen subjects still exhibited substantial concentrations (>10 mg/dL) 18 h after the once-daily 3000-mg dose.

The measured areas under the curves (AUC) at steady state (Table II) were proportional to the dose of I administered; the mean area computed over the 12-h interval after the subjects received 1500 mg of salicylate was about half the mean area calculated over the 24-h period after one 3000-mg dose was ingested at steady state.

The bioavailability of the single dose relative to that of the divided dose was 1.06. This value respresented the ratio of the AUC values (0–24 h/0–12 h) divided by the ratio of the respective doses (3000/1500) and did not differ significantly from the theoretical value of 1.0. Due to the very complex nonlinear pharmacokinetics of salicylate, the ratio of 1.06 can not be used as absolute evidence for equal absorption *via* the two dosage regimens. However, the data do suggest that the relative bioavailability from the two dosage regimens is probably very similar.

Two-way analyses of variance yielded the following significant differences between treatments in comparisons involving 24-h and 12-h observation periods for single 3000-mg and 1500-mg doses of salicylate, respectively: mean values for serum salicylate peak levels (C_{max}) and time to peak (t_{max}) were significantly higher ($p < 0.001$ and $p = 0.02$, respectively) with once-daily administration. No significant differences in elimination half-life ($t_{1/2\ (el)}$) or the elimination rate constant (k_{el}) was noted (Table I).

The incidence of apparently drug-related complaints was similar with both dosage schedules (Table III). They involved a total of eight subjects, three affected during the once-daily regimen only and four during the twice-daily schedule only; one volunteer experienced undesirable symptoms with both regimens (tinnitus with once-daily treatment and "stomach ache" with b.i.d. administration). The side effects were those generally expected to occur with salicylate use. They were usually transient despite continued treatment, in

Table III—Side Effects Associated with Repeated Administration of I

Salicylate Dosage Schedule[a]	Period	Subject	Side Effects
A	1	13	tinnitus
	1	18	tinnitus
	1	20	tinnitus
	2	22	tinnitus
	2	22	"stomach ache"
B	1	2	tinnitus
	1	6	"stomach pain"
	1	7	"upset stomach"
	2	18	"stomach ache"
	1	19	tinnitus

[a] A 7-d wash-out period intervened between dosage schedules. Schedule A is 3000 mg once daily for 6 d; Schedule B is 1500 mg twice daily for 6 d.

[1] Trilisate 750 tablets, lot no. P-55; The Purdue Frederick Co., Norwalk, Conn.

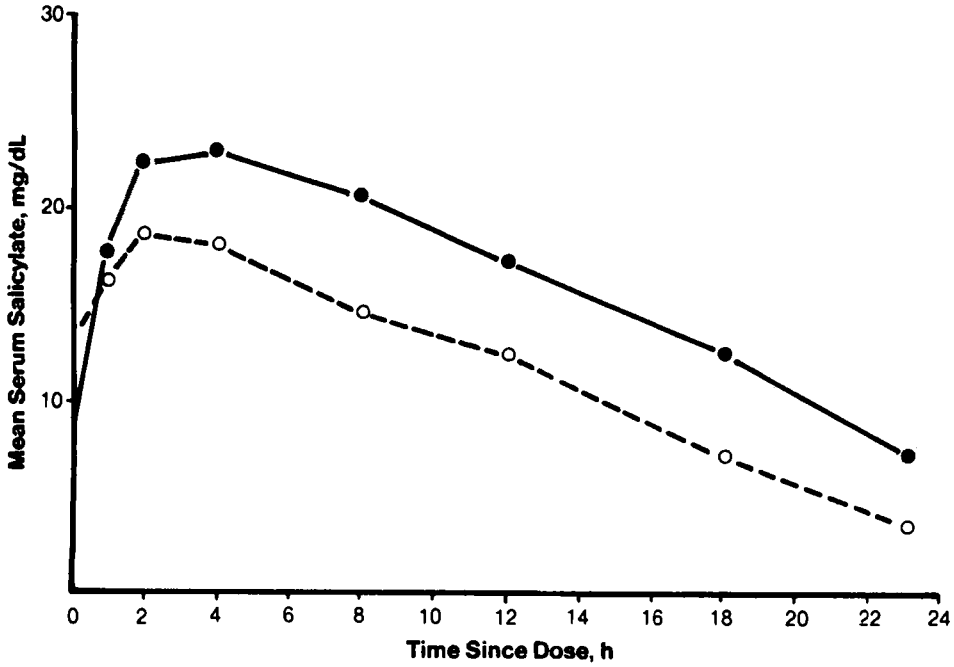

Figure 1—*Steady-state serum salicylate levels in 24 healthy subjects after final doses of two 6-d regimens of I administration. Key: (●) at the end of once-daily treatment with 3000 mg of salicylate; (○) at the end of twice-daily treatment with 1500 mg of salicylate.*

most cases occurred on a single day only, and did not require any of the subjects to leave the study. The complaints were more frequently voiced during the first phase of the study than during the second, regardless of treatment schedule.

DISCUSSION

Our results indicate the equal bioavailability of single daily and b.i.d. doses of I under the conditions of this trial and support the feasibility of once-daily treatment with this drug. They further show that daily ingestion of four-tablet doses yields mean "trough" and peak serum salicylate levels within the therapeutic range. However, since the pharmacokinetics of salicylate vary substantially from individual to individual, the choice of antiarthritic regimen should probably be individualized on the basis of blood concentrations and clinical response.

Once-daily use by arthritic patients is not known to be feasible with other salicylates now available, and hence, within this class of drugs, appears to be limited to choline magnesium trisalicylate (I). Obviously, drug safety is a major consideration in this respect. In the present study, physical examination and laboratory investigations, as well as analysis of reported side effects, indicated comparable safety of both dosage schedules of I in the healthy young males studied. While tinnitus appeared to be the predominating side effect during the once-daily regimen and GI symptoms occurred mainly with b.i.d. administration, the numbers of subjects involved were too small to indicate any trends in this regard.

REFERENCES

(1) D. B. Christensen, *Health Ser. Res.*, **13,** 171 (1978).

(2) M. S. Gatley, *J. R. Coll. Gen. Pract.*, **16,** 39 (1968).

(3) V. Wright and R. Hopkins, *Ann. Rheum. Dis.*, **35,** 174 (1976).

(4) G. Levy, *N. Engl. Soc. Allergy Proc.*, **2,** (Spring) 68 (1981).

(5) W. J. Blechman and B. L. Lechner, *Rheumatol. Rehab.*, **18,** 119 (1979).

(6) G. E. Ehrlich, S. B. Miller, and R. S. Zeiders, *Rheumatol. Rehab.*, **19,** 30 (1980).

(7) G. McLaughlin, *Curr. Ther. Res.*, **32,** 579 (1982).

(8) A. Goldenberg, R. D. Rudnicki, and M. L. Koonce, *Curr. Ther. Res.*, **24,** 245 (1978).

(9) G. W. Peng, M. A. F. Gadalla, V. Smith, A. Pen, and W. L. Chiou, *J. Pharm. Sci.* **67,** 710 (1978).

In Vivo Uptake of Polyisobutyl Cyanoacrylate Nanoparticles by Rat Liver Kupffer, Endothelial, and Parenchymal Cells

V. LENAERTS *, J. F. NAGELKERKE ‡, T. J. C. VAN BERKEL ‡, P. COUVREUR *x, L. GRISLAIN *, M. ROLAND *, and P. SPEISER §

Received November 10, 1982, from the *Laboratoire de Pharmacie Galénique, Université Catholique de Louvain, B-1200 Brussels, Belgium, the ‡Department Biochemistry 1, Erasmus University, 3000-DR Rotterdam, The Netherlands, and the §School of Pharmacy, Federal Institute of Technology, Zürich, Switzerland. Accepted for publication June 23, 1983.

Abstract □ Polyalkyl cyanoacrylate nanoparticles were previously developed as a biodegradable, ultrafine, solid drug carrier. Distribution studies in the rat showed an intense and rapid hepatic uptake. This liver accumulation appears to represent, to a certain extent, extracellularly bound nanoparticles. During liver perfusion, 15–20% of the liver-associated nanoparticles were washed out. The cellular distribution of strongly cell-associated nanoparticles was determined. At different intervals after injection of radioactive nanoparticles to rats, the cells were isolated according to a recently developed, low-temperature procedure during which processing of the carrier was inhibited. At all tested times, a relatively intense capture by Kupffer cells in comparison with endothelial and especially parenchymal cells was observed. This distribution pattern was not influenced by the size of the nanoparticles (0.08–0.215-μm diameter). This specific interaction of nanoparticles with Kupffer cells opens possibilities for the treatment of some parasitic diseases involving this cell type.

Keyphrases □ Nanoparticles—polyisobutyl cyanoacrylate, *in vivo* uptake, rat liver Kupffer, endothelial, and parenchymal cells □ Polyisobutyl cyanoacrylate—*in vivo* uptake of nanoparticles, rat liver Kupffer, endothelial, and parenchymal cells □ Distribution—*in vivo* uptake of polyisobutyl cyanoacrylate nanoparticles, rat liver Kupffer, endothelial, and parenchymal cells

The incorporation of a drug into a carrier such as liposomes, macromolecules, or solid colloidal nanoparticles modifies the body distribution of the drug (1–3). This change in the distribution pattern can be used to direct a drug specifically to the target tissue or to protect a tissue from the toxic effects of a drug. For this purpose a carrier consisting of polyalkyl cyanoacrylate nanoparticles was developed (4, 5). These submicroscopic spheres, <0.3 μm in diameter, are degraded under physiological conditions (6, 7). Associated with a cytostatic drug, they provoke an enhancement of the therapeutic activity (8) or a reduction of the toxicity (9). The body distribution of these carriers was studied, and, as for most carriers, an intense and rapid capture by the organs rich in reticuloendothelial cells was observed (10, 11).

Since the majority of nanoparticles were captured by the liver, the intrahepatic distribution of the carriers as a function of time is important. Whether the interaction between nanoparticles and parenchymal cells could be affected by administration of nanoparticles smaller than the fenestrated lining of the liver sinusoids (0.1 μm) was studied.

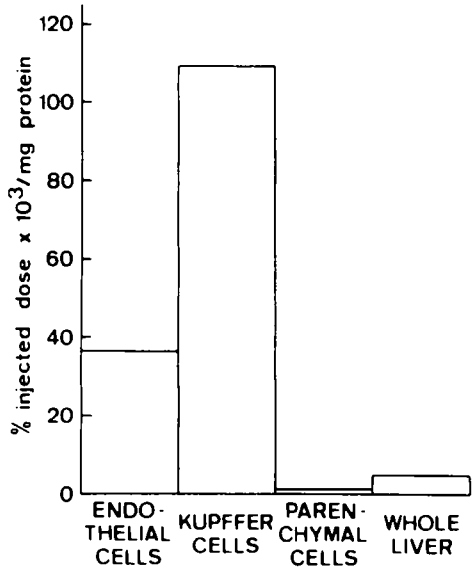

Figure 1—*Distribution of [^{14}C]polyisobutyl cyanoacrylate nanoparticles (0.215-μm diameter) in the rat liver Kupffer, endothelial, and parenchymal cells 30 min after intravenous administration.*

EXPERIMENTAL SECTION

Preparation of Radioactive Nanoparticles—Radioactive monomer was prepared according to a previously published method (12). [^{14}C]Formaldehyde was used in the synthesis; as a result, the monomer was tagged on the C-3 atom. The specific activity of the radioactive monomer[1] was 1.4 mCi/mL.

To a 10-mL solution of 1% dextran 70 and 0.05 M H_3PO_4 was added 0.1 mL of the radioactive monomer, with stirring. After 2 h of polymerization, the suspension was made isotonic with glucose and neutralized with 0.5 M NaOH. Smaller nanoparticles were prepared in a similar way, except the polymerization medium was a 5% glucose in 10^{-5} M HCl solution. The nanoparticles size was measured using a particle counter[2], based on laser beam scattering.

Isolation and Separation of Rat Liver Parenchymal, Kupffer, and Endothelial Cells—After intravenous administration of radioactive nanoparticles to rats (Wistar R1)[3], at different intervals, cell isolation was started by a liver perfusion, first with Ca^{2+}-free Hank's buffer at 8°C and then with 1 mM $CaCl_2$ Hank's buffer at 8°C containing either 0.5% (w/v) collagenase[4] for parenchymal cell isolation or 0.25% protease[5] for Kupffer and endothelial cell isolation. Further isolation was performed at 0°C to minimize degradation and redistribution of the internalized nanoparticles. Further purification of the Kupffer and endothelial cells was performed according to a modified version of a published method (13), which is described in detail elsewhere together with the parenchymal cells isolation technique (14). Kupffer and endothelial cells were obtained by, successively, 400×*g* centrifugation, metrizamide[6] density cushion centrifugation, and centrifugal elutriation[7].

The absence of parenchymal cell remnants was indicated by the absence of L-type pyruvate kinase (15, 16). The characterization of Kupffer and endothelial cell preparations was realized by light microscopic examination after staining for peroxidase activity with diaminobenzaldehyde (17) followed by a Papanicolaou counter-staining (18). After this treatment Kupffer cells were easily recognized by their brown appearance, while endothelial cells were blue. The purity of the endothelial cells preparations was >95%, while the purity of the Kupffer cells preparations was between 70 and 90%, the remainder being endothelial cells.

[1] I.R.E., Fleurus, Belgium.
[2] Nanosizer; Coulter Co. Ltd., Harpenden, England.
[3] C.P.B.; Erasmus University, Rotterdam, The Netherlands.
[4] 200 U/mg, type I; Sigma, St. Louis, Mo.
[5] Pronase, 50,000 PUK/mg, B-grade; Calbiochem-Behring, La Jolla, Calif.
[6] Metrizamide; Nyegaard and Co., A-S, Oslo, Norway.
[7] Beckman Elutriaton Rotor System; Beckman Instruments, Palo Alto, Calif.

0022-3549/84/0700-0980$01.00/0
© 1984, American Pharmaceutical Association

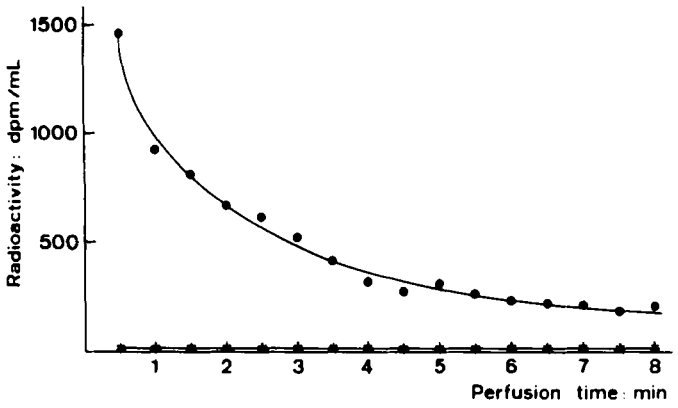

Figure 2—*Radioactivity present in fractions of the liquid collected from the rat liver during a perfusion with Hank's medium at 8°C started 30 min after intravenous administration of [^{14}C]polyisobutyl cyanoacrylate nanoparticles. Radioactivity was measured in the pellets (*) and supernatants (●) of the fractions after a 5-min centrifugation at 600×g.*

Parenchymal cells were isolated by repeated low-speed centrifugations, essentially in the same way as reported previously (19). The parenchymal cell preparations were free of other cell types, as checked by light microscopy.

The total liver value was calculated from the radioactivity present in a liver lobe which was tied off after an 8-min perfusion with Ca^{2+}-free Hank's buffer, just prior to perfusion with proteolytic enzymes. The liver lobe, isolated cells, and samples of the nanoparticle preparation were oxidized[8] and radioactivity was counted by liquid scintillation[9]. The protein content in the samples was determined according to the method of Lowry (20), using bovine serum albumin[10] as a standard.

To determine the amount of loosely bound nanoparticles, radioactivity was measured in the postperfusion medium during an 8-min perfusion with Hank's Ca^{2+}-free medium at 8°C. This perfusion was started 30 min after the injection of nanoparticles and just after a liver lobe had been tied-off and excised to serve as a nonperfusion control. Furthermore, the different samples were centrifuged at 600×*g* for 5 min to check whether the radioactivity was due to nonsediment nanoparticles or to nanoparticle-carrying cells. All these samples were then counted for radioactivity.

RESULTS AND DISCUSSION

Intrahepatic Distribution of Nanoparticles—Figure 1 shows the distribution of the 0.215-nm ^{14}C-labeled polyisobutyl cyanoacrylate nanoparticles between the different liver cell types 30 min after intravenous administration. Nanoparticles were recovered mainly in the Kupffer cells. The association of nanoparticles to Kupffer cells (expressed per milligram of cell protein) was

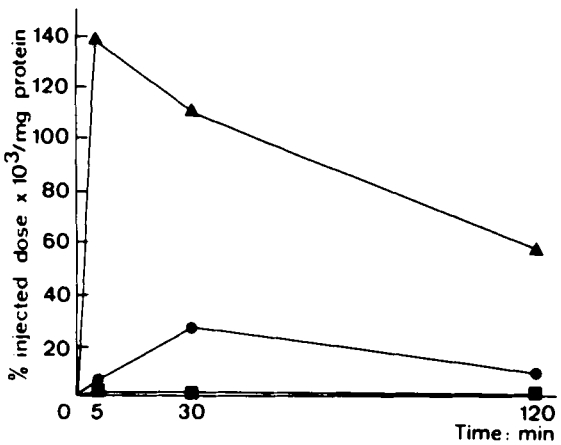

Figure 3—*Distribution of [^{14}C]polyisobutyl cyanoacrylate nanoparticles (0.215-μm diameter) in the Kupffer (▲), endothelial (●), and parenchymal (■) cells of a rat liver as a function of time after intravenous administration.*

[8] Packard Tri-Carb Oxidizer; Packard, Downers Grove, Ill.

[9] Packard Tri-Carb Liquid Scintillation Spectrometer; Packard, Downers Grove, Ill.

[10] Fraction V; Sigma, St. Louis, Mo.

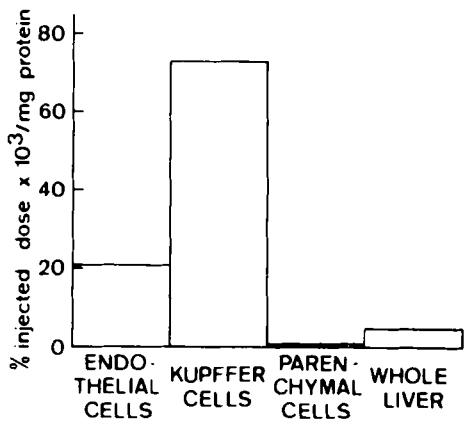

Figure 4—*Distribution of [^{14}C]polyisobutyl cyanoacrylate nanoparticles (0.08-μm diameter) in the rat liver Kupffer, endothelial, and parenchymal cells 30 min after intravenous administration.*

100-fold higher than with the major liver cell type (parenchymal cells). An intermediate cell accumulation value was observed for endothelial cell preparations.

Based on the relative contribution of Kupffer, endothelial, and parenchymal cells to total liver, the recovery of the radioactivity in the isolated cells as compared with that originally present in the whole liver can be calculated. This calculation indicates that the nanoparticles, present in the liver just before the perfusion with proteolytic enzymes, were quantitatively recovered in the isolated cells. This high recovery is only possible if the nanoparticles were either internalized or strongly associated with the liver cells. However, it was observed that during the Ca^{2+}-free perfusion, the loosely bound nanoparticles were removed (15–20% of the initial liver-associated radioactivity).

The total rat liver accumulation of radioactivity after an 8-min perfusion at 8°C was 13% of the injected dose. This value is somewhat lower than for the nonperfused liver (17% of the injected dose). This difference can only be explained by the release of loosely bound nanoparticles. Indeed, when the postperfusion medium was centrifuged at 600×*g* for 5 min, practically all radioactivity was found in the supernatant (Fig. 2). This result excludes the hypothesis of radioactive nanoparticle-containing cell release during the perfusion.

Liver Distribution as a Function of Time—Figure 3 shows the time course of the accumulation of nanoparticles into the different rat liver cell types. The association to Kupffer cells occurs very rapidly, while the maximal association to endothelial cells is clearly slower. However, at all time intervals tested, nanoparticles were always recovered mainly in the Kupffer cells. The radioactivity ratios of Kupffer to parenchymal cells were 173, 101, and 119, respectively, for intervals of 5, 30, and 120 min. For the same intervals, the ratios of Kupffer to endothelial cells were 21.2, 4.9, and 5.9.

Influence of Nanoparticle Size on Liver Distribution—The endothelial lining of the rat liver sinusoid contains fenestrae arranged in "sieve plates;" the pores of the fenestrae are ~0.1 μm in diameter (21). It can be argued that the low *in vivo* uptake of nanoparticles by the parenchymal cells is caused by this morphological barrier. If this is true, a drop in the particle size would enable an interaction with the parenchymal cells. For this purpose, the cellular distribution of particles with a mean diameter of 0.08 μm was studied 30 min after intravenous administration (Fig. 4). The uptake ratios of Kupffer to parenchymal cells and of Kupffer to endothelial cells were 92 and 3.6 for the 0.08-μm particles as compared with 101 and 4.2 for the 0.215-μm particles. These data indicate clearly that the interaction of nanoparticles with the different liver cells is not influenced by the size difference of the carrier.

CONCLUSIONS

After intravenous administration to rats, nanoparticles are localized in various compartments inside the liver. The data show that Kupffer cells are the major liver site for cell accumulation of the nanoparticles. This specific interaction is independent of the particle size in the range studied (0.08–0.215-μ diameter). Endothelial and especially parenchymal cells show a very low cell association with the nanoparticles. It is important to note that part of the nanoparticles remain loosely attached to the cells and can be released from their site by perfusion.

The interaction of nanoparticles with Kupffer cells should lead to specific drug delivery from this colloidal carrier. For the treatment of Kupffer cell-associated diseases, use of nanoparticles could be significant in achieving appropriate drug targeting.

REFERENCES

(1) G. Gregoriadis, E. Wills, C. Swain, and A. Tavill, *Lancet*, **i**, 1313 (1974).

(2) A. Trouet, D. Deprez-Decampeneere, M. Desmedt-Malengraux, and G. Atassi, *Eur. J. Cancer*, **10**, 405 (1974).

(3) P. Speiser, *Progr. Polym. Sci.*, **59**, 48 (1976).

(4) P. Couvreur, M. Roland, and P. Speiser, U.S. Patent 4,329,332 (1982).

(5) P. Couvreur, B. Kante, M. Roland, P. Guiot, P. Baudhuin, and P. Speiser, *J. Pharm. Pharmacol.*, **31**, 331 (1979).

(6) P. Couvreur, B. Kante, M. Roland, and P. Speiser, *J. Pharm. Sci.*, **68**, 1521 (1979).

(7) W. Vezin and A. Florence, *J. Biomed. Mat. Res.*, **14**, 93 (1980).

(8) F. Brasseur, P. Couvreur, B. Kante, L. Deckers-Passau, M. Roland, and C. Deckers, *Eur. J. Cancer*, **16**, 1441 (1980).

(9) P. Couvreur, B. Kante, L. Grislain, M. Roland, and P. Speiser, *J. Pharm. Sci.*, **71**, 790 (1982).

(10) B. Kante, P. Couvreur, V. Lenaerts, P. Guiot, M. Roland, P. Baudhuin, and P. Speiser, *Int. J. Pharm.*, **7**, 45 (1980).

(11) P. Couvreur, B. Kante, V. Lenaerts, V. Scailteur, M. Roland, and P. Speiser, *J. Pharm. Sci.*, **69**, 199 (1980).

(12) C. McKeever, U.S. Patent 2,912,454 (1959).

(13) D. P. Praaning-Van Dalen and D. L. Knook, *FEBS Letts.*, **141**, 2, (1982).

(14) J. F. Nagelkerke, K. P. Barto, T. J. C. Van Berkel, in "Sinusoidal Liver Cells," D. L. Knook and E. Wisse, Eds., Elsevier North-Holland Biomedical, Amsterdam, The Netherlands, 1983, pp. 319–326.

(15) T. J. C. Van Berkel, *Biochem. Biophys. Res. Comm.*, **61**, 204 (1974).

(16) J. F. Nagelkerke, K. P. Barto, T. J. C. Van Berkel, *Exp. Cell. Res.*, **138**, 183 (1982).

(17) H. D. Fahimi, *J. Cell Biol.* **47**, 247 (1970).

(18) L. G. Koss, in "Diagnostic Cytology," 3rd ed., Lippincott, Philadelphia, Pa. 1979, 1211–1222.

(19) M. N. Berry and D. S. Friend, *J. Cell Biol.*, **43**, 506 (1969).

(20) K. H. Lowry, N. J. Rosebrough, A. L. Farr, and R. J. Randall, *J. Biol. Chem.*, **193**, 265 (1951).

(21) E. Wisse in "Kupffer Cells and Other Sinusoidal Cells," E. Wisse and D. L. Knook, Eds., Elsevier North-Holland Biomedical Press, Amsterdam, The Netherlands, 1977, pp. 33–60.

ACKNOWLEDGMENTS

J.F.N. is supported by Grant 13-53-07 from the Foundation of Fundamental Medical Research (FUN 60). This work was supported by the Sopar S.A. Co. and by the Institut pour l'Encouragement de la Recherche Scientifique dans l'Industrie et l'Agriculture (I.R.S.I.A.). The kind support of the Assurances Générales de France was greatly appreciated.

The authors are thankful to Mr. Barto and Mrs. Duhamel for skillful assistance, to Mr. Vandiest for the drawings and the photographic work, and to Mrs. D'Heur for secretarial work.

Synthesis and Antimicrobial Activity of Novel Quinazolone Derivatives

N. S. HABIB * and M. A. KHALIL ‡x

Received February 14, 1983, from the **Pharmaceutical Chemistry Department, Faculty of Pharmacy, University of Alexandria, Egypt* and the ‡*College of Pharmacy, Florida A&M University, Tallahassee, FL 32307.* Accepted for publication May 11, 1983.

Abstract □ Three novel series of 4-oxoquinazoline derivatives were prepared and evaluated as potential antimicrobial agents. Evaluation of the antimicrobial activity of a variety of 4-substituted-1-thiosemicarbazides, 3,4-disubstituted thiazolines, and 3-substituted-5-thiazolidones reveals that the majority possess significant *in vitro* activity against Gram-positive organisms. Some derivatives also exhibited antifungal activity.

Keyphrases □ 4-Oxoquinazoline analogues—synthesis, antimicrobial activity, *in vitro* screen □ Antimicrobial agents—potential, 4-oxoquinazoline analogues, synthesis

There has been considerable interest in various 4-oxoquinazoline analogues. Some have shown a wide spectrum of biological effects (1–5) including antitubercular (6), antibacterial (7), and antifungal (8) activities. Thiazoline analogues were also reported to exhibit antitubercular (9) and antibacterial (10) activities. These observations prompted us to synthesize a variety of compounds containing the thiazoline nucleus and examine them for antimicrobial activity (11). Recently, the antimicrobial activities of some 4-oxoquinazoline thiosemicarbazides and thiazoline derivatives were investigated (12).

In a continuing effort to develop new antimicrobial agents, 1- [4- (2-methyl-4-oxoquinazoline-3-yl)benzoyl] -4-alkyl-, -aryl-, and -aralkyl-3-thiosemicarbazides (VII–X), 3,4-disubstituted thiazoline-2-oxo[4-(2-methyl-4-oxoquinazoline-3-yl)benzoyl]hydrazones (XI–XIV), and 3-substituted 5-thiazolidone-2-oxo-[4-(2-methyl-4-oxoquinazoline-3-yl)-benzoyl]hydrazones (XV–XVIII) were synthesized and evaluated as potential antimicrobial agents.

RESULTS AND DISCUSSION

Chemistry—Treatment of 2-substituted-4-oxoquinazolines, with hydrazine hydrate results in hydrazinolysis of the quinazolone ring to give 3-amino-2-substituted-4-oxoquinazolines (13). In the present investigation, as shown in Scheme I, heating 3-(4-carbethoxyphenyl)-2-methyl-4-oxoquinazolone (I) with hydrazine hydrate resulted in the formation of three products: *p*-aminobenzoic acid hydrazide (II), 4-(2-methyl-4-oxoquinazoline-3-yl)benzoic acid hydrazide (III) (as a minor product), and 3-amino-2-methyl-4-oxoquinazoline (IV). Compounds II and IV were identified by TLC, IR, and mixed melting point comparisons with authentic samples prepared by the previously reported methods (14, 15), while III was identified by IR spectrometry and elemental analysis. The formation of these three different products might indicate that hydrazine attacks first the ester side chain of I, then the quinazolone nucleus. This appears to be true since the treatment of III with hydrazine, resulted in the formation of II and IV. More evidence was obtained when we found that the hydrazine hydrate can replace substituted hydrazine from the quinazolone nucleus. This was shown by the hydrazinolysis of 3-(4-carbethoxyphenylamino)-2-methyl-4-oxoquinazoline (V) into IV and *p*-hydrazinobenzoic acid hydrazide (VI) (Scheme I).

In the present work, the intermediate 4-(2-methyl-4-oxoquinazoline-3-yl)benzoic acid hydrazide (III) was prepared in a higher yield, under carefully controlled reaction conditions by treating hydrazine hydrate with I at room temperature for 1 h. As outlined in Scheme II, treatment of III with the selected alkyl-, aryl-, or aralkylisothiocyanate in refluxing ethanol afforded the desired thiosemicarbazides (VII–X) (Table I). Reaction of the formed thiosemicarbazides with phenacyl bromide or ethyl bromoacetate gave the thiazoline (XI–XIV) or thiazolidone (XV–XVIII) derivatives, as shown in Table II and Table III, respectively. The products were identified by elemental

0022-3549/84/0700-0982$01.00/0

© 1984, American Pharmaceutical Association

REFERENCES

(1) G. Gregoriadis, E. Wills, C. Swain, and A. Tavill, *Lancet*, **i**, 1313 (1974).

(2) A. Trouet, D. Deprez-Decampeneere, M. Desmedt-Malengraux, and G. Atassi, *Eur. J. Cancer*, **10**, 405 (1974).

(3) P. Speiser, *Progr. Polym. Sci.*, **59**, 48 (1976).

(4) P. Couvreur, M. Roland, and P. Speiser, U.S. Patent 4,329,332 (1982).

(5) P. Couvreur, B. Kante, M. Roland, P. Guiot, P. Baudhuin, and P. Speiser, *J. Pharm. Pharmacol.*, **31**, 331 (1979).

(6) P. Couvreur, B. Kante, M. Roland, and P. Speiser, *J. Pharm. Sci.*, **68**, 1521 (1979).

(7) W. Vezin and A. Florence, *J. Biomed. Mat. Res.*, **14**, 93 (1980).

(8) F. Brasseur, P. Couvreur, B. Kante, L. Deckers-Passau, M. Roland, and C. Deckers, *Eur. J. Cancer*, **16**, 1441 (1980).

(9) P. Couvreur, B. Kante, L. Grislain, M. Roland, and P. Speiser, *J. Pharm. Sci.*, **71**, 790 (1982).

(10) B. Kante, P. Couvreur, V. Lenaerts, P. Guiot, M. Roland, P. Baudhuin, and P. Speiser, *Int. J. Pharm.*, **7**, 45 (1980).

(11) P. Couvreur, B. Kante, V. Lenaerts, V. Scailteur, M. Roland, and P. Speiser, *J. Pharm. Sci.*, **69**, 199 (1980).

(12) C. McKeever, U.S. Patent 2,912,454 (1959).

(13) D. P. Praaning-Van Dalen and D. L. Knook, *FEBS Letts.*, **141**, 2, (1982).

(14) J. F. Nagelkerke, K. P. Barto, T. J. C. Van Berkel, in "Sinusoidal Liver Cells," D. L. Knook and E. Wisse, Eds., Elsevier North-Holland Biomedical, Amsterdam, The Netherlands, 1983, pp. 319–326.

(15) T. J. C. Van Berkel, *Biochem. Biophys. Res. Comm.*, **61**, 204 (1974).

(16) J. F. Nagelkerke, K. P. Barto, T. J. C. Van Berkel, *Exp. Cell. Res.*, **138**, 183 (1982).

(17) H. D. Fahimi, *J. Cell Biol.* **47**, 247 (1970).

(18) L. G. Koss, in "Diagnostic Cytology," 3rd ed., Lippincott, Philadelphia, Pa. 1979, 1211–1222.

(19) M. N. Berry and D. S. Friend, *J. Cell Biol.*, **43**, 506 (1969).

(20) K. H. Lowry, N. J. Rosebrough, A. L. Farr, and R. J. Randall, *J. Biol. Chem.*, **193**, 265 (1951).

(21) E. Wisse in "Kupffer Cells and Other Sinusoidal Cells," E. Wisse and D. L. Knook, Eds., Elsevier North-Holland Biomedical Press, Amsterdam, The Netherlands, 1977, pp. 33–60.

ACKNOWLEDGMENTS

J.F.N. is supported by Grant 13-53-07 from the Foundation of Fundamental Medical Research (FUN 60). This work was supported by the Sopar S.A. Co. and by the Institut pour l'Encouragement de la Recherche Scientifique dans l'Industrie et l'Agriculture (I.R.S.I.A.). The kind support of the Assurances Générales de France was greatly appreciated.

The authors are thankful to Mr. Barto and Mrs. Duhamel for skillful assistance, to Mr. Vandiest for the drawings and the photographic work, and to Mrs. D'Heur for secretarial work.

Synthesis and Antimicrobial Activity of Novel Quinazolone Derivatives

N. S. HABIB * and M. A. KHALIL ‡x

Received February 14, 1983, from the **Pharmaceutical Chemistry Department, Faculty of Pharmacy, University of Alexandria, Egypt* and the ‡*College of Pharmacy, Florida A&M University, Tallahassee, FL 32307.* Accepted for publication May 11, 1983.

Abstract □ Three novel series of 4-oxoquinazoline derivatives were prepared and evaluated as potential antimicrobial agents. Evaluation of the antimicrobial activity of a variety of 4-substituted-1-thiosemicarbazides, 3,4-disubstituted thiazolines, and 3-substituted-5-thiazolidones reveals that the majority possess significant *in vitro* activity against Gram-positive organisms. Some derivatives also exhibited antifungal activity.

Keyphrases □ 4-Oxoquinazoline analogues—synthesis, antimicrobial activity, *in vitro* screen □ Antimicrobial agents—potential, 4-oxoquinazoline analogues, synthesis

There has been considerable interest in various 4-oxoquinazoline analogues. Some have shown a wide spectrum of biological effects (1–5) including antitubercular (6), antibacterial (7), and antifungal (8) activities. Thiazoline analogues were also reported to exhibit antitubercular (9) and antibacterial (10) activities. These observations prompted us to synthesize a variety of compounds containing the thiazoline nucleus and examine them for antimicrobial activity (11). Recently, the antimicrobial activities of some 4-oxoquinazoline thiosemicarbazides and thiazoline derivatives were investigated (12).

In a continuing effort to develop new antimicrobial agents, 1- [4- (2-methyl-4-oxoquinazoline-3-yl)benzoyl] -4-alkyl-, -aryl-, and -aralkyl-3-thiosemicarbazides (VII–X), 3,4-disubstituted thiazoline-2-oxo[4-(2-methyl-4-oxoquinazoline-3-yl)benzoyl]hydrazones (XI–XIV), and 3-substituted 5-thiazolidone-2-oxo-[4-(2-methyl-4-oxoquinazoline-3-yl)-benzoyl]hydrazones (XV–XVIII) were synthesized and evaluated as potential antimicrobial agents.

RESULTS AND DISCUSSION

Chemistry—Treatment of 2-substituted-4-oxoquinazolines, with hydrazine hydrate results in hydrazinolysis of the quinazolone ring to give 3-amino-2-substituted-4-oxoquinazolines (13). In the present investigation, as shown in Scheme I, heating 3-(4-carbethoxyphenyl)-2-methyl-4-oxoquinazolone (I) with hydrazine hydrate resulted in the formation of three products: *p*-aminobenzoic acid hydrazide (II), 4-(2-methyl-4-oxoquinazoline-3-yl)benzoic acid hydrazide (III) (as a minor product), and 3-amino-2-methyl-4-oxoquinazoline (IV). Compounds II and IV were identified by TLC, IR, and mixed melting point comparisons with authentic samples prepared by the previously reported methods (14, 15), while III was identified by IR spectrometry and elemental analysis. The formation of these three different products might indicate that hydrazine attacks first the ester side chain of I, then the quinazolone nucleus. This appears to be true since the treatment of III with hydrazine, resulted in the formation of II and IV. More evidence was obtained when we found that the hydrazine hydrate can replace substituted hydrazine from the quinazolone nucleus. This was shown by the hydrazinolysis of 3-(4-carbethoxyphenylamino)-2-methyl-4-oxoquinazoline (V) into IV and *p*-hydrazinobenzoic acid hydrazide (VI) (Scheme I).

In the present work, the intermediate 4-(2-methyl-4-oxoquinazoline-3-yl)benzoic acid hydrazide (III) was prepared in a higher yield, under carefully controlled reaction conditions by treating hydrazine hydrate with I at room temperature for 1 h. As outlined in Scheme II, treatment of III with the selected alkyl-, aryl-, or aralkylisothiocyanate in refluxing ethanol afforded the desired thiosemicarbazides (VII–X) (Table I). Reaction of the formed thiosemicarbazides with phenacyl bromide or ethyl bromoacetate gave the thiazoline (XI–XIV) or thiazolidone (XV–XVIII) derivatives, as shown in Table II and Table III, respectively. The products were identified by elemental

0022-3549/84/0700-0982$01.00/0

© 1984, American Pharmaceutical Association

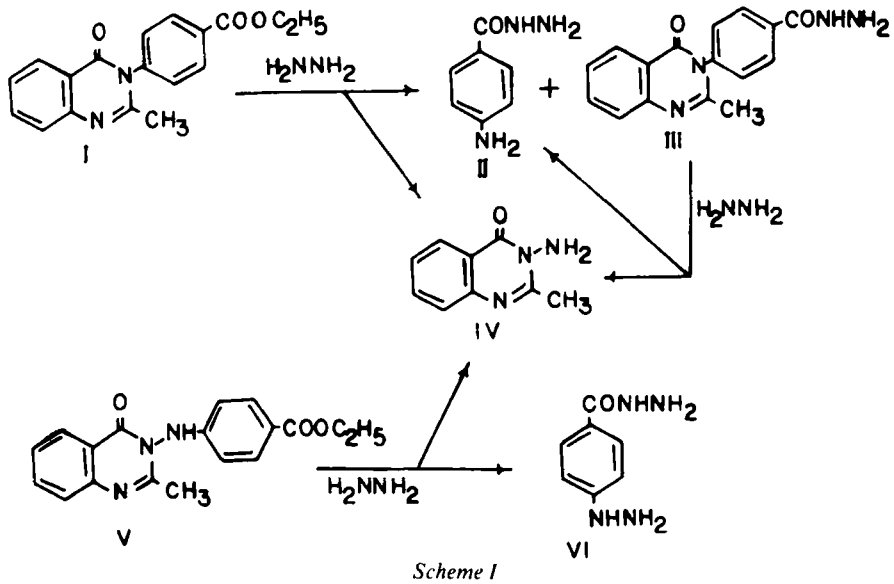

Scheme I

analyses, IR, and for some representative examples by H^1-NMR and MS. The H^1-NMR spectrum for thiazoline derivative XIV showed a singlet at δ 5.7 ppm characteristic for the thiazoline proton, while the spectrum for XVIII showed a singlet at δ 3.85 ppm characteristic of the thiazolidone protons. The mass spectra of both derivatives XIV and XVIII showed molecular ion, at *m/z* 543 and 483, respectively, and a base peak at *m/z* 91 corresponding to the tropylium ion.

Antimicrobial Activity—Compounds VII–XVIII were tested for antimicrobial activity by the agar diffusion method (16). The test organisms used were *Staphylococcus aureus* NCTC 4163, *Escherichia coli* NCTC 5933, and *Candida albicans* 3501[1]. The preliminary results obtained (Tables I–III) indicate that most of the tested compounds possess considerable antimicrobial activity against Gram-positive bacteria (*S. aureus*) and showed no activity against Gram-negative bacteria (*E. coli*). In addition, many of the tested compounds showed inhibitory activity against *C. albicans*.

EXPERIMENTAL SECTION[2]

3-(4-Carbethoxyphenyl)-2-methyl-4-oxoquinazoline (I) and 3-(4-Carbethoxyphenylamino)-2-methyl-4-oxoquinazoline (V)—Compounds I and V were prepared according to a previously reported method (17); I (80% yield), mp 169–170°C [lit. (17) mp 169–170°C]; V (72% yield) mp 149–150°C [lit. (17) mp 149–150°C].

Reaction of Hydrazine Hydrate with 2-(4-Carbethoxyphenyl)-2-methyl-4-oxoquinazoline (I)—A mixture of hydrazine hydrate (5 mL) and I (0.92 g, 3 mmol) in ethanol (15 mL) was refluxed for 30 min, diluted with water, and extracted with ethyl acetate. The organic phase was washed with water then dried over anhydrous sodium sulfate. The residue obtained after evaporation of the solvent to dryness, showed three spots on TLC. This mixture was chromatographed on a silica gel column [chloroform–ethanol (9:1)]. The first fraction afforded 3-amino-2-methyl-4-oxoquinazoline (IV) as white needle crystals from aqueous ethanol in 53% yield mp 149–151°C [lit. (15) mp 151–152°C]. The second fraction furnished *p*-aminobenzoic acid hydrazide (II) as white needles from ethanol in 35% yield, mp 221–223°C [lit. (14) mp 222°C]. The third fraction gave 4-(2-methyl-4-oxoquinazoline-3-yl)benzoic acid hydrazide (III) as white prisms from chloroform–benzene (10% yield), mp 220–221°C; IR: 3380–3350 (NH), 1670, and 1650 cm^{-1} (C=O).

Anal.—Calc. for $C_{16}H_{14}N_4O_2$: C, 65.31; H, 4.76; N, 19.05. Found: C, 65.20; H, 4.80; N, 19.30.

Reaction of Hydrazine Hydrate with III—A mixture of III (0.29 g, 0.001 mol) and hydrazine hydrate (2 mL) in ethanol (5 mL) was heated under reflux for 30 min, diluted with water, and extracted with ethyl acetate. The organic phase was washed with water, dried over anhydrous sodium sulfate, and the solvent was evaporated to dryness. The residue was chromatographed on silica gel [chloroform–ethanol (9:1)]. The initial fraction afforded IV, while the later fractions afforded II, identical in all respects with the aforementioned specimens.

Reaction of Hydrazine Hydrate with 3-(4-Carbethoxyphenylamino)-2-methyl-4-oxoquinazoline (V)—A mixture of V (0.32 g, 0.001 mol), hydrazine hydrate (2 mL), and ethanol (10 mL) was refluxed for 30 min. The mixture was treated in a manner similar to that above. The initial fraction afforded IV as white needles from aqueous ethanol (65% yield), mp 150–152°C [lit. (15) 151–152°C]. The later eluate furnished *p*-hydrazinobenzoic acid hydrazide (VI) as white needles from methanol (30% yield), mp 163–165°C [lit. (18) mp 165°C].

4-(2-Methyl-4-oxoquinazoline-3-yl)benzoic Acid Hydrazide (III)—Hydrazine hydrate (5 mL) was added to a solution of 3-(4-carbethoxyphenyl)-2-methyl-4-oxoquinazoline (I) (0.92 g, 3 mmol) in benzene (9 mL) and ethanol (1 mL). The mixture was stirred for 1 h at room temperature, then diluted with water. The remaining ester I was removed by extraction with benzene. The aqueous layer was then adjusted pH 6 with HCl and then extracted with chloroform. The extract was washed with water, dried over anhydrous sodium sulfate, and the solvent was evaporated *in vacuo* at room temperature. The residue was crystallized from chloroform–benzene to give III as white prisms; (33% yield), mp 220–221°C; IR: 3380–3350 (NH), 1670, and 1650 cm^{-1} (C=O).

Anal.—Calc. for $C_{16}H_{14}N_4O_2$: C, 65.31; H, 4.76; N, 19.05. Found: C, 65.20; H, 4.80; N, 19.30.

1-[4-(2-Methyl-4-oxoquinazoline-3-yl)benzoyl]-4-alkyl-, aryl-, or -aralkyl-3-thiosemicarbazides (VII–X)—A solution of equimolecular amounts of an alkyl-, aryl-, or aralkylisothiocyanate (2 mmol) and 4-(2-methyl-4-oxoquinazoline-3-yl)benzoic acid hydrazide (III) (0.58 g, 2 mmol) in ethanol (20 mL) was heated under reflux for 15 min. The mixture was concentrated, cooled, and left overnight at room temperature. The precipitate was removed by filtration and recrystallized from ethanol (only VII was recrystallized from aqueous ethanol). The yields and physical constants of the products are listed in Table I; IR: 3270–3140 (NH), 1700–1670 (C=O and C=N), and 1550–1520, 1340–1330, 1070–1050, and 870–830 cm^{-1} [—N—C=S I, II, III, and IV mixed-vibration bands, respectively (19)].

3,4-Disubstituted Thiazoline-2-oxo[4-(2-methyl-4-oxoquinazoline-3-yl)-benzoyl]hydrazones (XI–XIV)—A mixture of the appropriate thiosemicarbazides (VII–X) (0.01 mol), phenacyl bromide (0.01 mol), and anhydrous sodium acetate (0.04 mol) in absolute ethanol (40 mL) was refluxed for 2 h.

Table I—Properties and Antimicrobial Activity of 1-[4-(2-Methyl-4-oxoquinazoline-3-yl)benzoyl]-4-alkyl-, -aryl- or -aralkyl-3-thiosemicarbazides[a]

Compound	Yield, %	mp, °C	Molecular Formula	Antimicrobial Activity[b] *S. aureus*	*E. coli*	*C. albicans*
VII	70	141–142	$C_{21}H_{23}N_5O_2S$[c]	11	(–)	11
VIII	85	214–215	$C_{23}H_{19}N_5O_2S$	11	(–)	13
IX	85	225–226	$C_{24}H_{21}N_5O_2S$	12	(–)	14
X	75	145–146	$C_{24}H_{21}N_5O_2S$	11	(–)	12

[a] Compounds VII–X were analyzed for C, H, N, and S; unless otherwise noted, all results were within ±0.4% of the theoretical values. [b] Expressed in terms of *in vitro* inhibition zones in millimeters. [c] Calc. for S, 7.82; found, 7.40.

[1] The standard strain was obtained from the Institut of Microbiology, Göttingen, West Germany.

[2] All melting points were determined in open glass capillary tubes and are reported uncorrected. IR spectra were measured in Nujol mulls on a Beckman 4210 spectrophotometer. H^1-NMR spectra were obtained on a Bruker HX-270, and the chemical shift was expressed in ppm downfield from an internal tetramethylsilane standard. Mass spectra were recorded on a Finnigan 4510 GCMS at an electron energy of 70 eV.

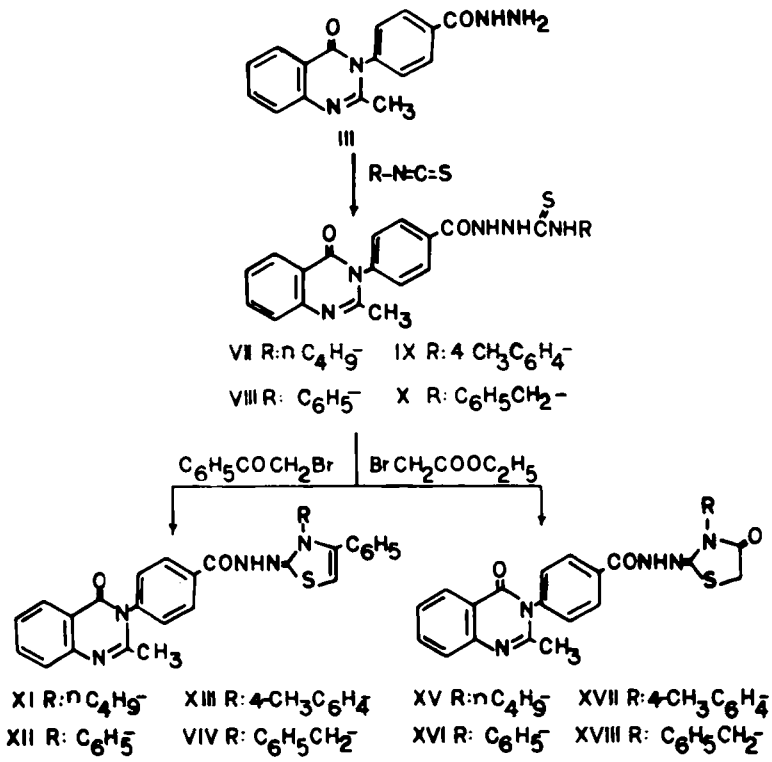

Scheme II

Table II—Properties and Antimicrobial Activity of 3,4-Disubstituted Thiazoline-2-oxo[4-(2-methyl-4-oxoquinazoline-3-yl)benzoyl]hydrazones[a]

Compound	Yield, %	Recrystallization Solvent	mp, °C	Molecular Formula	Antimicrobial Activity[b]		
					S. aureus	*E. coli*	*C. albicans*
XI	57	EtOH-H_2O	186-187	$C_{29}H_{27}N_5O_2S$	17	(−)	11
XII	64	$CHCl_3$-pet.ether	260-261	$C_{31}H_{23}N_5O_2S$	11	(−)	11
XIII	51	EtOH-H_2O	287-288	$C_{32}H_{25}N_5O_2S$	11	(−)	(−)
XIV	52	EtOH	120-121	$C_{32}H_{25}N_5O_2S$	13	(−)	10

[a] Compounds XI-XIV were analyzed for C, H, N, and S; all results were within ±0.4% of the theoretical values. [b] Expressed in terms of *in vitro* inhibition zones in millimeters.

Table III—Properties and Antimicrobial Activity of 3-Substituted 5-Thiazolidone-2-oxo[4-(2-methyl-4-oxoquinazoline-3-yl)benzoyl]hydrazones[a]

Compound	Yield, %	Recrystallization Solvent	mp, °C	Molecular Formula	Antimicrobial Activity[b]		
					S. aureus	*E. coli*	*C. albicans*
XV	91	EtOH-H_2O	96-7	$C_{23}H_{23}N_5O_3S$	12	(−)	10
XVI	87	$CHCl_3$-benzene	178-9	$C_{25}H_{19}N_5O_3S$	18	(−)	14
XVII	92	$CHCl_3$-pet.ether	255-6	$C_{26}H_{21}N_5O_3S$[c]	11	(−)	(−)
XVIII	91	benzene	139-40	$C_{26}H_{21}N_5O_3S$	15	(−)	10

[a] Compounds XV-XVIII were analyzed for C, H, N, and S; unless otherwise noted, all results were within ±0.4% of the theoretical values. [b] Expressed in terms of *in vitro* inhibition zones in millimeters. [c] Calc. for N, 14.49; found, 16.00.

The mixture was cooled, diluted with water, and allowed to stand. The solid material was removed by filtration and recrystallized from the appropriate solvent. The yields and physical constants of the products are summarized in Table II; IR: 3300-3200 (NH), 1680-1650 (C=O), 1543-1530 (NH), and 1330-1300 cm^{-1} (C—N); H^1-NMR for XIV ($CDCl_3$): δ 2.24 (s, 3, CH_3), 4.6 (s, 2, benzyl), 5.75 (s, 1, thiazoline proton), 7.39, 7.75, and 8.1 (3m, 19, ArH), and 8.3 ppm (br s, 1, N—H); MS for XIV, *m/z* (relative intensities): M^+ at 543 (0.06), 500 (0.02), 409 (38), 326 (0.29), 279 (2), 263 (12), 143 (24), 131 (2), 105 (13), 91 (100), and 76 (8).

2-Substituted 5-Thiazolidone-2-oxo[4-(2-methyl-4-oxoquinazoline-3-yl)-benzoyl]hydrazones (XV-XVIII)—These compounds were prepared by applying the same molar amounts and solvent volumes as in the preparation of XI-XIV, but using ethyl bromoacetate instead of phenacyl bromide. The yields and physical data of the products are recorded in Table III; IR: 3250-3200 (NH), 1740-1720 (C=O of thiazolidone), 1680-1650 (C=O), 1543-1530 (NH), and 1370-1320 cm^{-1} (C—N); H^1-NMR for XVIII ($CDCl_3$): δ 2.25 (s, 3, CH_3), 3.85 (s. 2, thiazolidone protons), 5.0 (s, 2 benzyl), 7.33, 7.76, and 8.05 (3 m, 13, ArH), and 8.49 ppm (br s, 1, N—H); MS for XVIII, *m/z* (%): M^+ at 483 (13), 409 (7), 279 (4), 263 (59), 236 (4), 143 (50), 121 (6), 116 (4), 105 (3), 91 (100), and 76 (14).

Antimicrobial Testing—Antimicrobial testing was performed by the agar diffusion method (16). The prepared compounds were dissolved in propylene glycol (2 mg/mL). Sterile nutrient agar (oxoid) was incubated with the test organisms (*S. aureus*, *E. coli*, and *C. albicans*). Each 100 mL of the medium received 1 mL of 24-hr broth culture, and 3 drops of the tested compound were placed separately in cups (8-mm diameter) cut in the agar. The plates were incubated at 37°C for 24 h and the resulting inhibition zones were measured (Tables I-III).

REFERENCES

(1) C. M. Gupta, A. P. Bhaduri, and N. M. Khanna, *J. Med. Chem.* **11**, 392 (1968).

(2) S. S. Tiwari, R. K. Satsangi, and S. Misra, *Indian J. Pharm. Sci.*, **40**, 60 (1978).

(3) K. H. Boltze, H. D. Dell, H.Lehwald, D. Lorenz, and M. Rueberg-Schweer, *Arznem. Forsch*, **13**, 688 (1963).

(4) C. Elliott, K. Betty, and R. V. James Jr., *J. Am. Chem. Soc.*, **81**, 5508 (1959).

(5) H. Lakham, *Chem. Pharm. Bull. (Jpn.)*, **17**, 2357 (1969).

(6) M. K. Jain and K. S. Narag, *J. Indian Chem. Soc.*, **30**, 711 (1953).
(7) L. Novacek, J. Belusa, V. Hruskova, and D. Vavrionova, *Cesk. Farm.*, **27**, 173 (1978); through *Chem. Abstr.*, **90**, 8145e (1979).
(8) S. K. V. Seshavataram and N. V. S. Rao, *Proc. Indian Acad. Sci. Sect. A.*, **85**, 81 (1977).
(9) R. H. Mizzoni and P. C. Eisman, *J. Am. Chem. Soc.*, **80**, 3471 (1958).
(10) I. Ishii, M. Katagiri, M. Sakazume, and T. Misata, *Nippon Nogei Kagaku Kaishi*, **40**, 437 (1966); through *Chem. Abstr.*, **66**, 92704w (1967).
(11) S. M. El-Khawass, M. A. Khalil, and G. G. Tawil, *Sci. Pharm.*, **48**, 219 (1980).
(12) A. Mohsen, M. E. Omar, S. A. Shams El-Dine, A. A. Ghobashy, and M. A. Khalil, *Eur. J. Med. Chem.*, **16**, 77 (1981).
(13) S. L. Mertsalov, N. N. Vereshchagina, and I. Ya. Postovskii, *Khim. Geterotsikl. Soedin., Akad. Nauk Latv. SSR*, **2**, 215-6 (1965) Russ; through *Chem. Abstr.*, **63**, 5643b (1965).
(14) L. N. Volovel'Skii and G. V. Knorozova, *Zh. Obshch Khim.*, **34**(1), 343 (1964); through *Chem Abstr.*, *60*, 12074h (1964).
(15) J. Klosa (Privatforschungslab, Berlin), *J. Prakt. Chem.*, **31**, 140 (1966).
(16) S. R. Jain and A. Kar, *Planta Med.*, **20**, 118 (1971).
(17) N. S. Habib and A. A. B. Hazzaa, *Sci. Pharm.*, **49**, 246 (1981).
(18) D. Libermann, N. Rist, F. Grumbach, M. Moyeux, B. Gauthier, A. Rouaix, J. Maillard, J. Himbert, and S. Cals (Inst. Pasteur, Paris). *Bull. Soc. Chim. France*, 1430 (1954); through *Chem. Abstr.*, **50**, 351h (1956).
(19) El-Sebai A. Ibrahim, A.-Mohsen M. E. Omar, and M. A. Khalil, *J. Pharm. Sci.*, **69**, 1346 (1980).

ACKNOWLEDGMENTS

The authors thank Dr. G. G. Tawil, Pharmaceutical Microbiology Department, Faculty of Pharmacy, University of Alexandria, for the microbiological testing.

Determination of Acetazolamide in Biological Fluids by Reverse-Phase High-Performance Liquid Chromatography

DENNIS J. CHAPRON *‡× and LORRAINE B. WHITE *

Received February 24, 1983, from the **School of Pharmacy, University of Connecticut, Storrs, CT 06268* and the *‡Clinical Pharmacokinetics Laboratory, University of Connecticut Health Center, Farmington, CT 06032.* Accepted for publication May 23, 1983.

Abstract □ A high-performance liquid chromatographic method for the determination of acetazolamide in whole blood, plasma, and urine was developed. Samples of biological fluids containing various concentrations of acetazolamide were spiked with the internal standard, sulfadiazine. Samples were then mixed with a 50% ammonium sulfamate solution. Whole blood samples were heated for 25 s in boiling water. All samples were extracted with ethyl acetate; a phosphate buffer (pH 8.0) was used to wash the extracts. Acetazolamide was back-extracted into a glycine buffer (pH 10.0), which was then washed with ether. Separation of acetazolamide and internal standard from other biological constituents was achieved on a 10-μm C_{18} reverse-phase column using an acetonitrile–methanol–acetate buffer (pH 4.0). The eluant was monitored at 254 nm. All calibration curves were linear, and the results from reproducibility studies were excellent. Application of the method to human pharmacokinetic studies was demonstrated.

Keyphrases □ Acetazolamide—biological fluids, reverse-phase HPLC, pharmacokinetics □ HPLC-acetazolamide, biological fluids, pharmacokinetics

Acetazolamide, a carbonic anhydrase inhibitor widely used in the medical management of glaucoma, lowers intraocular pressure by reducing the rate of aqueous humor formation. Acetazolamide is also used as an antiepileptic drug, where its effect is thought to result from inhibition of brain carbonic anhydrase. There is evidence that effective intraocular hypotensive and anticonvulsant actions are seen at plasma concentrations of 5–20 and 10 μg/mL, respectively (1–4). The drug is concentrated in erythrocytes, a site of action which has received little attention in the clinical literature. In humans, high erythrocyte levels have recently been associated with significant toxicity (4, 5). This is attributed to carbon dioxide retention resulting from inhibition of erythrocyte carbonic anhydrase, an important enzyme that greatly facilitates carbon dioxide exchange and transport in the capillary beds (6). Acetazolamide is completely eliminated unchanged *via* the kidney; determination of its clearance by this organ may prove useful for adjusting acetazolamide plasma concentrations.

Several high-performance liquid chromatographic (HPLC) assays have been published for determining acetazolamide levels in plasma or serum (7–9), and they have been an improvement on the older, less sensitive enzymatic assays (10, 11). A sensitive GC method is available, but it requires an electron-capture detector (12). Some of the recent HPLC procedures require repeated and/or successive extractions and dry-down procedures. None of the HPLC methods can quantitate acetazolamide in whole blood [erythrocytes indirectly (12)] or urine, fluids from which clinically important information may be ascertained.

The present report describes an HPLC method that (*a*) obviates time-consuming solvent evaporation steps, (*b*) displays excellent sensitivity and reproducibility, and (*c*) can be applied to several different biological fluids.

EXPERIMENTAL SECTION

Reagents and Materials—Acetazolamide[1] and sulfadiazine[2] were used as supplied. The solvents used for extraction and chromatography were all HPLC grade[3]. All chemicals were analytical reagent grade[4].

Standards—Separate stock solutions containing 1.0 mg/mL of acetazolamide and sulfadiazine (internal standard) were prepared weekly by dissolving these agents in 0.005 and 0.01 M NaOH, respectively. Aqueous solutions of lower concentrations (*i.e.*, 0.01–0.5 mg/mL) were prepared extemporaneously as needed from the stock solutions. Buffer solutions of 0.032 M glycine (pH 10.0) and 0.1 M phosphate buffer (pH 8.0) were prepared monthly. All solutions were stored at 4°C when not in use.

Extraction—Urine and heparinized whole blood were obtained from drug-free, normal, human volunteers. Plasma was obtained from an aliquot of whole blood using heparin as anticoagulant. Two hundred-microliter aliquots of plasma, whole blood, or urine (diluted 1:10) were added to 13 × 100-mm borosilicate glass tubes.

[1] Sigma Chemical Co., St. Louis, Mo.
[2] ICN Pharmaceuticals Inc., Cleveland, Ohio.
[3] Burdick and Jackson, Muskegon, Mich.
[4] Fisher Scientific, Fair Lawn, N.J.

0022-3549/84/0700-0985$01.00/0
© 1984, American Pharmaceutical Association

(6) M. K. Jain and K. S. Narag, *J. Indian Chem. Soc.*, **30**, 711 (1953).
(7) L. Novacek, J. Belusa, V. Hruskova, and D. Vavrionova, *Cesk. Farm.*, **27**, 173 (1978); through *Chem. Abstr.*, **90**, 8145e (1979).
(8) S. K. V. Seshavataram and N. V. S. Rao, *Proc. Indian Acad. Sci. Sect. A.*, **85**, 81 (1977).
(9) R. H. Mizzoni and P. C. Eisman, *J. Am. Chem. Soc.*, **80**, 3471 (1958).
(10) I. Ishii, M. Katagiri, M. Sakazume, and T. Misata, *Nippon Nogei Kagaku Kaishi*, **40**, 437 (1966); through *Chem. Abstr.*, **66**, 92704w (1967).
(11) S. M. El-Khawass, M. A. Khalil, and G. G. Tawil, *Sci. Pharm.*, **48**, 219 (1980).
(12) A. Mohsen, M. E. Omar, S. A. Shams El-Dine, A. A. Ghobashy, and M. A. Khalil, *Eur. J. Med. Chem.*, **16**, 77 (1981).
(13) S. L. Mertsalov, N. N. Vereshchagina, and I. Ya. Postovskii, *Khim. Geterotsikl. Soedin., Akad. Nauk Latv. SSR*, **2**, 215-6 (1965) Russ; through *Chem. Abstr.*, **63**, 5643b (1965).
(14) L. N. Volovel'Skii and G. V. Knorozova, *Zh. Obshch Khim.*, **34**(1), 343 (1964); through *Chem Abstr.*, *60*, 12074h (1964).
(15) J. Klosa (Privatforschungslab, Berlin), *J. Prakt. Chem.*, **31**, 140 (1966).
(16) S. R. Jain and A. Kar, *Planta Med.*, **20**, 118 (1971).
(17) N. S. Habib and A. A. B. Hazzaa, *Sci. Pharm.*, **49**, 246 (1981).
(18) D. Libermann, N. Rist, F. Grumbach, M. Moyeux, B. Gauthier, A. Rouaix, J. Maillard, J. Himbert, and S. Cals (Inst. Pasteur, Paris). *Bull. Soc. Chim. France*, 1430 (1954); through *Chem. Abstr.*, **50**, 351h (1956).
(19) El-Sebai A. Ibrahim, A.-Mohsen M. E. Omar, and M. A. Khalil, *J. Pharm. Sci.*, **69**, 1346 (1980).

ACKNOWLEDGMENTS

The authors thank Dr. G. G. Tawil, Pharmaceutical Microbiology Department, Faculty of Pharmacy, University of Alexandria, for the microbiological testing.

Determination of Acetazolamide in Biological Fluids by Reverse-Phase High-Performance Liquid Chromatography

DENNIS J. CHAPRON *‡× and LORRAINE B. WHITE *

Received February 24, 1983, from the **School of Pharmacy, University of Connecticut, Storrs, CT 06268* and the *‡Clinical Pharmacokinetics Laboratory, University of Connecticut Health Center, Farmington, CT 06032.* Accepted for publication May 23, 1983.

Abstract □ A high-performance liquid chromatographic method for the determination of acetazolamide in whole blood, plasma, and urine was developed. Samples of biological fluids containing various concentrations of acetazolamide were spiked with the internal standard, sulfadiazine. Samples were then mixed with a 50% ammonium sulfamate solution. Whole blood samples were heated for 25 s in boiling water. All samples were extracted with ethyl acetate; a phosphate buffer (pH 8.0) was used to wash the extracts. Acetazolamide was back-extracted into a glycine buffer (pH 10.0), which was then washed with ether. Separation of acetazolamide and internal standard from other biological constituents was achieved on a 10-μm C_{18} reverse-phase column using an acetonitrile–methanol–acetate buffer (pH 4.0). The eluant was monitored at 254 nm. All calibration curves were linear, and the results from reproducibility studies were excellent. Application of the method to human pharmacokinetic studies was demonstrated.

Keyphrases □ Acetazolamide—biological fluids, reverse-phase HPLC, pharmacokinetics □ HPLC-acetazolamide, biological fluids, pharmacokinetics

Acetazolamide, a carbonic anhydrase inhibitor widely used in the medical management of glaucoma, lowers intraocular pressure by reducing the rate of aqueous humor formation. Acetazolamide is also used as an antiepileptic drug, where its effect is thought to result from inhibition of brain carbonic anhydrase. There is evidence that effective intraocular hypotensive and anticonvulsant actions are seen at plasma concentrations of 5–20 and 10 μg/mL, respectively (1–4). The drug is concentrated in erythrocytes, a site of action which has received little attention in the clinical literature. In humans, high erythrocyte levels have recently been associated with significant toxicity (4, 5). This is attributed to carbon dioxide retention resulting from inhibition of erythrocyte carbonic anhydrase, an important enzyme that greatly facilitates carbon dioxide exchange and transport in the capillary beds (6). Acetazolamide is completely eliminated unchanged *via* the kidney; determination of its clearance by this organ may prove useful for adjusting acetazolamide plasma concentrations.

Several high-performance liquid chromatographic (HPLC) assays have been published for determining acetazolamide levels in plasma or serum (7–9), and they have been an improvement on the older, less sensitive enzymatic assays (10, 11). A sensitive GC method is available, but it requires an electron-capture detector (12). Some of the recent HPLC procedures require repeated and/or successive extractions and dry-down procedures. None of the HPLC methods can quantitate acetazolamide in whole blood [erythrocytes indirectly (12)] or urine, fluids from which clinically important information may be ascertained.

The present report describes an HPLC method that (*a*) obviates time-consuming solvent evaporation steps, (*b*) displays excellent sensitivity and reproducibility, and (*c*) can be applied to several different biological fluids.

EXPERIMENTAL SECTION

Reagents and Materials—Acetazolamide[1] and sulfadiazine[2] were used as supplied. The solvents used for extraction and chromatography were all HPLC grade[3]. All chemicals were analytical reagent grade[4].

Standards—Separate stock solutions containing 1.0 mg/mL of acetazolamide and sulfadiazine (internal standard) were prepared weekly by dissolving these agents in 0.005 and 0.01 M NaOH, respectively. Aqueous solutions of lower concentrations (*i.e.*, 0.01–0.5 mg/mL) were prepared extemporaneously as needed from the stock solutions. Buffer solutions of 0.032 M glycine (pH 10.0) and 0.1 M phosphate buffer (pH 8.0) were prepared monthly. All solutions were stored at 4°C when not in use.

Extraction—Urine and heparinized whole blood were obtained from drug-free, normal, human volunteers. Plasma was obtained from an aliquot of whole blood using heparin as anticoagulant. Two hundred-microliter aliquots of plasma, whole blood, or urine (diluted 1:10) were added to 13 × 100-mm borosilicate glass tubes.

[1] Sigma Chemical Co., St. Louis, Mo.
[2] ICN Pharmaceuticals Inc., Cleveland, Ohio.
[3] Burdick and Jackson, Muskegon, Mich.
[4] Fisher Scientific, Fair Lawn, N.J.

0022-3549/84/0700-0985$01.00/0
© 1984, American Pharmaceutical Association

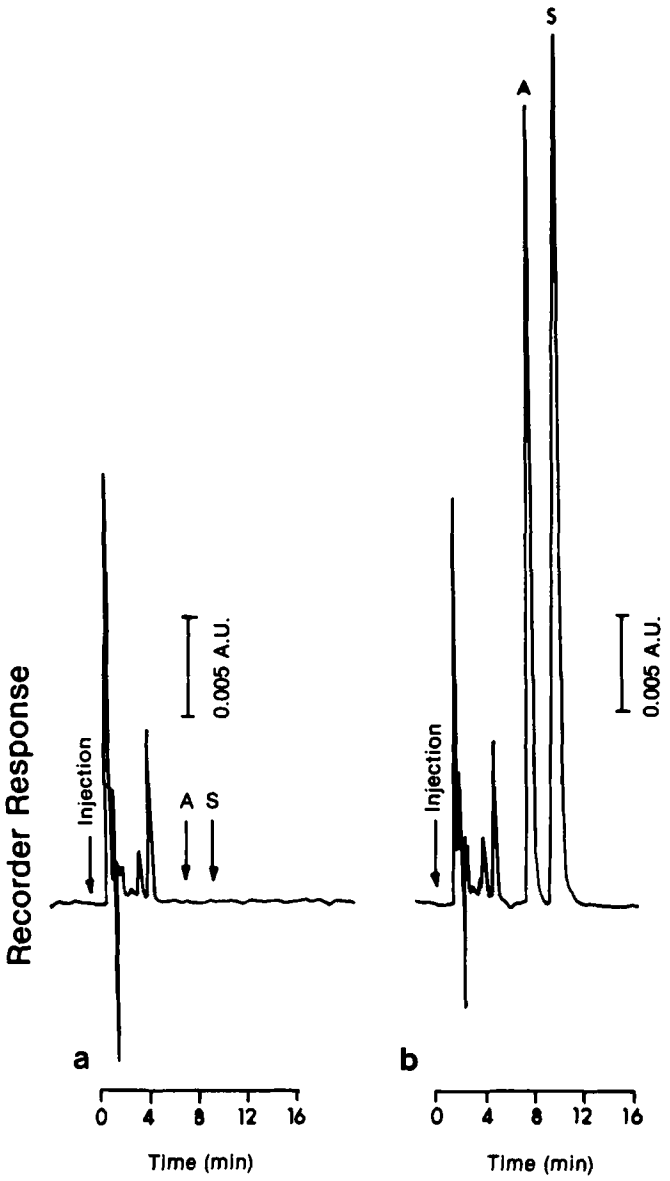

Figure 1—*Chromatograms of an extract of (a) blank whole blood and (b) an extract of whole blood containing 10.0 and 12.5 μg/mL of acetazolamide (A) and sulfadiazine (S), respectively.*

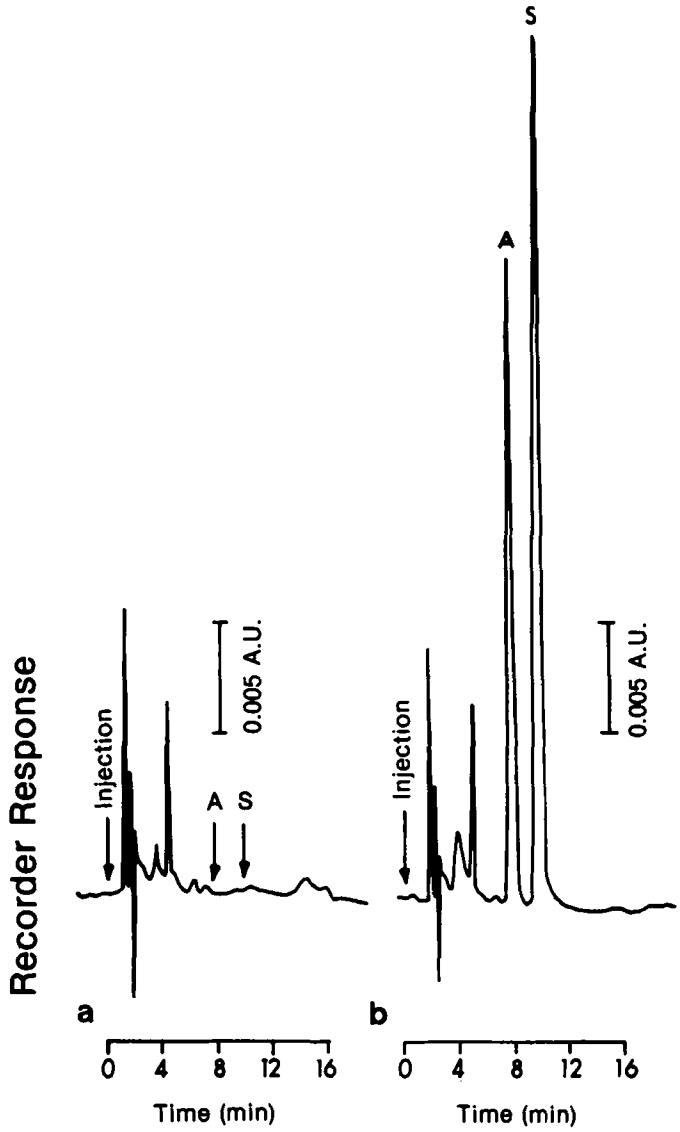

Figure 2—*Chromatograms of an extract of (a) blank plasma and (b) an extract of plasma containing 6.0 and 10.5 μg/mL of acetazolamide (A) and sulfadiazine (S), respectively.*

The tubes containing whole blood underwent two freeze-thaw cycles. Internal standard was then added (1–20 μL), the amount dependent on the range of concentrations expected in the unknown samples. One milliliter of a 50% solution of ammonium sulfamate was added, and the tubes were vortexed for a few seconds. The tubes containing whole blood were then placed in boiling water for 25 s, removed, and then quickly placed in cool water. One-half milliliter of water was added to the whole blood samples, and the tubes were vortexed for a few seconds.

Three milliliters of ethyl acetate was added to all tubes. The tubes were sealed with an extraction-tube plug[5] and shaken (200 oscillations/min) for 15 min. The phases were separated by centrifugation at 444×*g* for 5 min. The ethyl acetate layer was transferred to an identical tube containing 1.5 mL of pH 8.0 phosphate buffer (3.0 mL was used for urine workup). The tubes were then plugged and shaken, and the phases were separated by centrifugation as previously described. The organic phase was then transferred to tapered tubes[6] containing 200 μL of glycine buffer (pH 10.0), capped, and vortexed for 3 min. The phases were separated by centrifugation (444×*g*, 5 min), and the ethyl acetate layer was removed and discarded. To the remaining glycine layer, was added 1.0 mL of ether. The tubes were capped, vortexed for 2 min, the ether layer was removed and discarded, and the tubes were allowed to vent the ether vapors for ~15 min. An aliquot of the glycine phase (25–50 μL) was sampled from the tube and injected into the chromatograph.

Chromatography—The HPLC system consisted of a constant-flow pump[7], a variable-volume sampling valve[8], and a fixed-wavelength detector[9]. A 3.9 mm × 30-cm reverse-phase column[10] was used with a 2.3 × 3.9 mm guard column[11], which was packed with a commercially available bulk packing material[12]. The output from the detector was monitored on a 10-mV recorder[13].

Analyses were performed using a mobile phase of acetonitrile–methanol–0.05 M sodium acetate (3:2:95), the pH adjusted to 4.0 with glacial acetic acid. The mobile phase was deaerated before use. The system was operated at ambient temperature at a flow rate of 2.0 mL/min. The UV detector was fixed at a wavelength of 254 nm.

Calibration and Reproducibility—Known quantities of acetazolamide were added to blank plasma and whole blood. Samples (0.2 mL) were then assayed for acetazolamide. Calibration curves were constructed by plotting peak height ratio (acetazolamide-internal standard) *versus* the concentration of acetazolamide. Acetazolamide is rapidly eliminated from plasma; in order to accommodate a broad range of concentrations, two different standard curves

[5] Oxford Labs., Foster City, Calif.
[6] Corning centrifugation tube, Cat #8122.

[7] Model M6000A; Waters Associates, Milford, Mass.
[8] Model U6K; Waters Associates, Milford, Mass.
[9] Model 440; Waters Associates, Milford, Mass.
[10] μ-Bondapak C_{18}; Waters Associates, Milford, Mass.
[11] Waters Associates, Milford, Mass.
[12] Bondapak C_{18}/Corasil; Waters Associates, Milford, Mass.
[13] Omniscribe, model B5117-5; Houston Instruments, Austin, Tex.

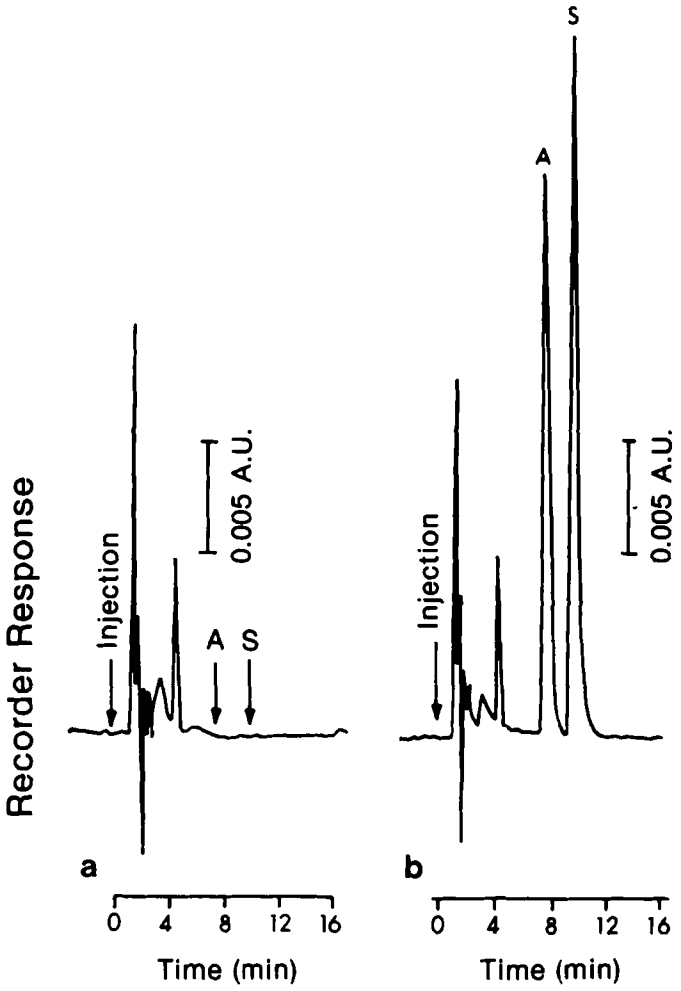

Figure 3—*Chromatograms of extracts of (a) blank urine and (b) urine containing acetazolamide (A) and sulfadiazine (S). Prior to extraction, each urine sample was diluted 1:10 with distilled water to yield final concentrations of 4.0 and 6.4 μg/mL for acetazolamide and sulfadiazine, respectively.*

were prepared. For plasma, standard calibration curve ranges were 0.05–1.5 μg/mL and 2.0–50.0 μg/mL. Because of significant accumulation and persistence of acetazolamide in erythrocytes, only a single calibration curve was needed for whole blood (*i.e.*, 1–50 μg/mL). Standard curves for urine were prepared in diluted urine (1:10) over the concentration range of 1–12 μg/mL. Day-to-day reproducibility and within-run precision of the analytical procedures were examined by processing spiked samples of plasma, whole blood, and urine.

Stability and Recovery—The stability of acetazolamide as a refrigerated aqueous solution (1 mg/mL), a frozen glycine extract, and frozen plasma and whole blood samples was assessed periodically by HPLC assay. Recovery of acetazolamide was calculated by comparing the peak height ratio of drug added to the biological fluid against the peak height ratio of drug added to the final glycine phase. In both treatments, the internal standard was added to the final glycine phase.

RESULTS AND DISCUSSION

Acetazolamide is a relatively polar drug [chloroform–water partition coefficient at pH 7.0 ≅ 0.001 (13)] which coextracts with endogenous blood and urinary constituents that create detection and quantification difficulties. The present results showed that a phosphate buffer washing step, which removes a moderate amount of acetazolamide, dramatically eliminates interfering endogenous substances. Blank urine, whole blood, and plasma (Figs. 1–3) do not show any endogenous interfering peaks. The retention times for acetazolamide and sulfadiazine were 7.6 and 9.8 min, respectively. Extraction of acetazolamide from whole blood was markedly improved by heating in boiling water for 25 s prior to processing. Perhaps heating irreversibly inactivates carbonic anhydrase and liberates the bound acetazolamide. Degradation of either acetazolamide or sulfadiazine does not occur during this heating step.

Table I—Calibration Curves for Acetazolamide in Various Biological Fluids

Fluid[a]	Concentration, μg/mL	r^2 [b]
Plasma	0.05–1.5	0.9984 ± 0.0025
	2.0–50	0.9988 ± 0.0022
Whole blood	1.0–50	0.9997 ± 0.0004
Urine	1.0–12	0.9996 ± 0.0004

[a] Based on five calibration curves. [b] Mean ± *SD*.

Calibration curves for all the biological fluids were linear over the concentrations described, and the intercepts were essentially zero. The mean coefficient of determination (r^2) for five successive calibration curves for urine, whole blood, and plasma are shown in Table I. Table II shows the coefficient of variation (*CV*) for the reproducibility studies. These data indicate the overall variability of the assay to be excellent, with all *CV* values <5.0%. With a 200-μL sample, the lowest quantifiable concentration providing reasonable reproducibility (*CV* ≤10%) was 0.05 μg/mL.

Absolute recoveries from plasma, whole blood, and urine were found to be 36, 33, and 20%, respectively. The significant loss of acetazolamide during processing was expected (acetazolamide has a pK_a of 7.4 and would be significantly ion-trapped in the phosphate buffer during the washing step) and considered very acceptable, because endogenous interfering substances were completely eliminated, sensitivity was adequate for human pharmacokinetic studies, and reproducibility of the assay was excellent. Absolute recovery can be increased by increasing the volume of ethyl acetate used for the initial extraction (*e.g.*, 4.0- and 5.0-mL ethyl acetate extraction of plasma provided absolute recoveries of 45 and 50%, respectively). We found it more convenient, however, to work with smaller extraction volumes. During sample processing the net loss of sulfadiazine was found to exceed that of acetazolamide. Across the biological matrices examined, sulfadiazine loss was found to parallel that of acetazolamide. A processed sample will produce a peak height ratio ~1 when initially spiked with a concentration of sulfadiazine 30% greater than that of acetazolamide.

Several stability studies were conducted. The aqueous refrigerated solution of acetazolamide (1 mg/mL) was found to be stable for ≤30 d. Frozen (−20°C) glycine extracts of acetazolamide and sulfadiazine were stable for ≤7 d. Acetazolamide in frozen plasma and whole blood was stable ≤180 d.

The HPLC procedures described have been successfully applied to pharmacokinetic studies of acetazolamide disposition in humans after intravenous administration. Figure 4 shows typical acetazolamide concentration–time curves following intravenous administration to a young female volunteer. Because urinary concentrations of the drug were expected to vary considerably, being very high initially and then rapidly declining thereafter, the following formula was used to estimate acetazolamide urinary concentrations:

$$\text{Estimated urinary acetazolamide concentration} = \frac{\text{AUC}\ (\mu\text{g}\cdot\text{min/mL}) \times CL\ (\text{mL/min})}{\text{Urine Volume (mL)}}$$

where AUC is the area under the acetazolamide plasma concentration–time curve and *CL* is its estimated clearance from plasma. Estimated urinary acetazolamide concentrations were then diluted to produce concentrations that would fall at the midpoint of the standard curve for urine (*i.e.*, 1–12 μg/mL). Cumulative urinary and excretion rate plots are shown in Fig. 5 for the same subject. It is noteworthy that 98.8% of the injected dose (320 mg) was recovered during a 72-h urine collection period. Studies designed to better define

Table II—Summary of Data for Reproducibility

Within-Run Precision[a]		Day-to-Day Reproducibility[b]	
Conc., μg/mL	*CV*, %	Conc., μg/mL	*CV*, %
	Plasma		
0.1	2.8	0.5	4.2
1.0	3.6	10.0	1.1
10.0	1.5		
20.0	2.0		
	Whole Blood		
1.0	1.3	10.0	3.7
10.0	1.6		
20.0	2.6		
	Urine		
5.0	1.2	6.0	1.3
10.0	1.5		

[a] $n = 8$. [b] $n = 6$.

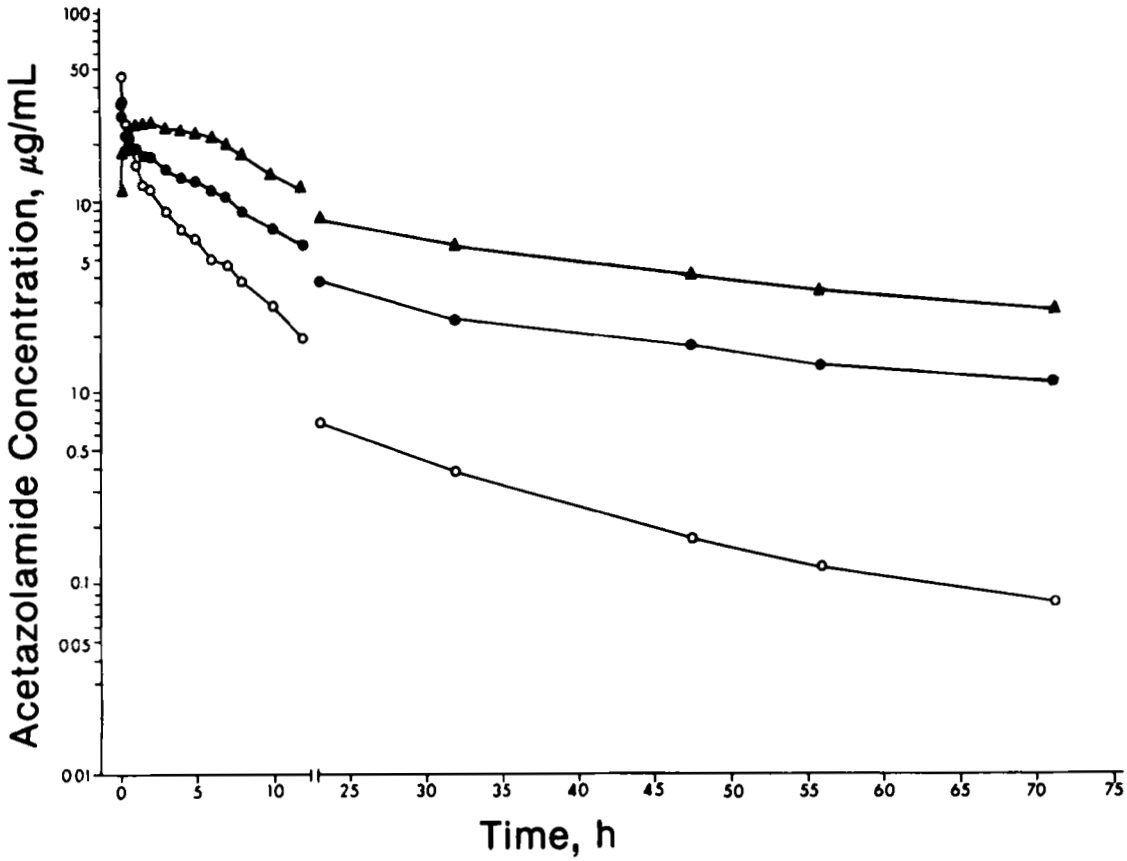

Figure 4—*Concentration-time profiles of acetazolamide in erythrocytes (▲), whole blood (●), and plasma (○) following an intravenous bolus injection of 320 mg.*

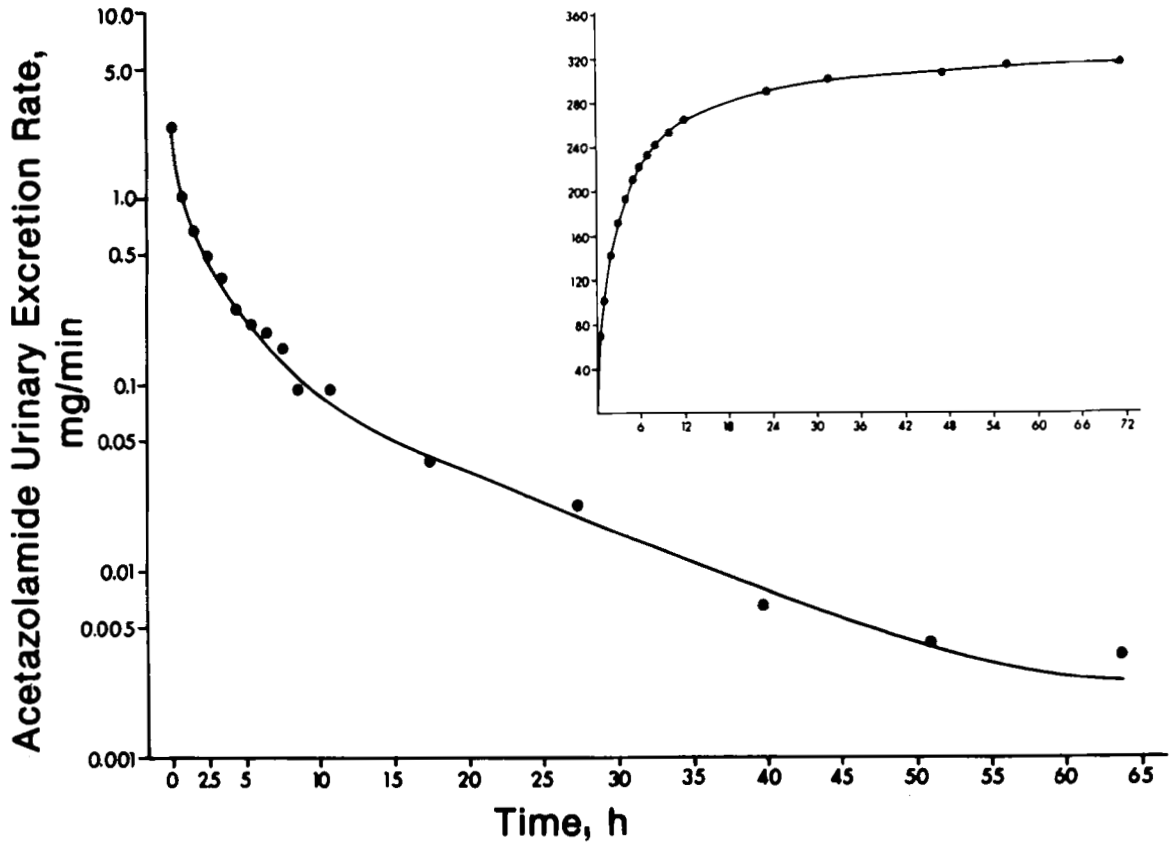

Figure 5—*Urinary excretion rate plot of acetazolamide following an intravenous bolus injection of 320 mg. The inset depicts cumulative amounts of acetazolamide excreted in urine (mg) over time (h) in the same subject.*

the factors that influence the disposition and response to acetazolamide are in progress.

REFERENCES

(1) B. Lehmann, E. Linner, and P. J. Wistrand, in "Schering Workshop in Pharmacokinetics," G. Raspe, Ed., Pergamon, Oxford, 1969, p. 197.

(2) B. R. Friedland, J. Mallonee, and D. R. Anderson, *Arch. Ophthalmol.*, **95**, 1809 (1977).

(3) F. G. Berson, D. L. Epstein, W. M. Grant, T. Hutchinson, and P. C. Dobbs, *Arch Ophthalmol.*, **98**, 1051 (1980).

(4) M. Inui, H. Azuma, T. Nishimura, and N. Hatada, in "Advances in Epileptology: XIIIth Epilepsy International Symposium," H. Akimoto, H. Kazamatsuri, M. Seino, and A. Ward, Eds., Raven, New York, N.Y., 1982, p. 307.

(5) D. M. Woodbury and J. W. Kemp, in "Antiepileptic Drugs," D. M. Woodbury, J. K Penry, and C. E. Pippenger, Eds., Raven Press, New York, N.Y., 1982, p. 771.

(6) J. B. West, "Respiratory Physiology," Williams and Wilkins Co., Baltimore, Md., 1979, p. 74.

(7) W. F. Bayne, G. Rogers, and N. Crisologo, *J. Pharm. Sci.*, **64**, 402 (1975).

(8) R. D. Hossie, N. Mouseau, S. Sved, and R. Brien, *J. Pharm. Sci.*, **69**, 348 (1980).

(9) D. M. Chambers, M. H. White, and H. B. Kostenbauder, *J. Chromatogr.*, **225**, 231 (1981).

(10) T. H. Maren, *J. Pharmacol. Exp. Ther.*, **130**, 26 (1960).

(11) G. J. Yakatan, C. A. Martin, and R. V. Smith, *Anal. Chim. Acta*, **84**, 173 (1976).

(12) S. M. Wallace, V. P. Shah, and S. Riegelman, *J. Pharm. Sci.*, **66**, 527 (1977).

(13) T. H. Maren, J. R. Haywood, S. K. Chapman, and T. J. Zimmerman, *Invest. Ophthalmol. Vis. Sci.*, **16**, 730 (1977).

Amperometric Determination of Hydralazine Hydrochloride in a Flowing Stream at the Glassy Carbon Electrode

MUMTAZ H. SHAH and JAMES T. STEWART ˣ

Received March 11, 1983, from the *Department of Medicinal Chemistry, College of Pharmacy, The University of Georgia, Athens, GA 30602.* Accepted for publication May 25, 1983.

Abstract □ A flow-injection method for the determination of hydralazine hydrochloride based on electrochemical oxidation at the glassy carbon electrode is presented. The amperometric method is highly specific and may be used to determine hydralazine hydrochloride in the presence of other drugs commonly found in its pharmaceutical dosage forms or administered concurrently in therapeutic situations. By using an electrode potential of +650 mV *versus* an Ag/AgCl reference electrode, a calibration curve was found to be linear in the 1–50-μg/mL concentration range, with minimum detectability at 10 ng (signal-to-noise ratio, 2). When the method was applied to the analysis of hydralazine hydrochloride in selected pharmaceutical dosage forms, it showed good accuracy and precision. Although automation was not used in this study, the method could readily be incorporated in automated systems because it employs the technique of continuous analysis in a flowing stream.

Keyphrases □ Hydralazine hydrochloride—amperometric determination in a flowing stream, glassy carbon electrode □ Flow-injection method—amperometric determination, hydralazine hydrochloride, glassy carbon electrode □ Electrochemical oxidation—glassy carbon electrode, flow-injection method, determination of hydralazine hydrochloride

Hydralazine hydrochloride, a widely prescribed antihypertensive agent, has been analyzed by diverse methodologies, including titrimetry (1, 2), spectrophotometry (3, 4), fluorometry (5), GC, and HPLC (6–10). Interest in this laboratory in the development of new continuous assay methods for drugs in flowing streams led us to investigate the oxidation of hydralazine at the glassy carbon electrode. There is almost no information in the literature concerning the electrochemistry of hydralazine. One report has indicated that the drug can be reduced at the dropping mercury electrode to give two half-wave potentials of −700 and −950 mV *versus* the standard calomel electrode (11). The reduction occurs in a solution containing 1 M HCl as a supporting electrolyte and gelatin as a surfactant. The report did not comment on the sensitivity, accuracy, precision, and specificity of the method. There appears to be no data in the literature on the electrochemical oxidation of the drug.

This laboratory has reported previously on continuous analysis in flowing streams by oxidation of drugs such as ascorbic acid and methyldopa at the tubular carbon electrode (12, 13). The glassy carbon electrode has supplanted the tubular carbon electrode and has shown general usefulness as a sensitive tool for the determination of oxidizable drugs in flowing stream systems such as HPLC (14–16). These kinds of electrodes can be easily incorporated into automated or semiautomated systems such as would be used in dosage form analysis.

In this report, amperometric determination of hydralazine hydrochloride in a flowing stream utilizing oxidation at the glassy carbon electrode is reported. The flow-injection method

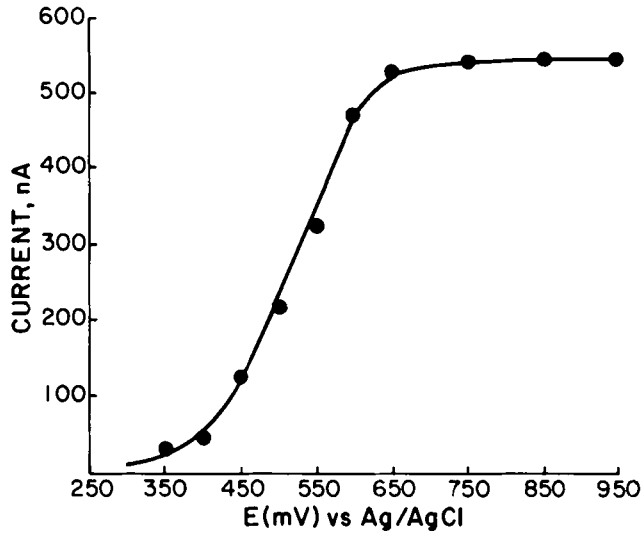

Figure 1—*Hydrodynamic voltammogram of hydralazine hydrochloride (50 μg/mL) in a 40:60 mixture of Walpole acetate buffer (pH 4.2)-absolute methanol at a flow rate of 1 mL/min.*

0022-3549/84/0700-0989$01.00/0
© 1984, American Pharmaceutical Association

the factors that influence the disposition and response to acetazolamide are in progress.

REFERENCES

(1) B. Lehmann, E. Linner, and P. J. Wistrand, in "Schering Workshop in Pharmacokinetics," G. Raspe, Ed., Pergamon, Oxford, 1969, p. 197.

(2) B. R. Friedland, J. Mallonee, and D. R. Anderson, *Arch. Ophthalmol.*, **95**, 1809 (1977).

(3) F. G. Berson, D. L. Epstein, W. M. Grant, T. Hutchinson, and P. C. Dobbs, *Arch Ophthalmol.*, **98**, 1051 (1980).

(4) M. Inui, H. Azuma, T. Nishimura, and N. Hatada, in "Advances in Epileptology: XIIIth Epilepsy International Symposium," H. Akimoto, H. Kazamatsuri, M. Seino, and A. Ward, Eds., Raven, New York, N.Y., 1982, p. 307.

(5) D. M. Woodbury and J. W. Kemp, in "Antiepileptic Drugs," D. M. Woodbury, J. K Penry, and C. E. Pippenger, Eds., Raven Press, New York, N.Y., 1982, p. 771.

(6) J. B. West, "Respiratory Physiology," Williams and Wilkins Co., Baltimore, Md., 1979, p. 74.

(7) W. F. Bayne, G. Rogers, and N. Crisologo, *J. Pharm. Sci.*, **64**, 402 (1975).

(8) R. D. Hossie, N. Mouseau, S. Sved, and R. Brien, *J. Pharm. Sci.*, **69**, 348 (1980).

(9) D. M. Chambers, M. H. White, and H. B. Kostenbauder, *J. Chromatogr.*, **225**, 231 (1981).

(10) T. H. Maren, *J. Pharmacol. Exp. Ther.*, **130**, 26 (1960).

(11) G. J. Yakatan, C. A. Martin, and R. V. Smith, *Anal. Chim. Acta*, **84**, 173 (1976).

(12) S. M. Wallace, V. P. Shah, and S. Riegelman, *J. Pharm. Sci.*, **66**, 527 (1977).

(13) T. H. Maren, J. R. Haywood, S. K. Chapman, and T. J. Zimmerman, *Invest. Ophthalmol. Vis. Sci.*, **16**, 730 (1977).

Amperometric Determination of Hydralazine Hydrochloride in a Flowing Stream at the Glassy Carbon Electrode

MUMTAZ H. SHAH and JAMES T. STEWART ˣ

Received March 11, 1983, from the *Department of Medicinal Chemistry, College of Pharmacy, The University of Georgia, Athens, GA 30602.* Accepted for publication May 25, 1983.

Abstract □ A flow-injection method for the determination of hydralazine hydrochloride based on electrochemical oxidation at the glassy carbon electrode is presented. The amperometric method is highly specific and may be used to determine hydralazine hydrochloride in the presence of other drugs commonly found in its pharmaceutical dosage forms or administered concurrently in therapeutic situations. By using an electrode potential of +650 mV *versus* an Ag/AgCl reference electrode, a calibration curve was found to be linear in the 1–50-μg/mL concentration range, with minimum detectability at 10 ng (signal-to-noise ratio, 2). When the method was applied to the analysis of hydralazine hydrochloride in selected pharmaceutical dosage forms, it showed good accuracy and precision. Although automation was not used in this study, the method could readily be incorporated in automated systems because it employs the technique of continuous analysis in a flowing stream.

Keyphrases □ Hydralazine hydrochloride—amperometric determination in a flowing stream, glassy carbon electrode □ Flow-injection method—amperometric determination, hydralazine hydrochloride, glassy carbon electrode □ Electrochemical oxidation—glassy carbon electrode, flow-injection method, determination of hydralazine hydrochloride

Hydralazine hydrochloride, a widely prescribed antihypertensive agent, has been analyzed by diverse methodologies, including titrimetry (1, 2), spectrophotometry (3, 4), fluorometry (5), GC, and HPLC (6–10). Interest in this laboratory in the development of new continuous assay methods for drugs in flowing streams led us to investigate the oxidation of hydralazine at the glassy carbon electrode. There is almost no information in the literature concerning the electrochemistry of hydralazine. One report has indicated that the drug can be reduced at the dropping mercury electrode to give two half-wave potentials of −700 and −950 mV *versus* the standard calomel electrode (11). The reduction occurs in a solution containing 1 M HCl as a supporting electrolyte and gelatin as a surfactant. The report did not comment on the sensitivity, accuracy, precision, and specificity of the method. There appears to be no data in the literature on the electrochemical oxidation of the drug.

This laboratory has reported previously on continuous analysis in flowing streams by oxidation of drugs such as ascorbic acid and methyldopa at the tubular carbon electrode (12, 13). The glassy carbon electrode has supplanted the tubular carbon electrode and has shown general usefulness as a sensitive tool for the determination of oxidizable drugs in flowing stream systems such as HPLC (14–16). These kinds of electrodes can be easily incorporated into automated or semiautomated systems such as would be used in dosage form analysis.

In this report, amperometric determination of hydralazine hydrochloride in a flowing stream utilizing oxidation at the glassy carbon electrode is reported. The flow-injection method

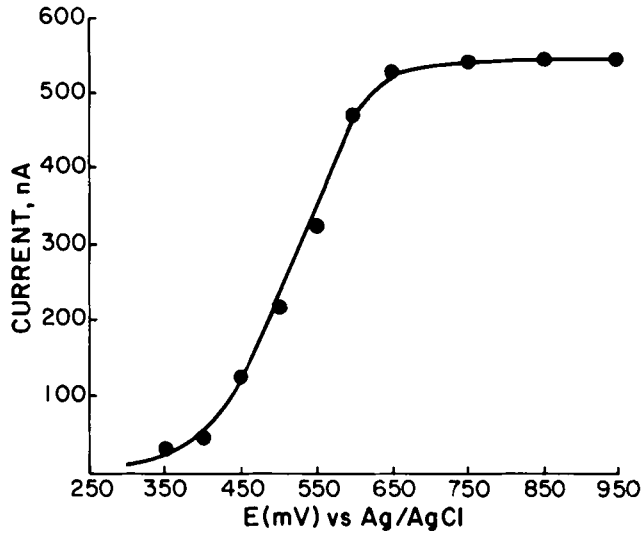

Figure 1—*Hydrodynamic voltammogram of hydralazine hydrochloride (50 μg/mL) in a 40:60 mixture of Walpole acetate buffer (pH 4.2)-absolute methanol at a flow rate of 1 mL/min.*

0022-3549/84/0700-0989$01.00/0
© 1984, American Pharmaceutical Association

Table I—Percent Recovery of Hydralazine Hydrochloride in Synthetic Drug Mixtures

Drug	Concentration, μg/mL[a]			
	8	16	32	100
Hydrochlorothiazide	99.79 ± 1.39	99.19 ± 1.25	99.19 ± 0.92	85.91 ± 1.52
Chlorothiazide	99.59 ± 0.60	99.39 ± 0.92	99.19 ± 0.92	90.52 ± 1.19
Reserpine	99.39 ± 0.92	99.38 ± 0.61	99.79 ± 1.39	78.96 ± 1.21
Propranolol hydrochloride	99.39 ± 0.92	99.19 ± 1.25	100.19 ± 0.61	99.99 ± 0.92
Triamterene	99.39 ± 0.92	99.99 ± 0.92	99.59 ± 1.21	99.19 ± 0.35
Methyldopa	99.59 ± 0.60	100.19 ± 0.61	99.99 ± 0.92	99.59 ± 1.21
Guanethidine monosulfate	99.39 ± 0.92	99.79 ± 1.39	99.19 ± 0.92	99.19 ± 0.35
Chlorthalidone	100.40 ± 0.35	100.60 ± 0.60	100.20 ± 0.35	100.20 ± 0.35

[a] Concentration of each drug in mixtures that also contained 16 μg/mL of hydralazine hydrochloride. Values represent mean percent recovery ± *SD* of hydralazine hydrochloride in the drug mixture. The data were based on quadruplicate determinations of each mixture.

detects the drug in the 1-50-μg/mL range with good accuracy, precision, and specificity. The procedure was shown to be applicable to the analysis of hydralazine hydrochloride in pharmaceutical dosage forms.

EXPERIMENTAL SECTION

Apparatus—Voltammograms and cyclic voltammetry measurements were made with a conventional three-electrode system[1] consisting of a glassy carbon working electrode, a platinum auxiliary electrode, and a silver-silver chloride reference electrode. A wall-jet-type methyl methacrylate electrochemical cell[2] and associated electronics[2] were used for the flowing stream analysis. The cell contained a glassy carbon working electrode, a silver-silver chloride reference electrode, and a second glassy carbon auxiliary electrode. The mobile phase was pumped through the cell at a fixed flow rate with a reciprocating pump[3]. Samples were manually injected into the sample injection system[4] with a microsyringe[5]. The pump, injector, and electrochemical cell were connected with standard HPLC stainless steel tubing (0.02 cm) and fittings. Cell currents were recorded at ambient temperature with a strip-chart recorder[6].

Chemicals—Hydralazine hydrochloride[7] powder was obtained for use in the analytical study. All other chemicals were commercially available and were used as received. A stock solution containing 0.1 mg/mL of hydralazine hydrochloride was prepared in Walpole acetate buffer, pH 4.2 (17). Further dilutions of the solution were made to provide working standards in the 1-50-μg/mL range.

Procedures—A 40:60 mixture of Walpole acetate buffer (pH 4.2)-absolute methanol was pumped through the electrochemical cell[2] at a flow rate of 1.0 mL/min. Aliquots (50 μL) of hydralazine hydrochloride solutions in acetate buffer were injected into the flowing stream, and the current was measured with an applied potential of +650 mV *versus* an Ag/AgCl reference electrode.

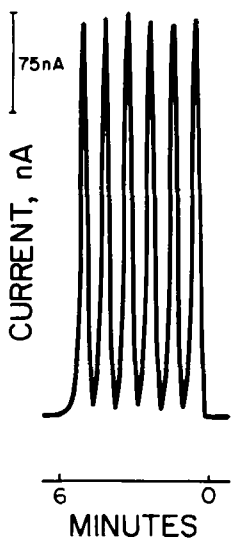

Figure 2—*Replicate injections of hydralazine hydrochloride (16 μg/mL) into the flowing stream system at a rate of 60 samples/h.*

To determine whether other antihypertensive drugs or compounds commonly found in dosage forms with hydralazine hydrochloride interfered with the assay by altering the current flow of the drug or were oxidized at the glassy carbon electrode, the following studies were performed. Individual solutions (0.1 mg/mL) of guanethidine monosulfate, reserpine, hydrochlorothiazide, chlorothiazide, triamterene, methyldopa, propranolol hydrochloride, and chlorthalidone were prepared in acetate buffer (pH 4.2)-methanol (40:60). Accurately pipetted aliquots of these solutions were then used to prepare various mixtures containing the individual drugs at the 8-100-μg/mL range, with the hydralazine concentration maintained at 16 μg/mL. Each mixture was then assayed for hydralazine content. The data obtained from each mixture were then compared with those of a pure solution of hydralazine hydrochloride to calculate the degree of interference, if any, at the various concentration levels of the added drugs.

Analysis of solid dosage form—Tablets and/or capsules containing hydralazine hydrochloride were sonicated in Walpole acetate buffer (pH 4.2). The resulting solution was then filtered, if necessary, and diluted to the 1-50-μg/mL range. An aliquot of the diluted solution was then assayed for hydralazine hydrochloride as described above.

RESULTS AND DISCUSSION

Figure 1 shows a hydrodynamic voltammogram of hydralazine hydrochloride (50 μg/mL) when subjected to electrochemical oxidation at the glassy carbon electrode in acetate buffer (pH 4.2)-methanol (40:60). A half-wave potential of +510 mV was observed. A potential of +650 mV was selected for the amperometric determination since it represented the point on the wave at which maximum drug sensitivity could be obtained.

By using the optimum electrode potential of +650 mV, a hydralazine hydrochloride calibration curve was obtained in the 1-50-μg/mL range. Linear regression analysis of the calibration data gave typical slope, intercept, and r values of 19.82, 8.79, and 0.9990 (n = 18), respectively.

To estimate the reproducibility of the electrode response by the amperometric method, eight replicate injections at hydralazine hydrochloride concentrations of 4-, 16-, and 40-μg/mL were run. Mean peak currents of 51 ± 1.15, 165.63 ± 1.25, and 367.50 ± 1.25 nA, respectively, were obtained. The

Table II—Analysis of Hydralazine Hydrochloride in Pharmaceutical Dosage Forms

Product Components	Hydralazine Declared/Sample, mg	Hydralazine Found/Sample, mg[a]	Recovery, %
Hydralazine hydrochloride	25	25.55 ± 0.25	102.10
Hydralazine hydrochloride Hydrochlorothiazide	25	24.98 ± 0.10	99.90
Hydralazine hydrochloride Reserpine	50	50.85 ± 0.52	101.70
Hydralazine hydrochloride Hydrochlorothiazide Reserpine	25	24.90 ± 0.42	99.35

[a] Values represent mean ± *SD* based on quadruplicate determinations of each sample.

[1] Model 174 A polarograph; Princeton Applied Research.
[2] Model EA-1096 plexiglas cell with Model E-611 detector; Metrohm.
[3] Model M-6000A Pump; Waters Associates, Milford, Mass.
[4] Model U6K Injector; Waters Associates, Milford, Mass.
[5] 50-μL syringe; Hamilton Co., Reno, Nev.
[6] Houston Omniscribe Recorder.
[7] CIBA-GEIGY Corp., Summit, N.J.

precision of these measurements is expressed by relative standard deviations of 2.30, 0.75, and 0.34% for the 4-, 16-, and 40-μg/mL levels, respectively.

Interference studies were performed to establish the specificity of the method for hydralazine hydrochloride in the presence of other drugs that might be found in its combination dosage forms. There was little or no interference from these miscellaneous compounds, except for hydrochlorothiazide, chlorothiazide, and reserpine, in which appreciable interference was noted when their concentrations were six- to sevenfold greater than the hydralazine level (Table I).

Applications of the method to the assay of hydralazine hydrochloride in commercial dosage forms was then studied. After sample preparation and dilution to the 1–50-μg/mL calibration range, the drug solutions were analyzed, and the concentration in each dosage form was calculated using the slope and intercept values generated from linear regression analysis of the hydralazine calibration data. The results of the assay shown in Table II indicate that hydralazine content in dosage forms can be conveniently determined by the amperometric method described herein with good accuracy and precision.

By using the parameters established for the assay, hydralazine samples can be injected into the flowing stream system at the rate of 60 samples/h (Fig. 2). The sensitivity of the assay, based on a signal-to-noise ratio of two, is 10 ng of drug.

REFERENCES

(1) "U.S. Pharmacopeia," 20th Rev., U.S. Pharmacopeial Convention, Rockville, Md., 1980, p. 377.

(2) R. Soliman and S. A. Belal, *J. Drug Res.*, **6**, 7 (1974).

(3) J. T. Stewart and Y. Chang, *J. Assoc. Off. Anal. Chem.*, **62**, 1107 (1979).

(4) S. B. Zak, M. F. Bartlett, W. E. Wagner, J. T. Gilleran, and G. Lukas, *J. Pharm. Sci.*, **63**, 225 (1974).

(5) D. V. Naik, B. R. Davis, K. M. Minnet, and S. G. Schulman, *J. Pharm. Sci.*, **65**, 274 (1976).

(6) K. D. Haegele, H. B. Skrdlant, N. W. Robie, D. Lalka, and J. L. McNay, *J. Chromatogr.*, **126**, 517 (1976).

(7) K. M. Smith, R. N. Johnson, and B. T. Kho, *J. Chromatogr.*, **137**, 431 (1977).

(8) D. B. Jack, S. Brechbuhler, P. H. Degen, Z. Zbinden, and W. Riess, *J. Chromatogr.*, **115**, 87 (1975).

(9) W. J. Proveaux, J. P. O'Donnell, and J. K. H. Ma, *J. Chromatogr.*, **176**, 480 (1979).

(10) T. M. Ludden, L. K. Goggin, J. L. McNay, R. D. Haegele, and A. M. M. Shepherd, *J. Pharm. Sci.*, **68**, 1423 (1979).

(11) Z. Modras, *Chem. Anal.*, **17**, 1349 (1973); through *Chem. Abstr.*, **78**, 128457g (1973).

(12) W. D. Mason, T. D. Gardner, and J. T. Stewart, *J. Pharm. Sci.*, **61**, 1301 (1972).

(13) J. T. Stewart, H. C. Loo, and W. D. Mason, *J. Pharm. Sci.*, **63**, 954 (1974).

(14) R. E. Shoup (Ed.), "Recent Reports on Liquid Chromatography with Electrochemical Detection," BAS Press, West Lafayette, Ind., 1981.

(15) D. D. Koch and P. T. Kissinger, *J. Chromatogr. Biomed. Appl.*, **164**, 441 (1979).

(16) L. A. Pachla and P. T. Kissinger, *Anal. Chem.*, **48**, 364 (1976).

(17) M. Brezina and P. Zuman, "Polarography in Medicine, Biochemistry and Pharmacy," Interscience, New York, N.Y., 1958, p. 731.

Rapid Gas Chromatographic Assay for Monitoring Valproic Acid and Valpromide in Plasma

MEIR BIALER ˣ, MICHAEL FRIEDMAN, and ABRAHAM RUBINSTEIN

Received July 1, 1982, from the *Department of Pharmacy, School of Pharmacy, Hebrew University, P.O. Box 12065, Jerusalem 91120, Israel.* Accepted for publication May 23, 1983.

Abstract □ A gas chromatographic (GC) method for monitoring valproic acid and valpromide in plasma was developed. The procedure involved a single solvent extraction of drugs from acidified plasma samples, followed by a GC injection of the organic phase. This rapid, sensitive, specific, and reproducible method is a key factor in pharmacokinetic and stability studies of valpromide. Pharmacokinetic application of the new GC method is presented by a simultaneous plasma monitoring of valpromide and valproic acid levels obtained after intravenous administration of valpromide to a dog.

Keyphrases □ Valproic acid—GC, plasma, valpromide □ Valpromide—GC, plasma, valproic acid

Valpromide (2-propylvaleramide), commonly used in clinical practice as an antiepileptic and antipsychotic drug (1–6), is a primary amide of the more widely known valproic acid, which is used to treat different types of epilepsy, particularly petit mal epilepsy (7, 8). Recent reports claimed that valpromide is biotransformed to valproic acid before reaching the systemic circulation. Only traces of valproic acid have been observed in patients who were on chronic oral treatment of valpromide (1, 4, 5); after treatment with valpromide (600 mg t.i.d.) to 42 epileptic patients, the therapeutic plasma concentrations of valproic acid ranged from 50 to 60 μg/mL with minimal fluctuations in plasma level (4). This is within the therapeutic range of valproic acid (8). After single oral administration of valpromide (600 mg) to humans, the plasma levels of valproic acid ranged from 7 to 20 μg/mL for >30 h after the valpromide administration (4, 5).

During the last decade various methods for analyzing valproic acid in biological fluids have been published (9, 10). Recently a gas chromatographic (GC) method for monitoring valpromide in plasma was reported (11). The aim of this work was to develop a rapid GC method for a routine valproic acid and valpromide assay in plasma. This assay is fundamental in pharmacokinetic and stability studies of valpromide, since valpromide may serve as a prodrug for valproic acid (1, 2).

EXPERIMENTAL SECTION

Reagents—Organic stock solutions of valproic acid[1] and valpromide[2] were prepared by dissolving the drugs separately in chloroform. Aqueous stock solutions were prepared by dissolving sodium valproate[1] and valpromide separately in water. The concentration of all stock solutions was 1 mg/mL. Caprylic acid[2] was used as an internal standard and was dissolved in chloroform at a concentration of 1 mg/mL. Stock solutions were stored at 4°C.

Apparatus—The gas chromatograph[3] was equipped with a flame-ionization detector and a recorder[4]. The glass column, 180 cm × 2 mm i.d., was packed with 5% free fatty acid phase[5] on 80–100 mesh Chrom Q. Flow rates were as follows: hydrogen, 40 mL/min; air, 400 mL/min; carrier gas (nitrogen), 40 mL/min. The system temperatures were: column, 175°C; injector, 180°C; detector, 220°C.

Extraction Procedure—To 1.0 mL of plasma spiked with the appropriate aliquots of valproic acid and valpromide aqueous solutions were added 480

[1] Labaz, Paris, France.
[2] BDH, Poole, England.
[3] Model 7421; Packard, Downers Grove, Ill.
[4] Unicorder 225; Panto, Kyoto, Japan.
[5] Applied Science Labs., State College, Pa.

0022-3549/84/0700-0991$01.00/0

© 1984, American Pharmaceutical Association

precision of these measurements is expressed by relative standard deviations of 2.30, 0.75, and 0.34% for the 4-, 16-, and 40-μg/mL levels, respectively.

Interference studies were performed to establish the specificity of the method for hydralazine hydrochloride in the presence of other drugs that might be found in its combination dosage forms. There was little or no interference from these miscellaneous compounds, except for hydrochlorothiazide, chlorothiazide, and reserpine, in which appreciable interference was noted when their concentrations were six- to sevenfold greater than the hydralazine level (Table I).

Applications of the method to the assay of hydralazine hydrochloride in commercial dosage forms was then studied. After sample preparation and dilution to the 1–50-μg/mL calibration range, the drug solutions were analyzed, and the concentration in each dosage form was calculated using the slope and intercept values generated from linear regression analysis of the hydralazine calibration data. The results of the assay shown in Table II indicate that hydralazine content in dosage forms can be conveniently determined by the amperometric method described herein with good accuracy and precision.

By using the parameters established for the assay, hydralazine samples can be injected into the flowing stream system at the rate of 60 samples/h (Fig. 2). The sensitivity of the assay, based on a signal-to-noise ratio of two, is 10 ng of drug.

REFERENCES

(1) "U.S. Pharmacopeia," 20th Rev., U.S. Pharmacopeial Convention, Rockville, Md., 1980, p. 377.

(2) R. Soliman and S. A. Belal, *J. Drug Res.*, **6**, 7 (1974).

(3) J. T. Stewart and Y. Chang, *J. Assoc. Off. Anal. Chem.*, **62**, 1107 (1979).

(4) S. B. Zak, M. F. Bartlett, W. E. Wagner, J. T. Gilleran, and G. Lukas, *J. Pharm. Sci.*, **63**, 225 (1974).

(5) D. V. Naik, B. R. Davis, K. M. Minnet, and S. G. Schulman, *J. Pharm. Sci.*, **65**, 274 (1976).

(6) K. D. Haegele, H. B. Skrdlant, N. W. Robie, D. Lalka, and J. L. McNay, *J. Chromatogr.*, **126**, 517 (1976).

(7) K. M. Smith, R. N. Johnson, and B. T. Kho, *J. Chromatogr.*, **137**, 431 (1977).

(8) D. B. Jack, S. Brechbuhler, P. H. Degen, Z. Zbinden, and W. Riess, *J. Chromatogr.*, **115**, 87 (1975).

(9) W. J. Proveaux, J. P. O'Donnell, and J. K. H. Ma, *J. Chromatogr.*, **176**, 480 (1979).

(10) T. M. Ludden, L. K. Goggin, J. L. McNay, R. D. Haegele, and A. M. M. Shepherd, *J. Pharm. Sci.*, **68**, 1423 (1979).

(11) Z. Modras, *Chem. Anal.*, **17**, 1349 (1973); through *Chem. Abstr.*, **78**, 128457g (1973).

(12) W. D. Mason, T. D. Gardner, and J. T. Stewart, *J. Pharm. Sci.*, **61**, 1301 (1972).

(13) J. T. Stewart, H. C. Loo, and W. D. Mason, *J. Pharm. Sci.*, **63**, 954 (1974).

(14) R. E. Shoup (Ed.), "Recent Reports on Liquid Chromatography with Electrochemical Detection," BAS Press, West Lafayette, Ind., 1981.

(15) D. D. Koch and P. T. Kissinger, *J. Chromatogr. Biomed. Appl.*, **164**, 441 (1979).

(16) L. A. Pachla and P. T. Kissinger, *Anal. Chem.*, **48**, 364 (1976).

(17) M. Brezina and P. Zuman, "Polarography in Medicine, Biochemistry and Pharmacy," Interscience, New York, N.Y., 1958, p. 731.

Rapid Gas Chromatographic Assay for Monitoring Valproic Acid and Valpromide in Plasma

MEIR BIALER ˣ, MICHAEL FRIEDMAN, and ABRAHAM RUBINSTEIN

Received July 1, 1982, from the *Department of Pharmacy, School of Pharmacy, Hebrew University, P.O. Box 12065, Jerusalem 91120, Israel.* Accepted for publication May 23, 1983.

Abstract □ A gas chromatographic (GC) method for monitoring valproic acid and valpromide in plasma was developed. The procedure involved a single solvent extraction of drugs from acidified plasma samples, followed by a GC injection of the organic phase. This rapid, sensitive, specific, and reproducible method is a key factor in pharmacokinetic and stability studies of valpromide. Pharmacokinetic application of the new GC method is presented by a simultaneous plasma monitoring of valpromide and valproic acid levels obtained after intravenous administration of valpromide to a dog.

Keyphrases □ Valproic acid—GC, plasma, valpromide □ Valpromide—GC, plasma, valproic acid

Valpromide (2-propylvaleramide), commonly used in clinical practice as an antiepileptic and antipsychotic drug (1–6), is a primary amide of the more widely known valproic acid, which is used to treat different types of epilepsy, particularly petit mal epilepsy (7, 8). Recent reports claimed that valpromide is biotransformed to valproic acid before reaching the systemic circulation. Only traces of valproic acid have been observed in patients who were on chronic oral treatment of valpromide (1, 4, 5); after treatment with valpromide (600 mg t.i.d.) to 42 epileptic patients, the therapeutic plasma concentrations of valproic acid ranged from 50 to 60 μg/mL with minimal fluctuations in plasma level (4). This is within the therapeutic range of valproic acid (8). After single oral administration of valpromide (600 mg) to humans, the plasma levels of valproic acid ranged from 7 to 20 μg/mL for >30 h after the valpromide administration (4, 5).

During the last decade various methods for analyzing valproic acid in biological fluids have been published (9, 10). Recently a gas chromatographic (GC) method for monitoring valpromide in plasma was reported (11). The aim of this work was to develop a rapid GC method for a routine valproic acid and valpromide assay in plasma. This assay is fundamental in pharmacokinetic and stability studies of valpromide, since valpromide may serve as a prodrug for valproic acid (1, 2).

EXPERIMENTAL SECTION

Reagents—Organic stock solutions of valproic acid[1] and valpromide[2] were prepared by dissolving the drugs separately in chloroform. Aqueous stock solutions were prepared by dissolving sodium valproate[1] and valpromide separately in water. The concentration of all stock solutions was 1 mg/mL. Caprylic acid[2] was used as an internal standard and was dissolved in chloroform at a concentration of 1 mg/mL. Stock solutions were stored at 4°C.

Apparatus—The gas chromatograph[3] was equipped with a flame-ionization detector and a recorder[4]. The glass column, 180 cm × 2 mm i.d., was packed with 5% free fatty acid phase[5] on 80–100 mesh Chrom Q. Flow rates were as follows: hydrogen, 40 mL/min; air, 400 mL/min; carrier gas (nitrogen), 40 mL/min. The system temperatures were: column, 175°C; injector, 180°C; detector, 220°C.

Extraction Procedure—To 1.0 mL of plasma spiked with the appropriate aliquots of valproic acid and valpromide aqueous solutions were added 480

[1] Labaz, Paris, France.
[2] BDH, Poole, England.
[3] Model 7421; Packard, Downers Grove, Ill.
[4] Unicorder 225; Panto, Kyoto, Japan.
[5] Applied Science Labs., State College, Pa.

0022-3549/84/0700-0991$01.00/0

© 1984, American Pharmaceutical Association

Table I—Recovery and Reproducibility of Valproic Acid and Valpromide in Human Plasma

Conc., μg/mL	Valproic Acid			Valpromide		
	Recovery[a], %	*SD*	*CV*, %	Recovery[a], %	*SD*	*CV*, %
5	104.25	7.18	6.89	104.14	5.70	5.42
10	100.32	5.58	5.57	102.09	5.37	5.26
20	104.49	6.46	6.19	100.54	7.48	7.44
30	102.73	7.29	8.49	99.43	8.56	8.61
40	103.45	7.89	7.63	98.85	7.98	8.07
50	104.19	6.69	6.42	99.76	8.59	8.62
60	104.21	6.85	6.57	99.81	7.64	7.66

[a] Mean of 10 determinations.

μL of chloroform, 20 μL of internal standard solution, and 0.5 mL of 1 M HCl. The sample was vortexed for 15 s, shaken for 15 min, and centrifuged at 4000 rpm for 15 min. Three microliters of the organic phase was injected into the gas chromatograph.

To determine the precision of the assay, 12 mL of human plasma was spiked with appropriate aliquots of the aqueous valproic acid and valpromide stock solutions and was stored at −20°C during the 3-month study. On different days 1-mL aliquots were taken from the various stored samples and analyzed against a fresh calibration curve made according to the extraction procedure on the same day.

RESULTS AND DISCUSSION

Typical chromatograms of extracts from plasma with reference to drug-free plasma samples is presented in Fig. 1. Under the assay conditions the following retention times were obtained: valproic acid, 0.96 min; internal standard, 1.8 min; and valpromide, 2.23 min. There was no interference from endogeneous plasma components.

Calibration curves from plasma extracts showed a linear correlation between peak height ratio (y) of valpromide or valproic acid against the internal standard and plasma concentration of the drugs (x). The linear calibration equation was $y = 0.0968x - 0.044$ ($r = 0.997$) for valproic acid and $y = 0.0713x + 0.0018$ ($r = 0.997$) for valpromide. A least-squares linear regression method was used to calculate these curves. The minimal detectable concentration was ~1-2 μg/mL in plasma.

Analytical recoveries of substances were established as follows. Various amounts (5, 10, 20, 30, 40, 50, and 60 μg taken from the aqueous stock solutions) of valproic acid and valpromide were dissolved in 1 mL of drug-free plasma. After acidification, plasma samples were extracted into 0.5 mL of chloroform which contained 20 μL of the internal standard solution. A series of external standards were prepared by adding 20 μL of the internal standard solution to 0.48 mL of chloroform which contained the various amounts taken from the organic stock solution (5, 10, 20, 30, 40, 50, and 60 μg) of valproic acid and valpromide. Recoveries were calculated by comparing peak height ratios of the extracted standard to the ratios of the external standards (Table I). The standard deviation of the analytical recoveries can serve as a good estimate for reproducibility.

Precision or accuracy of the assay was determined by performing 10 replicate analyses of five control samples containing 20, 30, 40, 50, and 60 μg/mL of both drugs on different days over a 3-month period (Table II). The recovery percentage of valpromide and valproic acid, as presented in Table I, does not have a statistically significant difference from 100% ($p > 0.05$). The observed values of the various valpromide and valproic acid concentrations (Table II) were not different statistically from the added concentrations ($p > 0.05$) (12).

In a preliminary pharmacokinetic study, valpromide (400 mg) was administered intravenously to a mongrel dog (20 kg). This 20-mg/kg dose was of the same order of magnitude as the therapeutic dose in humans, which is 900-1800 mg (13-26 mg/kg) in divided doses (6). The plasma levels of valpromide and valproic acid obtained in this study are presented in Fig. 2 (mean ± *SD* of three replicates). The curves presented in Fig. 2 were obtained after a computer fitting of the observed data using the NONLIN computer program (13). Valpromide was partly biotransformed to valproic acid, and the plasma levels of these two compounds were assayed by the proposed method throughout the duration of the 12-h study. The *CV* among the three replicates of each data point of valproic acid and valpromide was <10%. As in previous studies of valpromide, plasma levels of valpromide and valproic acid were

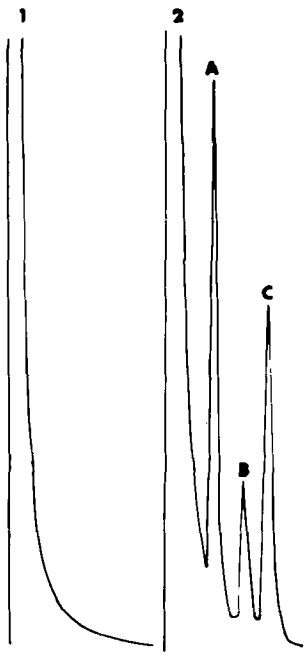

Figure 1—*Typical chromatograms of a human plasma blank (1) and valproic acid and valpromide in human plasma (2). Key: (A) valproic acid, 30 μg/mL; (B) IS, 10 μg/mL; (C) valpromide, 30 μg/mL.*

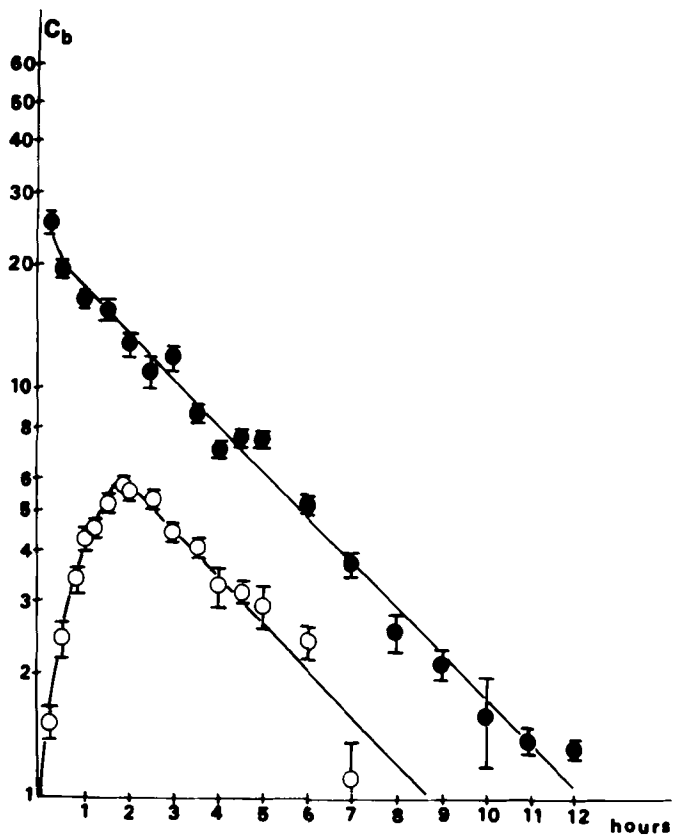

Figure 2—*Plasma levels of valpromide (●) and valproic acid (○) obtained after intravenous administration of 400 mg of valpromide to a dog.* C_b *is expressed in μg/mL.*

Table II—Precision of the Assay for Valproic Acid and Valpromide in Human Plasma

Conc., μg/mL	Valproic Acid: Conc. Found[a], μg/mL	Valproic Acid: SD	Valproic Acid: CV, %	Valpromide: Conc. Found[a], μg/mL	Valpromide: SD	Valpromide: CV, %
20	20.30	1.86	9.18	19.53	0.91	4.66
30	30.52	1.71	4.21	31.76	3.00	9.45
40	41.88	3.24	7.74	41.50	2.80	6.75
50	49.84	3.97	7.96	49.08	3.95	8.00
60	57.84	4.75	8.21	62.5	5.12	8.19

[a] Mean of 10 determinations.

assayed separately by two different systems (2, 4). The proposed method is very useful and advantageous in any pharmacokinetic or metabolic study of valpromide.

REFERENCES

(1) F. Pisani, A. Fazio, G. Oteri, and R. Di Perri, *Ther. Drug. Monit.*, **3**, 297 (1981).

(2) F. Pisani, A. Fazio, G. Oteri, and R. Di Perri, *J. Pharm. Pharmacol.*, **34**, 45 (1982).

(3) P. Favel, J. Cartier, J. P. Gratadou, and G. Gratadou, *Epilepsia*, **14**, 329 (1973).

(4) F. Pisani and R. Di Perri, *Ital. J. Neurol. Sci.*, **4**, 245 (1980).

(5) F. Pisani, A. A. D'Agostino, A. Fazio, G. Oteri, G. Primerano, and R. Di Perri, *Epilepsia*, **23**, 115 (1982).

(6) "Martindale, The Extra Pharmacopoeia," 27th ed. Pharmaceutical Press, London, 1977, p. 1752.

(7) R. M. Pinder, R. N. Brogden, T. M. Speight, and G. S. Avery, *Drugs*, **13**, 81 (1977).

(8) R. Gugler and E. von-Unruh, *Clin. Pharmacokinet.*, **5**, 67 (1980).

(9) A. Soufi, D. Colussi, and F. Marfil, *J. Chromatog.*, **182**, 241 (1980); and references cited therein.

(10) A. E. Hershey, J. R. Patton, and K. H. Dudley, *Ther. Drug. Monit.*, **1**, 217 (1979); and references cited therein.

(11) F. Pisani, R. Di Perri, and G. Nistico, *J. Chromatogr.*, **174**, 231 (1979).

(12) R. V. Smith and J. T. Stewart, "Textbook of Biopharmaceutic Analysis," Lea and Febiger, 1981, p. 79.

(13) C. M. Metzler, O. L. Elfind, and A. J. McEwen, "A User's Manual for NONLIN and Associated Program Research Biostatistics," The Upjohn Co., Kalamazoo, Mich., 1974.

ACKNOWLEDGMENTS

This work was supported by Grant Number 2127 from the Israel National Council for Research and Development, and is included in the dissertation project of Abraham Rubinstein, as a partial fulfilment of the Doctor of Philosophy degree requirements of the Hebrew University of Jerusalem.

The authors thank Miss Dana Lev for her skillful technical assistance.

Pharmacokinetics of Iohexol, a New Nonionic Radiocontrast Agent, in Humans

JEROME EDELSON ˣ, DAVID SHAW, and GERARD PALACE

Received Feburary 17, 1983, from *Sterling-Winthrop Research Institute, Rensselaer, NY 12144.* Accepted for publication May 20, 1983.

Abstract □ Sixteen healthy men received iohexol intravenously at a concentration of 346 mg of iodine/mL. Doses of 500, 750, 1000, and 1500 mg of iodine/kg of body weight were administered to four volunteers each. Neither clearance nor percent of dose excreted in the urine showed any significant correlation with size of the dose. The overall mean (±*SD*) renal and total body clearances were 120 ± 18.6 and 131 ± 18.6 mL/min, respectively. The overall mean apparent volume of distribution was 165 (±30.7) mL/kg. Urine contained 92.3 ± 4.4% of the dose. Most of the drug (89.9%) was excreted within the first 12 h. An open three-compartment body model gave the best fit to the experimental data. The mean apparent first-order terminal elimination (γ-phase) half-life was 12.6 h.

Keyphrases □ Iohexol—pharmacokinetics, intravenous administration, humans □ Pharmacokinetics—iohexol intravenous administration, humans □ Radiocontrast agents—iohexol, plasma and urine levels, intravenous administration, pharmacokinetics, humans

Ionic contrast media that are approved for human use are hyperosmolar to plasma. Administration of the large volumes necessary for visualization can result in large detrimental fluid shifts within the body. Prior to conducting intensive clinical trials with a new contrast medium, the route and rate of excretion must be adequately assessed. Previous studies with ionic contrast media have suggested that excretion occurs almost exclusively *via* the kidney at a rate that is consistent with passive handling by glomerular filtration (1).

Iohexol[1], 5-[acetyl(2,3-dihydroxypropyl)-amino]-*N*,*N*′-bis(2,3-dihydroxypropyl)-2,4,6-triiodo-1,3-benzenedicarboxamide, is a new nonionic radiographic contrast agent which is intended for vascular and intrathecal use in humans. The biological properties of iohexol (2) are similar to those of metrizamide, the first nonionic contrast medium approved for clinical use (3). A significant advantage of iohexol is its stability in solution to terminal heat sterilization, and its preparation as a ready-to-use solution.

This report describes the results of our investigations into the excretion of iohexol, and includes a nonlinear least-squares estimate of the pharmacokinetic parameters of iohexol following intravenous administration.

EXPERIMENTAL SECTION

Study in Human Volunteers—Four groups of four healthy male volunteers, between the ages of 18 and 50 years, received iohexol intravenously at doses

[1] Omnipaque; Sterling Drug, New York, N.Y.

© 1984, American Pharmaceutical Association

Table II—Precision of the Assay for Valproic Acid and Valpromide in Human Plasma

Conc., μg/mL	Valproic Acid: Conc. Found[a], μg/mL	Valproic Acid: SD	Valproic Acid: CV, %	Valpromide: Conc. Found[a], μg/mL	Valpromide: SD	Valpromide: CV, %
20	20.30	1.86	9.18	19.53	0.91	4.66
30	30.52	1.71	4.21	31.76	3.00	9.45
40	41.88	3.24	7.74	41.50	2.80	6.75
50	49.84	3.97	7.96	49.08	3.95	8.00
60	57.84	4.75	8.21	62.5	5.12	8.19

[a] Mean of 10 determinations.

assayed separately by two different systems (2, 4). The proposed method is very useful and advantageous in any pharmacokinetic or metabolic study of valpromide.

REFERENCES

(1) F. Pisani, A. Fazio, G. Oteri, and R. Di Perri, *Ther. Drug. Monit.*, **3**, 297 (1981).

(2) F. Pisani, A. Fazio, G. Oteri, and R. Di Perri, *J. Pharm. Pharmacol.*, **34**, 45 (1982).

(3) P. Favel, J. Cartier, J. P. Gratadou, and G. Gratadou, *Epilepsia*, **14**, 329 (1973).

(4) F. Pisani and R. Di Perri, *Ital. J. Neurol. Sci.*, **4**, 245 (1980).

(5) F. Pisani, A. A. D'Agostino, A. Fazio, G. Oteri, G. Primerano, and R. Di Perri, *Epilepsia*, **23**, 115 (1982).

(6) "Martindale, The Extra Pharmacopoeia," 27th ed. Pharmaceutical Press, London, 1977, p. 1752.

(7) R. M. Pinder, R. N. Brogden, T. M. Speight, and G. S. Avery, *Drugs*, **13**, 81 (1977).

(8) R. Gugler and E. von-Unruh, *Clin. Pharmacokinet.*, **5**, 67 (1980).

(9) A. Soufi, D. Colussi, and F. Marfil, *J. Chromatog.*, **182**, 241 (1980); and references cited therein.

(10) A. E. Hershey, J. R. Patton, and K. H. Dudley, *Ther. Drug. Monit.*, **1**, 217 (1979); and references cited therein.

(11) F. Pisani, R. Di Perri, and G. Nistico, *J. Chromatogr.*, **174**, 231 (1979).

(12) R. V. Smith and J. T. Stewart, "Textbook of Biopharmaceutic Analysis," Lea and Febiger, 1981, p. 79.

(13) C. M. Metzler, O. L. Elfind, and A. J. McEwen, "A User's Manual for NONLIN and Associated Program Research Biostatistics," The Upjohn Co., Kalamazoo, Mich., 1974.

ACKNOWLEDGMENTS

This work was supported by Grant Number 2127 from the Israel National Council for Research and Development, and is included in the dissertation project of Abraham Rubinstein, as a partial fulfilment of the Doctor of Philosophy degree requirements of the Hebrew University of Jerusalem.

The authors thank Miss Dana Lev for her skillful technical assistance.

Pharmacokinetics of Iohexol, a New Nonionic Radiocontrast Agent, in Humans

JEROME EDELSON ˣ, DAVID SHAW, and GERARD PALACE

Received Feburary 17, 1983, from *Sterling-Winthrop Research Institute, Rensselaer, NY 12144.* Accepted for publication May 20, 1983.

Abstract □ Sixteen healthy men received iohexol intravenously at a concentration of 346 mg of iodine/mL. Doses of 500, 750, 1000, and 1500 mg of iodine/kg of body weight were administered to four volunteers each. Neither clearance nor percent of dose excreted in the urine showed any significant correlation with size of the dose. The overall mean (±*SD*) renal and total body clearances were 120 ± 18.6 and 131 ± 18.6 mL/min, respectively. The overall mean apparent volume of distribution was 165 (±30.7) mL/kg. Urine contained 92.3 ± 4.4% of the dose. Most of the drug (89.9%) was excreted within the first 12 h. An open three-compartment body model gave the best fit to the experimental data. The mean apparent first-order terminal elimination (γ-phase) half-life was 12.6 h.

Keyphrases □ Iohexol—pharmacokinetics, intravenous administration, humans □ Pharmacokinetics—iohexol intravenous administration, humans □ Radiocontrast agents—iohexol, plasma and urine levels, intravenous administration, pharmacokinetics, humans

Ionic contrast media that are approved for human use are hyperosmolar to plasma. Administration of the large volumes necessary for visualization can result in large detrimental fluid shifts within the body. Prior to conducting intensive clinical trials with a new contrast medium, the route and rate of excretion must be adequately assessed. Previous studies with ionic contrast media have suggested that excretion occurs almost exclusively *via* the kidney at a rate that is consistent with passive handling by glomerular filtration (1).

Iohexol[1], 5-[acetyl(2,3-dihydroxypropyl)-amino]-*N*,*N*′-bis(2,3-dihydroxypropyl)-2,4,6-triiodo-1,3-benzenedicarboxamide, is a new nonionic radiographic contrast agent which is intended for vascular and intrathecal use in humans. The biological properties of iohexol (2) are similar to those of metrizamide, the first nonionic contrast medium approved for clinical use (3). A significant advantage of iohexol is its stability in solution to terminal heat sterilization, and its preparation as a ready-to-use solution.

This report describes the results of our investigations into the excretion of iohexol, and includes a nonlinear least-squares estimate of the pharmacokinetic parameters of iohexol following intravenous administration.

EXPERIMENTAL SECTION

Study in Human Volunteers—Four groups of four healthy male volunteers, between the ages of 18 and 50 years, received iohexol intravenously at doses

[1] Omnipaque; Sterling Drug, New York, N.Y.

© 1984, American Pharmaceutical Association

Table I—Pharmacokinetic Parameters in Volunteers Receiving Intravenous Iohexol

Subject	Regression-Dependent Parameters						Model-Independent Parameters		
	α, h^{-1}	β, h^{-1}	γ, h^{-1}	A, $\mu g/mL$	B, $\mu g/mL$	C, $\mu g/mL$	Volume of Distribution, mL/kg	AUC_0^{96}, $\mu g \cdot h/mL$	Renal Clearance, mL/min	Total Body Clearance, mL/min
					500 mg of Iodine/kg					
1	1.60	0.271	0.060	5190	2130	25.1	146	12,000	97.1	111
2	1.64	0.291	0.093	4800	2410	41.6	147	12,200	86.0	110
3	2.79	0.431	0.139	3570	2590	80.8	171	8,150	112	128
4	2.99	0.412	0.145	5810	3220	166	116	11,500	113	134
Mean ± *SD*	2.26 ± 0.738	0.351 ± 0.08	0.109 ± 0.048	4840 ± 945	2590 ± 462	78.4 ± 62.9	145 ± 22.5	11,000 ± 1900	102 ± 12.9	121 ± 12.1
					750 mg of Iodine/kg					
5	0.946	0.258	0.006	8400	1440	1.74	162	14,800	125	142
6	4.60	0.437	0.048	9690	5010	18.3	108	14,900	162	163
7	1.35	0.309	0.026	5680	2490	6.18	196	13,100	116	141
8	2.69	0.363	0.035	7300	4430	13.6	136	16,400	98.6	97.7
Mean ± *SD*	2.40 ± 1.65	0.342 ± 0.08	0.029 ± 0.018	7770 ± 1700	3340 ± 1660	9.96 ± 7.41	151 ± 37.5	14,800 ± 1350	125 ± 26.7	136 ± 27.4
					1000 mg of Iodine/kg					
9	1.49	0.340	0.051	9390	2990	18.1	172	16,100	127	133
10	1.75	0.345	0.061	7980	4440	21.1	172	18,800	145	165
11	1.22	0.297	0.030	5980	3770	11.3	219	18,900	129	141
12	1.55	0.339	0.030	10200	3790	8.68	152	18,900	108	111
Mean ± *SD*	1.50 ± 0.219	0.330 ± 0.02	0.043 ± 0.016	8390 ± 1850	3750 ± 593	14.8 ± 5.78	179 ± 28.4	18,200 ± 1380	127 ± 15.2	138 ± 22.3
					1500 mg of Iodine/kg					
13	1.56	0.303	0.039	11600	6200	20.4	179	29,900	116	115
14	1.32	0.324	0.031	12100	5770	8.45	179	28,400	130	130
15	2.64	0.351	0.081	9910	8950	62.0	169	31,800	131	130
16	0.632	0.224	0.006	13600	1330	1.36	214	25,600	119	138
Mean ± *SD*	1.54 ± 0.833	0.301 ± 0.06	0.039 ± 0.031	11,800 ± 1520	5560 ± 3150	23.1 ± 27.1	185 ± 19.7	28,900 ± 2620	124 ± 7.62	128 ± 9.60
Overall Mean ± *SD*	1.92 ± 0.988	0.331 ± 0.06	0.055 ± 0.041				165 ± 30.7		120 ± 18.6	131 ± 18.6

of 500, 750, 1000, and 1500 mg of iodine/kg. Iohexol was administered at a concentration of 346 mg of iodine/mL of solution at a temperature of 37°C. The injection was made into an antecubital vein at a rate that delivered the total dose in 3 min. Time zero ($t = 0$) is defined as the time at which the injection was completed. Blood samples were drawn from the contralateral antecubital vein. Plasma and urine samples were collected at appropriate intervals and stored frozen until analyzed.

Table II—Urinary Recovery of Intact Iohexol in Humans

Subject	Administered Dose, mg[a]	Iohexol Excreted in Urine (0–96 h), mg	Dose Excreted (0–96 h), %
	500 mg of Iodine/kg		
1	79,800	70,000	87.6
2	80,600	63,900	79.3
3	62,700	54,700	87.2
4	92,500	83,700	90.6
Mean ± *SD*			86.2 ± 4.83
	750 mg of Iodine/kg		
5	126,000	111,000	87.7
6	146,000	145,000	99.4
7	111,000	95,400	85.8
8	96,300	97,400	101.0
Mean ± *SD*			93.5 ± 7.83
	1000 mg of Iodine/kg		
9	129,000	123,000	94.8
10	186,000	163,000	87.9
11	160,000	146,000	91.3
12	126,000	122,000	96.9
Mean ± *SD*			92.7 ± 3.96
	1,500 mg of Iodine/kg		
13	206,000	207,000	101
14	221,000	221,000	100
15	248,000	250,000	100
16	212,000	183,000	86.1
Mean ± *SD*			96.8 ± 7.13
Overall Dose Excreted, %			92.3 ± 4.44

[a] Expressed as iohexol.

Appropriate institutional review and approval were obtained. No subject had a clinical history or laboratory findings that were suggestive of renal or hepatic dysfunction.

Assay Procedure—The analysis of plasma and urine for iohexol concentration was dependent on separation by HPLC. The mobile phase was a mixture of 0.01 M phosphate buffer, pH 7.4, and methanol; the column was a 5-μm Spherisorb ODS[2] column, 25 cm × 4.6 mm i.d. The UV detector was set at 254 nm. Details of the HPLC procedure will be reported elsewhere (4). Plasma and urine standards, which were prepared in normal human biological fluids, were processed and anlayzed with each set of samples from the subjects in the study. The concentrations of iohexol were determined by inverse prediction (5), using the linear regression of the peak height ratios of the standards. The minimum quantifiable level of iohexol was estimated as the concentration whose lower 80% confidence limit just encompassed zero (6).

Pharmacokinetic Calculations—The data obtained from the analysis of the plasma samples was described by an open three-compartment body model by means of a weighted nonlinear regression (NLIN) procedure using the Marquardt algorithm (7); the weighting factor was the reciprocal of the square of the concentration. The model was defined with the following equation:

$$C_p = Ae^{-\alpha t} + Be^{-\beta t} + Ce^{-\gamma t}$$

where C_p is the plasma concentration; A, B, and C are constants; and α, β, and γ are the hybrid rate constants for the three-compartment model.

In addition to the regression-dependent parameters, the plasma concentration data were used to calculate the area under the plasma concentration *versus* time curve during the 96-h study period (AUC_0^{96}). Both total body clearance and renal clearance were estimated by dividing the dose administered and the amount of drug excreted into the urine during 96 h, respectively, by the AUC_0^{96}.

RESULTS AND DISCUSSION

The concentrations of iohexol in the plasma samples from each of the volunteers were determined. After intravenous administration, the plasma concentrations declined triexponentially with time, suggesting that a three-compartment body model would be appropriate. Pharamacokinetic parameters were estimated for each subject after computer-fitting of the plasma data by

[2] Excalibar, Applied Science, State College, Pa.

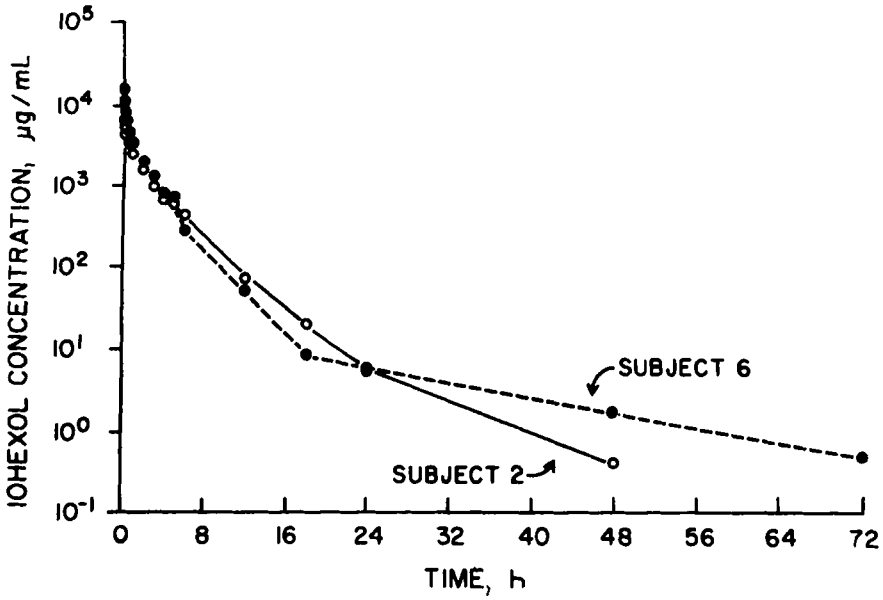

Figure 1—*Plasma concentration of iohexol in human volunteers after intravenous administration. Plasma concentrations were observed in subject 2 (○), and in subject 6 (●), with widely divergent renal clearance rates and concentrations predicted by the open three-compartment body model (lines).*

an iterative nonlinear least-squares regression technique (7). Despite the threefold range in both the total dose administered and the infusion rate, the same model was fitted to the plasma concentration data of each subject, with satisfactory results (Table I).

The mean apparent first-order terminal (γ-phase) elimination half-life for iohexol was ~12.6 h. The mean value for α, 1.92 h^{-1}, corresponds to a half-life of 22 min; the mean value for β, 0.331 h^{-1}, corresponds to a half-life of 2.1 h. The mean ($\pm SD$) apparent volume of distribution was 165 (±30.7) mL/kg of body weight. This value suggests that iohexol distributes into extracellular water.

The AUC during the 96-h study period was estimated by the trapezoidal method (Table I); linear regression analysis indicated a good correlation between the amount of drug injected and the AUC_0^{96} ($r = 0.94$; $p < 0.001$).

From the amount of drug excreted into the urine and the regression-independent AUC, the renal clearances were calculated (Table I). Although there is almost a twofold difference between the highest (subject 6) and lowest (subject 2) renal clearances, the observed concentration data were adequately described by the open three-compartment body model for both of these subjects. A comparison of the observed and predicted concentrations is shown in Fig. 1; the agreement between the observed values and those predicted by the pharmacokinetic model is apparent.

The urinary excretion of intact iohexol is summarized in Table II. The overall mean ($\pm SD$) percent of dose excreted into urine was 92.3 ± 4.4%; the recovery was not significantly different across doses ($p < 0.158$). Most of the drug was excreted into the urine within the first 12 h[3] with a mean of 89.9 ± 7.0%. As can be determined from the clearances presented in Table I, renal clearance accounts for 95% of the total body clearance; obviously, iohexol is not metabolized appreciably.

Iohexol was well tolerated in these subjects, in doses up to 1500 mg of iodine/kg of body weight. No drug-related adverse reactions were reported, although, in a few cases, a sensation of heat was recorded following injection of iohexol.

[3] Unpublished results.

REFERENCES

(1) E. W. McChesney, in "Radiocontrast Agents," Vol. 1, P. K. Knoefel, Ed., Pergamon, Oxford, 1971, p. 147.

(2) E. Lindgren (Ed.), "Iohexol," Acta Radiologica, Supplementum 362, Almqvist and Wiksell, Uppsala, Sweden, 1980.

(3) E. Lindgren (Ed.), "Metrizamide-Amipaque," Acta Radiologica, Supplementum 355, Almqvist and Wiksell, Uppsala, Sweden, 1977.

(4) J. Edelson, G. Palace, and G. Park, *J. Chromatogr.*, **274**, 428 (1983).

(5) R. R. Sokal and F. J. Rohlf, "Biometry," W. H. Freeman, San Francisco, Calif., 1969.

(6) R. W. Ross and H. Stander, "Some Statistical Problems in Drug Metabolism," Princeton Conference on Applied Statistics, December, 1975.

(7) J. T. Helwig and K. A. Council (Eds.), "SAS User's Guide," SAS Institute, Raleigh, N.C., 1979, pp. 317-329.

ACKNOWLEDGMENTS

The authors are grateful to the staff of the Quincy Research Center, Kansas City, Mo., for providing the plasma and urine samples.

High-Performance Liquid Chromatographic Assay for *N*-Acetylcysteine in Plasma and Urine

P. A. LEWIS ˣ, A. J. WOODWARD, and J. MADDOCK

Received February 22, 1983, from *Simbec Research Ltd, Merthyr Tydfil Industrial Park, Merthyr Tydfil, Mid Glamorgan, Wales, U.K.* Accepted for publication July 29, 1983.

Abstract □ A sensitive high-performance liquid chromatographic (HPLC) assay for *N*-acetylcysteine in human plasma and urine has been developed. The method employs a prechromatographic stage to produce the dinitrophenyl derivative of *N*-acetylcysteine, which is chromatographed on a 5-μm C_{18} bonded reverse-phase column using an external standard method. The derivatized *N*-acetylcysteine molecule has a retention time of ≃13 min at a flow rate of 1.0 mL/min for a mobile phase of methanol–aqueous 0.05 M citrate–0.001 M EDTA buffer pH 7.0 (30:70). In a multistep extraction procedure, which is slightly modified for the *N*-acetylcysteine assay in urine, the limits of sensitivity for the plasma and urine assays were found to be ≃60 ng/mL and ≃200 μg/mL, respectively. Preliminary data from pilot studies in human subjects are presented.

Keyphrases □ *N*-Acetylcysteine—HPLC, plasma and urine □ HPLC-*N*-acetylcysteine, plasma and urine

N-Acetylcysteine, when administered intravenously, has been shown to be effective as an antidote for the treatment of acetaminophen poisoning, giving protection against liver damage (1), and to influence the consistency and volume of sputum when administered orally to patients with chronic obstructive bronchitis (2). A further potential use of *N*-acetylcysteine is the inhibition of cyclophosphamide-induced bladder toxicity in rodents without adversely affecting the beneficial immunosuppressive action of cyclophosphamide (3).

Pharmacokinetic studies with *N*-acetylcysteine are confined to studies (4) employing material labeled with sulfur-35 which measured total radioactivity. Studies with unlabeled *N*-acetylcysteine have been hampered by the lack of a suitable analytical procedure to determine the compound in plasma and urine.

A GC procedure (5) has been reported but is unsuitable for determinations in plasma. A high-performance liquid chromatographic (HPLC) method for determining the compound in plasma ultrafiltrates has been published (6), but this method failed to detect *N*-acetylcysteine on every occasion and was unable to determine total plasma levels. *N*-Acetylcysteine has been determined (7) as *N*-(1-pyrene)maleimide and *N*-(7-dimethylamino-4-methyl-3-coumarinyl)maleimide derivatives, but the procedure can only be used for urinary measurements.

This paper describes a reliable and sensitive procedure for determining *N*-acetylcysteine in plasma and urine which is suitable for the study of the pharmacokinetics of the drug.

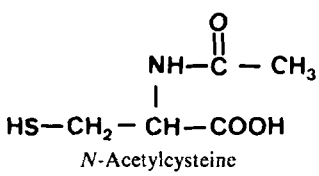

N-Acetylcysteine

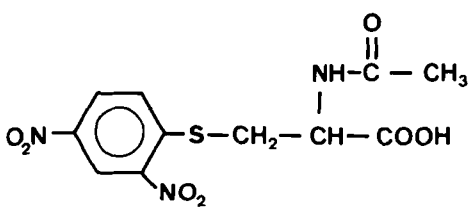

2,4-Dinitrophenyl Derivative

EXPERIMENTAL SECTION

Materials—Pure authentic *N*-acetylcysteine[1] was used as received without purification, as a standard. All chemicals used were of "Analar" [2] grade. All solvents used were of glass-distilled[3] or HPLC[3] grade. The ultrafiltration cones[4] used were of a membrane type.

Apparatus—The high-performance liquid chromatographic pump[5] was fitted with a loop injector[6] with a 50-μL loop and a variable-wavelength detector[7] set at 360 nm, attenuated at 0.02 AUFS for plasma and 0.5 AUFS for urine. The signal was recorded on a 10-mV recorder[8]. An "in-house" packed 25 cm × 0.46-mm i.d. column containing a reverse-phase (C_{18}) chemically bonded to 5-μm silica[9] was employed at ambient temperature.

Mobile Phase—The mobile phase was prepared by mixing an aqueous solution of 0.05 M trisodium citrate and 0.001 M EDTA, adjusted to pH 7.0 with a citric acid solution, with HPLC-grade methanol in a ratio of 70:30. (When performing the assay on urine samples, this solution may be modified by mixing the aqueous buffer with methanol in a 65:35 ratio.) This solution was filtered through a membrane filter[10] and deaerated by sonication in an ultrasonic bath[11]. Immediately prior to use the solution was purged with pure helium. The mobile phase was pumped isocratically through the column at ambient temperature with a flow rate of 1.0 mL/min, giving a back-pressure of ≃1000 psi.

Standard Solutions—Aqueous stock solutions of *N*-acetylcysteine were prepared daily and stored at 4°C. Plasma standard solution was prepared by dissolving authentic *N*-acetylcysteine in the mobile phase solution (25 mg/100 mL). Urine standard solution was prepared by dissolving authentic *N*-acetylcysteine in 2.0% sodium hydrogen carbonate solution (2.0 g/100 mL).

Plasma standards were produced by spiking 3.0-mL aliquots of fresh human plasma to give a range of calibrators with concentrations of *N*-acetylcysteine as follows: 0, 0.25, 0.50, 0.75, 1.0, 1.25, 1.50, 2.0, and 2.5 μg/mL. These standards were vortex-mixed for 30 s and then allowed to stand at ambient temperature for 15 min to equilibrate. Similarly, urine calibration standards were produced by spiking 100-μL aliquots of fresh human urine to give a range of concentrations of *N*-acetylcysteine as follows: 0, 0.25, 0.50, 0.75, 1.0, 1.25, and 1.50 mg/mL.

Each range of calibrators were taken through the appropriate complete extraction procedure as described below. In each instance, calibration curves were constructed by plotting the integrated peak area against the corresponding *N*-acetylcysteine standard concentration. Plasma and urine samples were similarly treated, and the measured peak areas (referred to the appropriate calibration curve) were used to determine the concentration of *N*-acetylcysteine present.

Chromatographic Method—Aliquots of plasma (3.0 mL) or urine (100 μL) diluted in 1 mL of glass-distilled water were pipetted into 10-mL polytef-lined screw-capped glass tubes. A 500-μL aliquot of 5-mg/mL dithiothreitol solution was added; the tubes were vortex-mixed for 10 sec, capped, and incu-

[1] Laboratories Bristol, France.
[2] BDH Ltd., Poole, Dorset, England.
[3] Rathburn Chemicals Ltd., Walkerburn, Peebleshire, Scotland.
[4] CF5OA Centriflo Cones; Amicon Ltd., Stonehouse, Gloucestershire, England.
[5] LDC Constametric III HPLC Pump; Milton Roy Corp., Fla.
[6] Rheodyne type 7125; Rheodyne Inc., Calif.
[7] LDC Spectromonitor III variable-wavelength detector; Milton Roy Corp., Fla.
[8] Rikadenki Mitsui Ltd., Machinery Sales, Chessington, Surrey, England.
[9] Hypersil ODS 5 μm, Shandon Ltd., Runcorn, Cheshire, England.
[10] Whatman PTFE Membrane Filters 0.5 μm; Whatman LabSales Ltd., Maidstone, Kent, England.
[11] Baird and Tatlock Ltd., Romford, Essex.

0022-3549/84/0700-0996$01.00/0
© 1984, American Pharmaceutical Association

Table I—Replicate Calibration Data for Plasma and Urinary *N*-Acetylcysteine by HPLC, Showing Linear Regression Analysis

Assay	Calibration Range	*n*	Slope	Intercept	*r*
Plasma	0.25–2.5 μg/mL	4	8.07	0.82	0.996
Urine	0.25–1.5 mg/mL	5	152.7	11.5	0.997

bated for 30 min at 37°C in a water bath. Following incubation 1.0 mL of 2% sodium hydrogen carbonate in water and 350 μL of 5.0% 2,4-dinitro-1-fluorobenzene in ethanol, which had been recrystallized from ether, was added to all tubes. The tubes were vortex-mixed for 10 s and incubated for 30 min at 60°C in a water bath.

The contents of each tube were then transferred to the membrane centrifuge cones, conditioned before use by immersion in double-glass-distilled water for 60 min and centrifuging for 5 min at 1000×*g* to remove excess water. The samples in the ultrafiltration cones were placed in labeled 20-mL glass vials and centrifuged at 1000×*g* for 20 min at 20°C. Aliquots (1.0 mL) of the ultrafiltrates were transferred to 25-mL extraction tubes, and 5 mL of water was added. The ultrafiltration step was omitted for the urine sample assays. Ether (10 mL) was added to all tubes, which were then capped and shaken mechanically[12] at 250 cpm for 5 min in the dark. Following centrifugation at 1000×*g* for 5 min at 10°C, the ether layers were transferred to clean glass vials and the solvent was evaporated to dryness under a gentle stream of nitrogen at room temperature. The dried residues were stored in capped vials at −20°C until just prior to chromatography, when the plasma and urine residues were reconstituted with 75 μL and 1.0 mL of mobile phase, respectively.

RESULTS AND DISCUSSION

The chromatographic conditions described were implemented in order to provide the best compromise between chromatographic resolution and peak symmetry and relatively short retention times, permitting the analysis of a large number of samples with good accuracy and precision. Under these HPLC conditions, the *N*-acetylcysteine derivative gives a retention time of ≃13 min, with a run time between injections of 20 min.

Figures 1 and 2 illustrate typical plasma and urine chromatograms, respectively, of spiked material, drug-free control material, and of material following dosing of the compound. Standard calibration lines were constructed by plotting the peak areas of *N*-acetylcysteine against the concentration of the compound in spiked standards. Typical calibration curve data is presented in Table I, showing linearity over the ranges employed with coefficients of variation of 12.6% at 0.25 mg/mL and 3.8% at 1.5 mg/mL for the urinary range and 11.9% at 0.25 μg/mL and 9.7% at 2.5 μg/mL for the plasma calibrations. These data show good precision despite the lack of an internal standard. A number of candidate substances were investigated for suitability as an internal standard, but none were acceptable for a variety of reasons.

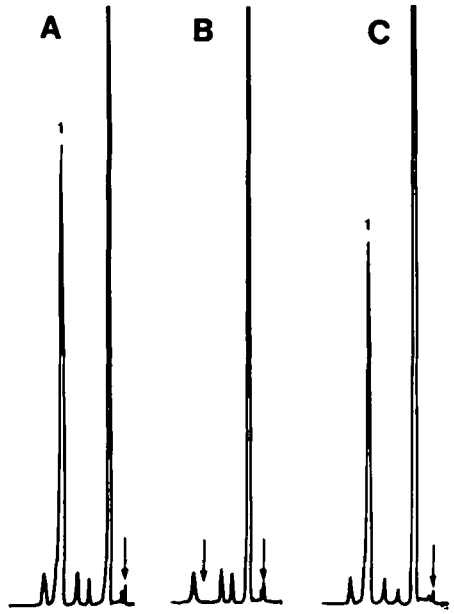

Figure 1—*Typical chromatograms of* N-*acetylcysteine in human plasma. Key: (A) a spiked plasma extract containing 2.0 μg/mL of* N-*acetylcysteine (1); (B) a drug-free control plasma extract; (C) a plasma extract from a subject receiving oral* N-*acetylcysteine.*

[12] Braun Lab-Shaker LSL; FT Scientific Ltd., Tewkesbury, England.

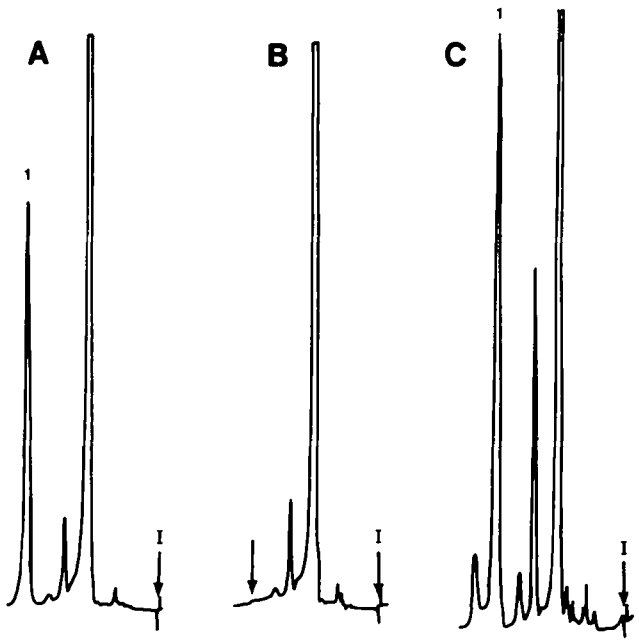

Figure 2—*Typical chromatograms of* N-*acetylcysteine in human urine. Key: (A) a spiked urine extract containing 1.5 mg/mL of* N-*acetylcysteine (1); (B) a control drug-free urine extract; (C) a test urinary collection 4–6 h following intravenous administration of* N-*acetylcysteine.*

Within- and between-batch data showed generally very favorable reproducibility. Ten replicate plasma controls each at 0.4, 1.1 and 1.9 μg/mL assayed the same day gave mean values of 0.43 ± 0.07 (*SD*), 0.99 ± 0.06 (*SD*), and 1.95 ± 0.22 (*SD*) μg/mL, respectively. Between-batch reproducibility ranged from 0.6 to 17.3% (mean 7.9%) for a series of seven control samples; however, occasional outliers were encountered, *e.g.*, a control spiked at 0.83 μg/mL gave a result of 1.15 μg/mL, a 38% error. Investigations of the stability of *N*-acetylcysteine in plasma on storage at −20°C lend further evidence of good overall reproducibility for the procedure. Plasma from a subject in receipt of a 1.0-g iv dose of *N*-acetylcysteine was assayed freshly and at 4, 5, 6, and 11 d of storage at −20°C. Samples withdrawn at 0.5, 1, 1.5, and 2.0 h postdose gave concentrations of 58.9, 25.0, 15.4, and 12.0 μg/mL when analyzed freshly, and the levels did not deteriorate on storage, giving *SD* values of 2.41, 2.48, 1.46, and 1.52, respectively, over the period.

Levels as low as 50 ng/mL can be seen over a baseline signal-to-noise ratio of 2.1. Although accurate detection limits have not been determined, sensitivity for the plasma and urine levels encountered were not a problem.

The measurement of free levels of *N*-acetylcysteine in plasma was investigated by omitting the dithiothreitol stage in order to produce ultrafiltrates containing free, unbound compound. Following derivatization and HPLC, no discernible free levels could be detected, even after oral doses of 800 mg of *N*-acetylcysteine. These data call into question that published by other workers who have reported free *N*-acetylcysteine in plasma. Our investigations demonstrate that a reduction employing dithiothreitol is essential to release *N*-acetylcysteine from binding sites on protein and to release the compound from disulfides, *e.g.*, bis-*N*-acetylcysteine. There is evidence to suggest that the latter is present, since our investigation of urinary *N*-acetylcysteine levels shows that very much lower levels of the compound are found when omitting the dithiothreitol stage. An ultrafiltration stage is incorporated in the plasma assay to remove excess 2,4-dinitro-1-fluorobenzene, which binds to plasma proteins and interferes with the chromatography.

The procedure described herein is being used to investigate the pharmacokinetics of *N*-acetylcysteine in adult healthy human subjects in receipt of intravenous and oral dosage forms. Preliminary data indicate that a rapid, specific, and precise procedure for determining *N*-acetylcysteine in biological fluids has been developed.

REFERENCES

(1) L. F. Prescott, R. N. Illingworth, J. A. J. H. Critchley, M. J. Stewart, R. D. Adam, and A. T. Proudfoot, *Br. Med. J.*, **2**, 1097 (1979).

(2) M. Aylward, J. Maddock, and P. M. Dewland, *Eur. J. Respir. Dis.*, **61** (Suppl. III), 81 (1980).

(3) L. Levy and R. Harris, *Biochem. Pharmacol.*, **26**, 1015 (1977).
(4) D. Rodenstein, A. DeCoster, and A. Gazzaniga, *Clin. Pharmacokinet.*, **3**, 247 (1978).
(5) H. Hannestad and B. Surba, *Clin. Chim. Acta*, **95**, 189 (1979).
(6) J. Maddock, *Eur. J. Respir. Dis.*, **61**, 52 (1980).
(7) B. Kagedal and M. Kallberg, *J. Chromatogr.*, **229**, 409 (1982).

ACKNOWLEDGMENTS

The authors thank Dr. M. Aylward and his Clinical Staff for their help in the recruiting and dosing of the human volunteers, Mr. P. Ho for his technical assistance, and Miss A. Jones and Miss D. A. Protheroe for their secretarial assistance.

Comparative Aspirin Absorption Kinetics after Administration of Sodium- and Potassium-Containing Buffered Solutions

WILLIAM D. MASON

Received March 28, 1983, from the *Pharmacokinetics Laboratory, University of Missouri-Kansas City, Schools of Pharmacy & Medicine, Kansas City, MO 64108.* Accepted for publication June 29, 1983.

Abstract □ Twelve fasting normal volunteers received three aspirin dosage forms in a single 325-mg dose in a complete crossover study; the plasma aspirin and salicylic acid levels and the urine salicylic acid and salicyluric acid levels were measured over 10 h. The three dosage forms included an unbuffered tablet and two effervescent solutions, one with sodium bicarbonate-citrate buffer and the other with potassium bicarbonate-citrate buffer. A significantly faster absorption rate was observed with the sodium bicarbonate-citrate buffer, when compared with the potassium bicarbonate-citrate buffer and the unbuffered tablets, which were equivalent. These differences were attributed primarily to gastric emptying rate differences. Urine pH and salicylate renal clearance were significantly affected by the single dose of antacid buffer. The area under the curve and urine accumulation comparisons suggested that ~25% more aspirin reaches the general circulation intact after administration of the unbuffered tablet than the two solutions, but that the total salicylate absorbed is equivalent for all three dosage forms. This difference in aspirin bioavailability is probably due to the fact that the two buffered solutions are predominantly absorbed through the intestine, in which presystemic hydrolysis occurs, whereas a significant portion of the tablet dose is absorbed through the gastric mucosa.

Keyphrases □ Aspirin—absorption kinetics after administration of sodium- and potassium-containing buffered solutions □ Salicylic acid—absorption kinetics after administration of sodium- and potassium-containing buffered solutions □ Absorption kinetics—aspirin after administration of sodium- and potassium-containing buffered solutions

Aspirin is the drug of choice when a mild analgesic-antipyretic effect is required. It is also a primary agent used in the chronic management of rheumatoid arthritis and osteoarthritis. After oral administration for pain, rapid absorption is desirable to provide the rapid onset of effects and to reduce contact time with the gastric mucosa. The potential influence of potassium ion *versus* sodium ion on the absorption kinetics of aspirin from two different effervescent solutions is the subject of this report.

BACKGROUND

A recent report (1) from this laboratory compared the absorption kinetics of aspirin from three commercially available dosage forms. Two of the dosage forms were extemporaneously prepared effervescent solutions containing either 1.825 or 3.808 g of sodium bicarbonate as a component of the buffer. It was concluded that a primary mechanism for the more rapid absorption of the solutions than the unbuffered tablet was more rapid gastric emptying. Also, the lower area under the aspirin curve for the solutions was attributed to a greater portion of the aspirin being absorbed through the intestine (*i.e.*, rather than through the stomach wall) and thus being subjected to a greater presystemic hydrolysis.

Patients on sodium-restricted diets may wish to take aspirin as a buffered effervescent solution. Absorption kinetics of the commercially available buffered effervescent solution was compared with that of a solution in which the sodium was replaced with potassium. A commercially available unbuffered tablet was also studied for comparison.

EXPERIMENTAL SECTION

Dosage Forms—Three dosage forms were used to provide equal doses of aspirin: a plain tablet containing 325 mg of aspirin[1]; an effervescent tablet containing 324 mg of aspirin, 1,904 g of sodium bicarbonate, and 1 g of citric acid[2]; and a prepared effervescent tablet containing 324 mg of aspirin, 2.26 g of potassium bicarbonate, and 1 g of citric acid.

Subjects—Twelve healthy volunteers (eight males and four females; ages 21–37 years; weight, 53.6–94.5 kg) were evaluated by a comprehensive physical examination, blood chemistry profile (including blood count and differential), and complete urinalysis. None of the subjects had a history of gastrointestinal disease or surgery. All subjects were free of any active disease process, and none had used any medication for 14 d before the study.

Method—A Latin-square design for three treatments in 12 subjects was employed. A 10-h fast preceded dosing and continued for 4 h postdose. At ~7 a.m., predose urine and blood samples were obtained, and a single dose of aspirin with 240 mL of water was administered. The effervescent tablets were dissolved in 140 mL of water 3 min before dosing and the mixture was then swallowed. The glass was rinsed with 100 mL of water, which also was swallowed. After dosing, 100 mL of water was administered at 1, 2, and 3 h, and a uniform meal was served after the 4-h sample was obtained, after which water was allowed *ad libitum*. Subjects remained standing or sitting through the day, and exercise was limited to walking about the room.

Blood was drawn into chilled vacuum containers[3] *via* an indwelling catheter at 5, 10, 15, 20, 30, and 45 min and 1, 1.5, 2, 3, 4, 6, 8, and 10 h. Plasma was separated by centrifugation at 1764×*g* at 4°C within 20 min of collection. All urine was collected at 2-h intervals over 10 h, the pH and volume were measured, and an acidified aliquot was saved for analysis. All samples were frozen at −30°C and assayed within 2 weeks of collection by the HPLC method described previously (2).

RESULTS

As shown in Tables I and II, both plasma aspirin and salicylic acid levels rise more rapidly after administration of the solution with sodium than the potassium solution or the tablet. This rank order and profile reflect the values for 11 of the 12 subjects and is statistically significant ($p < 0.05$). Plasma aspirin levels rise rapidly to a mean peak of 7.20 μg/mL at 17.5 min with the single 324-mg dose in a sodium-containing effervescent solution, whereas the potassium-substituted solution reaches only 5.26 μg/mL at 30.4 min, which is not significantly higher ($p < 0.05$) than for the tablet. The ultimate exposure

[1] Bayer Aspirin; Glenbrook Laboratories -Division of Sterling Drug Inc., New York.
[2] Alka-Seltzer; Miles Laboratories, Inc., Elkhart, Ind.
[3] Vacutainer BD, 278-069, 7.0 mL, containing 14 mg of potassium oxalate and 17.5 mg of sodium fluoride.

0022-3549/84/0700-0998$01.00/0
© 1984, American Pharmaceutical Association

(3) L. Levy and R. Harris, *Biochem. Pharmacol.*, **26**, 1015 (1977).
(4) D. Rodenstein, A. DeCoster, and A. Gazzaniga, *Clin. Pharmacokinet.*, **3**, 247 (1978).
(5) H. Hannestad and B. Surba, *Clin. Chim. Acta*, **95**, 189 (1979).
(6) J. Maddock, *Eur. J. Respir. Dis.*, **61**, 52 (1980).
(7) B. Kagedal and M. Kallberg, *J. Chromatogr.*, **229**, 409 (1982).

ACKNOWLEDGMENTS

The authors thank Dr. M. Aylward and his Clinical Staff for their help in the recruiting and dosing of the human volunteers, Mr. P. Ho for his technical assistance, and Miss A. Jones and Miss D. A. Protheroe for their secretarial assistance.

Comparative Aspirin Absorption Kinetics after Administration of Sodium- and Potassium-Containing Buffered Solutions

WILLIAM D. MASON

Received March 28, 1983, from the *Pharmacokinetics Laboratory, University of Missouri-Kansas City, Schools of Pharmacy & Medicine, Kansas City, MO 64108.* Accepted for publication June 29, 1983.

Abstract □ Twelve fasting normal volunteers received three aspirin dosage forms in a single 325-mg dose in a complete crossover study; the plasma aspirin and salicylic acid levels and the urine salicylic acid and salicyluric acid levels were measured over 10 h. The three dosage forms included an unbuffered tablet and two effervescent solutions, one with sodium bicarbonate-citrate buffer and the other with potassium bicarbonate-citrate buffer. A significantly faster absorption rate was observed with the sodium bicarbonate-citrate buffer, when compared with the potassium bicarbonate-citrate buffer and the unbuffered tablets, which were equivalent. These differences were attributed primarily to gastric emptying rate differences. Urine pH and salicylate renal clearance were significantly affected by the single dose of antacid buffer. The area under the curve and urine accumulation comparisons suggested that ~25% more aspirin reaches the general circulation intact after administration of the unbuffered tablet than the two solutions, but that the total salicylate absorbed is equivalent for all three dosage forms. This difference in aspirin bioavailability is probably due to the fact that the two buffered solutions are predominantly absorbed through the intestine, in which presystemic hydrolysis occurs, whereas a significant portion of the tablet dose is absorbed through the gastric mucosa.

Keyphrases □ Aspirin—absorption kinetics after administration of sodium- and potassium-containing buffered solutions □ Salicylic acid—absorption kinetics after administration of sodium- and potassium-containing buffered solutions □ Absorption kinetics—aspirin after administration of sodium- and potassium-containing buffered solutions

Aspirin is the drug of choice when a mild analgesic-antipyretic effect is required. It is also a primary agent used in the chronic management of rheumatoid arthritis and osteoarthritis. After oral administration for pain, rapid absorption is desirable to provide the rapid onset of effects and to reduce contact time with the gastric mucosa. The potential influence of potassium ion *versus* sodium ion on the absorption kinetics of aspirin from two different effervescent solutions is the subject of this report.

BACKGROUND

A recent report (1) from this laboratory compared the absorption kinetics of aspirin from three commercially available dosage forms. Two of the dosage forms were extemporaneously prepared effervescent solutions containing either 1.825 or 3.808 g of sodium bicarbonate as a component of the buffer. It was concluded that a primary mechanism for the more rapid absorption of the solutions than the unbuffered tablet was more rapid gastric emptying. Also, the lower area under the aspirin curve for the solutions was attributed to a greater portion of the aspirin being absorbed through the intestine (*i.e.*, rather than through the stomach wall) and thus being subjected to a greater presystemic hydrolysis.

Patients on sodium-restricted diets may wish to take aspirin as a buffered effervescent solution. Absorption kinetics of the commercially available buffered effervescent solution was compared with that of a solution in which the sodium was replaced with potassium. A commercially available unbuffered tablet was also studied for comparison.

EXPERIMENTAL SECTION

Dosage Forms—Three dosage forms were used to provide equal doses of aspirin: a plain tablet containing 325 mg of aspirin[1]; an effervescent tablet containing 324 mg of aspirin, 1,904 g of sodium bicarbonate, and 1 g of citric acid[2]; and a prepared effervescent tablet containing 324 mg of aspirin, 2.26 g of potassium bicarbonate, and 1 g of citric acid.

Subjects—Twelve healthy volunteers (eight males and four females; ages 21–37 years; weight, 53.6–94.5 kg) were evaluated by a comprehensive physical examination, blood chemistry profile (including blood count and differential), and complete urinalysis. None of the subjects had a history of gastrointestinal disease or surgery. All subjects were free of any active disease process, and none had used any medication for 14 d before the study.

Method—A Latin-square design for three treatments in 12 subjects was employed. A 10-h fast preceded dosing and continued for 4 h postdose. At ~7 a.m., predose urine and blood samples were obtained, and a single dose of aspirin with 240 mL of water was administered. The effervescent tablets were dissolved in 140 mL of water 3 min before dosing and the mixture was then swallowed. The glass was rinsed with 100 mL of water, which also was swallowed. After dosing, 100 mL of water was administered at 1, 2, and 3 h, and a uniform meal was served after the 4-h sample was obtained, after which water was allowed *ad libitum*. Subjects remained standing or sitting through the day, and exercise was limited to walking about the room.

Blood was drawn into chilled vacuum containers[3] *via* an indwelling catheter at 5, 10, 15, 20, 30, and 45 min and 1, 1.5, 2, 3, 4, 6, 8, and 10 h. Plasma was separated by centrifugation at 1764×*g* at 4°C within 20 min of collection. All urine was collected at 2-h intervals over 10 h, the pH and volume were measured, and an acidified aliquot was saved for analysis. All samples were frozen at −30°C and assayed within 2 weeks of collection by the HPLC method described previously (2).

RESULTS

As shown in Tables I and II, both plasma aspirin and salicylic acid levels rise more rapidly after administration of the solution with sodium than the potassium solution or the tablet. This rank order and profile reflect the values for 11 of the 12 subjects and is statistically significant ($p < 0.05$). Plasma aspirin levels rise rapidly to a mean peak of 7.20 μg/mL at 17.5 min with the single 324-mg dose in a sodium-containing effervescent solution, whereas the potassium-substituted solution reaches only 5.26 μg/mL at 30.4 min, which is not significantly higher ($p < 0.05$) than for the tablet. The ultimate exposure

[1] Bayer Aspirin; Glenbrook Laboratories -Division of Sterling Drug Inc., New York.
[2] Alka-Seltzer; Miles Laboratories, Inc., Elkhart, Ind.
[3] Vacutainer BD, 278-069, 7.0 mL, containing 14 mg of potassium oxalate and 17.5 mg of sodium fluoride.

0022-3549/84/0700-0998$01.00/0
© 1984, American Pharmaceutical Association

Table I—Mean Plasma Aspirin Levels and Kinetic Parameters [a]

Parameter	Na^+ solution	K^+ solution	Tablet
Mean conc, μg/mL			
5 min	1.04	0.71	0.94
10 min	4.17	1.84	2.17
15 min	6.43	2.97	3.42
20 min	6.27	3.56	3.98
30 min	4.41	4.34	4.22
45 min	1.99	2.65	3.34
60 min	1.10	1.56	2.70
90 min	0.36	0.52	1.28
120 min	0.30	0.30	0.80
Maximum conc., μg/mL	7.20*	5.27†	4.76†
Time of maximum conc., min	17.5*	30.4†	36.7†
Area under curve to 120 min, (μg·min/mL)	228.1*	211.4*	276.3†
to infinity, (μg·min/mL)	231.7*	216.6*	290.8†
$t_{1/2}$, min	19.6*	18.7*	24.7†

[a] A common symbol beside the mean indicates no significant difference ($p < 0.05$) by three-way analysis of variance and least significant difference.

to aspirin, as indicated by the area under the curve to infinity, is higher by ~25% for the tablet than for the two buffered solutions, which are equivalent.

Parameters that indicate the rate of absorption, maximum concentration, and time to maximum concentration for salicylic acid show the sodium-containing solution to be faster, with the potassium-containing solution being intermediate, and the tablet slowest. For salicylic acid, however, only the maximum concentration differs significantly ($p < 0.05$), whereas the renal clearance of salicylate is higher for the two buffered solutions (Table III). The overall contribution to total clearance is not sufficient to lower the area under the salicylate plasma curve over 10 h (Table II).

In Table III, the data obtained from urine samples are summarized, and the small differences in urine pH and salicylate renal clearance resulting from the buffered solutions are shown. Although urine pH was measured for 10 h, only during the first 2 h was there a significant difference between buffered and unbuffered dosages. Over a 10-h period, ~70% of the 325-mg dose was recovered in urine as salicylurate and salicylate, which demonstrates the equivalence of the extent of aspirin and/or salicylate absorption for all three dosage forms.

Table II—Mean Plasma Salicylic Acid Levels and Kinetic Parameter [a]

Parameter	Na^+ solution	K^+ solution	Tablet
Mean conc., μg/mL			
0.08 h	1.03	0.71	0.73
0.16 h	6.17	3.13	2.04
0.25 h	12.3	6.18	4.39
0.33 h	18.1	9.87	6.62
0.50 h	20.8	16.6	10.6
0.75 h	20.2	19.5	13.9
1.0 h	19.0	19.1	14.8
1.5 h	17.1	16.8	15.6
2 h	15.3	15.7	16.1
3 h	12.0	12.5	13.4
4 h	9.94	10.1	11.2
6 h	5.86	6.51	6.92
8 h	3.23	3.51	3.96
10 h	1.86	2.06	2.28
Maximum conc., μg/mL	21.8*	20.2*	17.2†
Time of maximum conc., h	0.59*	0.75*	1.50†
Area under curve to infinity, μg·h/mL	94.9*	95.6*	98.1*
$t_{1/2}$, h	2.42*	2.60*	2.91*

[a] A common symbol beside the mean indicates no significant difference ($p < 0.05$) for three-way analysis of variance and least significant difference.

Table III—Mean Urine Salicylate and Salicylurate Levels [a]

Parameter	Na^+ solution	K^+ solution	Tablet
Urine volume (0 → 2 h), L	0.131*	0.186*	0.170*
Urine pH (0 → 2 h)	6.63*	6.87*	6.11†
Salicylic acid renal clearance (0 → 2 h), L/h	0.31*	0.43*	0.14†
Urine volume (0 → 10 h), L	0.845*	0.918*	0.874*
Salicylic acid renal clearance (0 → 10 h), L/h	0.334*	0.353*	0.204†
Accumulation of salicylic acid (0 → 10 h), mg	28.7*	29.2*	17.1†
Accumulation of salicyluric acid (0 → 10 h), mg	214*	206*	221*
Percent aspirin dose (equivalent) recovered as salicylic acid and salicylurate to 10 h, %	72.3*	70.4*	69.9*

[a] A common symbol beside the mean indicates no significant difference ($p < 0.05$) for three-way analysis of variance and least significant difference.

DISCUSSION

Two significant results were obtained from this study. First, the rapid absorption rate of aspirin from a buffered solution is, in part, related to the sodium content, and potassium is not equivalent to sodium in this regard. This observed difference in absorption rate is most probably from the comparative effects of these two ions on gastric emptying kinetics. Before mixing with gastric secretion, the solutions are each ~100 mM in sodium or potassium ion with a total milliosmolarity of ~120[4]. In this concentration range, sodium has been shown to accelerate gastric emptying, whereas potassium inhibits gastric emptying (3, 4). Thus, although both solutions can raise gastric pH, which would speed gastric emptying, the inhibitory effect of potassium nullifies the pH effect, and the potassium-containing solution is emptied at about the same rate as the unbuffered tablet.

A second and more subtle observation is the extent to which aspirin reaches the general circulation unhydrolyzed, which is the same for both the sodium- and potassium-containing buffered solutions. Both are ~25% less bioavailable than the unbuffered tablet. This is consistent with the previously stated hypothesis (1) that the aspirin administered in a buffered solution is ionized in the stomach and little or no absorption occurs until it is emptied into the intestine. Intestinal absorption is associated with greater presystemic hydrolysis and, thus, a lower portion is bioavailable. These observations are consistent with the hypothesis that the potassium-containing solution is retained longer in the stomach and the antacid buffering is sufficient to reduce or inhibit gastric absorption.

It would appear that the replacement of sodium in extemporaneously prepared effervescent solutions of aspirin may slow absorption to equal that of a conventional tablet. However, the protection afforded the gastric mucosa by the elevated pH may be the same for both the sodium and potassium buffers.

REFERENCES

(1) W. D. Mason and N. Winer, *J. Pharm. Sci.*, **70**, 262 (1981).

(2) W. D. Mason and R. Gillilan, *Anal. Lett.*, **16** (B12), 903 (1983).

(3) J. N. Hunt and J. D. Pathak, *J. Physiol.*, **154**, 254 (1960).

(4) J. N. Hunt, *Gastroenterology*, **41**, 49 (1961).

[4] Personal communication; A. E. Troup, Miles Laboratories, Elkhart, Ind.

Plasma Protein Binding of Warfarin: Methodological Considerations

DENNIS MUNGALL *, YAN YAN WONG ‡, ROBERT L. TALBERT *, MICHAEL H. CRAWFORD §, JAMES MARSHALL ¶, DAVID W. HAWKINS *, and THOMAS M. LUDDEN *x

Received January 24, 1983, from the *College of Pharmacy, The University of Texas at Austin, Austin, Texas, and The University of Texas Health Science Center at San Antonio, San Antonio, TX 78284; ‡Department of Pharmaceutical Services, University of Chicago Hospital and Clinics, Chicago, IL 60637; §Department of Medicine, Division of Cardiology, The University of Texas Health Center and Veterans Administration Hospital, San Antonio, TX 78284; and ¶Veterans Administration Medical Center, Department of Clinical Pharmacy, Birmingham, AL 35209. Accepted for publication June 7, 1983.

Abstract □ Recent theoretical work has suggested that radiochemical impurities can significantly alter the binding results for highly protein-bound drugs. We compared protein binding of warfarin by ultrafiltration and equilibrium dialysis with 98% radiochemically pure [^{14}C]warfarin. Ultrafiltration and equilibrium dialysis were performed at 37°C and pH 7.45 on the plasma of patients receiving chronic warfarin therapy. Binding to plasma from seven patients was measured in duplicate by both a nonspecific radioisotopic technique and a specific HPLC technique. The nonspecific technique gave percentage of free warfarin values of 1.84 ± 0.11 (mean ± *SD*) and 1.59 ± 0.14 for ultrafiltration and equilibrium dialysis, respectively. The HPLC procedure yielded a percentage of free warfarin by ultrafiltration of 0.969 ± 0.203 and a value of 0.690 ± 0.095 by equilibrium dialysis ($p < 0.05$). The HPLC procedure for protein binding was performed on plasma samples from 12 additional patients and yielded a percentage of free warfarin of 1.01 ± 0.69 by ultrafiltration and 0.44 ± 0.34 by equilibrium dialysis ($p < 0.05$). It can be concluded that radiochemical impurities may lead to significant overestimation of the percentage of free warfarin. Ultrafiltration yielded a higher percentage of free warfarin than did equilibrium dialysis, but the ability to distinguish binding differences among patients was similar.

Keyphrases □ Warfarin—methodological considerations, plasma protein binding □ Plasma protein binding—methodological considerations, warfarin, radiochemical impurities □ Radiochemical impurities—methodological considerations, plasma protein binding of warfarin

A number of factors may affect the results of protein binding studies. These factors include the administration of heparin, the type of blood collection tubes, the system used for determining binding (equilibrium dialysis, ultrafiltration), and the radiochemical purity of the radiolabeled compound. Bjornsson *et al.* (1) have recently emphasized the importance of radiochemical purity of radiolabeled drugs used for determining plasma protein binding. Theoretically, radiochemical impurities that are poorly bound to plasma proteins could lead to significant overestimations of the free concentration of drugs that are highly bound. Warfarin is an agent which is highly protein bound, and its binding could be susceptible to measurement errors related to the presence of radiochemical impurities. [^{14}C]Warfarin is ~98.5% radiochemically pure. Studies with [^{14}C]warfarin for binding without a purification procedure (2–4) have reported a significantly higher percentage of free warfarin than studies in which a TLC assay procedure was utilized (5, 6). Yacobi and Levy (7) have found that a twofold error in the estimation of the percentage of free warfarin was made when radiochemically impure warfarin was used to determine protein binding in rats. No data on human plasma are available concerning this issue.

The majority of studies evaluating warfarin binding have utilized equilibrium dialysis, and no information is available comparing ultrafiltration with equilibrium dialysis. In the present study, the influence of radiochemical impurity on warfarin binding in human plasma is evaluated, and plasma binding as determined by ultrafiltration and equilibrium dialysis is compared.

Table I—Comparison of Ultrafiltration and Equilibrium Dialysis Methods for Measuring Warfarin Protein Binding [a]

Procedure	Mean Unbound ± *SD*, %
Ultrafiltration	1.010 ± 0.69
Equilibrium dialysis	0.44 ± 0.34

[a] Free and total concentrations were determined by the chromatographic procedure described in the text ($n = 12$).

EXPERIMENTAL SECTION

Initial attempts were made to purify racemic [^{14}C]warfarin[1] (specific activity, 50 mCi/mmol) before binding studies were performed. The major impurity could be separated by HPLC. Collection and assay of sequential fractions of the eluant revealed that 98.5% of the eluted radioactivity corresponded to warfarin, and ~1.5% corresponded to a chromatographic peak with a somewhat longer retention time. However, an overall recovery of only 20–25% could be obtained by collecting the eluant fraction corresponding to warfarin and extracting into ether. A second method with a sample preparation column[2] did not separate the impurity from the parent compound. Thus, it was necessary to perform the binding studies with the 98.5% pure [^{14}C]warfarin. However, the radioactive warfarin was measured in plasma, ultrafiltrate, or dialysate by the specific chromatographic procedure described below.

Preliminary studies were performed to assess binding of [^{14}C]warfarin to the ultrafiltration device[3] and the effect of *in vitro* heparin on the binding of warfarin. Binding of [^{14}C]warfarin to the ultrafiltration device was tested between the concentrations of 0.02 μg/mL and 2 mg/mL. Less than 10% binding to the device was found with these concentrations. No difference in binding was found between heparinized (*in vitro*) and nonheparinized samples. The time to reach equilibrium with the equilibrium dialysis system[4] was 4 h.

Plasma samples from 19 outpatients treated chronically with warfarin were collected in evacuated blood collection tubes[5] containing 143 U of lithium heparin per tube. Total warfarin concentrations ranged from ~1.0 to 4.3 μg/mL. The coefficient of variation of the HPLC assay was 10.0%. All plasma samples were stored at −20°C until assayed.

Equilibrium dialysis—Aliquots of plasma (1 mL) were dialyzed against 1 mL of 0.1 M phosphate buffer (pH 7.45) with polytef cells separated by dialysis membranes[3]. Radiolabeled [^{14}C]warfarin (0.5 μCi) was added to each plasma sample. The cells were rotated in a water bath at 37°C for 4 h.

Ultrafiltration—[^{14}C]Warfarin (1 μCi) was added to 1-mL plasma samples placed in the reservoir of the ultrafiltration device[3]. An initial 100-μL plasma sample was obtained for measurement of total radioactivity. The samples were placed in a centrifuge in an incubator maintained at 37°C. Samples were allowed to equilibrate for 15 min and were then centrifuged for 15 min at 1000×*g*.

Sample Analysis—For the dialysis experiments, 0.4 μg of phenprocoumon (the internal standard) and 10 μg of unlabeled warfarin (the carrier) were added to 250-μL samples of plasma and dialysate. For the ultrafiltration experiments, similar quantities of internal standard and carrier were added to 100-μL samples of plasma and ultrafiltrate. Each sample was then processed

[1] Amersham Corp., Arlington Heights, Ill.
[2] Sep-Pak; Waters Associates, Milford, Mass.
[3] MPS-1; Amicon Corp., Danvers, Mass.
[4] Spectrum Medical Industries, Los Angeles, Calif.
[5] Texfuno Medical Corp., Elkton, Md.

0022-3549/84/0700-1000$01.00/0
© 1984, American Pharmaceutical Association

and described by Fasco *et al.* (8). Each sample was extracted with 5 mL of ether, and the ether was evaporated to dryness at room temperature under a stream of nitrogen. The residue was diluted in 100 μL of mobile phase and injected onto a reverse-phase HPLC column[6]. The mobile phase was 40% acetonitrile in 1.5% acetic acid and was adjusted to pH 4.7 with ammonium hydroxide. The flow rate was 2 mL/min[7], and detection was at 309 nm[8].

The effluent which corresponded to the warfarin peak was collected in a liquid scintillation vial, mixed with 15 mL of scintillation fluid[9], and counted for 10 min in a liquid scintillation counter[10]. The percentage of [^{14}C]warfarin that was unbound was calculated as follows:

$$\% \text{ unbound} = (0.93A/B)100\% \qquad \text{(Eq. 1)}$$

where A is the net counts in dialysate or ultrafiltrate per internal standard peak height for dialysate or ultrafiltrate and B is the net counts in plasma per internal standard peak height for plasma. The correction factor of 0.93 was used to correct for the fact that plasma is ~93% water, and only this portion was available for the distribution of free drug.

Plasma samples of 7 of the 19 patients were used to determine the apparent percentage of free warfarin if the extraction and chromatography procedures were omitted. Aliquots of plasma and dialysate or filtrate were directly placed in scintillation fluid and counted. The percent unbound was calculated as follows:

$$\% \text{ unbound} = 100\% \frac{0.93 \text{ (net counts in dialysate or filtrate)}}{\text{net counts in plasma}} \qquad \text{(Eq. 2)}$$

For these seven patients, all procedures were performed in duplicate.

RESULTS AND DISCUSSION

Table I shows the mean binding values by ultrafiltration and equilibrium dialysis when the HPLC procedure was used. Ultrafiltration yielded a higher percentage of unbound warfarin than did equilibrium dialysis ($p < 0.05$).

Table II demonstrates the effect of the radiochemical impurities on warfarin plasma protein binding and compares the results obtained between ultrafiltration and equilibrium dialysis in seven additional patients. A significant difference in the percentage of unbound warfarin was found between the direct counting and the chromatographic procedures ($p < 0.05$). The samples counted directly yielded unbound values approximately twice those given by the more specific chromatographic procedure. These results are similar to those found by Yacobi and Levy (7) in rat plasma.

An important consideration in evaluating binding procedures is the relative ability of each to assess differences in the percentage of unbound warfarin between patients. This was evaluated in the present study by using the Spearman rank correlation coefficient (Rs). In the 12 patients in which equilibrium dialysis and ultrafiltration were performed singly and samples were assayed chromatographically, the Rs was 0.7 ($p < 0.05$). For the seven patients in which binding was determined in duplicate, these procedures yielded an Rs value of 0.81 ($p < 0.05$). An Rs of 0.63 ($p < 0.05$) was found between unchromatographed and chromatographed samples from the ultrafiltration procedure, and an Rs of 0.929 ($p < 0.05$) was found between unchromatographed and chromatographed samples from the equilibrium dialysis procedure. These results suggest that the same relative binding results may be obtained for equilibrium dialysis whether or not a cleanup procedure is used. Further study of a group of patients with greater differences in warfarin binding is needed.

This study demonstrates that radiochemical impurities can significantly alter the percentage of unbound warfarin as determined by ultrafiltration or equilibrium dialysis, and that equilibrium dialysis and ultrafiltration are similar in their ability to discriminate warfarin binding differences between patients.

Table II—Effect of Radiochemical Impurity on Protein Binding of Warfarin [a]

Procedure	Mean Unbound ± *SD*, %
Ultrafiltration (counted directly)	1.84 ± 0.11
Equilibrium dialysis (counted directly)	1.59 ± 0.14
Ultrafiltration (extracted, chromatographed)	0.97 ± 0.20
Equilibrium dialysis (extracted, chromatographed)	0.69 ± 0.10

[a] Comparisons in seven patients before and after HPLC cleanup procedure. All samples were performed in duplicate.

[6] μ-Bondapak C_{18}; Waters Associates, Milford, Mass.
[7] Model M-6000A; Waters Associates, Milford, Mass.
[8] Varichrom U-V detector; Varian Instrument Division, Palo Alto, Calif.
[9] Aquasol-2; New England Nuclear Corp., Boston, Mass.
[10] Beckman LS 7500; Beckman Instrument Co., Irvine, Calif.

REFERENCES

(1) T. D. Bjornsson, J. E. Brown, and C. Ts Chanz, *J. Pharm. Sci.*, **70**, 1372 (1981).

(2) I. Odar-Cederlog, *Clin. Pharmacokinet.*, **2**, 147 (1977).

(3) A. M. M. Shepherd, P. S. Hewick, T. A. Moreland, and I. H. Stevenson. *Br. J. Clin. Pharmacol.*, **4**, 315 (1977).

(4) P. A. Routledge, P. H. Chapman, D. M. Davies, and M. D. Rawlins, *Br. J. Clin. Pharmacol.*, **8**, 243 (1979).

(5) A. Yacobi, T. Lampman, and G. Levy, *Clin. Pharmacol. Ther.*, **21**, 283 (1976).

(6) A. Yacobi, J. A. Udall, and G. Levy, *Clin. Pharmacol. Ther.*, **20**, 300 (1976).

(7) A. Yacobi and G. Levy, *J. Pharmacokinet. Biopharm.*, **3**, 439 (1975).

(8) M. J. Fasco, L. J. Piper, and L. S. Kavrinsky. *J. Chromatogr.*, **131**, 365 (1977).

Penetration of Trolamine Salicylate into the Skeletal Muscle of the Pig

J. R. BALDWIN ˣ, R. A. CARRANO, and A. R. IMONDI

Received January 7, 1983, from *Adria Laboratories, Inc., Columbus, OH 43216.* Accepted for publication May 26, 1983.

Abstract □ Studies to determine the extent of local tissue penetration of topically applied trolamine [^{14}C]salicylate were conducted in domestic pigs. The preparation was applied onto a 100-cm^2 shaved area of skin overlying the biceps femoris at a concentration of 0.7 mg of salicylate/cm^2 to closely approximate the actual use in humans. At least 82% of the topically applied trolamine salicylate was absorbed over a 2-h period. Based on blood and muscle salicylate levels, a localization of the absorbed drug occurred in muscle underlying the treated area within 120 min. Muscle from the treated area had a concentration of salicylate that was 13 times that of blood and 49 times that of muscle taken from untreated areas. Blood samples taken from the treated area at 10, 20, and 30 min showed that salicylate levels ranged from 15.8 to 5.3 μg/g. Less than 0.5% of the applied drug was excreted in the urine during the 2-h period.

Keyphrases □ Trolamine salicylate—percutaneous absorption, local tissue penetration, domestic pigs □ Percutaneous absorption—trolamine salicylate, domestic pigs, local tissue penetration □ Tissue penetration—local, percutaneous absorption of trolamine salicylate, domestic pigs

Trolamine salicylate is the active ingredient in a number of topical analgesic creams that are used for sore muscles, joint stiffness, and strains. The creams are also used as a topical adjunct for arthritis and rheumatism therapy. Although the percutaneous absorption of salicylate is well known, only one published report on the penetration of salicylate into canine knee joints has shown that preferential uptake and localization of salicylate occurs in tissue and fluids beneath the area of salicylate application (1). This study was carried out to determine whether localization of trolamine salicylate could be demonstrated in the muscle of the domestic pig after topical administration.

The most commonly used laboratory species have loose-fitting skin, a heavy hair coat, and dermal vasculature that does not resemble that found in humans (2). The pig, on the other hand, has a sparse hair coat, close-fitting skin, a thick epidermis with a well-differentiated lower limit, a dermis with a distinct papillary body, a highly elastic tissue content (3, 4), and vascularization similar to that of humans (2, 5). These findings have been confirmed ultrastructurally by Karasek and Oehlert (6, 7). In addition, the thickness of the dermis and epidermis (8), the distributed enzymes (9), the keratinous proteins (10), and the permeability characteristics of pig skin closely resemble those of humans (11, 12).

EXPERIMENTAL SECTION

Materials—The [7-^{14}C]salicylic acid[1] had a specific activity of 0.37 mCi/mg. Scintillation fluid[2], carbon dioxide trapping agent[2], cellulose cups[2], powdered cellulose[3], ^{14}C-recovery standards[3], and scintillation fluid[4] were commercially obtained. All other materials were reagent grade, obtained from commercial sources, and used without further purification.

Animals—Six healthy female Yorkshire swine (weighing 23–40 kg), maintained on a commercial swine diet[5], were used.

Dosage Preparation—A trolamine [^{14}C]salicylate formulation based on a commercial topical cream[6] was prepared. The trolamine [^{14}C]salicylate was incorporated into a white hydrophilic cream base by dissolving [^{14}C]salicylate (1 μCi/mg) and trolamine in stoichiometric proportions in the aqueous phase of the cream. The oil phase of the cream was then added and thoroughly mixed. The final concentration of trolamine [^{14}C]salicylate was 10% (w/w).

Drug Treatment and Sample Collection—Before the experiment, each pig was dosed with acepromazine (1.1 mg/kg im) followed 30 min later by administration of pentobarbital[7] (30 mg/kg ip). Phenobarbital was administered intravenously as required during the experimental period. The animals were quickly washed with water and dried, and their hind quarters were clipped and carefully shaved. Shaving was performed with a safety razor and warm water. The trolamine [^{14}C]salicylate formulation was not applied until 45–60 min after shaving. During the 45–60-min pretreatment, the urinary bladder was catheterized with a polypropylene catheter, and a 10- × 10-cm area was marked over the biceps femoris. The radiolabeled cream was applied to this area with a syringe fitted with a 16-gauge blunt needle and spread evenly over the area by gentle rubbing. The syringe was calibrated to deliver 1.5 g of the preparation, which contained the equivalent of 72 mg of salicylic acid. This application closely approximates the amounts and conditions of application of trolamine salicylate applied in actual practice by humans.

In pigs 1 through 4, 30 min after the application of the dose, one-half of the 100-cm^2 area was washed with a damp paper towel until the cream was no longer visible. An incision of ~4 cm was then made in the center of the washed area with a scalpel. The scalpel blade was changed often during the cutting of the skin. The subcutaneous fat (when present) was then removed with scissors to expose the underlying muscle. Three samples of the exposed muscle (0.4–0.6 g) were then removed with scissors and pressed firmly between gauze to remove blood. Muscle was also taken from the contralateral side (control) by the same procedure. At the same time, blood samples were collected from the orbital sinus. The procedures were repeated at 120 min postdose. Skin wipes taken at 120 min were retained for analysis of carbon-14. Skin removed from the total area of application (10 × 10 cm) was assayed for carbon-14 in pigs 1 and 4.

The concentration of salicylate in blood at the site of application was determined in pigs 5 and 6. The area of drug application was cleaned as described above, and blood samples were taken from shallow incisions (1–1.5 mm) at 10, 20, and 30 min postdose.

All samples were placed in cellulose cups and allowed to air-dry for 48 h before combustion in an oxidizer[8]. The amount of radioactivity on the paper towel wipes was determined by placing the wipes into a 500-mL beaker containing a magnetic stirring bar and by adding 300 mL of toluene. The beaker was covered and placed on a magnetic stirrer to stir overnight. Duplicate 1-mL samples were removed the next morning and added to 10 mL of scintillation fluid[4]. The carbon-14 was quantitated by liquid scintillation counting.

RESULTS AND DISCUSSION

Skin wipes taken at 120 min after application of the dose indicated 7.9 ± 0.5% (mean ± *SEM*) of the dose remaining on the skin, whereas assays of skin tissue showed 9.3 ± 0.7% remaining in the skin. These figures were calculated from data obtained at the 120-min sampling time and multiplied by a factor of two, since one-half of the area remained at this time. Thus, at least 82% of the dose was found to be absorbed within 120 min after application. The excellent absorption of trolamine salicylate shown by the data was not a result of incomplete extraction of the paper towels. Extraction of paper towels containing a known amount of cream indicated that 49.1, 78.1, 90.7, 93.7, 97.7, 101.0, and 100% of the applied carbon-14 could be recovered at 30, 60, and 90 min and 2, 3, 4, and 7 h, respectively. The literature indicates that the absorption of salicylate after topical administration to humans varies considerably. Feldmann and Maibach have found that only 13% of the applied salicylate was absorbed in a 24-h period (13), whereas Taylor and Halprin have

[1] New England Nuclear Corp., Boston, Mass.
[2] Permafluor V, Carbosorb, Combusto Cones; Packard Instrument Co., Inc., Downers Grove, Ill.
[3] Packard Instrument Co., Downers Grove, Ill.
[4] Thrift-Solve; Kew Scientific, Inc., Columbus, Ohio.
[5] Yoeman, Plain City, Ohio.
[6] Myoflex creme (trolamine salicylate); Adria Laboratories, Inc., Dublin, Ohio.
[7] Nembutal.
[8] Model 306 Sample Oxidizer, Packard Instrument Co.

0022-3549/84/0700-1002$01.00/0
© 1984, American Pharmaceutical Association

Table I—Concentration of [^{14}C]Salicylate in Pig Muscle [a]

Sample	Pig	Drug Concentration, ng/g[b]		T/B[c]	
		30 min	120 min	30 min	120 min
Blood	1	56.4	38.7	—	—
	2	47.7	84.5	—	—
	3	35.4	—	—	—
	4	31.6	41.6	—	—
Control muscle	1	28.7	55.2	0.5	1.4
	2	0.0	8.6	0.0	0.1
	3	8.7	—	0.2	—
	4	6.8	23.8	0.2	0.6
Treated muscle	1	635.0	313.5	11.3	8.1
	2	150.9	582.3	3.2	6.9
	3	724.5	—	20.5	—
	4	236.8	560.1	7.5	13.5

[a] [^{14}C]Salicylate trolamine applied topically (0.6–0.7 mg of salicylic acid equivalents/cm^2) over biceps femoris (treated muscle). Biopsy from treated muscle and contralateral (control) muscle assayed for total carbon-14. Blood was taken from the orbital sinus. [b] Concentration of drug is expressed as free salicylic acid equivalents. [c] Ratio of tissue to blood.

Table II—Penetration of [^{14}C]Salicylate into Pig Muscle [a]

Parameter	Pig				Mean ± *SEM*
	1	2	3	4	
Concentration in muscle, ng/g[b]	635 (30 min)[c]	582 (120 min)	725 (30 min)[d]	560 (120 min)	625 ± 37
Carbon-14 Ratios					
Treated muscle/blood	11.3	6.9	20.5	13.5	13.1 ± 2.8
Control muscle/blood	0.5	0.1	0.2	0.6	0.4 ± 0.1
Treated muscle/control muscle	22.1	67.7	83.2	23.5	49.1 ± 15.5

[a] [^{14}C]Salicylate trolamine was applied topically (0.6–0.7 mg/cm^2) over biceps femoris (treated muscle). Biopsy from treated muscle and contralateral (control) muscle assayed for total carbon-14. Blood was taken from orbital sinus. [b] Concentration of drug is expressed as free salicylic acid equivalents. [c] Number in parentheses represents the time of biopsy (30 or 120 min) when concentration was higher. [d] Only data at 30 min were obtained. Animal died from anesthesia before 120-min sampling time.

shown that 60% of the dose was absorbed within a 24-h period (14). In the latter study, the peak plasma level occurred at 5 h. The extreme differences shown in the percentage of the dose absorbed between these two studies are probably due to the vehicle and the treatment of the dose after application. Feldmann and Maibach applied salicylate to the skin dissolved in a small volume of acetone, whereas Taylor and Halprin used 60% propylene glycol and 19.4% alcohol as a vehicle and occluded the areas for 10 h. However, not only the vehicle, but also the salt form of salicylate affect the rate of its percutaneous absorption. Gaudin has demonstrated that the percutaneous absorption of the trolamine salt of salicylate after 24 h is 1.7 times greater than that of the sodium salt form (15). The fact that the dose of salicylate applied to the skin of the pig in the present study was the trolamine salt in a hydrophilic cream base most likely accounts for the rapid absorption of the dose.

Although the dose was well absorbed, urinary excretion of carbon-14 was found to be minimal. Urine collected during the first 30 min postdose contained 0.13 ± 0.12% of the dose, and 0.45 ± 0.07% (mean ± *SEM*) of the dose was excreted after 2 h.

Data obtained from the blood and tissue samples taken at 30 and 120 min are shown in Table I. Greater concentrations of carbon-14 were observed in the treated area at 30 min of pigs 1 and 3, whereas pigs 2 and 4 were found to have a greater concentration of carbon-14 at 120 min. Pig 3 died from the anesthesia after the 30-min muscle biopsy, but the data obtained at that time were similar to those in pigs 1, 2, and 4, which had greater concentrations of carbon-14.

A summary of those data representing the greater concentration of salicylate in muscle is presented in Table II. Whether these data represent the highest concentrations of carbon-14 achieved during the experimental period is not known since samples were only obtained at 30 and 120 min to minimize the possible effects of local trauma.

Table II shows that [^{14}C]salicylate was detectable in muscle underlying the site of application in greater concentrations (49 times) than that taken from the contralateral (control) muscle. Gross differences in skin thickness were observed not only from pig to pig, but also from areas as close as 3.5 cm within the same pig. This may have influenced the differences in the time of detection of the greater concentration from pig to pig. Table II also shows the ratios of [^{14}C]salicylate levels in muscle to [^{14}C]salicylate levels in blood taken from the orbital sinus. The data show that the carbon-14 concentration was ~13 times greater in the muscle underlying the site of drug application than in the blood. The concentration of salicylate in pig muscle was low compared with that obtained in the dog (1). This difference may be attributed to the application of a much lower dose in the pig (1.5 *versus* 10 g) without massaging the preparation into the skin, as was done in the dog. However, despite methodological differences, preferential uptake and localization of salicylate in tissues underlying the area of drug application were found in both studies.

Analysis of blood taken from the applied area also indicated that the penetration of salicylate through the dermis to underlying muscle occurs fairly rapidly. Whether partitioning of the salicylate between the local vasculature and the muscle tissue accounts for the high concentration of salicylate in the muscle beneath the area treated with trolamine salicylate is not known. However, blood collected from shallow incisions in the dermis of pigs 5 and 6 had carbon-14 concentrations equivalent to 15.8 ± 4.6, 6.2 ± 3.3, and 5.3 ± 1.8 μg of salicylate/g (mean ± *SEM*) at 10, 20, and 30 min, respectively. Data obtained from control muscle demonstrate that salicylate has a muscle-blood partition coefficient of 0.1. If this coefficient is applicable in the tissues underlying the point of trolamine salicylate application, then the local blood salicylate concentrations of 5–16 μg/g would be expected to result in salicylate concentrations of 500–1600 ng/g in the treated muscle. This agrees with the mean value of 625 ng/g that was actually found.

Several studies have demonstrated the percutaneous absorption of salicylic acid and its ultimate excretion from the body. However, the significance of this absorption with regard to a local pharmacological effect on muscles or other tissues beneath the area of application has not been fully investigated. The present studies, as well as an earlier study (1), have indicated that salicylic acid does, indeed, penetrate the skin and is taken up by muscle tissue beneath the treated area. Although these studies shed little light on the pharmacological significance of the concentration of salicylic acid present in the muscle of the treated area, the fact that significant amounts of salicylate were transported through the local area and permeated the musculature provides a basis for the possible efficacy of topically applied trolamine salicylate.

REFERENCES

(1) J. Rabinowitz, E. Feldman, H. Weinberger, and R. Schumacher, *J. Clin. Pharmacol.*, **22**, 42 (1982).

(2) W. Montagna and P. Parakkal, "The Structure and Function of Skin," Academic, New York, N.Y., 1943, p. 142.

(3) W. Montagna and J. S. Yun, *J. Invest. Dermatol.*, **43**, 11 (1964).

(4) H. Q. Marcarian and M. L. Calhoun, *Am. J. Vet. Res.*, **27**, 765 (1966).

(5) P. D. Forbes, "Hair Growth, Advances in Biology of Skin," vol. 9, Pergamon, Oxford, 1969, p. 419.

(6) J. Karasek and W. Oehlert, *Z. Mikroshopisch-anatomische Forsch.*, **78**, 133 (1968).

(7) J. Karasek and W. Oehlert, *Z. Mikroshopisch-anatomische Forsch.*, **79**, 157 (1968).

(8) E. H. Rose, L. M. Vistnes, and G. A. Ksander, *Plastic Reconstr. Surg.*, **59**, 94 (1977).
(9) W. Meyer and K. Neurand, *Lab. Anim.*, **10**, 237 (1976).
(10) G. D. Weinstein, "Swine in Biomedical Research," Frayn, Seattle, Wash., 1966, p. 287.
(11) M. J. Bartek, J. A. LaBudde, and H. I. Maibach, *J. Invest. Dermatol.*, **58**, 114 (1972).
(12) C. Chow, A. K. Chow, R. H. Downie, and H. S. Buttar, *Toxicology*, **9**, 147 (1978).
(13) R. J. Feldmann and H. I. Maibach, *J. Invest. Dermatol.*, **54**, 399 (1970).
(14) J. R. Taylor and K. M. Halprin, *Arch. Dermatol.*, **111**, 740 (1975).
(15) O. Gaudin, U.S. Patent 2,596,674 (May 13, 1952).

ACKNOWLEDGMENTS

The authors thank Dr. M. Kustek, D. Shaeffer, and K. Broadnax for their excellent technical assistance and B. Green for clerical assistance.

Simultaneous Determination of Nitrate and Nitrite in Toothpastes by High-Performance Liquid Chromatography

H. LULLA, S. S. CHEN ˣ, and F. J. SENA

Received February 24, 1983, from *R & D Laboratories, Block Drug Co. Inc., Jersey City, NJ 07302.* Accepted for publication May 25, 1983.

Abstract □ A stability-indicating analytical method is described for the simultaneous determination of nitrate, and if present, its reductive degradation product, nitrite, in toothpastes. Nitrate and nitrite were extracted from the toothpaste using distilled water and separated from other water-soluble excipients by two RP-8 columns (250 mm × 4 mm i.d.) using a mobile phase containing 0.2% (w/v) sodium acetate and 2.5% (v/v) glacial acetic acid in distilled water. A UV detector set at 313 nm was used for quantitation. The method was applied to commercial toothpastes containing 5% potassium nitrate and yielded an average recovery of 100.1% with a relative standard deviation of 1.43%. Average recovery of nitrate and nitrite from spiked samples were 100.6% and 96.4%, respectively. The minimum detectable concentration for nitrite was 50 μg/g of toothpaste.

Keyphrases □ Nitrate—simultaneous determination with nitrite, toothpastes, HPLC □ Nitrite—simultaneous determination with nitrate, toothpastes, HPLC □ Dentifrices—simultaneous determination of nitrate and nitrite, HPLC

Potassium nitrate, reportedly a tooth desensitizing agent (1-3), is the active ingredient in commercial dentrifrices for the treatment of dental hypersensitivity. As nitrate ion can be converted to nitrite by reducing agents or bacteria, a simple, specific, and sensitive method for simultaneous determination of intact nitrate and its reductive degradation product is desirable for routine quality control and stability evaluation.

The widely used colorimetric procedures for nitrate (4, 5) and nitrite (6-12) are subject to interference by other ions and generally require tedious sample treatment. In addition, those methods involving the cadmium reduction of nitrate to nitrite (6, 7) prior to color development often suffer from nonstoichiometric conversion.

Methods involving derivatization followed by HPLC (13) or GC (14, 15) are lengthy. The potentiometric method with a nitrate ion-selective electrode (16-18), differential pulse polarography (19), and enthalpimetric analysis for nitrate (20) are specific, but they measure only one ion (nitrate or nitrite). The newly developed ion chromatography (21) and its variations (22-27) are selective, sensitive, and suitable for one-step differentiation and determination of nitrate and nitrite. However, the need for additional expensive instrumentation (an ion chromatography system with conductivity or electrochemical detector and ion-exchange columns) hinders the use of this technique.

Recently, Skelly (28) reported the use of an eluant containing the octylamine salt of a mineral acid to separate inorganic anions on a conventional reverse-phase column, with detection at 205 nm. Leuenberger *et al.* (29) and Cortes (30), using phosphate buffer as an eluant, have described the resolution of nitrate from nitrite on an amino normal-phase column. The separation mechanism of the former is dynamic ion-exchange, while the second is weak base ion-exchange. Both methods, which directly determined nitrate and nitrite by conventional HPLC with low-wavelength detection, are simple and sensitive, but they have not been applied to the toothpaste matrix.

The purpose of this paper is to report the separation and simultaneous determination of nitrate and nitrite by high-performance liquid chromatography (HPLC) using two RP-8 columns with acetate buffer as mobile phase. The separated nitrate and nitrite were monitored by a UV detector set at 313 nm. No sample treatment or cleanup was required, and the method was found to be simple, rapid, precise, and selective for the measurement of nitrate and nitrite in a complex toothpaste matrix.

EXPERIMENTAL SECTION

Chemicals and Reagents—Potassium nitrate[1] and sodium acetate[2] were used without further purification. Glacial acetic acid[3] and 0.1 M sodium nitrite solution[4] were used as received.

Apparatus—The liquid chromatograph[5] was fitted with a manual septumless injector[6], a fixed-wavelength UV detector (313 nm)[7], and a strip-chart recorder[8]. The recorder was connected to a laboratory data system[9] through an A/D converter[10]. Two 250 mm × 4.0-mm i.d. columns containing 10-μm Lichrosorb RP-8 packing[11] and one precolumn containing 37-40-μm octadecylsilane packing[12] were used.

Chromatographic Conditions—The chromatographic solvent was 0.2% (w/v) sodium acetate in distilled water containing 2.5% (v/v) glacial acetic acid, adjusted to pH 3.0 ± 0.1 with glacial acetic acid or sodium hydroxide. This solvent was vacuum-filtered[13] through a 0.45-μm filter[13] and deaerated

[1] Baker Analyzed Reagent, J. T. Baker Chemical Co., Phillipsburg, N.J.
[2] MCB Manufacturing Chemical Inc., Cincinnati, Ohio.
[3] VWR Scientific Inc., South Plainfield, N.J.
[4] Orion Research Inc., Cambridge, Mass.
[5] Model 6000 A Pump; Waters Associates, Milford, Mass.
[6] Valco Model CV6-UHpa-N6o, 7000 psi sample injection valve equipped with a 100-μL sampling loop.
[7] Model 440; Waters Associates, Milford, Mass.
[8] Houston Instrument, Austin, Tex.
[9] Model 21MX Computer with model 2645A terminal; Hewlett-Packard, Avondale, Pa., and model DP 8000 printer; Anadex, Chatsworth, Calif.
[10] Model 18652A; Hewlett-Packard, Avondale, Pa.
[11] Cat. #9318; Merck, Elmsford, N.Y.
[12] Waters Associates, Milford, Mass.
[13] Millipore Corp., Bedford, Mass.

0022-3549/84/0700-1004$01.00/0
© 1984, American Pharmaceutical Association

(8) E. H. Rose, L. M. Vistnes, and G. A. Ksander, *Plastic Reconstr. Surg.*, **59**, 94 (1977).
(9) W. Meyer and K. Neurand, *Lab. Anim.*, **10**, 237 (1976).
(10) G. D. Weinstein, "Swine in Biomedical Research," Frayn, Seattle, Wash., 1966, p. 287.
(11) M. J. Bartek, J. A. LaBudde, and H. I. Maibach, *J. Invest. Dermatol.*, **58**, 114 (1972).
(12) C. Chow, A. K. Chow, R. H. Downie, and H. S. Buttar, *Toxicology*, **9**, 147 (1978).
(13) R. J. Feldmann and H. I. Maibach, *J. Invest. Dermatol.*, **54**, 399 (1970).
(14) J. R. Taylor and K. M. Halprin, *Arch. Dermatol.*, **111**, 740 (1975).
(15) O. Gaudin, U.S. Patent 2,596,674 (May 13, 1952).

ACKNOWLEDGMENTS

The authors thank Dr. M. Kustek, D. Shaeffer, and K. Broadnax for their excellent technical assistance and B. Green for clerical assistance.

Simultaneous Determination of Nitrate and Nitrite in Toothpastes by High-Performance Liquid Chromatography

H. LULLA, S. S. CHEN ˣ, and F. J. SENA

Received February 24, 1983, from *R & D Laboratories, Block Drug Co. Inc., Jersey City, NJ 07302.* Accepted for publication May 25, 1983.

Abstract □ A stability-indicating analytical method is described for the simultaneous determination of nitrate, and if present, its reductive degradation product, nitrite, in toothpastes. Nitrate and nitrite were extracted from the toothpaste using distilled water and separated from other water-soluble excipients by two RP-8 columns (250 mm × 4 mm i.d.) using a mobile phase containing 0.2% (w/v) sodium acetate and 2.5% (v/v) glacial acetic acid in distilled water. A UV detector set at 313 nm was used for quantitation. The method was applied to commercial toothpastes containing 5% potassium nitrate and yielded an average recovery of 100.1% with a relative standard deviation of 1.43%. Average recovery of nitrate and nitrite from spiked samples were 100.6% and 96.4%, respectively. The minimum detectable concentration for nitrite was 50 μg/g of toothpaste.

Keyphrases □ Nitrate—simultaneous determination with nitrite, toothpastes, HPLC □ Nitrite—simultaneous determination with nitrate, toothpastes, HPLC □ Dentifrices—simultaneous determination of nitrate and nitrite, HPLC

Potassium nitrate, reportedly a tooth desensitizing agent (1-3), is the active ingredient in commercial dentrifrices for the treatment of dental hypersensitivity. As nitrate ion can be converted to nitrite by reducing agents or bacteria, a simple, specific, and sensitive method for simultaneous determination of intact nitrate and its reductive degradation product is desirable for routine quality control and stability evaluation.

The widely used colorimetric procedures for nitrate (4, 5) and nitrite (6-12) are subject to interference by other ions and generally require tedious sample treatment. In addition, those methods involving the cadmium reduction of nitrate to nitrite (6, 7) prior to color development often suffer from nonstoichiometric conversion.

Methods involving derivatization followed by HPLC (13) or GC (14, 15) are lengthy. The potentiometric method with a nitrate ion-selective electrode (16-18), differential pulse polarography (19), and enthalpimetric analysis for nitrate (20) are specific, but they measure only one ion (nitrate or nitrite). The newly developed ion chromatography (21) and its variations (22-27) are selective, sensitive, and suitable for one-step differentiation and determination of nitrate and nitrite. However, the need for additional expensive instrumentation (an ion chromatography system with conductivity or electrochemical detector and ion-exchange columns) hinders the use of this technique.

Recently, Skelly (28) reported the use of an eluant containing the octylamine salt of a mineral acid to separate inorganic anions on a conventional reverse-phase column, with detection at 205 nm. Leuenberger *et al.* (29) and Cortes (30), using phosphate buffer as an eluant, have described the resolution of nitrate from nitrite on an amino normal-phase column. The separation mechanism of the former is dynamic ion-exchange, while the second is weak base ion-exchange. Both methods, which directly determined nitrate and nitrite by conventional HPLC with low-wavelength detection, are simple and sensitive, but they have not been applied to the toothpaste matrix.

The purpose of this paper is to report the separation and simultaneous determination of nitrate and nitrite by high-performance liquid chromatography (HPLC) using two RP-8 columns with acetate buffer as mobile phase. The separated nitrate and nitrite were monitored by a UV detector set at 313 nm. No sample treatment or cleanup was required, and the method was found to be simple, rapid, precise, and selective for the measurement of nitrate and nitrite in a complex toothpaste matrix.

EXPERIMENTAL SECTION

Chemicals and Reagents—Potassium nitrate[1] and sodium acetate[2] were used without further purification. Glacial acetic acid[3] and 0.1 M sodium nitrite solution[4] were used as received.

Apparatus—The liquid chromatograph[5] was fitted with a manual septumless injector[6], a fixed-wavelength UV detector (313 nm)[7], and a strip-chart recorder[8]. The recorder was connected to a laboratory data system[9] through an A/D converter[10]. Two 250 mm × 4.0-mm i.d. columns containing 10-μm Lichrosorb RP-8 packing[11] and one precolumn containing 37-40-μm octadecylsilane packing[12] were used.

Chromatographic Conditions—The chromatographic solvent was 0.2% (w/v) sodium acetate in distilled water containing 2.5% (v/v) glacial acetic acid, adjusted to pH 3.0 ± 0.1 with glacial acetic acid or sodium hydroxide. This solvent was vacuum-filtered[13] through a 0.45-μm filter[13] and deaerated

[1] Baker Analyzed Reagent, J. T. Baker Chemical Co., Phillipsburg, N.J.
[2] MCB Manufacturing Chemical Inc., Cincinnati, Ohio.
[3] VWR Scientific Inc., South Plainfield, N.J.
[4] Orion Research Inc., Cambridge, Mass.
[5] Model 6000 A Pump; Waters Associates, Milford, Mass.
[6] Valco Model CV6-UHpa-N6o, 7000 psi sample injection valve equipped with a 100-μL sampling loop.
[7] Model 440; Waters Associates, Milford, Mass.
[8] Houston Instrument, Austin, Tex.
[9] Model 21MX Computer with model 2645A terminal; Hewlett-Packard, Avondale, Pa., and model DP 8000 printer; Anadex, Chatsworth, Calif.
[10] Model 18652A; Hewlett-Packard, Avondale, Pa.
[11] Cat. #9318; Merck, Elmsford, N.Y.
[12] Waters Associates, Milford, Mass.
[13] Millipore Corp., Bedford, Mass.

0022-3549/84/0700-1004$01.00/0
© 1984, American Pharmaceutical Association

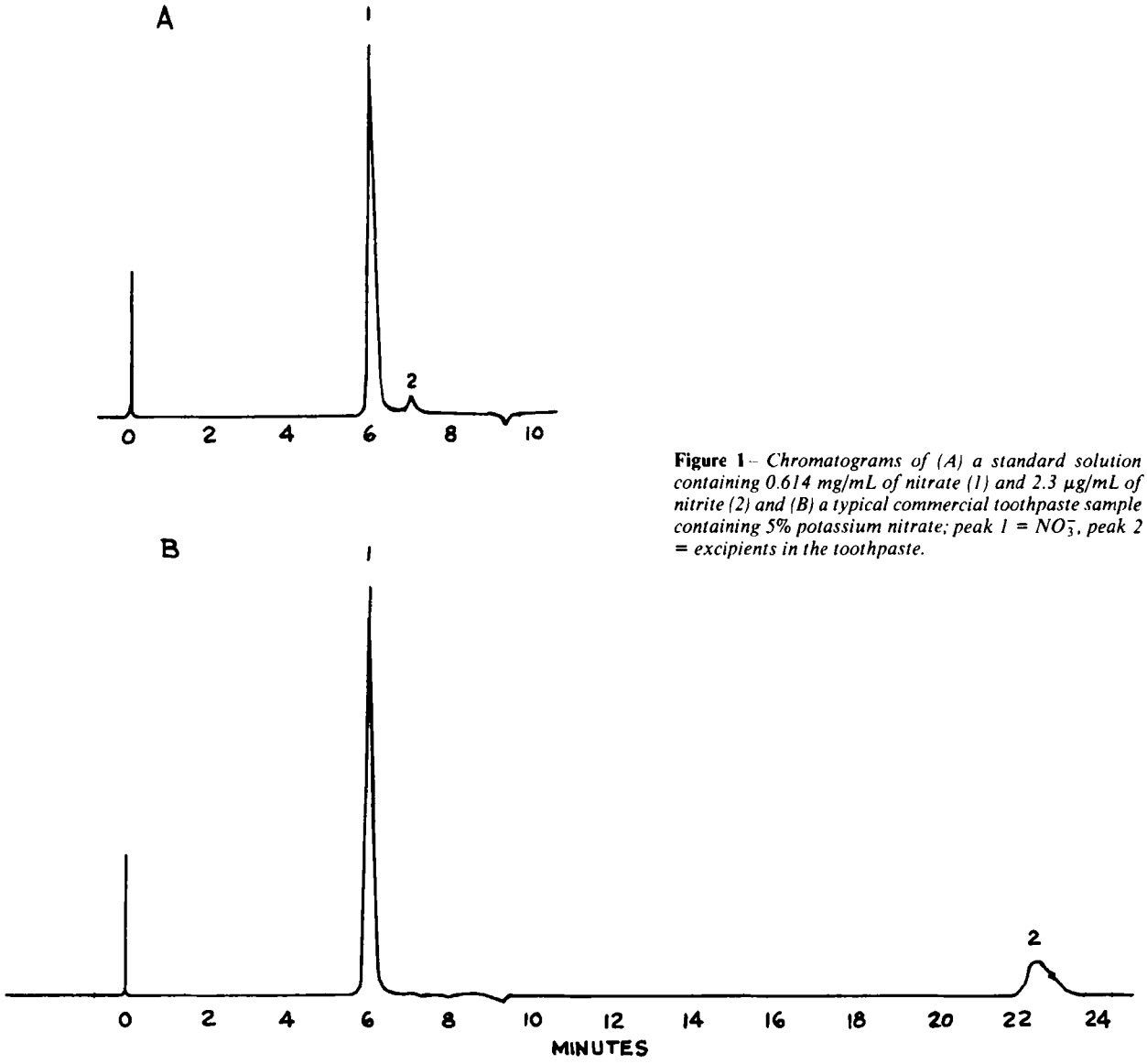

Figure 1—*Chromatograms of (A) a standard solution containing 0.614 mg/mL of nitrate (1) and 2.3 μg/mL of nitrite (2) and (B) a typical commercial toothpaste sample containing 5% potassium nitrate; peak 1 = NO_3^-, peak 2 = excipients in the toothpaste.*

for 5 min with stirring before use. The temperature was ambient, the solvent flow rate was 1.0 mL/min, and the inlet pressure was 1800 psi. The detector sensitivity was 0.1 AUFS, and the chart speed was 1.0 cm/min.

Standard Solutions—Three standard solutions containing 30.7, 61.4, and 92.1 mg of nitrate and, respectively, 115, 230, and 460 μg of nitrite per 100 mL were prepared in distilled water and filtered as described above prior to injection.

Assay for Commercial Products—An accurately weighed 2.0-g portion of the toothpaste was transferred to a 100-mL beaker, 20 mL of distilled water was added, and the contents were mixed with a spatula to complete dispersion. The dispersion was then quantitatively transfered to a 100-mL volumetric flask, diluted to volume with distilled water, and mixed well. A portion of this solution was centrifuged at 3000 rpm for 5 min and filtered through a 0.45-μm filter before injection.

Spiked Samples—Accurately measured quantities of nitrate and nitrite were admixed with a placebo portion of toothpaste. These mixtures were formulated to contain 30.7, 61.4, and 92.1 mg of NO_3 and 115, 230, and 460 μg of NO_2, respectively, per 2.0-g sample. These samples were assayed as described above for commercial products.

Quantitation—Since peak areas of nitrate and nitrite were found to be directly proportional to their concentrations, all results were calculated by interpolation from standard curves of peak areas *versus* concentrations.

Table I—Recovery Data for Nitrate from Spiked Samples

Amount Added, mg	Amount Found, mg	Recovery, %
0.5062	0.5167 (*RSD* = 0.69%, *n* = 3)	102.07
1.0124	1.0199 (*RSD* = 1.11%, *n* = 4)	100.75
1.5186	1.5045 (*RSD* = 1.72%, *n* = 3)	99.07
Mean *N* = 10		100.6
SD		1.63
RSD		1.62

RESULTS AND DISCUSSION

Linearity responses for nitrate and nitrite were observed, respectively, over the range of 0.307–0.921 mg/mL with a correlation coefficient of 0.999 and 1.15–9.2 μg/mL with a correlation coefficient of 0.999. The relationship of peak area to concentration can be presented by the linear regression equations

Table II—Assay Results for Toothpaste Containing 5% Potassium Nitrate

Sample	Potassium Nitrate Found, %	Percent of Label Claim
1	5.09	101.8
2	4.99	99.8
3	5.07	101.4
4	5.00	100.0
5	4.90	98.0
6	5.02	100.4
7	5.02	100.4
8	4.89	97.8
9	5.07	101.4
Mean		100.1
SD		1.43
RSD		1.43

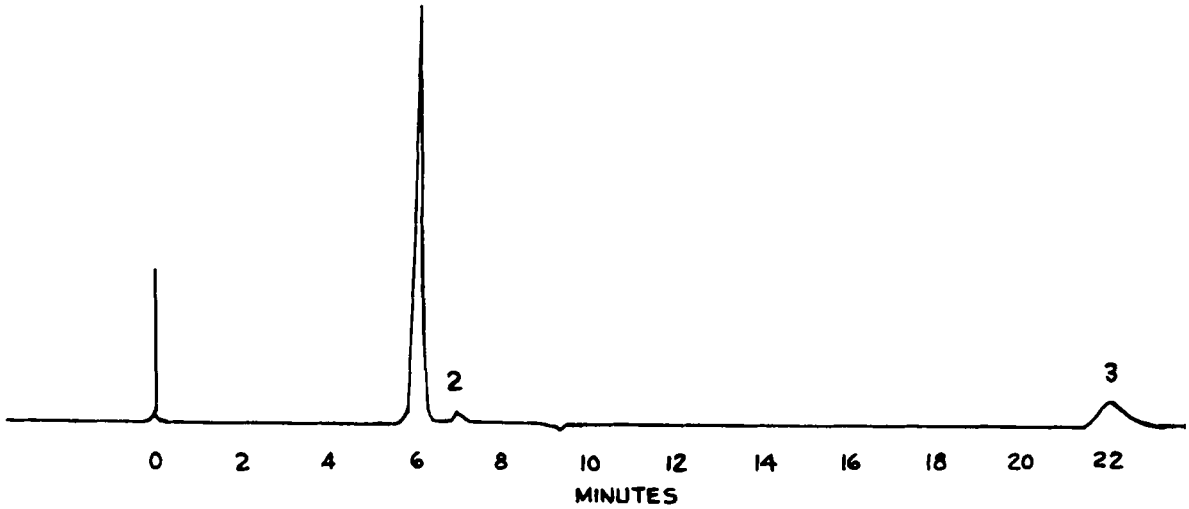

Figure 2—*Chromatogram of a toothpaste placebo spiked with both nitrate (1) and nitrite (2). The spiked placebo was prepared by adding 100 mg of potassium nitrate and 2 mL of 5.0 mM sodium nitrite solution into 2 g of toothpaste placebo; peak 3 = excipients in the toothpaste.*

$y = 35789.8x + 1127.5$ for nitrate and $y = 668322x + 312$ for nitrite, where y is the peak area obtained by the laboratory data system and x is the concentration in mg/mL.

Chromatograms obtained for a standard solution of nitrate and nitrite and for a typical commercial toothpaste containing 5% potassium nitrate are presented in Fig. 1A and B, respectively. The nitrate ion was well resolved from the other excipients, and the recovery data for nitrate from spiked samples of toothpaste (Table I) illustrate the validity of the method for these formulations. Average recovery for placebo dentifrices spiked with three concentration levels (50, 100, and 150% of label concentration) of nitrate was 100.6% with a standard deviation of 1.63%. This method has been used routinely in a product stability program and found to be accurate and precise with a relative standard deviation of 1.43% ($n = 9$). Representative data are summarized in Table II.

Although nitrite was not detected in any commercial toothpaste samples, it was necessary to demonstrate the selectivity of the method for nitrate in the presence of nitrite; therefore, spiked toothpaste samples containing both nitrate and nitrite were prepared and assayed. A representative chromatogram of a spiked sample containing 61.4 mg of nitrate and 115 μg of nitrite per 100 mL is reproduced in Fig. 2. Excellent resolution of nitrite from nitrate, an essential requirement for a stability-indicating assay, was obtained. Average recovery at the 2.3–9.2-μg/mL nitrite level was 96.4%, with a relative standard deviation of 6.7% ($n = 8$). The minimum detectable concentration of nitrite was 50 μg/g of toothpaste sample.

The retention of nitrate and nitrite on a reverse-phase column may be attributed to the interaction of these anions with the protonated silanol backbone of stationary phase at the acidic condition (pH 3.0 ± 0.1) employed in this experiment. In addition to this electrostatic attractive force, solute anions may also experience the steric exclusion provided by the hydrophobic long-chain octyl substituents of the stationary phase. The balance between these two opposing forces could determine the retention of anions on the column and the separation of one anion from the others. The unsatisfactory results obtained with an RP-18 column may be due to the overwhelming steric exclusion provided by the more hydrophobic octadecyl substituents of the stationary phase.

REFERENCES

(1) B. L. Green, M. L. Green, and W. T. McFall, Jr., *J. Periodontol*, **48**(10), 667 (1977).

(2) W. J. Tarbet, G. Silverman, J. M. Stolman, and P. A. Fratarcangelo, *J. Periodontol*, **51**(9), 535 (1980).

(3) M. Hodosh, *J. Am. Dent. Assoc.*, **88**, 831 (1974).

(4) F. B. Hora and P. J. Webber, *Analyst*, **85**, 567 (1960).

(5) F. L. Fisher, E. R. Ibert, and H. F. Beckman, *Anal. Chem.*, **30**, 1972 (1958).

(6) R. J. Elliott and A. G. Porter, *Analyst*, **96**, 522 (1971).

(7) W. Davison and C. Woof, *Analyst*, **104**, 385 (1979).

(8) J. Gabbay, Y. Almog, M. Davidson, and A. E. Donagi, *Analyst*, **102**, 371 (1977).

(9) M. K. Chau, T. Higuchi, and L. A. Sternson, *Anal. Chem.*, **50**, 1670 (1978).

(10) F. Fox and A. Okabe, *J. Assoc. Off. Anal. Chem.*, **65**, 157 (1982).

(11) J. A. Dongherty and G. A. Laban, *Anal. Chem.*, **47**, 1130 (1975).

(12) R. Raogaddle and B. Patel, *J. Soc. Cosmet. Chem.*, **30**, 385 (1970).

(13) H. Noda, M. Minemoto, A. Noda, K. Matsuyama, S. Iguchi, and T. Kohinata, *Chem. Pharm. Bull.*, **28**, 2541 (1980).

(14) M. Toyoda, H. Suzuki, Y. Ito, and M. Iwaida, *J. Assoc. Off. Anal. Chem.*, **61**, 508 (1978).

(15) K. Funazo, M. Tanaka, and T. Shono, *Anal. Chem.*, **52**, 1222 (1980).

(16) J. S. DiGregorio and M. D. Morris, *Anal. Chem.*, **42**, 94, (1970).

(17) D. G. Jehring, W. A. Dippel, and R. S. Boucher, *Anal. Chem.*, **42**, 1686 (1970).

(18) G. P. Morie, C. J. Ledford, and C. A. Glover, *Anal. Chim. Acta*, **60**, 397 (1972).

(19) S. W. Boese and V. S. Archer, *Anal. Chem.*, **49**, 479 (1977).

(20) L. D. Hansen, B. E. Richter, and D. J. Eatongh, *Anal. Chem.*, **49**, 1779 (1977).

(21) H. Small, T. S. Stevens, and W. C. Bauman, *Anal. Chem.*, **47**, 1801 (1975).

(22) D. T. Gjerde, J. S. Fritz, and G. Schmuckler, *J. Chromatogr.*, **186**, 590 (1979).

(23) D. T. Gjerde, G. Schmuckler, and J. S. Fritz, *J. Chromatogr.*, **187**, 35 (1980).

(24) F. A. Buytenhugs, *Chrompack Topics*, **8**, 4 (1981).

(25) R. J. Davenport and D. C. Johnson, *Anal. Chem.*, **46**, 1971 (1974).

(26) J. R. Thayer and R. C. Huffaker, *Anal. Biochem.*, **102**, 110 (1980).

(27) J. E. Girard and J. A. Glatz, *Am. Lab.*, **26**, (Oct.) (1981).

(28) N. Skelly, *Anal. Chem.*, **54**, 712 (1982).

(29) U. Leuenberger, R. Gauch, K. Rieder, and T. Baumgartner, *J. Chromatogr.*, **202**, 461 (1980).

(30) H. J. Cortes, *J. Chromatogr.*, **234**, 517 (1981).

Exchange of Sodium by Magnesium in Aluminum Hydroxycarbonate Gel

EDWARD C. SCHOLTZ *, JOSEPH R. FELDKAMP ‡, JOE L. WHITE ‡, and STANLEY L. HEM *x

Received April 11, 1983, from the *Departments of *Industrial and Physical Pharmacy and ‡Agronomy, Purdue University, West Lafayette, IN 47907. Accepted for publication June 5, 1983.

Abstract □ Approximately 90% of the sodium present in a washed aluminum hydroxycarbonate gel was removed by exchange with magnesium. This behavior supports recent structural studies which have suggested that cations such as sodium serve as counterions in aluminum hydroxycarbonate gel. However, sodium could not be removed from dihydroxyaluminum sodium carbonate by exchange with magnesium because sodium is part of the crystal structure. It is hypothesized that aluminum hydroxycarbonate gels which resist removal of sodium are actually mixtures containing dihydroxyaluminum sodium carbonate in addition to aluminum hydroxycarbonate.

Keyphrases □ Aluminum hydroxycarbonate gel—removal of sodium by magnesium □ Counterions—removal of sodium by magnesium in aluminum hydroxycarbonate gel

Structural studies have suggested (1, 2) that the acid-reactive aluminum hydroxide gel used in antacids has a planar structure in which the basic unit is a six-membered ring of aluminum atoms joined by double hydroxide bridges. Carbonate is specifically adsorbed at aluminum sites along the edge (3-5). This structure suggests that other cations which may be present simply function as counterions. To further test the structural model of aluminum hydroxycarbonate gel, the ability of magnesium ions to replace sodium ions was studied.

EXPERIMENTAL SECTION

The aluminum hydroxycarbonate gel was precipitated by reacting solutions of 0.5 M aluminum chloride and 2.0 M sodium carbonate at a constant pH of 7.0 (6). A gel composed of a mixture of aluminum hydroxycarbonate and dihydroxyaluminum sodium carbonate was precipitated from the same system at a constant pH of 8.5 (6).

Each gel was divided into two equal portions. One portion, designated as the control, was washed with distilled water by adding a volume of distilled water equal to the volume of the gel, mixing for 15 min, and centrifuging to produce a clear supernatant. The supernatant was tested for chloride by the silver nitrate test (7). The washing procedure was repeated until the supernatant was free of chloride as indicated by the silver nitrate test. The second portion was washed four times with a volume of 1 M $MgCl_2$, which was equal to the volume of the gel before washing with distilled water as described above, and is called the magnesium-exchanged portion.

The chloride-containing aluminum hydroxide gel was prepared by treating 0.5 M $AlCl_3$ with 1 M KOH (8). The equivalent aluminum oxide and magnesium content were determined by chelatometric titration (9).

The sodium content was determined by atomic absorption spectrometry[1]. A sample containing a 0.4-g equivalent of aluminum oxide was dissolved by adding 4 mL of 12 M HCl. Potassium chloride (95 mg) was added, and the final volume was adjusted to 25 mL with distilled water. Standards and blanks for the magnesium-exchanged samples contained the same quantity of magnesium ion as was present in the sample.

IR spectra[2] were recorded on air-dried samples with potassium bromide pellets (0.75-mg sample and 300 mg of KBr). X-ray diffractograms were obtained with air-dried samples in powder mounts (McCreery mounts). Diffractograms were recorded from 6 to 40° (2θ) under the following conditions[3]: CuK_α radiation, 30 kV, 28 mA, 2°/min. The acid neutralization reaction was monitored by an automated[4] pH-stat titration (10). The point of zero charge was determined by a continuous titration procedure (8).

RESULTS AND DISCUSSION

The control and magnesium-exchanged portions of the aluminum hydroxycarbonate gel each required four washings with distilled water to produce a negative test for chloride. The control contained 0.82 M (8.4%) equivalent aluminum oxide and 2.5×10^{-2} M (0.057%) sodium, which is equivalent to a sodium-aluminum molar ratio of 1.5×10^{-2}. The magnesium-exchanged portion contained 0.78 M (8.0%) equivalent aluminum oxide and 2.7×10^{-3} M (0.0062%) sodium, which is equivalent to a sodium-aluminum molar ratio of 1.7×10^{-3}. Thus, ~90% of the sodium present in the control was removed by the magnesium-exchange procedure.

The IR spectrum and X-ray diffraction pattern of the magnesium-exchanged portion were typical of aluminum hydroxycarbonate gel (11) and were identical with the control (Fig. 1A and B), indicating that no structural changes occurred due to the magnesium-exchange procedure.

The control aluminum hydroxycarbonate gel was free of magnesium, whereas the magnesium-exchanged portion contained 6.9×10^{-2} M (0.17%) magnesium, which is equivalent to a magnesium-aluminum molar ratio of 0.044. Thus, as suggested by recent structural studies (1-5), sodium appears to be a counterion in aluminum hydroxycarbonate gel and not a structural component.

It should be noted that the sodium content of the control was low in terms of the clinical use of aluminum hydroxycarbonate gel as an antacid. For example, if the control were used at a dosage regimen of 40 mEq/dose for seven daily doses, as occurs in high-intensity antacid therapy (12, 13), the aluminum hydroxycarbonate gel would contribute 32 mg of sodium/d to the sodium intake of the patient. This represents only 6.4% of the 500 mg (22 mmol) of sodium allowed in a strict sodium-restricted diet (14). The magnesium-exchanged aluminum hydroxycarbonate gel would only contribute 3.7 mg of sodium/d for the same dosage regimen (<1% of the sodium allowed in a strict sodium-restricted diet).

The ratio of milliequivalents of magnesium adsorbed to milliequivalents of sodium desorbed was 6.2. This ratio exceeds the expected value of 1. It is hypothesized that magnesium displaced some other cation, such as a proton, in addition to sodium. Magnesium ions could displace protons in the diffuse portion of the electrical double layer or perhaps from the Stern layer.

The hypothesis that magnesium exchanges for protons in addition to sodium was tested by titrating a chloride-containing aluminum hydroxide suspension with magnesium nitrate. The pH of the chloride-containing aluminum hydroxide suspension and the 6×10^{-4} M $Mg(NO_3)_2$ was adjusted to 9.6, which is the point of zero charge for the chloride-containing aluminum hydroxide. This was necessary to eliminate pH shifts in the suspension on addition of titrant, which could be attributed to a simple ionic strength effect (8). The pH of the chloride-containing aluminum hydroxide suspension decreased from pH 9.6 to 8.76 as a result of titration with 3 mL of 6×10^{-4} M $Mg(NO_3)_2$ (Table I). Titration with 3 mL of water adjusted to pH 9.6 only caused a pH change of 0.08. The decrease in pH on addition of $Mg(NO_3)_2$ is believed to be due to the exchange of magnesium for protons at the aluminum hydroxide surface. Normally, the pH of the aluminum hydroxide at its point of zero charge would be unaffected by an ionic strength change since the background salt usually behaves as an indifferent electrolyte. This suggests that magnesium specifically adsorbs as a Stern layer ion and displaces protons in the process.

The antacid properties of the magnesium-exchanged aluminum hydroxycarbonate gel are very similar to the control. Both portions reacted completely within 15 min, with the neutralization of three protons per aluminum ion. Thus, the presence of sodium as a counterion in aluminum hydroxycarbonate

[1] Model 290B; Perkin-Elmer Co., Norwalk, Conn.
[2] Model 180; Perkin-Elmer Co., Norwalk, Conn.
[3] Siemens A G Kristalloflex 4 generator, Type F diffractometer; Karlsrule, Federal Republic of Germany.
[4] PHM 26, TTT 60, ABU 12 (2.5 mL), TTA60, REA 160; Radiometer, Copenhagen, Denmark.

0022-3549/84/0700-1007$01.00/0
© 1984, American Pharmaceutical Association

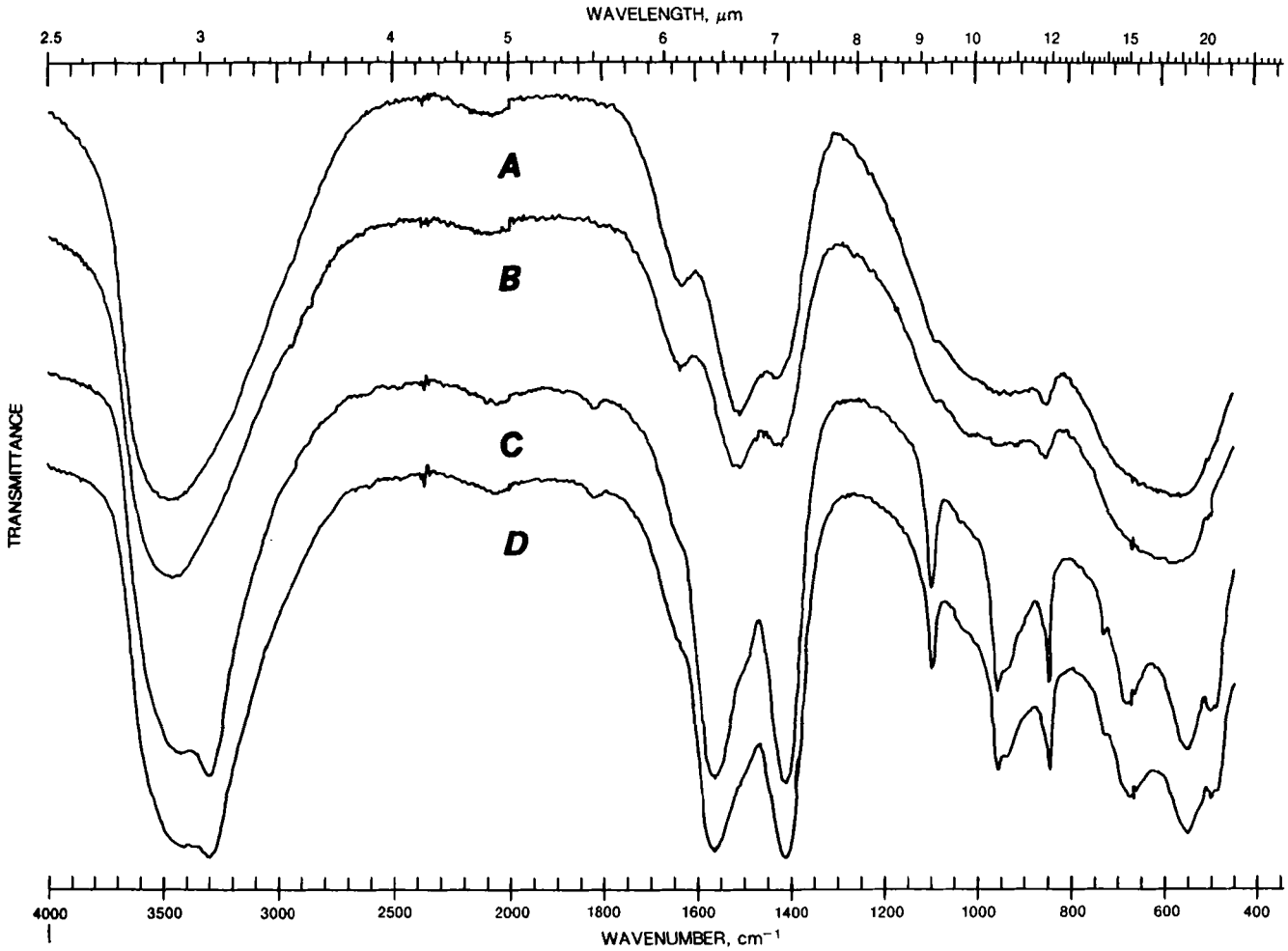

Figure 1—*IR spectra. Key: (A) control aluminum hydroxycarbonate gel; (B) magnesium-exchanged aluminum hydroxycarbonate gel; (C) control gel containing aluminum hydroxycarbonate gel and dihydroxyaluminum sodium carbonate; (D) magnesium-exchanged gel containing aluminum hydroxycarbonate gel and dihydroxyaluminum sodium carbonate.*

gel is unimportant in terms of antacid properties since the rate of acid neutralization is independent of sodium content (15).

The hypothesis that sodium is a counterion in aluminum hydroxycarbonate gel was further tested by attempting to exchange magnesium for sodium in a gel which is known to be a mixture of aluminum hydroxycarbonate and dihydroxyaluminum sodium carbonate. Dihydroxyaluminum sodium carbonate has the formula $NaAl(OH)_2CO_3$ and is known mineralogically as dawsonite (16). The precipitation conditions were altered to produce the desired mixture (6). The IR spectrum of the mixture (Fig. 1C) shows a wider split of the ν_3 mode of carbonate (1560 and 1410 cm^{-1}) than aluminum hydroxycarbonate (Fig. 1A). The IR spectrum of the mixture also contains bands which are characteristic of dawsonite at 3290, 1818, 955, 935, 846, and 550 cm^{-1} (17), in addition to the bands associated with aluminum hydroxycarbonate.

Table I—Titration of Aluminum Hydroxide [a] with 6×10^{-4} M Magnesium Nitrate

Sample[b]		Blank[b]	
pH	Titrant, mL	pH	Water, mL
9.60	0	9.63	0
9.52	0.1	9.61	0.1
9.44	0.2	9.60	0.5
9.36	0.3	9.58	1.0
9.30	0.4	9.56	2.0
9.21	0.6	9.55	3.0
9.12	0.8		
9.05	1.0		
8.96	1.4		
8.86	2.0		
8.76	3.0		

[a] At pH equal to the point of zero charge (9.6). [b] Aluminum hydroxide gel (100 mL) containing 1% equivalent aluminum oxide.

The sodium to aluminum molar ratio of the mixture was 0.50 after washing with water. The high sodium to aluminum molar ratio is due to the presence of dawsonite, which has a sodium-aluminum molar ratio of 1. The sodium-aluminum molar ratio of the mixture only decreased to 0.42 after magnesium exchange. It is believed that the sodium associated with aluminum hydroxycarbonate was exchanged with magnesium, but the sodium in dawsonite is part of the crystal structure and was not exchanged with magnesium.

In conclusion, cations such as sodium which are present in aluminum hydroxycarbonate gel function as counterions and can be removed by cation exchange. However, sodium cannot be removed by cation exchange from dihydroxyaluminum sodium carbonate. Thus, aluminum hydroxycarbonate gels which resist the removal of sodium by cation exchange may also contain dihydroxyaluminum sodium carbonate (dawsonite).

REFERENCES

(1) S. L. Nail, J. L. White, and S. L. Hem, *J. Pharm. Sci.*, **65**, 1188 (1976).

(2) S. L. Nail, J. L. White, and S. L. Hem, *J. Pharm. Sci.*, **65**, 1192 (1976).

(3) J. L. White and S. L. Hem, *J. Pharm. Sci.*, **64**, 468 (1975).

(4) C. J. Serna, J. L. White, and S. L. Hem, *J. Pharm. Sci.*, **67**, 1144 (1978).

(5) E. C. Scholtz, J. R. Feldkamp, J. L. White, and S. L. Hem, *J. Pharm. Sci.*, **73**, 209 (1984).

(6) E. C. Scholtz, Ph.D. Thesis, Purdue University, 1981, pp. 19–23.

(7) "The United States Pharmacopeia," 20th rev., United States Pharmacopeial Convention, Inc., Rockville, Md., 1980, p. 906.

(8) J. R. Feldkamp, D. N. Shah, S. L. Meyer, J. L. White, and S. L. Hem, *J. Pharm. Sci.*, **70**, 638 (1981).

(9) "The United States Pharmacopeia," 20th rev., United States Pharmacopeial Convention, Inc., Rockville, Md., 1980, p. 23.

(10) N. J. Kerkhof, R. K. Vanderlaan, J. L. White, and S. L. Hem, *J. Pharm. Sci.*, **66**, 1528 (1977).
(11) C. J. Serna, J. L. White, and S. L. Hem, *J. Pharm. Sci.*, **67**, 324 (1978).
(12) J. S. Fordtran, *N. Engl. J. Med.*, **298**, 1082 (1978).
(13) R. W. Welch, *Arch. Intern. Med.*, **138**, 1208 (1978).
(14) "The Merck Manual," 13th ed., Merck and Co., Rahway, N.J., 1977, p. 1132.
(15) S. L. Hem, J. L. White, J. D. Buehler, J. R. Luber, W. M. Grim, and E. A. Lipka, *Am. J. Hosp. Pharm.*, **39**, 1925 (1982).
(16) A. J. Frueh and J. P. Golightly, *Can. Mineral.*, **9**, 51 (1967).
(17) J. A. Gadsden, "Infrared Spectra of Minerals and Related Inorganic Compounds," Butterworth, Reading, Mass., 1975, p. 74.

ACKNOWLEDGMENTS

This study was supported in part by William H. Rorer, Inc. This report is Journal Paper 9493, Purdue University Agricultural Experiment Station, West Lafayette, IN 47907.

Rapid Quantitative Liquid Chromatographic Determination of Caffeine Levels in Plasma after Oral Dosing

S. E. O'CONNELL ˣ **and F. J. ZURZOLA**

Received May 6, 1983, from *Bristol-Myers Products, Hillside, NJ 07207.* Accepted for publication July 11, 1983.

Abstract □ A simple method is described for the rapid, quantitative analysis of caffeine in human plasma. Caffeine levels present in plasma following drug administration were determined by high-performance liquid chromatography with UV detection at 273 nm after plasma protein precipitation. Caffeine was detectable at levels as low as 0.1 μg/mL. Mean recoveries of 98% with a coefficient of variation of 3% were obtained for plasma standards, in which concentrations ranged from 0.1 to 8 μg/mL. Interassay variability of the slope of the standard curve had a coefficient of variation of 3%. Application of this method during human bioavailability studies is described.

Keyphrases □ Caffeine—HPLC, human plasma, bioavailability □ Bioavailability—caffeine, HPLC, human plasma, oral dosing

Caffeine is a commonly ingested drug that is present in foods, beverages, and medicaments. Its widespread use has stimulated an interest in the development of a simple and rapid plasma determination for caffeine suitable for analyzing multiple samples.

Although GC (1-3) and spectrophotometric (4) methods exist for caffeine determination in biological fluids, high-performance liquid chromatographic (HPLC) methods are relatively few, and those available suffer from the disadvantages of inadequate sensitivity (5), time-consuming extraction steps (5-7), dedicated equipment (8), inadequate sample cleanup, inadequate sensitivity for pharmacokinetic studies (9-11), and insufficient testing in human plasma (11).

The method described herein involves a single plasma protein precipitation followed by liquid chromatographic determination of caffeine in the clear supernatant. The plasma proteins were denatured and precipitated with 0.15 M $Ba(OH)_2$ and 5% $ZnSO_4$ solutions, as described previously (12). The use of this combination of reagents results in a supernatant with a neutral pH and a clean chromatographic profile due to efficient coprecipitation of both plasma proteins and excess reagents. The method is capable of detecting at least 0.1 μg/mL of caffeine, and the reproducibility eliminates the need for an internal standard. Furthermore, the ease and rapidity of sample workup make this method ideal for multiple-sample analyses.

This method has been used routinely on long-term human bioavailability studies, resulting in clean predose plasma chromatograms with no interference and no column deterioration after several hundred analyses, and has been found to be precise and accurate.

EXPERIMENTAL SECTION

Reagents—Standard solutions were prepared in distilled water. The 0.15 M $Ba(OH)_2$ and 5% $ZnSO_4$ solutions were obtained commercially[1].

Instrumentation and Operating Conditions—The analysis was performed with a high-performance liquid chromatograph[2] with a variable-wavelength UV detector[3] set at 273 nm, an automated injection system[4] fitted with a 75-μL loop, and a 30 cm × 4-mm i.d. reverse-phase, high-efficiency C_{18} col-

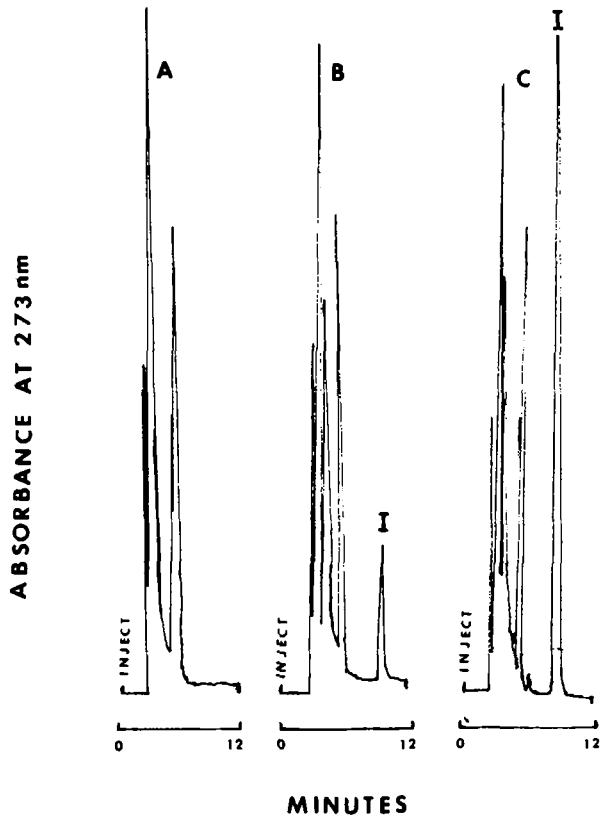

Figure 1—*Chromatograms for a typical subject. Key: (A) taken prior to caffeine (I) administration; (B) taken 10 min after oral administration of two 65-mg tablets; (C) taken 20 min postdose.*

[1] $ZnSO_4$ solution (lot SO-Z-10), $Ba(OH)_2$ solution (lot SO-B-138); Fisher Scientific Co.
[2] Model 6000; Waters Associates, Milford, Mass.
[3] Model 773; Kratos, Ramsey, N.J.
[4] Model 725; Mircomeritics, Norcross, Ga.

0022-3549/84/0700-1009$01.00/0
© 1984, American Pharmaceutical Association

(10) N. J. Kerkhof, R. K. Vanderlaan, J. L. White, and S. L. Hem, *J. Pharm. Sci.*, **66**, 1528 (1977).
(11) C. J. Serna, J. L. White, and S. L. Hem, *J. Pharm. Sci.*, **67**, 324 (1978).
(12) J. S. Fordtran, *N. Engl. J. Med.*, **298**, 1082 (1978).
(13) R. W. Welch, *Arch. Intern. Med.*, **138**, 1208 (1978).
(14) "The Merck Manual," 13th ed., Merck and Co., Rahway, N.J., 1977, p. 1132.
(15) S. L. Hem, J. L. White, J. D. Buehler, J. R. Luber, W. M. Grim, and E. A. Lipka, *Am. J. Hosp. Pharm.*, **39**, 1925 (1982).
(16) A. J. Frueh and J. P. Golightly, *Can. Mineral.*, **9**, 51 (1967).
(17) J. A. Gadsden, "Infrared Spectra of Minerals and Related Inorganic Compounds," Butterworth, Reading, Mass., 1975, p. 74.

ACKNOWLEDGMENTS

This study was supported in part by William H. Rorer, Inc. This report is Journal Paper 9493, Purdue University Agricultural Experiment Station, West Lafayette, IN 47907.

Rapid Quantitative Liquid Chromatographic Determination of Caffeine Levels in Plasma after Oral Dosing

S. E. O'CONNELL ˣ **and F. J. ZURZOLA**

Received May 6, 1983, from *Bristol-Myers Products, Hillside, NJ 07207.* Accepted for publication July 11, 1983.

Abstract □ A simple method is described for the rapid, quantitative analysis of caffeine in human plasma. Caffeine levels present in plasma following drug administration were determined by high-performance liquid chromatography with UV detection at 273 nm after plasma protein precipitation. Caffeine was detectable at levels as low as 0.1 μg/mL. Mean recoveries of 98% with a coefficient of variation of 3% were obtained for plasma standards, in which concentrations ranged from 0.1 to 8 μg/mL. Interassay variability of the slope of the standard curve had a coefficient of variation of 3%. Application of this method during human bioavailability studies is described.

Keyphrases □ Caffeine—HPLC, human plasma, bioavailability □ Bioavailability—caffeine, HPLC, human plasma, oral dosing

Caffeine is a commonly ingested drug that is present in foods, beverages, and medicaments. Its widespread use has stimulated an interest in the development of a simple and rapid plasma determination for caffeine suitable for analyzing multiple samples.

Although GC (1-3) and spectrophotometric (4) methods exist for caffeine determination in biological fluids, high-performance liquid chromatographic (HPLC) methods are relatively few, and those available suffer from the disadvantages of inadequate sensitivity (5), time-consuming extraction steps (5-7), dedicated equipment (8), inadequate sample cleanup, inadequate sensitivity for pharmacokinetic studies (9-11), and insufficient testing in human plasma (11).

The method described herein involves a single plasma protein precipitation followed by liquid chromatographic determination of caffeine in the clear supernatant. The plasma proteins were denatured and precipitated with 0.15 M $Ba(OH)_2$ and 5% $ZnSO_4$ solutions, as described previously (12). The use of this combination of reagents results in a supernatant with a neutral pH and a clean chromatographic profile due to efficient coprecipitation of both plasma proteins and excess reagents. The method is capable of detecting at least 0.1 μg/mL of caffeine, and the reproducibility eliminates the need for an internal standard. Furthermore, the ease and rapidity of sample workup make this method ideal for multiple-sample analyses.

This method has been used routinely on long-term human bioavailability studies, resulting in clean predose plasma chromatograms with no interference and no column deterioration after several hundred analyses, and has been found to be precise and accurate.

EXPERIMENTAL SECTION

Reagents—Standard solutions were prepared in distilled water. The 0.15 M $Ba(OH)_2$ and 5% $ZnSO_4$ solutions were obtained commercially[1].

Instrumentation and Operating Conditions—The analysis was performed with a high-performance liquid chromatograph[2] with a variable-wavelength UV detector[3] set at 273 nm, an automated injection system[4] fitted with a 75-μL loop, and a 30 cm × 4-mm i.d. reverse-phase, high-efficiency C_{18} col-

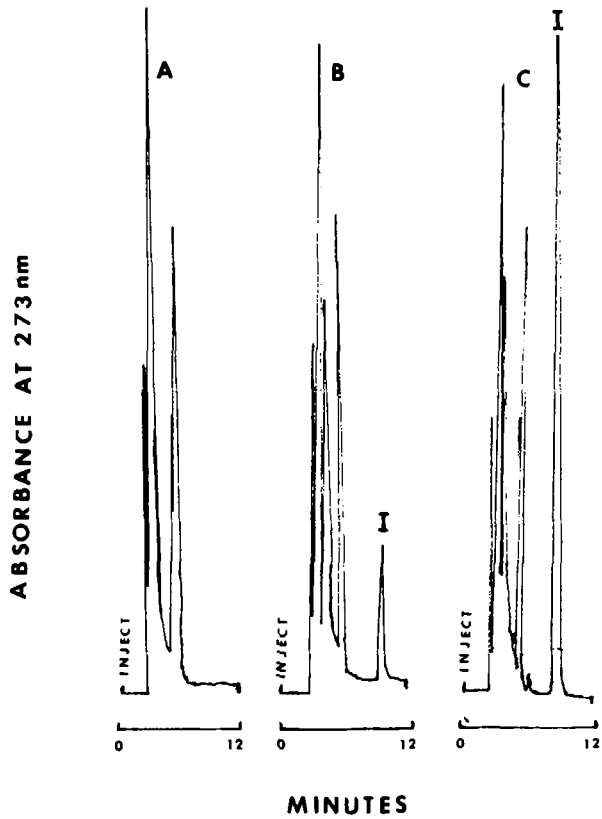

Figure 1—*Chromatograms for a typical subject. Key: (A) taken prior to caffeine (I) administration; (B) taken 10 min after oral administration of two 65-mg tablets; (C) taken 20 min postdose.*

[1] $ZnSO_4$ solution (lot SO-Z-10), $Ba(OH)_2$ solution (lot SO-B-138); Fisher Scientific Co.
[2] Model 6000; Waters Associates, Milford, Mass.
[3] Model 773; Kratos, Ramsey, N.J.
[4] Model 725; Mircomeritics, Norcross, Ga.

0022-3549/84/0700-1009$01.00/0
© 1984, American Pharmaceutical Association

Table I—Accuracy of HPLC Assay for Caffeine in Human Plasma

Amount Added, μg	Experiment 1 Amount Found, μg	1 Error, %	2 Amount Found, μg	2 Error, %	3 Amount Found, μg	3 Error, %	4 Amount Found, μg	4 Error, %	5 Amount Found, μg	5 Error, %
0	0.01		0.01		0		0		0	
0	0.01		0.01		0		0		0	
0.1	0.10	0.0	0.10	0.0	—		—		—	
0.1	0.11	10.0	0.10	0.0	—		—		—	
0.25	0.25	0.0	0.26	4.0	0.24	4.0	0.26	4.0	0.27	8.0
0.25	0.23	8.0	0.26	4.0	0.24	4.0	0.27	8.0	0.26	4.0
0.50	0.48	4.0	0.50	0.0	0.50	0.0	0.47	6.0	0.51	2.0
0.50	0.51	2.0	0.52	4.0	0.50	0.0	0.50	0.0	0.55	10.0
1.00	0.99	1.0	1.00	0.0	0.96	4.0	0.99	1.0	0.89	1.0
1.00	1.05	5.0	1.05	5.0	1.01	1.0	0.99	1.0	1.01	1.0
2.00	1.93	3.5	1.99	0.5	2.04	2.0	1.92	4.0	1.95	2.5
2.00	2.04	2.0	1.95	2.5	1.99	0.5	2.04	2.0	1.95	2.5
4.00	3.86	3.5	3.84	4.0	3.94	1.5	3.91	2.3	4.01	0.3
4.00	4.08	2.0	3.91	2.3	3.96	1.0	4.10	2.5	4.00	0.0
8.00	7.78	3.0	8.02	0.3	7.92	1.0	7.93	0.8	7.97	0.4
8.00	8.25	3.0	8.11	1.4	8.12	1.3	8.08	1.0	8.08	1.0

umn[5]. The mobile phase was methanol-water (30:70), which was filtered through a 0.45-μm pore-size filter[6] and was deaerated before use. The flow rate was 1.0 mL/min. The column was fitted with a precolumn packed with C_{18} Corasil, 37–50 μm[7]. This precolumn was repacked once a week during panel use, since particulate matter accumulated on the precolumn frit and started to increase the column pressure after a weekly load of 300–400 injections. The detector was set at a sensitivity of 0.02 AUFS.

Plasma Caffeine Study in Humans—Because the described method was so sensitive to low levels of caffeine, it became necessary to insist that panelists abstain from caffeine-containing food, drugs, and beverages for at least 72 h before dosing. The panelists were fasted overnight and then received a 130-mg oral dose of caffeine in the form of two multicomponent tablets[8] taken with 100 mL of water. It had been determined in earlier panels that coadministration of aspirin and acetaminophen do not result in drug or metabolite peaks which interfere with the caffeine peak. Venous blood specimens were withdrawn by syringe and discharged into centrifuge tubes containing heparin as an anticoagulant. Specimens were taken before and at specified times after drug administration through 4 h. Collected specimens were centrifuged immediately for 15 min at 3500 rpm in a bench-top centrifuge. Plasma was separated and analyzed for caffeine by the proposed method.

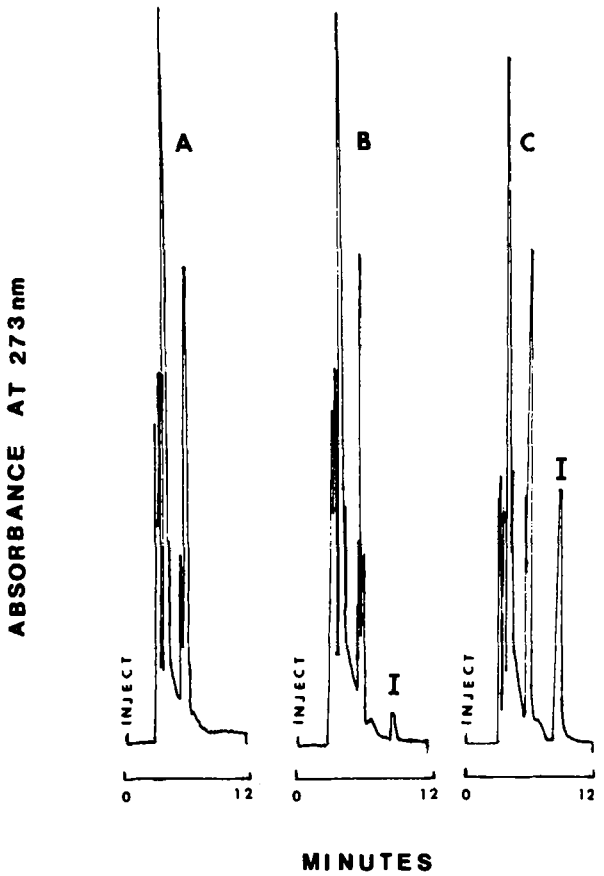

Figure 2—*Chromatograms of a 1-mL human plasma sample processed by the described precipitation method. The mobile phase was 30% methanol at a flow rate of 1.0 mL/min, and the chart speed was 15 cm/h. Key: (A) unspiked plasma; (B) plasma spiked with 0.1 μg of caffeine (I); (C) plasma spiked with 1 μg of I.*

Analysis—One milliliter of freshly drawn plasma was added to a screw-top culture tube (16 × 100 mm). To each tube was added 1 mL of the saturated 0.15 M $Ba(OH)_2$ solution. The tubes were vortexed for 2 min at sufficient speed on a multiple tube vortex mixer[9] to allow thorough mixing and sufficient reaction time. The addition of 1 mL of the 5% $ZnSO_4$ solution was made only after each sample became opaque in appearance. Each tube was then capped and vortexed at high speed for 1 min. The tubes were then centrifuged in a bench-top centrifuge at high speed for 10 min. The resulting clear, water-like supernatant was separated from the precipitate and filtered directly into an autoinjector vial with a Pasteur pipet plugged with glass wool. This ensured a minimal volume loss and a particulate-free sample.

Standard Curves—Calculations were carried out with standard curves constructed by analyzing 1-mL samples of the pooled predose plasma spiked with 0.1–8 μg of caffeine and by plotting the peak height *versus* the corresponding concentration. The standard curve data were subjected to least-squares linear regression analyses, and the resulting equation was utilized for the calculation of the drug concentration in the unknown samples.

RESULTS AND DISCUSSION

Typical chromatograms of a predose plasma sample (Fig. 1A) and the 10- and 20-min postdose plasma samples (Fig. 1B and C, respectively) obtained for a typical subject demonstrate the specificity of this method by the absence of interfering peaks. With 30% methanol in water as the eluant at a flow rate of 1.0 mL/min, the retention time for caffeine was 9 min.

Figure 2 represents the chromatograms of a 1-mL plasma blank, a 1-mL plasma sample spiked with 0.10 μg of caffeine, and a 1-mL plasma sample spiked with 1 μg of caffeine. The standards and samples are chromatographically clean to the extent that caffeine concentrations <0.1 μg/mL can be detected by this procedure. The adequate peak size and clean baseline resolution for a 75-μL sample injection containing 0.10 μg/mL of caffeine indicates the potential for detecting caffeine at concentrations of <0.1 μg/mL *via* an increased injection volume or more sensitive detector setting. Since the lowest caffeine level normally encountered in our therapeutic drug monitoring was ~0.25 μg/mL, the present sensitivity of this method is more than adequate for use in blood level and pharmacokinetic studies.

Recovery—The recovery of caffeine from plasma relative to its recovery from water, as measured by the ratio of the slopes of the standard curves in plasma and water, respectively, was 0.98 ± 0.03, with a coefficient of variation

[5] μ-Bondapak C_{18}, Waters Associates.
[6] Millipore Corp., Bedford, Mass.
[7] Waters Associates.
[8] Excedrin; Bristol-Myers Products, Hillside, N.J.
[9] Kraft Apparatus, Inc., Mineola, N.Y.

Table II—Caffeine Plasma Levels [a]

Subject	Caffeine Levels, μg/mL						
	10 min	20 min	40 min	60 min	120 min	180 min	240 min
Females							
1	0.7578	4.3575	3.9549	3.2918	2.2024	1.4683	1.0657
3	1.7288	4.3338	3.8839	3.5760	2.6524	2.1314	1.6814
5	2.3238	3.9185	3.8729	3.5312	3.0756	2.7566	2.5516
7	0.0000	1.1394	3.5811	4.2594	3.7439	3.3370	2.9843
9	2.9160	3.6563	3.2301	2.9160	2.5572	2.2431	1.9964
11	0.4561	2.6294	4.4807	4.2124	3.7026	3.1392	2.7367
13	1.7465	4.3202	4.0904	4.1134	3.5389	3.2632	3.2402
15	4.5783	5.6424	4.3555	3.8111	3.2172	2.7470	2.3015
17	0.3960	5.3454	5.0732	4.6030	3.8853	3.4646	3.1182
19	0.7061	3.1482	5.7374	5.6491	4.7370	4.0015	3.5601
21	2.0590	4.3696	3.8434	3.2715	2.5623	2.1276	1.7845
23	1.4077	4.7510	4.3771	4.0692	3.5853	3.1014	2.5955
25	4.2452	5.8676	5.0294	4.1912	3.0555	2.4065	1.8928
27	0.7842	6.8141	5.1376	4.5968	3.8126	3.3530	3.1907
29	0.1978	1.6808	2.6201	2.5954	2.3235	2.1011	1.9775
31	2.1887	4.3993	3.3050	2.8453	2.1231	1.5759	1.1819
33	2.3090	5.2018	3.9279	3.5032	2.7336	2.2293	1.9109
35	0.2261	1.2886	3.2555	3.1650	2.7807	2.6677	2.4868
37	4.2461	4.9246	4.3118	3.9178	3.3487	2.9329	2.7140
39	2.2933	4.5110	4.0826	3.7046	2.7974	2.3185	1.8397
Males							
2	0.8973	2.3553	3.4768	2.7815	2.3777	2.0188	1.8394
4	0.0000	1.4353	3.8478	2.4149	2.0276	1.8454	1.6631
6	1.4209	3.1971	2.7945	2.6998	2.3919	2.0603	1.7288
10	3.3641	4.4493	3.0657	2.6587	1.9533	1.5735	1.3022
12	0.6440	2.4148	2.6026	2.1197	1.7440	1.4757	1.3148
14	0.4455	2.0788	2.8955	2.7222	2.5242	2.2768	2.2025
16	1.8513	3.8977	2.6830	2.4952	2.5220	2.3342	2.1464
18	1.3558	3.9065	3.4929	3.3320	2.7575	2.7346	2.4588
20	1.6914	4.0158	3.7510	3.5744	3.1037	2.8389	2.4564
22	0.1352	1.0816	3.3259	3.1096	2.4065	2.0821	1.8387
24	0.6863	2.3792	3.7061	2.9054	2.1275	1.8073	1.6014
26	0.1730	1.2112	2.7437	3.3122	2.1752	1.6067	1.1865
28	0.1977	0.9887	2.5707	2.9415	2.5213	2.1258	1.8539
30	0.0000	0.9458	2.4855	2.1556	1.7157	1.4077	1.2318
34	2.1232	3.0521	2.8398	2.7071	2.4682	2.3355	2.3090
40	1.6416	3.2174	3.3050	2.9548	2.2106	1.9261	1.7729

[a] $n = 36$.

of 3%. Interassay variability of the slope of the standard curves generated during the bioavailability study had a coefficient of variation of <5%. A typical calibration regression line is $y = 44.33x - 0.37$, where x is concentration and y is peak height; this is linear over a concentration range of 0.1–8 μg/mL. The good linearity between the peak height and caffeine concentration in plasma is indicated by the correlation coefficient of >0.999.

Accuracy—Table I shows the actual amounts with which 1-mL blank plasma samples were spiked and the amounts found when the plasma was analyzed by the described method. The experiment was performed in duplicate on each of 5 d. The percent error for each unknown sample was calculated according to (13):

$$\text{percent error} = \left(\frac{\text{amount added} - \text{amount found}}{\text{amount added}}\right) \times 100$$

The average percent error was 3%. In no case did it exceed 10%.

Plasma Levels of Caffeine—A comparison was made of caffeine levels produced by two different caffeine-containing tablet formulations. The total caffeine dose administered was 130 mg. Table II shows the caffeine levels for one of the formulations for 36 subjects in a two-way crossover study with samples taken at 10, 20, 40, 60,120, 180, and 240 min postdose. The 10-min plasma levels indicate a slower absorption by male panelists, with the lowest detectable level of caffeine being slightly less than 0.2 μg/mL. A further inspection of the data reveals that caffeine was rapidly absorbed from the oral dose, reaching a peak plasma level of 3.6 μg/mL in <40 min.

The proposed method is extremely simple, inexpensive, and sensitive for the rapid determination of caffeine in plasma or blood at levels likely to be encountered after a usual 65- or 130-mg total dose. Plasma proteins are denatured by the addition of a saturated $Ba(OH)_2$ solution and then precipitated with a 5% $ZnSO_4$ solution. The resulting colorless clear supernatant is analyzed by HPLC with conventional 3.9-mm i.d. columns. The reproducibility, sensitivity, and selectivity of the method make the use of an internal standard unnecessary. The reproducibility and reliability of this method have been demonstrated in >500 determinations of plasma concentrations of caffeine.

REFERENCES

(1) R. L. Merriman, A. Swanson, M. W. Anders, and N. E. Sladek, *J. Chromatogr.*, **146**, 85 (1978).

(2) F. L. Grab and J. A. Reinstein, *J. Pharm. Sci.*, **57**, 1703 (1968).

(3) J. L. Cohen, C. Cheng, J. P. Henry, and Y. Chan, *J. Pharm. Sci.*, **67**, 1093 (1978).

(4) J. I. Routh, N. A. Shane, E. G. Arredondo, and W. D. Paul, *Clin. Chem.*, **15**, 661 (1969).

(5) C-N. Ou and V. L. Frawley, *Clin. Chem.*, **28**, 1671 (1982).

(6) A. A. Tin, S. Somani, H. Bada, and N. Khanna, *J. Anal. Toxicol.*, **3**, 26 (1979).

(7) D. B. Haughey, *J. Chromatogr.*, **229**, 387 (1982).

(8) Sj.van der Wal, S. J. Bannister, and L. R. Snyder, *J. Chromatogr. Sci.*, **20**, 250 (1982).

(9) J. Blanchard, J. Mohammadi, and K. Conrad, *Clin. Chem.*, **26**, 1351 (1980).

(10) J. Blanchard and J. Mohammadi, *J. Trang, Clin. Chem.*, **27**, 637 (1981).

(11) F. L. S. Tse and D. W. Szeto, *J. Chromatogr.*, **226**, 231 (1981).

(12) S. E. O'Connell and F. J. Zurzola, *J. Pharm. Sci.*, **71**, 1291 (1982).

(13) M. A. Schwartz and J. A. De Silva, in "Principles and Perspectives in Drug Bioavailability," J. Blanchard, R. W. Sawchuck, and B. B. Brodie, Eds., S. Karger, Basel, Switzerland, 1979, p. 92.

Antimicrobial Activity of Triethylammonium Chloride–*N*-Substituted *N'*-Cyano-*O*-(triphenylstannyl)-isourea Complexes

EUGENE J. KUPCHIK *[x], MICHAEL A. PISANO [‡], DILIPKUMAR K. PARIKH *, CAROLYN KREJCI [‡], and JONATHAN TAYLOR [‡]

Received January 31, 1983, from the **Department of Chemistry* and the [‡]*Department of Biological Sciences, St. John's University, New York, NY 11439.* Accepted for publication May 20, 1983.

Abstract □ The triethylammonium chloride complexes of *N*-substituted *N'*-cyano-*O*-(triphenylstannyl)isoureas were generally found to be better antifungal and antibacterial agents than the uncomplexed compounds.

Keyphrases □ *N*-Substituted *N'*-cyano-*O*-(triphenylstannyl)isoureas—complexes with triethylammonium chloride, antibacterial and antifungal activities □ Antimicrobial agents—*N*-substituted *N'*-cyano-*O*-(triphenylstannyl)isourea-triethylammonium chloride complexes, bacterial and fungal screens

Many biocidal applications have been found or suggested for organotin compounds (1, 2). Their use in agriculture as fungicides and pesticides (3–5) is of special interest because they degrade to nontoxic inorganic compounds and, therefore, appear to pose little threat to the environment (6–10). Recently, some diorganotin dihalide and di-pseudohalide complexes were shown to exhibit antitumor activity (11, 12).

It was previously found that triethylammonium (organocyanoamino)chlorotriphenylstannates (I), which are the triethylammonium chloride complexes of *N*-substituted *N*-(triphenylstannyl)cyanamides (II), exhibit higher antifungal activity than the II compounds (13). It was of interest to determine if the triethylammonium chloride complexes (III) (14) of some previously tested *N*-substituted *N'*-cyano-*O*-(triphenylstannyl)isourea compounds (IV) (15) would likewise exhibit higher antifungal activity than the IV compounds. It was also of interest to compare the antibacterial activity of the III and IV compounds.

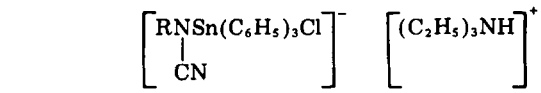

[I]

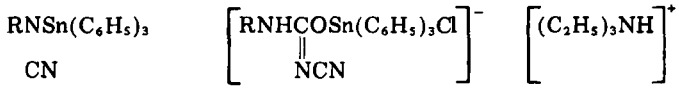

[II] [III]

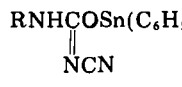

[IV]

EXPERIMENTAL SECTION

The series III compounds were individually dissolved in tetrahydrofuran. The preparation of sterile solutions of the compounds, the fungi employed, the antimicrobial testing procedures, and the determination of growth inhibition were reported previously (15). The preparation of the series III compounds was described previously (14).

Table I—Antifungal Activity of Triethylammonium Chloride–*N*-Substituted *N'*-Cyano-*O*-(triphenylstannyl)isourea Complexes (III) and *N*-Substituted *N'*-Cyano-*O*-(triphenylstannyl)isoureas (IV)

		Aspergillus niger (*ATCC 12845*)			*Chaetomium globosum* (*ATCC 6205*)			*Cladosporium carpophilum* (*ATCC 12117*)			*Fusarium monoliforme* (*ATCC 10052*)			*Myrothecium verrucaria* (*ATCC 9095*)			*Penicillium notatum* (*ATCC 9179*)			*Rhizopus stolonifer* (*ATCC 10404*)			*Saccharomyces cerevisiae* (*ATCC 9896*)			*Trichoderma viride* (*ATCC 8678*)			*Trichophyton mentagrophytes* (*ATCC 9129*)		
Compound	R	1[a]	10	100	1	10	100	1	10	100	1	10	100	1	10	100	1	10	100	1	10	100	1	10	100	1	10	100	1	10	100
IIIa	C_2H_5	+	+	+	+	+	+	+	+	+	+	+	+	+	+	+	+	+	+	−	−	−	+	+	+	−	−	−	+	+	+
IIIb	CH_2=CHC-H_2	+	+	+	+	+	+	+	+	+	+	+	+	+	+	+	+	+	+	−	−	−	+	+	+	−	−	−	+	+	+
IIIc	cyclo-C_6H_{11}	+	+	+	+	+	+	+	+	+	+	+	+	+	+	+	+	+	+	−	−	−	+	+	+	−	−	−	+	+	+
IIId	C_6H_5	+	+	+	+	+	+	+	+	+	+	+	+	+	+	+	+	+	+	−	−	−	+	+	+	−	−	−	+	+	+
IIIe	*p*-F C_6H_4	+	+	+	−	+	+	−	+	+	+	+	+	+	+	+	+	+	+	−	−	−	+	+	+	−	−	−	+	+	+
IVa	C_6H_5	−	+	+	−	+	+	−	+	+	−	+	+	+	+	+	−	+	+	−	+	+	−	−	2+	−	−	+	+	+	2+
IVb	cyclo-C_6H_{11}	−	+	2+	−	+	+	+	+	+	−	+	+	−	+	+	−	+	+	−	+	+	−	−	+	−	−	+	+	+	2+

[a] Concentrations of compounds employed in micrograms per milliliter; key: (−) no inhibition of growth; (+) partial inhibition of growth; (2+) complete inhibition of growth.

Table II—Antibacterial Activity of Triethylammonium Chloride–*N*-Substituted *N'*-Cyano-*O*-(triphenylstannyl)isourea Complexes (III) and *N*-Phenyl-*N'*-cyano-*O*-(triphenylstannyl)isourea (IVa)

		Escherichia coli[a]			*Micrococcus agilis*[a]			*Bacillus subtilis*[a]			*Staphylococcus aureus*[a]		
Compound	R	1[b]	10	100	1	10	100	1	10	100	1	10	100
IIIa	C_2H_5	−	−	−	2+	2+	2+	2+	2+	2+	−	−	+
IIIb	CH_2=$CHCH_2$	−	−	−	2+	2+	2+	2+	2+	2+	−	−	−
IIIc	cyclo-C_6H_{11}	−	−	−	2+	2+	2+	2+	2+	2+	+	2+	2+
IIId	C_6H_5	−	−	−	2+	2+	2+	+	2+	2+	−	2+	2+
IIIe	*p*-F C_6H_4	−	−	−	2+	2+	2+	2+	2+	2+	2+	2+	2+
IVa	C_6H_5	−	−	−	2+	2+	2+	+	2+	2+	−	+	2+

[a] Obtained from the culture collection of the Department of Biological Sciences, St. John's University. [b] Concentration of compounds employed, in micrograms per milliliter; key: (−) no inhibition of growth; (+) partial inhibition of growth; (2+) complete inhibition of growth.

0022-3549/84/0700-1012$01.00/0
© 1984, American Pharmaceutical Association

RESULTS AND DISCUSSION

The data in Table I show that each of the series III compounds behaved essentially identically toward each of the 10 test fungi. All of the series III compounds were inactive towards *Rhizopus stolonifer* and *Trichoderma viride* at all concentrations. In this regard they were inferior to the previously tested series IV compounds, which partially inhibited *R. stolonifer* at 10 μg/mL and *T. viride* at 100 μg/mL (15). With the exception of IIIe, the series III compounds partially inhibited the growth of the other eight test fungi at a concentration of 1 μg/mL. Employment of higher concentrations did not improve the antifungal activity. Compound IIIe differed from the other series III compounds only in that it was inactive towards *Chaetomium globosum* and *Cladosporium carpophilum* at 1 μg/mL. In comparison with the series III compounds, IVa was inactive towards *Aspergillus niger*, *Ch. globosum*, *Cl. carpophilum*, *Fusarium monoliforme*, *Penicillium notatum*, and *Saccharomyces cerevisiae* at 1 μg/mL. Compound IVb was also inferior to the series III compounds in that it was inactive towards *A. niger*, *Ch. globosum*, *F. monoliforme*, *Myrothecium verrucaria*, *P. notatum*, and *S. cerevisiae* at 1 μg/mL. Furthermore, the series IV compounds were inactive towards *S. cerevisiae* even at 10 μg/mL. Thus, the series III compounds generally exhibited higher antifungal activity than the series IV compounds.

The data in Table II show that all of the series III compounds were inactive towards the Gram-negative bacterium *Escherichia coli* at all concentrations. In this regard they resembled the previously tested IVa (15). All of the series III compounds behaved identically towards the two Gram-positive bacteria *Micrococcus agilis* and *Bacillus subtilis*, totally inhibiting the growth of these bacteria at a concentration of 1 μg/mL. In this regard they were somewhat better than IVa, which only partially inhibited *B. subtilis* at 1 μg/mL. The most effective series III compound against *Staphylococcus aureus* was IIIe, which totally inhibited the growth of this bacterium at 1 μg/mL. In contrast, IVa was inactive towards *St. aureus* at 1 μg/mL. Thus, the series III compounds generally exhibited higher antibacterial activity than IVa.

REFERENCES

(1) J. S. Thayer, *J. Organomet. Chem.*, **76**, 265 (1974).

(2) "Organotin Compounds: New Chemistry and Applications," J. J. Zuckerman, Ed., American Chemical Society, Washington, D.C., 1976.

(3) B. Sugavanam, *Tin Its Uses*, **126**, 4 (1980).

(4) F. E. Smith, *Tin Its Uses*, **126**, 6 (1980).

(5) S. Haynes, *Tin Its Uses*, **127**, 12 (1981).

(6) K.-D. Freitag and R. Bock, *Pestic. Sci.*, **5**, 731 (1974).

(7) R. D. Barnes, A. T. Bull, and R. C. Poller, *Pestic. Sci.*, **4**, 305 (1973).

(8) M. E. Getzendaner and H. B. Corbin, *J. Agr. Food Chem.*, **20**, 881 (1972).

(9) R. Bock and K.-D. Freitag, *Naturwissenschaften*, **59**, 165 (1972).

(10) A. J. Chapman and J. W. Price, *Int. Pestic. Control*, **1**, 11 (1972).

(11) A. J. Crowe and P. J. Smith, *Chem. Ind. (London)*, **200** (1980).

(12) A. J. Crowe, P. J. Smith, and G. Atassi, *Chem. Biol. Interact.*, **32**, 171 (1980).

(13) E. J. Kupchik, M. A. Pisano, A. M. Carroll, J. R. Lumpp, and J. A. Feiccabrino, *J. Pharm. Sci.*, **69**, 340 (1980).

(14) E. J. Kupchik and D. K. Parikh, *J. Organomet. Chem.*, **121**, 327 (1976).

(15) E. J. Kupchik, M. A. Pisano, D. K. Parikh, and M. A. D'Amico, *J. Pharm. Sci.*, **63**, 261 (1974).

Acylation of Hemoglobin by Aspirin-Like Diacyl Esters

SOLOMON E. MASSIL, GUEY-YUEH SHI, and IRVING M. KLOTZ ˣ

Received April 5, 1983 from the *Department of Chemistry, Northwestern University, Evanston, IL 60201.* Accepted for publication May 19, 1983.

Abstract □ Aspirin-like diacyl esters of different steric disposition have been prepared and compared with acetylsalicylate in their abilities to modify hemoglobin.

Keyphrases □ Diacyl esters—aspirin derivatives, acylation of hemoglobin □ Hemoglobin—acylation by aspirin-like diacyl esters, sickle cell anemia

In a previous paper (1), it has been shown that aspirin can acylate hemoglobin and thereby provide a novel approach to the alteration of sickle hemoglobin. Acetylsalicylate is the prototype of a general class of monoacyl esters of salicylic acid. Consequently, a variety of such esters have been synthesized (2) and examined for their effectiveness in modifying hemoglobin S and in inhibiting the aggregation process leading to sickling.

Among variants in aspirin-like derivatives are the diacyl esters of dihydroxybenzoic acids. These seem attractive because they would present two active acyl groups to the protein when it forms a reaction complex with a reagent molecule. We have prepared, therefore, a series of such diacyl ester compounds of different steric structure and compared their abilities to modify hemoglobin.

EXPERIMENTAL SECTION

A variety of hydroxybenzoic acids were purchased from commercial sources[1]. Their mono- and diacyl esters were synthesized by methods described in the literature (3-7). The derivatives prepared are listed in Table I.

[1] Aldrich Chemical Co., for example.

Of the compounds obtained, only 3,5-diacetoxybenzoic acetic anhydride (XI) has not been reported in the literature. It appeared as a by-product in the mother liquor (chloroform–petroleum ether) from the preparation of the diacetoxybenzoic anhydride (X). The fine white precipitate which appeared in the mother liquor after standing for several hours was removed by filtration, washed with petroleum ether, and dried without heat, mp 71–72°C. This product, insoluble in aqueous $NaHCO_3$ at room temperature, bubbled on heating. It did not give a positive $FeCl_3$ test for free phenol. ^{1}H-NMR and

Table I—Modification of Hemoglobin by Aspirin-like Mono- and Diacyl Esters

Compound	Concentration, mM	Modification of Oxyhemoglobin A[a], %
I	10	22.5
II	10	23.1
	20	34.2
III	10	26.3
	20	36.8
IV	10	27.7
	20	37.3
V	5	32.3
	10	49.3
VI	5	19.1
	10	37.4
VII	10	78.7
VIII	5	36.3
	10	53.0
IX	5	23.8
	10	46.7
X	5	26.3
XI	5	45.0
	10	79.2

[a] Hemoglobin concentration = 1 mM.

RESULTS AND DISCUSSION

The data in Table I show that each of the series III compounds behaved essentially identically toward each of the 10 test fungi. All of the series III compounds were inactive towards *Rhizopus stolonifer* and *Trichoderma viride* at all concentrations. In this regard they were inferior to the previously tested series IV compounds, which partially inhibited *R. stolonifer* at 10 μg/mL and *T. viride* at 100 μg/mL (15). With the exception of IIIe, the series III compounds partially inhibited the growth of the other eight test fungi at a concentration of 1 μg/mL. Employment of higher concentrations did not improve the antifungal activity. Compound IIIe differed from the other series III compounds only in that it was inactive towards *Chaetomium globosum* and *Cladosporium carpophilum* at 1 μg/mL. In comparison with the series III compounds, IVa was inactive towards *Aspergillus niger*, *Ch. globosum*, *Cl. carpophilum*, *Fusarium monoliforme*, *Penicillium notatum*, and *Saccharomyces cerevisiae* at 1 μg/mL. Compound IVb was also inferior to the series III compounds in that it was inactive towards *A. niger*, *Ch. globosum*, *F. monoliforme*, *Myrothecium verrucaria*, *P. notatum*, and *S. cerevisiae* at 1 μg/mL. Furthermore, the series IV compounds were inactive towards *S. cerevisiae* even at 10 μg/mL. Thus, the series III compounds generally exhibited higher antifungal activity than the series IV compounds.

The data in Table II show that all of the series III compounds were inactive towards the Gram-negative bacterium *Escherichia coli* at all concentrations. In this regard they resembled the previously tested IVa (15). All of the series III compounds behaved identically towards the two Gram-positive bacteria *Micrococcus agilis* and *Bacillus subtilis*, totally inhibiting the growth of these bacteria at a concentration of 1 μg/mL. In this regard they were somewhat better than IVa, which only partially inhibited *B. subtilis* at 1 μg/mL. The most effective series III compound against *Staphylococcus aureus* was IIIe, which totally inhibited the growth of this bacterium at 1 μg/mL. In contrast, IVa was inactive towards *St. aureus* at 1 μg/mL. Thus, the series III compounds generally exhibited higher antibacterial activity than IVa.

REFERENCES

(1) J. S. Thayer, *J. Organomet. Chem.*, **76**, 265 (1974).

(2) "Organotin Compounds: New Chemistry and Applications," J. J. Zuckerman, Ed., American Chemical Society, Washington, D.C., 1976.

(3) B. Sugavanam, *Tin Its Uses*, **126**, 4 (1980).

(4) F. E. Smith, *Tin Its Uses*, **126**, 6 (1980).

(5) S. Haynes, *Tin Its Uses*, **127**, 12 (1981).

(6) K.-D. Freitag and R. Bock, *Pestic. Sci.*, **5**, 731 (1974).

(7) R. D. Barnes, A. T. Bull, and R. C. Poller, *Pestic. Sci.*, **4**, 305 (1973).

(8) M. E. Getzendaner and H. B. Corbin, *J. Agr. Food Chem.*, **20**, 881 (1972).

(9) R. Bock and K.-D. Freitag, *Naturwissenschaften*, **59**, 165 (1972).

(10) A. J. Chapman and J. W. Price, *Int. Pestic. Control*, **1**, 11 (1972).

(11) A. J. Crowe and P. J. Smith, *Chem. Ind. (London)*, **200** (1980).

(12) A. J. Crowe, P. J. Smith, and G. Atassi, *Chem. Biol. Interact.*, **32**, 171 (1980).

(13) E. J. Kupchik, M. A. Pisano, A. M. Carroll, J. R. Lumpp, and J. A. Feiccabrino, *J. Pharm. Sci.*, **69**, 340 (1980).

(14) E. J. Kupchik and D. K. Parikh, *J. Organomet. Chem.*, **121**, 327 (1976).

(15) E. J. Kupchik, M. A. Pisano, D. K. Parikh, and M. A. D'Amico, *J. Pharm. Sci.*, **63**, 261 (1974).

Acylation of Hemoglobin by Aspirin-Like Diacyl Esters

SOLOMON E. MASSIL, GUEY-YUEH SHI, and IRVING M. KLOTZ ˣ

Received April 5, 1983 from the *Department of Chemistry, Northwestern University, Evanston, IL 60201.* Accepted for publication May 19, 1983.

Abstract □ Aspirin-like diacyl esters of different steric disposition have been prepared and compared with acetylsalicylate in their abilities to modify hemoglobin.

Keyphrases □ Diacyl esters—aspirin derivatives, acylation of hemoglobin □ Hemoglobin—acylation by aspirin-like diacyl esters, sickle cell anemia

In a previous paper (1), it has been shown that aspirin can acylate hemoglobin and thereby provide a novel approach to the alteration of sickle hemoglobin. Acetylsalicylate is the prototype of a general class of monoacyl esters of salicylic acid. Consequently, a variety of such esters have been synthesized (2) and examined for their effectiveness in modifying hemoglobin S and in inhibiting the aggregation process leading to sickling.

Among variants in aspirin-like derivatives are the diacyl esters of dihydroxybenzoic acids. These seem attractive because they would present two active acyl groups to the protein when it forms a reaction complex with a reagent molecule. We have prepared, therefore, a series of such diacyl ester compounds of different steric structure and compared their abilities to modify hemoglobin.

EXPERIMENTAL SECTION

A variety of hydroxybenzoic acids were purchased from commercial sources[1]. Their mono- and diacyl esters were synthesized by methods described in the literature (3-7). The derivatives prepared are listed in Table I.

[1] Aldrich Chemical Co., for example.

Of the compounds obtained, only 3,5-diacetoxybenzoic acetic anhydride (XI) has not been reported in the literature. It appeared as a by-product in the mother liquor (chloroform–petroleum ether) from the preparation of the diacetoxybenzoic anhydride (X). The fine white precipitate which appeared in the mother liquor after standing for several hours was removed by filtration, washed with petroleum ether, and dried without heat, mp 71–72°C. This product, insoluble in aqueous $NaHCO_3$ at room temperature, bubbled on heating. It did not give a positive $FeCl_3$ test for free phenol. ^{1}H-NMR and

Table I—Modification of Hemoglobin by Aspirin-like Mono- and Diacyl Esters

Compound	Concentration, mM	Modification of Oxyhemoglobin A[a], %
I	10	22.5
II	10	23.1
	20	34.2
III	10	26.3
	20	36.8
IV	10	27.7
	20	37.3
V	5	32.3
	10	49.3
VI	5	19.1
	10	37.4
VII	10	78.7
VIII	5	36.3
	10	53.0
IX	5	23.8
	10	46.7
X	5	26.3
XI	5	45.0
	10	79.2

[a] Hemoglobin concentration = 1 mM.

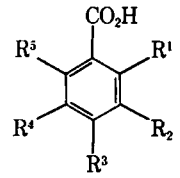

I R^1=$OCOCH_3$, R^2=R^3=R^4=R^5=H
II R^3=$OCOCH_3$, R^1=R^2=R^4=R^5=H
III R^1=OH, R^3=$OCOCH_3$, R^2=R^4=R^5=H
IV R^1=$OCOCH_3$, R^3=OH, R^2=R^4=R^5=H
V R^1=R^3=$OCOCH_3$, R^2=R^4=R^5=H
VI R^1=R^4=$OCOCH_3$, R^2=R^3=R^5=H
VII R^1=R^5=$OCOCH_3$, R^2=R^3=R^4=H
VIII R^2=R^3=$OCOCH_3$, R^1=R^4=R^5=H
IX R^2=R^4=$OCOCH_3$, R^1=R^3=R^5=H

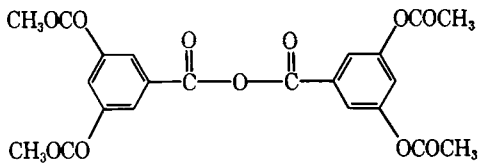

X

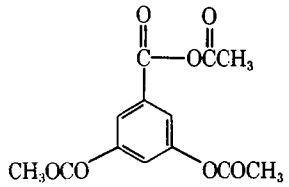

XI

microanalysis corresponded to expectations for XI. ^{1}H-NMR ($CDCl_3$-Me_4Si): δ 2.33 [d, 6, $(-O-COCH_3)_2$], 2.38 (s, 3, $-O-COCH_3$), and 7.2-7.75 ppm (m, 3, ArH).

Anal.—Calc. for $C_{13}H_{12}O_7$ (280.24): C, 55.72; H, 4.32. Found: C, 55.62; H, 4.17.

The preparation of hemoglobin and procedures for following its chemical modification by aspirin-like reagents have been described previously (2).

RESULTS AND DISCUSSION

In Table I, the efficacies of the diacyl esters in modifying hemoglobin are compared with those of corresponding monoacyl compounds. The following features are worthy of note.

Compound II, the *para* analogue of aspirin, is about as effective as I in acylating hemoglobin. Likewise the two positional monoacyl isomers of hydroxysalicylic acid, III and IV, are comparable in activity to each other and to aspirin (I). In contrast, the diacetoxy salicylic acid, V, is significantly more reactive, but the isomer VI is less so. By far the most effective of the diacyl hydroxysalicylic esters is VII, in which both acetyl groups are close to the anionic $-COO^-$ moiety. Alternative isomers of dihydroxybenzoic acids gave diacyl esters VIII and IX that did not compare in efficacy with VII, although VIII was significantly better than aspirin itself. Compound X, the anhydride of IX, was not better than aspirin, but the mixed anhydride XI was significantly better. In this series, therefore, the double *ortho* derivative VII is the most interesting compound and merits further investigation.

Previous studies (1, 8) have shown that aspirin-like reagents acylate sickle hemoglobin S just as extensively as they do hemoglobin A. Consequently effective compounds, such as 6-acetoxyacetylsalicylic acid (VII) of the present series, have potential as antisickling agents.

REFERENCES

(1) I. M. Klotz and J. W. O. Tam, *Proc. Natl. Acad. Sci.*, **70,** 1313 (1973).

(2) R. H. Zaugg, J. A. Walder, R. Y. Walder, J. M. Steele, and I. M. Klotz, *J. Biol. Chem.*, **255,** 2816 (1980).

(3) R. Lesser and G. Gad, *Ber. Dtsch. Chem. Ges.*, **59B,** 233 (1926).

(4) M. Bergmann and P. Dangschat, *Ber. Dtsch. Chem. Ges.*, **52B,** 371 (1919).

(5) E. Bernatek and I. Bø, *Acta Chem. Scand.*, **13,** 337 (1959).

(6) S. E. Hunt, J. Idris Jones, and A. S. Lindsey, *J. Chem. Soc.*, **1956,** 3099.

(7) R. Huls and A. Hubert, *Bull. Soc. Chim., Belg.*, **65,** 596 (1956).

(8) L. E. Wood, D. N. Haney, J. R. Patel, S. E. Clare, G.-Y. Shi, L. C. King, and I. M. Klotz, *J. Biol. Chem.*, **256,** 7046 (1981).

ACKNOWLEDGMENTS

This investigation was supported in part by Grant HL22719 from the National Heart, Lung, and Blood Institute, National Institutes of Health. S.E.M. was on leave from Makhteshim Chemical Works, Ltd., Beer-Sheva, Israel.

Liquid Chromatographic Analysis of Cimetidine with Procainamide as Internal Standard

Keyphrases □ Cimetidine—HPLC analysis in plasma and urine □ Liquid chromatography—analysis of cimetidine in plasma and urine

To the Editor:

We recently reported in this journal a simple and sensitive liquid chromatographic assay for cimetidine in plasma and urine (1). Chromatographic separation was performed on a radially compressed column[1], which allowed much faster and more efficient chromatography than previously described assays (1). However, since burimamide (the internal standard) is no longer manufactured, this has rendered our assay inapplicable by other investigators. We have therefore examined the chromatography of a wide variety of other compounds, including many other H_2-antagonist analogues, and found procainamide to be the most suitable alternative internal standard to burimamide. This results in minimal modification of our originally published assay.

In the analysis of plasma, procainamide hydrochloride[2] (20 μg/mL, 100 μL, in a 0.09% sodium metabisulfite solution), sodium hydroxide (2 M, 0.5 mL), and dichloromethane (20 mL) were added to 1.0 mL of plasma in a 30-mL glass tube. In the analysis of urine, procainamide hydrochloride[2] (1 mg/mL, 25 μL, in a 0.09% sodium metabisulfite solution), sodium hydroxide (2 M, 100 μL), and dichloromethane (5 mL) were added to 250 μL of urine in a 30-mL glass tube. Thereafter, the method of extraction and reconstitution of both plasma and urine samples was identical to that previously reported (1). The mobile phase, radial compression column[1], chromatographic conditions, and instrumentation were as reported previously (1). Procainamide (2.6-min retention) and cimetidine (3.8-min retention) were completely resolved. Cimetidine sulfoxide (1.5-min retention), the major metabolite of cimetidine (2), did not interfere with the assay. The analytical recoveries of cimetidine and procainamide were 60 and 59%, respectively. The coefficient of variation for within-day assays of plasma cimetidine levels was 1.8% at 1000 ng/mL (n = 6); for urine it was 0.53% at 50 μg/mL (n = 6). The coefficient of variation of between-day assays of plasma cimetidine levels over 4 weeks was 5.2% at 901 ng/mL (n = 7); for urine over 4 weeks the value was 5.4% at 51.0 μg/mL (n = 5).

The assay was applied to the measurement of plasma and urine samples obtained from a patient who underwent intravenous and oral cimetidine therapy in pharmacokinetic studies according to the protocol reported previously (1). The same samples were also analyzed for cimetidine by our original liquid chromatographic method (1) with burimamide as internal standard. There was good correlation between the two methods (r = 0.991), and the cimetidine levels did not significantly differ (paired t test, $p \geq 0.20$, df = 20) between the assays.

Thus, with a change in internal standard from burimamide to procainamide, this method can still be applied to the assay of cimetidine in biological fluids, without a major change in methodology.

[1] Rad Pak A and RCM-100, Waters Associates, Milford, Mass.
[2] Sigma Chemical Company, St. Louis, Mo.

(1) G. W. Mihaly, S. Cockbain, D. B. Jones, R. G. Hanson, and R. A. Smallwood, *J. Pharm. Sci.*, **71**, 590 (1982).
(2) D. C. Taylor, P. R. Creswell, and D. C. Bartlett, *Drug Metab. Dispos.*, **6**, 21 (1978).

Michael S. Ching[‡]
*George W. Mihaly**[x]
*D. Brian Jones**
*Richard A. Smallwood**

*Gastroenterology Unit, Department of Medicine, and [‡]Department of Surgery
University of Melbourne
Austin Hospital
Heidelberg 3084 Victoria, Australia

Received August 3, 1983.
Accepted for publication April 24, 1984.
This work was supported by the National Health and Medical Research Council of Australia. We thank Jane Bell for typing the manuscript.

BOOKS

A Textbook of Pharmaceutical Analysis, 3rd Ed. By KENNETH A. CONNORS. Wiley-Interscience, 605 Third Avenue, New York, NY 10016. 1982. 664 pp. 15 × 23 cm. Price $55.00.

This book is the latest revision in what is by now a classic text in pharmaceutical analysis for the undergraduate pharmacy curriculum. The first and second editions were issued in 1967 and 1975. The field of "pharmaceutical analysis" has undergone enormous changes over the 15 years this text has been used. Whether the sample be raw materials, dosage forms, or biological fluids, the methodology is more selective, more precise, and more accurate. As a reflection of modern developments, the latest edition includes a chapter on immunoassay and a substantially expanded chapter on liquid chromatography. Both of these subjects scarcely existed in 1967 (especially with respect to determination of pharmaceuticals), and now they are prominent in virtually every issue of this journal.

As was the case with previous editions, this book meets its objectives very well. I especially like Connor's focus on chemical reactions and his liberal use of examples, practice problems, and laboratory experiments. He is at his best when describing the interface between fundamental chemistry and instrumentation. It is delightful to see organic reaction mechanisms and stereochemistry taken into consideration. So many analytical chemistry texts are stuck on inorganic things and gadgets and thus miss the needs of many students.

The only fault I find with this book is that it is too much material for the undergraduate level and not quite enough to be useful as a graduate text for junior researchers. It just misses these audiences by dropping in between, a problem that can be solved by selective assignments and supplementary material. Overall, a job well done!

Reviewed by Peter T. Kissinger
Department of Chemistry
Purdue University
West Lafayette, IN 47907

0022-3549/84/0700-1015$01.00/0
© 1984, American Pharmaceutical Association

Liquid Chromatographic Analysis of Cimetidine with Procainamide as Internal Standard

Keyphrases □ Cimetidine—HPLC analysis in plasma and urine □ Liquid chromatography—analysis of cimetidine in plasma and urine

To the Editor:

We recently reported in this journal a simple and sensitive liquid chromatographic assay for cimetidine in plasma and urine (1). Chromatographic separation was performed on a radially compressed column[1], which allowed much faster and more efficient chromatography than previously described assays (1). However, since burimamide (the internal standard) is no longer manufactured, this has rendered our assay inapplicable by other investigators. We have therefore examined the chromatography of a wide variety of other compounds, including many other H_2-antagonist analogues, and found procainamide to be the most suitable alternative internal standard to burimamide. This results in minimal modification of our originally published assay.

In the analysis of plasma, procainamide hydrochloride[2] (20 μg/mL, 100 μL, in a 0.09% sodium metabisulfite solution), sodium hydroxide (2 M, 0.5 mL), and dichloromethane (20 mL) were added to 1.0 mL of plasma in a 30-mL glass tube. In the analysis of urine, procainamide hydrochloride[2] (1 mg/mL, 25 μL, in a 0.09% sodium metabisulfite solution), sodium hydroxide (2 M, 100 μL), and dichloromethane (5 mL) were added to 250 μL of urine in a 30-mL glass tube. Thereafter, the method of extraction and reconstitution of both plasma and urine samples was identical to that previously reported (1). The mobile phase, radial compression column[1], chromatographic conditions, and instrumentation were as reported previously (1). Procainamide (2.6-min retention) and cimetidine (3.8-min retention) were completely resolved. Cimetidine sulfoxide (1.5-min retention), the major metabolite of cimetidine (2), did not interfere with the assay. The analytical recoveries of cimetidine and procainamide were 60 and 59%, respectively. The coefficient of variation for within-day assays of plasma cimetidine levels was 1.8% at 1000 ng/mL (n = 6); for urine it was 0.53% at 50 μg/mL (n = 6). The coefficient of variation of between-day assays of plasma cimetidine levels over 4 weeks was 5.2% at 901 ng/mL (n = 7); for urine over 4 weeks the value was 5.4% at 51.0 μg/mL (n = 5).

The assay was applied to the measurement of plasma and urine samples obtained from a patient who underwent intravenous and oral cimetidine therapy in pharmacokinetic studies according to the protocol reported previously (1). The same samples were also analyzed for cimetidine by our original liquid chromatographic method (1) with burimamide as internal standard. There was good correlation between the two methods (r = 0.991), and the cimetidine levels did not significantly differ (paired t test, $p \geq 0.20$, df = 20) between the assays.

Thus, with a change in internal standard from burimamide to procainamide, this method can still be applied to the assay of cimetidine in biological fluids, without a major change in methodology.

[1] Rad Pak A and RCM-100, Waters Associates, Milford, Mass.
[2] Sigma Chemical Company, St. Louis, Mo.

(1) G. W. Mihaly, S. Cockbain, D. B. Jones, R. G. Hanson, and R. A. Smallwood, *J. Pharm. Sci.*, **71**, 590 (1982).
(2) D. C. Taylor, P. R. Creswell, and D. C. Bartlett, *Drug Metab. Dispos.*, **6**, 21 (1978).

Michael S. Ching[‡]
*George W. Mihaly**[x]
*D. Brian Jones**
*Richard A. Smallwood**

*Gastroenterology Unit, Department of Medicine, and [‡]Department of Surgery
University of Melbourne
Austin Hospital
Heidelberg 3084 Victoria, Australia

Received August 3, 1983.
Accepted for publication April 24, 1984.
This work was supported by the National Health and Medical Research Council of Australia. We thank Jane Bell for typing the manuscript.

BOOKS

A Textbook of Pharmaceutical Analysis, 3rd Ed. By KENNETH A. CONNORS. Wiley-Interscience, 605 Third Avenue, New York, NY 10016. 1982. 664 pp. 15 × 23 cm. Price $55.00.

This book is the latest revision in what is by now a classic text in pharmaceutical analysis for the undergraduate pharmacy curriculum. The first and second editions were issued in 1967 and 1975. The field of "pharmaceutical analysis" has undergone enormous changes over the 15 years this text has been used. Whether the sample be raw materials, dosage forms, or biological fluids, the methodology is more selective, more precise, and more accurate. As a reflection of modern developments, the latest edition includes a chapter on immunoassay and a substantially expanded chapter on liquid chromatography. Both of these subjects scarcely existed in 1967 (especially with respect to determination of pharmaceuticals), and now they are prominent in virtually every issue of this journal.

As was the case with previous editions, this book meets its objectives very well. I especially like Connor's focus on chemical reactions and his liberal use of examples, practice problems, and laboratory experiments. He is at his best when describing the interface between fundamental chemistry and instrumentation. It is delightful to see organic reaction mechanisms and stereochemistry taken into consideration. So many analytical chemistry texts are stuck on inorganic things and gadgets and thus miss the needs of many students.

The only fault I find with this book is that it is too much material for the undergraduate level and not quite enough to be useful as a graduate text for junior researchers. It just misses these audiences by dropping in between, a problem that can be solved by selective assignments and supplementary material. Overall, a job well done!

Reviewed by Peter T. Kissinger
Department of Chemistry
Purdue University
West Lafayette, IN 47907

0022-3549/84/0700-1015$01.00/0
© 1984, American Pharmaceutical Association

Drugs and Therapy: A Handbook of Psychotropic Drugs, 2nd Ed. By ALVIN SWONGER and LARRY CONSTANTINE. Little, Brown and Company, 34 Beacon Street, Boston, MA 02106 1983. 431 pp. 15.5 × 23.5 cm. Price $18.95 (paperback).

This book is unusual in that it is directed to nonmedical personnel. The "therapy" of the title refers not to those modalities that medical people generally consider therapy, but more specifically to psychosocial approaches to treatment. The authors are a faculty member of a school of pharmacy and a family therapist. The intended audience might be nurses, social workers, psychologists, or others not primarily concerned with the use of drugs in treatment, but who may need to know what types of drugs their clients are taking and what effects these drugs may have on them.

This second edition has been expanded to include new sections not in the first. It is organized around eight general topics, each of which is covered in a few short chapters: drugs in therapeutic perspective (again, meaning from the perspective of the psychotherapist); foundations of drug action (a review of basic neuropharmacology); drug use and abuse; drugs and the arousal state (referring to sedative-hypnotics, alcohol, stimulants, and psychedelics); psychiatric disorders and drugs (psychosis, anxiety, depression, and mania); motor functions and drugs; pain and its drug management; and drugs and consciousness (which includes anticonvulsants). Each section is headed by a short introduction indicating the aims of the several chapters that follow.

The book is well illustrated with figures and tables. Most of these have appeared in either the same or slightly different form in other books. Virtually all the references are also to books or book chapters. Thus, it appears that the authors have attempted a synthesis of much that has already been published, tailoring it to the needs of the prospective audience. Relatively little emphasis has been placed on how specific drugs are used, but each chapter that discusses a class of drugs finishes with a brief synopsis providing the generic and trade names of the drug, the class to which they belong, their usual indications, and the usual range of daily doses. The major emphases are on how the drugs work in the nervous system and how they may affect the behavior of interest to the psychotherapist.

The book is well written and generally free of errors. It should certainly meet the needs of its intended audience, but would probably be inadequate for pharmacists or physicians. The only other book that I can remember that addressed a similar audience was one that Honigfeld wrote many years ago. Thus, the present volume services a useful need. It would be well worth having as a reference handbook for those who need to know how drugs affect their clients.

Reviewed by Leo E. Hollister
Senior Medical Investigator
Veterans Administration Medical Center
Palo Alto, CA

Calcium Antagonism in Heart and Smooth Muscle: Experimental Facts and Therapeutic Perspectives. By ALBRECHT FLECKENSTEIN. John Wiley and Sons, Inc., One Wiley Drive, Somerset, NJ 08873. 1983. 399 pp. 17 × 24 cm. Price $60.00.

Calcium antagonists have generated considerable interest in the pharmaceutical sciences since nifedipine was reported to be effective in the treatment of Printzmetal angina. This book constitutes a major tool for understanding the role of calcium and calcium antagonism in the heart and smooth muscle. The reader will find important information about the pharmacological properties of verapamil and its derivative, nifedipine and its derivatives, and diltiazem. It is not the first book published on this subject; however, the author makes this one very original.

Dr. Albrecht Fleckenstein investigated this field for more than 20 years. He is recognized as one of the most important contributors to the advancement accomplished in this field. This book provides indispensable knowledge related to the role of calcium in myocardial and vascular smooth muscle contractions, the pacemaker activity in physiological and pathological conditions, allowing a much better understanding of the cardiovascular indications of this very attractive group of drugs. Finally, it is of special interest to find a classification of these drugs in relation to their specificity in affecting the calcium channel. Dr. Fleckenstein proposed classifying the calcium antagonists in three groups: Group A, specific calcium antagonists including verapamil, nifedipine, their derivatives, and diltiazem; Group B, calcium antagonists also affecting the movement of sodium including prenylamine, terodiline, fendiline, perhexiline, and caroverine; Group C, substances with calcium antagonistic side effects, including nitroglycerin, barbituric acid, etc. Such classification is based on a number of pharmacological criteria. There are so many drugs claimed to be specific calcium antagonists, but also interfere with movements of other ions.

This book is recommended as a major source of information concerning the pharmacological properties of calcium antagonists.

Reviewed by Jacques Chelly
Department of Pharmacology
University of Houston
Department of Anesthesiology
Baylor College of Medicine
Houston, TX 77030

Nicotinic Acid: Nutrient–Cofactor–Drug. (Clinical Pharmacology Series, Vol. 1). By MURRAY WEINER and JAN VAN EYS. Marcel Dekker, 270 Madison Avenue, New York, NY 10016. 1983. 308 pp. 16 × 24 cm. Price $55.00 (20% higher outside the U.S. and Canada).

This monograph provides a synthesis of existing knowledge from a wide variety of sources into a single, concise volume. Topics are not examined in excessive detail, but that was not a purpose of the book. Rather, it emerges as a strength in that it permits the diverse audience addressed to be informed readily in areas beyond particular disciplinary constraints. An index and extensive references facilitate acquisition of detailed information on the topics covered for interested readers. The book succeeds well in crossing disciplinary boundaries, and it frequently reveals provocative possibilities for future research. Exposition, organized by sections according to the title, is acceptably comprehensive and includes such newer developments as the nicotinamide coenzymes as donors in transribosylation reactions and in regulation of DNA repair and synthesis, use of nicotinic acid in cardiovascular and hyperlipidemic diseases (including pharmacokinetics and pharmacodynamics), and reexamination of the tryptophan-nicotinic acid relationship in a world in which protein hunger is a global problem of growing concern. For example, nonspecialists who identify pellagra with a simple niacin-tryptophan deficiency will be enlightened by the very first chapter.

The roles of nicotinic acid at the metabolic level are manifold. The most vital function of living material—the capacity to abstract and utilize energy from complex molecules—requires controlled oxidations linked to the nicotinic acid-derived coenzymes. Moreover, NAD participates in the generation of adenosine diphosphate robose polymers, which have a role in DNA metabolism and function. Indeed, in its coenzyme forms the physiological roles of nicotinic acid are pervasive and pivotal in the subcellular compartments of cytoplasm, nucleus, mitochondrion, and endoplasmic reticulum. The authors aver that "there are few areas of biochemistry in which pharmacology, nutritional biochemistry, and molecular biology are interwoven in such a coherent whole." Their monograph amply illuminates that statement. This overview of nicotinic acid and its variety of chemical and metabolic derivatives includes important biochemical, nutritional, pharmacological, and clinical aspects. In addition to life scientists and practitioners in those fields, the book should appeal to dieticians, pharmacists, and others interested in a concise and authoritative exposition of the functions and relationships of this critical cog in the metabolic machinery. It is an excellent contemporary reference for courses in all these disciplines, and it will be at home on laboratory benches due to its durable, stain-resistant binding.

There are relatively few printing errors and oversights for a first printing. Minor misspellings and errors in figures, such as the entry of the symbol for oxygen for that of coenzyme Q and a misplaced arrow (p. 219) and an exotically appended CO_2 on the NAM molecule (p. 19), are neither overly distracting nor misleading. Of somewhat more concern are the use of "niacin" in the second paragraph of p. 9 when "niacytin" is intended and strange displacements such as "substitutes" for "substrates" (p. 217).

This monograph is the first volume in a projected series in clinical pharmacology under the general editorial direction of Dr. Weiner. Three decades of distinguished research in many of the aspects of the metabolic roles of these compounds by Professor van Eys are evident in the clarity and insightful coverage which characterize this volume. If succeeding volumes maintain those qualities we will have much to look forward to and a wide audience stands much to gain.

Reviewed by Edwin S. Higgins
Department of Biochemistry
Medical College of Virginia
Virginia Commonwealth University
Richmond, VA 23298

Drugs and Therapy: A Handbook of Psychotropic Drugs, 2nd Ed. By ALVIN SWONGER and LARRY CONSTANTINE. Little, Brown and Company, 34 Beacon Street, Boston, MA 02106 1983. 431 pp. 15.5 × 23.5 cm. Price $18.95 (paperback).

This book is unusual in that it is directed to nonmedical personnel. The "therapy" of the title refers not to those modalities that medical people generally consider therapy, but more specifically to psychosocial approaches to treatment. The authors are a faculty member of a school of pharmacy and a family therapist. The intended audience might be nurses, social workers, psychologists, or others not primarily concerned with the use of drugs in treatment, but who may need to know what types of drugs their clients are taking and what effects these drugs may have on them.

This second edition has been expanded to include new sections not in the first. It is organized around eight general topics, each of which is covered in a few short chapters: drugs in therapeutic perspective (again, meaning from the perspective of the psychotherapist); foundations of drug action (a review of basic neuropharmacology); drug use and abuse; drugs and the arousal state (referring to sedative-hypnotics, alcohol, stimulants, and psychedelics); psychiatric disorders and drugs (psychosis, anxiety, depression, and mania); motor functions and drugs; pain and its drug management; and drugs and consciousness (which includes anticonvulsants). Each section is headed by a short introduction indicating the aims of the several chapters that follow.

The book is well illustrated with figures and tables. Most of these have appeared in either the same or slightly different form in other books. Virtually all the references are also to books or book chapters. Thus, it appears that the authors have attempted a synthesis of much that has already been published, tailoring it to the needs of the prospective audience. Relatively little emphasis has been placed on how specific drugs are used, but each chapter that discusses a class of drugs finishes with a brief synopsis providing the generic and trade names of the drug, the class to which they belong, their usual indications, and the usual range of daily doses. The major emphases are on how the drugs work in the nervous system and how they may affect the behavior of interest to the psychotherapist.

The book is well written and generally free of errors. It should certainly meet the needs of its intended audience, but would probably be inadequate for pharmacists or physicians. The only other book that I can remember that addressed a similar audience was one that Honigfeld wrote many years ago. Thus, the present volume services a useful need. It would be well worth having as a reference handbook for those who need to know how drugs affect their clients.

Reviewed by Leo E. Hollister
Senior Medical Investigator
Veterans Administration Medical Center
Palo Alto, CA

Calcium Antagonism in Heart and Smooth Muscle: Experimental Facts and Therapeutic Perspectives. By ALBRECHT FLECKENSTEIN. John Wiley and Sons, Inc., One Wiley Drive, Somerset, NJ 08873. 1983. 399 pp. 17 × 24 cm. Price $60.00.

Calcium antagonists have generated considerable interest in the pharmaceutical sciences since nifedipine was reported to be effective in the treatment of Printzmetal angina. This book constitutes a major tool for understanding the role of calcium and calcium antagonism in the heart and smooth muscle. The reader will find important information about the pharmacological properties of verapamil and its derivative, nifedipine and its derivatives, and diltiazem. It is not the first book published on this subject; however, the author makes this one very original.

Dr. Albrecht Fleckenstein investigated this field for more than 20 years. He is recognized as one of the most important contributors to the advancement accomplished in this field. This book provides indispensable knowledge related to the role of calcium in myocardial and vascular smooth muscle contractions, the pacemaker activity in physiological and pathological conditions, allowing a much better understanding of the cardiovascular indications of this very attractive group of drugs. Finally, it is of special interest to find a classification of these drugs in relation to their specificity in affecting the calcium channel. Dr. Fleckenstein proposed classifying the calcium antagonists in three groups: Group A, specific calcium antagonists including verapamil, nifedipine, their derivatives, and diltiazem; Group B, calcium antagonists also affecting the movement of sodium including prenylamine, terodiline, fendiline, perhexiline, and caroverine; Group C, substances with calcium antagonistic side effects, including nitroglycerin, barbituric acid, etc. Such classification is based on a number of pharmacological criteria. There are so many drugs claimed to be specific calcium antagonists, but also interfere with movements of other ions.

This book is recommended as a major source of information concerning the pharmacological properties of calcium antagonists.

Reviewed by Jacques Chelly
Department of Pharmacology
University of Houston
Department of Anesthesiology
Baylor College of Medicine
Houston, TX 77030

Nicotinic Acid: Nutrient–Cofactor–Drug. (Clinical Pharmacology Series, Vol. 1). By MURRAY WEINER and JAN VAN EYS. Marcel Dekker, 270 Madison Avenue, New York, NY 10016. 1983. 308 pp. 16 × 24 cm. Price $55.00 (20% higher outside the U.S. and Canada).

This monograph provides a synthesis of existing knowledge from a wide variety of sources into a single, concise volume. Topics are not examined in excessive detail, but that was not a purpose of the book. Rather, it emerges as a strength in that it permits the diverse audience addressed to be informed readily in areas beyond particular disciplinary constraints. An index and extensive references facilitate acquisition of detailed information on the topics covered for interested readers. The book succeeds well in crossing disciplinary boundaries, and it frequently reveals provocative possibilities for future research. Exposition, organized by sections according to the title, is acceptably comprehensive and includes such newer developments as the nicotinamide coenzymes as donors in transribosylation reactions and in regulation of DNA repair and synthesis, use of nicotinic acid in cardiovascular and hyperlipidemic diseases (including pharmacokinetics and pharmacodynamics), and reexamination of the tryptophan-nicotinic acid relationship in a world in which protein hunger is a global problem of growing concern. For example, nonspecialists who identify pellagra with a simple niacin-tryptophan deficiency will be enlightened by the very first chapter.

The roles of nicotinic acid at the metabolic level are manifold. The most vital function of living material—the capacity to abstract and utilize energy from complex molecules—requires controlled oxidations linked to the nicotinic acid-derived coenzymes. Moreover, NAD participates in the generation of adenosine diphosphate robose polymers, which have a role in DNA metabolism and function. Indeed, in its coenzyme forms the physiological roles of nicotinic acid are pervasive and pivotal in the subcellular compartments of cytoplasm, nucleus, mitochondrion, and endoplasmic reticulum. The authors aver that "there are few areas of biochemistry in which pharmacology, nutritional biochemistry, and molecular biology are interwoven in such a coherent whole." Their monograph amply illuminates that statement. This overview of nicotinic acid and its variety of chemical and metabolic derivatives includes important biochemical, nutritional, pharmacological, and clinical aspects. In addition to life scientists and practitioners in those fields, the book should appeal to dieticians, pharmacists, and others interested in a concise and authoritative exposition of the functions and relationships of this critical cog in the metabolic machinery. It is an excellent contemporary reference for courses in all these disciplines, and it will be at home on laboratory benches due to its durable, stain-resistant binding.

There are relatively few printing errors and oversights for a first printing. Minor misspellings and errors in figures, such as the entry of the symbol for oxygen for that of coenzyme Q and a misplaced arrow (p. 219) and an exotically appended CO_2 on the NAM molecule (p. 19), are neither overly distracting nor misleading. Of somewhat more concern are the use of "niacin" in the second paragraph of p. 9 when "niacytin" is intended and strange displacements such as "substitutes" for "substrates" (p. 217).

This monograph is the first volume in a projected series in clinical pharmacology under the general editorial direction of Dr. Weiner. Three decades of distinguished research in many of the aspects of the metabolic roles of these compounds by Professor van Eys are evident in the clarity and insightful coverage which characterize this volume. If succeeding volumes maintain those qualities we will have much to look forward to and a wide audience stands much to gain.

Reviewed by Edwin S. Higgins
Department of Biochemistry
Medical College of Virginia
Virginia Commonwealth University
Richmond, VA 23298

Drugs and Therapy: A Handbook of Psychotropic Drugs, 2nd Ed. By ALVIN SWONGER and LARRY CONSTANTINE. Little, Brown and Company, 34 Beacon Street, Boston, MA 02106 1983. 431 pp. 15.5 × 23.5 cm. Price $18.95 (paperback).

This book is unusual in that it is directed to nonmedical personnel. The "therapy" of the title refers not to those modalities that medical people generally consider therapy, but more specifically to psychosocial approaches to treatment. The authors are a faculty member of a school of pharmacy and a family therapist. The intended audience might be nurses, social workers, psychologists, or others not primarily concerned with the use of drugs in treatment, but who may need to know what types of drugs their clients are taking and what effects these drugs may have on them.

This second edition has been expanded to include new sections not in the first. It is organized around eight general topics, each of which is covered in a few short chapters: drugs in therapeutic perspective (again, meaning from the perspective of the psychotherapist); foundations of drug action (a review of basic neuropharmacology); drug use and abuse; drugs and the arousal state (referring to sedative-hypnotics, alcohol, stimulants, and psychedelics); psychiatric disorders and drugs (psychosis, anxiety, depression, and mania); motor functions and drugs; pain and its drug management; and drugs and consciousness (which includes anticonvulsants). Each section is headed by a short introduction indicating the aims of the several chapters that follow.

The book is well illustrated with figures and tables. Most of these have appeared in either the same or slightly different form in other books. Virtually all the references are also to books or book chapters. Thus, it appears that the authors have attempted a synthesis of much that has already been published, tailoring it to the needs of the prospective audience. Relatively little emphasis has been placed on how specific drugs are used, but each chapter that discusses a class of drugs finishes with a brief synopsis providing the generic and trade names of the drug, the class to which they belong, their usual indications, and the usual range of daily doses. The major emphases are on how the drugs work in the nervous system and how they may affect the behavior of interest to the psychotherapist.

The book is well written and generally free of errors. It should certainly meet the needs of its intended audience, but would probably be inadequate for pharmacists or physicians. The only other book that I can remember that addressed a similar audience was one that Honigfeld wrote many years ago. Thus, the present volume services a useful need. It would be well worth having as a reference handbook for those who need to know how drugs affect their clients.

Reviewed by Leo E. Hollister
Senior Medical Investigator
Veterans Administration Medical Center
Palo Alto, CA

Calcium Antagonism in Heart and Smooth Muscle: Experimental Facts and Therapeutic Perspectives. By ALBRECHT FLECKENSTEIN. John Wiley and Sons, Inc., One Wiley Drive, Somerset, NJ 08873. 1983. 399 pp. 17 × 24 cm. Price $60.00.

Calcium antagonists have generated considerable interest in the pharmaceutical sciences since nifedipine was reported to be effective in the treatment of Printzmetal angina. This book constitutes a major tool for understanding the role of calcium and calcium antagonism in the heart and smooth muscle. The reader will find important information about the pharmacological properties of verapamil and its derivative, nifedipine and its derivatives, and diltiazem. It is not the first book published on this subject; however, the author makes this one very original.

Dr. Albrecht Fleckenstein investigated this field for more than 20 years. He is recognized as one of the most important contributors to the advancement accomplished in this field. This book provides indispensable knowledge related to the role of calcium in myocardial and vascular smooth muscle contractions, the pacemaker activity in physiological and pathological conditions, allowing a much better understanding of the cardiovascular indications of this very attractive group of drugs. Finally, it is of special interest to find a classification of these drugs in relation to their specificity in affecting the calcium channel. Dr. Fleckenstein proposed classifying the calcium antagonists in three groups: Group A, specific calcium antagonists including verapamil, nifedipine, their derivatives, and diltiazem; Group B, calcium antagonists also affecting the movement of sodium including prenylamine, terodiline, fendiline, perhexiline, and caroverine; Group C, substances with calcium antagonistic side effects, including nitroglycerin, barbituric acid, etc. Such classification is based on a number of pharmacological criteria. There are so many drugs claimed to be specific calcium antagonists, but also interfere with movements of other ions.

This book is recommended as a major source of information concerning the pharmacological properties of calcium antagonists.

Reviewed by Jacques Chelly
Department of Pharmacology
University of Houston
Department of Anesthesiology
Baylor College of Medicine
Houston, TX 77030

Nicotinic Acid: Nutrient–Cofactor–Drug. (Clinical Pharmacology Series, Vol. 1). By MURRAY WEINER and JAN VAN EYS. Marcel Dekker, 270 Madison Avenue, New York, NY 10016. 1983. 308 pp. 16 × 24 cm. Price $55.00 (20% higher outside the U.S. and Canada).

This monograph provides a synthesis of existing knowledge from a wide variety of sources into a single, concise volume. Topics are not examined in excessive detail, but that was not a purpose of the book. Rather, it emerges as a strength in that it permits the diverse audience addressed to be informed readily in areas beyond particular disciplinary constraints. An index and extensive references facilitate acquisition of detailed information on the topics covered for interested readers. The book succeeds well in crossing disciplinary boundaries, and it frequently reveals provocative possibilities for future research. Exposition, organized by sections according to the title, is acceptably comprehensive and includes such newer developments as the nicotinamide coenzymes as donors in transribosylation reactions and in regulation of DNA repair and synthesis, use of nicotinic acid in cardiovascular and hyperlipidemic diseases (including pharmacokinetics and pharmacodynamics), and reexamination of the tryptophan-nicotinic acid relationship in a world in which protein hunger is a global problem of growing concern. For example, nonspecialists who identify pellagra with a simple niacin-tryptophan deficiency will be enlightened by the very first chapter.

The roles of nicotinic acid at the metabolic level are manifold. The most vital function of living material—the capacity to abstract and utilize energy from complex molecules—requires controlled oxidations linked to the nicotinic acid-derived coenzymes. Moreover, NAD participates in the generation of adenosine diphosphate robose polymers, which have a role in DNA metabolism and function. Indeed, in its coenzyme forms the physiological roles of nicotinic acid are pervasive and pivotal in the subcellular compartments of cytoplasm, nucleus, mitochondrion, and endoplasmic reticulum. The authors aver that "there are few areas of biochemistry in which pharmacology, nutritional biochemistry, and molecular biology are interwoven in such a coherent whole." Their monograph amply illuminates that statement. This overview of nicotinic acid and its variety of chemical and metabolic derivatives includes important biochemical, nutritional, pharmacological, and clinical aspects. In addition to life scientists and practitioners in those fields, the book should appeal to dieticians, pharmacists, and others interested in a concise and authoritative exposition of the functions and relationships of this critical cog in the metabolic machinery. It is an excellent contemporary reference for courses in all these disciplines, and it will be at home on laboratory benches due to its durable, stain-resistant binding.

There are relatively few printing errors and oversights for a first printing. Minor misspellings and errors in figures, such as the entry of the symbol for oxygen for that of coenzyme Q and a misplaced arrow (p. 219) and an exotically appended CO_2 on the NAM molecule (p. 19), are neither overly distracting nor misleading. Of somewhat more concern are the use of "niacin" in the second paragraph of p. 9 when "niacytin" is intended and strange displacements such as "substitutes" for "substrates" (p. 217).

This monograph is the first volume in a projected series in clinical pharmacology under the general editorial direction of Dr. Weiner. Three decades of distinguished research in many of the aspects of the metabolic roles of these compounds by Professor van Eys are evident in the clarity and insightful coverage which characterize this volume. If succeeding volumes maintain those qualities we will have much to look forward to and a wide audience stands much to gain.

Reviewed by Edwin S. Higgins
Department of Biochemistry
Medical College of Virginia
Virginia Commonwealth University
Richmond, VA 23298

Pain, Analgesia, and Addiction: The Pharmacologic Treatment of Pain. By BARRY STIMMEL. Raven Press, 1140 Avenue of the Americas, New York, NY 10036. 1983. 312 pp. 16 × 24 cm. Price $45.00.

This is an interesting volume presenting a multifaceted discussion of pain and its pharmacological management. The book appears to be written primarily with a pedagogic perspective and intent, presenting a rather broad survey of factors involved in the phenomenon of pain and of drugs used for relief of pain. It seems most useful for someone who is interested in pain and wishes to learn more about its various aspects, rather than for one who already has some expertise in the study or treatment of pain.

This book is organized into three distinct sections. The first deals with fundamental components of pain and analgesia, including the description and discussion of the anatomical pathways, neurochemical species, and psychological factors believed to be involved, as well as discussion of drug tolerance, dependence, and withdrawal. The second section deals with the clinical pharmacology of drugs used to relieve pain. Included in this are discussions of some unconventional agents such as stimulants, antidepressants, antipsychotic drugs, sedative-hypnotic-antianxiety agents, and marijuana. The discussions of pharmacological properties of the drug classes are broad, including description of effects on a number of organ systems, biodisposition, adverse effects, and drug interactions, rather than being confined to matters relating to pain and analgesia. This approach seems to diffuse the focus of the book somewhat, but may make it more useful for the clinician considering the use of these agents in a patient or encountering a patient already taking them. The third section offers a discussion of practical management of pain. It addresses such issues as the differences in management of acute *versus* chronic pain, management in "problem" populations such as the elderly, patients with malignancy, and drug-dependent patients, and the problem of iatrogenic drug dependence.

Included with each chapter is an ample list of references, but for some chapters more recent references are noticeably lacking. It also seems that the pharmacology section would have benefitted from more basic science references, especially some dealing with cellular actions and mechanisms of drugs, which would contribute to a better understanding of drug effects.

One strength of the volume, in spite of the preceding statement, is its combination and integration of basic and clinical sciences. The first section is done best in this regard. Another strength is the breadth of topics covered, including some not usually considered in texts dealing with pain or analgesic drugs. The author also applies his practical experience in discussion of the topics, which probably enhances the usefulness of the book for less experienced practitioners. The opinions of the author are expressed rather strongly in some of the "practical" sections of the book, and this expression could be viewed as being both a strength and weakness of the work. Weaknesses of the volume include a rather large number of typographical errors and some factual errors. While these are rather trivial relative to the content of the book as a whole, they are still somewhat bothersome. Other weaknesses, referred to earlier, include lack of currency in discussion of some topics and a paucity of basic science data in some discussions.

In summary, this volume deals with pain, analgesia, and related phenomena in considerable breadth and in sufficient depth to make it a useful source of information for both health scientists and clinicians who are interested in basic concepts concerning the nature of pain and analgesia and in the practical treatment of pain.

Reviewed by Graham A. Patrick
Department of Pharmacology and Toxicology
Medical College of Virginia
Virginia Commonwealth University
Richmond, VA 23298

Antibiotics: Assessment of Antimicrobial Activity and Resistance. (Society for Applied Bacteriology, Technical Series No. 18.) Edited by A. DENVER RUSSELL and LOUIS B. QUENSEL. Academic Press, Inc., 111 Fifth Avenue, New York, NY 10003. 1983. 384 pp. 15 × 23 cm. Price $48.00 (£29.00).

This volume, the 18th in the Society for Applied Bacteriology technical series, includes 23 lectures with contributions from 50 microbiologists presented at a Demonstration Meeting of the Society held at the Welsh School of Pharmacy, University of Science and Technology, Cardiff, in September 1981.

The invaluable medicinal properties of antibiotics are universally recognized, but the ability of many organisms to develop resistance to certain of these antibiotics is sometimes underestimated or ignored. One of the greatest challenges in drug development is the continued need to discover and develop new chemotherapeutic agents to which microorganisms are initially, and continue to be, highly sensitive. This volume discusses many of the details of microbial sensitivity and resistance to antibiotics.

An introductory chapter in the book briefly describes the various types of antibiotics, their mode(s) of action, and methods of assay for these compounds. Other topics considered include: sensitivity testing; effects of media composition on MIC values of antibiotics; sensitivity determination by the measurement of conductance; the effects of cell envelope composition on antibiotic activity; the use of ionophoric antibiotics as experiment tools in microbiology; the extraction, purification, detection, and identification of β-lactamases; methods for determining the stability of β-lactam antibiotics to β-lactamase extracts; the biochemical evaluation of β-lactamase inhibitors; detection methods for bacterial penicillin-binding proteins; means of detecting aminoglycoside-modifying strains of bacteria; assay methods for aminoglycosides; methods of studying plasmid-determined tetracycline resistance; methods of studying bacterial folate metabolism inhibition; *in vitro* methods for determining transferable resistance to antibiotics; phage typing and plasmid characterization in studying the epidemiology of multiresistant *Salmonella typhimurium;* measurement of combined antibiotic action; use of a biophotometer in determining the effects of antibiotics; use of high-voltage electrophoresis in the identification of antibiotics; testing antibiotics for sterility; and the detection of antibiotic residues in milk and animal tissues.

The volume contains both theoretical and practical information on a variety of analytical techniques, and many valuable tables, figures, and schemes are included. The articles presented are well referenced and are current up to 1982. This is an excellent publication which contains an enormous amount of information and is highly recommended as a reference book. The price, along with its incomplete coverage of all aspects of antibiotics, would limit its usefulness as a textbook.

Reviewed by Leonard R. Worthen
Department of Pharmacognosy and Environmental Health Sciences
College of Pharmacy
University of Rhode Island
Kingston, RI 02881

The Alkaloids: Chemistry and Pharmacology. Vol. 21. Edited by ARNOLD BROSSI. Academic Press, Inc., 111 Fifth Avenue, New York, NY 10003. 1983. 368 pp. 16 × 23.5 cm. Price $49.50.

This new volume in *The Alkaloids* series, the first to be edited by Arnold Brossi, is truly an exciting book. There is a sense of urgency and intensity about it which is hard to miss. It includes seven chapters, and in three of these the authors involved have deemed it necessary to add (at the end of their respective chapters) an addendum to bring the material presented completely up-to-date. In another chapter, a last minute change was made to round off the material presented.

In every instance, emphasis has been placed not only on occurrence, structural elucidation, and synthesis, but also on the most recent pharmacological results. One is thus led to realize that the justification for endeavors in natural products chemistry lies in the intrinsic interest and challenge of the chemical subject matter, as well as in the biological activity of natural products, particularly alkaloids.

Another characteristic of this volume of *The Alkaloids* is that the term "alkaloid" has been interpreted in broad terms, so that cyclic nitrogenous compounds produced by plants, micro-organisms, sponges, amphibians, and mammals are all discussed in detail.

Each of the presentations for the seven chapters is authoritative, precise, thorough, and above all permeated with enthusiasm. The authors who brought about this impressive *tour de force* in their chapters are: K. Gerzon and G. H. Svoboda: "Acridone Alkaloids"; J. Bergman: "Quinazolinocarboline Alkaloids"; T. Arai and A. Kubo: "Isoquinolinequinones"; J.-C. Cai and C. R. Hutchinson: "Camptothecin"; B. Witkop and E. Gossinger: "Amphibian Alkaloids"; J. Lundstrom: "Simple Isoquinolines"; and M. A. Collins: "Mammalian Alkaloids."

Incidentally, one of the twelve authors is supposed to be retired and has only a private address. Yet, he has shared in the writing of an excellent chapter.

Pain, Analgesia, and Addiction: The Pharmacologic Treatment of Pain. By BARRY STIMMEL. Raven Press, 1140 Avenue of the Americas, New York, NY 10036. 1983. 312 pp. 16 × 24 cm. Price $45.00.

This is an interesting volume presenting a multifaceted discussion of pain and its pharmacological management. The book appears to be written primarily with a pedagogic perspective and intent, presenting a rather broad survey of factors involved in the phenomenon of pain and of drugs used for relief of pain. It seems most useful for someone who is interested in pain and wishes to learn more about its various aspects, rather than for one who already has some expertise in the study or treatment of pain.

This book is organized into three distinct sections. The first deals with fundamental components of pain and analgesia, including the description and discussion of the anatomical pathways, neurochemical species, and psychological factors believed to be involved, as well as discussion of drug tolerance, dependence, and withdrawal. The second section deals with the clinical pharmacology of drugs used to relieve pain. Included in this are discussions of some unconventional agents such as stimulants, antidepressants, antipsychotic drugs, sedative-hypnotic-antianxiety agents, and marijuana. The discussions of pharmacological properties of the drug classes are broad, including description of effects on a number of organ systems, biodisposition, adverse effects, and drug interactions, rather than being confined to matters relating to pain and analgesia. This approach seems to diffuse the focus of the book somewhat, but may make it more useful for the clinician considering the use of these agents in a patient or encountering a patient already taking them. The third section offers a discussion of practical management of pain. It addresses such issues as the differences in management of acute *versus* chronic pain, management in "problem" populations such as the elderly, patients with malignancy, and drug-dependent patients, and the problem of iatrogenic drug dependence.

Included with each chapter is an ample list of references, but for some chapters more recent references are noticeably lacking. It also seems that the pharmacology section would have benefitted from more basic science references, especially some dealing with cellular actions and mechanisms of drugs, which would contribute to a better understanding of drug effects.

One strength of the volume, in spite of the preceding statement, is its combination and integration of basic and clinical sciences. The first section is done best in this regard. Another strength is the breadth of topics covered, including some not usually considered in texts dealing with pain or analgesic drugs. The author also applies his practical experience in discussion of the topics, which probably enhances the usefulness of the book for less experienced practitioners. The opinions of the author are expressed rather strongly in some of the "practical" sections of the book, and this expression could be viewed as being both a strength and weakness of the work. Weaknesses of the volume include a rather large number of typographical errors and some factual errors. While these are rather trivial relative to the content of the book as a whole, they are still somewhat bothersome. Other weaknesses, referred to earlier, include lack of currency in discussion of some topics and a paucity of basic science data in some discussions.

In summary, this volume deals with pain, analgesia, and related phenomena in considerable breadth and in sufficient depth to make it a useful source of information for both health scientists and clinicians who are interested in basic concepts concerning the nature of pain and analgesia and in the practical treatment of pain.

Reviewed by Graham A. Patrick
Department of Pharmacology and Toxicology
Medical College of Virginia
Virginia Commonwealth University
Richmond, VA 23298

Antibiotics: Assessment of Antimicrobial Activity and Resistance. (Society for Applied Bacteriology, Technical Series No. 18.) Edited by A. DENVER RUSSELL and LOUIS B. QUENSEL. Academic Press, Inc., 111 Fifth Avenue, New York, NY 10003. 1983. 384 pp. 15 × 23 cm. Price $48.00 (£29.00).

This volume, the 18th in the Society for Applied Bacteriology technical series, includes 23 lectures with contributions from 50 microbiologists presented at a Demonstration Meeting of the Society held at the Welsh School of Pharmacy, University of Science and Technology, Cardiff, in September 1981.

The invaluable medicinal properties of antibiotics are universally recognized, but the ability of many organisms to develop resistance to certain of these antibiotics is sometimes underestimated or ignored. One of the greatest challenges in drug development is the continued need to discover and develop new chemotherapeutic agents to which microorganisms are initially, and continue to be, highly sensitive. This volume discusses many of the details of microbial sensitivity and resistance to antibiotics.

An introductory chapter in the book briefly describes the various types of antibiotics, their mode(s) of action, and methods of assay for these compounds. Other topics considered include: sensitivity testing; effects of media composition on MIC values of antibiotics; sensitivity determination by the measurement of conductance; the effects of cell envelope composition on antibiotic activity; the use of ionophoric antibiotics as experiment tools in microbiology; the extraction, purification, detection, and identification of β-lactamases; methods for determining the stability of β-lactam antibiotics to β-lactamase extracts; the biochemical evaluation of β-lactamase inhibitors; detection methods for bacterial penicillin-binding proteins; means of detecting aminoglycoside-modifying strains of bacteria; assay methods for aminoglycosides; methods of studying plasmid-determined tetracycline resistance; methods of studying bacterial folate metabolism inhibition; *in vitro* methods for determining transferable resistance to antibiotics; phage typing and plasmid characterization in studying the epidemiology of multiresistant *Salmonella typhimurium;* measurement of combined antibiotic action; use of a biophotometer in determining the effects of antibiotics; use of high-voltage electrophoresis in the identification of antibiotics; testing antibiotics for sterility; and the detection of antibiotic residues in milk and animal tissues.

The volume contains both theoretical and practical information on a variety of analytical techniques, and many valuable tables, figures, and schemes are included. The articles presented are well referenced and are current up to 1982. This is an excellent publication which contains an enormous amount of information and is highly recommended as a reference book. The price, along with its incomplete coverage of all aspects of antibiotics, would limit its usefulness as a textbook.

Reviewed by Leonard R. Worthen
Department of Pharmacognosy and Environmental Health Sciences
College of Pharmacy
University of Rhode Island
Kingston, RI 02881

The Alkaloids: Chemistry and Pharmacology. Vol. 21. Edited by ARNOLD BROSSI. Academic Press, Inc., 111 Fifth Avenue, New York, NY 10003. 1983. 368 pp. 16 × 23.5 cm. Price $49.50.

This new volume in *The Alkaloids* series, the first to be edited by Arnold Brossi, is truly an exciting book. There is a sense of urgency and intensity about it which is hard to miss. It includes seven chapters, and in three of these the authors involved have deemed it necessary to add (at the end of their respective chapters) an addendum to bring the material presented completely up-to-date. In another chapter, a last minute change was made to round off the material presented.

In every instance, emphasis has been placed not only on occurrence, structural elucidation, and synthesis, but also on the most recent pharmacological results. One is thus led to realize that the justification for endeavors in natural products chemistry lies in the intrinsic interest and challenge of the chemical subject matter, as well as in the biological activity of natural products, particularly alkaloids.

Another characteristic of this volume of *The Alkaloids* is that the term "alkaloid" has been interpreted in broad terms, so that cyclic nitrogenous compounds produced by plants, micro-organisms, sponges, amphibians, and mammals are all discussed in detail.

Each of the presentations for the seven chapters is authoritative, precise, thorough, and above all permeated with enthusiasm. The authors who brought about this impressive *tour de force* in their chapters are: K. Gerzon and G. H. Svoboda: "Acridone Alkaloids"; J. Bergman: "Quinazolinocarboline Alkaloids"; T. Arai and A. Kubo: "Isoquinolinequinones"; J.-C. Cai and C. R. Hutchinson: "Camptothecin"; B. Witkop and E. Gossinger: "Amphibian Alkaloids"; J. Lundstrom: "Simple Isoquinolines"; and M. A. Collins: "Mammalian Alkaloids."

Incidentally, one of the twelve authors is supposed to be retired and has only a private address. Yet, he has shared in the writing of an excellent chapter.

Pain, Analgesia, and Addiction: The Pharmacologic Treatment of Pain. By BARRY STIMMEL. Raven Press, 1140 Avenue of the Americas, New York, NY 10036. 1983. 312 pp. 16 × 24 cm. Price $45.00.

This is an interesting volume presenting a multifaceted discussion of pain and its pharmacological management. The book appears to be written primarily with a pedagogic perspective and intent, presenting a rather broad survey of factors involved in the phenomenon of pain and of drugs used for relief of pain. It seems most useful for someone who is interested in pain and wishes to learn more about its various aspects, rather than for one who already has some expertise in the study or treatment of pain.

This book is organized into three distinct sections. The first deals with fundamental components of pain and analgesia, including the description and discussion of the anatomical pathways, neurochemical species, and psychological factors believed to be involved, as well as discussion of drug tolerance, dependence, and withdrawal. The second section deals with the clinical pharmacology of drugs used to relieve pain. Included in this are discussions of some unconventional agents such as stimulants, antidepressants, antipsychotic drugs, sedative-hypnotic-antianxiety agents, and marijuana. The discussions of pharmacological properties of the drug classes are broad, including description of effects on a number of organ systems, biodisposition, adverse effects, and drug interactions, rather than being confined to matters relating to pain and analgesia. This approach seems to diffuse the focus of the book somewhat, but may make it more useful for the clinician considering the use of these agents in a patient or encountering a patient already taking them. The third section offers a discussion of practical management of pain. It addresses such issues as the differences in management of acute *versus* chronic pain, management in "problem" populations such as the elderly, patients with malignancy, and drug-dependent patients, and the problem of iatrogenic drug dependence.

Included with each chapter is an ample list of references, but for some chapters more recent references are noticeably lacking. It also seems that the pharmacology section would have benefitted from more basic science references, especially some dealing with cellular actions and mechanisms of drugs, which would contribute to a better understanding of drug effects.

One strength of the volume, in spite of the preceding statement, is its combination and integration of basic and clinical sciences. The first section is done best in this regard. Another strength is the breadth of topics covered, including some not usually considered in texts dealing with pain or analgesic drugs. The author also applies his practical experience in discussion of the topics, which probably enhances the usefulness of the book for less experienced practitioners. The opinions of the author are expressed rather strongly in some of the "practical" sections of the book, and this expression could be viewed as being both a strength and weakness of the work. Weaknesses of the volume include a rather large number of typographical errors and some factual errors. While these are rather trivial relative to the content of the book as a whole, they are still somewhat bothersome. Other weaknesses, referred to earlier, include lack of currency in discussion of some topics and a paucity of basic science data in some discussions.

In summary, this volume deals with pain, analgesia, and related phenomena in considerable breadth and in sufficient depth to make it a useful source of information for both health scientists and clinicians who are interested in basic concepts concerning the nature of pain and analgesia and in the practical treatment of pain.

Reviewed by Graham A. Patrick
Department of Pharmacology and Toxicology
Medical College of Virginia
Virginia Commonwealth University
Richmond, VA 23298

Antibiotics: Assessment of Antimicrobial Activity and Resistance. (Society for Applied Bacteriology, Technical Series No. 18.) Edited by A. DENVER RUSSELL and LOUIS B. QUENSEL. Academic Press, Inc., 111 Fifth Avenue, New York, NY 10003. 1983. 384 pp. 15 × 23 cm. Price $48.00 (£29.00).

This volume, the 18th in the Society for Applied Bacteriology technical series, includes 23 lectures with contributions from 50 microbiologists presented at a Demonstration Meeting of the Society held at the Welsh School of Pharmacy, University of Science and Technology, Cardiff, in September 1981.

The invaluable medicinal properties of antibiotics are universally recognized, but the ability of many organisms to develop resistance to certain of these antibiotics is sometimes underestimated or ignored. One of the greatest challenges in drug development is the continued need to discover and develop new chemotherapeutic agents to which microorganisms are initially, and continue to be, highly sensitive. This volume discusses many of the details of microbial sensitivity and resistance to antibiotics.

An introductory chapter in the book briefly describes the various types of antibiotics, their mode(s) of action, and methods of assay for these compounds. Other topics considered include: sensitivity testing; effects of media composition on MIC values of antibiotics; sensitivity determination by the measurement of conductance; the effects of cell envelope composition on antibiotic activity; the use of ionophoric antibiotics as experiment tools in microbiology; the extraction, purification, detection, and identification of β-lactamases; methods for determining the stability of β-lactam antibiotics to β-lactamase extracts; the biochemical evaluation of β-lactamase inhibitors; detection methods for bacterial penicillin-binding proteins; means of detecting aminoglycoside-modifying strains of bacteria; assay methods for aminoglycosides; methods of studying plasmid-determined tetracycline resistance; methods of studying bacterial folate metabolism inhibition; *in vitro* methods for determining transferable resistance to antibiotics; phage typing and plasmid characterization in studying the epidemiology of multiresistant *Salmonella typhimurium;* measurement of combined antibiotic action; use of a biophotometer in determining the effects of antibiotics; use of high-voltage electrophoresis in the identification of antibiotics; testing antibiotics for sterility; and the detection of antibiotic residues in milk and animal tissues.

The volume contains both theoretical and practical information on a variety of analytical techniques, and many valuable tables, figures, and schemes are included. The articles presented are well referenced and are current up to 1982. This is an excellent publication which contains an enormous amount of information and is highly recommended as a reference book. The price, along with its incomplete coverage of all aspects of antibiotics, would limit its usefulness as a textbook.

Reviewed by Leonard R. Worthen
Department of Pharmacognosy and Environmental Health Sciences
College of Pharmacy
University of Rhode Island
Kingston, RI 02881

The Alkaloids: Chemistry and Pharmacology. Vol. 21. Edited by ARNOLD BROSSI. Academic Press, Inc., 111 Fifth Avenue, New York, NY 10003. 1983. 368 pp. 16 × 23.5 cm. Price $49.50.

This new volume in *The Alkaloids* series, the first to be edited by Arnold Brossi, is truly an exciting book. There is a sense of urgency and intensity about it which is hard to miss. It includes seven chapters, and in three of these the authors involved have deemed it necessary to add (at the end of their respective chapters) an addendum to bring the material presented completely up-to-date. In another chapter, a last minute change was made to round off the material presented.

In every instance, emphasis has been placed not only on occurrence, structural elucidation, and synthesis, but also on the most recent pharmacological results. One is thus led to realize that the justification for endeavors in natural products chemistry lies in the intrinsic interest and challenge of the chemical subject matter, as well as in the biological activity of natural products, particularly alkaloids.

Another characteristic of this volume of *The Alkaloids* is that the term "alkaloid" has been interpreted in broad terms, so that cyclic nitrogenous compounds produced by plants, micro-organisms, sponges, amphibians, and mammals are all discussed in detail.

Each of the presentations for the seven chapters is authoritative, precise, thorough, and above all permeated with enthusiasm. The authors who brought about this impressive *tour de force* in their chapters are: K. Gerzon and G. H. Svoboda: "Acridone Alkaloids"; J. Bergman: "Quinazolinocarboline Alkaloids"; T. Arai and A. Kubo: "Isoquinolinequinones"; J.-C. Cai and C. R. Hutchinson: "Camptothecin"; B. Witkop and E. Gossinger: "Amphibian Alkaloids"; J. Lundstrom: "Simple Isoquinolines"; and M. A. Collins: "Mammalian Alkaloids."

Incidentally, one of the twelve authors is supposed to be retired and has only a private address. Yet, he has shared in the writing of an excellent chapter.

The choice of Dr. Brossi as editor of *The Alkaloids* is particularly felicitous since he brings to his position an extensive and impressive background in natural products chemistry as well as pharmacology.

To minimize costs, the publishers have seen fit to let each group of authors draw their own chemical diagrams. This has worked out very satisfactorily, since the structures are well drawn and clearly layed out. The result is that this book of almost 400 pages, with a very large number of tables, charts and structures, is offered for a relatively modest $49.50. Not a bad deal!

Reviewed by Maurice Shamma
Department of Chemistry
The Pennsylvania State University
University Park, PA 16802

Compartmental Models and Their Application. By KEITH GODFREY. Academic Press Inc., 24-28 Oval Road, London NW1 7Dx, England. 1983. 293 pp. 15.5 × 23.5 Price $50.00 (£32.00).

The use of compartmental models to describe the disposition of drugs *in vivo* is a widely practiced art in the pharmaceutical sciences. These models very often provide a reasonable phenomenological description of the complex set of events and processes that determine the pharmacokinetics of a drug in mammalian systems. Less often, they also provide a means to interpret or discern what mechanisms are responsible for the observed performance. It is surprising, then, that the current texts on pharmacokinetics do not address the properties and problems associated with the models themselves. Godfrey's text attempts to do just that.

This book provides a comprehensive overview of compartmental models. The subjects can be roughly divided into three general areas (not corresponding to the individual chapters): the performance of linear systems; the problem of identifiability and parameter estimation; and the properties of more complex systems which display nonlinear, time variant, and stochastic behavior. The general layout includes a mathematical description of the various systems, comments concerning their performances, and many examples to illustrate applications. Two cautions must be voiced. First, while proofs have been eliminated, the vocabulary and notation are that of an applied mathematics-engineering approach. This, however, should not be a problem since the author carefully provides good descriptions throughout the text. Second, this is definitely not a pharmacokinetics text. While many of the examples are taken from that area, the emphasis is on the mathematical system and not on the phenomena being modeled. In this respect, the author provides a welcome service to the pharmacokinetics community.

In the first four chapters many linear compartmental systems are presented. The descriptions are straightforward and present an excellent overview. The various models are shown mathematically, their performances are illustrated by numerous calculations and graphical illustrations, and literature examples of actual applications are provided. The third section on nonlinear and time variant systems is similarly well described, to a depth not found elsewhere. The second section on identifiability and parameter estimation is by far the most important contribution of this book. Here, Dr. Godfrey provides an excellent analysis of whether particular models actually can be used to describe real data. Often we decide that a particular model effectively represents a set of data. Is the model unique? In most cases the answer is a resounding no. That fact is amply demonstrated by the use of Laplacian analysis as well as consideration of numerical problems. My only complaint is that the author does not go far enough; the emphasis is on the estimation of microconstants, not on integrated parameter estimation. The problem of correlation between parameters is barely considered; no mention of reparameterization is provided. Yet, this is a minor fault compared with the large assortment of warnings provided.

In summary, this book is an excellent reference document concerning the power and problems of lumped parameter systems composed of first-order differential equations. It is probably the best book on that subject available. The appropriateness of these models is up to us.

Reviewed by Kenneth J. Himmelstein
Inter$_x$ Research Corporation
2201 West 21st Street
Lawrence, KS 66044

Formaldehyde: Toxicology—Epidemiology—Mechanisms. Edited by JOHN J. CLARY, JAMES E. GIBSON, and RICHARD S. WARITZ. Marcel Dekker, 270 Madison Avenue, New York, NY 10016. 1983. 296 pp. 15 × 23 cm. Price $45.00 (20% higher outside the U.S. and Canada).

The Chemical Industry Institute of Toxicology (CIIT), Research Triangle Park, NC, sponsored conferences on formaldehyde toxicity in November 1980 and, with funding from the Formaldehyde Institute, on November 3, 1982. The papers and discussions of the latter conference are presented in this book.

There are eleven chapters by 26 contributors, of which half are from CIIT. Chapter titles are as follows: "Occupational Exposure to Formaldehyde—Recent NIOSH Involvement," "Mathematical Cancer Risk Assessment for Formaldehyde," "Case Control Study of Cancer Deaths in DuPont Workers with Potential Exposure to Formaldehyde," "Mortality of Ontario Undertakers: A First Report," "Skin Initiation/Promotion Study with Formaldehyde in Sencar Mice," "Skin Initiation/Promotion Study with Formaldehyde in CD-1 Mice," "Mutagenic Effects of Formaldehyde in Bacterial and Human Cells," "Formaldehyde and the Nasal Mucociliary Apparatus," "Reaction of Formaldehyde in the Rat Nasal Mucosa," "The Effect of Formaldehyde Exposure in Cytotoxicity and Cell Proliferation," and "Mechanisms of Formaldehyde Toxicity and Risk Evaluation."

In general these topics are well written, and the summaries of the discussions that follow the actual presentations are of interest. Literature is cited up to the time of publication including 1983 references and citations to manuscripts in press.

In summary of the information presented at this second CIIT conference—it is now well accepted that airborne formaldehyde leads to cancer in rats and mice, that formaldehyde has the potential to cause genetic toxicity, and that formaldehyde will bind to DNA *in vitro*. Clarification, however, is still required regarding the importance of binding *in vitro*, especially as related to detoxification pathways and repair mechanisms. Of prime importance was the need for the results of additional epidemiological studies. While this volume is of restricted interest in the pharmaceutical sciences, it should be of value to those in contact with formaldehyde and its products as well as to toxicologists.

Reviewed by Joseph E. Sinsheimer
College of Pharmacy
The University of Michigan
Ann Arbor, MI 48109

Methods in Industrial Microbiology. By B. SIKYTA. John Wiley & Sons, Inc. One Wiley Drive, Somerset, NJ 08873. 1983. 349 pp. 16 × 24 cm. Price $79.95.

This short textbook is aimed primarily at the microbiologist who is seeking a very broad and simplified introduction to industrial fermentation processes. The chapter headings: "Introduction," "Culture Equipment," "Sterilization of Media and Air," "Aeration and Mixing," "Substrates for Microbial Processes," "Kinetics of Microbial Processes," "Genetics of Industrial Microorganisms," "Development of Microbial Processes," "Measurement and Control of Microbial Processes," and "Isolation of Microbial Products" indicate that the author has attempted to condense a broad spectrum of biotechnology in a limited space. As a result, the subject matter is treated too superficially to make this a truly valuable reference source (*e.g.*, mass transfer scale-up in two and one-half pages).

The potentially useful aspects of this book might be the listing of the composition of various natural substances (*e.g.* cornsteep liquor) for material balance purposes and, possibly, the reference sources for their historical significance. Otherwise, the book should be of value to the layman interested in a broad view of the fermentation industry.

Reviewed by: H. Michael Koplove
Hoffmann-La Roche
Nutley, NJ 07110

The choice of Dr. Brossi as editor of *The Alkaloids* is particularly felicitous since he brings to his position an extensive and impressive background in natural products chemistry as well as pharmacology.

To minimize costs, the publishers have seen fit to let each group of authors draw their own chemical diagrams. This has worked out very satisfactorily, since the structures are well drawn and clearly layed out. The result is that this book of almost 400 pages, with a very large number of tables, charts and structures, is offered for a relatively modest $49.50. Not a bad deal!

Reviewed by Maurice Shamma
Department of Chemistry
The Pennsylvania State University
University Park, PA 16802

Compartmental Models and Their Application. By KEITH GODFREY. Academic Press Inc., 24-28 Oval Road, London NW1 7Dx, England. 1983. 293 pp. 15.5 × 23.5 Price $50.00 (£32.00).

The use of compartmental models to describe the disposition of drugs *in vivo* is a widely practiced art in the pharmaceutical sciences. These models very often provide a reasonable phenomenological description of the complex set of events and processes that determine the pharmacokinetics of a drug in mammalian systems. Less often, they also provide a means to interpret or discern what mechanisms are responsible for the observed performance. It is surprising, then, that the current texts on pharmacokinetics do not address the properties and problems associated with the models themselves. Godfrey's text attempts to do just that.

This book provides a comprehensive overview of compartmental models. The subjects can be roughly divided into three general areas (not corresponding to the individual chapters): the performance of linear systems; the problem of identifiability and parameter estimation; and the properties of more complex systems which display nonlinear, time variant, and stochastic behavior. The general layout includes a mathematical description of the various systems, comments concerning their performances, and many examples to illustrate applications. Two cautions must be voiced. First, while proofs have been eliminated, the vocabulary and notation are that of an applied mathematics-engineering approach. This, however, should not be a problem since the author carefully provides good descriptions throughout the text. Second, this is definitely not a pharmacokinetics text. While many of the examples are taken from that area, the emphasis is on the mathematical system and not on the phenomena being modeled. In this respect, the author provides a welcome service to the pharmacokinetics community.

In the first four chapters many linear compartmental systems are presented. The descriptions are straightforward and present an excellent overview. The various models are shown mathematically, their performances are illustrated by numerous calculations and graphical illustrations, and literature examples of actual applications are provided. The third section on nonlinear and time variant systems is similarly well described, to a depth not found elsewhere. The second section on identifiability and parameter estimation is by far the most important contribution of this book. Here, Dr. Godfrey provides an excellent analysis of whether particular models actually can be used to describe real data. Often we decide that a particular model effectively represents a set of data. Is the model unique? In most cases the answer is a resounding no. That fact is amply demonstrated by the use of Laplacian analysis as well as consideration of numerical problems. My only complaint is that the author does not go far enough; the emphasis is on the estimation of microconstants, not on integrated parameter estimation. The problem of correlation between parameters is barely considered; no mention of reparameterization is provided. Yet, this is a minor fault compared with the large assortment of warnings provided.

In summary, this book is an excellent reference document concerning the power and problems of lumped parameter systems composed of first-order differential equations. It is probably the best book on that subject available. The appropriateness of these models is up to us.

Reviewed by Kenneth J. Himmelstein
Inter$_x$ Research Corporation
2201 West 21st Street
Lawrence, KS 66044

Formaldehyde: Toxicology—Epidemiology—Mechanisms. Edited by JOHN J. CLARY, JAMES E. GIBSON, and RICHARD S. WARITZ. Marcel Dekker, 270 Madison Avenue, New York, NY 10016. 1983. 296 pp. 15 × 23 cm. Price $45.00 (20% higher outside the U.S. and Canada).

The Chemical Industry Institute of Toxicology (CIIT), Research Triangle Park, NC, sponsored conferences on formaldehyde toxicity in November 1980 and, with funding from the Formaldehyde Institute, on November 3, 1982. The papers and discussions of the latter conference are presented in this book.

There are eleven chapters by 26 contributors, of which half are from CIIT. Chapter titles are as follows: "Occupational Exposure to Formaldehyde—Recent NIOSH Involvement," "Mathematical Cancer Risk Assessment for Formaldehyde," "Case Control Study of Cancer Deaths in DuPont Workers with Potential Exposure to Formaldehyde," "Mortality of Ontario Undertakers: A First Report," "Skin Initiation/Promotion Study with Formaldehyde in Sencar Mice," "Skin Initiation/Promotion Study with Formaldehyde in CD-1 Mice," "Mutagenic Effects of Formaldehyde in Bacterial and Human Cells," "Formaldehyde and the Nasal Mucociliary Apparatus," "Reaction of Formaldehyde in the Rat Nasal Mucosa," "The Effect of Formaldehyde Exposure in Cytotoxicity and Cell Proliferation," and "Mechanisms of Formaldehyde Toxicity and Risk Evaluation."

In general these topics are well written, and the summaries of the discussions that follow the actual presentations are of interest. Literature is cited up to the time of publication including 1983 references and citations to manuscripts in press.

In summary of the information presented at this second CIIT conference—it is now well accepted that airborne formaldehyde leads to cancer in rats and mice, that formaldehyde has the potential to cause genetic toxicity, and that formaldehyde will bind to DNA *in vitro*. Clarification, however, is still required regarding the importance of binding *in vitro*, especially as related to detoxification pathways and repair mechanisms. Of prime importance was the need for the results of additional epidemiological studies. While this volume is of restricted interest in the pharmaceutical sciences, it should be of value to those in contact with formaldehyde and its products as well as to toxicologists.

Reviewed by Joseph E. Sinsheimer
College of Pharmacy
The University of Michigan
Ann Arbor, MI 48109

Methods in Industrial Microbiology. By B. SIKYTA. John Wiley & Sons, Inc. One Wiley Drive, Somerset, NJ 08873. 1983. 349 pp. 16 × 24 cm. Price $79.95.

This short textbook is aimed primarily at the microbiologist who is seeking a very broad and simplified introduction to industrial fermentation processes. The chapter headings: "Introduction," "Culture Equipment," "Sterilization of Media and Air," "Aeration and Mixing," "Substrates for Microbial Processes," "Kinetics of Microbial Processes," "Genetics of Industrial Microorganisms," "Development of Microbial Processes," "Measurement and Control of Microbial Processes," and "Isolation of Microbial Products" indicate that the author has attempted to condense a broad spectrum of biotechnology in a limited space. As a result, the subject matter is treated too superficially to make this a truly valuable reference source (*e.g.*, mass transfer scale-up in two and one-half pages).

The potentially useful aspects of this book might be the listing of the composition of various natural substances (*e.g.* cornsteep liquor) for material balance purposes and, possibly, the reference sources for their historical significance. Otherwise, the book should be of value to the layman interested in a broad view of the fermentation industry.

Reviewed by: H. Michael Koplove
Hoffmann-La Roche
Nutley, NJ 07110

The choice of Dr. Brossi as editor of *The Alkaloids* is particularly felicitous since he brings to his position an extensive and impressive background in natural products chemistry as well as pharmacology.

To minimize costs, the publishers have seen fit to let each group of authors draw their own chemical diagrams. This has worked out very satisfactorily, since the structures are well drawn and clearly layed out. The result is that this book of almost 400 pages, with a very large number of tables, charts and structures, is offered for a relatively modest $49.50. Not a bad deal!

Reviewed by Maurice Shamma
Department of Chemistry
The Pennsylvania State University
University Park, PA 16802

Compartmental Models and Their Application. By KEITH GODFREY. Academic Press Inc., 24-28 Oval Road, London NW1 7Dx, England. 1983. 293 pp. 15.5 × 23.5 Price $50.00 (£32.00).

The use of compartmental models to describe the disposition of drugs *in vivo* is a widely practiced art in the pharmaceutical sciences. These models very often provide a reasonable phenomenological description of the complex set of events and processes that determine the pharmacokinetics of a drug in mammalian systems. Less often, they also provide a means to interpret or discern what mechanisms are responsible for the observed performance. It is surprising, then, that the current texts on pharmacokinetics do not address the properties and problems associated with the models themselves. Godfrey's text attempts to do just that.

This book provides a comprehensive overview of compartmental models. The subjects can be roughly divided into three general areas (not corresponding to the individual chapters): the performance of linear systems; the problem of identifiability and parameter estimation; and the properties of more complex systems which display nonlinear, time variant, and stochastic behavior. The general layout includes a mathematical description of the various systems, comments concerning their performances, and many examples to illustrate applications. Two cautions must be voiced. First, while proofs have been eliminated, the vocabulary and notation are that of an applied mathematics-engineering approach. This, however, should not be a problem since the author carefully provides good descriptions throughout the text. Second, this is definitely not a pharmacokinetics text. While many of the examples are taken from that area, the emphasis is on the mathematical system and not on the phenomena being modeled. In this respect, the author provides a welcome service to the pharmacokinetics community.

In the first four chapters many linear compartmental systems are presented. The descriptions are straightforward and present an excellent overview. The various models are shown mathematically, their performances are illustrated by numerous calculations and graphical illustrations, and literature examples of actual applications are provided. The third section on nonlinear and time variant systems is similarly well described, to a depth not found elsewhere. The second section on identifiability and parameter estimation is by far the most important contribution of this book. Here, Dr. Godfrey provides an excellent analysis of whether particular models actually can be used to describe real data. Often we decide that a particular model effectively represents a set of data. Is the model unique? In most cases the answer is a resounding no. That fact is amply demonstrated by the use of Laplacian analysis as well as consideration of numerical problems. My only complaint is that the author does not go far enough; the emphasis is on the estimation of microconstants, not on integrated parameter estimation. The problem of correlation between parameters is barely considered; no mention of reparameterization is provided. Yet, this is a minor fault compared with the large assortment of warnings provided.

In summary, this book is an excellent reference document concerning the power and problems of lumped parameter systems composed of first-order differential equations. It is probably the best book on that subject available. The appropriateness of these models is up to us.

Reviewed by Kenneth J. Himmelstein
Inter$_x$ Research Corporation
2201 West 21st Street
Lawrence, KS 66044

Formaldehyde: Toxicology—Epidemiology—Mechanisms. Edited by JOHN J. CLARY, JAMES E. GIBSON, and RICHARD S. WARITZ. Marcel Dekker, 270 Madison Avenue, New York, NY 10016. 1983. 296 pp. 15 × 23 cm. Price $45.00 (20% higher outside the U.S. and Canada).

The Chemical Industry Institute of Toxicology (CIIT), Research Triangle Park, NC, sponsored conferences on formaldehyde toxicity in November 1980 and, with funding from the Formaldehyde Institute, on November 3, 1982. The papers and discussions of the latter conference are presented in this book.

There are eleven chapters by 26 contributors, of which half are from CIIT. Chapter titles are as follows: "Occupational Exposure to Formaldehyde—Recent NIOSH Involvement," "Mathematical Cancer Risk Assessment for Formaldehyde," "Case Control Study of Cancer Deaths in DuPont Workers with Potential Exposure to Formaldehyde," "Mortality of Ontario Undertakers: A First Report," "Skin Initiation/Promotion Study with Formaldehyde in Sencar Mice," "Skin Initiation/Promotion Study with Formaldehyde in CD-1 Mice," "Mutagenic Effects of Formaldehyde in Bacterial and Human Cells," "Formaldehyde and the Nasal Mucociliary Apparatus," "Reaction of Formaldehyde in the Rat Nasal Mucosa," "The Effect of Formaldehyde Exposure in Cytotoxicity and Cell Proliferation," and "Mechanisms of Formaldehyde Toxicity and Risk Evaluation."

In general these topics are well written, and the summaries of the discussions that follow the actual presentations are of interest. Literature is cited up to the time of publication including 1983 references and citations to manuscripts in press.

In summary of the information presented at this second CIIT conference—it is now well accepted that airborne formaldehyde leads to cancer in rats and mice, that formaldehyde has the potential to cause genetic toxicity, and that formaldehyde will bind to DNA *in vitro*. Clarification, however, is still required regarding the importance of binding *in vitro*, especially as related to detoxification pathways and repair mechanisms. Of prime importance was the need for the results of additional epidemiological studies. While this volume is of restricted interest in the pharmaceutical sciences, it should be of value to those in contact with formaldehyde and its products as well as to toxicologists.

Reviewed by Joseph E. Sinsheimer
College of Pharmacy
The University of Michigan
Ann Arbor, MI 48109

Methods in Industrial Microbiology. By B. SIKYTA. John Wiley & Sons, Inc. One Wiley Drive, Somerset, NJ 08873. 1983. 349 pp. 16 × 24 cm. Price $79.95.

This short textbook is aimed primarily at the microbiologist who is seeking a very broad and simplified introduction to industrial fermentation processes. The chapter headings: "Introduction," "Culture Equipment," "Sterilization of Media and Air," "Aeration and Mixing," "Substrates for Microbial Processes," "Kinetics of Microbial Processes," "Genetics of Industrial Microorganisms," "Development of Microbial Processes," "Measurement and Control of Microbial Processes," and "Isolation of Microbial Products" indicate that the author has attempted to condense a broad spectrum of biotechnology in a limited space. As a result, the subject matter is treated too superficially to make this a truly valuable reference source (*e.g.*, mass transfer scale-up in two and one-half pages).

The potentially useful aspects of this book might be the listing of the composition of various natural substances (*e.g.* cornsteep liquor) for material balance purposes and, possibly, the reference sources for their historical significance. Otherwise, the book should be of value to the layman interested in a broad view of the fermentation industry.

Reviewed by: H. Michael Koplove
Hoffmann-La Roche
Nutley, NJ 07110

The choice of Dr. Brossi as editor of *The Alkaloids* is particularly felicitous since he brings to his position an extensive and impressive background in natural products chemistry as well as pharmacology.

To minimize costs, the publishers have seen fit to let each group of authors draw their own chemical diagrams. This has worked out very satisfactorily, since the structures are well drawn and clearly layed out. The result is that this book of almost 400 pages, with a very large number of tables, charts and structures, is offered for a relatively modest $49.50. Not a bad deal!

Reviewed by Maurice Shamma
Department of Chemistry
The Pennsylvania State University
University Park, PA 16802

Compartmental Models and Their Application. By KEITH GODFREY. Academic Press Inc., 24-28 Oval Road, London NW1 7Dx, England. 1983. 293 pp. 15.5 × 23.5 Price $50.00 (£32.00).

The use of compartmental models to describe the disposition of drugs *in vivo* is a widely practiced art in the pharmaceutical sciences. These models very often provide a reasonable phenomenological description of the complex set of events and processes that determine the pharmacokinetics of a drug in mammalian systems. Less often, they also provide a means to interpret or discern what mechanisms are responsible for the observed performance. It is surprising, then, that the current texts on pharmacokinetics do not address the properties and problems associated with the models themselves. Godfrey's text attempts to do just that.

This book provides a comprehensive overview of compartmental models. The subjects can be roughly divided into three general areas (not corresponding to the individual chapters): the performance of linear systems; the problem of identifiability and parameter estimation; and the properties of more complex systems which display nonlinear, time variant, and stochastic behavior. The general layout includes a mathematical description of the various systems, comments concerning their performances, and many examples to illustrate applications. Two cautions must be voiced. First, while proofs have been eliminated, the vocabulary and notation are that of an applied mathematics-engineering approach. This, however, should not be a problem since the author carefully provides good descriptions throughout the text. Second, this is definitely not a pharmacokinetics text. While many of the examples are taken from that area, the emphasis is on the mathematical system and not on the phenomena being modeled. In this respect, the author provides a welcome service to the pharmacokinetics community.

In the first four chapters many linear compartmental systems are presented. The descriptions are straightforward and present an excellent overview. The various models are shown mathematically, their performances are illustrated by numerous calculations and graphical illustrations, and literature examples of actual applications are provided. The third section on nonlinear and time variant systems is similarly well described, to a depth not found elsewhere. The second section on identifiability and parameter estimation is by far the most important contribution of this book. Here, Dr. Godfrey provides an excellent analysis of whether particular models actually can be used to describe real data. Often we decide that a particular model effectively represents a set of data. Is the model unique? In most cases the answer is a resounding no. That fact is amply demonstrated by the use of Laplacian analysis as well as consideration of numerical problems. My only complaint is that the author does not go far enough; the emphasis is on the estimation of microconstants, not on integrated parameter estimation. The problem of correlation between parameters is barely considered; no mention of reparameterization is provided. Yet, this is a minor fault compared with the large assortment of warnings provided.

In summary, this book is an excellent reference document concerning the power and problems of lumped parameter systems composed of first-order differential equations. It is probably the best book on that subject available. The appropriateness of these models is up to us.

Reviewed by Kenneth J. Himmelstein
Inter$_x$ Research Corporation
2201 West 21st Street
Lawrence, KS 66044

Formaldehyde: Toxicology—Epidemiology—Mechanisms. Edited by JOHN J. CLARY, JAMES E. GIBSON, and RICHARD S. WARITZ. Marcel Dekker, 270 Madison Avenue, New York, NY 10016. 1983. 296 pp. 15 × 23 cm. Price $45.00 (20% higher outside the U.S. and Canada).

The Chemical Industry Institute of Toxicology (CIIT), Research Triangle Park, NC, sponsored conferences on formaldehyde toxicity in November 1980 and, with funding from the Formaldehyde Institute, on November 3, 1982. The papers and discussions of the latter conference are presented in this book.

There are eleven chapters by 26 contributors, of which half are from CIIT. Chapter titles are as follows: "Occupational Exposure to Formaldehyde—Recent NIOSH Involvement," "Mathematical Cancer Risk Assessment for Formaldehyde," "Case Control Study of Cancer Deaths in DuPont Workers with Potential Exposure to Formaldehyde," "Mortality of Ontario Undertakers: A First Report," "Skin Initiation/Promotion Study with Formaldehyde in Sencar Mice," "Skin Initiation/Promotion Study with Formaldehyde in CD-1 Mice," "Mutagenic Effects of Formaldehyde in Bacterial and Human Cells," "Formaldehyde and the Nasal Mucociliary Apparatus," "Reaction of Formaldehyde in the Rat Nasal Mucosa," "The Effect of Formaldehyde Exposure in Cytotoxicity and Cell Proliferation," and "Mechanisms of Formaldehyde Toxicity and Risk Evaluation."

In general these topics are well written, and the summaries of the discussions that follow the actual presentations are of interest. Literature is cited up to the time of publication including 1983 references and citations to manuscripts in press.

In summary of the information presented at this second CIIT conference—it is now well accepted that airborne formaldehyde leads to cancer in rats and mice, that formaldehyde has the potential to cause genetic toxicity, and that formaldehyde will bind to DNA *in vitro*. Clarification, however, is still required regarding the importance of binding *in vitro*, especially as related to detoxification pathways and repair mechanisms. Of prime importance was the need for the results of additional epidemiological studies. While this volume is of restricted interest in the pharmaceutical sciences, it should be of value to those in contact with formaldehyde and its products as well as to toxicologists.

Reviewed by Joseph E. Sinsheimer
College of Pharmacy
The University of Michigan
Ann Arbor, MI 48109

Methods in Industrial Microbiology. By B. SIKYTA. John Wiley & Sons, Inc. One Wiley Drive, Somerset, NJ 08873. 1983. 349 pp. 16 × 24 cm. Price $79.95.

This short textbook is aimed primarily at the microbiologist who is seeking a very broad and simplified introduction to industrial fermentation processes. The chapter headings: "Introduction," "Culture Equipment," "Sterilization of Media and Air," "Aeration and Mixing," "Substrates for Microbial Processes," "Kinetics of Microbial Processes," "Genetics of Industrial Microorganisms," "Development of Microbial Processes," "Measurement and Control of Microbial Processes," and "Isolation of Microbial Products" indicate that the author has attempted to condense a broad spectrum of biotechnology in a limited space. As a result, the subject matter is treated too superficially to make this a truly valuable reference source (*e.g.*, mass transfer scale-up in two and one-half pages).

The potentially useful aspects of this book might be the listing of the composition of various natural substances (*e.g.* cornsteep liquor) for material balance purposes and, possibly, the reference sources for their historical significance. Otherwise, the book should be of value to the layman interested in a broad view of the fermentation industry.

Reviewed by: H. Michael Koplove
Hoffmann-La Roche
Nutley, NJ 07110

A publication of the
American Pharmaceutical Association—
the National Professional Society
of Pharmacists

JOURNAL OF PHARMACEUTICAL SCIENCES

Volume 73, 1984

JPMSAE 73(1-12) 1-1910 (1984)
ISSN 0022-3549

Sharon G. Boots
Editor

Sue A. Kruger
Production Editor

Margaret M. Madeleine
Assistant Production Editor

Karen A. Blakney
Copy Editor

Edward G. Feldmann
Contributing Editor

Samuel W. Goldstein
Contributing Editor

Patricia A. Evich
Editorial Secretary

Editorial Advisory Board

Jordan L. Cohen
Kenneth A. Connors
Louis Diamond
Ho-Leung Fung
Milo Gibaldi
Everett N. Hiestand
W. Homer Lawrence
Ian W. Mathison
Carl M. Metzler
Robert E. Notari
Paul L. Schiff, Jr.
Jane E. Shaw

Published monthly under the supervision of the Board of Trustees

Good Public Policy Requires Good Science

Everyone knows that there are many different languages spoken around the world—a phenomenon that the Old Testament tells us was God's punishment to Noah's descendents who embarked on building the Tower of Babel after surviving the great flood.

But even though we all acknowledge the differences *between* languages—English, French, German, Russian, and so on—we seldom recognize, much less acknowledge, the difference *within* a language. And yet, there are differences and at times those differences can be highly significant.

For example, the vast majority of our readers are over 30 years of age. And those who are over 30 probably have encountered the difficulty in conversing with someone under 20 although they are both from the same country, and presumably speak the same native tongue; in fact, they may even be family members from the same household!

Similarly, there is a major difference between the language of the scientist and the language of the layperson—even though both claim to speak the same tongue or native language.

However, the language of scientists is really unique to them; it is very carefully precise and qualified; it often focuses on the exceptions—their occurrence, their frequency, their seriousness, etc. On the other hand, the layperson or the general public speaks another language—one that deals in simple absolutes, and also involves instincts, intuition, psychology, and moods.

The public asks whether a drug is effective or not; whether it is safe or not. The idea that it may be judged "effective" when it only works in three out of four patients, or 75% of the time, is incomprehensible. And the concept that a drug is classified as "safe" when it causes minor side effects in one out of five patients, major side effects in one out of a thousand patients, and death in one out of a hundred thousand patients, is mind-boggling to virtually everyone outside of the field of science.

We were recently reminded of this vast communication gap, as we read reports relating to the issuance of revised cancer guidelines from the White House Office of Science and Technology Policy (OSTP). The June 1 issue of the *Washington Post* headlined its article "Drastic Revision from 1982 Draft." The story itself then started out by describing the background to this report:

"The Reagan Administration has issued dramatically revised draft principles to guide federal policy-makers in cancer regulation, stating that cancer-causing substances can be dangerous even at extremely low levels.

"The massive White House science office document also says that materials that cause cancer in animals are 'suspected human carcinogens.'

"The report reverses many of the positions laid out in a draft issued 18 months ago, according to experts in the field. Designed as the basis for setting cancer policy across the federal government, it appears to have succeeded in creating consensus out of the chaos caused by earlier efforts."

The "earlier efforts" referred to was the former approach to the regulation of potential carcinogens as promoted most vigorously by the Environmental Protection Agency (EPA) during the very early days of the Reagan Administration.

Efforts were then felt necessary to overcome the "doomsday" interpretation that the public had come to associate with the theory that "everything and anything can be harmful and cause cancer if given in a large enough dose, for a long enough period of time, and via certain peculiar conditions of exposure" that was then being espoused by many scientists. The EPA responded by discounting the value of animal tests in determining the risk of cancer in humans; it criticized the way high doses given to animals were being used to predict human reactions; and it stated that a threshold probably existed below which doses of a suspected carcinogen would not cause cancer.

This approach calmed public fears and anxiety, but was roundly criticized by the scientific community at large.

The chief toxicologist for the Environmental Defense Fund is quoted as saying that the original policy draft "got blasted across the board because people were appalled at the bad science in it." A spokesman for the industry-supported American Industrial Health Council commented that the former policy draft "just wasn't accurate scientifically. It has to be defensible scientifically."

In contrast, the current draft comes close to drawing "rave reviews" from the great majority of scientists who have examined it to date. Moreover, those scientists represent the full spectrum of philosophical thinking from the environmental and consumer groups at one end, to the industrial and trade groups on the other end.

Specifically, the current report carefully describes the present state of knowledge as to how cancer is caused and to what degree science can determine whether a given substance is carcinogenic. It also provides a number of guidelines for federal agency use in helping agency officials decide how to regulate suspected carcinogens.

Although the document does not constitute binding policy or regulatory requirements, it does set benchmarks of agreement and understanding for those who regulate and those who are regulated. It also provides a standard of measurement for other interested parties such as consumer groups and environmental coalitions. For these reasons, there is general recognition of the significance of the report, despite its lack of obligatory standing. A key feature of the statement is the listing of 31 separate principles designed to help at least 10 different federal agencies prepare their own guidelines to shape their regulatory programs and activities.

OSTP Director George A. Keyworth II—who also serves as President Reagan's Science Advisor—characterized the document as "one of the most ambitious attempts yet to examine data on cancer causation and their implications for regulatory policy. It responds to society's need for better balance and objectivity in how we regulate man-made and naturally occurring chemicals that may cause cancer."

If there is a lesson to be learned from this experience, it is that good science is a basic need for good public policy. Furthermore, in communicating with the public, efforts must be made to enable the public to understand and comprehend the risks, the benefits, the costs, and so on that may be involved. And in doing so, great efforts must be made to translate the language of science into that which the public can grasp, understand, accept, and place in proper perspective. Finally, and most important, it is essential to maintain the factual accuracy and fundamental integrity of the information itself.

—EDWARD G. FELDMANN
American Pharmaceutical Association
2215 Constitution Avenue, N.W.
Washington, DC 20037

0022-3549/84/0800-1019$01.00/0
© 1984, American Pharmaceutical Association

JOURNAL OF PHARMACEUTICAL SCIENCES

AUGUST 1984
VOLUME 73 NUMBER 8

RESEARCH ARTICLES

Relationship of Chemical Structure to Corneal Penetration and Influence of Low-Viscosity Solution on Ocular Bioavailability

GEORGE M. GRASS and JOSEPH R. ROBINSON ˣ

Received May 2, 1983, from the *School of Pharmacy, University of Wisconsin, Madison, WI 53706.* Accepted for publication August 12, 1983.

Abstract □ Current understanding of the mechanism of corneal penetration by organic molecules proposes the epithelial layer as the rate-limiting membrane for water-soluble compounds and the stromal layer as rate limiting for lipid-soluble compounds. This suggests that the relationship between corneal permeability and the logarithm of oil/water partition coefficients, for a series of drugs, should not be the typical, single, continuous, parabolic-shaped curve. Corneal penetration studies have been conducted in unanesthetized albino rabbits using various organic compounds, representing five orders of magnitude in partition coefficient, at a constant concentration of 4×10^{-5} M dispensed in either a 1- or 90-centipoise (cps) solution. It has been shown that for non-ionizable compounds, a pair of bell-shaped curves were generated, one for lipid-soluble and one for water-soluble compounds. Small water-soluble species demonstrate very high apparent permeabilities, which may relate to the presence of aqueous pores or other paracellular drug movement. Penetration of ionizable compounds does not appear to correlate well with the structural relationships invoked for un-ionized compounds. Consistent with the proposed mechanisms of corneal penetration, oil-soluble drug substances show no improvement in drug bioavailability when dosed from a 90-cps solution, and water-soluble drugs show a modest improvement in ocular drug bioavailability. Small water-soluble substances demonstrate no improvement due to their already high bioavailability. The importance of nonproductive absorption and precorneal drainage on bioavailability is addressed.

Keyphrases □ Bioavailability, ocular—corneal penetration mechanisms, low-viscosity solutions □ Corneal penetration—ocular bioavailability, low-viscosity solutions

Although numerous studies on the penetration of organic compounds into the eye from topical dosing have been reported, these efforts have been limited in the majority of cases to the simple quantification of the amount of drug reaching the aqueous humor (1-3). None of these *in vivo* studies were designed to explore the relationship between drug structure and corneal penetration rate. On the other hand, there have been several reported *in vitro* studies which were expressly designed to explore corneal penetration rate and properties of the permeating species, especially the partition coefficient of the permeating species (4-6). In each of the *in vitro* studies, only a limited number of compounds and/or partition coefficient ranges was studied, and interpretation of the results generally ignored the mechanism of corneal penetration and precorneal disposition kinetics.

The intent of the present work is to explore corneal drug absorption as a function of drug properties, including the following specific aims: (*a*) an examination of vehicle effects (low-viscosity solutions) on drug bioavailability and the relationship of this effect, if any, to the mechanism(s) of corneal permeability, and (*b*) an investigation of the relationship of corneal penetration to physicochemical properties of the drug entity.

Several investigators (4-7) have postulated that the best predictor of corneal penetration rate of drugs is the oil/water (o/w) partition coefficient, and that an optimum partition coefficient exists for maximal penetration. Furthermore, several sources cite this optimal o/w partition coefficient for corneal penetration at a value of 10:1-1000:1 (4, 6), with the corresponding implication that very water-soluble drugs do not penetrate effectively. It has also been assumed that the charged forms of the drug, *i.e.*, ionized molecules, penetrate the cornea at a low rate that is essentially zero. In general, the studies upon which these assertions/assumptions have been based employed *in vitro* mounted corneas and either a restricted range of drugs (*i.e.*, a restricted range of partition coefficients) or a small number of drugs.

Based on published studies (8, 9) and the known structure of the cornea, a limiting-membrane mechanism for corneal penetration of small organic molecules, as depicted in Fig. 1, is proposed. When a drug with a high o/w partition coefficient is applied to the cornea, it quickly partitions into the "lipid-like" epithelial layers of the cornea. However, for such a drug, the aqueous stroma presents a rate-limiting membrane and, therefore, a small concentration gradient across this barrier is expected. Conversely, when a compound with a low o/w partition coefficient is applied to the corneal surface of high-

0022-3549/84/0800-1021$01.00/0
© 1984, American Pharmaceutical Association

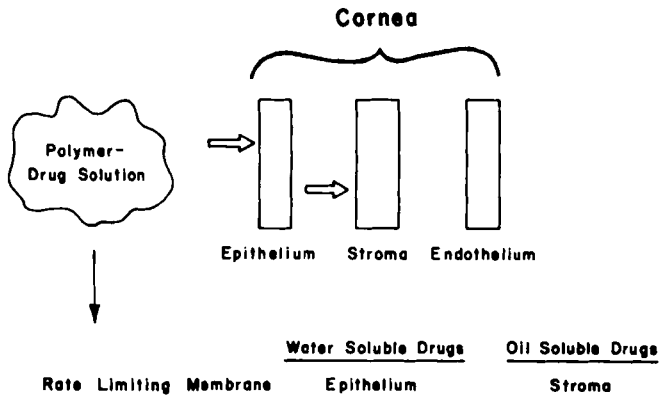

Figure 1—*Diagrammatic representation of proposed limiting-membrane mechanism for corneal penetration of small organic molecules based on oil/water partition coefficient for the penetrating species.*

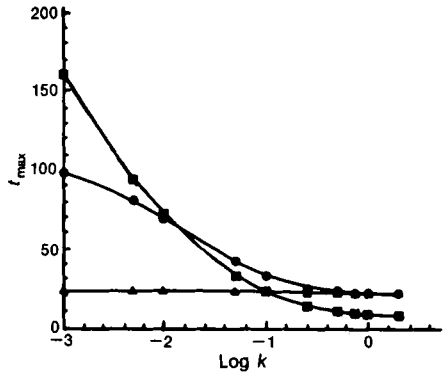

Figure 2—*Representation of the effects of changing rate constants on peak concentration (C_{max}) in the aqueous humor. Key: (●) k_{10}; (▲) k_{12}; (■) k_{23}.*

lipid character, this region serves as the rate-limiting membrane. Once across this barrier, the drug favorably partitions and quickly diffuses across the stroma. At some intermediate partition coefficient, it is likely that both membranes are rate limiting.

Directly related to this model are the anticipated effects of low-viscosity solutions on drug bioavailability. It is known that an increase in solution viscosity from 1 to 100 centipoises (cps) causes a decrease in precorneal drainage and, hence, increases corneal contact time for the drug. The decrease in the drainage rate constant, over this viscosity range, is ~10-fold in albino rabbits (10). For drugs with high o/w partition coefficients, little or no improvement in the bioavailability of the drug in the aqueous humor is expected, since the drug quickly partitions into the epithelium and the limited increase in contact time afforded by this solution should be of little or no benefit. However, water-soluble substances should show increased bioavailability due to the fact that any increase in contact time with the cornea allows continued flux of the drug across the rate-limiting membrane. Evidence of this result in rabbits has already been demonstrated for pilocarpine in low-viscosity polyvinyl alcohol and methylcellulose solutions (10–13).

A prediction of the effect of viscosity on bioavailability for compounds which possess both water and oil solubility (intermediate o/w partition coefficient) is difficult, since these drugs will most likely combine the above mechanisms. Predictions concerning ionizable compounds are equally difficult, since corneal penetration may involve mechanisms which are unrelated to the o/w partition coefficient. Expected corneal penetration mechanisms for the different drug types are summarized in Table I.

THEORETICAL SECTION

Pharmacokinetic Background—Many aspects of drug disposition in the eye have been reported (8, 15–17). Of particular interest is the precorneal fate and the rate of corneal absorption of various compounds. Extensive work in this area has been reported for pilocarpine, and this provides a substantial base from which to make predictions for other drugs (18).

One of the most important developments to come from the kinetic modeling of pilocarpine is the notion of a parallel loss process from the precorneal area. When a drug is placed in the precorneal area, in a simple solution, it experiences very short residence time. All corneal absorption of pilocarpine ceases after 4–5 min in rabbits (15). This, combined with the fact that most drugs demonstrate a relatively short time to reach peak levels in the aqueous humor, led early investigators to believe that the rate of corneal absorption was quite large (0.5 min^{-1}). However, this apparent rate constant and the true rate constant for corneal absorption have been demonstrated to be ~100 times smaller [~0.005 min^{-1} (15)]. The remaining rate of disappearance of drug from the precorneal area (0.495 min^{-1}) can be attributed to several loss processes, collectively referred to as the parallel loss function. This elimination step consists primarily of drainage coupled with tear turnover and nonproductive absorption. Since the rate constant for parallel elimination is ~100 times larger than the absorption rate constant, it is obvious that it is this larger rate constant which will control the time to reach peak drug levels in the cornea and the aqueous humor.

Since this is a parallel first-order process, the fraction of the dose absorbed can be calculated from:

$$(F_t) = \frac{k_{12}}{k_{12} + k_{10}} \qquad \text{(Eq. 1)}$$

where k_{12} is the true rate constant for corneal absorption and k_{10} is the rate constant for precorneal loss. A simple calculation using the determined rate constants for pilocarpine predicts that the fraction absorbed should be ~0.01, and this has been found to be a good estimate (15). Assuming that k_{10} is largely comprised of the drainage rate constant (19), changes in the fraction of dose absorbed should be a direct reflection of changes in k_{12}.

An initial premise of the present work is that the true corneal absorption rate should be related to the o/w partition coefficient of the specific drug. Assuming this is accurate, it should be possible to predict changes in the extent of absorption from changes in the o/w partition coefficient.

Directly related to the above discussion is the expected effect of instilled solution viscosity on the extent of corneal absorption. Previous work with methylcellulose has demonstrated that a 100-cps solution can improve precorneal residence time by a factor of ~10, with a corresponding doubling of the aqueous humor levels of pilocarpine (10). Since an increase in residence time is associated with a decreased drainage loss, with subsequent smaller influence of tear turnover, this allows a calculated estimate of the maximum increase expected for this dosage form. Decreasing k_{10} by a factor of 10 and then calculating Eq. 1 gives a fraction absorbed of 0.09, or about a ninefold increase. It is emphasized that this calculation is for the maximum improvement obtainable and is dependent on the absolute magnitude of the corneal absorption rate. Just as the available time for corneal absorption increases so will that for nonproductive absorption, thus increasing drug loss by this mechanism. Also, drugs which could attain saturation of the epithelial layer would show varying degrees of improvement less than this amount. Since the degree of this saturation should be related to the o/w partition coefficient of the absorbing drug, very oil-soluble drugs should demonstrate little or no improvement, while very water-soluble compounds should approach this maximal increase. A gradation of this effect is expected for compounds with an intermediate o/w partition coefficient.

Theoretical Pharmacokinetic Simulations—As shown in Scheme I, a simplified model of the eye, based on previously published work with pilocarpine, was chosen to assess the importance of the various rate constants on drug levels in the aqueous humor. Drug movement is designated in one direction only, since there is no evidence of significant back-diffusion.

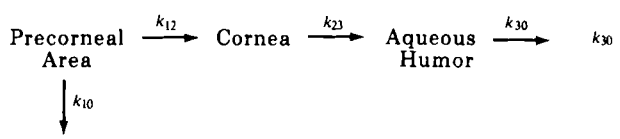

Scheme I—Model used to determine effects of parallel loss on C_{max} and t_{max} in aqueous humor

Table I—Expected Mechanism(s) of Corneal Penetration and Corresponding Viscosity Effects

Drug Type	Apparent Rate-Limiting Membrane	Mechanism	Low-Viscosity Polymer Influence
Water soluble	Epithelium	- Low oil/water partition into epithelium - High partition rate plus rapid diffusion through stroma-endothelium - Leaky channels do exist, *i.e.*, albumin (14) - Solute movement may be intercellular and/or transcellular	Increase in ocular bioavailability
Water and oil soluble	Epithelium–stroma	- Both mechanisms operate	Unknown
Oil soluble	Stroma	-High oil/water partition into epithelium and rapid diffusion through epithelium - Low oil/water partition into stroma	No effect
Ionizable	Epithelium or aqueous channel	- Mechanism not solely dependent on partition coefficient	Variable

The rate equation for appearance of drug in the aqueous humor is presented as:

$$dA/dt = k_{23}C - k_{30}A \qquad \text{(Eq. 2)}$$

where k_{23} is the rate constant for transfer from the cornea to the aqueous humor, k_{30} is the elimination rate constant from the aqueous humor, C is the amount of drug in the cornea, and A is the amount of drug in the aqueous humor at time t. C can be represented by:

$$C = \frac{Dk_{12}}{k_{12} + k_{10} - k_{23}} (e^{-k_{23}t} - e^{-(k_{12}+k_{10})t}) \qquad \text{(Eq. 3)}$$

as earlier derived (18), where D is the dose administered, k_{12} is the rate constant for corneal absorption, and k_{10} is the rate constant for precorneal loss. Equation 3 was integrated to give the amount of drug in the aqueous humor:

$$A = \frac{Dk_{12}k_{23}}{abc} (ae^{-k_{30}t} + be^{-k_{23}t} + ce^{-Kt}) \qquad \text{(Eq. 4)}$$

where a is $k_{23} - K$, b is $K - k_{30}$, C is $k_{30} - k_{23}$, and $K = k_{12} + k_{10}$. It should be noted that when D has a value of unity, A becomes the fraction of the applied dose in the aqueous humor at time t.

Simulations were conducted by solving for the fraction of dose in the aqueous humor at various times up to 60 min. Each rate constant was varied individually with the remaining values held constant, using the experimentally determined values for pilocarpine as starting values. A series of curves delineating the fraction of dose in aqueous humor *versus* time was generated for each rate constant examined. The elimination rate constant (k_{30}) was not varied.

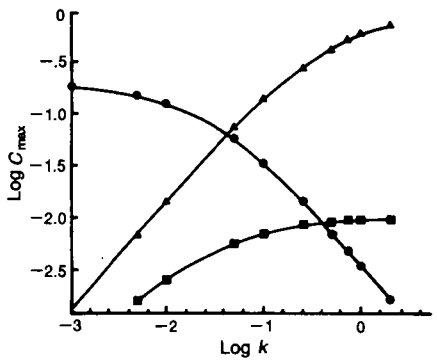

Figure 3—*Representation of the effects of changing rate constants on peak time (t_{max}) in the aqueous humor. Key: (●) k_{10}; (▲) k_{12}; (■) k_{23}.*

[1] Apple II+; Apple Computer, Cupertino, Calif.

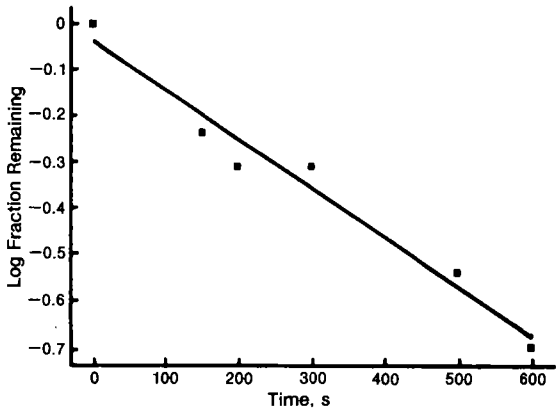

Figure 4—*Results of* in vitro *evaporation experiments for methanol conducted at 34°C. Note that the* SEM *is less than point size.*

In Figs. 2 and 3, the rate constant for parallel loss (k_{10}) is shown to affect both the time of peak concentration (t_{max}) and the magnitude of aqueous humor levels (C_{max}). The effect of decreasing the magnitude of this loss with, for example, a viscous solution or sustained-release system to a factor of 10 less, causes the expected increase in C_{max}. It is important to note that any decrease in k_{10} will be accompanied by a change in t_{max}. In this case, an order-of-magnitude decrease in k_{10} will result in an increase in peak time from the normal time of 20 min to ~40 min.

Results obtained for variations in the true absorption rate constant from its experimentally determined value of 0.005 min^{-1} demonstrate that the fraction of drug reaching the aqueous compartment is increased significantly with an increase in k_{12} (Fig. 3), as was expected from Eq. 1. Another result demonstrated in these simulations (Fig. 2), which would not be intuitively expected, is that t_{max} is minimally affected by increases in the range of values used for this rate constant. This is due to the fact that the changes in k_{12} are minimal when compared with the magnitude of k_{10}, which remains the controlling rate constant for precorneal processes. When k_{12} is increased by two orders of magnitude, this only doubles the sum of k_{10} and k_{12}; hence, the effects on t_{max} in this range of values are minimal. Therefore, it is expected that if changes in partitioning affect only the absorption rate constant, no effect on the time of peak levels in the aqueous humor should be observed. This is consistent with a previously presented theory (15).

The effects of a theoretical change in the rate constant for transfer of drug from the cornea to the aqueous humor (k_{23}) were as anticipated. At values below the experimentally determined value for pilocarpine (0.1 min^{-1}), t_{max} is increased and C_{max} is decreased. Conversely, t_{max} is decreased and C_{max} is increased for values >0.1 min^{-1}.

Summarizing the effects of changes in these rate constants on t_{max} and C_{max}, it may be concluded that an increase of the partition coefficient, which favors an increase in permeability through the corneal epithelium, will increase bioavailability of the compound (C_{max}), but should not influence the time to maximum aqueous humor concentration. This simulation does not allow for changes in nonproductive absorption due to changes in permeability from partitioning.

Table II—Characterization and Applied Concentration of Studied Compounds

Drug Name	Label	Supplier[a]	Specific Activity, Ci/mmol	Actual Applied Conc., $\times 10^{-5}$
Progesterone	Carbon-14	A	0.056	3.8
Fluorometholone	Tritium	A	23	4.01[b]
Fluorometholone acetate	Tritium	A	30	4.26
Hydrocortisone	Tritium	B	88	4.17
Hydrocortisone	Carbon-14	B	0.055	13.8
Prednisolone	Tritium	A	53	4.04
Methanol	Carbon-14	B	0.0036	46.80[b]
Ethanol	Carbon-14	B	0.021	7.64
Butanol	Carbon-14	B	0.0009	92.23[b]
Glycerol	Carbon-14	B	10	12.6[b]
Propranolol	Tritium	A	23	4.69
Pilocarpine	Tritium	B	6.95	4.00
Pyrilamine	Tritium	A	24.1	4.73

[a] A: New England Nuclear, Boston, Mass.; B: Amersham. [b] See text.

Table III—Thin-Layer Chromatography Results for Aqueous Humor Samples

Drug Name	Solvent System	Ratio	Metabolites Detected, %
Progesterone	Dichloromethane–acetone	4:1	<5.0
Progesterone	Ethyl acetate	—	<10.0
Fluorometholone acetate	Dichloromethane–acetone	4:1	<4.0
Fluorometholone acetate	Chloroform–ethyl acetate	3:1	<1.0
Hydrocortisone	Dichloromethane–acetone	1:1	<2.0
Hydrocortisone	Ethyl acetate	—	<1.0
Prednisolone	Ethyl acetate	—	<1.0
Glycerol	1-Butanol–water	9:1	<3.5

Factors which decrease the magnitude of drug loss will have a direct and almost linear effect on aqueous humor concentration and may increase the time to reach peak levels. A 10-fold decrease in k_{10} will result in a change in peak time from 20 min to ~40 min. Another factor of 10 decrease should result in a peak time of 90 min. It can be concluded, therefore, that a viscous solution that reduces the rate of loss from the precorneal area by a factor of 10, and increases C_{max}, should have a small effect on t_{max}. It is also notable that the second factor of 10 decrease in k_{10} (to a value of 0.005 min^{-1}) does not provide the same factor of nine increase in C_{max} decribed earlier, since it appears that for this rate constant an asymptotic value is reached (Fig. 3). This is reasonable and represents the ideal situation where no drug is lost, and k_{12} is the only precorneal rate constant for drug removal.

Due to the overwhelming magnitude of k_{10}, this rate constant has been proposed to control the peak time of drug in the aqueous humor. In cases where k_{10} is constant or decreases, this is valid. However, changes in k_{10} cannot induce a peak time in <20 min as demonstrated in Fig. 2. An increase in k_{23} is required to obtain a shorter peak time. The magnitude of k_{10} reaches an asymptotic value at 20 min. This value is obtained within the normal range of values expected for this rate constant, hence its control over C_{max}, t_{max} values below 20 min appear to be induced by an increase in the rate of transfer from the corneal epithelium to the following compartment. However, it is emphasized that the absolute magnitude of this asymptotic value of k_{10} is dependent on the fixed values of the remaining rate constants (k_{12} and k_{23}).

EXPERIMENTAL SECTION

Materials—Radiolabeled substances were obtained from commercial sources. All compounds were purified by vacuum distillation immediately prior to use. The original supplier, specific activity, and type of radiolabel are indicated in Table II for each compound. All other chemicals were either reagent or analytical grade and were used as received.

Male albino rabbits[2] (weight, 2.5–3.0 kg) were used throughout. Lighting and auditory background were maintained at a constant level in the caging facilities, and the animals were fed a regular diet with no restrictions on the amount of food or water consumed.

Preparation of Solutions—Drug solutions were prepared by the addition of purified, labeled material to a 4.0×10^{-5} M solution of the specific drug. The standard buffer solution was isotonic Sörenson's buffer at a pH of 7.4.

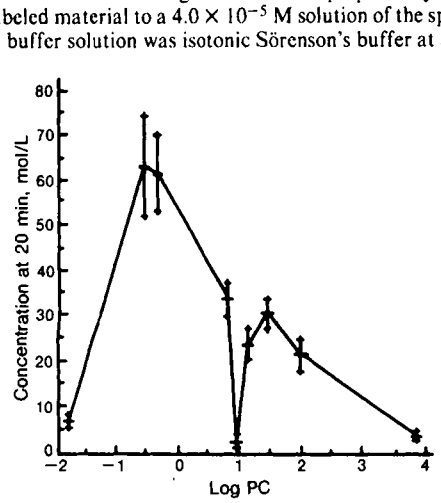

Figure 5– *Plot of molar concentration* versus *log partition coefficient for un-ionized species only.*

[2] Klubertanz, Edgerton, Wis.

Table IV—Effect of Solution Viscosity on Aqueous Humor Bioavailability

Compound	Log PC	C-20, × 10^9 1 cps	C-20, × 10^9 90 cps	Increase, %
Progesterone	3.89	3.25 (0.51)[a]	3.73 (0.38)	0[b]
Fluorometholone	2.00	23.72 (3.55)	29.84 (4.38)	0
Fluorometholone acetate	1.50	33.17 (10.57)	38.57 (6.83)	0
Propranolol	1.25	2.75 (0.34)	1.84 (0.25)	0
Hydrocortisone	1.20	25.80 (3.10)	33.46 (3.02)	0
Prednisolone	0.97	2.59 (0.57)	3.50 (0.48)	0
Pyrilamine	0.80	9.94 (1.44)	13.84 (1.53)	40[c]
Pilocarpine	0.22	5.56 (0.46)	10.84 (1.56)	95[d]
Methanol	−0.32	64.69 (10.90)	83.64 (18.90)	0
Glycerol	−1.79	6.84 (1.27)	8.15 (0.79)	0

[a] Numbers in parentheses represent *SEM*. [b] Percent increase was taken to be zero if no statistical difference was found between the means by t test. [c] $p < 0.01$. [d] $p < 0.001$.

Sufficient radioactive material was used to ensure good counting efficiency throughout the studies, *i.e.*, 100,000–400,000 cpm/μL of dosing solution. The actual final molar concentration of the solution was calculated from summation of the amount of unlabeled and labeled drug (Table II). Individual compounds, which resulted in high concentrations (Table II, footnote *b*) due to low specific activity, were also repeated at 20-min time points at another concentration to ensure linearity. All solution concentrations were normalized to 4×10^{-5} M for calculation and comparison purposes.

Ninety-centipoise solutions were prepared by the addition of methylcellulose[3] to a standard buffer solution until a final concentration of 0.8% polymer was reached. The viscosities of the solutions were determined with a viscometer[4].

Partition Coefficient Determinations—Oil/water partition coefficients were determined for all compounds listed in Table II. For lipid-soluble drugs, 4×10^{-5} M solutions of these compounds, with a sufficient amount of radiolabeled material added, were prepared in octanol. One hundred milliliters of this solution was added to an equivalent volume of isotonic Sörenson's buffer (pH 7.4) and allowed to reach equilibrium in a constant-temperature water bath at 34°C for 5–7 d. Both aqueous and octanol layers were sampled at 24-h intervals, and the samples placed in vials with scintillation cocktail for counting. The experimentally determined concentration was compared with the initial concentration in octanol, and an o/w partition coefficient was calculated. For water-soluble compounds, the procedure was the same except that the initial solution was prepared in the aqueous buffer phase.

Aqueous Humor Concentration Determinations—Rabbits were placed in restraining boxes to minimize movement. Doses (25 μL) were administered directly onto the corneas of both eyes with a micropipet. Animals were sacrificed at various times postdose by rapid injection of sodium pentobarbital solution through a marginal ear vein. The corneal surface was rinsed with buffer solution and carefully blotted dry with tissue. Aqueous humor samples were then tapped with a 1-mL syringe fitted with a 27-gauge needle.

Aqueous humor samples were transferred to glass vials, and scintillation cocktail[5] was added. Vials were dark-adapted for 24 h before counting to minimize chemiluminescence. Samples were counted with a liquid scintillation counter[6] and, after appropriate corrections, the final counts were converted to micrograms of drug per milliliter of aqueous humor.

Throughout the study, samples were removed as quickly as possible to minimize error due to redistribution and elimination. This is of particular importance for early time points and for drugs with apparently fast absorption kinetics. Rinsing the cornea prior to sampling and rapid surgery were methods used to minimize potential sources of error.

Metabolism Studies—Four aqueous humor samples were pooled, extracted with 1 mL of chloroform, and then centrifuged. The recovered chloroform was evaporated under nitrogen and then 10 μL of methanol was added. The methanol solution was spotted on silica gel plates[7] and developed in an appropriate solvent system. For water-soluble compounds (glycerol), aqueous humor was spotted directly without extraction. Control solutions were extracted, excepted glycerol, and treated in an identical manner. Dried plates were cut into 0.5-cm sections and then placed in scintillation vials containing 1 mL of methanol or water and mixed for 5 min. Scintillation cocktail was added and the samples counted after 24-h dark adaptation. Results were compared to TLC plates which had been spotted with nonradioactive solutions

[3] Methylcellulose E4-M Premium; Dow Chemical Co., Midland, Mich.
[4] Brookfield Engineering Labs., Stoughton, Mass.
[5] Aquasol; New England Nuclear, Boston, Mass.
[6] Packard Model 2002; Packard Instrument Co., Downers Grove, Ill.
[7] Polygram Sil G/UV_{254}; Brinkmann Instruments, Westbury, N.Y.

Table V—Molar Concentration of Drug in Aqueous Humor at Various Times Postdose

Compound	Log PC	Mol. Wt.	*C*-10, × 10^9 M	*C*-20, × 10^9 M	*C*-30, × 10^9 M	*C*-45, × 10^9 M
			Lipid Soluble			
Progesterone	3.89	314	1.62 (0.36)[a]	3.25 (0.51)	5.16 (1.31)	6.78 (1.55)
Fluorometholone	2.00	376	10.79 (1.62)	23.72 (3.56)	30.19 (4.45)	22.78 (3.71)
Fluorometholone acetate	1.50	418	—	33.17 (3.34)	—	—
Hydrocortisone	1.20	363	5.85 (0.89)	25.82 (3.10)	36.26 (7.41)	6.57 (1.34)
Prednisolone	0.97	360	3.04 (0.58)	2.59 (0.57)	3.84 (0.65)	2.89 (0.32)

			Water Soluble (Un-ionized) C-5 × 10^9 M	C-10 × 10^9 M	C-20 × 10^9 M	C-30 × 10^9 M
Butanol	0.88	74	—	56.43 (10.17)	35.47 (10.04)	—
Ethanol	−0.32	46	—	59.31 (10.57)	65.57 (8.71)	—
Methanol	−0.5	32	144.38 (12.55)	59.49 (13.97)	64.69 (10.88)	31.35 (11.45)
Glycerol	−1.79	92	—	3.12 (0.48)	6.84 (1.27)	6.32 (0.82)

				Water Soluble (Ionized) *C*-10,	*C*-20,	*C*-30,	*C*-45,
			pK_a	× 10^9 M	× 10^9 M	× 10^9 M	× 10^9 M
Propranolol	1.24	295	9.1	2.01 (0.50)	2.74 (0.34)	5.33 (0.76)	1.17 (0.24)
Pyrilamine	0.80	295	8.9	5.75 (0.99)	7.04 (1.01)	8.94 (1.86)	6.31 (1.01)
Pilocarpine	0.22	271	6.67	4.48 (0.37)	5.56 (0.46)	5.15 (0.73)	3.79 (0.54)

[a] Numbers in parentheses represent *SEM*.

and examined under UV light to determine R_f values for each drug in its specific solvent system.

***In Vitro* Evaporation Studies**—A 10.16-cm diameter petri dish was suspended in a water bath maintained at 34°C. Distilled water was added to just cover the inner surface of the dish. A 2.54-cm diameter watch glass was placed onto this arrangement and 25-μL samples of the test solution were placed on the watch glass and allowed to evaporate for ≤20 min. A separate watch glass was used for each determination to avoid contamination. At appropriate times, disks were rinsed with 3 mL of distilled water, and the rinsing solution was retained in a scintillation vial. Determinations of amount of compound remaining with respect to time were computed.

RESULTS

Drug Metabolism—Table III indicates, unexpectedly, that there is little or no metabolism occurring for the drugs examined over the time course of these studies. For example, published results (20) for prednisolone acetate demonstrate 100% metabolism under these conditions, and one would anticipate that fluorometholone acetate would behave similarly. Further comment on metabolism will be presented subsequently.

Viscosity Effects—Table IV gives the results of partition coefficient studies and aqueous humor levels for both 1- and 90-cps solutions. Results of partition coefficient studies correlate well with data available from Leo *et al.* (21). The percent bioavailability increase between 1- and 90-cps solutions was indicated as zero if there was no statistical difference ($p < 0.01$) in the mean values at 20 min as indicated by Student's *t* test. It is notable that a significant increase was demonstrated only for pilocarpine and pyrilamine. Additional studies for glycerol at both 20- and 30-min time points established that a change in t_{max}, expected from an increase in k_{10}, had not obscured the effects of viscosity on C_{max}.

Drug Concentrations in Aqueous Humor—Drug levels in the aqueous humor for the compounds studied are given in Table V. From the data, it appears that there is not a linear relationship between the partition coefficient and the amount of drug in the aqueous humor at 20 min. An order of magnitude increase in the partition coefficient does not coincide with a similar magnitude increase in the aqueous humor drug levels.

The low molecular weight alcohols (methanol, ethanol, and butanol) demonstrated peak times ≥10 min. Methanol and tritiated water data[8] from this laboratory had significantly ($p < 0.005$) higher levels in the aqueous humor at 5 min as compared with the 10-min levels. These compounds also have increased precorneal loss rates. *In vitro* determinations of evaporation rates for these compounds indicate that this is a significant mechanism of drug loss (methanol = 0.21 min^{-1}, water = 0.098 min^{-1}). An example of the evaporation study for methanol is given in Fig. 4. The rate constants of evaporation (k_{ev}) for these compounds were as expected, with the more volatile compound having the greater value. If these values represent an accurate approximation of evaporation rates *in vivo*, then the total rate constant for loss can be calculated as the sum of k_{10} and k_{ev}. For methanol, the total loss rate constant (0.71 min^{-1}) is ~40% higher than for nonvolatile compounds (0.5 min^{-1}).

To verify that methanol was not penetrating at a rapid rate due to toxic destruction of the corneal barrier, fluorometholone acetate was coadministered. Results were identical to fluorometholone acetate levels obtained without methanol.

The plots of C_{max} *versus* the log partition coefficient provide some insight into the relationships of the corneal penetration mechanism and the partition coefficient. Of particular interest is the observation that a clear dual-parabolic shape is demonstrated in the plot which includes only non-ionizable species (Fig. 5). This is consistent with predictions derived from the concept of the corneal epithelium or stroma as rate-limiting membranes depending on the partitioning properties of the absorbing drug. It is also important to note that on a molar basis, small molecular weight (water-soluble) species such as methanol and ethanol have greater corneal permeability than larger molecular weight compounds. This argues against the conclusions of some investigators, who have postulated that water-soluble compounds should show little or no corneal absorption. A similar relationship between partition coefficient and aqueous humor drug levels for ionized species is not clear, as shown in Fig. 6.

DISCUSSION

Vehicle Effects—Increasing vehicle viscosity from 1 to 90 cps did not result in an increase in aqueous humor levels for compounds whose log partition coefficients ranged from 1 to 4. This is consistent with the expectation that these lipid-soluble drugs quickly partition into the corneal epithelium. Thus, the limited increase in contact time afforded by low-viscosity solutions should not and does not improve their bioavailability. Propranolol data are also consistent with this expectation, since this compound has a relatively high partition coefficient. Despite the fact that propranolol is largely ionized at physiological pH, the favorable partition coefficient of the un-ionized species predicts that no effect is expected from an increase in viscosity of administered solution. It is anticipated that the un-ionized species will account for the majority of penetrating drug; therefore, the high degree of ionization also accounts for the decreased bioavailability of propranolol when compared with a steroid with a similar partition coefficient (such as hydrocortisone).

The effects of viscosity on water-soluble compounds indicate that, for these species, the mechanism(s) of corneal penetration are not well understood. Based on the partition coefficient alone, un-ionized water-soluble species such as glycerol or methanol are predicted to show modest increases in bioavail-

[8] Unpublished results.

ability from a viscous solution. Related processes, such as the possible water structuring of glycerol, may account for this discrepancy. Structured water could greatly inhibit transport of even a small molecule through a highly lipid membrane; also, water structuring may not be fully reflected in an equilibrium partition coefficient measurement.

For methanol, the apparently high rate of corneal penetration, in light of its small molecular size, suggests that this compound may be passing through aqueous channels. No significant improvement in bioavailability is demonstrated with a viscous solution. It is obvious that the rate of transfer from the epithelium to the stroma for this compound will be very high (high k_{23}). This explains the very short peak time and, to some extent, the substantial levels of compound in the aqueous humor. The lack of improvement with a low-viscosity solution for methanol suggests several possibilities. The first is that of a saturable mechanism within the epithelium, since a compound which already demonstrates saturable kinetics in the epithelial layer from a 1-cps solution should reflect little improvement from moderately increased precorneal residence time. This proposes that methanol enters the epithelium at a fairly fast rate to a maximum solubility of the compound. Partitioning across this barrier occurs, followed by very fast transfer from the epithelium to the stroma and aqueous humor. The relatively low partition coefficient and linear change in aqueous humor levels with changes in dosing concentration, however, argue against this explanation.

An alternate explanation for the lack of a viscosity effect on methanol bioavailability requires a calculated estimate for k_{12}. Using the peak concentration to give a rough estimate of the fraction of dose absorbed, since an accurate calculation of area under the curve is not possible, methanol demonstrates an ~30-fold increase over pilocarpine. Using Eq. 1, it is possible to calculate an estimate of k_{12}. For methanol, the total loss rate constant, including evaporation, is ~0.71 min^{-1}. This provides an estimate for k_{12} of 0.3 min^{-1}. Decreasing residence time by a factor of 10 and maintaining the evaporation rate constant reduces k_{10} to 0.26 min^{-1}. An estimate of the fraction absorbed from Eq. 1 predicts a value of 0.53 or a maximum increase of ~1.75. As with pilocarpine, this calculation represents the maximum increase expected with a 10-fold increase in precorneal residence time, neglecting all other precorneal factors. In light of the fact that pilocarpine demonstrates only a factor of two increase from a calculated maximum of nine, little increase should be expected with methanol. Close inspection of these calculations reveals that the increase in k_{10} is responsible for the dramatic decrease in the effect of viscosity. Since reduction of residence time should have no effect on the rate constant for evaporation (k_{ev}), the total loss rate constant remains relatively high. For example, if the approximation of the fraction of methanol absorbed has been overestimated by a factor of two (*i.e.*, k_{ev} decreases to 0.15 min^{-1}), this only changes the estimation of maximum benefit from a viscous solution to 2.1.

It is interesting that only pilocarpine and, to some extent, pyrilamine demonstrate vehicle effects in rabbits. Note that as the partition coefficient increases from that of pilocarpine to pyrilamine, the effect from a viscous solution decreases, as expected. Of importance also is the observation that as the percent increase falls below 50%, it becomes more difficult to discern statistical differences in the values between 1- and 90-cps solutions. This indicates that in an ideal situation, where errors in biological data were greatly reduced, the trends demonstrated for prednisolone and hydrocortisone could be the minimal increases in bioavailability expected for compounds with this range of partition coefficients. It should also be kept in mind that the rabbit, as a model for human ocular kinetics, apparently demonstrates much less sensitivity to viscous solutions than the human eye does for vehicles in this viscosity range (22).

Complicating the results for ionizable compounds is the possibility of penetration of ionized species through the cornea. Evidence of possible ionized drug movement through the cornea has been documented for cromolyn sodium[9]. This compound, with a pK_a of 2.0, is almost totally ionized at physiological pH; yet, significant drug levels in aqueous humor from solution dosing have been reported[9] in rabbits and confirmed in this laboratory.

In light of the results with compounds of relatively high log partition coefficients (1.0–4.0), one can visualize the epithelial layer acting in the same manner as a viscous solution for the ionizable water-soluble compounds, maintaining drug concentration at the rate-limiting membrane.

Partition Coefficient Relationships—The plot of aqueous humor drug concentration at 20 min *versus* partition coefficient for un-ionized compounds, Fig. 5, is a dual parabolic shape, consistent with expectations based on the proposed model of corneal penetration. In the high log partition coefficient range (1.0–4.0), a parabolic-shaped curve is indicated, although it is not as well defined as expected. It is obvious that compounds such as prednisolone and hydrocortisone do not penetrate the epithelial layer as well as fluorometholone or fluorometholone acetate, and that progesterone partitions well into the epithelial layer but has extremely poor partitioning characteristics from this layer to the stroma (decrease in k_{23}). The relatively low aqueous humor bioavailability for these drugs may be partially due to an increase in nonproductive absorption, since partitioning through these tissues, *e.g.*, the conjunctiva and nictitating membrane, will increase as partitioning increases into the epithelium.

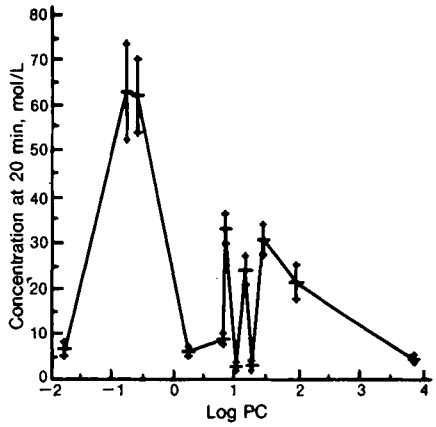

Figure 6—*Plot of molar concentration* versus *log partition coefficient for un-ionized and ionizable species.*

The curve depicted in Fig. 5 shows a much more defined peak than the *in vitro* data presented by Schoenwald and Ward (4). The reasons for this may be twofold. First, the plateau effect seen in the Schoenwald and Ward (4) data may be due to saturation of the system at partition coefficients near the "peak"; therefore, no defined peak is observed. Second, effects from changes in precorneal disposition cannot be accounted for in these *in vitro* studies. With a low partition coefficient, drug is lost to a greater extent by tear turnover and drainage. As the partition coefficient increases, corneal absorption increases in a relative manner, and relative drainage loss decreases. At very high partition coefficient values, nonproductive absorption greatly increases; hence, the sharp peak in the curve of the aqueous humor drug level *versus* the log partition coefficient.

As the o/w partition coefficient increases, the concept of a changing rate-limiting membrane predicts that the peak time should increase, since partitioning into the stroma becomes less favorable. This represents a decrease in k_{23} and should result in an increase in t_{max} and a corresponding decrease in C_{max}. It appears that this expected shift in peak time is obscured by the biological variability of the data. Although the means of the concentrations for the steroid compounds demonstrate a progressive increase in peak time with increasing partition coefficients, this is at a low level of significance ($p > 0.01$). In general, the expected decrease in C_{max} from a decrease in k_{23} appears offset by the increase in corneal absorption (k_{12}) due to favorable partitioning into the epithelium. The change in k_{12}, as previously noted, has no effect on peak time.

In the low log partition coefficient range (−2.0–1.0), a parabolic trend is also observed. This is most likely due to a combination of partitioning effects from the tears to the epithelium and then to the stroma. The peak in this region is due to the fact that compounds here have the best combination of partitioning characteristics in the water-soluble range. At the extreme ranges, drugs with the lowest partition coefficients cannot readily pass the epithelial layer (low k_{12}), and no matter how ideal their partitioning to the stroma (k_{23}), only low levels will be found in the aqueous humor. At the upper end of the water-soluble range, and the lower end of the oil-soluble range, it is probable that these compounds have both the epithelial layer and the stroma as rate-limiting membranes (low k_{12} and k_{23}), and therefore, have poor corneal permeability. The validity of the dual-parabolic shape of these results rests on the significance of the data for prednisolone and hydrocortisone. These data points are in substantial agreement with those of Schoenwald and Ward (4).

Water and Small Molecule Permeation—When low molecular weight alcohols were used, their rate of corneal penetration was much faster than the rate of most other molecules. Since the rate of elimination from the precorneal area by tear turnover should be essentially the same for these compounds as for all others, the shorter peak time observed must be due to an increase in transfer of drug from the epithelium to the stroma (k_{23}). Important to this discussion are results reported by Donn *et al.* (23) from a study utilizing $[^3H]H_2O$ and $[^{18}O]H_2O$. These investigators concluded that the transport for these two molecules was the same, within experimental error, thus ruling out the possibility of hydrogen ion transport as opposed to molecular transport

[9] V. H.-L. Lee, unpublished results.

for tritiated water. Significantly, they concluded that there is no active transport of water and that diffusion of water in the epithelium and endothelium is very close to the rate of diffusion for this molecule in the stroma, which is composed of 70–80% water. Since water and methanol are both compounds of small molecular size, the above comments concerning the possibility of paracellular penetration through the epithelium are strengthened. Such a pathway has been proposed by Kaiser and Maurice for fluorescein (24). This leads to a mechanistic picture of drug movement through the epithelium, where both transcellular and paracellular routes for drug permeation are possible and probable for water-soluble drugs. It is anticipated that transcellular drug penetration would be related to the partition coefficient, whereas paracellular movement would more likely be related to characteristics such as molecular size and aqueous diffusivity.

Ocular Metabolism—The results of metabolism studies in this work clearly indicate that, over the time period of 20–30 min in albino rabbits, the drug entities examined are not subject to appreciable degradation. Previously published work in the area of ocular metabolism must be considered before allowing such a simple conclusion. It is well documented that metabolism of pilocarpine is minimal in albino rabbits but increases in mixed breeds (25); since all work herein has been with albino species, this discussion will be restricted to studies using these animals. Studies in the area of ocular metabolism are limited in number, and the activity of different ocular enzymes appears variable; *i.e.*, pilocarpine undergoes minimal degradation, whereas dipivefrin demonstrates significant corneal metabolism (25, 26). The degradation of atropine is dependent on atropine esterase, which is inherited through an incompletely dominant trait (27). Mydriatic response to atropine is significantly less in a rabbit with positive esterase than one without the enzyme.

The area of steroid metabolism is equally confusing. One study (20) indicates that prednisolone acetate is metabolized completely to the parent alcohol, and one would therefore expect similar results with fluorometholone acetate. However, minimal metabolism was detected despite the fact that two different solvent systems were used which could potentially separate the acetate and alcohol forms. Another study (28) utilizing steroid alcohols and ketones, reports metabolites of $\leq 15\%$ from corneal and iris–ciliary tissue incubates. The results of these investigations agree with the present study for both hydrocortisone and progesterone. The subject of ocular metabolism, its mechanism and location, is one which requires additional research.

Dynamic *versus* Equilibrium Correlation—The original concept relating drug action to the partition coefficients, by Meyer (29) and Overton (30, 31), or to log partition coefficients, by Hansch and co-workers (32, 33), demonstrated relationships between lipophilic character and biological activity. Many of these examples deal with drugs that bind to enzymes, other proteins, or receptor sites. Current attempts to relate the partition coefficient and corneal penetration of compounds must rely on the fact that partitioning into the corneal layers mimics an equilibrium phenomenon: this is in fact difficult to imagine in the eye. Administered drugs have finite contact time with the corneal tissues. The dynamic aspect of corneal penetration is, therefore, being correlated with an equilibrium value of the partition coefficient; thus, one would not expect a good correlation between corneal absorption and the partition coefficient.

A significant rate of loss (k_{10}) controls the amount of drug reaching the target tissue, so steady-state kinetics, which should be accurately reflected by the partition coefficient, are not expected. Compounds with a very high rate of oil or water solubility can be expected to transfer more rapidly to their respective membrane of favorable partitioning. Therefore, some method of correlating the rate of partitioning with corneal penetration is desirable and is currently being pursued in this laboratory.

In summary, the present study has demonstrated that, as anticipated, a low-viscosity solution affords no benefit to compounds with a log partition coefficient >1.0. For these compounds, the rate-limiting membrane for corneal penetration is fairly well defined, although several factors influencing bioavailability, such as metabolism and nonproductive absorption, require further investigation and quantitation. Water-soluble compounds, on the other hand, are not as well understood.

REFERENCES

(1) C. Hanna and J. D. Sharp, *Arch. Ophthalmol.*, **88,** 196 (1972).

(2) A. Kupferman and H. M. Leibowitz, *Arch Ophthalmol.*, **93,** 425 (1975).

(3) I. H. Leopold, J. L. Sawyer, and H. Green, *Arch. Ophthalmol.*, **54,** 916 (1955).

(4) R. D. Schoenwald and R. L. Ward, *J. Pharm. Sci.*, **67,** 786 (1978).

(5) G. L. Mosher and T. J. Mikkelson, *Int. J. Pharm.*, **2,** 239 (1979).

(6) K. Kishida and T. Otori, *Jpn. J. Ophthalmol.*, **24,** 251 (1980).

(7) F. E. Ros, H. C. Inemee, and P. A. Van Zwieten, *Documenta Ophthalmol.*, **48,** 291 (1979).

(8) D. M. Maurice and S. Mishima, in "Pharmacology of the Eye," M. L. Sears, Ed., Springer-Verlag, New York, N.Y., 1984, pp. 19–116.

(9) S. Mishima and S. Nagataki, *Contact and Intraocular Lens Medical Journal*, Vol. 4, No. 3, Conrad Berens Memorial Lecture, p. 23, July/Sept. 1978.

(10) S. S. Chrai and J. R. Robinson, *J. Pharm. Sci.*, **63,** 1218 (1974).

(11) T. F. Patton and J. R. Robinson, *J. Pharm. Sci.*, **64,** 1312 (1975).

(12) C. A. Adler, D. M. Maurice, and M. E. Paterson, *Exp. Eye Res.*, **11,** 34 (1971).

(13) S. M. Blaug and A. J. Canada, Jr., *Am. J. Hosp. Pharm.*, **22,** 662 (1965).

(14) A. Bill, *Arch. Ophthalmol.*, **74,** 248 (1965).

(15) M. C. Makoid and J. R. Robinson, *J. Pharm. Sci.*, **68,** 435 (1979).

(16) D. M. Maurice and Y. Ota, *Jpn. J. Ophthalmol.*, **22,** 95 (1978).

(17) D. M. Maurice, *I.O.C.-Clinical Pharmacology of the Anterior Segment*, Fall 1980, Vol. 20, No. 3 by Little, Brown and Co., Boston, Mass.

(18) M. C. Makoid, Ph.D. Thesis, University of Wisconsin, Madison, Wis., 1976.

(19) V. H-L. Lee and J. R. Robinson, *J. Pharm. Sci.*, **68,** 673 (1979).

(20) H. Yamauchi, H. Kito, and K. Uda, *Jpn. J. Ophthalmol.*, **19,** 339 (1975).

(21) A. Leo, C. Hansch, and D. Elkins, *Chem. Rev.*, **71,** 525 (1971).

(22) M. F. Saettone *et al.*, *Pharm. Acta. Helv.*, **57,** 47 (1982).

(23) A. Donn, S. Miller, and N. Mallet, *Arch. Ophthalmol.*, **70,** 515 (1963).

(24) R. J. Kaiser and D. M. Maurice, *Exp. Eye Res.*, **3,** 156 (1964).

(25) V. H-L. Lee, V-W. Hui, and J. R. Robinson, *Invest. Ophthalmol.*, **19,** 210 (1980).

(26) J. A. Anderson, W. L. Davis, and C-P. Wei, *Invest. Ophthalmol.*, **19,** 817 (1980).

(27) N. Ambache, *Pharmacol. Rev.*, **7,** 476 (1955).

(28) A. L. Southren *et al.*, *Invest. Ophthalmol.*, **15,** 222 (1976).

(29) H. Meyer, *Arch. Exp. Pathol. Pharmakol.*, **42,** 109 (1899).

(30) E. Overton, *Vierteljahresschr. Naturforsch. Ges. Zeurich*, **44,** 88 (1899).

(31) E. Overton, "Studien Uber Die Narkose," Fischer, Jena, Germany, 1901.

(32) C. Hansch and W. J. Dunn, *J. Pharm. Sci.*, **61,** 1 (1972).

(33) C. Hansch and J. M. Clayton, *J. Pharm. Sci.*, **62,** 1 (1973).

ACKNOWLEDGMENTS

The authors are grateful to James C. Robinson for his excellent technical assistance.

Physical Model Approach in the Study of the Transport of Alkyl Amines Across a Silicone Rubber Membrane in a Two-Chamber Diffusion Cell

DINESH C. PATEL, JEFFREY L. FOX, and WILLIAM I. HIGUCHI *x

Received December 22, 1978, from the *College of Pharmacy, The University of Michigan, Ann Arbor, MI 48109.* Accepted for publication July 26, 1983. *Present address: Department of Pharmaceutics, College of Pharmacy, The University of Utah, Salt Lake City, UT 84112.

Abstract □ The transport of hexylamine and octylamine through a silicone rubber membrane was studied as a function of buffer (phosphate) concentration and pH. The results were interpreted using a physical model which assumed a steady-state rate of transport and which accounted for (*a*) the simultaneous diffusion and rapid equilibrium of all the aqueous species, (*b*) the possible diffusion of both the amine and its protonated form through the membrane, and (*c*) the effect of a stagnant aqueous diffusion layer on each side of the membrane. The following conclusions were reached: (*a*) The thickness of the aqueous diffusion layer is ~100 μm, which is about the same as that previously measured for benzoic acid in this system. Transport of octylamine at pH ≥ 10 is ~90% aqueous diffusion layer controlled, whereas hexylamine is ~50% aqueous diffusion layer controlled at high pH. (*b*) The membrane permeability of octylamine is ~15–20 times that of hexylamine. This gives an incremental π constant for the partition coefficient of ~0.61, as compared with the previously reported value of 0.56. (*c*) At low pH (≤5), the transport of the protonated species becomes important. The membrane permeabilities of these ammonium ions are about four or five orders of magnitude less than the membrane permeabilities of the corresponding amines. The membranes were examined at 30,000× with the scanning electron microscope, and no evidence of holes was found.

Keyphrases □ Diffusion—transport of alkyl amines across a silicone rubber membrane □ Hexylamine—transport across a silicone rubber membrane, octylamine, two-chamber diffusion cell □ Octylamine—transport across a silicone rubber membrane, hexylamine, two-chamber diffusion cell

There is a need for an experimental system in which the transport of weak organic acids and bases across a lipoidal membrane can be studied. There are many situations in biopharmaceutics and therapeutics, including situations involving binding of drugs to macromolecules and micelles, in which such a system would be useful. Stehle and Higuchi (1, 2) have conducted studies on the transport of weak acids and bases across lipoidal membranes; however, these were of a limited nature. They used fiberglass filter disks preloaded with oil-polymer mixtures as lipoidal membranes. These membranes were not entirely satisfactory, as experiments could not be performed in the totally diffusion-controlled region. Also, membrane permeability changes with time were found in some of the experiments which were attributed to changes in the lipid viscosity with time.

Accordingly, this investigation was carried out to develop a rugged experimental system for studying the transport of weak acids and bases across lipoidal membranes and, simultaneously, to develop theoretical methods for analyzing the experimental results on a quantitative basis. We selected a silicone rubber membrane as our model membrane, as several investigators (3–8) have found it suitable for studying drug transport, and employed a standard two-chamber diffusion cell. This membrane may be used in consecutive experiments without significant changes in its permeability characteristics. We modified and adopted the theoretical relationships developed previously by Stehle and Higuchi (1, 2) and Suzuki *et al.* (9, 10) and show how this experimental system and the theoretical relationships can be productively employed in evaluation of pH, buffer concentration, and chain-length effects on the transport of weak bases from aqueous solutions across lipoidal membranes.

It is hoped that the results of these studies can also be used for quantitative determination of macromolecular binding or micellar solubilization of weak acids and bases in aqueous media. It can be argued that, where possible, the use of a lipoidal membrane would be preferred over the cellulose dialysis membrane for studying micellar solubilization of weak acids and bases because of the Donnan membrane effects encountered with cellophane membrane dialysis methods. Also, we hope to use this technique in the study of species distribution and the mechanisms of action of the amine-type cholesterol dissolution rate accelerators (11) in bile.

THEORETICAL SECTION

A physical model approach was utilized to study the transport of hexylamine and octylamine through a silicone rubber membrane as a function of buffer (phosphate) concentration and pH. The model used in this study is very similar to the one developed by Stehle and Higuchi (1, 2), in which a membrane separates two aqueous compartments, with an aqueous diffusion layer on each side of the membrane.

The steady-state model for amine, RN, which is protonated to RNH^+ at lower pH values, is illustrated in Fig. 1. Steady-state diffusion is assumed between donor and receiver compartments, and all relevant equilibria (the various phosphate species, as well as the free and protonated amines) are accounted for. The model allows for diffusion of protonated amine, as well as free amine, through the membrane.

The following equations describe the model under steady-state conditions. G, the total flux of the amine species RN and RNH^+ through each barrier, I–III, is given by:

$$GI = \{D_{RN}[(RN)_L - (RN)_1] + D_{RNH^+}[(RNH^+)_L - (RNH^+)_1]\}/h_1 \quad \text{(Eq. 1)}$$

$$GII = \{P_{RN}[(RN)_1 - (RN)_2] + P_{RNH^+}[(RNH^+)_1 - (RNH^+)_2]\}/h_2 \quad \text{(Eq. 2)}$$

$$GIII = \{D_{RN}[(RN)_2 - (RN)_R)] + D_{RNH^+}[(RNH^+)_2 - (RNH^+)_R]\}/h_3 \quad \text{(Eq. 3)}$$

where the subscripts 1 and 2 indicate the left and right aqueous interfacial locations, respectively, and subscripts L and R refer to the borders of left and right bulk aqueous phases, respectively (Fig. 1). D_{RN} and D_{RNH^+} (cm^2/s) are the aqueous diffusion coefficients of RN and RNH^+, respectively; P_{RN} and P_{RNH^+} are the membrane permeabilities (defined as the product of partition coefficient and diffusion coefficient) of RN and RNH^+, respectively; h_1 and h_3 (cm) are the effective thicknesses of the unstirred aqueous diffusion layers; h_2 is the membrane thickness. G is expressed in $mmol/cm^2 \cdot s$. At steady state, $GI = GII = GIII$.

Since it is assumed that no buffer species can penetrate the lipid phase, the total net flux of the buffer species through each of the two aqueous diffusion layers is zero at steady state. Hence, the equations for J_B, the total net flux of buffer species in the aqueous barriers, can be written as follows:

$$J_{BI} = D_{H_3PO_4}[(H_3PO_4)_L - (H_3PO_4)_1] + D_{H_2PO_4}[(H_2PO_4)_L - (H_2PO_4)_1] + D_{HPO_4}[(HPO_4)_L - (HPO_4)_1] + D_{PO_4}[(PO_4)_L - (PO_4)_1] = 0 \quad \text{(Eq. 4)}$$

0022-3549/84/0800-1028$01.00/0
© 1984, American Pharmaceutical Association

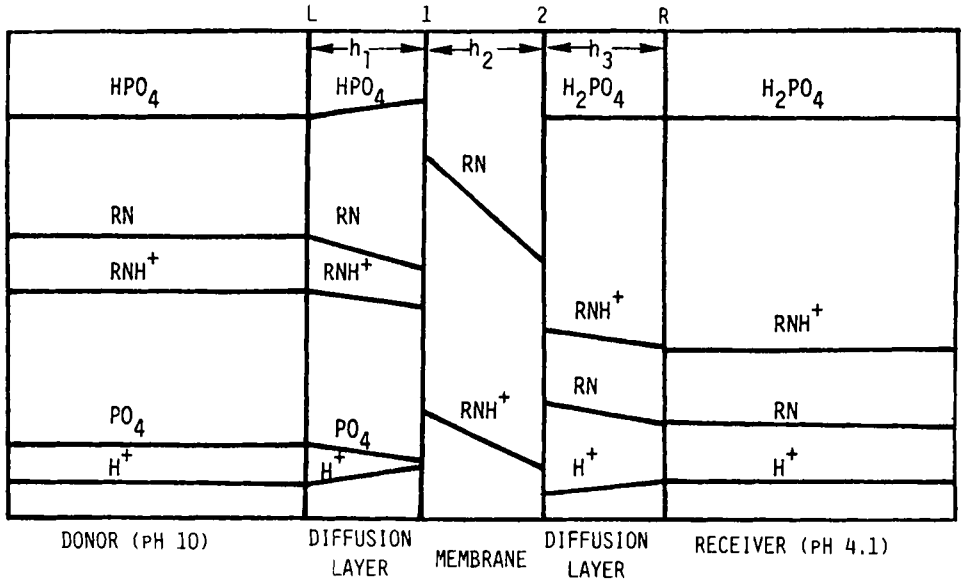

Figure 1—*Three-phase model showing schematic concentration profiles present in steady-state transport of amine, RN. RNH^+ is protonated amine; H_2PO_4, HPO_4, and PO_4 are buffer species (only the predominant species are shown in Fig. 1), and H^+ is hydrogen ion. h_1, h_2, and h_3 are diffusion barrier thicknesses in the three phases.*

$$J_B III = D_{H_3PO_4}[(H_3PO_4)_2 - (H_3PO_4)_R] + D_{H_2PO_4}[(H_2PO_4)_2 - (H_2PO_4)_R] + D_{HPO_4}[(HPO_4)_2 - (HPO_4)_R] + D_{PO_4}[(PO_4)_2 - (PO_4)_R] = 0 \quad \text{(Eq. 5)}$$

J_H, the net flux of H^+ minus the flux of OH^-, occurs *via* the transport of the protonated form of the amine, RNH^+, through the membrane and *via* the transport of all protonated species and also OH^- through the aqueous diffusion layers. The expressions for this quantity are given by:

$$J_{H^+}I = \{D_{RNH^+}[(RNH^+)_L - (RNH^+)_1] + 3D_{H_3PO_4}[(H_3PO_4)_L - (H_3PO_4)_1] + 2D_{H_2PO_4}[(H_2PO_4)_L - (H_2PO_4)_1] + D_{HPO_4}[(HPO_4)_L - (HPO_4)_1] + D_H[(H)_L - (H)_1] - D_{OH}[(OH)_L - (OH)_1]\}/h_1 \quad \text{(Eq. 6)}$$

$$J_{H^+}II = \{P_{RNH^+}[(RNH^+)_1 - (RNH^+)_2]\}/h_2 \quad \text{(Eq. 7)}$$

$$J_{H^+}III = \{D_{RNH^+}[(RNH^+)_2 - (RNH^+)_R] + 3D_{H_3PO_4}[(H_3PO_4)_2 - (H_3PO_4)_R] + 2D_{H_2PO_4}[(H_2PO_4)_2 - (H_2PO_4)_R] + D_{HPO_4}[(HPO_4)_2 - (HPO_4)_R] + D_H[(H)_2 - (H)_R] - D_{OH}[(OH)_2 - (OH)_R]\}/h_3 \quad \text{(Eq. 8)}$$

Analogous to the total amine flux, at steady state $J_HI = J_HII = J_HIII$. In the above equations, $D_{H_3PO_4}$, $D_{H_2PO_4}$, D_{HPO_4}, and D_{PO_4} (cm^2/s) are the aqueous diffusion coefficients of the H_3PO_4, H_2PO_4, HPO_4, and PO_4 buffer species, respectively, and D_H and D_{OH} (cm^2/s) are the aqueous diffusion coefficients of the hydrogen and hydroxyl ions, respectively.

In addition to satisfying the flux relationships expressed in Eqs. 1–8, a valid solution of the model must also satisfy all the chemical equilibrium constraints at each point in the system. These constraints can be written as follows (for n = 1, 2, L, R):

$$(HPO_4)_n = \frac{(H)_n(PO_4)_n}{K_{HPO_4}} \quad \text{(Eq. 9)}$$

$$(H_2PO_4)_n = \frac{(H)_n^2(PO_4)2_n}{K_{H_2PO_4}} \quad \text{(Eq. 10)}$$

$$(H_3PO_4)_n = \frac{(H)_n^3(PO_4)_n}{K_{H_3PO_4}} \quad \text{(Eq. 11)}$$

where $K_{HPO_4} = K_3$, $K_{H_2PO_4} = K_3 \cdot K_2$, and $K_{H_3PO_4} = K_3 \cdot K_2 \cdot K_1$ (K_1, K_2, and K_3 are the dissociation constants of phosphoric acid).

Similarly, for the amine (for n = 1, 2, L, R):

$$K_a = \frac{(RN)_n(H)_n}{(RNH^+)_n} \quad \text{(Eq. 12)}$$

where K_a is the dissociation constant of the protonated amine.

Given these relationships, the model can be used to calculate concentrations and fluxes of all the species at each point in the system when only the compositions of the bulk solutions on each side are given. This calculation is complicated by both the complex equilibria involved and the fact that a solution is sought for a system employing a trilaminar membrane. Nonetheless, the equations can be arranged in such a way that they can be rapidly solved with a digital computer if a program is available for the solution of systems of nonlinear algebraic equations. This particular problem can be reduced to a system of two equations in two unknowns by a number of different approaches. The algebraic approach employed here was to choose pH_1 and pH_2 (the pH values at the membrane surfaces) as the unknowns and, for a given set of values for pH_1 and pH_2, to calculate all the other quantities in such a way that all the problem constraints are satisfied, except for the constraint that $GI = GII = GIII$ at steady state. The nonlinear system solver then determines the values for pH_1 and pH_2 such that the equations $GI = GII$ and $GII = GIII$ are satisfied.

The algebraic procedure for calculating the species concentrations throughout the system for a given trial set of pH_1 and pH_2 values is as follows. First, the concentrations of all the species in the bulk solutions on each side of the membrane are calculated (for n = L, R):

$$(H)_n = 10^{-pH_n} \quad \text{(Eq. 13)}$$

$$(PO_4)_n = P_{tot_n} \Big/ \left(1 + \frac{(H)_n}{K_{HPO_4}} + \frac{(H)_n^2}{K_{H_2PO_4}} + \frac{(H)_n^3}{K_{H_3PO_4}}\right) \quad \text{(Eq. 14)}$$

$$(RN)_n = R_{tot_n} \Big/ \left(1 + \frac{(H)_n}{K_a}\right) \quad \text{(Eq. 15)}$$

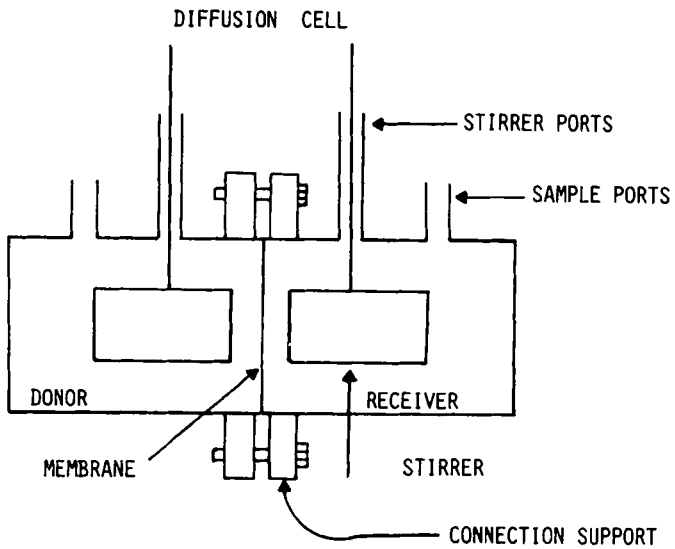

Figure 2—*Two-chamber diffusion cell used in transport studies. At predetermined intervals, donor and receiver solutions were totally replaced for analysis. Cross-sectional transport area was 2.10 cm^2.*

Table I—Typical Permeation Data [a]

Δ Time, h	Concentration, μg/mL Receiver	Donor	Flux, mmol/cm²·s [b]
0	0	546	—
2	9.9	514	5.654×10^{-11}
2	11.5	522	6.606×10^{-11}
2	13.2	519	7.562×10^{-11}
2	12.9	530	7.425×10^{-11}

[a] The system consisted of donor, 5 mM hexylamine, 0.1 M NaCl, and 0.1 M PO_4 (pH 8.5); receiver, 0.1 M NaCl and 0.1 M PO_4 (pH 4.1). [b] From the receiver data.

where P_{tot} and R_{tot} are total concentrations of the phosphate and amine, respectively. The concentrations of the other species can be readily calculated from $(H)_n$, $(PO_4)_n$, and $(RN)_n$ with Eqs. 9-12.

Next, the concentrations of the phosphate species at the membrane interfaces can be calculated by a suitable rearrangement of Eqs. 4 and 5 with appropriate substitutions from Eqs. 9-11. The concentrations of PO_4 at the interfaces are given by:

$$(PO_4)_1 = [D_{H_3PO_4}(H_3PO_4)_L + D_{H_2PO_4}(H_2PO_4)_L + D_{HPO_4}(HPO_4)_L + D_{PO_4}(PO_4)_L] \Big/ \left[D_{H_3PO_4}\frac{(H)_1^3}{K_{H_3PO_4}} + D_{H_2PO_4}\frac{(H)_1^2}{K_{H_2PO_4}} + D_{HPO_4}\frac{(H)_1}{K_{HPO_4}} + D_{PO_4}\right] \quad \text{(Eq. 16)}$$

and:

$$(PO_4)_2 = [D_{H_3PO_4}(H_3PO_4)_R + D_{H_2PO_4}(H_2PO_4)_R + D_{HPO_4}(HPO_4)_R + D_{PO_4}(PO_4)_R] \Big/ \left[D_{H_3PO_4}\frac{(H)_2^3}{K_{H_3PO_4}} + D_{H_2PO_4}\frac{(H)_2^2}{K_{H_2PO_4}} + D_{HPO_4}\frac{(H)_2}{K_{HPO_4}} + D_{PO_4}\right] \quad \text{(Eq. 17)}$$

and the concentrations of HPO_4, H_2PO_4, and H_3PO_4 follow from Eqs. 9-11.

Thus far, for given values of pH_1 and pH_2 we have determined concentrations of the various phosphate species at 1 and 2 so that the net total phosphate flux is zero. The remaining task is to determine the concentrations of RN and RNH^+ at these interfaces that satisfy the equations for total proton flux (Eqs. 6-8). This task is greatly facilitated by defining new variables *RI* and *RIII* such that:

$$RI = J_H I + \frac{D_{RNH^+}}{h_1}(RNH^+)_1 \quad \text{(Eq. 18)}$$

and

$$RIII = J_H III - \frac{D_{RNH^+}}{h_3}(RNH^+)_2 \quad \text{(Eq. 19)}$$

Table II—Model Parameters [a]

Parameter	Known	Computer Fitted
D_{OH}	5×10^{-5} cm²/s	
D_H	9×10^{-5} cm²/s	
D_{RN}, D_{RNH^+} (hexylamine)	1.087×10^{-5} cm²/s	
D_{RN}, D_{RNH^+} (octylamine)	9.880×10^{-6} cm²/s	
$D_{H_3PO_4}$, $D_{H_2PO_4}$, D_{HPO_4}, kD_{PO_4},	10^{-5} cm²/s	
h_1 and h_3	0.009 cm	0.01 cm
h_2	0.0127 cm	
K_1 (H_3PO_4)	7.50×10^{-3}	
K_2 (H_3PO_4)	6.20×10^{-8}	
K_3 (H_3PO_4)	2.10×10^{-13}	
K_a (hexylamine)	2.7542×10^{-11}	
K_a (octylamine)	2.2387×10^{-11}	
P_{RN} (hexylamine)		2.27×10^{-5} cm²/s
P_{RNH^+} (hexylamine)		4.130×10^{-9} cm²/s
P_{RN} (octylamine)		3.88×10^{-4} cm²/s
P_{RNH^+} (octylamine)		3.770×10^{-9} cm²/s

[a] Diffusivities for hexylamine and octylamine were determined experimentally; those for hydrogen and hydroxyl ions were calculated from mobility data. For the phosphate species, we assumed 10^{-5} cm²/s to be a reasonable estimate based on previous experience.

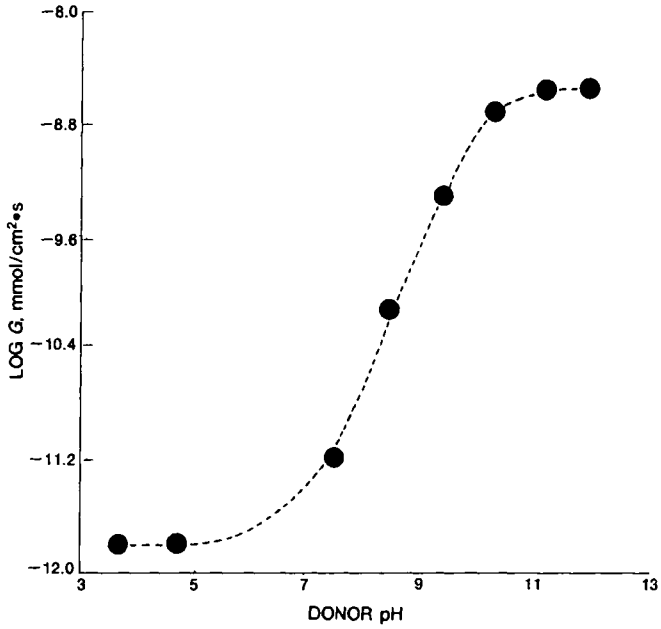

Figure 3—*pH-rate profile for hexylamine diffusing through the silicone rubber membrane into aqueous phase buffered at pH 4.1. The dashed line is a computer-generated line for* $h_1 = h_3 = 100$ *μm,* $h_2 = 127$ *μm,* $P_{RN} = 2.27 \times 10^{-5}$ *cm²/s, and* $P_{RNH^+} = 4.13 \times 10^{-9}$ *cm²/s.*

Numerical values for *RI* and *RIII* are readily obtained by substituting Eqs. 18 and 19 into Eqs. 6 and 8 and rearranging to get:

$$h_1 \cdot RI = D_{RNH^+}(RNH^+)_L + D_H[(H)_L - (H)_1] + D_{HPO_4}\left[(HPO_4)_L - \frac{(H)_1(P)_1}{K_{HPO_4}}\right] + 2D_{H_2PO_4}\left[(H_2PO_4)_L - \frac{(H)_1^2(PO_4)_1}{K_{H_2PO_4}}\right] + 3D_{H_3PO_4}\left[(H_3PO_4)_L - \frac{(H)_1^3(PO_4)_1}{K_{H_3PO_4}}\right] - D_{OH}[(OH)_L - (OH)_1] \quad \text{(Eq. 20)}$$

$$h_3 \cdot RIII = D_{RNH^+}(RNH^+)_R + D_H[(H)_R - (H)_2] + D_{HPO_4}\left[(HPO_4)_R - \frac{(H)_2(PO_4)_2}{K_{HPO_4}}\right] + 2D_{H_2PO_4}\left[(H_2PO_4)_R - \frac{(H)_2^2(PO_4)_2}{K_{H_2PO_4}}\right] + 3D_{H_3PO_4}\left[(H_3PO_4)_R - \frac{(H)_2^3(PO_4)_2}{K_{H_3PO_4}}\right] - D_{OH}[(OH)_R - (OH)_2] \quad \text{(Eq. 21)}$$

Consideration of Eqs. 6, 18, and 19 leads to:

$$h_2 \cdot h_1 \cdot RI = P_{RNH^+} \cdot h_1[(RNH^+)_1 - (RNH^+)_2] + h_2 \cdot D_{RNH^+}[RNH^+]_1 \quad \text{(Eq. 22)}$$

and

$$h_2 \cdot h_3 \cdot RIII = P_{RNH^+} \cdot h_3([RNH^+]_1 - [RNH^+]_2) - h_2 \cdot D_{RNH^+}[RNH^+]_2 \quad \text{(Eq. 23)}$$

or:

$$\begin{pmatrix} h_1 P_{RNH^+} \cdot h_2 D_{RNH^+} & -h_1 P_{RNH^+} \\ h_3 PRNH^+ & -h_3 P_{RNH^+} - h_2 D_{RNH^+} \end{pmatrix} \begin{pmatrix} [RNH^+]_1 \\ [RNH^+]_2 \end{pmatrix} = \begin{pmatrix} h_2 h_1 RI \\ h_2 h_3 RIII \end{pmatrix} \quad \text{(Eq. 24)}$$

Table III—Influence of the Aqueous Diffusion Layer

Donor pH	Receiver pH	Flux, mmol/cm²·s
	Hexylamine	
11.20	11.00	1.987×10^{-9}
11.20	4.10	2.975×10^{-9}
	Octylamine	
11.10	11.00	2.518×10^{-9}
11.10	4.10	4.951×10^{-9}

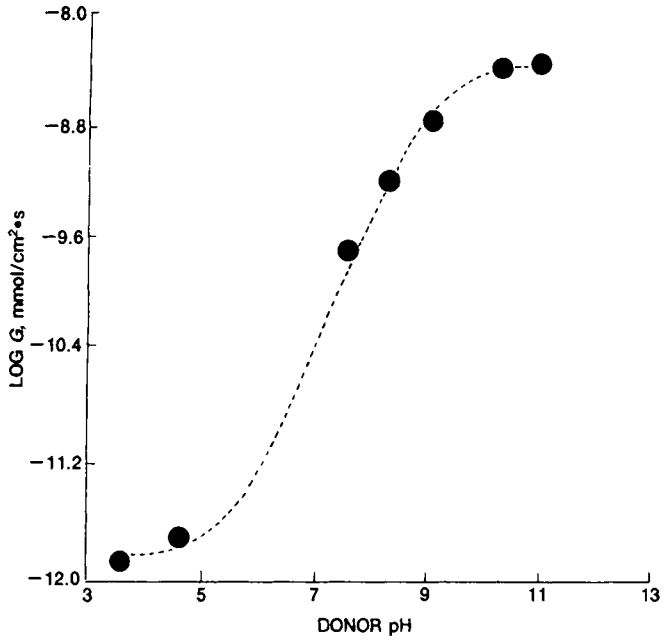

Figure 4—*pH-rate profile for octylamine diffusing through the silicone rubber membrane into aqueous phase buffered at pH 4.1. The dashed line is a computer-generated line for* $h_1 = h_3 = 100\ \mu m$, $h_2 = 127\ \mu m$, $P_{RN} = 3.88 \times 10^{-4}\ cm^2/s$, *and* $P_{RNH^+} = 3.77 \times 10^{-9}\ cm^2/s$.

where every quantity except $(RNH^+)_1$ and $(RNH^+)_2$ has been calculated. This equation is solved for $(RNH^+)_1$ and $(RNH^+)_2$, after which $(RN)_1$ and $(RN)_2$ are calculated from Eq. 12. Finally, *GI*, *GII*, and *GIII* are calculated from Eqs. 1-3 and the functions:

$$f_1 = GI - GII \qquad \text{(Eq. 25)}$$

and:

$$f_2 = GIII - GII \qquad \text{(Eq. 26)}$$

are evaluated. The procedure is repeated, with the nonlinear system solver adjusting the values of pH_1 and pH_2 until f_1 and f_2 are arbitrarily close to zero.

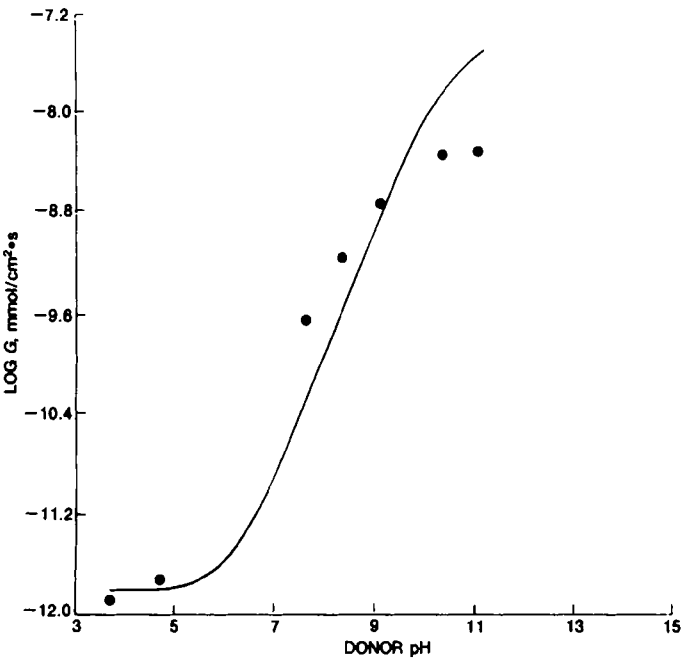

Figure 5—*pH-rate profile for octylamine diffusing through the silicone rubber membrane into aqueous phase buffered at pH 4.1. The solid line is a computer-generated line for* $h_1 = h_3 = 0\ \mu m$, $h_2 = 127\ \mu m$, $P_{RN} = 9.586 \times 10^{-5}\ cm^2/s$, *and* $P_{RNH^+} = 4.017 \times 10^{-9}\ cm^2/s$.

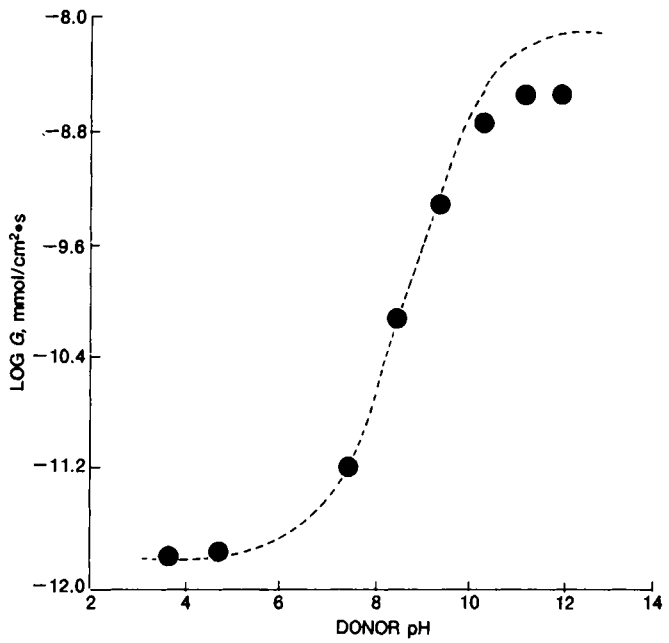

Figure 6—*pH-rate profile for hexylamine diffusing through the silicone rubber membrane into aqueous phase buffered at pH 4.1. The dashed line is a computer-generated line for* $h_1 = 0\ \mu m$, $h_2 = 127\ \mu m$, $h_3 = 100\ \mu m$, $P_{RN} = 2.27 \times 10^{-5}\ cm^2/s$, *and* $P_{RNH^+} = 4.13 \times 10^{-7}\ cm^2/s$.

EXPERIMENTAL SECTION

Experimental Design—The overall permeation procedure was designed such that depletion of the donor concentration was negligible during the course of the runs, and the receiver concentration was never an appreciable fraction of the donor concentration. Under these circumstances, the steady-state condition is readily attained.

The presence of the aqueous diffusion layer was studied by conducting studies in which the receiver compartment pH was maintained at pH 11.0 or 4.1. At high pH, the resistance of the aqueous diffusion layer causes a concentration gradient across the aqueous diffusion layer, and permeation of the weak base is reduced. At low pH, the aqueous diffusion layer is "short-circuited," *i.e.*, the aqueous diffusion layer offers no significant resistance to the transport of the weak base. When the aqueous diffusion layers are the main barriers for the weak base transport, elimination of half of the total aqueous diffusion layer resistance should result in ~100% increase in the permeation rate.

To study the influence of pH and buffer concentration on permeation, permeation was measured as a function of donor pH and donor buffer concentration. The pH of the donor compartment was closely monitored. The receiver compartment solution was buffered at pH 4.1 to ensure zero concentration of un-ionized drug; thus, perfect sink conditions were obtained.

Materials—*n*-Octylamine[1], *n*-hexylamine[2], sodium chloride[3], picric acid[4], dichloromethane[5], and sodium phosphate[5] (monobasic and dibasic) were reagent grade and used as received.

Preparation of Membrane—Membranes were cut from sheets of nonreinforced dimethylpolysiloxane[6], reportedly 0.127-cm thick, with a die made especially for the diffusion cell. Initially, they were washed in hot water, thoroughly rinsed with distilled water, and allowed to equilibrate overnight in receiver solution. Fresh membrane was used for each experiment.

Diffusion Cell—The diffusion cell consisted of two cylindrical half-cells, with inside diameters of ~1.5 cm and depths of ~5 cm. This gave a half-cell volume of ~9 mL. The cell halves were assembled, with the membrane between half-cells (Fig. 2), using polytef connection supports. The entire cell was immersed in a constant-temperature bath. The cell contents were stirred with small stirrers on shafts driven at 150 rpm by a constant-speed motor.

Permeation Procedure—Donor solution (9 mL) was placed in one half-cell, and 9 mL of receiver solution was placed in the other half-cell. The receiver solution consisted of 0.1 M NaCl and 0.1 M phosphate buffer. The donor

[1] Aldrich Chemical Co., Milwaukee, Wis.
[2] Eastman Kodak Co., Rochester, N.Y.
[3] Fisher Scientific Co., Fair Lawn, N.J.
[4] MCB, Norwood, Ohio.
[5] Mallinckrodt, St. Louis, Mo.
[6] Silastic; Dow Corning Corp., Midland, Mich.

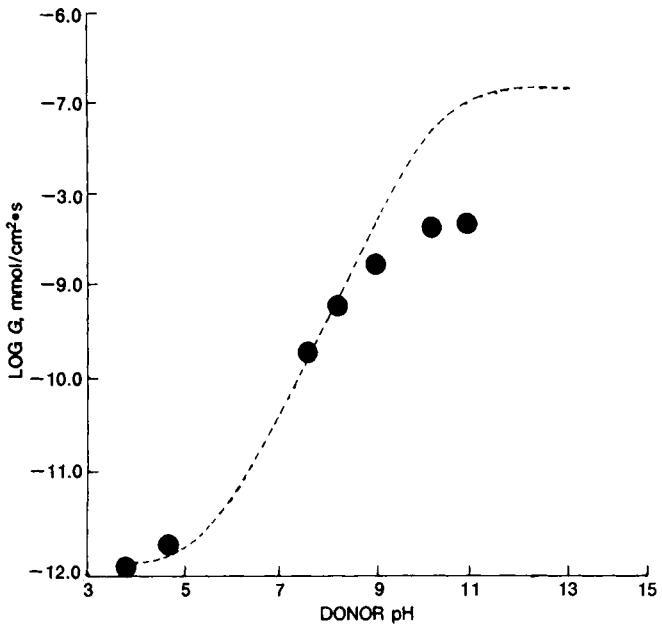

Figure 7—*pH-rate profile for octylamine diffusing through the silicone rubber membrane into aqueous phase buffered at pH 4.1. The dashed line is a computer-generated line for* $h_1 = 0$ *μm,* $h_2 = 127$ *μm,* $h_3 = 100$ *μm,* $P_{RN} = 3.88 \times 10^{-4}$ *cm²/s, and* $P_{RNH^+} = 3.77 \times 10^{-9}$ *cm²/s.*

solution consisted of the amine and 0.1 M NaCl in 0.1 M phosphate buffer. The contents of each half-cell were stirred at 150 rpm. At predetermined intervals, donor and receiver solutions were totally replaced for analysis. The total time involved in the exchange of the solutions was 1–2 min. The experiment was continued until the difference between two consecutive receiver compartment concentrations was <5%. The average of these concentrations was then used to calculate the flux under essentially steady-state conditions.

The amine analysis involved complexation of the amine with picric acid. The concentration of this picrate complex was determined spectrophotometrically. Receiver solution (5 mL) was shaken in a separatory funnel with two successive portions of 10 and 15 mL of a 0.2% solution of picric acid in dichloromethane. The two portions were drawn off, and the absorbance of these solutions was determined spectrophotometrically at a wavelength of 420 nm[7]. Picric acid was used as the reagent here for assaying the amines because it has a strong absorption spectrum and a single strong anionic functional group that has been shown to react quickly and quantitatively with the base (12, 13).

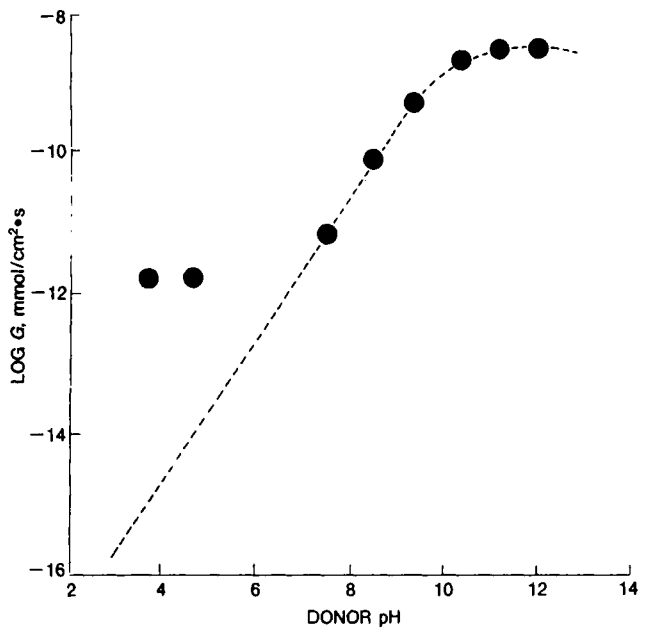

Figure 8—*pH-rate profile for hexylamine diffusing through the silicone rubber membrane into aqueous phase buffered at pH 4.1. The dashed line is a computer-generated line for* $h_1 = h_3 = 100$ *μm,* $h_2 = 127$ *μm,* $P_{RN} = 2.27 \times 10^{-5}$ *cm²/s, and* $P_{RNH^+} = 0$ *cm/2.*

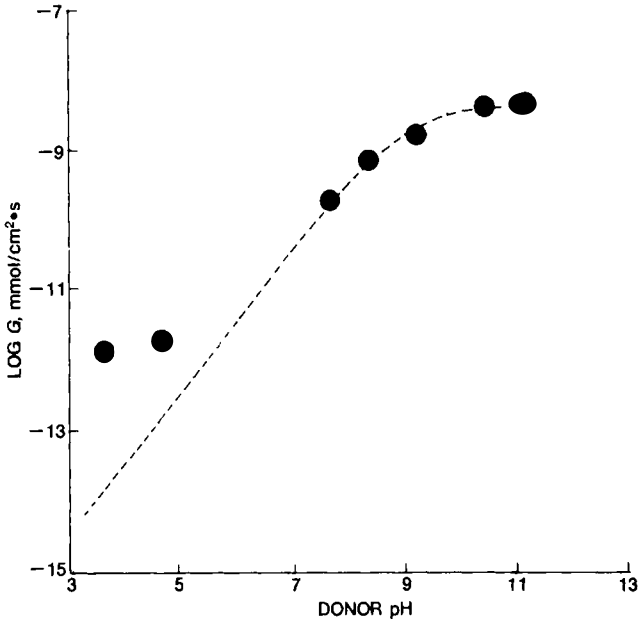

Figure 9—*pH-rate profile for octylamine diffusing through the silicone rubber membrane into aqueous phase buffered at pH 4.1. The dashed line is a computer-generated line for* $h_1 = h_3 = 100$ *μm,* $h_2 = 127$ *μm,* $P_{RN} = 3.88 \times 10^{-4}$ *cm²/s, and* $P_{RNH^+} = 0$ *cm²/s.*

Except at low pH (pH $\lesssim$ 6.0), the typical uncertainty in the flux determination was on the order of 5%. At low pH, because of the extremely low fluxes, the errors were relatively large (~25–50%).

RESULTS AND DISCUSSION

Table I shows typical transport data, from which it can be seen that a 5% error in the donor compartment would result in ~ ±26 μg/mL scatter; this scatter is greater than the amount transported across the membrane. Hence, it was decided to calculate the flux from the receiver compartment data only. Typically, steady-state conditions were attained within 2–4 h.

The initial steady-state flux into the receiver compartment is given by:

$$\text{Flux} = \frac{V}{A} \cdot \frac{dC}{dt} = k \cdot C_0 \text{ mmol/cm}^2 \cdot \text{s} \qquad \text{(Eq. 27)}$$

where V is the donor compartment volume, A is the diffusional area of the membrane, dC/dt is the rate at which drug permeates the membrane under steady-state conditions, C_0 is the concentration differential across the membrane (assumed to be initial donor concentration), and k is the permeability constant. Thus, k can be calculated from the experimental data by:

$$k = \frac{V \cdot \frac{dC}{dt}}{A \cdot C_0} \qquad \text{(Eq. 28)}$$

Variation in flux from run to run was 5–10% when the fluxes were $>10^{-11}$; for fluxes $<10^{-11}$ cm²/s, variation was 25–50%. Table II shows the values of various model parameters. Of the model parameters, the only unknown is the membrane permeability (defined as the partition coefficient multiplied by diffusivity) which is obtained by computer fitting (14).

Using nonlinear least-squares regression, best values were found for the membrane permeabilities and the aqueous diffusion layer thickness by the following technique. Trial values for the unknown parameters were assumed. Then, Eqs. 1–26 were solved, as described above, to calculate flux as a function of solution composition. The calculated values were compared with the experimentally observed fluxes, and the sum of the squares of the relative differences between calculated and observed fluxes was computed. Then, new values were chosen for the unknown parameters, and the procedure was re-

[7] Model 139, Hitachi Perkin-Elmer UV-V15 Spectrophotometer; Hitachi Ltd., Japan.

Table IV—Influence of Buffer Concentration on Hexylamine

Donor pH	Flux, mmol/cm²·s	
	0.1 M PO_4	0.01 M PO_4
12.05	3.334×10^{-9}	3.269×10^{-9}
9.50	5.210×10^{-10}	1.696×10^{-10}
7.50	7.154×10^{-12}	7.200×10^{-12}

peated. This entire cycle was repeated using a nonlinear least-squares fitting program until the sum of squares was minimized.

For both compounds, the diffusion layer thickness was found to be ~100 μm. The membrane permeabilities were as follows (cm²/s): free hexylamine, 2.27×10^{-5}; protonated hexylamine, 4.13×10^{-9}; free octylamine, 3.88×10^{-4}; protonated octylamine, 3.77×10^{-9}. Figures 3 and 4 show the experimental fluxes and theoretical fluxes based on parameter values shown in Table II. Over a range of more than 7 pH units and three orders of magnitude of flux, the model gives an essentially perfect fit to data.

Table III shows the influence of high and low pH in the receiver compartment on permeation. At low pH, the aqueous diffusion layer in the receiver compartment is essentially "short-circuited," *i.e.*, the effective transport resistance is very low. For octylamine under these conditions, this is an ~100% increase in flux, which indicates that the transport is essentially 100% aqueous diffusion layer controlled for this solute. However, for hexylamine, it can be seen that there is only an ~50% increase; this means that the membrane transport resistance is an appreciable part of the overall resistance in the case of hexylamine.

The thickness of the aqueous diffusion layer was independently evaluated by mounting a benzoic acid pellet onto the half-cell. The thickness was calculated from:

$$J/A = \frac{D(C_s - C_b)}{h} \qquad \text{(Eq. 29)}$$

where J is the dissolution rate (flux), A is the surface area of dissolving solid exposed to the solution, C_s is the concentration of the solute in the solution at saturation, C_b is the concentration of the solute in the bulk, D is the diffusion coefficient of the solute in the solvent (1.4×10^{-5} cm²/s at 37°C), and h is the Nernst effective diffusion layer thickness. Under sink conditions, $C_b = 0$; J/A and C_s were experimentally determined, and the value of D has been well documented previously (15). The thickness of the aqueous diffusion layer was found to be 90 μm. Hence, the computer-fit value of 100 μm is reasonable.

To determine whether the experimental data could fit a model in which there were no aqueous diffusion layers, *i.e.*, $h_1 = h_3 = 0$, best values were found for the membrane permeabilities using nonlinear least-squares regression and values listed in Table II, except for the membrane permeabilities and the aqueous diffusion layer thickness. Figure 5 shows the best fit when the aqueous diffusion layers are totally neglected. As can be seen under such circumstances, *i.e.*, when $h_1 = h_3 = 0$, the fit between the experimental values and the values predicted by the model is rather poor.

To assess the importance of the aqueous diffusion layers and the membrane permeabilities of the protonated species on the steady-state flux, computer simulations were made using the model parameters listed in Table II but excluding the parameter of interest. Figures 6 and 7 show that if the aqueous diffusion layer of the donor compartment is left out, the fluxes are significantly greater at the higher pH values. This shows that the aqueous diffusion layer is important, and significant errors in the analysis may result when it is ignored.

Figures 8 and 9 show the expected behavior if no protonated amine species were diffusing through the membrane. The theoretical fluxes were much smaller than the experimental fluxes at lower pH values. This clearly indicates that protonated amines are diffusing through the membrane, although they have much lower apparent membrane permeabilities than the free amines. These membranes were examined *via* scanning electron microscopy at 30,000×, and no evidence of holes was found, which supports the hypothesis of a true diffusion through the membrane of the protonated species.

Table IV shows the influence of buffer concentration on permeation. At pH values at which the buffer capacity is good (pH 12.05 and 7.50), the buffer concentration has no significant influence on permeation. At pH 9.5, at which the buffer capacity is poor, a lower flux was observed when the buffer strength was 0.01 M. This was the result of a drop in the bulk pH of ~1 pH unit at the lower buffer concentration, which was theoretically predicted and experimentally observed.

Figure 10 shows the effect of the alkylamine chain length. The membrane permeability of octylamine is 15–20 times that of hexylamine. If it is assumed that the membrane diffusivities of these two compounds are about equal, this leads to an incremental π constant for the partition coefficient per methylene group of ~0.61, which is in good agreement with the value of 0.56 reported by Flynn and Yalkowsky (16).

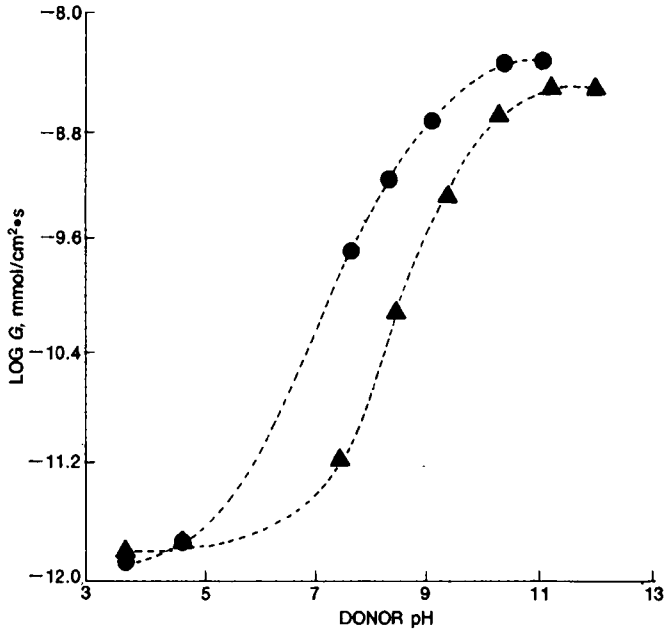

Figure 10—*Influence of chain length on flux. Assuming that the membrane diffusivities of these two compounds are approximately equal, it leads to an incremental π constant for the partition coefficient of ~0.61 per methylene group. Key: (●) octylamine; (▲) hexylamine.*

CONCLUSIONS

We have developed a rugged experimental system for studying the transport of weak acids and bases across a lipoidal membrane and developed theoretical methods for analyzing the experimental results on a quantitative basis. The experimental system consisted of the two aqueous phases separated by silicone rubber membrane. The experimental data were analyzed by utilizing theory, which takes into account the simultaneous diffusion and equilibria among all species (the various buffer species as well as the free and protonated amine), pH, and aqueous diffusion layers on both sides.

These results are conclusive evidence of the existence of aqueous diffusion barriers, as well as their effect on transport rates of solutes under varying conditions in a three-phase model. A true diffusion through the membrane of the protonated species was shown. The incremental π constant for the partition coefficient per methylene group was found to be 0.61, which is in good agreement with the value reported by Flynn and Yalkowsky (16).

Since charged bile acid micelles are not transported across the membrane, it should be possible to evaluate the degree of micellar solubilization of the amines if the study were carried out at pH 7.5–8.5, where aqueous diffusion layer effects are not important. As the un-ionized form of the amine is the major species diffusing through the membrane, the flux is the direct measurement of the thermodynamic activity of the un-ionized species and can be measured accurately, as the Donnan membrane effects encountered with cellophane membrane dialysis methods are absent.

REFERENCES

(1) R. G. Stehle and W. I. Higuchi, *J. Pharm. Sci.*, **61**, 1922 (1972).

(2) R. G. Stehle and W. I. Higuchi, *J. Pharm. Sci.*, **61**, 1931 (1972).

(3) E. R. Garrett and P. B. Chemburkar, *J. Pharm. Sci.*, **57**, 944 (1968).

(4) E. R. Garrett and P. B. Chemburkar, *J. Pharm. Sci.*, **57**, 1401 (1968).

(5) T. J. Roseman and W. I. Higuchi, *J. Pharm. Sci.*, **59**, 353 (1970).

(6) C. F. Most, *J. Appl. Polym. Sci.*, **11**, 1019 (1970).

(7) J. Haleblian, R. Runkel, N. Mueller, J. Christopherson, and K. Ng, *J. Pharm. Sci.*, **60**, 541 (1971).

(8) G. L. Flynn and T. J. Roseman, *J. Pharm. Sci.*, **60**, 1788 (1971).

(9) A. Suzuki, W. I. Higuchi, and N. F. H. Ho, *J. Pharm. Sci.*, **59**, 644 (1970).

(10) A. Suzuki, W. I. Higuchi, and N. F. H. Ho, *J. Pharm. Sci.*, **59**, 651 (1970).

(11) K. H. Kwan, W. I. Higuchi, A. M. Molokhia, and A. H. Hofmann, *J. Pharm. Sci.*, **66**, 1105 (1977).
(12) K. Gustavii and G. Schill, *Acta Pharm. Suec.*, **3**, 241 (1966).
(13) K. Gustavii, *Acta Pharm. Suec.*, **4**, 233 (1967).
(14) J. O'M. Bockris and A. K. N. Reddy, "Modern Electrochemistry," Plenum, New York, N.Y., 1970.
(15) W. I. Higuchi, S. Prakongpan, and F. Young, *J. Pharm. Sci.*, **62**, 945 (1973).
(16) G. L. Flynn and S. H. Yalkowsky, *J. Pharm. Sci.*, **61**, 838 (1972).

ACKNOWLEDGMENTS

This study was supported by Grant AM 16694 from the National Institute of Arthritis, Metabolism and Digestive Diseases.

Sintering Technique for the Preparation of Polymer Matrices for the Controlled Release of Macromolecules

JONATHAN COHEN *‡, **RONALD A. SIEGEL** §¶△, **and ROBERT LANGER** *¶‖x

Received September 13, 1982, from the *Department of Nutrition and Food Science, ‡Department of Materials Science and Engineering, §Department of Electrical Engineering and Computer Science, ¶Whitaker College of Health Sciences, Technology, and Management, Massachusetts Institute of Technology, Cambridge, MA 02139; and ‖Department of Surgery, Children's Hospital Medical Center, Boston, MA 02115. Accepted for publication July 28, 1983. △Present address: Department of Pharmaceutics, School of Pharmacy, University of California at San Francisco, San Francisco, CA 94143.

Abstract □ A new method for making polymeric systems for the controlled release of macromolecular drugs is described. The method consists of mixing drug and polymer (ethylene-vinyl acetate copolymer) powders below the glass transition temperature of the polymer and compressing the mixture at a temperature above the glass transition point. The macromolecule is not exposed to organic solvent during the fabrication process. Kinetic studies indicate that there is sustained release, and the bioactivity of macromolecules tested is unchanged throughout the sintering and release processes.

Keyphrases □ Copolymers—ethylene-vinyl acetate, controlled release of macromolecules □ Sustained release—macromolecules, ethylene-vinyl acetate copolymer □ Sintering technique—preparation of ethylene-vinyl acetate copolymer, controlled release of macromolecules

Previous studies (1, 2) have shown that controlled-release systems for macromolecules can be formulated by dissolution of ethylene-vinyl acetate copolymer in an organic solvent (dichloromethane), adding powdered macromolecule, casting the mixture in a mold at low temperature, and vacuum drying. However, the addition of solvent during the casting procedure may cause denaturation of certain macromolecules. In addition, the removal of the casting solvent in the drying step is time consuming and leads to shrinkage with possible shape distortion of the matrix. This report describes a 37°C sintering technique which takes advantage of the low glass transition temperature (−36.5°C) of ethylene-vinyl acetate copolymer and eliminates the need for solvent casting.

EXPERIMENTAL SECTION

Polymer Glass Transition Temperature—The glass transition temperature (T_g) of ethylene-vinyl acetate copolymer was determined with a differential scanning calorimeter[1] (3).

Matrix Preparation—Ethylene-vinyl acetate copolymer[2] was converted into a powder by one of two methods. The first method involved the dissolution of 3 g of ethylene-vinyl acetate copolymer in 20 mL of dichloromethane[3]. The solution was extruded dropwise, with a 50-mL syringe[4] fitted with a hypodermic needle[5], into a 250-mL beaker containing 100 mL of liquid nitrogen. From this point on, all instruments that came into contact with the frozen polymer solution were cooled with liquid nitrogen and, whenever possible, precooled in a freezer to minimize the quantity of liquid nitrogen needed for cooling.

The frozen droplets were ground for 5 min with a mortar and pestle. The powder was then spread evenly over three 20.3 × 20.3-cm glass sheets that were cooled to −10°C. The glass sheets were returned to a −10°C freezer for 2 h. At the end of that time, most of the solvent had evaporated, leaving a stringy powder. This powder was removed with a razor blade, bathed in a 100-mL beaker[6] with 30 mL of liquid nitrogen, and then ground to a fine powder with a mortar and pestle as described above. This powder was placed under vacuum for 2 h. The bulk powder was sieved to specific size ranges with a stack of graduated sieves[7]. Polymer powder prepared by this method is referred to here as powder I.

Powder I was produced under two aging conditions. In one set of experiments, the powder was dried under vacuum for 2 h at room temperature. This is referred to here as "fresh" powder I. In the other set of experiments, the powder was dried under vacuum for 2 h and then left in a covered petri dish for 1 week at room temperature. This is referred to here as "aged" powder I.

In the second method of powder preparation, 20 g of ethylene-vinyl acetate copolymer beads[2] were cooled in 40 mL of liquid nitrogen and placed in an electric mill[8]. The mill was set for 90-s grinding intervals. Between grindings, the polymer beads were cooled with 20-mL portions of liquid nitrogen. During the grinding process, cold nitrogen vapor was circulated around the sample chamber through the cooling ducts of the chamber. The powder collected around the outer edges of the sample chamber and could be extracted with a spatula after the second grinding and after every successive grinding. After the eighth grinding, ~4 g of frozen pellets was added to restore the sample to its original volume. This process was repeated until sufficient powder was collected to prepare the samples. The ground polymer powder was then sieved to specific size ranges with a stack of graduated sieves in an automatic sieve shaker[9] at −40°C. Polymer powder prepared by this second method is referred to here as powder II.

Studies were performed on both powders with either a specific particle size range (90–180 μm) or a mixture of sizes as described in Table I. To formulate the controlled-release system, macromolecular drug powder was sieved to a particle size range of 90–180 μm. Macromolecule and polymer powders, a total of 1.0 g, were placed in a plastic weighing boat[10], which was then

[1] Model DSC-II; Perkin-Elmer Corp., Norwalk, Conn.
[2] EVAc pellets, Elvax 40, prewashed to remove clay; DuPont Chemical Co., Wilmington, Del.
[3] Analytical reagent, Mallinckrodt, Inc.
[4] Becton, Dickenson and Co., Rutherford, N.J.
[5] 21-Gauge, 5.08 cm; Becton, Dickenson and Co.
[6] Pyrex; Corning Glass Works, Corning, N.Y.
[7] 450 90 μm; Newark Wire Cloth Co., Newark, N.J.
[8] Micromill model 550; Technilab Instruments, Pequannock, N.J.
[9] Portable sieve shaker; C. E. Tyler, Inc., Fisher Scientific Co., Philadelphia, Pa.
[10] Polyethylene, 75-mL capacity; VWR Scientific.

0022-3549/84/0800-1034$01.00/0
© 1984, American Pharmaceutical Association

(11) K. H. Kwan, W. I. Higuchi, A. M. Molokhia, and A. H. Hofmann, *J. Pharm. Sci.*, **66**, 1105 (1977).
(12) K. Gustavii and G. Schill, *Acta Pharm. Suec.*, **3**, 241 (1966).
(13) K. Gustavii, *Acta Pharm. Suec.*, **4**, 233 (1967).
(14) J. O'M. Bockris and A. K. N. Reddy, "Modern Electrochemistry," Plenum, New York, N.Y., 1970.
(15) W. I. Higuchi, S. Prakongpan, and F. Young, *J. Pharm. Sci.*, **62**, 945 (1973).
(16) G. L. Flynn and S. H. Yalkowsky, *J. Pharm. Sci.*, **61**, 838 (1972).

ACKNOWLEDGMENTS

This study was supported by Grant AM 16694 from the National Institute of Arthritis, Metabolism and Digestive Diseases.

Sintering Technique for the Preparation of Polymer Matrices for the Controlled Release of Macromolecules

JONATHAN COHEN *‡, **RONALD A. SIEGEL** §¶△, **and ROBERT LANGER** *¶‖x

Received September 13, 1982, from the *Department of Nutrition and Food Science, ‡Department of Materials Science and Engineering, §Department of Electrical Engineering and Computer Science, ¶Whitaker College of Health Sciences, Technology, and Management, Massachusetts Institute of Technology, Cambridge, MA 02139; and ‖Department of Surgery, Children's Hospital Medical Center, Boston, MA 02115. Accepted for publication July 28, 1983. △Present address: Department of Pharmaceutics, School of Pharmacy, University of California at San Francisco, San Francisco, CA 94143.

Abstract □ A new method for making polymeric systems for the controlled release of macromolecular drugs is described. The method consists of mixing drug and polymer (ethylene-vinyl acetate copolymer) powders below the glass transition temperature of the polymer and compressing the mixture at a temperature above the glass transition point. The macromolecule is not exposed to organic solvent during the fabrication process. Kinetic studies indicate that there is sustained release, and the bioactivity of macromolecules tested is unchanged throughout the sintering and release processes.

Keyphrases □ Copolymers—ethylene-vinyl acetate, controlled release of macromolecules □ Sustained release—macromolecules, ethylene-vinyl acetate copolymer □ Sintering technique—preparation of ethylene-vinyl acetate copolymer, controlled release of macromolecules

Previous studies (1, 2) have shown that controlled-release systems for macromolecules can be formulated by dissolution of ethylene-vinyl acetate copolymer in an organic solvent (dichloromethane), adding powdered macromolecule, casting the mixture in a mold at low temperature, and vacuum drying. However, the addition of solvent during the casting procedure may cause denaturation of certain macromolecules. In addition, the removal of the casting solvent in the drying step is time consuming and leads to shrinkage with possible shape distortion of the matrix. This report describes a 37°C sintering technique which takes advantage of the low glass transition temperature (−36.5°C) of ethylene-vinyl acetate copolymer and eliminates the need for solvent casting.

EXPERIMENTAL SECTION

Polymer Glass Transition Temperature—The glass transition temperature (T_g) of ethylene-vinyl acetate copolymer was determined with a differential scanning calorimeter[1] (3).

Matrix Preparation—Ethylene-vinyl acetate copolymer[2] was converted into a powder by one of two methods. The first method involved the dissolution of 3 g of ethylene-vinyl acetate copolymer in 20 mL of dichloromethane[3]. The solution was extruded dropwise, with a 50-mL syringe[4] fitted with a hypodermic needle[5], into a 250-mL beaker containing 100 mL of liquid nitrogen. From this point on, all instruments that came into contact with the frozen polymer solution were cooled with liquid nitrogen and, whenever possible, precooled in a freezer to minimize the quantity of liquid nitrogen needed for cooling.

The frozen droplets were ground for 5 min with a mortar and pestle. The powder was then spread evenly over three 20.3 × 20.3-cm glass sheets that were cooled to −10°C. The glass sheets were returned to a −10°C freezer for 2 h. At the end of that time, most of the solvent had evaporated, leaving a stringy powder. This powder was removed with a razor blade, bathed in a 100-mL beaker[6] with 30 mL of liquid nitrogen, and then ground to a fine powder with a mortar and pestle as described above. This powder was placed under vacuum for 2 h. The bulk powder was sieved to specific size ranges with a stack of graduated sieves[7]. Polymer powder prepared by this method is referred to here as powder I.

Powder I was produced under two aging conditions. In one set of experiments, the powder was dried under vacuum for 2 h at room temperature. This is referred to here as "fresh" powder I. In the other set of experiments, the powder was dried under vacuum for 2 h and then left in a covered petri dish for 1 week at room temperature. This is referred to here as "aged" powder I.

In the second method of powder preparation, 20 g of ethylene-vinyl acetate copolymer beads[2] were cooled in 40 mL of liquid nitrogen and placed in an electric mill[8]. The mill was set for 90-s grinding intervals. Between grindings, the polymer beads were cooled with 20-mL portions of liquid nitrogen. During the grinding process, cold nitrogen vapor was circulated around the sample chamber through the cooling ducts of the chamber. The powder collected around the outer edges of the sample chamber and could be extracted with a spatula after the second grinding and after every successive grinding. After the eighth grinding, ~4 g of frozen pellets was added to restore the sample to its original volume. This process was repeated until sufficient powder was collected to prepare the samples. The ground polymer powder was then sieved to specific size ranges with a stack of graduated sieves in an automatic sieve shaker[9] at −40°C. Polymer powder prepared by this second method is referred to here as powder II.

Studies were performed on both powders with either a specific particle size range (90–180 μm) or a mixture of sizes as described in Table I. To formulate the controlled-release system, macromolecular drug powder was sieved to a particle size range of 90–180 μm. Macromolecule and polymer powders, a total of 1.0 g, were placed in a plastic weighing boat[10], which was then

[1] Model DSC-II; Perkin-Elmer Corp., Norwalk, Conn.
[2] EVAc pellets, Elvax 40, prewashed to remove clay; DuPont Chemical Co., Wilmington, Del.
[3] Analytical reagent, Mallinckrodt, Inc.
[4] Becton, Dickenson and Co., Rutherford, N.J.
[5] 21-Gauge, 5.08 cm; Becton, Dickenson and Co.
[6] Pyrex; Corning Glass Works, Corning, N.Y.
[7] 450 90 μm; Newark Wire Cloth Co., Newark, N.J.
[8] Micromill model 550; Technilab Instruments, Pequannock, N.J.
[9] Portable sieve shaker; C. E. Tyler, Inc., Fisher Scientific Co., Philadelphia, Pa.
[10] Polyethylene, 75-mL capacity; VWR Scientific.

0022-3549/84/0800-1034$01.00/0
© 1984, American Pharmaceutical Association

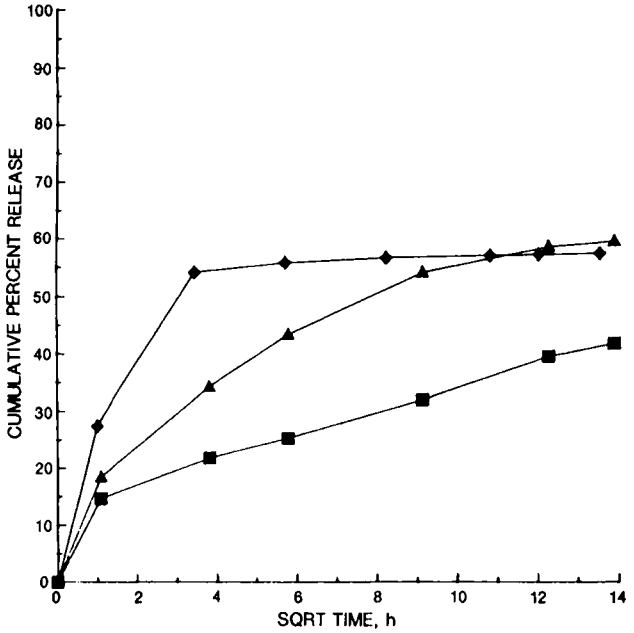

Figure 1—*Release kinetics for 25% (w/w) albumin slabs: effect of polymer powder type. Matrices were cast with a mixed particle size range (Table I) and with a formation pressure of 10.5 MPa. Key: (■) fresh powder I; (▲) aged powder I; (◆) powder II.*

transferred to a baking dish[11] containing liquid nitrogen at a depth of 1 cm. The powders were mixed in the weighing boat for 5 min with a spatula that was chilled with liquid nitrogen. After mixing, the powders were poured into a piston mold[12]. The mold was chilled in a −10°C freezer for 1 h and then chilled with 20 mL of liquid nitrogen immediately before the powder mixture was poured in. After the mixed powder was poured into the piston, the piston mold assembly was warmed to 37°C in an oven[13] for 1 h and then placed in a hydraulic press[14]. The pressure on the mold was increased over a 90-s interval from 0 Pa to the maximum pressure desired. After 30 min, the pressure was released, leaving a cohesive, heterogeneous slab.

The slab was removed from the mold with the aid of a scalpel[15] and forceps. A small amount (<2%) of the fused polymer mixture was extruded into the space between the moving piston and the jacket of the mold. The scalpel was used to trim any of the polymer mixture than may have leaked. The slab was then gently peeled from the mold with forceps.

Slabs were prepared separately at maximum pressures of 3.5, 7, and 10.5 MPa from each powder described above. Macromolecules tested for release were bovine serum albumin[16] and trypsin[17].

Kinetics—Each slab was ~1.4-mm thick. Four pieces, measuring ~7 × 7 × 1 mm each, were cut from each slab with a scalpel and tested for release as follows. Scintillation vials[18] were filled with 10 mL of physiological saline for albumin release studies and 10 mL of Tris[19] buffer for trypsin release studies. The matrix samples were attached to glass loops made from Pasteur pipets[20] that were fitted into scintillation vial caps. The samples were attached by passing a thread of 4/0 silk[21] through the sample in an orthogonal direction to its face. By tying the sample to the rod, it ensured that the sample was always bathed on all sides with fluid and provided an easy way to transfer the samples from vial to vial during the release study. Release kinetics for albumin, based on the amount of protein released, were determined by UV spectrophotometry at 220 nm on 144 samples cut from 36 25% (w/w) loaded slabs.

[11] Pyrex; Corning Glass Works.

[12] Accessory piston for Carver press (surface area, 2.54 cm²); Fred S. Carver, Inc., Menomonee, Wis.

[13] Stabiltherm constant temperature cabinet; Blue M Electric Co., Blue Island, Ill.

[14] Carver Laboratory press, model C; Fred S. Carver, Inc.

[15] Scalpel blade #22; Bard Parker, Rutherford, N.J.

[16] Catalog number T8253; Sigma Chemical Co., St. Louis, Mo.

[17] Catalog number A4503; Sigma Chemical Co.

[18] 20 mL; Fisher Scientific Co.

[19] Tris, 0.0115 M, Schwarz/Mann, Spring Valley, N.Y.; $CaCl_2$, 0.0115 M, Baker Chemical Co., Phillipsburgh, N.Y.; HCl (pH 8.0), Mallinckrodt.

[20] 13.61 cm × 7 mm, catalog number 14672-200; VWR Scientific. Loop was fashioned by heating the pipet over a bunsen burner. The shaft of pipet was fitted into the cap of a scintillation vial. A hole was drilled through the top of the cap wide enough to accomodate the shaft. The pipet was sealed into place with paraffin wax.

[21] Black braided; presoaked in saline for 1 week and dried; American Cyanamid, Pearl River, N.Y.

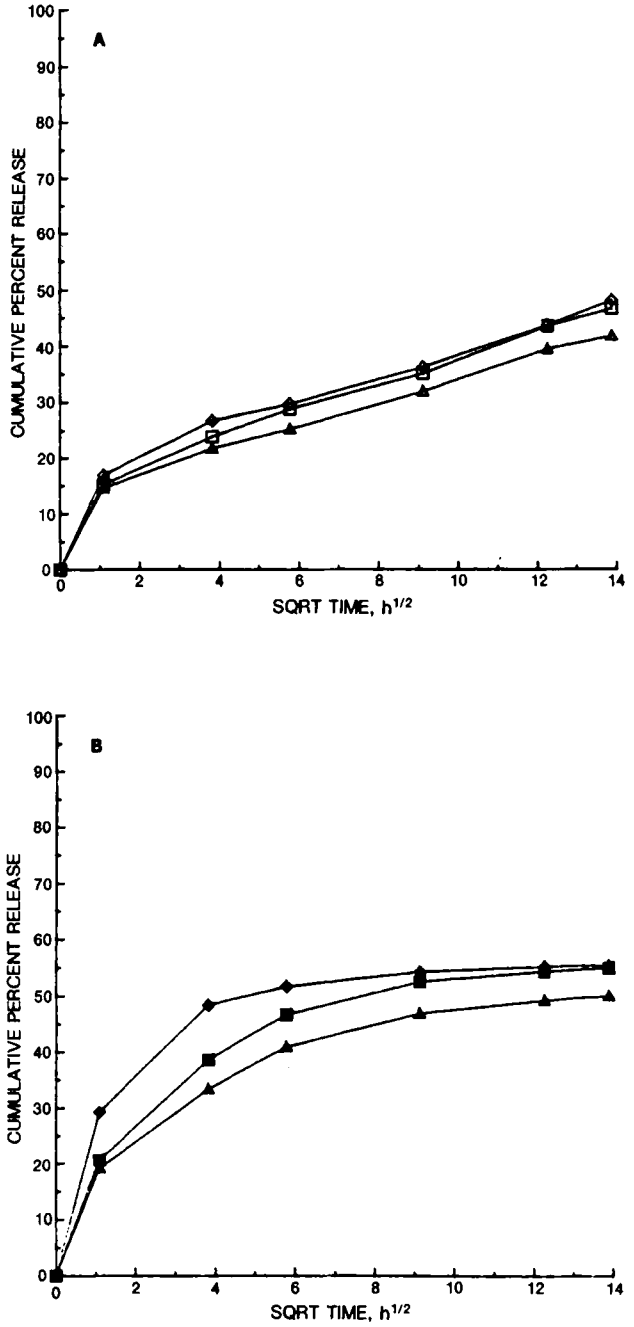

Figure 2—*Release kinetics for 25% (w/w) albumin slabs: effect of formation pressure. Key: (a) matrices cast with fresh powder I, a mixed particle size range (Table I), and with formation pressures of 3.5 (◇), 7.0 (□), and 10.5 MPa (△); (b) matrices cast with aged powder I, a fixed particle size range (90–180 μm), and with formation pressures of 3.5 (◆), 7.0 (■), and 10.5 MPa (▲).*

Trypsin release, also based on protein content, was determined by UV spectrophotometry at 220 nm on 18 samples cut from nine 18% loaded slabs.

Bioactivity—After trypsin release from the 18 samples was assayed (see above), the recovered enzyme was then diluted with Tris buffer to a concentration of 0.11 mg/mL. The enzyme turnover rate of the diluted trypsin solution on a tosyl-arginine methyl ester[22] substrate was then tested at 247 nm (4). The turnover rate of the test solution was compared with the turnover rate of a standard trypsin solution at the same concentration. The bioactivity index was taken to be the ratio of the two turnover rates.

Bioactivity was assessed at nine different times over a 310-h release period for two separate matrices cast with each powder (fresh powder I, aged powder I, and powder II) all at a pressure of 10.5 MPa. Bioactivity was also tested

[22] T4626, catalog number 1022-31; Sigma Chemical Co.

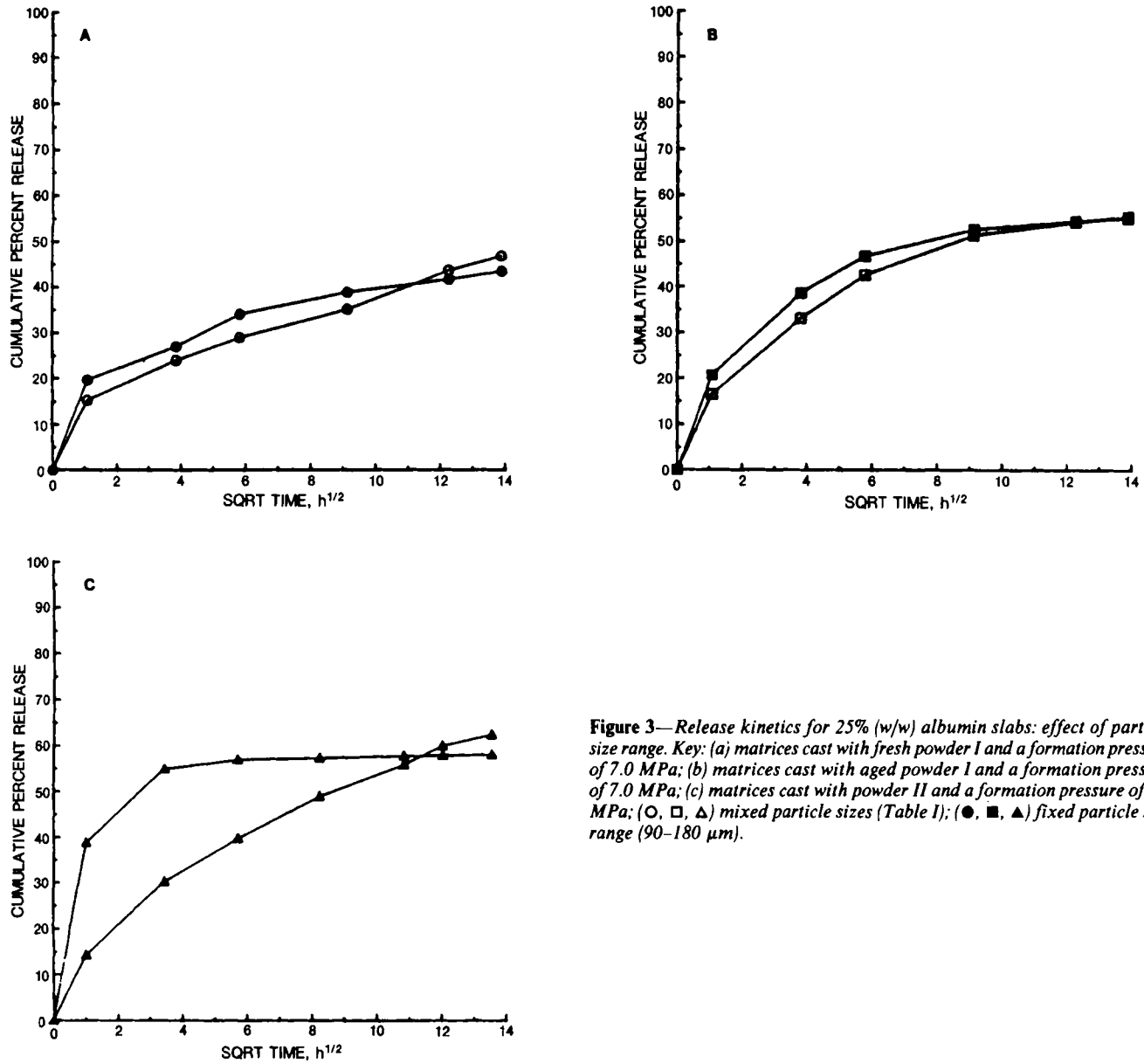

Figure 3—*Release kinetics for 25% (w/w) albumin slabs: effect of particle size range. Key: (a) matrices cast with fresh powder I and a formation pressure of 7.0 MPa; (b) matrices cast with aged powder I and a formation pressure of 7.0 MPa; (c) matrices cast with powder II and a formation pressure of 7.0 MPa; (○, □, △) mixed particle sizes (Table I); (●, ■, ▲) fixed particle size range (90–180 μm).*

for each powder on trypsin matrices cast at 3.5 and 7.0 MPa. For these matrices, bioactivity was assessed at only one time point (with release occurring between 24 and 36 h).

RESULTS

Polymer Glass Transition Temperature—The glass transition temperature was −36.5°C.

Kinetics—Figure 1 shows the release kinetics for slabs cast at 10.5 MPa with polymer powder granules with a mixed size range (Table I). Both the powder type and aging condition affect the rate of drug release. Specifically, powder II matrices release all of their releasable drug rapidly. Aged powder I matrices release drug at an intermediate rate, and fresh powder I matrices release drug at the slowest rate. Fresh powder I still releases at the same $t^{1/2}$ rate after 1 week.

In general, it was found that formation pressure has a small effect on release kinetics. When it does have an effect, it tends to be in the earliest stages of release, *i.e.*, the initial burst. Two examples of formation pressure dependence are shown in Fig. 2. The initial burst decreases with increasing pressure.

Similarly, the polymer powder particle size distribution generally does not dramatically affect release. Typical plots comparing release for the two polymer particle size distributions are shown in Fig. 3a. There is a slight tendency for matrices cast with mixed polymer particles to release more slowly and steadily than matrices cast with polymers cast with polymer particles of a single size range (90–180 μm). One case was observed in which the particle size mix had a pronounced effect (Fig. 3c).

Reproducibility between identically made slabs was within 8%. From samples cut from the same slab, reproducibility was within 6%[23].

Bioactivity—Table II shows the bioactivity index of released trypsin recovered during the time point corresponding to the release occurring between 24 and 36 h as a function of formation pressure and polymer powder type. The bioactivity index in all cases exceeded 96%. There appeared to be no difference between polymer powder types in their effect on enzyme activity. When the bioactivity index of released trypsin was measured for the amount of enzyme released from the matrix at later times, it exceeded 95% in every case.

DISCUSSION

The advantages of the sintering method used in this study, when compared with solvent casting methods used in previous studies, include (*a*) elimination of shrinkage; (*b*) elimination of the need for potentially expensive scale-up steps such as vacuum drying; (*c*) reduction of processing time [slabs were produced in 2 h[24] compared with 4 d required for solvent casting (1)]; and (*d*) lack of the necessity to expose the macromolecule to solvent.

Microscopic examination of the polymer particles of the two powder types reveals that they are similar in shape and are both white and translucent. They range in shape from a spherical form to an oblate spheroid form, in which the

[23] Reproducibility was determined by dividing the range of all points corresponding to a mean value by that mean value.

[24] These studies were performed on test slabs that were produced in 2 h. Since then, slabs have been produced in as little as 24 min.

Table I—Particle Size Distribution for Polymer Powder with a Mixture of Particle Sizes

Particle Size, μm	Weight, %
300-425	33
150-300	7
106-150	33
90-106	10
53-90	17

length is ~1.5 times the width. The only visually discernable differences between the powder types is surface topography. Powder I shows a roughened surface, with occasional folds and depressions. Powder II shows particles that are smoother with neither folds nor depressions. Some of the powder II particles have sharp, well-defined edges.

When stored at room temperature for 2 weeks and reexamined with a microscope, polymer powders produced by both of the methods described above showed the same surface morphology as the respective fresh powders. Neither fabrication procedure nor aging affected the adhesive quality of the polymer powder.

In the sintering method, the powdered drug and polymer were cooled to −200°C at which temperature they lose their adhesive properties. They were then mixed to give a homogenous blend. Warming the powders restored their elastic properties. Pressure applied at temperatures > −36.5°C caused the polymer particles to flow around the drug powder and merge together with other polymer particles. The result was a solid with drug powder locked into it.

Temperatures below T_g are essential for uniform mixing. Ethylene-vinyl acetate with 40% vinyl acetate by weight is a highly adhesive substance. Above T_g there are clumps of polymer powder that cannot be evenly mixed with the macromolecule. When fabrication was undertaken without cold mixing, some of the polymer particles clumped together. Substrate crystals adhered to these lumps in a nonuniform fashion. The mechanical strength of the slabs that were prepared without cold mixing was poor. Samples prepared in this way were fragile, pulled apart easily, and did not have evenly distributed substrates.

The polymer powder type seems to be the most important variable in determining release rates. The difference in the release kinetics for polymers cast with different powder types may be due to the fact that fresh powder I may contain residual solvent which might help fuse the boundaries between the polymer particles. Powder I granules also appear to have a folded surface. The extra surface area of the grains may allow for a more complete fusion to the solid matrix. Similarly, it is likely that aged powder I contains less solvent than fresh powder I, and this might explain why the fresh powder releases drug on a more sustained basis.

Increasing formation pressure often decreases the initial burst of release when both powder I and powder II are used. This is probably due to the requirement of high pressure to ensure fusion of polymer granules. At low formation pressure, the polymer matrix is grainy. The boundaries between polymer grains may provide extra channels (4) through which drug can diffuse.

Table II—Percent Bioactivity for Trypsin Release Averaged over Two Slabs for Each Formation Pressure and Powder Type

Pressure, MPa	Powder I, %		Powder II, %
	Fresh	Aged	
3.5	97.3	100	100
7.0	99.4	98.5	96.4
10.5	98.3	98.8	100

Using a mixture of varying polymer particle sizes can have the effect of prolonging release. This is probably due to the fact that the smaller particles fit into the interstitial spaces between the larger grains. The smaller particles might then help cement the larger polymer particles and thereby foster a more complete fusion. The small particles might also help fill spaces that would otherwise become small pores that would increase the release rate. It was noted, however, that there was only one case in which the particle size mixture had a significant effect on release rates (Fig. 3c). At present, we cannot ascertain whether the results shown in Fig. 3c are anomalous or whether there is some uncontrolled variable that caused the difference between the results shown in Fig. 3c and Fig. 3a and b.

It is well known (5) that diffusive release from slabs shows $t^{1/2}$ kinetics. Our results also follow $t^{1/2}$ kinetics. It has been shown that diffusive release with zero-order release kinetics is obtained from hemispheric drug–polymer pellets that are coated with an impermeable barrier, except for a small cavity in the center face (6). It is possible to form hemispheres by the sintering method presented here. Initial results with such sintered hemispheres have shown near-constant release of polypeptides such as insulin for >70 d (7).

REFERENCES

(1) W. D. Rhine, D. S. T. Hsieh, and R. S. Langer, *J. Pharm. Sci.*, **69**, 265 (1980).

(2) R. Langer, *Chemtech*, **12**, 98 (1982).

(3) F. W. Billmeyer, Jr., "Textbook of Polymer Science," 2nd ed., Wiley-Interscience, New York, N.Y., 1971.

(4) R. S. Langer, W. D. Rhine, D. S. T. Hsieh, and R. S. Bawa, in "Controlled Release of Bioactive Materials," R. Baker, Ed., Academic, New York, N.Y., 1980, pp. 83-98.

(5) J. Crank, "The Mathematics of Diffusion," 2nd ed., Clarendon, Oxford, 1975.

(6) D. S. T. Hsieh, W. D. Rhine, and R. Langer, *J. Pharm. Sci.*, **72**, 17, (1983).

(7) R. Siegel, J. Cohen, L. Brown, and R. Langer, in "Recent Advances in Drug Delivery Systems," J. Anderson and S. W. Kim, Eds., Plenum, New York, N.Y., in press.

ACKNOWLEDGMENTS

This work was funded by Grant GM26698 from the National Institutes of Health.

Renal Clearance and Serum Protein Binding of Acetaminophen and Its Major Conjugates in Humans

MARILYN E. MORRIS and GERHARD LEVY ˣ

Received April 4, 1983, from the *Department of Pharmaceutics, School of Pharmacy, State University of New York at Buffalo, Amherst, NY 14260.* Accepted for publication July 29, 1983.

Abstract □ The renal clearances of acetaminophen, acetaminophen glucuronide, and acetaminophen sulfate were determined in eight healthy adults 2 h after administration of 1.5 g of acetaminophen. The renal clearance ratios (relative to creatinine) were 0.058 ± 0.026, 0.890 ± 0.153, and 1.43 ± 0.250 (mean ± *SD*), respectively. The renal clearance of acetaminophen increased with increasing urine flow rate, and that of acetaminophen sulfate decreased with increasing serum concentration of the conjugate. A strong positive correlation was found between the renal clearances of acetaminophen glucuronide and acetaminophen sulfate, possibly due to blood perfusion rate-dependent renal tubular secretion of the two conjugates. The serum protein binding of acetaminophen (≃20%) and acetaminophen glucuronide (<10%) are minor. Acetaminophen sulfate is >50% protein bound, as determined by equilibrium dialysis and ultrafiltration. The results of these studies are (*a*) consistent with previous reports of animal studies, indicating that renal excretion of acetaminophen involves glomerular filtration and passive reabsorption and that acetaminophen sulfate is subject to active renal tubular secretion, and (*b*) compatible with the reported occurrence of renal tubular secretion of acetaminophen glucuronide in animals.

Keyphrases □ Acetaminophen—renal clearance, serum protein binding, glucuronide and sulfate metabolites □ Renal clearance—acetaminophen, serum protein binding glucuronide and sulfate conjugates □ Protein binding—acetaminophen, ligand and albumin concentration

Acetaminophen, the widely used nonnarcotic analgesic and antipyretic agent, is eliminated primarily by formation of the glucuronide and sulfate conjugates (1–3). These metabolites are excreted as such in the urine. While the renal clearance of the acetaminophen conjugates has been studied extensively in experimental animals (4–6), only limited information is available concerning their renal clearance in humans (7, 8). We have, therefore, determined the renal clearances of acetaminophen, acetaminophen glucuronide, and acetaminophen sulfate in normal humans of both sexes and examined the concentration dependence of, and the interrelationship between, these processes. Since proper interpretation of renal clearance data requires knowledge of the plasma or serum protein binding characteristics of the cleared substance, we have also determined the serum protein binding of acetaminophen and its two major metabolites, and the effect of ligand and albumin concentration, respectively, on the protein binding of these compounds.

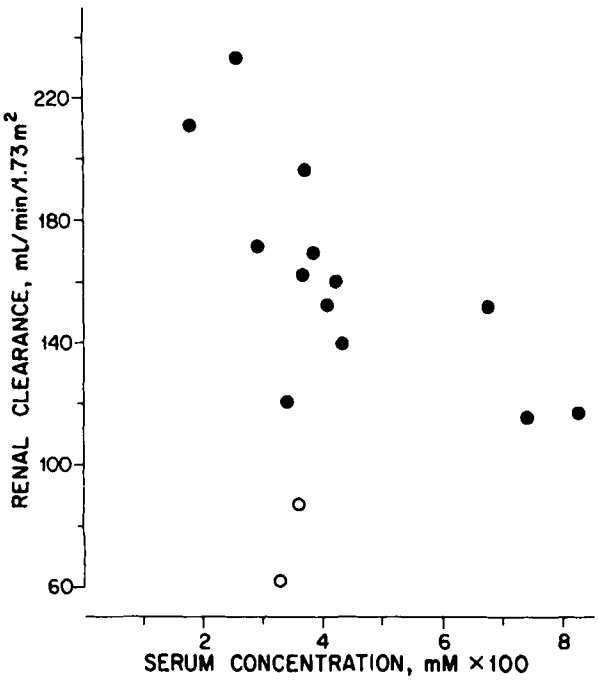

Figure 1—*Relationship between the apparent renal clearance of acetaminophen sulfate (normalized to a body surface area of 1.73 m²) and the serum concentration of acetaminophen sulfate; r = 0.718, p < 0.01. The open symbols are the data points of one outlier, which were not included in the statistical analysis; 0.01 mM acetaminophen = 1.51 μg/mL.*

EXPERIMENTAL SECTION

Eight adults in apparent good health (two females and six males, weighing 46–98 kg, 26–35 years old), received 1.5 g of acetaminophen in solution[1] orally, after an overnight fast. Seven of these subjects received acetaminophen a second time, 8 months later, after a light, low-fat breakfast (as part of another study). The subjects were drug-free for at least 4 d prior to the study. Urine was collected from 1 to 3 h after administration of the drug, and a blood sample was obtained at the midpoint of the urine collection period. Urine and serum samples were stored at −20°C until assayed. The concentrations of acetaminophen and its conjugates were determined by a slightly modified version of the HPLC assay of Adriaenssen and Prescott (9). A C_{18} column[2] with a mobile phase of 10% methanol and 1% acetic acid in 0.1 M potassium dihydrogen phosphate solution was used. The assay has a sensitivity limit of ~0.1 μg/mL (in terms of acetaminophen) for acetaminophen, acetaminophen sulfate, and acetaminophen glucuronide. Serum and urine were also assayed for creatinine by a modified picrate method[3].

Renal clearance values were determined by dividing the urinary excretion rate of acetaminophen, its conjugates, or creatinine by the midpoint serum concentration of the respective compound. Clearance ratios were calculated by dividing the clearance of acetaminophen or its conjugates by the creatinine clearance. Body surface area was estimated by means of a nomogram (10) based on body weight and height.

Multiple regression analysis was used to determine the relationships between the renal clearances of acetaminophen, or its conjugates, and urine flow rate, creatinine clearance, and serum concentration (11). Bivariate linear regression equations were determined by the perpendicular least-squares method, in which it is assumed that both variables are subject to error (12).

Serum protein binding measurements were made by equilibrium dialysis at 37°C against an equal volume, 0.3 mL, of 0.13 M phosphate buffer (pH 7.4) and by ultrafiltration. In the equilibrium dialysis studies, acetaminophen and its conjugates were added to the buffer phase in amounts designed to produce serum concentrations similar to those found in the study samples. The buffer solutions were dialyzed against pooled blank human serum or solutions of crystalline human albumin[4]; also, blank buffer was dialyzed against samples of pooled serum obtained in this study. Preliminary experiments showed that the optimal equilibration time for acetaminophen, acetaminophen glucuronide, and acetaminophen sulfate was 6–8 h. The protein binding of acetaminophen, acetaminophen glucuronide, and acetaminophen sulfate over the concentration ranges of 0.10–1.15 mM, 0.04–0.52 mM, and 0.11–1.22 mM, respectively, in human albumin solutions of varying concentrations (1.57–4.79 g/dL) was determined. Tris buffer (0.16 M) was used instead of phosphate buffer in some of these experiments.

[1] Tylenol Elixir; McNeil Lab, Inc., Fort Washington, Pa.
[2] μ-Bondapak C_{18}; Waters Associates, Milford, Mass.
[3] Creatinine Kit (No. 555-A); Sigma Chemical Co., St. Louis, Mo.
[4] Calbiochem-Behring, La Jolla, Calif.

0022-3549/84/0800-1038$01.00/0
© 1984, American Pharmaceutical Association

Table I—Renal Clearance of Acetaminophen, Acetaminophen Glucuronide, and Acetaminophen Sulfate in Normal Adults [a]

Excretion Product	Renal Clearance, mL/min/1.73 m²	Clearance Ratio[b]
Acetaminophen	6.32 ± 1.93 (3.26-8.92)	0.058 ± .026 (0.030-.103)
Acetaminophen glucuronide	100 ± 13.6 (80.9-120)	0.890 ± .153 (0.770 ± 1.16)
Acetaminophen sulfate	161 ± 30.6[c] (116-200)	1.43 ± .250[c] (1.05-1.86)

[a] Results expressed as mean ± *SD* (range), $n = 8$, based on clearance values for each subject, which are the average of two determinations made on separate occasions. The average renal clearance of creatinine ranged from 75.5 to 135 mL/min/1.73 m², and average urine flow rates ranged from 15 to 75 mL/h/1.73 m². [b] Relative to creatinine. [c] One outlier with an average renal clearance of 74.9 mL/min/1.73 m² and an average clearance ratio of 0.628 was excluded.

Ultrafiltration studies were performed with solutions of acetaminophen and its conjugates in pH 7.4 isotonic phosphate buffer (to examine the possibility of membrane binding) and with serum obtained following the administration of acetaminophen. Approximately 2 mL of buffer solution or serum was placed in cellulose tubing[5] (0.83 mm o.d., molecular exclusion limit of 12,000–14,000 Da) which was mounted in stoppered plastic centrifuge tubes. The tubes were centrifuged at 750×*g* for 30 min at 37°C, and 0.10–0.15 mL of ultrafiltrate was collected (13).

Acetaminophen sulfate was synthesized in our laboratory[6] by the method of Feigenbaum and Neuberg (14), and acetaminophen glucuronide was supplied[7] (15). Total protein concentrations were determined by the biuret method (16), and the albumin fraction was determined by electrophoresis[8].

RESULTS

The creatinine clearance values of the subjects in this study ranged from 74 to 139 mL/min/1.73 m². Urine flow rates ranged[9] from 15 to 110 mL/h/1.73 m². The renal clearance values for acetaminophen, acetaminophen glucuronide, and acetaminophen sulfate and the corresponding renal clearance ratios relative to creatinine are summarized in Table I[10]. The renal clearance ratio of acetaminophen sulfate was consistently larger than unity, indicative of net renal tubular secretion. The renal clearance ratio of acetaminophen was quite small, reflecting extensive renal tubular reabsorption since (as will be shown) the serum protein binding of the drug is very limited. The body surface area-normalized renal clearance of acetaminophen increased with increasing normalized urine flow rate ($r = 0.577$, $p < 0.05$), but the urine flow rate had no apparent effect on the renal clearances of acetaminophen glucuronide or acetaminophen sulfate.

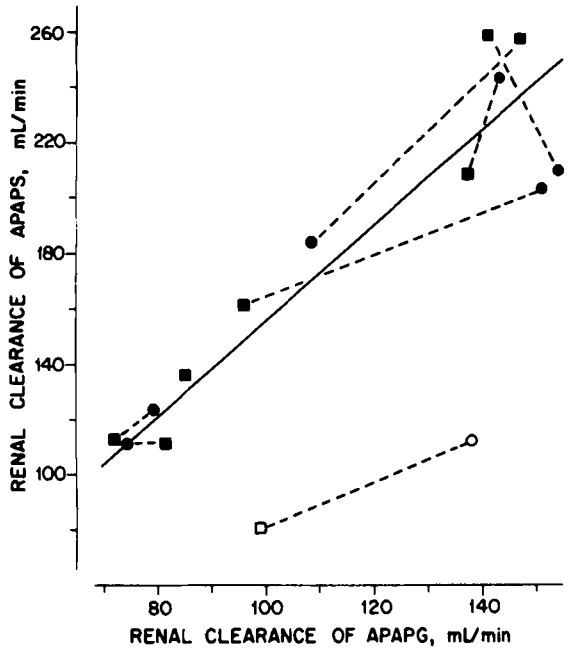

Figure 2—*Relationship between the apparent renal clearances of acetaminophen sulfate (APAPS) and acetaminophen glucuronide (APAPG); r = 0.928, p < 0.001. Seven of the eight subjects received acetaminophen on two separate occasions [first dose (■), second dose (●)], and the two data points for any one subject are connected by a dashed line. The open symbols are the data points for one outlier, which were not included in the statistical analysis.*

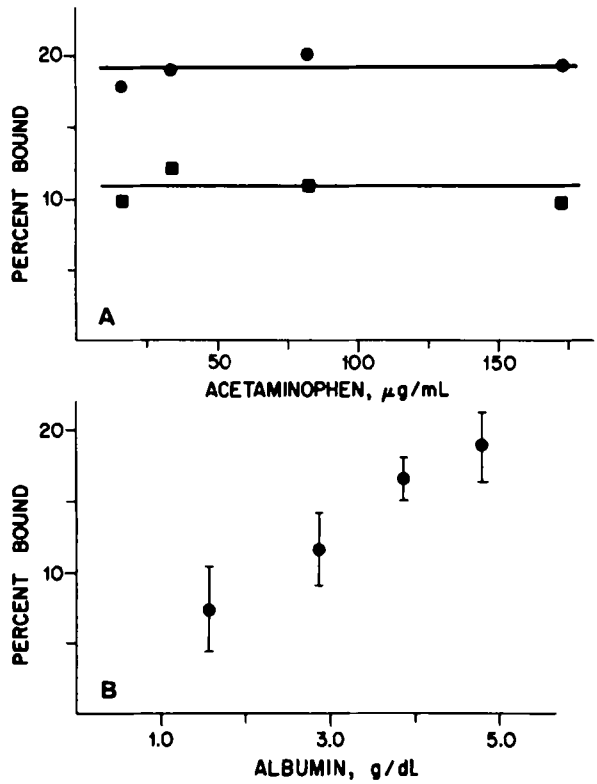

Figure 3—*Protein binding of acetaminophen in human albumin solution, determined by equilibrium dialysis. (A) Binding of acetaminophen over the concentration range of 15–174 μg/mL in 4.79 g/dL (●) and 2.88 g/dL (■) albumin solution. (B) Binding (mean ± SD, n = 9) of acetaminophen over the same drug concentration range in albumin solutions of 1.57, 2.88, 3.88, and 4.79 g/dL.*

The normalized renal clearance of acetaminophen sulfate decreased with increasing serum concentration of this conjugate (Table II and Fig. 1). A similar negative correlation ($r = -0.771$, $p < 0.01$) was found with respect to the acetaminophen sulfate-to-creatinine clearance ratio and acetaminophen sulfate serum concentration for concentrations <0.06 mM (this excludes a total of three sets of data from two subjects), but the correlation was not statistically significant when all data were included. There was no apparent correlation between normalized renal clearance and serum concentration in the cases of acetaminophen and acetaminophen glucuronide, respectively (Table II). Also, there was no statistically significant correlation between the normalized renal clearance of either conjugate and the serum concentration of acetaminophen.

The absolute renal clearances of acetaminophen glucuronide and acetaminophen sulfate for individual subjects (except one outlier) were strongly correlated (Fig. 2). A statistically significant correlation was found also with respect to normalized clearance values for the individual subjects ($r = 0.876$, $p < 0.001$), again excluding the one outlier. The latter individual yielded, on two occasions, significantly lower renal clearance values for acetaminophen sulfate than any of the other subjects in the study, but renal clearance values for acetaminophen glucuronide (Fig. 2) and the serum-free fraction of acetaminophen sulfate (≃0.4) for this subject were in the normal range.

Neither acetaminophen nor acetaminophen glucuronide was significantly protein bound in the serum of subjects who had taken acetaminophen or in human albumin solution and blank serum to which these compounds had been added *in vitro* (Table III). On the other hand, acetaminophen sulfate was

[5] Union Carbide Corp., New York, N.Y.
[6] By Dr. R. E. Galinsky.
[7] Dr. Leonard Weintraub of Bristol-Myers Products, Hillside, N.Y.
[8] Gelman Sepratek Electrophoresis System.
[9] This range is based on individual determinations while the ranges in Table I are averages of two determinations per subject.
[10] Individual urine and serum concentration data are available on request.

Table II—Concentration Dependence of the Renal Clearance and Clearance Ratio of Acetaminophen, Acetaminophen Glucuronide, and Acetaminophen Sulfate [a]

	Range of Serum Conc., mM	Range of Clearance, mL/min/1.73 m²	Range of Clearance Ratio[c]	Correlation Coefficient	
				Clearance	Clearance Ratio
Acetaminophen	0.070–0.200	3.26–11.3	0.030–0.127	0.095	0.229
Acetaminophen glucuronide	0.052–0.134	71.7–132	0.530–1.169	−0.104	−0.086
Acetaminophen sulfate[b]	0.018–0.083	115–233	0.889–2.12	−0.718[d]	−0.145

[a] Ranges and correlation analyses based on 15 individual sets of values from eight subjects (all but one subject participated in two studies). One mM of acetaminophen glucuronide and acetaminophen sulfate is equal to 327 mg/L and 231 mg/L, respectively. [b] One outlier (see footnote c in Table I) was excluded. [c] Relative to creatinine. [d] $p < 0.01$.

appreciably (>50%) protein bound in all of these fluids. These results, obtained by equilibrium dialysis, were confirmed by ultrafiltration experiments. For example, the serum free fraction value (mean ±*SD*, $n = 3$ or 4) of acetaminophen sulfate was 0.460 ± 0.021 by equilibrium dialysis and 0.425 ± 0.021 by ultrafiltration. Preliminary ultrafiltration experiments with protein-free aqueous solutions of acetaminophen and its two conjugates yielded average "free fraction" values consistently near unity (0.988–1.07), indicative of negligible binding to the cellophane membrane. Freezing and thawing of serum (one or two times) had no apparent effect on the protein binding of acetaminophen and its conjugates.

The albumin binding of acetaminophen was independent of drug concentration over a wide range, but increased with increasing albumin concentration (Fig. 3). On the other hand, the albumin binding of acetaminophen sulfate decreased with increasing concentration of the conjugate and increased with increasing albumin concentration (Fig. 4). The protein binding of acetaminophen glucuronide was very low (<10%) and not significantly affected by its concentration or by the concentration of albumin[11].

DISCUSSION

Acetaminophen, in nontoxic doses, has no apparent effect on renal creatinine clearance in humans (17) and on glomerular filtration rate and other indices of renal function in experimental animals (18–20). Consistent with previous reports (7, 8), the renal clearance of unmetabolized acetaminophen is quite low despite its negligible serum protein binding and is positively correlated with urine flow rate (7). It is also independent of acetaminophen concentration in the serum, at least under the conditions of this investigation. These observations confirm studies in dogs which have shown that acetaminophen undergoes glomerular filtration and renal tubular reabsorption by simple diffusion (4). The mean renal clearance of acetaminophen obtained in this investigation, 6.32 ± 1.93 mL/min/1.73 m², is somewhat lower than that reported by Prescott *et al.* (8) for 12 normal subjects (11.9 ± 4.9 mL/min/67 kg average body weight). This may be due to different urine flow rates in the two studies. In general, small differences in the average renal clearances of acetaminophen and its major metabolites, observed in this investigation and in that by Prescott *et al.* (8), may be due to the fact that the data reported here are based on a single serum concentration determination at the midpoint of a 2-h urine collection period while Prescott *et al.* employed the usually preferable area-under-the-curve method. However, the latter method would not reveal concentration dependence of renal clearance if the determinations are based on the total area under the plasma concentration–time curve and total urinary excretion. The conditions of the present study (*i.e.*, a constant absolute dose given to subjects of widely differing body weight) facilitated assessment of the possible serum concentration dependence of the renal clearances.

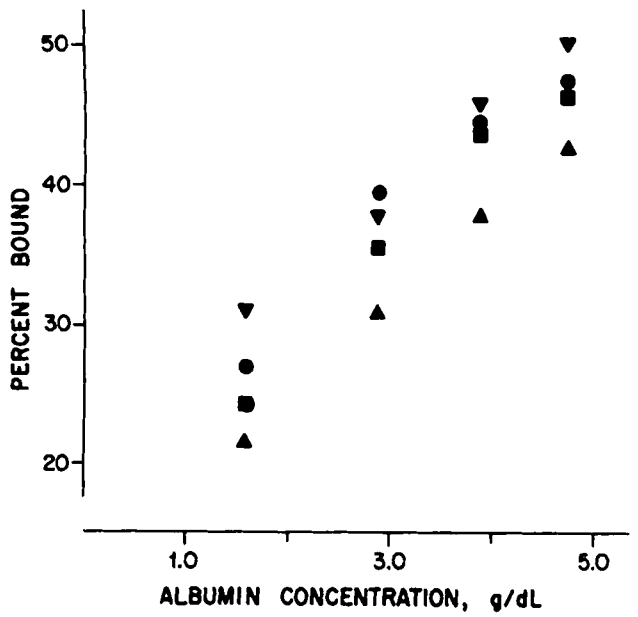

Figure 4—*Protein binding of acetaminophen sulfate in human albumin solutions (1.57, 2.88, 3.88, and 4.79 g/dL), determined by equilibrium dialysis, at acetaminophen sulfate concentrations of 1.22 ± 0.040 mM (mean ± SD) (▲), 0.564 ± 0.038 mM (■), 0.252 ± 0.021 mM (●), and 0.107 ± 0.007 mM (▼).*

[11] Unpublished results.

Renal clearance values for the acetaminophen glucuronide and sulfate conjugates determined following administration of acetaminophen, rather than of the conjugates themselves, must be considered, in principle, as estimates of apparent renal clearances. This is because studies on isolated perfused rat kidneys (18–20) and isolated rat kidney cells (21) have shown that renal tissues form acetaminophen glucuronide and sulfate conjugates, albeit at very low rates. These conjugates do not appear in the perfusate of isolated kidneys, but are immediately excreted in the urine. It is likely that the renal contribution to acetaminophen conjugation is also quantitatively negligible in humans since the elimination of acetaminophen by biotransformation is not impaired in anephric patients (22).

Previous studies by Duggin and Mudge in dogs (4) and by Lin and Levy in rats (6) have shown that the renal clearance of acetaminophen sulfate is substantially higher than glomerular filtration rate at low serum concentrations of the conjugate and that the renal clearance decreases with increasing serum concentration. The present study in humans also yielded renal clearance ratios, relative to creatinine, appreciably higher than unity. This demonstrates that acetaminophen sulfate is subject to renal tubular secretion. While, in theory, similar results may be obtained if the conjugate was excreted only by glomerular filtration and formed at a high rate in the renal tissues, that possibility is unlikely in view of the evidence reviewed in the preceding paragraph. Moreover, there was no relationship between the normalized apparent renal clearance of acetaminophen sulfate and the serum concentration of acetaminophen. A relationship would be expected had there been appreciable renal synthesis of the conjugate. The renal clearance value obtained in this study (161 ± 30.6 mL/min/1.73 m²) is in good agreement with that of Prescott *et al.* (166 ● 29 mL/min) in 12 healthy volunteers, with an average body weight of 67 kg, who received a single dose of acetaminophen, 20 mg/kg (8). More direct comparison is not possible since Prescott *et al.* did not report individual or normalized average values or glomerular filtration rates.

The apparent renal clearance of acetaminophen glucuronide determined in this study, 100 ± 13.6 mL/min/1.73 m², is also in reasonable agreement

Table III—Serum Protein Binding of Acetaminophen, Acetaminophen Glucuronide, and Acetaminophen Sulfate [a]

	Free Fraction		
	Acetaminophen	Acetaminophen Glucuronide	Acetaminophen Sulfate
Serum after administration of acetaminophen	0.819 ± 0.018	0.923 ± 0.009	0.460 ± 0.021
Human albumin, 5%	0.818 ± 0.013	0.928 ± 0.012	0.469 ± 0.019
Blank serum	0.780 ± 0.020	0.916 ± 0.019	0.391 ± 0.016
	0.844 ± 0.017[b]	0.954 ± 0.019[b]	0.387 ± 0.015[b]

[a] Results expressed as mean ±*SD* ($n = 3$). Serum was dialyzed for 6–8 h at 37°C against isotonic phosphate buffer, pH 7.4. The approximate concentrations of acetaminophen, acetaminophen glucuronide, and acetaminophen sulfate at equilibrium were 0.09, 0.06, and 0.05 mM, respectively, in serum from medicated subjects, and 0.2, 0.1, and 0.05 mM in albumin solution and blank serum. [b] Determined by 6-h dialysis against Tris buffer instead of phosphate buffer.

with that of Prescott *et al.* (8), 131 ± 22 mL/min, but did not, on the average, exceed creatinine clearance. However, there were four individual renal clearance ratio values (of two subjects) above unity: the highest of these was 1.17. Thus, the results of the present study do not provide strong evidence for renal tubular secretion of acetaminophen glucuronide, perhaps because of the opposing effects of tubular secretion and reabsorption. Duggin and Mudge (4) found that acetaminophen glucuronide is subject to both processes in the dog.

This investigation revealed a striking positive correlation between the renal clearances of acetaminophen glucuronide and acetaminophen sulfate in normal human subjects. Such correlation could reflect the existence of a common renal tubular secretory (transport) process for the two conjugates. Alternatively, the secretion rate of both conjugates could be blood flow rate dependent, either in terms of overall renal blood flow or with respect to the blood perfusion of the secretory region of the kidneys. We favor the second of these alternatives because of evidence suggesting separate renal transport processes for the two conjugates. First, probenecid has been found to inhibit the net renal tubular secretion of acetaminophen sulfate, but not that of the glucuronide, in dogs (4). Second, the present investigation identified one apparently healthy male subject, with normal creatinine, inorganic sulfate (17), and acetaminophen glucuronide renal clearances, but markedly subnormal renal clearance of acetaminophen sulfate during two experiments ~8 months apart. Such selectivity suggests a dissociation of the secretory processes for acetaminophen glucuronide and sulfate or, alternatively, the existence of separate specialized reabsorption processes together with a common or separate process(es) for renal tubular secretion of the two conjugates.

The serum protein binding of acetaminophen and acetaminophen glucuronide is very limited, so that correction of the renal clearance values of these compounds for protein binding will have only a quantitatively small effect. On the other hand, acetaminophen sulfate was found to be appreciably bound to serum proteins, so that its renal clearance referenced to the unbound metabolite would be more than double the value reported in Table III. While the limited protein binding of acetaminophen and acetominophen glucuronide is consistent with the results of previous studies (4, 22, 23), one of these studies had also indicated that acetaminophen sulfate binding to serum proteins is similarly negligible. Consequently, the protein binding of acetaminophen sulfate was examined in considerable detail in this investigation. Appreciable (>50%) binding was found by equilibrium dialysis and ultrafiltration, with good agreement between the results of the two methods. These binding experiments were performed on serum obtained from acetaminophen-treated subjects, blank serum with acetaminophen and its two major conjugates added *in vitro*, and human albumin solution with added acetaminophen and conjugates. All of these fluids yielded similar free fraction estimates. Moreover, protein binding was also determined in serum from rats pretreated with acetaminophen, with the following average results (percent binding, concentration): acetaminophen 23%, 0.55 mM; acetaminophen glucuronide 5%, 0.15 mM; acetaminophen sulfate 65%, 0.28 mM. Several studies by other investigators have shown that various organic sulfate esters are extensively bound to plasma proteins (24–26).

Acetaminophen is almost entirely metabolized to the glucuronide and sulfate conjugates under ordinary conditions, and these conjugates are excreted in the urine. Renal failure results, therefore, in substantial accumulation of these metabolites in plasma (22). The present study provides information relevant to the elimination of these metabolites by human subjects with normal renal function under conditions yielding serum concentrations of acetaminophen and its glucuronide and sulfate conjugates in the usual therapeutic range.

REFERENCES

(1) J. T. Slattery and G. Levy, *Clin. Pharmacol. Ther.*, **25,** 185 (1979).

(2) G. Levy and H. Yamada, *J. Pharm. Sci.*, **60,** 215 (1971).

(3) G. Levy and C.-G. Regardh, *J. Pharm. Sci.*, **60,** 608 (1971).

(4) G. G. Duggin and G. H. Mudge, *Br. J. Pharmacol.*, **54,** 359 (1975).

(5) R. E. Galinsky and G. Levy, *J. Pharmacol. Exp. Ther.*, **219,** 14 (1981).

(6) J. H. Lin and G. Levy, *J. Pharmacol. Exp. Ther.*, **225,** 653 (1983).

(7) L. F. Prescott and N. Wright, *Br. J. Pharmacol.*, **49,** 602 (1973).

(8) L. F. Prescott, J. A. J. H. Critchley, M. Balali-Mood, and B. Pentland, *Br. J. Clin. Pharmacol.*, **12,** 149 (1981).

(9) P. I. Adriaenssen and L. F. Prescott, *Br. J. Clin. Pharmacol.*, **6,** 87 (1978).

(10) K. Diem and C. Lentner (Eds.), "Documenta Geigy Scientific Tables," Ciba-Geigy Ltd., Basle, Switzerland, 1970, p. 537.

(11) J. Frane, in "BMDP Statistical Software, 1981," W. J. Dixon, Ed., University of California Press, Berkeley, 1981, pp. 264–277.

(12) D. S. Riggs, J. A. Guarnieri, and S. Adelman, *Life Sci.*, **22,** 1305 (1978).

(13) R. C. Chou and G. Levy, *J. Pharm. Sci.*, **71,** 471 (1982).

(14) J. Feigenbaum and C. A. Neuberg, *J. Am. Chem. Soc.*, **63,** 3529 (1941).

(15) L. Weintraub, S. R. Oles, A. Wilson, and L. Wilson, *J. Chem. Soc. C*, **1969,** 1562.

(16) A. G. Gornall, C. J. Bardawill, and M. M. David, *J. Biol. Chem.*, **177,** 751 (1948).

(17) M. E. Morris and G. Levy, *Clin. Pharmacol. Ther.*, **33,** 529 (1983).

(18) B. Ross, J. Tange, K. Emslie, S. Hart, M. Smail, and I. Calder, *Kidney Internat.*, **18,** 562 (1980).

(19) J. F. Newton, W. E. Braselton Jr., C.-H. Kuo, W. M. Kluwe, M. W. Gemborys, G. H. Mudge, and J. B. Hook, *J. Pharmacol. Exp. Ther.*, **221,** 76 (1982).

(20) K. R. Emslie, M. C. Smail, I. C. Calder, S. J. Hart, and J. D. Tange, *Xenobiotica*, **11,** 43 (1981).

(21) D. P. Jones, G.-B. Sundby, K. Ormstad, and S. Orrenius, *Biochem. Pharmacol.*, **28,** 929 (1979).

(22) D. T. Lowenthal, S. Øie, J. C. van Stone, W. A. Briggs, and G. Levy, *J. Pharmacol. Exp. Ther.*, **196,** 570 (1976).

(23) B. G. Gazzard, A. W. Ford-Hutchinson, M. J. H. Smith, and R. Williams, *J. Pharm. Pharmacol.*, **25,** 964 (1973).

(24) D. Y. Wang and R. D. Bulbrook, *J. Endocrinol.*, **39,** 405 (1967).

(25) J. E. Plager, *J. Clin. Invest.*, **44,** 1234 (1965).

(26) C. G. Curtis, D. J. Hearse, and G. M. Powell, *Xenobiotica*, **4,** 595 (1974).

ACKNOWLEDGMENTS

Supported in part by grant GM 19568 from the National Institute of General Medical Sciences, National Institutes of Health, and by a fellowship for M. E. Morris from the Graduate School of State University of New York at Buffalo.

Kinetics of Partitioning and Binding of Digoxin and Its Analogues in the Subcompartments of Blood

PETER H. HINDERLING

Received April 12, 1982, from the *Department of Pharmacology, Biocenter, University of Basle, 4056 Basle, Switzerland.* Accepted for publication March 10, 1983. Present address: F. Hoffmann-La Roche & Co., Grenzacherstrasse 124, Basle CH-4002, Switzerland.

Abstract □ The kinetics of digoxin and analogues (metabolites) in the subcompartments of blood, erythrocytes and plasma, were first order and concentration independent. The rate and extent of red blood cell partitioning of the tested compounds were, according to first-order kinetics, identical in the presence and absence of structurally related compounds and dependent on lipophilicity and temperature; red blood cell penetration was a reversible process. Erythrocyte partitioning of digoxin and its analogues was postulated to be by passive diffusion. There was significant intracellular binding of the compounds, and hemoglobin was the major ligand. The kinetics of red blood cell partitioning of the individual compounds were fitted according to a closed two- or three-compartment model. The latter indicated the existence of two kinetically separable compartments within the red blood cells. Model-independent mean transit times of red blood cell–plasma water partitioning of the compounds depended largely on the lipophilicity and were a thousand times greater for the least lipophilic analogues than for the most lipophilic derivatives. Red blood cell partitioning of digoxin and its metabolites under *in vivo* and *in vitro* conditions, were equivalent. Plasma protein binding of the tested compounds was concentration independent, unaltered in the presence of the analogues, and temperature independent between 24°C and 37°C. Binding to albumin in buffer solution was significantly larger than to albumin in plasma for all the compounds. Binding of digoxin and its analogues to albumin in buffer solution increased with increasing lipophilicity of the compounds.

Keyphrases □ Digoxin—kinetics of red blood cell partitioning, plasma protein binding, analogues □ Red blood cell partitioning—digoxin and analogues, kinetics, plasma protein binding □ Plasma protein binding—digoxin and analogues, kinetics of red blood cell partitioning □ Kinetics—digoxin and analogues in blood, plasma protein binding, red blood cell partitioning

The overall goal of the present study was the further (1) elucidation of the kinetics of digoxin (I) and its analogues (*i.e.*, metabolites) in the subcompartments of blood, plasma and red blood cells (Scheme I). The individual goals were to (*a*) delineate the kinetics of red blood cell partitioning, (*b*) investigate the influence of temperature and drug lipophilicity on cellular uptake, (*c*) assess the gross intracellular distribution of the compounds, and (*d*) make a comparative study of the binding of the compounds to albumin and plasma protein.

Special emphasis was put on the delineation of the kinetics of red blood cell partitioning of the tested compounds. A review of the pharmacokinetic literature on this subject indicated that the significance of the kinetics of drugs in this subcompartment of blood has not been adequately appreciated by pharmacokineticists. The extent of red blood cell uptake has been determined for drugs in some studies; the rate of such uptake has been studied only exceptionally (2). Often tacit assumptions have been made that either red blood cell partitioning of the drug is negligible or equilibration between plasma and cells is instantaneous if drug uptake into the erythrocytes is significant. Concentrations of drugs usually have been assessed in plasma, not whole blood, in pharmacokinetic studies. Obviously, temperature-independent red blood cell partitioning has been presumed for the drugs in most of the studies, since no effort appears to have been made to maintain the temperature of the blood samples after their withdrawal until separation of plasma and erythrocytes. This paper will show conclusively that these *a priori* assumptions are unwarranted and may lead to biased values of pharmacokinetic parameters.

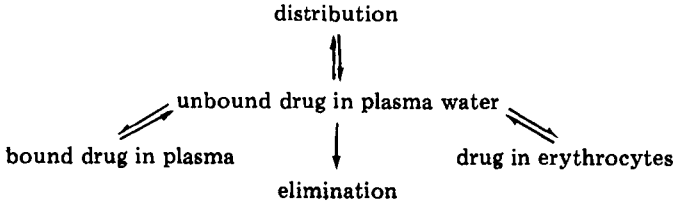

Scheme I—Drug in the blood compartments.

EXPERIMENTAL SECTION

Materials—The following unlabeled and labeled compounds were used: digoxin[1] (I), digitoxin[1] (II), β-methyldigoxin[1] (III), dihydrodigoxin[1] (IV), digoxigenin bis(digitoxoside)[1] (V), digoxigenin digitoxoside[1] (VI), epidigoxigenin[1], digitoxigenin bis(digitoxoside)[1], digitoxigenin digitoxoside[1], digoxin-16′-glucuronide[2] (VII), [12α-^{3}H]digoxin[1], β-methyl[12α-^{3}H]digoxin[1], [12α-^{3}H]digoxigenin bis(digitoxoside)[1], [12α-^{3}H]digoxigenin digitoxoside[1], [21,22-^{3}H]digitoxin[2], dihydro[12α-^{3}H]digoxin[2], and [12α-^{3}H]digoxin-16′-glucuronide[2]. The compounds with the label in the α-position were synthesized according to the method of von Wartburg *et al.* (3) and had the following specific activities: [^{3}H]I, 1460 μCi/mg; [^{3}H]III, 910 μCi/mg; [^{3}H]IV, 12,772 μCi/mg; [^{3}H]V, 552 μCi/mg; [^{3}H]VI, 457 μCi/mg; [^{3}H]VII, 1570 μCi/mg. [^{3}H]II was synthesized according to the method of Haberland and Merten (4) and had a specific activity of 509 μCi/mg. The radiochemical purities of the labeled compounds were investigated using different TLC systems, as described elsewhere (5, 6), and were: [^{3}H]I, >94.5%; [^{3}H]II, 100%; [^{3}H]III, >95.9%; [^{3}H]IV, 100%; [^{3}H]V, >92.5%; [^{3}H]VI, >95.9%; [^{3}H]VII, >98.0%.

n-Octanol was obtained commercially[3]; heparinized (5 USP U/mL) or citrated (3.69 mg/mL sodium citrate and 0.46 mg/mL citric acid) blood and plasma samples were obtained from healthy volunteers who had no prior drug intake[4] for 168 h. Human albumin (fraction V, fatty acid free) (AB_1[5] AB_2[6]) and hemoglobin (HB)[5] (type IV, crystalized twice) were purchased. Three different buffers were used: (*a*) 0.067 M KH_2PO_4, 0.067 M Na_2HPO_4, and 0.113 M NaCl (pH 7.4, 0.300 Osmol, ionic strength: 0.23) (7), (*b*) 0.001 M KH_2PO_4, 0.001 M Na_2HPO_4, 0.157 M NaCl, 0.006 M glucose, 0.004 M KCl, 0.003 M $CaCl_2$, and 0.002 M $MgCl_2$ (pH 7.2, 0.356 Osmol, ionic strength: 0.18), and (*c*) 0.05 M Tris, 0.042 M HCl, and 0.060 M NaCl (pH 7.4, 0.304 Osmol, ionic strength: 0.15). Buffers b and c represented a slight modification of the original buffers employed previously (8, 9).

Determination of Apparent Octanol–Water Partition Coefficients of Digoxin and Analogues—Partition coefficients were determined for [^{3}H]I–[^{3}H]VII at 24°C using twice-distilled water ([^{3}H]I–[^{3}H]VI) or phosphate buffer *a* ([^{3}H]VII). The octanol was allowed to equilibrate with water with gentle shaking for 24 h. Only water-saturated octanol and octanol-saturated water were used in the partitioning experiments. The experiments were performed in 15-mL tubes equipped with glass stoppers. The compounds were added to tubes containing, initially, only the water phase (2.5 mL) spiked with drug concentrations of 40 ng/mL ([^{3}H]I, [^{3}H]III–[^{3}H]VI), 100 ng/mL ([^{3}H]II), and 200 ng/mL ([^{3}H]VII); the octanol phases were added subsequently. The stoppered tubes were then shaken vigorously for 45 min. Preliminary experiments had indicated that this time permitted the compounds to reach equilibrium. After centrifugation, the phases were separated and aliquots (200 μL) were taken from both phases for determination of radioactivity. Two experiments were performed with each of the compounds tested.

[1] Boehringer Mannheim, FRG.
[2] Beiersdorf, Hamburg, FRG.
[3] Fluka AG, Buchs, Switzerland.
[4] Blood Bank, Kantonsspital, Basel, Switzerland.
[5] Miles Laboratories, Elkhart, Ind.
[6] Sigma Chemical Co., St. Louis, Mo.

0022-3549/84/0800-1042$01.00/0
© 1984, American Pharmaceutical Association

Table I—Apparent Erythrocyte–Buffer and Erythrocyte–Plasma Partition Coefficients for Digoxin and Analogues at Different Temperatures[a]

Compounds[b]	37°C	n[c]	24°C	n[c]	14°C	n[c]	4°C	n[c]
[^{3}H]II	2.51 ± 0.061	3	1.95 ± 0.097	5	1.59	1	1.23 ± 0.124	8
	0.090 (0.084, 0.097)	2	0.055 (0.046, 0.064)	2				
[^{3}H]III	1.28 (1.23, 1.33)	2	1.11 ± 0.027	3			0.877 ± 0.095	5
	0.946 (0.917, 0.976)	2	0.882 (0.842, 0.922)	2				
[^{3}H]IV	1.47 (1.44, 1.49)	2	1.34 ± 0.027	4			0.900 ± 0.104	4
	1.09 (1.03, 1.15)	2	1.02 ± 0.013	4				
[^{3}H]I	1.49 ± 0.031	3	1.29 ± 0.056	7			0.884 ± 0.032	7
	1.13 (1.06, 1.19)	2	0.997 ± 0.026	3				
[^{3}H]V	1.31 (1.30, 1.32)	2	1.15 ± 0.061	4			0.875 ± 0.009	4
	1.01 (0.95, 1.07)	2	0.862 ± 0.010	3				
[^{3}H]VI	1.21 ± 0.031	4	1.19 ± 0.032	3	1.02	1	0.932 ± 0.043	3
	0.966 ± 0.028	3	0.838 ± 0.045	3				
[^{3}H]VII	0.762	1						
	0.625	1						

[a] Mean ± *SD*; individual values are reported in parentheses. The upper value is P_{e/c_u}; the lower value is $P_{e/c}$. [b] In order of decreasing lipophilicity. [c] Number of mean values considered; averages of 3–5 individual determinations in blood of 1–7 donors.

Erythrocyte Partitioning of Digoxin and Analogues—The goals of these experiments were to investigate the red blood cell–buffer or –plasma distribution of the compounds prior to and at partition equilibrium, and to determine whether the partitioning was temperature dependent. The experiments used erythrocytes obtained from different donors (n = 2–8) for the partitioning of each individual compound.

Erythrocyte suspensions in buffer *a* or in plasma, with physiological hematocrits of 40% (10), were employed. The procedure used for the determination of drug partitioning into red blood cells was the centrifugal method, which has previously been described in detail (7). Briefly, the suspensions had volumes of 10 mL and were kept in 15-mL glass-stoppered tubes. Immediately after drug addition, the tubes containing the suspensions were shaken vigorously for 15 s and were then rotated for the duration of the experiments. Samples of the suspensions were taken as early as possible following drug addition (≥0.3 min) and at appropriate intervals thereafter. The samples were immediately centrifuged for intervals ranging from 0.5 (early samples) to 5 min (later samples). The time of removal of the separated buffer or plasma phases was taken as the sampling time. The concentrated erythrocyte phases had hematocrits ranging between 50 and 95%. Aliquots (100–500 μL) were taken from the separated erythrocyte, buffer, or plasma phases, and the radioactivity was determined.

Erythrocyte buffer partitioning studies were conducted at 37°C, 24°C, and 4°C with all the labeled compounds; additional experiments at 14°C were performed with [^{3}H]II and [^{3}H]VI. Erythrocyte plasma partitioning was investigated at 37°C and 24°C with all the labeled compounds. The temperatures were maintained throughout the experiments, including the final centrifugation of the red blood cell suspensions. The pH was in the 7.35–7.45 range. Only fresh erythrocyte suspensions were used. For a delineation of the type of kinetics involved, the partitioning of all the compounds with the exception of [^{3}H]VII was investigated systematically at 24°C at drug concentrations of 5, 10, and 100 ng/mL. Additional experiments at 24°C studied the red blood cell partitioning of the (labeled) compounds (10 ng/mL) in the presence of the (unlabeled) analogues (100 ng/mL each). Reversibility of red blood cell partitioning was checked at 24°C by resuspending drug-containing erythrocytes in fresh buffer *a* (11).

The stability of the compounds during their incubation with erythrocytes in buffer or plasma at 37°C was checked for all compounds except [^{3}H]II. Plasma and buffer aliquots taken at different times after incubation were analyzed by specific column chromatography or TLC, as described previously (6). The results showed that the compounds were stable under these experimental conditions. Estimates for the precision of the red blood cell partitioning values were obtained by repetitive determination of the ratios of the erythrocytes to buffer or plasma concentrations in suspensions with red blood cells from a particular donor. The coefficient of variation (CV) values ranged between 1 and 8% for the compounds, except [^{3}H]II. Considerably larger CV values (20–80%) were obtained for this compound with red blood cell plasma suspensions. This was due to the comparatively low erythrocyte concentrations of this drug in the plasma suspensions.

The possible influence of buffer composition on red blood cell partitioning of [^{3}H]I and its analogues was also studied. Red blood cells from different donors were divided up in equal parts and suspended either in buffer *a* or buffer *c*. Red blood cell partitioning from the two buffers at 37°C was then studied with all the compounds except [^{3}H]VII. The results of these experiments showed that red blood cell partitioning from buffer *a* was significantly larger than from buffer *c* for all the compounds tested, although the respective mean red blood cell-to-buffer concentration ratios differed by only 1–15%. These results indicated that red blood cell partitionings of the nonelectrolytic [^{3}H]I–[^{3}H]VI were influenced by buffer composition. Differences in ionic strength, pH, and molecular composition of the two buffers used may have been responsible for the observed discrepancy.

Only buffer *a* was used in the definitive partitioning experiments with [^{3}H]I and its analogues. Buffer *a* was preferred because it had been used successfully in the past (7, 12) in equivalent experiments with other compounds and guaranteed a pH equivalent to that in plasma water (13).

***In Vivo* Erythrocyte Partitioning of Digoxin and Metabolites**—Tritiated digoxin (0.6 and 1.2 mg) was administered intravenously (bolus) and orally to three healthy volunteers aged 21–25 years. Blood was obtained over a period of 144 h after administration of the drug. After blood withdrawal, there was a lapse of 30 min before separation of the plasma and erythrocytes. During this interval the samples were kept at a temperature of 24°C. Plasma of the samples was then divided into two parts. In one part [^{3}H]I and its separable, known, apolar metabolites ([^{3}H]IV–[^{3}H]VI) and unknown polar metabolites were assayed by specific methods (6); in the other part, total radioactivity was measured. Total radioactivity was also determined in the separated erythrocytes of the samples.

Binding of Digoxin and Analogues to Hemolysate, Hemoglobin, Albumin, and Plasma Protein—Details of the equilibrium dialysis method employed in these investigations have been reported previously (1). The experiments were performed at 37°C or 24°C and within a pH range of 7.30–7.50. The hemolysate suspensions and the protein solutions were dialyzed against buffer for 6.5 h. Equilibrium between the free drug concentrations in plasma and buffer was established within this time interval. Aliquots (100–500 μL) were then taken from both chambers of the dialysis apparatus, and the radioactivity was determined.

The binding to hemolysate and albumin was investigated for all the compounds. The binding to hemoglobin was studied with [^{3}H]I and [^{3}H]II. Plasma protein binding was investigated with [^{3}H]II, [^{3}H]III, and [^{3}H]VII. The results obtained with [^{3}H]I and [^{3}H]IV–[^{3}H]VI have been reported previously (1).

Hemolysate Binding—Red blood cells from one donor were separated from

Table II—Linearity of the Red Blood Cell Partitioning Kinetics of Digoxin and Analogues at 24°C

Compound[a]	P_{e/c_u}[b]			
	5 ng/mL	10 ng/mL	10 ng/mL[c]	100 ng/mL
[^{3}H]II	1.82 (1.75, 1.87)	2.03 (2.01, 2.06)	1.93 (1.88, 1.97)	2.06 (2.01, 2.10)
[^{3}H]III	1.10 (1.05, 1.14)	1.13 (1.13, 1.13)	1.19 (1.07, 1.30)	1.13 (1.13, 1.13)
[^{3}H]IV	1.39 (1.38, 1.39)	1.36 (1.33, 1.39)	1.31 (1.30, 1.33)	1.35 (1.32, 1.39)
[^{3}H]I	1.29 (1.22, 1.36)	1.35 (1.33, 1.37)	1.26 (1.24, 1.28)	1.31 (1.24, 1.37)
[^{3}H]V	1.15 (1.08, 1.22)	1.14 (1.13, 1.15)	1.17 (1.10, 1.24)	1.19 (1.16, 1.21)
[^{3}H]VI	1.19 (1.13, 1.25)	1.20 (1.18, 1.22)	1.23 (1.22, 1.24)	1.23 (1.22, 1.23)

[a] In the order of decreasing lipophilicity. [b] n (Number of individual values considered) = 2, obtained from one donor. Individual values are in parentheses. [c] Molar ratio of labeled drug to each of the unlabeled analogues = 0.1.

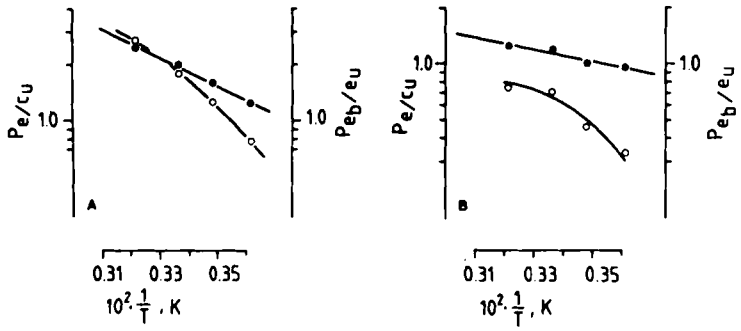

Figure 1—*Semilogarithmic plot of the averaged apparent red blood cell-buffer partition coefficient, P_{e/c_u} (●), and the averaged true red blood cell partition coefficient, P_{e_b/e_u} (○) against the reciprocal of the absolute temperature 1/T for [^{3}H]II (A) and [^{3}H]VI (B). There was an apparent linear dependency of P_{e/c_u} on 1/T in contrast to a nonlinear relationship between P_{e_b/e_u} and 1/T.*

plasma by centrifugation. After removal of the buffy coat, the cells were washed five times and suspended in buffer *a*. Lysis was then induced by exposing the red cells to a temperature of −20°C for 2 h. Membrane-free hemolysates (hemoglobin concentration 140 g/L) were then obtained by ultracentrifugation[7] at 20,000 rpm for 20 min. Binding and/or partitioning to hemolysate was determined for [^{3}H]II (20, 50, and 100 ng/mL) and [^{3}H]I and [^{3}H]III-[^{3}H]VII (20 ng/mL) at 37°C. There was significant net transport of fluid during dialysis, leading to a 10–20% decrease of the initial hemoglobin concentrations in the hemolysates. From 2 to 6 dialysis experiments were run in parallel with the hemolysates for each compound.

Hemoglobin Binding—The binding to hemoglobin was investigated with [^{3}H]I and [^{3}H]II (20 ng/mL) by dialysis against buffer *a* at 37°C. There was significant net transport of fluid during dialysis leading to a 10–20% decrease of the initial hemoglobin concentrations of 140 g/L. The binding to diluted hemoglobin (7 g/L) was also investigated. There was no net transport of fluid in these experiments. Two dialysis experiments were run in parallel.

Albumin Binding—Albumin binding was studied with all the compounds

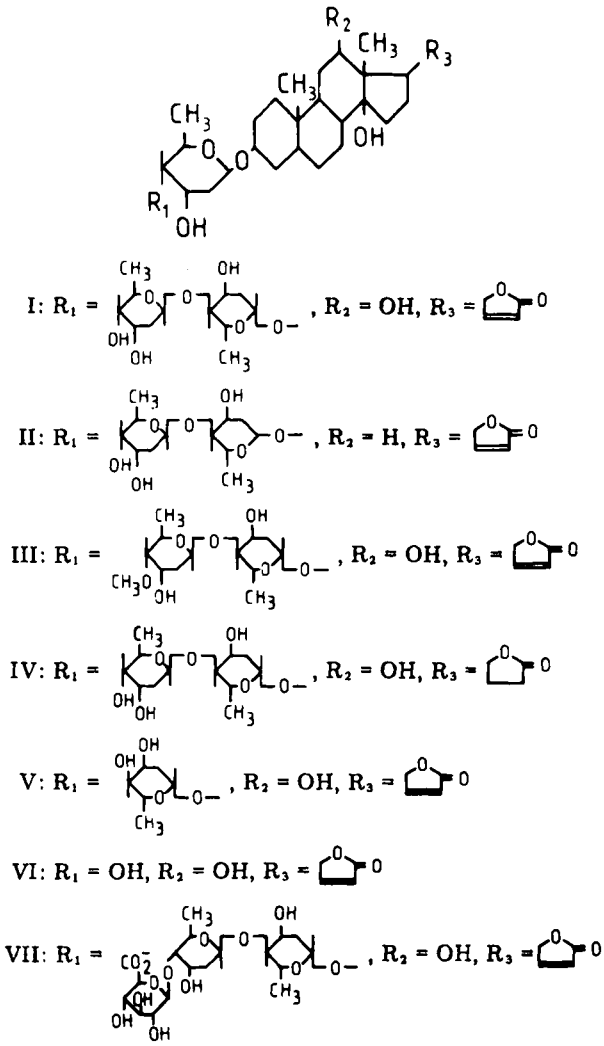

[7] Sorvall Ultracentrifuge, RC-2B; Ivan Sorvall Inc., USA.

(20 ng/mL) at a physiological concentration of the protein (45 g/L) (14). Buffer *a* was used, and the experiments were conducted at 37°C. Albumin AB_1 and AB_2 were employed in these studies: the binding of [^{3}H]II was with both albumins, the binding of [^{3}H]I and [^{3}H]IV-[^{3}H]VI with albumin AB_1, and the binding of [^{3}H]III and [^{3}H]VII with albumin AB_2. Between 2 and 10 dialysis experiments were run with albumin for each compound. The *CV* values of replicate albumin binding determinations were 1% for [^{3}H]II and 3–7% for the rest of the compounds.

Preliminary experiments had shown that binding of [^{3}H]I (20 ng/mL) to albumin was not influenced by the buffer used. [^{3}H]I was 34.2 ± 2.67% (n = 10) and 35.9% (35.2, 36.6; n = 2) bound to albumin when buffers *a* and *c* were used, respectively. This suggested that the [^{3}H]I-albumin interaction was not influenced by the phosphate ion concentration of buffer *a*.

Plasma Protein Binding—Plasma with physiological albumin content (42–54 g/L) (14) obtained from different donors was used. The binding of [^{3}H]III and [^{3}H]VII was studied at concentrations of 5, 10, and 100 ng/mL (initial concentrations after spiking plasma prior to initiation of dialysis) with the plasma of two donors. [^{3}H]II was investigated at concentrations of 100 and 1000 ng/mL with the plasma of seven donors. In addition, the plasma binding of these three labeled compounds in the presence of unlabeled analogues was studied. The plasma binding of [^{3}H]III and [^{3}H]VII (5 ng/mL) was studied in the presence of all the other analogues (unlabeled I–VII, 100 ng/mL each), and the plasma binding of [^{3}H]II (5 and 100 ng/mL) was determined in the presence of unlabeled digitoxigenin bis(digitoxoside) and digitoxigenin digitoxoside (100 ng/mL each). From 4 to 8 dialysis experiments were run in parallel with the plasma of a particular donor for each compound. The *CV* values for replicate determinations of the plasma protein binding were 1% for [^{3}H]II and 7–15% for the rest of the compounds.

Analytical Procedures—The details of the liquid scintillation method used have been given previously (10). Briefly, 100–500-μL aliquots from plasma buffers *a*, *b*, and *c* and octanol were analyzed in duplicate, either directly[8] or after combustion[9]. The radioactivity in erythrocytes, hemoglobin solutions, and hemolysates was measured only after combustion. The red blood cells were lysed prior to combustion. The hemoglobin concentrations in the hemoglobin and hemolysate binding studies were measured spectrophotometrically after transformation to hemoglobin cyanide (15).

RESULTS

The ± values given in the text and in the Tables refer to the standard deviation, *SD*, of the means, and n is the number of observations considered. Values for *SD* and n are only given in the text for mean values which are not listed in the Tables.

Octanol–Water Partition Coefficients of Digoxin and Analogues—Apparent octanol–water partition coefficients at 24°C (P) of [^{3}H]I and its analogues were calculated from the ratio of the concentration in the organic phase to the concentration in the aqueous phase at equilibrium. The mean P values for the individual compounds were (n = 2): [^{3}H]I, 16.6 (16.5, 16.7); [^{3}H]II, 98.2 (96.8, 99.5); [^{3}H]III, 38.6 (38.3, 38.8); [^{3}H]IV, 17.6 (17.5, 17.6); [^{3}H]V, 15.6 (15.2, 16.0); [^{3}H]VI, 11.6 (11.4, 11.8); [^{3}H]VII, 0.024 (0.023, 0.024).

Erythrocyte Partitioning of Digoxin and Analogues—*Equilibrium Kinetics*—Red blood cell–buffer and red blood cell–plasma partition coefficients, P_{e/c_u} and $P_{e/c}$, respectively, were obtained for the compounds under different experimental conditions and are listed in Tables I, II, and III as mean values for erythrocytes from different donors. Red blood cell partitioning of all the tested compounds was linear and concentration independent (Table II), indicating that first-order kinetics were operative. The values for P_{e/c_u} of the individual compounds were identical in the presence and absence of large concentrations of the respective analogues (Table II). This implied the exis-

[8] Packard Tri-Carb Nos. 3280 and 3255; Packard Instruments, Downers Grove, Ill.

[9] Model 4101; Intertechnique, Plaisir, France.

Table III—Reversibility of the Red Blood Cell Partitioning Kinetics of Digoxin and Analogues at 24°C

Compound	P_{e/c_u}[a] Suspension Experiments	n^b	Resuspension Experiments	n^b
[^{3}H]I	1.39 ± 0.040	8	1.38 ± 0.088	3
[^{3}H]V	1.07 (1.04, 1.10)	2	1.13 (1.11, 1.15)	2
[^{3}H]VI	1.16 ± 0.038	8	1.14 ± 0.061	4

[a] Mean ± *SD*; individual values in parentheses. [b] Number of individual values considered, obtained from one donor.

tence of binding and/or partitioning sites of large capacity within the red blood cells. The equivalency of P_{e/c_u} for the individual compounds in suspension and resuspension experiments (Table III) suggested reversibility of the red blood cell partitioning kinetics. For all the compounds tested, P_{e/c_u} is greater than P_{e/c_l}, indicating significant plasma protein binding of the compounds.

There was no clear-cut relationship between the magnitude of P_{e/c_u} and lipophilicity (P) of the compounds (Table I). Red cell partitioning from buffer or plasma was clearly temperature dependent and decreased with decreasing temperature (Table I). Semilogarithmic plots of P_{e/c_u} against $1/T$, the reciprocal of the absolute temperature, yielded apparent straight lines for all the compounds tested (Fig. 1). The P_{e/c_u} values of [^{3}H]I and its analogues in the experiments conducted at 4°C were >0.70 (Table I), the partition coefficient value predicted for compounds solely distributed within the intracellular water phase of the red blood cells (2, 16). This implied binding and/or partitioning of the compounds in nonaqueous phases within the red blood cells, even at this low temperature.

However, P_{e/c_u}, as defined, did not characterize the distribution of the compounds between a nonaqueous and an aqueous phase as required (17), but defined equilibrium conditions existing in mixed nonaqueous-aqueous (cellular) and aqueous (extracellular) phases. In conceiving the red blood cells as a two-phase (nonaqueous-aqueous) system, a true partition coefficient, P_{e_b/e_u}, was defined as the ratio of the bound/partitioned concentration in the nonaqueous phase to the unbound concentration in the aqueous phase of the cells. Values for P_{e_b/e_u} were calculated (see *Appendix I*). Similarly, the percentage of drug truly bound/partitioned within the nonaqueous phase of the red cells, β_E, was computed (see *Appendix I*) for the different compounds. The values obtained for P_{e_b/e_u} and β_E are listed in Table IV.

When P_{e_b/e_u} was plotted semilogarithmically against $1/T$, curves were obtained with all the compounds (Fig. 1). This was in contrast to the apparent linear relationship obtained previously with semilogarithmic plots of P_{e/c_u} against $1/T$ (Fig. 1).

Nonequilibrium Kinetics—Time-dependent concentration curves were not obtained for the compounds under all the experimental conditions. With the most hydrophilic compound of the series, [^{3}H]VII, erythrocyte partitionings at temperatures of 4°C and 24°C were such slow processes that substantial hemolysis occurred long before the red blood cell partitionings were at equilibrium. With the more lipophilic compounds, however, red blood cell uptake was so fast that partition equilibrium was nearly or completely reached within the interval needed for centrifuging the very first sample taken after admixing the compounds ([^{3}H]I-[^{3}H]V at 37°C, [^{3}H]II and [^{3}H]III at 24°C).

Semilogarithmic plots against time of $(B - B_{eq})/(B_0 - B_{eq})$ and of $(E_{eq} - E)/E_{eq}$, derived respectively from the experimental data obtained in erythrocytes and buffer (see *Appendix II*), gave equivalent results and could be fitted by the same line (Figs. 2 and 3). Red blood cell partitioning of the compounds was characterized by a single distribution phase in most of the experimental settings. However, two distribution phases were clearly distinguishable with [^{3}H]I and [^{3}H]IV-[^{3}H]VI (Fig. 3) at 4°C and with [^{3}H]VII at 37°C. The respective concentration-time data in the erythrocytes, e, in buffer, c_u, and in plasma, c, of all the experiments were fitted using the non-

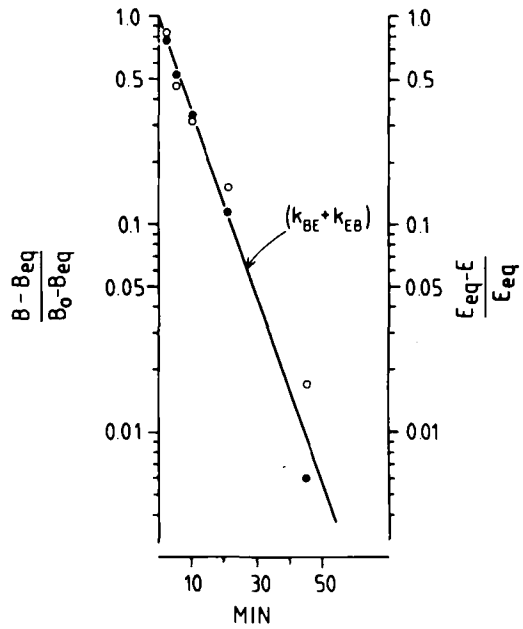

Figure 2—*Semilogarithmic plots of* $(B - B_{eq})/(B_0 - B_{eq})$ *and* $(E_{eq} - E)/E_{eq}$, *calculated from the experimental data for buffer and erythrocytes, respectively, for [^{3}H]III at 4°C. A red blood cell suspension in buffer was spiked with drug, and a single distribution phase was observed. The erythrocyte and buffer data could be fitted to the same line.*

linear least-squares estimation program TOPFIT (18). The program yielded values for the microscopic rate constants (Figs. 4–7) and equilibrium concentrations in erythrocytes, buffer, or plasma. The respective volumes of the red blood cell and buffer/plasma phases, hematocrit (Hc) and "plasmacrit" (1 − Hc), which were known in all the experiments, were fixed and not iterated.

Except for [^{3}H]VII, all data sets from the experiments were fitted individually and the fitting of the concentrations in erythrocytes, buffer, or plasma was simultaneous. The data sets obtained for [^{3}H]VII showed larger variability. The respective results of the two experiments performed with this compound in suspensions of red blood cells in buffer or in plasma were averaged and then fitted. Equal weights were given to all the erythrocyte, buffer, or plasma data. This was justified since the concentration range of all the experimental data was rather small. Attempts were made to fit all the data sets to a closed two-compartment model (Figs. 5–7); however, systematically deviating fits were obtained in those cases where two distribution phases had been seen previously in the graphic analysis of the data (Fig. 3). Adequate fits resulted when these data were fitted to a closed three-compartment model (Fig. 4).

A detailed analysis was performed with the data that had been fitted to the three-compartment model. Attempts were made to interpret, physiologically, the two erythrocyte compartments, E_1 and E_2, which were separable in these experiments (see the Scheme in Fig. 4). Plasma membrane, cellular water, and hemoglobin were expected to contain significant amounts/concentrations of the compounds (9, 19) and, thus, could be the physiological equivalents of the two erythrocyte compartments. However, it must be clearly realized that compartments E_1 and E_2 and the corresponding rate constants obtained in the kinetic analysis were interchangeable; these two compartments could be attributed to the cellular constituents and barriers as follows: (*a*) E_1 = plasma membrane + water, E_2 = hemoglobin; (*b*) E_1 = plasma membrane, E_2 =

Table IV—Compartmental Distribution and True Partitioning of Digoxin and Analogues in Red Blood Cells at 4°C[a]

Compound[b]	$(e_1/c_u)_{eq}$, × 10^2	$(e_2/c_u)_{eq}$, × 10^2	n^c	$(e_1/e)_{eq}$, × 10^2	$(e_2/e)_{eq}$, × 10^2	$(e_1/e_2)_{eq}$	P_{e_b/e_u}	β_E	n^d
[^{3}H]IV	26 (24, 28)	61 (56, 66)	2	30	70	0.43	0.29 ± 0.15	22 ± 8.8	4
[^{3}H]I	22 ± 4.5	62 ± 4.8	5	26	74	0.35	0.26 ± 0.05	21 ± 2.9	7
[^{3}H]V	16 ± 2.0	69 ± 6.1	6	19	81	0.23	0.25 ± 0.01	20 ± 0.8	4
[^{3}H]VI	19 ± 6.7	74 ± 6.5	4	20	80	0.25	0.33 ± 0.06	26 ± 3.6	3
[^{3}H]VII[e]	6.7	69	1	8.8	91	0.10			

[a] $e_{1,eq}$, $e_{2,eq}$, $e_{eq}[(e_1 + e_2)_{eq}]$, and $c_{u,eq}$, respectively the drug concentrations in the erythrocyte compartments (E_1, E_2, E) and plasma water (buffer) (B) at equilibrium, were obtained from fitting suitable data to the closed three-compartment model (see Fig. 4, *Appendix II*). The values for P_{e_b/e_u} and $\beta_E(e_b/e)_{eq}$ were predicted from P_{e/c_u}, depicting the red blood cells as consistingg of a nonaqueous and an aqueous phase of fractional volume 0.7. The values of $(e_1/e)_{eq}$ and $(e_1/e_2)_{eq}$ of the individual compounds should be compared, respectively, to P_{e_b/e_u} and β_E. The values are mean ± *SD*, with individual values in parentheses. [b] In order of decreasing lipophilicity. [c] Number of experiments performed in blood of different donors. [d] Number of mean values considered; averages of 3–5 individual determinations in blood of 3–7 donors.

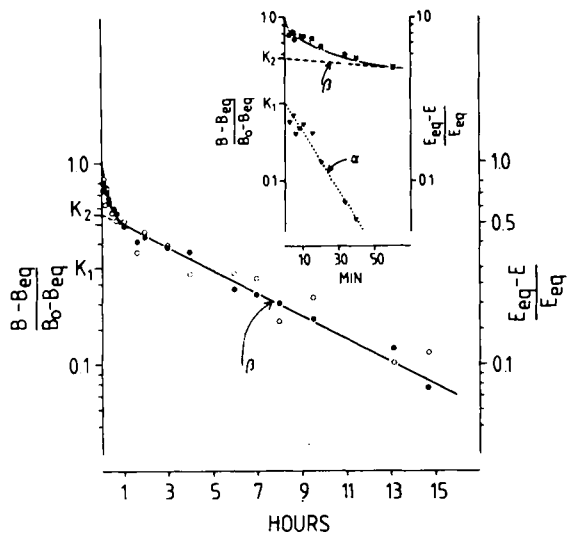

Figure 3 —*Semilogarithmic plot for [^{3}H]VI under same conditions as in Fig. 2. The inset is for the initial data on an expanded time scale. Two distribution phases were separable. The erythrocyte and buffer data could be fitted to the same line.*

water + hemoglobin; (*c*) E_1 = hemoglobin, E_2 = plasma membrane + water; and (*d*) E_1 = water + hemoglobin, E_2 = plasma membrane.

The respective concentrations in the red blood cell compartments, relative to the concentration in buffer [$(e_1/c_u)_{eq}$ and $(e_2/c_u)_{eq}$], were calculated from the microscopic rate constants obtained from the fits (see *Appendix II*). Similarly, the respective compartmental concentrations in the erythrocytes at equilibrium, as a percentage of the total concentration in the red blood cells, $10^2(e_1/e)_{eq}$ and $10^2(e_2/e)_{eq}$, and the ratio of the compartmental concentrations at equilibrium, $(e_1/e_2)_{eq}$, were computed (Table IV). It is interesting to note that, on average, $(e_2/c_u)_{eq}$ was 0.65 ± 0.05 for the tested compounds (Table IV), which is close to 0.7 (2, 16), the value predicted for the ratio of $(e_u/c_u)_{eq}$. In addition, $10^2(e_1/e)_{eq}$ of the individual compounds were similar to the predicted individual values for β_E (Table IV). Furthermore, the $(e_1/e_2)_{eq}$ values for the individual analogues agreed with the individually predicted P_{e_b/e_u} values (Table IV). This suggested that $(e_1)_{eq}$ and $(e_2)_{eq}$ obtained from the kinetic analysis on the assumption of a three-compartment model were equivalent, respectively, to e_b and e_u calculated on consideration of the physiology of erythrocytes and the P_{e/c_u} for the compounds. Hence, the most probable physiological equivalents of compartments E_1 and E_2 were, respectively, hemoglobin and cellular water + plasma membrane (alternative *c* above), on the assumption that the plasma membrane did not contain significant amounts of the drugs.

It became necessary to compare the partitioning kinetics of all the compounds under all the different experimental conditions. Hence, there was a need for a model-independent parameter. Mean transit time, $\bar{t}$, which has been used repeatedly in pharmacokinetic data analysis (20, 21), appeared to be most appropriate for this purpose. The $\bar{t}$ values for the individual experiments were calculated from the ratio of the area under the first moment curve ($AUMC_\infty$) to the area under the plasma concentration time curve (AUC_∞) (21) or from the microscopic rate constants obtained in the fits (see *Appendix II*). The values so obtained for $\bar{t}$ are listed in Table V. An upper limit for $\bar{t}$ was estimated in experiments where red blood cell partition equilibrium of the compounds was reached very quickly. There was wide variation among the $\bar{t}$ values obtained for the compounds in the different experimental settings; $\bar{t}$ ranged between <0.5 and 3800 min. Mean transit time clearly decreased with increasing lipophilicity (*P*) of the compounds (Table V, Fig. 8). For the experiments conducted at 4°C and 24°C, plots of log $(1/\bar{t})$ against log *P* yielded straight lines for the tested compounds (Fig. 8). Mean transit times of [^{3}H]I and its analogues were also highly dependent on absolute temperature. The quantitative evaluation of this dependency, using the data obtained with [^{3}H]VI and plotting log $(1/\bar{t})$ against $1/T$, showed that the relationship was nonlinear (Fig. 9).

The values obtained for $\bar{t}$ with erythrocyte buffer suspensions were significantly larger than with erythrocyte plasma suspensions for all the compounds tested; the differences ranged between 10–25% (Table IV). This implies that plasma protein binding and unbinding were not rate limiting and were much faster processes than red blood cell partitioning and repartitioning. Attempts were made to predict $(\bar{t})$, k_{PE}, and k_{EP} in red blood cell plasma suspension experiments at 24°C for [^{3}H]I and [^{3}H]IV–[^{3}H]VI from $\bar{t}$, k_{BE}, and k_{EB} in red blood cell buffer suspensions, which had been previously obtained in experiments conducted at an equivalent temperature (see *Appendix III*). There was good agreement between predicted and experimentally measured parameters for the tested compounds in the red blood cell plasma suspensions [$(\bar{t})_{pred}$ = 96.9 (±8.50)%·$(\bar{t})_{exp}$, $k_{PE,pred}$ = 103.1 (±10.4)%·$k_{PE,exp}$, and $k_{EP,pred}$ = 104.4 (±10.2)%·$k_{EP,exp}$ (n = 4)].

The similarity of the respectively obtained mean transit time values on partitioning of [^{3}H]VI from buffer into red blood cells ($\bar{t}$ = 5.1 min) and on repartitioning of the compound from erythrocytes into buffer ($\bar{t}$ = 4.9 min) (Fig. 6) suggested complete reversibility of the kinetics. Attempts were made to estimate mean transit times of repartitioning from red blood cells into buffer and plasma at 37°C for the compounds that reached partition equilibrium very quickly ([^{3}H]I–[^{3}H]V: $\bar{t}$ < 1.5 min, Table V). It was assumed that the temperature dependency of $\bar{t}$ for [^{3}H]VI in the range of 4°–37°C was also representative for the other analogues and that the equilibrium of the plasma protein interaction with the compounds was instantaneous. The estimated $\bar{t}$ values for the analogues in the red blood cell buffer suspensions at 37°C were: 0.008 min for [^{3}H]II; 0.036 min for [^{3}H]III; 0.307 min for [^{3}H]IV; 0.536 min for [^{3}H]I; and 1.39 min for [^{3}H]V (*Appendix III*). The corresponding values in the red blood cell plasma suspensions were smaller, on average 80% of the estimates obtained in the red blood cell buffer suspensions, for the slowly plasma-bound compounds ([^{3}H]I and [^{3}H]III–[^{3}H]V). In contrast, the estimated mean transit times in the two suspensions differed widely for the highly plasma-bound [^{3}H]II. The value in suspensions in plasma was clearly smaller [$(\bar{t})$ = 0.001 min] than in suspensions in buffer [$\bar{t}$ = 0.008].

Mean transit times for blood flowing through the sinusoids of the liver and the capillaries of the proximal tubules of the kidney were reported to be 10 and 2.5 s, respectively (22, 23). This suggested that, for the most lipophilic analogues ([^{3}H]II and [^{3}H]III), all of the amounts in the red blood cells could repartition during a single pass through the eliminating organs and, hence, could become available for extraction. For the least lipophilic analogues ([^{3}H]V–[^{3}H]VII), only small fractions of the amounts residing in the red blood cells could repartition and were available for extraction.

***In Vivo* Red Cell Partitioning of Digoxin and Metabolites**—Mean *in vivo*

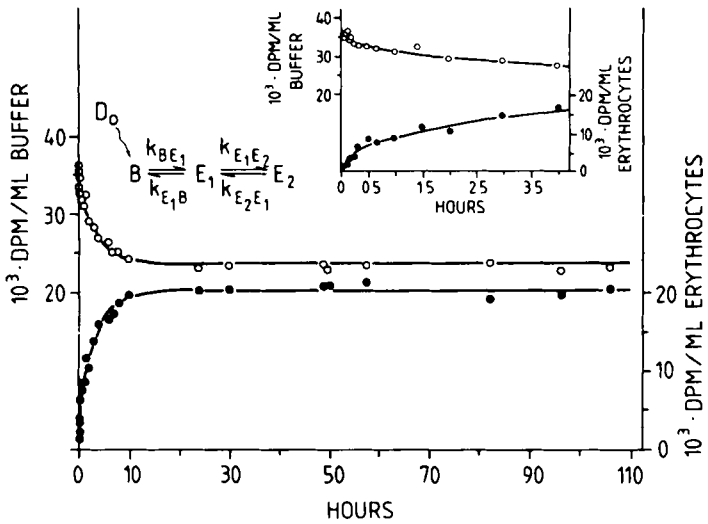

Figure 4—*Typical linear plot of the respective concentrations in erythrocytes (e) (●) and in buffer (c_u) (○) against time for [^{3}H]V at 4°C. A red blood cell suspension in buffer was spiked; the erythrocyte and buffer data were fitted simultaneously to the closed three-compartment model shown. The inset is a plot of the initial data on an expanded time scale.*

Table V—Mean Transit Time of Red Blood Cell Partitioning of Digoxin and Analogues from Buffer or Plasma at Different Temperatures

Compound[a]	$\bar{t}$ in Buffer or ($\bar{t}$) in Plasma, min[b] 4°C	n[c]	24°C	n[c]	37°C	n[c]
[^{3}H]II	1.65 ± 0.32	5	<0.50	2	<0.50	2
[^{3}H]III	7.46 ± 0.98	4	<0.50	2	<0.50	2
[^{3}H]IV	30.3 ± 1.29	3	1.14 (1.03, 1.24)	2	<0.50	2
			0.95 (0.91, 0.98)	2		
[^{3}H]I	63.1 ± 8.64	6	1.99 (1.56, 2.41)	2	<0.50	2
			1.59 (1.44, 1.73)	2		
[^{3}H]V	248 ± 39.1	6	5.17 (5.03, 5.31)	2	<0.50	2
			4.23 (3.85, 4.61)	2		
[^{3}H]VI	407 ± 43.3	4	7.35 (7.21, 7.49)	2		
			6.70 (6.05, 7.34)	2	1.70 (1.63, 1.78)	2
[^{3}H]VII					3807	1
					3098	1

[a] In the order of decreasing lipophilicity. [b] Mean ± *SD*; individual values in parentheses. When multiple values are given, the upper value is in buffer, the lower value in plasma; all single values are in buffer. [c] Number of experiments performed in blood of different donors.

red blood cell-plasma partition coefficients, $\bar{P}_{e/c}^{in\ vivo}$, were determined from the ratio of the total radioactivity in erythrocytes to total radioactivity in plasma in all the blood samples obtained in the pharmacokinetic studies. The $\bar{P}_{e/c}^{in\ vivo}$ values found were dose independent, but showed a clear time dependency: they were only constant for periods of ~2 h after intravenous and oral administration of the drug and increased significantly at later times. This was most probably due to a slow red blood cell partitioning of polar derivatives of [^{3}H]I, which were consistently measurable in the plasma samples of the volunteers. $\bar{P}_{e/c}^{in\ vivo}$ values obtained within the initial 2 h after drug administration were considered for a comparison with *in vitro* red blood cell partitioning values. Estimates for $\bar{P}_{e/c}^{in\ vitro}$ were made from the individual red cell partitioning values of [^{3}H]I and its apolar metabolites ([^{3}H]IV-[^{3}H]VI), previously obtained under *in vitro* conditions at 24°C ($P_{e/c,i}^{in\ vitro}$) and the concentrations of the individual compounds measured in plasma of the volunteers ($c_{eq}^{in\ vivo}$) in accordance with:

$$\bar{P}_{e/c}^{in\ vitro} = \frac{\sum_{i=1}^{4} (P_{e/c,i}^{in\ vitro}) \cdot c_{eq,i}}{\sum_{i=1}^{4} (c_{eq,i})}$$

It was assumed that $P_{e/c} \simeq 0$ for the measured polar derivatives of [^{3}H]I. This was in accordance with the insignificant red blood cell partitioning found for the polar [^{3}H]VII within comparable time intervals at 37°C.

Mean red blood cell partitioning *in vivo* and *in vitro* at 24°C were found to be similar in the intravenous experiments [$\bar{P}_{e/c}^{in\ vivo} = 0.943 \pm 0.154$ ($n = 6$), $\bar{P}_{e/c}^{in\ vitro} = 0.971 \pm 0.012$ ($n = 6$)] and oral experiments [$\bar{P}_{e/c}^{in\ vivo} = 0.975 \pm 0.148$ ($n = 6$), $\bar{P}_{e/c}^{in\ vitro} = 0.955 \pm 0.023$ ($n = 6$)]. This suggested that results on the kinetics of red blood cell partitioning obtained under *in vitro* conditions are valid and allow conclusions regarding *in vivo* conditions.

Binding of Digoxin and Analogues to Hemolysate, Hemoglobin, Albumin, and Plasma Protein—The percentage of drug bound to hemolysate ($\beta_{HB'}$), to hemoglobin (β_{HB}), to albumin (β_{AB}), and to plasma protein (β_{PB}) were obtained with the equilibrium dialysis method. The respective values are given in Table VI (see *Appendix I*). Estimates for β_{PB} of the compounds were also obtained by the red blood cell partitioning method and are included in Table VI (see *Appendix I*).

Binding to Hemolysate—Except for [^{3}H]VII, all the compounds showed significant binding to hemolysate (hemoglobin concentration, 110 g/L) at 37°C (Table VI). The $\beta_{HB'}$ values obtained for [^{3}H]I and its analogues ranged between 47.1% ([^{3}H]II) and −5.1% ([^{3}H]VII). The apparent negative value observed with [^{3}H]VII indicated that this compound was completely unbound and, hence, was excluded from volumes where binding of the other analogues occurred (12, 24). The binding of [^{3}H]II to hemolysate was concentration independent over the range studied (20–100 ng/mL). Estimates of $\beta_{HB'}$ in hemolysates (hemoglobin concentration, 110 g/L) were significantly and consistently smaller than β_E in intact cells (hemoglobin concentration, 330 g/L) (25) (Fig. 10), indicating a diminished binding capacity of the former. This was either due to the much lower hemoglobin concentration in the hemolysates or suggested additional binding/partitioning to constituents other than hemoglobin in the intact cells. There existed a significant positive linear correlation between the values obtained for β_E and $\beta_{HB'}$ [$\beta_E = 27.4\ (\pm 4.71) + 1.11\ (\pm 0.214) \cdot \beta_{HB'}$, $r = 0.919$ (Fig. 10)].

Binding to Hemoglobin—The respective values for the binding of [^{3}H]I and [^{3}H]II to hemoglobin (110 g/L) were $\beta_{HB} = 22.0$ and 71.4% (Table VI). The former value was in agreement with the value previously obtained for the binding of [^{3}H]I to hemolysate ($\beta_{HB'} = 19.7\%$). In contrast, binding of [^{3}H]II was much greater with hemoglobin ($\beta_{HB} = 71.4\%$) than with hemolysate ($\beta_{HB'} = 47.1\%$) (Table VI). It is possible that existing differences in conformation or aggregation of hemoglobin in the two preparations affect the highly bound [^{3}H]II more than the lesser-bound [^{3}H]I. The binding of [^{3}H]II to diluted hemoglobin (7 g/L) was significant [$\beta_{HB} = 19.0$ (15.6 and 22.3; $n = 2$)] and suggested that results on the membrane binding of compounds reported in the literature (19), which had been obtained with red cell ghosts not freed from hemoglobin (14 g/L), must be interpreted with due caution.

Binding to Albumin—The values for the binding of [^{3}H]I and its analogues to albumin are listed in Table VI. The bindings of [^{3}H]II to albumins AB_1 and AB_2 were $\beta_{AB_1} = 97.0\%$ and $\beta_{AB_2} = 97.9\%$. The similarity of these results implied equivalence of the two albumins. Binding of the compounds tested ranged between $\beta_{AB} = 97\%$ ([^{3}H]II) and $\beta_{AB} = 27\%$ ([^{3}H]VII). Albumin binding increased with increasing lipophilicity (P) of the compounds [$\beta_{AB} = 24.3\ (\pm 1.78) + 0.748\ (\pm 0.043) \cdot P$, $r = 0.992$].

Binding to Plasma Protein—The mean values obtained for the plasma protein binding of [^{3}H]II, [^{3}H]III, and [^{3}H]VII together with the previously reported (1) values for [^{3}H]I and [^{3}H]IV-[^{3}H]VI are given in Table VI. All the values were obtained with the equilibrium dialysis method. Plasma protein binding of [^{3}H]II, [^{3}H]III, and [^{3}H]VII was concentration independent over the range studied and was unaltered in the presence of large concentrations of analogues. This was in accordance with the binding characteristics previously found with [^{3}H]I and [^{3}H]IV-[^{3}H]VI (1). Plasma protein bindings of

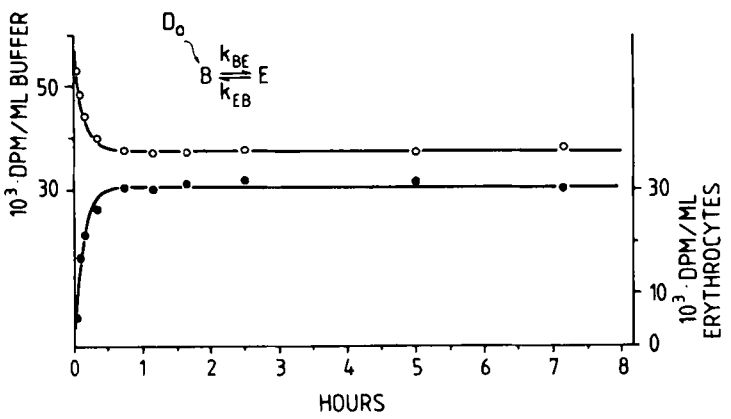

Figure 5—*Linear plot of the respective concentrations in erythrocytes (e) (●) and in buffer (c_u) (○) against time for [^{3}H]III at 24°C. A red blood cell suspension in buffer was spiked; the erythrocyte and buffer data were fitted simultaneously to the closed two-compartment model shown.*

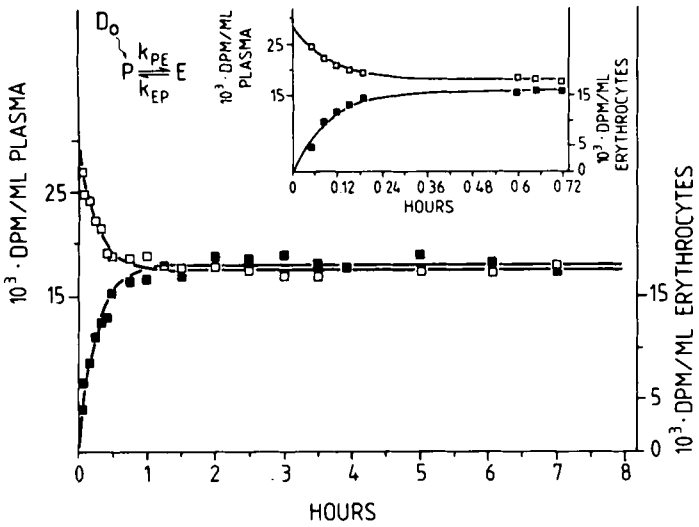

Figure 6—*Linear plot of the respective concentrations in erythrocytes (e) (■) and in plasma (c) (□) against time for [³H]V at 24°C. A red blood cell suspension in plasma was spiked; the data were fitted to the two-compartment model shown. The inset is a plot of the initial data on an expanded time scale.*

[³H]II at experimental temperatures of 24°C [β_{BP} = 96.7 ± 0.38% (n = 11)] and 37°C [β_{PB} = 95.1 ± 1.90% (n = 5)] were similar.

The binding to plasma protein was consistently smaller than to albumin for [³H]I and all the analogues tested (Table VI). A highly significant positive correlation existed between binding to albumin and to plasma protein for the compounds [$\beta_{AB} = -15.9\ (\pm 8.36) + 1.07\ (\pm 0.164)\ \beta_{PB}$, r = 0.894]. There was excellent agreement between the respective plasma protein binding estimates of the compounds obtained from the red blood cell partitioning procedure and the equilibrium dialysis method (Table VI). Plasma protein binding of [³H]I and its analogues using the red blood cell partitioning method was temperature independent within the tested range of 24–37°C (Table VI).

DISCUSSION

Octanol–Water Partition Coefficient of Digoxin and Its Analogues—The partition coefficient values obtained for [³H]I and its analogues in the present study were—except for [³H]II—in agreement with those reported previously by Cohnen *et al.* (26); a significantly higher P value was found for [³H]II in the present study. The reason for this discrepancy was not apparent, since equivalent experimental methods were used in both studies. A significant linear correlation existed between the R_m values by partition chromatography reported by Cohnen *et al.* (26) and the log P values obtained in the present study [$R_{m(30)} = 1.36\ (\pm 0.069) \cdot x - 1.47\ (\pm 0.091) \cdot \log P$, r = 0.995].

Erythrocyte Partitioning of Digoxin and Its Analogues—Red blood cell partitioning kinetics of [³H]I and its analogues were first order over a considerable concentration range, unaltered in the presence of large concentrations of analogues (Table II) and clearly temperature dependent (Table I). This suggested that red blood cell uptake of the compounds was a passive process. Its temperature dependency indicated that partitioning into the plasma membrane, diffusion through unstirred water layers, and/or interaction with hemoglobin could be rate limiting. Membrane diffusion through pores (27) was excluded for [³H]I and its analogues on consideration of the molecular weights of the compounds and the pore radius (4 Å) of the red blood cell plasma membrane (28–32).

The three-compartment model kinetics found for the less lipophilic analogues [³H]V and [³H]VI at 4°C (Figs. 3 and 4) and [³H]VII at 37°C indicated that two rate-limiting steps—one faster, one slower—were operative in these cases. Clearly the processes could be composite. In accordance with the previous physiological interpretation of the erythrocyte compartments, the slower process represented partitioning into the plasma membrane and/or diffusion through intracellular water; the faster process was equivalent to binding to hemoglobin. However, in considering the degree of acceleration of the kinetics of red blood cell partitioning of the compounds found on elevating the temperature, it was concluded that diffusion through water was most probably not a rate-limiting process (31). The three-compartment model collapsed into a two-compartment model with the more lipophilic analogues at the lowest temperature ([³H]II–[³H]III; Figs. 2 and 5) and with all the analogues except [³H]VII at the higher temperatures. This finding suggested that the slower of the two processes was accelerated by an increase in temperature or lipophilicity of the compounds and approached the rate of the faster process, so that apparently two-compartment kinetics with a single rate-limiting process evolved in these cases.

Equilibrium Kinetics—Red blood cell partition coefficients for [³H]-IV–[³H]VII have not been reported thus far in the literature; however, values for [³H]I–[³H]III have been published. Mean P_{e/c_u} and $P_{e/c}$ values of 0.97 (0.93, 1.01; n = 2) and 0.89 ± 0.030 (n = 3), respectively, had been obtained previously by Hinderling *et al.* (5). The latter value was confirmed by the results of the present study [$P_{e/c}$ = 0.88 (0.842, 0.922; n = 2)]; however, the former value was significantly smaller than the corresponding value of the present study [$P_{e/c_u} = 1.11 \pm 0.027$ (n = 3)]. Although it cannot be excluded that the discrepancy was caused by the use of plasma water instead of buffer a in the previous study, there was indications that the value of the former study was biased. Abshagen *et al.* (19), using radiolabeled compounds, reported mean red blood cell partitioning values of six donors for [³H]I and [³H]II at 37°C. The values were obtained on consideration of one drug concentration only ([³H]I: 51 ng/mL; [³H]II: 69 ng/mL). Their respective P_{e/c_u} and $P_{e/c}$ values were 0.90 and 0.90 for [³H]I and 1.37 and 0.09 for [³H]II. The former three values were significantly smaller than those found in the present study ([³H]I: P_{e/c_u} = 1.49, $P_{e/c}$ = 1.13; [³H]II: P_{e/c_u} = 2.51); there was agreement regarding the last value. Attempts to compute estimates for the plasma protein binding of the two compounds using the respective P_{e/c_u} and $P_{e/c}$ values (see *Appendix I*) of Abshagen *et al.* (19) yielded β_{PB} = 0% for [³H]I and β_{PB} = 93.1% for [³H]II. The former value was clearly lower than the values given in the literature for the plasma binding of [³H]I [β_{PB} = 23–29% (equilibrium dialysis, 37°C, normal human serum–plasma) (33–37)] and there was no ready explanation for this bias. The latter value was within the range of the

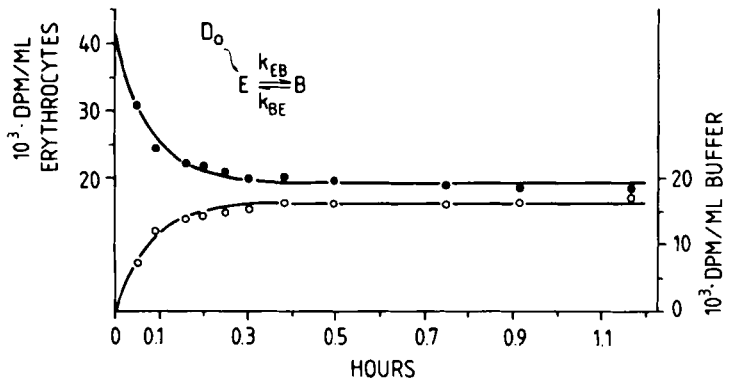

Figure 7—*Linear plot of the respective concentrations in buffer (c_u) (○) and in erythrocyte (e) (●) against time for [³H]VI at 24°C. Red blood cells suspended in buffer and spiked with the compound were separated centrifugally and then resuspended in fresh buffer. The data were fitted according to the two-compartment model shown.*

Table VI—Percent Binding of Digoxin and Analogues to Hemolysate, Albumin, and Plasma Protein at 37°C and 24°C [a]

Compound	β_{HB} 37°C [b]	n [c]	β_{AB} 37°C [b]	n [d]	β_{PB} 37°C [b]	n [e]	37°C [f]	24°C [f]
[^{3}H]II	47.1 (45.1, 49.2)	2	97.2 ± 0.690	12	95.6 ± 1.59	7	96.4	97.2
[^{3}H]III	12.3 (10.3, 14.2)	2	57.3 (55.6, 58.9)	2	25.1 (24.7, 25.4)	2	26.2	20.8
[^{3}H]IV	18.2 (18.0, 18.4)	2	33.9 ± 2.64	6	22.3 ± 2.00	3	25.9	23.8
[^{3}H]I	19.7 (18.8, 20.5)	2	34.2 ± 2.67	10	22.3 ± 1.43	3	24.2	22.8
[^{3}H]V	15.6 (13.4, 17.7)	2	33.0 (32.3, 33.6)	2	22.4 ± 2.55	3	23.0	24.9
[^{3}H]VI	7.45 (6.50, 8.40)	2	35.8 (34.9, 36.7)	2	26.2 ± 1.61	3	20.4	29.5
[^{3}H]VII	−5.05 (−2.10, −8.00)	2	26.8 (24.9, 28.7)	2	13.9 (13.6, 14.2)	2		

[a] Mean ± *SD*; individual values in parentheses. The compounds are listed in order of decreasing lipophilicity. [b] Equilibrium dialysis method. [c] Number of individual determinations considered, obtained in hemolysates of one donor. [d] Number of individual values considered obtained, in plasma of one donor. [e] Number of mean values considered; averages of two determinations in plasma of 2–7 donors. [f] Red blood cell partitioning method.

values reported in the literature for the plasma binding of [^{3}H]II [β_{PB} = 92–97% (equilibrium dialysis, 37°C, normal human serum–plasma) (33–35, 38)].

Nonequilibrium Kinetics—Gardner *et al.* (9) reported mean data on the kinetics of red blood cell partitioning for [^{3}H]I (9–94 ng/mL) at 37°C. An apparent $\bar{t}$ value of 13 min could be calculated from those results. This value was much larger than the corresponding estimate of $\bar{t} < 0.5$ min obtained in the present study. The discrepancy was possibly due to differences in the methods employed. The procedure of Gardner *et al.* used a different buffer and the red blood cell suspensions had much lower hematocrits (5–10%); the incubated red blood cell suspensions were repeatedly washed (at nonspecified temperatures) prior to the final ultracentrifugal separation of the cells and buffer. The surprisingly low values for P_{c/c_u} of 0.65 and 0.40 at concentrations of 9 and 94 ng/mL of the drug, respectively, calculated from their data, indicated that the washing procedure used may have led to a substantial loss of drug from the cells.

Binding of Digoxin and Its Analogues to Hemolysate, Hemoglobin, and Plasma Protein—Hemoglobin (*per se* and in hemolysate preparations) was shown to bind significantly all the compounds tested with the exception of [^{3}H]VII (Table VI). A statistically significant linear correlation existed between binding to hemolysate and binding to intact cells for [^{3}H]I–[^{3}H]VI (Fig. 10). These results suggested that hemoglobin was the major red blood cell constituent that interacted with the compounds. An important binding of the analogues to constituents other than hemoglobin could not be excluded; however, the finding that low concentrations of hemoglobin (7 g/L) bound substantial amounts of [^{3}H]II suggested that reported plasma membrane binding values (9, 19) could be overestimations, since the membrane preparations used in these studies were not free of hemoglobin.

The differences in the binding of [^{3}H]I and its analogues to hemolysate, hemoglobin, and suspensions of intact cells observed in the present study could be explained by the nonequivalence of the three preparations. The cell suspensions had larger hemoglobin concentrations and included additional constituents with binding potential. In addition, conformation and aggregation of hemoglobin in the different preparations were possibly not identical.

The binding of [^{3}H]I and its analogues in albumin preparations was consistently larger than in plasma. Albumin was reported to be the sole protein in plasma to interact with [^{3}H]I and [^{3}H]II (38, 39). The different binding performance observed could be due to a nonidentical conformation or aggregation of the commercially available albumin in buffer *a* and of the "natural" albumin in plasma water. Alternatively, and more likely, this discrepancy was due to a difference in the concentrations of free fatty acids in the albumin preparations and in the plasma used. Free fatty acids at physiological concentrations in plasma were shown to interfere with the binding of drugs to albumin (40). Elevated concentrations of free fatty acids were reported to decrease, significantly, the binding of [^{3}H]I and [^{3}H]II in plasma (41).

Data on the binding of [^{3}H]I and [^{3}H]II to albumin at 37°C, obtained with equilibrium dialysis methods, are reported in the literature. Lukas and de Martino (38) reported β_{AB} = 23% for [^{3}H]I, employing an albumin with a significant free fatty acid content. This value was clearly smaller than β_{AB} = 34.2% for [^{3}H]I found in the present study, which used a fatty acid-free albumin preparation (Table VI). Brock (39) reported a value of β_{AB} = 96.6% for [^{3}H]II with no specification as to the fatty acid content of the albumin used. This value was close to the β_{AB} = 97.2% obtained in the present study (Table VI).

Widely varying plasma protein binding values were reported for [^{3}H]I and [^{3}H]II in the literature (35). The discrepancies were most likely due to differences in the methodologies and experimental conditions used in the studies. For a discussion of the results of the present study, only those data reported in the literature that had been obtained on application of equivalent procedures (equilibrium dialysis, individual plasma of healthy volunteers, temperature 37°C, pH 7.4) were considered. The average percent plasma protein binding found for [^{3}H]II (β_{PB} = 95.6%, Table VI) in the present study was within the

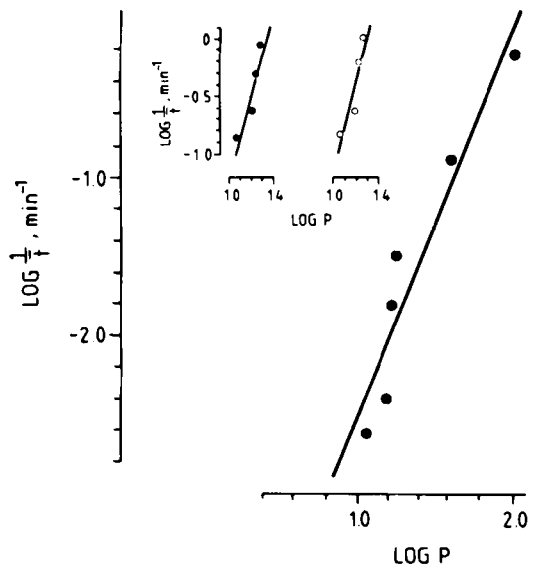

Figure 8—*Logarithmic plot of the reciprocal of the averaged mean transit time, $1/\bar{t}$, against the octanol–water partition coefficient, P, for [^{3}H]I–[^{3}H]VI at an experimental temperature of 4°C. Red blood cell suspensions in buffer were spiked with the compounds. There was an apparent linear dependency of log ($1/\bar{t}$) on log P [log ($1/\bar{t}$) = −5.00 (±0.608) + 2.49 (±0.0428) · log P, r = 0.995]. Corresponding plots are given in the inset for [^{3}H]I and [^{3}H]-IV–[^{3}H]VI in red blood cell–buffer suspensions (●) and in red blood cell–plasma suspensions (○) at an experimental temperature of 24°C.*

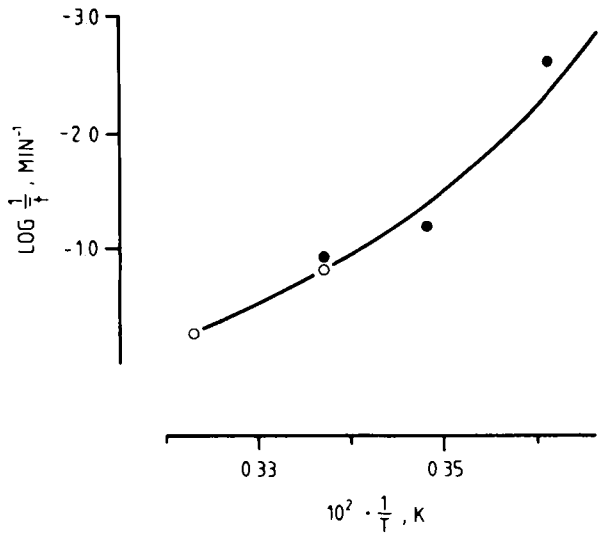

Figure 9—*Linear plot of the logarithm of the reciprocal of the averaged mean transit time, $1/\bar{t}$, against the reciprocal of the absolute temperature, 1/T, for [^{3}H]VI at 4°C, 14°C, 24°C, and 37°C. The relationship between log ($1/\bar{t}$) and 1/T was nonlinear. Key: (●) red blood cell–buffer suspensions; (○) red blood cell–plasma suspensions.*

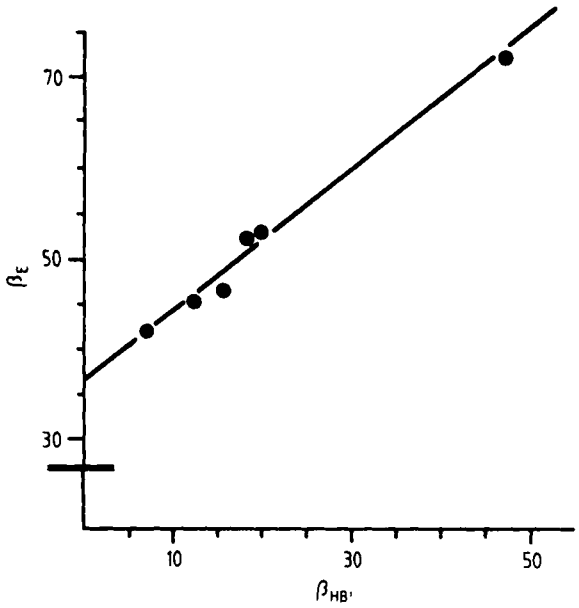

Figure 10—*Linear plot of the percentage bound in intact erythrocytes, β_E, against the percentage bound in hemolysate, $\beta_{HB'}$, for [^{3}H]I–[^{3}H]VI at 37°C. There was an apparent linear relationship between β_E and $\beta_{HB'}$ [β_E: 36.7 (±1.19) + 0.762 (±0.0502) · $\beta_{HB'}$, r = 0.992].*

range of the values given in the literature [92.3–97.3% (33–35, 38)]. The corresponding value for [^{3}H]III, β_{PB} = 25.1%, in the present study was close to the β_{PB} = 25.8% reported by Kramer *et al.* (34), but exceeded the value reported by Dengler *et al.* (42) (β_{PB} = 14%) for this drug. The plasma binding of [^{3}H]VII (β_{PB} = 13.9%) in the present study was similar to the sole value reported in the literature [β_{PB} = 16% (43)] for this drug. The temperature independence of the plasma binding of [^{3}H]I and its analogues for the range of 24–37°C observed in the present study was in agreement with equivalent findings of earlier studies with [^{3}H]II (35, 39).

CONCLUSIONS

The present study showed that red blood cell partitioning under *in vivo* and *in vitro* conditions gave equivalent results. The rate and extent of the red blood cell partitioning of [^{3}H]I and its analogues were according to first-order kinetics, identical in the presence and absence of structurally related compounds, and dependent on lipophilicity and temperature. The kinetics of red blood cell partitioning were reversible. Except for the rather strong temperature dependence found, the results were in accordance with passive diffusion as the underlying process (44, 45). The kinetics of red blood cell partitioning of the compounds from plasma could be predicted from the results obtained in analogous experiments with red blood cell buffer suspensions. The rate constants of red blood cell partitioning and repartitioning were much smaller than the rate constants of plasma protein binding and unbinding for the compounds tested.

Mean transit times of partitioning between red blood cells and plasma water were largely different for the compounds tested and varied at 37°C more than 1000-fold. Similarly, large differences in the kinetics of red blood cell partitioning were reported by Schanker *et al.* (2) for a series of basic compounds which differed in lipophilicity. Measured and estimated values for the mean transit time of the compounds at 37°C indicated that there could be significant repartitioning from red blood cells into plasma during a single passage of blood through the eliminatory organs with the more lipophilic analogues. In contrast, only insignificant red blood cell repartitioning occurred with the less lipophilic analogues.

Plasma membrane partitioning appeared to be the rate-limiting step in the red blood cell penetration of the compounds. All the compounds tested—with the exception of [^{3}H]VII—exerted significant binding/partitioning in a "nonaqueous" phase of the red blood cells. Hemoglobin was the major ligate among the erythrocyte constituents.

Plasma protein bindings of [^{3}H]I and its analogues were concentration independent and unaltered in the presence of structurally related compounds. Binding of [^{3}H]I and the analogues to plasma did not simply reflect the interaction between the individual compounds and albumin, but included the interfering action of fatty acids. Albumin binding of the compounds increased with increasing lipophilicity.

In contrast to plasma protein binding, erythrocyte partitioning of the tested compounds was temperature dependent within the range of 24–37°C. Temperature-dependent repartitioning of the compounds from the red blood cells into plasma on lowering the temperature from 37°C to 24°C was low for the tested compounds, leading to an increase in the plasma concentrations of 2–6%. However, it is entirely feasible that for drugs with more extensive red blood cell partitioning, temperature-dependent red blood cell repartitioning could lead to important artifactual changes in the plasma concentration.

The study demonstrated that the delineation of the kinetics of digoxin and analogues in the subcompartments of blood (erthrocytes and plasma) was mandatory and that *a priori* assumptions regarding the rate and extent of red blood cell partitioning of drugs are unwarranted. In defining clearance in the well-stirred (46) or parallel-tube models (47), it was assumed that drug repartitioning from red blood cells into plasma water was instantaneous, so that the unbound fraction was maintained during the passage of blood through the eliminatory organs. However, the results of this study suggest that this may not generally be true. Hence, in the reported literature, clearance values of drugs estimated without experimentally testing the kinetics of red blood cell partitioning may be biased.

APPENDIX I: Calculations for Partition Coefficients and Percentages Bound

Apparent Red Blood Cell–Buffer (P_{e/c_u}) and Red Blood Cell–Plasma Partition Coefficients ($P_{e/c}$)—Red blood cell–buffer and red blood cell–plasma partition coefficients of drugs have been defined previously (48):

$$P_{e/c_u} = \left(\frac{e}{c_u}\right)_{eq} \quad \text{(Eq. 1A)}$$

$$P_{e/c} = \left(\frac{e}{c}\right)_{eq} \quad \text{(Eq. 2A)}$$

where $c_{u,eq}$, c_{eq} [*i.e.*, $(c_u + c_b)_{eq}$], and e_{eq} [*i.e.*, $(e_u + e_b)_{eq}$] represent, respectively, the unbound concentration of a drug in plasma water (buffer), the total (bound + unbound) concentration in plasma, and the total (bound + unbound) concentration in red blood cells at equilibrium.

True Red Blood Cell Partition Coefficient—The red blood cell partition coefficient, P_{e_b/e_u}, may be defined as the ratio of the unbound to bound red blood cell concentration of a drug at equilibrium:

$$P_{e_b/e_u} = (e_b/e_u)_{eq} \quad \text{(Eq. 3A)}$$

On the assumption that the concentration of a nonelectrolytic drug in the aqueous phase of the red blood cells at equilibrium is equal to the known concentration in the surrounding plasma water (buffer), $c_{u,eq}$, and by setting the fractional volume of the red cell water phase equal to 0.7 (2, 16), e_u can be calculated:

$$e_{u,eq} = 0.7 \cdot c_{u,eq} \quad \text{(Eq. 4A)}$$

In substituting $e_{b,eq}$ with $(e - e_u)_{eq}$ and $e_{u,eq}$ with $0.7 \cdot c_{u,eq}$, an expression for P_{e_b/e_u} is obtained:

$$P_{e_b/e_u} = \frac{P_{e/c_u}}{0.7} - 1 \quad \text{(Eq. 5A)}$$

Percentage of Drug Bound and/or Partitioned in Red Blood Cells—The percentage of a compound bound to and/or partitioned into the nonaqueous phase of red cells, β_E, was defined according to:

$$\beta_E = 10^2 \cdot \left(\frac{e_b}{e}\right)_{eq} = 10^2\left[1 - \left(\frac{e_u}{e}\right)_{eq}\right] \quad \text{(Eq. 6A)}$$

On substitution of Eq. 4A into Eq. 6A an expression for β_E is obtained:

$$\beta_E = 10^2[1 - (0.7/P_{e/c_u})] \quad \text{(Eq. 7A)}$$

Respective Percentages of Drug Bound to Hemolysate, Hemoglobin, Albumin, and Plasma Protein—In the studies which employed the equilibrium dialysis method, the percentage of bound drug, β, was obtained from:

$$\beta = 10^2(c_b/c)_{eq} = 10^2[(c - c_u)/c]_{eq} \quad \text{(Eq. 8A)}$$

In the studies which used the red blood cell partitioning method to estimate plasma protein binding, β_{PB} was calculated from Eq. 9A as reported previously (7):

$$\beta_{PB} = 10^2[1 - (P_{e/c}/P_{e/c_u})] \quad \text{(Eq. 9A)}$$

APPENDIX II: Compartmental Models

Closed Two-Compartment Model (Figs. 4–6)—The integrated equations for this model and the initial conditions, $B = B_0$ and $E = 0$, are in accordance with (49):

$$B = \frac{B_0}{k_{BE} + k_{EB}} [k_{EB} + k_{BE} \cdot e^{-(k_{BE}+k_{EB})t}] \quad \text{(Eq. 10A)}$$

$$E = \frac{k_{BE}B_0}{k_{BE} + k_{EB}} [1 - e^{-(k_{BE}+k_{EB})t}] \quad \text{(Eq. 11A)}$$

where $B_0(D_0)$, B, and E represent the dose and the amounts of drug in the plasma water (buffer) and red blood cells, respectively. Equation 10A can be transformed into:

$$\frac{B(k_{BE} + k_{EB}) - k_{EB} \cdot B_0}{k_{BE} \cdot B_0} = e^{-(k_{BE}+k_{EB})t} \quad \text{(Eq. 12A)}$$

Solving Eqs. 10A and 11A for $t = \infty$ (at equilibrium) yields respectively:

$$k_{BE} + k_{EB} = \frac{k_{EB} \cdot B_0}{B_{eq}} \quad \text{(Eq. 13A)}$$

$$k_{BE} + k_{EB} = \frac{k_{BE} \cdot B_0}{E_{eq}} \quad \text{(Eq. 14A)}$$

where B_{eq} and E_{eq} are, respectively, the amounts in plasma water (buffer) and red blood cells at equilibrium. Substituting Eq. 13A into Eq. 12A and rearranging gives:

$$\frac{B - B_{eq}}{B_0 - B_{eq}} = e^{-(k_{BE}+k_{EB})t} \quad \text{(Eq. 15A)}$$

Equation 15A can be formulated in terms of the amounts of drug in the red blood cells:

$$\frac{E_{eq} - E}{E_{eq}} = e^{-(k_{BE}+k_{EB})t} \quad \text{(Eq. 16A)}$$

Plots of $\ln [(B - B_{eq})/(B_0 - B_{eq})]$ or $\ln [(E_{eq} - E)/E_{eq}]$ against time yield identical negative slopes of $(k_{BE} + k_{EB})$ and intercepts of 1.0 (see Fig. 2).

The mean transit time, $\bar{t}$, for the closed two-compartment model is obtained in accordance with (21):

$$\bar{t} = \frac{AUMC_\infty}{AUC_\infty} = \frac{[(B_0 - B_{eq})/(1 - Hc)]/(k_{BE} + k_{EB})^2}{[(B_0 - B_{eq})/(1 - Hc)]/(k_{BE} + k_{EB})} = \frac{1}{k_{BE} + k_{EB}} \quad \text{(Eq. 17A)}$$

Closed Three-Compartment Model (Fig. 4)—The integrated equations for this model and the initial conditions, $B = B_0$ and $E_1 = E_2 = 0$, are in accordance with (49):

$$B = B_0 \left\{ \frac{k_{E_1B} \cdot k_{E_2E_1}}{\alpha \cdot \beta} + \left[\frac{\alpha^2 - \alpha(k_{E_1B} + k_{E_1E_2} + k_{E_2E_1}) + k_{E_1B} \cdot k_{E_2E_1}}{\alpha(\alpha - \beta)} \right] \cdot e^{-\alpha t} + \left[\frac{\beta^2 - \beta(k_{E_1B} + k_{E_1E_2} + k_{E_2E_1}) + k_{E_1B} \cdot k_{E_2E_1}}{\beta(\beta - \alpha)} \right] \cdot e^{-\beta t} \right\} \quad \text{(Eq. 18A)}$$

$$E = E_1 + E_2 = k_{BE_1}B_0 \left\{ \frac{k_{E_2E_1} + k_{E_1E_2}}{\alpha \cdot \beta} + \left[\frac{k_{E_2E_1} + k_{E_1E_2} - \alpha}{\alpha(\alpha - \beta)} \right] \cdot e^{-\alpha t} + \left[\frac{k_{E_2E_1} + k_{E_1E_2} - \beta}{\beta(\beta - \alpha)} \right] \cdot e^{-\beta t} \right\} \quad \text{(Eq. 19A)}$$

where:

$$\alpha,\beta = \frac{1}{2} [k_{BE_1} + k_{E_1B} + k_{E_1E_2} + k_{E_2E_1} \pm \sqrt{(k_{BE_1} + k_{E_1B} + k_{E_1E_2} + k_{E_2E_1})^2 - 4k_{BE_1} \cdot k_{E_1E_2} + k_{E_1B} \cdot k_{E_2E_1} + k_{BE_1} \cdot k_{E_2E_1}}] \quad \text{(Eq. 20A)}$$

Equation 18A can be transformed and written in a form which is equivalent to Eqs. 15A and 16A of the two-compartment model:

$$\frac{B - B_{eq}}{B_0 \cdot B_{eq}} = \frac{E_{eq} - E}{E_{eq}} = K_1 \cdot e^{-\alpha t} + K_2 \cdot e^{-\beta t} \quad \text{(Eq. 21A)}$$

Similarly plots of $\ln [(B - B_{eq})/(B_0 - B_{eq})]$ or $\ln [(E_{eq} - E)/E_{eq}]$ against time have an intercept of 1.0 and a terminal logarithmic linear phase with a negative slope of β. By, respectively, extrapolating and using peeling-off techniques, the intercepts, K_2, K_1, and the slope α of the faster exponential term can be obtained (see Fig. 3).

The mean transit time for the closed three-compartment model with measurements in compartment B, $\bar{t}_B$, can be computed in accordance with (21):

$$\bar{t}_B = \frac{AUMC_{\infty,B}}{AUC_{\infty,B}} = \frac{[(B_0 - B_{eq})/(1 - Hc)]/(k_1/\alpha^2 + k_2/\beta^2)}{[(B_0 - B_{eq})/(1 - Hc)]/(k_1/\alpha + k_2/\beta)} = \frac{k_1/\alpha + k_2/\beta}{k_1/\alpha^2 + k_2/\beta^2} \quad \text{(Eq. 22A)}$$

Alternatively, $\bar{t}_B$, can be calculated and expressed in terms of the microscopic rate constants in accordance with:

$$\bar{t}_B = \frac{1}{k_{E_1B} + k_{E_1E_2} + k_{E_2E_1}} \cdot \left[\frac{(k_{E_1B} + k_{E_1E_2} + k_{E_2E_1})^2 - k_{E_1B} \cdot k_{E_2E_1} + k_{E_1B} \cdot k_{BE_1}}{k_{BE_1}(k_{E_1E_2} + k_{E_2E_1}) + k_{E_1B} \cdot k_{F_2E_1}} - \frac{k_{E_1B} \cdot k_{E_2E_1}}{(k_{E_1F_2} + k_{E_2E_1})^2 + k_{E_1B} \cdot k_{E_1E_2}} \right] \quad \text{(Eq. 23A)}$$

This alternative way of calculating $\bar{t}$ from the microscopic rate constants of compartmental systems will be presented in a forthcoming paper[10].

Calculation of Equilibrium Concentrations of Drugs in Erythrocytes ($e_{1,eq}$, $e_{2,eq}$, and e_{eq}) and Plasma Water/Buffer ($c_{u,eq}$) Using the Microscopic Rate Constants Obtained from the Fits (Table IV)—*Two-Compartment Model:*

$$e_{eq} = \frac{E_{eq}}{Hc} = \frac{k_{BE}}{k_{EB}} \cdot \frac{B_{eq}}{Hc} \quad \text{(Eq. 24A)}$$

$$c_{u,eq} = \frac{B_{eq}}{1 - Hc} = \frac{k_{EB}}{k_{BE}} \cdot \frac{E_{eq}}{1 - Hc} \quad \text{(Eq. 25A)}$$

$$P_{e/c_u} = \frac{k_{BE}}{k_{EB}} \cdot \frac{1 - Hc}{Hc} \quad \text{(Eq. 26A)}$$

Three-Compartment Model:

$$e_{1,eq} = \frac{E_{1,eq}}{Hc} = \left(\frac{k_{BE_1} \cdot k_{E_2E_1} \cdot B_0}{\alpha \cdot \beta} \right) \cdot \frac{1}{Hc} \quad \text{(Eq. 27A)}$$

$$e_{2,eq} = \frac{E_{2,eq}}{Hc} = \left(\frac{k_{BE_1} \cdot k_{E_1E_2} \cdot B_0}{\alpha \cdot \beta} \right) \cdot \frac{1}{Hc} \quad \text{(Eq. 28A)}$$

$$c_{u,eq} = \frac{B_{eq}}{1 - Hc} = \left(\frac{k_{E_1B} \cdot k_{E_2E_1} \cdot B_0}{\alpha \cdot \beta} \right) \cdot \frac{1}{1 - Hc} \quad \text{(Eq. 29A)}$$

$$(e_1/c_u)_{eq} = \frac{k_{BE_1}}{k_{E_1B}} \cdot \frac{1 - Hc}{Hc} \quad \text{(Eq. 30A)}$$

$$(e_2/c_u)_{eq} = \left(\frac{k_{BE_1} \cdot k_{E_1E_2}}{k_{E_1B} \cdot k_{F_2E_1}} \right) \left(\frac{1 - Hc}{Hc} \right) \quad \text{(Eq. 31A)}$$

$$P_{e/c_u} = (e/c_u)_{eq} = \left(\frac{k_{BE_1} \cdot k_{E_1E_2}}{k_{E_1B} \cdot k_{F_2E_1}} + \frac{k_{BE_1}}{k_{E_1B}} \right) \left(\frac{1 - Hc}{Hc} \right) \quad \text{(Eq. 32A)}$$

APPENDIX III: Prediction of Apparent Mean Transit Time and Rate Constants of a Drug in a Erythrocyte Plasma Suspension from Its True Mean Transit Time and Rate Constants in an Erythrocyte Buffer Suspension Assuming a Two-Compartment Model

The values of the apparent $(\bar{t})$, k_{PE}, and k_{EP} for a drug in a red blood cell plasma suspension are expected to be different from the values of the true $\bar{t}$, k_{BE}, and k_{EB} for the same drug in a red blood cell buffer suspension. Plasma protein binding affects extent and rate of drug partitioning into red blood cells in a suspension in plasma. On the assumption that drug binding to and unbinding from plasma protein is much faster than drug partitioning into and repartitioning from red blood cells, predictions of $(\bar{t})$, k_{PE}, and k_{EP} from $\bar{t}$, k_{BE}, and k_{EB}, respectively, are possible.

The plasma binding-induced alteration of the equilibrium conditions and its impact on the magnitude of the parameters in a red blood cell suspension in plasma relative to a red blood cell suspension in buffer is considered first. Equation 16A can be reformulated:

$$\frac{E_{eq}}{E_{eq} - E} = e^{t/\bar{t}} \quad \text{(Eq. 33A)}$$

for a red blood cell buffer suspension experiment and:

$$\frac{(E_{eq})}{(E_{eq}) - (E)} = e^{t/(\bar{t})} \quad \text{(Eq. 34A)}$$

for a red cell plasma suspension experiment. Solving Eqs. 33A and 34A for $t = \bar{t}$ and $t = (\bar{t})$, respectively, yields:

$$E_{t=\bar{t}}/E_{eq} = (1 - e^{-t/\bar{t}}) = 0.632 \quad \text{(Eq. 35A)}$$

$$(E_t)_{=(\bar{t})}/(E_{eq}) = (1 - e^{-t=(\bar{t})}) = 0.632 \quad \text{(Eq. 36A)}$$

[10] R. Sperb and P. H. Hinderling, unpublished results.

Equations 35A and 36A indicate that after a lapse of $\bar{t}$ after drug administration to buffer or of $(\bar{t})$ after administration of drug to plasma, 63.2% of the amounts, respectively, residing in the erythrocytes at partition equilibrium have reached the cells. (Analogously for a drug "administration" into red blood cells, after a lapse of $\bar{t}$ following drug administration, 63.2% of the amounts, respectively, residing in plasma at partition equilibrium have reached the plasma.)

In the following fractional equilibria $[E_{t=\gamma\bar{t}} = (1 - e^{-\gamma})\cdot E_{eq}, (E_t)_{=\gamma\cdot(\bar{t})} = (1 - e^{-\gamma})\cdot(E_{eq})]$ of a drug and the respective times for their attainment in red blood cell suspensions, $t = \gamma\cdot\bar{t}$ and $(t) = \gamma\cdot(\bar{t})$, where γ is a dimensionless fraction ($0 < \gamma \leq 1$), will be considered. The respective fractional equilibria in a red blood cell suspension in plasma and in buffer are not equivalent for a plasma protein-bound drug. The shift in the equilibrium toward the plasma site in the former suspension affects the magnitude of the parameters. This effect can, however, be assessed theoretically in an erythrocyte buffer suspension. Fractional equilibrium conditions equivalent to those in an erythrocyte plasma suspension are reached at some time, $t = \gamma\cdot\bar{t}'$, after addition of drug to a red blood cell buffer suspension $[E_{t=\gamma\bar{t}'} = (1 - e^{-\gamma})E'_{eq}]$. Intuitively, the corresponding new mean transit time, $\bar{t}'$, should be smaller than $\bar{t}$ (and accordingly k'_{BE}, and k'_{EB} should be larger than k_{BE} and k_{EB}) since the new fractional equilibrium is reached earlier than the true fractional equilibrium in a red blood cell in buffer suspension.

The ratio of $\gamma\cdot\bar{t}$ to $\bar{t}'$, r, can be calculated from:

$$r = \gamma\frac{\bar{t}}{\bar{t}'} = -\ln\left[\frac{E'_{eq} - E_{t=\gamma\cdot\bar{t}}}{E'_{eq}}\right] \qquad \text{(Eq. 37A)}$$

After substituting Eqs. 1A, 2A, 9A, 24A, 25A, and 35A and rearranging, Eq. 37A can be reformulated:

$$r = \gamma\frac{\bar{t}}{\bar{t}'} = -\ln\left\{1 - \left[(1 - e^{-\gamma}) \cdot \frac{[(1 - \beta_{PB}/10^2)\cdot P_{e/c_u}\cdot Hc] + (1 - Hc)}{(1 - \beta_{PB}/10^2)\cdot[P_{e/c_u}\cdot Hc + (1 - Hc)]}\right]\right\} \qquad \text{(Eq. 38A)}$$

and k'_{BE} and k'_{EB} are then obtained from:

$$k'_{BE} = k_{BE}\cdot\frac{r}{\gamma} \qquad \text{(Eq. 39A)}$$

$$k'_{EB} = k_{EB}\cdot\frac{r}{\gamma} \qquad \text{(Eq. 40A)}$$

The plasma binding-induced reduction of the amounts of drug that can partition into the red blood cells is now considered. In a red blood cell plasma suspension only the unbound drug fraction in plasma is available for cell partitioning. The magnitude of the apparent partitioning constant, k_{PE}, referenced to the total (bound + unbound) drug concentration in plasma, will be affected in accordance with:

$$k_{PE} = k'_{BE}\cdot\left(1 - \frac{\beta_{PB}}{10^2}\right) = k_{BE}\cdot\frac{r}{\gamma}\left(1 - \frac{\beta_{PB}}{10^2}\right) \qquad \text{(Eq. 41A)}$$

Hence, if plasma protein binding and red blood cell buffer partitioning of a drug are known, the apparent parameters $(\bar{t})$, k_{PE}, and k_{EP} in an erythrocyte plasma suspension can be predicted from the true parameters ($\bar{t}$, k_{BE}, and k_{EB}) obtained for the drug in an erythrocyte buffer suspension according to:

$$(\bar{t}) = \frac{1}{k_{PE} + k_{EP}} = \frac{1}{\frac{r}{\gamma}[k_{BE}(100 - \beta_{PB}) + k_{EB}]} \qquad \text{(Eq. 42A)}$$

$$k_{PE} = \frac{r}{\gamma}[k_{BE}(100 - \beta_{PB})] \qquad \text{(Eq. 43A)}$$

$$k_{EP} = \frac{r}{\gamma}\cdot k_{EB} \qquad \text{(Eq. 44A)}$$

REFERENCES

(1) P. H. Hinderling, *Agents Actions*, **7**, 379 (1977).

(2) L. W. Schanker, P. A. Nafpliotis, and J. M. Johnson, *J. Pharmacol.*, **133**, 325 (1961).

(3) A. von Wartburg, F. Kalberer, and J. Rutschmann, *Biochem. Pharmacol.*, **14**, 1883 (1965).

(4) G. Haberland and G. Maerten, *Naturwissenschaften*, **56**, 516 (1969).

(5) P. H. Hinderling, E. R. Garrett, and R. Wester, *J. Pharm. Sci.*, **66**, 314 (1977).

(6) O. Eichhorst and P. H. Hinderling, *J. Chromatogr.*, **224**, 67 (1981).

(7) A. Roos and P. H. Hinderling, *J. Pharm. Sci.*, **70**, 252 (1981).

(8) G. G. Belz, K. O. Vollmer, and J. H. Wissler, *Eur. J. Clin. Pharmacol.*, **4**, 92 (1972).

(9) J. D. Gardner, D. R. Kiino, T. J. Swartz, and V. P. Butler, *J. Clin. Invest.*, **52**, 1820 (1973).

(10) "Documenta Geigy, Scientific Tables," 7th ed., K. Diem and C. Lentner, Eds., Geigy Pharmaceuticals, Ardsley, N.Y., 1975, p. 617.

(11) P. H. Hinderling, J. Brès, and E. R. Garrett, *J. Pharm. Sci.*, **63**, 1684 (1974).

(12) M. Eckert and P. H. Hinderling, *Agents Actions*, **11**, 5 (1981).

(13) "Documenta Geigy, Scientific Tables," 7th ed., K. Diem and C. Lentner, Eds., Geigy Pharmaceuticals, Ardsley, N.Y., 1975, p. 560.

(14) "Documenta Geigy, Scientific Tables," 7th ed., K. Diem and C. Lentner, Eds., Geigy Pharmaceuticals, Ardsley, N.Y., 1975, p. 582.

(15) O. W. van Assenfeldt, W. G. Zijlstra, and E. J. van Kampen, *Proc. K. Ned. Akad. Wet. Ser. C*, **73**, 104 (1970).

(16) "Documenta Geigy, Scientific Tables," 7th ed., K. Diem and C. Lentner, Eds., Geigy Pharmaceuticals, Ardsley, N.Y., 1975, p. 561.

(17) A. N. Martin, J. Swarbrick, and A. Cammarata, "Physical Pharmacy," 3rd ed., Lea & Febiger, Philadelphia, Pa., 1970, p. 314.

(18) G. Heinzel, in "Pharmacokinetics during Drug Development, Data Analysis and Evaluation Techniques," J. van Rossum and G. Bozler, Eds., G. Fischer Verlag, Stuttgart, New York, 1982, p. 207.

(19) U. Abshagen, H. Kewitz, and N. Rietbrock, *Naunyn-Schmiedebergs Arch. Pharmak.*, **270**, 105 (1971).

(20) A. Rescigno and E. Gurpide, *J. Clin. Endocrinol. Metab.*, **36**, 263 (1973).

(21) K. Yamaoka, T. Nagakawa, and T. Uno, *J. Pharmacokinet. Biopharm.*, **6**, 547 (1978).

(22) C. A. Goresky, *Am. J. Physiol.*, **204**, 626 (1963).

(23) K. Kramer, K. Thurau, and P. Deetjen, *Pflügers Arch. Ges. Physiol.*, **270**, 251 (1960).

(24) E. Krüger-Thiemer, *J. Am. Pharm. Assoc., Sci. Ed.*, **49**, 311 (1960).

(25) "Documenta Geigy, Scientific Tables," 7th ed., K. Diem and C. Lentner, Eds., Geigy Pharmaceuticals, Ardsley, N.Y., 1975, p. 576.

(26) E. Cohnen, H. Flasch, N. Heinz, and F. W. Hempelmann, *Drug Res.*, **28**, 2179 (1978).

(27) W. Scheler and J. Blanck, in "Kinetics of Drug Action," J. M. van Rossum, Ed., Springer Verlag, Berlin, Heidelberg, New York, 1977, p. 11.

(28) C. V. Paganelli and A. K. Solomon, *J. Gen. Physiol.*, **41**, 259 (1957).

(29) R. I. Sha'afi, G. T. Rich, V. W. Sidel, W. Bossert, and A. K. Solomon, *J. Gen. Physiol.*, **50**, 1377 (1967).

(30) J. M. Plá-Delfina and J. Moreno, *J. Pharmacokinet. Biopharm.*, **9**, 191 (1981).

(31) E. M. Renkin and J. R. Pappenheimer, *Ergebn. Physiol.*, **49**, 59 (1957).

(32) J. S. Fordtran, F. C. Rector, Jr., M. F. Ewton, N. Soter, and J. Kinney, *J. Clin. Invest.*, **44**, 12 (1965).

(33) J. D. Baggot and L. E. Davis, *Res. Vet. Sci.*, **15**, 81, (1973).

(34) P. Kramer, E. Köthe, J. Saul, and F. Scheler, *Eur. J. Clin. Invest.*, **54**, 53 (1974).

(35) L. Storstein, *Clin. Pharmacol. Ther.*, **20**, 6 (1976).

(36) E. E. Ohnhaus, P. Spring, and L. Dettli, *Eur. J. Clin. Pharmacol.*, **5**, 34 (1972).

(37) D. C. Evered, *Eur. J. Pharmacol.*, **18**, 236 (1972).

(38) D. S. Lukas and A. G. de Martino, *J. Clin. Invest.*, **48**, 1041 (1969).

(39) A. Brock, *Acta Pharmacol. Toxicol.*, **36**, 13 (1975).

(40) A. A. Spector, E. C. Santos, J. D. Ashbrook, and J. E. Fletcher, *Ann. N.Y. Acad. Sci.*, **226**, 247 (1973).

(41) L. Storstein and H. Janssen, *Clin. Pharmacol. Ther.*, **20**, 15 (1976).

(42) H. J. Dengler, G. Bodem, and K. Wirth, *World Congr. Cardiol., Cardiovasc. Res., vol. VI*, 1970, p. 119.

(43) F. W. Hempelmann and N. Heinz, *Drug. Res.*, **28**, 25 (1978).

(44) W. Scheler and J. Blanck, in "Kinetics of Drug Action," J. M. van Rossum, Ed., Springer Verlag, Berlin, Heidelberg, New York, 1977, p. 12.

(45) P. Heintzen, *Pflügers Arch. Ges. Physiol.*, **266**, 207 (1958).

(46) G. R. Wilkinson and D. G. Shand, *Clin. Pharmacol. Ther.*, **18**, 377 (1975).

(47) K. S. Pang and M. Rowland, *J. Pharmacokinet. Biopharm.*, **5**, 625 (1977).

(48) E. R. Garrett and H. J. Lambert, *J. Pharm. Sci.*, **62**, 550 (1973).

(49) C. Capellos and B. H. J. Bielski, in "Kinetic Systems," Wiley-Interscience, New York, N.Y., 1972, pp. 32–35.

ACKNOWLEDGMENTS

Supported in part by a scholarship by the Sandoz Stiftung "zur Förderung der Medizinischen Wissenschaften," Sandoz Ltd., Basle, Switzerland.

The author thanks Professor W. Schaumann, Boehringer Mannheim Ltd., FRG, and Dr. H. Flasch, Beiersdorf Ltd., Hamburg, FRG, for the supply of the labeled and unlabeled digoxin and derivatives. The expert technical assistance of Rosmarie Leder is gratefully acknowledged.

Absorption and Disposition of Ethambutol in Rabbits

M. M. CHEN *, C. S. LEE ‡x, and J. H. PERRIN *

Received May 9, 1983, from the **Department of Pharmacy, University of Florida, Gainesville, FL 32610* and the ‡*Department of Pharmaceutics, University of Houston, Houston, TX 77030.* Accepted for publication July 13, 1983.

Abstract □ The absorption and disposition of ethambutol was examined in six rabbits in a three-way crossover study. Each rabbit received 45-mg/kg doses of ethambutol in three treatments: one intravenous injection, and two oral solutions, ethambutol alone and ethambutol in the presence of aluminum hydroxide (40 mg/kg). Half-lives of ethambutol ranged from 2.26 to 5.20 h when administered alone and 2.18 to 4.00 h when coadministered with the antacid; the difference was not significant ($p > 0.3$). Mean clearance after the oral administrations (189.2 mL/min/kg) was significantly greater than the mean intravenous clearance (43.7 mL/min/kg) ($p < 0.01$), suggesting a first-pass metabolism of ethambutol when administered nonparenterally to rabbits. The volume of distribution ranged from 5.5 to 17.8 L/kg, suggesting an extensive distribution of ethambutol outside the central compartment and, possibly, a localized deposit within the body tissues. Mean bioavailability of ethambutol was ~28% and was not affected by the presence of aluminum hydroxide. The rate of ethambutol absorption, however, was slightly delayed by the antacid.

Keyphrases □ Ethambutol—pharmacokinetics in rabbits, coadministration with aluminum hydroxide □ Aluminum hydroxide—effect on ethambutol absorption in rabbits □ Bioavailability—absorption of ethambutol in rabbits, coadministration with aluminum hydroxide

Ethambutol (I), an antitubercular agent, is prescribed alone or in combination with other drugs for the treatment of tuberculosis. The absorption and excretion of I has been studied in rats and mice (1), dogs (2, 3), and humans (4–6). The median lethal dose (LD_{50}) of racemic I in noninfected adult mice was 12,800 mg/kg when administered orally, 1600 mg/kg when administered subcutaneously, 800–1600 mg/kg when administered intraperitoneally, and 200–400 mg/kg when administered intravenously (1). Since I is well absorbed in mice and the drug metabolites are pharmacologically inactive (3), the remarkable discrepancies in LD_{50} following different administration routes suggest a first-pass metabolism of the drug when taken nonparenterally. A part of this study was thus designed to investigate the effect of first-pass metabolism on the availability of I in rabbits.

Pharmacokinetic studies comparing the intravenous and oral administrations of I to humans have demonstrated rapid and adequate absorption, with bioavailabilities of 70–80% (6, 7). The oral solution and tablets of I were equally well absorbed in humans (6), suggesting a gastric emptying rate- rather than dissolution rate-limited absorption of the drug. Aluminum ion is a known inhibitor of gastric emptying, and its effect on drug absorption has been documented (8). Mattila *et al.* (9) have investigated the effect of aluminum hydroxide on the absorption of I in humans; the results were erratic. Since the results of Matilla *et al.* (9) were inconclusive, this study also seeks to clarify the effect of aluminum hydroxide on the absorption of I using the rabbit model.

EXPERIMENTAL SECTION

Materials—All materials used in this study were the same as those used in a previous investigation (10).

Animal Experiments—Six male New Zealand White rabbits (weight, 2.8–4.1 kg) were studied in a three-way crossover manner. Each rabbit received 45-mg/kg doses of I in three separate treatments: as an intravenous injection, as an oral solution, and as an oral solution in the presence of aluminum hydroxide (40 mg/kg). Gastric emptying of solid food residues was induced by fasting for 38–42 h before drug administration. Water was allowed *ad libitum* during fasting; food and water were withheld over the experimental period. A 2-week washout interval was implemented between the crossover studies.

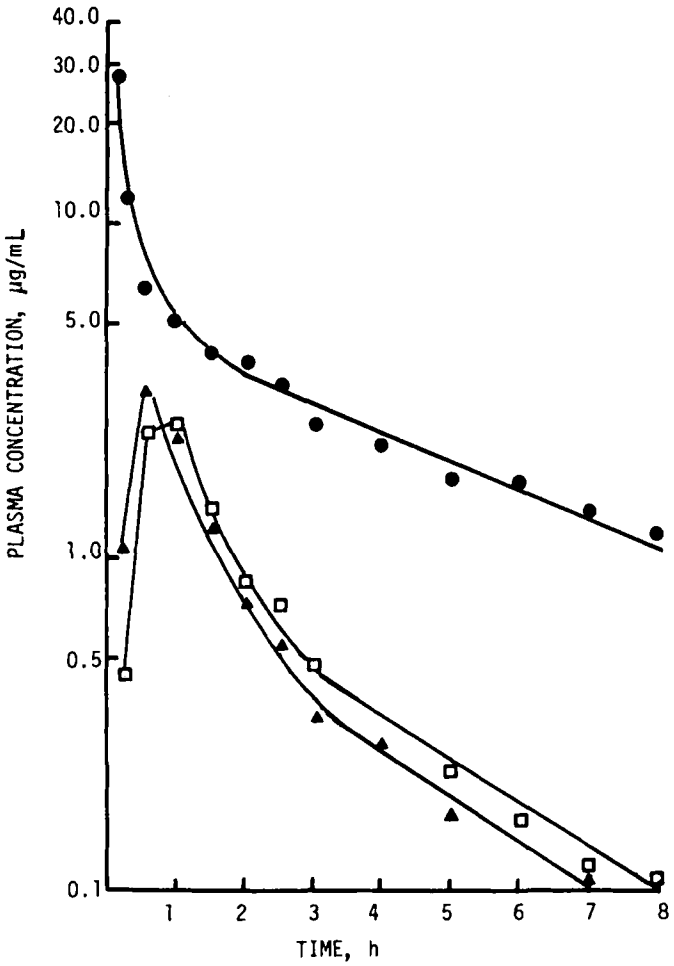

Figure 1—*Semilogarithmic plasma concentration* versus *time plots for rabbit 6 administered ethambutol (45 mg/kg) intravenously (●) and orally (▲, without aluminum hydroxide; □, with the antacid).*

0022-3549/84/0800-1053$01.00/0
© 1984, American Pharmaceutical Association

ACKNOWLEDGMENTS

Supported in part by a scholarship by the Sandoz Stiftung "zur Förderung der Medizinischen Wissenschaften," Sandoz Ltd., Basle, Switzerland.

The author thanks Professor W. Schaumann, Boehringer Mannheim Ltd., FRG, and Dr. H. Flasch, Beiersdorf Ltd., Hamburg, FRG, for the supply of the labeled and unlabeled digoxin and derivatives. The expert technical assistance of Rosmarie Leder is gratefully acknowledged.

Absorption and Disposition of Ethambutol in Rabbits

M. M. CHEN *, C. S. LEE ‡x, and J. H. PERRIN *

Received May 9, 1983, from the **Department of Pharmacy, University of Florida, Gainesville, FL 32610* and the ‡*Department of Pharmaceutics, University of Houston, Houston, TX 77030.* Accepted for publication July 13, 1983.

Abstract □ The absorption and disposition of ethambutol was examined in six rabbits in a three-way crossover study. Each rabbit received 45-mg/kg doses of ethambutol in three treatments: one intravenous injection, and two oral solutions, ethambutol alone and ethambutol in the presence of aluminum hydroxide (40 mg/kg). Half-lives of ethambutol ranged from 2.26 to 5.20 h when administered alone and 2.18 to 4.00 h when coadministered with the antacid; the difference was not significant ($p > 0.3$). Mean clearance after the oral administrations (189.2 mL/min/kg) was significantly greater than the mean intravenous clearance (43.7 mL/min/kg) ($p < 0.01$), suggesting a first-pass metabolism of ethambutol when administered nonparenterally to rabbits. The volume of distribution ranged from 5.5 to 17.8 L/kg, suggesting an extensive distribution of ethambutol outside the central compartment and, possibly, a localized deposit within the body tissues. Mean bioavailability of ethambutol was ~28% and was not affected by the presence of aluminum hydroxide. The rate of ethambutol absorption, however, was slightly delayed by the antacid.

Keyphrases □ Ethambutol—pharmacokinetics in rabbits, coadministration with aluminum hydroxide □ Aluminum hydroxide—effect on ethambutol absorption in rabbits □ Bioavailability—absorption of ethambutol in rabbits, coadministration with aluminum hydroxide

Ethambutol (I), an antitubercular agent, is prescribed alone or in combination with other drugs for the treatment of tuberculosis. The absorption and excretion of I has been studied in rats and mice (1), dogs (2, 3), and humans (4–6). The median lethal dose (LD_{50}) of racemic I in noninfected adult mice was 12,800 mg/kg when administered orally, 1600 mg/kg when administered subcutaneously, 800–1600 mg/kg when administered intraperitoneally, and 200–400 mg/kg when administered intravenously (1). Since I is well absorbed in mice and the drug metabolites are pharmacologically inactive (3), the remarkable discrepancies in LD_{50} following different administration routes suggest a first-pass metabolism of the drug when taken nonparenterally. A part of this study was thus designed to investigate the effect of first-pass metabolism on the availability of I in rabbits.

Pharmacokinetic studies comparing the intravenous and oral administrations of I to humans have demonstrated rapid and adequate absorption, with bioavailabilities of 70–80% (6, 7). The oral solution and tablets of I were equally well absorbed in humans (6), suggesting a gastric emptying rate- rather than dissolution rate-limited absorption of the drug. Aluminum ion is a known inhibitor of gastric emptying, and its effect on drug absorption has been documented (8). Mattila *et al.* (9) have investigated the effect of aluminum hydroxide on the absorption of I in humans; the results were erratic. Since the results of Matilla *et al.* (9) were inconclusive, this study also seeks to clarify the effect of aluminum hydroxide on the absorption of I using the rabbit model.

EXPERIMENTAL SECTION

Materials—All materials used in this study were the same as those used in a previous investigation (10).

Animal Experiments—Six male New Zealand White rabbits (weight, 2.8–4.1 kg) were studied in a three-way crossover manner. Each rabbit received 45-mg/kg doses of I in three separate treatments: as an intravenous injection, as an oral solution, and as an oral solution in the presence of aluminum hydroxide (40 mg/kg). Gastric emptying of solid food residues was induced by fasting for 38–42 h before drug administration. Water was allowed *ad libitum* during fasting; food and water were withheld over the experimental period. A 2-week washout interval was implemented between the crossover studies.

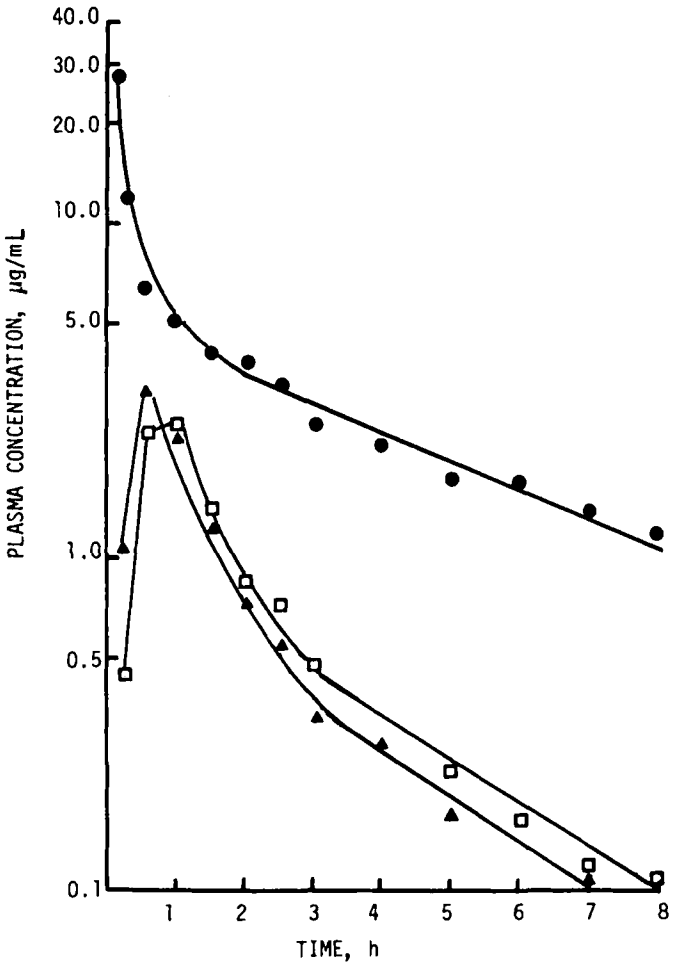

Figure 1—*Semilogarithmic plasma concentration* versus *time plots for rabbit 6 administered ethambutol (45 mg/kg) intravenously (●) and orally (▲, without aluminum hydroxide; □, with the antacid).*

0022-3549/84/0800-1053$01.00/0
© 1984, American Pharmaceutical Association

Table I—Mean Plasma I Levels after Single Doses of I (45 mg/kg) as Three Treatments

Treatment[a]	Plasma I Concentration, μg/mL												
	0.15 h	0.25 h	0.5 h	1.0 h	1.5 h	2.0 h	2.5 h	3.0 h	4.0 h	5.0 h	6.0 h	7.0 h	8.0 h
A													
Mean	20.23	10.84	5.34	4.09	3.11	2.21	2.13	1.64	1.66	1.35	0.90	0.77	0.70
SD	6.20	3.09	1.62	2.11	1.81	1.13	0.73	0.81	1.20	0.61	0.49	0.49	0.47
B													
Mean	—	0.74	2.44	1.52	0.76	0.55	0.37	0.29	0.26	0.18	0.18	0.13	0.12
SD	—	0.20	0.96	0.44	0.27	0.17	0.12	0.07	0.07	0.07	0.07	0.07	0.07
C													
Mean	—	0.74	1.73	1.56	0.81	0.56	0.46	0.37	0.24	0.19	0.15	0.12	0.09
SD	—	0.44	0.61	0.56	0.37	0.20	0.17	0.10	0.07	0.12	0.05	0.05	0.05

[a] Treatments: (A) intravenous injection; (B) oral solution with I alone; (C) oral solution with I and aluminum hydroxide; $n = 6$.

In the case of the intravenous injection, I was administered *via* the ear vein by a slow push over 5 min. As oral solutions, I was prepared in 70 mL of warm, deionized water and administered *via* the mouth by intubation. The intubation line was flushed with 30 mL of warm water to ensure that the complete dose was deposited into the stomach. Blood samples were collected from the ear vein at 0 (blank), 0.15 (injection only), 0.25, 0.5, 1.0, 1.5, 2, 2.5, 3, 4, 5, 6, 7, and 8 h. Hourly urine aliquots were collected from two rabbits by urethral catheter for the first 8 h; thereafter, cumulative 16-h urine samples were collected by natural voiding while rabbits were housed in the metabolism cage.

Blood Cell-to-Plasma Partition Ratio—Aliquots (1 mL) of heparinized whole blood were incubated with I (concentrations of 0.5, 1, and 2 μg/mL) at 37°C for 30 min. Immediately after incubation, plasma was separated by centrifugation and stored at −20°C until analysis. The blood cell-to-plasma partition ratio was calculated as $[C_b/C_p - (1 - H)]/H$, where H is the hematocrit.

Analytical Procedure—A GC procedure, as previously described, was used for sample analysis (10). The GC procedure normally provides a lower detection limit of 0.25 μg/mL. Since plasma levels of I after administration of the oral solutions were usually low, the procedure was manipulated to accommodate the concentration of 0.1 μg/mL.

Pharmacokinetic Analysis—The β-phase half-life ($t_{1/2\beta}$) was obtained by fitting the plasma data to a two-compartment model by the NONLIN program (11). Total body clearance (CL_t) and the noncompartmental steady-state volume of distribution (Vd_{ss}) were determined as:

$$CL_t = \text{dose}/\text{AUC}_\infty \qquad \text{(Eq. 1)}$$

$$Vd_{ss} = \text{dose}(\text{AUMC}_\infty)/(\text{AUC}_\infty)^2 \qquad \text{(Eq. 2)}$$

where AUC is the area under the plasma concentration *versus* time curve, and AUMC is the area under the first moment of the plasma curve (12). Both areas were calculated by the trapezoidal rule in conjunction with an area extrapolation method. The first plasma datum was assumed to be zero in the case of the oral administrations; the first plasma datum after intravenous administration was a NONLIN-generated initial concentration.

Bioavailability was determined by the AUC method, taking into account the half-life change due to alternate routes of drug administration:

$$F = \left(\frac{\text{AUC}_{po}}{\text{AUC}_{iv}}\right) \times \left(\frac{t_{1/2iv}}{t_{1/2po}}\right) \qquad \text{(Eq. 3)}$$

where iv indicates the intravenous administration route, and po indicates the oral administration route. In the two rabbits for which urine was collected at 24 h, bioavailability was also determined by the urinary recovery method:

$$F = \frac{(Ae,24 + CL_r \cdot \text{AUC}_{24\to\infty})_{po}}{(Ae,24 + CL_r \cdot \text{AUC}_{24\to\infty})_{iv}} \qquad \text{(Eq. 4)}$$

Table II—Half-lives of I after Single Doses of I (45 mg/kg) as Three Treatments [a]

Rabbit	Half-life, h		
	Treatment A	Treatment B	Treatment C
1	4.67	5.20	3.77
2	4.08	3.58	3.37
3	4.49	3.66	4.00
4	3.42	2.65	2.18
5	1.96	2.26	2.58
6	4.59	2.83	2.62
Mean ± *SD*	3.87 ± 1.03[b]	3.36 ± 1.05[b]	3.09 ± 0.73[b]

[a] Treatments: (A) intravenous injection; (B) oral solution with I alone; (C) oral solution with I and aluminum hydroxide. [b] Half-lives of I after treatments A, B, and C are not significantly different ($p > 0.3$); $n = 6$.

where $Ae,24$ is the amount of drug excreted in the 24-h urine sample, and CL_r is the average renal clearance as determined from the drug excretion rates during the first 8 h. The extrapolated area ($\text{AUC}_{24\to\infty}$) was calculated as $C_{p,24}/\beta$, where the 24-h plasma concentration was extrapolated from $C_{p,8}$ using the elimination rate constant, β.

Statistical Analysis—Mean pharmacokinetic parameters between any two treatments were tested for significance of difference by paired *t* test statistics.

RESULTS AND DISCUSSION

Table I describes the mean plasma data for rabbits that received I after treatment protocols A, B, and C. At the end of the 8-h sampling period, the residual level of I after intravenous injection was six times that after administration of the oral solutions. Figure 1 depicts a representative plasma profile in rabbit 6. During the first hour of intravenous injection, plasma concentrations of I dropped rapidly, indicating a fast distribution of the drug into the peripheral tissue compartment. Overall, the log-linear phase began at 1–3 h after drug injection and exhibited a half-life range of 1.96–4.67 h. After the oral administrations of I, a rapid distribution of the drug was also observed in all rabbits. Peak plasma concentrations were reached within 1 h, and a slightly delayed peak time was observed for I in combination with aluminum hydroxide. The log-linear phase did not begin until 1.5 h after oral solution administration, and the time to reach distribution equilibrium was as late as 3 h in some rabbits. It should be noted that the delayed stomach emptying as induced by fasting might lead to prolonged absorption and overestimation of half-life measurements (13). In the presence of aluminum hydroxide, I exhibited half-lives of 2.18–4.00 h, as compared with 2.26–5.20 h for I administered alone. The mean half-life of I was not significantly altered by the coadministration of aluminum hydroxide (3.36 ± 1.05 *versus* 3.09 ± 0.73 h; $p > 0.3$). In Table II, the mean half-lives of I in the three treatments are compared; all rabbits exhibited similar half-lives, irrespective of the route of administration and the presence of aluminum hydroxide.

Values for the steady-state volume of distribution of I, derived on the basis of venous data after intravenous administration, are shown in Table III. A wide range was observed for the volume of distribution of I (5.5–17.8 L/kg; mean, 8.5 ± 1.9 L/kg). Chiou (14) has reported that Vd_{ss} estimated with venous data could be 20–120% higher than that derived on the basis of arterial concentration. By taking into consideration the arteriovenous difference, the volume obtained is still several times the body weight of the rabbit (assuming a density of 1 g/mL). This indicates that in addition to the extensive distribution, I was probably deposited locally in the rabbit body tissues. Ethambutol has been known to be extensively distributed into the viscera and tissues of animals and humans. Pujet and Pujet (15) have reported a preferential distribution of I in the deep layers of the lung. Furthermore, *in vivo* and *in vitro*

Table III—Total Body Clearance and Volume of Distribution of I after Single Doses of I (45 mg/kg) as Three Treatments [a]

Rabbit	CL_t, mL/min/kg			Vd_{ss}, L/kg
	Treatment A	Treatment B	Treatment C	Treatment A
1	70.4	120.6	139.4	17.8
2	35.3	196.3	199.5	7.8
3	28.6	175.6	182.5	6.4
4	29.8	261.3	272.7	5.5
5	76.1	178.9	249.2	8.1
6	22.3	148.2	145.8	5.6
Mean ± *SD*	43.7 ± 23.2[b]	180.2 ± 46.0[b]	198.2 ± 54.0[b]	8.5 ± 4.6

[a] Treatments: (A) intravenous injection; (B) oral solution with I alone; (C) oral solution with I and aluminum hydroxide. [b] Oral clearances are not significantly different ($p > 0.1$); however, oral clearance and intravenous clearance are statistically different ($p < 0.01$); $n = 6$.

studies have demonstrated a favorable partition of I into erythrocytes in humans (4, 6). The blood-cell-to plasma partition ratio averaged 1.25 in all rabbits for the concenration range thus investigated.

Values for total body clearance of I after the three treatments are summarized in Table III. Two oral studies, I alone and I in combination with aluminum hydroxide, yielded virtually the same clearance (180.2 ± 47.9 *versus* 198.2 ± 54.0 mL/min/kg), indicating that aluminum hydroxide had no effect on the elimination of I. However, the total clearance after oral administration was significantly greater than the intravenous clearance (189.2 *versus* 43.7 mL/min/kg; $p < 0.01$), suggesting a first-pass metabolism for I. Previous studies with mice, rats, and dogs did not document first-pass metabolism of I since intravenous and oral studies were not carried out in a crossover manner (2, 3). The difference in LD_{50} among various routes of administration in mice could be due partly to the rate of absorption into the circulatory system. However, the magnitude of difference in LD_{50} observed (1) between oral and intravenous administrations (12,800 *versus* 400 mg/kg) supported our proposition of first-pass metabolism in rabbits. Poor absorption of I in rabbits could be an alternative argument; however, we found <15% of orally administered I in rabbit feces.

Renal excretion of I was studied in two rabbits after intravenous and oral administrations. Renal clearances, computed as $Ae,8/AUC_{0\to8}$, averaged 2.5 mL/min/kg. There was no significant change in renal clearance between studies utilizing the oral and intravenous administration routes. The fraction of I dose excreted unchanged after intravenous studies averaged 5.2%, which is considerably lower than the corresponding figures of 30 and 70% in dogs and humans, respectively (10).

The bioavailability data for I, alone and in combination with aluminum hydroxide, were calculated with Eq. 3 and are shown in Table IV. It should be noted that the validity of Eq. 3 is based on the assumption that $Vd_\beta(CL_t/\beta)$ remains the same, in spite of a change in β (16). Although the AUC method was used in all rabbits for bioavailability determination, the urinary recovery method was simultaneously applied to two rabbits for cross-examination. For rabbit 1, the urinary recovery method yielded a somewhat higher bioavailability than the AUC method (62.9 *versus* 57.5%), whereas for rabbit 5, both methods yielded virtually the same results (30.1 *versus* 30.0%). On the average, 28% of the oral I dose was bioavailable to the circulatory system. Without correction for half-life change with Eq. 3, the mean bioavailability was somewhat lower (25%). The low bioavailability also supported the hypothesis of first-pass metabolism of I in rabbits, as previously suggested on the basis of clearance measurements (Table III). As the hepatic blood flow (Q_b) in rabbits has been reported to be 60 mL/min/kg (17), the extent of hepatic first-pass effect for I was approximated as CL_t/Q_b where CL_t is the mean plasma clearance after intravenous administration. A mean of 73% (43.7 of 60) of the dose of I was estimated to undergo first-pass metabolism. This is consistent with the bioavailability of 25–28% in rabbits reported here.

The aluminum hydroxide dose of 40 mg/kg, as used in this study, was three times the therapeutic dose of the antacid used in humans on a weight basis. In the study of Mattila *et al.* (9), a 60-mg/kg dose was used. *In vitro*, aluminum ion at 5×10^{-4} M inhibits the contractile response of human and rat gastric strips to acetylcholine by >50% (18). The *in vitro* effect of aluminum ion on the contractile response of rabbit gastric strips has not been investigated. The aluminum concentration achieved *in vivo* in the stomach of rabbits receiving aluminum hydroxide (2×10^{-2} M) was much higher than that used *in vitro*. It was felt that such a concentration would be sufficient to significantly delay gastric emptying in rabbits.

With regard to the absorption of I, the rabbit may not be an ideal model for comparison with human data; however, rabbits demonstrated a consistent, although insignificant, response to aluminum hydroxide. On the contrary, humans responded to aluminum hydroxide erratically, making it difficult to make a conclusion on the effect of the antacid on the bioavailability of I. In summary, the concomitant administration of aluminum hydroxide appeared to have slightly delayed the absorption of I in some rabbits, as reflected by a prolonged peak time; the extent of absorption, however, was insignificantly altered by the presence of the antacid.

Table IV—Bioavailability of I after Two Oral Treatments [a]

Rabbit	Bioavailability, % of Intravenous Dose	
	Treatment B	Treatment C
1	52.40 (67.57)[b]	62.52 (58.30)[b]
2	20.48	21.38
3	19.97	17.58
4	14.71	17.12
5	36.87 (30.28)[b]	23.17 (29.98)[b]
6	24.44	26.82
Mean ± *SD*[c]	28.15 ± 14.01	28.10 ± 17.24

[a] Treatments: (B) solution with I alone; (C) solution with I and aluminum hydroxide. [b] Numbers in parentheses denote bioavailability determined by the urinary recovery method. [c] $n = 6$.

REFERENCES

(1) J. P. Thomas, C. O. Baughn, R. G. Wilkinson, and R. G. Shepherd, *Am. Rev. Resp. Dis.*, **83,** 891 (1961).

(2) E. A. Peets and D. A. Buyske, *Biochem. Pharmacol.*, **13,** 1403 (1964).

(3) D. A. Buyske, W. Sterling, and E. Peets, *Ann. N.Y. Acad. Sci.*, **135,** 711 (1966).

(4) E. A. Peets, W. M. Sweeney, W. A. Place, and D. A. Buyske, *Am. Rev. Resp. Dis.*, **91,** 51 (1965).

(5) T. G. Christopher, A. Blair, A. Forrey, and E. Cutler, *Proc. Dialy. Transpl. Forum.*, **3,** 96 (1975).

(6) C. S. Lee, J. G. Gambertoglio, D. C. Brater, and L. Z. Benet, *Clin. Pharmacol. Ther.*, **22,** 615 (1977).

(7) C. S. Lee, D. C. Brater, J. G. Gambertoglio, and L. Z. Benet, *J. Pharmacokinet. Biopharm.*, **8,** 335 (1980).

(8) A. Hurwitz, in "Drug Interactions," Raven, New York, N.Y., 1974, p. 27.

(9) M. J. Mattila, L. T. Seppala, and R. Kosbinen, *Br. J. Clin. Pharmacol.*, **5,** 161 (1978).

(10) C. S. Lee and A. Varughese, *J. Pharm. Sci.*, **73,** 787 (1984).

(11) C. M. Metzler, G. L. Elfring, and A. J. McEwen, *Biometrics*, **30,** 562 (1974).

(12) L. Z. Benet and R. L. Galeazzi, *J. Pharm. Sci.*, **68,** 1071 (1979).

(13) W. L. Chiou, S. Riegelman, and J. R. Amberg, *Chem. Pharm. Bull.*, **17,** 2170 (1969).

(14) W. L. Chiou, *Int. J. Clin. Pharmacol. Ther. Toxicol.*, **20,** 255 (1982).

(15) J. C. Pujet and C. Pujet, *Med. J. France (Suppl.)*, **79,** 7312 (1972).

(16) W. C. Chiou, C. Y. Lui, and G. Lam, *J. Pharm. Sci.*, **70,** 109 (1981).

(17) Ch. Balabaud, Mc. Roche, and J. Dangoumau, *Biomedicine*, **23,** 353 (1975).

(18) M. Hava and A. Hurwitz, *Eur. J. Pharm.*, **22,** 156 (1973).

ACKNOWLEDGMENTS

This work was presented in part at the 129th APhA Annual Meeting, Las Vegas, Nev., April 1982. The authors thank the Word Processing Center Staff of the University of Houston for assistance in manuscript preparation.

In Vitro Interaction of Neuroleptics and Tricylic Antidepressants with Coffee, Tea, and Gallotannic Acid

WILLIAM L. LASSWELL, JR. ˣ, STANLEY S. WEBER, and JOHN M. WILKINS

Received March 16, 1983, from the *College of Pharmacy, University of Rhode Island, Kingston, RI 02881.* Accepted for publication September 4, 1983.

Abstract □ The *in vitro* interaction of selected drugs with coffee, tea, gallic acid, and gallotannic acid was examined by mixing solutions of drug with each of these four preparations. Results of these experiments indicate that significant precipitation occurs for a variety of agents, including several phenothiazines, amitriptyline, haloperidol, imipramine, and loxapine. The strong complex which is formed between these drugs and tannins is probably the basis of the interaction of these drugs with coffee and tea. Although precipitates did occur with a number of neuroleptics, two members of this drug class, thiothixene and molindone, failed to interact with the solutions used.

Keyphrases □ Tricyclic antidepressants—*in vitro* interaction with coffee, tea, gallotannic acid, and gallic acid □ Neuroleptics—*in vitro* interaction with coffee, tea, gallotannic acid, and gallic acid

The interaction of certain antipsychotic agents with tea and coffee has received some attention in recent years. Mikkelsen (1) first reported that increased consumption of coffee may reduce the effectiveness of phenothiazines. Soon after, Hirsch (2) and Kulhaneck *et al.* (3) reported that *in vitro* mixing of a number of neuroleptics, including chlorpromazine, haloperidol, and fluphenazine (but not trifluoperazine), with coffee or tea led to the formation of a precipitate. Cheeseman and Neal (4) have studied the interaction of chlorpromazine with coffee and tea in more detail and have found that simultaneous oral administration of tea with chlorpromazine completely abolished the cataleptic effects of this drug in rats. Concern about the possible effects which precipitation of antipsychotics could have on their bioavailability in humans led Bowen *et al.* (5) to study the possible interaction of coffee and tea with these four drugs in female patients. Using a dopamine receptor assay (6), plasma drug concentrations were measured during sequential weekly periods of normal coffee and tea intake, abstinence from these beverages, and finally resumption of intake. On the basis of plasma drug levels and behavioral scores (7), they concluded that withdrawal of coffee and tea did not increase drug bioavailability. However, neither the amounts of coffee and tea used in this study nor the timing of beverage intake with respect to drug administration were specified. Furthermore, the time intervals used in the overall design of this experiment were questionable.

In the present study, we report results on the *in vitro* interaction of coffee, tea, gallotannic acid, and gallic acid with a variety of neuroleptic agents, as well as amitriptyline and imipramine.

EXPERIMENTAL SECTION

The drugs used in this study included amitriptyline hydrochloride[1], chlorpromazine hydrochloride[2], haloperidol[3], imipramine hydrochloride[2], loxapine hydrochloride[4], molindone hydrochloride[5], prochlorperazine hydrochloride[6], thioridazine hydrochloride[7], thiothixene hydrochloride[8], and trifluoperazine hydrochloride[2]. Gallotannic acid[9] and gallic acid[2] were commercially obtained. The buffer solutions used in these studies were McIlvaine's buffer (0.1 M citric acid–0.2 M sodium dihydrogen phosphate, pH 2–8) and Clark and Lub's buffer (0.1 M potassium chloride–0.1 M hydrochloric acid, pH 1).

pH Variability Studies—Portions (1 mL) of an aqueous solution of drug (20 mg/mL) were diluted with 1 mL of buffer. This solution was then added to a mixture of aqueous gallotannic acid (1 mL, 20 mg/mL) and buffer (3 mL) to achieve final concentrations of drug and gallotannic acid of 3.3 mg/mL each. The resulting precipitate was removed by filtration[10]. A portion of the filtrate (2 mL) was acidified by the addition of 2 M HCl in a dropwise manner and adjusted to pH 2 by addition of 2 mL of buffer. A saturated solution of lead acetate (2 mL) was added to the acidified filtrate, and the resulting precipitate was removed by filtration. The concentration of free drug in the filtrate was determined by comparing the UV absorbance of appropriately diluted samples with a standard curve of absorbance *versus* concentration. Experiments designed to study the interaction of gallotannic acid with various drugs at specific pH values were carried out in an identical manner. Studies assessing the effects of reduced drug concentration on precipitation were also carried out in an identical fashion with drug concentrations of 2 mg/mL (for a 1:10 dilution). Samples containing drug at a 1:10 dilution required an additional extraction step because of the high concentration of tannin relative to drug. During this step, 2 mL of the lead acetate filtrate was adjusted to pH 10 by addition of 1 M NaOH in a dropwise manner. This solution was then extracted three times with 2-mL portions of distilled ethyl acetate. The combined ethyl acetate fractions were washed with water, dried with anhydrous sodium sulfate, filtered, and evaporated. The remaining residue was dissolved in 4 mL of buffer (pH 2) before dilution and UV absorption measurement.

Studies to estimate the effects of mutual dilution of drug and tannin were conducted by using buffered solutions of drug and gallotannic acid which were diluted 1:5 with distilled water before mixing and filtration. The filtrate (2 mL) was then mixed with 2 mL of buffer (pH 2), treated with 2 mL of lead acetate, and filtered before UV absorption measurements.

Experiments with Coffee and Tea—Measurements of the interaction of coffee and tea with neuroleptic agents were carried out by mixing aqueous solutions of drugs with these beverages in the following proportions: for amitriptyline, haloperidol, and loxapine, 1 mL of drug solution (10 mg/mL) with 2.5 mL of beverage; for thiothixene, 1 mL of drug solution (5 mg/mL) with 0.65 mL of beverage. All other studies were conducted with 1 mL of drug solution (20 mg/mL) and 5 mL of beverage. Coffee was prepared by dissolving 2 g of instant coffee in 150 mL of boiling distilled water. Tea infusions were prepared by steeping one tea bag containing 2.5 g of black tea in 150 mL of boiling water for 5 min. The pH resulting from addition of drug to tea or coffee varied between 4.5 and 5.0. In the experiments with tea, the resulting precipitates were filtered, and 2-mL portions of the filtrate were diluted with buffer, treated with lead acetate, and filtered as described above. In the experiments with coffee, the drug precipitates and lead–tannin precipitates were removed by centrifugation at 4000 rpm for 8 min. Extractions and UV absorption measurements were then carried out as described above.

Other Studies—Studies designed to examine the reversibility of the interaction between chlorpromazine and gallotannic acid in an aqueous medium were conducted by mixing buffered (pH 5) solutions of drug and gallotannic acid as described above. The resulting suspension was placed in a dialysis bag made from benzoylated dialysis tubing[2] (exclusion range, 1200–2000). The bag was immersed in four volumes of buffer and stirred at room temperature for 24 h. The suspension within the dialysis bag was then filtered. Portions of this filtrate, as well as the dialysate, were then treated with lead acetate, filtered, and diluted in preparation for the UV absorption measurement. The

[1] Merck, Sharp and Dohme Co.
[2] Sigma Chemical Co., St. Louis, Mo.
[3] McNeill Laboratories, Inc.
[4] Lederle Laboratories.
[5] Endo, Inc.
[6] Smith Kline and French Laboratories.
[7] Sandoz Pharmaceuticals.
[8] Roerig.
[9] FCC grade; J.T. Baker Chemical Co.
[10] Whatman no. 1.

0022-3549/84/0800-1056$01.00/0
© 1984, American Pharmaceutical Association

Table I—Interactions of Neuroleptics and Antidepressants with Gallotannic Acid, Tea, Coffee, and Gallic Acid [a]

Drug [b]	Percent Drug Precipitated by Gallotannic Acid [c]		Percent Drug Precipitated by Tea		Percent Drug Precipitated by Coffee	Drug-Gallic Acid [d] Interactions
	20 mg/mL	2 mg/mL	20 mg/mL	2 mg/mL		
Amitriptyline hydrochloride (245 nm)	43 ± 2 (5)	nd [e]	12 ± 1	nd	nd	nr [f]
Chlorpromazine hydrochloride (305 nm)	91 ± 1 (6)	69 ± 1	51 ± 2	69 ± 1	19 ± 2	+
Haloperidol hydrochloride (252 nm)	41 ± 4 (6)	nd	3 ± 1	nd	nd	nr
Imipramine hydrochloride (252 nm)	64 ± 1 (6)	54 ± 1	62 ± 1	nd	nd	nr
Loxapine hydrochloride (295 nm)	80 ± 5 (6)	72 ± 4	nd	nd	nd	nr
Molindone hydrochloride	nr	nr	nr	nr	nr	nr
Prochlorperazine hydrochloride (305 nm)	98 ± 1 (5)	84 ± 1	84 ± 1	94 ± 1	65 ± 1	+
Thioridazine hydrochloride (312 nm)	91 ± 1 (4)	76 ± 2	71 ± 1	78 ± 1	55 ± 1 [g]	+
Thiothixene	nr	nr	nr	nr	nr	nr
Trifluoperazine hydrochloride (305 nm)	88 ± 1 (6)	61 ± 1	51 ± 2	80 ± 1	31 ± 1	+

[a] Values listed are averages of triplicate determinations taken at drug concentrations of 20 and 2 mg/mL. [b] Numbers in parentheses indicate wavelengths at which measurements were made. [c] Numbers in parentheses indicate pH vaues at which these determinations were made. The pH values represent the highest pH which could be used without precipitating the free base forms of these drugs. [d] All determinations were made with pH 5 buffer. [e] nd—Percent drug precipitated was not determined due to weak drug absorptions and interfering absorptions due to constituents in coffee and tea. In the case of loxapine, measurements were not made due to inability to extract drug into the organic phase. [f] nr—No precipitate was formed on mixture of these substances. [g] Duplicate experiments indicated that 67% drug precipitation occurred when the same brand of decaffeinated coffee was mixed with thioridazine.

resulting absorbances for these fractions were compared with those obtained from a dialysis experiment using chlorpromazine alone, which was dissolved in buffer (pH 5). A similar procedure was used to examine the reversibility of the interaction between chlorpromazine and the condensed tannins present in tea. A solution of drug and tea were mixed as described above, and this mixture was placed in a dialysis bag which was immersed in water for 24 h with stirring.

In a separate experiment, a buffered solution of chlorpromazine was mixed with tea or gallotannic acid. A portion of the resulting suspension was centrifuged at 4000 rpm for 8 min. The supernatant was decanted, and the remaining pellet was washed by resuspending in distilled water and centrifuging. After decanting the resulting supernatant, the drug precipitate was washed once more and then dissolved in 6 mL of a 1:1 methanol-water. Several drops of this solution were treated with 3% ferric chloride in 0.5 M HCl. Another portion of this solution was spotted on a TLC plate[11], which was developed in methanol and visualized under short-wavelength UV light.

RESULTS AND DISCUSSION

In Table I the interactions which occurred between the various drugs and the solutions are listed. Although drug precipitation was most pronounced with phenothiazines, it also occurred with other drugs as well. The observation of precipitate formation between trifluoperazine and coffee or tea is contrary to the results reported by Hirsch (2).

It is not surprising that tannins interact with many of the drugs examined in this study. Both hydrolyzable tannins (*e.g.*, gallotannic acid) and condensed tannins, such as those present in tea and coffee, are known for their ability to precipitate metals, proteins, and certain organic compounds (8–10). The historic use of gallotannic acid as an antidote for alkaloid poisoning is based on its ability to form precipitates with many such natural products (11). Gallotannic acid complexes with morphine and cyanocobalamin have been examined as possible sustained dosage forms (12, 13). The effects of tannins on the absorption of iron and thiamine have also been studied. Roy and Mukherjee (14) have studied the effects of food tannins on iron metabolism. Morck *et al.* (15) have recently demonstrated that both coffee and tea can inhibit iron absorption in humans. In studies of the interaction between gallotannic acid and thiamine (16), it has been suggested that excessive intake of tea can contribute to thiamine deficiency, possibly because the phenolic groups of the tannins found in tea participate in ring opening and oxidation reactions of thiamine (17).

The phenothiazines used in these studies formed a precipitate with gallic acid, which is a constituent of both condensed and hydrolyzable tannins. Cheeseman and Neal have reported precipitation of chlorpromazine with solutions of sodium benzoate and sodium salicylate (4). They have suggested that these agents could account for the observed interactions of neuroleptics with coffee and tea. However, the concentrations of the aromatic acids used in the studies of Cheeseman and Neal, as well as the gallic acid solutions used in this study, are much higher than those which could exist in coffee and tea. On the other hand, the concentrations of tannins found in tea are high enough to account for the degree of drug precipitation seen in Table I. The differences in the amounts of drug precipitated by coffee and tea reflect the differences in tannin content (tea, 10–15%; coffee, 3–5%). In addition, ferric chloride treatment of a washed chlorpromazine–tea precipitate resulted in the production of a dark-green color, which is indicative of polyphenolic compounds, such as the condensed tannins present in tea. Furthermore, tea which was pretreated with lead acetate to remove tannins failed to produce a precipitate when mixed with chlorpromazine.

Experiments were carried out by using thioridazine with regular and decaffeinated coffee to test the possible effects of caffeine on drug precipitation. The results show very little difference in the amount of drug precipitated with the two varieties of coffee. Thus, any competition which may exist between caffeine and drug in complexing with tannins results in a minimal decline in drug precipitation. Although caffeine may not alter drug precipitation in tea or coffee, it could exert significant influence on the therapeutic effects of phenothiazines by producing pharmacokinetic or pharmacodynamic interactions. Such interactions may result from effects of caffeine on microsomal metabolism of antipsychotics (18) or from possible pharmacological antagonism (19). Evidence for a pharmacological effect is conflicting. Morpurgo (20) has reported that caffeine citrate (10 mg/kg) totally inhibited the cataleptic effects of phenothiazines in rats within 1 h after administration. On the other hand, Cheeseman and Neal have found that the caffeine content in tea did not account for the total loss of chlorpromazine-induced catalepsy in rats when tea was administered simultaneously (4). The doses of chlorpromazine and caffeine used in this experiment were 8 and 15 mg/kg, respectively.

The effects of pH and dilution on drug precipitation were studied in some detail to learn more of the drug-tannin interaction. The results shown in Fig. 1 indicate that the percent precipitation of imipramine, loxapine, and thioridazine increases as the pH increases from 1 to 6. A similar trend holds for all other drugs listed in Table I when mixed with either gallotannic acid or tea. Furthermore, dilution studies indicate that a significant amount of chlorpromazine (59%) is precipitated, even when drug and gallotannic acid are both diluted 1:5 before mixing. Experiments with tea and chlorpromazine diluted 1:5 resulted in a 36% drug precipitation. As indicated in Table I, a 10-fold dilution of drug alone also had little effect on total drug precipitation. Such increases in drug precipitation which occur with dilution are consistent with the results of Cheeseman and Neal (4), who have reported increases in percent chlorpromazine precipitation as the chlorpromazine–tea ratio is reduced.

Additional experiments have indicated that the drug-tannin complex is strong in the sense that the majority of drug remains complexed with tannin after prolonged dialysis. Dialysis of the chlorpromazine–gallotannic acid precipitate at pH 5 for 24 h showed that 90% of total drug remained complexed. Dialysis of a chlorpromazine–tea precipitate showed that 62% of the drug remained complexed after 24 h. However, although the complex between chlorpromazine and tannins is strong, it is not irreversible, and it does not produce a modification of the drug molecule. Dissolution of the precipitate in methanol–water (1:1), followed by TLC showed the presence of chlorpromazine. This result is in agreement with the findings of Kulhaneck *et al.* (3), who have reported that fluophenazine and haloperidol were liberated unchanged by dissolving drug–tea precipitates in water.

CONCLUSIONS

The present studies identify tannins as the major contributory factor in the precipitation of various neuroleptics and tricyclic antidepressants by coffee and tea. They also indicate that tea and coffee can precipitate significant

[11] Silica gel 60 F-254.

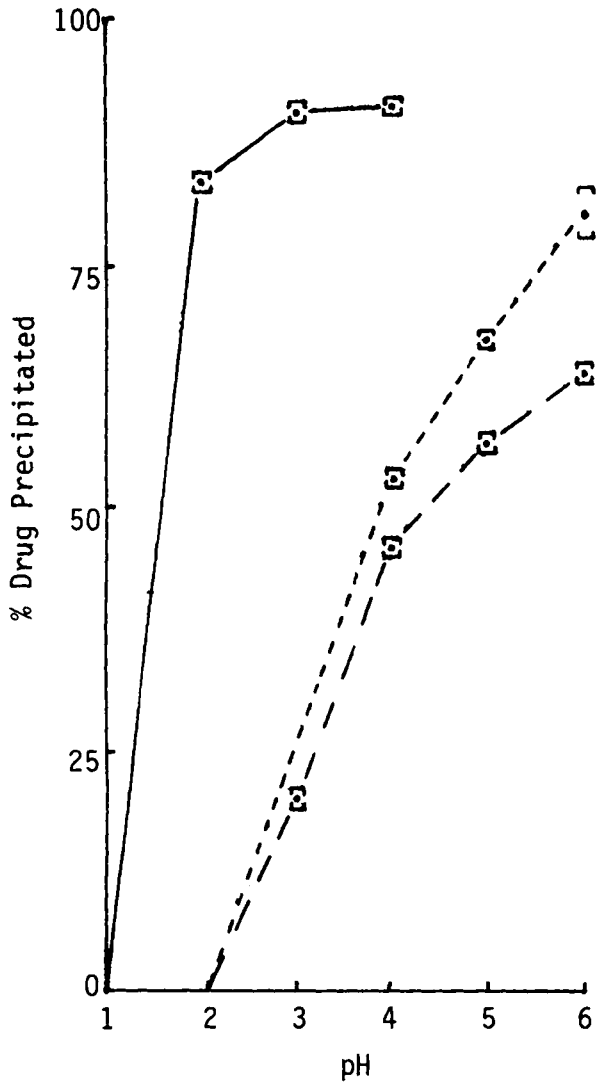

Figure 1—*pH variability of drug-gallotannic acid interaction. Plots represent results with thioridazine (—), loxapine (- - - -), and imipramine (— —). Each point represents the average of three determinations. At pH 3, loxapine produced a fine precipitate which could not be isolated by filtration or centrifugation. However, no precipitate was formed with this drug at pH 2.*

amounts of these drugs, especially phenothiazines. It is possible that the effects of gastric acidity, along with GI secretions and motility, may drastically reduce the amount of drug complexed in the intestine. However, studies on the effects of pH and dilution indicate that any drug-tannin complexation which may occur in the GI tract should be maximal in the intestine, where most drug absorption occurs. Furthermore, dilution studies indicate that gallotannic acid and tea precipitate significant amounts of drug even at somewhat diluted concentrations, suggesting that dilution in the intestine may not completely eliminate drug-tannin interactions. Finally, dialysis experiments show that the chlorpromazine-gallotannic acid complex is quite stable at nearly neutral pH. Thus, once formed, the drug-tannin precipitate may not be readily soluble in the intestine.

Studies in rats have shown that simultaneous administration of tea can abolish the cataleptic effects of chlorpromazine. Whether this effect is due to caffeine or other components in tea is open to question. Bowen *et al.* (5) have reported that abstinence from tea or coffee had no effect on the bioavailability of several neuroleptics studied. However, the time and amounts of coffee and tea intake in this study were not specified. It is interesting to note that Bogner and Walsh (21) have compared the absorption of a sustained-release complex of gallotannic acid and radiolabeled phenylephrine hydrochloride with that of phenylephrine hydrochloride alone in human volunteers. The results indicated that use of the drug-tannin complex prolonged the time at which peak radioactivity was observed in the blood and reduced levels of peak radioactivity. A reduction in total radioactivity *versus* time (~25%) also occurred during the 24-h period in which measurements were taken. Prolonged absorption such as that observed in this study may have an especially significant role in affecting blood and tissue levels of drugs, such as chlorpromazine, which undergo significant metabolism in the intestine (22, 23). More detailed studies need to be carried out on the possible *in vivo* interaction of coffee and tea with neuroleptics and tricyclic antidepressants.

REFERENCES

(1) E. J. Mikkelsen, *J. Clin. Psychiat.*, **39**, 732 (1978).

(2) S. R. Hirsch, *Lancet*, **ii**, 1130 (1979).

(3) F. Kulhaneck, O. K. Linde, and G. Meisenberg, *Lancet*, **ii**, 1130 (1979).

(4) H. J. Cheeseman and M. J. Neal, *Br. J. Clin. Pharm.*, **12**, 165 (1981).

(5) S. Bowen, K. M. Taylor, and I. A. McI. Gibb, *Lancet*, **i**, 1217 (1981).

(6) I. Creese and S. H. Sander, *Nature (London)*, **270**, 180 (1977).

(7) K. Nihira, R. Foster, M. Shellhaas, and H. Leland, "AAMD Adaptive Behavior Scale Manual," American Association of Mental Deficiency, Washington, D.C., 1975.

(8) E. Haslam, "The Chemistry of Vegetable Tannins," Academic, New York, N.Y., 1966.

(9) M. E. Wall, H. Taylor, L. Ambrosio, and K. Davis, *J. Pharm. Sci.*, **58**, 839 (1969).

(10) N. Kojima, D. Wallace, and G. W. Bates, *Am. J. Clin. Nutr.*, **34**, 1392 (1981).

(11) "U.S. Dispensatory," 25th Ed., Lippincott, Philadelphia, Pa., 1955, pp. 1379–1380.

(12) B. Brands, J. C. Baskerville, R. Herve, M. Hirst, and C. W. Gowdey, *Neuropharmacology*, **19**, 443 (1980).

(13) K. Kristensen and T. Hansen, *J. Pharm. Sci.*, **55**, 610 (1966).

(14) S. N. Roy and S. Mukherjee, *Ind. J. Biochem. Biophys.*, **16**, 93 (1979).

(15) T. A. Morck, S. R. Lynch, and J. D. Cook, *Am. J. Clin. Nutr.*, **37**, 416 (1983).

(16) K. Rungravngsak, P. Tosukhoweng, B. Panjipan, and S. L. Vimakesani, *J. Am. Diet. Assoc.*, **30**, 1680 (1977).

(17) B. Panjipan and K. Ratanaubalchai, *Int. J. Vit. Nutr. Res.*, **50**, 247 (1980).

(18) C. Mitoma, T. J. Sorich, and S. Neubauer, *Life Sci.*, **7**, 145 (1968).

(19) F. A. Freyhan, *Am. J. Psychiat.*, **115**, 577 (1959).

(20) C. Morpurgo, *Arch. Int. Pharmacodyn.*, **137**, 84 (1962).

(21) R. L. Bogner and J. M. Walsh, *J. Pharm. Sci.*, **53**, 617 (1964).

(22) L. Rivera-Calimlim, L. Castanneda, and L. Lasagna, *Clin. Pharmacol. Ther.*, **14**, 978 (1973).

(23) S. H. Curry, A. D'Mello, and G. P. Mould, *Br. J. Pharmacol.*, **42**, 403 (1971).

ACKNOWLEDGMENTS

The authors thank Ms. Sylvia Stoner for preparation of this manuscript.

Solid–Solid Reaction Between Sulfacetamide and Phthalic Anhydride

HO-LUN WENG and EUGENE L. PARROTT ˣ

Received May 23, 1983, from the *College of Pharmacy, The University of Iowa, Iowa City, IA 52240.* Accepted for publication September 30, 1983.

Abstract □ Thermal and kinetic data for the solid-state addition reaction of sulfacetamide and phthalic anhydride are presented. A compaction method was used so that the influence of some pharmaceutical parameters (compressional pressure, particle size, concentration, and temperature) on the reaction kinetics could be observed.

Keyphrases □ Sulfacetamide—solid-solid reaction with phthalic anhydride □ Phthalic anhydride—solid-solid reaction with sulfacetamide □ Solid-solid reactions—sulfacetamide and phthalic anhydride, thermal and kinetic analyses

The stability of a medicinal compound in a solid dosage form is routinely investigated in terms of the percentage of the medicinal compound that is unchanged after exposure to various temperatures (1–4). Although thermal decomposition is an important consideration in the processing, testing, and storage of solid dosage forms, only a limited number of reports in the pharmaceutical literature have been concerned with the physicochemical mechanism and kinetics of solid-state reactions (5–13). In general, the chemistry of solids has been presented in several texts (14–18). This study was initiated to present a simple model of a solid-state addition reaction so that some pharmaceutical factors (compressional pressure, concentration, particle size, and temperature) could be viewed in relation to their influence on the reaction.

EXPERIMENTAL SECTION

Samples of sulfacetamide[1] and phthalic anhydride[2] were individually separated into a 100/140-mesh-size fraction by means of U.S. standard sieves and a shaker[3]. Blends of the sulfacetamide and phthalic anhydride were prepared at 2:1, 1:1, and 1:2 molar ratios and were passed through a 200-mesh sieve. The thermal analytical data of the components and the blends were determined with a thermogravimetric analyzer[4] and a differential thermal analyzer[5]. Typical thermograms are given in Figs. 1 and 2.

For the study concerned with the effect of molar ratio on the reaction kinetics of sulfacetamide and phthalic anhydride, compacts with molar ratios of 1:1, 1:2, and 1:3 were used. An appropriate weight (400 mg) of a 100/140-mesh fraction of the blend was compressed for 1 min at a pressure of 3580 kg/cm^2 with an hydraulic press[6] fitted with a 1.27-cm punch and die set. Each compact was sealed under nitrogen in a glass vial and then immersed in a thermostated oil bath at 95 ± 0.5°C. At a given time, the reaction was quenched by immersion of the vial in ice, and the compact was then assayed. The reaction was conducted in triplicate. Typical data of the percent conversion of sulfacetamide to phthalylsulfacetamide are given in Table I.

For the study of the effect of particle size on the reaction kinetics, sulfacetamide was recrystallized from distilled water and then dried in a vacuum oven at 60°C. The purity of the sulfacetamide, as analyzed by differential scanning calorimetry[7], was 99.63%. With sieves and a shaker, the sulfacetamide was classified into 40/45-, 45/60-, 60/80-, 80/100-, and 100/140-mesh fractions. Blends with a 1:2 molar ratio of sulfacetamide and phthalic anhydride were prepared with phthalic anhydride of a 100–140-mesh fraction and the five sizes of sulfacetamide. An appropriate weight (2025 mg) of the blends was compressed for 1 min at a pressure of 35 kg/cm^2 with a hydraulic press fitted with a 2.857-cm punch and die set. Each compact, which corresponded to a specific particle size of sulfacetamide, was manually divided diametrically into six parts with a razor blade. Three parts were assayed for initial content, and the other parts were used for the kinetic study at 95°C. The percent conversion of sulfacetamide to phthalylsulfacetamide is shown in Table II.

For the study concerned with the effect of compressional pressure on reaction kinetics, a blend of an equimolar ratio of sulfacetamide and phthalic anhydride with a 100/140-mesh fraction was compressed for 1 min with a hydraulic press fitted with a 2.857-cm punch and die set at 35, 106, 283, 601, 1003, 2005, 3580, and 5371 kg/cm^2. The percent conversion is shown in Table III.

For the study concerned with the influence of temperature on the reaction kinetics, a blend of an equimolar ratio of sulfacetamide and phthalic anhydride with a 100/140-mesh fraction was compressed for 1 min in an hydraulic press fitted with a 1.27-cm punch and die set at a pressure of 3580 kg/cm^2. Each compact weighed 400 mg. The reaction was conducted at 85°C, 90°C, 95°C, 100°C, 105°C, and 110°C. Typical data are given in Table IV.

The unreacted sulfacetamide was colorimetrically analyzed by diazotization and a coupling reaction with *N*-naphthylethylenediamine dihydrochloride (19, 20). A standard concentration–absorbance curve was determined by transferring 0.5-, 1.0-, 2.0-, 3.0-, and 4.0-mL aliquots of a stock solution

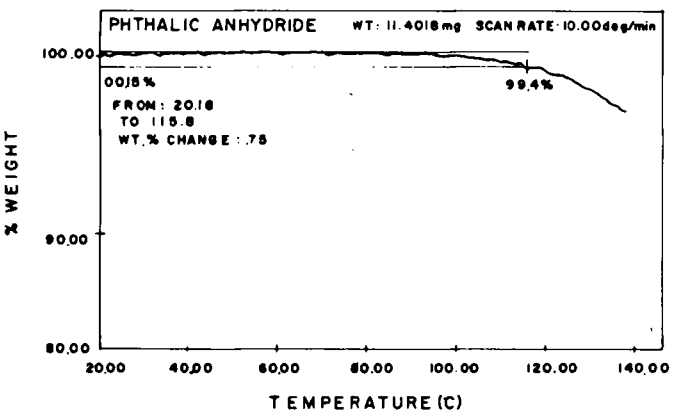

Figure 1—*Thermogram of phthalic anhydride showing its sublimation characteristics.*

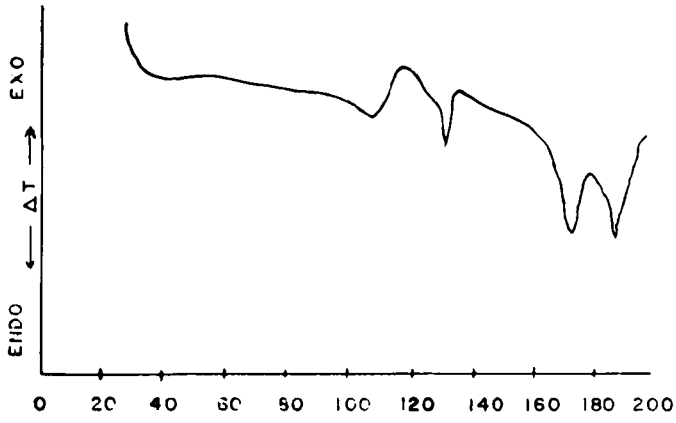

Figure 2—*DTA thermogram of a 2:1 molar ratio of sulfacetamide and phthalic anhydride. Reference, glass beads; heating rate, 20°C/min; atmosphere, N_2 (1 atm); sensitivity of* y*-axis, 0.2°C/cm.*

[1] Lot 59C-0276; Sigma Chemical Co.
[2] Reagent grade, lot 88C-0525; Fisher Scientific Co.
[3] Central Scientific Co.
[4] Model TGS-2; Perkin-Elmer.
[5] Model 900; E.I. duPont de Nemours & Co.
[6] Model C; Carver Press.
[7] Model DSC-2 differential scanning calorimeter; Perkin-Elmer.

0022-3549/84/0800-1059$01.00/0
© 1984, American Pharmaceutical Association

Table I—Conversion of Sulfacetamide to Phthalylsulfacetamide [a]

Time, min	Conversion, %	Mean Conversion ± SD, %
0	0	0
10	6.68	
	6.71	5.90 ± 1.38
	4.31	
20	8.19	
	5.45	6.05 ± 1.91
	4.52	
30	7.03	
	6.61	5.89 ± 1.62
	4.04	
60	9.14	7.33 ± 2.57
	5.51	
180	10.24[b]	
	8.28[b]	10.07 ± 0.72
	10.68[b]	
300	13.66[b]	
	16.00[b]	14.85 ± 1.17
	14.88[b]	

[a] At 95°C as a function of time for a 1:2 molar ratio of sulfacetamide and phthalic anhydride. [b] Corrected to include sublimed phthalic anhydride (0.51 and 1.10% of total compact weight for 180 and 300 min, respectively).

(prepared by dissolving 125.6 mg of sulfacetamide in 50 mL of 0.5 M NaOH and adjusting with distilled water to 250 mL in a volumetric flask) into sufficient distilled water to make 50 mL. From each dilution, 5.0 mL was transferred into a 50-mL volumetric flask and neutralized with 0.02 M HCl. Then, 5.0 mL of 0.5 M HCl and 5.0 mL of a 0.1% aqueous sodium nitrite solution were added to the flask. After 3 min, 5.0 mL of 0.5% ammonium sulfamate solution was added, and the volume was adjusted to 50 mL by the addition of distilled water. The absorbance was measured against a blank at 536 nm. A plot of absorbance against concentration showed a Beer's law relationship.

At each time period, the compact was triturated in a mortar, and the appropriate amount of powdered compact corresponding to 125 mg of sulfacetamide was accurately weighed and transferred to a 250-mL volumetric flask. The subsequent addition of reagents and the procedure have been described above. By means of the standard curve, the measured absorbance was used to determine the concentration of unreacted sulfacetamide. When sublimation occurred, a correction was made in the calculation of the percent conversion.

RESULTS AND DISCUSSION

Physicochemical Characteristics—As reports (14–18) have been published for single-solid decompositions, the reaction of sulfacetamide and phthalic anhydride was selected as an example of a solid–solid addition reaction for the simple model: A + B → AB. Samples of sulfacetamide maintained at 50°C, 90°C, and 110°C for 24 and 16 d and 5 h, respectively, showed no degradation within the variability (0.6%) of the analytical method.

Table II—Influence of Particle Size on Conversion of Sulfacetamide [a]

Particle Size[b] of Sulfacetamide, μm	Conversion, %[c]	Mean Conversion ± SD, %
128	22.45	
	18.47	21.54 ± 2.74
	23.71	
164	15.80	
	22.08	19.43 ± 3.25
	20.42	
214	14.49	
	20.23	17.25 ± 2.88
	17.03	
302	18.31	
	6.81	15.69 ± 7.90
	21.95	
387	11.90	
	4.25	9.34 ± 4.41
	11.88	

[a] After 3 h at 95°C. [b] Mean of U.S. Standard Sieve opening passed and retained. [c] Corrected to include sublimed phthalic anhydride.

Table III—Influence of Compression Pressure on Conversion of Sulfacetamide in an Equimolar Blend of Sulfacetamide and Phthalic Anhydride [a]

Compressional Pressure, kg/cm²	Conversion, %[b]	Mean Conversion ± SD, %
0	7.01	
	9.87	8.19 ± 1.49
	7.69	
35	19.92	
	23.78	19.40 ± 4.66
	14.51	
106	18.54	
	15.88	16.48 ± 1.84
	15.02	
283	17.83	
	17.98	17.28 ± 1.08
	16.04	
601	14.98	
	9.95	12.26 ± 2.54
	11.86	
1003	11.18	
	11.13	11.26 ± 0.19
	11.48	
2005	11.43	
	9.89	10.45 ± 0.85
	10.04	
3581	8.67	
	12.07	
	9.39	9.61 ± 1.76
	11.36	
	8.70	
	7.45	
5381	8.51	
	7.81	8.50 ± 0.69
	9.19	

[a] After 3 h at 95°C. [b] Corrected to include sublimed phthalic anhydride.

It has been demonstrated that the solid-state reaction of sulfathiazole and phthalic anhydride is an addition reaction with a 1:1 stoichiometry (21). Preliminary differential thermal analysis (DTA) of an equimolar ratio of sulfacetamide and phthalic anhydride showed that (*a*) the stoichiometry was 1:1, (*b*) the reaction product melted at 195°C [lit. mp of phthalylsulfacetamide (22) 196°C] and (*c*) decomposition occurred as the temperature exceeded 196°C. The anhydrous state of each reactant was determined by thermogravimetry. The weight loss of phthalic anhydride is due to sublimation, as the slope (*dW/dT*) (Fig. 1) is negatively increasing without discontinuity. The melting points of sulfacetamide and phthalic anhydride, as shown on the thermograms, were 185°C and 132.1°C, respectively [lit. mp (22) 182–184°C and 130.8°C, respectively].

Figure 2 is a typical thermogram of those determined on the blends of various molar ratios. The endothermic peak at 107°C is probably caused by fusion of the sulfacetamide and phthalic anhydride eutectic because a large exothermic peak ensues immediately. The exothermic peak at 117°C is due to the liquid-state addition reaction. At 131°C, the unreacted anhydride is completely melted and penetrates into the surface fissures of any solid sulfacetamide undergoing the addition reaction, as indicated by the broad exothermic peak between 135°C and 156°C. The endothermic peak at 172.5°C is likely caused by the melting of the sulfacetamide-phthalylsulfacetamide eutectic. After melting, a small exothermic peak occurs at 178.5°C and may be due to the liquid-state addition between sulfacetamide and the residual anhydride. Finally, the endothermic peak at 187°C may be caused by fusion of phthalylsulfacetamide (depressed by impurity).

At molar ratios of 1:1 and 1:2 sulfacetamide and phthalic anhydride, the thermograms (not shown to conserve space) are essentially the same as those for the 2:1 molar ratio at temperatures <160°C. The relatively small quantity of sulfacetamide in the 1:2 molar ratio has undergone addition, so there is no endothermic peak corresponding to the melting of sulfacetamide at 172.5°C. The final endothermic peaks are caused by the melting of impure phthalysulfacetamide; however, the quantity of impurity is different in the three ratios.

Influence of Concentration on Reaction Kinetics—Molar ratios of sulfacetamide to phthalic anhydride from 1:1 to 1:3 provide excess phthalic anhydride so that the initial contact area between the reactants is varied as the concentration of sulfacetamide is changed. The conversion (milligrams sulfacetamide per gram of anhydride) is shown as a function of time in Fig. 3.

Table IV—Conversion of Sulfacetamide to Phthalylsulfacetamide at 90°C as a Function of Time for an Equimolar Ratio of Sulfacetamide and Phthalic Anhydride

Time, min	Conversion, %[a]	Mean Conversion ± *SD*, %
0	0	0
10	1.53	
	1.94	
	2.28	
	4.85	2.62 ± 1.08
	2.79	
	2.23	
	2.73	
20	3.61	
	3.18	
	3.01	3.32 ± 0.74
	3.74	
	4.06	
30	4.58	
	3.19	
	3.66	3.81 ± 0.51
	3.92	
	3.69	
60	4.77	
	4.23	
	6.04	5.20 ± 0.46
	5.24	
	5.70	
180	5.63	
	8.18	
	7.07	7.84 ± 1.31
	9.34	
	8.98	
300	11.20[a]	
	8.87[a]	
	9.07[a]	10.64 ± 1.74
	10.97[a]	
	13.10[a]	

[a] Corrected to include sublimed phthalic anhydride (0.53% of weight of compact).

The conversion (milligrams of sulfacetamide per gram of anhydride) is greater for a high concentration of sulfacetamide than for a lower concentration as the reaction time is increased (Fig. 4). For example, a comparison of the 60- and 180-min curves shows that for the 1:1 molar ratio, an additional 33.7 mg of sulfacetamide/g of anhydride was converted during the 120-min interval, whereas for the same interval of time, only an additional 16.5 mg of sulfacetamide/g of anhydride was converted at the 1:3 molar ratio.

Influence of Particle Size on Reaction Kinetics—By using a 1:2 molar ratio of sulfacetamide to phthalic anhydride, compacts were prepared with several sizes of sulfacetamide. A low compressional pressure (35 kg/cm²) was used to retain the integrity of the particles. The percent conversion of sulfacetamide after 3 h at 95°C is given for the various sizes in Table II. It appears that a reduction of particle size increases the percent conversion.

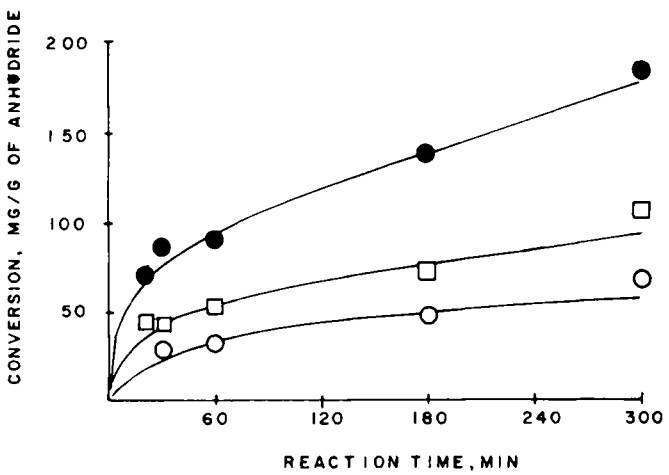

Figure 3—*Influence of concentration on the reaction at 95°C of sulfacetamide and phthalic anhydride prepared from 100/140-mesh fraction compressed at 3581 kg/cm². Key: (○) 1:3; (□) 1:2; (●) 1:1.*

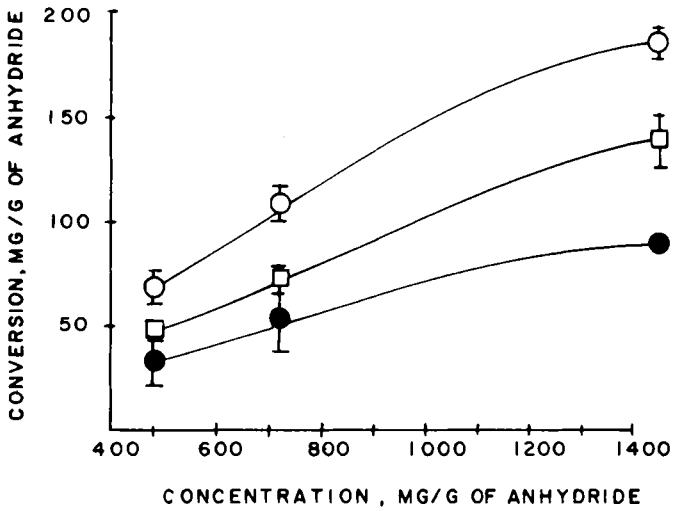

Figure 4—*Influence of concentration of sulfacetamide on weight conversion at various times at 95°C. Key: (●) 60 min; (□) 180 min; (○) 300 min. Bars represent* SD.

Although the conversion rate of sulfacetamide has been shown to be proportional to its concentration, it may be more meaningful to describe the kinetics of solid-solid reactions in terms of interfacial area of contact between the reactants (18, 23); however, the determination of actual area of contact is questionable. Since the actual area of contact is unknown but is probably proportional to the total surface area, reaction kinetics of a solid-solid system could be considered in terms of the total surface area of the sulfacetamide, because phthalic anhydride is the only mobile phase (21, 24) and is transported to the surface of the sulfacetamide by surface migration (21) and/or sublimation. Assuming that the particles of sulfacetamide are spherical, the total surface area per gram of blend was calculated and plotted against the percent conversion (Fig. 5).

Influence of Pressure on Reaction Kinetics—Compacts of an equimolar blend of sulfacetamide and phthalic anhydride were prepared at pressures up to 5380 kg/cm² and were maintained for 3 h at 95°C. The percent conversion of sulfacetamide increases to a maximum value (17%) as the compressional pressure is increased to 283 kg/cm² (Fig. 6), and then, with further increases in compressional pressure, the percent conversion decreases.

As the compressional pressure is increased, packing of the particles is more dense, and as bonding occurs, the porosity is decreased (25, 26). As consolidation occurs, the area of contact between the reactants is increased by fragmentation or deformation (27) until a maximum specific surface area, which provides more reaction sites between the sulfacetamide and phthalic anhydride, is attained. Additional increases in compressional pressure result in consolidation with a progressive decrease in specific surface area, which

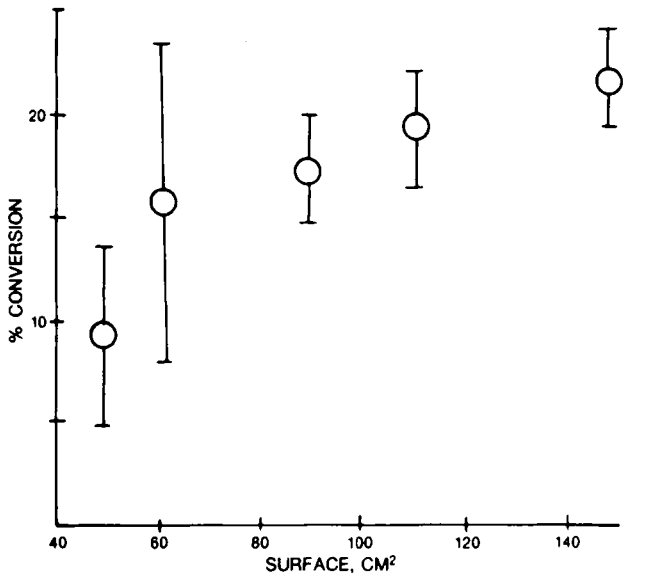

Figure 5—*Influence of total surface area of sulfacetamide on conversion after 3 h at 95°C. Bars represent* SD.

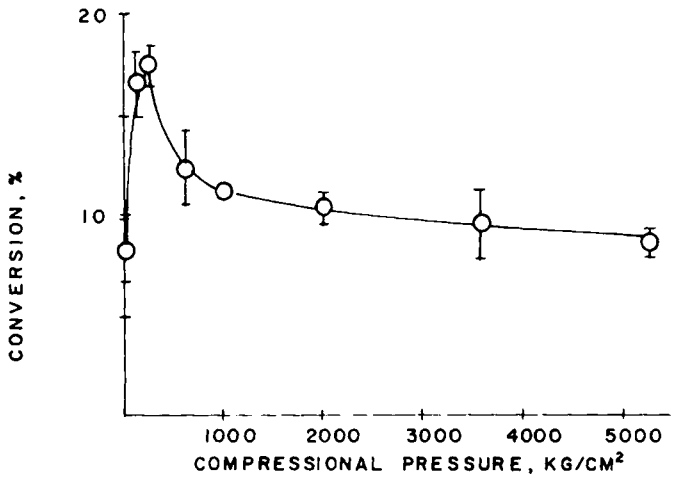

Figure 6—*Influence of compressional pressure on the conversion of sulfacetamide after 3 h at 95°C. Bars represent* SD.

provides fewer reaction sites. In addition, the transport rate of the anhydride by diffusion through the phthalylsulfacetamide layer (24), surface migration (21), and/or sublimation will be decreased. Both effects operate to decrease the percent conversion.

Influence of Temperature on Reaction Kinetics—Compacts compressed at a pressure of 3581 kg/cm² from an equimolar blend of sulfacetamide and phthalic anhydride of a 100/140-mesh fraction were exposed to six temperatures from 85°C to 110°C. The percent conversion of sulfacetamide at these temperatures is shown as a function of time in Fig. 7. At 100°C, 105°C, and 110°C, the curve attains a plateau in a very brief time because of the fast reaction. Based on the thermogram (Fig. 2), it is likely that the initial phase-boundary reaction proceeds mainly in the liquid state, in which a more vigorous chemical reaction would be expected according to the lever rule (28), which infers that the fraction of the melt at the interface between the reactants is approximately proportional to the reaction temperature. At 85°C, 90°C, and 95°C, there is a slowing of the reaction rate, possibly due to the fact that the reaction occurs primarily in the solid state, which requires more energy and is more restrictive of molecular movement than in the liquid-solid reaction.

In addition to the solid-solid interaction at the phase boundary, mass transport of the anhydride to the free sulfacetamide surface occurs simultaneously (21). Diffusion through a solid is slow, and after the phase-boundary reaction is completed, the conversion curve asymptotically approaches a plateau. Since the percent conversion at 85°C, 90°C, and 95°C significantly increases, although at a slower rate, it could be considered as phase-boundary reaction and treated mathematically (see *Appendix*). The reaction rate constants for given conditions at 85°C, 90°C, and 95°C were calculated by starting with an A value, which was set equal to the percent conversion at 300 min, and then sequentially, reaction rate constants were calculated by continuous increments of 0.5 to the previous A value. The value of the derived constant, A, was selected which best fit the experimental data.

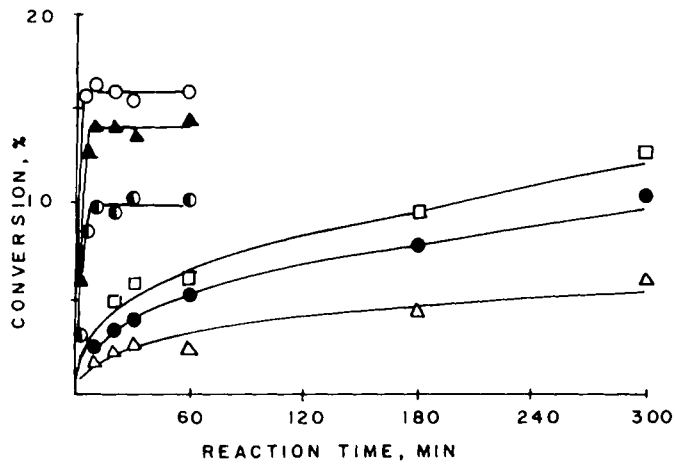

Figure 7—*Influence of temperature on the reaction kinetics of equimolar sulfacetamide and phthalic anhydride compacts prepared at 3581 kg/cm². Key: (△) 85°C; (●) 90°C; (□) 95°C; (◐) 100°C; (▲) 105°C; (○) 110°C.*

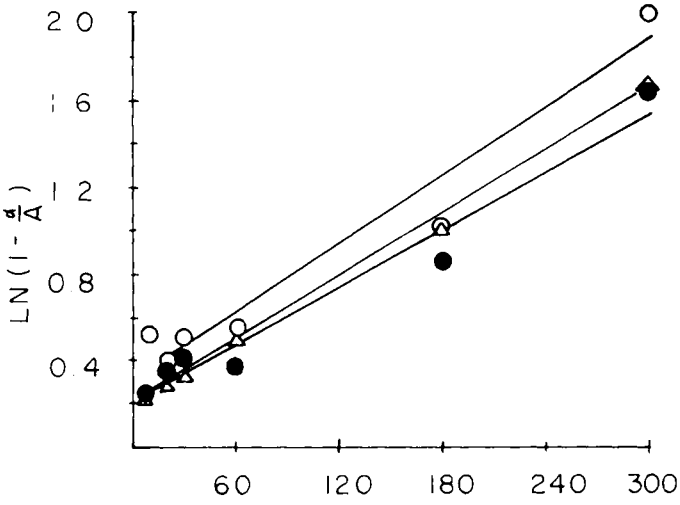

Figure 8—*Linear plot of $-\ln(1 - \alpha/A)$ against reaction time at various temperatures. Key: (●) 85°C; (△) 90°C; (○) 95°C.*

The best plot ($r = 0.9758$) of $-\ln[1 - (\alpha/A)]$ against time at 85°C is shown in Fig. 8 ($A = 7.75\%$; $k = 0.004704\ \text{min}^{-1}$). The experimental percent conversion at 85°C is compared in Fig. 9 with that calculated with the best set of values of A and k and Eq. 14 (see *Appendix*). The greatest deviation in the plot occurs at short reaction times and is obviously due to the omission in case 2 (see *Appendix*) of the second term of Eq. 12. Similar results occur if the data at 90°C ($A = 13.14\%$; $k = 0.004912\ \text{min}^{-1}$; $r = 0.9875$) and at 95°C ($A = 14.72\%$; $k = 0.005272\ \text{min}^{-1}$, $r = 0.9437$) are plotted.

As shown in Fig. 10, a plot of ln k against reciprocal temperature is linear with a slope of $-1502\ \text{K}^{-1}$. From the plot of ln k against reciprocal temperature over the range from 85°C to 95°C, it could be inferred that the reaction rate constants could be estimated at various temperatures; however, this concept has its limitations and may not be extended to other temperatures at which different physical parameters and mechanisms of transport and reaction occur (18).

APPENDIX

By assuming that the solid-solid reaction rate, $d\alpha/dt$, is proportional to the area of contact, X, between the reactants at time, t:

$$\frac{d\alpha}{dt} = \frac{k}{c}X \qquad \text{(Eq. 1)}$$

where k is the reaction rate constant and c is the proportionality constant. If the rate of generation of new contact area between the reactants is proportional to the free sulfacetamide surface, X_f, at time, t:

$$\frac{dX}{dt} = -kX + k_1X_f \qquad \text{(Eq. 2)}$$

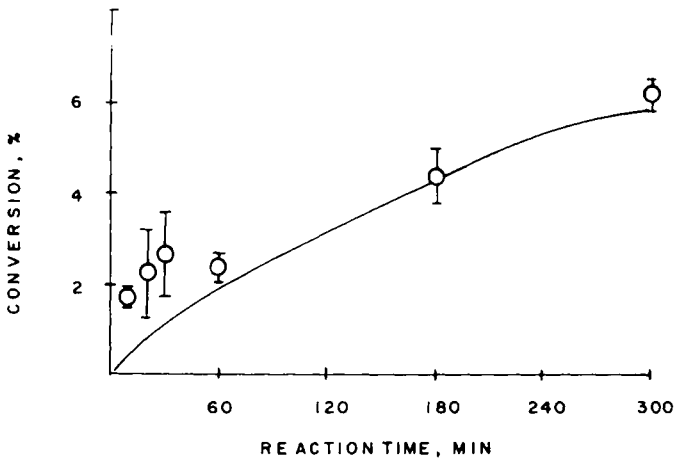

Figure 9—*Conversion curve at 85°C of equimolar sulfacetamide and phthalic anhydride compacts compressed at 3581 kg/cm². Solid curve represents theoretical values according to Eq. 14. Points are experimental values; bars represent* SD.

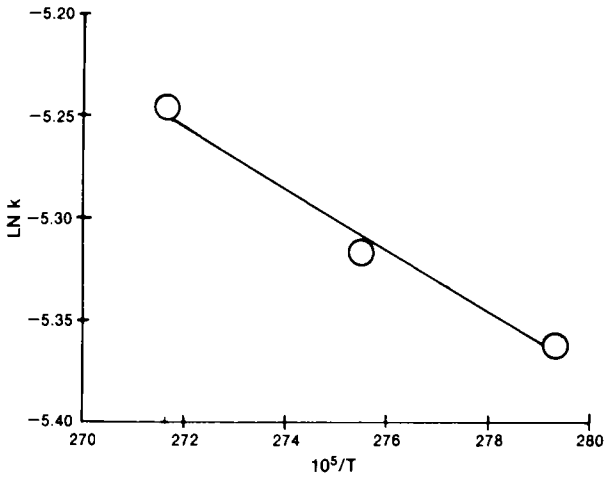

Figure 10—*Arrhenius plot of reaction rate constants and temperatures (T).*

where k_1 is the rate constant for the generation of new area of contact and is related to the mass transport of the anhydride. The changing rate of free sulfacetamide surface may be expressed as:

$$\frac{dX_f}{dt} = -k_1 X_f \qquad \text{(Eq. 3)}$$

The Laplace transformations of Eqs. 1–3 are:

$$s\bar{\alpha} = (k/c)\bar{X} \qquad \text{(Eq. 4)}$$

$$s\bar{X} - k_2X_0 = -k\bar{X} + k_1\bar{X}_f \qquad \text{(Eq. 5)}$$

$$s\bar{X}_f - k_2k_3X_{f,0} = -k_1\bar{X}_f \qquad \text{(Eq. 6)}$$

where s is the Laplace parameter, X_0 is the initial contact area between the reactants, $X_{f,0}$ is the initial free sulfacetamide area of contact, k_2 is the fraction of ultimately reacted area of contact, k_3 is the fraction of ultimately covered free sulfacetamide surface area, and $\bar{\alpha}$ is the Laplace transform of α. After combining the same terms in Eqs. 5 and 6:

$$\bar{X} = \frac{k_2X_0 + k_1\bar{X}_f}{s + k} \qquad \text{(Eq. 7)}$$

$$\bar{X}_f = \frac{k_4X_{f,0}}{s + k_1} \qquad \text{(Eq. 8)}$$

where $k_4 = k_2k_3$. By combining Eqs. 7 and 8 and substituting $\bar{X}$ into Eq. 4:

$$\bar{\alpha} = \frac{(k/c)k_2X_0s + (k/c)k_1k_2X_0 + (k/c)k_1k_4X_{f,0}}{s(s + k)(s + k_1)} \qquad \text{(Eq. 9)}$$

In Case 1, assume that $k \gg k_1$, and then the anti-Laplace transformation of $\bar{\alpha}$ in Eq. 4 would be:

$$\alpha = \frac{(kk_1k_2X_0 + kk_1k_4X_{f,0})/c}{kk_1} - \frac{(k^2k_2X_0 - kk_1k_2X_0 - kk_1k_4X_{f,0})/c}{k(k - k_1)} \cdot \exp(-kt) - \frac{(kk_1k_2X_0 - kk_1k_2X_0 - kk_1k_4X_{f,0})/c}{k_1(k - k_1)} \cdot \exp(-k_1t) \qquad \text{(Eq. 10)}$$

Because $k \gg k_1$, the second term on the right side of the equation rapidly becomes negligible, and in a short reaction time, Eq. 10 reduces to:

$$\alpha = (k_2X_0 + k_4X_{f,0})/c - (k_4X_{f,0}/c) \cdot \exp(-k_1t) \qquad \text{(Eq. 11)}$$

and at $t = 0$ and $\alpha = 0$, $k_2X_0/c = 0$. Since X_0 and c cannot be zero, the inference is that $k_2 = 0$ (no reaction occurred). Thus, the simplified form (Eq. 11) does not meet the initial condition, although it may apply when the reaction time is long enough to neglect the second term of Eq. 10. In addition, at a molar ratio of 1:3 sulfacetamide to phthalic anhydride, the sulfacetamide would be completely covered by the anhydride, and the third term of Eq. 10 would be operative. As shown in Fig. 9, the conversion is continuing. The value of k is relatively small, so the second term in Eq. 10 is not negligible throughout the 5-h reaction time.

In Case 2, assume that $k_1 \gg k$ and then:

$$\alpha = \frac{(kk_1k_2X_0 + kk_1k_4X_{f,0})/c}{kk_1} - \frac{(kk_1k_2X_0 - kk_1k_4X_{f,0} - kk_1k_2X_0)/c}{k_1(k_1 - k)} \cdot \exp(-k_1t) - \frac{(k^2k_2X_0 - kk_1k_2X_0 - kk_1k_4X_{f,0})/c}{k(k_1 - k)} \cdot \exp(-kt) \qquad \text{(Eq. 12)}$$

Because $k_1 \gg k$, the second term on the right side of the equation rapidly becomes negligible, so in a very short reaction time:

$$\alpha = (1/c)(k_2X_0 + k_4X_{f,0})[1 - \exp(-kt)] \qquad \text{(Eq. 13)}$$

or:

$$\alpha = A[1 - \exp(-kt)] \qquad \text{(Eq. 14)}$$

$$A = (1/c)(k_2X_0 + k_4X_{f,0}) \qquad \text{(Eq. 15)}$$

Thus, a plot of $-\ln[1 - (\alpha/A)]$ against time will produce a straight line with the slope equal to k.

REFERENCES

(1) E. R. Garrett, in "Advances in Pharmaceutical Sciences," vol. II, H. S. Bean, A. H. Beckett, and J. E. Carless, Eds., Academic, New York, N.Y., 1967, p. 77.

(2) J. Mollica, S. Ahuja, and J. Cohen, *J. Pharm. Sci.*, **67,** 443 (1978).

(3) L. Lachman, *J. Pharm. Sci.*, **54,** 1519 (1965).

(4) R. Tardif, *J. Pharm. Sci.*, **54,** 281 (1965).

(5) J. T. Carstensen, "Theory of Pharmaceutical Systems," vol. II, Academic, New York, N.Y., 1973, p. 295.

(6) J. T. Carstensen, *J. Pharm. Sci.*, **63,** 1 (1974).

(7) S. R. Byrn, *J. Pharm. Sci.*, **65,** 1 (1976).

(8) E. Garrett, E. L. Schumann, and M. F. Grostic, *J. Am. Pharm. Assoc., Sci. Ed.*, **48,** 684 (1959).

(9) J. T. Carstensen and M. N. Musa, *J. Pharm. Sci.*, **61,** 1112 (1972).

(10) P. Pothisiri and J. Carstensen, *J. Pharm. Sci.*, **64,** 1931 (1975).

(11) J. Carstensen and R. Kothari, *J. Pharm. Sci.*, **70,** 1095 (1981).

(12) S. S. Kornblum and B. J. Sciarrone, *J. Pharm. Sci.*, **53,** 935 (1964).

(13) J. Carstensen and P. Pothisiri, *J. Pharm. Sci.*, **64,** 37 (1975).

(14) W. P. Gomes and W. Dekeyser, in "Treatise on Solid State Chemistry," vol. 4, N. B. Hannay, Ed., Plenum, New York, N.Y., 1976, chap. 2.

(15) P. W. M. Jacobs and F. C. Tompkins, in "Chemistry of the Solid State," W. E. Garner, Ed., Butterworth, London, 1955, chap. 7.

(16) D. A. Young, "Decomposition of Solids," Pergamon, Long Island, N.Y., 1966.

(17) A. K. Galwey, "Chemistry of Solids," Chapman and Hall, London, 1967.

(18) C. H. Bamford and C. F. H. Tipper, "Reactions in the Solid State," Elsevier, Amsterdam, The Netherlands, 1980.

(19) A. C. Bratton and E. K. Marshall, Jr., *J. Biol. Chem.*, **128,** 537 (1939).

(20) T. Higuchi and E. Brochmann-Hanssen, "Pharmaceutical Analysis," Interscience, New York, N.Y., 1961, pp. 141–147.

(21) J. Tomas, E. Pereira, and J. Ronco, *Ind. Eng. Chem. Fund.*, **8,** 121 (1969).

(22) "The Merck Index," 9th ed., M. Windholz, Ed., Merck & Co., Inc., Rahway, N.J., 1976.

(23) S. S. Tamhankar and L. K. Doraiswamy, *AIChE J.*, **25,** 561 (1979).

(24) R. J. Arrowsmith and J. M. Smith, *Ind. Eng. Chem. Fund.*, **5,** 327 (1966).

(25) E. L. Parrott in "Pharmaceutical Dosage Forms: Tablets," vol. 2, H. A. Lieberman and L. Lachman, Eds., Dekker, New York, N.Y., 1981, chap. 4.

(26) T. Higuchi, A. N. Rao, L. W. Busse, and J. V. Swintosky, *J. Am. Pharm. Assoc., Sci. Ed.*, **42,** 194 (1953).

(27) P. W. Atkins, "Physical Chemistry," W. H. Freeman, San Francisco, Calif., 1978, p. 180.

(28) J. K. Guillory and T. Higuchi, *J. Pharm. Sci.*, **51,** 100 (1962).

ACKNOWLEDGMENTS

This study was abstracted in part from a dissertation submitted by Ho-Lun Weng to the Graduate College, University of Iowa, in partial fulfillment of the Doctor of Philosophy degree requirement.

Long-Term Controlled Navel Administration of Testosterone

YIE W. CHIEN

Received September 28, 1982, from the *Controlled Drug Delivery Research Center, Rutgers University, College of Pharmacy, Busch Campus, Piscataway, NJ 08854.* Accepted for publication June 29, 1983.

Abstract □ Male fertility has reportedly been regulated by the long-term, continuous administration of testosterone. To deliver the testosterone at a controlled rate for a month or longer, a bandage-type, testosterone-releasing, disk-shaped device was developed. *In vitro* drug elution studies demonstrated that a constant release profile of testosterone was achieved. *In vivo* studies in rhesus monkeys with the medicated device directly overlaying the navel for 46 d, yielded a fairly steady plasma level and also a constant urinary excretion rate for 32 d. A greater systemic bioavailability (more than twofold) was achieved as compared with drug disposition directly onto the navel or *via* the polacebo device (*i.e.*, drug is deposited onto the prefabricated placebo device). A fairly constant cumulative urinary recovery profile was achieved for longer than 1 month, in which >90% of the dose was administered. The *in vitro* and *in vivo* relationship was analyzed and discussed.

Keyphrases □ Testosterone—long-term controlled administration, navel, rhesus monkeys, bioavailability □ Controlled administration, navel—long-term, testosterone, rhesus monkeys, bioavailability □ Bioavailability—long-term controlled administration, navel, testosterone

It is known that the spermatogenesis is an androgen-dependent process which can be maintained in hypophysectomized rats by continuous administration of testosterone (1). Also, it was reported that male fertility can be regulated by the long-term, continuous administration of testosterone or testosterone derivatives (2–4).

Recently, several medicated bandages were successfully developed and approved by the FDA for marketing to provide a continuous transdermal administration of systemically active drugs through the intact skin (5–7). Following the development of a scopolamine-releasing system for 3-d prevention of motion sickness, four nitroglycerin-releasing transdermal therapeutic systems (system A[1], system B[2], system C[3], and system D[4]) were also developed to provide 24-h continuous protection against anginal attack (6, 7).

It was recently observed in this laboratory that the transdermal absorption of testosterone in six rhesus monkeys *via* the navel area produces a substantially greater systemic bioavailability than by forearm administration (79.9 *versus* 49.9%). Bioavailability of testosterone by intravenous administration was used as the control (22). In the present investigation, we evaluated the feasibility of using the navel as the site for a long-term application of a bandage-type controlled-release drug delivery system developed to provide a continuous transdermal administration of testosterone at a controlled rate.

EXPERIMENTAL SECTION

Preparation of the Testosterone-Releasing Transdermal Bandage—To deliver the testosterone at a controlled rate for a month or longer, a disk-shaped testosterone-releasing device was fabricated, using the methodology and process outlined for the preparation of microsealed drug delivery (MDD) systems (9–11), to contain a combination of 0.041% w/w of [^{14}C]testosterone and 0.252% w/w of nonradioactive testosterone in the medicated liquid compartments. The testosterone-saturated liquid compartments were dispersed homogeneously as discrete microscopic spheres in the cross-linked polymer matrix (Fig. 1).

For the *in vivo* studies, medicated MDD disks with a surface area closely resembling that of the navel of a rhesus monkey (with an apparent surface area of 0.2 cm^2 each) were fabricated to contain 4.41 ± 0.25 μCi of [^{14}C]-testosterone. Each of the disks was then glued onto the center of a piece of commercially available plastic adhesive[5] to form a testosterone-releasing transdermal bandage.

***In Vitro* Release Studies**—The *in vitro* drug elution system, used to characterize the mechanism and rates of testosterone release from each of the MDD disks, was essentially the same as that reported previously (12), except that the medicated MDD disk was mounted in a specially designed acrylic holder (Fig. 2). The whole assembly was then rotated at a constant angular rotation speed of 81 rpm, to achieve a constant hydrodynamic condition, in a perfect sink aqueous medium (with a constant volume of 150 mL) at 37°C. The medium contains 75% v/v of polyethylene glycol 400 to enhance the aqueous solubility of testosterone and to maintain a perfect sink, which simulates the biological sink achieved by blood perfusion. The amount of testosterone released daily was determined spectrophotometrically at the λ_{max} of 241 nm.

***In Vivo* Navel Absorption Studies**—Rhesus monkeys (4.85–5.0 kg) were immobilized by the injection of 1 mg/kg of phencyclidine hydrochloride[6]

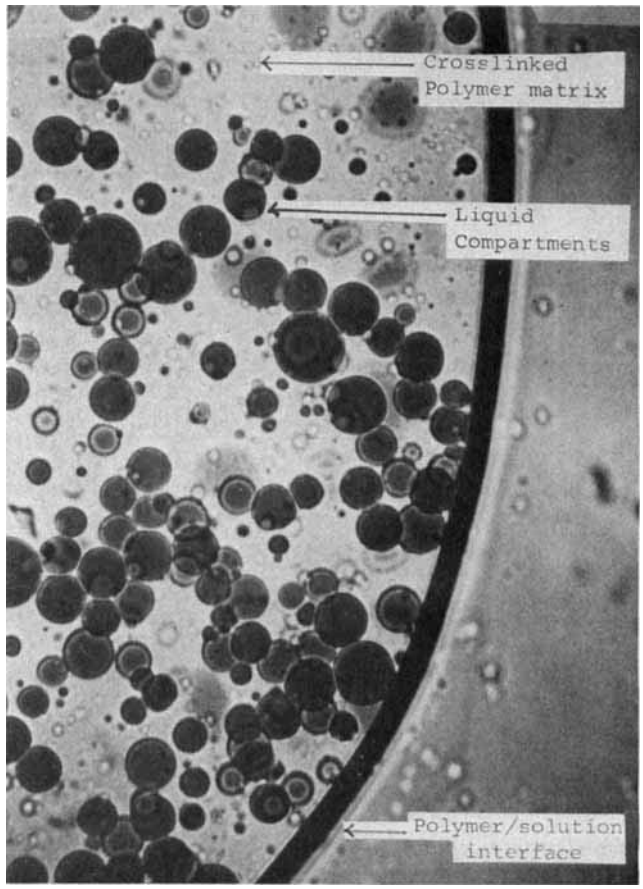

Figure 1 —*Photomicrograph (1300×) of the cross-sectional view of an MDD system. The microscopic liquid compartments (dark areas), which encapsulate drug particles, are homogenously dispersed as discrete, immobilized, unleachable spheres (with diameter <50 μm) in a cross-linked polymer matrix (light background area).*

[1] Nitrodisc; Searle Pharmaceuticals, Chicago, Ill.
[2] Nitro-Dur; Key Pharmaceuticals, Miami, Fla.
[3] Transderm-Nitro; Ciba Pharmaceutical Co., Summit, N.J.
[4] Deponit; Pharma-Schwarz GmbH.
[5] Johnson & Johnson, New Brunswick, N.J.
[6] Bio-ceutic Laboratories, St. Joseph, Mo.

0022-3549/84/0800-1064$01.00/0
© 1984, American Pharmaceutical Association

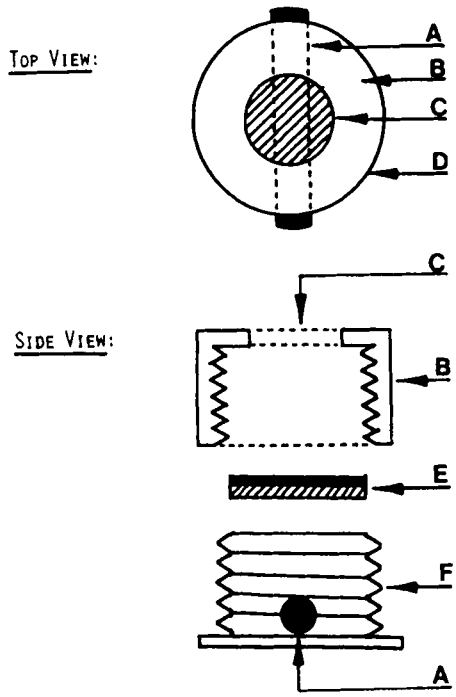

Figure 2—*Diagrammatic illustration of the acrylic holder which is specially designed for the mounting of the disk-shaped MDD system. The whole assembly can be rotated in a thermostated drug elution solution at constant rotation speed by a magnetic stirrer. Key: (A) magnetic spin bar; (B) acrylic cap; (C) opening; (D) acrylic holder; (E) MDD disk; (F) acrylic platform.*

solution. Testosterone was then administered to the navel area by the following methods.

Drug Disposition—Five microcuries (25 μg) of [^{14}C]testosterone[7] in 100 μL of acetone was applied dropwise to the navel, with the area of application controlled at 0.2 cm^2 by a template (an aluminum plate with a 0.2-cm^2 circular hole at the center). After all the drug solution was applied and quickly dried, a piece of plastic adhesive was placed over the application site and further reinforced with another plastic adhesive strip.

MDD Disk Application—One hundred microliters of drug-free acetone[8] was applied dropwise to the navel (this was done to correct for any possible effect of acetone on percutaneous absorption). After the solvent had dried, a unit of testosterone-releasing transdermal bandage was applied directly with the medicated MDD disk centered on the navel. It was then reinforced with another strip of plastic adhesive.

Placebo Disk Application—A placebo disk containing no testosterone was prepared in the same manner as described earlier for the MDD disk. After placing the placebo disk over the acetone-treated navel, 6 μCi (30 μg) of [^{14}C]testosterone in 10 μL of acetone was applied dropwise on the 0.2-cm^2 placebo disk. After drug solution was dried rapidly, a piece of plastic adhesive was placed over the placebo disk and further reinforced with another strip of plastic adhesive.

Each of the treated monkeys was placed into a jacket[9] and then secured in a metabolism chair. A 20-gauge catheter needle[10] was secured to the leg of the monkey to collect blood samples from the saphenous vein. Meanwhile, saline solution[11] was continuously infused through another catheter at a rate of 14 mL/h. Two-milliliter aliquots of blood were collected at 0.5, 1, 2, 3, 4, 5, 6, and 24 h and then every 24 h thereafter until the completion of a study. Urine was also collected on a daily basis.

At the end of each study, the plastic adhesive strips and MDD or placebo disks were removed and thoroughly extracted with methanol[8]. The area of drug application was also carefully washed to remove the residual, unabsorbed testosterone (both radioactive and nonradioactive). The extractions and washings were then combined for the analysis and determination of the fraction of dose not absorbed.

The blood samples were collected in heparinized tubes. After centrifugation, 200 μL of plasma were transferred from each sample and mixed with 5 mL of scintillation fluid[12]. Duplicate samples were prepared and their radioactivity was determined[13]. Conversion of counts per minute (cpm) to disintegrations per minute (dpm) was accomplished by the external standard channels ratio method. Data measured as dpm was recorded and converted to the corresponding total radioactivity in 100 mL of plasma (μCi/100 mL) at each sampling interval.

Samples (500 μL–1 mL) were taken in duplicate from a daily urine collection and mixed with 10 mL of scintillation fluid[12]. Total radioactivity in each sample was determined and calculated in the same manner as described earlier for plasma samples.

[7] New England Nuclear Corp., Boston, Mass.
[8] Reagent grade; MCB Manufacturing Chemists, Norwood, Ohio.
[9] Alice King Chatham, Medical Arts, Los Angeles, Calif.
[10] Longwell; Becton, Dickinson & Co., Rutherford, N.J.
[11] McGaw Laboratories, Glendale, Calif.

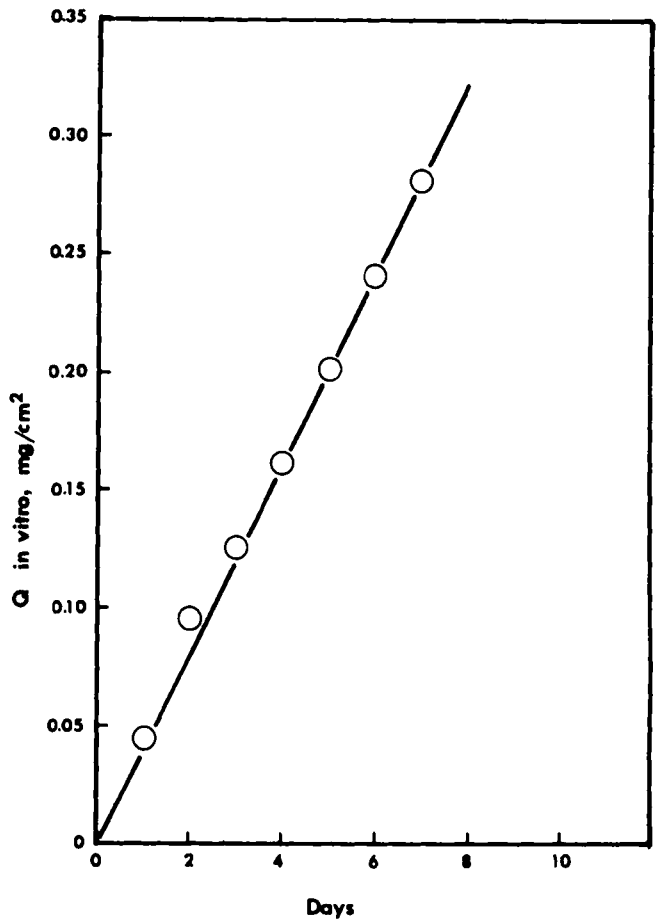

Figure 3—*Seven-day* in vitro *release of testosterone from the disk-shaped MDD system under a perfect sink condition at 37°C. The rate of release (Q/t) was determined to be 40.25 ± 0.64 μg/cm^2/d (mean ± SD).*

RESULTS AND DISCUSSION

***In Vitro* Release of Testosterone from MDD Disks**—A typical set of data on the *in vitro* release of testosterone from an MDD disk is illustrated in Fig. 3. The cumulated amount, Q, of testosterone released from a unit surface area of the MDD disk was found to be linearly proportional to the duration (in days) of elution in the elution solution. Apparently, a constant (zero-order) release profile was achieved. The observation is in good agreement with the controlled release of deoxycorticosterone acetate from the same type of MDD system (12). From the slope of the linear Q *versus* t plot, the rate of release, Q/t, of testosterone from the MDD disk was calculated to be 40.25 (±0.64) μg/cm^2/d (average of triplicate experiments with a coefficient of variation of 1.6%). The theoretical basis for the observed Q *versus* t relationship was analyzed previously (13).

Long-Term Navel Absorption of Testosterone—For the *in vivo* studies, a unit of testosterone-releasing transdermal bandage was applied to each of two rhesus monkeys with the medicated MDD disk (0.2 cm^2) directly overlaying the navel. Blood and urine samples were collected according to the protocol outlined earlier (*Experimental Section*) until all the testosterone dose incorporated was totally released (~46 d).

[12] PCS; T. M. Amersham/Searle Corp., Arlington Heights, Ill.
[13] Mark II Scintillation Counter; Searle Analytic, Inc., Des Plaines, Ill.

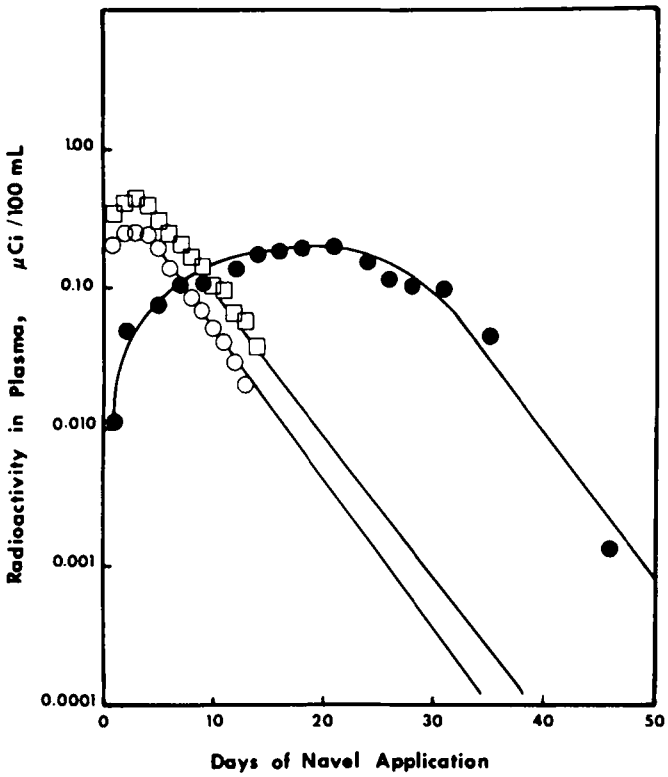

Figure 4—*Mean plasma radioactivity levels following the navel administration of [^{14}C]testosterone in two rhesus monkeys. Key: (○) drug alone (5.03 μCi); (□) disposition on a placebo disk (6.02 μCi), (●) microseal in an MDD disk (4.41 μCi). The first-order rate constants for elimination (β) were 0.0104, 0.0098, and 0.0101 h^{-1}, respectively.*

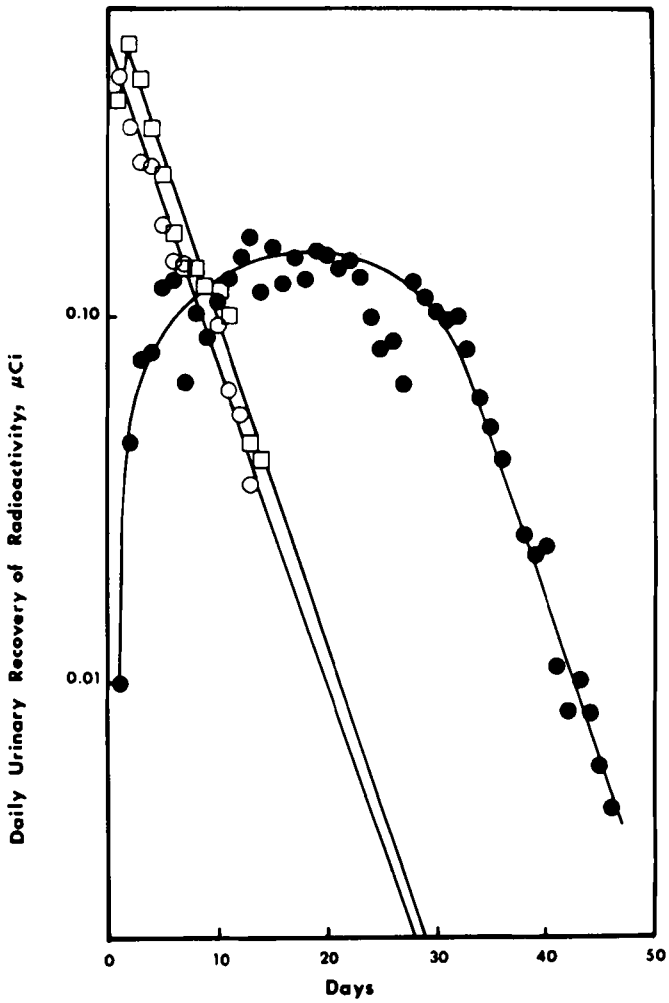

Figure 5—*Mean daily urinary recovery of radioactivity following the navel administration of [^{14}C]testosterone in two rhesus monkeys. Key: (○) drug alone (5.03 μCi); (□) disposition on a placebo disk (6.02 μCi); (●) microseal in an MDD disk (4.41 μCi). The first-order constants for urinary excretion (k_e) were 0.0085, 0.0087, and 0.0085 h^{-1}, respectively.*

Both plasma profiles (Fig. 4) and daily urinary recovery data (Fig. 5) demonstrated that the 46-d application of the MDD disk on the navel of the monkey maintained a fairly steady plasma radioactivity level at ~0.10 μCi/100 mL for a duration of slightly over 1 month and also a fairly constant urinary excretion rate of 0.10 μCi/d in the same period.

On the other hand, application of [^{14}C]testosterone directly onto the navel by the solution disposition technique or disposition of drug on a placebo MDD disk (without microsealed drug inside the device) at the time of navel application could not achieve or maintain either a steady plasma level or a constant daily urinary excretion rate of [^{14}C]testosterone (Figs. 4 and 5). The results suggested that the MDD system provides the controlled-release mechanisms to meter the release of a constant amount of [^{14}C]testosterone available for navel absorption.

The data in Figs. 4 and 5 also indicated that the rate constants for elimination (β) and for urinary excretion (k_e) of [^{14}C]testosterone were not altered by the controlled drug administration of the MDD system. These observations are expected since the β and k_e values are the intrinsic pharmacokinetic profiles of the drug and should not be modified in any way by the method of administration. Both with and without microsealed [^{14}C]testosterone in the device, the testosterone and its metabolites were eliminated and excreted basically at the same rates as those for drug alone. Testosterone and its metabolites were eliminated at a mean β value of 0.0101 ± 0.0003 h^{-1} and excreted at a mean k_e value of 0.0085 ± 0.0001 h^{-1}.

To determine the *in vivo* release rate of testosterone at the navel site, the cumulative urinary total radioactivity recovery data (expressed as percent of the administered dose) was plotted as a function of time (Fig. 6). As seen in the short-term (7-d) *in vitro* drug release studies (Fig. 3), a fairly constant urinary recovery profile was also observed in the navel absorption of testosterone when the combination of radioactive and nonradioactive testosterone was delivered by an MDD disk, for a period of ≤32 d. It was also noted that >90% of the administered dose of the radioactive testosterone was recovered in the urine during the 32-d zero-order transdermal controlled drug administration (Fig. 6).

On the other hand, it was observed that only one-half (~46%) of the administered dose was recovered from the urinary excretion when [^{14}C]testosterone was administered either by direct disposition on the navel or by depositing a placebo MDD disk (without microsealed compound in the liquid compartments) on the navel. The balance of the administered dose was recovered from the washings of the skin surface and from the extractions of the covering materials. The reasons for the low transdermal bioavailability observed are still not clear and require further study. In any case, a better systemic bioavailability of testosterone was achieved by use of the controlled-release MDD system, which released testosterone at the molecular level and controlled the amount of testosterone available for continuous transdermal administration through the navel.

As previously stated, each MDD disk contained a combination of 0.041% w/w [^{14}C]testosterone and 0.252% w/w nonradioactive testosterone. By calculation, the 32-d cumulative urinary radioactivity recovery data in Fig. 6 can be translated into the cumulative total amount (Q) of testosterone (radioactive and nonradioactive) absorbed by each of the rhesus monkeys investigated. Again, a fairly linear Q *versus* t relationship was achieved (Fig. 7), as seen in the *in vitro* drug release studies (Fig. 3). From the slope of this linearity, it was determined that the testosterone was released and absorbed from the MDD disk at an *in vivo* rate (Q/t) of 27.66 μg/cm^2/d.

***In Vitro–In Vivo* Relationships**—Comparison of this *in vivo* release rate (27.66 μg/cm^2/d) with the *in vitro* release rate (40.25 μg/cm^2/d) determined in Fig. 3 yields an *in vitro–in vivo* correlation coefficient of 0.69. The observation of a nonunity correlation coefficient, *e.g.*, 0.69, could be attributed to the existence of skin tissues in the *in vivo* situation, which act as an additional diffusion barrier for the permeation of drug molecules released from the medicated MDD disk. Drug molecules have to diffuse through this barrier before they can reach the biological sink for transport to a target organ[4]. The dissimilarity between *in vitro* and *in vivo* conditions may also contribute to the *in vitro–in vivo* correlation coefficient lower than unity. The sink condition established in the *in vitro* situation by the enhancement in saturation solubility may not simulate the interfacial partitioning of the drug from the drug delivery device toward the stratum corneum, which is a nonsink medium in nature.

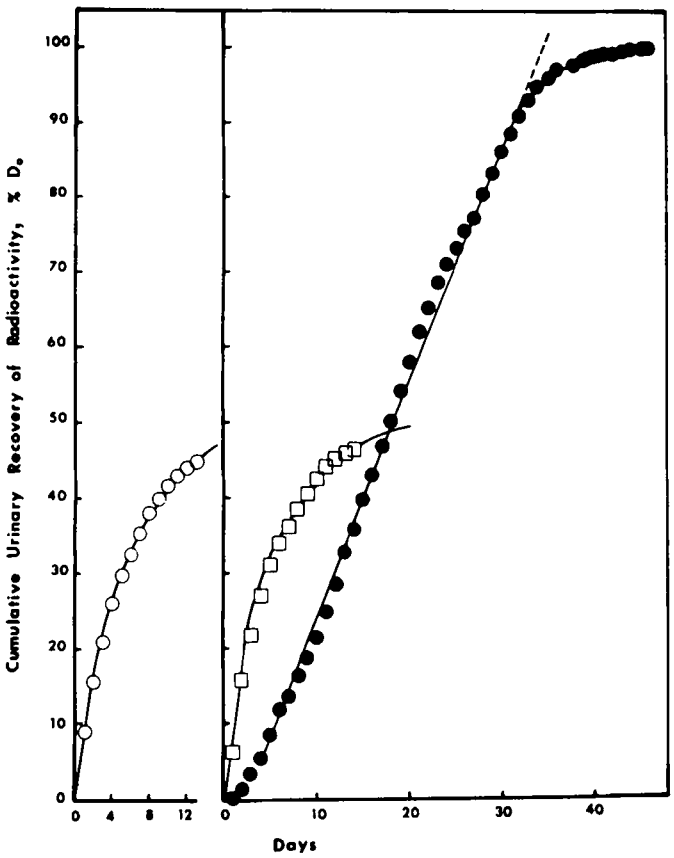

Figure 6—*Comparison of the time course for the cumulative urinary total recovery of radioactivity following the navel administration of [^{14}C]testosterone. Key: (○) drug only; (□) disposition on a placebo disk; (●) microseal in an MDD disk. The total urinary recovery is 44.8, 46.5, and 93.4%, respectively, of the administered dose (D_0).*

In a separate study with subcutaneously controlled administration of deoxycorticosterone acetate delivered by an identical MDD-type drug delivery system, an almost unity (1.09) *in vitro–in vivo* correlation coefficient was obtained (13), in which the stratum corneum does not exist between the drug delivery system and the biological sink.

However, the *in vitro–in vivo* correlation coefficient (0.69) obtained can be utilized as a working factor in the determination and projection of the long-term *in vivo* release rates from a short-term *in vitro* drug release study (13–17). This coefficient can be very useful in the development of a long-acting drug delivery system in that it can minimize the expense involved in the amount of testing required and the use of costly animals.

In conclusion, the bioavailability data generated in this investigation have clearly demonstrated that the navel can be a useful site for long-term transdermal administration of drugs, such as testosterone, *via* a bandage-type controlled-release drug delivery system [such as a microsealed drug delivery (MDD) system] to provide a prolonged plasma drug level for at least 1 month. The systemic bioavailability of the drug can also be enhanced substantially by the controlled drug-release mechanisms of the MDD system. The same conclusion was reached in the controlled subcutaneous administration of deoxycorticosterone acetate by a subdermal implant-type MDD system (13).

REFERENCES

(1) E. Steinberger, A. Steinberger, and M. Ficher, *Recent Prog. Horm. Res.*, **26**, 547 (1970).

(2) L. G. Stratton, L. L. Ewing, and C. Desjardins, *J. Reprod. Fert.*, **35**, 235 (1973).

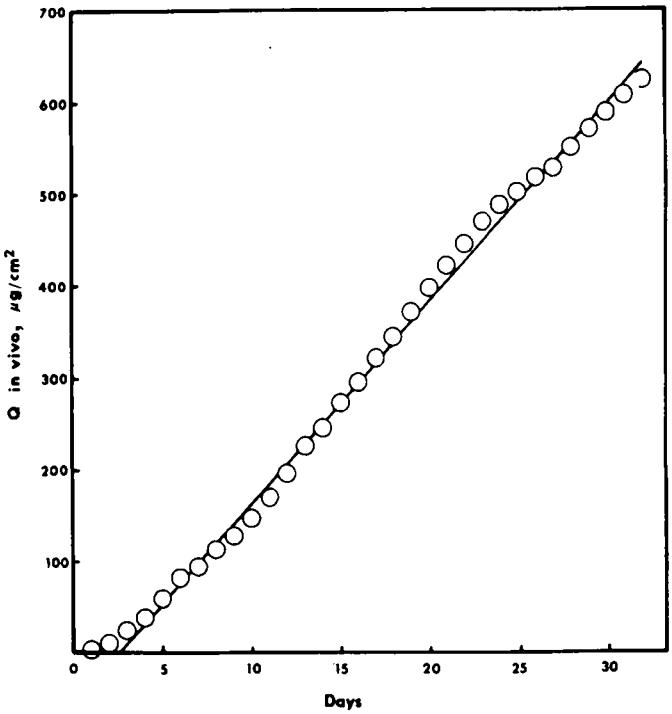

Figure 7—*Time course for the cumulative total amount of testosterone administered to the two rhesus monkeys during 32-d navel application of an MDD disk (0.2 cm^2). The data were calculated from Fig. 6 by converting the cumulative urinary radioactivity data into the total amount of testosterone administered/cm^2 of the MDD disk. The* in vivo *release rate (Q/t) was calculated to be 27.66 μg/cm^2/d.*

(3) M. Briggs and M. Briggs, *Nature* (*London*), **252**, 585 (1974).

(4) J. Mauss, G. Borsch, K. Bormacher, E. Richter, G. Legendecker, and W. Nocke, *Acta Endocrinol.*, **78**, 373 (1975).

(5) S. K. Chandrasekaran, W. Bayne, and J. E. Shaw, *J. Pharm. Sci.*, **67**, 1370 (1978).

(6) A. Gerardin, J. Hirtz, P. Frankhauser, and J. Moppert, "Abstracts," APhA/APS 31st. National Meeting **11**(2), 84 (1981).

(7) Y. W. Chien, *Drug Dev. Indust. Pharm.*, **9**(4), 497 (1983).

(8) Y. W. Chien, *J. Pharm. Sci.*, **73**, 283 (1984).

(9) Y. W. Chien and H. J. Lambert, U.S. Pat. 3,946,106 (March 23, 1976).

(10) Y. W. Chien and H. J. Lambert, U.S. Pat. 3,992,518 (Nov. 16, 1976).

(11) Y. W. Chien and H. J. Lambert, U.S. Pat.. 4,053,580 (Oct. 11, 1977).

(12) Y. W. Chien, H. J. Lambert, and D. E. Grant, *J. Pharm. Sci.*, **63**, 365 (1974).

(13) Y. W. Chien, L. F. Rozek, and H. J. Lambert, *J. Pharm. Sci.*, **67**, 214 (1978).

(14) Y. W. Chien, in "Recent Advances in Drug Delivery," J. M. Anderson and S. W. Kim, Eds., Plenum, New York, N.Y., 1984, pp. 367–387.

(15) Y. W. Chien and E. P. K. Lau, *J. Pharm. Sci.*, **65**, 488 (1976).

(16) Y. W. Chien, *Chem. Pharm. Bull.*, **24**, 1471 (1976).

(17) Y. W. Chien, "Novel Drug Delivery Systems: Fundamentals, Developmental Concepts and Biomedical Assessments," Dekker, New York, N.Y., 1982, chap. 9.

ACKNOWLEDGMENTS

The author extends his appreciation to Dr. B. Nicolova for her technical assistance and to Searle Laboratories for providing monkey research facilities.

Phenytoin Prodrugs III: Water-Soluble Prodrugs for Oral and/or Parenteral Use

S. A. VARIA *, S. SCHULLER, K. B. SLOAN ‡, and V. J. STELLA ˣ

Received December 22, 1982, from the *Department of Pharmaceutical Chemisty, School of Pharmacy, The University of Kansas, Lawrence, KS 66045.* Accepted for publication September 6, 1983. Present addresses: *Squibb Institute for Medical Research, New Brunswick, NJ 08903; ‡College of Pharmacy, University of Florida, Gainesville, FL 32610.

Abstract □ Various bioreversible derivatives of phenytoin, a poorly water soluble and erratically absorbed drug after both oral and parenteral dosing, were synthesized. Initial evaluation of these expected prodrugs, *i.e.*, their aqueous solubility, cleavage in the presence of various animal tissues, and anticonvulsant activity in mice, confirmed that a number of the derivatives did indeed behave as prodrugs. The more promising prodrugs were the disodium phosphate ester and various amino groups containing acyl esters of 3-(hydroxymethyl)-5,5-diphenylhydantoin.

Keyphrases □ Prodrugs—phenytoin, water-soluble, hydroxymethylation, anticonvulsants □ Anticonvulsants—phenytoin prodrugs, water-soluble, hydroxymethylation □ Phenytoin—water-soluble prodrug, hydroxymethylation

Phenytoin (I) is a high melting (293°C), weakly acidic (1, 2) drug exhibiting poor solubility (3–5) in water. These properties lead to erratic absorption after oral dosing with both the free acid and the sodium salt (Ia) (3, 6–19). For parenteral use, sodium phenytoin is formulated in an aqueous alkaline medium of pH ~12 containing 40% propylene glycol and 10% ethanol. The parenteral dosage form is hazardous if the intravenous injection is rapid (20, 21), and the free acid appears to precipitate at intramuscular injection sites (22–25). The parenteral dosage form has also presented handling problems, especially if admixing or dilution was desired (26, 27).

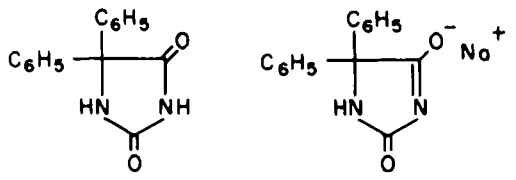

I Ia

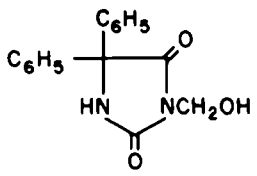

II

One solution to these problems was to develop prodrugs of phenytoin with more desirable physicochemical properties[1]. The overall goal of this study, therefore, was to synthesize various water-soluble phenytoin prodrugs and to evaluate their potential oral and parenteral use. Recently, interest has arisen in *N*-hydroxymethyl derivatives of hydantoins, amides, and imides (4, 5, 28–31). In the present study 3-(hydroxymethyl)-5,5-diphenylhydantoin or 3-(hydroxymethyl)phenytoin (II) was synthesized with the expressed purpose of providing a "synthetic handle" in the molecule to which various other potential bioreversible water-solubilizing functional groups could be added (esters III–X).

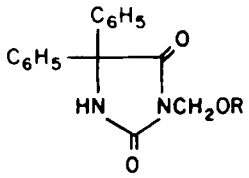

III: R = $COCH_3$
IV: R = $COCH_2\overset{+}{N}H(CH_3)_2\ CH_3SO_3^-$
V: R = $CO(CH_2)_2\overset{+}{N}H(C_2H_5)_2$ (2-naphthalenesulfonate)
VI: R = $CO_2(CH_2)_2\overset{+}{N}H(CH_3)_2\ CH_3SO_3^-$
VII: R = $PO_3^{2-}Na_2^+$
VIII: R = $SO_3^-Na^+$
IX: R = $CO(CH_2)_2CO_2^-Na^+$
X: R = $CO(CH_2)_3CO_2^-Na^+$

All the esters except III have an ionizable group in the ester moiety, and the salt forms of esters would be expected to have an increased aqueous solubility over that of phenytoin. Compounds IV–VI, IX, and X would be expected to be cleaved *in vivo* by esterases to II, which will be shown in this study to break down further to phenytoin and formaldehyde with a half-life of ~2 s at 37°C and pH 7.4, an observation consistent with an earlier study (5). Similarly, VII and VIII were expected to be catalytically hydrolyzed by phosphatase and sulfatase enzymes, respectively.

The evaluation of VIII as a potential prodrug of phenytoin has been presented elsewhere (32); VIII was found not to behave as a prodrug of phenytoin. The syntheses and preliminary evaluations of compounds IV–VII, IX, and X are presented herein.

EXPERIMENTAL SECTION

All compounds were synthesized by standard techniques. The specific details for the synthesis of each compound are presented below.

3-(Hydroxymethyl)phenytoin [II, 3-(Hydroxymethyl)-5,5-diphenylhydantoin]—A suspension of 20 g (0.08 mol) of phenytoin, 80 mL of formalin (1.07 mol, 37% formaldehyde in water), 1 g (0.007 mol) of potassium carbonate, and 720 mL of water were stirred at room temperature for 24 h. The mixture was filtered and the resulting white solid was washed with 3% aqueous formaldehyde, air dried for 24 h to give 21.5 g of II (92% yield), mp 187–189°C. ^{1}H-NMR (Me_2SO-d_6): δ 4.85 (d, CH_2), 6.4 (t, OH), 7.4 (s, 10), and 9.6 ppm (s, NH).

Anal.—Calc. for $C_{16}H_{14}N_2O_3$: C, 68.08; H, 5.00; N, 9.92. Found: C, 68.15; H, 4.93; N, 9.97.

3-(Hydroxymethyl)-5,5-diphenylhydantoin Acetate (Ester III)—A solution of 1.5 g (0.0058 mol) of II, 1 mL of acetic anhydride, and 10–20 μL of sulfuric acid was allowed to stand for 10 min. The solid precipitate was suspended in 10 mL of ether, filtered, washed with 30 mL of ether, and then recrystallized from ethanol to give 1.69 g of ester III (90% yield), mp 154–157°C. ^{1}H-NMR ($CDCl_3$): δ 2.0 (s, CH_3), 5.55 (s, CH_2), 7.4 (s, 10), and 7.7 ppm (s, NH).

Anal.—Calc. for $C_{18}H_{16}N_2O_4$: C, 66.65; H, 4.97; N, 8.64. Found: C, 66.66; H, 5.01; N, 8.61.

[1] Paper I in this series was published in "Prodrugs as Novel Drug Delivery Systems", ACS Symposium Series, No. 14, 1975, Chap. 3, paper II in *J. Pharm. Sci.*, **72**, 400 (1983).

0022-3549/84/0800-1068$01.00/0
© 1984, American Pharmaceutical Association

3-(Hydroxymethyl)-5,5-diphenylhydantoin Ester with *N,N*-Dimethylglycine, Monomethanesulfonate (IV)—A suspension of 3.65 g (0.035 mol) of *N,N*-dimethylglycine, 7.3 g (0.035 mol) of dicyclohexylcarbodiimide, and 10 g (0.035 mol) of II in 50 mL of dry pyridine was stirred at room temperature for 24 h. After evaporation under reduced pressure at 50°C, the syrupy contents were triturated with 100 mL of dichloromethane and the dicyclohexylurea was removed by filtration. The dichloromethane was removed under reduced pressure, and the trituration was repeated twice to produce a syrup, to which was added 50 mL of ether. After standing, the resulting precipitate was removed by filtration and washed with 25 mL of ether and dried *in vacuo* to give 11.3 g of IVa (88% yield), mp 133–137°C. ^{1}H-NMR and elemental analysis confirm the structure of the product as 3-(hydroxymethyl)-5,5-diphenylhydantoin ester with *N,N*-dimethylglycine (IVa). A solution of 1.92 g (0.005 mol) of IVa, 0.5 g (0.005 mol) of methanesulfonic acid, and 25 mL of dichloromethane was stirred, and the resulting precipitate was removed by filtration and recrystallized from ethanol–acetone–ether to give 2.15 g of IV (93% yield), mp 173–175°C. ^{1}H-NMR (D_2O): δ 3.05 (s, CH_3), 3.2 (s, 2, CH_3), 4.4 (s, CH_2), 5.85 (s, CH_2), and 7.5 ppm (s, 10).

Anal.—Calc. for $C_{21}H_{25}N_3O_7S$: C, 54.42; H, 5.44; N, 9.07. Found: C, 54.22; H, 5.40; N, 8.92.

3-(Hydroxymethyl)-5,5-diphenylhydantoin Ester with *N,N*-Diethyl-β-alanine, Mono-2-naphthalenesulfonate (V)—A suspension of 3.54 g (0.0195 mol) of 3-*N,N*-diethylaminopropionic acid hydrochloride, 4.02 g (0.0195 mol) of dicyclohexylcarbodiimide, and 5 g (0.0177 mol) of II in 20 mL of dry pyridine was stirred at room temperature for 20 h and filtered. The glassy residue was triturated with 100 mL of dichloromethane, and the suspended dicyclohexyl urea was removed by filtration. The dichloromethane was removed under reduced pressure and the trituration was repeated twice. The syrup was dissolved in 100 mL of water, the pH was lowered to 3 with dilute HCl, and the mixture was extracted twice with 100 mL of ether. The pH of the aqueous layer was raised to 9 with solid potassium carbonate, and the mixture was extracted with 100 mL of ether. The organic phase was dried (magnesium sulfate), and the solvent was removed under reduced pressure to yield 3-(hydroxymethyl)-5,5-diphenylhydantoin ester with *N,N*-diethyl-β-alanine (Va). A solution of 4.35 g (0.0106 mol) of Va and 2.6 g (0.0106 mol) of 2-naphthalenesulfonic acid, dissolved in a minimum amount of methanol, in 80 mL of dry ether was stirred until the precipitation of a white solid. The precipitate was removed by filtration, washed with 50 mL of ether, and dried in a vacuum desiccator to give 4.0 g of V (44.5% yield), mp 174–176°C. ^{1}H-NMR (Me_2SO-d_6): δ 1.15 (t, $2CH_3$), 3.1 (m, 8), 5.55 (s, CH_2), 7.4 (m, 17), and 9.9 ppm (s, NH).

Anal.—Calc. for $C_{33}H_{35}N_3O_7S$: C, 64.17; H, 5.17; N, 6.80. Found: C, 63.90; H, 5.72; N, 6.62.

3-(Hydroxymethyl)-5,5-diphenylhydantoin Ester with 2-(Dimethylamino)-ethyl Carbonate, Monomethanesulfonate (VI) *Via* 3-(Hydroxymethyl)-5,5-diphenylhydantoin, *p*-Nitrophenyl Carbonate (XI)—A solution of 6.78 g (0.033 mol) of *p*-nitrophenylchloroformate and 9.5 g (0.033 mol) of II in 30 mL of dry pyridine was stirred at room temperature for 5 h, poured with vigorous stirring into ice water, and acidified with 0.38 mol of sulfuric acid. The pale yellow solid was removed by filtration and dried in a vacuum oven at 40°C overnight to give 12.9 g of XI (88% yield), mp 191–193°C.

A solution of 4 mL of 2-(*N,N*-dimethylamino)ethanol, previously dried by distillation, and 4.5 g (0.01 mol) of XI in 25 mL of acetonitrile was stirred at room temperature for 5 h, poured into ice water, and extracted with 100 mL of dichloromethane. The organic layer was extracted twice with 25 mL of 5% aqueous potassium carbonate solution, dried over anhydrous magnesium sulfate, filtered, and evaporated under reduced pressure to give 1.42 g of a white glassy solid, (35% yield), mp 88–90°C (VIa).

The methanesulfonate salt of VIa (VI) was prepared in the same manner as IV from IVa, except that on filtration from dichloromethane, the salt was refluxed in acetone to remove phenytoin contamination (46% yield), mp 186–189°C. ^{1}H-NMR (D_2O): δ 3.05 (s, CH_3), 3.2 (s, $2CH_3$), 3.7 (t, CH_2), 4.75 (t, CH_2), 5.8 (s, CH_2), and 7.55 ppm (s, 10).

Anal.—Calc. for $C_{22}H_{27}N_3O_8S$: C, 53.57; H, 5.47; N, 8.51. Found: C, 53.2; H, 5.5; N, 8.3.

3-(Hydroxymethyl)-5,5-diphenylhydantoin Disodium Phosphate Ester (VII)—Sodium dibenzylphosphate and silver dibenzylphosphate were synthesized according to the method of Clark and Todd (33) from dibenzylphosphite[2].

3-(Chloromethyl)-5,5-diphenylhydantoin (XII)—A solution of 20 g (0.071 mol) of II and 6.2 mL of phosphorous trichloride in 100 mL of dichloromethane was stirred at room temperature for 24 h, diluted with a further 50 mL of dichloromethane, and extracted once with 100 mL of water and twice with 250 mL of 5% w/v aqueous sodium carbonate solution. The separated dichloromethane was dried over anhydrous magnesium sulfate, filtered, and evaporated under reduced pressure to give 13.1 g of a white solid (61% yield), mp 155.0–156.5°C.

[2] Aldrich Chemical Co., Milwaukee, Wis.

Table I—Aqueous Solubilities and pH Values of the Saturated Solutions of Phenytoin, II (in 1 M Aqueous Formaldehyde), and IV–VII at 25°C

Compound	pH	Solubility (Phenytoin Equivalent), mg/mL	Solubility Relative to Phenytoin
I	Neutral	0.02[a] (0.02)	1
II	Neutral	0.19[b] (0.17)	8.5
IV	~2	140 (76.2)	3810
V	~4	1.9 (0.78)	39
VI	~2	185 (94.6)	4730
VII	~9	142 (88.17)	4408.5

[a] Literature values vary from 0.01–0.04 mg/mL (1, 26). A value of 0.02 mg/mL was found in our studies. [b] The solubility was determined in aqueous formaldehyde (1 M).

3-(Hydroxymethyl)-5,5-diphenylhydantoin Dibenzyl Phosphate Ester (XIII)—A suspension of 13.13 g (0.034 mol) of silver dibenzylphosphate and 10 g (0.033 mol) of XII in 300 mL of benzene was refluxed for 2 h, hot-filtered under reduced pressure, extracted with 250 mL of 5% aqueous potassium carbonate, dried over magnesium sulfate, filtered, and evaporated under reduced pressure. The remaining syrup was triturated with 60 mL of ether and allowed to stand overnight; the white precipitate (XIII) which formed was removed by filtration, washed with 60 mL of ether, and dried in a vacuum oven to give 12 g of XIII (67% yield), mp 116–118°C.

Phosphate Ester of II (VIIa) and Its Disodium Salt (VII)—A suspension of 1 g of palladium (5%) on activated carbon[2] and 2 g (0.0037 mol) of XIII in 100 mL of ethyl acetate was subjected to hydrogenation[3] at 60 psi for 25 min (34). The suspension was filtered and the filtrate was evaporated under reduced pressure to give 0.7 g of a white solid (VIIa) which readily recrystallized from acetone (54.5% yield), mp 173–176.5°C.

Anal.—Calc. for $C_{16}H_{15}N_2O_6P$: C, 53.05; H, 4.17; N, 7.73. Found: C, 52.88; H, 4.02; N, 7.60.

A solution of 1.8 g (0.005 mol) of VIIa in 100 mL of methanol was titrated with 1 M NaOH to the second end point as determined by pH monitoring. The solution was filtered, evaporated under reduced pressure, and the white solid recrystallized from water–ethanol–acetone to give 1.1 g of VII (56% yield), mp 220°C (softens). ^{1}H-NMR (D_2O): δ 5.3 (d, CH_2) and 7.45 ppm (s, 10).

Anal.—Calc. for $C_{16}H_{13}N_2O_6PNa_2{\cdot}2H_2O$: C, 43.4; H, 3.87; N, 6.33. Found: C, 43.25; H, 3.82; N, 6.31.

3-(Hydroxymethyl)-5,5-diphenylhydantoin Sodium Succinate (Ester IX)—A solution of 10 g (0.035 mol) of II in 100 mL of dry pyridine was stirred at room temperature for 5 d with the gradual addition of 4.85 g (0.043 mol) of succinic anhydride. The solution was poured into 400 mL of 5% w/v aqueous sodium bicarbonate and immediately extracted with 250 mL of chloroform. The aqueous layer was isolated and the pH was lowered to 2 with hydrochloric acid; the aqueous layer was then rapidly extracted with 400 mL of chloroform. The chloroform layer was dried over anhydrous magnesium sulfate, filtered, and evaporated under reduced pressure; the resulting white solid (IXa) was triturated with ether and removed by filtration, mp 144.5–147.5°C. ^{1}H-NMR ($CDCl_3$): δ 2.6 (s, $2CH_2$), 5.55 (s, CH_2), 6.2 (s, 1), 7.4 (s, 10), and 7.6 ppm (s, 1).

Anal.—Calc. for $C_{20}H_{18}N_2O_6$: C, 62.83; H, 4.75; N, 7.33. Found: C, 62.74; H, 4.71; N, 7.20.

The sodium salt of IXa was prepared by titrating IXa with an equimolar solution of sodium methoxide in anhydrous methanol to give 8.8 g (62% yield), mp 141.5–146°C.

Anal.—Calc. for $C_{20}H_{17}N_2O_6Na{\cdot}0.5\ H_2O$: C, 58.13; H, 4.36; N, 6.78. Found: C, 57.87; H, 4.18; N, 6.57.

3-(Hydroxymethyl)-5,5-diphenylhydantoin Sodium Gluturate (Ester X)—Compound X was synthesized by allowing glutaric acid anhydride to react with II in dry pyridine and isolated by a method identical to that described for the synthesis of IX (30% yield), mp 137.5–144°C. ^{1}H-NMR of Xa ($CDCl_3$): 2.8 (m, 3 CH_3), 5.55 (s, CH_2), 6.6 (s, 1), 7.4 (s, 10), and 7.7 ppm (s, 1).

Anal.—Calc. for $C_{21}H_{20}N_2O_6$ (Xa): C, 63.6; H, 5.09; N, 7.07. Found: C, 62.87; H, 5.07; N, 6.91.

Anal.—Calc. for $C_{21}H_{19}N_2O_6Na{\cdot}H_2O$ (X): C, 57.81; H, 4.81; N, 6.41. Found: C, 57.71; H, 4.77; N, 5.47.

Aqueous Solubility of II and IV–VII—The aqueous solubility of II was determined by adding an excess of II to a solution of formaldehyde (1 M) in vials maintained at 25 ± 0.1°C in a constant-temperature water bath. The solubility was determined in 1 M formaldehyde solution in order to prevent

[3] Parr Instrument Co., Moline, Ill.

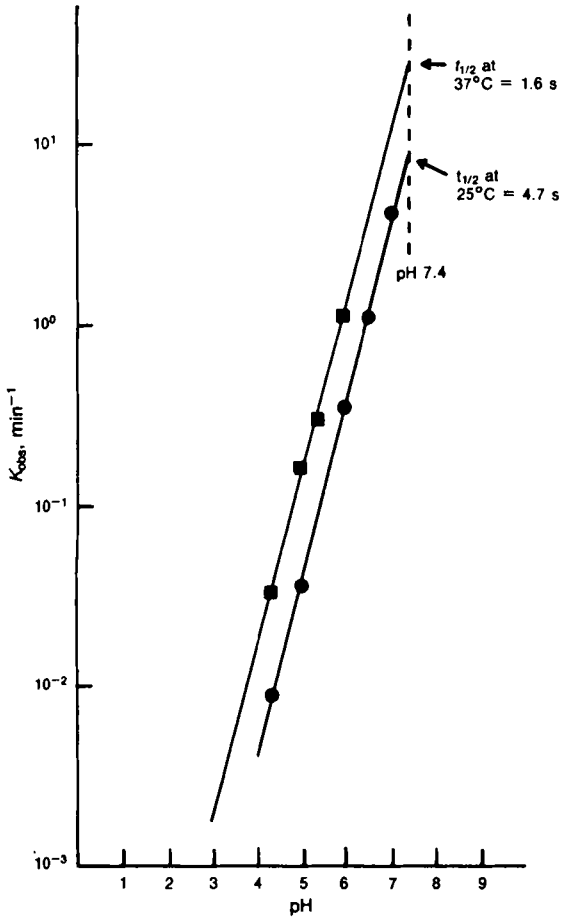

Figure 1—*pH-rate profile for the conversion of II to phenytoin at 25°C (●) and 37°C (■), μ = 0.5.*

the decomposition of II to phenytoin. The vials were shaken for 24 h so that equilibrium solubility was attained. The contents of the vials were then filtered. Appropriate dilutions of the filtrate with 1 M formaldehyde were made, and the absorbances of the diluted solutions at 260 nm were measured. The concentration of II was calculated from the measured absorbances by reference to standard curves. The aqueous solubilities of IV–VII were estimated at 25 ± 0.1°C by shaking an excess of the compound with a known volume of water, over a limited time period of 3–6 h to minimize the extent of degradation of the esters to phenytoin. The saturated solutions were filtered, diluted, and the concentrations of the esters were calculated from measured UV absorbances of the diluted solutions by reference to standard curves. The pH values of the saturated solutions were also measured.

Cleavage of IV–VII to Phenytoin in Biological Tissues—Conversion of IV–VII to phenytoin was carried out at 25°C and 37°C in plasma or whole blood obtained from rats[4], beagle dogs[5], and human subjects[6]. Blood was treated with EDTA to prevent coagulation. Plasma was obtained by centrifuging[7] blood for 15–20 min at 1000×*g*.

The conversion of VII to phenytoin was also studied in rat and dog tissue homogenates at 37°C. Sörensen's isotonic phosphate buffer (pH 7.4) was used to prepare the tissue homogenates and also to dilute plasma in cases where the reversion of the esters to phenytoin was too fast to follow in undiluted plasma. Reaction was initiated by injecting an appropriate amount of a stock solution of the ester in an appropriate solvent into temperature-equilibrated plasma, whole blood, or tissue homogenates. Samples obtained for the hydrolysis of IV–VI were quenched with *m*-phosphoric acid and assayed for phenytoin by the GC[8] method of Stella (35). In the case of the hydrolysis of VII, 100 μL of blood, plasma, or tissue homogenate samples were extracted directly into toluene containing the gas chromatography internal standard, 5-(*p*-methylphenyl)-5-phenylhydantoin, 0.7 μg/mL. The rest of the procedure

[4] Harlan Sprague-Dawley, Madison, Wis.
[5] Kindly supplied by INTERx Research Corp.
[6] Community Blood Bank, Kansas City, Mo.
[7] Dynac II; Beckton, Dickinson and Co.
[8] Varian model 2100 or 3700 gas chromatograph fitted with a flame-ionization detector.

Table II—Half-Lives for the Conversion of IV–VII to Phenytoin in Rat, Dog, and Human Plasma at 25°C and 37°C

Compound	Temperature, °C	Half-Life Rat	Dog	Human
IV	25	1.3 min	19.5 min	1.1 min
	37	16 s	10.7 min	23 s
V	25	27 s[a]	20.3 min	24.0 min
	37	—[c]	8.3 min	6.8 min
VI	25	1.1 min[b]	28.6 min	9.3 min
	37	33 s[b]	14.1 min	1.7 min

[a] In 10% rat plasma diluted with isotonic Sörenson's phosphate buffer, pH 7.4. [b] In 0.5% rat plasma diluted with isotonic Sörenson's phosphate buffer, pH 7.4. [c] Not determined.

was as described by Stella (35). Apparent first-order kinetics over 2–4 half-lives for the appearance of phenytoin were observed in all instances. Quantitative recovery (or conversion) of all the prodrugs were observed.

The tissue homogenates studied were rat and dog liver and rat intestinal homogenates prepared in pH 7.4, isotonic Sörensen's phosphate buffer (one part tissue to four parts buffer). The tissue was homogenized for 10 min using a 100-mL glass homogenizer with a polytef pestle having radial serrations[9]. The homogenizer was mechanically driven using a 3/8-hp variable-speed drill. The homogenates were centrifuged[10] for 90 min at 100,000×*g* at 5°C. The temperature was maintained between 5–10°C during the preparation of the tissue homogenate to prevent inactivation of the enzymes.

Hydrolysis of II to Phenytoin—The rates of decomposition of II in buffer solutions at 25°C and 37°C were studied spectrophotometrically[15] by recording the decrease[11] in absorbance at 255 nm. A 10-cm thermostated quartz cuvette was filled (30 mL) with pre-equilibrated buffer solutions [0.1 M acetate buffer (pH 3.0–5.0), 0.1 M phosphate buffer (pH 5.0–7.05), ionic strength 0.5], and the reaction was initiated by injecting a 25-μL aliquot of a stock solution of II in acetonitrile to yield a final concentration of II of 8×10^{-5} M. All reactions followed apparent first-order kinetics as determined from plots of log $(A_t - A_\infty)$ *versus* time, where A_t and A_∞ are the absorbance readings at time t and at completion of the reaction, respectively. In all cases the final spectrum corresponded to that of phenytoin. In a few studies, the effects of varying buffer concentrations at constant pH were evaluated. Since no buffer catalysis was noted at any pH value, no further studies on the effect of buffers were attempted.

Anticonvulsant Activity and Toxicological Evaluation of IV–VII—Compounds IV–VII were evaluated using the anticonvulsant drug screening program (36) conducted by the National Institute of Neurological and Communicative Disorders and Stroke at the National Institutes of Health, Bethesda, Md. All four compounds underwent the primary evaluation (phase I); in a minimal number of animals, the anticonvulsant activity of each compound was evaluated by the maximal electroshock test (MES) and the subcutaneous pentylenetetrazol test (ScMET); the CNS toxicity of each compound was evaluated by the rotorod test using mice[12] (36). After this initial evaluation, any potentially useful derivatives may be subjected to further comprehensive screening for activity and toxicity. Specifically, this consists of the phase II and phase IV studies. The phase II study requires administering the drug intraperitoneally to mice and determining the time of peak effect (activity and toxicity) by the MES and the rotorod test. From this, the effective dose 50% (ED_{50}) and toxic dose 50% (TD_{50}) for the prodrugs could be determined. The phase IV study is similar to the phase II study except that the drug is administered orally.

For specific details of the procedures used in the screening, the reader is directed to Ref. 36. With the current compounds, IV–VII underwent the initial screening (Phase I), VI underwent phase II, while IV and VII underwent both phase II and phase IV evaluations.

RESULTS AND DISCUSSION

Compounds IV–X were synthesized by standard procedures as indicated in the *Experimental Section*. All compounds were found to conform to the proposed structures and showed only one spot on TLC. Compounds IX and X showed less than theoretical values for carbon and nitrogen analyses. Recrystallization attempts did not improve the results. The precursors IXa and Xa gave reasonable C, H, N analyses, so it appears that during the formation

[9] Series 3431-E04; A. H. Thomas Co., Philadelphia, Pa.
[10] Beckman Model L-5-50 Ultracentrifuge, T-35 rotor.
[11] Cary Model 118; Varian Instruments.
[12] Carworth Farm # 1 mice.

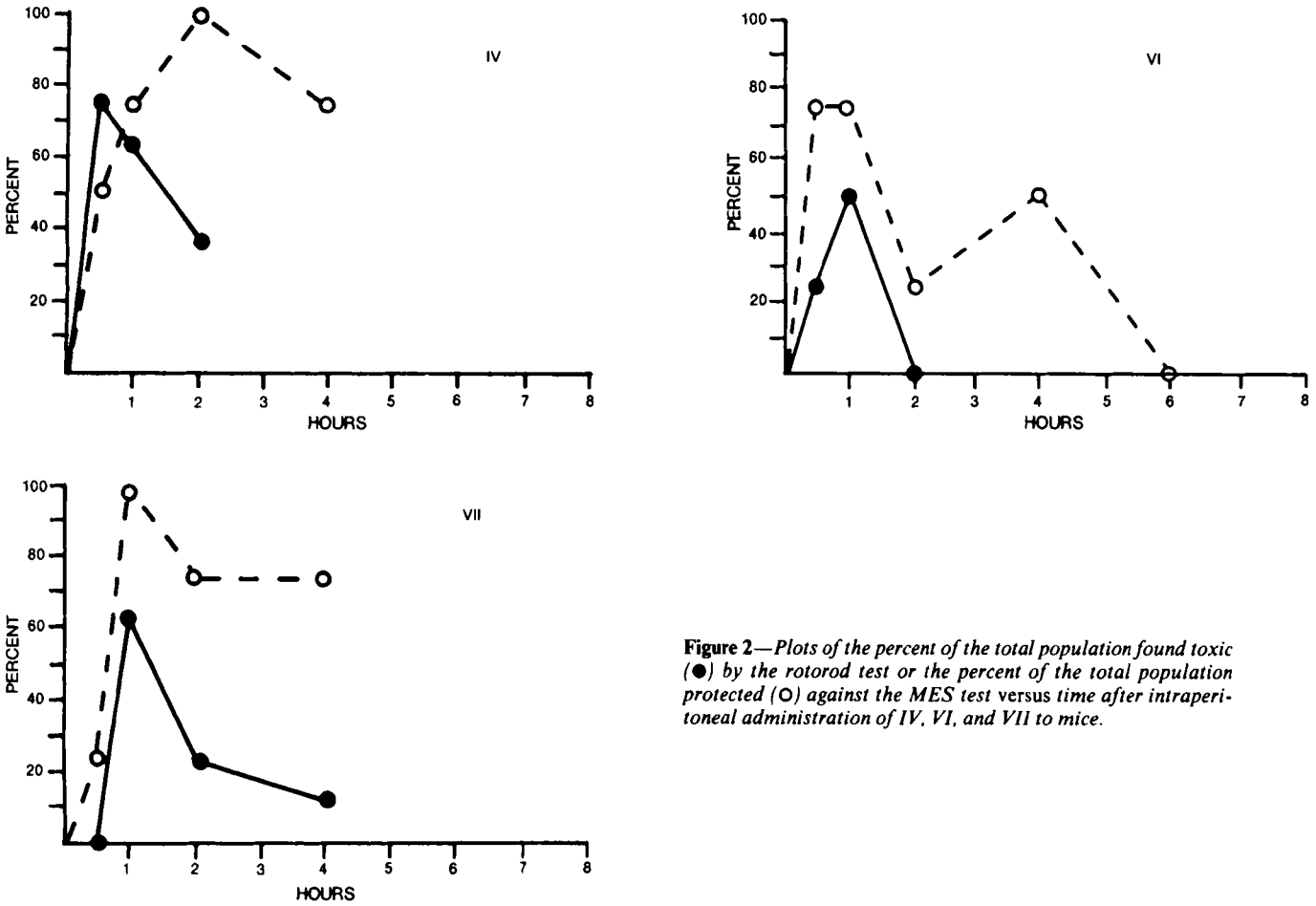

Figure 2—*Plots of the percent of the total population found toxic (●) by the rotorod test or the percent of the total population protected (○) against the MES test* versus *time after intraperitoneal administration of IV, VI, and VII to mice.*

of the sodium salts in methanol a certain amount of degradation took place and the final product may have been contaminated with small quantities of phenytoin.

The solubility of II in aqueous formaldehyde (1 M) and the solubilities of I and IV–VII in water at 25°C are shown in Table I. The increase in solubility of II over I of 8.5-fold may partly be attributed to the decreased intermolecular hydrogen bonding in the crystal lattice of II. This is reflected by the decrease in the melting point from 293°C for phenytoin (I) to 187–189°C for II. The reported solubilities of IV–VII are only approximate, as the prodrugs did begin to revert to phenytoin to some extent during the course of the solubility determinations, *i.e.*, the solid state is a mixture of prodrug and precipitated phenytoin. The methanesulfonate salts of IV, VI, and VII were prepared preferentially to the hydrochloride salts to prevent any common ion solubility problems on oral dosing with the prodrugs. Also, the hydrochloride salt of IV was very hygroscopic. The hydrochloride and methanesulfonate salts of V were prepared but were also found to be very hygroscopic; therefore, only the 2-naphthalenesulfonate salt was evaluated.

The solubilities of IX and X in water could not be determined because initial clear solutions rapidly began precipitating phenytoin acid, which was easily characterized on filtration by its melting behavior. This rapid precipitation of phenytoin from IX and X precluded the use of IX and X as parenteral forms of phenytoin and, therefore, IX and X were discarded as potentially useful prodrugs of I.

Compounds IV–VII were more soluble in water than phenytoin (Table I, last column). Based on this initial observation, IV, VI, and VII were considered possible candidates for parenteral and oral forms of phenytoin, while V was considered as a possible oral prodrug form of phenytoin.

For IV–VII to behave as true prodrugs of phenytoin, they must undergo cleavage to phenytoin under *in vivo* conditions. Therefore, the cleavage rates of IV–VII were studied in various rat, dog, and human tissues to give indications as to their *in vivo* behavior. The hydrolysis of esters IV–VI, 2×10^{-5} M, monitored by following the formation of phenytoin, exhibited pseudo-first-order kinetics in rat, dog, and human plasma. The half-lives are given in Table II. Esters IV–VI were quantitatively hydrolyzed to phenytoin in the plasma of all species studied. The hydrolysis of V and VI was determined in 10 and 0.5% rat plasma, respectively, because their cleavage rates were too fast to follow at higher plasma concentrations. Under comparable conditions in the absence of plasma, IV–VI hydrolyzed slowly to phenytoin; however, no attempts were made at this stage to unambiguously discriminate as to whether the acceleration in the cleavage rates in the presence of plasma was truly enzymatic in nature. Overall, the cleavage of the esters was slowest in dog plasma, consistent with findings of low overall esterase activity in various dog tissues relative to other animal species (37–39). The differences in the relative cleavage rates indicate that the spectrum of esterases present in plasma varies between the animal species.

An attempt was made to determine the hydrolysis of VII in the plasma of rats, dogs, and humans. No detectable cleavage was observed over a 3-h period. Since phosphatases are known to exist in red blood cells (40, 41), cleavage of

Table III—ED_{50} and TD_{50} of Phenytoin, IV, VI, and VII after Intraperitoneal and/or Oral Administration to Mice

Compound	Intraperitoneal Administration		Oral Administration	
	ED_{50} (MES)[a], mg/kg ± *SE*	TD_{50} (Rotorod)[a], mg/kg ± *SE*	ED_{50} (MES)[a], mg/kg ± *SE*	TD_{50} (Rotorod)[a], mg/kg ± *SE*
I[b]	9.50 (8.13–10.4)[c]	65.4 (52.5–72.1)[c]	9.04 (7.39–10.62)[c]	86.71 (80.39–96.09)[c]
IV	10.3 ± 2.35	46.2 ± 3.1	10.6 ± 1.1	80.7 ± 0.8
VI	7.9 ± 1.4	47.7 ± 1.02	—[d]	—[d]
VII	10.3 ± 2.2	42.1 ± 1.9	11.8 ± 1.4	81.6 ± 3.1

[a] All values are in phenytoin equivalents. [b] Reported by the Anticonvulsant Drug Screening program (36). [c] 95% confidence interval. [d] Not determined.

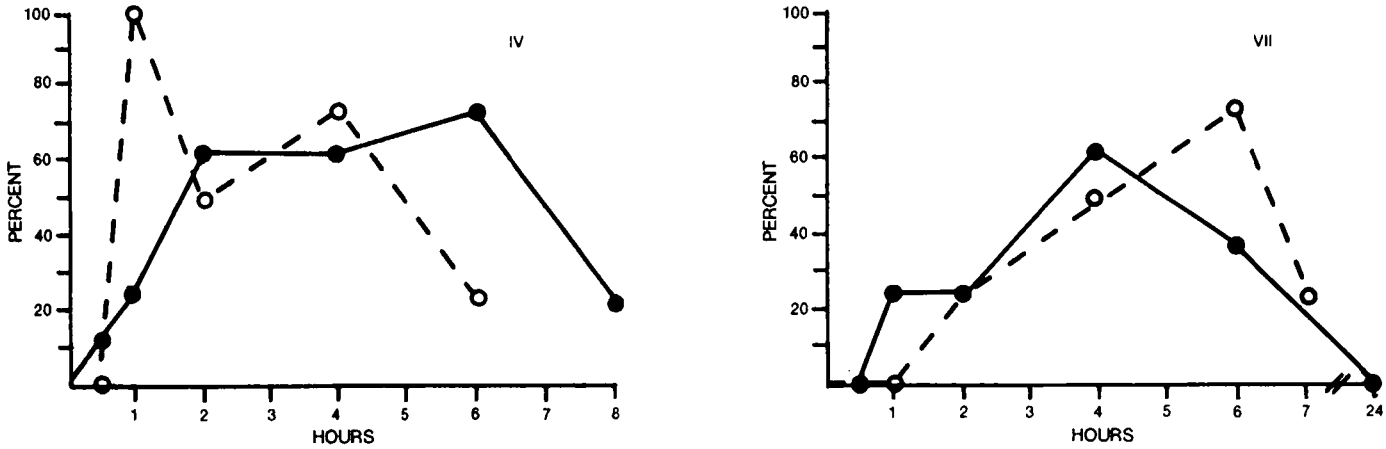

Figure 3—*Plots of the percent of the total population found toxic (●) by the rotorod test or the percent of the total population protected (○) against the MES test* versus *time after oral administration of IV and VII to mice.*

VII in rat, dog, and human whole blood was evaluated. Cleavage in rat whole blood was observed ($t_{1/2}$ = 2 h and 30 min at 25°C and 37°C, respectively). Slow cleavage in dog whole blood ($t_{1/2}$ > 24 h) was observed, but no significant cleavage was seen in human whole blood. These results tend to suggest that either the activity of the phosphatase enzymes was low in dog and human whole blood or that VII had poor accessibility to red blood cell phosphatases. The catalytic conversion of VII to phenytoin in the rat liver ($t_{1/2}$ < 30 s) and intestinal homogenates ($t_{1/2}$ < 30 s) and dog liver homogenate ($t_{1/2}$ = 57.5 min) were observed at 37°C.

It appears from these tissue studies that esters IV–VII would behave as prodrugs of phenytoin *in vivo* based on their reasonably facile cleavage *in vitro* in rat, dog, and human tissues. The only questionable candidate for quantitative conversion might be the phosphate ester VII, although there is adequate precedence in the literature for phosphate esters of various alcohols as prodrugs (42–50).

Mechanistically, the cleavage of esters IV–VII is expected to follow Scheme I, where k_1 represents the *in vitro* or *in vivo* cleavage of esters IV–X to II, which should then hydrolyze releasing formaldehyde[13]. The dehydroxymethylation of II to phenytoin was, therefore, studied in the pH range 4–7 at both 25°C and 37°C (μ = 0.5). As stated earlier, the hydrolysis followed pseudo-first-order kinetics, and no buffer catalysis was observed. Figure 1 shows the pH–rate profiles for the hydrolyses of II to phenytoin at 25°C and 37°C. The half-lives for the dehydroxymethylation extrapolated to pH 7.4 are also indicated in the figure. These data are quantitatively and qualitatively similar to those observed by Bundgaard and Johansen (5) who proposed a

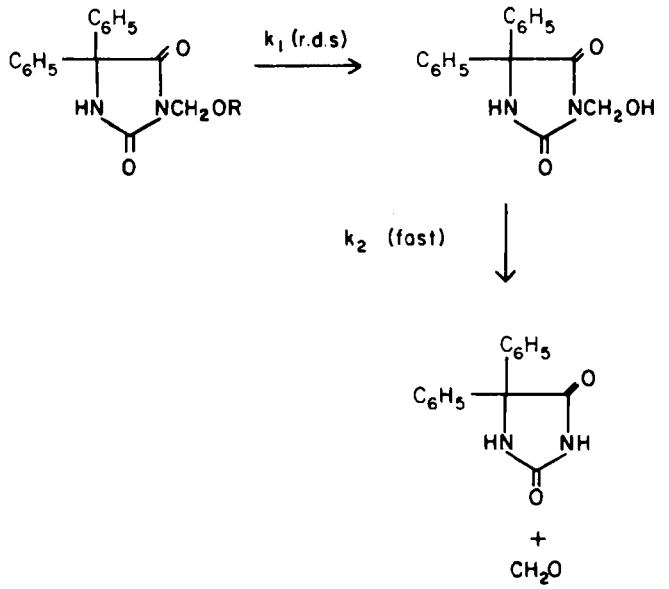

Scheme I

mechanism involving an initial fast ionization of the hydroxyl group (p*Ka* > 12) followed by a slower nitrogen–carbon bond cleavage step producing phenytoin and formaldehyde. The very rapid breakdown of II to phenytoin ($t_{1/2}$ < 2 s at pH 7.4 and 37°C) precludes the accumulation of II when esters IV–VII are cleaved *in vitro* or *in vivo*.

Compounds IV–VII underwent pharmacological evaluation in the anticonvulsant drug screening program operated by National Institute of Neurological and Communicative Disorders and Stroke (36). In the phase I (initial screen) study all compounds showed good anticonvulsant (antiseizure) activity after intraperitoneal administration in the MES evaluation, but (as expected) showed no activity in the ScMET test[14]. The least active prodrug was V, which showed no protection in the MES test at 30 mg/kg; all the other compounds were active at 30 mg/kg. From the results of this initial screen, IV, VI, and VII were subjected to phase II analysis, where the anticonvulsant activity, MES, and rotorod toxicity were evaluated after intraperitoneal administration of the prodrugs in a larger number of animals. Compounds IV and VII were also evaluated in a phase IV study, which involves administering the prodrugs orally. Table III summarizes the ED_{50} and TD_{50} data for IV, VI, and VII after intraperitoneal and oral administrations to mice.

As can be seen in Table III, all the prodrugs had equivalent activity when compared with phenytoin, but all displayed slightly higher toxicity (lower TD_{50} values). This may be consistent with the more rapid absorption of phenytoin in the form of the prodrugs or an elevated intrinsic toxicity by the prodrugs exacerbated by their expected more rapid absorption relative to phenytoin, *i.e.*, the TD_{50} values probably should be compared with the TD_{50} of intravenous phenytoin. Figures 2 and 3 are plots of the percent of the total mice population studied found to be toxic by the rotorod test (toxicity–time profile) and the percent of the total population protected against the MES (activity–time profile) *versus* time after intraperitoneal and oral administrations, respectively. In Fig. 2 (intraperitoneal data) prodrugs VI and VII show an early peaking in the activity- and toxicity-time profile, suggesting rapid release of phenytoin, providing that the anticonvulsant activity is attributable to phenytoin. Ester IV, however, shows maximum activity at 2 h and the toxicity peaking at 0.5 h postdose. This tends to suggest that IV may be undergoing slow hydrolysis, compared with VI and VII, and that the early toxicity peaking may be due to the intact ester IV.

The lack of early toxicity in the oral study (Fig. 3) for IV compared with its activity suggests that after oral dosing, IV may be hydrolyzed during the absorption process. The delayed peaking of both toxicity and activity for VII after oral dosing (compared with the intraperitoneal data), suggests that the activity and toxicity of VII are probably due to phenytoin and that VII is only slowly absorbed from the intestine; alternatively, VII may be cleaved slowly in the GI tract, releasing phenytoin which was subsequently absorbed.

Based on the findings presented in this paper, IV, VI, and VII were evaluated further with respect to other physicochemical properties (51) and their pharmacokinetic behavior after oral and intravenous administration to dogs compared with phenytoin (52). Compound VII was also evaluated after intramuscular and intravenous administration to rats (53).

REFERENCES

(1) P. A. Schwartz, C. T. Rhodes, and J. W. Cooper, Jr., *J. Pharm. Sci.*, **66**, 994 (1977).

[13] Formaldehyde toxicity may be raised as a problem with these types of prodrugs. Whether the quantity of formaldehyde generated here is sufficient to raise concerns will have to be evaluated.

[14] Phenytoin itself is inactive in the ScMET test.

(2) S. P. Agarwal and M. I. Blake, *J. Pharm. Sci.*, **57,** 1434 (1968).
(3) K. Arnold, N. Gerber, and G. Levy, *Can. J. Pharm. Sci.*, **5,** 89 (1970).
(4) M. Johansen and H. Bundgaard, *Arch. Pharm. Chem., Sci. Ed.*, **7,** 175 (1979).
(5) H. Bundgaard and M. Johansen, *Int. J. Pharmacol.*, **5,** 67 (1980).
(6) C. M. Martin, M. Rubin, W. E. O'Malley, V. F. Garagusi, and C. E. McCauley, *Pharmacologist*, **10,** 167 (1968).
(7) L. Rail, *Med. J. Australia*, **ii,** 339 (1968).
(8) T. Suzuki, T. Saitoh, and K. Nishihara, *Chem. Pharm. Bull.*, **18,** 405 (1970).
(9) J. I. Manson, S. M. Beal, A. Magarey, A. C. Pollard, W. J. O'Reilly, and L. N. Sansom, *Med. J. Australia*, **2,** 590 (1975).
(10) B. Rambeck, H.-E. Boenigk, and E. Stenzel, *Eur. J. Clin. Pharmacol.*, **12,** 285 (1977).
(11) P. J. Neuvonen, P. J. Pentikainen, and S. M. Elfving, *Int. J. Clin. Pharmacol.*, **15,** 84 (1977).
(12) P. J. Neuvonen, A. Bardy, and R. Lehtovaara, *Br. J. Clin. Pharmacol.*, **8,** 37 (1979).
(13) P. J. Pentikainen, P. J. Neuvonen, and S. M. Elfving, *Eur. J. Clin. Pharmacol.*, **9,** 213 (1975).
(14) H. Sekikawa, M. Nakano, M. Takada, and T. Arita, *Chem. Pharm. Bull.*, **28,** 2443 (1980).
(15) M. J. Stewart, B. R. Ballinger, E. J. Devlin, A. Y. Miller, and A. C. Ramsay, *Eur. J. Clin. Pharmacol.*, **9,** 209 (1975).
(16) S. Sved, R. D. Hosie, I. J. McGilveray, N. Beaudoin, and R. Brien, *Can. J. Pharm. Sci.*, **14,** 67 (1979).
(17) L. Lund, *Eur. J. Clin. Pharmacol.*, **7,** 119 (1974).
(18) P. Tammisto, K. Kauko, and M. Villkari, *Lancet*, **i,** 254 (1976).
(19) D. F. Kowalczyk, *J. Vet. Pharmacol. Ther.*, **3,** 237 (1980).
(20) S. Zoneraich, O. Zoneraich, and J. Siegel, *Am. Heart J.*, **91,** 375 (1976).
(21) A. J. Atkinson, Jr. and R. Davison, *Annu. Rev. Med.*, **25,** 99 (1974) and references therein.
(22) A. J. Wilensky and J. A. Lowden, *Neurology*, **23,** 318 (1973).
(23) H. B. Kostenbauder, R. D. Rapp, J. P. McGovren, T. S. Foster, D. G. Perrier, H. M. Blacker, W. C. Hulon, and A. W. Kinkel, *Clin. Pharmacol. Ther.*, **18,** 449 (1975).
(24) M. Dam and V. Olesen, *Neurology*, **16,** 288 (1966).
(25) B J. Wilder, E. E. Serrano, E. Ramsey, and R. A. Buchanan, *Clin. Pharmacol. Ther.*, **16,** 507 (1974).
(26) D. W. Newton and R. B. Kluza, *Am. J. Hosp. Pharm.*, **37,** 1647 (1980) and references therein.
(27) R. B. Salem, R. L. Yost, G. Torosian, F. T. Davis, and B. J. Wilder, *Drug Intel. Clin. Pharmacol.*, **14,** 605 (1980).
(28) M. Johansen and H. Bundgaard, *Arch. Pharm. Chem., Sci. Ed.*, **8,** 141 (1980).
(29) P. C. Bansal, I. H. Pitman, J. N. S. Tam, M. Mertes, and J. J. Kaminski, *J. Pharm. Sci.*, **70,** 850 (1981).
(30) P. C. Bansal, I. H. Pitman, and T. Higuchi, *J. Pharm. Sci.*, **70,** 855 (1981).
(31) H. Bundgaard, in "Optimization of Drug Delivery," H. Bundgaard, A. B. Hansen, and H. Kofod, Eds., Munksgaard, Copenhagen, Denmark 1982, pp. 178 198 and references therein.
(32) D. B. Williams, S. A. Varia, V. J. Stella, and I. H. Pitman, *Int. J. Pharmaceut.*, **14,** 113 (1983).
(33) V. M. Clark and A. R. Todd, *J. Chem. Soc.*, **1950,** 2023.
(34) M. Miyano and S. Funahashi, *J. Am. Chem. Soc.*, **77,** 3522 (1955).
(35) V. J. Stella, *J. Pharm. Sci.*, **66,** 1510 (1977).
(36) Anticonvulsant screening project: Antiepileptic Drug Development Program. U.S. Department of Health, Education, and Welfare, Public Health Service, NIH, DHEW Publication No. (NIH) 76-1093.
(37) K. Fukuda, M. Imai, H. Shindo, and V. Mizuhira, *Acta Histochem. Cytochem.*, **11,** 78 (1978).
(38) M. M. Nachlas and A. M. Seligman, *Anat. Rect.*, **105,** 677 (1949).
(39) H. Shindo, K. Fukuda, K. Kawai, and K. Tanaka, *J. Pharm. Dyn.*, **1,** 310 (1978).
(40) M. Martland and R. Robinson, *Biochem. J.*, **18,** 765 (1924).
(41) M. A. M. Abul-Fadl and E. J. King, *Biochem. J.*, **45,** 51 (1949).
(42) M. J. Cho, R. R. Kurtz, C. Lewis, S. M. Machkovech, and D. J. Houser, *J. Pharm. Sci.*, **71,** 410 (1982).
(43) J. C. Melby and M. St. Cyr, *Metabolism*, **10,** 75 (1961).
(44) K. J. Kripalani, A. I. Cohen, I. Weliky, and E. C. Schreiber, *J. Pharm. Sci.*, **64,** 1351 (1975).
(45) J. C. K. Loo, I. J. McGilveray, N. Jordan, and R. Brien, *Biopharm. Drug Dispos.*, **2,** 265 (1981).
(46) S. Miyabo, T. Nakamura, S. Kuwazima, and S. Kishida, *Eur. J. Clin. Pharmacol.*, **20,** 277 (1981).
(47) E. Novak, A. R. Disanto, C. E. Seckman, G. Elliot, J. G. Lee, and S. S. Stubbs, *J. Clin. Pharmacol.*, **17,** 324 (1977).
(48) L. E. Hare, K. C. Yeh, C. A. Ditzler, F. G. McMahon, and D. E. Duggan, *Clin. Pharmacol. Ther.*, **18,** 330 (1975).
(49) R. E. Kauffman, D. W. Shoeman, S. H. Wan, and D. L. Azarnoff, *Clin. Pharmacol. Ther.*, **13,** 704 (1972).
(50) R. M. DeHaan, C. M. Metzler, D. Schellenberg, and W. VanDenbosch, *J. Clin. Pharmacol.*, **13,** 190 (1973).
(51) S. A. Varia, S. Schuller, and V. J. Stella, *J. Pharm. Sci.*, **73,** 1074 (1984).
(52) S. A. Varia and V. J. Stella, *J. Pharm. Sci.*, **73,** 1080 (1984).
(53) S. A. Varia and V. J. Stella, *J. Pharm. Sci.*, **73,** 1087 (1984).

ACKNOWLEDGMENTS

Adapted in part from a dissertation submitted by S. A. Varia to The University of Kansas in partial fulfillment of the Doctor of Philosophy degree requirements.

This work was supported in part by the INTERx Research Corporation, a subsidiary of Merck Sharp & Dohme. The authors wish to express their appreciation to the National Institute of Neurological and Communicative Disorders and Stroke, National Institutes of Health, for evaluating some of the prodrugs in the Anticonvulsant Drug Screening program.

Phenytoin Prodrugs IV: Hydrolysis of Various 3-(Hydroxymethyl)phenytoin Esters

S. A. VARIA *, S. SCHULLER, and V. J. STELLA ˣ

Received December 22, 1982, from the *Department of Pharmaceutical Chemistry, The University of Kansas, Lawrence, KS 66045.* Accepted for publication July 6, 1983. *Present address: Squibb Institute for Medical Research, New Brunswick, NJ 08903.

Abstract □ The aqueous chemical stability of various bioreversible derivatives or prodrugs of phenytoin, a poorly water-soluble and erratically absorbed drug after both oral and intramuscular parenteral dosing, were evaluated. This study, together with assessments of other physicochemical properties including cleavage in the presence of various animal tissues and anticonvulsant activity in mice, helped identify a number of promising candidate prodrugs. Various amino groups containing acyl esters of 3-(hydroxymethyl)phenytoin [3-(hydroxymethyl)-5,5-diphenylhydantoin] were identified as potential orally and perhaps parenterally useful prodrugs, while the disodium phosphate ester of 3-(hydroxymethyl)phenytoin appears to be ideally suited as a parenteral form of phenytoin.

Keyphrases □ Prodrugs—water-soluble, phenytoin stability, pH profiles □ Phenytoin—water-soluble prodrugs, stability, pH profiles □ Anticonvulsants—phenytoin, water-soluble prodrugs, stability, pH profiles

The aqueous chemical stabilities of various selected prodrugs and model compounds of phenytoin (I), *i.e.*, various esters (III–VII) of 3-(hydroxymethyl)phenytoin [II, 3-(hydroxymethyl)-5,5-diphenylhydantoin], are presented in this paper. The synthesis and a preliminary evaluation (including aqueous solubility determination, cleavage rates in the presence of various animal tissues, the chemical degradation of II to I under simulated physiological conditions, and, in some cases, the anticonvulsant activity in mice) of II–VII and other potential prodrugs of phenytoin were presented in the previous paper (1).

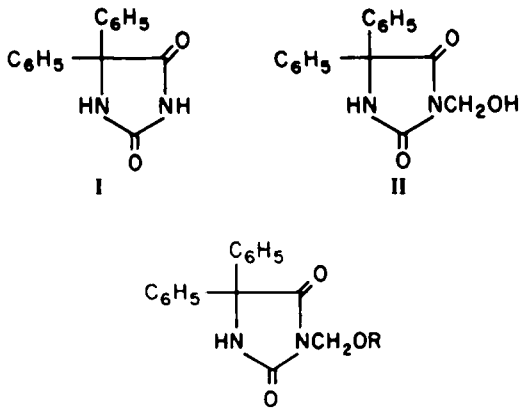

I

II

III: R = $COCH_3$
IV: R = $COCH_2\overset{+}{N}H(CH_3)_2CH_3SO_3^-$
V: R = $CO(CH_2)_2\overset{+}{N}H(C_2H_5)_2$
VI: R = $CO_2(CH_2)_2\overset{+}{N}H(CH_3)_2CH_3SO_3^-$
VII: R = $PO_3^{2-}Na_2^+$

The overall goal of this series of studies was to identify orally bioavailable phenytoin prodrugs with delivery characteristics superior to phenytoin itself, and parenterally useful prodrugs of phenytoin with good aqueous solubility and stability at a physiologically acceptable pH, a goal that was only partially achieved in a previous study (2).

Since any prodrug, to be useful as either an oral or parenteral form of phenytoin, must display adequate chemical stability, a study of the aqueous stability pH profiles for III–VII was undertaken. Because phenytoin has poor aqueous solubility (1, 3–6), the stability-limiting factor for a potential parenteral prodrug form of phenytoin was not considered to be maintenance of some percentage of the labeled amount of prodrug, but rather, the time that it takes for the poorly water-soluble phenytoin to begin precipitating from an aqueous solution of the prodrug on chemical degradation (2). This question will also be addressed briefly in this paper.

EXPERIMENTAL SECTION

Materials—Unless otherwise stated, all reagents used were analytical grade. Phenytoin was obtained from a commercial source[1]; the prodrugs were synthesized previously and were analytically pure (1). The water used in the stability studies was deionized (≤1-mho conductance) and charcoal-filtered prior to use or freshly distilled from an all-glass still. All buffers were prepared in carbonate-free (freshly boiled) deoxygenated (nitrogen-purge) water.

Kinetic Studies—Stock solutions of III in dry acetonitrile, IV–VII in water, and V in methanol–water were prepared immediately before use. An appropriate aliquot of the stock solution was mixed with the aqueous buffers to initiate kinetic runs. The final concentration of methanol in the case of V was <0.2% v/v and that of acetonitrile for III was <0.01% v/v.

All kinetic studies were carried out at a constant temperature maintained by a circulating-water bath[2]. The kinetics of conversion of IV–VI in the pH range of 3–5 and VII at all pH values were studied in aqueous buffers by the

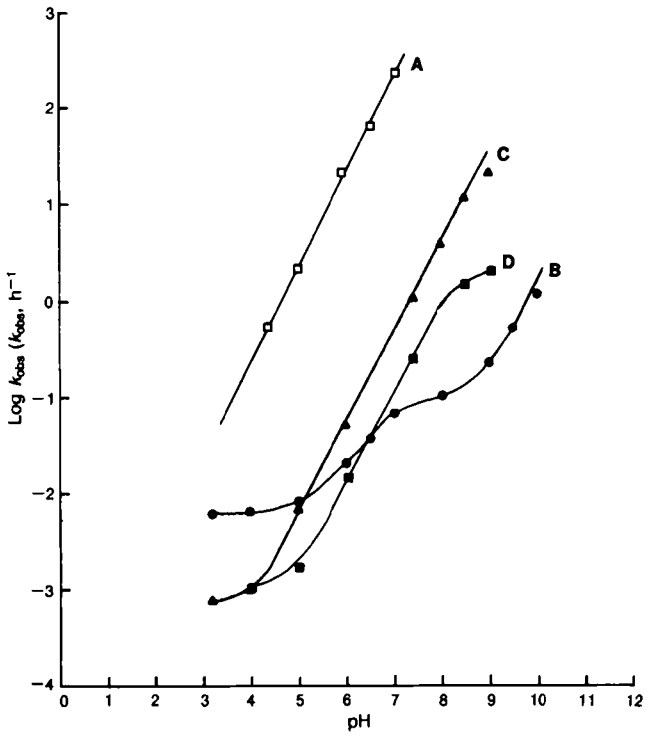

Figure 1—*pH-rate profiles for the hydrolysis of II (A), IV (B), V (C), and VI (D) to phenytoin at 25°C, μ = 0.5 M.*

[1] Sigma Chemical Co., St. Louis, Mo.
[2] Brinkman Model, Landa RC 20.

0022-3549/84/0800-1074$01.00/0
© 1984, American Pharmaceutical Association

Table I—Buffers Used in the Hydrolysis of the Esters III–VII at Various pH Values

pH Range	Buffer
3.0–5.0	Acetate
6.0–8.1	Phosphate
8.5–9.5	Borate
10.0	Carbonate
11.0–12.2	Sodium hydroxide

Table II—Observed First-Order Rate Constants for the Hydrolysis of III at Various pH Values [a]

pH[b]	Observed First-Order Rate Constant (k_{obs}), h^{-1}
12.19	39.7
11.92	17.2
11.8	15.3
11.5	11.08
11.1	3.24
11.01	3.34
10.8	2.01

[a] μ = 0.5, 25°C. [b] pH adjusted with sodium hydroxide.

initial rate method (7) since the half-lives of the esters under these conditions were long. The prodrugs in their stock solutions were mixed with the temperature-equilibrated buffer solution, and phenytoin production was followed until ~5% of the reaction was complete. All other kinetic studies were followed to completion by monitoring the appearance of phenytoin.

The chemical stability of III–VI was assessed in aqueous buffer solutions at 25 ± 0.1°C, and VII was studied at 70 ± 0.1°C (and at 50°C and 90°C at pH 7.4). A list of the buffers used at the various pH values is shown in Table I. The ionic strength was adjusted to 0.5 by the addition of potassium chloride. The stability studies were carried out at different buffer concentrations to allow for the determination of the rate constant at zero buffer concentration. Unless otherwise specified, all rate constants used in the pH–rate profiles were obtained by extrapolation to zero buffer concentration. The hydrolysis of III was monitored by UV spectroscopy[3], and the stability of VI–VII was studied by following the formation of phenytoin as a function of time using GC[4] as described previously by Stella (8).

Specifically, the rate of hydrolysis of III was studied at 25°C by following the decrease in absorbance at 256 nm. The initial concentration of the ester was 2×10^{-5} M. The reaction followed pseudo-first-order kinetics, and apparent first-order rate constants were determined from plots of log $(A_t - A_\infty)$ *versus* time, where A_t and A_∞ are the absorbance readings at time t and at the completion of the reaction, respectively. In all cases, the final spectrum corresponded to that of phenytoin. Conversion to phenytoin was also confirmed by TLC and GC.

The stability of IV–VII was studied by observing the appearance of phenytoin as a function of time using GC analysis (1, 8). In the case of esters possessing an amino group in the ester moiety (IV–VI), 100-μL samples were removed from the temperature-equilibrated reaction vessels at regular intervals and added to 100 μL of 10% metaphosphoric acid solution. The metaphosphoric acid helped quench the reaction due to the increased stability of these compounds under acidic conditions and also protonated the amino group of the ester, which prevented its extraction into toluene, the next step required for the work-up for the GC analysis (8).

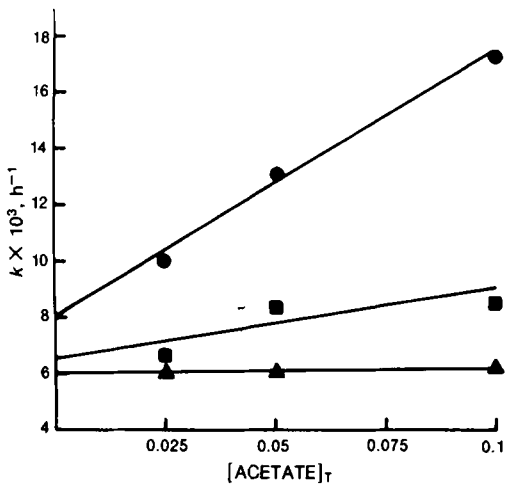

Figure 2—*Effect of acetate buffer concentration on the hydrolysis of IV at pH 3.2 (▲), 4.0 (■), and 5.0 (●); 25°C, μ = 0.5 M.*

[3] Cary Model 118, Varian Instruments.
[4] Varian Model 2100 or 3700 gas chromatograph.

Table III—Effect of Buffer Concentration on the Rates of Hydrolysis of IV at Various pH Values [a]

Buffer	Buffer Conc., M	Apparent First-Order Rate Constant (k), × 10^4 h^{-1}	k_{obs} at Zero Buffer Conc., × 10^4 h^{-1}
Acetate			
pH 3.2	0.025–0.1	60.4[b]	60.4
pH 4.0	0.025	66.7	
	0.05	83.9	
	0.1	85.7	65.8
pH 5.0	0.025	103.0	
	0.05	131.3	
	0.1	173.9	81.7
Phosphate			
pH 6.0	0.01	243	
	0.02	267	
	0.03	315	204.0
pH 6.5	0.01	422.5	
	0.02	468.2	
	0.03	515.1	376.0
pH 7.0	0.01	788	
	0.02	856	
	0.03	963	695.0
pH 8.0	0.01	1103.0	
	0.02	1194.0	
	0.03	1280.0	1015
Borate			
pH 9.0	0.02–0.04	2310[a]	2310
pH 9.5	0.01–0.04	5500[a]	5500
Carbonate			
pH 10.0	0.01	12882	12499.7
	0.03	13500	
	0.04	13980	

[a] μ = 0.5, 25°C. [b] No buffer catalysis.

For conversion of VII to phenytoin at elevated temperatures in aqueous buffer solutions, aliquots (100 μL) were removed from the reaction vessel at various intervals and transferred to tubes immersed in dry ice in order to quench the reaction. The samples were then assayed by the same technique used for following the hydrolysis of VII in tissue samples (1).

The conversion of the esters to phenytoin followed first-order kinetics. Apparent first-order rate constants for the production of phenytoin from the various prodrugs were determined from plots of log $(D_\infty - D_t)$ *versus* time where D_t and D_∞ are the concentrations of phenytoin at time t and infinity, respectively. The apparent first-order rate constants for the decompositions of IV–VI in the pH range of 3–5 and VII were determined by the initial rate method, in which <5% of the reaction was followed (7).

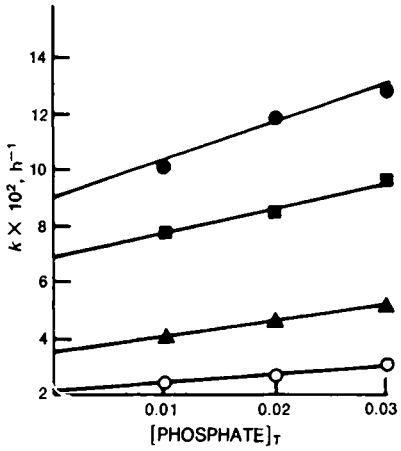

Figure 3—*Effect of phosphate buffer concentration on the hydrolysis of IV at pH 6.0 (○), 6.5 (▲), 7.0 (■), and 8.0 (●); 25°C, μ = 0.5 M.*

Table IV—Effect of Buffer Concentration on the Rates of Hydrolysis of V at Various pH Values [a]

Buffer	Buffer Conc., M	Apparent First-Order Rate Constant (k), × 10^4 h^{-1}	k_{obs} at Zero Buffer Conc., × 10^4 h^{-1}
Acetate			
pH 3.2	0.02	7.9	
	0.05	8.5	
	0.2	10.9	7.6
pH 4.0	0.025	10.7	
	0.1	12.6	
	0.2	15.2	10.0
pH 5.0	0.02	69.2	
	0.1	74.2	
	0.2	80.1	68.0
Phosphate			
pH 6.0	0.02-0.04	507.0[b]	507
pH 7.4	0.01-0.04	10,014.5[b]	10,014.5
pH 8.0	0.02-0.04	35,568.0[b]	35,568.0
Borate			
pH 8.5	0.02-0.04	112,200[b]	112,200
pH 9.0	0.02-0.04	221,405[b]	221,405

[a] μ = 0.5, 25°C. [b] No buffer catalysis.

Precipitation Time Study—This study was carried out to determine the time for precipitation of phenytoin from aqueous solutions of IV and VII. Various aqueous solutions of IV, *i.e.*, 1, 10, and 100 mg/mL, were prepared and filtered, and the pH values of the solutions were measured. Visual observations and spectral determinations of the precipitation times were recorded by the following technique. Three-milliliter aliquots of the solutions were placed in cylindrical 1-cm quartz spectrophotometer cells. These cells were then placed in a constant-temperature shaking water bath[5] and maintained at 25 ± 0.1°C. The absorbance of these solutions as a function of time was followed at 500 nm, a wavelength at which there was no absorbance due to the compounds, and the light absorption due to precipitate formation could be easily assessed. Plots of absorbance *versus* time were made and the precipitation time determined when a significant break occurred in the plot.

To determine the time for precipitation of phenytoin from a 61-mg/mL aqueous filtered solution of VII, visual observations were made. The solution was stored in sealed vials, and these were kept at ambient temperature (23-26°C). The vials were not subjected to any agitation during storage. The vials were inspected at regular intervals for the presence of any turbidity, in order to get an estimate of the time for phenytoin to precipitate from solution.

RESULTS AND DISCUSSION

Esters III-VII would be expected to revert to phenytoin in aqueous solution according to Scheme I, with the cleavage of the ester being the rate-determining step. The pH-rate profile for the cleavage of II to I was presented in the previous paper in this series (1), as well as by Bundgaard and Johansen (5). The log k_{obs} *versus* pH profile is reproduced in Fig. 1 (pH profiles at 25°C for II and IV-VI) to show that for all the esters at all the pH values studied, k_2 was indeed fast relative to k_1.

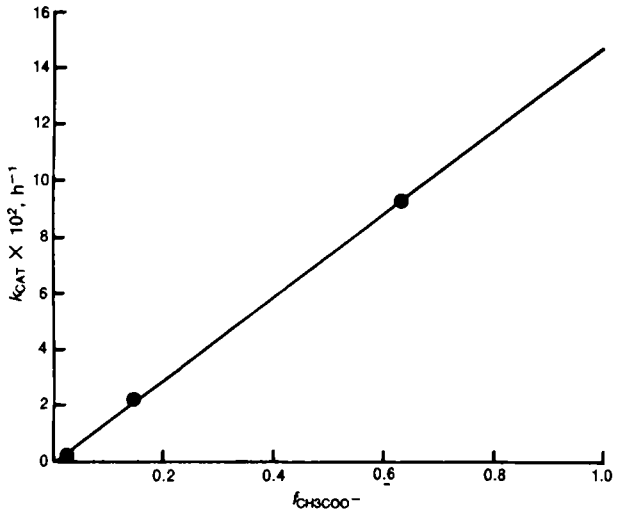

Figure 4—*Dependence of the catalytic constant,* k_{cat}, *on the fraction of acetate ion,* $f_{CH_3COO^-}$, *for the hydrolysis of IV.*

[5] AO Model No. 2156; American Optical Corp., Buffalo, N.Y.

Table V—Effect of Buffer Concentration on the Rates of Hydrolysis of VI at Various pH Values

Buffer	Buffer Conc., M	Apparent First-Order Rate Constant (k), × 10^4 h^{-1}	k_{obs} at Zero Buffer Conc., × 10^4 h^{-1}
Acetate			
pH 4.01	0.05	10.4	
	0.15	11.2	
	0.2	12.2	9.8
pH 4.98	0.1	18.2	
	0.15	19.4	
	0.2	20.7	15.7
Phosphate			
pH 6.0	0.01-0.03	143.6[b]	143.6
pH 7.4	0.01-0.03	2480[b]	2480
Borate			
pH 8.5	0.02-0.04	15180[b]	15180
pH 9.0	0.03-0.04	20550[b]	20550

[a] μ = 0.5, 25°C. [b] No buffer catalysis.

The observed pseudo-first-order rate constants (k_{obs}) for the hydrolysis of III to phenytoin at alkaline pH (μ = 0.5, 25°C) is given in Table II, and a plot of log k_{obs} *versus* pH was linear with a slope of 0.92, indicating a hydroxide ion-catalyzed reaction. The observed pseudo-first-order constant follows the form of:

$$k_{obs} = k_{OH}a_{OH} \qquad \text{(Eq. 1)}$$

where a_{OH} is the hydroxide ion activity (calculated from k_w/a_H) and k_{OH} is the second-order hydroxide ion-catalyzed rate constant for the hydrolysis of III. A value of 50.8 M^{-1} min^{-1} was calculated for k_{OH} at 25°C, which was consistent with similar findings by Bundgaard and Johansen (5) for the hydrolysis of III at 37°C.

The purpose of studying the hydrolysis of III was twofold: (*a*) to observe the hydrolysis rate of III as a standard for the accelerative effect of amino groups in the acyl function, *e.g.*, how much faster does IV cleave relative to III, and (*b*) the determination of k_{OH} for III allows an estimate of the pK_a' of the hydroxyl group of II. For example, Bruice *et al.* (9) have shown that a linear relationship exists between the logarithm of the second-order rate constants for the alkaline hydrolysis of various acetyl esters and the pK_a' for the corresponding leaving-group alcohol. This relationship is given by:

$$\log k_{OH} = -0.253 \cdot pK_a' + 4.9 \qquad \text{(Eq. 2)}$$

Substituting the k_{OH} value for III into this equation gives a pK_a' = 12.6, a

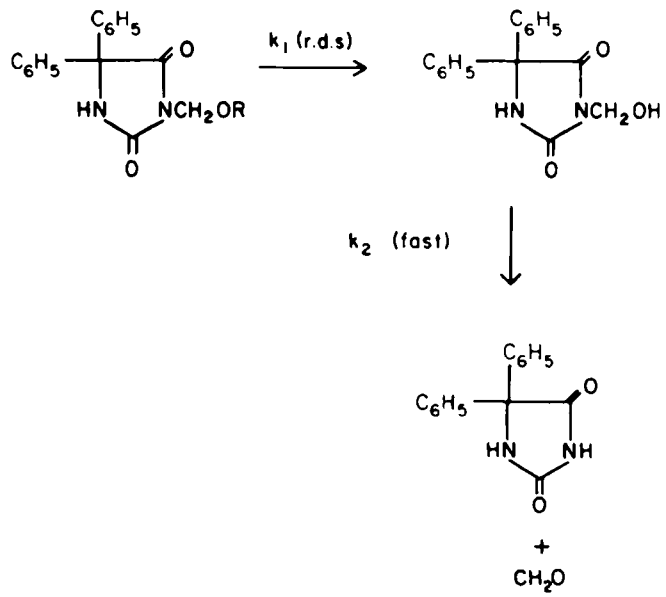

Scheme I

Table VI—Rate and Dissociation Constants for the Hydrolysis of IV–VI in Buffered Aqueous Solutions

	IV	V	VI
k_0, $\times 10^4$ h^{-1}	60.0	7.5	9.8
k_{OH}, $\times 10^{-6}$ $M^{-1}h^{-1}$	2.4	3.6	1.44
k'_{OH}, $\times 10^{-4}$ $M^{-1}h^{-1}$	1.2	ND[b]	ND
K_a, $\times 10^9$	253	<1	6.3
pK_a	6.60	>9.0	8.20

[a] μ = 0.5, 25°C. [b] ND = Not determinable.

Table VII—Effect of Buffer Concentration on the Rate of Hydrolysis of VII at Various pH Values[a]

Buffer	Buffer Conc., M	Apparent First-Order Rate Constant (k), $\times 10^4$ h^{-1}	k_{obs} at Zero Buffer Conc., $\times 10^4$ h^{-1}
Acetate			
pH 3.9	0.025	50.1	
	0.05	50.7	
	0.1	62.1	44.4
Phosphate			
pH 6.5	0.02	13.4	
	0.03	15.2	
	0.04	18.3	8.3
pH 7.4	0.01–0.04	2.9[b]	2.9
pH 8.1	0.02–0.04	1.1[b]	1.1

[a] μ = 0.5, 70°C. [b] No buffer catalysis.

value comparable to the apparent pK_a' of 13.1 at 37°C previously reported for *N*-(hydroxymethyl)benzamide (4).

In aqueous solution, IV–VI hydrolyzed to yield phenytoin quantitatively. The effect of pH and buffer concentration on the apparent first-order rate constants for the hydrolyses of IV–VI are shown in Tables III–V, respectively. The buffer-free apparent first-order rate constants (k_{obs}) at various pH values were obtained from intercepts of linear plots of the apparent first-order rate constants against the total buffer concentration (see Fig. 2). The slopes of these plots are the catalytic constants for buffer catalysis, k_{cat}. Figure 1 is a plot of the logarithm of k_{obs} *versus* pH for the hydrolysis of II and IV–VI to phenytoin at 25°C, μ = 0.5.

The pH–rate profiles for IV–VI are consistent with Scheme II, where R_1 = —CH_3 or —C_2H_5, n = 0–2, x = —CH_2— or —O— and can be adequately described by[6]:

$$k_{obs} = \frac{k_0 a_H}{K_a + a_H} + \frac{k_{OH} a_H}{K_a + a_H}[OH^-] + \frac{k'_{OH} K_a}{K_a + a_H}[OH^-] \qquad \text{(Eq. 3)}$$

where k_0 is the pseudo-first-order rate constant for the pH-independent hydrolysis of the protonated form of the ester (pH < 4), and k_{OH} and k'_{OH} are the second-order rate constants for the apparent attack of the hydroxide ion on the protonated and unprotonated form of the esters, respectively. K_a is the dissociation constant of the protonated amino group. Equation 3 predicts a break in the pH profile at around the pK_a if k_{OH} is significantly different from k'_{OH} (as expected). Breaks can be seen at pH values close to the expected pK_a' values of the amino group for IV and VI. Ester V did not show a break up to pH 9.0, suggesting its pK_a may be >9.0. The lines drawn for the pH–rate profiles for IV–VI in Fig. 1 were constructed from Eq. 3 and the appropriate rate constants given in Table VI. These pH profiles were similar to the pH–rate profile of phenyl-3-dimethylaminopropionate reported by Kirby and Lloyd (10), as well as other amino side-chain esters (11–15).

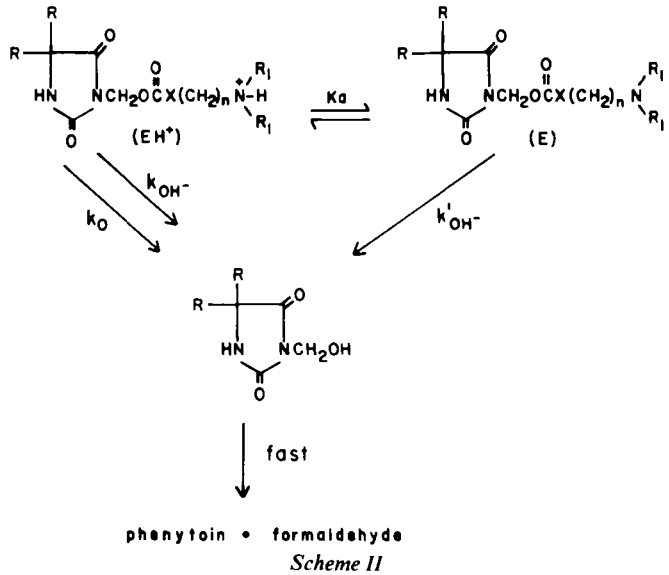

Scheme II

[6] It is recognized in this and subsequent cases that kinetically equivalent terms may be equally correct and indistinguishable.

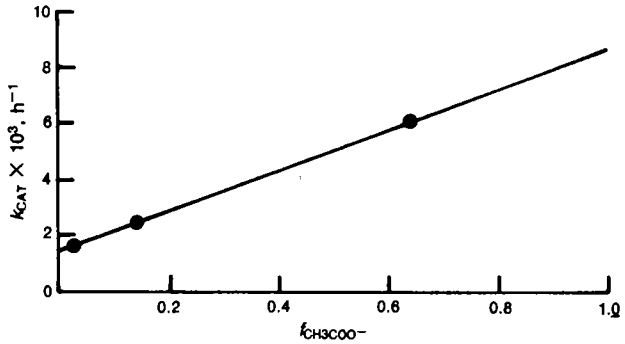

Figure 5—*Dependence of the catalytic constant, k_{cat}, on the fraction of acetate ion, $f_{CH_3COO^-}$, for the hydrolysis of V.*

Based on the pH profiles alone, it is difficult to assign mechanisms for these reactions. For example, the reaction term defined by k_{OH} in Scheme II and Eq. 3 is kinetically equivalent (mathematically equivalent) to the water-catalyzed hydrolysis of the unprotonated ester, perhaps facilitated intramolecularly through a general-base mechanism by the unprotonated tertiary amino group; alternatively, the possibility of an intramolecular nucleophilic attack by the tertiary amine on the acyl function displacing the alcohol has to be considered. A clue as to the possible mechanisms can be seen from an analysis of the buffer catalysis. The hydrolysis of IV exhibited buffer catalysis in the presence of acetate and phosphate buffers (see Figs. 2 and 3). Plots of k_{cat} *versus* the fraction of acetate ion $f_{CH_3COO^-}$ for each pH (Fig. 4) shows that the only catalytic species is the acetate ion. Similarly, reference to Fig. 3 shows that HPO_4^{2-} is a better catalyst than $H_2PO_4^-$. All these results are consistent with a general-base catalysis mechanism for these buffers, where the buffers are facilitating the attack by a water molecule on the acyl function or stabilizing a transition state.

In the case of V and VI, little or no buffer catalysis was observed, except in the case of acetate buffer for V. A plot of k_{cat} *versus* $f_{CH_3COO^-}$ (Fig. 5) for the cleavage of V again showed that general-base catalysis by the acetate anion was the primary catalyst; however, $k_{CH_3COO^-}$ for IV is 1.5×10^{-1} $M^{-1}h^{-1}$, while $k_{CH_3COO^-}$ for V is 8.5×10^{-3} $M^{-1}h^{-1}$, *i.e.*, acetate anion is a 17.6-fold better catalyst of IV hydrolysis compared with V. No significant buffer catalysis was seen for the hydrolysis of VI. It would appear from these results that the following mechanisms for the hydrolysis of IV–VI are operative:

1. At pH values <4, the primary reaction, k_0, involves water attack on the protonated ester, facilitated by general bases such as acetate and phosphate.

2. At pH values >5 but <pK_a, the primary reaction (defined mathematically in Eq. 3 as k_{OH}) is probably hydroxide ion attack on the protonated amine or attack of water on the unprotonated amine. The reason it is difficult to distinguish between these two mechanisms is that if the first mechanism is operative, no catalysis by buffers should be seen provided the rate-determining step is the actual attack on the acyl function by the hydroxide ion. This is usually seen with esters that have good leaving groups, *e.g.*, esters of activated phenols. Compound II should show behavior intermediate between a phenol and an aliphatic alcohol (a conclusion based on a pK_a of 12.6). Water

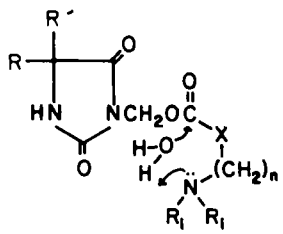

Scheme III

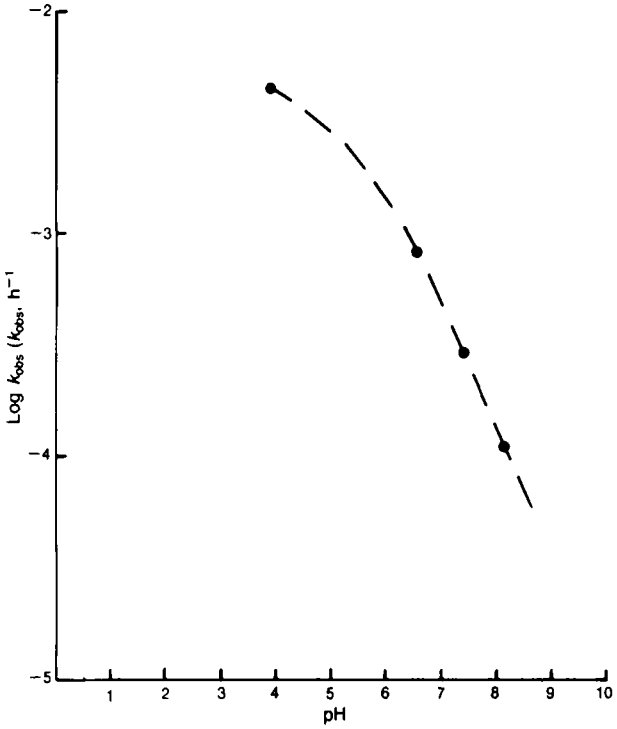

Figure 6—*pH-rate profile for the hydrolysis of VII at 70°C, μ = 0.5.*

attack on the unprotonated ester should be subject to general-base catalysis, but as seen in Scheme III intramolecular general-base catalysis by the dialkylamino group may be operative.

Such a mechanism is unfavorable for IV because a *five*-membered ring including a hydrogen bond would be required. Hydrogen-bonded systems favor a linear hydrogen bond (16) which, therefore, is not favored in a five-membered ring. Compounds V and VI form six- and seven-membered rings, respectively. Such cyclic structures are favorable for hydrogen-bond formation (16, 17). This type of intramolecular general-base catalysis has been shown by Kirby and Lloyd (10) to occur in the hydrolysis of other 3-dimethylaminopropionates. To fully differentiate between the two mechanisms, techniques such as proton inventory solvent isotope effects will have to be employed. Alternatively, ionic strength and solvent polarity changes could be used. However, interpretation of results obtained from such studies are complicated by changes in pK_a values, *etc.*

3. More than likely at pH > pK_a (*e.g.*, pH > 9 for IV), the major reaction is probably hydroxide attack on the unprotonated amine. Consistent with this is the lack of buffer catalysis by carbonate or borate[7] in the hydrolysis of IV.

Phosphate esters such as VII are of interest pharmaceutically because their polar nature provides a means of making water-soluble derivatives of sparingly soluble compounds such as those containing a hydroxyl group. In addition phosphate esters have been found to be chemically stable at neutral to slightly alkaline pH (18–22). The hydrolysis of such esters follow pseudo-first-order kinetics; it is assumed that VII would behave similarly.

Table VII contains the data on the rates of hydrolysis of VII to phenytoin at 70°C and various pH values and buffer concentrations, while Fig. 6 shows the pH–rate profile for the hydrolysis of VII at 70°C.

To determine the apparent energy of activation and the half-life for the hydrolysis of VII at 25°C and pH 7.4, rate constants were determined at various temperatures. Figure 7 shows the Arrhenius plot for the hydrolysis of VII, obtained by plotting the apparent first-order rate constants, determined at pH 7.4 and in 0.04 M phosphate buffer, *versus* the reciprocal of the absolute temperatures. From the slope of the Arrhenius plot, the apparent energy of activation and the half-life for the hydrolysis of VII at 25°C were calculated.

The data on the hydrolysis of VII suggests that it is catalyzed by acetate and phosphate buffers at pH 3.9 and 6.5. The pH–rate profile for VII is similar to the pH–rate profiles reported for the hydrolysis of various other phosphate monoesters (18–22). The rate of hydrolysis increases with decreasing pH suggesting that the monoanionic form of VII is the reactive species. The concentration of the monoanion would be at a maximum at pH ~4.0, as the

[7] This was also not unexpected, as borate is a poor general-base catalyst.

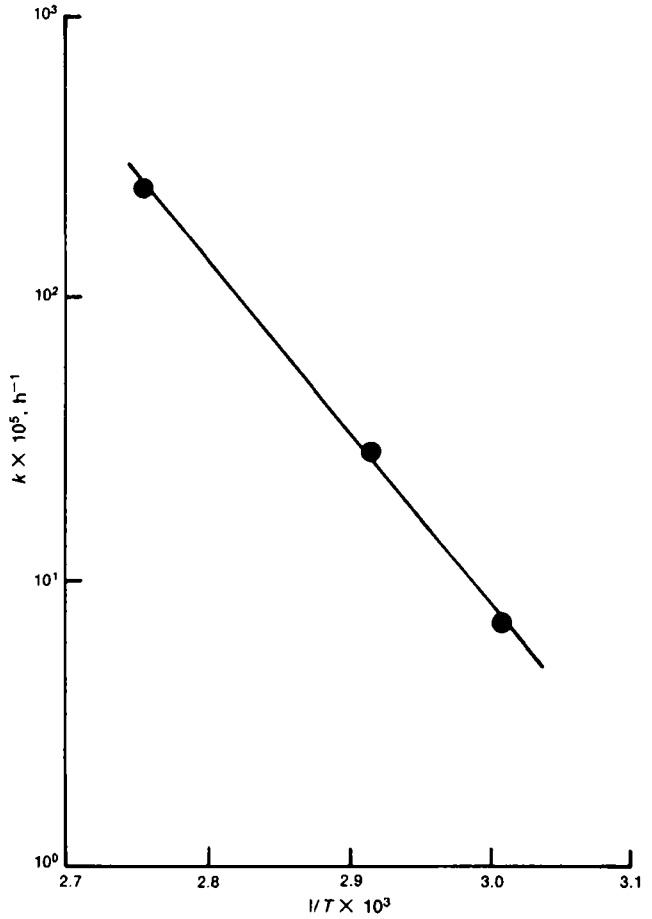

Figure 7—*Arrhenius plot for the hydrolysis of VII to phenytoin in 0.04 M phosphate buffer, pH 7.4, μ = 0.5.*

second pK_a of most phosphate esters is 6.0–6.5 (18–21) at this ionic strength. The pK_{a_2} of VII in water at 25°C was determined to be 6.2 by titration with hydrochloric acid. Thus, the pH–rate profile for VII began to plateau at pH 4.0; however, the rate of degradation of VII below pH 4.0 was not studied. The hydrolysis of other phosphate esters at pH <4.0 has been shown to increase (20) or decrease (23, 24) depending on the reactivity of the neutral species. The neutral species may undergo degradation, with carbon–oxygen bond cleavage. The mechanism for the hydrolysis of VII in the pH range 3.9–8.1 is probably similar to that proposed for the hydrolysis of other phosphate monoesters (20–22). The probable reaction mechanism is shown in Scheme IV. The mechanism involves the negative charge on the phosphate oxygen acting as the driving force for the reaction. Proton transfer to the alkoxide group occurs by formation of a six-membered ring through hydrogen

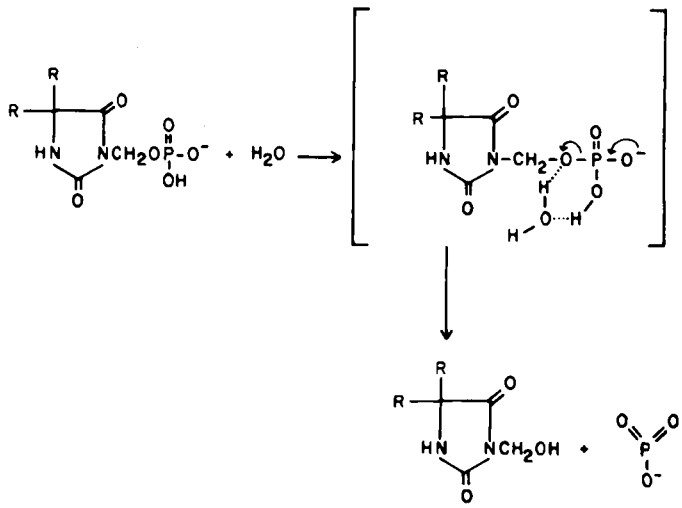

Scheme IV

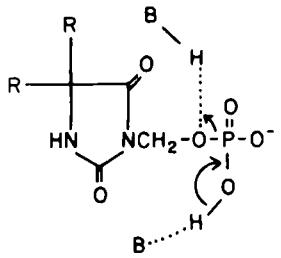

Scheme V

bonding with a single water molecule. This would be consistent with the dianion being less susceptible to hydrolysis, as observed in the pH-rate profile.

Another concerted mechanism can be proposed to explain the buffer catalysis observed at pH 3.9 and 6.5 (Scheme V). The mechanism involves the buffer acting as both a proton donor and a proton acceptor.

The apparent energy of activation of 20.5 kcal·mol^{-1} obtained for the hydrolysis of VII was consistent with the activation energies reported for other phosphate esters (18). Ester VII had a long half-life of ~6800 d at 25°C and pH 7.4, which is characteristic of most phosphate esters.

Based on the pH profiles (Figs. 1 and 7) and the data presented in the rest of this study, esters IV–VII hydrolyze to phenytoin *via* pseudo-first-order kinetics at fixed pH values with no accumulation of the decomposition intermediate, II. The amino acyl esters exhibit maximum stability in the pH range 3–4 (Table VIII), which is within the physiologically acceptable range for parenteral dosage forms. The superior stability of VII over IV–VI makes it an attractive prodrug candidate for parenteral administration provided it is nontoxic and rapidly and quantitatively reverts to phenytoin *in vivo*.

Table VIII points out the $t_{90\%}$ (time for 90% of the ester remaining at the indicated pH values), perhaps suggesting that this may be the determining factor controlling the shelf life of a reconstituted dosage form of these prodrugs if they were to be formulated as reconstituted parenteral dosage forms (sterile powder or freeze-dried powder). However, as pointed out earlier, the $t_{90\%}$ will probably not be the stability-limiting factor for these products, since hydrolysis of the esters produces the sparingly soluble parent drug, phenytoin. For example, if a 50-mg/mL solution (phenytoin equivalents) of IV is prepared, then theoretically, when 0.02 mg/mL of phenytoin is produced, phenytoin should begin precipitating from solution; *i.e.*, the reaction would only have to proceed to the extent of 0.04% before problems could occur. For this reason, and because IV and VII (25, 26) were considered to be the two most likely candidates as oral/parenteral and parenteral prodrugs, respectively, a limited study[8] on the theoretical and observed precipitation times for phenytoin was undertaken

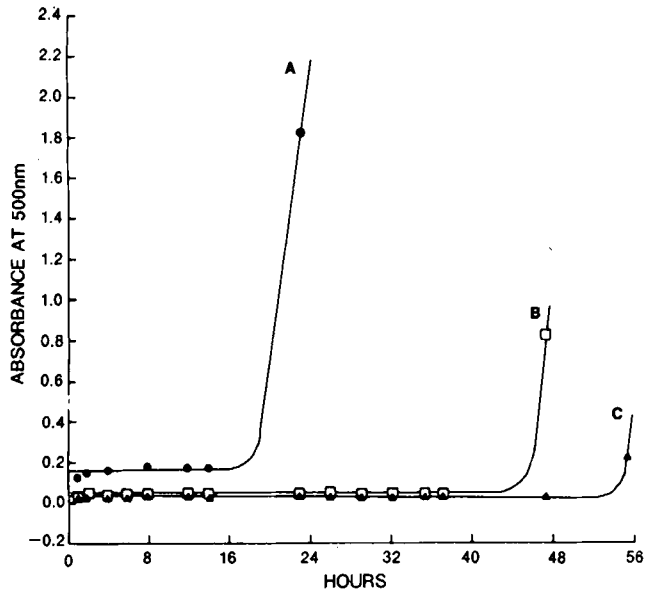

Figure 8—*Plot of change in the absorbance at 500 nm of aqueous solutions of IV due to precipitation of phenytoin. Solutions are 100 (A), 10 (B), and 1 mg/mL (C) of IV.*

[8] A more comprehensive study of this problem of precipitation is currently underway in our laboratory. Results will be formally presented in a later paper.

Table VIII—Time for 10% Hydrolysis ($t_{90\%}$) of IV–VI at pH Values of Maximum Stability and of VII at pH 7.4 [a]

Compound	pH	$t_{90\%}$, h
IV	3.2	17.4
V	3.2	138.1
VI	4.0	107.1
VII	7.4	24,769.0 (2.8 years)

[a] μ = 0.5, 25°C.

Table IX—Theoretical ($t_{ppt,calc}$) and Experimental ($t_{ppt,obs}$) Precipitation Times for the Formation of Phenytoin from Aqueous Solutions of IV and VII, Determined at 25°C

Compound	Initial Conc. of Ester (Phenytoin equivalent), mg/mL	pH of Solution	$t_{ppt,calc}$	$t_{ppt,obs}$
IV	1 (0.54)	3.86	6 h[a]	~55 h
IV	10 (5.44)	2.85	0.6 h[a]	~43 h
IV	100 (54.43)	1.94	0.06 h[a]	~19 h
VII	61.3 (38.1)	8.5	13.7 d[b]	>114 d[c]

[a] The half-life for the degradation of IV to phenytoin was taken as 115.0 h at pH 3.2 and 25°C. [b] The apparent first-order rate constant for the degradation of VII to phenytoin was taken as 68.9 × 10^{-8} h^{-1} at pH 8.5 and 25°C. [c] No precipitation was observed at the end of the 114-d period.

using aqueous solutions of 1–100 mg/mL of IV at 25 ± 0.1°C and a 61.3-mg/mL aqueous solution of VII at pH ~8.5 and ambient room temperature.

In the case of IV, 1-, 10-, and 100-mg/mL solutions of IV were prepared and the presence of a precipitate was detected by following absorbance changes at 500 nm (Fig. 8). The break in the absorbance *versus* time plots was due to the light absorption by the solid phenytoin when it began to precipitate from solution. In the case of VII, only periodic visual inspection over a 114-d period was attempted. Table IX summarizes the calculated and observed times for phenytoin to precipitate from aqueous solutions of esters IV and VII. The calculated times were based on the assumption that the rate constant for hydrolysis was independent of initial concentration and that precipitation would occur when a 7.9 × 10^{-5} M (20-μg/mL) solution of phenytoin was produced at 25°C. It was also assumed that the prodrug solutions contained no phenytoin as an initial impurity.

The results shown in Table IX show no correlation between the calculated (theoretical) and observed precipitation times. Possible explanations for this behavior have appeared in the literature (2). In an extension of the results presented in Table IX, we have tentatively shown[8] that the following processes contribute to this lack of correlation.

1. In the case of IV, associated solutions (probably micellar) occur at ~3–5 mg/mL of IV, resulting in a slowing of the rate of phenytoin production at concentrations >3–5 mg/mL than would be predicted by the dilute solution kinetics. This contributes approximately a factor of two to the discrepancy between $t_{ppt,calc}$ and $t_{ppt,obs}$.

2. Phenytoin is significantly solubilized by IV at concentrations >3–5 mg/mL, *e.g.*, a 50-mg/mL solution of IV has been shown to dissolve ~1.6 mg/mL of phenytoin[8], an increase in aqueous solubility of phenytoin of ~80-fold over water alone. This increased solubility by the prodrug, along with the processes mentioned above, can account for all but about a factor of three in the discrepancy between the theoretical and observed precipitation times. A similar study with VII showed that in the presence of 74 mg/mL of VII, the solubility of phenytoin was approximately double that in water[8].

3. Therefore, it appears from our preliminary results that there may also be a contribution from supersaturation (a factor of two to five).

Based on the data presented in this paper and the solubility data on IV–VII presented in the previous paper (1), it seems that all the compounds should be sufficiently stable for oral usage, especially in solid dosage forms; *i.e.*, the compounds do not appear to be excessively unstable in aqueous solution. It also seems likely that any injectable form of IV, VI[9], and VII would have to be of the reconstitutable type, although there may be a chance that VII maintained at pH ~9–9.5 would be sufficiently stable as a constituted injectable[10]. Based on stability considerations alone, the best candidate for an injectable form of phenytoin appears to be the phosphate ester, VII.

[9] Compound VI will be rejected later due to toxicity concerns. Compound V had already been rejected as a parenteral form due to its low aqueous solubility.

[10] Such studies on VII are ongoing.

REFERENCES

(1) S. A. Varia, S. Schuller, K. B. Sloan, and V. J. Stella, *J. Pharm. Sci.*, **73**, 1068 (1984).

(2) V. Stella, T. Higuchi, A. Hussain, and J. Truelove, in "Prodrugs as Novel Drug Delivery Systems," T. Higuchi and V. Stella, Eds., American Chemical Society Symposium Series #14, 1975, pp. 154–183.

(3) K. Arnold, N. Gerber, and G. Levy, *Can. J. Pharm. Sci.*, **5**, 89 (1970).

(4) M. Johansen and H. Bundgaard, *Arch. Pharm. Chem., Sci. Ed.*, **7**, 175 (1979).

(5) H. Bundgaard and M. Johansen, *Int. J. Pharm.*, **5**, 67 (1980).

(6) D. W. Newton and R. B. Kluza, *Am. J. Hosp. Pharm.*, **37**, 1647 (1980).

(7) A. A. Frost and R. G. Pearson, in "Kinetics and Mechanism," 2nd ed., Wiley, New York, N.Y., 1960, p. 28.

(8) V. J. Stella, *J. Pharm. Sci.*, **66**, 1510 (1977).

(9) T. C. Bruice, T. H. Fife, J. J. Bruno, and N. E. Brandon, *Biochemistry*, **1**, 7 (1962).

(10) A. J. Kirby and G. J. Lloyd, *J. Chem. Soc., Perkin II*, **1976**, 1748.

(11) T. Higuchi, A. Havinga, and L. W. Busse, *J. Am. Pharm. Assoc., Sci. Ed.*, **39**, 405 (1950).

(12) M. Johansen and H. Bundgaard, *Arch. Pharm. Chem., Sci. Ed.*, **9**, 43 (1981).

(13) P. Y. Bruice and H. G. Mautner, *J. Am. Chem. Soc.*, **95**, 1582 (1973).

(14) T. C. Bruice and S. J. Benkovic, *J. Am. Chem. Soc.*, **85**, 1 (1963).

(15) J. P. Patel and A. J. Repta, *Int. J. Pharm.*, **9**, 29 (1981).

(16) S. S. Minor and R. L. Schowen, *J. Am. Chem. Soc.*, **95**, 2279 (1973).

(17) M. D. Joesten and L. J. Schaad, "Hydrogen Bonding," Dekker, New York, N.Y., 1974, chap. 5, pp. 253–279.

(18) G. L. Flynn and D. J. Lamb, *J. Pharm. Sci.*, **59**, 1433 (1970).

(19) T. O. Oesterling and E. L. Rowe, *J. Pharm. Sci.*, **59**, 175 (1970).

(20) J. Kumamoto and F. H. Westheimer, *J. Am. Chem. Soc.*, **77**, 2515 (1955).

(21) C. A. Bunton, D. R. Llewellyn, K. G. Oldham, and C. A. Vernon, *J. Chem. Soc.*, **1958**, 3574.

(22) W. W. Butcher and F. H. Westheimer, *J. Am. Chem. Soc.*, **77**, 2420 (1955).

(23) M. C. Bailley, *Bull. Soc. Chim. France*, **9**, 340 (1942).

(24) A. Desjobert, *Bull. Soc. Chim. France*, **14**, 809 (1947).

(25) S. A. Varia and V. J. Stella, *J. Pharm. Sci.*, **73**, 1080 (1984).

(26) S. A. Varia and V. J. Stella, *J. Pharm. Sci.*, **73**, 1087 (1984).

ACKNOWLEDGMENTS

The paper is adapted in part from a dissertation submitted by S. A. Varia to The University of Kansas in partial fulfillment of the Doctor of Philosophy degree requirements. This work was supported in part by INTERx Research Corp., a subsidiary of Merck Sharp & Dohme.

Phenytoin Prodrugs V: *In Vivo* Evaluation of Some Water-Soluble Phenytoin Prodrugs in Dogs

S. A. VARIA * and V. J. STELLA ˣ

Received December 22, 1982, from the *Department of Pharmaceutical Chemistry, School of Pharmacy, The University of Kansas, Lawrence, KS 66045.* Accepted for publication September 6, 1983. *Present address: Squibb Institute for Medical Research, New Brunswick, NJ 08903.

Abstract □ Phenytoin bioavailability was evaluated in beagle dogs after oral and intravenous administrations of sodium phenytoin and two amino acyl esters and a disodium phosphate ester of 3-(hydroxymethyl)phenytoin (three prodrugs of phenytoin). Phenytoin displayed nonlinear pharmacokinetics in the dogs, complicating the determination of the absolute bioavailability of phenytoin from sodium phenytoin and the prodrugs. All three prodrugs essentially released phenytoin after intravenous administration in a quantitative manner, and all gave plasma levels of phenytoin after oral administration greater than those found after administration of sodium phenytoin. Based on the behavior in dogs and the earlier determination of the physicochemical properties of the prodrugs, it was concluded that one of the amino acyl esters, 3-(hydroxymethyl)-5,5-diphenylhydantoin *N,N*-dimethylglycine ester methanesulfonate, would be the most useful prodrug for oral administration, while 3-(hydroxymethyl)-5,5-diphenylhydantoin disodium phosphate ester would be the most useful for parenteral administration.

Keyphrases □ Prodrugs—phenytoin, bioavailability, dogs □ Phenytoin—hydroxymethyl esters, prodrugs, bioavailability, dogs □ Bioavailability—phenytoin prodrugs, dogs

Phenytoin (I), because of its weakly acid nature (1–4) and poor aqueous solubility (3–5), shows erratic absorption patterns after oral administration of either the sodium salt (Ia) or the free acid in both humans (6–19) and dogs (20, 21). Sodium phenytoin (Ia) in the parenteral dosage form is hazardous if rapidly injected intravenously (22, 23), and the free acid appears to precipitate at intramuscular injection sites (24–29), leading to prolonged and marginal phenytoin release.

In the previous papers in this series (5, 30), a number of water-soluble prodrugs of phenytoin were evaluated with respect to their physicochemical properties (*e.g.*, solubility and stability), their cleavage to phenytoin in animal tissues, and their anticonvulsant activity in mice. Based on those studies, three of the prodrugs, 3-(hydroxymethyl)-5,5-diphenylhydantoin *N,N*-dimethylglycine ester methanesulfonate (II)[1], 3-(hydroxymethyl)-5,5-diphenylhydantoin *N,N*-dimethylaminoethyl carbonate methanesulfonate (III)[1], and 3-(hydroxymethyl)-5,5-diphenylhydantoin disodium phosphate

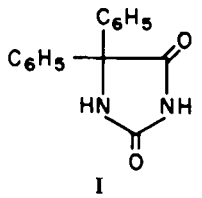

I

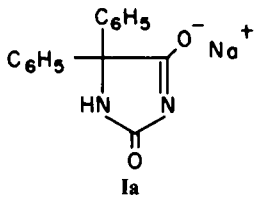

Ia

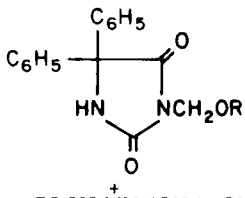

II: R = $-COCH_2\overset{+}{N}H(CH_3)_2\ CH_3SO_3^-$

III: R = $-CO_2(CH_2)_2\overset{+}{N}H(CH_3)_2\ CH_3SO_3^-$

IV: R = $-PO_3^{2-}\ Na_2^+$

[1] Compounds II, III, and IV are equivalent to IV, VI, and VII, respectively, in papers III and IV in this series.

0022-3549/84/0800-1080$01.00/0

© 1984, American Pharmaceutical Association

REFERENCES

(1) S. A. Varia, S. Schuller, K. B. Sloan, and V. J. Stella, *J. Pharm. Sci.*, **73**, 1068 (1984).

(2) V. Stella, T. Higuchi, A. Hussain, and J. Truelove, in "Prodrugs as Novel Drug Delivery Systems," T. Higuchi and V. Stella, Eds., American Chemical Society Symposium Series #14, 1975, pp. 154–183.

(3) K. Arnold, N. Gerber, and G. Levy, *Can. J. Pharm. Sci.*, **5**, 89 (1970).

(4) M. Johansen and H. Bundgaard, *Arch. Pharm. Chem., Sci. Ed.*, **7**, 175 (1979).

(5) H. Bundgaard and M. Johansen, *Int. J. Pharm.*, **5**, 67 (1980).

(6) D. W. Newton and R. B. Kluza, *Am. J. Hosp. Pharm.*, **37**, 1647 (1980).

(7) A. A. Frost and R. G. Pearson, in "Kinetics and Mechanism," 2nd ed., Wiley, New York, N.Y., 1960, p. 28.

(8) V. J. Stella, *J. Pharm. Sci.*, **66**, 1510 (1977).

(9) T. C. Bruice, T. H. Fife, J. J. Bruno, and N. E. Brandon, *Biochemistry*, **1**, 7 (1962).

(10) A. J. Kirby and G. J. Lloyd, *J. Chem. Soc., Perkin II*, **1976**, 1748.

(11) T. Higuchi, A. Havinga, and L. W. Busse, *J. Am. Pharm. Assoc., Sci. Ed.*, **39**, 405 (1950).

(12) M. Johansen and H. Bundgaard, *Arch. Pharm. Chem., Sci. Ed.*, **9**, 43 (1981).

(13) P. Y. Bruice and H. G. Mautner, *J. Am. Chem. Soc.*, **95**, 1582 (1973).

(14) T. C. Bruice and S. J. Benkovic, *J. Am. Chem. Soc.*, **85**, 1 (1963).

(15) J. P. Patel and A. J. Repta, *Int. J. Pharm.*, **9**, 29 (1981).

(16) S. S. Minor and R. L. Schowen, *J. Am. Chem. Soc.*, **95**, 2279 (1973).

(17) M. D. Joesten and L. J. Schaad, "Hydrogen Bonding," Dekker, New York, N.Y., 1974, chap. 5, pp. 253–279.

(18) G. L. Flynn and D. J. Lamb, *J. Pharm. Sci.*, **59**, 1433 (1970).

(19) T. O. Oesterling and E. L. Rowe, *J. Pharm. Sci.*, **59**, 175 (1970).

(20) J. Kumamoto and F. H. Westheimer, *J. Am. Chem. Soc.*, **77**, 2515 (1955).

(21) C. A. Bunton, D. R. Llewellyn, K. G. Oldham, and C. A. Vernon, *J. Chem. Soc.*, **1958**, 3574.

(22) W. W. Butcher and F. H. Westheimer, *J. Am. Chem. Soc.*, **77**, 2420 (1955).

(23) M. C. Bailley, *Bull. Soc. Chim. France*, **9**, 340 (1942).

(24) A. Desjobert, *Bull. Soc. Chim. France*, **14**, 809 (1947).

(25) S. A. Varia and V. J. Stella, *J. Pharm. Sci.*, **73**, 1080 (1984).

(26) S. A. Varia and V. J. Stella, *J. Pharm. Sci.*, **73**, 1087 (1984).

ACKNOWLEDGMENTS

The paper is adapted in part from a dissertation submitted by S. A. Varia to The University of Kansas in partial fulfillment of the Doctor of Philosophy degree requirements. This work was supported in part by INTERx Research Corp., a subsidiary of Merck Sharp & Dohme.

Phenytoin Prodrugs V: *In Vivo* Evaluation of Some Water-Soluble Phenytoin Prodrugs in Dogs

S. A. VARIA * and V. J. STELLA ˣ

Received December 22, 1982, from the *Department of Pharmaceutical Chemistry, School of Pharmacy, The University of Kansas, Lawrence, KS 66045.* Accepted for publication September 6, 1983. *Present address: Squibb Institute for Medical Research, New Brunswick, NJ 08903.

Abstract □ Phenytoin bioavailability was evaluated in beagle dogs after oral and intravenous administrations of sodium phenytoin and two amino acyl esters and a disodium phosphate ester of 3-(hydroxymethyl)phenytoin (three prodrugs of phenytoin). Phenytoin displayed nonlinear pharmacokinetics in the dogs, complicating the determination of the absolute bioavailability of phenytoin from sodium phenytoin and the prodrugs. All three prodrugs essentially released phenytoin after intravenous administration in a quantitative manner, and all gave plasma levels of phenytoin after oral administration greater than those found after administration of sodium phenytoin. Based on the behavior in dogs and the earlier determination of the physicochemical properties of the prodrugs, it was concluded that one of the amino acyl esters, 3-(hydroxymethyl)-5,5-diphenylhydantoin *N,N*-dimethylglycine ester methanesulfonate, would be the most useful prodrug for oral administration, while 3-(hydroxymethyl)-5,5-diphenylhydantoin disodium phosphate ester would be the most useful for parenteral administration.

Keyphrases □ Prodrugs—phenytoin, bioavailability, dogs □ Phenytoin—hydroxymethyl esters, prodrugs, bioavailability, dogs □ Bioavailability—phenytoin prodrugs, dogs

Phenytoin (I), because of its weakly acid nature (1–4) and poor aqueous solubility (3–5), shows erratic absorption patterns after oral administration of either the sodium salt (Ia) or the free acid in both humans (6–19) and dogs (20, 21). Sodium phenytoin (Ia) in the parenteral dosage form is hazardous if rapidly injected intravenously (22, 23), and the free acid appears to precipitate at intramuscular injection sites (24–29), leading to prolonged and marginal phenytoin release.

In the previous papers in this series (5, 30), a number of water-soluble prodrugs of phenytoin were evaluated with respect to their physicochemical properties (*e.g.*, solubility and stability), their cleavage to phenytoin in animal tissues, and their anticonvulsant activity in mice. Based on those studies, three of the prodrugs, 3-(hydroxymethyl)-5,5-diphenylhydantoin *N,N*-dimethylglycine ester methanesulfonate (II)[1], 3-(hydroxymethyl)-5,5-diphenylhydantoin *N,N*-dimethylaminoethyl carbonate methanesulfonate (III)[1], and 3-(hydroxymethyl)-5,5-diphenylhydantoin disodium phosphate

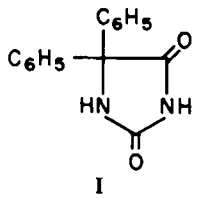

I

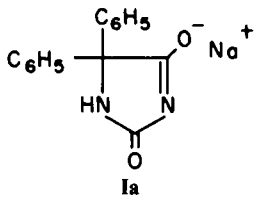

Ia

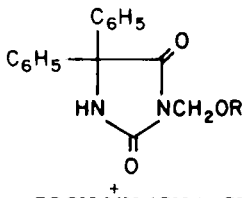

II: R = $-COCH_2\overset{+}{N}H(CH_3)_2\ CH_3SO_3^-$

III: R = $-CO_2(CH_2)_2\overset{+}{N}H(CH_3)_2\ CH_3SO_3^-$

IV: R = $-PO_3^{2-}\ Na_2^+$

[1] Compounds II, III, and IV are equivalent to IV, VI, and VII, respectively, in papers III and IV in this series.

0022-3549/84/0800-1080$01.00/0

© 1984, American Pharmaceutical Association

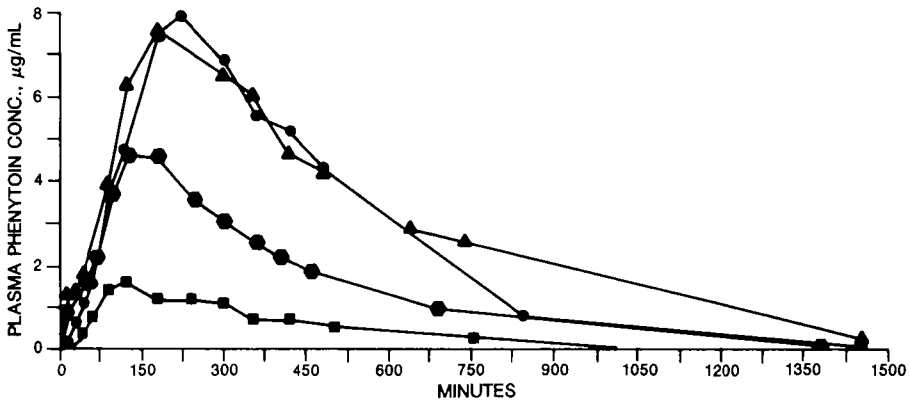

Figure 1—*Plasma levels of phenytoin in dog 20 following oral administration of Ia (■), II (●), III (▲), and IV (●) in capsule form. Doses (phenytoin equivalents) were 15 mg/kg.*

ester (IV)[1] were chosen for further evaluation in the beagle dog.

Compounds II and III were evaluated as possible oral-delivery forms of phenytoin because of their aqueous solubility (~150 mg/mL), pK_a values (6.60 and 8.20, respectively), and because they are readily cleaved enzymatically to phenytoin. However, the chemical stability of II and III indicated that there could be some difficulty in preparing suitably stable injectable dosage forms (30). Ester IV was chosen primarily as a parenteral candidate but was also evaluated for oral delivery of phenytoin, since recent evidence has suggested that dexamethasone phosphate quantitatively releases dexamethasone after oral dosing (31). Beagle dogs were chosen for this study because of their ease of handling and because phenytoin has been shown to be marginally bioavailable in dogs (20, 21), probably because of their short GI transit times (20). Dogs, therefore, may be a good model for pediatric patients, where phenytoin absorption has been shown to be particularly erratic (10, 19).

EXPERIMENTAL SECTION

Prodrugs II–IV were analytically pure and were prepared as previously described (5). Phenytoin and sodium phenytoin were obtained from a commercial source[2].

Gas Chromatographic Analysis of Phenytoin—Venous whole blood obtained from dogs was immediately centrifuged for 15–20 min at 1000×*g* and plasma was collected. In the case of II and III, a 100-μL plasma sample was immediately treated with 100 μL of a 10% metaphosphoric acid solution and assayed for phenytoin by GC according to the method of Stella (32). A second plasma sample was allowed to stand at 37°C for >1–2 h and then was assayed as described above. Any II or III in dog plasma is cleaved to phenytoin during this period (5). This procedure allowed for the analysis of phenytoin (first sample) and phenytoin plus prodrug (second sample), whereby prodrug concentration could be determined by difference. None of the samples (after both oral and parenteral dosings), contained any significant levels of II or III.

The procedure for IV was modified. The first plasma sample was not quenched with metaphosphoric acid, but was extracted into toluene, the first step in preparation for the GC assay. The second plasma sample was diluted with 100 μL of 10% amylase[3], maintained at 37°C overnight, and then assayed for phenytoin as described above. Only in the case of the 5–15-min samples were any levels of IV detectable after intravenous administration of IV; IV could not be detected after oral dosing.

Oral and Intravenous Evaluation Studies in Dogs—Four adult female beagle dogs, ranging in weight from 8 to 13 kg, were used for two crossover studies employing a Latin-square design. The intravenous and oral studies were carried out according to Table I. Each dog received 15-mg/kg (phenytoin equivalent) doses of sodium phenytoin, II, III, and IV orally and intravenously. The dogs were fasted overnight prior to drug administration, but were allowed water *ad libitum*. The dogs were rested for at least 1 week between studies.

For the intravenous study, fresh aqueous solutions of II, III, and IV were used. Phenytoin was administered intravenously as the sodium salt in a solvent system of propylene glycol–alcohol–water (4:1:5). The pH of this solution was adjusted to ~11.5–12.0 with sodium hydroxide. The injection volumes ranged from 2–3.5 mL and were administered into the leg vein over a period of 1–2 min.

In the oral study the compounds were administered in hard gelatin capsules without any excipients. After administering the compound, sufficient water to guarantee that the capsule had been swallowed (100–200 mL) was administered. The dogs were then returned to their respective cages.

After administration of the drug, serial venous blood samples were taken at appropriate times from the neck vein. The samples were withdrawn into 2-ml containers[4] containing 3 mg of EDTA. The blood samples were immediately centrifuged, and the separated plasma samples were analyzed for phenytoin and prodrug as described earlier.

Dose-Dependent Pharmacokinetics in Dogs—The evaluation of plasma concentration time curves of phenytoin, after administration of sodium phenytoin and the prodrugs of phenytoin at 15 mg/kg (phenytoin equivalents), suggested that phenytoin at a dose of 15 mg/kg displayed nonlinear pharmacokinetics. To confirm this, dogs 20 and 21, used in the 15-mg/kg study, were each administered 10-mg/kg and 6.6- or 5.5-mg/kg (phenytoin equivalent) doses of sodium phenytoin intravenously; plasma samples were assayed for phenytoin as described earlier.

RESULTS AND DISCUSSION

Figure 1 is a representative plot of the plasma phenytoin concentration *versus* time obtained after oral administrations of 15-mg/kg (phenytoin equivalent) doses of sodium phenytoin (Ia) and II–IV to dog 20. Dog 22 consistently rejected III, and hence, data for III for that particular dog could not be obtained. The areas under the plasma phenytoin concentration *versus* time curves (AUC_0^∞) after oral administration of Ia and II–IV were evaluated by the trapezoidal method (33) (Table II). Statistical analysis by one-way ANOVA showed that there was significant difference ($p < 0.05$) between the mean AUC_0^∞ values obtained after oral administration of the prodrugs and the mean AUC_0^∞ obtained after oral administration of sodium phenytoin (Ia). However, there was no significant difference ($p > 0.05$) in the mean AUC_0^∞ values between the prodrugs. Figures 2 and 3 show two representative plots of the plasma phenytoin concentration *versus* time after intravenous administration of the prodrugs and sodium phenytoin to dogs 19 and 20. Dogs 21 and 22 were not administered the intravenous injection of III, since the compound was observed to cause pain and toxic manifestations in dogs 19 and 20. Intravenous administration of III to dog 20 appeared to be incomplete, since pain and swelling around the injection site suggested that some of the dose may not have been placed directly in the vein.

Prodrugs II–IV, on oral administration, produced higher plasma phenytoin levels than the levels obtained after oral administration of Ia. The poor availability of phenytoin from Ia was probably due to the precipitation of phenytoin acid in the acidic environment of the stomach as well as the poor dosage form used, *i.e.*, sodium phenytoin in a hard gelatin capsule. Phenytoin has a low aqueous solubility and, thus, the slow and incomplete redissolution probably results in low plasma levels of phenytoin.

The primary purpose of the intravenous and oral administration of the prodrugs to the beagle dogs was to determine (*a*) if the prodrugs quantitatively released phenytoin and (*b*) the extent of absorption of phenytoin from the prodrugs on oral administration. Such an evaluation of the prodrugs of phenytoin is difficult since the elimination kinetics of phenytoin may be

[2] Sigma Chemical Co., St. Louis, Mo.

[3] Diatase or clarase, a phosphatase enzyme preparation, was found to cleave IV with a half-life of <1 h; Fisher Scientific Co., Fair Lawn, N.J.

[4] Vacutainers, No. 6496; Becton, Dickinson and Co., Rutherford, N.J.

Table I—Intravenous and Oral Studies Using a Latin-Square Design Carried out in Beagle Dogs

Experiment	Dog 19	Dog 20	Dog 21	Dog 22
Intravenous				
1	III[a]	IV	Ia	II
2	II	III[b]	IV	Ia
3	Ia	II	III[c]	IV
4	IV	Ia	II	III[c]
Oral				
5	Ia	II	IV	III[d]
6	III	Ia	II	IV
7	IV	III	Ia	II
8	II	IV	III	Ia

[a] Produced severe toxic reactions in the dog including salivation, dilatation of the pupils, and hypotension. [b] Appeared to cause severe pain on administration, thus resulting in incomplete administration of the dose. [c] Not administered due to toxicity seen in Experiments 1 and 2. [d] Dog 22 rejected III three times. Further attempts to administer III orally to dog 22 were therefore terminated.

nonlinear (34, 35), probably due to the saturation of the enzyme system responsible for the metabolism of phenytoin to 5-*p*-hydroxyphenyl-5-phenylhydantoin (36). Dayton *et al.* (34) and Frey and Loseher (35) have shown that phenytoin exhibits dose-dependent kinetics in the dog. It was reported (35) that after intravenous administration of 20, 10, and 5 mg/kg (phenytoin equivalents) of Ia to dogs, the apparent elimination half-life of phenytoin decreased from 11.2 to 6.1 to 4.3 h, respectively. A plot of the logarithm of the plasma phenytoin concentration *versus* time was curvilinear at the three doses studied. Such a curvilinear plot is typical of drugs with Michaelis–Menten kinetics with a capacity-limited pathway of elimination or for drugs exhibiting product inhibition (37–41). In the present study, the nonlinear behavior of phenytoin in the beagle dog is apparent from the curvilinear shape observed in the plot of the logarithm of the plasma phenytoin concentration *versus* time obtained after intravenous administration of a 15-mg/kg (phenytoin equivalent) dose of Ia (Fig. 4).

In its simplest form, the pharmacokinetic model in Scheme I can be proposed for phenytoin and its prodrugs. Since phenytoin seems to exhibit nonlinear elimination kinetics in the dog (34, 35) at a dose of 15 mg/kg (phenytoin equivalents) of either Ia or the prodrug, quantitation of the extent of conversion of the prodrugs to phenytoin is difficult. This is because the elimination rate and the clearance of phenytoin (and thus the area under the plasma phenytoin concentration *versus* time profiles) depends on its input rate. This, in turn, depends on either the absorption rate of the prodrug after oral dosing and/or the metabolic conversion rate of the prodrug to phenytoin.

To confirm the nonlinear behavior of phenytoin in the beagle dog, a pharmacokinetic study involving variation of the dose of Ia was carried out in dogs 20 and 21. Dog 20 was administered 15-, 10-, and 6.6-mg/kg (phenytoin equivalent) doses of Ia intravenously and dog 21 was administered 15-, 10-, and 5.5-mg/kg (phenytoin equivalent) doses of Ia intravenously. The AUC_0^∞ values obtained after intravenous administration of the different doses of Ia were determined by the trapezoidal method. A plot of the AUC_0^∞ values *versus* the dose is shown in Fig. 5. The plot shows that the relationship between AUC_0^∞ and the dose is nonlinear. In the case of drugs obeying linear pharmacokinetics,

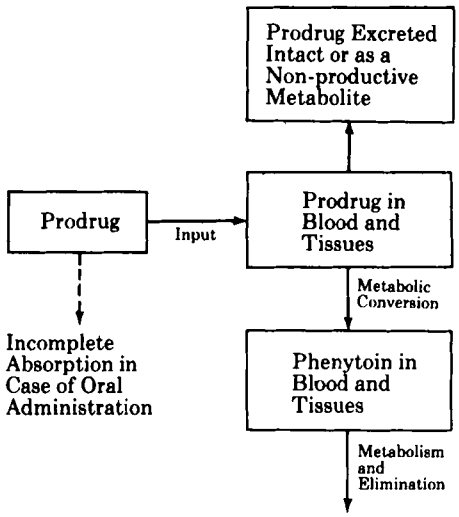

Scheme I

the AUC_0^∞ obtained after intravenous administration of the drug is directly proportional to the intravenous dose:

$$AUC_0^\infty = \frac{D_{iv}}{CL} \qquad \text{(Eq. 1)}$$

where D_{iv} is the intravenous dose and CL is the total body clearance of the drug. Thus, the AUC_0^∞ would increase proportionately with dose if the clearance remains constant. The elimination half-life of the drug should also be independent of the dose for drugs obeying linear pharmacokinetics. Hence, the nonlinear relationship between AUC_0^∞ *versus* dose and the increase in the apparent elimination half-life with increasing dose observed in this study (Table III) confirms the dose dependency and nonlinear behavior of phenytoin in the current study.

The absolute bioavailability of drugs (or prodrugs) exhibiting linear pharmacokinetics is normally determined by calculating the ratio of the AUC_0^∞ of the parent drug obtained after oral administration of the drug (or prodrug) and the AUC_0^∞ obtained after intravenous administration of the parent drug (33). Also, the availability of the parent drug after intravenous administration of a prodrug could be determined by calculating the ratio of the AUC_0^∞ values obtained after intravenous administration of the prodrug and those obtained after intravenous administration of an equivalent dose of the parent drug. Table IV summarizes the AUC_0^∞ values, calculated by the trapezoidal method, of the plasma phenytoin concentration *versus* time profiles obtained after intravenous administration of molar equivalent doses of Ia and II–IV. If phenytoin did exhibit linear pharmacokinetics, then the ratio of the AUC_0^∞ obtained after intravenous administration of the prodrugs and the AUC_0^∞ obtained after intravenous administration of Ia (Table V) would give the extent of conversion of the prodrugs to phenytoin. Similarly, the ratio of the AUC_0^∞ values obtained after oral administration of the prodrug and those obtained

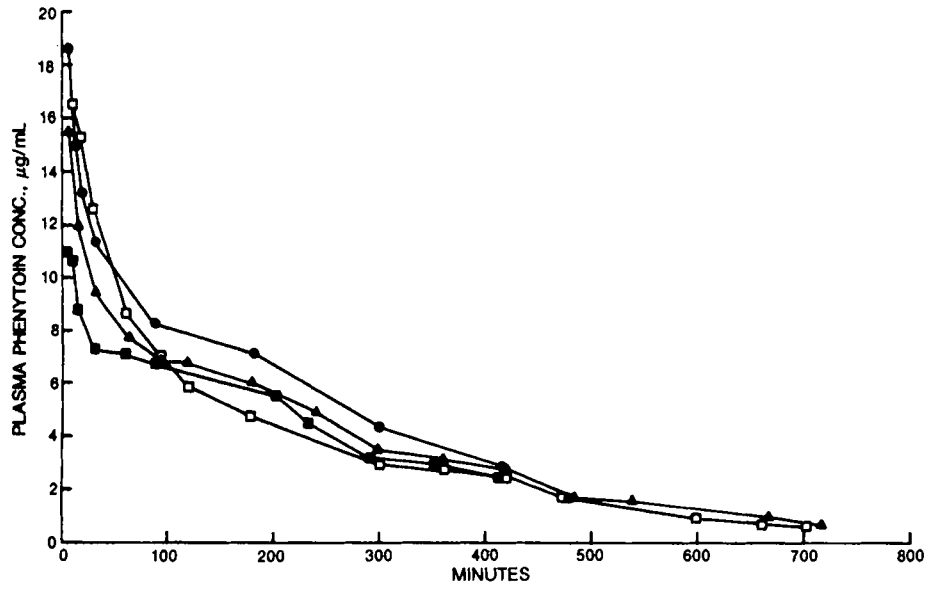

Figure 2—*Plots of the plasma phenytoin concentrations* versus *time obtained after intravenous administration of Ia (●), II (■), III (□), and IV (▲) to dog 19. Doses (phenytoin equivalents) were 15 mg/kg.*

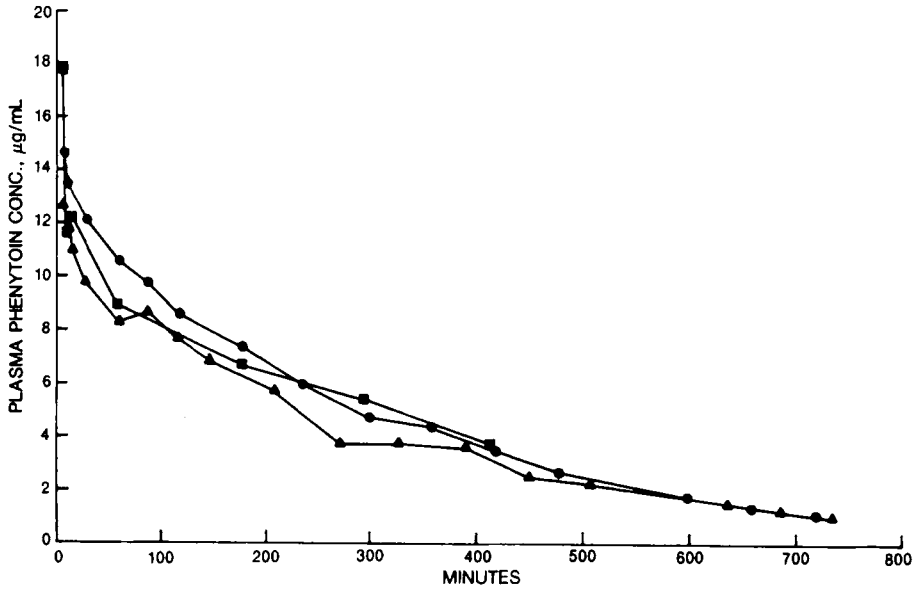

Figure 3—*Plots of the plasma phenytoin concentrations* versus *time obtained after intravenous administration of Ia (●), II (■), and IV (▲) to dog 20. Doses (phenytoin equivalents) were 15 mg/kg.*

after intravenous administration of Ia (Table VI) would give the absolute bioavailability of the prodrugs. However, since phenytoin exhibits nonlinear behavior, the ratios summarized in Tables V and VI are only apparent values of the bioavailabilities of the prodrugs compared with Ia.

To determine the bioavailabilities of the prodrugs, the model shown in Scheme II is proposed, representing a one-compartment model. Although phenytoin does exhibit two-compartmental behavior, the distribution phase in the dog is insignificant; most authors[5] (35, 42, 43), therefore, describe the kinetics of phenytoin according to a one-compartment model[6]. According to the model, elimination of phenytoin, after an intravenous or oral dose D, is assumed to occur by a capacity-limited process. It will be assumed that the capacity-limited process, described by the Michaelis–Menten equation for a one-enzyme reaction, is applicable to phenytoin elimination in the dog.

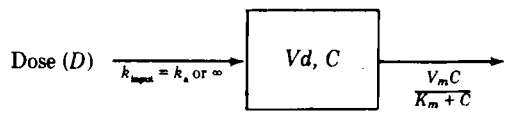

Scheme II

Following intravenous administration of a dose (D_{iv}) of phenytoin, the differential equation describing the concentration of phenytoin at any time t in the body is:

$$\frac{-dC}{dt} = \frac{V_m C}{K_m + C} \qquad \text{(Eq. 2)}$$

where V_m is the theoretical maximum velocity per unit volume of distribution of the capacity-limited process (and in the present case has the units of μg/mL/min) and K_m represents the Michaelis–Menten constant (and has the units of concentration, μg/mL). Numerical values of V_m and K_m for dogs 20 and 21 were obtained by nonlinear least-squares iteration of the integrated form of Eq. 2, *i.e.*:

$$C_1 - C + K_m \cdot \ln (C_1/C) = V_m(t - t_1) \qquad \text{(Eq. 3)}$$

using the SIMPLEX program; data was obtained at three different intravenous doses of sodium phenytoin. C_1 is the first plasma phenytoin concentration point chosen by inspection in the elimination phase at time t_1.

The volume of distribution, Vd (really Vd extrapolated) was obtained from:

$$Vd = \frac{D_{iv}}{C_0} \qquad \text{(Eq. 4)}$$

where C_0 is the time zero plasma phenytoin concentration, determined by back extrapolation of the elimination phase of the plasma phenytoin concentration *versus* time profile obtained after intravenous administration of Ia.

The values of V_m, K_m, and Vd obtained are shown in Table VII. Figures 6 and 7 show the semilogarithmic plots of the plasma phenytoin concentration *versus* time in dogs 20 and 21, respectively, after administration of the three different doses of Ia; the solid lines were computer-generated from Eq. 2 using the individual V_m and K_m values determined at the different doses. The solid lines in Fig. 4 are the theoretical lines obtained using Eq. 3 and the mean V_m and K_m values shown in Table VII.

To determine the true bioavailability of the prodrugs in dogs 20 and 21, the method described by Martis and Levy (39) and Jusko *et al.* (38) for calculating the bioavailability of drugs exhibiting dose-dependent elimination due to enzyme saturation was employed. The method assumes a one-compartment pharmacokinetic system with a constant volume of distribution and a capacity-limited pathway of elimination. The volume of distribution of phenytoin, shown in Table VII, is practically constant. Following oral administration of

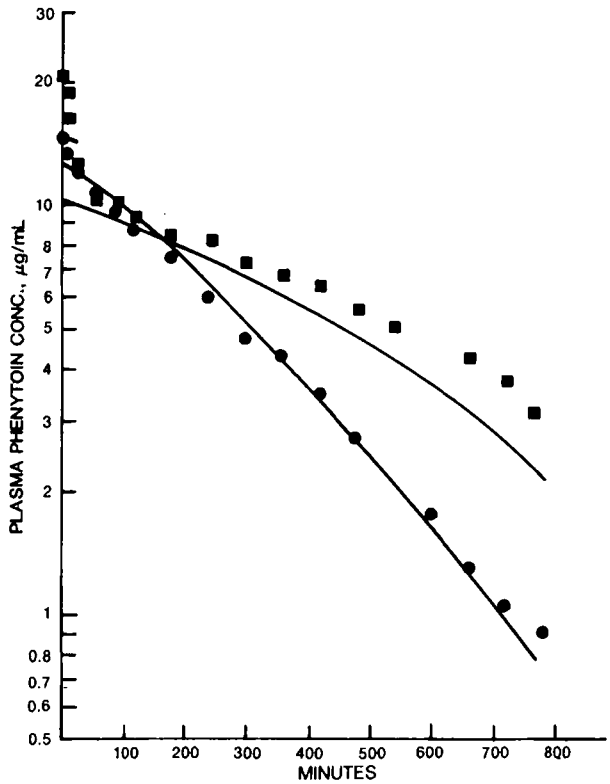

Figure 4—*Semilogarithmic plots of plasma phenytoin concentrations* versus *time after an intravenous dose of 15 mg/kg (phenytoin equivalents) of sodium phenytoin to dog 20 (●) and dog 21 (■). (——) theoretical line using mean* V_m *and* K_m *values.*

[5] D. F. Kowalczyk, unpublished results.

[6] The differences in AUC^{∞}_0 values between assuming a distribution phase and disregarding the distribution phase is only 0.5 and 3.8% in dogs 20 and 21, respectively, for the 15-mg/kg data.

Table II—Area under the Plasma Phenytoin Concentration *versus* Time Curve After Oral Administration of a Dose Equivalent to 15 mg/kg of Phenytoin

Compound	AUC_0^∞, μg·min/mL[a]				
	Dog 19	Dog 20	Dog 21	Dog 22	Mean ± *SD*
Ia	376	668	921	659	656 ± 222
II	2569	3724	2975	2576	2961 ± 543
III	3306	4438	1869	—[b]	3204 ± 1287[c]
IV	1714	2065	4190	2151	2530 ± 1123

[a] Calculated *via* the trapezoidal method. [b] Compound III was rejected three times by dog 22. [c] Mean obtained from results of 3 dogs.

the prodrugs and Ia, the rate of change of phenytoin concentration in the body can be expressed by:

$$\frac{dC}{dt} = \frac{k_a F D_{iv} e^{-K_a t}}{Vd} - \frac{V_m C}{K_m + C} \qquad \text{(Eq. 5)}$$

where k_a is the first-order absorption rate constant and F represents the fraction of the dose absorbed. D_{iv} is the intravenous dose, and this is equal to the oral dose, *i.e.*, 15 mg/kg. The rate of elimination of phenytoin from the body after oral administration is given by:

$$\frac{1}{Vd} \times \frac{dA_e}{dt} = \frac{V_m C}{K_m + C} \qquad \text{(Eq. 6)}$$

where A_e is the amount of phenytoin eliminated at any time t. If the total amount of drug eliminated is equal to the amount absorbed, then:

$$\int_0^\infty \frac{dA_e}{dt} dt = F D_{oral} \qquad \text{(Eq. 7)}$$

where D_{oral} is the oral dose. However, from Eq. 6:

$$\int_0^\infty \frac{dA_e}{dt} dt = Vd \int_0^\infty \frac{V_m C}{K_m + C} dt \qquad \text{(Eq. 8)}$$

Combining Eqs. 7 and 8, the following equality is obtained:

$$Vd \int_0^\infty \frac{V_m C}{K_m + C} dt = F D_{oral} \qquad \text{(Eq. 9)}$$

Dividing Eq. 9 by the intravenous dose, D_{iv}, gives:

$$\frac{\int_0^\infty \frac{V_m C}{K_m + C} dt}{D_{iv}/Vd} = \frac{F D_{oral}}{D_{iv}} \qquad \text{(Eq. 10)}$$

Since equivalent doses are administered intravenously and orally, Eq. 10 reduces to:

$$\frac{\int_0^\infty \frac{V_m C}{K_m + C} dt}{D_{iv}/Vd} = F \qquad \text{(Eq. 11)}$$

where F is the corrected bioavailability. Equation 11 can also be used to determine the availability of phenytoin after an intravenous dose of the prodrug relative to an equivalent intravenous dose of Ia.

To obtain the numerator of Eq. 11, the area under the plot of $V_m C/(K_m + C)$ *versus* time from zero to the last time point (t_L) was determined by the trapezoidal method (33). The concentration at the last time point in the plasma phenytoin concentration *versus* time profile after oral and intravenous administration of the prodrugs was very low. The contribution of the $AUC_{t_L}^\infty$ of a plot of $V_m C/(K_m + C)$ *versus* time would, therefore, be very small. Thus, $AUC_0^{t_L}$ would be approximately equal to AUC_0^∞, which is equal to the numerator of Eq. 11.

The results of the determination of the corrected true bioavailability of intravenously administered prodrugs II and IV in dogs 20 and 21 relative to intravenously administered Ia are summarized in Table VIII, and corrected bioavailabilities of prodrugs II–IV in dogs 20 and 21 after oral dosing are shown in Table IX. Similar calculations could be done to determine the corrected bioavailabilities of oral and intravenously administered prodrugs, respectively, in dogs 19 and 22 if the V_m and K_m values could have been accurately estimated.

Comparison of the AUC_0^∞ values to determine the availability of phenytoin after intravenous administration of its prodrugs relative to Ia can result in an underestimation in the case of drugs like phenytoin, which exhibit nonlinear pharmacokinetics. The extent of underestimation will depend on the rate of conversion of the prodrugs to phenytoin. If the rate of hydrolysis of the prodrugs is slow, the input rate of phenytoin will be slow. This in turn will show a decreased degree of saturation of the enzyme system responsible for metabolism of phenytoin compared with the saturation that would be exhibited by an equivalent intravenous dose of Ia. Similarly, the bioavailability of the prodrugs calculated by determining the ratio of AUC_0^∞ obtained after oral administration of the prodrugs and the AUC_0^∞ obtained after intravenous administration of an equivalent dose of Ia can result in an underestimation. If the input rate of phenytoin (*i.e.*, the absorption and conversion of the prodrug) is slow, the apparent absolute bioavailability is considerably underes-

Table III—Apparent Elimination Half-Lives of Phenytoin after Intravenous Administration of Three Different Doses [a]

Dog	Dose, mg/kg[a]			
	15	10	6.6	5.5
20	3.2 h	2.6 h	2.3 h	—
21	6.7 h	4.4 h	—	2.9 h

[a] Doses of sodium phenytoin, expressed as phenytoin equivalents. Linear kinetics are assumed.

Table IV—Area under the Plasma Phenytoin Concentration *versus* Time Curves after Intravenous Administration of a Dose Equivalent to 15 mg/kg of Phenytoin

Compound	AUC_0^∞, μg·min/mL[a]			
	Dog 19	Dog 20	Dog 21	Dog 22
Ia	3697	3889	7225	4720
II	2499	3808	3070	4873
III	2762	—[b]	—[c]	—[c]
IV	3008	3491	4452	3150

[a] Calculated *via* the trapezoidal method. [b] Unable to administer complete dose due to excessive pain on administration. [c] Compound III was not administered.

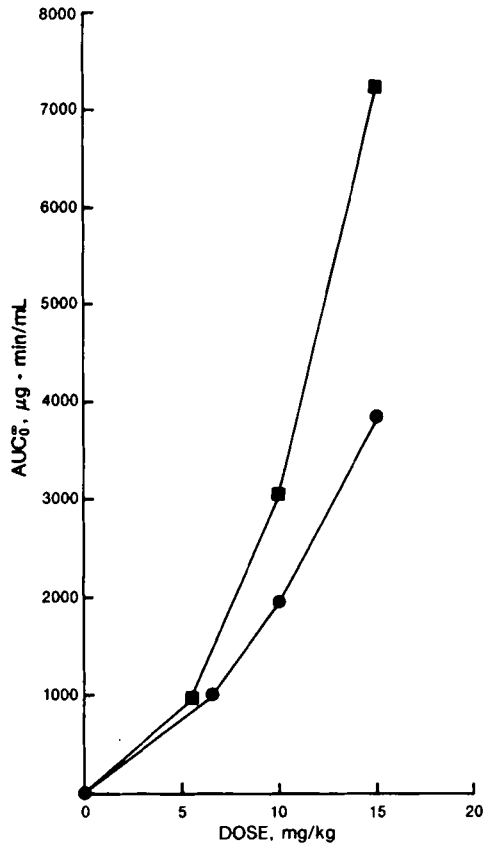

Figure 5—*Plot of the area under the plasma phenytoin concentration* versus *time curve, AUC_0^∞, as a function of the intravenous dose of sodium phenytoin administered to dog 20 (●) and dog 21 (■). Doses are in phenytoin equivalents.*

Table V—Apparent Bioavailability of Phenytoin after Intravenous Administration of Prodrugs II–IV [a]

Compound	F^{abs}_{app}, %[b] Dog 19	Dog 20	Dog 21	Dog 22
II	67	98	42	103
III	75	—[c]	—[d]	—[d]
IV	81	90	62	67

[a] Relative to Ia. [b] Calculated as $[AUC^{\infty}_{0,iv}$ (prodrug)$/AUC^{\infty}_{0,iv}$ (Ia)$] \times 100$. [c] Unable to administer complete dose due to excessive pain on administration. [d] Compound III was not administered.

Table VI—Apparent Bioavailability of Phenytoin after Oral Administration of Ia and II–IV [a]

Compound	F^{abs}_{app}, %[b] Dog 19	Dog 20	Dog 21	Dog 22
Ia	10	17	13	14
II	69	96	41	55
III	89	114	26	—[c]
IV	46	53	58	46

[a] Relative to intravenously administered Ia. [b] Calculated as $[AUC^{\infty}_{0,po}$ (Ia and prodrugs)$/AUC^{\infty}_{0,iv}$ (Ia)$] \times 100$. [c] Compound III was rejected by dog 22.

timated. This is apparent from the results summarized in Tables VIII and IX. The corrected bioavailabilities show that in dog 21, the apparent bioavailabilities are drastic underestimations. This is consistent with the larger change in the AUC^{∞}_{0} and the apparent elimination half-life of phenytoin with dose observed in dog 21 compared with the change observed in dog 20 (Table III),

Table VII—V_m, K_m, and the Apparent Volume of Distribution (Vd) Calculated from the Data Obtained after Intravenous Administration of Sodium Phenytoin

Parameters	Dose mg/kg[a] 15	10	5.5	Mean ± SD
		Dog 20		
K_m, μg/mL	25.3	15.9	7.9	16.4 ± 8.7
V_m, μg/mL/min	0.1	0.087	0.045	0.077 ± 0.03
Vd, L/kg[b]	1.15	1.15	1.28	1.19 ± 0.07
		Dog 21		
K_m, μg/mL	4.5	2.7	4.7	3.99 ± 1.1
V_m, μg/mL/min	0.016	0.016	0.02	0.018 ± 0.003
Vd, L/kg[b]	1.41	1.43	1.77	1.54 ± 0.20

[a] Doses are in phenytoin equivalents. [b] Volume of distribution extrapolated.

suggesting that dog 21 is more susceptible to enzyme saturation than is dog 20 (lower K_m value observed for dog 21).

The corrected bioavailability of both orally and intravenously administered II in dog 20 is ~100%; in dog 21, it is ~60%. This suggests that in dog 20, II undergoes quantitative hydrolysis to phenytoin and is completely absorbed from the GI tract. However, in dog 21, it seems that the complete oral dose of II may be absorbed from the GI tract, but the prodrug may not undergo quantitative conversion to phenytoin, *i.e.*, the ester may be undergoing a nonproductive metabolic pathway such as hydroxylation of the hydantoin phenyl ring followed then by the cleavage of the ester. This pathway may be

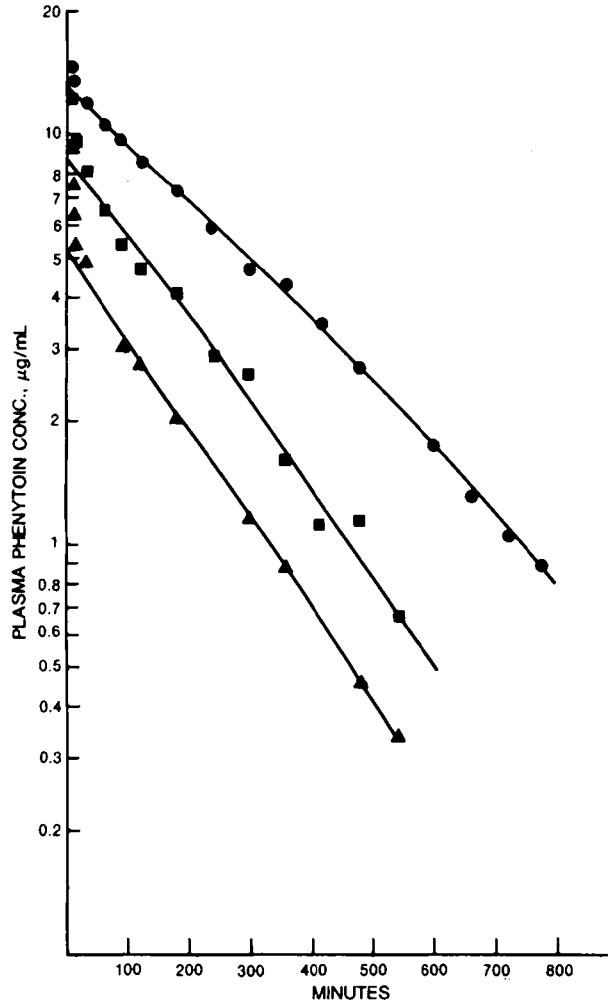

Figure 6—*Semilogarithmic plots of plasma phenytoin concentrations* versus *time following intravenous administration of 15 (●), 10 (■), and 6.6 (▲) mg/kg (phenytoin equivalents) of sodium phenytoin to dog 20; (—) computer-fitted lines.*

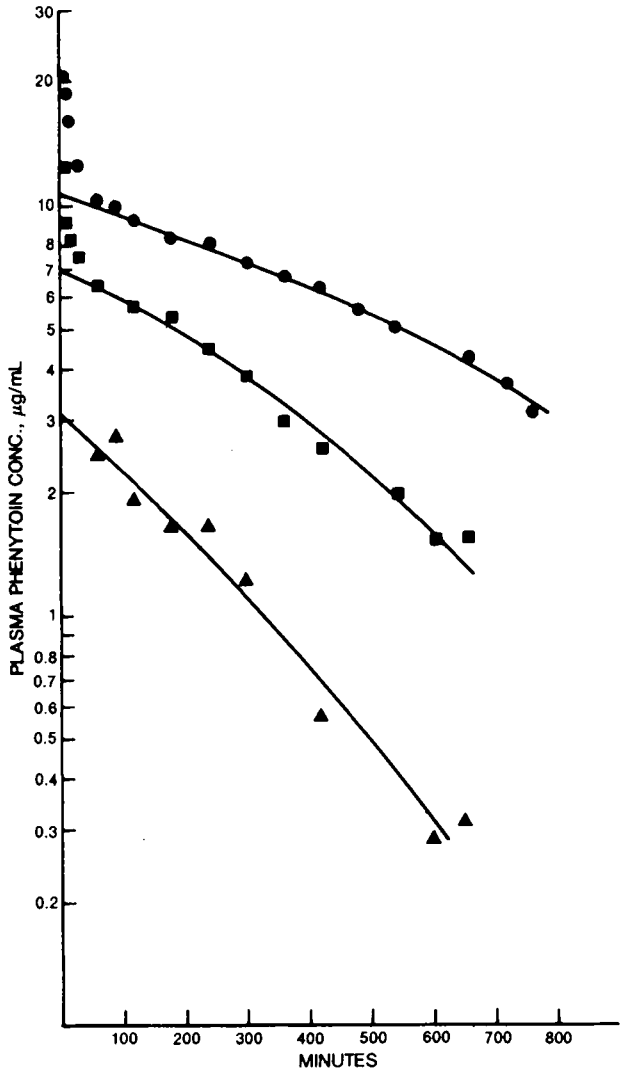

Figure 7—*Semilogarithmic plots of plasma phenytoin concentrations* versus *time following intravenous administration of 15 (●), 10 (■), and 5.5 (▲) mg/kg (phenytoin equivalents) of sodium phenytoin to dog 21; (—) computer-fitted lines.*

Table VIII—Calculation of the Corrected Bioavailability of Phenytoin [a] after Intravenous Administration of II and IV to Two Beagle Dogs

Compound	$\int_0^\infty \frac{V_m C}{K_m + C} dt$		F_{app}^{abs}, %[b]		Corrected F, %[c]	
	Dog 20	Dog 21	Dog 20	Dog 21	Dog 20	Dog 21
II	13.8	6.4	98	42	106	60.2
IV	12.8	10.1	90	62	98.7	95.3

[a] Corrected for enzyme saturation. [b] Calculated by $[AUC_{0,iv}^{\infty}$ (prodrug)$/AUC_{0,iv}^{\infty}$ (Ia)$] \times 100$. [c] Based on Eq. 11.

Table IX—Calculation of the Corrected Bioavailability of Phenytoin [a] after Oral Administration of Ia and II–IV to Two Beagle Dogs

Compound	$\int_0^\infty \frac{V_m C}{K_m + C} dt$		F_{app}^{abs}, %[b]		Corrected F, %[c]	
	Dog 20	Dog 21	Dog 20	Dog 21	Dog 20	Dog 21
Ia	2.5	2.3	17	13	19.5	21.9
II	16.3	6.8	96	41	125.4	64.1
III	16.1	4.5	1114	26	123.8	42.9
IV	8.2	9.2	53	58	63.2	86.8

[a] Corrected for enzyme saturation. [b] Calculated by $[AUC_{0,po}^{\infty}$ (Ia and prodrugs)$/AUC_{0,iv}^{\infty}$ (Ia)$] \times 100$. [c] Based on Eq. 11.

competing with the hydrolysis of the ester to phenytoin. Another possibility is that the esterase activity in dog 21 may be low. Prodrug III also seems to show a bioavailability of only ~45% in dog 21, whereas, in dog 20, the corrected bioavailability of III is ~100%.

The results in Table VIII suggest that IV is quantitatively hydrolyzed to phenytoin on intravenous dosing to dogs 20 and 21. However, the corrected bioavailability of IV on oral dosing in dogs 20 and 21 was ~65 and ~90%, respectively. This suggests that the ester may be incompletely absorbed from the GI tract, probably because of its polar nature.

In all the calculations and discussions to date, it was assumed that phenytoin does not exhibit presystemic clearance in the dog and that orally or intravenously administered prodrugs do not exhibit a sequential first-pass effect (44); *i.e.*, if the prodrugs are cleaved to phenytoin prior to reaching systemic circulation, then the formed phenytoin may be further metabolized prior to release to systemic circulation. For dogs 20 and 21, presaturation clearances could be calculated from:

$$CL = \frac{VdV_m}{K_m} \qquad \text{(Eq. 12)}$$

For dog 20, the approximate phenytoin clearance is 5.6 mL/min/kg, while for dog 21 a clearance of ~6.9 mL/min/kg is calculated. If it is assumed that phenytoin readily equilibrates between red blood cells and plasma, that the metabolism of phenytoin occurs only in the liver, and that liver blood flow in dogs is 40–45 mL/min/kg (45), then it can be estimated that phenytoin at presaturation doses may exhibit a first-pass effect of ~12–14% and 15–17% in dogs 20 and 21, respectively. Obviously, this is not sufficient to account for the poor oral performance of Ia, but it may account for the <100% availability of phenytoin from the prodrugs, even correcting for the nonlinear kinetics.

It can be concluded that II would be a better oral-delivery form of phenytoin than Ia. Compound III caused nausea, vomiting on oral dosing, and pain and hematoma on intravenous dosing. This would make it less favorable as a prodrug candidate for either oral or parenteral use. Compound II would probably be quantitatively hydrolyzed to phenytoin on oral administration to humans, since the esterase activity of the intestinal mucosa of dogs is poor relative to other mammalian species (46). Oral administration of II would help in overcoming the problem of low and erratic bioavailability of phenytoin associated with the oral administration of Ia.

The long shelf life of IV (30) and its high aqueous solubility at physiological pH (5) would render it useful as a parenteral dosage form for the delivery of phenytoin in humans, provided it is quantitatively hydrolyzed to phenytoin (as was observed in the dog). This would aid in overcoming the hazards associated with intravenous administration of sodium phenytoin.

REFERENCES

(1) P. A. Schwartz, C. T. Rhodes, and J. W. Cooper, Jr., *J. Pharm. Sci.*, **66,** 994 (1977).

(2) S. P. Agarwal and M. I. Blake, *J. Pharm. Sci.*, **57,** 1434 (1968).

(3) H. Bundgaard and M. Johansen, *Int. J. Pharm.*, **5,** 67 (1980).

(4) D. W. Newton and R. B. Kluza, *Am. J. Hosp. Pharm.*, **37,** 1647 (1980).

(5) S. A. Varia, S. Schuller, K. B. Sloan,and V. J. Stella, *J. Pharm. Sci.*, **73,** 1068 (1984).

(6) K. Arnold, N. Gerber, and G. Levy, *Can. J. Pharm. Sci.*, **5,** 89 (1970).

(7) C. Martin, M. Rubin, W. E. O'Malley, V. F. Garagusi, and C. E. McCauley, *Pharmacologist*, **10,** 167 (1968).

(8) L. Rail, *Med. J. Aust.*, **ii,** 339 (1968).

(9) T. Suzuki, Y. Saitoh, and K. Nishihara, *Chem. Pharm. Bull.*, **18,** 405 (1970).

(10) J. I. Manson, S. M. Beal, A. Magarey, A. C. Pollard, W. J. O'Reilly, and L. N. Sansom, *Med. J. Aust.*, **2,** 590 (1975).

(11) B. Rambeck, H.-E. Bochnick, and E. Stenzel, *Eur. J. Clin. Pharmacol.*, **12,** 285 (1977).

(12) P. J. Neuvonen, P. J. Pentikainen, and S. M. Elfving, *Int. J. Clin. Pharmacol.*, **15,** 84 (1977).

(13) P. J. Neuvonen, A. Bardy, and R. Lehtovaara, *Br. J. Clin. Pharmacol.*, **8,** 37 (1979).

(14) P. J. Pentikainin, P. J. Neuvonen, and S. M. Elfving, *Eur. J. Clin. Pharmacol.*, **9,** 213 (1975).

(15) M. J. Stewart, B. R. Ballinger, E. J. Devlin, A. Y. Miller, and A. C. Ramsay, *Eur. J. Clin. Pharmacol.*, **9,** 209 (1975).

(16) S. Sved, R. D. Hosie, I. J. McGilveray, N. Beaudoin, and R. Brien, *Can. J. Pharm. Sci.*, **14,** 67 (1979).

(17) L. Lund, *Eur. J. Clin. Pharmacol.*, **7,** 119 (1974).

(18) P. Tammisto, K. Kauko, and M. Villkari, *Lancet*, **i,** 254 (1976).

(19) J. G. Lagos, *J. Am. Med. Assoc.*, **5,** 726 (1972).

(20) D. F. Kowalczyk, *J. Vet. Pharmacol. Ther.*, **3,** 237 (1980).

(21) D. Shinkuma, T. Hamaguchi, C. Muro, F. Ohto, Y. Yamanaka, and N. Mizuno, *Int. J. Pharm.*, **9,** 17 (1981).

(22) S. Zoneraich, O. Zoneraich, and J. Siegel, *Am. Heart J.*, **91,** 375 (1976).

(23) A. J. Atkinson, Jr. and R. Davison, *Annu. Rev. Med.*, **25,** 99 (1974) and references therein.

(24) A. J. Wilensky and J. A. Lowden, *Neurology*, **23,** 318 (1973).

(25) H. B. Kostenbauder, R. D. Rapp, J. P. McGovren, T. S. Foster, D. G. Perrier, H. M. Blacker, W. C. Hulon, and A. W. Kinkel, *Clin. Pharmacol. Ther.*, **18,** 449 (1975).

(26) M. Dam and V. Olesen, *Neurology*, **16,** 288 (1966).

(27) B. J. Wilder, E. E. Serrano, E. Ramsey, and R. A. Buchanan, *Clin. Pharmacol. Ther.*, **16,** 507 (1974).

(28) P. L. Morselli and R. F. Morselli, *Pharmacol. Ther.*, **10,** 65 (1980).

(29) E. E. Serrano and B. J. Wilder, *Arch. Neurol.*, **31,** 276 (1974).

(30) S. A. Varia, S. Schuller, and V. J. Stella, *J. Pharm. Sci.*, **73,** 1074 (1984).

(31) J. C. K. Loo, I. J. McGilveray, N. Jordan, and R. Brien, *Biopharm. Drug Dispos.*, **2,** 265 (1981).

(32) V. J. Stella, *J. Pharm. Sci.*, **66,** 1510 (1977).

(33) M. Gibaldi and D. Perrier, "Pharmacokinetics," J. Swarbrick, Ed., Dekker, New York, N.Y., 1975, pp. 293–296.

(34) P. G. Dayton, S. A. Cucinell, M. Weiss, and J. M. Perel, *J. Pharmacol. Exp. Ther.*, **158,** 305 (1967).

(35) H. H. Frey and W. Loseher, *Am. J. Vet. Res.*, **41,** 1635 (1980).

(36) A. J. Atkinson, J. Macgee, J. Strong, D. Garteiz, and T. E. Gaffney, *Biochem. Pharmacol.*, **19,** 2483 (1970).

(37) N. Gerber and J. G. Wagner, *Res. Commun. Chem. Pathol. Pharmacol.*, **3,** 455 (1972).

(38) W. J. Jusko, J. R. Koup, and G. Alvain, *J. Pharmacokinet. Biopharm.*, **4,** 327 (1976).

(39) L. Martis and R. Levy, *J. Pharmacokinet. Biopharm.*, **1**, 283 (1973).
(40) C. H. Lawyer, N. Gerber, R. K. Lynn, and R. G. Dickinson, *Res. Commun., Chem. Pathol. Pharmcol.*, **27**, 469 (1980).
(41) D. Perrier, J. J. Ashley, and G. Levy, *J. Pharmacokinet. Biopharm.*, **1**, 231 (1973).
(42) J. E. Sander and R. A. Yeary, *J. Am. Vet. Med. Assoc.*, **172**, 153 (1978).
(43) K. Arnold and N. Gerber, *Clin. Pharmacol. Ther.*, **11**, 121 (1970).
(44) K. S. Pang and J. R. Gillette, *J. Pharmacokinet. Biopharm.*, **7**, 275 (1979).
(45) H. Boxenbaum, *J. Pharmacokinet. Biopharm.*, **8**, 165 (1980).
(46) M. Inoue, M. Morikawa, M. Tsuboi, and M. Sugiura, *Jpn. J. Pharmacol.*, **29**, 9 (1979).

ACKNOWLEDGMENTS

This paper was adapted in part from a dissertation submitted by S. A. Varia to The University of Kansas in partial fulfillment of the Doctor of Philosophy degree requirements. This work was supported in part by INTERx Research Corporation, a subsidiary of Merck Sharp and Dohme.

Phenytoin Prodrugs VI: *In Vivo* Evaluation of a Phosphate Ester Prodrug of Phenytoin after Parenteral Administration to Rats

S. A. VARIA * and V. J. STELLA ˣ

Received December 22, 1982, from the *Department of Pharmaceutical Chemistry, School of Pharmacy, The University of Kansas, Lawrence, Kansas 66045.* Accepted for publication September 6, 1983. *Present address: Squibb Institute for Medical Research, New Brunswick, NJ 08903.

Abstract □ Tissue damage caused by subcutaneous and intramuscular administration of three phenytoin prodrugs to rats was assessed. Since two of the prodrugs caused significant irritation, only 3-(hydroxymethyl)-5,5-diphenylhydantoin disodium phosphate ester might be useful as a nonirritant phenytoin prodrug suitable for parenteral administration. To confirm the release of phenytoin from this prodrug, phenytoin availability after intramuscular and intravenous administrations of the phosphate prodrug was evaluated in rats and compared with sodium phenytoin. The prodrug quantitatively released phenytoin after intravenous administration, and phenytoin levels from intramuscular administration of the prodrug were far superior to those generated from similarly administered sodium phenytoin. Based on this and earlier studies, it was concluded that this prodrug should be further assessed as a parenteral form of phenytoin.

Keyphrases □ Phenytoin—phosphate prodrug, parenteral administration, rats □ Prodrugs—phenytoin, phosphate ester, parenteral administration, rats □ Anticonvulsants—phenytoin, phosphate prodrug, parenteral administration, rats

The parenteral form of the anticonvulsant drug phenytoin (I), *i.e.*, sodium phenytoin (Ia) dissolved in a vehicle consisting of 40% propylene glycol and 10% alcohol at pH ~12, is hazardous if too rapidly injected intravenously (1, 2); intramuscular injection results in delayed release of phenytoin from the precipitated phenytoin acid at the injection site (3–8). We recently evaluated the potential usefulness of a series of phenytoin prodrugs (9–11). Based on those studies, II–IV were thought to be possible parenteral forms of phenytoin because of their superior solubility properties compared with phenytoin (9). In a dog study, these prodrugs quantitatively released phenytoin after intravenous injection (11), although III was observed to cause significant acute toxicity in the dog and II had only marginal chemical stability (10). It was concluded that IV would be the best candidate among prodrugs II–IV (11) for parenteral administration.

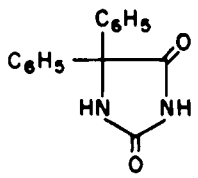

I

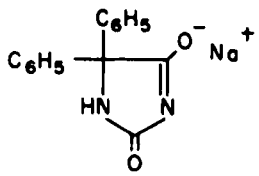

Ia

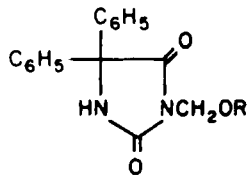

II: R = $-COCH_2\overset{+}{N}H(CH_3)_2\ CH_3SO_3^-$
III: R = $-CO_2(CH_2)_2\overset{+}{N}H(CH_3)_2\ CH_3SO_3^-$
IV: R = $-PO_3^{2-}\ Na_2^+$

Presented here are two further studies, designed to evaluate the possible utility of II–IV as parenteral forms of phenytoin. First, an evaluation of the tissue damage after subcutaneous and intramuscular injection of prodrugs II–IV to rats was initiated. Based on these findings (significant irritation seen with both II and III but not IV) a second study, the intravenous and intramuscular availability of phenytoin from IV in rats, was addressed. The results of the two studies are presented in this paper.

EXPERIMENTAL SECTION

Evaluation of the Tissue Damage Caused by Subcutaneous and Intramuscular Administration of II–IV—Male Sprague-Dawley rats[1], weighing between 250–275 g, were used; twelve rats were used for each ester studied. Fresh aqueous solutions of esters II–IV (9), 25 mg/kg (phenytoin equivalents), were prepared, and each of six groups of six rats received an ester injected intramuscularly in the thigh muscle or an ester injected subcutaneously under the thigh skin. The injection volume did not exceed 200 μL. After administration, the rats were placed in metabolism cages with access to food and water. At 24 h postdose, three rats administered drug intramuscularly and three rats administered drug subcutaneously for each ester were sacrificed, and the extent of tissue damage was evaluated. The extent of tissue damage in the remaining six rats was evaluated after 7 d postdose. Visual observations were made to determine the extent of tissue damage. The rats were observed externally to check for any skin damage after the subcutaneous injection. The animals were then checked for internal damage by exposing the thigh muscle (intramuscular administration) or the muscles underlying the skin at the injection site (subcutaneous injection).

***In Vivo* Evaluation of IV as a Prodrug of Phenytoin in Rats**—The availability of phenytoin after intramuscular administration of IV was studied in

[1] Harlan Sprague-Dawley, Madison, Wis.

0022-3549/84/0800-1087$01.00/0
© 1984, American Pharmaceutical Association

(39) L. Martis and R. Levy, *J. Pharmacokinet. Biopharm.*, **1**, 283 (1973).
(40) C. H. Lawyer, N. Gerber, R. K. Lynn, and R. G. Dickinson, *Res. Commun., Chem. Pathol. Pharmcol.*, **27**, 469 (1980).
(41) D. Perrier, J. J. Ashley, and G. Levy, *J. Pharmacokinet. Biopharm.*, **1**, 231 (1973).
(42) J. E. Sander and R. A. Yeary, *J. Am. Vet. Med. Assoc.*, **172**, 153 (1978).
(43) K. Arnold and N. Gerber, *Clin. Pharmacol. Ther.*, **11**, 121 (1970).
(44) K. S. Pang and J. R. Gillette, *J. Pharmacokinet. Biopharm.*, **7**, 275 (1979).
(45) H. Boxenbaum, *J. Pharmacokinet. Biopharm.*, **8**, 165 (1980).
(46) M. Inoue, M. Morikawa, M. Tsuboi, and M. Sugiura, *Jpn. J. Pharmacol.*, **29**, 9 (1979).

ACKNOWLEDGMENTS

This paper was adapted in part from a dissertation submitted by S. A. Varia to The University of Kansas in partial fulfillment of the Doctor of Philosophy degree requirements. This work was supported in part by INTERx Research Corporation, a subsidiary of Merck Sharp and Dohme.

Phenytoin Prodrugs VI: *In Vivo* Evaluation of a Phosphate Ester Prodrug of Phenytoin after Parenteral Administration to Rats

S. A. VARIA * and V. J. STELLA ˣ

Received December 22, 1982, from the *Department of Pharmaceutical Chemistry, School of Pharmacy, The University of Kansas, Lawrence, Kansas 66045.* Accepted for publication September 6, 1983. *Present address: Squibb Institute for Medical Research, New Brunswick, NJ 08903.

Abstract □ Tissue damage caused by subcutaneous and intramuscular administration of three phenytoin prodrugs to rats was assessed. Since two of the prodrugs caused significant irritation, only 3-(hydroxymethyl)-5,5-diphenylhydantoin disodium phosphate ester might be useful as a nonirritant phenytoin prodrug suitable for parenteral administration. To confirm the release of phenytoin from this prodrug, phenytoin availability after intramuscular and intravenous administrations of the phosphate prodrug was evaluated in rats and compared with sodium phenytoin. The prodrug quantitatively released phenytoin after intravenous administration, and phenytoin levels from intramuscular administration of the prodrug were far superior to those generated from similarly administered sodium phenytoin. Based on this and earlier studies, it was concluded that this prodrug should be further assessed as a parenteral form of phenytoin.

Keyphrases □ Phenytoin—phosphate prodrug, parenteral administration, rats □ Prodrugs—phenytoin, phosphate ester, parenteral administration, rats □ Anticonvulsants—phenytoin, phosphate prodrug, parenteral administration, rats

The parenteral form of the anticonvulsant drug phenytoin (I), *i.e.*, sodium phenytoin (Ia) dissolved in a vehicle consisting of 40% propylene glycol and 10% alcohol at pH ~12, is hazardous if too rapidly injected intravenously (1, 2); intramuscular injection results in delayed release of phenytoin from the precipitated phenytoin acid at the injection site (3–8). We recently evaluated the potential usefulness of a series of phenytoin prodrugs (9–11). Based on those studies, II–IV were thought to be possible parenteral forms of phenytoin because of their superior solubility properties compared with phenytoin (9). In a dog study, these prodrugs quantitatively released phenytoin after intravenous injection (11), although III was observed to cause significant acute toxicity in the dog and II had only marginal chemical stability (10). It was concluded that IV would be the best candidate among prodrugs II–IV (11) for parenteral administration.

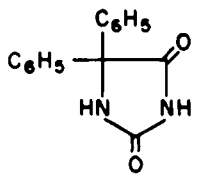

I

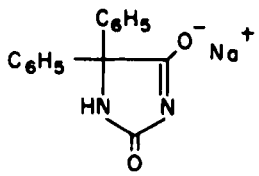

Ia

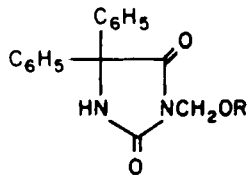

II: R = $-COCH_2\overset{+}{N}H(CH_3)_2\ CH_3SO_3^-$
III: R = $-CO_2(CH_2)_2\overset{+}{N}H(CH_3)_2\ CH_3SO_3^-$
IV: R = $-PO_3^{2-}\ Na_2^+$

Presented here are two further studies, designed to evaluate the possible utility of II–IV as parenteral forms of phenytoin. First, an evaluation of the tissue damage after subcutaneous and intramuscular injection of prodrugs II–IV to rats was initiated. Based on these findings (significant irritation seen with both II and III but not IV) a second study, the intravenous and intramuscular availability of phenytoin from IV in rats, was addressed. The results of the two studies are presented in this paper.

EXPERIMENTAL SECTION

Evaluation of the Tissue Damage Caused by Subcutaneous and Intramuscular Administration of II–IV—Male Sprague-Dawley rats[1], weighing between 250–275 g, were used; twelve rats were used for each ester studied. Fresh aqueous solutions of esters II–IV (9), 25 mg/kg (phenytoin equivalents), were prepared, and each of six groups of six rats received an ester injected intramuscularly in the thigh muscle or an ester injected subcutaneously under the thigh skin. The injection volume did not exceed 200 μL. After administration, the rats were placed in metabolism cages with access to food and water. At 24 h postdose, three rats administered drug intramuscularly and three rats administered drug subcutaneously for each ester were sacrificed, and the extent of tissue damage was evaluated. The extent of tissue damage in the remaining six rats was evaluated after 7 d postdose. Visual observations were made to determine the extent of tissue damage. The rats were observed externally to check for any skin damage after the subcutaneous injection. The animals were then checked for internal damage by exposing the thigh muscle (intramuscular administration) or the muscles underlying the skin at the injection site (subcutaneous injection).

***In Vivo* Evaluation of IV as a Prodrug of Phenytoin in Rats**—The availability of phenytoin after intramuscular administration of IV was studied in

[1] Harlan Sprague-Dawley, Madison, Wis.

0022-3549/84/0800-1087$01.00/0
© 1984, American Pharmaceutical Association

Table I—Extent of Tissue Damage[a] Observed at the End of 1 and 7 d after Subcutaneous and Intramuscular Injections of II–IV to Rats[a]

Compound	Observations after Subcutaneous Administration	Observations after Intramuscular Administration
II	Externally, a white patch at the injection site Severe tissue damage and necrosis of the skin	Slight necrosis with inflammation at site of injection
III	Build up of scar tissue and severe skin necrosis	Inflammation at injection site
IV[a]	No visible damage	No visible damage

[a] Doses were 25 mg/kg (phenytoin equivalents). [b] It is realized that more elaborate studies including histopathology would be needed if considerations were given to testing IV clinically. However, these clear-cut findings probably eliminate further evaluation of II and III clinically.

the rat model. Specifically, three different types of crossover studies were carried out on male Sprague–Dawley rats in an effort to evaluate the quantitative nature of the conversion of IV to phenytoin after intravenous and intramuscular dosing. The crossover studies comprised of: (*a*) three rats which received phenytoin-equivalent doses of 7 mg/kg im of IV[2] and 10 mg/kg im of sodium phenytoin; (*b*) three rats which received 7 mg/kg im of IV[2] and 10 mg/kg iv of sodium phenytoin, and a second group of three rats which received 10 mg/kg im of IV and 10 mg/kg iv of sodium phenytoin; and (c) two rats which received 10 mg/kg iv of IV and 10 mg/kg iv of sodium phenytoin. The rats weighed between 250–300 g. Each rat was used for only one crossover study, at the end of which it was sacrificed. The rats were rested for at least 1 week between doses and were fed standard laboratory diet and water *ad libitum*.

Prior to a study, the rats were weighed and anesthetized with 60 mg/kg ip of sodium pentobarbital. The animals were kept on a heated surgical table (38°C) to maintain their normal body temperature. The rats were kept unconscious throughout the experiment by administering smaller doses of sodium pentobarbital (30 mg/kg) whenever the animal showed signs of regaining consciousness.

The jugular vein was exposed by means of a small incision on the ventral side of the neck region. The right jugular vein was used to administer aqueous solutions of IV and also to obtain blood samples at various time intervals. At the end of the experiment the area of incision was cleaned with ethanol, and the incision was closed using a nonabsorbable, sterile, surgical silk suture[3].

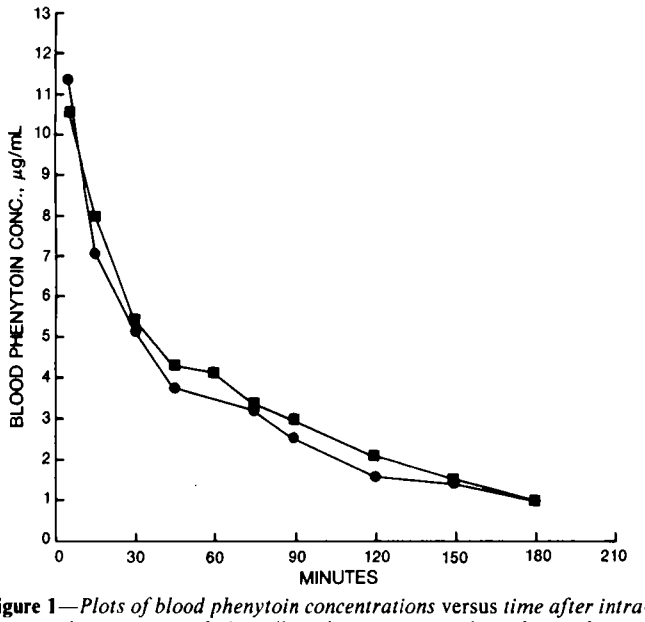

Figure 1—*Plots of blood phenytoin concentrations* versus *time after intravenous administration of 10-mg/kg (phenytoin equivalent) doses of Ia (●) and IV (■) to the same rat.*

[2] After having carried out these two partial studies, it was found that one particular batch of IV (prepared just before this *in vivo* study) was only 70% pure as confirmed by GC and TLC (9). The impurity was determined to be inorganic in nature. Hence, instead of administering 10 mg/kg (phenytoin equivalents) of IV, rats in study a and the first study b received a 7-mg/kg (phenytoin equivalent) dose of IV. This was the only batch of IV that was so contaminated. Earlier batches reported (9–11) were pure.

[3] Sutupak, SA-63H; Etgicon, Inc., Somerville, N.J.

Table II—Area under the Blood Phenytoin Concentration *versus* Time Curves for Ia and IV after Intramuscular Administration of 10 and 7 mg/kg[a]

Compound	AUC_0^{210}, μg·min/mL[b] Rat 1	Rat 2	Rat 3	Mean ± *SD*
Ia	30	189	75	97.8 ± 82.0
IV	348	343	329	339.8 ± 9.7

[a] Doses expressed as phenytoin equivalents. [b] Calculated *via* the trapezoidal method.

The rats were then placed in metabolism cages with access to food and water.

Administration of sodium phenytoin intravenously and intramuscularly leads to precipitation of phenytoin at the injection site. If blood samples were obtained after intravenous administration of sodium phenytoin from the same vein where sodium phenytoin had been administered, it may show erroneous blood levels of the drug. To overcome this problem, sodium phenytoin was administered intravenously through the exposed femoral vein and blood samples were obtained from the left jugular vein.

The various routes of administration of sodium phenytoin and IV were as follows.

1. For IV, fresh aqueous solutions were intravenously administered into the right jugular vein, with blood samples from the same vein; intramuscular administration was into the thigh muscle, with blood sampling also from the right jugular vein.

2. For sodium phenytoin, the drug was dissolved in a solvent of propylene glycol–alcohol–water (4:1:5) with the pH adjusted to 11.5–12 with sodium hydroxide. This was administered intravenously into a femoral vein, and blood was sampled from the left jugular vein. Intramuscular administration was into the thigh muscle, with blood sampling also from the left jugular vein. The volume administered did not exceed 250 μL. Intravenous injections of sodium phenytoin and IV were infused slowly over a 1-min period.

Blood samples obtained from the jugular vein were transferred to containers[4] containing 3 mg of EDTA and were immersed in an ice bath. A measured quantity (usually 100–200 μL) of blood was extracted into 2 mL of toluene containing the internal standard. The GC procedure described earlier (12) for the determination of phenytoin was then followed. No effort was made to determine the presence of the prodrug, as earlier studies had indicated rapid conversion of IV to phenytoin in rat tissues (9).

RESULTS AND DISCUSSION

Compound IV has been shown to have physicochemical properties that are ideal for a prodrug of phenytoin for parenteral use (9–11). Although prodrugs II and III had been projected as possible oral delivery forms of phenytoin (9, 10), they may also be potentially useful parenteral prodrugs.

Emergency use of parenteral phenytoin, *e.g.*, in cases of controlling seizures in patients with head injuries, may require the administration of the prodrug intramuscularly. A study was undertaken, therefore, to qualitatively assess the extent of the localized tissue damage caused by prodrugs II–IV after intramuscular and subcutaneous administration to rats.

To be clinically acceptable, intramuscular administration of a drug should cause minimal tissue damage at the injection site. Intramuscular administration of sodium phenytoin has been reported to be painful, probably due to the precipitation of phenytoin (7). It has also been shown to cause hemorrhage, hematoma, and necrosis at the injection site in cats and rabbits (3, 8).

Table I summarizes the extent of tissue damage observed after subcutaneous and intramuscular administration of II–IV to rats. There were only some minor qualitative differences between the 1- and 7-d observations; the results were, therefore, summarized together. Esters II and III cause tissue damage after subcutaneous as well as intramuscular administration. The tissue damage may have been caused by the ester or the products formed on hydrolysis of the ester. Recently, Adachi *et al.* (13) have shown that aged solutions of cephalothin caused pain when administered intraperitoneally to mice, which was attributed to the acetic acid produced on hydrolysis of cephalothin. The possibility of irritation and tissue damage caused by the acids produced on hydrolysis of the esters cannot be ruled out. Another possibility for the cause of the tissue damage was the methanesulfonate anion of II and III. Administration of the hydrochloride salt of 3-(hydroxymethyl)-5,5-diphenylhydantoin *N*,*N*-dimethylglycine ester was found to cause tissue damage comparable to that caused by II[5]. Many parenteral dosage forms of amine drugs for intramuscular use are administered as their hydrochloride salts and have

[4] Vacutainers, No. 6496; Becton, Dickinson and Co., Rutherford, N.J.

[5] The hydrochloride salt was not extensively evaluated with respect to its physicochemical properties because of its hygroscopic properties. It was prepared in a small quantity specifically for this test.

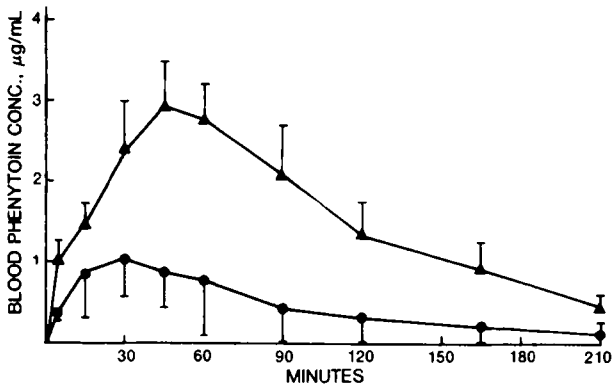

Figure 2—*Blood concentrations of phenytoin in rats* (n = 3) *following intramuscular administration of Ia* (●) *and IV* (▲). *Doses (phenytoin equivalents) were 10 mg/kg of Ia and 7 mg/kg of IV; Bars represent* SD.

not been reported to cause any specific tissue damage due to the choice of the hydrochloride salt. Thus, it seems that the counter anion of II and III does not cause the observed tissue damage.

Ester IV did not exhibit any tissue damage after subcutaneous or intramuscular administration. Thus, IV could be a suitable prodrug candidate for intramuscular delivery of phenytoin, providing that the ester is well absorbed from the site of injection and is quantitatively converted to phenytoin *in vivo*.

The bioavailability of phenytoin after intramuscular and intravenous injections of IV to rats was studied. The specific aims of this study were to (*a*) determine whether IV was quantitatively converted to phenytoin *in vivo* after its intravenous administration, (*b*) compare the levels of phenytoin obtained after intramuscular administration of IV with those obtained after intramuscular administration of sodium phenytoin (Ia), and (*c*) determine the absolute bioavailability of IV after intramuscular administration. All the studies carried out in rats were crossover studies, as described in the *Experimental Section*. Crossover studies were used instead of a single treatment per rat in order to minimize the effects of differences in the elimination half-lives of phenytoin due to variations in the extent of protein binding of phenytoin among rats (14).

Gerber *et al.* (15), Ashley and Levy (16, 17) and Vicuna *et al.* (18) have shown that phenytoin displays dose-dependent or nonlinear kinetics in rats. The apparent half-lives of phenytoin after intravenous administrations of 10-, 25-, and 40-mg/kg doses of phenytoin to rats increased from 0.6 to 1.2 to 2.5 h, respectively (15). There is considerable controversy as to whether the dose dependency exhibited by phenytoin in rats is due to saturation of the enzyme system responsible for metabolism of phenytoin to 5-(*p*-hydroxyphenyl)-5-phenylhydantoin (*p*-HPPH) or to product inhibition in which *p*-HPPH can have an inhibitory effect on the biotransformation of phenytoin. However, it has been reported by a number of workers (15-18) that the pharmacokinetics of phenytoin approaches linear elimination kinetics in rats after a 10-mg/kg iv dose of phenytoin. Thus, for the present study, doses of 10 mg/kg (administration equivalent) of IV and Ia were used, and the data was evaluated assuming linear phenytoin elimination kinetics.

To determine whether IV reverted quantitatively to phenytoin *in vivo*, a crossover study in which each rat received either a 10-mg/kg (phenytoin equivalent) dose of IV or a 10-mg/kg (phenytoin equivalent) dose of Ia intravenously was undertaken. Figure 1 is a linear plot of blood phenytoin concentrations as a function of time in one rat after intravenous administrations of Ia and IV. Semilogarithmic plots of blood phenytoin *versus* time after intravenous administrations of IV and Ia showed that phenytoin exhibited two-compartmental pharmacokinetics in the rat, which is consistent with the results obtained by other workers (14, 16, 17). Compound IV produced plasma phenytoin levels similar to those obtained after the intravenous administration of an equivalent dose of Ia. The percentage ratios of the areas under the plasma concentration *versus* time profiles from 0 to 180 min after intravenous administrations of IV and Ia were 109.7 and 91.2% in the two rats studied. This suggests that IV was completely hydrolyzed to phenytoin in these rats.

The evaluation of IV as an intramuscular form for the delivery of phenytoin required the determination of blood levels of phenytoin after intramuscular administration of the prodrug and Ia. Figure 2 shows a plot of the mean blood concentrations of phenytoin *versus* time obtained after intramuscular administrations of IV and Ia at doses of 7 and 10 mg/kg (phenytoin equivalents), respectively, to three rats. Table II summarizes the area under the blood phenytoin concentration *versus* time curves from 0 to 210 min obtained in each rat after intramuscular administrations of IV and Ia. Statistical analysis of the mean phenytoin blood level data using the paired *t* test showed that the

Table III—Area under the Blood Phenytoin Concentration *versus* Time Curve Obtained in Rats after Administration of IV Intramuscularly and Ia Intravenously [a]

Rat	Intramuscular Administered IV AUC_0^∞, μg·min/mL[b]	Intravenous Administered Ia AUC_0^∞, μg·min/mL[c]	F[d]
4	522	723	1.0
5	527	786	1.0
6	330	578	0.8
7	837	763	1.1
8	2209	2695	0.8
9	552	467	1.2

[a] Rats 4-6 received 7 mg/kg of IV intramuscularly; rats 7-9 received 10 mg/kg of IV intramuscularly. Compound Ia was administered at a dose of 10 mg/kg. All doses were phenytoin equivalents. [b] AUC_0^∞ was calculated using the trapezoidal method. [c] AUC_0^∞ was calculated using $(A/\alpha) + (B/\beta)$. [d] Calculated by AUC_0^∞/Dose (intramuscular) ÷ AUC_0^∞/Dose (intravenous).

blood levels of phenytoin at 5, 30, 45, and 60 min after intramuscular administrations of IV and Ia were significantly different ($p < 0.05$). The one-way ANOVA showed the mean area under the blood phenytoin concentration *versus* time curve from 0 to 210 min was significantly different ($p < 0.01$).

To determine the absolute bioavailability of intramuscularly administered IV, a crossover study was initiated in which the rats received an intramuscular injection of IV followed 1 week later by an intravenous dose of Ia. The same order of administration of IV and Ia was maintained in all the rats (see *Experimental Section* for explanation). The results are reported in two groups of three rats each. The first group of rats received 7 mg/kg (phenytoin equivalents) of IV intramuscularly and the second group of rats received 10 mg/kg (phenytoin equivalents) of IV. The division into two groups occurred as the first group was administered an impure batch of IV[2]; *i.e.*, the ester was only 70% pure, with the other 30% of the dose as inorganic impurities. Thus, instead of administering a 10-mg/kg (phenytoin equivalent) dose of IV, the rats in group 1 were inadvertently administered a 7-mg/kg (phenytoin equivalent) dose of IV. Both the groups received 10-mg/kg (phenytoin equivalent) dose of Ia intravenously. The blood phenytoin concentration *versus* time profiles for a rat in group 2 is shown in Fig. 3. Table III summarizes the areas under the blood phenytoin concentration *versus* time curves (AUC_0^∞) obtained after intramuscular injection of IV, calculated using the trapezoidal method (19). The blood phenytoin concentration (C) *versus* time profile after intravenous administration of Ia was computer-fitted to Eq. 1 using the AUTOAN-NONLIN library program (20, 21):

$$C = Ae^{-\alpha t} + Be^{-\beta} \qquad \text{(Eq. 1)}$$

Equation 1 describes a two-compartment open model. The parameters A, α, B, and β were then used to calculate AUC_0^∞ using:

$$AUC_0^\infty = \frac{A}{\alpha} + \frac{B}{\beta} \qquad \text{(Eq. 2)}$$

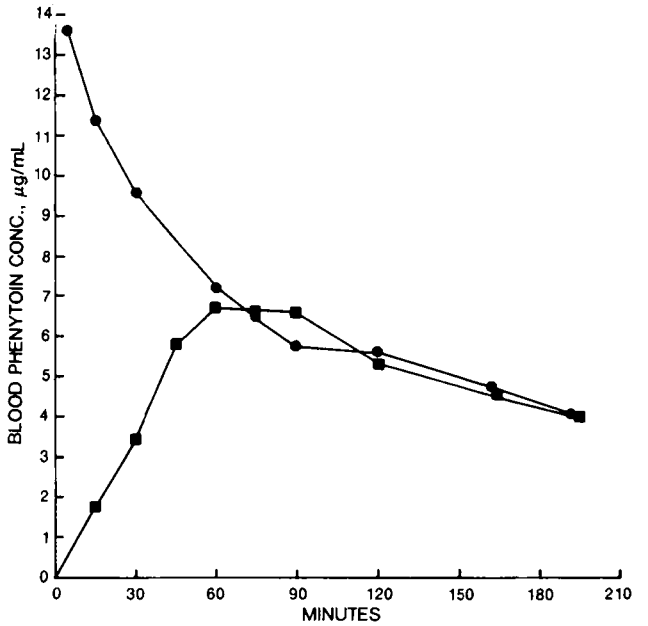

Figure 3—*Plots of the blood phenytoin concentrations* versus *time following administration of 10-mg/kg doses of IV intramuscularly* (■) *and of Ia intravenously* (●) *to rat 8. Doses are in phenytoin equivalents.*

The absolute bioavailability was determined by dividing the AUC_0^∞ values obtained after intramuscular administration of IV by those obtained after intravenous administration of Ia, corrected for dose.

Compound IV was rapidly and quantitatively hydrolyzed following intravenous administration to rats, producing blood levels of phenytoin similar to those obtained after intravenous administration of an equivalent dose of Ia. This is consistent with the rapid and quantitative hydrolysis of IV observed in an *in vitro* rat liver homogenate study (9). Thus, IV must be metabolized catalytically by phosphatase enzymes at a rate faster than the rate at which the ester would be eliminated by other mechanisms. Intramuscular administration of IV showed a higher area under the blood phenytoin concentration *versus* time profile compared with that obtained after intramuscular administration of Ia. The large standard deviation in the AUC_0^{240} value observed after intramuscular administration of Ia reflects the erratic and unpredictable absorption of phenytoin from Ia. This has been attributed to the precipitation of phenytoin at the site of injection. It has been shown that the intramuscular administration of Ia is much less effective, and doses of ~2–3 times higher than the oral dose may be necessary to achieve comparable plasma concentrations on single dose administration (5, 6). Intramuscular administration of IV produced higher blood phenytoin levels, which peaked within 45–60 min; this showed that IV was rapidly cleared from the site of injection. The mean absolute bioavailability of intramuscular administered ester IV was determined, assuming linear pharmacokinetics, to be 98.4%. This suggested that the administered dose of IV was completely absorbed from the site and was quantitatively converted to phenytoin *in vivo*. This is consistent with the quantitative conversion of IV observed after intravenous administration of this prodrug.

Based on rat data presented in this paper, earlier physicochemical studies (9, 10), and an *in vivo* evaluation in dogs (11), it can be concluded that IV would be an ideal prodrug for the parenteral delivery of phenytoin provided it is quantitatively hydrolyzed to phenytoin in humans. Compound IV could be administered intravenously or intramuscularly as an aqueous solution in emergency cases to control seizures. The use of IV as a parenteral delivery form would overcome the problems of precipitation of phenytoin associated with intravenous and intramuscular administration (3, 4, 8) of sodium phenytoin (Ia). It should also be free of the toxic cardiac effects seen after rapid intravenous injections of sodium phenytoin and the tissue damage reported to occur after intramuscular administration of sodium phenytoin.

REFERENCES

(1) S. Zoneraich, O. Zoneraich, and J. Siegel, *Am. Heart J.*, **91,** 375 (1976).

(2) A. J. Atkinson, Jr. and R. Davison, *Ann. Rev. Med.*, **25,** 99 (1974) and references therein.

(3) A. J. Wilensky and J. A. Lowden, *Neurology*, **23,** 318 (1973).

(4) H. B. Kostenbauder, R. D. Rapp, J. P. McGovren, T. S. Foster, D. G. Perrier, H. M. Blacker, W. C. Hulon, and A. W. Kinkel, *Clin. Pharmacol. Ther.*, **18,** 449 (1975).

(5) M. Dam and V. Olesen, *Neurology*, **16,** 288 (1966).

(6) B. J. Wilder, E. E. Serrano, E. Ramsey, and R. A. Buchanan, *Clin. Pharmacol. Ther.*, **16,** 507 (1974).

(7) P. L. Morselli and R. F. Morselli, *Pharm. Ther.*, **10,** 65 (1980).

(8) E. E. Serrano and B. J. Wilder, *Arch. Neurol.*, **31,** 276 (1974).

(9) S. A. Varia, S. Schuller, K. B. Sloan and V. J. Stella, *J. Pharm. Sci.*, **73,** 1068 (1984).

(10) S. A. Varia, S. Schuller and V. J. Stella, *J. Pharm. Sci.*, **73,** 1074 (1984).

(11) S. A. Varia and V. J. Stella, *J. Pharm. Sci.*, **73,** 1080 (1984).

(12) V. J. Stella, *J. Pharm. Sci.*, **66,** 1510 (1977).

(13) Y. Adachi, C. Nakamura, N. Yohkoh, M. Ikeda, A. Kato, and K. Shimada, *Yakagaku Zasshi*, **100,** 1104 (1980).

(14) W. A. Colburn and M. Gibaldi, *J. Pharmacol. Exp. Ther.*, **203,** 500 (1977).

(15) N. Gerber, W. L. Weller, R. Lynn, R. E. Rangno, B. J. Sweetman, and M. T. Bush, *J. Pharmacol. Exp. Ther.*, **178,** 567 (1971).

(16) J. Ashley and G. Levy, *J. Pharmacokinet. Biopharm.*, **1,** 99 (1973).

(17) J. Ashley and G. Levy, *Res. Commun. Chem. Pathol. Pharmacol.*, **4,** 297 (1972).

(18) A. Vicuna, D. Lacka, P. duSouich, N. Vicuna, T. M. Ludden, and M. J. McLean, *Res. Commun. Chem. Pathol. Pharmacol.*, **28,** 3 (1980).

(19) M. Gibaldi and D. Perrier, "Pharmacokinetics," J. Swarbrick, Ed., Dekker, New York, N.Y., 1975, pp. 293–296.

(20) A. J. Sedman and J. G. Wagner, "Autoan Manual," distributed by J. G. Wagner, Upjohn Center for Clinical Pharmacology, University of Michigan Medical Center, Ann Arbor, Mich.

(21) C. M. Metzler, G. L. Elfring, and A. J. McEwen, "A Users Manual for Nonlin Associated Programs," Red. Ed., The Upjohn Co., Kalamazoo, Mich., 1976.

ACKNOWLEDGMENTS

This paper was adapted in part from a dissertation submitted by S. A. Varia to The University of Kansas in partial fulfillment of the Doctor of Philosophy degree requirements. This work was supported in part by $INTER_x$ Research Corporation, a subsidiary of Merck Sharp and Dohme.

Labeling Suspended Aerosol Particles with Short-Lived Radionuclides for Determination of Particle Deposition

MARY FAYE SMITH ‡, SHELLEY BRYANT §, SIMON WELCH *§, and GEORGE A. DIGENIS *x

Received February 10, 1983, from the *Division of Medicinal Chemistry and Pharmacognosy, College of Pharmacy, University of Kentucky, Lexington, KY 40536-0053, ‡Pharmaceutical Research and Development Laboratories, Burroughs Wellcome Co., Greenville, NC 27834, and §Lederle Laboratories, Pearl River, NY 10965. Accepted for publication July 29, 1983.

Abstract □ Radiotracer techniques were developed to examine parameters that characterize pressurized aerosols designed to deliver insoluble particles suspended in the aerosol formulation. Microaggregated bovine serum albumin microspheres that were to be suspended were labeled with iodine-131 ($t_{1/2}$ = 8 d). This iodination procedure (>80% effective) is also applicable to iodine-123, which possesses superior characteristics for external imaging and further *in vivo* studies. This report shows that for pressurized aerosols containing suspended particles, each metered dose is approximately equal (not including the priming doses and the emptying doses). Increase in the delivery of the albumin particles out of the canister was best achieved by pretreating the valve assembly with a solution of 2% (w/v) bovine serum albumin in phosphate buffer. Use of a cascade impactor delineated the particle size distribution of the microspheres, with the majority of particles ranging in size from 2 to 8 μm. The data disclosed here indicate that the techniques developed with short-lived radionuclides can be used to (*a*) quantitate each metered dose, (*b*) characterize the particle size distribution profile of the aerosol contents, and (*c*) determine the extent of deposition of the particles in the aerosol canister and all of its components.

Keyphrases □ Radionuclides—short-lived, determination of particle deposition □ Aerosol particles—labeling with short-lived radionuclides, determination of particle deposition □ Particle deposition—determination with short-lived radionuclide labeling, suspended aerosol particles

In recent years, several reports have appeared that deal with the deposition of aerosols in the lungs of rats (1) and humans (2). Previous studies in this area have utilized liquid droplets delivered from nebulizers (3) and liquid droplets or solid particles delivered from pressurized aerosols (2, 4). Various equipment has also been developed for use in the determination of radioactive aerosol retention in the lungs of rabbits (5), as well as in studies designed to observe increased whole lung deposition of particles (6). Studies have also been performed to improve the deposition of aerosols in the lungs by controlling the breathing pattern of the patient (6). Oral adaptor extension devices have been shown to decrease the delivery of an aerosol to the oropharyngeal area (7). These devices are important not only because aerosols are used for site-specific drug delivery (2, 4), but also because the sizes of the aerosolized particles determine their distribution in the respiratory tract (2, 3).

Consequently, some studies have been performed to ascertain the amount of a compound, whether it is a solid or a liquid, that has actually been released in any individual metered dose. Several experimental techniques have been used for these determinations. In one study, weighing of a pressurized aerosol container before and after a designated number of actuations to measure the reproducibility of metered doses from a random sampling of the manufactured canisters has been reported (8). Davies *et al.* (9) have reported that there is great reproducibility and uniformity of delivery in random samples of manufactured pressurized aerosols. Those studies were performed on aerosols in a particle-size analyzer which is dependent on light-scattering techniques. In another study, the measured volume of propellant containing a known amount of particulate matter per dose has been reported (2). In yet another report, the size distribution of particles in commercially available cosmetic aerosols were delineated by microscopy, cascade impaction, and single-particle aerodynamic relaxation time analysis (10). Each of these are reliable accounts, but better quantitation can be achieved with short-lived radionuclides.

The most reliable method for the determination of reproducibility of all delivered doses from any given aerosol at any time, as well as the distribution of the size of particles released and the deposition of the compound in an aerosol canister, is by radioactive tracer methodology. Utilization of short-lived radionuclides in the assessment of quantitation techniques of aerosol particles has been reported in the past. For some time, the incorporation of a radioactive tag has been the major hindrance, due to the techniques needed for tagging the aerosol particle to be studied. Garrard *et al.* (11) have used ^{99m}Tc-labeled Fe_2O_3 colloid in experimentation, whereas Moren (4), Newman *et al.* (2), and Agnew *et al.* (12) have utilized technetium-99m incorporated into synthetic polymer particles. Isawa *et al.* (13) have published results of an aerosol study in which ^{99m}Tc-labeled serum albumin aerosols were scrutinized, although the tagging technique was not disclosed.

In this study, bovine microaggregated serum albumin microspheres labeled with iodine-131 were utilized as the suspended particles of the aerosol formulation. The chemical procedure developed for the labeling of the microspheres with iodine-131 is applicable to iodine-123, which possesses superior characteristics for external imaging (14). Unlike the previously studied synthetic particles (2, 4, 12), the iodinated albumin microspheres, which are currently used in nuclear medicine, can be degraded by the body and, therefore, are available for *in vivo* experimentation.

This report describes techniques which show how short-lived radionuclides can be used in (*a*) quantitation of each metered dose, (*b*) characterization of particle size distribution by the aerosol, and (*c*) determination of the extent of deposition of the particles in the canister and all of its components.

EXPERIMENTAL SECTION

Iodination of Microaggregated Albumin Microspheres—The prepared microaggregated albumin microspheres[1] were first washed with phosphate buffer (pH 8.0) for use in the subsequent experiments. The microspheres were mixed in a mixer[2] and then centrifuged in a tabletop centrifuge[3]. The supernatant was removed, and the microspheres were resuspended in the phosphate buffer. The washing process was repeated a total of five times. To determine the weight of the microspheres, a representative sample was obtained, allowed to dry, and then weighed. The weight of microspheres per volume of solution was then determined and recorded.

The microspheres suspended in the phosphate buffer were then transferred

[1] Microaggregated albumin microspheres (diameter, 3-8 μm) were suspended in a 2% Tween 80 solution in ethanol; Lederle Laboratories, Division of American Cyanamid Co., Pearl River, N.Y.

[2] Super Mixer, model 4722; Cole Parmer, Chicago, Ill.

[3] Clinical tabletop centrifuge; IEC Co., Needham Heights, Mass.

0022-3549/84/0800-1091$01.00/0
© 1984, American Pharmaceutical Association

Table I—Determination of the Metered Doses Actuated from an Aerosol Canister as a Function of Number of the Actuation

Actuation[a]	Total Recovered Activity[b], % of dose		
	Experiment 1	Experiment 2	Experiment 3
1	1.05		0.04
2	2.04	4.12	2.69
3	4.49	5.24	3.10
4	4.50	4.72	12.40
5	6.83	8.29	5.22
6	5.93	3.48	2.84
7	6.11	2.51	6.29
8	6.23	2.38	6.00
9	7.06	7.41	5.15
10	6.07	2.78	6.25
11	8.63	4.08	4.77
12	4.07	5.71	2.89
13	8.40	7.40	4.66
14	4.35	4.21	6.39
15	7.08	3.22	4.56
16	8.13	3.34	8.85
17	4.59	0.91	4.76
18	1.28	2.62	4.02
19	2.10	1.99	1.04

[a] A canister was filled with propellant and ^{131}I-labeled microaggregated albumin microspheres and crimped. After temperature equilibration, the canister was emptied by releasing the contents, actuation by actuation, into appropriately labeled scintillation vials. [b] Values listed are percentages of each dose to the total activity recovered in all the actuations from each of three aerosol canisters.

to a 1.0-mL glass vial with a magnetic spin-vane stirrer[4] and capped with a plastic cap containing a multiple-delivery rubber septum. The radionuclide was introduced into the closed system, and then *N*-chloro-4-methylbenzenesulfonamide sodium salt[5] (5 mg dissolved in 0.5 mL of buffer solution) was added such that the total concentration was 1–10 μg of microspheres. The reaction was stirred continuously for 5 min on a magnetic stirrer[6], and then sodium metabisulfite[7] in buffer solution (10 mg/0.25 mL) was added, so that the final ratio was 5 μg of sodium metabisulfite[7] to 10 μg of microspheres. The contents of the vial[4] were mixed for an additional 5 min and then transferred quantitatively to a conical centrifuge tube by repeated washings of the vial[4] with the phosphate buffer. The sample was then centrifuged for 8 min, the supernatant was removed, and the labeled microspheres were washed two more times with fresh phosphate buffer.

To determine the efficiency of iodination of the microspheres, two test methods were used. In the first method, the iodinated microspheres were precipitated with 20% trichloroacetic acid[8] and then centrifuged and washed repeatedly with the phosphate buffer. The radioactivity found in the precipitate was considered to be bound to the albumin microspheres. A second test involved the use of a dialysis bag[9] in phosphate buffer. The radioactivity remaining in the dialysis bag and in the total dialysate after 62 h was quantitated.

Preparation of the Aerosol Containers—The iodinated microspheres were suspended in ethanol[10] for use in the modified aerosol canister[11]. The canister was fitted with an insert made of aluminum, stainless steel, or plastic[12] so that when filled it would deliver 20 metered doses of 65 μg/dose (the similar commercially available canister is designed to deliver 200 metered doses).

The freshly prepared albumin microspheres[1] were placed in the plastic[12] insert in a canister and supercooled to −65°C in an acetone–dry ice bath. The propellant, dichlorodifluoromethane[13] (1.3 g), was added, and the valve[14] was put in place and crimped[15]. The closed canister was placed in a warm water bath, *i.e.*, 55°C, to test for crimping leaks. After successfully passing the leak test, the canister was allowed to equilibrate to room temperature for use in the deposition studies.

Determination of the Radioactive Species—By testing the interaction of the canister insert, valves, and contents singly and combined, determination of the radioactive species was attempted. That is, attempts were made to check whether the quantitated activity was due to free iodine, iodinated propellant, or the labeled microspheres. By varying the different parameters, the radioactive deposition was proven.

Experiment 1—Three aluminum canisters were filled with propellant and a known, weighed amount of unlabeled albumin microspheres, crimped closed, and then allowed to equilibrate to room temperature after successfully passing the leak test. The contents of each were then actuated into scintillation vials for later determination by the ninhydrin assay for the amount of protein present.

Experiment 2—Again, three aluminum aerosol containers were used, with the first containing ^{131}I-iodinated microspheres and propellant. After crimping, the canister was warmed to room temperature, cooled to −60°C, and then opened. After evaporation of the propellant, the activity was quantitated. The second canister contained only [^{131}I]NaI and unlabeled microspheres. Propellant was added, the system was crimped hydraulically and allowed to warm to room temperature. After supercooling (−60°C) the aerosol container, the valve assembly was removed, and the contents were permitted to evaporate. The final canister in this portion of the experiment contained only [^{131}I]NaI and propellant that was allowed to evaporate without the crimping, warming, and cooling procedure.

Experiment 3—One of the two canisters containing iodinated microspheres and propellant was crimped closed, heated to 50°C, cooled to −60°C, and opened by removing the valve to allow the contents to evaporate. The other canister was filled with iodinated microspheres and propellant, which were then allowed to evaporate at room temperature.

Metered Dose Determinations—The canister was shaken manually for dispersion, and subsequently, the contents were emptied into plastic scintillation vials[16] lined with gauze. After each actuation, the canister was shaken vigorously for 2–3 s. The end of the valve stem was held with needle-nose pliers, and each metered dose was delivered into a separate appropriate vial. The collection of actuations was continued until the canister was empty. The canister was then dismantled, the inside of the plastic[12] insert was washed exhaustively, and the valve was dismantled to quantitate the deposition of the radioactivity.

Cascade Impaction—Filled and leak-tested aerosol canisters containing the radiolabeled albumin microspheres[1] were also used in the second experiment. An appropriate oral adaptor was fitted onto the canister and the valve stem, and subsequently, the aerosol was actuated in a cascade impactor[17]. A pressure of 18 psi was applied to the cascade impactor with a vacuum pump[18]. The canister was shaken before each actuation into the impactor, and the vacuum was run for an additional 5 min after the last actuation to ensure complete impaction. The glass slides for collecting the sized particles were removed and washed with 3 M NaOH[19]. All washings were collected, and the radioactivity was quantitated.

RESULTS AND DISCUSSION

This study was undertaken to examine several parameters which characterize pressurized aerosols in which the drug used is in the form of an insoluble particle suspended in the aerosol formulation. These parameters include (*a*) accurate quantitation of metered doses, (*b*) characterization of the size distribution of particles ejected from the aerosol, and (*c*) the deposition profile of the aerosol particles in the canister and component parts.

To achieve these goals, microaggregated bovine albumin microspheres (ranging from 3 to 8 μm in diameter) were labeled with iodine-131 by the general methods of McConahey and Dixon (15), Greenwood *et al.* (16), and Hughes and Straessle (17) adapted for use with microspheres in this experiment. The microspheres, which were suspended in phosphate buffer (pH 8.0), were placed in a glass vial[4], and the radioactivity, in this case [^{131}I]NaI, was added. *N*-Chloro-4-methylbenzenesulfonamide sodium salt was added, the mixture was stirred for 5 min, and the reducing agent, sodium metabisulfite, was added to halt the iodination procedure. The radiolabeled microspheres were then washed with phosphate buffer to remove any residual radioactivity.

To ascertain that the iodine was covalently bonded to the protein backbone, the microaggregated albumin microspheres were precipitated with trichloroacetic acid. The total radioactivity found in the supernatant and in the precipitated protein indicated an 80–90% efficiency of iodination. To further determine the covalent linkage of the iodine to the microspheres, an identical sample of the microspheres was dialyzed[9]. The results indicate that 12% of the total radioactivity was found in the dialysate and the dialysis bag, confirming that the majority (>80%) of the radioactivity is associated with the microspheres.

[4] Minivial and stirrer; Reliance Glass Work Co., Bensenville, Ill.
[5] Chloramine-T; Eastman Kodak Co., Rochester, N.Y.
[6] Model PC-351; Corning Glass Works, Corning, N.Y.
[7] Mallinckrodt, Inc., Paris, Ky.
[8] J. T. Baker Chemical Co., Phillipsburg, N.J.
[9] Spectropor Membrane Tubing (molecular weight cut off ~3500); Spectrum Medical Industries Inc., Los Angeles, Calif.
[10] U.S. Industrial Chemical, Louisville, Ky.
[11] Cebal canister; Lederle Laboratories.
[12] Teflon, Dupont.
[13] Freon-12; Racon Inc., Wichita, Kan.
[14] Valois valve; Lederle Laboratories.
[15] J & G Crimper, Paterson, N.J.
[16] Packard Instrument Co., Downers Grove, Ill.
[17] Delron DCI; Delron Research Products Co., Powell, Ohio.
[18] Gast Manufacturing Co., Benton Harbor, Mich.
[19] Fisher Scientific Co., Fair Lawn, N.J.

Table II—Effect of Various Treatments Involving Aerosol Valves and Canister Contents on the Delivery of Iodinated Microspheres [a]

Canister	Valve Treatment	Surfactant	Percent Radioactivity In Valve	Percent Radioactivity In Insert [b]
1		2% (v/v) Tween 80 in EtOH	79.9	8.9
2	2% (w/v) BSA [c] in phosphate buffer pipetted into valve	2% (v/v) Tween 80 in EtOH	51.4	11.3
3	4% (w/v) BSA [c] in phosphate buffer pipetted into valve	2% (v/v) Tween 80 in EtOH	89.8	4.5
4	10% (w/v) Tween 80 in phosphate buffer pipetted in valve	2% (v/v) Tween 80 in EtOH	57.5	5.8
5	4% (v/v) Tween 80 in phosphate buffer pipetted in valve	10% (v/v) Tween 80 in EtOH	89.9	4.3
6	10% (v/v) Tween 80 in phosphate buffer pipetted in valve	10% (v/v) Tween 80 in EtOH	83.5	6.9
7		2% (v/v) Tween 80 in EtOH	94.1	1.9
8		10% (v/v) Tween 80 in EtOH	83.2	7.9
9	Silylated with 1% (v/v) organosilane [d] in dioxane by immersion		77.4	10.2
10	Silylated with 1% (v/v) organosilane [d] in methanol by immersion		75.1	4.2
11	Silylated with 1% (v/v) organosilane [d] in distilled water by immersion		74.5	4.8
12	2% (w/v) BSA [c] in phosphate buffer pipetted into valve		54.6	6.2
13	5% (w/v) BSA [c] in phosphate buffer pipetted into valve		59.2	8.5
14	10% (w/v) BSA [c] in phosphate buffer pipetted into valve		71.2	8.7
15	Silylated with 100% (v/v) trimethylchlorosilane by immersion		82.9	6.4

[a] Numbers represent percent of total radioactivity delivered from the aerosol. [b] Teflon; DuPont. [c] Bovine serum albumin. [d] Prosil-8; PCR Research Chemicals, Inc.

When the labeled microspheres were photographed[20] under a microscope[21] before and after the labeling process, it was found that their spherical geometry remained unaltered by the iodination procedure.

The labeled microspheres were introduced into an aerosol canister[11] (a plastic insert was used to decrease the fill volume), the propellant[13] was added, and the canister was crimped closed with the valve[14] in place. Leak tests in warm water provided proof of good crimps with no gas leaks, and the filled canisters were subsequently allowed to equilibrate to room temperature for 15 min before use in the experiments.

Experiments were devised to determine the reproducibility of each metered dose from the canister. The aerosol container was shaken; each actuation was collected in individual scintillation vials[16] lined with gauze and quantitated.

The percentage of the total radioactivity collected from each actuation is listed in Table I. In all three experiments, the first three actuations (necessary to prime the valve) had suboptimal amounts of solid particles, as indicated by the smaller amounts of radioactivity delivered. The last three doses also showed lower amounts of radioactivity. The total radioactivity released from the canister represented only 5% of the total quantitated. The majority of the activity was found in the valve. Several attempts were made to improve the delivery of the labeled microspheres from the aerosol canister. These included impregnation of the valve with (*a*) 2, 5, or 10% bovine serum albumin in phosphate buffer, (*b*) 4 or 10% Tween 80 in phosphate buffer, and (*c*) 1% organosilane[22] in dioxane, methanol, or distilled water. The best results (Table II) were obtained when the valve was impregnated with 2% bovine serum albumin in phosphate buffer. A total of 0.4 mL was applied directly into the valve, and it was allowed to air dry at room temperature for 1 h before use. Approximately 50% of the total activity was found in the valve after the albumin pretreatment, indicating an improvement in delivery of the labeled microspheres of ~40%.

The amount of protein present in unlabeled microspheres delivered from the aerosol canister was determined using the ninhydrin assay (4.31 mg), indicating that ~20% had been actuated out of an untreated aerosol container. This value is higher than the reported value of 5% for the radiolabeled microspheres released from the canister by acutating the valve. Further experiments with (a) labeled microspheres and propellant, (*b*) unlabeled microspheres, [^{131}I]NaI, and propellant, and (*c*) [^{131}I]NaI and propellant demonstrated that iodine-131 alone was not responsible for the activity present in the valve assembly, but the iodinated microspheres represented the radioactive species quantitated.

To determine the particle size distribution of the aerosol, a cascade impactor[17] was utilized. Either 2 or all 20 actuations (metered doses) were passed through a cascade impactor[17] subjected to a vacuum of 18 psi[18]. Due to the aerodynamic design of this particle size analyzer, the microspheres exhibited a size distribution profile as shown in Table III. Stage 1, with the largest opening, collected the heaviest or largest particles, whereas stage 6 collected those particles which traveled the fastest, that is, the smallest particles. The size determination provided by the cascade impactor[17] showed that the majority of particles (stages 3-5, Table III), had sizes ranging from 2 to 8 μm.

Dismantling of the emptied canister and quantitation of the residual radioactivity constituted the final aspect of the study. The valve was removed from the canister and separated into six component parts. Approximately 90% of the total radioactivity in the aerosol container was found in the valve[14], with the spring accounting for the highest amount counted (95%). Impregnation of the valve decreased the amount of radioactivity in the spring to 46%. Radioactivity was also present in the plastic[12] insert, and direct counting of the insert with the residue present led to quantitation of the particles that had not been aerosolized (2-10%).

The major drawback in this study was the tendency of the ^{131}I-labeled albumin microspheres to adhere to the various components of the aerosol container. A substantial amount of the total radioactivity was located in the valve apparatus, and therefore, this type of suspended microsphere aerosol system is not practical for drug delivery. However, the data obtained concerning the quantitation of metered doses and the determination of size distribution of particles illustrate the usefulness of tracer methodology in aerosol research.

Table I shows that reasonably equal doses can be delivered in actuations 5-16. The first four primer doses delivered lesser quantities of the formulation. This is probably due to the fact that these primer doses rid the valve of any water in the stem after the leak test and fill the valve chamber with the propellant. The last three doses shown are also smaller. As the pressure decreases, the quantity of particles delivered becomes less because the weight of the microspheres is too great for the amount of propellant remaining.

In the particular valve system utilized, each metered dose delivered is 65 μg. Therefore, determination of a single dose by the conventional weighing-by-difference method would be difficult.

Table III—Determination of Particle Size Distribution Profile of Microspheres Delivered from an Aerosol [a]

Cascade Impactor Stage	Known particle Size Impacted, μm	Particle size, % of total [b] Experiment 1	Particle size, % of total [b] Experiment 2
1	32	15.18	16.59
2	16	9.14	11.30
3	8	23.02	24.06
4	4	24.59	17.42
5	2	14.73	15.80
6	1	9.21	10.59
Filter paper	0.5	4.14	4.24

[a] Data were obtained from ^{131}I-labeled microaggregated albumin microspheres pulled through a cascade impactor with 18 psi pressure applied by two in-line vacuum pumps. [b] Values listed are percentages of total radioactivity recovered on all six glass slides of the impactor plus the filter paper at the bottom of the cascade impactor.

[20] Model N35A camera; Nikon.
[21] Reichert microscope, Vienna, Austria.
[22] ProSil-8; PCR Research Chemicals, Inc., Gainesville, Fla.

The variability of the amount delivered per actuation could be due to inadequate shaking of the aerosol container. The method of collection of the labeled microspheres could also cause the valve stem to be blocked, thus detrimentally affecting the results.

The cascade impactor, which was used to delineate the particle size distribution profile, showed that the majority of microspheres had sizes ranging from 2 to 8 μm. The size profile seen in Table III lists microspheres with sizes greater than the reported prepared size of 3 to 8 μm, indicating aggregation of the smaller particles into heavier larger clusters. These aggregates were deposited onto the glass slides of the first two stages of the impactor, as dictated by the aerodynamic parameters of this particle-size analyzer. Again, the radiotracer method proved superior to the classical weighing-by-difference procedure for quantitation of the amount of particulate matter present on each slide after only one actuation of the aerosol.

The deposition of the microspheres onto the components of the valve constituted the final portion of this study. Untreated valves permitted the release of ~5–10% of the total radioactivity. By pretreating the valves with albumin solutions, the adherence of the iodinated albumin microspheres to the plastic parts of the valve and the metal spring was significantly decreased. The delivery of the activity from the treated canister, however, was found not to exceed 50% of the total dose. These results indicate that much more work must be done before microspheres utilized as a drug delivery system can be released effectively from present aerosol canisters.

CONCLUSIONS

The advantages of radiotracer methodology described in the study of aerosols are multifold: (*a*) single doses of an aerosol delivered from a canister can be analyzed, rather than multiple doses as required in previous studies, (*b*) short-lived isotopes can be disposed of easily after the passing of an appropriate decay period, and (*c*) by proper choice of the radionuclide label, rapid and accurate data may be obtained both in *in vivo* and *in vitro* studies. Since aerosols are designed to deliver a metered amount of drug to the patient, the elucidation of the size of the dose and its deposition in the patient is an important consideration. The technique outlined here should prove to be useful in answering these problems.

REFERENCES

(1) J. Halik, V. Lenger, V. Klimet, and P. Voboril, *J. Hyg. Epidemiol. Microbiol. Immunol.*, **24**, 405 (1980).

(2) S. P. Newman, D. Pavia, F. Moren, N. F. Sheahan, and S. W. Clarke, *Thorax*, **36**, 52 (1981).

(3) D. L. Swift, *Am. Rev. Respir. Dis.*, **122**, 71 (1980).

(4) F. Moren, *Int. J. Pharm.*, **8**, 1 (1981).

(5) R. B. Schlesinger, B. Naumann, and L. Chen, *Health Phys.*, **42**, 73 (1982).

(6) S. P. Newman, F. Moren, D. Pavia, F. Little, and S. W. Clarke, *Am. Rev. Respir. Dis.*, **124**, 317 (1981).

(7) S. P. Newman, D. Pavia, and S. W. Clarke, *Chest*, **80**, 909 (1981).

(8) A. Cutie, J. Burger, C. Clawans, D. Dolinsky, W. Feinstein, B. Gupta, A. Grueneberg, and J. Sciarra, *J. Pharm. Sci.*, **70**, 1085 (1981).

(9) P. J. Davies, K. K. Amin, and G. A. Mott, *Drug Dev. Ind. Pharm.*, **6**, 653 (1980).

(10) M. K. Halbert, M. K. Mazumder, and R. L. Bond, *Food Cosmet. Toxicol.*, **19**, 85 (1981).

(11) C. S. Garrard, T. R. Gerrity, J. D. Schreiner, and D. B. Yeates, *Arch. Environ. Health*, **36**, 184 (1981).

(12) J. E. Agnew, D. Pavia, and S. W. Clarke, *Eur. J. Respir. Dis.*, **62**, 239 (1981).

(13) T. Isawa, T. Teshima, T. Hirano, E. Ebina, and K. Konno, *Tokoho J. Exp. Med.*, **134**, 245 (1981).

(14) G. B. Saha, "Fundamentals of Nuclear Pharmacy," Springer-Verlag, New York, N.Y., 1979, p. 85.

(15) P. J. McConahey and F. J. Dixon, *Int. Arch. Allergy*, **29**, 185 (1966).

(16) F. C. Greenwood, W. M. Hunter, and J. S. Glover, *Biochem. J.*, **89**, 114 (1963).

(17) W. L. Hughes, Jr. and R. Straessle, *J. Am. Chem. Soc.*, **72**, 452 (1950).

Effects of Solvent Medium on Solubility III: Hydrophilic–Lipophilic Character Exhibited by Some Functional Groups Having Oxygen or Nitrogen in Ethanol–Water

RUBEN H. MANZO ˣ, AMELIA A. AHUMADA, and ERNESTINA LUNA

Received August 12, 1981, from the *Departamento de Farmacia, Facultad de Ciencias Químicas, Universidad Nacional de Córdoba, Sucursal 16, CC 61, 5016 Córdoba, Argentina.* Accepted for publication June 16, 1983.

Abstract □ Solubility data of nine derivatives of the structure p-X_1—C_6H_4—X_2 in ethanol-water at 25°C are reported. The correlation of such sets of data by $\log S_y = P_y \cdot \log S_x + C$ yields the medium effect parameter P_y for a variety of functional groups possessing either oxygen or nitrogen. P_y accounts for the hydrophilic-lipophilic character exhibited by each group.

Keyphrases □ Solubility—effects of solvent medium, hydrophilic-lipophilic character, ethanol-water □ Solvent medium—effects on solubility, hydrophilic-lipophilic character, ethanol-water □ Hydrophilic-lipophilic character—effects of solvent medium, solubility, ethanol-water

The existence of linear relationships between the logarithms of the solubility equilibria of structurally related crystalline compounds, as they vary with changes in solvent or solvent composition has been shown previously (1, 2). Such linear free energy relationships (LFER) are conveniently expressed by:

$$\log S_y = P_y \cdot \log S_x + C \qquad \text{(Eq. 1)}$$

where S_y and S_x are sets of solubility data of compounds A_y and A_x, respectively. By taking a proper solvent condition as reference, Eq. 1 becomes:

$$\log S_y - \log S_y^0 = P_y(\log S_x - \log S_x^0) \qquad \text{(Eq. 2)}$$

or

$$\Delta\log S_y = P_y \cdot \Delta\log S_x \qquad \text{(Eq. 3)}$$

The medium effect parameter P_y depends on the structural difference between A_y and A_x on the one side and on the effects of the solvent change on the solubility of the substrate series (*i.e.*, on the sign of Δlog S) on the other. To illustrate this point, Fig. 1 shows a typical LFER plot of a pair of p-aminobenzoic esters which pass through a solubility maximum when they move from the first to the last solvent condition. There, as the solvent system increases in lipophilicity, the solubility

0022-3549/84/0800-1094$01.00/0

© 1984, American Pharmaceutical Association

The variability of the amount delivered per actuation could be due to inadequate shaking of the aerosol container. The method of collection of the labeled microspheres could also cause the valve stem to be blocked, thus detrimentally affecting the results.

The cascade impactor, which was used to delineate the particle size distribution profile, showed that the majority of microspheres had sizes ranging from 2 to 8 μm. The size profile seen in Table III lists microspheres with sizes greater than the reported prepared size of 3 to 8 μm, indicating aggregation of the smaller particles into heavier larger clusters. These aggregates were deposited onto the glass slides of the first two stages of the impactor, as dictated by the aerodynamic parameters of this particle-size analyzer. Again, the radiotracer method proved superior to the classical weighing-by-difference procedure for quantitation of the amount of particulate matter present on each slide after only one actuation of the aerosol.

The deposition of the microspheres onto the components of the valve constituted the final portion of this study. Untreated valves permitted the release of ~5–10% of the total radioactivity. By pretreating the valves with albumin solutions, the adherence of the iodinated albumin microspheres to the plastic parts of the valve and the metal spring was significantly decreased. The delivery of the activity from the treated canister, however, was found not to exceed 50% of the total dose. These results indicate that much more work must be done before microspheres utilized as a drug delivery system can be released effectively from present aerosol canisters.

CONCLUSIONS

The advantages of radiotracer methodology described in the study of aerosols are multifold: (*a*) single doses of an aerosol delivered from a canister can be analyzed, rather than multiple doses as required in previous studies, (*b*) short-lived isotopes can be disposed of easily after the passing of an appropriate decay period, and (*c*) by proper choice of the radionuclide label, rapid and accurate data may be obtained both in *in vivo* and *in vitro* studies. Since aerosols are designed to deliver a metered amount of drug to the patient, the elucidation of the size of the dose and its deposition in the patient is an important consideration. The technique outlined here should prove to be useful in answering these problems.

REFERENCES

(1) J. Halik, V. Lenger, V. Klimet, and P. Voboril, *J. Hyg. Epidemiol. Microbiol. Immunol.*, **24**, 405 (1980).

(2) S. P. Newman, D. Pavia, F. Moren, N. F. Sheahan, and S. W. Clarke, *Thorax*, **36**, 52 (1981).

(3) D. L. Swift, *Am. Rev. Respir. Dis.*, **122**, 71 (1980).

(4) F. Moren, *Int. J. Pharm.*, **8**, 1 (1981).

(5) R. B. Schlesinger, B. Naumann, and L. Chen, *Health Phys.*, **42**, 73 (1982).

(6) S. P. Newman, F. Moren, D. Pavia, F. Little, and S. W. Clarke, *Am. Rev. Respir. Dis.*, **124**, 317 (1981).

(7) S. P. Newman, D. Pavia, and S. W. Clarke, *Chest*, **80**, 909 (1981).

(8) A. Cutie, J. Burger, C. Clawans, D. Dolinsky, W. Feinstein, B. Gupta, A. Grueneberg, and J. Sciarra, *J. Pharm. Sci.*, **70**, 1085 (1981).

(9) P. J. Davies, K. K. Amin, and G. A. Mott, *Drug Dev. Ind. Pharm.*, **6**, 653 (1980).

(10) M. K. Halbert, M. K. Mazumder, and R. L. Bond, *Food Cosmet. Toxicol.*, **19**, 85 (1981).

(11) C. S. Garrard, T. R. Gerrity, J. D. Schreiner, and D. B. Yeates, *Arch. Environ. Health*, **36**, 184 (1981).

(12) J. E. Agnew, D. Pavia, and S. W. Clarke, *Eur. J. Respir. Dis.*, **62**, 239 (1981).

(13) T. Isawa, T. Teshima, T. Hirano, E. Ebina, and K. Konno, *Tokoho J. Exp. Med.*, **134**, 245 (1981).

(14) G. B. Saha, "Fundamentals of Nuclear Pharmacy," Springer-Verlag, New York, N.Y., 1979, p. 85.

(15) P. J. McConahey and F. J. Dixon, *Int. Arch. Allergy*, **29**, 185 (1966).

(16) F. C. Greenwood, W. M. Hunter, and J. S. Glover, *Biochem. J.*, **89**, 114 (1963).

(17) W. L. Hughes, Jr. and R. Straessle, *J. Am. Chem. Soc.*, **72**, 452 (1950).

Effects of Solvent Medium on Solubility III: Hydrophilic–Lipophilic Character Exhibited by Some Functional Groups Having Oxygen or Nitrogen in Ethanol–Water

RUBEN H. MANZO ˣ, AMELIA A. AHUMADA, and ERNESTINA LUNA

Received August 12, 1981, from the *Departamento de Farmacia, Facultad de Ciencias Químicas, Universidad Nacional de Córdoba, Sucursal 16, CC 61, 5016 Córdoba, Argentina.* Accepted for publication June 16, 1983.

Abstract □ Solubility data of nine derivatives of the structure p-X_1—C_6H_4—X_2 in ethanol-water at 25°C are reported. The correlation of such sets of data by $\log S_y = P_y \cdot \log S_x + C$ yields the medium effect parameter P_y for a variety of functional groups possessing either oxygen or nitrogen. P_y accounts for the hydrophilic-lipophilic character exhibited by each group.

Keyphrases □ Solubility—effects of solvent medium, hydrophilic-lipophilic character, ethanol-water □ Solvent medium—effects on solubility, hydrophilic-lipophilic character, ethanol-water □ Hydrophilic-lipophilic character—effects of solvent medium, solubility, ethanol-water

The existence of linear relationships between the logarithms of the solubility equilibria of structurally related crystalline compounds, as they vary with changes in solvent or solvent composition has been shown previously (1, 2). Such linear free energy relationships (LFER) are conveniently expressed by:

$$\log S_y = P_y \cdot \log S_x + C \qquad \text{(Eq. 1)}$$

where S_y and S_x are sets of solubility data of compounds A_y and A_x, respectively. By taking a proper solvent condition as reference, Eq. 1 becomes:

$$\log S_y - \log S_y^0 = P_y(\log S_x - \log S_x^0) \qquad \text{(Eq. 2)}$$

or

$$\Delta\log S_y = P_y \cdot \Delta\log S_x \qquad \text{(Eq. 3)}$$

The medium effect parameter P_y depends on the structural difference between A_y and A_x on the one side and on the effects of the solvent change on the solubility of the substrate series (*i.e.*, on the sign of Δlog S) on the other. To illustrate this point, Fig. 1 shows a typical LFER plot of a pair of p-aminobenzoic esters which pass through a solubility maximum when they move from the first to the last solvent condition. There, as the solvent system increases in lipophilicity, the solubility

0022-3549/84/0800-1094$01.00/0

© 1984, American Pharmaceutical Association

Table I—Derivatives of p-X_1—C_6H_4—X_2 Used in the Solubility Determinations

Compound	X_1	X_2	mp, °C Experimental[a]	mp, °C Literature
I	H_2N—	—$COOCH_3$	113-114.5	114 (8)
II	H_2N—	—$CONHCH_3$	181-181.5	180 (9)
III	CH_3CONH—	—H	112-113	113-115 (10)
IV	CH_3CONH—	—OH	169-171	169-170.5 (10)
V	CH_3CONH—	—$COOCH_3$	128.5-129.5	130 (6)
VI	$(CH_3)_2N$—	—$COOCH_3$	100-101	102 (6)
VII	HO—	—$COOCH_3$	131	131 (10)
VIII	CH_3COO—	—$COOCH_3$	80-80.5	—
IX	CH_3O—	—$COOCH_3$	47.5-48.5	48-48.5 (11)

[a] Uncorrected.

of the propyl ester A_y increases at a faster rate (part B, ethanol-water) and decreases more slowly (part A, ethanol-cyclohexane) than that of the methyl ester A_x, as a result of its greater lipophilic portion.

In this study, the purpose has been to use this methodology to get information about the hydrophilic-lipophilic properties of a variety of functional groups possessing either oxygen or nitrogen. These were selected because the information available, mainly obtained from partition coefficient (PC) measurements, regards the high sensitivity of the properties of these atoms to the structural environment (3, 4). Hence, a set of oxygen and nitrogen analogues was obtained by the appropriate variation of the basic structure p-X_1 —C_6H_4—X_2 as indicated in Table I, and their solubility equilibria were measured in hydroxylic mixtures. In such systems, the specific solute-solvent interactions through hydrogen bridges are recognized to play a major role among the factors that determine the solubility behavior of the substrates.

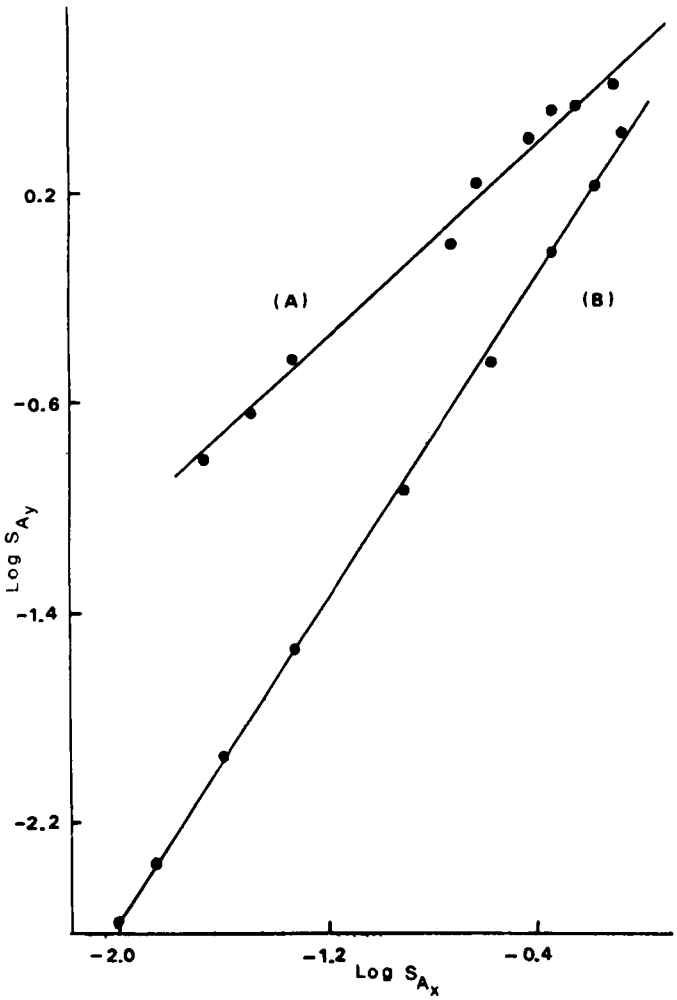

Figure 1—*LFER plot of propyl ester (A_y) and methyl ester (A_x) of* p-*hydroxybenzoic acid in ethanol-water (B) and ethanol-cyclohexane (A); data taken from Ref. 2.*

EXPERIMENTAL SECTION

Substrates—The calculated and literature melting points (mp) of all derivatives are reported in Table I. The following compounds were commercial products, purified by recrystallization: I[1], III[2], IV[2], and VII[2]. Compounds II, V, VI, VIII, and IX were prepared by adequate structural variation of the available derivatives through known techniques (5-7). All products were characterized by their melting points. In addition, for II and VIII, it was considered appropriate to report ^{1}H-NMR[3] and MS[4] data.

Solvents—Mixtures were prepared by mixing exactly measured volumes of absolute ethanol and water, *i.e.*, ethanol-water (40:60).

Solubility Determination and Correlation Procedure—The method employed for the solubility measurements was reported previously (1, 2). For all compounds, a spectrophotometric determination of substrate concentration at λ_{max} was performed. From the values of Table II, the corresponding molalities were calculated, and their logarithms were used in the correlations. The linear regression parameters reported in Table III were calculated by the least-squares method.

RESULTS AND DISCUSSION

Table II reports the solubility of I-IX in ethanol-water mixtures at 25°C. At low solubility conditions, small changes in solvent composition produce significant solubility variations; on the other hand, the lower the substrate

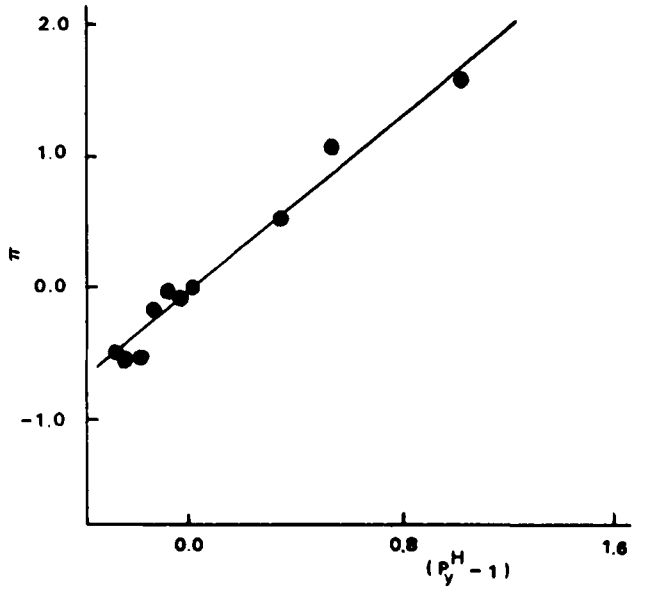

Figure 2—*Plot of the lipophilic constant π (octanol-water) against the medium effect parameter (P_y^H − 1) in ethanol-water for different functional groups.*

[1] R. Hellman.
[2] Aldrich.
[3] Varian T 60.
[4] Finnigan 3300F-100.

Table II—Solubility in Ethanol–Water at 25°C

Solvent Composition		Solubility, mg/g_{soln}								
Ethanol	Water	I	II	III[a]	IV	V	VI	VII	VIII	IX
00.0	100	1.45	8.64	6.38	15.1	1.35	0.112	2.89	0.621	0.753
10.0	90.0	2.05	13.2	9.64	25.6	2.39	0.168	3.81	0.889	1.19
20.0	80.0	3.70	17.9	14.4	35.7	4.63	0.338	6.73	1.25	2.19
30.0	70.0	6.94	26.1	36.3	62.8	12.0	0.866	20.5	2.73	5.82
40.0	60.0	18.3	39.4	52.6	113	19.9	2.85	49.3	6.63	17.6
50.0	50.0	38.0	55.3	76.5	160	40.0	8.79	123	15.7	—
60.0	40.0	63.5	72.4	141	203	116	17.0	196	28.0	—
70.0	30.0	89.6	80.5	206	247	158	29.8	265	45.9	—

[a] Solubility of III in ethanol-water has been reported early (12). Present results are in good agreement with those.

Table III—Correlation of Solubility Data According to Eq. 1 [a]

Compounds Correlated	Range	n	Slope	Intercept	r	δ_y	δ_{sl}
VI/I	0-70	8	1.334	−0.542	0.999	0.029	0.016
IV/III	0-70	8	0.851	0.188	0.992	0.066	0.043
V/IV	0-70	8	1.559	−0.681	0.989	0.125	0.095
VIII/VII	0-70	8	0.870	−1.014	0.997	0.062	0.028
V/I	0-70	8	1.107	0.138	0.992	0.108	0.058
V/III	0-70	8	1.347	−0.377	0.997	0.066	0.043
II/I	0-70	8	0.520	−0.104	0.994	0.043	0.023
V/VIII	0-70	8	1.079	0.647	0.991	0.111	0.058
VI/IX	0-40	5	1.024	−0.815	0.999	0.017	0.016
VIII/IX	0-40	5	0.746	−0.758	0.999	0.025	0.023
IX/VII	0-40	5	1.050	−0.497	0.997	0.049	0.047
I/VII	0-70	8	0.855	−0.520	0.998	0.044	0.018

[a] r is the regression coefficient, δ_{sl} is the standard deviation of the slope, and δ_y is the standard deviation of the points from the regression line in the y direction.

concentration, the lower the probability of particular solute–solute interactions. Therefore, to correlate solubility data by Eq. 1, those values corresponding to lower solubilities are preferred to the ones obtained under conditions of higher solubility—near the maximum solubility. A composition variation covering 0–70% of ethanolic content was considered appropriate.

Going from water to ethanol through a series of ethanol-water mixtures, the increase of the ethanolic content increases the lipophilic character of the mixture and raises the solubility of all the substrates studied [(+)$\Delta\log S$]. For a given correlation, a medium effect parameter P_y higher or lower than the unity means that A_y is respectively more lipophilic or hydrophilic than A_x.

Table III reports the results obtained by the correlation according to Eq. 1 when adequately selected pairs of compounds were matched together. As can be seen, good linear correlations were obtained in all cases affording the corresponding P_y parameters.

To get a uniform set of P_y values, the hydrogen atom attached to the aromatic ring was taken as the reference functional group ($P_{yH} = 1$). When direct calculation was not possible, the following procedure was used:

$$P_y = \Delta\log S_{Ar-Y}/\Delta\log S_{Ar-X} \qquad \text{(Eq. 4)}$$

and

$$P_x = \Delta\log S_{Ar-X}/\Delta\log S_{Ar-H} \qquad \text{(Eq. 5)}$$

Table IV—Hydrophilic–Lipophilic Character of Different Functional Groups Attached to the Benzene Ring

Functional Group	$(P_y^H - 1)$	π
$-CONHCH_3$	−0.33	
$-NH_2$	−0.28	−0.49[a]
CH_3COO-	−0.26	−0.58[b]
CH_3CONH-	−0.20	−0.56[b]
$-OH$	−0.15	−0.16[a]
CH_3O-	−0.09	−0.03[b]
$(CH_3)_2N-$	−0.05	−0.08[b]
$-H$	0.00	0.00
$-COOCH_3$	0.33	0.49[c]
$-CH_2-CH_2-$[d]	0.53	1.08
$-COO(CH_2)_2CH_3$	1.04	1.57[c]

[a] Calculated from log PC (octanol-water) of I (1.63) and VII (1.96), respectively, using as reference log PC of benzoic acid methyl ester (2.12); all data from Ref. 3. [b] Values from Ref. 13. [c] Calculated respectively from log PC of VII or log PC of *p*-hydroxybenzoic acid propyl ester using as reference log PC of phenol; all data from Ref. 3. [d] Concerned with the extension of the alkyl chain. The random value of P_y arises from propyl and methyl esters of both *p*-hydroxy- and *p*-aminobenzoic acids (2), while π is the difference between $\pi_{-COO(CH_2)_2CH_3}$ and π_{-COOCH_3}.

then

$$P_y^H = P_y \cdot P_x = \Delta\log S_{Ar-Y}/\Delta\log S_{Ar-H} \qquad \text{(Eq. 6)}$$

Table IV contains the calculated hydrophilic-lipophilic character of each functional group, which is expressed as $(P_y^H - 1)$. There, a negative value means higher hydrophilic character, while a positive value indicates higher lipophilic character than hydrogen.

Therefore, the inspection of the figures in Table IV reveals the higher hydrophilicity of the aromatic primary amino group with respect to the phenolic hydroxy group, while the respective acetyl derivatives exhibit a reverse order. However, the comparison of the aryl carboxy derivatives (*i.e.*, I and II) again shows a remarkably higher hydrophilic character of the nitrogenated derivative. On the other hand, the methoxy group appears to be more hydrophilic than the fully methylated tertiary amino.

The use of $(P_y^H - 1)$ is a convenient way to express the hydrophilic-lipophilic properties of the functional groups since, as it has been previously stated (1), it is directly related to the expected PC parameter π'_y by:

$$P_y - 1 = \frac{\Delta\log S_y - \Delta\log S_x}{\Delta\log S_x} = \frac{\pi'_y}{\Delta\log S_x} \qquad \text{(Eq. 7)}$$

π'_y has also been regarded as a lipophilic variable (1) whose meaning extends the concept of the lipophilic constant π (3) and hydrophobic constant (14) which arise from partition coefficient measurements.

In addition, Table IV also contains literature values of π for the octanol-water partitioning system, which also consists of two hydroxylic solvents. Because inspection of the columns suggests a parallel variation of both sets of figures, it was considered of interest to match them together in a plot. Therefore, Fig. 2 shows the agreement between the results obtained from medium effects on solubility in ethanol-water mixtures and those obtained from octanol-water partition coefficients.

The results quoted show how LFER applied to solubility equilibria measurements yields reliable information about the hydrophilic-lipophilic properties of different functional groups. It appears that this simple methodology would be a useful and versatile tool to extend our present knowledge of solubility behavior to a wide variety of solvent systems. In addition, the use of Eqs. 2–7 as a means of predicting medium effects on solubility appears to be attractive for the pharmaceutical sciences.

REFERENCES

(1) R. H. Manzo, *J. Pharm. Pharmacol.*, **34**, 486 (1982).

(2) R. H. Manzo, *An. Assoc. Quim. Argentina*, **71**, 47 (1983).

(3) A. Leo, C. Hansch, and D. Elkins, *Chem. Rev.*, **71**, 525 (1971).

(4) S. S. Davis, T. Higuchi, and J. H. Rytting, *Adv. Pharm. Sci.*, **4**, 104 (1974).
(5) "Vogel's Textbook of Practical Organic Chemistry," 4th ed., Longman, London and New York, 1978.
(6) P. Grammaticakis, *Bull. Soc. Chim. Fr.*, **1951**, 220.
(7) K. A. Connors, "A Textbook of Pharmaceutical Analysis," 2nd ed., Wiley, New York, N.Y., 1975, pp 455-459.
(8) "Handbook of Chemistry and Physics," 56th ed., CRC Press, 1975-1976.
(9) H. Wenker, *J. Am. Chem. Soc.*, **60**, 1081 (1938).
(10) "The Merck Index," 8th ed., Merck & Co. Inc, Rahway, N.J., 1968.
(11) T. C. Corby and P. H. Elworthy, *J. Pharm. Pharmacol.*, **23**, Suppl., 39 S (1971).
(12) E. J. Cohn, *Chem. Rev.*, **19**, 241 (1936).
(13) S. M. Sicardi, "Farmacologia Molecular," Centro Editor Argentino, 1981.
(14) R. F. Rekker and H. M. de Kort, *Eur. J. Med. Chem.-Chim. Ther.*, **14**, 479 (1979).

ACKNOWLEDGMENTS

The authors thank the Consejo de Investigaciones Cientlficas y Technológicas de la Provincia de Córdoba for financial support (Grant 064/82).

Acute Intravenous Infusion of Disodium Dihydrogen (1-Hydroxyethylidene)diphosphonate: Mechanism of Toxicity

MARION D. FRANCIS ˣ **and CANDICE L. SLOUGH**

Received September 20, 1982, from the *Miami Valley Laboratories, 2N142, Proctor & Gamble Co., Cincinnati, OH 45247.* Accepted for publication July 26, 1983.

Abstract □ The acute intravenous toxicity of disodium dihydrogen (1-hydroxyethylidene)diphosphonate (etidronate disodium; I) and the mechanism of this toxic response have been investigated in 40 beagle dogs. The intravenous toxicity of I is dependent on the total dose administered and the length of the infusion interval. The toxicity of I is directly related to the ability of the drug to bind or complex with the circulating calcium in the blood. Maximum depressions in ionized calcium coincide in time with peak blood levels of I, and at lethal doses electrocardiographic changes indicative of hypocalcemia are observed. For a 2-min infusion of 2 mg of I/kg, no effect is observed on ionized calcium levels, and the electrocardiogram remains normal. At doses of 16 and 32 mg/kg, coincident with an immediate fall in ionized calcium levels, there is a transient rise in total calcium and a fall in phosphorus levels. The ionized calcium level rises, and total calcium level falls and stabilizes at baseline levels within 30 min after the infusion. However, the phosphorus level rises and exceeds the baseline value, reaching 3-4 times normal by 72 h after the infusion. With proven lethal doses of I (60 mg/kg infused over 2 min) and the simultaneous infusion of an ionized calcium salt such as calcium gluconate (20 mg of Ca^{2+}/kg), electrocardiograms remain normal and death is prevented. Thus, an effective antidote in the event of an overdose or too rapid an infusion of I can be employed to prevent acute toxic effects.

Keyphrases □ Etidronate disodium—hypercalcemia, intravenous toxicity, dogs □ Hypercalcemia—treatment with etidronate disodium and calcium gluconate, toxicity, dogs □ Calcium gluconate—hypercalcemia, use with etidronate disodium, dogs

Disodium dihydrogen (1-hydroxyethylidene)diphosphonate (etidronate disodium; I) is a substance which has both therapeutic (1-4) and diagnostic (5, 6) uses in metabolic bone disease. Clinically, the ability of orally administered drug[1] to reduce elevated bone turnover prompted speculation that the drug might be used intravenously to control other disease processes such as hypercalcemia secondary to malignancy or hyperparathyroidism. Studies to examine physiological and pharmacological responses to varying intravenous doses of diphosphonates were therefore undertaken.

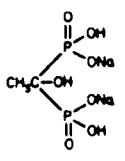

I

The mechanism of intravenous toxicity of I might be expected to be similar to that of ethylenediaminetetraacetic acid (II) and polyphosphate compounds (III) because of the chelating properties (7-10) of each of these compounds. However, I differs from II and III in several respects, which could markedly alter its effect on calcium homeostasis.

At physiological pH, I is a less-effective simple chelator of calcium than II and, unlike II, forms polynuclear complexes (11) which can reach molecular weights of ≥20,000. There is some evidence for this formation *in vivo*, but their biological activity is unknown. In addition, I is cleared from the blood both by adsorption on the hydroxyapatite of bone (12) and by renal clearance, whereas II is cleared only by renal excretion. There are also differences in the p*K* values of I, II, and III. Furthermore, although III are adsorbed on hydroxyapatite like I, III are rapidly hydrolyzed *in vivo* to the natural orthophosphate metabolites (HPO_4^{2-}, $H_2PO_4^-$), while I is not metabolized (13). Based on the above differences, the present study was undertaken to establish a broader safety profile for I by clearly defining the acute intravenous toxicity of I and demonstrating the relationship between acute intravenous toxicity, serum ionized and total calcium levels, and diphosphonate blood levels. Subsequent to these studies, intravenously administered I and another diphosphonate (dichloromethylenediphosphonate) have been shown to effectively reduce hypercalcemia associated with malignant disease and hyperparathyroidism in humans (14-18).

EXPERIMENTAL SECTION

Purebred adult male and female beagle dogs weighing 5.7-13.9 kg were used in four experiments. It was necessary to conduct the initial studies in unanesthetized animals to ensure that no signs or symptoms of toxicity were masked by the anesthetic. However, in subsequent experiments, animals receiving toxic doses of I were anesthetized with sodium pentobarbital unless its use was contraindicated.

[1] Didronel; Procter & Gamble Co., Cincinnati, Ohio.

0022-3549/84/0800-1097$01.00/0
© 1984, American Pharmaceutical Association

(4) S. S. Davis, T. Higuchi, and J. H. Rytting, *Adv. Pharm. Sci.*, **4**, 104 (1974).
(5) "Vogel's Textbook of Practical Organic Chemistry," 4th ed., Longman, London and New York, 1978.
(6) P. Grammaticakis, *Bull. Soc. Chim. Fr.*, **1951**, 220.
(7) K. A. Connors, "A Textbook of Pharmaceutical Analysis," 2nd ed., Wiley, New York, N.Y., 1975, pp 455-459.
(8) "Handbook of Chemistry and Physics," 56th ed., CRC Press, 1975-1976.
(9) H. Wenker, *J. Am. Chem. Soc.*, **60**, 1081 (1938).
(10) "The Merck Index," 8th ed., Merck & Co. Inc, Rahway, N.J., 1968.
(11) T. C. Corby and P. H. Elworthy, *J. Pharm. Pharmacol.*, **23**, Suppl., 39 S (1971).
(12) E. J. Cohn, *Chem. Rev.*, **19**, 241 (1936).
(13) S. M. Sicardi, "Farmacologia Molecular," Centro Editor Argentino, 1981.
(14) R. F. Rekker and H. M. de Kort, *Eur. J. Med. Chem.-Chim. Ther.*, **14**, 479 (1979).

ACKNOWLEDGMENTS

The authors thank the Consejo de Investigaciones Cientlficas y Technológicas de la Provincia de Córdoba for financial support (Grant 064/82).

Acute Intravenous Infusion of Disodium Dihydrogen (1-Hydroxyethylidene)diphosphonate: Mechanism of Toxicity

MARION D. FRANCIS ˣ **and CANDICE L. SLOUGH**

Received September 20, 1982, from the *Miami Valley Laboratories, 2N142, Proctor & Gamble Co., Cincinnati, OH 45247.* Accepted for publication July 26, 1983.

Abstract □ The acute intravenous toxicity of disodium dihydrogen (1-hydroxyethylidene)diphosphonate (etidronate disodium; I) and the mechanism of this toxic response have been investigated in 40 beagle dogs. The intravenous toxicity of I is dependent on the total dose administered and the length of the infusion interval. The toxicity of I is directly related to the ability of the drug to bind or complex with the circulating calcium in the blood. Maximum depressions in ionized calcium coincide in time with peak blood levels of I, and at lethal doses electrocardiographic changes indicative of hypocalcemia are observed. For a 2-min infusion of 2 mg of I/kg, no effect is observed on ionized calcium levels, and the electrocardiogram remains normal. At doses of 16 and 32 mg/kg, coincident with an immediate fall in ionized calcium levels, there is a transient rise in total calcium and a fall in phosphorus levels. The ionized calcium level rises, and total calcium level falls and stabilizes at baseline levels within 30 min after the infusion. However, the phosphorus level rises and exceeds the baseline value, reaching 3-4 times normal by 72 h after the infusion. With proven lethal doses of I (60 mg/kg infused over 2 min) and the simultaneous infusion of an ionized calcium salt such as calcium gluconate (20 mg of Ca^{2+}/kg), electrocardiograms remain normal and death is prevented. Thus, an effective antidote in the event of an overdose or too rapid an infusion of I can be employed to prevent acute toxic effects.

Keyphrases □ Etidronate disodium—hypercalcemia, intravenous toxicity, dogs □ Hypercalcemia—treatment with etidronate disodium and calcium gluconate, toxicity, dogs □ Calcium gluconate—hypercalcemia, use with etidronate disodium, dogs

Disodium dihydrogen (1-hydroxyethylidene)diphosphonate (etidronate disodium; I) is a substance which has both therapeutic (1-4) and diagnostic (5, 6) uses in metabolic bone disease. Clinically, the ability of orally administered drug[1] to reduce elevated bone turnover prompted speculation that the drug might be used intravenously to control other disease processes such as hypercalcemia secondary to malignancy or hyperparathyroidism. Studies to examine physiological and pharmacological responses to varying intravenous doses of diphosphonates were therefore undertaken.

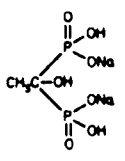

I

The mechanism of intravenous toxicity of I might be expected to be similar to that of ethylenediaminetetraacetic acid (II) and polyphosphate compounds (III) because of the chelating properties (7-10) of each of these compounds. However, I differs from II and III in several respects, which could markedly alter its effect on calcium homeostasis.

At physiological pH, I is a less-effective simple chelator of calcium than II and, unlike II, forms polynuclear complexes (11) which can reach molecular weights of ≥20,000. There is some evidence for this formation *in vivo*, but their biological activity is unknown. In addition, I is cleared from the blood both by adsorption on the hydroxyapatite of bone (12) and by renal clearance, whereas II is cleared only by renal excretion. There are also differences in the p*K* values of I, II, and III. Furthermore, although III are adsorbed on hydroxyapatite like I, III are rapidly hydrolyzed *in vivo* to the natural orthophosphate metabolites (HPO_4^{2-}, $H_2PO_4^-$), while I is not metabolized (13). Based on the above differences, the present study was undertaken to establish a broader safety profile for I by clearly defining the acute intravenous toxicity of I and demonstrating the relationship between acute intravenous toxicity, serum ionized and total calcium levels, and diphosphonate blood levels. Subsequent to these studies, intravenously administered I and another diphosphonate (dichloromethylenediphosphonate) have been shown to effectively reduce hypercalcemia associated with malignant disease and hyperparathyroidism in humans (14-18).

EXPERIMENTAL SECTION

Purebred adult male and female beagle dogs weighing 5.7-13.9 kg were used in four experiments. It was necessary to conduct the initial studies in unanesthetized animals to ensure that no signs or symptoms of toxicity were masked by the anesthetic. However, in subsequent experiments, animals receiving toxic doses of I were anesthetized with sodium pentobarbital unless its use was contraindicated.

[1] Didronel; Procter & Gamble Co., Cincinnati, Ohio.

0022-3549/84/0800-1097$01.00/0
© 1984, American Pharmaceutical Association

Electrocardiography—Electrocardiograms were obtained according to standard procedures (19) on an electrocardiograph unit[2]. Serial six-lead electrocardiograms were obtained immediately prior to dosing and at 5, 10, 15, and 60 min after the start of the infusion. In all experiments, a continuous lead II electrocardiogram was obtained during and for 1–3 min after the start of the infusion.

Infusions—Indwelling catheters[3] were inserted percutaneously into the cephalic vein to facilitate infusions. Dose solutions were delivered manually from a syringe. In the "rescue" study, I was infused into one cephalic vein, and the calcium solution was infused simultaneously into the other cephalic vein.

Dose Solutions—All solutions of I were prepared in sterile distilled water and adjusted to pH 7.4. Solutions were filtered[4] (0.22 μm) into sterile serum bottles. The concentrations of the dose solutions varied with the intended dose level. The diphosphonate concentrations employed were (x to y mg of I/mL, z mg/kg): 1.9 to 4.0, 2; 5.7 to 5.8, 4; 14.5 to 14.7, 8; 27.0 to 32.0, 16; 38.3 to 49.4, 28; 41.1 to 64.0, 32; and 52.8 to 58.4, 37 and 44, and 55.3, 60.

Ten percent calcium gluconate for injection[5] was used as supplied; the concentration of calcium was 9.2 mg/mL. Physiological saline[6] was used as the control infusion solution.

Experiment I—Part 1 of experiment I was designed to determine the acute toxicity of I when doses of 2, 4, 8, 16, and 32 mg of I/kg (two dogs per dose level) were administered intravenously over a 15-s interval. Six males and four females were used. Part 2 of experiment I was a determination of the acute toxicity of I using doses of 2, 4, 8, 16, 28, 37, and 44 mg of I/kg (two dogs per dose level) administered intravenously over a 2-min interval. Nine males and five females were used. These two studies were designed to examine the toxic effects and influence of the duration of the infusion on the toxicity of intravenously administered I.

Experiment II—This experiment was designed to examine the relationship between diphosphonate blood levels and the physiological response to three nonlethal dose levels (2, 16, and 32 mg of I/kg) administered intravenously over a 2-min interval. Six dogs (one male and one female per dose level) were used. In this experiment silicone rubber cannulas were surgically implanted into the jugular vein on the day prior to the infusion to facilitate serial blood sampling. The cannulas were kept patent with heparinized saline (125–250 U/mL).

The diphosphonate dose solution was labeled with carbon-14 in the 1-position, [^{14}C]I, so that the diphosphonate blood level could be monitored by standard radioassay procedures using a scintillation fluid[7]. Total calcium and total orthophosphate were analyzed on an autoanalyzer. Calcium was determined using calcein (20), phosphorus was determined colorimetrically (21), and ionized calcium was determined with a calcium electrode. Serial blood samples were collected immediately prior to the start of the infusion and then at the following intervals: 0.5, 1, 1.5, 2, 3, 5, 10, 15, and 30 min, 1, 2, 4, 24, 48, and 72 h, and 1 week. All analyses were performed on the serum.

Experiment III—A calcium "rescue" experiment was designed to determine if the effects of a lethal intravenous dose of I could be prevented by the simultaneous intravenous infusion of an ionized calcium salt. Preliminary infusions using two dogs (one male and one female) confirmed the lethality of 60 mg of I/kg administered over a 2-min interval. Two other dogs (one male and one female) received only calcium gluconate at 20 mg of Ca^{2+}/kg in order to determine generalized and electrocardiographic responses to 2-min infusions of an ionized calcium salt. Subsequent to the above, two female dogs received infusions of 60 mg of I/kg simultaneously with calcium gluconate (20 mg of Ca^{2+}/kg) over a 2-min interval.

Experiment IV—This experiment served as a control for the preceding series of experiments. Four dogs (two males and two females) received 2-min intravenous infusions of physiological saline.

General Reactions and Anesthesia—The reactions of the dogs to infusions of I were monitored by continuous observation during and immediately after the infusion, and daily for up to 2 weeks. These data were considered important in defining the potential hazards of intravenous administration of I in humans.

Sodium pentobarbital decreases respiration and may affect the cardiovascular system such that the electrocardiogram and distribution of I would be altered (22–24); therefore, anesthesia was not employed in experiments I and II. Having established the relationship between calcium and I in the blood, and the coincident electrocardiographic changes in the conscious dog, dogs receiving lethal doses of I were anesthetized for experiment III.

[2] Burdich Model EKS; Kauffman-Goodwin, Columbus, Ohio.
[3] Sherwood Medical Industries, St. Louis, Mo.
[4] Millipore Corp., Bedford, Mass.
[5] W. A. Butler, Cincinnati, Ohio.
[6] Abbott Laboratories, North Chicago, Ill.
[7] Triton X-100; Rohm & Haas.

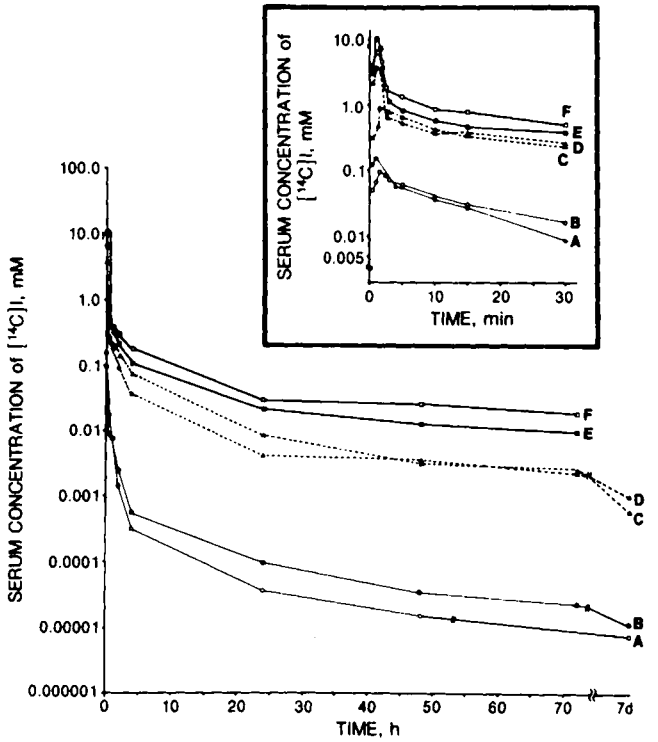

Figure 1—*Concentration of [^{14}C]I in the serum of dogs during and after 2-min intravenous infusions of 2 (A,B), 16 (C,D), and 32 (E,F) mg of [^{14}C]I/kg. Inset shows the first 30 min during and after the infusion.*

RESULTS

Acute Toxicity Studies (Experiment I)—*15-s Infusions*—No drug-related electrocardiographic effects were observed during or after infusions of 2–8 mg of I/kg. At a dose level of 16 mg/kg, an increased respiratory rate and a transient increase in heart rate were observed in both dogs during the infusion. The heart rate returned to normal within 5 min after the start of the infusion. Daily observations, lasting up to 2 weeks, did not reveal adverse effects in dogs receiving up to 16 mg/kg. At a dose level of 32 mg/kg, clonic contractions preceded death, which was observed in both dogs as a cessation of respiration. Electrocardiographically, both animals receiving 32 mg of I/kg developed lethal ventricular arrhythmias within 2–3 min after starting the infusion; tachycardia, QT prolongation, heart block, premature ventricular contractions, and finally, ventricular fibrillation were noted sequentially in both dogs.

2-min Infusions—No significant electrocardiographic effects were observed during or after infusions of 2–8 mg of I/kg. At doses of 16 or 28 mg of I/kg, transient tachycardia was the only consistent electrocardiographic effect and, in all dogs, the heart rate had returned to normal within 5 min after the start of the infusion. As the dose level increased to 37, and finally to 44, mg of I/kg, the dogs resisted restraint and electrocardiographic changes became evident. Electrocardiographically, slight, persistent sinus tachycardia occurred at a dose level of 37 mg of I/kg. Dogs that received 44 mg of I/kg exhibited severe, persistent tachycardia, T waves of increased magnitude, prolonged QRS intervals, ST segment elevation, and premature ventricular contractions. At a dose level of 44 mg of I/kg, one of the two dogs died.

Physiological Response to Nonlethal Doses of I (Experiment II)—*2-min Infusion*—The electrocardiograms of dogs receiving 2 mg of [^{14}C]I/kg appeared essentially normal. At a dose of 16 mg of [^{14}C]I/kg there was a transient increase in heart rate and a prolongation of the QT interval in both dogs. Within 5 min after start of the infusion, these had returned to normal (predose) values. At 32 mg of [^{14}C]I/kg a predominant sinus tachycardia and a prolongation of the QT interval occurred in both dogs. In one dog, these had returned to normal within 5 min, but in the other dog the tachycardia persisted for 30 min. In the latter dog, premature ventricular contractions were observed between 2 and 3 min after the start of the infusion. In dogs receiving 32 mg of I/kg, respiratory rates increased and the dogs resisted restraint. These reactions were absent within 1 min after cessation of the infusion. No toxic symptoms were observed the day after infusion in any dog, and all dogs survived.

Diphosphonate, Total and Ionic Calcium, and Total Phosphorus Levels in Serum—The peak [^{14}C]I serum levels occurred for all dose levels within the 2-min infusion interval and then decreased exponentially (Fig. 1). The

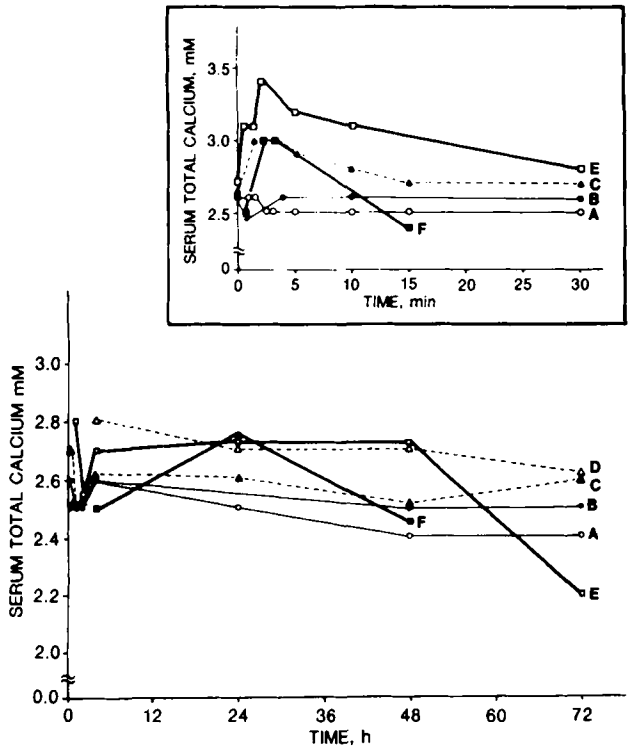

Figure 2—*Concentration of total calcium in serum of dogs during and after 2-min intravenous infusions of 2 (A,B), 16 (C,D), and 32 (E,F) mg of [^{14}C]-I/kg. Inset shows the first 30 min during and after the infusion.*

highest peak serum concentration achieved at each dose level was: 0.15 mM (2 mg of [^{14}C]I/kg), 3.8 mM (16 mg of [^{14}C]I/kg), and 10 mM (32 mg of [^{14}C]I/kg).

At the two highest dose levels (16 and 32 mg of [^{14}C]I/kg) total serum calcium increased 0.4–0.7 mM within 5 min after the start of infusion (Fig. 2), while serum phosphorus for these same animals decreased 0.2–0.5 mM within 15 min (Fig. 3). There was a decrease in ionic calcium within the 2-min infusion interval that was proportional to the serum [^{14}C]I level (Fig. 4). For example, the highest [^{14}C]I serum level (10 mM) corresponded to the lowest

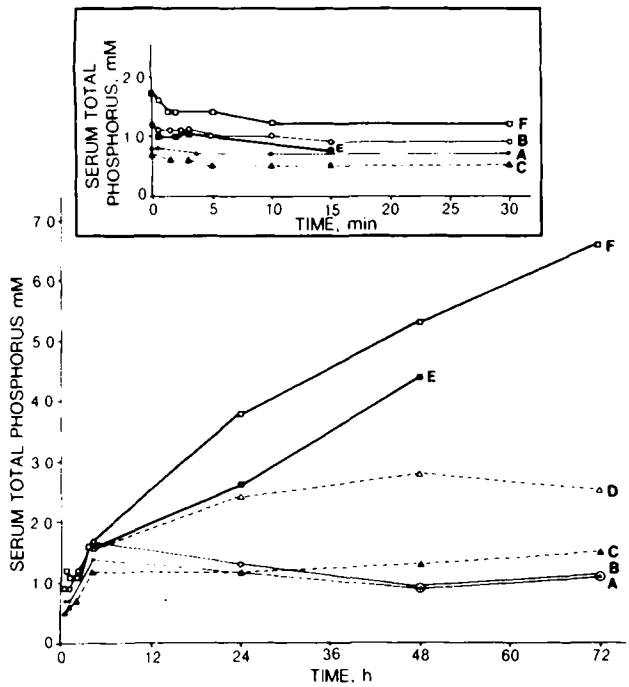

Figure 3—*Concentration of serum orthophosphate in dogs during and after 2-min intravenous infusions of 2 (A,B), 16 (C,D) and 32 (E,F) mg of [^{14}C]I/kg. Inset shows the first 30 min during and after the infusion.*

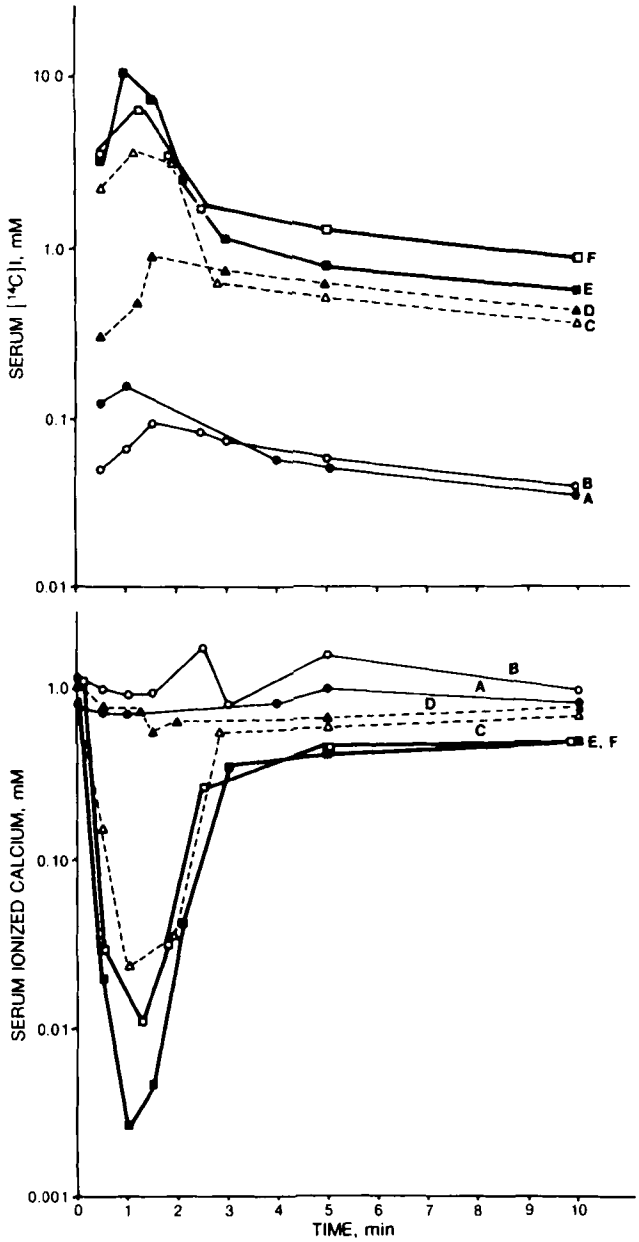

Figure 4—*Concentration of [^{14}C]I and of ionized calcium in the serum of dogs during and after 2-min intravenous infusions of 2 (A,B), 16 (C,D), and 32 (E,F) mg of [^{14}C]I/kg.*

ionized calcium level attained (0.001 mM). The lowest [^{14}C]I blood levels were achieved with a dose of 2 mg of [^{14}C]I/kg and did not alter the baseline ionized calcium (~1 mM). In dogs receiving the two highest levels of bisphosphonate, ionized calcium fell precipitously and then rose rapidly to normal levels within 5 min after the start of the infusion (Fig. 4), while total calcium, after increasing, did not return to normal levels until ~30 min after the start of the infusion (Fig. 2). In these same dogs, serum phosphorus (as orthophosphate) showed a progressive and steady increase (Fig. 3) up to 72 h after the start of infusion (up 5.4 mM). In the dog which exhibited the greatest increase in serum phosphorus, there was a concomitant decrease in both total and ionized calcium at the 72-h evaluation.

Calcium "Rescue" (Experiment III)—Both dogs infused with 60 mg of I/kg died. Within 1 min after initiation of the infusion, tachycardia was evident in both dogs. Electrocardiographic changes were similar to those which occurred with lethal doses in experiment I. Infusions of calcium gluconate, on the other hand, were associated with emesis and transient electrocardiographic changes consistent with hypercalcemia.

Animals that received a combination of I and calcium gluconate did not display any significant electrocardiographic effects during the first 5 min of the experiment. Sinus tachycardia was observed in one dog 1 h postdose. Negative P waves and second degree atrioventricular block were observed in the other dog through the 15-min tracing, but this arrhythmia was absent in

the 1-h tracing. The dogs that received I plus calcium gluconate appeared normal during the 2-week postdose observation period.

Control Infusions (Experiment IV)—No general reactions were observed in response to 2-min intravenous infusions of saline. No significant electrocardiographic changes were observed in these dogs.

DISCUSSION

The intravenous administration of high doses of I can produce rapid death; however, the toxic effect is both time and dose dependent. The lethal toxicity of I relates directly to the concentration of I achieved in the blood. Identical doses administered over a shorter period of time produce a higher blood concentration and result in higher toxicity.

The toxicity of I is directly related to its ability to bind or complex with the circulating calcium of the blood. For a given infusion interval, when the intravenous dose of [^{14}C]I was increased, the concentration in the blood rose proportionally (Fig. 1). At the two highest dose levels (16 and 32 mg of [^{14}C]I/kg), the concentration of ionized calcium in the blood fell, with the maximum depressions of ionized calcium coinciding in time with the peak blood levels of [^{14}C]I (Fig. 4). The ionized calcium returned rapidly to near-normal concentrations within 5 min, despite the significant concentration of I beyond this time. The use of electrocardiography during infusions of increasing diphosphonate doses was found to be a useful diagnostic tool for detecting progressive signs of increasing cardiotoxic effects. The electrocardiographic effects observed at the high dose levels of I are consistent with depressions in ionized calcium and indicate the sensitivity of heart muscle to low ionized calcium levels, in spite of elevations in total calcium (Fig. 2). No effect on ionized calcium levels was seen at the 2-mg/kg dose of I administered over a 2-min interval, and no significant electrocardiographic changes were observed in these dogs.

The rise in total calcium observed with high parenteral doses of I (Fig. 2) has been observed previously (25). For the animals showing the greatest rise in total calcium, serum phosphorus fell (Fig. 3). The rise in total calcium reflects mobilization of calcium to satisfy ionized calcium homeostasis in the blood. The fall in serum phosphorus levels probably does not relate to the rise in total calcium since ionized calcium fell. The fall in phosphorus is probably effected by stimulation of parathyroid hormone release (26) with consequent clearance of phosphorus by the kidneys. After returning rapidly to normal (as did the total calcium and ionized calcium levels), serum phosphorus increased slowly and steadily above normal for up to 72 h after the infusion (Fig. 3), reaching a maximum level that was 3–4 times normal in dogs receiving the highest dose of I. This delayed and elevated serum phosphorus level has been observed on numerous occasions in humans given high daily oral doses of I (20 mg of I/kg), and is attributed to an increased tubular reabsorption of orthophosphate by the kidney (27).

The lethal effects (depression in ionized calcium) of the very high doses of I can be overcome by simultaneous infusion of an ionized calcium salt, such as calcium gluconate. Similar studies with another diphosphonate (disodium dichloromethylenediphosphonate) have confirmed this "rescue" effect[8]. In these studies, calcium gluconate maintained normal serum ionized calcium, while total calcium rose above normal until shortly after the infusion period. In the present study, in the absence of calcium gluconate, maximum depression in ionized calcium would be expected during the first 5 min after the start of infusion (see Fig. 4). During this period, electrocardiographic changes were observed but, with simultaneous infusion of calcium gluconate, normal electrocardiographic patterns were obtained. Calcium chloride can achieve the same effects as calcium gluconate[8], but the gluconate salt is preferred (28), since toxic effects of calcium administration have been reported and the chloride salt seems more toxic than the gluconate salt.

This series of studies describes the lethal and sublethal toxic responses of I administered over two infusion intervals. The studies define the dose levels of I which can be administered safely by intravenous injection. In addition, the studies provide insight into the mechanism of toxicity, and describe a means to prevent death associated with lethal doses of intravenously administered disodium dihydrogen (1-hydroxyethylidene)diphosphonate.

[8] M. D. Francis and C. L. Slough; unpublished results.

REFERENCES

(1) R. D. Altman, C. Johnston, M. R. A. Khairi, H. Wellman, A. N. Serafini, and R. R. Sankey, *N. Engl. J. Med.*, **289,** 1380 (1973).

(2) R. G. G. Russell, R. Smith, C. Preston, R. J. Walton, and C. G. Woods, *Lancet*, **7863,** 894 (1974).

(3) S. J. Stover, H. R. Hahn, and J. M. Miller, *Paraplegia*, **14,** 46 (1976).

(4) G. A. M. Finerman, W. F. Krengel, J. D. Lowell, W. R. Murray, R. G. Volz, J. W. Bowerman, and R. H. Gold, in "Proceedings of the Fifth Open Scientific Meeting of the Hip Society," C. V. Mosby, St. Louis, Mo., 1977, p. 222.

(5) E. B. Silberstein, E. Saenger, A. J. Tofe, G. W. Alexander, and H. M. Park, *Radiology*, **107,** 551 (1973).

(6) H. N. Wellman, A. Browne, M. Kavula, R. Khairi, P. Anger, A. J. Tofe, and M. D. Francis, "Radiopharmaceuticals and Labelled Compounds," IAEA/SM-171/52, Copenhagen, 1973.

(7) M. I. Kabachnik, R. P. Lastovskii, T. Ya. Medved, V. V. Medyntsev, I. D. Kolpakova, and N. M. Dyatlova, *Dokl. Akad. Nauk., SSSR*, **177,** 582 (1967).

(8) M. D. Francis and R. L. Centner, *J. Chem. Ed.*, **55,** 760 (1978).

(9) A. Catsch and A.-E. Harmuth-Hoene, *Biochem. Pharmacol.*, **24,** 1557 (1975).

(10) J. R. Van Wazer, "Phosphorus and Its Compounds," Interscience, New York, N.Y., 1958, p. 419.

(11) R. J. Grabenstetter and W. A. Cilley, *J. Phys. Chem.*, **75,** 676 (1971).

(12) M. D. Francis, *Calc. Tissue Res.*, **3,** 151 (1969).

(13) W. R. Michael, W. R. King, and J. M. Wakim, *Toxicol. Appl. Pharmacol.*, **21,** 503 (1972).

(14) J. I. Zweig, *J. Am. Med. Assoc.*, **244,** 437 (1980).

(15) A. Jung, C. Van Ouwenaller, A. Chantraine, and B. Courvoisier, *Cancer*, **48**(8), 1922 (1981).

(16) T. P. Jacobs, E. S. Siris, J. P. Bilezikian, D. C. Boquiran, E. Shane, and R. E. Canfield, *Ann. Internal Med.*, **94**(3), 312 (1981).

(17) E. Shane, T. P. Jacobs, E. S. Siris, S. F. Steinberg, K. Stoddart, R. E. Canfield, and J. P. Bilezikian, *Am. J. Med.*, **72,** 939 (1982).

(18) R. R. Martodam, T. J. Taylor, T. E. Davis, and H. M. Golomb, "Abstracts XVII," European Symposium Calcif. Tissue, 1983.

(19) S. J. Ettinger and P. F. Suter, "Canine Cardiology," W. B. Saunders, Philadelphia, Pa., 1970, p. 109.

(20) B. F. Fingerhut, A. Poock, and H. Miller, *Clin. Chem.*, **15,** 870 (1969).

(21) C. H. Fiske and Y. Subbarow, *J. Biol. Chem.*, **66,** 375 (1925).

(22) L. M. Jones, N. H. Booth and L. E. McDonald, "Veterinary Pharmacology and Therapeutics," 4th ed., Iowa State University Press, Ames, Iowa, 1977, p. 241.

(23) H. L. Price, *Physiol. Rev.*, **40,** 187 (1960).

(24) S. F. Vatner and E. Braunwald, *N. Engl. J. Med.*, **293,** 970 (1975).

(25) H. Fleisch, S. Bisaz, A. D. Care, R. C. Muhlbauer, and R. G. G. Russell, "Calcitonin, 1969, Proceedings of the Second International Symposium," Springer-Verlag, New York, N.Y., 1969, p. 409.

(26) H. Rasmussen, "Textbook of Endocrinology," W. B. Saunders, Philadelphia, Pa., 1968, p. 881.

(27) R. G. Walton, R. G. G. Russell, and R. Smith, *Clin. Sci. Mol. Med.*, **49,** 45 (1975).

(28) R. J. Garner, "Veterinary Toxicology," Bailliere, Tundall and Cox, London, 1957, p. 60.

ACKNOWLEDGMENTS

The authors wish to acknowledge the assistance of G. G. Cloyd D. V. M. in designing and carrying out these experiments.

In Vitro Dehalogenation of *para*-Substituted Aromatic Halides in Rat Liver Preparations

M. T. SCOTT * and J. E. SINSHEIMER ˣ

Received December 27, 1982, from the *College of Pharmacy, The University of Michigan, Ann Arbor, MI 48109.* Accepted for publication August 4, 1983. *Present address: Analytical Research and Development, DuPont Pharmaceuticals, Garden City, NY 11530.

Abstract □ The *in vitro* dehalogenation of a series of *para*-substituted halobenzenes was studied using HPLC separation followed by scintillation counting or neutron-activation analysis. Microsomal and cytosolic deiodination were established for iodobenzene substrates whose *para*-substituents were CO_2H, CHO, NO_2, OH, and C_6H_5 but not for *para*-iodobenzonitrile. A nonglutathione cytosolic deiodinase was only indicated with 4-iodobiphenyl as the substrate. *In vitro* dehalogenation could not be established for 4-bromobiphenyl using neutron-activation analysis.

Keyphrases □ Dehalogenation—rat liver *in vitro* studies, microsomal, cytosolic □ Aromatic halides—effect of *para*-substitution on *in vitro* dehalogenation □ Glutathione—role in *in vitro* dehalogenation, *N*-ethylmaleimide inhibition

There has been considerable human exposure to aromatic halides due to their use in medicine as well as their widespread applications in industry and agriculture. In addition to the medicinal use of thyroxine and iodohydroxyquin preparations, acyl iodides have been employed as radiopaque diagnostic agents. Also, ^{131}I- or increasingly, ^{123}I-labeled aromatic iodides have been synthesized as potential tumor-imaging agents (1–4). Polychlorinated and polybrominated biphenyls are ubiquitous environmental pollutants with well-established toxicities (5–10).

The possibility of contact with these compounds is evident and has prompted numerous investigations, especially with the biphenyl compounds. *In vivo* dehalogenation plays a small but significant role in the metabolism of these compounds (11–13). Therefore, it was basic to an understanding of their potential toxicity to study the mechanism and extent of *in vitro* dehalogenation in the rat by direct measurement of liberated halide. *para*-Substituted aromatic halides labeled with iodine-125 or chlorine-36, or containing unlabeled bromine or chlorine, were chosen as the model compounds.

EXPERIMENTAL SECTION

Apparatus—The liquid chromatograph consisted of a microprocessor controller[1], two pumps[2], a dynamic-flow mixer[3], and an injection valve[4]. A reverse-phase C_{18} column[5] was used for radiohalide detection by either a radiochemical detector in a liquid scintillation mode[6] or by liquid scintillation counting[7] of the eluant. A cumene-based cocktail[8], at a flow rate of 3.0 mL/min, was used with the radiochemical detector, while a xylene-based cocktail[9] was used for liquid scintillation counting of the eluant.

Synthesis—^{125}I-labeled compounds, except for [4,4′-^{125}I]diiodobiphenyl, were synthesized by an exchange reaction using a melt procedure (14). Labeled 4,4′-diiodobiphenyl was synthesized as previously described (15). Radiochemical purity was established by reverse isotopic dilution analysis and HPLC.

General Melt Procedure—The unlabeled iodo compound (25 mg) and acetamide (100 mg) were added to a flask followed by sodium[^{125}I]iodide[10] (1–2 mCi) in acetone. Sodium thiosulfate (10^{-7} M, 20 μL) and ammonium chloride (10^{-7} M, 20 μL) were also added to prevent oxidation of the iodide and to prevent degradation of the reactant, respectively. Reaction conditions for specific compounds and their yields are outlined in Table I. Water (4 mL) was added, and the mixture was extracted with chloroform (4 × 4 mL), dried over sodium sulfate, and evaporated to dryness under a stream of nitrogen. The solid was dissolved in a small volume (~1 mL) of chloroform and passed through a small silica gel column[11] to remove inorganic iodide-125. The eluant was evaporated using nitrogen, and the solid was recrystallized in methanol (except for the iodobiphenyl compounds, which were recrystallized in ethanol).

Reverse Isotopic Dilution Analysis—A known amount of radiolabeled material was added to 500–1000 mg of accurately weighed unlabeled material. Mixtures were recrystallized until a constant specific activity of ±5% was achieved. From each recrystallization, three 10-mg aliquots, accurately weighed, were counted (Table I).

Radiochemical Purity by Liquid Chromatography—A reverse-phase C_{18} column[12], with methanol–water (90:10) as the mobile phase, was used to determine the purity of the ^{125}I-labeled substrates. The presence of any inorganic iodide-125 in the ethanolic or buffer solutions is listed in Table I.

Pretreatment of Animals—Male Sprague–Dawley rats[13] (250–300 g) were quarantined for 2 d before a single intraperitoneal injection of a commercial mixture of polychlorinated biphenyls[14] [500 mg/kg (16)] in corn oil. Rats had free access to food and water for 4 d, after which time the food was removed. The rats were killed on day 5 by asphyxiation using carbon dioxide.

Liver Fractions—Preparation of microsomal and cytosolic fractions were carried out as previously described (15). The procedure of Levine and Murphy (17) was used for the preparation of glutathione-depleted cytosol.

Incubation Procedures—The incubation conditions were modifications of those previously described (15), and studies with *N*-ethylmaleimide[15] and glutathione-depleted cytosol were performed. Mixtures of 20 μL of the ethanolic substrate solution (containing at least 40,000 cpm of substrate), 460 μL of homogenate, and 20 μL of buffer (0.01 M Na_2HPO_4–0.25 M sucrose, pH 7.4) or microsomal additive solution were incubated for 2 h at 37°C. Microsomal additive solutions consisted of magnesium chloride (15 μmol), nicotinamide (20 μmol), and NADPH (0.05 μmol) contained in 20 μL of buffer. *N*-Ethylmaleimide was added to selected substrate solutions to inactivate cytosolic glutathione such that the final concentration of imide was 0.0025 M. Five experimental and three control values were run for each experiment. Controls consisted of immersing the homogenate for 5 min in boiling water, cooling, and then following the incubation procedure as above.

Analytical Procedures—*Deiodination Studies*—The enzymatic reaction was stopped by the addition of 150 μL of 20% trichloroacetic acid. Following centrifugation (2000×*g*) and removal of the supernatant, the pellet was washed with 0.5 mL of buffer. After recentrifugation the two supernatants were combined, and the total supernatant was centrifuged and filtered through a 0.45-μm membrane[16] prior to injection into the liquid chromatograph. Samples were stored frozen until HPLC analysis.

To separate inorganic iodide from unreacted substrates and metabolites, 1.0 mL of *in vitro* solution was injected into the liquid chromatograph and eluted with a mobile phase of methanol–water (20:80) using a reverse-phase C_{18} column[5]. With the radiochemical detector, cpm measurements were taken every minute for 5 min after injection. When a scintillation counter was used, the first 4 mL of eluant was collected in a scintillation vial and counted for 5 min following the addition of 1 mL of methanol. The methanol was used to preserve a homogeneous solution with the cocktail (14 mL). Between injections, the chromatograph was flushed with methanol (30 mL) and equilibrated again with the solvent system.

[1] Model 421; Altex, Berkeley, Calif.
[2] Model 110A; Altex, Berkeley, Calif.
[3] Altex, Berkeley, Calif.
[4] Model 7125, 2.0-mL loop; Rheodyne, Berkeley, Calif.
[5] RP-18, 30 × 4.6 mm i.d., Brownlee, Santa Clara, Calif.
[6] Model Flo-One DR; Radiomatic, Tampa, Fla.
[7] Model 9000; Beckman, Berkeley, Calif.
[8] Flo-Scint II; Radiomatic, Tampa, Fla.
[9] ACS, Amersham, Arlington Heights, Ill.
[10] New England Nuclear, Boston, Mass.
[11] Sep-Pak; Waters Associates, Milford, Mass.
[12] ODS-3, 250 × 4.6 mm i.d.; Whatman, Clifton, N.J.
[13] Charles River, Portage, Mich.
[14] Aroclor 1254; Monsanto, St. Louis, Mo.
[15] Sigma, St. Louis, Mo.
[16] Metricel GA-6; Gelman Scientific, Ann Arbor, Mich.

0022-3549/84/0800-1101$01.00/0
© 1984, American Pharmaceutical Association

Table I—Synthesis of ^{125}I-Labeled Substrates [a]

Compound	Reaction Conditions: Max. Temp., °C (for Time, h)	Reaction Conditions: Total Heating Time, h	Specific Activity, mCi/mmol [b]	Radiochemical [c] Purity, %	Inorganic Iodine-125, %: Ethanol	Inorganic Iodine-125, %: Buffer [d]
p-Iodobenzoic Acid	180–190 (1)	2.5	4.13 (12.5)	95.4 ± 5.2	0.0152	0.0139 ± 0.00652 [e]
p-Iodobenzaldehyde	110–120 (1)	2.5	0.111 (3.52)	95.3 ± 2.4	0.668 ± 0.0848	0.903 ± 0.070
p-Iodobenzonitrile	110–120 (1.5)	3.0	0.427 (1.75)	99.5 ± 3.0	0.505 ± 0.00402	0.577 ± 0.0724
p-Iodonitrobenzene	145 (1.5)	3.5	0.973 (3.0)	91.6 ± 1.5	0.0949 ± 0.0403	0.0747 ± 0.0561
p-Iodophenol	100–110 (1.25)	3.5	7.022 (17.47)	98.1 ± 0.75	0.151 ± 0.0244	0.333 ± 0.146
4-Iodobiphenyl	130–135 (1.5)	3.0	1.734 (13.86)	98.4 ± 1.2	0.0708 ± 0.00465	0.108 ± 0.0075
4,4′-Diiodobiphenyl [f]	225 (48)	48.5	17.97 (82.5)	98.6 ± 1.6		

[a] Synthesized by the method of Elias and Lotterhos (14). [b] Radiochemical yield, expressed as percentage, in parentheses. [c] Reverse isotopic dilution. [d] Incubation in pH 7.4 phosphate buffer for 2 h at 37°C. [e] Mean of three experimental values ± SD. [f] Synthesized as previously described (16).

Debromination and Dechlorination Studies of Unlabeled Substrates—The enzymatic reaction was stopped with the addition of 150 μL of 35% H_2SO_4. The aforementioned procedure for iodide was then followed except that Tris-sucrose buffer was used; the HPLC procedure for separation of inorganic bromide and chloride was identical to that for iodide. The eluant (4 mL) was condensed by lyophilization after addition of 160 μL of concentrated ammonium hydroxide to prevent charring.

For bromide analysis, the residue was transferred to quartz tubes[17] with 1.0 mL of deionized water. Following lyophilization overnight, ≤0.5 mL of deionized water was added and the tubes were sealed. They were placed in the reactor at a neutron flux of 1.5×10^{13} neutrons/cm^2/s for 50 h. Bromide was determined by gamma-ray analysis of bromide-82 ($t_{1/2}$ = 35.34 h, 554.3, 619.0, and 776.5 keV) using two Canberra 22% coaxial Ge (Li) detectors and two multichannel analyzers[18].

For chloride analysis, the lyophilized material was transferred to small polyethylene tubes[19] with deionized water (0.25 mL). Tubes were placed in the reactor core at a flux of 1.5×10^{13} neutrons/cm^2/s for 15 min. Chloride was determined as chloride-38 ($t_{1/2}$ = 37.3 min, 1642.0 and 2167.5 keV) with the aforementioned instrumentation.

Glutathione-*S*-Transferase Assay—Glutathione-*S*-transferase was assayed by the method of Habig *et al.* (18). The concentration of *p*-nitrobenzyl chloride in the final solution was 0.00025 M, and the concentration of glutathione, when required, was 0.005 M in 0.5 M Na_2HPO_4 buffer, pH 7.4. The substrate was delivered in 25 μL of acetonitrile. Cytosol (100 μL) was used and UV absorbance measurements were taken at 310 nm every minute for 10 min.

Glutathione Determination—Glutathione was determined by the Ellman thiol assay (19) as modified by Benke *et al.* (20). A glutathione stock solution (0.002 M) was prepared in 0.1 M Na_2HPO_4 buffer (pH 8.0) containing 0.5% trichloroacetic acid and 0.001 M EDTA (tetrasodium salt). Four hundred microliters of stock solution was added to 4.55 mL of buffer, followed by the addition of 50 μL of 0.01 M 5,5′-dithiobis(2-nitrobenzoic acid). The absorbance was measured at 420 nm

RESULTS AND DISCUSSION

Analytical System—A reverse-phase HPLC technique similar to the systems previously reported for iodide (21, 22) was developed for separating inorganic halide from unreacted substrates and metabolites. Liquid scintillation counting of the eluant, following injection of sodium [^{36}Cl]chloride[10] in a simulated incubation mixture, resulted in quantitative recovery of inorganic chloride-36. Recovery of chloride-36 was independent of solvent composition from 10 to 90% methanol.

The analysis of inorganic iodide-125 required that carrier sodium iodide be added to the samples. Quantitative recovery was independent of solvent composition from 10 to 90% methanol. *para*-Iodobenzoic acid was chosen to determine the optimal solvent composition because resolution of this polar substrate and inorganic iodide could pose a difficult problem. Methanol–water (20:80) was suitable for all the substrates since complete resolution of inorganic and organically bound iodide was obtained in a minimal amount of time (~5 min).

Stability of Substrates—*In vitro* dehalogenation was expected to liberate trace quantities of halide; therefore, the purity of the labeled substrates, and the stability of the carbon–iodine-125 bond in ethanolic substrate solution and in buffer under incubation conditions, was of crucial importance if statistically significant levels of deiodination were to be obtained. Table I shows the percent inorganic iodide-125 found for the substrates in ethanol and in buffer under incubation conditions. The percentage of inorganic iodide in ethanol was determined by injection of an aliquot of an ethanolic solution of substrate containing 500 μg of carrier sodium iodide.

All solutions were freshly prepared and injected into the chromatograph within 5 min of preparation. Deiodination in buffer was carried out by incubating an aliquot of ethanolic substrate solutions in pH 7.4 sodium phosphate buffer (0.010 M) under the same conditions used in the *in vitro* experiments. HPLC conditions were also as described for *in vitro* dehalogenation studies.

Deiodination in ethanol was about the same as that in buffer under incubation conditions. Deiodination of [*p*-^{125}I]iodobenzaldehyde was statistically greater (Student's *t* test, $p \leq 0.05$) in buffer than in ethanol; there was no statistical difference in deiodination of the phenol in ethanol or buffer.

Dechlorination and Debromination Studies Using Neutron-Activation Analysis—Neutron-activation analysis was an attractive alternative to using radiolabeled substrates for *in vitro* debromination and dechlorination studies. Therefore, a feasibility study was undertaken using simulated incubation mixtures containing ammonium bromide or ammonium chloride and the reverse-phase HPLC conditions described above. These samples contained bromide and chloride equivalent to 0.5, 1.0, and 2.0% biotransformations, based on the incubation of 100 μg of 4-bromobiphenyl or 4-chlorobiphenyl. Bromide analysis at 554.0 and 776.9 keV was used. Results of analysis at 619.0 keV were not used due to interference from another radioisotope. HPLC analysis at either 554.0 or 776.9 keV of blanks containing no ammonium bromide did not show statistically significant bromide levels; therefore, bromide contamination as a result of the workup and analysis was not a problem. Statistically significant levels of bromide were observed for all three of the simulated biotransformations.

Neutron-activation analyses at 1641.3 and 2165.9 keV of simulated, dechlorinated samples indicated high background levels which were consistent with known interference in this method by other elements, particularly sodium and potassium in the measurement of chloride. It was estimated that there would have to be at least a 3% biotransformation for detection of chloride in this background. Therefore, while neutron-activation analysis of bromide was a viable technique for study of debromination, this technique was not useful under the conditions of our incubations for chloride measurements.

Neutron-activation analysis of the HPLC effluent following injection of the supernatant of the incubation medium of 4-bromobiphenyl with cytosol (for three sets of determinations) gave 0.206 ± 0.032% *versus* 0.169 ± 0.032% for the respective control at 553.8 keV and 0.209 ± 0.032% *versus* 0.156 ± 0.019% at 776.0 keV. Neither measurement, compared to the respective control, was statistically significant at $p \leq 0.05$.

Debromination (~1%) of 4,4′-dibromobiphenyl has been reported in the rabbit (12) and pig (13). However, Safe *et al.* (12) did not detect any debrominated metabolites of 4-bromobiphenyl after administration to pigs or rabbits. Analysis of the *in vitro* incubation of tritiated 4-bromobiphenyl with rabbit liver microsomes also showed no debrominated metabolite (12). Thus, while debromination is known to occur, it has not been detected with 4-bromobiphenyl previously or in this study. Analysis of *in vitro* debromination studies was hampered by low substrate solubility. *In vitro* debromination was expected to be less than deiodination based on aromatic carbon–bromine bond strength compared with that of the carbon–iodine bond.

Microsomal Deiodination—The results of deiodination in microsomes are shown in Table II. Each substrate exhibited statistically significant deiodination above its control value except for [*p*-^{125}I]iodobenzonitrile. The relatively high variance of the control values and the low amount of substrate activity prevented detection of a statistically significant difference in deiodination between microsomal samples and the respective controls. Control values, in general, agreed with those found in Table I for incubation in buffer.

Deiodination of the substrates was ≥ ~2%, and there was no unique specificity of the microsomes for any of the substrates. The results for [*p*-^{125}I]-iodonitrobenzene and [4-^{125}I]iodobiphenyl generally agreed with previous

[17] T21 Supersil-7 mm; Harris-Amersil Co., Sayerville, N.J.
[18] Models-4420 and 6660; Nuclear Data, Schaumberg, Ill.
[19] Cole-Palmer, Chicago, Ill.

Table II—Percent Deiodination of p-^{125}I—C_6H_4—R

R	Microsomal		Cytosolic					
	Experimental	Control	No additives	Control	*N*-ethyl-maleimide	Control	Glutathione-Depleted[a]	Control
—CO_2H	0.225 ± 0.0162 (4)[b,c]	0.0332 ± 0.0120 (3)	0.244 ± 0.0079 (5)[b]	0.0046 ± 0.0081 (3)	0.175 ± 0.0994 (4)[d]	0.172 ± 0.00078 (2)[d]	—[e]	—
—CHO	1.37 ± 0.0655 (4)[b]	0.848 ± 0.0685	1.48 ± 0.126 (5)[b]	1.08 ± 0.102 (3)	0.854 ± 0.134 (5)	0.951 ± 0.151 (3)	—	—
—CN	0.625 ± 0.0850 (5)	0.594 ± 0.0680	0.695 ± 0.090 (5)[b]	0.550 ± 0.051 (3)	0.451 ± 0.079 (5)	0.576 ± 0.064 (3)	—	—
—NO_2	1.97 ± 0.499 (4)[b]	0.181 ± 0.0393	28.8 ± 3.02 (5)[b]	1.51 ± 0.0839 (3)	0.498 ± 0.0645 (5)	0.487 ± 0.046 (3)	—	—
—OH	1.32 ± 0.345 (4)[b]	0.459 ± 0.0540	1.89 ± 0.194 (4)[b]	0.857 ± 0.109 (3)	2.21 ± 0.068 (5)[b]	0.735 ± 0.105 (3)	0.358 ± 0.029 (5)	0.381 ± 0.020 (3)
—C_6H_5	1.12 ± 0.348 (5)[b]	0.143 ± 0.0108	0.273 ± 0.0087 (5)[b]	0.182 ± 0.0241 (3)	0.213 ± 0.0087 (5)[b]	0.170 ± 0.0184 (3)	0.137 ± 0.006 (5)[b]	0.113 ± 0.011 (3)
—$C_6H_4{}^{125}I$[f]	0.00	0.00	—	—	—	—	—	—

[a] Depleted by the method of Levine and Murphy (17). [b] Statistically significant above control values ($p \leq 0.05$). [c] Percent deiodination ±*SD*, with the number of determinations in parentheses. [d] Adjusted enzyme activity from a different source for this cytosolic fraction, by comparison of cytosolic activities with the nitro compound as the substrate. [e] Not determined. [f] Substrate could not be incorporated into the medium without excessive loss of enzymatic activity.

results determined in this laboratory: 2.5 ± 0.52% for labeled *p*-iodonitrobenzene and 0.6 ± 0.04% for [4-^{125}I]iodobiphenyl (15).

The microsomal deiodination of these compounds can be explained by considering them as substrates for the mixed-function oxygenase system with arene oxide formation at the iodocarbon. The possible loss of iodide during a subsequent "N.I.H. shift" (23) involving this arene oxide would be analogous to the mechanism proposed for the loss of bromide or chloride in polyhalogenated biphenyl compounds (12, 13).

No correlation was found between microsomal deiodination and the electron-withdrawing character of *para*-substituents, as indicated by their Hammett values (24). Furthermore, no correlation was found between microsomal deiodination and the lability of the carbon-iodine bond as evidenced by the radiochemical yield in the exchange reaction used in their preparation.

Cytosolic Deiodination—Results of cytosolic deiodination are also shown in Table II. Six of the seven substrates exhibited deiodinations that were statistically significantly greater than the control values ([4,4′-^{125}I]diiodobiphenyl did not). [*p*-^{125}I]Iodonitrobenzene deiodinated to the greatest extent above the respective control value, indicating a unique specificity of glutathione-*S*-transferase for the nitro compound. The extent of this transformation, although large, was not unexpected. The metabolism of *p*-chloronitrobenzene resulted in ~7% of the dose being excreted as the mercapturic acid (25). The more labile carbon-iodine bond would facilitate increased deiodination. Cytosolic control values generally agreed with those in buffer and ethanol (Table I), although control values for the benzoic acid, nitro, 4-iodobiphenyl, and phenol substrates were significantly higher than their deiodination in buffer. Nonenzymatic glutathione conjugation of the nitro compound was believed to account for the high amount of deiodination found in the respective control. The reduction in deiodination when free glutathione levels were reduced with the addition of *N*-ethylmaleimide would further substantiate this belief. Pabst *et al.* (26) have established that nonenzymatic conjugation of glutathione with *p*-nitrobenzyl chloride and 1,2-dichloro-4-nitrobenzene was significant at or near physiological pH in the rat. Deiodination of the *p*-nitro and 4-iodobiphenyl substrates agreed well with values previously reported from this laboratory (15). No correlation was found between cytosolic deiodination and the electron-withdrawing character of the *para*-substituent for the acid, aldehyde, nitrile, nitro, phenol, or 4-iodobiphenyl substrates as measured by their Hammett values (24). There was also no correlation with the radiochemical yield of the syntheses of these compounds.

Kraus (27) reported the dechlorination of α-hexachlorocyclohexane in rat liver cytosol by a mechanism that was not dependent on glutathione and by a glutathione-*S*-transferase mechanism. Our previous studies also indicated a second cytosolic dehalogenase (16). An efficient means of inhibiting glutathione-*S*-transferase was sought in order to explore the nature of this second cytosolic dehalogenase system.

N-Ethylmaleimide is known to bind to thiols (28). [p-^{125}I]Iodonitrobenzene was incubated as described with 0.1–40.0 mM *N*-ethylmaleimide to determine the optimal concentration for the inhibition of glutathione-*S*-transferase. Deiodination decreased as the concentration of *N*-ethylmaleimide increased up to 2.5 mM. Increasing its concentration >2.5 mM resulted in no statistically significant decrease in deiodination. Thus, 2.5 mM *N*-ethylmaleimide was chosen as the optimal concentration in the final incubation mixture. Confirmation of the inhibition of glutathione-*S*-transferase was also established by measuring the concentration of glutathione in cytosol with and without *N*-ethylmaleimide. The standard Ellman thiol assay (19) as modified by Benke (20) showed that glutathione was below detectable levels with the addition of 2.5 mM *N*-ethylmaleimide.

Results of cytosolic deiodination with *N*-ethylmaleimide present are shown in Table II. [4-^{125}I]Iodobiphenyl and [*p*-^{125}I]iodophenol were the only substrates to exhibit statistically significant deiodination above the respective control values.

These two possible indications of a second nonglutathione cytosolic deiodinase were also studied by the use of an anion-exchange preparation (17) of glutathione-depleted cytosol. Glutathione concentration was again assayed by the Ellman procedure (20) and found to be below detectable limits. Further evidence of the efficiency of glutathione removal was demonstrated by determining the glutathione-*S*-transferase activity of intact and glutathione-depleted cytosol. The procedure of Habig *et al.* (18) with *p*-nitrobenzyl chloride as the substrate was used to follow the UV absorbance of the glutathione conjugate. Formation of the conjugate did not increase with time when glutathione-depleted cytosol was used. When the depleted cytosol was reconstituted with glutathione (5 mM), the rate of formation of the conjugate was not statistically different from that of intact cytosol. Therefore, this depletion procedure inhibited glutathione activity, but did not adversely affect glutathione-*S*-transferase.

The results of deiodination of [*p*-^{125}I]iodophenol and [4-^{125}I]iodobiphenyl using glutathione-depleted cytosol are shown in Table II. The deiodination of the biphenyl was statistically significant above the respective control value, but this was not the case for the phenolic compound. Thus, this confirmation of the presence of a cytosolic nonglutathione dehalogenase could only be established for the iodobiphenyl substrate. The microsomal and cytosolic glutathione systems were the more generally applicable deiodination mechanisms.

REFERENCES

(1) R. E. Counsell, T. D. Smith, V. V. Ranade, O. P. D. Noronha, and P. Desai, *J. Med. Chem.*, **16,** 684 (1973).

(2) R. E. Counsell, R. H. Seevers, N. Korn, and S. W. Schwende, *J. Med. Chem.*, **24,** 5 (1981).

(3) R. H. Seevers, Jr., Ph.D. Thesis, The University of Michigan, 1981.

(4) R. P. Spencer (Ed.), "Radiopharmaceuticals," Stratton, New York, N.Y., 1981.

(5) R. D. Kimbrough, R. A. Squire, R. E. Linder, J. D. Strandberg, R. J. Montali, and V. W. Burse, *J. Natl. Cancer Inst.*, **55,** 1453 (1975).

(6) L. Fishbein, *Ann. Rev. Pharmacol.*, **14,** 139 (1974).

(7) R. D. Kimbrough, *CRC Critical Rev. Toxicol.*, **2,** 445 (1974).

(8) A. C. Kolbye in "Health Effects of Polychlorinated and Polybrominated Biphenyls," U.S. HEW Report (1976).

(9) R. D. Kimbrough and R. E. Linder, *J. Natl. Cancer Inst.*, **53,** 547 (1974).

(10) S. D. Aust, G. A. Dannin, S. D. Sleight, P. J. Fraker, R. K. Ringer, and D. Polin, Symposium on Health and Ecological Effects of Chlorinated Hydrocarbons: Hepatotoxicity of Halogenated Hydrocarbons. Second Chemical Congress of the North American Continent, Las Vegas, Nev., August 24-29, 1980.

(11) O. Hutzinger, W. D. Jamieson, S. Safe, L. Paulmann, and R. Ammon, *Nature (London)*, **252**, 698 (1974).
(12) S. Safe, D. Jones, and O. Hutzinger, *J. Chem. Soc. (Perkin I)*, **4**, 357 (1976).
(13) J. Kohli and S. Safe, *Chemosphere*, **5**, 433 (1976).
(14) H. Elias and H. T. Lotterhos, *Chem. Ber.*, **109**, 1580 (1976).
(15) J. E. Sinsheimer, T. Wang, S. Röder, and Y. Y. Shun, *Biochem. Biophys. Res. Commun.*, **83**, 281 (1978).
(16) B. N. Ames, J. McCann, and E. Yamasaki, *Mutat. Res.*, **31**, 347 (1975).
(17) B. S. Levine and S. D. Murphy, *Toxicol. Appl. Pharmacol.*, **40**, 393, (1977).
(18) W. H. Habig, M. J. Pabst, and W. B. Jakoby, *J. Biol. Chem.*, **249**, 7130 (1974).
(19) G. L. Ellman, *Arch. Biochem. Biophys.*, **82**, 70 (1959).
(20) G. M. Benke *et al.*, *Toxicol. Appl. Pharmacol.*, **28**, 97 (1974).
(21) U. A. H. Hadi, D. J. Malcolme-Lawes, and G. Oldham, *Int. J. Appl. Rad. Isotop.*, **28**, 747 (1978).
(22) Y. C. J. Wang, *J. Pharm. Sci.*, **69**, 671 (1980).
(23) J. W. Daly, D. M. Jerina, and B. Witkop, *Experientia*, **28**, 1129 (1972).
(24) D. H. McDaniel and H. C. Brown, *J. Org. Chem.*, **23**, 420 (1958).
(25) H. G. Bray, S. P. James, and W. V. Thorpe, *Biochem. J.*, **67**, 607 (1957).
(26) M. J. Pabst, W. H. Habig, and W. B. Jakoby, *J. Biol. Chem.*, **249**, 7140 (1974).
(27) P. Kraus, *Naunyn-Schmiedeberg's Arch. Pharmacol.*, **291**, 79 (1975).
(28) F. Oesch and J. Daly, *Biochem. Biophys. Res. Commun.*, **46**, 1713 (1972).

ACKNOWLEDGMENTS

The authors would like to thank William Harrity and Amy Khan, National Science Foundation Undergraduate Research Participants, Grants No. SPI 7826914 and SPI 8026361, respectively, and Randy Olenyk for their laboratory assistance. This study was supported in part by a Training Grant 5-T32-GM07767 from the National Institutes of Health.

The authors are grateful to Mr. John Jones and The University of Michigan's Phoenix Memorial Laboratory for their cooperation in conducting our neutron-activation analyses.

Determination of Bupropion and Its Major Basic Metabolites in Plasma by Liquid Chromatography With Dual-Wavelength Ultraviolet Detection

THOMAS B. COOPER ˣ, RAYMOND F. SUCKOW, and ALEXANDER GLASSMAN

Received March 11, 1983, from the *Analytical Psychopharmacology Laboratory, New York State Psychiatric Institute, New York, NY 10032.* Accepted for publication September 14, 1983.

Abstract □ A method for the determination of bupropion and its three major basic metabolites in plasma is described. Following an extraction from alkaline plasma into 1.5% v/v isoamyl alcohol in *n*-heptane, a portion of the acid-backwashed extract was injected onto a column packed with trimethylsilyl reverse-phase material and eluted with a phosphate buffer–acetonitrile (80:20) mobile phase containing an ion-pairing reagent and triethylamine. The compounds were detected with a dual-wavelength UV detector (214 and 254 nm) to optimize sensitivity and facilitate simultaneous detection. The method provides an absolute recovery of ~85% for bupropion and ~98% for the metabolites. Day-to-day reproducibility did not exceed 4.0% for all compounds. The detection limits were ~5 ng/mL for bupropion and 100 ng/mL for the major metabolites. The limit of 100 ng/mL for metabolite quantitation is imposed by the internal standard concentration selected for steady-state studies. In single-dose pharmacokinetic studies, 10% of the steady-state concentration of internal standard was used; this permitted a 10-ng/mL lower limit of detection. Steady-state plasma levels of bupropion and the metabolites from eight different patients are presented.

Keyphrases □ Bupropion—metabolites, HPLC, dual-wavelength UV detection □ Antidepressants—bupropion and its metabolites, HPLC, dual-wavelength UV detection

Bupropion hydrochloride[1] [(±)-2-*tert*-butylamino-3′-chloropropiophenone hydrochloride], a chemically unique antidepressant currently undergoing clinical evaluation, appears to be free of any significant anticholinergic or cardiovascular effects (1–3). The assay of bupropion in biological fluids has been limited to RIA (4) and high-performance liquid chromatography (HPLC) (5). The RIA procedure appears to be sensitive (<1 ng/mL) and specific for bupropion, whereas the HPLC method is less sensitive (50 ng/mL). However, neither method quantitates metabolites.

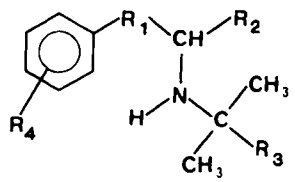

I: R_1 = C=O, R_2 = R_3 = CH_3, R_4 = 3-Cl
II: R_1 = C=O, R_2 = CH_3, R_3 = CH_2OH, R_4 = 3-Cl
III: R_1 = CHOH, R_2 = R_3 = CH_3, R_4 = 3-Cl (*erythro*)
IV: R_1 = CHOH, R_2 = R_3 = CH_3, R_4 = 3-Cl (*threo*)
V: R_1 = CHOH, R_2 = CH_3, R_3 = CH_2OH, R_4 = 3-Cl (*erythro*)
VI: R_1 = C=O, R_2 = C_2H_5, R_3 = CH_3, R_4 = 4-F
VII: R_1 = C=O, R_2 = C_3H_7, R_3 = CH_3, R_4 = 4-F

Current interest in biologically active metabolites of psychotropic drugs led us to develop an HPLC procedure which separates and quantitates bupropion and its major basic metabolites in plasma with dual-wavelength UV detection.

EXPERIMENTAL SECTION

Apparatus—Chromatography was performed with a dual-piston solvent delivery pump[2] with either a manual injector[3] or an automatic sample processor[4]. The column was 25 cm × 4.6 mm i.d. packed with 5-μm particle size trimethylsilyl material[5]. The effluent was monitored at 254 and 214 nm by

[1] Wellbutrin.

[2] Model 6000A; Water Associates, Milford, Mass.
[3] U6K Injector; Waters Associates.
[4] Wisp 710B; Waters Associates.
[5] LC-1; Supelco, Bellafonte, Pa.

0022-3549/84/0800-1104$01.00/0
© 1984, American Pharmaceutical Association

(11) O. Hutzinger, W. D. Jamieson, S. Safe, L. Paulmann, and R. Ammon, *Nature (London)*, **252**, 698 (1974).
(12) S. Safe, D. Jones, and O. Hutzinger, *J. Chem. Soc. (Perkin I)*, **4**, 357 (1976).
(13) J. Kohli and S. Safe, *Chemosphere*, **5**, 433 (1976).
(14) H. Elias and H. T. Lotterhos, *Chem. Ber.*, **109**, 1580 (1976).
(15) J. E. Sinsheimer, T. Wang, S. Röder, and Y. Y. Shun, *Biochem. Biophys. Res. Commun.*, **83**, 281 (1978).
(16) B. N. Ames, J. McCann, and E. Yamasaki, *Mutat. Res.*, **31**, 347 (1975).
(17) B. S. Levine and S. D. Murphy, *Toxicol. Appl. Pharmacol.*, **40**, 393, (1977).
(18) W. H. Habig, M. J. Pabst, and W. B. Jakoby, *J. Biol. Chem.*, **249**, 7130 (1974).
(19) G. L. Ellman, *Arch. Biochem. Biophys.*, **82**, 70 (1959).
(20) G. M. Benke *et al.*, *Toxicol. Appl. Pharmacol.*, **28**, 97 (1974).
(21) U. A. H. Hadi, D. J. Malcolme-Lawes, and G. Oldham, *Int. J. Appl. Rad. Isotop.*, **28**, 747 (1978).
(22) Y. C. J. Wang, *J. Pharm. Sci.*, **69**, 671 (1980).
(23) J. W. Daly, D. M. Jerina, and B. Witkop, *Experientia*, **28**, 1129 (1972).
(24) D. H. McDaniel and H. C. Brown, *J. Org. Chem.*, **23**, 420 (1958).
(25) H. G. Bray, S. P. James, and W. V. Thorpe, *Biochem. J.*, **67**, 607 (1957).
(26) M. J. Pabst, W. H. Habig, and W. B. Jakoby, *J. Biol. Chem.*, **249**, 7140 (1974).
(27) P. Kraus, *Naunyn-Schmiedeberg's Arch. Pharmacol.*, **291**, 79 (1975).
(28) F. Oesch and J. Daly, *Biochem. Biophys. Res. Commun.*, **46**, 1713 (1972).

ACKNOWLEDGMENTS

The authors would like to thank William Harrity and Amy Khan, National Science Foundation Undergraduate Research Participants, Grants No. SPI 7826914 and SPI 8026361, respectively, and Randy Olenyk for their laboratory assistance. This study was supported in part by a Training Grant 5-T32-GM07767 from the National Institutes of Health.

The authors are grateful to Mr. John Jones and The University of Michigan's Phoenix Memorial Laboratory for their cooperation in conducting our neutron-activation analyses.

Determination of Bupropion and Its Major Basic Metabolites in Plasma by Liquid Chromatography With Dual-Wavelength Ultraviolet Detection

THOMAS B. COOPER ˣ, RAYMOND F. SUCKOW, and ALEXANDER GLASSMAN

Received March 11, 1983, from the *Analytical Psychopharmacology Laboratory, New York State Psychiatric Institute, New York, NY 10032.* Accepted for publication September 14, 1983.

Abstract □ A method for the determination of bupropion and its three major basic metabolites in plasma is described. Following an extraction from alkaline plasma into 1.5% v/v isoamyl alcohol in *n*-heptane, a portion of the acid-backwashed extract was injected onto a column packed with trimethylsilyl reverse-phase material and eluted with a phosphate buffer–acetonitrile (80:20) mobile phase containing an ion-pairing reagent and triethylamine. The compounds were detected with a dual-wavelength UV detector (214 and 254 nm) to optimize sensitivity and facilitate simultaneous detection. The method provides an absolute recovery of ~85% for bupropion and ~98% for the metabolites. Day-to-day reproducibility did not exceed 4.0% for all compounds. The detection limits were ~5 ng/mL for bupropion and 100 ng/mL for the major metabolites. The limit of 100 ng/mL for metabolite quantitation is imposed by the internal standard concentration selected for steady-state studies. In single-dose pharmacokinetic studies, 10% of the steady-state concentration of internal standard was used; this permitted a 10-ng/mL lower limit of detection. Steady-state plasma levels of bupropion and the metabolites from eight different patients are presented.

Keyphrases □ Bupropion—metabolites, HPLC, dual-wavelength UV detection □ Antidepressants—bupropion and its metabolites, HPLC, dual-wavelength UV detection

Bupropion hydrochloride[1] [(±)-2-*tert*-butylamino-3′-chloropropiophenone hydrochloride], a chemically unique antidepressant currently undergoing clinical evaluation, appears to be free of any significant anticholinergic or cardiovascular effects (1–3). The assay of bupropion in biological fluids has been limited to RIA (4) and high-performance liquid chromatography (HPLC) (5). The RIA procedure appears to be sensitive (<1 ng/mL) and specific for bupropion, whereas the HPLC method is less sensitive (50 ng/mL). However, neither method quantitates metabolites.

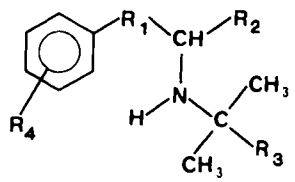

I: R_1 = C=O, R_2 = R_3 = CH_3, R_4 = 3-Cl
II: R_1 = C=O, R_2 = CH_3, R_3 = CH_2OH, R_4 = 3-Cl
III: R_1 = CHOH, R_2 = R_3 = CH_3, R_4 = 3-Cl (*erythro*)
IV: R_1 = CHOH, R_2 = R_3 = CH_3, R_4 = 3-Cl (*threo*)
V: R_1 = CHOH, R_2 = CH_3, R_3 = CH_2OH, R_4 = 3-Cl (*erythro*)
VI: R_1 = C=O, R_2 = C_2H_5, R_3 = CH_3, R_4 = 4-F
VII: R_1 = C=O, R_2 = C_3H_7, R_3 = CH_3, R_4 = 4-F

Current interest in biologically active metabolites of psychotropic drugs led us to develop an HPLC procedure which separates and quantitates bupropion and its major basic metabolites in plasma with dual-wavelength UV detection.

EXPERIMENTAL SECTION

Apparatus—Chromatography was performed with a dual-piston solvent delivery pump[2] with either a manual injector[3] or an automatic sample processor[4]. The column was 25 cm × 4.6 mm i.d. packed with 5-μm particle size trimethylsilyl material[5]. The effluent was monitored at 254 and 214 nm by

[1] Wellbutrin.

[2] Model 6000A; Water Associates, Milford, Mass.
[3] U6K Injector; Waters Associates.
[4] Wisp 710B; Waters Associates.
[5] LC-1; Supelco, Bellafonte, Pa.

0022-3549/84/0800-1104$01.00/0
© 1984, American Pharmaceutical Association

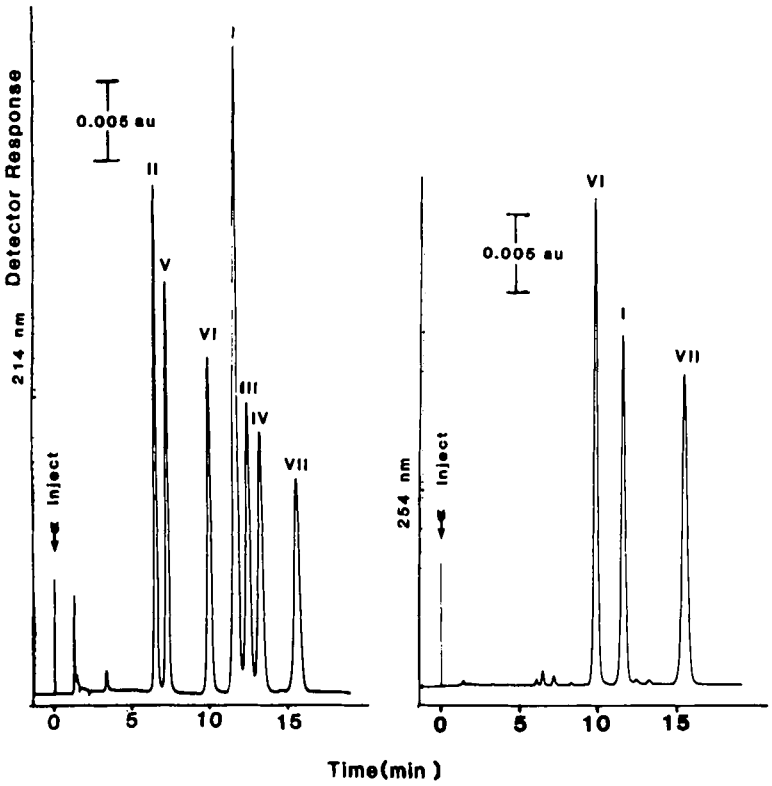

Figure 1—*Dual chromatogram of a standard aqueous solution containing 400 ng each of I, its major metabolites (II, III, and IV), a possible urinary metabolite (V), and internal standards (VI and VII). The compounds were detected at 214 and 254 nm simultaneously.*

a dual (in series) UV detector system[6], a signal recorder[7], and a laboratory data acquisition system[8]. The column temperature was controlled with an aluminum block devised to fit this column and with a circulating water pump[9].

Reagents—Phosphoric acid[10], monobasic potassium phosphate[10], sodium carbonate[10], and sodium bicarbonate[10] were all analytical reagent grade. Sodium heptanesulfonate[11] and triethylamine[12] were used as received. UV-grade acetonitrile[13] and *n*-heptane[10] were used without further purification. Isoamyl alcohol[14] was distilled before use. Distilled water was passed through a water purification system[15] before use.

Standards—Bupropion hydrochloride (I), 3'-chloro-2-(2-hydroxy-1,1-dimethylethylamino)propiophenone hydrochloride (II), (+)(*R**,*S**)-2-(*tert*-butylamino)-1-(3-chlorophenyl)propanol (III), (*R**,*R**)-2-(*tert*-butylamino)-1-(3-chlorophenyl)propanol (IV), (±)(*R**,*S**)-1-(3-chlorophenyl)-2-(2-hydroxy-1,1-dimethylethylamino)propanol (V), 2-(*tert*-butylamino)-4'-fluorobutyrophenone hydrochloride (VI), and 2-(*tert*-butylamino)-4'-fluorovalerophenone hydrochloride (VII) stock solutions (1 mg/mL) were prepared in 0.01 M HCl. Working solutions were further diluted to 1 ng/μL in 0.01 M HCl for I and V, and to 10 ng/μL in 0.01 M HCl for II, III, IV, VI, and VII. The structures and activities of these metabolites have been described elsewhere (3).

Extraction—To 1.0 mL of plasma, 800 ng of internal standard VI and 150 ng of internal standard VII were added to 1.0 mL of 0.6 M carbonate buffer (pH 9.5) and 10 mL of 1.5% v/v isoamyl alcohol in *n*-heptane. The mixture was shaken for 15 min and centrifuged at 1500×*g* for 10 min. The organic layer was then transferred to a 15-mL tube containing 250 μL of 0.1 M HCl. After mixing for 10 min and centrifuging at 1500×*g* for 10 min, the organic layer was removed by aspiration. Suitable aliquots of the aqueous phase were injected for chromatographic separation.

Chromatographic Conditions—The mobile phase consisted of 0.05 M monobasic potassium phosphate–acetonitrile (80:20), with 0.007 M sodium heptanesulfonate and 0.01 M triethylamine added. The final pH of the aqueous portion was brought to 3.0 by the addition of phosphoric acid. The mixture was filtered and deaerated prior to use. The flow rate was 2.3 mL/min, and the column temperature was set at 30°C. The effluent was monitored with a dual UV detector system at 254 and 214 nm in series.

Quantitation—All determinations were performed by calculating the peak height and/or area ratios of each compound to the internal standard. A linear regression analysis for each of the standard curves was performed with an on-line data acquisition system resulting in the computation of the slope, *x*-intercept, correlation coefficient, and standard error. Compound I was quantitated at 254 nm with internal standard VII. Metabolites II, III, and IV were quantitated at 214 nm with internal standard VI.

RESULTS AND DISCUSSION

Bupropion (I) and its major metabolites in plasma were separated and quantitated by HPLC with a dual-wavelength UV detector system. Although all compounds absorb at 214 nm, only I and the two internal standards (VI and VII) absorb at 254 nm (Fig. 1). Since it was found that the steady-state plasma concentration of I was low in comparison to its metabolites, simultaneous quantitation was not possible for all compounds at 214 nm. The major metabolite of I (*i.e.*, II) is usually found at concentrations 10–100 times that of bupropion. Thus, I was quantitated at 254 nm with internal standard VII.

All compounds were adequately resolved and eluted within a 20-min period (Fig. 1). An actual spiked plasma sample is shown in Fig. 2. A drug-free patient plasma sample did not show any interfering endogenous peaks at either wavelength (Fig. 3). Although V is reported to be a urinary metabolite (6), no detectable levels were found in steady-state plasma samples obtained from patients (Fig. 4). Therefore, this metabolite was not included in the precision and accuracy tests in plasma. Figure 2 illustrates that V could be coextracted, separated, and quantitated, thus making this method possibly useful in metabolite studies in urine.

In general, it was found that the addition of triethylamine enhanced peak symmetry. Other amine modifiers such as *n*-butylamine or nonylamine did not afford the resolution needed. Other columns such as an octyldecylsilyl and an octylsilyl-bonded column resulted in longer retention times and inadequate resolution between III and IV.

The detection limit for I is ~5 ng/mL of plasma, and the detector response remained linear at least up to 400 ng. The detection limit for II, III, and IV in this assay was 100 ng/mL, and the detector response showed linearity from 100 to at least 3000 ng.

The limit of 100 ng/mL for metabolite quantitation is imposed by the internal standard concentration selected for steady-state studies. In single-dose pharmacokinetic studies, 10% of the concentration of internal standard used for steady state was utilized; this permitted a 10-ng/mL lower limit of detection.

[6] Model 440 (254 nm) with extended wavelength module (214 nm); Waters Associates.
[7] Houston Omniscribe model B5217B-2; Houston Instruments, Austin, Tex.
[8] PDP 11/34 "Peak II" System; Digital Equipment Co., Maynard, Mass.
[9] Model FE; Haake Co., Saddlebrook, N.J.
[10] Fisher Scientific Co., Fair Lawn, N.J.
[11] Eastman Kodak Co., Rochester, N.Y.
[12] Aldrich Chemical Co., Milwaukee, Wis.
[13] Burdick and Jackson Laboratories, Muskegon, Mich.
[14] Sigma Chemical Co., St. Louis, Mo.
[15] Milli-Q; Millipore Corp., Bedford, Mass.

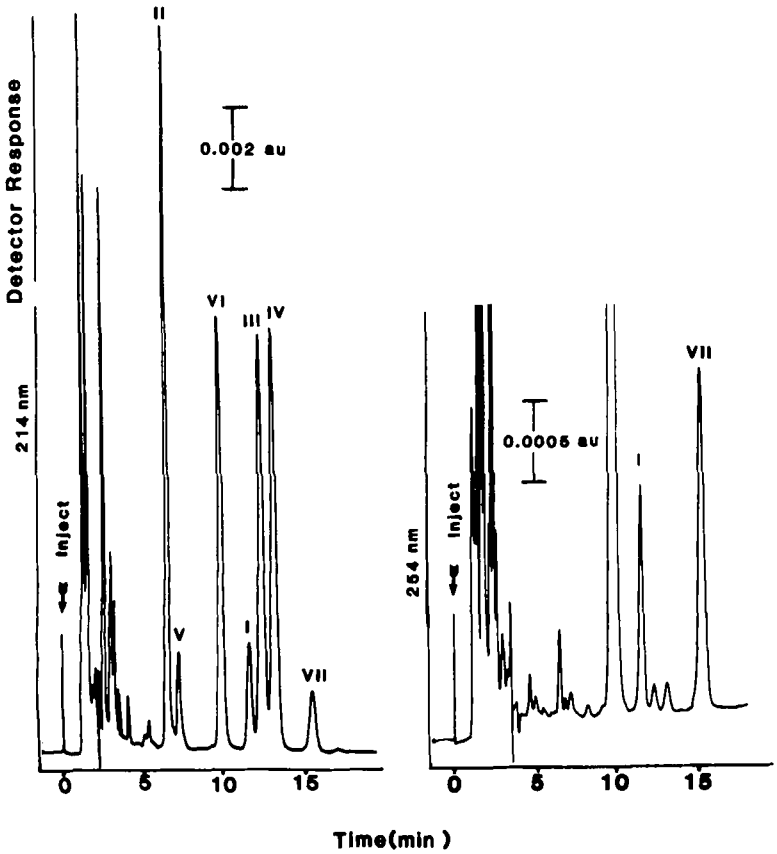

Figure 2—*Dual chromatogram of a 1-mL spiked plasma extract containing 100 ng of I and metabolite V and 1000 ng of II, III, and IV. Fifty microliters of the acid extract was injected. Compounds VI and VII are the internal standards.*

In preliminary single-dose studies, the major metabolites (II and IV) were present at 30 min postdose, reaching a maximum of 2–3 times that of bupropion. Furthermore, inspection of these data clearly indicates that the metabolites have markedly different (longer) half-lives of elimination[16].

The absolute recovery was determined by preparing a solution of known

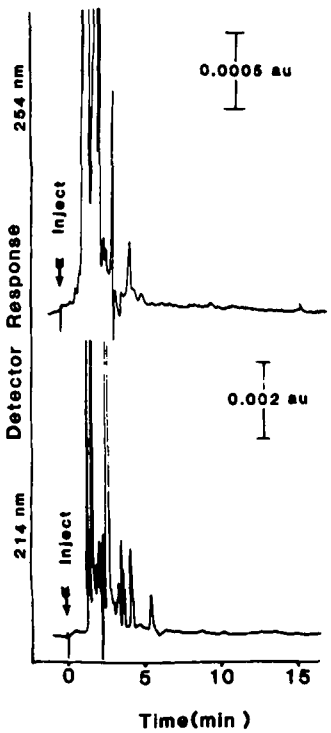

Figure 3—*Dual chromatogram of a 1-mL plasma extract from a drug-free patient. The volume injected was 100 μL.*

[16] Unpublished results.

Table I—Recovery of I and Metabolites from 1 mL of Plasma

Compound	Recovery, %[a] 3000 ng/mL	1000 ng/mL	400 ng/mL	100 ng/mL	12.5 ng/mL
I	—	—	82 ± 3.2	87 ± 2.9	85 ± 10.4
II	95 ± 2.2	96 ± 3.8	—	97 ± 10.0	—
III	98 ± 2.4	102 ± 2.8	—	97 ± 9.3	—
IV	99 ± 2.4	104 ± 3.0	—	97 ± 9.7	—

[a] Mean ± *RSD*; $n = 8$.

Table II—Precision of Assay for I and Metabolites Based on Peak Height Ratios[a]

Concentration, ng/mL	*RSD*, % I	II	III	IV
3000		±0.8	±1.1	±1.2
1500		±2.3	±2.6	±2.7
1000		±1.3	±1.1	±1.2
500		±3.3	±3.7	±4.0
400	±2.9			
250		±4.0	±3.6	±4.4
200	±2.0			
100	±4.7	±5.0	±8.2	±3.9
50	±4.3			
25	±2.5			
10	±6.0			

[a] $n = 8$.

Table III—Reproducibility of Assay Based on Slopes of the Linear Regression Curves[a]

Compound	Slope, ng/mL	*RSD*, %
I	147.8	±3.3
II	627.4	±3.1
III	1074.8	±2.7
IV	1066.4	±4.0

[a] Data computed from five consecutive standard curves.

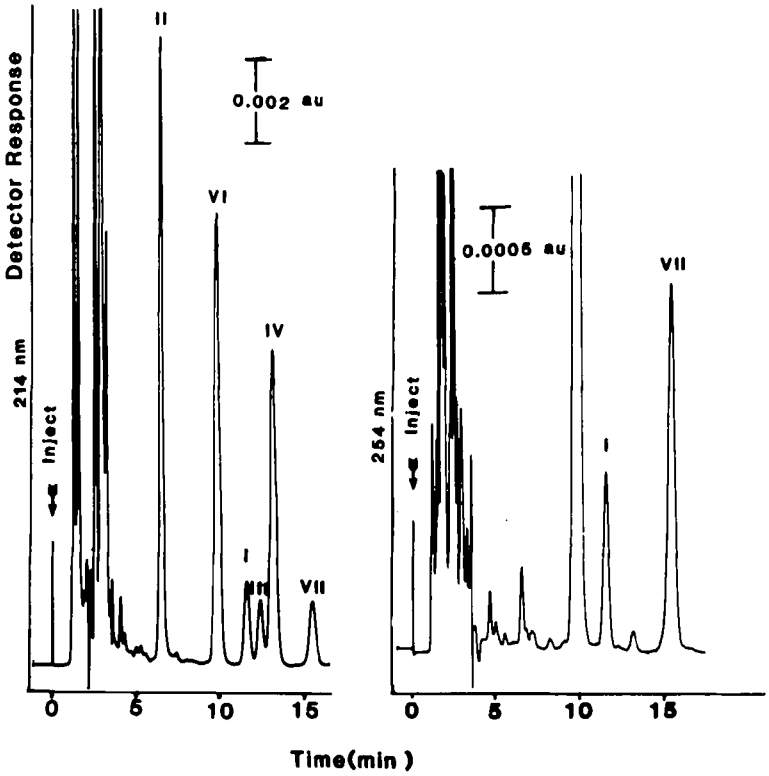

Figure 4—*Dual chromatogram of a 1-mL plasma extract from a patient receiving bupropion. Fifty microliters of the acid extract was injected. The plasma levels were calculated to be 72 ng of bupropion, 831 ng of II, 151 ng of III, and 743 ng of IV. Compounds VI and VII are the internal standards.*

concentration of all compounds. The internal standards were added to each solution, and the sample was injected into the chromatograph. The same standards were added to 1 mL of plasma and processed routinely, except for the internal standards. To 100 μL of the final acid extract, 100 μL of internal standard solution containing twice the usual concentration was added. The tube was capped, thoroughly mixed, and then injected. The difference between the ratios of the standards to internal standards in the processed samples *versus* direct injection samples gave a measure of overall recovery (Table I).

The precision of the method was determined by spiking eight standards; the sample was processed as described above. The percent relative standard deviations for various concentrations are reported in Table II.

A measure of the stability of the assay was demonstrated by the variability in the slope of the linear regression curves on 5 consecutive days (Table III). Accuracy was further assessed by comparing plasma concentrations of bupropion from two single-dose pharmacokinetic studies determined by this method and an RIA procedure (4). Twenty-eight samples (range, 5–130 ng/mL) were analyzed. Least-squares linear regression analysis resulted in the following: slope, 0.93; x-intercept, 2.2 ng/mL; and correlation coefficient, 0.987, where y and x were the bupropion concentrations by HPLC and RIA, respectively. Metabolite concentrations could not be compared since no other method has, as of now, been established.

Several psychotropic drugs and their metabolites were tested to determine potential interference in the assay. All commonly used tricyclic antidepressant compounds (imipramine, desipramine, amitriptyline, nortriptyline, doxepin, and desmethyldoxepin) and the new antidepressant drugs maprotiline, trazodone, mianserin, amoxapine, and chlorimipramine have much longer retention times than VII. Similarly, the major neuroleptic compounds such as chlorpromazine, thioridazine, loxapine, fluphenazine, perphenazine, and haloperidol do not interfere.

Compounds that may interfere are the hydroxy metabolites of amitriptyline, chlordiazepoxide and its *N*-demethyl metabolite, and nordiazepam.

Until now, there has been no reported human steady-state plasma level data for bupropion or its metabolites. The pharmacokinetics of bupropion has been reported (7), but metabolite determinations were not performed. Table IV is a summary of plasma concentration of bupropion and its major metabolites in eight different patients being treated for depression. The dose varied from patient to patient (100–450 mg/d). Although bupropion plasma concentrations averaged 50 ng/mL, the major metabolite (II) was found to be ~50 times higher (2500 ng/mL). The two diastereoisomers (III and IV) were also found in considerably higher concentrations (the *threo* isomer was always present in amounts 3–5 times greater than the *erythro* isomer).

Table IV—Typical Steady-State Plasma Concentrations of I and Metabolites in Eight Depressed Patients [a]

Patient	Dose, mg/24 h	Concentration, ng/mL I	II	III	IV
1	450	68	2784	103	453
2	350	43	3111	542	2226
3	100	24	1006	123	483
4	450	66	2931	368	1715
5	450	51	1931	379	1959
6	300	41	2801	348	1146
7	300	33	1512	174	552
8	350	35	2581	218	997

[a] All samples were collected immediately prior to morning dose. Dosage range, 100–450 mg/d.

REFERENCES

(1) H. J. Leighton and R. A. Maxwell, *Fed. Proc. Fed. Am. Soc. Exp. Biol.*, **37**, 481 (1978).

(2) J. P. Feighner, *J. Clin. Psychiat.*, **44**, 5(2), 49 (1983).

(3) R. A. Maxwell, W. B. Mehta, W. E. Tucker, Jr., D. H. Schroeder, and W. C. Stern in "Pharmacological and Biochemical Properties of Substances," vol. 3, *Am. Pharmaceutical Assoc.*, Washington, D.C., 1981, pp. 1–55.

(4) R. F. Butz, D. H. Schroeder, R. M. Welch, N. B. Mehta, A. P. Phillips, and J. W. A. Findlay, *J. Pharmacol. Exp. Ther.*, **217**, 602 (1981).

(5) D. H. Schroeder, M. L. Hinton, P. G. Smith, C. A. Nichol, and R. M. Welch, *Fed. Proc. Fed. Am. Soc. Exp. Biol.*, **37**, 691 (1978).

(6) D. H. Schroeder, J. L. Eiseman, N. B. Mehta, D. A. Brent, F. E. Soroko, and R. M. Welch, *Pharmacologist*, **16**, 191 (1979).

(7) J. W. A. Findlay, J. Vanwyck Fleet, P. G. Smith, R. F. Butz, M. L. Hinton, M. R. Blum, and D. H. Schroeder, *Eur. J. Clin. Pharmacol.*, **21**, 127 (1981).

ACKNOWLEDGMENTS

This work was made possible by a grant-in-aid to T.B.C. by Burroughs-Wellcome Co., Research Triangle Park, NC 27709. Help from the following Burroughs-Wellcome senior staff scientists is especially acknowledged: Dr. Warren C. Stern for generously supplying bupropion, metabolites, and the compounds used as internal standards and for his continuing advice and support; and Drs. A. A. Lai and D. H. Schroeder for supplying the plasma from bupropion-treated depressed patients and single-dose bupropion samples from normal volunteers.

Pharmacokinetics of Bumetanide Following Intravenous, Intramuscular, and Oral Administrations to Normal Subjects

A. A. HOLAZO *x, W. A. COLBURN *, J. H. GUSTAFSON *, R. L. YOUNG ‡, and M. PARSONNET §

Received May 5, 1983, from the *Department of Pharmacokinetics and Biopharmaceutics, ‡Department of Biochemistry and Drug Metabolism, and §Department of Clinical Pharmacology, Hoffmann-La Roche Inc., Nutley, NJ 07110. Accepted for publication August 22, 1983.

Abstract □ The pharmacokinetics of bumetanide was studied in 12 normal subjects after 1-mg intravenous, intramuscular, oral solution, and tablet administrations in a random four-treatment crossover design. Plasma and urine concentrations of intact bumetanide were analyzed by a sensitive and specific RIA. The pharmacokinetics of bumetanide after intravenous administration was characterized by a biexponential equation, including an initial disposition phase ($t_{1/2,\alpha}$ = 5.1 min), followed by a slower elimination phase ($t_{1/2,\beta}$ = 44 min). Bumetanide pharmacokinetics after intramuscular and oral administration could be described by a biexponential equation with first-order absorption and elimination. Bumetanide is rapidly absorbed *via* the intramuscular and oral routes, with mean ± *SD* maximum plasma concentrations of 38.2 ± 9.8 (intramuscular), 34.0 ± 10.6 (oral solution), and 30.9 ± 14.6 ng/mL (tablet) achieved within 0.34 ± 0.23, 0.76 ± 0.27, and 1.8 ± 1.2 h after dosing, respectively. The drug is rapidly eliminated from the body after intravenous, intramuscular, oral solution, and oral tablet administrations, with half-lives ranging from 24–86, 47–139, 27–71, and 26–99 min, respectively. Approximately 70% of a parenteral dose and 60% of an oral dose are excreted as intact drug in urine taken 0–24 h after administration. The extent of bioavailability of bumetanide from the tablet and oral solution dosage forms are equivalent, and the absolute bioavailability of the intramuscular and oral preparations are ~100 and 80%, respectively. This is consistent with the predicted limited extent of first-pass metabolism after complete absorption of an oral dose. The pharmacokinetic and pharmacodynamic data support the conclusion that bumetanide is galenically available from the tablet dosage form and that comparable cumulative diuretic activity is obtained, regardless of the route and mode of administration.

Keyphrases □ Pharmacokinetics—bumetanide, intravenous, intramuscular, and oral administration □ Bumetanide—pharmacokinetics, intravenous, intramuscular, and oral administration, □ Diuretics—bumetanide, pharmacokinetics following intravenous, intramuscular, and oral administration □ Bioavailability—bumetanide, intravenous, intramuscular, and oral administration

Bumetanide, 3-(butylamino)-4-phenoxy-5-sulfamoylbenzoic acid, a new potent sulfonamide diuretic, produces a rapid diuretic response with a short duration of action in humans. The major site of action is on the ascending limb of Henle's loop, in addition to further action on the proximal tubule (1–3). The diuretic effects of bumetanide are as extensive as those of other "loop" diuretics but at oral doses of 1 mg, as compared with 40–60 mg of furosemide (4–8). Although pharmacokinetic studies in humans after intravenous and oral administration of bumetanide have been reported (6, 9–12), the pharmacokinetics and bioavailability of intramuscularly administered bumetanide have not.

The purpose of this study was to determine primary pharmacokinetic parameters of bumetanide following intravenous, intramuscular, and oral administrations and to assess the bioavailability of the intramuscular, oral tablet, and oral solution preparations of bumetanide relative to intravenous administration.

EXPERIMENTAL SECTION

Clinical Protocol—Twelve healthy adult male and female volunteers [23–40 years old (mean 30); weight, 54–96 kg (mean 70)] were selected for the study. Subjects were considered normal by medical history, physical examination, and blood and urine laboratory tests. An informed written consent was obtained from each volunteer before the study.

Single 1-mg doses of bumetanide were administered to each subject as intravenous, intramuscular, oral solution, and tablet preparations. Subjects were randomly assigned to the four treatments, and there were at least 2 weeks between dosage administrations. The drug was supplied in 0.25-mg/mL ampules for parenteral and oral solution administrations. The intravenous dose was administered over a 2-min period, and the intramuscular dose was injected into the lateral thigh with an intramuscular administration needle. The oral solution dose was administered in a 4-mL solution given with 250 mL of water, and the oral tablet was given with 250 mL of water.

Subjects fasted for 8 h prior to drug administration and remained fasting until the 4-h blood sample was collected. A hospital-prepared lunch, supper, and a bedtime snack were served. No additional salt or highly salted foods were permitted. Water was permitted *ad libitum*.

Blood samples (10 mL) were drawn through an indwelling cannula or by separate venipuncture into oxalated tubes prior to drug administration and at 0.1, 0.25, 0.5, 0.75, 1, 1.5, 2, 2.5, 3, 4, 5, 6, 7, 8, 10, 12, and 24 h after drug administration. Plasma was separated and stored at −17°C until assayed. All urine voided over 12 h before dose and 0–2, 2–4, 4–6, 6–8, 8–12, and 12–24 h after drug administration was collected, and 50-mL aliquots were stored at −17°C until assayed.

Analytical Procedures—Plasma and urine samples were assayed for intact bumetanide using a slight modification of the sensitive and specific RIA procedure of Dixon *et al.* (13). In the present study, the precipitated antibody-bound fraction was quantitated rather than the unbound fraction, and the data were calculated as outlined by Rodbard (14), with a digital computer used for iterative weighted linear regression analysis of logit B/B_0 *versus* log dose. The RIA had a limit of sensitivity of 3 ng/mL of bumetanide with 0.1 mL of plasma or urine.

Pharmacokinetic Analysis—Plasma concentrations following intravenous administration were curve-fitted as follows (15):

$$C_p(t) = Ae^{-\alpha t} + Be^{-\beta t} \quad \text{(Eq. 1)}$$

and concentrations after intramuscular and oral administration were fitted with the following (15):

$$C_p(t) = A'[e^{-\beta(t-t_0)} - e^{-k_a(t-t_0)}] \quad \text{(Eq. 2)}$$

where $C_p(t)$ is the plasma concentration of bumetanide at time t; A, A', and B are coefficients; α is the initial disposition rate constant; β is the terminal elimination rate constant; k_a is the apparent absorption rate constant; and t_0 is the lag time preceding initiation of absorption. A weighted ($1/C_p$) nonlinear regression program [NONLIN (16)] was used to calculate the best estimates of the pharmacokinetic parameters.

The model-estimated parameters were used to calculate the theoretical area under the plasma concentration–time curve (AUCTh), the apparent volume of the central compartment (V_c), and volume of distribution in the postdistributive phase (Vd_{area}) as follows:

$$\text{AUCTh (intravenous)} = A/\alpha + B/\beta \quad \text{(Eq. 3)}$$

$$\text{AUCTh (intramuscular, oral)} = A'/\beta - A'/k_a \quad \text{(Eq. 4)}$$

$$V_c \text{ (intravenous)} = \text{Dose}/(A + B) \quad \text{(Eq. 5)}$$

$$Vd_{area} \text{ (intravenous)} = \text{Dose}/(\text{AUCTh}\cdot\beta) \quad \text{(Eq. 6)}$$

The maximum plasma concentration (C_{max}) and the time (t_{max}) of its occurrence following intramuscular and oral administrations were read directly from the observed plasma concentration–time data. The area under the plasma concentration–time curve from time zero to infinity (AUCTr) were calculated as follows:

$$\text{AUCTr} = \text{AUC}_{0\to t} + C_p(t)/\beta \quad \text{(Eq. 7)}$$

where $\text{AUC}_{0\to t}$ is the area calculated by trapezoidal summation from time zero to the time, t, of the last measurable plasma concentration, $C_p(t)$. For

0022-3549/84/0800-1108$01.00/0
© 1984, American Pharmaceutical Association

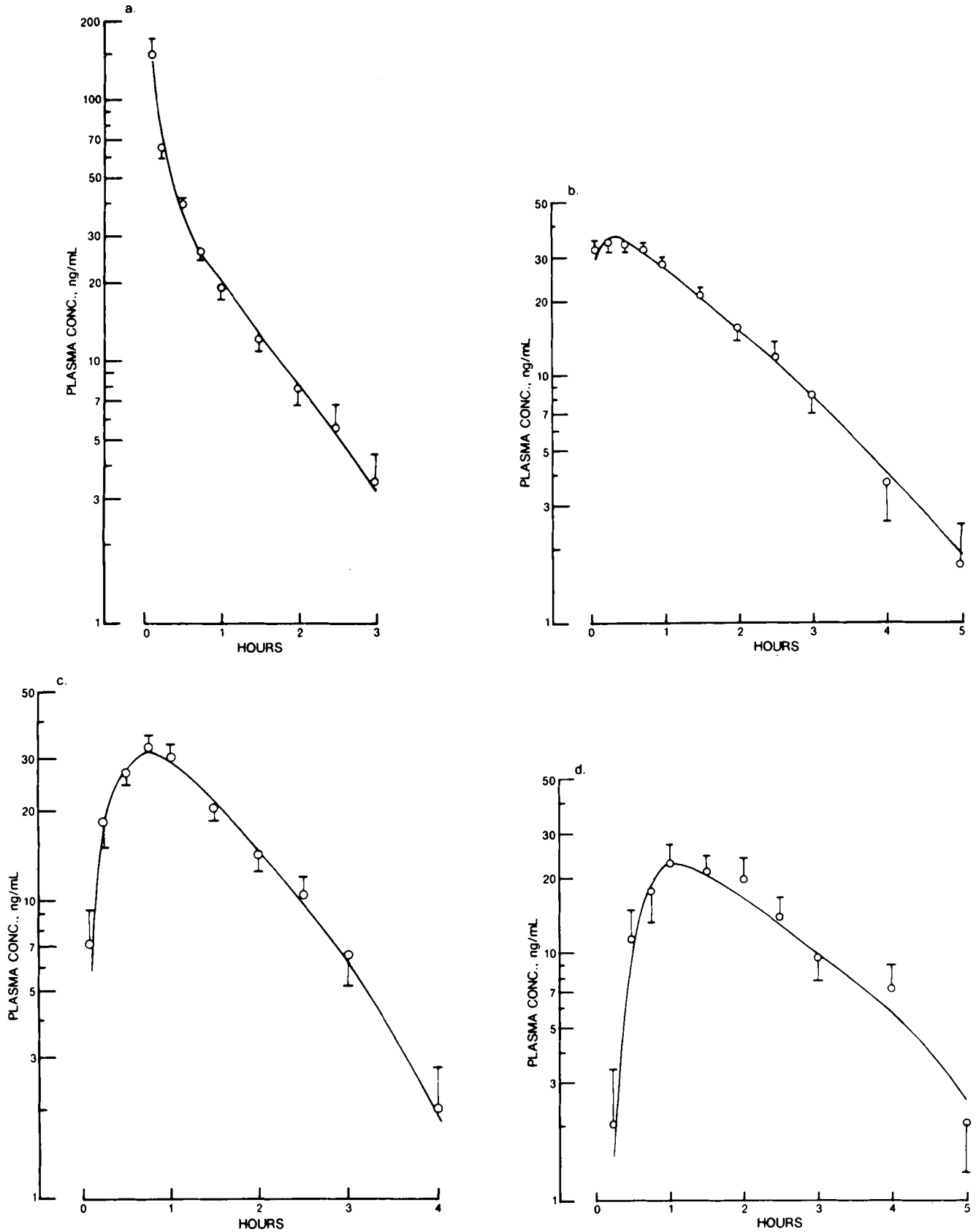

Figure 1—*Mean plasma concentration–time profiles of bumetanide following administrations of 1 mg of bumetanide to 12 normal subjects. The circles are actual data points (mean ±SE), and the solid lines are the fitted curves. Key: (a) intravenous; (b) intramuscular; (c) oral solution; (d) oral tablet.*

intravenous administration, the plasma concentration at time zero was extrapolated graphically.

The volume of distribution at steady-state (Vd_{ss}), systemic plasma clearance (CL_p), apparent oral clearance (CL_o), renal clearance (CL_r), and nonrenal clearance (CL_{nr}) were calculated by model-independent methods from the following relationships:

$$Vd_{ss}\text{ (intravenous)} = \text{Dose (AUMCTr)}/(\text{AUCTr})^2 \quad \text{(Eq. 8)}$$

$$CL_p\text{ (intravenous, intramuscular)} = \text{Dose}/\text{AUCTr} \quad \text{(Eq. 9)}$$

Table I—Pharmacokinetic Parameters[a] of Bumetanide Estimated by Curve-Fitting Intravenous Plasma Concentration–Time Data to Eq. 1

Subject	A, ng/mL	α, h^{-1}	B, ng/mL	β, h^{-1}	$t_{1/2,\alpha}$, min	$t_{1/2,\beta}$, min	V_c, L	Vd_{area}, L	AUCTh, ng·h/mL	r
1	161	6.3	52	0.482	7	86	4.7	15.4	134	0.999
2	117	9.1	74	1.09	5	38	5.2	11.4	81	1.000
3	122	5.7	36	0.797	7	52	6.3	18.9	67	1.000
4	477	7.2	42	0.664	6	62	1.9	11.6	130	0.999
5	329	9.9	32	0.926	4	45	2.8	15.8	68	0.999
6	105	7.0	40	0.854	6	49	6.9	19.0	62	1.000
7	236	6.9	52	0.771	6	54	3.5	12.8	101	0.998
8	157	7.4	46	1.06	5	39	4.9	14.5	65	0.999
9	99	8.5	36	0.909	5	46	7.4	21.6	51	0.999
10	228	8.2	61	0.991	5	42	3.5	11.2	90	1.000
11	81	14.8	84	1.75	3	24	6.1	10.7	54	0.999
12	320	6.7	61	1.01	6	41	2.6	9.1	109	1.000
Mean	203	8.1	51	0.942	5.1[b]	44[b]	4.7	14.3	84	
SD	±120	±2.4	±16	±0.308			±1.8	±3.9	±29	

[a] Parameters are defined in the text. [b] Harmonic mean.

Table II—Model-Independent Pharmacokinetic Parameters Determined from Plasma Concentration–Time Data and Urinary Excretion Data Following 1-mg Doses of Bumetanide[a]

Parameter	Intravenous	Intramuscular	Oral Solution	Oral Tablet
C_{max} (ng/mL)	—	38.2 ± 9.8	34.0 ± 10.6	30.9 ± 14.6
t_{max} (h)	—	0.34 ± 0.23	0.76 ± 0.27	1.8 ± 1.2
AUCTr, (ng·h/mL)	89 ± 30	80 ± 25	64 ± 27	66 ± 28
Vd_{ss} (L)	9.8 ± 3.4	—	—	—
CL_p (mL/min)	208 ± 65	223 ± 59	—	—
CL_o (mL/min)	—	—	299 ± 100	310 ± 165
CL_r (mL/min)	146 ± 59	146 ± 32	169 ± 61	178 ± 99
CL_{nr} (mL/min)	62 ± 24	78 ± 37	130 ± 55	132 ± 71
Percent dose in urine (0–24 h)	69 ± 11	66 ± 9	57 ± 12	58 ± 7
Absolute bioavailability				
Area method	—	0.94 ± 0.25	0.74 ± 0.23	0.78 ± 0.33
Urinary excretion method	—	0.98 ± 0.16	0.84 ± 0.16	0.86 ± 0.13
Relative bioavailability				
Area method	—	—	—	1.0 ± 0.3
Urinary excretion method	—	—	—	1.0 ± 0.2

[a] Parameters are defined in the text. Values are mean ±*SD*; n = 12.

$$CL_o = F\cdot\text{Dose}/\text{AUCTr} \quad \text{(Eq. 10)}$$

$$CL_r = Ae(0\text{–}24\text{ h})/\text{AUCTr} \quad \text{(Eq. 11)}$$

$$CL_{nr} = (CL_p - CL_r) \text{ or } (CL_o - CL_r) \quad \text{(Eq. 12)}$$

where AUMCTr is the area under the first moment of the plasma concentration–time curve, *i.e.*, the area under the curve when the product of time and plasma concentration are plotted against time (17); F is the fraction of the dose that is available for absorption as intact drug (F = 1, assuming complete absorption of the oral dose); and Ae(0–24 h) is the amount of intact bumetanide excreted in the urine over 0–24 h, assuming complete elimination during this interval.

Assessment of the absolute bioavailability of intramuscularly and orally administered bumetanide relative to intravenously administered bumetanide and the relative bioavailability of the oral tablet compared with the oral solution were determined by area ratios and urinary excretion ratios as follows:

Absolute bioavailability

$$= \frac{(\text{AUCTr})\text{ im, oral}}{(\text{AUCTr})\text{ iv}}, \frac{Ae(0\text{–}24\text{ h})\text{ im, oral}}{Ae(0\text{–}24\text{ h})\text{ iv}} \quad \text{(Eq. 13)}$$

Relative bioavailability

$$= \frac{(\text{AUCTr})\text{ tablet}}{(\text{AUCTr})\text{ solution}}, \frac{Ae(0\text{–}24\text{ h})\text{ tablet}}{Ae(0\text{–}24\text{ h})\text{ solution}} \quad \text{(Eq. 14)}$$

RESULTS AND DISCUSSION

Intravenous Administration—The mean observed plasma concentration–time profile and the fitted curve following intravenous administration of bumetanide are shown in Fig. 1a, and the pharmacokinetic parameters estimated by curve-fitting plasma concentration to Eq. 1 are presented in Table I. The mean ±*SD* model-independent pharmacokinetic parameters are presented in Table II. The plasma concentration–time data after intravenous administration were fitted well with a biexponential equation, including disposition and elimination phases in all the 12 subjects. The goodness of fit of the individual data to the equation is shown by correlation coefficients of 0.998–1.000 and the close agreement between the theoretical area [mean ±*SD* = 84 ± 29 ng·h/mL (Table I)] and the model-independent trapezoidal area [mean ± *SD* = 89 ± 30 ng·h/mL (Table II)].

The biphasic plasma concentration–time curve is characterized by a rapid α-phase with a harmonic mean half-life of 5.1 min, followed by a slower β-phase with a harmonic mean half-life of 44 min (Table I; Fig. 1a). Following intravenous administration, bumetanide is rapidly distributed into a small central compartment with a mean volume of 4.7 L ± 1.8 (*SD*) which is roughly comparable to the blood volume in an adult. The mean ±*SD* values for Vd_{area} and Vd_{ss} were 14.3 ± 3.9 and 9.8 ± 3.4 L, respectively. The disposition of intravenously administered [^{14}C]bumetanide in humans has been described by a triexponential equation in an earlier study (11). The mean values reported for $t_{1/2,\alpha}$ (5.9 min), $t_{1/2,\beta}$ (46 min), and V_c (5.5 L) are comparable to the mean values in our present study. However, the reported mean Vd_{area} value of 62.5 L is much higher than the mean Vd_{area} of 14.3 L determined in our study. In the study with labeled drug, the reported Vd_{area} represented the volume of distribution during the terminal phase (γ), which accounted for only 17% of the AUC for bumetanide. In a recent study (12), in which a two-compartment model was shown to adequately fit the data following intravenous administration of bumetanide, the mean values reported for $t_{1/2,\alpha}$ (5.75 min), V_c (3.53 L), and Vd_{ss} (9.45 L) were of the same magnitude as the values obtained in the present study. Their reported mean elimination half-life of 64 min, however, is slightly longer than the mean value of 44 min determined in our study.

Bumetanide is ~96%[1] bound to plasma protein in humans over the therapeutic plasma concentration range. High plasma binding contributes to the relatively small volume of distribution for bumetanide and may contribute to its high renal clearance. Although glomerular filtration is restricted to the free concentration of drug in the blood, active tubular secretion has been shown to act on both free and bound drug concentrations (18, 19). Therefore, binding decreases the volume of distribution of bumetanide, resulting in larger concentrations of drug being delivered to the kidney for possible secretion.

The mean ±*SD* plasma clearance and renal clearance of bumetanide were 208 ± 65 and 146 ± 59 mL/min, respectively (Table II). Lower renal clearance values relative to plasma clearance have been observed in other intra-

[1] Unpublished results; Hoffmann-La Roche, Inc., Nutley, N.J.

Table III—Pharmacokinetic Parameters[a] of Bumetanide Estimated by Curve-Fitting Intramuscular Plasma Concentration–Time Data to Eq. 2

Subject	A', ng/mL	k_a, h^{-1}	β, h^{-1}	t_{lag}, min	$t_{1/2,k_a}$, min	$t_{1/2,\beta}$, min	AUCTh, ng·h/mL	r
1	67	9.6	0.441	0	4	94	146	0.999
2	69	3.1	0.626	0	14	67	88	0.990
3	39	21.1	0.575	0	2	73	65	1.000
4	25	19.2	0.300	0	2	139	80	0.998
5	54	94.9	0.882	0	1	47	61	0.996
6	41	43.8	0.735	0	1	56	55	0.996
7	45	18.8	0.426	0	2	98	103	0.998
8	67	6.1	0.752	0	7	55	78	0.997
9	38	11.9	0.444	4	4	94	82	0.999
10	59	18.1	0.673	0	2	62	84	0.998
11	38	11.5	0.675	0	4	62	53	0.996
12	81	3.2	0.809	0	13	52	75	0.996
Mean	52	21.8	0.612	0	1.9[b]	68[b]	81	
SD	±17	±25.5	±0.177	±0			±25	

[a] Parameters are defined in the text. [b] Harmonic mean.

Table IV—Pharmacokinetic Parameters[a] of Bumetanide Estimated by Curve-Fitting Oral Solution Plasma Concentration–Time Data to Eq. 2

Subject	A', ng/mL	k_a, h^{-1}	β, h^{-1}	t_{lag}, min	$t_{1/2,k_a}$, min	$t_{1/2,\beta}$, min	AUCTh, ng·h/mL	r
1	86	3.8	0.585	4	11	71	124	0.996
2	135	2.3	0.889	3	18	47	93	0.998
3	66	3.1	0.928	3	13	45	50	0.995
4	834	1.7	1.54	4	25	27	53	0.999
5	62	4.1	0.882	2	10	47	55	0.997
6	38	5.1	0.778	4	8	53	41	0.997
7	120	2.5	0.811	0	16	51	100	0.994
8	287	1.7	1.37	13	25	31	40	0.995
9	292	1.9	1.41	8	22	29	56	0.989
10	40	29.5	0.710	26	1	59	55	0.999
11	59	2.6	0.989	12	16	42	37	0.999
12	603	1.0	0.958	1	40	43	50	0.971
Mean	219	4.9	0.988	6.7	8.5[b]	42[b]	63	
SD	±254	±7.8	±0.297	±7.3			±27	

[a] Parameters are defined in the text. [b] Harmonic mean.

venous studies (6, 11, 12) and have been attributed to nonrenal elimination of the drug. The absolute values reported in a recent study (12), however, are much lower than the values in our present study. Evidence that hepatic metabolism and biliary excretion contribute to the total clearance of bumetanide have been reported in previous studies with ^{14}C-labeled bumetanide. After intravenous administration, metabolites of bumetanide accounted for ~30–35% of the total radioactivity excreted into the urine (10, 11), whereas ~14% of an oral dose was recovered in the feces, mostly in the form of metabolites identical to those found in bile (9).

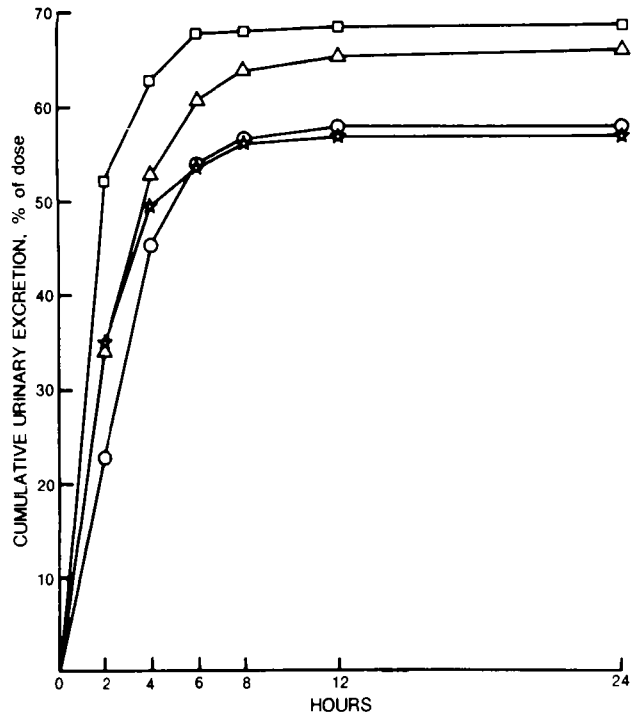

Figure 2—*Mean cumulative urinary excretion of intact bumetanide following administrations of 1 mg of bumetanide to 12 normal subjects. Key: (□) intravenous; (△) intramuscular; (★) oral solution; (○) oral tablet.*

The cumulative urinary excretion of intact bumetanide is shown in Fig. 2. The mean 0–24 h urinary recovery of intact drug following intravenous administration was 69 ± 11%. As shown in Fig. 2, more than one-half of the dose was excreted within 2 h of dosing, and urinary excretion was virtually complete 8 h after drug administration. This rapid excretion of intact drug is consistent with the short duration of action of bumetanide.

Intramuscular Administration—The mean observed plasma concentration–time profile and fitted curve following intramuscular administration are shown in Fig. 1b, and the pharmacokinetic parameters estimated by curve-fitting the plasma concentration–time data to Eq. 2 are presented in Table III. Fits of the intramuscular data to a biexponential equation, including first-order absorption and elimination were good in all 12 subjects, as shown by r values of 0.990–1.000. The goodness of fit of the individual data is supported by the virtually identical mean ±*SD* model-dependent and -independent AUC values (81 ± 25 and 80 ± 25 ng·h/mL, respectively).

Bumetanide was rapidly absorbed following intramuscular administration, with measurable concentrations of intact drug observed in the plasma within 6 min after drug administration. In all but one subject, there was no lag time in the onset of absorption (Table III). The large absorption rate constant (k_a = 21.8 ± 25.5 h^{-1}) further indicates the rapid absorption of bumetanide when administered intramuscularly. After reaching maximum plasma concentrations of 22.5 to 55.4 ng/mL (mean 38.2) within 0.1–0.75 h (mean 0.34) after dosing, plasma concentrations declined rapidly, with a harmonic mean elimination half-life of 68 min. This mean value is longer than the mean of 44 min observed after intravenous administration (Table I). The elimination of bumetanide from the body after intramuscular administration may be absorption rate limited, resulting in a slower apparent elimination rate relative to that after intravenous administration.

The observed mean ±*SD* values for CL_p, CL_r, CL_{nr}, and percentage for the dose recovered as intact drug in the urine were 223 ± 59 mL/min, 146 ± 32 mL/min, 78 ± 37 mL/min, and 66 ± 9%, respectively. These values agree closely with corresponding values observed after intravenous administration (Table II), suggesting that bumetanide is, in fact, completely absorbed into the systemic circulation after intramuscular injection. The absolute bioavailabilities after intramuscular administration were 0.94 ± 0.25 and 0.98

Table V—Pharmacokinetic Parameters[a] of Bumetanide Estimated by Curve-Fitting Oral Tablet Plasma Concentration-Time Data to Eq. 2

Subject	A', ng/mL	k_a, h^{-1}	β, h^{-1}	t_{lag}, min	$t_{1/2,k_a}$, min	$t_{1/2,\beta}$, min	AUCTh, ng·h/mL	r^b
1	72	5.4	0.564	41	8	74	114	0.997
2	77	5.5	0.754	25	8	55	88	0.997
3	40	12.1	0.748	25	8	56	51	0.999
4	389	0.5	0.419	89	83	99	54	0.987 (0.991)
5	128	3.3	1.34	14	13	31	57	0.999
6	64	2.2	0.677	4	19	61	66	0.992
7	637	0.9	0.786	25	46	53	99	0.983 (0.993)
8	262	1.1	0.960	24	38	43	41	0.996
9	241	1.0	0.750	35	42	55	72	0.988
10	261	0.5	0.478	48	83	87	65	0.987 (0.997)
11	443	1.8	1.60	38	23	26	23	0.998
12	40	4.9	0.723	28	9	58	47	0.999
Mean	221	3.3	0.817	33	12.6[c]	51[c]	65	
SD	±190	±3.4	±0.342	±21			±26	

[a] Parameters are defined in the text. [b] Values in parentheses are for zero-order fit. [c] Harmonic mean.

± 0.16 (based on the trapezoidal AUC and the 0–24-h urinary excretion, respectively), indicating that intramuscularly administered bumetanide is completely available relative to intravenously administered bumetanide.

Oral Administration—The mean observed and fitted plasma concentration-time curves following administration of the oral solution and the oral tablet are shown in Fig. 1c and d, respectively. The respective pharmacokinetic parameters estimated by curve-fitting the plasma concentration-time data to Eq. 2 are presented in Tables IV and V. The plasma concentration-time data after administration of both oral formulations were fitted with a biexponential equation, including first-order absorption and elimination. Good fits were obtained in all 12 subjects for the oral solution and in 9 subjects for the tablet. Although the oral tablet data from the other three subjects were also fitted with Eq. 2, there was a slight improvement in the fits when the plasma concentration-time data were fitted with a monoexponential equation with zero-order absorption (Table V). The goodness of fit of the data to the equation selected is shown by r values ranging from 0.971 to 0.999 and 0.983 to 0.999 for the oral solution and tablet, respectively. The good agreement of the model-independent AUC values (Table II) and the AUC values estimated from the curve-fitted parameters (Tables IV and V) further supports the reliability of the equation to fit the data.

After lag times of 0–26 and 4–89 min following administration of the oral solution and tablet, respectively, the harmonic mean half-lives of absorption ($t_{1/2,k_a}$) were 8.5 and 12.6 min, respectively. Mean ±*SD* C_{max} and t_{max} values for the oral solution were 34.0 ± 10.6 ng/mL and 0.76 ± 0.27 h, respectively, whereas the corresponding values for the tablet were 30.9 ± 14.6 ng/mL and 1.8 ± 1.2 h. The mean C_{max} and t_{max} values observed for the tablet are in good agreement with the values for C_{max} of 30 ng/mL and t_{max} of 1.5 h observed in a previous study following a 1-mg oral dose of bumetanide (6). Comparable mean t_{max} values (1.4 h) but higher mean C_{max} values (48 ng/mL) have been reported for a 1-mg oral dose of bumetanide in another study (12). Although absorption from the GI tract was rapid for both formulations, the later mean peak time observed for the tablet reflects the longer lag time, as well as a somewhat slower rate of absorption from the tablet relative to the oral solution. The plasma concentrations declined rapidly after reaching maximum concentrations, with harmonic mean elimination half-lives of 42 min for the oral solution and 51 min for the tablet. The mean half-lives observed after oral administration are comparable to the mean half-life observed after intravenous administration, indicating that the apparent elimination rate of bumetanide from the body is independent of this route of administration, *i.e.*, it is not absorption rate limited.

The mean ±*SD* AUC, CL_o, and percent urinary recovery of intact bumetanide for the oral solution were 64 ± 27 ng·h/mL, 299 ± 100 mL/min, and 57 ± 12%, respectively (Table II). The corresponding values for the tablet were 66 ± 28 ng·h/mL, 310 ± 165 mL/min, and 58 ± 7%. Comparison of the respective areas and urinary excretion values between the two oral formulations showed a mean (tablet-solution) ratio of 1.0 (Table II), indicating that the extent of absorption of bumetanide from the tablet and solution oral dosage forms are equivalent, and that galenic availability was not a problem for the oral tablet. The similar apparent oral clearance values for both oral formulations further supports the assumption of complete absorption of bumetanide from the tablet. However, urinary excretion of intact bumetanide indicated absolute bioavailabilities of 0.84 and 0.86 for the oral solution and tablet, respectively, when compared with the intravenous dose. The respective bioavailabilities calculated from the AUCTr values were 0.74 and 0.78. Since the fraction of the dose excreted in the urine as intact bumetanide is large and the elimination of the drug from the plasma is fast, the urinary excretion method of estimating bioavailability is probably a more reliable method for bumetanide. A recent study (12), however, showed that there was no difference in the bioavailability values calculated by either the AUC or the urinary excretion method (0.90 and 0.89, respectively).

The diminished availability of intact drug to the systemic circulation following oral admninistration tends to suggest that bumetanide undergoes first-pass clearance. In support of this observation, the first-pass metabolism

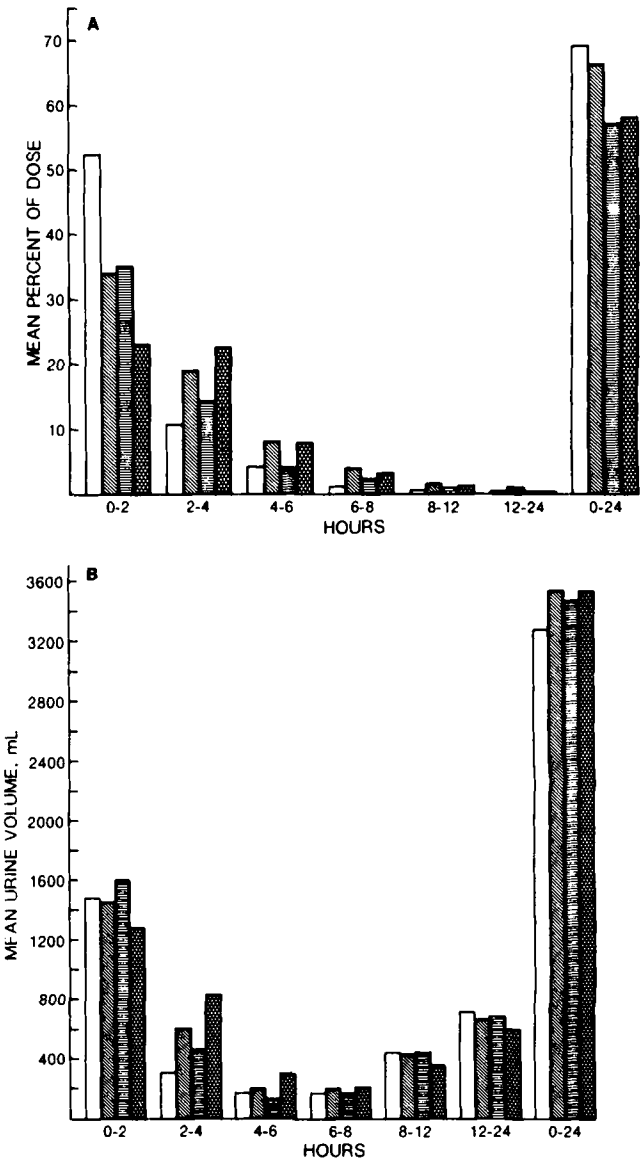

Figure 3—*Mean urinary excretion of intact bumetanide (A) and mean urine volume (B) following administrations of 1 mg of bumetanide to 12 normal subjects. Key: (□) intravenous; (▨) intramuscular; (▤) oral solution; (■) oral tablet.*

predicted for an oral dose, assuming linear kinetics, would be 10–20% (20). First-pass metabolism would also account for the higher mean oral clearance observed for both solution and tablet relative to the mean plasma clearance after intravenous and intramuscular administrations. Since ~70% of a parenteral dose and 60% of an oral dose are excreted as intact drug in the 0–24-h urine samples, the 10% difference as a function of the oral route of administration is consistent with the predicted limited extent of first-pass metabolism of the oral dose. These findings are consistent with the results of previous studies (10, 12), which have reported urinary recoveries for intact bumetanide of 60 ± 3% (10) and 66 ± 3% (12) from the intravenous dose, but only 49 ± 5% (10) and 59 ± 3% (12) from the oral dose.

The mean urinary excretion of intact bumetanide and the corresponding mean urinary volume following the four treatments are shown in Fig. 3. The diuretic effect of bumetanide following 1-mg iv, im, oral solution, and oral tablet doses was clearly evident in the first 2-h period, with mean urine volumes ranging from 1270 mL (tablet) to 1600 mL (oral solution). The diuretic activity lasted for ~4–8 h for all treatments, and the mean cumulative diuresis after 24 h was the same for the four treatments. The diuresis profile of bumetanide parallels the urinary excretion profile of intact bumetanide in that the major portion of intact bumetanide was excreted during the first 2 h following drug administration (Fig. 3). This confirms previous observations (9, 21) that the diuretic activity of bumetanide is closely associated with the concentration of intact drug in the kidney. The fact that the oral formulations are as effective diuretics as the parenteral preparations presumably reflects the maintenance of a minimum effective plasma or renal tubule concentration of bumetanide (22).

REFERENCES

(1) E. Bourke, M. J. A. Asbury, S. O'Sullivan, and P. B. B. Gatenby, *Eur. J. Pharmacol.*, **23**, 283 (1973).

(2) S. G. Karlander, R. Henning, and O. Lundvall, *Eur. J. Clin. Pharmacol.*, **6**, 220 (1973).

(3) J. B. Puschett, *J. Clin. Pharmacol.*, **21**, 575 (1981).

(4) M. J. Asbury, P. B. B. Gatenby, S. O'Sullivan, and E. Bourke, *Br. Med. J.*, **1**, 211 (1972).

(5) K. H. Olesen, B. Sigurd, E. Steiness, and A. Leth, *Acta. Med. Scand.*, **193**, 119 (1973).

(6) D. L. Davies, A. F. Lant, N. R. Millard, A. J. Smith, J. W. Ward, and G. M. Wilson, *Clin. Pharmacol. Ther.*, **15**, 141 (1974).

(7) W. R. Murdoch and W. H. R. Auld, *Postgrad. Med. J.*, **51**, 10 (1975).

(8) A. Whelton, *J. Clin. Pharmacol.*, **21**, 591 (1981).

(9) S. C. Halladay, I. G. Sipes and D. E. Carter, *Clin. Pharmacol. Ther.*, **22**, 179 (1977).

(10) P. J. Pentikainen, A. Penttila, P. J. Neuvonen, and G. Gothoni, *Br. J. Clin. Pharmacol.*, **4**, 39 (1977).

(11) P. J. Pentikainen, P. J. Neuvonen, M. Kekki and A. Penttila, *J. Pharmacokinet. Biopharm.*, **8**, 219 (1980).

(12) L. A. Marcantonio, W. H. R. Auld, G. G. Skellern, C. A. Howes, W. R. Murdoch, and R. Purohit, *J. Pharmacokinet. Biopharm.*, **10**, 393 (1982).

(13) W. R. Dixon, R. L. Young, A. Holazo, M. L. Jack, R. E. Weinfeld, K. Alexander, A. Liebman, and S. A. Kaplan, *J. Pharm. Sci.*, **65**, 701 (1976).

(14) D. Rodbard, *Clin. Chem.*, **20**, 1255 (1974).

(15) M. Gibaldi and D. Perrier, "Pharmacokinetics," Dekker, New York, N.Y., 1975.

(16) C. M. Metzler, G. L. Elfring, and A. J. McEwen, *Biometrics*, **30**, 562 (1974).

(17) L. Z. Benet and R. L. Galeazzi, *J. Pharm. Sci.*, **68**, 1071 (1979).

(18) G. Levy, *J. Pharm. Sci.*, **69**, 482 (1980).

(19) E. J. Cafruny, *Am. J. Med.*, **62**, 490 (1977).

(20) M. Rowland, *J. Pharm. Sci.*, **61**, 70 (1972).

(21) P. W. Feit, K. Roholt, and H. Sorensen, *J. Pharm. Sci.*, **62**, 375 (1973).

(22) H. W. Smith, "The Kidney," Oxford University Press., New York, N.Y., 1951, pp. 241–408.

ACKNOWLEDGMENTS

The authors wish to thank Mrs. W. Morley and Mrs. J. Webster for their assistance in the preparation of the manuscript.

Determination of Total Captopril in Human Plasma by Gas Chromatography–Mass Spectrometry with Selected-Ion Monitoring After Reduction of Disulfides

EUGENE IVASHKIV *, DORIS N. McKINSTRY ‡, and ALLEN I. COHEN *x

Received January 10, 1983, from the **Department of Analytical Research, The Squibb Institute for Medical Research, New Brunswick, NJ 08903* and ‡*Department of Clinical Pharmacology, The Squibb Institute for Medical Research, Princeton, NJ 08540.* Accepted for publication August 19, 1983.

Abstract □ Captopril is liberated from covalently protein-bound disulfides and other disulfide metabolites in human plasma by reduction with tri-*n*-butyl-phosphine. The captopril is then treated with *N*-ethylmaleimide, purified on XAD-2 resin, eluted with ethyl acetate, and methylated prior to its determination by gas chromatography–mass spectrometry with selected-ion monitoring. The limit of detection is 20 ng/mL of plasma.

Keyphrases □ Captopril—reduction of disulfides, GC–MS, selected-ion monitoring □ GC MS—selected-ion monitoring, total captopril in human plasma, reduction of disulfides

Captopril (I), an orally active angiotensin I-converting enzyme inhibitor (1, 2), is currently marketed for the treatment of hypertension (3, 4). Because of the extreme reactivity of thiols in biological systems, captopril is quantitatively converted to a derivative, such as the *N*-ethylsuccimide derivative (II), prior to analysis (5). The reaction product was determined by a gas chromatographic–mass spectrometric (GC–MS) method (6, 7) with selected-ion monitoring for captopril in whole blood and by a radiometric-thin-layer chromatographic (RTLC) procedure for establishing the biological disposition of captopril (8, 9). The latter method has been used in various metabolism and pharmacokinetic studies (10–12). Other reported methods for the determination of captopril employ GC (13), HPLC (14–17), and most recently GC–MS with selected-ion monitoring (18).

Metabolites of captopril identified so far include captopril disulfide (III), the mixed cysteine and glutathione disulfides of I (IV and V, respectively), and the *S*-methyl (VI) and *S*-methyl sulfoxide (VII) metabolites (9, 10, 12, 19). A substantial proportion of the captopril radioactivity in human blood after oral administration of radioactively labeled I was associated with the plasma fraction (8), which was covalently bound as plasma protein disulfides. It is believed that the plasma proteins and mixed disulfides with endogenous thiol-

0022-3549/84/0800-1113$01.00/0

© 1984, American Pharmaceutical Association

predicted for an oral dose, assuming linear kinetics, would be 10–20% (20). First-pass metabolism would also account for the higher mean oral clearance observed for both solution and tablet relative to the mean plasma clearance after intravenous and intramuscular administrations. Since ~70% of a parenteral dose and 60% of an oral dose are excreted as intact drug in the 0–24-h urine samples, the 10% difference as a function of the oral route of administration is consistent with the predicted limited extent of first-pass metabolism of the oral dose. These findings are consistent with the results of previous studies (10, 12), which have reported urinary recoveries for intact bumetanide of 60 ± 3% (10) and 66 ± 3% (12) from the intravenous dose, but only 49 ± 5% (10) and 59 ± 3% (12) from the oral dose.

The mean urinary excretion of intact bumetanide and the corresponding mean urinary volume following the four treatments are shown in Fig. 3. The diuretic effect of bumetanide following 1-mg iv, im, oral solution, and oral tablet doses was clearly evident in the first 2-h period, with mean urine volumes ranging from 1270 mL (tablet) to 1600 mL (oral solution). The diuretic activity lasted for ~4–8 h for all treatments, and the mean cumulative diuresis after 24 h was the same for the four treatments. The diuresis profile of bumetanide parallels the urinary excretion profile of intact bumetanide in that the major portion of intact bumetanide was excreted during the first 2 h following drug administration (Fig. 3). This confirms previous observations (9, 21) that the diuretic activity of bumetanide is closely associated with the concentration of intact drug in the kidney. The fact that the oral formulations are as effective diuretics as the parenteral preparations presumably reflects the maintenance of a minimum effective plasma or renal tubule concentration of bumetanide (22).

REFERENCES

(1) E. Bourke, M. J. A. Asbury, S. O'Sullivan, and P. B. B. Gatenby, *Eur. J. Pharmacol.*, **23**, 283 (1973).

(2) S. G. Karlander, R. Henning, and O. Lundvall, *Eur. J. Clin. Pharmacol.*, **6**, 220 (1973).

(3) J. B. Puschett, *J. Clin. Pharmacol.*, **21**, 575 (1981).

(4) M. J. Asbury, P. B. B. Gatenby, S. O'Sullivan, and E. Bourke, *Br. Med. J.*, **1**, 211 (1972).

(5) K. H. Olesen, B. Sigurd, E. Steiness, and A. Leth, *Acta. Med. Scand.*, **193**, 119 (1973).

(6) D. L. Davies, A. F. Lant, N. R. Millard, A. J. Smith, J. W. Ward, and G. M. Wilson, *Clin. Pharmacol. Ther.*, **15**, 141 (1974).

(7) W. R. Murdoch and W. H. R. Auld, *Postgrad. Med. J.*, **51**, 10 (1975).

(8) A. Whelton, *J. Clin. Pharmacol.*, **21**, 591 (1981).

(9) S. C. Halladay, I. G. Sipes and D. E. Carter, *Clin. Pharmacol. Ther.*, **22**, 179 (1977).

(10) P. J. Pentikainen, A. Penttila, P. J. Neuvonen, and G. Gothoni, *Br. J. Clin. Pharmacol.*, **4**, 39 (1977).

(11) P. J. Pentikainen, P. J. Neuvonen, M. Kekki and A. Penttila, *J. Pharmacokinet. Biopharm.*, **8**, 219 (1980).

(12) L. A. Marcantonio, W. H. R. Auld, G. G. Skellern, C. A. Howes, W. R. Murdoch, and R. Purohit, *J. Pharmacokinet. Biopharm.*, **10**, 393 (1982).

(13) W. R. Dixon, R. L. Young, A. Holazo, M. L. Jack, R. E. Weinfeld, K. Alexander, A. Liebman, and S. A. Kaplan, *J. Pharm. Sci.*, **65**, 701 (1976).

(14) D. Rodbard, *Clin. Chem.*, **20**, 1255 (1974).

(15) M. Gibaldi and D. Perrier, "Pharmacokinetics," Dekker, New York, N.Y., 1975.

(16) C. M. Metzler, G. L. Elfring, and A. J. McEwen, *Biometrics*, **30**, 562 (1974).

(17) L. Z. Benet and R. L. Galeazzi, *J. Pharm. Sci.*, **68**, 1071 (1979).

(18) G. Levy, *J. Pharm. Sci.*, **69**, 482 (1980).

(19) E. J. Cafruny, *Am. J. Med.*, **62**, 490 (1977).

(20) M. Rowland, *J. Pharm. Sci.*, **61**, 70 (1972).

(21) P. W. Feit, K. Roholt, and H. Sorensen, *J. Pharm. Sci.*, **62**, 375 (1973).

(22) H. W. Smith, "The Kidney," Oxford University Press., New York, N.Y., 1951, pp. 241–408.

ACKNOWLEDGMENTS

The authors wish to thank Mrs. W. Morley and Mrs. J. Webster for their assistance in the preparation of the manuscript.

Determination of Total Captopril in Human Plasma by Gas Chromatography–Mass Spectrometry with Selected-Ion Monitoring After Reduction of Disulfides

EUGENE IVASHKIV *, DORIS N. McKINSTRY ‡, and ALLEN I. COHEN *x

Received January 10, 1983, from the **Department of Analytical Research, The Squibb Institute for Medical Research, New Brunswick, NJ 08903* and ‡*Department of Clinical Pharmacology, The Squibb Institute for Medical Research, Princeton, NJ 08540.* Accepted for publication August 19, 1983.

Abstract □ Captopril is liberated from covalently protein-bound disulfides and other disulfide metabolites in human plasma by reduction with tri-*n*-butyl-phosphine. The captopril is then treated with *N*-ethylmaleimide, purified on XAD-2 resin, eluted with ethyl acetate, and methylated prior to its determination by gas chromatography–mass spectrometry with selected-ion monitoring. The limit of detection is 20 ng/mL of plasma.

Keyphrases □ Captopril—reduction of disulfides, GC–MS, selected-ion monitoring □ GC MS—selected-ion monitoring, total captopril in human plasma, reduction of disulfides

Captopril (I), an orally active angiotensin I-converting enzyme inhibitor (1, 2), is currently marketed for the treatment of hypertension (3, 4). Because of the extreme reactivity of thiols in biological systems, captopril is quantitatively converted to a derivative, such as the *N*-ethylsuccimide derivative (II), prior to analysis (5). The reaction product was determined by a gas chromatographic–mass spectrometric (GC–MS) method (6, 7) with selected-ion monitoring for captopril in whole blood and by a radiometric-thin-layer chromatographic (RTLC) procedure for establishing the biological disposition of captopril (8, 9). The latter method has been used in various metabolism and pharmacokinetic studies (10–12). Other reported methods for the determination of captopril employ GC (13), HPLC (14–17), and most recently GC–MS with selected-ion monitoring (18).

Metabolites of captopril identified so far include captopril disulfide (III), the mixed cysteine and glutathione disulfides of I (IV and V, respectively), and the *S*-methyl (VI) and *S*-methyl sulfoxide (VII) metabolites (9, 10, 12, 19). A substantial proportion of the captopril radioactivity in human blood after oral administration of radioactively labeled I was associated with the plasma fraction (8), which was covalently bound as plasma protein disulfides. It is believed that the plasma proteins and mixed disulfides with endogenous thiol-

0022-3549/84/0800-1113$01.00/0

© 1984, American Pharmaceutical Association

containing compounds (*e.g.*, glutathione) may act as a reservoir from which captopril is liberated over time to exert pharmacological effects (12, 20). It would not be practical to measure each metabolite separately, nor would it be possible to adequately measure the protein-bound levels by a nonradiometric method. Consequently, a method for measuring total captopril in plasma has been developed by treating the plasma fraction with the disulfide-reducing agent tri-*n*-butylphosphine (21), followed by reaction with *N*-ethylmaleimide to form II, which is then methylated and measured by GC–MS with selected-ion monitoring (7).

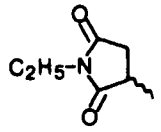

$C_6H_8NO_2$

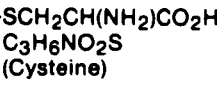

$-SCH_2CH(NH_2)CO_2H$
$C_3H_6NO_2S$
(Cysteine)

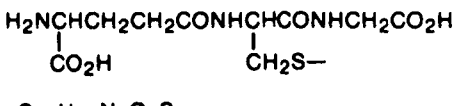

$C_{10}H_{16}N_3O_6S$
(glutathione)

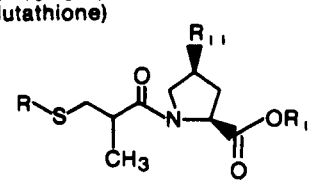

I:R = $R_1 = R_{11} = H$
II:R = $C_6H_8NO_2$ $R_1 = R_{11} = H$
III:R = $C_9H_{14}NO_3S$ $R_1 = R_{11} = H$
IV:R = $C_3H_6NO_2S$ $R_1 = R_{11} = H$
V:R = $C_{10}H_{16}N_3O_6S$ $R_1 = R_{11} = H$
VI:R = CH_3 $R_1 = R_{11} = H$
VII:R = CH_3(*S*-oxide) $R_1 = R_{11} = H$
VIII:R = H $R_1 = H\ R_{11} = F$
IX:R = $C_6H_8NO_2$ $R_1 = H\ R_{11} = F$
X:R = $C_6H_8NO_2$ $R_1 = CH_3\ R_{11} = H$
XI:R = $C_6H_8NO_2$ $R_1 = CH_3\ R_{11} = F$

EXPERIMENTAL SECTION

Apparatus—A mass spectrometer[1] with a data acquisition system, gas chromatograph, and an interface was used as reported by Cohen *et al.* (7). A centrifuge[2] with stainless steel adapters, drug-screen columns[3], a water bath[4] set at 50°C, two sample concentrators[5], dry-block heating baths[6,7], a column mounting plate[8], an aspirator trough[8], 1-mL reaction vessels[9], vial seals[10], 100-μL micropipets[11], and 1-, 3-, 5-, and 10-mL dispensers[12] were used. Samples were agitated on a heavy-duty shaker[13]. Screw-capped 150-mm culture tubes with polytef-faced liners, 20-mL scintillation vials, 21-gauge syringe needles, a vial crimper, a desiccator, 15-cm disposable Pasteur pipets, a vortex mixer, 13 × 100-mm disposable glass tubes, and 1- and 5-mL disposable serological pipets were obtained commercially[13].

Reagents—Acetone, ethyl acetate, hydrochloric acid, phosphoric acid, *N*-ethylmaleimide, dimethylformamide, Tris, urea, dibasic sodium phosphate, sodium chloride, EDTA (disodium salt), neutral alumina Brockman Activity I (80–200 mesh), and sodium bicarbonate were reagent grade. An *N*-ethylmaleimide solution was prepared daily by dissolving 0.5 g of reagent in 1.5 mL of dimethylformamide. A 20% v/v solution of tri-*n*-butylphosphine was prepared with redistilled reagent[14] and acetone. A buffer was prepared by dissolving 12.1 g of Tris in 980 mL of distilled water, and the pH was adjusted to 8.2 with phosphoric acid. To 26 g of urea, was added 65 mL of the pH 8.2 buffer. This solution was prepared each day as required. A pH 7.0 buffer was prepared by dissolving 40 g of dibasic sodium phosphate heptahydrate in 1960 mL of distilled water, adjusting the pH with phosphoric acid. A diluted column activator solution[3] was prepared by diluting 35–500 mL with distilled water. The solution was refrigerated and used for not more than 1 week. The plasma used for experiments was prepared from commercially obtained blood[15]. Methanolic hydrochloride was prepared as described previously (6, 7). Captopril (I), captopril disulfide (III), and the fluoro analogue internal reference (VIII) were pharmaceutical-grade materials[16].

Standard Solutions—Captopril disulfide (III) solutions were prepared at concentrations of 10 and 40 μg/mL in methanol and stored in a refrigerator. A solution of II was prepared by treating 50 mg of I with 250 mg of *N*-ethylmaleimide in 10 mL of pH 7.0 buffer for 15 min, diluting to 100 mL with acetone, and filtering through a fine-porosity sintered glass filter. An unextracted control solution was prepared from II and IX, with respective final concentrations equivalent to 40 μg of I and VIII per mL of solution. The solution was stored in a refrigerator. For calibration, appropriate solution concentrations of III in methanol were prepared.

Preparation of Standard Curves—To each of six 20-mL scintillation vials, was added 1 mL of plasma. With 100-μL syringes, varying amounts (between 0 and 1 μg) of III and 1 μg of internal reference standard VIII were added. To another set of six 20-mL scintillation vials containing 1 mL of plasma, between 0 and 8 μg of III and 4 μg of VIII were added. These standards were immediately reduced or stored in a freezer with the samples until required.

Reduction—Aliquots (1 mL) of a thawed, well-mixed plasma sample were transferred to separate 20-mL scintillation vials and 5 mL of urea pH 8.2 buffer solution was added to each vial. To vial 12, 1 mL of blank plasma and the appropriate amount of control solution containing III and VIII were added. To plasma samples collected from 0.25 to 6 h after oral administration of a 100-mg tablet of captopril, was added 4 μg of VIII; 1 μg of VIII was added to all other plasma samples. The respective additions to controls were 4 μg of III and VIII and 1 μg of III and VIII. To each vial (located under a hood), 0.1 mL of 20% v/v tri-*n*-butylphosphine solution was added. The vials, covered with tin foil-lined caps, were mixed on a vortex mixer. These samples and standards were allowed to stand in the dark at 50°C for 1 h.

Reaction of Reduced Captopril with *N*-Ethylmaleimide—The aforementioned vials were cooled in the hood for 15 min and uncapped; to each vial, was added 25 mg of *N*-ethylmaleimide in 0.1 ml of dimethylformamide, and the vials were recapped. The samples were vortexed for 10 s, the vials were set aside for 5 min, and then the samples were treated with 5 mL of 0.67 M H_3PO_4.

Isolation and Purification of Samples—Prior to use, the required number of XAD-2 columns were activated with 5 mL of diluted activator solution, treated with 5 mL 0.1 M HCl, and 21-gauge syringe needles were attached. Each sample solution was decanted into an individual column, and the solution was allowed to percolate through the column; 5 ml of 0.1 M HCl was added to a scintillation vial, mixed, and decanted to the column after the original solution had eluted. The syringe needle was removed, and the column was washed first with a 10-mL aliquot and then with a 20-mL aliquot of 0.1 M HCl[17]. The columns were placed on a column mounting plate and dried under reduced pressure for 1 h; this was followed by eluting II and the fluoro analogue (IX) first with 10 mL and then with 15 mL of purified ethyl acetate. To each test tube containing the ethyl acetate eluant was added 3 mL of 5% sodium bicarbonate solution; this was shaken for 5 min to effect the transfer of II and IX into the aqueous layer, followed by centrifugation at 2000 rpm for 5 min. The upper ethyl acetate layer was discarded and 1 mL of 2 M phosphoric acid and 3 g of sodium chloride were added and the sample was mixed for 5 min. The sample was reextracted into ethyl acetate by adding 5 mL of the purified solvent, shaking, and centrifuging for the required times as indicated above. The entire contents of each test tube were decanted to new 13- × 100-mm test tubes, and the upper ethyl acetate layer (~4.8 mL) was transferred to a 20-mL scintillation vial with a 5-mL serological pipet. The solvent was then evaporated with a sample concentrator set at 65°C. The sample was transferred quantitatively, first with 0.5 mL and then with 0.2 mL of purified ethyl acetate, to a 1-mL reaction vial with a Pasteur pipet. An unextracted control solution containing 4 μg each of II and IX was added to a clean reaction vial and evaporated to dryness with a concentrator, along with extracted samples and the control. The vials were then dried under reduced pressure in a desiccator for 15 min. Samples were redissolved and methylated to X and XI as previously described (6, 7).

[1] Model HP 5985B; Hewlett Packard, Palo Alto, Calif.
[2] Model IEP 2741; International, Scientific Products Co.
[3] XAD-2 with Column Activator A; Brinkmann Instruments.
[4] Organomation Associates, Inc.
[5] Model SC 248; Brinkmann Instruments.
[6] Techne, SC-3.
[7] Techne, DB-3.
[8] Biochemical Diagnostics.
[9] Supelco Inc., Bellefonte, Pa.
[10] Hewlett-Packard Instruments, Palo Alto, Calif.
[11] Scientific Manufacturing Industries.
[12] Lab Industries.
[13] Fisher Scientific Co.
[14] Strem Chemicals, Inc.
[15] New Jersey Blood Services.
[16] E. R. Squibb & Sons, Princeton, N.J.
[17] Sometimes it is necessary to initiate flow with the palm of the hand or a rubber bulb.

Table I—Covalent Binding of Captopril and Its Metabolites in Plasma as a Function of Storage Temperature and Time

Drug	Sample	Storage Temp., °C	Extractable Drug with Methanol, ng/vial[a]		
			Initial	1 Week	4 Weeks
[^{14}C]I	1	5	3240	2230 (68)	1250 (38)
	2	5	3390	2250	1290
	1	−20	—	940 (28)	430 (13)
	2	−20	—	920	420
[^{14}C]III	1	5	3920	3960 (101)	2250 (58)
	2	5	3940	2710 (69)	2280
	1	−20	—	3650 (93)	2140 (55)
	2	−20	—	3820 (100)	2180
[^{14}C]IV	1	5	3420	1980 (59)	nil
	2	5	3450	2040	nil
	1	−20	—	2030 (57)	870 (23)
	2	−20	—	1910	720
[^{14}C]VI	1	5	1630	1580 (97)	1590 (99)
	2	5	1600	1560	1600
	1	−20	—	1560 (98)	1590 (98)
	2	−20	—	1610	1590

[a] Values in parentheses are the percentages of the initial values.

Table II—Reduction of Captopril Disulfide As Function of pH

Solution	pH	Reduction, %
0.1 M HCl	1.1	47.5
~0.67 M H_3PO_4	1.6	67.8
0.1 M phosphate Buffer	7.0	79.5
	8.0	81.9
0.1 M Tris buffer	8.2	90.5
8 M Urea in 0.1 M Tris buffer	8.2	97.0
Tris buffer–propanol, 1:1	8.2	98.0
Tris buffer–propanol, 3:1	8.2	97.8
(~0.1 M NaOH)	12.5	64.0

Selected-Ion Monitoring—Approximately 1–2 μL of solution added to the tip of a GC solids injector[18] was allowed to evaporate. The appropriate ion profiles (m/z 230.1, m/z 248.1) were obtained by selected-ion monitoring. The maximum peak heights were measured by using a program written especially for the batch processing of the data (7). The program selects the baseline-corrected maximum peak heights of the requested ions. The mean ratio (R_n^*), and standard deviation for three to five injections of the control sample bracketing the samples were determined for subsequent use in correcting the data for differences in response from the calibration slope (k_n). The adjustment factor (A) is related to the calibration slope and the measured ratio of the control (R_n^*), by:

$$A = \frac{R_n^*}{I_n + k_n}$$

The data were processed as previously described (7).

RESULTS AND DISCUSSION

Captopril undergoes extensive biotransformation to form covalently protein-bound disulfides (21) in addition to the disulfides III, IV, and V (9, 10, 12, 21). When captopril is added to plasma and stored at either 5°C or −20°C, 62 and 87% of I is bound to protein (Table I). The greater binding at the lower temperature may result from an increase in protein thiols from freezing and thawing of the plasma. Approximately 43% of the disulfide III was bound to the protein, presumably due to interchange and disulfide formation with protein. The only captopril-related product not bound was *S*-methyl captopril (VI), a potential metabolite. The use of *N*-ethylmaleimide as a thiol alkylating agent in whole blood, plasma, and urine is the most effective method of preventing the formation of protein-bound captopril (5–7). It is not feasible to measure unbound captopril, because a significant amount of captopril is converted to protein-bound compound during the production of serum or plasma from whole blood and during storage prior to analysis.

Plasma or serum was subsequently processed to liberate I bound to proteins and mixed disulfides by reduction with tri-*n*-butylphosphine[19]. This reagent was previously used to reduce captopril disulfides in urine (14, 21). The great depot of protein disulfides required a tri-*n*-butylphosphine concentration of 20 mg/mL of plasma to achieve 98% reduction. Only 85 and 50% reduction could be obtained at tri-*n*-butylphosphine concentrations of 10 and 2 mg/mL, respectively. Nearly complete reduction is obtained in solutions more basic than pH 8 (Table II). The rate of reduction and the yield are also influenced by temperature. At 50°C, it takes ~30 min to reduce III with 20 mg/mL of tri-*n*-butylphosphine and 45 min to reduce protein-bound I. At temperatures greater than 60°C, III is reduced in <15 min, but some sample decomposition occurs. Up to 10 mL of urea buffer, used as a plasma-solubilizing agent, did not effect the reduction efficiency when 1 mL of plasma was used. When >1 mL of plasma was used, the yield decreased. Only 90% disulfide reduction could be achieved with whole blood samples, but decreased whole blood volumes yielded satisfactory reduction efficiency. Although excellent reductions have been obtained from 50% propanol solutions (22), the solvent causes interferences in the isolation procedure. When added to plasma, I, III, IV, and V are essentially quantitatively converted and subsequently measured as the methyl ester of II by the GC–MS procedure with selected-ion monitoring (Table III). Plasma samples of I, III, and IV stored for 4 weeks either at 5°C or −20°C yield substantially all of the available reducible compound (Table IV).

The precision of measurement was improved by adding 1000 ng of internal reference to the samples with lower concentrations (within a range of 0–1000 ng/mL); 4000 ng was added to those samples expected to have >1000 ng of reducible captopril. Samples collected from human subjects at 0.25 to 6 h after administration of a single 100-mg tablet of captopril were treated as high-concentration samples, whereas the 0-h samples and those collected at ≥8 h were treated as low-concentration samples. The methylated sample extracts were measured by essentially the same methods as used for free I (6, 7). Calibration curves of standard disulfide III, extracted from plasma, demonstrated a linear response–concentration relationship for reduction and extraction. The slope and intercept, 2.084 and 0.0667, respectively, are identical to the values reported for free I in whole blood (6). The extracted control was used as a single-point calibration (6, 7). The mean of three to five values was

Table III—Recovery of Captopril and Disulfides from Plasma [a]

	Plasma, μg/mL[b]		
	Added	Found	Reduction, %
Captopril Disulfide (III)	5	4.82	96.4
	2.5	2.41	96.4
	1.0	0.98	98.0
	0.5	0.48	97.0
	0.25	0.23	92.0
Captopril (I)	5.12	4.89	95.5
	2.56	2.48	96.7
	1.02	0.9	96.0
	0.51	0.48	93.0
	0.25	0.26	102.
Captopril–cysteine (IV)	8	7.79	97.4
	4	3.87	96.8
	2	1.93	96.0
Captopril–glutathione (V)	12	11.7	97.7
	6	5.75	95.8
	3	2.96	98.5
Plasma Blank	0	0	—

[a] Captopril was used as standard. [b] As percentage of captopril equivalents.

[18] SI-IRDS; Scientific Glass Equipment Co., Penzias Associates, Roslyn Heights, N.Y.

[19] Tri-*n*-butylphosphine is a toxic substance, and all procedures should be carried out in a hood. As it is readily oxidized by air, it should be refrigerated under nitrogen, with acetone solutions prepared daily.

Table IV—Recovery of Captopril from Plasma Stored at 5°C and −20°C for 4 Weeks

Drug	Sample	Storage Temp., °C	Recovery, ng/vial		
			Initial	Final	Percent of Initial
[^{14}C]I	1	5	3240	3020	91
	2	5	3390	3270	99
	1	−20	—	2950	90
	2	−20	—	2920	88
[^{14}C]III	1	5	3920	3730	95
	2	5	3940	3830	97
	1	−20	—	3900	99
	2	−20	—	3890	99
[^{14}C]IV	1	5	3420	3170	92
	2	5	3450	3090	90
	1	−20	—	3260	95
	2	−20	—	3160	92

Table V—Bioavailability Data for Captopril[a]

Time, h	Bioavailability (F) in Blood, ng/mL[b]	$^1/_2T$, ng/mL[c]	Disulfides ($^1/_2T - F$), ng/mL[d]	Bioavailability in Plasma, ng/mL[b]
0.5	350 ± 100	390	40	780 ± 230
1.0	900 ± 140	1300	400	2590 ± 420
1.5	720 ± 110	1480	760	2960 ± 390
2.0	360 ± 50	1240	880	2480 ± 320
2.5	230 ± 40	980	750	1960 ± 220
3.0	170 ± 40	800	630	1600 ± 120
4.0	100 ± 20	570	470	1130 ± 80
5.0	80 ± 50	490	410	980 ± 220
6.0	30 ± 10	370	340	740 ± 110
8.0	10 ± 3	250	240	490 ± 50
12.0	4 ± 1	130	130	260 ± 20
16.0	1 ± 0.3	80	80	160 ± 10
24		40	40	70 ± 10

[a] Single oral administration of 100 mg of captopril; nine healthy male subjects were treated. [b] ± *SEM* for nine healthy male subjects. [c] One-half total volume for plasma (blood equivalent). [d] Difference is equivalent to disulfides in blood.

used to adjust for the small variation in the response (6, 7). The data for total captopril are of the same quality as those for free captopril in whole blood (7). For total captopril values, the estimated precision from 0 to 100 ng/mL of plasma is 20 ng/mL; between 100 and 1000 ng/mL the precision is ~50 ng/mL; and at >1000 ng/mL the precision is 3%. The distribution of the measured total plasma levels of 27 plasma samples taken at 0, 12, 16, and 24 h is a demonstration of the sensitivity of the method (Fig. 1). Recorded to the nearest decade, 90% of the 0-h samples were determined to have 0 ng/mL, whereas the range of the 24-, 16-, and 12-h samples fell into groups of 40–100, 110–210, and 180–370 ng/mL, respectively. The mean values were also nearly equally spaced, with respective values of 70 (σ_n = 20), 130 (σ_n = 25), and 240 (σ_n = 50) ng/mL. A limit of detection of 20 ng/mL more than adequately reflects these data, and a sensitivity of 30 ng/mL appears to be readily achievable.

The mean bioavailability of I in whole blood and the total reducible captopril plasma levels of nine healthy subjects given a single oral 100-mg dose of captopril is shown as a typical example (Table V). The maximum concentration occurs at 1 h for free captopril, which is 900 (±140) ng/mL of whole blood, and at 1.5 h for total captopril in plasma, which is nearly 3000 ng/mL. To relate the total captopril levels in plasma to the whole blood equivalent, the plasma values were divided by 2 to adjust for the volume difference between the whole blood and plasma fractions. The difference between one-half the total captopril value and the free captopril value is the reducible captopril in whole blood. This parameter peaks at 2 h after drug administration. In a recent kinetic study of captopril in humans (20), it was suggested that captopril bound to plasma proteins and mixed disulfides with endogenous thiol-containing compounds may act as a reservoir from which captopril is slowly released. This possibility has also been cited in a captopril binding study (12). Future studies in which the total captopril method combined with the method for free captopril (7) are used should help in the refinement of the pharmacokinetics of captopril.

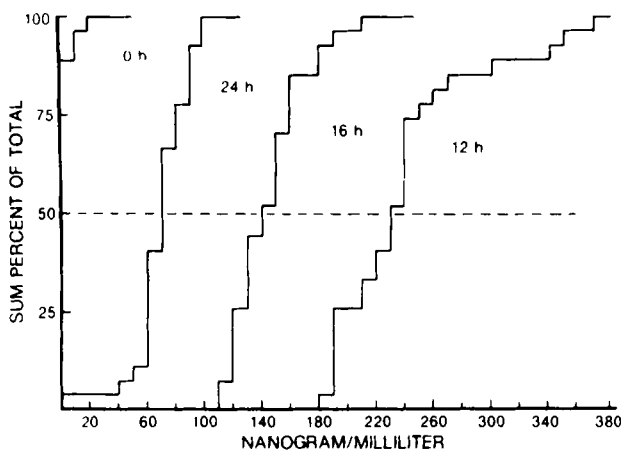

Figure 1—*Distribution and concentration range of total captopril in 0-, 24-, 16-, and 12-h plasma samples.*

REFERENCES

(1) M. A. Ondetti, B. Rubin, and D. W. Cushman, *Science*, **196**, 441 (1977).

(2) D. W. Cushman, H. S. Cheung, E. F. Sabo, and M. A. Ondetti, *Biochemistry*, **16**, 5484 (1977).

(3) *Drugs Future*, **5**, 576 (1980).

(4) J. Koch-Weser, D. G. Vidt, E. L. Bravo, and F. M. Fouad, *N. Engl. J. Med.*, **306**, 214 (1982).

(5) A. I. Cohen and K. J. Kripalani, U.S. Patent 4,179,568, December 18, 1979.

(6) P. T. Funke, E. Ivashkiv, M. F. Malley, and A. I. Cohen, *Anal. Chem.*, **52**, 1086 (1980).

(7) A. I. Cohen, R. G. Devlin, E. Ivashkiv, P. T. Funke, and T. McCormick, *J. Pharm. Sci.*, **71**, 1251 (1982).

(8) K. J. Kripalani, D. N. McKinstry, S. M. Singhvi, D. A. Willard, R. A. Vukovich, and B. H. Migdalof, *Clin. Pharmacol. Ther.*, **27**, 636 (1980).

(9) B. H. Migdalof, S. M. Singhvi, and K. J. Kripalani, *J. Liq. Chromatogr.*, **3**, 857 (1980).

(10) T. Ikeda, T. Komai, K. Kawai, and H. Shindo, *Chem. Pharm. Bull.*, **29**, 1416 (1981).

(11) T. Komai, T. Ikeda, K. Kawai, E. Kameyama, and H. Shindo, *J. Pharm. Dyn.*, **4**, 677 (1981).
(12) B. K. Park, P. S. Grabowski, J. H. K. Yeung, and A. M. Breckenridge, *Biochem. Pharmacol.*, **31**, 1755 (1982).
(13) Y. Matsuki, K. Fukuhara, T. Ito, H. Ono, N. Ohara, T. Yui, and T. Nambara, *J. Chromatogr.*, **188**, 177 (1980).
(14) Y. Kawahara, M. Hisaoka, Y. Yamazaki, A. Inage, and T. Morioka, *Chem. Pharm. Bull.*, **29**, 150 (1981).
(15) B. Jarrott, A. Anderson, R. Hooper, and W. J. Louis, *J. Pharm. Sci.*, **70**, 665 (1981).
(16) K. Shimada, M. Tanaka, T. Nambara, Y. Imai, K. Abe, and K. Yoshinaga, *J. Chromatogr.*, **227**, 445 (1982).
(17) D. Perrett and P. L. Drury, *J. Liq. Chromatogr.*, **5**, 97 (1982).
(18) Y. Matsuki, T. Ito, K. Fukahara, T. Nakamura, M. Kimura, and H. Ono, *J. Chromatogr.*, **239**, 585 (1982).
(19) O. H. Drummer, B. Jarrott, and W. J. Louis, *Clin. Exp. Pharmacol. Physiol., Suppl.* **7**, 81 (1982).
(20) K. L. Duchin, S. M. Singhvi, D. A. Willard, B. H. Migdalof, and D. N. McKinstry, *Clin. Pharmacol. Ther.*, **31**, 452 (1982).
(21) H. Shindo, T. Komai, T. Ikeda, K. Kawai, W. Kawamata, and S. Kameyama, Proceedings of the 11th Symposium on Drug Metabolism and Action, Nogoya, Japan, November 6–7, 1979.
(22) B. J. Sweetman and J. A. Maclaren, *Aust. J. Chem.*, **19**, 1247 (1967).

ACKNOWLEDGMENTS

The authors thank P. Egli for the radioactive compounds used in the binding studies, T. McCormick for the MS data, and H. Roberts for stability data.

Pharmacokinetics of Pentobarbital, Quinidine, Lidocaine, and Theophylline in the Thermally Injured Rat

RICHARD J. FRUNCILLO ˣ and G. JOHN DIGREGORIO

Received February 2, 1983, from the *Department of Pharmacology, Hahnemann Medical College and Hospital, Philadelphia, PA 19102.* Accepted for publication August 4, 1983.

Abstract □ Previous studies have shown that rats with 15% third-degree burns show a severe depression in various *in vitro* hepatic drug-metabolizing enzymes. This effect was assessed *in vivo* by measuring the disposition of four liver-metabolized drugs in 16% third-degree burned rats at 7 d postburn. Compared with pair-fed control rats, pentobarbital demonstrated a significantly prolonged clearance and elimination half-life without a change in volume of distribution. Quinidine demonstrated a significantly increased volume of distribution and a significantly decreased clearance without a change in elimination half-life. Lidocaine showed a significantly increased volume of distribution. Theophylline, which is only 50% metabolized in the rat, showed no changes in any pharmacokinetic parameters. The free drug fractions of quinidine and lidocaine were found to be significantly decreased at 1 d postburn and normal at 7 d postburn. These results warrant pharmacokinetic studies in human burn patients.

Keyphrases □ Pentobarbital—pharmacokinetics in thermally injured rats □ Quinidine—pharmacokinetics in thermally injured rats □ Lidocaine—pharmacokinetics in thermally injured rats □ Theophylline—pharmacokinetics in thermally injured rats □ Thermal injury—phramacokinetics of pentobarbital, quindine, lidocaine, and theophylline, rats

Thermal injury can produce numerous pathophysiological alterations in an organism which may modify the absorption, distribution, metabolism, and renal excretion of therapeutic agents (1). Such changes would be directly reflected in the derived pharmacokinetic parameters for a given drug (2). Recently, our laboratory has presented evidence of a generalized depression in various *in vitro* liver drug-metabolizing enzymes in rats subjected to 15–16% third-degree burns (3–5). Also, this phenomenon may occur in human thermal injury, as demonstrated by significantly decreased levels of D-glucaric acid in human burn victims (6). However, such data on drug metabolism in which *in vitro* liver homogenates and D-glucaric acid are used may not reflect the pharmacokinetic characteristics of a drug in an intact organism. Besides the activity of hepatic microsomal drug-metabolizing enzymes, other factors such as alterations in hepatic blood flow and changes in drug binding by plasma proteins may significantly contribute to the overall process of hepatic drug clearance (7). Thus, the present study was undertaken in a rodent model with a 16% third-degree burn to assess the effects of thermal injury on the *in vivo* disposition of four liver-metabolized drugs commonly used for burn patients.

EXPERIMENTAL SECTION

Animals—Adult male Sprague-Dawley rats[1] (weight, 220–250 g) received 16% full-thickness burns as described below. They were housed in plastic cages in groups of one or two over corncob bedding in a room maintained at 24 ± 0.5°C with a constant 12-h light and dark cycle. Pharmacokinetic experiments were done 7 d after the burning. Control rats housed alone were carefully pair-fed[2] daily with the burned rats to adjust for the slight anorexic effect of the burn wound.

Burn Procedure—A full-thickness burn was produced on the rats by the method of Arturson (8). This type of burn completely destroys all dermal appendages and epithelial elements, including sensory nerve endings, resulting in a virtually pain-free preparation (9). The animals were anesthetized with sodium pentobarbital (50 mg/kg) and shaved with electric clippers. Each rat was placed in a plastic mold with a hole cut out that corresponded to ~16% of the total body surface area. This value was arrived at by skinning burned rats and measuring the area of the burn and the total body area by tracing these areas onto graph paper and counting the squares. It was found that this particular mold consistently delivered an approximate 16% burn for animals in the weight range of 220–250 g. The burns were inflicted by placing the mold (containing the bare rat skin protruding through the hole) in 90 ± 1°C water for 20 s. This procedure produced a burn with sharp edges that did not impair the mobility of the animals. The animals awoke from the procedure in no apparent distress and did not require analgesics. At no time during the study did any burned animal exhibit gross signs of infection. Control animals were shaved and anesthetized but not immersed in water.

Biochemical Parameters—Estimations of the serum levels of proteins, enzymes, and other constituents were done on six 16% burned and six pair-fed control rats by sending 5 mL of serum from the pooled blood of two rats to a commercial laboratory[3]. The serum was analyzed with a standard serum multiple analyzer, with normal rat serum used as standards. Serum was ob-

[1] Charles River Breeding Laboratories, Wilmington, Mass.
[2] Rodent Chow; Ralston Purina Inc., St. Louis, Mo.
[3] Vet Path Veterinary Laboratories, Teterboro, N.J.

0022-3549/84/0800-1117$01.00/0
© 1984, American Pharmaceutical Association

(11) T. Komai, T. Ikeda, K. Kawai, E. Kameyama, and H. Shindo, *J. Pharm. Dyn.*, **4**, 677 (1981).
(12) B. K. Park, P. S. Grabowski, J. H. K. Yeung, and A. M. Breckenridge, *Biochem. Pharmacol.*, **31**, 1755 (1982).
(13) Y. Matsuki, K. Fukuhara, T. Ito, H. Ono, N. Ohara, T. Yui, and T. Nambara, *J. Chromatogr.*, **188**, 177 (1980).
(14) Y. Kawahara, M. Hisaoka, Y. Yamazaki, A. Inage, and T. Morioka, *Chem. Pharm. Bull.*, **29**, 150 (1981).
(15) B. Jarrott, A. Anderson, R. Hooper, and W. J. Louis, *J. Pharm. Sci.*, **70**, 665 (1981).
(16) K. Shimada, M. Tanaka, T. Nambara, Y. Imai, K. Abe, and K. Yoshinaga, *J. Chromatogr.*, **227**, 445 (1982).
(17) D. Perrett and P. L. Drury, *J. Liq. Chromatogr.*, **5**, 97 (1982).
(18) Y. Matsuki, T. Ito, K. Fukahara, T. Nakamura, M. Kimura, and H. Ono, *J. Chromatogr.*, **239**, 585 (1982).
(19) O. H. Drummer, B. Jarrott, and W. J. Louis, *Clin. Exp. Pharmacol. Physiol., Suppl.* **7**, 81 (1982).
(20) K. L. Duchin, S. M. Singhvi, D. A. Willard, B. H. Migdalof, and D. N. McKinstry, *Clin. Pharmacol. Ther.*, **31**, 452 (1982).
(21) H. Shindo, T. Komai, T. Ikeda, K. Kawai, W. Kawamata, and S. Kameyama, Proceedings of the 11th Symposium on Drug Metabolism and Action, Nogoya, Japan, November 6–7, 1979.
(22) B. J. Sweetman and J. A. Maclaren, *Aust. J. Chem.*, **19**, 1247 (1967).

ACKNOWLEDGMENTS

The authors thank P. Egli for the radioactive compounds used in the binding studies, T. McCormick for the MS data, and H. Roberts for stability data.

Pharmacokinetics of Pentobarbital, Quinidine, Lidocaine, and Theophylline in the Thermally Injured Rat

RICHARD J. FRUNCILLO ˣ and G. JOHN DIGREGORIO

Received February 2, 1983, from the *Department of Pharmacology, Hahnemann Medical College and Hospital, Philadelphia, PA 19102.* Accepted for publication August 4, 1983.

Abstract □ Previous studies have shown that rats with 15% third-degree burns show a severe depression in various *in vitro* hepatic drug-metabolizing enzymes. This effect was assessed *in vivo* by measuring the disposition of four liver-metabolized drugs in 16% third-degree burned rats at 7 d postburn. Compared with pair-fed control rats, pentobarbital demonstrated a significantly prolonged clearance and elimination half-life without a change in volume of distribution. Quinidine demonstrated a significantly increased volume of distribution and a significantly decreased clearance without a change in elimination half-life. Lidocaine showed a significantly increased volume of distribution. Theophylline, which is only 50% metabolized in the rat, showed no changes in any pharmacokinetic parameters. The free drug fractions of quinidine and lidocaine were found to be significantly decreased at 1 d postburn and normal at 7 d postburn. These results warrant pharmacokinetic studies in human burn patients.

Keyphrases □ Pentobarbital—pharmacokinetics in thermally injured rats □ Quinidine—pharmacokinetics in thermally injured rats □ Lidocaine—pharmacokinetics in thermally injured rats □ Theophylline—pharmacokinetics in thermally injured rats □ Thermal injury—phramacokinetics of pentobarbital, quindine, lidocaine, and theophylline, rats

Thermal injury can produce numerous pathophysiological alterations in an organism which may modify the absorption, distribution, metabolism, and renal excretion of therapeutic agents (1). Such changes would be directly reflected in the derived pharmacokinetic parameters for a given drug (2). Recently, our laboratory has presented evidence of a generalized depression in various *in vitro* liver drug-metabolizing enzymes in rats subjected to 15–16% third-degree burns (3–5). Also, this phenomenon may occur in human thermal injury, as demonstrated by significantly decreased levels of D-glucaric acid in human burn victims (6). However, such data on drug metabolism in which *in vitro* liver homogenates and D-glucaric acid are used may not reflect the pharmacokinetic characteristics of a drug in an intact organism. Besides the activity of hepatic microsomal drug-metabolizing enzymes, other factors such as alterations in hepatic blood flow and changes in drug binding by plasma proteins may significantly contribute to the overall process of hepatic drug clearance (7). Thus, the present study was undertaken in a rodent model with a 16% third-degree burn to assess the effects of thermal injury on the *in vivo* disposition of four liver-metabolized drugs commonly used for burn patients.

EXPERIMENTAL SECTION

Animals—Adult male Sprague-Dawley rats[1] (weight, 220–250 g) received 16% full-thickness burns as described below. They were housed in plastic cages in groups of one or two over corncob bedding in a room maintained at 24 ± 0.5°C with a constant 12-h light and dark cycle. Pharmacokinetic experiments were done 7 d after the burning. Control rats housed alone were carefully pair-fed[2] daily with the burned rats to adjust for the slight anorexic effect of the burn wound.

Burn Procedure—A full-thickness burn was produced on the rats by the method of Arturson (8). This type of burn completely destroys all dermal appendages and epithelial elements, including sensory nerve endings, resulting in a virtually pain-free preparation (9). The animals were anesthetized with sodium pentobarbital (50 mg/kg) and shaved with electric clippers. Each rat was placed in a plastic mold with a hole cut out that corresponded to ~16% of the total body surface area. This value was arrived at by skinning burned rats and measuring the area of the burn and the total body area by tracing these areas onto graph paper and counting the squares. It was found that this particular mold consistently delivered an approximate 16% burn for animals in the weight range of 220–250 g. The burns were inflicted by placing the mold (containing the bare rat skin protruding through the hole) in 90 ± 1°C water for 20 s. This procedure produced a burn with sharp edges that did not impair the mobility of the animals. The animals awoke from the procedure in no apparent distress and did not require analgesics. At no time during the study did any burned animal exhibit gross signs of infection. Control animals were shaved and anesthetized but not immersed in water.

Biochemical Parameters—Estimations of the serum levels of proteins, enzymes, and other constituents were done on six 16% burned and six pair-fed control rats by sending 5 mL of serum from the pooled blood of two rats to a commercial laboratory[3]. The serum was analyzed with a standard serum multiple analyzer, with normal rat serum used as standards. Serum was ob-

[1] Charles River Breeding Laboratories, Wilmington, Mass.
[2] Rodent Chow; Ralston Purina Inc., St. Louis, Mo.
[3] Vet Path Veterinary Laboratories, Teterboro, N.J.

0022-3549/84/0800-1117$01.00/0
© 1984, American Pharmaceutical Association

tained 7 d postburning or pair-feeding by needle puncture of the surgically exposed jugular veins in rats anesthetized with sodium pentobarbital (50 mg/kg ip).

Quinidine, Lidocaine, and Theophylline Pharmacokinetics—Both burned and pair-fed rats were anesthetized with 1.7 g/kg of urethane, an anesthetic that does not inhibit drug metabolism (10) and which has been reported to maintain hepatic blood flow at a level equal to that of an awake animal (11). The right and left jugular veins were surgically exposed by superficial skin incisions in the areas of both clavicles, and 25 mg/kg of quinidine (free base), 15 mg/kg of lidocaine hydrochloride, or 15 mg/kg of theophylline (18.75 mg/kg of aminophylline) was injected intravenously through the right jugular vein. Blood samples (0.4 mL) were taken at 0.5, 1, 2, 3, and 4 h postinjection for quinidine; at 10, 20, 30, 40, and 50 min postinjection for lidocaine; and at 1, 2, 3, 4, and 5 h postinjection for theophylline. Samples were obtained by venipuncture of the left jugular vein through the pectoris major muscle with a 1-mL heparinized tuberculin syringe.

Pentobarbital Pharmacokinetics—Both 16% burned and pair-fed rats were lightly anesthetized with ether, and their ventral tail veins were cannulated with a piece of heparinized polyethylene tubing[4]. After securing the tubing in the vein with silk ligatures, the animals were placed in restraint cages and allowed to become fully awake. The rats were kept in the restraint cages for at least 3 h before the pharmacokinetic experiment was run, since it has been shown that brief exposure to ether can inhibit drug metabolism in the immediate postexposure period (10). After this 3-h recovery period, 40 mg/kg of sodium pentobarbital was injected intravenously through the tail vein cannula. Once the rats were in deep anesthesia, they were removed from the restraint cages, and the right jugular vein was exposed as described above. Blood samples were taken at 0.5, 1.0, 1.5, 2.0, and 2.5 h postinjection by venipuncture of the jugular vein with a 1-mL heparinized tuberculin syringe. Samples ranged in volume from 0.6 to 1.0 mL and did not exceed 3.0 mL of blood before the withdrawal of the last sample. After the 2.0-h sample was taken, 1.0 mL of saline was injected into the rat through the tail vein cannula in an attempt to partially restore some of the blood volume.

Drug Analysis—Quinidine, lidocaine, and theophylline plasma concentrations were measured by commercially available enzyme immunoassay kits[5] as described previously (12). The plasma concentrations of pentobarbital were determined by a modification of the GC method of Watson and Kalman (13). A gas chromatograph[6] equipped with a hydrogen flame-ionization detector was used for this study. Glass columns (~183 cm × 4 mm i.d.), packed with 3% OV-17 Gas Chrom Q, were used under the following conditions: injection port temperature, 200°C; column temperature, 180°C; detector temperature, 215°C; carrier gas, nitrogen at a flow rate of 20 mL/min. The sensitivity settings were 2 × 1.

The extraction procedure was as follows. Into a 13-mL glass centrifuge tube with a ground glass stopper were placed 0.3–0.6 mL of unknown plasma and 100 μL of barbital standard (200 μg of barbital/mL of distilled water). Saturated potassium dihydrogen phosphate (0.6 mL) was added, and the tubes were shaken lightly. Dichloromethane (0.5 mL) was then added, the stopper was replaced, and the tube was inverted manually 40 times. The layers were separated by centrifuging at 4000 rpm for 5 min, and the protein-containing aqueous layer was removed by aspiration. The organic layer (3.0 mL) was then transferred to a second 13-mL glass centrifuge tube, and the solvent was evaporated under a stream of nitrogen in a water bath at 45–50°C. The sides of the tube were washed with 0.5 mL of dichloromethane, and the solvent was again evaporated off. Chloroform (50 μL) was added and swirled around the tube, and 2 μL of the reconstituted sample was injected into the gas chromatograph.

Equilibrium Dialysis Experiments—A modification of the method of Woo and Greenblatt (14) was employed. Sixteen percent burns were inflicted as described above, and serum from 1- and 7-d postburn rats was compared with pair-fed controls. Whole blood was obtained by allowing decapitated rats to bleed into a large beaker without anticoagulant. The serum obtained after centrifugation was stored at −20°C and thawed just before dialysis.

Quinidine and lidocaine were dialyzed against pH 7.4 potassium phosphate buffer with added sodium chloride, prepared by dissolving 14.11 g of K_2HPO_4, 2.59 g of KH_2PO_4, and 1.99 g of NaCl in distilled water to make 1 L of solution. Lengths (19 cm) of cellulose dialysis tubing[7], with a molecular weight cut off of 10,000–14,000, were boiled in distilled water for 4 h and then rinsed with cold distilled water. Serum (1 mL) was added to the tubing, and both ends were sealed with double knots. The resultant dialysis bags were then placed in culture tubes holding 10 mL of buffer containing either 1.6 μg/mL of quinidine (free base) or 1.6 μg/mL of lidocaine (free base). The culture tubes were placed in a shaking water bath at 37°C for 20 h to reach equilibrium. Serum and buffer quinidine and lidocaine concentrations were determined by the enzyme immunoassay method[5], and the free drug percentage was calculated by:

$$\text{percent free drug} = \frac{\text{drug concentration in buffer} \times 100}{\text{drug concentration in serum}}$$

Mathematical Calculations—Pharmacokinetic parameters were calculated by utilizing the one-compartment open model which assumes very rapid initial distribution of the drug (15). The plasma disappearance of all four drugs was considered to follow the exponential function $C_p(t) = Ae^{-\lambda t}$, where $C_p(t)$ is the plasma concentration at time t, A is the zero-time intercept, and λ is the elimination rate constant. The elimination half-life ($t_{1/2}$) was calculated by $t_{1/2} = 0.693/\lambda$, the volume of distribution (Vd) was calculated by Vd = dose/A, and the clearance (CL) was calculated by $CL = Vd \cdot \lambda$. The parameters were calculated for each animal by linear regression analysis of a semilogarthmic plot of drug concentration *versus* time. All data were compared by the unpaired Student's t test, with $p > 0.05$ being statistically insignificant.

Table I—Biochemical Parameters in 16% Burned *versus* Pair-Fed Control Rats[a]

Parameters	Control	Burn
Serum glutamic oxaloacetic transaminase, IU/L	175 ± 30	200 ± 18
Serum glutamic pyruvic transaminase, IU/L	57 ± 8	59 ± 11
γ-Glutamyltransferase, IU/L	3.5 ± 2.1	6 ± 3
Total Bilirubin, mg/dL	0.59 ± .25	0.52 ± .25
Albumin, g/dL	2.80 ± .10	1.96 ± .06[b]
Total Protein, g/dL	6.0 ± 0.3	4.8 ± 0.2[b]
Blood urea nitrogen, mg/dL	13.7 ± 0.6	14.6 ± 1.1
Creatinine, mg/dL	1.5 ± 0.3	1.3 ± 0.1
Blood urea nitrogen–creatinine	9.1 ± 0.4	11.2 ± 1.2

[a] Values are means ± *SD* of six burned and six control animals compared at 7 d postburn. [b] $p < 0.0005$.

RESULTS

Biochemical laboratory parameters for pair-fed control rats and 16% burned rats 7 d postburn are listed in Table I. The serum albumin and total protein concentrations were significantly lower in the burned rats as compared with

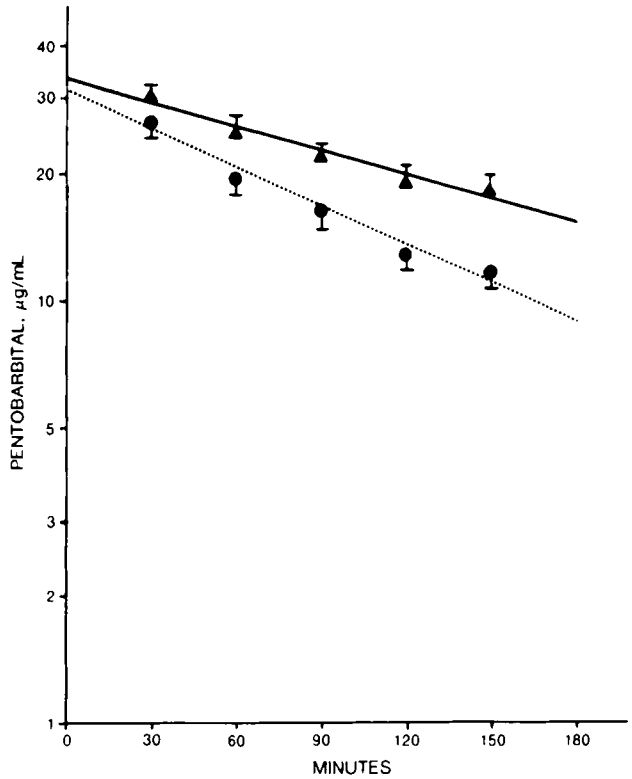

Figure 1—*Plasma disappearance curves of pentobarbital after a 40-mg/kg iv administration in 16% burned male rats at 7 d postburn (▲) and pair-fed control rats (●). Values are mean ± SE, with n = 5 or 6 at each point.*

[4] PE-50 tubing; Becton, Dickinson and Co., Parsippany, N.J.
[5] EMIT system; Syva Co., Palo Alto, Calif.
[6] Model 3920; Perkin-Elmer Corp., Norwalk, Conn.
[7] Fisher Scientific Co., King of Prussia, Pa.

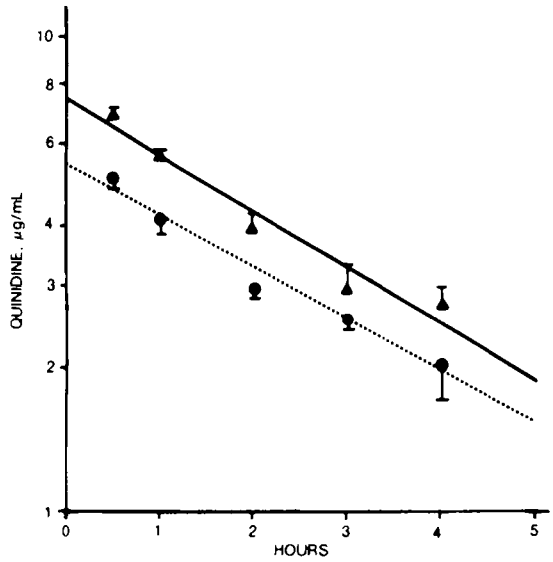

Figure 2—*Plasma disappearance curves of quinidine after 25 mg/kg (free base) iv administration in 16% burned male rats at 7 d postburn (▲) and pair-fed control rats (●). Values are mean ± SE, with n = 4 at each point.*

the control groups. There was no significant difference in the concentrations of the various liver enzymes measured between the two groups or in the concentrations of total bilirubin, creatinine, or blood urea nitrogen.

Figures 1–4 illustrate the respective average plasma disappearance curves for pentobarbital, quinidine, lidocaine, and theophylline for pair-fed controls and 16% burned rats 7 d postburn, and Table II shows the derived pharmacokinetic parameters and weight changes for these same animals. For each drug group tested, the burned rats gained a significantly lower amount of weight over the 7-d period than their corresponding controls, even though each control animal received the same amount of food daily as its paired burned animal. Thermal injury produced a significant 69% prolongation in pentobarbital elimination half-life and a correspondingly significant 43% reduction in total pentobarbital clearance. There was no significant difference in the volume of distribution observed for pentobarbital. For quinidine, the burned animals exhibited a significant reduction (24%) in total clearance and a significant reduction (25%) in volume of distribution, with an unchanged elimination half-life. The burned rats receiving lidocaine demonstrated a significant decrease (27%) in volume of distribution without significant changes in either total clearance or elimination half-life. For theophylline, thermal injury did not significantly alter total clearance, volume of distribution, or elimination half-life.

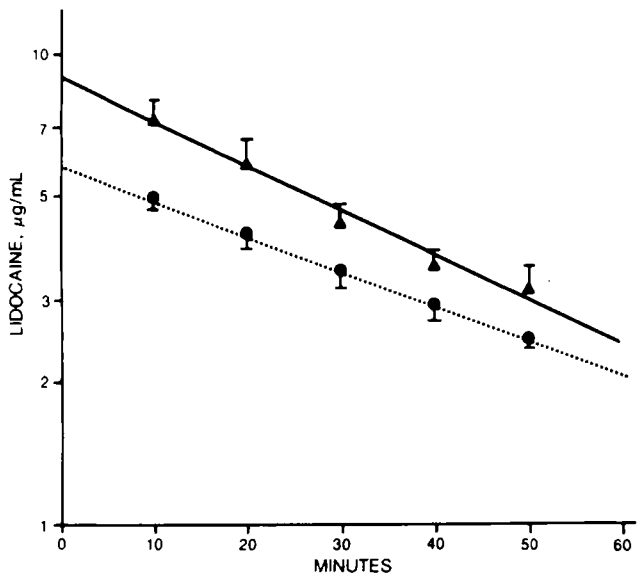

Figure 3—*Plasma disappearance curves of lidocaine after a 15-mg/kg (free base) iv administration in 16% burned male rats at 7 d postburn (▲) and pair-fed control rats (●). Values are mean ±SE, with n = 5 at each point.*

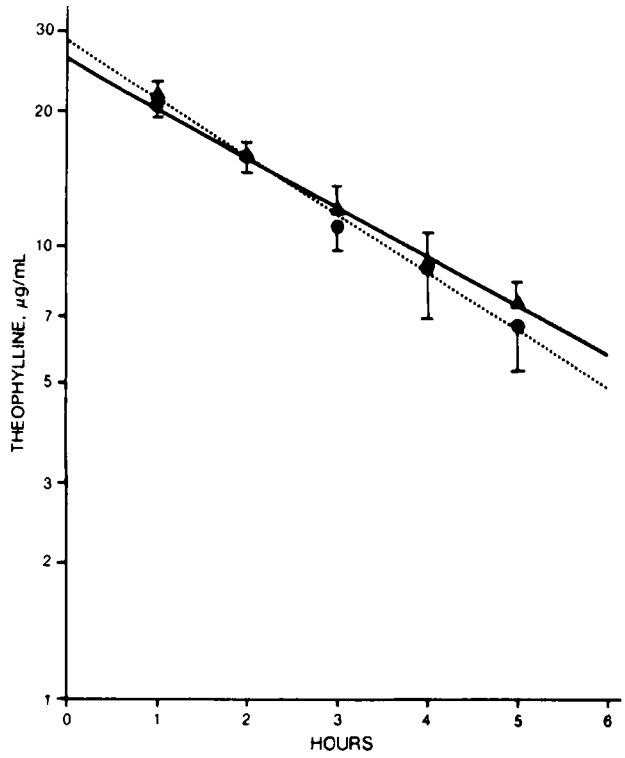

Figure 4—*Plasma disappearance curves of theophylline after a 15-mg/kg iv administration in 16% burned male rats at 7 d postburn (▲) and pair-fed control rats (●). Values are mean ± SE, with n = 4 at each point.*

To determine whether changes in drug protein binding contributed to the observed alterations in the volumes of distribution of quinidine and lidocaine at 7 d postburn, equilibrium dialysis studies were performed with quinidine and lidocaine in 16% burned and pair-fed control rats at 7 d postburn and also at 1 d postburn to serve as a comparison. At 7 d postburn, there was no significant difference in free drug percentages or total drug concentrations of either quinidine or lidocaine compared with controls (Table III). However, at 1 d postburn, there was a significant decrease (18%) in the free drug percentage of quinidine and a significant decrease (27%) in the free drug percentage of lidocaine, which resulted in a significant increase (20%) in total quinidine concentration and a significant increase (37%) in total lidocaine concentration.

Table II—Pharmacokinetic Parameters of Various Drugs in 16% Burned *versus* Pair-Fed Control Rats[a]

Parameter	Control	Burn
	Pentobarbital (40 mg/kg iv)[b]	
$t_{1/2}$, min	102.9 ± 27.8	173.9 ± 40.1[c]
Vd, L/kg	1.21 ± 0.16	1.20 ± 0.19
CL, mL/min/kg	8.59 ± 2.39	4.94 ± 0.90[c]
Percent weight change[d]	+17.5 ± 2.6	+4.1 ± 9.6[c]
	Quinidine (25 mg/kg iv)[e]	
$t_{1/2}$, h	2.65 ± 0.57	2.63 ± 0.48
Vd, L/kg	4.58 ± 0.47	3.45 ± 0.24[f]
CL, mL/min/kg	20.5 ± 3.3	15.5 ± 2.8[g]
Percent weight change[d]	+15.9 ± 3.5	+3.0 ± 4.4[f]
	Lidocaine (15 mg/kg iv)[h]	
$t_{1/2}$, min	38.6 ± 4.7	34.5 ± 6.5
Vd, L/kg	2.52 ± 0.27	1.84 ± 0.42[c]
CL, mL/min/kg	46.7 ± 9.1	37.5 ± 9.4
Percent weight change[d]	+10.4 ± 3.7	+1.8 ± 6.2[g]
	Theophylline (15 mg/kg iv)[e]	
$t_{1/2}$, h	2.19 ± 0.38	2.33 ± 0.36
Vd, L/kg	0.50 ± 0.05	0.57 ± 0.10
CL mL/min/kg	2.70 ± 0.66	2.83 ± 0.66
Percent weight change[d]	+14.0 ± 5.1	−1.2 ± 12.2[g]

[a] Mean ± *SD* measured 7 d postburn. [b] *n* = 5 for the controls, 6 for the burn group. [c] Significantly different from the controls at $p < 0.01$. [d] Calculated by [(wt. at day 7 − wt. at day 0)/wt. at day 0] × 100. [e] *n* = 4 for both groups. [f] Significantly different from the controls at $p < 0.005$. [g] Significantly different from the controls at $p < 0.05$. [h] *n* = 5 for both groups.

Table III—Equilibrium Dialysis Results in 16% Burned *versus* Pair-Fed Control Rats [a]

	Control	Day 1 Postburn	Day 7 Postburn
	Percent Free Drug		
Quinidine	29.9 ± 5.1	24.4 ± 2.3[b]	31.1 ± 2.4
Lidocaine	52.5 ± 6.0	38.1 ± 1.8[c]	52.5 ± 4.8
	Total Drug Concentration, μg/mL		
Quinidine	4.13 ± 0.71	4.96 ± 0.45[b]	3.98 ± 0.48
Lidocaine	2.46 ± 0.24	3.38 ± 0.23[c]	2.48 ± 0.18

[a] Mean ± *SD*; $n = 6$. [b] Significantly different from the controls at $p < 0.05$. [c] Significantly different from the controls at $p < 0.0005$.

DISCUSSION

In this study, it has been demonstrated that thermal injury can alter pharmacokinetic parameters for various liver-metabolized drugs in rats. Previous studies in this laboratory have shown that third-degree burns can depress various components of the hepatic mixed-function oxidase system in rats (3-5) and D-glucaric acid excretion in humans (6). A manifestation of this effect *in vivo* would be a decrease in the total clearance of a drug. However, as stated previously, in addition to levels of hepatic drug-metabolizing enzymes, total clearance can also be affected by changes in hepatic blood flow and free drug fraction (7).

The significant reduction (43%) in pentobarbital clearance can probably be attributed to a reduction in the level of liver enzymes that metabolize pentobarbital. Although a decrease in the free fraction of pentobarbital could also cause a decreased total clearance (7), this event was unlikely since albumin is the main serum protein that binds pentobarbital (16), and it has been shown that the serum albumin concentration is decreased in the burned rats (Table I). This decrease in serum albumin should cause, if anything, an increased and not a decreased free drug concentration (7). Also, the observed total plasma pentobarbital clearance of 8.59 mL/min/kg in control rats is considerably less than the estimated literature values for hepatic plasma flow of ~40 mL/min/kg in similar rats (17). Thus, it can be assumed that pentobarbital clearance is relatively independent of hepatic blood flow changes in the rat (7).

For quinidine, there was a significant decrease (24%) in total clearance ($p < 0.05$), and for lidocaine there was a 20% reduction in total clearance ($p < 0.1$). Although these two drugs have total clearances in humans which are dependent on liver blood flow and drug-metabolizing enzyme activity (7), the relationship of total clearance to renal clearance, liver blood flow, and enzyme activity is unknown in rats. Thus, it is not possible to attribute the observed differences in total clearance for these drugs in the burned rats to any one particular factor. However, changes in drug protein binding did not play a part, as both drugs demonstrated unchanged free drug fractions at 7 d postburn (Table III).

For theophylline, the unchanged total clearance may not be due to a lack of effect of thermal injury on drug-metabolizing enzymes, since the disposition of theophylline differs markedly in rats as compared with humans, in that 46% of the drug is excreted unchanged by the kidneys in rats (18), as compared with less than 10% in humans (19). Thus, the renal route in rats may compensate for any reduction in hepatic clearance.

Since the concentrations of quinidine, lidocaine, and theophylline were measured by enzyme immunoassay, the possibility exists that certain metabolites in rat plasma may cross-react with the parent compounds in the assay and, thus, cause falsely higher values for intact quinidine, lidocaine, or theophylline to be reported. If such a situation were present, the values for drug concentrations and pharmacokinetic parameters in both burned and control rats would be altered slightly from their true values. However, any difference in these values would still be preserved. The only situation that could occur which would make the observed differences between burned and control rats artifactual would be that in which the burned rats metabolized the parent compound through a different metabolic pathway, producing different metabolites from the controls with a higher cross-reactivity for intact drug. Although such a situation cannot be completely ruled out, its occurrence seems unlikely.

For both the basic drugs, quinidine and lidocaine, there were significant decreases in volume of distribution in the burned animals at 7 d postburn (Table II). Increased plasma protein binding of these drugs was not the causative factor for these changes (Table III). A possible explanation is a displacement of drug from tissue-binding sites by substances released at the burn site. For these same drugs, there was a significant decrease in the free drug fraction and a significant increase in total drug concentration when serum taken from rats 1 d postburn was used for equilibrium dialysis studies. Quinidine and lidocaine are examples of drugs that bind more strongly to a specific plasma protein, α_1-acid glycoprotein, than to albumin (20). A number of inflammatory conditions, including burns, have been shown to elevate α_1-acid glycoprotein levels in humans (21) and to increase the plasma protein binding of various drugs (20). The results shown in Table III are consistent with the observation of a rapid rise in α_1-acid glycoprotein levels 24 h postburn in the male rat and a fall to normal levels by 7 d postburn.

In recent years, it has become increasingly apparent that various methodological artifacts could cause errors in the interpretation of data from protein binding experiments with equilibrium dialysis (22). Of particular relevance to this study is the possibility that the free drug fractions reported here after an 18-h dialysis may be larger than those after a shorter dialysis period due to possible deterioration of α_1-acid glycoprotein with time or dilution of this protein by an osmotic influx of water during the dialysis. Although no dialysis experiments were done at shorter time intervals, the control free drug fraction of quinidine reported here (30%) compares favorably with a literature value of 31% in the rat done over a shorter dialysis interval (23). However, the control free fraction of lidocaine (53%) is higher than an estimated literature value of 44% in the rat based on saliva-plasma lidocaine levels (24) and, thus, may have been influenced by the aforementioned factors.

Despite careful daily pair-feeding of burned animals with control animals, all of the burned rats in the four drug groups had a significantly slower rate of weight gain compared with the pair-fed controls (Table II). This finding is consistent with the hypermetabolic response and increased basal metabolic rate found previously both in burn patients and experimental animals (25).

The pathophysiological alterations caused by thermal injury can produce variable changes in the kinetic and dynamic behavior of drugs in humans. An increased elimination rate was found for the renally eliminated aminoglycosides gentamicin (26), tobramycin (27), and amikacin (28). This effect was probably due to a burn-induced increase in the glomerular filtration rate (27). For the nondepolarizing neuromuscular blocking agents tubocurarine (29) and metocurine (30), two- to fivefold increases in plasma drug concentrations were required to give normal muscle relaxation in burn patients. This effect could not be explained by increased drug protein binding and was probably related to a burn-related change in the neuromuscular junction receptors (31). The liver-metabolized drug diazepam has recently been shown to have a reduced free clearance in burn patients (32); however, all patients in this study received cimetidine, a drug known to inhibit diazepam clearance (33). Thermal injury in humans has also been shown to lower plasma protein concentrations (34) and to alter the protein binding of a number of drugs (35). A pharmacokinetic study in 15% burned rats has shown that thermal injury can increase the free phenytoin fraction with a corresponding increase in total phenytoin clearance (36). However, no calculation of free phenytoin clearance was done.

In conclusion, the results of this study and previous investigations suggest that the complex dynamic state of thermal injury can affect numerous aspects of drug disposition and action. Further pharmacokinetic studies with liver-metabolized drugs in burn patients are needed to determine whether altered hepatic drug metabolism plays a part in the disposition of drugs in human thermal injury.

REFERENCES

(1) R. J. Sawchuk and T. S. Rector, *Clin. Pharmacokinet.*, **5**, 548 (1980).

(2) L. B. Sheiner and T. N. Tozer, in "Clinical Pharmacology," 2nd ed., K. L. Melmon and H. F. Morelli, Eds., Macmillan, New York, N.Y. 1978, pp. 71-109.

(3) E. I. Ciaccio and R. J. Fruncillo, *Biochem. Pharmacol.*, **28**, 3151 (1979).

(4) L. Durlofsky and R. J. Fruncillo, *J. Trauma*, **22**, 950 (1982).

(5) R. J. Fruncillo and G. J. DiGregorio, *J. Trauma*, **23**, 523 (1983).

(6) E. I. Ciaccio and R. J. Fruncillo, *Clin. Pharmacol. Ther.*, **25**, 340 (1979).

(7) M. Rowland and T. N. Tozer, in "Clinical Pharmacokinetics," Lea and Febiger, Philadelphia, Pa., 1980, pp. 48-76.

(8) G. Arturson, *Acta Chir. Scand. (Suppl.)*, **274**, 1 (1961).

(9) C Teplitz, in "Burns: A Team Approach," C. P. Artz, J. A. Moncrief and B. A. Pruitt, Eds., W. B. Saunders, Philadelphia, Pa., 1979, pp. 45-94.

(10) T. Umeda and T. Inaba, *Can. J. Physiol. Pharmacol.*, **56**, 241 (1978).

(11) C. R. Hiley, M. S. Yates, and D. J. Bock, *Experientia*, **34**, 1061 (1978).

(12) R. J. Bastiani, R. C. Phillips, and R. S. Schneider, *Am. J. Med. Tech.*, **39**, 211 (1973).

(13) E. Watson and S. M. Kalman, *Clin. Chim. Acta*, **38**, 33 (1972).

(14) E. Woo and D. J. Greenblatt, *J. Pharm. Sci.*, **68**, 466 (1979).

(15) S. E. Mayer, K. L. Melmon, and A. G. Gilman, in "The Pharmacological Basis of Therapeutics," 6th ed., A. G. Goodman, L. S. Goodman, and A. Gilman, Eds., Macmillan, New York, N.Y., 1980, pp. 761-792.
(16) S. Harvey, in "The Pharmacological Basis of Therapeutics," 6th ed., A. G. Goodman, L. S. Goodman, and A. Gilman, Eds., MacMillan, New York, N.Y., 1980, pp. 339-375.
(17) D. Lebrec, L. Blanchet, and S. Lacroix, *Eur. J. Physiol.*, **391,** 353 (1981).
(18) J. F. Williams, S. Lowitt, and A. Szentivanyi, *Biochem. Pharmacol.*, **28,** 2935 (1979).
(19) J. W. Jenne, H. T. Nagasawa, and R. D. Thompson, *Clin. Pharmacol. Ther.*, **19,** 373 (1976).
(20) D. J. Edwards, D. Lalka, F. Cerra, and R. L. Slaughter, *Clin. Pharmacol. Ther.*, **31,** 62 (1982).
(21) S. Sevitt, in "Reactions to Injury and Burns and their Clinical Importance," J.B. Lippencott, Philadelphia, Pa., 1974, pp. 22-36.
(22) F. D. Boudinot and W. J. Jusko, *J. Pharm. Sci.*, **73,** 774 (1984).
(23) D. Fremstod, S. Jacobsen, and P. K. Lunde, *Acta Pharmacol. Toxicol.*, **41,** 161 (1977).
(24) G. J. DiGregorio, A. J. Piraino, and E. Ruch, *J. Pharm. Sci.*, **68,** 1192 (1979).
(25) D. W. Wilmore, A. D. Mason, and D. W. Johnson, *J. Appl. Physiol.*, **38,** 593 (1975).
(26) D. E. Zaske, R. J. Sawchuk, D. N. Gerding, and R. G. Strate, *J. Trauma*, **16,** 824 (1976).
(27) P. Loirat, J. Rohan, A. Baillet, F. Beaufils, R. David, and A. Chapman, *N. Engl. J. Med.*, **299,** 915 (1978).
(28) D. E. Zaske, R. J. Sawchuk, and R. G. Strate, *Surgery*, **84,** 603 (1978).
(29) J. A. J. Martyn, S. K. Szyfelbein, H. H. Ali, R. S. Matteo, and J. J. Savarese, *Anesthesiology*, **52,** 352 (1980).
(30) J. A. J. Martyn, N. G. Goudsouzian, R. S. Matteo, L. M. Liu, S. K. Szyfelbein, and R. F. Kaplan, *Br. J. Anaesth.*, **55,** 263 (1983).
(31) W. S. Leibel, J. A. J. Martyn, S. K. Szyfelbein, and K. W. Miller, *Anesthesiology*, **54,** 378 (1982).
(32) J. A. J. Martyn, D. J. Greenblatt, and W. C. Quinby, *Anesth. Analg.*, **62,** 293 (1983).
(33) U. Klotz and I. Riemann, *N. Engl. J. Med.*, **302,** 1012 (1980).
(34) H. Zetterstrom and G. Arturson, *Acta Anaesth. Scand.*, **24,** 288 (1980).
(35) D. C. Bloedow, T. C. Hardin, M. A. Simons, and J. F. Hansbrough, *Clin. Pharmacol. Ther.*, **31,** 204 (1982).
(36) A. Bowdle, G. D. Neal, R. H. Levy, and D. M. Heimbach, *J. Pharmacol. Exp. Ther.*, **213,** 97 (1980).

ACKNOWLEDGMENTS

This study was supported by a grant from the Hahnemann Medical College and Hospital Biomedical Research Support Grant No. 5-S07-RR05413 and certified by the Hahnemann Medical College Animal Welfare Committee as meeting the guidelines of the National Institutes of Health for the care and use of laboratory animals.

The authors thank Mrs. Linda Bush and Ms. Joanne Addario for their help in the preparation of this manuscript.

Comparative *In Vivo* and *In Vitro* Studies of Phenytoin Protein Binding and *In Vitro* Lipolysis in Plasma of Pregnant and Nonpregnant Rats

RUBY C. CHOU and GERHARD LEVY ˣ

Received June 17, 1983, from the *Department of Pharmaceutics, School of Pharmacy, State University of New York at Buffalo, Amherst, NY 14260.* Accepted for publication October 3, 1983.

Abstract □ This investigation was designed to determine the cause of the changes in drug protein binding that occur in rat plasma, particularly in plasma from pregnant animals, during *in vitro* drug-protein binding measurements. *In vivo* estimates of phenytoin binding in plasma were obtained from steady-state CSF-plasma concentration ratios in pregnant and nonpregnant rats. Immediate ultrafiltration of heparin- or EDTA-anticoagulated plasma yielded phenytoin free fraction values that were in good agreement with *in vivo* estimates for nonpregnant rats but that were about one-third higher than *in vivo* estimates for pregnant animals. *In vitro* free fraction values tended to increase during incubation of plasma and/or during equilibrium dialysis. The concentrations of the four major endogenous free fatty acids were similar in plasma of pregnant and nonpregnant rats if determined immediately after blood collection. Six hours of incubation at 37°C caused fatty acid concentrations to increase about fivefold and twofold in heparin-anticoagulated plasma from pregnant and nonpregnant animals, respectively. The corresponding increases in EDTA-anticoagulated plasma were only about twofold and 1.14-fold, respectively. These changes were associated with decreased plasma protein binding of phenytoin. The *in vivo* differences between pregnant and nonpregnant rats with respect to phenytoin binding in plasma are not due to differences in fatty acid concentrations, but the *in vitro* differences are due primarily to corresponding differences in free fatty acid concentrations if extensive *in vitro* lipolysis occurs.

Keyphrases □ Phenytoin—plasma protein binding, lipolysis, pregnant and nonpregnant rats □ Lipolysis—*in vitro* and *in vivo* comparisons, plasma protein binding, pregnant and nonpregnant rats □ Anticoagulants—heparin, EDTA, plasma protein binding, *in vitro* and *in vivo* comparisons, pregnant and nonpregnant rats

Pregnancy is known to be associated with quantitative changes of drug biotransformation (1) and drug-protein binding in plasma or serum (2). Properly designed studies of the effect of pregnancy on the pharmacokinetics of drugs, therefore, require measurement of unbound drug in plasma, to differentiate between pharmacokinetic changes due solely to drug binding alterations and those due to altered intrinsic clearance or to a combination of both types of effects. Unfortunately, the drug-protein binding characteristics of plasma from pregnant rats and, to a lesser extent, from pregnant women are quite unstable (3, 4). A lack of appreciation of this problem can lead to serious misinterpretations in pharmacokinetic studies, particularly in the assessment of intrinsic drug clearance and drug concentration–pharmacological activity relationships.

This investigation was designed to determine the causes of *in vitro* alterations in protein binding of drugs in plasma from pregnant and nonpregnant rats and to assess the effects of the *in vitro* anticoagulant and of the methodology used for protein binding determinations. The study protocol also permitted a comparative determination of the effect of pregnancy on the total clearance and *in vivo* plasma protein binding of phenytoin in rats.

EXPERIMENTAL SECTION

Pregnant (day 20 of gestation) and nonpregnant Lewis rats[1] (the latter ≃ 200 g) received a loading dose of phenytoin, 14.7 mg/kg, by rapid injection

[1] Charles River Breeding Laboratories, Wilmington, Mass.

0022-3549/84/0800-1121$01.00/0
© 1984, American Pharmaceutical Association

(15) S. E. Mayer, K. L. Melmon, and A. G. Gilman, in "The Pharmacological Basis of Therapeutics," 6th ed., A. G. Goodman, L. S. Goodman, and A. Gilman, Eds., Macmillan, New York, N.Y., 1980, pp. 761-792.
(16) S. Harvey, in "The Pharmacological Basis of Therapeutics," 6th ed., A. G. Goodman, L. S. Goodman, and A. Gilman, Eds., MacMillan, New York, N.Y., 1980, pp. 339-375.
(17) D. Lebrec, L. Blanchet, and S. Lacroix, *Eur. J. Physiol.*, **391,** 353 (1981).
(18) J. F. Williams, S. Lowitt, and A. Szentivanyi, *Biochem. Pharmacol.*, **28,** 2935 (1979).
(19) J. W. Jenne, H. T. Nagasawa, and R. D. Thompson, *Clin. Pharmacol. Ther.*, **19,** 373 (1976).
(20) D. J. Edwards, D. Lalka, F. Cerra, and R. L. Slaughter, *Clin. Pharmacol. Ther.*, **31,** 62 (1982).
(21) S. Sevitt, in "Reactions to Injury and Burns and their Clinical Importance," J.B. Lippencott, Philadelphia, Pa., 1974, pp. 22-36.
(22) F. D. Boudinot and W. J. Jusko, *J. Pharm. Sci.*, **73,** 774 (1984).
(23) D. Fremstod, S. Jacobsen, and P. K. Lunde, *Acta Pharmacol. Toxicol.*, **41,** 161 (1977).
(24) G. J. DiGregorio, A. J. Piraino, and E. Ruch, *J. Pharm. Sci.*, **68,** 1192 (1979).
(25) D. W. Wilmore, A. D. Mason, and D. W. Johnson, *J. Appl. Physiol.*, **38,** 593 (1975).
(26) D. E. Zaske, R. J. Sawchuk, D. N. Gerding, and R. G. Strate, *J. Trauma*, **16,** 824 (1976).
(27) P. Loirat, J. Rohan, A. Baillet, F. Beaufils, R. David, and A. Chapman, *N. Engl. J. Med.*, **299,** 915 (1978).
(28) D. E. Zaske, R. J. Sawchuk, and R. G. Strate, *Surgery*, **84,** 603 (1978).
(29) J. A. J. Martyn, S. K. Szyfelbein, H. H. Ali, R. S. Matteo, and J. J. Savarese, *Anesthesiology*, **52,** 352 (1980).
(30) J. A. J. Martyn, N. G. Goudsouzian, R. S. Matteo, L. M. Liu, S. K. Szyfelbein, and R. F. Kaplan, *Br. J. Anaesth.*, **55,** 263 (1983).
(31) W. S. Leibel, J. A. J. Martyn, S. K. Szyfelbein, and K. W. Miller, *Anesthesiology*, **54,** 378 (1982).
(32) J. A. J. Martyn, D. J. Greenblatt, and W. C. Quinby, *Anesth. Analg.*, **62,** 293 (1983).
(33) U. Klotz and I. Riemann, *N. Engl. J. Med.*, **302,** 1012 (1980).
(34) H. Zetterstrom and G. Arturson, *Acta Anaesth. Scand.*, **24,** 288 (1980).
(35) D. C. Bloedow, T. C. Hardin, M. A. Simons, and J. F. Hansbrough, *Clin. Pharmacol. Ther.*, **31,** 204 (1982).
(36) A. Bowdle, G. D. Neal, R. H. Levy, and D. M. Heimbach, *J. Pharmacol. Exp. Ther.*, **213,** 97 (1980).

ACKNOWLEDGMENTS

This study was supported by a grant from the Hahnemann Medical College and Hospital Biomedical Research Support Grant No. 5-S07-RR05413 and certified by the Hahnemann Medical College Animal Welfare Committee as meeting the guidelines of the National Institutes of Health for the care and use of laboratory animals.

The authors thank Mrs. Linda Bush and Ms. Joanne Addario for their help in the preparation of this manuscript.

Comparative *In Vivo* and *In Vitro* Studies of Phenytoin Protein Binding and *In Vitro* Lipolysis in Plasma of Pregnant and Nonpregnant Rats

RUBY C. CHOU and GERHARD LEVY ˣ

Received June 17, 1983, from the *Department of Pharmaceutics, School of Pharmacy, State University of New York at Buffalo, Amherst, NY 14260.* Accepted for publication October 3, 1983.

Abstract □ This investigation was designed to determine the cause of the changes in drug protein binding that occur in rat plasma, particularly in plasma from pregnant animals, during *in vitro* drug-protein binding measurements. *In vivo* estimates of phenytoin binding in plasma were obtained from steady-state CSF-plasma concentration ratios in pregnant and nonpregnant rats. Immediate ultrafiltration of heparin- or EDTA-anticoagulated plasma yielded phenytoin free fraction values that were in good agreement with *in vivo* estimates for nonpregnant rats but that were about one-third higher than *in vivo* estimates for pregnant animals. *In vitro* free fraction values tended to increase during incubation of plasma and/or during equilibrium dialysis. The concentrations of the four major endogenous free fatty acids were similar in plasma of pregnant and nonpregnant rats if determined immediately after blood collection. Six hours of incubation at 37°C caused fatty acid concentrations to increase about fivefold and twofold in heparin-anticoagulated plasma from pregnant and nonpregnant animals, respectively. The corresponding increases in EDTA-anticoagulated plasma were only about twofold and 1.14-fold, respectively. These changes were associated with decreased plasma protein binding of phenytoin. The *in vivo* differences between pregnant and nonpregnant rats with respect to phenytoin binding in plasma are not due to differences in fatty acid concentrations, but the *in vitro* differences are due primarily to corresponding differences in free fatty acid concentrations if extensive *in vitro* lipolysis occurs.

Keyphrases □ Phenytoin—plasma protein binding, lipolysis, pregnant and nonpregnant rats □ Lipolysis—*in vitro* and *in vivo* comparisons, plasma protein binding, pregnant and nonpregnant rats □ Anticoagulants—heparin, EDTA, plasma protein binding, *in vitro* and *in vivo* comparisons, pregnant and nonpregnant rats

Pregnancy is known to be associated with quantitative changes of drug biotransformation (1) and drug-protein binding in plasma or serum (2). Properly designed studies of the effect of pregnancy on the pharmacokinetics of drugs, therefore, require measurement of unbound drug in plasma, to differentiate between pharmacokinetic changes due solely to drug binding alterations and those due to altered intrinsic clearance or to a combination of both types of effects. Unfortunately, the drug-protein binding characteristics of plasma from pregnant rats and, to a lesser extent, from pregnant women are quite unstable (3, 4). A lack of appreciation of this problem can lead to serious misinterpretations in pharmacokinetic studies, particularly in the assessment of intrinsic drug clearance and drug concentration–pharmacological activity relationships.

This investigation was designed to determine the causes of *in vitro* alterations in protein binding of drugs in plasma from pregnant and nonpregnant rats and to assess the effects of the *in vitro* anticoagulant and of the methodology used for protein binding determinations. The study protocol also permitted a comparative determination of the effect of pregnancy on the total clearance and *in vivo* plasma protein binding of phenytoin in rats.

EXPERIMENTAL SECTION

Pregnant (day 20 of gestation) and nonpregnant Lewis rats[1] (the latter ≃ 200 g) received a loading dose of phenytoin, 14.7 mg/kg, by rapid injection

[1] Charles River Breeding Laboratories, Wilmington, Mass.

0022-3549/84/0800-1121$01.00/0
© 1984, American Pharmaceutical Association

Table I—Plasma Protein Binding of Phenytoin in Pregnant and Nonpregnant Rats: Effect of Methodology and *In Vitro* Anticoagulant on Free Fraction Determination [a]

	Pregnant Rats		Nonpregnant Rats	
	EDTA	Heparin	EDTA	Heparin
Total phenytoin in plasma, μg/mL	15.8 ± 1.7	16.9 ± 3.6	12.3 ± 4.7	12.4 ± 3.0
CSF-plasma conc. ratio × 100	19.1 ± 2.3	17.0 ± 0.9[b]	12.6 ± 2.3	13.8 ± 0.9[b]
Free fraction × 100				
Immediate ultrafiltration	25.5 ± 4.2	23.4 ± 7.3[e]	12.4 ± 1.5	13.7 ± 1.8
Ultrafiltration after 6 h	31.9 ± 4.9[d]	39.4 ± 12.9[d, e]	12.5 ± 1.8[c]	13.9 ± 1.9[c]
Equilibrium dialysis	26.2 ± 3.2	28.5 ± 7.3[d, e]	15.2 ± 1.4[d]	17.5 ± 1.9[c,d]

[a] Mean ±*SD*, $n = 6$ except pregnant-heparin group where $n = 5$. [b] $n = 4$ since CSF could not be obtained from one or two animals. [c] $n = 5$ due to loss of sample or inadequate plasma volume. [d] The method of protein binding measurement had a significant effect on free fraction values, as determined by two-way ANOVA for pregnant and nonpregnant rats considered separately. The superscript indicates that the free fraction value differs significantly ($p < 0.05$ by Newman-Keuls test) from the CSF-plasma concentration ratio × 100. [e] One rat had only three fetuses and yielded unusually low free fraction values. Without that animal, the free fraction × 100 values for immediate ultrafiltration, ultrafiltration after 6 h, and equilibrium dialysis were 25.9 ± 4.3, 44.4 ± 4.5, and 31.3 ± 2.6, respectively.

Table II—Concentrations of Free Fatty Acids in Plasma of Pregnant and Nonpregnant Rats: Effect of Ultrafiltration and *In Vitro* Anticoagulant [a]

	Pregnant Rats		Nonpregnant Rats	
	EDTA	Heparin	EDTA	Heparin
Palmitic Acid[b]				
0 h	196 ± 48	179 ± 38	167 ± 26	152 ± 19
6 h	371 ± 119	792 ± 67	183 ± 29	260 ± 29
Ratio, 6 h/0 h	1.94 ± 0.58	4.54 ± 0.79	1.10 ± 0.14	1.75 ± 0.37
Stearic Acid				
0 h	58.8 ± 26.8	54.9 ± 23.6	51.0 ± 14.3	49.2 ± 9.9
6 h	89.4 ± 28.1	156 ± 27	64.6 ± 18.4	95.6 ± 24.5
Ratio, 6 h/0 h	1.65 ± 0.50	3.12 ± 0.93	1.42 ± 0.73	2.05 ± 0.73
Oleic Acid				
0 h	152 ± 78	130 ± 53	127 ± 44	118 ± 37
6 h	321 ± 137	743 ± 110	127 ± 28	209 ± 37
Ratio 6 h/0 h	2.27 ± 0.68	6.25 ± 1.76	1.09 ± 0.44	1.97 ± 0.81
Linoleic Acid				
0 hr	77.5 ± 45.4	65.7 ± 27.0	67.7 ± 26.0	66.1 ± 23.1
6 h	178 ± 88	379 ± 74	89.2 ± 38.5	145 ± 31
Ratio 6 h/0 h	2.49 ± 0.91	6.28 ± 1.84	1.37 ± 0.49	2.45 ± 0.99
Total fatty acids[c]				
0 h	484 ± 196	430 ± 125	422 ± 122	385 ± 87
6 h	960 ± 364	2071 ± 578	463 ± 105	709 ± 94
Ratio 6 h/0 h	2.08 ± 0.62	5.10 ± 1.20	1.14 ± 0.32	1.95 ± 0.62

[a] Mean ±*SD*, $n = 6$ except pregnant-heparin group where $n = 5$. All concentrations are expressed as μM/L. [b] Assayed immediately after blood collection (0 h) or after 6 h incubation of the plasma at 37°C, before ultrafiltration (6 h). [c] Based on the sum of the concentrations of the four individual free fatty acids.

and then a continuous infusion of phenytoin, 195 μg/min/kg, through a jugular vein cannula. Only saline solution without anticoagulant was used to maintain cannula patency before the experiment. CSF and blood (for plasma) from the abdominal aorta were obtained at 2 h after the beginning of the infusion and were assayed for phenytoin by HPLC. Details of these procedures have been described previously (5). The blood was collected in a plastic syringe[2] containing either heparin[3] or EDTA in amounts such that their concentrations in the blood were ~20 U/mL or 2 mg/mL, respectively. The syringes had been dried overnight at 37°C to remove the solvent from the anticoagulant solutions. Plasma was separated immediately after blood collection by centrifuging at 15,600×*g* for 1 min. Two microliters were ultrafiltered (3) immediately at 37°C to yield ≃ 90 μL of filtrate, and another portion of the plasma was similarly ultrafiltered after 6-h incubation (in a capped glass vial) in a waterbath at 37°C. A third portion of the plasma was used for equilibrium dialysis at 37°C for 6 h against an equal volume of isotonic sodium-potassium phosphate buffer, pH 7.4 (5). The cellophane membrane[4] used for these procedures had a pore permeability cut-off of between 12,000 and 14,000 Da. Phenytoin concentrations in the protein binding experiments were measured by an HPLC method, with a detection limit of ~1 μg/mL (5).

One hundred-microliter portions of plasma were taken before and after incubation for analysis of free fatty acid concentrations. The "before incubation" sample was extracted into hexane within 5 min after blood collection to minimize *in vitro* lipolysis. Fatty acid concentrations were determined by GC after extraction and derivatization as described by others (6) except that *n*-heptadecanoic acid was used as the internal standard and sample volumes were reduced.

To determine the effect of *in vitro* addition of free fatty acids to serum on phenytoin protein binding, 200 μL of an ethanolic solution of fatty acids (palmitic, ≃40 mM; stearic, ≃8 mM; oleic, ≃60 mM; linoleic, ≃25 mM) was added to 20 mL of pooled rat serum (from 10 nonpregnant female animals) containing added phenytoin, 23 μg/mL. Another portion of that serum with only ethanol added was used as a control. Protein binding of phenytoin was determined by ultrafiltration at 37°C of seven aliquots of each pooled serum portion.

RESULTS

The results of the phenytoin infusion studies on pregnant and nonpregnant rats are summarized in Table I. Based on the plasma concentrations, which should be at steady state under the experimental conditions (5), the total clearance of phenytoin was significantly lower in the pregnant rats (12.2 ± 2.0 mL/min/kg; mean ±*SD*) than in the nonpregnant rats (17.1 ± 4.9 mL/min/kg; $p < 0.01$). This was also the case for the total clearance of free drug (70.0 ± 14.9 *versus* 136 ± 35 mL/min/kg; $p < 0.001$) which was calculated on the basis of the *in vivo* free fraction of phenytoin (*i.e.*, CSF concentration–plasma concentration ratio). These results represent the combined data obtained from the EDTA and heparin experiments because of their excellent replication and the identical *in vivo* experimental conditions, and were analyzed statistically by the unpaired *t* test.

The CSF-plasma concentration ratio of phenytoin was significantly higher in pregnant than in nonpregnant rats ($p < 0.001$ by *t* test for the combined EDTA and heparin data). There was excellent agreement between this ratio and the *in vitro* phenytoin free fraction in plasma from nonpregnant rats that was ultrafiltered within 5 min after blood collection (Table I). On the other hand, the *in vitro* free fraction of phenytoin in plasma from pregnant rats, determined under the same conditions, was about one-third higher than the CSF-plasma concentration ratio in these animals. Free fraction values of phenytoin determined by ultrafiltration after incubating plasma from pregnant rats for 6 h at 37°C were even higher. Equilibrium dialysis for 6 h at 37°C also yielded appreciably higher free fraction values than the *in vivo* estimates (CSF-plasma concentration ratio), for both pregnant and nonpregnant rats. The statistical significance of these differences are indicated in Table I.

Table II contains a summary of the results of the assays of the plasma samples for palmitic, stearic, oleic, and linoleic acids. The concentrations of these endogenous free fatty acids in plasma assayed within 5 min after blood

[2] Plastipak; Becton, Dickinson and Co., Rutherford, N.J.
[3] Heparin from beef lungs, 1000 U/mL solution; The Upjohn Co., Kalamazoo, Mich.
[4] Visking; Union Carbide Corp., Chicago, Ill.

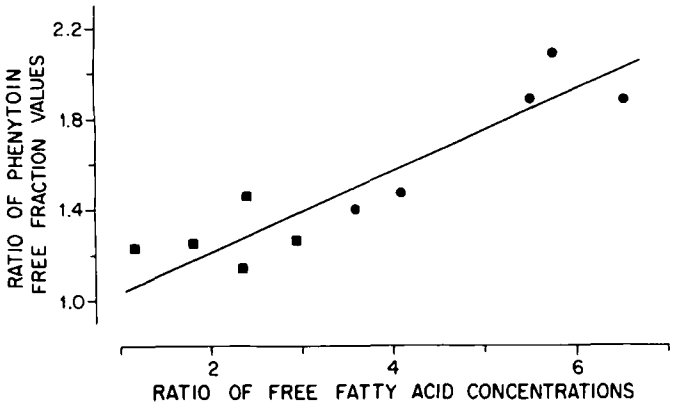

Figure 1—*Relationship between the ratios of the phenytoin free fraction values obtained by ultrafiltration (after 6 h incubation at 37°C-immediately, without incubation) and the ratios of the total free fatty acid concentrations (measured concomitantly in plasma of rats at day 20 of gestation) when either EDTA (■) or heparin (●) was used as the* in vitro *anticoagulant (r = 0.90, p < 0.001).*

collection were similar in pregnant and nonpregnant animals, irrespective of the anticoagulant used. However, heparin-anticoagulated plasma underwent pronounced lipolysis during 6 h of incubation, particularly plasma from the pregnant rats. Total free fatty acid concentrations increased by an average of 410% in plasma from pregnant rats and 95% in plasma from nonpregnant rats during incubation. These changes were much smaller in EDTA-anticoagulated plasma: 108% and 14%, respectively. The relative increase in fatty acid concentrations was associated with a corresponding relative increase in the free fraction of phenytoin in plasma from pregnant rats (Fig. 1). Addition of a mixture of the four free fatty acids, similar in proportion to that found *in vivo*, to serum from nonpregnant rats caused an increase of phenytoin free fraction values similar in relative magnitude to that found on lipolysis (Fig. 2).

DISCUSSION

The therapeutic management of pregnant patients with seizure disorders is difficult (7). The most frequently used drug for this purpose is phenytoin. Pregnancy may be associated with alterations in the pharmacokinetics of phenytoin and in the phenytoin concentration–effect relationship. Investigations of these possibilities in patients and in intact animals must be designed to distinguish between apparent effects referable to pregnancy-associated

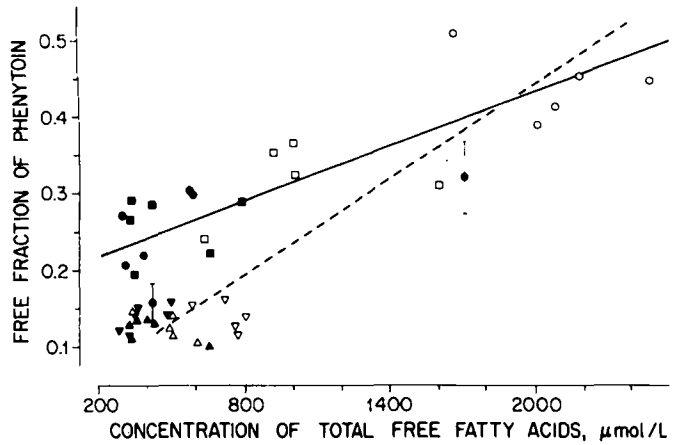

Figure 2—*Relationship between free fraction values of phenytoin and concentration of total free fatty acids in plasma. The lines were determined by bivariate linear regression. The two closed circles with the vertical bars (±SD) are the free fraction values obtained with serum from nonpregnant rats with and without addition of a physiological mixture of free fatty acids. Key: (——) relationship for pregnant rats at day 20 of gestation (r = 0.85, p < 0.001); (- - -) relationship for both nonpregnant and pregnant rats after incubation of plasma for 6 h at 37°C (r = 0.86, p < 0.001); (■,□) plasma from pregnant rats with EDTA as anticoagulant; (●,○) plasma from pregnant rats with heparin as anticoagulant; (▲,△) plasma from nonpregnant rats with EDTA as anticoagulant; (▼,▽) plasma from nonpregnant rats with heparin as anticoagulant. Closed symbols: before incubation; open symbols: after 6-h incubation at 37°C.*

decreased plasma protein binding of phenytoin and actual changes in intrinsic clearance of the drug and in the relationship between biophasic drug concentration and pharmacological response. It became evident in the course of such an investigation (8) that the protein binding of phenytoin in plasma from pregnant rats undergoes rapid and pronounced alterations *in vitro* during the time between blood collection and plasma protein binding determination (3). The present study was designed to determine the cause of these alterations and to explore possibilities for minimizing them.

An important, although incidental, result of this investigation is the demonstration of a decreased steady-state plasma clearance of phenytoin by pregnant as compared with nonpregnant rats. The clearance of free (unbound) phenytoin in nonpregnant (control) animals was about twice as high as that in pregnant rats when both groups of animals received infusions of the drug at the same rate per unit of body weight. Since phenytoin pharmacokinetics are nonlinear and subject to product inhibitory effects in rats (9, 10), quantitatively different results may have been obtained if the clearance determinations had been made at comparable plasma concentrations rather than at comparable infusion rates. The results of more detailed and extensive studies of the effect of pregnancy on phenytoin elimination kinetics in rats will be presented in another report and a discussion of the subject will, therefore, be deferred.

Unbound phenytoin in plasma equilibrates readily with phenytoin in CSF; the CSF–plasma concentration ratio of the drug represents, therefore, its free fraction value in plasma under *in vivo* conditions (5). It was found that the free fraction of phenytoin in rat plasma is substantially (≃50%) increased in late pregnancy. This result is not a consequence of the higher phenytoin concentrations in the pregnant animals, since the protein binding of phenytoin in rat serum is independent of concentration over a wide range (11). Nor are these *in vivo* results subject to uncertainties due to the technical problems and possible artifacts associated with *in vitro* protein binding determinations.

The ability of nonesterified (free) fatty acids to affect (usually decrease) the plasma protein binding of drugs is well established (12). Recent research emphasis has been on the elevation of fatty acid concentrations in plasma after systemic administration of heparin; this elevation is now recognized to be largely an *in vitro* artifact due to continuing lipolysis in plasma during the time between blood collection and the determination of fatty acid concentrations (13, 14). While injected heparin mobilizes and activates lipases which then cause formation of free fatty acids from triglycerides in plasma, even plasma from individuals (humans and rats) who have not received heparin contains appreciable lipolytic activity (15–17). Consequently, the concentrations of free fatty acids increase *in vitro* even in plasma of individuals who have not been treated with heparin (4, 18–22), albeit at a much lower rate than in post-heparin plasma.

The free fatty acids that accumulate in plasma *in vitro* derive from triglycerides as well as from lecithin (19, 23, 24). The plasma concentrations of these sources of fatty acids increase substantially during pregnancy (25), thereby increasing both the absolute rate and the extent of *in vitro* free fatty acid formation in pregnancy plasma. Such increase apparently does not occur to any significant extent *in vivo*, probably due to distribution of the formed free fatty acids from blood to extravascular sites and metabolic clearance. Neither distribution nor clearance occur *in vitro* so that accumulation of free fatty acids in plasma can be substantial under *in vitro* conditions.

The four fatty acid concentrations quantitatively determined in this investigation (palmitic, stearic, oleic, and linoleic acids) account for most (≃90%) of the fatty acids in human plasma (20, 26), and the sum of their concentrations is probably a reasonable estimate of total fatty acid concentration in rat plasma. It is desirable, however, to determine the concentrations of these fatty acids individually, because they may have quantitatively different displacing effects on drugs bound to plasma proteins. By the same token, confirmatory protein binding experiments involving *in vitro* addition of free fatty acids to plasma should be carried out with fatty acid mixtures with a composition and ratio of concentrations similar to that found *in vivo*. The effect of free fatty acids on the plasma protein binding of different drugs is a function of the capacity of the binding sites, the relative concentrations and affinity of the ligands, and other variables. Consequently, the rate and extent of protein binding alterations of phenytoin reported here apply to that drug only.

The results of this investigation show that the concentrations of free fatty acids in plasma from nonpregnant rats increase about twofold within 6 h at 37°C, *i.e.*, under conditions typical of equilibrium dialysis, if heparin is used as the *in vitro* anticoagulant. This lipolysis is almost prevented by use of EDTA instead of heparin. Total free fatty acid concentrations in heparinized plasma from pregnant rats increase about fivefold during 6 h at 37°C; use of EDTA instead of heparin reduces this increase to twofold. When EDTA and heparin are used together, the extent of lipolysis is similar to that in heparinized plasma[5]. This is consistent with reports that EDTA is not a good lipoprotein

[5] Unpublished results.

lipase inhibitor (14, 27) and indicates that *in vitro* heparin increased lipolytic activity, particularly in pregnancy plasma, under our experimental conditions. According to the literature, heparin may activate or inhibit lipases, depending on its concentration (28, 29). To significantly reduce the *in vitro* accumulation of free fatty acids in plasma, it will be necessary to inhibit not only the lipolysis of triglycerides but also the formation of fatty acids from phospholipids (23, 24).

The rapid and pronounced *in vitro* lipolysis in the plasma of pregnant rats can easily lead to artifactual overestimation of *in vivo* free fatty acid concentrations. One group of investigators reported total plasma free fatty acid concentrations of $\simeq$360, 565, and 848 μM in heparinized plasma from nonpregnant rats, rats at day 19 of gestation, and rats at day 21 of gestation, respectively (30). The control value is similar to that in this study ($\simeq$400 μM), but the values for the pregnant rats are substantially higher than that for rats on day 20 of gestation determined in this study ($\simeq$430 μM) under conditions that minimize *in vitro* lipolysis. When proper precautions are taken to avoid artifacts, there appears to be no appreciable difference in plasma free fatty acid concentrations of pregnant and nonpregnant rats. This is also true for humans (26).

While plasma free fatty acid concentrations are of direct biochemical and physiological interest, their significance in pharmacology and pharmacokinetics relates principally to their effect on the plasma protein binding of drugs (12, 31). This effect is clearly evident in the strong correlation between the relative increase in the phenytoin free fraction and the relative increase of total free fatty acid concentrations in plasma found in the present investigation (Fig. 1). Moreover, direct addition of a physiological mixture of fatty acids to serum from nonpregnant rats, thereby duplicating the elevation of fatty acid concentrations found in the plasma of pregnant rats after 6 h of incubation at 37°C, results in an increase of the phenytoin free fraction to a value similar to that of the incubated pregnancy plasma (Fig. 2).

It is easy to come to the erroneous conclusion that pregnancy-associated changes of *in vivo* plasma protein binding of phenytoin (or other drugs) are due to the displacing effect of increased concentrations of free fatty acids. The dashed regression line in Fig. 2 represents the relationship between phenytoin free fraction value and total free fatty acids concentration in plasma from both pregnant and nonpregnant rats when that plasma had been incubated for 6 h at 37°C (*i.e.*, under conditions typical of equilibrium dialysis). The correlation is strong ($r = 0.86$) and highly significant ($p < 0.001$), but the conclusion is incorrect because it is based on inappropriate experimental conditions.

The solid symbols in Fig. 2 demonstrate that, when *in vitro* lipolysis is minimized, the protein binding of phenytoin is much less pronounced in plasma of pregnant rats than in plasma of nonpregnant controls at comparable free fatty acid concentrations. Viewed from another perspective, *in vivo* plasma protein binding of phenytoin is much less in pregnant than in nonpregnant rats (Table I), even though fatty acid concentrations are similar in the two groups when measured under conditions that minimize *in vitro* lipolysis (Table II). The notion that the diminished *in vivo* plasma protein binding of drugs during pregnancy is due to elevated fatty acid concentrations is, therefore, untenable. Lower plasma albumin concentrations during pregnancy (2, 32), possible accumulation of endogenous displacers other than fatty acids, and possible conformational changes of albumin are more likely causes of decreased plasma protein binding of albumin-bound drugs during pregnancy (11).

The *in vitro* lipolysis and corresponding changes in drug–protein binding demonstrated here with respect to plasma from rats in late pregnancy have also been investigated in humans (4, 33). The degree of *in vitro* lipolysis in plasma obtained from pregnant women during 6 h of equilibrium dialysis was, generally, somewhat less pronounced than in plasma from pregnant rats while the protein binding changes associated with the increased fatty acid concentrations ranged from negligible (phenytoin), to modest (salicylate, ibuprofen), to pronounced (diazepam). Rapid *in vitro* lipolysis may also occur in plasma from other species and in other states of altered physiology. It will be necessary to identify or rule out these factors in investigations of drug kinetics and dynamics in disease states.

Unfortunately, an *in vivo* estimation of plasma protein binding based on the steady-state CSF-plasma concentration ratio is not always feasible, because not all drugs equilibrate to equal concentrations in CSF and plasma water (5). Rapid separation of plasma after blood collection (which is facilitated by use of a high speed centrifuge), use of EDTA (or other suitable compounds) rather than heparin as the *in vitro* anticoagulant (provided that EDTA does not interfere with the drug–protein binding), and rapid ultrafiltration will minimize *in vitro* lipolysis and thereby reduce the likelihood of artifactual protein binding estimates. Particularly, if ultrafiltration is not feasible due to membrane binding or other technical problems and equilibrium dialysis must be used, determinations of fatty acid concentrations in plasma immediately after blood collection and again after dialysis (33) will provide an indication of the magnitude of *in vitro* lipolysis under the experimental conditions.

REFERENCES

(1) B. Krauer, F. Krauer, and F. E. Hytten, *Pharmacol. Ther.*, **10**, 301 (1980).

(2) M. Dean, B. Stock, R. J. Patterson, and G. Levy, *Clin. Pharmacol. Ther.*, **28**, 253 (1980).

(3) R. C. Chou and G. Levy, *J. Pharm. Sci.*, **71**, 471 (1982).

(4) R. C. Chou, U. W. Wiegand, A. S. Lele, and G. Levy, *J. Pharm. Sci.*, **72**, 716 (1983).

(5) R. C. Chou and G. Levy, *J. Pharmacol. Exp. Ther.*, **219**, 42 (1981).

(6) S. D. Brunk and J. R. Swanson, *Clin. Chem.*, **27**, 924 (1981).

(7) D. Janz, M. Dam, A. Richens, L. Bossi, H. Helge, and D. Schmidt (Eds.), "Epilepsy, Pregnancy, and the Child," Raven, New York, N.Y., 1982.

(8) R. C. Chou, Ph.D. Dissertation, State University of New York at Buffalo, 1983.

(9) J. J. Ashley and G. Levy, *J. Pharmacokinet. Biopharm.*, **1**, 99 (1973).

(10) G. Levy and J. J. Ashley, *J. Pharm. Sci.*, **62**, 161 (1973).

(11) B. Stock, M. Dean, and G. Levy, *J. Pharmacol. Exp. Ther.*, **212**, 264 (1980).

(12) W. J. Jusko and M. Gretch, *Drug Metab. Rev.*, **5**, 43 (1976).

(13) K. M. Giacomini, S. E. Swezey, J. C. Giacomini, and T. F. Blaschke, *Life Sci.*, **27**, 771 (1980).

(14) J. E. Brown, B. B. Kitchell, T. D. Bjornsson, and D. G. Shand, *Clin. Pharmacol. Ther.*, **30**, 636 (1981).

(15) H. Engelberg, *Proc. Soc. Exp. Biol. Med.*, **99**, 489 (1958).

(16) H. Engelberg, *Am. J. Cardiol.*, **14**, 8 (1964).

(17) Y. Gabr, M. Mahfouz, E. Soliman, and F. Mansour, *Int. J. Biochem.*, **14**, 155 (1982).

(18) Y. Gabr, F. Mansour, and N. Amin, *Lancet*, **ii**, 196 (1966).

(19) R. Berlin, C. O. Oldfelt, and O. Vikrot, *Acta Med. Scand.*, **185**, 427 (1969).

(20) D. Sampson and W. J. Hensley, *Clin. Chim. Acta*, **61**, 1 (1975).

(21) T. Moilanen and T. Nikkari, *Clin. Chim. Acta*, **114**, 111 (1981).

(22) T. A. Bowdle, I. H. Patel, R. H. Levy, and A. J. Wilensky, *Eur. J. Clin. Pharmacol.*, **23**, 343 (1982).

(23) J. A. Glomset, F. Parker, M. Tjaden, and R. H. Williams, *Biochim. Biophys. Acta*, **58**, 398 (1962).

(24) W. C. Vogel and L. Zieve, *Proc. Soc. Exp. Biol. Med.*, **111**, 538 (1962).

(25) R. Punnonen, *Br. J. Obstet. Gynaecol.*, **84**, 838 (1977).

(26) R. G. McDonald-Gibson, M. Young, and F. E. Hytten, *Br. J. Obstet. Gynaecol.*, **82**, 460 (1975).

(27) J. Augustin and H. Greten, *Prog. Biochem. Pharmacol.*, **15**, 5 (1979).

(28) E. D. Korn and T. W. Quigley, Jr., *J. Biol. Chem.*, **226**, 833 (1957).

(29) R. S. Elkeles, *Horm. Metab. Res.*, **6**, 151 (1974).

(30) R. H. Knopp, C. D. Saudek, R. A. Arky, and J. B. O'Sullivan, *Endocrinology*, **92**, 984 (1973).

(31) R. C. Chou, U. W. Wiegand, D. M. Soda, and G. Levy, *J. Pharm. Sci.*, **72**, 1230 (1983).

(32) E. Perucca, M. Ruprah, and A. Richens, *J. Royal Soc. Med.*, **74**, 422 (1981).

(33) M. J. Ridd, K. F. Brown, R. G. Moore, and R. L. Nation, *Int. J. Pharm.*, **11**, 11 (1982).

ACKNOWLEDGMENTS

Supported in part by Grant GM 20852 from the National Institute of General Medical Sciences, National Institutes of Health.

Systematic Error Associated with Apparatus 2 of the USP Dissolution Test V: Interaction of Two Tableted Prednisone Formulations with Glass and Plastic Vessels

DON C. COX ˣ and WILLIAM B. FURMAN

Received June 17, 1983, from the *Food and Drug Administration, National Center for Drug Analysis, St. Louis, MO 63101.* Accepted for publication September 22, 1983.

Abstract □ Recently marketed glass vessels that are uniform and pass USP specifications were compared with uniform plastic vessels that also pass USP specifications. Two lots of prednisone tablets, Tablet 1 and Tablet 2, were tested in both types of vessels. Tablet 1 gave higher results (+12.7% of label claim) in glass vessels at 50 rpm but gave equivalent results in either vessel at 75 rpm. Tablet 2 gave equivalent results in either vessel at 50 rpm but gave higher results (+22% of label claim) in glass vessels at 75 rpm. The type of vessel used to obtain dissolution results for tablets should be specified.

Keyphrases □ USP Dissolution Apparatus 2—error associated with use of glass and plastic vessels □ Dissolution—systematic error associated with USP dissolution Apparatus 2, use of glass and plastic vessels

In a previous report (1), it has been shown that glass and plastic vessels may give different results when dissolution of prednisone tablets is measured with USP Apparatus 2. In the earlier work, the glass vessels[1] used had nonuniform inside bottom curvatures and did not conform to the USP specification (2) of spherical curvature; the inside bottom curvatures of the plastic vessels[2] were more uniform and approximated spherical curvature. It was thus concluded (1) that use of the plastic vessels would reduce systematic error in the USP Apparatus 2.

Glass vessels[3] advertised to meet USP specifications were recently introduced, and five were purchased for evaluation. To permit direct comparisons, the previously used techniques and tablet lots were employed to evaluate the suitability of the new glass vessels in the USP dissolution test for prednisone tablets (3), and the results are reported here.

EXPERIMENTAL SECTION

Tablets—In this laboratory, two commercial lots of prednisone tablets that originally gave wide ranges in dissolution results with Apparatus 2 have been used extensively. The dissolution rates of Tablet 1 (5-mg prednisone tablets) and Tablet 2 (10-mg prednisone tablets) are affected to an unusual degree by minor variations in the test. In this respect, they are not typical of prednisone tablets currently available to the public but are very useful for measurement of apparatus variations. The dissolution rate of Tablet 1 responds to variations in the physical alignment of the equipment (4) and vessel curvature (1). The dissolution rate of Tablet 2 is less affected by these variations but is increased considerably if gas concentrations in the dissolution medium exceed a critical value (5, 6). Tablet 2 has been collaboratively studied in 11 laboratories (7). Both lots exhibit similar physical dissolution behavior; disintegration takes place within 2 min, and the disintegrated tablet material stays on the bottom of the vessel, where it gathers into a dynamic conical mass. Undesirable changes in test conditions alter the fluid flow in the vicinity of the conical mass; the conical mass is displaced or dispersed, and higher dissolution results are obtained. In this laboratory, the dissolution results from Tablet 2 are currently used as an indicator to determine whether the dissolution equipment and medium are suitable for testing tablets by the procedure with the USP Apparatus 2.

Apparatus—A six-spindle dissolution drive[4] was used. The drive was mounted on an acrylic water bath equipped with levelers. A circulator-heater[5], mounted externally to the bath, maintained the bath temperature at 37.5 ± 0.1°C. The base of the drive was leveled[6], and the paddle shafts were aligned vertically[6]. A specially designed tool (8) was used to center the vessels around the paddle shafts[7]. Each vessel was held in place with three cam lugs. Each paddle was adjusted with a depth gauge[8] to provide 25 mm of clearance above the bottom of the vessel. Paddle rotation was maintained within ±1.7% of the nominal value.

Procedure—A 20-L carboy was filled with deionized water. To achieve the desired equilibrium of gases, air was drawn through the water for 15 min at 145 mm Hg (6). The water was siphoned into 500-mL volumetric flasks[9], which were placed in a water bath at 37.5°C until their contents had reached that temperature. The contents were then transferred to the dissolution vessels in a 37.5°C water bath. The tablets were dropped into the vessels with the paddles rotating. After 30 min, aliquots were taken and filtered. (The water temperatures were 37.0 and 36.5°C in the glass and plastic vessels, respectively.) The absorbance of each filtrate was measured at 242 nm in a 1-cm cell.

Reevaluation of Glass and Plastic Vessels—Dissolution data for Tablet 1 were obtained with the same six glass vessels[1] previously evaluated (1). A different set of six plastic vessels was used, however, because the plastic vessels used in the previous evaluation were not available for this study.

Evaluation of New Glass Vessels—The new glass vessels[3] have graduations from 500 to 1000 mL in 50-mL increments. Inside diameters were measured with inside calipers. The bottom curvatures were measured with a mechanic's depth gauge and plaster of Paris (1). The glass vessels were numbered 1 through 5 and placed in the dissolution drive with one plastic vessel. Two sets of six tablets each were subjected to the dissolution test. The vessels were then moved one position in a clockwise direction, and two more sets of six tablets each were subjected to the test. This procedure was continued until each vessel had been tested twice in each position of the dissolution drive for a total of 72 results. Twelve results were associated with each vessel, which were sequentially placed in all six positions. Likewise, 12 sets of results were associated with each position in which all six vessels had been sequentially placed. The experiment was conducted only with Tablet 1.

Plastic-Coated Glass Vessels—Ten grams of plastic from a broken plastic vessel was dissolved in 100 mL of chloroform. This solution was poured into a clean, dry, glass vessel[3]. The vessel was tilted and rotated until its inside surface was brought in contact with the solution. The solution was poured from the vessel, and the vessel was inverted and placed on a cork ring in a draft hood overnight. The inside of the glass vessel was coated with a thin layer of plastic. The vessels had to be recoated after each dissolution test because the plastic did not adhere to the glass. Tablet 1 and Tablet 2 were tested in these coated vessels.

Glass Vessels with Different Bottom Curvatures—Dissolution results for Tablet 1 were taken from a glass vessel[10], in which the bottom curvature came to a blunted point (1), and from a flat-bottom glass vessel[11] that was positioned in the dissolution apparatus in a manner similar to that for the other vessels.

Dissolution Results at Different Stirring Rates—Three plastic vessels and three glass vessels[3] were placed in alternating positions in the dissolution apparatus. The dissolution test was conducted at stirring rates from 25 to 100 rpm for Tablet 1 and Tablet 2.

Dissolution Results from One or More Tablets Per Vessel—Three plastic vessels and three glass vessels[3] were placed in alternating positions as before.

[1] Model No. 33730; Kimble, Div. of Owens-Illinois, Vineland, N.J. (currently available).
[2] Model No. EQ1900; Eli Lilly and Co., Indianapolis, Ind.
[3] Model No. V1000A; Applied Analytical Industries, Wilmington, N.C.
[4] Built by the Winchester Engineering and Analytical Center; Food and Drug Administration, Winchester, Mass.
[5] Haake, Model E52; Fisher Scientific Co., Pittsburgh, Pa.
[6] Nine-inch (22.86 cm) torpedo level; Stanley Tools, New Britain, Conn.
[7] Hanson Research Corp., Northridge, Calif.
[8] Van-Kel Industries, Chatham, N.J.
[9] Model No. 28045-500; Kimble, Div. of Owens-Illinois.
[10] Model No. 33730; Kimble, Div. of Owens-Illinois (discontinued in 1978).
[11] Model No. BSF-1000; Virtis Co., Gardiner, N.Y.

0022-3549/84/0800-1125$01.00/0
© 1984, American Pharmaceutical Association

Table I—Dissolution Data [a] for Tablet 1 from Five Glass Vessels (Rearranged for Two-Way ANOVA)

Vessel	Percent of Label Claim at Position: 1	2	3	4	5	6	Mean ± SD[b]
1	54.2	49.5	55.7	52.0	55.7	54.0	
	53.1	51.6	54.4	52.5	53.1	53.8	53.3 ± 1.76
2	55.0	51.0	53.2	55.7	51.8	52.6	
	52.4	55.6	55.4	54.1	51.4	51.7	53.3 ± 1.76
3	52.3	53.0	54.6	50.9	51.3	49.9	
	51.8	52.5	52.2	51.6	52.0	52.0	52.0 ± 1.15
4	52.5	55.0	51.5	51.3	49.5	50.9	
	52.6	53.0	51.6	52.2	49.5	52.0	51.8 ± 1.50
5	57.2	49.9	53.1	50.4	52.7	53.0	
	52.1	53.6	54.3	50.3	53.8	54.8	52.9 ± 2.09
Position Mean	53.3	52.5	53.6	52.1	52.1	52.5	
Position *SD*	1.69	2.01	1.51	1.69	1.88	1.49	

[a] Percent of label claim dissolved at 30 min. [b] Mean ± *SD* of 12 individual tablets.

Table II—Dissolution Data [a] for Tablet 1 from One Plastic Vessel Carried Through ANOVA Experiment

Percent of Label Claim at Position: 1	2	3	4	5	6	Mean ± SD[b]
39.0	41.2	45.1	40.4	41.1	38.9	
40.8	38.5	43.3	41.1	40.2	41.1	40.9 ± 1.85

[a] Percent of label claim dissolved at 30 min. [b] Mean ± *SD* of 12 individual tablets.

One or several tablets were dropped into each vessel. The test was conducted at 50 and 75 rpm for Tablet 1 and Tablet 2, respectively.

RESULTS AND DISCUSSION

Physical Dimensions—The five glass vessels[3] had inside diameters that ranged from 103.0 to 103.5 mm. The bottom curvatures of the vessels corresponded to those of spheres of diameters from 102.4 to 105.2 mm. Plaster of Paris casts of the bottom curvatures revealed no irregularities. The depth of the vessels was 165 mm. The vessels thus met USP specifications.

The dimensions of the glass vessels[3] differ from those of the plastic vessels in two respects. For the glass and plastic vessels, the outside diameters of the flanges are ~122 and 135 mm, respectively. The outer edge of the flange is lopsided with respect to the outer wall of the glass vessel, but is symmetrical with the outer wall of the plastic vessel. This difference in flange dimension required larger cam lugs on the dissolution apparatus to hold each glass vessel centered around its paddle axis. The flanges were marked so that they could always be oriented in the same configuration before use.

The glass vessels[3] have parallel sides, but the plastic vessels are tapered toward the bottom. Both types of vessel have essentially the same inside diameter at the top (103 mm), but the plastic vessel has a diameter of 101 mm just above the start of its bottom curvature. This difference in internal dimension causes the glass vessel to have a slightly flatter bottom curvature and to hold a slightly larger volume of liquid at a specified depth.

Selection of Tablets for Evaluation—With Tablet 1, significant differences among glass and plastic vessels (1) were revealed when the amount of dissolved drug, expressed as a percentage of the amount purported to be in the tablet, was measured at 30 min. The difference between mean results from the two types of vessels was dramatic for Tablet 1 but slight for Tablet 2. Tablet 1 was therefore selected to be used to detect differences among the five new glass vessels[3].

Tablet 1 had not been tested for 3 years. New dissolution results were collected from the six glass vessels[1] evaluated previously (1) and from six plastic vessels. The mean results obtained for 12 tablets were 54.7 and 41.2% of label claim in glass and plastic vessels, respectively. The corresponding standard deviations were 1.68 and 2.23% of label claim. These results compare favorably with the results previously obtained from the four positions of the dissolution drive that had vertical shafts[12]. Thus, Tablet 1 had not deteriorated, and direct comparisons could be made between the results collected 3 years ago and those from the new glass vessels[3].

Analysis of Variance—The data collected in the test of five glass vessels[3] and one plastic vessel were rearranged for an analysis of variance (Tables I and II). The data in the rows are associated with the individual vessels, and the data in the columns are associated with the individual positions in the dissolution apparatus.

[12] The Hanson dissolution drive used in the previous study (1) had two paddle shafts that were nonparallel with the other four shafts; results from the two nonparallel (nonvertical) positions were considered to be anomalous.

Table III shows the ANOVA. The *F* ratios indicate that at the 95% confidence level, there were no significant differences among the positions on the dissolution apparatus. However, the chance that Tablet 1 would give the same results in each of the glass[3] vessels is only ~1 in 40. The maximum range of the 12-tablet means associated with the glass vessels[3] is only 1.5% of label (Table I). The maximum ranges obtained previously (1) were 4.1% of label for six glass vessels[1] and 4.9% of label for six plastic vessels. Therefore, the dissolution data from Tablet 1 indicate that the new glass vessels[3] are more uniform than either type of vessel previously evaluated.

The overall mean of dissolution results for Tablet 1 in the new glass vessels[3] (52.7% of label claim; Table I) agrees well with the mean from the previously evaluated glass vessels[1] (54.7% of label claim). Neither of these means agree with the mean from plastic vessels (~41% of label claim; Table II), yet both the glass[3] and plastic vessels met USP specifications.

Results from Coated Vessels—It has been observed in this laboratory that at the beginning of the dissolution test, certain tablets seem to become more centered in glass vessels than in plastic vessels, which suggests that friction between a tablet and the wetted vessel surface may be greater for plastic than glass. Also, certain tablets become more centered in glass vessels cleaned with soap and water than in those rinsed with water and 95% ethanol, which suggests that a tablet may interact with residual films on the glass surface. Thus, certain tablets may interact differently with wetted plastic and glass surfaces.

The glass vessels[3] were coated with the material from which the plastic vessels were made. Five tablets of Tablet 1 were individually tested in plastic-coated vessels. A mean of 55.1% of label claim with an *SD* of 1.05% of label claim was obtained. These results indicate that the plastic coating had little or no effect.

Vessel Curvature—A correlation has been established between the dissolution data obtained for Tablet 1 and the shape of the bottom curvature of glass vessels (1). A glass vessel with an oblate deformation produces a higher dissolution result than one with a prolate deformation. Tablet 1 was used to estimate a maximum magnitude of this curvature effect; a single tablet was tested in a molded glass dissolution vessel[10] that possessed a bottom curvature that came to a blunted point, and a single tablet was tested in a flat-bottom glass vessel[11] similar to those used in the spinning-filter dissolution apparatus (9). Results were 38.9 and 70.3% of label claim, respectively. The extreme difference in vessel curvature gave a difference of ~31% of label claim which supports the idea that the difference in curvature between the glass[3] and the plastic vessels may have an effect. This supposition could not be further investigated because of the lack of glass vessels that have exactly the same dimensions as the plastic vessels.

Different Stirring Rates—Unlike Tablet 1, Tablet 2 does not give a large difference in dissolution results in glass and plastic vessels at 50 rpm. Results reported earlier (5) suggest that Tablet 2 would respond differently at 100 rpm. Tablet 1 and Tablet 2 were tested in glass and plastic vessels at stirring rates from 25 to 100 rpm (Table IV). For Tablet 1, the largest divergence in results between glass and plastic vessels occurred at 50 rpm, and the results converged at higher stirring rates. For Tablet 2 the dissolution results did not begin to diverge until stirring rates >50 rpm were attained.

Individual tablets from Tablet 2 were tested simultaneously at 75 rpm in three plastic-coated glass vessels[3] and three plastic vessels. The mean dissolution results (±*SD*) as percentage of label claim were 55.4 (4.68) and 60.7 (4.30) from plastic and plastic-coated glass vessels, respectively. Comparison of these results with those in Table IV (Tablet 2, 75 rpm) indicates that the plastic surface does interact with Tablet 2.

Volume of Disintegrated Tablet Material—The higher dissolution results obtained for Tablet 1 and Tablet 2 in glass vessels suggest that these tablets are subjected to higher fluid flow rates in glass vessels. During the dissolution

Table III—ANOVA for Six Apparatus Positions and Five Glass Vessels

Source	Sum of Squares	df[a]	Mean Square	F ratio	F (0.95)	F (0.975)
Position means	20.40	5	4.08	2.15	2.53	—
Vessel means	25.08	4	6.27	3.30	2.69	3.25
Interaction	77.97	20	3.90	2.05	1.93	—
Within means	56.97	30	1.90	—	—	—
Total	180.42	59	3.06	—	—	—

[a] Degrees of freedom.

Table IV—Effect of Stirring Rate on Dissolution Data[a] for Tablet 1 and Tablet 2 from Glass and Plastic Vessels[b]

Stirring Rate, rpm	Percent of Label Claim for Tablet 1			Percent of Label Claim for Tablet 2		
	Glass	Plastic	Difference[c]	Glass	Plastic	Difference[c]
25	24.7 ± 1.15	30.3 ± 1.76	−5.6	14.6 ± 0.17	17.0 ± 2.57	−2.4
35	35.3 ± 1.66	31.4 ± 1.44	3.9	—	—	—
50	52.9 ± 1.47	40.2 ± 1.17	12.7	34.0 ± 1.65	35.7 ± 1.42	−1.7
60	—	—	—	46.1 ± 2.51	47.2 ± 4.43	−1.1
70	—	—	—	66.4 ± 6.70	54.2 ± 2.14	12.2
75	66.3 ± 1.76	65.0 ± 1.73	1.3	81.5 ± 4.76	59.5 ± 5.36	22.0
100	71.2 ± 2.20	70.0 ± 0.58	1.2	97.2 ± 1.17	73.6 ± 6.52	23.6

[a] Percent of label claim dissolved at 30 min. Three individual tablets were tested in each type of vessel. [b] Mean ± SD. [c] Difference of mean values obtained using glass and mean values obtained using plastic.

Table V—Dissolution Data[a] for Increasing Loads of Tablet 1 and Tablet 2 in Glass and Plastic Vessels

Tablets/Vessel	Percent of Label Claim for Tablet 1[b]		Percent of Label Claim for Tablet 2[c]	
	Glass	Plastic	Glass	Plastic
1	53.3	41.0	87.2	55.2
2	56.2	43.9	84.0	62.1
4	54.5	45.0	66.6	66.9
8	55.9	43.5	—	—

[a] Percent of label claim per tablet at 30 min. [b] At 50 rpm. [c] At 75 rpm.

test of a single tablet, the volume of the conical mass of disintegrated tablet material on the bottom of the vessel from Tablet 2 is about three times that from Tablet 1. It was speculated that this difference in volume could cause Tablet 1 to be more sensitive to slight differences among vessels because there might be less tendency for the tablet material to pack together at a specified stirring rate, *i.e.*, fewer particles would have greater freedom of movement in a given space.

The data in Table V show that this speculation is false for Tablet 1, but true for Tablet 2. For Tablet 1 at 50 rpm, the amount of drug dissolved per tablet remains relatively constant as the number of tablets per vessel is increased. For Tablet 2 at 75 rpm, the amount of drug dissolved per tablet decreases for the glass vessels[3] and increases for the plastic vessels until the amounts converge at about four tablets per vessel.

CONCLUSIONS

The glass vessels[3] are uniform and comply with USP specifications. At a given stirring rate, certain tablets may give higher dissolution rates in glass[3] than in plastic vessels. Although the results from Tablet 1 indicate that the vessel material is not important, the results from Tablet 2 indicate that tablets may significantly interact with the plastic or glass surface. Tablet 1 and Tablet 2 are affected to an unusual degree by minor changes in the test. However, if reproducible results are to be obtained for a wide range of products, it is important to specify which type of vessel was used in the dissolution test.

REFERENCES

(1) D. C. Cox, C. E. Wells, W. B. Furman, T. S. Savage, and A. C. King, *J. Pharm. Sci.*, **71**, 395 (1982).

(2) "Third Supplement to USP XX and NF XV," U.S. Pharmacopeial Convention, Inc., Rockville, Md., 1982, p. 310.

(3) "The United States Pharmacopeia," 20th rev., U.S. Pharmacopeial Convention, Inc., Rockville, Md., 1980, p. 655.

(4) D. C. Cox and W. B. Furman, *J. Pharm. Sci.*, **71**, 451 (1982).

(5) D. C. Cox, W. B. Furman, L. K. Thornton, T. W. Moore, and E. H. Jefferson, *J. Pharm. Sci.*, **72**, 910 (1983).

(6) D. C. Cox, W. B. Furman, and D. P. Page, *J. Pharm. Sci.*, **72**, 1061 (1983).

(7) D. C. Cox and W. B. Furman, *J. Pharm. Sci.*, **73**, 670 (1984).

(8) A. Serino, *J. Pharm. Sci.*, **71**, 725 (1982).

(9) A. C. Shah, C. B. Peat, and J. F. Ochs, *J. Pharm. Sci.*, **62**, 671 (1973).

Sulpiride Pharmacokinetics in Humans After Intramuscular Administration at Three Dose Levels

FRANÇOISE BRESSOLLE *x, JANINE BRES *, MARIE DOMINIQUE BLANCHIN *, and ROBERTO GOMENI ‡

Received June 21, 1982, from the *Groupe de Recherche en Pharmacocinétique, Laboratoire de Chimie Analytique, Faculté de Pharmacie, Université de Montpellier, Montpellier 34060 and the ‡Laboratoires d'Etudes et de Recherches, Synthélabo-58, rue de la Glacière, Paris 75013, France. Accepted for publication July 1, 1983.

Abstract □ Pharmacokinetics of the disinhibitory psychotropic agent sulpiride was investigated in 9 healthy male subjects after intramuscular administrations of 50, 100, and 200 mg in a 3 × 3 Latin square design. Plasma and urine concentrations were measured by HPLC for 36 and 48 h, respectively. The lowest detectable concentration was 10 ng/mL. Plasma concentration *versus* time and urinary excretion rate *versus* time curves were consistent with an open two-compartment body model, where mean ±*SD* apparent half-lives of the absorption from muscle, λ_1 distribution, and λ_2 elimination phases were 6.96 ± 2.64 min, 0.220 ± 0.120 h, and 6.74 ± 2.67 h, respectively. The initial volume of distribution was 0.145 ± 0.063 L/kg, the steady-state volume of distribution was 0.639 ± 0.184 L/kg, and the total clearance was 89.8 ± 22.3 mL/min. The microscopic rate constants were $k_{12} = 2.53 \pm 1.13\ h^{-1}$, $k_{21} = 0.674 \pm 0.197\ h^{-1}$, and $k_{10} = 0.635 \pm 0.298\ h^{-1}$. Comparison of total clearance (89.8 mL/min), renal clearance (83.0 mL/min), and renal clearance of unbound drug (97.6 mL/min, $f = 0.15$) indicated that sulpiride is mainly excreted unchanged by the renal route, 93.1 ± 6.6% of the administered dose being recovered unchanged in urine. Statistical evaluation of all the above parameters, determined at the three dosage levels, did not show any variations related to dose; the pharmacokinetics of sulpiride, over the dose range tested, was therefore linear and independent of dose. The two-compartment body model proposed was validated by digital computer simulation on a small digital computer (32K).

Keyphrases □ Sulpiride—intramuscular administration, pharmacokinetics, humans □ Pharmacokinetics—intramuscular sulpiride, humans, HPLC

Sulpiride, 5-(aminosulfonyl)-*N*-[(1-ethyl-2-pyrrolidinyl)-methyl]-2-methoxybenzamide, a disinhibitory psychotropic drug belonging to the *o*-anisamide or substituted benzamide class of antipsychotic agents, is rapidly becoming an important psychotherapeutic agent in many parts of the world. Sulpiride is indicated mainly for the treatment of psychiatric disorders, peptic ulcers, and vertigo. At high dosage levels, it is a major nonsedative neuroleptic for use in acute psychosis, obsessional neurosis, and behavioral disorders. Sulpiride is characterized by its low incidence of extrapyramidal side effects, although it can induce endocrine effects, amenorrhea, or galactorrhea, probably as a result of direct interaction with prolactin cells. Benakis *et al.* (1) and Stefan *et al.* (2) demonstrated that the drug is specifically distributed into the pituitary.

Optimization of treatment with sulpiride requires knowledge of its bioavailability, pharmacokinetics, and metabolism in humans. The pharmacokinetic parameters determined after a single dose can then be used for adjustment of the dosage regimen and individualization of therapy.

The model which best describes the pharmacokinetics of a drug is that determined after intravenous administration or, when this is not possible, after administration by another route if absorption by this route is known to be rapid and total. Only then will the pharmacokinetic parameters determined be relevant. Sulpiride pharmacokinetics was investigated in humans after intravenous administration by Wiesel *et al.* (3, 4) and after intramuscular administration by Bres *et al.* (5–7) in order to choose the most appropriate model to describe the fate of sulpiride in humans and to determine the absolute bioavailability of several sulpiride preparations for oral administration. In bioavailability studies (5, 6), the intramuscular route was selected as the reference, following demonstration by the authors of bioequivalence between the intravenous and the intramuscular routes in the dog (8). All of these studies were conducted at one dose level only [1.5 mg/kg (3, 4), 6 mg/kg (5, 6), or 2.6 mg/kg (6)] and the linearity of the kinetics in humans was never truly demonstrated, as it had been in the dog (8). In the study presented here, the pharmacokinetics of intramuscularly administered sulpiride was evaluated at three dose levels (50, 100, and 200 mg) in nine healthy volunteers to determine the relationships between plasma levels, areas under the curve, rate constants, volumes of distribution, clearances, amounts of sulpiride recovered unchanged in urine, and the administered doses, and to ascertain whether all data deduced from sulpiride plasma levels and urinary excretion rate data were consistent with the two-compartment model with first-order transfer among compartments and first-order elimination.

Plasma and urine concentrations of sulpiride were determined by an original HPLC technique (7), since it has been shown that HPLC is a valid method for assay of benzamides in biological fluids (3, 4, 9–11). This technique has an increase in specificity compared with the spectrofluorometric determination of Kleimola *et al.* (12–14) and an increase in sensitivity compared with the quantitative TLC method developed for our earlier studies (5, 6, 8, 15–17).

EXPERIMENTAL SECTION

Drug Products and Materials—Sulpiride[1], sulpiride ampules[2] for intramuscular injection (100 mg/2 mL) were furnished. Nicotinamide[3] (used as an internal standard) was purchased. All chemicals and solvents were of analytical grade. Methanol and chloroform were twice-distilled in an all-glass apparatus before use. These solvents and distilled water were filtered through a 0.45-μm filter[4] before use.

Subjects—The study was conducted with nine male Caucasian subjects (25.6 ± 3.2 years) in good health as determined by screening, laboratory tests including hematology, urinalysis, blood chemistry (SMA-12), electrocardiogram, history, physical examination, and creatinine clearance. They were within the normal range for height (179 ± 6 cm) and weight (68.7 ± 5.0 kg) and had no history of recent drug intake or allergy. All laboratory parameters were monitored before and once during the study. The subjects were fully informed of study design and were given all available data on sulpiride clinical and toxicological studies.

Study Design—Each subject received three different treatments, randomly allocated according to three series of 3 × 3 Latin squares (Table I); at least 7 d were allowed between treatments. Each person received no medication for at least 48 h before the drug administration. They fasted for 12 h prior to and 4 h after each drug administration. Food and water were then taken as usual. Water (300 mL) was taken before each dosage administration.

Each subject received a single dose of 50, 100, or 200 mg im of sulpiride into the upper outer quadrant of the gluteus muscle. A catheter was placed in a forearm vein and a continuous drip was maintained for the first 6 h after

[1] Delagrange, Paris, France.
[2] Dogmatil; Delagrange, Paris, France.
[3] Nicotinamide, Niacinamide; Sigma Chemical Co., St. Louis, Mo.
[4] Millipore Corp., Bedford, Mass.

0022-3549/84/0800-1128$01.00/0
© 1984, American Pharmaceutical Association

Table I—Subject Data and Treatment Schedule

Subject	Age, years	Weight, kg	Height, m	Creatinine Clearance, mL/min	Order of Administered Doses[a] 50 mg	100 mg	200 mg
1	26	74.0	1.87	104	1	2	3
2	24	71.0	1.80	110	2	3	1
3	28	64.5	1.74	223	2	3	1
4	23	72.0	1.81	113	3	1	2
5	29	63.5	1.85	145	1	2	3
6	31	69.0	1.76	143	3	1	2
7	21	60.0	1.68	128	3	1	2
8	24	74.5	1.80	115	1	2	3
9	24	69.5	1.83	292	2	3	1

[a] Randomized with a 3 × 3 Latin square design.

drug administration, during which time the subjects were nonambulatory.

Blood samples were obtained by venipuncture immediately before and 5, 10, 15, 20, 25, 30, 35, 40, 45, 60, 90 min, 2, 3, 4, 5, 6, 8, 10, 12, 16, 24, 30 and 36 h after each injection. Urine specimens were collected before drug administration and for the following intervals after the injection: 0-1, 1-2, 2-3, 3 4, 4-5, 5-6, 6-8, 8-10, 10-12, 12-16, 16-24, 24 28, 28-32, 32-36, and 36-48 h.

Sample Collection—Blood samples were collected in heparinized tubes and immediately centrifuged; the plasma was removed and immediately frozen. The voided urine was collected, the total volume recorded, and an aliquot was placed in vials and stored frozen until analysis.

Assay Method—*Instrumentation*—The chromatograph[5] was connected to a 10-μL automatic loop injection system, a multiple-wavelength detector[6], and a computing integrator[7]. Chromatography was performed on a reverse-phase column[8] (filled in-house) with a precolumn[9], to extend column life.

The mobile phase contained 30 parts of methanol and 70 parts of 0.1 M ammonium acetate. The temperature was ambient, and the flow rate was 1.0 mL/min. The detector was set at 0.002 AUFS (197 nm), and the chart speed was 0.25 cm/min.

Sample Preparation—Plasma or urine (1-4 mL) was treated with 0.5 M NaOH (0.2 mL) and the pH was adjusted to 10. After extraction with 15 mL of chloroform for 20 min and centrifugation, a 15-mL aliquot of the organic phase was retained. After further extraction with 5 mL of chloroform, an additional 5 mL of the organic phase was retained. An internal standard was added (0.4 mL of nicotinamide at 1 mg/L in methanol for plasma and 1.0 mL of nicotinamide at 10 mg/L in methanol for urine) to the combined organic phases, and the extracts were evaporated to dryness. Before HPLC analysis, 0.3 mL of the mobile phase was added. After ultrasonic mixing[10], 10 μL of this solution was injected into the column by the automatic loop injection system.

The peak area ratio of sulpiride to nicotinamide (internal standard) was used as the assay parameter. Calibrations curves in control plasma (4 mL) were prepared for each two experiments from spiked pooled plasma samples of two subjects at concentrations of 20, 40, 50, 100, and 150 ng/mL. Calibration curves in control urine (2 mL) were prepared for each experiment from spiked urine samples of each subject at the concentrations of 0.5, 1.25, 6.25, 12.5, and 25 μg/mL. They were processed in the same manner as the *in vivo* samples.

Data Analysis—The plasma concentration of sulpiride for each subject was modeled using a two-compartment open model (Scheme I) with first-order absorption after intramuscular administration. The structural model describing the serum concentration C_p at time t is given by (18, 19):

$$C_p = \frac{k_a F D}{Vd_1}\left[\frac{(k_{21}-\lambda_1)e^{-\lambda_1 t}}{(k_a-\lambda_1)(\lambda_2-\lambda_1)} + \frac{(k_{21}-\lambda_2)e^{-\lambda_2 t}}{(k_a-\lambda_2)(\lambda_1-\lambda_2)} + \frac{(k_{21}-k_a)e^{-k_a t}}{(\lambda_1-k_a)(\lambda_2-k_a)}\right] \quad \text{(Eq. 1)}$$

where Vd_1 is volume of distribution in the central compartment, F is fraction

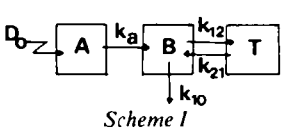

Scheme I

of dose D absorbed, λ_1 and λ_2 are first-order disposition rate constants in the distribution and elimination phases, k_{21} is the first-order transfer rate constant from the tissue compartment to the central compartment, and k_a is the first-order absorption rate constant from the muscle. Equation 1 is equivalent to:

$$C_p = -C_1' e^{-k_a t} + C_1 e^{-\lambda_1 t} + C_2 e^{-\lambda_2 t} \quad \text{(Eq. 2)}$$

The coefficients and exponents of the exponential terms were determined by an extended least-squares method..

The dispersion error on the measured concentrations was not known, so we decided to estimate the structural model parameters minimizing the log-likelihood function:

$$L = \sum_{i=1}^{N} \frac{(y_i - C_{pi})^2}{V_i} + \ln V_i \quad \text{(Eq. 3)}$$

where V_i is the error variance of the ith observation C_{pi}. Note that usually weighted least squares are appropriately used when it is assumed that the error variance is known up to a proportional factor. In our case the error variance is not known, so according to Sheiner (20) the following variance model was assumed:

$$V_i = a \times C_{pi}^b \quad \text{(Eq. 4)}$$

where a and b are variance model parameters. This is a reasonable model because it generalizes the usual weighting scheme applied to the weighted regression analysis, *e.g.*, for $a = 1$ and $b = 1$ the variance model becomes $V_i = C_{pi}^2$ and the weight is $1/y^2$. The exponential parameters as well as the error model parameters were estimated using the AUTOMOD II program (21-23) using a computer[11].

The microscopic rate constants k_{12} (first-order transfer rate constant from the central compartment to the tissue compartment), k_{21} (as previously determined), and k_{10} (first-order elimination rate constant from the central compartment) were determined from the coefficients and exponents of Eq. 2 (20). The total area under the plasma drug concentration-time curve (AUC_∞) was calculated from $AUC_{36\,h} + C_{36\,h}/\lambda_2$; $AUC_{36\,h}$ was calculated by the trapezoidal rule. Total body clearance, CL_{tot}, of sulpiride was calculated from the ratio of the dose of sulpiride and AUC_∞. The renal clearance, CL_r, of sulpiride was estimated either from the ratio of the amount of sulpiride eliminated unchanged in urine and the total area under the curve or from the slope of the plot of excretion rate *versus* plasma drug concentration at the midpoint of the drug excretion intervals.

The volume of distribution in the central compartment was evaluated by $Vd_1 = D \times k_a/[C_2 \times (k_a - \lambda_2)] + [C_1 \times (k_a - \lambda_1)]$; the volume of distribution in equilibrated tissues was evaluated by $Vd = CL_{tot}/\lambda_2$, and the steady-state volume of distribution was evaluated by $Vd_{ss} = Vd_1 \times (1 + k_{12}/k_{21})$. A pharmacokinetic analysis of the urinary excretion rate of sulpiride *versus* time curves (rate plot) and of amount of sulpiride remaining to be excreted *versus* time curves (σ^- plot) was undertaken for each subject using the GPHARM (24) computer program[12]. In some subjects three rate constants could then be determined for the absorption from muscle (phase 1), distribution (phase 2), and elimination (phase 3) processes, but in most of the subjects only the two latter phases could be measured with accuracy.

Digital Computer Simulations—Multicompartmental simulations on a small digital computer (32K)[12] was performed employing the GPHARM computer program (18, 24). The dose is introduced into an absorption compartment ($A = 5$). It then reaches the central compartment ($B = 1$), is distributed between the central and tissue compartments ($T = 2$), and is eliminated in urine ($U = 3$) or by another route of elimination ($E = 4$) (Scheme II).

The experimentally obtained sulpiride concentrations (in μg/mL) in plasma were expressed as percent of administered dose per milliliter of plasma and multiplied, for the three doses studied, by the mean initial volume of distri-

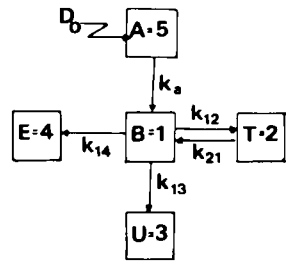

Scheme II

[5] Liquid chromatograph SP 8000; Spectra Physics, Orsay, France.
[6] Spectroflow monitor SF 770; Schoeffel Instruments, Cunow, Clichy, France.
[7] Computing integrator SP 4000; Spectra Physics, Orsay, France.
[8] Column Hypersil ODS 5 μm, 2.50 × 4.6 mm i.d.
[9] Precolumn Hypersil ODS 5μm, 50 × 1.5 mm i.d.
[10] Bandelin Snorex TK 52, Chrompack, Orsay, France.
[11] Model HP 1000; Hewlett-Packard, Orsay, France.
[12] Computing graphic system model 4051 with interactive digital plotter model 4662; Tektronix, Orsay, France.

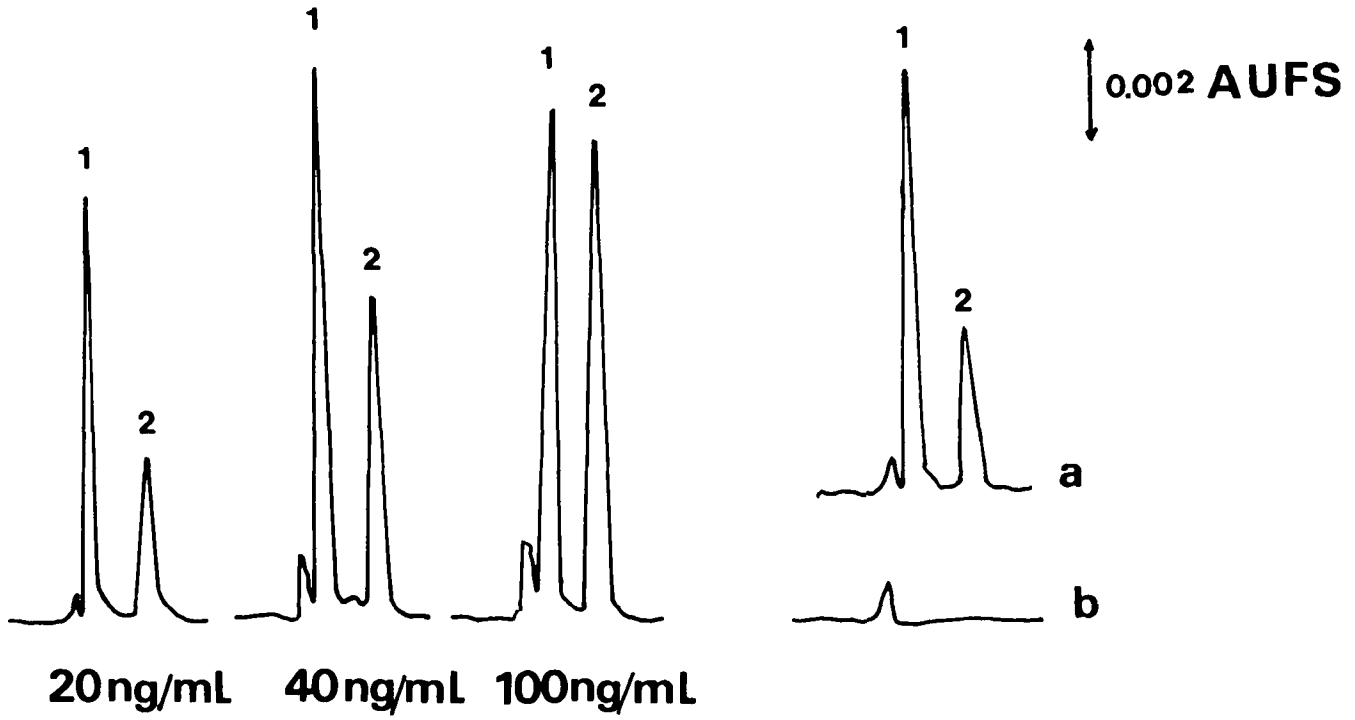

Figure 1—*Typical chromatograms obtained after injection on a Hypersil ODS column of 10-μL aliquots of the chloroform extracts of 4 mL of plasma spiked with sulpiride (20, 40, and 100 ng/mL) or taken from subject 3 before (b) and after (a) intramuscular administration of 96 mg of sulpiride.*

bution Vd_1 in order to obtain sulpiride amounts in the central compartment in terms of percent of administered dose (with the assumption that $F = 1$). For each subject, and for the three doses studied, these values and the experimentally obtained amounts of sulpiride excreted in urine as percent of administered dose were plotted against time. To account for the elimination of the remaining dose, another route of elimination from the central compartment was introduced into the model, so that at all times the mass balance was 100% of the dose.

For each subject, the mean microscopic rate constants obtained after pharmacokinetic analyses at the three dosage levels were taken as a first estimate for the simulations. They were then slightly modified to obtain the best fit between the curves generated with these values for plasma and urine and the experimentally obtained sulpiride amounts in plasma and urine at all times for the three doses.

Statistical Analysis—An analysis of variance on a randomized 3 × 3 Latin square design was performed on all the pharmacokinetic parameters determined to test variability between sequence of administrations, between doses, and between subjects.

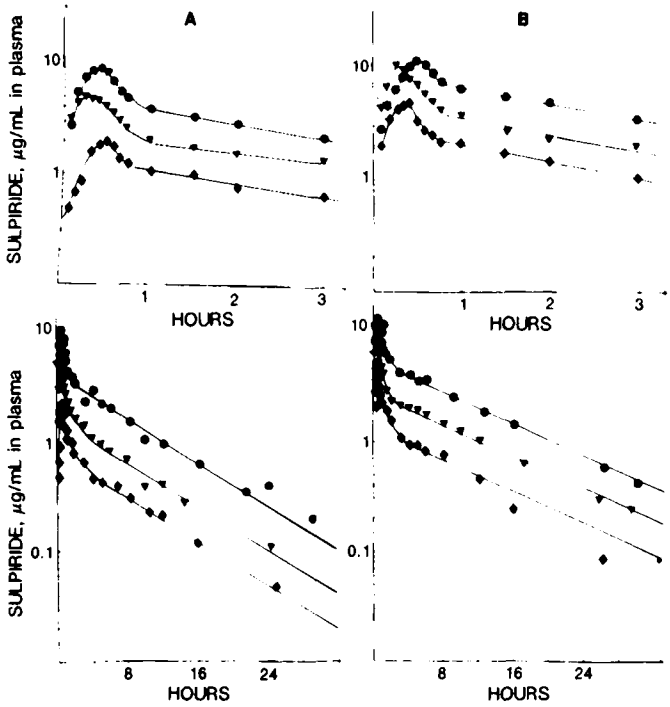

Figure 2—*Sulpiride plasma levels in two subjects following intramuscular administration of 50, 100, and 200 mg of sulpiride. The lines were obtained when the experimental data were fitted to a two-compartment model. Key: (A) subject 6: (♦) 52.24 mg; (▼) 94.53 mg; (●) 195.60 mg; (B) subject 5: (♦) 52.00 mg; (▼) 94.55 mg; (●) 196.15 mg.*

RESULTS

Sensitivity and Reliability of the Analytical Method—Retention times were 12 min for sulpiride and 6.8 min for the internal standard nicotinamide. There were no major interfering peaks in control plasma and urine samples at the retention times of the aforementioned compounds (Fig. 1). To improve the reliability of the assay, each sample was injected in triplicate. Detection limits, evaluated by the amounts of samples yielding a detector response equal to twice the detector noise, was 10 ng/mL. Recovery after extraction from the plasma and urine was 98%. A five-point calibration curve was run with every set of 50 samples, and the method was validated with spiked samples every 10 samples throughout the duration.

In plasma, the peak area ratio (R) of sulpiride over the internal standard varied linearly with concentration over the range used. These calibration curves passed through the origin with a slope $\pm SD$ of $146.4 \pm 0.54 \times 10^{-4}$ ng^{-1} mL and a coefficient of the linear regression analysis of 0.9998 ± 0.0001 ($n = 10$) (Fig. 1). The intercept was not significantly different from zero ($13.8 \pm 4.48 \times 10^{-3}$). For the urine samples the reliability of the assay was of the same magnitude, with a slope of $579 \pm 1.9 \times 10^{-3}$ ng^{-1} mL, an intercept of $12.7 \pm 10.1 \times 10^{-3}$, and a correlation coefficient of 0.999979 ± 0.000013 ($n = 10$).

A stability study of plasma and urine samples stored at −20°C showed that sulpiride was stable over 3 months. Storage of samples during the present studies did not exceed 3 months.

Pharmacokinetic Analysis—After the maximum, sulpiride plasma concentration follows a biexponential decay. For each subject, the three curves obtained after 50-, 100-, and 200-mg im administrations were parallel when concentration units were μg/mL (Fig. 2), and superimposable when concentrations are expressed as percent of administered dose per milliliter of plasma (Fig. 3). These results are consistent with a two-compartment body model with first-order transfers among compartments and first-order elimination (Scheme I). All the pharmacokinetic parameters included in this model were first evaluated by the residual method or "exponential stripping" using the GPHARM program (24), and their values have been reported by Blanchin

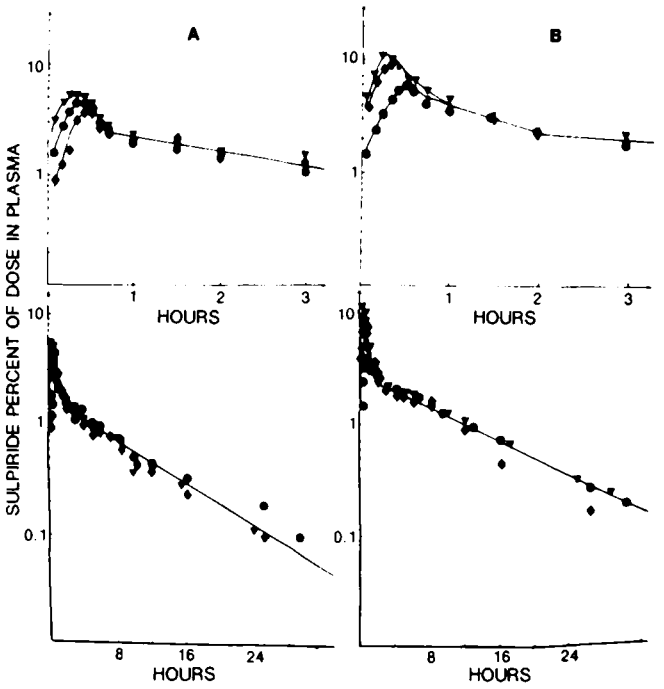

Figure 3—*Sulpiride plasma levels expressed as percent of the administered dose per milliliter in plasma, in two subjects, following intramuscular administrations of 50, 100, and 200 mg of sulpiride. Key as in Fig. 2.*

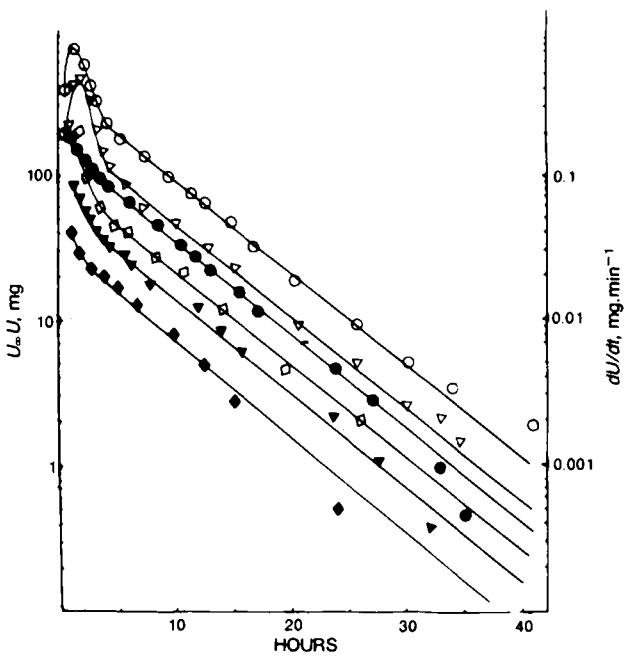

Figure 4—*Sulpiride urinary excretion rate (open symbols) and amount remaining to be excreted in form of unchanged sulpiride (closed symbols) following intramuscular administrations of 50, 100, and 200 mg of sulpiride to subject 6. Key: (◇, ◆) 52.24 mg; (▽, ▼) 94.53 mg; (○, ●) 195.60 mg.*

(7). The parameters so estimated were used as starting values for the more refined extended least-squares maximum-likelihood method to obtain the best possible evaluation (20-23) (Table II).

Absorption from muscle is fast and complete, but an important inter- and intrasubject variability was observed. The lag time determined in each case with the program used was always negligible. The mean half-lives of the λ_1 distribution and λ_2 disposition phases were 0.220 ± 0.120 and 6.74 ± 2.67 h, respectively; these values are in good agreement with those reported by Imondi *et al.* (25) and Wiesel *et al.* (3), but they differ from those we reported previously (5, 6).

Distribution in peripheral tissues was rapid (k_{12} = 2.53 ± 1.13 h^{-1}), with a rate of transfer from tissue to plasma of the same order of magnitude (k_{21} = 0.674 ± 0.197 h^{-1}) as the elimination rate constant (k_{10} = 0.635 ± 0.298 h^{-1}). The apparent volume of distribution of the central compartment, Vd_1 = 0.145 ± 0.063 L/kg, was very close to the extracellular water volume (from 0.15 to 0.20 L/kg in humans), while the apparent volume of distribution at steady state, Vd_{ss} = 0.639 ± 0.184 L/kg, seemed to correspond to total water, which varies in humans from 0.45 to 0.65 L/kg. Total plasma clearance was 89.8 ± 22.3 mL/min. For each subject the cumulative urinary excretion curves as percent of administered dose were superimposable; the rate and extent of sulpiride elimination in urine in the form of unchanged drug does not, therefore, seem to depend on the dose administered (Table II).

Elimination of sulpiride after intramuscular administration was mainly *via* the renal route, since 93.1 ± 6.6% was recovered unchanged in the urine. Renal clearance, evaluated from total amount of sulpiride eliminated unchanged in urine divided by AUC_∞, was 83.0 ± 19.8 mL/min, while the renal clearance evaluated from the slope of the plot of urinary excretion rate *versus* plasma concentration at the midpoint of the drug excretion interval was 62.3 ± 22.3 mL/min. Sulpiride renal clearance was 83.0 mL/min when total sulpiride (free and bound) was assayed in plasma. If the fraction bound to plasma protein was f = 0.15 (26), free sulpiride clearance would be 97.6 mL/min.

The apparent rate contants of the absorption, distribution, and elimination phases, determined from the variations with time of the urinary excretion rate (rate method) or from the variations with time of the amount remaining to be excreted (σ^- method), were close to those determined from plasma data (Fig. 4, Table II). Mean elimination half-lives determined by these two methods were 5.58 ± 1.41 and 5.68 ± 1.52 h, respectively.

Linearity—To test the linearity of sulpiride pharmacokinetics all the individual data were normalized by the dose administered and fitted to the full model of data (structural and error model). Using 3 × 3 Latin-square analysis of variance, the following parameters were then compared: time to peak and peak plasma levels, area under the time concentration curve, amount of drug excreted unchanged in the urine, λ_1, λ_2, k_a, k_{12}, k_{10}, total clearance, and renal clearance. The analyses did not show any sequence nor dose effects. While the interindividual variations with dose of all parameters are small, large variations are observed between subjects (Table III). Of all the parameters tested, clearance was the most variable within subjects and for a same subject within administration (Fig. 5). The system is linear and time invariant, because all the pharmacokinetic parameters are independent of drug concentration and time. It would appear that distribution and elimination kinetics of sulpiride in humans are linear over the dose range tested.

Validation of the Proposed Model by Digital Simulation—The two-compartment model was validated by digital simulation employing the mean microscopic rate constants determined for each subject after intramuscular administration at the three dosage levels. The good fit obtained between the simulated curves (percent of dose in the central compartment) and the experimental points after the maximum, at the three dosage levels, allowed a single value for each parameter to be given for each subject.

These values were for all subjects in the study (Table IV): k_a = 9.36 ± 1.84 h^{-1}, k_{12} = 1.36 ± 0.47 h^{-1}, k_{21} = 0.61 ± 0.15 h^{-1}, k_{10} = 0.53 ± 0.13 h^{-1}, Vd_1 = 0.18 ± 0.02 L/kg, and Vd_{ss} = 0.57 ± 0.08 L/kg. Simulated curves for the peripheral compartment showed that marked distribution in tissues did not occur. At the maximum tissue level, 40-60% of the administered dose was present in tissues (Fig. 6); after this maximum and up to 10 h, the total amount of sulpiride in the tissues was ~1.5-2 times higher than that in the central

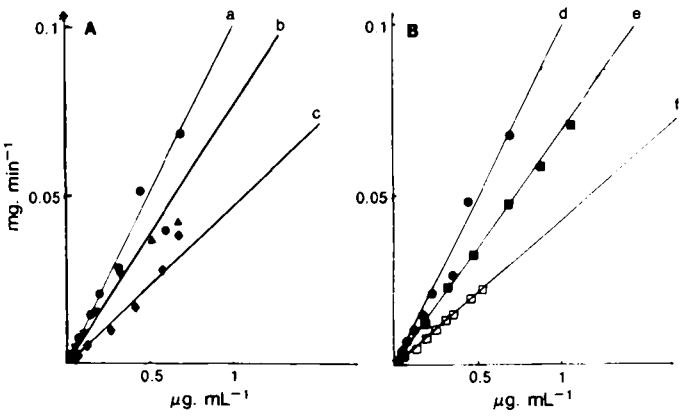

Figure 5—*Renal clearance of sulpiride in one subject for different administered doses (A) and for a same dose and for three different subjects (B), illustrating the large variations. Key: (A) subject 1: (◆) 47.55 mg; (▼) 97.90 mg; (●) 182.95 mg; (B) (●) subject 1; (■) subject 3; (□) subject 5. Rates: (a) 99 mL/min; (b) 77 mL/min; (c) 47 mL/min; (d) 99 mL/min; (e) 69.5 mL/min; (f) 43 mL/min.*

Table II—Pharmacokinetic Parameters After Intramuscular Administration of Sulpiride at 50, 100, and 200 mg

	Subject 1			Subject 2			Subject 3			Subject 4			Subject 5		
D_0[a]															
mg	47.55	95.90	182.95	52.17	97.32	193.88	50.00	96.00	172.42	47.71	95.33	149.90	52.00	94.55	196.15
mg/kg	0.643	1.296	2.472	0.709	1.333	2.810	0.769	1.488	2.673	0.673	1.288	2.026	0.813	1.501	3.114
k_a, h^{-1}	6.70	5.68	6.90	10.2	3.64	4.50	7.87	7.87	7.90	9.51	7.36	9.61	8.67	11.7	11.7
λ_1, h^{-1}	4.69	4.41	5.15	2.48	2.62	3.57	6.07	5.87	6.82	5.37	5.00	4.84	2.83	2.60	2.98
λ_2, h^{-1}	0.104	0.109	0.101	0.0702	0.044	0.0476	0.115	0.137	0.139	0.138	0.135	0.142	0.120	0.0845	0.0893
$t_{1/2}$, h Absorption	0.104	0.122	0.100	0.0681	0.190	0.154	0.0881	0.0881	0.0877	0.0728	0.0942	0.0721	0.0799	0.059	0.0595
$t_{1/2}$, h Distribution	0.148	0.157	0.135	0.279	0.264	0.194	0.114	0.118	0.102	0.129	0.139	0.143	0.245	0.267	0.233
$t_{1/2}$, h Elimination	6.66	6.34	6.89	9.87	15.6	14.6	6.00	5.08	4.98	5.03	5.12	4.90	5.78	8.20	7.76
k_{12}, h^{-1}	3.40	3.11	3.81	1.69	2.01	2.70	4.36	3.94	5.01	3.77	3.45	3.33	1.76	1.76	1.98
k_{21}, h^{-1}	0.575	0.602	0.678	0.527	0.337	0.280	0.587	0.538	0.978	0.829	0.952	0.768	0.718	0.503	0.720
k_{10}, h^{-1}	0.815	0.806	0.756	0.329	0.311	0.637	1.24	1.53	0.977	0.907	0.735	0.882	0.473	0.413	0.373
Vd_1, L/kg	0.0744	0.0892	0.0900	0.209	0.160	0.0976	0.075	0.0704	0.117	0.0941	0.117	0.0946	0.108	0.0973	0.125
Vd, L/kg	0.600	0.650	0.822	0.962	1.22	1.18	0.777	0.755	0.795	0.585	0.604	0.568	0.410	0.491	0.509
Vd_{ss}, L/kg	0.514	0.551	0.773	0.881	1.11	1.04	0.632	0.586	0.713	0.523	0.543	0.505	0.370	0.439	0.469
AUC, mg · h/L															
Observed	9.57	17.5	28.9	8.86	18.1	41.6	8.12	14.0	23.8	7.88	15.5	24.8	15.8	33.2	65.2
To infinity	10.3	18.3	29.8	10.5	24.9	50.0	8.61	14.4	24.2	8.33	15.8	25.1	16.5	36.2	68.5
$AUC_{(1\ mg/kg)}$; h/L/kg	16.1	14.1	12.1	14.8	18.7	17.8	11.2	9.69	9.07	12.4	12.3	12.4	20.3	24.1	22.0
CL, mL/min															
Total	76.9	87.3	102	82.8	65.1	64.6	96.8	111	119	95.5	100	99.5	52.5	43.5	47.7
Renal[b]	64.2	71.5	90.8	81.5	65.2	47.7	95.9	96.4	112	83.2	91.3	90.3	59.9	45.1	46.3
	(47.0)	(77.0)	(99.0)	(77.0)	(40.0)	(22.0)	(50.0)	(65.0)	(70.0)	(49.0)	(46.5)	(92.0)	(55.0)	(39.5)	(43.0)
Cumulative amount															
in urine (U_∞), %	83.4	81.9	88.7	98.4	100	73.8	99.1	86.8	94.0	87.1	90.8	90.7	96.8	97.9	97.0
Rate constant from rate plot, h^{-1}															
Absorption (phase 1)	—	—	—	—	5.72	—	—	2.09	—	—	—	3.19	—	—	—
Distribution (phase 2)	0.512	1.17	0.423	0.667	1.68	1.44	0.825	1.81	0.595	1.69	0.694	2.73	0.786	0.750	0.386
Elimination (phase 3)	0.126	0.0811	0.0898	0.120	0.0790	0.096	0.149	0.119	0.116	0.125	0.135	0.137	0.105	0.0916	0.0912
Rate constant from σ^- plot, h^{-1}															
Absorption (phase 1)	—	—	—	—	—	—	—	—	—	—	—	2.01	—	—	3.59
Distribution (phase 2)	0.742	1.56	0.282	0.574	0.666	1.14	0.652	0.793	0.634	1.99	0.786	0.635	0.819	0.860	2.19
Elimination (phase 3)	0.109	0.0816	0.0813	0.114	0.0833	0.084	0.106	0.116	0.118	0.119	0.135	0.129	0.0990	0.0956	0.103

Table II—*Continued*

	Subject 6			Subject 7			Subject 8			Subject 9		
D_0[a]												
mg	52.24	94.53	195.60	53.11	98.03	194.70	59.90	94.37	198.29	62.33	88.70	193.36
mg/kg	0.757	1.370	2.835	0.885	1.634	3.245	0.719	1.258	2.680	0.897	12.76	2.782
k_a, h^{-1}	4.19	5.57	4.30	4.97	4.18	4.50	6.82	4.70	2.91	6.76	6.18	9.35
λ_1, h^{-1}	3.62	4.20	3.41	3.81	3.34	3.11	4.35	1.26	1.19	1.84	3.15	2.03
λ_2, h^{-1}	0.121	0.138	0.0952	0.137	0.125	0.122	0.125	0.116	0.118	0.113	0.124	0.119
$t_{1/2}$, h Absorption	0.165	0.125	0.161	0.139	0.166	0.154	0.102	0.148	0.239	0.103	0.112	0.0741
$t_{1/2}$, h Distribution	0.191	0.165	0.203	0.182	0.207	0.223	0.159	0.550	0.585	0.378	0.220	0.342
$t_{1/2}$, h Elimination	5.71	5.02	7.28	5.05	5.53	5.68	5.54	5.97	5.89	6.14	5.57	5.83
k_{12}, h^{-1}	2.36	2.80	2.34	2.46	2.03	1.98	2.97	0.602	0.554	1.00	1.98	1.10
k_{21}, h^{-1}	0.903	0.809	0.624	0.889	1.01	0.746	0.718	0.384	0.382	0.619	0.833	0.696
k_{10}, h^{-1}	0.481	0.726	0.547	0.600	0.430	0.500	0.787	0.394	0.374	0.327	0.453	0.350
Vd_1, L/kg	0.206	0.121	0.144	0.211	0.213	0.162	0.123	0.155	0.164	0.315	0.200	0.276
Vd, L/kg	0.786	0.587	0.803	0.907	0.703	0.667	0.716	0.502	0.505	0.934	0.813	0.795
Vd_{ss}, L/kg	0.742	0.543	0.692	0.798	0.643	0.593	0.570	0.398	0.403	0.828	0.672	0.710
AUC, mg · h/L												
Observed	7.53	16.4	35.0	6.93	18.4	39.1	8.39	20.9	43.5	8.07	13.6	29.0
To infinity	7.96	16.9	37.1	7.13	18.6	39.9	8.92	21.6	45.0	8.50	13.9	29.4
$AUC_{(1\ mg/kg)}$, h/L/kg	10.52	12.3	13.1	8.06	11.4	12.3	12.4	17.2	16.8	9.48	10.9	10.6
CL, mL/min												
Total	109	93.2	87.9	124	87.8	81.3	112	72.8	73.4	122	106	110
Renal[b]	109	94.4	87.3	103	84.4	76.9	86.5	69.3	69.5	115	102	103
	(80.0)	(56.0)	(37.0)	(105)	(68.0)	(49.5)	(80.0)	(63.5)	(18.0)	(74.0)	(71.0)	(97.0)
Cumulative amount												
in urine (U_∞), %	100	101	93.3	83.2	96.0	94.5	85.9	95.2	94.6	91.6	95.5	93.6
Rate constant from rate plot, h^{-1}												
Absorption (phase 1)	—	2.55	—	—	—	—	—	—	—	—	—	—
Distribution (phase 2)	1.49	1.42	0.706	—	4.67	0.719	—	0.860	1.04	—	0.683	0.785
Elimination (phase 3)	0.150	0.133	0.149	0.180	0.158	0.167	0.182	0.139	0.135	0.140	0.159	0.153
Rate constant from σ^- plot, h^{-1}												
Absorption (phase 1)	—	—	—	—	—	—	—	—	—	—	—	—
Distribution (phase 2)	1.51	1.04	0.923	—	0.825	0.527	—	0.983	0.811	—	0.420	0.885
Elimination (phase 3)	0.151	0.153	0.150	0.195	0.153	0.168	0.227	0.148	0.137	0.135	0.149	0.146

[a] The administered dose was determined by weighing the syringe before and after the injection. [b] Renal clearance estimated from slope of the plot of excretion rate *versus* plasma drug concentration at midpoint of the drug excretion intervals is indicated in parentheses.

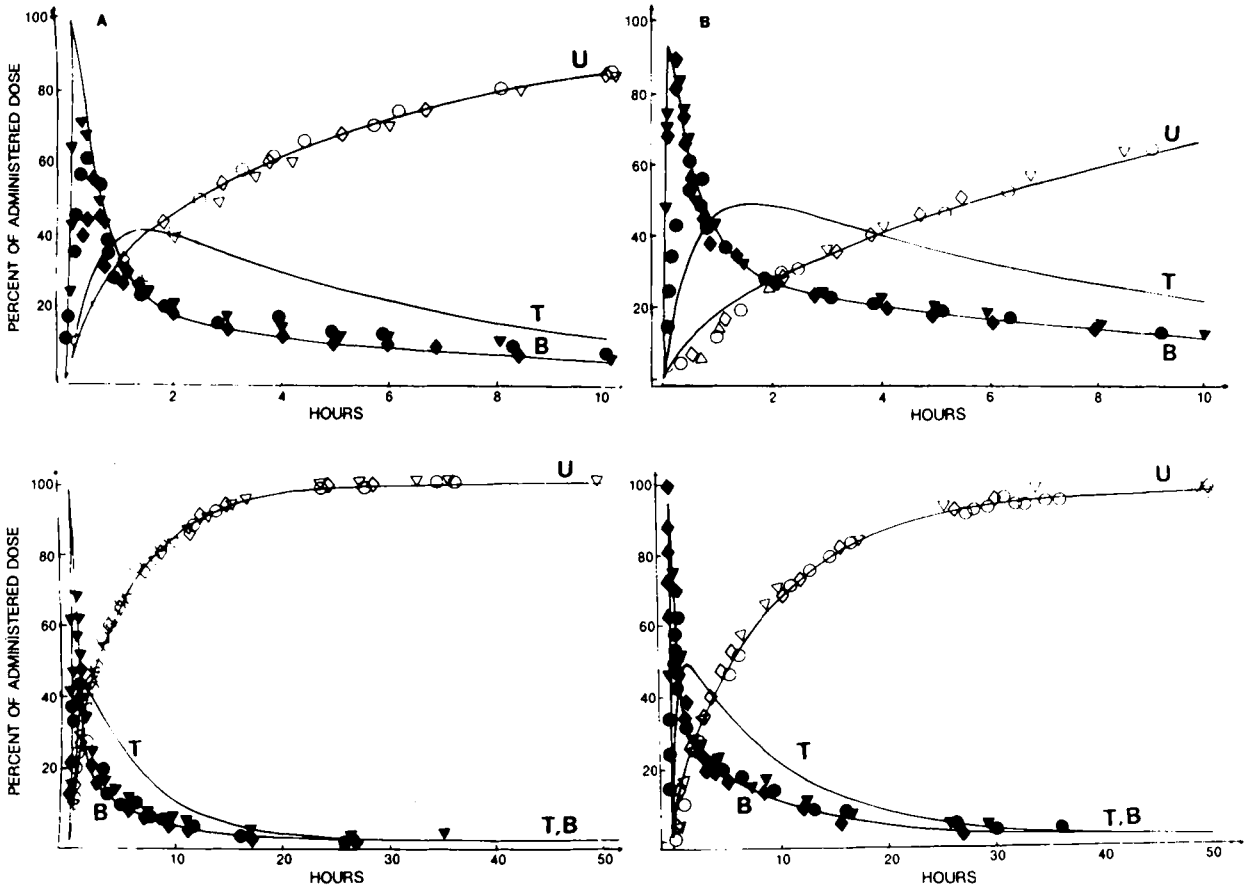

Figure 6—*Digital computer-fitting of sulpiride plasma (B) and urine (U) data following intramuscular administration of sulpiride, 50 (♦, ◇), 100 (▼, ▽), 200 mg (●, ○), to subjects 6 (A) and 5 (B). The curves labeled T are computer-generated amounts of sulpiride in the tissues in accordance with an open two-compartment model with first-order rates of transfer and elimination.*

compartment. The good fit obtained between the experimental points for urine and the curves generated from plasma data, at the three dosage levels, validates the proposed model.

DISCUSSION

Distribution in Peripheral Tissues—Distribution in the peripheral tissues can be estimated from the pharmacokinetic model consistent with sulpiride fate in humans. After intravenous (3) or intramuscular administration (5–7), plasma sulpiride levels follow a biexponential decay in most of the subjects. Two apparent rate constants can be determined for the λ_1 distribution and λ_2 elimination phases (Table V), since after intramuscular administration, absorption from the muscle is rapid and total. These results are consistent with a two-compartment open model with first-order transfer between compartments and first-order elimination from the central compartment. In four subjects (one male and three female), Bres *et al.* (5, 6) reported that only one phase of elimination was apparent since the distribution was too rapid to be detectable and the data were consistent with a one-compartment body model. Wiesel *et al.* (3) reported for two subjects, after intravenous administration, a triexponential decay consistent with a three-compartment body model. The terminal log-linear phase had half-lives of 11 and 13.9 h for the two subjects, respectively. The deep compartment added to fit the data in these cases did not modify the distribution rate constants between the central compartment and the shallow compartment (k_{12} and k_{21}).

Table III—Results of Statistical Analyses using a Replicated Latin Square Design [a]

Parameter	Period	Subjects	Dose
C_{max}/D_0, mg/L/kg	$F = 1.575$ (NS)	$F = 5.282$ ($p < 0.01$)	$F = 1.077$ (NS)
t_{max}, h	$F = 2.284$ (NS)	$F = 4.208$ ($p < 0.01$)	$F = 1.706$ (NS)
$t_{1/2,\lambda_1}$, h	$F = 1.842$ (NS)	$F = 5.369$ ($p < 0.01$)	$F = 0.776$ (NS)
$t_{1/2,\lambda_2}$, h	$F = 0.232$ (NS)	$F = 13.080$ ($p < 0.001$)	$F = 1.350$ (NS)
k_{12}, h^{-1}	$F = 1.945$ (NS)	$F = 9.236$ ($p < 0.001$)	$F = 0.793$ (NS)
k_{21}, h^{-1}	$F = 2.872$ (NS)	$F = 4.270$ ($p < 0.01$)	$F = 0.413$ (NS)
k_{10}, h^{-1}	$F = 0.070$ (NS)	$F = 5.111$ ($p < 0.01$)	$F = 1.218$ (NS)
AUC/D_0, h/L/kg	$F = 0.689$ (NS)	$F = 17.747$ ($p < 0.001$	$F = 2.636$ (NS)
CL, mL/min	$F = 0.253$ (NS)	$F = 8.203$ ($p < 0.001$)	$F = 1.788$ (NS)
Renal			
Total	$F = 0.696$ (NS)	$F = 6.942$ ($p < 0.01$)	$F = 1.958$ (NS)
U_∞, %	$F = 0.700$ (NS)	$F = 1.387$ (NS)	$F = 0.363$ (NS)

[a] NS = not significant.

Rate Constants of Transfer Between Compartments—The microscopic rate constant of transfer from the central compartment to the peripheral tissues (k_{12}), which regulates the amount going to tissues, had a values of 2.19 h^{-1} (5, 6), 2.29 h^{-1} (3), and 2.53 h^{-1} (Table V). The rates of transfer from tissues to plasma (k_{21}), which regulates output from tissues, were 1.24 h^{-1} (5, 6), 0.703 h^{-1} (3), and 0.674 h^{-1} (in this study). These values were of the same magnitude as the elimination microscopic rate constant, k_{10}. The values found in this study were consistent with those found in our earlier study and the values reported by Wiesel *et al.* (3) with different routes of administration and final sampling times.

In our earlier studies (5, 6), the large number of samples taken up to 10 h allowed good determination of k_{10}, even if the value of λ_2 was overestimated. The differences for k_{10} reported in these three studies, 0.73, 0.686, or 0.635 (mean) h^{-1}, were smaller than the differences reported for λ_2 (0.22, 0.103, or 0.103 (mean) h^{-1}; Table V).

Table IV—Individual Pharmacokinetic Parameters Obtained from Digital Computer Simulations and Fitting of Plasma and Urine Data When Sulpiride was Administered at Three Dose Levels

Parameter	Subject 1	2	3	4	5	6	7	8	9	Mean ± *SD*
Weight, kg	74.0	69.0	61.0	71.0	62.0	69.5	60.0	75.0	69.5	67.89 ± 5.57
Vd_1, L/kg	0.17	0.17	0.16	0.16	0.16	0.19	0.20	0.16	0.23	0.18 ± 0.024
Vd_{ss}, L/kg	0.66	0.64	0.65	0.58	0.43	0.53	0.61	0.48	0.54	0.57 ± 0.08
k_{12}, h^{-1}	1.61	1.20	1.63	2.36	1.00	0.90	1.50	1.00	1.00	1.36 ± 0.47
k_{21}, h^{-1}	0.56	0.43	0.53	0.90	0.60	0.50	0.73	0.50	0.74	0.61 ± 0.15
k_{10}, h^{-1}	0.45	0.60	0.59	0.73	0.30	0.58	0.64	0.47	0.41	0.53 ± 0.13
k_a, h^{-1}	10.9	6.0	11.0	10.5	9.3	10.0	6.5	10.0	10.0	9.36 ± 1.84
U_∞, %	89.7	90.8	93.3	89.6	97.0	100.0	92.7	92.0	93.6	93.18 ± 3.42

Table V—Sulpiride Distribution

Route of Administration	Dose, mg	Dose, mg/kg	$t_{1/2,\lambda_1}$, h	$t_{1/2,\lambda_2}$, h	λ_2, h^{-1}	*CL*, mL/min, Total	*CL*, mL/min, Renal	Vd_1, L/kg	Vd_{ss}, L/kg	k_{12}, h^{-1}	k_{21}, h^{-1}	k_{10} h^{-1}
Intramuscular[a]	300-500	6-7	0.17 (0.05)	3.11 (0.21)	0.223 (0.016)	220 (63)	190 (63)	0.30 (0.11)	1.06 (0.11)	2.19 (1.05)	1.24 (0.30)	0.73 (0.34)
Intravenous[b]	100	1.3-1.7		6.75 (1.78)		415 (84)	310 (91)	0.53 (0.10)	2.72 (0.66)	2.29 (0.91)	0.703 (0.213)	0.686 (0.197)
Intramuscular[c]	50	0.78	0.158 (0.063)	6.20 (1.47)	0.116 (0.0203)	96.8 (23.2)	88.7 (19.0)	0.157 (0.0822)	0.651 (0.171)	2.64 (1.08)	0.707 (0.141)	0.662 (0.302)
	100	1.38	0.232 (0.130)	6.94 (3.39)	0.113 (0.0307)	85.2 (21.5)	80.0 (18.5)	0.136 (0.0494)	0.609 (0.207)	2.41 (1.02)	0.663 (0.246)	0.644 (0.377)
	200	2.74	0.240 (0.147)	7.09 (2.98)	0.108 (0.0290)	87.3 (22.9)	80.4 (22.7)	0.141 (0.0577)	0.655 (0.192)	2.53 (1.37)	0.652 (0.209)	0.600 (0.231)
Mean			0.220 (0.120)	6.74 (2.67)	0.112 (0.0262)	89.8 (22.3)	83.0 (19.8)	0.145 (0.063)	0.639 (0.184)	2.53 (1.13)	0.674 (0.197)	0.635 (0.298)

[a] Blood (0-10 h) and urine (0-24 h) were collected from 1 male and 11 female subjects; the amount of drug was determined by quantitative TLC with UV detection (plasma). The data were fit to a one- or two-compartment model (5, 6). [b] Blood and urine were collected for 0-36 h from three male and three female subjects; the amount of drug was determined by HPLC with fluorometric detection (serum). The data were fit to a two- or three-compartment model (3). [c] Blood (0-30 h) and urine (0-48 h) were collected from nine male subjects; the amount of drug was determined by HPLC with UV detection (plasma). The data were fit to a two-compartment model (this research).

Volumes of Distribution—Large variations were apparent in the values reported by the authors for the volume of distribution of the central compartment and for the volume of distribution at steady state (Table V). The apparent volume of distribution of the central compartment (Vd_1) was very close to extracellular water (0.15 to 0.20 L/kg) in humans; the apparent volumes of distribution at steady state (Vd_{ss}) of 1.06 and 0.639 L/kg seemed to correspond with total body water, which ranges from 0.45 to 0.65 L/kg in humans. The slightly higher value reported by Imondi *et al.* (25), 1.8 L/kg, is overestimated. Since sulpiride was administered orally, the calculated volume of distribution (Vd/F), would give a value of 0.6 L/kg for Vd if the absorption coefficient F were 0.30.

These results are in accordance with the very low lipophilic properties of sulpiride, which should lead to a poor distribution in tissues and thus to a volume of distribution close to total body water volume. The high value of Vd_1 (0.53 L/kg) and Vd_{ss} (2.7 L/kg) found by Wiesel *et al.* (3) are related to the low plasma levels found either after oral or intravenous administration by these authors. It could be that within-subject variations of the distribution parameters gave rise to these differences between the populations studied. In our earlier study (5, 6), all the subjects but one were females and the volume of distribution was significantly higher than in the recent study conducted exclusively in male subjects. In three female and one male subject, the distribution phase was not apparent after intramuscular administration (5, 6). There could be sex-related variations in the distribution pattern of sulpiride in humans.

Total Elimination from Plasma—*Half-Life of Elimination*—The half-life of sulpiride elimination from the body was evaluated either from plasma data by the slope of the log-linear terminal part of the plasma concentration *versus* time curve (Table V), from the urinary excretion rate *versus* time curve plot (rate plot), and the amount remaining to be excreted *versus* time plot (σ^- plot) (Table VI). The mean values obtained by these three methods were very close and ranged from 6 to 8 h.

Wiesel *et al.* (3) obtained elimination half-lives of 6.75 h (λ_2) and 7.15 h (dU/dt) after intravenous administration. In this study, we report elimination half-lives after intramuscular administration of 6.87 h (λ_2), 5.58 h (dU/dt), and 5.68 h ($U_\infty - U$). These values, obtained either after intramuscular or intravenous administration, with a sample collection lasting up to 36 h, should be the closest values to the true ones. When plasma and urine samples were collected for a shorter period than in these studies, the terminal log-linear part of the curves was not reached and the half-life was underestimated (the rate constant was overestimated). Bres *et al.* (5, 6) reported elimination half-lives after intramuscular administration of 3.11 h (λ_2), 3.73 h (dU/dt), and 3.33 h ($U_\infty - U$), while after oral administration these values were 3.0, 3.6, and 3.0 h, respectively (Table VI).

Total Clearance—Total plasma clearances, estimated from the ratio of dose/AUC were 415 mL/min after intravenous administration (3) and 220 mL/min (5, 6) or 89.8 mL/min (this study) after intramuscular administration. The large differences observed in these three studies were related to variations in the volumes of distribution at steady state (Table V).

Excretion in Urine in the Form of Unchanged Sulpiride—*Extent of Sulpiride Elimination in Urine*—Sulpiride is mainly eliminated from plasma by the renal route. After intravenous administration of the drug, Wiesel *et al.* (3) found 72.3 ± 8.9% of the administered dose in urine over a 36-h period. After intramuscular administration, Bres *et al.* (5, 6) found 82.9 ± 7.4% of administered dose in urine (24-h collection). In this study, 93.1 ± 6.6% was found in urine, almost all the administered dose (48-h collection; Table VI).

Rate Constant of Elimination—The rate of elimination of sulpiride in urine was identical to the rate of disappearance of sulpiride from the plasma. The fraction of administered dose eliminated unchanged in urine is close to 1.0; nevertheless, another route of elimination had to be introduced for the simulations (Scheme II, with $k_{10} = k_{13} + k_{14}$).

Renal Clearance—The renal clearances of sulpiride were 310 mL/min after intravenous administration (3) and 190 mL/min (5, 6) or 83.0 mL/min (this study) after intramuscular administration. The large variations observed in these studies and the interindividual variations, estimated from the standard deviations, are mainly related to changes in the sulpiride apparent volume of distribution within subjects. The renal clearance of sulpiride, while slightly lower than the total clearance, is a good reflection of the sulpiride total

Table VI—Sulpiride Elimination[a]

Route of Administration	Dose, mg	Dose, mg/kg	k_e, h^{-1} $\frac{dU/dt}{U_\infty - U}$		$t_{1/2}$, h $\frac{dU/dt}{U_\infty - U}$		U_∞, %
Intramuscular	300-500	6 to 7	0.186	0.208	3.73	3.33	82.9 ± 7.4
Intravenous	100	1.3 for men 1.7 for women	0.097		7.15		72.3 ± 8.9
Intramuscular	50	0.78	0.144	0.143	4.95	5.21	92.3 ± 6.8
	100	1.38	0.122	0.124	6.09	5.95	94.1 ± 6.2
	200	2.74	0.111	0.124	5.77	5.92	91.8 ± 7.5
Mean			0.131	0.157	5.58	5.68	93.1 ± 6.6

[a] See Table V for collection procedures.

clearance from plasma. Since renal clearances of sulpiride and creatinine were simultaneously evaluated in all subjects in this study (Table I), we attempted to correlate these two values. With the large intraindividual variability (Table II, Fig. 5) in sulpiride renal clearance, it was not possible to find a positive correlation with creatinine clearance, but subjects 3 and 9 who had the highest sulpiride clearances also had the highest creatinine clearances.

REFERENCES

(1) A. Benakis and Ch. Rey, *J. Pharmacol. (Paris)*, **77**, 367 (1976).

(2) Y. Stefan and A. Benakis, *J. Pharmacol. (Paris)*, **77**, 379 (1976).

(3) F. A. Wiesel, G. Alfredsson, M. Ehrnebo, and G. Sedvall, *Eur. J. Clin. Pharmacol.*, **17**, 385 (1980).

(4) G. Alfredsson, G. Sedvall, and F. A. Wiesel, *J. Chromatogr.*, **164**, 187 (1979).

(5) J. Bres, F. Bressolle, M. D. Blanchin, and E. Rechencq, Congrès hispano-français de Biopharmacie et de Pharmacocinétique, Barcelona, Spain, April 1979, vol. III, pp. 23–38.

(6) J. Bres, F. Bressolle, D. Monsoncles, and M. D. Blanchin, Premier Congrès Européen de Biopharmacie et de Pharmacocinétique, Clermont-Ferrand, France, April 1981, vol. II, pp. 335–345.

(7) M. D. Blanchin, Thèse de 3ème Cycle, Montpellier, France, July 1981.

(8) J. Bres, F. Bressolle, M. D. Blanchin, and E. Rechencq, Congrès hispano-français de Biopharmacie et de Pharmacocinétique, Barcelona, Spain, April 1979, vol. III, pp. 11–23.

(9) N. Verbiese Genard, M. Hanocq, and L. Molle, *Chromatogr. Symp. Sci.*, **1**, 79 (1979).

(10) N. Verbiese Genard, M. Hanocq, M. Van Damme, and L. Molle, *Int. J. Pharm.*, **2**, 155 (1979).

(11) N. Verbiese Genard, M. Hanocq, and L. Molle, *J. Pharm. Belg.*, **1**, 24 (1980).

(12) T. Kleimola, O. Leppanen, J. Kanto, R. Mantyla, and E. Syvalahti, *Ann. Clin. Res.*, **8**, 104 (1976).

(13) J. K. Salminen, V. Lehtonen, H. Allonen, and J. Kanto, *Curr. Ther. Res.*, **27**, 109 (1980).

(14) L. Bjerkenstedt, C. Harnryd, and G. Sedvall, *Psychopharmacology*, **64**, 135 (1979).

(15) F. Bressolle, J. Bres, S. Brun, and E. Rechencq, *J. Chromatogr.*, **174**, 421 (1979)

(16) J. Bres, A. F. Gaillot, D. Monsoncles, J. C. Penochet, and G. Vidal, "Progress in Clinical Pharmacy," vol. III, H. Turraka and E. Van Der Kleijn, Eds., Elsevier North Holland, 1981, pp. 61–70.

(17) F. Bressolle, J. Bres, E. Fuseau, and A. M. Siouffi, *J. Pharm. Clin.*, **2**, 127 (1982).

(18) M. Rowland and T. N. Tozer, "Clinical Pharmacokinetics," Lea and Febiger, Philadelphia, Pa., 1980.

(19) M. Gibaldi and D. Perrier, in "Drugs and the Pharmaceutical Sciences," Vol. I, J. Swarbrick, Ed., Dekker, New York, N.Y., 1975.

(20) L. B. Sheiner, "ELSFIT Users Manual," Division of Clinical Pharmacology, University of California, San Francisco, 1981.

(21) R. Gomeni, "The Impact of Computer Technology on Drug Information," P. Manell and S. G. Johansson, Eds., Elsevier North Holland, 1982, p. 32.

(22) L. B. Sheiner, B. Rosenberg, and K. L. Melmon, *Comput. Biomed. Res.*, **5**, 441 (1972).

(23) H. D. Vinod and A. Ullah, "Recent Advances in Regression Methods," Dekker, New York, N.Y., 1981, pp. 1–9.

(24) C. Gomeni and R. Gomeni, *Comput. Biomed. Res.*, **11**, 345 (1978).

(25) A. R. Imondi, A. S. Alam, J. J. Brennan, and L. M. Hagerman, *Arch. Int. Pharmacodyn.*, **232**, 79 (1978).

(26) A. S. Alam, A. R. Imondi, J. Udinsky, and L. M. Hagerman, *Arch. Int. Pharmacodyn.*, **242**, 4 (1979).

ACKNOWLEDGMENTS

The authors gratefully acknowledge support of this work by Delagrange (Paris, France).

Pulmonary Absorption and Excretion of Compounds in the Gas Phase: Theoretical Pharmacokinetic and Toxicokinetic Analysis

PETER VENG-PEDERSEN

Received September 1, 1982, from *Division of Pharmacokinetics, School of Pharmacy, Purdue University, West Lafayette, IN 47907.* Accepted for publication July 29, 1983. Present address: College of Pharmacy, University of Iowa, Iowa City, IA 52242.

Abstract □ Kinetic equations were derived that describe the plasma concentration of an inhaled compound during and following single or repeated regular and irregular pulmonary exposures. The equations are based on a diffusional type of input function and assume a linear disposition with a biexponential unit-impulse response. The use of linear system analysis avoids the complexity of modeling the disposition processes; yet, the effect of these processes is still accounted for mathematically. The approach, therefore, appears to be more general and rational than approaches based on linear compartmental modeling. The ways in which the kinetic equations can be readily applied in pharmacokinetic or toxicokinetic analyses to obtain valuable parameters that enable kinetic predictions of the cumulation during prolonged exposure are discussed. The toxicokinetic problem of comparing the effect of different work schedules in occupational environments with air contaminants is discussed. Formulas derived from considerations of the blood plasma kinetics are presented for the calculation of an adjustment factor for the adjustment of the contaminant threshold limit value for abnormal work weeks. The use of these formulas appears to be more rational than that of similar formulas that have been proposed.

Keyphrases □ Absorption—pulmonary, excretion, theoretical pharmacokinetic and toxicokinetic analyses □ Pharmacokinetics—pulmonary absorption and excretion, toxicokinetics □ Toxicokinetics—pulmonary absorption and excretion, pharmacokinetics

Little attention has been given to the pharmacokinetic-toxicokinetic characterization of the pulmonary absorption and excretion of compounds in the gas phase. The kinetic investigations of the volatile drugs used in general anesthetics has been limited mainly to empirical quantitative analysis of uptake, metabolism, and pulmonary excretion (1–3), without a formal mathematical, pharmacokinetic analysis of the plasma level-time profile (4, 5).

The study of pulmonary absorption kinetics is also of particular interest in environmental toxicology (6–9). Special attention has been given to the risk assessment of work place exposures to vaporous air contaminants. Of particular concern

0022-3549/84/0800-1136$01.00/0

© 1984, American Pharmaceutical Association

clearance from plasma. Since renal clearances of sulpiride and creatinine were simultaneously evaluated in all subjects in this study (Table I), we attempted to correlate these two values. With the large intraindividual variability (Table II, Fig. 5) in sulpiride renal clearance, it was not possible to find a positive correlation with creatinine clearance, but subjects 3 and 9 who had the highest sulpiride clearances also had the highest creatinine clearances.

REFERENCES

(1) A. Benakis and Ch. Rey, *J. Pharmacol. (Paris)*, **77**, 367 (1976).

(2) Y. Stefan and A. Benakis, *J. Pharmacol. (Paris)*, **77**, 379 (1976).

(3) F. A. Wiesel, G. Alfredsson, M. Ehrnebo, and G. Sedvall, *Eur. J. Clin. Pharmacol.*, **17**, 385 (1980).

(4) G. Alfredsson, G. Sedvall, and F. A. Wiesel, *J. Chromatogr.*, **164**, 187 (1979).

(5) J. Bres, F. Bressolle, M. D. Blanchin, and E. Rechencq, Congrès hispano-français de Biopharmacie et de Pharmacocinétique, Barcelona, Spain, April 1979, vol. III, pp. 23–38.

(6) J. Bres, F. Bressolle, D. Monsoncles, and M. D. Blanchin, Premier Congrès Européen de Biopharmacie et de Pharmacocinétique, Clermont-Ferrand, France, April 1981, vol. II, pp. 335–345.

(7) M. D. Blanchin, Thèse de 3ème Cycle, Montpellier, France, July 1981.

(8) J. Bres, F. Bressolle, M. D. Blanchin, and E. Rechencq, Congrès hispano-français de Biopharmacie et de Pharmacocinétique, Barcelona, Spain, April 1979, vol. III, pp. 11–23.

(9) N. Verbiese Genard, M. Hanocq, and L. Molle, *Chromatogr. Symp. Sci.*, **1**, 79 (1979).

(10) N. Verbiese Genard, M. Hanocq, M. Van Damme, and L. Molle, *Int. J. Pharm.*, **2**, 155 (1979).

(11) N. Verbiese Genard, M. Hanocq, and L. Molle, *J. Pharm. Belg.*, **1**, 24 (1980).

(12) T. Kleimola, O. Leppanen, J. Kanto, R. Mantyla, and E. Syvalahti, *Ann. Clin. Res.*, **8**, 104 (1976).

(13) J. K. Salminen, V. Lehtonen, H. Allonen, and J. Kanto, *Curr. Ther. Res.*, **27**, 109 (1980).

(14) L. Bjerkenstedt, C. Harnryd, and G. Sedvall, *Psychopharmacology*, **64**, 135 (1979).

(15) F. Bressolle, J. Bres, S. Brun, and E. Rechencq, *J. Chromatogr.*, **174**, 421 (1979)

(16) J. Bres, A. F. Gaillot, D. Monsoncles, J. C. Penochet, and G. Vidal, "Progress in Clinical Pharmacy," vol. III, H. Turraka and E. Van Der Kleijn, Eds., Elsevier North Holland, 1981, pp. 61–70.

(17) F. Bressolle, J. Bres, E. Fuseau, and A. M. Siouffi, *J. Pharm. Clin.*, **2**, 127 (1982).

(18) M. Rowland and T. N. Tozer, "Clinical Pharmacokinetics," Lea and Febiger, Philadelphia, Pa., 1980.

(19) M. Gibaldi and D. Perrier, in "Drugs and the Pharmaceutical Sciences," Vol. I, J. Swarbrick, Ed., Dekker, New York, N.Y., 1975.

(20) L. B. Sheiner, "ELSFIT Users Manual," Division of Clinical Pharmacology, University of California, San Francisco, 1981.

(21) R. Gomeni, "The Impact of Computer Technology on Drug Information," P. Manell and S. G. Johansson, Eds., Elsevier North Holland, 1982, p. 32.

(22) L. B. Sheiner, B. Rosenberg, and K. L. Melmon, *Comput. Biomed. Res.*, **5**, 441 (1972).

(23) H. D. Vinod and A. Ullah, "Recent Advances in Regression Methods," Dekker, New York, N.Y., 1981, pp. 1–9.

(24) C. Gomeni and R. Gomeni, *Comput. Biomed. Res.*, **11**, 345 (1978).

(25) A. R. Imondi, A. S. Alam, J. J. Brennan, and L. M. Hagerman, *Arch. Int. Pharmacodyn.*, **232**, 79 (1978).

(26) A. S. Alam, A. R. Imondi, J. Udinsky, and L. M. Hagerman, *Arch. Int. Pharmacodyn.*, **242**, 4 (1979).

ACKNOWLEDGMENTS

The authors gratefully acknowledge support of this work by Delagrange (Paris, France).

Pulmonary Absorption and Excretion of Compounds in the Gas Phase: Theoretical Pharmacokinetic and Toxicokinetic Analysis

PETER VENG-PEDERSEN

Received September 1, 1982, from *Division of Pharmacokinetics, School of Pharmacy, Purdue University, West Lafayette, IN 47907.* Accepted for publication July 29, 1983. Present address: College of Pharmacy, University of Iowa, Iowa City, IA 52242.

Abstract □ Kinetic equations were derived that describe the plasma concentration of an inhaled compound during and following single or repeated regular and irregular pulmonary exposures. The equations are based on a diffusional type of input function and assume a linear disposition with a biexponential unit-impulse response. The use of linear system analysis avoids the complexity of modeling the disposition processes; yet, the effect of these processes is still accounted for mathematically. The approach, therefore, appears to be more general and rational than approaches based on linear compartmental modeling. The ways in which the kinetic equations can be readily applied in pharmacokinetic or toxicokinetic analyses to obtain valuable parameters that enable kinetic predictions of the cumulation during prolonged exposure are discussed. The toxicokinetic problem of comparing the effect of different work schedules in occupational environments with air contaminants is discussed. Formulas derived from considerations of the blood plasma kinetics are presented for the calculation of an adjustment factor for the adjustment of the contaminant threshold limit value for abnormal work weeks. The use of these formulas appears to be more rational than that of similar formulas that have been proposed.

Keyphrases □ Absorption—pulmonary, excretion, theoretical pharmacokinetic and toxicokinetic analyses □ Pharmacokinetics—pulmonary absorption and excretion, toxicokinetics □ Toxicokinetics—pulmonary absorption and excretion, pharmacokinetics

Little attention has been given to the pharmacokinetic-toxicokinetic characterization of the pulmonary absorption and excretion of compounds in the gas phase. The kinetic investigations of the volatile drugs used in general anesthetics has been limited mainly to empirical quantitative analysis of uptake, metabolism, and pulmonary excretion (1–3), without a formal mathematical, pharmacokinetic analysis of the plasma level-time profile (4, 5).

The study of pulmonary absorption kinetics is also of particular interest in environmental toxicology (6–9). Special attention has been given to the risk assessment of work place exposures to vaporous air contaminants. Of particular concern

0022-3549/84/0800-1136$01.00/0

© 1984, American Pharmaceutical Association

has been the effect of the work schedule on the toxicokinetic effect (10–15). It is recognized that an assessment of the toxic effect cannot simply be determined on the basis of exposure level and total exposure time. Two different work schedules with the same exposure level and the same total hours of exposure may give substantially different plasma and tissue levels resulting in different toxic effects. Therefore, attempts have been made to predict and compare the biological effect of different work schedules by using the exposure limits established by the U.S. government, since these limits are based on exposures of a normal work week schedule (16, 17). However, the formulas that have been proposed are based on a one-compartment kinetic model, despite the fact that most gases show definite biphasic kinetics (10–14). The shortcomings of conceiving the body as exhibiting properties of a single compartment are well recognized (18). The formulas that have been proposed inappropriately deal with "the body burden" (the total amount of substance in the body) instead of plasma concentration (10, 11). Not only is it virtually impossible to experimentally determine "the body burden," but it is also misleading and inaccurate to conceive the body as a "homogeneous box," ignoring the pronounced tissue distribution of volatile lipophilic substances. The formulas presented are essentially "one-point comparisons" that only consider the peak "body burdens" (10, 11). No attempts have been made to describe the complete kinetics (10, 11).

The work presented here should overcome the shortcomings of previous analyses through a rigorous pharmacokinetic analysis that is based on more realistic and rational kinetic assumptions. A linear system-analysis approach is used to account for the disposition kinetics. This model-independent system approach requires fewer assumptions and is more general than conventional classical compartmental approaches and, therefore, should provide a more rational toxicokinetic basis for the development of exposure guidelines. By giving a complete pharmacokinetic description of the plasma level–time profile during and following multiple daily or weekly exposures, the analysis allows criteria other than peak plasma levels to be considered in a toxicokinetic assessment. By using this analysis, the daily and weekly accumulation effects are isolated and considered, thereby facilitating the assessment of prolonged exposures.

THEORETICAL SECTION

Single-Exposure Kinetics—The mass transfer rate $f(t)$ of a gas into the blood plasma from inhaled air containing a gas at a concentration C_g can be described by:

$$f(t) = K_1[C_g - K_2 \cdot c(t)] \qquad (0 \le t > T) \qquad \text{(Eq. 1)}$$

during the exposure period and:

$$f(t) = 0 \qquad (t \ge T) \qquad \text{(Eq. 2)}$$

in the postexposure period.

K_1 is a positive constant, and K_2 is the air/plasma partition coefficient of the gas. The plasma concentration of the gas [$c(t)$] depends on the input rate $f(t)$, as well as the disposition (distribution, metabolism, and excretion) of the gas in the body. It is assumed that the disposition processes result in a linear kinetic system in the sense that the superposition principle holds, so that the plasma response $c(t)$ is related to the systemic input rate, $f(t)$, by[1]:

$$c(t) = \int_0^t f(u)c_\delta(t-u)du \qquad \text{(Eq. 3)}$$

where $c_\delta(t)$ is the unit impulse response.

[1] See references 19–22 for a discussion of linear system analysis in pharmacokinetics.

The pulmonary excretion of gases appears to be well characterized by a biexponential decay, indicating that the unit-impulse response can be described by a biexponential expression:

$$c_\delta(t) = Ae^{-\alpha t} + Be^{-\beta t} \qquad (A, B, \alpha, \beta > 0) \qquad \text{(Eq. 4)}$$

The choice of Eq. 4 is also supported by the fact that most volatile drugs show a biexponential response to a bolus input.

Insertion of Eqs. 1 and 4 into Eq. 3 yields:

$$c(t) = \int_0^t K_1[C_g - K_2c(u)][Ae^{-\alpha(t-u)} + Be^{-\beta(t-u)}]du \qquad (t < T)$$

$$\text{(Eq. 5)}$$

Equation 5 is recognized as a Volterra integral equation of the second kind with a convolution-type kernel and can therefore be solved by Laplace transforms giving:

$$c(t) = K_1C_g[A'(1 - e^{-\alpha' t}) + B'(a - e^{-\beta' t})] \qquad (t < T) \qquad \text{(Eq. 6)}$$

where $-\alpha'$ and $-\beta'$ are the roots of the polynomial:

$$P(s) = (s + \alpha)(s + \beta) + K_1K_2[A(s + \beta) + B(S + \alpha)] \qquad \text{(Eq. 7)}$$

[$P(-\alpha') = P(-\beta') = 0$], and A' and B' are given by:

$$A' = \frac{A(\beta - \alpha') + B(\alpha - \alpha')}{\alpha'(\beta' - \alpha')} \qquad \text{(Eq. 8)}$$

$$B' = \frac{A(\beta - \beta') + B(\alpha - \beta')}{\beta'(\alpha' - \beta')} \qquad \text{(Eq. 9)}$$

Equation 6 describes the plasma level of the gas during the exposure period only. The plasma level in the postexposure period is subsequently obtained from the following:

$$c(t) = \int_0^T K_1[C_g - K_2c(u)][Ae^{-\alpha(t-u)} + Be^{-\beta(t-u)}]du \qquad (t \ge T)$$

$$\text{(Eq. 10)}$$

where the $c(u)$ term is given by Eq. 6 by substituting t with the dummy integration variable u.

Equation 10 then gives:

$$c(t) = K_1C_gAe^{-\alpha t}\left[\frac{K_1K_2A'}{\alpha - \alpha'} \cdot e^{(\alpha-\alpha')T} + \frac{K_1K_2B'}{\alpha - \beta'} \cdot e^{(\alpha-\beta')T} + \frac{\beta}{\alpha'\beta'} \cdot e^{\alpha T}\right] + K_1C_gBe^{-\beta t}\left[\frac{K_1K_2A'}{\beta - \alpha'} \cdot e^{(\beta-\alpha')T} + \frac{K_1K_2B'}{\beta - \beta'} \cdot e^{(\beta-\beta')T} + \frac{\alpha}{\alpha'\beta'} \cdot e^{\beta T}\right] \qquad \text{(Eq. 11)}$$

where $t \ge T$. The exposure solution (Eq. 6, $t < T$) and the postexposure solution (Eq. 11, $t \ge T$) can be combined to yield the following final equation, which describes the plasma concentration of the gas at any time during or after a single pulmonary exposure:

$$c(t) = A_T(t) \cdot e^{-\alpha(t-T)_+} + B_T(t) \cdot e^{-\beta(t-T)_+} \qquad \text{(Eq. 12)}$$

where:

$$A_T(t) = K_1C_gA\left(\frac{K_1K_2A'}{\alpha - \alpha'} \cdot e^{-\alpha' t'} + \frac{K_1K_2B'}{\alpha - \beta'} \cdot e^{-\beta' t'} + \frac{\beta}{\alpha'\beta'}\right) \qquad \text{(Eq. 13)}$$

$$B_T(t) = K_1C_gB\left(\frac{K_1K_2A'}{\beta - \alpha'} \cdot e^{-\alpha' t'} + \frac{K_1K_2B'}{\beta - \beta'} \cdot e^{-\beta' t'} + \frac{\alpha}{\alpha'\beta'}\right) \qquad \text{(Eq. 14)}$$

and

$$t' = t \text{ (for } t < T) \qquad \text{(Eq. 15)}$$

$$t' = T \text{ (for } t \ge T) \qquad \text{(Eq. 16)}$$

$$(t - T)_+ = 0 \text{ (for } t < T) \qquad \text{(Eq. 17)}$$

$$(t - T)_+ = t - T \text{ (for } t \ge T) \qquad \text{(Eq. 18)}$$

$A_T(t)$ and $B_T(t)$ are constants [$A_T(T)$, $B_T(T)$] in the postexposure phase ($t \ge T$); thus, Eq. 12 predicts a simple biexponential decay in this phase. The time coefficients in the decay are equal to those of the unit-impulse-response function (Eq. 4).

If the unit-impulse-response function is described by a single-exponential expression, $Ae^{-\alpha t}$, then Eq. 12 simplifies to:

$$c(t) = A_T'(t) \cdot e^{-\alpha(t-T)_+} \qquad \text{(Eq. 19)}$$

where:

$$A_T'(t) = \frac{K_1 C_g A}{\alpha + K_1 K_2 A} \cdot (1 - e^{-(\alpha + K_1 K_2 A)t'}) \quad \text{(Eq. 20)}$$

Multiple-Exposure Kinetics—*Regular Dosing Cycle*—Consider a repeated exposure cycle consisting of an exposure period of length T followed by a postexposure period of length H. The plasma kinetics during the first cycle are described by Eq. 12. At the start of the second cycle, there is a residual concentration of gas in the plasma equal to:

$$c_2(0) = A_T(T) \cdot e^{-\alpha H} + B_T(T) \cdot e^{-\beta H} \qquad (t_r = 0) \quad \text{(Eq. 21)}$$

The notation $c_n(t_r)$ is introduced here to denote the plasma concentration of the gas in the nth exposure cycle at a time t_r, measured relative to the start of the cycle (*i.e.*, relative to the start of the most recent exposure period).

Due to the superposition principle of linear systems, the plasma concentration of the gas in the second cycle is given by:

$$c_2(t_r) = A_T(T) \cdot e^{-\alpha(H+t_r)} + B_T(T) \cdot e^{-\beta(H+t_r)} + A_T(t_r) \cdot e^{-\alpha(t_r-T)+} + B_T(t_r) \cdot e^{-\beta(t_r-T)+} \quad \text{(Eq. 22)}$$

Thus, the residual plasma concentration at the start of the third exposure cycle is:

$$c_3(0) = A_T(T) \cdot e^{-\alpha(H+L)} + B_T(T) \cdot e^{-\beta(H+L)} + A_T(T) \cdot e^{-\alpha H} + B_T(T) \cdot e^{-\beta H} \quad \text{(Eq. 23)}$$

where L is the length of the exposure cycle:

$$L = T + H \quad \text{(Eq. 24)}$$

By deduction from Eqs. 21–23, it is concluded that:

$$c_n(t_r) = A_T(T) \cdot e^{-\alpha(H+t_r)} \sum_{j=0}^{n-2} e^{-jL\alpha} + B_T(t) \cdot e^{-\beta(H+t_r)} \sum_{j=0}^{n-2} e^{-jL\beta} + A_T(t_r) \cdot e^{-\alpha(t_r-T)+} + B_T(t_r) \cdot e^{-\beta(t_r-T)+} \quad \text{(Eq. 25)}$$

Equation 25 simplifies to the following final equation that describes the plasma concentration of the gas at any time (t_r) in any exposure cycle (n) during (or any time after) a regular repeated pulmonary exposure:

$$c_n(t_r) = \frac{1 - e^{-(n-1)L\alpha}}{1 - e^{-L\alpha}} A_T(T) \cdot e^{-\alpha(H+t_r)} + \frac{1 - e^{-(n-1)L\beta}}{1 - e^{-L\beta}} B_T(T) \cdot e^{-\beta(H+t_r)} + A_T(t_r) \cdot e^{-\alpha(t_r-T)+} + B_T(t_r) \cdot e^{-\beta(t_r-T)+} \quad \text{(Eq. 26)}$$

To simplify the notation and better conceptualize the cumulative effect of multiple exposures, it is convenient to introduce and define the function:

$$\phi_i(x) = \frac{1 - e^{-ix}}{1 - e^{-x}} = \sum_{j=0}^{i-1} e^{-jx} \quad \text{(Eq. 27)}$$

It can be seen in Eq. 26 that the first two terms of this equation represent the cumulation from the previous $(n-1)$ exposure cycles. Therefore, it appears to be more descriptive to present Eq. 26 in the following simplified form:

$$c_n(t_r) = A_T(t_r) \cdot e^{-\alpha(t_r-T)+} + B_T(t_r) \cdot e^{-\beta(t_r-T)+} + P_{n-1}(t_r) \quad \text{(Eq. 28)}$$

$P_{n-1}(t_r)$, the cumulation from the previous exposure cycles can, according to Eqs. 26 and 27, be simplified as:

$$P_{n-1}(t_r) = \phi_{n-1}(L\alpha) \cdot A_T(T) \cdot e^{-\alpha(H+t_r)} + \phi_{n-1}(L\beta) \cdot B_T(T) \cdot e^{-\beta(H+t_r)} \quad \text{(Eq. 29)}$$

Irregular Dosing Cycle Case.—In the context of occupational exposure to toxic substances, Eq. 28 is limited to a description of the kinetics during and following exposure to a gas for a single work week (or any fraction thereof). If there is a significant residual concentration left after the exposure-free weekend, then Eq. 28 should not be used for the second or subsequent work weeks. The following derivation includes cumulations from previous work weeks.

Consider a work schedule consisting of N working days (*i.e.*, N exposure cycles) and M nonworking days ($N + M = 7$). On each working day, the subject is exposed for T hours to a constant concentration (C_g) of a gas in the air. There are H hours between the exposure periods ($T + H = L = 24$), except for the period of nonworking days where there are ($H + M \cdot L$) hours without exposure. According to the superposition principle of linear systems, the plasma gas concentration at time t_r in the nth exposure cycle[2] in the mth work week is:

$$c_{n,m}(t_r) = c_n(t_r) + Q_{m-1}(t_r) \quad \text{(Eq. 30)}$$

where $c_n(t_r)$ is given by Eq. 28, and $Q_{m-1}(t_r)$ is given by Eq. 38. The function $Q_{m-1}(t_r)$ in Eq. 30, which is given by:

$$Q_{m-1}(t_r) = \sum_{i=1}^{m-1} c_N[(M+1)L + (m-i-1)7L + (n-1)L + t_r] \quad \text{(Eq. 31)}$$

represents the cumulations from the $(m-1)$ previous weeks. The residue from the exposure in week i ($i = 1, \ldots, m-1$) is derived as follows. The concentration left from this exposure is $c_N(t_i)$, where t_i is the time elapsed since the start of the last exposure cycle of the ith work week, and $c_N(\ )$ is given by Eq. 28 substituting n with N where N is the total number of exposure cycles in the work week. The time span t_i can be considered to consist of the following three components:

1. $(M+1)L$ is the time from the start of the last exposure cycle of week i to the start of the first exposure cycle of week $(i+1)$.
2. $(m-i-1)7L$ is the time from the start of the first exposure cycle of week $(i+1)$ to the start of the first exposure cycle of week m.
3. $(n-1)L + t_r$ is the time from the start of the first exposure cycle of week m to the current time t_r, where t_r as previously defined is measured relative to the start of the current exposure cycle, *i.e.*, cycle n. Thus:

$$t_i = (M+1)L + (m-i-1)7L + (n-1)L + t_r \quad \text{(Eq. 32)}$$

which is in agreement with Eq. 31.

The time span t_i stretches beyond the last exposure period of week i. Thus, according to Eqs. 28, 29, and 16, $c_N(t_i)$ becomes:

$$c_N(t_i) = A_T(T) \cdot e^{-\alpha(t_i-T)} + B_T(T) \cdot e^{-\beta(t_i-T)} + \phi_{N-1}(L\alpha) \cdot A_T(T) \cdot e^{-\alpha(H+t_i)} + \phi_{N-1}(L\beta) \cdot B_T(T) \cdot e^{-\beta(H+t_i)} \quad \text{(Eq. 33)}$$

According to $L = T + H$, Eq. 33 can be written:

$$c_N(t_i) = [1 + e^{-L\alpha} \cdot \phi_{N-1}(L\alpha)] A_T(T) \cdot e^{\alpha T} \cdot e^{-\alpha t_i} + [1 + e^{-L\beta} \cdot \phi_{N-1}(L\beta)] B_T(T) \cdot e^{\beta T} \cdot e^{-\beta t_i} \quad \text{(Eq. 34)}$$

This equation can be further simplified[3]:

$$c_N(t_i) = \phi_N(L\alpha) \cdot A_T(T) \cdot e^{-\alpha(t_i-T)} + \phi_N(L\beta) \cdot B_T(T) \cdot e^{-\beta(t_i-T)} \quad \text{(Eq. 35)}$$

To simplify the expression for the cumulation function $Q_{m-1}(t_r)$, it is convenient to rewrite the summation in Eq. 31 so that the formula in Eq. 27 can be employed:

$$Q_{m-1}(t_r) = \sum_{i=0}^{m-2} c_N(x_i) \quad \text{(Eq. 36)}$$

where:

$$x_i = (M-n)L + (m-2)7L - i7L + t_r \quad \text{(Eq. 37)}$$

When t_i is substituted by x_i in Eq. 35 and this equation is subsequently inserted in Eq. 36, the following final expression for the cumulation term in Eq. 30 is obtained:

$$Q_{m-1}(t_r) = \phi_N(L\alpha) \cdot \phi_{m-1}(7L\alpha) \cdot e^{-(M+n)L\alpha} \cdot A_T(T) \cdot e^{-\alpha(t_r-T)} + \phi_N(L\beta) \cdot \phi_{m-1}(7L\beta) \cdot e^{-(M+n)L\beta} \cdot B_T(T) \cdot e^{-\beta(t_r-T)} \quad \text{(Eq. 38)}$$

In deriving Eq. 37, the following property of the ϕ function was used:

$$e^{-(i-1)x} \cdot \phi_i(-x) = \phi_i(x) \quad \text{(Eq. 39)}$$

RESULTS AND DISCUSSION

The analysis described above is based on certain kinetic assumptions. It is assumed that the compound is present in the inhaled air at a constant concentration during the exposure. It is also assumed that the transport of the agent into the pulmonary blood plasma is proportional to the difference between the partial pressures of the agent in the inhaled air and in the blood plasma. It is assumed that the compound shows a linear disposition in the body in the sense that the linear superposition principle holds, so that input and plasma level response are functionally related through a convolution. Furthermore, it is assumed that the system is time invariant with a unit-impulse response that is well approximated by a biexponential expression. These assumptions that form the basis for the fundamental Eqs. 1–4 appear fairly well justified. The kinetics of gas diffusion is well understood, and many drugs and compounds have been shown to exhibit a linear disposition. In fact, a linear disposition is expected most often for compounds that are only slightly me-

[2] Note that the nth working day usually contains part of exposure cycle $(n-1)$ and cycle n, so it would be misleading in general to define n as the nth working day.

[3] Note that the ϕ function has the simple progression formula $e^{-x}\phi_{i-1}(x) = \phi_i(x) - 1$.

tabolized, such as the volatile, lipophilic compounds used in general anesthetics. The choice of a biexponential expression to represent the unit-impulse response appears to be appropriate, since this leads to kinetic equations that agree with the typical biexponential pulmonary excretion decay that is often observed. A biexponential expression also agrees with the elimination behavior most frequently seen in pharmacokinetic studies. The very distinct advantages of using a linear system approach instead of a classical compartmental approach have been discussed previously (19–22).

Three main equations have been derived that describe the plasma concentration of a gas at any time during or after (*a*) a single pulmonary exposure (Eq. 12), (*b*) a series of regular, constant exposures (Eq. 28), and (*c*) 1 or more weeks of exposures to a gas during the working days of the week (Eq. 30).

Single-Exposure Kinetics—The kinetic equation for a single pulmonary exposure (Eq. 12) is of particular pharmacokinetic interest, as it deals with the type of drug exposure found in general anesthetics. The equation also forms the basis for the multiexposure equations (Eqs. 28 and 30) that are of special toxicokinetic interest. An important use of the equation is in nonlinear regression analysis of single exposure data to obtain useful pharmacokinetic parameters. The data can be obtained either from a blood gas analysis or from excretion data obtained from the postexposure phase by analyzing the expired air for the gas.

Kinetic Analysis Based on Sampling of Expired Air—Pulmonary excretion data are typically in the form of the cumulative amount of gas excreted at various times, $M(t)$. According to Eq. 1, the rate of pulmonary excretion in the postexposure phase is $K_1K_2 \cdot c(t)$. Integration of Eq. 12 gives:

$$M(t) = \int_T^t K_1K_2 \cdot c(t)dt = K_1K_2 \frac{A_T(t)}{\alpha}[1 - e^{-\alpha(t-T)}] + K_1K_2 \frac{B_T(T)}{\beta}[1 - e^{-\beta(t-T)}] \qquad (t \geq T) \quad \text{(Eq. 40)}$$

In its simplest form, this equation is uniquely defined by only four quantities [$\alpha, \beta, K_1K_2 \cdot A_T(T)$, and $K_1K_2 \cdot B_T(T)$]. Therefore, it is not possible to determine all of the six basic parameters (*Appendix*) from pulmonary excretion data alone. However, Eq. 40 allows the two important parameters, α and β, to be accurately determined.

Although general kinetic predictions require that all six basic parameters (see *Appendix*) be determined, a closer analysis of Eq. 40 reveals that some important predictions can still be made from pulmonary excretion data alone. For example, it can be predicted how much the plasma concentration in the postexposure phase increases in multiple exposures relative to that resulting from a single exposure, *i.e.*, the ratio $c_n(t_r)/c(t_r)$, where $t_r > T$, can be predicted. To prove this, it is convenient to rewrite Eq. 28 in the following form[3]:

$$c_n(t_r) = \phi_n(L\alpha) \cdot A_T(T) \cdot e^{-\alpha(t_r-T)} + \phi_n(L\beta) \cdot B_T(T) \cdot e^{-\beta(t_r-T)} \qquad (t_r \geq T) \quad \text{(Eq. 41)}$$

By multiplying this equation and Eq. 12 ($t \geq T$) by K_1K_2, the following ratio is obtained:

$$\frac{c_n(t_r)}{c(t_r)} = \frac{\phi_n(L\alpha) \cdot [K_1K_2A_T(T)] \cdot e^{-\alpha(t_r-T)} + \phi_n(L\beta) \cdot [K_1K_2B_T(T)] \cdot e^{-\beta(t_r-T)}}{[K_1K_2A_T(t)] \cdot e^{-\alpha(t_r-T)} + [K_1K_2B_T(T)] \cdot e^{-\beta(t_r-T)}} \qquad (t_r \geq T) \quad \text{(Eq. 42)}$$

Fitting Eq. 40 to pulmonary excretion data yields values for $\alpha, \beta, K_1K_2 \cdot A_T(T)$, and $K_1K_2 \cdot B_T(T)$, so that Eq. 42 can be calculated at any time $t_r > T$ for any values of n and L. Thus, excretion data from a single exposure provide quite extensive and valuable information about the plasma accumulation of the compound. In particular, such data allow a comparison of the maximum plasma concentration by letting $t_r = T$ in Eq. 42:

$$\frac{\max c_n(t_r)}{\max c(t_r)} = \frac{c_n(T)}{c(T)} = \frac{\phi_n(L\alpha) \cdot [K_1K_2 \cdot A_T(T)] + \phi_n(L\beta) \cdot [K_1K_2 \cdot B_T(T)]}{[K_1K_2 \cdot A_T(T)] + [K_1K_2 \cdot B_T(T)]} \quad \text{(Eq. 43)}$$

A comparison of the minimum values is achieved by letting $t_r = L = (T + H)$ in Eq. 42, noting that $\min c_{n+1}(t_r) = c_{n+1}(0) = c_n(L)$:

$$\frac{\min c_{n+1}(t_r)}{c(L)} = \frac{\phi_n(L\alpha) \cdot [K_1K_2 \cdot A_T(T)] \cdot e^{-\alpha H} + \phi_n(L\beta) \cdot [K_1K_2 \cdot B_T(T)] \cdot e^{-\beta H}}{[K_1K_2 \cdot A_T(T)] \cdot e^{-\alpha H} + [K_1K_2 \cdot B_T(T)] \cdot e^{-\beta H}} \quad \text{(Eq. 44)}$$

Although the above analyses (Eqs. 42 and 43) are limited to the postexposure phase ($t \geq T$), the characterization is complete enough to get an adequate assessment of the accumulation tendency of the compound. It is particularly valuable to be able to determine the relative change in the maximum (Eq. 43) and minimum (Eq. 44) plasma level concentrations.

Kinetic Analysis Based on Blood Sampling—Plasma level data in the exposure phase provide a more comprehensive kinetic characterization than pulmonary excretion data. All six basic kinetic parameters are determined by fitting Eq. 6 to the plasma level data[4]. Thus, once these parameters are determined by a suitable nonlinear regression technique, then predictions can be made as to which plasma-time profiles or accumulations can be reasonably expected from other single or multiple exposures (Eqs. 12, 28, and 30).

If the plasma level data are obtained only in the postexposure phase ($t \geq T$), then it is not possible to determine more than two (α and β) of the six basic parameters. However, despite this, some useful predictions can still be made.

The postexposure phase, according to Eq. 12, is described by:

$$c(t) = A_T(T) \cdot e^{-\alpha(t-T)} + B_T(T) \cdot e^{-\beta(t-T)} \qquad (t \geq T) \quad \text{(Eq. 45)}$$

By fitting this equation to the data, values for $\alpha, \beta, A_T(T)$, and $B_T(T)$ are obtained which, according to Eqs. 42 and 43, permit the following predictions to be made from the single exposure response, $c(t)$:

$$c_n(t_r) = \left[\frac{\phi_n(L\alpha) \cdot A_T(T) \cdot e^{-\alpha(t_r-T)} + \phi_n(L\beta) \cdot B_T(T) \cdot e^{-\beta(t_r-t)}}{A_T(T) \cdot e^{-\alpha(t_r-T)} + B_T(T) \cdot e^{-\beta(t_r-T)}}\right] c(t) \qquad (t \geq T) \quad \text{(Eq. 46)}$$

$$\max c_n(t_r) = c_n(T) = \left[\frac{\phi_n(L\alpha) \cdot A_T(T) + \phi_n(L\beta) \cdot B_T(T)}{A_T(T) + B_T(T)}\right] c(t) \quad \text{(Eq. 47)}$$

$$\min c_{n+1}(t_r) = \left[\frac{\phi_n(L\alpha) \cdot A_T(T) \cdot e^{-\alpha H} + \phi_n(L\beta) \cdot B_T(T) \cdot e^{-\beta H}}{A_T(T) \cdot e^{-\alpha H} + B_T(T) \cdot e^{-\beta H}}\right] c(L) \quad \text{(Eq. 48)}$$

Thus, although pulmonary excretion data in the postexposure phase allow only relative comparisons (Eqs. 42–44), plasma data obtained in the same phase permit absolute predictions (Eqs. 46–48). In both cases, the predictions can only be made for exposure duration(s) of the same length, T, as in the single-exposure experiment. This limitation is not found when data are obtained during the exposure. Equations analogous to Eqs. 42–48 are readily obtained from Eq. 30 to extend the analysis to irregular exposures.

The single-exposure equation (Eq. 12) shows an interesting, unusual kinetic behavior. The exponential time coefficients in the exposure phase (α' and β') are different from those in the postexposure phase (α and β). This is in contrast to the equations of classical linear compartmental modeling, which have constant time coefficients (the eigenvalues). The different kinetic behavior is due to the use in pharmacokinetics of input functions that do not depend on the concentration or the amount of drug in the blood. Such input functions are likely to be encountered during oral absorption, because the GI concentration is much greater than the plasma concentration. However, in pulmonary absorption, the plasma concentration cannot be ignored in defining the input function. The concentration (partial pressure) gradient in the absorption path is considerably smaller because of an often very low concentration of the gas, a slow nonpulmonary elimination, and a rapid tissue equilibration.

The simple diffusional pulmonary absorption and excretion of a gas is intrinsically very regular and much less erratic and complex than the GI absorption and metabolism and renal excretion of regular drugs. A much smaller intra- and intersubject variability is expected. Kinetic predictions and estimations such as those described above should, therefore, be considerably more accurate than those made in general pharmacokinetic practice.

Multiple-Exposure Kinetics with Regular Dosing Cycle—Similar to the above (Eq. 40), the cumulative amount of gas excreted in the postexposure phase can be determined by integration of Eq. 41:

$$M_n(t_r) = \int_T^{t_r} K_1K_2 \cdot c_n(t)dt = \phi_n(L\alpha) \cdot \left[K_1K_2 \frac{A_T(T)}{\alpha}\right]\left[1 - e^{-\alpha(t_r-T)}\right] + \phi_n(L\beta) \cdot \left[K_1K_2 \frac{B_T(T)}{\beta}\right]\left[1 - e^{-\beta(t_r-T)}\right] \qquad (t_r \geq T) \quad \text{(Eq. 49)}$$

[4] Equation 6 is the explicit $c(t)$ function obtained directly from the implicit relationship in Eq. 5 which contains all six basic parameters. Equation 6, therefore, contains the exact same basic parameters as Eq. 5. The basic parameters are related to the macroparameters A', α', B', β' (introduced for simplification) through Eqs. 7–9. Determination of the macroparameters and their basic parameters by least-squares regression of Eq. 6 poses no real problem. The procedure is completely analogous to the determination of macroparameters and micro-rate constants in classical linear compartmental modeling, which is routinely done with well-established computer programs.

By fitting this expression to pulmonary excretion data, the same quantities [α, β, $K_1K_2 \cdot A_T(T)$, and $K_1K_2 \cdot B_T(T)$] as in the single-exposure case (Eq. 40) can be determined. Thus, the same predictions (Eqs. 42-44) can be made as before. Similarly, if plasma level data are obtained in the postexposure phase ($t_r \geq T$), then by fitting Eq. 41, the quantitites α, β, $A_T(T)$, and $B_T(T)$ are obtained and predictions can be made as before (Eqs. 46-48).

Irregular Dosing Cycle—By combining Eqs. 30, 41, and 38, the following expression for the plasma level in the postexposure phase is obtained:

$$c_{n,m}(t_r) = [\phi_n(L\alpha) + \phi_N(L\alpha) \cdot \phi_{m-1}(7L\alpha) \cdot e^{-(M+n)L\alpha}]A_T(T) \cdot e^{-\alpha(t_r-T)} + [\phi_n(L\beta) + \phi_N(L\beta) \cdot \phi_{m-1}(7L\beta) \cdot e^{-(M+n)L\beta}]B_T(T) \cdot e^{-\beta(t_r-T)} \quad (t_r \geq T) \quad \text{(Eq. 50)}$$

By integrating this equation, the cumulative amount of gas excreted in the postexposure phase can be described as:

$$M_{n,m}(t_r) = [\phi_n(L\alpha) + \phi_N(L\alpha) \cdot \phi_{m-1}(7L\alpha) \cdot e^{-(M+n)L\alpha}] \left[K_1K_2 \frac{A_T(T)}{\alpha}\right] [1 - e^{-\alpha(t_r-T)}] + [\phi_n(L\beta) + \phi_N(L\beta) \cdot \phi_{m-1}(7L\beta) \cdot e^{-(M+n)L\beta}] \left[K_1K_2 \frac{B_T(T)}{\beta}\right] [1 - e^{-\beta(t_r-T)}] \quad (t_r \geq T) \quad \text{(Eq. 51)}$$

In analogy to the regular dosing cycle case, the quantities α, β, $K_1K_2 \cdot A_T(T)$, and $K_1K_2 \cdot B_T(T)$ can be determined by fitting Eq. 51 to pulmonary excretion data. Similarly α, β, $A_T(T)$, and $B_T(T)$ are obtained from plasma level data by Eq. 50.

Thus, a kinetic analysis of data in the postexposure phase(s) of multiple exposures provides the same basic kinetic information as an analysis of postexposure data from a single exposure.

Occupational Exposure Limit Adjustment in Unusual Work Schedules—The regulatory threshold limit values (TLV) for exposure in air contaminants administered by the Occupational Safety and Health Administration are based on exposure during a normal work week of five 8-h days (16). If a person with a non-normal work week is not going to be exposed to a greater toxic burden than allowed, if may be appropriate to consider a different TLV. There is no general consensus of how to best compare the toxic burden from different exposure schemes. One approach that seems to have received particular interest is based on a comparison of the predicted maximum amount of the contaminant in the body (10). Such an approach appears to be unsatisfactory because of the experimental difficulties of estimating such a quantity and because of the kinetic misconception of treating the body as a homogeneous "box."

A more appropriate approach would be based on a comparison of peak plasma levels predicted from kinetic equations based on rational assumptions. In the comparison of two exposure schemes (denoted with superscripts I and II), it is of interest to determine a TLV adjustment factor, F, defined as follows. The maximum plasma level of the contaminant predicted for exposure scheme II with contamination level C_g^{II} is the same as that predicted for scheme I with contamination level C_g^{I} when:

$$C_g^{II}F \cdot C_g^{I} \quad \text{(Eq. 52)}$$

An analysis of Eq. 30 reveals that $c_{n,m}$ is directly proportional to the contamination level C_g. The adjustment factor F can therefore be calculated from the relationship:

$$F = \frac{\max c_{n,m}{}^{I}}{\max c_{n,m}{}^{II}} \quad \text{(Eq. 53)}$$

where

$$\max c_{n,m} = c_{N,m}(T) \quad \text{(Eq. 54)}$$

The predicted maximum plasma level, max $c_{n,m}$, can be calculated by Eq. 50:

$$\max c_{n,m} = \phi_N(L\alpha) \cdot [1 + \phi_{m-1}(7L\alpha) \cdot e^{-(M+n)L\alpha}] \cdot A_T(T) + \alpha_N(L\beta) \cdot [1 + \alpha_{m-1}(7L\beta) \cdot e^{-(M+n)L\beta}] \cdot B_T(T) \quad \text{(Eq. 55)}$$

If there is no more than one work week exposure ($m = 1$), Eq. 55 reduces to the regular dosing cycle case:

$$\max c_{n,1} = \phi_N(L\alpha) \cdot A_T(T) + \phi_N(L\beta) \cdot B_T(T) \quad \text{(Eq. 56)}$$

Although the above equations used to calculate the adjustment factor may appear complex and demanding in kinetic terms, F can be determined most simply from two sets of pulmonary excretion data; one set can be determined from a single or multiple exposure with an exposure period T^{I}, and another set can be determined with an exposure period T^{II}. By fitting a simple biexponential expression to the two sets of data, values for α, β, $K_1K_2 \cdot A_T(T)^{I}$, $K_1K_2 \cdot A_T(T)^{II}$, $K_1K_2 \cdot B_T(T)^{I}$, and $K_1K_2 \cdot B_T(T)^{II}$ can then be determined as previously discussed. In calculating F, it is important to realize that it is not necessary to know $A_T(T)$ and $B_T(T)$. It is sufficient to know the products $K_1K_2 \cdot A_T(T)$ and $K_1K_2 \cdot B_T(T)$, since in forming the ratio in Eq. 53, it makes no difference if $A_T(T)$ and $B_T(T)$ are replaced with the products.

The above analysis of the pulmonary kinetics is for the non-steady-state case. The steady-state cases are easily considered by letting n or $m = \infty$ and by noting that:

$$\phi_\infty(x) = \frac{1}{1 - e^{-x}} \quad \text{(Eq. 57)}$$

For most practical purposes, it is adequate to approximate the unit-impulse response by a biexponential equation (Eq. 4). However, the analysis can be readily extended to consider any number of exponential terms in the approximation.

APPENDIX: GLOSSARY

Basic Kinetic Parameters:

K_1	Mass transfer constant for transport of the inhaled gas into the blood plasma (Eq. 1)
K_2	Partition coefficient between air and blood plasma for the inhaled gas; $K_2c(t)$ is the partial pressure of the gas in plasma (Eq. 1)
A,B,α, β	Parameters defining the unit-impulse response of the gas in the subject, *i.e.*, the parameters describing the plasma concentration-time profile if a unit amount of the gas was introduced momentarily into the plasma (Eq. 4)

Parameters Defining the Exposure:

C_g	Concentration of gas in the inhaled air (Eq. 1)
T	Duration of single or multiple exposures (Eq. 1)
H	Duration between regular exposures (T) (Eq. 22)
t_r	Time elapsed since the start of the most recent exposure for multiple exposures (Eq. 21)
n	Number of the current exposure cycle (n runs from 1 to N each week for exposure for multiple weeks) (Eq. 25)
m	Number of the current week ($m = 1$ for exposure for the first week) (Eq. 30)
N	Total number of exposure periods in each week for exposure for multiple weeks (Eq. 31)
M	Number of exposure-free periods in each week for exposure for multiple weeks (Eq. 32)
L	$T + H$

Auxilliary Functions and Parameters:

α', β'	Parameters calculated from the fundamental parameters K_1, K_2, A, B, α, and β according to Eq. 7
A',B'	Parameters calculated from the fundamental parameters K_1, K_2, A, B, α, and β; A' and B' are calculated according to Eqs. 8 and 9 after α' and β' are calculated
$(x)_+$	Truncation function equal to x for $x \geq 0$ and 0 for $x < 0$ (Eqs. 17 and 18)
$A_T(t)/B_T(t)$	Functions introduced to simplify the mathematical notation [note that these functions are constant ($A_T(T)$,$B_T(T)$) for $t_r \geq T$ (Eqs. 13-16)]
t'	min (t,T) (Eqs. 15 and 16)
$\phi_i(x)$	Function introduced to simplify the mathematical notation (Eq. 27)
$P_{n-1}(t_r)$	Function describing the plasma accumulation of gas at time t_r resulting from the previous ($n - 1$) exposure periods (Eq. 29)
$Q_{m-1}(t_r)$	Function describing the plasma accumulation of the gas at time t_r resulting from the previous ($m - 1$) weeks of exposure (Eq. 38)

REFERENCES

(1) R. A. VanDyke, M. D. Chenoweth, and A. Van Poznak, *Biochem. Pharmacol.*, **13**, 1239 (1964).

(2) E. N. Cohen, *Anesthesiology*, **35**, 193 (1971).

(3) V. Fiserova-Bergerova and D. A. Holaday, *Drug Metab. Rev.*, **9**(1), 43 (1979).

(4) E. M. Paper and R. J. Kitz (Eds.), "Uptake and Distribution of Anesthetic Agents," McGraw-Hill, New York, N.Y., 1963.
(5) S. S. Kety, *Pharmacol. Rev.*, **3**, 1 (1951).
(6) K. Nomiyama and H. Nomiyama, *Int. Arch. Arbeitsmed.*, **32**, 75 (1974).
(7) M. E. Andersen, M. L. Gargas, R. A. Jones, and L. J. Jenkins, *Toxicol. Appl. Pharmacol.*, **54**, 100 (1980).
(8) I. Astrand, *Scand. J. Work Environ. Health*, **1**, 199 (1975).
(9) I. Astrand and F. Gamberale, *Environ. Res.*, **15**, 1 (1978).
(10) J. L. S. Hickey and C. Reist, *Am. Ind. Hyg. Assoc. J.*, **38**, 613 (1977).
(11) J. L. S. Hickey and C. Reist, *Am. Ind. Hyg. Assoc. J.*, **40**, 727 (1979).
(12) J. W. Mason and H. Dershin, *J. Occup. Med.*, **18**, 603 (1976).
(13) S. A. Roach, *Am. Ind. Hyg. Assoc. J.*, **27**, 1 (1966).
(14) S. A. Roach, *Am. Ind. Hyg. Assoc. J.*, **39**, 345 (1978).
(15) R. D. Stewart, H. H. Gay, D. S. Erley, C. L. Hake, and J. E. Peterson, *J. Occup. Med.*, **3**, 586 (1961).
(16) "Occupational Safety and Health Standards: Title 9 Code of Federal Regulations, Part 1910," Occupational Safety and Health Administration, Washington, D.C., 1976.
(17) "Threshold Limit Values for Chemical Substances and Physical Agents in the Workroom Environment with Intended Changes for 1976," American Conference Industrial Hygiene, Cincinnati, Ohio, 1976.
(18) S. Riegelman, J. C. Loo, and M. Rowland, *J. Pharm. Sci.*, **57**, 117 (1968).
(19) P. Veng-Pedersen, *J. Pharm. Sci.*, **69**, 298 (1980).
(20) P. Veng-Pedersen, *J. Pharm. Sci.*, **69**, 305 (1980).
(21) P. Veng-Pedersen, *J. Pharmacokinet. Biopharm.*, **8**, 463 (1980).
(22) D. J. Cutter, *J. Pharmacokinet. Biopharm.*, **6**, 243 (1973).

Synthesis of 4-Substituted Aminoquinoline-3-carboxylates as Potential Antimicrobial Agents

PAUL E. MARECKI *x and RONALD E. BAMBURY

Received March 7, 1983, from *SDS Biotech Corporation, World Headquarters, Concord Township, Painesville, OH 44077.* Accepted for publication July 19, 1983. *Present address: Ohio Medical Anesthetics, AIRCO Central Research Laboratories, Murray Hill, NJ 07974.

Abstract □ A series of 4-substituted aminoquinoline-3-carboxylates was prepared and evaluated for antimicrobial activity. Four of the compounds (VIII, XIII, XV, and XXIII) exhibited low activity against *Staphylococcus aureus*.

Keyphrases □ 4-Substituted aminoquinoline-3-carboxylates—synthesis, antimicrobial activity □ Antimicrobial agents—potential, 4-substituted aminoquinoline-3-carboxylates

The structural similarity between the coccidiostat buquinolate (I) (1) and the antimalarial 4-aminoquinolines (*e.g.*, chloroquin; II) (2) raised the question as to whether combination of the major functional groups of each class might lead to useful agents. This work sought to determine if the quinoline-3-carboxylate moiety of the coccidiostats could be successfully combined with 4-amino substituents, some of which have shown promise in antimalarial quinolines. A series of 4-aminoquinoline-3-carboxylates (III) was necessary, and a search of the literature revealed that these compounds had not previously been synthesized. To determine if antibacterial properties were associated with this new substituent pattern, the synthesis of several examples was undertaken.

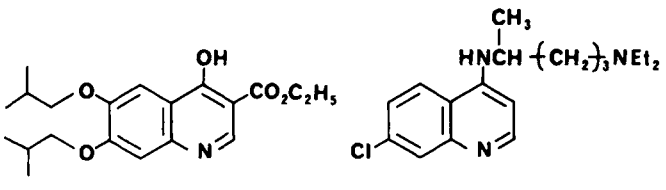

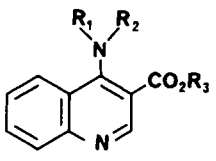

III

R_1, R_2 = H, alkyl, aralkyl
R_3 = K, C_2H_5

RESULTS AND DISCUSSION

Ethyl 4-chloroquinoline-3-carboxylate, IV (3), was the key intermediate from which the target compounds were prepared (Scheme I). The immediate precursor to IV, ethyl 4-hydroxyquinoline-3-carboxylate V, was prepared in satisfactory yield by the method of Gould and Jacobs (4) as modified by Price and Roberts (5) and by Riegel *et al.* (6). The importance of short reaction times in the preparation of V was noted (7); yields of V decrease for reaction times exceeding 30 min. Reaction of V with phosphorus oxychloride smoothly led to IV (3).

Nucleophilic displacement of the 4-chloro substituent occurred in high yield after a few hours in refluxing toluene; several cases were noted where the reaction started while still at room temperature. The relative ease of displace-

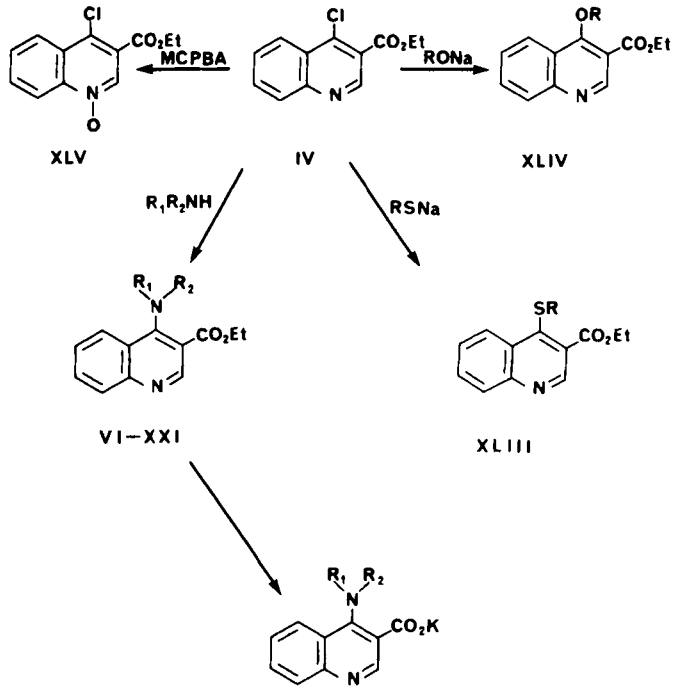

Scheme I

0022-3549/84/0800-1141$01.00/0
© 1984, American Pharmaceutical Association

(4) E. M. Paper and R. J. Kitz (Eds.), "Uptake and Distribution of Anesthetic Agents," McGraw-Hill, New York, N.Y., 1963.
(5) S. S. Kety, *Pharmacol. Rev.*, **3**, 1 (1951).
(6) K. Nomiyama and H. Nomiyama, *Int. Arch. Arbeitsmed.*, **32**, 75 (1974).
(7) M. E. Andersen, M. L. Gargas, R. A. Jones, and L. J. Jenkins, *Toxicol. Appl. Pharmacol.*, **54**, 100 (1980).
(8) I. Astrand, *Scand. J. Work Environ. Health*, **1**, 199 (1975).
(9) I. Astrand and F. Gamberale, *Environ. Res.*, **15**, 1 (1978).
(10) J. L. S. Hickey and C. Reist, *Am. Ind. Hyg. Assoc. J.*, **38**, 613 (1977).
(11) J. L. S. Hickey and C. Reist, *Am. Ind. Hyg. Assoc. J.*, **40**, 727 (1979).
(12) J. W. Mason and H. Dershin, *J. Occup. Med.*, **18**, 603 (1976).
(13) S. A. Roach, *Am. Ind. Hyg. Assoc. J.*, **27**, 1 (1966).
(14) S. A. Roach, *Am. Ind. Hyg. Assoc. J.*, **39**, 345 (1978).
(15) R. D. Stewart, H. H. Gay, D. S. Erley, C. L. Hake, and J. E. Peterson, *J. Occup. Med.*, **3**, 586 (1961).
(16) "Occupational Safety and Health Standards: Title 9 Code of Federal Regulations, Part 1910," Occupational Safety and Health Administration, Washington, D.C., 1976.
(17) "Threshold Limit Values for Chemical Substances and Physical Agents in the Workroom Environment with Intended Changes for 1976," American Conference Industrial Hygiene, Cincinnati, Ohio, 1976.
(18) S. Riegelman, J. C. Loo, and M. Rowland, *J. Pharm. Sci.*, **57**, 117 (1968).
(19) P. Veng-Pedersen, *J. Pharm. Sci.*, **69**, 298 (1980).
(20) P. Veng-Pedersen, *J. Pharm. Sci.*, **69**, 305 (1980).
(21) P. Veng-Pedersen, *J. Pharmacokinet. Biopharm.*, **8**, 463 (1980).
(22) D. J. Cutter, *J. Pharmacokinet. Biopharm.*, **6**, 243 (1973).

Synthesis of 4-Substituted Aminoquinoline-3-carboxylates as Potential Antimicrobial Agents

PAUL E. MARECKI *x and RONALD E. BAMBURY

Received March 7, 1983, from *SDS Biotech Corporation, World Headquarters, Concord Township, Painesville, OH 44077.* Accepted for publication July 19, 1983. *Present address: Ohio Medical Anesthetics, AIRCO Central Research Laboratories, Murray Hill, NJ 07974.

Abstract □ A series of 4-substituted aminoquinoline-3-carboxylates was prepared and evaluated for antimicrobial activity. Four of the compounds (VIII, XIII, XV, and XXIII) exhibited low activity against *Staphylococcus aureus*.

Keyphrases □ 4-Substituted aminoquinoline-3-carboxylates—synthesis, antimicrobial activity □ Antimicrobial agents—potential, 4-substituted aminoquinoline-3-carboxylates

The structural similarity between the coccidiostat buquinolate (I) (1) and the antimalarial 4-aminoquinolines (*e.g.*, chloroquin; II) (2) raised the question as to whether combination of the major functional groups of each class might lead to useful agents. This work sought to determine if the quinoline-3-carboxylate moiety of the coccidiostats could be successfully combined with 4-amino substituents, some of which have shown promise in antimalarial quinolines. A series of 4-aminoquinoline-3-carboxylates (III) was necessary, and a search of the literature revealed that these compounds had not previously been synthesized. To determine if antibacterial properties were associated with this new substituent pattern, the synthesis of several examples was undertaken.

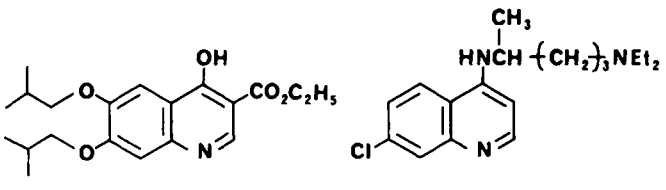

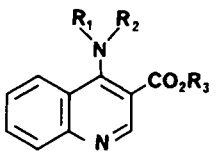

III

R_1, R_2 = H, alkyl, aralkyl
R_3 = K, C_2H_5

RESULTS AND DISCUSSION

Ethyl 4-chloroquinoline-3-carboxylate, IV (3), was the key intermediate from which the target compounds were prepared (Scheme I). The immediate precursor to IV, ethyl 4-hydroxyquinoline-3-carboxylate V, was prepared in satisfactory yield by the method of Gould and Jacobs (4) as modified by Price and Roberts (5) and by Riegel *et al.* (6). The importance of short reaction times in the preparation of V was noted (7); yields of V decrease for reaction times exceeding 30 min. Reaction of V with phosphorus oxychloride smoothly led to IV (3).

Nucleophilic displacement of the 4-chloro substituent occurred in high yield after a few hours in refluxing toluene; several cases were noted where the reaction started while still at room temperature. The relative ease of displace-

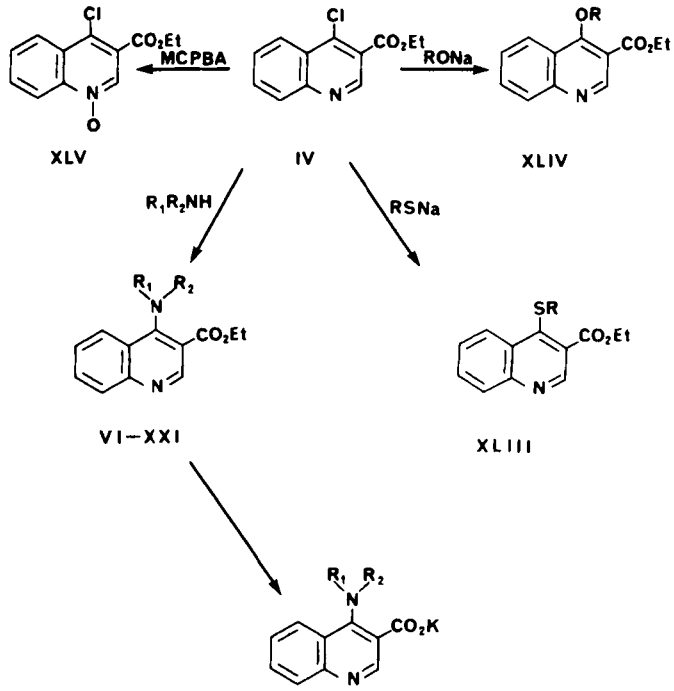

Scheme I

0022-3549/84/0800-1141$01.00/0
© 1984, American Pharmaceutical Association

Table I—Properties of 4-Aminoquinoline-3-carboxylates (III)[a]

Compound	R_1	R_2	R_3	Yield, %	mp, °C	MIC Against *Staph. aureus*, ppm
VI	H	H	C_2H_5	76	205–207	
VII[b]	C_2H_5	C_2H_5	C_2H_5	96	oil	
VIII[c]	n-C_3H_7	n-C_3H_7	C_2H_5	30	oil	62.5
IX	H	C_2H_5	C_2H_5	69	65–68	
X	H	n-C_3H_7	C_2H_5	85	63–65	
XI	H	$CH_2CH{=}CH_2$	C_2H_5	83	79–81	
XII	H	$CH_2C{\equiv}CH$	C_2H_5	68	115.0–117.5	
XIII[d]	H	C_6H_5	C_2H_5	60	102.5–104.5	50
XIV	H	$CH_2C_6H_5$	C_2H_5	84	98.5–100.5	
XV	H	CH_2-p-C_6H_4Cl	C_2H_5	68	124–126	25
XVI	H	CH_2-p-$C_6H_4NO_2$	C_2H_5	49	133–135	
XVII	$-CH_2CH_2CH_2CH_2-$		C_2H_5	68	75.5–78.0	
XVIII	$-CH_2CH_2CH_2CH_2CH_2-$		C_2H_5	95	oil	
XIX[e]	$-CH_2CH_2-O-CH_2CH_2-$		C_2H_5	91	oil	
XX	$-CH{=}CH-N{=}CH-$		C_2H_5	72	115.5–117.0	
XXI	$-CH_2CH_2NHCH_2CH_2-$		C_2H_5	76	120.0–121.5	
XXII	C_2H_5	C_2H_5 HCl Salt	C_2H_5	34	145–147	
XXIII	n-C_3H_7	n-C_3H_7 HCl Salt	C_2H_5	75	95–98	50
XXIV[f]	H	$CH_2CH_2CH_2N(CH_3)_2$ HCl Salt	C_2H_5	77	219–220	
XXV	$-CH_2CH_2CH_2CH_2CH_2-$	HCl Salt	C_2H_5	78	174.5–176.0	
XXVI[g]	$-CH_2CH_2OCH_2CH_2-$	HCl Salt	C_2H_5	67	204.5–206.0	
XXVII[g]	H	H	K	97	>350	
XXVIII[h]	C_2H_5	C_2H_5	K	66	258–260	
XXIX[i]	n-C_3H_7	n-C_3H_7	K	29	174–176	
XXX[h]	H	C_2H_5	K	90	275–277	
XXXI[h]	H	n-C_3H_7	K	94	250.0–252.5	
XXXII[j]	H	$CH_2CH{=}CH_2$	K	87	249.5–251.5	
XXXIII[k]	H	$CH_2C{\equiv}CH$	K	93	340 (dec.)	
XXXIV[l]	H	$CH_2CH_2CH_2N(CH_3)_2$	K	72	78–83	
XXXV[h]	H	C_6H_5	K	71	331–332	
XXXVI[m]	H	$CH_2C_6H_5$	K	71	293.5–295.0	
XXXVII[n]	H	CH_2-p-C_6H_4Cl	K	94	278.0–279.5	
XXXVIII[o]	$-CH_2CH_2CH_2CH_2-$		K		>250	
XXXIX[p,q]	$-CH_2CH_2CH_2CH_2CH_2-$		K	83	274–277	
XL[p]	$-CH_2CH_2OCH_2CH_2-$		K	82	>330	
XLI[o]	$-CH{=}CHN{=}CH-$		K			
XLII[n]	$-CH_2CH_2NHCH_2CH_2-$		K	74	210–213	
XLIII	C-4	$SCH_2C_6H_5$	C_2H_5	51	34–36	
XLIV[r]	C-4	OC_2H_5	C_2H_5	53	34–36	
XLV	C-4 N-oxide	Cl	C_2H_5	49	102–104 bp 125–128 (0.01 mm Hg)	
V[s]	C-4	OH	C_2H_5			
IV[t]	C-4	Cl	C_2H_5		44–46 bp 133–135 (0.5 mm Hg)	

[a] In all cases the spectral data agreed with the structure illustrated. Compounds VI–XLIII and XLV underwent elemental analyses for C, H, and N; XLIII and XLV were also analyzed for S and Cl, respectively. Unless otherwise noted, the values were within ±0.4% of the theoretical values. [b] Calc. for C, 70.56; N, 10.29. Found: C, 69.88; N, 10.91. [c] Calc. for N, 9.33; found, 10.20. [d] See Ref. 11; lit. mp 99–100°C. [e] Seven attempts were made to determine microanalytical data for this oil after evaporative distillation and vigorous pumping at high vacuum. All determinations of carbon were erratic, for unknown reasons. The spectroscopic evidence was excellent. [f] Calc. for C, 54.55; found, 54.00. [g] 0.25 H_2O. [h] 1.0 H_2O. [i] Microanalyses were done on the benzylisothiuronium salt. [j] 1.25 H_2O. [k] 1.75 H_2O. [l] 3.5 H_2O. Calc. for H, 6.73; found, 7.20. [m] 2.25 H_2O. [n] 2.0 H_2O. [o] Deliquescent. [p] 1.5 H_2O. [q] Calc. for N, 8.60; found, 9.24. [r] See Ref. 10; lit. mp 32–34°C. [s] See Ref. 6; lit. mp 269–270°C. [t] See Ref. 3; lit. mp 46–47°C, bp 128–129°C (0.2 mm Hg).

ment is presumably due to the activating effect of the carboxylic ester adjacent to the reaction center. A similar effect has been observed for halogen displacement of 3-nitro-4-chloroquinolines (8). Table I lists the ethyl 4-aminoquinoline-3-carboxylates obtained in this manner. Preparation of VI required a slight modification. When the normal reaction conditions were employed with a constant, steady stream of ammonia passing through the reaction solution, no VI was obtained; however, when the reaction was carried out in liquid ammonia at 115–130°C a good yield of VI resulted.

Several of the amino esters were viscous oils which could not be purified either by evaporative distillation or by chromatography. These compounds were converted to the corresponding hydrochloride salts (XXII–XXVI) which, in some cases, could be purified by crystallization. Some of the salts, notably XXV and XXVI, were hygroscopic and did not give satisfactory microanalysis results after several attempts.

Ester hydrolysis using an equivalent amount or a slight excess of potassium hydroxide in ethanol afforded salts XXVII–XLII (Table I). The potassium carboxylates were hygroscopic, making acquisition of microanalytical data difficult. In the extreme cases of XXXVIII and XLI, the compounds were deliquescent. The remaining salts were also hygroscopic, but most could be equilibrated with atmospheric moisture to yield a hydrate of constant, although often nonstoichiometric, composition. The method of Donleavy (9) for preparation of solid derivatives of waxy fatty acids was helpful in some cases. Formation of the pseudouronium salt of the quinoline carboxylates in some instances gave nonhygroscopic salts suitable for microanalysis, but this method was by no means applicable to each compound. Structural assignments were confirmed by ^{1}H-NMR and IR spectrometry, and each ester showed one spot on TLC.

Nucleophilic displacement of the halogen in IV also readily occurred when IV was treated with a sodium thiolate to give XLIII and with ethoxide anion to give XLIV (10). In addition, the *N*-oxide XLV was prepared by treating IV with *m*-chloroperoxybenzoic acid.

Each compound was tested in an *in vitro* assay against a range of microorganisms to determine a general activity profile. The organisms used were *Escherichia coli* ATCC 23540, *Salmonella choleraesuis* ATCC 13312, *Streptococcus faecalis* ATCC 19433, *Staphylococcus aureus* (Smith) Merck 2949, *Pseudomonas aeruginosa* PS-44, *Proteus mirabilis* PR-91, and *Clostridium perfringens* ATCC 3624. Dimethyl sulfoxide was used to aid the dissolution of test compounds in Mueller-Hinton broth at 50 ppm. Inoculated broths, prepared with a semiautomated dispenser and inoculator[1], were incubated for 18 h at 37°C, then examined and assigned a general rating of active, slightly active, or inactive. Measurement of the minimum inhibitory concentrations (MIC) was accomplished by the same method using successive twofold dilutions of the test compound, starting at a concentration of 62.5 ppm.

The target compounds showed no remarkable *in vitro* antibacterial activity, although small amounts of growth inhibition by several members of the series

[1] Model MIC 2000; Dynatech.

was observed. Four of the active compounds (X, XVIII, XXV, and XLIII) were slightly active against *C. perfringens* with minimum inhibitory concentrations of ≥62.5 ppm. Another subgroup of four compounds showed general activity against *Staph. aureus*.

The four compounds active against *Staph. aureus* were examined further by measurement of the MIC values (Table I). Since XXIII is the salt of VIII, it is not surprising that both species have the same order of activity. However, the presence of XIII and XV, which bear no structural relationship to the tertiary amines VIII and XXIII, makes it difficult to draw a structural relationship with the *in vitro* antimicrobial activity.

EXPERIMENTAL SECTION[2]

Ethyl 4-Aminoquinoline-3-carboxylate (VI)—A solution of 23.5 g (0.1 mol) of IV, 250 mL of toluene, and 21 mL (1.0 mol) of liquid ammonia was scaled in a high-pressure reaction vessel, then heated at 120–125°C for 4 h. The vessel was cooled, opened, and the ammonia was allowed to evaporate. The residue was suction-filtered, and the solid was partitioned between chloroform and water. The organic phase was dried (Na_2SO_4), and the solvent was removed under reduced pressure to give 17.4 g of white needles. Recrystallization from ethyl acetate afforded 14.9 g (69%) of VI as white needles, mp 205.0–207.5°C. IR (KBr): 1669 cm^{-1} (C=O); ^{1}H-NMR (Me_2SO-d_6): δ 8.90 (s, 1, quinoline C-2 H), 7.33–8.50 (m, 6, ArH and NH), 4.33 (q, 2, J = 7 Hz, OCH_2), and 1.36 ppm (t, 3, J = 7 Hz, CH_3).

General Procedure for Preparation of Ethyl 4-Alkylamino- and Ethyl 4-Aralkylaminoquinoline-3-carboxylates (VII–XXI)—The general method is illustrated by the synthesis of VII. A solution of 5.89 g (25 mmol) of IV and 9.17 g (125 mmol) of diethylamine in 50 mL of toluene was stirred and heated at reflux for 35 h. The mixture was cooled to room temperature and the salt was removed by filtration. The solvent was removed under reduced pressure to give 7.5 g of a cloudy oil, which was chromatographed on silica gel (5 × 40 cm, ether) to give 6.59 g (96%) of VII as a clear yellow oil. IR ($CHCl_3$): 1698 cm^{-1} (C=O); ^{1}H-NMR ($CDCl_3$): δ 8.90 (s, 1, C-2 H), 7.25–8.22 (m, 4, ArH), 4.43 (q, 2, J = 7 Hz, OCH_2), 3.43 (q, 4, J = 7 Hz, CH_2NCH_2), 1.41 (t, 3, J = 7 Hz, ester CH_3), and 1.15 ppm (t, 6, J = 7 Hz, aminoethyl CH_3).

General Procedure for Preparation of Hydrochloride Salts (XXII–XXVI)—The general method is illustrated by the synthesis of XXII. To a stirred solution of 15.2 g (55.8 mmol) of VII in 250 mL of ether was added 200 mL of dry, ethereal hydrogen chloride. The resulting mixture was filtered, and the solid was recrystallized several times from dichloromethane–ether and then from ethyl acetate. The solid was sublimed to give 5.83 g (34%) of XXII as a fine yellow powder, mp 145–147°C. IR ($CHCl_3$): 1712 cm^{-1} (C=O); ^{1}H-NMR ($CDCl_3$): δ 8.93 (s, 1, C-2 H), 7.61–8.72 (m, 4, ArH), 4.50 (q, 2, J = 7 Hz, OCH_2), 3.87 (q, 4, J = 7 Hz, CH_2NCH_2), 1.47 (t, 3, J = 7 Hz, ester CH_3), and 1.40 ppm (t, 6, J = 7 Hz, aminoethyl CH_3).

General Procedure for Preparation of Potassium Salts (XXVII–XLII)—The general method is illustrated by the synthesis of XXVIII. A solution of 14.9 g (54.8 mmol) of VII and 5.37 g (82.2 mmol) of potassium hydroxide in 150 mL of ethanol was stirred and heated at reflux for 4 h. The mixture was cooled to room temperature, and the solid material was removed by filtration. The solvent was removed under reduced pressure to give 16.9 g of a tan solid. Recrystallization from ethyl acetate–acetone afforded 10.9 g (70%) of XXVIII as fine needles, mp 258–260°C; ^{1}H-NMR (Me_2SO-d_6): δ 8.76 (s, 1, C-2 H), 7.30–8.43 (m, 4, ArH), 3.61 (s, 2, H_2O), 3.33 (q, 4, J = 7 Hz, CH_2NCH_2), and 1.06 ppm (t, 6, J = 7 Hz, CH_3).

[2] Boiling and melting points are uncorrected. Melting points were measured with a Thomas-Hoover Unimelt capillary melting point apparatus. IR spectra were measured with a Perkin-Elmer model 137 spectrophotometer. NMR spectra were measured with a Varian 56/60D or a Hitachi Perkin-Elmer R-24B spectrometer in the stated solvent using tetramethylsilane as internal standard. Microanalyses were performed by the Analytical Department, Diamond Shamrock Corp.

Ethyl 4-Benzylthioquinoline-3-carboxylate (XLIII)—A mixture of 1.65 g (72 mg-atoms) of sodium and 75 mL of absolute ethanol was stirred at room temperature under an argon atmosphere. To the resulting solution of sodium ethoxide was added, over a period of 10 min, a solution of 8.7 g (70 mmol) of benzylmercaptan in 50 mL of absolute ethanol. The mixture was stirred at room temperature for 25 min, and then a solution of 16.5 g (70 mmol) of IV in 75 mL of absolute ethanol was added. The stirring was continued at room temperature for 27 h. The mixture was poured into 150 mL of water, the phases were separated, and the aqueous phase was extracted with ether (3 × 150 mL). The organic phases were combined, washed with water and then with brine, and dried (Na_2SO_4). Removal of the solvent under reduced pressure gave a solid-oil mixture. The oil was decanted, and the solid was recrystallized from hexane to afford 11.4 g (51%) of XLIII as pale yellow prisms, mp 34–36°C. IR ($CHCl_3$): 1724 cm^{-1} (C=O); ^{1}H-NMR ($CDCl_3$): δ 8.97 (s, 1, C-2 H), 7.33–8.62 (m, 4, ArH quinoline), 7.05 (s, 5, ArH), 4.43 (q, 2, J = 7 Hz, OCH_2), 4.12 (s, 2, SCH_2), and 1.42 ppm (t, 3, J = 7 Hz, CH_3).

Ethyl 4-Ethoxyquinoline-3-carboxylate (XLIV)—The method of Markees (10) was employed with slight modification. Dimethylformamide was not used as cosolvent, and the entire reaction was allowed to take place at room temperature rather than for a brief period at reflux. This gave a 53% yield of XLIV as colorless needles, mp 34–36°C, bp 125–128°C (0.1 mm Hg) [lit. (10) mp 32–34°C, bp 160–162°C (1.4 mm Hg)].

Ethyl 4-Chloroquinoline-3-carboxylate-*N*-oxide (XLV)—A solution of 22.3 g (0.11 mol) of *m*-chloroperoxybenzoic acid and 23.5 g (0.1 mol) of IV in 350 mL of dichloromethane was stirred in an ice bath for 1 h, then at room temperature for 66 h. The solution was then stirred with 50 mL of 10% Na_2HSO_3 until a negative starch–iodide test was observed. The phases were separated, and the organic phase was washed with 7.5% $NaHCO_3$ and then brine, and dried (Na_2SO_4). Removal of the solvent under reduced pressure gave 22.2 g of an orange solid, which was recrystallized from ether to give 12.4 g (49%) of XLV as pale yellow plates, mp 102–104°C. IR ($CHCl_3$): 1739 cm^{-1} (C=O); ^{1}H-NMR ($CDCl_3$): δ 7.55–9.00 (m, 5, ArH), 4.50 (q, 2, J = 7 Hz, OCH_2), and 1.47 ppm (t, 3, J = 7 Hz, CH_3).

REFERENCES

(1) E. J. Watson, Jr., U.S. Pat. No. 3,267,106 (1964).

(2) T. R. Sweeny and R. E. Stube in "Burger's Medicinal Chemistry," 4th ed., Part II, M. E. Wolff, Ed., Interscience, New York, N.Y., 1979, chap. 18.

(3) C. E. Kaslow and W. R. Clark, *J. Org. Chem.*, **18,** 55 (1953).

(4) R. G. Gould, Jr. and W. A. Jacobs, *J. Am. Chem. Soc.*, **61,** 2890 (1939).

(5) C. C. Price and R. M. Roberts, *J. Am. Chem. Soc.*, **68,** 1204 (1946).

(6) B. Riegel, G. R. Lappin, G. H. Adelson, R. I. Jackson, C. J. Albisette, Jr., R. M. Dodson, and R. H. Baker, *J. Am. Chem. Soc.*, **68,** 1264 (1946).

(7) G. Jones (Ed.), "Quinolines Part I," Interscience, New York, N.Y., 1977, p. 139.

(8) A. R. Surrey and R. A. Cutler, *J. Am. Chem. Soc.*, **73,** 2413 (1951).

(9) J. J. Donleavy, *J. Am. Chem. Soc.*, **58,** 1004 (1936).

(10) D. G. Markees, *J. Org. Chem.*, **31,** 4253 (1966).

(11) W. O. Kermack and N. E. Storey, *J. Chem. Soc.*, **1951,** 1389.

ACKNOWLEDGMENTS

The authors thank Daniel T. Feeley for performing the general antimicrobial screen and for measurement of the MIC values.

Subnanogram Quantitation of Chlorpheniramine in Plasma by a New Radioimmunoassay and Comparison With a Liquid Chromatographic Method

K. K. MIDHA ˣ, G. RAUW, G. McKAY, J. K. COOPER, and J. McVITTIE

Received June 2, 1983, from the *College of Pharmacy, University of Saskatchewan, Saskatoon, Saskatchewan S7N 0W0 Canada.* Accepted for publication September 7, 1983.

Abstract □ A new radioimmunoassay (RIA) procedure for the quantitation of chlorpheniramine in plasma is described. The assay allows the determination of chlorpheniramine levels up to 96 h after oral administration of a single 4-mg tablet to healthy volunteers. This procedure was sensitive to a 156-pg/mL plasma concentration when a 100-μL plasma sample was used. The mean coefficient of variation over the linear range of the assay from 0.156 to 20 ng/mL was 3.79%. The specificity of the assay was investigated, and the antisera showed 7% cross-reactivity with the *N,N*-didemethyl analogue and 17% cross-reactivity with the *N*-demethyl analogue. This high degree of specificity was also evident from the findings that the plasma concentrations determined by this newly described RIA procedure in samples of two healthy male volunteers who were administered 4 mg of chlorpheniramine maleate orally gave a strong correlation (r^2 = 0.88) with values obtained by an HPLC-UV procedure. The antiserum cross-reacted 100% with brompheniramine and, thus, can be used for its analysis in plasma. The described RIA procedure is precise, simple, and capable of handling a large number of plasma samples with a minimal turnaround time.

Keyphrases □ Radioimmunoassay—chlorpheniramine, plasma, comparison with HPLC-UV □ Chlorpheniramine—subnanogram quantitation in plasma, RIA, comparison with HPLC-UV

Chlorpheniramine (2-[*p*- chloro -α-[2-(dimethylamino)ethyl]-benzyl]pyridine), a potent antihistaminic drug widely used for relief of symptoms of the common cold and other allergic reactions, is a common ingredient in nonprescription antihistamine preparations. It is generally recommended for use in relatively low doses (1). Recent studies have established that the assay methods of this drug should be sensitive at least to the low nanogram range to adequately follow the plasma concentrations for thorough, reliable pharmacokinetic investigations (2-6) in children.

The various methods for the quantitation of chlorpheniramine that have been used include TLC with liquid scintillation counting (7), TLC followed by chemical conversion to an azo dye and subsequent colorimetric analysis (8), GC (9-15), HPLC (16, 17), and GC-MS (18, 19). Most of the earlier methods were developed to assay the drug in dosage forms or in urine; only a few procedures (15, 17-19) have the necessary sensitivity to quantitate normal plasma levels of chlorpheniramine after single doses of the drug. The GC procedure using electron-capture detection (15) is complicated because it requires the liquid chromatographic separation of the drug from its metabolites and an oxidation reaction as preliminary steps. The HPLC (17) and GC-MS procedures (18, 19) have adequate sensitivity to determine 1-2-ng/mL plasma concentrations after single doses; however, they all require extraction of the drug from plasma and/or sophisticated instrumentation such as GC-MS and are generally cumbersome for routine analysis. Radioimmunoassay (RIA) procedures, on the other hand, are usually simple, sensitive, and readily applicable to routine analysis. They generally do not require either extraction of the drug from plasma or expensive instrumentation. Such an RIA method for chlorpheniramine, which is sensitive to 0.156 ng/mL and requires only a 100-μL plasma sample, has been developed and is reported here. This report also describes the comparison of the RIA with a new HPLC procedure.

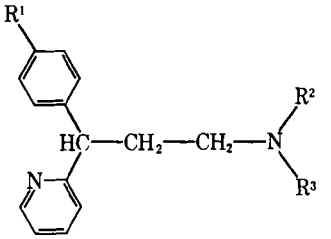

(I): R^1=Br; R^2=R^3=CH_3
(II): R^1=Cl; R^2=R^3=H
(III): R^1=Cl; R^2=CH_3; R^3=H
(IV): R^1=Cl; R^2=R^3=CH_3
(V): R^1=Cl; R^2=CH_3; R^3= $-CH_2CH_2-COOH$

EXPERIMENTAL SECTION

Materials—Chlorpheniramine maleate[1], prochlorperazine dimaleate[2], 2-[*p*-chloro-α-(2-aminoethyl)benzyl]pyridine (II)[3], 2-[*p*-chloro-α-[2-(methylamino)ethyl]benzyl]pyridine (III)[3], and brompheniramine maleate[4] were used. All solvents were HPLC grade, and all other chemicals were commercial analytical reagent grade. The tracer solution was tritiated chlorpheniramine with a specific activity of 14.6 Ci/mmol, prepared by catalytic exchange with tritium gas[5]. The following reagents were used without modification: 0.2 M phosphate buffer (pH 7.2) and dextran-coated charcoal suspension [prepared by the method of Powell *et al.* (20)]. A scintillation fluid[6] was used for liquid scintillation counting.

Apparatus—A liquid chromatographic pump[7] fitted with a valve-loop (500 μL) injector[8] was connected to a variable-wavelength detector[9] operated at 229 nm. A Spherisorb 5-μm cyano column (250 mm × 4.6 mm i.d.)[10] was used at ambient temperature with a flow rate of 3 mL/min. The mobile phase consisted of 30% 0.05 M ammonium acetate in acetonitrile. It was deaerated by filtration[11] before use. Scintillation counting was carried out with a liquid scintillation counter equipped with an automatic quench compensation[12].

Liquid Chromatographic Internal Standard—A stock solution of prochlorperazine dimaleate (100 μg/mL, calculated as free base) was prepared in double-distilled water and stored in the absence of UV light at 4°C; this was prepared fresh monthly. Dilutions of 200 ng/mL were prepared daily.

Preparation of Standard Curves—An aqueous solution of chlorpheniramine maleate (100 μg/mL, calculated as free base) was prepared monthly in double-distilled deionized water and stored at 4°C. Appropriate dilutions of the stock solutions were made in plasma. For RIA, this plasma was obtained from drug-free volunteers. For HPLC, outdated plasma[13] was used.

[1] Schering Corp. Ltd., Pointe Claire, Quebec, Canada
[2] Rhône-Poulenc Ltd., Montreal, Quebec, Canada.
[3] Smith Kline & French Laboratories, Philadelphia, Pa.
[4] A. H. Robins, Canada Ltd.
[5] Nuclear Research Center, Negev, Beer-Sheva, Israel.
[6] Ready-Solve MP; Beckman Instruments, Canada.
[7] Model M-45; Waters Scientific Co., Mississauga, Ontario, Canada.
[8] Model 7125, Rheodyne; Technical Marketing Associates, Calgary, Alberta, Canada.
[9] Waters Scientific Co., Mississauga, Ontario, Canada.
[10] Spherisorb Phase Separations Ltd., Deeside Industrial Estate, Queensferry, Clwyd, U.K.
[11] Millipore Corp., Bedford, Mass.
[12] Model 1215; LKB Rackbeta; Fisher Scientific Co, Canada.
[13] Obtained from the Red Cross.

0022-3549/84/0800-1144$01.00/0
© 1984, American Pharmaceutical Association

Table I—RIA Estimation of Chlorpheniramine Added to Plasma [a]

Concentration, ng/mL	n	Mean, B/B_0, %	SD, ng	RSD[b]
0.156	9	93.3	0.0016	1.05
0.313	7	86.8	0.0070	2.24
0.625	7	75.6	0.0137	2.19
1.25	8	59.2	0.0488	3.90
2.5	6	42.7	0.0608	2.43
5	8	25.8	0.2785	5.57
10	7	15.7	0.4560	4.56
20	6	9.7	1.672	8.36

[a] Composite standard curve where logit $y = M \cdot \log_{10} x + I$; $M = -2.329$, $I = 0.6686$, $r^2 = 0.999$. [b] Mean RSD = 3.79%.

For RIA, calibration curves were constructed by the following:

$$\text{Logit } y = \text{Log}_e \frac{B/B_0}{1 - B/B_0} = M \cdot \text{Log}_{10} C + I \qquad \text{(Eq. 1)}$$

where B is percentage bound, B_0 is the percentage bound at zero concentrations, M is the slope, C is the concentration (ng/mL), and I is the intercept.

Liquid Chromatographic Extraction of Samples—The extraction procedure was similar to that previously described for chlorpromazine (21, 22). To a 10-mL polytef-lined screw-capped centrifuge tube (13 × 100 mm) were added 2.0 mL of plasma (spiked or from dosed volunteers), 1.0 mL of prochlorperazine internal standard (100 ng/mL), and 0.5 mL of saturated sodium carbonate solution. The tube was mixed for 5 s, and 5 mL of 3% isopropyl alcohol in pentane was added. The tube was tightly capped and mixed[14] for 15 min and centrifuged[15] 10 min at 1725×g at ambient temperature.

The organic layer was transferred to a clean 10-mL tube, and the extraction was repeated with another 5.0 mL of 3% isopropyl alcohol in pentane. The combined organic extracts were evaporated at 65°C in a dry bath[16]. The dried residue was dissolved in 200 μL of acetonitrile, and 100 μL was injected into the chromatograph.

Synthesis of Drug Protein Conjugate and Production of Antisera—Antisera were raised in New Zealand White rabbits to an immunogen synthesized by covalent linkage of bovine serum albumin to *N*-(2-carboxyethyl)demethylchlorpheniramine employing the mixed anhydride condensation reaction (23, 24). A blank was prepared in the same manner without demethylchlorpheniramine. The number of hapten residues per mole of bovine serum albumin was determined to be 4 by a UV method (23, 24).

The hapten *N*-(2-carboxyethyl)demethylchlorpheniramine was prepared by alkaline hydrolysis of *N*-(2-methoxycarbonylethyl)demethylchlorpheniramine, a compound synthesized by refluxing equimolar amounts of methyl acrylate and III (25). The addition of III to methyl acrylate was monitored by GC, in which the absence of the peak due to III indicated completion of addition.

Four rabbits were each given one intradermal injection of 1.0 mg of the immunogen emulsified with 0.5 mL of Freund's complete adjuvant and 0.5 mL of isotonic saline. The rabbits were given four injections at 2-week intervals with the same amount of immunogen emulsified with Freund's incomplete adjuvant. Four intravenous boosters of 1.0 mg of immunogen dissolved in 0.25 mL of isotonic saline were given. After the second booster, titers of 1:500 were produced in three of the rabbits, and titers of 1:1000 were produced in the fourth. Subsequent injections did not increase the titer. The antiserum from each of the rabbits was characterized for its cross-reactivity and sensitivity. The antiserum employed in the present study was lyophilized and stored at −20°C. An aliquot of 25 mg was weighed out and reconstituted with 31.25 mL of phosphate buffer (pH 7.2). The cross-reactions (50% inhibition of binding at zero drug concentration) for the metabolites and other drugs were determined by the criteria of Abraham (26).

Radioimmunoassay—The assay was done in subdued light and an ice water bath so as to maintain the temperature at 4°C. To a 12 × 75-mm polystyrene tube containing 100 μL of plasma sample (standard or from dosed volunteer) was added 250 μL of tritiated chlorpheniramine (22,000 dpm) diluted in 0.2 M phosphate buffer (pH 7.2). The tube contents were mixed[17] for 5 s. An aliquot of 250 μL of the antiserum (80 mg in 100 mL) was added, and the tube contents were mixed[17] once more for 5 s and incubated at 4°C for 60 min. To this incubated solution was added 1.0 mL of a cold dextran-coated charcoal suspension (4°C). The tube contents were mixed[17] again for 5 s and incubated for 30 min at 4°C. The sample was then centrifuged[15] at 1720×g for 10 min at 4 °C. The supernatant was decanted into a scintillation vial containing 10 mL of cocktail[6] and then counted.

[14] SMI, Multitube Shakers; Canlab, Edmonton, Alberta, Canada.
[15] TJ6 Centrifuge; Beckman Instruments, Canada.
[16] Thermolyne Dri-Bath; Fisher Scientific Co.
[17] Vortex Genie; Fisher Scientific Co., Canada.

Table II—Cross-Reactivity of Chlorpheniramine Antiserum

Compound Tested	Cross-Reactivity, %
Brompheniramine (I)	100
2-[*p*-Chloro-α-(2-amino ethyl)benzyl]pyridine (II)	7
2-[*p*-Chloro-α-[2-(methylamino)ethyl]benzyl]pyridine (III)	17
Chlorpheniramine (IX)	100
N-(2-Carboxyethyl)demethylchlorpheniramine (V)	—

Plasma Level Study—A 4-mg dose of a commercial preparation of chlorpheniramine maleate[18] was given orally with 250 mL of water to each of two volunteers (weight, 56 and 60 kg, respectively). Blood samples were collected from each of the volunteers over a 96-h period in evacuated glass tubes[19] and centrifuged, and separated plasma was stored at 4°C for a maximum of 7 d. During collection of the venous samples, care was taken to avoid contact of the blood with the rubber stopper of the evacuated tube. For three of these blood samples for each volunteer, one extra tube of blood was collected in the conventional manner in which blood was allowed to come into contact with the rubber stopper.

Recovery Study for Liquid Chromatography—For the determination of chlorpheniramine recovery, blank plasma was spiked with 5 or 20 ng of chlorpheniramine/mL. The tritiated chlorpheniramine (10,400 dpm/mL) was also added to the spiked plasma. This brought the total concentration of chlorpheniramine added to 5.25 or 20.25 ng/mL. The samples were extracted as previously described, except that the organic layers were transferred to a 20-mL borosilicate glass scintillation vial and dried. Cocktail[6] (10 mL per vial) was also added, mixed, and then counted. Recovery of chlorpheniramine was determined by counting the radioactivity recovered *versus* the amount added.

Analytical Recovery for Radioimmunoassay—Tritiated chlorpheniramine was added to plasma samples containing chlorpheniramine and incubated with buffer in accordance with the procedure described above. The solutions were then decanted into scintillation fluid, and the radioactivity was measured. The recoveries of 0.156–20 ng were ~95%, which are similar to the values reported for another basic drug, trifluoperazine (27). It should be emphasized that during the decanting technique, small amounts of the sample adhere to the sides of the tube; thus, actual recoveries may be greater. When the tracer was added directly to the polystyrene tube without using plasma, >40% of the tracer was lost, probably due to adsorption onto the surface of the tube. Thus, all standards at a low nanogram range of chlorpheniramine were prepared in plasma.

RESULTS

Radioimmunoassay—The amount bound at zero concentration of chlorpheniramine was determined at incubation times of 30, 60, and 90 min and at temperatures of 4°C and 37°C for the first incubation step in the assay. From the results of these experiments, the optimal conditions for the assay were found to be an incubation time of 60 min at 4°C, and B_0 was 23%. The concentrations of unknown samples were estimated by running a calibration curve with each set of unknown samples.

Table I shows a composite standard curve covering the range of 0.156 to 20 ng/mL, which is definable by:

$$\text{Logit } y = -2.329 \cdot \log_{10} x + 0.6686 \; (r^2 = 0.999) \qquad \text{(Eq. 2)}$$

Specificity—The cross-reactivity of the available metabolites of chlorpheniramine, as well as the related drug brompheniramine, as assessed by the criteria of Abraham, is recorded in Table II. Brompheniramine, as expected, did cross-react 100%. Thus, this antiserum can be used for the development of an RIA for brompheniramine. The *N*-demethyl and *N*,*N*-didemethyl metabolites of chlorpheniramine cross-reacted 17 and 7%, respectively. The significant cross-reactivity of the pharmacologically active *N*-demethyl metabolite (17%) was not surprising since the antisera were raised to a drug–protein conjugate prepared by coupling to this secondary amine. This also may explain the 7% cross-reactivity of the *N*,*N*-didemethyl metabolite. This relative cross-reactivity of 7% of the *N*,*N*-didemethyl metabolite was the same as that observed in the case of the chlorpromazine RIA (28). In the chlorpromazine RIA, the antisera raised in New Zealand White rabbits to the bovine serum

[18] Chlor-Tripolon; Schering Inc., Canada.
[19] Vacutainers, each containing 143 USP units of sodium heparin; Becton, Dickinson and Co., Mississauga, Ontario, Canada.

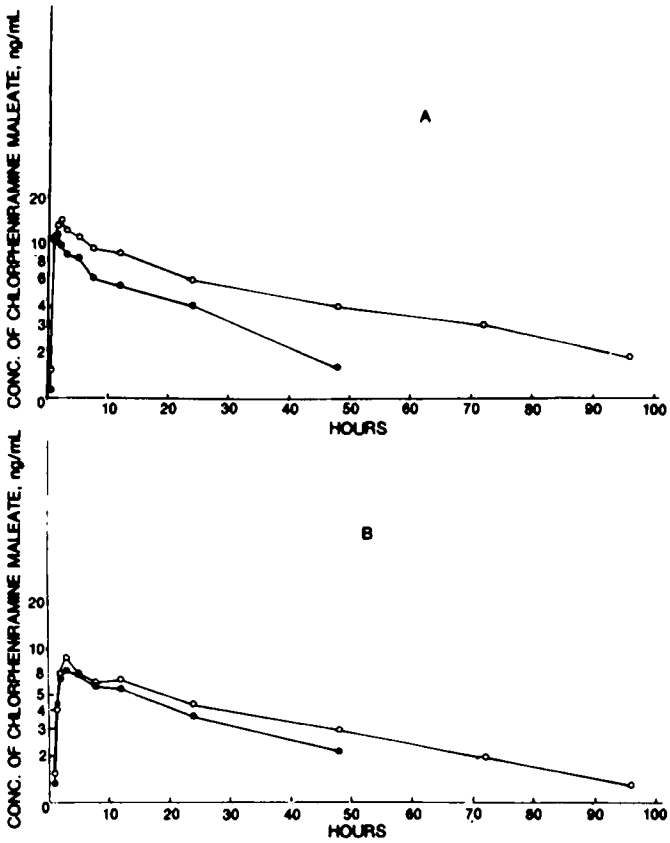

Figure 1—*Plasma concentrations* versus *time profiles obtained by RIA (○) and HPLC (●) for two healthy volunteers (A and B) weighing 56 and 60 kg, respectively, each of whom received a 4-mg dose of chlorpheniramine maleate.*

albumin conjugate of *N*-(2-carboxyethyl)demethylchlorpromazine cross-reacted 7% with the *N*,*N*-didemethyl metabolite.

The detection limit is <15.6 pg, which corresponds to 0.156 ng/mL if a 100-μL plasma sample is used. This sensitivity is greater than any method reported for chlorpheniramine. Thus, this RIA should be ideal for samples from infants and children, as the plasma volume needed does not exceed 0.2 mL for duplicate analyses of each sample.

Precision—The coefficient of variation for the replicate analyses of various concentrations of chlorpheniramine from 0.156 to 20 ng/mL is shown in Table I. The coefficient of variation of 0.156 ng/mL (n = 9) was ~1.05%.

Influence of Plasma Volume on Standard Curves—Standard curves were prepared by use of 50-, 100-, and 200-μL volumes of plasma. The slopes and intercepts derived were identical, thereby suggesting that plasma volumes did not affect the assay.

Capacity and Application of the Procedure—One technician can assay 50 samples in triplicate in a normal working day. Concentrations in plasma measured in two healthy volunteers (weight, 56 and 60 kg) after oral administration of a single 4-mg dose of the maleate salt of the drug are illustrated in Fig. 1. Note that the assay can easily quantitate the drug and/or its *N*-dealkylated metabolites in specimens collected as late as 96 h after a single oral dose.

Effect of Rubber Stoppers of the Evacuated Glass Tubes on Plasma Concentration Determination—To establish whether the measurement of the weakly basic lipophilic compound, chlorpheniramine [pK_a 8.99, (29)], is affected by contact with the rubber stoppers of the evacuated glass tubes, the duplicate samples of blood from the two dosed subjects were collected at three different times as described above. In each case, the first sample was collected with the evacuated tube held vertically so that the blood did not touch the rubber stopper at any time, whereas the second sample was collected immediately, with the tube held horizontally so that the blood did touch the stoppers. Plasma was prepared from the duplicate samples, which were analyzed in parallel by the RIA procedure. There was substantial reduction (18–30%) of the apparent plasma concentration of chlorpheniramine in all six samples when the blood was allowed to touch the stoppers. This significant lowering of apparent plasma concentration in chlorpheniramine is similar to that reported for other weakly basic lipophilic drugs (30). Therefore, for chlorpheniramine, during blood collection procedures, contact with the rubber stoppers should be avoided.

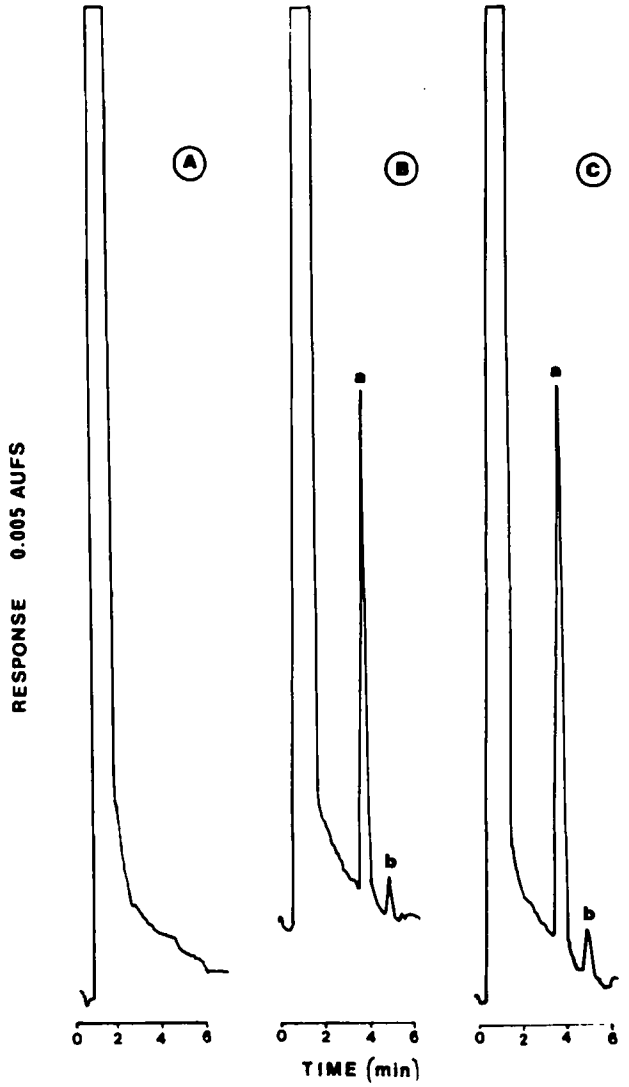

Figure 2—*Chromatograms of extracts from 2.0 mL of plasma. Key: (A) blank plasma; (B) plasma spiked with chlorpheniramine (b, 5.0 ng/mL) and internal standard prochlorperazine (a, 100.0 ng/mL); (C) plasma sample from a volunteer (56 kg) 7.5 h postdose (chlorpheniramine maleate, 4 mg), estimated to contain 6.1 ng of the drug per mL of plasma.*

High-Performance Liquid Chromatography—Under the HPLC conditions described above, chlorpheniramine and the internal standard prochlorperazine gave sharp and symmetrical peaks that eluted in 6 min (Fig. 2). No interference from endogenous plasma constituents was observed. Figure 2B shows a chromatogram of a spiked plasma sample containing 5.0 ng of chlorpheniramine/mL and 100 ng of prochlorperazine/mL. Figure 2C shows a chromatogram of a 7.5-h postdose plasma sample (2 mL) from a volunteer (56 kg) who received 4 mg of chlorpheniramine maleate orally, with the chlorpheniramine concentration estimated as 6.1 ng/mL. *N*-Demethylchlorpheniramine and *N*,*N*-didemethylchlorpheniramine do not interfere in the assay, as they are eluted at 4.2 and 3.1 min, respectively, as compared with chlorpheniramine and the internal standard, which elute with retention times of 5.7 and 4.7 min, respectively. Brompheniramine may also be amenable to analysis by the described HPLC assay, as it elutes at a retention time of 5.4 min.

Table III shows a composite standard curve for the quantitation of chlorpheniramine by HPLC from plasma. The curve is linear with a negligible intercept over the concentration range of 5–25 ng/mL. The ratios of chlorpheniramine to prochlorperazine peak heights plotted against chlorpheniramine concentrations gave a straight line passing through the origin (r^2 = 0.999). A mean slope value of 0.0102 ± 0.00089 was obtained. The sensitivity at 229 nm for chlorpheniramine (Fig. 2) is such that the HPLC assay can quantitate 2.5 ng/mL of the drug in plasma. This sensitivity is comparable

Table III—HPLC Estimation of Chlorpheniramine Added to Plasma [a]

Concentration, ng/mL	n	Mean Peak Height Ratio	SD	RSD, %[b]
5	6	0.0517	0.0017	3.39
10	6	0.1024	0.0060	5.90
15	6	0.1552	0.0085	5.47
20	7	0.2051	0.0054	2.64
25	8	0.2555	0.0130	5.08

[a] $y = mx$, where $m = 0.0102 \pm 0.00089$ and $r^2 = 0.99996$. [b] Mean $RSD = 4.5\%$.

with that reported for chlorpheniramine by a reverse-phase system with UV detection at 254 nm (17).

The overall recoveries of chlorpheniramine obtained from seven determinations, each at two concentrations (5.25- and 20.25-ng/mL of plasma) were 78.15 ± 2.71 and 78.43 ● 5.92, respectively. A mean percent recovery of 78.29 ± 4.32 was considered satisfactory.

Application of the described HPLC procedure to plasma concentration determinations in two healthy volunteers (56 and 60 kg), each of whom received a single oral dose of a commercial preparation[19] containing 4 mg of chlorpheniramine maleate, is shown in Fig. 1. As can be seen, the method is of sufficient sensitivity to analyze specimens obtained up to 48 h after this low oral dose, whereas the RIA procedure could measure the plasma concentrations in the specimens up to 96 h.

DISCUSSION

Sensitive, specific, and reproducible procedures are essential in order to carry out pharmacokinetic investigations of drugs which are given in small doses. Rapidity, high sample turnover, and low cost would be advantageous in encouraging clinicians to monitor plasma levels in individuals who do not respond to a certain dose of a drug.

For chlorpheniramine, two such methods are described here. The RIA procedure has the simplicity and sensitivity to measure plasma concentrations of chlorpheniramine and/or its *N*-dealkylated metabolites in specimens collected as late as 96 h after administration of single low doses, such as 4 mg. Because of its sensitivity, the RIA procedure is well suited to determine plasma chlorpheniramine levels in infants and children where the available plasma volume may not be large. The described HPLC procedure could measure concentrations up to 48 h after administration of single low doses in the two volunteers studied here. The plasma half-lives of chlorpheniramine after the single oral dose of 4 mg of the maleate salt in these two volunteers were estimated by the HPLC method to be 17 and 23 h, which are comparable with previous reports (2, 3). However, these half-lives were estimated by the RIA procedure for these volunteers as 35 h in each case. This over-estimation in half-lives is probably due to the cross-reactivity (17%), especially of the active *N*-demethyl metabolite with the antiserum used. Similarly, area under the plasma concentration time curves up to 48 h (AUC_0^{48}) by RIA for the two subjects were 330 and 222 ng·h/mL, respectively, whereas these values by HPLC were 205 and 187 ng·h/mL, respectively. This overestimation of AUC_0^{48} and 1.5–2.0-fold increase in half-life values between RIA and HPLC suggest that the RIA may not be useful in pure pharmacokinetic studies of chlorpheniramine.

The increases of 61 and 19% in the AUC_0^{48} value when measured by RIA probably represent the contributions due to the *N*-demethyl and, to a lesser extent, the *N*,*N*-didemethyl metabolites. The *N*-demethyl and *N*,*N*-didemethyl metabolites could not be detected by Huang *et al.* (2) in plasma after single oral doses. After both single and multiple doses of chlorpheniramine, the *N*-demethyl and *N*,*N*-didemethyl metabolites constitute 22 and 3%, respectively, of the total administered dose of the drug excreted in urine. This raises the possibility that there may be other unknown metabolites, which are responsible, at least in part, for the difference in results from RIA and HPLC. In spite of the cross-reactivity of the antiserum to the *N*-demethyl metabolite (17%), the RIA procedure, when compared with the HPLC method, gave a slope of 1.21 with a positive intercept of 0.46 and a correlation coefficent of 0.88 in plasma samples from the two healthy volunteers, who were each given orally a single dose of chlorpheniramine maleate.

The described RIA procedure is simple, precise, and capable of handling a large number of samples. This RIA may be useful for comparative bioequivalency studies of different formulations and for monitoring compliance. The HPLC method is reliable and should be well suited for pure pharmacokinetic studies.

REFERENCES

(1) "The Pharmacological Basis of Therapeutics," L. S. Goodman and A. Gilman, Eds., Macmillan, New York, N.Y., 1980, p. 623.

(2) S. M. Huang, N. K. Athanikar, K. Sridhar, Y. C. Huang, and W. L. Chiou, *Eur. J. Clin. Pharmacol.*, **22,** 359 (1982).

(3) J. A. Kotzam, J. J. Valner, J. T. Stewart, W. J. Brown, C. T. Viswanathan, T. E. Needham, S. V. Dighe, and R. Malinowski, *J. Pharm. Sci.*, **71,** 919 (1982).

(4) J. A. Thompson, D. C. Bloedow, and F. H. Leffert, *J. Pharm. Sci.*, **70,** 1284 (1981).

(5) K. J. Simons, G. H. Luciuk, and F. E. R. Simons, Abstracts, A. Ph.A. Academy of Pharmaceutical Sciences Meeting, Orlando, Fla., November 1981.

(6) A. Yacobi, R. G. Stoll, G. C. Chao, J. W. Carter, D. M. Baaske, B. L. Kamath, A. H. Amann, and C.-M. Lai, *J. Pharm. Sci.*, **69,** 1077 (1980).

(7) E. A. Peets, M. Jackson, and S. Symchowicz, *J. Pharmacol. Exp. Ther.*, **180,** 464 (1972).

(8) P. Haefelfinger, *J. Chromatogr.*, **124,** 351 (1976).

(9) A. H. Beckett and G. R. Wilkinson, *J. Pharm. Pharmacol.*, **17,** 256 (1965).

(10) P. Kabasakalian, M. Taggart, and E. Townley, *J. Pharm. Sci.*, **57,** 621 (1968).

(11) P. Kabaskalian, M. Taggart, and E. Townley, *J. Pharm. Sci.*, **57,** 856 (1968).

(12) J. J. Kamm, C. R. Ferullo, D. Miller, and E. J. VanLoon, *Biochem. Pharmacol.*, **18,** 659 (1969).

(13) E. Townley, I. Perez, and P. Kabasakalian, *Anal. Chem.*, **42,** 1759 (1970).

(14) S. Hanna and A. Tang, *J. Pharm. Sci.*, **63,** 1954 (1974).

(15) J. W. Barnhart and J. D. Johnson, *Anal. Chem.*, **49,** 1085 (1977).

(16 C. M. Lai, R. G. Stoll, Z. M. Look, and A. Yacobi, *J. Pharm. Sci.*, **68,** 1243 (1979).

(17) N. K. Athanikar, G. W. Peng, R. L. Nation, S.-M. Huang, and W. L. Chiou, *J. Chromatogr.*, **162,** 367 (1979).

(18) H. Miyazaki and H. Abuki, *Chem. Pharm. Bull.*, **24,** 2572 (1976).

(19) J. A. Thomson and F. H. Leffert, *J. Pharm. Sci.*, **69,** 707 (1980).

(20) B. Powell, R. E. Garola, G. C. Chammess, and W. L. McGuire, *Cancer Res.*, **39,** 1678 (1979).

(21) G. McKay, K. Hall, J. K. Cooper, E. M. Hawes, and K. K. Midha, *J. Chromatogr.*, **232,** 275 (1982).

(22) J. K. Cooper, G. McKay, and K. K. Midha, *J. Pharm. Sci.*, **72,** 1259 (1983).

(23) B. F. Erlanger, F. Borek, S. M. Beiser, and S. Lieberman, *J. Biol. Chem.*, **200,** 713 (1957).

(24) B. F. Erlanger, F. Borek, S. M. Beiser, and S. Lieberman, *J. Biol. Chem.*, **234,** 1090 (1957).

(25) J. W. Hubbard, K. K. Midha, I. J. McGilveray, and J. K. Cooper, *J. Pharm. Sci.*, **67,** 1563 (1978).

(26) G. E. Abraham, *Br. J. Clin. Endocrinol. Metab.*, **29,** 866 (1969).

(27) K. K. Midha, J. W. Hubbard, J. K. Cooper, E. M. Hawes, S. Fournier, and P. Yeung, *Br. J. Clin. Pharmacol.*, **12,** 189 (1981).

(28) K. K. Midha, J. C. K. Loo, J. W. Hubbard, M. L. Rowe, and I. J. McGilveray, *Clin. Chem.*, **25,** 166 (1979).

(29) L. G. Chatten (Ed.), "Pharmaceutical Chemistry," Vol. 1, Dekker, New York, N.Y., 1966, p. 85.

(30) K. K. Midha, J. K. Cooper, Y. D. Lapierre, and J. W. Hubbard, *Can. Med. Assoc. J.*, **124,** 263 (1981).

ACKNOWLEDGMENTS

This study was supported by medical Research Council of Canada Grant MT-7838 to K.K.M., and the Saskatchewan Health Research Board is acknowledged for the fellowship to G.M. The authors gratefully acknowledge Dr. E. M. Hawes, College of Pharmacy, University of Saskatchewan, Saskatoon, Canada, for helpful discussions and Smith Kline & French, Philadelphia, Pa., for the gift of *N*-demethylchlorpheniramine maleate and *N*,*N*-didemethylchlorpheniramine maleate.

Studies on the Formation of Electrostatic Complexes Between Benzethonium Chloride and Anionic Polymers

EDWARD A. TAVSS ˣ, ABDUL GAFFAR, and WILLIAM J. KING *

Received April 20, 1983, from the *Colgate-Palmolive Research Center, Piscataway, NJ 08854.* Accepted for publication September 7, 1983. * Present address: Department of Dental Research, Fairleigh Dickinson University School of Dentistry, Hackensack, NJ 07601.

Abstract □ The chemistry of a mixture of benzethonium chloride and a copolymer of methoxyethylene-maleic anhydride was investigated. This mixture was of interest because it was effective in reducing dental plaque, calculus, and gingival inflammation *in vivo*. Evidence from dialysis, pH measurements, and stoichiometry demonstrated that the benzethonium cation and the anion of the hydrolyzed copolymer formed an electrostatic complex. An emulsion was produced when a stoichiometric excess of either component was present, but this mixture coacervated at stoichiometric quantities. The stability of the complex was pH dependent, and it did not form in 50% acetone. The complex was decomposed by simulated saliva, mainly due to calcium and magnesium ions, but was unaffected by salivary proteins. Other anionic polymers also formed this type of complex.

Keyphrases □ Electrostatic complexes—reaction of benzethonium chloride and methoxyethylene-maleic anhydride copolymer □ Polyanions—complex formation with long-chain quaternary ammonium ion □ Benzethonium chloride—electrostatic complex with methoxyethylene-maleic anhydride copolymer

The antibacterial compound benzethonium chloride has been shown to be an effective inhibitor of dental plaque formation in humans (1). In a subsequent study, a mixture of benzethonium chloride and a copolymer of methoxyethylene-maleic anhydride (mol. wt. 500,000) was evaluated *in vitro* for antibacterial activity and *in vivo* (beagle dogs) for inhibition of plaque, gingivitis, and calculus formation (2–4). The results demonstrated that the combination was as effective as benzethonium chloride alone in antibacterial activity and in the reduction of plaque and gingivitis. A difference did exist, however, in the effect on calculus. Benzethonium chloride significantly increased calcified deposits on teeth as compared with the water control group, whereas the mixture showed significantly less calculus. Hence, the mixture was as effective as benzethonium chloride for the inhibition of plaque and gingivitis and had the advantage of inhibiting calculus formation rather than enhancing it. It was, therefore, of interest to elucidate the chemistry of the complex.

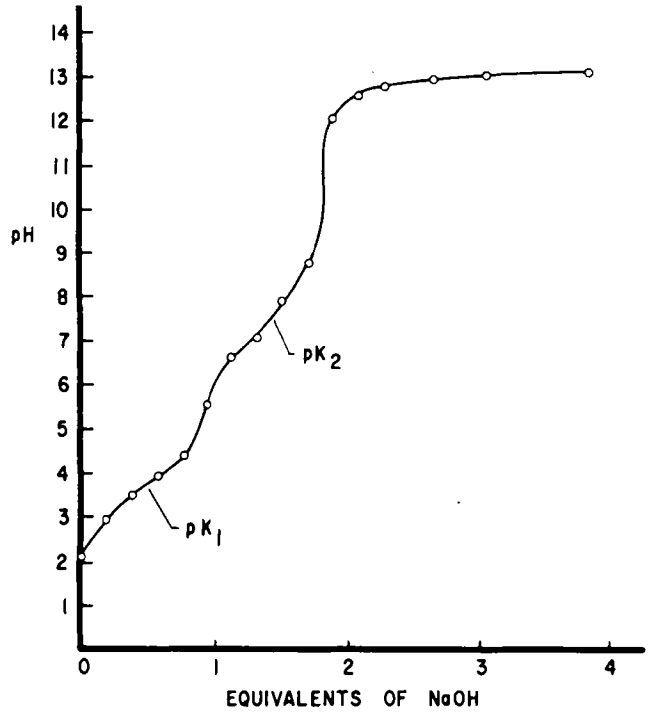

Figure 1—*Titration curve of the methoxyethylene-maleic anhydride copolymer.*

A number of investigators have studied the interactions of cations with polymers. Ackart *et al.* have investigated carboxyl-containing copolymers, such as the copolymer of ethylene-acrylic acid, and quaternary ammonium compounds, such as benzalkonium cations (5). They have suggested that the carboxyl-containing copolymer can be neutralized directly by the benzalkonium hydroxide or that the partial sodium salt of the copolymer could be ion-exchanged with benzalkonium chlorides. No evidence was presented, however, for the formation of electrostatic complexes. Rölla *et al.* have demonstrated interactions of another cationic antibacterial agent, chlorhexidine, with acidic salivary proteins (6). They hypothesized that this precipitate was an insoluble salt of the negatively charged protein and the positively charged chlorhexidine cations. Saito has studied interactions of tetra-alkyl ammonium chlorides with polyacrylic acid (7). By measuring the surface tension, he demonstrated that the quaternary compound became bound to the negatively charged polymer, neutralizing the surface and causing precipitation. Further addition of the quaternary cation coated the neutral surface of the coagulum, causing it to become charged and water soluble. Interactions of the alkaloid cation with the negatively charged ionized group of biocolloids were determined by coagulation observations and measurements of the direction of electrolytic transport by Jong and Meer (8). They demonstrated that there was an increase in interaction with increasing charge density on the colloid anion. Michaels and Miekka studied the interaction between sodium polystyrene sulfonate and polyvinylbenzyltrimethyl ammonium chloride (9). They have demonstrated that when the two were mixed in water, a precipitate formed which contained almost exactly stoichiometric proportions of the component polyions and, furthermore, contained virtually none of the sodium and chloride counterions associated with the individual polymers.

Table I—Formula for Simulated Saliva [a]

Component	Weight, g/L
$CaCl_2 \cdot 2H_2O$ [b]	0.228
$MgCl_2 \cdot 6H_2O$ [b]	0.061
NaCl [b]	1.017
$K_2CO_3 \cdot 1\frac{1}{2}H_2O$ [b]	0.603
$Na_2HPO_4 \cdot 7H_2O$ [b]	0.204
$NaH_2PO_4 \cdot H_2O$ [b]	0.273
Submaxillary Mucin [c]	1.000
α-Amylase [d]	2.000

[a] See Refs. 17 and 18. [b] J.T. Baker Chemical Co., Bricktown, N.J. [c] Worthington Biochemical Corp., Freehold, N.J. [d] ICN Nutritional Biochemicals, Life Science Group, Plainview, N.J.

0022-3549/84/0800-1148$01.00/0
© 1984, American Pharmaceutical Association

Table II—Equilibrium Dialysis of Aqueous Mixture of Ammonia, Benzethonium Chloride, and Methoxyethylene–Maleic Anhydride Copolymer

Cation	Theoretical for 100% Electrostatic Complex	Theoretical for 0% Electrostatic Complex	Found
		Inside Dialysis Bag	
Benzethonium[a]	0.10% (2.2 mM)	0.05% (1.1 mM)	0.11% (2.4 mM)
Ammonium[b]	2×10^{-4}% (0.1 mM)	20×10^{-4}% (1.2 mM)	2×10^{-4}% (0.1 mM)
		Outside Dialysis Bag	
Benzethonium[a]	None	0.05% (1.1 mM)	0.003% (0.06 mM)
Ammonium[b]	3.8×10^{-3}% (2.2 mM)	2.0×10^{-3}% (1.2 mM)	3.1×10^{-3}% (1.8 mM)

[a] Calculated as benzethonium chloride. [b] Calculated as ammonia.

Studies have been done on the degree of binding of negatively charged polymers with small positively charged ions (10). Increased binding at a particular polymer carboxylate site resulted in decreased negative charge density at that site. This resulted in reduced energy requirements for nearby carboxylic acid groups to ionize and, therefore, in a lowering of the pH (11). This decrease in pH has, in fact, been used to establish the magnitude of binding of counterions to polyanions (12–15).

The studies described above, taken together, strongly suggest the formation of electrostatic complexes between polyanions and cations. The evidence for interaction with long-chain quaternary ammonium salts such as benzethonium chloride, however, is nonexistent. Furthermore, evidence of this kind of interaction with a type of copolymer such as methoxyethylene–maleic anhydride is lacking. Therefore, an investigation was undertaken to determine the nature of the mixture of benzethonium chloride and methoxyethylene–maleic anhydride copolymer.

EXPERIMENTAL SECTION

Preparation of Benzethonium Chloride–Polymer Mixtures in Water—Methoxyethylene–maleic anhydride copolymer[1] (100 mg) was added to deionized, distilled water at 50°C. The pH was adjusted with 3 M NH_4OH to 5.0, and the solution was diluted to 100 mL. An equal volume of a 0.2% solution of benzethonium chloride[2] in water was slowly added while maintaining the pH at 5.0–5.1 with 3 M NH_4OH. The final concentration was 0.0023 M NH_4^+, 0.0022 M benzethonium chloride, and 0.0032 M methoxyethylene–maleic acid repeating units. A 5% solution of the polymer was used for titration studies with 4 M NaOH (Fig. 1). Copolymer and benzethonium chloride were used as received.

Other benzethonium chloride–polymer mixtures were prepared in the same manner, but without pH adjustment, to provide the same concentrations of repeating units as described above. The complex was also prepared in 50% acetone by mixing equal volumes of 0.2% benzethonium chloride in acetone with 0.016–0.4% aqueous solutions of the copolymer at room temperature.

Dialysis—Cellulose acetate dialysis tubing[3], with a molecular weight cutoff of 12,000, was washed with distilled, deionized water. Equilibrium dialysis was performed at room temperature, with solvent inside and outside of the bag identical in composition and pH, under the following conditions: (*a*) equal volumes outside and inside the bag; (*b*) four times the volume outside as inside the bag; and (*c*) 19 times the volume outside as inside the bag.

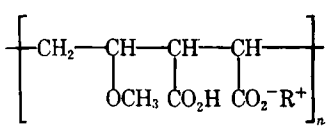

I: $R^+ = NH_4^+$

II: $R^+ = (CH_3)_3CCH_2C(CH_3)_2$—C$_6H_4$—$(OCH_2CH_2)_2\overset{+}{N}(CH_3)_2$ with $CH_2C_6H_5$

[1] Gantrez 139; GAF Corp., Wayne, N.J.
[2] Hyamine 1622; Rohm and Haas, Philadelphia, Pa.
[3] Arthur H. Thomas Co., Philadelphia, Pa.

Advantages of the high ratio were that it allowed more unbound ions to dialyze out of the bag and there was a reduction of the Donnan effect. The disadvantage, however, was that any material of interest outside the bag was diluted. The ratio used depended on the optimum requirement for a particular experiment.

Dialysis was performed for 18–24 h with constant stirring. Before analysis of components under condition *c*, the volume of solution was concentrated to the volume found inside the bag.

Effect of Salivary Components—Four solutions, each containing some of the salivary components from simulated saliva (16, 17), were prepared (Table I). The solutions were: (A) calcium and magnesium salts, (B) potassium and sodium salts, (C) all saliva salts included in A and B; (D) proteins. For the salt reactions, 1 volume of these solutions or water was added to 3 volumes of 0.1% benzethonium chloride–polymer mixture and dialyzed. On the outside of the dialysis bag was a mixture of the salts with the same concentration as inside the bag. Dialysis proceeded according to condition *c*.

For the protein reactions, 1 volume of protein solution was added to 3 volumes of benzethonium chloride or the benzethonium chloride–polymer mixture and dialyzed according to condition *a*.

Analysis of Benzethonium Chloride—Benzethonium chloride was determined by anionic titration with sodium lauryl sulfate, using disulphine blue–dimidium bromide as an end point indicator (18).

Analysis of Ammonia—Ammonia was determined with an ammonium ion-selective electrode[4].

RESULTS AND DISCUSSION

Equilibrium Dialysis—An aqueous mixture of benzethonium chloride and ammonia-adjusted hydrolyzed methoxyethylene–maleic acid copolymer contained 0.0023 M ammonia, 0.0022 M benzethonium chloride, and 0.0032 M copolymer repeating units. This mixture was equilibrium dialyzed by using dialysis condition *c*. If all the benzethonium cations formed an electrostatic complex with the polymer anions, which by virtue of its molecular weight (500,000) would not pass through the membrane, then one would have expected to find all the benzethonium cations (0.0022 M) and only 0.05% of the ammonium ions (0.0001 M) inside the dialysis bag. On the other hand, if there was no selective binding of the benzethonium cation to the polymer counterion, then half of the benzethonium cation (0.0011 M) and half of the ammonium cation (0.0012 M) would have remained inside the bag to maintain charge neutrality with that portion of the polymer which is ionized (0.0023 M).

The results (Table II) show that approximately all the benzethonium cations (0.0024 M) and only 0.0001 M ammonium ions remained inside the dialysis bag. Virtually no benzethonium cations and most of the ammonium ions were found outside the bag. The ammonium ion concentration outside the bag would probably have been even higher if not for the likely loss of ammonia during the concentration step. These results indicate selective electrostatic binding of the benzethonium cations to the copolymer anions, *i.e.*, formation of an electrostatic complex.

pH Drop—The pH of a 0.20% benzethonium chloride concentrate rose slightly after being diluted to 0.10%, as would be expected for a twofold dilution. Similarly, after a 0.10% ammonia-adjusted copolymer concentrate was adjusted to 0.05%, the pH also rose slightly. When the two concentrates were diluted by mixing together, however, the pH decreased to below that of the individual components (Table III). This could be due to the fact that the benzethonium cation had a higher affinity than NH_4^+ for the polymer anion. This, in effect, reduces the amount of negative charge on the neutralized carboxylate group, permitting the adjacent carboxylic acid group to ionize, thus lowering the pH.

Stoichiometry—In Table IV, a study of precipitation conditions for the mixture is presented. It shows that when one equivalent of benzethonium chloride was mixed with one equivalent of active carboxylic acid (pK_a 3.7),

[4] Orion Research, Cambridge, Mass.

Table III—pH Drop in Mixing Benzethonium Chloride and Methoxyethylene–Maleic Anhydride Copolymer

Mixture Composition	pH
0.10% Benzethonium chloride	6.38
0.05% Ammonia-adjusted methoxyethylene-maleic anhydride copolymer	5.82
0.10% Benzethonium chloride and 0.05% ammonia-adjusted methoxyethylene-maleic anhydride copolymer (from respective stock solutions)	5.37

Table IV—Stoichiometry of Precipitation of Benzethonium Chloride and Active Methoxyethylene–Maleic Acid Copolymer Carboxylic Acids

Mixture Composition	Ratio of Equivalents of Mixture to Active Carboxylic Acid	Appearance
0.1% Benzethonium chloride + 0.050% polymer	1:1.5	Emulsion
0.1% Benzethonium chloride + 0.033% polymer	1:1	Precipitate
0.1% Benzethonium chloride + 0.025% polymer	1:0.75	Emulsion
0.1% Benzethonium chloride + 0.017% polymer	1:0.50	Emulsion
0.1% Benzethonium chloride + 0.009% polymer	1:0.25	Emulsion
0.1% Benzethonium chloride	1:0	Clear Solution

a precipitate formed, but an excess of either reactant resulted in formation of an emulsion. This can be explained by formation of an electrostatic complex between the reactants, which would tend to reduce the effective charge on each of the components, thereby decreasing water solubility. At the same time, a large, hydrophobic molecule is produced, which would also tend to have minimal water solubility.

Formation of an emulsion at any other ratio is readily explainable. With an excess of copolymer, the surplus negative charge keeps the material partially suspended in water. With an excess of benzethonium chloride, the positively charged, surface-active benzethonium chloride acts an an emulsifying agent.

Other Anionic Polymers—The effect of polymer molecular weight was investigated as a possible parameter of interaction with benzethonium chloride; dialysis condition *c* was used. The methoxyethylene-maleic anhydride copolymers used all have the same structure but average molecular weights of 250,000[5] (A), 500,000[1] (B), and 1,250,000[6] (C), respectively. Table II shows the theoretical results expected for 100 and 0% electrostatic complexation of benzethonium chloride with copolymer B (used throughout this research). These values also apply for copolymers A and C. The observed results (Table V) show that in all three cases, approximately all of the benzethonium cation stayed inside the membrane and approximately all of the ammonium ion was released. That is, within the limits investigated, formation of an electrostatic complex proceeded to completion independent of molecular weight.

The possibility of electrostatic complex formation was also investigated for benzethonium chloride and other polycarboxylic acids. Benzethonium chloride was mixed with several different types of anionic polymers. Two changes were observed (Table VI) which are similar to those observed with benzethonium chloride and copolymer B. These changes were marked increases in turbidity and, generally, decreases in pH to below that of either of the individual components. The pH of the benzethonium chloride solution was 6.38. The pH of the polymer solutions are listed in Table VI.

These two effects are consistent with formation of an electrostatic complex. Production of turbidity was explained above. Decrease in pH by formation of an electrostatic complex is also easily explained. Methoxyethylene-maleic anhydride copolymer, polyacrylic acid, and ethylacrylate-methacrylic acid copolymer yield hydrochloric acid, a relatively strong acid, as a by-product of the reaction. (As explained above, for copolymer B the decrease in the pK_a of the less active acid should also contribute to the decrease in pH.) For the diisobutylene-maleic acid and vinyl alcohol-acrylic acid copolymers, in which sodium chloride rather than hydrochloric acid would be expected to be released during the formation of an electrostatic complex, no decrease in pH was observed. One of these polymers, the disodium salt of the copolymer of diisobutylene-maleic acid, was further investigated by equilibrium dialysis. After equilibrium was attained, 98% of the benzethonium cation remained inside the membrane, demonstrating electrostatic complex formation. Dialysis was not attempted with the sodium salt of the vinyl alcohol-acrylic acid copolymer because of difficulties anticipated due to the precipitate.

[5] Gantrez 119; GAF Corp.
[6] Gantrez 169; GAF Corp.

Table V—Equilibrium Dialysis of Aqueous Mixture of Ammonia, Benzethonium Chloride, and Three Copolymers of Different Molecular Weights

Cation	Mol. Wt. 250,000	Mol. Wt. 500,000	Mol. Wt. 1,250,000
Benzethonium[a]	0.105[b]	0.107	0.108
Ammonium	0.0002[b]	0.0002	0.0002

[a] Calculated as benzethonium chloride. [b] Inside membrane, %.

Effect of Acetone—To elucidate the driving force of the reaction, it was of interest to determine the effect of other solvents on the benzethonium-copolymer complex. The reaction mixture was made with water-acetone (50:50) as solvent. The ratios of equivalents of benzethonium chloride-active carboxylic acid groups ranged from excess benzethonium chloride (1:0.25, for 0.1% benzethonium chloride and 0.008% copolymer) to excess carboxylic acid groups (1:6.00, for 0.1% benzethonium chloride and 0.200% copolymer). The solutions were dialyzed according to condition *b*. The degree of complexation was determined by analysis of the benzethonium cation inside and outside the membrane. The observed values were compared with theoretical values calculated *via* Donnan's equilibria.

The results (Table VII) show very good agreement between the observed ratio and that calculated for 0% complexation, indicating that, surprisingly, reaction did not occur, which is in contrast to the corresponding situation in water in which the reaction went to completion. This would suggest that a driving force of the reaction in acetone is different than in water. It has been suggested that in water, charged species (polyanions and polycations) show an increase in entropy (9). Molecules tend to occupy as much space as possible. Movement of the polymer microions is restricted due to the limited movement of the polyelectrolyte chain. Therefore, there is an "escaping tendency" of the microions. This escaping tendency is overcome by two oppositely charged polyions coming together, thereby liberating the microions from the polyelectrolyte. One would expect the reaction also to occur in aqueous acetone because the same escaping tendency should be present. However, the reaction did not occur in aqueous acetone.

This suggests a second possibility with respect to the driving force of the reaction. Benzethonium chloride forms micelles in water due to the incompatibility of the hydrophobic tails with water. The extent of this micelle formation is limited because of the repulsion among the positively charged benzethonium head groups. This can be overcome, however, by the oppositely charged field exerted by the polyanion. That is, strong attraction of the positively charged head groups on the benzethonium cation with the negatively charged field exerted by the polyanion tends to reduce the repulsion of the benzethonium cations with each other, allowing increased formation of micelles. This could be the driving force for the reaction in water. In acetone, however, there is no incompatibility between the benzethonium hydrophobic tails and the solvent and, therefore, no micelle formation. The reaction, therefore, should not, and did not, take place in acetone. Hence, a driving force for the reaction that is consistent with the facts is increased hydrophobic interactions of the long chains rather than increased freedom of the microions. Both could cause an increase in entropy.

Influence of pH—The effect of pH on the stability of aqueous benzethonium-copolymer complex was studied (Table VIII). The mixture was treated with either dilute hydrochloric acid or ammonium hydroxide to achieve the desired pH. Virtually no difference in appearance was observed at pH 4.0, 5.0, and 8.0. A decrease in pH to 3.6, however, by slow addition of hydrochloric acid led to complete clarification of the supernatant and concomitant formation of a precipitate. On the other hand, when hydrochloric acid was rapidly added to the pH 5.0 emulsion until it was at pH 2.0, a clear solution resulted without ever going through a precipitate stage. At pH 1.0, the clear solution separated into an oil and a clear supernatant.

Analysis of the dispersions or clear supernatants before dialysis showed the theoretical amount of benzethonium cation at pH 2.0, 4.0, 5.0, and 8.0, but not at pH 1.0 and 3.6. This suggests that there was a meaningful amount of benzethonium cation in the oil (pH 1.0) and solid precipitate (pH 3.6).

The mixtures of pH 2.0, 4.0, 5.0, and 8.0 were treated according to dialysis condition *b*. The results demonstrate that at pH $\geq$ 4.0, approximately all of the benzethonium cation is retained inside the membrane; however, at pH 2.0, within experimental error, the benzethonium cation is evenly distributed on both sides of the membrane. The formation of a precipitate at pH 3.6 can be explained by the fact that protons react with any excess negatively charged

Table VI—Comparison of pH and Appearance of Polymers Before and After Addition of Benzethonium Chloride

Polymer	pH of Polymer		Appearance of Polymer	
	Without Benzethonium Chloride	With Benzethonium Chloride	Without Benzethonium Chloride	With Benzethonium Chloride
Methoxyethylene-maleic anhydride	3.45	2.78	Clear Solution	Cloudy + Precipitate
Polyacrylic acid[a]	3.89	3.20	Clear Solution	Cloudy
Ethylacrylate-methacrylic acid copolymer[a]	5.15	3.47	Clear Solution	Cloudy
Diisobutylene-maleic acid disodium salt copolymer[a]	10.23	10.30	Clear Solution	Cloudy
Vinyl alcohol-acrylic acid sodium salt copolymer[a]	9.40	8.75	Clear Solution	Cloudy + Precipitate

[a] Rohm and Haas, Philadelphia, Pa.

Table VII—Benzethonium-Copolymer Complexation in Aqueous Acetone Studied by Equilibrium Dialysis

Complex Composition	Benzethonium Cation Inside-Benzethonium Cation Outside		
	Theoretical		
	100% Complexation	0% Complexation	Observed
0.1% Benzethonium chloride	—	1.0	1.0
0.1% Benzethonium chloride and 0.008% methoxyethylene-maleic anhydride	2.0	1.6	1.5
0.1% Benzethonium chloride and 0.017% methoxyethylene-maleic anhydride	3.6	2.2	2.4
0.1% Benzethonium chloride and 0.025% methoxyethylene-maleic anhydride	6.0	2.8	2.8
0.1% Benzethonium chloride and 0.033% methoxyethylene-maleic anhydride	11.2	3.3	3.5
0.1% Benzethonium chloride and 0.050% methoxyethylene-maleic anhydride	∞	4.2	3.9
0.1% Benzethonium chloride and 0.200% methoxyethylene-maleic anhydride	∞	12.2	7.8

Table VIII—pH Effect on Stability of the Benzethonium-Copolymer Complex

pH	Appearance	Benzethonium Cation, %[a]		
		Before Dialysis	After Dialysis	
			Inside Tube	Outside Tube
1.0	Clear supernatant and oil	0.011[b]	—	—
2.0	Clear solution	0.103	0.024	0.019
3.6	Clear supernatant and solid precipitate	0.010[b]	—	—
4.0	Dispersion	0.100	0.116	0.001
5.0	Dispersion	0.105	0.101	0.001
8.0	Dispersion	0.104	0.096	<0.001

[a] Calculated as benzethonium chloride. [b] Virtually only the supernatants were analyzed.

groups on the complex, thereby making the complex less water soluble. Formation of a clear solution at pH 2.0, in which the benzethonium cation was approximately evenly distributed inside and outside of the membrane, can be explained by the fact that the hydrogen and chloride ions of the hydrochloric acid successfully compete with the reactants for the charged sites on the complex. Hence, at pH 2.0, the benzethonium-polymer complex dissociated to form the soluble protonated polymer and soluble benzethonium chloride, and the benzethonium chloride passed through the dialysis bag. At pH 1.0, the same situation as at pH 2.0 existed, except that benzethonium chloride was insoluble at low pH. The results of the studies at pH 4–8 demonstrated that at these pH values, stable emulsions formed.

Effect of Saliva—Since the ultimate use of the benzethonium-copolymer complex was for a mouth rinse or dentifrice, it was important to determine whether it remained intact in the presence of saliva. Saliva contains mainly salts and glycoproteins. Due to experimental difficulties in working with whole saliva containing both salts and proteins, simulated saliva was made containing either one or the other.

Salivary Salts—After it was shown in a preliminary experiment that, indeed, the complex dissociated considerably in the presence of saliva salts under exaggerated conditions (in terms of contact time and concentrations of salts), it was of interest to determine which salts in the saliva were responsible for this dissociation. The reaction of the benzethonium-copolymer complex with salivary salts was studied by equilibrium dialysis condition *c*. The composition inside the dialysis tube roughly simulated in-use conditions, *i.e.*, dilution of a mouth wash by 25% with the saliva salt solution. This saliva salt solution had approximately the same composition as found in saliva. Benzethonium chloride and the benzethonium-copolymer complex diluted by 25% with water, were used as controls.

Table IX—Effect of Salivary Salts on Decomposition of Benzethonium-Copolymer Complex[a]

Reaction Mixture	Benzethonium Cation Inside of Bag After Dialysis, %[b]
Benzethonium chloride[a]	0.004
Benzethonium-copolymer complex	0.079
Benzethonium-copolymer complex and potassium and sodium salts	0.071
Benzethonium-copolymer complex and calcium and magnesium salts	0.064
Benzethonium-copolymer complex and all saliva salts	0.023

[a] 0.075% with respect to benzethonium chloride. [b] Calculated as benzethonium chloride.

The data (Table IX) show that the 0.075% benzethonium chloride was not held back by the dialysis membrane and was diluted ~20-fold by the dialysis solution. The 0.075% benzethonium-copolymer control was essentially maintained completely (0.079%) inside the membrane. In the presence of either the monovalent or divalent salts, little effect was apparent, with final concentrations of 0.071 and 0.064%, respectively. But when the monovalent and divalent salts were combined, a marked dissociation of the complex resulted. It appeared that a combination of calcium and magnesium salts and high ionic strength had a synergistic effect, giving a significant dissociation of the benzethonium-copolymer complex.

The contribution of calcium and magnesium ions was also studied by atomic absorption (Table X). The data show that the number of moles of calcium and magnesium ions which became bound to the copolymer was approximately equal to the sum of the carboxylate groups which contained sodium and am-

Table X—Relationship Between Available Copolymer Carboxylates and Binding of Calcium and Magnesium Ions

	Available Carboxylate[a], mol × 10^{-5}/100 mL	Bound Ca and Mg, mol × 10^{-5}/100 mL
Before salt reaction	8	—
After salt reaction	19	20

[a] Available carboxylate groups before the reaction are those containing sodium or ammonium counterions; available carboxylate groups after the reaction include the ones with sodium or ammonium counterions as well as those in which the benzethonium cations were displaced.

Table XI—Effect of Salivary Protein on Stability of the Benzethonium–Copolymer Complex

Mixture Composition	Benzethonium Cation After Dialysis, %[a]	
	Inside Bag	Outside Bag
Benzethonium chloride	0.038	0.038
Benzethonium chloride and mucin	0.034	0.032
Benzethonium chloride and α-amylase	0.038	0.038
Benzethonium-copolymer complex	0.071	0.000
Benzethonium-copolymer complex and mucin	0.074	0.001
Benzethonium-copolymer complex and α-amylase	0.071	0.002

[a] Calculated as benzethonium chloride.

monium ions and those groups which were freed of benzethonium cations. This suggests a direct relationship between the amount of benzethonium cation released from the polymer and the amount of divalent cations taken up.

The dissociation of the complex in the presence of saliva salts can be represented by Scheme I:

$$Bt^+G^- + M^+X^- \rightleftharpoons Bt^+X^- + M^+G^-$$

Scheme I

where Bt represents benzethonium, G represents the copolymer, M represents the saliva salt cations, and X represents the saliva salt anions.

These results provide a reasonable explanation for the mode of action of the benzethonium-copolymer complex in the oral cavity (2). Simply, the calcium-magnesium ions of the saliva displace the benzethonium cation in the benzethonium-copolymer electrostatic complex. Slow release of the benzethonium cations by the saliva salts explains the low plaque and gingivitis values since benzethonium chloride is an active antimicrobial compound. Complexation of calcium ions from the saliva by the copolymer explains the low calculus value.

Salivary Proteins—The stability of the benzethonium-copolymer complex with another type of salivary component, the proteins, was also studied by equilibrium dialysis (condition *a*). Benzethonium chloride and the benzethonium-copolymer complex were mixed with salivary proteins and dialyzed. The results (Table XI) show that the benzethonium cations from benzethonium chloride solutions were approximately evenly distributed inside and outside the dialysis bags, not being affected by the proteins, and the benzethonium cation from the benzethonium-copolymer emulsions remained inside the bag, not being released by the proteins.

If a complex formed between the proteins and the benzethonium cation, then the benzethonium cation would have been trapped with the protein inside the bag, since the molecular weight cutoff of the membrane is 12,000. The fact that in the benzethonium chloride-protein cells, the benzethonium cation was not trapped indicated that the salivary proteins had little or no affinity for the benzethonium cation. If the proteins formed some sort of complex with the copolymer, thereby dissociating the benzethonium-copolymer complex, then the benzethonium cation would have been found in the dialysate. It was not. Hence, although the complex dissociated in the presence of salivary salts, it did not dissociate in the presence of saliva proteins.

CONCLUSIONS

A mixture of benzethonium chloride and methoxyethylene-maleic anhydride copolymer formed an electrostatic complex of the benzethonium cation and the anion of the hydrolyzed polymer, as determined by dialysis, pH, and stoichiometric evidence. An emulsion of the complex was stable in the presence of an excess of either constituent and at pH > 4. The complex was unstable at pH < 4, precipitated at stoichiometric quantities, and did not form in 50% acetone. It was decomposed by simulated saliva because of calcium and magnesium ions in saliva and was unaffected by saliva proteins.

REFERENCES

(1) A. R. Volpe, L. J. Kupczak, J. H. Brant, W. J. King, R. C. Kestenbaum, and H. J. Schlissel, *J. Dent. Res.*, **48**, 832 (1969).

(2) A. Gaffar, M. C. Solis-Gaffar, E. Tavss, H. W. Marcussen, and K. N. Rustogi, *J. Dent. Res.*, **60**, 1897 (1981).

(3) A. Gaffar, M. C. Gaffar, H. W. Marcussen, and K. Rustogi, *IADR Progr. Abstr.*, **56**, Abstr. No. 486 (1978).

(4) M. Dichter, D. Mangaraj, and W. J. King, U.S. Pat. No. 3,956,480 (1976).

(5) W. B. Ackart, R. L. Camp, W. C. Wheelwright, and J. S. Byck, *J. Biomed. Mater. Res.*, **9**, 55 (1975).

(6) G. Rölla, H. Loe, and C. R. Schiott, *J. Periodontal Res.*, **5**, 90 (1970).

(7) S. Saito, *Kolloid Z.*, **143**, 66 (1955).

(8) H. G. D. B. Jong and C. V. D. Meer, *Proc. Nederland Akad. Wetensch.*, **45**, 593 (1942).

(9) A. S. Michaels and R. G. Miekka, *J. Phys. Chem.*, **65**, 1765 (1961).

(10) H. P. Gregor and M. Frederick, *J. Polym. Sci.*, **23**, 451 (1957).

(11) R. W. Armstrong and U. P. Strauss, *Encycl. Polym. Sci. Technol.*, **10**, 822 (1969).

(12) H. P. Gregor, L. B. Luttinger, and E. M. Loebl, *J. Phys. Chem.*, **59**, 34 (1955).

(13) H. Morawetz, A. M. Kotliar, and H. Mark, *J. Phys. Chem.*, **58**, 619 (1954).

(14) A. M. Kottliar and H. Morawetz, *J. Am. Chem. Soc.*, **77**, 3692 (1955).

(15) M. Mandel and J. C. Leyte, *J. Polym. Sci. A*, **1**, 2883 (1964).

(16) A. Davies, *J. Periodontal Res.*, **12**, Suppl. 68 (1973).

(17) R. E. Davis, C. W. Hartman, and J. H. Fincher, *J. Pharm. Sci.*, **60**, 429 (1971).

(18) D. C. Cullum, *Third Int. Congr. Surface Activity (Cologne)*, **3**, 42 (1960).

Increased Skin Permeability for Lipophilic Molecules

EUGENE R. COOPER

Received July 30, 1982, from *The Procter & Gamble Co., Miami Valley Laboratories, Cincinntai, OH 45247.* Accepted for publication August 25, 1983. Present address: Alcon Laboratories, Fort Worth, TX 76134.

Abstract □ Treatment of the epidermis with surfactants can markedly increase the transport of polar molecules but only marginally increases the transport of nonpolar (lipophilic) molecules. Thus, other vehicle systems are needed to increase the transport of lipophilic molecules. One method to accomplish this increased transport is to add small quantities of polar lipids to a base vehicle containing propylene glycol. The transport of nonpolar materials such as salicylic acid can be increased by an order of magnitude by the addition of small amounts of fatty acids or alcohols to a formulation. The effect of this mixed system is much greater than the effect of any of the agents alone.

Keyphrases □ Transport systems—increased skin permeability, lipophilic molecules □ Lipophilic molecules—transport systems, increased skin permeability

The stratum corneum, which is the main barrier to cutaneous transport (1), is structurally a complex membrane, and thus, transport probably takes place through a variety of pathways. It has been suggested in a study of the effect of temperature on the penetration of alcohols (2) that there are at least two pathways for transport across the skin: a polar pathway and a nonpolar pathway. The polar pathway is associated with the protein component of the stratum corneum and might be envisioned as aqueous channels in the protein; the nonpolar pathway is associated with the lipid component.

In recent studies (3), the attempt has been made to clarify and support the hypothesis that there are at least two parallel pathways for transport by using surfactant treatment, which greatly increases the transport of polar molecules but only slightly increases the transport of nonpolar molecules. For example, it has been found that treatment of the human epidermis with decylmethyl sulfoxide greatly increases the transport of salicylic acid at pH 9.9 (ionized or polar form) but only slightly increases salicylic acid transport at pH 2.65 (un-ionized or nonpolar form). Other studies have shown that the transport of 1-propanol is greater than that of propylene glycol or glycerol. That is, even though propylene glycol has a much higher oil–water partition coefficient than glycerol (4), its cutaneous flux from aqueous solution is only slightly greater than that of glycerol but much less than that of 1-propanol. Thus, as the polarity of a molecule is increased, *i.e.*, its oil–water partition coefficient decreases, a polarity exists for which the oil–water partition coefficient is not related to transport. These results differ noticeably from those obtained previously (2), in which even 1-pentanol is claimed to transport *via* a polar pathway.

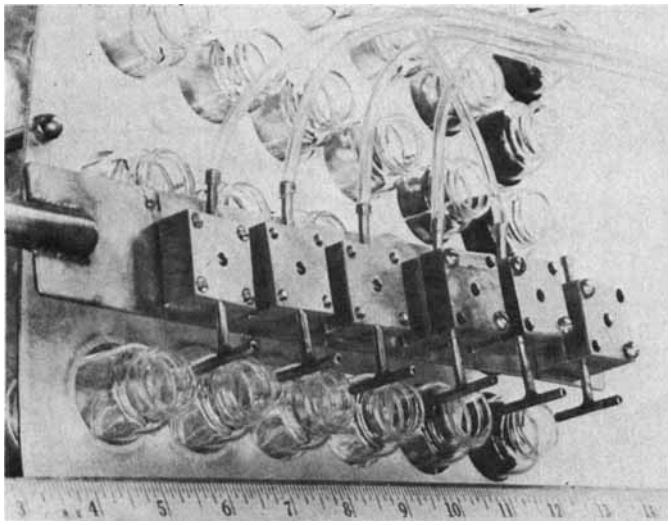

Figure 1—*Diffusion cell.*

The existence of multiple transport pathways in skin points to the possibility for design of vehicles to alter the permeability of the skin *via* the different pathways, as the surfactants seem to uniquely alter the polar pathway. Certain two-component systems have been found which alter transport differently from the way the components behave individually. The purpose of this report is to describe the effects of these vehicle systems on the transport of nonpolar molecules across skin. Salicylic acid was used as a prototype nonpolar compound, but similar results were obtained on many other nonpolar compounds. A model is proposed to interpret these findings, but the mechanism by which these vehicles alter transport is still unknown.

EXPERIMENTAL SECTION

Materials—Salicylic acid[1], [^{14}C-carboxylate]salicylic acid[2], the fatty acids and alcohols[3], propylene glycol[4], diethylene glycol[5], and the polyethylene glycols[6] were obtained commercially. The sulfoxides (purity >95%) were synthesized[7], and the dimethyl polysiloxane[8] rubber membranes were cast on a large stainless steel plate. All other chemicals used were of reagent grade.

Diffusion Studies—*Epidermis Preparation*—Full-thickness human ab-

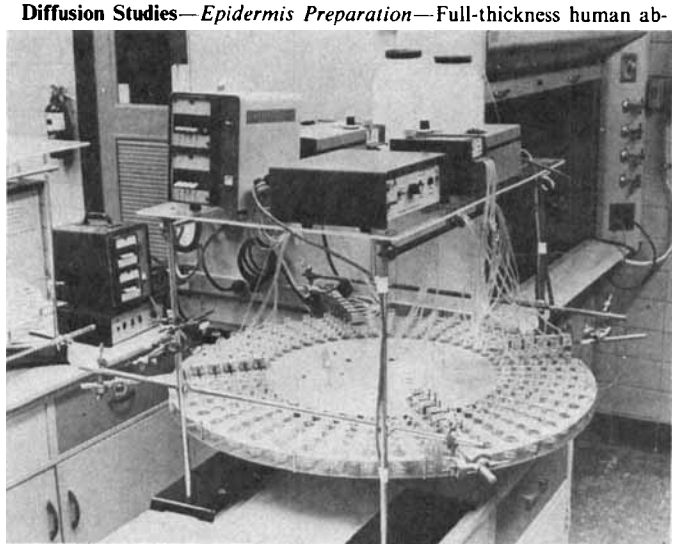

Figure 2—*Diffusion Apparatus.*

[1] Fisher Scientific Co., Cincinnati, Ohio.
[2] ICN Chemicals, Radioisotope Division, Irvine, Calif.
[3] Nu-Chek Prep, Inc., Elysian, Minn.
[4] J. T. Baker Chemical Co., Phillipsburg, N.J.
[5] Aldrich Chemical Co., Inc., Metuchen, N.J.
[6] Ventron Corp., Danvers. Mass.
[7] Miami Valley Laboratories.
[8] MDX-4-4210 elastomer and MDX-4-4210 curing agent; Dow Corning, Midland, Mich.

0022-3549/84/0800-1153$01.00/0
© 1984, American Pharmaceutical Association

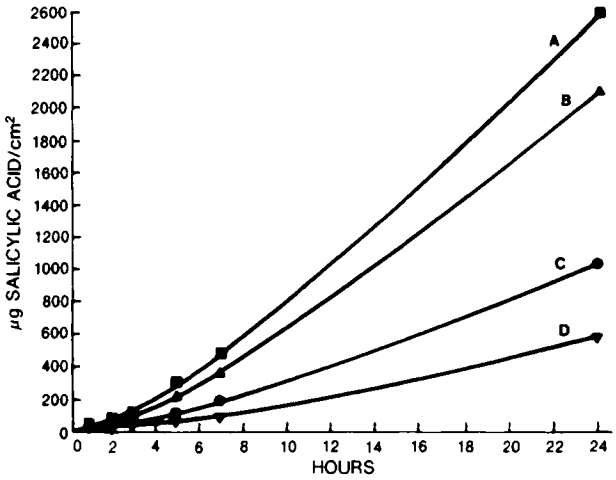

Figure 3—*Effect of polar solvents on salicylic acid transport across human epidermis. Key: (A) 24% salicylic acid in diethylene glycol; (B) 19% salicylic acid in propylene glycol; (C) 30% salicylic acid in tetraethylene glycol; (D) 27% salicylic acid in pentaethylene glycol.*

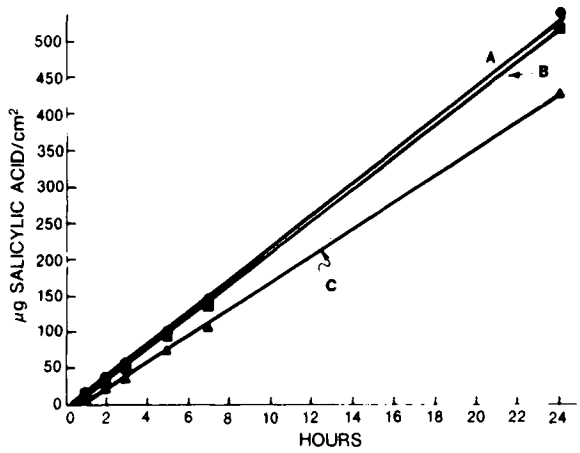

Figure 4—*Effect of polar solvents on salicylic acid transport across silicone rubber. Key: (A) 30% salicylic acid in tetraethylene glycol; (B) 19% salicylic acid in propylene glycol and 24% salicylic acid in diethylene glycol; (C) 27% salicylic acid in pentaethylene glycol.*

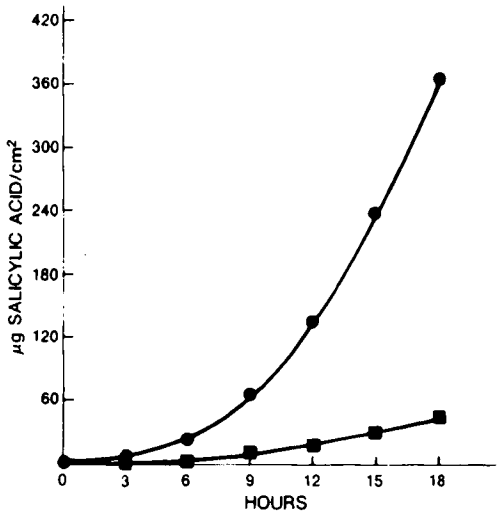

Figure 5—*Penetration of 1% salicylic acid across human epidermis. Key: (●) 0.1 M oleic acid in propylene glycol; (■) propylene glycol.*

dominal skin was obtained at autopsy and frozen until ready for use. The subcutaneous fat was removed with a scalpel, and the skin was placed in water at 60°C for 80 s. The epidermis was carefully removed and mounted (outer surface up) on aluminum foil before rinsing in 0°C hexane for 10 s to remove

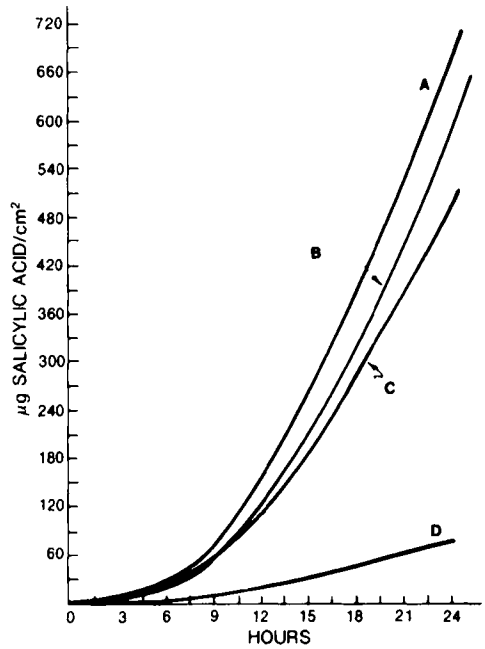

Figure 6—*Effect of the addition of* cis*-unsaturated fatty acids on the penetration of 1% salicylic acid in propylene glycol across human epidermis. Key: (A) 0.1 M myristoleic acid; 0.1 M palmitoleic acid; (C) 0.1 M oleic acid; (D) propylene glycol.*

any fat contamination. The epidermis was either used immediately or wrapped in a plastic sheet[9] and frozen.

Experimental Apparatus—The epidermis was mounted in diffusion cells as pictured in Fig. 1. The flat surfaces of the cell provide a pressure seal after the epidermis is placed between the two compartments, which are bolted together. Up to 100 µL of solution can be placed in the chamber above the skin. The area for transport is 0.122 cm². Water was pumped *via* a multichannel peristaltic pump through the lower compartment at 3.5 mL/h and collected in scintillation vials placed in a programmable rotating fraction collector. Figure 2 shows the entire assembly. The volume of water in the chamber beneath the skin is ~5 µL, so the volume beneath the skin is replaced ~100 times/h. The temperature of the experiments was that of the laboratory, 22 ± 1°C.

Assay for Penetration—Approximately 1 µCi of radioactive tracer was used for each diffusion cell. The quantity of radioactive tracer transported

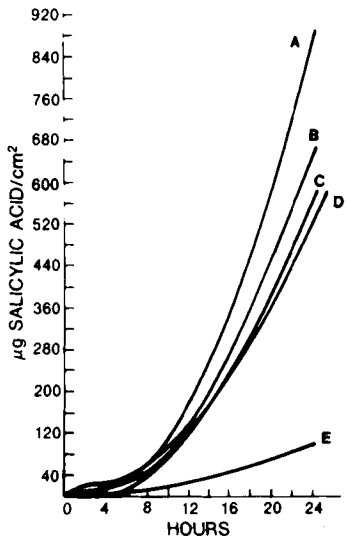

Figure 7—*Effect of the addition of* cis*-unsaturated fatty acids on the penetration of 1% salicylic acid in propylene glycol across human epidermis. Key: (A) 0.1 M vaccenic acid; (B) 0.1 M 10-heptadecanoic acid; (C) 0.1 M petroselenic acid; (D) 0.1 M eicosenoic acid; (E) propylene glycol.*

[9] Saran Wrap.

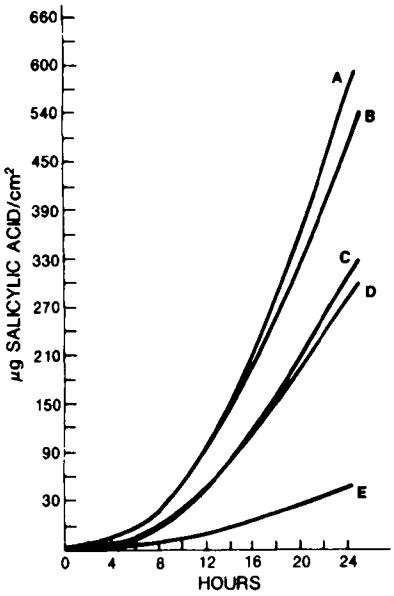

Figure 8—*Effect of the addition of polyunsaturated fatty acids on the penetration of 1% salicylic acid in propylene glycol across human epidermis. Key: (A) 0.1 M linolenic acid; (B) 0.1 M linoleic acid; (C) 0.1 M vaccenic acid; (D) 0.1 M linoelaidic acid; (E) propylene glycol.*

across the skin and collected in the scintillation vials was determined by liquid scintillation counting. The scintillation counting solution (10 mL), added to each 7-mL sample, consisted of cocktail stock solution. The latter consisted of 2,5-diphenyloxazole (8 g) and 1,4-bis(4-methyl-5-phenyloxazol-2-yl) benzene (0.16 g) per liter of toluene.

Variation in Data—The epidermal transport from each vehicle was determined in quadruplicate, and the variation in the data was ±25%. Data on each graph represent separate experiments run on different days with different epidermal samples.

RESULTS AND DISCUSSION

The vehicles described in this paper are two-component systems consisting of a polar solvent, such as propylene glycol, and a lipid, such as oleic acid. The choice of polar solvent is important, since there is a wide range in the effects of polar solvents. For example, it can be seen in Fig. 3 that propylene glycol and diethylene glycol support a high rate of transport of salicylic acid but that the flux drops off some as the number of ethylene oxide groups is increased. (Note that comparisons are made among saturated solutions to ensure equal thermodynamic activity.) Transport of salicylic acid across a dimethyl polysiloxane membrane (Fig. 4) was essentially the same from each of these

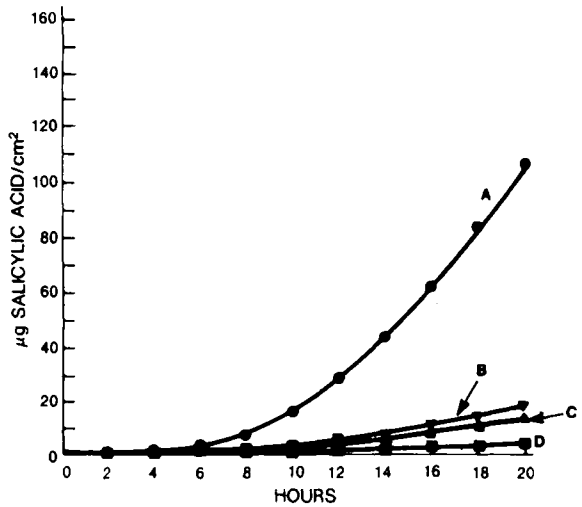

Figure 9—*Effect of the addition of fatty acids on the penetration of 1% salicylic acid in propylene glycol across human epidermis. Key: (A) 0.1 M oleic acid in propylene glycol; (B) 0.1 M lauric acid in propylene glycol; (C) 0.1 M decanoic acid in propylene glycol; (D) propylene glycol (control).*

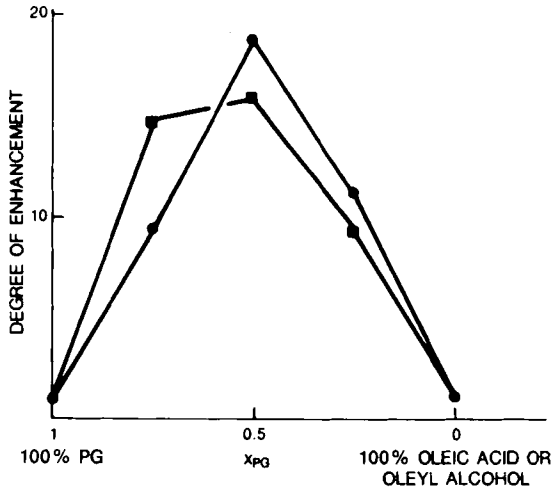

Figure 10—*Degree of enhancement of salicylic acid steady-state flux as a function of propylene glycol mole fraction ($X_{propylene\ glycol}$) from saturated solutions. Key: (■) oleyl alcohol; (●) oleic acid.*

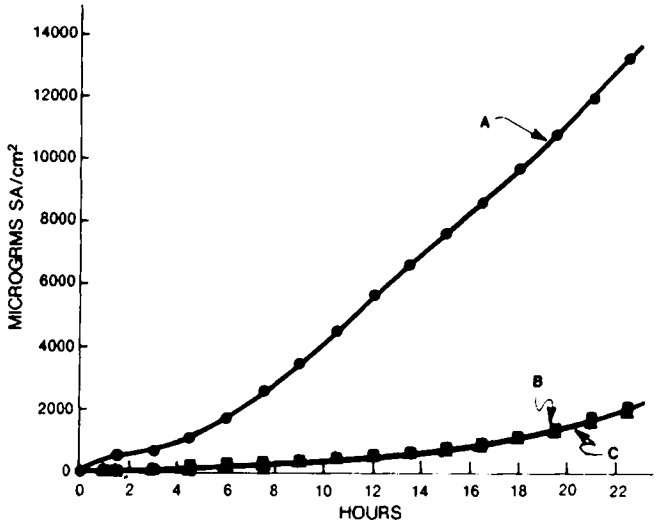

Figure 11—*Effect of sulfoxides on salicylic acid transport across human epidermis. Key: (A) 24% salicylic acid in propylene glycol plus 0.1 M oleyl methyl sulfoxide; (B) 21% salicylic acid in propylene glycol; (C) 22% salicylic acid in propylene glycol plus 1 M decyl methyl sulfoxide.*

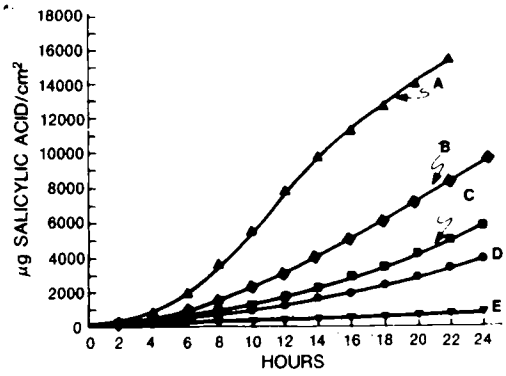

Figure 12—*Penetration of salicylic acid at saturation from propylene glycol–alcohol vehicles across human epidermis. Key: (A) 21% salicylic acid in 0.25 mole fraction decanol–propylene glycol; (B) 22% salicylic acid in 0.25 mole fraction hexanol–propylene glycol; (C) 22% salicylic acid in 0.25 mole fraction octanol–propylene glycol; (D) 22% salicylic acid in 0.25 mole fraction butanol–propylene glycol; (E) 20% salicylic acid in propylene glycol.*

solvents. This result indicates that polar solvents interact differently with skin and that the variations in transport are not due to solution phenomena.

The addition of a small amount of oleic acid to propylene glycol provides for a rather large increase in salicylic acid transport (Fig. 5). (Similar increases

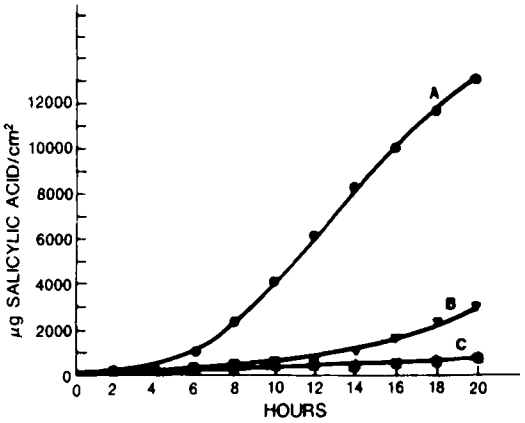

Figure 13—*Penetration of salicylic acid at saturation from oleic acid–propylene glycol or –1,2-butanediol vehicles across human epidermis. Key: (A) 15% salicylic acid in 0.25 mole fraction oleic acid–propylene glycol; (B) 15% salicylic acid in 0.25 mole fraction oleic acid–1,2-butanediol; (C) 23% salicylic acid in propylene glycol or 1,2-butanediol.*

in transport were also observed for the other polar solvents, but only the results for propylene glycol are presented.) Other unsaturated fatty acids give a similar result. Figures 6–8 show the effects of chain length and number and type of double bonds. The effect is reduced for saturated fatty acids (Fig. 9). Long-chain saturated fatty acids are too insoluble in propylene glycol for any effect on transport to be observed.

As the concentration of oleic acid (or oleyl alcohol) is increased, the transport of salicylic acid is also increased, up to a point. As the concentration of lipid is further increased, the flux of salicylic acid decreases (Fig. 10). Here, as mentioned above, transport from saturated solutions is compared to ensure equal driving force (chemical potential). The transport of salicylic acid from saturated solutions of propylene glycol (~22%) and oleic acid (~4%) [or water (0.2%)] are the same. However, use of a mixture of the two materials gives a ~20-fold increase in the transport rate.

The hydrocarbon chain seems to be the important factor as to whether a lipid will increase transport. For example, it can be seen (Fig. 11) that only the unsaturated methyl sulfoxide increases transport. Stearyl methyl sulfoxide also had no effect on transport. However, for alcohols, even the saturated chains can increase transport (Fig. 12). Here, the longer chains are more effective at increasing transport until the length of the chain exceeds 14. At this point, solubility of the alcohol becomes too small for an effect on transport to be observed. Other diols also exhibit this synergism with lipids, but the effect is less pronounced as the chain length is increased (Figs. 13 and 14).

The mechanism by which the epidermal barrier properties are altered is

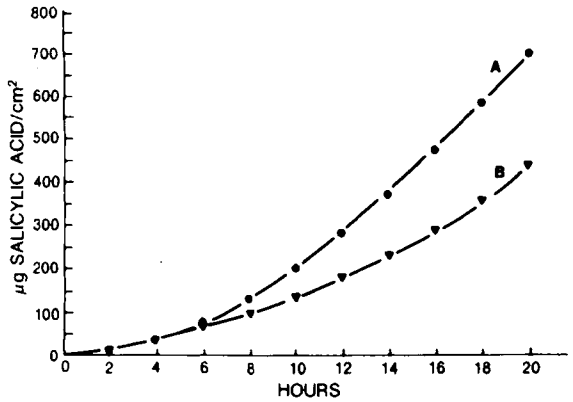

Figure 14—*Penetration of salicylic acid at saturation from oleic acid–1,2-hexanediol vehicles across human epidermis. Key: (A) 24% salicylic acid in 0.25 mole fraction oleic acid–1,2-hexanediol; (B) 14% salicylic acid in 1,2-hexanediol.*

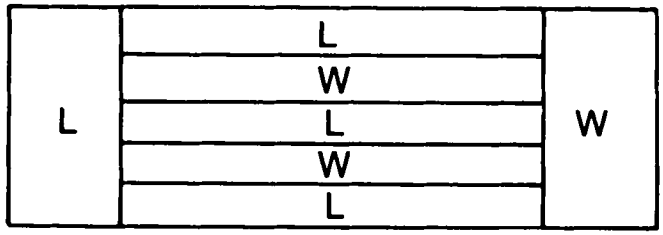

Figure 15—*Model for skin transport.*

not known, but differential scanning calorimetry studies of the stratum corneum[10] indicate that the two-component systems result in an increased fluidization of the stratum corneum lipids. This effect could then result in more rapid diffusion of the molecules across skin. The use of two different solvents to increase solute solubility has been known for some time as "cosolvency" and "blending" (5), and there might be a connection between cosolvency and the effects observed in this study on skin transport.

Regardless of the detailed mechanism by which these vehicles act, the results presented here open the door to the investigation of multicomponent systems to alter the barrier properties of skin. The penetration-aid guidelines obtained from this study and an earlier report (3) indicate that, for polar molecules, the head groups dominate (ionic > zwitterionic > nonionic) and for nonpolar molecules (polar solvent plus lipid), the hydrocarbon chains dominate. It was predicted that branched-chain lipids would be as effective as unsaturated lipids; this was, indeed, the case for isostearic acid.

A general way to categorize the pathways for transport in skin is depicted in Fig. 15, in which no attempt was made to assign a pathway to a particular morphological structure. J_s, the flux at steady state, can be written as:

$$J_s = a_w J_w + a_{Lw} J_{Lw} + (1 - a_w - a_{Lw}) J_L$$

where a_w is the area fraction of the aqueous pathway, a_{Lw} is the area function of the lipid–water pathway, J_w is the flux across the aqueous pathway, J_{Lw} is the flux across the lipid–water pathway, and J_L is the flux across the lipid pathway. It seems clear that there exists a continuous polar pathway, because the flux (at constant concentration) levels off with a decreasing oil–water partition coefficient and because surfactants act primarily to increase the transport of polar molecules. The pathway with the largest area fraction is probably the lipid–water pathway because molecules that have high solubility in both oil and water have the greatest transport. The lipid continuous pathway is included to account for the transport of very lipophilic molecules (such as benzyl salicylate), for which water becomes a major barrier to transport. The two-component systems described in this report act primarily on the lipid barriers, but they may have some effect on the polar pathway.

REFERENCES

(1) R. J. Scheuplein and I. H. Blank, *Physiol. Rev.*, **51**, 702 (1971).

(2) I. H. Blank, R. J. Scheuplein, and D. J. MacFarlane, *J. Invest. Derm.*, **49**, 582 (1967).

(3) E. R. Cooper, in "Solution Behavior of Surfactants: Theoretical and Applied Aspects," K. L. Mittal and E. J. Fendler, Eds., Plenum, New York, N.Y., 1982.

(4) E. M. Wright and J. R. Diamond, *Proc. R. Soc. B.*, **172**, 227 (1969).

(5) K. Shinoda, "Principles of Solution and Solubility," Dekker, New York, N.Y., 1978, chap. 10.

ACKNOWLEDGMENTS

The author would like to acknowledge Patricia Sprong and Gregory Albright for conducting many of the experiments presented in this paper and Bret Berner for pointing out the similarity between cosolvency and blending and the results observed for skin transport.

[10] Experiments were performed in collaboration with Randy Wickett at the Miami Valley Laboratories.

Fluorescence Determination of Microconcentrations of Chlorambucil after Photoactivation

L. G. BERNIER *x, R. C. GAUDREAULT ‡, M. PAGE *, and L. P. JOLY ‡

Received March 9, 1983, from the *Department of Biochemistry, Faculty of Medicine and the ‡School of Pharmacy, Université Laval, Québec, G1K 7P4, Canada. Accepted for publication May 20, 1983.

Abstract □ A fluorescence assay is described which measures the alkylating activity of chlorambucil or its isocyanate derivative after photoactivation in the presence of dimethyl sulfoxide. This assay has a lower limit of sensitivity of 100 ng/mL and *RSD* of <10% for chlorambucil. The method requires <5 μg of alkylating agent and the fluorophore produced is stable for at least 24 h.

Keyphrases □ Chlorambucil—isocyanate derivative, alkylating activity, fluorescence assay □ Nitrogen mustards—chlorambucil and its isocyanate derivatives, alkylating activity, fluorescence assay

Bifunctional alkylating agents are used extensively in the chemotherapeutic treatment of neoplastic and autoimmune diseases. Several colorimetric methods for the determination of specific nitrogen mustards have been described (1–5). These methods are based on the first report by Epstein *et al.* (6) who first showed the reaction of alkylating agents with nitrobenzylpyridine. A fluorometric method has also been described (7) which has a greater sensitivity, but it was not applicable to chlorambucil.

Gaudreault (8) reported that chlorambucil dissolved in dimethyl sulfoxide and exposed to UV light yielded a mixture of products. The fluorescence of the mixture was proportional to the amount of chlorambucil present. Perhydrothiazocine was the most important fluorophore; its structure was determined by mass spectrometry (8).

We describe here the use of this reaction (Scheme I) for the quantitative determination of chlorambucil. This method is sensitive while requiring little material.

EXPERIMENTAL SECTION

Chlorambucil[1] was dissolved in dimethyl sulfoxide[2]. The isocyanate of chlorambucil, 3-{4-[bis(2-chloroethyl)amino]phenyl}propyl-isocyanate, was produced in-house using a literature method (9).

A 200-W UV lamp[3] supplied by a power unit[4] was used for the photoactivation. A UV meter[5] was used to check the UV lamp periodically. Quartz cuvettes[6] (10-mm path length) were placed circularly at 10 cm around the lamp to expose the samples; the fluorescence was then read in the same cuvettes. A spectrophotofluorometer[7] was used to measure the fluorescence of the samples at 434 nm for emission after an excitation at 358 nm.

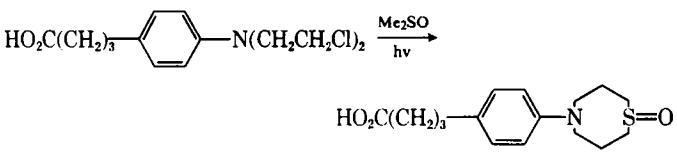

Scheme I

[1] Sigma Chemical Co., St. Louis, Mo.
[2] Spectrophotometric grade; Aldrich Chemical Co., Milwaukee, Wis.
[3] Super Pressure Mercury Lamp HBO; OSRAM Gmb, Berlin-Munich, F.R.G.
[4] Model HB200 Mercury Burner Power Unit; Otto Watzka & Co., Montreal.
[5] Model J-225; Blak-Ray, San Gabriel, Calif.
[6] Fluorescence Open Cuves; Fisher Scientific Co.
[7] Model 4-0202; Aminco-Bowmann, Silver Spring, Md.

Chlorambucil (1 mg/mL) was dissolved in dimethyl sulfoxide and stored at −20°C until use. Standards from 0.1 to 20 μg/mL were freshly prepared by dilution of the stock solution with dimethyl sulfoxide. Two milliliters of the standard was placed in quartz cuvettes and the background fluorescence was read. Samples were placed for 30 min in the UV illuminator (Fig. 1). They were then allowed to cool for 20 min and the fluorescence was read again. The difference in the fluorescence was plotted against the concentration of chlorambucil. The method was also applied to the isocyanate of chlorambucil.

RESULTS

Standard Curves—Following the assay procedure described above, we found a linear relationship between the fluorescence and chlorambucil concentrations varying from 0.1 to 1 μg/mL ($r = 0.986$) and from 1 to 20 μg/mL ($r = 0.999$). We also found a very good linear relationship using the isocyanate of chlorambucil ($r = 0.999$) for concentrations varying from 1 to 10 μg/mL. The lower

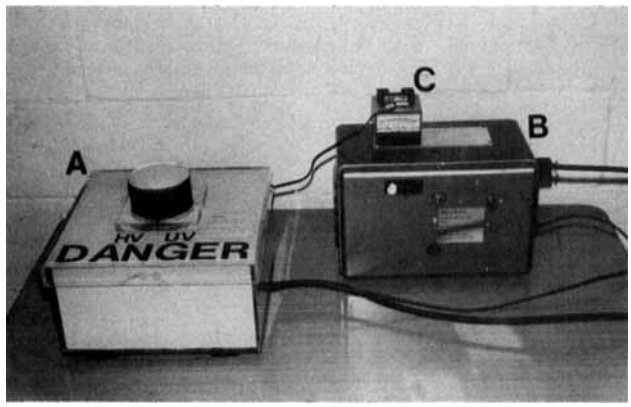

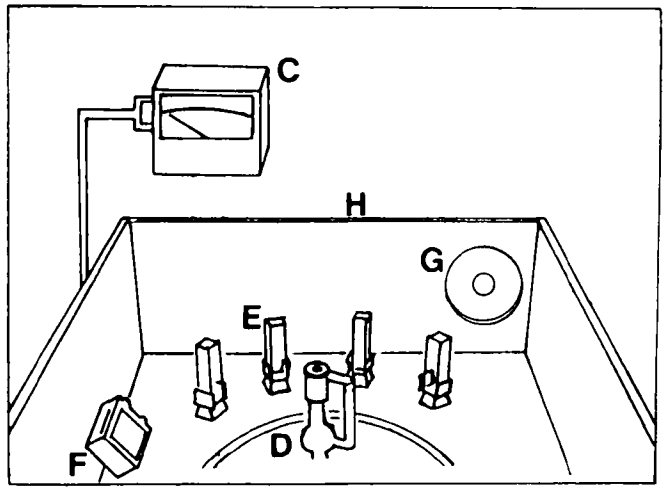

Figure 1—*UV illuminator for the photoactivation of chlorambucil. Key: (A) illuminator; (B) power unit; (C) UV meter; (D) UV lamp; (E) quartz cuvettes; (F) UV detector; (G) ventilator; (H) fiberglass box covered on the inside surface with reflecting material.*

0022-3549/84/0800-1157$01.00/0
© 1984, American Pharmaceutical Association

Table I—Intra- and Interassay Relative Standard Deviations for Two Concentrations of Chlorambucil and Isocyanate of Chlorambucil

Assay	Conc., μg/mL	Mean of Fluorescence	*RSD*, % Intra-assay	*RSD*, % Interassay
Chlorambucil				
1	2	11.9 ± 0.854	7.17	
2	2	11.6 ± 1.25	10.7	9.25
3	2	11.5 ± 1.08	9.39	
4	2	9.63 ± 0.479	4.97	
1	5	48.2 ± 1.41	2.92	
2	5	52.1 ± 1.93	3.70	8.79
3	5	58.0 ± 1.73	2.98	
4	5	57.8 ± 2.66	4.60	
Isocyanate of Chlorambucil				
1	2	20.3 ± 1.60	7.88	
2	2	20.3 ± 1.20	5.91	
3	2	13.6 ± 0.980	7.21	21.1
4	2	14.5 ± 1.17	8.07	
1	5	51.1 ± 1.65	3.23	
2	5	50.0 ± 1.73	3.46	
3	5	48.9 ± 1.03	2.11	5.25
4	5	45.2 ± 1.16	2.57	

limit of sensitivity of 0.1 μg/mL found with this method was 50-fold lower than the one obtained with the nitrobenzylpyridine method (5).

Reproducibility of the Assay—We found intra-assay *RSD* of 8.1 and 3.6%, respectively, at 2 and 5 μg/mL. The interassay *SD* was determined on four fluorescence measurements at 2 and 5 μg/mL and we found *SD* of 9.3 and 8.8%, respectively. The intra- and interassay relative standard deviations were also obtained with the isocyanate derivative of chlorambucil at the same concentrations (Table I).

Fluorophore Stability—Contrary to the nitrobenzylpyridine assay, the fluorescence could be read several hours after the photoactivation of the samples by UV. When the fluorophore produced was kept in the dark, it was stable for at least 24 h. We found a variation of only 5% in the fluorescence during the 24-h period at room temperature. This is an advantage over the nitrobenzylpyridine method, which yields a highly unstable chromophore.

DISCUSSION

The method presented above offers many advantages over the existing method for measuring alkylating activity. This fluorescence method is at least 50 times as sensitive as the nitrobenzylpyridine colorimetric procedure proposed by Balazs *et al.* (5). The interassay relative standard deviations given may represent the variations in the intensity of the UV lamp and the daily variations in the fluorometer light source; these deviations are much lower when a standard curve is used for each assay. This assay may be performed in protein-containing solutions, in contrast to the other assays available which require incubation at 85°C and cause protein precipitation.

Since alkylating activity is measured in this assay, it is essential that the assay is performed with an active alkylating agent; therefore, chlorambucil must be kept in a desiccator to prevent hydrolysis and formation of the hemimustard. The method proposed above measures the alkylating activity of chlorambucil; it should be useful for studying the metabolism of this compound in biological fluids.

REFERENCES

(1) O. Klatt, A. C. Griffin, and J. S. Stehlin, Jr., *Proc. Soc. Exp. Biol. Med.*, **104**, 629 (1960).

(2) H. G. Petering and G. J. Van Giessen, *J. Pharm. Sci.*, **52**, 1159 (1963).

(3) A. M. Agree and R. L. Meeker, *Talanta*, **13**, 1151 (1966).

(4) R. Truhaut, E. Delacoux, G. Brûlé, and C. Bohuon, *Clin. Chim. Acta*, **8**, 235 (1963).

(5) M. K. Balazs, C. A. Anderson, R. H. Iwamoto, and P. Lim, *J. Pharm. Sci.*, **59**, 563 (1970).

(6) J. Epstein, R. W. Rosenthal, and R. J. Ess, *Anal. Chem.*, **27**(9), 1435 (1955).

(7) M. A. Chirigos and J. A. R. Mead, *Anal. Chem.*, **7**, 259 (1964).

(8) R. C. Gaudreault, M.Sc. Thesis, Université Laval, Québec, 1979.

(9) R. C. Gaudreault, Ph.D. Thesis, Université Laval, Québec, 1983.

ACKNOWLEDGMENTS

This work was supported by the Fondation Dr. Georges Phénix with a studentship to L. G. Bernier and by the C.R.S.Q. with a studentship to R. C. Gaudreault. The technical assistance of Pierre De Grandpré is acknowledged.

Quantitation of Phenobarbital and Phenobarbital Sodium in Pharmaceutical Dosage Forms

V. DAS GUPTA

Received April 11, 1983, from the *Department of Pharmaceutics, University of Houston, Houston, TX 77030.* Accepted for publication July 29, 1983.

Abstract □ A reverse-phase high-performance liquid chromatographic method for the quantitation of phenobarbital and phenobarbital sodium in pharmaceutical dosage forms (elixir, injection, and tablets) was developed. The method is precise and accurate with percent relative standard deviations of 0.9 (without an internal standard) and 0.7 (with an internal standard) based on six injections. The method is stability indicating and is more sensitive than the revised USP–NF method. The products of decomposition showed two new peaks in the chromatogram.

Keyphrases □ Phenobarbital—quantitation with phenobarbital sodium in pharmaceutical dosage forms □ Phenobarbital sodium—quantitation with phenobarbital in pharmaceutical dosage forms

Phenobarbital (I) and phenobarbital sodium (II), extensively used as sedatives, are available in a variety of dosage forms, including capsules, elixir, injectable, tablets, *etc.* The literature for the quantitation of phenobarbital has been surveyed by Schmidt and Pennington (1). According to this report, investigations in which reverse-phase HPLC have been used without the addition of a counterion have not been successful. A reverse-phase HPLC assay procedure for phenobarbital with 0.01 M tetramethylammonium chloride as the counterion has been reported (1); however, the use of counterions usually shortens column life (2).

The revised USP–NF method for the quantitation of phenobarbital appeared in USP Supplement 3 (3), and use of a mobile phase of pH 4.5 is recommended.

The purpose of this investigation was to develop a stability-indicating assay method for the quantitation of phenobarbital and phenobarbital sodium in pharmaceutical dosage forms at neutral or weakly basic pH without the addition of a counterion to the mobile phase.

EXPERIMENTAL SECTION

Chemicals and Reagents—All chemicals and reagents were USP, NF, or ACS quality and used without further purification. The USP-quality powders of phenobarbital[1] and phenobarbital sodium[1] were used as received.

[1] American Chemical and Drug Co., Los Angeles, Calif.

0022-3549/84/0800-1158$01.00/0

© 1984, American Pharmaceutical Association

Table I—Intra- and Interassay Relative Standard Deviations for Two Concentrations of Chlorambucil and Isocyanate of Chlorambucil

Assay	Conc., μg/mL	Mean of Fluorescence	*RSD*, % Intra-assay	*RSD*, % Interassay
Chlorambucil				
1	2	11.9 ± 0.854	7.17	
2	2	11.6 ± 1.25	10.7	9.25
3	2	11.5 ± 1.08	9.39	
4	2	9.63 ± 0.479	4.97	
1	5	48.2 ± 1.41	2.92	
2	5	52.1 ± 1.93	3.70	8.79
3	5	58.0 ± 1.73	2.98	
4	5	57.8 ± 2.66	4.60	
Isocyanate of Chlorambucil				
1	2	20.3 ± 1.60	7.88	
2	2	20.3 ± 1.20	5.91	
3	2	13.6 ± 0.980	7.21	21.1
4	2	14.5 ± 1.17	8.07	
1	5	51.1 ± 1.65	3.23	
2	5	50.0 ± 1.73	3.46	
3	5	48.9 ± 1.03	2.11	5.25
4	5	45.2 ± 1.16	2.57	

limit of sensitivity of 0.1 μg/mL found with this method was 50-fold lower than the one obtained with the nitrobenzylpyridine method (5).

Reproducibility of the Assay—We found intra-assay *RSD* of 8.1 and 3.6%, respectively, at 2 and 5 μg/mL. The interassay *SD* was determined on four fluorescence measurements at 2 and 5 μg/mL and we found *SD* of 9.3 and 8.8%, respectively. The intra- and interassay relative standard deviations were also obtained with the isocyanate derivative of chlorambucil at the same concentrations (Table I).

Fluorophore Stability—Contrary to the nitrobenzylpyridine assay, the fluorescence could be read several hours after the photoactivation of the samples by UV. When the fluorophore produced was kept in the dark, it was stable for at least 24 h. We found a variation of only 5% in the fluorescence during the 24-h period at room temperature. This is an advantage over the nitrobenzylpyridine method, which yields a highly unstable chromophore.

DISCUSSION

The method presented above offers many advantages over the existing method for measuring alkylating activity. This fluorescence method is at least 50 times as sensitive as the nitrobenzylpyridine colorimetric procedure proposed by Balazs *et al.* (5). The interassay relative standard deviations given may represent the variations in the intensity of the UV lamp and the daily variations in the fluorometer light source; these deviations are much lower when a standard curve is used for each assay. This assay may be performed in protein-containing solutions, in contrast to the other assays available which require incubation at 85°C and cause protein precipitation.

Since alkylating activity is measured in this assay, it is essential that the assay is performed with an active alkylating agent; therefore, chlorambucil must be kept in a desiccator to prevent hydrolysis and formation of the hemimustard. The method proposed above measures the alkylating activity of chlorambucil; it should be useful for studying the metabolism of this compound in biological fluids.

REFERENCES

(1) O. Klatt, A. C. Griffin, and J. S. Stehlin, Jr., *Proc. Soc. Exp. Biol. Med.*, **104**, 629 (1960).

(2) H. G. Petering and G. J. Van Giessen, *J. Pharm. Sci.*, **52**, 1159 (1963).

(3) A. M. Agree and R. L. Meeker, *Talanta*, **13**, 1151 (1966).

(4) R. Truhaut, E. Delacoux, G. Brûlé, and C. Bohuon, *Clin. Chim. Acta*, **8**, 235 (1963).

(5) M. K. Balazs, C. A. Anderson, R. H. Iwamoto, and P. Lim, *J. Pharm. Sci.*, **59**, 563 (1970).

(6) J. Epstein, R. W. Rosenthal, and R. J. Ess, *Anal. Chem.*, **27**(9), 1435 (1955).

(7) M. A. Chirigos and J. A. R. Mead, *Anal. Chem.*, **7**, 259 (1964).

(8) R. C. Gaudreault, M.Sc. Thesis, Université Laval, Québec, 1979.

(9) R. C. Gaudreault, Ph.D. Thesis, Université Laval, Québec, 1983.

ACKNOWLEDGMENTS

This work was supported by the Fondation Dr. Georges Phénix with a studentship to L. G. Bernier and by the C.R.S.Q. with a studentship to R. C. Gaudreault. The technical assistance of Pierre De Grandpré is acknowledged.

Quantitation of Phenobarbital and Phenobarbital Sodium in Pharmaceutical Dosage Forms

V. DAS GUPTA

Received April 11, 1983, from the *Department of Pharmaceutics, University of Houston, Houston, TX 77030.* Accepted for publication July 29, 1983.

Abstract □ A reverse-phase high-performance liquid chromatographic method for the quantitation of phenobarbital and phenobarbital sodium in pharmaceutical dosage forms (elixir, injection, and tablets) was developed. The method is precise and accurate with percent relative standard deviations of 0.9 (without an internal standard) and 0.7 (with an internal standard) based on six injections. The method is stability indicating and is more sensitive than the revised USP–NF method. The products of decomposition showed two new peaks in the chromatogram.

Keyphrases □ Phenobarbital—quantitation with phenobarbital sodium in pharmaceutical dosage forms □ Phenobarbital sodium—quantitation with phenobarbital in pharmaceutical dosage forms

Phenobarbital (I) and phenobarbital sodium (II), extensively used as sedatives, are available in a variety of dosage forms, including capsules, elixir, injectable, tablets, *etc.* The literature for the quantitation of phenobarbital has been surveyed by Schmidt and Pennington (1). According to this report, investigations in which reverse-phase HPLC have been used without the addition of a counterion have not been successful. A reverse-phase HPLC assay procedure for phenobarbital with 0.01 M tetramethylammonium chloride as the counterion has been reported (1); however, the use of counterions usually shortens column life (2).

The revised USP–NF method for the quantitation of phenobarbital appeared in USP Supplement 3 (3), and use of a mobile phase of pH 4.5 is recommended.

The purpose of this investigation was to develop a stability-indicating assay method for the quantitation of phenobarbital and phenobarbital sodium in pharmaceutical dosage forms at neutral or weakly basic pH without the addition of a counterion to the mobile phase.

EXPERIMENTAL SECTION

Chemicals and Reagents—All chemicals and reagents were USP, NF, or ACS quality and used without further purification. The USP-quality powders of phenobarbital[1] and phenobarbital sodium[1] were used as received.

[1] American Chemical and Drug Co., Los Angeles, Calif.

0022-3549/84/0800-1158$01.00/0

© 1984, American Pharmaceutical Association

Table I—Assay Results of Dosage Forms

Type of Dosage Form	Active Ingredient	Percent of Label Claim Found 230 nm[a]	245 nm[b]
Elixir			
Lot 1	I (4 mg/mL)	99.0	99.0
Lot 2	I (4 mg/mL)	99.8	100.2
Lot 3	I (4 mg/mL)	99.2	99.3
Injection			
Lot 1	II (65 mg/mL)	100.8	100.8
Lot 2	II (130 mg/mL)	99.4	99.6
Lot 3	II (65 mg/mL)	100.0	100.1
Lot 4	II (130 mg/mL)	101.2	101.0
Tablets			
Lot 1	I (15 mg)	98.8	98.9
Lot 2	I (30 mg)	100.2	99.9
Lot 3	I (60 mg)	100.0	100.4
Lot 4	I (100 mg)	99.2	99.2
Lot 5	I (16.2 mg) With 10.8 mg of belladonna extract per tablet	100.1	100.5
Lot 6	I (30 mg)	98.8	99.1
	Recovery Data of Synthetic Mixtures		
Mixture			
1	I (60 mg/200 mg of lactose)	99.8	—[c]
2	II (80 mg/300 mg of lactose)	100.0	—[c]
3	I (4 mg/mL)[d]	100.9	—[c]
Decomposed sample			
1	~4 min boiling	78.2%	—[c]
2	~30 min boiling	15.4%	—[c]

[a] With internal standard. [b] Without internal standard. [c] Not determined at this wavelength. [d] In aqueous solution containing 15% ethanol (v/v) and 45% glycerol (v/v).

Apparatus—The chromatograph[2] was equipped with a multiple-wavelength detector[3], a recorder[4], and a digital integrator[5]. A semipolar column[6] (30 cm × 4 mm i.d.) was used. The mobile phase contained 35% (v/v) of methanol in 0.02 M aqueous ammonium acetate. The flow rate was 2.0 mL/min, and the temperature was ambient. The sensitivity was set at either 0.2 (245 nm) or 0.1 (230 nm), and the chart speed was 30.5 cm/h.

Preparation of Stock and Standard Solutions—The stock solutions of phenobarbital (2.0 mg/mL in methanol), phenobarbital sodium (2.0 mg/mL in water) and the internal standard, mezlocillin sodium[7] (10.0 mg/mL in water) were prepared fresh daily. The standard solutions were prepared by diluting the appropriate quantities of stock solutions with water, methanol, or a mixture of both, as needed. All standard solutions of phenobarbital sodium were diluted with water. The standard solution of phenobarbital for assays at 230 nm contained 10% methanol (final concentration, v/v) in water, and pure methanol was used for diluting all solutions for assays at 245 nm. No internal standard was used for assays at 245 nm due to very poor absorbance at this wavelength. For assays at 230 nm, the concentration of the internal standard was 600.0 μg/mL.

Preparation of Assay Solutions—For assay at 230 nm, an appropriate quantity (3.75 mL) of phenobarbital elixir USP (4.0 mg/mL) was mixed with 10 mL of methanol and 6.0 mL of stock solution of the internal standard and brought to volume with water (100 mL). For assay at 245 nm, 6.25 mL of elixir was diluted to 25.0 mL with methanol.

Injections—An appropriate quantity of the injection of phenobarbital sodium was diluted with water to contain either 0.15 or 1.0 mg/mL of the drug for assays at 230 and 245 nm, respectively. The solution for assay at 230 nm also contained 0.6 mg/mL of mezlocillin sodium (internal standard).

Tablets—An appropriate quantity of the fine powder representing 200.0 mg of the phenobarbital powder was thoroughly mixed with 80 mL of methanol and shaken for 5 min. The mixture was brought to volume (100 mL) with methanol and filtered[8]. The first 15 mL of the filtrate was rejected and then collected for assay. For assays at 230 nm, 7.5 mL of the clear filtrate was mixed with 2.5 mL of methanol and 6.0 mL of the internal standard stock solution and brought to volume (100 mL) with water. For assays at 245 nm, a 12.5-mL quantity of the clear filtrate was diluted to 25 mL with methanol.

Assay Solutions of Decomposed Phenobarbital Sodium—A 30.0-mg sample of phenobarbital sodium powder was mixed with ~2 mL of ~1 M NaOH solution in a 150-mL beaker. The mixture was boiled on a hot plate for (*a*) ~4 min and (*b*) ~30 min; additional water was added as needed, and the mixture was cooled to room temperature and neutralized (pH ~6–8) with ~4 mL of ~0.5 M HCl. A 12.0-mL quantity of the stock solution of the internal standard was added, and the mixture was brought to volume (200 mL) with water. These solutions were assayed only at 230 nm.

Chromatographic Procedure—A 20-μL aliquot of the assay solution was injected into the chromatograph at the conditions described (solutions with internal standard, 230 nm; others, 245 nm). For comparison, an identical volume of the standard solution containing an identical concentration of the drug was injected after the assay solution was eluted.

Calculations—Since the peak heights (ratio of the peak heights when internal standard was added) were directly related to concentrations, the results were calculated by the equation:

$$100 \times \frac{R_{pha}}{R_{phs}} = \text{percent of the label claim}$$

where R_{pha} is the peak height (ratio of the peak height of drug to internal standard for assays at 230 nm) of the assay solution and R_{phs} is the peak height of the standard solution.

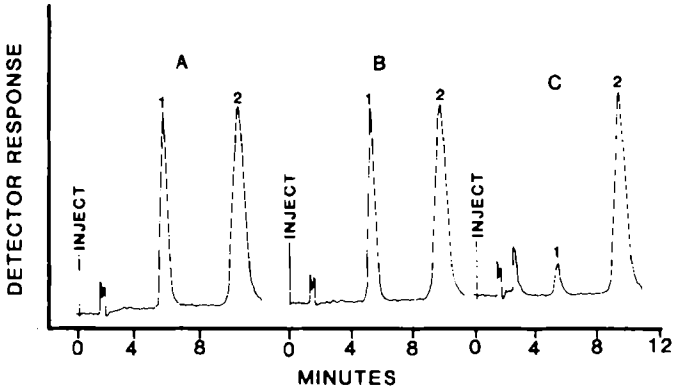

Figure 1—*Typical chromatograms at 230 nm. Peaks 1 and 2 are from phenobarbital sodium (II) and mezlocillin sodium (internal standard), respectively. Key: (A) standard solution; (B) injection containing 130 mg/mL of II; (C) decomposed solution (~30 min boiling, see text).*

[2] Model ALC 202 equipped with a U6K universal injector; Waters Associates, Milford, Mass.
[3] Spectroflow monitor SF770; Schoeffel Instrument Corp., Ramsey, N.J.
[4] Omniscribe 5213-12; Houston Instruments, Austin, Tex.
[5] Autolab minigrator; Spectra-Physics, Santa Clara, Calif.
[6] μ-Bondapak phenyl (catalog no. 27198); Waters Associates, Milford, Mass.
[7] Miles Pharmaceutical, West Haven, Conn.
[8] Whatman no. 1 filter paper.

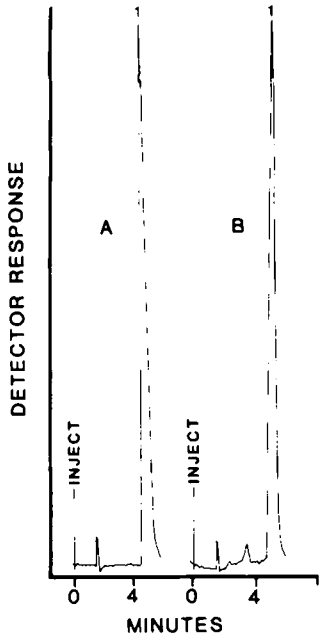

Figure 2—*Typical chromatograms at 245 nm. Peak 1 is from phenobarbital sodium (II). Key: (A) standard solution; (B) injection containing 130 mg/mL of II.*

RESULTS AND DISCUSSION

The assay results indicate (Table I) that the proposed HPLC method can be adopted for the quantitation of phenobarbital and phenobarbital sodium in pharmaceutical dosage forms. The method is accurate and precise. The percent relative standard deviations based on six injections were 0.9 and 0.7 at 245 and 230 nm (with internal standard), respectively. The internal standard was not used for assays at 245 nm due to poor absorption of mezlocillin at this wavelength. However, the results by both assay methods were similar (Table I). The concentrations *versus* peak heights were directly related in the 7- to 21-μg range at 245 nm. The ratio of peak heights (drug to internal standard) were directly related to drug concentrations at the 1.5- to 4.5-μg range at 230 nm. The method is ~1.7 times more sensitive at 230 than at 245 nm, as determined by using a standard solution (300 μg/mL in water) and a sensitivity of 0.1. Moreover, the method is at least two times more sensitive than the USP-NF method (3), as determined by UV spectrometry with the two mobile phases. The elixirs and injections can be simply diluted and assayed for phenobarbital and phenobarbital sodium. A simple preliminary extraction procedure is required to assay phenobarbital in tablets. There was no interference from excipients present in the tablets and the red colorant of the elixir (Table I).

The decomposed samples of phenobarbital sodium showed a new peak (peak 1, Fig. 1C) in the chromatogram, and the potency of the drug remaining intact was only 15.4% after ~30 min of boiling (see above). After ~4 min of boiling, there were two small peaks (side by side) in the chromatogram at about the same location as peak 1, Fig. 1C. The scheme of decomposition has been reported previously in the literature (4). It is interesting to point out that there were two additional peaks when the same lot of phenobarbital was assayed at 245 nm *versus* only one peak when assayed at 230 nm. It is perhaps due to the facts that (*a*) the concentration of excipients was 3.33 times higher (also considering AUFS of 0.2 at 245 nm and 0.1 at 230 nm) at 245 *versus* 230 nm and (*b*) there was poor or no absorption from one of the excipients at 230 nm. Furthermore, the same lot of phenobarbital sodium injection showed a small additional peak (Fig. 2B) when assayed at 245 nm *versus* almost none (Fig. 1B) when assayed at 230 nm.

REFERENCES

(1) W. F. Schmidt and L. J. Pennington, *J. Pharm. Sci.*, **71**, 954 (1982).

(2) R. Gloor and E. L. Johnson, *J. Chromatogr. Sci.*, **15**, 413 (1977).

(3) Third Supplement to USP XX and to NF XV, The U.S. Pharmacopeial Convention, Rockville, Md., 1982, pp. 216–217.

(4) K. A. Connors, G. L. Amidon, and L. Kennon, "Chemical Stability of Pharmaceuticals—A Handbook for Pharmacists," Wiley, New York, N.Y., 1979, p. 280.

Mesophase Formation During Cholesterol Gallstone Dissolution in Human Bile: Effect of Bile Acid Composition

C. C. SU ‡, W. I. HIGUCHI *x, I. T. GILMORE §, R. G. DANZINGER ¶, and A. F. HOFMANN §

Received February 14, 1983, from the **College of Pharmacy, University of Utah, Salt Lake City, UT 84112*, ‡*College of Pharmacy, University of Michigan, Ann Arbor, MI 48105*, §*University of California at San Diego, San Diego, CA 92103, and* ¶*St. Boniface General Hospital, Winnipeg, Manitoba, Canada.* Accepted for publication July 8, 1983.

Abstract □ Duodenal bile obtained from patients with gallstones who were acutely infused with chenodeoxycholic acid, ursodeoxycholic acid, or cholic acid were examined for the propensity toward the formation of a liquid crystalline mesomorphic phase when cholesterol gallstones were incubated in these bile acids. Bile taken from patients infused with ursodeoxycholic acid was found to be enriched in ursodeoxycholic acid; mesophase formation was detected in these samples but not in bile from patients infused with chenodeoxycholic acid or cholic acid.

Keyphrases □ Cholesterol—gallstone dissolution in human bile, effect of bile acid composition □ Gallstone dissolution—human bile, effect of bile acid composition □ Bile acids—mesophase formation during cholesterol gallstone dissolution

Clinical investigations have shown that ursodeoxycholic acid is as effective or more effective than chenodeoxycholic acid in gallstone dissolution. From the physicochemical standpoint, these results are interesting, because ursodeoxycholic acid (1) and its conjugates are generally not as effective as chenodeoxycholic acid and its conjugates in solubilizing cholesterol in the bile acid or the bile acid–lecithin solution (2). We have recently suggested (2, 3) that during *in vitro* dissolution of cholesterol monohydrate in the form of powder, compressed disks, single crystals, or in gallstones, a transition from the micellar phase to the liquid crystalline phase occurs when the dissolution media contain lecithin and predominantly ursodeoxycholic acid conjugates, but not chenodeoxycholic acid or cholic acid conjugates.

It was shown that mesophase formation and subsequent dispersion may contribute to the total dissolution/disintegration of cholesterol in the solid phase. To determine whether mesophase formation would occur during the *in vitro* disso-

0022-3549/84/0800-1160$01.00/0
© 1984, American Pharmaceutical Association

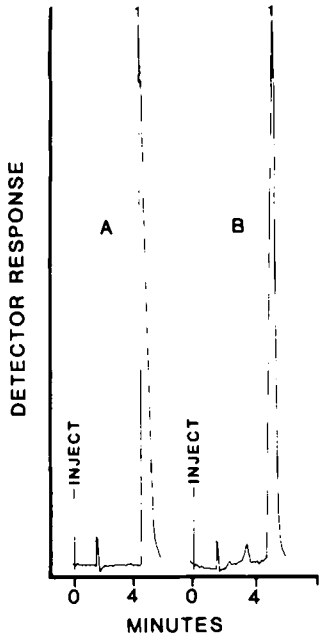

Figure 2—*Typical chromatograms at 245 nm. Peak 1 is from phenobarbital sodium (II). Key: (A) standard solution; (B) injection containing 130 mg/mL of II.*

RESULTS AND DISCUSSION

The assay results indicate (Table I) that the proposed HPLC method can be adopted for the quantitation of phenobarbital and phenobarbital sodium in pharmaceutical dosage forms. The method is accurate and precise. The percent relative standard deviations based on six injections were 0.9 and 0.7 at 245 and 230 nm (with internal standard), respectively. The internal standard was not used for assays at 245 nm due to poor absorption of mezlocillin at this wavelength. However, the results by both assay methods were similar (Table I). The concentrations *versus* peak heights were directly related in the 7- to 21-μg range at 245 nm. The ratio of peak heights (drug to internal standard) were directly related to drug concentrations at the 1.5- to 4.5-μg range at 230 nm. The method is ~1.7 times more sensitive at 230 than at 245 nm, as determined by using a standard solution (300 μg/mL in water) and a sensitivity of 0.1. Moreover, the method is at least two times more sensitive than the USP-NF method (3), as determined by UV spectrometry with the two mobile phases. The elixirs and injections can be simply diluted and assayed for phenobarbital and phenobarbital sodium. A simple preliminary extraction procedure is required to assay phenobarbital in tablets. There was no interference from excipients present in the tablets and the red colorant of the elixir (Table I).

The decomposed samples of phenobarbital sodium showed a new peak (peak 1, Fig. 1C) in the chromatogram, and the potency of the drug remaining intact was only 15.4% after ~30 min of boiling (see above). After ~4 min of boiling, there were two small peaks (side by side) in the chromatogram at about the same location as peak 1, Fig. 1C. The scheme of decomposition has been reported previously in the literature (4). It is interesting to point out that there were two additional peaks when the same lot of phenobarbital was assayed at 245 nm *versus* only one peak when assayed at 230 nm. It is perhaps due to the facts that (*a*) the concentration of excipients was 3.33 times higher (also considering AUFS of 0.2 at 245 nm and 0.1 at 230 nm) at 245 *versus* 230 nm and (*b*) there was poor or no absorption from one of the excipients at 230 nm. Furthermore, the same lot of phenobarbital sodium injection showed a small additional peak (Fig. 2B) when assayed at 245 nm *versus* almost none (Fig. 1B) when assayed at 230 nm.

REFERENCES

(1) W. F. Schmidt and L. J. Pennington, *J. Pharm. Sci.*, **71**, 954 (1982).

(2) R. Gloor and E. L. Johnson, *J. Chromatogr. Sci.*, **15**, 413 (1977).

(3) Third Supplement to USP XX and to NF XV, The U.S. Pharmacopeial Convention, Rockville, Md., 1982, pp. 216–217.

(4) K. A. Connors, G. L. Amidon, and L. Kennon, "Chemical Stability of Pharmaceuticals—A Handbook for Pharmacists," Wiley, New York, N.Y., 1979, p. 280.

Mesophase Formation During Cholesterol Gallstone Dissolution in Human Bile: Effect of Bile Acid Composition

C. C. SU ‡, W. I. HIGUCHI *x, I. T. GILMORE §, R. G. DANZINGER ¶, and A. F. HOFMANN §

Received February 14, 1983, from the **College of Pharmacy, University of Utah, Salt Lake City, UT 84112*, ‡*College of Pharmacy, University of Michigan, Ann Arbor, MI 48105*, §*University of California at San Diego, San Diego, CA 92103, and* ¶*St. Boniface General Hospital, Winnipeg, Manitoba, Canada.* Accepted for publication July 8, 1983.

Abstract □ Duodenal bile obtained from patients with gallstones who were acutely infused with chenodeoxycholic acid, ursodeoxycholic acid, or cholic acid were examined for the propensity toward the formation of a liquid crystalline mesomorphic phase when cholesterol gallstones were incubated in these bile acids. Bile taken from patients infused with ursodeoxycholic acid was found to be enriched in ursodeoxycholic acid; mesophase formation was detected in these samples but not in bile from patients infused with chenodeoxycholic acid or cholic acid.

Keyphrases □ Cholesterol—gallstone dissolution in human bile, effect of bile acid composition □ Gallstone dissolution—human bile, effect of bile acid composition □ Bile acids—mesophase formation during cholesterol gallstone dissolution

Clinical investigations have shown that ursodeoxycholic acid is as effective or more effective than chenodeoxycholic acid in gallstone dissolution. From the physicochemical standpoint, these results are interesting, because ursodeoxycholic acid (1) and its conjugates are generally not as effective as chenodeoxycholic acid and its conjugates in solubilizing cholesterol in the bile acid or the bile acid–lecithin solution (2). We have recently suggested (2, 3) that during *in vitro* dissolution of cholesterol monohydrate in the form of powder, compressed disks, single crystals, or in gallstones, a transition from the micellar phase to the liquid crystalline phase occurs when the dissolution media contain lecithin and predominantly ursodeoxycholic acid conjugates, but not chenodeoxycholic acid or cholic acid conjugates.

It was shown that mesophase formation and subsequent dispersion may contribute to the total dissolution/disintegration of cholesterol in the solid phase. To determine whether mesophase formation would occur during the *in vitro* disso-

0022-3549/84/0800-1160$01.00/0
© 1984, American Pharmaceutical Association

Table I—Biliary Lipid Composition During Infusion with Chenodeoxycholic, Ursodeoxycholic, and Cholic Acid [a]

Bile Acid Infused	Bile Acid, mol %	Phospholipids, mol %	Cholesterol, mol %	Phospholipids-Cholesterol Molar Ratio
Chenodeoxycholic acid	87.2	8.3	4.5	1.84
Ursodeoxycholic acid	86.2	11.4	2.4	4.75
Cholic acid	89.2	6.7	4.1	1.63

[a] Averages of two samples are presented.

lution of cholesterol gallstones in human bile, we studied the mesophase formation tendency with gallstones in human bile samples which were selectively enriched with conjugates of ursodeoxycholic acid, chenodeoxycholic acid, or cholic acid by prior infusion of these bile acids into the jejunum of patients with gallstones.

EXPERIMENTAL SECTION

Materials—A triple-lumen orojejunal tube was placed into the patient with gallstones fluoroscopically[1], and synthetically prepared conjugates of chenodeoxycholic, ursodeoxycholic, or cholic acids were infused into the jejunum at 2 mmol/h for 8 h (3). Bile was aspirated from the duodenal port, beginning at 8 h, at which time replacement of the bile acid pool by the infused bile acid was 69–90% complete. Bile was collected in 60-min pools for the subsequent 28 h and frozen. Each bile acid was infused in random order in three consecutive 72-h periods. Before the experiments, the bile samples were freeze-dried, weighed, and reconstituted to predetermined concentrations by equilibrating in water at 37°C for 3 d. After inactivating the enzymes by heating at 60°C for 30 min, the reconstituted bile was filtered through a 0.45-μm filter[2]. The biliary lipid compositions were determined by enzymatic methods[3] (4, 5).

Gallstones were obtained at routine cholecystectomy from patients[1] who had not taken a gallstone-dissolving bile acid. Gallstones were washed free of bile and mucus and stored for short periods in normal saline solutions under nitrogen at 4°C in the dark.

Mesophase Detection—Two gallstones were placed in 2.5 mL of the filtered bile in a test tube. The test tube was flushed with nitrogen, capped, and then shaken with a wrist-action shaker in a water bath at 37°C. At predetermined intervals, samples of the dissolution media were taken and examined immediately under a polarizing microscope. The observation of birefringent spherules was interpreted to mean that the formation of a liquid crystalline phase had occurred.

RESULTS AND DISCUSSION

The effect of infused ursodeoxycholic acid on hepatic secretion of biliary lipids is shown in Table I. The better suppression of hepatic cholesterol output during ursodeoxycholic acid infusion than under the other experimental conditions has also been reported in healthy volunteers either acutely infused with (6, 7) or chronic enterally administered this bile acid and in patients with radiolucent gallstones (8). It is interesting to note that acute administration of ursodeoxycholic acid increased the amount of phospholipids secreted per mole of cholesterol (6). Table II indicates that during infusion with ursodeoxycholic acid, this bile acid increased to 73% of the bile, whereas chenodeoxycholic acid decreased to 11.5% of the total biliary bile acids. An even higher (>80%) enrichment of ursodeoxycholic acid in bile has recently been reported by others (6) in patients during the postreplacement phase of ursodeoxycholic acid studies.

Table III presents the results of the mesophase formation studies performed with the polarizing microscope. A transition from the micellar phase to the liquid crystalline phase was detected in the ursodeoxycholic acid-enriched bile samples but not in the chenodeoxycholic acids or cholic acid-enriched bile (Table III).

Table II—Bile Acid Composition in Reconstituted Duodenal Bile

Bile Acid Infused	Molar % Chenodeoxycholic Acid	Ursodeoxycholic Acid	Cholic Acid	Deoxycholic Acid	Lithocholic Acid
Chenodeoxycholic acid	51.1	37.4	10.5	0.6	0.4
Ursodeoxycholic acid	11.5	73.1	12.0	3.0	0.4
Cholic acid	1.3	—	98.2	0.5	—

Table III—Mesophase Formation in Reconstituted Duodenal Bile

Bile Acid Infused	Bile Acid, mM	Phospholipid, mM	Cholesterol, mM	Time Mesophase Observed
Chenodeoxycholic acid				
Sample 1	87.2	8.1	4.3	—[a]
Sample 2	142.5	13.9	7.6	—
Ursodeoxycholic acid				
Sample 3	81.3	13.2	2.1	<10 d
Sample 4	123.6	12.7	3.9	<2 d
Cholic acid				
Sample 5	52.6	4.2	2.1	—
Sample 6	90.4	6.4	4.6	—

[a] Not observed.

Although these bile samples were obtained from patients with acute infusion of bile acids and although ursodeoxycholic acid concentrations in these bile samples appear to be higher than those taken from patients taking ursodeoxycholic acid orally (8), these results provide the first insights regarding the possibility of mesophase formation during ursodeoxycholic acid administration *in vivo* in patients undergoing ursodeoxycholic acid therapy for gallstone dissolution. Mesophase formation is believed (3) to be the consequence of thermodynamics favoring the formation of a lecithin-cholesterol-rich mesophase from cholesterol monohydrate in the presence of aqueous bile acid–lecithin solutions when the bile acid is an ursodeoxycholic acid conjugate. The subsequent dispersion of the mesophase may then contribute to the total dissolution/disintegration of cholesterol in the solid phase (2, 3), and this process may effect mass transfer significantly beyond the micellar phase saturation limit. Thus, this finding that ursodeoxycholic acid conjugates, but not chenodeoxycholate conjugates, induced the formation of mesophases during the gallstone dissolution process in the conjugated ursodeoxycholic acid-enriched bile may relate to the equal or superior clinical efficacy of ursodeoxycholic acid compared with chenodeoxycholic acid.

REFERENCES

(1) H. Igimi and M. C. Carey, *J. Lipid Res.*, **22**, 254 (1981).

(2) O. I. Corrigan, C. C. Su, W. I. Higuchi, and A. F. Hofmann, *J. Pharm. Sci.*, **69**, 869 (1980).

(3) C. C. Su, J. Y. Park, W. I. Higuchi, M. H. Alkan, O. I. Corrigan, A. F. Hofmann, and R. G. Danzinger, *J. Pharm. Sci.*, **70**, 713 (1981).

(4) I. T. Gilmore, K. Stokes, A. F. Hofmann, D. Gurantz, and D. Lorenzo, *Gastroenterology*, **79**, 1023 (1980).

(5) H. Dam, I. Kruse, I. Prange, H. E. Kallehauge, H. J. Fenger, and M. Krogh Jensen, *Z. Ernaehrungswiss.*, **10**, 160 (1971).

(6) C. Sama, N. F. Larusso, V. Lopez del Pino, and J. L. Thistle, *Gastroenterology*, **82**, 515 (1982).

(7) T. Schersten and L. Lindblad, in "Biological Effects of Bile Acids," G. Paumgartner, A. Stiehl, and W. Gerok, Eds., MTP Press, Lancaster, England, 1978, pp. 53–60.

(8) K. von Bergmann, M. Gutsfeld, K. Schulze-Hagen, and G. von Unruh, in "Biological Effects of Bile Acids," G. Paumgartner, A. Stiehl, and W. Gerok, Eds., MTP Press, Lancaster, England, 1978, pp. 61–66.

ACKNOWLEDGMENTS

This study was supported by Public Health Service Grants AM16694, AM32472, and AM16770 from the National Institutes of Health.

[1] Dr. A. F. Hofmann, University of California, San Diego, Calif.; written informed consent and institutional human subjects committee approval were obtained.

[2] Millipore Corp., Bedford, Mass.

[3] Cholesterol Reagent Set; Bio-Dynamics/bmc, Indianapolis, Ind; Sterognost-3 Set; Accurate Chemical & Scientific Corp., Hicksville, N.Y.; PL Kit-K; Nippon Shouji Kaisha Ltd., Osaka, Japan.

Liquid Chromatographic Chiral Stationary Phases in Pharmaceutical Analysis: Determination of Trace Amounts of the (−)-Enantiomer in (+)-Amphetamine

IRVING W. WAINER ˣ, THOMAS D. DOYLE, and WILLIAM M. ADAMS

Received December 23, 1982, from the *Division of Drug Chemistry, Food and Drug Administration, Washington, DC 20204.* Accepted for publication June 8, 1983.

Abstract □ A rapid and accurate method was developed for the determination of the enantiomeric composition of amphetamine preparations. Amide derivatives of the amphetamine enantiomers are first formed by using achiral 2-naphthoyl chloride. The resulting enantiomeric amides are then chromatographed on a commercially available chiral stationary phase. The capacity factors (k') of (−)- and (+)-2-naphthoylamphetamine are 20 and 22, respectively, and the separation factor (α) for the two enantiomers is 1.08. The method allows detection of as little as 0.5% of the (−)-enantiomer in (+)-amphetamine and is applicable to both bulk drug and single-tablet analyses.

Keyphrases □ Enantiomers—(+)- and (−)-amphetamine, HPLC, trace amounts □ Chiral stationary phases—HPLC, determination of trace amounts of (+)- and (−)-amphetamine □ Amphetamine—(+)- and (−)-enantiomers, HPLC, trace amounts

Amphetamine (α-methylphenethylamine) is a pharmacologically active asymmetric molecule whose (S) and (R) enantiomeric forms, (+)- and (−)-amphetamine, respectively, have different biological activities (1). Accordingly, the resolution and quantification of the amphetamine enantiomers have received a great deal of attention.

The most common approach to this analytical problem involves the synthesis and separation by GC of diastereoisomeric amides of amphetamine (2–9). Although this technique has been successfully utilized, it suffers from a number of inherent problems which hinder the development of methods for the determination of trace amounts of one enantiomer in the presence of the other.

The most serious drawback is that the synthesis of diastereoisomers necessarily involves the use of a chiral derivatizing agent. Any isomeric impurity in this reagent will result in spurious results. Liu and Ku (9) have discussed this problem in detail for the case of L-prolyl-derivatives of amphetamine and were able to correct for it by resolving the diastereoisomers into their enantiomeric pairs on a GC chiral stationary phase. An additional complication is that enantiomers may have quite different rates and/or equilibrium constants when they react with another chiral molecule, resulting in the generation of two diastereoisomeric products in proportions that differ from the starting enantiomeric composition (10).

Both of these problems can be avoided by resolving the enantiomeric pair as enantiomers by utilizing chromatography on chiral stationary phases. In such a case, if a derivative is to be formed and if the derivatizing agent is not an optically active molecule, there is no question of trace isomeric contamination. Furthermore, all enantiomers react with an optically inactive reagent to the same extent, *i.e.*, they have the same rate constants and the same equilibrium constants (10). Therefore, complete reaction is not a requirement. Direct resolution of enantiomeric amphetamine derivatives has been accomplished by GC (9, 11) and most recently by Wainer and Doyle *via* high-performance liquid chromatography (HPLC) (12).

In this report the application of direct HPLC resolution (12) to the determination of the enantiomeric composition of bulk drug and commercial preparations of amphetamine is described. The method involves the synthesis of the 2-naphthoyl amide of amphetamine and its resolution by HPLC on a commercially available chiral stationary phase containing (*R*)-*N*-(3,5-dinitrobenzoyl)phenylglycine. It is rapid and accurate and can detect the presence of as little as 0.5% of the (−)-enantiomer in (+)-amphetamine.

EXPERIMENTAL SECTION

Apparatus—The liquid chromatograph[1] was equipped with a data system[2], a fixed-wavelength detector[3] (280 nm), a temperature-controlled column compartment, and a 20-μL fixed-loop injector[4]. All analyses were performed with a 25-cm × 4.6-mm i.d. stainless steel column packed with a covalently bonded chiral stationary phase[5] and a 50-mm × 4.6-mm i.d. stainless steel guard column packed with 35–50-μm silica.

Materials—Hexane[6], isopropyl alcohol[6], and acetonitrile[6] were HPLC grade and were used as purchased. The 2-naphthoyl chloride[7], (+)-amphetamine sulfate (reference standard)[8], and (+)-, (−)-, and (±)-amphetamine sulfate (bulk drug)[9] were also used as purchased. Pharmaceutical preparations of (+)-amphetamine sulfate as capsule[10] and syrup[11], (+)-amphetamine-(±)-amphetamine sulfate capsule[12], and (±)-amphetamine sulfate capsule[13] were purchased commercially.

Structural Determinations—Structural determinations were made with a 200-MHz NMR spectrometer[14], a gas chromatograph–mass spectrometer[15], and an IR spectrophotometer[16]. The ^{1}H-NMR spectra ($CDCl_3$) contained the following peaks: δ 1.24 (d, 3), 2.80–3.02 (m, 2), 4.44–4.58 (m, 1), 6.19 (d, 1), and 7.22–8.20 ppm (m, 12). The mass spectra contained a molecular ion peak at m/z 289 and a base peak at m/z 155. The IR spectra (CH_2Cl_2) contained a sharp peak at 1655 cm^{-1}. The following melting points for the derivatives were obtained: (+)-2-naphthoylamphetamine, 152–155°C; (−)-2-naphthoylamphetamine, 152–155°C; (±)-2-naphthoylamphetamine, 162–165°C.

General Procedure—The bulk drug (10 mg) or the pharmaceutical preparation (one 10-mg tablet or capsule or 10 mL of a 1-mg/mL syrup) was placed in 5 mL of 20% NaOH solution and ultrasonicated until dissolved. The solution was then transferred to a 30-mL separatory funnel. Ten milliliters of a 0.01 M solution of 2-naphthoyl chloride in dichloromethane was added, and the mixture was shaken for 1 min. The organic phase was transferred to another 30-mL separatory funnel. The aqueous phase was washed with a 5-mL

[1] Model SP3500 chromatograph; Spectra-Physics, Santa Clara, Calif.
[2] Model SP4000 data system; Spectra-Physics.
[3] Model SP8200 detector; Spectra-Physics.
[4] Valco injector; Spectra-Physics.
[5] Pirkle Covalent Phenylglycine column; Regis Chemical Co., Morton Grove, Ill.
[6] Distilled-in-glass; Burdick & Jackson Laboratories, Muskegon, Mich.
[7] Pfaltz & Bauer, Stamford, Conn.
[8] United States Pharmacopeial Convention, Rockville, Md.
[9] ICN K&K Laboratories, Plainview, N.Y.
[10] Dexedrine timed-release capsule, 10 mg; Smith, Kline, and French Laboratories, Philadelphia, Pa.
[11] Dexedrine syrup, 1 mg/mL; Smith, Kline, and French Laboratories.
[12] Biphetamine, capsule, 10 mg; Penwalt Pharmaceutical Division, Rochester, N.Y.
[13] Benzedrine capsule, 10 mg; Smith, Kline, and French Laboratories.
[14] Varian Model XL-200 NMR spectrometer; Varian Associates, Palo Alto, Calif.
[15] Finnigan Model 4023-T GC/MS/DS; Finnigan MAT, San Jose, Calif.
[16] Perkin-Elmer Model 599B IR spectrophotometer: Perkin-Elmer, Norwalk, Conn.

0022-3549/84/0800-1162$01.00/0
© 1984, American Pharmaceutical Association

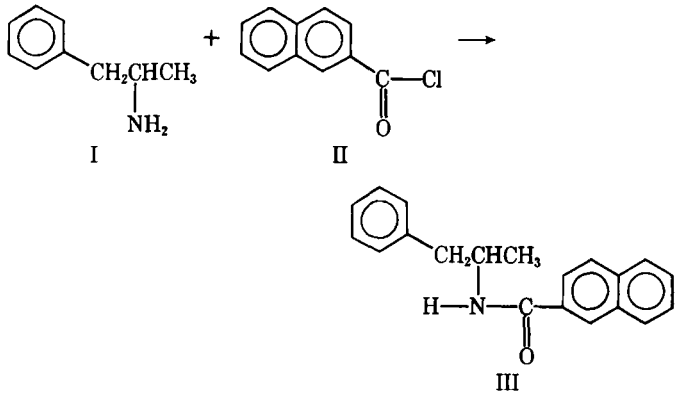

Scheme I—Reaction of amphetamine free base (I) and 2-naphthoyl chloride (II) to yield 2-naphthoylamphetamine (III).

portion of dichloromethane, and the organic layers were combined. The dichloromethane was extracted with two 5-mL portions of 0.01 M sulfuric acid, filtered through a cotton plug, and injected onto the HPLC column.

Chromatographic Conditions—The mobile phase was hexane–isopropyl alcohol–acetonitrile (97:3:0.5) at a flow rate of 2 mL/min. A column temperature of 20°C was maintained throughout the analyses.

Standard Curves—Two standard curves were constructed by combining (+)-amphetamine reference standard and (±)-amphetamine in various proportions by weight. The enantiomeric composition of one standard curve ranged from 50 parts (−)-amphetamine sulfate–50 parts (+)-amphetamine sulfate to 10 parts (−)-amphetamine sulfate–90 parts (+)-amphetamine sulfate. The other curve measured from 10 parts (−)-amphetamine sulfate–90 parts (+)-amphetamine sulfate to 0.5 parts (−)-amphetamine sulfate–99.5 parts (+)-amphetamine sulfate. The ratio of the integrated peak area of the (−)-isomer to the integrated peak area of the (+)-isomer was plotted *versus* the known enantiomeric composition.

RESULTS AND DISCUSSION

The reaction of amphetamine (I) with 2-naphthoyl chloride (II) proceeded rapidly under Schotten–Baumann conditions. When USP reference standard (+)-amphetamine sulfate was reacted under these conditions, a single product was isolated. The product was recrystallized from methanol and identified as the 2-naphthoylamide [III-(+)] by NMR, MS, and IR analyses (Scheme I). The amide was chromatographed on the chiral stationary phase; the chromatogram contained a single sharp peak with a capacity factor (k') of 22.

A series of five reactions with the USP reference standard and 2-naphthoyl chloride was carried out, and the crude reaction mixture was analyzed for amide concentration by using the crystalline product prepared as described above as an external standard. In this manner, the yield of the reaction was determined to be 82%. No attempt was made to increase the yield of the reaction, since the use of an achiral acid chloride ensures that both enantiomers react equally.

Table I—Enantiomeric Composition of Commercial Amphetamine Preparations

Sample	Assay 1, %	Assay 2, %	Average, %	Label, %
(+)-Amphetamine (bulk drug)				
(−)-Isomer	8.9	9.6	9.3	0
(+)-Isomer	91.1	90.4	90.8	100
(−)-Amphetamine (bulk drug)				
(−)-Isomer	98.4	99.3	98.9	100
(+)-Isomer	1.6	0.7	1.2	0
(+)-Amphetamine (timed-release capsule)				
(−)-Isomer	1.2	1.5	1.4	0
(+)-Isomer	98.7	98.5	98.9	100
(+)-Amphetamine (syrup)				
(−)-Isomer	1.4	0.8	1.1	0
(+)-Isomer	98.6	99.1	98.9	100
(+)-,(±)-Amphetamine (capsule)				
(−)-Isomer	25.4	25.5	25.5	25
(+)-Isomer	74.7	74.5	74.6	75
(±)-Amphetamine (capsule)				
(−)-Isomer	49.1	49.5	49.3	50
(+)-Isomer	50.8	50.4	50.7	50

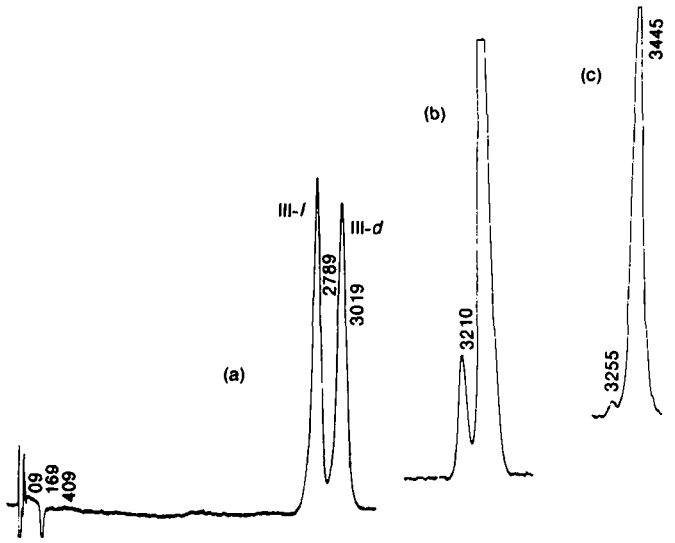

Figure 1—*Chromatograms of mixtures of (−)-2-naphthoylamphetamine [III-(−)] and (+)-2-naphthoylamphetamine [III-(+)]. Key: (a) III-(−)-III-(+), 50:50; (b) III-(−)-III-(+), 10:90; (c) III-(−)-III-(+), 1:99.*

The reaction of (−)-amphetamine bulk drug and 2-naphthoyl chloride afforded, on recrystallization, a product with the same NMR, MS, and IR spectral features as (+)-2-naphthoylamphetamine; this product was identified as the (−)-enantiomer [III-(−)]. The HPLC chromatogram of the recrystallized product contained two sharp peaks with capacity factors of 20 and 22, respectively. The first peak in the chromatogram, that of the (−)-enantiomer, contained 99% of the integrated area of the chromatogram, and the second peak, that of the (+)-enantiomer, contained 1% (Table I).

Two series of mixtures of (+)- and (−)-amphetamine were prepared by combining USP reference standard (+)-amphetamine sulfate and (±)-amphetamine sulfate in various proportions by weight. Enantiomeric proportions in the first series ranged from (±)-amphetamine sulfate (a 50:50 mixture of the two isomers) to a (+)-amphetamine sulfate–(−)-amphetamine sulfate mixture of 90:10. Proportions in the second series ranged from a (+)-amphetamine sulfate–(−)-amphetamine sulfate mixture of 90:10 to a 99.5:0.5 mixture. All solutions were derivatized and analyzed, and standard curves were constructed (Fig. 1). The curves were linear over both concentration ranges. The first standard curve (50:50–90:10) had a standard error of 0.0170 and a correlation coefficient of 0.998. The second curve had a standard error of 0.0077 and a correlation coefficient of 0.982. The separation factor (α) averaged 1.08.

Four pharmaceutical preparations of (+)-amphetamine and of (+)-amphetamine–(−)-amphetamine mixtures were purchased commercially and analyzed (Table I). A single 10-mg capsule or 10 mL of a 1-mg/mL syrup was used in the assays. By this method 1% of the (−)-isomer was detected in the (+)-amphetamine preparations; the expected enantiomeric ratios were detected in the other preparations.

The assay is a rapid (requiring no more than 2 h) and accurate method for the determination of the isomeric content of amphetamine bulk drug and commercial pharmaceutical preparations. It utilizes an achiral derivatizing reagent, 2-naphthoyl chloride, and a chiral stationary phase HPLC column which are both commercially available.

REFERENCES

(1) T. C. Daniels and E. C. Jorgensen, in "Textbook of Organic Medicinal and Pharmaceutical Chemistry," 7th ed., C. O. Wilson, O. G. Gisvold, and R. F. Doerge, Eds., J. B. Lippincott, Philadelphia, Pa., 1977, p. 416.

(2) C. E. Wells, *J. Assoc. Off. Anal. Chem.*, **53**, 113 (1970).

(3) A. H. Beckett and B. Testa, *J. Chromatogr.*, **69**, 285 (1972).

(4) L. R. Pohl and W. F. Trager, *J. Med. Chem.*, **16**, 475 (1973).

(5) S. B. Matin, M. Rowland, and N. Castognoli, *J. Pharm. Sci.*, **62**, 821 (1973).

(6) S. B. Matin, S. H. Wan, and J. B. Knight, *Biomed. Mass Spectrom.*, **4**, 118 (1977).

(7) J. Gol, *J. Pharm. Sci.*, **66**, 169 (1977).

(8) R. W. Souter, *J. Chromatogr.*, **108**, 265 (1975).

(9) J. H. Liu and W. W. Ku, *Anal. Chem.*, **53**, 2180 (1981).

(10) F. S. Krull, in "Advances in Chromatography," vol. 16, J. C. Giddings,

E. Grushka, J. Cazes, and P. R. Brown, Eds., Dekker, New York, N.Y., 1978, p. 176.

(11) C. H. Lochmüller and J. V. Hinshaw, *J. Chromatogr.*, **202**, 363 (1980).

(12) I. W. Wainer and T. D. Doyle, *J. Chromatogr.*, **259**, 465 (1983).

ACKNOWLEDGMENTS

Presented in part at the 96th Annual International Meeting of the Association of Official Analytical Chemists in Washington, D.C., October 1982.

Dipole Moments and Conformational Equilibrium in Some Substituted 1-Phenyl-1-fluoro-2-halogenoethanes

C. CHARLON *, A.-M. GALY ‡, C. LUU DUC *, and J. BARBE ‡x

Received March 21, 1983, from the **Service de Chimie Pharmacie, UER des Sciences Biologiques et Pharmaceutiques, Domaine de la Merci, 38700 La Tronche* and the ‡*Service de Chimie Minérale, UER de Pharmacie, 27 Boulevard Jean-Moulin, 13385 Marseille Cedex 5, France.* Accepted for publication July 5, 1983.

Abstract □ Experimental dipole moments of substituted 1-phenyl-1-fluoro-2-halogenoethanes are compared with the vectorially and the theoretically calculated values using the CNDO/2 method. Results support the existence of a conformational mixture of these compounds as solutes; *gauche* structures are the prevailing conformations as in the related catecholamines.

Keyphrases □ Phenylfluorohalogenoethanes—substituted, dipole moments, conformations as solutes □ Dipole moments—substituted phenylfluorohalogenoethanes as solutes □ Conformations—phenylfluorohalogenoethanes as solutes

Potentially antiarrhythmic drugs can be prepared from substituted 1-phenyl-1-fluoro-2-halogenoethanes, because the latter are structurally related to catecholamines. However, conformations of these intermediates have to be portrayed. For this purpose, their experimental dipole moments and the vectorially as well as the theoretically calculated moments were compared in this report.

EXPERIMENTAL SECTION

Materials—The following compounds were studied: 1-phenyl-1-fluoro-2-chloroethane (I), 1-phenyl-(4′-bromo)-1-fluoro-2-chloroethane (II), 1-phenyl-(4′-chloro)-1-fluoro-2-chloroethane (III), 1-phenyl-(2′-bromo)-1-fluoro-2-bromoethane (IV), 1-phenyl-(2′-chloro)-1-fluoro-2-bromoethane (V), 1-phenyl-(2′,4′-dichloro)-1-fluoro-2-chloroethane (VI), 1-phenyl-(2′,-5′-dichloro)-1-fluoro-2-chloroethane (VII), and 1-phenyl-(2′,6′-dichloro)-1-fluoro-2-bromoethane (VIII). These compounds were prepared from the corresponding alcohols, in accordance with the process previously described (1).

Methods—The dipole moments of the compounds as solutes in anhydrous benzene were measured at 25.00 ± 0.05°C. The permittivity[1] and refractive index[2] of the solutions were extrapolated to infinite dilution according to Guggenheim (2) and Smith (3). The quantity $(\epsilon_{12} - n_{12}^2) - (\epsilon_1 - n_1^2)$ was plotted *versus* the molar concentration, C, of the solute. The slope of the curve at $C = 0$ was then used to calculate the dipole moment, μ, by:

$$\mu^2 = \frac{9kT}{4\pi N} \cdot \frac{3}{(\epsilon_1 + 2)(n_1^2 + 2)} \cdot \frac{(\epsilon_{12} - n_{12}^2) - (\epsilon_1 - n_1^2)}{C} \qquad \text{(Eq. 1)}$$

where k is the Boltzmann constant, N is Avogadro's number, T is the absolute temperature, and ϵ_i and n_i are the permittivities and refractive indexes, respectively, of the solutes (Index 1) and of the solutions (Index 12).

RESULTS AND DISCUSSION

The molecular geometry of the compounds studied is schematized in Fig. 1. Hence, six limit-conformers have to be considered, because of the presumable restricted rotation around the C_1—C_2 bond. These conformers, presented in Fig. 2, are noted (A) when bonds are staggered and (B) when bonds are opposed. The following bond increments were then used for vectorial calculations: H—$C_{sp}3$, 0.25 *D* (4); $C_{sp}3$—Br, 1.38 *D*; $C_{sp}3$—Cl, 1.46 *D*; $C_{sp}3$—F, 1.41 *D* (5); $C_{sp}3$—$C_{sp}2$, 0.4 *D*; $C_{sp}2$—Br, 1.54 *D*; and $C_{sp}2$—Cl, 1.58 *D* (6).

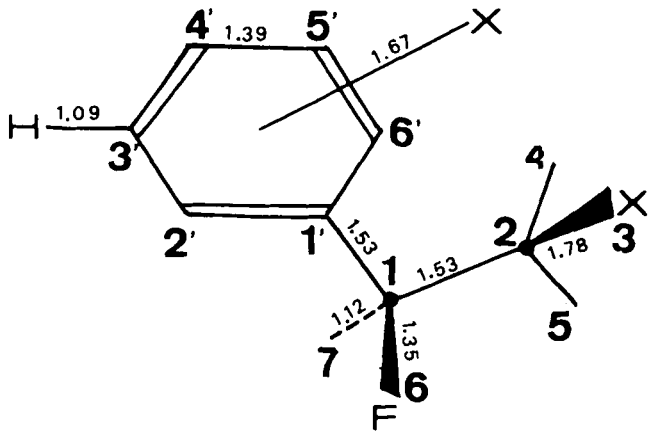

Figure 1—*Molecular geometry of the compounds studied.*

As regards the vectorial pattern of the molecules, it must be emphasized that spatial orientation of the phenyl ring *versus* the C_1—F bond is of no importance, except with the *ortho*-substituted derivatives. In the latter case, four possible orientations must be taken into account in accordance either with

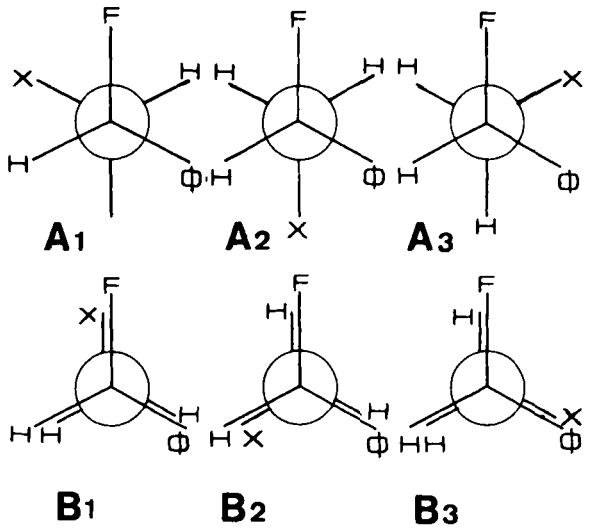

Figure 2—*Schemes of the staggered and the opposed limit-conformers used in the calculations.*

[1] W.T.W. DM 01 dipolmeter with a DFL 1 cell.
[2] O.P.L. Abbe type refractometer.

0022-3549/84/0800-1164$01.00/0
© 1984, American Pharmaceutical Association

E. Grushka, J. Cazes, and P. R. Brown, Eds., Dekker, New York, N.Y., 1978, p. 176.

(11) C. H. Lochmüller and J. V. Hinshaw, *J. Chromatogr.*, **202**, 363 (1980).

(12) I. W. Wainer and T. D. Doyle, *J. Chromatogr.*, **259**, 465 (1983).

ACKNOWLEDGMENTS

Presented in part at the 96th Annual International Meeting of the Association of Official Analytical Chemists in Washington, D.C., October 1982.

Dipole Moments and Conformational Equilibrium in Some Substituted 1-Phenyl-1-fluoro-2-halogenoethanes

C. CHARLON *, A.-M. GALY ‡, C. LUU DUC *, and J. BARBE ‡x

Received March 21, 1983, from the **Service de Chimie Pharmacie, UER des Sciences Biologiques et Pharmaceutiques, Domaine de la Merci, 38700 La Tronche* and the ‡*Service de Chimie Minérale, UER de Pharmacie, 27 Boulevard Jean-Moulin, 13385 Marseille Cedex 5, France.* Accepted for publication July 5, 1983.

Abstract □ Experimental dipole moments of substituted 1-phenyl-1-fluoro-2-halogenoethanes are compared with the vectorially and the theoretically calculated values using the CNDO/2 method. Results support the existence of a conformational mixture of these compounds as solutes; *gauche* structures are the prevailing conformations as in the related catecholamines.

Keyphrases □ Phenylfluorohalogenoethanes—substituted, dipole moments, conformations as solutes □ Dipole moments—substituted phenylfluorohalogenoethanes as solutes □ Conformations—phenylfluorohalogenoethanes as solutes

Potentially antiarrhythmic drugs can be prepared from substituted 1-phenyl-1-fluoro-2-halogenoethanes, because the latter are structurally related to catecholamines. However, conformations of these intermediates have to be portrayed. For this purpose, their experimental dipole moments and the vectorially as well as the theoretically calculated moments were compared in this report.

EXPERIMENTAL SECTION

Materials—The following compounds were studied: 1-phenyl-1-fluoro-2-chloroethane (I), 1-phenyl-(4′-bromo)-1-fluoro-2-chloroethane (II), 1-phenyl-(4′-chloro)-1-fluoro-2-chloroethane (III), 1-phenyl-(2′-bromo)-1-fluoro-2-bromoethane (IV), 1-phenyl-(2′-chloro)-1-fluoro-2-bromoethane (V), 1-phenyl-(2′,4′-dichloro)-1-fluoro-2-chloroethane (VI), 1-phenyl-(2′,-5′-dichloro)-1-fluoro-2-chloroethane (VII), and 1-phenyl-(2′,6′-dichloro)-1-fluoro-2-bromoethane (VIII). These compounds were prepared from the corresponding alcohols, in accordance with the process previously described (1).

Methods—The dipole moments of the compounds as solutes in anhydrous benzene were measured at 25.00 ± 0.05°C. The permittivity[1] and refractive index[2] of the solutions were extrapolated to infinite dilution according to Guggenheim (2) and Smith (3). The quantity $(\epsilon_{12} - n_{12}^2) - (\epsilon_1 - n_1^2)$ was plotted *versus* the molar concentration, C, of the solute. The slope of the curve at $C = 0$ was then used to calculate the dipole moment, μ, by:

$$\mu^2 = \frac{9kT}{4\pi N} \cdot \frac{3}{(\epsilon_1 + 2)(n_1^2 + 2)} \cdot \frac{(\epsilon_{12} - n_{12}^2) - (\epsilon_1 - n_1^2)}{C} \qquad \text{(Eq. 1)}$$

where k is the Boltzmann constant, N is Avogadro's number, T is the absolute temperature, and ϵ_i and n_i are the permittivities and refractive indexes, respectively, of the solutes (Index 1) and of the solutions (Index 12).

RESULTS AND DISCUSSION

The molecular geometry of the compounds studied is schematized in Fig. 1. Hence, six limit-conformers have to be considered, because of the presumable restricted rotation around the C_1—C_2 bond. These conformers, presented in Fig. 2, are noted (A) when bonds are staggered and (B) when bonds are opposed. The following bond increments were then used for vectorial calculations: H—$C_{sp}3$, 0.25 *D* (4); $C_{sp}3$—Br, 1.38 *D*; $C_{sp}3$—Cl, 1.46 *D*; $C_{sp}3$—F, 1.41 *D* (5); $C_{sp}3$—$C_{sp}2$, 0.4 *D*; $C_{sp}2$—Br, 1.54 *D*; and $C_{sp}2$—Cl, 1.58 *D* (6).

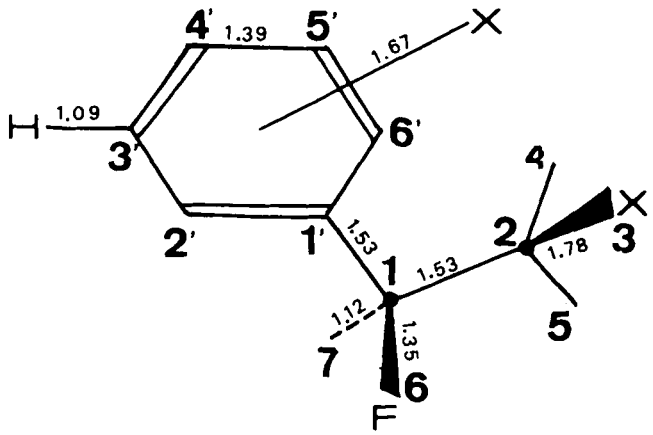

Figure 1—*Molecular geometry of the compounds studied.*

As regards the vectorial pattern of the molecules, it must be emphasized that spatial orientation of the phenyl ring *versus* the C_1—F bond is of no importance, except with the *ortho*-substituted derivatives. In the latter case, four possible orientations must be taken into account in accordance either with

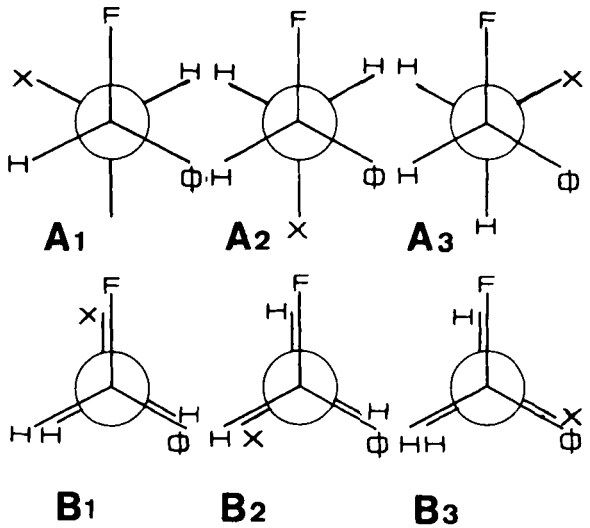

Figure 2—*Schemes of the staggered and the opposed limit-conformers used in the calculations.*

[1] W.T.W. DM 01 dipolmeter with a DFL 1 cell.
[2] O.P.L. Abbe type refractometer.

0022-3549/84/0800-1164$01.00/0
© 1984, American Pharmaceutical Association

Table I—Experimental and Calculated Dipole Moments [a]

Compound	μ_{exp}	Ring Orientation	Method	Calculated Moments: Conformers A-1	A-2	A-3	B-1	B-2	B-3	μ_{theor}	Conformer Population [b]: A-1	A-2	A-3
I	2.54	1-4	Vect	2.24	0.67	2.82	2.92	0.99	1.98	2.21			
		1	PCILO	2.80	0.64	2.96				2.57	0.54	0.20	0.26
		1	CNDO/2	3.30	1.14	3.12				2.94			
II	1.90	1-4	Vect	1.59	2.22	3.51	2.77	0.89	3.28	2.40	0.48	0.25	0.27
III	1.93	1-4	Vect	1.60	2.26	3.54	2.79	0.94	3.32	2.42	0.50	0.23	0.27
		2	CNDO/2	1.65	1.72	3.29				2.25			
IV	2.65	1a	Vect	3.63	1.35	3.99	4.34	2.16	2.73	3.65			
		1b	Vect	2.46	1.30	1.37	2.17	2.13	0.61	2.08			
		2a	Vect	2.71	1.33	2.99	3.20	1.76	2.16	2.74			
		2b	Vect	3.48	1.53	3.08	3.69	2.54	1.96	3.25			
		3a	Vect	3.50	1.42	4.05	4.29	2.01	2.86	3.60	0.58	0.07	0.35
		3b	Vect	2.75	1.36	1.77	2.55	2.29	0.91	2.38			
		4a	Vect	3.68	1.40	3.88	4.29	2.31	2.61	3.64			
		4b	Vect	2.21	1.37	1.35	1.97	1.98	0.92	1.91			
V	2.71	1a	Vect	3.67	1.38	4.03	4.37	2.20	2.76	3.64			
		1b	Vect	2.48	1.34	1.34	2.17	2.17	0.58	2.06			
		2a	Vect	2.73	1.36	3.00	3.22	1.79	2.18	2.72			
		2b	Vect	3.52	1.57	3.09	3.72	2.58	1.98	3.23			
		3a	Vect	3.54	1.45	4.08	4.33	2.05	2.89	3.59	0.56	0.10	0.34
		3b	Vect	2.77	1.40	1.76	2.56	2.33	0.90	2.35			
		4a	Vect	3.72	1.46	3.91	4.33	2.35	2.64	3.63			
		4b	Vect	2.23	1.41	1.33	1.95	2.01	0.91	1.89			
VI	1.65	1a	Vect	2.94	1.93	4.33	4.13	1.41	3.48	3.49			
		1b	Vect	1.17	1.99	1.99	1.50	1.49	2.20	1.63			
		1b	CNDO/2	1.72	2.19	1.26				1.61			
		2a	Vect	1.67	2.01	3.40	2.87	0.84	3.08	2.53			
		2b	Vect	2.68	1.98	3.38	3.33	1.89	2.80	2.92	0.50	0.10	0.40
		3a	Vect	2.87	2.11	4.45	4.14	1.37	3.66	3.53			
		3b	Vect	1.80	2.10	2.52	2.10	1.80	2.36	2.15			
		4a	Vect	3.07	2.05	4.25	4.11	1.75	3.42	3.52			
		4b	Vect	0.83	2.17	2.11	1.36	1.45	2.42	1.61			
VII	2.39	1-4	Vect	2.24	0.67	2.82	2.92	0.99	1.98	2.40	0.51	0.10	0.39
VIII	3.09	1-4	Vect	3.47	0.94	2.84	3.62	2.44	1.39	2.80	0.56	0.34	0.10

[a] In Debye units. [b] According to NMR data (17).

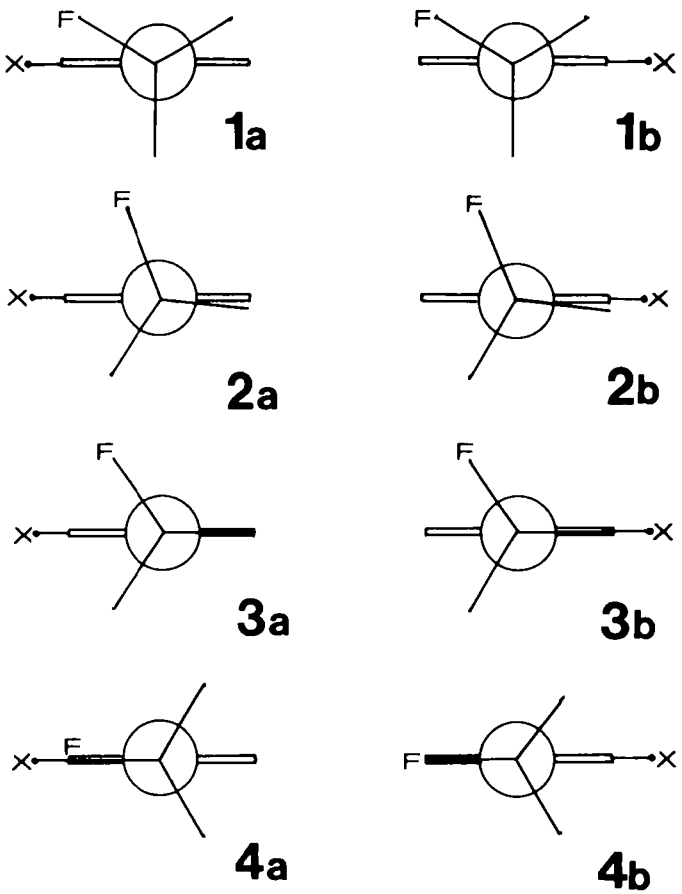

Figure 3—*Ring orientations* versus *the fluorine-carbon bond, in case of orthohalogeno(X)-substituted derivatives.*

experimental results concerning benzyl fluorides [Fig. 3, part 1 (7); Fig. 3, part 3 (8); Fig. 3, part 4 (9)] or crystallographic data about homologues of the compounds studied (Fig. 3, part 2)[3].

Experimental dipole moments and the vectorially calculated moments as well as some values theoretically calculated by means of the CNDO/2 (10) or PCILO (11) methods are given in Table I. On the one hand, all the calculated values are in satisfactory agreement, whatever are methods of calculation. The slight deviations noted are due to the bond increments herein used in the vectorial calculations instead of molecular increments. Under these conditions, atomic interactions through either bonds (12) or space (13) are neglected, although they lead to an inductive moment to be added or subtracted to the bond moments (14).

On the other hand, every vectorially calculated value can be alternately compared with the measured value of the dipole moments. In so doing, structures labeled "B" can be left out. This latter hypothesis directly proceeds from the conformational energy mapping (15), where energy minima only correspond to the "A" conformers. Under these conditions, it follows from the comparison that *gauche* structures (quoted as A-1 or A-3) prevail. However, existence of a conformational mixture cannot be ignored, because of the difference between experimental and calculated values. This is in agreement with the IR results (16). Nevertheless, relative populations cannot be then readily calculated using dielectric data, contrary to NMR data. Indeed, the coupling constants J^{t}_{HH}, J^{g}_{HF}, and J^{t}_{HF} calculated from the latter lead to values of conformational populations (17). Therefore, by using these values, theoretical dipole moments of each compound can be calculated according to the following:

$$\mu_{theor} = \sqrt{\mu^2_{A\text{-}1} \cdot P_1 + \mu^2_{A\text{-}2} \cdot P_2 + \mu^2_{A\text{-}3} \cdot P_3} \qquad \text{(Eq. 2)}$$

These results are also presented in Table I.

The conformational multiplicity is then confirmed by the good relationships noted between the theoretical and the experimental moments. Added to this, the spatial orientation of the phenyl ring can now be figured for IV, V, and VI. Indeed, experimental dipole moments of these molecules are pointed out in Fig. 4, referring to the theoretical moments calculated for the various orientations previously quoted. In the cases of IV and V, the geometrical structure intermediate between 2b and 3b is certainly favored because of the

[3] B. Chion, C. Charlon, and C. Luu Duc, unpublished results.

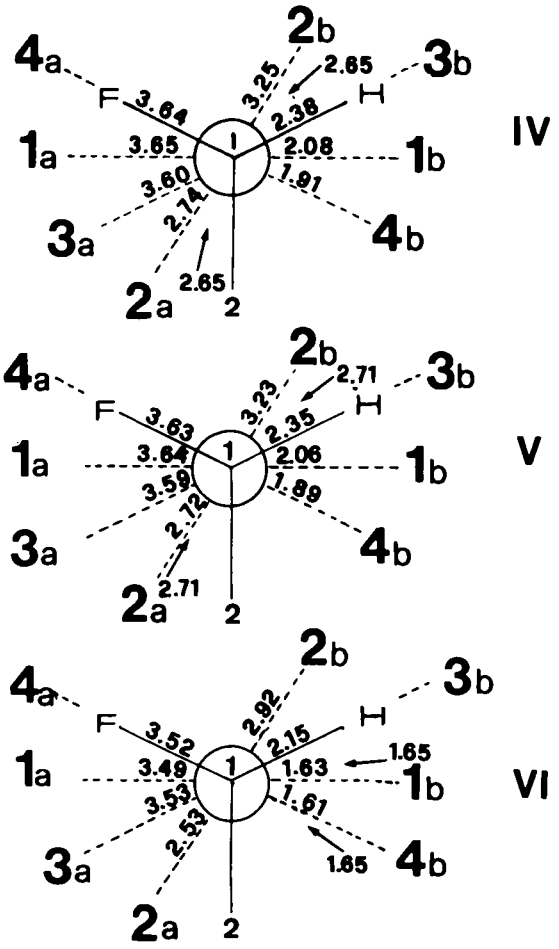

Figure 4—*Experimental dipole moments (values with arrows) and theoretical moments calculated for each ring orientation for IV, V, and VI.*

steric hindrances between halogens in the 2a structure. Conversely, structures 1b and 4b would have to be equally possible for VI, because the C_1—F and the C_2—X bonds are practically *anti* in each case. However, as steric hindrances between the halogen bonded to C-2 and the phenyl ring are minimized in position 1b, the latter will be more stable. These results are in close agreement with ^{13}C-NMR data (18).

REFERENCES

(1) C. Beguin, C. Charlon, C. Coulombeau, and C. Luu Duc, *J. Fluorine Chem.*, **8**, 531 (1976).

(2) E. A. Guggenheim, *Trans. Faraday Soc.*, **45**, 714 (1949).

(3) J. W. Smith, *Trans. Faraday Soc.*, **46**, 394 (1950).

(4) V. I. Minkin, O. A. Osipov and Y. A. Zdanov, "Dipole Moments in Organic Chemistry," Plenum, New York, N.Y., 1970.

(5) C. P. Smith, *J. Phys. Chem.*, **41**, 209 (1937).

(6) C. P. Smith, "Dielectric Behaviour and Structure," McGraw-Hill, New York, N.Y., 1955.

(7) C. Beguin and E. Gout-Mallaret, *J. Fluorine Chem.*, **8**, 279 (1976).

(8) R. J. Abraham, R. A. Hearmon, M. Traetteberg, and P. Bakken, *J. Mol. Struct.*, **57**, 149 (1979).

(9) T. Schaefer, J. B. Rowbotham, W. J. E. Parr, K. Marat, and A. F. Janzen, *Can. J. Chem.*, **54**, 1322 (1976).

(10) Program 141, Quantum Chemistry Program Exchange, Indiana Univ., Bloomington.

(11) Program 220/221, Quantum Chemistry Program Exchange, Indiana Univ., Bloomington.

(12) A. Caristan, P. Bothorel, and H. Bodot, *J. Chim. Phys.*, **66**, 1009 (1969).

(13) M. Camail and D. D. Dicko, *Comptes Rendus*, **272C**, 1188 (1971).

(14) C. P. Smyth and W. S. Walls, *J. Am. Chem. Soc.*, **54**, 1854 (1932).

(15) Cartolab, Automatic Mapping Program, J. L. Mallet, Univ. Nancy, France.

(16) J. P. Lere-Porte, A. Bonniol, J. Petrissans, C. Charlon, and C. Luu Duc, *J. Mol. Struct.*, **98**, 77 (1983).

(17) S. Hamman, C. Beguin, C. Charlon, and C. Luu Duc, *Org. Magn. Reson.*, **21**, 361 (1983).

(18) C. Charlon, Thesis, UER Pharm., University of Grenoble, 1983.

Synthesis and Biological Evaluation of New 2,3-Dihydrothiazole Derivatives for Antimicrobial, Antihypertensive, and Anticonvulsant Activities

A.-MOHSEN M. E. OMAR ˣ and NABIL H. ESHBA

Received December 2, 1982, from the *Pharmaceutical Chemistry Department, Faculty of Pharmacy, University of Alexandria, Egypt.* Accepted for publication August 2, 1983.

Abstract □ A novel series of 2-arylimino-2,3-dihydrothiazole derivatives, substituted in the 3-position with a β-phenethyl moiety and the 4-position with substituted aryl functions, was synthesized as potential antimicrobial, antihypertensive and anticonvulsive agents. While no antimicrobial or significant antihypertensive activity was observed for the products, XII, XIII, and XXI displayed potent anticonvulsant activity.

Keyphrases □ 2,3-Dihydrothiazole derivatives—synthesis antimicrobial, antihypertensive, and anticonvulsant properties □ Antimicrobial activity—2,3-dihydrothiazole derivatives, antihypertensive and anticonvulsant properties

The synthesis and pharmacological properties of a variety of thioureas (1-3), thiosemicarbazones (4-6), thiosemicarbazides (1, 7, 8), thiazoles (2, 6, 7), and thiadiazines (9) derived from various biologically active nuclei (1-5, 8), aromatic (6), and heterocyclic compounds (7, 9) have been recently described in connection with our studies on the structure-activity relationships of certain thio compounds. The high bactericidal activity displayed by some 3,4-diarylthiazolin-2-oxo-(3-substituted 4-oxoquinazolin-2-yl)hydrazones (7) prompted the investigation of a novel series of 2-arylimino-2,3-dihydrothiazoles (VIII-XXXIII) which bear a structural similarity to such active thiazolines with respect to the substituents in the 4-position. This paper reports the synthesis and evaluation of these materials for antimicrobial, antihypertensive, and anticonvulsant activities.

RESULTS AND DISCUSSION

Chemistry—The *N*-substituted *N'*-(2-phenethyl)thiourea derivatives (II-VII), Scheme I, were synthesized (Table I) by treating 2-phenethylamine (I) with the appropriate aryl- or aralkylisothiocyanate in refluxing ethanol

0022-3549/84/0800-1166$01.00/0

© *1984, American Pharmaceutical Association*

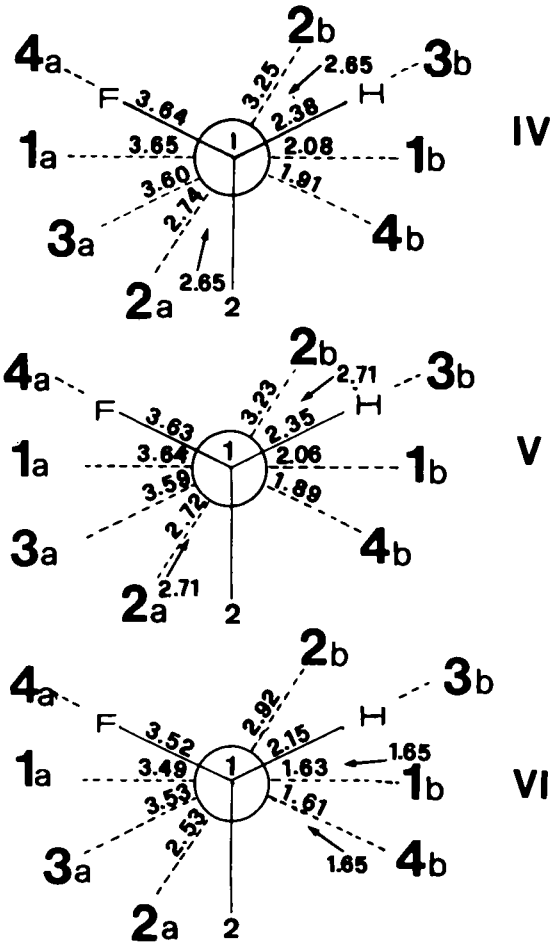

Figure 4—*Experimental dipole moments (values with arrows) and theoretical moments calculated for each ring orientation for IV, V, and VI.*

steric hindrances between halogens in the 2a structure. Conversely, structures 1b and 4b would have to be equally possible for VI, because the C_1—F and the C_2—X bonds are practically *anti* in each case. However, as steric hindrances between the halogen bonded to C-2 and the phenyl ring are minimized in position 1b, the latter will be more stable. These results are in close agreement with ^{13}C-NMR data (18).

REFERENCES

(1) C. Beguin, C. Charlon, C. Coulombeau, and C. Luu Duc, *J. Fluorine Chem.*, **8**, 531 (1976).

(2) E. A. Guggenheim, *Trans. Faraday Soc.*, **45**, 714 (1949).

(3) J. W. Smith, *Trans. Faraday Soc.*, **46**, 394 (1950).

(4) V. I. Minkin, O. A. Osipov and Y. A. Zdanov, "Dipole Moments in Organic Chemistry," Plenum, New York, N.Y., 1970.

(5) C. P. Smith, *J. Phys. Chem.*, **41**, 209 (1937).

(6) C. P. Smith, "Dielectric Behaviour and Structure," McGraw-Hill, New York, N.Y., 1955.

(7) C. Beguin and E. Gout-Mallaret, *J. Fluorine Chem.*, **8**, 279 (1976).

(8) R. J. Abraham, R. A. Hearmon, M. Traetteberg, and P. Bakken, *J. Mol. Struct.*, **57**, 149 (1979).

(9) T. Schaefer, J. B. Rowbotham, W. J. E. Parr, K. Marat, and A. F. Janzen, *Can. J. Chem.*, **54**, 1322 (1976).

(10) Program 141, Quantum Chemistry Program Exchange, Indiana Univ., Bloomington.

(11) Program 220/221, Quantum Chemistry Program Exchange, Indiana Univ., Bloomington.

(12) A. Caristan, P. Bothorel, and H. Bodot, *J. Chim. Phys.*, **66**, 1009 (1969).

(13) M. Camail and D. D. Dicko, *Comptes Rendus*, **272C**, 1188 (1971).

(14) C. P. Smyth and W. S. Walls, *J. Am. Chem. Soc.*, **54**, 1854 (1932).

(15) Cartolab, Automatic Mapping Program, J. L. Mallet, Univ. Nancy, France.

(16) J. P. Lere-Porte, A. Bonniol, J. Petrissans, C. Charlon, and C. Luu Duc, *J. Mol. Struct.*, **98**, 77 (1983).

(17) S. Hamman, C. Beguin, C. Charlon, and C. Luu Duc, *Org. Magn. Reson.*, **21**, 361 (1983).

(18) C. Charlon, Thesis, UER Pharm., University of Grenoble, 1983.

Synthesis and Biological Evaluation of New 2,3-Dihydrothiazole Derivatives for Antimicrobial, Antihypertensive, and Anticonvulsant Activities

A.-MOHSEN M. E. OMAR ˣ and NABIL H. ESHBA

Received December 2, 1982, from the *Pharmaceutical Chemistry Department, Faculty of Pharmacy, University of Alexandria, Egypt.* Accepted for publication August 2, 1983.

Abstract □ A novel series of 2-arylimino-2,3-dihydrothiazole derivatives, substituted in the 3-position with a β-phenethyl moiety and the 4-position with substituted aryl functions, was synthesized as potential antimicrobial, antihypertensive and anticonvulsive agents. While no antimicrobial or significant antihypertensive activity was observed for the products, XII, XIII, and XXI displayed potent anticonvulsant activity.

Keyphrases □ 2,3-Dihydrothiazole derivatives—synthesis antimicrobial, antihypertensive, and anticonvulsant properties □ Antimicrobial activity—2,3-dihydrothiazole derivatives, antihypertensive and anticonvulsant properties

The synthesis and pharmacological properties of a variety of thioureas (1-3), thiosemicarbazones (4-6), thiosemicarbazides (1, 7, 8), thiazoles (2, 6, 7), and thiadiazines (9) derived from various biologically active nuclei (1-5, 8), aromatic (6), and heterocyclic compounds (7, 9) have been recently described in connection with our studies on the structure-activity relationships of certain thio compounds. The high bactericidal activity displayed by some 3,4-diarylthiazolin-2-oxo-(3-substituted 4-oxoquinazolin-2-yl)hydrazones (7) prompted the investigation of a novel series of 2-arylimino-2,3-dihydrothiazoles (VIII-XXXIII) which bear a structural similarity to such active thiazolines with respect to the substituents in the 4-position. This paper reports the synthesis and evaluation of these materials for antimicrobial, antihypertensive, and anticonvulsant activities.

RESULTS AND DISCUSSION

Chemistry—The *N*-substituted *N'*-(2-phenethyl)thiourea derivatives (II-VII), Scheme I, were synthesized (Table I) by treating 2-phenethylamine (I) with the appropriate aryl- or aralkylisothiocyanate in refluxing ethanol

0022-3549/84/0800-1166$01.00/0

© *1984, American Pharmaceutical Association*

Table I—Synthesized *N,N'*-Disubstituted Thiourea (II-VII) and 4-Thiazoline Derivatives (VIII-XXXIII), and Their Anticonvulsant Activities [a]

Compound	Yield, %	mp, °C	Molecular Formula	Anticonvulsant Activity, % Protection [b]
II	82	118-120	$C_{16}H_{18}N_2S$	—
III	85	106-107 [c]	$C_{15}H_{16}N_2S$	—
IV	79	101-102	$C_{16}H_{18}N_2S$	—
V	85	124-126	$C_{16}H_{18}N_2S$	—
VI	80	135-137	$C_{15}H_{15}ClN_2S$	—
VII	83	130-132	$C_{15}H_{15}BrN_2S$	—
VIII	84	166-167	$C_{24}H_{23}BrN_2S$	+13
IX	89	207-208	$C_{24}H_{22}Br_2N_2S$	−20
X	87	230-231	$C_{24}H_{22}BrN_3O_2S$	+12
XI	81	180-181	$C_{25}H_{25}BrN_2S$	+53
XII	86	226-227	$C_{24}H_{22}BrClN_2S$	+91 [d]
XIII	88	229-230	$C_{23}H_{21}BrN_2S$	+162
XIV	88	230-231	$C_{23}H_{20}Br_2N_2S$	+25
IV	93	266-267	$C_{23}H_{20}BrN_3O_2S$	+12
XVI	100	209-210	$C_{24}H_{23}BrN_2S$	+23
XVII	82	219-220	$C_{24}H_{23}BrN_2S$	+5
XVIII	86	240-241	$C_{24}H_{22}Br_2N_2S$	+37
XIX	85	266-267	$C_{24}H_{22}BrN_3O_2S$	+1
XX	79	204-205	$C_{25}H_{25}BrN_2S$	−17
XXI	93	235-236	$C_{24}H_{23}BrN_2S$	+94
XXII	96	266-267	$C_{24}H_{22}Br_2N_2S$	−22
XXIII	95	274-275	$C_{24}H_{22}BrN_3O_2S$	+24
XXIV	91	233-234	$C_{25}H_{25}BrN_2S$	−5
XXV	94	269-270	$C_{23}H_{20}BrClN_2S$	+1
XXVI	98	270-271	$C_{23}H_{19}Br_2ClN_2S$	−8
XXVII	94	279-280	$C_{23}H_{19}BrClN_3O_2S$	−5
XXVIII	92	269-270	$C_{24}H_{22}BrClN_2S$	−15
XXIX	100	264-265	$C_{23}H_{19}BrCl_2N_2S$	+19
XXX	91	265-266	$C_{23}H_{20}Br_2N_2S$	+17
XXXI	98	267-268	$C_{23}H_{19}Br_3N_2S$	+6
XXXII	94	275-276	$C_{23}H_{19}Br_2N_3O_2S$	+25
XXXIII	91	263-264	$C_{24}H_{22}Br_2N_2S$	−7

[a] All compounds underwent elemental analyses for C and H. Compounds II VIII, XI, XIV-XVI, XXII, XXIII, XXVII, and XXIX-XXXI were also analyzed for N; II, V, VIII, X, XIII, XV-XVII, XX, XXI, XXIII-XXV, XXVIII, and XXX-XXXIII were analyzed for S; and IX, XIV, XXII, XXXI, and XXXII were analyzed for Br. All values were within ±0.4% of the theoretical values. [b] Percentages of protection for diazepam (5 mg/kg po) and chlordiazepoxide (10 mg/kg po) were +174 and +185, respectively. [c] Reported (13) mp 111 °C, without confirmation of elemental analysis. [d] Associated with symptoms of toxicity.

(10). The products were treated with either phenacyl bromide or the properly substituted phenacyl bromide in boiling ethanol to give the required 2,3-dihydrothiazole derivatives (VIII-XXXIII) as hydrobromide salts (see Table I).

Biological Screening[1]—*Antimicrobial Activity*—Using the serial dilution method in Mueller Hinton agar (6), VIII-XXXIII did not show antimicrobial effect against *Escherichia coli* NCTC 10418, *Klebsiella aerogene* A, *Pseudomonas aeroginosa* NCTC 10662, *Serratia marcescens* US32, *Staphylococcus aureus* Oxford, *Candida albicans* W97, and *Bacteroides fragilis* BC4, NCTC 8560, and B3.

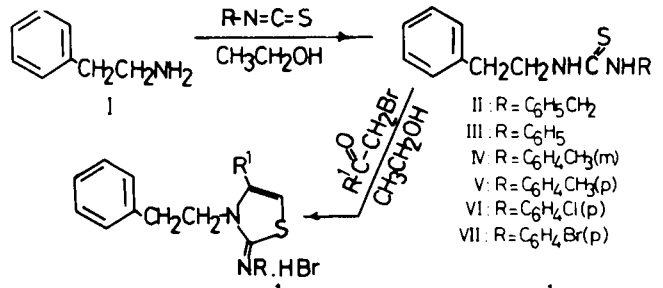

	R	R'		R	R'
VIII:	$C_6H_5CH_2$	C_6H_5	IX:	$C_6H_5CH_2$	$C_6H_4Br(p)$
X:	$C_6H_5CH_2$	$C_6H_4NO_2(p)$	XI:	$C_6H_5CH_2$	$C_6H_4CH_3(p)$
XII:	$C_6H_5CH_2$	$C_6H_4Cl(p)$	XIII:	C_6H_5	C_6H_5
XIV:	C_6H_5	$C_6H_4Br(p)$	XV:	C_6H_5	$C_6H_4NO_2(p)$
XVI:	C_6H_5	$C_6H_4CH_3(p)$	XVII:	$C_6H_4CH_3(m)$	C_6H_5
XVIII:	$C_6H_4CH_3(m)$	$C_6H_4Br(p)$	XIX:	$C_6H_4CH_3(m)$	$C_6H_4NO_2(p)$
XX:	$C_6H_4CH_3(m)$	$C_6H_4CH_3(p)$	XXI:	$C_6H_4CH_3(p)$	C_6H_5
XXII:	$C_6H_4CH_3(p)$	$C_6H_4Br(p)$	XXIII:	$C_6H_4CH_3(p)$	$C_6H_4NO_2(p)$
XXIV:	$C_6H_4CH_3(p)$	$C_6H_4CH_3(p)$	XXV:	$C_6H_4Cl(p)$	C_6H_5
XXVI:	$C_6H_4Cl(p)$	$C_6H_4Br(p)$	XXVII:	$C_6H_4Cl(p)$	$C_6H_4NO_2(p)$
XXVIII:	$C_6H_4Cl(p)$	$C_6H_4CH_3(p)$	XXIX:	$C_6H_4Cl(p)$	$C_6H_4Cl(p)$
XXX:	$C_6H_4Br(p)$	C_6H_5	XXXI:	$C_6H_4Br(p)$	$C_6H_4Br(p)$
XXXII:	$C_6H_4Br(p)$	$C_6H_4NO_2(p)$	XXXIII:	$C_6H_4Br(p)$	$C_6H_4CH_3(p)$

Scheme I

Antihypertensive Activity—The 2-phenylimino-3-phenyl-4-phenyl-2,3-dihydrothiazole (XIII) caused a slight fall in blood pressure 6 h after administration of a dose of 100 mg/kg in spontaneously hypertensive rats. The 2,3-dihydrothiazoles XI and XX (at a dose of 5 mg/kg) and XXI (at a dose of 100 mg/kg), as the other selected examples of the series, did not exhibit antihypertensive activity.

Anticonvulsant Activity—The oral administration of VIII-XXXIII in doses of 100 mg/kg in mice 60 min prior to induction of convulsions by pentylenetetrazol[2] (8 mg/mL in saline), gave variable anticonvulsant activities ranging from +162 to −22% protection (Table I). The 2,3-dihydrothiazoles XIII and XXI were the most potent, causing +162 and +94% protection, respectively. The +91% protection exhibited by XII was accompanied by symptoms of toxicity.

Such results, as compared with those recently reported for the thiazoline-2-hydrazonoquinazolones (7), are indicative of the effect of the bulky phenethyl group, which is a constant substituent, on the supression of the antimicrobial activity of all products (12). The insignificant antihypertensive effect displayed by XIII as well as the general lack of anticonvulsant activity, despite the observed potency of XII, XIII, and XXI, could not lead to reliable structure-activity relationships in these 2,3-dihydrothiazoles.

EXPERIMENTAL SECTION[3]

N-Aryl-N'-(2-phenethyl)thiourea Derivatives (II-VII)—A mixture of 2-phenethylamine (I) (1.2 g, 0.01 mol) and the appropriate aryl- or aralkylisothiocyanate (0.01 mol) in ethanol (20 mL) was heated at reflux for 1 h. The mixture was concentrated under reduced pressure, and the material which separated on cooling was removed by filtration, washed with 10% HCl, dried, and recrystallized from ethanol. The yields and physical constants of the products (II-VII) are presented in Table I. IR (mineral oil) ν: 3370 and

[1] Performed in accordance with the protocol of the biological screening of the Chemotherapeutic Research Centre, Beecham Pharmaceuticals, Brockham Park, Betchworth, Surrey, RH3 7AJ, U.K.

[2] Metrazol; Sigma, U.K.

[3] All melting points are uncorrected. IR spectra were measured on a Beckman 4210 IR Spectrophotometer. ^{1}H-NMR spectra were measured on a Varian A-90, and mass spectra on a Finnigan 3200.

3250-3160 (NH), 1550-1525, 1345, 1320-1305, and 945-910 cm^{-1} (NCS I, II, III, and IV amide bands, respectively) (11); ^{1}H-NMR of II ($CDCl_3$): δ 2.82 (t, 2, J = 7.5 Hz, $C_6H_5CH_2CH_2$—), 3.68 (q, 2, J = 7.5 Hz, $C_6H_5CH_2CH_2$—), 4.41 (d, 2, J = 5 Hz, $C_6H_5CH_2$—), 5.64 (s, distorted, 1, 2-phenethyl-NH, exchangeable), 6.07 (s, distorted, 1, benzyl-NH, exchangeable), and 7.13 ppm (m, 10, ArH).

2-Arylimino-4-aryl-3-(2-phenethyl)-2,3-dihydrothiazole Hydrobromides (VIII–XXXIII)—A mixture of *N*-aryl-*N'*-(2-phenethyl)thioureas (II–VII) (0.001 mol) and phenacyl bromide or the appropriately substituted phenacyl bromide (0.0011 mol) in absolute ethanol (10 mL) was heated at reflux for 4 h. Some of the products separated during the heating, while others crystallized after cooling the mixture. The products were removed by filtration, dried, and recrystallized from benzene containing a few drops of absolute ethanol. The yields and physical constants of the products (VIII–XXXIII) are listed in Table I. IR (mineral oil) ν: 2780–2670 (—NH) and 1610–1590 cm^{-1} (C=N); ^{1}H-NMR of XXIII (Me_2SO-d_6): δ 2.41 (s, 3, CH_3), 2.94 (t, 2, J = 7.5 Hz, $C_6H_5CH_2CH_2$—), 4.46 (t, 2, J = 7.5 Hz, $C_6H_5CH_2CH_2$—), 7.26 (m, 10, ArH and C_5—H of the thiazoline ring), 7.70 (d, 2, J = 9 Hz, ArH, *meta* to nitro group), and 8.44 ppm (d, 2, J = 9 Hz, ArH, *ortho* to nitro group); ^{1}H-NMR for XXVIII: δ 2.41 (s, 3, CH_3), 2.87 (t, 2, J = 7.5 Hz, $C_6H_5CH_2CH_2$—), 4.34 (t, 2, J = 7.5 Hz, $C_6H_5CH_2CH_2$—), 6.87 (s, 1, C_5-thiazoline proton), and 7.25 ppm (m, 13, ArH); ^{1}H-NMR for XXX: δ 2.81 (t, 2, J = 7.5 Hz, $C_6H_5CH_2CH_2$—), 4.27 (t, 2, J = 7.5 Hz, $C_6H_5CH_2CH_2$—), 6.80 (s, 1, C_5-thiazoline proton), and 7.29 ppm (m, 14, ArH). MS, *m/z* (relative abundance %) for XXIII: M^+ at 415(7), 312(22), 311(100), 310(20), 134(19), 105(47), 104(22), 103(26), 91(49), and 89(28). For XXVIII: M^+ at 404 and M + 2 at 406(8), 302(36), 301(22), 300(100), 299(15), 149(27), 148(51), 147(74), 134(27), 118(31), 115(28), 105(52), 104(21), 103(29), and 91(48). For XXX: M^+ at 435 and M + 2 at 437(0.9), 332(57), 331(17), 330(50), 139(22), 135(31), 134(100), 105(41), 104(49), 103(32), 102(23), 91(86), 90(24), 89(20), and 82(16).

Antihypertensive Testing—Rats, maintained in an incubator (32–35°C) for 20–40 min, were restrained to measure systolic blood pressure and heart rate indirectly by the tail cuff method[4]. Each determination was the mean of at least six recordings. Groups of four animals were used, and measurements were made predose (time zero) 1, 2, 4, and 6 h after administration of the products, with occasional readings at 24 h.

Anticonvulsant Testing—The compounds suspended in 1% methylcellulose were administered orally (1 mL/100 g) to CD-1 male mice (18–25 g), 10 per group, 1 h before intravenous infusion of 8 mg/mL of pentylenetetrazol in saline at a rate of 0.5 mL/min. The time of infusion required to elicit a tonic extensor spasm was noted, and the dose of pentylenetetrazol administered was calculated. The results (Table I) are expressed as the percentage change compared with controls treated with vehicle only. Statistical significance was determined using the Student's t test.

[4] W, W8005 B.P. recorder.

REFERENCES

(1) A.-M. M. E. Omar, A. M. Farghaly, A. A. B. Hazza, N. H. Eshba, F. M. Sharabi, and T. T. Daabees, *J. Pharm. Sci.*, **70**, 1075 (1981).

(2) El-S. A. Ibrahim, A.-M. M. E. Omar, N. S. Habib, O. M. Aboul-Wafa, S. M. El-Sewedy, and J. Bourdais, *J. Pharm. Sci.*, **72**, 1205 (1983).

(3) A.-M. M. E. Omar, O. M. AboulWafa, and G. Leclercq, *J. Pharm. Sci.*, in press.

(4) A.-M. M. E. Omar, S. M. El-Khawass, A. B. Makar, N. M. Bakry, and T. T. Daabees, *Pharmazie*, **33**, 577 (1978).

(5) A.-M. M. E. Omar and N. S. Habib, *Pharmazie*, **33**, 81 (1978).

(6) A.-M. M. E. Omar, I. M. Labouta, G. M. Kassem, and J. Bourdais, *J. Pharm. Sci.*, **72**, 1226 (1983).

(7) A.-M. M. E. Omar, S. A. Shams El-Din, A. A. Ghobashy, and M. A. Khalil, *Eur. J. Med. Chem.*, **16**, 77 (1981).

(8) El-S. A. Ibrahim, A.-M. M. E. Omar, M. A. Khalil, M. A. Makar, M. T. I. Soliman, and T. T. Daabees, *Pharmazie*, **35**, 80 (1980).

(9) M. A. El-Dawy, A.-M. M. E. Omar, A. M. Ismail, and A. A. B. Hazzaa, *J. Pharm. Sci.*, **72**, 45 (1983).

(10) A. A. B. Hazzaa, A.-M. M. E. Omar, and M. S. Ragab, *Pharmazie*, **28**, 364 (1973).

(11) A.-M. M. E. Omar and S. A. Osman, *Pharmazie*, **28**, 30 (1973).

(12) E. B. Akerblom, *J. Med. Chem.*, **17**, 609 (1974).

(13) C. Braun, *Chem. Ber.*, **45**, 2192 (1912).

ACKNOWLEDGMENTS

Supported in part by Pharco Pharmaceuticals, Cairo, Egypt. The authors thank the members of the Chemotherapeutic Research Centre, Beecham Pharmaceuticals, Brockham Park, Betchworth, Surrey, RH3 7AJ, U.K. for the biological screening of the products, and the members of the Microanalytical Unit, Faculty of Science, Cairo University, for the analytical data. They are also indebted to Dr. Farouk S. El-Feraly, Department of Pharmacognosy, School of Pharmacy, The University of Mississippi, University, Miss. for the NMR and MS data.

Synthesis of *N*,*N'*-Disubstituted *N''*-2-(2-Quinolinylmethylthio)ethylguanidines as Potential Anticancer Agents

WILLIAM O. FOYE *x, SEUNG HO AN *§, and TIMOTHY J. MAHER ‡

Received April 25, 1983, from the **Samuel M. Best Research Laboratory* and the ‡*Department of Pharmacology, Massachusetts College of Pharmacy and Allied Health Sciences, Boston, MA 02115.* Accepted for publication June 1, 1983.

§Present address: Roswell Park Memorial Institute, Buffalo, N.Y.

Abstract □ A simple method for obtaining the title compounds was found in the alkaline rearrangement of *S*-2-aminoethylisothiouronium salts, which were obtained from the condensation of thiourea or substituted thioureas with 2-bromoethylamine hydrobromide. No activity was found for the substituted guanidines against P388 lymphocytic leukemia in mice, or as H_2-receptor antagonists.

Keyphrases □ *N,N'*-Disubstituted *N''*-2-(2-quinolinylmethylthio)ethylguanidines—anticancer activity, potential H_2-receptor antagonist □ Anticancer agents—potential, *N,N'*-disubstituted *N''*-2-(2-quinolinylmethylthio)ethylguanidines, H_2-receptor antagonist activity

A number of strongly basic compounds have shown appreciable anticancer activity. Bis(guanidines) and guanylhydrazones are active in leukemia systems (1, 2), and bis(guanylhydrazones) of anthracene-9,10-dicarboxaldehydes (3) have a particularly broad spectrum of anticancer activity. Recently, synthesized bis(*S*-alkyl) (4), and *S*-alkyl cycloalkylamino (5) derivatives of *N*-methylquinolinium dithioacetic acid showed reproducible activity against P388 lymphocytic leukemia in mice, the best activity being shown by one of the basic (morpholino) derivatives. It appeared that further increase in basicity of this series was warranted. The basic side chain of the cimetidine molecule was selected for inclusion in the quinoline-2-methyl structure because of the reported cytostatic and immunosuppressive activities of some guanidine derivatives (6). Modification of the basicity by inclusion of electron-attracting or -releasing functions on the guanidine moiety was

0022-3549/84/0800-1168$01.00/0

© 1984, American Pharmaceutical Association

3250-3160 (NH), 1550-1525, 1345, 1320-1305, and 945-910 cm^{-1} (NCS I, II, III, and IV amide bands, respectively) (11); ^{1}H-NMR of II ($CDCl_3$): δ 2.82 (t, 2, J = 7.5 Hz, $C_6H_5CH_2CH_2$—), 3.68 (q, 2, J = 7.5 Hz, $C_6H_5CH_2CH_2$—), 4.41 (d, 2, J = 5 Hz, $C_6H_5CH_2$—), 5.64 (s, distorted, 1, 2-phenethyl-NH, exchangeable), 6.07 (s, distorted, 1, benzyl-NH, exchangeable), and 7.13 ppm (m, 10, ArH).

2-Arylimino-4-aryl-3-(2-phenethyl)-2,3-dihydrothiazole Hydrobromides (VIII–XXXIII)—A mixture of *N*-aryl-*N'*-(2-phenethyl)thioureas (II–VII) (0.001 mol) and phenacyl bromide or the appropriately substituted phenacyl bromide (0.0011 mol) in absolute ethanol (10 mL) was heated at reflux for 4 h. Some of the products separated during the heating, while others crystallized after cooling the mixture. The products were removed by filtration, dried, and recrystallized from benzene containing a few drops of absolute ethanol. The yields and physical constants of the products (VIII–XXXIII) are listed in Table I. IR (mineral oil) ν: 2780–2670 (—NH) and 1610–1590 cm^{-1} (C=N); ^{1}H-NMR of XXIII (Me_2SO-d_6): δ 2.41 (s, 3, CH_3), 2.94 (t, 2, J = 7.5 Hz, $C_6H_5CH_2CH_2$—), 4.46 (t, 2, J = 7.5 Hz, $C_6H_5CH_2CH_2$—), 7.26 (m, 10, ArH and C_5—H of the thiazoline ring), 7.70 (d, 2, J = 9 Hz, ArH, *meta* to nitro group), and 8.44 ppm (d, 2, J = 9 Hz, ArH, *ortho* to nitro group); ^{1}H-NMR for XXVIII: δ 2.41 (s, 3, CH_3), 2.87 (t, 2, J = 7.5 Hz, $C_6H_5CH_2CH_2$—), 4.34 (t, 2, J = 7.5 Hz, $C_6H_5CH_2CH_2$—), 6.87 (s, 1, C_5-thiazoline proton), and 7.25 ppm (m, 13, ArH); ^{1}H-NMR for XXX: δ 2.81 (t, 2, J = 7.5 Hz, $C_6H_5CH_2CH_2$—), 4.27 (t, 2, J = 7.5 Hz, $C_6H_5CH_2CH_2$—), 6.80 (s, 1, C_5-thiazoline proton), and 7.29 ppm (m, 14, ArH). MS, *m/z* (relative abundance %) for XXIII: M^+ at 415(7), 312(22), 311(100), 310(20), 134(19), 105(47), 104(22), 103(26), 91(49), and 89(28). For XXVIII: M^+ at 404 and M + 2 at 406(8), 302(36), 301(22), 300(100), 299(15), 149(27), 148(51), 147(74), 134(27), 118(31), 115(28), 105(52), 104(21), 103(29), and 91(48). For XXX: M^+ at 435 and M + 2 at 437(0.9), 332(57), 331(17), 330(50), 139(22), 135(31), 134(100), 105(41), 104(49), 103(32), 102(23), 91(86), 90(24), 89(20), and 82(16).

Antihypertensive Testing—Rats, maintained in an incubator (32–35°C) for 20–40 min, were restrained to measure systolic blood pressure and heart rate indirectly by the tail cuff method[4]. Each determination was the mean of at least six recordings. Groups of four animals were used, and measurements were made predose (time zero) 1, 2, 4, and 6 h after administration of the products, with occasional readings at 24 h.

Anticonvulsant Testing—The compounds suspended in 1% methylcellulose were administered orally (1 mL/100 g) to CD-1 male mice (18–25 g), 10 per group, 1 h before intravenous infusion of 8 mg/mL of pentylenetetrazol in saline at a rate of 0.5 mL/min. The time of infusion required to elicit a tonic extensor spasm was noted, and the dose of pentylenetetrazol administered was calculated. The results (Table I) are expressed as the percentage change compared with controls treated with vehicle only. Statistical significance was determined using the Student's t test.

[4] W, W8005 B.P. recorder.

REFERENCES

(1) A.-M. M. E. Omar, A. M. Farghaly, A. A. B. Hazza, N. H. Eshba, F. M. Sharabi, and T. T. Daabees, *J. Pharm. Sci.*, **70**, 1075 (1981).

(2) El-S. A. Ibrahim, A.-M. M. E. Omar, N. S. Habib, O. M. Aboul-Wafa, S. M. El-Sewedy, and J. Bourdais, *J. Pharm. Sci.*, **72**, 1205 (1983).

(3) A.-M. M. E. Omar, O. M. AboulWafa, and G. Leclercq, *J. Pharm. Sci.*, in press.

(4) A.-M. M. E. Omar, S. M. El-Khawass, A. B. Makar, N. M. Bakry, and T. T. Daabees, *Pharmazie*, **33**, 577 (1978).

(5) A.-M. M. E. Omar and N. S. Habib, *Pharmazie*, **33**, 81 (1978).

(6) A.-M. M. E. Omar, I. M. Labouta, G. M. Kassem, and J. Bourdais, *J. Pharm. Sci.*, **72**, 1226 (1983).

(7) A.-M. M. E. Omar, S. A. Shams El-Din, A. A. Ghobashy, and M. A. Khalil, *Eur. J. Med. Chem.*, **16**, 77 (1981).

(8) El-S. A. Ibrahim, A.-M. M. E. Omar, M. A. Khalil, M. A. Makar, M. T. I. Soliman, and T. T. Daabees, *Pharmazie*, **35**, 80 (1980).

(9) M. A. El-Dawy, A.-M. M. E. Omar, A. M. Ismail, and A. A. B. Hazzaa, *J. Pharm. Sci.*, **72**, 45 (1983).

(10) A. A. B. Hazzaa, A.-M. M. E. Omar, and M. S. Ragab, *Pharmazie*, **28**, 364 (1973).

(11) A.-M. M. E. Omar and S. A. Osman, *Pharmazie*, **28**, 30 (1973).

(12) E. B. Akerblom, *J. Med. Chem.*, **17**, 609 (1974).

(13) C. Braun, *Chem. Ber.*, **45**, 2192 (1912).

ACKNOWLEDGMENTS

Supported in part by Pharco Pharmaceuticals, Cairo, Egypt. The authors thank the members of the Chemotherapeutic Research Centre, Beecham Pharmaceuticals, Brockham Park, Betchworth, Surrey, RH3 7AJ, U.K. for the biological screening of the products, and the members of the Microanalytical Unit, Faculty of Science, Cairo University, for the analytical data. They are also indebted to Dr. Farouk S. El-Feraly, Department of Pharmacognosy, School of Pharmacy, The University of Mississippi, University, Miss. for the NMR and MS data.

Synthesis of *N*,*N'*-Disubstituted *N''*-2-(2-Quinolinylmethylthio)ethylguanidines as Potential Anticancer Agents

WILLIAM O. FOYE *x, SEUNG HO AN *§, and TIMOTHY J. MAHER ‡

Received April 25, 1983, from the **Samuel M. Best Research Laboratory* and the ‡*Department of Pharmacology, Massachusetts College of Pharmacy and Allied Health Sciences, Boston, MA 02115.* Accepted for publication June 1, 1983.

§Present address: Roswell Park Memorial Institute, Buffalo, N.Y.

Abstract □ A simple method for obtaining the title compounds was found in the alkaline rearrangement of *S*-2-aminoethylisothiouronium salts, which were obtained from the condensation of thiourea or substituted thioureas with 2-bromoethylamine hydrobromide. No activity was found for the substituted guanidines against P388 lymphocytic leukemia in mice, or as H_2-receptor antagonists.

Keyphrases □ *N,N'*-Disubstituted *N''*-2-(2-quinolinylmethylthio)ethylguanidines—anticancer activity, potential H_2-receptor antagonist □ Anticancer agents—potential, *N,N'*-disubstituted *N''*-2-(2-quinolinylmethylthio)ethylguanidines, H_2-receptor antagonist activity

A number of strongly basic compounds have shown appreciable anticancer activity. Bis(guanidines) and guanylhydrazones are active in leukemia systems (1, 2), and bis(guanylhydrazones) of anthracene-9,10-dicarboxaldehydes (3) have a particularly broad spectrum of anticancer activity. Recently, synthesized bis(*S*-alkyl) (4), and *S*-alkyl cycloalkylamino (5) derivatives of *N*-methylquinolinium dithioacetic acid showed reproducible activity against P388 lymphocytic leukemia in mice, the best activity being shown by one of the basic (morpholino) derivatives. It appeared that further increase in basicity of this series was warranted. The basic side chain of the cimetidine molecule was selected for inclusion in the quinoline-2-methyl structure because of the reported cytostatic and immunosuppressive activities of some guanidine derivatives (6). Modification of the basicity by inclusion of electron-attracting or -releasing functions on the guanidine moiety was

0022-3549/84/0800-1168$01.00/0

© 1984, American Pharmaceutical Association

Table I—Physical Properties of *N,N'*-Disubstituted *N''*-2-(2-Quinolinylmethylthio)ethylguanidines (I·HX) and Antileukemic Activities in Mice [a]

Compound	R	R'	HX	Formula[b]	mp, °C	Yield, %	Dose, mg/kg[c]	Weight Difference (T − C)	Median Survival Time, T/C%[d]
Ia	H	H	2HCl	$C_{13}H_{16}N_4S\cdot 2HCl\cdot 1.5H_2O$	189–191	44[e]	100.0	−1.1	101
							50.0	0.6	94
Ib	H	CH_3	2HCl	$C_{14}H_{18}N_4S\cdot 2HCl\cdot 3H_2O$	220–223	43[f]			
Ic	CH_3	CH_3	2HCl	$C_{15}H_{20}N_4S\cdot 2HCl\cdot H_2O$	158–160	63[g]	50.0	−3.3	112
							25.0	−0.5	118
							12.5	−0.5	115
Id	CH_3	$C_6H_5CH_2$	2HCl	$C_{21}H_{24}N_4S\cdot 2HCl\cdot 1.5H_2O$	122 (dec.)	84[h]	50.0	−2.0	101
							25.0	−0.3	109
							12.5	−0.4	98
Ie	CH_3	$C_6H_5SO_2$	2HBr	$C_{20}H_{22}N_4O_2S_2\cdot 2HBr\cdot 2H_2O$	80–90 (dec.)	77	200.0	−0.5	100
							100.0	0.4	106
							50.0	0.7	106
If	CH_3	CN		$C_{15}H_{17}N_5S$		93	100.0	−1.2	94
							50.0	0.0	115

[a] CD_2F_1 mice were inoculated with P388 lymphocytic leukemia. [b] All compounds were analyzed for C, H, and N; in addition, Ia was analyzed for Cl, and Ib–d were analyzed for S. All values were within ±0.4% of the theoretical values. [c] Drugs were administered intraperitoneally on days 1, 5, and 9. [d] A T/C% value of ≥125 is considered a positive result. [e] Recrystallized from MeOH. [f] Recrystallized from MeOH–EtOAc. [g] Recrystallized from acetone–water. [h] Recrystallized from ether.

made, giving compounds of the I series. Since quinoline-2-methyl analogues of cimetidine have not been prepared or tested as H_2-receptor antagonists, this activity was also investigated for these derivatives.

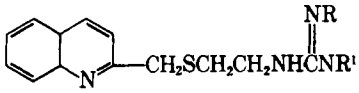

R=H, CH_3, $C_6H_5CH_2$ CN, $C_6H_5SO_2$
R'=H, CH_3

I

DISCUSSION

Chemistry—Most synthetic methods used for cimetidine analogues have involved the use of cyanamide (7, 8) or a derivative such as *N*-cyanoiminodithiocarbonic acid dimethyl ester (9) or *N*-methyldicyanodiamide (10) and treatment with appropriate amines or halides. It was found more convenient to synthesize the guanidinoethylmercapto moiety by alkaline rearrangement of *N,N'*-disubstituted *S*-2-aminoethylisothiouronium salts (11). These were prepared by condensation of *N,N'*-disubstituted thioureas with 2-bromoethylamine hydrobromide. When an electron-withdrawing function was present on the thiourea, salts were not formed, and rearrangement was carried out on the neutral molecule. The resulting mercapto compounds were converted to the sodium salts and condensed with 2-chloromethylquinoline. Yields of the *N*-2-(2-quinolinylmethylthio)ethylguanidines ranged from 42 to 93%, based on the isothiuronium compounds. Physical constants of the compounds obtained are recorded in Table I. This method of synthesis is shown in Scheme I. It may be considered an improvement over previously used methods for cimetidine analogues because of fewer synthetic steps and more stable starting materials.

^{1}H-NMR spectra of the products agreed with the proposed structures. Quinoline protons appeared at δ 8.46–8.60 ppm as salts and at δ 7.68–7.76 ppm as neutral molecules. The 2-quinolinylmethyl protons appeared as singlets at δ 4.52–4.64 ppm for the salts and at δ 3.90–3.99 ppm for the neutral molecules. The S—CH_2 protons were seen at δ 2.78–3.55 ppm for the salts and at δ 2.59–2.65 ppm for the neutral compounds. The N—CH_2 protons had chemical shifts at δ 3.50–3.55 ppm for the salts and at δ 3.41–3.43 ppm for the nonsalt forms. The N—CH_3 protons were found at δ 2.75–2.96 ppm for the salts and at δ 2.74–2.78 ppm for the nonsalts. The doublet of the N—CH_3 protons became a singlet in the presence of D_2O, indicating the proximity of N—H.

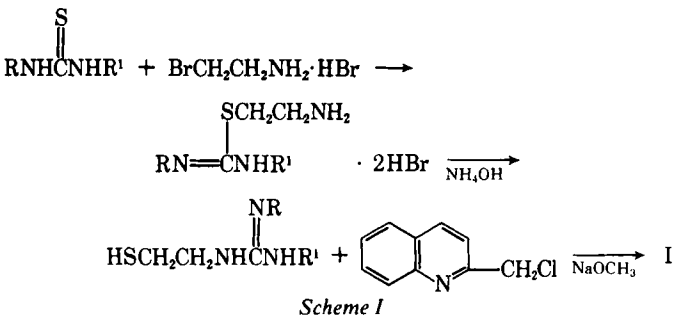

Scheme I

Biological Test Results—Antileukemia testing of the *N*-2-(2-quinolinylmethylthio)ethylguanidines was done at the National Cancer Institute in mice with P388 lymphocytic leukemia using the NCI protocol (12). Details regarding dose and survival of the treated animals are recorded in Table I. None of the compounds showed positive activity (a T/C × 100 ratio of ≥125), and all were appreciably toxic. Doses >100 mg/kg were generally fatal.

Screening of the compounds for possible H_2-receptor antagonism was carried out with guinea pig atria at doses of 10^{-4}–10^{-5} M. Cimetidine and tripelennamine were employed as H_2- and H_1-antagonists, respectively, and histamine was used as the H_2-agonist. None of the compounds had the ability to interact with the H_2-receptor, as determined by an isolated right atrial preparation from the guinea pig. The *N*-benzyl-*N'*-methylguanidine derivative slowed atrial rate but was not acting *via* an H_2-receptor.

EXPERIMENTAL SECTION[1]

***N*-Methyl-*S*-2-aminoethylisothiouronium Bromide Hydrobromide**—A mixture of *N*-methylthiourea (4.5 g, 0.05 mol) and absolute ethanol (50 mL) was refluxed for 30 min, 2-bromoethylamine hydrobromide (10.25 g, 0.05 mol) was added, and the mixture was refluxed for 2 h. The mixture was cooled, and the white precipitate was removed by filtration, dried at reduced pressure, and recrystallized from methanol to give 13.39 g (91%), mp 220–222°C; R_f 0.60. IR(KBr): 3300, 3260, 3080 (NH, NH_2^+, and NH_3^+), 1940 (amine·HBr), and 1648 (N—C=N) cm^{-1}; ^{1}H-NMR: δ 8.90 (br s, 6, NH, NH_2^+ and NH_3^+), 3.55 (t, 2, N—CH_2), 3.19 (t, 2, S—CH_2), and 2.99 ppm (s, 3, CH_3).

Anal.—Calc. for $C_4H_{11}N_3S\cdot 2HBr$: C, 16.28; H, 4.44; N, 14.24. Found: C, 16.43; H, 4.61; N, 14.37.

***N,N'*-Dimethyl-*S*-2-aminoethylisothiouronium Bromide Hydrobromide**—To a solution of *N,N'*-dimethylthiourea (5.20 g, 0.05 mol) in absolute ethanol (50 mL) was added 2-bromoethylamine hydrobromide (10.25 g, 0.05 mol) and the solution was refluxed for 2 h. The mixture was cooled (ice-bath), and the white solid was isolated and dried at reduced pressure. Recrystallization from methanol gave 12.59 g (82%), mp 215–216°C (dec.); R_f 0.59. IR(KBr): 3260, 3120, 3070 (NH_2^+, NH_3^+), 2020 (amine·HBr), 1630, and 1620 (N—C=N, NH_3^+) cm^{-1}; ^{1}H-NMR: δ 8.70 (br s, 5, NH_2^+ and NH_3^+), 3.68 (t, 2, N—CH_2), 3.18 (t, 2, S—CH_2), and 3.04 ppm (s, 6, $2CH_3$).

Anal.—Calc. for $C_5H_{13}N_3S\cdot 2HBr$: C, 19.43; H, 4.89; N, 13.60. Found: C, 19.65; H, 5.01; N, 13.46.

***N*-Benzyl-*N'*-methyl-*S*-2-aminoethylisothiouronium Bromide Hydrobromide**—*N*-Benzyl-*N'*-methylthiourea was prepared in 95% yield from benzylamine and methyl isothiocyanate in methanol, stirring for 20 h and recrystallizing from aqueous methanol to give white crystals, mp 71–73°C. The thiourea (9.01 g, 0.05 mol) was refluxed in absolute ethanol (50 mL) for 30 min, 2-bromoethylamine hydrobromide (10.25 g, 0.05 mol) was added, and

[1] Melting points were determined in capillary tubes with a Mel-Temp block and are uncorrected. ^{1}H-NMR spectra were obtained in Me_2SO-d_6 with a Varian T-60 spectrometer using Me_4Si as internal standard. IR spectra were obtained on a Perkin-Elmer 457A grating spectrophotometer using KBr pellets. TLC was carried out using Eastman silica gel plates with fluorescent indicator and a solvent system of 1-butanol–acetone–water (4:5:1). Elemental analyses were done by F. B. Strauss, Oxford, England. Organic reagents were supplied by Aldrich Chemical Co. and Fisher Scientific Co., and the hydrogen chloride by Matheson Gas Products.

the mixture was refluxed until it became homogeneous. It was cooled (ice-bath), and the white precipitate was removed by filtration and dried at reduced pressure. A second crop resulted on reducing the volume of the filtrate to 20 mL and cooling at −20°C. The combined solids were recrystallized from methanol to give 13.66 g (72%), mp 219–221°C; R_f 0.65. IR(KBr): 3330, 3230, 3100 (NH_2^+ and NH_3^+), 2020 (amine·HBr), 1620, and 1615 (N—C=N, NH_3^+) cm^{-1}; ^{1}H-NMR: δ 8.53 (bs, 5, NH_2^+ and NH_3^+), 7.93 (s, 5, ArH), 4.74 (s, 2, CH_2), 3.67 (t, 2, N—CH_2), 3.18 (t, 2, S—CH_2), and 3.09 ppm (s, 3, CH_3).

Anal.—Calc. for $C_{11}H_{17}N_3S{\cdot}2HBr$: C, 34.30; H, 4.97; N, 10.91. Found: C, 34.52; H, 5.18; N, 10.82.

***N*-Benzenesulfonyl-*N'*-methyl-*S*-2-aminoethylisothiourea**—To a solution of benzenesulfonamide (8.65 g, 0.055 mol) in dimethylformamide (30 mL) at 4°C was added a solution of sodium hydroxide (2.22 g) in water (3 mL) and methyl isothiocyanate (4.02 g, 0.055 mol), and the solution was stirred for 30 min. 2-Bromoethylamine hydrobromide (10.25 g, 0.05 mol) in dimethylformamide (20 mL) was added and stirring was continued at room temperature for 7 h. The mixture was added to water (500 mL) and extracted with 1-butanol (350 mL), and the extract was washed with water (2 × 250 mL). The organic phase was evaporated and the resulting syrup solidified on storage at −20°C. The white solid was recrystallized from methanol, to yield 4.23 g (28%), mp 114–116°C; R_f 0.50. IR(KBr): 3340, 3260 (NH and NH_2), 1570 (NH), 1200, and 1135 (SO_2) cm^{-1}; ^{1}H-NMR: δ 7.62 (m, 5, ArH), 7.20 (br t, 2, NH_2), 3.35 (m, 2, N—CH_2), 2.72 (d, 3, CH_3), and 2.60 ppm (m, 2, S—CH_2).

***N*-Cyano-*N'*-methyl-*S*-2-aminoethylisothiourea**—To a solution of cyanamide (2.31 g, 0.055 mol) in dimethylformamide (30 mL) at 4°C were added a solution of sodium hydroxide (2.2 g) in water (3 mL) and methyl isothiocyanate (4.02 g, 0.055 mol), and the solution was stirred for 30 min. 2-Bromoethylamine hydrobromide (10.25 g, 0.05 mol) in dimethylformamide (20 mL) was added, and the mixture was stirred at room temperature for 18 h. The solvent was evaporated at reduced pressure and the residue was extracted with 1-butanol (2 × 30 mL). The extract was washed with water (2 × 30 mL), and the organic phase was evaporated at reduced pressure to give 4.50 g (52%) of a syrup; R_f 0.81. IR(KBr film): 3350, 3240, 3170 (NH and NH_2), 2180 (CN), 1580; and 1540 (NH and NH_2) cm^{-1}; ^{1}H-NMR: δ 6.80 (br s, 3, NH and NH_2), 3.35 (m, 2, N—CH_2), 2.72 (d, 3, CH_3), and 2.60 ppm (m, 2, S—CH_2).

Representative Procedures for the Preparation of *N,N'*-Disubstituted *N''*-2-(2-Quinolinylmethylthio)ethylguanidines—*N-2-(2-Quinolinylmethylthio)ethylguanidine Dihydrochloride*—*S*-2-Aminoethylisothiouronium bromide hydrobromide (11) (28.10 g, 0.1 mol) in 50 mL of water was treated with concentrated ammonium hydroxide (15 mL, 0.25 mol) and stirred at room temperature for 2 h. The mixture was evaporated to dryness, and the residue was dried at reduced pressure. This material was dissolved in 25 mL of methanol, and a solution of sodium methoxide (5.40 g, 0.1 mol) in methanol (50 mL) was added. To the solution of the sodium salt of 2-mercaptoethylguanidine was added a solution of 2-chloromethylquinoline, prepared from the hydrochloride (21.41 g, 0.1 mol) and sodium methoxide (5.40 g, 0.1 mol), in methanol (50 mL). The mixture was stirred at room temperature for 18 h, the sodium chloride was removed by filtration, and the filtrate was evaporated to dryness. The residue was extracted with water (75 mL) and ether (75 mL), and the residual oil was reextracted with water (50 mL) and ether (50 mL). The aqueous extracts were evaporated to a syrup and dried at reduced pressure. The residue was treated with methanolic hydrogen chloride (75 mL), prepared by saturation at 0°C for 20 h. The methanol was evaporated, and the residue was recrystallized from methanol to give 14.59 g (44%) of beige crystals, mp 189–191°C; R_f 0.52. IR(KBr): 3380, 3300, 3120 (NH and NH_2), 2720–2600 (amine·HCl), and 1630 (N—C=N and NH_3^+) cm^{-1}; ^{1}H-NMR: δ 11.58 (br s, 1, quinoline·NH^+), 8.47 (m, 6, quinoline), 7.48 (br s, 5, NH, NH_2, and NH_2^+), 4.59 (s, 2, CH_2), 3.50 (q, 2, N—CH_2), 3.20 (s, H_2O), and 2.78 ppm (t, 2, S—CH_2).

N-Benzenesulfonyl-N'-methyl-N''-2-(2-quinolinylmethylthio)ethylguanidine Hydrobromide—*N*-Benzenesulfonyl-*N'*-methyl-*S*-2-aminoethylisothiourea (2.73 g, 0.01 mol) was added to 30 mL of methanol saturated with ammonia at 0°C, and stirred at 0°C for 18 h. The mixture was evaporated to dryness, and the residue was treated with acetone (20 mL) and sodium hydroxide (0.4 g) in water (10 mL). To the resulting solution was added 2-chloromethylquinoline (1.78 g, 0.01 mol) and stirring was continued at room temperature for 4 h. The mixture was evaporated to half volume, water (20 mL) was added, and the solution was extracted with 1-butanol (2 × 30 mL). The extract was washed with water (2 × 30 mL), evaporated to a syrup, and dried at reduced pressure to give 3.21 g (77%), which was converted to the hydrobromide, mp 68°C (color change), 80–90°C (dec.); R_f 0.84. ^{1}H-NMR ($CDCl_3$): δ 7.68 (m, 11, ArH), 6.60 (br s, 2, 2 NH), 3.90 (s, 2, CH_2), 3.41 (q, 2, N—CH_2), 2.74 (d, 3, CH_3), and 2.59 ppm (t, 2, S—CH_2).

N-Cyano-N'-methyl-N''-2-(2-quinolinylmethylthio)ethylguanidine—*N*-Cyano-*N'*-methyl-*S*-2-aminoethylisothiourea (3.35 g, 0.021 mol) was added to methanol (30 mL) saturated with ammonia at 0°C, and stirred at 0°C for 18 h. The mixture was evaporated to a syrup and dried at reduced pressure. The residue was added to a solution of sodium methoxide (0.81 g) in methanol (30 mL), 2-chloromethylquinoline (2.67 g, 0.015 mol) was added, and the solution was stirred at room temperature for 3 h. The mixture was filtered, and the filtrate was evaporated to a syrup which was dried at reduced pressure. The residue was extracted with 1,2-dichloroethane (50 mL), washed with water (2 × 30 mL), dried (Na_2SO_4), and filtered. The filtrate was evaporated to a syrup and dried at reduced pressure to give 4.18 g (93%); R_f 0.84. IR (film): 3280, 3160 (NH), and 2170 (CN) cm^{-1}; ^{1}H-NMR ($CDCl_3$): δ 7.76 (m, 6, quinoline), 6.18 (br s, 2, 2 NH), 3.99 (s, 2, CH_2), 3.43 (m, 2, N—CH_2), 2.78 (d, 3, CH_3), and 2.65 ppm (m, 2, S—CH_2).

H_2-Receptor Antagonist Test—Compounds were tested for H_2-receptor antagonist activity using the guinea pig right atrial preparation described by Yellen *et al.* (13) and Lumley and Broadley (14). The isolated atrium was placed in a 50-mL tissue bath at 30°C and filled with Krebs-bicarbonate solution oxygenated with oxygen-carbon dioxide (95:5). Connected to a Grass Force displacement transducer, a 750-mg tension was applied to the atrium, and the tissue was allowed to equilibrate for 60–90 min. Cumulative dose-response curves were constructed using 10^{-7} 10^{-4} M histamine[2] in the presence or absence of cimetidine[3], tripelennamine dihydrochloride[2], or propranolol hydrochloride[4]. None of the compounds tested was capable of shifting the cumulative dose-response curve to histamine.

REFERENCES

(1) E. Mihich, C. Dane, J. Soucek, A. I. Mulhern, and M. J. Ehrke, "Proceedings of the 6th International Congress of Chemotherapy," vol. 2, 1970, p. 190.

(2) S. A. Schepartz, *Cancer Chemother. Rep.*, **2**, 3 (1971).

(3) K. C. Murdock, R. G. Child, Y. Lin, J. D. Warren, P. F. Fabio, V. J. Lee, P. T. Izzo, S. A. Lang, Jr., R. B. Angier, R. V. Citarella, R. E. Wallace, and F. E. Durr, *J. Med. Chem.*, **25**, 505 (1982).

(4) W. O. Foye and J. M. Kauffman, *J. Pharm. Sci.*, **68**, 336 (1979).

(5) W. O. Foye and J. M. Kauffman, *J. Pharm. Sci.*, **69**, 477 (1980).

(6) M. Konieczny and D. Charytonowicz, *Arch. Immunol. Ther. Exp.*, **26**, 951 (1978); D. Kieronska, B. Rozalska, B. Marczyk, and B. Zablocki, *Arch. Immunol. Ther. Exp.*, **26**, 959 (1978).

(7) H. J. Petersen, *J. Med. Chem.*, **21**, 773 (1978).

(8) G. J. Durant, J. C. Emmett, and C. R. Ganellin, Ger. Pat. No. 2,344,779 (1974).

(9) J. J. Lewis and R. L. Webb, Ger. Pat. No. 2,649,059 (1977); G. J. Durant, J. C. Emmett, and C. R. Ganellin, U.S. Pat. No. 4,024,271 (1977).

(10) C. F. Saat, M. S. Regas, and P. A. Agnesetti, Span. Pat. No. 479,083 (1979).

(11) W. O. Foye, J. Mickles, R. N. Duvall, and J. R. Marshall, *J. Med. Chem.*, **6**, 509 (1963).

(12) R. I. Geran, N. H. Greenberg, M. M. MacDonald, A. M. Schumacher, and B. J. Abbott, *Cancer Chemother. Rep.* (Part 3), **3**, 1 (1972).

(13) T. O. Yellen, J. W. Sperow, and S. H. Buck, *Nature (London)*, **253**, 561 (1975).

(14) P. Lumley and K. J. Broadley, *Eur. J. Pharmacol.*, **34**, 207 (1975).

ACKNOWLEDGMENTS

Supported by funds from the John R. and Marie K. Sawyer Memorial Fund, Massachusetts College of Pharmacy and Allied Health Sciences. The authors are indebted to the Division of Cancer Treatment, National Cancer Institute for the antileukemia test results.

[2] Sigma Chemical Co.
[3] Generously supplied by Smith, Kline and Beckman.
[4] Generously supplied by Ayerst Laboratories.

Direct Chloride Measurement of [4-^{36}Cl]Chlorobiphenyl and [4,4′-^{36}Cl]Dichlorobiphenyl Dechlorination in the Rat

M. T. SCOTT * **and J. E. SINSHEIMER** ˣ

Received December 27, 1982 from the *College of Pharmacy, University of Michigan, Ann Arbor, MI 48109.* Accepted for publication August 4, 1983. *Present address: Analytical Research and Development, Du Pont Pharmaceuticals, Garden City, NY 11530.

Abstract □ A reverse-phase HPLC system was used for the determination of inorganic chloride liberated *in vivo* from two biphenyl compounds in the rat. Oral administration of [4-^{36}Cl]chlorobiphenyl resulted in a total yield of 27.6% of the original dose excreted over 10 d in the urine and included 1.7% of the dose as inorganic chloride. For [4,4′-^{36}Cl]dichlorobiphenyl, the radioactivity of the original dose in the urine was 39.8% after 10 d, which included 11.5% of the dose as inorganic chloride. These results appear to represent the first direct determination of dechlorination by measurement of the inorganic chloride and suggest that biodechlorination plays a greater role in the metabolism of these compounds than previously expected.

Keyphrases □ Dechlorination—chloride in rat urine, 4-chloro- and 4,4′-dichlorobiphenyl □ Chloride determination—rat urine, 4-chloro- and 4,4′-dichlorobiphenyl □ 4-Chlorobiphenyl—*in vivo* dechlorination in rats □ 4,4′-Dichlorobiphenyl—*in vivo* dechlorination in rats.

The metabolism of polychlorinated biphenyls (PCBs), the ubiquitous environmental pollutants, leading to macromolecular binding (1-3) and mutagenicity (3) has been reported. Although metabolic activation appears to involve arene oxides (1-3), biodechlorination may play a role in the formation of bound metabolites and subsequent toxicity. Metabolic dehalogenation has been noted for polychlorinated biphenyls (4-6), bromobiphenyls (4-6), and iodobiphenyl (7). This paper describes an extension of these *in vivo* dehalogenation studies to ^{36}Cl-labeled 4-chlorobiphenyl and 4,4′-dichlorobiphenyl in an effort to assess the extent of biodehalogenation by direct chloride measurement.

EXPERIMENTAL SECTION

Copper(II) [^{36}Cl]Chloride—[^{36}Cl]Hydrochloride[1] (1.4 M, 1.0 mL, 50 μCi) and copper(II) oxide (55.9 mg, 1.7 mmol) were slowly heated to 115-125°C in a closed flask. This temperature was maintained for 8 h and then the vessel was cooled, opened, heated to dryness at 150°C for 3 h, and then stored in a desiccator. The brown product was redried immediately before use at 25°C and 0.3 mm pressure for 12 h.

[4-^{36}Cl]Chlorobiphenyl—In a modification of the general procedure of Doyle *et al.* (8) unlabeled copper(II) chloride (1.1976 g, 8.9 mmol) and isoamyl nitrate (2.812 g, 24.0 mmol) were added to [^{36}Cl]$CuCl_2$. After anhydrous acetonitrile (20 mL) was added, the mixture was maintained at 0°C to −5°C with stirring for 25 min before 4-aminobiphenyl (1.3528 g, 8.0 mmol) in anhydrous acetonitrile (10 mL) was slowly added. The mixture was stirred for 2 h at 0°C to −5°C and then for 3 h at room temperature before it was poured into 150 mL of 20% HCl and extracted with ether (3 × 150 mL). The ether was dried over sodium sulfate and the solvent was removed under reduced pressure. The aqueous phase was neutralized (pH 6-7) with 40% NaOH and extracted with ether. The ether was dried and the solvent removed as before. The resulting solid was then combined with the original solid. The product was isolated by column chromatography using silica gel and hexane as the mobile phase. After removal of the solvent, 925 mg (61.3%) of product with a specific activity of 2.24 μCi/mmol was obtained (mp 76-77°C). The IR, melting point, and NMR data of the product (synthesized in the same manner but with unlabeled $CuCl_2$) were identical with spectra of a known, pure (>99%) sample of 4-chlorobiphenyl[2].

[4,4′-^{36}Cl]Dichlorobiphenyl—Copper(II) oxide (62.0 mg, 1.89 mmol) and 1.0 mL of 1.54 M [^{36}Cl]hydrochloride (61 μCi) were mixed as described to produce labeled copper(II) chloride. Unlabeled copper(II) chloride (1.0819 g, 8.0 mmol) and isoamyl nitrite (2.812 g, 24.0 mmol) were added to labeled copper(II) chloride with the aid of 20 mL of anhydrous acetonitrile. Benzidine (740.2 mg, 4.0 mmol) in 15 mL of anhydrous acetonitrile was added slowly to the mixture which was at 0°C to −5°C. The mixture was stirred for 5 h at that temperature. Workup was as described for [4-^{36}Cl]chlorobiphenyl with a yield of 502.1 mg (56.3%) of white solid, mp 144.5-147.0°C (reference compound[2], 147-148°C). The specific activity was 4.61 μCi/mmol. The chromatographic behavior of the product that was synthesized in the same manner, except using unlabeled copper(II) chloride, matched the behavior of the known, pure (>99%) reference sample of 4,4′-dichlorobiphenyl[2]. Both labeled chlorobiphenyl compounds were found to be free of inorganic chloride-36 by HPLC using a C_{18} column and methanol-water (90:10).

***In Vivo* Studies**—Male Sprague-Dawley rats weighing 250 300 g were quarantined for 2 d prior to administration of substrates by gastric intubation. The dosing regimens of substrates in corn oil were as follows: three rats were dosed with 0.5 mL of [4-^{36}Cl]chlorobiphenyl, containing 197,000 dpm of substrate; three rats were dosed with 0.9 mL of [4,4′-^{36}Cl]dichlorobiphenyl, containing 60,000 dpm; another rat was given twice the dose of the others. Rats were allowed food and water *ad libitum*. Urine was collected daily and stored frozen.

Chlorine-36 Analysis—*Total Activity*—Urine (100 μL) was measured for total radioactivity by scintillation counting[3]. A storage period of 24 h in the dark, after addition of the cocktail[4] (10 mL) and before counting, was required to avoid chemiluminescence.

Inorganic Chloride—Urine was acidified to pH 6-7 with dilute sulfuric acid and centrifuged. The supernatant was combined with the supernatant resulting from recentrifugation of the washed pellet (0.5 mL of water), and 1.0 mL was injected into a C_{18} HPLC system (9). The mobile phase consisted of methanol-water-glacial acetic acid (12.5:86.5:1.0) at a flow rate of 1 mL/min. Inorganic chloride-36 was determined in the eluant 2-6 min after injection; methanol (1.0 mL) and cocktail[4] (14 mL) were added with counting for 10 min. Between injections the HPLC system was flushed with methanol (30 mL) and reequilibrated with mobile phase.

RESULTS AND DISCUSSION

Analytical System—The metabolism of the chlorinated biphenyls was expected to yield phenols (5) and their glucuronides (10). Therefore, an HPLC procedure that would separate inorganic chloride prior to highly polar metabolites was desired. We used the system devised by Mitchell *et al.* (11) for the separation of metabolic conjugates which happened to be similar to a system we have used for the determination of inorganic halides (9). In a test mixture of chloride in the presence of the glucuronide and sulfate of *p*-nitrophenol, chloride was recovered quantitatively well before completely resolved peaks for these conjugates.

***In Vivo* Dechlorination**—*[4-^{36}Cl]Chlorobiphenyl*—Figure 1 outlines the excretion of total urinary radioactivity expressed as an average of the percentage of dose for three rats. The excretion of radioactive substances (17.7 ± 6.45%) after the first day constituted at least half the total radioactivity over 10 d and agreed with the data in the literature [25.8 ± 13.3% (12)] for oral administration. Excretion of total radioactivity after intravenous administration has been reported (12, 13) to be even more rapid, with 80% of the dose excreted within 24 h and almost total excretion after 2 d. In the present study, urinary excretion of radioactivity decreased to 2.5 ± 1.5% for the second day and remained relatively constant through day 10.

Injection of an aliquot of a composite urine sample from each of the three rats indicated that 1.7 ± 0.5% (mean for three animals, 11 injections) of the dose of [4-^{36}Cl]chlorobiphenyl was excreted as inorganic chloride-36 over a 10-d period. This was less than the *in vivo* deiodination of [4-^{125}I]iodobiphenyl (14), as expected, due to the stronger carbon-chloride bond. The low levels of total radioactivity in daily urine samples prevented determination of liberated chloride-36 on a daily basis.

[1] New England Nuclear, Boston, Mass.
[2] Aldrich Chemical Co., Milwaukee, Wis.
[3] Model 9000 scintillation counter; Beckman, Berkeley, Calif.
[4] ACS; Amersham, Arlington Heights, Ill.

0022-3549/84/0800-1171$01.00/0
© 1984, American Pharmaceutical Association

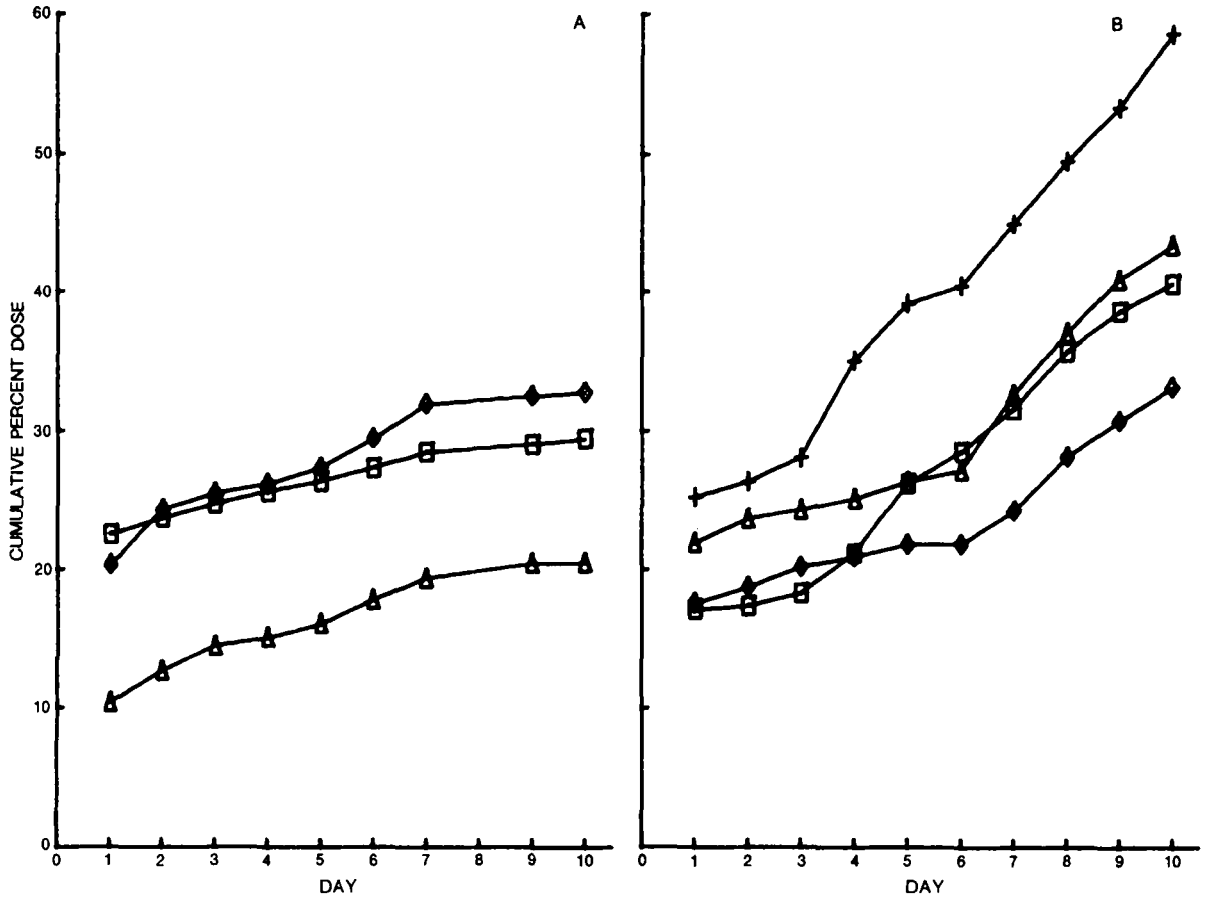

Figure 1—*Cumulative total urinary radioactivity expressed as a percentage of dose from [4-^{36}Cl]chlorobiphenyl (A) for 3 rats and [4,4'-^{36}Cl]dichlorobiphenyl (B) from 4 rats where the rat denoted with a "+" received twice the dose.*

These results appear to be the first to show dechlorination of 4-chlorobiphenyl and the first to follow dechlorination by direct determination of inorganic chloride. Previous studies in the rabbit (10) and in a variety of other species (5) reported no dechlorinated metabolites. The rapid excretion of total radioactivity coupled with the slow rate and low percentage of dechlorination may explain why no dechlorinated metabolites have been found in these *in vivo* studies.

[4,4'-^{36}Cl]Dichlorobiphenyl—The cumulative daily excretion of total radioactivity (percent of dose) for the four rats tested is summarized in Fig. 1. The total urinary radioactivity for the first day was 20.5 ± 3.9%, which agrees with the literature value of 22.9 ± 3.1% (12). Daily excretion of total radioactivity decreased rapidly, so that the day 2 through day 10 excretion ranged between 1 and 4.25% daily. This resulted in a small but continuous rise in the cumulative total urinary radioactivity for the dichloro compound in comparison to an earlier leveling off of radioactivity with 4-chlorobiphenyl for the 10-d period studied.

A composite urine sample for each of four rats was analyzed for chloride by HPLC, and the percentage of original dose was found to be 11.5 ± 2.7% (the mean of three measurements for each of four animals). This was 10-fold more dechlorination than found for [4-^{36}Cl]chlorobiphenyl. In addition to the twofold greater amount of original chloride, this increased dechlorination might have been a result of the increased importance of the dechlorination of an intermediate 3-hydroxy,4-chloro metabolite.

Tulp *et al.* (15) have shown that 4-chloro-3'-hydroxybiphenyl is an intermediate in the metabolism of 4,4'-dichlorobiphenyl and that the *ortho* hydroxy group in this metabolite and related compounds (16) activates dehalogenation. In the present study it is assumed that such activated dehalogenation would be more important in the 4,4'-dichlorobiphenyl than in the 4-chlorobiphenyl compound. In the former case there would be greater opportunity for the presence of a hydroxy group *ortho* to the increased number of chlorides. In the latter compound, there is the established (5, 10) hydroxylation of the unsubstituted ring with the elimination of the compound prior to the formation of 3-hydroxy-4-chlorobiphenyl.

The direct measurements of dechlorination for both 4-chloro- and 4,4'-dichlorobiphenyl would indicate that aromatic dechlorination plays a more important role in the metabolism of these compounds than previously noted.

REFERENCES

(1) T. Shimada, *Bull. Environ. Contam. Toxicol.*, **16**, 25 (1976).

(2) T. Shimada and R. Sato, *Biochem. Pharmacol.*, **27**, 581 (1978).

(3) C. Wyndham, J. Devenish, and S. Safe, *Res. Commun. Chem. Pathol. Pharmacol.*, **15**, 1563 (1976).

(4) S. Safe, D. Jones, and O. Hutzinger, *J. Chem. Soc. (Perkin I)*, **4**, 357 (1976).

(5) G. Sundström, O. Hutzinger, and S. Safe, *Chemosphere*, **5**, 267 (1976).

(6) J. Kohli, C. Wyndham, M. Smylie, and S. Safe, *Biochem. Pharmacol.*, **27**, 1245 (1978).

(7) J. E. Sinsheimer, T. Wang, S. Röder, and Y. Y. Shum, *Biochem. Biophys., Res. Commun.*, **83**, 281 (1978).

(8) M. P. Doyle, B. Siegfried, and J. F. Delaria, Jr., *J. Org. Chem.*, **42**, 2426 (1976).

(9) M. T. Scott and J. E. Sinsheimer, *J. Pharm. Sci.*, **73**, 1101 (1984).

(10) W. D. Block and H. H. Cornish, *J. Biol. Chem.*, **234**, 330 (1959).

(11) A. R. Buckpitt, D. E. Rollins, S. D. Nelson, R. B. Franklin, and J. R. Mitchell, *Anal. Biochem.*, **83**, 168 (1977).

(12) H. B. Matthews and M. W. Anderson, *Drug Metab. Dispos.*, **3**, 371 (1975).

(13) J. R. Hass, L. T. Jao, N. K. Wilson, and H. B. Matthews, *J. Agric. Food Chem.*, **25**, 1330 (1977).

(14) J. E. Sinsheimer and Y. Y. Shum, *J. Pharm. Sci.*, **70**, 546 (1981).

(15) M. Th. M. Tulp, G. Sundström, and O. Hutzinger, *Chemosphere*, **6**, 425 (1976).

(16) M. Th. M. Tulp, W. A. Bruggeman, and O. Hutzinger, *Experientia*, **33**, 1134 (1977).

ACKNOWLEDGMENTS

This study was supported in part by Training Grant 5-T32 GM-07767 from the National Institutes of Health.

Assay of Adinazolam in Plasma by Liquid Chromatography

GEOFFREY W. PENG

Received June 17, 1983, from the *Drug Metabolism Research, The Upjohn Company, Kalamazoo, MI 49001* Accepted for publication August 1, 1983.

Abstract □ A procedure for the quantitative determination of adinazolam in plasma was developed. The drug, an *N*-demethylated metabolite, and an internal standard were extracted from basified plasma into ethyl acetate. After evaporation, the residue was dissolved in toluene which was washed with sodium hydroxide. The toluene was evaporated and the residue was dissolved in a mixture of acetonitrile, methanol, and water for chromatography. The concentrations of the drug and the metabolite were determined using reverse-phase liquid chromatography with UV detection at 254 nm. The assay methodology showed good peak height ratio-concentration linearity, precision, and accuracy and has been used to analyze plasma samples collected from human subjects after oral administration of adinazolam mesylate in compressed tablets. The low plasma background interferences allowed the quantitative determination of concentrations as low as ~5 ng/mL.

Keyphrases □ Adinazolam and *N*-demethyl metabolite—liquid chromatographic assay in plasma □ Liquid chromatographic assay—adinazolam and *N*-demethyl metabolite in plasma

A number of compounds of the triazolobenzodiazepine class have been found to have important pharmacological properties (1, 2), *i.e.*, the antianxiety activity of alprazolam (3) and the hypnotic activity of triazolam (4) and estazolam (1, 5). More recently, adinazolam mesylate, the methanesulfonate salt of 8-chloro-1-[(dimethylamino)methyl]-6-phenyl-4*H*-*s*-triazolo[4,3-*a*][1,4]benzodiazepine (I), was shown to have both antidepressant and antianxiety properties (6–8).

Adinazolam mesylate is currently undergoing clinical testing for the treatment of depression in humans (9). Since little is known about the pharmacokinetic disposition of adinazolam, such an understanding would facilitate the design and evaluation of clinical efficacy studies. For this purpose, a liquid chromatographic method was developed for the separation and quantitative determination of adinazolam in human plasma samples. 8-Chloro-1-[(methylamino)-methyl]-6-phenyl-4*H*-*s*-triazolo[4,3-*a*][1,4]benzodiazepine (II) (8), an *N*-demethylated metabolite of adinazolam, found in abundant amounts in the plasma samples, were simultaneously analyzed.

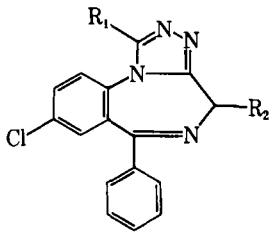

I: $R_1 = CH_2N(CH_3)_2$, $R_2 = H$
II: $R_1 = CH_2NHCH_3$, $R_2 = H$
III: $R_1 = CH_2CH_3$, $R_2 = CH_2N(CH_3)_2$

EXPERIMENTAL SECTION

Materials—Adinazolam (I) mesylate, the *N*-demethyl metabolite (II), and the internal standard, 8-chloro-1-ethyl-4[(dimethylamino)methyl]-6-phenyl-4*H*-*s*-triazolo[4,3-*a*][1,4]benzodiazepine (III) (6) were used as received[1]. Acetonitrile and methanol were distilled-in-glass grade[2]. All other solvents and chemicals were reagent grade. Plasma samples were obtained from volunteer human subjects after oral administration of compressed tablets of adinazolam mesylate.

Sample Preparation—Aliquots of 1-mL plasma samples in 15-mL culture tubes equipped with polytef-lined screw caps[3] were supplemented with internal standard, basified with 1 mL of 0.1 M dibasic potassium phosphate[4], and extracted with 5 mL of ethyl acetate[2]. After shaking on a horizontal shaker for ~5 min and centrifuging at 2000 rpm for 5 min, these tubes were placed in a shallow bath of dry ice–acetone mixture to freeze the aqueous phase. The ethyl acetate was transferred to clean tubes and evaporated under a stream of nitrogen[5]. The residues were taken up in toluene[2], (2-mL aliquots) which were in turn washed with 2 mL of 2.0 M NaOH by shaking and centrifugation. After freezing the aqueous layer, the toluene extracts were transferred to clean tubes and evaporated under nitrogen at a temperature <50°C. The residues from the toluene extracts were dissolved in 0.1 mL of acetonitrile–methanol–water (1:1:2, v/v/v), mixed on a vortex mixer[3], and centrifuged prior to chromatography. Calibration standard samples were prepared by supplementing aliquots of blank human plasma with the drug, its metabolite, and the internal standard. These standard samples were similarly extracted and concurrently chromatographed with the plasma samples.

Chromatography—The liquid chromatographic system consisted of a solvent delivery pump[6], a fixed-wavelength UV absorbance detector[7], and a sample injection valve with a 100-μL loop[8]. The prepared plasma samples and the standard samples were chromatographed on a prepacked reverse-phase column[9] using acetonitrile–methanol–phosphate buffer (30:20:85, v/v/v) as the mobile phase. The phosphate buffer contained 0.06 M monobasic ammonium phosphate and 0.02% phosphoric acid. The mobile phase was filtered, deaerated, and pumped through the system at a flow rate of 2 mL/min. The chromatograms monitored by UV absorbance at 254 nm were recorded on a strip chart recorder[10]. The adinazolam–internal standard and *N*-demethyl metabolite–internal standard peak height ratios were measured for quantitative determination. The chromatography was carried out at ambient temperature (20–22°C).

RESULTS AND DISCUSSION

The recovery of adinazolam from the plasma samples by the extraction procedure was investigated by comparison of the chromatograms of the drug standards and the chromatograms of the extracts of plasma samples supplemented with the same quantities of adinazolam mesylate. The internal standard was added to these samples just prior to chromatography, and the peak height ratios measured from the resulting chromatograms were used to estimate the extraction recovery. The solvent extraction recovery of adinazolam from plasma was found to be ~82% in the concentration range of ~10–800 ng/mL of adinazolam mesylate and was essentially independent of the concentration. The extraction of the *N*-demethyl metabolite appeared to be less efficient than the parent drug because of the higher polarity of the metabolite. The extraction procedure was satisfactory for the preparation of the plasma samples for the chromatographic separation of the drug and the metabolite. Ethyl acetate extraction gave very good recovery of the drug and the metabolite from the plasma samples, but the high background interferences rendered the chromatographic separation unsuitable for quantitative determination of these compounds. Toluene extraction gave poor recovery of the metabolite, but the background interference was minimal. The two-step extractions using ethyl acetate and toluene were necessary to remove background interferences and to allow the quantitative determination of the drug and the metabolite at ~5 ng/mL levels.

Figure 1 shows the chromatograms of the extracts of plasma samples collected shortly before (Fig. 1A) and 4 h after (Fig. 1B) the administration of

[1] The Upjohn Company, Kalamazoo, Mich.
[2] Burdick and Jackson Laboratory, Muskegon, Mich.
[3] Fisher Scientific Co., Fair Lawn, N.J.
[4] Mallinckrodt, Inc., St. Louis, Mo.
[5] Multivap; Organomation Associates, Inc., Northborough, Mass.
[6] Model 6000A; Waters Associates, Milford, Mass.
[7] Model 440; Waters Associates, Milford, Mass.
[8] Valco Instruments Co., Inc., Houston, Tex.
[9] μ-Bondapak C_{18}; Waters Associates, Milford, Mass.
[10] Linear Instruments Corp., Irvine, Calif.

0022-3549/84/0800-1173$01.00/0
© 1984, American Pharmaceutical Association

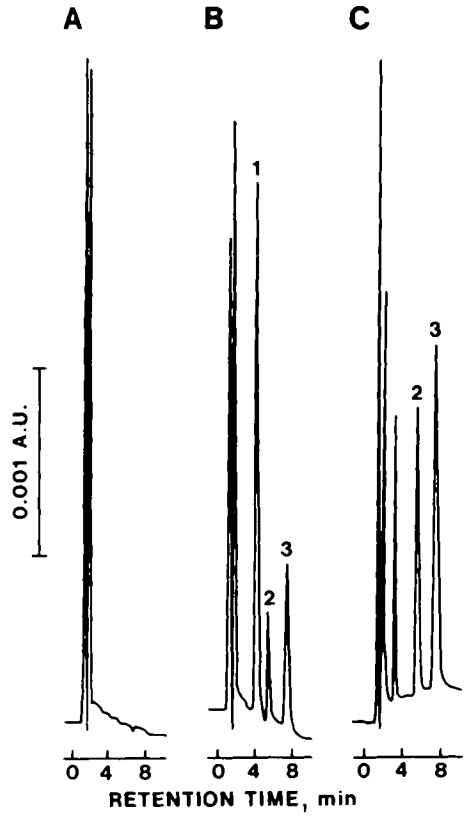

Figure 1—*Chromatograms of the extracts of plasma samples collected from a human subject shortly before (A) and 4 h after (B) the administration of a 20-mg dose of adinazolam mesylate in tablets, and the chromatogram of the extract of a blank plasma sample supplemented with adinazolam mesylate and internal standard (C). Key: (1) N-demethyl metabolite; (2) adinazolam; (3) internal standard.*

adinazolam mesylate. Both samples were obtained from the same human subject who received orally a single 20-mg dose of the drug in compressed tablets. Clinical studies showed that ≤30 mg of adinazolam mesylate three times a day for a total daily dose of 90 mg was efficacious in treatment of depression (9). Figure 1 also shows a chromatogram of the extract of a sample

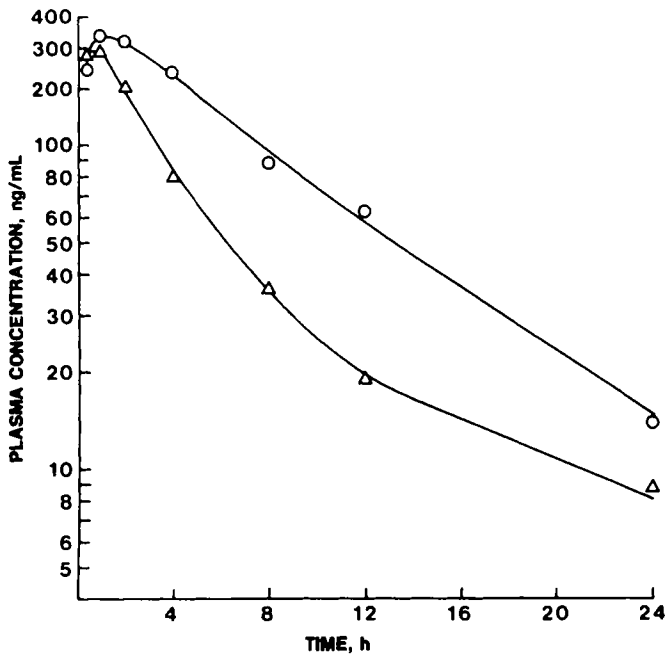

Figure 2—*Plasma concentration-time profiles of adinazolam (△) and the N-demethyl metabolite (○) after administration of a 30-mg dose of adinazolam mesylate in tablets to a human subject.*

of blank plasma with added adinazolam mesylate and the internal standard (Fig. 1C). Samples of blank plasma from several sources showed minimal interferences during the chromatographic separation. The chromatographic separation eluted adinazolam and the internal standard with retention volumes of ~11.2 and 16 mL, respectively. In the post-medication samples, an additional drug-related peak with a retention volume of ~8.8 mL was found (Fig. 1C). This peak was later identified as the *N*-demethyl metabolite of the parent drug. No other material could be identified as drug related in the chromatograms under the experimental conditions. The retention volumes of these sample components varied slightly from day-to-day and were especially sensitive to the changes in the proportions of acetonitrile, the concentrations of ammonium phosphate, and the pH of the buffer in the mobile phase. These compounds were more retentive on the column[9] using mobile phase with a lower proportion of organic solvents, a lower concentration of ammonium phosphate in the buffer, or a higher pH of the buffer. This knowledge was used to optimize the chromatographic separation by adjusting the mobile phase compositions. The limitations of these modifications were the excessive peak tailing and the prolongation of the retention times.

Like other benzodiazepines, the triazolobenzodiazepines undergo reversible ring-opening reactions in acidic media involving the hydrolysis of the azomethine linkage. These reversible reactions have been reported for triazolam (10) and estazolam (11). Adinazolam also showed similar ring-opening reactions in acidic solutions. At the pH of the buffer for the chromatographic mobile phase (pH 2.5–4.0), and in the mobile phase containing organic solvents, adinazolam was hydrolyzed to its ring-open form to a large extent. However, chromatographic separation using the acidic mobile phase indicated that essentially no ring-opening reaction took place by eluting adinazolam through the reverse-phase column as monitored by the UV detector. Under the same conditions, when an acidic solution of adinazolam was chromatographed, the intact drug and its ring-open form were separated: the ring-open form was much less retentive on the column than the intact drug. The reason for the discrepancy between the apparent stability of adinazolam during the acidic reverse-phase column separation and its instability in acidic solution was uncertain. It is possible that with the acid-catalyzed hydrolysis of the azomethine linkage, the environment inside the column was different from a simple acidic solution of a mixture of the buffer and organic solvents.

The adinazolam-internal standard and the *N*-demethylated metabolite-internal standard peak-height ratios showed good linear relationships with their corresponding concentrations. The linear regression of the peak height ratio-concentration data of both compounds usually resulted in calibration curves with correlation coefficients >0.998 and with positive or negative intercepts statistically zero, judging from 95% confidence limits. The slopes of the calibration curves were quite reproducible from day-to-day. For example, 12 sets of the calibration curves of adinazolam prepared over a period of three weeks showed a *RSD* of 4.3%, and eight sets of the calibration curves of the metabolite prepared over the same period showed a *RSD* of 9.7%. These data indicated the good interassay reproducibility for these compounds. The intra-assay reproducilibity and the accuracy of this methodology were also very good; *i.e.*, in the analyses of aliquots of blank plasma samples supplemented with 12, 74.5, 165, and 462 ng/mL of adinazolam mesylate, the concentrations found were 11.9 ± 0.38, 73.6 ± 1.0, 164.6 ± 17.24, and 462.5 ± 2.33 ng/mL, respectively. The relative *SD* of these replicate assays (N = 4) were from 0.5 to 10.5%.

The assay methodology has been used to analyze the plasma samples collected from human subjects after oral administration of adinazolam in compressed tablets. The plasma concentration of the parent drug reached its peak usually at ~1 h postdose and then declined following a biexponential pattern. In the same sample, the concentration of the *N*-demethyl metabolite was higher than the parent drug at most sampling times. A representative set of data, demonstrating the utility of the assay methodology, is shown in Fig. 2.

REFERENCES

(1) J. B. Hester, Jr., A. D. Rudzik, and B. V. Kamdar, *J. Med. Chem.*, **14**, 1078 (1971).

(2) A. D. Rudzik, J. B. Hester, A. H. Tang, R. N. Straw, and W. Friis, in "The Benzo-diazepines," S. Garattini, E. Mussini, and L. O. Randall, Eds., Raven, New York, N.Y., 1973, pp. 285–293.

(3) T. M. Itil, N. Polvan, S. Egilmer, B. Saletu, and J. Sarasa, *Curr. Ther. Res.*, **15**, 603 (1973).

(4) R. I. Wang and S. L. Stockdale, *J. Int. Med. Res.*, **1**, 600 (1973).

(5) K. Meguro and Y. Kuwada, *Tetrahedron Lett.*, **1970**, 4039.

(6) J. B. Hester, Jr., *J. Org. Chem.*, **44**, 4165 (1979).

(7) J. B. Hester, Jr., *J. Heterocycl. Chem.*, **17**, 575 (1980).

(8) J. B. Hester, Jr., A. D. Rudzik, and P. F. VonVoigtlander, *J. Med. Chem.*, **23**, 392 (1980).

(9) R. E. Pyke, J. B. Cohn, J. P. Feighner, and W. T. Smith, *Psychopharmacol. Bull.* **19**, 96 (1983).
(10) M. Konishi, K. Hirai, and Y. Mori, *J. Pharm. Sci.*, **71**, 1328 (1982).
(11) N. Inotsume and M. Nakano, *Chem. Pharm. Bull.* **28**, 2536 (1980).

Potential Antitumor Agents X: Synthesis and Antitumor Activity of Two Nitrogen Mustard Derivatives Related to Ketocaine

ALDO ANDREANI *x, DANIELA BONAZZI *, MIRELLA RAMBALDI *, IRAKLIS GALATULAS ‡, and ROSARIA BOSSA ‡

Received July 19, 1982, from the **Istituto di Chimica Farmaceutica e Tossicologica, University of Bologna* and the ‡*Istituto di Farmacologia, University of Milan, Italy.* Accepted for publication May 23, 1983.

Abstract □ The synthesis of two nitrogen mustard derivatives (VIII and IX) related to the well-known local anesthetic ketocaine (III) is reported. These compounds were tested in mice implanted with Ehrlich ascites tumor cells, and the antitumor activity was compared with that of two previously synthesized analogues (I and II) lacking the nitro group and with that of doxorubicin. The monofunctional compound IX was inactive, but the bifunctional compound VIII showed potent antitumor activity (%T/C > 254 at 20 mg/kg).

Keyphrases □ Antitumor agents—potential, nitrogen mustard derivatives, Ehrlich ascites carcinoma screen □ Nitrogen mustard derivatives—antitumor agents, potential, Ehrlich ascites carcinoma screen

In a previous paper of this series (1), we reported the synthesis of I and II, two analogues of the well-known local anesthetic ketocaine (III). This work was based on the hypothesis that the *in vitro* antimitotic activity of ketocaine is related to its effect on oxygen consumption by tissues with prevailing anaerobic metabolism; this, in turn, demonstrates the ability of ketocaine to pass through the cell membrane (2). While ketocaine does not show antitumor activity, I and II were active (1). On the other hand, a series of butyrophenone derivatives showed that ketocaine and one of its nitro derivatives had analogous behavior to oxygen consumption (3). This study describes the nitration of *o*-hydroxybutyrophenone and the subsequent alkylation of the nitro derivative with tris(2-chloroethyl)amine hydrochloride, as previously described (1). The antitumor activity and the effect on oxygen consumption of these substances were compared with those of the previously described I and II.

RESULTS AND DISCUSSION

The nitration of *o*-hydroxybutyrophenone always gave a mixture of IV–VI. These materials were separated by column chromatography and identified by means of spectrometric data (see *Experimental Section*). The reaction between the nitro derivative (IV) and tris(2-chloroethyl)amine hydrochloride (VII) gave VIII and IX, as well as X (Scheme I). Compounds VIII and IX were tested, as the hydrochlorides, for antitumor activity.

The bifunctional compound VIII inhibited tumor growth and prolonged the life span of mice bearing Ehrlich ascites carcinoma beyond that of the untreated animals. The %T/C at 4 mg/kg ip was 144, and it was >254 at 20 mg/kg. The monofunctional compound IX was inactive. Table I reports the antitumor activity of VIII and IX compared with that of the previously reported I and II (1) and doxorubicin.

Compounds I, II, VIII, and IX also affected the oxygen consumption of tumor cells. Figure 1 shows a difference in the respiratory inhibition that may be related to the different lipophilicity of the four compounds: in fact respiratory inhibition is a linear function of lipophilicity in a series of 4-hydroxyquinoline-3-carboxylic acids (4). The potent antitumor activity of VIII under the experimental conditions employed is evident. From the results so far available it appears that VIII is also active against other experimental tumors.

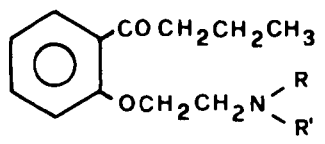

I R = R' = $-CH_2CH_2Cl$

II R = $-CH_2CH_2Cl$; R' = $-CH_2CH_2O-$ (with $COCH_2CH_2CH_3$)

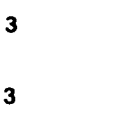

III R = R' = $-CH(CH_3)_2$

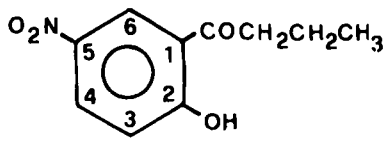

IV

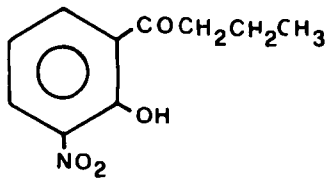

V

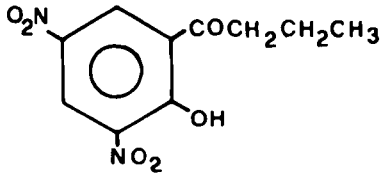

VI

0022-3549/84/0800-1175$01.00/0
© 1984, American Pharmaceutical Association

(9) R. E. Pyke, J. B. Cohn, J. P. Feighner, and W. T. Smith, *Psychopharmacol. Bull.* **19**, 96 (1983).
(10) M. Konishi, K. Hirai, and Y. Mori, *J. Pharm. Sci.*, **71**, 1328 (1982).
(11) N. Inotsume and M. Nakano, *Chem. Pharm. Bull.* **28**, 2536 (1980).

Potential Antitumor Agents X: Synthesis and Antitumor Activity of Two Nitrogen Mustard Derivatives Related to Ketocaine

ALDO ANDREANI *x, DANIELA BONAZZI *, MIRELLA RAMBALDI *, IRAKLIS GALATULAS ‡, and ROSARIA BOSSA ‡

Received July 19, 1982, from the **Istituto di Chimica Farmaceutica e Tossicologica, University of Bologna* and the ‡*Istituto di Farmacologia, University of Milan, Italy.* Accepted for publication May 23, 1983.

Abstract □ The synthesis of two nitrogen mustard derivatives (VIII and IX) related to the well-known local anesthetic ketocaine (III) is reported. These compounds were tested in mice implanted with Ehrlich ascites tumor cells, and the antitumor activity was compared with that of two previously synthesized analogues (I and II) lacking the nitro group and with that of doxorubicin. The monofunctional compound IX was inactive, but the bifunctional compound VIII showed potent antitumor activity (%T/C > 254 at 20 mg/kg).

Keyphrases □ Antitumor agents—potential, nitrogen mustard derivatives, Ehrlich ascites carcinoma screen □ Nitrogen mustard derivatives—antitumor agents, potential, Ehrlich ascites carcinoma screen

In a previous paper of this series (1), we reported the synthesis of I and II, two analogues of the well-known local anesthetic ketocaine (III). This work was based on the hypothesis that the *in vitro* antimitotic activity of ketocaine is related to its effect on oxygen consumption by tissues with prevailing anaerobic metabolism; this, in turn, demonstrates the ability of ketocaine to pass through the cell membrane (2). While ketocaine does not show antitumor activity, I and II were active (1). On the other hand, a series of butyrophenone derivatives showed that ketocaine and one of its nitro derivatives had analogous behavior to oxygen consumption (3). This study describes the nitration of *o*-hydroxybutyrophenone and the subsequent alkylation of the nitro derivative with tris(2-chloroethyl)amine hydrochloride, as previously described (1). The antitumor activity and the effect on oxygen consumption of these substances were compared with those of the previously described I and II.

RESULTS AND DISCUSSION

The nitration of *o*-hydroxybutyrophenone always gave a mixture of IV–VI. These materials were separated by column chromatography and identified by means of spectrometric data (see *Experimental Section*). The reaction between the nitro derivative (IV) and tris(2-chloroethyl)amine hydrochloride (VII) gave VIII and IX, as well as X (Scheme I). Compounds VIII and IX were tested, as the hydrochlorides, for antitumor activity.

The bifunctional compound VIII inhibited tumor growth and prolonged the life span of mice bearing Ehrlich ascites carcinoma beyond that of the untreated animals. The %T/C at 4 mg/kg ip was 144, and it was >254 at 20 mg/kg. The monofunctional compound IX was inactive. Table I reports the antitumor activity of VIII and IX compared with that of the previously reported I and II (1) and doxorubicin.

Compounds I, II, VIII, and IX also affected the oxygen consumption of tumor cells. Figure 1 shows a difference in the respiratory inhibition that may be related to the different lipophilicity of the four compounds: in fact respiratory inhibition is a linear function of lipophilicity in a series of 4-hydroxyquinoline-3-carboxylic acids (4). The potent antitumor activity of VIII under the experimental conditions employed is evident. From the results so far available it appears that VIII is also active against other experimental tumors.

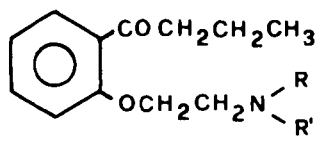

I R = R' = $-CH_2CH_2Cl$

II R = $-CH_2CH_2Cl$; R' = $-CH_2CH_2O-$ (with $COCH_2CH_2CH_3$)

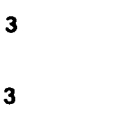

III R = R' = $-CH(CH_3)_2$

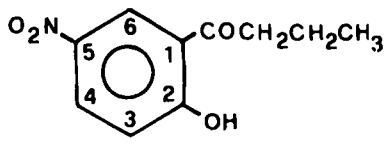

IV

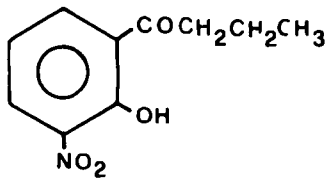

V

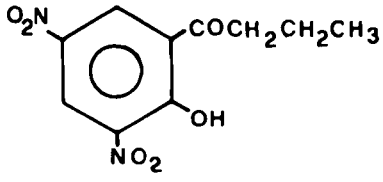

VI

0022-3549/84/0800-1175$01.00/0
© 1984, American Pharmaceutical Association

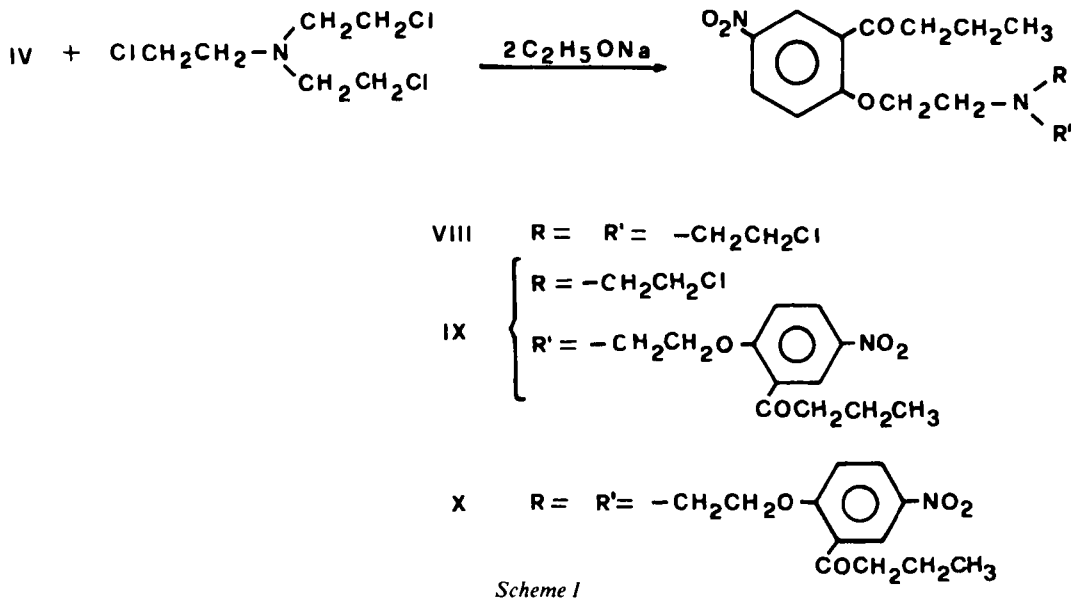

Scheme I

Table I—Antitumor Activity of Ketocaine Analogues Against Ehrlich Ascites Carcinoma in Mice

Compound	Dose on Day 1, mg/kg ip	n^a	MST[b]	%T/C[c]	LTS[d]
Control[e]	—	10	16.0	—	
I	1	5	15.0	93.7	
	5	5	23.8	148.7	
	20	5	†[f]	—	
II	10	5	19.6	122	
	50	5	27.4	171.2	
	200	5	†[f]	—	
VIII	4	10	23.1	144.3	
	20	10	40.7	>254	4
	100	10	†[f]	—	
IX	20	10	16.6	103.7	
	100	10	15.6	97.5	
	200	10	17.6	110	
Doxorubicin	1	10	36.6	>228	3

[a] Number of animals per group. [b] Mean survival time (d). [c] %T/C ≥125 denotes significant activity. [d] Long-term survivors (>60 d). [e] Saline. [f] †— Death due to drug-related toxicity.

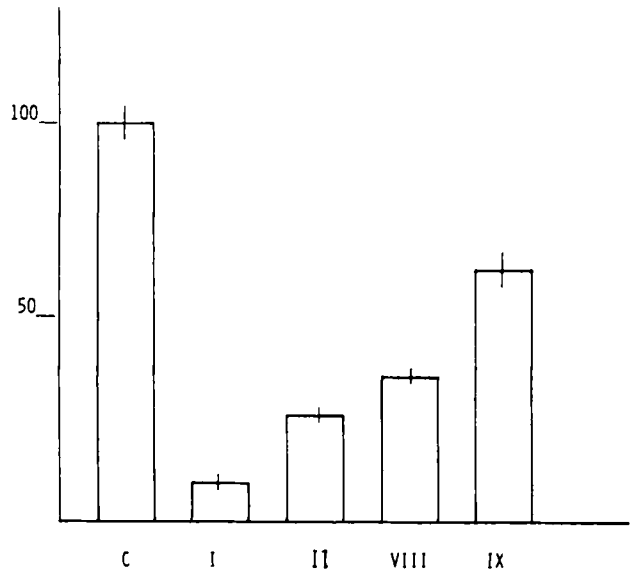

Figure 1—*Effect of oxygen consumption induced in Ehrlich ascites tumor cells by I, II, VIII, and IX at 50 μg/10⁶ cells. Controls (C) = 100 (means of at least six determinations).*

EXPERIMENTAL SECTION[1]

Chemistry—*Nitration of o-Hydroxybutyrophenone*—A cold solution of 90% HNO_3 (5.2 mL, 110 mmol) in acetic anhydride (15 mL) was slowly added with stirring to a cold solution of *o*-hydroxybutyrophenone (14.8 g, 90 mmol) in 20 mL of acetic anhydride. The temperature was maintained below 15°C. The mixture was then stirred for 1 h at room temperature and poured onto ice. A densitometric TLC analysis of the precipitate gave the following percentages: 60% IV, 30% V, and 10% VI similar results were obtained by using acetic acid or sulfuric acid in place of acetic anhydride. The three compounds were isolated by means of column chromatography.

2-Hydroxy-5-nitrobutyrophenone (IV)—Compound IV was obtained as yellow needles, mp 108–110°C (petroleum ether). IR (nujol): 3080, 1638, and 810 cm^{-1}; ^{1}H-NMR: δ 8.85 (d, 1, J = 3.0 Hz, H-6); 8.43 (q, 1, J = 9.6 Hz, 3.0 Hz, H-4); 7.15 (d, 1, J = 9.6 Hz, H-3); and 3.15, 1.83, and 1.06 ppm (7, $—CH_2CH_2CH_3$).

Anal.—Calc. for $C_{10}H_{11}NO_4$: C, 57.41; H, 5.30; N, 6.70. Found: C, 57.70; H, 5.31; N, 6.69.

2-Hydroxy-3-nitrobutyrophenone (V)—Compound V was obtained as yellow needles, mp 43–45°C (petroleum ether). IR (nujol): 3080, 1642, and 1030 cm^{-1}; ^{1}H-NMR: δ 8.26 (q, 1, J = 8.0 Hz, 2.0 Hz, H-6); 8.20 (q, 1, J = 9.0 Hz, 2.0 Hz, H-4); 7.10 (q, 1, J = 9.0 Hz, 8.0 Hz, H-5); and 3.08, 1.83, and 1.03 ppm (7, $—CH_2CH_2CH_3$).

Anal.—Calc. for $C_{10}H_{11}NO_4$: C, 57.41; H, 5.30; N, 6.70. Found: C, 57.18; H, 5.35; N, 6.60.

2-Hydroxy-3,5-dinitrobutyrophenone (VI)—Compound VI was obtained as yellow needles, mp 118–120°C (ethanol). IR (nujol): 3070, 1645, and 1610 cm^{-1}; ^{1}H-NMR: δ 8.96 (d, 2, J = 2.4 Hz, H-4 + H-6) and 3.15, 1.83, and 1.06 ppm (7, $—CH_2CH_2CH_3$).

Anal.—Calc. for $C_{10}H_{10}N_2O_6$: C, 47.25; H, 3.96; N, 11.02. Found: C, 47.08; H, 3.76; N, 10.82.

Synthesis of VIII–X—Compound IV (6.3 g, 30 mmol), dissolved in 60 mL of absolute ethanol, was added to a solution of C_2H_5ONa (60 mmol) in absolute ethanol (50 mL). Tris(2-chloroethyl)amine hydrochloride (VII; 7.3 g, 30 mmol) was then added with stirring. The mixture was refluxed for 5 h, and then the solvent was removed under reduced pressure. The residue was extracted with chloroform. The organic phase was washed with water, dried (Na_2SO_4), and the solvent was removed under reduced pressure. A densitometric TLC analysis of the residue gave the following percentages: 35% (IV), 40% (VIII), 20% (IX), and 5% (X). The four compounds were separated by column chromatography and VIII and IX were converted into the corresponding hydrochlorides.

N-[2-(2-Butanoyl-4-nitro)phenoxyethyl]-N,N-bis(2-chloroethyl)amine Hydrochloride (VIII-HCl)—The compound was a white powder, mp 113–115°C (absolute ethanol); IR (KBr): 1695, 1610, and 1580 cm^{-1}.

[1] Melting points are uncorrected. Bakerflex plates (silica-gel IB2-F) were used for the TLC. For column chromatography Kieselgel 60 (Merck) was used, activated at 120°C for 2 h, in the proportion of 40 g/g of mixture; the eluant was petroleum ether (bp 60–80°C)/acetone (80:20). The IR spectra were recorded on a Perkin-Elmer 298 spectrometer. The ^{1}H-NMR spectra were recorded in $CDCl_3$ on a Varian XL-100 instrument using Me_4Si as internal standard.

Anal.—Calc. for $C_{16}H_{22}Cl_2N_2O_4 \cdot HCl$: C, 46.45; H, 5.60; N, 6.77. Found: C, 46.46; H, 5.70; N, 6.59.

N,N-*Bis*[*2-(2-butanoyl-4-nitro)phenoxyethyl*]-N-(*2-chloroethyl*)*amine Hydrochloride* (*IX·HCl*)—The compound was a white powder, mp 160–165°C (absolute ethanol); IR (KBr): 1685, 1605, and 1580 cm^{-1}.

Anal.—Calc. for $C_{26}H_{32}ClN_3O_8 \cdot HCl$: C, 53.25; H, 5.67; N, 7.16. Found: C, 53.49; H, 5.83; N, 7.05.

N,N,N-*Tris*[*2-(2-butanoyl-4-nitro)phenoxyethyl*]*amine* (*X*)—Compound X was a white powder, mp 87–90°C (ethanol); IR (KBr): 1670, 1605, and 1580 cm^{-1}.

Anal.—Calc. for $C_{36}H_{42}N_4O_{12}$: C, 59.82; H, 5.86; N, 7.75. Found: C, 59.56; H, 5.80; N, 7.63.

Pharmacology—*Antitumor Test*—Female Swiss mice (average weight 21 ± 1 g) were implanted on day 0 with 10^6 Ehrlich ascites tumor cells from donor mice. After 24 h the animals were treated with VIII (4, 20, or 100 mg/kg ip) or IX (20, 100, or 200 mg/kg ip) dissolved in dimethyl sulfoxide; the amount of dimethyl sulfoxide, previously used in analogous experiments, did not affect tumor growth. Doxorubicin (1 mg/kg ip) was used as a positive control. Deaths were recorded for a period of 60 d. The activity was measured as the ratio of the mean survival time of the test animals to that of the control expressed as a percentage (%T/C). Significant activity is achieved with an increased life span of 25% (T/C ≥ 125).

Respirometric Test—Oxygen consumption by Ehrlich ascites tumor cells was performed by placing in each flask of a Warburg's apparatus 4×10^7 Ehrlich carcinoma cells suspended in 1.8 mL of Ringer's solution and 0.2 mL of distilled water or the same volume of solution of the test compound (the final concentration in each flask was 1 mg/mL). Ehrlich ascites carcinoma cells were obtained from the ascitic fluid removed from mice 7–9 d after transplantation (female Swiss mice with weekly transplantations of 10^6 cells). Viability of cells was assayed by trypan blue dye test. Flasks containing the cell suspension were equilibrated for 10 min and respiration was measured for 60 min (temperature: 37°C; gas phase: air).

REFERENCES

(1) A. Andreani, G. Scapini, I. Galatulas, and R. Bossa, *J. Pharm. Sci.*, **72**, 814 (1983).

(2) R. Bossa, F. Dubini, I. Galatulas, and M. Taniguchi, *Arch. Ital. Pat. Clin. Tumori*, **13**, 135 (1970).

(3) F. Ardizzone, I. Galatulas, A. Longhi, and P. Pomarelli, *Arzneim.-Forsch.*, **20**, 1794 (1970).

(4) E. A. Coats, K. J. Shah, S. R. Milstein, C. S. Genther, D. M. Nene, J. Roesener, J. Schmidt, M. Pleiss, E. Wagner, and J. K. Baker, *J. Med. Chem.*, **25**, 57 (1982).

ACKNOWLEDGMENTS

Presented in part at the XXI Congress of the Italian Pharmacological Society in Naples, June 1982.

Gas Chromatographic–Mass Spectrometric Assay for the Ultra-Short-Acting β-Blocker Esmolol

CHECK Y. SUM ˣ and AVRAHAM YACOBI *

Received November 15, 1982, from *Research and Development, American Critical Care, McGaw Park, IL 60085.* Accepted for publication May 19, 1983. *Present address: Lederle Laboratories, Pearl River, NY 10965.

Abstract □ Esmolol is an ultra-short-acting β-blocker currently in Phase II clinical trials. The ester functionality in esmolol results in rapid metabolism of the β-blocker into an acidic metabolite and methanol. Dichloromethane was used to denature blood esterases and quantitatively extract esmolol from the blood. A deuterated analogue of esmolol was selected as the internal standard, and both compounds were chromatographed as the trimethylsilyl derivatives. Blood levels of esmolol were quantitated by gas chromatography–mass spectrometry with selective-ion monitoring, focusing on specific ions corresponding to esmolol and the internal standard. The lower limit of sensitivity of the assay was 2.5 ng/mL. Using the assay, blood samples from a dose-ranging study in humans were analyzed for concentrations of esmolol. Steady-state blood levels of esmolol after intravenous infusion rates of 40, 100, 200, 300, 450, and 650 μg/kg/min were 0.202, 0.464, 0.977, 1.31, 1.92, and 2.97 μg/mL of blood. The elimination $t_{1/2}$ and total body clearance were estimated to be ~10 min and 220 mL/kg/min, respectively. The high clearance of esmolol suggested that metabolism by blood esterase(s) was the primary determinant of the duration of action of the drug.

Keyphrases □ Esmolol—GC-MS, ultra-short-acting β-blocker □ Beta-blocker—ultra-short-acting, esmolol, GC-MS.

The concept and advantages of ultra-short-acting β-adrenergic receptor blockers have been presented recently (1). Briefly, in critical care settings like emergency rooms and intensive cardiac-care units, an ultra-short-acting β-blocker would be superior to conventional β-blockers with long durations of action, since therapeutic effects of the drug can be altered rapidly in either direction to meet changing cardiovascular responses.

Development of esmolol, methyl-3-[4-[2-hydroxy-3-(isopropylamino)propoxy]phenyl]propionate hydrochloride, as a novel ultra-short-acting β-blocker is based on the enzymatic instability of an ester function and incorporation of this functionality into a chemical structure that has β-blocking properties. Hydrolysis of the ester linkage in esmolol by blood and tissue esterases transforms the β-blocker into an acidic metabolite and methanol.

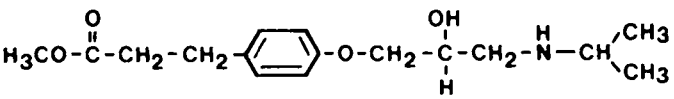

ESMOLOL

Esmolol has been shown to be cardioselective and to possess a duration of action of ~15 min in dogs (1). Since blood levels of esmolol were anticipated to decrease very rapidly after stopping administration of the drug, a sensitive assay was needed in order to conduct detailed preclinical and clinical pharmacodynamic and pharmacokinetic studies. This report describes a gas chromatographic–mass spectrometric (GC-MS) method for the quantitation of esmolol in whole blood. Application of the method to the analysis of blood samples from a dose-ranging study in humans is also presented.

EXPERIMENTAL SECTION

Chemicals—Esmolol and the deuterated internal standard, methyl-3-[4-[2-hydroxy-3-(isopropylamino)propoxy]phenyl][1,2-$^2H_2$]propionate hydrochloride, were synthesized in-house[1]. Dichloromethane[2] was spectro grade.

[1] Medicinal Chemistry Section, American Critical Care, McGaw Park, Ill.
[2] Matheson, Coleman, and Bell, Norwood, Ohio.

0022-3549/84/0800-1177$01.00/0

© 1984, American Pharmaceutical Association

Anal.—Calc. for $C_{16}H_{22}Cl_2N_2O_4 \cdot HCl$: C, 46.45; H, 5.60; N, 6.77. Found: C, 46.46; H, 5.70; N, 6.59.

N,N-*Bis*[*2-(2-butanoyl-4-nitro)phenoxyethyl*]-N-(*2-chloroethyl*)*amine Hydrochloride* (*IX·HCl*)—The compound was a white powder, mp 160–165°C (absolute ethanol); IR (KBr): 1685, 1605, and 1580 cm^{-1}.

Anal.—Calc. for $C_{26}H_{32}ClN_3O_8 \cdot HCl$: C, 53.25; H, 5.67; N, 7.16. Found: C, 53.49; H, 5.83; N, 7.05.

N,N,N-*Tris*[*2-(2-butanoyl-4-nitro)phenoxyethyl*]*amine* (*X*)—Compound X was a white powder, mp 87–90°C (ethanol); IR (KBr): 1670, 1605, and 1580 cm^{-1}.

Anal.—Calc. for $C_{36}H_{42}N_4O_{12}$: C, 59.82; H, 5.86; N, 7.75. Found: C, 59.56; H, 5.80; N, 7.63.

Pharmacology—*Antitumor Test*—Female Swiss mice (average weight 21 ± 1 g) were implanted on day 0 with 10^6 Ehrlich ascites tumor cells from donor mice. After 24 h the animals were treated with VIII (4, 20, or 100 mg/kg ip) or IX (20, 100, or 200 mg/kg ip) dissolved in dimethyl sulfoxide; the amount of dimethyl sulfoxide, previously used in analogous experiments, did not affect tumor growth. Doxorubicin (1 mg/kg ip) was used as a positive control. Deaths were recorded for a period of 60 d. The activity was measured as the ratio of the mean survival time of the test animals to that of the control expressed as a percentage (%T/C). Significant activity is achieved with an increased life span of 25% (T/C ≥ 125).

Respirometric Test—Oxygen consumption by Ehrlich ascites tumor cells was performed by placing in each flask of a Warburg's apparatus 4×10^7 Ehrlich carcinoma cells suspended in 1.8 mL of Ringer's solution and 0.2 mL of distilled water or the same volume of solution of the test compound (the final concentration in each flask was 1 mg/mL). Ehrlich ascites carcinoma cells were obtained from the ascitic fluid removed from mice 7–9 d after transplantation (female Swiss mice with weekly transplantations of 10^6 cells). Viability of cells was assayed by trypan blue dye test. Flasks containing the cell suspension were equilibrated for 10 min and respiration was measured for 60 min (temperature: 37°C; gas phase: air).

REFERENCES

(1) A. Andreani, G. Scapini, I. Galatulas, and R. Bossa, *J. Pharm. Sci.*, **72**, 814 (1983).

(2) R. Bossa, F. Dubini, I. Galatulas, and M. Taniguchi, *Arch. Ital. Pat. Clin. Tumori*, **13**, 135 (1970).

(3) F. Ardizzone, I. Galatulas, A. Longhi, and P. Pomarelli, *Arzneim.-Forsch.*, **20**, 1794 (1970).

(4) E. A. Coats, K. J. Shah, S. R. Milstein, C. S. Genther, D. M. Nene, J. Roesener, J. Schmidt, M. Pleiss, E. Wagner, and J. K. Baker, *J. Med. Chem.*, **25**, 57 (1982).

ACKNOWLEDGMENTS

Presented in part at the XXI Congress of the Italian Pharmacological Society in Naples, June 1982.

Gas Chromatographic–Mass Spectrometric Assay for the Ultra-Short-Acting β-Blocker Esmolol

CHECK Y. SUM ˣ and AVRAHAM YACOBI *

Received November 15, 1982, from *Research and Development, American Critical Care, McGaw Park, IL 60085.* Accepted for publication May 19, 1983. *Present address: Lederle Laboratories, Pearl River, NY 10965.

Abstract □ Esmolol is an ultra-short-acting β-blocker currently in Phase II clinical trials. The ester functionality in esmolol results in rapid metabolism of the β-blocker into an acidic metabolite and methanol. Dichloromethane was used to denature blood esterases and quantitatively extract esmolol from the blood. A deuterated analogue of esmolol was selected as the internal standard, and both compounds were chromatographed as the trimethylsilyl derivatives. Blood levels of esmolol were quantitated by gas chromatography–mass spectrometry with selective-ion monitoring, focusing on specific ions corresponding to esmolol and the internal standard. The lower limit of sensitivity of the assay was 2.5 ng/mL. Using the assay, blood samples from a dose-ranging study in humans were analyzed for concentrations of esmolol. Steady-state blood levels of esmolol after intravenous infusion rates of 40, 100, 200, 300, 450, and 650 μg/kg/min were 0.202, 0.464, 0.977, 1.31, 1.92, and 2.97 μg/mL of blood. The elimination $t_{1/2}$ and total body clearance were estimated to be ~10 min and 220 mL/kg/min, respectively. The high clearance of esmolol suggested that metabolism by blood esterase(s) was the primary determinant of the duration of action of the drug.

Keyphrases □ Esmolol—GC-MS, ultra-short-acting β-blocker □ Beta-blocker—ultra-short-acting, esmolol, GC-MS.

The concept and advantages of ultra-short-acting β-adrenergic receptor blockers have been presented recently (1). Briefly, in critical care settings like emergency rooms and intensive cardiac-care units, an ultra-short-acting β-blocker would be superior to conventional β-blockers with long durations of action, since therapeutic effects of the drug can be altered rapidly in either direction to meet changing cardiovascular responses.

Development of esmolol, methyl-3-[4-[2-hydroxy-3-(isopropylamino)propoxy]phenyl]propionate hydrochloride, as a novel ultra-short-acting β-blocker is based on the enzymatic instability of an ester function and incorporation of this functionality into a chemical structure that has β-blocking properties. Hydrolysis of the ester linkage in esmolol by blood and tissue esterases transforms the β-blocker into an acidic metabolite and methanol.

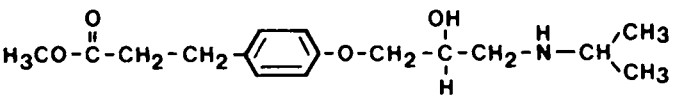

ESMOLOL

Esmolol has been shown to be cardioselective and to possess a duration of action of ~15 min in dogs (1). Since blood levels of esmolol were anticipated to decrease very rapidly after stopping administration of the drug, a sensitive assay was needed in order to conduct detailed preclinical and clinical pharmacodynamic and pharmacokinetic studies. This report describes a gas chromatographic–mass spectrometric (GC-MS) method for the quantitation of esmolol in whole blood. Application of the method to the analysis of blood samples from a dose-ranging study in humans is also presented.

EXPERIMENTAL SECTION

Chemicals—Esmolol and the deuterated internal standard, methyl-3-[4-[2-hydroxy-3-(isopropylamino)propoxy]phenyl][1,2-$^2H_2$]propionate hydrochloride, were synthesized in-house[1]. Dichloromethane[2] was spectro grade.

[1] Medicinal Chemistry Section, American Critical Care, McGaw Park, Ill.
[2] Matheson, Coleman, and Bell, Norwood, Ohio.

0022-3549/84/0800-1177$01.00/0

© 1984, American Pharmaceutical Association

Dibasic potassium phosphate[3], hydrochloric acid[4], and bis(trimethylsilyl)-trifluoroacetamide[5] were reagent grade.

Instrumentation—Quantitation of esmolol was accomplished using a 2-m × 2-mm i.d. stainless steel column packed with 3% SP-2250 on 100–200-mesh Supelcoport[6]. The GC–MS system consisted of a gas chromatograph[7] coupled to a mass spectrometer[8]. The GC conditions were as follows: injector, column, and detector temperatures were set at 280°C, 230°C, and 290°C, respectively.

Electron-impact mass spectra were obtained at 70 eV, and the mass spectrometer was programmed in the selective-ion mode, focusing on ions at *m/z* 251 and 253 (corresponding to esmolol and the internal standard, respectively). The major fragments (>15% relative abundance) of esmolol were: *m/z* 101 (59.3), 103 (20.4), 107 (23.7), 116 (20.4), 120 (15.5), 131 (29.8), 145 (21.9), 147 (24.9), 188 (36.2), 251 (base peak, 100), 252 (20.4), 336 (16.4), 352 ($M^+ - 15$, 36.5), and 367 (M^+, 1.8). For the deuterated internal standard, the major fragments were: *m/z* 101 (72.6), 108 (23.4), 116 (22.8), 122 (15.2), 132 (30.1), 146 (21.1), 188 (36.5), 253 (base peak, 100), 254 (17.9), 338 (15.2), 354 ($M^+ - 15$, 36.7), and 369 (M^+, 1.7).

Clinical Protocol—Six healthy male subjects, 20–30 years old (mean 23.2 years) and weighing 67.5–82.5 kg (mean 73.4 kg), received constantly increasing intravenous infusions of 10, 40, 100, 150, 200, 300, 450, and 650 μg/kg/min of esmolol for 60 min on 8 consecutive days. The minimum period between treatments was 23 h. In each treatment, blood samples were collected into heparinized tubes 1 min before and 30 and 60 min after initiation of the infusion, and at 5 and 15 min after cessation of the infusion.

Blood Sample Processing and Analysis—Immediately after collection of blood, a 1.0-mL aliquot was transferred into a 20- × 150-mm extraction tube containing 10.0 mL of dichloromethane and an appropriate amount of the deuterated internal standard. The tube was then shaken vigorously by hand for 10 s and then placed into a mechanical shaker[9] for 10 min. The two phases were separated by centrifugation in a refrigerated table-top centrifuge[10] at 1700×*g* for 10 min. After centrifugation, the reddish aqueous phase, which contained the polar metabolites, was removed. After tilting the tube to loosen the protein plaque, a serological pipet was carefully inserted into the organic phase, and 9.0 mL of dichloromethane was removed and transferred into another extraction tube containing 2.0 mL of 0.02 M HCl. The tube was shaken and centrifuged to separate the phases. The resultant aqueous phase was transferred into another tube and the pH was raised to 8.0 by addition of 200 μL of a 1.0 M potassium phosphate buffer (pH 8.0). Five milliliters of dichloromethane was added to the tube, and the tube was shaken and centrifuged. The organic phase was quantitatively removed and concentrated to ~100 μL under a stream of dry nitrogen. Then, 50 μL of bis(trimethylsilyl)trifluoroacetamide was added and the resultant mixture was heated at 60°C for 30 min. Two microliters of the final solution was injected into the GC–MS system for analysis. Using the selective extraction steps, the resultant final solution was devoid of any biological contaminants and the final recovery was 73%.

Quantitation of esmolol in the samples was accomplished by adding varying amounts of esmolol and a constant amount of the deuterated internal standard to blank human blood samples prior to the addition of 10 mL of dichloromethane. The standard curve samples were then processed and analyzed according to the aforementioned procedures.

RESULTS

The mass spectrum of esmolol (data not shown) showed that the molecular ion (*m/z* = 367) was present at a relative abundance of 1.8% indicating that only one trimethylsilyl group was attached. Analysis of the mass fragments suggested that the trimethylsilyl group was attached to the amino nitrogen. In addition, the base peak at *m/z* = 251 contained the propionate portion of the molecule. Thus, an internal standard was prepared by substituting the hydrogen atoms at the 1,2-positions of the propionate portion of the molecule with deuterium. In the mass spectrum of the deuterated internal standard (data not shown), the molecular ion was shifted two mass units higher to *m/z* = 369 and the base peak was shifted to 253. Using selective-ion monitoring, focusing on *m/z* = 251 and *m/z* = 253, the contribution of esmolol to *m/z* = 253 was determined to be ~7% and the contribution of the deuterated internal standard to *m/z* = 251 was <1%. This finding indicated that the deuterium in the internal standard did not exchange with hydrogen during sample processing and analysis. By selecting the concentration of internal standard to be always greater than or equal to the highest esmolol concentration in the standard curve, the small "cross-talk" was neglected.

Table I—Standard Curve of Esmolol

Conc., ng/mL	Peak Area Ratio[a]	Mean ± *SD* *CV*
2.5	0.006, 0.009, 0.010, 0.007, 0.007	0.008 ± 0.002 25.0
5.0	0.012, 0.016	0.014 ± 0.003 21.4
10	0.029, 0.033	0.031 ± 0.003 9.6
25	0.063, 0.067, 0.051, 0.063, 0.064	0.062 ± 0.006 9.7
50	0.094, 0.101	0.098 ± 0.005 5.1
100	0.211, 0.205	0.208 ± 0.004 1.9
250	0.483, 0.494	0.489 ± 0.008 1.6
250	0.067, 0.074	0.071 ± 0.005 7.0
500	0.117, 0.112	0.115 ± 0.004 3.5
1,000	0.220, 0.223, 0.224, 0.223, 0.221	0.222 ± 0.002 0.9
2,500	0.546, 0.540	0.543 ± 0.004 0.7
10,000	1.99, 1.98	1.99 ± 0.0007 0.4

[a] Peak area ratio of *m/z* 251–253 (esmolol/esmolol-d_2). The first set contained 500 ng/mL of esmolol-d_2 and the second set contained 5000 ng/mL of esmolol-d_2.

Table I summarizes the reproducibility of the assay. At the lower limit of sensitivity (2.5 ng/mL of blood), the coefficient of variation of six different determinations was 25%; at 25 ng/mL blood, the coefficient of variation was 10%; and at 1.0 μg/mL blood, the coefficient of variation was 1%.

After establishing its validity, the GC–MS method was used to analyze blood samples from a dose-ranging study in humans. The blood concentration-time profile of esmolol is shown in Fig. 1. The concentration of esmolol was approaching or was at steady state after 60 min of intravenous infusion with all the doses that were examined. Blood levels of esmolol decreased very rapidly after stopping the infusion, so that in 15 min blood levels had decreased by >50%. Figure 2 shows the linear relationship between the average blood

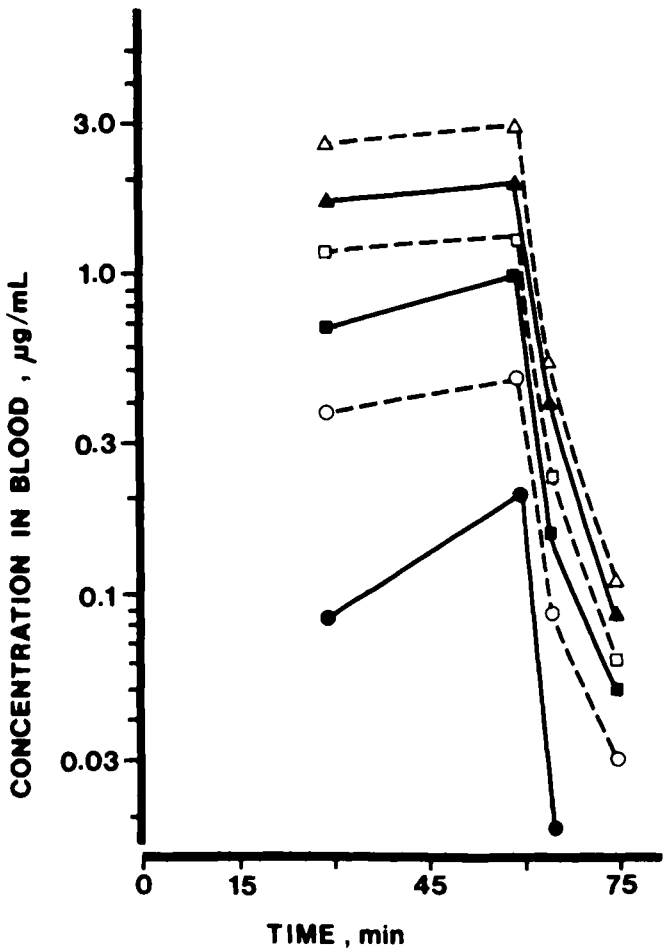

Figure 1—*Average blood concentration* versus *time profile of esmolol in normal subjects* (n = 1–6) *during and after a 1-h infusion of 40 (●), 100 (○), 200 (■), 300 (□), 450 (▲), and 650 (△) μg/kg/min.*

[3] Mallinckrodt, Paris, Ky.
[4] Eastman Kodak Co., Rochester, N.Y.
[5] Aldrich Chemical Co., Milwaukee, Wis.
[6] Supelco, Bellefonte, Pa.
[7] Model 5840A; Hewlett-Packard, Palo Alto, Calif.
[8] Model 5985A; Hewlett-Packard.
[9] Model 6000; Eberbach Corp., Ann Arbor, Mich.
[10] Model Centra-7R; International Equipment Co., Needham Heights, Mass.

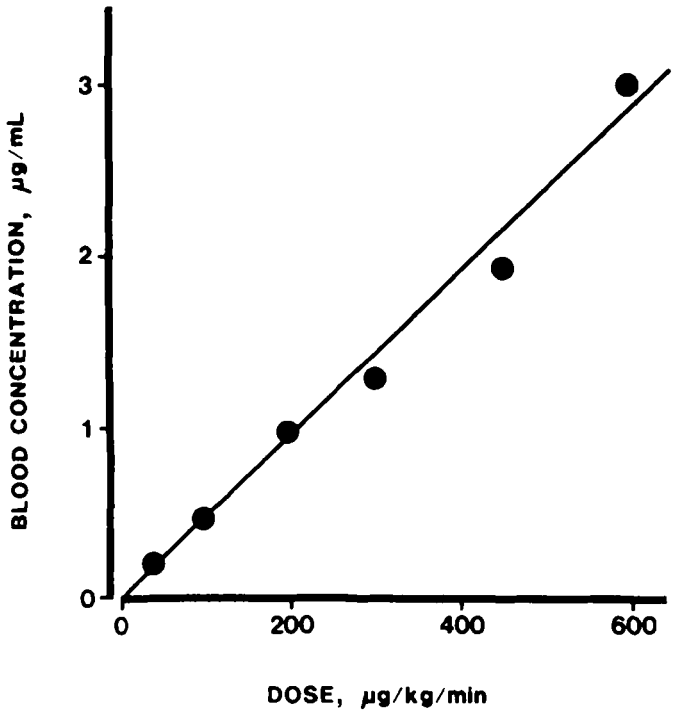

Figure 2—*Average blood concentrations (n = 1-6) of esmolol at the conclusion of a 1-h infusion of esmolol as a function of dose in normal subjects.*

concentrations of esmolol at the conclusion of a 1-h infusion and the doses of esmolol. These results suggest that over the dose range examined esmolol appeared to follow linear pharmacokinetics.

Assuming that blood concentrations of esmolol had reached steady state, model-independent analyses of blood data indicated that the total body clearance (C_{ss}/infusion rate) averaged 220 mL/kg/min (Table II). A rough graphic determination indicated an extremely short elimination half-life for esmolol, averaging ~10 min.

Tble II—Summary of Estimated Pharmacokinetic Parameters of Esmolol in Humans

Dose, μg/kg/min	n^a	$C_{ss}{}^b$, μg/mL	Clearance^c, mL/kg/min	$t_{1/2}$, min
40	3	0.202 ± 0.038	198	≤10
100	3	0.464 ± 0.170	216	≤10
200	6	0.977 ± 0.201	205	≤10
300	1	1.31	229	≤10
450	3	1.92 ± 0.500	234	≤10
650	1	2.97	219	≤10
Mean ± *SD*	—	—	217 ± 13.7	≤10

[a] *n* = number of subjects. [b] Concentration of esmolol observed in blood sample collected 60 min after the start of infusion at the indicated doses. [c] Clearance = dose/C_{ss}.

DISCUSSION

Most drugs are relatively stable in the presence of blood components for some time at room temperature. After removal of the drug from the body *via* blood sampling, there is reasonable assurance that levels of the drug in blood will not change until the sample is frozen or processed and analyzed. Even though blood does not appear to contain any of the oxidative enzymes which are abundant in the liver, it does contain high levels of esterases, which are found in red blood cells and plasma. Thus, drugs containing an ester functionality can potentially be rapidly metabolized by blood esterases.

Traditionally, very specific inhibitors were used to slow down or stop blood esterase activity. Assays for compounds such as chloroprocaine (2) were developed using this approach. Strong acids or bases have also been used to stop enzymatic activity, but the chemical lability of most ester linkages to high or low pH makes this approach undesirable. *In vivo* (1) and *in vitro* (3) studies with esmolol indicate that the compound is rapidly metabolized by blood esterase(s). To obtain reproducible results, blood esterases must be rapidly inactivated after blood sample collection. Dichloromethane was used to denature blood proteins, including esterase(s), and to partition esmolol into the organic layer away from the enzymatic activity.

The rapid decrease in blood levels of esmolol after stopping the infusion observed in the dose-ranging study in humans is consistent with results obtained in dogs (1). This rapid decrease in blood levels and concomitant dissipation of effects would be advantageous in critical-care settings. The high total clearance value of esmolol (220 mL/kg/min) in humans is three times greater than the cardiac output (5 L/min or 70 mL/min/kg in a 70-kg man) and 20 times greater than the hepatic blood flow (4). These results indicate that the primary determinant of the duration of action of esmolol in humans is blood esterases and not esterase activities in the liver and other tissues. The liver may still, however, play a role in the elimination of esmolol, since esterases and other plasma proteins which may bind esmolol are synthesized in the liver.

REFERENCES

(1) J. Zaroslinski, R. J. Borgman, J. P. O'Donnell, W. G. Anderson, P. W. Erhardt, S. T. Kam, R. D. Reynolds, R. J. Lee, and R. J. Gorczynski, *Life Sci.*, **31**, 899 (1982).

(2) J. E. O'Brien, V. Abbey, O. Hinsvark, J. Perel, and M. Finster, *J. Pharm. Sci.*, **68**, 75 (1979).

(3) C. Y. Sum, H. F. Stampfli, C. M. Lai, S. T. Kam, P. E. Erhardt, C. Woo, and A. Yacobi, *Proceedings of the 33rd National Meeting of the Academy of Pharmaceutical Sciences*, **12**, 36 (1982).

(4) A. C. Clayton, "Textbook of Medical Physiology," 4th ed., W. B. Saunders, New York, N.Y., 1971, p. 369.

ACKNOWLEDGMENTS

The authors thank Dr. Doris Hung of the Department of Chemistry, Northwestern University, for operating the GC–MS system and Dr. Paul Erhardt of Berlex Laboratories for synthesis of the deuterated esmolol.

Effect of Folic Acid on the Pharmacokinetics of Acutely Administered Phenytoin in Pregnant and Nonpregnant Rats

RUBY C. CHOU and GERHARD LEVY ˣ

Received June 27, 1983, from the *Department of Pharmaceutics, School of Pharmacy, State University of New York at Buffalo, Amherst, N.Y. 14260.* Accepted for publication August 19, 1983.

Abstract □ The concentrations of both total and free phenytoin in the plasma of epileptic women tend to decrease during pregnancy, suggestive of a pregnancy-associated increase in the metabolic clearance of the drug. On the other hand, the metabolic clearance of free (unbound) phenytoin decreases during pregnancy in rats. One possible reason for this species difference is the routine dietary supplementation of folic acid in human pregnancy and the apparent ability of folic acid to lower phenytoin plasma concentrations even in nonpregnant humans. The purpose of this investigation was to determine the effect of treatment with folic acid on the pharmacokinetics of phenytoin in pregnant and female nonpregnant rats. In one experiment, the treated animals received folic acid in the drinking water, ~100–150 μg/kg/d, for 19 d. There was no apparent difference between the treated and untreated rats in the pharmacokinetics of a 10-mg/kg iv dose of phenytoin (which was administered to the pregnant rats on the 20th day of gestation), regardless of pregnancy status. In another experiment, pregnant and female nonpregnant rats received either folic acid, 400 μg/kg/d, or an equal volume of the solvent only, by gastric intubation for 19 d. The next day (which was the 20th day of gestation for the pregnant rats), the animals received an intravenous injection of phenytoin, 30 mg/kg. Again, pretreatment with folic acid had no apparent effect on the pharmacokinetics of phenytoin in both pregnant and nonpregnant rats. However, the results of this investigation confirm previous observations of dose-dependent phenytoin pharmacokinetics in rats and of decreased clearance of free phenytoin in late pregnancy. It is possible that the qualitative difference between humans and rats with respect to the effect of pregnancy on the pharmacokinetics of phenytoin may be due, at least in part, to a species difference in response to folic acid.

Keyphrases □ Pharmacokinetics—acutely administered phenytoin, folic acid, pregnant and nonpregnant rats □ Phenytoin—acutely administered, effect of folic acid on, pregnant and nonpregnant rats □ Folic acid—effect on acutely administered phenytoin, pregnant and nonpregnant rats

Long term use of phenytoin by epileptic patients is associated with decreased concentrations of folic acid or folate activity in serum, erythrocytes, and cerebrospinal fluid (1–3). Decreased folate activity has also been observed during pregnancy in nonepileptic women who are not taking phenytoin or other drugs (4, 5). Pregnant women taking phenytoin are, therefore, considered to be at particular risk of folate deficiency, and it is customary to give them supplementary folic acid.

Plasma concentrations of total and free phenytoin tend to decrease in women during pregnancy (6). The occurrence of decreased concentrations of free phenytoin suggests that the intrinsic metabolic clearance of the drug is increased in human pregnancy. The opposite is found in rats, *i.e.*, the metabolic clearance of free phenytoin is decreased during pregnancy (7). The reasons for this unusual, qualitative, apparent species difference are unclear (7), particularly since both humans and rats eliminate phenytoin primarily by the same metabolic pathway, *i.e.*, *p*-hydroxylation. One possibility is that it may be related to the dietary supplementation of folate in pregnant women. A number of studies on nonpregnant human subjects have shown that administration of folic acid can cause phenytoin plasma concentrations to decrease (8–11). The question arises, therefore, whether folate administration to rats will alter the pharmacokinetics of phenytoin in these animals, particularly during pregnancy.

EXPERIMENTAL SECTION

Female inbred Lewis rats were used in this investigation. Some of the animals were mated while others were designated as nonpregnant controls. The rats were then housed individually in suspended wire cages to prevent or minimize coprophagy. In one experiment, some of the pregnant and nonpregnant animals had folic acid and sodium bicarbonate, 1 μg/mL each, added to the drinking water while the others received drinking water containing only sodium bicarbonate. After 10 d, the folic acid concentration in the drinking water of pregnant animals was increased to 1.2 μg/mL in case these rats did not increase their water intake in proportion to their increased body weight. The total period of folic acid administration was 19 d; on the 20th day (day 20 of gestation of the pregnant rats) the rats received an intravenous injection of phenytoin, 10 mg/kg. Venous blood samples were collected periodically for determination of plasma phenytoin concentrations by HPLC. A large volume of blood was obtained from the abdominal aorta at the end of the experiment for determination of the plasma free fraction of phenytoin by immediate ultrafiltration at 37°C. The anticoagulant was heparin for the serial blood samples intended for phenytoin assay and EDTA for the large sample intended for plasma ultrafiltration.

In another experiment, some of the pregnant and nonpregnant rats received folic acid, 400 μg/kg as a 200 μg/mL freshly prepared aqueous solution containing 200 μg/mL sodium bicarbonate, daily for 19 d by gastric intuba-

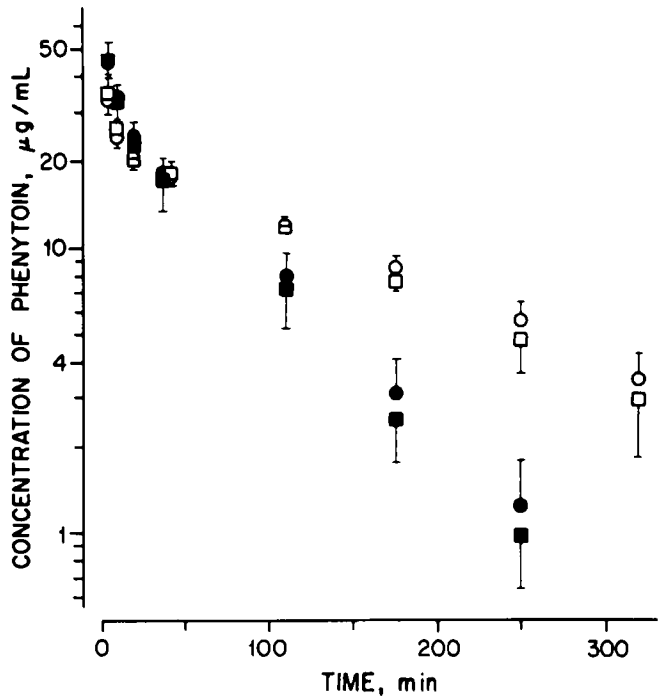

Figure 1—*Effect of pretreatment with folic acid (400 μg/kg/d orally for 19 d) on the pharmacokinetics of a 30-mg/kg iv dose of phenytoin in pregnant (day 20 of gestation) (open symbols) and nonpregnant (solid symbols) rats. Key: (□, ■) folic acid pretreated rats; (○, ●) rats that did not receive supplementary folic acid. Mean of 5 animals per group; vertical bars indicate + or − SD.*

0022-3549/84/0800-1180$01.00/0
© 1984, American Pharmaceutical Association

Table I—Effect of Treatment with Folic Acid on the Pharmacokinetics of a 10 mg/kg Dose of Phenytoin in Pregnant (Day 20 of Gestation) and Female Nonpregnant Inbred Lewis Rats [a]

Variable	Pregnant		Nonpregnant	
	Folic Acid Treated	Untreated	Folic Acid Treated	Untreated
Number of animals	4	3	7	6
Body weight, g	301 ± 31	303 ± 23	246 ± 17	229 ± 24
Hematocrit, %	37.1 ± 2.5	36.5 ± 1.5	44.4 ± 2.0	45.0 ± 2.1
Total plasma clearance, mL/min	4.90 ± 0.48	4.98 ± 0.35	3.85 ± 1.02	4.24 ± 0.63
mL/min/kg	16.3 ± 1.0	16.5 ± 0.9	15.7 ± 4.3	18.5 ± 1.9
Apparent volume of distribution, mL	297 ± 66	309 ± 100	180 ± 25	169 ± 22
mL/kg	979 ± 119	1009 ± 245	733 ± 94	745 ± 116
Plasma free fraction, %	21.7 ± 4.2	20.2 ± 4.5	13.5 ± 1.1	15.3 ± 2.5
Apparent volume of distribution of free drug, mL/kg	4594 ± 711	4987 ± 186	5419 ± 394	4949 ± 1008
Half-life, min	41.9 ± 6.6	42.7 ± 11.6	33.8 ± 6.9	28.1 ± 4.9
Free plasma clearance, mL/min	22.9 ± 2.4	25.3 ± 4.0	28.4 ± 7.0	27.9 ± 4.0
mL/min/kg	77.2 ± 14.9	84.4 ± 18.9	116 ± 29	123 ± 21

[a] Results are reported as mean ±*SD*. The treated animals received approximately 100–150 μg/kg/d of folic acid in drinking water for 19 d before the experiment. There were no statistically significant differences between treated and untreated pregnant or nonpregnant animals.

Table II—Effect of Treatment with Folic Acid on the Pharmacokinetics of a 30 mg/kg Dose of Phenytoin in Pregnant (Day 20 of Gestation) and Female Nonpregnant Inbred Lewis Rats [a]

Variable	Pregnant		Nonpregnant	
	Folic Acid Treated	Untreated	Folic Acid Treated	Untreated
Number of animals	5	5	5	5
Body weight, g	278 ± 11	281 ± 6	226 ± 5	222 ± 10
Hematocrit, %	36.5 ± 1.7	35.6 ± 1.8	44.9 ± 1.8	45.4 ± 1.6
Total plasma clearance, mL/min	2.13 ± 0.20	2.02 ± 0.13	2.79 ± 0.69	2.47 ± 0.37
mL/min/kg	7.64 ± 0.64	7.18 ± 0.54	12.3 ± 2.8	11.1 ± 1.7
Apparent volume of distribution, mL	339 ± 81	356 ± 41	199 ± 41	195 ± 23
mL/kg	1210 ± 257	1268 ± 147	878 ± 163	874 ± 91
Plasma free fraction, %	24.3 ± 3.7	23.9 ± 3.1	15.3 ± 1.8	14.8 ± 1.4
Apparent volume of distribution of free drug, mL/kg	4958 ± 478	5368 ± 898	5769 ± 1126	5898 ± 400
Half-life, min	111 ± 31	123 ± 21	49.7 ± 2.8	55.5 ± 9.5
Free plasma clearance, mL/min	8.96 ± 1.79	8.57 ± 1.43	18.4 ± 4.8	16.7 ± 2.7
mL/min/kg	32.3 ± 6.9	30.5 ± 5.3	81.0 ± 19.3	75.2 ± 11.6

[a] Results are reported as mean ±*SD*. The treated animals received 400 μg/kg/d of folic acid by gavage for 19 d before the experiment. There were no statistically significant differences between treated and untreated pregnant or nonpregnant animals.

tion. The other animals received only the solvent. On the 20th day (day 20 of gestation of the pregnant rats), a single intravenous injection of phenytoin, 30 mg/kg, was administered, and blood samples were collected periodically for assay and a large terminal sample was collected for ultrafiltration. All technical details of the pharmacokinetic study were identical to those already described (7).

RESULTS

The nonpregnant rats consumed 26.8 ± 2.8 (mean ± *SD*) mL/d of folic acid solution (equivalent to 109 ± 15 μg/kg/d of folic acid), 28.0 ± 2.4 mL/d of sodium bicarbonate solution, or 28.3 ± 3.3 mL/d of pure water (the latter determined in rats not used in the pharmacokinetic study). The pregnant rats consumed increasingly larger volumes of water with increasing gestation time: 16.3 ± 3.3, 23.5 ± 3.0, and 36.8 ± 6.3 mL/d on the 4th, 10th, and 15th day of gestation, respectively. These are combined figures for folic acid and sodium bicarbonate solutions since there were no apparent differences between the two. The average dose of folic acid ingested with the drinking water was 151 ± 21 μg/kg/d at the end of gestation.

The results of the pharmacokinetic study with the 10 mg/kg dose of phenytoin are summarized in Table I. There was no statistically significant difference between the folic acid treated and untreated rats in any of the parameters that describe the pharmacokinetics of phenytoin, including the plasma protein binding. This applies to pregnant and to nonpregnant rats, considered separately. A comparison of phenytoin pharmacokinetics in untreated pregnant and nonpregnant rats, with a larger number of animals per group, has been reported (7).

The results of the pharmacokinetic study with a 30 mg/kg dose of phenytoin are summarized in Table II, and the average plasma concentration *versus* time profiles are presented in Fig. 1. As already reported (7), the plasma clearance of the 30 mg/kg dose is considerably lower than that of the 10 mg/kg dose and is significantly decreased in pregnancy; but again, supplementation with folic acid had *no* apparent effect on the pharmacokinetics of phenytoin in either the pregnant or the nonpregnant animals. Nor did folic acid treatment affect body weight, hematocrit, or plasma protein binding of phenytoin.

One out of 10 folic acid treated and 4 out of 12 sodium bicarbonate treated impregnated (spermatozoa-positive vaginal smear) rats were not pregnant on the 20th day after mating, most likely due to resorption of fetuses. The difference between the two groups is not statistically significant by comparison of two success probabilities (12). Only the rats that were actually pregnant were used in the pharmacokinetic studies.

DISCUSSION

Female Sprague–Dawley rats fed a diet containing 1.6-mg folic acid per kg of feed[1] had 52% lower serum folate concentrations on the 21st day of pregnancy than did nonpregnant controls (13). The type of cages used to house these animals was not specified. The rats in the present investigation were fed a diet[2] containing 0.89-mg folic acid per kg of feed[1], and they were housed in suspended wire-mesh cages to minimize coprophagy, by which the animals could obtain folate synthesized by intestinal bacteria (14). It is not practical to put pregnant rats on a folate-deficient diet since this results in a high incidence of fetal resorption (15).

Blake *et al.* (16) have determined the effect of folic acid supplementation (100 μg/kg daily by gavage, from the 7th to the 20th day of gestation) on the *in vitro* activity of hepatic microsomal phenytoin hydroxylase in pregnant Sprague–Dawley rats on a diet containing 1.7 mg folic acid per kg of feed[1]. Enzyme activity per gram of liver increased fourfold relative to that of rats that did not receive folic acid supplementation. The authors concluded that this may explain the decreased plasma phenytoin concentrations observed when patients receive extra folic acid. Contrary to the *in vitro* findings by Blake *et al.* (16), the results of the present *in vivo* investigation indicate that

[1] Information obtained from the manufacturer's product literature.
[2] RMA 1000; Charles River.

folic acid supplementation has no apparent effect on the pharmacokinetics of phenytoin in pregnant as well as in nonpregnant rats. Significantly, neither of these two studies involved prior or chronic administration of phenytoin.

The published clinical data concerning decreased phenytoin plasma concentrations during pregnancy were obtained, necessarily, from patients on a chronic oral regimen of the drug. While it would seem feasible to administer a single intravenous tracer dose of stable isotope labeled phenytoin to these individuals before, during, and after pregnancy, this has apparently not been done. In an acute (single dose) clinical study on nonpregnant individuals, pretreatment with 15- or 30-mg folic acid orally everyday for several weeks had no effect on the biological half-life of phenytoin (17). Plasma concentrations of phenytoin in male Wistar rats 1.5 and 5 h after a single intraperitoneal dose of phenytoin, were similar in animals given a single concomitant oral dose of folic acid, 5 mg/kg, and in controls (18).

One possibility not explored in the present investigation is that folic acid supplementation affects the *in vivo* clearance of phenytoin only in rats that have been treated chronically with phenytoin. If that possibility can be excluded, then the qualitative species difference between humans and rats, with respect to the effect of pregnancy on the pharmacokinetics of phenytoin, may be due, at least in part, to the difference in response to folate. If, however, increased dietary folic acid causes an increase in the metabolic clearance of phenytoin in both humans and rats on chronic phenytoin therapy, then the apparent species difference in the effect of pregnancy on phenytoin pharmacokinetics may be related to the common practice of supplementing the diet of pregnant women, but not of pregnant rats, with folate.

REFERENCES

(1) J. Preece, E. H. Reynolds, and A. L. Johnson, *Epilepsia*, **12**, 335 (1971).

(2) D. Labadarios, J. W. T. Dickerson, D. V. Parke, E. G. Lucas, and G. H. Obuwa, *Br. J. Clin. Pharmacol.*, **5**, 167 (1978).

(3) E. H. Reynolds, R. H. Mattson, and B. B. Gallagher, *Neurology*, **22**, 841 (1972).

(4) D. Rothman, *Am. J. Obstet. Gynecol.*, **108**, 149 (1970).

(5) B. A. Cooper, *Clin. Haematol.*, **2**, 461 (1973).

(6) S.-S. Chen, E. Perucca, J.-N. Lee, and A. Richens, *Br. J. Clin. Pharmacol.*, **13**, 547 (1982).

(7) R. C. Chou and G. Levy, *J. Pharmacol. Exp. Ther.*, **229**, 351 (1984).

(8) M. Furlanut, P. Benetello, A. Avogaro, and R. Dainese, *Clin. Pharmacol. Ther.*, **24**, 294 (1978).

(9) K. A. Makki, E. Perucca, and A. Richens, *Br. J. Clin. Pharmacol.*, **9**, 304P (1980).

(10) E. M. Baylis, J. M. Crowley, J. M. Preece, P. E. Sylvester, and V. Marks, *Lancet*, **1**, 62 (1971).

(11) R. H. Mattson, B. B. Gallagher, E. H. Reynolds, and D. Glass, *Arch. Neurol.*, **29**, 78 (1973).

(12) B. W. Brown, Jr. and M. Hollander, "Statistics, A Biomedical Introduction," Wiley, New York, N.Y., 1977, pp. 173–193.

(13) G. R. DeVore and D. M. Woodbury, *Epilepsia*, **18**, 387 (1977).

(14) R. Beaulieu, J. Bachevalier, and P. Sekaly, "Folic Acid in Neurology, Psychiatry and Internal Medicine," M. I. Botez and E. H. Reynolds, Eds., Raven, New York, N.Y., 1979, pp. 89–94.

(15) D. C. Hill, "Folic Acid in Neurology, Psychiatry and Internal Medicine," M. I. Botez and E. H. Reynolds, Eds., Raven, New York, N.Y., 1979, pp. 229–235.

(16) D. A. Blake, J. M. Collins, B. C. Miyasaki, and F. Cohen, *Drug Metab. Dispos.*, **6**, 246 (1978).

(17) P. Buch Andreasen, J. Mølholm Hansen, L. Skovsted, and K. Siersbaek-Nielsen, *Acta Neurol Scand.*, **47**, 117 (1971).

(18) H. van Rees, G. A. H. Telkers-Duijts, and E. L. Noach, *Arch. Int. Pharmacodyn. Ther.*, **261**, 16 (1983).

ACKNOWLEDGMENTS

Supported in part by grant GM 20852 from the National Institute of General Medical Sciences, National Institutes of Health.

NOTE ADDED IN PROOF

Subsequent to the submission of this manuscript, Carl and Smith (19) reported that oral folate supplementation (20 mg/kg/d for 6 d, then every 12 h for 4 d) had no apparent effect on phenytoin concentrations in the liver, brain, and plasma of male Sprague-Dawley rats who received oral phenytoin (100 mg/kg/d) for 6 d, then every 12 h for 4 d) concomitantly. In a prospective study of epileptic women during pregnancy, Hiilesmaa *et al.* (20) found a negative correlation between folate and phenytoin concentrations in serum ($r = -0.56$, $p = 0.002$, $n = 39$) but no association between serum folate concentrations and the number of seizures during pregnancy.

(19) G. F. Carl and D. B. Smith, *Epilepsia*, **24**, 494 (1983).

(20) V. K. Hiilesmaa, K. Teramo, M.-L. Granström, and A. H. Bardy, *Brit. Med. J.*, **287**, 577 (1983).

Synthesis of Methyl 2,3-*Bis*(hydroxymethyl)-5-phenyl-7-oxabicyclo[2.2.1]hepta-2,5-diene-6-carboxylate *Bis*(*N*-methylcarbamate) Derivatives as Potential Antitumor Agents

WAYNE K. ANDERSON ˣ and BIPI MULUMBA

Received August 2, 1982, from the *Department of Medicinal Chemistry, School of Pharmacy, State University of New York at Buffalo, Buffalo, NY 14260.* Accepted for publication July 29, 1983.

Abstract □ Methyl 2,3-*bis*(hydroxymethyl)-5-phenyl-7-oxabicyclo[2.2.1]-hepta-2,5-diene-6-carboxylate *bis*(*N*-methylcarbamate) along with the *p*-chlorophenyl and *p*-nitrophenyl analogues were synthesized using a Diels Alder reaction. The title compound and the *p*-chlorophenyl analogue were inactive against murine P388 lymphocytic leukemia.

Keyphrases □ *Bis*-carbamates—synthesis, antitumor activity □ 7-Oxabicyclo[2.2.1]hepta-2,5-diene derivatives—synthesis, antitumor activity

The discovery that certain derivatives of 7-oxabicyclo[2.2.1]heptane (1) showed cytotoxic activity in the 9KB tissue culture assay led to the synthesis and evaluation of related compounds. Dimethyl 2,3-*bis*(acetoxymethyl)-7-oxa-

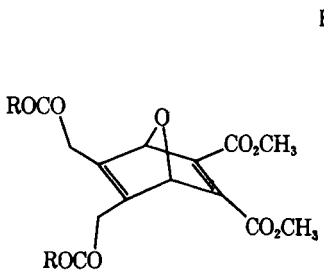

IA: R=CH_3,
IB: R=NH-*N*-C_4H_9,

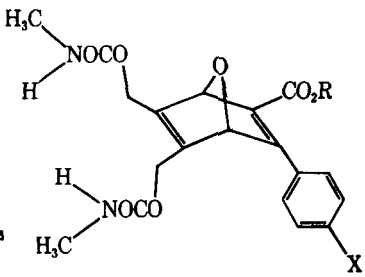

IIA: X=H; R=C_2H_5,
IIB: X=Cl; R=CH_3,
IIC: X=NO_2; R=CH_3,

0022-3549/84/0800-1182$01.00/0

© 1984, American Pharmaceutical Association

folic acid supplementation has no apparent effect on the pharmacokinetics of phenytoin in pregnant as well as in nonpregnant rats. Significantly, neither of these two studies involved prior or chronic administration of phenytoin.

The published clinical data concerning decreased phenytoin plasma concentrations during pregnancy were obtained, necessarily, from patients on a chronic oral regimen of the drug. While it would seem feasible to administer a single intravenous tracer dose of stable isotope labeled phenytoin to these individuals before, during, and after pregnancy, this has apparently not been done. In an acute (single dose) clinical study on nonpregnant individuals, pretreatment with 15- or 30-mg folic acid orally everyday for several weeks had no effect on the biological half-life of phenytoin (17). Plasma concentrations of phenytoin in male Wistar rats 1.5 and 5 h after a single intraperitoneal dose of phenytoin, were similar in animals given a single concomitant oral dose of folic acid, 5 mg/kg, and in controls (18).

One possibility not explored in the present investigation is that folic acid supplementation affects the *in vivo* clearance of phenytoin only in rats that have been treated chronically with phenytoin. If that possibility can be excluded, then the qualitative species difference between humans and rats, with respect to the effect of pregnancy on the pharmacokinetics of phenytoin, may be due, at least in part, to the difference in response to folate. If, however, increased dietary folic acid causes an increase in the metabolic clearance of phenytoin in both humans and rats on chronic phenytoin therapy, then the apparent species difference in the effect of pregnancy on phenytoin pharmacokinetics may be related to the common practice of supplementing the diet of pregnant women, but not of pregnant rats, with folate.

REFERENCES

(1) J. Preece, E. H. Reynolds, and A. L. Johnson, *Epilepsia*, **12**, 335 (1971).

(2) D. Labadarios, J. W. T. Dickerson, D. V. Parke, E. G. Lucas, and G. H. Obuwa, *Br. J. Clin. Pharmacol.*, **5**, 167 (1978).

(3) E. H. Reynolds, R. H. Mattson, and B. B. Gallagher, *Neurology*, **22**, 841 (1972).

(4) D. Rothman, *Am. J. Obstet. Gynecol.*, **108**, 149 (1970).

(5) B. A. Cooper, *Clin. Haematol.*, **2**, 461 (1973).

(6) S.-S. Chen, E. Perucca, J.-N. Lee, and A. Richens, *Br. J. Clin. Pharmacol.*, **13**, 547 (1982).

(7) R. C. Chou and G. Levy, *J. Pharmacol. Exp. Ther.*, **229**, 351 (1984).

(8) M. Furlanut, P. Benetello, A. Avogaro, and R. Dainese, *Clin. Pharmacol. Ther.*, **24**, 294 (1978).

(9) K. A. Makki, E. Perucca, and A. Richens, *Br. J. Clin. Pharmacol.*, **9**, 304P (1980).

(10) E. M. Baylis, J. M. Crowley, J. M. Preece, P. E. Sylvester, and V. Marks, *Lancet*, **1**, 62 (1971).

(11) R. H. Mattson, B. B. Gallagher, E. H. Reynolds, and D. Glass, *Arch. Neurol.*, **29**, 78 (1973).

(12) B. W. Brown, Jr. and M. Hollander, "Statistics, A Biomedical Introduction," Wiley, New York, N.Y., 1977, pp. 173–193.

(13) G. R. DeVore and D. M. Woodbury, *Epilepsia*, **18**, 387 (1977).

(14) R. Beaulieu, J. Bachevalier, and P. Sekaly, "Folic Acid in Neurology, Psychiatry and Internal Medicine," M. I. Botez and E. H. Reynolds, Eds., Raven, New York, N.Y., 1979, pp. 89–94.

(15) D. C. Hill, "Folic Acid in Neurology, Psychiatry and Internal Medicine," M. I. Botez and E. H. Reynolds, Eds., Raven, New York, N.Y., 1979, pp. 229–235.

(16) D. A. Blake, J. M. Collins, B. C. Miyasaki, and F. Cohen, *Drug Metab. Dispos.*, **6**, 246 (1978).

(17) P. Buch Andreasen, J. Mølholm Hansen, L. Skovsted, and K. Siersbaek-Nielsen, *Acta Neurol Scand.*, **47**, 117 (1971).

(18) H. van Rees, G. A. H. Telkers-Duijts, and E. L. Noach, *Arch. Int. Pharmacodyn. Ther.*, **261**, 16 (1983).

ACKNOWLEDGMENTS

Supported in part by grant GM 20852 from the National Institute of General Medical Sciences, National Institutes of Health.

NOTE ADDED IN PROOF

Subsequent to the submission of this manuscript, Carl and Smith (19) reported that oral folate supplementation (20 mg/kg/d for 6 d, then every 12 h for 4 d) had no apparent effect on phenytoin concentrations in the liver, brain, and plasma of male Sprague-Dawley rats who received oral phenytoin (100 mg/kg/d) for 6 d, then every 12 h for 4 d) concomitantly. In a prospective study of epileptic women during pregnancy, Hiilesmaa *et al.* (20) found a negative correlation between folate and phenytoin concentrations in serum ($r = -0.56$, $p = 0.002$, $n = 39$) but no association between serum folate concentrations and the number of seizures during pregnancy.

(19) G. F. Carl and D. B. Smith, *Epilepsia*, **24**, 494 (1983).

(20) V. K. Hiilesmaa, K. Teramo, M.-L. Granström, and A. H. Bardy, *Brit. Med. J.*, **287**, 577 (1983).

Synthesis of Methyl 2,3-*Bis*(hydroxymethyl)-5-phenyl-7-oxabicyclo[2.2.1]hepta-2,5-diene-6-carboxylate *Bis*(*N*-methylcarbamate) Derivatives as Potential Antitumor Agents

WAYNE K. ANDERSON ˣ and BIPI MULUMBA

Received August 2, 1982, from the *Department of Medicinal Chemistry, School of Pharmacy, State University of New York at Buffalo, Buffalo, NY 14260.* Accepted for publication July 29, 1983.

Abstract □ Methyl 2,3-*bis*(hydroxymethyl)-5-phenyl-7-oxabicyclo[2.2.1]-hepta-2,5-diene-6-carboxylate *bis*(*N*-methylcarbamate) along with the *p*-chlorophenyl and *p*-nitrophenyl analogues were synthesized using a Diels Alder reaction. The title compound and the *p*-chlorophenyl analogue were inactive against murine P388 lymphocytic leukemia.

Keyphrases □ *Bis*-carbamates—synthesis, antitumor activity □ 7-Oxabicyclo[2.2.1]hepta-2,5-diene derivatives—synthesis, antitumor activity

The discovery that certain derivatives of 7-oxabicyclo[2.2.1]heptane (1) showed cytotoxic activity in the 9KB tissue culture assay led to the synthesis and evaluation of related compounds. Dimethyl 2,3-*bis*(acetoxymethyl)-7-oxa-

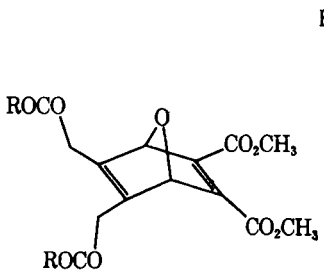

IA: R=CH_3,
IB: R=NH-*N*-C_4H_9,

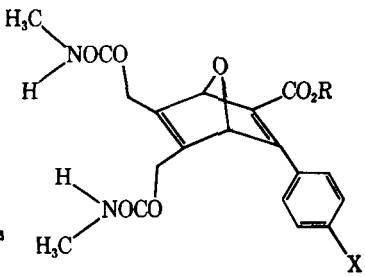

IIA: X=H; R=C_2H_5,
IIB: X=Cl; R=CH_3,
IIC: X=NO_2; R=CH_3,

0022-3549/84/0800-1182$01.00/0

© 1984, American Pharmaceutical Association

bicyclo[2.2.1]hepta-2,5-diene-5,6-dicarboxylate (Ia) exhibited potent activity against L1210 leukemia in tissue culture assays, but failed to show any *in vivo* activity (2). The *bis*-carbamate (Ib) showed marginal activity against P388 lymphocytic leukemia *in vivo*, but this result was difficult to reproduce. This report describes an attempt to prepare derivatives of 2,3-*bis*(hydroxymethyl)-7-oxabicyclo[2.2.1]hepta-2,5-diene which show significant reproducible antineoplastic activity *in vivo*.

EXPERIMENTAL SECTION[1]

Ethyl 2,3-*bis*(hydroxymethyl)-5-phenyl-7-oxabicyclo[2.2.1]hepta-2,5-diene-6-carboxylate *bis*(*N*-methylcarbamate) (IIa) and its *p*-chloro (IIb) and *p*-nitro (IIc) analogues were prepared as follows. A mixture of 3,4-*bis*-(trimethylsilyloxymethyl)furan (2) (0.0147 mol), ethyl phenylpropiolate (0.0206 mol), and toluene (20 mL) was heated under reflux for 40 h. (Note, methyl *p*-methoxyphenylpropiolate failed to react under these conditions.) The mixture was concentrated under reduced pressure and the residue was treated with ethanol–water (1:1, 80 mL) at 60°C for 30 min. The hot mixture was filtered to remove the insoluble phenylpropiolate ester, and the filtrate was concentrated under reduced pressure. The residue was dried under high vacuum (P_2O_5) to give the unstable diol in 90–95% yield.

A solution of the diol (0.0059 mol) and triethylamine (0.2 mL) in dichloromethane (10 mL) was treated with methylisocyanate (2 mL), and the mixture was heated at reflux for 36 h. The reaction mixture was concentrated to dryness under reduced pressure and the residue was crystallized from ethyl acetate–isopropyl ether to give IIa in 60% yield, mp 140–143°C. IR: 3350, 2950, 1700, 1550, 1250, 1150, 1000, and 850 cm^{-1}; ^{1}H-NMR: δ 1.30 (t, 3, J = 8 Hz), 2.60 (d, 3, J = 6 Hz), 2.80 (d, 3, J = 6 Hz), 4.40 (q, 2, J = 8 Hz), 4.90 (s, 4), 5.70 (s, 2), and 7.20–7.80 ppm (m, 5).

Anal.—Calc. for $C_{20}H_{23}N_2O_7$: C, 60.56; H, 5.80; N, 6.72. Found: C, 60.45; H, 5.88; N, 6.69.

The chloro and nitro derivatives (IIb and IIc), as ethyl esters, were prepared in the same manner. Compound IIb, obtained in 72% yield, had mp 176–178°C (ethyl acetate–isopropyl ether). IR: 3350, 2950, 1700, 1540, and 1260 cm^{-1}; ^{1}H-NMR: δ 2.60 (d, 3, J = 6 Hz), 2.80 (d, 3, J = 6 Hz), 3.75 (s, 3), 4.85 (s, 4), 5.65 (s, 2), and 7.2–7.8 ppm (m, 4).

Anal.—Calc. for $C_{20}H_{22}ClN_2O_7$: C, 54.98; H, 4.84; N, 6.41; Cl, 8.11. Found: C, 54.92; H, 4.91; N, 6.35; Cl, 8.14.

Compound IIc (68%) had mp 172–176°C (ethyl acetate–isopropyl ether). IR: 3550, 2950, 1700, 1550, 1250, 975, and 850 cm^{-1}; ^{1}H-NMR: δ 2.60 (d, 3, J = 6 Hz), 2.80 (d, 3, J = 6 Hz), 3.75 (s, 3), 4.85 (s, 4), 5.65 (s, 2), and 7.2–7.8 ppm (m, 4).

Anal.—Calc. for $C_{20}H_{22}N_3O_9$: C, 53.69; H, 4.73; N, 9.39. Found: C, 53.74; H, 4.76; N, 9.34.

RESULTS AND DISCUSSION

The rationale for the design of I was based on two factors. These were, first, the electrophilicity of the allylic esters, which can react by an alkyl–oxygen cleavage mechanism (3, 4) and, second, the neighboring group participation

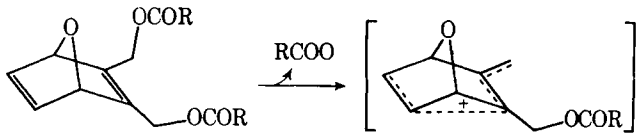

Scheme I

of C=C π-bonds in nucleophilic substitution reactions. These two factors are summarized in Scheme I.

The 5,6-double bond in I is substituted with two electron-withdrawing groups [for $-CO_2CH_3$ the Swain–Lupton resonance (R) and field (F) contributions are 0.552 and 0.140, respectively]. Compounds of the general structure II were designed to have a 5,6-double bond which was less electron-deficient than I (the phenyl substituent has F = 0.139 and R = −0.088). Thus, compounds of the general structure II should be more reactive than I.

These *bis*-carbamates were prepared in a reaction sequence which began with a Diels Alder reaction between 3,4-*bis*(trimethylsilyloxymethyl)furan (2) and the appropriate phenylpropiolic acid derivative. The trimethylsilyl-protected diol was used because it could be removed from the reaction mixture by distillation at a sufficiently low temperature to avoid decomposition of the product. The phenylpropiolic acid derivatives were prepared from the appropriate cinnamic acid by a bromination–dehydrobromination sequence (5–9).

The silyl blocking groups were removed from the Diels Alder adducts (ethanol–water), and the diols were converted to the *bis*-carbamates by treatment with methylisocyanate in the presence of triethylamine. The intermediate diols were unstable and attempts to purify these compounds led to extensive decomposition; thus, the diols were used directly in the next step.

Two of the compounds, selected as "lead" structures, were tested against P388 lymphocytic leukemia in mice under the auspices of the National Cancer Institute (10). The *p*-chloro compound (IIb) was inactive over the dose range of 1.56–200 mg/kg, and IIa was inactive over the dose range of 12.5–400 mg/kg. Compound IIa was toxic at the 400-mg/kg dose; three of the six test animals died before the fifth day of the test (the animals were given once daily intraperitoneal injections). Only one of six animals died before day 5 at the 200-mg/kg level with both IIa and IIb; however, IIb appeared to be more toxic as judged by the weight losses of the treated animals.

The reactivity of II was greater than I, as evidenced by the greater instability of II. Nevertheless, the reactivity is still not sufficient to confer *in vivo* antitumor activity to *bis*-carbamate derivatives in the oxabicyclic series.

REFERENCES

(1) W. K. Anderson and R. H. Dewey, *J. Med. Chem.*, **20**, 306 (1977).

(2) W. K. Anderson, R. H. Dewey, and B. Mulumba, *J. Med. Chem.*, **22**, 1270 (1979).

(3) W. K. Anderson and P. F. Corey, *J. Med. Chem.*, **20**, 812 (1977).

(4) W. K. Anderson, *Cancer Res.*, **42**, 2168 (1982).

(5) M. S. Newman and S. H. Merill, *J. Am. Chem. Soc.*, **77**, 5549 (1955).

(6) F. G. Baddar, *J. Chem. Soc.*, **1955**, 461.

(7) G. Rychler, *Bull. Soc. Chim. Fr.*, **17**, 512 (1897).

(8) F. G. Baddar and El Assal, *J. Chem. Soc.* **1948**, 1267.

(9) J. Banghiat and E. I. Becker, *J. Org. Chem.*, **23**, 885 (1958).

(10) R. I. Geran, N. H. Greenberg, M. M. McDonald, A. M. Schumacher, and B. J. Abbott, *Cancer Chemother. Rep., Part 3*, **3**(2), 1 (1972).

[1] Melting points (uncorrected) were determined in open capillary tubes with a Thomas-Hoover Unimelt apparatus. IR spectra were determined for KBr wafers with a Perkin-Elmer 727 spectrophotometer. ^{1}H-NMR spectra were determined for deuterochloroform solutions containing ~1% (v/v) tetramethylsilane as the internal standard with a Varian T-60A spectrometer. Microanalyses were performed by Atlantic Microlabs, Inc., Atlanta, Ga.

Colorimetric Determination of Procainamide in Injectable Preparations

J. E. WHITAKER * and A. M. HOYT, JR. ‡x

Received October 13, 1981, from the *University of Oregon, Eugene, OR 97403 and the ‡Department of Chemistry, University of Central Arkansas, Conway, AR 72032. Accepted for publication August 30, 1983.

Abstract □ A simple, rapid colorimetric method is described which determines procainamide in commercially available, injectable solutions. It is based on complexing the drug with cupric ion and then measuring the absorption at 380 nm. The reaction is fast and the metal–drug ratio in the complex is 1:1. The pH optimum for maximum reaction is 4.0–4.5 which is maintained by an acetate buffer. Linear standard curves were obtained from 1.52 to 6.06 mg/mL. Analysis of 29 commercial samples resulted in an average of 97.3% of the label claim.

Keyphrases □ Procainamide—colorimetric determination, injectable preparations, cupric ion complexing □ Colorimetry—procainamide, injectable preparations, cupric ion complexing

Procainamide (I) is an antiarrhythmic agent used to treat cardiac disorders. Dosages and plasma concentrations as well as half-life and ultimate fate have been the subject of previous studies (1, 2). All of these studies require an analytical method for the analysis of I, and there exists an obvious need for such a method in manufacturing and quality control.

A large volume of literature exists on the determination of I in pharmaceutical and biological systems. One of the most favored techniques is HPLC (3–5), although gas chromatography (6), TLC (7), spectrophotofluorometry (8, 9), and even polarography (10) have been used. Some of the claimed advantages in specificity are not realized (11), and some of the methods are quite tedious and time-consuming.

Spectrophotometric procedures which involve diazotization and coupling reactions have been reported (12, 13). A colorimetric procedure for I that requires less manipulation and fewer reactions would be useful and more convenient. The text describes such a colorimetric method for I based on the formation of a complex between procainamide and cupric ion. This colorimetric method for the drug is shown to have sufficient sensitivity and adequate specificity, especially for relatively pure samples. The suitability of this colored complex for analytical purposes, and the application of this colorimetric method are also described.

EXPERIMENTAL SECTION

Materials—Procainamide hydrochloride[1] (II), *N*-acetylprocainamide[1], procaine hydrochloride[1], sulfuric and acetic acids[2] (reagent grade), sodium hydroxide[2] (50% solution), iron(III) nitrate[2], cobalt(II) chloride[2], and sodium acetate[2] (ACS grade), and chlorides[2] of copper(II), nickel(II), and chromium(III) were obtained commercially. The injectable vials[3] were obtained through local retail outlets.

Preliminary work was done on a recording UV-visible light instrument[4], but later analytical work was carried out using a single-beam spectrophotometer[5]. pH measurements were made on an instrument[6] which was standardized daily with commercially prepared biphthalate buffers.

Complex Formation—Screening of various metal ions for potential use was carried out by adding a few drops of ~2M solutions of the various metal ions (cobalt(II), nickel(II), chromium(III), copper(II) chlorides, and iron(III) nitrate) to ~1 mL of a 10-mg/mL solution of II in a spot plate. The only visible color change occurred with cupric ion; a green color became apparent on addition of the metal.

Spectra of solutions of II were obtained from 330–550 nm both in the presence and absence of the cupric ion, as shown in Fig. 1. Using the absorption generated at 380 nm, the formula of the complex was obtained by the continuous variations method (14). The absorption at 380 nm was maximized at $X_{Cu} = 0.5$, where X_{Cu} is the mole fraction of cupric ion.

pH Dependence of the Complex—The optimum pH for the complex was established by mixing 0.10 M solutions of II and cupric chloride, adjusting to a measured pH of 1.5 with concentrated sulfuric acid, and then gradually neutralizing the solution with dropwise addition of 10% NaOH, after measurement of absorbance at 380 nm. A plot of absorbance *versus* pH (Fig. 2) shows a maximum at pH 4. Increasing the pH >4.3–4.6 causes a white to light blue precipitate to form; therefore, a pH of 4.0 was selected for further studies.

Linearity Studies—A pH 4.0 acetate buffer (prepared by addition of sodium acetate to a 1 M solution of acetic acid) was used as the solvent for these studies. A series of solutions of the complex in acetate buffer were prepared; the solutions each contained a constant, excess level (10.5 mg/mL) of the cupric ion, and varying (1.52, 3.04, 4.55, and 6.06 mg/mL) amounts of II. This series of solutions was prepared by mixing three solutions in various ratios: 37.87 mg/mL II, 131.1 mg/mL cupric ion, and the buffer. Measurements of the absorbances of these solutions and their respective concentrations are shown in Table I.

Analysis of Injectable Solutions—A series of standards of II were prepared that are similar to those in the linearity studies; the absorbances were measured and a least-square line prepared from the data. Concurrently, 100 mg/mL commercial samples were analyzed by withdrawing 1 mL of the liquid, mixing with 4 mL of the 131.1 mg/mL cupric ion solution, and diluting to 50 mL with pH 4 acetate buffer. The absorbances of these solutions were also determined at 380 nm, and their concentrations calculated from the slope and intercept of the least-square line described above. As shown in Table II, recoveries varied from a low of 88.4% to a high of 107.9% based on label claims.

RESULTS AND DISCUSSION

Cupric ion complexed instantly with the procainamide molecule, the 1:1 coordination resulting in a visible absorption with a maximum at 380 nm. The complex formed most completely at a pH value of 4.0–4.5; a precipitate formed near the upper pH limit. Attempts to form the complex at pH 5.0 gave a dark blue precipitate which dissolved on long standing. The curve shape shown in Fig. 2 was reproduced by later experiments in which II in water (pH 4.5) was acidified, as opposed to the acid to neutral direction reported in the *Experi-*

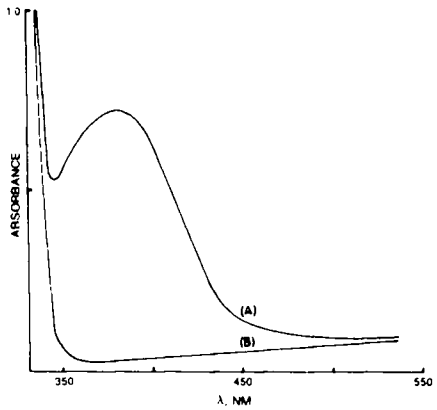

Figure 1—*Visible spectrum of II in presence (A) and absence (B) of the cupric ion.*

[1] ICN K & K Labs, Plainview, N.Y.
[2] Fisher Scientific Co., Fair Lawn, N.J.
[3] Pronestyl; E. R. Squibb & Sons, Inc., Princeton, N.J.
[4] Model 618-900; Perkin-Elmer Corp., Norwalk, Conn.
[5] Spectronic 70; Bausch & Lomb, Rochester, N.Y.
[6] Model 7; Corning Glass Works, Corning, N.Y.

0022-3549/84/0800-1184$01.00/0
© 1984, American Pharmaceutical Association

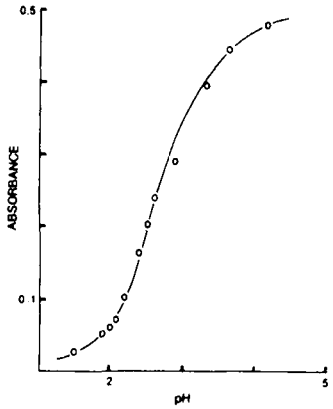

Figure 2—*380 nm Absorption of the cupric ion–procainamide complex as a function of pH.*

mental Section. The anion present with copper did not affect complex formation and the sulfate salt was used routinely in later work.

An acetate buffer, pH 4.0, was found to be an excellent medium for analytical work; however, unbuffered solutions, as well as those buffered with biphthalate, were also tried and found to give linearly increasing absorbance at 380 nm with increasing levels of II. Biphthalate, however, repressed complex formation (as evidenced by the lower-than-expected absorbances), probably by competing with II for the cupric ion. Repetition of the above experiment showed that the concentration of acetate buffer was not critical; however, for reproducible results, the pH must be kept constant. This is most easily accomplished by preparing and using large quantities of buffer. It was also discovered, in later experiments, that the amount of excess copper was not critical; but, a minimum of two-threefold excess was used throughout. This observation indicates that the equilibrium constant for formation is very favorable and, thus, well-suited for an analytical technique.

The reported experiment on the analyses of injectable vials was carried out on four different days; each repetition gave a linear standard curve, and recoveries of the samples (all were guaranteed 100 mg/mL) varied from a low of 88.4% to a high of 107.9% on the results from 29 different samples. Between sets of samples there was a slight day-to-day variation in recovery; within a set the results were remarkably consistent (the highest *SD* within a set was 2.6%, the lowest was 0.5%, based on recovery figures). The variation between sets can be attributed to slight pH differences in different batches of buffer, therefore, it is suggested that large amounts of buffer be made to promote uniformity.

To address the question of the specificity of this procedure, a spot plate test of procaine hydrochloride and *N*-acetylprocainamide showed that the color is not unique to procainamide. Procaine gave the color, the *N*-acetylprocainamide did not. Procaine is the most chemically similar drug available, so the presence of color, not altogether surprising, was the most stringent test possible. *N*-Acetylprocainamide was selected because it is chemically similar to I, and, in addition, is the major metabolite in humans (15). The involvement of nitrogen atoms in coordination with copper is also suggested by the lack of color with the *N*-acetyl compound. The lack of absolute specificity was not viewed as a serious drawback, since use in laboratory was limited to the injectable sample only.

Table I—380 nm Absorbance Values of Varying Concentrations of the Copper–Procainamide Complex

Conc. of Procainamide, mg/mL	Absorbance
0	0.063
1.52	0.388
3.04	0.705
4.55	1.01
6.06	1.28

Table II—Concentrations of Pronestyl Injectables Calculated from Absorbance Data

Sample Number	Conc., mg/mL	Sample Number	Conc., mg/mL
1	102	16	89.5
2	91.2	17	96.8
3	89.0	18	93.6
4	89.2	19	99.6
5	89.7	20	96.0
6	90.7	21	88.4
7	89.0	22	88.5
8	99.3	23	104.4
9	100.5	24	107.1
10	101.4	25	104.6
11	107.5	26	106.8
12	102.6	27	107.9
13	92.5	28	106.5
14	100.9	29	105.7
15	88.8		

REFERENCES

(1) C. L. Winek, *Clin. Chem.*, **22,** 832 (1976).

(2) B. L. Kamath, C. Lai, S. D. Gupta, M. J. Durrani, and A. Yacobi, *J. Pharm. Sci.*, **70,** 299 (1981).

(3) P. M. Kabra, S. Chen, and L. J. Marton, *Ther. Drug Monit.*, **3,** 91 (1981).

(4) K. Carr, R. L. Woosley, and J. A. Oates, *J. Chromatogr.*, **129,** 363 (1976).

(5) R. M. Rocco, D. C. Abbott, R. W. Giese, and B. L. Karger, *Clin. Chem.*, **23,** 705 (1977).

(6) K. J. Simons and R. H. Levy, *J. Pharm. Sci.*, **64,** 1967 (1975).

(7) B. Wesley-Hadzija and A. M. Matlocks, *J. Chromatogr.*, **143,** 307 (1977).

(8) J. M. Sterling and W. G. Haney, *J. Pharm. Sci.*, **63,** 1448 (1974).

(9) H. Tan, S. S. McEnany, and A. C. Glasser, *Microchem. J.*, **24,** 395 (1979).

(10) L. A. Kiseleva and Y. E. Orlov, *Farmatsiya (Moscow)*, **26,** 38 (1977).

(11) A. Marion, L. J. Lesko, and C. Oliver, *Ther. Drug Monit.*, **3,** 107 (1981).

(12) J. C. Hamm, *J. Assoc. Off. Anal. Chem.*, **95,** 807 (1976).

(13) J. Koch-Weser and S. W. Klein, *J. Am. Med. Assoc.*, **215,** 1454 (1971).

(14) C. T. Kenner and K. W. Busch, "Quantitative Analysis," MacMillan, New York, N.Y., 1979, p. 325.

(15) J. Dreyfuss, J. J. Ross, and E. C. Schreiber, *Arzneim.-Forsch.*, **21,** 948 (1971).

Decrease in the Rate of Capsule Dissolution Due to Formaldehyde from Polysorbate 80 Autoxidation

Keyphrases □ Dissolution, capsule—rate decrease, formation of formaldehyde, polysorbate 80 autoxidation □ Polysorbate 80—autoxidation, formation of formaldehyde, decreased dissolution rate, capsules

To the Editor:

Dissolution studies on some stability samples of gemfibrozil capsules showed a significant decrease in dissolution rate with time of storage and exposure to humidity. Observations of these slowly dissolving samples during the tests showed that the capsule contents were held together by a thin, tough, water-insoluble film, the disruption of which was seen to be the dissolution rate-limiting factor for the drug product. A bioavailability study of such film-forming gemfibrozil capsules showed them to be bioequivalent to the readily dissolving product. Thus, the decrease in dissolution rate in the *in vitro* test is an anomaly because it does not correlate with *in vivo* results. This communication describes studies which established that film formation is due to denaturation of the inner surface of the capsule by formaldehyde, formed by trace autoxidation of the polysorbate 80 used as an excipient.

Polysorbate 80 had been useful in our laboratories as a wetting agent in capsule formulations of hydrophobic drugs. It was convenient to prepare a 1:2 dispersion by drying an alcohol solution of polysorbate 80 mixed with colloidal silica. The silica aided in powder flow, facilitating high-speed encapsulation. This dispersion was used in several capsule formulations of investigational drugs, all of which exhibited film formation when stored under high-humidity conditions. Studies on experimental capsule formulations (Table I) made with constituents of the gemfibrozil capsule formula and stored at 37°C, 37°C with 80% relative humidity (RH), and 45°C and tested after 1, 2, and 3 months showed that film formation occurred only when polysorbate 80 was present. All of the capsules containing polysorbate 80 showed film formation during testing after 1 month at 37°C with 80% RH.

The reaction of formaldehyde and other aldehydes with proteins is well known (1, 2). Cross-linking of the amino groups in gelatin results in its denaturation to an insoluble protein (3). Since formaldehyde could result from autoxidation of the end groups in polysorbate 80 and acetaldehyde could be produced by oxidation of alcohol used in preparation of polysorbate 80–silica dispersion, the hypothesis that one or both of these aldehydes was responsible for film formation was tested. Formation of aldehydes would be facilitated by the immense surface area of the silica, so the results in Table I are consistent with the hypothesis.

Table I—Experimental Capsule Formulations [a]

Ingredients, mg	Formulation a	b[b]	c	d[c]	e[d]	f[d]	g[e]	h[d]
Gemfibrozil	171	171	171	171	171	171	—	—
Polysorbate 80 on Silica	5	10	—	—	—	—	150	—
Cornstarch NF	99	94	102	100	97	104	—	—
Polysorbate 80 NF	—	—	2	4	—	—	—	—
Silica Gel NF	—	—	—	—	7	—	—	90
Fill weight, mg	275	275	275	275	275	275	150	90

[a] No. 2 snap-fit white opaque 999 capsules, Lot 162 (Capsugel), were used for all formulations. [b] Questionable film formation at 3 months at 45°C. [c] Film formation 3 months at 37°C. [d] No film formation. [e] Film formation 1 month at 37°C.

Table II—Assay of Formaldehyde in Polysorbate 80 on Silica

Lot	Formaldehyde, μg/g of Sample Taken HPLC	Fluorometric	Colorimetric
1	20	163	260
2	13	55	170
3	13	—	75
4	18	—	100
5	27	111	200
6	36	163	110

Six lots of polysorbate 80–silica dispersion were analyzed for formaldehyde by three methods. The HPLC method (4) is based on the reaction of aldehydes with 2-diphenylacetyl-1,3-indanedione-1-hydrazone and afforded a separation of formaldehyde and acetaldehyde derivatives. The fluorometric method (5), based on the Hantzsch reaction, is much more sensitive for formaldehyde than for acetaldehyde. The same sample preparation was used for both; however, the fluorometric method provided significantly higher numbers. (This was determined later to be a result of lower reaction rate for the sample than the standard in the HPLC method.) The colorimetric microdiffusion method (6) was much simpler, with a weighed amount of dispersion in the outer ring of a microdiffusion chamber and chromotropic acid reagent in the inner ring. Table II shows results establishing that formaldehyde is present in all of the samples, half of which showed equivalent amounts of acetaldehyde by the HPLC method. For the purposes of this study, the qualitative results of the tests were much more important than the quantitative results. Obtaining reliable quantitative methods for the lower aldehydes in heterogeneous systems is difficult, owing to their volatility and reactivity; however, further work on this methodology has shown promise and may be reported elsewhere.

The highest estimate of formaldehyde content presented in Table II is <0.08% of the polysorbate 80 content of the dispersion. Thus, elucidation of the film-forming phenomenon provides a further example of the profound effect that trace decomposition may have on a drug product (7). Although the artifact has no bioavailability significance, it requires development of an alternative dissolution method for quality assurance, one where the film is digested or disrupted. Based on these studies, dissolution testing at 1 month of capsules stored at 37°C with 80% RH should provide a reliable indication of potential problems due to aldehydes. Whether film formation occurs in the presence of trace aldehydes likely depends on the reactivity of other constituents of the formulation, the internal moisture content, pH, and other factors. Certainly, the use of aldehyde-generating excipients in capsule formulations should be circumvented wherever possible.

(1) J. F. Walker, "Formaldehyde," 2nd ed. American Chemical Society Monograph Series, Waverly Press, Baltimore, Md., 1953, pp. 311–317.

0022-3549/84/0800-1186$01.00/0
© 1984, American Pharmaceutical Association

(2) Kirk-Othmer, "Encyclopedia of Chemical Technology," 3rd ed., Vol. 11, Wiley, New York, N.Y., 1980, p. 911.
(3) E. M. Marks, D. Toutellotte, and A. Andux, *Food Technol.*, **22**, 1433 (1968).
(4) S. J. Swarin and F. Lipari, *J. Liq. Chromatogr.*, **6**, 425 (1983).
(5) S. Belman, *Anal. Chim. Acta.*, **29**, 120 (1963).
(6) V. P. Hollander, S. Dimowro, and O. H. Pearson, *Endocrinology*, **49**, 617 (1951).
(7) L. Chafetz and J. Philip, *J. Pharm. Sci.*, **71**, 470 (1982).

Lester Chafetz ˣ
Wen-hai Hong
Dimitri C. Tsilifonis
Anne K. Taylor
Jose Philip
Product Development Laboratories
Warner-Lambert
Parke-Davis Pharmaceutical Research Division
Morris Plains, NJ 07950

Received February 29, 1984.
Accepted for publication June 12, 1984.
The authors are grateful to Michael Hitscherich and Joseph Preziosi for skillful technical assistance.

Does Cimetidine Impair Nitroreduction?

Keyphrases □ Cimetidine—possible nitroreduction, nitrazepam □ Nitrazepam—nitroreduction, possible interference by cimetidine

To the Editor:

A recent report by Ochs *et al.* (1) demonstrated that cimetidine reduced the clearance of nitrazepam in human subjects from a mean of 1.41 mL/min/kg in the control state to 1.17 mL/min/kg during cimetidine treatment. Cimetidine had no effect on the absorption kinetics or on volume of distribution of nitrazepam. These observations, in conjunction with the belief that nitroreduction accounts for most of nitrazepam clearance, prompted Ochs and co-workers to conclude that cimetidine impairs the nitroreduction of nitrazepam. Furthermore, the authors suggested that such metabolic inhibition by cimetidine may interfere with the elimination of other drugs biotransformed by nitroreduction (1).

While the effect of cimetidine on nitrazepam clearance (1) is clear, we suggest that the above conclusion by Ochs *et al.* regarding the inhibition of nitroreduction by cimetidine may be premature. Our doubts are based on a review of published studies (2–5) of the metabolic fate of nitrazepam in humans. These studies reveal that while nitroreduction is an important biotransformation pathway for nitrazepam, it accounts for only a limited amount of the administered dose in humans. For example, Sawada and Shinohara found (2) that 17% of an oral dose of nitrazepam was excreted as nitro-reduced metabolites in the urine of human subjects in 5 d. Unchanged drug (1%) and a ring-opened metabolite (2%) were also detected, but 80% of the administered dose was not recovered (2). Kangas (3) isolated unchanged drug (1%) and nitro-reduced metabolites (52%) from the 7-d urine samples of human subjects administered nitrazepam, but could not account for nearly one-half of the administered dose. Nitro-reduced metabolites recovered from 72-h human urine samples represented only 6% of the administered nitrazepam dose in another study (4). Rieder and Wendt found (5) that ~7% of an administered oral radioactively labeled nitrazepam dose appeared in the 24-h urine specimen as nitro-reduced metabolites. Ring-opened metabolites accounted for an additional 9%, and traces of unchanged drug were also isolated. Other metabolites, which represented 21% of the administered dose, were also present but could not be identified. Thus, a total of 37% of the administered dose was excreted in the 24-h urine sample, and much of it was not identified (5). Although the recovery of total radioactivity increased to 65–70% after oral dosing and to 94% following intravenous administration during the subsequent 100 h, the proportion of the identified metabolites did not change significantly. Rieder and Wendt also demonstrated the accumulation of large amounts of unidentified metabolites in the plasma of human subjects after oral doses of this drug (5). Quantitative differences among the above-described studies may be due to differences in analytical methods and/or to inclusion *versus* omission of conjugated metabolites. Nevertheless, nitroreduction in humans has been shown to account, at most, for ~50% (3) of total nitrazepam elimination, and for much less in most studies (2, 4, 5). Since negligible amounts of unchanged drug are excreted (2–5), unidentified metabolites probably account (3, 5) for the remainder of nitrazepam elimination.

Cimetidine is known (6) to inhibit oxidative biotransformation of many drugs and, therefore, the following question must be raised: Is the effect of cimetidine on the clearance of nitrazepam due to the inhibition of some unidentified *oxidative* biotransformation rather than to inhibition of nitroreduction? This alternative explanation is supported by the isolation of small amounts of oxidized metabolites of nitrazepam from urine samples after the administration of the drug to humans (2, 5). Furthermore, oxidation may also be involved (7, 8) in the ring-opening biotransformation of benzodiazepines which may be an important metabolic pathway for nitrazepam (5).

Thus, it is clear that previous work has not accounted for a large fraction of the nitrazepam dose, and it appears that oxidative biotransformations may be responsible for a portion of nitrazepam clearance. There is insufficient data to determine whether nitrazepam nitroreduction or some hitherto unidentified oxidative metabolic pathway is impaired by cimetidine. Therefore, we feel that it is premature to suggest (1) that the ability of cimetidine to impair drug oxidation in humans should be extended to include inhibition of nitroreduction. There are several important drugs with a nitro group in their structure (*e.g.*, chloramphenicol, clonazepam, nitrofurantoin, and metronidazole), and some of these compounds have been shown to be metabolized *via* nitroreduction. We are concerned that the suggestion by Ochs *et al.* (1) may foster a general belief that cimetidine—a widely used agent—impairs the elimination of such drugs *via* nitroreduction, a belief for which there is, as yet, no firm evidence.

Perhaps cimetidine will be shown in the future to inhibit one or more of the several distinct nitroreductases known [*e.g.*, cytochrome P_{450}, whose oxidative function is inhibited by cimetidine (9), can also function as a nitroreductase (10)]. However, to demonstrate inhibition of nitroreduction, studies of the effects of cimetidine on specific biotransformations and on metabolite formation will be required. It will be interesting to watch developments in this area.

(1) H. R. Ochs, D. J. Greenblatt, R. Gugler, G. Munteferig, A. Locniskar, and D. R. Abernathy, *Clin. Pharmacol. Ther.*, **34**, 227 (1983).

0022-3549/84/0800-1187$01.00/0
© 1984, American Pharmaceutical Association

(2) H. Sawada and K. Shinohara, *Arch. Toxikol.*, **28,** 214 (1971).
(3) L. Kangas, *Acta Pharmacol. Toxicol.*, **45,** 16 (1979).
(4) K.-H. Beyer and W. Sadee, *Arzneim.-Forsch.*, **19,** 1929 (1969).
(5) J. Rieder and G. Wendt, in "The Benzodiazepines," S. Garratini, E. Mussini, and L. O. Randall, Eds., Raven, New York, N.Y., 1973, pp. 99-127.
(6) A. Somogyi and R. Gugler, *Clin. Pharmacokinet.*, **7,** 23 (1982).
(7) S. F. Sisenwine, C. O. Tio, S. R. Shrader, and H. W. Ruelius, *Arzneim.-Forsch.*, **22,** 682 (1972).
(8) B. Testa and P. Jenner, "Drug Metabolism: Chemical and Biochemical Aspects," Dekker, New York, N.Y., 1976, pp. 161, 231, 232.
(9) S. Rendic, F. Kajfez, and H.-H. Ruf, *Drug Metab. Dispos.*, **11,** 137 (1983).
(10) P. G. Wislocki, G. T. Miwa and A. Y. H. Lu, in "Enzymatic Basis of Detoxication," Vol. I, W. B. Jakoby, Ed., Academic, New York, N.Y., 1980, p. 165.

Joseph Gal ˣ
Allen J. Sedman
Division of Clinical Pharmacology and Department of Emergency Medicine
School of Medicine
University of Colorado Health Sciences Center
Denver, CO 80262

Received January 30, 1984.
Accepted for publication June 11, 1984.

BOOKS

Review of Organic Functional Groups: Introduction to Medicinal Organic Chemistry. By THOMAS L. LEMKE. Lea and Febiger, Philadelphia, PA. 1983. 131 pp. 15 × 23 cm. Price $10.50.

The objective of this book is to provide a self-paced review of the nomenclature, physical properties, chemical properties, and metabolism of organic functional groups that are important in medicinal chemistry. The book is designed for use as supplemental material for a pharmacy course in medicinal chemistry as well as a concise reference for students and professional practitioners in pharmacy, medicine, nursing, dentistry, and veterinary medicine. After a general chapter on water solubility and chemical bonding, subsequent chapters focus on specific functional groups. Organic functional groups covered include alkanes, alkenes, aromatic hydrocarbons, halogenated hydrocarbons, alcohols, phenols, ethers, aldehydes, ketones, amines, carboxylic acids and their derivatives, sulfonic acids and sulfonamides, and heterocycles. A chapter on empirical and analytical methods of determining water solubility and an appendix on acidity and basicity are also included. Review questions are placed at the end of chapters to reinforce concepts presented in the text.

Chapters on individual functional groups are concise, and adhere to an outline format where the three major subheadings are Nomenclature, Physical-Chemical Properties, and Metabolism. There are adequate examples and tables of physical data given to illustrate the major points. The sections on nomenclature and physical-chemical properties are especially clearly written and complete. Most of the sections on metabolism are also clear and concise. However, the metabolism sections on aromatic hydrocarbons, halogenated hydrocarbons, and amines may be confusing since they contain several statements which contradict information found in drug metabolism chapters of current medicinal chemistry textbooks.

The major emphasis of this book is in areas of medicinal chemistry which many undergraduate pharmacy students find difficult. The sections on nomenclature and physical-chemical properties should be very helpful to those students who have difficulty extracting information from general organic chemistry textbooks that is directly pertinent to medicinal chemistry. Therefore, this book fills a distinct need in undergraduate medicinal chemistry instruction. As long as weaknesses in some metabolism sections are recognized, this book should be an excellent supplement to most undergraduate pharmacy courses in medicinal chemistry as well as a concise review for students and practitioners of other health professions.

Reviewed by Michael W. Duffel
Division of Medicinal Chemistry and Natural Products
College of Pharmacy
University of Iowa
Iowa City, IA 52242

Applied Clinical Pharmacokinetics. Edited by DENNIS R. MUNGALL. Raven Press, 1140 Avenue of the Americas, New York, NY 10036. 1983. 448 pp.

This book represents the most recent compilation of information related to the discipline of therapeutic drug monitoring. As stated in the preface, the major objective of this text is "to offer students and clinicians in pharmacy, medicine, pharmacology, and clinical chemistry a practical guide to clinical pharmacokinetics." Although a brief introductory chapter discusses general concepts and basic pharmacokinetic principles, students without previous pharmacokinetic course work may have difficulty applying the information presented in the remainder of the textbook. The subsequent chapter which examines protein binding and free drug concentrations is complete, reasonably well referenced, and a good review of the pertinent drug-protein binding literature. However, this chapter cannot be recommended for students because it contains several misleading statements and very minor yet bothersome errors.

The remaining chapters are primarily devoted to the discussion of individual therapeutic agents and include: procainamide, quinidine, digoxin, anticonvulsants, theophylline, aminoglycosides, warfarin, antihypertensives, lithium, tricyclic antidepressants, benzodiazepines, salicylates, and antineoplastics. The absence of a chapter addressing the pharmacokinetics of lidocaine is a limitation of the text and certainly would have proven more useful to the clinician than a chapter discussing antihypertensive agents.

Each of the drugs reviewed has a chapter to itself with the format designed to cover important aspects of clinical pharmacology, pharmacokinetics, plasma concentration and response relationships, dosage regimen design, and assay methods. The book is quite readable in this format and appears to be relatively free from errors. Most chapters contain practice problems along with detailed solutions. The information on each drug is, for the most part, well detailed and referenced. The concluding chapter is devoted to the use of programmable calculators in clinical pharmacokinetics. Included in this chapter is a group of calculator programs that may prove useful to those individuals who utilize such devices in their clinical practice.

On the whole, this book provides a reasonable compilation of the published literature in the areas addressed by the authors. However, this text is not unique in its area of emphasis and a more rigorous and comprehensive examination is available as a reference source. While the practicing clinician may find certain areas of this book of interest, (*e.g.* practice problems, calculator programs) its general appeal is limited; therefore, the student in either introductory or advanced courses will find currently available texts of greater benefit.

Reviewed by Thomas J. Nester
Division of Pharmacy Practice
College of Pharmacy
The Ohio State University
Columbus, OH 43210

Decrease in the Rate of Capsule Dissolution Due to Formaldehyde from Polysorbate 80 Autoxidation

Keyphrases □ Dissolution, capsule—rate decrease, formation of formaldehyde, polysorbate 80 autoxidation □ Polysorbate 80—autoxidation, formation of formaldehyde, decreased dissolution rate, capsules

To the Editor:

Dissolution studies on some stability samples of gemfibrozil capsules showed a significant decrease in dissolution rate with time of storage and exposure to humidity. Observations of these slowly dissolving samples during the tests showed that the capsule contents were held together by a thin, tough, water-insoluble film, the disruption of which was seen to be the dissolution rate-limiting factor for the drug product. A bioavailability study of such film-forming gemfibrozil capsules showed them to be bioequivalent to the readily dissolving product. Thus, the decrease in dissolution rate in the *in vitro* test is an anomaly because it does not correlate with *in vivo* results. This communication describes studies which established that film formation is due to denaturation of the inner surface of the capsule by formaldehyde, formed by trace autoxidation of the polysorbate 80 used as an excipient.

Polysorbate 80 had been useful in our laboratories as a wetting agent in capsule formulations of hydrophobic drugs. It was convenient to prepare a 1:2 dispersion by drying an alcohol solution of polysorbate 80 mixed with colloidal silica. The silica aided in powder flow, facilitating high-speed encapsulation. This dispersion was used in several capsule formulations of investigational drugs, all of which exhibited film formation when stored under high-humidity conditions. Studies on experimental capsule formulations (Table I) made with constituents of the gemfibrozil capsule formula and stored at 37°C, 37°C with 80% relative humidity (RH), and 45°C and tested after 1, 2, and 3 months showed that film formation occurred only when polysorbate 80 was present. All of the capsules containing polysorbate 80 showed film formation during testing after 1 month at 37°C with 80% RH.

The reaction of formaldehyde and other aldehydes with proteins is well known (1, 2). Cross-linking of the amino groups in gelatin results in its denaturation to an insoluble protein (3). Since formaldehyde could result from autoxidation of the end groups in polysorbate 80 and acetaldehyde could be produced by oxidation of alcohol used in preparation of polysorbate 80–silica dispersion, the hypothesis that one or both of these aldehydes was responsible for film formation was tested. Formation of aldehydes would be facilitated by the immense surface area of the silica, so the results in Table I are consistent with the hypothesis.

Table I—Experimental Capsule Formulations [a]

Ingredients, mg	Formulation a	b[b]	c	d[c]	e[d]	f[d]	g[e]	h[d]
Gemfibrozil	171	171	171	171	171	171	—	—
Polysorbate 80 on Silica	5	10	—	—	—	—	150	—
Cornstarch NF	99	94	102	100	97	104	—	—
Polysorbate 80 NF	—	—	2	4	—	—	—	—
Silica Gel NF	—	—	—	—	7	—	—	90
Fill weight, mg	275	275	275	275	275	275	150	90

[a] No. 2 snap-fit white opaque 999 capsules, Lot 162 (Capsugel), were used for all formulations. [b] Questionable film formation at 3 months at 45°C. [c] Film formation 3 months at 37°C. [d] No film formation. [e] Film formation 1 month at 37°C.

Table II—Assay of Formaldehyde in Polysorbate 80 on Silica

Lot	Formaldehyde, μg/g of Sample Taken HPLC	Fluorometric	Colorimetric
1	20	163	260
2	13	55	170
3	13	—	75
4	18	—	100
5	27	111	200
6	36	163	110

Six lots of polysorbate 80–silica dispersion were analyzed for formaldehyde by three methods. The HPLC method (4) is based on the reaction of aldehydes with 2-diphenylacetyl-1,3-indanedione-1-hydrazone and afforded a separation of formaldehyde and acetaldehyde derivatives. The fluorometric method (5), based on the Hantzsch reaction, is much more sensitive for formaldehyde than for acetaldehyde. The same sample preparation was used for both; however, the fluorometric method provided significantly higher numbers. (This was determined later to be a result of lower reaction rate for the sample than the standard in the HPLC method.) The colorimetric microdiffusion method (6) was much simpler, with a weighed amount of dispersion in the outer ring of a microdiffusion chamber and chromotropic acid reagent in the inner ring. Table II shows results establishing that formaldehyde is present in all of the samples, half of which showed equivalent amounts of acetaldehyde by the HPLC method. For the purposes of this study, the qualitative results of the tests were much more important than the quantitative results. Obtaining reliable quantitative methods for the lower aldehydes in heterogeneous systems is difficult, owing to their volatility and reactivity; however, further work on this methodology has shown promise and may be reported elsewhere.

The highest estimate of formaldehyde content presented in Table II is <0.08% of the polysorbate 80 content of the dispersion. Thus, elucidation of the film-forming phenomenon provides a further example of the profound effect that trace decomposition may have on a drug product (7). Although the artifact has no bioavailability significance, it requires development of an alternative dissolution method for quality assurance, one where the film is digested or disrupted. Based on these studies, dissolution testing at 1 month of capsules stored at 37°C with 80% RH should provide a reliable indication of potential problems due to aldehydes. Whether film formation occurs in the presence of trace aldehydes likely depends on the reactivity of other constituents of the formulation, the internal moisture content, pH, and other factors. Certainly, the use of aldehyde-generating excipients in capsule formulations should be circumvented wherever possible.

(1) J. F. Walker, "Formaldehyde," 2nd ed. American Chemical Society Monograph Series, Waverly Press, Baltimore, Md., 1953, pp. 311–317.

0022-3549/84/0800-1186$01.00/0
© 1984, American Pharmaceutical Association

(2) Kirk-Othmer, "Encyclopedia of Chemical Technology," 3rd ed., Vol. 11, Wiley, New York, N.Y., 1980, p. 911.
(3) E. M. Marks, D. Toutellotte, and A. Andux, *Food Technol.*, **22**, 1433 (1968).
(4) S. J. Swarin and F. Lipari, *J. Liq. Chromatogr.*, **6**, 425 (1983).
(5) S. Belman, *Anal. Chim. Acta.*, **29**, 120 (1963).
(6) V. P. Hollander, S. Dimowro, and O. H. Pearson, *Endocrinology*, **49**, 617 (1951).
(7) L. Chafetz and J. Philip, *J. Pharm. Sci.*, **71**, 470 (1982).

Lester Chafetz ˣ
Wen-hai Hong
Dimitri C. Tsilifonis
Anne K. Taylor
Jose Philip
Product Development Laboratories
Warner-Lambert
Parke-Davis Pharmaceutical Research Division
Morris Plains, NJ 07950

Received February 29, 1984.
Accepted for publication June 12, 1984.
The authors are grateful to Michael Hitscherich and Joseph Preziosi for skillful technical assistance.

Does Cimetidine Impair Nitroreduction?

Keyphrases □ Cimetidine—possible nitroreduction, nitrazepam □ Nitrazepam—nitroreduction, possible interference by cimetidine

To the Editor:

A recent report by Ochs *et al.* (1) demonstrated that cimetidine reduced the clearance of nitrazepam in human subjects from a mean of 1.41 mL/min/kg in the control state to 1.17 mL/min/kg during cimetidine treatment. Cimetidine had no effect on the absorption kinetics or on volume of distribution of nitrazepam. These observations, in conjunction with the belief that nitroreduction accounts for most of nitrazepam clearance, prompted Ochs and co-workers to conclude that cimetidine impairs the nitroreduction of nitrazepam. Furthermore, the authors suggested that such metabolic inhibition by cimetidine may interfere with the elimination of other drugs biotransformed by nitroreduction (1).

While the effect of cimetidine on nitrazepam clearance (1) is clear, we suggest that the above conclusion by Ochs *et al.* regarding the inhibition of nitroreduction by cimetidine may be premature. Our doubts are based on a review of published studies (2–5) of the metabolic fate of nitrazepam in humans. These studies reveal that while nitroreduction is an important biotransformation pathway for nitrazepam, it accounts for only a limited amount of the administered dose in humans. For example, Sawada and Shinohara found (2) that 17% of an oral dose of nitrazepam was excreted as nitro-reduced metabolites in the urine of human subjects in 5 d. Unchanged drug (1%) and a ring-opened metabolite (2%) were also detected, but 80% of the administered dose was not recovered (2). Kangas (3) isolated unchanged drug (1%) and nitro-reduced metabolites (52%) from the 7-d urine samples of human subjects administered nitrazepam, but could not account for nearly one-half of the administered dose. Nitro-reduced metabolites recovered from 72-h human urine samples represented only 6% of the administered nitrazepam dose in another study (4). Rieder and Wendt found (5) that ~7% of an administered oral radioactively labeled nitrazepam dose appeared in the 24-h urine specimen as nitro-reduced metabolites. Ring-opened metabolites accounted for an additional 9%, and traces of unchanged drug were also isolated. Other metabolites, which represented 21% of the administered dose, were also present but could not be identified. Thus, a total of 37% of the administered dose was excreted in the 24-h urine sample, and much of it was not identified (5). Although the recovery of total radioactivity increased to 65–70% after oral dosing and to 94% following intravenous administration during the subsequent 100 h, the proportion of the identified metabolites did not change significantly. Rieder and Wendt also demonstrated the accumulation of large amounts of unidentified metabolites in the plasma of human subjects after oral doses of this drug (5). Quantitative differences among the above-described studies may be due to differences in analytical methods and/or to inclusion *versus* omission of conjugated metabolites. Nevertheless, nitroreduction in humans has been shown to account, at most, for ~50% (3) of total nitrazepam elimination, and for much less in most studies (2, 4, 5). Since negligible amounts of unchanged drug are excreted (2–5), unidentified metabolites probably account (3, 5) for the remainder of nitrazepam elimination.

Cimetidine is known (6) to inhibit oxidative biotransformation of many drugs and, therefore, the following question must be raised: Is the effect of cimetidine on the clearance of nitrazepam due to the inhibition of some unidentified *oxidative* biotransformation rather than to inhibition of nitroreduction? This alternative explanation is supported by the isolation of small amounts of oxidized metabolites of nitrazepam from urine samples after the administration of the drug to humans (2, 5). Furthermore, oxidation may also be involved (7, 8) in the ring-opening biotransformation of benzodiazepines which may be an important metabolic pathway for nitrazepam (5).

Thus, it is clear that previous work has not accounted for a large fraction of the nitrazepam dose, and it appears that oxidative biotransformations may be responsible for a portion of nitrazepam clearance. There is insufficient data to determine whether nitrazepam nitroreduction or some hitherto unidentified oxidative metabolic pathway is impaired by cimetidine. Therefore, we feel that it is premature to suggest (1) that the ability of cimetidine to impair drug oxidation in humans should be extended to include inhibition of nitroreduction. There are several important drugs with a nitro group in their structure (*e.g.*, chloramphenicol, clonazepam, nitrofurantoin, and metronidazole), and some of these compounds have been shown to be metabolized *via* nitroreduction. We are concerned that the suggestion by Ochs *et al.* (1) may foster a general belief that cimetidine—a widely used agent—impairs the elimination of such drugs *via* nitroreduction, a belief for which there is, as yet, no firm evidence.

Perhaps cimetidine will be shown in the future to inhibit one or more of the several distinct nitroreductases known [*e.g.*, cytochrome P_{450}, whose oxidative function is inhibited by cimetidine (9), can also function as a nitroreductase (10)]. However, to demonstrate inhibition of nitroreduction, studies of the effects of cimetidine on specific biotransformations and on metabolite formation will be required. It will be interesting to watch developments in this area.

(1) H. R. Ochs, D. J. Greenblatt, R. Gugler, G. Munteferig, A. Locniskar, and D. R. Abernathy, *Clin. Pharmacol. Ther.*, **34**, 227 (1983).

0022-3549/84/0800-1187$01.00/0
© 1984, American Pharmaceutical Association

(2) H. Sawada and K. Shinohara, *Arch. Toxikol.*, **28,** 214 (1971).
(3) L. Kangas, *Acta Pharmacol. Toxicol.*, **45,** 16 (1979).
(4) K.-H. Beyer and W. Sadee, *Arzneim.-Forsch.*, **19,** 1929 (1969).
(5) J. Rieder and G. Wendt, in "The Benzodiazepines," S. Garratini, E. Mussini, and L. O. Randall, Eds., Raven, New York, N.Y., 1973, pp. 99-127.
(6) A. Somogyi and R. Gugler, *Clin. Pharmacokinet.*, **7,** 23 (1982).
(7) S. F. Sisenwine, C. O. Tio, S. R. Shrader, and H. W. Ruelius, *Arzneim.-Forsch.*, **22,** 682 (1972).
(8) B. Testa and P. Jenner, "Drug Metabolism: Chemical and Biochemical Aspects," Dekker, New York, N.Y., 1976, pp. 161, 231, 232.
(9) S. Rendic, F. Kajfez, and H.-H. Ruf, *Drug Metab. Dispos.*, **11,** 137 (1983).
(10) P. G. Wislocki, G. T. Miwa and A. Y. H. Lu, in "Enzymatic Basis of Detoxication," Vol. I, W. B. Jakoby, Ed., Academic, New York, N.Y., 1980, p. 165.

Joseph Gal ˣ
Allen J. Sedman
Division of Clinical Pharmacology and Department of Emergency Medicine
School of Medicine
University of Colorado Health Sciences Center
Denver, CO 80262

Received January 30, 1984.
Accepted for publication June 11, 1984.

BOOKS

Review of Organic Functional Groups: Introduction to Medicinal Organic Chemistry. By THOMAS L. LEMKE. Lea and Febiger, Philadelphia, PA. 1983. 131 pp. 15 × 23 cm. Price $10.50.

The objective of this book is to provide a self-paced review of the nomenclature, physical properties, chemical properties, and metabolism of organic functional groups that are important in medicinal chemistry. The book is designed for use as supplemental material for a pharmacy course in medicinal chemistry as well as a concise reference for students and professional practitioners in pharmacy, medicine, nursing, dentistry, and veterinary medicine. After a general chapter on water solubility and chemical bonding, subsequent chapters focus on specific functional groups. Organic functional groups covered include alkanes, alkenes, aromatic hydrocarbons, halogenated hydrocarbons, alcohols, phenols, ethers, aldehydes, ketones, amines, carboxylic acids and their derivatives, sulfonic acids and sulfonamides, and heterocycles. A chapter on empirical and analytical methods of determining water solubility and an appendix on acidity and basicity are also included. Review questions are placed at the end of chapters to reinforce concepts presented in the text.

Chapters on individual functional groups are concise, and adhere to an outline format where the three major subheadings are Nomenclature, Physical-Chemical Properties, and Metabolism. There are adequate examples and tables of physical data given to illustrate the major points. The sections on nomenclature and physical-chemical properties are especially clearly written and complete. Most of the sections on metabolism are also clear and concise. However, the metabolism sections on aromatic hydrocarbons, halogenated hydrocarbons, and amines may be confusing since they contain several statements which contradict information found in drug metabolism chapters of current medicinal chemistry textbooks.

The major emphasis of this book is in areas of medicinal chemistry which many undergraduate pharmacy students find difficult. The sections on nomenclature and physical-chemical properties should be very helpful to those students who have difficulty extracting information from general organic chemistry textbooks that is directly pertinent to medicinal chemistry. Therefore, this book fills a distinct need in undergraduate medicinal chemistry instruction. As long as weaknesses in some metabolism sections are recognized, this book should be an excellent supplement to most undergraduate pharmacy courses in medicinal chemistry as well as a concise review for students and practitioners of other health professions.

Reviewed by Michael W. Duffel
Division of Medicinal Chemistry and Natural Products
College of Pharmacy
University of Iowa
Iowa City, IA 52242

Applied Clinical Pharmacokinetics. Edited by DENNIS R. MUNGALL. Raven Press, 1140 Avenue of the Americas, New York, NY 10036. 1983. 448 pp.

This book represents the most recent compilation of information related to the discipline of therapeutic drug monitoring. As stated in the preface, the major objective of this text is "to offer students and clinicians in pharmacy, medicine, pharmacology, and clinical chemistry a practical guide to clinical pharmacokinetics." Although a brief introductory chapter discusses general concepts and basic pharmacokinetic principles, students without previous pharmacokinetic course work may have difficulty applying the information presented in the remainder of the textbook. The subsequent chapter which examines protein binding and free drug concentrations is complete, reasonably well referenced, and a good review of the pertinent drug-protein binding literature. However, this chapter cannot be recommended for students because it contains several misleading statements and very minor yet bothersome errors.

The remaining chapters are primarily devoted to the discussion of individual therapeutic agents and include: procainamide, quinidine, digoxin, anticonvulsants, theophylline, aminoglycosides, warfarin, antihypertensives, lithium, tricyclic antidepressants, benzodiazepines, salicylates, and antineoplastics. The absence of a chapter addressing the pharmacokinetics of lidocaine is a limitation of the text and certainly would have proven more useful to the clinician than a chapter discussing antihypertensive agents.

Each of the drugs reviewed has a chapter to itself with the format designed to cover important aspects of clinical pharmacology, pharmacokinetics, plasma concentration and response relationships, dosage regimen design, and assay methods. The book is quite readable in this format and appears to be relatively free from errors. Most chapters contain practice problems along with detailed solutions. The information on each drug is, for the most part, well detailed and referenced. The concluding chapter is devoted to the use of programmable calculators in clinical pharmacokinetics. Included in this chapter is a group of calculator programs that may prove useful to those individuals who utilize such devices in their clinical practice.

On the whole, this book provides a reasonable compilation of the published literature in the areas addressed by the authors. However, this text is not unique in its area of emphasis and a more rigorous and comprehensive examination is available as a reference source. While the practicing clinician may find certain areas of this book of interest, (*e.g.* practice problems, calculator programs) its general appeal is limited; therefore, the student in either introductory or advanced courses will find currently available texts of greater benefit.

Reviewed by Thomas J. Nester
Division of Pharmacy Practice
College of Pharmacy
The Ohio State University
Columbus, OH 43210

(2) H. Sawada and K. Shinohara, *Arch. Toxikol.*, **28,** 214 (1971).
(3) L. Kangas, *Acta Pharmacol. Toxicol.*, **45,** 16 (1979).
(4) K.-H. Beyer and W. Sadee, *Arzneim.-Forsch.*, **19,** 1929 (1969).
(5) J. Rieder and G. Wendt, in "The Benzodiazepines," S. Garratini, E. Mussini, and L. O. Randall, Eds., Raven, New York, N.Y., 1973, pp. 99-127.
(6) A. Somogyi and R. Gugler, *Clin. Pharmacokinet.*, **7,** 23 (1982).
(7) S. F. Sisenwine, C. O. Tio, S. R. Shrader, and H. W. Ruelius, *Arzneim.-Forsch.*, **22,** 682 (1972).
(8) B. Testa and P. Jenner, "Drug Metabolism: Chemical and Biochemical Aspects," Dekker, New York, N.Y., 1976, pp. 161, 231, 232.
(9) S. Rendic, F. Kajfez, and H.-H. Ruf, *Drug Metab. Dispos.*, **11,** 137 (1983).
(10) P. G. Wislocki, G. T. Miwa and A. Y. H. Lu, in "Enzymatic Basis of Detoxication," Vol. I, W. B. Jakoby, Ed., Academic, New York, N.Y., 1980, p. 165.

Joseph Gal ˣ
Allen J. Sedman
Division of Clinical Pharmacology and Department of Emergency Medicine
School of Medicine
University of Colorado Health Sciences Center
Denver, CO 80262

Received January 30, 1984.
Accepted for publication June 11, 1984.

BOOKS

Review of Organic Functional Groups: Introduction to Medicinal Organic Chemistry. By THOMAS L. LEMKE. Lea and Febiger, Philadelphia, PA. 1983. 131 pp. 15 × 23 cm. Price $10.50.

The objective of this book is to provide a self-paced review of the nomenclature, physical properties, chemical properties, and metabolism of organic functional groups that are important in medicinal chemistry. The book is designed for use as supplemental material for a pharmacy course in medicinal chemistry as well as a concise reference for students and professional practitioners in pharmacy, medicine, nursing, dentistry, and veterinary medicine. After a general chapter on water solubility and chemical bonding, subsequent chapters focus on specific functional groups. Organic functional groups covered include alkanes, alkenes, aromatic hydrocarbons, halogenated hydrocarbons, alcohols, phenols, ethers, aldehydes, ketones, amines, carboxylic acids and their derivatives, sulfonic acids and sulfonamides, and heterocycles. A chapter on empirical and analytical methods of determining water solubility and an appendix on acidity and basicity are also included. Review questions are placed at the end of chapters to reinforce concepts presented in the text.

Chapters on individual functional groups are concise, and adhere to an outline format where the three major subheadings are Nomenclature, Physical-Chemical Properties, and Metabolism. There are adequate examples and tables of physical data given to illustrate the major points. The sections on nomenclature and physical-chemical properties are especially clearly written and complete. Most of the sections on metabolism are also clear and concise. However, the metabolism sections on aromatic hydrocarbons, halogenated hydrocarbons, and amines may be confusing since they contain several statements which contradict information found in drug metabolism chapters of current medicinal chemistry textbooks.

The major emphasis of this book is in areas of medicinal chemistry which many undergraduate pharmacy students find difficult. The sections on nomenclature and physical-chemical properties should be very helpful to those students who have difficulty extracting information from general organic chemistry textbooks that is directly pertinent to medicinal chemistry. Therefore, this book fills a distinct need in undergraduate medicinal chemistry instruction. As long as weaknesses in some metabolism sections are recognized, this book should be an excellent supplement to most undergraduate pharmacy courses in medicinal chemistry as well as a concise review for students and practitioners of other health professions.

Reviewed by Michael W. Duffel
Division of Medicinal Chemistry and Natural Products
College of Pharmacy
University of Iowa
Iowa City, IA 52242

Applied Clinical Pharmacokinetics. Edited by DENNIS R. MUNGALL. Raven Press, 1140 Avenue of the Americas, New York, NY 10036. 1983. 448 pp.

This book represents the most recent compilation of information related to the discipline of therapeutic drug monitoring. As stated in the preface, the major objective of this text is "to offer students and clinicians in pharmacy, medicine, pharmacology, and clinical chemistry a practical guide to clinical pharmacokinetics." Although a brief introductory chapter discusses general concepts and basic pharmacokinetic principles, students without previous pharmacokinetic course work may have difficulty applying the information presented in the remainder of the textbook. The subsequent chapter which examines protein binding and free drug concentrations is complete, reasonably well referenced, and a good review of the pertinent drug-protein binding literature. However, this chapter cannot be recommended for students because it contains several misleading statements and very minor yet bothersome errors.

The remaining chapters are primarily devoted to the discussion of individual therapeutic agents and include: procainamide, quinidine, digoxin, anticonvulsants, theophylline, aminoglycosides, warfarin, antihypertensives, lithium, tricyclic antidepressants, benzodiazepines, salicylates, and antineoplastics. The absence of a chapter addressing the pharmacokinetics of lidocaine is a limitation of the text and certainly would have proven more useful to the clinician than a chapter discussing antihypertensive agents.

Each of the drugs reviewed has a chapter to itself with the format designed to cover important aspects of clinical pharmacology, pharmacokinetics, plasma concentration and response relationships, dosage regimen design, and assay methods. The book is quite readable in this format and appears to be relatively free from errors. Most chapters contain practice problems along with detailed solutions. The information on each drug is, for the most part, well detailed and referenced. The concluding chapter is devoted to the use of programmable calculators in clinical pharmacokinetics. Included in this chapter is a group of calculator programs that may prove useful to those individuals who utilize such devices in their clinical practice.

On the whole, this book provides a reasonable compilation of the published literature in the areas addressed by the authors. However, this text is not unique in its area of emphasis and a more rigorous and comprehensive examination is available as a reference source. While the practicing clinician may find certain areas of this book of interest, (*e.g.* practice problems, calculator programs) its general appeal is limited; therefore, the student in either introductory or advanced courses will find currently available texts of greater benefit.

Reviewed by Thomas J. Nester
Division of Pharmacy Practice
College of Pharmacy
The Ohio State University
Columbus, OH 43210

(2) H. Sawada and K. Shinohara, *Arch. Toxikol.*, **28,** 214 (1971).
(3) L. Kangas, *Acta Pharmacol. Toxicol.*, **45,** 16 (1979).
(4) K.-H. Beyer and W. Sadee, *Arzneim.-Forsch.*, **19,** 1929 (1969).
(5) J. Rieder and G. Wendt, in "The Benzodiazepines," S. Garratini, E. Mussini, and L. O. Randall, Eds., Raven, New York, N.Y., 1973, pp. 99-127.
(6) A. Somogyi and R. Gugler, *Clin. Pharmacokinet.*, **7,** 23 (1982).
(7) S. F. Sisenwine, C. O. Tio, S. R. Shrader, and H. W. Ruelius, *Arzneim.-Forsch.*, **22,** 682 (1972).
(8) B. Testa and P. Jenner, "Drug Metabolism: Chemical and Biochemical Aspects," Dekker, New York, N.Y., 1976, pp. 161, 231, 232.
(9) S. Rendic, F. Kajfez, and H.-H. Ruf, *Drug Metab. Dispos.*, **11,** 137 (1983).
(10) P. G. Wislocki, G. T. Miwa and A. Y. H. Lu, in "Enzymatic Basis of Detoxication," Vol. I, W. B. Jakoby, Ed., Academic, New York, N.Y., 1980, p. 165.

Joseph Gal ˣ
Allen J. Sedman
Division of Clinical Pharmacology and Department of Emergency Medicine
School of Medicine
University of Colorado Health Sciences Center
Denver, CO 80262

Received January 30, 1984.
Accepted for publication June 11, 1984.

BOOKS

Review of Organic Functional Groups: Introduction to Medicinal Organic Chemistry. By THOMAS L. LEMKE. Lea and Febiger, Philadelphia, PA. 1983. 131 pp. 15 × 23 cm. Price $10.50.

The objective of this book is to provide a self-paced review of the nomenclature, physical properties, chemical properties, and metabolism of organic functional groups that are important in medicinal chemistry. The book is designed for use as supplemental material for a pharmacy course in medicinal chemistry as well as a concise reference for students and professional practitioners in pharmacy, medicine, nursing, dentistry, and veterinary medicine. After a general chapter on water solubility and chemical bonding, subsequent chapters focus on specific functional groups. Organic functional groups covered include alkanes, alkenes, aromatic hydrocarbons, halogenated hydrocarbons, alcohols, phenols, ethers, aldehydes, ketones, amines, carboxylic acids and their derivatives, sulfonic acids and sulfonamides, and heterocycles. A chapter on empirical and analytical methods of determining water solubility and an appendix on acidity and basicity are also included. Review questions are placed at the end of chapters to reinforce concepts presented in the text.

Chapters on individual functional groups are concise, and adhere to an outline format where the three major subheadings are Nomenclature, Physical-Chemical Properties, and Metabolism. There are adequate examples and tables of physical data given to illustrate the major points. The sections on nomenclature and physical-chemical properties are especially clearly written and complete. Most of the sections on metabolism are also clear and concise. However, the metabolism sections on aromatic hydrocarbons, halogenated hydrocarbons, and amines may be confusing since they contain several statements which contradict information found in drug metabolism chapters of current medicinal chemistry textbooks.

The major emphasis of this book is in areas of medicinal chemistry which many undergraduate pharmacy students find difficult. The sections on nomenclature and physical-chemical properties should be very helpful to those students who have difficulty extracting information from general organic chemistry textbooks that is directly pertinent to medicinal chemistry. Therefore, this book fills a distinct need in undergraduate medicinal chemistry instruction. As long as weaknesses in some metabolism sections are recognized, this book should be an excellent supplement to most undergraduate pharmacy courses in medicinal chemistry as well as a concise review for students and practitioners of other health professions.

Reviewed by Michael W. Duffel
Division of Medicinal Chemistry and Natural Products
College of Pharmacy
University of Iowa
Iowa City, IA 52242

Applied Clinical Pharmacokinetics. Edited by DENNIS R. MUNGALL. Raven Press, 1140 Avenue of the Americas, New York, NY 10036. 1983. 448 pp.

This book represents the most recent compilation of information related to the discipline of therapeutic drug monitoring. As stated in the preface, the major objective of this text is "to offer students and clinicians in pharmacy, medicine, pharmacology, and clinical chemistry a practical guide to clinical pharmacokinetics." Although a brief introductory chapter discusses general concepts and basic pharmacokinetic principles, students without previous pharmacokinetic course work may have difficulty applying the information presented in the remainder of the textbook. The subsequent chapter which examines protein binding and free drug concentrations is complete, reasonably well referenced, and a good review of the pertinent drug-protein binding literature. However, this chapter cannot be recommended for students because it contains several misleading statements and very minor yet bothersome errors.

The remaining chapters are primarily devoted to the discussion of individual therapeutic agents and include: procainamide, quinidine, digoxin, anticonvulsants, theophylline, aminoglycosides, warfarin, antihypertensives, lithium, tricyclic antidepressants, benzodiazepines, salicylates, and antineoplastics. The absence of a chapter addressing the pharmacokinetics of lidocaine is a limitation of the text and certainly would have proven more useful to the clinician than a chapter discussing antihypertensive agents.

Each of the drugs reviewed has a chapter to itself with the format designed to cover important aspects of clinical pharmacology, pharmacokinetics, plasma concentration and response relationships, dosage regimen design, and assay methods. The book is quite readable in this format and appears to be relatively free from errors. Most chapters contain practice problems along with detailed solutions. The information on each drug is, for the most part, well detailed and referenced. The concluding chapter is devoted to the use of programmable calculators in clinical pharmacokinetics. Included in this chapter is a group of calculator programs that may prove useful to those individuals who utilize such devices in their clinical practice.

On the whole, this book provides a reasonable compilation of the published literature in the areas addressed by the authors. However, this text is not unique in its area of emphasis and a more rigorous and comprehensive examination is available as a reference source. While the practicing clinician may find certain areas of this book of interest, (*e.g.* practice problems, calculator programs) its general appeal is limited; therefore, the student in either introductory or advanced courses will find currently available texts of greater benefit.

Reviewed by Thomas J. Nester
Division of Pharmacy Practice
College of Pharmacy
The Ohio State University
Columbus, OH 43210

A publication of the
American Pharmaceutical Association—
the National Professional Society
of Pharmacists

JOURNAL OF PHARMACEUTICAL SCIENCES

Volume 73, 1984

JPMSAE 73(1-12) 1-1910 (1984)
ISSN 0022-3549

Sharon G. Boots
Editor

Sue A. Kruger
Production Editor

Margaret M. Madeleine
Assistant Production Editor

Karen A. Blakney
Copy Editor

Edward G. Feldmann
Contributing Editor

Samuel W. Goldstein
Contributing Editor

Patricia A. Evich
Editorial Secretary

Editorial Advisory Board

Jordan L. Cohen
Kenneth A. Connors
Louis Diamond
Ho-Leung Fung
Milo Gibaldi
Everett N. Hiestand
W. Homer Lawrence
Ian W. Mathison
Carl M. Metzler
Robert E. Notari
Paul L. Schiff, Jr.
Jane E. Shaw

Published monthly under the supervision of the Board of Trustees

A Drug Is A Drug—Or Is It?

A matter of significant recent controversy is referred to by the public news media as "the use of prescription drugs in executions." Indeed, this subject has become so controversial that the matter is to be weighed by the U.S. Supreme Court this fall.

Capital punishment is also a controversial issue in itself, but the question of using "prescription drugs" to carry out the process of execution is a completely separate and distinct matter.

The current issue at hand was concisely summarized in a recent issue of APhA's weekly newsletter, *apharmacy weekly:*

"The court (U.S. Supreme Court) will hear oral arguments in a suit filed against the federal government by eight Texas and Oklahoma prisoners awaiting executions by lethal injection. The inmates are asking FDA to ban the use of prescription drugs for other than medical purposes.

"Currently, 14 states permit such executions, though only two (Texas and North Carolina) have carried any out. The executions typically involve the use of potassium chloride to stop the heart, a muscle relaxant to stop breathing, and a barbiturate to cause unconsciousness.

"To date, FDA has tried to sidestep the issue, saying it has an enforcement role only in instances which endanger the public health or involve fraud."

Other press reports have gone on to state that the prisoners have further claimed that FDA should not permit such use of these "drugs" because there has not been clinical demonstration of their effectiveness and safety for this particular use, as required by federal law for any new use of an otherwise approved and marketed drug.

Years ago, the *United States Pharmacopeia* and the *National Formulary* were faced with similar dilemmas. Substances such as sodium chloride, sucrose, rose water ointment, magnesium trisilicate, microcystalline cellulose, polysorbate, saccharin, carbon tetrachloride, and so on, all had multiple uses. They all had certain distinct uses as drug dosage form ingredients: either for the physiological activity they provided *per se*, or as pharmaceutical adjuncts that contributed to the overall suitability and activity of various drug dosage forms. But, in addition, they had certain other commercial uses that were clearly "non-therapeutic" or "non-drug" in nature: as foods, cosmetics, solvents, cleaning agents, and so on.

However, neither the drug laws nor the USP-NF made any distinction; in fact, the law as well as the official compendia appeared to specifically blanket all such substances under the broad obligation of meeting USP-NF standards and specifications. The wording in the General Notices section of both compendia read that: "The standards apply equally to articles bearing the official titles ... whether or not the added designation 'USP' (or 'NF') is used."

When the officials responsible for revising the compendia and maintaining their currency became aware of this unintended broad interpretation, they promptly introduced a clarifying new statement reading: "Articles listed herein are official and the standards set forth in the monographs apply to them only when the articles are intended or labeled for use as drugs or medical devices and when bought, sold, or dispensed for these purposes."

This means that a box of sodium chloride—whether it is labeled "USP" or not—must meet USP standards if it is intended for use as a drug or therapeutic agent. If, however, it is intended for use as a food, or as an agent in ice cream manufacture, or to melt road ice, then it is not obliged to meet the compendial standards.

Similarly, barbiturates are used as drugs and also as laboratory buffering agents; certain anticoagulants are used therapeutically and also as rat poison; and other examples might be cited as well. In each such case, it is the intended use of the substance—rather than what it is chemically—that determines whether it is a "drug," and therefore must meet the applicable drug requirements.

Applying this line of reasoning, the situation with regard to the substances used for execution *via* lethal injection seems quite obvious; namely, the substances are not drugs because their intended use is clearly otherwise, despite the fact that these same substances may also be labeled and used as drugs under another set of circumstances.

Ironically, however,the FDA itself is largely responsible for confusing what should be a clearly differentiated situation. Approximately 20 years ago, the FDA seized shipments of paper disks impregnated with various antibiotic agents which were intended for clinical laboratory use in determining whether cultures of isolated organisms were inhibited by one or more of the antibiotic agents. This FDA enforcement action was challenged by the manufacturer (Difco Laboratories), and the case went to trial.

In the personal view of this writer, the antibiotic-impregnated disks were only a diagnostic aid at most—they were not used in any therapeutic manner and, hence, were not drugs. Although they happened to contain trace amounts of antibiotic substances, their use made them no different than other reagents used in the clinical laboratory. On this basis, we testified as an expert witness in Federal District Court on behalf of Difco Laboratories and in opposition to the position taken by the FDA.

The case was a most difficult one, and was eventually decided by the U.S. Supreme Court in a landmark decision. The FDA had fought tenaciously to protect all aspects of its antibiotic certification program which was then in effect—but which has recently been abolished—and convinced the court of the necessity of "certifying" these test disks. In turn, this required the court to determine that the disks were "drugs" although they never came near the patient, and in themselves have no effect on the course of the patient's disease or condition of the patient.

It appears to us that the conclusion of the court was terribly erroneous and that many absurd interpretations mutually follow when the court's general conclusion is applied to other articles and to other situations that have subsequently arisen.

Perhaps the court, in reviewing the lethal injetion tissue, will see fit to review the Difco decision. If so, we believe that the wise course of action would be to reverse the unfortunate conclusion reached by an earlier panel of jurists some 15 years ago.

—EDWARD G. FELDMANN
American Pharmaceutical Association
2215 Constitution Avenue, NW
Washington, DC 20037

Editor's Note: Dr. Feldmann's editorials are an expression of personal opinion and do not necessarily reflect views or policies of APhA. The editorials are intended to be provocative and to stimulate thinking. Readers having reactions, either pro or con, are invited to submit them for publication in the Open Forum section.

0022-3549/84/0900-1189$01.00/0
© 1984, American Pharmaceutical Association

JOURNAL OF PHARMACEUTICAL SCIENCES

SEPTEMBER 1984
VOLUME 73 NUMBER 9

RESEARCH ARTICLES

Alcoholism and Mortality Kinetics

HAROLD BOXENBAUM *x and DOMENIC CIRAULO ‡

Received March 31, 1983, from the *Pharmaceutics Section, School of Pharmacy, University of Connecticut, Storrs, CT 06268, and ‡Psychiatry Service, Veterans Administration Medical Center, Newington, CT 06111. Accepted for publication, September 8, 1983.

Abstract □ Gompertz plots of age-specific mortality rates *versus* age were compared in alcoholics and the general population. Alcoholism had a dual effect, apparently increasing vulnerability to death while slowing the aging rate (longevity is a two-dimensional function). It was hypothesized that the apparent slowing of the aging rate was an artifact, resulting from population heterogeneity in vulnerability. It is recommended that in future studies, attempts be made to categorize alcoholic subjects with respect to alcoholic habit. Longitudinal studies would also be useful.

Keyphrases □ Kinetics, mortality—effects of alcoholism □ Alcoholism—effects on mortality kinetics

It has long been recognized that alcoholism has serious consequences for health and longevity. Excess mortality in alcoholics has been reported for all major disease categories, particularly cirrhosis, cancers of the upper respiratory and digestive tracts, accidents, and suicide (1). The alcoholic environment probably promotes injury by exacerbating existing pathological tendencies, with the extent of deterioration being a weighted sum of the several kinds of injury produced in the constituent systems. The progressive and irreversible accumulation of informational entropy is hastened in alcoholism, and chances for survival are lessened. Death occurs when one or more subsystem is incapable of meeting the demands placed on it, producing a fluctuation in the physiological state of the organism of such magnitude as to exceed the limits within which homeostatic regulation can occur (2-6). The cybernetic failure or escape of one of these subsystems to a more likely configuration (death) is analogous to the transition of an activated complex over the activation energy barrier, implying an inherently stochastic component to the process. The situation is similar to a group of identical radioactive atoms, in which each atom has λdt probability of disintegrating in the interval dt. Alcoholic subjects are characterized by a hypothetical mean physiological state[1], which is more unstable than that in normal subjects and, therefore, more likely to undergo a biological fluctuation that produces death. This increased actuarial risk could result from two kinds of parameters governing longevity: rate of aging and vulnerability (7). These parameters are investigated in this report.

THEORETICAL SECTION

The measure of age-specific mortality rate is the actuary's q_x (7-10):

$$q_x = \frac{1}{h}\frac{L_x - L_{x+h}}{L_x} \qquad \text{(Eq. 1)}$$

where h is the length of the time interval, L_x is the number living at age x, and

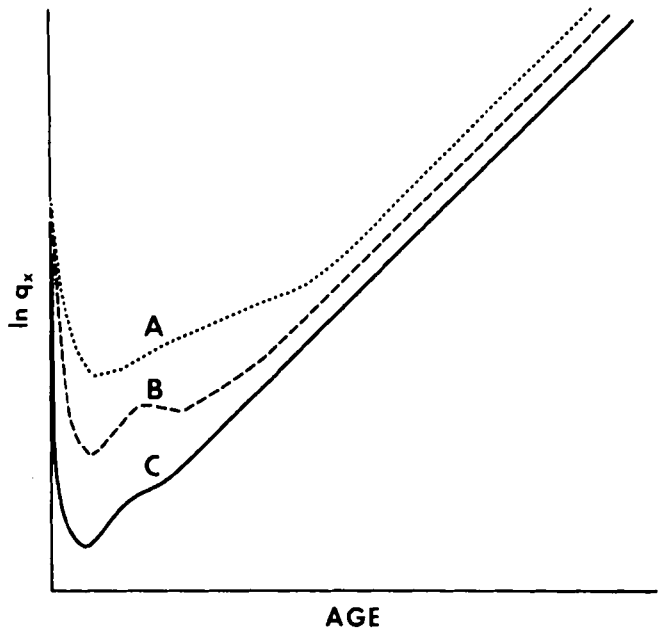

Figure 1—*Age-specific mortality rate plotted semilogarithmically against age for three populations; all populations have the same aging rate parameter but differ with respect to the vulnerability parameter (see text for discussion).*

[1] Mean physiological state can be described by specifying the mean values of certain essential physiological variables in a theoretical as opposed to an operational sense (see Refs. 3 and 5 for development of this concept).

0022-3549/84/0900-1191$01.00/0
© 1984, American Pharmaceutical Association

Table I—Parameter Estimates for the Gompertz Equations in Alcoholics and General Populations [a]

Population	Sex	Reference	Regression Line: Slope, years^{-1}	Regression Line: Intercept, years^{-1}	T_d, years^{-1}	1000 q_0, years^{-1}	Ratio, Alcoholic:Population: T_d	Ratio, Alcoholic:Population: q_0	t-Test: Slopes [b]	t-Test: Intercepts [b]
South Africa										
Caucasion alcoholics	M	23	0.0423 (0.0160[c])	1.46 (0.728)	16.4	4.32[c]				
Caucasion population	M	23	0.0816 (0.00228)[c]	−1.72 (0.118)	8.49	0.178[c]	1.93	24.3	$0.025 < p < 0.05$	$p < 0.001$
Ontario, Canada										
Alcoholics[d]	M	24, 25	0.0599 (0.00576)[c]	−0.0197 (0.309)	11.6	0.980[c]				
General Population[e]	M	24, 25	0.0931 (0.00251)[c]	−2.56 (0.142)	7.45	0.0775[c]	1.56	12.6	$p < 0.001$	$p < 0.001$
Alcoholics[d]	F	24-26	0.0301 (0.0118)[f]	1.36 (0.583)	23.0	3.89[f]				
General Population[e]	F	24-26	0.0918 (0.000638)[f]	−3.05 (0.0364)	7.55	0.0474[f]	3.05	82.1	$p < 0.001$	$p < 0.001$
Working class alcoholics[g]	81% M	27	0.0587 (0.00941)	−0.264 (0.489)	11.8	0.768				
Working class population[h]	M, F	27	0.0967 (0.00182)	−2.82 (0.0988)	7.17	0.0599	1.65	12.8	$0.001 < p < 0.005$	$p < 0.001$
Middle class alcoholics[g]	79% M	27	0.0556 (0.00854)	0.234 (0.442)	12.5	1.26				
Middle class population[h]	M, F	27	0.0966 (0.00199)	−2.79 (0.109)	7.18	0.0614	1.74	20.5	$p < 0.001$	$p < 0.001$
England and Wales										
Alcoholics[i]	M	28	0.0437 (0.00365)[c]	1.25 (0.198)	15.9	3.49[c]				
General Population[j]	M	28	0.0981 (0.00198)[c]	−2.97 (0.126)	7.07	0.0515[c]	2.25	67.8	$p < 0.001$	$p < 0.001$
Alcoholics[i]	F	28	0.0482 (0.00406)[f]	0.837 (0.222)	14.4	2.31[f]				
General Population[j]	F	28	0.0987 (0.00150)[f]	−3.53 (0.0957)	7.02	0.0292[f]	2.05	79.1	$p < 0.001$	$p < 0.001$

[a] Numbers in parentheses are *SD*s of the parameter estimates. [b] All tests are between alcoholics *versus* the general population. [c] Male data fitted by Eq. 4; see text for discussion. [d] A t test of slopes for male *versus* female alcoholics detected differences ($p < 0.05$), whereas a t test of intercepts failed to detect differences ($p > 0.05$). [e] A t test of slopes for male *versus* female populations failed to detect differences ($p > 0.6$), whereas a t test of intercepts detected differences ($p < 0.005$). [f] Female data fitted by Eq. 4; see text for discussion. [g] t Tests of slopes and intercepts for working class *versus* middle class alcoholics failed to detect differences ($p > 0.4$). [h] t Tests of slopes and intercepts for working class *versus* middle class populations failed to detect differences ($p > 0.8$). [i] t Tests of slopes and intercepts for male *versus* female alcoholics failed to detect differences ($p > 0.4$ and $p > 0.1$, respectively). [j] A t test of slopes for male *versus* female populations failed to detect differences ($p > 0.8$), whereas a t test of intercepts detected differences ($p < 0.005$).

L_{x+h} is the number living at age $x + h$. This is an estimate of the instantaneous mortality rate or force of mortality, $\rho(x)$ (5, 9):

$$\rho(x) = -\frac{1}{N(x)}\frac{dN(x)}{dx} \qquad \text{(Eq. 2)}$$

where $N(x)$ is the number of individuals surviving to age x. $\rho(x)$ is also the probability of an individual of age x dying over the interval from x to $x + dx$. Characteristically, q_x is high during infancy, falls to a minimum at ~10 years of age, and increases at an accelerated rate thereafter. Figure 1 illustrates typical semilogarithmic age-specific mortality curves for different populations. Goldman (11) has noted the similarity of these curves to failure curves for manufactured articles. High values of q_x occur during infancy and may be due to birth defects, immune deficiencies, incomplete gestation, *etc.* These are analogous to initial failures of manufactured products, resulting from faulty steps in the manufacturing process, defective parts, *etc.* After the curve bottoms out, but before it becomes exponential, chance failures predominate. In mortality curves and for manufactured goods, these chance failures are due to factors which are just as likely to be operative at any one time as at any other[2]. In mortality curves, this could be due to rare but fatal exposure to toxicants (chemicals, bacteria, *etc.*), accidents, *etc.* At some point in time, chance failures become exceedingly small relative to first-order wear-out failures, and the curve becomes exponential. Wear-out failures in manufactured articles are due to the effects of the duration of the service of the article. In mortality kinetics, wear-out failures are due to biological changes induced by processes we collectively lump under the heading of aging. In those Western societies with good standards of living, first-order mortality kinetics are generally first observed between the ages of 30 and 35 years. The appropriate mathematical relationship, termed the Gompertz equation, is (5, 7, 9, 12-17):

$$q_x = q_0 \cdot e^{\alpha x} \qquad \text{(Eq. 3)}$$

where q_x is the death rate at age x (age-specific death rate), q_0 is the extrapolated value of the death rate at age zero, and α is an aging rate parameter. The q_0 term is a measure of the initial vulnerability (7, 15) of the population to senescent-mediated causes of death in adults, *i.e.*, it measures the vulnerability of the population before the onset of aging. It is not an estimate of the death rate at birth, but rather is a theoretical parameter that is indicative of environmental influences and vigor of the genotype. Note in Fig. 1 that group A is more vulnerable than group B or C. The α term specifies the rate of increase of age-specific mortality; the doubling time (T_d) of age-specific mortality rates is equal to $(\ln 2)/\alpha$. In humans, T_d is ~8.5 years[3] (18). In a homogeneous population, an 8.5-year T_d means that a typical 50-year-old individual has twice the probability of dying during the course of one 24-h period than does a typical 41.5-year-old individual.

Sacher (7) has investigated the effects of various treatments (ionizing radiation, drugs, *etc.*) that contribute to the shortening and prolongation of life and has noted that although some treatments may affect both vulnerability (q_0) and rate of aging (α), most treatments affect predominantly one or the other (pharmacological agents usually affect q_0). In life prolongation, efficacious pharmacological therapies such as chronic procaine administration

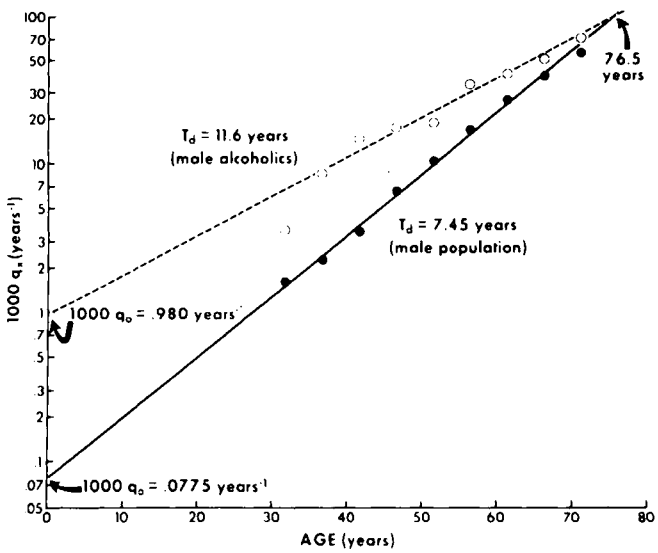

Figure 2—*Gompertz plots of age-specific mortality rates* versus *age for male alcoholics and the male general population in Ontario, Canada. See Fig. 3 for sample sizes and statistical weights in alcoholics (data are from Refs. 25 and 26).*

[2] This zero-order loss accounts for the age-independent term in the so-called Gompertz-Makeham equation (7, 12, 13), $q_x = q_0 e^{\alpha x} + A$, which characterizes age-specific mortality in this region and beyond; q_0 and α are defined with Eq. 3, and A is the zero-order component to mortality.

[3] In the data collated by Strehler and Mildvan (12), T_d ranged from 5.82 years in people from Trinidad and Tobago to 11.3 years for Algerian Moslems.

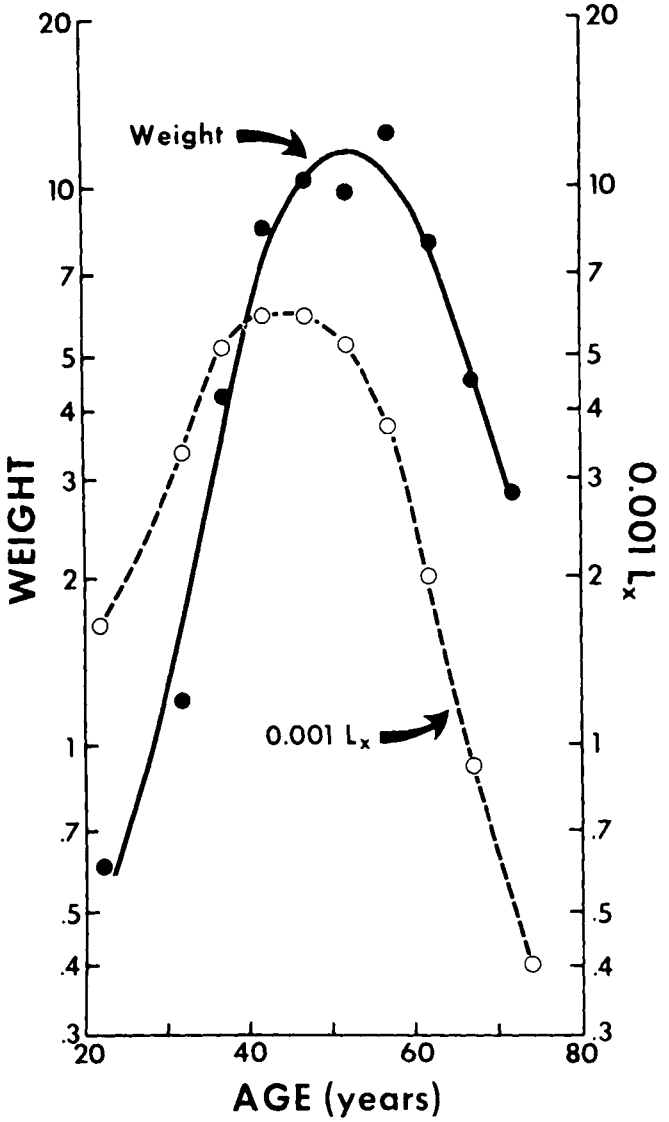

Figure 3—*Statistical weights and sample sizes (L_x) for alcoholic age-specific mortality data in Fig. 2 (data are from Refs. 25 and 26).*

achieve their effects by reducing q_0, whereas smoking in humans (7, 19) shortens life by increasing q_0. Strehler and Mildvan (12), on the other hand, have developed a general theory of mortality and aging which predicts an inverse relationship between q_0 and α.

Although the disease we term alcoholism is not generally regarded as a pharmacological treatment, mortality kinetics arising from it can be analyzed and discussed in that context; the results of such an analysis are reported.

EXPERIMENTAL SECTION

Mortality data in alcoholics was acquired by exhaustively searching the literature; this search ended in December 1982. In all cases, data were also presented on the general population as a whole[4], including all individuals of the same sex living in designated geographical areas.

Literature mortality data were generally collated for individuals in 5-year age groups; age-specific mortality rates were plotted semilogarithmically against age (Gompertz plot), where age was taken as the midpoint for the group. Data prior to the exponential phase were not used. Generally, this meant using only data obtained at or beyond the age of 32 years. A linear transformation of Eq. 3 is:

$$\ln q_x = \alpha x + \ln q_0 \qquad \text{(Eq. 4)}$$

Equation 5 was fitted to each set of data by the method of weighted, linear least-squares (21); parameter estimates and standard deviations were obtained for α and q_0. The weighting factor used for $\ln q_x$ was the reciprocal of its variance, and this was estimated by (9):

$$w = \frac{1}{v} \cong \frac{N_x P_x (\ln P_x)^2}{1 - P_x} \qquad \text{(Eq. 5)}$$

where w is the statistical weight, v is the sampling variance, N_x is the sample size, and P_x is the calculated probability of surviving the interval ($1 - P_x = q_x$). Differences between parameter estimates for alcoholics *versus* the general population were detected by t tests (Eq. 17 in Ref. 22).

[4] The population itself contains alcoholics, and a popular estimate of the point prevalence of alcoholism in Western societies is 7% (20). The lifetime prevalence rate is higher.

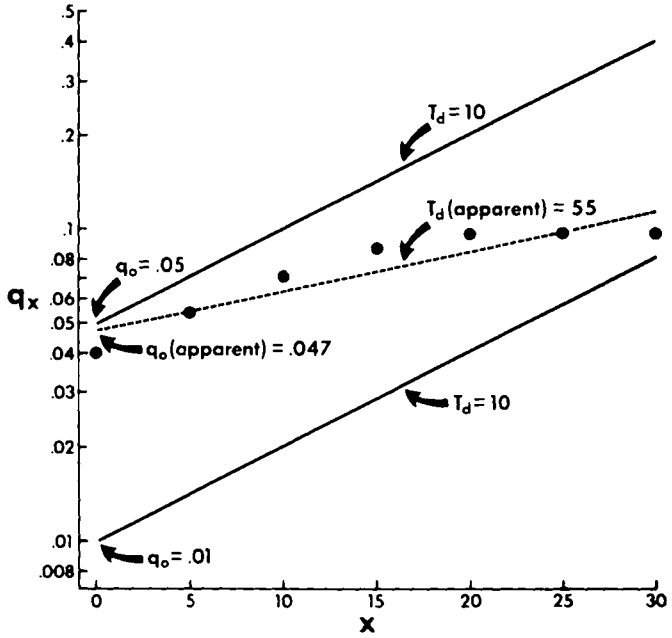

Figure 4—*Hypothetical Gompertz curves (—) for two strata of alcoholic subjects (arbitrary units). One group ($q_0 = 0.05$) is highly vulnerable to the mortality effects of alcohol, whereas the other group ($q_0 = 0.01$) mimics the general population; both groups have a T_d of 10. By taking the vulnerable group to comprise 75% of the alcoholic population and the invulnerable group to comprise 25%, pooling of the alcoholic subject data gives rise to the q_x data points between the two solid lines. The dashed line arises from a linear least-squares analysis of the pooled data. Note that the T_d (apparent) is considerably increased (see text for discussion).*

RESULTS AND DISCUSSION

Influence of Alcoholism on Vulnerability and Aging—Parameter estimates obtained from analysis of Gompertz plots are summarized in Table I. Curves for alcoholics and the general population from one representative study are shown in Fig. 2. Figure 3 depicts sample size and statistical weights for those data points from alcoholics in Fig. 2. A cursory examination of these data indicates two significant effects of alcoholism on the Gompertz parameters. First, the vulnerability parameter, q_0, is ~10-80 times higher in the alcoholic populations. Second, there appears to be a concomitant reduction in the aging rate parameter, α (see below). Although T_d in the general male population is ~7.7 years, an ostensible T_d of ~14.6 years is noted for male alcoholics.

The apparent increases noted for q_0 and T_d in male alcoholics are also seen in females. In the one study in which alcoholic subjects were categorized as either "working class" or "middle class," there were no differences in Gompertz plot slopes ($p > 0.8$) or intercepts ($p > 0.4$); in working class *versus* middle class general populations, slope ($p > 0.9$) and intercept ($p > 0.8$) values also did not differ.

Considerable variability exists between q_0 values in both normal male and female populations (an approximate threefold range). Aside from the genetic component, q_0 is affected by environmental factors (air and water quality, disease-carrying insects, *etc.*) and medical intervention (inoculations against disease, antibiotic therapy, *etc.*). Variability is also seen in a comparison of the influences of alcoholism on the T_d and q_0 parameters, particularly the latter. Values of q_0 are increased 12.6-fold over normal values in male alcoholics from Ontario, Canada, whereas there is a 67.8-fold increase in male alcoholics from England and Wales. Part of this diversity may be due to the variables mentioned above, as well as genetic factors predisposing individuals to alcoholism. In addition, several types of alcoholism do exist. Jellinek (29)

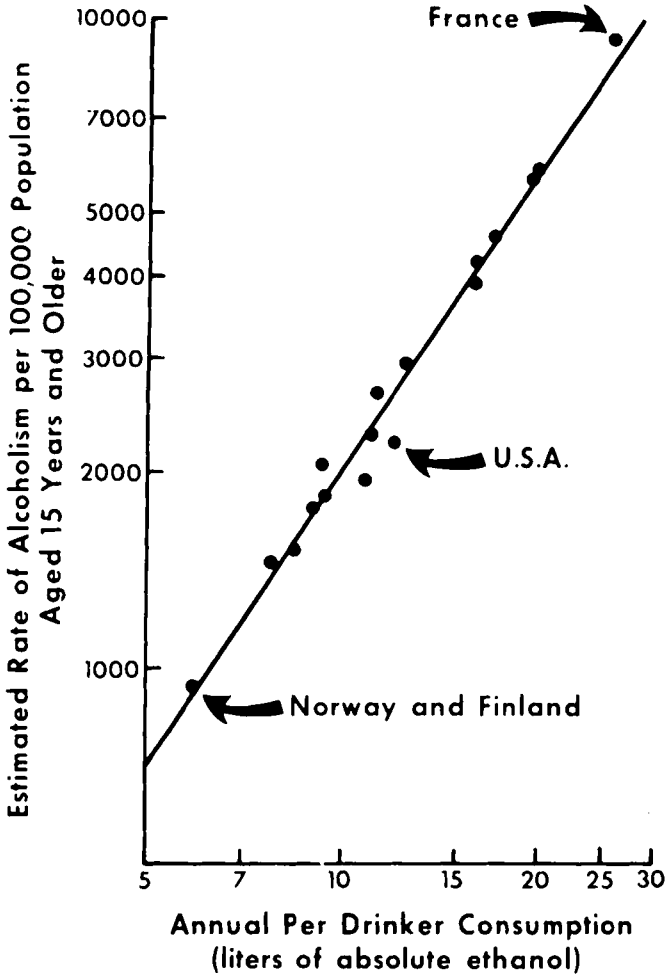

Figure 5—*Double logarithmic plot of the estimated rate of alcoholism in a country* versus *the annual per drinker consumption of alcohol. The equation consistent with this plot* ($y = \theta_1 y^{\theta_2}$) *was fitted by least-squares analysis (data from Ref. 30) and is* $y = 61.5\ x^{1.52}$; $r = 0.990$; $p < 0.01$.

has divided alcoholics into four major and several minor categories. The four major classifications are: (*a*) alpha alcoholism, a purely psychological continued dependence on the effects of alcohol to relieve bodily or emotional pain; (*b*) beta alcoholism, a condition in which alcoholic complications such as polyneuropathy, gastritis, and cirrhosis of the liver may occur without either physical or psychological dependence on alcohol; (*c*) gamma alcoholism, physical dependence and loss of control over the use of alcohol, a disease in and of itself; and (*d*) delta alcoholism, which is similar to gamma alcoholism, except instead of loss of control, there is inability to abstain (inveterate drinking)[5]. Therefore, alcoholics constitute a markedly heterogeneous group, with different drinking pattern and disease entities. Additionally, it is well known that the risk of getting cancer, cirrhosis of the liver, *etc.*, due to excessive alcohol use varies greatly among individuals. Those alcoholics who survive the age of, for example, 60 years in effect will be the least vulnerable, and their average vulnerability should be much lower than the average vulnerability in the general population at the same age. The range increases observed for q_0 in different populations probably reflects this heterogeneity[6].

To help explain this anomaly of an apparent slowing of aging in alcoholics, consider a hypothetical situation in which the alcoholic population consists of two strata, one highly vulnerable and one invulnerable to the effects of alcohol. In the latter group, the Gompertz curve is identical to that for the general population. In the former, the aging rate (α) is the same, but the vulnerability parameter is larger. For all alcoholics taken together, age-specific mortality rates will lie somewhere in between the two subgroups. This is illustrated in Fig. 4, in which q_0 for the invulnerable group is 0.01 (arbitrary units), and for the vulnerable group is 0.05. Note that the doubling times (T_d values) for the two subgroups are identical ($T_d = 10$ arbitrary units). If we take the vulnerable group ($q_0 = 0.05$) to comprise 75% of the alcoholic population and the invulnerable group ($q_0 = 0.01$) to comprise 25% of the alcoholic population, pooling of the data results in the q_x data points observed between the two Gompertz functions. Although the data points are best characterized by a curve, a linear function may be reasonably well fitted to the data, and this is indicated by the dashed line ($r = 0.92$) (Fig. 4). Note that the apparent T_d is now 55. After a number of years, the vulnerable alcoholics will become more or less extinct, and only the invulnerable ones will remain. At this age, the curve for all alcoholics would conicide with the one for the invulnerable group and, therefore, also for the general population. The larger the average vulnerability of the alcoholic group, as compared with the general population, the greater the apparent increase in T_d. This hypothetical illustration is no doubt simplistic (there are probably several strata), but it does serve to illustrate how an erroneously high T_d for alcoholics could be obtained. Although other possibilities exist to explain the increase in T_d, the grouping of heterogeneous alcoholic population is, by far, the most likely explanation.

If we assume the unlikely possibility that alcoholics are relatively homogeneous with respect to mortality parameters, we conclude that those factors causing or resulting from alcoholism also slow the aging rate. The Strehler–Mildvan theory of mortality and aging (12), mentioned above, interrelates the values of q_0 and α and predicts that a high initial mortality rate (q_0) should be associated with as low rate of increase of mortality rate (reduced α); this represents yet another interpretation of the data.

In future studies of alcoholic mortality, attempts should be made to categorize the various types of alcoholics. Another problem is that all studies have heretofore been based on age-group cohorts (not longitudinal data). Data from chronic, progressive alcoholics are therefore lumped with those from individuals who have a fluctuating course or a limited single alcoholic episode. This may have contributed to the postulated heterogeneity in vulnerability, producing the postulated artifactual increase in T_d. Longitudinal studies, therefore, would be very useful.

Drinking Habits, Alcoholism, and Aging—The fact that alcoholism affects apparent values of α and q_0 suggests that there might be some correlation between drinker consumption of alcohol in a given country and these parameters. Data from 16 countries (12, 30) were used to test this hypothesis. Correlation analyses were conducted on data for per drinker consumption *versus* α or q_0. Correlation coefficients were <0.02, indicating no correlations whatsoever. Similar results were obtained when rates of alcoholism in various countries were compared with α or q_0. This analysis implies that the drinking habits of a nation will not affect the overall Gompertz parameters for that nation. As expected, annual drinker consumption of alcohol did correlate with the rate of alcoholism (Fig. 5). For each twofold increase in per drinker alcohol consumption, alcoholism increases 2.87-fold.

REFERENCES

(1) S. Pell and C. A. D'Alonzo, *J. Occup. Med.*, **15,** 120 (1973).

(2) G. A. Sacher, *J. Natl. Cancer Inst.*, **15,** 1125 (1955).

(3) G. A. Sacher, *Radiology*, **67,** 250 (1956).

(4) B. L. Strehler, in "The Biology of Aging," B. L. Strehler, Ed., publication no. 6, American Institute of Biological Sciences, Washington, D.C., 1960, pp. 309–314.

(5) G. A. Sacher and E. Trucco, *Ann. N.Y. Acad. Sci.*, **96,** 985 (1962).

(6) H. A. Johnson, *Science*, **141,** 910 (1963).

(7) G. A. Sacher, in "Handbook of the Biology of Aging," C. E. Finch and L. Hayflick, Eds., Van Nostrand Reinhold, New York, N.Y., 1977, pp. 582–638.

(8) L. I. Dublin, A. J. Lotka, and M. Spiegelman, in "Length of Life," 2nd ed., Ronald Press, New York, N.Y., 1949.

(9) G. A. Sacher, in "Radiation and Ageing: Proceedings of a Colloquium held in Semmering, Austria, June, 1966," P. J. Lindop and G. A. Sacher, Eds., Taylor and Francis, London, 1966, pp. 411–441.

(10) C. L. Chiang, "Introduction to Stochastic Processes in Biostatistics," Wiley, New York, N.Y., 1968.

(11) S. Goldman, *Perspect. Biol. Med.*, **12,** 12 (1968).

(12) B. L. Strehler and S. Mildvan, *Science*, **132,** 14 (1960).

(13) A. Comfort, in "The Biology of Senescence," 3rd ed., Elsevier/North-Holland, New York, N.Y., 1964, pp. 23–24.

(14) B. L. Strehler, *Quart. Rev. Biol.*, **34,** 117 (1959).

(15) G. A. Sacher and R. W. Hart, in "Genetic Effects on Aging," D. H. Harrison, Ed., A. R. Liss, New York, N.Y., 1977, pp. 73–98.

[5] Current research programs are investigating the possibilities of several other or different types of alcoholism.

[6] Considerable heterogeneity also exists within each of the major categories with respect to the following variables: age of onset of heavy drinking, cumulative period of drinking, alcohol consumption, smoking habits, social and financial status, marital status, availability and cost of alcohol, social mores, genetic constitution, geographical location, treatment intervention, ethnicity, accessibility and availability of health care, amount of exercise and sleep, and environmental stress.

(16) G. A. Sacher, in "Genetics of Ageing," E. L. Schneider, Ed., Plenum, New York, N.Y., 1978, pp. 151-168.
(17) B. Gompertz, *Philosophical Transactions*, **27**, 513 (1825); reproduced in "Mathematical Demography," D. Smith and N. Keyfitz, Eds., Springer-Verlag, Berlin, 1977, pp. 279-288.
(18) H. Jones, in "Basic Mechanisms in Radiobiology. V. Mammalian Aspects," H. J. Curtis and H. Quastler, Eds., National Academy of Science—National Research Council, Washington, D.C., 1957, pp. 102-170.
(19) W. F. Forbes and J. F. Gentleman, *J. Gerontol.*, **28**, 302 (1973).
(20) R. M. Costello, in "Encyclopedic Handbook of Alcoholism," E. M. Pattison and E. Kaufman, Eds., Gardner Press, New York, N.Y., 1982, pp. 1197-1210.
(21) N. R. Draper and H. Smith, "Applied Regression Analysis," Wiley, New York, N.Y., 1966.
(22) H. G. Boxenbaum, S. Riegelman, and R. M. Elashoff, *J. Pharmacokinet. Biopharm.*, **2**, 123 (1974).
(23) L. S. Gillis, *South African Med. J.*, **43**, 230 (1969).
(24) W. Schmidt and J. de Lint, *Q. J. Stud. Alcohol*, **30**, 112 (1969).
(25) W. Schmidt and J. de Lint, *Q. J. Stud. Alcohol*, **33**, 171 (1972).
(26) J. de Lint and T. Levinson, *Can. Med. Assoc. J.*, **113**, 385 (1975).
(27) W. Schmidt and J. de Lint, *Br. J. Addict.*, **64**, 327 (1970).
(28) A. Adelstein and G. White, *Popul. Trends.*, **6**, 7 (1976).
(29) E. M. Jellinek, "The Disease Concept of Alcoholism," Hillhouse Press, New Haven, Conn., 1960.
(30) J. de Lint and W. Schmidt, in "Biological Basis of Alcoholism," Y. Israel and J. Mardones, Eds., Wiley-Interscience, New York, N.Y., 1971, pp. 423-442.

ACKNOWLEDGMENTS

This work was supported in part by Grant 2P50AA03510-06 from NIAAA. The authors thank Susan Mercik, Robert Ronfeld, and the reviewer for assistance and critical comments.

Solubility and Complexation Behavior of Griseofulvin in Fatty Acid–Isooctane Mixtures

MEHDI MEHDIZADEH and DAVID J. W. GRANT ˣ

Received January 17, 1983, from the *Faculty of Pharmacy, University of Toronto, Toronto, Ontario M5S 1A1 Canada.* Accepted for publication August 1, 1983.

Abstract □ The influence of complex formation on the solubility behavior of griseofulvin in the straight-chain fatty acids was investigated by using phase solubility analysis in isooctane (2,2,4-trimethylpentane) at 25°C. The apparent molar solubility of the proton acceptor griseofulvin ($[A]_t$) was determined spectrophotometrically in the presence of various total molar concentrations ($[D]_t$) of each of the proton donors (acetic, propanoic, butanoic, hexanoic, and octanoic acids). Increasing $[D]_t$ caused a pronounced increase in $[A]_t$ according to a biphasic log-log relationship, suggesting the formation of two complexes, AD_m and AD_n. The data are in close agreement with a simple mathematical model which assumes that two complexes, AD_m and AD_n, are formed and that $[D]_t \approx 2[D_2]$, where D_2 refers to the fatty acid dimer. Linear regression analysis showed that the data best fit the complexation models with $n = 5$ or 6 and $m = 0$, 1, or 2, depending on the fatty acid. Assuming values of the dimerization constants of the fatty acids as reported in the literature, the stability constants of the complexes, K_n and K_m, were calculated and found to decrease with increasing chain length of the fatty acids. The proposed model was critically appraised. An alternative model, which takes into full account the fatty acid monomer while assuming that only one complex is formed, leads to unacceptable conclusions.

Keyphrases □ Molecular complexes—griseofulvin and straight-chain alkanoic acids, isooctane solution, solubility □ Carboxylic acid dimerization—influence on molecular complexation, griseofulvin and straight-chain fatty acids, isooctane solution □ Griseofulvin—solubility in isoocatane solution, straight-chain fatty acids

Complex formation, a valuable method for increasing the solubility, dissolution rate, and bioavailability of sparingly soluble drugs (1), also leads to a modification of the rate of transfer of certain drugs through lipid barriers (2). Griseofulvin (I) exhibits a poor bioavailability due to its low aqueous solubility (3). The stable crystal lattice of griseofulvin can, however, be broken down by proton-donating solvents, such as chloroform (4) and the fatty acids (5), which presumably form hydrogen-bonded complexes. Some of these complexes appear to exist in the solid state as solvates or inclusion compounds (6–8). Phenobarbital, a weak acid, also forms a solid complex with griseofulvin (9). Soluble complexes are formed between griseofulvin and phenols in carbon tetrachloride (10) and between certain steroidal drugs and organic solvents (11).

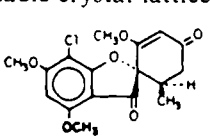

I

The purpose of the present work is to investigate further the complexation of griseofulvin with the straight-chain alkanoic acids. The solubility method of Kostenbauder and Higuchi (12) was employed, and isooctane (2,2,4-trimethylpentane) was used as the inert solvent.

EXPERIMENTAL SECTION

Materials—Griseofulvin[1] was >99% pure, as described previously (5). Chloroform[2], acetic acid[3], *n*-butanoic acid[3], and *n*-octanoic acid[3] were reported to be >99% pure. Propanoic acid[4] and *n*-hexanoic acid[3] were distilled by using a glass apparatus. Isooctane (2,2,4-trimethylpentane)[4] was ≥99% pure.

Solubility Determinations—A mixture of griseofulvin (in excess of its solubility) and 5 mL of isooctane–fatty acid was shaken at 25.0 ± 0.05°C. Aliquots of 0.1–1.0 mL were diluted with chloroform, and the concentration of griseofulvin was determined (in duplicate) spectrophotometrically[5] at λ_{max} = 289.5 nm[6]. Saturation equilibrium was attained in <24 h. Each value (*e.g.*, $[A]_t$) is the mean of three separate determinations.

Analysis of the Solid Phases—A sample of the solid was removed from the equilibrated saturated solution, and the crystals were immediately placed on filter paper. The following methods of analysis were applied to all samples: X-ray diffraction (9), hot-stage microscopy (9), thermogravimetry (8), and

[1] ICI Ltd., Pharmaceuticals Division, Macclesfield, Cheshire, U.K.
[2] J.T. Baker Chemical Co.
[3] BDH Chemicals Ltd.
[4] Fisher Scientific Co. Ltd.
[5] Model PMQ II UV-visible spectrophotometer; Zeiss.
[6] Model 118 UV-visible spectrophotometer; Cary.

0022-3549/84/0900-1195$01.00/0
© 1984, American Pharmaceutical Association

(16) G. A. Sacher, in "Genetics of Ageing," E. L. Schneider, Ed., Plenum, New York, N.Y., 1978, pp. 151-168.
(17) B. Gompertz, *Philosophical Transactions*, **27**, 513 (1825); reproduced in "Mathematical Demography," D. Smith and N. Keyfitz, Eds., Springer-Verlag, Berlin, 1977, pp. 279-288.
(18) H. Jones, in "Basic Mechanisms in Radiobiology. V. Mammalian Aspects," H. J. Curtis and H. Quastler, Eds., National Academy of Science—National Research Council, Washington, D.C., 1957, pp. 102-170.
(19) W. F. Forbes and J. F. Gentleman, *J. Gerontol.*, **28**, 302 (1973).
(20) R. M. Costello, in "Encyclopedic Handbook of Alcoholism," E. M. Pattison and E. Kaufman, Eds., Gardner Press, New York, N.Y., 1982, pp. 1197-1210.
(21) N. R. Draper and H. Smith, "Applied Regression Analysis," Wiley, New York, N.Y., 1966.
(22) H. G. Boxenbaum, S. Riegelman, and R. M. Elashoff, *J. Pharmacokinet. Biopharm.*, **2**, 123 (1974).
(23) L. S. Gillis, *South African Med. J.*, **43**, 230 (1969).
(24) W. Schmidt and J. de Lint, *Q. J. Stud. Alcohol*, **30**, 112 (1969).
(25) W. Schmidt and J. de Lint, *Q. J. Stud. Alcohol*, **33**, 171 (1972).
(26) J. de Lint and T. Levinson, *Can. Med. Assoc. J.*, **113**, 385 (1975).
(27) W. Schmidt and J. de Lint, *Br. J. Addict.*, **64**, 327 (1970).
(28) A. Adelstein and G. White, *Popul. Trends.*, **6**, 7 (1976).
(29) E. M. Jellinek, "The Disease Concept of Alcoholism," Hillhouse Press, New Haven, Conn., 1960.
(30) J. de Lint and W. Schmidt, in "Biological Basis of Alcoholism," Y. Israel and J. Mardones, Eds., Wiley-Interscience, New York, N.Y., 1971, pp. 423-442.

ACKNOWLEDGMENTS

This work was supported in part by Grant 2P50AA03510-06 from NIAAA. The authors thank Susan Mercik, Robert Ronfeld, and the reviewer for assistance and critical comments.

Solubility and Complexation Behavior of Griseofulvin in Fatty Acid–Isooctane Mixtures

MEHDI MEHDIZADEH and DAVID J. W. GRANT ˣ

Received January 17, 1983, from the *Faculty of Pharmacy, University of Toronto, Toronto, Ontario M5S 1A1 Canada.* Accepted for publication August 1, 1983.

Abstract □ The influence of complex formation on the solubility behavior of griseofulvin in the straight-chain fatty acids was investigated by using phase solubility analysis in isooctane (2,2,4-trimethylpentane) at 25°C. The apparent molar solubility of the proton acceptor griseofulvin ($[A]_t$) was determined spectrophotometrically in the presence of various total molar concentrations ($[D]_t$) of each of the proton donors (acetic, propanoic, butanoic, hexanoic, and octanoic acids). Increasing $[D]_t$ caused a pronounced increase in $[A]_t$ according to a biphasic log-log relationship, suggesting the formation of two complexes, AD_m and AD_n. The data are in close agreement with a simple mathematical model which assumes that two complexes, AD_m and AD_n, are formed and that $[D]_t \approx 2[D_2]$, where D_2 refers to the fatty acid dimer. Linear regression analysis showed that the data best fit the complexation models with $n = 5$ or 6 and $m = 0$, 1, or 2, depending on the fatty acid. Assuming values of the dimerization constants of the fatty acids as reported in the literature, the stability constants of the complexes, K_n and K_m, were calculated and found to decrease with increasing chain length of the fatty acids. The proposed model was critically appraised. An alternative model, which takes into full account the fatty acid monomer while assuming that only one complex is formed, leads to unacceptable conclusions.

Keyphrases □ Molecular complexes—griseofulvin and straight-chain alkanoic acids, isooctane solution, solubility □ Carboxylic acid dimerization—influence on molecular complexation, griseofulvin and straight-chain fatty acids, isooctane solution □ Griseofulvin—solubility in isoocatane solution, straight-chain fatty acids

Complex formation, a valuable method for increasing the solubility, dissolution rate, and bioavailability of sparingly soluble drugs (1), also leads to a modification of the rate of transfer of certain drugs through lipid barriers (2). Griseofulvin (I) exhibits a poor bioavailability due to its low aqueous solubility (3). The stable crystal lattice of griseofulvin can, however, be broken down by proton-donating solvents, such as chloroform (4) and the fatty acids (5), which presumably form hydrogen-bonded complexes. Some of these complexes appear to exist in the solid state as solvates or inclusion compounds (6–8). Phenobarbital, a weak acid, also forms a solid complex with griseofulvin (9). Soluble complexes are formed between griseofulvin and phenols in carbon tetrachloride (10) and between certain steroidal drugs and organic solvents (11).

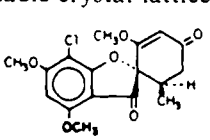

I

The purpose of the present work is to investigate further the complexation of griseofulvin with the straight-chain alkanoic acids. The solubility method of Kostenbauder and Higuchi (12) was employed, and isooctane (2,2,4-trimethylpentane) was used as the inert solvent.

EXPERIMENTAL SECTION

Materials—Griseofulvin[1] was >99% pure, as described previously (5). Chloroform[2], acetic acid[3], *n*-butanoic acid[3], and *n*-octanoic acid[3] were reported to be >99% pure. Propanoic acid[4] and *n*-hexanoic acid[3] were distilled by using a glass apparatus. Isooctane (2,2,4-trimethylpentane)[4] was ≥99% pure.

Solubility Determinations—A mixture of griseofulvin (in excess of its solubility) and 5 mL of isooctane–fatty acid was shaken at 25.0 ± 0.05°C. Aliquots of 0.1–1.0 mL were diluted with chloroform, and the concentration of griseofulvin was determined (in duplicate) spectrophotometrically[5] at λ_{max} = 289.5 nm[6]. Saturation equilibrium was attained in <24 h. Each value (*e.g.*, $[A]_t$) is the mean of three separate determinations.

Analysis of the Solid Phases—A sample of the solid was removed from the equilibrated saturated solution, and the crystals were immediately placed on filter paper. The following methods of analysis were applied to all samples: X-ray diffraction (9), hot-stage microscopy (9), thermogravimetry (8), and

[1] ICI Ltd., Pharmaceuticals Division, Macclesfield, Cheshire, U.K.
[2] J.T. Baker Chemical Co.
[3] BDH Chemicals Ltd.
[4] Fisher Scientific Co. Ltd.
[5] Model PMQ II UV-visible spectrophotometer; Zeiss.
[6] Model 118 UV-visible spectrophotometer; Cary.

0022-3549/84/0900-1195$01.00/0
© 1984, American Pharmaceutical Association

Table I—UV Spectral Data of Griseofulvin in Various Solvents at 25°C

Solvent	$\lambda_{max,1}$, nm	ϵ_1, 10^3 M^{-1} cm^{-1}	$\lambda_{max,2}$, nm	ϵ_2, 10^3 M^{-1} cm^{-1}
Isooctane	248.5	13.3	317	2.71
Chloroform in isooctane (50% v/v)	289.0	16.5	321	5.03
Chloroform	289.5	23.8	321	5.30
Acetic acid	288.5	23.3	320	5.17
Propanoic acid	287.5	24.1	320	5.45
Butanoic acid	287.2	23.0	320	5.23
Hexanoic acid	287.0	19.4	319	5.07
Methanol[a]	291.0	24.1	324	5.47
Ethanol[b]	292.0	24.9	325	5.53

[a] From Ref. 13. [b] From Ref. 14.

Table II—Apparent Molar Solubility of Griseofulvin ($[A]_t$) in Isooctane Containing Various Total Molar Concentrations of Fatty Acids ($[D]_t$) at 25°C

Donor, % (v/v)	Acetic Acid		Propanoic Acid		Butanoic Acid		Hexanoic Acid		Octanoic Acid	
	$[D]_t$, M	$[A]_t$, M × 10^5	$[D]_t$, M	$[A]_t$, M × 10^5	$[D]_t$, M	$[A]_t$, M × 10^5	$[D]_t$, M	$[A]_t$, M × 10^5	$[D]_t$, M	$[A]_t$, M × 10^5
0	0	0.9358[a]	0	0.9358[a]	0	0.9358[a]	0	0.9358[a]	0	0.9358[a]
2	0.3476	2.7580	0.2605	2.6187	0.2095	1.5217	0.1632	2.3173	0.1271	2.7170
4	0.6952	6.2499	0.5146	4.5701	0.4168	2.8545	0.3121	3.2021	0.2533	3.6332
6	1.0428	9.6369	0.7708	7.2094	0.6191	4.5350	0.4648	4.1777	0.3794	4.8125
8	1.3904	17.922	1.0189	10.256	0.8241	7.0268	0.6297	6.2423	0.5062	5.5706
10	1.7380	26.807	1.2778	12.418	1.0211	9.4026	0.7839	7.7623	0.6280	7.1758
20	3.4759	185.35	2.6771	66.812	2.1798	29.339	1.5594	20.902	1.2338	12.631
30	5.2139	540.76	4.0173	117.21	3.2608	88.639	2.3478	43.084	1.8670	25.186
40	6.9519	1209.0	5.3612	302.02	4.3523	145.56	3.1179	77.581	2.4724	34.941
50	8.6898	2170.7	6.712	505.91	5.4329	249.86	3.9043	128.39	3.1073	53.863
60	10.428	3697.9	8.052	905.49	6.4994	424.78	4.6932	207.16	3.7195	80.505
70	12.166	5261.5	9.357	1491.1	7.5687	644.98	5.5410	319.74	4.3491	110.40
80	13.904	7675.9	10.658	2017.5	8.6098	976.96	6.3159	435.18	4.7815	138.99
90	15.642	10,349	12.023	3002.6	9.6715	1349.8	7.1204	622.85	5.5349	185.35
100	17.380	13,034	13.381	4160.5	10.826	1855.8	7.8545	858.98	6.1604	254.89

[a] The molar solubility of griseofulvin in pure isooctane ($[A]_0$) is 9.358 μM.

differential scanning calorimetry[7] (DSC). For DSC, a 2–3-mg sample was encapsulated and heated at a rate of 10 mcal·s^{-1}, with alumina as the reference material, helium as the gas phase, and indium as the calibrating standard. The data indicated that the samples removed from the saturated solutions were essentially unsolvated crystals of griseofulvin.

THEORETICAL SECTION

Griseofulvin (I) contains two keto groups, four ether oxygen atoms, and an aromatic ring, each of which can accept protons to form a hydrogen bond. Since griseofulvin has no proton-donating groups, it acts only as a proton acceptor, A.

Fatty acids act as proton donors, D. Since each acid molecule has only one proton, whereas griseofulvin has multiple acceptor sites, the total molar concentration of acid ($[D]_t$) and griseofulvin ($[A]_t$) in solution can be expressed by the following mass balance equations:

$$[A]_t = [A]_0 + [AD] + [AD_2] + [AD_3] + \ldots + [AD_z] \quad \text{(Eq. 1)}$$

$$[D]_t = [D] + 2[D]_2 + [AD] + 2[AD_2] + 3[AD_3] + \ldots + z[AD_z] \quad \text{(Eq. 2)}$$

where $[A]_0$ is the molar concentration of uncomplexed griseofulvin and is equal to the solubility in isooctane, $[AD_n]$ is the molar concentration of a complex of stoichiometric number n, $[D]$ is the molar concentration of fatty acid monomers, and $[D_2]$ is the molar concentration of fatty acid dimers.

If the standard state of each dissolved species (X) is assumed to be a hypothetical 1 M solution, which is assumed to behave as if it were infinitely dilute, then the activity of X, $\{X\}$, is given by:

$$\{X\} = \gamma_x[X] \quad \text{(Eq. 3)}$$

where γ_x is the molarity-based activity coefficient.

The formation of each complex can be represented as follows:

$$A + nD \rightleftharpoons AD_n \quad \text{(Eq. 4)}$$

$$\{AD_n\} = K_{1:n}\{A\}\{D\}^n \quad \text{(Eq. 5)}$$

$$[AD_n] = (K_{1:n}\{A\}\gamma_D^n/\gamma_{AD_n})[D]^n \quad \text{(Eq. 6)}$$

$$[AD_n] = K_n[D]^n \quad \text{(Eq. 7)}$$

where $K_{1:n}$ is the thermodynamic stability constant (based on activity), and K_n is the apparent stability constant (based on concentration), such that:

$$K_n = K_{1:n}\{A\}\gamma_D^n/\gamma_{AD_n} \quad \text{(Eq. 8)}$$

Dimerization of the fatty acid donor may be represented as:

$$2D \rightleftharpoons D_2 \quad \text{(Eq. 9)}$$

$$\{D_2\} = K_D\{D\}^2 \quad \text{(Eq. 10)}$$

$$[D_2] = (K_D\gamma_D^2/\gamma_{D_2})[D]^2 \quad \text{(Eq. 11)}$$

$$[D_2] = K_d[D]^2 \quad \text{(Eq. 12)}$$

where K_D is the thermodynamic dimerization constant (based on activity) and K_d is the apparent dimerization constant (based on concentration), such that:

$$K_d = K_D\gamma_D^2/\gamma_{D_2} \quad \text{(Eq. 13)}$$

Equations 7 and 12 can be combined as follows:

$$[AD_n] = (K_n/K_d^{n/2})[D_2]^{n/2} \quad \text{(Eq. 14)}$$

Two-Complex Model—If the two complexes, AD_m and AD_n, are present, Eq. 1 becomes:

$$[A]_t - [A]_0 = [AD_m] + [AD_n] \quad \text{(Eq. 15)}$$

$$= (K_m \cdot K_d^{-m/2})[D_2]^{m/2} + (K_n \cdot K_d^{-n/2})[D_2]^{n/2} \quad \text{(Eq. 16)}$$

whereas Eq. 2 becomes:

$$[D]_t = [D] + 2[D_2] + m[AD_m] + n[AD_n] \quad \text{(Eq. 17)}$$

Expressing $[D]$, $[AD_m]$, and $[AD_n]$ in terms of $[D_2]$ using Eqs. 12 and 14 affords:

$$[D]_t = K_d^{-1/2}[D_2]^{1/2} + 2[D_2] + (m \cdot K_m \cdot K_d^{-m/2})[D_2]^{m/2} + (n \cdot K_n \cdot K_d^{-n/2})[D_2]^{n/2} \quad \text{(Eq. 18)}$$

Two-Complex Model with Predominance of the Fatty Acid Dimer—In the presence of all but the lowest concentrations of fatty acid in a hydrocarbon

[7] DSC-2C differential scanning calorimeter; Perkin-Elmer.

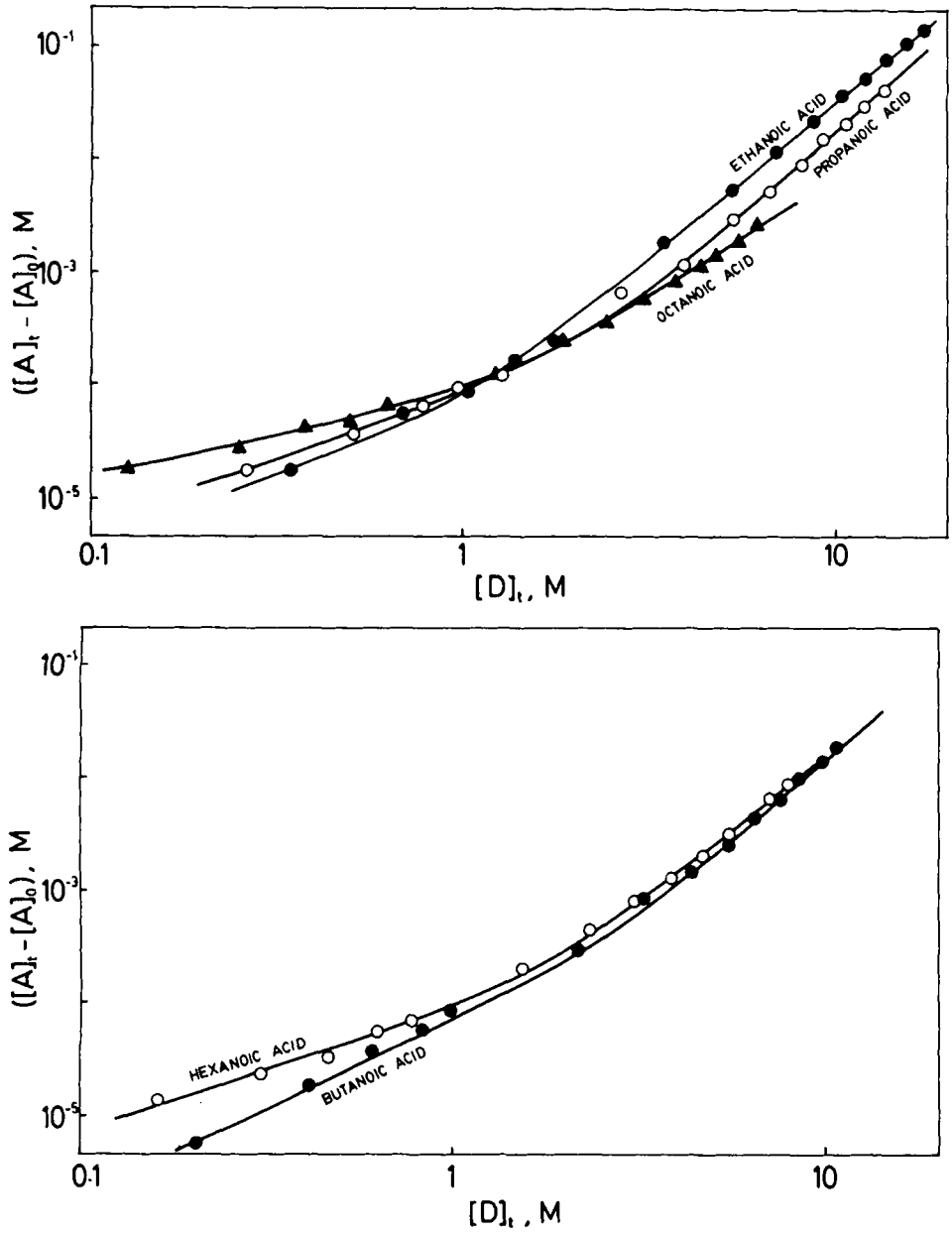

Figure 1—*Plots of log ([A]$_t$ − [A]$_0$) against log [D]$_t$, where ([A]$_t$ − [A]$_0$) is the increase in the apparent molar solubility of griseofulvin brought about by the presence of the following straight-chain alkanoic acids of total molar concentration, [D]$_t$, in isooctane at 25°C.*

solvent, $[D] \ll [D_2]$, because K_d in Eq. 12 has values of the order of 10^4 M^{-1}. Since the solubility of griseofulvin is always much smaller than the concentration of the fatty acid, $[AD_m] \ll [D_2]$ and $[AD_n] \ll [D_2]$. Equation 17 then simplifies to:

$$[D]_t \approx 2[D_2] \qquad \text{(Eq. 19)}$$

and Eq. 16 then becomes:

$$[A]_t - [A]_0 \approx (K_m \cdot K_d^{-m/2} \cdot 2^{-m/2})[D]_t^{m/2} + (K_n \cdot K_d^{-n/2} \cdot 2^{-n/2})[D]_t^{n/2} \qquad \text{(Eq. 20)}$$

Therefore:

$$[A]_t - [A]_0 \approx p[D]_t^{m/2} + q[D]_t^{n/2} \qquad \text{(Eq. 21)}$$

where:

$$p = K_m \cdot K_d^{-m/2} \cdot 2^{-m/2},\ q = K_n \cdot K_n^{-n/2} \cdot 2^{-n/2} \qquad \text{(Eq. 22)}$$

Therefore:

$$([A]_t - [A]_0)/[D]_t^{m/2} \approx p + q[D]_t^{(n-m)/2} \qquad \text{(Eq. 23)}$$

Thus, if two donor–acceptor complexes are present, $([A]_t - [A]_0)/[D]_t^{m/2}$ is expected to be a linear function of $[D]_t^{(n-m)/2}$. The slope q and intercept p afford the apparent stability constants, K_n and K_m, of the respective complexes, provided that the apparent dimerization constant, K_d, is known.

Single-Complex Model with Predominance of the Fatty Acid Dimer—If only one complex species, AD_m, is considered, Eqs. 1, 15, 20, and 21 reduce to:

$$[A]_t - [A]_0 = [AD_m] = (K_m \cdot K_d^{-m/2})[D_2]^{m/2} \qquad \text{(Eq. 24)}$$

$$\approx (K_m \cdot K_d^{-m/2} \cdot 2^{-m/2})[D]_t^{m/2} \qquad \text{(Eq. 25)}$$

$$[A]_t - [A]_0 \approx p[D]_t^{m/2} \qquad \text{(Eq. 26)}$$

The increase in solubility of the acceptor ($[A]_t - [A]_0$) is then expected to be proportional to the $m/2$ power of the total concentration of donor, $[D]_t^{m/2}$. The proportionality constant affords the apparent stability constant K_m of the complex if the apparent dimerization constant K_d is known. By taking logarithms, Eq. 26 yields:

$$\log([A]_t - [A]_0) \approx \log(K_m \cdot K_d^{-m/2} \cdot 2^{-m/2}) + (m/2) \cdot \log [D]_t \qquad \text{(Eq. 27)}$$

The linear regression of $\log([A]_t - [A]_0)$ against $\log [D]_t$ enables the stoichiometric number m of the complex to be determined from the regression coefficient (slope) and K_m to be determined from the intercept.

Single-Complex Model Allowing for all Donor Species Including the Monomer—Alternative models may be constructed which take into full account all species containing the fatty acid, including the monomer D. The approximate equation (Eq. 19) is clearly inappropriate here. For simplicity,

Table III—Linear Regression Analyses [a]

Donor	m	n	r [a]	$100s$ [b]	$10^5 p$	$10^5 q$
Acetic acid	0	4	0.9949	14.35	−385.3	42.49
	0	5	0.9997	3.52	−43.45	10.52
	0	6	0.9966	11.79	230.0	2.578
	1	5	0.9996	3.79	−19.16	10.55
	1	6	0.9957	12.04	72.56	28.88
	2	5	0.9992	4.45	−8.587	10.59
	2	6	0.9944	12.03	25.53	2.590
	3	5	0.9975	6.62	−3.732	10.63
	3	6	0.9932	10.84	11.57	2.540
	4	6	0.9806	11.27	8.597	2.166
Propanoic acid	0	5	0.9964	12.93	−67.64	6.127
	0	6	0.9997	3.75	9.529	1.723
	0	7	0.9976	10.54	74.26	0.4807
	1	5	0.9947	14.16	−21.82	6.070
	1	6	0.9996	4.14	10.78	1.724
	2	5	0.9906	16.18	−5.493	5.938
	2	6	0.9991	4.92	6.195	1.679
	3	5	0.9696	21.02	1.782	5.431
	3	6	0.9936	9.73	7.022	1.525
	4	6	0.5166	37.30	10.43	0.6557
Butanoic acid	0	5	0.9977	10.05	−21.91	4.695
	0	6	0.9997	3.44	13.51	1.470
	0	7	0.9964	12.60	43.25	0.4545
	1	5	0.9964	11.27	6.771	4.645
	1	6	0.9996	3.96	7.897	1.457
	2	5	0.9932	13.02	−0.6602	4.520
	2	6	0.9992	4.49	5.927	1.419
	3	5	0.9778	16.37	2.786	4.055
	3	6	0.9966	6.43	6.020	1.261
	4	6	0.5874	23.21	8.430	0.4527
Hexanoic acid	0	5	0.9976	9.99	−4.015	4.727
	0	6	0.9992	5.92	11.88	1.730
	0	7	0.9960	12.88	25.01	0.6289
	1	5	0.9968	10.17	0.7631	4.639
	1	6	0.9989	6.06	8.542	1.702
	2	5	0.9927	11.84	4.040	4.354
	2	6	0.9991	4.16	7.996	1.599
	3	5	0.8724	25.34	9.091	2.981
	3	6	0.9241	19.81	10.55	1.125
	4	6	−0.3866	15.91	19.78	−1.637
Octanoic acid	0	4	0.9963	10.97	−0.3622	6.254
	0	5	0.9988	6.32	6.168	2.597
	0	6	0.9941	13.79	11.38	1.068
	1	5	0.9988	5.03	6.301	2.468
	1	6	0.9940	11.13	9.047	1.017
	2	5	0.9781	12.01	8.879	1.906
	2	6	0.9905	7.92	10.04	0.7977
	3	5	−0.3132	53.17	17.64	−1.175
	3	6	−0.2141	54.69	16.30	−0.3239
	4	6	−0.5381	129.36	37.30	−7.222

[a] Linear regression analysis of $([A]_t - [A]_0)/[D]^{m/2} = p + q[D]_t^{(n-m)/2}$ corresponding to the formation of two complexes of stoichiometry AD_m and AD_n, where $[D]_t$ is the total molar concentration of donor fatty acid in isooctane and $([A]_t - [A]_0)$ is the increase in the apparent molar solubility of the acceptor, griseofulvin, brought about by the presence of the donor in isooctane solution. It is assumed here that $[D_2] \approx 2[D]_t$. [b] Residual standard deviation per mean value of $([A]_t - [A]_0)[D]_t^{-m/2}$.

only one complex, AD_n, may be assumed, in which case the third term on the right in each equation (Eqs. 17 and 18) is ignored, so that:

$$[D]_t = K_d^{-1/2}[D_2]^{1/2} + 2[D_2] + (n \cdot K_n \cdot K_d^{-n/2})[D_2]^{n/2} \quad \text{(Eq. 28)}$$

Equation 24 is applied to AD_n instead of AD_m; thus:

$$[A]_t - [A]_0 = (K_n \cdot K_d^{-n/2})[D_2]^{n/2} \quad \text{(Eq. 29)}$$

Eliminating $[D_2]$ from Eqs. 28 and 29 affords:

$$[D]_t = c_1([A]_t - [A]_0)^{1/n} + c_2([A]_t - [A]_0)^{2/n} + n([A]_t - [A]_0) \quad \text{(Eq. 30)}$$

where:

$$c_1 = K_n^{-1/n} \text{ and } c_2 = 2K_n^{-1/n} \cdot K_d^{1/2} \quad \text{(Eq. 31)}$$

Rearranging Eq. 30 into a form suitable for linear regression analysis, we obtain:

$$\frac{[D]_t - n([A]_t - [A]_0)}{([A]_t - [A]_0)^{1/n}} = c_1 + c_2([A]_t - [A]_0)^{1/n} \quad \text{(Eq. 32)}$$

where c_1 is the intercept, and c_2 is the slope. This model, if valid, enables both the stability constant (K_n) and the dimerization constant (K_d) to be calculated directly from the intercept and the slope. Thus, from Eq. 31, we obtain:

$$K_n = (c_1)^{-n}, \quad K_d = (c_2/2c_1)^2 \quad \text{(Eq. 33)}$$

RESULTS AND DISCUSSION

UV Spectra and the Nature of the Griseofulvin–Fatty Acid Interactions—The choice of chloroform as the spectrophotometric solvent for the determination of dissolved griseofulvin was based on the UV absorption[6] data presented in Table I. Griseofulvin gave a high molar absorptivity which was unaffected by the presence of small amounts of fatty acids or isooctane. However, to measure the very low solubility of griseofulvin in isooctane alone, dilution with an equal volume of chloroform was preferable to optimize sensitivity and accuracy. In each determination, the linear (Beer's law) region of the appropriate absorbance–concentration calibration was employed.

Proton-donating solvents cause small but consistent red shifts to the UV spectrum of griseofulvin and increase the molar absorptivities about twofold, as compared with the noninteractive solvent, isooctane (Table I). These transitions are therefore $\pi \rightarrow \pi^*$ (15) and suggest that each protic solvent forms a hydrogen-bonded complex with the lone pair of electrons on the ether oxygen atom and/or the carbonyl oxygen atom, all of which are conjugated with the π electrons in an unsaturated or aromatic center in the griseofulvin molecule (I).

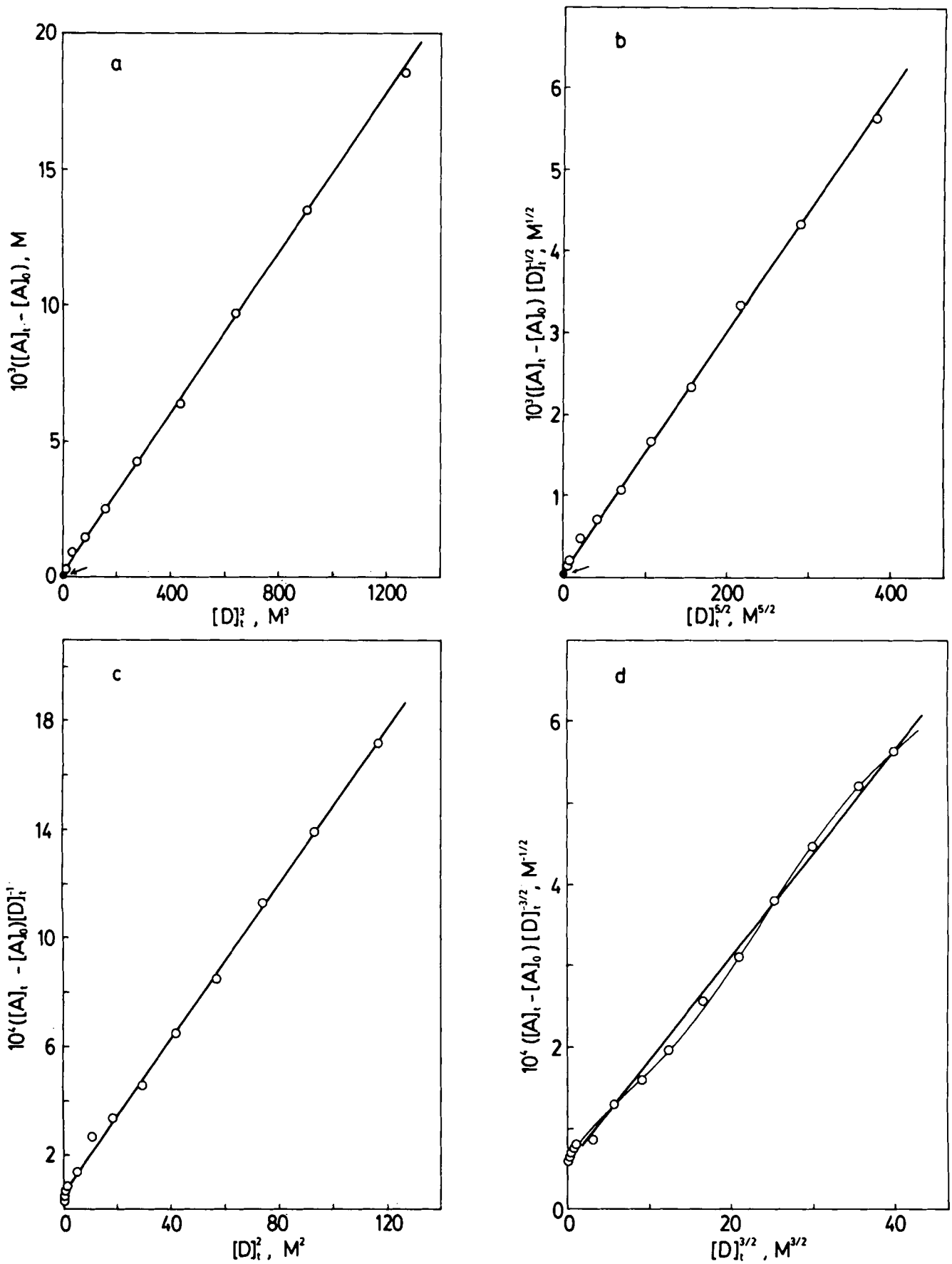

Figure 2—*Plots of various functions of* $([A]_t - [A]_0)$ *and* $[D]_t$, *where* $([A]_t - [A]_0)$ *is the increase in the apparent molar solubility of griseofulvin brought about by the presence of butanoic acid of total molar concentration* $[D]_t$, *in isooctane at 25°C. These plots correspond to linear regressions assuming the formation of the following complexes: (a)* AD_6 *alone; (b)* AD *and* AD_6; *(c)* AD_2 *and* AD_6; *(d)* AD_3 *and* AD_6.

Table IV—Stability Constants of Each of the Two Complexes Whose Stoichiometries Provide the Best Fit to the Solubility Data of Griseofulvin (A)[a]

Fatty Acid	K_d, M^{-1}	AD_m	K_m (Molarity Based)	AD_n	K_n (Molarity Based)
Acetic acid	37000[c]	AD	Very small[d]	AD_5	1.57×10^8
Propanoic acid	12000[b]	AD	0.0167	AD_6	2.38×10^8
Butanoic acid	9000[e]	AD	0.0106	AD_6	8.49×10^7
Hexanoic acid	6000[e]	AD_2	0.959	AD_6	2.76×10^7
Octanoic acid	5800[c]	AD	0.0068	AD_5	3.58×10^5

[a] In isooctane containing various concentrations of several fatty acids at 25°C. [b] Dimerization constant in cyclohexane at 25°C (from Ref. 19) is assumed to represent the corresponding value in isooctane at 25°C. [c] Dimerization constant in heptane at 23°C and 30°C (from Refs. 17 and 18) are assumed to represent the corresponding values in isooctane at 25°C. [d] Cannot be estimated from the negative intercept. [e] Determined by interpolation of the K_d values from Refs. 17–20.

Determination of the Stoichiometry of the Complexes—Table II presents the solubility data. The apparent molar solubility of griseofulvin in isooctane ($[A]_t$) increases rapidly with increasing molar concentrations of each acidic donor ($[D]_t$) from the value in isooctane, $[A]_0 = 9.358\ \mu M$. Plots of the logarithm of the increase in molar solubility, $\log([A]_t - [A]_0)$, against $\log [D]_t$ in Fig. 1 show two approximately linear regions: at $[D]_t < \sim 1$ M and at $[D]_t > \sim 2$ M. Each of these linear regions may be attributed to a complex between A and D, *e.g.*, AD_m or AD_n, according to Eq. 27. Regression analysis of the linear regions in Fig. 1 indicates high correlation coefficients ($r \geq 0.99$) and small residual standard deviations ($s < 1\%$). From each slope in Fig. 1, approximate values of the stoichiometric number, m or n, of fatty acid (D) molecules in each complex were calculated. Reference to Eq. 21 suggests that this is possible if m and n differ sufficiently such that at low $[D]_t$, the $[D]_t^{n/2}$ term is relatively small, whereas at high $[D]_t$, the $[D]_t^{m/2}$ term is relatively insignificant. Estimated stoichiometries are $m \simeq 1.7$–3.3 and $n \simeq 4.5$–5.9, depending on the fatty acid. However, the approximate nature of this treatment should be emphasized, especially with regard to the estimates of m for the lower-order complexes.

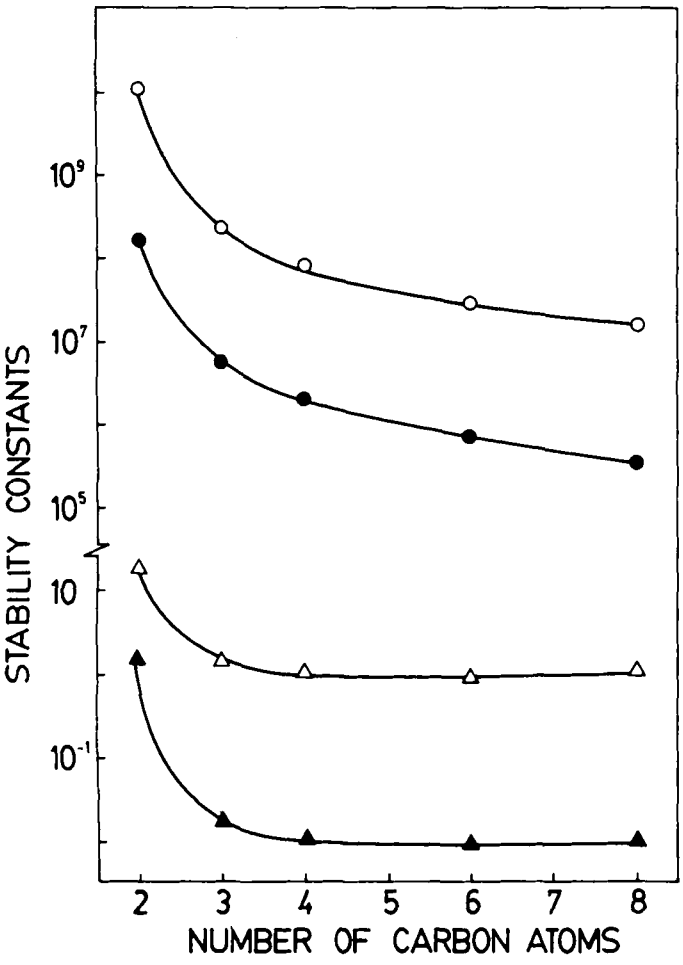

Figure 3—*Influence of the chain length of various straight-chain alkanoic acids on the molarity-based stability constants* K *of their complexes with griseofulvin. Key: (▲)* K_1 *for* AD *with* AD_6; *(△)* K_2 *for* AD_2 *with* AD_6; *(●)* K_5 *for* AD_5 *with* AD; *(○)* K_6 *for* AD_6 *with* AD.

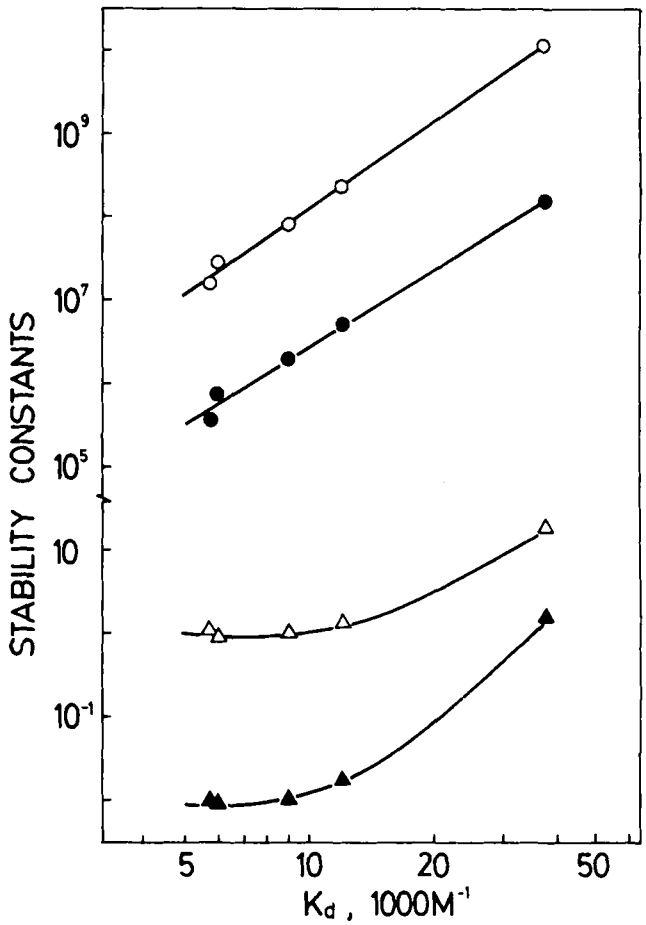

Figure 4—*Logarithmic relationships between the molarity-based dimerization constants* K_d *of various straight-chain alkanoic acids and the molarity-based stability constants* K *of their complexes* AD_n *with griseofulvin. Key: (▲)* K_1 *for* AD *with* AD_6; *(△)* K_2 *for* AD_2 *with* AD_6; *(●)* K_5 *for* AD_5 *with* AD; *(○)* K_6 *for* AD_6 *with* AD.

By using the approximate values of m and n as a guide, the solubility data were reanalyzed in terms of two stoichiometric complexes, AD_m and AD_n, by means of linear regressions represented by Eq. 23 (Table III). For this purpose, various probable and possible complexation models were assumed, with each corresponding to a certain pair of integral m and n values of greater or smaller magnitude than the approximate quantities, and the fatty acid dimers were generally assumed to predominate over all other species. For each acidic donor, the statistically most probable model (or pair of m and n values) corresponds to the linear regression with the highest correlation coefficient and the lowest residual standard deviation. Table III shows that these models are (m, n) 0,5 for acetic acid; 0,6 for propanoic and butanoic acids; 0,6 or 2,6 for hexanoic acid; and 1,5 for octanoic acid. When, however, the linear regressions were plotted (Fig. 2) for butanoic acid, the models for which $m = 0$ gave points that were crowded together at low $[D]_t$ and widely separated at high $[D]_t$ (Fig. 2a), whereas the models for which $m = 1$ or 2 gave points which were better separated (Fig. 2b–d). Therefore, the statistics of linear regression may be misleading at low $[D]_t$. Furthermore, the log-log plots in Fig. 1 clearly show two approximately linear regions, indicating $m > 0$. If, however, a value of m is selected that is too high, the correlation deteriorates (as shown by r and s in Table III), and the experimental points follow a sigmoidal curve on either side of the regression line. This is apparent in the case of the 3,6 model for butanoic acid (Fig. 2d) and is beginning to show in the 2,6 model (Fig. 2c). Bearing in mind all of these considerations, the preferred models (AD_m, AD_n) for each fatty acid donor with griseofulvin are summarized in Table IV.

To calculate the stability constants K_m and K_n of the complexes (Table IV) from the intercept (p) and slope (q) of each linear regression (Eqs. 20–22), the dimerization constant (K_d) of the fatty acid donor must be known.

Table V—Linear Regression Analyses [a]

Donor	n	r	$100s$ [b]	c_1	c_2	c_1^{-n} [c]	$c_2/2c_1^2$ [d]
Acetic acid	4	0.9702	10.08	7.12	36.97	3.9×10^{-4}	6.7
	5	0.9938	5.85	0.845	37.04	2.3	480
	6	0.9987	3.01	−3.06	36.58	1.2×10^{-3}	36
	7	0.9985	3.45	−6.00	36.46	-3.6×10^{-6}	9.2
	8	0.9967	5.37	−8.46	36.69	3.8×10^{-8}	4.7
	9	0.9945	7.19	−10.64	37.18	-5.7×10^{-10}	3.1
Propanoic acid	5	0.9808	11.28	−1.52	54.01	-1.2×10^{-1}	314
	6	0.9933	7.29	−5.36	49.01	4.2×10^{-5}	21
	7	0.9977	4.54	−8.21	46.26	-4.0×10^{-7}	8.5
	8	0.9988	3.41	−10.59	44.81	6.3×10^{-9}	4.9
	9	0.9985	3.89	−12.70	44.18	-1.2×10^{-10}	3.3
Butanoic acid	5	0.9892	8.71	−2.51	62.31	-1.0×10^{-2}	153
	6	0.9966	5.32	−5.85	53.32	2.5×10^{-5}	20
	7	0.9980	4.28	−8.26	48.33	-3.8×10^{-7}	8.5
	8	0.9972	5.29	−10.25	45.44	8.2×10^{-9}	4.9
	9	0.9956	6.87	−11.99	43.79	-1.9×10^{-10}	3.3
Hexanoic acid	5	0.9901	8.81	−4.73	69.30	-4.2×10^{-4}	54
	6	0.9973	4.96	−7.38	56.49	6.2×10^{-6}	14
	7	0.9993	2.63	−9.33	49.62	-1.6×10^{-7}	7.1
	8	0.9993	2.69	−10.95	45.66	4.8×10^{-9}	4.3
	9	0.9985	4.08	−12.41	43.30	-1.4×10^{-10}	3.0
Octanoic acid	4	0.9840	11.21	−7.26	168.08	3.6×10^{-4}	134
	5	0.9951	6.72	−10.47	106.26	-8.0×10^{-6}	26
	6	0.9983	4.13	−12.38	80.23	2.8×10^{-7}	11
	7	0.9988	3.58	−13.88	66.97	-1.0×10^{-8}	5.8
	8	0.9983	4.43	−15.22	59.42	3.5×10^{-10}	3.8
	9	0.9975	5.58	−16.48	54.83	-1.1×10^{-10}	2.8

[a] Linear regression analysis of $\{[D]_t - n([A]_t - [A]_0)\}([A]_t - [A]_0)^{-1/n} = c_1 + c_2([A]_t - [A]_0)^{1/n}$ corresponding to the single complex model allowing for all donor species, including the monomer, where $[D]_t$ is the total molar concentration of donor fatty acid in isooctane, and $[A]_t - [A]_0$ is the increase in the apparent molar solubility of the acceptor, griseofulvin, brought about by the presence of the donor in isooctane solution at 25°C. The single complex is represented by AD_n, where n corresponds to the stoichiometric number. [b] Residual standard deviation per mean value of ordinate. [c] $c_1^{-n} = K_n$, the stability constant of AD_n, if the model is correct. [d] $c_2/2c_1^2 = K_d$, the dimerization constant of D, if the model is correct.

Dimerization Constants of the Fatty Acid Donors—Equilibrium constants for hydrogen bonding, such as K_d, are usually largest in solvents of the saturated hydrocarbon type and do not differ much from one solvent to another within this group (16). They are not very dependent on temperature within a few degrees, because the negative enthalpies of hydrogen bonding are relatively small (<40 kJ·mol^{-1}, *i.e.*, <10 kcal·mol^{-1}). Consequently, the values of K_d for acetic, propanoic, and octanoic acids were taken to be the corresponding values in heptane and cyclohexane (17–19), whereas those for butanoic and hexanoic acids were obtained by interpolating the available data for six *n*-alkanoic acids (17–20) in these hydrocarbons (Table IV).

Although these values of K_d and the stability constants K_m and K_n (which are calculated from K_d and from the respective experimental quantities p and q) are only approximate (Table IV), the approximations will not affect the stoichiometry of complexation, since they are applied after the statistically favored complexation model has been selected from Table III.

Stability Constants of the Complexes—The stability constants of the various complexes plotted on a $\log_{10}$ scale against the chain length of the fatty acids are presented in Fig. 3. For the lower-order complexes AD and AD_2, the stability constants K_1 and K_2 are influenced by the stoichiometry of the accompanying higher-order complex and, for the purposes of comparison in Fig. 3, were calculated for the 1,6 and 2,6 models to form a self-consistent series. The values of K_1 and K_2 are, respectively, of the order 10^{-2}–10^{-1} M^{-1} and 1–10 M^{-2}, which are so small as to be accounted for by nonspecific, nonhydrogen-bonding interactions between D and A (21, 22). Values of $K_1 < \sim 1$ M^{-1} may be expected in nonbonding situations on a purely statistical analysis of the nearest neighbors (23, 24). K_1 and K_2 are preferably regarded as empirical quantities, reflecting an enhancement of the solubility of griseofulvin in isooctane by the presence of low concentrations of fatty acids interacting nonspecifically.

K_1 and K_2 are relatively independent of the chain length of the donor from propanoic to octanoic acid. The relatively high values of K_1 and K_2 for acetic acid may arise from deficiencies in the model, as reflected by the negative values of p, which have no physical meaning. The dimerization constants (K_d) also show relatively little dependence on the alkyl chain length (Table IV). Evidently, the flexible hydrocarbon chain has little effect on the stability of the smaller species (D_2, AD, or AD_2) derived from the fatty acids.

For the higher-order complexes AD_5 and AD_6, the values of the constants K_5 and K_6 are insensitive to the stoichiometry of the accompanying lower-order complex (AD_2, AD, or none) and are large, indicating powerful interactions between the fatty acids and griseofulvin. This reflects the strength of the donor and acceptor species and perhaps also the cooperative nature of hydrogen bonding. Griseofulvin has six obvious acceptor sites. The favored stoichiometries of the higher-order complexes suggest that these sites are saturated in AD_6 and not fully saturated in AD_5. Saturation of acceptor sites is probably accompanied by steric crowding, since K_6 decreases markedly with an increasing number of carbon atoms of the donor. This also reflects the increasing disruptive effect of the flexible hydrocarbon chain on the stability of the complex. The effect on K_5 is less pronounced, probably because one fewer acceptor site is occupied, thereby reducing the crowding and disruptive influences of the longer chains of the donor.

The concepts described above also explain why the relationships between $\log_{10} K_m$ or $\log_{10} K_n$ and the number of carbon atoms are not linear, as might be expected if a linear free energy relationship were obeyed (25). The gradient of the tangent to the curves in Fig. 3 represents the methylene-group contribution of the donor to the standard free energy of complexation; thus:

$$\Delta G_n^\theta = -RT \cdot \ln K_n \qquad \text{(Eq. 34)}$$

This contribution is not constant but decreases with increasing number of carbon atoms, reflecting the increasing disturbance to the griseofulvin–carboxyl group interactions by the longer hydrocarbon chains and perhaps the partial replacement of these interactions by weaker dispersion forces between the hydrocarbon chains and griseofulvin (5).

The statistically favored stoichiometry of the higher-order complex (Tables III and IV) for propanoic, butanoic, and hexanoic acids is AD_6; for octanoic acid it is AD_5, reflecting the steric crowding resulting from the larger size of the donor molecule in the latter case. The favored AD_5 stoichiometry for acetic acid is unexpected and is attributed tentatively to variations in the activity coefficients (γ in Eqs. 6, 8, 11, and 13), which are assumed to be constant.

In Fig. 4 are shown distinct linear free energy relationships between $\log_{10} K_5$ and $\log_{10} K_d$ and between $\log_{10} K_6$ and $\log_{10} K_d$. The linearity of these plots might result from the fact that the stability constants were calculated from K_d by Eq. 22. However, K_1 and K_2 were also calculated from K_d, but nonlinear relationships are found between their logarithms and $\log_{10} K_d$. Therefore, we suggest that the linear relationships between $\log_{10} K_6$ and $\log_{10} K_d$ and between $\log_{10} K_5$ and $\log_{10} K_d$ arise from the similarities of the intermolecular interactions, namely, hydrogen bonding, between D and A in the complexes AD_5 and AD_6 and between two fatty acid molecules in the dimer D_2. On the other hand, the nonlinearity of the relationships involving $\log_{10} K_1$, $\log_{10} K_2$, and $\log_{10} K_d$ probably reflect nonspecific interactions between A and D, in contrast to the specific interactions in the dimer.

Poor correlations are, however, found between $\log_{10} K_5$, $\log_{10} K_6$, $\log_{10} K_2$, $\log_{10} K_1$, and $\log_{10} K_d$, on the one hand, and the pK_a of the fatty acids (26) on the other hand. This is not unexpected, since ionization involves different intermolecular effects than interactions of the donor–acceptor type between D and A and two D molecules.

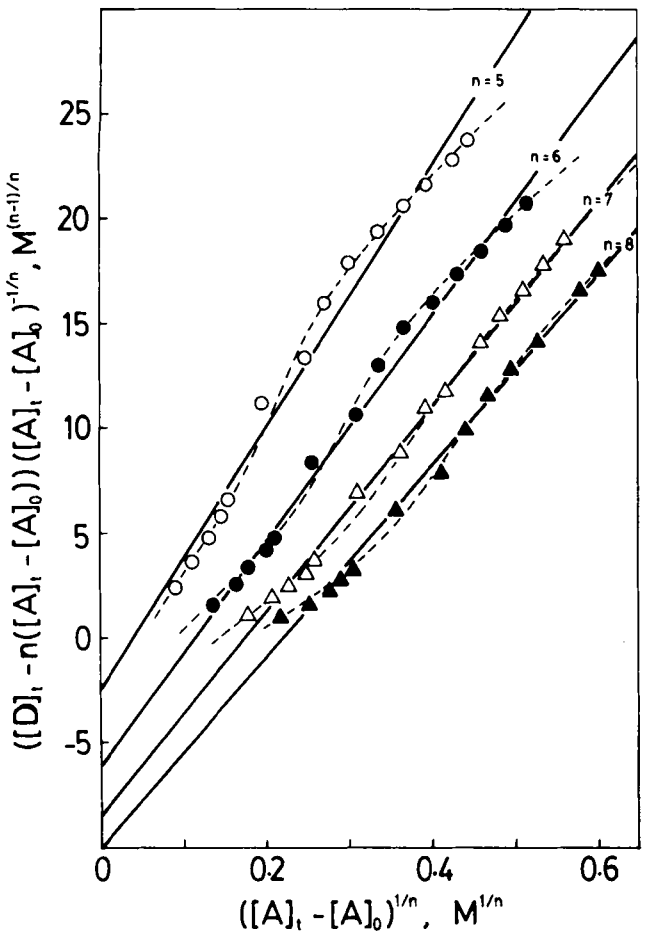

Figure 5—*Plots of* $\{[D]_t - n([A]_t - [A]_0)\}\{[A]_t - [A]_0\}^{-1/n}$ *against* $([A]_t - [A]_0)^{1/n}$, *corresponding to the single complex model allowing for all donor species, including the monomer. The stoichiometric number,* n, *of the single complex,* AD_n, *is as follows:* (○) n = 5; (●) n = 6; (△) n = 7; (▲) n = 8.

Critical Appraisal of the Proposed Models—The solubility behavior of griseofulvin in fatty acid–isooctane mixtures appears to conform to simple donor-acceptor models involving one or two complexes, AD_m and AD_n, which are summarized by Eqs. 20–27. These models are based on the following major assumptions: (*a*) the activity coefficient (γ) of each dissolved species (*e.g.*, in Eqs. 6, 8, 11, and 13) is constant and independent of the concentration terms, particularly $[D]_t$; (*b*) the activity of the solid which is in equilibrium with every saturated solution consisting of each fatty acid and isooctane (*e.g.*, in Eqs. 5, 6, and 8) is a constant equal to the activity of pure griseofulvin $\{A\}$; (*c*) the total amount of fatty acid is present almost exclusively as the dimer according to Eq. 19.

The assumption of constant activity coefficients becomes less reliable with increasing $[D]_t$, and the deviations become increasingly positive. In other words, with increasing concentrations of the highly polar fatty acid molecules in nonpolar isooctane solution, their activity or escaping tendency probably increases more rapidly than their concentration increases. Thus, although AD_6 is probably, for structural reasons, the real activity-based stoichiometry for the lower straight-chain alkanoic acids (C_2–C_6) as donors, the concentration-based stoichiometric number of D derived from the statistical treatment may be slightly less than the integral values of 6, as seen in Table III. When, however, acetic acid is present as the donor at volume fractions >60%, its molar concentration (>10 M; Table II) is so high that very large positive deviations from the ideal laws are expected, and the concentration-based stoichiometry which emerges from the statistical treatment is apparently AD_5 (Table III). The positive deviations, corresponding to $\gamma > 1$, may simply account for the negative values of p, which occur most commonly with acetic acid (Table III).

The activity of solid griseofulvin ($\{A\}$) depends on the nature of the solid phase which is in equilibrium with the saturated solution. When griseofulvin is allowed to crystallize from supersaturated solutions in each of the straight-chain alkanoic acids (except propanoic acid), new solid phases are obtained which contain both griseofulvin and the fatty acid (7, 8). Analysis of the excess of solid griseofulvin which stood in contact with each saturated solution in the solubility measurements, however, corresponded to that of the original griseofulvin crystals whose surface was moistened with liquid solution. The techniques used were DSC of five samples, which had previously been equilibrated with different mixtures of each fatty acid and isooctane, and differential thermal analysis and X-ray powder diffraction of one sample after equilibration with each neat fatty acid. This was confirmed by the inclusion of propanoic acid as a negative control which did not form solvates and which gave solubility data that were qualitatively no different from those of the other acids. We therefore conclude that $\{A\}$ was essentially constant in all the solubility measurements in the presence of each fatty acid and that solvates or inclusion compounds are not formed by allowing griseofulvin merely to stand in contact with each fatty acid.

The assumption that $[D]_t \approx 2[D_2]$ by Eq. 19 agrees with the experimental data. An alternative single-complex model in which $[D]_t$ accounts for the monomer, dimer, and complex leads to Eq. 32. The experimental data fit this equation also (Table V, Fig. 5 for butanoic acid), and it would appear that the statistically favored complexes correspond to $n = 6$, 7, or 8, depending on the fatty acid donor. However, except for statistically disfavored values of n for acetic acid, the data give negative values of c_1, which correspond to unacceptable negative values of the stability constant K_n (Eq. 33, Table V). In theory, this model should yield values of the dimerization constant K_d, but unacceptably small values are derived from the experimental data (*cf.* Table IV and V). Thus, this model, which accounts for the fatty acid monomer and a single complex, is totally unsatisfactory. Nevertheless, fatty acid monomers are undoubtedly present when fatty acids are dissolved in isooctane, and their relative concentration and influence increase as $[D]_t$ decreases. There is also evidence (27) that fatty acids in nonpolar solvents can form trimers, and perhaps also higher oligomers, in which the concentration is likely to increase with increasing $[D]_t$. If, however, all fatty acid species, with the exception of the dimer, are ignored, the solubility of griseofulvin in isooctane containing low concentrations of fatty acid can be explained by the presence of the lower-order complex, AD_m (in which $m = 1$ or 2). No doubt the most comprehensive model would involve a range or spectrum of AD_n complexes (Eq. 1) together with monomers, dimers, and perhaps even higher-order-associated species of fatty acids. Such a model would be algebraically complicated and would involve so many adjustable constants that it would be capable of fitting virtually any experimental data.

REFERENCES

(1) A. J. Repta, in "Techniques of Solubilization of Drugs," S. H. Yalkowsky, Ed., Dekker, New York, N.Y., 1981, p. 135.

(2) G. Levy and E. J. Mroszczak, *J. Pharm. Sci.*, **57**, 235 (1968).

(3) P. H. Elworthy and F. J. Lipscomb, *J. Pharm. Pharmacol.*, **20**, 790 (1968).

(4) K. Sekiguchi, K. Ito, E. Owada, and K. Ueno, *Chem. Pharm. Bull. (Tokyo)*, **12**, 1192 (1964).

(5) D. J. W. Grant and I. K. A. Abougela, *J. Pharm. Pharmacol.*, **34**, 766 (1982).

(6) "Martindale, The Extra Pharmacopoeia," 27th ed., A. Wade, Ed., The Pharmaceutical Press, London, 1977, p. 635.

(7) I. K. A. Abougela and D. J. W. Grant, *J. Pharm. Pharmacol.*, **31**, Suppl., 49P (1979).

(8) D. J. W. Grant and I. K. A. Abougela, *J. Pharm. Pharmacol.*, **33**, 619 (1982).

(9) I. K. A. Abougela, D. J. Bigford, I. McCorquodale, and D. J. W. Grant, *Proceedings of the 1st International Conference on Pharmaceutical Technology (Paris)*, **5**, 142 (1977).

(10) T. Higuchi, J. H. Richards, S. S. Davis, A. Kamada, J. P. Hou, M. Nakano, N. I. Nakano, and I. H. Pitman, *J. Pharm. Sci.*, **58**, 661 (1969).

(11) K. C. James and M. Mehdizadeh, *J. Pharm. Pharmacol.*, **33**, 9 (1981).

(12) H. B. Kostenbauder and T. Higuchi, *J. Am. Pharm. Assoc., Sci. Ed.*, **45**, 518 (1956).

(13) E. R. Townley, in "Analytical Profiles of Drug Substances," vol. 8, K. Florey, Ed., Academic, New York, N.Y., 1979, p. 219.

(14) M. A. Hassan and E. A. Aboutabl, in "Analytical Profiles of Drug Substances," vol. 9, K. Florey, Ed., Academic, New York, N.Y., 1980, p. 583.

(15) M. Jauquet and P. Laszlo, in "Solutions and Solubilities," Part I, M. R. J. Dack, Ed., Wiley, New York, N.Y., 1975, p. 195.

(16) G. C. Pimentel and A. L. McClellan, in "The Hydrogen Bond," Wm. Freeman, San Francisco, 1960, pp. 348, 368.

(17) D. S. Goodman, *J. Am. Chem. Soc.*, **80**, 3887 (1958).

(18) H. A. Pohl, M. E. Hobbs, and P. M. Gross, *J. Chem. Phys.*, **9**, 408 (1941).

(19) U. Jentschura and E. Lippert, *Ber. Bunsenges. Phys. Chem.*, **75**, 782 (1971).
(20) F. Thyrion and D. Decroocq, *C.R. Acad. Sci. (Paris)*, **260**, 2797 (1965).
(21) W. B. Person, *J. Am. Chem. Soc.*, **87**, 167 (1965).
(22) D. A. Deranleau, *J. Am. Chem. Soc.*, **91**, 4044, 4050 (1969).
(23) T. Higuchi and K. A. Connors, *Adv. Anal. Chem. Instrum.*, **4**, 117 (1965).
(24) B. D. Anderson, J. H. Rytting, and T. Higuchi, *J. Pharm. Sci.*, **69**, 676 (1980).
(25) S. S. Davis, T. Higuchi, and J. H. Rytting, *Adv. Pharm. Sci.*, **4**, 73 (1974).
(26) J. J. Christensen, M. D. Slade, D. E. Smith, R. M. Izatt, and J. Tsang, *J. Am. Chem. Soc.*, **92**, 4164 (1970).
(27) O. Levy, G. Y. Markovits, and I. Perry, *J. Phys. Chem.*, **79**, 239 (1975).

ACKNOWLEDGMENTS

This study was supported in part by The Atkinson Charitable Foundation and by the Medical Research Council of Canada, to whom we express our thanks. The authors also thank Mr. Joseph Go for skilled technical assistance and Mrs. Vivienne Hinds for typing the manuscript.

pH–Solubility Profile of Papaverine Hydrochloride and Its Relationship to the Dissolution Rate of Sustained-Release Pellets

ABU T. M. SERAJUDDIN ˣ and MORTON ROSOFF*

Received January 28, 1983, from the *Pharmacy Research and Development Department, Research and Development Division, Revlon Health Care Group, Tuckahoe, NY 10707.* Accepted for publication August 16, 1983. *Present address: Arnold and Marie Schwartz College of Pharmacy and Health Sciences, Brooklyn, NY 11201.

Abstract □ The pH–solubility profile of papaverine hydrochloride (I) was determined using the phase-solubility technique and equilibrium solubilities in buffers. The release of I from sustained-release pellets consisting of a shellac-based matrix was determined by the USP basket technique and was found to exhibit zero-order kinetics. Release rates at various pH values of the permeating solvent were compared with the pH–solubility profile and were directly proportional to the solubility below, but not above, the apparent pH_{max} (3.9). This lack of proportionality was also shown by the intrinsic dissolution rates. The effect was attributed to the self-buffering action of I and the metastability of the papaverine salt–base system in the vicinity of pH_{max}. It is postulated that the outer layer of polymer and filler on the surface of the pellets forms a barrier which determines the rate of release. The inner matrix serves as a drug reservoir in which the internal pH may not be the same as the bulk pH.

Keyphrases □ Papaverine hydrochloride—pH–solubility profile, supersaturation effect, common-ion effect, solubility–dissolution rate ratio, self-buffering effect □ Shellac-based matrix—sustained-release dosage forms, solubility–dissolution rate ratios, internal self-buffering effect □ Mechanism of release—matrix model, effect of filler

The solubility of a hydrochloride salt and its base may vary greatly in the GI pH range, depending on the solubilities of ionized and un-ionized forms and the pK_a of the compound (1). Kramer and Flynn (2) have investigated the solubility interrelationships of hydrochloride salts and their bases. They observed that instead of giving a smooth curve, the solubility curves of a salt and its base intersect at a sharp angle at the pH of maximum solubility (pH_{max}) of both forms. Chowhan (3) has also noticed a similar relationship between organic acids and their salts.

The release of papaverine hydrochloride (I) from commercial sustained-release preparations has been reported to be significantly affected by pH (1). A partial pH–solubility profile showed that the drug solubility reached a maximum at pH ~4.5, and a common-ion effect owing to the addition of excess chloride ion was noticed at low pH.

In the present investigation, the pH–solubility profile of I and the interrelationships betwen the solubility of its salt and base forms were studied. Experiments were then conducted to study the dissolution of I from sustained-release pellets[1] in relation to the pH–solubility profile.

EXPERIMENTAL SECTION

Materials—Papaverine hydrochloride[2] (I) was used as received. The papaverine base (II) was prepared by increasing the pH of an aqueous solution of I to at least 12.0, washing the resultant precipitate four to five times with water, and drying under reduced pressure over phosphorus pentoxide. The identity of II was established by elemental analysis.

Commercial sustained-release papaverine hydrochloride capsules were used as the dosage forms. Each capsule contained ~500 pellets. The diameter of each individual pellet was 0.9 ± 0.1 mm. The diameter of sugar granules around which I was embedded in a shellac-based matrix by a coating process in a conventional rotating pan (4) was ~0.6 mm. The outermost layers of pellets were formed by the addition of drug-free shellac and filler.

The citric acid–phosphate buffers (pH 2.2–7.8) were prepared by mixing 0.1 M citric acid and 0.2 M disodium phosphate. All other reagents used were of analytical grade.

pH–Solubility Profile—The solubility profile of I and its base was determined by the phase-solubility technique of Dittert *et al.* (5). The pH of I in saturated aqueous solution was 3.0. The solubilities at pH <3.0 were determined by titrating dropwise with 1 M HCl, stirring with an overhead stirrer for 1 h at 37°C in a water bath, recording the pH, and then collecting a suitable aliquot. To attain a higher pH, 1 M NaOH was similarly added. Throughout the titration, care was taken to maintain an excess of solid in equilibrium with the solution. The aliquots were filtered[3] immediately, diluted with 0.1 M HCl, and analyzed spectrophotometrically[4] at 310 nm. The solubility was calculated in terms of the hydrochloride salt. A preliminary study showed that the solubility did not change significantly if the equilibration of solution was continued for more than 1 h after each addition of titrant.

The solubility in a citric acid–phosphate buffer was determined by adding an excess of I to ~15 mL of the buffer in a 50-mL volumetric flask, shaking overnight with a wrist-action shaker[5] in a water bath at 37°C, and analyzing the aliquot as described above. The saturation solubility in 0.01 and 0.1 M HCl was determined in the same manner.

[1] Cerespan, (lot no. 56370; 150 mg); USV Pharmaceutical Corp., Tuckahoe, N.Y.
[2] USVP no. 29745; USV Pharmaceutical Corp., Tuckahoe, N.Y.
[3] Millipore filter, Type HA; Millipore Corp., Bedford, Mass.
[4] Model 25; Beckman Instruments, Fullerton, Calif.
[5] Burrell Corp., Pittsburgh, Pa.

0022-3549/84/0900-1203$01.00/0
© 1984, American Pharmaceutical Association

(19) U. Jentschura and E. Lippert, *Ber. Bunsenges. Phys. Chem.*, **75**, 782 (1971).
(20) F. Thyrion and D. Decroocq, *C.R. Acad. Sci. (Paris)*, **260**, 2797 (1965).
(21) W. B. Person, *J. Am. Chem. Soc.*, **87**, 167 (1965).
(22) D. A. Deranleau, *J. Am. Chem. Soc.*, **91**, 4044, 4050 (1969).
(23) T. Higuchi and K. A. Connors, *Adv. Anal. Chem. Instrum.*, **4**, 117 (1965).
(24) B. D. Anderson, J. H. Rytting, and T. Higuchi, *J. Pharm. Sci.*, **69**, 676 (1980).
(25) S. S. Davis, T. Higuchi, and J. H. Rytting, *Adv. Pharm. Sci.*, **4**, 73 (1974).
(26) J. J. Christensen, M. D. Slade, D. E. Smith, R. M. Izatt, and J. Tsang, *J. Am. Chem. Soc.*, **92**, 4164 (1970).
(27) O. Levy, G. Y. Markovits, and I. Perry, *J. Phys. Chem.*, **79**, 239 (1975).

ACKNOWLEDGMENTS

This study was supported in part by The Atkinson Charitable Foundation and by the Medical Research Council of Canada, to whom we express our thanks. The authors also thank Mr. Joseph Go for skilled technical assistance and Mrs. Vivienne Hinds for typing the manuscript.

pH–Solubility Profile of Papaverine Hydrochloride and Its Relationship to the Dissolution Rate of Sustained-Release Pellets

ABU T. M. SERAJUDDIN ˣ and MORTON ROSOFF*

Received January 28, 1983, from the *Pharmacy Research and Development Department, Research and Development Division, Revlon Health Care Group, Tuckahoe, NY 10707.* Accepted for publication August 16, 1983. *Present address: Arnold and Marie Schwartz College of Pharmacy and Health Sciences, Brooklyn, NY 11201.

Abstract □ The pH–solubility profile of papaverine hydrochloride (I) was determined using the phase-solubility technique and equilibrium solubilities in buffers. The release of I from sustained-release pellets consisting of a shellac-based matrix was determined by the USP basket technique and was found to exhibit zero-order kinetics. Release rates at various pH values of the permeating solvent were compared with the pH–solubility profile and were directly proportional to the solubility below, but not above, the apparent pH_{max} (3.9). This lack of proportionality was also shown by the intrinsic dissolution rates. The effect was attributed to the self-buffering action of I and the metastability of the papaverine salt–base system in the vicinity of pH_{max}. It is postulated that the outer layer of polymer and filler on the surface of the pellets forms a barrier which determines the rate of release. The inner matrix serves as a drug reservoir in which the internal pH may not be the same as the bulk pH.

Keyphrases □ Papaverine hydrochloride—pH–solubility profile, supersaturation effect, common-ion effect, solubility–dissolution rate ratio, self-buffering effect □ Shellac-based matrix—sustained-release dosage forms, solubility–dissolution rate ratios, internal self-buffering effect □ Mechanism of release—matrix model, effect of filler

The solubility of a hydrochloride salt and its base may vary greatly in the GI pH range, depending on the solubilities of ionized and un-ionized forms and the pK_a of the compound (1). Kramer and Flynn (2) have investigated the solubility interrelationships of hydrochloride salts and their bases. They observed that instead of giving a smooth curve, the solubility curves of a salt and its base intersect at a sharp angle at the pH of maximum solubility (pH_{max}) of both forms. Chowhan (3) has also noticed a similar relationship between organic acids and their salts.

The release of papaverine hydrochloride (I) from commercial sustained-release preparations has been reported to be significantly affected by pH (1). A partial pH–solubility profile showed that the drug solubility reached a maximum at pH ~4.5, and a common-ion effect owing to the addition of excess chloride ion was noticed at low pH.

In the present investigation, the pH–solubility profile of I and the interrelationships betwen the solubility of its salt and base forms were studied. Experiments were then conducted to study the dissolution of I from sustained-release pellets[1] in relation to the pH–solubility profile.

EXPERIMENTAL SECTION

Materials—Papaverine hydrochloride[2] (I) was used as received. The papaverine base (II) was prepared by increasing the pH of an aqueous solution of I to at least 12.0, washing the resultant precipitate four to five times with water, and drying under reduced pressure over phosphorus pentoxide. The identity of II was established by elemental analysis.

Commercial sustained-release papaverine hydrochloride capsules were used as the dosage forms. Each capsule contained ~500 pellets. The diameter of each individual pellet was 0.9 ± 0.1 mm. The diameter of sugar granules around which I was embedded in a shellac-based matrix by a coating process in a conventional rotating pan (4) was ~0.6 mm. The outermost layers of pellets were formed by the addition of drug-free shellac and filler.

The citric acid–phosphate buffers (pH 2.2–7.8) were prepared by mixing 0.1 M citric acid and 0.2 M disodium phosphate. All other reagents used were of analytical grade.

pH–Solubility Profile—The solubility profile of I and its base was determined by the phase-solubility technique of Dittert *et al.* (5). The pH of I in saturated aqueous solution was 3.0. The solubilities at pH <3.0 were determined by titrating dropwise with 1 M HCl, stirring with an overhead stirrer for 1 h at 37°C in a water bath, recording the pH, and then collecting a suitable aliquot. To attain a higher pH, 1 M NaOH was similarly added. Throughout the titration, care was taken to maintain an excess of solid in equilibrium with the solution. The aliquots were filtered[3] immediately, diluted with 0.1 M HCl, and analyzed spectrophotometrically[4] at 310 nm. The solubility was calculated in terms of the hydrochloride salt. A preliminary study showed that the solubility did not change significantly if the equilibration of solution was continued for more than 1 h after each addition of titrant.

The solubility in a citric acid–phosphate buffer was determined by adding an excess of I to ~15 mL of the buffer in a 50-mL volumetric flask, shaking overnight with a wrist-action shaker[5] in a water bath at 37°C, and analyzing the aliquot as described above. The saturation solubility in 0.01 and 0.1 M HCl was determined in the same manner.

[1] Cerespan, (lot no. 56370; 150 mg); USV Pharmaceutical Corp., Tuckahoe, N.Y.
[2] USVP no. 29745; USV Pharmaceutical Corp., Tuckahoe, N.Y.
[3] Millipore filter, Type HA; Millipore Corp., Bedford, Mass.
[4] Model 25; Beckman Instruments, Fullerton, Calif.
[5] Burrell Corp., Pittsburgh, Pa.

0022-3549/84/0900-1203$01.00/0
© 1984, American Pharmaceutical Association

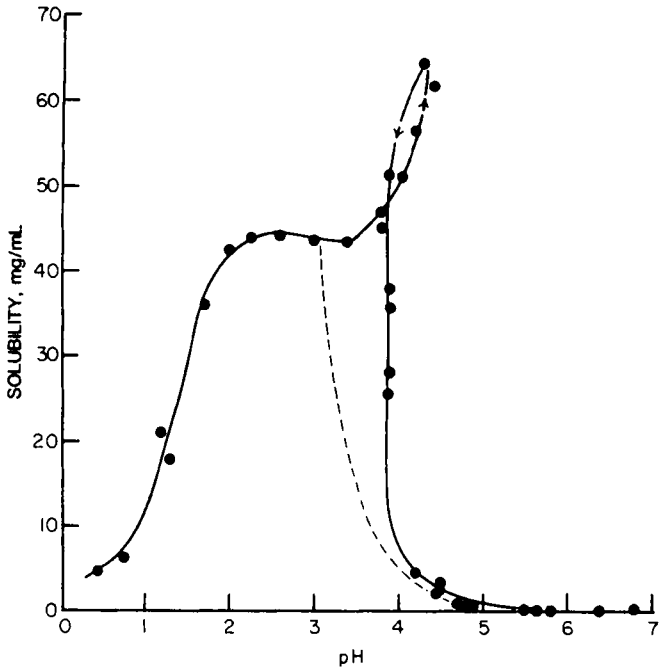

Figure 1—*Solubility of I in water at 37°C as a function of pH determined by adjusting the pH with 1 M HCl at pH <3.0 or with 1 M NaOH at pH >3.0. Each point represents one experimental value. All data were calculated in terms of hydrochloride salt equivalent. The broken line shows the theoretical solubility profile according to Eq. 3.*

The pH of the buffers with initial values >4 shifted to lower values on addition of I; consequently, the solubilities at these pH values were determined by using II, which gave no significant change in pH. The pH values of 0.01 and 0.1 M HCl media remained practically unchanged in the presence of I.

Analysis of Chloride Ion—During the determination of the solubility of I by the addition of 1 M HCl or 1 M NaOH, the analysis of chloride ion was made with selected aliquots. For the determination of chloride concentration, the aliquots were diluted 50 or 100 times with water, and 2 mL of 5 M $NaNO_3$ for each 100 mL of the diluted solution was added. The electrode potential in millivolts was measured with a pH meter[6] fitted with a chloride-sensitive electrode[7]. The standard calibration curve of log $[Cl^-]$ *versus* millivolts was obtained with sodium chloride solutions containing 2 mL of 5 M $NaNO_3$/100 mL.

Determination of pK_a—The apparent pK_a values of papaverine reported in the literature are 5.95 (6), 6.95 (7), and 6.40 (8). Since variations were noticed, the pK_a was determined in this study by recording the UV spectra of 0.015-mg/mL solutions of I in citric acid–phosphate buffer under various pH conditions. The average pK_a value obtained from the absorbances at 310 nm, using the following equation, was 6.5:

$$pK_a = pH - \log\left[\frac{A_{obs} - A_{BH^+}}{A_B - A_{obs}}\right] \qquad \text{(Eq. 1)}$$

where A_{BH^+} and A_B are the absorbances of the ionized and un-ionized species, respectively, and A_{obs} is the observed absorbance at the particular pH.

Dissolution from Papaverine Sustained-Release Pellets—A method using the USP dissolution apparatus[8] was developed for measuring the dissolution rates of papaverine hydrochloride-containing pellets. The contents of one capsule were placed in a dissolution basket, and the basket was immersed in 900 mL of dissolution medium previously warmed to 37°C. The basket was rotated at 100 rpm, and aliquots were taken from a point near the upper end of the basket and midway between the cylindrical edge of the basket and the wall of the vessel. The aliquots were analyzed spectrophotometrically at 310 nm, and the concentrations of the drug were determined from the extinction coefficients at the particular pH.

Intrinsic Dissolution of I—The intrinsic dissolution rates of I were determined using the dissolution apparatus described by Wood *et al.* (9). About 700 mg of the sample was compressed in a die with a hydraulic press[9] at a pressure of 4540 kg. The assembly was immersed in 300 mL of the medium at 37°C and stirred at 220 rpm. The surface of the pellet exposed to buffer had an area of 0.95 cm^2. The drug was assayed by removing suitable aliquots, diluting with 0.1 M HCl, and reading the absorbance spectrophotometrically at 310 nm.

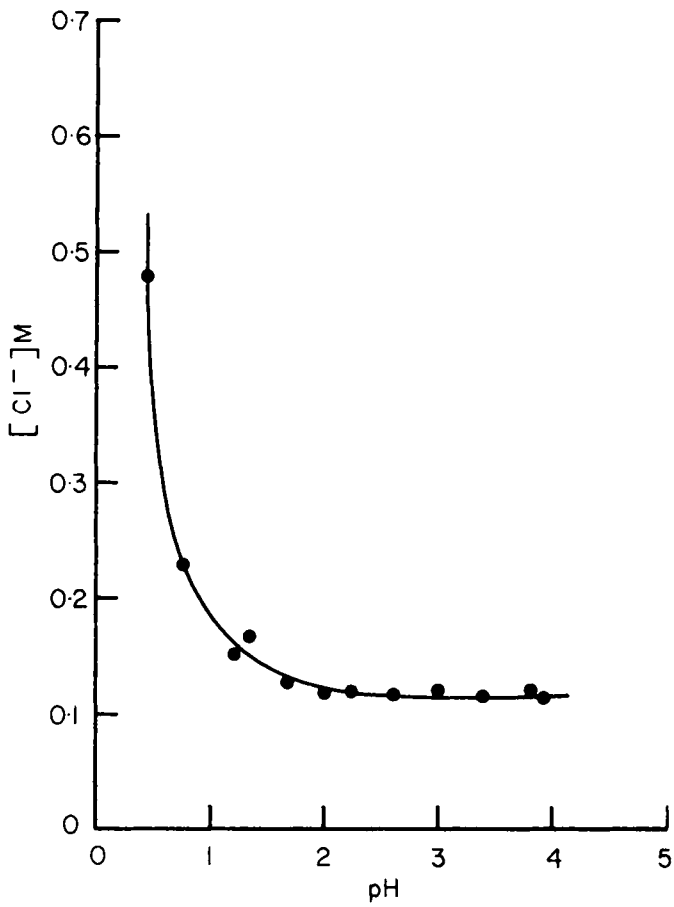

Figure 2—*The concentrations of chloride ion in the saturated solutions of I plotted as a function of pH (pH < apparent pH_{max}).*

Determination of the Effect of I on the pH of Buffers—The change in buffer pH in contact with I was determined in two ways. First, the citric acid–phosphate buffer, with pH 5, 6, or 7, was added to 1 g of I and stirred with a magnetic stirrer. The pH was recorded when stabilized, after the addition of 4 mL of the buffer and after 2-mL additions. Alternatively, the solid form of I was added in 0.1-g aliquots to 50 mL of a pH 6 buffer. The stabilized pH was recorded after each addition of solid.

Photomicroscopy of the Cross Sections of Pellets—The pellets were embedded in paraffin, and sections at a thickness of 10 μm were cut with a rotary microtome[10] using a diamond knife. The midsections of pellets were affixed to glass slides with egg albumin, and photomicrographs[11] were taken under UV light.

Determination of Density and Porosity—The densities of I and the sustained-release pellets were measured with a null pycnometer[12] using helium gas. Helium was purged through the samples for 12–15 min at the rate of 2–3 bubbles/s prior to the density measurement. The porosity of the pellets was determined by a mercury intrusion porosimeter[13].

RESULTS AND DISCUSSION

Solubility of I—The solubility of I at 37°C as a function of pH determined with the salt is shown in Fig. 1. It is observed from this figure that supersaturated solutions with a pH between 3.9 and 4.5 were formed; the pH of the supersaturated solution rose to 4.5 with the addition of 1 M NaOH before the precipitation of papaverine base (II) ensued; the pH finally stabilized at 3.9 (apparent pH_{max}). Elemental analysis of the solid phase precipitating at pH

[6] Digital 110; Corning Instruments, Medfield, Mass.
[7] Model 96-17; Orion Research, Cambridge, Mass.
[8] Model 72-RL; Hanson Research, Northridge, Calif.
[9] Fred S. Carver; Inc., Monomonee Falls, Wis.
[10] Model 820; American Optical Corp., Buffalo, N.Y.
[11] Series 10 microscope; American Optical Corp.
[12] Model PY-5; Quantachrome Corp., Syosset, N.Y.
[13] Model J5-7125D; American Instrument Co., Silver Spring, Md.

Table I—Dissolution Rates from Sustained-Release Pellets, Intrinsic Dissolution Rates, and Ratios of Rates to Solubilities of Papaverine Hydrochloride at Various pH Values

Medium	pH_{bulk}	Solubility of I at pH_{bulk} at 37°C	Dissolution Rate from Pellets, mg/min	Ratio of Dissolution Rate from Pellets to Solubility	Intrinsic Dissolution Rate of I, $mg \cdot cm^{-2} \cdot min^{-1}$	Ratio of Intrinsic Dissolution Rate to Solubility
0.1 M HCl	1.1	19.9	0.6	0.030	2.6	0.131
0.01 M HCl	2.0	42.1	1.6	0.038	6.3	0.150
Citric Acid-Phosphate Buffer	2.2	62.0	2.3	0.037	10.2	0.163
	3.0	60.5	2.5	0.041	—	—
	4.0	62.5	2.5	0.040	9.8	0.157
	5.0	0.41	2.2	5.4	9.0	22.0
	5.4	0.16	1.1	6.9	—	—
	6.0	0.047	0.24	5.1	4.1[a]	87.2
	7.0	0.016	0.11	6.9	—	—

[a] Rate may have been affected by the deposition of a porous film on the dissolving surface.

3.9 revealed that the solid consisted of II only. The applicable equations (2) to express the total solubility (S_T) of salt and base at any pH are:

$$S_{T(pH < pH_{max})} = [BH^+]_s + [B] = [BH^+]_s\left(1 + \frac{K_a}{[H_3O^+]}\right) \quad \text{(Eq. 2)}$$

$$S_{T(pH > pH_{max})} = [BH^+] + [B]_s = [B]_s\left(1 + \frac{[H_3O^+]}{K_a}\right) \quad \text{(Eq. 3)}$$

where $[BH^+]$ and $[B]$ are the concentrations of the ionized and un-ionized species, respectively. The subscripts $pH < pH_{max}$ and $pH > pH_{max}$ indicate that the equations are applicable for pH values less than and greater than pH_{max}, respectively. The subscripts indicates a saturated species, and K_a is the apparent dissociation constant. Each of these equations describes an independent curve limited by the solubility of one of the two species, and pH_{max} is the juncture of the two curves. The solid phases in equilibrium with the solutions at a pH lower or higher than the pH_{max} are salt and base, respectively. By using the apparent pK_a of 6.5 and a solubility of 0.015 mg/mL for the base, the theoretical curve corresponding to Eq. 3 is also drawn in Fig. 1. The experimental values agree with Eq. 3 only at a pH >4.6. Below this pH, the experimental points are higher than the theoretical line, and the calculated pH_{max} (3.0) is lower than the apparent value (3.9).

The supersaturation at pH values of 3.9–4.5 in Fig. 1 is released by nucleation when the pH shifts to either side of the apparent pH_{max}. This was proven by the rapid precipitation observed when a supersaturated solution of salt was nucleated with solid base or *vice versa*.

According to Eq. 2, the total solubility below pH_{max} should remain constant,

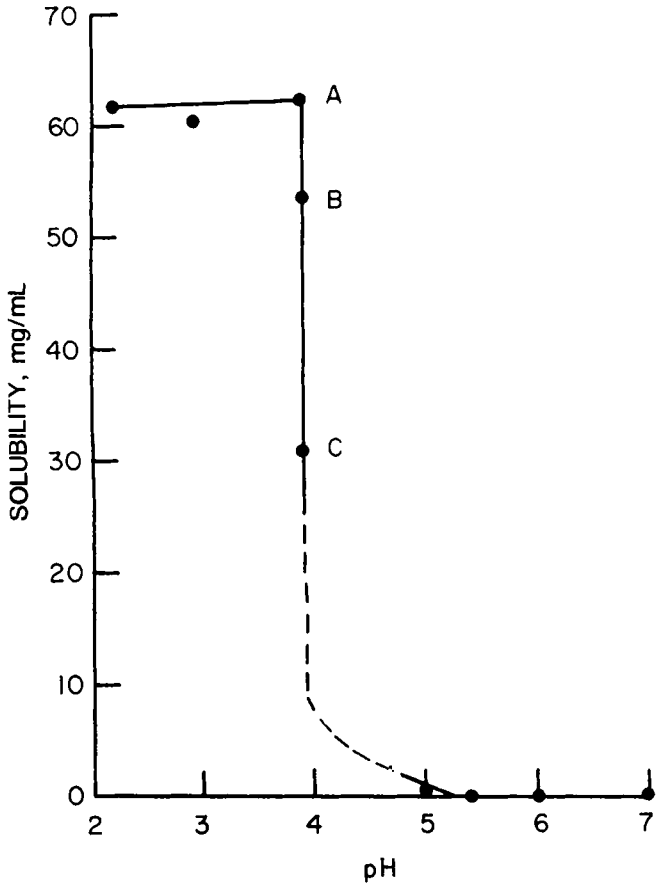

Figure 3—*The solubility of I in citric acid-phosphate buffers. A, B, and C were obtained when an excess of I was added to buffers of pH 4.0, 5.0, and 5.4, respectively. The solubility at pH ≥5 was determined with II. Each point represents one experimental value. All data were calculated in terms of hydrochloride salt equivalent.*

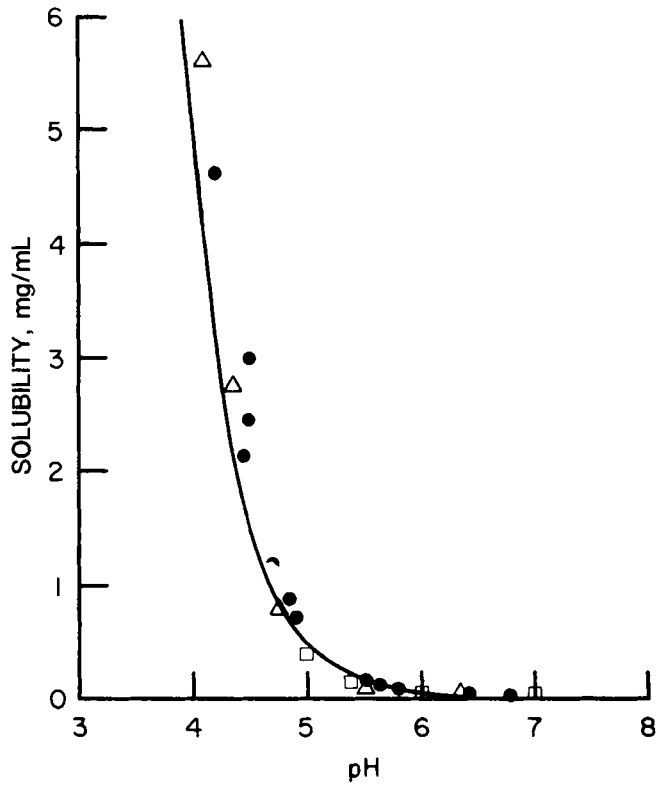

Figure 4—*The solubility of I and II at pH higher than pH_{max} shown with an expanded scale. The solubility was determined by increasing the pH of a solution of I with 1 M NaOH (●), by decreasing the pH of a solution of II with 1 M HCl (△), and by adding II to citric acid-phosphate buffer (□). The solid line was generated theoretically according to Eq. 3.*

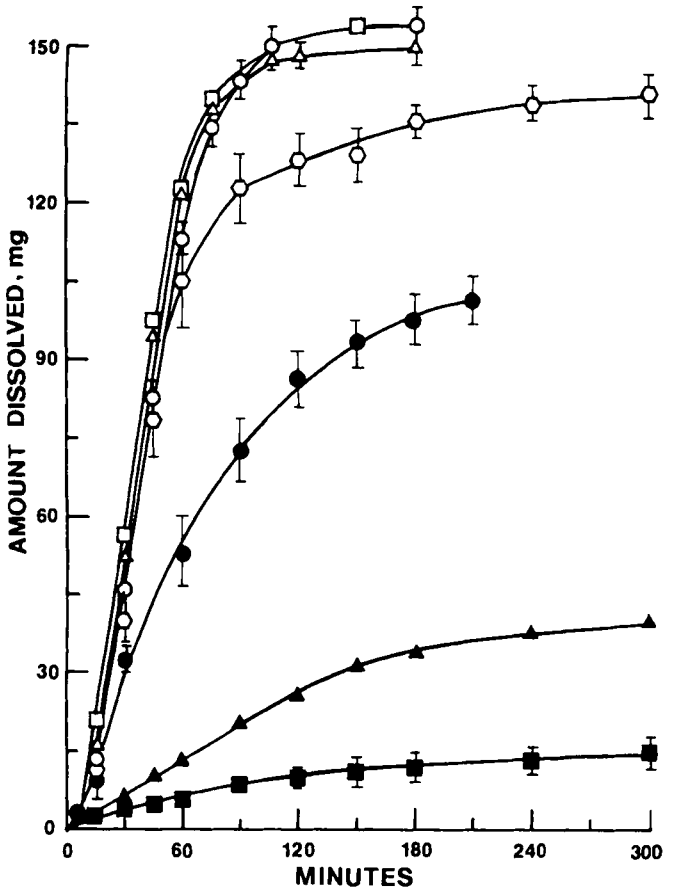

Figure 5 —*Dissolution of I from papaverine sustained-release pellets in citric acid–phosphate buffers. Key: (○) pH 2.2; (△) pH 3; (□) pH 4; (○) pH 5; (●) pH 5.4; (▲) pH 6; (■) pH 7. Each point represents mean ± SD of three experimental values, except for pH 6, for which the mean of duplicate determinations was plotted.*

i.e., equal to the solubility of the salt. The solubility of I, however, dropped gradually on lowering the pH below 2 with the addition of 1 M HCl. The chloride concentrations of solutions with pH values lower than pH_{max} are plotted in Fig. 2. Between pH 2 and 4, the chloride concentration remained constant, along with the constant solubility exhibited over this range (Fig. 1). A sharp increase in chloride ion concentration below pH 2 showed that the decline in solubility in Fig. 1 was due to a common-ion effect.

Solubility in Buffers— The pH–solubility of profile I in citric acid–phosphate buffers is presented in Fig. 3. As in Fig. 1, the apparent pH_{max} was 3.9 (higher than the theoretical pH_{max}), but the solubility of the salt at pH values between 2.2 and 3.9 was higher than that in the unbuffered solutions. Equilibrium solubility determinations in buffer showed no supersaturation effect around the apparent pH_{max}. The increase in solubility, however, over that obtained by the addition of acid or base between pH 3.3 and 3.9 may be due to salt formation with the buffer components. When an excess of I was added to the buffers with an initial pH higher than the apparent pH_{max}, the pH dropped to the latter value. The data points A, B, and C (Fig. 3) were obtained by adding an excess of I to buffers of pH 4, 5, and 5.4, respectively. Since the profile could not be extended below pH 2.2 in the citric acid–phosphate buffer system, no common-ion effect was noticed.

The solubilities above the apparent pH_{max} determined by (*a*) increasing the pH of a solution of I, (*b*) decreasing the pH of a solution of II, and (*c*) adding II to citric acid–phosphate buffer are shown with an expanded scale in Fig. 4. The line drawn is a theoretical value based on Eq. 3. As noted earlier, the solubility below pH 4.6 lies higher than the theoretical line.

Equilibrium solubility values determined by overnight shaking were plotted in Fig. 3, whereas Fig. 1 was generated by titration. An apparent pH_{max} of 3.9 in both cases, which is higher than the value of 3.0 derived theoretically, suggests that the positive deviation in solubility profile observed in Fig. 1 was not due to nonequilibrium conditions. Bogardus and Blackwood (10) have also observed similar nonideal behavior in the pH–solubility profile of doxycycline hydrochloride and have suggested that this might be due to self-association of the solute.

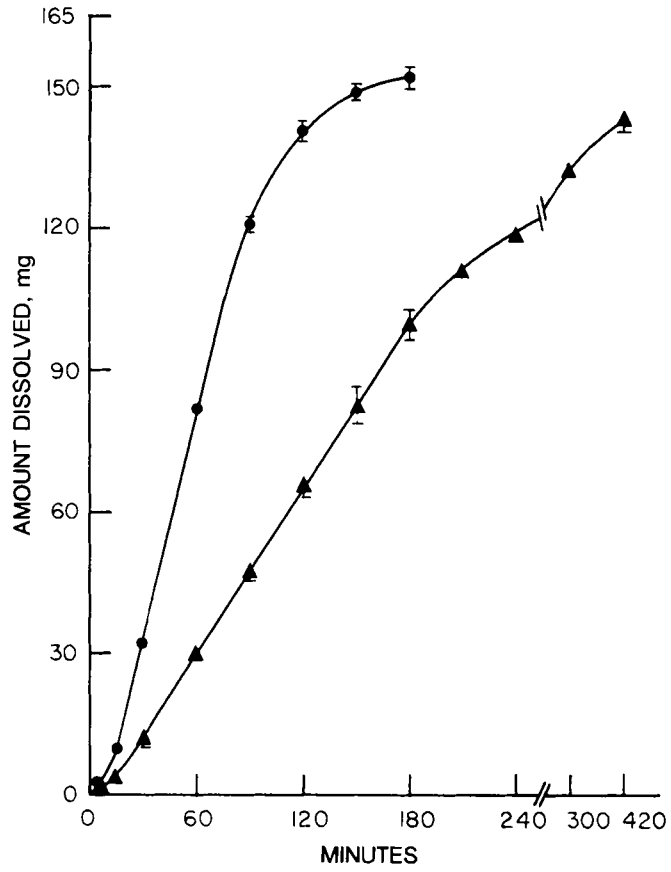

Figure 6—*Dissolution of I from papaverine sustained-release pellets in 0.01 M HCl (●) and 0.1 M HCl (▲). Each point represents mean ± SD of the three experimental values.*

Dissolution from Papaverine Sustained-Release Pellets— The dissolution of I from sustained-release pellets of I in citric acid–phosphate buffers at pH values of 2.2, 3.0, 4.0, 5.0, 5.4, 6.0, and 7.0 is shown in Fig. 5. The graphs in the pH region between 2.2 and 5.0 showed linearity after certain initial lag periods. This implies that the release rates were zero order for the periods corresponding to the linearity. At pH 2.2, 3.0, and 4.0, 100% of the drug was

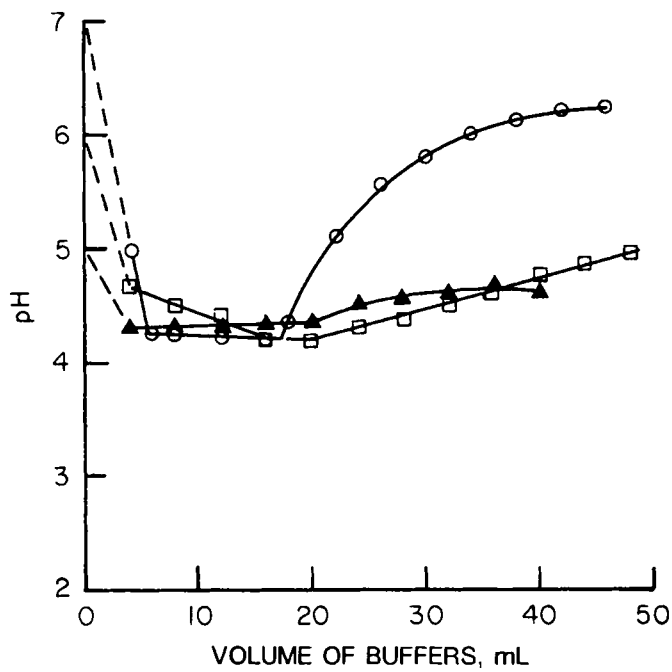

Figure 7— *Changes of pH of citric acid–phosphate buffers added to 1 g of I. Key: (▲) pH 5; (□) pH 6; (○) pH 7.*

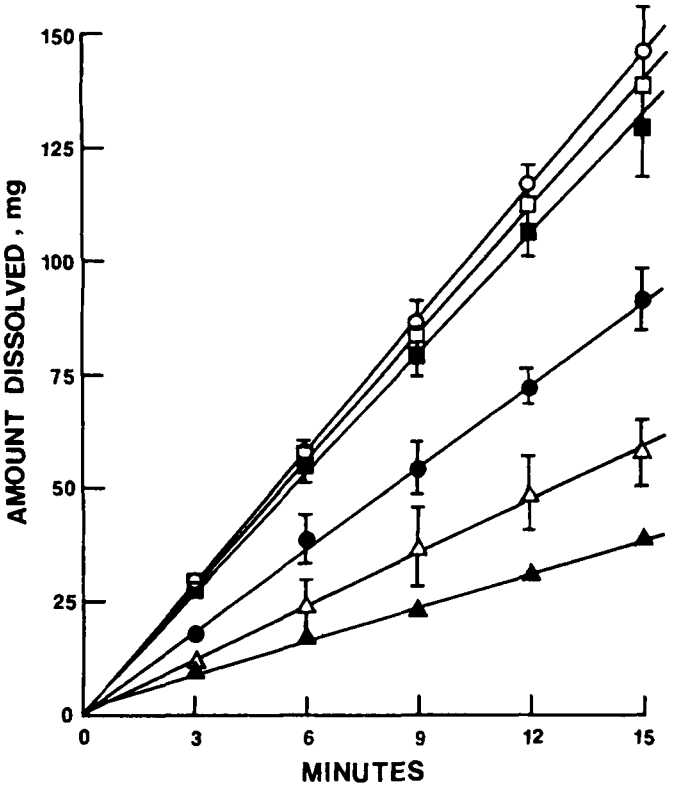

Figure 8—*Dissolution profiles of I from a constant surface area of 0.95 cm^2 at 37°C in various buffers. Each point represents mean ± SD of three experimental values. Key: (▲) pH 1.1; (●) pH 2.0; (○) pH 2.2; (□) pH 4.0; (■) pH 5.0; (△) pH 6.0. Deposition of a porous film of papaverine base was observed on the surface of I at pH 6.0.*

released from the pellets, whereas at pH ≥5.0, the dissolution profiles leveled off before complete release.

The zero-order rates in the pH range between 2.2 and 5.0 were calculated from the straight-line portions of the graphs. The release rates at pH 5.4, 6.0, and 7.0 were calculated from the initial portions of the graphs (<60 min) since sink conditions were not fulfilled. The rate constants, the solubilities, and their ratios at various pH are shown in Table I. According to Fig. 3, the saturation solubility between pH 2.2 and 3.9 was almost constant. This agrees with a similar constancy in dissolution rates at pH 2.2, 3.0, and 4.0. The dissolution of the pellets was also measured in 0.01 and 0.1 M HCl to study the effect of solubility on release rates (Fig. 6, Table I). In these two media, the saturation solubilities were 42 and 20 mg/mL, and the zero-order dissolution rates were 1.6 and 0.6 mg/min, respectively. Thus, at the apparent pH_{max} and lower, the dissolution rates were approximately proportional to the solubilities.

Similar proportional relationships between the solubility and the dissolution rate did not exist at higher pH. For example, although the solubilities at pH 5.0 and 5.4 were 152 and 390 times lower, respectively, than the solubility in the pH range of 2.2–3.9, the dissolution rates decreased only by factors of 1.1 and 2.3. This effect is further illustrated in Table I by the ratios of dissolution rate from pellets to solubility. At pH ≤4, the ratios were very small and almost constant, whereas at higher pH, the ratios were much larger. The discontinuity between the two sets of ratios occurred at the apparent pH_{max}.

Self-Buffering Action of I—The larger dissolution rate to solubility ratio at pH values higher than the apparent pH_{max} may be related to the effect of an excess of I on the pH of the buffer solutions. When buffers of pH 5.0, 6.0, and 7.0 were added to solid drug, the pH always dropped to a level between 4.0 and 4.5 and remained at this level until a considerable excess of buffer was added to raise the pH (Fig. 7). The same effect was also observed when an excess of I in solid form was added to pH 6 buffer, causing the pH to drop to 3.9. As long as an excess of I in solid form was present, the pH of the solution remained between 3.9 and 4.5, although the initial pH values of the buffers were higher. This pH range corresponds to the apparent pH_{max} and the supersaturation range of I (Fig. 1). The self-buffering action of I inside the pellets may increase the effective drug solubility, thus giving higher release rates at external pH values greater than the apparent pH_{max}. The increase in solubility due to the self-buffering action of I may not be identical when buffers of different pH values are used as the dissolution media. This is apparent from Fig. 3, in which points B and C represent the saturation solubilities of I in citric acid–phosphate buffers of pH 5.0 and 5.4, respectively.

The dissolution profiles of I from constant surfaces in selected media are shown in Fig. 8, and the results are tabulated in Table I along with those from sustained-release pellets. The profiles showed apparent linearity, although sink conditions should not exist at pH 5.0 and 6.0. According to the Noyes–Whitney equation (11), the dissolution rate (J) of a compound is proportional to the saturation solubility (C_s), and J/C_s is constant if the surface area, diffusion layer thickness, and diffusion coefficient are assumed to be constant. However, due to the self-buffering action in the diffusion layer (12, 13), the intrinsic dissolution rates of I at pH > pH_{max} were not proportional to the solubilities. This similarity with the dissolution from pellets confirms that the self-buffering action of I was involved in the dissolution from sustained-release pellets.

Mechanism of Release from Sustained-Release Pellets—The linearity of the drug release with time and the extended duration indicate zero-order kinetics for the dissolution rate. The structure of the pellets, consisting of I dispersed in a matrix of shellac with added filler, suggests a mechanism involving the leaching of the drug from the matrix (14). The equation describing the heterogeneous diffusion-controlled matrix model is:

$$Q = \left[\frac{D\epsilon C_s}{\tau}(2A - \epsilon C_s)t\right]^{1/2} \qquad \text{(Eq. 4)}$$

where Q is the amount of drug released per unit area from a matrix of porosity ϵ, tortuosity τ, and initial drug concentration A at the time t. D and C_s are the diffusion coefficient and solubility of the drug in the permeating solvent, respectively. Figure 9a and b show photomicrographs of the cross sections of pellets. The diameter of the core is ~0.6 mm, as compared with the diameter of 0.9 mm for the pellet. The outermost layer produced by the addition of shellac and filler cannot be clearly identified in Fig. 9a, because slight migration of I to this layer during spraying of the shellac solution obscures the distinction under UV light. However, the outermost barrier layer is distinguishable and remains intact after total leaching of I (Fig. 9b); the thickness of this layer is estimated to be 20–30 μm. From the core volume and papaverine hydrochloride charge, A was estimated at 700 mg/mL, and the condition $A \gg C_s$ was satisfied. Porosimetry measurements of pellets allowed computation of the average porosity of the penetrated portion of the matrix, which

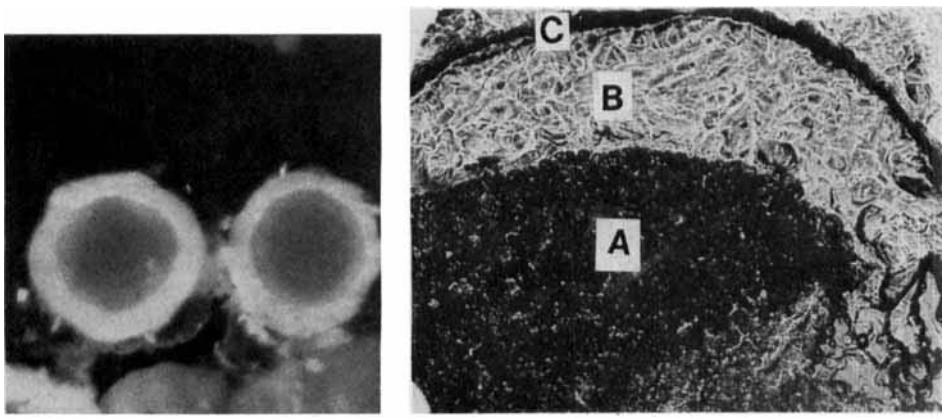

Figure 9—*Photomicrographs of (a) cross-sections of gross pellets (magnification, 30×) showing internal sugar beads and fluorescence of the papaverine hydrochloride annulus and (b) microtomed cross sections of leached-out pellets (magnification, 100×). Key: (A) sugar core; (B) leached-out annulus filled with paraffin; (C) outer shellac-filled layer.*

was ~0.6[14]. The tortuosity term must be high, particularly since additional shellac and filler were added in the final stages of pellet preparation. From the dissolution rate of pellets without added filler, a value of 30 was estimated for τ by Eq. 4. By assuming from the pellet core dimensions a matrix thickness of 150 μm and a boundary layer thickness of 100 μm, the ratio of resistances of matrix to unstirred layer is of the order of ~75, so matrix-controlled release proportional to $t^{1/2}$ would be predicted. The zero-order release rates that were observed, however, imply a constant activity of drug in a reservoir, due possibly to a barrier layer on the surface of the pellet where a constant concentration is maintained. Diffusion at constant concentrations through such a barrier layer may be the rate-determining step which results in release being linear with time. This mechanism was confirmed by dissolution from thick films of I dispersed in a shellac-based matrix in the same proportion as in the pellets but without the final drug-free layer. The release was found to be linear with $t^{1/2}$ and agreed with the heterogeneous matrix model. Moreover, the release from pellets made without the outer layer of shellac and filler also adhered to the $t^{1/2}$ relationship.

The sensitivity of the release rates to pH of the external solvent at pH < pH_{max} confirms that the leaching process takes place within a granular matrix. However, the expected decrease of release rate based on the decreased solubility at higher pH was not observed. These results were explained by the self-buffering action of the drug and the tendency to revert toward the apparent pH_{max} in the media of low buffer capacity.

The results of the present investigation indicate that the variability in the dissolution rate of a drug within the GI pH range due to differences in solubility may be reduced by designing controlled-release dosage forms. The importance of internal pH within the polymer matrices in controlling the solubility of drug and hence the dissolution rate has also been noted by Jambhekar and Cobby (15).

[14] The maximum porosity when all of the active drug is dissolved is given by $\epsilon + A(1 - \epsilon)$, where ϵ is the porosity of the pellet equal to 0.07, and A is the concentration of drug in the matrix.

REFERENCES

(1) R. J. Timko and N. G. Lordi, *J. Pharm. Sci.*, **67,** 496 (1978).
(2) S. F. Kramer and G. L. Flynn, *J. Pharm. Sci.*, **61,** 1896 (1972).
(3) Z. T. Chowhan, *J. Pharm. Sci.*, **67,** 1257 (1978).
(4) M. Robinson, in "The Theory and Practice of Industrial Pharmacy," 2nd ed., L. Lachman, H. A. Lieberman, and J. L. Kanig, Eds., Lea & Febiger, Philadelphia, Pa., 1976, p. 456.
(5) L. W. Dittert, T. Higuchi, and D. R. Reese, *J. Pharm. Sci.*, **53,** 1325 (1964).
(6) I. M. Kolthoff, *Biochem. Z.*, **162,** 289 (1925).
(7) V. H. Veley, *J. Chem. Soc.*, **95,** 758 (1909).
(8) A. I. Biggs, *Trans. Faraday Soc.*, **50,** 800 (1954).
(9) J. H. Wood, J. E. Syarto, and H. Letterman, *J. Pharm. Sci.*, **54,** 1068 (1965).
(10) J. B. Bogardus and R. K. Blackwood, *J. Pharm. Sci.*, **68,** 188 (1979).
(11) A. A. Noyes and W. R. Whitney, *J. Am. Chem. Soc.*, **19,** 930 (1897).
(12) E. Nelson, *J. Am. Pharm. Assoc., Sci. Ed.*, **46,** 607 (1957).
(13) K. G. Mooney, M. A. Mintun, K. J. Himmelstein, and V. J. Stella, *J. Pharm. Sci.*, **70,** 13 (1981).
(14) T. Higuchi, *J. Pharm. Sci.*, **52,** 1145 (1963).
(15) S. Jambhekar and J. Cobby, Abstracts, Academy of Pharmaceutical Sciences 29th National Meeting, **10**(2), 86 (1980).

ACKNOWLEDGMENTS

The authors wish to thank Mr. J. Breitbart for measurements of the dissolution rates of papaverine hydrochloride from films and Dr. D. Mufson for his encouragement and advice throughout the course of this study and for critical review of the manuscript.

Serum and Myocardial Kinetics of Amiodarone and Its Deethyl Metabolite After Intravenous Administration in Rabbits

R. KANNAN *x, N. IKEDA ‡, R. WAGNER ‡, M. DRACHENBERG ‡, and B. N. SINGH *

Received July 5, 1983, from the **Department of Cardiology, Veterans Administration Medical Center, West Los Angeles, CA 90073* and the ‡*Department of Medicine, UCLA School of Medicine, Los Angeles, CA.* Accepted for publication October 6, 1983.

Abstract □ The serum kinetics of amiodarone and its major metabolite the deethyl analogue were studied in rabbits after intravenous administration. The elimination of the drug and the metabolite from serum occurred as a biexponential function. Both compounds exhibited a rapid distribution phase (6.5 and 4.4 min, respectively) and had elimination half-lives of 136 and 235 min, respectively. There was a rapid uptake of both drugs by the myocardium, with maximal concentrations at 5 and 15 min. The myocardial concentrations were higher than the respective serum concentrations and declined with time. There was a wide scatter in myocardium-serum ratios, which ranged from 1 to 11 for amiodarone and 12 to 29 for the metabolite. Neither the drug nor the metabolite produced significant changes in the surface electrocardiogram after intravenous administration. These data suggest that accumulation of the metabolite does not account for the slow onset of action of amiodarone.

Keyphrases □ Kinetics—serum and myocardial, amiodarone and its metabolite, rabbits □ Amiodarone—serum and myocardial kinetics, rabbits □ Deethyl metabolite—amiodarone, serum and myocardial kinetics, rabbits

Plasma drug levels are commonly used to monitor the efficacy and toxicity of antiarrhythmic compounds. Such an approach is based on the assumption that the drug level in the myocardium, the presumed site of action of cardioactive agents, is in equilibrium with that in plasma. However, this assumption may not necessarily be valid under conditions of rapidly changing plasma levels of drugs (1). The significance of the myocardium–plasma drug ratios in the interpretation of the pharmacological responses of antidysrhythmic agents such as lidocaine (2), quinidine (3), verapamil (4), disopyramide (5), and *n*-acetylprocainamide (6) has been emphasized. Such studies are particularly relevant in the case of amiodarone, a potent class III antiarrhythmic drug (7), in light of our recent finding which demonstrates a lack of correlation between serum drug concentrations and suppression of premature ventricular contractions in patients with cardiac arrhythmias (8). Chronic amiodarone therapy results in the accumulation of a metabolite, the deethyl analogue, in serum (9). However, neither the pharmacokinetics nor the pharma-

0022-3549/84/0900-1208$01.00/0

© 1984, American Pharmaceutical Association

was ~0.6[14]. The tortuosity term must be high, particularly since additional shellac and filler were added in the final stages of pellet preparation. From the dissolution rate of pellets without added filler, a value of 30 was estimated for τ by Eq. 4. By assuming from the pellet core dimensions a matrix thickness of 150 μm and a boundary layer thickness of 100 μm, the ratio of resistances of matrix to unstirred layer is of the order of ~75, so matrix-controlled release proportional to $t^{1/2}$ would be predicted. The zero-order release rates that were observed, however, imply a constant activity of drug in a reservoir, due possibly to a barrier layer on the surface of the pellet where a constant concentration is maintained. Diffusion at constant concentrations through such a barrier layer may be the rate-determining step which results in release being linear with time. This mechanism was confirmed by dissolution from thick films of I dispersed in a shellac-based matrix in the same proportion as in the pellets but without the final drug-free layer. The release was found to be linear with $t^{1/2}$ and agreed with the heterogeneous matrix model. Moreover, the release from pellets made without the outer layer of shellac and filler also adhered to the $t^{1/2}$ relationship.

The sensitivity of the release rates to pH of the external solvent at pH < pH_{max} confirms that the leaching process takes place within a granular matrix. However, the expected decrease of release rate based on the decreased solubility at higher pH was not observed. These results were explained by the self-buffering action of the drug and the tendency to revert toward the apparent pH_{max} in the media of low buffer capacity.

The results of the present investigation indicate that the variability in the dissolution rate of a drug within the GI pH range due to differences in solubility may be reduced by designing controlled-release dosage forms. The importance of internal pH within the polymer matrices in controlling the solubility of drug and hence the dissolution rate has also been noted by Jambhekar and Cobby (15).

[14] The maximum porosity when all of the active drug is dissolved is given by $\epsilon + A(1 - \epsilon)$, where ϵ is the porosity of the pellet equal to 0.07, and A is the concentration of drug in the matrix.

REFERENCES

(1) R. J. Timko and N. G. Lordi, *J. Pharm. Sci.*, **67,** 496 (1978).
(2) S. F. Kramer and G. L. Flynn, *J. Pharm. Sci.*, **61,** 1896 (1972).
(3) Z. T. Chowhan, *J. Pharm. Sci.*, **67,** 1257 (1978).
(4) M. Robinson, in "The Theory and Practice of Industrial Pharmacy," 2nd ed., L. Lachman, H. A. Lieberman, and J. L. Kanig, Eds., Lea & Febiger, Philadelphia, Pa., 1976, p. 456.
(5) L. W. Dittert, T. Higuchi, and D. R. Reese, *J. Pharm. Sci.*, **53,** 1325 (1964).
(6) I. M. Kolthoff, *Biochem. Z.*, **162,** 289 (1925).
(7) V. H. Veley, *J. Chem. Soc.*, **95,** 758 (1909).
(8) A. I. Biggs, *Trans. Faraday Soc.*, **50,** 800 (1954).
(9) J. H. Wood, J. E. Syarto, and H. Letterman, *J. Pharm. Sci.*, **54,** 1068 (1965).
(10) J. B. Bogardus and R. K. Blackwood, *J. Pharm. Sci.*, **68,** 188 (1979).
(11) A. A. Noyes and W. R. Whitney, *J. Am. Chem. Soc.*, **19,** 930 (1897).
(12) E. Nelson, *J. Am. Pharm. Assoc., Sci. Ed.*, **46,** 607 (1957).
(13) K. G. Mooney, M. A. Mintun, K. J. Himmelstein, and V. J. Stella, *J. Pharm. Sci.*, **70,** 13 (1981).
(14) T. Higuchi, *J. Pharm. Sci.*, **52,** 1145 (1963).
(15) S. Jambhekar and J. Cobby, Abstracts, Academy of Pharmaceutical Sciences 29th National Meeting, **10**(2), 86 (1980).

ACKNOWLEDGMENTS

The authors wish to thank Mr. J. Breitbart for measurements of the dissolution rates of papaverine hydrochloride from films and Dr. D. Mufson for his encouragement and advice throughout the course of this study and for critical review of the manuscript.

Serum and Myocardial Kinetics of Amiodarone and Its Deethyl Metabolite After Intravenous Administration in Rabbits

R. KANNAN *x, N. IKEDA ‡, R. WAGNER ‡, M. DRACHENBERG ‡, and B. N. SINGH *

Received July 5, 1983, from the **Department of Cardiology, Veterans Administration Medical Center, West Los Angeles, CA 90073* and the ‡*Department of Medicine, UCLA School of Medicine, Los Angeles, CA.* Accepted for publication October 6, 1983.

Abstract □ The serum kinetics of amiodarone and its major metabolite the deethyl analogue were studied in rabbits after intravenous administration. The elimination of the drug and the metabolite from serum occurred as a biexponential function. Both compounds exhibited a rapid distribution phase (6.5 and 4.4 min, respectively) and had elimination half-lives of 136 and 235 min, respectively. There was a rapid uptake of both drugs by the myocardium, with maximal concentrations at 5 and 15 min. The myocardial concentrations were higher than the respective serum concentrations and declined with time. There was a wide scatter in myocardium-serum ratios, which ranged from 1 to 11 for amiodarone and 12 to 29 for the metabolite. Neither the drug nor the metabolite produced significant changes in the surface electrocardiogram after intravenous administration. These data suggest that accumulation of the metabolite does not account for the slow onset of action of amiodarone.

Keyphrases □ Kinetics—serum and myocardial, amiodarone and its metabolite, rabbits □ Amiodarone—serum and myocardial kinetics, rabbits □ Deethyl metabolite—amiodarone, serum and myocardial kinetics, rabbits

Plasma drug levels are commonly used to monitor the efficacy and toxicity of antiarrhythmic compounds. Such an approach is based on the assumption that the drug level in the myocardium, the presumed site of action of cardioactive agents, is in equilibrium with that in plasma. However, this assumption may not necessarily be valid under conditions of rapidly changing plasma levels of drugs (1). The significance of the myocardium–plasma drug ratios in the interpretation of the pharmacological responses of antidysrhythmic agents such as lidocaine (2), quinidine (3), verapamil (4), disopyramide (5), and *n*-acetylprocainamide (6) has been emphasized. Such studies are particularly relevant in the case of amiodarone, a potent class III antiarrhythmic drug (7), in light of our recent finding which demonstrates a lack of correlation between serum drug concentrations and suppression of premature ventricular contractions in patients with cardiac arrhythmias (8). Chronic amiodarone therapy results in the accumulation of a metabolite, the deethyl analogue, in serum (9). However, neither the pharmacokinetics nor the pharma-

0022-3549/84/0900-1208$01.00/0

© 1984, American Pharmaceutical Association

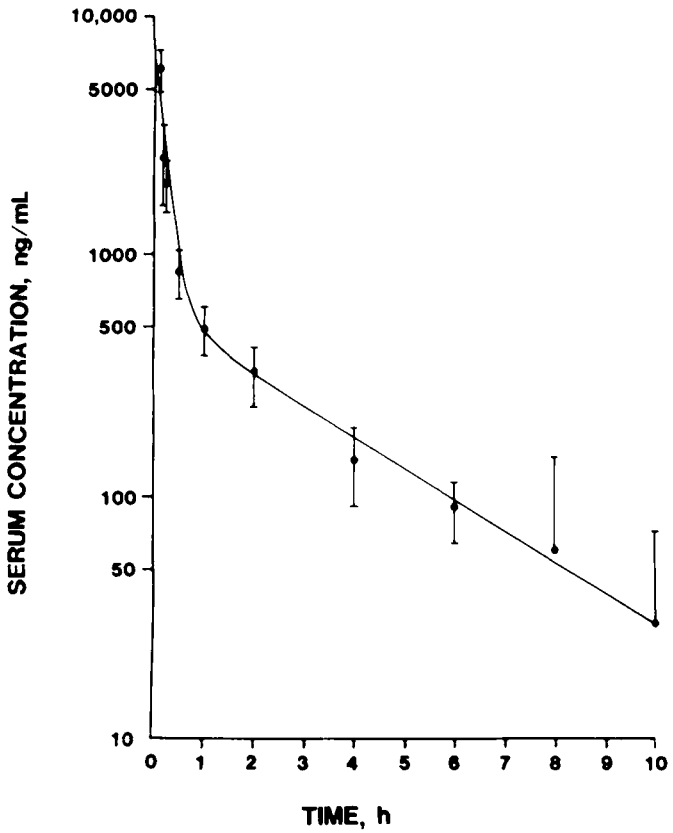

Figure 1—*Semilogarithmic plot of the elimination kinetics of amiodarone after intravenous administration to rabbits. The data represent mean values (±95% confidence limits) from 6 to 14 determinations per time point. The curve drawn is a two-exponential fit to the data.*

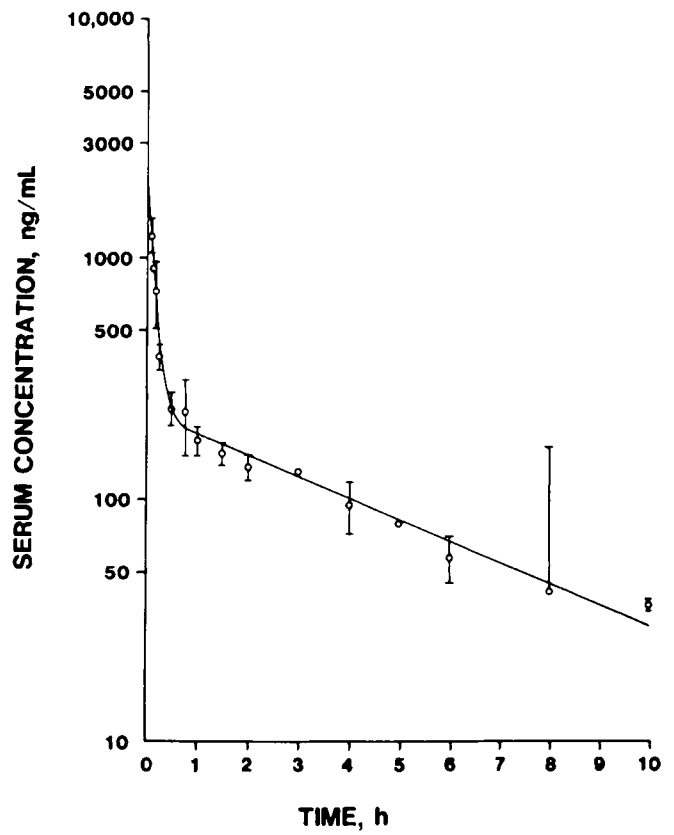

Figure 2—*Semilogarithmic plot of the elimination kinetics of the deethyl analogue after intravenous administration to rabbits. The data represent mean values (±95% confidence limits) from 3 to 9 values per time point. The curve drawn is a two-exponential fit to the data.*

cological properties of the metabolite are known. The purpose of the present study was twofold: first, to make a comparative evaluation of the serum elimination kinetics of amiodarone and its major metabolite after intravenous administration in rabbits and, second, to determine the myocardial concentrations of amiodarone and its deethyl metabolite as a function of time after an intravenous dose and to correlate the tissue levels with the electrocardiographic changes.

EXPERIMENTAL SECTION

Experimental Design—The kinetic and electrophysiological studies were conducted using female New Zealand White rabbits. For the study of amiodarone kinetics, 15 rabbits [body weight, 1.9 ± 0.2 kg (mean ± *SD*)] were used. One rabbit died after the administration of amiodarone, and data from that rabbit were not included in the final analysis. The kinetics of the deethyl analogue were evaluated in 15 rabbits (2.42 ± 0.33 kg). However, three rabbits were excluded since they died from either anesthesia ($n = 1$) or drug ($n = 2$). All animals were anesthetized with pentobarbital[1] (20 mg/kg). Either 5% aqueous amiodarone hydrochloride[2] at a dose of 10 mg/kg or the deethyl analogue as the hydrochloride[2] in 50% ethanol (1.5% solution) at a dose of 10 mg/kg was injected as a single intravenous bolus dose in the marginal vein of the left ear. The total volume of injectant did not exceed 0.30–0.52 mL for amiodarone and 0.7–1.3 mL for the metabolite. Serial blood samples (1–1.7 mL) were drawn from the right ear vein. Up to eight serial blood samples were obtained at the following sampling times: 5, 10, 15, 30, 45, and 60 min and 1.5 h, 2, 4, 6, 8, and 10 h. Blood collected before the drug was injected served as the blank in drug assays. In some rabbits, blood samples were also taken at 2.5, 7.5, and 12.5 min. To obtain myocardial tissue samples, all 15 rabbits used in the amiodarone serum kinetics studies were sacrificed as groups of two to three rabbits each at 5 and 15 min and 1, 2, and 6 h. Similarly, groups of three to four rabbits were sacrificed at 15 min and 2, 4, 6, and 10 h in the metabolite studies. After dissection, the heart tissue was blotted dry, weighed, and kept frozen. Blood samples were spun at 10,000 rpm, after which the serum was separated and stored frozen until analysis. Electrocardiograms (ECGs) were recorded[3] with standard limb leads immediately before injection of the drug and at 15 and 30 min and 1, 3, 4, and 6 h postdose. ECGs of control rabbits that were injected with either equivalent volumes of sterile distilled water or 50% ethanol were recorded for up to 6 h.

Table I—Kinetic Parameters of Amiodarone and its Metabolite, the Deethyl Analogue, After Intravenous Administration in Rabbits [a]

	$t_{1/2,\alpha}$ min	$t_{1/2,\beta}$ min	Vd_{ss}, L/kg	CL, L/min/kg
Amiodarone	6.5 ± 1.2	136 ± 20	6.7	0.055
Deethyl analogue	4.4 ± 0.6	235 ± 7	34.4	0.116

[a] These data are derived from the serum elimination curves for amiodarone and the metabolite shown in Figs. 1 and 2.

Drug Analysis—Analyses were carried out in a liquid chromatograph[4] equipped with a solvent delivery system[5], a valve-type injector[6], a normal-phase silica column[7], and a variable-wavelength UV detector[8] set a 240 nm. Serum concentrations of amiodarone and its metabolite were determined by using a recent modification (10) of the procedure described by Flanagan *et al.* (11). The serum volumes for analysis varied from 0.25 to 0.75 mL, depending on the expected drug concentrations, with corresponding increase in the volume of the extracting solvent, methyl *tert*-butyl ether. The combined ether extract from two extractions was dried under a stream of nitrogen and reconstituted in 25 μL of methanol, of which 20 μL was injected into the liquid chromatograph.

For the measurement of myocardial concentrations of amiodarone and its metabolite, 100–250 mg of ventricular muscle was homogenized with 5 mL of deionized distilled water by sonication, and the homogenate was centrifuged

[1] Nembutal, Abbott.
[2] Labaz Inc., Brussels, Belgium.
[3] Gould Brush 280; Grass Instruments, Quincy, Mass.
[4] Waters Associates, Milford, Mass.
[5] Model 6000A; Waters Associates.
[6] U6K; Waters Associates.
[7] Beckman Instruments, Palo Alto, Calif.
[8] M450; Waters Associates.

Table II—Mean Concentrations of Amiodarone and Its Deethyl Analogue in Serum and Myocardium after Intravenous Administration in Rabbits [a]

Time after Injection	Concentration		Myocardium-Serum Ratio (range) [b]
	Serum, ng/mL	Myocardium, ng/g	
		Amiodarone	
5 min	6050 ± 2200 (14)	8100 ± 4000 (3)	1.2 (0.3–1.7)
15 min	1990 ± 680 (11)	14,400 ± 2800 (3)	5.8 (4.9–7.6)
1 h	490 ± 170 (11)	7000 ± 1900 (3)	11.1 (9.6–12.0)
2 h	320 ± 120 (10)	530 ± 430 (2)	1.3 (0.5–2.1)
6 h	90 ± 30 (6)	362 ± 431 (3)	2.3 (0.7–5.5)
		Deethyl Analogue	
15 min	389 ± 64 (9)	10,800 ± 7850 (3)	28.8 (24.0–33.6)
2 h	136 ± 21 (8)	3444 ± 2910 (3)	26.9 (3.7–47.1)
4 h	95 ± 21 (6)	2590 ± 1150 (2)	25.9 (18.7–33.0)
6 h	58 ± 11 (6)	1006 ± 620 (3)	17.0 (8.6–28.7)
10 h	37 ± 1 (3)	445 ± 358 (4)	11.7 (1.8–24.4)

[a] Data are mean ± *SD*; number of rabbits is given in parentheses. [b] Ratios are presented only for those rabbits for which both serum and myocardial concentrations were available.

at 10,000 rpm for 10 min. Aliquots (2 mL) of the supernatant were extracted twice with 1 mL of methyl *tert*-butyl ether. Further processing of the sample was the same as described above for serum. The extraction efficiency of amiodarone and the metabolite from ventricular muscle of control rabbits was 71.2 ± 2.7% (n = 6), which did not differ from that found in serum (74.0 ± 9.8%; n = 8).

Data Analysis—Mean serum concentrations of amiodarone and the deethyl metabolite were fitted by nonlinear least-squares regression analysis (12). Clearance (CL) and volume of distribution at steady state (Vd_{ss}) were determined by using model-independent calculations (13). The ECG parameters were derived manually from records at 125-mm/s paper speed, and the resulting data were compared at each time point with an ANOVA program.

RESULTS

Serum Kinetics of Amiodarone and the Deethyl Analogue in Rabbits—In Figs. 1 and 2 are shown the serum elimination kinetics of amiodarone and the metabolite, respectively, in rabbits after intravenous administration. The data shown are from 14 rabbits administered amiodarone and 15 rabbits administered the metabolite; in both series of experiments, both serum and myocardial kinetics were studied. A biexponential fall in serum concentrations was observed for the parent drug and the metabolite. The serum concentrations 5 min after administration of the intravenous dose were 6050 and 2660 ng/mL for amiodarone and the metabolite, respectively, and fell to 30 and 38 ng/mL, respectively, in 10 h. The kinetic parameters of serum kinetics of amiodarone and the deethyl analogue are listed in Table I. Both drugs had a rapid distribution phase ($t_{1/2,\alpha}$ 6.5 and 4.4 min for amiodarone and the metabolite, respectively). The elimination half-lives ($t_{1/2,\beta}$) were 136 min for amiodarone and 235 min for the metabolite. The mean volumes of distribution and clearance for amiodarone were 6.7 L/kg and 0.055 L/min/kg, respectively. The corresponding values for the metabolite were 34.4 L/kg and 0.116 L/min/kg, respectively (Table I).

In Table II, the myocardial concentrations of amiodarone and the metabolite in rabbits as a function of time after intravenous administration are summarized. We used ventricular muscle as a representative tissue sample for the determination of the myocardial concentrations. The myocardial concentrations of the parent drug and the metabolite expressed as nanograms per gram of wet tissue were higher than the respective serum concentrations that were obtained throughout the time course of the study. In the postdistributive phase, myocardial concentrations of the metabolite declined approximately parallel to those of serum. Such a similarity was not apparent for amiodarone, partly due to the limited number of data points (2 and 6 h) for myocardial levels of amiodarone in the postdistributive phase. The myocardium-serum ratios (Table II) are derived from only those rabbits for which both serum and myocardial concentrations were available. Although the myocardium-serum ratios of amiodarone and the metabolite overlapped, the ratios for the metabolite (range, 11.7–28.8) were higher than for amiodarone (range 1.3–11.3). The large scatter in the ratios was a result of wide variations in myocardial concentrations.

Electrocardiographic Changes—Electrocardiographic changes accompanying intravenous administration of amiodarone and the metabolite were compared between rabbits injected with drug and a control group (n = 5) injected with the vehicle alone. All rabbits were mildly anesthetized with pentobarbital before administration of the appropriate drug or the vehicle and at other times during the study to obtain ECG recordings that were free of technical artifacts. An analysis of variance among the three groups showed that intravenous administration of either amiodarone or the metabolite did not cause any significant changes in RR, PQ, QRS, and QT_c intervals[9] as compared with the control group, except for an increase in the QRS intervals of the animals treated with the metabolite 15 min after administration of the drug (37.2 ± 4.0 *versus* 29.6 ± 2.8 ms in the controls). However, this increase is only of borderline significance. There were fluctuations in the values of the QRS intervals both in the control and drug-treated groups, although the values of the QRS intervals did not differ significantly from those of the controls at other time points studied.

DISCUSSION

We have determined the serum elimination kinetics and myocardial distribution of amiodarone in rabbits after intravenous administration. The pharmacokinetics of the major metabolite of amiodarone, the deethyl analogue, was compared with those of the parent drug for the first time. The short and long elimination half-lives of amiodarone in patients after acute and chronic oral administrations have been determined by us and others (9, 14, 15). It has been suggested that amiodarone equilibrates rapidly with tissues, such as the myocardium, after acute administration, and the rapid repartitioning between tissue and serum results in a short half-life. On the other hand, the long elimination half-life after chronic administration is attributed to the slowly equilibrating tissues, mainly adipose tissue and muscle. We found that amiodarone was rapidly eliminated from the serum of rabbits after intravenous administration, with an elimination half-life of 136 min, which is similar to that found in dogs (16, 17) but different from that found in rats (18). The disappearance of the intravenously administered metabolite from the serum of rabbits is also rapid ($t_{1/2,el}$ 235 min). There is a rapid uptake of both the drug and its metabolite by the myocardium. Although our limited data did not allow us to determine the precise time of maximal uptake of amiodarone and the metabolite by the myocardium, it can be estimated to be between 5 and 15 min. The myocardial concentrations of amiodarone and the metabolite decreased with time. This decline in myocardial concentrations was approximately parallel to that detected for the metabolite in serum but not for amiodarone. For both the drug and the metabolite, the myocardial concentrations were higher than the respective serum concentrations used throughout the study.

Latini *et al.* (16, 17) have recently reported a detailed investigation on serum kinetics and myocardial disposition of amiodarone in dogs. The mean serum elimination half-life of amiodarone after intravenous administration in dogs (3.01 h) was similar to that in rabbits, as determined in the present study. They observed a large interanimal variability in myocardium-serum ratios in dogs. The average ratio of myocardium-plasma amiodarone concentration was much higher in dogs (range, 34–134) than that in rabbits (range, 1.2–11.3). Whether this represents a species difference or differential binding characteristics of amiodarone is not certain at present. Interestingly, Latini *et al.* (17) have shown by computer simulation, that peak myocardial concentrations were achieved between 15 and 20 min after intravenous administration of amiodarone to dogs. Our limited data on rabbit myocardial levels appear to be in accord with their findings. In spite of high concentrations of amiodarone and the metabolite in the myocardium, no appreciable ECG changes were observed for up to 6 h after intravenous administration, suggesting a complex

[9] Definitions: (RR) duration between two successive heart beats; (PQ) time from the beginning of atrial depolarization to the beginning of ventricular depolarization; (QRS) duration of ventricular depolarization; (QT_c) duration of ventricular repolarization normalized or corrected for heart rate.

pharmacological action of the parent drug and possibly the metabolite. This finding is consistent with our previous observation of no significant alterations in the action potentials of rabbit sinoatrial node, atrioventricular node, and atrial fibers after a 1-h superfusion with therapeutically meaningful concentrations of amiodarone suspended in homologous plasma (19). Although similar studies with microelectrodes will be needed to establish the electrophysiological properties of the metabolite, our preliminary data on ECG changes suggest that the behavior of the metabolite is similar to that of the parent drug under acute conditions. However, this lack of the acute effect does not exclude the possibility that the accumulation of metabolite during chronic therapy may contribute significantly to the pharmacological and electrophysiological action of amiodarone. Thus, more definitive electrophysiological studies in rabbits treated chronically with amiodarone and its metabolite will be required to estimate the contribution of the metabolite to the observed pharmacological action of amiodarone during chronic administration.

In summary, both amiodarone and its major metabolite, the deethyl analogue, have similar serum kinetics after intravenous administration in rabbits and are rapidly taken up by the myocardium. Neither the parent drug nor its metabolite produces significant electrophysiological changes under acute conditions in concentrations that are therapeutically relevant. The data do not exclude the possibility that the metabolite exerts pharmacological effects that are similar to those of the parent compound during chronic dosing.

REFERENCES

(1) R. E. Kates and P. Jaillon, *J. Pharmacol. Exp. Ther.*, **214**, 31 (1980).

(2) N. Benowitz, R. P. Forsyth, K. L. Melmon, and M. Rowland, *Clin. Pharmacol. Ther.*, **16**, 87 (1974).

(3) Y. W. Cho, *Am. Heart J.*, **85**, 648 (1973).

(4) D. L. Keefe and R. E. Kates, *J. Pharmacol. Exp. Ther.*, **220**, 91 (1982).

(5) E. Patterson, P. Stetson, and B. R. Lucchesi, *J. Cardiovasc. Pharmacol.*, **5**, 541 (1979).

(6) A. Yacobi, H. F. Stampfli, C. M. Lai, and B. L. Kamath, *Drug Metab. Dispos.*, **9**, 193 (1981).

(7) K. Nademanee, J. A. Hendrickson, R. Kannan, and B. N. Singh, *Am. Heart J.*, **103**, 950 (1982).

(8) B. N. Singh, K. Nademanee, N. Ikeda, and R. Kannan, in "New Aspects in the Medical Treatment of Tachyarrhythmias," G. Breithardt and F. Loogen, Eds., Urben and Schwarzenberg, Munich, Federal Republic of Germany, 1983, p. 46.

(9) R. Kannan, K. Nademanee, J. A. Hendrickson, H. Rostami, and B. N. Singh, *Clin. Pharmacol. Ther.*, **31**, 438 (1982).

(10) G. C. A. Storey, D. W. Holt, P. Holt, and P. V. L. Curry, *Ther. Drug Monit.*, **4**, 385 (1982).

(11) R. J. Flanagan, G. C. A. Storey, and D. W. Holt, *J. Chromatogr.*, **187**, 391 (1980).

(12) C. M. Metzler, NONLIN, Upjohn Co. Tech. Rep. 7292/69/7291/005, 1974.

(13) M. Gibaldi and D. Perrier, in "Pharmacokinetics," Dekker, New York, N.Y., 1982, p. 412.

(14) L. Harris, W. J. McKenna, E. Rowland, G. C. A. Storey, D. M. Krikler, and D. W. Holt. *Circulation*, **64**, Suppl. IV, 263 (1982).

(15) F. Andreason, H. Agerback, P. Bjergaard, and H. Hotzche, *Eur. J. Clin. Pharmacol.*, **19**, 293 (1981).

(16) R. Latini, S. Conolly, R. Kernoff, and R. E. Kates, *Circulation*, **66**, Suppl. II, 223 (1982).

(17) R. Latini, S. J. Conolly, and R. E. Kates *J. Pharmacol. Exp. Ther.*, **224**, 603 (1982).

(18) E. Riva, M. Gerna, P. Neyroz, R. Urso, I. Bartozek, and A. Guaitani, *J. Cardiovasc. Pharmacol.*, **4**, 270 (1982).

(19) R. Kannan, N. Ikeda, K. Prasad, M. Ookhtens, and B. N. Singh, *Circulation*, **64**, Suppl. IV, 69 (1981).

ACKNOWLEDGMENTS

This work was supported by a grants-in-aid award from the American Heart Association, Los Angeles affiliate (756 G1-2) and by the Medical Research Service of the Veterans Administration. M. Drachenberg was a summer Research Trainee of the American Heart Association. We thank Dr. Keith Muir of the University of Southern California for helpful suggestions.

Analysis of Carprofen Dosage Forms and Drug Substance by High-Performance Liquid Chromatography

A. J. ROSS, M. D. DEL MAURO, H. K. SOKOLOFF, and D. L. CASEY ˣ

Received August 19, 1983, from the *Pharmaceutical Research Products Section, Quality Control Department, Hoffmann-La Roche, Inc., Nutley, NJ 07110.* Accepted for publication September 26, 1983.

Abstract □ A high-performance liquid chromatographic method for the analysis of carprofen in solid dosage forms and as the bulk drug substance was developed. The simple, accurate, reproducible, and stability-indicating method was shown to be applicable to drug substance and dosage form stability studies, as well as the quality control of carprofen dosage forms.

Keyphrases □ Carprofen—analysis of dosage forms and drug substances, HPLC □ HPLC—analysis of carprofen dosage forms and drug substance

Carprofen [(±)-6-chloro-α-methylcarbazole-2-acetic acid (I)], under development as a nonsteroidal anti-inflammatory agent (1–9), has been formulated as a solid oral dosage form. Analytical procedures for the analysis of carprofen in biological fluids have appeared in the literature (10–16). However, since carprofen is a relatively new drug entity, analytical procedures suitable for the analysis and control of carprofen drug substance and dosage forms have not appeared in the literature or the USP.

The purpose of this work was to provide specific, accurate, and reproducible liquid chromatographic (HPLC) methods which would be applicable to various quality control functions, *i.e.*, drug substance stability studies, potency and content uniformity assays of dosage forms, and dosage form stability studies. To satisfy these criteria, it was necessary to develop a method which would separate I from all known impurities and potential degradation products and separate the impurities and potential degradation products from each other.

0022-3549/84/0900-1211$01.00/0

© 1984, American Pharmaceutical Association

pharmacological action of the parent drug and possibly the metabolite. This finding is consistent with our previous observation of no significant alterations in the action potentials of rabbit sinoatrial node, atrioventricular node, and atrial fibers after a 1-h superfusion with therapeutically meaningful concentrations of amiodarone suspended in homologous plasma (19). Although similar studies with microelectrodes will be needed to establish the electrophysiological properties of the metabolite, our preliminary data on ECG changes suggest that the behavior of the metabolite is similar to that of the parent drug under acute conditions. However, this lack of the acute effect does not exclude the possibility that the accumulation of metabolite during chronic therapy may contribute significantly to the pharmacological and electrophysiological action of amiodarone. Thus, more definitive electrophysiological studies in rabbits treated chronically with amiodarone and its metabolite will be required to estimate the contribution of the metabolite to the observed pharmacological action of amiodarone during chronic administration.

In summary, both amiodarone and its major metabolite, the deethyl analogue, have similar serum kinetics after intravenous administration in rabbits and are rapidly taken up by the myocardium. Neither the parent drug nor its metabolite produces significant electrophysiological changes under acute conditions in concentrations that are therapeutically relevant. The data do not exclude the possibility that the metabolite exerts pharmacological effects that are similar to those of the parent compound during chronic dosing.

REFERENCES

(1) R. E. Kates and P. Jaillon, *J. Pharmacol. Exp. Ther.*, **214**, 31 (1980).

(2) N. Benowitz, R. P. Forsyth, K. L. Melmon, and M. Rowland, *Clin. Pharmacol. Ther.*, **16**, 87 (1974).

(3) Y. W. Cho, *Am. Heart J.*, **85**, 648 (1973).

(4) D. L. Keefe and R. E. Kates, *J. Pharmacol. Exp. Ther.*, **220**, 91 (1982).

(5) E. Patterson, P. Stetson, and B. R. Lucchesi, *J. Cardiovasc. Pharmacol.*, **5**, 541 (1979).

(6) A. Yacobi, H. F. Stampfli, C. M. Lai, and B. L. Kamath, *Drug Metab. Dispos.*, **9**, 193 (1981).

(7) K. Nademanee, J. A. Hendrickson, R. Kannan, and B. N. Singh, *Am. Heart J.*, **103**, 950 (1982).

(8) B. N. Singh, K. Nademanee, N. Ikeda, and R. Kannan, in "New Aspects in the Medical Treatment of Tachyarrhythmias," G. Breithardt and F. Loogen, Eds., Urben and Schwarzenberg, Munich, Federal Republic of Germany, 1983, p. 46.

(9) R. Kannan, K. Nademanee, J. A. Hendrickson, H. Rostami, and B. N. Singh, *Clin. Pharmacol. Ther.*, **31**, 438 (1982).

(10) G. C. A. Storey, D. W. Holt, P. Holt, and P. V. L. Curry, *Ther. Drug Monit.*, **4**, 385 (1982).

(11) R. J. Flanagan, G. C. A. Storey, and D. W. Holt, *J. Chromatogr.*, **187**, 391 (1980).

(12) C. M. Metzler, NONLIN, Upjohn Co. Tech. Rep. 7292/69/7291/005, 1974.

(13) M. Gibaldi and D. Perrier, in "Pharmacokinetics," Dekker, New York, N.Y., 1982, p. 412.

(14) L. Harris, W. J. McKenna, E. Rowland, G. C. A. Storey, D. M. Krikler, and D. W. Holt. *Circulation*, **64**, Suppl. IV, 263 (1982).

(15) F. Andreason, H. Agerback, P. Bjergaard, and H. Hotzche, *Eur. J. Clin. Pharmacol.*, **19**, 293 (1981).

(16) R. Latini, S. Conolly, R. Kernoff, and R. E. Kates, *Circulation*, **66**, Suppl. II, 223 (1982).

(17) R. Latini, S. J. Conolly, and R. E. Kates *J. Pharmacol. Exp. Ther.*, **224**, 603 (1982).

(18) E. Riva, M. Gerna, P. Neyroz, R. Urso, I. Bartozek, and A. Guaitani, *J. Cardiovasc. Pharmacol.*, **4**, 270 (1982).

(19) R. Kannan, N. Ikeda, K. Prasad, M. Ookhtens, and B. N. Singh, *Circulation*, **64**, Suppl. IV, 69 (1981).

ACKNOWLEDGMENTS

This work was supported by a grants-in-aid award from the American Heart Association, Los Angeles affiliate (756 G1-2) and by the Medical Research Service of the Veterans Administration. M. Drachenberg was a summer Research Trainee of the American Heart Association. We thank Dr. Keith Muir of the University of Southern California for helpful suggestions.

Analysis of Carprofen Dosage Forms and Drug Substance by High-Performance Liquid Chromatography

A. J. ROSS, M. D. DEL MAURO, H. K. SOKOLOFF, and D. L. CASEY ˣ

Received August 19, 1983, from the *Pharmaceutical Research Products Section, Quality Control Department, Hoffmann-La Roche, Inc., Nutley, NJ 07110.* Accepted for publication September 26, 1983.

Abstract □ A high-performance liquid chromatographic method for the analysis of carprofen in solid dosage forms and as the bulk drug substance was developed. The simple, accurate, reproducible, and stability-indicating method was shown to be applicable to drug substance and dosage form stability studies, as well as the quality control of carprofen dosage forms.

Keyphrases □ Carprofen—analysis of dosage forms and drug substances, HPLC □ HPLC—analysis of carprofen dosage forms and drug substance

Carprofen [(±)-6-chloro-α-methylcarbazole-2-acetic acid (I)], under development as a nonsteroidal anti-inflammatory agent (1–9), has been formulated as a solid oral dosage form. Analytical procedures for the analysis of carprofen in biological fluids have appeared in the literature (10–16). However, since carprofen is a relatively new drug entity, analytical procedures suitable for the analysis and control of carprofen drug substance and dosage forms have not appeared in the literature or the USP.

The purpose of this work was to provide specific, accurate, and reproducible liquid chromatographic (HPLC) methods which would be applicable to various quality control functions, *i.e.*, drug substance stability studies, potency and content uniformity assays of dosage forms, and dosage form stability studies. To satisfy these criteria, it was necessary to develop a method which would separate I from all known impurities and potential degradation products and separate the impurities and potential degradation products from each other.

0022-3549/84/0900-1211$01.00/0

© 1984, American Pharmaceutical Association

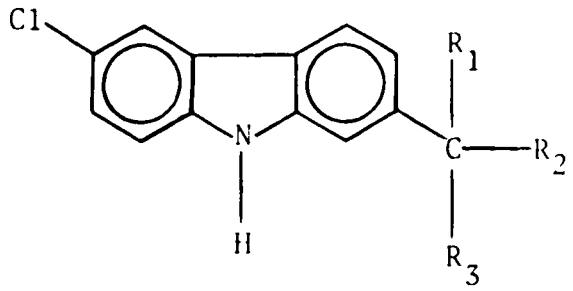

I: $R_1 = CH_3$, $R_2 = COOH$, $R_3 = H$
II: $R_1 = CH_3$, $R_2 = R_3 = CO_2C_2H_5$
III: $R_1 = CH_3$, $R_2 = CO_2C_2H_5$, $R_3 = H$
IV: $R_1 = CH_3$, $R_2 = OH$, $R_3 = H$
V: $R_1 = CH_3$, $R_2 = O$
VI: $R_1 = CH_3$, $R_2 = R_3 = H$

The dosage form assay procedure was designed to be amenable to either manual or automated injection. It was also designed so that quantification could be done either by a computer data acquisition system or by manual calculation of peak response.

EXPERIMENTAL SECTION

Materials—Benzophenone[1], anthraquinone[2], and glacial acetic acid[3] were all analytical reagent grade and were used as received. The methanol[4] and acetonitrile[4] used were distilled in glass. Water used in the preparation of mobile phases was doubly distilled.

Mobile Phase—The mobile phases used were prepared by mixing appropriately measured volumes of methanol and 1% acetic acid. The mobile phase selected for the assay was methanol-water (1% acetic acid) (65:35). All mobile phases were filtered before use.

Instrumentation—Portions of the present study were conducted with several different HPLC systems. The early developmental work on the dosage form assay was done with a constant-pressure single-piston pump[5], a fixed-loop injector[6], and a UV detector[7] set at 254 nm. The early developmental work on the drug substance stability assay was done with an HPLC system consisting of two constant-flow solvent-metering pumps[8], a solvent programmer[9], an injector[10], and an UV detector[11]. The major portion of the work was done with a 10-μm particle size octadecylsilane column[12]. Quantifications associated with developmental work on the dosage form assay were done with manual peak height measurements. Those associated with the drug substance stability study were done using peak area measurements obtained with an electronic integrator[13]. Subsequent to the earlier work, both dosage form and drug substance analyses were automated with an autosampler[14] and a more sophisticated computer data acquisition system[15].

Methods Development—Carprofen (I) and its known impurities (II and III) were chromatographed under various conditions until a suitable column–mobile phase combination was obtained that was capable of separating all compounds of interest. Samples from accelerated degradation studies were also chromatographed in this initial system to make certain that the system was also capable of separating potential degradation products. Compounds IV, V, and VI were isolated and identified as the major potential decomposition products[16]. These compounds were formed only under accelerated storage conditions. A study was also conducted in which the mobile phase composition was varied to determine the sensitivity of the separation to changes in mobile phase composition.

Dosage Form Assay Procedures—All solutions containing I were prepared by using low-actinic glassware and acetonitrile-water (50:50) as the diluent.

Internal Standard Solution—Benzophenone (380 mg) was accurately weighed into a 2-L volumetric flask and dissolved in 1 L of acetonitrile. Once dissolved, the resulting solution was diluted to volume with distilled water.

Standard Solution—Approximately 40 mg of carprofen reference standard was accurately weighed into a 100-mL volumetric flask. The standard was then dissolved and diluted to volume with the internal standard solution.

Sample Preparation for Potency Assay—Twenty tablets were combined and finely powdered with a mortar and pestle. From the composite, a tablet mass equivalent to 40 mg of I was accurately weighed into a 100-mL volumetric flask. The sample was dissolved in the internal standard solution by shaking for 15 min. After shaking, the sample was diluted to volume with the internal standard solution and filtered through a 5-μm filter[17].

System Suitability Test—Six injections of the standard solution were chromatographed, and the carprofen–internal standard response ratio was calculated for each injection. The system precision was considered to be adequate if the *RSD* for the six response ratio values did not exceed 1.5%.

The resolution factor (R^1) was calculated for the separation between the benzophenone and carprofen peaks according to the USP. The resolution was acceptable if R^1 was >3.5.

Potency Assay Procedure—The sample solutions were injected into the chromatograph using 20-μL injections. The carprofen content per tablet was then calculated by using the standard response ratio from the system suitability test, the respective peak heights in the sample chromatogram, the sample weight, and the appropriate dilution factor. Alternatively, peak areas obtained from a suitable computer system can be substituted for peak heights throughout the calculations.

Content Uniformity Sample Preparations—The same assay procedure as described above was applied to conduct content uniformity tests. For content uniformity measurements, the following sample preparation was substituted. One tablet was placed in each of ten 100-mL volumetric flasks. To each flask, 50 mL of the internal standard solution was added, and the flasks were shaken on a mechanical shaker for 1 h. Samples were then diluted to volume with internal standard solution and filtered as described above. Depending on the dosage strength, the samples were then appropriately diluted to obtain a final carprofen concentration of ~0.4 mg/mL. The final sample solutions were then chromatographed as described above, and the carprofen content per tablet was calculated.

Drug Substance Stability Assay Procedure—The same HPLC system was applied to drug substance stability testing. Several modifications in terms of sample preparation, amount of carprofen injected, and quantification techniques were necessary when the assay was to be used in bulk substance stability studies. For these assays, ~10 mg of carprofen was accurately weighed into a 10-mL volumetric flask, dissolved, and diluted to volume with the internal standard solution. Anthraquinone was used as an internal standard in some studies. During subsequent studies, it was discovered that use of benzophenone as an internal standard would shorten the analysis time. Either internal standard gave acceptable results. The carprofen concentration was determined by using an internal standard quantification technique, and the impurity and degradation product levels were estimated by using an area percent technique corrected for the presence of the internal standard in the chromatogram.

Validation—Both the dosage form assay and the drug substance stability assay were validated with respect to specificity, linearity, precision, and accuracy. The methods were also validated with both manual and automated

Table I—Method Precision of the Carprofen Dosage Form Assay

Sample Weighing	Assay Value, mg/Tablet[a]
1	150.6
2	149.3
3	149.5
4	150.7
5	150.0
6	150.3
7	151.3
8	150.1
9	149.7
10	149.3
11	150.9

[a] Mean, 150.2 mg per tablet; 101% of claim; *RSD*, 0.45%. Determined by internal standard quantification techniques; manual (loop) injection and manually measured peak heights.

[1] Fluka A. G., Buchs S. G., Switzerland.
[2] Pfaltz and Bauer Inc., Stamford, Conn.
[3] J. T. Baker Chemical Co., Phillipsburg, N.J.
[4] Burdick and Jackson, Muskegon, Mich.
[5] LDC mini-pump; Laboratory Data Control, Riviera Beach, Fla.
[6] Model 7010; Rheodyne, Inc.
[7] Model 1285; Laboratory Data Control.
[8] Model 6000A; Waters Associates, Milford, Mass.
[9] Model 660; Waters Associates.
[10] Model U6K; Waters Associates.
[11] Model 440 set at 254 nm; Waters Associates.
[12] Chromegabond C-18; E. S. Industries, Marlton, N.J.
[13] Model 3385A; Hewlett-Packard, Avondale, Pa.
[14] WISP Model 710B, Waters Associates.
[15] Computer Inquiry Systems, Waldwick, N.J.
[16] The full details of the isolation and identification of these compounds and studies on the degradation pathway of carprofen are the subject of a separate report.
[17] Type LS5; Millipore Corp., Bedford, Mass.

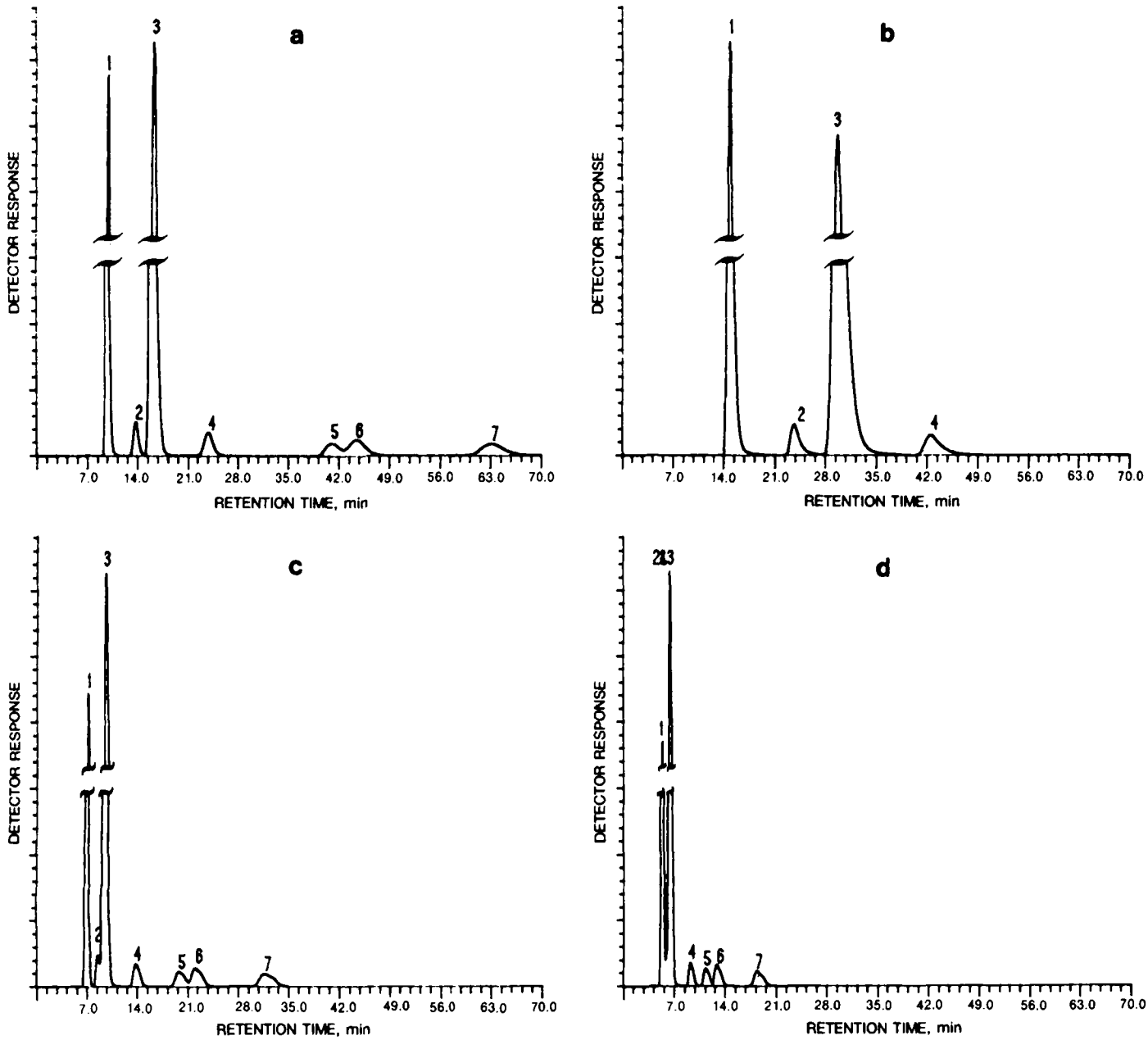

Figure 1—*Chromatograms of carprofen and related compounds* versus *the following percent methanol–water (1% acetic acid) in the mobile phase: (a) 65:35; (b) 60:40; (c) 70:30; (d) 75:25. Key: (1) benzophenone; (2) IV; (3) carprofen; (4) V; (5) III; (6) II; (7) VI.*

injection devices and by using both internal and external standard techniques.

RESULTS AND DISCUSSION

During preliminary methods development experiments, the carprofen peak exhibited marked tailing when chromatographed on a number of reverse-phase columns. This was believed to be due to partial ionization of the carboxylic acid function of the molecule in the mobile phase. Consequently, acetic acid was added to the mobile phase to suppress ionization and improve peak shape.

Since the intended purpose of the method was to supply a reliable and reproducible procedure suitable for assay, content uniformity, and stability studies, various columns and mobile phase compositions were carefully studied to achieve baseline resolution between carprofen, the internal standard, known impurities, and potential degradation products. The column[12] originally selected for the dosage form assay and used in the validation of the method was one that provided the desired separation within a reasonable analysis time and was commercially available at the time the method was developed. A chromatogram showing the separation between all possible components obtained with this column and the specified mobile phase composition is given in Fig. 1a. The sensitivity of that separation to variations in the mobile phase composition was studied with the same column (Fig. 1b–d). The data obtained were used to design an appropriate system suitability test for the dosage form assay. The separation most adversely affected by variations in mobile phase composition and most critical to the specificity of the dosage form assay is the separation between IV and carprofen (Fig. 1). Direct assurance of adequate separation between these two components could be obtained by specifying a minimum resolution factor between these two compounds in a system suitability test. However, this would require that all laboratories have access to a reference standard of IV. To make the method generally applicable for any laboratory and to eliminate the need for a reference standard of IV, an alternative approach was taken. The resolution factors R^1 (carprofen–internal standard) and R^2 (IV–carprofen) were obtained and plotted as a function of mobile phase composition (Fig. 2). For symmetrical peaks, minimum baseline resolution between two peaks should yield a resolution factor >1.0. By using the plot in Fig. 2, the appropriate resolution factor (R^1) which would simultaneously yield an R^2 value ≥ 1.0 was determined. The value for R^1 selected and included in the system suitability test was $R^1 \geq 3.5$. With the column specified, all mobile phase compositions which resulted in an R^1 value ≥ 3.5 also produced an R^2 value > 1.0 (Fig. 2). Therefore, by performing the system suitability test with the specified column and adjusting the mobile phase

Table II—System Precision of the Carprofen Dosage Form Assay

Injection	RR/Internal Standard[a]	RR/Internal Standard[b]	RR/Internal Standard[c]	External Standard[d]	External Standard[e]
1	0.4478	0.9177	1.683	429.3	23664
2	0.4445	0.9239	1.683	434.6	23744
3	0.4468	0.9220	1.683	436.2	23793
4	0.4449	0.9241	1.681	438.3	23816
5	0.4474	0.9237	1.682	437.3	23838
6	0.4470	0.9259	1.682	438.9	23737
Mean	0.4464	0.9234	1.682	435.8	23765
RSD	0.31%	0.39%	0.05%	0.81%	0.27%

[a] Response ratio (RR) by internal standard technique; manual (loop) injections and manually determined peak heights. [b] By internal standard technique; automatic injection and computer-generated peak heights. [c] By internal standard technique; automatic injection and computer-generated peak areas. [d] By external standard technique; automatic injection and computer-generated peak heights. [e] By external standard technique; automatic injection and computer-generated peak areas.

composition to achieve a resolution factor $R^1 \geq 3.5$ between internal standard (commercially available) and carprofen, any laboratory can perform the assay and be assured of adequate resolution between all possible components.

The specificity of the method was examined in several ways. The method was shown to separate all known synthetic impurities. Solutions of carprofen subjected to accelerated degradation studies were chromatographed, and the method was shown to be capable of separating several potential degradation products. To establish the carprofen peak integrity in these accelerated degradation study chromatograms, several injections were made, and the carprofen peak was collected as it eluted from the column. After removal of the mobile phase under a stream of nitrogen followed by lyophilization, NMR analysis demonstrated that the peak assigned to carprofen appeared to be only one substance. The collected carprofen fractions also showed one spot on TLC.

The precision of the method was examined by repeating the entire assay procedure with several weighings of the same composite sample (Table I). The method was shown to be reproducible, with an *RSD* of 0.45%, by manual injection, manual peak height measurements, and the internal standard quantification technique. The system precision was evaluated by making several injections of the same standard solution. The *RSD* of the response ratios obtained was 0.31% (Table II). Subsequent to the initial validation, the method was automated. The system precision was examined using automated injection by both peak areas and peak height measurements and both internal standard and external standard quantification techniques (Table II). The system precision was acceptable by any of the quantification methods described above.

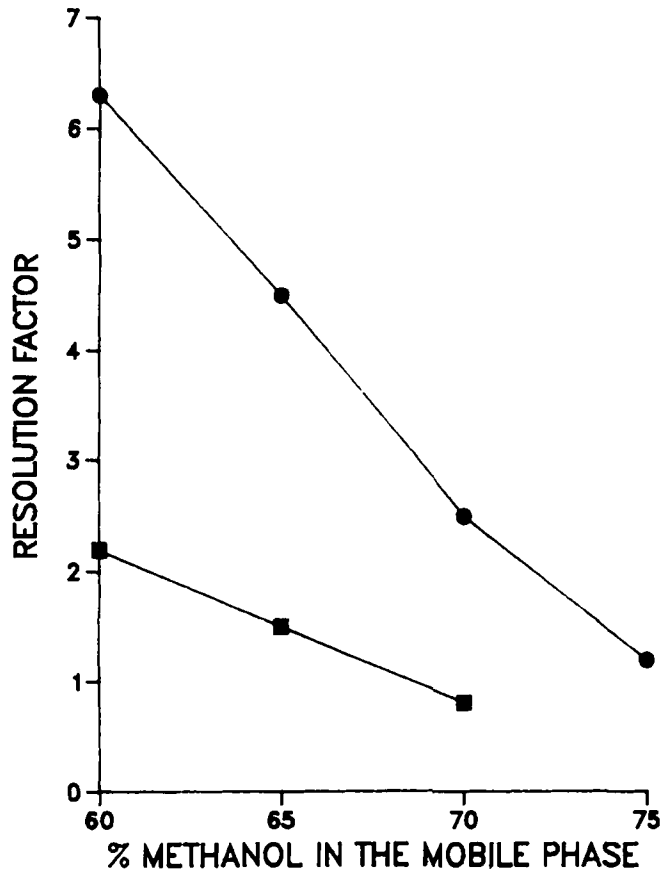

Figure 2—*Plot of resolution factors* versus *percent methanol in the mobile phase. Key: (●) resolution factor (R^1) between carprofen and internal standard; (■) resolution factor (R^2) between carprofen and IV.*

The linearity of the method was also studied. For the dosage form assay, samples containing carprofen concentrations spanning 50–150% of the expected working range were analyzed by the method. Plots of peak response ratios (carprofen–internal standard) *versus* carprofen concentration were generated. Similar plots were generated by using both peak heights (measured manually) and computer-calculated peak areas. The linearity of each plot was determined by using a computer program, LIN, to fit the observed data to a curve of the form $y = mx^n + b$. For perfect linearity, $n = 1.0$. The program also calculated the maximum error to be expected by the deviations from perfect linearity (17). When the observed data from the linearity plots was subjected to the LIN program, the value of n was between 0.95 and 1.0 in all cases. The maximum relative percent error due to nonlinearity over the assay range was also calculated by use of the LIN program and was found to be <0.3% in all cases.

The accuracy of the dosage form assay was also examined. Synthetic samples of carprofen tablets were prepared, covering 50–133% of the theoretical dosage range. The samples were prepared in such a way as to approach the average tablet weight of 365 mg. Appropriate weights of placebo tablet mass were mixed with known weights of carprofen spanning the range given above. These samples were analyzed by the described method. The recovery of carprofen from the tablet matrix is presented in Table III; the data show that excellent recoveries were obtained at all levels.

This HPLC system was also applied to drug substance stability testing, with several aforementioned modifications. For this application, emphasis was placed on the estimation of degradation products with reasonable accuracy, as well as quantification of intact carprofen in the stability study samples. Because of these joint objectives, the sample preparation was adjusted so that the concentration of carprofen in the sample injected was as high as possible without exceeding the linear range of the detector. This allowed accurate determination of the carprofen content and, at the same time, maximized the detector response for any impurities or degradation products present. For this purpose, a separate linearity study was conducted. The results show that carprofen concentrations as high as 2.0 mg/mL (20-μL injections) could be used while remaining within the linear range of the detector.

As mentioned above, various quantification techniques were studied for use with this method. The appropriate quantification technique depends both on the intended use of the method and on the instrumental and data acquisition systems available to the analytical laboratory.

Since the original developmental work on the dosage form assay was carried out by using manual injection and manual peak height measurements, it was believed that an internal standard quantification technique was appropriate. Since that time, state-of-the-art autosamplers and computer data acquisition systems have continually become more readily available. Because of this, the system precision of the dosage form assay was revalidated by other quantification techniques so that the assay procedure could be performed by any laboratory, regardless of the degree of sophistication of its automation and

Table III—Percent Recovery and Dosage Form Assay for Synthetic Tablet Mix

Placebo, mg	Carprofen, mg	Carprofen Found, mg	Recovery, %
340.35	26.08	27.02	103.6
314.90	49.80	50.26	100.9
264.45	101.45	101.88	100.4
214.70	150.36	145.92	97.0
165.42	203.25	203.93	100.3

data acquisition. The data with which the system precision of the dosage form analysis was compared by various quantification techniques is presented in Table II. The precision obtained by any of the quantification techniques was quite acceptable. Since external standard techniques require fewer calculations and are more convenient in terms of sample preparation, those laboratories in which automated equipment is used may select this as the preferred quantification technique.

Two different quantification techniques were used when the method was applied to drug substance stability studies. In such studies, the amount of carprofen in each sample was determined by using internal standard calculations similar to those used in the dosage form assay. However, the quantifications performed to estimate the impurity and degradation product levels were carried out by using an area percent calculation method corrected for the presence of the internal standard in the chromatogram. This technique has been found to be particularly useful when conducting drug substance stability studies on compounds in early phases of development. An underlying assumption with such a quantification technique is that potential degradation products and impurities have the same absorptivity as the parent compound at the chosen detector wavelength. Although this assumption may not always be valid, in many cases it is reasonable. It eliminates the need for reference standards of all impurities and degradation products, which are usually not available during the early stages of development. Considering this restriction, the technique described above is certainly acceptable for demonstrating stability trends. When reference materials become available, the data generated by using the area percent method can be refined or recalculated to take into account any differences in absorptivity. The area percent technique is also useful if an outside laboratory (without access to reference standards of potential impurities and degradation products) is conducting the assay.

The method described has been shown to be accurate, precise, and broadly applicable to all control and analysis laboratories and functions. The sample preparations are simple, and the method can easily be automated.

REFERENCES

(1) L. O. Randall and H. Baruth, *Arch. Int. Pharmacodyn. Ther.*, **220,** 94 (1976).

(2) T. F. Yu and J. Perel, *J. Clin. Pharmacol.*, **20,** 347 (1980).

(3) R. A. Dickey, A. Wasserman, E. Evans, and J. Proctor, Abstracts of the International Meeting on Inflammation, Verona, Italy, 1979, p. 75.

(4) R. A. Dickey and R. L. Lipson, Abstracts of the International Meeting on Inflammation, Verona, Italy, 1979, p. 85.

(5) H. A. Silverman, T. G. Lawrence, and J. D. Holloman, 14th International Congress on Rheumatology, San Francisco, Calif., 1977, p. 258.

(6) R. A. Dickey and J. A. Huleatt, Abstracts of the International Symposium on Rheumatoid Arthritis, Verona, Italy, 1980, p. 113.

(7) E. M. Jensen, J. Fossgreen, B. Kirchheiner, J. Kryger, P. Holm, and K. Mollenbach, *Curr. Ther. Res. Clin. Exp.*, **28,** 882 (1980).

(8) B. Kirchheiner, J. Fossgreen, E. M. Jensen, J. Kryger, P. Holm, and K. Mollenbach, *Curr. Ther. Res. Clin. Exp.*, **28,** 875 (1980).

(9) A. Lussier, L. Rouleau, M. Caron, and L. Tetreault, *Int. J. Clin. Pharmacol. Ther. Toxicol.*, **18,** 482 (1980).

(10) J. A. F. de Silva, N. Strojny, and M. A. Brooks, *Anal. Chim. Acta*, **73,** 283 (1974).

(11) N. Strojny and J. A. F. de Silva, *J. Chromatogr. Sci.*, **13,** 583 (1975).

(12) C. V. Puglisi, J. C. Meyer, and J. A. F. de Silva, *J. Chromatogr.*, **136,** 391 (1977).

(13) B. J. Hodshon, W. A. Garland, C. W. Perry, and G. J. Bader, *Biomed. Mass Spectrom.*, **6,** 325 (1979).

(14) G. Palmskog and E. Hultman, *J. Chromatogr.*, **140,** 310 (1977).

(15) W. A. Garland and M. L. Powell, *J. Chromatogr. Sci.*, **19,** 392 (1981).

(16) J. K. Stoltenborg, C. V. Puglisi, F. Rubio, and F. M. Vane, *J. Pharm. Sci.*, **70,** 1207 (1981).

(17) E. Debesis, J. P. Boehlert, T. E. Givand, and J. C. Sheridan, *Pharm. Tech.*, **1982,** p. 120.

ACKNOWLEDGMENTS

The authors thank Dr. P. Bhattacharyya and Ms. A. Grant for help in obtaining and interpretation of NMR spectral data. The authors also thank Ms. F. Manalili and Mr. G. Clark for technical assistance, and Ms. J. Comment for the typing of this manuscript.

Development and Evaluation of Enteric-Coated Penicillamine Tablets

WALTER G. CHAMBLISS, DIANA A. CHAMBLISS, ROBERT W. CLEARY, ALAN B. JONES, ERNEST C. HARLAND, and ARTHUR H. KIBBE* ˣ

Received February 18, 1983, from the *Department of Pharmaceutics, University of Mississippi, University, MS 38677.* Accepted for publication September 26, 1983. * Present address: Chief, Pharmaceutical Development Services, Building 10, Room 1D37, Clinical Center, National Institutes of Health, Bethesda, MD 20205.

Abstract □ Commercially available 250-mg penicillamine tablets were converted into enteric-coated tablets. Based on *in vitro* dissolution and disintegration tests, tablets coated with five layers of a cellulose acetate phthalate formulation by a modified pan coating technique were judged to be superior to other coated tablets. These tablets resisted disintegration in simulated gastric fluid over a 4-h period and disintegrated in an average of 21 min in simulated intestinal fluid. Enteric-coated penicillamine tablets were tested *in vivo* in nine weanling pigs divided into three groups: a negative control group, a test group dosed with enteric-coated penicillamine tablets, and a positive control group dosed with uncoated tablets. The incidence of GI tract bleeding, as determined by daily occult blood tests of the stools, was significantly less in the animals receiving the enteric-coated tablets when compared with the positive control group. The enteric-coated dosage form appeared to decrease GI tract irritation caused by penicillamine. Plasma concentration–time curves for penicillamine in the pigs were similar in shape to those reported in humans. Atypical double peaks occur in both species. Relative bioavailability of the enteric-coated tablet was found to be 67% when compared with the uncoated tablet. This apparent reduction is probably due to a large intrasubject variation in areas under the plasma concentration–time curves and not to a dosage form effect.

Keyphrases □ Penicillamine—development and evaluation of enteric-coated tablets □ Formulations—penicillamine, development and evaluation of enteric-coated tablets

Penicillamine has been used for many years in the treatment of Wilson's disease and cystinuria. More recently, the drug has been approved for the treatment of rheumatoid arthritis. Due to severe adverse reactions, penicillamine therapy in the arthritic patient is normally limited to those who have been previously treated unsuccessfully by conventional therapy (1).

It has been estimated that up to one-third of the patients

0022-3549/84/0900-1215$01.00/0

© 1984 American Pharmaceutical Association

data acquisition. The data with which the system precision of the dosage form analysis was compared by various quantification techniques is presented in Table II. The precision obtained by any of the quantification techniques was quite acceptable. Since external standard techniques require fewer calculations and are more convenient in terms of sample preparation, those laboratories in which automated equipment is used may select this as the preferred quantification technique.

Two different quantification techniques were used when the method was applied to drug substance stability studies. In such studies, the amount of carprofen in each sample was determined by using internal standard calculations similar to those used in the dosage form assay. However, the quantifications performed to estimate the impurity and degradation product levels were carried out by using an area percent calculation method corrected for the presence of the internal standard in the chromatogram. This technique has been found to be particularly useful when conducting drug substance stability studies on compounds in early phases of development. An underlying assumption with such a quantification technique is that potential degradation products and impurities have the same absorptivity as the parent compound at the chosen detector wavelength. Although this assumption may not always be valid, in many cases it is reasonable. It eliminates the need for reference standards of all impurities and degradation products, which are usually not available during the early stages of development. Considering this restriction, the technique described above is certainly acceptable for demonstrating stability trends. When reference materials become available, the data generated by using the area percent method can be refined or recalculated to take into account any differences in absorptivity. The area percent technique is also useful if an outside laboratory (without access to reference standards of potential impurities and degradation products) is conducting the assay.

The method described has been shown to be accurate, precise, and broadly applicable to all control and analysis laboratories and functions. The sample preparations are simple, and the method can easily be automated.

REFERENCES

(1) L. O. Randall and H. Baruth, *Arch. Int. Pharmacodyn. Ther.*, **220,** 94 (1976).

(2) T. F. Yu and J. Perel, *J. Clin. Pharmacol.*, **20,** 347 (1980).

(3) R. A. Dickey, A. Wasserman, E. Evans, and J. Proctor, Abstracts of the International Meeting on Inflammation, Verona, Italy, 1979, p. 75.

(4) R. A. Dickey and R. L. Lipson, Abstracts of the International Meeting on Inflammation, Verona, Italy, 1979, p. 85.

(5) H. A. Silverman, T. G. Lawrence, and J. D. Holloman, 14th International Congress on Rheumatology, San Francisco, Calif., 1977, p. 258.

(6) R. A. Dickey and J. A. Huleatt, Abstracts of the International Symposium on Rheumatoid Arthritis, Verona, Italy, 1980, p. 113.

(7) E. M. Jensen, J. Fossgreen, B. Kirchheiner, J. Kryger, P. Holm, and K. Mollenbach, *Curr. Ther. Res. Clin. Exp.*, **28,** 882 (1980).

(8) B. Kirchheiner, J. Fossgreen, E. M. Jensen, J. Kryger, P. Holm, and K. Mollenbach, *Curr. Ther. Res. Clin. Exp.*, **28,** 875 (1980).

(9) A. Lussier, L. Rouleau, M. Caron, and L. Tetreault, *Int. J. Clin. Pharmacol. Ther. Toxicol.*, **18,** 482 (1980).

(10) J. A. F. de Silva, N. Strojny, and M. A. Brooks, *Anal. Chim. Acta*, **73,** 283 (1974).

(11) N. Strojny and J. A. F. de Silva, *J. Chromatogr. Sci.*, **13,** 583 (1975).

(12) C. V. Puglisi, J. C. Meyer, and J. A. F. de Silva, *J. Chromatogr.*, **136,** 391 (1977).

(13) B. J. Hodshon, W. A. Garland, C. W. Perry, and G. J. Bader, *Biomed. Mass Spectrom.*, **6,** 325 (1979).

(14) G. Palmskog and E. Hultman, *J. Chromatogr.*, **140,** 310 (1977).

(15) W. A. Garland and M. L. Powell, *J. Chromatogr. Sci.*, **19,** 392 (1981).

(16) J. K. Stoltenborg, C. V. Puglisi, F. Rubio, and F. M. Vane, *J. Pharm. Sci.*, **70,** 1207 (1981).

(17) E. Debesis, J. P. Boehlert, T. E. Givand, and J. C. Sheridan, *Pharm. Tech.*, **1982,** p. 120.

ACKNOWLEDGMENTS

The authors thank Dr. P. Bhattacharyya and Ms. A. Grant for help in obtaining and interpretation of NMR spectral data. The authors also thank Ms. F. Manalili and Mr. G. Clark for technical assistance, and Ms. J. Comment for the typing of this manuscript.

Development and Evaluation of Enteric-Coated Penicillamine Tablets

WALTER G. CHAMBLISS, DIANA A. CHAMBLISS, ROBERT W. CLEARY, ALAN B. JONES, ERNEST C. HARLAND, and ARTHUR H. KIBBE* ˣ

Received February 18, 1983, from the *Department of Pharmaceutics, University of Mississippi, University, MS 38677.* Accepted for publication September 26, 1983. * Present address: Chief, Pharmaceutical Development Services, Building 10, Room 1D37, Clinical Center, National Institutes of Health, Bethesda, MD 20205.

Abstract □ Commercially available 250-mg penicillamine tablets were converted into enteric-coated tablets. Based on *in vitro* dissolution and disintegration tests, tablets coated with five layers of a cellulose acetate phthalate formulation by a modified pan coating technique were judged to be superior to other coated tablets. These tablets resisted disintegration in simulated gastric fluid over a 4-h period and disintegrated in an average of 21 min in simulated intestinal fluid. Enteric-coated penicillamine tablets were tested *in vivo* in nine weanling pigs divided into three groups: a negative control group, a test group dosed with enteric-coated penicillamine tablets, and a positive control group dosed with uncoated tablets. The incidence of GI tract bleeding, as determined by daily occult blood tests of the stools, was significantly less in the animals receiving the enteric-coated tablets when compared with the positive control group. The enteric-coated dosage form appeared to decrease GI tract irritation caused by penicillamine. Plasma concentration–time curves for penicillamine in the pigs were similar in shape to those reported in humans. Atypical double peaks occur in both species. Relative bioavailability of the enteric-coated tablet was found to be 67% when compared with the uncoated tablet. This apparent reduction is probably due to a large intrasubject variation in areas under the plasma concentration–time curves and not to a dosage form effect.

Keyphrases □ Penicillamine—development and evaluation of enteric-coated tablets □ Formulations—penicillamine, development and evaluation of enteric-coated tablets

Penicillamine has been used for many years in the treatment of Wilson's disease and cystinuria. More recently, the drug has been approved for the treatment of rheumatoid arthritis. Due to severe adverse reactions, penicillamine therapy in the arthritic patient is normally limited to those who have been previously treated unsuccessfully by conventional therapy (1).

It has been estimated that up to one-third of the patients

0022-3549/84/0900-1215$01.00/0

© 1984 American Pharmaceutical Association

Table I—Enteric Coating Formulations

Formulation Ingredients	% w/w
Cellulose acetate phthalate coating	
Cellulose acetate phthalate	12.0
Diethyl phthalate	3.0
Ethyl acetate	42.5
Isopropyl alcohol	42.5
Polyvinyl acetate phthalate coating	
Polyvinyl acetate phthalate	10.0
Polyethylene glycol 400	1.0
Methanol	89.0

treated orally with penicillamine must discontinue use because of adverse reactions such as gastric distress (2). Gastric upset, which is normally decreased by coadministering food or antacids with the drug, is not possible in this case because the drug chelates magnesium, calcium, and iron (1). In previous work, it has been shown that plasma levels of the unchanged drug are reduced in humans when penicillamine is given with a meal (3).

Enteric-coated dosage forms release drugs in the intestine and have been shown to decrease gastric irritation (4). In this study, an enteric-coated penicillamine tablet is described, and this dosage form is evaluated *in vitro* and *in vivo* in weanling pigs.

EXPERIMENTAL SECTION

Materials– Penicillamine tablets[1], cellulose acetate phthalate[2], and polyvinyl acetate phthalate[3] were obtained commercially. Simulated gastric and intestinal fluids were made as directed in USP XX (5).

Coating Methods– *Dip Coating*—The capsule-shaped tablet was held at one end with tweezers and dipped a little over one-half way into 50 mL of 10% w/w cellulose acetate phthalate in acetone. The tablet was withdrawn after 10 s, and its free end was touched to the lip of the beaker to remove excess solution. The tablet was held in the air for 2 min to dry. The procedure was repeated until both halves of the tablet were coated three times. Twenty tablets were coated by this procedure. The tablets were placed in an evaporating dish and dried at 50°C for 16 h.

Pan Coating—A 15-cm diameter stainless steel coating pan was used. Two aluminum baffles were mounted in the pan to promote a smooth tumbling action of the tablets. The 11.4 × 0.64-cm baffles extended from the inside of the pan rim to 3.8 cm from the bottom center. They were equally spaced, 180° apart. The baffles were bent to fit the curvature of the pan and sloped in the direction of the pan rotation. The pan was rotated at 32 rpm.

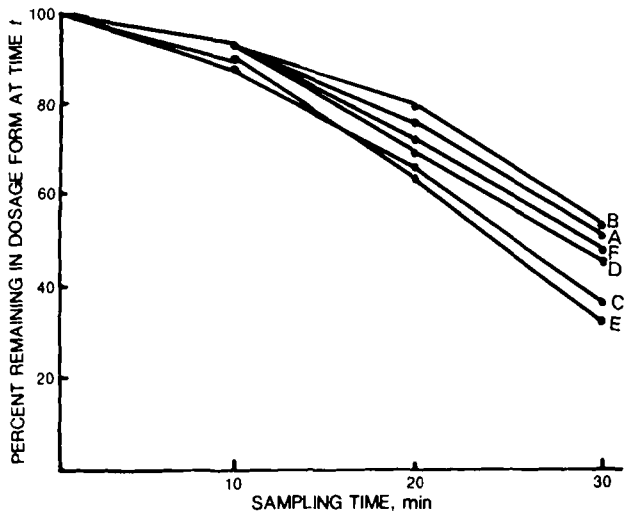

Figure 1—*Effect of storage at 50°C on the dissolution of enteric-coated penicillamine tablets at pH 6.0. Key to storage times: (A) 0 d; (B) 15 d; (c) 30 d; (D) 45 d; (E) 60 d; (F) 75 d.*

[1] Depen (250 mg); Wallace Laboratories.
[2] Eastman Kodak.
[3] Colorcon, Inc.

Table II—Mean Disintegration Time for Enteric-Coated and Uncoated Tablets as Compared with Coat Thickness[a]

Tablet Group	Coat Thickness, cm	Disintegration Time, min	
		Gastric Fluid[b]	Intestinal Fluid
Uncoated	0.000	28	21
Cellulose acetate phthalate			
5 coats	0.010	>60 (*b*)	20
7 coats	0.012	>60 (*a*)	20
10 coats	0.013	>60 (*a*)	22
Polyvinyl acetate phthalate			
5 coats	0.007	>60 (*d*)	13
10 coats	0.010	>60 (*c*)	16
15 coats	0.013	>60 (*c*)	17
20 coats	0.018	>60 (*b*)	21
25 coats	0.023	>60 (*b*)	14
30 coats	0.030	>60 (*a*)	18

[a] $n = 6$. [b] Key: (*a*), no damage to coat; (*b*), some softening of coat and slight pitting; (*c*), obvious coat damage, deep pits; (*d*), partial tablet core disintegration.

Table I contains the two formulations that were applied to the tablets by the pan coating procedure. The cellulose acetate phthalate formulations (200 g) were prepared by mixing 95.0 mL of ethyl acetate and 180.6 mL of isopropyl alcohol in a 600-mL beaker. The solution was vigorously stirred with a magnetic stirrer, and 24.0 g of cellulose acetate phthalate was dissolved in the solution followed by the addition of 2.7 mL of diethyl phthalate; the solution was continuously stirred for 20 min.

The polyvinyl acetate phthalate formulation was prepared by slowly adding 10.0 g of polyvinyl acetate phthalate to 75.0 mL of methanol over a 15-min period. The solution was vigorously stirred with a magnetic stirrer. After the polyvinyl acetate phthalate was added, 0.9 mL of polyethylene glycol 400 was added, and the solution was stirred for 10 min. The weight of the solution was adjusted to 100.0 g by the addition of methanol. The solution was stirred for an additional 10 min.

A typical batch of 90 tablets was placed in a 1000-mL beaker, and 3 mL of the formulation was added. The tablets were stirred by hand for 1 min and then transferred to the pan. The pan was rotated for 10 min at 32 rpm. The tablets were stirred by hand during the first 2 min of rotation to prevent clumping. When the coat was dry, the tablets were returned to the 1000-mL beaker. The procedure was repeated until the required number of coats were applied. After receiving the final coating, the tablets were placed on a drying tray in a 50°C oven for 16 h. The number of coats used were 5, 7, and 10 for the cellulose acetate phthalate formulation and 5, 10, 15, 20, 25, and 30 for the polyvinyl acetate phthalate formulation.

***In Vitro* Tests of Enteric-Coated Tablets**—*Uniformity Test*—Tablets from each batch were visually inspected for uniformity in appearance, smoothness of coat, and absence of cracks. Twenty tablets in each batch were individually weighed, and the mean weight and *SD* were determined.

A micrometer was used to determine the average length, width, and thickness of the 20 tablets from each batch. The mean thickness of the enteric coat was calculated by:

$$\text{Coat Thickness} = \frac{(L_c - L_n) + (W_c - W_n) + (T_c - T_n)}{(2) \cdot (3)}$$

where L_c is the length of coated tablet, W_c is the width of coated tablet, T_c is the thickness of coated tablet, L_n is the length of uncoated tablet, W_n is the width of uncoated tablet, and, T_n is the thickness of uncoated tablet. The numerator of the equation sums the differences between the coated and uncoated tablets in three dimensions (length, width, and thickness). The denominator contains two correction factors: the three dimensions and the two sides of the tablet contained in each measurement.

Disintegration Test—The USP XX (6) disintegration test for enteric-coated tablets was used to evaluate the penicillamine tablets coated by either the dip coating or pan coating procedure. A standard six-tube basket-rack assembly[4] was used for all the determinations. After 1 h of operation using simulated gastric fluid as the disintegration fluid, the basket was lifted from the fluid, and the tablets were inspected for signs of disintegration, cracking, or softening. The condition of the coated tablets was rated by the following scale: (*a*) no obvious damage, (*b*) some softening of the coat and slight pitting, (*c*) obvious coat damage, deep pits, (*d*) partial tablet core disintegration, and (*e*) total tablet disintegration. The medium was then changed to simulated

[4] USP disintegration apparatus; Fisher Scientific Co.

Table III—Dissolution of Enteric-Coated and Uncoated Tablets at pH 1.2 [a]

Sampling Time, min	Dissolution, % Remaining ± *SD*					
		Cellulose Acetate Phthalate			Polyvinyl Acetate Phthalate	
	Uncoated	5 Coats	7 Coats	10 Coats	25 Coats	30 Coats
5	76.4 ± 6.9	—[b]	—	—	—	
10	65.0 ± 5.2	—	—	—	—	—
15	55.5 ± 7.5	—	—	—	—	—
20	46.3 ± 4.8	—	—	—	—	—
30	38.5 ± 2.9	99.7 ± 0.6	100 ± 0	100 ± 0	97.1 ± 2.8	98.2 ± 1.7
60	—	96.8 ± 3.0	100 ± 0	100 ± 0	91.5 ± 1.3	98.3 ± 0.6
120	—	94.9 ± 2.6	100 ± 0	97.8 ± 3.8	82.6 ± 2.8	96.4 ± 2.8
180	—	92.7 ± 1.3	100 ± 0	97.8 ± 3.2	74.8 ± 4.5	94.5 ± 1.1
240	—	90.0 ± 3.4	98.6 ± 0.6	93.4 ± 5.8	71.1 ± 4.0	92.6 ± 2.8

[a] $n = 3$. [b] No sample taken.

intestinal fluid and disks were added to each tube. The disintegration time for each of the six tablets was noted to the nearest minute.

Dissolution Test—A USP rotating-basket dissolution apparatus[5] was used for all dissolution studies. A single enteric-coated or uncoated tablet was placed into the 40-mesh basket and lowered into the specified medium such that the basket was 2.0 cm from the bottom of the vessel. The basket was rotated at 100 rpm. Each dissolution test was run in triplicate.

Three dissolution media were used. A pH 1.2 solution (0.063 M HCl) was used to simulate gastric fluid. A pH 6.0 sodium phosphate buffer was used to simulate intestinal fluid in the duodenum. A pH 8.0 sodium phosphate buffer was used to simulate intestinal fluid with a pH in the upper range.

A colorimetric assay developed by Mann and Mitchell (7) was used to quantitate penicillamine in the dissolution medium. The absorbance was determined at 412 nm with a spectrophotometer[6]. The amount of penicillamine contained in the sample was determined from a standard curve prepared for penicillamine in each of the dissolution solutions. A linear relationship held over the concentration range tested.

Stability of the Enteric Coat—The effect of storage at different temperatures on the enteric-coated tablet was investigated. Enteric-coated tablets with five layers of the cellulose acetate phthalate formulation, prepared by the pan coating procedure, were stored and tested along with uncoated tablets so that changes in the tablet core could be determined. Samples of each tablet were stored in ~118-mL amber glass prescription bottles at 4°C, 25°C, 37°C, or 50°C. Eighteen tablets were removed from each bottle at various times during a 75-d period for testing.

The USP disintegration test for enteric-coated tablets was performed on six tablets from the enteric-coated group at each sampling period. The tablets were inspected for signs of disintegration, cracking, or softening after 1 h in simulated gastric fluid. The disintegration time in simulated intestinal fluid was then noted to the nearest minute. The disintegration time of six uncoated tablets in simulated intestinal fluid was determined to the nearest minute.

The procedure described above was used to test the dissolution of the coated and noncoated tablets at pH 1.2 and 6.0. Samples were removed at 0, 10, 20, and 30 min from the pH 6.0 solution and at 0, 30, and 60 min from the pH 1.2 solution. The concentration of penicillamine in each dissolution medium was determined by colorimetry, as described above. Each test was performed on three tablets.

Experimental Animals—Nine disease-free, acclimated, Yorkshire pigs (5–8 weeks old) were randomly divided into three groups by using color-coded tags. Control pigs, pigs receiving uncoated penicillamine tablets, and pigs receiving enteric-coated penicillamine tablets were housed in separate pens and fed ~2.2 kg of commercial hog feed daily. Food was offered for at least 4 h after dosing and was removed at least 12 h before the next dose was given. Each pen was equipped with an automatic watering device which allowed water *ad libitum*.

A dosing syringe was designed to administer the tablets to the pigs. The device consisted of a 26.6-cm flexible plastic tube (0.7 cm i.d. and 1.1 cm o.d.), with a 31-cm, flexible polytef rod (0.6-cm diameter) which was inserted into the tube and used as a plunger. The entire apparatus was bent to promote insertion past the throat of the pig. Before dosing, the plunger and the outside of the tube were coated with a water-soluble lubricant. The penicillamine tablet was placed into the end of the dosing syringe, and the tube was inserted 10–15 cm down the esophagus of the pig, where the tablet was injected. Each pig received several milliliters of 50% w/v sucrose solution before dosing; the mouth was flushed with the sucrose solution after dosing, and a small slice of apple was then given to decrease the incidence of tablet regurgitation. Another tablet was administered if the first one was rejected.

[5] Erweka Dissolution apparatus (type DT); Chemical and Pharmaceutical Industry Co.

[6] Spectronic 20 colorimeter/spectrophotometer; Bausch and Lomb.

The control pigs were treated in an identical fashion except that no tablet was loaded into the dosing apparatus. Dosing occurred daily for a period of 2 months.

Bioavailability Study—The study was conducted on 2 d, 1 week apart. On the first day, one animal from each treatment group was used. The other pigs were dosed as usual for an additional week and then used in the study.

Each animal received an appropriate 250-mg penicillamine tablet (uncoated or enteric coated) and was prepared for surgery immediately after dosing. A catheter was surgically placed in the jugular vein such that the tip was in the anterior vena cava; the catheter was exteriorized behind the base of the ear and attached to a 15-gauge needle, which was taped to the neck to allow access.

Blood samples were obtained at 0.5-h intervals for 12 h. The catheter was aspirated until fresh blood entered the syringe. One milliliter of blood was collected with a fresh 3-mL syringe containing 100 U of heparin, and the catheter was flushed with 2–3 mL of heparinized saline (100 U/mL). The blood was centrifuged at 500×*g* for 10 min. Plasma (500 μL) was transferred to another centrifuge tube, 100 μL of 20% w/v trichloroacetic acid was added, and the contents of the tube were gently mixed. The sample was centrifuged at 500×*g* for an additional 10 min. The protein-free supernatant was decanted and stored at 20°C until assayed; all samples were analyzed within 7 d.

A procedure developed by Bergstrom *et al.* (8) to assay penicillamine in

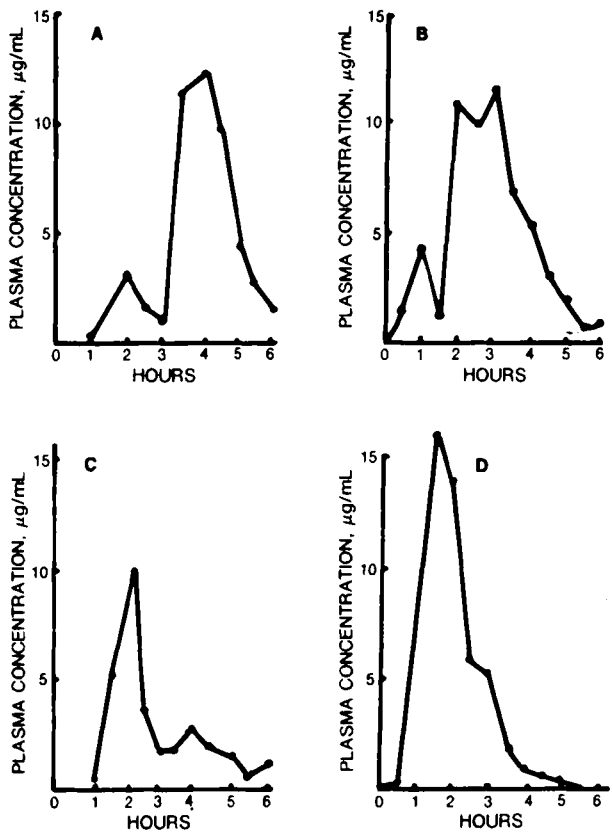

Figure 2—*Plasma concentration–time curves for penicillamine in pigs. Key: (A) pig C28 (19.8 kg); (B) pig B24 (18.5 kg); (C) pig C26 (24.0 kg); (D) pig B23 (29.0 kg).*

Table IV—Dissolution of Enteric-Coated and Uncoated Tablets at pH 6.0 [a]

Group	Dissolution, % Remaining ± *SD*			
	5 min	10 min	15 min	20 min
Uncoated	70.1 ± 5.0	49.5 ± 5.7	31.6 ± 4.0	19.3 ± 3.9
Cellulose acetate phthalate				
5 coats	97.0 ± 2.6	77.5 ± 3.3	58.7 ± 4.0	34.2 ± 9.3
7 coats	97.9 ± 1.8[b]	95.5 ± 2.2[b]	92.0 ± 3.1[b]	84.5 ± 2.0[b]
10 coats	100.0 ± 0.0[b]	97.5 ± 2.3[b]	94.8 ± 4.6[b]	90.3 ± 6.6[b]
Polyvinyl acetate phthalate				
25 coats	88.5 ± 2.0	81.1 ± 2.3[b]	63.3 ± 7.8	46.9 ± 7.0
30 coats	94.2 ± 1.3	85.0 ± 2.6[b]	72.5 ± 7.2[b]	63.5 ± 6.2[b]

[a] $n = 3$. [b] Significantly different from uncoated group at $p = 0.001$.

Table V—Dissolution of Enteric-Coated and Uncoated Tablets at pH 8.0 [a]

Group	Dissolution, % Remaining ± *SD*			
	5 min	10 min	15 min	20 min
Uncoated	75.7 ± 1.9	57.3 ± 3.4	31.8 ± 4.4	20.5 ± 3.0
Cellulose acetate phthalate				
5 coats	80.1 ± 4.8	64.0 ± 7.3	50.7 ± 12.0	37.8 ± 9.4
7 coats	83.7 ± 10.5	67.2 ± 8.6	53.1 ± 3.0	42.5 ± 4.2
10 coats	90.9 ± 4.2	72.8 ± 8.7	56.7 ± 15.6	47.5 ± 15.7
Polyvinyl acetate phthalate				
25 coats	83.7 ± 2.4	67.6 ± 2.5	48.3 ± 5.5	35.0 ± 6.0
30 coats	87.7 ± 1.4[b]	72.4 ± 3.6	56.7 ± 8.0	48.7 ± 7.3

[a] $n = 3$. [b] Significantly different from uncoated group at $p = 0.001$.

plasma with a liquid chromatograph[7], which was equipped with a cation-exchange analytical column[8] and an electrochemical detector[9], was used. The detector consisted of a thin-layer electrochemical cell[10] containing a mercury-gold amalgam working electrode, a glassy carbon auxiliary electrode, and a silver-silver chloride reference electrode. The potential of the working electrode was set at +0.1 V *versus* the reference electrode. The range on the detector was varied from 5 to 20 nA, depending on the sample concentration. The mobile phase consisted of a 0.035 M citric acid–0.005 M disodium phosphate buffer. The buffer was filtered and deaerated before use. Penicillamine has an average retention time of 3.34 min at a flow rate of 2 mL/min.

A standard curve of peak height ratios, prepared with plasma samples obtained from the control animals, was linear. The plasma samples were treated as described above. One previously prepared standard was analyzed with each set of samples. A total of 20 μL of the standard was injected into the liquid chromatograph approximately every 0.5 h during sample analysis. The peak height of an unknown plasma sample was then compared with the average peak height of the standards injected before and after the sample. Duplicate 20-μL injections of each unknown plasma samples were made.

Occult Blood Tests—Stool samples were collected from each pen daily before drug administration. The stool samples were tested for occult blood with a commercially available kit[11]. The incidence of positive tests after 55 d of dosing was determined for each group.

Tissue Sample Collection—Immediately after sacrificing the animals, tissue sections were removed from the GI tract, including glandular and nonglandular stomach, duodenum, jejunum, colon, and a mesenteric lymph node. The tissues were preserved in buffered formalin, embedded in paraffin, sectioned, and mounted on slides. The slides were stained with hematoxylin and eosin for routine histological examination.

RESULTS AND DISCUSSION

Coating Method— Two methods of coating the penicillamine tablets were investigated. The dip coating procedure was slow and tedious, requiring approximately 2 h to coat 20 tablets. Although the coating solution overlapped at the center of the tablets, causing a nonuniform coat, these tablets performed well in the USP disintegration test. No damage to the coat was apparent after 1 h of testing in simulated gastric fluid, and six tablets disintegrated in an average of 20 min in simulated intestinal fluid.

The pan coating procedure provided an excellent method of coating the tablets. The procedure was easy and quick; it produced tablets with uniform coats and proved to be the method of choice.

Evaluation of Coated Tablets—The enteric-coated tablets prepared in this study were judged on ease of preparation, appearance, uniformity, and performance in disintegration and dissolution tests. Tablets coated with polyvinyl acetate phthalate and cellulose acetate phthalate by a pan coating procedure were evaluated.

The polyvinyl acetate phthalate formulation was much more difficult to work with than the cellulose acetate phthalate formulation. Polyvinyl acetate phthalate solutions are tacky and are more suited to a spray coating procedure. Tablets pan-coated with this formulation tended to clump together and to stick to the side of the pan. Tablet sticking can normally be controlled by the use of a dusting powder. Penicillamine, however, chelates with magnesium, calcium, and aluminum, which eliminates the possibility of using common dusting powders, such as magnesium stearate and talc. Tablets coated with cellulose acetate phthalate had clean coats with a high gloss. Due to the tackiness of polyvinyl acetate phthalate, the tablets coated with this polymer were not smooth.

Both formulations provided coated tablets of uniform size and weight. The average dimensions of 20 tablets from each batch had <1% variation in any dimension. The thickness of the coat increased with increasing number of coats.

The results of the disintegration tests are given in Table II. All of the enteric-coated tablets resisted disintegration in gastric fluid after 1 h of testing. Cellulose acetate phthalate coating was thicker than polyvinyl acetate phthalate for the same number of coats.

The condition of the coated tablets, as indicated by the alphabetical rating (Table II), varied with the polymer used for coating and the number of coats. Thirty coats of the polyvinyl acetate phthalate formulation were required to provide complete protection to the tablet. Only seven coats of the cellulose acetate phthalate formulation were required. The tablets with five coats of cellulose acetate phthalate showed some signs of coat softening after 1 h in the gastric fluid. Tablet core disintegration, however, did not occur in this group after testing for 4 h in the gastric fluid. All batches had an average disintegration time in intestinal fluid of ≤22 min. There appeared to be no relationship between the number of coats and disintegration times.

The following criteria were established to help in the selection of the best coating material and the ideal number of coats based on dissolution testing:

1. Less than 10% of the drug should be released after 4 h at pH 1.2.
2. The enteric coat should not alter dissolution of the tablet at pH 6.0. There should be no significant difference in percent remaining in the uncoated or enteric-coated tablets at selected sampling times.
3. The enteric coat should not alter dissolution of the tablet at pH 8.0. There should be no significant difference in percent remaining in the uncoated or enteric-coated tablets at selected sampling times.

The dissolution profiles for the uncoated tablets and five batches of enteric-coated tablets at pH 1.2 are given in Table III. All of the coated formulations, except for polyvinyl acetate phthalate with 25 coats, retained ≥90% of the drug in the dosage form after 4 h of dissolution testing at pH 1.2. Less than 40% of the drug remained in the uncoated tablets after 30 min of testing.

A *t* test ($p = 0.001$) was used to determine whether criteria 2 and 3 were met by any of the formulations. The results of the analysis for pH 6.0 and pH 8.0 are given in Tables IV and V, respectively. Differences between the groups were more evident with the pH 6.0 buffer. Only tablets coated with five layers of cellulose acetate phthalate showed no difference at each sampling time when compared with the uncoated tablet group. By using the pH 8.0 buffer, only the 5-min sample of tablets coated with 30 coats of polyvinyl acetate phthalate differed from the uncoated group.

Table VI—Mean Disintegration Times for Enteric-Coated and Uncoated Tablets in Intestinal Fluid After Storage [a]

Temperature, °C	Mean Disintegration Time, min					
	0 d	15 d	30 d	45 d	60 d	75 d
	Enteric-Coated Tablets					
4	21	—[b]	21	—	21	20
25	21	—	20	—	21	21
37	21	—	22	21	22	20
50	21	29	20	20	17	18
	Uncoated Tablets					
4	21	—	15	—	18	20
25	21	—	19	—	25	25
37	21	—	19	19	20	20
50	21	17	16	19	17	17

[a] $n = 3$. [b] No sample taken.

[7] Model 4200 aerograph; Varian Associates.
[8] Partisil-10-SCXR; Whatman, Inc.
[9] LC-4A amperometric controller; Bioanalytical Systems, Inc.
[10] LC-19 flow cell; Bioanalytical Systems, Inc.
[11] Hemoccult slides; Smith Kline Diagnostics.

Table VII—Relationship Between Animal Weight and t_{max}

Animal	Weight, kg	C_{max}, μg/mL	t_{max}, h
C26	24.0	10.18	2.0
B23	29.0	16.46	1.5
C28	19.8	12.55	4.0
B24	18.5	11.84	3.0

Selection of the Best Coat—In general, the formulation containing cellulose acetate phthalate was more suited to the pan coating procedure than was the formulation which contained polyvinyl acetate phthalate. The tablets coated with cellulose acetate phthalate did not stick together and required fewer applications. Tablets coated with 5 layers of this formulation were judged to be better than tablets coated with 7 or 10 coats. Five applications prevented disintegration after 4 h of testing in simulated gastric fluid, although some damage occurred after 1 h. This batch of tablets was the only one to meet the specifications set for the dissolution study. The addition of two more layers improved the performance in the disintegration test but drastically altered dissolution at pH 6.0.

Stability of the Coat—Disintegration and dissolution tests were used to determine whether storage at different temperatures altered the release of drug from uncoated and enteric-coated penicillamine tablets. All enteric-coated tablets resisted disintegration in simulated gastric fluid after 1 h of testing. The degree of coat damage during the disintegration test varied from no obvious damage to some softening of the coat. There was no relationship between temperature or storage time and the amount of coat damage.

Storage had no effect on the disintegration time of enteric-coated tablets in intestinal fluid (Table VI). These results compare favorably with those reported previously by Luce (9). In that study, tablets coated with cellulose acetate phthalate showed no change in disintegration time after storage at room temperature for 1 year.

No changes in dissolution of the uncoated or enteric-coated tablets was seen at pH 1.2. Changes did occur in the dissolution of both the coated and uncoated tablets at pH 6. As shown by a typical profile (Fig. 1), the changes in dissolution were random. No relationship could be established between storage time or temperature. The apparent changes in dissolution could not be attributed to the presence of the enteric coat.

Plasma Concentrations—The plasma concentration-time curves for four animals are shown in Fig. 2. Data from one animal in each group were not included because the samples were not assayed until 10 d after collection, and degradation of the samples was suspected.

The curves show atypical double peaks. Similarly shaped curves have been reported after oral administration of penicillamine in a mongrel dog (10) and in normal human subjects (3). The multiple peaks did not occur after intravenous administration of the drug in the dog (10) or when given with food in humans (3). Double peaks after oral administration of cimetidine (11) and phenytoin (12) have also been reported in the literature. Explanations for these types of curves have included a GI transit-time effect (3) and an enterohepatic cyclic-process effect (11).

Examination of the plasma concentration-time curves (Fig. 2) reveals two types of curves, which differ in the size and location of the double peaks. The curve shape was independent of the type of tablet administered. Although the number of subjects was low, it appears that the shape may be related to the weight of the animal. In Table VII, the relationship between animal weight and the time (t_{max}) to reach the maximum plasma concentration (C_{max}) is shown. The lag time seen in the group receiving the enteric-coated tablet group was ~1 h.

The same two types of plasma concentration-time curves have been observed by Bergstrom *et al.* (3) and appear to be related to the weight of the subject. The areas under the plasma concentration-time curves (AUC) from 0 to 6 h were calculated by the trapezoidal rule. The average AUC from pigs that received enteric-coated tablets was compared with the average AUC from pigs that received uncoated tablets. Since the drug was not given on a milligram per kilogram basis, each AUC was normalized to a body weight of 24.0 kg. Both the calculated and normalized AUC values are given in Table VIII.

The mean, normalized, AUC for animals that received uncoated tablets was 27.61 mg·h/mL, as compared with 18.36 μg·h/mL for the animals that received enteric-coated tablets. The relative bioavailability of the enteric-coated tablet as compared with the uncoated tablet was 66.5%. The overall difference in AUC between the two groups was due primarily to the large difference between animals C26 and B23. A study with a larger number of subjects and a crossover design would be necessary to determine whether the bioavailability is reduced by the enteric formulation.

Table VIII—AUC from Pigs Receiving Either Uncoated or Enteric-Coated Penicillamine Tablets

Animal	AUC, μg·h/mL	Weight, kg	Normalized AUC, μg·h/mL
B23	26.95	29.0	32.56
B24	29.40	18.5	22.67
C26	16.15	24.0	16.15
C28	24.93	19.8	20.57

Occult Blood Tests—Stool specimens from each group of pigs were checked for occult blood daily for 55 d. The incidence of positive tests in the control group was 13%. Pigs receiving uncoated penicillamine tablets had positive tests on 44% of the days. The group receiving enteric-coated penicillamine tablets had 24% positive tests. An outbreak of vibrionic dysentery during the middle of the study was probably responsible for some of the positive tests. The *Vibrio coli* organism can cause bleeding from the GI tract (13). If the 21 d in which the animals were treated for dysentery are omitted, the percentage of positive tests for the control group, animals receiving uncoated tablets, and animals receiving enteric-coated tablets become 5.8, 35.3, and 11.8%, respectively. The incidence of blood in the stool of the group receiving uncoated tablets was significantly higher using either set of data. It appears, therefore, that less GI bleeding occurred in the pigs which were given enteric-coated penicillamine tablets than those given the uncoated tablets.

Tissue Analysis—No significant mucosal damage was noted in any of the groups.

REFERENCES

(1) "The American Hospital Formulary Service," vol. 2, American Society of Hospital Pharmacists, Inc., Washington, D.C., 1979, p. 64:00.

(2) "Meyler's Side Effects of Drugs," 9th ed., M. N. G. Dukes, Ed., Excerpta Medica, Amsterdam, 1980, pp. 383–388.

(3) R. F. Bergstrom, D. R. Kay, T. M. Harkcom, and J. G. Wagner, *Clin. Pharmacol. Exp. Ther.* **30,** 404 (1981).

(4) J. G. Wagner, "Biopharmaceutics and Relevant Pharmacokinetics," Drug Intelligence Publications, Hamilton, Ill., 1971, pp. 158–165.

(5) "United States Pharmacopeia XX, National Formulary XV," United States Pharmacopeial Convention, Inc., Rockville Md., 1979, p. 1105.

(6) "United States Pharmacopeia XX, National Formulary XV," United States Pharmacopeial Convention, Inc., Rockville, Md., 1979, pp. 958–959.

(7) J. Mann and P. D. Mitchell, *J. Pharm. Pharmacol.*, **31,** 420 (1979).

(8) R. F. Bergstrom, D. R. Kay, and J. G. Wagner, *J. Chromatogr.*, **222,** 445 (1981).

(9) G. T. Luce, *Manuf. Chem. Aerosol News*, **49,** 50 (1978).

(10) R. F. Bergstrom, D. R. Kay, and J. G. Wagner, *J. Pharmacokinet. Biopharm.*, **9,** 603 (1981).

(11) P. Veng-Pedersen, *J. Pharm. Sci.* **70,** 32 (1981).

(12) A. Melander, G. Brante, O. Johansson, T. Lindberg, and F. Wahlin-Boll, *Eur. J. Clin. Pharmacol.* **15,** 269 (1979).

(13) "The Merck Veterinary Manual," 4th ed., O. H. Siegmund and C. M. Frazier, Eds., Merck and Co., Inc., Rahway, N.J., 1973, pp. 411–412.

ACKNOWLEDGMENTS

This study was abstracted from a dissertation submitted by Walter Chambliss to the University of Mississippi in partial fulfillment of the Doctor of Philosophy degree requirements. The dissertation was directed by Dr. Arthur H. Kibbe.

This study was supported by the Research Institute of Pharmaceutical Sciences, School of Pharmacy, University of Mississippi, University, MS 38677.

Pharmacokinetics of Mitomycin C in Dogs: Application of a High-Performance Liquid Chromatographic Assay

R. H. BARBHAIYA ˣ, E. A. PAPP, D. R. VAN HARKEN, and R. D. SMYTH

Received April 11, 1983, from the *Metabolism and Pharmacokinetics Department, Pharmaceutical Research and Development Division, Bristol-Myers Co., Syracuse, NY 13201.* Accepted for publication September 4, 1983.

Abstract □ A normal-phase high-performance liquid chromatographic (HPLC) assay was developed for the determination of mitomycin C in plasma and urine. The method involves extraction of mitomycin C from plasma or urine into ethyl acetate-2-propanol-chloroform (70:15:15) with UV detection at 365 nm. Quantitation was performed with an internal standard (porfiromycin) by the peak height ratio method. Excellent correlation was obtained between the HPLC assay and the established microbiological cup-plate bioassay. The pharmacokinetics of mitomycin C were investigated in beagle dogs following a 1-mg/kg iv (22-mg/m^2) bolus dose. The plasma mitomycin C concentration *versus* time data were analyzed by using an open three-compartment model. The average volume of distribution was 1.90 L or 17% of body weight for the central compartment and 7.7 L or 68% of body weight for the terminal elimination phase. The volumes of distribution at steady state, calculated by model-dependent and -independent methods, compared very well with each other and were 6.5 L or 58% of body weight. Total body clearance averaged 112 mL/min, and the mean terminal plasma half-life was 53 min. The 0–24-h urinary excretion of intact mitomycin C accounted for 19% of the dose. The terminal half-life and percent urinary recovery of mitomycin C in dogs is similar to that in humans. Based on these observations, the dog appears to be a good model for studying the disposition of mitomycin C.

Keyphrases □ Mitomycin C—pharmacokinetics in dogs, HPLC □ Pharmacokinetics—mitomycin C in dogs, HPLC

Mitomycin C, an anticancer antibiotic, was first introduced for clinical trials in the United States over two decades ago, but its use was limited due to bone marrow toxicity. The development of high-dosage, intermittent schedules and its use in combination with other anticancer agents has improved the therapeutic index of mitomycin C against a variety of tumors (1–3). The therapeutic index and toxicity are reported to be dependent on dose and schedule (4).

The pharmacokinetics of mitomycin C in animals and humans have not been fully described, mainly due to the lack of a sensitive and specific assay. Preliminary pharmacokinetics of mitomycin C have been reported in humans (5, 6) and rabbits (6). Recently, assay methodologies involving high-performance liquid chromatography (HPLC) (6, 7) and enzyme immunoassay (8) have been described for the determination of mitomycin C in serum.

The HPLC assays utilize reverse-phase columns with UV detection at 365 nm. One of the HPLC assays (7) has a sensitivity of 40 ng/mL in plasma, making it unsuitable for pharmacokinetic studies. In addition, the assay involves acidification of plasma prior to the extraction of mitomycin C into ethyl acetate. As mitomycin C is unstable in acidic and basic solutions (5, 9, 10), it may degrade before being extracted. A modified, stability-indicating HPLC assay involving extraction of mitomycin C at neutral pH in plasma has been reported (5). The disadvantage of this method relates to the fact that no internal standard is used in the assay. In a third HPLC assay (6), a nonionic exchange resin column is utilized for the extraction of mitomycin C and the internal standard. The assay has a sensitivity of ~5–10 ng/mL; however, it is expensive to run on a routine basis because of the cost of the resin columns. The enzyme immunoassay (8) may lack the necessary specificity for pharmacokinetic studies.

In the present study, a normal-phase HPLC assay for mitomycin C in plasma and urine was developed, compared with an established microbiological cup-plate assay (11), and applied to a study of the pharmacokinetics of mitomycin C after intravenous bolus administration in beagle dogs.

EXPERIMENTAL SECTION

Reagents—Mitomycin C[1], porfiromycin[2], tetrahydrofuran[3], dichloromethane[4] (glass distilled), ethyl acetate[3] (glass distilled), isooctane[5] (pesticide grade), 2-propanol[4] (glass distilled), methanol[5] (certified ACS), and chloroform[4] (glass distilled) were used as received from the suppliers.

Animals—Three healthy female beagle dogs (weight, 10.7–12 kg) were used in the study. Each dog was restrained in a sling; the urinary bladder was catheterized, and indwelling venous catheters were placed in the saphenous veins of both hind legs.

Dose Preparation and Administration—To each vial[6], containing 20 mg of mitomycin C and 40 mg of mannitol, was added 40 mL of sterile distilled water. The vials were gently shaken until a clear solution of mitomycin C was obtained. A 1-mg/kg dose was administered by a rapid bolus (1-min) injection through a saphenous vein catheter.

Sample Collection—Samples of venous blood (8 mL) were collected in heparinized tubes just before dosing and at 2, 5, 10, 15, 20, 30, and 45 min, and 1, 1.5, 2, 3, 4, 5, 6, and 7 h after drug administration. A venous catheter placed contralaterally to the one used for intravenous administration of the drug was used for all blood collections. Blood samples were centrifuged immediately after collection, and the plasma was separated and stored at −20°C. Urine samples were collected in a graduated cylinder and immersed in crushed ice before dosing and 1, 3, 5, 7, and 24 h after dosing. After each collection interval, the volume of urine was recorded, and 10 mL of urine was stored at −20°C.

Extraction of Mitomycin C from Plasma and Urine—The extraction solvent consisted of ethyl acetate-2-propanol-chloroform (70:15:15). The reconstitution solvent was chloroform-methanol (9:1). The internal standard was 1000-ng of porfiromycin/mL in methanol.

Plasma (2 mL) or urine (0.2 mL), 1.0 mL of distilled water, 7.0 mL of the extraction solvent, and 0.1 mL of the internal standard solution were transferred into a 16 × 125-mm screw-capped tube. The tube was capped with a polytef-lined screw cap and gently rotated[7] for 20 min. The tube was centrifuged[8] at 3000 rpm for 10 min and the upper organic phase was transferred into a clean 16 × 125-mm tube. The solvent was evaporated to dryness under nitrogen. The residue was dissolved in 50 μL of the reconstitution solvent, and 25 μL was injected on the liquid chromatograph.

Chromatography—The HPLC system was the same for mitomycin plasma and urine assays and consisted of a solvent pump[9], an injector[10], a 10-μm particle size normal-phase silica column[11], a fixed-wavelength UV detector[12]

[1] Lot no. 11210; Bristol Laboratories, Syracuse, N.Y.
[2] Lot no. 6891; Bristol Laboratories.
[3] MCB Manufacturing Chemist, Inc., Cincinnati, Ohio.
[4] Burdick and Jackson, Inc., Muskegon, Mich.
[5] Fisher Scientific Co., Fair Lawn, N.J.
[6] Mutamycin, 20 mg for injection, lot no. D1C01; Bristol Laboratories.
[7] Model 343, Roto-Rack; Fisher, Springfield, N.J.
[8] International Centrifuge, model UV; Scientific Glass, Bloomfield, N.J.
[9] Model M-45 solvent delivery system; Waters Associates, Milford, Mass.
[10] Model U6K injector; Waters Associates.
[11] μPorasil P/N 27477 N/SA no. 115735, Waters Associates.
[12] Model 441 UV absorbance detector; Waters Associates.

0022-3549/84/0900-1220$01.00/0
© 1984, American Pharmaceutical Association

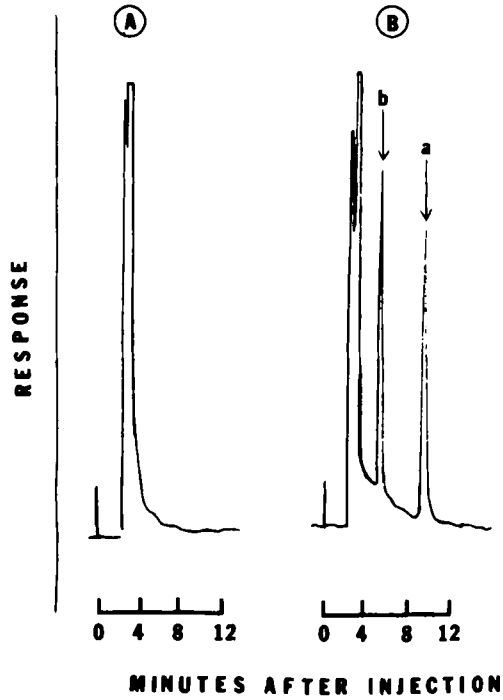

Figure 1—*Chromatograms from plasma containing no drugs (A) and plasma containing 116 ng of mitomycin C/mL (a in B) and 48 ng of porfiromycin/mL (b in B).*

with a 365-nm filter, and a guard column[13]. The mobile phase consisted of tetrahydrofuran-methanol-isooctane-dichloromethane (3:7:15:75). The solvent flow rate was maintained at 1.0 mL/min. HPLC analysis was performed at ambient temperature.

Data Processing—The peak heights were measured manually or with an automated laboratory data system[14], and the ratio of the mitomycin C to porfiromycin peaks for each chromatogram was calculated. After each series of injections, the regression of peak height ratio *versus* concentration of mitomycin C standard was calculated by least-squares analysis, and the concentration of mitomycin C in each plasma or urine sample was estimated by inverse prediction.

Comparison with Bioassay—Samples of plasma and urine from dogs have also been assayed by a cup-plate bioassay (11), with *Escherichia coli B* A22636 as the test organism. The assay was sensitive to 10 ng/mL of mitomycin C on plasma or urine.

Pharmacokinetic Calculations—After intravenous administration, unchanged mitomycin C concentration-time curves showed a triexponential decay on a semilogarithmic graph. Thus, an open three-compartment model, with elimination occurring from the central compartment, was proposed to describe mitomycin C kinetics (Scheme I).

The data were fitted according to:

$$C_p = Pe^{-\pi t} + Ae^{-\alpha t} + Be^{-\beta t} \qquad \text{(Eq. 1)}$$

where C_p is the concentration of mitomycin C in plasma at time t; π, α, and β are the exponential coefficients during the three phases; and P, A, and B are the concentrations of the exponential terms at time zero. Estimates of these parameters were first obtained by standard graphical analysis and then by computer program P-AUTOAN which is a combination of the programs

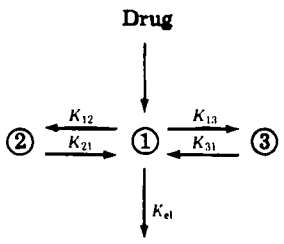

Scheme 1—*Linear three-compartment model with elimination from the central compartment.*

[13] 2.54 cm long packed with 37–50 μCorasil; Waters Associates.
[14] Model 3354; Hewlett Packard, Avondale, Pa.

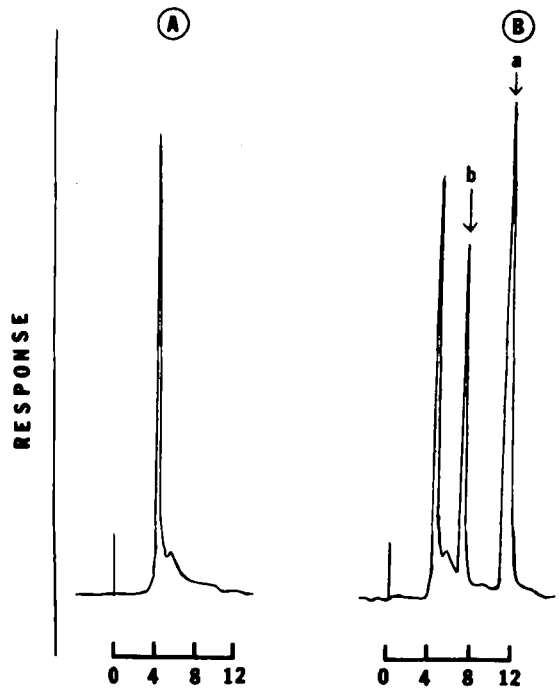

Figure 2—*Chromatograms from urine containing no drugs (A) and urine containing 878 ng of mitomycin C/mL (a in B) and 77 ng of porfiromycin/mL (b in B).*

CSTRIP (12) and GUESS (13). For computer analysis, all plasma level data were squared, weighted according to their reciprocals, and fitted to mono-, bi-, tri-, and tetraexponential equations. The model equation with Akaike's minimum information criterion (14) was chosen as the best representation for the time course data. The values obtained for each parameter were then used to calculate other kinetic parameters, such as intercompartment rate constants (k_{12}, k_{21}, k_{13}, and k_{31}), the overall elimination rate constant (k_{el}), terminal elimination phase and central compartment volumes of distribution (Vd_β and V_c, respectively), and total (CL_{tot}) and renal (CL_r) clearances, using conventional methods (15). The steady-state volume of distribution (Vd_{ss}) was calculated by model-dependent (16) and -independent (17) equations (Eqs. 2 and 3, respectively):

$$Vd_{ss} = (1 + k_{12}/k_{21} + k_{13}/k_{31})V_c \qquad \text{(Eq. 2)}$$

$$Vd_{ss} = \frac{\text{Dose} \cdot \left(\int_0^\infty t\, C_p dt\right)}{\left(\int_0^\infty C_p dt\right)^2} \qquad \text{(Eq. 3)}$$

The areas under the plasma concentration-time curves (AUC) were calculated by the trapezoidal rule with extrapolation to infinite time.

RESULTS AND DISCUSSION

Assay—Mitomycin C and the internal standard (porfiromycin) can be readily extracted into organic solvent from plasma and urine at neutral pH. As mitomycin C and porfiromycin are very stable at neutral pH and are subjected to rapid decomposition in acid and base (5, 9, 10), extraction was carried out at neutral pH. The extraction efficiency of mitomycin C and the internal standard in plasma and urine was not significantly affected between pH 7.0 and 7.9 and was >90% with a phase volume ratio of plasma extractant of at least 1:3.5. The normal-phase chromatographic procedure was developed to separate mitomycin C from endogenous plasma and urine components, the internal standard, and possible metabolite(s). A mobile phase consisting of ethyl acetate–2-propanol–chloroform (70:15:15) was found to be most suitable for the selective determination of mitomycin C in plasma and urine. Mitomycin C has maximum UV absorbance at 365 nm (5); detection at 254 nm resulted in decreased sensitivity and increased interference at or near the mitomycin C or porfiromycin peaks. A 365-nm UV filter was therefore selected for the optimum sensitivity and specificity.

Typical chromatograms obtained from blank plasma samples and from

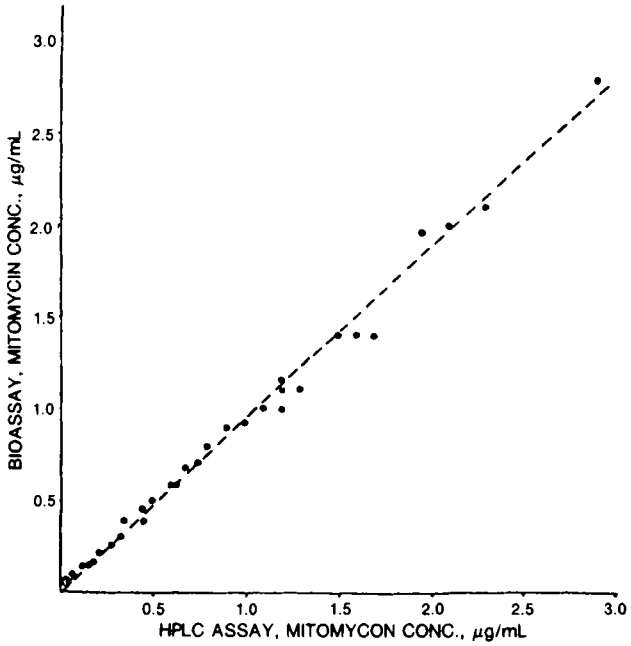

Figure 3—*Comparison of HPLC assay and bioassay of mitomycin C in plasma: slope 0.93; intercept, 0.008; r = 0.996.*

plasma samples containing mitomycin C and porfiromycin are shown in Fig. 1. Mitomycin C was completely separated from porfiromycin, and there was no interference from any endogenous substance in the plasma samples obtained from dogs. The retention times for mitomycin C and porfiromycin were 10.5 and 5.6 min, respectively, and the response (concentration *versus* peak height ratio) was linear in the range of 1–2000 ng of mitomycin C per mL. Standard curves obtained from repeated determinations of plasma standards were $y = 0.009x + 0.033$, $r = 0.999$. Typical chromatograms obtained from blank urine samples and from urine samples containing mitomycin C and porfiromycin are shown in Fig. 2. The retention times for mitomycin C and porfiromycin were the same as in the plasma assay. The urine assay for mitomycin C was linear in the range of 200–2000 ng/mL. Standard curves obtained from repeated determinations of urine standards were $y = 0.0008x - 0.027$, $r = 0.999$.

A set of 10 plasma samples was prepared to contain 5 ng of mitomycin C/mL and carried through the assay procedure for determining accuracy and precision of the assay. The estimated sample concentrations were then used to calculate the observed mean (5.3 ng/mL), *SD* (0.61), *RSD* (11.0%) and mean recovery (106%).

A set of 10 urine samples was prepared to contain 1000 ng of mitomycin C/mL and carried through the assay procedure for determining accuracy and precision of the assay. The estimated sample concentrations were then used to calculate the observed mean (1019 ng/mL), *SD* (35), *RSD* (3.39%), and mean recovery (102%).

Comparison of the Liquid Chromatographic Assay and the Bioassay—Since the lower limit of detection for the plasma bioassay was 10 ng/mL, values of <10 ng/mL found by the HPLC assay were excluded from the comparison of the two assays. The paired assay values of mitomycin C by HPLC assay and bioassay were highly correlated, with a correlation coefficient of 0.996 (Fig. 3). Excellent correlation between the HPLC assay and bioassay suggests that both assays are specific, and metabolite(s) of mitomycin C may not be microbiologically active. Pharmacokinetic calculations were performed by employing the values obtained from the plasma HPLC assay because of its greater sensitivity (1 ng/mL).

Pharmacokinetics of Mitomycin C in Dogs—Following the bolus intravenous administration of mitomycin C, a triexponential plasma level curve was observed in all three dogs (Fig. 4). The graphic and computer analyses of the data suggest that the pharmacokinetic evaluation would require a three-compartment open-model system (Scheme I), assuming that all processes are linear and that elimination occurs from the central compartment (plasma) which is connected to two peripheral compartments. The summary of pharmacokinetic parameters is shown in Table I.

The rate constants associated with the rapidly and relatively slowly equilibrating sites in the peripheral compartments ranged from 27.6 to 42.2 h^{-1} for π and from 3.73 to 7.86 h^{-1} for α, respectively. These values correspond to apparent half-life ranges of 1–1.5 and 5–11 min, respectively. The terminal elimination rate constant (β) ranged from 0.66 to 0.89 h^{-1}, corresponding to an apparent half-life range of 47–63 min. The magnitude of the three hybrid rate constants π, α, and β reflect an extremely rapid initial distribution of mitomycin C and a relatively slow elimination rate of the drug from plasma.

The individual rate constants k_{12}, k_{21}, k_{13}, and k_{31} reflect the rate of distribution into and out of the shallow and deep peripheral compartments. The mean ratio of k_{21}/k_{12} of 1.4, which reflects the return and entry of the drug within the shallow peripheral compartment, suggests rapid equilibration and free transfer of the drug between the central and shallow peripheral compartments. The mean ratio of k_{31}/k_{13} of 0.66, which reflects the return and entry of the drug within the deep peripheral compartment, suggests somewhat slower equilibration plus the possibility of drug binding to tissues or protein sites in this compartment, with a corresponding slower return of the drug to the central compartment. The mean ratio of β/k_{el} of 0.23 indicates that only 23% of the mitomycin C in the body is in the central compartment and available for elimination at any time (18).

The volume of distribution of mitomycin C in the central compartment (V_c) was calculated to be 16, 14, and 22% of body weight for dogs 17637, 17876, and 17516, respectively. The Vd_{ss} calculated by model-dependent (16) and -independent (17) methods were in agreement with each other and ranged from 35 to 62% of body weight in the three dogs. The values calculated for Vd_β were higher than Vd_{ss} and ranged from 58 to 78% of body weight.

The 24-h excretion of intact mitomycin C in urine ranged from 19.2 to 19.8% of the dose, most of which was excreted in the first 7 h. The total body clearance for mitomycin C ranged from 90 to 129 mL/min, and renal clear-

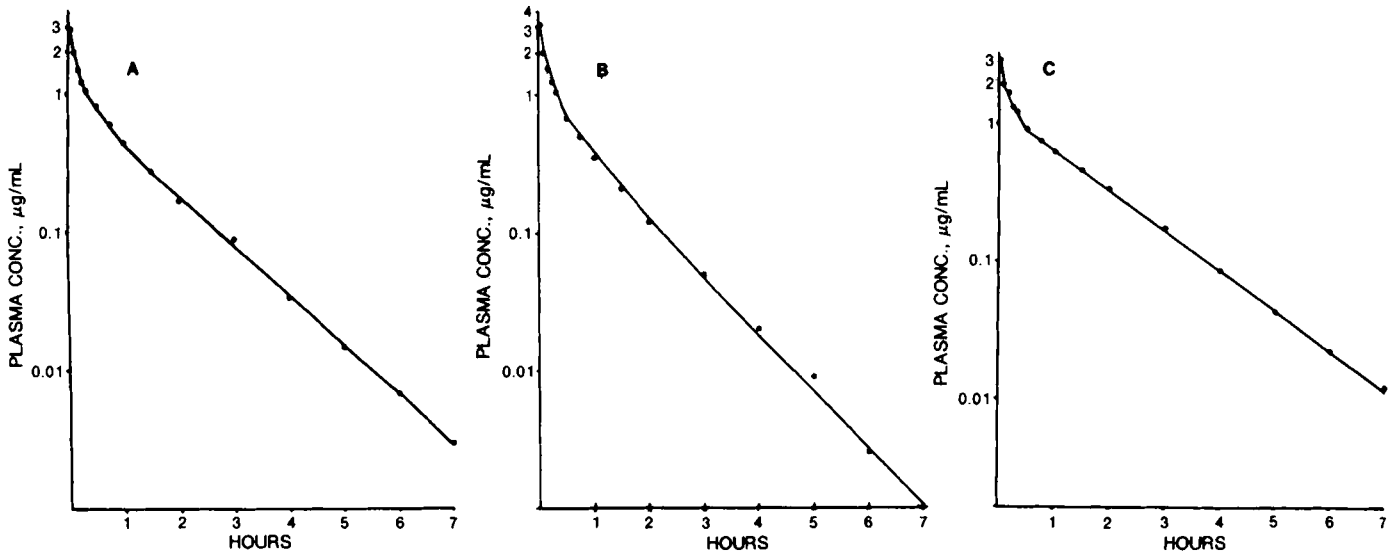

Figure 4—*Plasma levels of mitomycin C in three dogs after a single 1-mg/kg intravenous dose. Key: (●) experimental values; (—) computer-predicted curve; (A) dog 17516; (B) dog 17637; (C) dog 17874.*

Table I—Pharmacokinetic Profiles of Mitomycin C in Dogs after Single Intravenous Doses

Parameters	Dog 17637	Dog 17874	Dog 17516	Mean
Dose, mg	10.7	12.0	11.0	11.2
Dose, mg/kg	1	1	1	1
P, μg/mL	3.61	3.69	2.37	3.22
A, μg/mL	1.74	2.11	1.16	1.67
B, μg/mL	0.96	1.23	0.94	1.04
π, h^{-1}; $t_{1/2\pi}$, h	42; 0.016	38; 0.018	28; 0.025	36; 0.02
α, h^{-1}; $t_{1/2\alpha}$, h	4.8; 0.14	7.86; 0.09	3.73; 0.18	5.5; 0.14
β, h^{-1}; $t_{1/2\beta}$, h	0.89; 0.78	0.66; 1.05	0.82; 0.85	0.79; 0.89
k_{12}, h^{-1}	18.1	11.9	10.8	13.6
k_{21}, h^{-1}	20.0	21.1	14.3	18.5
k_{13}, h^{-1}	3.2	7.3	2.2	4.2
k_{31}, h^{-1}	2.2	3.0	2.0	2.4
k_{el}, h^{-1}	4.5	3.2	2.9	3.5
Ratio β/k_{el}	0.20	0.20	0.28	0.23
AUC, μg/mL/h	1.5267	2.2197	1.5477	1.7647
V_c, L; % of body weight	1.7; 16	1.7; 14	2.4; 22	1.9; 17
Vd_{ss}, L; % of body weight[a]	5.9; 55	4.2; 35	6.8; 62	5.6; 51
Vd_{ss}, L; % of body weight[b]	5.8; 54	6.8; 57	6.8; 62	6.5; 58
Vd_{β}, L; % of body weight	6.2; 58	8.2; 68	8.6; 78	7.7; 68
Percent of Dose Excreted in Urine (0-24 h)	19.2	19.2	19.8	19.4
Cl_{tot}, mL/min	129	90	118	112
Cl_r, mL/min	22	17	23	21

[a] Calculated by the model-independent method. [b] Calculated by the model-dependent method.

ance ranged from 17 to 23 mL/min in the three dogs. The large differences between renal and plasma clearances can be attributed to extensive biliary and/or metabolic clearances of mitomycin C. The terminal half-life and percent recovery of the mitomycin C dose in the urine of dogs is very similar to those values in humans (19).

The HPLC assay described for mitomycin C in plasma is sensitive to 1 ng/mL and should be suitable for elucidating the pharmacokinetics of mitomycin C in humans after therapeutic doses. There appears to be no interference from any metabolite in dogs. Drug-free human plasma and urine samples from different individuals do not have any interfering peak with mitomycin C or porfiromycin. However, possible interference from other drugs which may be coadministered with mitomycin C must be determined before use of this assay in humans. The pharmacokinetic data of mitomycin C in dogs are similar to preliminary pharmacokinetic data in humans (19). The dog may, therefore, be a good model for studying the disposition of mitomycin C.

REFERENCES

(1) W. W. Sutow, J. R. Wilbur, T. J. Vietti, P. Vuthilhagdee, T. Fujimoto, and A. Watanabe, *Cancer Chemother. Rep.*, **55**, 285 (1971).

(2) T. E. Godfrey and D. W. Wilbur, *Cancer*, **29**, 1647 (1972).

(3) M. L. Gutierrez, A. Evans, T. Rohrbaugh, J. Belasco, and F. H. Lee, *Med. Pediatr. Oncol.*, **9**, 405 (1981).

(4) S. K. Carter and S. T. Crooke, in "Mitomycin C, Current Status and New Developments," Academic, New York, N.Y., 1979 p. 3.

(5) J. den Hartigh, W. J. van Oort, M. C. Y. H. Bocken, and H. M. Pinedo, *Anal Chim. Acta*, **127**, 47 (1981).

(6) G. A. van Hazel and J. S. Kovach, *Cancer Chemother. Pharmacol.*, **8**, 189 (1982).

(7) A. Kono, Y. Hara, S. Eguchi, and M. Tanaka, *J. Chromatogr.*, **164**, 404 (1979).

(8) K. Fujiwara, H. Saikusa, M. Yasuno, and T. Kitagawa, *Cancer Res.*, **42**, 1487 (1982).

(9) E. R. Garrett, *J. Med. Chem.*, **6**, 488 (1963).

(10) D. Edwards, A. B. Selkirk, and R. B. Taylor, *Int. J. Pharm.*, **4**, 21 (1979).

(11) D. C. Grove and W. A. Randall, in "Assay Methods of Antibiotics: A Laboratory Manual," Medical Encyclopedia, New York, N.Y., 1955.

(12) A. J. Sedman and J. G. Wagner, *J. Pharm. Sci.*, **65**, 1006 (1976).

(13) E. Ackerman, L. C. Gatewood, J. W. Rosevear, and G. D. Molnar, in "Concepts and Models of Biomathematics," F. Heinmetr, Ed., Dekker, New York, N.Y., 1969, pp. 131-156.

(14) K. Yamaoka, T. Nakagawa, and T. Uno, *J. Pharmcokinet. Biopharm.*, **6**, 165, (1978).

(15) M. Gibaldi and D. Perrier, "Pharmacokinetics," Dekker, New York, N.Y., 1978.

(16) J. G. Wagner, *J. Pharmacokinet. Biopharm.*, **4**, 443 (1976).

(17) L. Z. Benet and R. L. Galeazzi, *J. Pharm. Sci.*, **68**, 1071 (1979).

(18) M. Gibaldi, R. Nagashima, and G. Levy, *J. Pharm. Sci.*, **58**, 193 (1969).

(19) J. den Hartigh, M. C. Y. H. Bocken, H. Gall, G. Simonetti, R. Kroes, J. G. McVie, W. J. van Oort, and H. M. Pinedo, American Association for Cancer Research Proceedings, vol. 23, abstract no. 494, 1982, p. 126.

ACKNOWLEDGMENTS

The authors would like to thank Shirley Sutton for development and Suzanne Connors for performance of the microbiological cup-plate assays.

Mass and Heat Transfer in Vial Freeze-Drying of Pharmaceuticals: Role of the Vial

M. J. PIKAL ˣ, M. L. ROY, and SAROJ SHAH

Received April 25, 1983, from the *Lilly Research Laboratories, Eli Lilly and Company, Indianapolis, IN 46285.* Accepted for publication June 8, 1983.

Abstract □ Flow of water vapor is impeded by three barriers or resistances: resistance of the dried-product layer, resistance of the semistoppered vial, and resistance of the chamber. The relationship between heat flow and temperature difference may be described by a vial heat transfer coefficient which has contributions from three parallel mechanisms: (*a*) direct conduction from the shelf to the vial *via* points of direct contact between the vial and shelf, (*b*) conduction through the vapor between the vial bottom and the shelf, and (*c*) radiative heat transfer. This report describes experimental studies of the resistance of semistoppered vials, the resistance of the chamber, and vial heat transfer coefficients. Mass transfer through the semistoppered vial has significant contributions from both Knudsen- and viscous-flow mechanisms. Stopper and chamber resistances are of the same magnitude and are about a factor of 10 less than the dried product resistance. All three heat transfer mechanisms are significant, the relative contributions depending on both the chamber pressure and the type of vial. Vial heat transfer coefficients are sensitive to the geometry of the vial bottom, and even vials of nominally the same specifications may differ significantly in heat transfer characteristics. Vials from the same lot are relatively uniform in their heat transfer characteristics, the relative standard deviation of the vial heat transfer coefficient being only ~4%. The temperature distribution in the frozen product is adequately described by a constant temperature gradient in the vertical direction and the thermal conductivity of ice.

Keyphrases □ Freeze-drying—vial heat transfer coefficients, measurement of resistance to mass transfer □ Heat transfer coefficients—freeze-drying, experimental measurement, mechanisms

Freeze-drying, or lyophilization, is the process by which the solvent, normally water, is removed from a frozen solution by sublimation. The freeze-drying process may be divided into three stages: freezing, primary drying, and secondary drying. For pharmaceutical products, the solution is normally filled into vials and then stoppers are partially inserted into the vial necks (semistoppered position), such that openings for vapor flow are present. Next, the vials are placed on temperature-controlled shelves in the freeze-drying chamber. After freezing, the chamber is evacuated to the desired pressure, normally in the range of 30–500 μm, and the shelf temperature is increased to provide energy for sublimation of ice during primary drying. Secondary drying, which is removal of water from the solute phase, begins in a local region of the sample when the ice has been removed from that region and normally continues for some time after all of the ice has been removed from the sample.

Due to high equipment costs, there is considerable economic motivation to minimize process times (1) while maintaining a low level of product loss arising from either eutectic melt or collapse (2). Optimization of the primary-drying stage requires a knowledge of the maximum allowable product temperature, which is either the eutectic temperature (for a crystalline solute) or the collapse temperature (for an amorphous solute), and also requires a determination of the optimum shelf temperature and chamber pressure–time profile required to maintain the product temperature slightly lower than the maximum allowable temperature during all of primary drying. In practice, the shelf temperature and chamber pressure–time relationship is often determined by trial and error. Since, in principle, optimization of this relationship is a problem in coupled mass and heat transfer, a better fundamental understanding of mass and heat transfer in primary drying would allow greater efficiency in process development and minimize problems encountered on scaleup to production operations.

Passing from the frozen product to the condenser, the flow of water vapor is impeded by three barriers or resistances: (*a*) resistance of the dried-product layer above the frozen product, which in addition to being product dependent is also dependent on the vial used (both the area of the ice–vapor interface and the thickness of the dried-product layer) (3), (*b*) resistance of the semistoppered vial, and (*c*) resistance in transfer from the drying chamber to the condenser. Heat for sublimation must be transferred to the product on the vial bottom from the surface upon which the vial rests and through the frozen solution to the subliming ice. For purposes of this discussion, it will be assumed that the vials are placed directly on the dryer shelf. The relationship between heat flow and temperature difference may be characterized by a vial heat transfer coefficient which has contributions from three parallel mechanisms for heat flow: direct conduction from the surface to the vial *via* points of direct contact between the vial and the shelf, conduction through the vapor between the vial bottom and the shelf, and by radiation heat transfer.

The resistance of the dried product was the subject of an earlier experimental study from this laboratory (3), while several aspects of heat transfer have been addressed by Nail (4). He demonstrated that, for a system of vials in a metal tray placed on a heated shelf, the sublimation rate increased as the chamber pressure was increased. Theoretical arguments were used to demonstrate that the temperature differences across the frozen product, across the glass at the vial bottom, and across the metal tray bottom are small and, therefore, the largest temperature differences, or thermal resistances, were across the vapor boundaries between surfaces. In this case, there were two vapor boundaries, one between the vial bottom and the tray surface upon which the vials rested, and the other between the tray bottom and the shelf. However, since Nail's methodology did not allow the thermal resistances for the two vapor boundaries to be evaluated separately, vial heat transfer coefficients could not be determined.

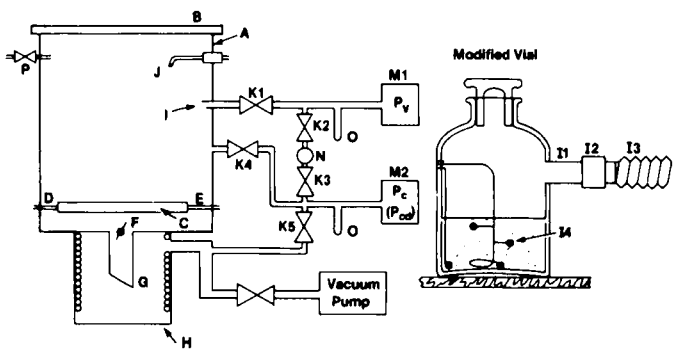

Figure 1—*Schematic of the laboratory freeze-dryer (see text for key).*

0022-3549/84/0900-1224$01.00/0
© *1984, American Pharmaceutical Association*

Table I—Geometric Parameters of Vials

Vial	A_v, cm^2	A_p, cm^2	Neck Finish, mm	Contact o.d., cm	Print Thickness, cm	l_{max}, cm
W5800	4.71	3.80	20	1.90	0.05	0.12
K5800	4.71	3.80	20	1.75	0.12	0.07
W5811	4.71	3.80	20	1.88	0.07	0.04
W5816	6.83	5.71	20	2.24	0.07	0.11
K5816	6.83	5.71	20	2.30[a]	—[a]	0.04
W, K5303	17.2	14.3	28	3.74	0.08	0.22
K5304	8.3	6.72	13	2.60	0.03	0.17

[a] These vials frequently show two concentric prints with the procedure used. The diameter given is the outer diameter of the largest print.

This research describes experimental studies which evaluate: (*a*) mass transfer coefficients (resistances) for several stoppers in the semistoppered configurations, (*b*) resistance of the chamber-to-condenser pathway in a laboratory dryer, and (*c*) vial heat transfer coefficients as a function of chamber pressure for seven types of vials, including examples of both tubing and molded vials. With the aid of a theoretical model for heat transfer, the relative contributions of the three mechanisms of heat flow are examined. Further, since variability in heat transfer coefficients within a given lot of vials is an important consideration in process development, the standard deviation of heat transfer coefficients is determined at selected chamber pressures for six of the seven types of vials studied.

THEORETICAL SECTION

Definition of Mass Transfer Coefficients—Mass transfer is discussed in terms of resistance offered by a given barrier. Resistance, rather than permeability, is used since the total resistance is the sum of component resistances in series. Assuming the usual proportion between flow rate through the barrier and driving force for the process, resistance is defined as the ratio of driving force to flow rate. Since the driving force for both sublimation at the ice-vapor interface and Knudsen flow (3–5)[1] of vapor through the small pores of a dried product is a difference in partial pressures of water (5), the difference between the equilibrium vapor pressure of subliming ice and the partial pressure of water above the dried product is taken as the driving force in the definition of the resistance of the dried product. For vapor flow through the semistoppered vial neck and through the chamber condenser pathway, the driving force is more appropriately taken as a difference in total pressure, to be consistent with the driving force for viscous flow of a fluid (5)[1].

The resistance of the dried-product layer, R_p, is defined by:

$$R_p = (P_0 - x_1^v P_v)/\dot{m} \quad \text{(Eq. 1)}$$

where P_0 is the equilibrium vapor pressure (mm Hg) of the subliming ice, x_1^v is the mole fraction of water vapor in the vial, P_v is the total pressure in the vial (mm Hg), and $\dot{m}$ is the sublimation rate (g/h/vial). As will be shown later, $x_1^v \approx 1$. The normalized product resistance, $\hat{R}_p$, is an area-normalized quantity (independent of product area) given by:

$$\hat{R}_p = A_p R_p \quad \text{(Eq. 2)}$$

where A_p is the geometric cross-sectional area of the product normal to the direction of water vapor flow (computed from the internal diameter of the vial).

The resistance of the semistoppered vial, R_s, is defined by:

$$R_s = (P_v - P_c)/\dot{m} \quad \text{(Eq. 3)}$$

where P_c is the chamber pressure (mm Hg). The resistance of the chamber to condenser pathway, R_c, is defined similarly:

$$R_c = (P_c - P_{cd})/\dot{m}N \quad \text{(Eq. 4)}$$

where N is the number of vials in the dryer and P_{cd} is the pressure in the condenser chamber.

Assuming $x_1^v = 1$, the combination of Eqs. 1–4 yields:

$$\dot{m} = R_T^{-1}(P_0 - P_{cd}) \quad \text{(Eq. 5)}$$

where the total resistance to flow from a given vial to the condenser chamber, R_T, is:

$$R_T = R_p + R_s + NR_c \quad \text{(Eq. 6)}$$

Thus, the contributions to total resistance offered by the dried product, stopper, and chamber are, respectively: R_p, R_s, and NR_c. The quantity NR_c, is a "scaled" chamber resistance and, in effect, is the chamber resistance per vial.

Since the mean free path of water vapor in the dried product is large compared with pore dimensions in the dried product, flow in this region is free molecular or Knudsen flow and the dried-product resistance (R_p) is, therefore, independent of pressure (3, 5). However, the mean free path is smaller than the channels in the stopper and the chamber through which vapor must flow and, hence, the flow mechanism is expected to be predominantly viscous flow with perhaps some contribution from Knudsen flow. Therefore, the stopper and chamber resistances should be pressure dependent and are expected (5) to be of the form:

$$R_i^{-1} = a_0 + a_1\bar{P}_i, \; i = s, c \quad \text{(Eq. 7)}$$

where R_i refers to either R_s or R_c and $\bar{P}_i$ is the mean pressure across the barrier. For example, for $i = s$, $\bar{P}_s = (P_v + P_c)/2$.

The form of Eq. 7 assumes that viscous flow may be described by Poiseuille's law. For viscous flow in short tubes, a correction to Poiseuille's law (5) leads to an additional term in Eq. 7 which is proportional to the product of the sublimation rate and the mean pressure. However, the equations presented by Dushman (5) indicate that the short tube correction is small for both closure resistance and resistance of the laboratory dryer chamber. A preliminary study of closure resistance data (3) suggests that the sublimation rate dependence of the closure resistance is negligible. Thus, although not rigorous, Eq. 7 should serve as a useful first approximation.

Definition of Heat Transfer Coefficients—A heat transfer coefficient is defined as the ratio of the area-normalized heat flow to the temperature difference between heat source and heat sink. For the case of vials resting directly on the freeze-dryer shelf, the vial heat transfer coefficient, K_v, is defined by:

$$\dot{Q} = A_v K_v (T_s - T_b) \quad \text{(Eq. 8)}$$

where $\dot{Q}$ (cal/s) is the heat flow from the shelves to the product in a given vial, A_v is the cross-sectional area of the vial calculated from the vial outer diameter, T_s is the temperature of the shelf surface, and T_b is the temperature of the product at the bottom center of the vial. If the vials are resting on a tray bottom, the temperature T_s refers to the tray surface temperature. Equation 8 assumes the surface above the vials is also at T_s and further assumes the normal situation of a small temperature differential between subliming ice and ice at the vial bottom.

The vial heat transfer coefficient may be expressed as the sum of three terms:

$$K_v = K_c + K_r + K_g \quad \text{(Eq. 9)}$$

[1] When the mean free path is large compared with the dimensions of the pores or tubes constituting the physical system responsible for resistance to flow, as is the case with flow through a dried product (3), collisions of water molecules with the pore or tube walls are responsible for resistance to flow, and the flow mechanism is said to be free molecular flow or Knudsen flow (5). Here, the driving force is the difference in partial pressure of the flowing gas under discussion. When the mean free path is small compared with pore or tube dimensions, collisions between gas molecules are much more frequent than collisions of gas molecules with pore or tube walls, and the resistance is due to momentum transfer between gas molecules, or viscous "forces." The flow mechanism is "viscous flow" (5), and the driving force is the difference in total pressure. The distinction between partial pressure and total pressure is obviously not important when the gas phase is essentially pure water. As data to be presented later will show, the mole fractions of water in the vial and in the chamber are close to unity. The mole fraction of water vapor in the condenser, however, is significantly less than unity. Thus, if flow from the chamber to the condenser were predominantly Knudsen flow, the chamber resistance, defined using the total pressure difference between chamber and condenser as the driving force, might behave anomalously with variations in chamber pressure. However, as will be demonstrated later, the pressure dependence of the chamber resistance is of the expected form, and, therefore, the selection of the driving force seems appropriate.

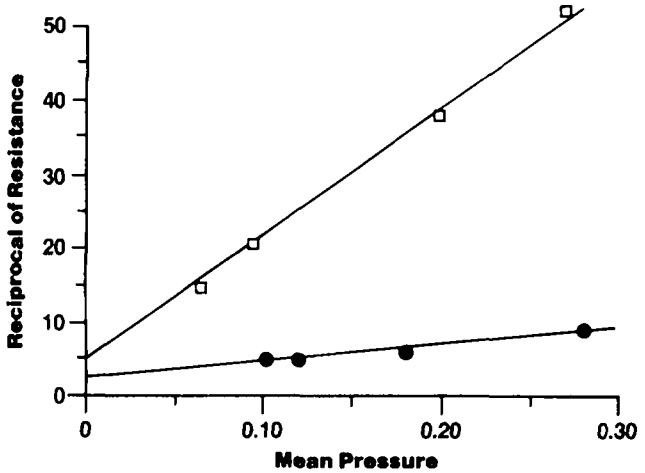

Figure 2—*Reciprocal of closure resistance* versus *pressure. Key: (□) 20-mm closure, (●) 13-mm closure.*

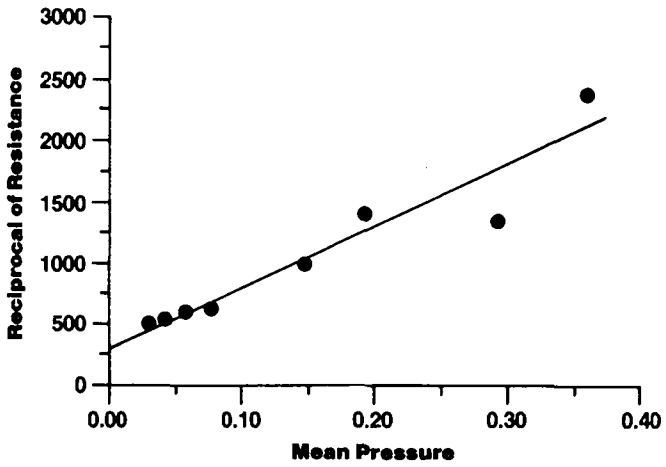

Figure 3—*Reciprocal of chamber resistance* versus *pressure.*

where K_c is the contribution resulting from direct conduction from shelf to glass at the points of contact, K_r is the contribution from radiative heat transfer, and K_g is the contribution from conduction through the gas between the shelf and the vial bottom. Both K_c and K_r are independent of pressure, but K_g increases with increasing gas pressure. Using the Smoluchowski theory as outlined by Dushman (5), and assuming the gap between the vial bottom and the shelf may be characterized by a constant "effective" distance, l, the gas conduction term may be written:

$$K_g = \frac{\alpha\Lambda_0 P}{1 + l(\alpha\Lambda_0/\lambda_0)P} \qquad \text{(Eq. 10)}$$

where Λ_0 is the free molecular heat conductivity of the gas at 0°C, λ_0 is the heat conductivity of the gas at ambient pressure, P is the gas pressure, and α is a function of the energy accommodation coefficient (a_c) and the absolute temperature of the gas (T):

$$\alpha = \frac{a_c}{2 - a_c} \cdot \sqrt{\frac{273.2}{T}} \qquad \text{(Eq. 11)}$$

The radiation term is a sum of two contributions, radiative heat transfer between the shelf and the vial bottom and radiative heat transfer between the shelf above the vial and the top of the vial. Radiative heat flow Q_r, depends on the difference in the fourth powers of the absolute temperatures of the two surfaces:

$$\dot{Q}_r = A_v \bar{e} \sigma (T_2^4 - T_1^4) \qquad \text{(Eq. 12)}$$

where σ is the Stefan-Boltzmann constant and $\bar{e}$ is the "effective" emissivity for the heat exchange, which depends on the relative areas of the two surfaces, their emissivities, and a geometrical view factor (4). For modest temperature differences between the two surfaces:

$$\dot{Q}_r \cong A_v \bar{e} \sigma 4\overline{T}^3 (T_2 - T_1) \qquad \text{(Eq. 13)}$$

where $\overline{T}$ is the mean temperature. For temperatures normally used in freeze-drying, the product, $\sigma 4\overline{T}^3$, is $\sim 1.0 \times 10^{-4}$. For radiation from the shelf upon which the vials rest (bottom radiation), the view factor is approximately unity, and since the emissivity of glass is near unity (4), the effective emissivity for bottom radiation is essentially the emissivity of the shelf surface, e_s, and T_1 is essentially the temperature at the vial bottom, T_b. For radiation from the top, the shelf area view factor of the vial top is much greater than the vial area, and one therefore expects (4) the effective emissivity to be essentially independent of the emissivity of the shelf above the vials. An exact evaluation of $\bar{e}$ for top radiation is not possible, and we treat the effective emissivity for top radiation, denoted e_v, as an experimental quantity to be evaluated by vial heat transfer experiments.

Since Q_r for top radiation is the heat transferred to the subliming ice, an empirically defined e_v should be based on an identification of T_1 as the temperature of subliming ice. In general, temperature differences within the product are small and, as a satisfactory approximation in most cases, T_1 may be taken as T_b. With the definitions of e_s and e_v given above, use of Eq. 13 and the approximation, $\sigma 4\overline{T}^3 \approx 1.0 \times 10^{-4}$, the radiative heat transfer coefficient, K_r, becomes:

$$K_r = 1.0 \times 10^{-4}(e_v + e_s) \qquad \text{(Eq. 14)}$$

In the case of vials resting on a tray bottom, an equation similar to Eq. 8 may be used to define a tray heat transfer coefficient, K_{TR}. Here the area, A_v, is replaced by the ratio of the tray area to the number of vials in the tray, and T_b is replaced by the temperature of the tray bottom. The meaning of $\dot{Q}$ and T_s is the same as in Eq. 8. The components of K_{TR} are given by the right side of Eq. 9, with the form of K_g identical to Eq. 10, although the value of the accommodation coefficient could differ from the value applicable to heat transfer between shelf and vial.

Since most of the heat input flows from the bottom of the vial to the subliming ice, the temperature of the product decreases as the distance from the bottom of the vial, X, increases. The usual proportionality between heat flow and temperature gradient may be used to define the effective thermal conductivity of the product, K_I:

$$\dot{Q}_B = -A_v K_I \cdot \frac{dT}{dX} \qquad \text{(Eq. 15)}$$

where $\dot{Q}_B$ is the heat flow (cal/s) through the bottom of the vial and T is the temperature of the frozen product in the vial. Since the total area available for heat transfer, A_v, is in part glass and in part frozen solution, one would expect K_I to be an area-weighted sum of the thermal conductivities of glass, κ_G, and frozen product, κ_p:

$$K_I \cong \frac{A_v - A_p}{A_v} \cdot \kappa_G + \frac{A_p}{A_v} \cdot \kappa_p \qquad \text{(Eq. 16)}$$

where A_p is the cross-sectional area of the frozen product calculated from the inner diameter of the vial. For dilute solutions, one would expect κ_p to be close to the value for pure ice (6, 7).

EXPERIMENTAL SECTION

Materials—Chemicals used were either reagent or USP grade and were used without further purification, except for filtration of the solutions prepared through a 0.45-μm filter to remove particulate matter. Solutions were prepared by weighing the appropriate quantities of distilled water and solute. Studies involving pure water used distilled water[2].

The rubber closures[3] have two openings for vapor passage in the semi-stoppered position. The 20-mm finish closure has two openings of ~0.4 cm in diameter, while the 13-mm finish closure has openings of ~0.2 cm in diameter.

The vials used were of commercial origin[4] and, except for the limited studies with 5304 vials, were selected to yield a representative cross section of vials produced during a given production run. All of the vials were type I glass; the 5303 and 5304 vials were molded and the others were tubing vials. The relevant vial geometric parameters are summarized in Table I. The contact-print parameters refer to the imprint created by first placing the vial bottom on an ink pad and then placing the vial on a sheet of paper resting on cardboard. Moderate pressure is applied by placing a 500-g weight on top of the vial. While reproducible, the thickness of the contact print is obviously procedure sensitive and does not represent, except in a relative sense, the actual area of physical contact between the vial and a hard surface. The entry in the last column, l_{max}, is the maximum separation distance between the vial bottom

[2] Water for Injection, Eli Lilly and Co.
[3] West Co.
[4] The vials with designation K were obtained from the Kimble Glass Co. and those with designation W were obtained from the Wheaton Glass Co.

Table II—Comparison of Resistances [a]

Product	Closure	Sublimation Rate, g/h[b]	Total Resistance, h·mm Hg/g	Relative Resistance, Percent of Total		
				Product	Closure	Chamber
KCl	None	0.523	1.38	91.5	0	6.5
KCl	20 mm	0.506	1.42	90.8	3.0	6.2
KCl	13 mm	0.458	1.56	82.7	11.7	5.6
I[c]	None	0.321	2.18	96.3	0	3.7
I	20 mm	0.315	2.22	94.6	2.0	3.4
I	13 mm	0.294	2.37	88.6	8.1	3.3

[a] Calculated for a vial of 3.8 cm^2 internal area, a dried product thickness of 0.5 cm, a chamber pressure of 0.1 mm Hg, an ice temperature of −20°C, and the laboratory freeze-dryer with a load of 60 vials of 4.7 cm^2 external area. [b] Sublimation rate per vial. [c] System I is dobutamine hydrochloride (dobutrex) and mannitol in a 1.12:1 weight ratio with total solids being 53 mg/mL.

and a flat surface, obtained simply by direct measurement with a metric ruler. Thus, this parameter is subject to a measurement error of ± ~0.02 cm.

Freeze-Dryers—The laboratory freeze-dryer was a highly modified commercial unit[5] (3) illustrated schematically in Fig. 1. A stainless steel cylinder (A) constituted the drying chamber wall, and the top of the unit (B) was a transparent plastic lid which formed a vacuum-tight seal with the chamber walls *via* a rubber gasket. Temperature control of the shelf (C) was provided by rapid circulation of fluid (methanol) from a thermostat (not shown) into the shelf (D) and out of the shelf (E); the fluid flowed through channels in the shelf interior. The chamber walls and top were covered with 2 cm of rubber foam insulation. However, under the usual conditions of ice sublimation, the dryer walls and top run warmer than the shelf. With a 5°C shelf, the walls were ~15°C while the top was ~12°C. The shelf surface used in these experiments was a thin (1-mm) metal plate in good thermal contact with the original shelf *via* a thin coat of high-vacuum silicone grease impregnated with copper dust. Unless specifically indicated otherwise, the shelf surface was a polished 316 stainless steel plate with a measured emissivity, e_s, of 0.28[6].

The temperature of the shelf surface was measured by thermocouple sensors (30-gauge wire) designed for surface temperature measurements. A welded copper-constantan thermocouple junction was silver-soldered to a copper disk ~1 mm thick and 1.5 cm in diameter. A 2-mm thick disk of foam insulation was glued to the copper disk, and an empty 10-mL glass vial was then glued to the insulation, thus insulating the thermocouple junction from the vial. Good thermal contact between the copper disk and the shelf surface was obtained by applying a thin coat of high-vacuum silicone stopcock grease to the bottom of the copper disk. The shelf surface temperature readings were accurate within ±0.5°C.

Without grease at the interface between the copper disk and shelf surface, the shelf sensors gave readings that were dependent on chamber pressure and were 2–3°C lower than the greased sensors. The shelf surface temperature was normally independent of position on the shelf, within ±0.5°C. The difference between fluid temperature and shelf surface temperature increased as the total sublimation rate increased (*i.e.*, increased heat flow), but was in the 1–2°C range for most of the experiments.

A butterfly valve (F) separated the drying chamber from a tube (G) (2.3 cm diameter, 25 cm length) leading to the condenser chamber (H). A tube (I) connected the interior of a modified vial with a pressure sensor external to the drying chamber (M1 or M2) by suitable manipulation of valves (K1, K2, K3, K4, and K5). A pressure-tight seal between the vial and a glass tube (I1) was made with silicone rubber glue. The glass tube was connected to a flexible stainless steel tube (I3) with a high-vacuum union[7]. The flexible tube was then connected with tube I *via* another high-vacuum union. Temperature measurements were made at four locations within the frozen product using copper-constantan thermocouples (30-gauge wire) (I4). Ten additional thermocouple leads (J) were also available. Differential capacitance manometers (M1, M2)[8] were used for quantitative measurements of absolute pressure, although a thermocouple vacuum gauge (N) was also included in the apparatus. Pressures and temperatures in the vial and chamber were continuously displayed as a function of time on a 24-channel recorder[9].

Studies requiring a larger shelf area than that available in the laboratory dryer were carried out using a pilot scale dryer[10] with condensers in the drying chamber. The dryer contained three shelves of 2800 cm^2 area separated from the condensers by radiation shields. Only the middle shelf was used in the experiments. The shelf surface was painted black and the surface temperature was uniform within 3°C: several shelf temperature sensors were used and care was taken to locate the sensors at positions where the average recorded temperature represented the true average shelf temperature. The temperature of the surface above the vials was colder than the shelf surface upon which the vials rested. Temperature measurements taken near the center of the top shelf indicated a mean difference of 4.3°C for the experiments performed.

Procedures—*Calibrations*—The differential capacitance manometers were calibrated against a precision McCloud gauge[11]. Deviations were less than the stated accuracy of the McCloud gauge (±3%) and no corrections were used. The thermocouple temperature sensors were calibrated at the ice point and at −25°C against a mercury-in-glass thermometer (±0.1°C).

Vapor Composition Measurement—Vapor composition was measured by comparing the pressure of a fixed quantity of vapor at room temperature with the corresponding pressure at dry ice temperature (−78°C), where the pressure of water is negligible. For example, the vapor composition in the vial was measured by first determining the total pressure in the vial with pressure gauge M1 (Fig. 1). Valves K1 and K2 were opened, valve K3 was closed, and the cold finger (O) was at ambient temperature. Next, valve K1 was closed to isolate the sample of vapor, representing the composition of vapor in the vial, and a dry ice–acetone bath was placed around the cold finger. Within a few minutes essentially all water vapor was condensed, and the residual pressure was due only to air[12]. This residual pressure was slightly lower than the air pressure in the original vapor since the air in the cold finger was at a lower temperature. The original air pressure was obtained from the measured residual pressure, using an empirically determined correction factor (1.044). The correction factor was determined by measuring the pressure reduction after placing the dry-ice bath on the cold finger at high pressure in a "dry" system, where essentially all the vapor was air. With the total pressure and the air pressure determined, the water vapor pressure in the sample was obtained by difference. The mole fraction of water in the vapor sample was calculated as the ratio of water partial pressure to the total pressure. When the pressure measurements were complete, the dry-ice bath was removed, and, by appropriate manipulation of valves, the vapor sample was pumped directly into the condenser chamber. The valves were then returned to their normal operating position for pressure monitoring. This procedure was believed to result in more rapid equilibration of the system following a composition measurement.

Mass Transfer Coefficients—Closure resistance at given mean pressure was determined by measuring the average pressure difference across the closure during sublimation of a known quantity of ice at constant chamber pressure. The mean pressure, $\bar{P}$, is the mean of the vial pressure and chamber pressure over the time interval of the experiment. The mean sublimation rate was calculated from the mass of ice sublimed and the time required for sublimation. The closure resistance was then obtained from Eq. 3. Similarly, the chamber resistance was evaluated from the chamber pressure, P_c, pressure in the condenser chamber, P_{cd}, and the total sublimation rate (all vials), $N \cdot \dot{m}$, using Eq. 4. Since both chamber and closure resistance measurements are sensitive to small pressure measurement errors (the pressure differences were small), care was taken to ensure that the pressure sensors (M1 and M2, Fig. 1) gave the same reading when connected to the same source, and a number of replicate experiments were made at each mean pressure to obtain the final data sets.

Heat Transfer Experiments—Two types of vial heat transfer experiments were performed. Experiments where data were collected on a single vial over a wide range of shelf temperatures and chamber pressures in a single experiment were denoted "single vial experiments." Experiments designed to measure both the mean heat transfer coefficient for a set of nominally identical vials and their corresponding standard deviation in heat transfer coefficients were referred to as "multivial experiments." All experiments, except those multivial experiments that used larger vials, were carried out using a full shelf

[5] Virtis Unitrap.
[6] Determined by adjusting the emissivity control on a hand-held optical pyrometer until the temperature readout of the instrument agreed with the thermocouple-measured surface temperature of the shelf.
[7] Cajon Ultra Torr Union; Cajon Co., Solon, Ohio.
[8] MKS Model 220 Baratron; MKS Instruments, Inc., Burlington, Mass.
[9] Esterline Angus Speed Servo II.
[10] REPP; Virtis Co.
[11] Kontes Glass Co., Vineland, N.J.
[12] The vapor pressure of ice at −78°C is only 0.6 μm.

Table III—Vapor Composition in Freeze-Drying [a]

Rate Per Vial, g/h	Shelf Temp., °C	Chamber Pressure, mm Hg	Mole Fraction of H_2O [b] Vial	Chamber
		Pure H_2O [c]		
0.23	−16	0.068	0.94	0.78 ± 0.08
0.26	−16	0.490 [d]	0.96	0.89
0.52	+12	0.093	0.96	0.78 ± 0.04
0.90	+12	0.493 [d]	0.97	0.94
		Mannitol, 50 mg/mL		
0.16	−21	0.045	0.85	0.78
0.22	−21	0.127 [d]	0.92	0.90
0.33	−21	0.228 [d]	0.95	0.92
0.42	− 6	0.232 [d]	0.95	0.93

[a] Full load of 60 vials (2.4 cm o.d.) in the laboratory freeze-dryer. [b] Estimated uncertainty ± 0.02 unless specifically indicated otherwise. [c] Mean of four replicate experiments. [d] Controlled air leak into the drying chamber.

of vials in the laboratory dryer. In both types of experiments, a small precision bore stainless steel tube (length 1.497 cm, 0.217 cm i.d.) was inserted in each stopper, and the stopper was inserted fully into the vial neck[13]. This procedure accomplished several purposes:

1. The pressure difference across the closure, which was needed to evaluate the sublimation rate in a single vial experiment, was increased over that found with stoppers in the usual semistoppered position, thereby decreasing the relative error in the pressure difference measurement.

2. The closure resistance was fixed by the geometry of the tube and the chamber pressure and, therefore, was not subject to variation arising from slight variations in stopper placement or geometry. Uniformity in resistance to mass transfer in a set of vials is critical when the standard deviation in heat transfer coefficient is measured.

The resistance of the metal tube used with the modified vial (Fig. 1) was determined as a function of mean pressure by a procedure identical to that used to determine closure resistance. The tube resistance, R_{TB}, is given by:

$$R_{TB}^{-1} = 0.2478 + 1.944\,\bar{P} \qquad \text{(Eq. 17)}$$

where $\bar{P}$ is $(P_v + P_c)/2$, and the numerical coefficients are a result of regression analysis of four data points over a range of $\bar{P}$ from 0.2 to 0.5 mm Hg, yielding a correlation coefficient of 0.9965. The numerical coefficients were in satisfactory agreement with the corresponding coefficients calculated strictly from theory[14].

A fill volume equivalent to a liquid depth of ~2 cm was used for all heat transfer studies. With pure water, a redistribution of ice within the vial occurred such that ice near the vial wall and ice near the thermocouple wire was preferentially removed. As a result of this phenomenon, measurements of temperature distribution in the ice had to be completed early in the experiment, before the assumption of a planar ice-vapor interface was seriously violated. Accurate temperature distribution data was obtained until ~15% of the ice had been removed. The vial heat transfer coefficient is defined assuming the ice at the vial bottom is in good thermal contact with the glass. Normally, with vials filled with pure water, partial loss of thermal contact occurs after sublimation of 35–50% of the ice. Thus, duration of a heat transfer experiment is limited to a time corresponding to sublimation of ~25% of the ice. Loss of thermal contact is rarely a problem when a frozen solution is dried.

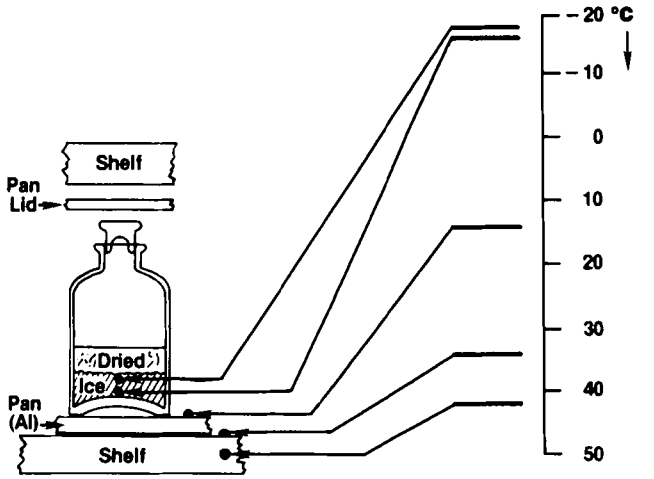

Figure 4—*Temperature profile in primary drying using dobutamine hydrochloride–mannitol (1:1) (10 mL) in 5304 molded vials (8.3 cm²) in an aluminum tray; heat flux = 42 cal/cm²·h, chamber pressure 0.10 mm Hg.*

[13] Experiments with the 5304 vials represented our first attempt at heat transfer coefficient measurement and used 13-mm freeze-drying stoppers in the semistoppered position.

[14] Using the theoretical relationships for gas flow in tubes (5), the resistance of the tube, in mm Hg·h/g, is given in terms of the tube cross-sectional area, A, tube radius, a, and tube length, l, by $R_{TB}^{-1} = [150 \cdot A\,(a/l)]/[1 + 8/3\,(a/l)] + 7965A\,(a^2/l)\bar{P}$. Substitution of the measured values of a and l (in cm) gives $R_{TB}^{-1} = 0.338 + 2.329\,\bar{P}$. While the agreement between theory and experiment is not quantitative, uncertainty in the measured value of a and uncertainty in the experimental coefficients could account for the difference.

Table IV—Evaluation of Heat Transfer by Top Radiation: Effective Emissivity, e_v

Product	N	A_v	$e_v \pm \sigma_m$
H_2O	7	4.71	0.83 ± 0.04
H_2O	3	6.83	0.94 ± 0.02
H_2O	3	17.2	0.79 ± 0.03
KCl (l = 0)	2	4.71	0.88
KCl (l = 0.3)	1	4.71	0.97
KCl (l = 0)	1	20.8	0.58
KCl (l = 0.2)	1	20.8	0.80
Mean			0.84

For single vial heat transfer studies, a representative vial from a given lot of vials was modified as shown in Fig. 1. After filling, normally with pure water, the modified vial and other vials of the same lot, all equipped with "identical" metal tubes, were loaded into the laboratory dryer, the liquid was frozen, and the chamber was evacuated. The procedure then involved a series of heat transfer measurements under steady-state conditions at selected shelf temperatures and chamber pressures. An operational definition of steady state is taken as constant temperatures (±0.2°C) and pressures (±2 μm) for a period of 10–15 min. The sublimation rate, $\dot{m}$, is calculated from the observed steady-state pressure readings using Eq. 3 with the closure resistance given by the tube resistance, Eq. 17. The heat transfer rate, $\dot{Q}$, is then calculated:

$$\dot{Q}\ (\text{cal/s}) = 0.1833\dot{m}\ (\text{g/h}) \qquad \text{(Eq. 18)}$$

where 660 cal/g is used for the heat of sublimation (8).

The first shelf temperature setting was adjusted to be equal to the ice temperature at the vial bottom. Heat transfer from the shelf to the vial was zero, and any residual heat transfer was due to radiative heat transfer from the dryer lid and/or possible contributions from conduction through the thermocouple wires and the pressure measurement tube (I, Fig. 1). Normally, shelf temperature settings of −10°C, 5°C, and 25°C were used in the balance of the experiment with four chamber pressures studied at each shelf temperature. The first pressure setting was the minimum pressure attainable with the leak valve closed (0.05–0.10 mm Hg). Higher pressures (0.2, 0.4, and 0.6 mm Hg) were obtained by manual adjustment of the controlled-leak valve (P, Fig. 1).

The advantages of the single vial experiment were that, during one ~6-h experiment, heat transfer could be studied over a wide range of shelf temperatures and chamber pressures, and the effect of radiation from the dryer lid could be directly measured. Since this procedure characterized the heat transfer for only one vial in a given experiment, the procedure was not designed to examine the variation in the heat transfer coefficient in a set of nominally equivalent vials. Moreover, it is difficult to select a "typical" vial and, even if this selection is successful, the presence of the pressure measurement tube makes it difficult to place the vial absolutely flat on the shelf with no downward force on the vial. Even a slight tilt of the vial would have decreased the area of actual contact between the glass and the shelf and would, therefore, decrease the contact conduction term, K_c (Eq. 9). The value of the separation distance, l (Eq. 10), may also be increased. Conversely, good contact with an excessive downward force on the vial may actually increase the value of K_c over that characteristic of a free-standing vial (9). Thus, particularly for the smaller vials where the contact problems were most severe, the single vial procedure was not the method of choice for determining the heat-transfer coefficient of an average vial in normal contact with the shelf.

Single vial data are, however, an accurate representation of the heat transfer for the vial used and the degree of vial–shelf contact experienced in the experiment performed. Thus, single vial data were used to efficiently and accurately investigate various assumptions in the defining equation for vial heat transfer coefficients (Eq. 8), to verify the theoretical form of the pressure dependence of K_v (Eqs. 9, 10), to characterize radiative heat transfer from the dryer lid, and to determine the effective thermal conductivity of the product (Eq. 15).

The equation defining the vial heat transfer coefficient, Eq. 8, assumes the

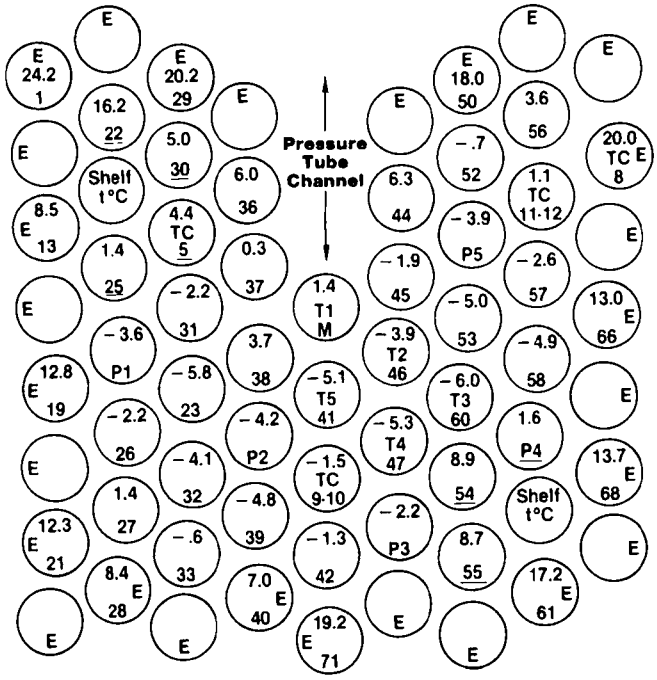

Figure 5—*Vial placement on the shelf and mean percent deviations in sublimation rates for components of the variance study. (See* Appendix I *for discussion.)*

temperature of the surface above the vials is the same as the temperature of the surface upon which the vials rest. While this assumption is valid for most freeze-dryers, the surface above the vials in the laboratory dryer (Fig. 1) was the chamber lid, which was not temperature controlled. Thus, the calculation of K_v from heat transfer data accumulated on the laboratory dryer involves a correction for the atypical radiative heat transfer from the dryer lid to the top of the vials. The heat transfer rate, $\dot{Q}$, for vials in the laboratory dryer may be written:

$$\dot{Q} = A_v(K_c + 1.10^{-4}e_s + K_g)(T_s - T_b) + A_v e_v \sigma(T_L^4 - T^4) \quad \text{(Eq. 19)}$$

where T_L is the lid temperature and T is the temperature of the subliming ice. The effective emissivity for top radiation (e_v) is assumed to be a property of the vial only. Thus, to convert heat transfer data from the laboratory dryer to K_v data defined by Eqs. 8 and 14, e_v must be evaluated.

Data for e_v were generated by using the single vial procedure and adjusting the shelf temperature so that $T_s = T_b$. Under these conditions, the heat transfer was due to the top radiation term only, and e_v data may be evaluated by determining $\dot{Q}$, T_L, and T. The value of T_L is obtained by direct measurement, $\dot{Q}$ is determined from P_v and P_c as outlined earlier, and T is calculated using one of the following procedures. When pure ice is in the vial, the resistance to mass transfer between the sublimation interface and the chamber is almost entirely due to the metal tube in the closure. The pressure in the vial, P_v, is essentially equal to the equilibrium vapor pressure of the subliming ice, and the temperature of the subliming ice, T, may be evaluated from the measured P_v data[15]. However, when a solution is freeze-dried, the vial pressure is much less than the equilibrium vapor pressure of ice, and the value of T is calculated using the measured product temperature near the sublimation interface[16].

Multivial heat transfer studies were used to determine the mean vial heat transfer coefficient as a function of pressure as well as to obtain the standard deviation in heat transfer coefficients for a set of nominally equivalent vials. All vials investigated were filled with pure water to a depth of ~2 cm, and each vial was weighed (±0.2 mg). After loading and freezing, the shelf temperature

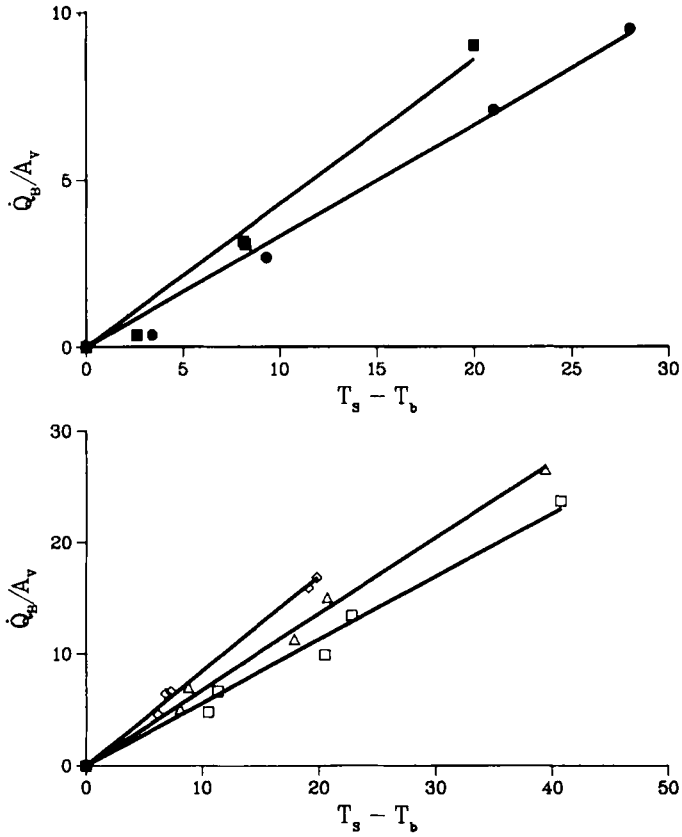

Figure 6—*Proportionality between heat transfer rate and temperature difference. Key: 5303 vials, (●) 0.1 mm Hg and (■) 0.2 mm Hg; W5800 vials, (□) 0.2 mm Hg, (△) 0.4 mm Hg, and (◇) 0.6 mm Hg.*

(and product temperature) were adjusted to the expected steady-state sublimation temperature for that experiment, and the chamber was quickly evacuated to the desired chamber pressure by manual adjustment of the leak valve. Once the pressure decreased below ~1 mm Hg and sublimation began, the shelf temperature was quickly increased to +5°C. The entire experiment was conducted under conditions of constant shelf temperature (5°C) and constant chamber pressure. After ~2 g of ice was sublimed, the dryer was vented, and each vial was weighed to obtain the mass loss for each vial. The average sublimation rate for each vial is calculated as the mass loss divided by the time period of sublimation. Calculations of the heat transfer coefficients and the corresponding standard deviation from the raw sublimation rate and temperature data are described in *Appendix I.*

RESULTS AND DISCUSSION

Closure Resistance—Two types of closures of similar design were studied. The smaller closure was designed for use with vials that had 13-mm o.d. necks, while the larger closure was used with vials that had 20-mm o.d. necks. Both closures had two openings in the semistoppered position with effective diameters of 0.2 cm for the 13-mm size and 0.4 cm for the 20-mm size. The experimental data (Fig. 2) demonstrate that the reciprocal of closure resistance is a linear function of mean pressure, as expected (Eq. 7). The mean pressure is the mean of the vial and chamber pressures. Each point is the mean of at least two replicate experiments, while the solid lines represent smoothed data from Eq. 7 with the coefficients determined by regression analysis:

$$R_s^{-1} = 2.3 + 22.4\bar{P} \text{ (13 mm)} \quad \text{(Eq. 20)}$$

$$R_s^{-1} = 4.8 + 169\bar{P} \text{ (20 mm)} \quad \text{(Eq. 21)}$$

The resistance of the 13-mm closure was roughly a factor of 5 higher than the 20-mm closure at corresponding pressures over the pressure range normally encountered in practice, a ratio close to that predicted theoretically[17]. The

[15] The vapor pressure of ice, in mm Hg, as a function of absolute temperature (8), may be expressed as $\ln P = -6144.96/T + 24.01849$.

[16] Although we cannot directly measure temperature at the sublimation interface, the temperature variation within the product is negligible between locations where temperature is measured (Fig. 1); thus, both methods of determining T should yield the same result when the product is pure water. However, we find that the value of T determined from P_v is systematically ~1.8°C lower than the corresponding measured product temperature. Evidently, a temperature gradient exists very near the sublimation surface, at least when the sample is pure water. However, a temperature error of 1.8°C produces an error in e_v of only 0.03, so even if the same error is present with a solution, the error introduced into the e_v data is slight.

[17] If each closure opening is approximated as a tube of radius a and length l, the same equation used to calculate resistance of the metal tubes[14] may be used to estimate the coefficients in Eq. 7. The estimated values of a and l are $a = 0.2$ cm, $l = 0.4$ cm (20 mm) and $a = 0.1$ cm, $l = 0.3$ cm (13 mm). Thus, the theoretical equivalents of Eqs. 20 and 21 are $R_s^{-1} = 1.7 + 17\bar{P}$ (13 mm) and $R_s^{-1} = 8.1 + 200\bar{P}$ (20 mm).

Table V—Vial Heat Transfer Coefficients for 10-mL Vials (A_v = 4.71 cm²) in Laboratory Dryer

Experiment	Vial	Chamber Pressure, mm Hg	Mean $\dot{m}$, g/h	$\hat{\sigma}(\dot{m})$, %	$10^4 K_v$, cal/s·cm²·°C	$\sigma(K_v)$, %
			Polished Stainless Steel Shelf Surface			
R[a]	W5800	0.2	0.3782	4.5	6.19	5.1
1[b]	W5800	0.1	0.3472	3.7	4.89	2.0
1[b]	K5800	0.1	0.3727	4.8	5.45	5.2
2[b]	W5800	0.2	0.4061	3.3	6.10	2.1
2[b]	K5800	0.2	0.4339	4.2	6.78	4.7
3[b]	W5800	0.4	0.4509	3.9	7.89	4.6
3[b]	K5800	0.4	0.4824	4.5	8.83	6.1
4[b]	W5800	0.1	0.3440	4.0	4.79	2.8
4[b]	W5811	0.1	0.3632	3.9	5.21	2.9
5[b]	W5800	0.2	0.4051	3.9	6.17	3.8
5[b]	W5811	0.2	0.4335	4.1	6.86	4.4
6[b]	W5800	0.4	0.4508	3.2	7.69	2.8
6[b]	W5811	0.4	0.4849	3.0	8.65	2.4
			Painted Black Shelf Surface			
7[c]	W5811	0.2	0.4451	4.7	7.43	6.1

[a] Mean data from six replicate experiments; N = 36, A = 5; SD in calculated $10^4 \times K_v$ is ±0.14; N is the total number of vials in the sample and A is the number of vials located adjacent to a shelf temperature sensor (see *Appendix I* and Fig. 5). [b] N = 15, A = 6. [c] N = 35, A = 12.

intercept (Fig. 2) at $P = 0$ represents the contribution of Knudsen flow, and the ratio R_s^{-1} ($P = 0$) to R_s^{-1} at any given pressure represents the relative contribution of Knudsen flow to the total vapor flow at that pressure. Thus, at >0.03 mm Hg for the 20-mm closure and >0.1 mm Hg for the 13-mm closure, Knudsen flow was <50% of the total flow, and the flow mechanism became predominantly viscous flow or bulk-fluid flow.

Chamber Resistance—The reciprocal of the chamber resistance of the laboratory dryer is a linear function of the mean pressure (the mean of the chamber and condenser pressures) within the precision of the data (Fig. 3). Each data point is the mean of at least two, and usually more than four, replicate experiments. The solid line gives the best fit of the data to Eq. 7 with $a_0 = 320 \pm 230$ and $a_1 = 4960 \pm 650$, where the uncertainty represents the standard error in the coefficient. As with closure resistance, the intercept (Fig. 3) at $P = 0$ represents the contribution of Knudsen flow while the ratio R_c^{-1} ($P = 0$)/R_c^{-1} gives the relative contribution of Knudsen flow to total vapor flow. Due to the considerable uncertainty in the experimental value of a_0, it is not possible to make a definitive comment on the relative contribution of Knudsen flow.

Assuming that the chamber resistance is due entirely to the tube separating the chamber from the condenser, theoretical values of a_0 and a_1 may be calculated[14]: a_0 = 124 and a_1 = 28,639. While the experimental and theoretical values of a_0 agree within the uncertainty in the data, the experimental value of a_1 is a factor of ~6 less than the theoretical estimate. Thus, the pressure-dependent term in R_c^{-1}, which is due to the viscous flow mechanism, was much smaller than expected, and the resistance to viscous flow in the laboratory dryer appeared to be anomalously high.

Since the chamber resistance depends on the dryer dimensions, the chamber resistance of a production scale dryer obviously will be much less than the chamber resistance of the laboratory dryer. However, the total resistance to flow from a given vial (Eq. 6) depends on the scaled chamber resistance, NR_c, where N is the number of vials in the dryer. The pressure drop between chamber and condenser for a given sublimation rate per vial depends on the scaled chamber resistance (Eq. 4). If the laboratory dryer is a satisfactory model for a production scale dryer, the scaled resistances should be comparable for the two dryers. Although sparse, the production data available suggest that at a mean pressure of 0.1 mm Hg, the scaled chamber resistance (N = 30,000) is ~0.05 mm Hg·h/g, while the corresponding scaled resistance for the laboratory dryer (N = 70) is 0.086 mm Hg·h/g.

Comparison of Resistances—Using the data presented in Figs. 2 and 3 and dried product resistances generated from vial data in a previous study (3), the resistance to passage of water vapor from the sublimation surface in a given vial to the condenser chamber may be calculated for each barrier: dried product, closure, and chamber–condenser pathway. The mean pressures needed to evaluate closure and chamber resistances are evaluated by solving Eqs. 1, 3, and 7 or Eqs. 1, 4, and 7, with 0.1 mm Hg as the chamber pressure.

The dried-product resistance was the dominant resistance, accounting for nearly 80% of the mass transfer resistance even when the small (13-mm) closures were used (Table II). Closure and chamber resistances were of the same order of magnitude, the chamber resistance was less than the resistance of a 13-mm closure, but greater than the resistance of a 20-mm closure.

Vapor Composition—The gas present in the vial and the chamber was mostly water vapor under all conditions studied (Table III). Even when the chamber pressure was increased by a controlled air leak, the vapor in the chamber was predominantly water. These observations, which are in qualitative agreement with literature data (10), are a direct result of the low pumping speed of the system for air relative to the pumping speed for a considerable vapor (H_2O). An air leak increases the total pressure in the condenser chamber (mostly air) and, because the chamber pressure is related to the condenser pressure by Eq. 4, the chamber pressure also increases. However, even with an air leak sufficient to increase the condenser pressure significantly, the molar flow rate of air is still much smaller than the molar flow rate of water vapor, and the chamber gas is, therefore, predominantly water. Thus, as a first approximation, the heat conductivity parameters Λ_0 and λ_0 (Eq. 10) refer to water vapor.

Temperature Profile in Primary Drying—A temperature profile measured during primary drying in the pilot dryer is illustrated by Fig. 4. In this experiment, the vials were placed in an aluminum tray with a flat 5-mm thick bottom and a tray lid containing open channels for vapor passage. Only the middle shelf was used. The temperature data (Fig. 4) refer to mean temperatures recorded at 50% completion of primary drying, and the heat transfer rate is the average heat transfer rate calculated from the total amount of ice sublimed and the primary-drying time.

Heat transfer may be described in terms of four barriers or resistances to heat flow: (*a*) the shelf itself, with a temperature difference of 8°C between the shelf interior and the shelf surface; (*b*) the pan or tray, with a temperature

Table VI—Vial Heat Transfer Coefficients for 20-mL Vials (A_v = 6.83 cm²) in Laboratory Dryer[a]

Experiment	Vial	Chamber Pressure, mm Hg	$\dot{m}$, g/h	$\hat{\sigma}(\dot{m})$, %	$10^4 K_v$, cal/s·cm²·°C	$\sigma(K_v)$, %
1	W5816	0.068	0.3664	3.4	3.47	4.0
1	K5816	0.068	0.3875	3.5	3.79	4.2
2	W5816	0.100	0.4209	3.2	4.22	3.8
2	K5816	0.100	0.4503	4.0	4.69	5.1
3	W5816	0.200	0.4879	3.0	5.40	3.6
3	K5816	0.200	0.5285	4.0	6.14	5.5
4	W5816	0.400	0.5520	2.3	6.89	2.4
4	K5816	0.400	0.6113	3.2	8.18	4.4
5	K5816	0.400	0.6159	4.7	8.13	6.9

[a] Polished stainless steel shelf. A = 0; N = 14 (K5816), N = 13 (W5816); see Table V footnote *a* for definitions of A and N.

Table VII—Vial Heat Transfer Coefficients for 100-mL 5303 Vials (A_v = 17.2) in Pilot Dryer [a]

Experiment	Chamber Pressure, mm Hg	$\dot{m}$, g/h	$\hat{\sigma}(\dot{m})$, %	$10^4 K_v$, cal/s·cm²·°C	$\sigma(K_v)$, %
1	0.100	0.5342	4.1	3.1	3.0
2	0.200	0.7470	4.0	4.2	3.3
3	0.200	0.7968	3.0	4.6	1.7
4	0.400	0.7696	4.2	5.0	3.8

[a] Both W5303 and K5303 vials gave the same mean K_v (within 0.2%), and $\hat{\sigma}(\dot{m})$ is essentially the same for the pooled data set as for each data set considered individually.

difference of 20°C between the shelf surface and the top surface of the tray bottom; (*c*) the vial, with a temperature difference of 30°C between the pan surface and the product in the bottom of the vial; and (*d*) the frozen product, with a temperature difference of ~2°C between the ice at the vial bottom and the ice at the sublimation interface. The thermal resistance of a barrier may be defined as the ratio of temperature difference across the barrier and the area-normalized heat flow (4). Thus, the largest thermal resistance (50%) is the vial-tray interface, but both the tray-shelf interface and the shelf itself contribute significantly to the total resistance, 33.3 and 13.3%, respectively.

As defined here, the thermal resistance of the vial includes the thermal resistance of the glass in the vial bottom. Likewise, the tray resistance includes the thermal resistance of the aluminum in the tray bottom. However, as shown by Nail (4), the thermal resistance of the metal in an aluminum tray bottom is essentially zero. Therefore, the tray resistance is due to the tray-shelf interface resistance. The thermal resistance of the glass, even for molded vials where the glass is several millimeters thick, is generally less than the thermal resistance of the frozen product (4), and the vial thermal resistance is nearly all due to the tray-vial interface resistance. In Fig. 4, the thermal resistance of the glass (3.5 mm thick) is ~5% of the defined vial resistance and <3% of the total thermal resistance. For tubing vials, the glass thickness is usually ~1 mm, and the corresponding contribution of the glass to thermal resistance is even less. Consequently, the thickness of the glass is not a significant factor in vial heat transfer and the usual variations in glass thickness may be ignored.

Heat transfer coefficients for the tray, K_{TR}, and the shelf itself, K_S, may be defined by equations analogous to the defining equation for vial heat transfer coefficients (Eq. 8). Theoretically, the tray heat transfer coefficient may be described as a sum of contact, radiation, and gas conduction terms (Eq. 9), where the gas conduction term depends on pressure in the same manner as the corresponding term in the vial heat transfer coefficient (Eq. 10). For the aluminum tray studied, the tray temperature is uniform throughout the tray bottom, and the calculated value of $K_{TR} = 5.8 \times 10^{-4}$ cal/s²·cm²·°C at 0.1 mm Hg. Similar measurements with a stainless steel tray of the same geometry, but with a warped bottom (with ~4 mm maximum distance between the shelf and the tray bottom) showed significant tray temperature differences (≈5°C) between zones over a maximum warp and zones near a shelf-tray contact point. The mean tray heat transfer coefficient at 0.1 mm Hg is 3.3×10^{-4} cal/s·cm²·°C, but in a zone of maximum warp, the coefficient decreased to 2.4×10^{-4} cal/s·cm²·°C.

The shelf heat transfer coefficient, K_S, calculated from the temperature difference between shelf interior and shelf surface (Fig. 4) is 1.5×10^{-3} cal/s·cm²·°C. The reciprocal of K_S is the thermal resistance for flow of heat from the shelf interior to the surface and probably represents a combination of limited fluid flow through the shelf interior and a finite thermal conductivity of the shelf material itself. Thus, the shelf heat transfer coefficient is expected to be independent of chamber pressure and is probably quite sensitive to dryer design.

Vial Heat Transfer: Radiation Effects/Driving Force for Heat Flow—*Contribution of Radiation*- The parameter, e_v, represents the effect of radiation heat transfer from the surface above the vials. The e_v data obtained (Table IV) show no systematic trend as the vial size (value of A_v) increased[18]. The experiments with potassium chloride were carried out to determine whether the development of a dried-product layer above the sublimation interface would act as a thermal barrier and reduce the heat transfer *via* top radiation. Thus, measurements of e_v were made at the beginning of sublimation where the dried-product thickness, l, is essentially zero, and later in the same experiment after a dried product layer developed ($l > 0$). The data clearly do not show a decrease in e_v as l increases; indeed, there appears to be a small increase in e_v as l increases, a result for which we cannot offer a reasonable interpretation. In summary, the data appear to be adequately interpreted in terms of a value of e_v equal to 0.84, independent of vial size and thickness of the dried-product layer.

The definition of the vial heat transfer coefficient assumes the vial is completely surrounded by other vials. Clearly, this assumption is not valid for those vials forming the perimeter of a group of vials. Such "edge" vials may show a significantly higher sublimation rate than "interior" vials due to radiative heat transfer from the surface facing the vial perimeter. The additional heat transfer rate for edge vials, $\Delta\dot{Q}_E$, may be written:

$$\Delta\dot{Q}_E = A_c e_E \sigma (T_w^4 - T_b^4) \qquad \text{(Eq. 22)}$$

where A_c is the vial area exposed to the extra radiation effects, taken as one-half the cylindrical area of the vial, T_w is the absolute temperature of the heat source (*i.e.*, the chamber wall), and T_b is the absolute temperature of the product. The parameter, e_E, denotes the effective emissivity for radiative heat transfer between the edge vial and the heat source. Numerical analysis[19] of the experimental data (Appendix I; Fig. 5) yields, $e_E = 0.21$. Since edge vials are atypical, edge vial data are excluded from heat transfer data analysis.

Proportionality Between Heat Transfer Rate and Temperature Difference—The definition of the vial heat transfer coefficient assumes that the heat transfer rate is proportional to the temperature difference between the shelf surface and the temperature in the product at the bottom of the vial (Eq. 8). Thus, the driving force for heat flow is taken as the temperature difference, $T_s - T_b$. The corresponding assumption for heat transfer in the laboratory dryer is a direct proportion between heat transfer rate from the shelf, denoted $\dot{Q}_B$, and the same temperature difference. The value of $\dot{Q}_B$ is obtained from the total heat transfer rate by subtraction of the top radiation contribution. The top radiation contribution is calculated using the term in Eq. 19 involving e_v with $e_v = 0.84$. Data are obtained at constant pressure as a function of $T_s - T_b$ by varying the shelf temperature in single vial studies. Representative results for two types of vials are shown in Fig. 6 at selected chamber pressures. As expected, $\dot{Q}_B$ is directly proportional to $T_s - T_b$ within the uncertainty in the data. Further, the slopes of the plots were observed to increase as the chamber pressure increased, which is consistent with the expected increase in conduction through the vapor phase as pressure increases.

Vial Heat Transfer Coefficients *Phenomenological Results*—The results of the multivial studies (Tables V-VII) are identified by experiment number (first column), vial type (second column), and chamber pressure (third column). In general, two vial types were studied in the same experiment, thereby providing greater accuracy for the comparison of K_v between the two vial samples under identical conditions. Thus, while the precision in K_v for a given set of vials is ± ~2%, as measured by the standard deviation in a series of replicate experiments (laboratory dryer), the ratio of K_v data for the two sets of vials is precise within ± ~0.5%.

The vial number (*e.g.*, 5800) defines the vial specifications while the letter (*i.e.*, W or K) defines the supplier. Thus, although W5800 and K5800 vials are nominally identical, vial heat transfer coefficients for K5800 vials are significantly higher than K_v for W5800 vials at corresponding pressures (Table V). For the 5800 vials studied, the K_v ratio is 1.115, independent of pressure within ±0.5%. The analogous K_v ratios for 5816 vials (Table VI) increases smoothly from 1.092 at 0.068 mm Hg to 1.187 at 0.4 mm Hg. Again, although both W5816 and K5816 vials are nominally identical, the K vials have significantly higher vial heat transfer coefficients than the W vials. Contrary to the K *versus* W bias found for tubing vials (5800 and 5816), the large molded 5303 vials studied show no supplier bias in K_v (footnote *a* in Table VII). The mean K_v values are identical, within ±0.2%, for K5303 and W5303 vials at corresponding pressures.

The mean K_v data reported are evaluated using a finite number of vials

[18] If a significant amount of heat were conducted down the thermocouple wires or through the pressure measurement tube, a term in Eq. 19, independent of vial area, would be needed. The experimental value of e_v would include a term inversely proportioned to A_v, which would then result in the measured e_v data decreasing as A_v increases. Regression analysis of all the pure water data (13 experiments) gives: $e_v = 0.82 + 0.14/A_v$, with a correlation coefficient of 0.10. Thus, heat conduction through the thermocouple wires (30-gauge) and/or the pressure measurement tube is small and may be ignored.

[19] Under the conditions of the experiment (*Appendix I*), the 15.0% sublimation rate bias between edge vials and interior vials yields $\Delta\dot{Q}_E = 0.0106$ cal/s. The W5800 vial is a cylinder of height ~4 cm and radius 1.22 cm. The observed value of T_b is 254.7 K. Since the shelf is actually a shallow box with a height of 1 cm, the heat source is the shelf, 275.5 K, for the first 1 cm of vial height and is the chamber wall, 288 K, for the remaining 3 cm of vial height. Thus, $\Delta\dot{Q}_E = \pi(1.22)e_E \cdot \sigma[1\cdot(275.5^4 - T_b^4) + 3\cdot(288^4 - T_b^4)]$, and the calculated value of e_E is 0.21.

Table VIII—Vial Heat Transfer Parameters[a] with Accommodation Coefficient, a_c, of 0.67 and Effective Top Emissivity, e, of 0.84

Vial	Contact Parameter 10^4K_c	Separation Distance (l), cm
W5800[b]	1.24 ± .08[e]	0.0471 ± 0.0018[e]
K5800[b]	1.70 ± 0.11	0.0396 ± 0.0021
W5811[b]	1.58 ± 0.11	0.0395 ± 0.0021
W5816[b]	0.63 ± 0.08	0.0513 ± 0.0024
K5816[b]	0.87 ± 0.08	0.0372 ± 0.0013
5303[c]	0.4 ± 0.4	0.090 ± 0.028
5304[d]	0.7 ± 0.2	0.067 ± 0.008

[a] Parameters evaluated using heat conductivity values for pure water taken from the literature (5, 11): $\Lambda_0 = 6.34 \cdot 10^{-3}$ cal/s·cm²·°C·mm Hg; $\lambda_0 = 4.29 \times 10^{-5}$ cal/s·°C·cm. [b] Data from multivial studies (Tables V and VI). [c] Datum is mean of the multivial study ($10^4K_c = 0 \pm 0.6$, $l = 0.103 \pm 0.040$) and the single vial study ($10^4K_c = 0.8 \pm 0.1$, $l = 0.078 \pm 0.009$). [d] Datum from the single vial studies with two vials. [e] Uncertainty given is the standard error of the parameter as given by the MLAB program output and does not reflect absolute error. The value of K_c is sensitive to the choice of a_c and also depends on the mathematical form chosen for K_g.

(normally ~15) randomly selected from one lot of vials. Thus, the reported K_v value is an accurate representation of the mean of the lot within a standard error, $\sigma(K_v)/\sqrt{N}$, where N is the number of vials studied. Using the $\sigma(K_v)$ data reported, the corresponding standard error in the K_v ratio between K vials and W vials averages ~1.5%. Therefore, the K_v ratios calculated from the reported data are an accurate representation of the lots studied, within ~1.5%, and probably reflect differences in geometry of the vial bottoms (Table I). Vial heat transfer data for different lots from the same supplier are needed to verify that the lots investigated in this study are typical of the total output from a given supplier. At present, such data are not available, but the differences in vial bottoms noted in Table I appear to be consistent, suggesting that the K_v ratios determined in this study do indeed indicate a supplier difference rather than a lot-to-lot variation within a given product.

The differences in K_v between K and W vials are of no practical significance in freeze-drying, as long as vials from only one supplier are used for a given product. A slightly lower K_v simply requires a slightly higher shelf temperature in the freeze-drying process. The supplier bias is particularly important if circumstances can arise where both K and W vials are used for the same pharmaceutical product lot. Since the K *versus* W bias in K_v is significantly greater than nonuniformity in K_v for a given vial type, measured by $\sigma(K_v)$, a significant increase in nonuniformity of heat input would result whenever both K and W vials are used in the same freeze-drying run. The consequence could well be a large product loss arising from collapse or eutectic melt, although the severity of the problem encountered would depend on both the nature of the product and the process design.

The relative standard deviation in K_v, $\sigma(K_v)$, is a measure of the uniformity of heat transfer coefficients within a given lot of vials. Since the $\sigma(K_v)$ data are based on data from a relatively small number of vials (~15), one expects a sizable uncertainty in a given value of $\sigma(K_v)$[20]. Based on the differences in $\sigma(K_v)$ between replicate experiments (Tables V–VII), the uncertainty (SD) in a reported value of $\sigma(K_v)$ is ~1.2%.

While the $\sigma(K_v)$ data are only semiquantitative, several generalizations appear valid. First, all vial types have a surprisingly uniform heat transfer coefficient; the average value of $\sigma(K_v)$ is only 4%. Second, the uniformity in K_v is systematically slightly better for W tubing vials than for the corresponding K vials (Tables V and VI). The data for 5800 and 5816 vials show a mean $\sigma(K_v)$ of 3.4 ± 0.3% for W vials, while the corresponding value for K vials is 5.3 ± 0.3%. The uncertainties given are standard deviations of the means. Third, while a small but significant pressure dependence in $\sigma(K_v)$ could be obscured by the scatter of the data, the data are not consistent with a pressure dependence of more than a factor of ~2 over the pressure range studied. The pressure dependence in $\sigma(K_v)$ will be addressed later from a theoretical point of view.

While histograms constructed from the sublimation rate data do appear consistent with a normal distribution of K_v data in a set of vials, the data available are not sufficient for a critical test. Experiments involving a very large number of vials in a freeze-dryer with no significant position effects would be needed for a definitive study of the distribution function. Thus, one should exercise caution in assuming a normal distribution for the vial heat transfer coefficients.

Mechanisms of Heat Transfer—In principle, the contribution of each of the parallel mechanisms of heat transfer from shelf to vial may be evaluated by regression analysis of K_v data as a function of pressure using the mathematical model defined by Eqs. 9–11 and 14. The zero pressure intercept of K_v *versus* pressure defines the sum of the radiative and the contact conduction contributions. The radiative contribution (Eq. 14) is evaluated independently by evaluation of the effective emissivity for top radiation, $e_v = 0.84$ (Table IV), and by measurement of the emissivity of the shelf surface (0.28 for polished stainless steel, 0.95 for painted black shelf). The contact contribution, K_c, is calculated from the zero pressure intercept of K_v and the calculated value of the radiative contribution, K_r. Both heat conductivity parameters, Λ_0 and λ_0, are available from the literature (5, 11). The gas conduction term, K_g (Eq. 10), is therefore determined by the accommodation coefficient, a_c (Eq. 11) and the effective mean separation distance between the bottom of the vial and the shelf, l. Thus, three parameters, K_c, a_c, and l, are determined by regression analysis of the data. However, the multivial K_v data set for any type of vial consists of K_v values at only three or four different pressures, which is insufficient data to evaluate the three parameters with acceptable accuracy. In theory (12), the accommodation coefficient is a function of the natures of the gas, the shelf surface, and the vial surface. The gas is independent of the vial studied, the vial surface is always glass, and, with the exception of one study with the pilot dryer, the shelf surface is polished stainless steel. Therefore, the accommodation coefficient is assumed to be a constant and is evaluated by simultaneous regression analysis of all data sets, where K_c and l are vial specific, but the accommodation coefficient is independent of the type of vial. Both single vial-generated data, fit to Eq. 19, and multivial data, fit to Eqs. 9–11 and 14, were used to determine the accommodation coefficient. Although single vial data may yield inaccurate values of K_c and l (see *Experimental Section*), these data are suitable for evaluation of the accommodation coefficient.

Table IX—Vial Heat Transfer: Comparison of Heat Transfer Mechanisms for Vials on a Polished Stainless Steel Shelf

Vial	Contribution to Heat Flow, % of Total					
	P = 0.1 mm Hg			P = 0.4 mm Hg		
	Radiation	Contact	Gas	Radiation	Contact	Gas
K5800	21	32	47	13	19	68
W5816	27	16	57	16	9	75
5303	32	11	57	22	8	70

Single vial heat transfer data for the 5303, W5816, W5800, K5800, and W5811 vials are well represented by the theoretical model (Eq. 19) with a single accommodation coefficient of 0.72 ± 0.07. The uncertainty given is the standard error provided by the MLAB[21] fit program. The data are the result of replicated experiments consisting of 132 data points at chamber pressures from 0.06 mm Hg to 0.6 mm Hg and at shelf temperatures from −15°C to 25°C. The computer fit provided 11 parameters, including the accommodation coefficient, with a relative SD in $\dot{Q}$ of 7.7%, which is within the anticipated

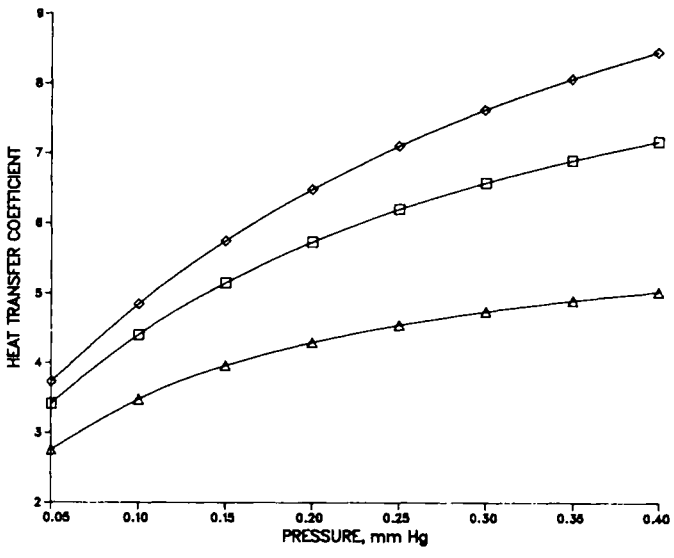

Figure 7—*Pressure dependence of vial heat transfer coefficients for selected vials. Key: (□) W5816, (◇) K5816, and (△) 5303.*

[20] The variance in a standard deviation estimate based on N measurements is approximately $\sigma^2/2N$ (14), where σ^2 is the variance in the measured quantity. Thus, the SD in $\hat{\sigma}(\dot{m})$ is $\approx \hat{\sigma}(\dot{m})/\sqrt{2N}$. Assuming that in the evaluation of $\sigma(K_v)$ from $\hat{\sigma}(\dot{m})$, the only uncertainty of consequence originates in the uncertainty in $\hat{\sigma}(\dot{m})$; numerical calculations give 1.6% for the average uncertainty (SD) in $\sigma(K_v)$.

[21] MLAB is a general purpose model fitting a computer program package available from the Division of Computer Research and Technology, National Institutes of Health, Bethesda, Md.

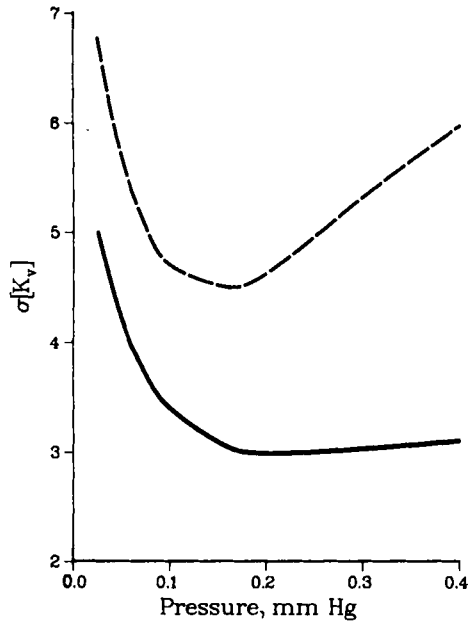

Figure 8—*Calculated pressure dependence of the relative standard deviation in vial heat transfer coefficients. Key: (—) mean of W tubing vials, and (- - -) mean of K tubing vials.*

experimental error. The multivial data set, consisting of 22 (K_v, P) data pairs, is also well represented by the theoretical model. Eleven parameters, including a single accommodation coefficient, $a_c = 0.62 \pm 0.05$, are obtained. The *SD* of the fit for 10^4K_v is ±0.10, which is within the precision of the data. The agreement between the single vial results and the multivial results for a_c is satisfactory, and the mean value, 0.67, is taken as the effective accommodation coefficient for vial heat transfer. When a_c is fixed at 0.67, and the regression analysis of single vial and multivial data are repeated, the quality of the fit obtained is essentially identical to that found when a_c is an adjustable parameter. The resulting K_c and l parameters are listed in Table VIII.

Since multivial data are generally a more accurate representation of the heat transfer characteristics of the mean of a set of vials, only multivial-derived parameters are listed for the tubing vials (5800, 5816, 5811). The parameters for the 5304 vials are derived from single vial studies with two "typical" vials since multivial results are not available. In general, K_v data from single vial studies are in satisfactory agreement with the correspondingly more accurate multivial data; the mean relative deviation in K_v is <6%. For the 5303 vials, the agreement between multivial and single vial data is less satisfactory, and this lack of agreement in K_v data is reflected in a comparison of the heat transfer parameters (K_c and l) obtained from the two data sets (Table VIII, footnote *c*). Moreover, the standard error in l derived from the multivial data is unusually large. Lacking a satisfactory explanation for these observations, the K_c and l parameters reported (Table VIII) for the 5303 vials represent means of the results of single vial- and multivial-derived parameters.

The values of l (Table VIII) correlate reasonably well with the l_{max} data from Table I, where l_{max} is the approximate maximum separation distance between the vial surface and a flat surface. Linear regression gives:

$$l = 0.023 + 0.273\, l_{max} \qquad \text{(Eq. 23)}$$

with a correlation coefficient of 0.958. The values of K_c might be expected to correlate with the ratio of the contact area to the total vial area, denoted f_c, where the contact area is calculated from the diameter and thickness of the contact print. As a rough approximation, $10^4K_c = 12f_c$, but the correlation coefficient is only 0.76.

The uncertainties given (Table VIII) are standard errors provided by the computer output and are a useful indication of uncertainty only when data in Table VIII are compared. The value of K_c is particularly sensitive to changes in a_c and may also depend on the mathematical form chosen for K_g. An increase of 0.05 in a_c results in a decrease in 10^4K_c of 0.20. With the mathematical form of K_g fixed by Eq. 10, the standard error in a_c is ± ~0.05, corresponding to an absolute uncertainty in 10^4K_c of ±0.2. Note, however, that if the value of a_c is really 0.72 instead of 0.67, all values of 10^4K_c in Table VIII decrease by 0.2. The mathematical form of K_g (Eq. 10) is derived for two surfaces separated by a constant distance, l. The separation distance between the vial and the shelf is not a constant, but generally decreases as the radial distance from the center of the vial increases, until the contact print region is reached. As the radial distance increases further, the separation distance

Table X—Variation in Vial Heat Transfer Coefficients: Components of $\sigma(K_v)$ Defined by Eq. 25

Vial	RSD	
	Constant Term, $\sigma(K_K)$	Separation Distance, $\sigma(l)$
W5800	5.0	8.9
K5800	8.8	14.4
W5811	6.7	5.5
W5816	7.9	3.6
K5816	8.9	13.8
5303	4.6	7.0

increases sharply up to a maximum value characteristic of the vial. An alternate mathematical model for K_g (denoted model II), based on the vial bottom geometry discussed above, produces an extremely complex mathematical form for K_g[22]. Regression analysis of single vial and multivial data using K_g from model II yields an accommodation coefficient of 0.84 ± 0.04 and gives contact parameters, 10^4K_c, which are in good agreement with the corresponding parameters given in Table VIII. The quality of the fit is the same as that found using Eq. 10 for K_g. The absolute value of the difference between the corresponding values of 10^4K_c averages 0.14, as the parameters from model II are systematically lower. Thus, it appears that as long as the form of K_g provides a good fit to the data, the values of the contact parameter obtained are not extremely sensitive to the precise form of K_g used. We conclude that the systematic error in 10^4K_c introduced by the combination of uncertainty in a_c and uncertainty in the form of K_g is > ± ~0.3.

The energy accommodation coefficient, a_c, measures the efficiency of energy transfer in a collision between a gas molecule and a surface. For an elastic collision no energy is transferred and $a_c = 0$, while for a perfect inelastic collision, the gas molecule "equilibrates" with the temperature of the surface and $a_c = 1$. Since both the vial and shelf surfaces are involved in energy transfer, the accommodation coefficient for vial heat transfer reflects an average accommodation coefficient for gas molecule collisions with the two surfaces. For freeze-drying, the gas is nearly pure water vapor (Table III), and the error in a_c introduced by assuming the vapor is 100% H_2O is negligible[23]. Thus, although the value of a_c determined from the data may depend slightly on the model chosen for K_g, 0.67 ± 0.05 for Eq. 10 *versus* 0.84 ± 0.04 for Model II, both models suggest incomplete energy transfer ($a_c < 1$) for the collision of a water molecule with one (or both) of the surfaces involved. Due to the difficulties in evaluating an accommodation coefficient from vial heat transfer data, the conclusion, $a_c < 1$, must be regarded as tentative. Unfortunately, the accommodation coefficient data in the literature (12), do not include data for water vapor or glass surfaces.

Theoretically, the accommodation coefficient could depend on the nature of the shelf surface; however, at least for the two surfaces investigated, polished stainless steel and black paint, the K_v data (Table V) suggest such a dependence is minimal. The increase in K_v obtained with a black painted shelf (experiment 7 *versus* experiment 5, Table V), $\Delta 10^4K_v = 0.57 \pm 0.14$, is fully consistent with the observed increase in shelf emissivity, $\Delta e_s = 0.67 \pm 0.10$.

The relative importance of the three heat transfer mechanisms (radiation, contact conduction, and gas conduction) are compared in Table IX. Although the contact contributions are somewhat uncertain due to the possible systematic errors in K_c discussed earlier, it does appear that all three heat transfer mechanisms can make significant contributions to the total heat flow in freeze-drying. The dominant mechanism depends on both the chamber pressure and the type of vial considered. At chamber pressures >0.1 mm Hg, the dominant mechanism is gas conduction, but even at 0.4 mm Hg, both radiation and contact conduction can be important for some vials.

[22] Model II assumes that the vial bottom curvature near the shoulder is described by a semicircle of radius k_s while the curvature in the middle of the vial may be approximated by the arc of a circle. The arc and semicircle meet at $r = a$ (near the contact print region). Thus, K_g is obtained by integration of Eq. 10 over the radial distance $0 \le r \le r_v$, where r_v is the vial radius, $\sqrt{A_v/\pi}$, and the separation distance, l, is a function of r. For $0 \le r \le a$, the equation for an arc is used to obtain $l(r)$, while for $a \le r \le r_v$, the equation of a semicircle is used to evaluate $l(r)$. The value of a is calculated from $r_v = a + k_s$, where k_s is measured from the vial geometry and found to be 0.25 cm (10-mL vials), 0.32 cm (20-mL vials), and 0.44 cm (5303 vials). The resulting expression for K_g may be written in the form: $K_g = [(\lambda_0/h)/(1 + k_s/a)^2] \cdot \ln [1 + (\Lambda_0/\lambda_0)\alpha hP] + [2(ks/a)\Lambda_0\alpha P/(1 + ks/a)^2] \int_0^1 [1 + (ks/a)x]dx/[1 + (ks\Lambda_0\alpha P/\lambda_0)(1 - \sqrt{1 - x^2})]$ where h is the distance between the shelf and the vial bottom at the vial center (r = 0), and x is a dummy variable. The remaining symbols are as previously defined. The definite integral is a function of pressure, P, which must be evaluated by numerical procedures. Regression analysis of the data using the model II function for K_g gives an excellent fit to the data, but the values of h determined from the regression analysis are consistently a factor of ~2 larger than the measured separation distances (Table I).

[23] The average mole fraction of air (Table III) is ~0.15. Assuming that the value of Λ_0 is a weighted average of the Λ_0 data for water vapor and air, with the mole fraction of each component as the corresponding weight, the value of Λ_0 is calculated as 5.98×10^{-3} (P in mm Hg), compared with 6.34×10^{-3} for pure H_2O. Using 5.98×10^{-3} for Λ_0 increases the value of a_c determined from the data by only 0.03.

Table XI—Variation in Sublimation Rate Attributable to Tube Variation

Tube/Vial	Percent Deviation from Run Mean M	46	60	47	41	Row Mean
1	−0.17	−3.40	−5.42	−4.26	−5.06	−3.66
2	2.66	−4.97	−5.73	−4.63	−4.42	−3.44
3	2.14	−3.94	−5.70	−5.11	−3.92	−3.35
4	0.79	−3.93	−6.40	−5.64	−4.88	−4.01
5	−2.60	−3.42	−5.98	−4.84	−6.38	−4.64
Column Mean	0.56	−3.93	−5.91	−4.90	−4.93	−3.82

Analysis of Variance

Component	Variance, %²
Total, $\hat{\sigma}^2(\dot{m})$	6.42
Column Average (vial), $\hat{\sigma}_{\bar{c}}^2$	6.49
Row Average (tube), $\hat{\sigma}_{\bar{R}}^2$	0.27
Measurement Error, σ^2	1.18[a]
Column Effect (σ_c^2), σ_c^2	6.25
Row effect (tube), σ_R^2	0.03[a]

[a] Excluding M vial: $\sigma^2 = 0.44$, $\sigma_R^2 = 0.05$.

The pressure dependence of K_v is illustrated in Fig. 7 for several vials. The data shown are evaluated from the parameters in Table VIII. The curvature is a reflection of the importance of the separation distance, l, which is highly vial specific. Thus, particularly at high pressure, the vial heat transfer coefficient is quite sensitive to the geometry of the vial bottom.

Intervial Variability in K_v*: Pressure Dependence*—While there is no obvious pressure dependence in the $\sigma(K_v)$ data, theoretical considerations suggest a small but significant pressure dependence may be obscured by the lack of precision in the data. Assuming the variation in K_v arises from both variation in the pressure-independent term, $K_r + K_c$, and from variation in the separation distance, l, the variance in K_v is written:

$$\sigma^2(K_v) = \left(\frac{\partial \ln K_v}{\partial \ln K_K}\right)^2 \cdot \sigma^2(K_K) + \left(\frac{\partial \ln K_v}{\partial \ln l}\right)^2 \cdot \sigma^2(l) \qquad \text{(Eq. 24)}$$

where K_K denotes the pressure independent part of K_v, $K_K = K_r + K_c$, and the sigmas represent *RSD* values. Equation 24 also assumes that the deviations in K_K and l are not correlated. Evaluation of the derivatives in Eq. 24 then gives:

$$\sigma^2(K_v) = \sigma^2(K_K)G1(P) + \sigma^2(l)G2(P) \qquad \text{(Eq. 25)}$$

where $G1$ and $G2$ are functions of pressure:

$$G1(P) = (1 + k_D \cdot P)^2/[1 + (k_D + k_p/k_K)P]^2 \qquad \text{(Eq. 26)}$$

$$G2(P) = (k_p/k_K)^2 \left[\frac{k_p \cdot P^2}{1 + k_D P}\right]^2/[1 + (k_D + k_p/k_K)P]^2 \qquad \text{(Eq. 27)}$$

where $k_D = (\Lambda_0/\lambda_0)\alpha \cdot l$, $k_p = \Lambda_0\alpha$, and the other symbols have their usual meanings. The functions, $G1$ and $G2$, depend on vial type as well as pressure, but at low pressure $G1 \gg G2$, and at 0.4 mm Hg, $G2$ is slightly larger than $G1$.

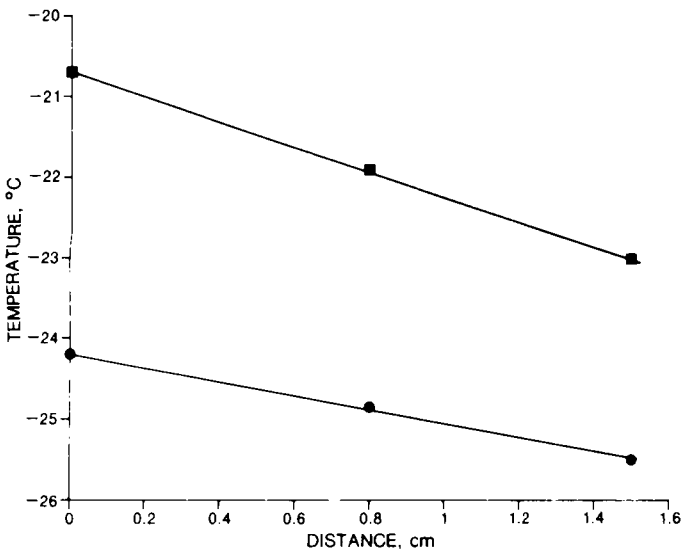

Figure 9—*Product temperature as a function of distance from the vial bottom. Key: (●) heat flux = 5.4 mcal/cm²·s, (■) heat flux = 10.6 mcal/cm²·s.*

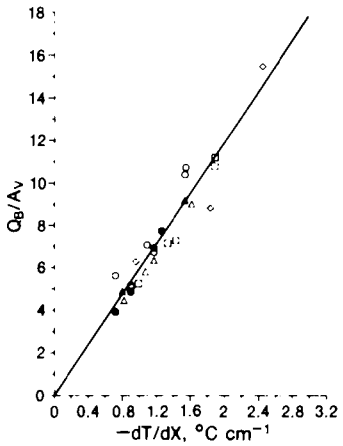

Figure 10—*Heat flux as a function of temperature gradient in the frozen product;* $\dot{Q}_B = \Lambda_r K_I[-dT/dx]$*;* $10^3 K_I = 5.9 \pm 0.4$*. Key: (○) W5800, (●) W5800 (5% KCl), (□) K5800, (△) W5811, (◇) W5816.*

Formally, Eq. 25 gives $\sigma^2(K_v)$ as a function of two variables, $G1$ and $G2$, with $\sigma(K_K)$ and $\sigma(l)$ as parameters. Regression analysis of the $\sigma(K_v)$ data, according to Eq. 25, produces "experimental" values for $\sigma(K_K)$ and $\sigma(l)$ (Table X). Presumably, variation in the contact term is the major contributor to $\sigma(K_K)$. The data are well represented by Eq. 25, but neither the precision nor the extent of the data is sufficient to establish the validity of Eqs. 25–27. Rather, provided one assumes the theoretical analysis in Eqs. 25–27 is valid, the data are sufficient to establish both $\sigma(K_K)$ and $\sigma(l)$ for each vial type with slightly better accuracy than the accuracy in the input $\sigma(K_v)$ data. The means of $\sigma(K_K)$ and $\sigma(l)$ for all W tubing vials are 6.5 and 6.0, respectively; the corresponding means for K tubing vials are 8.8 and 14.1, respectively. Thus, the K vials display somewhat greater relative variability, particularly in the separation distance. Calculated values of $\sigma(K_v)$, Eq. 25, for the average W and average K vials do show a pressure dependence (Fig. 8), the variability in K_v passing through a minimum at ~0.15 mm Hg. Particularly with K tubing vials where the minimum is relatively pronounced, primary drying will be more uniform if the chamber pressure is maintained between 0.1 and 0.2 mm Hg.

Intravial Temperature Distribution—The temperature of the frozen mass in the vial is routinely measured at four locations (Fig. 1) during all single vial experiments. No significant temperature difference is observed between the bottom center and bottom edge of the vial, suggesting that radial heat flow is minimal. As expected, however, the temperature decreases linearity with distance, X, from the vial bottom (Fig. 9), the slope increasing in magnitude as the heat flow through the bottom of the vial increases. Theoretically, the heat flow rate through the bottom of the vial, $\dot{Q}_B$, should be directly proportional to the temperature gradient, $\partial T/\partial X$ (Eq. 15). Evaluating $\dot{Q}_B$ as previously described yields the data shown in Fig. 10. Within the precision in the data, the heat flux, $\dot{Q}_B/A_v$, is directly proportional to the measured temperature gradient. The scatter in the data is largely a consequence of the uncertainty in temperature measurement. The slope appears to be independent of vial type; moreover, the data for KCl solutions do not deviate significantly from the data obtained using pure water. It appears that, independent of the vial type or product, the temperature distribution in a vial may be characterized by Eq. 15 with a constant value for the effective product thermal conductivity, K_I. Regression analysis yields $10^3 K_I = 5.9 \pm 0.4$. Theoretically, K_I contains contributions from both the frozen mass and the glass, Eq. 16. From the vial dimensions (Table I) and the thermal conductivity of glass (13), the thermal conductivity of the frozen product, κ_p, is calculated: $10^3\kappa_p = 6.6 \pm 0.5$ cal/s-cm-°C, in excellent agreement with literature data for ice (6, 7) at corresponding temperatures (−25°C).

CONCLUSIONS

The vial is an extremely important variable in the primary-drying stage of the freeze-drying process. Although the direct effect of the vial on mass transfer (*via* closure resistance) is slight, the nature of the vial does significantly affect the rate of heat transfer to the product and is a major factor in determining the product temperature and drying time for a given set of chamber pressure–shelf temperature settings. Vial heat transfer coefficients increase with increasing chamber pressure, but the pressure dependence is nonlinear. At high pressures, the coefficients are less sensitive to changes in pressure. The magnitude of the vial heat transfer coefficient is sensitive to the geometry of the vial bottom. While the thickness of the glass in the vial bottom

Table XII—Variation in Sublimation Rate Attributable to Vial Position

Position/ Vial[a]	Percent Deviation from Run Mean 24	16	48	59	7	Row Mean
1	−4.12	−5.87	−2.41	−3.13	−2.74	−3.65
2	−5.64	−5.46	−0.56	−4.86	−4.69	−4.24
3	−2.22	−4.49	3.77	−4.58	−3.73	−2.25
4	4.56	−1.48	3.30	−0.72	2.25	1.58
5	−3.18	−3.66	−1.62	−6.08	−5.06	−3.92
Column Mean	−2.12	−4.19	0.50	−3.87	−2.79	−2.50

Analysis of Variance

Component	Variance Including Position 4	Excluding Position 4
Total, $\hat{\sigma}^2(\dot{m})$	9.52	5.14
Column Mean, $\hat{\sigma}_{\bar{C}}^2$	3.49	3.62
Row Mean, $\hat{\sigma}_{\bar{R}}^2$	5.77	0.77
Measurement Error, σ^2	2.70	1.48
Column Effect (σ_v^2), σ_c^2	2.95	3.25
Row Effect (Position), σ_R^2	5.23	0.47

[a] Position 4 is class A (adjacent to shelf temperature sensor); all others are class H.

is not important, both the average separation distance between the vial bottom and the shelf and the degree of physical contact between the vial and the shelf are critical factors. The *RSD* in vial heat transfer coefficients, reflecting variability within a given lot of vials, is rather small (≈4%). However, large differences in vial heat-transfer coefficients exists between different types of vials. Even vials of nominally the same specifications, manufactured by different suppliers, differ significantly in their heat transfer characteristics. A freeze-drying cycle, optimized using one type of vial, cannot be expected to perform satisfactorily with a different vial. Indeed, circumstances may arise where a product is routinely freeze-dried with excellent yield, but a change of supplier for vial stock results in significant product loss arising from eutectic melt. Clearly, heat transfer characteristics must be given serious consideration when vial specifications are determined.

APPENDIX I: Data Analysis for K_v and $\sigma(K_v)$ Evaluation

Evaluation of Intervial Variability $\sigma(K_v)$—The multivial experiment directly yields the estimated variance in the sublimation rate for a given set of vials, $\hat{\sigma}^2(\dot{m})$. The desired parameter is the *RSD* in the vial heat transfer coefficients, $\sigma(K_v)$, and considerable data reduction is needed to extract $\sigma(K_v)$ from the raw data. First, components of variance in $\dot{m}$, due to causes unrelated to the vial heat transfer coefficient, must be subtracted from the estimated variance in $\dot{m}$, $\hat{\sigma}^2(\dot{m})$, to obtain the variance in $\dot{m}$ due to variation in the vials, σ_v^2. Second, the calculated value of σ_v must be converted into the corresponding value of $\sigma(K_v)$.

In addition to variation in vial heat transfer coefficients, three sources of variation in sublimation rate are possible: (*a*) variation in the mass transfer coefficients of the metal tubes, (*b*) variations due to location of the vial on the shelf originating from variations in shelf surface temperature and variations in radiation effects, and (*c*), measurement error or intrinsic variation in the procedure itself, probably resulting mostly from variability in the surface area and contour of the ice-vapor interface[24].

A series of six multivial experiments at a chamber pressure of 0.2 mm Hg were designed to evaluate the various components of variance in sublimation rate. The entire series of experiments were carried out with the same set of W5800 vials in the laboratory dryer. For most of the vials, the vial number, the metal tube used, and the shelf position were held constant throughout the series to allow evaluation of the intrinsic variation or "error" component of the variance, σ^2. For the first five experiments, a subgroup of five vials and corresponding positions were fixed, and the five metal tubes were rotated among the subgroup to determine the effect of variation in metal tube on the sublimation rate. A second subgroup of five vials, with corresponding metal tubes, were rotated among five selected shelf positions to determine the effect of shelf positions on the sublimation rate. The vial placement used in these studies is shown in Fig. 5, where each vial is shown as a circle. The term "pressure tube channel" denotes the space occupied by the tube connecting

[24] Particularly with pure ice, the ice-vapor interface does not remain perfectly planar during the entire experiment. While the mass transfer resistance of the solid to vapor phase transition is small, it is not zero (3), and variation in surface area will therefore have a small effect on the overall mass transfer resistance. Moreover, the effective thickness of the ice plug for heat transmission from the vial bottom may vary slightly between vials or between replicate experiments with the same vial. Thus, even for fixed K_v and fixed T_s, the sublimation rate will vary slightly within a given set of vials.

Table XIII—Sublimation Rate Variation in Pilot Dryer: Percent Deviation from Mean Sublimation Rate Related to Vial Position[a]

Row/ Column	Percent Deviation from Run Mean 1	2	3	4	5	Row Mean, $\bar{R}_i$
1	−4.17	−4.64	−4.47	−3.60	1.79	−3.02
2	−3.47	−7.14	−1.85	−3.75	0.41	−3.16
3	−2.21	−3.52	−4.79	−4.78	0.15	−3.03
4	−1.59	0.14	−7.20	1.08	1.20	−1.27
5	−6.61	1.85	1.26	−0.79	2.46	−0.37
6	−0.28	3.48	5.48	5.51	−1.74	2.49
7	5.66	1.29	4.71	3.75	3.34	3.75
8	−1.22	1.74	3.15	5.22	13.58	4.49
9	1.16	1.31	2.55	2.13	6.55	2.74
10	−4.28	−3.91	0.00	−0.50	4.04	−0.93
11	−0.14	−5.12	−2.26	−3.96	3.23	−1.65
Column Average, $\bar{C}j$	−1.56	−1.32	−0.31	0.03	3.18	0.00

Analysis of Variance

Component	Variance
Total, $\hat{\sigma}^2(\dot{m})$	16.28
Column Average, $\hat{\sigma}_{\bar{C}}^2$	3.60
Row Average, $\hat{\sigma}_{\bar{R}}^2$	8.16
Measurement Error, σ^2	1.99
Column Effects, σ_c^2	3.41
Row Effects, σ_R^2	7.76
Vial, σ_v^2	5.83

[a] 5303 vials, 0.2 mm Hg.

the interior of the modified vial to the pressure sensor. Vials on the edge of the shelf, which are exposed to the chamber walls, are marked with an E. All other (interior) vials are divided into two classes: class A, which represents those vials adjacent to a shelf temperature sensor, and class H, where the vial is in a hexagonal close-packed configuration with other vials, as would be found in normal loading of a freeze-dryer. Vials adjacent to the pressure tube channel are not rigorously in a hexagonal configuration, but the results of this series of experiments and subsequent multivial experiments indicate that vials adjacent to the pressure tube channel show no measureable position bias when compared with hexagonally packed vials. The vial identification number is given in the lower part of the circle, and the class A vials have a bar underlining the vial number. [The modified vial (Fig. 1) is denoted M.] The symbols P_1, P_2, P_3, P_4, and P_5, refer to the positions used in the position rotation study while the symbols T_1, T_2, . . . , refer to vials-positions used in the tube rotation study. Thermocouple-containing vials have the designation TC, followed by the thermocouple identification numbers, or numbers in the case of multiple-thermocouple vials. The number in the top part of the circle, containing a decimal point, is the percent deviation of the mean sublimation rate for that vial-position combination from the corresponding mean for the total interior set of vials. The deviations recorded for the P vials correspond to the mean deviation for that position as found in the position rotation study.

The edge vial deviations represent the results of a single experiment but clearly show a higher sublimation rate than the interior vials. The mean deviation in sublimation rate for the edge vials is 15.0 ± 1.5%, where the uncertainty is the *SD* of the mean. The higher sublimation rate for edge vials is undoubtedly due to radiation effects from the edge of the shelf and chamber wall. Since edge vials are atypical, edge vial data are excluded from the data analysis. It should also be noted that vial 22 (Fig. 5, upper left corner) behaves anomalously. The edge vials surrounding vial 22 displayed a tendency to move away from it during the course of the experiment, presumably due to vibrations, giving vial 22 some characteristics of an edge vial. Thus, vial 22 is also excluded from data analysis.

The raw data and corresponding analysis of variance for the metal tube rotation portion of the experiment (Table XI) show essentially zero variance in sublimation rate caused by variation in the mass transfer coefficient of the metal tubes. All standard deviations (σ) are relative standard deviations. The estimated or directly measured *SD* in the first three rows of the analysis of variance section are evaluated with $N - 1$ weighting from the raw data. The value of $\hat{\sigma}_{\bar{C}}$ is computed from the column means while the value of $\hat{\sigma}_{\bar{R}}$ is computed from the row means. The last three rows in the analysis of variance section are calculated variances for an infinite set of vials evaluated from the variances in the first three rows using the appropriate corrections for degrees of freedom (14). The measurement error component, σ^2, represents the intrinsic variability in the experiment while the column effect, σ_c^2, gives the variance originating from vial-position variability. The variance component giving the row effect, σ_R^2, represents the contributions to the variance in sublimation rate originating from variation in metal tubes. Clearly, variation in the mass-transfer coefficient of the metal tubes is negligible.

The results of the position rotation experiment (Table XII) indicate a significant position effect, but nearly all of this effect is due to a difference between class A and class H interior shelf positions. Indeed, when position 4 (class A) is excluded from the analysis, the remaining four positions yield a position variance of only 0.47. Thus, the shelf temperature uniformity appears to be excellent.

The mean bias between position 4 and the other positions is 5.1 ± 1.0%, where the uncertainty is the standard error in the bias estimate. Additional multivial experiments comparing class A positions with class H positions yield a bias of 3.6 ± 1.0%, in reasonable agreement with the value obtained from the data in Table XII. The higher sublimation rate for vials adjacent to a shelf sensor is probably a result of radiative heat transfer from the shelf sensor, at roughly the shelf temperature, to the vial. We write[25]:

$$\Delta\dot{Q}_A \cong A_v S_a \times 10^{-4} (T_s - T_b) \qquad \text{(Eq. 28)}$$

where $\Delta\dot{Q}_A$ is the extra heat flow coming from the shelf sensor. The parameter, S_a, evaluated from the data is 0.31.

The measurement error variance, σ^2, is estimated from the replication data for those vials where the vial position is held fixed for the series of six experiments. Using $N - 1$ weighting, the estimated variance is calculated for each vial, and the mean variance of each vial class is taken as the measurement error variance for that class. For class A vials $\sigma^2 = 4.3$, while for class H vials, $\sigma^2 = 2.6$.

For a set of N vials of which A vials are adjacent to a shelf temperature sensor, the total estimated variance in $\dot{m}$, $\hat{\sigma}^2(\dot{m})$, where $\hat{\sigma}(\dot{m})$ is the estimated *RSD* in $\dot{m}$, with $N - 1$ weighting, may be approximated by:

$$\hat{\sigma}^2(\dot{m}) = \sigma_v^2 + \sigma_{SP}^2 + (A/N)\sigma_{EA}^2 + (1 - A/N)\sigma_{EH}^2 + (A/N)(1 - A/N)r^2 \qquad \text{(Eq. 29)}$$

here, σ_v^2 is the variance component from variation in the vial heat transfer coefficient, σ_{SP}^2 is the variance component from shelf position variation for class H vials [0.47 (Table XII)], σ_{EA}^2 and σ_{EH}^2 are the measurement error components for class A (4.3) and class H (2.6) vials, respectively. The term in r gives the variance component originating in the class bias between class A and class H vials where:

$$r = 10^2 \frac{\Delta\dot{m}_A}{\langle\dot{m}\rangle} = \frac{0.0545\, A_v S_a (T_s - T_b)}{\langle\dot{m}\rangle} \qquad \text{(Eq. 30)}$$

The term, $\Delta\dot{m}_A$, is the difference in sublimation rate (g/h) between a class A vial and the mean sublimation rate for the entire set, $\langle\dot{m}\rangle$. From the variance data obtained in the series of preliminary experiments described in Tables XI, XII and Fig. 5, and the experimental value of $\hat{\sigma}^2(\dot{m})$ obtained for a given experiment, the corresponding variance due to variation in the vial transfer coefficient, σ_v^2, may be calculated. When A/N is ~0.5, the position bias term in Eq. 29 is large and may be the largest component of variance, thus limiting the accuracy with which σ_v^2 may be determined.

Equation 29 is an approximation where the most serious problem arises from the assumption that the measurement error variances and class bias do not vary between experiments. Clearly, the accuracy in σ_v^2 would be greatly improved with an experimental design where A/N is zero without decreasing N significantly. Originally, we were concerned with potential shelf temperature variation with position and chose to employ two shelf sensors at central locations on the shelf (A/N is ~0.4). However, experience has shown that shelf temperature variation is not a problem with the laboratory dryer, and our current experiment design uses only one shelf sensor at an edge vial location and does not use the modified (M) vial. Thus, the pressure tube channel is filled with vials. The net result is that only one vial from a set of ~15 is adjacent to the shelf sensor, and this vial is excluded from the data analysis. Only vials in a truly hexagonal packing arrangement are used in the data analysis.

The *RSD* in sublimation rate is slightly smaller than the corresponding *RSD* in the vial heat transfer coefficient. The sublimation rate is proportional to the product of K_v and the temperature difference, $T_s - T_b$. A given positive deviation in K_v produces a corresponding increase in T_b, thereby decreasing slightly the temperature difference, $T_s - T_b$, resulting in a net relative increase in $\dot{m}$ smaller than the relative increase in K_v. The *RSD* in K_v, $\sigma(K_v)$, may be related to the *RSD* in $\dot{m}$, σ_v by:

$$\sigma(K_v) = \sigma_v \cdot \frac{d \ln K_v}{d \ln \dot{m}} \qquad \text{(Eq. 31)}$$

where:

$$\frac{d \ln K_v}{d \ln \dot{m}} \cong 1.2 + 400\, K_v \qquad \text{(Eq. 32)}$$

Since K_v is of the magnitude 5×10^{-4}, the value of $\sigma(K_v)$ is ~50% greater than σ_v. The derivation of Eq. 32 is given in *Appendix II*.

Due to significant shelf position effects, evidently originating, at least in part, from nonuniformity of shelf temperature, the statistical analysis for data generated with the pilot dryer differs slightly from the analysis (Eq. 29) given data from the laboratory dryer. The procedure used with data from the pilot dryer is outlined in Table XIII. Here, the rows and columns represent vial locations on the dryer shelf. The numbers within the row-column matrix are percent deviations of the sublimation rate for a given vial-position from the mean sublimation rate of all interior vials. The *RSD* ($\hat{\sigma}(\dot{m})$, $\hat{\sigma}_{\bar{c}}$, and $\hat{\sigma}_{\bar{R}}$) are evaluated directly from the raw data as described previously in the discussion of Table XI. The last four rows in the analysis of variance section of Table XIII are calculated data (14)[26] using $\sigma^2 = 1.99$. This value of σ^2 is determined from a series of replication experiments with 5303 vials in the pilot dryer. Note that the column position effect, σ_c^2, and row position effect, σ_R^2, are major contributors to the total variance. The term of interest, the variance in $\dot{m}$ due to vial heat transfer variations, σ_v^2, is <50% of the total variance.

Evaluation of Vial Heat Transfer Coefficients From Multivial Data—The vial heat transfer coefficient is formally defined by Eq. 8 when the surface above the vials is at the temperature of the shelf. For both the laboratory and pilot dryers, the temperature of the surface above the vials differs somewhat from the shelf temperature. Moreover, although the average sublimation rate is measured, from which the mean heat transfer rate may be calculated, the temperature difference $T_s - T_b$ is measured for a limited number of vials, normally four. Therefore, the average temperature difference corresponding to the average heat-transfer rate is not directly measurable, and an indirect calculation procedure is used to evaluate the average heat transfer coefficient.

First, the mean heat transfer rate corresponding to heat flow through the vial bottom, $\langle\dot{Q}_B\rangle$, is evaluated from the mean heat transfer rate, $\langle\dot{Q}\rangle$, by subtraction of the top radiation contribution:

$$\langle\dot{Q}_B\rangle = \langle\dot{Q}\rangle - A_v e_v \sigma (T_L^4 - T^4) \qquad \text{(Eq. 33)}$$

where σ is the Stefan-Boltzmann constant, T_L is the temperature of the surface above the vials, and e_v is taken as 0.84 (Table IV). The value of $\langle\dot{Q}\rangle$ in cal/s is calculated from the mean sublimation rate in g/h by $\langle\dot{Q}\rangle = 0.1833\langle\dot{m}\rangle$. The temperature, T_L, is directly measured, and the temperature of subliming ice, T, is evaluated indirectly from the mean sublimation rate and the chamber pressure. Since the gas in the vial is essentially pure water vapor at the equilibrium vapor pressure of the subliming ice, the mean sublimation rate, mean vapor pressure, and chamber pressure are related (Appendix II, Eq. 41). Thus, the mean vapor pressure is determined from the mean sublimation rate, and the corresponding mean ice temperature, $\langle T\rangle$, is evaluated from the mean vapor pressure[15]. Equation 33 is used to evaluate the mean heat transfer rates for both the set of thermocouple-containing vials and the complete vial set.

That portion of the vial heat transfer coefficient representing heat transfer from the shelf to the vial bottom, denoted K_{vB}, is evaluated for the set of thermocouple-containing vials:

$$\langle K_{vB}\rangle_{TC} = \langle\dot{Q}\rangle_{TC}/A_v\langle T_s - T_b\rangle \qquad \text{(Eq. 34)}$$

where the subscript TC denotes the mean of the thermocouple vial set. The mean of K_{vB} for all vials, denoted $\langle K_{vB}\rangle$, is obtained indirectly. In general, the value of $\langle\dot{Q}_B\rangle_{TC}$ is slightly different from the corresponding mean of all the vials, $\langle\dot{Q}_B\rangle$. Treating this small difference as a differential, $d\langle\dot{Q}_B\rangle \cong \langle\dot{Q}_B\rangle - \langle\dot{Q}_B\rangle_{TC}$, the corresponding differential in $\langle K_{vB}\rangle$, $d\langle K_{vB}\rangle = \langle K_{vB}\rangle - \langle K_{vB}\rangle_{TC}$, may be evaluated from the value of the derivative, $d \ln K_{vB}/d \ln \dot{Q}_B$ (Appendix II, Eq. 45). Thus, the value of $\langle K_{vB}\rangle$ is given by:

$$\langle K_{vB}\rangle = \langle K_{vB}\rangle_{TC}\,[1 + (1.2 + 400\,\langle K_{vB}\rangle_{TC}) \cdot (\langle\dot{Q}_B\rangle/\langle\dot{Q}_B\rangle_{TC} - 1)] \qquad \text{(Eq. 35)}$$

The value of $\langle K_{vB}\rangle$ calculated from Eq. 35 refers to the mean of all vials and, therefore, includes the effects of atypical radiation heat transfer from the shelf sensor for the class A vials. The result of Eq. 35 is corrected to represent only class H (normal position) vials by subtracting the term, $S_a \times 10^{-4}\,(A/N)$, (see Eq. 28) from $\langle K_{vB}\rangle$. Finally, the total vial heat transfer coefficient, as defined by Eq. 8, is obtained by adding $e_v \times 10^{-4}$ to the corrected result from

[25] Heat flow from the shelf sensor to the vial is probably proportional to the "cylinder" area of the vial, A_c. However, for the vials studied, A_c is approximately proportional to the cross-sectional vial area, A_v.

[26] For a matrix of deviations containing p rows and q columns, where the rows and columns represent position effects, the random component of variance is the sum, $\sigma_v^2 + \sigma^2$, which may be evaluated from (14): $\sigma_v^2 + \sigma^2 = [(pq - 1)/(p - 1)(q - 1)]\hat{\sigma}^2(\dot{m}) - p/(p - 1)\hat{\sigma}_{\bar{c}}^2 - [q/(q - 1)]\,\hat{\sigma}_{\bar{R}}^2$.

Eq. 35 to provide for the correct top radiation term under the conditions of Eq. 8. Thus, the mean value of K_v for the vial set is:

$$K_v = \langle K_{vB} \rangle - S_a \times 10^{-4} (A/N) + e_v \times 10^{-4} \qquad \text{(Eq. 36)}$$

where $\langle K_{vB} \rangle$ is given by Eq. 35, S_a is taken as 0.31, and e_v is 0.84 (Table IV).

APPENDIX II: Relationship of Relative Standard Deviation in K_v with Relative Standard Deviation in $\dot{m}$

The relationship of $\sigma(K_v)$ to $\hat{\sigma}(\dot{m})$ depends on the derivative, $d\ln K_v/d\ln \dot{m}$ according to Eq. 31. This derivative may be evaluated with sufficient accuracy assuming the temperature of the source of top radiation is equal to the shelf temperature, T_s. With this assumption, the sublimation rate, $\dot{m}$ (g/h) may be written:

$$\dot{m} = \frac{3600\, A_v K_v}{\Delta \overline{H}_s} (T_s - T_b) \qquad \text{(Eq. 37)}$$

where $\Delta \overline{H}_s$ is the heat of sublimation and the factor, 3600, converts sublimation rate from g/s to g/h. Similarly, the sublimation rate may be related to the temperature difference between the bottom of the vial and the temperature of subliming ice using the approximation:

$$\dot{m} \cong \frac{3600\, A_v K_I}{\Delta \overline{H}_s} \frac{(T_b - T)}{l_i} \qquad \text{(Eq. 38)}$$

where l_i is the thickness of the ice plug and T is the temperature of the subliming ice. The relationship given by Eq. 38 is rigorous only when all heat flow comes through the vial bottom. However, the error introduced by using Eq. 38 does not seriously affect the results of this section. Differentiation of Eq. 37 yields:

$$\frac{d \ln K_v}{d \ln \dot{m}} = 1 + 3600 \frac{A_v K_v}{\Delta \overline{H}_s} \left(\frac{d\dot{m}}{dT} \cdot \frac{dT}{dT_b} \right)^{-1} \qquad \text{(Eq. 39)}$$

while differentiation of Eq. 38 gives:

$$\left[\frac{dT}{dT_b} \right]^{-1} = 1 + \left(\frac{l_i \Delta \overline{H}_s}{3600 A_v K_I} \right) \cdot \frac{d\dot{m}}{dT} \qquad \text{(Eq. 40)}$$

The sublimation rate may also be related to the pressure in the vial using Eqs. 3, 7, and 17. Since in multivial experiments with pure water, the pressure in the vial is approximately equal to the equilibrium vapor pressure of ice (P_0), one may write:

$$\dot{m} = a_0 (P_0 - P_c) + \frac{a_1}{2} (P_0^2 - P_c^2) \qquad \text{(Eq. 41)}$$

with $a_0 = 0.2478$ and $a_1 = 1.944$. Thus, since $d\dot{m}/dT = (d\dot{m}/dP_0)(dP_0/dT)$:

$$\frac{d\dot{m}}{dT} = (0.2478 + 1.944\, P_0) \frac{dP_0}{dT} \qquad \text{(Eq. 42)}$$

Combining Eqs. 39-42 and using $dP_0/dT \approx 0.1\, P_0^{1.5}$:

$$\frac{d \ln K_v}{d \ln \dot{m}} = 1 + \frac{l_i}{K_I} K_v + \frac{3.6 \times 10^4 A_v K_v}{\Delta \overline{H}_s (0.2478 + 1.944 P_0) P_0} \qquad \text{(Eq. 43)}$$

Numerical evaluation of the term involving P_0 demonstrates that this term is nearly constant at 0.2 for all multivial experiments conducted. Thus, with $l_i \approx 2.3$ cm and $K_I = 5.9 \times 10^{-3}$ (Fig. 9), Eq. 43 simplifies to:

$$\frac{d \ln K_v}{d \ln \dot{m}} = 1.2 + 400\, K_v \qquad \text{(Eq. 44)}$$

A derivation nearly identical to that given above may be given to evaluate the derivative $d \ln K_{vB}/d \ln \dot{Q}_B$, where K_{vB} is that portion of the heat transfer coefficient describing heat transfer from the shelf to the vial bottom, and $\dot{Q}_B$ is the heat flow from the shelf to the vial bottom. The result is also nearly identical to Eq. 44 and may be written:

$$\frac{d \ln K_{vB}}{d \ln \dot{Q}_B} = 1.2 + 400\, K_{vB} \qquad \text{(Eq. 45)}$$

Equation 45 is used in the evaluation of vial heat transfer coefficients from the raw data.

REFERENCES

(1) T. A. Jennings, *Drug Cosmet. Ind.*, **127**, 43 (1980).

(2) A. P. MacKenzie, *Ann. N.Y. Acad. Sci.*, **125**, 522 (1965).

(3) M. J. Pikal, S. Shah, D. Senior, and J. E. Lang, *J. Pharm. Sci.*, **72**, 635 (1983).

(4) S. L. Nail, *J. Parenter. Drug Assoc.*, **34**, 358 (1980).

(5) S. Dushman and J. M. Lafferty. "Scientific Foundations of Vacuum Technique," 2nd ed., Wiley, New York, N.Y., 1962.

(6) R. W. Powell, *Adv. Phys.*, **7**, 235 (1958).

(7) T. Ashworth, Proceeding International Cryogenic Engineering Conference, 4th ed., IPC Sci. Technol. Press, Ltd., Guilford, Engl., 1972, p. 377.

(8) G. Janesco, J. Pupezin, and W. A. VanHook, *J. Phys. Chem.*, **74**, 2984 (1970).

(9) F. P. Incropera and D. P. DeWitt, "Fundamentals of Heat Transfer," Wiley, New York, N.Y., 1981.

(10) J. Amoignon, "Freeze Drying and Advanced Food Technology," Academic, London, 1975, p. 445.

(11) J. R. Partington, "An Advanced Treatise on Physical Chemistry," vol. 1, Wiley, New York, N.Y., 1949.

(12) F. O. Goodman and H. Y. Wachman, "Dynamics of Gas-Surface Scattering," Academic, New York, N.Y., 1976.

(13) "International Critical Tables," vol. 4, McGraw-Hill, New York, N.Y., 1929, p. 217.

(14) C. A. Bennett and N. L. Franklin, "Statistical Analysis in Chemistry and the Chemical Industry," Wiley, New York, N.Y., 1954.

Determination of the Chemical Constituents and Spectral Properties of Commercial and NF Reference Standard Potassium Guaiacolsulfonate: Implications of the Findings on Compendial Analytical Methodology

PAKTIYA TANGTATSAWASDI and S. EDWARD KRIKORIAN ˣ

Received June 1, 1983, from the *Department of Medicinal Chemistry/Pharmacognosy, School of Pharmacy, University of Maryland, Baltimore, MD 21201.* Accepted for publication September 26, 1983.

Abstract □ HPLC analysis confirmed a difference in the chemical composition of commercial *versus* NF reference standard potassium guaiacolsulfonate. After separation by fractional crystallization, the two constituents comprising the former sample were identified by ^{1}H-NMR as potassium guaiacol-4- and -5-sulfonate, respectively. The former isomer predominated. The reference standard material was identified as the 4-sulfonate salt by HPLC, NMR, IR, and UV. This difference raises questions concerning the validity of the compendial identification tests and assay procedure for the drug, which are based on methods requiring direct comparison between it and the reference standard. In fact, the IR test has now been shown to be unreliable as a rigorous criterion for identification, in light of significant differences found in the fingerprint regions of the spectra of the two isomers. However, because the two isomers exhibit identical UV absorption characteristics in solutions of pH ≤7 (but not in alkaline solution), the compendial UV identification test and assay procedure appear to be valid under the conditions specified. The pK_a values of the isolated isomers were estimated by a spectrophotometric method to be 8.74 and 9.16 for the phenolic group of potassium guaiacol-4- and -5-sulfonate, respectively.

Keyphrases □ Potassium guaiacolsulfonate—chemical constituents, spectral properties, commercial and NF reference standard □ Isomers—potassium guaiacolsulfonate, determination of chemical constituents and spectral properties, commercial and NF reference standard

Since the first reported synthesis of potassium guaiacolsulfonate *via* sulfonation of guaiacol with concentrated sulfuric acid (1), there has been disagreement over product composition. Some workers have suggested that a single product is formed (2–4); however, others have described isomeric mixtures (1, 5–8). The identification of the mixture as the 1-hydroxy-2-methoxybenzene-4- and -5-sulfonic acid salts by Paul (5) has been accepted (9, 10) and confirmed by others who examined both commercial samples and formulated drug products (11–13).

However, discrepancies in several drug listings (14–16) have persisted. The National Formulary (NF) has failed to be specific about the composition of the officially recognized drug entity (I) with no reference to a mixture of isomers (17). The original analytical methodology introduced in NF XII appears to be based on methodology (18) which (*a*) failed to take into account the fact that the drug may be an isomeric mixture and (*b*) proposed a reference standard prepared by recrystallization of the commercial sample from water or alcohol, which could lead to a product of uncertain composition, since solubility differences between the isomeric components of the mixture of potassium guaiacolsulfonates are known to exist (9, 11).

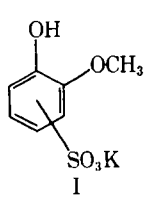

I

Although potassium guaiacolsulfonate (I) is no longer included in the official compendium, its commercial use in cough and cold remedies as an expectorant is still widespread. In this study, a commercial sample and an NF reference standard of potassium guaiacolsulfonate are characterized, and the NF XIII methodology (17) is evaluated.

EXPERIMENTAL SECTION

Materials—Commercial[1] and NF reference standard[2] potassium guaiacolsulfonate were used as received. All solvents and standard chemicals employed were reagent grade.

High-Performance Liquid Chromatography—The apparatus consisted of a single-piston reciprocating solvent delivery pump with integral pulse dampener[3]; a valve injector[4] fitted with a 25-μL sample loop; a 30 cm × 4-mm stainless steel column packed with a chemically bonded octadecylsilane reverse-phase packing[5]; a variable-wavelength UV–visible spectrophotometer[6] operated at 278 nm and fitted with an 8-μL, 1-cm path length, quartz flow cell[7] as detector; and a recorder[8].

The mobile phase consisted of 0.005 M tetrabutylammonium hydroxide, adjusted to pH 7.15 with 86% H_3PO_4, and contained 10% (v/v) methanol. It was deaerated by stirring under reduced pressure. The flow rate was maintained at ~1.4 mL/min.

All solutions of potassium guaiacolsulfonate analyzed by HPLC were prepared at a concentration of ~1.3 mg/mL in water. Analysis of the commercial sample of I under the conditions described above resulted in a chromatogram with two baseline-resolved peaks (R_s = 1.7) at retention times (t_R) near 11 and 14 min, respectively, in the area ratio[9] 1.5:1 (Fig. 1). Analysis of the NF reference standard of I under identical conditions yielded a chromatogram containing only a single peak with a retention time of 11 min, which was shown by mixture analysis to be identical with the t_R of the earlier-eluting (major) peak of the commercial sample.

Spectrometric Measurements—^{1}H-NMR spectra were recorded[10] in D_2O[11] containing 1% sodium 3-trimethylsilyl-1-propanesulfonate (DSS)[12]. To generate the phenolate anions of the I isomers, a few drops of NaOD solution[13] were added to the D_2O solutions. Chemical shifts are reported as δ values in parts per million relative to DSS.

IR spectra[14] were run as KBr pellets. UV spectra[15] were recorded at a concentration of 0.02 mg/mL in water, 0.1 M HCl, and pH 7.0 potassium phosphate buffer and at 0.01 mg/mL in 0.1 M NaOH. Molar absorptivities (ε) of the isomers at the wavelengths of maximum absorption in the pH 7.0 phosphate buffer solution were determined from the slopes of Beer's law plots derived from absorbance measurements of seven solutions over the concentration range 8×10^{-5} to 3×10^{-4} M.

[1] ICN Pharmaceuticals, K & K Labs Division, Plainview, N.Y.
[2] USP authentic substance, Lot F; U.S. Pharmacopeial Convention, Inc., Rockville, Md.
[3] Milton Roy Co., Laboratory Data Division, Riviera Beach, Fla.
[4] Valco Instruments Co., Houston, Tex.
[5] μ-Bondapak C_{18}; Waters Associates, Milford, Mass.
[6] Unicam SP1800; Pye-Unicam Ltd., Cambridge, England.
[7] Hellma Cells, Inc., Jamaica, N.Y.
[8] Model EU-20B; Heath Co., Benton Harbor, Mich.
[9] Peak areas were calculated from the product of peak height times the width of the peak at half height.
[10] Model T-60A NMR spectrometer; Varian Instruments.
[11] 99.75 atom% of deuterium; J. T. Baker Chemical Co., Phillipsburg, N.J.
[12] Norell Chemical Co., Landisville, N.J.
[13] 40% in D_2O; Stohler Isotope Chemicals, Rutherford, N.J.
[14] Model IR8 IR spectrophotometer; Beckman Instruments.
[15] Model DB spectrophotometer with laboratory recorder; Beckman Instruments.

0022-3549/84/0900-1238$01.00/0
© 1984, American Pharmaceutical Association

Preparative Isolation of the Constituents of Commercial I by Fractional Crystallization—The commercial sample (90 g) was dissolved in 120 mL of boiling water, and the solution was filtered while hot, cooled to room temperature, and refrigerated overnight. The resulting white crystals were removed by filtration and recrystallized from water to give isomer A (41 g), which has previously been described as the "less-soluble" salt (9).

To the mother liquor (80 mL) from the aforementioned first crystallization was added slowly with stirring 95 mL of absolute ethanol. A white solid precipitated (4 g), which was removed by filtration. This material was purified by suspending in boiling absolute ethanol (125 mL) and then adding sufficient aqueous ethanol (25% ethanol–water), while heating, to completely dissolve the solid. The solution was cooled and allowed to stand overnight. The resulting precipitate was removed by filtration and washed with aqueous ethanol, and then absolute ethanol, to give (after drying) 2 g of isomer B, the "more-soluble" salt.

1-*O*-Acetyl Derivatives of the Isomeric Potassium Guaiacolsulfonates—Each of the aforementioned isomers A and B (200 mg, 0.8 mmol) was refluxed with 10 mL of acetic anhydride and 2 mL of pyridine for 30 min and then cooled. The white crystals were removed by filtration, washed with acetone, and dried, to give 160 mg of potassium 4-(acetyloxy)-3-methoxybenzenesulfonate (acetylated isomer A) [IR(KBr): 1760 cm^{-1} (C=O); ^{1}H-NMR (D_2O): δ 2.36 (s, CH_3CO), 3.92 (s, CH_3O), 7.25 (d, ArH), 7.51 (d of d, ArH), and 7.55 ppm (d, ArH)] and 150 mg of potassium 3-(acetyloxy)-4-methoxybenzenesulfonate (acetylated isomer B) [IR(KBr): 1760 cm^{-1} (C=O); ^{1}H-NMR (D_2O): δ 2.36 (s, CH_3CO), 3.86 (s, CH_3O), 7.24 (d, ArH), 7.60 (d, ArH), and 7.79 ppm (d of d, ArH)].

Anal.[16]—Calc. for $C_9H_9O_6SK$: C, 38.02; H, 3.19; S, 11.28. Found for acetylated isomer A: C, 37.72; H, 3.47; S, 11.21. Found for acetylated isomer B: C, 37.75; H, 3.41; S, 10.99.

Spectrometric Estimation of the pK_a Values of the Isomers of I—Eleven solutions of each isomer were prepared (0.02 mg/mL), covering the pH range of 5.6–10.0, with 0.1 M potassium phosphate and sodium borate buffer systems. The analytical wavelengths employed were selected by comparison of the spectra of the free phenol and phenolate anion forms of the isomers in pH 5.6 buffer and 0.1 M NaOH solution, respectively, with 257 nm being chosen for isomer A and 296 nm for isomer B. From absorbance measurements of each of the 11 solutions and for the pure anion and free phenol form of each isomer at the selected wavelengths, the ratio $[A^-]/[HA]$ was calculated (19) at each pH[17]. The pK_a of the phenol group was then determined graphically (linear regression analysis) as the *y*-intercept of the linear plot of pH *versus* log $[A^-]/[HA]$ ($r > 0.99$, with unit slope for each determination).

RESULTS AND DISCUSSION

The results of paired-ion HPLC analysis of the commercial and NF reference standard samples of I clearly demonstrate the dissimilarity in their chemical compositions. Furthermore, determination of the retention times of the isolated pure isomers A and B show that the former represents the major constituent in the commercial sample and the sole constituent of the NF reference standard I, whereas isomer B represents the later-eluting peak in the chromatogram of the commercial sample. The structural identities of the two isomers then remain to be established.

Structure Determination of the Isomers of I by ^{1}H-NMR—The aromatic region of the ^{1}H-NMR spectra of isomers A and B both featured an upfield *ortho*-split doublet (H_a, δ 7.00, J = 9 Hz) and a lower-field doublet of doublets (H_b, J_{ortho} = 9 Hz, J_{meta} = 2 Hz) overlapping a *meta*-split doublet (H_c, J = 2 Hz). This pattern of absorption bands establishes that the three substituents on the aromatic ring of both isomers must be oriented asymmetrically [1,2,4 (II) and 1,2,5 (III)] rather than vicinally (1,2,3 or 1,2,6).

In order to assign structures II and III specifically to isomers A and B, respectively, the positions of the three ring protons relative to the ring substituents need to be differentiated for each compound. This was accomplished by determining the effect on the chemical shifts of the ring protons of changing the electronic character of the hydroxyl group of each of the isomers by converting it to its phenoxide ion and acetyl derivative. It is known that the chemical shifts of ring protons *ortho* and *para* to the hydroxyl group are most affected by such changes and *meta* protons are affected less (20). For the derivatives of isomer A, the greatest chemical shift changes were observed for the high-field doublet due to H_a (0.38 ppm upfield in the phenoxide ion, 0.25 ppm downfield in the acetate ester), with the corresponding changes for the absorptions due to H_b and H_c being approximately half as large. For the derivatives of isomer B, the greatest chemical shift changes were observed for the absorptions due to H_b and H_c (0.41 and 0.37 ppm upfield, respectively, in the phenoxide ion; 0.45 and 0.30 ppm downfield, respectively, in the acetate ester), with the corresponding changes in the high-field doublet due to H_a being much smaller (0.09 ppm upfield and 0.22 ppm downfield in the respective derivatives). These results leave no doubt that for isomer A, H_a must be *ortho* to the hydroxy group (*i.e.*, the 6-position) and that for isomer B, H_b and H_c must be *para* and *ortho*, respectively, to the hydroxy group (*i.e.*, the 4- and 6-positions, respectively) (20). Therefore, isomer A, the "less-soluble" salt which represents the earlier-eluting (major) HPLC peak from the commercial sample is potassium guaiacol-4-sulfonate (II) and isomer B is potassium guaiacol-5-sulfonate (III).

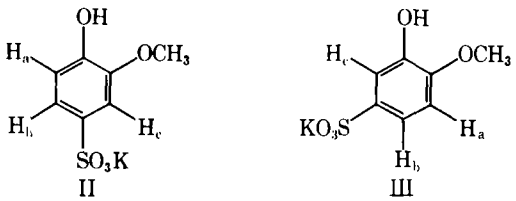

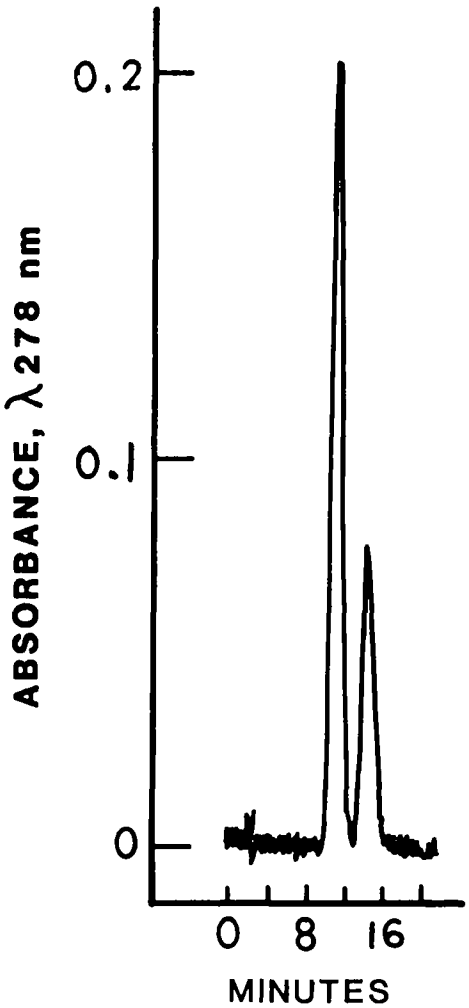

Figure 1—*Paired-ion high-performance liquid chromatogram of commercial sample of I. The major peak corresponds to isomer A (II), and the minor peak corresponds to isomer B (III), which were subsequently isolated from the sample by fractional crystallization.*

With the identity of the two constituents of the commercial sample of I established, it was concluded that the NF reference standard consisted solely of potassium guaiacol-4-sulfonate, inasmuch as its NMR and IR (see below) spectra were identical to those for II, and the retention time of its single HPLC peak coincided with that for II (see above).

The obvious difference in the compositions of the commercial sample of I and the NF reference standard raises some concern regarding the reliability of the identification tests and assay procedure described in NF XIII (17), since the methodologies involved rely on direct comparison of the drug with the reference standard. It was important, therefore, that the accuracy of these methods be reevaluated.

[16] Performed by Galbraith Laboratories, Inc., Knoxville, Tenn.
[17] Zeromatic IV pH meter; Beckman Instruments.

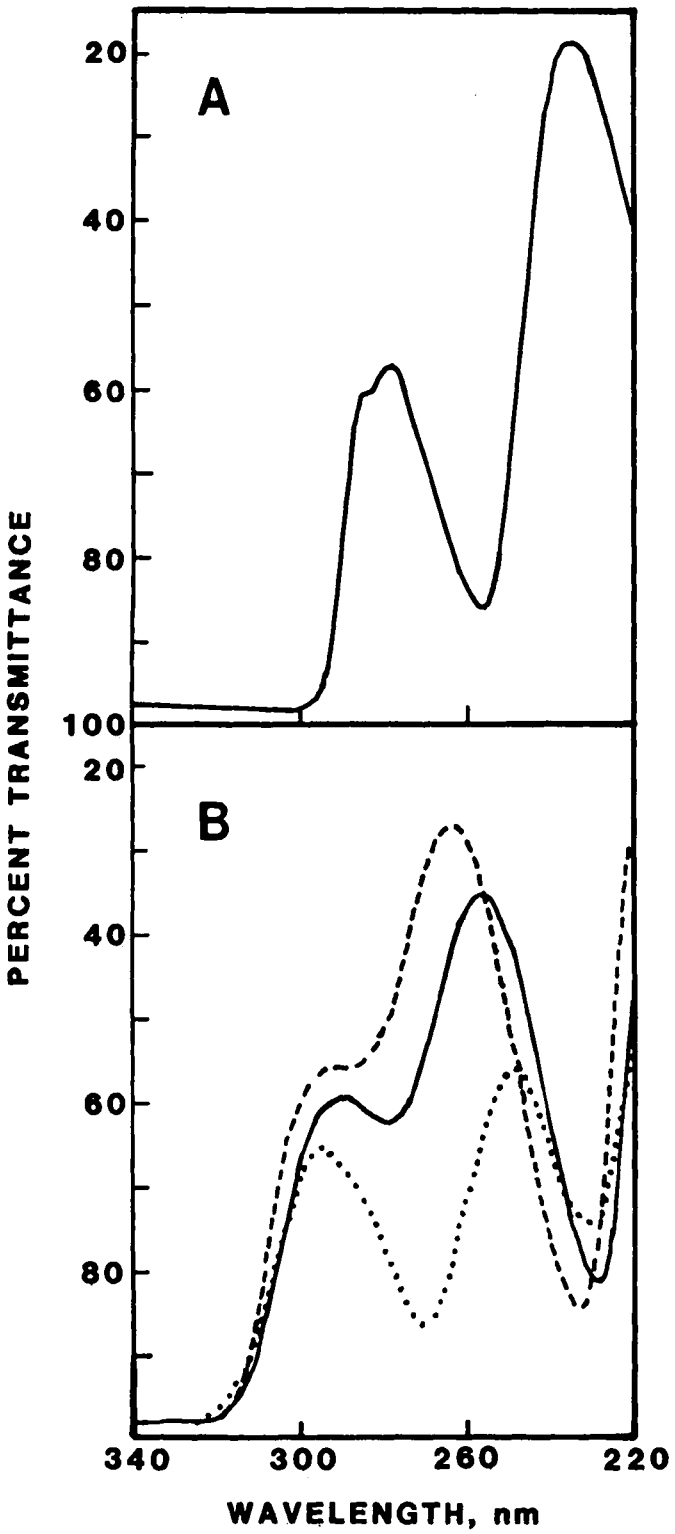

Figure 2—*(A) The identical UV spectra (1-cm path length cells) of 0.02-mg/mL solutions of II, III, and a commercial preparation of I in water, 0.1 M HCl, and pH 7.0 phosphate buffer. (B) UV spectra (1-cm path length cells) of 0.01-mg/mL solutions of II (- - - -), III (• • • •), and a commercial preparation of I (——) in 0.1 M NaOH.*

Evaluation of the NF IR Absorption Identification Test for I (17)—As expected, the IR spectra of KBr dispersions of pure II and the NF reference standard I proved to be superimposable, confirming the chemical identity of the standard as the single pure compound. However, the IR spectrum for the commercial preparation of I differed markedly from that of the reference standard in the fingerprint region (especially around 1100–1300 cm^{-1}) due to the contribution of absorption bands from its second constituent, III. Therefore, it must be concluded that comparison of the IR spectra of commercial and reference standard samples of I cannot be used as a rigorous criterion for the reliable identification of unknown samples of the drug.

Evaluation of the NF UV Absorption Identification Test and Assay Procedure for I (17)—Dabrowski and Patel (18), although not acknowledging that they were comparing different materials, claimed that their reference standard and commercial preparations of I exhibited the same UV behavior in aqueous solution at pH ≤ 7, and on this basis proposed an assay for the drug which was adopted by the NF. This methodology is only valid provided that isomers II and III have identical UV absorption characteristics.

Indeed, the UV spectra of II, III, and the commercial sample of I in aqueous solution all appear to be identical at pH ≤ 7 (Fig. 2A), with absorption maxima at 236 and 279 nm, as previously reported for the commercial preparation of I (18, 21, 22). However, in 0.1 M NaOH, the spectra for the two pure isomers differ substantially (Fig. 2B), with II exhibiting absorption at λ_{max} of 264 and 293 nm and III exhibiting absorption at λ_{max} of 249 and 296 nm. The spectrum for the commercial preparation of I (Fig. 2B) is clearly a composite of the contributions from its two isomeric constituents, with absorption maxima at 257 and 290 nm. Based on these results, it can be concluded that despite the difference in their compositions, comparison of the UV spectra of the commercial mixture and NF reference standard in pH 7.0 buffer solution (but not in alkaline solution), as specified in NF XIII, is a valid identification test. However, the same comparison for quantitation of I is only reliable provided that the absorptivities of the two isomeric constituents, II and III, are identical at the wavelength of analysis (279 nm).

Determination of the molar absorptivities of the two isomers from the slopes of the respective Beer's law plots ($r > 0.999$, with intercepts passing through the origin verified by t test) yielded values of ϵ of $3.07 \times 10^3 \pm 0.03 \times 10^3$ and $2.97 \times 10^3 \pm 0.01 \times 10^3$ L mol^{-1}-cm^{-1} for II and III, respectively, at λ_{max} of 279 nm in pH 7.0 buffer solution. Statistical comparison of these values by a two-tailed t test revealed that their difference is not significant at the $p = 0.05$ level but is significant at the $p = 0.1$ level. Thus, if a 95% or higher probability level of significance is acceptable, the two absorptivities can be considered to be not different, and therefore, the UV spectrometric quantitation of the commercial drug by direct comparison with the single-constituent NF reference standard appears to be justified under the specified conditions.

Spectrometric Estimation of the pK_a Values of the Isomers of I—The aforementioned differences in the UV spectra of the acidic and basic forms of II and III could be taken advantage of to determine their pK_a values (phenol group). The values obtained were 8.74 ± 0.05 for II and 9.16 ± 0.04 for III, which compare with a pK_a of 9.98 for guaiacol (23). The greater acidity of the 4-sulfonate *versus* the 5-sulfonate derivative is consistent with the relative acidities of *p*- and *m*-methylsulfonylphenol, which have pK_a values of 7.83 and 8.40, respectively (23).

CONCLUSIONS

The determination of the composition of the commercial preparation of I to be a mixture of the guaiacol-4- and -5-sulfonate salts, whereas the NF reference standard of I has been shown to be only pure potassium guaiacol-4-sulfonate, has raised questions concerning the reliability of direct comparison of the two materials for the identification and assay of the drug as specified in NF XIII. However, based on the present work, it appears that as long as the UV assay procedure is carried out in neutral or acidic solutions of the drug, valid quantitative results can be obtained. In contrast, comparison of the IR spectra of commercial *versus* reference standard I is not strictly reliable as an identification test for the drug, because significant differences in the fingerprint regions which distinguish the two pure isomers from each other also cause the commercial sample to present a composite spectrum which is different from that of the pure, single-component reference standard.

REFERENCES

(1) F. Tiemann and P. Koppe, *Ber. Dtsch. Chem. Ges.*, **14**, 2015 (1881).

(2) L. Rosenthaler, "Neue Arzneimittel Organischer Natur," Springer, Berlin, 1906, p. 95.

(3) N. Evers, "The Chemistry of Drugs," Van Nostrand, New York, N.Y., 1926, p. 41.

(4) J. Schwyzer, "Die Fabrikation Pharmazeutischer und Chemisch-Technischer Produkte," Springer, Berlin, 1931, p. 214.

(5) L. Paul, *Ber. Dtsch. Chem. Ges.*, **39**, 2773 (1906).

(6) A. Rising, *Ber. Dtsch. Chem. Ges.*, **39**, 3685 (1906).

(7) C. M. Suter, "The Organic Chemistry of Sulfur—Tetravalent Sulfur Compounds," Wiley, New York, N.Y., 1944, p. 242.

(8) E. A. Abarenkova and A. K. Guman, *Tr. Leningr. Inzh.-Ekon. Inst.*, **46**, 92 (1963); through *Chem. Abstr.* **61**, 8220*a* (1964).

(9) "Beilsteins Handbuch der Organischen Chemie," vol. 11, 4th ed., Springer, Berlin, 1928, p. 295, and succeeding supplements.
(10) O. Anselmino and E. Gilg, Eds., "Kommentar zum Deutschen Arzneibuch," 6th ed., vol. 1, Springer, Berlin, 1928, p. 840.
(11) E. Rupp and A. V. Brixen, *Arch. Pharm. Ber. Dtsch. Pharm. Ges.*, **264**, 698 (1926).
(12) A. H. Clark and E. Kirch, *J. Am. Pharm. Assoc., Sci. Ed.*, **24**, 564 (1935).
(13) S. Pfeifer, *Pharmazie*, **13**, 12 (1958).
(14) "The Merck Index," 9th ed., Merck & Co., Rahway, N.J., 1976, p. 991 with 8th ed., 1968, p. 854 and 7th ed., 1960, p. 841.
(15) "Remington's Pharmaceutical Sciences," 16th ed., Mack Publishing Co., Easton, Pa., 1980, p. 808 with 15th ed., 11975, p. 803, and 14th ed., 1970, p. 874.
(16) A. Wade, Ed., "Martindale: The Extra Pharmacopoeia," 27th ed., Pharmaceutical Press, London, 1977, p. 604.
(17) "The National Formulary," 13th ed., American Pharmaceutical Association, Washington, D.C., 1970, p. 574.
(18) R. Dabrowski and D. M. Patel, *J. Pharm. Sci.*, **54**, 1662 (1965).
(19) A. Albert and E. P. Serjeant, "The Determination of Ionization Constants," 2nd ed., Chapman and Hall, London, 1971, chap. 4.
(20) L. M. Jackman and S. Sternhell, "Applications of Nuclear Magnetic Resonance Spectroscopy in Organic Chemistry," 2nd ed., Pergamon, Oxford, 1969, p. 204, and references therein.
(21) L. Jung and P. Cordier, *Bull. Soc. Pharm. Strasbourg*, **8**, 89 (1965); through *Chem. Abstr.*, **66**, 31992 (1967).
(22) K. Pawelczyk, R. Adamski, and E. Stepien, *Farm. Pol.*, **28**, 285 (1972); through *Chem. Abstr.*, **77**, 39352 (1972).
(23) A. Albert and E. P. Serjeant, "The Determination of Ionization Constants," 2nd ed., Chapman and Hall, London, 1971, p. 87.

ACKNOWLEDGMENTS

The authors thank William M. Ment and Sharon R. Reed of the Baltimore District Laboratory, U.S. Food and Drug Administration, for calling attention to the possibility of the problem addressed in this study.

Synthesis of Bridged Catechol–Homocysteine Derivatives as Potential Inhibitors of Catechol *O*-Methyltransferase

O. WILLIAM LEVER, JR.ˣ, CLIFTON HYMAN, and HELEN L. WHITE

Received July 8, 1983, from the *Wellcome Research Laboratories, Burroughs Wellcome Co., Research Triangle Park, NC 27709.* Accepted for publication September 14, 1983.

Abstract □ Catechol derivatives, covalently joined to homocysteine by sulfide or sulfonium linkages, were synthesized as potential catechol *O*-methyltransferase multisubstrate inhibitors which might bridge the enzymatic binding sites for the catechol substrate and the amino acid portion of the methyl donor *S*-adenosylmethionine. These compounds were found to be less effective inhibitors than the product inhibitor *S*-adenosylhomocysteine.

Keyphrases □ Catechol homocysteine derivatives - bridged, synthesis, inhibition of catechol *O*-methyltransferase □ Catechol *O*-methyltransferase - potential inhibitors, bridged catechol-homocysteine derivatives

Catechol *O*-methyltransferase (COMT; EC 2.1.1.6) catalyzes methyl transfer from *S*-adenosyl-L-methionine (SAM, I) to catechol substrates and plays an important role in the inactivation of catecholamines (1, 2). COMT inhibitors offer opportunities for control of catecholamine levels and have potential for treatment of disorders thought to arise from catecholamine deficiencies (3). For example, by decreasing the formation of *O*-methylated metabolites of levodopa and dopamine, COMT inhibitors may enhance the effectiveness of levodopa therapy for Parkinsonism (3–5).

One approach to design of inhibitors of SAM-dependent methylases has focused on analogues of SAM or the product inhibitor *S*-adenosyl-L-homocysteine (SAH, II) (6–12). However, analogues of SAM and SAH may not be highly specific inhibitors for a single methylase since many methyltransferases utilize SAM as the methyl donor and are also subject to potent product inhibition by SAH (1). Although inhibitor specificity for COMT might be more readily achieved with catechol analogues, a number of potent *in vitro* inhibitors of this type are limited in clinical potential by poor *in vivo* activity and/or by unacceptable toxicity (3).

An intriguing alternative approach to COMT inhibitor design emanates from consideration of the proposed mechanism for methyl transfer by COMT. The mechanism appears to involve an S_N2-like nucleophilic attack by the catechol on the methyl group of SAM (13, 14) with a transition state which may be depicted as shown in III. This suggests that compounds such as IV and V, in which a catechol is covalently joined to homocysteine by sulfide or sulfonium linkages, might bridge the enzymatic binding sites for the catechol and for the amino acid portion of SAM and thus might function as multisubstrate (15), or rudimentary transition-state (16, 17), inhibitors of COMT.

The direct transition state analogue IV (n = 1) would not be expected to be sufficiently stable to permit study in an aqueous environment. In an earlier study (18), this problem was circumvented by isosteric replacement of one of the catechol oxygen atoms by a methylene group (*cf.* VI, n = 1). The adducts thus obtained were stable, but were not potent COMT

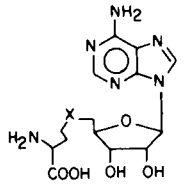

I X = $\overset{+}{S}$Me [SAM]
II X = S [SAH]

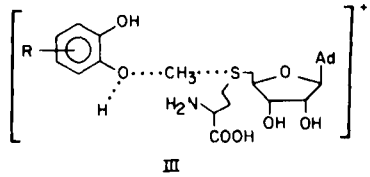

III

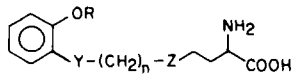

IV Y = O; Z = $\overset{+}{S}$Me
V Y = O; Z = S
VI Y = CH_2; Z = S or $\overset{+}{S}$Me

© 1984, American Pharmaceutical Association

(9) "Beilsteins Handbuch der Organischen Chemie," vol. 11, 4th ed., Springer, Berlin, 1928, p. 295, and succeeding supplements.
(10) O. Anselmino and E. Gilg, Eds., "Kommentar zum Deutschen Arzneibuch," 6th ed., vol. 1, Springer, Berlin, 1928, p. 840.
(11) E. Rupp and A. V. Brixen, *Arch. Pharm. Ber. Dtsch. Pharm. Ges.*, **264**, 698 (1926).
(12) A. H. Clark and E. Kirch, *J. Am. Pharm. Assoc., Sci. Ed.*, **24**, 564 (1935).
(13) S. Pfeifer, *Pharmazie*, **13**, 12 (1958).
(14) "The Merck Index," 9th ed., Merck & Co., Rahway, N.J., 1976, p. 991 with 8th ed., 1968, p. 854 and 7th ed., 1960, p. 841.
(15) "Remington's Pharmaceutical Sciences," 16th ed., Mack Publishing Co., Easton, Pa., 1980, p. 808 with 15th ed., 11975, p. 803, and 14th ed., 1970, p. 874.
(16) A. Wade, Ed., "Martindale: The Extra Pharmacopoeia," 27th ed., Pharmaceutical Press, London, 1977, p. 604.
(17) "The National Formulary," 13th ed., American Pharmaceutical Association, Washington, D.C., 1970, p. 574.
(18) R. Dabrowski and D. M. Patel, *J. Pharm. Sci.*, **54**, 1662 (1965).
(19) A. Albert and E. P. Serjeant, "The Determination of Ionization Constants," 2nd ed., Chapman and Hall, London, 1971, chap. 4.
(20) L. M. Jackman and S. Sternhell, "Applications of Nuclear Magnetic Resonance Spectroscopy in Organic Chemistry," 2nd ed., Pergamon, Oxford, 1969, p. 204, and references therein.
(21) L. Jung and P. Cordier, *Bull. Soc. Pharm. Strasbourg*, **8**, 89 (1965); through *Chem. Abstr.*, **66**, 31992 (1967).
(22) K. Pawelczyk, R. Adamski, and E. Stepien, *Farm. Pol.*, **28**, 285 (1972); through *Chem. Abstr.*, **77**, 39352 (1972).
(23) A. Albert and E. P. Serjeant, "The Determination of Ionization Constants," 2nd ed., Chapman and Hall, London, 1971, p. 87.

ACKNOWLEDGMENTS

The authors thank William M. Ment and Sharon R. Reed of the Baltimore District Laboratory, U.S. Food and Drug Administration, for calling attention to the possibility of the problem addressed in this study.

Synthesis of Bridged Catechol–Homocysteine Derivatives as Potential Inhibitors of Catechol *O*-Methyltransferase

O. WILLIAM LEVER, JR.ˣ, CLIFTON HYMAN, and HELEN L. WHITE

Received July 8, 1983, from the *Wellcome Research Laboratories, Burroughs Wellcome Co., Research Triangle Park, NC 27709.* Accepted for publication September 14, 1983.

Abstract □ Catechol derivatives, covalently joined to homocysteine by sulfide or sulfonium linkages, were synthesized as potential catechol *O*-methyltransferase multisubstrate inhibitors which might bridge the enzymatic binding sites for the catechol substrate and the amino acid portion of the methyl donor *S*-adenosylmethionine. These compounds were found to be less effective inhibitors than the product inhibitor *S*-adenosylhomocysteine.

Keyphrases □ Catechol homocysteine derivatives - bridged, synthesis, inhibition of catechol *O*-methyltransferase □ Catechol *O*-methyltransferase - potential inhibitors, bridged catechol-homocysteine derivatives

Catechol *O*-methyltransferase (COMT; EC 2.1.1.6) catalyzes methyl transfer from *S*-adenosyl-L-methionine (SAM, I) to catechol substrates and plays an important role in the inactivation of catecholamines (1, 2). COMT inhibitors offer opportunities for control of catecholamine levels and have potential for treatment of disorders thought to arise from catecholamine deficiencies (3). For example, by decreasing the formation of *O*-methylated metabolites of levodopa and dopamine, COMT inhibitors may enhance the effectiveness of levodopa therapy for Parkinsonism (3–5).

One approach to design of inhibitors of SAM-dependent methylases has focused on analogues of SAM or the product inhibitor *S*-adenosyl-L-homocysteine (SAH, II) (6–12). However, analogues of SAM and SAH may not be highly specific inhibitors for a single methylase since many methyltransferases utilize SAM as the methyl donor and are also subject to potent product inhibition by SAH (1). Although inhibitor specificity for COMT might be more readily achieved with catechol analogues, a number of potent *in vitro* inhibitors of this type are limited in clinical potential by poor *in vivo* activity and/or by unacceptable toxicity (3).

An intriguing alternative approach to COMT inhibitor design emanates from consideration of the proposed mechanism for methyl transfer by COMT. The mechanism appears to involve an S_N2-like nucleophilic attack by the catechol on the methyl group of SAM (13, 14) with a transition state which may be depicted as shown in III. This suggests that compounds such as IV and V, in which a catechol is covalently joined to homocysteine by sulfide or sulfonium linkages, might bridge the enzymatic binding sites for the catechol and for the amino acid portion of SAM and thus might function as multisubstrate (15), or rudimentary transition-state (16, 17), inhibitors of COMT.

The direct transition state analogue IV (n = 1) would not be expected to be sufficiently stable to permit study in an aqueous environment. In an earlier study (18), this problem was circumvented by isosteric replacement of one of the catechol oxygen atoms by a methylene group (*cf.* VI, n = 1). The adducts thus obtained were stable, but were not potent COMT

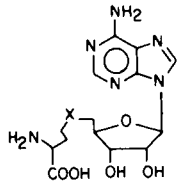

I X = $\overset{+}{S}$Me [SAM]
II X = S [SAH]

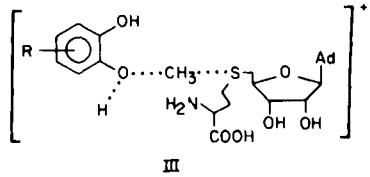

III

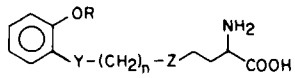

IV Y = O; Z = $\overset{+}{S}$Me
V Y = O; Z = S
VI Y = CH_2; Z = S or $\overset{+}{S}$Me

© 1984, American Pharmaceutical Association

Table I—Inhibition of Catechol-*O*-Methyltransferase [a]

Compound	Percent Inhibition at 100 μM
XXIV	--[b]
XXV	14.9
XV	13.2
XVI	9.0
XVII	12.1
XVIII	5.6
IX	17.3
X	14.0
XI	5.9
XII	Stimulates[c]
XIX	4.7
II	72.2

[a] Rat liver COMT was incubated with 0.1 mM [^{14}C-methyl]*S*-adenosyl-L-methionine (0.3 Ci/mol), 0.25 mM 3,4-dihydroxybenzoic acid, 1 mM $MgCl_2$, 0.5 mM dithiothreitol, and 50 mM Tris-HCl buffer, pH 7.8, for 30 min at 37°C. [b] No significant inhibition observed. [c] Apparent stimulation of activity by 26.4% at 100 μM XII.

inhibitors (18), possibly because COMT is highly specific for the catechol functionality in substrates and in most inhibitors (2, 3). Retention of both catecholic oxygen atoms, for possible coordination at the catechol binding site, might facilitate multisubstrate binding. This could be accomplished by insertion of one or more additional methylenes in the briding chain. The bridging link would thereby be one or two units longer than required for an exact transition-state analogue (*cf.* III). However, a bridging length greater than that suggested by precise transition state mimicry led to increased potency in multisubstrate kinase inhibitors (19), and the expanded bridging chain in the present case might thus be an acceptable structural feature. Accordingly, sulfides and sulfonium salts of types IV and V were synthesized for *in vitro* evaluation as COMT inhibitors.

RESULTS AND DISCUSSION

Chemistry—The synthesis of the sulfides and sulfonium salts with *o*-methoxy substituents are outlined in Scheme I. The only salt obtained from reaction of iodide VIII with dimethyl sulfide was trimethylsulfonium iodide; none of the desired salt XII could be isolated. This type of reversion-ligand exchange process is well documented for sulfonium salts (20, 21), and has recently been adapted as a synthetic method for symmetrical and unsymmetrical organic sulfides (22). This problem was circumvented by preforming

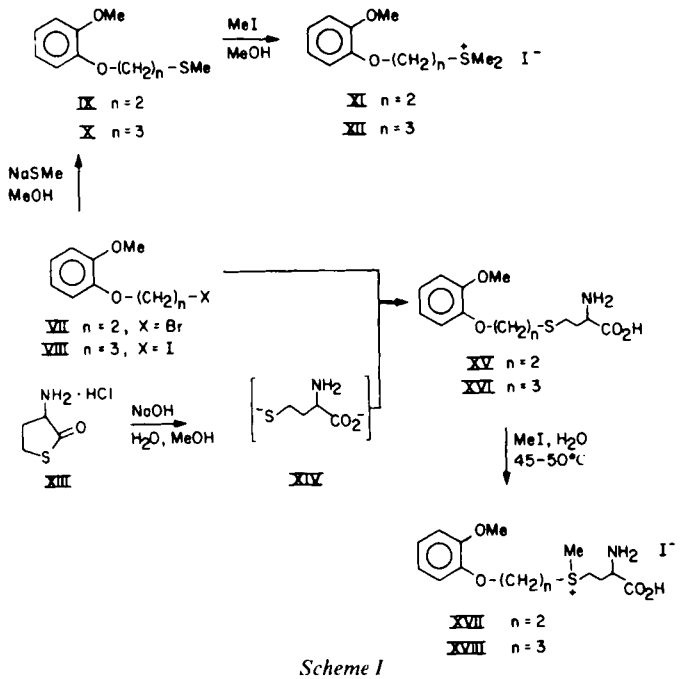

Scheme I

sulfides IX and X followed by their alkylation with methyl iodide. The unsuitability of iodide VIII for direct formation of sulfonium salts was again noted in unsuccessful attempts to form bridged salt XVIII from VIII and methionine, although *S*-methyl methionine XIX was readily formed from methionine and methyl iodide under acidic (23) or neutral (24), *i.e.* zwitterionic amino acid, conditions. We then developed an alternative route to XVII and XVIII utilizing thiolactone XIII. Dianion XIV was generated from XIII by a method similar to those previously reported (25-27) and was alkylated with halides VII and VIII to provide sulfides XV and XVI. The resulting alkyl homocysteines were then alkylated with methyl iodide under neutral conditions (24), which led to specific methylation of the sulfide linkage in the presence of the unprotected amino acid moiety.

The *o*-hydroxy sulfides XXIV and XXV were prepared by similar methods to those in Scheme I. Alkylation of *o*-benzyloxyphenol with 1,3-dibromopropane followed by reductive debenzylation provided the phenolic bromide XXII, which afforded sulfide XXV on treatment with dianion XIV. In the preparation of dimethylene analogue XXIV, protection of the phenol as the acid-labile tetrahydropyranyl group (*cf.* XXIII) was required to avoid intramolecular cyclization (28) of the unprotected phenolic bromide to benzodioxane XX during the reaction with dianion XIV. The free phenol was liberated during acidic workup.

Enzyme Inhibition Studies—Sulfides and sulfonium salts prepared in this study were evaluated as COMT inhibitors by a radiochemical assay (29). The inhibition results listed in Table I indicate that these compounds are at least fourfold less effective inhibitors of COMT than the potent product inhibitor *S*-adenosylhomocysteine (II), and that the inhibition is not greatly affected by the type of bridging atom (sulfide or sulfonium), the length of the bridge (di- or trimethylene), or the nature of the *o*-substituent (hydroxy *versus* methoxy). Our goal was to enhance affinity and specificity of candidate COMT inhibitors by incorporation of portions of SAM (or SAH) into a catechol structure to increase the number of binding sites. Both the level and the narrow range of inhibition shown by the compounds in Table I, along with the results from the related study by Coward and co-workers (18), suggest that a multisubstrate approach to potentially clinically significant COMT inhibitors is likely to require a higher level of molecular complexity than that offered by bridged catechol-homocysteine structures. The additional presence of significant portions of the nucleoside moiety of SAM or SAH may be essential.

EXPERIMENTAL SECTION[1]

2-(2-Methoxyphenoxy)ethyl Bromide (VII)—A mixture of 2-methoxyphenol (124 g, 1.0 mol), 1,2-dibromoethane (379.7 g, 2.0 mol), and aqueous NaOH (48 g, 1.2 mol, in 300 mL of H_2O) was stirred overnight at 80°C. The product was extracted into $CHCl_3$ and the extracts were washed three times with 5% aqueous NaOH and then with water. The solvent was removed under reduced pressure, and the residue was distilled twice through a Vigreux column (15 cm). The fraction boiling at 125°C (0.25 mm) was dissolved in EtOH and the solution was cooled to provide crystals of VII as white needles (112.7 g, 49% yield), mp 45-46°C; ^{1}H-NMR ($CDCl_3$): δ 3.60 (t, 2, J = 7 Hz), 3.81 (s, 3), 4.30 (t, 2, J = 7 Hz), and 6.86 ppm (s, 4); UV (MeOH) λ_{max}: 271.5 (ε 2300) and 220.5 (ε 7400) nm; TLC (silica, $CHCl_3$): R_f 0.57.

Anal.—Calc. for $C_9H_{11}BrO_2$: C, 46.77; H, 4.80; Br, 34.58. Found: C, 46.75; H, 4.80; Br, 34.53.

3-(2-Methoxyphenoxy)propyl Iodide (VIII)—3-(2-Methoxyphenoxy)propyl bromide (51% yield; bp 110-118°C, 0.3 mm Hg) was prepared from 2-methoxyphenol and 1,3-dibromopropane in ethanolic aqueous sodium hydroxide essentially as described for VII. The bromide (51.5 g, 0.21 mol) was

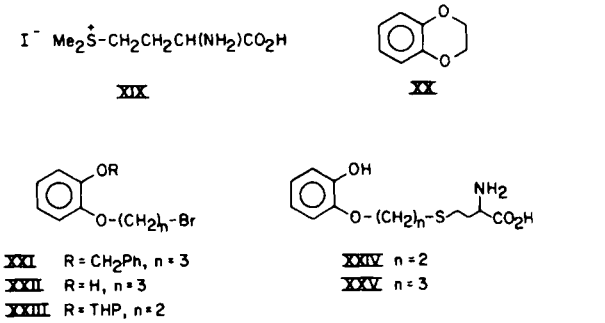

[1] Melting points were determined with a Buchi melting point apparatus and are uncorrected. Elemental analyses were performed by Atlantic Microlab, Inc., Atlanta, Ga. ^{1}H-NMR spectra were determined with Varian T-60, XL-100, and CFT20 and Hitachi Perkin-Elmer R-24B spectrometers with tetramethylsilane as internal standard. COMT inhibition data were obtained by a radiochemical assay (29).

then refluxed with sodium iodide (44.4 g, 0.3 mol) in methyl ethyl ketone (350 mL) for 21 h. The mixture was filtered and the solvent removed under reduced pressure. The residue was dissolved in ether, and on addition of hexane there was deposited 31.4 g (51% yield) of VIII. A portion (6.9 g) of this product was chromatographed on silica gel (Et_2O) and then was recrystallized from ether–hexane to give 4.4 g of VIII as white needles, mp 39–41°C; ^{1}H-NMR ($CDCl_3$): δ 2.31 (quintet, 2, J = 6 Hz), 3.39 (t, 2, J = 6 Hz), 3.85 (s, 3), 4.08 (t, 2, J = 6 Hz), and 6.91 ppm (s, 4); UV (MeOH) λ_{max}: 273.5 (ε 2700, sh) and 224.5 (ε 7200) nm; TLC (silica, $CHCl_3$): R_f 0.58.

Anal.—Calc. for $C_{10}H_{13}IO_2$: C, 41.11; H, 4.49; I, 43.45. Found: C, 41.31; H, 4.53; I, 43.22.

2-(2-Methoxyphenoxy)-1-methylthioethane (IX)—A solution of bromide VII (23.1 g, 0.10 mol) in MeOH (60 mL) was added over a 0.5-h period to a cold (0°C) stirred solution of NaOMe (16.5 g, 0.30 mol) and methanethiol (25 g, 0.52 mol) in MeOH (125 mL). After 0.5 h, the mixture was concentrated under reduced pressure and the residue was extracted with ether. The extracts were concentrated and the residue was distilled (oven 95–115°C, 0.025–0.045 mm Hg) to give IX (18.7 g, 92% yield) as a colorless oil; ^{1}H-NMR ($CDCl_3$): δ 2.19 (s, 3), 2.89 (t, 2, J = 7 Hz), 3.83 (s, 3), 4.17 (t, 2, J = 7 Hz), and 6.88 ppm (s, 4); UV (MeOH) λ_{max}: 272.5 (ε 2600, sh) and 222.5 (ε 8200) nm; TLC (silica, $CHCl_3$): R_f 0.77.

Anal.—Calc. for $C_{10}H_{14}O_2S$: C, 60.57; H, 7.12; S, 16.17. Found: C, 60.52; H, 7.16; S, 16.11.

3-(2-Methoxyphenoxy)-1-methylthiopropane (X)—Sulfide X was prepared in 79% yield from iodide VIII by the same procedure as described above for IX. Sulfide X was isolated as a colorless oil, bp 155°C (oven), 0.32 mm Hg; ^{1}H-NMR ($CDCl_3$): δ 2.10 (m, 5), 2.72 (t, 2, J = 6 Hz), 3.85 (s, 3), 4.14 (t, 2, J = 6 Hz), and 6.92 ppm (s, 4); UV (MeOH) λ_{max}: 272.5 (ε 2400, sh) and 222.5 (ε 7500) nm; TLC [silica, $CHCl_3$–EtOAc (2:1)]: R_f 0.61.

Anal—Calc. for $C_{11}H_{16}O_2S$: C, 62.23; H, 7.60; S, 15.10. Found: C, 62.47; H, 7.67; S, 14.94.

[2-(2-Methoxyphenoxy)ethyl]dimethylsulfonium Iodide (XI)—A solution of sulfide IX (2.97 g, 0.015 mol) and methyl iodide (2.74 g, 0.019 mol) in MeOH (10 mL) was stoppered and allowed to stand in the dark at ambient temperature for 17 h. Addition of ether precipitated sulfonium salt XI as an off-white powder, mp 100–101°C; ^{1}H-NMR (D_2O): δ 2.93 (s, 6), 3.73 (s, 3), 3.61 (t, 2, J = 6 Hz), 4.37 (t, 2, J = 6 Hz), and 6.93 ppm (m, 4); UV (MeOH) λ_{max}: 271.5 (ε 2500, sh) and 219.0 (ε 21,200) nm; TLC [silica, $CHCl_3$–MeOH–NH_4OH–H_2O (40:30:10:3)]: R_f 0.79.

Anal.—Calc. for $C_{11}H_{17}IO_2S$: C, 38.83; H, 5.04; I, 37.30; S, 9.43. Found: C, 38.83; H, 5.06; I, 37.33; S, 9.43.

[3-(2-Methoxyphenoxy)propyl]dimethylsulfonium Iodide (XII)—Sulfonium salt XII was prepared from sulfide X in 72% yield by the procedure described above for preparation of XI. Salt XII was isolated as an off-white microcrystalline solid, mp 98–99°C; ^{1}H-NMR (D_2O): δ 2.34 (br quintet, 2), 2.94 (s, 6), 3.50 (t, 2, J = 7 Hz), 3.87 (s, 3), 4.22 (t, 2, J = 6 Hz), and 7.06 ppm (br s, 4); UV (MeOH) λ_{max}: 271.5 (ε 4200, sh) and 219.5 (ε 23,900) nm; TLC [silica, $CHCl_3$–MeOH–H_2O, (40:30:3)]: R_f 0.78.

Anal.—Calc. for $C_{12}H_{19}IO_2S$: C, 40.68; H, 5.41; I, 35.82; S, 9.05. Found: C, 40.59; H, 5.41; I, 35.70; S, 9.01.

2-Amino-4-[2-(2-methoxyphenoxy)ethylthio]butyric Acid (XV)—DL-Homocysteinethiolactone hydrochloride XIII (12.24 g, 0.08 mol) was heated for 1.5 h at 65°C under nitrogen with a solution of NaOH (9.6 g, 0.24 mol) in 11% aqueous MeOH (88 mL). A solution of bromide VII (19.4 g, 0.084 mol) in MeOH (60 mL) was then added dropwise during a 0.5-h period. After an additional 3.5 h at 65°C, the mixture was concentrated under reduced pressure, the residue was dissolved in hot water, and the mixture was filtered. After cooling, the aqueous solution was extracted twice with ether and then adjusted to pH 7 with concentrated HCl. The resulting precipitate was collected and treated with EtOH. The mixture was filtered, and the filtrate was cooled to provide amino acid XV (11.7 g, 51% yield) as a white powder, mp 221–224°C; ^{1}H-NMR (Me_2SO-d_6): δ 1.92 (m, 2), 2.83 (t, 4, J = 7 Hz), 3.28 (br t, 1, J = 7 Hz), 3.72 (s, 3), 4.09 (t, 2, J = 7 Hz), and 6.90 ppm (s, 4); UV (MeOH) λ_{max}: 272 (ε 2600, sh) and 222.5 (ε 8000) nm; TLC (silica, MeOH): R_f 0.41.

Anal.—Calc. for $C_{13}H_{19}NO_4S$: C, 54.71; H, 6.71; N, 4.91; S, 11.24. Found: C, 54.47; H, 6.77; N, 4.84; S, 11.17.

2-Amino-4-[3-(2-methoxyphenoxy)propylthio]butyric Acid (XVI)—In the same manner as described for preparation of XV, the dianion of DL-homocysteine thiolactone was formed in aqueous methanol at 70°C. Iodide VIII was added as a warm oil and after 0.5 h at 70°C the solution was evaporated, the residue was washed with ether, treated with isopropyl alcohol, and the mixture was filtered. The filtrate was evaporated and the residue was dissolved in water. The pH was adjusted to 7.9 and the resulting precipitate was recrystallized from ethanol to give a 23% yield of XVI as a pale-yellow powder, mp 221–224°C; ^{1}H-NMR (Me_2SO-d_6): δ 1.95 (m, 4), 2.37–2.85 (m, 4), 3.32 (m, 1), 3.74 (s, 3), 4.01 (t, 2, J = 6 Hz), 4.6–6.8 (v br, 3), and 6.93 ppm (s, 4); UV (MeOH) λ_{max}: 272.5 (ε 2500, sh) and 222.5 (ε 7600) nm; TLC (silica, MeOH): R_f 0.54.

Anal.—Calc. for $C_{14}H_{21}NO_4S$: C, 56.16; H, 7.07; N, 4.68; S, 10.71. Found: C, 55.87; H, 7.12; N, 4.73; S, 10.79.

(3-Amino-3-carboxypropyl)[2-(2-methoxyphenoxy)ethyl]methylsulfonium Iodide (XVII)—Methyl iodide (1.88 g, 13.2 mmol) was added to a warm solution of sulfide XV (1.71 g, 6 mmol) in water (40 mL). The mixture was stirred at 50°C for 4 h followed by 12 h at 25°C. A cold condenser (~5°C) was used throughout. The residue, after evaporation under reduced pressure, was dissolved in 50% aqueous ethanol. The solution was filtered and cooled to provide salt XVII (1.00 g, 39% yield) as a pale yellow powder, mp 131–133°C; ^{1}H-NMR (D_2O): δ 2.34 (q, 2, J = 7 Hz), 2.99 (s, 3), 3.36–3.88 (m, 8), 3.77 (s, 3), 4.46 (t, 2, J = 6 Hz), and 6.96 ppm (m, 4); UV (MeOH) λ_{max}: 272 (ε 4900, sh) and 219 (ε 40,000) nm; TLC [silica, $CHCl_3$–MeOH–NH_4OH–H_2O (40:30:10:3)]: R_f 0.71.

Anal.—Calc. for $C_{14}H_{22}INO_4S$: C, 39.35; H, 5.19; I, 7.50; N, 3.28; S, 29.70. Found: C, 39.07; H, 5.20; I, 7.44; N, 3.22; S, 29.51.

(3-Amino-3-carboxypropyl)[3-(2-methoxyphenoxy)propyl]methylsulfonium Iodide (XVIII)—Methyl iodide (1.69 g, 12 mmol) was added to a warm (45°C) mixture of sulfide XVI and water (40 mL) in an apparatus protected with a cold water (~5°C) condenser. After 2 h at 45°C, an additional quantity (1.69 g, 12 mmol) of methyl iodide was added and stirring was continued for 3 h at 45°C and 14 h at ambient temperature. The mixture was filtered and evaporated, and the residue was dissolved in water. Ethanol was added, and the resulting solid was collected and dried to provide 2.77 g (63% yield) of salt XVIII as an off-white powder, mp 126–130°C; ^{1}H-NMR (D_2O): δ 2.39 (m, 4), 3.00 (s, 3), 3.58 (m, 4), 3.86 (s, 3), 3.91 (t, 1, J = 6 Hz), 4.22 (t, 2, J = 6 Hz), and 7.06 ppm (s, 4); UV (MeOH) λ_{max}: 298 (ε 190, sh), 272.5 (ε 2700), and 219.5 (ε 20,000) nm; TLC [silica, $CHCl_3$–MeOH–NH_4OH–H_2O (40:30:10:3)]: R_f 0.61.

Anal.—Calc. for $C_{15}H_{24}INO_4S$: C, 40.82; H, 5.48; I, 7.27; N, 3.17; S, 28.76. Found: C, 40.71; H, 5.52; I, 7.26; N, 3.14; S, 28.65.

(L-Methionine)methylsulfonium Iodide (XIX)—In a manner similar to that described for the preparation of the methyl sulfonium salt from racemic methionine (24), a mixture of L-methionine (3.7 g, 0.025 mol), water (20 mL), and methyl iodide (3.9 g, 0.027 mol) was stirred at 40°C for 18 h. The mixture was taken to dryness under reduced pressure, and the residue was triturated with ethanol. The resulting solid was recrystallized from aqueous ethanol, and the product was washed with hot methanol to provide 5.0 g (68% yield) of XIX as a white microcrystalline solid, mp 185°C (dec.) [the mp for the corresponding salt from racemic methionine has been reported as 150°C (dec.) (23, 24) and 156–157°C (dec.) (30); we are unaware of a specific mp citation for the optically active form, although an elemental analysis has been reported previously (31)]; ^{1}H-NMR (D_2O): δ 2.28–2.50 (m, 2), 2.98 (s, 6), 3.42–3.60 (m, 2), and 3.91 ppm (t, 1, J = 7 Hz); UV (MeOH) λ_{max}: 217.5 nm (ε 61,800); $[\alpha]_D^{20}$ 17.70°; TLC [silica, $CHCl_3$–MeOH–NH_4OH–H_2O (40:30:10:3)]: R_f 0.63.

Anal.—Calc. for $C_6H_{14}INO_2S$: C, 24.75; H, 4.85; I, 43.59; N, 4.81; S, 11.01. Found: C, 24.78; H, 4.89; I, 43.59; N, 4.80; S, 11.00.

1-(2-Benzyloxyphenoxy)-3-bromopropane (XXI)—To a stirred solution of 2-benzyloxyphenol (30.0 g, 0.15 mol) and 1,3-dibromopropane (60.5 g, 0.30 mol) in ethanol (100 mL) was added a solution of NaOH (6 g, 0.15 mol) in water (150 mL). The mixture was refluxed for 9 h, allowed to stand overnight, and then extracted with $CHCl_3$. The organic layer was washed with aqueous NaOH and then with water. The extract was dried (Na_2SO_4) and concentrated, and the residue was distilled to provide an oil (bp 157°C, 0.002 mm Hg) which was crystallized with ether–hexane to give 20.5 g (42% yield) of the bromide as a white powder, mp 29–30°C; ^{1}H-NMR ($CDCl_3$): δ 2.30 (quintet, 2, J = 6 Hz), 3.60 (t, 2, J = 6 Hz), 4.15 (t, 2, J = 6 Hz), 5.10 (s, 2), 6.92 (s, 4), and 7.40 ppm (m, 5); UV (MeOH) λ_{max}: 275 nm (ε 2750); TLC [silica, $CHCl_3$–hexane (1:1)]: R_f 0.44.

Anal.—Calc. for $C_{16}H_{17}BrO_2$: C, 59.81; H, 5.33; Br, 24.89. Found: C, 60.01; H, 5.39; Br, 24.70.

3-(2-Hydroxyphenoxy)propyl Bromide (XXII)—A solution of the benzyloxy compound XXI (44.9 g, 0.14 mol) in ethanol (100 mL) was hydrogenated at 40 psi over 20% $Pd(OH)_2$ on charcoal until hydrogen uptake ceased. The catalyst was removed by filtration, and the solution was evaporated under reduced pressure to provide XXII as an oil, which was used directly in the preparation of sulfide XXV. In another experiment the oil crystallized to give long off-white prisms, mp 52–54°C [lit. (28) mp 57–58°C]; ^{1}H-NMR ($CDCl_3$): δ 2.27 (quintet, 2, J = 6 Hz), 3.52 (t, 2, J = 6 Hz), 4.13 (t, 2, J = 6 Hz), 5.46 (br s, 1), and 6.84 ppm (m, 4).

2-(2-(2-Tetrahydropyranyloxy)phenoxy)ethyl Bromide (XXIII)—A mixture of 2-(2-tetrahydropyranyloxy)phenol (19.4 g, 0.10 mol), NaOH (4.4 g, 0.11 mol), 1,2-dibromoethane (75.1 g, 0.40 mol), and 20% aqueous EtOH (100 mL) was heated at 80°C for 4.5 h. The solvent was removed under reduced pressure, and the residue was treated with $CHCl_3$. The extract was washed

with 5% aqueous NaOH, then water, and concentrated under reduced pressure. Distillation of the residue gave 10.2 g (34% yield) of XXIII as a colorless oil, bp 105–130°C, 0.2 mm Hg; ^{1}H-HMR ($CDCl_3$): δ 1.3–2.3 (m, 6), 3.56 (t, 2, J = 6 Hz), 3.90 (m, 2), 4.25 (t, 2, J = 6 Hz), 5.37 (br s, 1), and 6.2–7.2 ppm (m, 4).

2-Amino-4-[2-(2-hydroxyphenoxy)ethylthio]butyric Acid (XXIV)—A mixture of DL-homocysteinethiolactone hydrochloride (XIII, 4.59 g, 0.03 mol) and NaOH (3.6 g, 0.09 mol) in 20% aqueous MeOH (45 mL) was stirred under nitrogen at 25°C for 18 h, then heated at 65°C for 2 h. Bromide XXIII (9.90 g, 0.033 mol) was then added, and after 3 h at 65°C and 17 h at room temperature, the mixture was concentrated, the residue was treated with isopropyl alcohol, and the mixture was filtered. The filtrate was evaporated, and the residue was dissolved in water. The resulting aqueous solution was washed twice with ether. The aqueous phase was adjusted to pH 8 (1 M HCl), and the precipitate which formed was collected and then suspended in water. The aqueous solution was adjusted to pH 6 (1 M HCl), and the mixture was stirred for 0.75 h. The deprotected product, precipitated by adjustment to pH 7, was washed with a small amount of absolute EtOH followed by ether. This afforded 3.31 g (41% yield) of sulfide XXIV as a white powder, mp 206–209°C; ^{1}H-NMR (Me_2SO-d_6): δ 1.9 (m, 2), 2.68 (t, 2, J = 7 Hz), 2.83 (t, 2, J = 7 Hz), 3.33 (t, 1, J = 6 Hz), 4.05 (t, 2, J = 7 Hz), 6.5–7.0 (m, 4), and 7.9 ppm (v br, 4); UV (MeOH) λ_{max}: 274 (ε 2800, sh), and 215 (ε 7200) nm; TLC (silica, MeOH): R_f 0.51.

Anal.—Calc. for $C_{12}H_{17}NO_4S$: C, 52.25; H, 6.39; N, 5.08; S, 11.62. Found: C, 52.24; H, 6.34; N, 5.05; S, 11.67.

2-Amino-4-[3-(2-hydroxyphenoxy)propylthiobutyric Acid (XXV)—A mixture of DL-homocysteinethiolactone hydrochloride (XIII; 12.24 g, 0.08 mol) and NaOH (9.6 g, 0.24 mol) in 20% aqueous MeOH (60 mL) was stirred under nitrogen at 25°C for 18 h, then heated at 65°C for 2 h. Bromide XXII (15.0 g, 0.065 mol) was added, followed by a solution of NaOH (5.2 g, 0.13 mol) in 20 mL of 50% aqueous MeOH. After the addition of a second portion of XXII (15.0 g, 0.065 mol), the mixture was stirred at 25°C for 18 h and the solvent was removed under reduced pressure. The residue was dissolved in water, and the solution was extracted three times with $CHCl_3$. The aqueous phase was brought to pH ~2 with 6 M HCl and extracted twice with $CHCl_3$. The aqueous phase was brought to pH 7 with 1 M NaOH, and product XXV was collected as a white powder (8.93 g, 39% yield), mp 218–221°C; ^{1}H-NMR (Me_2SO-d_6): δ 1.90 (m, 4), 2.4–2.8 (m, 4), 3.25 (t, 1, J = 6 Hz), 3.96 (t, 2, J = 6 Hz), 6.55–6.95 (m, 4), and 7.9 ppm (v br, 3); UV (MeOH) λ_{max}: 274.5 (ε 2900), 279 (ε 2500), and 215 (ε 6800) nm; TLC (silica, MeOH): R_f 0.51.

Anal.—Calc. for $C_{13}H_{19}NO_4S$: C, 54.71; H, 6.71; N, 4.91; S, 11.24. Found: C, 54.56; H, 6.78; N, 4.91; S, 11.22.

REFERENCES

(1) E. Usdin, R. T. Borchardt, and C. R. Creveling, Eds., "Transmethylation," Elsevier-North Holland, New York, N.Y., 1979.

(2) R. T. Borchardt, in "Enzymatic Basis of Detoxication," Vol. II, W. B. Jakoby, Ed., Wiley, New York, N.Y., 1980, p. 43.

(3) H. C. Guldberg and C. A. Marsden, *Pharmacol. Rev.*, **27,** 135 (1975).

(4) S. Fahn, R. Comi, S. R. Snider, and A. L. N. Prasad, *Biochem. Pharmacol.*, **28,** 1221 (1979).

(5) A. Reches, D. Jiang, and S. Fahn, *Naunyn-Schmiedeberg's Arch. Pharmacol.*, **320,** 34 (1982).

(6) R. T. Borchardt, Y. S. Wu, and B. S. Wu, *J. Med. Chem.*, **21,** 1307 (1978).

(7) R. T. Borchardt, Y. S. Wu, J. A. Huber, and A. F. Wycpalek, *J. Med. Chem.*, **19,** 1104 (1976).

(8) R. T. Borchardt, J. A. Huber, and Y. S. Wu, *J. Med. Chem.*, **19,** 1094 (1976).

(9) J. K. Coward, D. L. Bussolotti, and C. D. Chang, *J. Med. Chem.*, **17,** 1286 (1974).

(10) C. D. Chang and J. K. Coward, *J. Med. Chem.*, **19,** 684 (1976).

(11) R. W. Fuller and R. Nagarajan, *Biochem. Pharmacol.*, **27,** 1981 (1978).

(12) R. T. Borchardt, *J. Med. Chem.*, **23,** 347 (1980).

(13) R. W. Woodard, M. D. Tsai, H. G. Floss, P. A. Crooks, and J. K. Coward, *J. Biol. Chem.*, **255,** 9124 (1980).

(14) M. F. Hegazi, R. T. Borchardt, and R. L. Schowen, *J. Am. Chem. Soc.*, **101,** 4359 (1979).

(15) J. S. Heller, E. S. Canellakis, D. L. Bussolotti, and J. K. Coward, *Biochem. Biophys. Acta*, **403,** 197 (1975).

(16) R. W. Wolfenden, *Ann. Rev. Biophys. Bioeng.*, **5,** 271 (1976).

(17) R. N. Lindquist, in "Drug Design," Vol. V, E. J. Ariens, Ed., Academic, New York, N.Y., 1975, p. 23.

(18) G. L. Anderson, D. L. Bussolotti, and J. K. Coward, *J. Med. Chem.*, **24,** 1271 (1981).

(19) G. E. Lienhard and I. I. Secemski, *J. Biol. Chem.*, **248,** 1121 (1973).

(20) C. J. M. Stirling, in "Organic Chemistry of Sulfur", S. Oae, Ed., Plenum, New York, N.Y., 1977, p. 473.

(21) F. E. Ray and I. Levine, *J. Org. Chem.*, **2,** 267 (1937).

(22) A. J. H. Labuschagne, J. S. Malherbe, C. J. Meyer, and D. F. Schneider, *J. Chem. Soc., Perkin I*, **1978,** 956.

(23) G. Toennies and J. J. Kolb, *J. Am. Chem. Soc.*, **67,** 849 (1945).

(24) R. O. Atkinson and F. Poppelsdorf, *J. Chem. Soc.*, **1951,** 1378.

(25) H. M. Kolenbrander, *Can. J. Chem.*, **47,** 3271 (1969).

(26) J. A. Duerre and C. H. Miller, *Anal. Biochem.*, **17,** 310 (1966).

(27) M. D. Armstrong and J. D. Lewis, *J. Org. Chem.*, **16,** 749 (1951).

(28) G. Illuminati, L. Mandolini, and B. Masci, *J. Am. Chem. Soc.*, **96,** 1422 (1974).

(29) H. L. White and J. C. Wu, *Biochem. J.*, **145,** 135 (1975).

(30) K. Fukui, K. Kanai, and H. Kitano, *J. Org. Chem.*, **25,** 804 (1960).

(31) M. Mazelis, B. Levin, and N. Mallison, *Biochim. Biophys. Acta*, **106,** 105 (1965).

Effects of Divalent Amino Acids on Iron Absorption

JOHN M. CHRISTENSEN ˣ, MUSA GHANNAM, and JAMES W. AYRES

Received May 2, 1983, from the *School of Pharmacy, Oregon State University, Corvallis, OR 97331.* Accepted for publication August 30, 1983.

Abstract □ Solutions of each of 10 amino acids or ascorbic acid were mixed with iron and orally administered to rats. Iron was absorbed to a statistically significantly greater extent ($p < 0.05$) when mixed with asparagine, glycine, serine, or ascorbic acid as compared with a control solution of iron. The largest effects were for asparagine and glycine, which also increased iron absorption to a significantly greater extent ($p < 0.001$) than did serine or ascorbic acid. No statistically significant increase in iron absorption occurred when any of the other amino acids was mixed with iron. The extent of iron absorption from each test solution, as measured by area under the concentration of iron-59 in the blood-time curve ($r^2 = 0.0002$), and the initial rate of iron absorption for each test solution ($r^2 = 0.01$) showed no correlation with the stability constant of the amino acid-iron complex.

Keyphrases □ Absorption—iron, effects of divalent amino acids □ Iron—absorption, effects of divalent amino acids □ Amino acids—divalent, effects on iron absorption □ Complexes—iron-divalent amino acids, effect on iron absorption

Some products are available on the market in which amino acids or protein are combined with iron[1] in the hope of promoting iron absorption. Amino acids chelate with iron (1–3), and under certain circumstances, the resultant chelate enhances iron absorption from the GI tract (4–9). Low molecular weight chelates have been postulated to be essential for iron absorption by keeping iron in solution and preventing hydrolysis or precipitation of iron (10–12).

It has been proposed (8, 9) that amino acids which form the most stable complexes with iron are the most effective in increasing iron absorption from the GI tract, and failure of certain amino acids to promote iron absorption *in vivo* is due to their inability to chelate iron strongly enough to compete with water. Thus, they do not prevent hydrolysis and subsequent precipitation of iron. These data also suggest that amino acids with high stability constants should enhance iron absorption better than amino acids with lower stability constants.

These conclusions were reached based on data obtained for trivalent amino acids only (8). In some previous experiments conducted to study the effects of amino acids on iron absorption (4–9), phosphate buffers were used which have been reported to decrease iron absorption both *in vivo* and *in vitro* (13, 14). The conclusion of these reports that amino acid–iron complexes administered in phosphate buffer increase iron absorption may not be quantitatively correct since iron is known to form insoluble phosphate salts which might result in decreased iron absorption. Also, Monsen and Page (15) have studied some "iron absorption promoting agents," including aspartic acid which is an amino acid that forms a high-affinity iron chelate, and reported no increase in iron absorption.

This study was initiated to define the effect of selected divalent amino acids on iron absorption and to determine whether increased iron absorption with amino acids is related to the stability constant of the amino acid–iron complex. Ascorbic acid, an agent which is reported to enhance iron absorption (16, 17), was also tested to compare its effect on enhancing iron absorption with that of amino acids.

[1] Fe-Plus, a soy-protein iron complex; Miller, Inc.; and Ronium capsules, an amino acid–iron complex; Pasadena, Inc.

EXPERIMENTAL SECTION

Determination of Stability Constants of 10 Amino Acid Complexes with Iron—Glycine, L-proline, D,L-tryptophan, L-asparagine, D,L-alanine, D,L-phenylalanine, D-serine, D,L-methionine, D,L-leucine, and L-isoleucine were obtained commercially. Stability constants were determined by using a standard method for the determination of chelation between amino acids and metals (1–3). The amino acids described above were all dried at 60°C under reduced pressure for 1 h. Each amino acid (50 mL of a 0.01 M aqueous solution) was titrated with 0.1 M KOH first in the absence of metals and then in the presence of one equivalent of the ferrous sulfate salt (0.005 M). Thus, the molar ratio of the complex-forming agent to metal was 2:1 for all bivalent ions. The amount of alkali used in each titration was 5 mL (*i.e.*, the equivalent of the amount of complex-forming agent), and this was added in 10 equal portions of 0.5 mL each.

Experiments were conducted by using a water bath maintained at 37°C, and the amino acid solution was stirred continuously with nitrogen to maintain an inert atmosphere above the solutions. Boiled water was used since air must be removed from the system to avoid change in base concentration. The pH was recorded after each addition.

Preparation of the Buffer—A potassium hydrogen phthalate–sodium hydroxide buffer solution was prepared with a final pH of 6.0. Such a buffer contained 50 mL of 0.1 M potassium hydrogen phthalate and 43.7 mL of 0.1 M NaOH diluted to 100 mL. This buffer system was used because it did not precipitate iron from solution as did the phosphate buffer.

The ferrous ion was the important ion, and the potassium hydrogen phthalate buffer system maintained the iron in the ferrous state. This was determined throughout the study by taking a small portion of the solution, filtering it, and counting the radioactivity (iron-59) in solution. The ferric ion eventually forms and precipitates at pH 6.0 and does not stay in solution. The iron never precipitated in potassium hydrogen phthalate buffer throughout the study. The ferrous ion did not hydrolyze to form the ferric ion in potassium hydrogen phthalate buffer, and the iron was administered as the ferrous ion.

Procedure with Rats—Sprague–Dawley rats were bred and raised at the Oregon State University Animal Resource Center. The rats were housed in

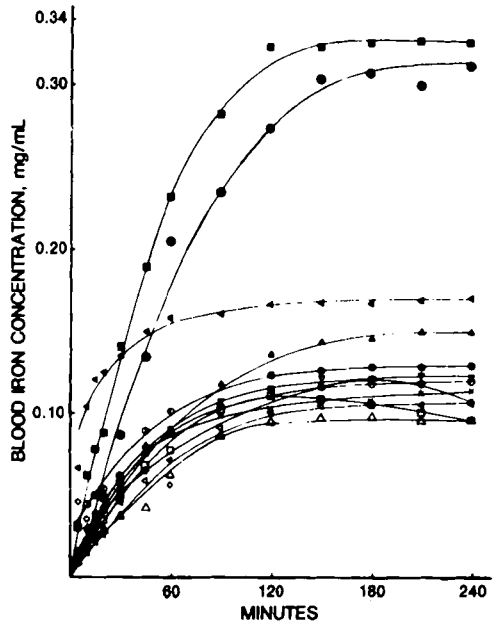

Figure 1—*Comparison of blood iron-59 concentrations-time curves when 0.2 M ferrous sulfate was given as control (△) and with amino acids and ascorbic acid added. Key: (■) asparagine; (●) glycine; (◀) serine; (▲) alanine; (⊖) proline; (▽) isoleucine; (○) leucine; (x) methionine; (◇) ascorbic acid; (◁) phenylalanine; (□) tryptophan; (△) control.*

0022-3549/84/0900-1245$01.00/0
© 1984, American Pharmaceutical Association

Table I—Formula of the Rat Feed

Ingredient	Pounds/Ton of Feed
Alfalfa (ground)	200
Bentonite (as a binder)	50
Corn (ground)	546
Barley (ground)	600
Soybean meal (44% crude protein)	240
Fish meal	100
Feather meal	40
Whey (dried)	200
Trace mineralized salt	10
Tricalcium phosphate	14
Vitamin A (1,000,000 IU/g)	3 g
Vitamin D (36,000 IU/g)	13.6 g

pairs in metal cages (~25.4 × 20.3 cm) for 3 months before use, with a 12-h light/12-h dark cycle. The rats were allowed food and water *ad libitum* prior to fasting. The rat food was a special feed developed at Oregon State University. The formula for the food is presented in Table I.

Solutions of iron (as $^{59}FeSO_4$)[2] as a control solution and complexed with each of 10 amino acids or ascorbic acid were administered orally to groups of six rats each. Male albino rats (weight, 250–270 g each) were used. Rats were fasted for 24 h before the start of the experiment to minimize the occurrence of extraneous complexing agents, present as food constituents in the intestinal lumen, which may affect iron absorption (4). All test solutions were prepared by adding an amino acid and $^{59}FeSO_4$ to aliquots of the buffer so that the resulting iron-59 activity was 10 μCi/mL. The amino acid concentration was 0.4 M. The ascorbic acid concentration was 0.5 M, and the ferrous sulfate concentration was 0.2 M (10 μCi/mL). A control solution was prepared by the same procedure, but it did not contain amino acid or ascorbic acid.

An oral intubation tube[3] was used to deliver 1 mL of test or control solution into the stomach. The tube was then removed, and the rat was kept under anesthesia (ether) during the entire experiment.

At 5, 10, 20, 30, 45, 60, 90, 120, 150, 180, 210, and 240 min after administration of the solution, 20-μL samples of blood were collected from a toe of the rat by clipping the skin and collecting blood in capillary tubes. The capillary tubes were then placed into counting vials. Each sample was counted for 10 min in a solid scintillation counter chamber[4].

At the end of 4 h, the animals were sacrificed by overdose of ether. Liver, kidney, heart, brain, and muscle samples were collected from the animals, weighed, and then counted for 10 min[4].

RESULTS AND DISCUSSION

The concentration of iron-59 in blood *versus* time curves of iron-59 absorbed from all amino acid–iron, ascorbic acid–iron, and control solutions are shown in Fig. 1. All test solutions of amino acid and ascorbic acid with iron produced concentrations of iron-59 in blood higher than that in the control solution. It is known that blood or serum iron *versus* time curves cannot be used alone for quantitative and reliable iron absorption measurements (15–17). Other tissue iron concentrations should be included with concentrations of iron-59 in blood so that the total iron absorbed can be measured or estimated from the tissues sampled. The concentration and amount of iron-59 in tissues sampled 4 h after administration of all the amino acid–iron solutions, the ascorbic acid solution, and the control solution are shown in Table II.

The concentration of iron-59 was highest in tissues of animals receiving asparagine–iron and glycine–iron solutions, whereas it was lower in the tissues of animals receiving the other amino acid–iron solutions or the ascorbic acid–iron solution. The fact that the concentrations of iron-59 in blood and tissue at the end of the experiment were higher in the animals receiving amino acid–iron solutions than control solutions indicates that the elevated concentrations of iron-59 in blood in these animals is an accurate reflection of increased absorption from the GI tract.

In the tissues, the iron-59 concentration was highest in the heart, and the largest amount was found in muscle (due to large muscle mass in the body). High concentrations of iron-59 were also found in the liver and kidney, and generally, there were very small concentrations in the muscle and brain. This was consistent for the control experiments as well as for all 10 amino acid–iron complexes and the ascorbic acid–iron solution. Stores of iron are mainly in reticuloendothelial cells and, thus, are found in organs rich in such cells, especially the liver (18, 19). The heart is also an organ that has been reported

[2] New England Nuclear Corp., Boston, Mass.
[3] Popper and Sons, Inc., New York.
[4] Tracer Northern T-1705 NCA 40 mL NaI (Tl) detector.

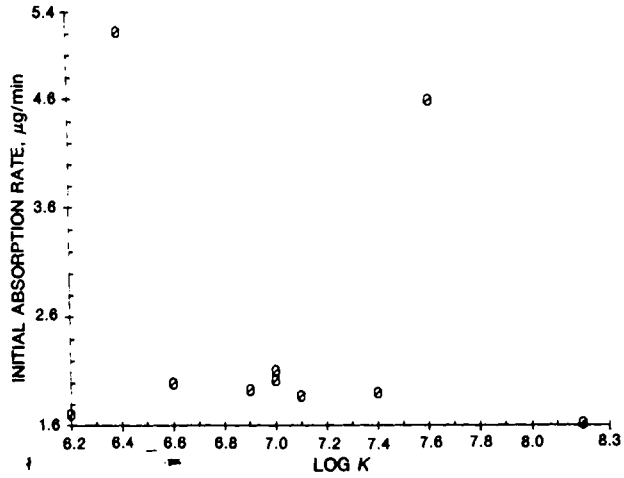

Figure 2—*Initial rate of absorption* versus *log* K *for each of the amino acids.*

(20, 21) to be high in iron content, which is most likely due to the heart being an organ high in iron sulfur proteins and cytochrome enzymes. Cytochrome *c*, for example, contains 1 g of iron/mol (20). The amount of stored iron varies with sources and also with demands made on it for hemoglobin formation. Glycine and asparagine increased iron-59 absorption to the greatest extent ($p < 0.001$) as compared with the control solution. Although the increase of iron-59 absorption over that of the control by serine and ascorbic acid was statistically significant (by ANOVA, $p < 0.05$), the increase was minimal, only 72.7 and 54.5%, respectively, compared with 309% for glycine and 345% for asparagine. These data are consistent with the data of Forth and Rummel, who observed a 300% increase in the amount of iron absorbed from the gut *in situ* in rats with glycine–phosphate buffer compared with iron–phosphate buffer (9) alone. Diets for chicks that were low in glycine but adequate in iron caused a marked reduction in the amount of iron absorbed *versus* diets in which glycine and iron were present in adequate amounts (22).

The concentration of iron-59 in tissues of animals receiving amino acid–iron solutions, control solution, or the ascorbic acid–iron solution was consistent with concentrations of iron-59 in the blood obtained from each test or control solution. Therefore, the concentration of iron-59 in blood *versus* time curves were used to compare the chelating affinity of the amino acid to iron (stability constant) with the ability of the amino acid to increase the rate or an approximated relative extent of iron absorption. This was done by comparing the initial rate of absorption with the stability constant of the amino acid–iron complex or by comparing the area under the concentration of iron-59 in blood *versus* time curve (0–4 h) with the stability constant of the amino acid complex. For all amino acid–iron complexes, the concentration of iron-59 in the blood *versus* time (Fig. 1) was fit to a trinomial equation (r^2 range, 0.9857–0.9991). Figure 1 shows the plot of the experimentally observed *versus* calculated concentrations of iron-59 in blood for each test solution. An empirical equation which describes the concentrations of iron-59 in blood curves, therefore, is:

$$y = B_0 + B_1 t + B_2 t^2 + B_3 t^3 \qquad \text{(Eq. 1)}$$

where t is time. This equation was used to fit the data so that the initial rate of absorption could be estimated.

The initial rate of absorption is approximated by the tangent to the concentration of iron-59 in blood curve at time zero and is equal to B_1 after differentiating dy/dt. The initial rates of iron-59 absorption, in decreasing order starting with the amino acid that increased the initial rate of absorption most, were: asparagine, glycine, serine, leucine, methionine, isoleucine, tryptophan, alanine, phenylalanine, and proline (Table III).

The effects of different amino acids on iron-59 absorption from time zero to 4 h were compared with the control by comparing the area under the concentration of iron-59 in blood *versus* time curve (AUC) for each amino acid–iron complex from time zero to 4 h. When integrating the above equation over the experimental period of 4 h, the area under the concentrations of iron-59 in blood time curve ($AUC_{0\text{-}240\ min}$) for each amino acid iron complex can be obtained as:

$$\int_{y_0}^{y_{240}} y\,dt = \int_{t=0}^{t=240} (B_0 + B_1 t + B_2 t^2 + B_3 t^3)\,dt \qquad \text{(Eq. 2)}$$

$$= 240\,B_0 + 28{,}800 B_1 + 4608 \times 10^3 B_2 + 82{,}944 \times 10^4 B_3$$

The values of B_0, B_1, B_2 and B_3 for each amino acid were obtained by curve

Table II—Iron in Tissues Sampled 4 h after Oral Administration of Test Solution to Rats

Test Solution	Average Concentration of Iron, μg/g of tissue					Conc. of Iron Remaining in GI Tract, μg/g of tissue[a]	Total Amount of Iron Absorbed, mg[b]
	Liver	Heart	Kidney	Muscle	Brain		
Iron alone	3.4 ± 0.3	4.5 ± 1.0	0.81 ± 0.15	0.81 ± 0.06	0.29 ± 0.05	- -	1.1 ± 0.1
Glycine-iron	16.4 ± 2.0	14.0 ± 2.4	3.58 ± 1.45	2.02 ± 0.44	0.68 ± 0.10	—	3.4 ± 0.2[c]
Leucine-iron	3.7 ± 0.1	5.2 ± 0.1	0.59 ± 0.11	0.96 ± 0.08	0.21 ± 0.17	—	1.3 ± 0.1
Tryptophan-iron	4.5 ± 1.2	5.2 ± 0.6	1.41 ± 0.38	1.01 ± 0.17	0.33 ± 0.04	–	1.1 ± 0.1
Asparagine-iron	21.7 ± 2.1	23.1 ± 0.9	13.19 ± 1.66	2.54 ± 0.22	0.36 ± 0.15	1.02 ± 2.6	3.8 ± 0.2[c]
Serine-iron	4.9 ± 0.3	6.9 ± 0.2	1.44 ± 0.17	1.25 ± 0.18	0.45 ± 0.08	—	1.9 ± 0.1[d]
Proline-iron	3.8 ± 0.3	5.6 ± 0.3	0.94 ± 0.19	0.98 ± 0.16	0.30 ± 0.07	—	1.4 ± 0.1
Methionine-iron	3.6 ± 0.2	5.1 ± 0.2	0.90 ± 0.12	0.84 ± 0.11	0.32 ± 0.04	45.2 ± 2.4	1.2 ± 0.1
Alanine-iron	3.9 ± 0.3	6.3 ± 0.8	0.93 ± 0.11	1.01 ± 0.17	0.33 ± 0.06	—	1.6 ± 0.1
Isoleucine-iron	3.8 ± 0.1	5.2 ± 0.4	0.78 ± 0.08	0.94 ± 0.10	0.37 ± 0.07	—	1.3 ± 0.1
Phenylalanine-iron	3.6 ± 0.2	4.9 ± 0.2	0.85 ± 0.13	0.84 ± 0.15	0.32 ± 0.02	46.8 ± 5.1	1.1 ± 0.1
Ascorbic Acid-iron	4.3 ± 0.2	5.2 ± 0.2	1.27 ± 0.18	1.08 ± 0.18	0.40 ± 0.07	—	1.7 ± 0.1[d]

[a] After 4 h. [b] After 4 h. Calculations assume homogenous iron content throughout the tissues sampled. Also, the skeletal and adipose tissues are assumed to have the same iron content as the muscle tissue. Tissue mass was not determined in this study, but published (23) averages values for specific tissue masses, corrected for rat weights, were used in these estimations. Although these assumptions may not be totally accurate for estimating total iron absorbed, they are adequate because the actual values of iron absorbed would only be all scaled-up or -down in proportion to the relative values listed. The dose of iron administered was 11.2 mg. [c] $p < 0.001$. [d] $p < 0.005$.

fitting[5], and the area (Table III) under the concentrations of iron-59 in blood–time curve (0–4 h) was then calculated for each test solution.

Table III lists stability constants determined experimentally for each amino acid–iron complex, as well as the initial rate of iron absorption and the area under the concentration of iron-59 in blood *versus* time curves.

Figure 2 is a plot of the initial rate of iron absorption *versus* stability constant for each amino acid–iron complex, and Fig. 3 is a plot of AUC *versus* stability constant for each amino acid–iron complex. No useful correlation between either the initial rate of absorption ($r^2 = 0.01$) or area under the concentration of iron-59 in blood *versus* time curve ($r^2 = 0.000208$) (Fig. 2) and the stability constants of the appropriate amino acid–iron complex was observed (Fig. 3). This is contrary to the earlier hypothesis that amino acids which have larger amino acid–iron complex stability constants should increase iron absorption (8, 9). Although the amino acids reported to increase iron absorption had high stability constants, neither glycine nor asparagine have high stability constants, but both were effective in increasing iron absorption from the GI tract. What may have been measured in the earlier experiments was the ability of those amino acids that have large iron-complex stability constants to protect iron from precipitating with phosphates. It is interesting to note that EDTA forms a more stable complex than any of the amino acids tested, yet it does not facilitate increased iron absorption (9, 16, 17) and is even reported to negate any iron absorption enhancement produced by an iron absorption-promoting agent.

As another measure of the ability of the amino acid to increase iron absorption, the amount of iron-59 in gut tissue was determined after administration of phenylalanine–iron and methionine–iron complexes, in which the increase in iron absorption was lowest, and asparagine–iron complexes, in which it was highest. The amount of iron-59 in gut tissue (Table II) was much higher in the case of the phenylalanine–iron and methionine–iron complexes. This, too, is an indication that the elevated concentration of iron-59 in blood in the rats is a reflection of increased absorption from the GI tract. Conversely, when iron absorption is lower, the iron is retained in the gut tissue.

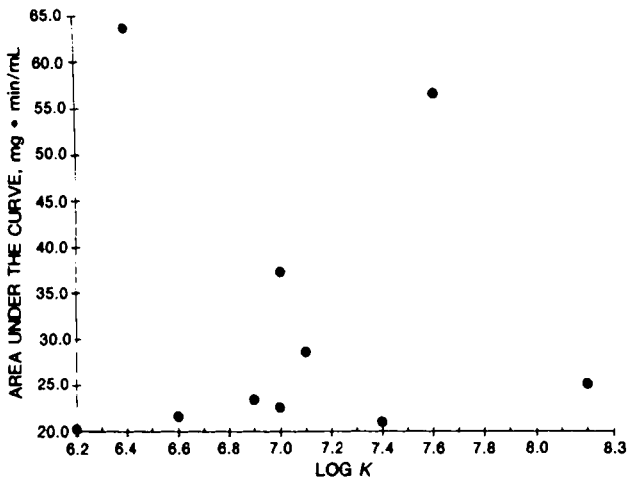

Figure 3—*AUC from time zero to 4 h of blood iron-59 concentration–time profile* versus *log K for each of the amino acids tested.*

Protein repeatedly has been reported to promote iron absorption (4–8, 24–26). This effect may account for the high fraction of iron in meat that is absorbed and for the enhancement of iron absorption from vegetables with simultaneous ingestion of meat (24–27). However, protein has also been reported to have a negative effect on iron absorption. Egg protein retards the absorption of iron (23, 27); it is not known whether the effect is related to its content of conalbumin. Conalbumin forms a stable complex with iron *in vitro* that drastically reduces the transfer of iron in jejunal segments of anemic rats (10). Egg yolk also contains phosphoproteins that form stable complexes with iron and prevent iron absorption (13, 23). The differential effects of proteins on absorption of iron may be attributed to the degree of proteolysis that occurs in the different experiments (23). All the data suggest that iron chelation does not always promote iron absorption.

Several products on the market have iron-chelating agents that are reported to promote iron absorption. These products, which contain agents reported to promote iron absorption, vary from protein hydrolysate to combinations of amino acids to a single amino acid. The iron absorption-promoting ability of these mixtures of agents needs to be investigated and compared with the ability of each one to promote iron absorption. It may be that only certain amino acids are responsible for enhanced iron absorption, and others can be omitted from iron product formulations; the result may be further increased iron absorption. A product containing only glycine and/or asparagine with iron may be sufficient to produce significantly increased iron absorption compared with other mixtures.

The amount of amino acids used in this study (or what would be used for an iron preparation for adult human use) is far too little to maintain a good nitrogen balance. Also, use of a single or a few selected amino acids as dietary supplements has caused significant shifts toward a negative nitrogen balance

Table III—Stability Constants, Initial Absorption Rates, and AUC for Each Amino Acid Tested

	log *K* Stability		Initial Absorption Rate, μg/min[b]	AUC, mg·min/mL[c]
	Experimental	Literature[a]		
Asparagine	6.4	6.5	5.21	63.59
Glycine	7.6	7.8	4.57	56.51
Serine	7.0	7.0	2.10	37.31
Leucine	7.0	6.9	2.02	22.60
Methionine	6.6	6.7	1.99	21.71
Isoleucine	6.9	7.1	1.93	23.48
Tryptophan	7.4	7.6	1.9	21.05
Alanine	7.1	7.3	1.87	28.64
Phenylalanine	6.2	6.3	1.70	20.24
Proline	8.2	8.3	1.62	25.22

[a] Values are from Refs. 1–3. [b] Calculated from Eq. 1. [c] Calculated from Eq. 2; time, 0–4 h.

[5] The organization and analysis of the data base associated with this investigation were carried out in part using the PROPHET system, a unique national resource sponsored by the National Institutes of Health. Information about PROPHET, including how to apply for access, can be obtained from the Director, Chemical/Biological Information-Handling Program, Division of Research Resources, National Institutes of Health, Bethesda, MD 20205.

in individuals (29). Therefore, individuals taking amino acid–iron complexes should be made aware that such products do not have value as protein supplements or replace the need for dietary protein. In addition, depending on the quantity and essentiality of the amino acids ingested from the supplement, protein metabolism may be adversely affected.

A consensus has been reached that amino acids considered to be essential are isoleucine, leucine, lysine, methionine, phenylalanine, threonine, tryptophan, and valine for children and adults. Histidine is an essential amino acid for infants, but it is not considered essential for children or adults (30). It is important to note that the amino acids that appear to increase the absorption of iron are not considered to be essential amino acids. Nitrogen balance is maintained by an adequate diet of protein and not by an iron supplement containing one or two amino acids in very low quantities (29, 30). Likewise, increasing the dosage of the amino acid by taking more tablets of an amino acid–iron preparation could cause iron toxicity.

REFERENCES

(1) A. Albert, *Biochem J.*, **47**, 531 (1950).

(2) A. Albert, *Biochem J.*, **50**, 690 (1952).

(3) A. Albert, *Biochem J.*, **76**, 621 (1960).

(4) D. Kroe, T. D. Kinney, N. Kaufman, and J. V. Klavins, *Blood*, **21**, 546 (1963).

(5) D. Kroe, T. D. Kinney, N. Kaufman, and J. V. Klavins, *Am. J. Physiol.*, **211**, 414 (1966).

(6) D. Van Campen and E. Gross, *J. Nutr.*, **99**, 69 (1969).

(7) D. Van Campen, *J. Nutr.*, **102**, 165 (1972).

(8) D. Van Campen, *J. Nutr.*, **103**, 139 (1973).

(9) W. Forth and W. Rummel, in "International Encyclopedia of Pharmacology and Therapeutics," Vol. II, Pergamon, Great Britain, 1975, p. 599.

(10) M. C. Linder and H. N. Munro, *Fed. Proc., Fed. Am. Soc. Exp. Biol.*, **36**, 2015 (1977).

(11) H. J. Helbeck and P. Saltman, *Biochim. Biophys. Acta*, **135**, 979 (1967).

(12) E. R. Monsen and J. D. Cook, *Am. J. Clin Nutr.*, **29**, 442 (1976).

(13) T. Peters, L. Apt, and J. F. Ross, *Gastroenterology*, **61**, 315 (1971).

(14) H. C. Heinrich, H. Bartel, E. E. Gabbe, G. Kugler, and K. H. Oppitz, *Arzneim-Forsch.*, **22**, 1091 (1972).

(15) E. R. Monsen and J. F. Page, *J. Agric. Food Chem.* **126**, 223 (1978).

(16) F. E. Viteri, R. Garcia-Ibanez, and B. Torum, *Am. J. Clin. Nutr.*, **31**, 961 (1978).

(17) H. C. Heinrich, in "Clinical Symposium on Iron Deficiency," L. Hallbreg, H. G. Harwerth, and A. Vannotti, Eds., Academic, New York, N.Y., 1970, p. 213.

(18) F. H. Meyers, E. Jawetz, and A. Goldfien, "Medical Pharmacology," 6th ed., Lange Medical Publications, New York, N.Y., 1975, p. 457.

(19) A. D. A. Miski and F. H. Kretzner, *J. Nutr.* **107**, 24 (1977).

(20) A. L. Lehninger, "Biochemistry," 2nd ed., Worth Publishers, New York, N.Y., 1975, p. 488.

(21) V. Herbert, in "The Pharmacological Basis of Therapeutics," 4th ed., L. S. Goodman and A. Gilman, Eds., MacMillan, New York, N.Y., 1970, p. 1398.

(22) M. Layrisse, J. D. Cook, C. Martines-Torres, M. Roche, J. A. Kuhn, and C. A. Finch, *Blood*, **33**, 430 (1969).

(23) O. Greengard, A. Sentenan, and N. Mendelsohn, *Biochem. Biophys.*, **90**,406 (1964).

(24) C. Martines-Torres and M. Layrisse, *Am. J. Clin. Nutr.*, **24**, 531 (1971).

(25) L. Hallburg and L. Rossander, *Am. J. Clin. Nutr.* **35**, 502 (1982).

(26) R. B. Chodos, I. F. Ross, L. Apt, M. Pollycore, and I. Hallett, *J. Clin. Invest.*, **36**, 314 (1957).

(27) P. C. Elwood, D. Newton, J. D. Eakins, and P. A. Brown, *Am. J. Clin. Nutr.*, **21**, 1162 (1968).

(28) L. Jansky and J. S. Hart, *Can. J. Physiol. Pharmacol.*, **46**, 653 (1968).

(29) M. I. Irwin, *J. Nutr.* **101**, 385 (1970).

(30) M. I. Irwin and D. M. Hegsted, *J. Nutr.* **101**, 539 (1971).

ACKNOWLEDGMENTS

This work was performed as partial fulfillment of a Master of Science degree in Pharmacy at Oregon State University School of Pharmacy. This work was supported in part by a Sigma Xi Scholarship to M. Ghannam.

Evaluation of High-Performance Liquid Chromatography and Gas Chromatography for Quantitation of Dextromethorphan Hydrobromide in Cough–Cold Syrup Preparations

V. GIBBS ˣ **and Z. ZAIDI**

Received May 27, 1983 from the *R & D Laboratories, Block Drug Co., Inc., Jersey City, NJ 07302.* Accepted for publication October 6, 1983.

Abstract □ A rapid and sensitive high-performance liquid chromatographic (HPLC) procedure is described for the analysis of the antitussive dextromethorphan hydrobromide in several cough–cold syrup preparations and compared with a gas chromatographic (GC) procedure. In the HPLC procedure, the active ingredient is analyzed as the hydrobromide salt by dilution in the mobile phase and separation on a reverse-phase cyano column. In the GC method, the active ingredient is analyzed as the free base, in which an aqueous solution of the antitussive is made alkaline and extracted with dichloromethane before injection onto the GC column. Excellent resolution of the antitussive agent was obtained by both systems; however, the HPLC assay is preferred for routine analysis (*RSD* 1%), as compared with the GC assay (*RSD* 4%).

Keyphrases □ Dextromethorphan hydrobromide—HPLC, GC □ Antitussive agents—dextromethorphan hydrobromide, HPLC, GC □ Formulations—cough–cold syrup, analyses by HPLC and GC

Dextromethorphan hydrobromide [(+)-3-methoxy-17 methyl-9α,13α,14α-morphinan hydrobromide monohydrate (I)] is commonly used an an antitussive agent in many commercial cough–cold syrup preparations. There are several clinically active compounds classified as morphinans. All have the drawbacks of morphine: its dependence liability and respiratory-depressant characteristics (1). However, the side effects of some morphinans are not as severe as those of morphine. As a result, dextromethorphan hydrobromide has gained wide acceptance as a nonaddictive antitussive agent because it is nearly devoid of any analgesic activity (2).

Dextromethorphan hydrobromide has been separated by

0022-3549/84/0900-1248$01.00/0

© 1984, American Pharmaceutical Association

in individuals (29). Therefore, individuals taking amino acid–iron complexes should be made aware that such products do not have value as protein supplements or replace the need for dietary protein. In addition, depending on the quantity and essentiality of the amino acids ingested from the supplement, protein metabolism may be adversely affected.

A consensus has been reached that amino acids considered to be essential are isoleucine, leucine, lysine, methionine, phenylalanine, threonine, tryptophan, and valine for children and adults. Histidine is an essential amino acid for infants, but it is not considered essential for children or adults (30). It is important to note that the amino acids that appear to increase the absorption of iron are not considered to be essential amino acids. Nitrogen balance is maintained by an adequate diet of protein and not by an iron supplement containing one or two amino acids in very low quantities (29, 30). Likewise, increasing the dosage of the amino acid by taking more tablets of an amino acid–iron preparation could cause iron toxicity.

REFERENCES

(1) A. Albert, *Biochem J.*, **47**, 531 (1950).

(2) A. Albert, *Biochem J.*, **50**, 690 (1952).

(3) A. Albert, *Biochem J.*, **76**, 621 (1960).

(4) D. Kroe, T. D. Kinney, N. Kaufman, and J. V. Klavins, *Blood*, **21**, 546 (1963).

(5) D. Kroe, T. D. Kinney, N. Kaufman, and J. V. Klavins, *Am. J. Physiol.*, **211**, 414 (1966).

(6) D. Van Campen and E. Gross, *J. Nutr.*, **99**, 69 (1969).

(7) D. Van Campen, *J. Nutr.*, **102**, 165 (1972).

(8) D. Van Campen, *J. Nutr.*, **103**, 139 (1973).

(9) W. Forth and W. Rummel, in "International Encyclopedia of Pharmacology and Therapeutics," Vol. II, Pergamon, Great Britain, 1975, p. 599.

(10) M. C. Linder and H. N. Munro, *Fed. Proc., Fed. Am. Soc. Exp. Biol.*, **36**, 2015 (1977).

(11) H. J. Helbeck and P. Saltman, *Biochim. Biophys. Acta*, **135**, 979 (1967).

(12) E. R. Monsen and J. D. Cook, *Am. J. Clin Nutr.*, **29**, 442 (1976).

(13) T. Peters, L. Apt, and J. F. Ross, *Gastroenterology*, **61**, 315 (1971).

(14) H. C. Heinrich, H. Bartel, E. E. Gabbe, G. Kugler, and K. H. Oppitz, *Arzneim-Forsch.*, **22**, 1091 (1972).

(15) E. R. Monsen and J. F. Page, *J. Agric. Food Chem.* **126**, 223 (1978).

(16) F. E. Viteri, R. Garcia-Ibanez, and B. Torum, *Am. J. Clin. Nutr.*, **31**, 961 (1978).

(17) H. C. Heinrich, in "Clinical Symposium on Iron Deficiency," L. Hallbreg, H. G. Harwerth, and A. Vannotti, Eds., Academic, New York, N.Y., 1970, p. 213.

(18) F. H. Meyers, E. Jawetz, and A. Goldfien, "Medical Pharmacology," 6th ed., Lange Medical Publications, New York, N.Y., 1975, p. 457.

(19) A. D. A. Miski and F. H. Kretzner, *J. Nutr.* **107**, 24 (1977).

(20) A. L. Lehninger, "Biochemistry," 2nd ed., Worth Publishers, New York, N.Y., 1975, p. 488.

(21) V. Herbert, in "The Pharmacological Basis of Therapeutics," 4th ed., L. S. Goodman and A. Gilman, Eds., MacMillan, New York, N.Y., 1970, p. 1398.

(22) M. Layrisse, J. D. Cook, C. Martines-Torres, M. Roche, J. A. Kuhn, and C. A. Finch, *Blood*, **33**, 430 (1969).

(23) O. Greengard, A. Sentenan, and N. Mendelsohn, *Biochem. Biophys.*, **90**,406 (1964).

(24) C. Martines-Torres and M. Layrisse, *Am. J. Clin. Nutr.*, **24**, 531 (1971).

(25) L. Hallburg and L. Rossander, *Am. J. Clin. Nutr.* **35**, 502 (1982).

(26) R. B. Chodos, I. F. Ross, L. Apt, M. Pollycore, and I. Hallett, *J. Clin. Invest.*, **36**, 314 (1957).

(27) P. C. Elwood, D. Newton, J. D. Eakins, and P. A. Brown, *Am. J. Clin. Nutr.*, **21**, 1162 (1968).

(28) L. Jansky and J. S. Hart, *Can. J. Physiol. Pharmacol.*, **46**, 653 (1968).

(29) M. I. Irwin, *J. Nutr.* **101**, 385 (1970).

(30) M. I. Irwin and D. M. Hegsted, *J. Nutr.* **101**, 539 (1971).

ACKNOWLEDGMENTS

This work was performed as partial fulfillment of a Master of Science degree in Pharmacy at Oregon State University School of Pharmacy. This work was supported in part by a Sigma Xi Scholarship to M. Ghannam.

Evaluation of High-Performance Liquid Chromatography and Gas Chromatography for Quantitation of Dextromethorphan Hydrobromide in Cough–Cold Syrup Preparations

V. GIBBS ˣ **and Z. ZAIDI**

Received May 27, 1983 from the *R & D Laboratories, Block Drug Co., Inc., Jersey City, NJ 07302.* Accepted for publication October 6, 1983.

Abstract □ A rapid and sensitive high-performance liquid chromatographic (HPLC) procedure is described for the analysis of the antitussive dextromethorphan hydrobromide in several cough–cold syrup preparations and compared with a gas chromatographic (GC) procedure. In the HPLC procedure, the active ingredient is analyzed as the hydrobromide salt by dilution in the mobile phase and separation on a reverse-phase cyano column. In the GC method, the active ingredient is analyzed as the free base, in which an aqueous solution of the antitussive is made alkaline and extracted with dichloromethane before injection onto the GC column. Excellent resolution of the antitussive agent was obtained by both systems; however, the HPLC assay is preferred for routine analysis (*RSD* 1%), as compared with the GC assay (*RSD* 4%).

Keyphrases □ Dextromethorphan hydrobromide—HPLC, GC □ Antitussive agents—dextromethorphan hydrobromide, HPLC, GC □ Formulations—cough–cold syrup, analyses by HPLC and GC

Dextromethorphan hydrobromide [(+)-3-methoxy-17 methyl-9α,13α,14α-morphinan hydrobromide monohydrate (I)] is commonly used an an antitussive agent in many commercial cough–cold syrup preparations. There are several clinically active compounds classified as morphinans. All have the drawbacks of morphine: its dependence liability and respiratory-depressant characteristics (1). However, the side effects of some morphinans are not as severe as those of morphine. As a result, dextromethorphan hydrobromide has gained wide acceptance as a nonaddictive antitussive agent because it is nearly devoid of any analgesic activity (2).

Dextromethorphan hydrobromide has been separated by

0022-3549/84/0900-1248$01.00/0

© 1984, American Pharmaceutical Association

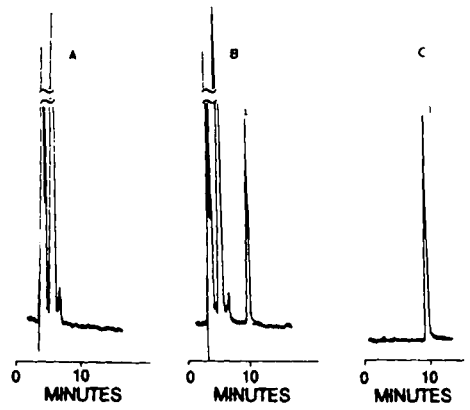

Figure 1—*Chromatograms of a typical HPLC run of placebo (A), sample syrup (B), and standard (C). Key: (1) dextromethorphan hydrobromide.*

use of various chromatographic procedures when present alone (3) and in combination (4–10) with other active ingredients. Foremost in this category is high-performance liquid chromatography (HPLC), employing either ion-pair (6, 9) or buffer systems (8, 10). Since cough–cold syrups usually contain a combination of many active ingredients, the ability to analyze a full range of amine ingredients in cough–cold syrups by a single assay has been emphasized by most of these methods, as opposed to one single active ingredient in a range of multicomponent cough–cold syrup preparations. In our laboratory, the application of several of these HPLC procedures to various marketed cough–cold syrups containing dextromethorphan hydrobromide was unsuccessful in separating the active ingredient each time. In addition, excessive retention times and peak tailing were also experienced in some cases. To our knowledge, we are unaware of any reported chromatographic procedure which is broadly applicable to the analysis of dextromethorphan hydrobromide in a variety of cough–cold syrups containing several active ingredients, as well as various excipients, dyes, and/or sugar bases. Reported gas chromatographic (GC) methods usually involve an extraction step and prove to be better at resolving dextromethorphan hydrobromide from various excipients present in cough–cold syrups. However, sufficient recovery data have not been reported (4, 5).

The purpose of this study was to develop a rapid and sensitive method for analyzing dextromethorphan hydrobromide in several cough–cold syrup preparations, regardless of formula subtleties and, subsequently, to compare the efficiency of GC and HPLC for completing this task. In this paper, the application of HPLC and GC to several different cough syrups containing dextromethorphan hydrobromide as an active ingredient is described.

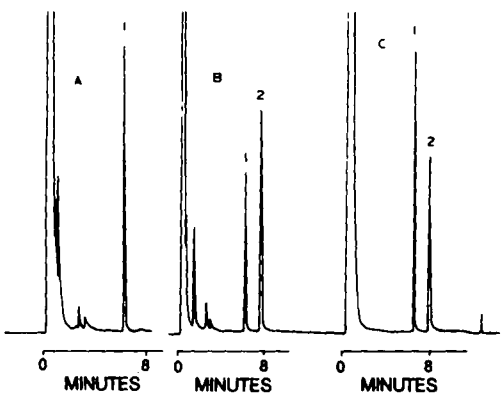

Figure 2—*Chromatograms of a typical GC run for placebo with internal standard (A), spike placebo (B), and standard (C). Key: (1) O-methoxyphenyl benzoate; (2) dextromethorphan hydrobromide.*

Table I—Recoveries by High-Performance Liquid Chromatography

Formulation I[a]			Formulation II[b]		
Amount Added, mg	Amount Found, mg	Recovery, %	Amount Added, mg	Amount Found, mg	Recovery, %
1.01	1.02	100.9	1.01	1.01	100.0
3.03	3.00	99.0	3.03	3.04	100.3
5.04	5.06	100.4	5.04	4.99	99.0
			7.24	7.29	100.7
			8.28	8.36	100.9
			10.35	10.37	100.2
			15.52	15.63	100.7
Mean		100.1			100.2
RSD, %		0.98			0.64

[a] 10 mL of placebo was spiked with the added amount of standard; I, contained no other active ingredients. [b] 5 mL of placebo was spiked with the added amount of standard; II, contained 12.5 mg of phenylpropanolamine hydrochloride and 20% alcohol.

EXPERIMENTAL SECTION

Chemicals and Reagents—Methanol, acetonitrile, and dichloromethane were distilled in glass[1] (HPLC grade). Perchloric acid (60% v/v), potassium nitrate, and anhydrous sodium sulfate were either ACS or analytical reagent grade[2].

High-Performance Liquid Chromatography—The liquid chromatograph[3] was fitted with an automatic injector[4] and a variable-wavelength UV detector[5] set at 280 nm. A microparticulate cyano column[6] (25 cm × 4.6 mm i.d.), containing 5-μm particles, was used.

Chromatographic Conditions—The mobile phase was 0.05 M potassium nitrate in acetonitrile–water (25:75), with the pH adjusted to 3.0 ± 0.1 with 60% v/v perchloric acid; the flow rate was 1.5 mL/min. The mobile phase was filtered[7] and deaerated before use. The inlet pressure was approximately 2900 psi. Detector sensitivity was 0.2 AUFS, the chart speed was 0.25 cm/min, and the injection volume was 10 μL.

Standard Preparation—Three working standard solutions were prepared by diluting 3, 5, and 8 mL of dextromethorphan hydrobromide[8] stock standard solution (1 mg/mL), respectively, to 100 mL with the mobile phase in volumetric flasks. Solutions were mixed and filtered[7].

Sample Preparation—Samples (2–10 mL, depending on label claim) were accurately transferred to 100-mL volumetric flasks and diluted to volume with the mobile phase. Solutions were mixed and filtered.

Gas Chromatography—The gas chromatograph[9] was a dual column modular system equipped with 1–10-mV recorder[10].

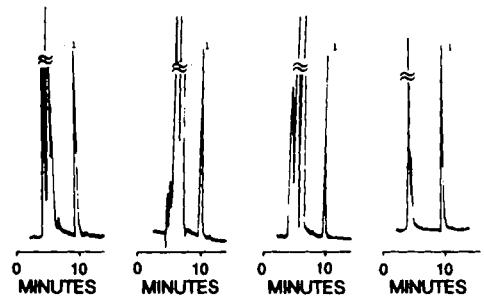

Figure 3—*HPLC analysis of four different commercial cough–cold syrups containing dextromethorphan hydrobromide. Key: (1) dextromethorphan hydrobromide.*

[1] MCB Manufacturing Chemists, Cincinnati, Ohio.
[2] J. T. Baker Chemical Co., Phillipsburg, N.J.
[3] Model SP 8000 equipped with a printer/plotter; Spectra Physics, Santa Clara, Calif.
[4] Auto Injector model 725; Micromeritics Instruments, Norcross, Ga.
[5] Spectroflow Monitor SF 770; Schoeffel Instruments, Westwood, N.J.
[6] IBM Instruments, Danbury, Conn.
[7] Hydrophilic type HV filter, 0.45-μm pore size; Millipore Corp., Bedford, Mass.
[8] USP reference standard or house-calibrated standard.
[9] Aerograph model 3700 TC-FID gas chromatograph; Varian Instruments Associates, Walnut Creek, Calif.
[10] Omniscribe Linear Recorder; Houston Instruments, Austin, Tex.

Table II—Recoveries by Gas Chromatography

Formulation II[a]			Formulation III[a]		
Amount Added, mg	Amount Found, mg	Recovery, %	Amount Added, mg	Amount Found, mg	Recovery, %
3.05	3.32	108.8	3.59	3.62	100.8
5.08	5.18	101.9	5.59	5.80	103.7
5.19	5.15	99.32	8.39	9.05	107.8
7.11	7.72	104.8	10.68	10.92	102.2
15.48	16.13	104.2	11.68	12.66	108.4
			16.28	16.95	104.1
Mean		103.8			104.5
RSD, %		3.4			2.9

[a] 5 mL of placebo was spiked with the added amount of standard; II, contained 12.5 mg of phenylpropanolamine hydrochloride and 20% alcohol; III, contained 20% alcohol.

Chromatographic Conditions—A glass column[11] (~1.8 m × 2 mm i.d.) packed with 3% OV-17 on Chromasorb Q[12] (100–120 mesh) was used. The column temperature was maintained at 110°C for 2 min and programmed to 230°C for 4 min at 30°C/min. The flow rate of the helium carrier gas was 25 mL/min, with an inlet pressure of 30 psi. The injector port temperature was 220°C. The detector temperature was 260°C, with a hydrogen flow rate of 30 mL/min and an air flow rate of 300 mL/min. Detector sensitivity was 10^{-9} with a chart speed of ~0.5 cm/min. The temperature program was initiated with each 5-μL injection[13]. The column was allowed to condition overnight at 240°C before use.

Standard Preparations—Standard solutions of dextromethorphan hydrobromide were prepared by accurately weighing 1–15 mg of dextromethorphan hydrobromide standard into a 60-mL separatory funnel containing 25 mL of 0.1 M NaOH. The separatory funnel was stoppered and shaken gently to dissolve the solid, and the free base was extracted with three 15-mL portions of dichloromethane. After each addition of the organic solvent, the separatory funnel was stoppered and shaken vigorously for 15 min. The organic layer was transferred to a 50-mL volumetric flask *via* a funnel containing 200 mg of sodium sulfate supported by glass wool. Two milliliters of a 2.5-mg/mL solution of *O*-methoxyphenyl benzoate[14] in chloroform was added as internal standard to each flask before diluting to volume with dichloromethane.

Sample Preparations—Samples (5–10 mL, depending on label claim) were accurately transferred to 60-mL separatory funnels and extracted in the same manner as described above for the standards.

Assay Procedure and Quantitation—Under the chromatographic conditions described for HPLC and GC, injections of the sample and standard solutions were made. Results were calculated from the linear regression of the three standards, relating peak height ratios (standard-internal standard) and concentration.

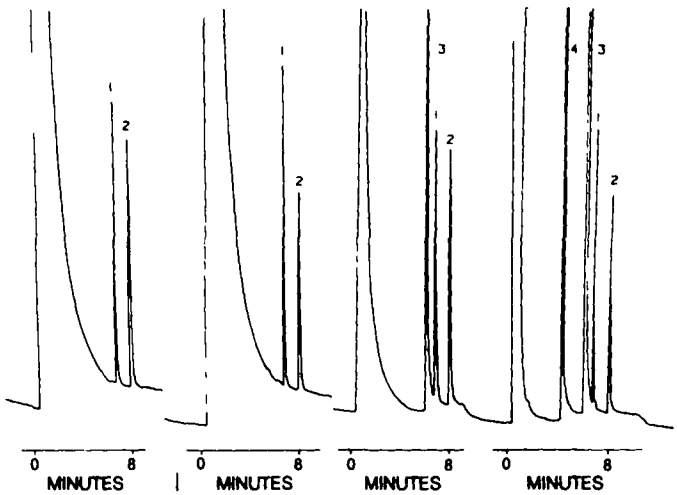

Figure 4—*Chromatograms of a typical GC run of four different commercial cough-cold syrups. Key: (1) O-methoxyphenyl benzoate; (2) dextromethorphan hydrobromide; (3) guaifenesin; (4) pseudoephredine hydrochloride.*

[11] Supelco, Bellefonte, Pa.
[12] Applied Science Laboratories, College Park, Pa.
[13] Microliter syringe, 701N; Hamilton Co., Reno, Nev.
[14] Pfaltz and Bauer Chemical Co., Stamford, Conn.

Table III—Comparative Analysis of Dextromethorphan Hydrobromide by HPLC and GC

	Precision Data				
	HPLC[a]			GC[a]	
Sample	I	II	III	I	III
1	2.46	5.17	15.52	2.57	16.73
2	2.43	5.19	15.50	2.61	16.26
3	2.42	5.18	15.57	2.65	16.61
4	2.38	5.26	15.52	2.49	14.99
5	2.47	5.29	15.59	2.66	16.52
6	2.42	5.31	15.43	2.61	16.87
7	2.42	5.22	15.59	2.77	16.77
8	2.46	5.27	15.43	2.76	17.10
9	2.42	5.28	15.61	2.75	16.06
Mean	2.43	5.24	15.53	2.65	16.43
RSD, %	1.15	0.90	0.43	3.5	3.8

[a] Formulation I, contains no other active ingredients; formulation II, contains 12.5 mg of phenylpropanolamine hydrochloride and 20% alcohol; formulation III, contains 20% alcohol.

RESULTS AND DISCUSSION

Preliminary studies involved testing of several mobile phase compositions for effective separation of dextromethorphan hydrobromide in a cough-cold syrup base. A 25:75 ratio of acetonitrile–water was finally found to be suitable for all the products analyzed. Peak tailing was minimized by using 0.05 M potassium nitrate and adjusting to pH 3.0. Several microparticulate reverse-phase columns with octadecylsilane (C_{18}) and cyano (CN) packings were tried from various manufacturers. In the past, C_{18} columns have been widely used by other workers for the separation of amines in cough-cold syrup preparations. In our experience, these columns (30 cm × 3.9 mm i.d. of 10-μm particle size) did not give suitable separation of dextromethorphan hydrobromide in some of the products analyzed. Finally, a cyano column (5-μm particle size; 25 cm × 4.6 mm i.d.) was used and was found to be more selective for the antitussive agent and, hence, provided better separation of the active ingredient from other excipients. Since the ultimate objective was to develop a method which would work for other commercially available products as well, column selection was considered to be an important factor.

Typical chromatograms of a placebo and sample run by HPLC are shown in Fig. 1. Construction of a standard curve from injections of dextromethorphan hydrobromide standard solutions ranging from 1 to 10 mg demonstrated the linearity of the HPLC procedure. The average peak height response was 8.98 cm for a 5-mg standard solution (*RSD* 1.6%). The limit of detection was 0.005 mg/mL for a steady baseline at 280 nm. The GC procedure offered comparable detection, and the standard curve was also found to be linear for solutions ranging from 1 to 15 mg. The average peak height response was 8.56 cm for a 5-mg standard solution (*RSD* 3.5%). Chromatograms of a GC run are shown in Fig. 2.

Data generated from the recovery studies by HPLC and GC are outlined in Tables I and II, respectively. The recoveries were performed by an external standard addition method. To evaluate the precision of the two methods, multiple injections of a single lot of cough syrup were made (Table III). For each formulation under investigation, the *RSD* was <1.5% for the HPLC assay and <4.0% for the GC assay. Although the HPLC assay is an external standard method, it was believed that the addition of an internal standard would not significantly improve the precision of the assay procedure. However, if an internal standard is desired, methaphenilene hydrochloride and promethazine can be used for this purpose. The retention times are 14.0 and 20.0 min, respectively, relative to dextromethorphan hydrobromide, which has a retention time of 10.0 min.

The second phase of the study involved the evaluation of both assay pro-

Table IV—Comparative Analysis of Dextromethorphan Hydrobromide in Commercial Products

		HPLC		GC	
Product[a]	Claim, mg	Found, mg[b]	Percent Label Claim	Found, mg	Percent Label Claim
A	15	14.95	99.6	14.82	98.8
B	10	10.18	101.8	10.92	109.2
C	10	9.99	99.9	10.82	108.2
D	30	29.08	96.9	30.31	101.0

[a] A, contained 100 mg of guaifenesin/5 mL and 1.4% alcohol; B, contained 5% alcohol; C, contained 100 mg of guaifenesin and 30 mg of pseudoephedrine hydrochloride/5 mL and 2.4% alcohol; D, contained 9.5% alcohol. [b] Results are the average of duplicate determinations.

cedures (HPLC and GC) for determining dextromethorphan hydrobromide from other commercially available cough syrups. Chromatograms obtained for these products were representative of the assay procedure and gave resolution and/or separation similar to that of dextromethorphan hydrobromide in the products under investigation. Typical chromatograms are shown in Figs. 3 and 4 for HPLC and GC, respectively, and the results are compared in Table IV.

The results obtained by the GC procedure were higher for all the products analyzed and, hence, reflected the difficulty in extracting the free base with organic solvents (10). This difficulty was experienced with the standard and sample solutions as well. It is believed that the partitioning behavior (11) of the antitussive agent is the major cause for this problem rather than the complexity of the cough syrup formulations. The GC procedure involved a lengthy sample preparation and required more analysis time as compared with the HPLC procedure. Finally, the HPLC procedure gave results that were in better agreement with label claims for all the products evaluated and was a more precise assay procedure.

CONCLUSION

Although excellent resolution of the antitussive agent was obtained by both the HPLC and GC systems, further examination of the applicability of either method for routine analysis of dextromethorphan hydrobromide revealed that the HPLC procedure described is simple, rapid, and precise for the quantitation of the antitussive agent in several commercially available cough-cold syrups. The GC procedure does not seem to be the method of choice for quantitation of dextromethorphan hydrobromide in cough syrups due to the difficulty in extracting the free base and the time involved in sample preparation.

REFERENCES

(1) Alfred Burger, "Medicinal Chemistry," part II, 3rd ed., Wiley-Interscience, New York, N.Y. 1970.

(2) R. Grewe and A. Mondon, *Chem. Ber.*, **91**, 279 (1948).

(3) E. J. Kubiak and J. W. Munson, *J. Pharm. Sci.*, **69**, 1380 (1980).

(4) J. L. Fabregas and A. Margalet, *J. Pharm. Sci.*, **64**, 1005 (1975).

(5) E. R. Kaplan and A. A. Spark, *So. African J. Sci.*, **71**, 241 (1975).

(6) G. W. Halstead, *J. Pharm. Sci.*, **71**, 1108 (1982).

(7) G. W. Schieffer and D. E. Hughes, *J. Pharm. Sci.*, **72**, 55 (1983).

(8) W. O. McSharry and I. V. E. Savage, *J. Pharm. Sci.*, **69**, 212 (1980).

(9) M. K. Chao, I. J. Holcomb, and S. A. Fusari, *J. Pharm. Sci.*, **68**, 1463 (1979).

(10) A. Menyhareth, F. P. Mahn, and J. E. Heveran, *J. Pharm. Sci.*, **63**, 431 (1974).

(11) T. Higuchi *et al.*, *Anal. Chem.*, **39**, 974 (1967).

(12) P. Mukerjee, *Anal. Chem.*, **28**, 870 (1956).

Nasal Drug Delivery System of a Quaternary Ammonium Compound: Clofilium Tosylate

KENNETH S. E. SU ˣ, KRISTINA M. CAMPANALE, and CHRISTIAN L. GRIES

Received September 9, 1983, from the *Pharmaceutical Research Department and Pathology Division, Lilly Research Laboratories, Eli Lilly and Co., Indianapolis, IN 46285.* Accepted for publication October 12, 1983.

Abstract □ The blood levels of the [^{14}C]clofilium ion in rats after various routes of administration of clofilium tosylate were compared. The results indicate that the blood levels after nasal administration were not statistically different from levels after intravenous administration ($p > 0.05$). Administration by the oral route resulted in considerably lower blood levels. Nasal administration of clofilium tosylate appeared to be superior to oral administration. Histological examinations of nasal mucosa were conducted. At the lower concentration, mild necrosis was observed, and large areas of mucosa were unaffected. However, necrosis of large areas of mucosa occurred after exposure to the higher concentration. Levels of radioactivity in heart, liver, lung, and kidney tissue, as a function of time, were also studied. Unlike the blood levels after nasal administration, the levels of radioactivity were persistent in heart tissue. The data suggest that the [^{14}C]clofilium ion and/or metabolite concentrate in the heart and that blood levels of radioactivity may not be an accurate index of cardiac levels or biological response.

Keyphrases □ Clofilium tosylate—nasal drug delivery □ Drug delivery systems—clofilium tosylate, nasal administration

Clofilium tosylate, [4-(*p*-chlorophenyl)butyl]diethylheptylammonium tosylate, is a newly synthesized quaternary ammonium compound that has been shown to selectively increase refractoriness of cardiac tissue in dogs and humans (1-3). It is known that oral administration of quaternary ammonium compounds results in low and varied blood levels (4). Predictably, the oral absorption of clofilium tosylate in rats was poor (5). A total of 0.35% of the dose was excreted in the urine and 79% was excreted in the feces within 72 h after oral administration. All tissues had extremely low levels of radioactivity and low rates of absorption after oral administration of clofilium tosylate. The pharmacokinetics and bioavailabilities of quaternary ammonium compounds given by various routes have been studied previously (4-7). However, nasal administration of a quaternary ammonium compound has not yet been evaluated. It was the object of this study to report the results on the nasal absorption of clofilium tosylate in rats. The tissue disposition of radioactivity after nasal administration of [^{14}C]clofilium tosylate is also reported.

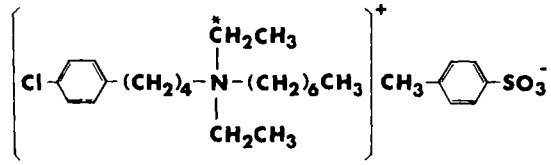

EXPERIMENTAL SECTION

Synthesis of [^{14}C]Clofilium Tosylate—[^{14}C]Clofilium tosylate was prepared in this laboratory by Dr. F. J. Marshall. *N*-[^{14}C]Acetyl-*N*-heptyl-(4-chlorophenyl)butylamine was prepared as follows: 104.4 mg (1.33 mmol) of [^{14}C]acetyl chloride was introduced by vacuum transfer into a flask containing 804.8 mg (2.86 mmol) of 4-(4-chlorophenyl)butylamine in 13 mL of dry toluene. The mixture was then stirred for 3 h and warmed gently for 1 h in a stoppered flask. The solution was washed with 10 mL of a 1 M HCl-water-saturated sodium chloride solution and then dried with magnesium sulfate and the organic phase was evaporated to dryness under reduced pressure. The resulting material was dissolved in chloroform and purified by preparative TLC (ethyl acetate, silica gel[1]). A total of 277 mg (64% yield) of the amide was obtained. This material was reduced to the tertiary amine as follows. With cooling in ice water, a solution of 277 mg (0.855 mmol) of the aforementioned

[1] 60-F254; E. Merck, Darmstadt, Federal Republic of Germany.

0022-3549/84/0900-1251$01.00/0

© 1984, American Pharmaceutical Association

cedures (HPLC and GC) for determining dextromethorphan hydrobromide from other commercially available cough syrups. Chromatograms obtained for these products were representative of the assay procedure and gave resolution and/or separation similar to that of dextromethorphan hydrobromide in the products under investigation. Typical chromatograms are shown in Figs. 3 and 4 for HPLC and GC, respectively, and the results are compared in Table IV.

The results obtained by the GC procedure were higher for all the products analyzed and, hence, reflected the difficulty in extracting the free base with organic solvents (10). This difficulty was experienced with the standard and sample solutions as well. It is believed that the partitioning behavior (11) of the antitussive agent is the major cause for this problem rather than the complexity of the cough syrup formulations. The GC procedure involved a lengthy sample preparation and required more analysis time as compared with the HPLC procedure. Finally, the HPLC procedure gave results that were in better agreement with label claims for all the products evaluated and was a more precise assay procedure.

CONCLUSION

Although excellent resolution of the antitussive agent was obtained by both the HPLC and GC systems, further examination of the applicability of either method for routine analysis of dextromethorphan hydrobromide revealed that the HPLC procedure described is simple, rapid, and precise for the quantitation of the antitussive agent in several commercially available cough-cold syrups. The GC procedure does not seem to be the method of choice for quantitation of dextromethorphan hydrobromide in cough syrups due to the difficulty in extracting the free base and the time involved in sample preparation.

REFERENCES

(1) Alfred Burger, "Medicinal Chemistry," part II, 3rd ed., Wiley-Interscience, New York, N.Y. 1970.

(2) R. Grewe and A. Mondon, *Chem. Ber.*, **91**, 279 (1948).

(3) E. J. Kubiak and J. W. Munson, *J. Pharm. Sci.*, **69**, 1380 (1980).

(4) J. L. Fabregas and A. Margalet, *J. Pharm. Sci.*, **64**, 1005 (1975).

(5) E. R. Kaplan and A. A. Spark, *So. African J. Sci.*, **71**, 241 (1975).

(6) G. W. Halstead, *J. Pharm. Sci.*, **71**, 1108 (1982).

(7) G. W. Schieffer and D. E. Hughes, *J. Pharm. Sci.*, **72**, 55 (1983).

(8) W. O. McSharry and I. V. E. Savage, *J. Pharm. Sci.*, **69**, 212 (1980).

(9) M. K. Chao, I. J. Holcomb, and S. A. Fusari, *J. Pharm. Sci.*, **68**, 1463 (1979).

(10) A. Menyhareth, F. P. Mahn, and J. E. Heveran, *J. Pharm. Sci.*, **63**, 431 (1974).

(11) T. Higuchi *et al.*, *Anal. Chem.*, **39**, 974 (1967).

(12) P. Mukerjee, *Anal. Chem.*, **28**, 870 (1956).

Nasal Drug Delivery System of a Quaternary Ammonium Compound: Clofilium Tosylate

KENNETH S. E. SU ˣ, KRISTINA M. CAMPANALE, and CHRISTIAN L. GRIES

Received September 9, 1983, from the *Pharmaceutical Research Department and Pathology Division, Lilly Research Laboratories, Eli Lilly and Co., Indianapolis, IN 46285.* Accepted for publication October 12, 1983.

Abstract □ The blood levels of the [^{14}C]clofilium ion in rats after various routes of administration of clofilium tosylate were compared. The results indicate that the blood levels after nasal administration were not statistically different from levels after intravenous administration ($p > 0.05$). Administration by the oral route resulted in considerably lower blood levels. Nasal administration of clofilium tosylate appeared to be superior to oral administration. Histological examinations of nasal mucosa were conducted. At the lower concentration, mild necrosis was observed, and large areas of mucosa were unaffected. However, necrosis of large areas of mucosa occurred after exposure to the higher concentration. Levels of radioactivity in heart, liver, lung, and kidney tissue, as a function of time, were also studied. Unlike the blood levels after nasal administration, the levels of radioactivity were persistent in heart tissue. The data suggest that the [^{14}C]clofilium ion and/or metabolite concentrate in the heart and that blood levels of radioactivity may not be an accurate index of cardiac levels or biological response.

Keyphrases □ Clofilium tosylate—nasal drug delivery □ Drug delivery systems—clofilium tosylate, nasal administration

Clofilium tosylate, [4-(*p*-chlorophenyl)butyl]diethylheptylammonium tosylate, is a newly synthesized quaternary ammonium compound that has been shown to selectively increase refractoriness of cardiac tissue in dogs and humans (1-3). It is known that oral administration of quaternary ammonium compounds results in low and varied blood levels (4). Predictably, the oral absorption of clofilium tosylate in rats was poor (5). A total of 0.35% of the dose was excreted in the urine and 79% was excreted in the feces within 72 h after oral administration. All tissues had extremely low levels of radioactivity and low rates of absorption after oral administration of clofilium tosylate. The pharmacokinetics and bioavailabilities of quaternary ammonium compounds given by various routes have been studied previously (4-7). However, nasal administration of a quaternary ammonium compound has not yet been evaluated. It was the object of this study to report the results on the nasal absorption of clofilium tosylate in rats. The tissue disposition of radioactivity after nasal administration of [^{14}C]clofilium tosylate is also reported.

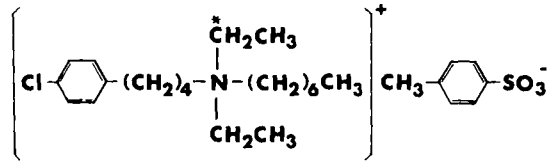

EXPERIMENTAL SECTION

Synthesis of [^{14}C]Clofilium Tosylate—[^{14}C]Clofilium tosylate was prepared in this laboratory by Dr. F. J. Marshall. *N*-[^{14}C]Acetyl-*N*-heptyl-(4-chlorophenyl)butylamine was prepared as follows: 104.4 mg (1.33 mmol) of [^{14}C]acetyl chloride was introduced by vacuum transfer into a flask containing 804.8 mg (2.86 mmol) of 4-(4-chlorophenyl)butylamine in 13 mL of dry toluene. The mixture was then stirred for 3 h and warmed gently for 1 h in a stoppered flask. The solution was washed with 10 mL of a 1 M HCl-water-saturated sodium chloride solution and then dried with magnesium sulfate and the organic phase was evaporated to dryness under reduced pressure. The resulting material was dissolved in chloroform and purified by preparative TLC (ethyl acetate, silica gel[1]). A total of 277 mg (64% yield) of the amide was obtained. This material was reduced to the tertiary amine as follows. With cooling in ice water, a solution of 277 mg (0.855 mmol) of the aforementioned

[1] 60-F254; E. Merck, Darmstadt, Federal Republic of Germany.

0022-3549/84/0900-1251$01.00/0

© 1984, American Pharmaceutical Association

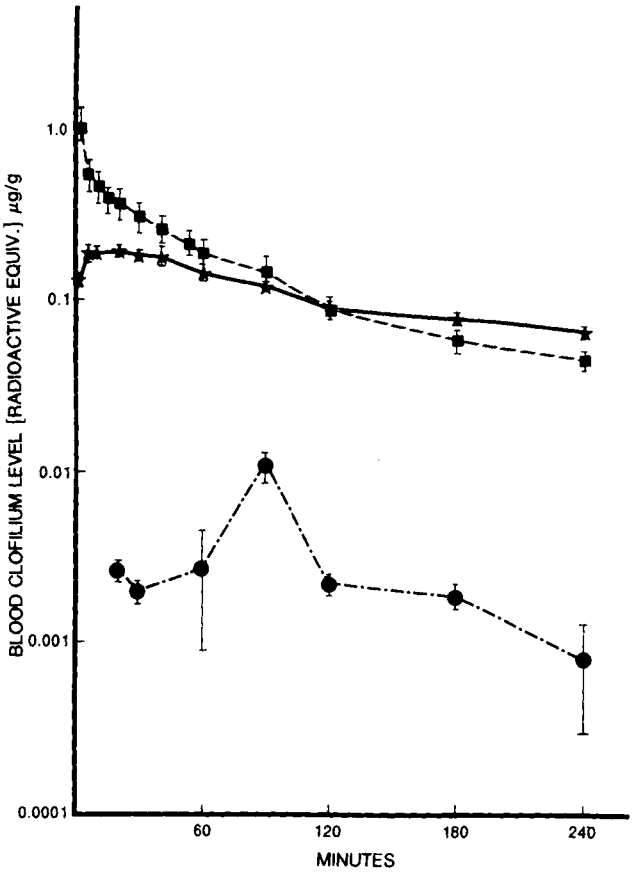

Figure 1—*[^{14}C]Clofilium ion in blood of male Sprague-Dawley rats after various routes of administration of a 1.2-mg/kg dose (n = 3). Key (1) intranasal administration; (2) intravenous administration; (3) oral administration.*

amide in 8 mL of tetrahydrofuran was added dropwise to 5.25 mL of a 1 M solution of diborane in tetrahydrofuran. The mixture was refluxed gently for about 20 h, cooled in ice water, and 7 mL of methanol was cautiously added. The mixture was stirred for a few minutes, and 11 mL of 1 M HCl and 3 mL of concentrated HCl were added. The mixture was heated for 3 h. After cooling in ice water, it was made strongly basic by the addition of 5 M NaOH. The product was extracted with ether, and the extract was washed with water-saturated sodium chloride solution and dried with magnesium sulfate. The ether was removed under reduced pressure. The tertiary amine was purified by preparative TLC as described above (ethyl acetate-triethylamine, 30:1) to give 206 mg (78% yield) of material which showed one spot on TLC. The quaternary tosylate was prepared as follows: 206 mg (0.665 mmol) of the ^{14}C-labeled tertiary amine was refluxed with 159.6 mg (0.797 mmol) of ethyl-*p*-toluenesulfonate in 3.2 mL of 1,2-dichloroethane for 96 h. The solvent was removed under reduced pressure, and the residue was recrystallized from acetone-ethyl acetate to give 226 mg of colorless crystals of [^{14}C][4-(*p*-chlorophenyl)butyl]diethylheptylammonium tosylate, mp 98–101°C. The product appeared to be 97.5% pure by TLC and autoradiography.

Formulation—[^{14}C]Clofilium tosylate was dissolved in NaCl for injection USP (8) and sonicated before administration to rats.

Animal Absorption Studies—Male Sprague-Dawley rats (average weight, 275 g) were anesthetized during the entire course of the intravenous and nasal absorption studies. For intravenous administration, the rats were anesthetized with pentobarbital by intraperitoneal injection, and the drug solution was administered by bolus injection into the femoral vein. For nasal administration, the surgical procedure conducted on the rats was that described previously (9, 10) with some modifications. The drug solution was delivered to the nasal cavity through the esophagus cannulation tubing by means of a syringe. For oral administration, the rats were not anesthetized, and the drug solution was administered by gavage. Blood samples were taken from the tail vein periodically and acid-digested in 0.2 mL of 70% $HClO_4$ and 0.4 mL of 30% H_2O_2 at 70°C for 1 h in scintillation vials. The samples were cooled and counted in scintillation fluid[2].

[2] Ready-Solv MP; Beckman.

Figure 2—*Nasal mucosa of necropsy A; control rat.*

Histological Examination of Nasal Mucosa in Rats—After the absorption phase of the study, the rats were killed, decapitated, and the nasal passages were flushed with 10% buffered formalin. After fixation by immersion, the heads were decalcified, and four cross sections of the nasal cavity of each rat were stained and examined (11).

Tissue Distribution of the [^{14}C]Clofilium Ion after Nasal Administration of [^{14}C]Clofilium Tosylate—At various times after nasal administration of the drug, tissues were dissected, rinsed, blotted, and weighed. Samples (100–260 mg) were digested in 0.2 mL of 70% $HClO_4$ and 0.4 mL of 30% H_2O_2 at 70°C for 1 h in scintillation vials. The samples were cooled and counted in scintillation fluid[2].

RESULTS AND DISCUSSION

The disappearance of radioactivity in the blood of rats administered [^{14}C]clofilium tosylate by the three administration routes is shown in Fig. 1. The variations in blood levels as well as the low absorption rate following administration of the oral dose are clearly demonstrated. Nasal administration of the drug resulted in much higher levels of radioactivity than levels after oral administration. The blood radioactivity levels of the clofilium ion after oral administration of the tosylate were ~1% of the levels obtained from the dose, whereas the radioactivity levels after nasal administration were 70% of those obtained from the dose (Table I). Furthermore, the difference in levels following intravenous and nasal administrations were statistically insignificant ($p > 0.05$).

The data on the effect of the clofilium ion concentration indicate that the area under the curve of the blood radioactivity level increased with dose in a nonlinear manner when administered nasally (Table II). However, a linear dose-response relationship appeared in the lower ranges. The nonlinear portion of the curve and good absorption rate at the concentration of 1.2 mg/kg were possibly attributable to damage to the nasal mucosa with exposure of the submucosal vasculature to the quaternary ammonium compound. Inspection of the blood kinetics of the radioactivity levels (Table III) suggested that, even at this lower dose, the drug was slowly absorbed and/or diffused through epithelial cells into the systemic circulation. At 0.3–0.6 mg/kg, the absorption

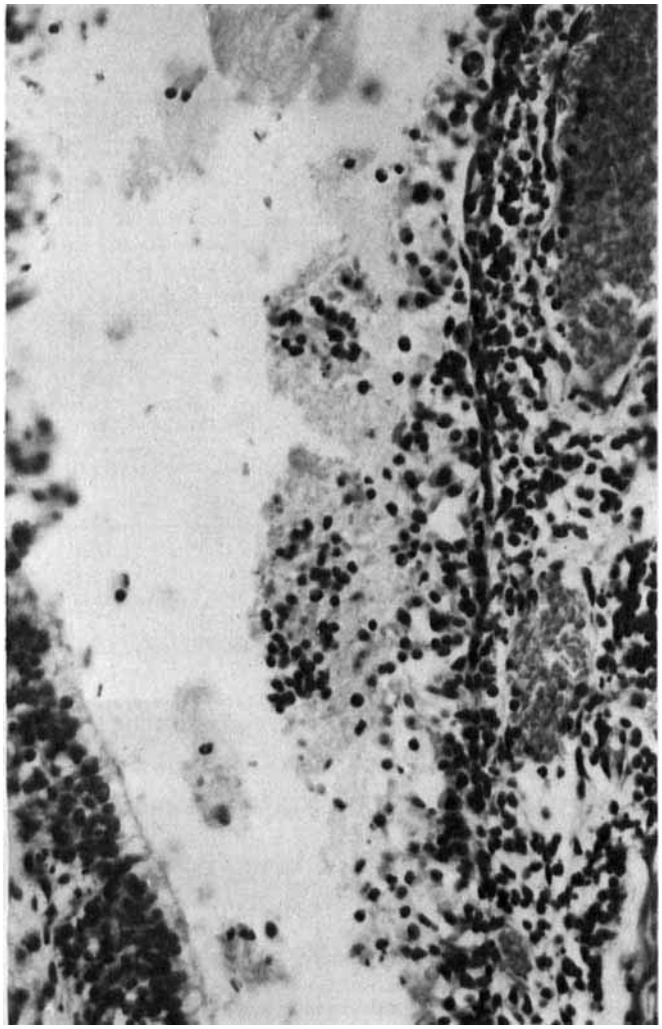

Figure 3—*Nasal mucosa of necropsy B; the rat was given a 1.2-mg/kg dose.*

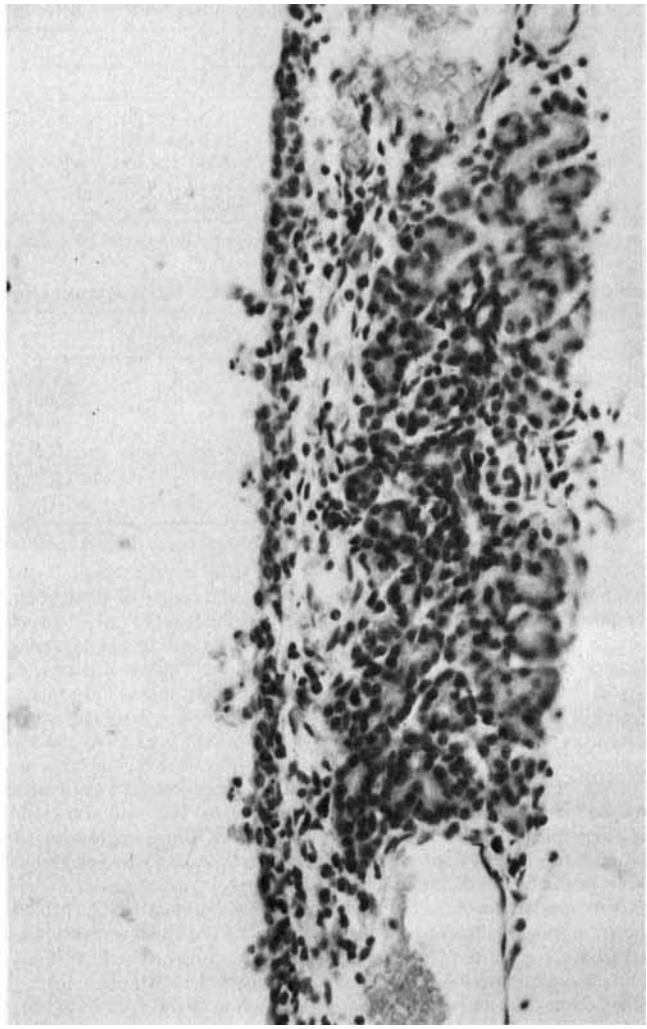

Figure 4—*Nasal mucosa of necropsy C; the rat was given a 0.6-mg/kg dose.*

under the AUC per unit dose remained constant (Table II). Thus, the amount of drug absorbed was directly proportional to the concentration in accordance with the law of diffusion. The observations are in agreement with those reported previously; that is, quaternary ammonium compounds are absorbed by a diffusion mechanism (6). Still, by administering a 0.3-mg/kg dose nasally, the nasal absorption was ~21-fold greater than the oral absorption. In these studies, it was indicated that clofilium tosylate was rapidly absorbed from the nasal mucosa. The peak blood level was attained ≤10 min after nasal instillation. A nasal drug delivery system for quaternary ammonium compounds appears to be feasible for this antiarrhythmic agent or for other applications.

Quaternary ammonium salts are often used as surface-active agents when dissolved in water for antimicrobial and/or antiseptic purposes (12, 13). The possibility that nasal absorption of clofilium tosylate could be attributable

Table I—Comparison of [^{14}C]Clofilium Ion Blood Levels [a] in Rats [b] after Various Routes of Administration

Route of Administration	Dose, mg/kg[c]	AUC, μg·min/g[d]	Absorption, %[e]	p[f]
Intravenous	1.2	39.5 ± 4.98	—	—
Oral	1.2	0.53[g] ± 0.097	1.3	0.001
Nasal	1.2	27.5[h] ± 1.30	69.6	0.08

[a] Expressed as microgram equivalents of carbon-14 per gram of blood. [b] Harlan Sprague-Dawley male rats, $n = 3$. [c] Formulated in solution form. [d] Mean ± *SEM* of three rats. [e] Percentage of intravenous dose. [f] Probability value (Student's t test), compared with intravenous administration route data. [g] $p < 0.05$, compared with nasal administration route data. [h] $p > 0.05$, compared with intravenous administration route data.

Table II—Comparison of [^{14}C]Clofilium Ion Blood Levels [a] in Rats—Effect of Dose

Route of Administration	Dose, mg/kg[b]	AUC, μg·min/g[c]	Mean Specific AUC[d]	Absorption, %
Intravenous	1.2	39.5 ± 4.98	32.9	—
Nasal	1.2	27.5 ± 1.30	22.9	69.6
Nasal	0.6	5.70 ± 1.06	9.50	28.9
Nasal	0.3	2.81[e] ± 0.28	9.37	28.5

[a] Expressed as microgram equivalents of carbon-14 per gram of blood. [b] Formulated in solution form. [c] Mean ± *SEM* of three rats. [d] Mean specific AUC: (μg·min/g)/(mg/kg) = mean AUC/administered dose. [e] $p > 0.05$, compared with an AUC of 0.6 mg/kg.

Table III—Tissue Distribution [a] of [^{14}C]Clofilium Ion [b] in Rats [c] after Intranasal Administration of a 0.3-mg/kg Dose of Clofilium Tosylate

Tissue	Time after Dose, h				
	0.5	1	2	4	6
Blood	12.06 ± 1.80	9.30 ± 0.34	14.88 ± 1.44	11.80 ± 1.20	14.40 ± 3.80
Heart	82.12 ± 12.54	88.09 ± 4.10	1785.16 ± 23.10	227.80 ± 22.50	263.70 ± 27.00
Lung	58.95 ± 8.42	49.47 ± 4.69	83.88 ± 8.90	97.06 ± 15.20	112.10 ± 15.00
Liver	221.31 ± 29.19	218.24 ± 12.20	328.60 ± 36.30	482.90 ± 39.80	271.90 ± 36.00
Kidney	475.13 ± 87.60	609.42 ± 20.59	944.40 ± 85.50	1116.00 ± 106.80	813.00 ± 110.00

[a] Each value represents the mean ± *SEM* of three animals. [b] Expressed as nanogram equivalents of carbon-14 per gram of tissue. [c] Harlan Sprague-Dawley male rats; $n = 3$.

Table IV—Summary of Histological Examination of Nasal Mucosa after Intranasal Administration of Clofilium Tosylate to Rats

Necropsy	Dose, mg/kg	Exposure, h	Microscopic Findings[a]
A	Control	0	No significant lesions.
B	1.2	6	About one-half of the mucosa was necrotic or missing. Occasional microabscesses were present in the mucosa. The lumens of affected turbinates contained debris formed of neutrophils and sloughed mucosa.
C	0.6	6	Mild necrosis was characterized by occasional eosinophilic, round, mucosal cells with pycnotic nuclei. Minimal amount of luminal debris.
D	0.3	6	Similar to that for the 0.6-mg/kg dose.

[a] Summarized from the observation from four cross sections of the nasal cavity of each rat and from a total of three rats in each study.

to damage to the mucosa was realized during the course of these studies. Therefore, histopathological studies were conducted. To avoid physical damage to any part of the nasal mucosa, the drug solution was delivered to the nasal cavity through the esophagus cannulation tubing with a syringe. Typical lesions of the exposed specimens of rat nasal mucosa are reported (Figs. 2-4). In general, large portions of mucosa that were in contact with the highest concentration of clofilium tosylate became necrotic. At the lower concentrations, only occasional epithelial cells were necrotic, and large areas of mucosa were unaffected. No histological differences between nasal mucosa exposed to the 0.3- or 0.6-mg/kg dose were detected. The results observed in the nasal mucosa of rats after administration of clofilium tosylate are summarized in Table IV. Control groups were also exposed to the vehicle.

The time course of the clofilium ion radioactivity in various tissues following nasal administration of clofilium tosylate in rats is summarized in Table III. The absorption kinetics of the radioactivity from the blood contrasted with that from some tissues. One hour after nasal administration, high levels of radioactivity relative to the blood were observed in the heart, lung, liver, and kidney tissues. There was a gradual accumulation of the drug in the heart, with a peak occurring between 4 and 6 h based on the experimental design. Radioactivity levels in the heart appeared to be very persistent. By 6 h after nasal administration, the total radioactivity in the heart was about 18-fold greater than that in the blood. The results are consistent with the previously reported gradual uptake by the myocardium after intravenous administration of the drug in rats and dogs (14). Distribution in blood and the relationship between tissue and blood concentrations appear to be similar, regardless of whether administration is intravenous or nasal. Other quaternary ammonium antiarrhythmic agents, such as bretylium and 1-(dimethylisopropylamino)-3-(1-naphthyloxy)-2-propanol methochloride (UM-272), are also known to have a high affinity for myocardial tissue relative to plasma (15, 16). The biological response of clofilium tosylate correlates with the levels of radioactivity in the heart (14). These data re-emphasize the fact that for the clofilium ion, and possibly other quaternary ammonium antiarrhythmic agents, blood levels are an insufficient indicator for estimating cardiac levels and thus pharmacological effect.

REFERENCES

(1) M. I. Steinberg and B. B. Molly, *Life Sci.*, **25**, 1397 (1979).

(2) M. I. Steinberg, M. E. Sullivan, S. A. Wiest, F. W. Rockhold, and B. B. Molly, *J. Cardiovasc. Pharmacol.*, **3**, 881 (1981).

(3) E. Platia and P. R. Reid, *Circulation*, **62**, 153 (1980).

(4) E. R. Garrett, J. R. Green, and M. Bialer, *Biopharm. Drug Dispos.*, **3**, 129 (1982).

(5) M. I. Steinberg, in "New Drug Annual," Raven Press, New York, N.Y., 1984, p. 103.

(6) J. A. Hemberger and L. S. Schanker, *Drug Metab. Dispos.*, **II**, 73 (1983).

(7) B. L. Kamath, H. F. Stampfli, C. M. Lai, and A. Yacobi, *J. Pharm. Sci.*, **70**, 667 (1981).

(8) "U.S. Pharmacopeia XX," U.S. Pharmacopeial Convention, Rockville, Md., 1980, p. 727.

(9) A. Hussain, S. Hirai, and R. Bawarshi, *J. Pharm. Sci.*, **69**, 1411 (1980).

(10) S. Hirai, T. Yashiki, and T. Matsuzawa, presented at the 98th Annual Meeting of the Pharmaceutical Society of Japan, April 1978.

(11) J. T. Young, *Fund. Appl. Toxicol.*, **1**, 309 (1981).

(12) R. M. E. Richards and R. H. Cavill, *J. Pharm. Sci.*, **65**, 76 (1976).

(13) J. P. Remington, in "Remington's Pharmaceutical Sciences," 14th ed., Mack Publishing Co., Easton, Pa., 1970, p. 315.

(14) T. D. Lindstrom, P. J. Murphy, J. K. Smallwood, S. A. Wiest, and M. I. Steinberg, *J. Pharmacol. Exp. Ther.*, **221**, 584 (1982).

(15) D. H. Namm, C. M. Wang, S. El-Sayad, F. C. Capp, and R. A. Maxwell, *J. Pharmacol. Exp. Ther.*, **193**, 194 (1975).

(16) E. Patterson, P. Stetson, and B. R. Lucchesi, *J. Pharmacol. Exp. Ther.*, **214**, 449 (1980).

ACKNOWLEDGMENTS

This study was presented to the Basic Pharmaceutics Section, American Pharmaceutical Association Academy of Pharmaceutical Sciences 35th National Meeting, Miami Beach, Fla., November 1983.

The authors thank Dr. T. D. Linstrom for helpful discussions and Mrs. C. Lammers for assistance in preparing the manuscript.

Methods for *In Vitro* Percutaneous Absorption Studies III: Hydrophobic Compounds

ROBERT L. BRONAUGH ˣ **and RAYMOND F. STEWART**

Received May 9, 1983, from the *Division of Toxicology, Food and Drug Administration, Washington, DC 20204.* Accepted for publication September 8, 1983.

Abstract □ The absorption of two hydrophobic compounds through rat skin was measured by *in vivo* and *in vitro* techniques. The permeation of the fragrance ingredients 3-phenyl-2-propenyl 2-aminobenzoate (I) and 1-(3-ethyl-5,6,7,8-tetrahydro-5,5,8,8-tetramethyl-2-naphthalenyl)ethanone (II) was measured from a petrolatum and an acetone vehicle. Increases in permeation of 8-fold (I) and 95-fold (II) were observed when the compounds were tested *in vivo* under conditions similar to *in vitro* procedures. The apparent inability of the compounds to freely enter the diffusion cell receptor fluid was partially reversed by replacing normal saline with other fluids: rabbit serum, 3% bovine serum albumin, organic solvents, and dilutions of four nonionic surfactants. The effect of the receptor fluids on the integrity of the skin barrier was assessed by measuring the permeability of control compounds (cortisone, urea, and water). A 6% solution of polyethylene glycol 20 oleyl ether was the receptor fluid of choice. Without apparent damage to the skin, 61% (petrolatum vehicle) or 73% (acetone vehicle) of the *in vivo* absorption of I was obtained. With II, only 32% of the *in vivo* absorption was achieved (petrolatum vehicle). Even when the surfactant solution is used, significant differences may still remain between *in vivo* and *in vitro* results.

Keyphrases □ Absorption—percutaneous, *in vitro*, hydrophobic compounds □ Hydrophobic compounds—*in vitro* percutaneous absorption

For a number of compounds, good agreement is found between the results of *in vivo* and *in vitro* skin permeability studies (1-10). The *in vitro* values determined by Franz (1, 2) compared favorably with the *in vivo* permeability results of Feldmann and Maibach (3) for 12 organic compounds in human skin when considerations were made for experimental differences. Bronaugh *et al.* (4) have measured both the *in vivo* and *in vitro* absorption of three compounds through rat skin. Again, the diffusion cell studies were accurate in their prediction of *in vivo* absorption.

For a certain type of compound, however, erroneous results may be obtained when standard diffusion cell techniques are used. Compounds that are essentially insoluble in water may not partition freely from excised skin into an aqueous receptor fluid. When applied to skin *in vivo*, however, these compounds may readily leave the barrier layers of the skin because of their solubility in biological fluids. In the *in vivo* and *in vitro* absorption comparisons of Tsuruta (8, 9), values much lower than expected were obtained for *in vitro* permeability measurements of organic solvents with the lowest water solubility.

The problem was alluded to by Franz (1), who in selecting compounds for study, omitted highly water-insoluble compounds to avoid results that were "artificially limited due to insolubility in the dermal bathing solution." Brown and Ulsamer (11) have found that the skin permeation of the hydrophobic compound hexachlorophene increased twofold when normal saline was replaced with 3% bovine serum albumin (in a physiological buffer) in the diffusion cell receptor. This new receptor fluid had a 500-fold greater solubility for hexachlorophene. In a recent study (12), a nonionic surfactant (poloxamer 188[1]) was used to enhance the solubility of linoleic acid in the diffusion cell receptor medium. Although the potential problem inherent in the partitioning of a hydrophobic compound from skin is now recognized, no systematic studies to characterize and attempt to solve this problem have been carried out.

In determining the skin absorption of two fragrance materials, it seemed that their hydrophobic nature might cause difficulties in an *in vitro* analysis. The water solubilities of 3-phenyl-2-propenyl 2-aminobenzoate (cinnamyl anthranilate; I) and 1-(3-ethyl-5,6,7,8-tetrahydro-5,5,8,8-tetramethyl-2-naphthalenyl)ethanone (acetyl ethyl tetramethyl tetralin; II) were 0.23 and 0.012 mg/L, respectively. Therefore, percutaneous absorption of these compounds was initially determined *in vivo* in rats. Lipophilic receptor fluids were substituted for normal saline to try to enhance absorption and approximate the *in vivo* results without damage to the permeability barrier. Rabbit serum and aqueous dilutions of serum albumin, organic solvents, and four commonly used nonionic surfactants were utilized as the lipophilic receptor fluids.

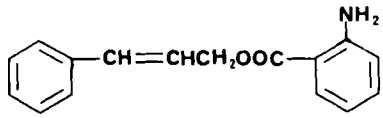

I

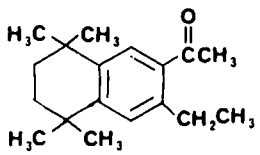

II

EXPERIMENTAL SECTION

Materials—The following radiolabeled compounds were used to facilitate quantitation of skin absorption (specific activity): [^{14}C]II[2] (2.40 mCi/mmol); [^{14}C]I[2] (10.5 mCi/mmol); [^{3}H]cortisone[4] (43.0 Ci/mmol); [^{14}C]urea[4] (57.0 mCi/mmol); and tritiated water (55.5 mCi/mmol). All compounds were determined to have a radiochemical purity of 98%. Agents used in the receptor fluids, polyethylene glycol 20 oleyl ether (PEG-20 oleyl ether)[5], octoxynol 9[6], poloxamer 188, polysorbate 80[7], and bovine serum albumin[8], were prepared in distilled water at the indicated concentrations. All agents (except albumin) are commonly used nonionic surfactants.

***In Vitro* Studies**—Percutaneous absorption measurements were made in a one-chambered static diffusion cell as described previously (13). The receptor fluid was stirred with a magnetic stirring bar in a constant-temperature water bath maintained at 32°C.

The skin on the back was lightly shaved and then excised from 3- to 7-month-old female Osborne-Mendel rats. In some experiments, subcutaneous tissue was removed, and full-thickness skin was fixed in the diffusion cell. For most experiments, split-thickness skin (350 μm) was prepared with a dermatome[9]. Test compounds were applied to the epidermal surface of the skin

[1] Pluronic F-68; BASF-Wyandotte, Wyandotte, Mich.

[2] Arthur D. Little, Cambridge, Mass.

[3] Division of Cosmetics Technology, Food and Drug Administration, Washington, D.C.

[4] New England Nuclear Corp., Boston, Mass.

[5] Volpo 20; Croda, Inc., New York, N.Y.

[6] Triton X-100; Rohm and Haas Co., Philadelphia, Pa.

[7] Tween 80; Fisher Scientific Co., Fair Lawn, N.J.

[8] Sigma Chemical Co., St. Louis, Mo.

[9] Padgett Dermatome, Kansas City, Mo.

0022-3549/84/0900-1255$01.00/0
© 1984, American Pharmaceutical Association

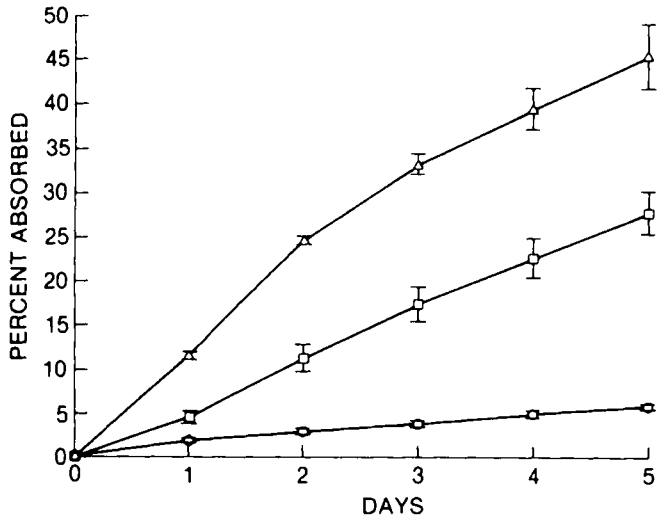

Figure 1—*Absorption of I from a petrolatum vehicle. Key: (Δ) in vivo results; (○) in vitro (saline in receptor); (□) in vitro (6% PEG-20 oleyl ether in receptor). At 5 d, 13% of the in vivo absorption was obtained by in vitro techniques, using saline in the diffusion cell receptor. Absorption was increased to 61% of the in vivo results by substituting 6% PEG-20 oleyl ether as the receptor fluid.*

dissolved in either a petrolatum or acetone vehicle. The 1.13-cm^2 area of skin was completely covered by the vehicle (30 mg of petrolatum, 20 μL of acetone). Aliquots of receptor fluid were removed from a side arm at various intervals, and the radioactivity was determined in a liquid scintillation counter[10].

Cortisone permeation was determined to monitor the effect of the receptor fluid on the integrity of the skin barrier. In most experiments, the permeability of the ^{14}C-labeled fragrance and the [^3H]cortisone was determined simultaneously by dual-label techniques. The absorption of the fragrances (I and II) was expressed as a percentage of the amount applied to the skin to facilitate comparison with the *in vivo* results. Cortisone permeation from the petrolatum vehicle was expressed as a permeability constant (steady-state absorption rate divided by the applied concentration). Other percutaneous absorption values were expressed as the percent dose absorbed and/or permeability constants.

***In Vivo* Studies**—The skin absorption of I and II was determined in rats by *in vivo* methods described previously (4). The back skin of the rats was lightly clipped and a nylon ring (inside area, 2 cm^2) was glued to the back with a cyanoacrylate adhesive. The rats were partially restrained with rubber tube collars, and the test compounds were applied inside the protective device on the back. Because of significant excretion in the feces expected with the lipophilic compounds, absorption was estimated by summing the amounts of compound excreted in the urine and feces (14). These samples were collected at 24-h intervals in metabolism cages for 5 d. Radioactivity in the samples was determined by liquid scintillation counting. Percutaneous absorption was expressed as the percentage of the applied dose excreted during the collection periods.

Statistical analysis was by the Student's *t* test. The significance of increased absorption of compounds resulting from changes in the receptor fluid was determined by using a one-tailed probability.

RESULTS

In vitro percutaneous absorption measurements, using a normal saline receptor solution, resulted in values that were much lower than the corresponding *in vivo* data for I and II. This difference is shown in the time course for the absorption of I (Fig. 1). In initial studies, the effect of different receptor fluids on the absorption of I was determined by comparing values obtained after 5 d (Table I). Only 12.7% of I absorbed *in vivo* during the 5-d period was obtained in a corresponding *in vitro* experiment, using normal saline receptor fluid and split-thickness rat skin. A 1.5% solution of the nonionic surfactant PEG-20 oleyl ether enhanced by threefold the skin permeability to I; the cortisone permeation determined simultaneously in the dual-label experiment was not altered. When full-thickness rat skin was used, no increase in the absorption of I was obtained with the PEG-20 oleyl ether. The optimal concentration of the surfactant was 6%. A fivefold increase in the absorption of I was obtained without altering the permeation of the cortisone control.

Rabbit serum and bovine serum albumin had no effect on the integrity of the barrier, but they were also less effective in increasing the absorption of I than PEG-20 oleyl ether. A methanol–water solution and 6% octoxynol 9 were equal or superior to 6% PEG-20 oleyl ether, but significant damage to the skin was indicated by the increased cortisone permeation since the absorption of cortisone is not limited by a lack of solubility in the normal saline receptor fluid. A 6% solution of poloxamer 188 in the receptor resulted in slight enhancement of both I and cortisone permeation.

An even greater difference was seen between the *in vivo* absorption of II and the diffusion cell data (Table I). Results similar to those determined with I were obtained by altering the receptor fluid. The enhanced absorption with 1.5% PEG-20 oleyl ether required the use of a dermatome skin section. Best results were obtained with 6% PEG-20 oleyl ether in the receptor, and no increase was observed in the permeation of the cortisone control. Use of a glycerol–water solution in the receptor resulted in permeability data similar to those obtained with normal saline. As was previously found when a methanol–water solution was used, the ethanol–water receptor fluid enhanced the penetration not only of II, but also of the cortisone control.

When I was applied to rat skin in an acetone vehicle, greater absorption was obtained than with a petrolatum vehicle (Table II). A 6% PEG-20 oleyl ether receptor fluid in the diffusion cells greatly increased the permeation of I without a significant effect on the permeation of cortisone.

The *in vitro* absorption of II and cortisone (acetone vehicle) was measured for 43 h to determine the effect on skin permeation of three nonionic surfactants (Table II). Use of 6% PEG-20 oleyl ether resulted in the greatest increase in the absorption of II without an increase in that of the cortisone control. At the same concentration (6%), both polysorbate 80 and octoxynol 9 resulted in increased cortisone permeation when compared with the value obtained with normal saline.

The effect of 6% PEG-20 oleyl ether on the absorption of water and urea

Table I—Effect of Diffusion Cell Conditions on the Absorption of I and II (Cortisone Control)[a]

Receptor Fluid	Percent Applied Dose Absorbed in 5 d	Cortisone Permeability Constant × 10^5
	Compound I	
Normal saline (4)[b]	5.0 ± 0.3	3.8 ± 0.7
1.5% PEG-20 oleyl ether (4)[b]	5.4 ± 0.9	–
Normal saline (4)	5.8 ± 0.4	7.1 ± 0.5
1.5% PEG-20 oleyl ether (10)	15.5 ± 1.2[c]	6.1 ± 0.5
6% PEG-20 oleyl ether (8)	27.9 ± 1.8[c,d]	7.0 ± 0.9
20% PEG-20 oleyl ether (8)	18.3 ± 1.8[c]	9.3 ± 0.9
Rabbit serum (4)	8.8 ± 0.6[c]	6.8 ± 0.8
3% Bovine serum albumin (4)	12.1 ± 1.2[c]	5.4 ± 0.2
50:50 Methanol–water (4)	27.1 ± 2.0[c]	17.2 ± 0.2[e]
1.5% Octoxynol 9 (4)	17.9 ± 1.1[c]	10.8 ± 0.5[e]
6% Octoxynol 9 (4)	38.4 ± 2.9[c]	14.5 ± 1.3[e]
6% Poloxamer 188 (4)	7.3 ± 1.3	9.8 ± 0.6[e]
	Compound II	
Normal saline (6)[b]	0.08 ± 0.01	3.8 ± 0.7[e]
1.5% PEG-20 oleyl ether (6)[b]	0.24 ± 0.07	–
Normal saline (4)	0.20 ± 0.06	6.3 ± 0.3
1.5% PEG-20 oleyl ether (4)	2.3 ± 0.4[c]	4.9 ± 0.2
6% PEG-20 oleyl ether (4)	6.0 ± 0.9[c,f]	7.0 ± 0.9[e]
50:50 Glycerol–water (3)	0.14 ± 0.03	4.7 ± 0.9
40:60 Ethanol–water (4)	6.1 ± 1.2[c,g]	21.7 ± 3.3[e]

[a] Values are the mean ± *SE*; the number of determinations is in parentheses. For most experiments, a 350-μm section from the surface of whole rat skin was prepared with a dermatome. Compounds were applied to the skin in a petrolatum vehicle. *In vivo* absorption of I was 45.6%; *in vivo* absorption of II was 18.9%. [b] Whole skin. [c] Significant increase when compared with results from the appropriate saline control (dermatome section) by one-tailed Student's *t* test, $p < 0.05$. [d] Significant increase when compared with results from all receptor fluid for I except methanol–water and 6% octoxynol 9 by one-tailed Student's *t* test, $p < 0.05$. [e] Value determined in experiments with I. [f] Significant increase when compared with results from all receptor fluids for II except ethanol–water by one-tailed Student's *t* test, $p < 0.05$. [g] Value determined at 4 d.

[10] Model LS 9000; Beckman Instruments, Fullerton, Calif.

Table II—Effect of Nonionic Surfactants on I, II, and Cortisone Absorption[a]

Receptor Fluid	Percent Absorbed (5 d) I	Cortisone
Compound I[b]		
Normal Saline (9)	14.1 ± 1.3	21.5 ± 2.5
6% PEG-20 oleyl ether (8)	44.1 ± 4.3[c]	24.8 ± 3.2
Compound II		
Receptor Fluid	Percent Absorbed (43 h) II	Cortisone
Normal Saline (12)	0.7 ± 0.1	7.2 ± 0.9
6% PEG-20 oleyl ether (8)	7.5 ± 1.4[c]	6.0 ± 0.5
6% Polysorbate 80 (4)	4.1 ± 0.6[c]	10.6 ± 1.5[c]
6% Octoxynol 9 (4)	11.9 ± 1.8[c]	15.1 ± 1.0[c]

[a] Values are the mean ± *SE*; the number of determinations is in parentheses. Compounds were applied *in vitro* to rat skin (350-μm section) in an acetone vehicle. [b] *In vivo* absorption of I (acetone vehicle) was 60.7%. [c] Significant increase when compared with the appropriate saline control by one-tailed Student's *t* test, $p < 0.05$.

was examined with rat skin in diffusion cells (Table III). No significant increase was seen in the percutaneous absorption of these two additional control compounds.

DISCUSSION

A comparison of the *in vivo* and *in vitro* percutaneous absorption data for the fragrance ingredients I and II reveals the underestimation of absorption that can occur by using diffusion cell techniques with hydrophobic compounds. Increases of 8-fold (I) and 95-fold (II) in permeation were obtained when the compounds were tested *in vivo* under similar conditions.

In vitro absorption was therefore increased by substituting more lipophilic receptor fluids for normal saline. A physiological-based solution to the problem, it seemed, might result from the use of serum or serum proteins in the diffusion cell receptor. However, the use of rabbit serum as the receptor fluid did not substantially increase absorption of the fragrances. This failure may be the result of the absence of a continual replacement of the bathing medium, as occurs *in vivo* with blood flow through the skin. Use of 3% bovine serum albumin was more effective than serum, but only about a twofold increase in I absorption was obtained. Brown and Ulsamer (11) have observed a similar increase in hexachlorophene permeation through excised human stratum corneum when 3% bovine albumin was added to the receptor. The penetration rate of hexachlorophene correlated with the solubility of the compound in different buffer-albumin mixtures.

Nonionic surfactants have a relatively mild effect on skin, with a much lower irritation potential than ionic agents (15). Aqueous dilutions of a series of nonionic surfactants were evaluated in the diffusion cell system. The fact that split-thickness skin was required for an increase in I and II absorption with 1.5% PEG-20 oleyl ether indicates that a more physiological value may be obtained with this preparation of skin. A major portion of systemic uptake occurs in the highly vascular upper dermis; thus, use of full-thickness skin *in vitro* can introduce an artificial barrier, which is of importance particularly with hydrophobic compounds.

More than 60% of the absorption of I that occurred *in vivo* was obtained by using diffusion cells with a 6% solution of PEG-20 oleyl ether (Table I). The permeability constant for cortisone was unaffected. Attempts to increase the absorption of I with a 20% solution of the surfactant resulted in a slight increase in cortisone permeation and an unexpected decrease in absorption of I. The high viscosity of a 20% solution makes it difficult to use experimentally. Solutions of octoxynol 9, poloxamer 188, and polysorbate 80 resulted in enhanced permeation of the cortisone control in experiments with I and II, even at concentrations at which lower amounts of these hydrophobic compounds were absorbed than with the PEG-20 oleyl ether (Tables I and II). A 6% solution of PEG-20 oleyl ether was found to be the receptor fluid of choice.

Table III—Effect of PEG-20 Oleyl Ether on the Absorption of Water and Urea[a]

Receptor Fluid	Water Permeability Constant × 10^3	Percent Absorbed (43 h) Water	Urea
Normal Saline	2.5 ± 0.6	21.0 ± 5.4	9.3 ± 3.2
6% PEG-20 oleyl ether	2.7 ± 0.6[b]	23.5 ± 5.5[b]	10.3 ± 3.4[b]

[a] Values are the mean ± *SE* of eight determinations. Compounds were applied to rat skin (350-μm section) in 600 μL of water. [b] No significant increase when compared with saline controls by one-tailed Student's *t* test, $p < 0.05$.

Table IV—Comparison of Solubility Properties and the Effect of PEG-20 Oleyl Ether on Percutaneous Absorption

Compound	Water Solubility, mg/L	Octanol-Water, K	Skin Permeation Ratio[a]
Urea	1×10^6	0.002	1.1[b]
Cortisone	280	44	1.2[c]
Testosterone	11	2089	2.3[d]
I	0.23	652	3.1[c]
II	0.012	3589	30.0[e]

[a] 6% PEG-20 oleyl ether/saline. The skin permeation ratio was determined by comparing the amount of compound absorbed in experiments in which the two receptor fluids were used. [b] Water vehicle, 43 h. [c] Acetone vehicle, 5 d. [d] Acetone vehicle, 43 h. [e] Petrolatum vehicle, 5 d.

The use of cortisone as a control in many of the experiments was based on its good solubility in the petrolatum vehicle, reasonable water solubility, and ready availability in the tritiated form for dual-label experiments. It was considered important to establish additionally that the permeation of other molecules was also unaffected by the use of 6% PEG-20 oleyl ether as a receptor fluid. The percutaneous absorption of two small polar molecules (water and urea) was not significantly increased by the use of the surfactant solution (Table III).

The use of an acetone vehicle resulted in better agreement between the *in vitro* data for I and the diffusion cell results with PEG-20 oleyl ether as the receptor fluid (Table II). *In vitro* permeation of I after 5 d was 73% of that found in the corresponding *in vivo* experiment. This result may be due to higher levels of I absorbed into the skin in the absence of the lipophilic petrolatum layer.

The increase in absorption resulting from the use of 6% PEG-20 oleyl ether instead of saline in the receptor is presented in Table IV along with the octanol and water solubility properties of selected compounds. No significant effect of using PEG-20 oleyl ether was obtained with the more water-soluble compounds. The greatest increase in permeation was obtained with II, an extremely hydrophobic compound with a large octanol-water partition coefficient. Compounds that are essentially insoluble in water (solubility, ~10 mg/L or less) and more soluble in lipoidal media may partition only slightly from skin into a normal saline solution. For these types of compounds, caution must be exercised in interpreting *in vitro* absorption data.

In a system in which split-thickness rat skin is used as the membrane, the use of a surfactant in the receptor fluid was advantageous for absorption measurements of several hydrophobic compounds. Although results identical to *in vivo* values were not obtained, dramatic increases in absorption were achieved without apparent damage to the skin. Obviously, one receptor fluid is not beneficial to the same degree for all hydrophobic compounds. The permeation of compounds like II, which are extremely lipophilic and hydrophobic, will be increased to the greatest extent, but even so, <50% of the *in vivo* absorption may be obtained. For compounds with a lower lipid-water partition coefficient, values more closely in agreement with *in vivo* results should be achieved.

REFERENCES

(1) T. J. Franz, *J. Invest. Dermatol.*, **52**, 190 (1975).

(2) T. J. Franz, *Curr. Probl. Dermatol.*, **7**, 58 (1978).

(3) R. J. Feldmann and H. I. Maibach, *J. Invest. Dermatol.*, **54**, 399 (1970).

(4) R. L. Bronaugh, R. F. Stewart, E. R. Congdon, and A. L. Giles, Jr., *Toxicol. Appl. Pharmacol.*, **62**, 474 (1982).

(5) G. E. Burch and T. Winsor, *Arch. Intern. Med.*, **74**, 437 (1944).

(6) M. Ainsworth, *J. Soc. Cosmet. Chem.*, **11**, 69 (1960).

(7) D. Sekura and J. Scala, in "Pharmacology and the Skin," W. Mon-

tagna, E. Van Scott, and R. Stoughton, Eds., Appleton-Century-Crofts, New York, N.Y., 1972, p. 257.
(8) H. Tsuruta, *Ind. Health*, **13**, 227 (1975).
(9) H. Tsuruta, *Ind. Health*, **15**, 131 (1977).
(10) N. H. Creasey, J. Battensby, and J. A. Fletcher, *Curr. Probl. Dermatol.*, **95**, 95 (1978).
(11) D. W. C. Brown and A. G. Ulsamer, *Food Cosmet. Toxicol.*, **13**, 81 (1975).
(12) A. Hoelgaard and B. Mollgaard, *J. Pharm. Pharmacol.*, **34**, 610 (1982).
(13) R. L. Bronaugh, E. R. Congdon, and R. J. Scheuplein, *J. Invest. Dermatol.*, **76**, 94 (1981).
(14) K. E. Anderson, H. I. Maibach, and M. D. Anjo, *Br. J. Dermatol.*, **102**, 447 (1980).
(15) A. B. J. Lansdown and P. Grasso, *Br. J. Dermatol.*, **86**, 361 (1972).

Kinetics of Aspirin Absorption Following Oral Administration of Six Aqueous Solutions with Different Buffer Capacities

WILLIAM D. MASON

Received October 29, 1982, from the *Pharmacokinetics Laboratory, Schools of Pharmacy and Medicine, University of Missouri-Kansas City, Kansas City, MO 64108.* Accepted for publication September 13, 1983.

Abstract □ Fifteen volunteers each received two of six aspirin solutions in a balanced incomplete block design. The solutions contained 0, 3, 6, 10, 16, and 34 mEq of sodium bicarbonate-citric acid buffer and 650 mg of aspirin. Plasma aspirin levels were measured in blood samples collected frequently during the first 2.5 h, and the accumulation of aspirin, salicylic acid, and salicyluric acid were measured over 2 and 24 h. The most rapid absorption rates occurred with solutions which contained small quantities of the antacid buffer. The 3- and 6-mEq antacid buffers had mean maximal aspirin concentrations of 17.3 and 17.8 μg/mL, respectively. In the absence of the buffering agent, the 650 mg of aspirin failed to dissolve completely and gave a mean maximal plasma concentration of 13.4 μg/mL. With 34 mEq of a buffering agent, a delay in the onset of absorption occurred and the presystemic hydrolysis increased. This was probably because more aspirin was emptied into and absorbed from the small intestine with higher concentrations of the buffering agent.

Keyphrases □ Aspirin—pharmacokinetics, oral administration, sodium bicarbonate-citric acid buffer, humans □ Pharmacokinetics—aspirin, sodium bicarbonate-citric acid buffer, oral administration, humans

Aspirin, the drug of choice when a mild analgesic-antipyretic is required, is also the primary agent in the chronic management of rheumatoid arthritis and osteoarthritis. After oral administration, rapid absorption beneficially provides rapid onset of effects and reduces the contact time with the gastric mucosa.

In an earlier report from this laboratory (1) the literature relating to the administration of aspirin in buffered solutions was reviewed, and data comparing an unbuffered tablet to two different buffered solutions was presented. The three dosage forms were an unbuffered tablet, an effervescent solution with 16 mEq of buffer, and an effervescent solution with 34 mEq of buffer. Significant differences in the aspirin absorption rate were observed: the solution of 16 mEq of buffer was fast, the solution of 34 mEq of buffer was intermediate, and the unbuffered tablet was slow. These differences were attributed primarily to gastric emptying and the rate of tablet dissolution.

It may be desirable to optimize the amount of buffer components to provide rapid absorption and to reduce gastric irritation through minimal alkalinization of urine and sodium intake. Thus, this study was undertaken to evaluate aspirin absorption kinetics over a range of buffer strengths.

EXPERIMENTAL SECTION

Dosage Forms—A series of soluble tablets were prepared that contained 650 mg of aspirin and sufficient sodium bicarbonate-citric acid buffer to provide 0, 3, 6, 10, 16, and 34 mEq of buffering. Just prior to administration, the tablets were placed in 140 mL of water and mechanically stirred to effect dissolution. The unbuffered tablet contained some undissolved particles in suspension, while all buffered tablets dissolved completely. Immediately following administration, the containers were rinsed with 100 mL of water which was also swallowed by the volunteers.

Subjects—Fifteen healthy volunteers, 21–33 years old and weighing 56.4–81.8 kg, were screened by a comprehensive physical examination, complete blood chemistry, complete blood count with differential, and urinalysis. All were free of any active disease such as influenza, and denied any use of medication for 14 d prior to the study. None of the subjects had a history of GI disease or surgery.

Method—The balanced incomplete block design, Table I, in which each of the 15 subjects received two of the six dosage forms with a 6-d washout between treatments, was employed. A 10-h fast preceeded dosing and continued 4 h postdose, except for water. Predose urine and blood samples were obtained, and a single dose of aspirin (650 mg) with 240 mL of water was administered as described. After dosing, 100 mL of water was administered at 1-, 2-, and 3-h intervals, and a uniform meal was served after 4 h. Subjects remained standing or sitting throughout the first 4 h, and exercise was limited to walking about the room.

Blood was drawn into chilled vacuum containers[1] *via* an indwelling catheter at 5, 10, 15, 20, 30, and 45 min and at 1, 1.5, 2, and 2.5 h. Plasma was separated by centrifugation at 1764×*g* within 20 min of collection. All urine was collected over a 0–2-h interval, the pH and volume were measured, and a 4-mL aliquot was taken for analysis. In addition, all urine was collected for 24 h. All plasma and urine samples were handled as described previously (2), which included storage at −20°C and HPLC analysis within 2 weeks. The HPLC method was updated by using a 5-μm octadecasilane column[2], measuring absorbance at 237 nm, and replacing the benzene with butyl chloride. These changes improved the sensitivity, safety, and reproducibility of the method over that reported previously (2); the statistics of the revised method will be the subject of a subsequent report.

Plasma aspirin concentration *versus* time plots for each dose to each subject were evaluated, and estimates for several kinetic parameters were obtained. The highest observed plasma concentration (C_{max}) and the time after dosing (t_{max}) to reach C_{max} were read directly from each plot. A terminal rate constant (k) and corresponding half-life ($t_{1/2}$) were computed by linear regression analysis of the natural logarithm of plasma concentration *versus* the time for all times greater than twice t_{max}. The trapezoid method was used to compute the area under the curve to the last measured concentration (C) and the value

[1] Vacutainer BD, 278-069, 7.0-mL capacity containing 14 mg of potassium oxalate and 17.5 mg of sodium fluoride.
[2] Altex Ultrasphere, ODS 5 μm; Altex Scientific Inc., Berkeley, Calif.

0022-3549/84/0900-1258$01.00/0
© 1984, American Pharmaceutical Association

tagna, E. Van Scott, and R. Stoughton, Eds., Appleton-Century-Crofts, New York, N.Y., 1972, p. 257.
(8) H. Tsuruta, *Ind. Health*, **13**, 227 (1975).
(9) H. Tsuruta, *Ind. Health*, **15**, 131 (1977).
(10) N. H. Creasey, J. Battensby, and J. A. Fletcher, *Curr. Probl. Dermatol.*, **95**, 95 (1978).
(11) D. W. C. Brown and A. G. Ulsamer, *Food Cosmet. Toxicol.*, **13**, 81 (1975).
(12) A. Hoelgaard and B. Mollgaard, *J. Pharm. Pharmacol.*, **34**, 610 (1982).
(13) R. L. Bronaugh, E. R. Congdon, and R. J. Scheuplein, *J. Invest. Dermatol.*, **76**, 94 (1981).
(14) K. E. Anderson, H. I. Maibach, and M. D. Anjo, *Br. J. Dermatol.*, **102**, 447 (1980).
(15) A. B. J. Lansdown and P. Grasso, *Br. J. Dermatol.*, **86**, 361 (1972).

Kinetics of Aspirin Absorption Following Oral Administration of Six Aqueous Solutions with Different Buffer Capacities

WILLIAM D. MASON

Received October 29, 1982, from the *Pharmacokinetics Laboratory, Schools of Pharmacy and Medicine, University of Missouri-Kansas City, Kansas City, MO 64108.* Accepted for publication September 13, 1983.

Abstract □ Fifteen volunteers each received two of six aspirin solutions in a balanced incomplete block design. The solutions contained 0, 3, 6, 10, 16, and 34 mEq of sodium bicarbonate-citric acid buffer and 650 mg of aspirin. Plasma aspirin levels were measured in blood samples collected frequently during the first 2.5 h, and the accumulation of aspirin, salicylic acid, and salicyluric acid were measured over 2 and 24 h. The most rapid absorption rates occurred with solutions which contained small quantities of the antacid buffer. The 3- and 6-mEq antacid buffers had mean maximal aspirin concentrations of 17.3 and 17.8 μg/mL, respectively. In the absence of the buffering agent, the 650 mg of aspirin failed to dissolve completely and gave a mean maximal plasma concentration of 13.4 μg/mL. With 34 mEq of a buffering agent, a delay in the onset of absorption occurred and the presystemic hydrolysis increased. This was probably because more aspirin was emptied into and absorbed from the small intestine with higher concentrations of the buffering agent.

Keyphrases □ Aspirin—pharmacokinetics, oral administration, sodium bicarbonate-citric acid buffer, humans □ Pharmacokinetics—aspirin, sodium bicarbonate-citric acid buffer, oral administration, humans

Aspirin, the drug of choice when a mild analgesic-antipyretic is required, is also the primary agent in the chronic management of rheumatoid arthritis and osteoarthritis. After oral administration, rapid absorption beneficially provides rapid onset of effects and reduces the contact time with the gastric mucosa.

In an earlier report from this laboratory (1) the literature relating to the administration of aspirin in buffered solutions was reviewed, and data comparing an unbuffered tablet to two different buffered solutions was presented. The three dosage forms were an unbuffered tablet, an effervescent solution with 16 mEq of buffer, and an effervescent solution with 34 mEq of buffer. Significant differences in the aspirin absorption rate were observed: the solution of 16 mEq of buffer was fast, the solution of 34 mEq of buffer was intermediate, and the unbuffered tablet was slow. These differences were attributed primarily to gastric emptying and the rate of tablet dissolution.

It may be desirable to optimize the amount of buffer components to provide rapid absorption and to reduce gastric irritation through minimal alkalinization of urine and sodium intake. Thus, this study was undertaken to evaluate aspirin absorption kinetics over a range of buffer strengths.

EXPERIMENTAL SECTION

Dosage Forms—A series of soluble tablets were prepared that contained 650 mg of aspirin and sufficient sodium bicarbonate-citric acid buffer to provide 0, 3, 6, 10, 16, and 34 mEq of buffering. Just prior to administration, the tablets were placed in 140 mL of water and mechanically stirred to effect dissolution. The unbuffered tablet contained some undissolved particles in suspension, while all buffered tablets dissolved completely. Immediately following administration, the containers were rinsed with 100 mL of water which was also swallowed by the volunteers.

Subjects—Fifteen healthy volunteers, 21–33 years old and weighing 56.4–81.8 kg, were screened by a comprehensive physical examination, complete blood chemistry, complete blood count with differential, and urinalysis. All were free of any active disease such as influenza, and denied any use of medication for 14 d prior to the study. None of the subjects had a history of GI disease or surgery.

Method—The balanced incomplete block design, Table I, in which each of the 15 subjects received two of the six dosage forms with a 6-d washout between treatments, was employed. A 10-h fast preceeded dosing and continued 4 h postdose, except for water. Predose urine and blood samples were obtained, and a single dose of aspirin (650 mg) with 240 mL of water was administered as described. After dosing, 100 mL of water was administered at 1-, 2-, and 3-h intervals, and a uniform meal was served after 4 h. Subjects remained standing or sitting throughout the first 4 h, and exercise was limited to walking about the room.

Blood was drawn into chilled vacuum containers[1] *via* an indwelling catheter at 5, 10, 15, 20, 30, and 45 min and at 1, 1.5, 2, and 2.5 h. Plasma was separated by centrifugation at 1764×*g* within 20 min of collection. All urine was collected over a 0–2-h interval, the pH and volume were measured, and a 4-mL aliquot was taken for analysis. In addition, all urine was collected for 24 h. All plasma and urine samples were handled as described previously (2), which included storage at −20°C and HPLC analysis within 2 weeks. The HPLC method was updated by using a 5-μm octadecasilane column[2], measuring absorbance at 237 nm, and replacing the benzene with butyl chloride. These changes improved the sensitivity, safety, and reproducibility of the method over that reported previously (2); the statistics of the revised method will be the subject of a subsequent report.

Plasma aspirin concentration *versus* time plots for each dose to each subject were evaluated, and estimates for several kinetic parameters were obtained. The highest observed plasma concentration (C_{max}) and the time after dosing (t_{max}) to reach C_{max} were read directly from each plot. A terminal rate constant (k) and corresponding half-life ($t_{1/2}$) were computed by linear regression analysis of the natural logarithm of plasma concentration *versus* the time for all times greater than twice t_{max}. The trapezoid method was used to compute the area under the curve to the last measured concentration (C) and the value

[1] Vacutainer BD, 278-069, 7.0-mL capacity containing 14 mg of potassium oxalate and 17.5 mg of sodium fluoride.
[2] Altex Ultrasphere, ODS 5 μm; Altex Scientific Inc., Berkeley, Calif.

0022-3549/84/0900-1258$01.00/0
© 1984, American Pharmaceutical Association

Table I—Balanced Incomplete Block Design

Subject Number	Antacid Buffering Agent, mEq	
	1st Dose	2nd Dose
1	16	6
2	3	16
3	34	10
4	10	6
5	6	0
6	0	16
7	0	34
8	34	3
9	16	34
10	10	0
11	16	10
12	6	3
13	34	6
14	3	0
15	10	3

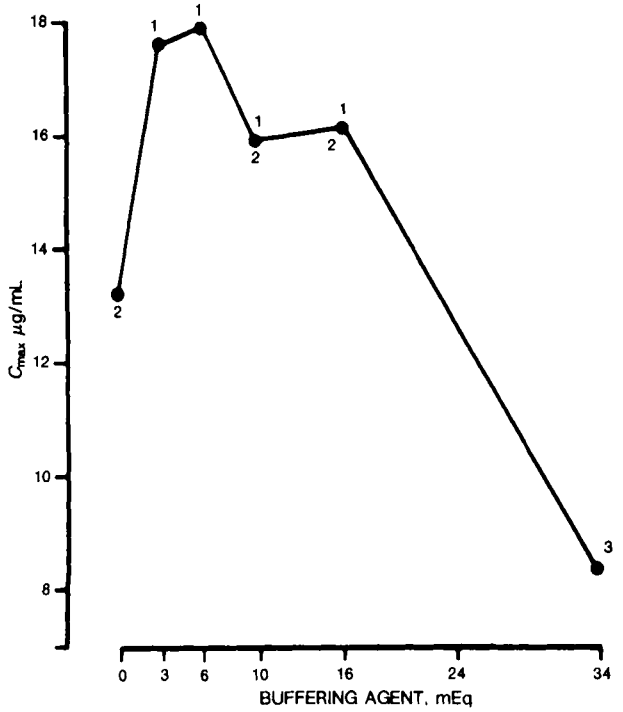

Figure 1—*A plot of C_{max} for aspirin as a function of buffer strength. A common number shared by two or more points indicates no significant difference ($p < 0.1$) for those points.*

C/k was added to estimate the area to infinity (AUC_∞). The renal clearance for aspirin (CL_r) was computed by dividing the amount of aspirin accumulated in the urine during the first 0–2-h interval by the area under the plasma curve for the corresponding time interval. Statistical moments (1, 3, 4) were used to compute the mean residence time for aspirin (MRT). An estimate of the residence time in the GI tract (MAT) for each dose was obtained by subtracting 16.2 min from each MRT value; 16.2 min approximates (4) the reported mean residence time for aspirin following intravenous administration and does not reflect experimental data from this report.

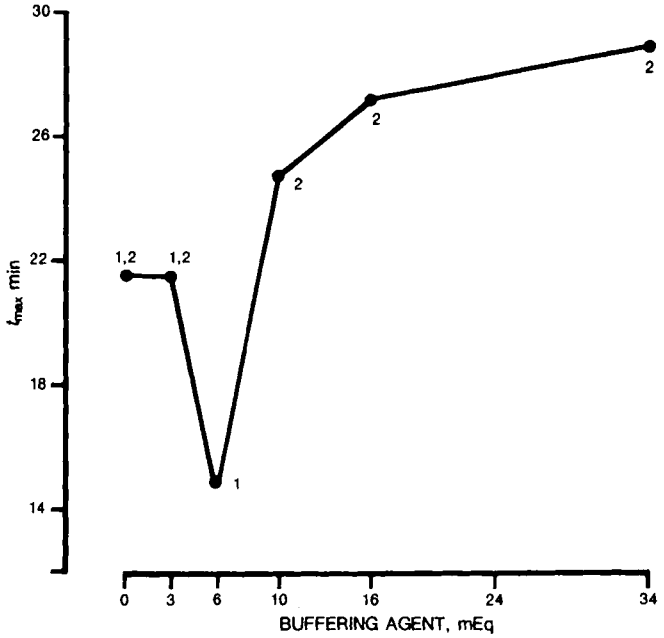

Figure 2—*A plot of t_{max} for aspirin as a function of buffer strength. A common number shared by two or more points indicates no significant difference ($p < 0.1$) for those points.*

RESULTS

In this study, the assay method had a lower limit of quantitation of 0.25 µg/mL and a relative coefficient of variation of 5%. Significant differences in the plasma aspirin concentration *versus* time curves, as presented in Table II, were observed for the various amounts of buffer in the dose. Although adjusted means (*i.e.*, least-square means) are employed in the balanced incomplete block design, these plots accurately reflect the plots for individual subjects. Unbuffered doses provided the highest aspirin concentration at the 5-min sample, while those with small amounts (*i.e.*, 3, 6, and 10 mEq) of buffer presented the most rapid rise between 5 and 10 min. With 34 mEq of the buffering agent there is a definite lag time preceding the appearance of aspirin in the plasma, followed by a rapid rise between the 10- and 20-min samples. All curves reached a maximum before 45 min with a subsequent monoexponential decay for which the mean half-lives ranged between 17.0 and 22.5 min across the six treatments.

Estimates of the comparative rate of aspirin absorption among the six different buffer strengths were obtained by referring to the mean C_{max}, t_{max}, MRT, and MAT values presented in Table III, and plotted in Figs. 1, 2, and 3. Although only some of the values are statistically significant ($p < 0.10$), the doses with 3 and 6 mEq of the buffer appear to provide higher C_{max} and lower t_{max} than unbuffered doses and for those doses with greater amounts of the buffering agent. This same trend is reflected in the statistical moment computations as expressed by the MAT and MRT values. The use of a 0.1 level of significance in computing the least significant differences is justified because the observations at each buffer level are not isolated; rather, they are

Table II—Plasma Aspirin Concentrations [a]

Time, min	Antacid Buffering Agent, mEq					
	0	3	6	10	16	34
Predose	—[b]	—[b]	—[b]	—[b]	—[b]	—[b]
5	5.00	0.84	2.61	4.50	3.56	0.49
10	7.29	7.60	12.6	8.98	6.70	1.97
15	10.7	13.9	13.8	13.8	12.1	5.47
20	11.8	17.3	16.0	10.5	12.5	7.49
30	11.3	12.7	11.3	9.26	9.91	8.15
45	6.71	6.16	4.72	6.94	7.04	5.86
60	3.70	3.17	2.22	4.12	3.53	3.84
90	1.38	1.11	0.72	1.38	0.90	1.16
120	0.43	0.40	0.25	0.60	0.41	0.42
150	—[b]	—[b]	—[b]	—[b]	—[b]	—[b]

[a] Adjusted means are least-squares means for the balanced incomplete block design. [b] Below detectable limit of 0.25 µg/mL.

Table III—Adjusted Means for Plasma Aspirin Parameters [a]

Parameters[b]						
AUC_∞, μg·min/mL						
Buffer, mEq	3	0	10	6	16	34
Adjusted Mean	599	586	578	560	554	420
C_{max}, μg/mL						
Buffer, mEq	6	3	16	10	0	34
Adjusted Mean	17.8	17.3	16.2	15.8	13.4	8.6
t_{max}, min						
Buffer, mEq	6	3	0	10	16	34
Adjusted Mean	14.8	21.5	21.5	24.8	27.3	29.0
Urine, pH, 0–2 h						
Buffer, mEq	6	16	0	3	10	34
Adjusted Mean	5.5	5.5	5.7	5.9	6.0	7.1
CL_r, L/h						
Buffer, mEq	6	0	10	3	16	34
Adjusted Mean	0.80	0.84	0.84	0.92	1.33	1.96
24-h Dose, %[c]						
Buffer, mEq	16	10	3	6	0	34
Adjusted Mean	60.4	63.2	64.5	66.3	70.6	71.0
MRT, min						
Buffer, mEq	6	3	16	0	10	34
Adjusted Mean	32.9	36.3	38.4	40.1	42.5	45.7
MAT[c], min						
Buffer, mEq	6	3	16	0	10	34
Adjusted Mean	16.7	20.1	22.2	23.9	26.3	29.5
$t_{1/2}$, min						
Buffer, mEq	3	0	6	16	10	34
Adjusted Mean	17.0	18.0	18.5	18.8	21.3	22.6

[a] Least-squares means for balanced incomplete block design; a line under two or more values indicates no significant difference ($p < 0.1$). [b] See text for definition of terms. [c] Sum of aspirin, salicylic acid, and salicyluric acid recovered in urine and corrected for formula weight.

integral members of a sequence of buffer strengths. To require each to meet the 0.05 level of significance, independently, would be an excessively severe test.

Estimation of the extent to which aspirin reaches the circulatory system requires consideration of both the AUC_∞ and the CL_r for aspirin. The significantly lower AUC_∞ for aspirin with 34 mEq of the buffering agent, compared with aspirin with lesser amounts of the buffering agent, as presented in Table I, can partially be attributed to an increased renal clearance as the pH of the urine increased. While the observed increase in renal clearance from 0.84 L/h, with no buffering, to 1.96 L/h, with 34 mEq of the buffering, is significant ($p < 0.10$), the overall maximal increase in systemic aspirin clearance in urine is ~2–3%, if the systemic clearance is ~40 L/h as previously reported for similar subjects (1, 5). Based on these clearance changes one might expect a 2–3% lower AUC_∞ with 34 mEq of the buffering agent, rather than the 28% lower AUC_∞ shown in Table III. These data suggest that adding 34 mEq of the buffering agent to the aspirin dose results in about 25% less aspirin reaching the circulatory system.

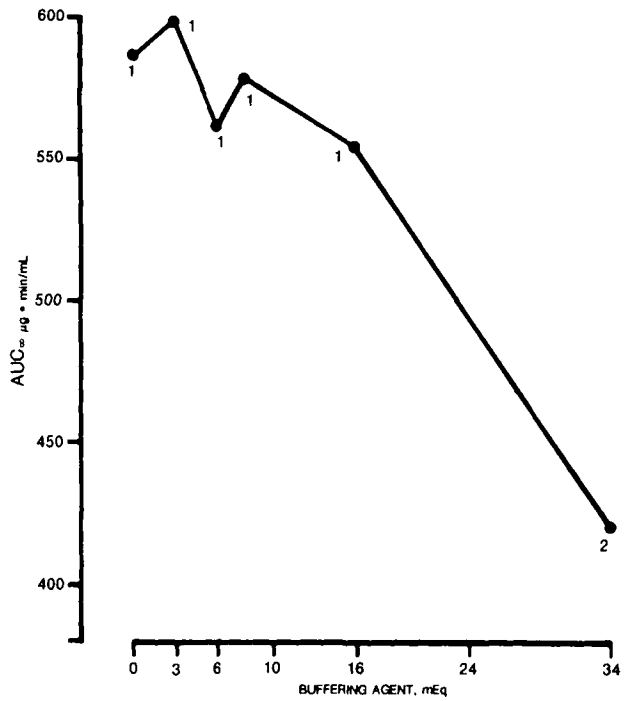

Figure 3—*A plot of AUC_∞ for aspirin as a function of buffer strength. A number shared by two or more points indicates no significant difference ($p < 0.1$) for those points.*

Although less aspirin reaches the circulatory system with the 34 mEq of the buffering agent, the total salicylate (*i.e.*, aspirin, salicylic acid, and salicyluric acid) which accumulates in the urine over 24 h is not decreased. Combining these observations suggests that the absorption of aspirin is not diminished by added buffering agents, but that the presystemic hydrolysis is increased. This is due to a greater portion of aspirin being emptied into and absorbed from the small intestine, where significant esterase activity has been reported to exist (6).

DISCUSSION

Aspirin was rapidly absorbed from all of the solutions, while the rate and extent of the bioavailability was dependent on buffer strength. Small quantities of the antacid buffering agent were associated with the most rapid rise in plasma aspirin, with mean maximal concentrations of 17.8 and 17.3 μg/mL for 6 and 3 mEq, respectively. This rapid rate of absorption was probably due to the increased solubility of the aspirin, with only a small increase in the pH of gastric contents and, thus, a minimal suppression of gastric absorption. In the absence of buffering the aspirin was only partly dissolved before reaching the stomach, which provided a rapid rate of absorption over the first few minutes only.

With 34 mEq of the antacid buffer, the gastric pH may rise above six and suppress absorption through the gastric mucosa (7, 8). Indeed, absorption would be predominately delayed until the aspirin was emptied into the small intestine, where the buffering effect of the antacid would be diminished and the surface area is much larger. The actual delay in absorption due to the increased gastric pH was only ~5 min, which was probably due to the acceleration of gastric emptying that is generally associated with administration of the sodium citrate-bicarbonate antacid (8).

The greater presystemic hydrolysis observed with the 34 mEq of buffering is consistent with the above hypothesis (*i.e.*, that the antacid can shift the absorption from the stomach to the intestine). Studies in dogs (9) and rats (10) support the supposition that a significant portion of the first-pass hydrolysis of aspirin occurs in the gut wall (6). With the gap between the 16- and 34-mEq strengths of the buffering agent used in the present study, one can only conclude that buffer quantities in excess of 16 mEq are required to significantly alter aspirin absorption kinetics.

Repeated contact with aspirin has been reported (11) to alter the gastric

membrane, allowing hydrogen-ion back-diffusion, which results in irritation, bleeding, and possible ulceration. If this mechanism is correct, then the rapid onset of absorption obtained with unbuffered solutions or solutions with less than 16 mEq of antacid buffering may not reduce the incidence of untoward effects as effectively as those containing a greater quantity of antacid buffering.

REFERENCES

(1) W. D. Mason and N. Winer, *J. Pharm. Sci.*, **70**, 262 (1981).

(2) E. N. Amick and W. D. Mason, *Anal. Lett.*, **12**, 629 (1979).

(3) K. Yamaoka, T. Nakagawa, and T. Uno, *J. Pharmacokinet. Biopharm.*, **6**, 547 (1978).

(4) S. Riegelman and P. Collier, *J. Pharmacokinet. Biopharm.*, **8**, 509 (1980).

(5) M. Rowland and S. Riegelman, *J. Pharm. Sci.*, **57**, 1313 (1968).

(6) M. Rowland, S. Riegelman, P. Harris, and S. Sholkoff, *J. Pharm. Sci.*, **61**, 379 (1972).

(7) A. Cooke and J. Hunt, *Guy's Hosp. Rep.*, **120**, 221 (1971).

(8) J. Hunt, *Am. J. Dig. Dis.*, **8**, 885 (1963).

(9) P. Harris and S. Riegelman, *J. Pharm. Sci.*, **58**, 71 (1969).

(10) K. Iwamoto, M. Takei, and J. Watanabe, *J. Pharm. Pharmacol.*, **34**, 176 (1981).

(11) B. M. Rothschild, *Clin. Pharmacol. Ther.*, **26**, 145 (1979).

Determination of Ethoxzolamide in the Iris/Ciliary Body of the Rabbit Eye by High-Performance Liquid Chromatography: Comparison of Tissue Levels Following Intravenous and Topical Administrations

MARK G. ELLER and R. D. SCHOENWALD ˣ

Received March 3, 1983, from the *Pharmaceutics Division, College of Pharmacy, University of Iowa, Iowa City, IA 52242.* Accepted for publication September 22, 1983.

Abstract □ A specific high-performance liquid chromatographic method is described for ethoxzolamide following the extraction of the material from iris/ciliary body eye tissue in rabbits. The steps consist of base extraction and protein and enzyme deactivation, followed by acid treatment, extraction into ethyl acetate, evaporation, and solubilization with a 50% aqueous methanol solution. The samples were chromatographed on a reverse-phase phenyl column with a mobile phase consisting of 50% methanol in 1% acetic acid. The recovery was 74.3% over a 10-fold range of tissue concentrations. The sensitivity was 0.03 μg/mL, and the response was linear over the concentration range (0.03–0.5 μg/mL) used in the study. Intravenous (2.0- and 6.0-mg/kg) and topical (1% suspension) doses of ethoxzolamide were administered to rabbits. Iris/ciliary body tissues were excised 45 min after drug administration. The tissue levels after a dose of 6 mg/kg were statistically greater than the levels obtained after a dose of 2 mg/kg. The smaller intravenous dose represented the lowest dose for which a reduction in intraocular pressure could be measured. An initial transitory drop in intraocular pressure was detected for the topical dose. Iris/ciliary body levels in the treated eye could be detected for the 2-mg/kg iv and topical doses.

Keyphrases □ Ethoxzolamide—determination in the iris/ciliary body, rabbits, HPLC, GC □ Dosage forms—intravenous and topical administration of ethoxzolamide, iris/ciliary body of rabbit eyes, HPLC, GC

Ethoxzolamide, a carbonic anhydrase inhibitor used in glaucoma to lower intraocular pressure (IOP), is effective orally but not when administered topically to the eye, presumably due to inadequate drug levels at the active site. In recent studies, the anatomical location of carbonic anhydrase with the anatomical location of aqueous humor formation in the ciliary body have been identified (1, 2). Friedlander and Muther (3) have utilized the high binding affinity of [^{3}H]-acetazolamide for carbonic anhydrase to demonstrate the distribution of carbonic anhydrase in the epithelium of the ciliary body. The greater specificity of ethoxzolamide for the enzyme was shown by displacing [^{3}H]acetazolamide with a high concentration of unlabeled ethoxzolamide.

Although Maren (4) have devised a sensitive method for the determination of carbonic anhydrase and its inhibitors, the assay measures drug activity; therefore, specificity is always in doubt. It is also tedious and time consuming. It was the purpose of this study to develop a high-performance liquid chromatographic (HPLC) procedure for the determination of ethoxzolamide in the iris/ciliary body tissue of rabbit eyes. Data are also presented which compare tissue concentrations after administration by the topical and intravenous routes.

EXPERIMENTAL SECTION

Chemicals—Ethoxzolamide, a gift from a commercial source[1], was used as received. The substances used in the preparation of the various buffers and vehicles were of analytical or USP quality, and included monobasic sodium phosphate[2], dibasic sodium phosphate[3], sodium carbonate[2], hydrochloric acid[2], sodium chloride[4], polysorbate 80[5], and *N*,*N*-dimethylacetamide[2]. Ethyl acetate[6] was used as the organic phase in the extraction procedure. Acetic acid[7], methanol[8], and distilled deionized water were used to prepare the chromotographic mobile phase. The distilled deionized water was also used to make all aqueous dilutions.

Apparatus—The chemicals and tissues were weighed on an electronic[9] or analytical[10] balance. The pH values of the various solutions were measured[11] when necessary.

The HPLC system consisted of a solvent delivery pump[12], a syringe-loading sample injector[13] fitted with a 100-μL loop[14], a reverse-phase phenyl column[15], and a fixed-wavelength UV detector[16] operating at 313 nm. Chromatograms were recorded on a chart recorder[17] operating at 0.5 cm/min. The mobile phase consisting of methanol–1% aqueous acetic acid (50:50, v/v) was deaerated before use; the flow rate was 1.5 mL/min.

[1] The Upjohn Co.
[2] Certified ACS; Fisher Scientific Co., Fair Lawn, N.J.
[3] Baker Analyzed Reagent; J. T. Baker Chemical Co., Phillipsburg, N.J.
[4] USP grade; J. T. Baker Chemical Co.
[5] USP grade; Ruger Chemical Co., Inc., Irvington, N.J.
[6] Analytical Reagent ACS; Mallinckrodt Inc., Paris, Ky.
[7] Certified ACS; Mallinckrodt Inc.
[8] HPLC grade; Burdick & Jackson Laboratories, Inc., Muskegon, Mich.
[9] Model 4100; Cahn Instruments, Paramount, Calif.
[10] Model B6; Mettler Instruments Corp., Hightstown, N.J.
[11] Model 701; Orion Research Corp., Cambridge, Mass.
[12] Model 6000A; Waters Associates, Milford, Mass.
[13] Model 7125; Rheodyne Inc., Cotati, Calif.
[14] Catalog no. 724; Rheodyne Inc.
[15] P/N 27198, S/N μ-Bondapak Phenyl; Waters Associates.
[16] Model 440 absorbance detector; Waters Associates.
[17] Model A5211-1; Omniscribe, Houston Instruments, Austin, Tex.

0022-3549/84/0900-1261$01.00/0

© 1984, American Pharmaceutical Association

membrane, allowing hydrogen-ion back-diffusion, which results in irritation, bleeding, and possible ulceration. If this mechanism is correct, then the rapid onset of absorption obtained with unbuffered solutions or solutions with less than 16 mEq of antacid buffering may not reduce the incidence of untoward effects as effectively as those containing a greater quantity of antacid buffering.

REFERENCES

(1) W. D. Mason and N. Winer, *J. Pharm. Sci.*, **70**, 262 (1981).

(2) E. N. Amick and W. D. Mason, *Anal. Lett.*, **12**, 629 (1979).

(3) K. Yamaoka, T. Nakagawa, and T. Uno, *J. Pharmacokinet. Biopharm.*, **6**, 547 (1978).

(4) S. Riegelman and P. Collier, *J. Pharmacokinet. Biopharm.*, **8**, 509 (1980).

(5) M. Rowland and S. Riegelman, *J. Pharm. Sci.*, **57**, 1313 (1968).

(6) M. Rowland, S. Riegelman, P. Harris, and S. Sholkoff, *J. Pharm. Sci.*, **61**, 379 (1972).

(7) A. Cooke and J. Hunt, *Guy's Hosp. Rep.*, **120**, 221 (1971).

(8) J. Hunt, *Am. J. Dig. Dis.*, **8**, 885 (1963).

(9) P. Harris and S. Riegelman, *J. Pharm. Sci.*, **58**, 71 (1969).

(10) K. Iwamoto, M. Takei, and J. Watanabe, *J. Pharm. Pharmacol.*, **34**, 176 (1981).

(11) B. M. Rothschild, *Clin. Pharmacol. Ther.*, **26**, 145 (1979).

Determination of Ethoxzolamide in the Iris/Ciliary Body of the Rabbit Eye by High-Performance Liquid Chromatography: Comparison of Tissue Levels Following Intravenous and Topical Administrations

MARK G. ELLER and R. D. SCHOENWALD ˣ

Received March 3, 1983, from the *Pharmaceutics Division, College of Pharmacy, University of Iowa, Iowa City, IA 52242.* Accepted for publication September 22, 1983.

Abstract □ A specific high-performance liquid chromatographic method is described for ethoxzolamide following the extraction of the material from iris/ciliary body eye tissue in rabbits. The steps consist of base extraction and protein and enzyme deactivation, followed by acid treatment, extraction into ethyl acetate, evaporation, and solubilization with a 50% aqueous methanol solution. The samples were chromatographed on a reverse-phase phenyl column with a mobile phase consisting of 50% methanol in 1% acetic acid. The recovery was 74.3% over a 10-fold range of tissue concentrations. The sensitivity was 0.03 μg/mL, and the response was linear over the concentration range (0.03–0.5 μg/mL) used in the study. Intravenous (2.0- and 6.0-mg/kg) and topical (1% suspension) doses of ethoxzolamide were administered to rabbits. Iris/ciliary body tissues were excised 45 min after drug administration. The tissue levels after a dose of 6 mg/kg were statistically greater than the levels obtained after a dose of 2 mg/kg. The smaller intravenous dose represented the lowest dose for which a reduction in intraocular pressure could be measured. An initial transitory drop in intraocular pressure was detected for the topical dose. Iris/ciliary body levels in the treated eye could be detected for the 2-mg/kg iv and topical doses.

Keyphrases □ Ethoxzolamide—determination in the iris/ciliary body, rabbits, HPLC, GC □ Dosage forms—intravenous and topical administration of ethoxzolamide, iris/ciliary body of rabbit eyes, HPLC, GC

Ethoxzolamide, a carbonic anhydrase inhibitor used in glaucoma to lower intraocular pressure (IOP), is effective orally but not when administered topically to the eye, presumably due to inadequate drug levels at the active site. In recent studies, the anatomical location of carbonic anhydrase with the anatomical location of aqueous humor formation in the ciliary body have been identified (1, 2). Friedlander and Muther (3) have utilized the high binding affinity of [^{3}H]-acetazolamide for carbonic anhydrase to demonstrate the distribution of carbonic anhydrase in the epithelium of the ciliary body. The greater specificity of ethoxzolamide for the enzyme was shown by displacing [^{3}H]acetazolamide with a high concentration of unlabeled ethoxzolamide.

Although Maren (4) have devised a sensitive method for the determination of carbonic anhydrase and its inhibitors, the assay measures drug activity; therefore, specificity is always in doubt. It is also tedious and time consuming. It was the purpose of this study to develop a high-performance liquid chromatographic (HPLC) procedure for the determination of ethoxzolamide in the iris/ciliary body tissue of rabbit eyes. Data are also presented which compare tissue concentrations after administration by the topical and intravenous routes.

EXPERIMENTAL SECTION

Chemicals—Ethoxzolamide, a gift from a commercial source[1], was used as received. The substances used in the preparation of the various buffers and vehicles were of analytical or USP quality, and included monobasic sodium phosphate[2], dibasic sodium phosphate[3], sodium carbonate[2], hydrochloric acid[2], sodium chloride[4], polysorbate 80[5], and *N*,*N*-dimethylacetamide[2]. Ethyl acetate[6] was used as the organic phase in the extraction procedure. Acetic acid[7], methanol[8], and distilled deionized water were used to prepare the chromotographic mobile phase. The distilled deionized water was also used to make all aqueous dilutions.

Apparatus—The chemicals and tissues were weighed on an electronic[9] or analytical[10] balance. The pH values of the various solutions were measured[11] when necessary.

The HPLC system consisted of a solvent delivery pump[12], a syringe-loading sample injector[13] fitted with a 100-μL loop[14], a reverse-phase phenyl column[15], and a fixed-wavelength UV detector[16] operating at 313 nm. Chromatograms were recorded on a chart recorder[17] operating at 0.5 cm/min. The mobile phase consisting of methanol–1% aqueous acetic acid (50:50, v/v) was deaerated before use; the flow rate was 1.5 mL/min.

[1] The Upjohn Co.
[2] Certified ACS; Fisher Scientific Co., Fair Lawn, N.J.
[3] Baker Analyzed Reagent; J. T. Baker Chemical Co., Phillipsburg, N.J.
[4] USP grade; J. T. Baker Chemical Co.
[5] USP grade; Ruger Chemical Co., Inc., Irvington, N.J.
[6] Analytical Reagent ACS; Mallinckrodt Inc., Paris, Ky.
[7] Certified ACS; Mallinckrodt Inc.
[8] HPLC grade; Burdick & Jackson Laboratories, Inc., Muskegon, Mich.
[9] Model 4100; Cahn Instruments, Paramount, Calif.
[10] Model B6; Mettler Instruments Corp., Hightstown, N.J.
[11] Model 701; Orion Research Corp., Cambridge, Mass.
[12] Model 6000A; Waters Associates, Milford, Mass.
[13] Model 7125; Rheodyne Inc., Cotati, Calif.
[14] Catalog no. 724; Rheodyne Inc.
[15] P/N 27198, S/N μ-Bondapak Phenyl; Waters Associates.
[16] Model 440 absorbance detector; Waters Associates.
[17] Model A5211-1; Omniscribe, Houston Instruments, Austin, Tex.

0022-3549/84/0900-1261$01.00/0

© 1984, American Pharmaceutical Association

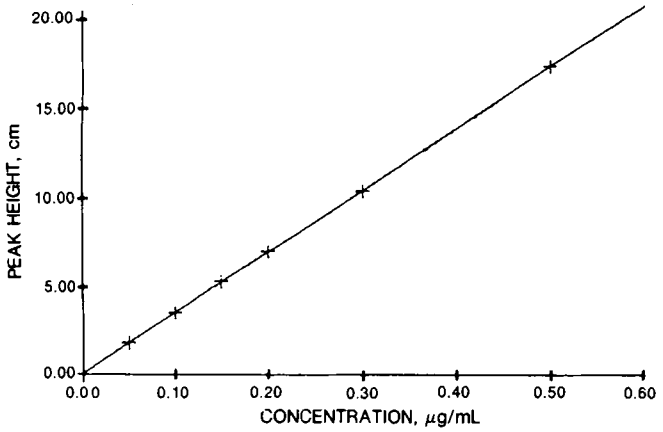

Figure 1—*Typical standard curve for ethoxzolamide over a concentration range of 0.03–0.5 μg/mL (single determinations).*

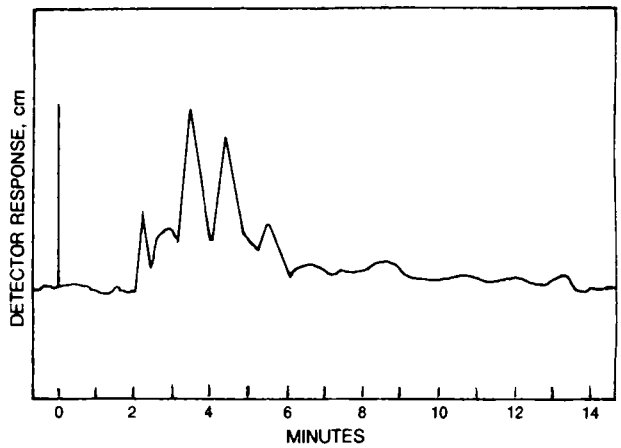

Figure 2—*Chromatograms of 100 μL of tissue extract devoid of drug (AUFS = 0.005).*

Drug Administration—New Zealand White rabbits[18] of either sex (age, 3–4 months; weight 2.0–3.5 kg) were administered ethoxzolamide by intravenous injection into the marginal ear vein or by topical application to the conjunctival sac of the eye. Because of the limited aqueous solubility of ethoxzolamide, a mixed solvent consisting of 60% *N,N*-dimethylacetamide–40% water was used for intravenous administration. With this vehicle, concentrations of up to 20 mg/mL could be injected. The intravenous dose of ethoxzolamide was either 2 or 6 mg/kg. The formulation was prepared immediately before use.

Ethoxzolamide was applied topically as a 1% suspension in Sörensen's modified phosphate buffer (5), to which 0.5% polysorbate 80 was added as a wetting agent. The pH of this vehicle was 7.2. The formulation was prepared ~8 h before use and was stirred continuously on a magnetic stir plate. A 50-μL volume of the suspension was applied every 2 min to one eye for a total of three doses; the blank vehicle was similarly applied to the other eye.

The rabbits were sacrificed 45 min after either intravenous or topical instillation by injecting a bolus of air into the marginal ear vein. The iris/ciliary tissue was immediately excised and weighed. This time interval was chosen to represent nearly the maximal IOP response. Preliminary studies in which ethoxzolamide was administered intravenously showed that a maximal pharmacological response (lowering of intraocular pressure) occurred at 45 min.

Tissue Extraction Procedure—Although the ciliary body has been identified as the active site (2, 3), it is difficult to excise precisely in the rabbit. The iris is easily removed, and the ciliary body remains attached to it when the iris is excised from the rabbit eye. Consequently, tissue levels, as reported here, represent an average level of the combined tissues. The wet tissue was cut into smaller segments and homogenized (30 rpm for 1.5 min) in centrifuge tubes[19] with dry ice; the latter disrupted cellular structure to facilitate extraction. A total of 5 mL of 0.025 M sodium carbonate solution was added to the tubes containing the homogenized tissue. The mixture was vigorously shaken[20] for 1 h at room temperature. The high pH and hypotonicity of the sodium carbonate solution promoted dissociation of the drug from carbonic anhydrase (6) and partitioning into the aqueous phase. The homogenate was then heated to 100°C for 5 min to denature and precipitate the tissue proteins. Identical treatment without iris/ciliary body tissue showed that the drug did not decompose. The mixture was cooled to room temperature, and 1 mL of 0.5 M HCl containing an additional 75 mg of NaCl/mL was added. The acid converted drug to the un-ionized form, and the salt aided in phase separation. Ethyl acetate (3 mL) was added to the mixture, which was shaken on a vortex mixer[21] and centrifuged[22] for 0.5 h. After centrifugation, the top layer, consisting of nearly 3 mL of ethyl acetate and containing drug, was transferred to a 5-mL vial[23]. The extraction was repeated twice with 3 mL of ethyl acetate each time; the ethyl acetate phases were then combined. The ethyl acetate solution was subsequently warmed[24] to 30°C and evaporated to dryness under a stream of nitrogen. To the residue was added 1 mL of 50% methanol to solubilize the drug. The 50% methanol solution containing drug was refrigerated until just before assay by HPLC. To assess the validity of the assay, iris/ciliary tissues were spiked with various known amounts of ethoxzolamide and treated by the extraction and assay procedure described above.

Chromatographic Assay Conditions—One hundred microliters of sample or standard was injected onto the column with the loop injector. Peak heights from five to seven known concentrations of ethoxzolamide, ranging from 0.03 to 0.75 μg/mL, were determined. A standard curve was constructed from these data, relating peak height to concentration. The standard curve was repeated whenever a set of unknowns was assayed. Also, standard concentrations were interspersed after approximately every third unknown sample to assess whether changes in column integrity, mobile phase, or detectors were occurring. The attenuation was 0.005 for all determinations.

Intraocular Pressure—A separate group of New Zealand White rabbits (n = 24) were maintained on 0.3% NaCl solution in place of drinking water for at least 3 weeks before the determination of IOP, because it has been shown that a diet deficient in sodium ion produces a variable IOP response to this class of drugs. Commercial rabbit chow does not provide a sufficient NaCl content compared with the diet available to rabbits in their natural habitat (7). Numerous measurements of IOP were made over 3 weeks to familiarize the rabbits with this procedure before drug administration. Baseline IOP measurements were determined by tonometry[25], followed by either intravenous or topical administration of ethoxzolamide (1% suspension). In each intravenous experiment, 25–50% of the rabbits received vehicle only; the observations were made on a "blind" basis. Whenever ethoxzolamide was administered topically, one eye was dosed as described above, and the opposite eye received vehicle only. Again, observations were made on a "blind" basis. IOP measurements were determined at 20-min intervals for 3 h.

RESULTS AND DISCUSSION

The standard curve (Fig. 1) was found to be linear over the concentration range (0.03–0.5 μg/mL) used in the study. The sensitivity of the assay was determined by analyzing progressively lower concentrations until the coefficient of variation for multiple determinations reached 10%. This occurred at a concentration of 0.03 μg/mL. This value also represented about five times the height of the baseline noise at 0.005 AUFS.

Figures 2 and 3 represent typical chromatograms for the analysis of ethoxzolamide in iris/ciliary body tissue. As shown in the chromatogram (Fig. 3), good separation was achieved from endogenous tissue components. When no drug was present, the baseline was observed (Fig. 2). A metabolite was not apparent in any of the observed chromatograms. The retention time for the drug was 7 min.

To determine the recovery and reproducibility of the assay procedure, iris/ciliary body tissue from the rabbits was spiked with known amounts of ethoxzolamide. The amount of drug was varied from 0.05 to 0.6 μg (Table I); the tissue weight also varied. The known amount of drug was first dissolved in 4 mL of distilled water, to which a freshly extracted tissue sample was added. A 12-mL test tube contained the mixture, which was incubated for ≥3 h at room temperature. Longer incubation periods (up to 72 h) did not increase the percent recovery. After incubation, 1 mL of 0.125 M sodium carbonate solution was added to the mixture to produce a final concentration of 0.025 M. The extraction procedure was continued from this step as described above. Identical extraction experiments were also conducted without the addition

[18] Morrison Rabbitry; West Branch, Iowa.
[19] Tissue grinder (10 mL); Potter-Elvehjem.
[20] Model E-1, Vibromixer; Chemapec Inc., Hoboken, N.J.
[21] Vortex Geni Mixer; American Hospital Supply, McGaw Park, Ill.
[22] Model CS; International Equipment Co., Needham Heights, Mass.
[23] ReactiVials; Pierce Chemical Co., Rockford, Ill.
[24] ReactiTherm; Pierce Chemical Co.

[25] Applanation Pneumatonograph; Alcon Labs, Fort Worth, Tex.

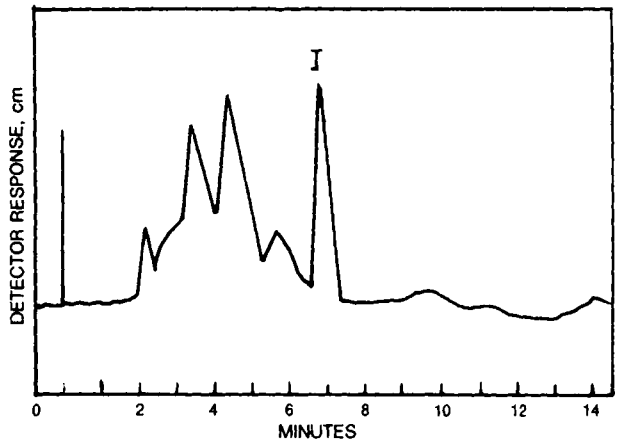

Figure 3—*Chromatograms of 100 μL of tissue extract containing ethoxzolamide (AUFS = 0.005); peak I is ethoxzolamide.*

of iris/ciliary body tissue but with varying amounts of drug (0.05–10 μg). Without added tissue, 85.8 ± 4.97% of the added drug could be extracted. When tissue was added, 74.3 ± 7.83% of the drug could be recovered. The presence of tissue was responsible for a significant increase in the extraction variability.

Without the presence of drug but including tissue, no ethoxzolamide peaks were observed in the chromatograms. A linear increase in the amount of drug recovered was detected by:

$$y = 0.099 + 0.706x \qquad (n = 31, r^2 = 0.995) \qquad \text{(Eq. 1)}$$

where x is the nanograms of drug added per milligram of tissue, and y is the nanograms of drug recovered per milligram of tissue. Although the mean percentage of drug extracted in the recovery experiments could be used to correct for the fraction of drug unavailable for extraction, its use would be somewhat less precise than the use of Eq. 1. This occurs because the calibration equation incorporates the weight of the tissue on a per-unit basis and because the variance can be expressed at every point on the regressed line.

Assay Application—The method described above was developed to compare iris/ciliary body concentrations of ethoxzolamide after intravenous and topical dosing to the eye.

Intraocular Pressure—Before tissue was extracted, a minimum dose was established which produced a significant reduction in IOP. This was accomplished by linear and quadratic regression analysis. If the IOP dropped below baseline values, a negative statistically significant slope from zero indicated a drug effect. Baseline measurements were made by measuring IOP repeatedly over 20 min just before dosing. Two intravenous doses were given. At 2 mg/kg, only 3 of 10 rabbits showed a response over 2 h, whereas at 6 mg/kg, 6 of 10 rabbits yielded a response, which at 45 min was 1.5 to 2 mm Hg lower than from 2 mg/kg. The maximum response occurred at 45 min after intravenous administration and at 40 min after topical administration (Table II).

When a 1% suspension of ethoxzolamide was administered topically to the eyes of 24 rabbits, a small but statistically significant drop in IOP was observed at 20–60 min. The criteria for observing a change in response was based on a statistical difference in IOP between the treated and untreated eyes at each time interval. Equation 2 expresses a change in IOP brought about by corneal penetration only. The responses measured for the two routes of administration are not directly comparable. For the topical route, a difference in response in treated and untreated eyes was measured over time, whereas by the intravenous route, both eyes responded so that changes were made relative to the baseline (*i.e.*, $t = 0$):

$$\text{IOP Changes} = (IOP_{DET} - IOP_{CET}) - (IOP_{DEO} - IOP_{CEO}) \qquad \text{(Eq. 2)}$$

where IOP_{DET} is the IOP measurement (mm Hg) of the dosed or treated eye at time t, IOP_{DEO} is the IOP measurement (mm Hg) of the treated eye at $t = 0$ but before receiving the dose, IOP_{CET} is the IOP measurement (mm Hg) of the control (nontreated) eye at time t, and IOP_{CEO} is the IOP measurement (mm Hg) of the control (nontreated) eye at time $t = 0$. By subtracting the IOP response from the nontreated eye at each time interval, the reduction in IOP occurring from systemic absorption is subtracted.

Interestingly, various manufacturers of carbonic anhydrase inhibitors have repeatedly been unable to detect a lowering of IOP from direct application to the eye[26]. These studies were often conducted with single doses in a small number of rabbits that had not been maintained on a diet sufficient in sodium chloride. This latter factor is most important in attempting to measure a small but detectable IOP response. These results, along with previously published reports (8, 9), have prompted researchers to conclude that intravenous doses of carbonic anhydrase inhibitors, including ethoxzolamide, were acting only centrally. More recently (1, 2, 10, 11), it has been shown that carbonic anhydrase inhibition occurs at the ciliary body. Nevertheless, studies (12, 13) have indicated that systemic acidosis, another effect of carbonic anhydrase inhibitors, contributes to a reduction in IOP. Maren *et al.* (12) have proposed that the acidotic effect of the lowering of the IOP and the direct effect on aqueous humor secretion are additive.

Tissue Levels—Tissue levels were determined in both eyes after either intravenous or topical administration (Tables III and IV, respectively). At each intravenous dose, the right and left eyes showed similar concentrations of ethoxzolamide. At 2 and 6 mg/kg (10 replications were conducted at each level), a statistically significant higher concentration was measured for 6 mg/kg.

[26] Unpublished results.

Table I—Recovery of Ethoxzolamide With the Addition of Known Amounts of Drug to Iris/Ciliary Body Tissue

Ethoxzolamide Added, μg	Tissue Weight, mg	Mean Recovery ± *SD*, %
0.1–10.0[a]	0	85.8 ± 4.97
0.05–0.60[b]	40.9 ± 12.4	74.3 ± 7.83

[a] Increments added are 0.1, 0.2, 0.4, 2.0, 4.0, and 10.0 μg; n = 2–4 for each determination. [b] Increments added are 0.05, 0.1, 0.15, 0.2, 0.3, 0.4, 0.5, and 0.6 μg; n = 2–4 for each determination.

Table II—Intraocular Pressure Measurement Changes after Topical Administration[a] of 1% Ethoxzolamide to Rabbit Eyes

Time Postdose, min	Change, mm[c]	$p^{b,d}$
0	--	--
20	−0.795 (0.63)	0.019
40	−1.085 (0.68)	0.0012
60	−0.955 (0.81)	0.010
80	−0.295 (0.72)	0.21
100	0.085 (0.75)	0.59
120	0.085 (0.76)	0.59
140	0.625 (0.79)	0.94
160	0.045 (0.86)	0.54
180	0.085 (0.71)	0.59

[a] 50 μL q 2 min × 3 (n = 24). [b] $p < 0.02$. [c] See Eq. 2 in text; values in parentheses represent the 95% confidence interval. [d] Probability determined from paired t test.

Table III—Iris/Ciliary Body Levels of Ethoxzolamide after Intravenous Administration to Rabbits

Dose, mg/kg iv	n^b	Ethoxzolamide Level, ng/mg[a] Left Eye	Right Eye	Pooled[c]
2.0	10	2.67 ± 1.91	2.27 ± 1.00	2.48 ± 1.50
6.0	10	10.08 ± 1.84	10.43 ± 1.94	10.26 ± 1.83

[a] Nanograms of drug per milligram of iris/ciliary body tissue; mean ± *SD*. [b] Number of determinations for either the left or the right eye. [c] Pooled data for the left and right eyes (n = 20).

Table IV—Iris/Ciliary Body Levels of Ethoxzolamide after Topical Administration

Rabbit	Ethoxzolamide Level, ng/mg[a] Treated Eye	Untreated Eye
1	5.64	2.08
2	3.50	0
3	1.60	0.30
4	1.87	0.29
5	2.20	0
6	1.83	0
7	0.444	0
8	0.544	0
9	1.94	0
10	1.76	0
Mean ± *SD*	2.13 ± (1.50)	0.27 ± (0.65)

[a] Nanograms of drug per milligram of iris/ciliary body tissue.

The results for the topical dose (Tables II and IV) show that ethoxzolamide could be detected in the untreated eye in 3 of 10 rabbits and in the treated eye in all of the rabbits. An outlier value of 2.08 ng/mg was determined for rabbit 1 in the untreated eye (Table III). The measurement in the untreated eye likely represents systemic absorption. The pooled treated eyes yielded iris/ciliary body levels of 2.13 ± 1.5 ng/mg (n = 10). The mean level is statistically lower ($p < 0.05$) than the mean value obtained for dosing at 6 mg/kg iv but not statistically different from tissue levels obtained at 2 mg/kg iv.

For an average-sized rabbit (2.5 kg), the minimum intravenous dose to produce a response (2 mg/kg) represents a 3.3-fold higher dose than that administered by the topical route. Thus, the nearly equal tissue levels shown in Tables III and IV for the two routes of administration suggest that the tissue levels detected from the smaller topical dose are, at least in part, a consequence of corneal transport and not primarily systemic absorption. Although our results do not differentiate between the direct and systemic effects of the drug, they do add credence to the possibility of a contribution from the corneal pathway.

REFERENCES

(1) E. Luten-Drecoll and G. Lonnerholm, *Invest. Ophthalmol. Visual Sci.*, **21**, 782 (1981).

(2) P. J. Wistrand and L. C. Garg, *Invest. Ophthalmol. Visual Sci.*, **18**, 802 (1979).

(3) B. R. Friedlander and T. M. Muther, in "Autoradiographic Localization of Carbonic Anhydrase in the Ciliary Body," Association for Research and Vision in Ophthalmology, Abstracts, 1978, p. 162.

(4) T. H. Maren, *J. Pharmacol. Exp. Ther.*, **130**, 26 (1960).

(5) E. L. Parrott, in "Pharmaceutical Technology," Burgess Publishing, Minneapolis, Minn., 1970, p. 236.

(6) J. E. Coleman, *J. Biol. Chem.*, **242**, 5212 (1967).

(7) V. Kinsey, E. Camacho, G. A. Cavanaugh, M. Constant, and D. A. McGinty, *Arch. Ophthalmol.*, **53**, 680 (1955).

(8) B. Becker, *Am. J. Ophthalmol.*, **39**, 177 (1955).

(9) J. Gloster and E. S. Perkins, *J. Physiol.*, **130**, 665 (1955).

(10) T. H. Maren, *Invest. Ophthalmol. Visual Sci.*, **13**, 479 (1974).

(11) G. Bietti, M. Virno, and J. Pecori-Giraldi, *Am. J. Ophthalmol.*, **80**, 360 (1975).

(12) T. H. Maren, J. R. Haywood, S. K. Chapman, and T. J. Zimmerman, *Invest. Ophthalmol. Visual Sci.*, **16**, 730 (1977).

(13) P. C. Dobbs, D. L. Epstein, and P. J. Anderson, *Invest. Ophthalmol. Visual Sci.*, **18**, 867 (1979).

ACKNOWLEDGMENTS

This study was supported by Grant EY003297 from the Eye Institute, National Institutes of Health, and Allergan Pharmaceuticals, Irvine, Calif.

Factors Affecting Quinidine Protein Binding in Humans

DAVID J. EDWARDS *, JAMES E. AXELSON ¶, RICHARD L. SLAUGHTER, ‡§, ALFRED T. ELVIN *, and DAVID LALKA *§x

Received June 27, 1983, from the *Departments of *Pharmaceutics and ‡Pharmacy, School of Pharmacy, State University of New York at Buffalo, Amherst, NY 14260*, the *§Clinical Pharmacokinetics Laboratory, Buffalo General Hospital, Buffalo, NY 14260*, and the *¶Division of Pharmaceutics, Faculty of Pharmaceutical Sciences, University of British Columbia, British Columbia V6T 1W5, Canada.* Accepted for publication September 27, 1983.

Abstract □ The free (unbound) concentration of drug in plasma is often an important determinant of pharmacological and toxicological effects. Unfortunately, studies examining the factors influencing the free fraction of quinidine in plasma have yielded inconsistent results. It is probable that differences in the type of blood collection tubes utilized and the analytical procedure employed biased some of these estimates of quinidine binding. The present study was executed in a manner free of factors now known to introduce artifacts into estimates of the free fraction of quinidine. In healthy volunteers, the free fraction of quinidine (1.0 μg/mL) was 0.129 ± 0.019 (mean ± SD) and was constant throughout the therapeutic range. A high-affinity, low-capacity binding site ($K = 1.17 \times 10^5$ M^{-1}; $nP = 3.49 \times 10^{-5}$ M) and a low-affinity, high-capacity binding site ($K = 1.33 \times 10^3$ M^{-1}; $nP = 3.14 \times 10^{-3}$ M) were identified. The characteristics of quinidine binding in a 4.5-g/dL solution of human serum albumin ($K = 3.05 \times 10^3$ M^{-1}; $nP = 1.36 \times 10^{-3}$ M) suggested that the low-affinity, high-capacity binding site was on this protein. In the presence of tris(butoxyethyl) phosphate (75 μg/mL), the quinidine free fraction increased from 0.114 to 0.231. A lidocaine concentration of 250 μg/mL caused a similar increase. Patients suffering traumatic injury had a significant increase in α_1-acid glycoprotein concentration (197 mg/dL) and a decreased quinidine free fraction (0.075 ± 0.019). Patients with hyperlipidemia had free fractions similar to those observed in healthy individuals (0.118 ± 0.019). These data suggest that the high-affinity, low-capacity binding site is on α_1-acid glycoprotein and that lipoproteins are of little importance in the protein binding of quinidine.

Keyphrases □ Protein binding—quinidine, humans □ Quinidine—protein binding, humans

Despite the recent development of a number of new agents, quinidine continues to be a mainstay of oral antiarrhythmic therapy. Effective concentrations of quinidine in serum range between 1 and 5 μg/mL (1, 2). However, much interindividual variability in the concentration necessary for arrhythmia suppression has been noted (2). Studies with other antiarrhythmic drugs, such as disopyramide (3) and propranolol (4), have demonstrated that the free drug concentration in plasma correlates better with the pharmacological effect than does the total concentration. These observations support the principle that free drug in plasma is in equilibrium with drug at receptor sites (*i.e.*, that which is responsible for the pharmacological effect). Furthermore, alterations in the degree of protein binding can also affect the pharmacokinetic properties of a drug. Fremstad *et al.* (5) have demonstrated a significant positive correlation between the free fraction of quinidine and both volume of distribution and total body clearance. For these reasons, a thorough understanding of the determinants of the protein binding of quinidine is important.

Unfortunately, studies in which the factors influencing quinidine protein binding have been examined have yielded inconsistent results. The mean free fraction in studies with healthy volunteers has been reported to be 0.10 (6), 0.105 (7), 0.141 (8), 0.246 (9), and 0.288 (10). Albumin, α_1-acid glycoprotein, and lipoproteins have all been reported to be important for quinidine binding, but their relative roles have been disputed (10–12). Some of the discrepancies between studies may have been due to methodological differences, as several factors have been found to influence quinidine binding *in vitro*. Quinidine free fraction is two- to three-fold higher when blood is collected in evacuated blood collection tubes[1] rather than glass syringes (6). Other factors influencing estimates of

0022-3549/84/0900-1264$01.00/0

© 1984, American Pharmaceutical Association

The results for the topical dose (Tables II and IV) show that ethoxzolamide could be detected in the untreated eye in 3 of 10 rabbits and in the treated eye in all of the rabbits. An outlier value of 2.08 ng/mg was determined for rabbit 1 in the untreated eye (Table III). The measurement in the untreated eye likely represents systemic absorption. The pooled treated eyes yielded iris/ciliary body levels of 2.13 ± 1.5 ng/mg (n = 10). The mean level is statistically lower ($p < 0.05$) than the mean value obtained for dosing at 6 mg/kg iv but not statistically different from tissue levels obtained at 2 mg/kg iv.

For an average-sized rabbit (2.5 kg), the minimum intravenous dose to produce a response (2 mg/kg) represents a 3.3-fold higher dose than that administered by the topical route. Thus, the nearly equal tissue levels shown in Tables III and IV for the two routes of administration suggest that the tissue levels detected from the smaller topical dose are, at least in part, a consequence of corneal transport and not primarily systemic absorption. Although our results do not differentiate between the direct and systemic effects of the drug, they do add credence to the possibility of a contribution from the corneal pathway.

REFERENCES

(1) E. Luten-Drecoll and G. Lonnerholm, *Invest. Ophthalmol. Visual Sci.*, **21**, 782 (1981).

(2) P. J. Wistrand and L. C. Garg, *Invest. Ophthalmol. Visual Sci.*, **18**, 802 (1979).

(3) B. R. Friedlander and T. M. Muther, in "Autoradiographic Localization of Carbonic Anhydrase in the Ciliary Body," Association for Research and Vision in Ophthalmology, Abstracts, 1978, p. 162.

(4) T. H. Maren, *J. Pharmacol. Exp. Ther.*, **130**, 26 (1960).

(5) E. L. Parrott, in "Pharmaceutical Technology," Burgess Publishing, Minneapolis, Minn., 1970, p. 236.

(6) J. E. Coleman, *J. Biol. Chem.*, **242**, 5212 (1967).

(7) V. Kinsey, E. Camacho, G. A. Cavanaugh, M. Constant, and D. A. McGinty, *Arch. Ophthalmol.*, **53**, 680 (1955).

(8) B. Becker, *Am. J. Ophthalmol.*, **39**, 177 (1955).

(9) J. Gloster and E. S. Perkins, *J. Physiol.*, **130**, 665 (1955).

(10) T. H. Maren, *Invest. Ophthalmol. Visual Sci.*, **13**, 479 (1974).

(11) G. Bietti, M. Virno, and J. Pecori-Giraldi, *Am. J. Ophthalmol.*, **80**, 360 (1975).

(12) T. H. Maren, J. R. Haywood, S. K. Chapman, and T. J. Zimmerman, *Invest. Ophthalmol. Visual Sci.*, **16**, 730 (1977).

(13) P. C. Dobbs, D. L. Epstein, and P. J. Anderson, *Invest. Ophthalmol. Visual Sci.*, **18**, 867 (1979).

ACKNOWLEDGMENTS

This study was supported by Grant EY003297 from the Eye Institute, National Institutes of Health, and Allergan Pharmaceuticals, Irvine, Calif.

Factors Affecting Quinidine Protein Binding in Humans

DAVID J. EDWARDS *, JAMES E. AXELSON ¶, RICHARD L. SLAUGHTER, ‡§, ALFRED T. ELVIN *, and DAVID LALKA *§x

Received June 27, 1983, from the *Departments of *Pharmaceutics and ‡Pharmacy, School of Pharmacy, State University of New York at Buffalo, Amherst, NY 14260*, the *§Clinical Pharmacokinetics Laboratory, Buffalo General Hospital, Buffalo, NY 14260*, and the *¶Division of Pharmaceutics, Faculty of Pharmaceutical Sciences, University of British Columbia, British Columbia V6T 1W5, Canada.* Accepted for publication September 27, 1983.

Abstract □ The free (unbound) concentration of drug in plasma is often an important determinant of pharmacological and toxicological effects. Unfortunately, studies examining the factors influencing the free fraction of quinidine in plasma have yielded inconsistent results. It is probable that differences in the type of blood collection tubes utilized and the analytical procedure employed biased some of these estimates of quinidine binding. The present study was executed in a manner free of factors now known to introduce artifacts into estimates of the free fraction of quinidine. In healthy volunteers, the free fraction of quinidine (1.0 μg/mL) was 0.129 ± 0.019 (mean ± SD) and was constant throughout the therapeutic range. A high-affinity, low-capacity binding site ($K = 1.17 \times 10^5$ M^{-1}; $nP = 3.49 \times 10^{-5}$ M) and a low-affinity, high-capacity binding site ($K = 1.33 \times 10^3$ M^{-1}; $nP = 3.14 \times 10^{-3}$ M) were identified. The characteristics of quinidine binding in a 4.5-g/dL solution of human serum albumin ($K = 3.05 \times 10^3$ M^{-1}; $nP = 1.36 \times 10^{-3}$ M) suggested that the low-affinity, high-capacity binding site was on this protein. In the presence of tris(butoxyethyl) phosphate (75 μg/mL), the quinidine free fraction increased from 0.114 to 0.231. A lidocaine concentration of 250 μg/mL caused a similar increase. Patients suffering traumatic injury had a significant increase in α_1-acid glycoprotein concentration (197 mg/dL) and a decreased quinidine free fraction (0.075 ± 0.019). Patients with hyperlipidemia had free fractions similar to those observed in healthy individuals (0.118 ± 0.019). These data suggest that the high-affinity, low-capacity binding site is on α_1-acid glycoprotein and that lipoproteins are of little importance in the protein binding of quinidine.

Keyphrases □ Protein binding—quinidine, humans □ Quinidine—protein binding, humans

Despite the recent development of a number of new agents, quinidine continues to be a mainstay of oral antiarrhythmic therapy. Effective concentrations of quinidine in serum range between 1 and 5 μg/mL (1, 2). However, much interindividual variability in the concentration necessary for arrhythmia suppression has been noted (2). Studies with other antiarrhythmic drugs, such as disopyramide (3) and propranolol (4), have demonstrated that the free drug concentration in plasma correlates better with the pharmacological effect than does the total concentration. These observations support the principle that free drug in plasma is in equilibrium with drug at receptor sites (*i.e.*, that which is responsible for the pharmacological effect). Furthermore, alterations in the degree of protein binding can also affect the pharmacokinetic properties of a drug. Fremstad *et al.* (5) have demonstrated a significant positive correlation between the free fraction of quinidine and both volume of distribution and total body clearance. For these reasons, a thorough understanding of the determinants of the protein binding of quinidine is important.

Unfortunately, studies in which the factors influencing quinidine protein binding have been examined have yielded inconsistent results. The mean free fraction in studies with healthy volunteers has been reported to be 0.10 (6), 0.105 (7), 0.141 (8), 0.246 (9), and 0.288 (10). Albumin, α_1-acid glycoprotein, and lipoproteins have all been reported to be important for quinidine binding, but their relative roles have been disputed (10–12). Some of the discrepancies between studies may have been due to methodological differences, as several factors have been found to influence quinidine binding *in vitro*. Quinidine free fraction is two- to three-fold higher when blood is collected in evacuated blood collection tubes[1] rather than glass syringes (6). Other factors influencing estimates of

0022-3549/84/0900-1264$01.00/0

© 1984, American Pharmaceutical Association

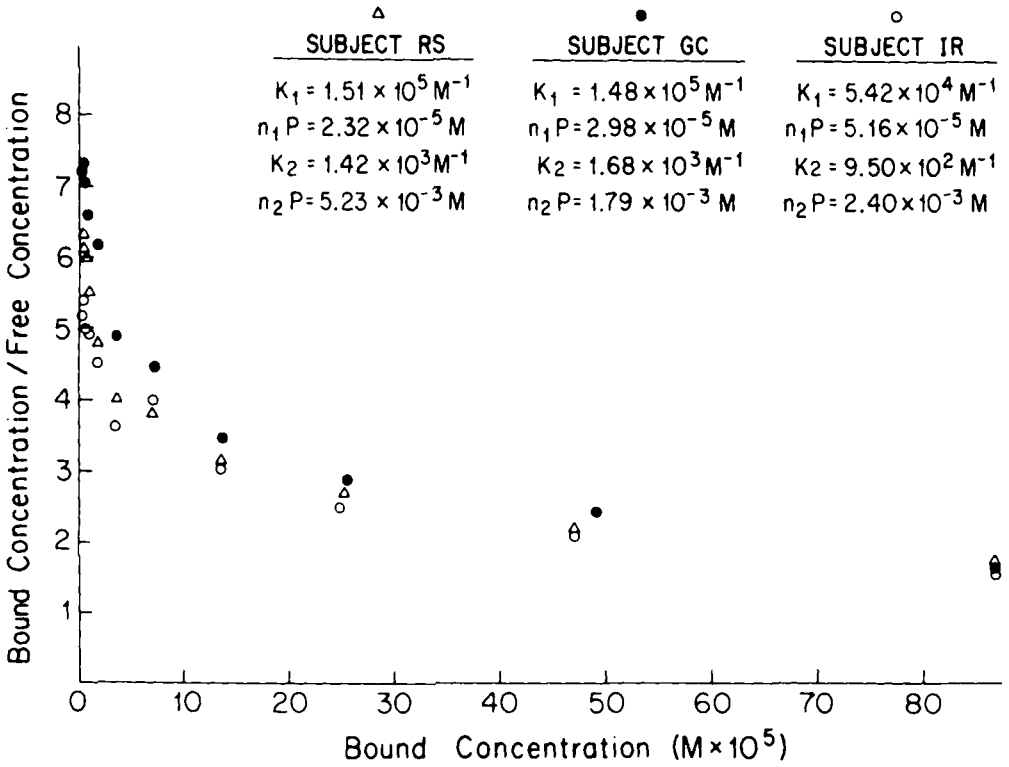

Figure 1—*Relationship between bound concentration/free concentration and bound concentration of quinidine in the serum of three healthy male volunteers.*

quinidine free fraction include the addition of heparin to blood *in vitro* (6), conditions under which equilibrium dialysis is performed (13), and the presence of dihydroquinidine, which is a common impurity in quinidine preparations (14). A principal purpose of the present investigation was to examine and clarify several aspects of quinidine protein binding in humans by using methods which do not bias estimates of the quinidine free fraction.

EXPERIMENTAL SECTION

Materials—Quinidine base was prepared from quinidine sulfate[2] by TLC (20% acetone in methanol) to separate quinidine from contaminants (primarily dihydroquinidine). [^{3}H]Quinidine[3] was also purified by this system, and a final purity of >98% was achieved.

Equilibrium Dialysis—Aliquots (400 μL) of phosphate buffer solution (pH 7.4, 0.134 M) containing quinidine (unlabeled, as well as a trace amount of radiolabeled drug) were dialyzed for 5 h at 37°C against an equal volume of serum in plexiglass cells. Postdialysis quinidine concentrations on each side of the dialysis membrane[4] were determined by liquid scintillation counting. All samples were assayed in triplicate, and the average coefficient of variation by this method was 2.97%. HPLC, coupled with liquid scintillation counting of the eluant, demonstrated that no degradation of quinidine occurred during the dialysis period.

Determination of Quinidine Binding Parameters: Rosenthal Analysis—Venous blood was obtained from three nonsmoking healthy male volunteers using glass syringes. The blood was transferred to glass tubes with polytef-lined screw caps and allowed to clot. The serum was removed after centrifugation and stored at 4°C. The serum was not frozen because of the possibility of structural alterations in lipoproteins (15). In all cases, binding studies were performed within 72 h of sample collection. The free fraction of quinidine was determined over a 2000-fold range of concentrations (initial quinidine concentrations, 0.5–1000 μg/mL), with the results plotted by the method of Rosenthal (16). The computer program PBNON[5] was used to estimate binding parameters. Quinidine binding in a solution of crystalline human serum albumin[6] (4.5 g/dL in phosphate buffer) was also determined over the same range of quinidine concentrations.

Effects of Potential Displacing Agents on Quinidine Binding—Serum obtained from a healthy volunteer was spiked with tris(butoxyethyl) phosphate[7] at a concentration of 75 μg/mL. Quinidine binding was studied over a range of concentrations from 0.5 to 1000 μg/mL, and the binding parameters obtained were compared with those from normal serum. Quinidine binding at a concentration of 1.0 μg/mL was also determined in serum containing lidocaine[8] at concentrations ranging from 1.0 to 500 μg/mL.

Effect of Hyperlipidemia and Trauma on the Serum Binding of Quinidine—Serum from six patients with elevated concentrations of lipoproteins and five healthy, nonsmoking male volunteers was obtained as described above and stored at 4°C for a maximum of 72 h before analysis. Quinidine binding was examined at an initial concentration of 1.0 μg/mL. In addition, quinidine binding was determined in two serum samples from each of four patients several days after traumatic injury (motor vehicle accidents). These samples were obtained as part of another investigation on the effect of trauma on α_1-acid glycoprotein concentration (17) and were handled in an identical manner to samples used in this investigation, with the exception that they were stored at −20°C. All samples were assayed for α_1-acid glycoprotein concentration by using a radial immunodiffusion procedure with commercially prepared kits[6]. Cholesterol and triglyceride concentrations were determined with an autoanalyzer by using the Liebermann–Burchard reagent and glycerol kinase method, respectively.

RESULTS

The quinidine serum protein binding data from three healthy volunteers are plotted (Fig. 1), by the method of Rosenthal (16). Two classes of binding sites are apparent over the concentration range studied. The affinity and capacity constants for each site are also shown (Fig. 1). At a concentration of 1.0 μg/mL, the free fraction of quinidine varied among individuals from 0.119 to 0.157 (mean, 0.138 ± 0.018). No evidence for clinically significant concentration-dependent changes in free fraction was observed within the usual therapeutic range (1–5 μg/mL). In isolated human serum albumin solution, quinidine binding was found to have characteristics consistent with those of the low-affinity, high-capacity class of sites in serum, with an observed value of 3.05×10^3 M^{-1} for the association constant (K) and 1.36×10^{-3} M for its binding capacity (nP; see Fig. 1).

[1] Vacutainer; Becton, Dickinson & Co.
[2] A. H. Robins Co., Richmond, Va.
[3] 100 mg of quinidine was supplied to New England Nuclear Corp., Boston, Mass. and was randomly tritiated by a catalytic exchange process (specific activity of the product, 0.24 mCi/mg).
[4] Spectrapor 2; Spectrum Medical Industries, Los Angeles, Calif.
[5] PBNON is a modification of the program MACMOL (written by Priore and Rosenthal in 1975) and generates protein binding parameters from the best nonlinear approximation of the data.
[6] Calbiochem-Behring, San Diego, Calif.
[7] Aldrich Chemical Co., Milwaukee, Wis.
[8] Astra Pharmaceutical Products, Inc., Worcester, Mass.

Table I—Mean Values for Quinidine Free Fraction and Concentration of Relevant Substances in Serum from Healthy Volunteers and Patients with Hyperlipidemia

	Mean ± *SD* Quinidine Free Fraction		
	Healthy Volunteers[a]	Hyperlipidemic Patients[b]	Statistical Significance[c]
Quinidine free fraction	0.129 ± 0.019	0.118 ± 0.019	NS[d]
Albumin, g/dL	4.8 ± 0.4	4.7 ± 0.3	NS
α_1-Acid glycoprotein, mg/dL	70 ± 16	99 ● 34	NS
Cholesterol, mg/dL	178 ± 14	313 ± 71	$p < 0.01$
Triglycerides, mg/dL	125 ± 32	245 ± 107[e]	$p < 0.05$

[a] $n = 5$. [b] $n = 6$. [c] t Test for independent samples. [d] Not significant. [e] The triglyceride value for one patient with a concentration of 2330 mg/dL was not included, as this would result in a badly skewed distribution of data.

Figure 2 contains the Rosenthal plot for quinidine binding in serum from a normal healthy male with and without the addition of tris(butoxyethyl) phosphate. The addition of this compound appeared to eliminate the high-affinity class of binding sites, resulting in a single class of sites with $K = 2.26 \times 10^3\ M^{-1}$ and $nP = 1.22 \times 10^{-3}$ M. In the presence of lidocaine, the quinidine free fraction increased with increasing lidocaine concentration, with a maximal value of 0.229 at a lidocaine concentration of 500 μg/mL[9]. This value is consistent with that observed at therapeutic quinidine concentrations in the presence of tris(butoxyethyl) phosphate (0.231) and with the predicted value; assuming the complete absence of the high-affinity class of binding sites in serum (0.272).

In the serum from patients suffering trauma, the mean α_1-acid glycoprotein concentration was 197 mg/dL (corresponding value in healthy volunteers, 70 mg/dL). The quinidine free fraction ranged from 0.049 to 0.113, with a mean value of 0.075 ± 0.019. The relationship between the quinidine binding ratio and the α_1-acid glycoprotein concentration is shown in Fig. 3. A strong correlation was observed, and the relationship was found to be quite consistent with that predicted by using the mean binding parameters shown in Fig. 1 (assuming that the high-affinity, low-capacity class of binding sites is on α_1-acid glycoprotein). Patients with hyperlipidemia had a mean cholesterol concentration of 313 mg/dL and a mean triglycerides concentration of 245 mg/dL (Table I). The free fraction of quinidine in these patients was 0.118 ± 0.019 and was not significantly different from the free fraction observed in healthy individuals (0.129 ± 0.019). In one patient with a triglyceride concentration of 2330 mg/dL, the quinidine free fraction was 0.128.

DISCUSSION

The protein binding of quinidine has been the subject of a number of previous investigations, many of which have yielded conflicting results. The recent identification of a number of factors which may artificially alter estimates of the quinidine free fraction prompted the present investigation, with the goal of obtaining definitive and clinically useful data.

The mean free fraction of quinidine in healthy volunteers has varied widely among studies (range, 0.10–0.29). The value of 0.129 observed in this investigation is near the lower limit of previously reported values. Two main classes of binding sites were identified in the serum from healthy volunteers, with both sites contributing nearly equally to the fraction of drug bound at therapeutic concentrations of quinidine. Because of this, one would predict that the free fraction would only double in the complete absence of one or the other of these classes of sites.

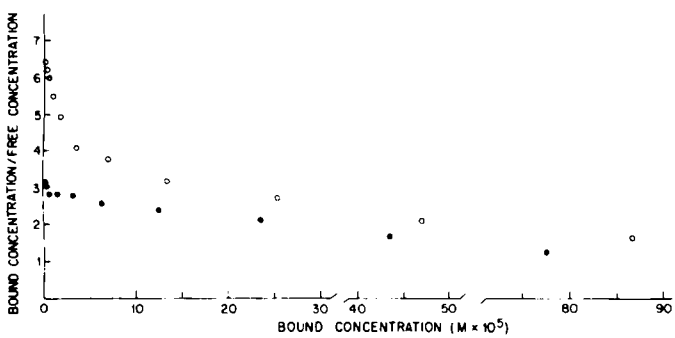

Figure 2—*Relationship between bound concentration/free concentration and bound concentration of quinidine in serum from a healthy male volunteer (○) and identical serum, to which tris(butoxyethyl) phosphate (●) at 75 μg/mL was added.*

Knowledge of the identity and characteristics of the binding proteins allows the prediction of the consequences of pathophysiological or pharmacological changes in the binding milieu. In this investigation, the binding of quinidine in an isolated albumin solution was found to have characteristics similar to the binding of quinidine to the low-affinity class of binding sites in serum. However, previous investigations have suggested that α_1-acid glycoprotein and lipoproteins, as well as albumin, contribute significantly to quinidine binding (11, 12). In attempting to establish the relative contributions of these proteins, quinidine binding was studied in the presence of tris(butoxyethyl) phosphate, a compound known to displace basic drugs from α_1-acid glycoprotein binding sites (18). The quinidine free fraction increased in a manner that was consistent with the absence of binding to the high-affinity class of sites. Because little is known about the specificity of tris(butoxyethyl) phosphate protein binding (*i.e.*, it could possibly also displace quinidine from lipoproteins), lidocaine was also studied as a potential displacer of quinidine. Lidocaine is known to be bound primarily to α_1-acid glycoprotein, with some binding to albumin and no demonstrable affinity for lipoproteins (17, 19). The ability of lidocaine to displace quinidine to the same extent as tris(butoxyethyl) phosphate suggests that interactions between quinidine and lipoproteins do not influence the free fraction of this drug.

The results of the quinidine binding studies in the trauma patients and hyperlipidemic patients support our conclusions concerning the identity of the binding sites. Trauma patients have been shown to have high concentrations of α_1-acid glycoprotein and increased binding of lidocaine (17). In this study, quinidine free fraction was reduced by >40% at a mean α_1-acid glycoprotein concentration of 197 mg/dL. Since concentrations of this magnitude are observed in several common conditions (acute myocardial infarction, rheumatoid arthritis, and cancer), similarly reduced quinidine free fractions are likely in many patients receiving the drug (20). A reduced free fraction has been reported in surgical patients (21) and in survivors of cardiac arrest (22). Using computer simulations, Kates *et al.* (10) have predicted that elevated concentrations of lipoproteins would have little effect on the quinidine binding ratio. Our results support this conclusion, as the small difference in

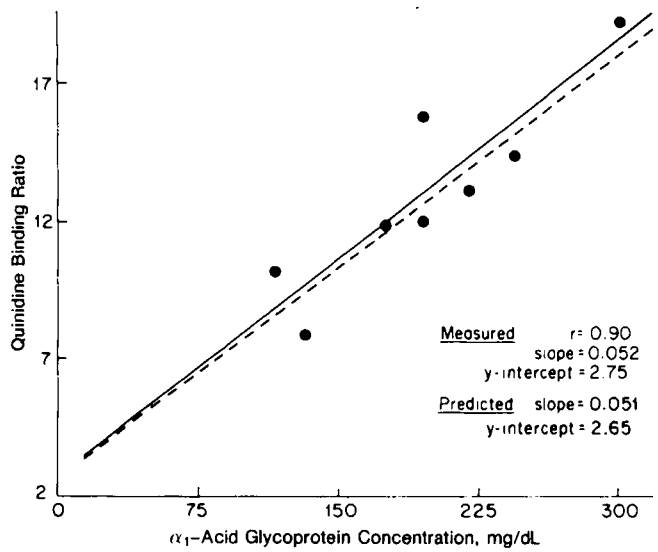

Figure 3—*Relationship between quinidine binding ratio (bound concentration/free concentration) and α_1-acid glycoprotein concentration in serum obtained from patients after traumatic injury. Predicted relationship (- - -) was obtained with the mean constants from Fig. 1 and by assuming site 1 to be on α_1-acid glycoprotein; (——) the best-fit line by linear regression analysis (measured).*

[9] Unpublished results.

free fraction between the hyperlipidemic patients and the healthy volunteers can be accounted for by slightly higher α_1-acid glycoprotein concentrations in the former group.

It appears, therefore, that the important binding proteins for quinidine are α_1-acid glycoprotein and albumin. Using the mean binding parameters for these proteins (Fig. 1), one can predict that at least a 50% decrease in albumin concentration would be necessary to obtain a 20% increase in quinidine free fraction. Clinically significant changes in quinidine binding are more likely to be due to changes in α_1-acid glycoprotein concentration, since serum levels of this protein may be increased in patients suffering from a number of common diseases.

REFERENCES

(1) K. M. Kessler, D. T. Lowenthal, M. Warner, T. Gibson, W. Briggs, and M. M. Reidenberg, *N. Engl. J. Med.*, **290**, 706 (1974).

(2) N. H. Carliner, M. L. Fisher, W. G. Crouthamel, P. K. Narang, and G. D. Plotnick, *Am. Heart J.*, **100**, 483 (1980).

(3) J.-D. Huang and S. Øie, *J. Pharmacol. Exp. Ther.*, **223**, 469 (1982).

(4) D. G. McDevitt and D. G. Shand, *Clin. Pharmacol. Ther.*, **18**, 708 (1975).

(5) D. Fremstad, O. G. Nilsen, L. Storstein, J. Amlie, and S. Jacobsen, *Eur. J. Clin. Pharmacol.*, **15**, 187 (1979).

(6) K. M. Kessler, R. C. Leech, and J. F. Spann, *Clin. Pharmacol. Ther.*, **25**, 204 (1979).

(7) M. Perez-Mateo and S. Erill, *Eur. J. Clin. Pharmacol.*, **11**, 225 (1977).

(8) M. Affrime and M. M. Reidenberg, *Eur. J. Clin. Pharmacol.*, **8**, 267 (1975).

(9) E. Woo and D. J. Greenblatt, *J. Pharm. Sci.*, **68**, 466 (1979).

(10) R. E. Kates, T. D. Sokoloski and T. J. Comstock, *Clin. Pharmacol. Ther.*, **23**, 30 (1978).

(11) O. G. Nilsen, *Biochem. Pharmacol.*, **25**, 1007 (1976).

(12) O. G. Nilsen, P. Leren, I. Aakesson, and S. Jacobsen, *Biochem. Pharmacol.*, **27**, 871 (1978).

(13) T. W. Guentert and S. Øie, *J. Pharm. Sci.*, **71**, 325 (1982).

(14) C. T. Ueda and M. C. Makoid, *J. Pharm. Sci.*, **68**, 448 (1979).

(15) National Heart and Lung Institute, National Institutes of Health, Manual of Laboratory Operations, Lipid Research Clinics Programs, Department of Health, Education and Welfare, publication no. 75-628.

(16) H. E. Rosenthal, *Anal. Biochem.*, **20**, 525 (1967).

(17) D. J. Edwards, D. Lalka, F. Cerra, and R. L. Slaughter, *Clin. Pharmacol. Ther.*, **31**, 62 (1982).

(18) O. Borga, K. M. Piafsky, and O. G. Nilsen, *Clin. Pharmacol. Ther.*, **22**, 539 (1977).

(19) P. J. McNamara, R. L. Slaughter, J. A. Pieper, M. G. Wyman, and D. Lalka, *Anesth. Analg.*, **60**, 395 (1981).

(20) K. M. Piafsky, *Clin. Pharmacokinet.*, **5**, 246 (1980).

(21) D. Fremstad, K. Bergerud, J. F. W. Haffner, and P. K. M. Lunde, *Eur. J. Clin. Pharmacol.*, **10**, 441 (1976).

(22) C. Conde, K. M. Kessler, B. Lisker, J. Silver, P. Ho-Tung, B. Cerny, D. Cooper, and R. J. Myerburg, *Circulation*, **64**, IV-36 (1981).

ACKNOWLEDGMENTS

This study was supported in part by Grant 65-0566 from the British Columbia Heart Foundation and by Public Health Service Grant GM-20852 from the Institute of General Medical Sciences, National Institutes of Health.

Simple, Rapid Method for Comparing the Self-Emulsifiability of Hydrocarbon Oils

T. A. IRANLOYE *x and N. PILPEL ‡

Received October 25, 1982, from the **Department of Pharmaceutics, University of Ife, Ile-Ife, Nigeria* and the ‡*Department of Pharmacy, Chelsea College, University of London, Manresa Road, London SW3, U.K.* Accepted for publication May 12, 1983.

Abstract □ A simple and rapid method for comparing the degree of self-emulsifiability of different hydrocarbon oils is described. The method involved measurement of the intensity of light scattered at an angle of 31° to the incident radiation by the sample. The extent or degree of self-emulsification of selected hydrocarbon oils was observed to be affected by the nature of the oil as well as by the type and concentration of the surfactants employed. The method is useful when screening surfactant–hydrocarbon oil combinations as potential vehicles for drugs in the pharmaceutical industry or herbicides and pesticides for agricultural purposes.

Keyphrases □ Emulsions—surfactant-hydrocarbon oil, self-emulsifiability, measurement by laser nephelometry □ Laser nephelometry—self-emulsifiability, surfactant-hydrocarbon oil mixtures □ Hydrocarbon oils—self-emulsifiability, effect of added surfactants, measurement by laser nephelometry

Self-emulsifiable oils (also known as emulsifiable concentrates), widely used in the chemical and allied industries because they readily form emulsions without the need for powerful or sophisticated emulsification equipment, serve as vehicles for herbicides and pesticides and are used for cutting and rolling metals into thin sheets. They are also employed as lubricants in the textile industry and are currently being used for the recovery and processing of crude oils.

Self-emulsifiable oils have some potential applications in the drug industry. Solutions of drugs in oils have been administered to patients in soft gelatin capsules since the early part of the 19th century. In its modern form, this dosage is claimed to be advantageous since the accuracy, stability, and patient convenience is greater than that for the corresponding tableted form of a given drug. These oily solutions readily emulsify when released into the aqueous environment of the stomach. The generation of a large surface area means an optimum condition for extraction and absorption of the drug. The main requirement would be a suitable combination of nontoxic surfactants in bland oils.

It has been reported that the oil droplets in self-emulsifiable systems can be very small, ~1 μm (1). Measurement of droplet sizes in the submicrometer range has proved to be very tedious and/or time consuming (2). It is anticipated that the laser nephelometer[1], when used judiciously, can reduce the number of problems associated with particle size characterization in dispersed systems.

THEORETICAL SECTION

Several theories of light scattering by small particles (3–5) have appeared in the literature since the pioneering work of Rayleigh (6, 7) in this field. Recently, Bagchi and Vold (8) have commented on the limitations of some of these theories. In the present work, it is assumed that the basic equation

[1] Hyland Laser Nephelometer PDQ; Travenol Laboratories.

0022-3549/84/0900-1267$01.00/0

© 1984, American Pharmaceutical Association

free fraction between the hyperlipidemic patients and the healthy volunteers can be accounted for by slightly higher α_1-acid glycoprotein concentrations in the former group.

It appears, therefore, that the important binding proteins for quinidine are α_1-acid glycoprotein and albumin. Using the mean binding parameters for these proteins (Fig. 1), one can predict that at least a 50% decrease in albumin concentration would be necessary to obtain a 20% increase in quinidine free fraction. Clinically significant changes in quinidine binding are more likely to be due to changes in α_1-acid glycoprotein concentration, since serum levels of this protein may be increased in patients suffering from a number of common diseases.

REFERENCES

(1) K. M. Kessler, D. T. Lowenthal, M. Warner, T. Gibson, W. Briggs, and M. M. Reidenberg, *N. Engl. J. Med.*, **290**, 706 (1974).

(2) N. H. Carliner, M. L. Fisher, W. G. Crouthamel, P. K. Narang, and G. D. Plotnick, *Am. Heart J.*, **100**, 483 (1980).

(3) J.-D. Huang and S. Øie, *J. Pharmacol. Exp. Ther.*, **223**, 469 (1982).

(4) D. G. McDevitt and D. G. Shand, *Clin. Pharmacol. Ther.*, **18**, 708 (1975).

(5) D. Fremstad, O. G. Nilsen, L. Storstein, J. Amlie, and S. Jacobsen, *Eur. J. Clin. Pharmacol.*, **15**, 187 (1979).

(6) K. M. Kessler, R. C. Leech, and J. F. Spann, *Clin. Pharmacol. Ther.*, **25**, 204 (1979).

(7) M. Perez-Mateo and S. Erill, *Eur. J. Clin. Pharmacol.*, **11**, 225 (1977).

(8) M. Affrime and M. M. Reidenberg, *Eur. J. Clin. Pharmacol.*, **8**, 267 (1975).

(9) E. Woo and D. J. Greenblatt, *J. Pharm. Sci.*, **68**, 466 (1979).

(10) R. E. Kates, T. D. Sokoloski and T. J. Comstock, *Clin. Pharmacol. Ther.*, **23**, 30 (1978).

(11) O. G. Nilsen, *Biochem. Pharmacol.*, **25**, 1007 (1976).

(12) O. G. Nilsen, P. Leren, I. Aakesson, and S. Jacobsen, *Biochem. Pharmacol.*, **27**, 871 (1978).

(13) T. W. Guentert and S. Øie, *J. Pharm. Sci.*, **71**, 325 (1982).

(14) C. T. Ueda and M. C. Makoid, *J. Pharm. Sci.*, **68**, 448 (1979).

(15) National Heart and Lung Institute, National Institutes of Health, Manual of Laboratory Operations, Lipid Research Clinics Programs, Department of Health, Education and Welfare, publication no. 75-628.

(16) H. E. Rosenthal, *Anal. Biochem.*, **20**, 525 (1967).

(17) D. J. Edwards, D. Lalka, F. Cerra, and R. L. Slaughter, *Clin. Pharmacol. Ther.*, **31**, 62 (1982).

(18) O. Borga, K. M. Piafsky, and O. G. Nilsen, *Clin. Pharmacol. Ther.*, **22**, 539 (1977).

(19) P. J. McNamara, R. L. Slaughter, J. A. Pieper, M. G. Wyman, and D. Lalka, *Anesth. Analg.*, **60**, 395 (1981).

(20) K. M. Piafsky, *Clin. Pharmacokinet.*, **5**, 246 (1980).

(21) D. Fremstad, K. Bergerud, J. F. W. Haffner, and P. K. M. Lunde, *Eur. J. Clin. Pharmacol.*, **10**, 441 (1976).

(22) C. Conde, K. M. Kessler, B. Lisker, J. Silver, P. Ho-Tung, B. Cerny, D. Cooper, and R. J. Myerburg, *Circulation*, **64**, IV-36 (1981).

ACKNOWLEDGMENTS

This study was supported in part by Grant 65-0566 from the British Columbia Heart Foundation and by Public Health Service Grant GM-20852 from the Institute of General Medical Sciences, National Institutes of Health.

Simple, Rapid Method for Comparing the Self-Emulsifiability of Hydrocarbon Oils

T. A. IRANLOYE *x and N. PILPEL ‡

Received October 25, 1982, from the **Department of Pharmaceutics, University of Ife, Ile-Ife, Nigeria* and the ‡*Department of Pharmacy, Chelsea College, University of London, Manresa Road, London SW3, U.K.* Accepted for publication May 12, 1983.

Abstract □ A simple and rapid method for comparing the degree of self-emulsifiability of different hydrocarbon oils is described. The method involved measurement of the intensity of light scattered at an angle of 31° to the incident radiation by the sample. The extent or degree of self-emulsification of selected hydrocarbon oils was observed to be affected by the nature of the oil as well as by the type and concentration of the surfactants employed. The method is useful when screening surfactant–hydrocarbon oil combinations as potential vehicles for drugs in the pharmaceutical industry or herbicides and pesticides for agricultural purposes.

Keyphrases □ Emulsions—surfactant-hydrocarbon oil, self-emulsifiability, measurement by laser nephelometry □ Laser nephelometry—self-emulsifiability, surfactant-hydrocarbon oil mixtures □ Hydrocarbon oils—self-emulsifiability, effect of added surfactants, measurement by laser nephelometry

Self-emulsifiable oils (also known as emulsifiable concentrates), widely used in the chemical and allied industries because they readily form emulsions without the need for powerful or sophisticated emulsification equipment, serve as vehicles for herbicides and pesticides and are used for cutting and rolling metals into thin sheets. They are also employed as lubricants in the textile industry and are currently being used for the recovery and processing of crude oils.

Self-emulsifiable oils have some potential applications in the drug industry. Solutions of drugs in oils have been administered to patients in soft gelatin capsules since the early part of the 19th century. In its modern form, this dosage is claimed to be advantageous since the accuracy, stability, and patient convenience is greater than that for the corresponding tableted form of a given drug. These oily solutions readily emulsify when released into the aqueous environment of the stomach. The generation of a large surface area means an optimum condition for extraction and absorption of the drug. The main requirement would be a suitable combination of nontoxic surfactants in bland oils.

It has been reported that the oil droplets in self-emulsifiable systems can be very small, ~1 μm (1). Measurement of droplet sizes in the submicrometer range has proved to be very tedious and/or time consuming (2). It is anticipated that the laser nephelometer[1], when used judiciously, can reduce the number of problems associated with particle size characterization in dispersed systems.

THEORETICAL SECTION

Several theories of light scattering by small particles (3–5) have appeared in the literature since the pioneering work of Rayleigh (6, 7) in this field. Recently, Bagchi and Vold (8) have commented on the limitations of some of these theories. In the present work, it is assumed that the basic equation

[1] Hyland Laser Nephelometer PDQ; Travenol Laboratories.

0022-3549/84/0900-1267$01.00/0

© 1984, American Pharmaceutical Association

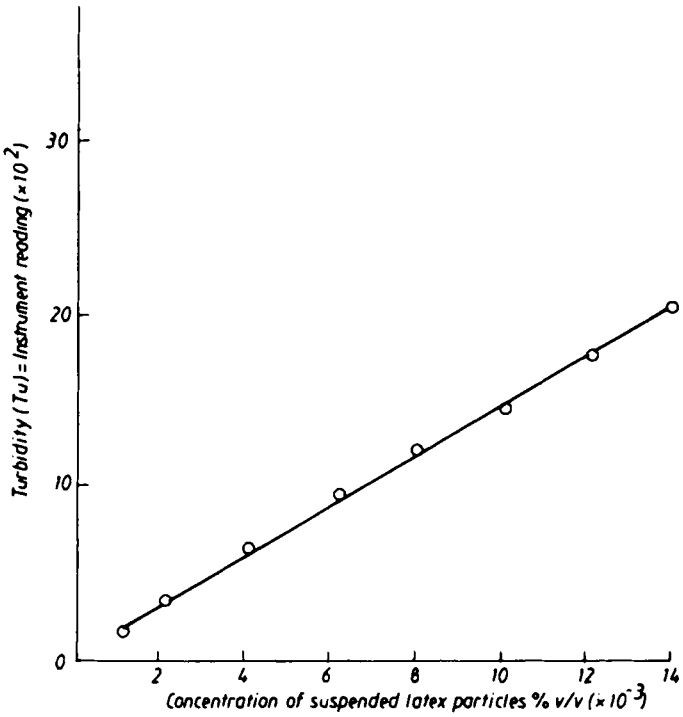

Figure 1—*Turbidity as a function on concentration of suspended latex particles. Nominal (manufacturer's) particle diamter = 0.24 μm.*

of Rayleigh (6) given by:

$$I_s(\theta) = \frac{9\pi NV^2}{2d^2\lambda^4} \cdot \frac{(n_i^2 - n_{ii}^2)}{(n_i^2 + 2n_{ii}^2)} \cdot (1 + \cos^2\theta) I_0 \qquad \text{(Eq. 1)}$$

is applicable. In this equation, $I_s(\theta)$ is the intensity of light scattered at angle θ, N is the number of particles in volume V, d is the distance between the measuring unit and the sample, n_i and n_{ii} are the refractive indices of the dispersed and continuous phases, respectively, and λ is the wavelength of the incident light of intensity I_0.

Lee and Groves (9) have shown that with the laser nephelometer, some factors (such as d and θ) may be regarded as constant, due to the design of the instrument, and they represented the measured intensity of scattered light by:

$$I_s(\theta) = fNV \cdot fn \cdot f(n_i - n_{ii}) \qquad \text{(Eq. 2)}$$

V is related to φ (*i.e.*, the volume fraction of the dispersed phase). The measured turbidity, Tu, is:

$$\text{Tu} = \frac{I_s(\theta)}{(n_i - n_{ii})\varphi} = f(\text{mean particle size}) \qquad \text{(Eq. 3)}$$

EXPERIMENTAL SECTION

Monosize latex[2] particles were used as received. High purity *n*-hydrocarbon[3] oils and a hydrocarbon mixture (I)[4] were purified further by repeated percolation through beds of fuller's earth[5] until their physical properties agreed closely with literature values. Surfactant mixture II[6] was used at a 1:1 ratio; surfactant mixture III[7] was used as 1:1 and 3:2 mixtures. Water was triple distilled from an all glass apparatus (surface tension, $\gamma a/w = 71.9$ mNm^{-1} at 25°C).

The laser nephelometer[1] utilizes a low-powered (0.5 mW) neon laser (λ = 632.8 nm) and an arbitrary scale of 0–200 to indicate increasing scattering intensity or turbidity, and was operated according to the manufacturer's manual (15).

[2] Rhône-Poulenc Polymeres, Aubervilliers, France.
[3] British Drug Houses, Poole, England.
[4] Dobane JN; Shell Chemicals. It is a mixture of aromatic (15%), naphtheneic (14%), and paraffinic (44%) hydrocarbons (10).
[5] Adsorption grade; Hopkin and Williams, Romford, England.
[6] Mixture of a water-soluble, phosphated nonylphenol ethoxylate (11) and an oil-soluble, phosphated fatty alcohol ethoxylate (12); Lankro Chemicals, Manchester, England.
[7] Mixture of Arylan PWS [a straight-chain, water-soluble dedecyl benzene sulfonate derivative (13)] and Ethylan D254 [an oil-soluble fatty alcohol ethoxylate (14)]; Lankro Chemicals, Manchester, England.

Table I—Composition of Emulsifiable Oils

Total Conc. of Surfactants[a], % w/w	Conc. of Hydrocarbon Oil, % w/w
10	90
20	80
30	70
40	60
50	50

[a] Mixture II was used as a 1:1 ratio; mixture III was either a 1:1 or a 3:2 ratio.

Serial dilutions of suspensions of the latex particles in water were made. Emulsifiable oils were prepared by adding the hydrocarbon oils to the surfactant mixtures; all preparations were made on a weight basis, as indicated in Table I. Emulsions were prepared by adding 1 mL of the emulsifiable oil to 99 mL of water in a 100-mL graduated cylinder, which was then gently inverted until the dispersion was homogeneous. Serial dilutions of the emulsions were then made.

Sample tubes containing the dilute suspensions of the latex particles or the emulsions were placed, in turn, in the low-power laser beam, and the turbidity as indicated by the instrument reading was recorded after a scanning period

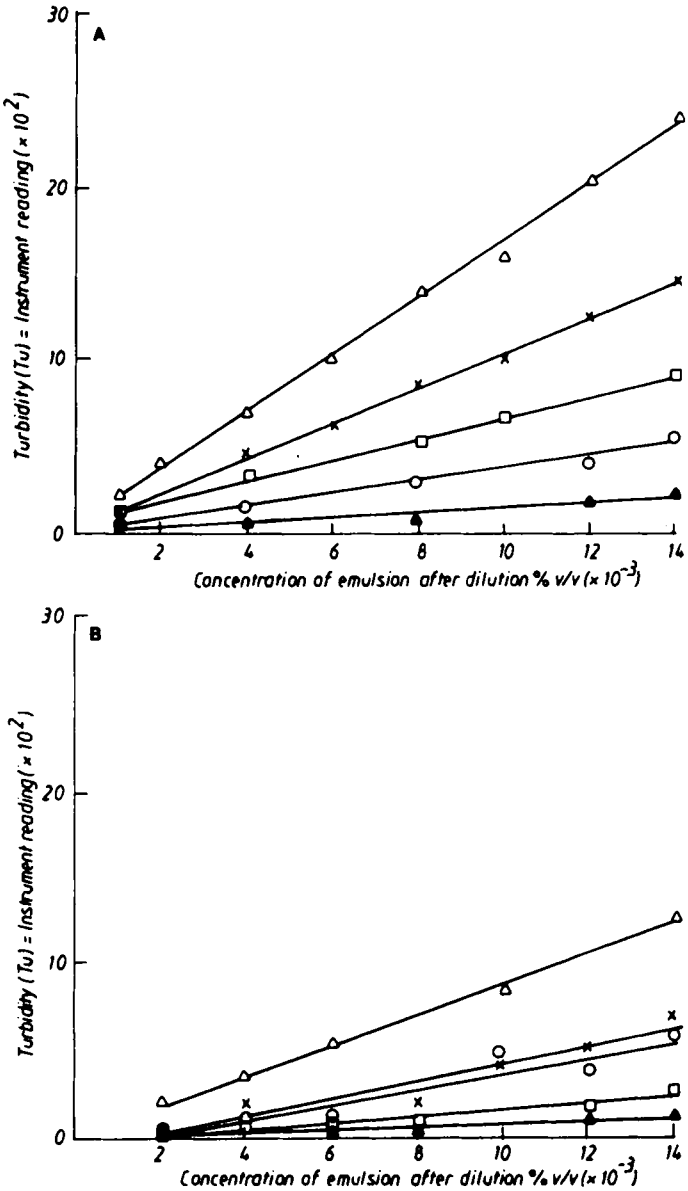

Figure 2—*Turbidity as a function of concentration of emulsions prepared from emulsifiable oils consisting of III (1:1) and I (A) and II (1:1) and n-hexane (B). Key: (□) 10% w/w; (△) 20% w/w; (×) 30% w/w; (○) 40% w/w; (▲) 50% w/w.*

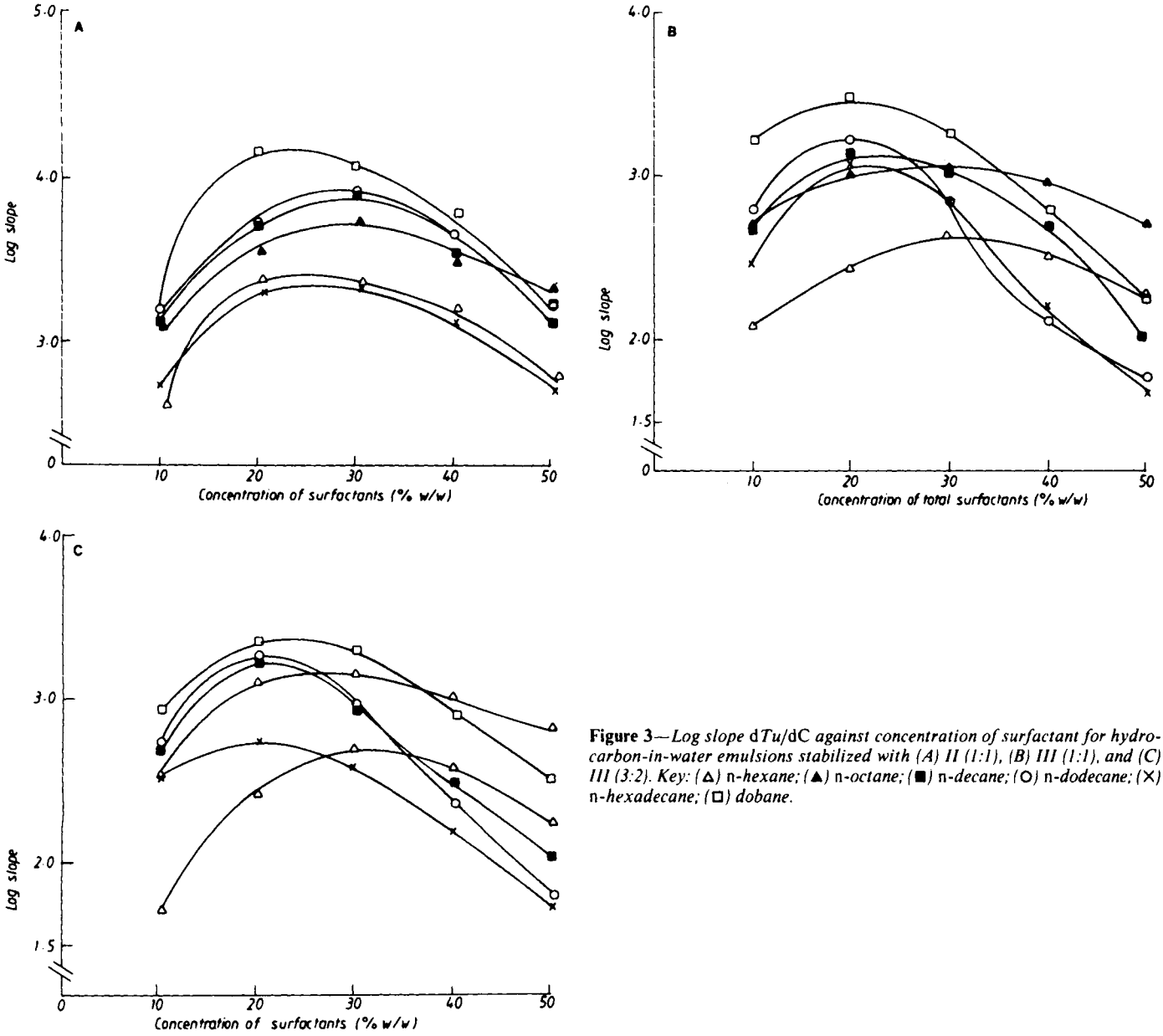

Figure 3—*Log slope* d*Tu*/d*C against concentration of surfactant for hydrocarbon-in-water emulsions stabilized with (A) II (1:1), (B) III (1:1), and (C) III (3:2). Key: (△) n-hexane; (▲) n-octane; (■) n-decane; (○) n-dodecane; (×) n-hexadecane; (□) dobane.*

of 5 s. At least 10 samples from each suspension or emulsion were analyzed and the results averaged.

RESULTS AND DISCUSSION

Graphs were plotted between turbidity (instrument reading) and concentration of latex particles or emulsions; representative results are shown in Figs. 1 and 2, respectively. The graphs were rectilinear within the range of concentrations examined. This observation conforms with Beer's law, which states that the decrease in intensity of radiation is related exponentially to the concentration of an absorbing substance in solution through which the radiation passes provided the light is monochromatic and the material homogenous.

To quantify the extent of emulsification of each hydrocarbon oil, slopes (*i.e.*, $d\mathrm{Tu}/dC$) were determined. The logarithms of the slopes (to accommodate the range) were then plotted against the concentration of surfactants in the emulsifiable oil (see Table I). Representative results[8] are shown in Fig. 3.

It can be seen that as the total concentration of the surfactants was increased, there was an increase in the value of the slope for each hydrocarbon oil until a maximum was reached, after which there was a decrease. The increase in slope (as a function of surfactant concentration) was probably the result of increased adsorption of surfactant molecules at the oil-water interface leading to an increase in the stabilization of the interfacial area until a maximum was reached. The fall in slope at higher concentrations of surfactants could be due to formation of associated structures with a corresponding decrease in translucency.

At any particular total concentration of surfactants, the numerical value of the slope (log $d\mathrm{Tu}/dC$) is a measure of the amount of light scattered by the system and, hence, a measure of its self-emulsifiability. Thus, from Fig. 3A it is seen that I is more readily emulsified by II (1:1) than *n*-hexane because at all concentrations of these emulsifiers, the curve for the former is above that of the latter. This observation is supported by recent work (16), which showed that droplets of *n*-hexane stabilized with equal weight ratios of these surfactants were larger and fewer than those of I.

When comparing the efficiency of II (1:1) with III (1:1) as an emulsifier for *n*-hexane, it can be said that the former is more efficient, since at each total concentration of surfactants the value of $d\mathrm{Tu}/dC$ with II (1:1) is higher than with III (1:1).

CONCLUSIONS

The objective in any formulation exercise should be to achieve a maximum value of $d\mathrm{Tu}/dC$ at the lowest convenient total concentration of surfactants. The present equipment and technique should prove suitable for comparing the relative self-emulsifiabilities of different oil-surfactant combinations.

REFERENCES

(1) M. J. Groves and H. S. Yalabik, *Powder Tech.*, **12**, 233 (1975).

[8] To minimize crossing of lines.

(2) M. J. Groves and D. C. Freshwater, *J. Pharm. Sci.*, **57**, 1273 (1968).
(3) G. Mie, *Ann. Physik.*, **25**, 377 (1908).
(4) M. Van der Waarden, *J. Colloid Sci.*, **9**, 215 (1954).
(5) M. Kerker, "The Scattering of Light and other Electromagnetic Radiation," Academic, New York, N.Y., 1969.
(6) L. Rayleigh, *Phil. Mag.*, **44**, 28 (1897).
(7) L. Rayleigh, *Phil. Mag.*, **47**, 375 (1899).
(8) P. Bagchi and R. D. Vold, *J. Colloid Interface Sci.*, **53**, 194 (1975).
(9) G. W. J. Lee and M. J. Groves, *Powder Tech.*, **28**, 49 (1981).
(10) N. Pilpel, *Insulation*, **May** 63 (1968).
(11) M. J. Groves, R. M. A. Mustafa, and J. E. Carless, *J. Pharm. Pharmacol.*, **24**, 104 (1972).
(12) M. J. Groves, R. M. A. Mustafa, and J. E. Carless, *J. Pharm. Pharmacol.*, **25**, 736 (1973).
(13) T. A. Iranloye, Ph.D. thesis, University of London, London, 1981, p. 45.
(14) T. A. Iranloye, Ph.D. thesis, University of London, London, 1981, p. 46.
(15) Operators instructions: PDQ Laser Nephelometer, Travenol Laboratories, Deerfield, Ill.
(16) T. A. Iranloye, N. Pilpel, and M. J. Groves, *J. Dispersion Sci. Technol.*, **4**, 109 (1983).

ACKNOWLEDGMENTS

T. A. Iranloye is grateful to University of Ife for granting him study leave.

Analytical Methods for the Determination of Sulindac and Metabolites in Plasma, Urine, Bile, and Gastric Fluid by Liquid Chromatography Using Ultraviolet Detection

D. G. MUSSON[x], W. C. VINCEK, M. L. CONSTANZER, and T. E. DETTY

Received March 15, 1983 from the *Merck Sharp & Dohme Research Laboratories, West Point, PA 19486.* Accepted for publication October 17, 1983.

Abstract □ A high-performance liquid chromatographic method using a linear elution gradient has been developed for the analysis of sulindac, sulindac sulfone, and sulindac sulfide in plasma, urine, bile, and gastric fluid. The methodology uses reverse-phase, radial compression chromatography with gradient elution, and UV detection. Sulindac and its metabolites in plasma can be quantitated at 0.25 μg/mL with a mean *CV* of 6.0 ● 2.9%; urine, bile, and gastric fluid (0.5 μg/mL) yield a mean *CV* of 5.5 ± 1.9%.

Keyphrases □ Sulindac—metabolites, liquid chromatography with UV detection, human plasma, urine, bile, and gastric fluid □ Liquid chromatography—sulindac and its metabolites, human plasma, urine, bile and gastric fluid

Sulindac (*cis*-5-fluoro-2-methyl-1-[*p*-(methylsulfinyl)-benzylidene]indene-3-acetic acid; I) is an anti-inflammatory drug with analgesic and antipyretic properties. Metabolites include sulindac sulfide (II) the active species (I), and sulindac sulfone (III). Sulindac and its metabolites are detected in plasma, while sulindac, sulindac sulfone, and their respective conjugates are the major constituents excreted in urine (2).

Previous methods of analysis include an isotope dilution radioimmunoassay (3), a computerized mass spectral assay (4), and a high-performance liquid chromatographic assay (HPLC) (5), and appear to be restricted to serum or plasma. A stepwise isocratic HPLC assay has been recently reported (6) for plasma and urine determination; however, it involves tedious extraction procedures and is not free of interfering substances.

Preliminary investigations using the Dusci and Hackett method (5) led to incomplete resolution of sulindac and its metabolites from endogenous substances. Modifying this method with gradient elution afforded an assay that is applicable for measuring total levels of sulindac and its metabolites in plasma, urine, bile, and gastric fluid, and one that appears to be free from interfering substances.

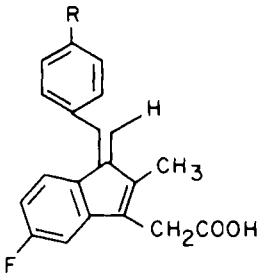

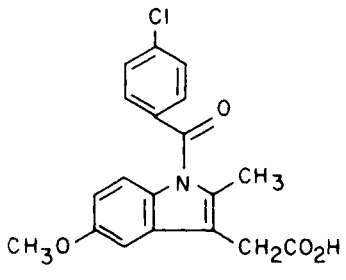

IV

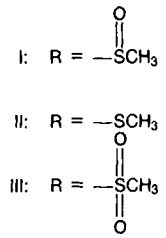

EXPERIMENTAL SECTION

Apparatus—The chromatography was performed on HPLC equipment which included two solvent delivery systems[1], an auto sampler[2], a fixed-wavelength absorbance detector with a 340-nm filter[3], and a solvent programmer[4]. The absorbance responses were recorded by a computing integrator[5] (attenuation 16 mV full scale; chart speed 0.5 cm/min).

Materials—Sulindac[6], sulindac sulfone[6], sulindac sulfide[6], and indomethacin[6] (IV, internal standard) were used as received (7, 8); acetonitrile,

[1] Model 6000A Solvent Delivery Systems; Waters Associates.
[2] WISP 710B auto sampler; Waters Associates.
[3] Model 440 Absorbance Detector; Waters Associates.
[4] Model 660 Solvent Programmer; Waters Associates.
[5] SP4100 Computing Integrator; Spectra Physics.
[6] Merck Sharp & Dohme Research Laboratories. Purity for sulindac and metabolites was determined by HPLC and elemental analysis. Sulindac sulfide: calc. for $C_{20}H_{17}FO_2S$: C, 70.6; H, 5.00. Found: C, 71.0; H, 4.68. Sulindac sulfone: calc. for $C_{20}H_{17}FO_4S$: C, 64.5; H, 4.57. Found: C, 64.3; H, 4.48. Sulindac: calc. for $C_{20}H_{17}FO_3S$: C, 67.4; H, 4.81. Found: C, 67.4; H, 4.72.

0022-3549/84/0900-1270$01.00/0
© 1984, American Pharmaceutical Association

(2) M. J. Groves and D. C. Freshwater, *J. Pharm. Sci.*, **57**, 1273 (1968).
(3) G. Mie, *Ann. Physik.*, **25**, 377 (1908).
(4) M. Van der Waarden, *J. Colloid Sci.*, **9**, 215 (1954).
(5) M. Kerker, "The Scattering of Light and other Electromagnetic Radiation," Academic, New York, N.Y., 1969.
(6) L. Rayleigh, *Phil. Mag.*, **44**, 28 (1897).
(7) L. Rayleigh, *Phil. Mag.*, **47**, 375 (1899).
(8) P. Bagchi and R. D. Vold, *J. Colloid Interface Sci.*, **53**, 194 (1975).
(9) G. W. J. Lee and M. J. Groves, *Powder Tech.*, **28**, 49 (1981).
(10) N. Pilpel, *Insulation*, **May** 63 (1968).
(11) M. J. Groves, R. M. A. Mustafa, and J. E. Carless, *J. Pharm. Pharmacol.*, **24**, 104 (1972).
(12) M. J. Groves, R. M. A. Mustafa, and J. E. Carless, *J. Pharm. Pharmacol.*, **25**, 736 (1973).
(13) T. A. Iranloye, Ph.D. thesis, University of London, London, 1981, p. 45.
(14) T. A. Iranloye, Ph.D. thesis, University of London, London, 1981, p. 46.
(15) Operators instructions: PDQ Laser Nephelometer, Travenol Laboratories, Deerfield, Ill.
(16) T. A. Iranloye, N. Pilpel, and M. J. Groves, *J. Dispersion Sci. Technol.*, **4**, 109 (1983).

ACKNOWLEDGMENTS

T. A. Iranloye is grateful to University of Ife for granting him study leave.

Analytical Methods for the Determination of Sulindac and Metabolites in Plasma, Urine, Bile, and Gastric Fluid by Liquid Chromatography Using Ultraviolet Detection

D. G. MUSSON[x], W. C. VINCEK, M. L. CONSTANZER, and T. E. DETTY

Received March 15, 1983 from the *Merck Sharp & Dohme Research Laboratories, West Point, PA 19486.* Accepted for publication October 17, 1983.

Abstract □ A high-performance liquid chromatographic method using a linear elution gradient has been developed for the analysis of sulindac, sulindac sulfone, and sulindac sulfide in plasma, urine, bile, and gastric fluid. The methodology uses reverse-phase, radial compression chromatography with gradient elution, and UV detection. Sulindac and its metabolites in plasma can be quantitated at 0.25 μg/mL with a mean *CV* of 6.0 ● 2.9%; urine, bile, and gastric fluid (0.5 μg/mL) yield a mean *CV* of 5.5 ± 1.9%.

Keyphrases □ Sulindac—metabolites, liquid chromatography with UV detection, human plasma, urine, bile, and gastric fluid □ Liquid chromatography—sulindac and its metabolites, human plasma, urine, bile and gastric fluid

Sulindac (*cis*-5-fluoro-2-methyl-1-[*p*-(methylsulfinyl)-benzylidene]indene-3-acetic acid; I) is an anti-inflammatory drug with analgesic and antipyretic properties. Metabolites include sulindac sulfide (II) the active species (I), and sulindac sulfone (III). Sulindac and its metabolites are detected in plasma, while sulindac, sulindac sulfone, and their respective conjugates are the major constituents excreted in urine (2).

Previous methods of analysis include an isotope dilution radioimmunoassay (3), a computerized mass spectral assay (4), and a high-performance liquid chromatographic assay (HPLC) (5), and appear to be restricted to serum or plasma. A stepwise isocratic HPLC assay has been recently reported (6) for plasma and urine determination; however, it involves tedious extraction procedures and is not free of interfering substances.

Preliminary investigations using the Dusci and Hackett method (5) led to incomplete resolution of sulindac and its metabolites from endogenous substances. Modifying this method with gradient elution afforded an assay that is applicable for measuring total levels of sulindac and its metabolites in plasma, urine, bile, and gastric fluid, and one that appears to be free from interfering substances.

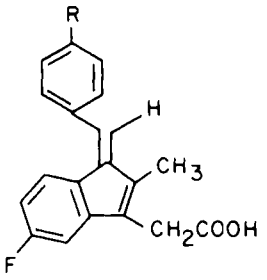

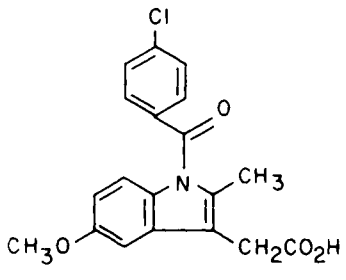

IV

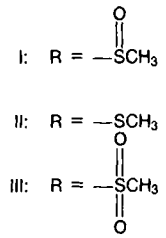

EXPERIMENTAL SECTION

Apparatus—The chromatography was performed on HPLC equipment which included two solvent delivery systems[1], an auto sampler[2], a fixed-wavelength absorbance detector with a 340-nm filter[3], and a solvent programmer[4]. The absorbance responses were recorded by a computing integrator[5] (attenuation 16 mV full scale; chart speed 0.5 cm/min).

Materials—Sulindac[6], sulindac sulfone[6], sulindac sulfide[6], and indomethacin[6] (IV, internal standard) were used as received (7, 8); acetonitrile,

[1] Model 6000A Solvent Delivery Systems; Waters Associates.
[2] WISP 710B auto sampler; Waters Associates.
[3] Model 440 Absorbance Detector; Waters Associates.
[4] Model 660 Solvent Programmer; Waters Associates.
[5] SP4100 Computing Integrator; Spectra Physics.
[6] Merck Sharp & Dohme Research Laboratories. Purity for sulindac and metabolites was determined by HPLC and elemental analysis. Sulindac sulfide: calc. for $C_{20}H_{17}FO_2S$: C, 70.6; H, 5.00. Found: C, 71.0; H, 4.68. Sulindac sulfone: calc. for $C_{20}H_{17}FO_4S$: C, 64.5; H, 4.57. Found: C, 64.3; H, 4.48. Sulindac: calc. for $C_{20}H_{17}FO_3S$: C, 67.4; H, 4.81. Found: C, 67.4; H, 4.72.

0022-3549/84/0900-1270$01.00/0
© 1984, American Pharmaceutical Association

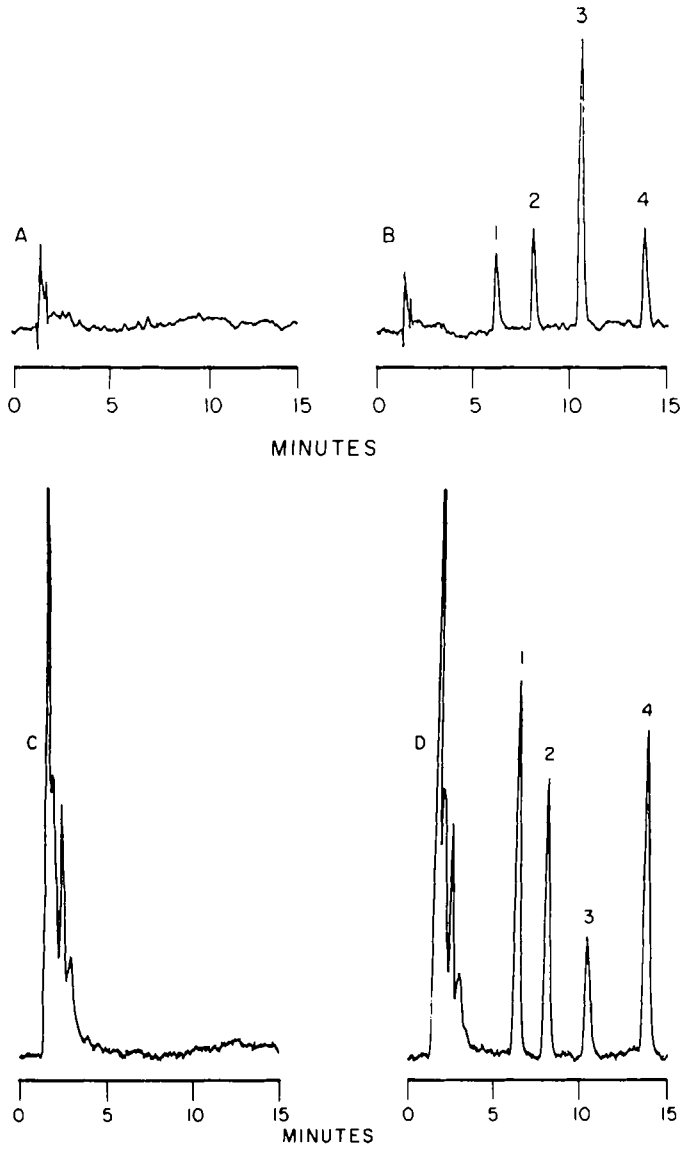

Figure 1—*Chromatograms from a stainless steel C_{18} column. Key: (A) is a plasma control blank; (B) is a plasma sample containing sulindac (1) at 1.5 μg/mL, sulindac sulfone (2) at a 1.7 μg/mL, sulindac sulfide (4)(at 1.2 μg/mL, and indomethacin (3) at 37.5 μg/mL; (C) is a urine blank; (D) is a urine sample containing sulindac at 2.7 μg/mL, sulindac sulfone at 2.0 μg/mL, sulindac sulfide at 2.3 μg/mL, and internal standard at 37.5 μg/mL.*

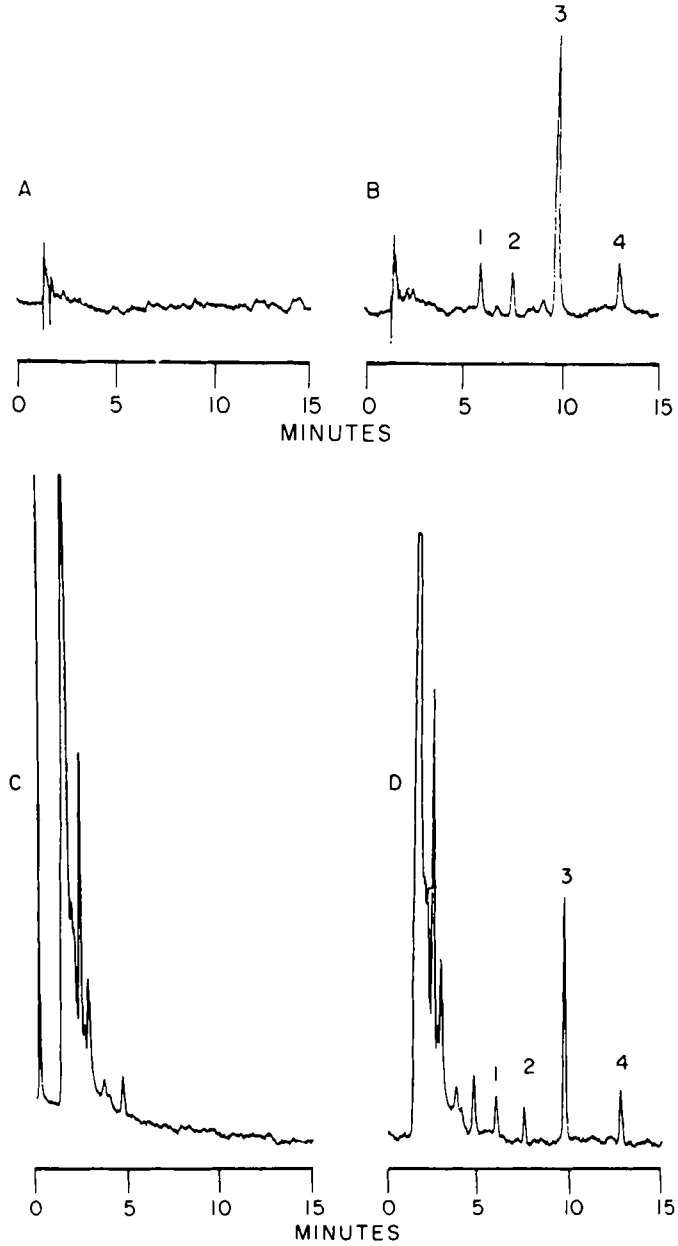

Figure 2—*Chromatograms from a radially compressed C_{18} column. Key: (A) is a control plasma blank; (B) is a plasma standard containing sulindac and its metabolites; (C) is a control urine; (D) is a urine standard. All concentrations of sulindac and its metabolites are at 0.5 μg/mL; the internal standard concentrations are 40.0 μg/mL for plasma and urine standards.*

HPLC grade[7], was filtered[8]; and water was purified[9]. Heparinized control plasma was collected and prepared in-house[6].

A C_{18} stainless steel column (30 cm × 3.9 mm i.d., 10 μm)[10], a C_{18} plastic cartridge (10 cm × 8 mm i.d., 10 μm) housed in a radial compression module[11], and a reverse-phase guard column[12] were used.

Prepared Solutions—Standard stock solutions of I, II, and III were prepared weekly by dissolving 2.0 mg of the appropriate compound in 2 mL of absolute ethanol and 8 mL of sodium borate buffer, pH 7.2 (12.4-g boric acid, 10.0-mL 1 M NaOH diluted to 1 L with purified[9] water). Working standards were mixed with appropriate dilutions from the stock solution with the boric acid buffer. Internal standard stock solutions were prepared weekly by dissolving indomethacin in the sodium borate buffer, pH 7.2 (300 μg/mL).

Chromatographic Conditions— The mobile phase gradients for the plasma, urine, bile, and gastric fluid assays were: a potassium phosphate buffer, pH 3.0 (6.8-g KH_2PO_4 in 1000 mL water with the pH adjusted to 3.0 with 85% phosphoric acid) and a mixture of acetonitrile and the phosphate buffer (70:30 v/v). Both solutions were filtered (cellulose, 0.5 μm) and kept under a helium atmosphere. During a gradient run the two solutions were mixed at 53:47, respectively, and changed to 7:93 over 10 min (linear gradient time) at 2 mL/min. The final solvent ratio continued to run for 5 min. The radial C_{18} column was reequilibrated for 5 min, with the initial mobile phase conditions, before the next sample run. Due to chromatographic interferences in the bile of certain patients in clinical studies, the gradient conditions for the bile assay required a 15-min gradient time and a 3-min hold.

Plasma Preparation—A 0.3-mL plasma sample was spiked with the internal standard, indomethacin (40.0 μL). One milliliter of acetonitrile was mixed with the plasma aliquot on a vortex mixer (30 s). The tube was then centrifuged (3500 rpm)[13], and the liquid sample was transferred to a tapered tube. The volume was reduced to 0.1 mL with a stream of nitrogen and a warm water bath (50°C) and then analyzed by HPLC (20-μL injection volume).

Urine, Bile, and Gastric Fluid Preparation—A 0.3-mL fluid sample of urine, bile, or gastric fluid was mixed with 0.1 mL of 5 M NaOH. The sample was

[7] Burdick & Jackson Laboratories.
[8] 0.5 μg Zeflor filter; Rainin.
[9] Milli-Q Water Purification System; Millipore Corp.
[10] μ-Bondapak C_{18} column; Waters Associates.
[11] RCM-100 containing a Radial-PAK C18 cartridge; Waters Associates.
[12] Microguard column; Bio-Rad.
[13] International Centrifuge, Size 2, Model K.

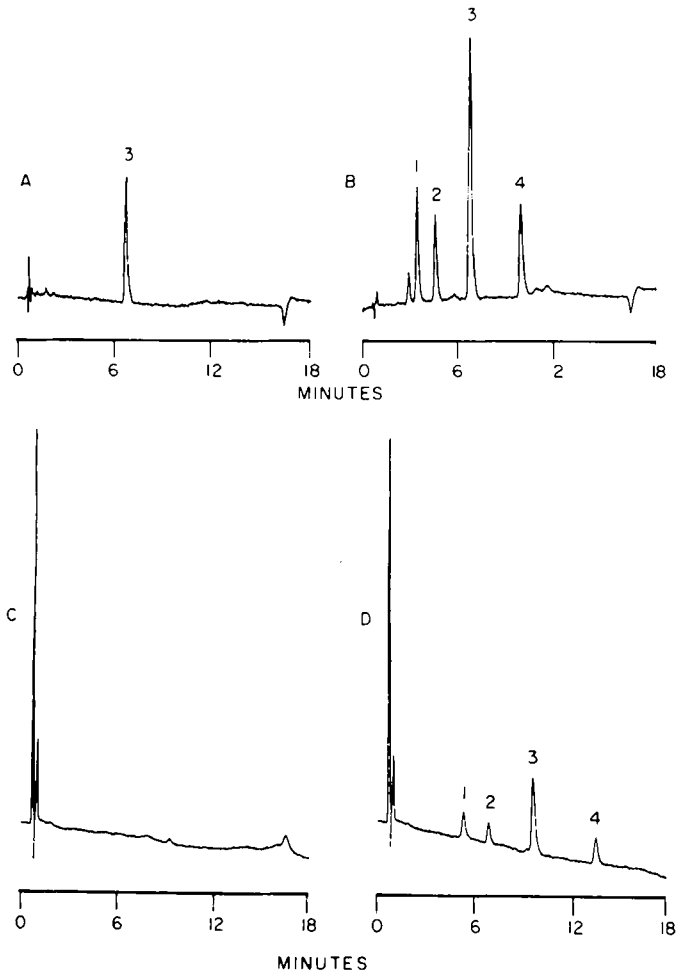

Figure 3—*Chromatograms from a radially compressed C_{18} column. Key: (A) is a control gastric fluid blank containing internal standard; (B) is a gastric fluid standard; (C) is a control bile blank; (D) is a bile standard. All concentrations of sulindac and its metabolites are at 0.5 μg/mL; the internal standard concentrations are 6.0 μg/mL for gastric and 25.0 μg/mL for bile standards.*

incubated at room temperature (25–27°C) for 15 min. The pH was then adjusted with the addition of 0.1 mL of phosphoric acid (28.3%). The internal standard (40 μL for urine, 6 μL for gastric fluid, and 25.0 μL for bile) and 1 mL of acetonitrile (1.5 mL for gastric and intestinal fluids) was mixed with the sample. In all cases, the samples were vortex-mixed (30 s) and centrifuged (3500 rpm)[13]. The organic layer was transferred to a tapered tube, the volume was reduced to 0.1 mL, and then it was analyzed by HPLC (20-μL injection volume for urine, 35-μL for bile, and 40-μL for gastric fluid).

Standard Curves—Plasma standards were prepared by mixing 1 mL of control plasma with the internal standard and appropriate volumes of I, II, and III to achieve concentrations from 0.25 to 10 μg/mL, *e.g.*, 0.25, 0.5, 1.0, 2.5, 5.0, and 10.0 μg/mL. From these standards, 0.3-mL aliquots were removed and processed as above.

Urine, bile, and gastric fluid standards (1 mL) were prepared similarly but without the internal standard, which is unstable under the basic conditions required for conjugate hydrolysis. The samples were hydrolyzed, pH adjusted, spiked with internal standard, and processed as above.

The standard curves were plotted with peak height ratios *versus* concentrations. A validation curve consisted of the above concentrations with six replicates per concentration (each replicate was prepared separately). A daily standard curve was assayed with the samples; unknown sample concentrations were interpolated from these daily curves.

Recovery Values—Recovery values were measured by comparing the amount of labeled material prepared in a standard sample with the amount detected in acetonitrile after deproteination and/or extraction. Standards of labeled sulindac ([2-^{14}C]acetic acid, 26 μCi/mg)[14], and sulindac sulfone ([^{3}H]methylene, vinyl, 50 μCi/mg), and sulindac sulfide ([^{3}H]methylene, 256 μCi/mg) were prepared in concentrations of 0.25, 1.0, and 10.0 μg/mL (3, 9) and processed. The acetonitrile extracts were measured for volume and counted for radioactivity. The radioactivity measured for the extracts was divided by the radioactivity of the standard solutions.

Table I—Linear Regression Parameters

	Slope	Intercept	r^2	Range, μg/mL
Plasma				
Sulindac	0.3703	−0.0232	0.9999	0.25–10
Sulindac Sulfone	0.3119	0.0326	0.9999	0.25–10
Sulindac Sulfide	0.3517	0.0084	0.9998	0.25–10
Urine				
Sulindac	0.2942	0.0072	0.9996	0.5–10
Sulindac Sulfone	0.2647	−0.0006	0.9996	0.5–10
Sulindac Sulfide	0.2677	−0.0123	0.9980	0.5–10
Bile				
Sulindac	0.0967	0.0345	0.9999	0.5–10
Sulindac Sulfone	0.0955	0.0011	0.9998	0.5–10
Sulindac Sulfide	0.1147	−0.0139	0.9995	0.5–10
Gastric				
Sulindac	1.0202	−0.0880	0.9998	0.5–5.0
Sulindac Sulfone	0.7213	−0.0402	0.9996	0.5–5.0
Sulindac Sulfide	0.8423	−0.1231	0.9950	0.5–2.5

Table II—Precision of the Assay

	CV, %[a]		
	Sulindac	Sulindac Sulfone	Sulindac Sulfide
Plasma Standards			
0.25	8.76	6.34	3.01
1.0	7.76	3.67	6.75
10.0	1.63	1.84	2.69
Urine Standards			
0.5	4.23	9.10	6.01
2.5	5.66	7.56	6.77
10.0	4.22	4.29	6.50
Intestinal Fluid			
0.5	6.4	6.3	2.9
2.5	10.4	7.3	8.4
10.0	11.8	8.1	8.6
Gastric Fluid			
0.5	5.2	6.3[b]	3.2
1.0	5.3	[b]	3.2
2.5	6.5	4.8	5.9
5.0	3.6	5.7	—[c]

[a] $n = 6$. [b] No replicates run. [c] Standard curve upper limit 2.5 μg/mL.

RESULTS AND DISCUSSION

This assay, a modification of an isocratic, reverse-phase HPLC method for the determination of sulindac in plasma (5), involves the use of a linear elution gradient to resolve sulindac and its metabolites from interfering peaks found in clinical plasma samples and other human fluids, *e.g.*, urine, bile, and gastric fluid. The mobile phase of acetonitrile and potassium phosphate buffer (pH 3.0) was adjusted so that separation from endogenous substances was achieved, the resolution of the sulfone metabolites and sulindac was enhanced, and the elution of the sulfide metabolite was hastened.

Chromatographic separation using a linear elution gradient was achieved, initially, for plasma and urine on a stainless steel C_{18} column[10] at 40:60 acetonitrile–potassium phosphate buffer (2 mL/min) changing to 65:35 over 10 min. Hold time and equilibration delay were set at 5 min. These HPLC conditions gave an assay applicable only to plasma and urine fluids (Fig. 1). Adaptation of the mobile phase conditions to a radially compressed C_{18} cartridge resulted in an assay applicable to plasma, urine, bile, and gastric fluid. This latter assay elutes and resolves sulindac and its metabolites in a chromatographic manner similar to the former assay with the stainless steel column. The chromatograms of plasma, urine, bile, and gastric fluid blanks did not show endogenous substances that would interfere with sulindac, its me-

[14] [^{14}C]Sulindac, (*Z*)-5-fluoro-2-methyl-1-[[4-(methyl-sulfinyl)phenyl] methylene]-1*H*-indene-3-[2-^{14}C]acetic acid, was prepared by Mr. Gregory, J. Gatto, and Miss Jane Chan in the Radiochemical Synthesis Laboratory of MSDRL, Rahway, N.J. under the direction of Dr. Holly E. Mertel. The procedure is unpublished. Labeled carbon was introduced by treating cyano[2-^{14}C]acetic acid (American Radiochemical Co., Sanford, Fla.) with 6-fluoro-2-methyl-1-indone, followed by hydrolysis and decarboxylation steps. The resulting 5-fluoro-2-methyl-1*H*-indene-3-[2-^{14}C]acetic acid was condensed with *p*-methyl-sulfinylbenzaldehyde to furnish the title tracer compound. A description of a related sequence is found in Canadian patent 1,027,967, March 14, 1978, (to John M. Chemerda and Seemon H. Pines).

Table III—Human Urine, Bile, and Gastric Fluid Levels of Sulindac and Metabolites (200 mg im of Sulindac)

Time[a]	Sulindac, μg/mL	Sulindac Sulfone, μg/mL	Sulindac Sulfide, μg/mL
Urine			
−1-0	0	0	0
0-6	34.60	9.15	0
6-24	11.60	14.90	0
Bile			
0-60	0	0	0
60-80	1.31	0.56	0
80-100	2.42	1.55	0
100-120	4.02	2.61	0
120-140	8.73	5.85	0
140-160	8.24	5.50	0
160-180	8.75	5.90	0
180-200	8.42	5.87	0
200-220	9.92	7.69	0
220-240	8.42	7.24	0.52
240-260	7.98	7.11	0.55
260-280	7.67	7.32	0.62
280-300	9.40	8.84	0.80
Gastric Fluid[d]			
0-160	—[c]	0	0
160-180	3.96	3.66	0
180-200	5.59	5.49	0
200-220	4.83	4.96	0
220-240	2.29	2.43	0
240-260	7.92	9.49	0
260-280	7.82	9.62	0
280-300	6.39	8.16	0
300-320	5.13	6.59	0
320-340	1.74	2.47	0

[a] Time period: for urine in hours, for bile and gastric fluid in minutes. [b] 20-min period collections gave 0.0 conc. [c] Only sulindac was found in the 100–120-min interval (1.55 μg/mL). [d] The gastric fluid levels of sulindac and its metabolites are due to the reflux of bile into the stomach.

tabolites, or indomethacin. Sulindac, sulindac sulfone, sulindac sulfide, and indomethacin were completely resolved (Figs. 2 and 3).

Acetonitrile deproteination of plasma (4) provided a method with acceptable reproducibility and linearity. Organic extraction techniques (*e.g.*, diethyl ether) consistently gave coefficients of variation of intraday replicates exceeding 10%.

Standard curves for I, II, and III in plasma were linear over the concentration range of 0.25–10.0 μg/mL; urine and bile gave linear curves over the range of 0.5–10 μg/mL; gastric fluid gave a linear curve over the range of 0.5–5 μg/mL (Table I). Concentrations at 0.1 μg/mL in plasma and in urine could be detected, but poor reproducibility restricted the low concentrations to 0.5 μg/mL. Linearity is lost at the higher concentrations (tested at 20 and 40 μg/mL) due to lower absorbance responses.

The *CV* measured for the plasma assay of the three components gave an average of 4.7 ± 2.7% over the linear concentration range. The urinary, bile, and gastric fluid assays gave average *CV* values of 6.04 ± 1.6%, 7.80 ± 2.5%, and 4.87 ± 1.24%. Representative *CV* are listed in Table II.

Recoveries of I, II, and III from plasma *via* acetonitrile protein precipitation are 39.9 ± 4.2%, 49.8 ± 6.7%, and 86.3 ± 3.7%, respectively. Similarly, representative recovery values for acetonitrile extraction (urine) are 58.2 ± 7.4%, 65.1 ± 9.9%, and 96.7 ± 6.9%. These values are means over three concentrations.

The hydrolysis of urine conjugates for total sulindac and its two metabolites by base catalysis were studied over time. Peak height values for sulindac and its metabolites reached a maximum in the first 15 min and began to decline

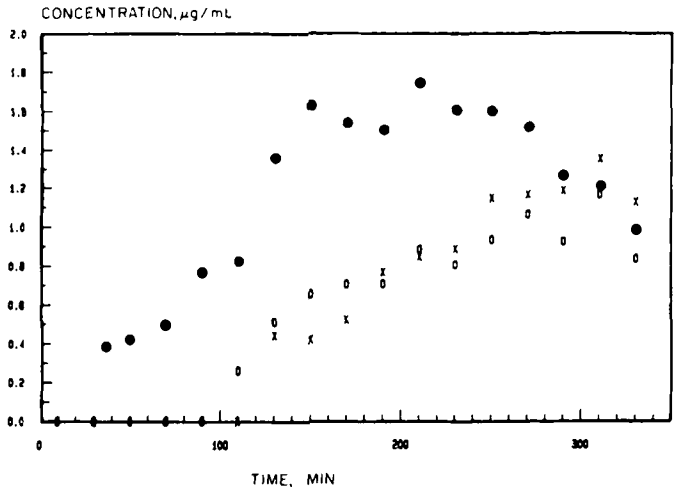

Figure 4—*Plasma levels of sulindac and its two metabolites in one subject administered a single 200-mg im injection of sulindac. Key: (●) sulindac; (○) sulindac sulfone; (X) sulindac sulfide.*

at 60 min. Reaction conditions were set with a 15-min incubation period at room temperature. Similar results were found for bile and gastric fluid.

Concentrations of sulindac and its metabolites in human plasma, urine, bile, and gastric fluid are represented in Fig. 4 and Table III. The data are of one subject who received a single intramuscular injection of sulindac (200 mg).

CONCLUSIONS

Gradient elution with acetonitrile and potassium phosphate buffer over a radially compressed, reverse stationary phase provides the necessary selectivity of the assay for quantitation of sulindac and its metabolites in plasma, urine, bile, and gastric fluid. The advantages of this gradient system over other available isocratic assays (5, 6) are: (*a*) a cleaner chromatogram for the plasma medium, (*b*) a shorter cleanup procedure for plasma and urine, and (*c*) a broader application of the assay to other biological fluids.

REFERENCES

(1) D. E. Duggan, K. F. Hooke, E. A. Risley, T. Y. Shen, and C. G. Van Arman, *J. Pharmacol. Exp. Ther.*, **201**, 8 (1977).

(2) K. C. Kwan, D. E. Duggan, G. G. Van Arman, and T. Y. Shen, *Eur. J. Rheumatol. Inflam.*, **1**, 9 (1978).

(3) L. E. Hare, C. A. Ditter, M. Hichens, A. Rosegay, and D. E. Duggan, *J. Pharm. Sci.*, **66**, 414 (1977).

(4) R. W. Walker, V. F. Gruber, A. Rosenberg, F. J. Wolf, and W. J. A. VandenHeuvel, *Anal. Biochem.*, **95**, 579 (1979).

(5) L. J. Dusci and L. P. Hackett, *J. Chromatogr.*, **171**, 490 (1979).

(6) B. N. Swanson and V. K. Boppana, *J. Chromatogr.*, **225**, 123 (1981).

(7) T. Y. Shen, H. Jones, and B. E. Witzel, U.S. Pat. 3,654,349.

(8) T. Y. Shen, T. B. Windholz, A. Rosegay, B. E. Witzel, A. N. Wilson, J. D. Willett, W. J. Holtz, R. L. Ellis, A. R. Matzack, S. Lucas, C. H. Stanner, F. W. Holly, L. H. Sarrett, E. A. Risley, G. W. Nuss, and C. A. Winter, *J. Am. Chem. Soc.*, **85**, 488 (1963).

(9) H. B. Hucker, S. C. Stauffer, S. D. White, R. E. Rhodes, B. H. Arison, E. R. Umbenhauer, R. J. Bower, and F. G. McMahon, *Drug Metab. Dispos.*, **1**, 721 (1973).

Physicochemical Model for Dose-Dependent Drug Absorption

J. B. DRESSMAN *x, D. FLEISHER *, and G. L. AMIDON *

Received July 11, 1983, from *INTERx, Merck Sharp & Dohme Research Laboratories, Lawrence, KS 66044*, and *The University of Kansas, Lawrence, KS 66045*. Accepted for publication October 5, 1983. *Present address: College of Pharmacy, University of Michigan, Ann Arbor, MI 48109.

Abstract □ A two-tank perfect-mixing tank model was used to simulate GI absorption. The effect of drug parameters (pK_a, solubility, and intrinsic wall permeability) and system parameters (pH profile, volume of intestinal contents, and intestinal flow rate) on drug absorption were studied by numerical data simulation. When the dose did not exceed the solubility of the drug in the intestinal lumen, the fraction absorbed depended on the transit rate relative to the absorption rate and the pK_a relative to the pH profile, but was independent of drug dose. Saturation of one or both tanks led to dose-dependent absorption. The model was used to simulate absorption of chlorothiazide. Good agreement between simulated and experimental data led to the conclusion that the physical characteristics of chlorothiazide, rather than a saturable transport mechanism at the intestinal wall, may be responsible for the dose-dependent absorption observed for this drug. The model was also used to simulate hydrochlorothiazide absorption. By applying the same system parameters used for chlorothiazide, the model simulation correctly predicted the dose proportionality of hydrochlorothiazide absorption. The lack of dose dependency in this case may be attributed to the higher solubility and pK_a of hydrochlorothiazide compared with chlorothiazide.

Keyphrases □ Absorption—GI dose-dependent, physicochemical model □ Chlorothiazide—physicochemical model, dose-dependent GI absorption □ Hydrochlorothiazide—physicochemical model, dose-independent GI absorption

Dose-dependent drug absorption is often attributed to absorption *via* a saturable (carrier-mediated) mechanism or to the existence of a so-called absorption window for the drug. In many cases, however, an alternative approach, which takes into account the physical and chemical factors of the drug and GI tract, provides a more reasonable explanation of the observed behavior. Shore *et al.* (1) were the first to recognize the importance of physical parameters to drug absorption in their classical pH-partition hypothesis of GI absorption. They postulated that the rate of absorption is fastest when the drug is in its un-ionized form, with the degree of ionization being a function of pH and, hence, location in the GI tract. Solubility and dissolution rate effects on absorption were studied by Stricker (2, 3) using mechanical *in vitro* systems to simulate absorption. Among his conclusions was the finding that variability in absorption of some sulfonamides could be attributed to their limited and pH-dependent solubilities.

Physiological parameters such as gastric emptying rate may also influence absorption. Clements *et al.* (4) have shown that for drugs, such as acetaminophen, which are poorly absorbed in the stomach, gastric emptying can be the rate-limiting step in absorption. If, in such a case, gastric emptying does not follow a monoexponential relationship, the apparent absorption rate will not be first order, even though the drug is absorbed by passive diffusion. In this report, it is demonstrated that the physicochemical properties of a drug, *i.e.*, its solubility, pK_a, and intrinsic absorption rate, can play a significant role in the determination of the relationship between the dose administered and the oral bioavailability. The drugs chosen as examples are chlorothiazide and hydrochlorothiazide. For chlorothiazide, the fraction absorbed orally is known to decrease substantially with increasing dose. By contrast, hydrochlorothiazide exhibits dose-proportional absorption (5–7).

THEORETICAL SECTION

A two-tank mixing tank model (Fig. 1) provides a simple but useful picture of intestinal absorption. Tank 1 represents the duodenum and, hence, has a smaller volume and lower pH than tank 2, which represents the jejunum and ileum. The following assumptions are incorporated into the model:

1. Absorption from the stomach is minor compared with intestinal absorption. The model could be extended to a three mixing-tank model to accommodate cases in which this assumption is invalid.
2. The drug dose is delivered to the duodenum as a bolus. Dissolution is considered to be instantaneous compared with other processes such as absorption and transit rate. The dissolution rate may, in fact, play an important role in determining the percentage absorbed; its effects will be examined in a future study.
3. Uptake by the intestinal wall is a first-order process which does not involve a saturable carrier mechanism.
4. Absorption of the ionized form is negligible compared with that of the un-ionized form.
5. Transit is a first-order process.

Depending on the drug and the dose administered, three general cases apply:

1. Neither tank becomes saturated after drug is administered.
2. One tank becomes saturated after drug is administered.
3. Both tanks become saturated after drug is administered.

The three cases are illustrated in Figs. 2, 3, and 4, respectively. The basic set of parameters used in the simulations is listed in the *Appendix;* deviations from these values are noted where appropriate in the figure legends. The following symbols are used: X_{Ti}, the amount of drug in tank i; V_i, volume of tank i; f_{ui}, fraction un-ionized in tank i; Q, flow or transit rate; k_{ai}, intrinsic absorption rate in tank i; X_0, dose administered; C_{si}, saturation concentration in tank i; X_{si}, $X_{si} = C_{si} \cdot V_i$; $R_i = X_{si}$, apparent absorption rate under saturated conditions in tank i; τ_1, time at which $X_{T1} = X_{s1}$; τ_{2A}, time at which $X_{T2} = X_{s2}$ (X_{T2} increasing); and τ_{2B}, time at which $X_{T2} = X_{s2}$ (X_{T2} decreasing).

Case 1—In this case, X_{T1}/V_1 and X_{T2}/V_2 are always less than the saturation concentrations. Loss from tank 1 is given by:

$$-\frac{\partial X_{T1}}{\partial t} = (k_{a1}f_{u1} + Q_1/V_1)X_{T1} \qquad \text{(Eq. 1)}$$

whereas loss from tank 2 is given by:

$$-\frac{\partial X_{T2}}{\partial t} = (Q_2/V_2 + k_{a2}f_{u2})X_{T2} - Q_1X_{T1}/V_1 \qquad \text{(Eq. 2)}$$

Transit out of tank 2 represents drug which is not absorbed, *i.e.*:

$$\frac{\partial X_{t\text{-OUT}}}{\partial t} = Q_2X_{T2}/V_2 \qquad \text{(Eq. 3)}$$

These equations can be solved by using Laplace transforms to yield (for $X_{T1} = X_0$ at $t = 0$):

$$X_{T1} = X_0e^{-At} \qquad \text{(Eq. 4)}$$

$$X_{T2} = \frac{Q_1X_0}{V_1(B-A)}(e^{-At} - e^{-Bt}) \qquad \text{(Eq. 5)}$$

$$X_{t\text{-OUT}} = \frac{Q_2Q_1X_0}{V_2V_1B}\left(\frac{1}{A} + \frac{e^{-Bt}}{B-A} - \frac{Be^{-At}}{A(B-A)}\right) \qquad \text{(Eq. 6)}$$

where $A = k_{a1}f_{u1} + Q_1/V_1$ and $B = k_{a2}f_{u2} + Q_2/V_2$. The fraction of dose absorbed is then given by:

$$F = 1 - \frac{X^{\infty}_{t\text{-OUT}}}{X_0} = 1 - \frac{Q_2Q_1}{V_1V_2(k_{a1}f_{u1} + Q_1/V_1)(k_{a2}f_{u2} + Q_2/V_2)} \qquad \text{(Eq. 7)}$$

This result shows that the fraction absorbed depends on transit rate, intrinsic absorption rate of the un-ionized form, pK_a of the drug, and gastrointestinal pH profile. Variations in transit rate and gastrointestinal pH profile can affect the fraction absorbed in this case, but bioavailability is not dependent on the dose of the drug *per se*.

0022-3549/84/0900-1274$01.00/0
© 1984, American Pharmaceutical Association

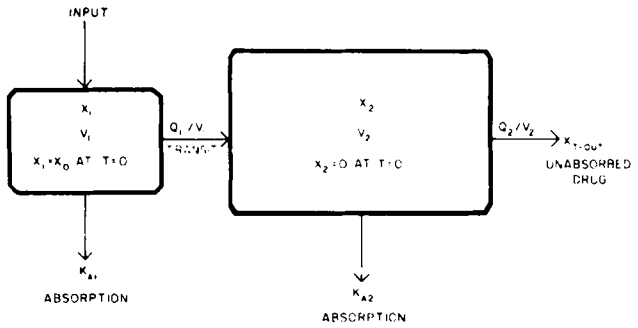

Figure 1—*Schematic of the two-tank perfect mixing tank model for oral drug absorption.*

Case 2—An example of the case in which one of the tanks becomes saturated occurs when the drug initially saturates tank 1 but levels in tank 2 never reach saturation, *e.g.*, absorption of a poorly soluble weak acid. In this case, it is convenient to split the derivation into two parts: (*a*) from $t = 0$ to $t = \tau_1$, the time at which concentration in tank 1 drops back below saturation, and (*b*) at times longer than τ_1. The second part is essentially described by the equations derived for case 1 by applying the appropriate boundary condition, *i.e.*, $X_{T1}/V_1 = C_s$ at $t = \tau_1$.

Equations for times shorter than τ_1 are:

$$-\frac{\partial X_{T1}}{\partial t} = R_1 + Q_1 X_{T1}/V_1 \qquad \text{(for tank 1)} \qquad \text{(Eq. 8)}$$

$$-\frac{\partial X_{T2}}{\partial t} = -Q_1 X_{T1}/V_1 + (k_{a2} f_{u2} + Q_2/V_2) X_{T2} \text{ (for tank 2)} \qquad \text{(Eq. 9)}$$

$$\frac{\partial X_{t\text{-OUT}}}{\partial t} = Q_2 X_{T2}/V_2 \qquad \text{(for unabsorbed drug)} \qquad \text{(Eq. 10)}$$

Solution of these equations by using Laplace transforms yields:

$$X_{T1} = -\frac{R_1 V_1}{Q_1} + e^{-Q_1 t/V_1}\left(X_0 + \frac{R_1 V_1}{Q_1}\right) \qquad \text{(Eq. 11)}$$

$$X_{T2} = -\frac{R_1}{B} - e^{-Q_1 t/V_1}\left(\frac{R_1 + Q_1 X_0/V_1}{Q_1/V_1 - B}\right) + e^{-Bt}\left(\frac{R_1 + BX_0}{B(Q_1/V_1 - B)}\right)\frac{Q_1}{V_1} \qquad \text{(Eq. 12)}$$

$$X_{t\text{-OUT}} = \frac{-Q_2 R_1 t}{BV_2} + (1 - e^{-Bt})\frac{Q_2}{V_2 B}\left[\frac{Q_1}{V_1 B}\frac{(R_1 + BX_0)}{(Q_1/V_1 - B)}\right] + (e^{-Q_1 t/V_1} - 1)\frac{Q_2 V_1}{V_2 Q_1}\left[\frac{R_1 + Q_1 X_0/V_1}{Q_1/V_1 - B}\right] \qquad \text{(Eq. 13)}$$

$$\tau_1 = \frac{-2.303 V_1}{Q_1}\log\left[\frac{Q_1 X_{s1}/V_1 + R_1}{Q_1 X_0/V_1 + R_1}\right] \qquad \text{(Eq. 14)}$$

The fraction of the dose absorbed can be determined by calculating τ_1 and then evaluating $X^{0\to\tau_1}_{t\text{-OUT}}$ by using Eq. 13 for $t = 0 \to \tau$ and Eq. 3 for $t = \tau_{1\to\infty}$ (solved with initial conditions $X_{T2} = X^{\tau_1}_{T2}$ and $X_{t\text{-OUT}} = X^{\tau_1}_{t\text{-OUT}}$ at $t = \tau_1$, the values of which are found from Eqs. 12 and 13, respectively); that is:

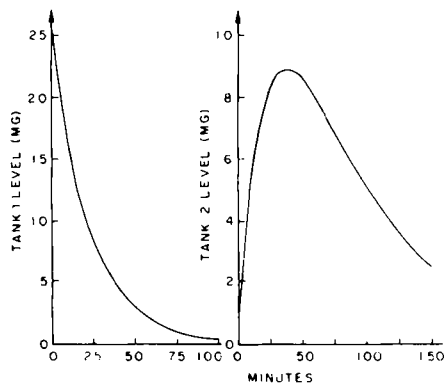

Figure 2—*Theoretical levels of drug in tanks 1 and 2 with time after administration of a dose lower than the saturation level in either tank. Case 1 equations apply throughout; the dosage is 25 mg.*

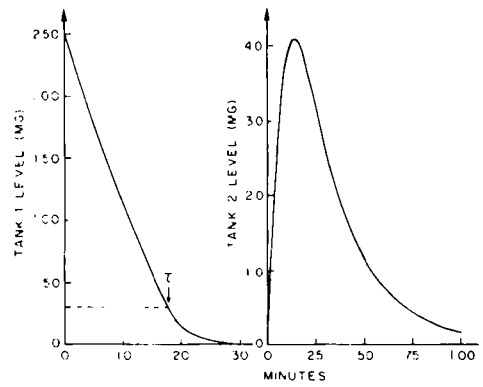

Figure 3—*Theoretical levels of drug in tanks 1 and 2 with time after administration of a dose which exceeds the saturation level in tank 1 only (τ_1 = 17.4 min). The intrinsic absorption rate constant is 0.3 min^{-1} for this simulation; the dosage is 250 mg. Case 2 equations apply from* t = 0 *to* t = τ_1.

$$X^{\tau_1\to\infty}_{t\text{-OUT}} = \frac{Q_2 X^{\tau_1}_{T2}}{V_2 B} + \frac{Q_1 X_0 Q_2}{V_1 V_2}\left(\frac{1}{AB}\right) \qquad \text{(Eq. 15)}$$

Then, the fraction absorbed is given by:

$$F_{abs} = 1 - \left(\frac{X^{0\to\tau_1}_{t\text{-OUT}} + X^{\tau_1\to\infty}_{t\text{-OUT}}}{X_0}\right) \qquad \text{(Eq. 16)}$$

Since the term for $X^{0\to\tau_1}_{t\text{-OUT}}$ is a function of the dose administered in addition to the factors listed under case 1, it appears that drugs which exceed their saturation solubilities in the GI tract will exhibit dose-dependent bioavailability. As expected, Eq. 13 indicates that as the dose increases, the fraction absorbed decreases.

Case 3—In this case, both tanks achieve levels greater than saturation. Assuming that tank 1 starts out above saturation, the times during which tank 2 becomes saturated ($\tau_{2A} \to \tau_{2B}$) may or may not overlap the time, τ_1, at which tank 1 falls below solubility, as this will depend on the flow rate relative to the absorption rate, solubility at the tank pH values, and the differences in tank volumes.

Differential equations governing drug levels when both tanks are saturated are:

$$-\frac{\partial X_{T1}}{\partial t} = R_1 + Q_1 X_{T1}/V_1 \qquad \text{(Eq. 17)}$$

$$-\frac{\partial X_{T2}}{\partial t} = R_2 + Q_2 X_{T2}/V_2 - Q_1 X_{T1}/V_1 \qquad \text{(Eq. 18)}$$

$$\frac{\partial X_{t\text{-OUT}}}{\partial t} = Q_2 X_{T2}/V_2 \qquad \text{(Eq. 19)}$$

By using the example in which $\tau_{2A} < \tau_{2B} < \tau_1$, the explicit solutions are as follows when $\tau_{2A} < t < \tau_{2B}$:

$$X_{T1} = [\mu(\tau_{2B}) - \mu(\tau_{2A})]\left\{-\frac{R_1 V_1}{Q_1} + e^{-Q_1(t-\tau_{2A})/V_1} \times \left[X_{T1}(\tau_{2A}) + \frac{R_1/V_1}{Q_1}\right]\right\} \qquad \text{(Eq. 20)}$$

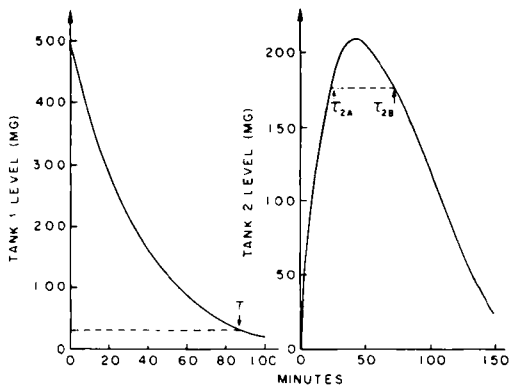

Figure 4—*Theoretical levels of drug in tanks 1 and 2 with time after administration of a dose which exceeds the saturation level in both tanks (τ_{2A} = 23, τ_{2B} = 71, τ_1 = 87 min). Case 3 equations apply from* t = τ_{2A} *to* t = τ_{2B}. *For this simulation, the dosage is 500 mg; pH_2 = 7.0.*

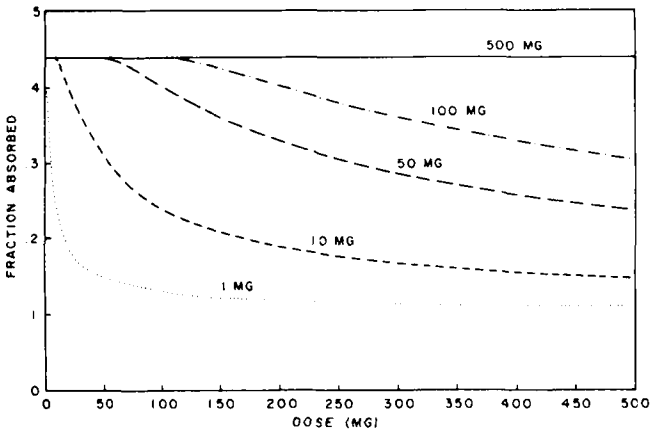

Figure 5—*Effect of solubility on the fraction of dose absorbed. Solubilities are expressed as the amount of drug required to saturate tank 1.*

$$X_{T2} = [\mu(\tau_{2B}) - \mu(\tau_{2A})]\left\{\frac{-(R_2 + R_1)V_2}{Q_2} + e^{-Q_1(t-\tau_{2A})/V_1} \times \left[\frac{Q_1 X_{T1}(\tau_{2A})/V_1 + R_1}{Q_2/V_2 - Q_1/V_1}\right] + e^{-Q_2(t-\tau_{2A})/V_2} \times \left[X_{s2} - \frac{Q_1 X_{T1}(\tau_{2A})/V_1}{Q_2/V_2 - Q_1/V_1} - \frac{Q_1 R_1/V_1}{Q_2/V_2(Q_2/V_2 - Q_1/V_1)} + \frac{R_2 V_2}{Q_2}\right]\right\} \quad \text{(Eq. 21)}$$

$$X_{t\text{-OUT}} = [\mu(\tau_{2B}) - \mu(\tau_{2A})]\left\{-(R_1 + R_2)(t - \tau_{2A}) - \frac{Q_2 V_1}{V_2 Q_1}\left[\frac{R_1 + Q_1 X_{T1}(\tau_{2A})/V_1}{Q_2/V_2 - Q_1/V_1}\right][e^{-Q_1(t-\tau_{2A})/V_1} - 1] + [1 - e^{-Q_2(t-\tau_{2A})/V_2}]\left[X_{s2} - \frac{Q_1 X_{T1}(\tau_{2A})/V_1}{Q_1/V_1 - Q_2/V_2} - \frac{Q_1 R_1/V_1}{Q_2/V_2(Q_2/V_2 - Q_1/V_1)} + \frac{R_2 V_2}{Q_2}\right]\right\} \quad \text{(Eq. 22)}$$

where $[\mu(\tau_{2B}) - \mu(\tau_{2A})] = 0$ at $t < \tau_{2A}$, $t > \tau_{2B}$ and 1 for $\tau_{2A} < t < \tau_{2B}$. In this instance, τ_{2A} is found by substituting X_{s2} for X_{T2} in Eq. 12 and solving for t. Similarly, τ_{2B} is found by substituting X_{s2} for X_{T2} in Eq. 21. At times $\tau_{2B} < t < \tau_1$, case 2 differential equations apply, and at $t > \tau_1$, the system reverts to case 1. A second possible order for τ_1, τ_{2A}, and τ_{2B} would be $\tau_{2A} < t_1 < \tau_{2B}$. The analogous set of equations for this order of τ values may be found by applying appropriate initial conditions.

A BASIC program incorporating initial value problem conditions for all possible orders of τ_1, τ_{2A}, and τ_{2B} and a zero-finding routine to determine the τ values was used to numerically evaluate the concentration–time profile and fraction absorbed for any given circumstance (see *Appendix*).

RESULTS AND DISCUSSION

Data were simulated under various conditions for the fraction absorbed *versus* dose plots. To cover the usual dosage range for most drugs, doses of 0–500 mg were studied. Parameters were initially chosen to simulate absorption for a poorly absorbed, weakly acidic drug. The effect of changing each drug and system parameter was then investigated. A discussion of initial parameter choices may be found in the *Appendix*.

Drug-Related Parameters—*Solubility*—Figure 5 depicts the influence of drug solubility on the fraction absorbed. For this simulation, solubility refers to the level required to saturate tank 1. For weak acids, tank 1 is saturated at lower levels than tank 2, in which the pH is higher and the volume is larger. Figure 5 shows that the solubility has a very pronounced effect on the relationship between the fraction absorbed and the dose administered. At very high solubility, the fraction absorbed is independent of dose since neither tank becomes saturated. In this case, the fraction absorbed depends on pK_a, pH profile, relative absorption, and transit rates but not on dose, since case 1 applies. When the dose exceeds the solubility, case 2 equations apply, and the fraction absorbed varies with dose. The form of the function varies with the drug solubility. The sharpest decrease in the fraction absorbed occurs at doses slightly above the solubility. At doses well above the solubility, the fraction absorbed is low and varies little with dose. Therefore, the dose dependency of absorption depends on the dosage range administered in relation to the solubility. If the doses given are near the solubility, marked dependency of the fraction absorbed on the dose may occur, but if the doses given exceed the solubility by a large amount, absorption will be poor and vary little with dose.

Drug pK_a—Variation in drug pK_a also causes a large effect on fraction absorbed as a function of dose (Fig. 6). Absorption of weakly acidic drugs with pK_a values ranging from 3.5 to 10.0 was simulated. Simulations indicate that drugs with low pK_a values (3.5 or 4.5) combined with poor intrinsic absorption rates would exhibit very poor absorption from the small intestine, with little dependency on dose. Even though the high pH relative to the drug pK_a ensures adequate solubility, the fraction un-ionized is very low, and so little absorption occurs during the drug residence time. The high solubility in both tanks results in case 1 conditions at all doses studied, which means that the percentage absorbed is independent of dose. Simulations for weaker acids indicate that absorption would be dose dependent in these cases. The fraction absorbed increases with increasing pK_a because the fraction of drug available for absorption, *i.e.*, in the un-ionized form, increases. When the pK_a of the drug is similar to or above the simulated intestinal pH, a high dose relative to the drug intrinsic solubility results in saturation in both tanks and, hence, case 3 equations apply. This occurs for $pK_a = 7.9$ at doses of >275 mg and for $pK_a = 10$ at doses of >225 mg under the conditions chosen (Fig. 6). When both tanks become saturated, the fraction absorbed decreases more rapidly with increasing dose than when only tank 1 is saturated. This is due to the further decrease in fraction available for absorption when both tanks are saturated. Overall, the drug pK_a affects both the form of the fraction absorbed *versus* dose function and the percentage of drug absorbed.

Intrinsic Absorption Rate Relative to Flow Rate—Figure 7 shows the impact of changing the ability of the drug to penetrate the membrane relative to the residence time of the drug in the system. The ratio of flow rate to intrinsic absorption rate was varied from 1:1 to 500:1. The absorption rates were chosen to represent a large spectrum of intestinal wall permeabilities. The flow rate was varied from 2 mL/min, which represents an approximate minimum flow in the human jejunum after a meal (8), up to 10 mL/min [maximum flow rate observed in dogs and sheep is ~6 mL/min (9)], thus covering the usual range of physiological values. When the absorption rate is on the same order as the flow rate, the fraction of dose absorbed is very high and virtually in-

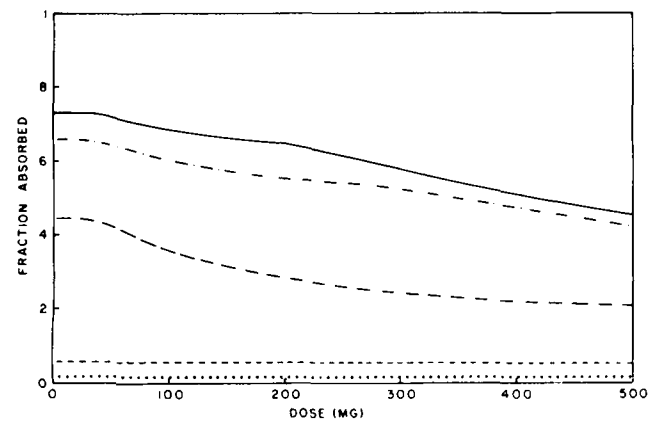

Figure 6—*Effect of drug* pK_a *on fraction of dose absorbed. Key to* pK_a *values: (• • •) 3.5; (– – –) 4.5; (— —) 6.7; (• — •) 7.9; (—) 10.0.*

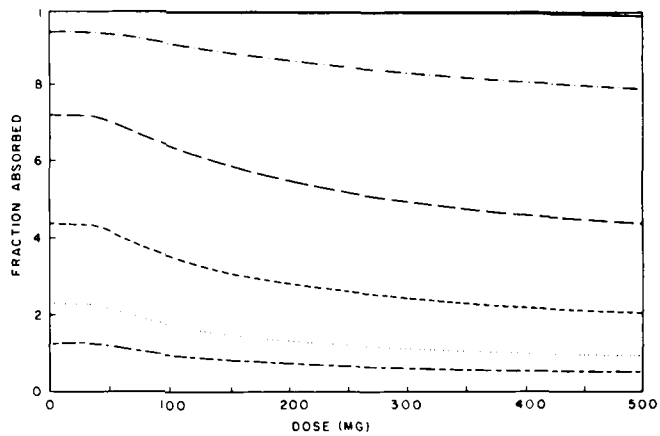

Figure 7—*Effect of absorption and transit rate on the fraction of dose absorbed. Key: (• — •)* $Q = 2$ *mL/min,* $k_a = 2$ *min*$^{-1}$*; (— —)* $Q = 2$ *mL/min,* $k_a = 0.2$ *min*$^{-1}$*; (– – –)* $Q = 2$ *mL/min,* $k_a = 0.017$ *min*$^{-1}$*; (• • •)* $Q = 5$ *mL/min,* $k_a = 0.017$ *min*$^{-1}$*; (– — –)* $Q = 10$ *mL/min,* $k_a = 0.017$ *min*$^{-1}$.

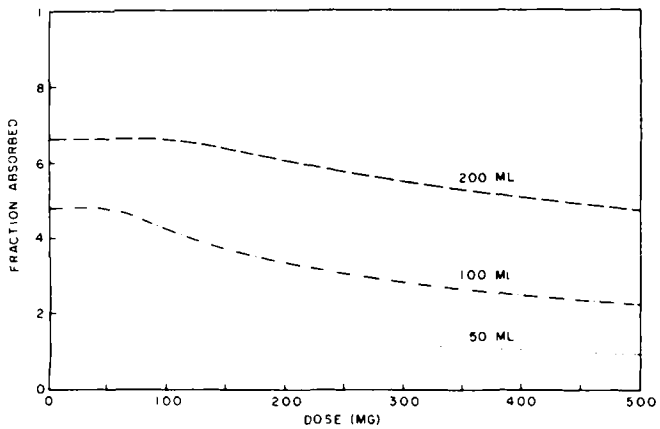

Figure 8— *Effect of tank volumes on fraction of dose absorbed. Equal volumes were used in the three simulations.*

dependent of dose. However, when the flow rate is large compared with the absorption rate, absorption is much poorer and more dose dependent. At very high flow rates, the residence time of the drug in the system is too short for extensive drug absorption. In this case, the percentage of dose absorbed is low at all doses and less dose dependency occurs. The major effect of changing the intrinsic absorption rate relative to the flow rate appears to be a shift in the fraction absorbed *versus* dose relationship. At extreme values, the form of the relationship is also affected.

System Parameters—*Tank Volumes*—Figure 8 shows the effect of increasing tank volumes on the fraction absorbed *versus* dose relationship. Equal tank volumes were used, ranging from 50 to 200 mL per tank. Increasing the tank volume has two effects. First, the level of drug required to saturate the tank increases. This changes to some degree the range of doses over which dose-dependent absorption occurs. Second, the drug residence time increases, so the drug is available for absorption for a longer period. This causes an upward shift in the fraction absorbed. The combined effect is that increasing the tank volume increases the fraction absorbed and decreases the dependency of absorption on dose. In the analogous *in vivo* situation, ingestion of a large volume of fluid with a poorly absorbed drug may improve the degree of absorption. However, the effect may be attenuated if there is a concomitant increase in flow rate in the intestine.

The effect of changing the relative tank volumes is shown in Fig. 9. Tank volume ratios were varied from 1:1 to 1:10. Although the jejunum is much longer than the duodenum, substantial water reabsorption occurs throughout the upper intestine. Therefore, the relative volume in the duodenum compared with the jejunum is not as low as would be suggested from a purely geometrical calculation. The volume ratios studied reflect these considerations. From the simulations, an increase in the tank volume ratio causes a small vertical shift in the fraction absorbed but has little effect on the shape of the curve. The shift is due to the increase in residence time with increasing total volume. The simulations shown in Fig. 9 all fell in the case 2 category, *i.e.*, only the first tank was saturated. Since the tank 1 volume was held constant, the lack of change in the degree of dose dependency with volume ratio change is reasonable. Overall, changing the relative tank volumes appears to have little

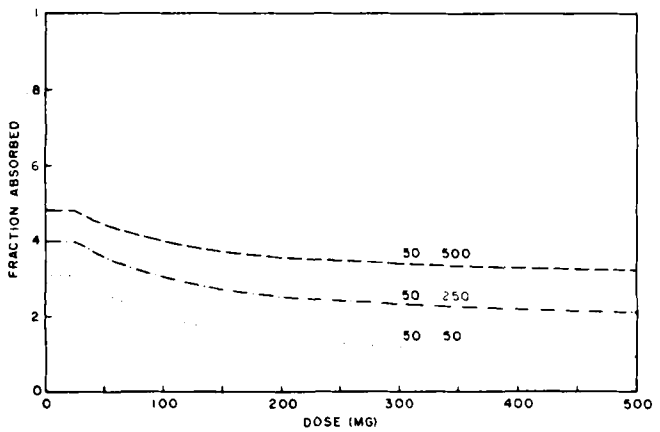

Figure 9— *Effect of relative tank volumes on the fraction of dose absorbed. The ratio is shown as tank 1:tank 2.*

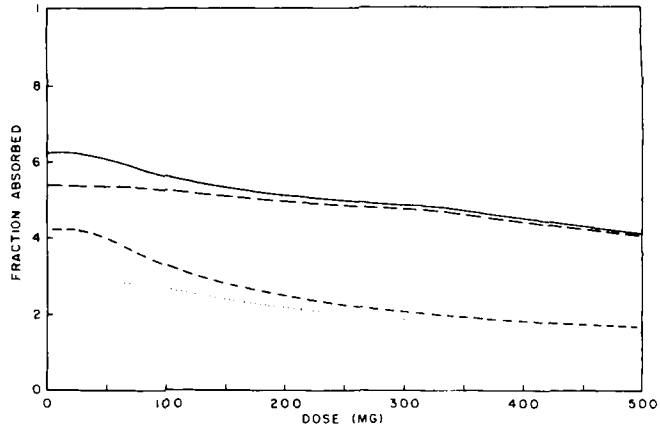

Figure 10—*Effect of pH profile on fraction of dose absorbed. Key: (—) pH_1 = 5.0, pH_2 = 6.7; (— —) pH_1 = 6.7, pH_2 = 6.7; (- - -) pH_1 = 5.0, pH_2 = 8.0; (· · ·) pH_1 = 6.7, pH_2 = 8.0.*

effect on the dose dependency of absorption over a reasonable range of volume ratios.

pH Profile—Simulations of drug absorption with several pH profiles are shown in Fig. 10. These represent the range of pH profiles one might reasonably expect to encounter in a normal patient population: low pH (5.0-6.7), high pH (6.7-8.0), flat pH profile (6.7), and sharp pH profile (5.0, 8.0) were simulated at a fixed drug pK_a of 6.7. The pH in tank 1 is the dominant factor in the determination of the shape of the fraction absorbed *versus* dose relationship. Within 2 units of the pK_a, the lower the tank 1 pH relative to the pK_a, the greater the fraction absorbed. This results from the higher fraction in the un-ionized, absorbable form when the pH is below the pK_a. The effect is only significant at doses in the vicinity of the solubility in tank 1 and below, since at high doses the solubility rather than the fraction un-ionized becomes the absorption-limiting factor. The pH in the second tank appears to determine the fraction absorbed. When the pH in tank 2 is similar to the pK_a, solubility may be low enough to cause case 3 behavior. When the pH in tank 2 is above the pK_a, solubility is higher due to ionization, and case 2 conditions will be operative.

From these simulations it appears that day-to-day and patient-to-patient variation in intestinal pH profile can play a significant role in the determination of the extent of absorption for incompletely absorbed drugs. This explains in part the observation that drugs which are poorly absorbed often exhibit variable absorption.

Model Assumptions—The assumptions made in the mixing tank model affect the simulations of the fraction absorbed *versus* dose. For instance, it is assumed that there is bolus delivery to the duodenum and that dissolution is instantaneous in both tanks while the concentration is below saturation. This provides a rather crude approximation of the input and dissolution functions which occur after oral drug administration. Passage of monolithic dosage forms out of the stomach intact would be an example of bolus input, but in most cases, the dosage form breaks up in the stomach so that delivery to the duodenum occurs over an interval of at least several minutes. The dissolution rate may be slow even for dosage forms designed for immediate drug release and particularly so for drugs with low solubility in intestinal fluids. If the dissolution rate is slow compared with the transit rate, absorption will be poorer than predicted by the mixing tank model analysis.

There are three assumptions which pertain to the absorption characteristics of the drug. First, absorption is negligible in the stomach as compared with the small intestine. It has been shown experimentally that for weak acids, such as sulfonamides and barbiturates which would be expected to be relatively well absorbed from the stomach (from pH-partition considerations), absorption occurs 5–10 times faster in the small intestine (10). Second, drug absorption occurs principally in the un-ionized rather than the ionized form. This is the basis of the pH-partition hypothesis (1). Both of these assumptions tend to underestimate the fraction absorbed, since absorption in the stomach or absorption of ionized drug would add to the overall extent of absorption. The third assumption with respect to drug absorption is that the drug is absorbed by a first-order process. First-order absorption applies to a broad range of drugs and is a reasonable assumption in the absence of specific data indicating that a saturable mechanism is in effect.

System assumptions pertain to the selection of values for the pH profile, the volume in the intestine, and the flow rate. The pH profile is constrained by the range of values which occurs physiologically. The volume and flow rate are interrelated. The flow rate in the intestine changes with ingestion of food and fluids, due to changes in gut motility and reabsorption of water. The as-

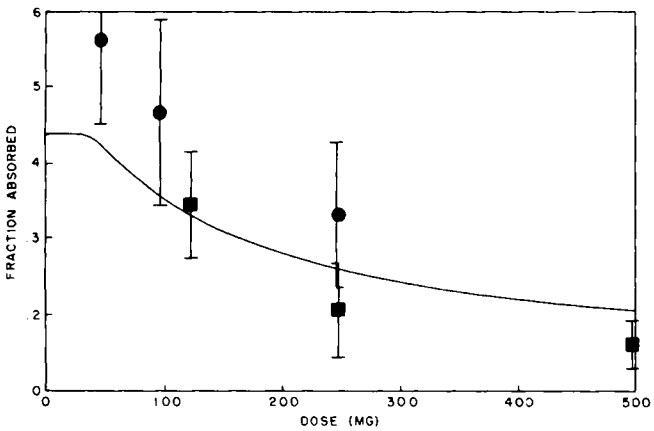

Figure 11—*Fraction absorbed* versus *dose simulated for chlorothiazide absorption. Data are taken from Refs. 5 (●) and 6 (■). Error bars indicate standard deviations. The solid line is the simulated data, using parameter values listed in the* Appendix.

sumption that the flow rate is constant throughout the small intestine therefore represents a simplified view of intestinal transit.

Simulation of Chlorothiazide Oral Absorption -Figure 11 shows a simulation for oral absorption of chlorothiazide. The selection of parameters used in this simulation is discussed in the *Appendix*. The experimental data were taken from two studies by Welling *et al.* (5, 6) in which solutions of chlorothiazide (prepared with the salt) were administered orally at different dosages. In the first study, doses of 50, 100, and 250 mg were administered. In the second study, the doses were 125, 250, and 500 mg. Although the relationship between the fraction absorbed and dose followed the same form in both studies, the actual extent of absorption seemed to be lower overall in the high-dose-range study, even when the same dosage was administered. The apparent displacement of the results of the second study from those of the first study may partly be explained by a difference in volume and transit rate in the two studies since the fluid intake protocol was not identical in both cases. Meyer and Straughn (11) and Welling and Barbhaiya (12) have shown that increasing the transit time of chlorothiazide in the GI tract, *via* concomitant administration of corn oil emulsion or a meal, resulted in substantial improvement in chlorothiazide bioavailability. A modest increase in fluid intake (12) had only a small effect, however, suggesting that volume/transit rate effects cannot explain all of the difference between the two studies. Comparison of both sets of data with the simulation curve indicates that the form of the fraction absorbed *versus* dose relationship is well described by the mixing tank model. Therefore, the dose-dependent absorption of chlorothiazide may be attributable to solubility ionization-permeability effects rather than a saturable transport mechanism in the intestinal wall. In particular, dose dependency of chlorothiazide may be attributable to limited solubility. Additionally, inspection of the pK_a simulation (Fig. 6) suggests that the low ionization constant is a major limitation to the extent of absorption.

Simulation of Hydrochlorothiazide Absorption—Figure 12 shows a simulation for oral absorption of hydrochlorothiazide. System parameters used

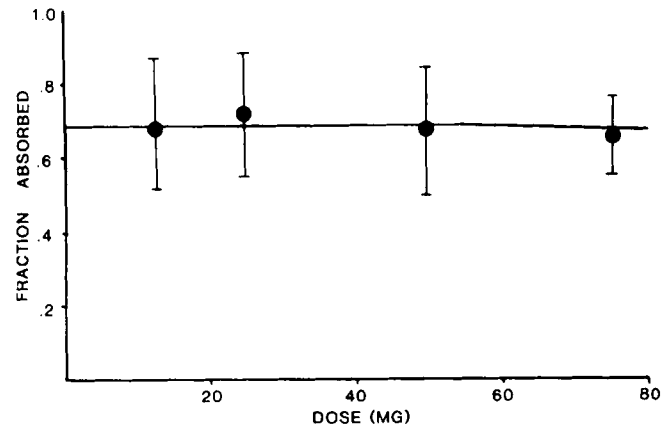

Figure 12—*Fraction absorbed* versus *dose simulated for hydrochlorothiazide absorption. Data are taken from Ref. 12. Error bars indicate standard deviations. The solid line is the simulated data, using parameter values listed in the* Discussion *and the* Appendix.

for chlorothiazide were kept the same for hydrochlorothiazide. The drug parameters were changed to literature values of intrinsic solubility (609 mg/L) (13) and pK_a (8.8) (13) and a lower estimate of the absorption rate constant (0.015 min^{-1}) to reflect the higher polarity of hydrochlorothiazide. The experimental data were taken from a study of eight subjects by Beerman and Groschinsky-Grind (14). Doses of 12.5, 25, 50, and 75 mg were administered orally. Urinary excretion data indicated that absorption was dose proportional, ~68% of the amount administered at each dose. Simulation of the dose-fraction absorbed relationship using the model correctly predicted the dose proportionality of hydrochlorothiazide absorption.

The difference in absorption behavior of hydrochlorothiazide from that of chlorothiazide is partly attributable to its higher solubility-dose ratio and partly due to the higher pK_a. Hydrochlorothiazide is in the un-ionized, absorbable form to at least a 90% extent in both the duodenum and the jejunum, whereas chlorothiazide is mainly in the ionized form at jejunal pH. These factors lead to the higher efficiency of absorption of hydrochlorothiazide that is observed clinically.

APPENDIX: Numerical Analysis and Parameter Value Selection

Although the initial value problems for cases 1 and 2 are analytically solvable with respect to their individual concentration-time profiles, the determination of τ_{2A} and τ_{2B} in case 3 is most conveniently achieved by using a zero-finding routine. In a given trial, the particular case followed depends on the values of the parameters such as solubility, dose, pK_a, flow rate, and intrinsic absorption rate of the drug. Also, case switching may occur with time as levels exceed or fall below saturation in the tanks. To accomodate all possibilities, a BASIC program was written that incorporated the three cases and allowed for case switching at τ_1, τ_{2A}, and τ_{2B}. Appropriate initial conditions were set for each case, depending on the order of τ_1, τ_{2A}, and τ_{2B}. It was thereby possible to examine the effects on the concentration-time profile and fraction absorbed for a wide variety of parameter values.

System parameters	V_i	volume of tank i
	pH_i	pH of tank i
	Q_i	flow rate from tank i
Derived system parameters	KT	Q_1/V_1
	KE	Q_2/V_2
Drug parameters	pK_a	
	solubility (intrinsic)	
Derived drug parameters	k_{ai}	intrinsic absorption rate constant in tank i
	C_{si}	total drug solubility in tank i
	f_{ui}	fraction un-ionized in tank i
Drug variable	X_0	dose
Independent variable	t	time
Dependent variables	X_i	amount in tank i at time t
	$X_{t\text{-OUT}}$	amount existing unabsorbed at time t
Derived variables dictating initial value problem switching	τ_1	time when X_1/V_1 falls below C_{s1}
	τ_{2A}	time when X_2/V_2 first exceeds C_{s2}
	τ_{2B}	time when X_2/V_2 falls below C_{s2}
Derived system/drug parameters	$R_i = k_{ai}f_{ui}C_{si}$	

The HP BASIC programs written for an HP 87 system are available on request from the authors. For the simulation of the chlorothiazide dose-dependent absorption, pH, and volumes in the two mixing tanks were chosen to simulate duodenum and jejunum: $pH_1 = 5.5$, $V_1 = 75$ mL; $pH_2 = 7.7$, $V_2 = 150$ mL. This flow rate was 2 mL/min, which is representative of physiological conditions (8). The pK_a [6.7 (15)], solubility [0.4 g/L at pH 4, 0.65 g/L at pH 7 (16)], and the usual range of doses [50 500 mg (5, 6)] were taken from the literature. The intrinsic absorption rate constant (0.017 min^{-1}) was estimated on the basis of the effective permeability and the surface area to volume ratio, *i.e.*, $k_{ai} = (SA_i/V_i)\cdot P_{eff}$, where $1/P_{eff} = (1/P_{aq}) + (1/P_w)$. Effective permeability is considered to be a function of the drug and independent of the segment of small intestine under consideration. For chlorothiazide, P_{eff} was estimated to be 7×10^{-5} cm/min. The ratio of surface area available for absorption to volume was estimated to be 250, a value between the value calculated on a geometric basis using a filled cylinder model and the value calculated by dividing the estimated total intestinal surface area (including villi surface area) by the cylinder model volume.

These parameter values were also used as a basis for simulations of levels in tanks 1 and 2 in the *Theoretical Section* and for the fraction absorbed *versus*

dose curves in the *Results*. Where other values were used, they are noted in the appropriate figure legends. In the *Results*, values of important drug and system parameters were varied systematically to ascertain their effects on the dose dependency of absorption.

REFERENCES

(1) P. A. Shore, B. B. Brodie, and C. A. M. Hogben, *J. Pharmacol. Exp. Ther.*, **119**, 361 (1957).

(2) H. Stricker, *Drugs Made Ger.*, **13**, 35 (1970).

(3) H. Stricker, *Drugs Made Ger.*, **14**, 93 (1971).

(4) J. A. Clements, R. C. Heading, W. S. Nimmo, and L. F. Prescott, *Clin. Pharmacol. Ther.*, **24**, 420 (1978).

(5) M. A. Osman, R. B. Patel, D. S. Irwin, W. A. Craig, and P. G. Welling, *Biopharm. Drug. Dispos.*, **3**, 89 (1982).

(6) P. G. Welling, R. H. Barbhaiya, R. B. Patel, T. S. Foster, V. P. Shah, J. P. Hunt, and V. K. Prasad, *Curr. Ther. Res.*, **31**, 379 (1982).

(7) J. E. Baer, H. L. Leidy, A. V. Brooks, and K. H. Beyer, *J. Pharmacol. Exp. Ther.*, **125**, 295 (1959).

(8) H. Davenport, in "Physiology of the Digestive Tract," 4th ed., Yearbook Medical Publishers, Chicago, Ill., 1980, p. 63.

(9) L. Bueno, J. Fioramonti, and Y. Ruckebusch, *J. Physiol.*, **249**, 69 (1975).

(10) W. G. Crouthemal, G. H. Tan, L. W. Dittert, and J. T. Doluisio, *J. Pharm. Sci.*, **60**, 1160 (1971).

(11) M. C. Meyer and A. B. Straughn, *Curr. Ther. Res.* **22**, 573 (1977).

(12) P. G. Welling and R. H. Barbhaiya, *J. Pharm. Sci.*, **71**, 32 (1982).

(13) H. P. Deppeler, in "Analytical Profiles of Drug Substances," Vol. 10, K. Florey, Ed., Academic, New York, N.Y., 1981, p. 405.

(14) B. Beerman and M. Groschinsky-Grind, *Eur. J. Clin. Pharmacol.*, **12**, 297 (1977).

(15) "Martindale: The Extra Pharmacopoeia," 27th ed., A. Wade, Ed., The Pharmaceutical Press, London, 1978, p. xxvii.

(16) "The Merck Index" 9th ed., M. Windholz, Ed., Merck and Co., Rahway, N.J., 1976, p. 277.

Microcalorimetric Investigation of the Binding of Some Chemotherapeutic Agents and Related Molecules to Calf Thymus DNA

WILLIAM R. VINCENT *, LEONARD S. ROSENBERG, and STEPHEN G. SCHULMAN ˣ

Received May 24, 1982, from the *College of Pharmacy, University of Florida, Gainesville, FL 32601.* Accepted for publication January 10, 1983.

*Present address: Arnold & Marie Schwartz College of Pharmacy and Health Science, Long Island University, Brooklyn, NY 11201.

Abstract □ Batch microcalorimetry was used to estimate directly the standard enthalpies of the binding of small molecules to DNA. These values were compared with those obtained from spectrophotometric binding constants and van't Hoff plots. The close agreement between the independently obtained enthalpies indicates that the appropriate (best) binding model has four phosphates per binding site. Thermodynamic binding constants were obtained from apparent binding constants measured at different ionic strengths. From these and the measured standard enthalpies, standard free energies and standard entropies of binding were calculated. The weak, presumably external, binding alleged to occur at high formal molar concentration ratios of ligand to DNA bases could not be detected by a measurable heat of binding.

Keyphrases □ Microcalorimetry—binding of chemotherapeutic agents and related molecules to calf thymus DNA □ Binding—chemotherapeutic agents and related molecules to calf thymus DNA, microcalorimetry □ DNA—microcalorimetry, binding of some chemotherapeutic agents and related molecules to calf thymus DNA

The binding of certain aromatic cations to nucleic acids for some time has been implicated as a primary process in antibacterial, antiprotozoal, antiviral, mutagenic, and antineoplastic activity (1–7). The changes in the thermal stability and the hydrodynamic and spectroscopic properties of DNA to which aromatic cations are bound have been suggested to indicate that at high ratios of formal DNA base to cation concentrations, intercalation of the flat aromatic portion of the ligand between adjacent base pairs on DNA occurs (8). Intercalation (also called type I binding) entails insertion of the flat aromatic portion of the ligand between base pairs (8–10) or bases (11–12) on DNA, accompanied by a partial unwinding of the double helix. In crystalline samples, X-ray diffraction spectrometry has provided direct evidence for the intercalation of the fungal antibiotic, dactinomycin, between the adjacent base pairs of DNA (13, 14).

The intercalative mode of binding does not appear to extend to all ligand molecules bound to a DNA helix (4). Rather, it is believed that only one molecule of ligand can be accommodated in an intercalative fashion for every four or five phosphate groups of the DNA helix. When nearly all intercalative binding sites of a DNA double helix are occupied, further interaction of the DNA with excess ligand is still able to occur. However, this binding is weaker than the intercalative binding, is not accompanied by hydrodynamic changes in the DNA solutions, and is believed to entail the electrostatic association of the cationic ligands with the anionic phosphodiester linkages at the surface of the helix. This is referred to as external (or type II) binding and occurs in solutions of low DNA base to ligand formal concentration ratios. At high ligand concentrations, some of the larger polycyclic aromatic molecules appear to be bound to the surface of DNA as dimers, because complexes can be spectroscopically distinguished in which there are two ligand molecules bound for each DNA phosphate group (15). The apparent relationship of the reversible reactions of aromatic cations with nucleic acids to the antimicrobial, antineoplastic, and mutagenic activities of the former has resulted in considerable interest in the qualitative and quantitative investigation of these interactions. These studies have usually been concerned with the stoichiometries and formation constants of the complexes formed between the ligands and the nucleic acids (1–22), although more recent work has been centered about the kinetics of binding (16, 21). Techniques such as electronic absorption spectrophotometry, fluorometry, differential spectrophotometry, and circular dichroic spectrophotometry have been employed to determine the amounts of bound and free ligand at each point in the titration of a so-

0022-3549/84/0900-1279$01.00/0

© 1984, American Pharmaceutical Association

dose curves in the *Results*. Where other values were used, they are noted in the appropriate figure legends. In the *Results*, values of important drug and system parameters were varied systematically to ascertain their effects on the dose dependency of absorption.

REFERENCES

(1) P. A. Shore, B. B. Brodie, and C. A. M. Hogben, *J. Pharmacol. Exp. Ther.*, **119**, 361 (1957).

(2) H. Stricker, *Drugs Made Ger.*, **13**, 35 (1970).

(3) H. Stricker, *Drugs Made Ger.*, **14**, 93 (1971).

(4) J. A. Clements, R. C. Heading, W. S. Nimmo, and L. F. Prescott, *Clin. Pharmacol. Ther.*, **24**, 420 (1978).

(5) M. A. Osman, R. B. Patel, D. S. Irwin, W. A. Craig, and P. G. Welling, *Biopharm. Drug. Dispos.*, **3**, 89 (1982).

(6) P. G. Welling, R. H. Barbhaiya, R. B. Patel, T. S. Foster, V. P. Shah, J. P. Hunt, and V. K. Prasad, *Curr. Ther. Res.*, **31**, 379 (1982).

(7) J. E. Baer, H. L. Leidy, A. V. Brooks, and K. H. Beyer, *J. Pharmacol. Exp. Ther.*, **125**, 295 (1959).

(8) H. Davenport, in "Physiology of the Digestive Tract," 4th ed., Yearbook Medical Publishers, Chicago, Ill., 1980, p. 63.

(9) L. Bueno, J. Fioramonti, and Y. Ruckebusch, *J. Physiol.*, **249**, 69 (1975).

(10) W. G. Crouthemal, G. H. Tan, L. W. Dittert, and J. T. Doluisio, *J. Pharm. Sci.*, **60**, 1160 (1971).

(11) M. C. Meyer and A. B. Straughn, *Curr. Ther. Res.* **22**, 573 (1977).

(12) P. G. Welling and R. H. Barbhaiya, *J. Pharm. Sci.*, **71**, 32 (1982).

(13) H. P. Deppeler, in "Analytical Profiles of Drug Substances," Vol. 10, K. Florey, Ed., Academic, New York, N.Y., 1981, p. 405.

(14) B. Beerman and M. Groschinsky-Grind, *Eur. J. Clin. Pharmacol.*, **12**, 297 (1977).

(15) "Martindale: The Extra Pharmacopoeia," 27th ed., A. Wade, Ed., The Pharmaceutical Press, London, 1978, p. xxvii.

(16) "The Merck Index" 9th ed., M. Windholz, Ed., Merck and Co., Rahway, N.J., 1976, p. 277.

Microcalorimetric Investigation of the Binding of Some Chemotherapeutic Agents and Related Molecules to Calf Thymus DNA

WILLIAM R. VINCENT *, LEONARD S. ROSENBERG, and STEPHEN G. SCHULMAN ˣ

Received May 24, 1982, from the *College of Pharmacy, University of Florida, Gainesville, FL 32601.* Accepted for publication January 10, 1983.

*Present address: Arnold & Marie Schwartz College of Pharmacy and Health Science, Long Island University, Brooklyn, NY 11201.

Abstract □ Batch microcalorimetry was used to estimate directly the standard enthalpies of the binding of small molecules to DNA. These values were compared with those obtained from spectrophotometric binding constants and van't Hoff plots. The close agreement between the independently obtained enthalpies indicates that the appropriate (best) binding model has four phosphates per binding site. Thermodynamic binding constants were obtained from apparent binding constants measured at different ionic strengths. From these and the measured standard enthalpies, standard free energies and standard entropies of binding were calculated. The weak, presumably external, binding alleged to occur at high formal molar concentration ratios of ligand to DNA bases could not be detected by a measurable heat of binding.

Keyphrases □ Microcalorimetry—binding of chemotherapeutic agents and related molecules to calf thymus DNA □ Binding—chemotherapeutic agents and related molecules to calf thymus DNA, microcalorimetry □ DNA—microcalorimetry, binding of some chemotherapeutic agents and related molecules to calf thymus DNA

The binding of certain aromatic cations to nucleic acids for some time has been implicated as a primary process in antibacterial, antiprotozoal, antiviral, mutagenic, and antineoplastic activity (1–7). The changes in the thermal stability and the hydrodynamic and spectroscopic properties of DNA to which aromatic cations are bound have been suggested to indicate that at high ratios of formal DNA base to cation concentrations, intercalation of the flat aromatic portion of the ligand between adjacent base pairs on DNA occurs (8). Intercalation (also called type I binding) entails insertion of the flat aromatic portion of the ligand between base pairs (8–10) or bases (11–12) on DNA, accompanied by a partial unwinding of the double helix. In crystalline samples, X-ray diffraction spectrometry has provided direct evidence for the intercalation of the fungal antibiotic, dactinomycin, between the adjacent base pairs of DNA (13, 14).

The intercalative mode of binding does not appear to extend to all ligand molecules bound to a DNA helix (4). Rather, it is believed that only one molecule of ligand can be accommodated in an intercalative fashion for every four or five phosphate groups of the DNA helix. When nearly all intercalative binding sites of a DNA double helix are occupied, further interaction of the DNA with excess ligand is still able to occur. However, this binding is weaker than the intercalative binding, is not accompanied by hydrodynamic changes in the DNA solutions, and is believed to entail the electrostatic association of the cationic ligands with the anionic phosphodiester linkages at the surface of the helix. This is referred to as external (or type II) binding and occurs in solutions of low DNA base to ligand formal concentration ratios. At high ligand concentrations, some of the larger polycyclic aromatic molecules appear to be bound to the surface of DNA as dimers, because complexes can be spectroscopically distinguished in which there are two ligand molecules bound for each DNA phosphate group (15). The apparent relationship of the reversible reactions of aromatic cations with nucleic acids to the antimicrobial, antineoplastic, and mutagenic activities of the former has resulted in considerable interest in the qualitative and quantitative investigation of these interactions. These studies have usually been concerned with the stoichiometries and formation constants of the complexes formed between the ligands and the nucleic acids (1–22), although more recent work has been centered about the kinetics of binding (16, 21). Techniques such as electronic absorption spectrophotometry, fluorometry, differential spectrophotometry, and circular dichroic spectrophotometry have been employed to determine the amounts of bound and free ligand at each point in the titration of a so-

0022-3549/84/0900-1279$01.00/0

© 1984, American Pharmaceutical Association

lution of the free ligand with a concentrated solution of nucleic acid.

THEORETICAL SECTION

Methods for evaluating equilibrium association constants for the binding of small molecules to DNA are generally derived from the independent-site model, developed by Scatchard (23), to deal with the binding of small molecules to proteins and the extension of this model by McGhee and von Hippel (24) to include ligand cooperativity. Peacocke and Skerrett (25) redefined the parameters of the Scatchard equations to allow their application to nucleic acids. In this approach, the ligand is titrated with a solution of DNA of known phosphate concentration, and the concentration of free ligand [B] is determined at each point in the titration either by direct spectrophotometry or by spectrophotometry subsequent to separation of free and bound ligand by equilibrium dialysis or some other suitable method. From the formal ligand concentration C_B, the former DNA phosphate concentration C_P, and the equilibrium free ligand concentration, the average number of bound ligand molecules (occupied binding sites) per phosphate (r) is calculated at each point in the titration:

$$r = \frac{C_B - [B]}{C_P} \qquad \text{(Eq. 1)}$$

For two classes of independent, noninteracting binding sites I (intercalative) and II (external):

$$r = \frac{n_I K_I [B]}{1 + K_I [B]} + \frac{n_{II} K_{II} [B]}{1 + K_{II} [B]} \qquad \text{(Eq. 2)}$$

where n_I and n_{II} are the reciprocals of the numbers of phosphates in each type of binding site and K_I and K_{II} are the equilibrium association constants, belonging to class I and class II binding, respectively. The reactions characterized by K_I and K_{II} may be written:

$$B + S_I \rightleftarrows BS_I \qquad \text{(Eq. 3)}$$

and:

$$B + S_{II} \rightleftarrows BS_{II} \qquad \text{(Eq. 4)}$$

where S_I and S_{II} are the type I and type II binding sites on DNA. The equilibria may be written:

$$K_I = \frac{[BS_I]}{[B][S_I]} \qquad \text{(Eq. 5)}$$

and:

$$K_{II} = \frac{[BS_{II}]}{[B][S_{II}]} \qquad \text{(Eq. 6)}$$

A plot of $r/[B]$ *versus* r is then constructed. This plot is generally hyperbolic in appearance, and if the components of the system are sufficiently dilute so that no ligand aggregation occurs on the polymer, the plot is usually considered to represent a superposition of the type I and type II processes. If K_I and K_{II} differ by at least an order of magnitude, the type I and type II binding may be resolved into straight lines at the high and low $r/[B]$ extrema, respectively, of the $r/[B]$ *versus* r plot. In this case, the extrema of the hyperbola are linearly extrapolated to the $r/[B]$ and r axes. The line of steep slope (at low values of r) is associated with the type I (intercalative) binding and has a slope $-K_I$ and an intercept on the $r/[B]$ axis of $K_I n_I + K_{II} n_{II}$. The line of shallow slope (at high values of r) associated with the type II (external) binding has a slope of $-K_{II}$ and an intercept on the r-axis of $n_I + n_{II}$.

However, the extrapolation of the legs of the hyperbolic plot to obtain slopes and intercepts places an inordinately high degree of reliance on the data at the extrema of the titrations. It is at the extrema that the data, regardless of how they were obtained, are the least precise.

During the course of investigations in this laboratory (26) of the binding of the singly charged cation of 3-aminoacridine, at pH 5.9 ($pK_a = 8.04$) and ionic strength 5.0×10^{-3}, to double-stranded calf thymus DNA, it was found that at high values of $r/[B]$, there was sufficient curvature in the extremum of the plot of $r/[B]$ *versus* r that it was very difficult to make reasonable linear extrapolation to the $r/[B]$-axis. This led us to hypothesize that the reaction represented by Eqs. 3 and 5 might be inappropriate to represent, even qualitatively, the type I binding. An attempt was made to rewrite the type I binding reaction in a way that might fit the experimental data. A reaction of the form:

$$B + qS \rightleftarrows B(S)q \qquad \text{(Eq. 7)}$$

was chosen, in which an integral number of binding sites, q, would react with BH^+ to form the type I complex $B(S)q$. The equilibrium expression corresponding to Eq. 7 would then be:

$$K = \frac{[B(S)q]}{[B][S]^q} \qquad \text{(Eq. 8)}$$

Since n phosphates are associated with each type I complex:

$$m \cdot q = n \qquad \text{(Eq. 9)}$$

where m is the number of phosphates associated with one type I site, S. In most binding studies, it has been demonstrated that the type I binding is characterized by $n = 4$ or 5. However, in our empirical approach, values of $q = 1$-4 and of $m = 1$-6 were tried in Eqs. 8 and 9. It was found that the best straight lines could be obtained when $m = 2$ and $q = 2$ (*i.e.*, two sites per complex, each site having two phosphates). Hence, for the type I binding of the 3-aminoacridinium monocation:

$$K = \frac{[B(S)_2]}{[B][S]^2} \qquad \text{(Eq. 10)}$$

corresponding to the essentially termolecular overall reaction:

$$B + 2S \rightleftarrows B(S)_2 \qquad \text{(Eq. 11)}$$

The reaction shown in Eq. 11 is difficult to rationalize if both sites which react with B lie on the same DNA molecule, as indeed they must, unless intercalation involves the bridging of ligand between two distinct macromolecules. To test the thermodynamic feasibility of the variously proposed reaction models ($q = 1$, $m = 4$; $q = 1$, $m = 5$; and $q = 2$, $m = 2$) for the intercalative binding of small molecules to DNA, it was decided to attempt to determine the standard enthalpy of binding ($\Delta H°$) for the reactions of several cationic drugs and dyes with calf thymus DNA. These values of $\Delta H°$ could be determined from van't Hoff plots of the appropriately calculated apparent binding constants as a function of temperature. It should be mentioned that the occurrence of a reasonably linear van't Hoff plot alone might be an indication of the chemical significance of the way in which the equilibrium expression is written. The values of $\Delta H°$ taken from the van't Hoff plots could then be compared with enthalpies of reaction (ΔH) determined directly by microcalorimetry. Since the standard state for a solute in dilute solution is taken to be the infinitely dilute solution at standard conditions, the calorimetrically determined values of ΔH may be taken to approximate $\Delta H°$ very well in each case because the concentrations of the reactants will be kept very low ($\sim 10^{-4}$-10^{-3} M). Agreement between the graphically and calorimetrically determined values of $\Delta H°$ then should lend support to the validity of the model used in the calculation of the equilibrium constants giving the best values of $\Delta H°$. Additionally, once the appropriate intercalative binding model is known and the best values of $\Delta H°$ are in hand, it should be possible to determine thermodynamic binding constants by extrapolation to infinite dilution and then to determine the standard entropy of binding ($\Delta S°$). Assessments of the relative importance of DNA-ligand interactions and ligand-water interactions in the binding process could then be attempted. With these objectives in mind, the following study of the binding of four compounds to calf thymus DNA was undertaken.

EXPERIMENTAL SECTION

The pH was maintained throughout this study at 5.50 with an acetic acid-sodium acetate buffer to ensure that all ligands utilized were in only one state of protonation and thereby obviate the necessity to correct for competitive prototropic equilibria.

Ethidium bromide[1] and 9-aminoacridine hydrochloride[2] were recrystallized from 95% ethanol. Doxorubicin hydrochloride[3] was used without further purification. 3-Aminoacridine was prepared by the procedure of Martin and Tong (27). The sodium salt of calf thymus DNA[4] was used without further purification.

The molar absorptivity of each ligand was determined by accurately weighing and dissolving each compound in a 10-mL volumetric flask and then delivering successive 50-μL aliquots of this stock solution into 9.00 mL of pH 5.50 buffer and recording the long-wavelength absorption spectra. A Beer's law plot was constructed for each ligand, with the final concentration of ligand equal to or greater than the final concentration employed in the determination of the DNA-ligand binding constants. Linearity was observed in all cases, indicating that aggregation of the free ligand in solution was negligible within the concentration range employed.

[1] Aldrich Chemical Co., Milwaukee, Wis.
[2] Pfaltz and Bauer, Stanford, Conn.
[3] Gift from Adria Laboratories, Columbus, Ohio.
[4] Calbiochem, La Jolla, Calif.

The molar absorptivity of the intercalated form of each ligand was determined analogously by adding the stock solution to a concentrated solution of DNA and recording the absorption spectra after each addition. A Beer's law plot was then constructed and found to be linear. This indicates that successively bound ligands have identical molar absorptivities, irrespective of the degree of saturation of polymer. The final concentration of bound ligand was equal to or greater than the concentration used in the determination of the intrinsic association constant. Variation of temperature and/or ionic strength had no effect on the measured molar absorptivities. The exact molar absorptivity of native calf thymus DNA is disputed in the literature (28–30). Values range from 6300 $L \cdot mol^{-1} \cdot cm^{-1}$ (29) to 6600 $L \cdot mol^{-1} \cdot cm^{-1}$ (31), with the wavelength maximum at either 259 (31) or 260 nm (29). Throughout this study, the concentrations of DNA solutions were determined absorptiometrically at 259 nm with a corresponding molar absorptivity of 6500 $L \cdot mol^{-1} \cdot cm^{-1}$. All absorptiometric measurements were carried out on a recording UV-visible spectrophotometer[5], using cylindrical 5-cm quartz cells.

The intrinsic association constants of all ligands with native double-stranded DNA were determined as a function of temperature and ionic strength. A measured volume and concentration of ligand was added to a known volume and concentration of DNA prior to the titration. Absorption spectra of the preequilibrated DNA-ligand solution were then recorded at temperatures and ionic strengths corresponding to those from which intrinsic association constants were calculated. The titration was then carried out differentially by placing an identical volume of the preequilibrated DNA solution in both the sample and reference compartments. The preequilibration of the DNA solution with ligand ensures that the concentration of unbound ligand is measurable from the outset and allows the differential spectral technique to be optimized for that region of the titration. Aliquots of the known concentration of ligand solution were then added with a micropipet[6] to the sample cell, and the resulting rise in the absorption spectra was recorded. The transfer of ligand solutions was found to be more reproducible than the more commonly used method of transferring the DNA solution, owing to the relatively high viscosity of the latter. Absorption spectra of all ligands during the titration were recorded starting at wavelengths at least 20 nm greater than the first observable absorbance and ending ~20 nm below the analytical wavelength of choice. Analytical wavelengths were chosen according to the ligand and were at the long-wavelength maxima of the free drug. The titrations were performed in duplicate for at least three temperatures between 15°C and 40°C for each ligand and at ionic strengths of 0.1, 0.05, and 0.01. The temperature in the absorbance cell was monitored by a submersible temperature probe and maintained with a constant-temperature bath[7] and a jacketed cell compartment. At least 10 points, and usually 20 points, were acquired in each titration.

The conservation of mass of the ligand requires that:

$$C_B = [B] + [BS] \qquad \text{(Eq. 12)}$$

where B and BS are the free and bound ligand, respectively, and C_B is the total concentration of ligand. At any point in the titration, assuming no aggregative binding, the absorbance is:

$$A_T = \epsilon_B[B]l + \epsilon_{BS}[BS]l \qquad \text{(Eq. 13)}$$

where A_T is the total absorbance at the analytical wavelength of choice, and l is the optical path length of the sample cell. Combination of Eqs. 12 and 13 gives:

$$[B] = \frac{A_T - \epsilon_{BS}C_B l}{(\epsilon_B - \epsilon_{BS})l} \qquad \text{(Eq. 14)}$$

and:

$$[BS] = \frac{\epsilon_B C_B l - A_T}{(\epsilon_B - \epsilon_{BS})l} \qquad \text{(Eq. 15)}$$

for the concentration of free and bound ligand at any point in the titration.

The heat generated by the binding of the ligands by DNA was measured with a batch microcalorimeter[8]. The reaction cells employed in the batch microcalorimeter are of the mixing type, each having two compartments into which liquid reactant can be introduced. The maximum volume that can be contained within each divided cell is 4.5 and 2.5 mL to minimize the heat of dilution and maximize concentration. DNA was introduced into the 4.5-mL compartment, and the ligand was introduced into the 2.5-mL chamber. The temperature within the microcalorimeter was maintained at 25.00 ± 0.01°C with a thermostatically controlled air bath[9] with an external adjunct water bath[10]. The temperature inside the sealed microcalorimeter was checked with a calibrated thermostat embedded in a heat sink. The microcalorimeter at thermal equilibrium was rotated, allowing the reactants to mix, and the heat of reaction was recorded. The output from the microcalorimeter was recorded on a linear strip chart recorder with a disk-driven integrator[11]. The microcalorimeter was calibrated with an electrical calibration current which passed through the reactant cell for a measured period of time[12]. A comparison of the signal from the calibration run with that measured for the heat of reaction of ligand with DNA yields an exact molar enthalpy of reaction. The heat of dilution of both reactants was measured and subtracted from the measured heat of reaction. The apparent enthalpy of binding can be calculated from:

$$\Delta H = \frac{Q}{C_B V_i f_{BS}} \qquad \text{(Eq. 16)}$$

where Q is the measured heat, V_i is the initial volume of ligand, C_B is the initial concentration of ligand, and f_{BS} is the fraction of the total ligand bound by the DNA at the end of the reaction. An *a priori* knowledge of the intrinsic association constant at the same temperature and ionic strength is necessary to calculate f_{BS}. However, to a first approximation, the value of the binding is not necessary since an excess of DNA was used, such that f_{BS} was >0.95. The error incurred in this assumption is <5% of the final value. The heat of binding for each compound was measured at ionic strengths of 0.1, 0.05, and 0.01. Data were analyzed using the facilities of the Northeast Regional Data Center[13].

RESULTS AND DISCUSSION

Intercalative binding of a cationic ligand with native DNA entails the slipping of the aromatic drug in between adjacent base pairs on the double helix. Concomitantly, the molar absorptivity of the ligand decreases dramatically. The concentration of free and bound ligand can be evaluated at each point in the titrations by Eqs. 14 and 15. These values were subsequently used for the evaluation of apparent binding constants from Eqs. 8 and 9 with values of $m = 1$–6 and $q = 1$–4, as described previously (26). Particular attention was paid to the values of $m = 4$, $q = 1$ and $m = 5$, $q = 1$ (corresponding to the modified Scatchard treatment of type I binding), $m = 3$, $q = 1$ (corresponding to the suggested stoichiometry for type II binding), and $m = 2$, $q = 2$ [for the termolecular treatment of type I binding (26)]. Of these, only values of $m = 4$, $q = 1$ and $m = 2$, $q = 2$ yielded binding constants which did not exhibit systematic variance and were positive over the entire titration interval. In addition, the values of $m = 4$, $q = 1$ gave estimated errors in the binding constants which were consistently less than those calculated by using values of $m = 2$, $q = 1$. However, both models gave feasible results, and each must be considered further.

Binding data for each compound at a different absolute temperature (T) were treated in the manner described above, with values of $m = 4$, $q = 1$ (bimolecular overall reaction) and $m = 2$, $q = 2$ (termolecular overall reaction). The logarithms of the apparent binding constants calculated therefrom are plotted against reciprocal absolute temperature (van't Hoff plots) in Figs. 1 and 2, respectively. The best first-order least-squares lines for these data are also shown, the slopes of which should be $-\Delta H°/2.303R$, where R is the universal gas constant. The calculated values of $\Delta H°$ are listed in Table I. The van't Hoff plots are apparently linear, with the deviations from linearity being very similar for both models. If the linearity of the plots is taken as a criterion for the validity of a binding model, then both models appear to be equally correct. However, a major difference between them is the magnitudes of the resultant values of $\Delta H°$ which are significantly larger for the termolecular model than those from the bimolecular model. Thus, to establish the appropriate model, the standard enthalpies of binding of each compound to DNA must be measured by an independent experimental procedure.

The calorimetric measurement of the binding enthalpies was therefore performed by batch microcalorimetry. The major advantage of batch microcalorimetry over the more commonly used flow calorimetry is the relatively small amounts of reagents required for the analysis. The heats of binding were found to be virtually identical at three ionic strengths and were subsequently averaged, and the resulting standard enthalpies for each compound were calculated (Table I). The calorimetrically determined enthalpies are in agreement with the values described above for the bimolecular model and significantly different from the termolecular values. This agreement of the standard enthalpies of binding, which were determined independently by

[5] Model 219; Varian-Cary.
[6] Finnpipette.
[7] Lauda K-2/R; Brinkmann.
[8] Model 2107-111; LKB.
[9] Model 2107-210; LKB.
[10] Lauda K-2/R; Brinkmann.
[11] *Omniscribe*; Houston Instruments, Houston, Tex.
[12] Control Unit 2107-310; LKB.
[13] 470 v/6-11 computer; Amdahl.

Table I—Thermodynamic Parameters of the Binding of Ligands to DNA

Ligand	$\Delta H°$, kcal·mol^{-1} [a,b]	$\Delta H°$, kcal·mol^{-1} [a,c]	ΔH, kcal·mol^{-1} [d]	$\Delta G°$, kcal·mol^{-1}	$\Delta S°$, cal·deg^{-1}mol^{-1}
Ethidium bromide	6.2 ± 0.5	10 ± 1	−7.5 ± 0.2	−9.30 ± 0.04	6.0 ± 0.7
9-Aminoacridine	6.3 ± 0.5	13 ± 2	−6.1 ± 0.2	−8.70 ± 0.07	8.7 ± 0.7
3-Aminoacridine	7 ± 1	11 ± 2	−6.9 ± 0.2	−7.69 ± 0.05	2.6 ± 0.7
Doxorubicin	5.3 ± 0.5	6.6 ± 0.7	−5.4 ± 0.3	−9.9 ± 0.1	15 ± 1

[a] From the least-squares slope of the van't Hoff plot. [b] Bimolecular model ($m = 4, q = 1$). [c] Termolecular model ($m = 2, q = 2$). [d] From calorimetry.

spectrophotometry and calorimetry, is strong evidence for the bimolecular model with four bases per binding site ($m = 4, q = 1$).

The determination of enthalpic contributions to the binding process inevitably leads to questions about the corresponding entropic contributions and to the standard free energy of the system. To calculate the standard free energy of binding from the association constant for the DNA-ligand interaction, the thermodynamic association constant must be known. Only from the thermodynamic constant can the standard free energy of binding ($\Delta G°$) be calculated. The standard entropy of binding ($\Delta S°$) can then be calculated from $\Delta G°$ and the standard enthalpy of binding, $\Delta H°$, using:

$$\Delta S° = \frac{\Delta G° - \Delta H°}{T} \qquad \text{(Eq. 17)}$$

The majority of reported association constants in the literature for DNA-ligand interactions are apparent equilibrium association constants. The use of an apparent association constant in the calculation of the free energy of binding does not yield $\Delta G°$ but rather an entity which varies with the ionic strength. The calculated entropy of binding will then also appear to fluctuate with ionic strength. However, the determination of a thermodynamic affinity constant extrapolated to zero ionic strength allows the direct and unambiguous determination of $\Delta G°$ and, subsequently, $\Delta S°$, which are thermodynamic constants of the reaction.

The Debye-Hückel relationship (Eq. 18) can serve as a starting point from which to correct the apparent association constants for ionic screening of the various reactants. The activity coefficient of the ith species can be calculated from:

$$-\log \gamma_i = \frac{AZ_i^2\mu^{1/2}}{1 + \mu^{1/2}} \qquad \text{(Eq. 18)}$$

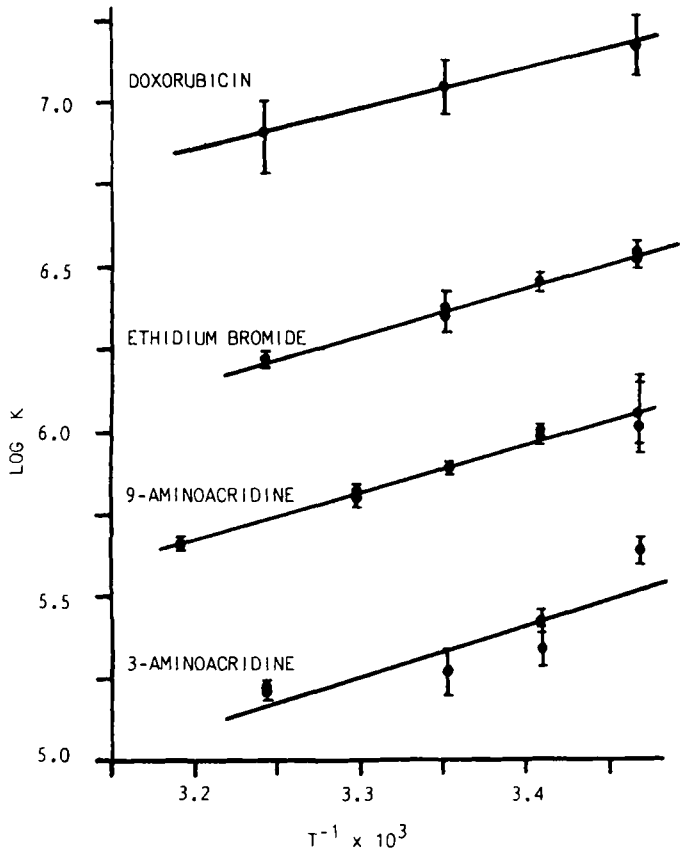

Figure 1—*Van't Hoff plots for the indicated compounds, assuming a bimolecular model* (m = 4, q = 1).

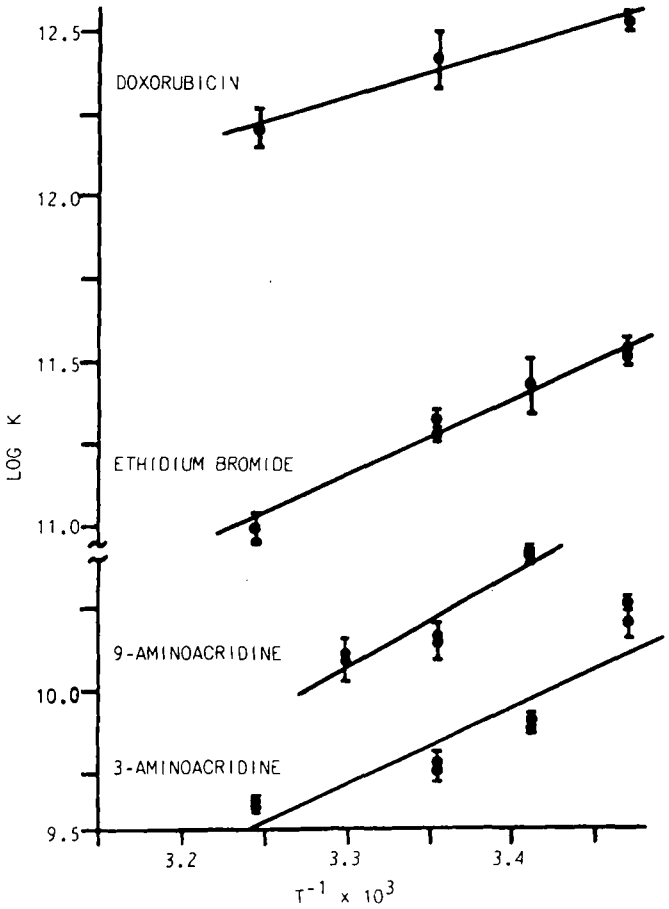

Figure 2—*Van't Hoff plots for the indicated compounds, assuming a termolecular model* (m = 2, q = 2).

where A is a constant dependent on the temperature and dielectric constant of the solute, Z_i is the charge on the ith species in solution, and μ is the ionic strength of the solution.

The thermodynamic equilibrium constant $K°$ can be related to the apparent constant K by:

$$K° = K\frac{\gamma_{BS}}{\gamma_B\gamma_S} \qquad \text{(Eq. 19)}$$

where the subscripts of the activity coefficients refer to the reactant species. Combination of Eqs. 18 and 19 yields, in logarithmic form:

$$\log K = \log K° + C\frac{\mu^{1/2}}{1 + \mu^{1/2}} \qquad \text{(Eq. 20)}$$

It is then possible to extract a thermodynamic association constant. Even if the Debye-Hückel equation is not quite correct for DNA solutions, the fact that log $K°$ is an intercept and not a slope minimizes the dependence on how γ_i is calculated. The apparent association constants at three ionic strengths and the thermodynamic association constant taken from the corresponding least-squares intercept are given for each ligand in Table II. The association constants agree well with the results of other workers (32–36). Values for all thermodynamic parameters are given in Table I. Note that the precision of the calorimetrically obtained enthalpies is better than that which could be obtained from spectrophotometric data.

Examination of the thermodynamic parameters gives some insight into the molecular forces which control the binding process. A favorable enthalpy of binding should be evident with large, planar, aromatic molecules. Their pla-

Table II—Parameters For the Binding of Ligands to DNA

Ligand	Wavelength, nm	Molar Absorptivity × 10^{-3} L·mol^{-1}·cm^{-1}		Log K^a			Log K° [b]
		Free	Bound	μ = 0.100	μ = 0.050	μ = 0.010	
Ethidium bromide	480	5.60 ± 0.06	2.46 ± 0.04	5.61 ± 0.02	5.93 ± 0.02	6.36 ± 0.04	6.82 ± 0.03
9-Aminoacridine	422	7.48 ± 0.16	2.84 ● 0.02	5.08 ± 0.07	5.54 ± 0.02	5.87 ± 0.01	6.38 ± 0.05
3-Aminoacridine	452	12.60 ± 0.11	8.50 ± 0.06	4.70 ± 0.03	4.95 ± 0.01	5.28 ± 0.05	5.64 ± 0.04
Doxorubicin	480	10.00 ± 0.15	5.96 ± 0.02	6.60 ± 0.07	6.80 ± 0.03	7.00 ± 0.09	7.25 ± 0.07

[a] Apparent equilibrium association constants. [b] Equilibrium association constants extrapolated to μ = 0.

Table III—Variation in the Measured Heat of Binding Due to the Fraction of Ligand Bound [a]

Percent Bound	Concentration, ×10^{-5} M				Molar Enthalpy of Binding, kcal/mol
	Total Drug	Bound Drug	Free Drug	Total DNA	
99	3.36	3.33	0.03	6.74	−6.2
95	3.50	3.33	0.170	2.39	−6.2
90	3.70	3.33	0.370	1.82	−6.1
85	3.92	3.33	0.590	1.64	−6.3
80	4.16	3.33	0.803	1.55	−6.2
70	4.76	3.33	1.43	1.46	−6.2
60	5.55	3.33	2.22	1.41	−6.3
50	6.66	3.33	3.33	1.39	−6.2

[a] T = 25°C; μ = 0.010 for 9-aminoacridine.

narity allows their insertion into the DNA helix with minimal disturbance of the DNA structure. Larger compounds enhance the opportunity for the van der Waals binding interaction between the ligand and the DNA bases. The largest binding enthalpy for ligands studied herein is that of ethidium bromide. In contrast to 9-aminoacridine and 3-aminoacridine, which also contain tricyclic aromatic ring systems, ethidium bromide has an exocyclic phenyl substituent which might at first be expected to sterically inhibit its intercalation. However, the observed large enthalpy of binding relative to those of the aminoacridines suggests that the phenyl ring of ethidium bromide reinforces binding. This would seem to indicate that the phenyl substituent serves to extend the area of the ligand which is bound to the DNA base pairs, perhaps by becoming coplanar with the aromatic nucleus of the ligand. In contrast, doxorubicin, which exhibits the least-favorable binding enthalpy, has a nonplanar ring linearly annulated with the aromatic system and an exocyclic amino sugar group. The weakness of the enthalpic binding contribution may be attributed to either the steric inhibition of the insertion of the planar portion of the molecule into the DNA helix or to the disruption of the DNA structure by the intercalation of the buckled ring segment or the amino sugar side chain.

The entropy of binding is probably influenced mainly by changes in the translational freedom due to the binding or release of solvent molecules by the ligands and/or the DNA. This is evidenced by the entropy of binding for doxorubicin which is much larger than that observed for the other ligands. The binding of the doxorubicin can be expected to displace water from its amino sugar side chain. In addition, the structure of the DNA helix and its accompanying waters of hydration may be disrupted significantly if the buckled ring or the amino sugar group makes contact with the double helix. Because of the limited number of compounds investigated in this study and the substantial structural differences between them, it would probably be premature and excessively speculative to attempt to account for the differences between their enthalpies and entropies of binding to DNA in any but those most obvious examples just cited.

Batch microcalorimetry can be used to investigate type II binding as well. The only condition necessary for the separation of type I and type II binding is that their heats of complexation be different and measurable. In that type II binding becomes prevalent in the presence of an excess concentration of free ligand, type II binding should demonstrate a heat of interaction in this region of titration, and an enthalpy of binding should be measurable by microcalorimetry. By using excess DNA, the heat for intercalative binding can be accurately calculated at any known concentration of DNA and ligand. By using these calculated values as a reference and by repeating the measurement with excess free ligand, any deviation from the reference value will be taken as being due to external binding. Table III shows the results of this experiment. Even in the presence of an excess free ligand concentration, which is equal to the total concentration of bound ligand, the measured enthalpy of binding is invariant from the reference value for intercalative binding. The heats of binding were checked at a number of bound ligand–free ligand concentrations, and in all cases the resulting enthalpy was equal to the reference value within experimental error.

The lack of a measurable heat of binding for type II interactions can be explained in two ways. First, type II binding may have a small, unmeasurable heat of complexation, such that the batch microcalorimeter cannot detect this heat above the reference value. Second, type II binding may be an artifact of the Scatchard plot. As such, external binding may not occur for nonaggregating ligands. For ligands which aggregate, if the concentration is maintained at a low value, external binding again may not occur.

The inaccuracy in measuring the exact concentration of free and bound ligand, when either is in a large excess, is great. Such is the case for external binding, in which it is an excess of free ligand that creates the difficulties. The curvature in the modified Scatchard plots is probably due to this inability to accurately measure free and bound ligand concentrations.

REFERENCES

(1) R. I. DeMars, *Nature (London)*, **172**, 964 (1953).

(2) J. Hurwitz, J. J. Furth, M. Malamy, and M. Alexander, *Proc. Natl. Acad. Sci. U.S.A.*, **48**, 1222 (1962).

(3) C. S. Woese, R. Naono, R. Soffer, and F. Gros, *Biochem. Biophys. Res. Commun.*, **11**, 435 (1963).

(4) A. Blake and A. R. Peacocke, *Biopolymers*, **6**, 1225 (1968).

(5) A. R. Peacocke in "Heterocyclic Compounds: Acridines," vol. 9, R. M. Acheson, Ed. Interscience, New York, N.Y., 1973, pp. 723–757.

(6) E. R. Lochmann and A. Micheler in "Physico-Chemical Properties of Nucleic Acids," vol. 1, J. Duchesne, Ed., Academic, New York, N.Y., 1973, pp. 223–267.

(7) S. Georghiou, *Photochem. Photobiol.*, **26**, 59 (1977).

(8) L. S. Lerman, *J. Mol. Biol.*, **3**, 18 (1961).

(9) L. S. Lerman, *Proc. Natl. Acad. Sci. U.S.A.*, **49**, 94 (1963).

(10) L. S. Lerman, *J. Cell. Comp. Physiol.*, Suppl. 1, **64**, 1 (1964).

(11) N. J. Pritchard, A. Blake, and A. R. Peacocke, *Nature (London)*, **212**, 1360 (1966).

(12) D. S. Drummond, V. F. W. Simpson-Gildemeister, and A. R. Peacocke, *Biopolymers*, **3**, 135 (1965).

(13) H. M. Sobell and S. C. Jain, *J. Mol. Biol.*, **68**, 21 (1972).

(14) H. M. Sobell, *Prog. Nucleic Acid Res. Mol. Biol.*, **13**, 153 (1973).

(15) E. Frederica and M. Houssier, *Biopolymers*, **10**, 2281 (1972).

(16) J. H. Li and D. M. Crothers, *J. Mol. Biol.*, **39**, 461 (1968).

(17) M. Sakoda, K. Hiromi, and K. Akasaka, *Biopolymers*, **10**, 1003 (1971).

(18) K. Akasaka, M. Sakoda, and K. Hiromi, *Biochem. Biophys. Res. Commun.*, **40**, 1239 (1970).

(19) M. Sakoda, K. Hiromi, and K. Akasaka, *J. Biochem.*, **71**, 891 (1972).

(20) J. L. Bresloff and D. M. Crothers, *J. Mol. Biol.*, **95**, 103 (1975).

(21) P. Davanloo and D. M. Crothers, *Biochemistry*, **15**, 5299 (1976).

(22) G. Duportail, Y. Mauss, and J. Chambron, *Biopolymers*, **16**, 1397 (1977).

(23) G. Scatchard, *Ann. N.Y. Acad. Sci.*, **51**, 660 (1948).

(24) J. D. McGhee and P. H. von Hippel, *J. Mol. Biol.*, **86**, 469 (1974).

(25) A. R. Peacocke and J. N. H. Skerrett, *Trans. Faraday Soc.*, **52**, 261 (1956).

(26) A. C. Capomacchia and S. G. Schulman, *J. Pharm. Sci.*, **67**, 89 (1978).
(27) R. F. Martin and J. H. Y. Tong, *Aust. J. Chem.*, **22**, 487 (1969).
(28) E. Frederica and C. Houssier, *Biopolymers*, **11**, 2281 (1972).
(29) G. Felsenfeld and S. Z. Hirschman, *J. Mol. Biol.*, **13**, 407 (1965).
(30) N. N. Zhadin and V. L. Rapoport, *Mol. Biol.*, **9**, 187 (1975).
(31) H. R. Mahler and D. D. Mehrotra, *J. Mol. Biol.*, **9**, 801 (1964).
(32) M. Waring, *J. Mol. Biol.*, **13**, 269 (1965).
(33) C. M. Lee, C. T. Chang, and J. G. Wetmur, *Biopolymers*, **12**, 1099 (1973).
(34) S. Aktipis and A. Kindelis, *Biochemistry*, **12**, 1213 (1973).
(35) P. S. Drummond, N. J. Pritchard, V. F. W. Simpson-Gildemeister, and A. R. Peacocke, *Biopolymers*, **4**, 1091 (1966).
(36) S. R. Byrn and G. D. Dolch, *J. Pharm. Sci.*, **67**, 688 (1978).

Antiradiation Compounds XIX: Metal-Binding Abilities of Thioureas

WILLIAM O. FOYE ˣ and CHING-CHIU CHAO

Received July 13, 1983, from the *Samuel M. Best Research Laboratory, Massachusetts College of Pharmacy and Allied Health Sciences, Boston, MA 02115.* Accepted for publication August 5, 1983.

Abstract □ Metal-binding stability constants for a series of *N*- and *N,N'*-substituted thioureas with Cu(II), Ni(II), Al(III), and Fe(III) ions were determined by potentiometric titration. The sequence of constants for thiourea, *N*-methylthiourea, and *N,N'*-dimethylthiourea indicated steric effects of the methyl groups and that both nitrogen and sulfur were involved in the complexation. The magnitude of the constants was somewhat lower than those of the simple peptides. The mechanism of protection against ionizing radiation by thioureas is probably due to hydrogen-atom transfer rather than binding of metal ions that catalyze cellular oxidations.

Keyphrases □ Thioureas—metal-ion complexes, stability constants, antiradiation protection □ Antiradiation protection—thioureas, metal-ion complexes, stability constants □ Stability constants—thioureas, metal-ion complexes, antiradiation protection

Metal-ion complexation has been shown or postulated to be involved in a number of biological activities. The effect of complexing agents such as dithiocarbamates (1) and some thioureas (2) on the inhibition of dopamine-β-oxidase, a copper-containing enzyme, is well known. Metal-ion complexation has also been postulated for the antithyroid activity of thiouracil (3), the inhibitory effects of dithiocarbamates against *Mycobacterium tuberculosis* (4), and the fungistatic effects of dithiocarbamates and other complexing agents (5). The nitrate reductase complex of *Neurospora crassa* is also sensitive to inhibition by metal-binding agents, including thiourea (6), and polyphenol oxidase is also inhibited by thiosinamine (allylthiourea) (7).

Several postulations (8–10) regarding the protective effects of a number of metal-binding radiation-protective agents have also been made. Although thiourea and its simple derivatives have some protective ability for whole-body irradiation of animals, these effects have not been appreciable. Thioureas have, however, shown substantial radiation-protective effects in other systems, such as mouse lung (11), human erythrocytes (12), T_2 phage (13), Ehrlich ascites cells (14), and macromolecules (15) (Table I). The radiation-protective effects of thiourea have been attributed to metal binding (11).

With such a significant number of postulations involving the metal-binding aspects of thioureas, it is surprising to find that, other than for thiourea itself (16), metal-binding abilities of substituted thioureas have not been determined. Stability constants for a series of cyclic thioureas, including mercaptoimidazoles and mercaptouracils, were determined with copper, iron, and aluminum ions (17), and the constants were surprisingly high. It was considered important, therefore, to measure the metal-binding stability constants for a series of alkyl, aralkyl, and cyclic thioureas. Knowledge of the magnitude of the constants would indicate whether thiourea complexes were capable of existence in the presence of cellular complexing agents, such as peptides, or whether thiourea might function as a transient metal complexer.

Compounds of the general structures I–III were measured for binding abilities to Cu(II), Ni(II), Al(III) and Fe(III) ions using the method of potentiometric titration.

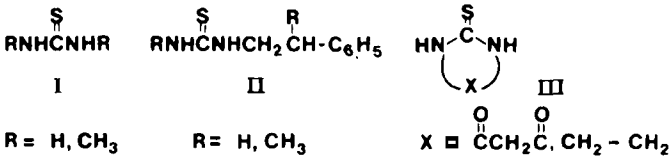

EXPERIMENTAL SECTION

Materials—Analytical reagent-grade[1] aluminum chloride hexahydrate, cupric chloride dihydrate, ferric nitrate nonahydrate, and nickel(II) chloride hexahydrate were used for the metal complexation determination. Carbonate-free 0.01 M KOH was prepared according to the method of Armstrong (18). Solutions of the metal salts were prepared in boiled distilled water and stored in polyethylene bottles under nitrogen; they were diluted quantitatively with carbon dioxide-free water just prior to use. Normalities were checked against potassium biphthalate.

The organic ligands were obtained commercially[2]. *N*-Methyl-*N'*-phenethylthiourea was reported previously (19), and *N*-methyl-*N'*-phenyl-2-propylthiourea was described earlier (20). Purity was ascertained by TLC using chromagram sheets[3]. Solutions (0.1%) of the compounds in ethanol were spotted, and the sheets were developed with benzene–methanol (8:2); spots were detected with iodine vapor.

Ionization Constants—The method of Albert and Serjeant (21) was used, which consisted of titrations of 0.001 M solutions of the compounds in 95% ethanol with 0.01 M KOH in 0.5-mL portions. The pH was recorded with a pH meter[4] with glass and calomel electrodes after each addition. Each titration thus yielded 10 pH values, giving 10 values for the pK_a, which were averaged (Table II). Since most of the pH values fell outside the 5–9 range, corrections were made for hydrogen-ion concentrations.

Stability Constants—Potentiometric titrations were carried out under nitrogen in 95% ethanol at 25°C with the described pH meter. Volumes of 50 mL of the 0.001 M solutions of the organic ligands were titrated with 0.01 M KOH in 0.5-mL portions, first in the absence of metal ions, and then in the

[1] J. T. Baker Analyzed Reagents.
[2] Aldrich Chemical Co., Eastman Organic Chemicals, or Fisher Scientific Co.
[3] Eastman Organic Chemicals.
[4] Beckman Instruments.

0022-3549/84/0900-1284$01.00/0
© 1984, American Pharmaceutical Association

(26) A. C. Capomacchia and S. G. Schulman, *J. Pharm. Sci.*, **67**, 89 (1978).
(27) R. F. Martin and J. H. Y. Tong, *Aust. J. Chem.*, **22**, 487 (1969).
(28) E. Frederica and C. Houssier, *Biopolymers*, **11**, 2281 (1972).
(29) G. Felsenfeld and S. Z. Hirschman, *J. Mol. Biol.*, **13**, 407 (1965).
(30) N. N. Zhadin and V. L. Rapoport, *Mol. Biol.*, **9**, 187 (1975).
(31) H. R. Mahler and D. D. Mehrotra, *J. Mol. Biol.*, **9**, 801 (1964).
(32) M. Waring, *J. Mol. Biol.*, **13**, 269 (1965).
(33) C. M. Lee, C. T. Chang, and J. G. Wetmur, *Biopolymers*, **12**, 1099 (1973).
(34) S. Aktipis and A. Kindelis, *Biochemistry*, **12**, 1213 (1973).
(35) P. S. Drummond, N. J. Pritchard, V. F. W. Simpson-Gildemeister, and A. R. Peacocke, *Biopolymers*, **4**, 1091 (1966).
(36) S. R. Byrn and G. D. Dolch, *J. Pharm. Sci.*, **67**, 688 (1978).

Antiradiation Compounds XIX: Metal-Binding Abilities of Thioureas

WILLIAM O. FOYE ˣ and CHING-CHIU CHAO

Received July 13, 1983, from the *Samuel M. Best Research Laboratory, Massachusetts College of Pharmacy and Allied Health Sciences, Boston, MA 02115.* Accepted for publication August 5, 1983.

Abstract □ Metal-binding stability constants for a series of *N*- and *N,N'*-substituted thioureas with Cu(II), Ni(II), Al(III), and Fe(III) ions were determined by potentiometric titration. The sequence of constants for thiourea, *N*-methylthiourea, and *N,N'*-dimethylthiourea indicated steric effects of the methyl groups and that both nitrogen and sulfur were involved in the complexation. The magnitude of the constants was somewhat lower than those of the simple peptides. The mechanism of protection against ionizing radiation by thioureas is probably due to hydrogen-atom transfer rather than binding of metal ions that catalyze cellular oxidations.

Keyphrases □ Thioureas—metal-ion complexes, stability constants, antiradiation protection □ Antiradiation protection—thioureas, metal-ion complexes, stability constants □ Stability constants—thioureas, metal-ion complexes, antiradiation protection

Metal-ion complexation has been shown or postulated to be involved in a number of biological activities. The effect of complexing agents such as dithiocarbamates (1) and some thioureas (2) on the inhibition of dopamine-β-oxidase, a copper-containing enzyme, is well known. Metal-ion complexation has also been postulated for the antithyroid activity of thiouracil (3), the inhibitory effects of dithiocarbamates against *Mycobacterium tuberculosis* (4), and the fungistatic effects of dithiocarbamates and other complexing agents (5). The nitrate reductase complex of *Neurospora crassa* is also sensitive to inhibition by metal-binding agents, including thiourea (6), and polyphenol oxidase is also inhibited by thiosinamine (allylthiourea) (7).

Several postulations (8–10) regarding the protective effects of a number of metal-binding radiation-protective agents have also been made. Although thiourea and its simple derivatives have some protective ability for whole-body irradiation of animals, these effects have not been appreciable. Thioureas have, however, shown substantial radiation-protective effects in other systems, such as mouse lung (11), human erythrocytes (12), T_2 phage (13), Ehrlich ascites cells (14), and macromolecules (15) (Table I). The radiation-protective effects of thiourea have been attributed to metal binding (11).

With such a significant number of postulations involving the metal-binding aspects of thioureas, it is surprising to find that, other than for thiourea itself (16), metal-binding abilities of substituted thioureas have not been determined. Stability constants for a series of cyclic thioureas, including mercaptoimidazoles and mercaptouracils, were determined with copper, iron, and aluminum ions (17), and the constants were surprisingly high. It was considered important, therefore, to measure the metal-binding stability constants for a series of alkyl, aralkyl, and cyclic thioureas. Knowledge of the magnitude of the constants would indicate whether thiourea complexes were capable of existence in the presence of cellular complexing agents, such as peptides, or whether thiourea might function as a transient metal complexer.

Compounds of the general structures I–III were measured for binding abilities to Cu(II), Ni(II), Al(III) and Fe(III) ions using the method of potentiometric titration.

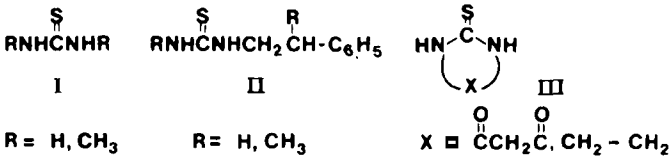

EXPERIMENTAL SECTION

Materials—Analytical reagent-grade[1] aluminum chloride hexahydrate, cupric chloride dihydrate, ferric nitrate nonahydrate, and nickel(II) chloride hexahydrate were used for the metal complexation determination. Carbonate-free 0.01 M KOH was prepared according to the method of Armstrong (18). Solutions of the metal salts were prepared in boiled distilled water and stored in polyethylene bottles under nitrogen; they were diluted quantitatively with carbon dioxide-free water just prior to use. Normalities were checked against potassium biphthalate.

The organic ligands were obtained commercially[2]. *N*-Methyl-*N'*-phenethylthiourea was reported previously (19), and *N*-methyl-*N'*-phenyl-2-propylthiourea was described earlier (20). Purity was ascertained by TLC using chromagram sheets[3]. Solutions (0.1%) of the compounds in ethanol were spotted, and the sheets were developed with benzene–methanol (8:2); spots were detected with iodine vapor.

Ionization Constants—The method of Albert and Serjeant (21) was used, which consisted of titrations of 0.001 M solutions of the compounds in 95% ethanol with 0.01 M KOH in 0.5-mL portions. The pH was recorded with a pH meter[4] with glass and calomel electrodes after each addition. Each titration thus yielded 10 pH values, giving 10 values for the pK_a, which were averaged (Table II). Since most of the pH values fell outside the 5–9 range, corrections were made for hydrogen-ion concentrations.

Stability Constants—Potentiometric titrations were carried out under nitrogen in 95% ethanol at 25°C with the described pH meter. Volumes of 50 mL of the 0.001 M solutions of the organic ligands were titrated with 0.01 M KOH in 0.5-mL portions, first in the absence of metal ions, and then in the

[1] J. T. Baker Analyzed Reagents.
[2] Aldrich Chemical Co., Eastman Organic Chemicals, or Fisher Scientific Co.
[3] Eastman Organic Chemicals.
[4] Beckman Instruments.

0022-3549/84/0900-1284$01.00/0
© 1984, American Pharmaceutical Association

Table I—Radiation Protection by Thioureas

Compound	Test System	Radiation Dose	Protection	Ref.
Thiourea	Mice	875 rad	Increased lifespan	31
Methylthiourea	Mice	650–700 rad	No effect on lifespan	32
Allylthiourea	Mice	700 rad	No effect on lifespan	8
Phenylthiourea	Mice	650–700 rad	No effect on lifespan	32
α-Naphthylthiourea	Mice	200 rad	No effect on lifespan	33
Ethyl isothiourea	Mice	800 rad	Increased lifespan	34
Sulfanilylthiourea	Mice	900 rad	Increased lifespan	35
Guanylthiourea	Mice	900 rad	Increased lifespan	35
Thiourea	Human erythrocytes	84 krad	Protection	12
Thiourea	T_2 phage	1000 rad/s	Protection	13
Thiourea	Ehrlich ascites cells	4000 rad	Protection	14
Allylthiourea	Human erythrocytes	84 krad	Protection	12

Table II—Ionization Constants [a]

Compound	pK_a
Thiourea	2.54[b]
N-Methylthiourea	3.06
N,*N*′-Dimethylthiourea	2.98
N-Methyl-*N*′-phenethylthiourea	3.12
N-Methyl-*N*′-phenyl-2-propylthiourea	3.04
2-Imidazolidinethione	3.08
2-Thiobarbituric acid	4.15
Thioacetamide	3.34

[a] Determined in 95% ethanol at 25°C. [b] Literature value (H_2O) is 2.03: T. J. Lane, J. A. Ryan, and J. L. Walter, *J. Am. Chem. Soc.*, **78**, 5560 (1956).

presence of 0.0005 mol of divalent metal salt or 0.00033 mol of trivalent metal salt.

Volumes of 50 mL of the same quantities of the metal salts were also titrated with 0.01 M KOH. The pH readings were recorded 2 min after each addition of titrant to allow equilibrium to be reached. Solvent concentration at the end of the titrations (if all 10 additions were made) was ~72% ethanol.

Calculations were performed as previously described (17) with a computer. The log K values obtained for the divalent metal complexes are recorded in Table III; values for the trivalent metal complexes are recorded in Table IV. Values for K_1, K_2, and K_3 were obtained from Eqs. 1–3, according to Flood and Loras (22) and Albert (23):

$$K_1 = \frac{\bar{n}}{(1-\bar{n})[L^-]} \quad \text{(Eq. 1)}$$

$$K_2 = \frac{(\bar{n}-1)}{(2-\bar{n})[L^-]} \quad \text{(Eq. 2)}$$

$$K_3 = \frac{(\bar{n}-2)}{(3-\bar{n})[L^-]} \quad \text{(Eq. 3)}$$

where $\bar{n}$ is the average number of ligand molecules bound by a metal ion at any stage in complex formation and $[L^-]$ is the concentration of the free chelating species.

Formation curves were plotted ($\bar{n}$ *versus* $-\log L^-$) to show whether stepwise complexation may have taken place. No steps were shown in the plots, probably because of the closeness of the log K values.

RESULTS AND DISCUSSION

The K_1 values for the Al(III) and Fe(III) complexes were not uncovered, with the exception of the ferric complex of thioacetamide, possibly because of lack of stepwise complexation (no values for $\bar{n}$ below 1 were obtained). No values for the ferric complex of 2-thiobarbituric acid were obtained because of precipitate formation at the beginning of the titration. Values for K_2 for the Cu(II) and Ni(II) complexes were not obtained because of the formation of precipitates, with the exception of the complexes of 2-thiobarbituric acid. Although log β values could not be obtained in most cases, for the purposes of comparison and for determining whether thiourea complexes are capable of existence in the presence of cellular complexing agents, the constants found should suffice.

The sequence of stability constants of thiourea, *N*-methylthiourea, and *N*,*N*′-dimethylthiourea allow some conclusions regarding structure of the complexes. The complexes of *N*-methylthiourea showed decreased stability constants, compared with those of thiourea, for the aluminum and ferric systems, but increased constants for the cupric and nickel systems. For the latter systems, where only K_1 values were observed, steric effects of the methyl group would be minimal. For the aluminum and ferric systems, the decrease in stability constants may be attributed to steric effects, since 2:1 and 3:1 complexes are involved. These sequences suggest that both the sulfur and a nitrogen atom are involved in bond formation of the complexes.

With the complexes of *N*,*N*′-dimethylthiourea, the additional methyl group caused a decrease in constants for all four metal ions observed. Two methyl groups apparently cause steric hindrance of the 1:1 complexes as well. The longer-chain substituents gave somewhat higher constants than the methyl groups, so the α-methylene groups were less interfering than the methyl groups. For the cyclic thioureas, particularly 2-thiobarbituric acid, where steric hindrance would be less than for the open-chain complexes, the stability constants were the largest of the series. It is also possible that some degree of aromaticity is possible with 2-thiobarbituric acid.

Table III—Stability Constants for Cu(II) and Ni(II) Complexes (25°C)

Compound	Cu(II) Complexes[a]			Ni(II) Complexes		
	log K_1	log K_2	log β_2	log K_1	log K_2	log β_2
Thiourea	1.38[b]			1.00		
N-Methylthiourea	1.67			1.39		
N,*N*′-Dimethylthiourea	1.35			1.33		
N-Methyl-*N*′-phenethylthiourea	1.51			1.47		
N-Methyl-*N*′-phenyl-2-propylthiourea	1.44			1.45		
2-Imidazolidinethione	1.66			1.40		
2-Thiobarbituric acid	4.35	3.79	8.14	3.76	3.18	6.94
Thioacetamide	2.30			1.69		

[a] The product of Cu(II) and thiourea is claimed to be a Cu(I) complex: E. I. Onstott and H. A. Laitinen, *J. Am. Chem. Soc.*, **72**, 4724 (1950). [b] The log β_2 for Cu(II) and thiourea was estimated by Bjerrum to be ~2: L. G. Sillén and A. E. Martell, "Stability Constants of Metal-Ion Complexes," The Chemical Society, London, 1964, p. 359.

Table IV—Stability Constants for Al(III) and Fe(III) Complexes (25°C)

Compound	Al(III) Complexes		Fe(III) Complexes			
	$\log K_2$	$\log K_3$	$\log K_1$	$\log K_2$	$\log K_3$	$\log \beta_3$
Thiourea	3.01	1.69		3.55	2.16	
N-Methylthiourea	2.73	1.90		3.00	2.16	
N,N'-Dimethylthiourea	2.61	1.81		2.87	2.28	
N-Methyl-*N'*-phenethylthiourea	3.79	2.21		3.59	2.41	
N-Methyl-*N'*-phenyl-2-propylthiourea	3.59	2.21			2.84	
2-Imidazolidinethione	3.61	2.12		3.92	2.40	
2-Thiobarbituric acid	5.15	3.29				
Thioacetamide	3.06	2.23	4.12	3.40	2.25	9.77

It has been shown previously (17) that stability constants for metal complexes of 2-mercaptoimidazoles and mercaptopyrimidines were relatively high, and that both sulfur and nitrogen were involved in bond formation to give four-membered rings. Four-membered metal chelate rings have also been reported for dithiocarbamates and xanthates (24), and for dithiocarboxylates (25). Ruthenium complexes of thioureas have also been postulated to involve the sulfur and nitrogen in four-membered rings (26).

If complexation to sulfur alone were involved, the presence of *N*-methyl substituents would be expected to increase stability constants by electron release. But the probable effect of steric hindrance by the methyl groups, as indicated for the decreased stability of 2:1 and 3:1 Al(III) and Fe(III) complexes, allow the postulation of four-membered chelate rings involving bonding to both sulfur and nitrogen (IV and V).

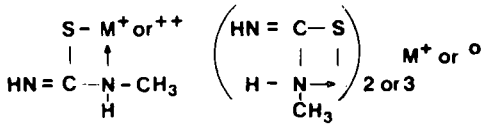

IV V

The magnitude of the metal-binding stability constants observed is somewhat lower than that for simple peptides. Log K_1 values reported for the Cu(II) and Ni(II) complexes of glycyl-DL-alanine, for instance, are 5.92 and 4.08, respectively (27). Although metal complexes of thioureas, with the possible exception of cyclic thioureas, should not be expected to exist in the presence of cellular peptides for any appreciable period, they should be capable of binding to the metal constituents of metalloenzymes.

Wheeler and Ribot (28) observed the protective effect of thiourea and methylthioureas for radiation damage to a synthetic polymer. Presence of the methyl groups distinctly lowered the protective ability of thiourea. It would not appear in this system that metal ions are involved in the radiation damage, which must be due largely to the radicals resulting from radiolysis of water. In this case, the ability of the thioureas to act similarly to the thiol radiation-protectors, in transferring hydrogen atoms to the radiation-produced radicals (29), would appear to offer a more probable mechanism of protection. The ability of thioureas to enter a thione–thiol equilibrium would make hydrogen atom transfer a realistic possibility, and in view of the rather low metal-binding stability constants for thioureas, a more likely mechanism than the ability to bind copper or iron ions, which catalyze cellular oxidations. A previous attempt to relate metal-binding ability to radiation protection of a series of aminoalkyl disulfides and thiosulfates did not give a positive correlation (30).

Involvement of thioureas with metalloenzymes, such as dopamine-β-oxidase, nitrate reductase, or polyphenol oxidase, is still a likely possibility by complexation of the metal constituent, however. A correlation between metal-binding ability and the antimicrobial effects of cyclic thioureas has already been observed (17), possibly through the inhibition of metalloenzyme activity.

REFERENCES

(1) S. Friedman and S. Kaufman, *J. Biol. Chem.*, **240,** 4763 (1965).

(2) G. A. Johnson, S. J. Boukma, and E. G. Kim, *J. Pharmacol. Exp. Ther.*, **168,** 229 (1969).

(3) M. J. Seven and L. A. Johnson, "Metal-Binding in Medicine," J. B. Lippincott, Philadelphia, Pa., 1960, p. 321.

(4) S. Garattini and A. Leonardi, *Giorn. Ital. Chemterap.*, **2,** 18 (1955).

(5) A. K. Sijpesteijn, M. J. Janssen, and G. J. VanderKerk, *Biochim. Biophys. Acta*, **23,** 550 (1957).

(6) R. H. Garrett and P. Greenbaum, *Biochim. Biophys. Acta*, **302,** 33 (1973).

(7) H. Less, *Nature (London)*, **158,** 97 (1946).

(8) P. Alexander, Z. M. Bacq, S. F. Cousens, M. Fox, A. Herve, and J. Lazar, *Radiat. Res.*, **2,** 392 (1955).

(9) M. M. Jones, *Nature (London)*, **185,** 96 (1960).

(10) W. O. Foye and J. Mickles, "Progress in Biochemical Pharmacology," vol. 1, Butterworths, Washington, D.C., 1965, pp. 152–160.

(11) H. Langendorff, R. Koch, and U. Hagen, *Arch. Intern. Pharmacodyn.*, **100,** 1 (1954).

(12) K. Flemming, *Folia Haemat. (Leipzig)*, **77,** 147 (1960); through *Chem. Abstr.*, **55,** 3687 (1961).

(13) P. Howard-Flanders and P. Jockey, *Int. J. Radiat. Biol.*, **2,** 361 (1960).

(14) V. Drasil, *Biol. Eff. Ioniz. Radiat. Mol. Level, Proc. Symp., 1962*, **91–7;** through *Chem. Abstr.*, **58,** 14413, (1963).

(15) A. Charlesby and P. M. Kopp, *Proc. Roy. Soc., Ser. A*, **291,** (1424), 113 (1966).

(16) L. G. Sillén and A. E. Martell, "Stability Constants of Metal-Ion Complexes," Suppl. 1, The Chemical Society, London, 1971, pp. 238–240.

(17) W. O. Foye and J.-R. Lo, *J. Pharm. Sci.*, **61,** 1209 (1972).

(18) D. M. G. Armstrong, *Chem. Ind. (London)*, **1955,** 1405.

(19) W. O. Foye and J. C. Anderson, *J. Pharm. Sci.*, **58,** 1558 (1969).

(20) W. O. Foye and J. N. Sane, *J. Pharm. Sci.*, **66,** 923 (1977).

(21) A. Albert and E. P. Serjeant, "The Determination of Ionization Constants," Chapman and Hall, London, 1971.

(22) H. Flood and V. Loras, *Tidsskr. Kjemi Bergv. Met.*, **4,** 35 (1944); through *Chem. Abstr.*, **41,** 6488 (1947).

(23) A. Albert, *Biochem. J.*, **47,** 531 (1950).

(24) J. Chatt, L. A. Duncanson, and L. M. Venanzi, *Nature (London)*, **177,** 1042 (1956).

(25) B. G. Werden, E. Billig, and H. B. Gray, *Inorg. Chem.*, **5,** 78 (1966).

(26) R. P. Yaffe and A. F. Voigt, *J. Am. Chem. Soc.*, **74,** 2503 (1952).

(27) L. G. Sillén and A. E. Martell, "Stability Constants of Metal-Ion Complexes," Suppl. 1, The Chemical Society, London, 1971, p. 386.

(28) O. H. Wheeler and R. A. Ribot, *Chem. Ind. (London)*, **30,** 1017 (1969).

(29) W. O. Foye, *Int. J. Sulfur Chem.*, **8,** 161 (1973).

(30) W. O. Foye and J.-M. Hu, *J. Pharm. Sci.*, **68,** 202 (1979).

(31) R. H. Mole, J. St. L. Philpot, and J. R. V. Hodges, *Nature (London)*, **166,** 515 (1950).

(32) L. F. Semenov and E. A. Prokudina, *Med. Radiol. (Moscow)*, **1/4,** 70 (1956); through *Chem. Abstr.*, **51,** 13212 (1957).

(33) H. Langendorff, R. Koch, and U. Hagen, *Arch. Int. Pharmacodyn.*, **104,** 57 (1955).

(34) J. F. Noble, V. J. Plzak, R. M. Dowben, and J. Doull, *Fed. Proc. Fed. Am. Soc. Exp. Biol.*, **16,** 325 (1957).

(35) K. Stratton and E. M. Davis, *Int. J. Radiat. Biol.*, **5,** 105 (1962).

ACKNOWLEDGMENTS

Abstracted in part from a thesis submitted by C.-C. Chao to the Massachusetts College of Pharmacy and Allied Health Sciences in partial fulfillment of the Master of Science degree requirements. Part XVIII of this series is W. O. Foye and J.-M. Hu, *J. Pharm. Sci.* **68,** 202 (1979).

Percutaneous Absorption of Corticosteroids: Age, Site, and Skin-Sectioning Influences on Rates of Permeation of Hairless Mouse Skin by Hydrocortisone

CHARANGIT R. BEHL *, GORDON L. FLYNN ˣ, EDWARDS E. LINN, and WARD M. SMITH

Received July 25, 1983, from the *College of Pharmacy, The University of Michigan, Ann Arbor, MI 48109.* Accepted for publication October 5, 1983. *Present address: Pharmacy Research, Hoffmann-LaRoche, Inc., Nutley, NJ 07110.

Abstract □ As part of a long-range plan to decipher the mechanism of mass transfer of corticosteroids across skin, the permeation of [^{3}H]hydrocortisone through hairless mouse skin was characterized by *in vitro* diffusion cell techniques. Age and anatomical site-related behaviors were explored mainly with whole skin but also with skin stripped of its horny layer. Permeability of the mouse skin was low shortly after birth and increased during the singular normal hair cycle exhibited by the SKH-hr^{-1} mouse strain. The return to a hairless state over a period of 20–35 d was accompanied by decreased permeability of hydrocortisone. A permeability coefficient of $\sim 2 \times 10^{-4}$ cm/h was found for the mature mouse. For whole skin, there was no difference in the permeabilities of dorsal and abdominal skin sections, but for stratum corneum-free membranes and dermal membranes, the abdominal site appeared to be more permeable, which is consistent with its thinner dimensions. Totally stripped skin and isolated dermis are ~500 and ~1000 times more permeable than intact skin, respectively; the unaltered stratum corneum of the hairless mouse is thus shown to be the major barrier to the mass transfer of hydrocortisone.

Keyphrases □ Absorption, percutaneous—hydrocortisone, influence of age, site, and skin sectioning on permeation rates, hairless mouse skin □ Hydrocortisone—percutaneous absorption, influences of age, site, and skin sectioning on permeation rates, hairless mouse skin

In previously published studies on the absorption through skin of hydrocortisone (the prototype of the corticosteroids), it was noted that the process is highly sensitive to the manner of treatment of the skin sample. The first evidence of its absorption was skin atrophy on repetitive applications to rat skin (1). When ^{14}C-labeled hydrocortisone became available, direct proof of its passage through skin in the form of radioisotope collected in urine after topical applications to human volunteers was gathered (2). By such methods, it was possible to show that only tiny fractions of the applied steroid passed through intact skin (2, 3), but that absorption through diseased and inflamed skin was far more facile (4). Occlusion was demonstrated to improve absorption by several times that without occlusion (3), and stripping of skin had exaggerated effects of enhancement (3, 5). By using a similar technique in monkeys, the influences of the amount of hydrocortisone applied to a specified area and the frequency of application have been described (6), and the important conclusion that absorption of hydrocortisone through skin is increased on long, continuous application has been reached (7). Along these lines, hairless mouse epidermal sections excised from animals treated with UV light and acetic acid–retinoic acid (vitamin A), all of which were under circumstances that induced epidermal hyperplasia, were measurably more permeable to hydrocortisone than were the skin samples used as controls (8). Excised skin (human) has also been used to study vehicle effects (9, 10). Hydrocortisone has also been shown in human volunteers to be a relatively feeble inhibitor of induced inflammation when directly compared with its intermediate-chain-length 21-alkyl esters (11).

All of the mentioned absorption-related phenomena and influences can be put to stringent, quantitative testing by *in vitro* diffusion cell methods. Yet, to date, only Scheuplein *et al.* (12) have characterized the permeabilities of such compounds, finding human epidermal permeability coefficients of 3×10^{-6} cm/h for hydrocortisone and 1×10^{-5} cm/h for cortisone. It is the specific purpose of this study to obtain, by using the hairless mouse model system, baselines on the absorption of hydrocortisone as a prelude to factoring the degree of permeation dependency of corticosteroid pharmacological responses.

EXPERIMENTAL SECTION

Chemicals—The tritiated hydrocortisone[1] used in these studies had a stated radiochemical purity of >99% and a specific radioactivity of 95.2 Ci/mmol. Sodium chloride irrigation[2] was used as an isotonic medium in which to prepare the hydrocortisone solutions and as the medium of the receptor compartment of the diffusion cell. [^{3}H]Hydrocortisone stock solutions, with a radiochemical activity of ~100 μCi/mL, were prepared. These solutions were diluted roughly 15-fold during the course of charging the donor compartment of the cell. Final concentrations of hydrocortisone in the chamber of the diffusion cell were $<10^{-5}$ M.

Membrane Preparation—The basic techniques for prepartion of the membranes and for running of the permeation experiments have been previously reported (13–16) and, therefore, are only briefly described herein. In most studies, the membranes were full-thickness skin sections from the abdominal and dorsal surfaces of hairless mice, SKH-hr^{-1} strain[3]. Male hairless mice of known ages were sacrificed by spinal cord dislocation. Rectangular sections of skin, several centimeters in each dimension, were excised from the animal, and the adhering fat and other visceral debris were removed. After trimming each excised skin section into an oversized, rough circle, the tissue was placed in a diffusion cell. Stretching of the skin, as evidenced by distortion or expansion of the circular marking, was corrected, and the cell halves were made fast with a spring clamp. The area available for diffusion between compartments was ~0.6 cm^2.

For some experiments, the skin surface, while still on the animal carcass, was stripped repeatedly of its stratum corneum cells by fastening adhesive tape[4] smoothly and securely to the surface with light pressure from the fingers. Attempts were made to obtain adhesion over the entire covered surface before the tape was abruptly removed. This procedure was repeated many times on each site with fresh pieces of adhesive tape used for each stripping.

Dermal sheets were prepared for the permeation studies by soaking excised skin sections for ~24 h, at which time the epidermis could be separated from the dermis by peeling carefully with the blade of a spatula. The isolated dermis layer was mounted in the diffusion chamber.

Diffusion Cells—Small glass diffusion cells, the dimensions of which have been reported previously, were employed (13–16). The cells were assembled with the freshly excised mouse skin between the half-cells. The assembled cells were then immersed in constant-temperature baths. The cell contents were stirred at 150 rpm.

Permeation Procedure—Each half-cell was partially filled (~1 mL) with saline, evacuated with a syringe, and filled with 1.4 mL of saline. The contents were mixed for 5 min to ensure temperature equilibration. Samples (100 μL) were withdrawn from each side; the samples were assayed to ensure that no residual radioactivity remained from previous runs. At this point, the donor

[1] Lot no. NET-396; New England Nuclear Corp., Boston, Mass.
[2] Abbott Laboratories, North Chicago, Ill.
[3] Skin Cancer Hospital, Philadelphia, Pa.
[4] Scotch Brand cellophane tape; 3M Co., Minneapolis, Minn.

0022-3549/84/0900-1287$01.00/0
© 1984, American Pharmaceutical Association

Table I—Permeability Coefficients and Lag Times of Hydrocortisone as a Function of Age and Anatomical Site

Mouse Age, d	n	Weight, g	Site[a]	$P_I \times 10^4$, cm/h[b]	Range of P_I	$t_{L,I}$, h[c]	Range of $t_{L,I}$	$P_{II} \times 10^4$, cm/h[b]	Range of P_I	$t_{L,II}$, h[c]	Range of $t_{L,II}$
5	3	3.67 ± 0.52	A	1.0 ± 0.3	0.7-1.2	7.6 ± 1.0	6.8-8.8	4.1	2.9-5.2	21.5[d]	18.3-24.6
			D	1.2 ± 0.1	1.1-1.3	9.9 ± 0.6	9.2-10.4	2.4 ± 0.2	2.3-2.6	17.8 ± 2.2	16.1-20.3
			C	1.1 ± 0.2	—	8.7 ± 1.5	—	3.1 ± 1.2	—	1.93 ± 3.4	—
15	5	7.8 ± 0.44	A	3.7 ± 1.3	2.5-5.2	4.4 ± 1.6	2.5-6.4	—	—	—	—
			D	4.5 ± 2.4	3.1-8.7	7.8 ± 2.4	5.2-11.4	—	—	—	—
			C	4.1 ± 1.9	—	6.1 ± 2.6	—	—	—	—	—
20	5	10.4 ± 0.65	A	3.4 ± 1.5[b]	2.3-5.5	5.3 ± 0.7	4.3-5.9	—	—	—	—
			D	4.4 ± 1.6	3.0-5.8	6.2 ± 1.5[d]	3.6-7.0		—	—	—
—			C	3.9 ± 1.3	—	5.8 ± 1.2	—	—	—	—	—
35	2	21.5 (21,22)	A	3.1	3.0-3.1	5.9	5.7-6.2	15.7	13.0-18.4	24.7	23.7-25.8
			D	3.1	3.0 3.2	7.4	6.7-8.1	20.8	18.5-23.1	25.9	25.5-26.4
			C	3.1 ± 1.0	—	6.7 ± 1	—	18.3 ± 4.1	—	25.3 ± 1.2	—
516	3	40.7 ± 1.5	A	2.4 ± 0.5	1.9-2.8	6.9 ± 0.7	6.1-7.4	—	—	—	—
			D	1.6 ± 0.4	1.3-2.0	8.6 ± 3.2	6.1-12.2	—	—	—	—
			C	2.0 ± 0.6	—	7.7 ± 2.3	—	—	—	—	—
657	2	41.0 (41,41)	A	1.7	1.2-2.1	11.8	9.3-14.2	—	—	—	—
			D	1.7	1.2-2.2	11.0	9.6-12.5	—	—	—	—
			C	1.7 ± 0.6	—	11.4 ± 2.4	—	—	—	—	—
80-100[e]		—	—	~3.0	—	~10	—	~90	—	~45	—

[a] A, D, and C represent abdominal, dorsal, and combined sites, respectively. [b] P_I and P_{II} are the permeability coefficients in phases I and II, respectively. [c] $t_{L,I}$ and $t_{L,II}$ are the lag times of phases I and II, respectively. [d] Average of one less value than the number of mice is indicated; an anomalous value was discarded. [e] Independent studies with an HPLC assay with nonradiolabeled hydrocortisone are to be presented in another report.

Table II—Permeability Coefficients of Hydrocortisone through Stripped Skin and Dermal Sections

No. of Strippings	Mouse Age, d	n	Site[a]	$P \times 10^4$, cm/h ± SD[b]	Range of $P \times 10^4$, cm/h	Average Ratio (D/A) of P[c]	Average P over Both Sites $\times 10^4$, cm/h
25	62	3	A	1080 ± 150	990-1250	0.58	855
			D	630 ± 210	390-790		
50	65	3	A	1310 ± 110	1190-1390	0.70	1110
			D	900 ± 55	850-950		
100	65	2	A	1560 ± 190	1360-1740	0.72	1340
			D	1110 ± 66	1060-1160		
Dermis	150	1	A	1890	—	0.81	1710
			D	1530	—		

[a] A and D represent abdominal and dorsal surfaces, respectively. [b] P is presented to allow direct comparisons to be made with data in Table I. [c] Average of the individual ratios for each mouse.

compartment was charged with 100 μL of the stock solution. Saline (100 μL) was added to the receiver. At predetermined intervals, samples were withdrawn from the respective compartments, transferred to vials containing scintillation cocktail[5] (10 mL), and assayed on a liquid scintillation counter[6].

The moment of charging the donor half-cell marked the zero time point for the diffusional run. Two minutes elapsed before the initial donor sample was withdrawn to allow for uniform mixing, and the concentration of this sample was used as the initial donor cell concentration. The overall procedure was designed to maintain an essentially fixed concentration across the membrane during the course of a run. The permeation entered pseudo steady state, and the permeability coefficients of the steroids were readily ascertained.

Analysis of Data—The data were plotted as counts collected in the receptor compartment as a function of time. Correction was made for sampling, which in all cases was done by replacing with saline. The permeability coefficient for a given run was calculated from:

$$J_T = P \cdot A \cdot \Delta C = V\frac{dC}{dt}$$

where J_T is the total pseudo-steady-state flux (in cpm/s) across the skin, P is the permeability coefficient (in cm/s); A is the diffusional area (in cm^2); ΔC is the concentration differential across the membrane, which was taken to be equal to the donor phase concentration, (in cpm/mL); V is the half-cell volume and volume of the receptor compartment (in mL); and dC/dt is the steady-state slope in terms of cpm/mL/s.

RESULTS

Some representative permeation plots obtained from runs with full-thickness skin sections taken from mice at 5, 20, 35, and 516 d of age are shown in Fig. 1. All runs were carried out for ~40 h. At 5 and 35 d, such plots were of a biphasic nature. Two lag times and two permeability coefficients were recorded in such instances. Data from runs such as these are summarized in Table I.

Table II is a compilation of data obtained on processed skins, *i.e.*, skins stripped of stratum corneum and dermis isolated by soaking overnight in saline. All data in Tables I and II were collected at 37°C.

DISCUSSION

Effect of Age—The permeabilities of the SKH-hr^{-1} hairless mouse skin to alkanols have previously been shown to pass through a cycle over the first 3 weeks of life (17), which is coincident with the development of a coat of fur. Similar behavior is evident for hydrocortisone, even within the limited number of age points available (Fig. 2). At 5 d (before the first appearance of hair), the permeability was low. By 15 d (slightly past midcycle and about the point in time of the first shedding of the coat), the permeability coefficient was ~3.7 times larger than the value at 5 d, and it remained high to near the end of the hair cycle (20 d). The overall averages at the latter two time points are statistically larger than the greater 5-d average (Student t test; $p < 0.01$). Based on permeability coefficients measured in the early phase of permeability of skins from 35-d-old mice and older, the permeability of hydrocortisone through the intact skin declined slightly after shedding of the furry coat, which was more or less complete at 25 d of age. The permeability coefficients of hydrocortisone through unbroken, mature mouse skin of the specified strain is on the order of 2×10^{-4} cm/h.

Permeability of Processed Skin Sections—In these studies, some skin samples were stripped 25, 50, and 100 times with adhesive tape and others were soaked overnight to remove the entire epidermal layer from the skin, leaving sheets comprised strictly of dermis and a thin film of protective tissue covering the undersurface of the dermis. The overall averages for the permeability coefficients of these processed tissues (Table II) are plotted against the number of strippings (Fig. 3). The isolated dermis represents infinite stripping. This plot indicates a systematic increase in permeability as the

[5] Aquasol; New England Nuclear Corp.

[6] Model 200 or 9000 scintillation counter; Beckman Instruments Co., Fullerton, Calif.

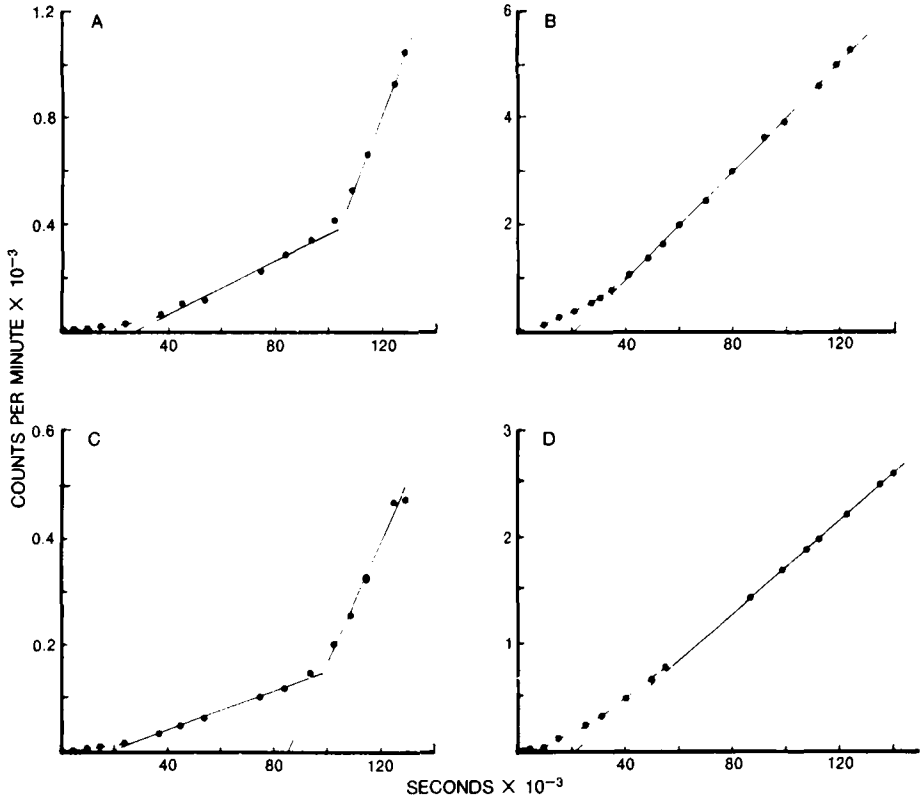

Figure 1—*Representative plots of counts per minute* versus *time for the permeation of hydrocortisone through the skins of hairless mice, aged 5 d (A), 20 d (B), 35 d (C), and 516 d (D).*

strippings become more numerous, but even at 100 strippings, the skin appears to be less permeabile than the dermis alone. The bulk of the barrier impairment is accomplished with 25 strippings, however, and the permeability coefficient is increased by roughly 300 times relative to the intact skin at this point. Seventy-five more tape strippings only doubled the coefficient again, whereas removal of the entire epidermis produced only a 2.5-fold additional increase. Past work with alkanols has indicated that 25 strippings effectively removed the entire stratum corneum. At first impression, the data obtained with hydrocortisone suggest that this may not be so. However, the stripping procedure is laborious and it is suspected that wear and tear of the resident living epidermal matrix, and possibly the dermis, may be responsible for increased permeability after exaggerated stripping rather than further removal of horny cells. As with all previous permeating species, the isolated dermal membrane is from 1.5 to 2 times more permeable than stripped skin, which is consistent with a resistance in the viable epidermis of the same order of magnitude as that of the dermis, which is much thicker. Finally, the absolute permeability coefficients of skin stripped 25 times (~0.085 cm/h) and isolated dermis (~0.17 cm/h) are roughly one-half the values found for the alkanols (14, 18) and for phenol (19) with tissue prepared in a comparable manner from mice of comparable age. On the other hand, neomycin, a larger molecule than hydrocortisone, is less permeable than the corticosteroid (20). There is a readily evident molecular size dependency to diffusion across these processed skin sections.

Anatomical Site as a Permeability Variable—Among all the studies, dorsal and abdominal skin sections from the same animals were studied in tandem. As far as we could determine, the permeabilities of full-thickness skin sections taken from these locations were the same. In contrast, stripped skin sections and isolated dermal sections from the abdomen appear to be one-third more permeable than comparably prepared sections from the back of the animals. Given that the intact skin section is several hundred times less permeable than the least-permeable sample of processed tissue, the implication is clear that the horny layers on the two sites have essentially the same barrier property. When the stratum corneum is removed, back sections evidence slightly greater diffusional resistance because they are, based on previous measurement (17), 40–50% thicker at 65 d of age.

Hairless Mouse–Human Comparison—Scheuplein *et al.* (12) have reported 3×10^{-6} cm/h as the 25°C value for the permeability coefficient of hydrocortisone through human epidermal membranes under similar experimental conditions. Considering that the 37°C permeability coefficient for hairless mouse skin lies somewhere between 1.1×10^{-4} and 4.1×10^{-4} cm/h (Table I, early phase or P_1 values), it appears as if this tissue in its normal state is many

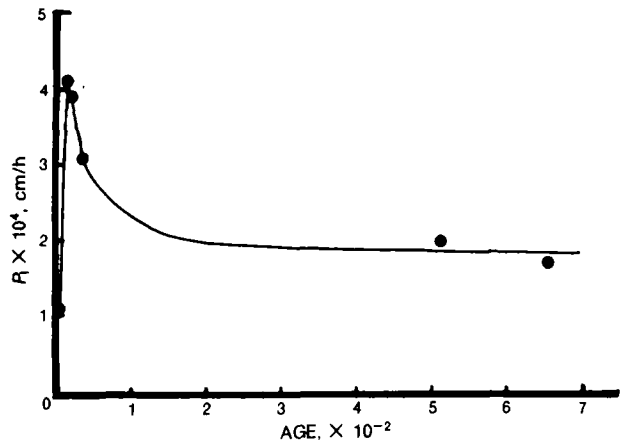

Figure 2—*Permeability coefficients (P_1 values) of hydrocortisone through hairless mouse skin as a function of mouse age.*

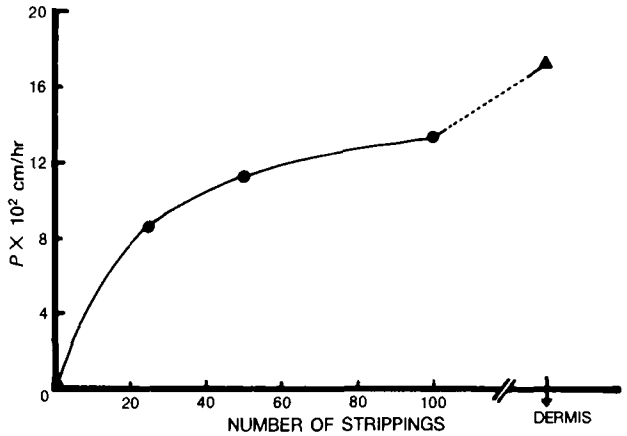

Figure 3—*Permeability coefficients of hydrocortisone through hairless mouse skin as a function of number of strippings. Data are also presented for the dermis. All data points represent average values of the abdominal and dorsal permeability coefficients.*

times more permeable to hydrocortisone than human skin. Assignment of an exact factor to this difference is made difficult, as the representativeness of the human epidermal value is uncertain, with there being no statistical data provided, nor are the temperature sensitivities of the permeation of hydrocortisone through the tissues known (but they can be assumed to be large). Nevertheless, this appears to be the first clear demonstration that to some permeating species, intact human and hairless integuments offer quantitatively different mass transfer resistances, with human skin being at least one logarithmic order less permeable. Previous diffusion cell-generated data for the alkanols (13, 14, 16) and phenol (19) have left the impression that the two skin types were, for practical purposes, identical in permeability.

Biphasic Character in Some Permeability Plots—A most unusual feature of some of these data is the biphasic quality of the permeability plots obtained with mice 5 and 35 d old. At 35 d of age, this aspect of the data was unequivocal. Like other researchers (8), we at first assumed that the skin membranes were deteriorating. However, when the permeability coefficient of a single section of skin was repetitively assessed approximately every 12 h over a 100-h period, using a previously outlined "hydration" protocol (16), the permeability coefficient remained constant at 2.5×10^{-4} cm/h. Subsequently, additional evidence has been gathered on skin of older animals which shows these same qualities (21), and it now appears that if a run is long and continuous, two distinct phases of permeation will be evident, with the second, more permeable, phase being as reproducible in its time of onset and permeability rate as the first. However, the onset of the second phase is at >40 h with the older skin sections, which is, by chance, the arbitrarily selected duration for the experiments reported here and which explains why the second phase was not apparent with the older skin sections. Also, the permeability coefficient of the second phase seems to increase dramatically with mouse age (consider the data for 5- and 35-d-old mice presented here). We suspect it was not evident after 5 d but not until 35 d because permeability in the early phase dominated events at 15 and 20 d. The physicochemical implication that this represents two separate and parallel permeability pathways through the stratum corneum with different dependencies on animal age is clear. This concept is mechanistically important and is thus being put to rigorous experimental testing.

REFERENCES

(1) F. D. Malkinson, *J. Soc. Cosmet. Chem.*, **11**, 146 (1960).

(2) F. D. Malkinson and E. H. Ferguson, *J. Invest. Dermatol.*, **25**, 281 (1955).

(3) R. J. Feldman and H. I. Maibach, *Arch. Dermatol.*, **91**, 661 (1965).

(4) C. S. Livingood, *J. Invest. Dermatol.* **31**, 27 (1958); in discussion of Ref. 5.

(5) F. D. Malkinson, *J. Invest. Dermatol.* **31**, 19 (1958).

(6) R. C. Wester, P. K. Noonan, and H. I. Maibach, *Arch. Dermatol.*, **113**, 620 (1977).

(7) R. C. Wester, P. K. Noonan, and H. I. Maibach, *Arch. Dermatol.*, **116**, 186 (1980).

(8) A. E. Solomon and N. J. Lowe, *Br. J. Dermatol.*, **100**, 717 (1979).

(9) H. Shinkai and I. Tanaka, *Yakugaku Zasshi*, **89**, 1283 (1969).

(10) H. Shinkai, *Yakugaku Zasshi*, **89**, 365 (1969).

(11) C. A. Schlagel, *Adv. Biol. Skin*, **12**, 339 (1972).

(12) R. J. Scheuplein, I. H. Blank, G. J. Brauner, and D. J. MacFarlane, *J. Invest. Dermatol.*, **52**, 63 (1969).

(13) H. Durrheim, G. L. Flynn, W. I. Higuchi, and C. R. Behl, *J. Pharm. Sci.*, **69**, 781 (1980).

(14) G. L. Flynn, H. Durrheim, and W. I. Higuchi, *J. Pharm. Sci.*, **70**, 52 (1981).

(15) C. R. Behl, G. L. Flynn, T. Kurihara, W. Smith, O. Gatmaitan, W. I. Higuchi, N. F. H. Ho, and C. L. Pierson, *J. Invest. Dermatol.*, **75**, 340 (1980).

(16) C. R. Behl, G. L. Flynn, T. Kurihara, N. Harper, W. Smith, W. I. Higuchi, N. F. H. Ho, and C. L. Pierson, *J. Invest. Dermatol.*, **75**, 346 (1980).

(17) C. R. Behl, G. L. Flynn, T. Kurihara, W. M. Smith, N. Bellantine, O. G. Gatmaitan, C. L. Pierson, W. I. Higuchi, and N. F. H. Ho, *J. Soc. Cosmet. Chem.*, **35**, 237 (1984).

(18) C. R. Behl, M. Barrett, G. L. Flynn, T. Kurihara, K. A. Walters, O. G. Gatmaitan, N. Harper, W. I. Higuchi, N. F. H. Ho, and C. L. Pierson, *J. Pharm. Sci.*, **71**, 229 (1982).

(19) C. R. Behl, E. E. Linn, G. L. Flynn, C. L. Pierson, W. I. Higuchi, and N. F. H. Ho, *J. Pharm. Sci.*, **72**, 391 (1983).

(20) E. E. Linn, Ph.D. Thesis, "Thermotropic Effects on Skin Permeability," University of Michigan, Arbor, Mich., 1982.

(21) W. M. Smith, Ph.D. Thesis, "An Inquiry into the Mechanism of Percutaneous Absorption of Hydrocortisone and its 21-*n*-alkyl Esters," University of Michigan, Ann Arbor, Mich., 1982.

ACKNOWLEDGMENTS

This work was presented in part at the 127th Annual Meeting of the American Pharmaceutical Association, Washington, D.C., April 1980 (Basic Pharmaceutics Section Abstract No. 100).

Determination of Minoxidil in Bulk Drug and Pharmaceutical Formulations by Ion-Pairing High-Performance Liquid Chromatography

P. A. ASMUS ˣ, J. B. LANDIS, M. E. GRANT, and H. A. HAVEL

Received June 8, 1983, from *Control Analytical Research and Development, The Upjohn Company, Kalamazoo, MI 49001.* Accepted for publication September 23, 1983.

Abstract □ An ion-pairing liquid chromatographic method with UV detection is described for the determination of minoxidil in bulk drug, compressed tablet, and topical solution formulations. The chromatographic system consists of a microparticulate octadecylsilica column and a mobile phase composed of sodium dioctylsulfosuccinate in aqueous methanol (pH 3). The bulk drug and the topical solution samples are prepared by the dissolution of the drug in internal standard solution. Sample preparation for the compressed tablet formulation involves dissolving the drug from an aliquot of pulverized sample and centrifuging to remove insoluble excipients. Quantitative recovery of minoxidil from formulation excipients was demonstrated; assay precision was <1% *CV*.

Keyphrases □ Minoxidil—compressed tablets, topical solution and bulk drug, HPLC □ HPLC—minoxidil, compressed tablets, topical solution, and bulk drug

Minoxidil (I), 2,4-diamino-6-piperidinopyrimidine 3-oxide, a potent, orally active antihypertensive agent, is commercially available as a compressed tablet formulation[1]. There are, as yet, no published methods for the determination of minoxidil in bulk drug or dosage forms. A simple, precise, and specific assay method for minoxidil in these matrices was needed for quality control activities. For use in accelerated stability studies, potential decomposition products of minoxidil must be separated from the drug peak. Minoxidil is quite stable, decomposing only at high temperatures to form 2,4-di-

[1] Loniten, The Upjohn Co., Kalamazoo, Mich.

0022-3549/84/0900-1290$01.00/0

© 1984, American Pharmaceutical Association

times more permeable to hydrocortisone than human skin. Assignment of an exact factor to this difference is made difficult, as the representativeness of the human epidermal value is uncertain, with there being no statistical data provided, nor are the temperature sensitivities of the permeation of hydrocortisone through the tissues known (but they can be assumed to be large). Nevertheless, this appears to be the first clear demonstration that to some permeating species, intact human and hairless integuments offer quantitatively different mass transfer resistances, with human skin being at least one logarithmic order less permeable. Previous diffusion cell-generated data for the alkanols (13, 14, 16) and phenol (19) have left the impression that the two skin types were, for practical purposes, identical in permeability.

Biphasic Character in Some Permeability Plots—A most unusual feature of some of these data is the biphasic quality of the permeability plots obtained with mice 5 and 35 d old. At 35 d of age, this aspect of the data was unequivocal. Like other researchers (8), we at first assumed that the skin membranes were deteriorating. However, when the permeability coefficient of a single section of skin was repetitively assessed approximately every 12 h over a 100-h period, using a previously outlined "hydration" protocol (16), the permeability coefficient remained constant at 2.5×10^{-4} cm/h. Subsequently, additional evidence has been gathered on skin of older animals which shows these same qualities (21), and it now appears that if a run is long and continuous, two distinct phases of permeation will be evident, with the second, more permeable, phase being as reproducible in its time of onset and permeability rate as the first. However, the onset of the second phase is at >40 h with the older skin sections, which is, by chance, the arbitrarily selected duration for the experiments reported here and which explains why the second phase was not apparent with the older skin sections. Also, the permeability coefficient of the second phase seems to increase dramatically with mouse age (consider the data for 5- and 35-d-old mice presented here). We suspect it was not evident after 5 d but not until 35 d because permeability in the early phase dominated events at 15 and 20 d. The physicochemical implication that this represents two separate and parallel permeability pathways through the stratum corneum with different dependencies on animal age is clear. This concept is mechanistically important and is thus being put to rigorous experimental testing.

REFERENCES

(1) F. D. Malkinson, *J. Soc. Cosmet. Chem.*, **11**, 146 (1960).

(2) F. D. Malkinson and E. H. Ferguson, *J. Invest. Dermatol.*, **25**, 281 (1955).

(3) R. J. Feldman and H. I. Maibach, *Arch. Dermatol.*, **91**, 661 (1965).

(4) C. S. Livingood, *J. Invest. Dermatol.* **31**, 27 (1958); in discussion of Ref. 5.

(5) F. D. Malkinson, *J. Invest. Dermatol.* **31**, 19 (1958).

(6) R. C. Wester, P. K. Noonan, and H. I. Maibach, *Arch. Dermatol.*, **113**, 620 (1977).

(7) R. C. Wester, P. K. Noonan, and H. I. Maibach, *Arch. Dermatol.*, **116**, 186 (1980).

(8) A. E. Solomon and N. J. Lowe, *Br. J. Dermatol.*, **100**, 717 (1979).

(9) H. Shinkai and I. Tanaka, *Yakugaku Zasshi*, **89**, 1283 (1969).

(10) H. Shinkai, *Yakugaku Zasshi*, **89**, 365 (1969).

(11) C. A. Schlagel, *Adv. Biol. Skin*, **12**, 339 (1972).

(12) R. J. Scheuplein, I. H. Blank, G. J. Brauner, and D. J. MacFarlane, *J. Invest. Dermatol.*, **52**, 63 (1969).

(13) H. Durrheim, G. L. Flynn, W. I. Higuchi, and C. R. Behl, *J. Pharm. Sci.*, **69**, 781 (1980).

(14) G. L. Flynn, H. Durrheim, and W. I. Higuchi, *J. Pharm. Sci.*, **70**, 52 (1981).

(15) C. R. Behl, G. L. Flynn, T. Kurihara, W. Smith, O. Gatmaitan, W. I. Higuchi, N. F. H. Ho, and C. L. Pierson, *J. Invest. Dermatol.*, **75**, 340 (1980).

(16) C. R. Behl, G. L. Flynn, T. Kurihara, N. Harper, W. Smith, W. I. Higuchi, N. F. H. Ho, and C. L. Pierson, *J. Invest. Dermatol.*, **75**, 346 (1980).

(17) C. R. Behl, G. L. Flynn, T. Kurihara, W. M. Smith, N. Bellantine, O. G. Gatmaitan, C. L. Pierson, W. I. Higuchi, and N. F. H. Ho, *J. Soc. Cosmet. Chem.*, **35**, 237 (1984).

(18) C. R. Behl, M. Barrett, G. L. Flynn, T. Kurihara, K. A. Walters, O. G. Gatmaitan, N. Harper, W. I. Higuchi, N. F. H. Ho, and C. L. Pierson, *J. Pharm. Sci.*, **71**, 229 (1982).

(19) C. R. Behl, E. E. Linn, G. L. Flynn, C. L. Pierson, W. I. Higuchi, and N. F. H. Ho, *J. Pharm. Sci.*, **72**, 391 (1983).

(20) E. E. Linn, Ph.D. Thesis, "Thermotropic Effects on Skin Permeability," University of Michigan, Arbor, Mich., 1982.

(21) W. M. Smith, Ph.D. Thesis, "An Inquiry into the Mechanism of Percutaneous Absorption of Hydrocortisone and its 21-*n*-alkyl Esters," University of Michigan, Ann Arbor, Mich., 1982.

ACKNOWLEDGMENTS

This work was presented in part at the 127th Annual Meeting of the American Pharmaceutical Association, Washington, D.C., April 1980 (Basic Pharmaceutics Section Abstract No. 100).

Determination of Minoxidil in Bulk Drug and Pharmaceutical Formulations by Ion-Pairing High-Performance Liquid Chromatography

P. A. ASMUS ˣ, J. B. LANDIS, M. E. GRANT, and H. A. HAVEL

Received June 8, 1983, from *Control Analytical Research and Development, The Upjohn Company, Kalamazoo, MI 49001.* Accepted for publication September 23, 1983.

Abstract □ An ion-pairing liquid chromatographic method with UV detection is described for the determination of minoxidil in bulk drug, compressed tablet, and topical solution formulations. The chromatographic system consists of a microparticulate octadecylsilica column and a mobile phase composed of sodium dioctylsulfosuccinate in aqueous methanol (pH 3). The bulk drug and the topical solution samples are prepared by the dissolution of the drug in internal standard solution. Sample preparation for the compressed tablet formulation involves dissolving the drug from an aliquot of pulverized sample and centrifuging to remove insoluble excipients. Quantitative recovery of minoxidil from formulation excipients was demonstrated; assay precision was <1% *CV*.

Keyphrases □ Minoxidil—compressed tablets, topical solution and bulk drug, HPLC □ HPLC—minoxidil, compressed tablets, topical solution, and bulk drug

Minoxidil (I), 2,4-diamino-6-piperidinopyrimidine 3-oxide, a potent, orally active antihypertensive agent, is commercially available as a compressed tablet formulation[1]. There are, as yet, no published methods for the determination of minoxidil in bulk drug or dosage forms. A simple, precise, and specific assay method for minoxidil in these matrices was needed for quality control activities. For use in accelerated stability studies, potential decomposition products of minoxidil must be separated from the drug peak. Minoxidil is quite stable, decomposing only at high temperatures to form 2,4-di-

[1] Loniten, The Upjohn Co., Kalamazoo, Mich.

0022-3549/84/0900-1290$01.00/0

© 1984, American Pharmaceutical Association

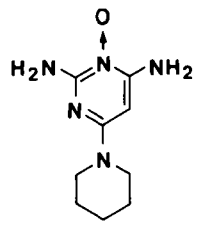

I

amino-6-piperidinopyrimidine (the deoxy product).

This paper reports the development of a reversed-phase ion-pairing high-performance liquid chromatographic (HPLC) assay method for minoxidil in several formulations and bulk drug. Since the work of Schill and co-workers (1, 2), Haney *et al.* (3, 4), and Knox *et al.* (5, 6), many workers have found that reversed-phase ion-pairing with alkylsulfates of alkylsulfonates is effective in reducing tailing and also for adjusting retention and selectivity (7-14). The method is simple, precise, and specific for minoxidil in the presence of possible decomposition products and several synthetic intermediates.

EXPERIMENTAL SECTION

Materials—Minoxidil[2], 2-*N*-dicyano-*N'*,*N'*-pentamethylene acetoamidine[2], 2,4-diamino-6-chloropyrimidine 3-oxide[2], 2,4-diamino-6-chloropyrimidine[2], 2,4-diamino-6-piperidinopyrimidine[2], and sodium dioctylsulfosuccinate[3] were >95% pure by HPLC and used as received. The internal standard, medroxyprogesterone acetate, was USP-NF quality. The methanol[4] and water used in the mobile phases were distilled. All other chemicals were reagent grade.

Apparatus—Experiments were conducted on a modular HPLC consisting of a reciprocating piston pump[5], a loop injection valve[6], a UV detector[7] (254 nm), and a recorder[8]. For quantitation, data were collected and processed by a digital computer[9].

Mobile Phase—The mobile phase was prepared as follows. Sodium dioctylsulfosuccinate (3.0 g) and 10 mL of glacial acetic acid were dissolved in 700 mL of methanol. Stirring was continued and 300 mL of water was added. The apparent pH was adjusted to 3.0 with concentrated perchloric acid. The solution was filtered through a 0.45 μm filter[10] before use.

The separation between minoxidil and the internal standard, medroxyprogesterone acetate, could be increased without affecting selectivity by decreasing the methanol concentration of the mobile phase.

The volume of the mobile phase in the column, V_m, which is equal to the retention volume of an unretained compound, was estimated by the retention volume of sodium nitrate (20 mg/mL in the mobile phase). The retention times of the compounds studied were measured using 1 mg/mL solutions of authentic standards. Capacity factors, k', were determined using the equation: $k' = V_R - V_m/V_m$, where V_R is the retention volume of the compound being measured. The separation factors were calculated by taking the ratio of the capacity factor of the compound to the capacity factor of minoxidil.

Column—The microparticulate octadecylsilane column[11] (10-μm particles, 300 × 3.9 mm) used was washed with methanol–water (80:20, v/v) and stored in the same solvent when not in use. The column temperature was ambient, the column pressure was ~1500 psi, the injection volume was ~10 μL, and the flow rate was 1.0 mL/min.

Sample Preparation—Standards and bulk drug samples were prepared by accurately weighing ~5 mg of the sample and dissolving it in 20 mL of internal standard solution (~0.2 mg/mL medroxyprogesterone acetate in mobile phase). For compressed tablet samples, 10 tablets were weighed and then pulverized to a fine powder. An accurately weighed aliquot of the powder containing ~5 mg of minoxidil was dissolved in 20 ml of internal standard solution, and insoluble excipients were separated by centrifugation. The clear supernatant was separated for analysis. Topical solution samples were prepared by accurately measuring an amount of solution containing ~50 mg minoxidil and diluting to 50 mL with mobile phase. Five milliliters of this solution was dissolved in 20 mL of the internal standard solution.

[2] The Upjohn Co.
[3] Eastman Kodak Co., Rochester, N.Y.
[4] Burdick & Jackson Laboratories, Muskegon, Mich.
[5] Model 110A; Altex Corp., Berkeley, Calif.
[6] Model 7125; Rheodyne Inc., Cotati, Calif.
[7] Model UVIII; Laboratory Data Control, Riviera Beach, Fl.
[8] Model XKR; Sargent Welch Co., Skokie, Ill.
[9] PDP 11; Digital Equipment Co., Maynard, Mass.
[10] Type HA; Millipore Corp., Bedford, Mass.
[11] μ-Bondapak C_{18}, Waters Associates, Milford, Mass.

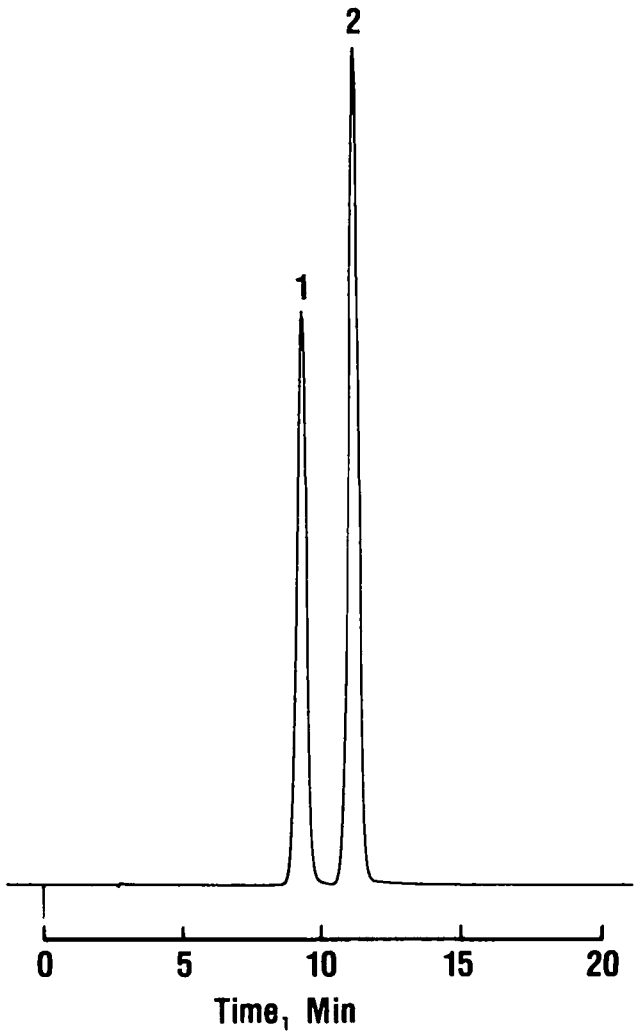

Figure 1—*Chromatogram of a compressed tablet preparation of minoxidil. The mobile phase was 6.7 mM sodium dioctylsulfosuccinate and 175 mM acetic acid in 70% methanol, pH 3.0; the flow rate was 1.0 mL/min; the temperature was ambient; the attenuation was 0.512 AUFS. Key: (1) medroxyprogesterone acetate (internal standard); (2) minoxidil.*

RESULTS AND DISCUSSION

A typical chromatogram of a minoxidil compressed tablet sample preparation is shown in Fig. 1. No excipient peaks are observed even though no sample clean-up steps were employed. The minoxidil peak was symmetrical and an adequate number of theoretical plates (3500) were generated. Retention and selectivity data for minoxidil and related compounds are shown

Table I—Retention and Selectivity Data for Minoxidil and Related Compounds

Compound	Retention Time, min	Capacity Factor	Separation Factor
2-*N*-Dicyano-*N'*,*N'*-pentamethylene acetoamidine	3.41	0.34	0.12
2,4-Diamino-6-chloropyrimidine 3-oxide	4.13	0.63	0.22
2,4-Diamino-6-chloropyrimidine	6.25	1.46	0.51
Medroxyprogesterone acetate (internal standard)	8.57	2.37	0.82
Minoxidil	9.87	2.89	1.00
2,4-Diamino-6-piperidinopyrimidine	12.4	3.88	1.35

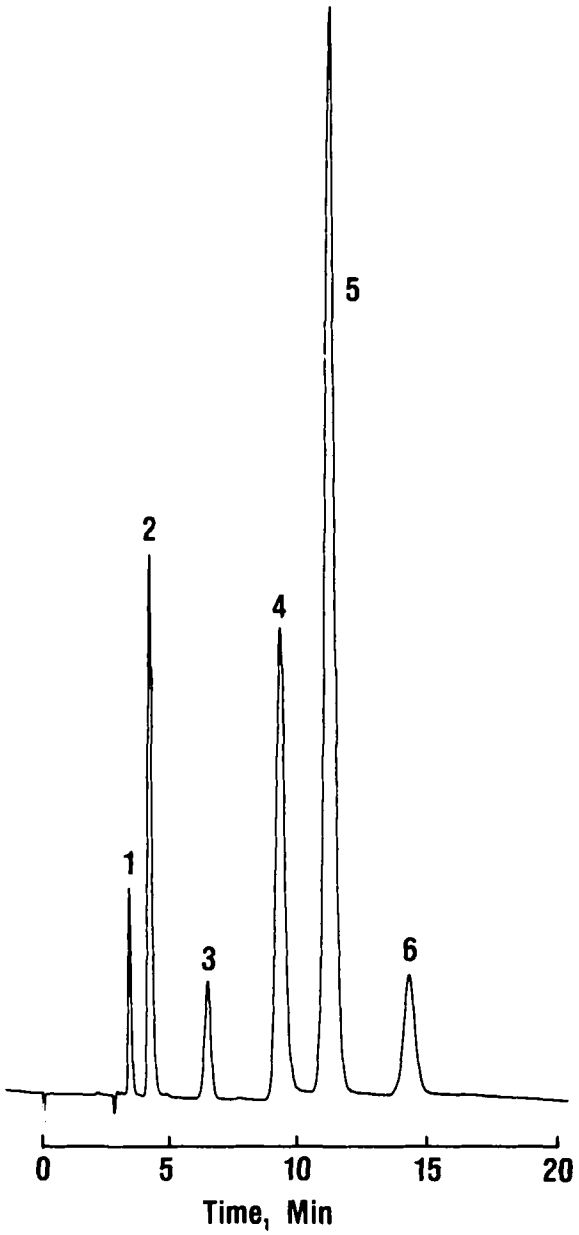

Figure 2—*Chromatogram of minoxidil and related compounds. Key: (1) 0.065 μg 2-N-dicyano-N′,N′-pentamethylene acetoamidine; (2) 1.5 μg 2,4-diamino-6-chloropyrimidine 3-oxide; (3) 0.5 μg 2,4-diamino-6-chloropyrimidine; (4) 0.9 μg medroxyprogesterone acetate; (5) 2.3 μg minoxidil; (6) 0.4 μg 2,4-diamino-6-piperidinopyrimidine. See Fig. 1 for mobile phase composition. Attenuation was 0.256 AUFS.*

in Table I. The sample preparation involved dissolution of the drug from a powdered tablet using the mobile phase which contained the internal standard. Insoluble excipients were separated by centrifugation and the supernatant was chromatographed.

The specificity of the chromatographic system was evaluated by chromatographing a mixture of minoxidil and its possible impurities. Figure 2 shows the very good resolution obtained between all components. This degree of specificity was achieved by manipulation of the mobile phase constituents, *i.e.*, the ion-pairing reagent concentration, the organic modifier concentration, and the pH.

Sodium dioctylsulfosuccinate was chosen as the ion-pairing reagent after several alkylsulfates and alkylsulfonates were tried. The dioctylsulfosuccinate anion is a large hydrophobic sulfonic acid containing 20 carbon atoms, of which 18 can be considered alkyl chain carbons. It has, therefore, a very large affinity for the alkyl groups on the packing material surface. Ion-pairing reagents with smaller carbon chain lengths allowed the minoxidil peak to tail. Sodium dioctylsulfosuccinate has been successfully used as an ion-pairing reagent in several other HPLC assay methods (10–14).

The relationship between retention and the dioctylsulfosuccinate concentration in the mobile phase was studied for minoxidil and related compounds (Fig. 3). In accordance with well known reversed-phase ion-pairing behavior, retention of all the basic compounds was proportional to the dioctylsulfosuccinate concentration. The concentration of dioctylsulfosuccinate was 6.7 mM, since adequate retention and resolution was observed at that level. Selectivity was not affected enough to cause peak reversal over a 1–25 mM dioctylsulfosuccinate concentration range.

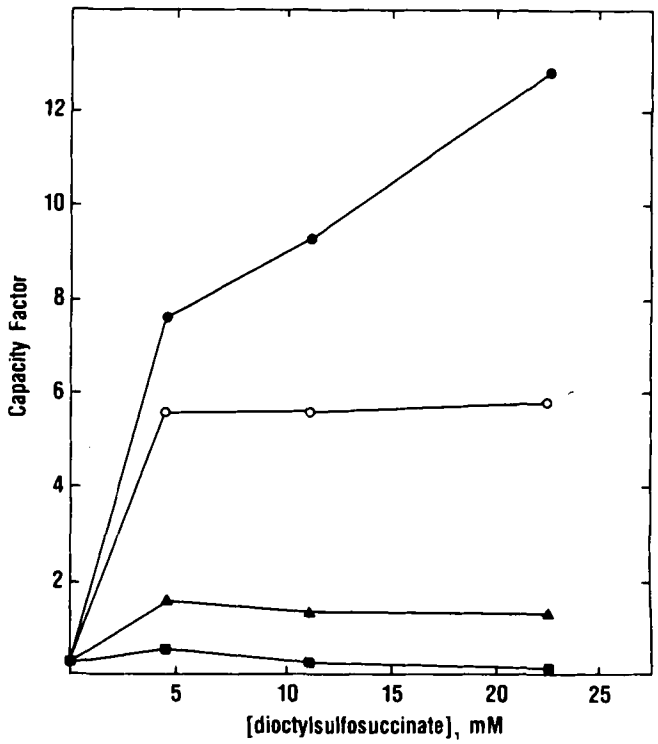

Figure 3—*Effect of mobile phase dioctylsulfosuccinate concentration on retention. Key: (■) 2-N-dicyano-N′,N′-pentamethylene acetoamidine and 2,4-diamino-6-chloropyrimidine 3-oxide; (▲) 2,4-diamino-6-chloropyrimidine; (○) minoxidil; (●) 2,4-diamino-6-piperidinopyrimidine. The mobile phase was 175 mM acetic acid in 70% methanol, pH 3.0.*

The mobile phase contained methanol as the organic modifier. The dependence of retention on its concentration was studied, and the results are

Table II—Recovery of Minoxidil Added to Compressed Tablet Placebo

Amount Added, mg	Amount Found, mg	Recovery, %
1.388	1.401	100.9
2.964	2.973	100.3
4.213	4.286	101.7
6.039	6.061	100.4
9.852	9.757	99.0
Mean		100.5

Table III—Analyses of Minoxidil Formulations

Lot No.	Labeled Amount, mg	Assay Result, mg
Tablets		
A	0.3	0.30
B	1.0	1.01
C	2.5	2.45
D	5.0	4.97
E	10.0	9.83
F	15.0	15.0
G	25.0	24.6
Topical Solutions[a]		
A	10.0	10.3
B	30.0	31.3
C	50.0	52.2

[a] Expressed as mg/mL for topical solutions.

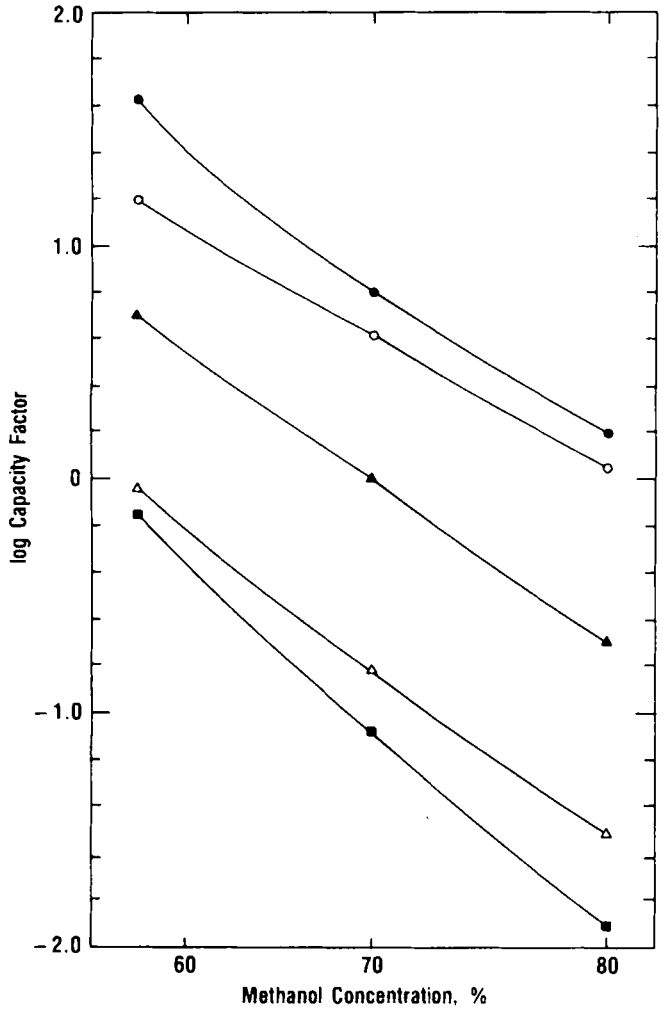

Figure 4—*Effect of mobile phase methanol concentration on retention. Key: (■) 2-N-dicyano-N′,N′-pentamethylene acetoamidine; (△) 2,4-diamino-6-chloropyrimidine 3-oxide; (▲) 2,4-diamino-6-chloropyrimidine, (○) minoxidil, (●) 2,4-diamino-6-piperidinopyrimidine. The mobile phase was 6.7 mM sodium dioctylsulfosuccinate and 175 mM acetic acid, pH 3.0.*

shown in Fig. 4. As expected, retention varies linearly with the log of the methanol concentration. It can be seen that selectivity does not change as the methanol concentration varies. The mobile phase methanol concentration can, therefore, be reduced to compensate for reduced retention as the column ages.

In reversed-phase ion-pairing liquid chromatography, the mobile phase pH is an important variable. The retention behavior of the compounds was studied as a function of the apparent pH of the mobile phase (Fig. 5). From this experiment, an apparent pH of 3.0 was chosen for the best separation of all compounds. At that pH, the ion-pairing reagent was ionized and the solutes were fully protonated. In the pH region of 4–7, the retention of minoxidil decreased due to deprotonation of the molecule, which decreased the magnitude of the interaction between minoxidil and dioctylsulfosuccinate. Glacial acetic acid and perchloric acid were added to the mobile phase to obtain an apparent pH of 3. The effect of the acetic acid concentration on retention is minimal.

Linearity of the assay for bulk drug was determined over a range of 75–125% of the amount called for in this procedure. The regression equation for the line was: minoxidil found = (1.014 ± 0.038) (minoxidil added) + (−0.102 ± 0.196). Tablet placebo samples were spiked with minoxidil, mixed in the

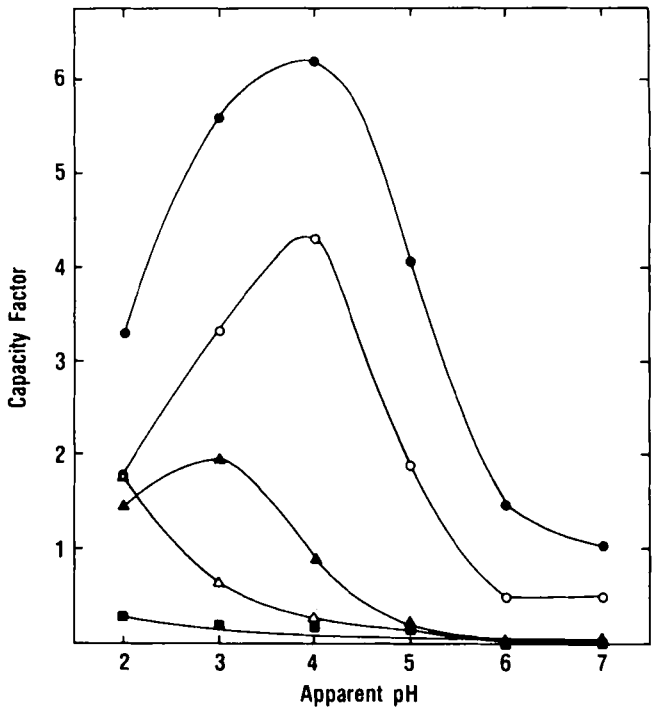

Figure 5—*Effect of mobile phase apparent pH on retention. See Fig. 3 for the key. The mobile phase was 6.7 mM sodium dioctylsulfosuccinate and 175 mM acetic acid in 70% methanol; pH from 2.0 to 3.5 adjusted with perchloric acid and from 3.5 to 7.0 adjusted with ammonium hydroxide.*

solid state, and analyzed by this method to measure recovery. Quantitative recovery of minoxidil was observed over the range of ~1.4–9.9 mg/0.13 g of compressed tablet placebo (Table II). This range corresponds roughly to 30–200% of the label claim for a 10 mg compressed tablet formulation. Replicate analyses of a single lot of 5-mg compressed tablets gave a method precision of 0.6% *RSD*. Results from the analyses of several lots of compressed tablets and topical solution formulations of various strengths are shown in Table III. Good agreement between assay results and the label claim amount was observed in all cases.

REFERENCES

(1) G. Schill, R. Modin, and B. Persson, *Acta Pharm. Suec.*, **2**, 119 (1965).

(2) G. Schill, *Acta Pharm. Suec.*, **2**, 13 (1965).

(3) D. P. Wittmer, N. O. Nuessle, and W. G. Haney, Jr., *Anal. Chem.*, **47**, 1422 (1975).

(4) S. P. Sood, L. F. Sartori, D. P. Wittmer, and W. G. Haney, Jr., *Anal. Chem.*, **48**, 796 (1976).

(5) J. H. Knox and G. R. Laird, *J. Chromatogr.*, **122**, 17 (1976).

(6) J. H. Knox and J. Jurrard, *J. Chromatogr.*, **125**, 89 (1976).

(7) C. Olieman, *J. Chromatogr.*, **133**, 385 (1977).

(8) H. F. Proeless, H. J. Lohmann, and D. G. Miles, *Clin. Chem.*, **24**, 1948 (1978).

(9) S. L. Pierson, J. J. Hanigan, R. E. Taylor, and J. E. McClurg, *J. Pharm. Sci.*, **68**, 1550 (1979).

(10) J. T. Stewart, I. L. Honingberg, J. P. Brant, W. A. Murray, J. L. Webb, and J. B. Smith, *J. Pharm. Sci.*, **65**, 1536 (1976).

(11) S. Sood, D. P. Wittmer, S. A. Ismaiel, and W. G. Haney, *J. Pharm. Sci.*, **66**, 40 (1977).

(12) P. A. Hartman, *J. Assoc. Off. Anal. Chem.*, **62**, 1099 (1979).

(13) E. J. Kubiak and J. W. Munson, *J. Pharm. Sci.*, **69**, 1380 (1980).

(14) G. W. Halstead, *J. Pharm. Sci.*, **71**, 1108 (1982).

Controlled Release of a Luteinizing Hormone-Releasing Hormone Analogue from Poly(*d*,*l*-lactide-co-glycolide) Microspheres

L. M. SANDERS *x, J. S. KENT *, G. I. McRAE *,
B. H. VICKERY *, T. R. TICE ‡, and D. H. LEWIS ‡

Received July 18, 1983, from the *Institutes of Pharmaceutical and Biological Sciences, Syntex Research, Palo Alto, CA 94304 and ‡Southern Research Institute, Birmingham, AL 35255. Accepted for publication October 3, 1983.

Abstract □ The performance *in vivo* of nafarelin acetate, a potent analogue of luteinizing hormone-releasing hormone, microencapsulated in poly(*d*,*l*-lactide-co-glycolide), was evaluated. The influence of polymer composition and molecular weight on the estrus-suppressing activity of the microspheres in female rats was determined. Compound release was shown to be effected by polymer erosion rather than by diffusion. A triphasic release of compound was observed, which was adjusted by altering the critical parameters of the polymer. A mechanism for the release of the compound was proposed. The primary release phase was compound loss by diffusion from the surface of the microspheres. The secondary phase of subeffective rates of release occurred concomitantly with polymer hydrolysis and a decrease in its molecular weight, although it remained insoluble. Dissolution of low-molecular weight fragments and erosion of the bulk of the polymer then initiated the tertiary phase of release of compound.

Keyphrases □ Microencapsulation—nafarelin acetate in poly(*d*,*l*-lactide-co-glycolide) □ Nafarelin acetate—microencapsulation in poly(*d*,*l*-lactide-co-glycolide) □ Controlled-release formulations—microencapsulation of nafarelin acetate in poly(*d*,*l*-lactide-co-glycolide)

Poly(*d*,*l*-lactide-co-glycolide) and its homopolymers have a long history of use in such products as biodegradable sutures (1) and bone plates (2, 3) and have more recently been used to achieve controlled release of pharmaceuticals. A great deal has been done with narcotic antagonists such as naltrexone (4–7), local anesthetics (8), and steroids (9). A system consisting of norethisterone microencapsulated in poly(*d*,*l*-lactide-co-glycolide) has recently been shown to provide controlled release in clinical studies over 6 months (10). These systems all share a common feature in that the kinetics of compound release are diffusion controlled, through the polymer continuum and/or through channels formed within the device which are achieved by a high loading level of active material.

In this report, the controlled release of nafarelin acetate (I), an analogue of luteinizing hormone-releasing hormone (II) is described. Compound I has high biological potency, ~200 times that of II (11).

(Pyro)Glu-His-Trp-Ser-Tyr-3-(2-naphthyl)D-alanine-Leu-Arg-Pro-Gly-NH_2
I

(Pyro)Glu-His-Trp-Ser-Tyr-Gly-Leu-Arg-Pro-Gly-NH_2
II

The system described is controlled by erosion, with the kinetics of compound release determined by parameters of the copolymer.

EXPERIMENTAL SECTION

Materials—Poly(*d*,*l*-lactide-co-glycolide) and microspheres were prepared in-house[1] and used as supplied. Intrinsic viscosity (η_i) which is a measure of relative molecular weight, was determined by measuring the flow times of solutions of the copolymer with concentrations of 1.0–10.0 mg/mL in chloroform through a viscometer[2] at 30°C. Specific viscosities were calculated by:

$$\eta_{sp} = \frac{t_s - t_0}{t_0} \qquad \text{(Eq. 1)}$$

where t_s is the time required for a solution to pass through the viscometer, and t_0 is the time required for the pure solvent to pass through the viscometer. The plot of η_{sp}/C *versus* C was extrapolated back to the ordinate, where the intercept represents the intrinsic viscosity and C is the concentration.

The microsphere-suspending vehicle consisted of 0.5% carboxymethylcellulose[3]–0.8% sodium chloride USP 0.1% polysorbate 80 USP[4], in aqueous solution.

[1]Southern Research Institute.

Table I—Estrus Suppression Activity of I in the Female Rat by Twice-Daily Injection and Continuous Infusion

Total Daily Dose, μg	Percentage of Animals Displaying Complete Estrus Suppression[a]: Twice-Daily Subcutaneous Injection[b]	Continuous Subcutaneous Infusion[c]
0.05	0	0
0.10	50	0
0.20	80	60
0.40	100	100

[a]From 4 d after start of treatment and lasting for the full 14 d of treatment. [b]n = 10. [c]With Alzet minipumps, model 2002, lot 0888; n = 5.

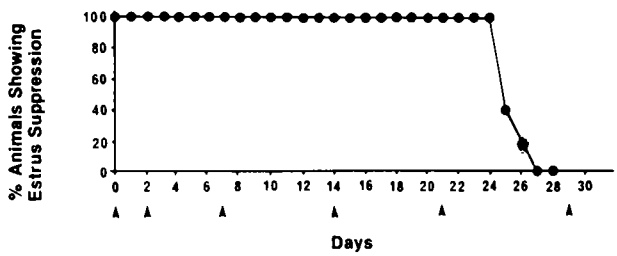

Figure 1—*Biological profile of 50:50 copolymer (η_i = 0.38 dL/g) microspheres containing 1% I injected subcutaneously in female rats at a 300-μg compound dose (n = 30).*

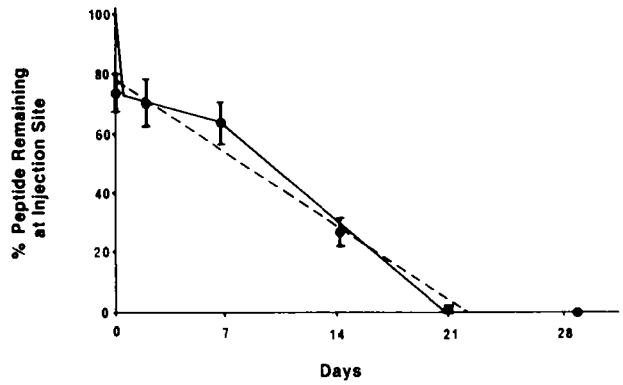

Figure 2—In vivo *release profile of naferelin acetate from 50:50 copolymer microspheres. Key: (——) triphasic kinetics; (- - -), zero-order kinetics.*

[2]Size 75; Cannon-Fenske.
[3]500 cps; Hercules.
[4]Tween 80, ICI Americas, Inc.

0022-3549/84/0900-1294$01.00/0
© 1984, American Pharmaceutical Association

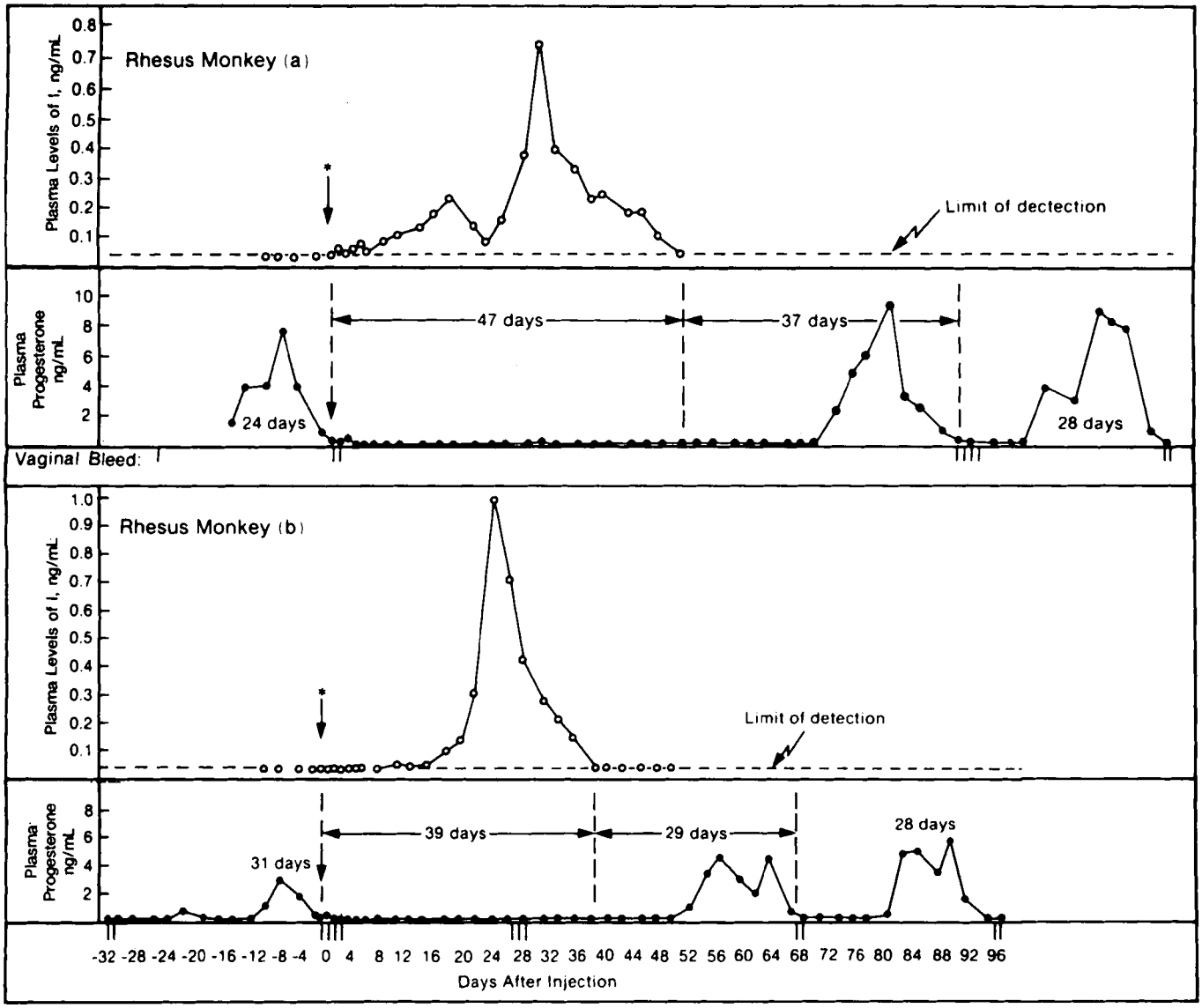

Figure 3—*Plasma levels of nafarelin acetate and progesterone in rhesus monkeys after a single subcutaneous injection of 1.0 mg of nafarelin acetate microencapsulated in 50:50 copolymer. The asterisks represent injection times.*

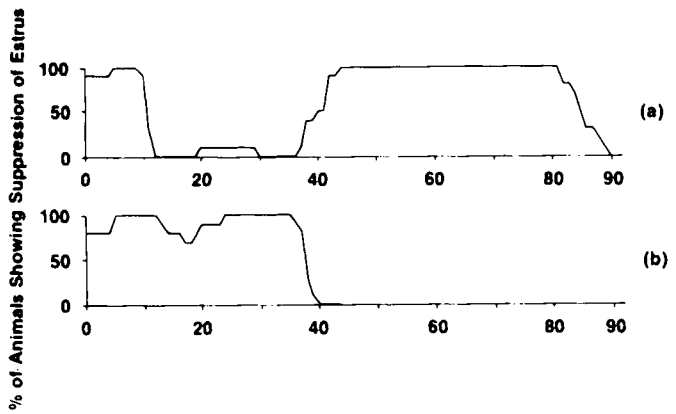

Figure 4—*Estrus suppression profiles provided by (a) 69:31 (η_i = 0.97 dL/g) and by (b) 50:50 (η_i = 1.52 dL/g) copolymer mixtures.*

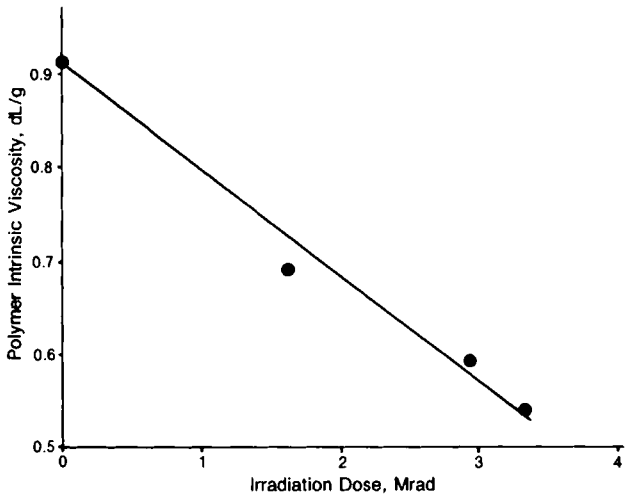

Figure 5—*Effect of gamma-irradiation on intrinsic viscosity of 69:31 copolymer.*

Animals—The rats used were mature females derived from the Sprague–Dawley line (weight, 155–165 g). Adult female rhesus monkeys (*Macaca mulatta*) that had menstrual cycles of predictable length based on prior history were also used.

Microencapsulation of I in Poly(*d,l*-lactide-co-glycolide)—Preparation of microspheres was by phase separation. An aqeous solution of I and a solution of the copolymer in dichloromethane were coemulsified to form a water-in-oil emulsion. A nonsolvent for the copolymer was then added to precipitate out the polymer around the aqueous droplets. The suspension of semi-formed

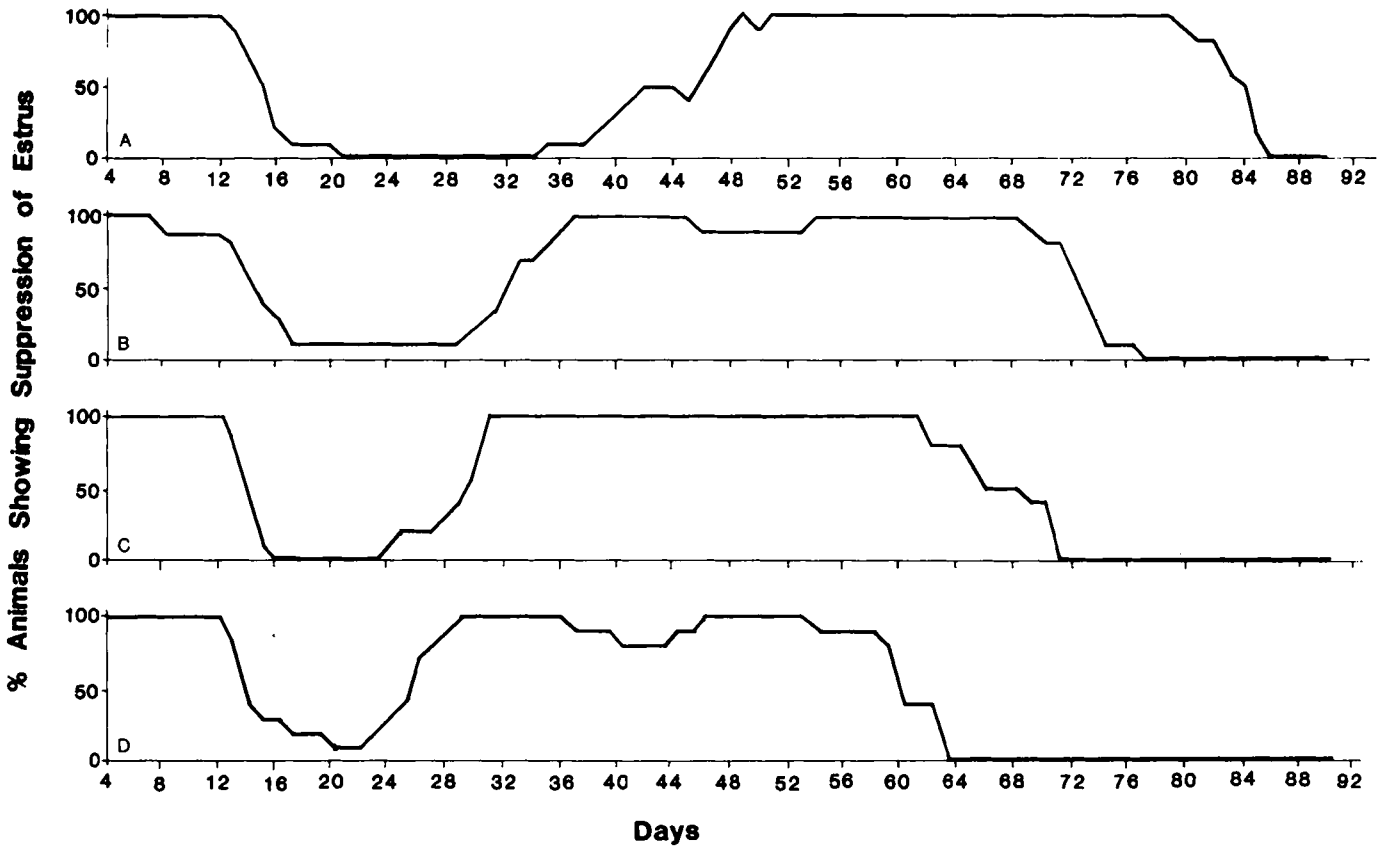

Figure 6—*Effect of irradiation on the biological activity of 69:31 copolymer microspheres (10–40 μm) containing I; n = 10. Key to irradiation: (A) none; (B) 1.6 Mrad; (C) 2.9 Mrad; (D) 3.3 Mrad.*

microspheres was added to a large volume of nonsolvent to cause them to harden and to complete the extraction of dichloromethane. The microspheres were then sieved, washed, and dried. Microspheres were thus prepared to contain ~1% (w/w) I.

Assay of I in Microspheres—A quantity of microspheres containing ~500 μg of I was dissolved in 3.3 mL of acetonitrile–water (9:1), in which both the copolymer and I are sufficiently soluble. Aqueous potassium dihydrogen phosphate (0.184 M) was added to 10.0 mL to precipitate the copolymer, and the suspension was stirred until the precipitate coalesced into a single mass. The supernatant was then assayed by reverse-phase HPLC by using a C_{18} 10-μm column[5], with a mobile phase[6] flow rate of 1.2 mL/min, an injection volume of 100 μL, and a detector wavelength of 225 nm. Compound recovery was 100 ± 1.5%.

Biological Assay—The microspheres were evaluated *in vivo* by using a rat estrus suppression model. It was shown that twice daily injection or continuous subcutaneous administration of ~0.4 μg/d is sufficient to maintain suppression of estrus in this model (Table I). Microspheres containing 300 μg of I were suspended in 0.5 mL of suspension vehicle and administered by a single subcutaneous injection. The animals were monitored for suppression of estrus by daily examination of vaginal smears. This model provides a reliable indication of the duration of compound release, although not of the release rate.

It was not possible to measure plasma levels of I in the rat since the compound is not sufficiently stable in rat plasma *in vitro*. Release kinetics in the rat were, therefore, determined by sequential sacrifice of treated animals, followed by excision of the injection sites and assay of the level of I remaining.

Biological efficacy of I in the female rhesus monkey was evaluated by monitoring menstrual bleeding and by measuring plasma levels of progesterone by RIA (12) after a single subcutaneous injection of microspheres containing 1.0 mg of I on day 1 of the menstrual cycle of the animal. The release profile of the compound was determined by the measurement of plasma levels of I by RIA (13).

Assay of I in Tissue Samples—The tissue samples, *i.e.*, excised injection sites, were frozen for ease of handling and sectioned into thin slices. They were vortexed with 5 mL of acetonitrile–water (9:1) periodically over 4 h. Potassium dihydrogen phosphate (0.184 M; 10 mL) was added, and the suspensions were vortexed over ~4 h. The samples were centrifuged at 1000 × *g* for 20 min and assayed by HPLC as described above. Compound recovery was 83 ± 5%.

[5]μ-Bondapak; Waters Associates.

[6]Acetonitrile–0.175 M aqueous potassium dihydrogen phosphate (30:70).

RESULTS AND DISCUSSION

Injection of rats with microspheres of a low intrinsic viscosity (0.38 dL/g), 50:50 mol% copolymer produced continuous suppression of estrous cyclicity for 24 d, followed by an abrupt resumption of normal estrous cycling (Fig. 1). In this experiment, 30 animals were injected at time zero, and 5 animals were sacrificed at each of the six indicated times. Assay of the excised injection sites indicated a compound release profile (Fig. 2) that exhibited complex kinetic behavior, possibly reflecting a triphasic release mechanism. Overall, release kinetics were quite satisfactory, as indicated by comparison with zero-order kinetics, with exhaustion of the compound from the injection sites at ~22 d. Plasma levels of I in female rhesus monkeys a and b, which received 1 mg of compound in the same 50:50 copolymer, were detectable (*i.e.*, >0.05 ng/mL) for 47 and 39 d, respectively, during which time ovulation was completely inhibited (Fig. 3). Ovulation in these monkeys, as indicated by a rise in plasma progesterone levels, occurred at 19 and 14 d, respectively, after the disappearance of I in the plasma; normal menstrual cycling resumed thereafter.

A high molecular weight 50:50 copolymer (η_i = 1.52 dL/g) and a 69:31 copolymer (η_i = 0.97 dL/g) were screened in the rat estrus suppression model and gave efficacy profiles with degrees of partial or complete discontinuity at an intermediate point of the release cycle (Fig. 4). The data are consistent with the release of compound by homogeneous polymer erosion. A 69:31 copolymer of relatively high intrinsic viscosity gives a clearly triphasic compound release over 90 d (Fig. 4a). It is postulated that the primary phase of compound release is by dissolution from the superficial regions of the microspheres. A secondary, latent period of some 25 d then follows, during which time <0.4 μg/d is released. The copolymer hydrates and hydrolyzes *in situ* and decreases in molecular weight, although it remains water insoluble. There are no grossly observable changes and no release of the compound. The duration of this latent phase is controlled by both the initial molecular weight and by the composition of the polymer, which determines hydrophilicity and the inherent hydrolysis rate of the polymer *in vivo*. When the molecular weight decreases to a point at which there is significant water solubility, the polymer begins to erode homogeneously, and both the compound and polymer degradation products

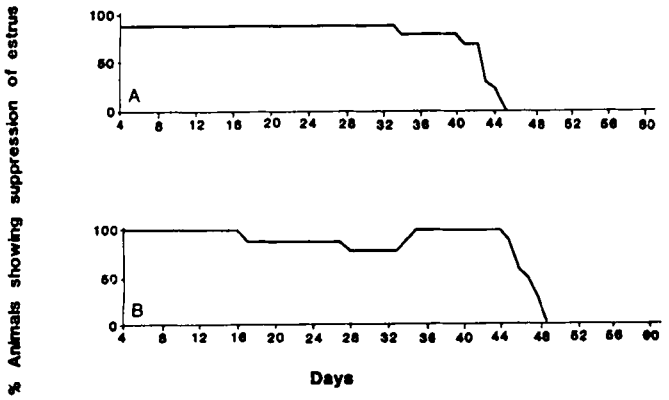

Figure 7—*Effect of size of 55:45 copolymer microspheres on duration of efficacy in female rats; n = 10. Key (A) large, 80–150 μg and (B) small, 30–50 μg.*

diffuse away from the loosening polymer matrix. This phase is diffusion controlled, although an increase in the permeability of the polymer as it erodes tends to compensate for an anticipated decrease in compound release with time. The system providing the plasma profile (Fig. 4a) demonstrates a clear definition of these three phases. When the composition is adjusted to 50:50 mol% *d,l*-lactide-co-glycolide (Fig. 4b) there is partial overlap of the primary and tertiary phases, and when the intrinsic viscosity is then decreased (Fig. 1), there is complete overlap. However, even in the system providing continuous efficacy in the rat (Fig. 1), the data clearly indicate a triphasic compound release, as shown by the release profile (Fig. 2) and by nonlinearity in the plasma profiles (Fig. 3a).

This postulated release mechanism was further supported by a study of the effects of gamma-irradiation on the intrinsic viscosity of a 69:31 copolymer (Fig. 5) and of the performance *in vivo* of the microspheres made from that polymer (Fig. 6). There was a decrease in the intrinsic viscosity of the polymer with an increase in radiation dose and, as would be predicted, a concomitant shortening of the secondary phase and a decrease in the time of onset of the tertiary phase.

The size of the microspheres was shown to have an insignificant influence on the duration of action *in vivo* (Fig. 7). This confirms the homogeneous or bulk nature of hydrolysis of this polymer and indicates that hydration is not a rate-limiting step in polymer degradation.

REFERENCES

(1) E. J. Frazza and E. E. Schmidt, *J. Biomed. Mater. Res. Symp.*, **1**, 43 (1971).

(2) R. K. Kulkarni, K. C. Pani, C. Neuman, and F. Leonard, *Arch. Surg.* **93**, 839 (1966).

(3) D. E. Cutwright, B. Perez, J. D. Beasley, W. J. Larson, and W. R. Posey, *Oral Surg.*, **37**, 142 (1974).

(4) A. C. Sharon and D. L. Wise, *NIDA Res. Monogr.*, **28**, 194 (1981).

(5) R. H. Reuning, S. H. T. Liao, and A. E. Staubus, *NIDA Res. Monogr.*, **28**, 172 (1981).

(6) J. H. R. Woodland, M. Helrich, and F. J. Meyer, *J. Med. Chem.*, **16**, 897 (1973).

(7) S. E. Harrigan, D. A. McCarthy, R. Reuning, and C. Thies, *Midl. Macromol. Monogr.*, **5** (Polym. Delivery Systems), 91 (1978).

(8) N. Wakiyama, K. Juni, and M. Nakano. *Chem. Pharm. Bull.*, **30**, 3719 (1982).

(9) D. L. Wise, H. Rosenkrantz, J. B. Gregory, and H. J. Esber. *J. Pharm. Pharmacol.*, **32**, 399 (1980).

(10) L. R. Beck, V. C. Pope, C. E. Flowers, D. R. Cowsar, T. R. Tice, R. L. Dunn, A. B. Moore, and R. M. Gilley, *Biol. Rep.*, **28**, 186 (1983).

(11) J. J. Nestor, T. L. Ho, R. A. Simpson, B. L. Horner, G. H. Jones, G. I. McRae, and B. H. Vickery, *J. Med. Chem.*, **25**, 795 (1982).

(12) B. Vickery and G. McRae, *Biol. Rep.*, **22**, 438 (1980).

(13) C. Nerenberg, J. Foreman, and S. Kushinsky, "Abstracts of the Annual Meeting of the Endocrinology Society," San Antonio, Tex, 1983.

ACKNOWLEDGMENTS

The authors acknowledge the excellent technical assistance of Mark T. Yost, Karen Bergstrom, Anne Worden, Richard Seidenberg, Clint Nerenberg, and Agnes Bajka of Syntex and Thomas J. Smitherman and David F. Peters of Southern Research Institute.

Improved Bioassay for Glucagon by Continuous Glucose Monitoring

CHANA R. KOWARSKI *, MING YU LIAOU *, DAVID KOWARSKI ‡, JEFFREY WEIZER *, DUTTON BOYNES *, and A. AVINOAM KOWARSKI §x

Received July 15, 1983 from the *Temple University School of Pharmacy, Philadelphia, PA 19140, ‡The University of Pennsylvania School of Medicine, Philadelphia, PA, and §The University of Maryland School of Medicine, Baltimore, MD 21201. Accepted for publication September 22, 1983.

Abstract □ A simplified and rapid *in vivo* bioassay for glucagon is described. The test involves continuous monitoring of blood glucose which makes possible an exact rendering of the glucose peaks induced by intravenous injection of glucagon. Two injections of known amounts of glucagon (0.002 and 0.004 U) are followed by an intravenous injection of a solution containing an unknown amount of glucagon for testing. The whole procedure can be completed in 8 h. The interassay variability of 6 bioassay procedures was ±12.4%. The intra-assay variability was ±3%.

Keyphrases □ Glucagon—*in vivo* bioassay, continuous glucose monitoring, dogs □ Glucose monitoring—glucagon, *in vivo* bioassay, dogs □ *In vivo* bioassay—glucagon, continuous glucose monitoring, dogs

Measurement of glucagon and its synthetic analogues by radioimmunoassay (1–3) does not necessarily reflect their biological activity, since there is no relationship between the binding affinity of glucagons to antibodies and their biological activity. There are several established *in vitro* bioassays for glucagon that are based on: (*a*) the *in vitro* release of glucose by liver slices; (*b*) the stimulation of adenyl cyclase in subcellular particles of the dog liver (4); and (*c*) the relaxing action on strips of rabbit renal artery (5).

Although these *in vitro* bioassays are more specific than the immunoassays, they do not necessarily reflect biological activity *in vivo*. Consequently, the USP bioassay of glucagon requires measurements of the *in vivo* hyperglycemic effect of glucagon (6). The USP bioassay also calls for multiple assays of the glucose levels in eight fasting adult cats and requires four intravenous injections of glucagon to each cat (two injections of a standard solution and two injections of assay samples). Two blood samples are taken after each injection.

The purpose of this study is to describe a simplified and rapid *in vivo* bioassay for glucagon, which can be completed in 8 h and requires only one dog.

EXPERIMENTAL SECTION

Animals—Six female hound dogs, weighing 17 kg, were used. The test was repeated six times on each dog at 2-week intervals. The dogs were anesthetized with intravenous sodium pentobarbital[1] (150-mg initial dose, 25 mg every 30 min for maintenance). Continuous glucose monitoring was then initiated, using a nonthrombogenic catheterization of the front paw.

Instruments—The glucose monitoring instrument consisted of systems for blood withdrawal and glucose measurement. The blood withdrawal system included a disposable sterile intravenous catheter connected to a peristaltic pump. Coating the inside of the catheter with triiododecylmethylammonium chloride complexed with heparin created a nonthrombogenic surface. The blood that was withdrawn continuously (at a rate of 8 mL/h) from a vein through the nonthrombogenic catheter was diluted in the plexiglass mixing chamber with 6 volumes of simultaneously withdrawn phosphate buffer solution (0.15 M, pH 7.4) and moved into the sensory chamber.

[1] Nembutal.

Table I—Six Repeated Bioassays of 0.003 U Glucagon after Intravenous Injection of Glucagon

	Blood Glucose Levels, mg/dL			
Dogs	Peak 1, 0.002 U	Peak 2, 0.004 U	Peak 3, 0.003 U	Bioactivity of 0.003 U of Glucagon
1	129	155	147	0.00 33
2	125	148	133	0.00 26
3	109	121	115	0.00 28
4	95	105	97	0.00 23
5	108	128	120	0.00 30
6	108	135	124	0.00 30
Mean	112.3	132	122.7	0.00 28
±*SD*	12.5	18.2	16.8	0.00 035
CV, %	11.12	13.70	13.60	12.4

The glucose measuring system included a plexiglass mixing chamber, a glucose-sensing probe, a digital display and a microprocessor-controlled digital graphic recorder. The glucose probe was a Clark electrode (7). A membrane impregnated with glucose oxidase covered the tip of the probe. Enzymatic oxidation of glucose diffusing through the glucose oxidase membrane generated hydrogen peroxide at a rate proportional to the concentration of glucose. Thus, current flow through the electrode was linearly related to the concentration of blood glucose. The level of blood glucose was exhibited by a digital display and by the digital graphic recorder.

Reagents—A glucagon standard solution for intravenous injection was prepared in accordance with the USP (6).

Bioassay Method—The hyperglycemic peak induced by intravenous injection of glucagon was accurately depicted in real time, using the nonthrombogenic glucose monitor. The assay consisted of comparing the hyperglycemic peak, induced by an unknown amount of glucagon, to the peaks induced by two intravenous injections of a known amount of glucagon.

The blood level of glucose was first monitored for at least 0.5 h in order to establish a baseline level of glucose. After establishing a steady baseline, the dog was given the first standard amount of glucagon. The glucagon was administered as an intravenous injection in a rapid bolus which was immediately flushed with 10 mL of saline. The first peak of glucose was recorded by the glucose monitor within 14 min after the injection of glucagon. A period of 41 min following a peak was allowed for restabilization of the glucose baseline. This procedure was then repeated using a second standard amount of glucagon. The second standard was usually higher than the first standard. After recording the second peak of glucose, a third injection of an unknown amount of glucagon was administered. The level of "unknown" glucagon was then calculated by linear regression of semilogarithmic paper of the three peak levels P_1, P_2, and P_3.

RESULTS

Interassay Variability—The bioassay was repeated six times using standards of 0.002 and 0.004 U of glucagon and an injection of 0.003 U to represent the unknown. The results are given in Table I. The interassay variability of the six consecutive assays was 12.4%.

Intra-assay Variability—The intra-assay variability of the bioassay was measured by comparing the variability of five consecutive peaks by a constant amount of glucagon. Two assays of intra-assay variabilities were carried out: one with 0.002 U, the other with 0.004 U. The results are recorded in Tables

0022-3549/84/0900-1298$01.00/0
© 1984, American Pharmaceutical Association

Table II—Variability of Peaks after Repeated Intravenous Injection of 0.002 U of Glucagon

	Blood Glucose Levels, mg/dL					Intra-assay Variability		
	Peak 1	Peak 2	Peak 3	Peak 4	Peak 5	Mean	±*SD*	*CV*, %
1	107	105	111	105	104	106.4	2.79	2.62
2	101	102	98	97	93	98.2	3.56	3.62
3	131	130	127	129	127	128.2	1.79	1.38
4	96	111	114	113	110	108.8	7.33	6.73
5	100	104	101	101	102	101.6	1.50	1.47
6	118	111	121	114	112	115.2	4.21	3.65
Mean	108.8	110.5	112	109.8	108	109.8	3.53	3.24
±*SD*	13.2	10.25	10.25	11.4	11.4			
CV, %	12.13	9.27	9.00	10.5	10.5			

Table III—Variability of Peak after Repeated Intravenous Injection of 0.004 U of Glucagon

	Blood Glucose Levels, mg/dL					Intra-assay Variability		
	Peak 1	Peak 2	Peak 3	Peak 4	Peak 5	Mean	±*SD*	*CV*, %
1	125	122	119	119	123	121.6	2.60	2.14
2	123	124	116	115	117	119	4.18	3.51
3	108	102	97	104	107	103.6	4.40	4.24
4	106	95	110	107	109	105.4	6.02	5.71
5	141	145	154	146	145	146.2	4.77	3.26
6	112	116	119	118	118	116.6	2.60	2.24
Mean	119.2	117.3	119.2	118.2	114.8	117.6	4.09	3.52
±*SD*	13.20	17.70	19.08	14.90	13.60			
CV, %	11.07	15.08	16.12	12.60	11.35			

II and III. The intra-assay variability of the assay using 0.002 U of glucagon was 3.2%. The intra-assay variability of the assay using 0.004 U was 3.5%.

The time interval from the intravenous injection of 0.002 U of glucagon to the peak level of glucose was 10.0 ± 1.2 min (mean ±1 *SD*), while the time to peak of 0.004 U glucagon was 11.9 ± 2.5 min. The peak level of glucose was maintained for 100 ± 69 s after 0.002 U of glucagon and 92 ± 49 s after 0.004 U of glucagon.

DISCUSSION

This new bioassay of glucagon is very similar to a previously published improved bioassay for insulin (8). Similar to the insulin bioassay, the improved accuracy of the bioassay for glucagon is based on the ability to obtain a continuous and almost instantaneous record of the changing levels of blood glucose. The continuous glucose monitor made possible an accurate determination of the glucagon-induced peaks of blood glucose, even though it lasted only for a few minutes and occurred at unpredictable times.

The USP bioassay depends on sampling of blood for glucose at predetermined times (6) which almost never occurred at the precise moment of the glucose peak. We have found the actual peaks of blood glucose, which were induced by a repeated but constant dose of glucagon, to be markedly consistent. The time to peak, on the other hand, was highly variable in relation to its duration. Thus, it is obvious that the USP bioassay, which depends on blood sampling for glucose levels at predetermined times, is inherently less accurate. This new bioassay procedure would be more practical, less expensive, and more accurate than the USP bioassay for the standardization of USP preparations of glucagon, provided the actual dose used for injection is adjusted to range from 0.002 to 0.004 U.

REFERENCES

(1) R. H. Unger, A. M. Eisentraut, M. S. McCall, L. L. Madison, K. R. Sims, L. Timm, and L. Patman, *J. Clin. Invest.*, **40**, 1280 (1961).

(2) R. H. Unger, A. M. Eisentraut, L. L. Madison, K. R. Sims, and N. Whissen, *J. Clin. Invest.*, **42**, 1031 (1963).

(3) E. Samols and D. Bilkus, *Proc. Soc. Exp. Biol. Med.*, **115**, 79 (1978).

(4) M. H. Makman and E. W. Sutherland, Jr., *Endocrinology*, **75**, 127 (1964).

(5) G. Gagnon, D. Regoli, and F. Rioux, *Br. J. Pharmacol.*, **64**, 99 (1978).

(6) "The United States Pharmacopeia" 20th rev., U.S. Pharmacopeial Convention, Rockville, Md., p. 900.

(7) W. L. Clark and J. V. Santiago, *Artif. Organs*, **1**, 78 (1977).

(8) C. R. Kowarski, D. Kowarski, B. D. Bick, H. Stein, D. Rudavich, and A. A. Kowarski, *J. Clin. Endocrinol. Metab.* **53**, 1145 (1981).

ACKNOWLEDGMENTS

This work was supported by Grant HD-16077 of the National Institutes of Health, U.S. Public Health Service.

Nasal Absorption of Testosterone in Rats

ANWAR A. HUSSAIN, RYOHEI KIMURA, and CHONG HENG HUANG

Received July 22, 1983 from the *College of Pharmacy, University of Kentucky, Lexington, KY 40536-0053.* Accepted for publication September 19, 1983.

Abstract □ Testosterone levels in the blood were determined in rats following nasal, intravenous, and intraduodenal administration of 25-μg and 50-μg doses. The results indicated that the drug levels after nasal and intravenous administration were similar, whereas intraduodenal administration resulted in considerably lower levels. The bioavailability of the nasally administered drug was calculated to be 99% and 90% at the 25-μg and 50-μg doses, respectively. The intraduodenal bioavailability was only 1% at the dose studied.

Keyphrases □ Testosterone—nasal absorption, rats □ Nasal absorption—testosterone, rats

Testosterone is considered to be the most potent of the natural male sex hormones. This androgen is readily absorbed orally, but it is ineffective when so administered because of extensive metabolism in the GI tract and the liver before reaching systemic circulation (1). The esters of testosterone are similarly metabolized (1). Consequently, testosterone and its esters are generally administered by intramuscular injection. Other routes of administration, for example, buccal, transdermal, and subcutaneous implantation, have been attempted, but success has been limited (1).

Previous studies by Hussain and co-workers have shown that selected drugs, for example, propranolol and progesterone, are efficiently and completely absorbed following nasal absorption in animals and man (2–5). To enhance testosterone bioavailability from non-parenteral routes, the nasal route was examined. This report presents results on the nasal administration of testosterone in rats as compared to intravenous and intraduodenal administration of the drug.

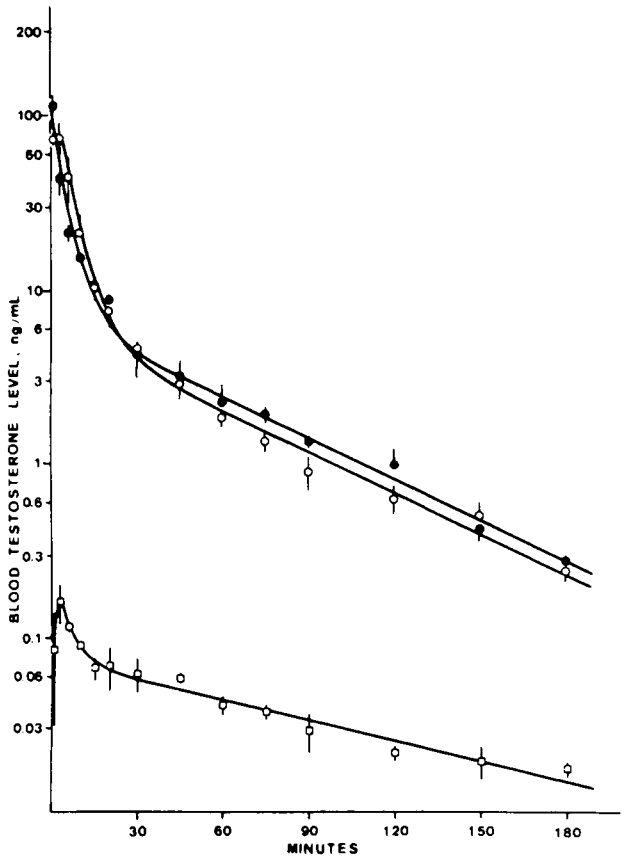

Figure 1—*Mean blood levels of testosterone in rats following nasal (○), intravenous (●), and intraduodenal (□) administration of 25-μg testosterone per rat. Points represent mean values of 3 animals ±SEM.*

Table I—Area Under Blood Level Curve (AUC) Following Intravenous, Nasal, and Intraduodenal Administration of Testosterone in Rats

Dose, μg	Route	AUC, ng·h/mL[a]	AUC (nasal, intraduodenal) / AUC (intravenous)
25	Intravenous	900.6 ± 90.9	—
	Nasal	890.5 ± 168.0	0.99
	Intraduodenal	8.9 ± 0.19	0.01
50	Intravenous	1716.3 ± 47.2	—
	Nasal	1545.7 ± 168.6	0.90

[a] Mean ± *SEM* (n = 3).

EXPERIMENTAL SECTION

Animal Studies—Male Sprague-Dawley rats, each weighing approximately 300 g, were anesthetized with pentobarbital (50 mg/kg). The surgical operation carried out on the rats was that described by Hussain *et al.* (2). For nasal administration of [^{3}H]testosterone[1], an incision was made in the neck of the animals, and the trachea was cannulated with a polyethylene tube. A closed tube was inserted through the esophagus to the posterior part of the nasal cavity. The nasopalatine passage was closed with an adhesive agent to prevent drainage of the drug from the nasal cavity to the mouth. Two doses of 25 and 50 μg of [^{3}H]testosterone, each containing 20 μCi of [^{3}H]testosterone in 0.1 mL of 1% polysorbate 80-saline solution, were administered to the nasal cavity by means of micropipet, and the nostrils were then closed with an adhesive agent. For intravenous administration, the same doses were injected through the femoral vein. For intraduodenal administration, the abdomen was opened by a midline incision, and the 25-μg dose in 0.1 mL of 1% polysorbate 80-saline solution was injected directly through the duodenum.

Analytical Method—The blood samples were placed in polyethylene tubes, to which 0.2 g of NaCl, 200 μL of nonradioactive testosterone solution (1.25 mg/mL) in ethyl acetate, and 5 mL of ether were added. After shaking and centrifugation, the tube was frozen in a dry ice–acetone mixture. The ether layer was decanted into another tube and evaporated to dryness. The residue was then dissolved in 60 μL of methanol and 40 μL was spotted on TLC plates and developed using chloroform–acetone (9:1, v/v). The spot that corresponded to unchanged testosterone was then scraped off the plate, and the powder was suspended in 10 mL of scintillation cocktail for a radioactivity count. The developing solvent system was shown to separate unchanged testosterone from its metabolites.

RESULTS AND DISCUSSION

The levels of testosterone in the blood after nasal administration increased rapidly and attained the peak level within 2 min, whereas the intraduodenal administration resulted in considerably lower blood levels. The blood levels following nasal administration were similar to those following intravenous administration, and the half-life of elimination for the two routes was ~40 min.

The nasal bioavailability, calculated from the ratio of the area under the blood level–time curve [(nasal/intravenous) × 100], was 99% at the 25-μg dose and 90% at the 50-μg dose; the intraduodenal bioavailability was only 1% of that of the intravenous bioavailability at the dose studied (Table I; Fig. 1).

The results of this study strongly suggest that the natural male sex hormone, testosterone, is rapidly absorbed from the nasal mucosa into systemic blood

[1] [1β,2β-^{3}H]Testosterone (40 Ci/mmol); New England Nuclear, Boston, Mass.

0022-3549/84/0900-1300$01.00/0
© 1984, American Pharmaceutical Association

without first-pass metabolism. The nasal route may be of practical value for the administration of this hormone.

REFERENCES

(1) "The Pharmacological Basis of Therapeutics," 6th ed., A. G. Gilman, L. S. Goodman and A. Gilman, Eds., Macmillan, New York, N.Y., 1980, Chap. 62.

(2) A. Hussain, S. Hirai, and R. Bawarshi, *J. Pharm. Sci.*, **68**, 1196 (1979).

(3) A. Hussian, S. Hirai, and R. Bawarshi, *J. Pharm. Sci.*, **69**, 1411 (1980).

(4) A. Hussian, S. Hirai, and R. Bawarshi, *J. Pharm. Sci.*, **70**, 466 (1981).

(5) A. Hussain, T. Foster, S. Hirai, T. Kashihara, R. Batenhorst, and M. Jones, *J. Pharm. Sci.*, **69**, 1240 (1980).

Colorimetric Determination of Gentamicin, Kanamycin, Tobramycin, and Amikacin Aminoglycosides with 2,4-Dinitrofluorobenzene

JAMES A. RYAN

Received March 29, 1983, from the *Department of Pharmaceutical Research and Development, Merck Sharp and Dohme Research Laboratories, Division of Merck and Company, Inc. West Point, PA 19486.* Accepted for publication August 3, 1983.

Abstract □ The reaction of 2,4-dinitrofluorobenzene (Sanger's reagent) is used to form colored products with aminoglycoside antibiotics. Stopping the progress of the reaction with acid after a fixed time allows aqueous solubility to be maintained while discharging any color due to excess reactant. The choice of an appropriate analytical wavelength results in adherence to Beer's law. Although this colorimetric method is not expected to be stability-indicating, it is convenient and should be useful in content uniformity determinations for pharmaceutical dosage forms (*e.g.*, ointments).

Keyphrases □ Colorimetry—aminoglycosides, 2,4-dinitrofluorobenzene □ Aminoglycosides—2,4-dinitrofluorobenzene, colorimetric determination

Most assays for monitoring aminoglycoside antibiotics which are mentioned in the Federal Register (1) are plate-cup bioassays. A number of chemical assays (2) have been developed for use with pharmaceutical dosage forms and content determinations. These assays are useful, in some cases, as rapid control procedures featuring high precision, but do not actually measure bioactivity; most are amine reagents (3). We found in our preliminary work that certain pharmaceutical formulation excipients do not react with 2,4-dinitrofluorobenzene (Sanger's reagent) (4–6); therefore, this reagent could be useful when determining aminoglycosides. Sanger's reagent was originally used to detect terminal amino groups in insulin, and was utilized recently (7) for postcolumn HPLC-derivatization and detection of neomycin sulfate.

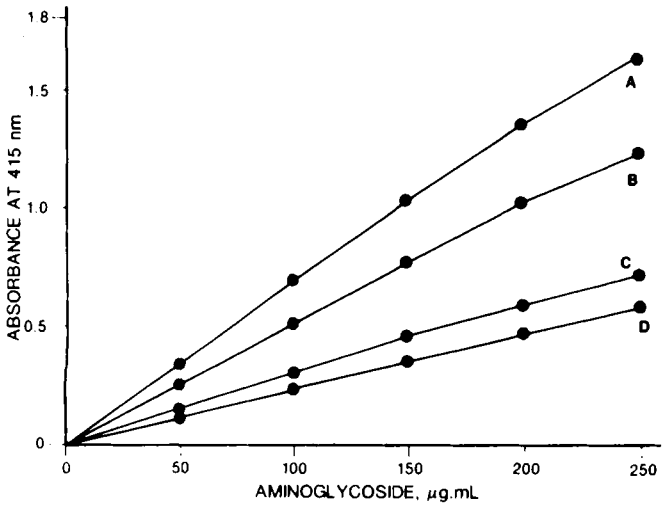

Figure 1—*Absorbance of aminoglycosides at 415 nm with 20-min reaction time. Key: (A) amikacin, (B) tobramycin, (C) kanamycin, (D) gentamicin.*

This paper reports the direct one-phase determination of gentamicin sulfate, kanamycin sulfate, tobramycin, and amikacin. The reaction was allowed to proceed under ambient conditions and then it was stopped, after an appropriate time, by acidification. The analytical wavelength chosen was not the absorption maximum, but one which permitted measurement in the aqueous-alcoholic medium without problem precipitation and with adherence to Beer's law over the range of 0–1000 μg/mL (Fig. 1). A typical reaction profile of gentamicin sulfate is outlined in Fig. 2.

EXPERIMENTAL SECTION[1]

Colorimetric Measurement—Exactly 5.0 mL of an aqueous solution containing ~500 μg of the aminoglycoside being tested was transferred to a 10-mL glass-stoppered flask or tube. Similarly, a series of flasks or tubes containing

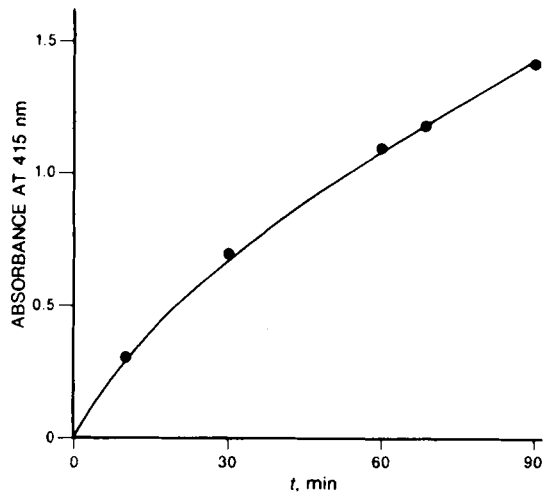

Figure 2—*Gentamicin sulfate reaction profile.*

[1] Gentamicin sulfate (lot GMC-6M-6024, potency 581 μg/mg) was obtained from the Schering Corp., Kenilworth, N.J. Kanamycin sulfate (lot 76F-140, potency 780 mg/mL) and amikacin (lot 74F-1805, potency 934 mg/mL) were both obtained from Bristol Labs., Syracuse, N.Y. The tobramycin (lot OCU55, potency 960 μg/mg) was made available through the courtesy of Eli Lilly and Co., Indianapolis, Ind. Sanger's reagent, 2,4-dinitrofluorobenzene (lot 101547, purity 98%), was obtained from the Aldrich Chemical Co., Milwaukee, Wis. Measurements were made on a Cary Model 15 UV-visible spectrophotometer.

0022-3549/84/0900-1301$01.00/0
© 1984, American Pharmaceutical Association

without first-pass metabolism. The nasal route may be of practical value for the administration of this hormone.

REFERENCES

(1) "The Pharmacological Basis of Therapeutics," 6th ed., A. G. Gilman, L. S. Goodman and A. Gilman, Eds., Macmillan, New York, N.Y., 1980, Chap. 62.

(2) A. Hussain, S. Hirai, and R. Bawarshi, *J. Pharm. Sci.*, **68**, 1196 (1979).

(3) A. Hussian, S. Hirai, and R. Bawarshi, *J. Pharm. Sci.*, **69**, 1411 (1980).

(4) A. Hussian, S. Hirai, and R. Bawarshi, *J. Pharm. Sci.*, **70**, 466 (1981).

(5) A. Hussain, T. Foster, S. Hirai, T. Kashihara, R. Batenhorst, and M. Jones, *J. Pharm. Sci.*, **69**, 1240 (1980).

Colorimetric Determination of Gentamicin, Kanamycin, Tobramycin, and Amikacin Aminoglycosides with 2,4-Dinitrofluorobenzene

JAMES A. RYAN

Received March 29, 1983, from the *Department of Pharmaceutical Research and Development, Merck Sharp and Dohme Research Laboratories, Division of Merck and Company, Inc. West Point, PA 19486.* Accepted for publication August 3, 1983.

Abstract □ The reaction of 2,4-dinitrofluorobenzene (Sanger's reagent) is used to form colored products with aminoglycoside antibiotics. Stopping the progress of the reaction with acid after a fixed time allows aqueous solubility to be maintained while discharging any color due to excess reactant. The choice of an appropriate analytical wavelength results in adherence to Beer's law. Although this colorimetric method is not expected to be stability-indicating, it is convenient and should be useful in content uniformity determinations for pharmaceutical dosage forms (*e.g.*, ointments).

Keyphrases □ Colorimetry—aminoglycosides, 2,4-dinitrofluorobenzene □ Aminoglycosides—2,4-dinitrofluorobenzene, colorimetric determination

Most assays for monitoring aminoglycoside antibiotics which are mentioned in the Federal Register (1) are plate-cup bioassays. A number of chemical assays (2) have been developed for use with pharmaceutical dosage forms and content determinations. These assays are useful, in some cases, as rapid control procedures featuring high precision, but do not actually measure bioactivity; most are amine reagents (3). We found in our preliminary work that certain pharmaceutical formulation excipients do not react with 2,4-dinitrofluorobenzene (Sanger's reagent) (4–6); therefore, this reagent could be useful when determining aminoglycosides. Sanger's reagent was originally used to detect terminal amino groups in insulin, and was utilized recently (7) for postcolumn HPLC-derivatization and detection of neomycin sulfate.

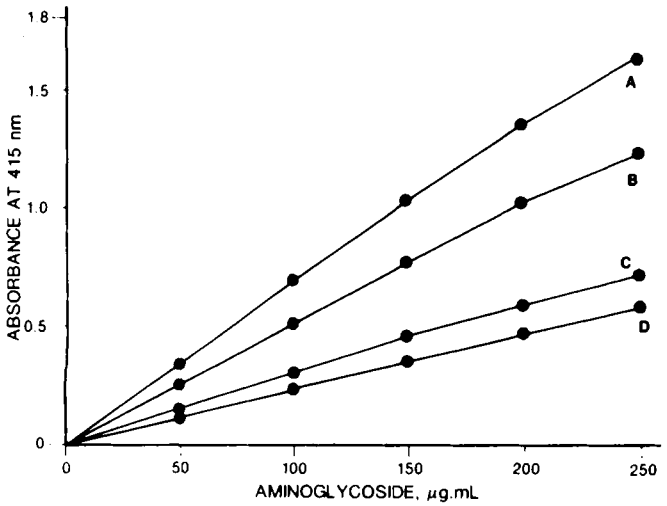

Figure 1—*Absorbance of aminoglycosides at 415 nm with 20-min reaction time. Key: (A) amikacin, (B) tobramycin, (C) kanamycin, (D) gentamicin.*

This paper reports the direct one-phase determination of gentamicin sulfate, kanamycin sulfate, tobramycin, and amikacin. The reaction was allowed to proceed under ambient conditions and then it was stopped, after an appropriate time, by acidification. The analytical wavelength chosen was not the absorption maximum, but one which permitted measurement in the aqueous-alcoholic medium without problem precipitation and with adherence to Beer's law over the range of 0–1000 μg/mL (Fig. 1). A typical reaction profile of gentamicin sulfate is outlined in Fig. 2.

EXPERIMENTAL SECTION[1]

Colorimetric Measurement—Exactly 5.0 mL of an aqueous solution containing ~500 μg of the aminoglycoside being tested was transferred to a 10-mL glass-stoppered flask or tube. Similarly, a series of flasks or tubes containing

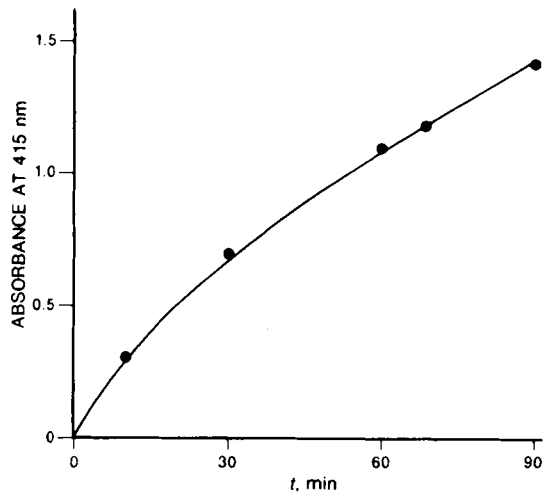

Figure 2—*Gentamicin sulfate reaction profile.*

[1] Gentamicin sulfate (lot GMC-6M-6024, potency 581 μg/mg) was obtained from the Schering Corp., Kenilworth, N.J. Kanamycin sulfate (lot 76F-140, potency 780 mg/mL) and amikacin (lot 74F-1805, potency 934 mg/mL) were both obtained from Bristol Labs., Syracuse, N.Y. The tobramycin (lot OCU55, potency 960 μg/mg) was made available through the courtesy of Eli Lilly and Co., Indianapolis, Ind. Sanger's reagent, 2,4-dinitrofluorobenzene (lot 101547, purity 98%), was obtained from the Aldrich Chemical Co., Milwaukee, Wis. Measurements were made on a Cary Model 15 UV-visible spectrophotometer.

0022-3549/84/0900-1301$01.00/0
© 1984, American Pharmaceutical Association

Table I—Stability of Developed Color after Acidification

	Absorbance Values	
	Initial	$T + 17$ h at Room Temperature
Blank	0.066	0.069
Gentamicin sulfate	0.321	0.318
Kanamycin sulfate	0.419	0.419
Amikacin	0.747	0.747
Tobramycin	0.586	0.586

5-mL aliquots of standard solutions containing 250, 500, 750, 1000, 1250 μg per 5.00 mL of the aminoglycoside were prepared. Using a definite sequence and a convenient but reproducible time interval between reagent additions, the following operations were performed on each sample and standard solution.

One milliliter of a 2% aqueous $NaHCO_3$ solution was added to each tube. The tubes were stoppered and mixed. Exactly 2.0 mL of a freshly prepared ethanolic (95%) solution of 2,4-dinitrofluorobenzene[2] (5, 6) containing 0.25 mL/100 mL was added to each tube. The contents of the tube were mixed thoroughly. After 20 min for tobramycin, amikacin, and kanamycin sulfate, or 30 min for gentamicin sulfate, the solution was neutralized by the addition of 0.5 mL 1 M HCl. After tapping the cell gently to remove any CO_2 bubbles, the absorbance was determined at 415 nm in the spectrophotometer using 1 cm cells and distilled water as a reference liquid.

RESULTS AND DISCUSSION

Inasmuch as adherence to Beer's law was obtained, the concentration of each aminoglycoside was determined by direct ratio to the diluted reference standard. Since the yellow color, due to excess reagent, is discharged by the acid solutions, no reagent blank was required when assaying colorless solutions. The *RSD* of each of the aminoglycosides tested was: gentamicin sulfate ±1.4%, kanamycin sulfate ±0.86%, tobramycin ±1.6%, and amikacin ±1.1%. The color that developed after acidification was found to be stable for at least 17 h (Table I). Use of filter photometers or other instruments with wide spectral band-pass may possibly result in deviations from Beer's law at 415 nm.

A probe experiment was also conducted to check the stability of the response of aqueous solutions of these antibiotics to the assay. Dilutions of the individual antibiotics in unbuffered aqueous solutions were prepared at levels of ~10 mg/100 mL. The solutions were sampled for their color response and then rechecked after 35 d under ambient conditions (~21.5°C in laboratory light) (Table II).

Compatibility of the Method with Various Pharmaceutical Excipients used for Topical Administration of the Antibiotics—Five grams of an ointment base[3] was mixed for 5 min with 20 mL of water and filtered[4]. The clear filtrate was used as a gentamicin sulfate diluent instead of water in the assay method and compared to a standard in distilled water. The average of three consecutive comparisons of these gentamicin solutions showed water extract absorbance values only 100.5% of those obtained with distilled water diluent solutions which demonstrates the lack of significant interference from the excipients.

Phosphate buffers are often used in connection with the bioassays of aminoglycosides such as gentamicin sulfate, however, they were found to interfere with the color development reaction. Those studied were 0.1–1.0 M buffers adjusted to pH 7.0. An average of eight measurements of four buffer strengths at pH 7 produced only 31.2% of the color development of a sample in distilled water.

Potential Automated Modifications—The requirement for precise timing during the initial reaction step and the need for caution to prevent exposure of Sanger's reagent to the skin indicates that, if automated, this method might reasonably be expected to have wide application.

Table II—Color Responses of Amino Functions after 35 d at 21.5°C in Unbuffered Aqueous Solutions

	Initial mg/mL	Final mg/mL	% Initial
Gentamicin sulfate	10.1	10.1	100
Kanamycin sulfate	9.74	10.5	107
Amikacin	10.3	10.2	99.0
Tobramycin	10.7	11.1	104

[2] Exercise appropriate caution; handle in hood with protective gloves and clothing.

[3] Ointment consisted of: 0.267 g of Wool Alcohols B.P., 0.8015 g of Amerchol C, 1.87 g of Multivax W445 White Wax, and 2.06 g of isopropyl myristate.

[4] Selas Flotronics Ag filter (0.2 μg apertures).

REFERENCES

(1) Federal Register, 21 CFR 436.105, U.S. Government Printing Office, Washington, D.C.

(2) D. W. Hughes, A. Vilim, and W. L. Wilson, *Can. J. Pharm. Sci.*, **13,** 21 (1978).

(3) D. Benjamin, J. McCormack, and D. Gump, *Anal. Chem.*, **45,** 1531 (1973).

(4) F. Sanger, *Biochem. J.*, **39,** 507 (1945).

(5) M. J. Levitt, and C. Bon, *Chem. Eng. News*, **55,** 30 (1977).

(6) Olin Safety Data Sheet, Olin Research Center, New Haven, Conn.

(7) K. Tsuji, J. Goetz, W. Van Meter, and K. Gusicora, *J. Chromatogr.* **175,** 141 (1979).

ACKNOWLEDGMENTS

The author acknowledges the assistance and/or encouragement willingly supplied by the following individuals: Mr. Warren Hagerman, Dr. Gerald Brenner, Dr. Edward M. Cohen, and members of the Merck Publications Review Committee for critical reviews.

High-Performance Liquid Chromatographic Determination of The Nitrate Esters Isosorbide Dinitrate, Pentaerythritol Tetranitrate, and Erythrityl Tetranitrate in Various Tablet Forms

CAROLYN S. OLSEN ˣ **and HENRY S. SCROGGINS**

Received April 11, 1983, from the *Food and Drug Administration, 4298 Elysian Fields Avenue, New Orleans, LA 70122.* Accepted for publication June 22, 1983.

Abstract □ A reliable, sensitive, and specific assay for isosorbide dinitrate, pentaerythritol tetranitrate, and erythrityl tetranitrate in sublingual, uncoated, sustained-release, and chewable dosage forms, using high-performance liquid chromatography, is described. The nitrate ester dosage forms were dissolved in methanol, filtered, and injected directly into the liquid chromatograph. A variable-wavelength UV detector, operated at 220 nm, and a reverse-phase C_{18} microporous silica column were employed. The mobile phase was methanol–water (40:60). The proposed method is quantitative and reproducible.

Keyphrases □ Isosorbide dinitrate—HPLC, tablet forms □ Pentaerythritol tetranitrate—HPLC, tablet forms □ Erythrityl tetranitrate—HPLC, tablet forms

Isosorbide dinitrate (I), pentaerythritol tetranitrate (II), and erythrityl tetranitrate (III) are members of a group of vasodilator drugs that are useful in the treatment of angina pectoris and ischemia of skeletal muscles. Since these nitrate esters have a slower onset of action and their duration is longer than nitroglycerin (IV), they are beneficial in the prevention of attacks, but not in the management of the acute attack (1).

Nitrate esters have been determined by polarographic (2–4), IR, spectrophotometric (5–8), and colorimetric (9–11) procedures. The basis for several procedures (12, 13) is nitration of phenoldisulfonic acid with the nitrate moiety of the ester and subsequent formation of a colored ion in a basic solution. These standard methods are time consuming and complex, and the colorimetric method is nonspecific for the active ingredient.

The objective of this investigation was to devise a simple, rapid, and specific procedure that would be applicable to the three nitrate esters cited above and to the majority of other nitrate esters. High-performance liquid chromatography (HPLC) as a determinative technique offered the best approach (14, 15). This straightforward procedure has already been successfully used to quantitatively determine IV (16, 17). This paper presents a method for the analysis of I, II, and III in various dosage forms by reverse-phase HPLC with IV as the internal standard. This method is simple, rapid, and reproducible.

EXPERIMENTAL SECTION

Reagents and Materials—HPLC-grade methanol[1] and water[1] were used. All other chemicals and solvents were reagent grade and were used without further purification. Ten percent of II[2], 10% of III[3], and 25% of I[4], all as lactose triturates, were used as reference standards; II and III were assayed by the USP phenoldisulfonic acid method (18). A 10% IV[5] triturate was used as an internal standard.

Instrumentation—The liquid chromatographic system consisted of a dual-head reciprocating piston positive-displacement pump[6], a septumless syringe-loaded loop injector with a 20-μL loop[7], a variable-wavelength UV detector[8], operated at 220 nm, and a 10-mV recorder[9]. A 30 cm × 3.9-mm i.d. 10-μm C_{18} microparticulate column[10] with a 4 cm × 4.6-mm guard column packed with pellicular octadecyl reverse-phase material[11] was used at ambient temperature. The mobile phase was methanol–water (40:60). The flow rate was 1 mL/min with a pressure of 1600 psi.

Solution Preparation—The internal standard, IV, was prepared as a 75-μg/mL solution in methanol and filtered through 0.7-μm filter paper[12]. To prepare a standard solution, 1 mg of I, 2 mg of II, or 3 mg of III was accurately weighed into a 50-mL glass-stoppered Erlenmeyer flask and diluted with 10.0 mL of internal standard solution. The desired solution was sonicated for 2 min, mechanically shaken for 30 min, and then filtered through 0.7-μm filter paper[12]. Samples of each drug were prepared by weighing and finely powdering 20 tablets. An accurately weighed portion of the powder, equivalent to 1 mg of I, 2 mg of II, or 3 mg of III, was transfered to a 50-mL glass-stoppered Erlenmeyer flask and diluted with 10.0 mL of internal standard solution,

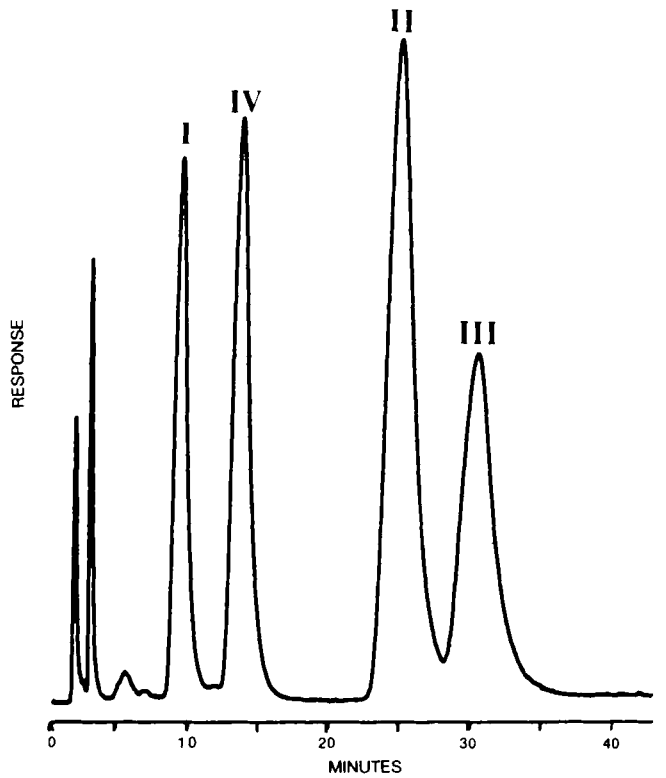

Figure 1—*Chromatogram of nitrate ester mixture. Key: (I) isosorbide dinitrate; (IV) nitroglycerin; (II) pentaerythritol tetranitrate; (III) erythrityl tetranitrate.*

[1] J. T. Baker Chemical Co., Phillipsburg, N.J.
[2] Atlas Chemical Industries, Wilmington, Del.
[3] Burroughs Wellcome, Research Triangle Park, N.C.
[4] USP Reference Standard, United States Pharmacopeial Convention, Rockville, Md.
[5] ICI Americas, Wilmington, Del.
[6] Model 100A; Altex Scientific, Berkeley, Calif.
[7] Model 210 injector with 210-06 loop; Altex Scientific, Berkeley, Calif.
[8] Model 155-40; Altex Scientific, Berkeley, Calif.
[9] B-D-41; Kipp & Zonen, Delft, The Netherlands.
[10] μ-Bondapak C_{18} (10 μm); Waters Associates, Milford, Mass.
[11] μ-Bondapak C_{18}/Corasil; Waters Associates, Milford, Mass.
[12] Gilman Instrument Co., Ann Arbor, Mich.

0022-3549/84/0900-1303$01.00/0
© 1984, American Pharmaceutical Association

Table I—Assay Results for Tablet Forms

Dosage Form	Tablet Conc., mg	Found, mg	Found, %
	Isosorbide Dinitrate		
Sublingual	2.5	2.34	93.6
Sublingual	2.5	2.40	96.0
Sustained-release	40	40.57	101.4
Sustained-release	40	38.53	96.3
	Pentaerythritol Tetranitrate		
Uncoated	10	9.04	90.4
Uncoated	10	10.05	100.5
Uncoated	10	9.17	91.7
Sustained-release	80	84.00	105.0
	Erythrityl Tetranitrate		
Chewable	10	10.80	108.0
Sublingual	10	10.13	101.3
Sublingual	10	10.36	103.6

sonicated for 2 min, mechanically shaken for 30 min, and filtered through 0.7-μm filter paper[12].

Assay of Standard and Sample—Using the HPLC parameters described, three 20-μL portions of the standard and sample filtrates were chromatographed. The calculation of the peak area ratio, R, was determined from the area of I/the area of internal standard peak. The concentration of I (C) was then determined from:

$$C_{sample} = C_{standard} \times (R_{sample}/R_{standard})$$

The percent of I was determined from the percent of label = (sample concentration/theoretical sample concentration) × 100.

Precision and Accuracy Studies—Twenty tablets were weighed and triturated to a fine powder. From this powder, seven samples were weighed and treated as described above. Triplicate injections were made of each sample. The spiked samples of each dosage form were prepared using standard addition procedures. Weighed amounts of the triturate were added to previously assayed dosages containing the active ingredient. These preparations were then analyzed as described (19).

RESULTS AND DISCUSSION

Figure 1 shows a typical chromatogram of a mixture of 2 μg of I, 4 μg of II, and 6 μg of III, using 1.5 μg of IV as the internal standard. The retention time with 40% methanol in water was ~10 min for I, 14 min for IV, 25 min for II, and 30 min for III.

During the development of this method, a number of variations were tried. Methanol was chosen as the extracting solvent because of its ability to solubilize the nitrate ester from its excipients in the various dosage forms. Methanol and acetonitrile performed equally well as the mobile phase; however, methanol was chosen because it is less costly. Compound IV was chosen as the internal standard because it does not interfere with the nitrate esters or any of the excipients present in the various dosage forms.

The various nitrate esters were separated by the HPLC method described. Detection with 220 nm gave twice the sensitivity with quantitative results compared with those obtained at 254 nm. Commercial preparations were analyzed by the proposed HPLC method. Results are given in Table I.

Quantitation was based on the nitrate ester-to-internal standard peak area ratio. Linearity was obtained between 0.2–40 μg of I, 0.4–50 μg of II, and 0.6–50 μg of III. The correlation coefficients were 0.9980, 0.9999, and 0.9999 for I, II, and III, respectively. The precision of the method showed an *RSD* of 1.56% ($n = 7$) (Table II). The overall percent recoveries (±*SD*) from the spiked sample mixtures were 100.8 (±1.4) for I, 101.1 (±0.5) for II, and 101.5 (±0.6) for III.

Table II—Precision of HPLC Assay of Isosorbide Dinitrate

Tablet	Absorbance[a]	Found, mg	Percent of Label Found
1	0.5500	2.43	97.2
2	0.5618	2.48	99.2
3	0.5694	2.51	100.4
4	0.5793	2.56	102.4
5	0.5657	2.50	100.4
6	0.5616	2.48	99.2
7	0.5656	2.50	100.0
Mean			99.8
SD (σ) =			1.56
RSD[b]			1.57%

[a] Factor = 4.4145. [b] *RSD* derived from 100 ($\sigma/\bar{x}$).

The HPLC assay provides a rapid, sensitive, and specific method for the determination of the nitrate esters in the various dosage forms. This method is faster and more specific than the present official methods.

REFERENCES

(1) P. Needleman and E. M. Johnson, Jr., in "The Pharmacological Basis of Therapeutics," L. S. Goodman and A. Gilman, Eds., Macmillan, New York, N.Y., 1980, p. 819.

(2) "The United States Pharmacopeia," 20th rev., U.S. Pharmacopeial Convention, Rockville, Md., 1980, p. 434.

(3) G. C. Whitnack, J. N. Nielson, and E. St. Clair Gantz, *J. Am. Chem. Soc.*, **74**, 4997 (1952).

(4) G. C. Whitnack, M. M. Mayfield, and E. St. Clair Gantz, *Anal. Chem.*, **27**, 899 (1955).

(5) "Official Methods of Analysis of the Association of Official Analytical Chemists," 13th ed., Association of Official Analytical Chemists, Arlington, Va., 1980, p. 679.

(6) J. Carol. *J. Assoc. Offic. Agr. Chem.*, **43**, 259 (1960).

(7) J. Rosenstein, *J. Assoc. Offic. Agr. Chem.*, **47**, 469 (1964).

(8) H. L. Fung, P. Dalecki, E. Tse, and C. T. Rhodes, *J. Pharm. Sci.*, **62**, 696 (1973).

(9) "The United State Pharmacopeia," 20th rev., U.S. Pharmacopeial Convention, Rockville, Md., 1980, p. 288.

(10) "The United State Pharmacopeia," 20th rev., U.S. Pharmacopeial Convention, Rockville, Md., 1980, p. 597.

(11) F. K. Bell, *J. Pharm. Sci.*, **53**, 752 (1964).

(12) J. R. Hohmann and J. Levine, *J. Assoc. Offic. Agr. Chem.*, **47**, 471 (1964).

(13) E. Sarnoff, *J. Assoc. Offic. Agr. Chem.*, **39**, 630 (1956).

(14) W. G. Crouthamel and B. J. Dorsch, *J. Pharm. Sci.*, **68**, 237 (1979).

(15) D. M. Baaske, J. E. Carter, and A. H. Amann, *J. Pharm. Sci.*, **68**, 481 (1979).

(16) C. S. Olsen and H. S. Scroggins, *J. Pharm. Sci.*, **72**, 963 (1983).

(17) L. Gelber, *J. Pharm. Sci.*, **69**, 1084 (1980).

(18) "The United States Pharmacopeia," 20th rev., U.S. Pharmacopeial Convention, Rockville, Md., 1980, p. 552.

(19) C. Ko, F. Marzian, and C. Janicki, *J. Pharm. Sci.*, **69**, 1081 (1980).

Determination of Ethylene Oxide, Ethylene Chlorohydrin, and Ethylene Glycol in Aqueous Solutions and Ethylene Oxide Residues in Associated Plastics

N. A. BALL

Received May 31, 1983 from *Fisons plc, London Road, Holmes Chapel, Crewe, Cheshire, England.* Accepted for publication September 8, 1983.

Abstract □ A gas chromatographic (GC) method was developed for the determination of ethylene oxide and its two reaction products, ethylene chlorohydrin and ethylene glycol, in aqueous ophthalmic solutions. Propylene oxide was used as an internal standard. All three components were determined in one isothermal chromatographic analysis in <15 min. An extraction method for the determination of ethylene oxide residues in plastic components was also developed, and certain plastics with different ethylene oxide retention characteristics were identified.

Keyphrases □ Gas chromatography—determination of three components in one analysis, ethylene oxide residues □ Ethylene oxide residues—GC, determination of three components in one analysis

The Food and Drug Administration published guidelines in 1978 for the levels of ethylene oxide and its hydrolysis products in ophthalmic solutions; ethylene oxide was used to sterilize plastic components. Manufacturers are now required to control the levels of ethylene oxide (I), ethylene chlorohydrin (II), and ethylene glycol (III) in their ophthalmic products for sale in the United States.

Many papers have been published on the analysis of ethylene oxide (1–7), ethylene chlorohydrin, and/or ethylene glycol (8–13). Very few papers deal with the analysis of all three compounds (14–16), and, of these, the analyses either involve two different gas chromatography (GC) columns (14, 15) or two analyses on one column (16).

EXPERIMENTAL SECTION

Apparatus—The gas chromatograph[1] was equipped with a flame-ionization detector and a glass column, 3% Carbowax 20M on Chromosorb 101 (80–100 mesh), 200 cm × 3 mm i.d. The gas chromatograph was linked to a data station[2] which controlled the temperatures and flow rates and processed the peak area data. The column was conditioned at 170°C under a nitrogen flow of 30 mL · min^{-1} for 14–16 h, at which time the temperature was reduced to 150°C, and several 1-μL injections of water were made before analysis commenced. This temperature and flow rate was maintained throughout the analysis. The injector temperature was 300°C and the detector temperature was 250°C.

Compounds I[3], II[3], III[4], and propylene oxide (IV)[3] were used as received.

Extraction Procedure—Approximately 15 g of cut-up plastic was weighed into a 500-mL conical flask; 100 mL of 1 M HCl was added and the flask was stoppered and sealed[5]. The flask was then placed in a water bath for 14–16 h at 80°C. The resultant solution was transferred to a 200-mL flask, neutralized to pH 7.0 ± 1.0 (using 1 M NaOH) and made to volume with water.

Approximately 15 g of plastic was exposed to an atmosphere of ethylene oxide under a pressure of 15 psi for 6 h and then sampled immediately for extraction.

Solution Preparation—Standards I and IV were prepared by accurately weighing ~50 μL of cold liquid (0–5°C) into a 10-mL flask, containing 3 mL of water, using a previously cooled (0–5°C) 100-μL syringe. The solution was then transferred quantitatively to a 100-mL flask and made to volume with water. Standards II and III were prepared in a similar way; however, the cooling stage was not necessary. A working standard was prepared by adding 1 mL of each solution to a 10-mL flask and diluting to volume with water. Standard IV was the internal standard.

The sample was prepared with 1 mL of IV which was added to a 10-mL flask and made to volume with sample solution.

RESULTS AND DISCUSSION

Column conditioning was found to be very important in achieving reproducible retention times. A high injection temperature of 300°C was used to achieve a sharper ethylene glycol peak. The peak shape was improved further by using a "hot needle" injection technique. Using a 5-μL syringe, a small volume of air was drawn into the barrel both before and after the uptake of 1 μL of sample solution. The needle was then placed in the injection port (300°C) for 5 s, the sample injected, left for a further 5 s in the port, and, finally, withdrawn. The ghosting phenomenon encountered by some authors (16) was not manifested in this analysis.

From the standard chromatogram, it can be seen that the I and IV peaks are very close to the solvent, *i.e.*, water peak. By using a peak skimming technique it was possible to achieve accurate and precise values for I content to 1 ppm.

Water flow peaks in GC are more intense with ophthalmic products. None of the ophthalmic products tested using this method gave rise to a sufficiently intense water flow peak as to overwhelm the ethylene oxide peak. The ophthalmic products[6] were tested with and without 2-phenylethanol.

The ethylene glycol peak was broad and, by altering the integration period during the analysis, accurate and precise figures for III content of samples down to 6 ppm were achieved. Below this level, III values become nonlinear. Without the advanced peak processing techniques inherent in the micro-

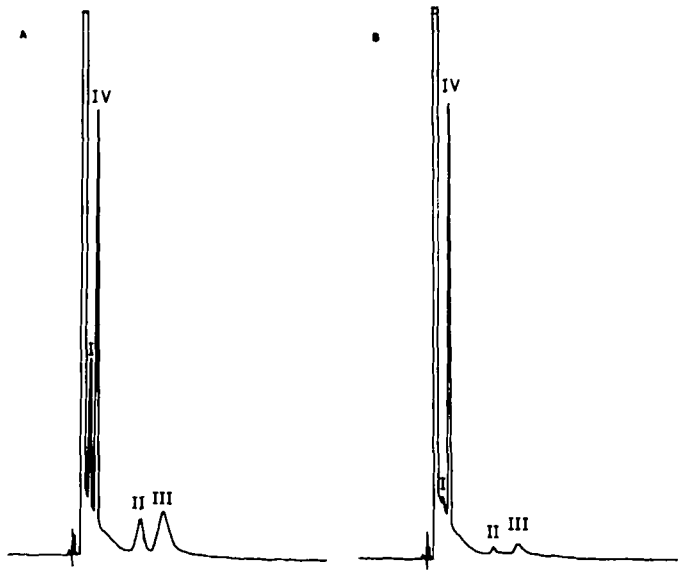

Figure 1—*Typical chromatograms of I–IV. Key: (A) 10 ppm of I, 20 ppm of II, 60 ppm of III, and 15 ppm of IV; (B) 1 ppm of I, 2 ppm of II, 6 ppm of III, and 15 ppm of IV.*

[1] Sigma 1; Perkin-Elmer.
[2] Sigma 10 Data Station; Perkin-Elmer.
[3] BDH Chemicals Ltd., Poole, Dorset.
[4] FSA Ltd., Loughborough, Leicestershire.
[5] Parafilm.
[6] Lomusol and Opticrom; registered trademarks of Fisons plc.

0022-3549/84/0900-1305$01.00/0
© 1984, American Pharmaceutical Association

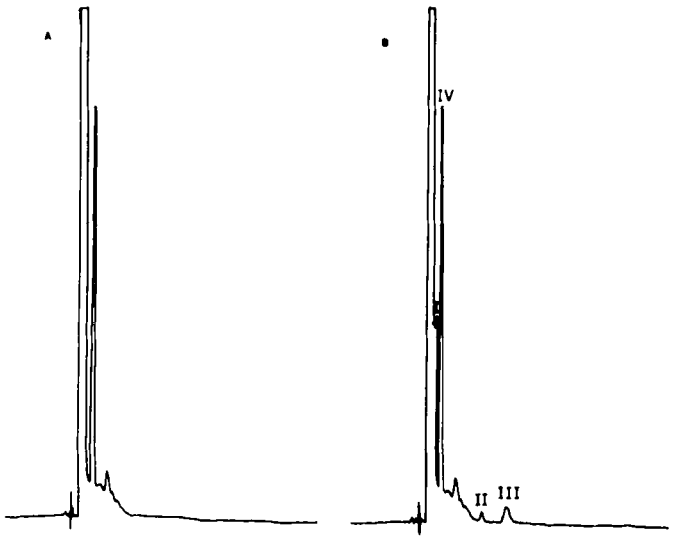

Figure 2—*Chromatograms of an ophthalmic solution (A) and an ophthalmic solution spiked with 2 ppm of I, 4 ppm of II, and 10 ppm of III (B).*

computer software, it would have been impossible to achieve the analysis in one isothermal run.

Coefficients of variation of 3.7, 2.1, and 5.7% for I, II, and III, respectively, were determined at concentrations of 18, 21, and 70 ppm, and coefficients of variation of 1.2, 1.3, and 6.2% were determined at concentrations of 90, 105, and 127 ppm, respectively. The limits of detection were 1, 2, and 6 ppm for I, II, and III, respectively (Fig. 1). Figure 2 shows a chromatogram of an ophthalmic solution and a chromatogram of an ophthalmic solution "spiked" with 2 ppm of I, 4 ppm of II, and 10 ppm of III.

Table I shows recovery data for I–III. For I and III, the recovery was worse at lower levels due to a shouldering of peaks and nonlinearity of response. Recovery values for II are very satisfactory at all levels. The system was calibrated at 10 ppm for I, 20 ppm for II, and 60 ppm for III.

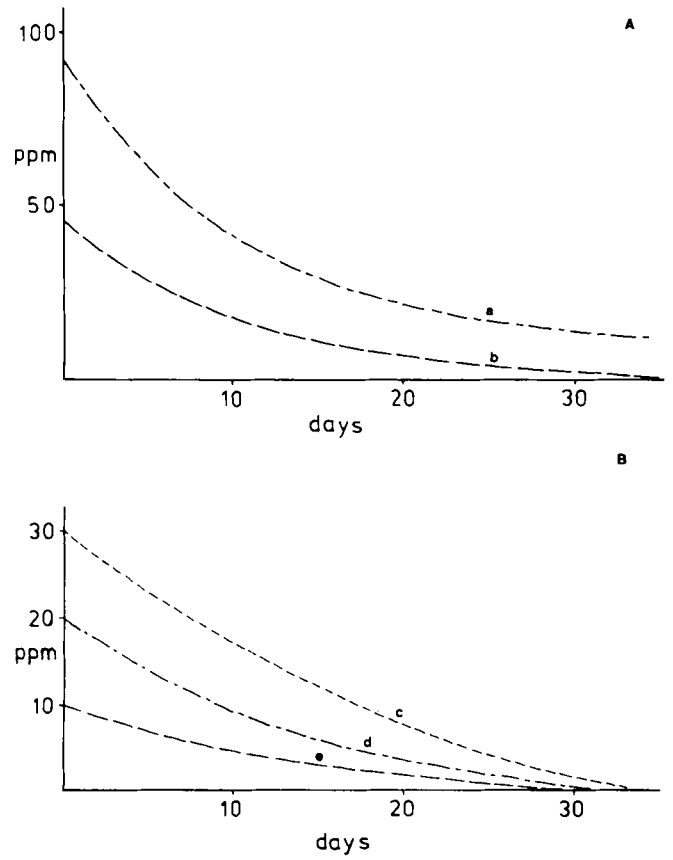

Figure 3—*Ethylene oxide hydrolysis at 25°C. Key: (A) (a) 100 ppm, (b) 50 ppm; (B) (c) 30 ppm, (d) 20 ppm, (e) 10 ppm.*

Table I—Recovery Data for Compound Additions to Control Ophthalmic Solution

Compound	Amount Added, μg/g	Amount Found, μg/g	Amount Recovered, %
I	8	6	75.0
	15	13	86.6
	30	28	93.3
	60	58	96.7
	150	150	100.0
II	13	13	100.0
	26	26	100.0
	52	51	98.1
	104	105	101.0
III	30	28	93.3
	60	59	98.3
	90	91	101.1
	120	122	101.1

This method was also employed to produce ethylene oxide hydrolysis curves in aqueous solution at 25°C (Fig. 3). It can be seen that ethylene oxide hydrolyzes steadily to ethylene glycol in solution, the reaction going to completion in <40 d at 30 ppm. At 80°C ethylene oxide fully hydrolyzes in <16 h.

An acidic medium was chosen for the extraction of ethylene oxide from plastics for two reasons. First, acid extracts I faster from plastic than does an entirely aqueous medium. Using an acid medium at 80°C, consistent ethylene oxide contents for plastics were achieved after 16 h, whereas an aqueous medium at 80°C required 7 d. At 25°C, recoveries of 18% after 16 h and 37% after 7 d were achieved for both media. Second, by choosing hydrochloric acid, the ethylene oxide thus extracted will be converted to II rather than III. Compound II is both easier to quantify and has a lower detection limit. Thus, by combining 1 M HCl with an elevated temperature (80°C), an efficient extraction procedure was developed. The retention characteristics of different plastics were studied in this way.

Solutions equivalent to 10, 20, and 30 ppm of ethylene oxide in 1 M HCl were prepared. After only 12 h at 80°C, ethylene oxide was fully converted to ethylene chlorohydrin. The recoveries ranged from 94 to 98% (Fig. 4).

The retention characteristics of polystyrene, high-density polyethylene, and low-density polyethylene were tested. The plastics had ethylene oxide contents of 430, 280, and 53 μg/g, respectively, after fumigation with ethylene oxide for 6 h at 15 psi. It was found that polystyrene retains a greater amount of I than does high-density polyethylene, which retains more I than does

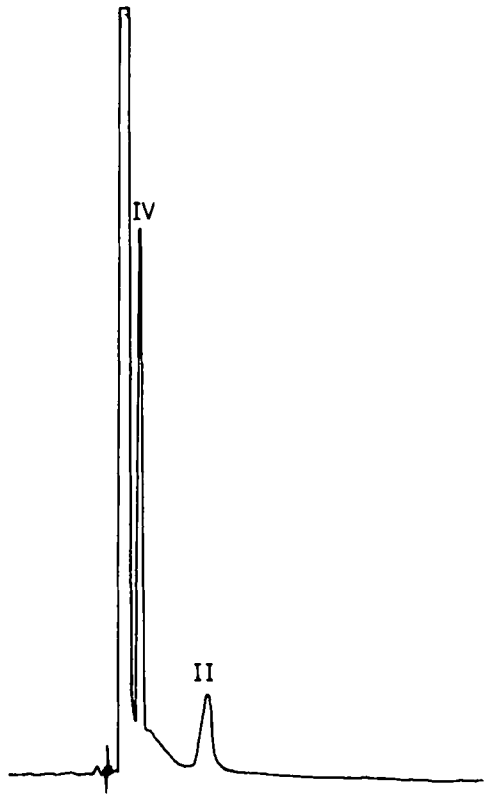

Figure 4—*Chromatogram showing complete conversion of I to II in 1 M HCl.*

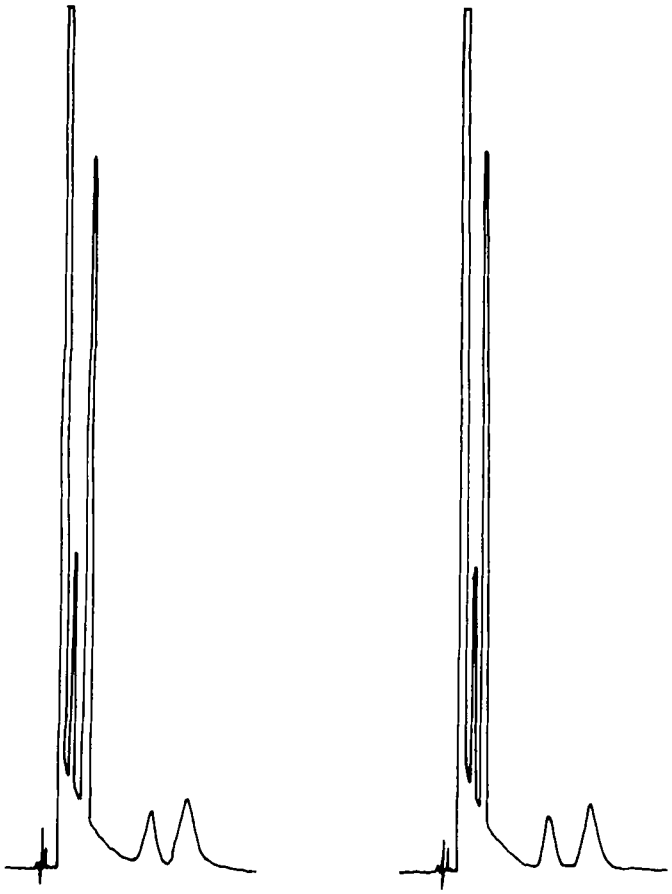

Figure 5 —*Duplication of the chromatographic column.*

low-density polyethylene. The average thickness for the materials were 1.26 mm for polystyrene and high-density polyethylene and 1.00 mm for low-density polyethylene.

When using polystyrene for manufacturing plastic components which are to be sterilized with ethylene oxide, there is the possibility of a "mesh" effect due to the composite nature of the plastic; the presence of bulky phenyl groups gives the plastic many interstitial spaces. Ethylene oxide may enter these spaces within the plastic and remain there, dissipating slowly over a long time period. Obviously, elevated temperature and reduced pressure will increase the rate of dissipation. Likewise, high-density polyethylene plastic components retain more ethylene oxide than low-density polyethylene plastics due to their higher density, where it is less likely that the fumigant will penetrate the plastic.

A most satisfying feature of this method has been the extraordinary longevity of the column. This method of analysis has been used routinely for 18 months with only two replacement columns, giving ~1000 injections per column life. The end of the useful life of a column manifests itself in the broadening of the ethylene glycol peak and a drift in retention times. Duplication of the chromatographic column has been achieved several times with no adverse effects on the separation of the components (Fig. 5). Since this method uses only one isothermal column run for the analysis of all three components and no elaborate sample preparation is necessary, it would appear that this method is ideal for use in quality control laboratories of companies which need to comply with the Food and Drug Administration proposals.

REFERENCES

(1) S. G. Heuser and K. A. Scudamore, *Analyst (London)*, **93**, 252 (1968).

(2) B. Warren, *J. Pharm. Pharmacol.*, **23**, 170S (1971).

(3) J. A. Mogenhan, J. E. Whitbourne, and R. R. Ernst, *J. Pharm. Sci.*, **60**, 222 (1971).

(4) L. A. Zagar, *J. Pharm. Sci.*, **61**, 1801 (1972).

(5) S. J. Romano, J. A. Renner, and P. M. Leitner, *Anal. Chem.*, **45**, 2327 (1973).

(6) J. D. White and T. J. Bradley, *J. Pharm. Sci.*, **62**, 1634 (1973).

(7) S. J. Romano and J. A. Renner, *J. Pharm. Sci.*, **64**, 1412 (1975).

(8) N. Adler, *J. Pharm. Sci.*, **54**, 735 (1965).

(9) E. P. Ragelis, B. S. Fisher, B. A. Klimeck, and C. Johnson, *J. Assoc. Off. Anal. Chem.*, **51**, 709 (1968).

(10) J. E. Whitbourne, J. A. Mogenhan, and R. R. Ernst, *J. Pharm. Sci.*, **58**, 1024 (1969).

(11) D. J. Brown, *J. Assoc. Off. Anal. Chem.*, **53**, 263, (1970).

(12) K. M. Brobst and H. Tai, *J. Assoc. Off. Anal. Chem.*, **54**, 1093 (1971).

(13) J. Weinberger, *J. Pharm. Sci.*, **60**, 545 (1971).

(14) H. D. Spitz and J. Weinberger, *J. Pharm. Sci.*, **60**, 271 (1971).

(15) P. A. Hartman and P. B. Bowman, *J. Pharm. Sci.*, **66**, 789 (1977).

(16) G. J. Manius, *J. Pharm. Sci.*, **68**, 1547 (1979).

Anti-Influenza A Activity of Some *N*-Substituted Bicyclo[3.2.1]octane-3-spiro-3′-pyrrolidine Hydrochlorides: Synthesis and Structure

ELENA DE LA CUESTA, PALOMA BALLESTEROS, and GREGORIO G. TRIGO[x]

Received March 9, 1983, from the *Departamento de Quimica Organica y Farmaceutica, Facultad de Farmacia, Universidad Complutense, Madrid-3, Spain.* Accepted for publication July 19, 1983.

Abstract □ Some *N*-substituted bicyclo[3.2.1]octane-3-spiro-3′-pyrrolidine hydrochlorides (IX–XII) prepared from bicyclo[3.2.1]octan-3-one (I), were assayed *in vitro* against influenza A viruses. All materials showed activity similar to 1-adamantanamine hydrochloride. A ^{1}H-NMR study revealed only one isomer at the spiro carbon atom.

Keyphrases □ *N*-Substituted bicyclo[3.2.1]octane-3-spiro-3′-pyrrolidine hydrochlorides — synthesis, structure, antiviral activity against influenza A □ Antiviral agents—potential, *N*-substituted bicyclo[3.2.1]octane-3-spiro-3′-pyrrolidine hydrochlorides, influenza A

Since Davis *et al.* (1) described the antiviral activity of 1-adamantanamine (amantadine) against influenza A viruses, a wide variety of derivatives have been prepared (for review; 2). Among them, some spiropyrrolidine derivatives of adamantane and other cyclic systems (3, 4) have been reported to show amantadine-like antiviral activity.

In this report we describe the synthesis of the *N*-substituted bicyclo[3.2.1]octane-3-spiro-3′-pyrrolidine hydrochlorides

0022-3549/84/0900-1307$01.00/0

© 1984, American Pharmaceutical Association

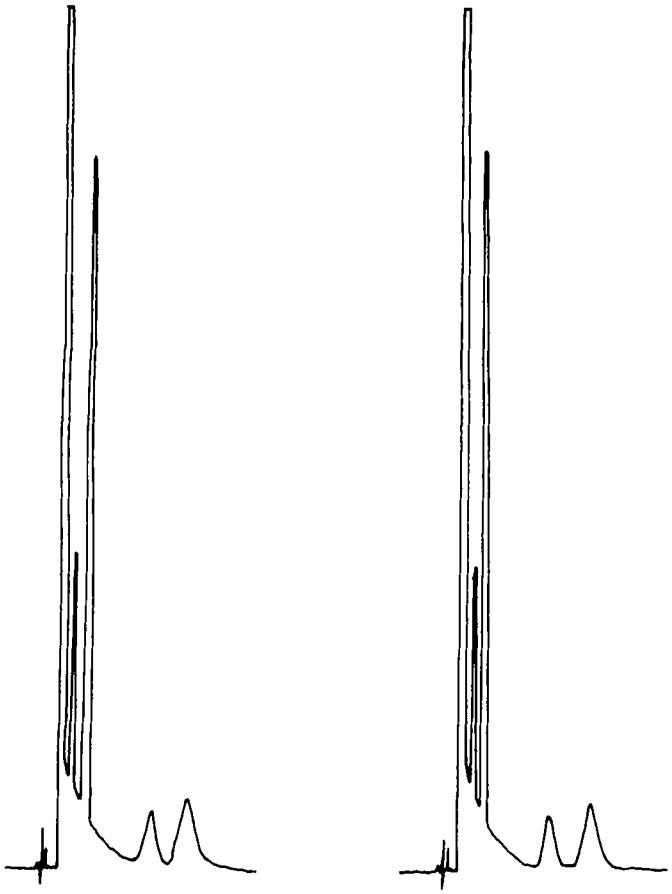

Figure 5 —*Duplication of the chromatographic column.*

low-density polyethylene. The average thickness for the materials were 1.26 mm for polystyrene and high-density polyethylene and 1.00 mm for low-density polyethylene.

When using polystyrene for manufacturing plastic components which are to be sterilized with ethylene oxide, there is the possibility of a "mesh" effect due to the composite nature of the plastic; the presence of bulky phenyl groups gives the plastic many interstitial spaces. Ethylene oxide may enter these spaces within the plastic and remain there, dissipating slowly over a long time period. Obviously, elevated temperature and reduced pressure will increase the rate of dissipation. Likewise, high-density polyethylene plastic components retain more ethylene oxide than low-density polyethylene plastics due to their higher density, where it is less likely that the fumigant will penetrate the plastic.

A most satisfying feature of this method has been the extraordinary longevity of the column. This method of analysis has been used routinely for 18 months with only two replacement columns, giving ~1000 injections per column life. The end of the useful life of a column manifests itself in the broadening of the ethylene glycol peak and a drift in retention times. Duplication of the chromatographic column has been achieved several times with no adverse effects on the separation of the components (Fig. 5). Since this method uses only one isothermal column run for the analysis of all three components and no elaborate sample preparation is necessary, it would appear that this method is ideal for use in quality control laboratories of companies which need to comply with the Food and Drug Administration proposals.

REFERENCES

(1) S. G. Heuser and K. A. Scudamore, *Analyst (London)*, **93**, 252 (1968).

(2) B. Warren, *J. Pharm. Pharmacol.*, **23**, 170S (1971).

(3) J. A. Mogenhan, J. E. Whitbourne, and R. R. Ernst, *J. Pharm. Sci.*, **60**, 222 (1971).

(4) L. A. Zagar, *J. Pharm. Sci.*, **61**, 1801 (1972).

(5) S. J. Romano, J. A. Renner, and P. M. Leitner, *Anal. Chem.*, **45**, 2327 (1973).

(6) J. D. White and T. J. Bradley, *J. Pharm. Sci.*, **62**, 1634 (1973).

(7) S. J. Romano and J. A. Renner, *J. Pharm. Sci.*, **64**, 1412 (1975).

(8) N. Adler, *J. Pharm. Sci.*, **54**, 735 (1965).

(9) E. P. Ragelis, B. S. Fisher, B. A. Klimeck, and C. Johnson, *J. Assoc. Off. Anal. Chem.*, **51**, 709 (1968).

(10) J. E. Whitbourne, J. A. Mogenhan, and R. R. Ernst, *J. Pharm. Sci.*, **58**, 1024 (1969).

(11) D. J. Brown, *J. Assoc. Off. Anal. Chem.*, **53**, 263, (1970).

(12) K. M. Brobst and H. Tai, *J. Assoc. Off. Anal. Chem.*, **54**, 1093 (1971).

(13) J. Weinberger, *J. Pharm. Sci.*, **60**, 545 (1971).

(14) H. D. Spitz and J. Weinberger, *J. Pharm. Sci.*, **60**, 271 (1971).

(15) P. A. Hartman and P. B. Bowman, *J. Pharm. Sci.*, **66**, 789 (1977).

(16) G. J. Manius, *J. Pharm. Sci.*, **68**, 1547 (1979).

Anti-Influenza A Activity of Some *N*-Substituted Bicyclo[3.2.1]octane-3-spiro-3′-pyrrolidine Hydrochlorides: Synthesis and Structure

ELENA DE LA CUESTA, PALOMA BALLESTEROS, and GREGORIO G. TRIGO[x]

Received March 9, 1983, from the *Departamento de Quimica Organica y Farmaceutica, Facultad de Farmacia, Universidad Complutense, Madrid-3, Spain.* Accepted for publication July 19, 1983.

Abstract □ Some *N*-substituted bicyclo[3.2.1]octane-3-spiro-3′-pyrrolidine hydrochlorides (IX–XII) prepared from bicyclo[3.2.1]octan-3-one (I), were assayed *in vitro* against influenza A viruses. All materials showed activity similar to 1-adamantanamine hydrochloride. A ^{1}H-NMR study revealed only one isomer at the spiro carbon atom.

Keyphrases □ *N*-Substituted bicyclo[3.2.1]octane-3-spiro-3′-pyrrolidine hydrochlorides — synthesis, structure, antiviral activity against influenza A □ Antiviral agents—potential, *N*-substituted bicyclo[3.2.1]octane-3-spiro-3′-pyrrolidine hydrochlorides, influenza A

Since Davis *et al.* (1) described the antiviral activity of 1-adamantanamine (amantadine) against influenza A viruses, a wide variety of derivatives have been prepared (for review; 2). Among them, some spiropyrrolidine derivatives of adamantane and other cyclic systems (3, 4) have been reported to show amantadine-like antiviral activity.

In this report we describe the synthesis of the *N*-substituted bicyclo[3.2.1]octane-3-spiro-3′-pyrrolidine hydrochlorides

0022-3549/84/0900-1307$01.00/0

© 1984, American Pharmaceutical Association

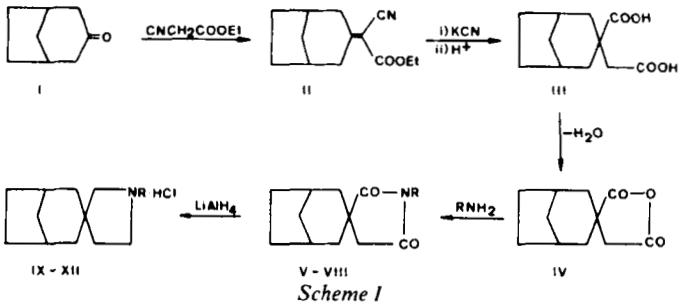

Scheme I

(IX-XII) (Scheme I) and their evaluation as potential antiviral agents.

EXPERIMENTAL SECTION[1]

Chemistry—Bicyclo[3.2.1]octan-3-one (I) was obtained according to a general literature method (5), using phase-transfer catalysis for the dichlorocarbene addition (6). Spiropyrrolidine hydrochlorides (IX-XII) were synthesized from I according to Scheme I.

Ethyl Bicyclo[3.2.1]octan-3′-yliden Cyanoacetate (II)—A solution of I (16.6 g, 0.133 mol), ethyl cyanoacetate (15.12 g, 0.133 mol), ammonium acetate (2.10 g, 0.026 mol), and glacial acetic acid (6.8 mL) in benzene (50 mL) was refluxed for 24 h using a Dean-Stark water separator. The mixture was cooled, washed with water, and dried over anhydrous Na_2SO_4. The benzene was removed under reduced pressure, and the residue was distilled *in vacuo* to yield 29.2 g (89%) of a colorless liquid, bp 103°C (0.5 mm Hg). IR (neat film): ν 2220 (C≡N) and 1725 cm^{-1} (C=O); ^{1}H-NMR (C_6D_6): δ 4.00 (q, 2, CH_2), 2.10 and 1.20 (two m, 12, cyclic H), and 1.00 ppm (t, 3, CH_3).

Anal.—Calc. for $C_{13}H_{17}NO_2$: C, 71.2; H, 7.8; N, 6.4. Found: C, 70.9; H, 7.8; N, 6.3.

3-Carboxybicyclo[3.2.1]octane-3-acetic Acid (III)—To a solution of ester II (17.25 g, 0.078 mol) in ethanol (170 mL), a solution of KCN (13.36 g, 0.2 mol) in water (34 mL) was added. After stirring for 5 d, the solvent was removed at reduced pressure. The residue was heated at reflux for 48 h with concentrated HCl (134 mL). The mixture was diluted with an equal volume of water and cooled overnight. The precipitate was removed by filtration and washed with water. The crude product was dissolved in a boiling saturated solution of $KHCO_3$, decolorized with charcoal, filtered, and the product was precipitated by the addition of concentrated HCl to yield 11.8 g (71%) of III as a white solid, mp 156-157°C. IR (KBr): ν 3100-2500 (COOH) and 1725 and 1700 cm^{-1} (COOH); ^{1}H-NMR (Me_2SO-d_6): δ 12.00 (br s, 2, COOH), 2.40 (s, 2, CH_2—COOH), and 2.15 and 1.50-1.15 ppm (two m, 12, cyclic H).

Anal.—Calc. for $C_{11}H_{16}O_4$: C, 62.6; H, 7.5. Found: C, 62.3; H, 7.8.

Bicyclo[3.2.1]octane-3-spiro-3′-succinic Anhydride (IV)—Carboxylic acid III (7.0 g, 0.033 mol) and acetic anhydride (20 mL) were refluxed for 2 h. The mixture was concentrated to dryness and crystallized from petroleum ether to give 6.02 g (94%) of the anhydride IV as a white solid, mp 57°C. IR (KBr): ν 1860 and 1790 cm^{-1} (C=O); ^{1}H-NMR ($CDCl_3$, 250 MHz): δ 2.80 (s, 2, CH_2—CO), 2.34 (br s, 2, $C_{1(5)}H_X$), 2.18 (dd, 2, J_{BA} = −14.34 Hz, $C_{2(4)}H_B$), 1.96 (dd, 2, $J_{B'A'}$ = −8.09 Hz, $C_{6(7)}H_{B'}$), 1.80 (dd, 2, J_{AB} = −14.34 Hz, $C_{2(4)}H_A$), and 1.70 ppm (dd, 2, $J_{A'B'}$ = −8.09 Hz, $C_{6(7)}H_{A'}$).

Anal.—Calc. for $C_{11}H_{14}O_3$: C, 68.04; H, 7.21. Found: C, 68.31; H, 7.55.

***N*-Substituted Bicyclo[3.2.1]octane-3-spiro-3′-succinimides**—*General Procedure*—To a solution of anhydride IV (0.15 mol) in hot benzene (50 mL), the corresponding amine (0.15 mol) in benzene (30 mL) was added with vigorous stirring at 60-65°C. After standing for 0.5 h at 60-65°C, the mixture was cooled, and the precipitate was removed by filtration and washed with benzene. The carboxyamide was heated for 1 h at 220-225°C. After cooling, the residue was crystallized giving the corresponding succinimides.

N-Benzyl Bicyclo[3.2.1]octane-3-spiro-3′-succinimide (*V*)—Yield: 78%; mp 68-69°C (white prisms, absolute ethanol). IR ($CHBr_3$): ν 1740 and 1714 cm^{-1} (C=O); ^{1}H-NMR (CCl_4): δ 7.15 (s, 5, ArH), 4.40 (s, 2, $CH_2C_2H_5$), 2.40 (s, 2, $C_{4'}H_2$), and 2.20, 1.80, and 1.40 ppm (m, 12, cyclic H).

Anal.—Calc. for $C_{18}H_{21}NO_2$: C, 76.3; H, 7.4; N, 4.9. Found: C, 76.3; H, 7.7; N, 5.0.

N-Cyclohexyl Bicyclo[3.2.1]octane-3-spiro-3′-succinimide (*VI*)—Yield: 58%; mp 78-79°C (white prisms, absolute ethanol). IR ($CHBr_3$): ν 1775 and 1700 cm^{-1} (C=O); ^{1}H-NMR ($CDCl_3$): δ 3.90 (m, 1, CH—N), 2.50 (s, 2, $C_{4'}H_2$), and 2.20, 1.80 and 1.40 ppm (m, 22, cyclic H).

Anal.—Calc. for $C_{17}H_{25}NO_2$: C, 74.2; H, 9.1; N, 5.1. Found: C, 73.9; H, 9.3; N, 5.0.

N-n-Butyl Bicyclo[3.2.1]octane-3-spiro-3′-succinimide (*VII*)—Yield: 66%; mp 86-87°C (white prisms, absolute ethanol). IR ($CHBr_3$): ν 1770 and 1700 cm^{-1} (C=O); ^{1}H-NMR (CCl_4): δ 3.35 (t, 2, CH_2—N), 2.50 (s, 2, $C_{4'}H_2$), 2.25, 1.80, and 1.35 (m, 18, cyclic H), and 1.00 ppm (t, 3, CH_3).

Anal.—Calc. for $C_{15}H_{23}NO_2$: C, 72.3, H, 9.3; N, 5.6. Found: C, 72.6; H, 9.5; N, 5.6.

N-β-Hydroxyethyl Bicyclo[3.2.1]octane-3-spiro-3′-succinimide (*VIII*)—Yield: 39%; mp 98-99°C (white plates, absolute ethanol). IR ($CHBr_3$): ν 3450 (OH), and 1775 and 1700 cm^{-1} (C=O); ^{1}H-NMR ($CDCl_3$-CCl_4): δ 3.55 (s, 4, CH_2—OH and CH_2—N), 3.00 (s, 1, OH), 2.60 (s, 2, $C_{4'}H_2$), and 2.25, 1.80, and 1.40 ppm (m, 12, cyclic H).

Anal.—Calc. for $C_{13}H_{19}NO_3$: C, 65.8; H, 8.2; N, 5.9. Found: C, 65.6; H, 8.3; N, 5.7.

***N*-Substituted Bicyclo[3.2.1]octane-3-spiro-3′-pyrrolidine Hydrochlorides**—*General Procedure*—A solution of the corresponding succinimide (0.08 mol) in ether was slowly added with stirring to a suspension of lithium aluminum hydride (0.32 mol) in ether. The mixture was stirred overnight, decomposed, filtered, and dried over anhydrous Na_2SO_4. The solvent was removed at reduced pressure, and the pyrrolidine was distilled. Pyrrolidine hydrochlorides were formed by treatment of the bases with 3 M HCl. After concentration under reduced pressure, the hydrochloride was crystallized.

N-Benzyl Bicyclo[3.2.1]octane-3-spiro-3′-pyrrolidine Hydrochloride (*IX*)—Yield: 83%; mp 265-266°C (white prisms, isopropyl alcohol). IR ($CHBr_3$): ν 2500 (N—H), and 1450, 1435, and 1410 cm^{-1} (aromatic); ^{1}H-NMR ($CDCl_3$): δ 7.65-7.35 (m, 5, ArH), 4.30 (s, 2, $CH_2C_6H_5$), 3.65-3.00 (m, 4, $C_{2'}H_2$ and $C_{5'}H_2$), and 2.25, 1.65, and 1.50 ppm (m, 14, $C_{4'}H_2$ and cyclic H).

Anal.—Calc. for $C_{18}H_{26}ClN$: C, 74.1; H, 8.9; N, 4.8. Found: C, 73.8; H, 9.0; N, 5.0.

N-Cyclohexyl Bicyclo[3.2.1]octane-3-spiro-3′-pyrrolidine Hydrochloride (*X*)—Yield: 57%; mp 178-179°C (white prisms, acetone). IR ($CHBr_3$): ν 2500 cm^{-1} (N—H); ^{1}H-NMR ($CDCl_3$): δ 3.65-2.95 (m, 5, $C_{2'}H_2$, $C_{5'}H_2$, and CH—N), and 2.00, 1.70, and 1.40 ppm (m, 24, cyclic H).

Anal.—Calc. for $C_{17}H_{30}ClN$: C, 71.9; H, 10.6; N, 4.9. Found: C, 71.6; H, 10.3; N, 4.8.

N-n-Butyl Bicyclo[3.2.1]octane-3-spiro-3′-pyrrolidine Hydrochloride (*XI*)—Yield: 39%; mp 186-187°C (white prisms, acetone). IR ($CHBr_3$): ν 2500 cm^{-1} (N—H); ^{1}H-NMR ($CDCl_3$): δ 3.76-2.90 (m, 6, $C_{2'}H_2$, $C_{5'}H_2$, and CH_2—N), 2.25, 1.90, 1.70, and 1.40 [m, 18, $(CH_2)_2$ and cyclic H], and 1.00 ppm (t, 3, CH_3).

Anal.—Calc. for $C_{15}H_{28}ClN$: C, 69.9; H, 10.9; N, 5.4. Found: C, 69.6; H, 10.6; N, 5.1.

N-β-Hydroxyethyl Bicyclo[3.2.1]octane-3-spiro-3′-pyrrolidine Hydrochloride (*XII*)—Yield: 74%; mp 160-161°C (white prisms, absolute ethanol). IR ($CHBr_3$): ν 3280 (OH) and 2500 cm^{-1} (N—H); ^{1}H-NMR (D_2O): δ 3.60 (t, 2, CH_2—OH), 3.20 (m, 6, CH_2—N, $C_{2'}H_2$, and $C_{5'}H_2$), 2.00, 1.50, and 1.15 ppm (m, 14, $C_{4'}H_2$ and cyclic H).

Anal.—Calc. for $C_{13}H_{24}ClNO$: C, 63.5; H, 9.4; N, 5.7. Found: C, 63.8; H, 9.7; N, 5.4.

RESULTS AND DISCUSSION

Structural Assignment—Due to the rigid structure of the bicyclo[3.2.1]-octane system, two different isomers (XIII and XIV) are possible. On the basis of the ^{1}H-NMR spectrum of the anhydride IV, only the configuration shown (XIII) appears to be present.

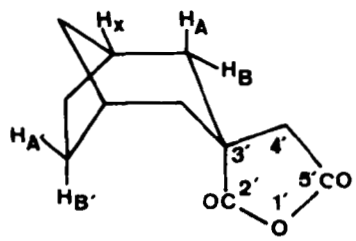

From the 250-MHz ^{1}H-NMR spectrum of anhydride IV, only one isomer is observed from the presence of only one singlet at δ 2.80 ppm for the $C_{4'}$-methylene group. The presence of two isomers should be evidenced by the

[1] All melting points were taken in open capillary tubes. Melting and boiling points are uncorrected. IR spectra were carried out on a Perkin-Elmer 577 spectrophotometer. ^{1}H-NMR spectra were recorded in $CDCl_3$ solution at room temperature using Bruker WM-250 (250 MHz) and Varian EM 360-A (60 MHz) spectrometers (Me_4Si as internal reference): (s) singlet; (d) doublet; (t) triplet; (m) multiplet; (br s) broad signal; (dd) doublet-doublet.

Table I—Inhibition of Growth of Influenza A Viruses by IX-XII and 1-Adamantanamine Hydrochloride

Inhibitor[a]	Titration of Infection[b], Plaque-Forming Units/mL	Inhibition[c]
None	2×10^7	—
IX	1×10^6	−1.30
X	7×10^5	−1.45
XI	1×10^7	−0.30
XII	7×10^6	−0.45
1-Adamantanamine hydrochloride	2×10^6	−1.00

[a] Inhibitors were administered at a concentration of 100 μM in an alcohol-water solution. [b] Plaque assay and primary isolation of influenza A viruses were carried out in an established line of canine kidney cells (MDCK), in the presence of trypsin (7). [c] Inhibition is expressed as the decimal logarithm of the quotient of plaque-forming units in the presence of inhibitor to that found in the absence of inhibitor: $\log_{10}$ [(pfu/mL of inhibitor)/(pfu/mL of control)].

appearance of two singlets, one each for the *endo* and *exo* $C_{4'}$-methylene groups. The same feature was observed in the NMR spectra of succinimides V-VIII.

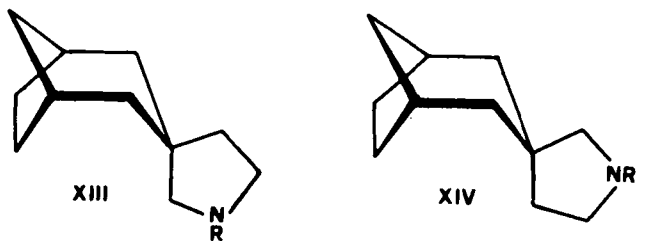

Protons $H_AH_BH_{A'}H_{B'}H_X$ behave as two different ABX and A'B'X systems. The influence of the deshielding effect of the *endo* $C_{2'}$-carbonyl group on protons H_B and $H_{B'}$ is shown by the downfield chemical shift of these protons at $\delta H_B = 2.18$ ppm and $\delta H_{B'} = 1.96$ ppm relative to those of the less-affected protons H_A and $H_{A'}$, which appear upfield at δ 1.80 and 1.70 ppm, respectively. Assignation of H_B and $H_{B'}$ has been done on the basis of the observable geminal coupling constants $J_{BA} = -14.34$ Hz and $J_{B'A'} = -8.09$ Hz, which are in agreement with reported values for cyclohexane and cyclopentane, respectively (8).

X-ray diffraction data of succinimide VI (9) conclusively confirm that the $C_{2'}$-carbonyl group is attached on the *endo*-position. In this case the spirocyclohexane ring appears to adopt a boat conformation to avoid the steric interaction between the $C_{2'}$-carbonyl group and the $C_{6(7)}$-methylene groups.

Biology—According to results shown in Table I, IX-XII, especially the *N*-benzyl and *N*-cyclohexyl derivatives (IX and X), show antiviral activity against influenza A viruses similar to or greater than that shown by 1-adamantanamine hydrochloride.

REFERENCES

(1) W. L. Davis, R. R. Gruvert, R. F. Haff, J. W. McGahen, E. M. Neumayer, M. Paulshock, J. C. Watts, T. R. Wood, and E. C. Herrmann, *Science*, **144**, 862 (1964).

(2) J. S. Oxford and A. Gilbraith, *Pharmacol. Ther.*, **11**, 181 (1980).

(3) K. Lundahl, J. Schut, J. L. M. A. Schalatmann, G. B. Paerels, and A. Peters, *J. Med. Chem.*, **15**, 129 (1972).

(4) R. van Hes, A. Smit, T. Kralt, and A. Peters, *J. Med. Chem.*, **15**, 132 (1972).

(5) C. W. Jefford, J. Gunsher, P. T. Hill, P. Brun, J. Legras, and B. Waegell, *Org. Synth.*, **51**, 60 (1971).

(6) G. C. Joshi, N. Singh, and L. M. Pande, *Tetrahedron Lett.*, **1972**, 1461.

(7) K. Tobita, A. Sugiura, C. Enomoto, and M. Furuyama, *Med. Microbiol. Inmunol.*, **162**, 9 (1975).

(8) E. Pretsh, T. Clerc, J. Seibl, and W. Simon, "Tabellen zur Strukturaufklarung Organischer Verbindungen mit Spektroskopischen Metoden," Springer Verlag, Berlin-Heidelberg-New York, 1976.

(9) F. Florencio, P. Smith-Verdier, and S. Garcia-Blanco, *Acta Crystallogr.*, **B38**, 2301 (1982).

ACKNOWLEDGMENTS

The authors are indebted to Dr. J. Ortin of Centro de Biologia Molecular of Madrid for supplying the *in vitro* antiviral results.

Distribution and Elimination of Polymethyl Methacrylate Nanoparticles After Peroral Administration to Rats

MARIJKE NEFZGER *, JÖRG KREUTER ‡x, ROLF VOGES §, EKKE LIEHL *, and RUDOLF CZOK *

Received March 7, 1983 from the **Sandoz Forschungsinstitut GmbH, Brunner Strasse 59, A 1235 Vienna, Austria*, the ‡*Department of Pharmaceutics, Swiss Federal Institute of Technology, Clausiusstrasse 25, CH 8092 Zurich, Switzerland*, and the §*Pharmaceutical Division, Sandoz Ltd., CH 4002 Basle, Switzerland.* Accepted for publication September 13, 1983.

Abstract □ Polymethyl [1-^{14}C]methacrylate nanoparticles were administered orally to bile cannulated rats. Ten to fifteen percent of the administered radioactivity was absorbed and found in the bile and urine. Within 48 h, 94 97% of the absorbed radioactivity had been eliminated from the body. After 8 d, the highest residual radioactivity was found in the bone marrow, fatty renal tissue, stomach, liver, and lymph nodes.

Keyphrases □ Polymethyl methacrylate—peroral administration, distribution, elimination, rats □ Peroral administration—polymethyl methacrylate, elimination and distribution, rats

A possible pathway of absorption is the uptake of colloidal particulate materials by the GI tract in liquid (pinocytosis) or solid (endocytosis) form. This uptake pathway was suggested for fat absorption by Frazer (1, 2). The uptake of corn starch and some other particulate materials by endocytosis was extensively studied by Volkheimer (3). No uptake of polymethyl methacrylate particles (labeled with a fluorescent dye and ranging in size from 10 nm–1.2 μm) was observed by Juhlin (4). This may, however, be due to leakage of the label or to the small size of the particles, which prevented optical observation. For this reason, ^{14}C-labeled polymethyl methacrylate nanoparticles of a mean size of 130 nm were employed in this study. These particles were shown to be taken up by the reticuloendothelial system after intravenous administration (5). After subcutaneous administration, the particles stayed at the injection site for about 200 d. After this time, the beginning of redistribution and elimination was observed (6).

Oral administration of these nanoparticles seems to be of

© 1984, American Pharmaceutical Association

Table I—Inhibition of Growth of Influenza A Viruses by IX-XII and 1-Adamantanamine Hydrochloride

Inhibitor[a]	Titration of Infection[b], Plaque-Forming Units/mL	Inhibition[c]
None	2×10^7	—
IX	1×10^6	−1.30
X	7×10^5	−1.45
XI	1×10^7	−0.30
XII	7×10^6	−0.45
1-Adamantanamine hydrochloride	2×10^6	−1.00

[a] Inhibitors were administered at a concentration of 100 μM in an alcohol-water solution. [b] Plaque assay and primary isolation of influenza A viruses were carried out in an established line of canine kidney cells (MDCK), in the presence of trypsin (7). [c] Inhibition is expressed as the decimal logarithm of the quotient of plaque-forming units in the presence of inhibitor to that found in the absence of inhibitor: $\log_{10}$ [(pfu/mL of inhibitor)/(pfu/mL of control)].

appearance of two singlets, one each for the *endo* and *exo* $C_{4'}$-methylene groups. The same feature was observed in the NMR spectra of succinimides V-VIII.

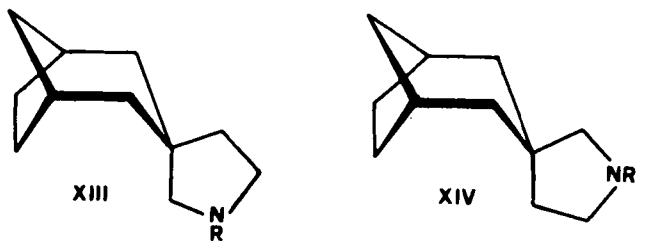

Protons $H_AH_BH_{A'}H_{B'}H_X$ behave as two different ABX and A'B'X systems. The influence of the deshielding effect of the *endo* $C_{2'}$-carbonyl group on protons H_B and $H_{B'}$ is shown by the downfield chemical shift of these protons at $\delta H_B = 2.18$ ppm and $\delta H_{B'} = 1.96$ ppm relative to those of the less-affected protons H_A and $H_{A'}$, which appear upfield at δ 1.80 and 1.70 ppm, respectively. Assignation of H_B and $H_{B'}$ has been done on the basis of the observable geminal coupling constants $J_{BA} = -14.34$ Hz and $J_{B'A'} = -8.09$ Hz, which are in agreement with reported values for cyclohexane and cyclopentane, respectively (8).

X-ray diffraction data of succinimide VI (9) conclusively confirm that the $C_{2'}$-carbonyl group is attached on the *endo*-position. In this case the spirocyclohexane ring appears to adopt a boat conformation to avoid the steric interaction between the $C_{2'}$-carbonyl group and the $C_{6(7)}$-methylene groups.

Biology—According to results shown in Table I, IX-XII, especially the *N*-benzyl and *N*-cyclohexyl derivatives (IX and X), show antiviral activity against influenza A viruses similar to or greater than that shown by 1-adamantanamine hydrochloride.

REFERENCES

(1) W. L. Davis, R. R. Gruvert, R. F. Haff, J. W. McGahen, E. M. Neumayer, M. Paulshock, J. C. Watts, T. R. Wood, and E. C. Herrmann, *Science*, **144**, 862 (1964).

(2) J. S. Oxford and A. Gilbraith, *Pharmacol. Ther.*, **11**, 181 (1980).

(3) K. Lundahl, J. Schut, J. L. M. A. Schalatmann, G. B. Paerels, and A. Peters, *J. Med. Chem.*, **15**, 129 (1972).

(4) R. van Hes, A. Smit, T. Kralt, and A. Peters, *J. Med. Chem.*, **15**, 132 (1972).

(5) C. W. Jefford, J. Gunsher, P. T. Hill, P. Brun, J. Legras, and B. Waegell, *Org. Synth.*, **51**, 60 (1971).

(6) G. C. Joshi, N. Singh, and L. M. Pande, *Tetrahedron Lett.*, **1972**, 1461.

(7) K. Tobita, A. Sugiura, C. Enomoto, and M. Furuyama, *Med. Microbiol. Inmunol.*, **162**, 9 (1975).

(8) E. Pretsh, T. Clerc, J. Seibl, and W. Simon, "Tabellen zur Strukturaufklarung Organischer Verbindungen mit Spektroskopischen Metoden," Springer Verlag, Berlin-Heidelberg-New York, 1976.

(9) F. Florencio, P. Smith-Verdier, and S. Garcia-Blanco, *Acta Crystallogr.*, **B38**, 2301 (1982).

ACKNOWLEDGMENTS

The authors are indebted to Dr. J. Ortin of Centro de Biologia Molecular of Madrid for supplying the *in vitro* antiviral results.

Distribution and Elimination of Polymethyl Methacrylate Nanoparticles After Peroral Administration to Rats

MARIJKE NEFZGER *, JÖRG KREUTER ‡x, ROLF VOGES §, EKKE LIEHL *, and RUDOLF CZOK *

Received March 7, 1983 from the **Sandoz Forschungsinstitut GmbH, Brunner Strasse 59, A 1235 Vienna, Austria*, the ‡*Department of Pharmaceutics, Swiss Federal Institute of Technology, Clausiusstrasse 25, CH 8092 Zurich, Switzerland*, and the §*Pharmaceutical Division, Sandoz Ltd., CH 4002 Basle, Switzerland.* Accepted for publication September 13, 1983.

Abstract □ Polymethyl [1-^{14}C]methacrylate nanoparticles were administered orally to bile cannulated rats. Ten to fifteen percent of the administered radioactivity was absorbed and found in the bile and urine. Within 48 h, 94 97% of the absorbed radioactivity had been eliminated from the body. After 8 d, the highest residual radioactivity was found in the bone marrow, fatty renal tissue, stomach, liver, and lymph nodes.

Keyphrases □ Polymethyl methacrylate—peroral administration, distribution, elimination, rats □ Peroral administration—polymethyl methacrylate, elimination and distribution, rats

A possible pathway of absorption is the uptake of colloidal particulate materials by the GI tract in liquid (pinocytosis) or solid (endocytosis) form. This uptake pathway was suggested for fat absorption by Frazer (1, 2). The uptake of corn starch and some other particulate materials by endocytosis was extensively studied by Volkheimer (3). No uptake of polymethyl methacrylate particles (labeled with a fluorescent dye and ranging in size from 10 nm–1.2 μm) was observed by Juhlin (4). This may, however, be due to leakage of the label or to the small size of the particles, which prevented optical observation. For this reason, ^{14}C-labeled polymethyl methacrylate nanoparticles of a mean size of 130 nm were employed in this study. These particles were shown to be taken up by the reticuloendothelial system after intravenous administration (5). After subcutaneous administration, the particles stayed at the injection site for about 200 d. After this time, the beginning of redistribution and elimination was observed (6).

Oral administration of these nanoparticles seems to be of

© 1984, American Pharmaceutical Association

Table I—Amount of Radioactivity Excreted after Peroral Administration (Percent of the Administered Dose)

Animal No.	1017	1018	1020	1024	1025	
Sex	F	F	M	M	M	
Body Weight, g	294	302	370	275	181	Mean, ±*SD*
Bile	7.0	5.4	6.6	8.4	6.4	6.8 ± 1.1
Urine	5.2	5.5	4.2	6.2	4.0	5.0 ± 0.9
Feces	89.3	86.5	86.0	116.1	72.8	83.7 ± 7.3[a]
Total	101.5	97.4	96.8	130.6	83.2	94.7 ± 8.0[a]
Amount Absorbed[b]	12.2	10.9	10.8	14.5	10.4	11.8 ± 1.7
Excreted within 24 h[c]	86	90	90	65	83	82.8 ± 10.4
Excreted within 48 h[c]	94	96	97	94	96	95.4 ± 1.3

[a] Calculation without rat 1024. [b] Bile + urine = amount absorbed. [c] Percentage of the total amount absorbed excreted within 24 or 48 h.

interest for the administration of certain vaccines. For example, good protection was observed with an inactivated rabies vaccine adsorbed to polymethyl methacrylate nanoparticles, whereas no protection was obtained with different control vaccines[1]. These particles might also be useful as cytostatic carriers against tumors of the GI tract.

EXPERIMENTAL SECTION

Preparation of Polymethyl [1-^{14}C]methylacrylate nanoparticles—Polymethyl [1-^{14}C]methacrylate was produced as described by Kreuter *et al.* (6). The monomer was dissolved in phosphate buffered saline, with or without influenza virions, to yield 0.5% polymethyl [1-^{14}C]methacrylate solutions. Nanoparticles were produced by polymerization of these monomer solutions using γ-irradiation with 500 krad (2.2 krad/min) in a cobalt-60 source. The resulting suspension had an activity of (5.22 ± 0.46) × 10^8 dpm/mL. The physicochemical characteristics of similar nonradioactive nanoparticles were described by Bentele *et al.* (7) and Kreuter (8).

Excretion and Tissue Distribution after Peroral Administration—Two female and three male bile-cannulated Sprague–Dawley rats weighing 181–370 g were administered 0.5 mL of the well-stirred virus containing nanoparticle suspension with a stomach tube. The animals were kept in metabolism cages with free access to food and a salt solution containing 0.9% sodium chloride, 0.04% potassium chloride, 0.017% calcium dichloride dihydrate, and 0.02% sodium hydrogen carbonate.

Urine was collected in dry ice. The storage container contained 100 μL of diethylamine in order to keep the urine at a pH ≥ 9, thus assuring the binding of the carbon-14 activity excreted as carbonate. After each collection period, the cage was rinsed with water (30–40 mL) to wash out dried urine residues. Samples of 400–500 μL were assayed for radioactivity. The collected feces was homogenized with about the same amount of water. Three samples (200–400 mg) of each homogenate were analyzed. The bile was collected in ice-cooled containers. Samples of 40 (0–8 h) and 100 μL (24–192 h) were assayed for radioactivity.

Eight days after administration, the activity in the organs was measured after sacrificing the animals with an intraperitoneal injection of ~0.5 mL of a euthanasia solution[2]. From the adrenal glands, epididymis, ovary, thyroid gland, lymph nodes, and bone marrow, one 7–130 mg sample was taken; from the other organs, two 50–400 mg samples were taken.

The radioactivity of the excreta, blood, plasma, and organs was determined after combustion in a sample oxidizer[3] (recovery of standard radioactivity: 92–100%). The resulting carbon dioxide was absorbed in a mixture of absorber solution and scintillation liquid[4]. The samples were then counted in a liquid scintillation counter for 20 min. The counting efficiency was determined by an automatic external standardization and previously prepared quench curves. The detection limit was 4 ng/g for the bone marrow, lymph nodes, and thyroid gland and 2 ng/g for all other organs and tissues.

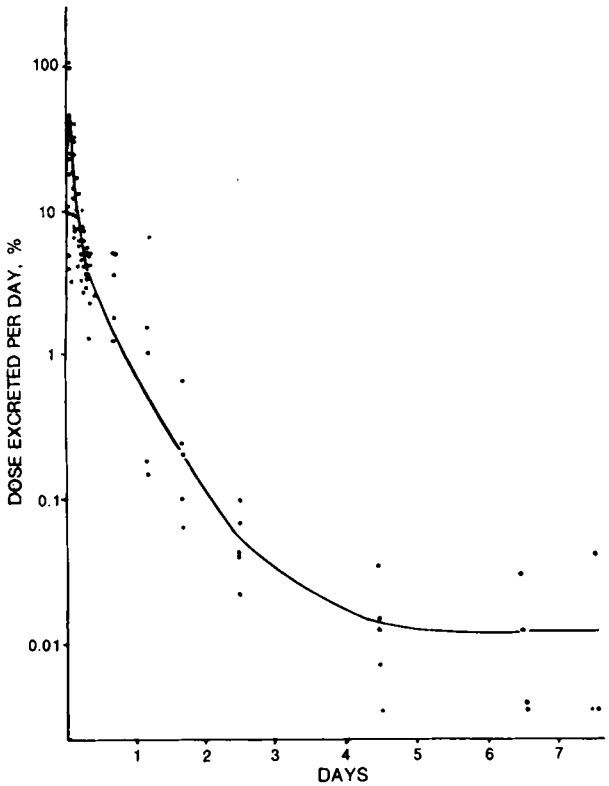

Figure 1—*Rate of biliary excretion of carbon-14 after peroral administration of ^{14}C-labeled polymethyl methacrylate nanoparticles to rats (n = 5).*

RESULTS AND DISCUSSION

Bile-cannulated rats were used so that the amount of radioactivity excreted *via* the bile could be determined. Within 8 d, between 5 and 8% of the administered dose was excreted *via* the bile and 4–6% *via* the urine (Table I).

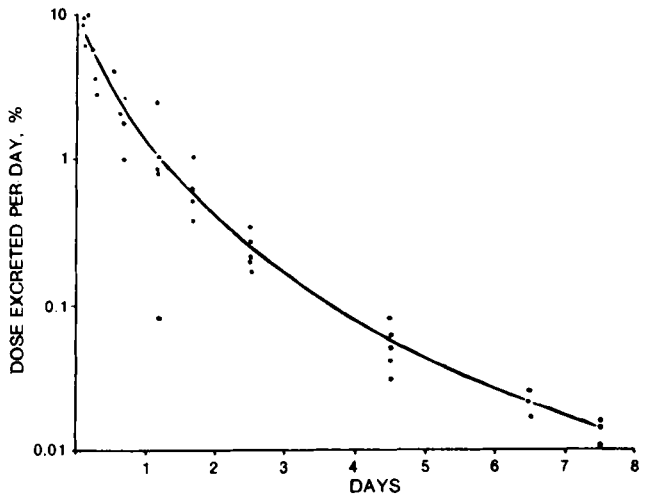

Figure 2—*Rate of urinary excretion of carbon-14 after peroral administration of ^{14}C-labeled polymethyl methacrylate nanoparticles to rats (n = 5).*

[1] Unpublished results.

[2] T-61 (each mL contains: 200 mg *N*-[2-(*m*-methoxy-phenyl)-2-ethyl-butyl-(1)]-gamma-hydroxybutyramide, 50 mg 4,4′-methylene-*bis*(cyclohexyl-trimethyl-ammonium)iodide, and 5 mg tetracaine hydrochloride with 0.6 mL dimethylformamide in distilled water). Farbwerke Hoechst, Frankfurt/Main, West Germany.

[3] Sample oxidizer; Packard Instruments, Downers Grove, Ill.

[4] Carbosorb and Permafluor; Packard Instruments.

Table II—Distribution of Carbon-14 in Organs 8 d after Peroral Administration of ^{14}C-Labeled Polymethyl Methacrylate Nanoparticles to Rats

	ng/g[a]
Blood	5.9 ± 1.6
Plasma	3.6 ± 1.1
Liver	12.7 ± 3.7
Spleen	5.1 ± 1.3
Pancreas	11.9 ± 4.6
Kidneys	9.6 ± 2.3
Adrenals	11.4 ± 6.2
Fatty renal tissue	24.5 ± 14.4
Testicles[b]	4.5
Uterus[c]	7.2
Epididymis[b]	9.0
Ovary[c]	7.0
Colon	5.0 ± 1.34
Stomach	14.5 ± 11.2
Small intestine	4.2 ± 0.6
Salivary glands	4.2 ± 1.4
Lymph nodes	13.3 ± 4.2
Thyroid glands	10.0 ± 4.8
Lungs	3.9 ± 1.4
Heart	4.1 ± 1.5
Muscles	2.6 ± 1.9
Bone marrow	66.5 ± 30.1
Skin	12.5 ± 7.1
Brain	4.3 ± 1.8
Stomach content	4.9 ± 2.3
Small intestine content	4.3 ± 1.6
Colon content	4.6 ± 2.7

[a] $n = 3$; mean, ±*SD*. [b] $n = 1$. [c] $n = 2$.

Since little radioactivity remained in the body after 8 d (Table II), the total absorption amounted to ~10–15% of the administered dose.

The absorption and excretion occurred rather rapidly. The biliary excretion rate reached a maximum after 1 h (Fig. 1) and then declined in a hyperbolic fashion. The maximal urinary excretion rate probably was reached within 2 h (Fig. 2) followed by a hyperbolic decline. Within 1 d ~83% and within 2 d ~95% of the total amount absorbed were eliminated from the body.

After 8 d, <0.5% of the administered dose remained in the body. The highest radioactivity (10 times more than in blood) was found in bone marrow. Higher levels of radioactivity were observed in renal fatty tissue, liver, pancreas, skin, adrenals, and the lymph nodes than in the blood. The values from the lymph nodes, however, give only an estimate of the actual value, due to the very small amounts of material available for the determination of the radioactivity in these organs.

The small amount of radioactivity absorbed from the GI tract probably consisted of low molecular weight components in the polymer. The figure of 10–15% is very similar to the 13% that was rapidly excreted after subcutaneous injection (6) and was, as mentioned above, attributed to low molecular weight components of the nanoparticle material. Whether these components can be used as carriers for nonabsorbable drugs is still an open question. The main part of the nanoparticle material, though capable of a carrier function, is not absorbable by rats. Because of the enhanced endocytotic activity of tumor cells (9), nanoparticles loaded with cytostatic carriers may be useful for the treatment of carcinomas of the GI tract.

REFERENCES

(1) A. C. Frazer "Surface Phenomena in Chemistry and Biology," J. F. Danieli, K. G. A. Pankhurst, and A. C. Riddiford, Eds., Pergamon, London, 1958, pp. 299–308.

(2) A. C. Frazer, *Br. Med. Bull.*, **14**, 212 (1958).

(3) G. Volkheimer, "Persorption," G. Thieme Verlag, Stuttgart, 1972, p. 2.

(4) L. Juhlin, *Acta Physiol. Scand.*, **47**, 365 (1959).

(5) J. Kreuter, U. Täuber, and V. Illi, *J. Pharm. Sci.*, **68**, 1443 (1979).

(6) J. Kreuter, M. Nefzger, R. Voges, E. Liehl, and R. Czok, *J. Pharm. Sci.*, **72**, 1146 (1983).

(7) V. Bentele, U. Berg, and J. Kreuter, *Int. J. Pharm.*, **13**, 109 (1983).

(8) J. Kreuter, *Int. J. Pharm.*, **14**, 43 (1983).

(9) P. Couvreur, P. Tulkens, M. Roland, A. Trouet, and P. Speiser, *FEBS Lett.*, **84**, 323 (1977).

High-Performance Liquid Chromatographic Determination of Acetylcholine in a Pharmaceutical Preparation

FRANK T. TAO ˣ, JOAN S. THURBER, and DANIEL M. DYE

Received September 7, 1982, from the *Analytical Development Department, CooperVision Pharmaceutical, Inc., Mountain View, CA 94043.* Accepted for publication September 22, 1983.

Abstract □ A simple and rapid method for quantitating acetylcholine in a lyophilized preparation by high-performance liquid chromatography (HPLC) is described. A reverse-phase column with a refractive index detector was utilized for the assay. The HPLC system was able to separate acetylcholine from choline, a major degradation product, which was verified by running a degraded sample of a commercial preparation. The HPLC results were compared with the results obtained by a spectrophotometric procedure.

Keyphrases □ Acetylcholine—high-performance liquid chromatographic determination, lyophilized preparation □ High-performance liquid chromatography—determination of acetylcholine □ Lyophilized preparation—acetylcholine, high-performance liquid chromatographic determination

Acetylcholine is an endogenous parasympathomimetic agent thought to play an important role in the transmission of nerve impulses at synapses and myoneural junctions. Because the action of this parasympathetic stimulation is abrupt and fleeting, acetylcholine has limited therapeutic use. However, this unique property is presently being used to advantage in an intraocular irrigating fluid to obtain complete miosis instantaneously after delivery of the lens in cataract surgery. The product[1] is in a vial of two compartments: the lower chamber contains a lyophilized preparation of acetylcholine chloride with mannitol as a tonicity adjusting agent. The upper chamber contains sterile water for injection, and the two chambers are separated by a rubber plug. Since aqueous solutions of acetylcholine are unstable, the drug is reconstituted in sterile water just prior to use.

There have been several reports on chemical assays for acetylcholine. An excellent review of the current chemical methods has been published (1). The classical colorimetric method (2) suffers from lack of specificity.

Several gas chromatographic procedures have been reported. Primary means of detection have been either flame ionization (3) or mass spectrometry (4). In all cases, they involve volatilizing acetylcholine either by demethylation (5)

[1] Miochol, CooperVision, Inc.

0022-3549/84/0900-1311$01.00/0

© 1984, American Pharmaceutical Association

Table II—Distribution of Carbon-14 in Organs 8 d after Peroral Administration of ^{14}C-Labeled Polymethyl Methacrylate Nanoparticles to Rats

	ng/g[a]
Blood	5.9 ± 1.6
Plasma	3.6 ± 1.1
Liver	12.7 ± 3.7
Spleen	5.1 ± 1.3
Pancreas	11.9 ± 4.6
Kidneys	9.6 ± 2.3
Adrenals	11.4 ± 6.2
Fatty renal tissue	24.5 ± 14.4
Testicles[b]	4.5
Uterus[c]	7.2
Epididymis[b]	9.0
Ovary[c]	7.0
Colon	5.0 ± 1.34
Stomach	14.5 ± 11.2
Small intestine	4.2 ± 0.6
Salivary glands	4.2 ± 1.4
Lymph nodes	13.3 ± 4.2
Thyroid glands	10.0 ± 4.8
Lungs	3.9 ± 1.4
Heart	4.1 ± 1.5
Muscles	2.6 ± 1.9
Bone marrow	66.5 ± 30.1
Skin	12.5 ± 7.1
Brain	4.3 ± 1.8
Stomach content	4.9 ± 2.3
Small intestine content	4.3 ± 1.6
Colon content	4.6 ± 2.7

[a] $n = 3$; mean, ±*SD*. [b] $n = 1$. [c] $n = 2$.

Since little radioactivity remained in the body after 8 d (Table II), the total absorption amounted to ~10–15% of the administered dose.

The absorption and excretion occurred rather rapidly. The biliary excretion rate reached a maximum after 1 h (Fig. 1) and then declined in a hyperbolic fashion. The maximal urinary excretion rate probably was reached within 2 h (Fig. 2) followed by a hyperbolic decline. Within 1 d ~83% and within 2 d ~95% of the total amount absorbed were eliminated from the body.

After 8 d, <0.5% of the administered dose remained in the body. The highest radioactivity (10 times more than in blood) was found in bone marrow. Higher levels of radioactivity were observed in renal fatty tissue, liver, pancreas, skin, adrenals, and the lymph nodes than in the blood. The values from the lymph nodes, however, give only an estimate of the actual value, due to the very small amounts of material available for the determination of the radioactivity in these organs.

The small amount of radioactivity absorbed from the GI tract probably consisted of low molecular weight components in the polymer. The figure of 10–15% is very similar to the 13% that was rapidly excreted after subcutaneous injection (6) and was, as mentioned above, attributed to low molecular weight components of the nanoparticle material. Whether these components can be used as carriers for nonabsorbable drugs is still an open question. The main part of the nanoparticle material, though capable of a carrier function, is not absorbable by rats. Because of the enhanced endocytotic activity of tumor cells (9), nanoparticles loaded with cytostatic carriers may be useful for the treatment of carcinomas of the GI tract.

REFERENCES

(1) A. C. Frazer "Surface Phenomena in Chemistry and Biology," J. F. Danieli, K. G. A. Pankhurst, and A. C. Riddiford, Eds., Pergamon, London, 1958, pp. 299–308.

(2) A. C. Frazer, *Br. Med. Bull.*, **14**, 212 (1958).

(3) G. Volkheimer, "Persorption," G. Thieme Verlag, Stuttgart, 1972, p. 2.

(4) L. Juhlin, *Acta Physiol. Scand.*, **47**, 365 (1959).

(5) J. Kreuter, U. Täuber, and V. Illi, *J. Pharm. Sci.*, **68**, 1443 (1979).

(6) J. Kreuter, M. Nefzger, R. Voges, E. Liehl, and R. Czok, *J. Pharm. Sci.*, **72**, 1146 (1983).

(7) V. Bentele, U. Berg, and J. Kreuter, *Int. J. Pharm.*, **13**, 109 (1983).

(8) J. Kreuter, *Int. J. Pharm.*, **14**, 43 (1983).

(9) P. Couvreur, P. Tulkens, M. Roland, A. Trouet, and P. Speiser, *FEBS Lett.*, **84**, 323 (1977).

High-Performance Liquid Chromatographic Determination of Acetylcholine in a Pharmaceutical Preparation

FRANK T. TAO ˣ, JOAN S. THURBER, and DANIEL M. DYE

Received September 7, 1982, from the *Analytical Development Department, CooperVision Pharmaceutical, Inc., Mountain View, CA 94043.* Accepted for publication September 22, 1983.

Abstract □ A simple and rapid method for quantitating acetylcholine in a lyophilized preparation by high-performance liquid chromatography (HPLC) is described. A reverse-phase column with a refractive index detector was utilized for the assay. The HPLC system was able to separate acetylcholine from choline, a major degradation product, which was verified by running a degraded sample of a commercial preparation. The HPLC results were compared with the results obtained by a spectrophotometric procedure.

Keyphrases □ Acetylcholine—high-performance liquid chromatographic determination, lyophilized preparation □ High-performance liquid chromatography—determination of acetylcholine □ Lyophilized preparation—acetylcholine, high-performance liquid chromatographic determination

Acetylcholine is an endogenous parasympathomimetic agent thought to play an important role in the transmission of nerve impulses at synapses and myoneural junctions. Because the action of this parasympathetic stimulation is abrupt and fleeting, acetylcholine has limited therapeutic use. However, this unique property is presently being used to advantage in an intraocular irrigating fluid to obtain complete miosis instantaneously after delivery of the lens in cataract surgery. The product[1] is in a vial of two compartments: the lower chamber contains a lyophilized preparation of acetylcholine chloride with mannitol as a tonicity adjusting agent. The upper chamber contains sterile water for injection, and the two chambers are separated by a rubber plug. Since aqueous solutions of acetylcholine are unstable, the drug is reconstituted in sterile water just prior to use.

There have been several reports on chemical assays for acetylcholine. An excellent review of the current chemical methods has been published (1). The classical colorimetric method (2) suffers from lack of specificity.

Several gas chromatographic procedures have been reported. Primary means of detection have been either flame ionization (3) or mass spectrometry (4). In all cases, they involve volatilizing acetylcholine either by demethylation (5)

[1] Miochol, CooperVision, Inc.

0022-3549/84/0900-1311$01.00/0

© 1984, American Pharmaceutical Association

Table I—Comparison of Colorimetric and HPLC Methods for the Determination of Acetylcholine in Lyophilized Preparations

Lot	Acetylcholine Chloride, mg/vial	
	HPLC	Colorimetric
A	21.53	21.56
	21.22	
Mean	21.38	
B	21.90	20.67
	21.28	
Mean	21.59	
C	22.19	22.79
	21.84	
Mean	22.02	

or by pyrolysis in order to transform the molecule to the gas phase (6, 7).

A high-performance liquid chromatographic (HPLC) procedure (8) has been reported using a normal-phase column with phosphate buffered picrate ion as the stationary phase and with chloroform–butanol as the mobile phase. Separation of choline and acetylcholine has been achieved by cation-exchange chromatography (9).

This paper describes the application of a reverse-phase, paired-ion HPLC analysis of acetylcholine in the pharmaceutical preparation described above. The procedure is quick, specific, and stability indicating since it separates the drug from the principle degradation products, choline and acetic acid. A comparison of the results of HPLC and colorimetric methods was made.

EXPERIMENTAL SECTION

Chemicals and Reagents—Acetylcholine chloride[2], choline chloride[3], and mannitol[4] were used as received from the suppliers without further purification. Acetonitrile[5] was HPLC grade. Ammonium hydroxide[6] and acetic acid[6] were ACS grade or equivalent. The water used was glass distilled.

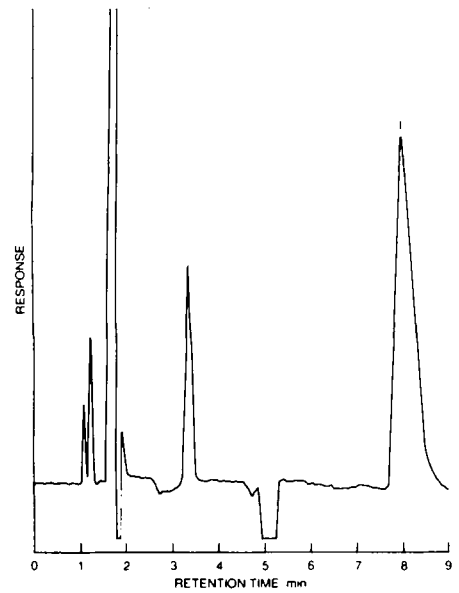

Figure 1—*Chromatogram of 50 μL injection of acetylcholine (I) standard (2 μg/μL).*

[2] Siegfried, Ltd.
[3] Eastman Kodak Co.
[4] J. T. Baker Chemical Co.
[5] Burdick & Jackson Labs., Inc.
[6] Fisher Scientific Co.

Table II—Precision Data for Acetylcholine in Lyophilized Preparations

Sample	Acetylcholine Chloride, mg/vial
1	21.62
2	21.22
3	22.04
4	21.23
5	21.70
6	20.96
Mean	21.46
SD	0.40
RSD, %	1.86

Instrumentation—The HPLC system consisted of a pump[7] capable of producing pressures of 6000 psi, a universal loop injector[8], a microparticulate reverse-phase column[9], a refractive index detector[10], and a microprocessor-controlled data system[11].

Mobile Phase—The mobile phase was prepared by adding sodium 1-heptanesulfonate[12] to 900 mL of water. After thorough mixing, 6 M ammonium hydroxide was added to adjust the pH to 4.0. After addition of 50 mL of acetonitrile, the solution was made up to 1 L with water.

Standard Stock Solution—Acetylcholine chloride, previously dried at 105°C for 4 h, was weighed (100 mg) into a 10.0-mL volumetric flask and dissolved in 5 mL of water. After mixing, the solution was brought to mark with water to make the stock standard solution.

Standard Solution—The standard solutions were prepared by pipetting 1.0, 2.0, and 3.0 mL of the stock standard solution to individual 10.0-mL volumetric flasks and bringing to mark with the mobile phase.

Decomposition of Acetylcholine—To prepare samples for heat stressing, the lyophilized solid in the commercial package was reconstituted in the sterile water. The solution was transferred quantitatively to a 10-mL clear glass ampule and the vial was washed with 1 mL of water; the wash solution was transferred to the ampule. After flame sealing, the ampule was placed in an oven at 130°C for 19 h. After cooling the ampule, the solution was transferred quantitatively to a 10.0-mL volumetric flask and was brought to the mark with the mobile phase.

Chromatographic Conditions—The volumetric flow rate was 2.0 mL/min, and the column temperature was ambient.

Standard Curve and Sample Analysis—Fifty-microliter volumes of each

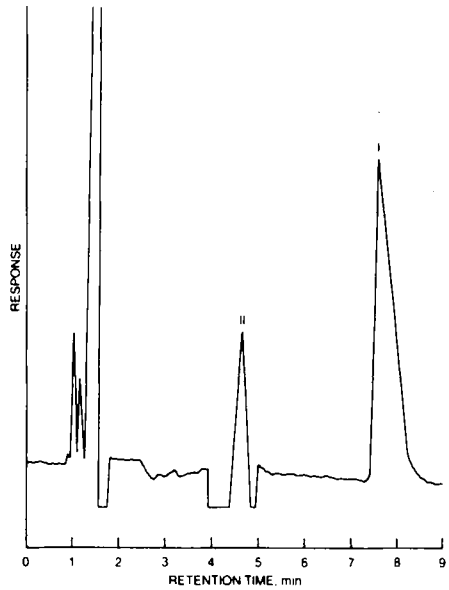

Figure 2—*Chromatogram of a heat-stressed sample of lyophilized preparation of acetylcholine chloride. The sample was heated at 130°C for 19 h. The final concentration of acetylcholine chloride was determined to be 11.13 mg/vial (55.65% of label claim). Key: (I) acetylcholine; (II) choline.*

[7] Model 6000A; Waters Associates.
[8] Model U6K; Waters Associates.
[9] μ-Bondapak C_{18}; Waters Associates.
[10] Model 401; Waters Associates.
[11] Model 4100; Spectra Physics.
[12] PIC Reagent B-7; Waters Associates.

of the three standard solutions were injected consecutively into the HPLC. With the aid of the data system, a three point linear calibration curve was constructed which plotted the weight (μg) of acetylcholine chloride injected as a function of area under the peak. The sample was quantitated by injecting 50 μL of the test solution and the weight (μg) of acetylcholine chloride obtained from the calibration curve. The test solution was prepared by transferring quantitatively the reconstituted solution into a 10.0-mL volumetric flask. The flask was brought to the mark with the mobile phase.

RESULTS AND DISCUSSION

Reverse-phase paired-ion HPLC was useful in separating intact acetylcholine from its decomposition products and its excipient, mannitol. Use of the mobile phase described gave a sharp, well resolved peak. The refractive index detector was the detector of choice since the drug lacks a chromophore; the sensitivity of the detector was more than adequate in quantitating acetylcholine chloride in the preparation.

Figure 1 illustrates the elution profile of acetylcholine. The retention time varied with the amount injected. The retention time increased with decreasing amounts of acetylcholine and ranged from 8.2 to 7.9 min for 50–150 μg of the acetylcholine standard. The variation in retention time is probably a manifestation of nonlinearity in the interaction of acetylcholine in the mobile phase with the stationary phase (reduction in interaction with increasing amounts of the drug). However, the variation of the retention time with the amount of acetylcholine injected did not negate the usefulness of the assay, since excellent linear curves were obtained. A standard curve constructed from 50, 100, and 150 g of the drug injected had a correlation coefficient of 0.9996.

Choline, acetic acid, and mannitol were shown not to interfere with the determination of acetylcholine (Fig. 2). One the the peaks in the sample displayed the same retention time, 5 min, as that of the authentic choline chloride solution. Acetic acid eluted with the solvent front and mannitol was retained on the column.

Three lots of the pharmaceutical preparation were analyzed by HPLC in duplicate and the results were compared with those from the hydroxylamine colorimetric method (2) (Table I). Precision data for the HPLC assay is presented in Table II. These results demonstrate the utility of the HPLC procedure; the method is simple, fast, specific, and stability indicating.

REFERENCES

(1) "Choline and Acetylcholine: Handbook of Chemical Assay Method," I. Hanin, Ed., Raven, New York, N.Y., 1974.

(2) S. Hestrin, *J. Biol. Chem.*, **180**, 249 (1949).

(3) J. W. Kosh, M. B. Smith, J. W. Sowell, and J. J. Freeman, *J. Chromatogr.*, **163**, 206 (1979).

(4) D. J. Jenden, M. Roch, and R. A. Booth, *Anal. Biochem.*, **55**, 438 (1973).

(5) D. J. Jenden, R. A. Booth, and M. Roch, *Anal. Chem.*, **44**, 1979 (1972).

(6) Y. Maruyama, M. Kusaka, J. Mori, A. Horikawa, and Y. Kaseyawa, *J. Chromatogr.*, **164**, 121 (1979).

(7) Y. Hasegawa, M. Kunihara, and Y. Maruyama, *J. Chromatogr.*, **239**, 375 (1982).

(8) B. Ulin, K. Gustavii, and B. A. Persson, *J. Pharm. Pharmacol.*, **28**, 672 (1976).

(9) R. Stein, *J. Chromatogr.*, **219**, 148 (1981).

ACKNOWLEDGMENTS

The authors thank Dr. W. F. Bayne for his guidance and encouragement.

Electron-Capture Capillary Gas Chromatographic Determination of Phenylpropanolamine in Human Plasma Following Derivatization with Trifluoroacetic Anhydride

N. CRISOLOGO, D. DYE ˣ, and W. F. BAYNE ‡

Received July 25, 1983 from the *ALZA Corporation, Palo Alto, CA 94303.* Accepted for publication September 26, 1983. ‡ Present address: Merck Sharp & Dohme Research Laboratories, West Point, PA 19486.

Abstract □ A capillary gas chromatographic analysis of phenylpropanolamine in human plasma, following extraction and derivatization with trifluoroacetic anhydride, is presented. Using an electron-capture detector, the method was sensitive enough to quantitate as little as 1 ng of drug/mL of plasma. The coefficient of variation from 5–262 ng/mL varied between 5.6 and 1.6%, respectively. Plasma concentration data following one 25-mg dose of phenylpropanolamine hydrochloride in four healthy volunteers illustrates the suitability of this analytical method for monitoring plasma levels after oral administration of a typical dosage form.

Keyphrases □ Capillary gas chromatography—phenylpropanolamine, human plasma, trifluoroacetic anhydride derivatization □ Phenylpropanolamine—capillary gas chromatography, human plasma, trifluoroacetic anhydride derivatization □ Derivatization—trifluoroacetic anhydride, capillary gas chromatography, human plasma

Previously reported methods for the determination of phenylalkanolamines and related compounds in biological fluids include gas chromatography (GC) after extraction and formation of perfluoroacyl or pentafluorobenzylimine-trimethylsilyl derivatives (1–10), GC after formation of a pentafluorophenyloxazolidine derivative (11), GC after extraction and detection with a nitrogen-selective detector (12), and HPLC following extraction and precolumn derivatization with *o*-phthalaldehyde (13), 4-chloro-7-nitrobenz-2,1,3-oxadiazole and sodium naphthaquinone-4-sulfonate (14), and phenyl isothiocyanate (15).

A procedure for extraction of phenylpropanolamine and an internal standard from plasma, derivatization with trifluoroacetic anhydride, separation by capillary GC, and detection by electron capture is presented in this report. The achievable detection limit of the method is 1 ng/mL. Plasma concentrations >5 ng/mL can be determined with accuracy and precision suitable for pharmacokinetic studies.

EXPERIMENTAL SECTION

Instrumentation—The gas chromatograph[1] was equipped with a capillary inlet system and an 8-mCi Ni^{63} electron-capture detector connected to an integrator-calculator[2]. The fused silica capillary column (0.25 mm i.d. × 30 m) was coated with polymethyl (5% phenyl) siloxane[3] to a final thickness of 0.25 μm.

The chromatographic conditions were as follows: injection volume of the

[1] 3700 Series gas chromatograph with a model 1070 capillary inlet system and pneumatics; Varian Instrument, Palo Alto, Calif.

[2] Model 4100; Spectra-Physics, Santa Clara, Calif.

[3] J & W Scientific, Rancho Cordova, Calif.

0022-3549/84/0900-1313$01.00/0

© 1984, American Pharmaceutical Association

of the three standard solutions were injected consecutively into the HPLC. With the aid of the data system, a three point linear calibration curve was constructed which plotted the weight (μg) of acetylcholine chloride injected as a function of area under the peak. The sample was quantitated by injecting 50 μL of the test solution and the weight (μg) of acetylcholine chloride obtained from the calibration curve. The test solution was prepared by transferring quantitatively the reconstituted solution into a 10.0-mL volumetric flask. The flask was brought to the mark with the mobile phase.

RESULTS AND DISCUSSION

Reverse-phase paired-ion HPLC was useful in separating intact acetylcholine from its decomposition products and its excipient, mannitol. Use of the mobile phase described gave a sharp, well resolved peak. The refractive index detector was the detector of choice since the drug lacks a chromophore; the sensitivity of the detector was more than adequate in quantitating acetylcholine chloride in the preparation.

Figure 1 illustrates the elution profile of acetylcholine. The retention time varied with the amount injected. The retention time increased with decreasing amounts of acetylcholine and ranged from 8.2 to 7.9 min for 50–150 μg of the acetylcholine standard. The variation in retention time is probably a manifestation of nonlinearity in the interaction of acetylcholine in the mobile phase with the stationary phase (reduction in interaction with increasing amounts of the drug). However, the variation of the retention time with the amount of acetylcholine injected did not negate the usefulness of the assay, since excellent linear curves were obtained. A standard curve constructed from 50, 100, and 150 g of the drug injected had a correlation coefficient of 0.9996.

Choline, acetic acid, and mannitol were shown not to interfere with the determination of acetylcholine (Fig. 2). One the the peaks in the sample displayed the same retention time, 5 min, as that of the authentic choline chloride solution. Acetic acid eluted with the solvent front and mannitol was retained on the column.

Three lots of the pharmaceutical preparation were analyzed by HPLC in duplicate and the results were compared with those from the hydroxylamine colorimetric method (2) (Table I). Precision data for the HPLC assay is presented in Table II. These results demonstrate the utility of the HPLC procedure; the method is simple, fast, specific, and stability indicating.

REFERENCES

(1) "Choline and Acetylcholine: Handbook of Chemical Assay Method," I. Hanin, Ed., Raven, New York, N.Y., 1974.

(2) S. Hestrin, *J. Biol. Chem.*, **180**, 249 (1949).

(3) J. W. Kosh, M. B. Smith, J. W. Sowell, and J. J. Freeman, *J. Chromatogr.*, **163**, 206 (1979).

(4) D. J. Jenden, M. Roch, and R. A. Booth, *Anal. Biochem.*, **55**, 438 (1973).

(5) D. J. Jenden, R. A. Booth, and M. Roch, *Anal. Chem.*, **44**, 1979 (1972).

(6) Y. Maruyama, M. Kusaka, J. Mori, A. Horikawa, and Y. Kaseyawa, *J. Chromatogr.*, **164**, 121 (1979).

(7) Y. Hasegawa, M. Kunihara, and Y. Maruyama, *J. Chromatogr.*, **239**, 375 (1982).

(8) B. Ulin, K. Gustavii, and B. A. Persson, *J. Pharm. Pharmacol.*, **28**, 672 (1976).

(9) R. Stein, *J. Chromatogr.*, **219**, 148 (1981).

ACKNOWLEDGMENTS

The authors thank Dr. W. F. Bayne for his guidance and encouragement.

Electron-Capture Capillary Gas Chromatographic Determination of Phenylpropanolamine in Human Plasma Following Derivatization with Trifluoroacetic Anhydride

N. CRISOLOGO, D. DYE ˣ, and W. F. BAYNE ‡

Received July 25, 1983 from the *ALZA Corporation, Palo Alto, CA 94303.* Accepted for publication September 26, 1983. ‡ Present address: Merck Sharp & Dohme Research Laboratories, West Point, PA 19486.

Abstract □ A capillary gas chromatographic analysis of phenylpropanolamine in human plasma, following extraction and derivatization with trifluoroacetic anhydride, is presented. Using an electron-capture detector, the method was sensitive enough to quantitate as little as 1 ng of drug/mL of plasma. The coefficient of variation from 5–262 ng/mL varied between 5.6 and 1.6%, respectively. Plasma concentration data following one 25-mg dose of phenylpropanolamine hydrochloride in four healthy volunteers illustrates the suitability of this analytical method for monitoring plasma levels after oral administration of a typical dosage form.

Keyphrases □ Capillary gas chromatography—phenylpropanolamine, human plasma, trifluoroacetic anhydride derivatization □ Phenylpropanolamine—capillary gas chromatography, human plasma, trifluoroacetic anhydride derivatization □ Derivatization—trifluoroacetic anhydride, capillary gas chromatography, human plasma

Previously reported methods for the determination of phenylalkanolamines and related compounds in biological fluids include gas chromatography (GC) after extraction and formation of perfluoroacyl or pentafluorobenzylimine-trimethylsilyl derivatives (1–10), GC after formation of a pentafluorophenyloxazolidine derivative (11), GC after extraction and detection with a nitrogen-selective detector (12), and HPLC following extraction and precolumn derivatization with *o*-phthalaldehyde (13), 4-chloro-7-nitrobenz-2,1,3-oxadiazole and sodium naphthaquinone-4-sulfonate (14), and phenyl isothiocyanate (15).

A procedure for extraction of phenylpropanolamine and an internal standard from plasma, derivatization with trifluoroacetic anhydride, separation by capillary GC, and detection by electron capture is presented in this report. The achievable detection limit of the method is 1 ng/mL. Plasma concentrations >5 ng/mL can be determined with accuracy and precision suitable for pharmacokinetic studies.

EXPERIMENTAL SECTION

Instrumentation—The gas chromatograph[1] was equipped with a capillary inlet system and an 8-mCi Ni^{63} electron-capture detector connected to an integrator-calculator[2]. The fused silica capillary column (0.25 mm i.d. × 30 m) was coated with polymethyl (5% phenyl) siloxane[3] to a final thickness of 0.25 μm.

The chromatographic conditions were as follows: injection volume of the

[1] 3700 Series gas chromatograph with a model 1070 capillary inlet system and pneumatics; Varian Instrument, Palo Alto, Calif.

[2] Model 4100; Spectra-Physics, Santa Clara, Calif.

[3] J & W Scientific, Rancho Cordova, Calif.

0022-3549/84/0900-1313$01.00/0

© 1984, American Pharmaceutical Association

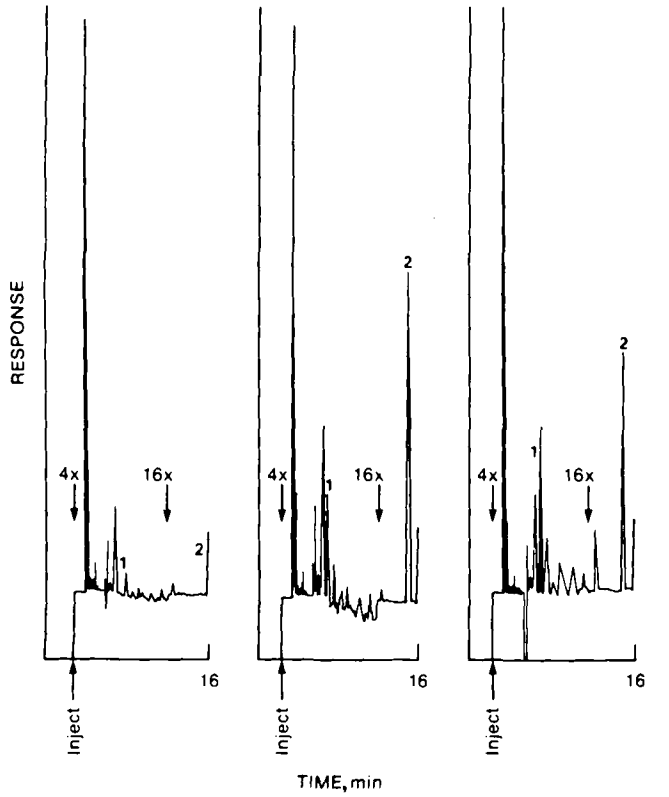

Figure 1 —*Chromatogram of an analysis of a plasma blank (A), a plasma sample with added phenylpropanolamine and internal standard (5.2 and 200 ng/mL, respectively) (B), and a plasma sample from a subject dosed with 25 mg of phenylpropanolamine hydrochloride with added internal standard (18 and 200 ng/ml, respectively) (C). Key: (1) phenylpropanolamine (retention time = 10.8 min); (2) internal standard, 2-amino-3-phenyl-1-propanol, (retention time = 15.3 min). (Note: Chart speed was 0.1 cm/min until 9 min into each run, and 0.5 cm/min thereafter.)*

sample, 1-2 μL; injector temperature, 220°C; detector temperature, 250°C; column temperature, initially at 117°C for 10 min, programmed at 3°C/min to 125°C, followed by a 6-min hold at 125°C; helium (high purity) carrier gas flow, 0.3 mL/min; nitrogen (high purity) make-up gas flow, 30 mL/min. Injections were made in the split mode; the split ratio was 1:50.

Reagents—Phenylpropanolamine hydrochloride[4] and internal standard 2-amino-3-phenyl-1-propanol hydrochloride[5] were used to prepare standard solutions. 4-Dimethylaminopyridine[5], trifluoroacetic anhydride[6], and toluene[7] (UV grade, distilled in glass) were used as received. All other reagents were reagent grade.

Standard Solutions—The stock standard solutions (1 mg/mL) of phenylpropanolamine hydrochloride and 2-amino-3-phenyl-1-propanol hydrochloride were prepared in water and stored at 4°C.

Preparation and Extraction of Plasma Standards and Samples—Varying microliter volumes of a 0.001 dilution of phenylpropanolamine hydrochloride stock standard solution in water were added to 1-mL plasma aliquots to obtain concentrations of 5.2, 20.9, 104.7, 157.1, and 261.8 ng/mL of plasma. An aliquot (200 μL) of a 0.001 dilution of 2-amino-3-phenyl-1-propanol hydrochloride stock standard solution in water was added to each plasma standard and the sample (1 mL) for a final concentration of 200 ng/mL.

To the plasma standards and samples contained in 12-mL polytef-stoppered conical centrifuge tubes (silanized with 5% dimethyldichlorosilane[8] in toluene) were added 0.2 mL of 0.5 M KH_2PO_4 buffer (adjusted to pH 11.0 with NaOH) and 3 mL of toluene. The tubes were sealed and shaken gently for 30 min at room temperature on a horizontal shaker[9]. After centrifugation at 2000 rpm for 5 min, the organic layers were transferred to another set of 12-mL centrifuge tubes and concentrated to ~0.5 mL under nitrogen in a 40°C water bath. 4-Dimethylaminopyridine (0.2 mg dissolved in 50 μL of toluene, added as a catalyst) and trifluoroacetic anhydride (70 μL) were then added; the tubes were then stoppered and heated for 30 min in a 60°C water bath. Two milliliters of 0.5 M Na_2HPO_4 buffer (pH 6.0) was then added, followed by vortex-mixing for 15 s. Aliquots (1-2 μL) of the toluene layer were injected into the gas chromatograph.

[4] Sigma Chemical Co., St. Louis, Mo.
[5] Aldrich Chemical Co., Milwaukee, Wis.
[6] Pierce Chemical Co., Rockford, Ill.
[7] Burdick & Jackson Laboratory, Muskegon, Mich.
[8] Applied Science Division, Milton Roy Laboratory Group, State College, Pa.
[9] Eberbach Corp., Ann Arbor, Mich.

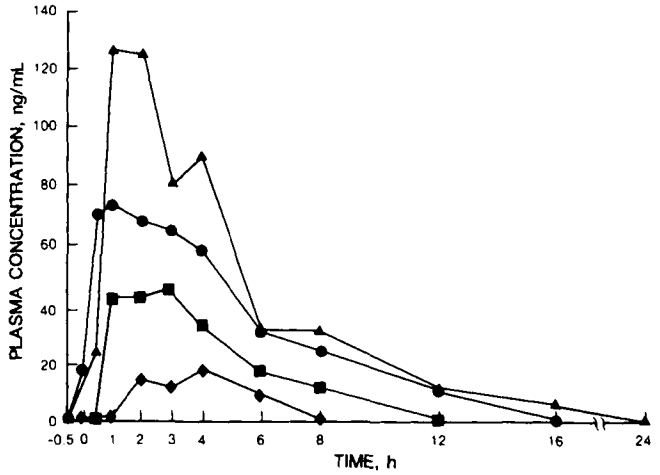

Figure 2—*Plasma levels of phenylpropanolamine base in four subjects following ingestion of 25 mg of phenylpropanolamine hydrochloride in water. Key: (●) subject 1; (▲) subject 2; (■) subject 3; (◆) subject 4.*

Standard Curve—The retention times of the di-trifluoroacetyl derivatives of phenylpropanolamine and 2-amino-3-phenyl-1-propanol were 10.8 and 15.3 min, respectively. The area responses for these chromatographic peaks were used to construct standard curves by plotting area ratio of phenylpropanolamine-internal standard against the respective phenylpropanolamine plasma concentration.

Clinical Study—As part of a clinical study, normal healthy subjects received a single 25-mg dose of phenylpropanolamine hydrochloride in water. Blood samples were collected at −0.5, 0, 0.5, 1, 2, 3, 4, 6, 8, 16, and 24 h in heparin-containing vacuum containers[10]. The plasma was separated immediately by centrifugation and frozen within 30 min. All samples were stored at −20°C until assayed.

RESULTS AND DISCUSSION

Figure 1 shows a typical chromatogram for phenylpropanolamine in spiked human plasma and in plasma obtained from a human subject after oral ingestion of 25 mg of phenylpropanolamine hydrochloride. Analysis of predose plasma samples from 24 human subjects presented no chromatographic peaks that interfered with either phenylpropanolamine or the internal standard. Plots of peak area ratios (phenylpropanolamine to internal standard) against phenylpropanolamine concentrations were linear. Typical standard curves for phenylpropanolamine in plasma had correlation coefficients of 0.9997.

The derivatization reaction was quantitative under the conditions described. This was determined in recovery experiments by monitoring the disappearance of underivatized drug in the reaction mixture. The reaction rate was increased several fold when 4-dimethylaminopyridine was present as a catalyst. The efficiency of extraction of drug from plasma was 60% due to the high water solubility of the phenylpropanolamine.

The coefficients of variation for five replicate assays at 5.2, 20.9, 104.7, 157.1, and 261.8 ng/mL of plasma were ±5.6, ±1.8, ±6.5, ±1.6, and ±1.6%, respectively. The lowest standard routinely used was 5 ng/mL, although the achievable detection limit of the assay was 1 ng/mL.

Figure 2, which shows typical plasma phenylpropanolamine levels following a single oral dose of 25 mg of phenylpropanolamine hydrochloride in water, demonstrates that the method is adequate for use in bioavailability studies.

REFERENCES

(1) P. Cancalon and J. D. Klingman, *J. Chromatogr. Sci.*, **10**, 253 (1972).

(2) L. M. Cummins and M. J. Fourier, *Anal. Lett.*, **2**, 403 (1969).

(3) J. Dickerson, D. Perrier, M. Mayersohn, and R. Bressler, *Eur. J. Clin. Pharmacol.*, **14**, 253 (1978).

(4) A. Yacobi, R. G. Stoll, G. C. Chao, J. E. Carter, D. M. Baaske, B. L. Kamath, A. H. Amann, and C. M. Lai, *J. Pharm. Sci.*, **69**, 1077 (1980).

[10] Vacutainers; Beckton, Dickinson and Co., Rutherford, N.J.

(5) R. B. Bruce and W. R. Maynard, Jr., *Anal. Chem.*, **41**, 977 (1969).
(6) L. J. Dombrowski, P. M. Comi, and E. L. Pratt, *J. Pharm. Sci.*, **62**, 1761 (1973).
(7) G. R. Wilkinson, *Anal. Lett.*, **3**, 289 (1970).
(8) T. Walle and H. Ehrsson, *Acta Pharm. Suec.*, **8**, 27 (1971).
(9) D. J. Edwards and K. Blau, *Anal. Biochem.*, **45**, 387 (1972).
(10) J. C. Lhuguenot and B. F. Maume, *J. Chromatogr. Sci.*, **12**, 411 (1974).
(11) L. Neelakantan and H. B. Kostenbauder, *J. Pharm. Sci.*, **65**, 740 (1976).
(12) H. Kinsun, M. A. Moulin, and E. C. Savini, *J. Pharm. Sci.*, **67**, 118 (1978).
(13) W. D. Mason and E. N. Amick, *J. Pharm. Sci.*, **70**, 707 (1981).
(14) B. M. Farrell and T. M. Jefferies, *J. Chromatogr.*, **272**, 111 (1983).
(15) F. T. Noggle, Jr., *J. Assoc. Off. Anal. Chem.*, **63**, 702 (1980).

ACKNOWLEDGMENTS

We thank Dr. Pieter Bonsen for critically reviewing this manuscript and Ms. Rose Wright for her extensive literature research.

Determination of Sodium Levothyroxine in Bulk, Tablet, and Injection Formulations by High-Performance Liquid Chromatography

JAMES F. BROWER ˣ, DUCKHEE Y. TOLER, and JOHN C. REEPMEYER

Received July 15, 1983, from the *National Center for Drug Analysis, Food and Drug Administration, St. Louis, MO 63101.* Accepted for publication September 28, 1983.

Abstract □ Sodium levothyroxine was determined in bulk drugs, tablets, and injections by high-performance liquid chromatography (HPLC). Levothyroxine was separated from excipients and impurities on a 10-μm cyanoalkyl column using an acetonitrile–water–phosphoric acid mobile phase. The HPLC method is shown to be linear, accurate, and precise, and the results obtained by the HPLC and USP XX methods are compared.

Keyphrases □ Sodium levothyroxine—HPLC, determination of bulk, tablet, and injection formulations □ HPLC—sodium levothyroxine, determination of bulk, tablet, and injection formulations

In a survey[1] of sodium levothyroxine products and formulations, 63 samples of tablets, representing 20 formulations from 5 manufacturers, 9 samples of injections from 2 manufacturers, and 6 samples of bulk sodium levothyroxine from 5 manufacturers, were analyzed in this labroatory. The purpose of the survey was to evaluate the quality of sodium levothyroxine products on the market and the adequacy of present compendial standards and methods. Methodology was developed for content uniformity analysis of sodium levothyroxine by high-performance liquid chromatography (HPLC). This method, unlike the official compendial method (1), differentiates levothyroxine from iodinated impurities and degradation products.

Previously developed methods for the determination of sodium levothyroxine (2–13) were evaluated and tested. A modification of the HPLC procedure described by Garnick *et al.* (13), using a cyanoalkyl bonded phase column, was selected. This method offers advantages over those already in the literature by avoiding buffers in the mobile phase, no sample derivatization, faster analysis times, greater sensitivity due to shorter retention times, lower flow rates, and 229 nm detection. A sample solvent was selected that readily dissolved sodium levothyroxine without degradation from tablet formulations. This method and the results obtained on the survey sample are reported here.

[1] This study was a national survey for the Food and Drug Administration.

EXPERIMENTAL SECTION

Apparatus A modular high-performance liquid chromatograph[2] (HPLC) was equipped with a fixed-wavelength (229 nm) cadmium lamp UV detector[3], an automated injector[4], a microprocessor controller[5], and a recorder-integrator[6]. A stainless steel column (3.9 mm × 30 cm) was packed with irregular 10-μm silica particles to which a layer of cyanoalkyl silane was chemically bonded[7].

The mobile phase consisted of acetonitrile–water–phosphoric acid (350:650:1). This solution was passed through a 0.45-μm filter[8], deaerated, and then pumped through the HPLC system at a rate of 1 mL/min.

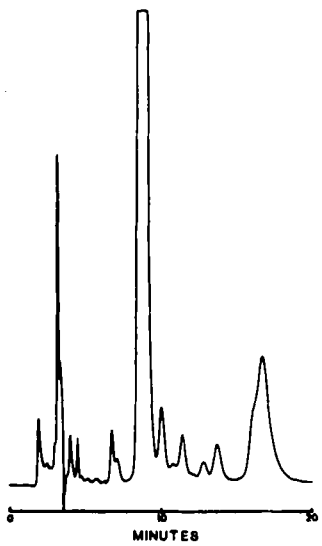

Figure 1—*Chromatogram of sodium levothyroxine bulk drug decomposed by heating in air; detector at 229 nm and 0.02 AUFS. Key: (1) sodium levothyroxine at a level of ~100 μg/mL.*

[2] Model ALC 204; Waters Associates.
[3] Model 441; Waters Associates.
[4] Model 710B WISP; Waters Associates.
[5] Model 720 System Controller; Waters Associates.
[6] Model 730 Data Module; Waters Associates.
[7] μ-Bondapak-CN; Waters Associates.
[8] Durapore UVLPO4700; Millipore Corp., Bedford, Mass.

0022-3549/84/0900-1315$01.00/0
© 1984, American Pharmaceutical Association

(5) R. B. Bruce and W. R. Maynard, Jr., *Anal. Chem.*, **41**, 977 (1969).
(6) L. J. Dombrowski, P. M. Comi, and E. L. Pratt, *J. Pharm. Sci.*, **62**, 1761 (1973).
(7) G. R. Wilkinson, *Anal. Lett.*, **3**, 289 (1970).
(8) T. Walle and H. Ehrsson, *Acta Pharm. Suec.*, **8**, 27 (1971).
(9) D. J. Edwards and K. Blau, *Anal. Biochem.*, **45**, 387 (1972).
(10) J. C. Lhuguenot and B. F. Maume, *J. Chromatogr. Sci.*, **12**, 411 (1974).
(11) L. Neelakantan and H. B. Kostenbauder, *J. Pharm. Sci.*, **65**, 740 (1976).
(12) H. Kinsun, M. A. Moulin, and E. C. Savini, *J. Pharm. Sci.*, **67**, 118 (1978).
(13) W. D. Mason and E. N. Amick, *J. Pharm. Sci.*, **70**, 707 (1981).
(14) B. M. Farrell and T. M. Jefferies, *J. Chromatogr.*, **272**, 111 (1983).
(15) F. T. Noggle, Jr., *J. Assoc. Off. Anal. Chem.*, **63**, 702 (1980).

ACKNOWLEDGMENTS

We thank Dr. Pieter Bonsen for critically reviewing this manuscript and Ms. Rose Wright for her extensive literature research.

Determination of Sodium Levothyroxine in Bulk, Tablet, and Injection Formulations by High-Performance Liquid Chromatography

JAMES F. BROWER ˣ, DUCKHEE Y. TOLER, and JOHN C. REEPMEYER

Received July 15, 1983, from the *National Center for Drug Analysis, Food and Drug Administration, St. Louis, MO 63101.* Accepted for publication September 28, 1983.

Abstract □ Sodium levothyroxine was determined in bulk drugs, tablets, and injections by high-performance liquid chromatography (HPLC). Levothyroxine was separated from excipients and impurities on a 10-μm cyanoalkyl column using an acetonitrile–water–phosphoric acid mobile phase. The HPLC method is shown to be linear, accurate, and precise, and the results obtained by the HPLC and USP XX methods are compared.

Keyphrases □ Sodium levothyroxine—HPLC, determination of bulk, tablet, and injection formulations □ HPLC—sodium levothyroxine, determination of bulk, tablet, and injection formulations

In a survey[1] of sodium levothyroxine products and formulations, 63 samples of tablets, representing 20 formulations from 5 manufacturers, 9 samples of injections from 2 manufacturers, and 6 samples of bulk sodium levothyroxine from 5 manufacturers, were analyzed in this labroatory. The purpose of the survey was to evaluate the quality of sodium levothyroxine products on the market and the adequacy of present compendial standards and methods. Methodology was developed for content uniformity analysis of sodium levothyroxine by high-performance liquid chromatography (HPLC). This method, unlike the official compendial method (1), differentiates levothyroxine from iodinated impurities and degradation products.

Previously developed methods for the determination of sodium levothyroxine (2–13) were evaluated and tested. A modification of the HPLC procedure described by Garnick *et al.* (13), using a cyanoalkyl bonded phase column, was selected. This method offers advantages over those already in the literature by avoiding buffers in the mobile phase, no sample derivatization, faster analysis times, greater sensitivity due to shorter retention times, lower flow rates, and 229 nm detection. A sample solvent was selected that readily dissolved sodium levothyroxine without degradation from tablet formulations. This method and the results obtained on the survey sample are reported here.

[1] This study was a national survey for the Food and Drug Administration.

EXPERIMENTAL SECTION

Apparatus A modular high-performance liquid chromatograph[2] (HPLC) was equipped with a fixed-wavelength (229 nm) cadmium lamp UV detector[3], an automated injector[4], a microprocessor controller[5], and a recorder-integrator[6]. A stainless steel column (3.9 mm × 30 cm) was packed with irregular 10-μm silica particles to which a layer of cyanoalkyl silane was chemically bonded[7].

The mobile phase consisted of acetonitrile–water–phosphoric acid (350:650:1). This solution was passed through a 0.45-μm filter[8], deaerated, and then pumped through the HPLC system at a rate of 1 mL/min.

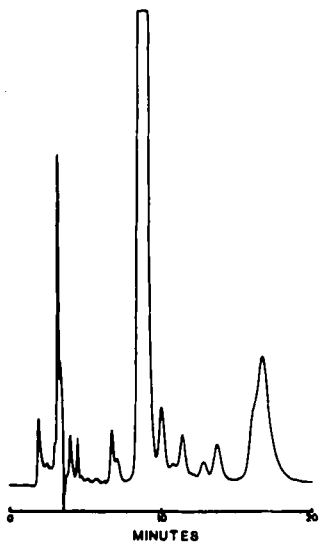

Figure 1—*Chromatogram of sodium levothyroxine bulk drug decomposed by heating in air; detector at 229 nm and 0.02 AUFS. Key: (1) sodium levothyroxine at a level of ~100 μg/mL.*

[2] Model ALC 204; Waters Associates.
[3] Model 441; Waters Associates.
[4] Model 710B WISP; Waters Associates.
[5] Model 720 System Controller; Waters Associates.
[6] Model 730 Data Module; Waters Associates.
[7] μ-Bondapak-CN; Waters Associates.
[8] Durapore UVLPO4700; Millipore Corp., Bedford, Mass.

0022-3549/84/0900-1315$01.00/0
© 1984, American Pharmaceutical Association

Table I—Sodium Levothyroxine Determined by HPLC and USP XX Procedures

Manufacturer[a]	Dosage Form, mg	Label Claim, % C.U.[b]	Label Claim, % Composite Assay HPLC	Label Claim, % Composite Assay USP
A	Tablet, 0.025	96.7 (1.2) 30		
	Tablet, 0.025	97.6 (1.6) 30		
	Tablet, 0.050	90.8 (1.8) 30		
	Tablet, 0.050	94.3 (2.1) 30		
	Tablet, 0.100	96.7 (1.8) 30		
	Tablet, 0.100	95.8 (1.3) 30		
	Tablet, 0.100	97.2 (1.9) 30		
	Tablet, 0.100	97.5 (2.5) 30		
	Tablet, 0.125	97.6 (1.7) 30		
	Tablet, 0.125	98.4 (0.8) 30		
	Tablet, 0.150	97.8 (2.0) 30		
	Tablet, 0.150	104.4 (2.0) 10		
	Tablet, 0.150	95.0 (1.8) 10		
	Tablet, 0.175	95.0 (1.8) 30		
	Tablet, 0.200	97.4 (1.3) 10		
	Tablet, 0.200	100.0 (2.5) 30		
	Tablet, 0.200	100.6 (1.9) 30		
	Tablet, 0.200	98.5 (1.7) 10	96.5	104.9
	Tablet, 0.300	102.0 (1.4) 10	97.8	109.2
	Tablet, 0.300	102.5 (2.6) 10	100.8	106.3
	Bulk drug		100.2	98.4
	Tablet, 0.050	80.7 (1.2) 10	Past expiration date	
	Tablet, 0.100	99.1 (1.7) 10	Past expiration date	
	Tablet, 0.175	88.3 (2.2) 10	Past expiration date	
	Tablet, 0.300	90.9 (1.9) 10	Past expiration date	
B	Tablet, 0.100	92.4 (2.6) 10	94.3	97.4
	Tablet, 0.100	89.5 (6.7) 10	95.7	96.6
	Tablet, 0.200	99.1 (5.2) 10	102.5	105.2
	Bulk drug		100.9	96.8
C	Tablet, 0.100	99.4 (3.2) 20		
	Tablet, 0.100	99.6 (2.1) 20		
	Tablet, 0.200	94.7 (1.8) 10	97.4	113.6
	Tablet, 0.200	90.2 (2.5) 20	95.6	111.7
	Bulk drug		100.7	96.4
D	Tablet, 0.100	63.9 (2.5) 20	62.3	101.8
	Tablet, 0.300	100.8 (1.5) 10	101.7	104.3
	Bulk drug		98.1	97.1
E	Tablet, 0.025	99.7 (3.7) 10		
	Tablet, 0.025	99.1 (2.9) 10		
	Tablet, 0.025	97.8 (2.7) 10		
	Tablet, 0.025	97.8 (2.1) 10		
	Tablet, 0.050	102.0 (2.1) 10		
	Tablet, 0.050	101.5 (3.7) 10		
	Tablet, 0.050	106.1 (1.4) 10		
	Tablet, 0.050	102.6 (2.3) 10		
	Tablet, 0.100	94.5 (1.4) 10		
	Tablet, 0.100	104.3 (2.3) 10		
	Tablet, 0.100	105.1 (2.7) 10		
	Tablet, 0.100	104.3 (1.9) 10		
	Tablet, 0.100	104.8 (2.0) 10		
	Tablet, 0.100	105.5 (2.0) 10		
	Tablet, 0.150	102.1 (1.5) 10		
	Tablet, 0.150	102.9 (1.2) 10		
	Tablet, 0.150	105.6 (1.2) 10		
	Tablet, 0.150	103.7 (1.4) 10		
	Tablet, 0.150	105.2 (1.6) 10		
	Tablet, 0.150	104.4 (1.8) 10		
	Tablet, 0.200	88.7 (1.5) 10		108.2
	Tablet, 0.200	106.3 (3.0) 10		106.6
	Tablet, 0.200	104.4 (2.7) 10		
	Tablet, 0.200	105.8 (2.3) 10		
	Tablet, 0.200	103.6 (3.3) 10		
	Tablet, 0.200	105.0 (2.7) 10		
	Tablet, 0.200	105.1 (1.8) 10		
	Tablet, 0.300	102.0 (1.8) 10		
	Inj., 0.100	84.1 (1.5) 5	86.5	
	Inj., 0.100	94.2 (2.9) 5		
	Inj., 0.100	89.0 (4.8) 5	94.4	
	Inj., 0.200	94.4 (4.7) 5		
	Inj., 0.200	95.5 (2.8) 5		
	Inj., 0.200	97.5 (1.3) 5		
	Inj., 0.500	95.5 (0.5) 5		
	Inj., 0.500	93.4 (3.6) 5		
	Bulk drug		97.8	95.4
	Bulk drug		99.2	98.0
F	Inj., 0.500	83.8 (9.4) 3		

[a] (A) Armour Pharmaceutical Co., Scottsdale, Ariz.; (B) Chelsea Laboratories Inc., Inwood, N.Y.; (C) Generic Pharmaceutical, Palisades Park, N.J.; (D) Western Research Laboratories, Denver, Colo.; (E) Travenol Laboratories, Deerfield, Ill.; (F) Carter-Glogau Laboratories, Glendale, Ariz. [b] Content uniformity by HPLC, mean; *RSD* in parentheses; number of units tested.

Reagents—Methanol[9], acetonitrile[9], phosphoric acid[10], and sodium hydroxide[11] were used as received. Deionized water was supplied by a commercial[12] water system. Samples and standards were prepared in 0.01 M sodium hydroxide in 50% methanol.

Standard Preparation—About 10 mg of USP levothyroxine reference standard was accurately weighed into a 50-mL volumetric flask, dissolved, and diluted to volume with 0.01 M methanolic sodium hydroxide. (This stock solution is stable for several weeks when refrigerated.) Two milliliters of this solution was pipetted into a 100-mL volumetric flask and diluted to volume with 0.01 M methanolic sodium hydroxide.

Sample Preparation—*Tablets*—One tablet was placed in a glass-stoppered flask and accurately diluted with 0.01 M methanolic sodium hydroxide to ~4 μg/mL. The flask was placed in an ultrasonic bath[13] until the tablet disintegrated; the tablet was then mechanically shaken[14] for 30 min. The solution was then filtered[15] into a vial for injection.

Powdered Composites and Lyophilized Injections—An accurately weighed portion of the powdered sample, equivalent to ~400 μg of sodium levothyroxine, was placed in a 100-mL volumetric flask. Fifty milliliters of 0.01 M methanolic sodium hydroxide was added, and the flask was placed in an ultrasonic bath for 1 min. The flask was shaken for 5 min; the contents were diluted to volume with 0.01 M methanolic sodium hydroxide and mixed well. The solution was then filtered[15] into a vial for injection.

Bulk Drug Substances—A sample of bulk drug substance was prepared in the same manner as the standard.

Determination—Fifty microliters each of the standard and sample solutions were injected into the liquid chromatograph, and the chromatograms were recorded. Sodium levothyroxine was calculated on the basis of peak areas.

RESULTS AND DISCUSSION

Linearity, Reproducibility, and Recovery—A series of validation tests were performed on the HPLC method. A linear response was obtained when four standard solutions containing from 1 to 8 μg/mL were tested. Placebo samples, based on the batch formulation of the manufacturers, were spiked with various levels of the standard. The recoveries ranged from 99.5 to 100.6%. The reproducibility of the method was determined by consecutively injecting 10 aliquots of standard solution. The *RSD* was 0.2%.

Decomposition and Stability Studies—In the course of the survey, it was found that the bulk drug substances were sensitive to the conditions of the USP drying procedure (60°C in a vacuum over P_2O_5). If the vacuum was not maintained below 10 mm Hg, sodium levothyroxine decomposed rapidly (10–15% in 4 h). Undried bulk drug samples were used in the analyses because of this problem, and corrections were made for moisture content. Figure 1 shows a chromatogram of sodium levothyroxine bulk drug dried in the presence of air. Some decomposition products can be seen in the chromatogram; these were not observed in the chromatograms of an unheated sample of sodium levothyroxine measured at the same sensitivity. In addition, there are probably other decomposition products in the heated sample which are not eluted from the column. The identity of these decomposition products will be investigated at a later time.

To test the stability of sodium levothyroxine in the sample solvent (0.01 M methanolic sodium hydroxide), solutions of the bulk drug samples were stored at 5°C and assayed periodically (*versus* freshly prepared reference standards) over a six month period. The assay values remained constant over the entire testing period, indicating little or no decomposition.

[9] Matheson, Coleman and Bell, Cincinnati, Ohio.
[10] NF Grade; Mallinckrodt Inc., St. Louis, Mo.
[11] AR Grade; Mallinckrodt Inc.
[12] Milli-Q; Millipore Corp.
[13] Model SC400T; Randall Mfg. Co., Inc., Hillside, N.J.
[14] Oscillating shaker; Eberbach Corp., Ann Arbor, Mich.
[15] Nylon-66, 13-mm diameter, 0.45-μm pore size; Rainin Instrument Co., Woburn, Mass.

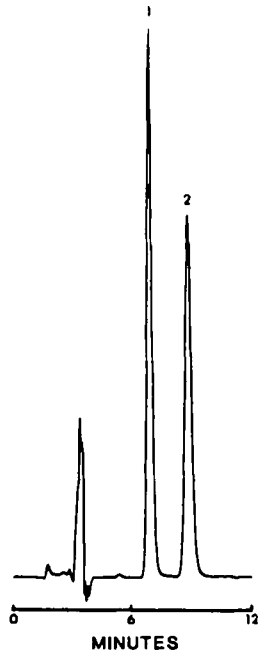

Figure 2—*Chromatogram of sodium levothyroxine and sodium liothyronine; detector at 229 nm and 0.02 AUFS. Key: (1) sodium liothyronine; (2) sodium levothyroxine, each at a level of ~4 μg/mL.*

The chromatographic system parameters were adequate to separate sodium levothyroxine from sodium liothyronine for testing the bulk drug substances for impurities; Fig. 2 shows a chromatogram of this separation. Liothyronine was found at levels of 0.04–0.96% in five sodium levothyroxine bulk drug samples analyzed by HPLC.

Sample Analysis—Table I lists the results obtained from survey by the HPLC procedure. A comparison of results for composite samples, obtained with the HPLC and the USP XX methods, shows that the latter gave a higher result in practically every case. This is not surprising since the USP XX assay is nonspecific for levothyroxine and measures total iodine content. However, the difference in assay values could not be totally accounted for by a total area summation of HPLC peaks. The major impurities and degradation products probably are not eluted from the column with this mobile phase.

Low assay values were a problem experienced by most manufacturers; this problem would not be recognized if the assays were based only on the results from the USP method. Some tablet composite samples gave suitable assay values for total iodine by the USP method, but gave extremely low assays for sodium levothyroxine by HPLC. All samples which gave low assay values by HPLC gave suitable assays by the USP method. This fact indicates that the problems of low assays of marketed sodium levothyroxine are, in all probability, attributable to sodium levothyroxine instability.

REFERENCES

(1) "The United States Pharmacopeia XX," U.S. Pharmacopeial Convention, Rockville, Md., 1980, pp. 446–447.

(2) B. L. Karger and S. C. Su, *J. Chromatogr. Sci.*, **12**, 678 (1974).

(3) F. Nachtmann, G. Knapp, and H. Spitzy, *J. Chromatogr.*, **149**, 693 (1978).

(4) M. T. W. Hearn, W. S. Hancock, and C. A. Bishop, *J. Chromatogr.*, **157**, 337 (1978).

(5) N. M. Alexander and M. Nishimoto, *Clin. Chem.*, **25**, 1757 (1979).

(6) R. S. Rapaka, P. W. Knight, V. P. Shah, and V. K. Prasad, *Anal. Lett.*, **12**, 1201 (1979).

(7) E. P. Lankmayr and K. W. Budna, *J. Chromatogr.*, **198**, 471 (1980).

(8) D. J. Smith and J. H. Graham, *J. Assoc. Off. Anal. Chem.*, **62**, 818 (1980).

(9) B. R. Hepler, S. G. Weber, and W. C. Purdy, *Anal. Chim. Acta*, **113**, 269 (1980).

(10) D. J. Smith, M. Biesmeyer, and C. Yaciw, *J. Chromatogr. Sci.*, **19**, 72 (1981).

(11) E. P. Lankmayr, B. Maichin, and G. Knapp, *J. Chromatogr.*, **224**, 239 (1981).

(12) I. D. Hay, T. M. Annesley, N. S. Jiang, and C. A. Gorman, *J. Chromatogr.*, **226**, 383 (1981).

(13) R. L. Garnick, G. F. Burt, F. R. Borger, J. P. Aldred, J. W. Bastian, and D. A. Long, in "Hormone Drugs, Proceedings of the FDA-USP Workshop on Drug and Reference Standards for Insulins, Somatropins, and Thyroid-Axis Hormones," U.S. Pharmacopeial Convention, Rockville, Md., 1983, pp. 504–516.

ACKNOWLEDGMENTS

The authors thank Dr. Thomas P. Layloff and Donald P. Page for assistance during the survey.

Determination of Isosorbide 5-Mononitrate in Human Plasma by Capillary Column Gas Chromatography

P. STRAEHL and R. L. GALEAZZI ˣ

Received February 22, 1983, from the *University of Bern, Department of Medicine, Inselspital, CH-3010 Bern, Switzerland.* Accepted for publication August 25, 1983.

Abstract □ An electron-capture gas chromatographic method for the determination of isosorbide 5-mononitrate in human plasma using a capillary column is described. Isosorbide 5-mononitrate and the internal standard (isosorbide dinitrate) are extracted from the alkalinized plasma with ether. The lower limit of detection for isosorbide 5-mononitrate is 1 ng/mL of plasma.

Keyphrases □ Gas chromatography—isosorbide 5-mononitrate, human plasma □ Isosorbide 5-mononitrate—GC, human plasma

Isosorbide 5-mononitrate [1,4:3,6-dianhydro-D-glucitol 5-nitrate (I)] is the primary metabolite of isosorbide dinitrate [1,4:3,6-dianhydro-D-glucitol dinitrate (II)] which has been used for many years in the treatment of angina pectoris and congestive heart failure. Recent studies of the hemodynamic effect of the mononitrate (1) indicate that, after acute administration, cardiac work load decreases at rest and during exercise. Pharmacokinetic studies (2–4) showed that the mononitrate is rapidly and completely absorbed from the GI tract without undergoing first-pass elimination. The maximum concentrations were reached within 1 h after oral administration, and the substance was eliminated with a half-life of ~4 h. Thus, the mononitrate has a half-life which is at least four times as long as the half-life of the dinitrate (5). Published gas chromatography (GC) assays (2, 6, 7), using older column

0022-3549/84/0900-1317$01.00/0
© 1984, American Pharmaceutical Association

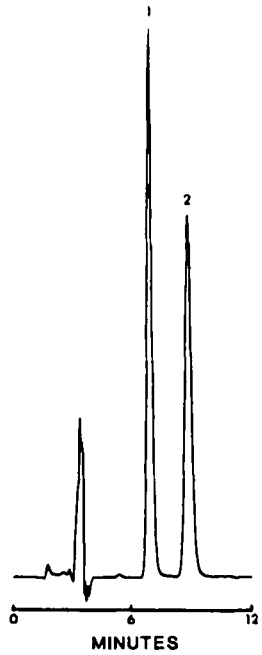

Figure 2—*Chromatogram of sodium levothyroxine and sodium liothyronine; detector at 229 nm and 0.02 AUFS. Key: (1) sodium liothyronine; (2) sodium levothyroxine, each at a level of ~4 μg/mL.*

The chromatographic system parameters were adequate to separate sodium levothyroxine from sodium liothyronine for testing the bulk drug substances for impurities; Fig. 2 shows a chromatogram of this separation. Liothyronine was found at levels of 0.04–0.96% in five sodium levothyroxine bulk drug samples analyzed by HPLC.

Sample Analysis—Table I lists the results obtained from survey by the HPLC procedure. A comparison of results for composite samples, obtained with the HPLC and the USP XX methods, shows that the latter gave a higher result in practically every case. This is not surprising since the USP XX assay is nonspecific for levothyroxine and measures total iodine content. However, the difference in assay values could not be totally accounted for by a total area summation of HPLC peaks. The major impurities and degradation products probably are not eluted from the column with this mobile phase.

Low assay values were a problem experienced by most manufacturers; this problem would not be recognized if the assays were based only on the results from the USP method. Some tablet composite samples gave suitable assay values for total iodine by the USP method, but gave extremely low assays for sodium levothyroxine by HPLC. All samples which gave low assay values by HPLC gave suitable assays by the USP method. This fact indicates that the problems of low assays of marketed sodium levothyroxine are, in all probability, attributable to sodium levothyroxine instability.

REFERENCES

(1) "The United States Pharmacopeia XX," U.S. Pharmacopeial Convention, Rockville, Md., 1980, pp. 446–447.

(2) B. L. Karger and S. C. Su, *J. Chromatogr. Sci.*, **12**, 678 (1974).

(3) F. Nachtmann, G. Knapp, and H. Spitzy, *J. Chromatogr.*, **149**, 693 (1978).

(4) M. T. W. Hearn, W. S. Hancock, and C. A. Bishop, *J. Chromatogr.*, **157**, 337 (1978).

(5) N. M. Alexander and M. Nishimoto, *Clin. Chem.*, **25**, 1757 (1979).

(6) R. S. Rapaka, P. W. Knight, V. P. Shah, and V. K. Prasad, *Anal. Lett.*, **12**, 1201 (1979).

(7) E. P. Lankmayr and K. W. Budna, *J. Chromatogr.*, **198**, 471 (1980).

(8) D. J. Smith and J. H. Graham, *J. Assoc. Off. Anal. Chem.*, **62**, 818 (1980).

(9) B. R. Hepler, S. G. Weber, and W. C. Purdy, *Anal. Chim. Acta*, **113**, 269 (1980).

(10) D. J. Smith, M. Biesmeyer, and C. Yaciw, *J. Chromatogr. Sci.*, **19**, 72 (1981).

(11) E. P. Lankmayr, B. Maichin, and G. Knapp, *J. Chromatogr.*, **224**, 239 (1981).

(12) I. D. Hay, T. M. Annesley, N. S. Jiang, and C. A. Gorman, *J. Chromatogr.*, **226**, 383 (1981).

(13) R. L. Garnick, G. F. Burt, F. R. Borger, J. P. Aldred, J. W. Bastian, and D. A. Long, in "Hormone Drugs, Proceedings of the FDA-USP Workshop on Drug and Reference Standards for Insulins, Somatropins, and Thyroid-Axis Hormones," U.S. Pharmacopeial Convention, Rockville, Md., 1983, pp. 504–516.

ACKNOWLEDGMENTS

The authors thank Dr. Thomas P. Layloff and Donald P. Page for assistance during the survey.

Determination of Isosorbide 5-Mononitrate in Human Plasma by Capillary Column Gas Chromatography

P. STRAEHL and R. L. GALEAZZI ˣ

Received February 22, 1983, from the *University of Bern, Department of Medicine, Inselspital, CH-3010 Bern, Switzerland.* Accepted for publication August 25, 1983.

Abstract □ An electron-capture gas chromatographic method for the determination of isosorbide 5-mononitrate in human plasma using a capillary column is described. Isosorbide 5-mononitrate and the internal standard (isosorbide dinitrate) are extracted from the alkalinized plasma with ether. The lower limit of detection for isosorbide 5-mononitrate is 1 ng/mL of plasma.

Keyphrases □ Gas chromatography—isosorbide 5-mononitrate, human plasma □ Isosorbide 5-mononitrate—GC, human plasma

Isosorbide 5-mononitrate [1,4:3,6-dianhydro-D-glucitol 5-nitrate (I)] is the primary metabolite of isosorbide dinitrate [1,4:3,6-dianhydro-D-glucitol dinitrate (II)] which has been used for many years in the treatment of angina pectoris and congestive heart failure. Recent studies of the hemodynamic effect of the mononitrate (1) indicate that, after acute administration, cardiac work load decreases at rest and during exercise. Pharmacokinetic studies (2–4) showed that the mononitrate is rapidly and completely absorbed from the GI tract without undergoing first-pass elimination. The maximum concentrations were reached within 1 h after oral administration, and the substance was eliminated with a half-life of ~4 h. Thus, the mononitrate has a half-life which is at least four times as long as the half-life of the dinitrate (5). Published gas chromatography (GC) assays (2, 6, 7), using older column

0022-3549/84/0900-1317$01.00/0
© 1984, American Pharmaceutical Association

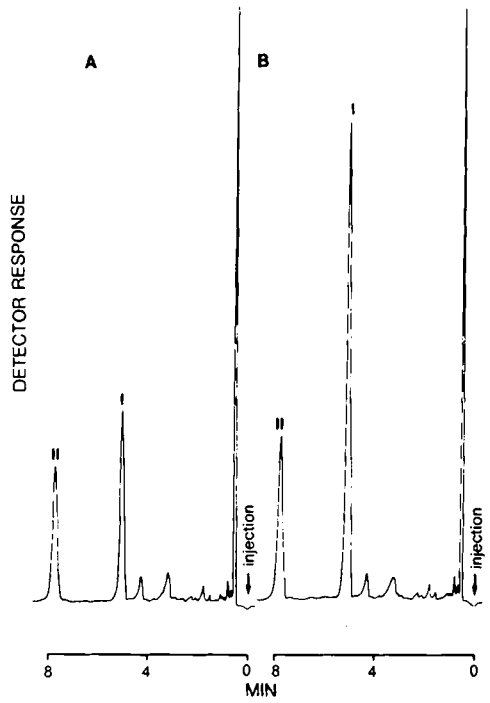

Figure 1—*Chromatograms of 1-mL human plasma extracts. Key: (A) plasma spiked with 25 ng of isosorbide 5-mononitrate (I) and 20 ng of isosorbide dinitrate (II); (B) plasma spiked with 50 ng of I and 20 ng of II.*

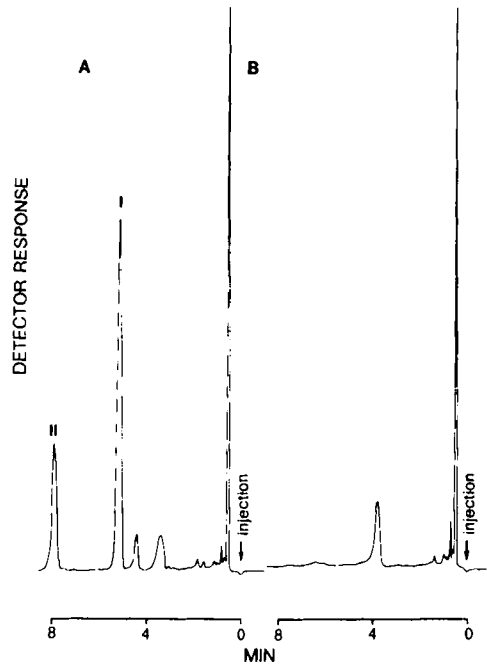

Figure 2—*Chromatograms of 1-mL plasma sample extracts obtained from a subject before (B) and 40 min after (A) an infusion of 5 mg of isosorbide 5-mononitrate; 20 ng of isosorbide dinitrate was added as the internal standard (A).*

coating or packing (OV-17, QF_1) and complicated extraction procedures, lack sufficient sensitivity and fail to give reproducible results.

EXPERIMENTAL SECTION

Apparatus—The analysis was performed on a GC[1] with a Grob-type, nonvaporizing, specially cooled on-column injector and equipped with a nickel-63 electron-capture detector.

Column—A wall-coated open tubular (WCOT) capillary column (16 m × 0.33 mm i.d.), with immobilized stationary phase SE-54[2], was used. Acidic leaching, silylation, and static coating, including immobilization, was carried out according to the method of Grob and Grob (8, 9). The film thickness was ~0.8 μm.

Reagents—The ethyl acetate[3] was pesticide grade, while the ether[3] and potassium carbonate[4] were analytical grade. Compounds I and II were used as received[5].

Instrumental Conditions—The carrier gas was helium with a flow rate of ~4 mL/min. The detector was operated with argon gas and 5% methane (v/v) at a flow rate of ~20 mL/min. The column was 160°C, the injector port was 200°C, and the electron-capture detector was 225°C. Direct on-column injection was used.

Procedure—Isosorbide dinitrate [the internal standard (20 ng in 50 μL of 0.9% NaCl)], 1 mL of patient plasma, 2 mL of saturated solution of potassium carbonate (pH 12.2), and 2 mL of ether were shaken in a 10-mL glass tube, with a polytef-lined screw cap, for 40 min at low speed (~25 rpm). After centrifugation (10 min at 4000 rpm) the organic phase was removed by aspiration in a conical tube. The solvent was evaporated to dryness under a gentle stream of nitrogen at room temperature. The residue was redissolved in 10–50 μL of ethyl acetate to give the desired concentration, and 0.4 μL of the solution was injected. All glassware was cleaned in an ultrasonic bath but not silanized; no plastic material was used.

Calibration—For calibration, human plasma (1 mL) was spiked with increasing concentrations of I (5–400 ng in 50 μL of 0.9% NaCl) and the internal standard, II (20 ng in 50 μL of 0.9% NaCl). Two milliliters of a saturated solution of potassium carbonate and 2 mL of ether were added to each solution. Extraction was performed as described above. The ratios of the peak heights of the mononitrate to the internal standard were plotted *versus* the concentrations of the mononitrate. Values of unknown plasma drug concentrations were determined from this calibration curve. Calibration chromatograms are shown in Fig. 1.

RESULTS AND DISCUSSION

This GC assay provides a method for determining I in plasma following a single extraction. A linear calibration curve, determined daily, was obtained for concentrations between 5 and 200 ng/mL of plasma. The mean slope was 0.058 ± 0.001 (peak height ratio/ng·mL^{-1} ± *SD*) and the mean intercept was 0.077 ± 0.09 (peak height ratio ± *SD*). The reproducibility from day-to-day analyses gave a coefficient of variation of 3.03% for 10 control plasma samples of 78 ng/mL of the mononitrate (78.71 ± 3.9), which were assayed on different days over 2 months. Within-day precision was assessed by analyses of five replicate plasma samples to which 10 and 50 ng/mL of I were added. The coefficients of variation were 1.6% for 10 ng (10.30 ± 0.165) and 1.49% for 50 ng (49.61 ± 0.793).

The use of a chemically similar drug as the internal standard, the quality of our column, and the on-column injection technique are probably the main reasons for the good reproducibility of the results. The attempted use of glyceryl trinitrate as internal standard was a failure because of its instability.

The recoveries for I and II were similar, varying between 70 and 75%. The retention times were 5.2 min for the mononitrate (mp 89°C) and 7.8 min for the dinitrate (mp 71°C). The lower limit of detection was ~1 ng/mL of plasma for the mononitrate and 0.5 ng/mL for the dinitrate. In some cases, small amounts of the mononitrate (<5 ng) were difficult to determine due to an unknown interfering peak. The use of peak height ratios was sufficient because the calibration curve passed through the origin and was linear up to 200 ng/mL. The column was washed every month with dichloromethane[3] and pentane[3], analytical grade.

Two chromatograms of human plasma extracts are shown in Fig. 2: a blank plasma extract and a plasma extract from the same subject 40 min after an infusion of 5 mg of the mononitrate. The dinitrate was added as an internal standard before analysis. Apart from an unknown peak with the retention time of 4.3 min (which always occurred), there is a second peak with about the same retention time as isosorbide 2-mononitrate (3.2 min). This peak, due to a contaminant in the internal standard, was eliminated later by recrystallization of isosorbide dinitrate.

Further investigations showed that this method could easily be adapted to determine the concentrations of the dinitrate and isosorbide 2-mononitrate by using the chemically similar substances isomannide dinitrate and isoidide dinitrate as internal standards, respectively. The use of pure solvents for ex-

[1] Fractovap 4160 series; Carlo Erba, Milano, Italy.
[2] Supelco, Bellefonte, Pa.
[3] Merck, Darmstadt, Federal Republic of Germany.
[4] Fluka, Buchs SG, Switzerland.
[5] A gift of the Schweizerische Sprengstoffabrik Dottikon, Switzerland.

traction and chromatography is essential for good results. The capillary column with an immobilized stationary phase and the possibility of solvent washing was also a big advantage in this assay.

REFERENCES

(1) W. Jansen, A. Osterspey, M. Tauchert, and H. Hilger, *Deut. Med. Wochenschr.*, **107**, 1499 (1982).

(2) T. Taylor, L. F. Chasseaud, R. Mayor, and E. Doyle, *Biopharm. Drug Dispos.*, **2**, 255 (1981).

(3) U. Abshagen, G. Betzien, R. Endele, and B. Kaufmann, *Eur. J. Clin. Pharmacol.*, **20**, 269 (1981).

(4) U. Abshagen and S. Spörl-Radun, *Eur. J. Clin. Pharmacol.*, **19**, 423 (1981).

(5) R. Platzer, G. Reutemann, and R. L. Galeazzi, *J. Pharmacokinet. Biopharm.*, **10**, 575 (1982).

(6) M. T. Rosseel and M. G. Bogaert, *J. Pharm. Sci.*, **68**, 659 (1979).

(7) E. Doyle, L. F. Chasseaud, and T. Taylor, *Biopharm. Drug Dispos.*, **1**, 141 (1980).

(8) K. Grob and G. Grob, *J. Chromatogr.*, **213**, 211 (1981).

(9) K. Grob and G. Grob, *J. Chromatogr.*, **244**, 197 (1982).

ACKNOWLEDGMENTS

The authors thank Prof. M. Soliva and Dr. G. Karlaganis for helpful advice during the development of this assay. The expert technical assistance of Mrs. L. Lüthi is kindly appreciated. This work was supported by a grant from the Swiss National Science Foundation and the Swiss Society of Cardiology.

Binding of Sulfadimethoxine to Isolated Human Blood Protein Fractions

J. W. HUBBARD *x, C. J. BRIGGS ‡, C. SAVAGE ‡, and D. SMITH ‡

Received January 24, 1983, from the **College of Pharmacy, University of Saskatchewan, Saskatoon, Saskatchewan, S7N 0W0, Canada* and the ‡*Faculty of Pharmacy, University of Manitoba, Winnipeg, Manitoba, R3T 2N2, Canada.* Accepted for publication September 8, 1983.

Abstract □ The binding of sulfadimethoxine to selected human blood protein fractions and to fresh serum has been examined by means of a new equilibrium dialysis technique which minimizes experimental error and permits the evaluation of low-level binding. Certain α-globulin fractions, containing mixtures of proteins, were found to bind the drug. Scatchard analysis of the binding of sulfadimethoxine to fresh serum, calculated as though all of the binding is due to albumin, gives a different result from that obtained with isolated albumin. This may be a reflection of the contribution of the α-globulins to the overall binding of sulfadimethoxine in fresh serum. Although sulfadimethoxine is amphoteric, it did not bind to the α_1-acid glycoprotein. The drug behaves as an acidic compound when binding to the blood proteins.

Keyphrases □ Sulfadimethoxine—blood fraction binding, equilibrium dialysis, humans □ Blood fraction binding—humans, sulfadimethoxine, equilibrium dialysis

Sulfadimethoxine is a long-acting sulfanilamide antibacterial drug which is extensively bound to the proteins of the blood (1, 2). It has been shown that the antibacterial activity and rate of metabolic *N*-acetylation of sulfanilamide drugs depend on the concentration of free, unbound drug in the plasma (3, 4). Nonlinearity in the pharmacokinetics of sulfadimethoxine has been associated with dose-dependent changes in the percentage of the drug bound to plasma proteins (5). Furthermore, the volume of distribution of sulfadimethoxine is altered significantly by small changes in the concentration of plasma albumin (6).

Albumin is the most important of the blood proteins in the binding of sulfanilamide drugs (2, 6–11), although the involvement of other plasma proteins has been implied (12). Sulfadimethoxine is an amphoteric compound (13) with an acidic center at the sulfonamide (pK_a 6.7) and a basic center at the aniline-like primary amino group (pK_b 11.98). The isoelectric point is at pH 4.36. Albumin is effective in binding acidic drugs such as warfarin (14–16), fenoprofen (17, 18) and phenylbutazone (19). Unlike these compounds, basic drugs such as imipramine (20), alprenolol (21), propranolol, (22) and lidocaine (23) bind significantly to α_1-acid glycoprotein and lipoproteins in addition to albumin. The individual contributions of different proteins to the binding of drugs becomes significant in disease states which lead to changes in the concentration of one or more of the blood proteins (24–27). The present study was undertaken to determine whether proteins other than albumin are involved in the overall binding of the amphoteric drug sulfadimethoxine.

The binding of sulfadimethoxine to isolated human plasma protein fractions was measured by a newly developed equilibrium dialysis technique (28). This method employs calibration and control procedures that minimize artifactual errors and permit statistical evaluation of control and test data. This stringent control technique also permits correction to be made for concentration-dependent binding to the dialysis membrane or other equipment; thus, it is possible to demonstrate statistically significant binding at low levels (<10%).

EXPERIMENTAL SECTION

Equilibrium dialysis was performed using 20-cm strips of dialysis tubing[1], 1-cm diameter, 4.8-nm pore diameter, with a molecular weight cut-off of 12,000. These membranes were immersed in boiling water and then stirred for 2 h as they cooled. The tubing was then stirred with 70% methanol for 30 min, stored in 50% methanol overnight, rinsed with distilled water, and soaked in phosphate buffer (pH 7.4) for 2–3 h prior to use. The membranes were used immediately after preparation. The tubing was tied with a double knot at one end, and then filled with 2 mL of protein solution in phosphate buffer (pH 7.4) containing sulfadimethoxine. The protein solutions were as follows: Cohn Fraction I (fibrinogen)[2] 0.34% (w/v); Cohn Fraction II (α-globulin)[3], 0.74% (w/v); Cohn Fraction IV-1 (α-globulin)[3], 0.81% (w/v); Cohn Fraction IV-4 (α-globulin)[3], 0.81% (w/v); Cohn Fraction V (albumin)[3], 4% (w/v); Cohn Fraction VI (α_1-acid glycoprotein)[3], 0.1% (w/v); lyophilized serum[3], 7.3%; and fresh serum[4], reduced to half volume by ultrafiltration. Except for the fresh serum, the protein solutions were prepared initially at double strength in buffer and then diluted with an equal volume of buffer containing sulfadimethoxine. The fresh serum, concentrated to half volume, was diluted with

[1] Fisher Scientific Co., Toronto, Ontario, Canada.
[2] ICN Pharmaceuticals Inc., Cleveland, Ohio.
[3] United States Biochemical Corp., Cleveland, Ohio.
[4] Collected from a healthy young-adult male volunteer.

0022-3549/84/0900-1319$01.00/0

© 1984, American Pharmaceutical Association

traction and chromatography is essential for good results. The capillary column with an immobilized stationary phase and the possibility of solvent washing was also a big advantage in this assay.

REFERENCES

(1) W. Jansen, A. Osterspey, M. Tauchert, and H. Hilger, *Deut. Med. Wochenschr.*, **107**, 1499 (1982).

(2) T. Taylor, L. F. Chasseaud, R. Mayor, and E. Doyle, *Biopharm. Drug Dispos.*, **2**, 255 (1981).

(3) U. Abshagen, G. Betzien, R. Endele, and B. Kaufmann, *Eur. J. Clin. Pharmacol.*, **20**, 269 (1981).

(4) U. Abshagen and S. Spörl-Radun, *Eur. J. Clin. Pharmacol.*, **19**, 423 (1981).

(5) R. Platzer, G. Reutemann, and R. L. Galeazzi, *J. Pharmacokinet. Biopharm.*, **10**, 575 (1982).

(6) M. T. Rosseel and M. G. Bogaert, *J. Pharm. Sci.*, **68**, 659 (1979).

(7) E. Doyle, L. F. Chasseaud, and T. Taylor, *Biopharm. Drug Dispos.*, **1**, 141 (1980).

(8) K. Grob and G. Grob, *J. Chromatogr.*, **213**, 211 (1981).

(9) K. Grob and G. Grob, *J. Chromatogr.*, **244**, 197 (1982).

ACKNOWLEDGMENTS

The authors thank Prof. M. Soliva and Dr. G. Karlaganis for helpful advice during the development of this assay. The expert technical assistance of Mrs. L. Lüthi is kindly appreciated. This work was supported by a grant from the Swiss National Science Foundation and the Swiss Society of Cardiology.

Binding of Sulfadimethoxine to Isolated Human Blood Protein Fractions

J. W. HUBBARD *[x], C. J. BRIGGS [‡], C. SAVAGE [‡], and D. SMITH [‡]

Received January 24, 1983, from the **College of Pharmacy, University of Saskatchewan, Saskatoon, Saskatchewan, S7N 0W0, Canada* and the [‡]*Faculty of Pharmacy, University of Manitoba, Winnipeg, Manitoba, R3T 2N2, Canada.* Accepted for publication September 8, 1983.

Abstract □ The binding of sulfadimethoxine to selected human blood protein fractions and to fresh serum has been examined by means of a new equilibrium dialysis technique which minimizes experimental error and permits the evaluation of low-level binding. Certain α-globulin fractions, containing mixtures of proteins, were found to bind the drug. Scatchard analysis of the binding of sulfadimethoxine to fresh serum, calculated as though all of the binding is due to albumin, gives a different result from that obtained with isolated albumin. This may be a reflection of the contribution of the α-globulins to the overall binding of sulfadimethoxine in fresh serum. Although sulfadimethoxine is amphoteric, it did not bind to the α_1-acid glycoprotein. The drug behaves as an acidic compound when binding to the blood proteins.

Keyphrases □ Sulfadimethoxine—blood fraction binding, equilibrium dialysis, humans □ Blood fraction binding—humans, sulfadimethoxine, equilibrium dialysis

Sulfadimethoxine is a long-acting sulfanilamide antibacterial drug which is extensively bound to the proteins of the blood (1, 2). It has been shown that the antibacterial activity and rate of metabolic *N*-acetylation of sulfanilamide drugs depend on the concentration of free, unbound drug in the plasma (3, 4). Nonlinearity in the pharmacokinetics of sulfadimethoxine has been associated with dose-dependent changes in the percentage of the drug bound to plasma proteins (5). Furthermore, the volume of distribution of sulfadimethoxine is altered significantly by small changes in the concentration of plasma albumin (6).

Albumin is the most important of the blood proteins in the binding of sulfanilamide drugs (2, 6–11), although the involvement of other plasma proteins has been implied (12). Sulfadimethoxine is an amphoteric compound (13) with an acidic center at the sulfonamide (pK_a 6.7) and a basic center at the aniline-like primary amino group (pK_b 11.98). The isoelectric point is at pH 4.36. Albumin is effective in binding acidic drugs such as warfarin (14–16), fenoprofen (17, 18) and phenylbutazone (19). Unlike these compounds, basic drugs such as imipramine (20), alprenolol (21), propranolol, (22) and lidocaine (23) bind significantly to α_1-acid glycoprotein and lipoproteins in addition to albumin. The individual contributions of different proteins to the binding of drugs becomes significant in disease states which lead to changes in the concentration of one or more of the blood proteins (24–27). The present study was undertaken to determine whether proteins other than albumin are involved in the overall binding of the amphoteric drug sulfadimethoxine.

The binding of sulfadimethoxine to isolated human plasma protein fractions was measured by a newly developed equilibrium dialysis technique (28). This method employs calibration and control procedures that minimize artifactual errors and permit statistical evaluation of control and test data. This stringent control technique also permits correction to be made for concentration-dependent binding to the dialysis membrane or other equipment; thus, it is possible to demonstrate statistically significant binding at low levels (<10%).

EXPERIMENTAL SECTION

Equilibrium dialysis was performed using 20-cm strips of dialysis tubing[1], 1-cm diameter, 4.8-nm pore diameter, with a molecular weight cut-off of 12,000. These membranes were immersed in boiling water and then stirred for 2 h as they cooled. The tubing was then stirred with 70% methanol for 30 min, stored in 50% methanol overnight, rinsed with distilled water, and soaked in phosphate buffer (pH 7.4) for 2–3 h prior to use. The membranes were used immediately after preparation. The tubing was tied with a double knot at one end, and then filled with 2 mL of protein solution in phosphate buffer (pH 7.4) containing sulfadimethoxine. The protein solutions were as follows: Cohn Fraction I (fibrinogen)[2] 0.34% (w/v); Cohn Fraction II (α-globulin)[3], 0.74% (w/v); Cohn Fraction IV-1 (α-globulin)[3], 0.81% (w/v); Cohn Fraction IV-4 (α-globulin)[3], 0.81% (w/v); Cohn Fraction V (albumin)[3], 4% (w/v); Cohn Fraction VI (α_1-acid glycoprotein)[3], 0.1% (w/v); lyophilized serum[3], 7.3%; and fresh serum[4], reduced to half volume by ultrafiltration. Except for the fresh serum, the protein solutions were prepared initially at double strength in buffer and then diluted with an equal volume of buffer containing sulfadimethoxine. The fresh serum, concentrated to half volume, was diluted with

[1] Fisher Scientific Co., Toronto, Ontario, Canada.
[2] ICN Pharmaceuticals Inc., Cleveland, Ohio.
[3] United States Biochemical Corp., Cleveland, Ohio.
[4] Collected from a healthy young-adult male volunteer.

0022-3549/84/0900-1319$01.00/0

© 1984, American Pharmaceutical Association

Table I—Sulfadimethoxine Binding

	Total Concentration of Sulfadimethoxine, nmol/mL				
	322.6	451.6	580.6	806.5	1096.8
Fresh serum					
% bound	95.9 ± 1.4[b]	96.9 ± 0.3	95.6 ± 0.5	92.1 ± 0.3	86.5 ± 0.4
nmole/mL bound	309.3 ± 4.4	437.4 ± 1.4	555.4 ± 2.7	742.9 ± 2.5	948.7 ± 4.7
Cohn Fraction V Albumin					
% bound	93.2 ± 0.5	90.5 ± 0.1[c]	87.2 ± 0.5	77.5 ± 0.3[c]	72.8 ± 0.04[b]
nmol/mL bound	300.7 ± 1.6	408.4 ± 0.6	506.4 ± 2.9	625.1 ± 2.2	798.8 ± 1.8
Cohn Fraction IV-1					
% bound	10.3 ± 1.1	11.8 ± 1.5	11.0 ± 1.3[d]	11.6 ± 0.8	13.7 ± 0.7
nmol/mL bound	33.2 ± 3.5	53.1 ± 6.9	64.2 ± 7.8	93.3 ± 6.5	150.3 ± 7.1
Cohn Fraction IV-4					
% bound	17.6 ± 0.8	16.0 ± 0.5	15.3 ± 1.1	12.2 ± 0.6	12.3 ± 1.0
nmol/mL bound	56.7 ± 2.4	72.4 ± 2.3	88.6 ± 6.4	98.6 ± 4.6	135.4 ± 11.1
Lyophilized serum					
% bound	17.8 ± 1.1[c]	20.8 ± 0.4	18.6 ± 0.8	16.6 ± 0.7	18.4 ± 0.4
nmol/mL bound	57.4 ± 3.5	93.7 ± 1.9	107.9 ± 4.9	133.7 ± 5.5	201.8 ± 4.2

[a] Unless otherwise noted each value is the mean of five replicates, ±*SE*; all values are significantly different from control values; $p < 0.001$. [b] $n = 3$. [c] $n = 4$. [d] $p < 0.01$.

an equal volume of buffer containing sulfadimethoxine. Albumin concentrations in fresh serum and lyophilized serum were measured by the method of Mancini *et al.* (29). The drug concentrations were 100, 140, 180, 250, and 340 μg/mL.

The following procedure was adopted for each of the solutions described above. The tubing was sealed and placed in a glass culture tube (16 × 125 mm) with a polytetrafluorethylene cap. Four milliliters of phosphate buffer (pH 7.4) were placed in each culture tube, and the solutions were dialyzed for 24 h at 37°C[5]. The tubes were rotated vertically through 360°, 12 times per minute using a rotary mixer[6]. The protein solution and dialysate were assayed for sulfadimethoxine using the Bratton-Marshall method (30), and absorbance was measured at 420 nm. Five replicates of each test concentration were dialyzed. A set of five controls was prepared for each sulfadimethoxine concentration studied and placed in the rotary mixer next to the test samples. Controls were identical to the test samples, except that the solution inside the dialysis membrane contained no protein. Glassware and buffer were autoclaved[7] prior to use. Preparation and transfer of solutions was carried out under aseptic conditions in a laminar airflow hood[8]. The dialysate was tested for the absence of protein visually (absence of frothing) and by means of a semiquantitative colorimetric indicator[9].

RESULTS AND DISCUSSION

For each of the protein-sulfadimethoxine systems described above, mean optical density values ($n = 5$) were calculated for tests and controls after dialysis. The percentage of binding was calculated for subtracting the mean test optical density from that of the control and expressing the result as a percentage of control, as previously described (28).

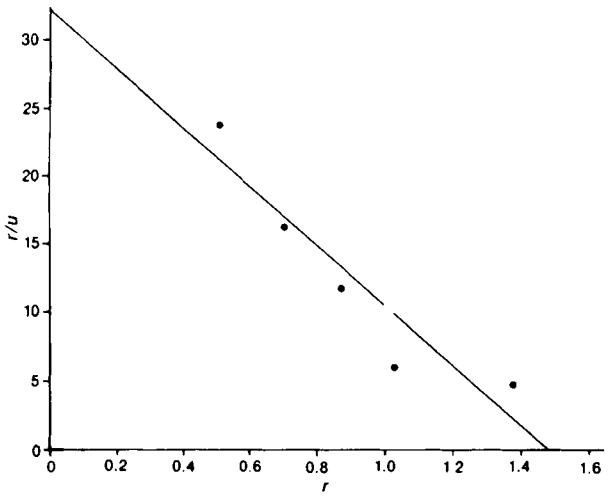

Figure 1—*A Scatchard plot of the binding of sulfadimethoxine to Cohn Fraction V albumin.*

There was a negative linear correlation between the concentration of sulfadimethoxine and the percentage binding to fresh serum (Table I; $y = -0.01316x + 102.0$; $r = -0.9475$, $p < 0.02$) and to isolated albumin (Table I; $y = -0.02807x + 102.5$; $r = 0.9863$, $p < 0.01$). This give the impression that the "degree of protein binding decreases with increasing concentration of sulfonamide" (3). However, the number of moles of sulfadimethoxine bound to fresh serum or to isolated albumin actually increased in a linear manner with increasing concentrations of drug (Table I; fresh serum: $y = 0.8223x + 62.97$; $r = 0.9978$, $p < 0.001$: albumin: $y = 0.6281x + 118.6$; $r = 0.9964$, $p < 0.001$). It is also important to realize that the concentration of free, unbound drug increased with total concentration of drug (fresh serum: $y = 0.1778x - 62.96$; $r = 0.9556$, $p < 0.02$; albumin: $y = 0.3719x - 118.6$; $r = 0.9899$, $p < 0.01$).

The results of the study of the binding of sulfadimethoxine to fresh serum (Table 1) are comparable to those published by Walker (1). Scatchard analysis (31) of the data was carried out in the same manner used by Walker who assumed that all of the binding was due to albumin (mol. wt. 69,000). In the present study, the concentration of albumin in the serum (44.25 mg/mL) was measured by radial immune diffusion (29). The five point linear regression equation ($y = -34361x + 61411$; $r = -0.8900$, $p < 0.05$) gave an x-axis intercept value of 1.8. A double reciprocal plot (32) derived from the same data ($y = 0.00002688x + 0.7377$; $r = 0.9893$, $p < 0.001$) gave a value of $n = 2.1$. This corresponds to the much quoted value of 2.0 binding sites for sulfadimethoxide per mole of albumin (1). In the study by Walker, the concentration of albumin in the serum was estimated to be 0.63 mM (43.47 mg/mL). Working from the published data (1), however, we obtained a value of 2.0 binding sites per mole only if we assumed the albumin concentration to be 40.00 mg/mL ($n = 2.1$ by Scatchard analysis; $n = 2.0$ by double reciprocal plot analysis).

In our studies on the binding of sulfadimethoxine to isolated albumin, the concentration of the protein was held constant at 40.00 mg/mL, an albumin concentration which is commonly employed in binding studies. The binding data cannot be compared directly because the isolated albumin was at a slightly different concentration from that in the fresh serum. The intercept values of Scatchard or reciprocal plot analysis can be compared, however, because these techniques are concerned with the number of moles of ligand bound per mole of protein. Therefore, if all the binding in serum was attributable to albumin, Scatchard plots of the respective data should give the same x-axis intercept value for serum as for isolated albumin. However, Scatchard analysis of the data (Table I), for the binding of sulfadimethoxine to isolated human albumin ($y = -22357x + 32829$; $r = 0.9511$, $p < 0.01$), gave an x-axis intercept value of 1.5. A double reciprocal plot derived from the same data ($y = 00002688x + 0.7377$; $r = 0.9893$, $p < 0.001$) gave a value of $n = 1.4$. There is a discrepancy between the corresponding values obtained with fresh serum, in the present study, and in the study by Walker (1). This suggests that (*a*) isolation of albumin from other serum constituents may alter the binding characteristics from those which prevail *in situ*, and/or (*b*) proteins other than albumin may be involved in the binding of the drug in serum.

The Scatchard plot (Fig. 1) of the binding of sulfadimethoxine to isolated albumin shows that the first four data points appear to fall on a straight line ($y = -31258x + 39244$; $r = -0.9958$, $p < 0.001$; x-axis intercept value 1.26), while the fifth point deviates considerably from this line. The study was not designed to investigate the binding of sulfisoxazole to albumin at high saturation, but the Scatchard plot does suggest that more than one binding site

[5] Thelco Model 4 Incubator; Fisher Scientific Co., Toronto, Ontario, Canada.
[6] Hematology/Chemistry Mixer Model 346; Fisher Scientific Co., Toronto, Ontario, Canada.
[7] Castle Autoclave; Fisher Scientific Co., Toronto, Ontario, Canada.
[8] Enviralab Sterility Module; Bio-Dynamics, Burlington, Ontario, Canada.
[9] Albustix; Ames Co. Division, Miles Laboratories, Rexdale, Ontario, Canada.

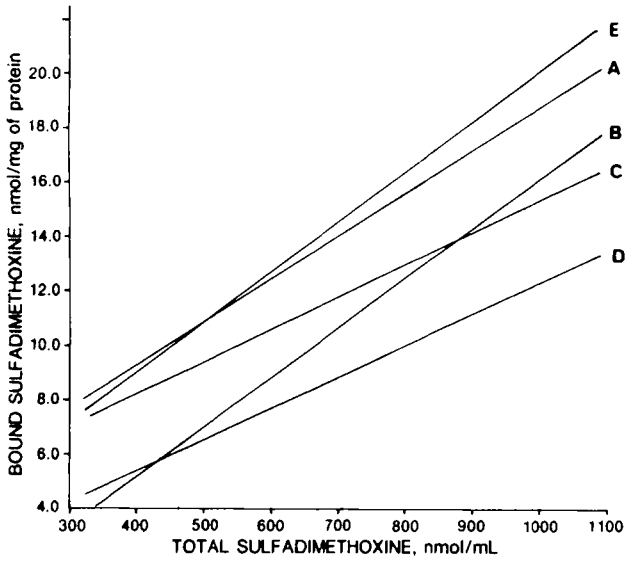

Figure 2—*The binding of sulfadimethoxine expressed in nmol/mg. Key: (A) Cohn Fraction V albumin,* $y = 0.01570x + 2.972$; $r = 0.9964$, $p < 0.001$. *(B) Cohn Fraction IV-1 α-globulin,* $y = 0.01817x - 2.1102$; $r = 0.9911$, $p < 0.01$, *(C) Cohn Fraction IV-4 α-globulin,* $y = 0.09612x + 27.69$; $r = 0.9883$, $p < 0.01$. *(D) Fresh serum, with calculations based on a total protein concentration of 72.5 mg/mL,* $y = 0.01133x + 0.8679$; $r = 0.9978$, $p < 0.001$. *(E) Fresh serum, calculated as if all the binding were due to albumin at a concentration of 44.25 mg/mL,* $y = 0.0186x + 1.422$; $r = 0.9978$, $p < 0.001$.

is involved. It is possible that at low saturation ($r < 1$), the drug binds primarily to a high affinity site, while at a higher saturation ($r > 1$), a lower affinity site will also bind sulfadimethoxine. At high saturation, however, the binding of the drug *in vivo* would be further complicated by the presence of other binding proteins.

Sulfadimethoxine showed low-level, but statistically significant, binding to two Cohn Fractions (33) of human plasma-serum, as shown in Table I. There were positive linear correlations between the concentration of sulfadimethoxine and the number of moles of the drug bound to Cohn Fraction IV-1 (α-globulin) ($y = 0.1472x - 17.0846$; $r = 0.9912$, $p < 0.001$) and to Cohn Fraction IV-4 (α-globulin) ($y = 0.09612x + 27.69$; $r = 0.9883$, $p < 0.01$). Unfortunately, it was not possible to carry out Scatchard analysis on these data because both α-globulin fractions are complicated mixtures of proteins (33), and there is no way of selecting a molecular weight with which to work.

Figure 2 suggests, however, that when the binding of sulfadimethoxine is expressed in terms of nanomoles bound per milligram of protein, the α-globulins have a significant capacity to bind the drug. Consequently, their contribution to the overall binding of the drug may be augmented in disease states, where plasma concentrations are elevated relative to albumin. Similar conclusions have been drawn about the role of lipoproteins in the overall binding of quinidine (34).

In Fig. 2, line E represents the binding of sulfadimethoxine to fresh serum, calculated as if all the binding were due to albumin alone. Line A represents the binding of the drug to isolated albumin. Note that the slopes of lines A and E are different and that there are larger discrepancies between binding values as the concentration of the drug increases. This may be an indication of increasing contributions by the α-globulin fractions (lines B and C) to the overall binding of the drug in serum as the concentration of sulfadimethoxine increases. Line D represents the binding of sulfadimethoxine to fresh serum based on the total concentration of protein in the serum (72.5 mg/mL). In this case, the values obtained are low because the binding proteins are diluted with protein materials which do not bind the drug.

There was no significant difference between tests and controls for the binding of sulfadimethoxine to Cohn Fractions I (fibrinogen), II (α-globulin), or VI (α_1-acid glycoprotein). These, and all of the other isolated protein fractions were comparable to their natural concentration ranges in the blood (35). Unfortunately, Cohn Fractions III^3 (β-globulin), and III-0^3 (β-lipoprotein) could not be reconstituted at or near physiological concentration and were, therefore, not examined.

Anomalous results were obtained when the binding of sulfadimethoxine to reconstituted lyophilized serum was examined. It was expected that the binding profile would be similar to that of fresh serum (Table 1), but the values obtained experimentally were ~20% of those of fresh serum. This discrepancy was undoubtedly due to low albumin concentration (15.50 mg/mL) in the reconstituted lyophilized serum. Total protein concentration was only 42 mg/mL (Biuret method), whereas normal fresh serum contains ~70 mg/mL of total protein (35).

In the experiment, care was taken to standardize the manipulative procedures in order to minimize experimental error. The use of tubes with polytetrafluoroethylene caps avoided the problem of plasticizers which can leach molecules from rubber or polyvinyl chloride-lined caps and cause displacement of drugs from protein binding sites (21, 36, 37). All solutions and glassware were sterilized before use, and solution transfers were made under aseptic conditions in a laminar airflow hood. This eliminated the possibility of microbial growth during dialysis and permitted the experiment to be conducted for 24 h without the use of preservatives, which could have influenced binding characteristics. All dialysates were checked for the absence of protein, both visually (absence of frothing) and by the use of a semiquantitative colorimetric indicator.

The concentration range of sulfadimethoxide was selected to include the reported plasma concentration obtained 4 h after an oral dose (38). Protein concentrations were held constant within normal physiological concentrations because binding parameters obtained with dilute albumin solutions have been shown to predict a higher degree of binding than those obtained by direct measurement (6–8). This phenomenon may be significant in disease states which cause hypoalbuminaemia (6), as may the role of minor binding proteins such as the α-globulins.

The plasma protein binding profile of sulfadimethoxine resembles that of an acidic drug although it is amphoteric. It did not bind to α_1-acid glycoprotein, which binds many basic drugs. This is presumably brought about by the predominance of the acidic center of sulfadimethoxine (pK_a 6.7) over the much weaker basic center (pK_b 11.98). Basic drugs, such as imipramine and propranolol, which binds strongly to α_1-acid glycoprotein, appear to have pK_b values which fall roughly within the range of 4–6. Presumably, the basic center of sulfadimethoxine is too weak to permit interaction with α_1-acid glycoprotein.

CONCLUSIONS

Sulfadimethoxine is an amphoteric drug which behaves like an acidic compound in its serum protein binding profile. Albumin is the protein largely responsible for the binding of the drug in blood, although there is also a significant amount of α-globulin binding of sulfadimethoxine in fresh serum.

REFERENCES

(1) S. R. Walker, *J. Pharm. Pharmacol.*, **22,** 574 (1970).

(2) T. Nishihata, N. Yata, and A. Kamada, *Chem. Pharm. Bull.*, **26,** 3353 (1978).

(3) B. B. Newbould and R. Kilpatrick, *Lancet*, *i*, 887 (1960).

(4) A. H. Anton, *J. Pharmacol. Exp. Ther.*, **129,** 282 (1960).

(5) O. Ladefoged, *Acta Pharmacol. Toxicol.*, **43,** 43 (1978).

(6) O. Ladefoged, *Acta Pharmacol. Toxicol.*, **43,** 174 (1978).

(7) H. Miese, W. E. Müller, and U. Wollert, *Arch. Int. Pharmacodyn. Ther.*, **236,** 18 (1978).

(8) S. W. Boobis and C. F. Chignell, *Biochem. Pharmacol.*, **28,** 751 (1979).

(9) R. Zini, P. d'Athis, A. Hoareau, and J. P. Tillement, *Eur. J. Clin. Pharmacol.*, **10,** 139 (1976).

(10) T. Fujita, *J. Med. Chem.*, **15,** 1049 (1972).

(11) R. Elofsson, S. O. Nilsson, and B. Kluczykowska, *Acta Pharm. Suec.*, **1,** 473 (1970).

(12) J. Clausen, *J. Pharmacol. Exp. Ther.*, **153,** 167 (1966).

(13) A. Suzuki, W. I. Higuchi, and N. F. H. Ho, *J. Pharm. Sci.*, **59,** 651 (1970).

(14) R. A. O'Reilly, *J. Clin. Invest.*, **48,** 193 (1969).

(15) R. A. O'Reilly, *Ann. N.Y. Acad. Sci.*, **226,** 293 (1973).

(16) R. A. O'Reilly, *Mol. Pharmacol.*, **7,** 209 (1971).

(17) J. H. Perrin, *J. Pharm. Pharmacol.*, **25,** 208 (1975).

(18) A. Rubin, P. Warrick, R. L. Wolen, S. M. Chernish, A. S. Ridolfo, and C. M. Gruber, *J. Pharmacol. Exp. Ther.*, **183,** 449 (1972).

(19) C. F. Chignell, *Mol. Pharmacol.*, **5,** 244 (1969).

(20) M. L. Kornguth, L. G. Hutchins, and B. S. Eichelman, *Biochem. Pharmacol.*, **30,** 2435 (1981).

(21) O. Borgå, K. M. Piafsky, and D. G. Nilsen, *Clin. Pharmacol. Ther.*, **22,** 539 (1977).

(22) G. Sager, D. G. Nilsen, and S. Jacobsen, *Biochem. Pharmacol.*, **28,** 905 (1979).

(23) P. A. Routledge, D. G. Shand, A. Barchowsky, G. Wagner, and W. W. Stargel, *Clin. Pharmacol. Ther.*, **30,** 154 (1981).

(24) J. P. Tillement, F. Lhoste, and J. F. Guidicelli, *Clin. Pharmacokinet.*, **3**, 144 (1978).
(25) R. Varma, A. Y. Hoshino, and J. R. Veraellotti, *Carbohydr. Res.*, **82**, 343 (1980).
(26) K. M. Piafsky, *Clin. Pharmacokinet.*, **5**, 246 (1980).
(27) I. Sjöholm, A. Kober, I. Odar-Cederlof, and O. Borgå, *Biochem. Pharmacol.*, **25**, 1205 (1976).
(28) C. J. Briggs, J. W. Hubbard, C. Savage, and D. Smith, *J. Pharm. Sci.*, **72**, 918 (1983).
(29) G. Mancini, A. O. Carbonara, and J. F. Heremans, *Immunochemistry* **2**, 235 (1965).
(30) A. C. Bratton and E. K. Marshall, *J. Biol. Chem.*, **128**, 537 (1939).
(31) G. Scatchard, *Ann. N.Y. Acad. Sci.*, **51**, 660 (1949).
(32) I. M. Klotz, *Arch. Biochem.*, **9**, 109 (1946).
(33) E. J. Cohn, L. E. Strong, W. L. Hughes Jr., D. J. Mulford, J. W. Ashworth, M. Melin, and H. L. Taylor, *J. Am. Chem. Soc.*, **68**, 459 (1946).
(34) R. E. Kates, T. D. Sokoloski, and T. J. Comstock, *Clin. Pharmacol. Ther.*, **23**, 30 (1977).
(35) "Geigy Scientific Tables," 7th ed. J. R. Geigy, S. A., Basel, Switzerland, (1970).
(36) K. K. Midha, J. K. Cooper, Y. D. Lapierre, and J. W. Hubbard, *Can. Med. J.*, **124**, 264 (1980).
(37) M. W. Wiegand, K. L. Hintze, J. T. Slattery, and G. Levy, *Clin. Pharmacol. Ther.*, **27**, 297 (1980).
(38) J. A. Prior and S. Saslaw, *J. Lab. Clin. Med.*, **38**, 420 (1951).

ACKNOWLEDGMENTS

The authors acknowledge financial support from the University of Manitoba Research Board and the Medical Research Council of Canada for the award of a summer studentship to Catherine Savage. The authors are grateful to Dr. A. D. Friesen of the Winnipeg Rh Institute Inc., Winnipeg, Manitoba, Canada, for the measurement of protein concentrations and for helpful discussions.

Degradation of Crystalline Ergocalciferol [Vitamin D_2, (3β,5*Z*,22*E*)-9,10-Secoergosta-5,7,10(19),22-tetraen-3-ol]

B. A. STEWART, S. L. MIDLAND, and S. R. BYRN ˣ

Received June 15, 1981, from the *Department of Medicinal Chemistry and Pharmacognosy, School of Pharmacy and Pharmacal Sciences, Purdue University, West Lafayette, IN 47907.* Accepted for publication October 17, 1983.

Abstract □ The products of the degradation of crystalline ergocalciferol were investigated. These studies showed that numerous acidic and neutral oxidation products were formed resulting in the complete destruction of the triene functionality. Separation of the neutral products by preparative TLC led to material identified as the Windaus ketone IIa, 2,3,3a,4,5,6,7,7aβ-octahydro-7aα-methyl-1*R*-(1α,1*R*,4*R*,5-trimethyl-2*E*-hexenyl)-4*H*-inden-4-one.

Keyphrases □ Ergocalciferol—crystal degradation products, liquid chromatography, identification of a Windaus ketone □ Liquid chromatography—determination of the crystal degradation products of ergocalciferol

Solid-gas reactions are often catalyzed by heat and/or light; thus, these reactions are of importance when studying the mechanism of drug degradation (1-6). This paper reports studies on a specific class of solid-gas reactions: solid-oxygen reactions. A review (1) reports our preliminary studies on the complex heat- and light-catalyzed solid-oxygen reactions of vitamin D_2, ergocalciferol (Ia). This paper presents these studies in greater detail.

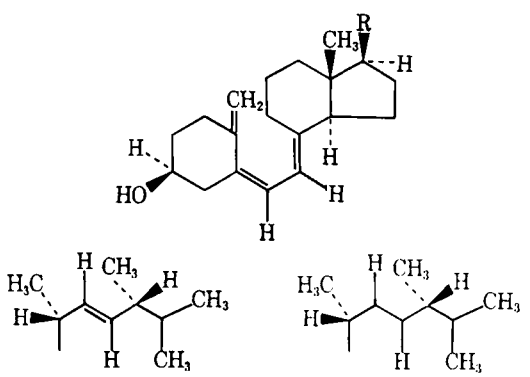

Ia, R = Ib, R =

The oxidative degradation of ergocalciferol has been known for over 40 years (7-11); however, the structures of the solid-state degradation products have not been elucidated. Thus, it is the aim of this study to isolate and unequivocally identify these products. Initially, the decomposition of ergocalciferol in room fluorescent light and air was investigated, resulting in the identification of the Windaus ketone (IIa).

EXPERIMENTAL SECTION

Reagents—Ergocalciferol[1] purchased in sealed ampules was used in all experiments. All reagents employed were of either reagent, spectral, or ACS grade. Methanol used in recrystallization of compounds was purified by reflux with magnesium and iodine followed by distillation over molecular sieves.

Apparatus—All melting points were obtained on a hot stage[2] and are uncorrected. IR spectra[3] were determined neat or as KBr pellets. NMR spectra were obtained using a 60-MHz instrument[4] with either $CDCl_3$ or acetone-d_6 as the solvent and 1% tetramethylsilane as the internal standard. Low-[5] and

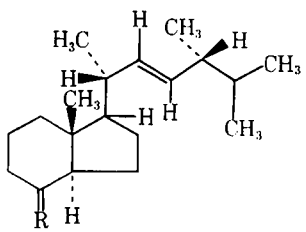

Ia, R = 0
Ib, R = NNHCONH$_2$

[1] Sigma Chemical Co., St. Louis, Mo.
[2] Kofler Hot Stage.
[3] Beckman IR-33; Beckman Instruments, Irvine, Calif.
[4] Varian Anaspect EM 360; Varian Associates, Palo Alto, Calif.
[5] Determined by Dr. I. Jardine and associates using a DuPont 21-492B mass spectrometer.

0022-3549/84/0900-1322$01.00/0
© 1984, American Pharmaceutical Association

(24) J. P. Tillement, F. Lhoste, and J. F. Guidicelli, *Clin. Pharmacokinet.*, **3**, 144 (1978).
(25) R. Varma, A. Y. Hoshino, and J. R. Veraellotti, *Carbohydr. Res.*, **82**, 343 (1980).
(26) K. M. Piafsky, *Clin. Pharmacokinet.*, **5**, 246 (1980).
(27) I. Sjöholm, A. Kober, I. Odar-Cederlof, and O. Borgå, *Biochem. Pharmacol.*, **25**, 1205 (1976).
(28) C. J. Briggs, J. W. Hubbard, C. Savage, and D. Smith, *J. Pharm. Sci.*, **72**, 918 (1983).
(29) G. Mancini, A. O. Carbonara, and J. F. Heremans, *Immunochemistry* **2**, 235 (1965).
(30) A. C. Bratton and E. K. Marshall, *J. Biol. Chem.*, **128**, 537 (1939).
(31) G. Scatchard, *Ann. N.Y. Acad. Sci.*, **51**, 660 (1949).
(32) I. M. Klotz, *Arch. Biochem.*, **9**, 109 (1946).
(33) E. J. Cohn, L. E. Strong, W. L. Hughes Jr., D. J. Mulford, J. W. Ashworth, M. Melin, and H. L. Taylor, *J. Am. Chem. Soc.*, **68**, 459 (1946).
(34) R. E. Kates, T. D. Sokoloski, and T. J. Comstock, *Clin. Pharmacol. Ther.*, **23**, 30 (1977).
(35) "Geigy Scientific Tables," 7th ed. J. R. Geigy, S. A., Basel, Switzerland, (1970).
(36) K. K. Midha, J. K. Cooper, Y. D. Lapierre, and J. W. Hubbard, *Can. Med. J.*, **124**, 264 (1980).
(37) M. W. Wiegand, K. L. Hintze, J. T. Slattery, and G. Levy, *Clin. Pharmacol. Ther.*, **27**, 297 (1980).
(38) J. A. Prior and S. Saslaw, *J. Lab. Clin. Med.*, **38**, 420 (1951).

ACKNOWLEDGMENTS

The authors acknowledge financial support from the University of Manitoba Research Board and the Medical Research Council of Canada for the award of a summer studentship to Catherine Savage. The authors are grateful to Dr. A. D. Friesen of the Winnipeg Rh Institute Inc., Winnipeg, Manitoba, Canada, for the measurement of protein concentrations and for helpful discussions.

Degradation of Crystalline Ergocalciferol [Vitamin D_2, (3β,5*Z*,22*E*)-9,10-Secoergosta-5,7,10(19),22-tetraen-3-ol]

B. A. STEWART, S. L. MIDLAND, and S. R. BYRN ˣ

Received June 15, 1981, from the *Department of Medicinal Chemistry and Pharmacognosy, School of Pharmacy and Pharmacal Sciences, Purdue University, West Lafayette, IN 47907.* Accepted for publication October 17, 1983.

Abstract □ The products of the degradation of crystalline ergocalciferol were investigated. These studies showed that numerous acidic and neutral oxidation products were formed resulting in the complete destruction of the triene functionality. Separation of the neutral products by preparative TLC led to material identified as the Windaus ketone IIa, 2,3,3a,4,5,6,7,7aβ-octahydro-7aα-methyl-1*R*-(1α,1*R*,4*R*,5-trimethyl-2*E*-hexenyl)-4*H*-inden-4-one.

Keyphrases □ Ergocalciferol—crystal degradation products, liquid chromatography, identification of a Windaus ketone □ Liquid chromatography—determination of the crystal degradation products of ergocalciferol

Solid-gas reactions are often catalyzed by heat and/or light; thus, these reactions are of importance when studying the mechanism of drug degradation (1-6). This paper reports studies on a specific class of solid-gas reactions: solid-oxygen reactions. A review (1) reports our preliminary studies on the complex heat- and light-catalyzed solid-oxygen reactions of vitamin D_2, ergocalciferol (Ia). This paper presents these studies in greater detail.

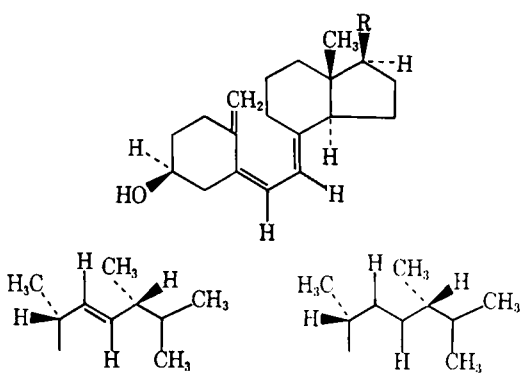

Ia, R = Ib, R =

The oxidative degradation of ergocalciferol has been known for over 40 years (7-11); however, the structures of the solid-state degradation products have not been elucidated. Thus, it is the aim of this study to isolate and unequivocally identify these products. Initially, the decomposition of ergocalciferol in room fluorescent light and air was investigated, resulting in the identification of the Windaus ketone (IIa).

EXPERIMENTAL SECTION

Reagents—Ergocalciferol[1] purchased in sealed ampules was used in all experiments. All reagents employed were of either reagent, spectral, or ACS grade. Methanol used in recrystallization of compounds was purified by reflux with magnesium and iodine followed by distillation over molecular sieves.

Apparatus—All melting points were obtained on a hot stage[2] and are uncorrected. IR spectra[3] were determined neat or as KBr pellets. NMR spectra were obtained using a 60-MHz instrument[4] with either $CDCl_3$ or acetone-d_6 as the solvent and 1% tetramethylsilane as the internal standard. Low-[5] and

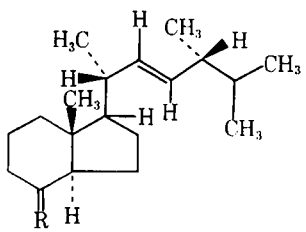

Ia, R = 0
Ib, R = NNHCONH$_2$

[1] Sigma Chemical Co., St. Louis, Mo.
[2] Kofler Hot Stage.
[3] Beckman IR-33; Beckman Instruments, Irvine, Calif.
[4] Varian Anaspect EM 360; Varian Associates, Palo Alto, Calif.
[5] Determined by Dr. I. Jardine and associates using a DuPont 21-492B mass spectrometer.

0022-3549/84/0900-1322$01.00/0
© 1984, American Pharmaceutical Association

high-resolution[6] mass spectra were determined using mass spectrometers operated in both the electron-impact and chemical-ionization modes.

Chromatography—Thin-layer silica gel chromatography plates containing fluorescent indicator[7] were used. Mixtures were applied to the preparative layer silica gel chromatography plates[8] with an applicator[9].

Synthesis of 2,3,3a,4,5,6,7,7aβ-octahydro-7aα-methyl-1*R*-(1α,1*R*,4*R*,5-trimethyl-2*E*-hexenyl)-4*H*-inden-4-one (IIa) and Its Semicarbazone (IIb)—Compounds IIa and IIb were synthesized according to the procedure of Windaus and Grundman (12). Compound IIb was crystallized as a white solid, mp 222°C [lit. (12) mp 222°C]; IR (KBr): 3440, 3240, 3170 (NHC=O amide), 1680 (primary amide), 1570 (secondary amide), and 960 cm^{-1} (*trans* RHC=CHR); ^{1}H-NMR (acetone-d_6): δ 0.57 (s, 3, C-18 CH_3), 0.80 (d, 6, C-26,27 CH_3), 0.90 (d, 3, C-28 CH_3), 1.1 (d, 3, C-21 CH_3), 1.1–2.9 (m, 15), 5.2 (m, 2, 22-H, 23-H), 5.6 (d, 2, H_2N—C=O), and 8.2 ppm (s, 1, HNC=O); MS: *m/z* 333 (M^+, 58%).

Anal.—Calc. for $C_{20}H_{35}N_3O$: C, 72.03; H, 10.57; N, 12.60; O, 4.80. Found: C, 71.91; H, 10.68; N, 12.80[10].

Degradation of Ergocalciferol in the Solid State—The experiments, performed in triplicate by different investigators at different times of the year, led to similar results. Crystalline ergocalciferol from a newly opened refrigerated ampule was spread in a petri dish and left exposed to artificial light and room air (with average humidity, room temperature, and atmospheric pressure). The colorless needles gradually changed to an orange powder. The IR and NMR spectra of the degrading compound gradually changed for the first 6 months and then remained unchanged after 6 months.

A sample of ergocalciferol (0.81 g), which had been stored for 6 months at room temperature, chloroform (150 mL), and a 10% $NaHCO_3$ solution (150 mL) were stirred for 5 min at room temperature. The organic phase was removed at reduced pressure. Thin-layer chromatography of the residue [cyclohexane–ethyl acetate–chloroform–acetic acid (5:2:1:1)] indicated three fractions ($R_f \times 100$: 0, 31, 53):

1. Material *A* R_f (× 100) 0; 0.038 g; 46% of the recovered material was an amber oil that could not be crystallized. IR (neat): 3400 (broad), 1700 (C=O, broad), and 1620 cm^{-1} (C=C); MS (C.I.): *m/z* 309 (5.7%), 279 (11.0), 153 (11.0), 143 (28.0), and 91 (100.0).
2. Material *B* R_f (× 100) 31; 0.023 g; 28% of the recovered material was an amber oil that could not be crystallized. IR (neat): 3400 (ROH), 1710 (C=O, broad), and 1620 cm^{-1} (C=C); MS (C.I.): *m/z* 309 (40.5%), 307 (33.8), 294 (22.3), 293 (100.0), 292 (24.3), 291 (86.5), 279 (27.0), 275 (72.3), and 125 (21.6).
3. Material *C* R_f (× 100) 53; 0.021 g; 26% of the recovered material was an amber oil that could not be crystallized. IR (neat): 2490 (C—H), 1700 (C=O), and 1630 cm^{-1} (C=C); MS (C.I.): *m/z* 209 (11.3%), 278 (22.6), and 277 (100). The exact mass of the 276 peak was determined to be 276.247.

Material *C* and IIa co-chromatographed on silica gel plates using a three solvent system: cyclohexane–ethyl acetate chloroform–glacial acetic acid (5:2:1:1); chloroform–methanol (9:1); and ethanol.

Preparation of the Semicarbazone Derivative of Material *C*—A mixture of material *C* (0.04 g), semicarbazide hydrochloride (0.26 g, 0.002 mol), sodium acetate (0.41 g, 0.01 mol), and methanol (10 mL) was heated to a reflux temperature in an 80°C oil bath. Water (0.5 mL) was added dropwise over a 5 min period. The mixture was refluxed for 0.5 h, then cooled. Recrystallization of the material from methanol gave a white crystalline solid (0.005 g), mp 220°C, the IR spectrum (KBr) of which was identical to that of the aforementioned semicarbazone, IIb.

[6] Determined by the Purdue University Spectral Services Department using a Hitachi RMV-6A mass spectrometer.

[7] Silica Gel 60 F-254 plates, 0.25 mm; E. Merck A. G., Darmstadt, West Germany.

[8] Silica Gel GF Prep Pre-Coat plates, 1.0 mm; Camag, Inc., Milwaukee, Wis.

[9] Kontes Chromaflex Streaker; Kontes Glass Co., Vineland, N.J.

[10] Microanalyses were performed by Dr. C. S. Yeh and associates, Purdue University, West Lafayette, Ind.

RESULTS AND DISCUSSION

Degradation of ergocalciferol in ordinary fluorescent light at average room temperature and humidity results in the oxidation and fragmentation of the triene functionality. The ^{1}H-NMR spectrum of degraded ergocalciferol showed that the peaks assigned to the vinyl protons of the triene system at δ 4.7, 5.0, 5.94, and 6.14 ppm had disappeared while the peaks assigned to the vinyl protons of the C-22 to C-23 olefinic bond remained unchanged (13). In addition, carbonyl absorption appeared in the IR spectrum of the degraded material. In the NMR spectrum the peak attributed to the C-18 CH_3 absorption had decreased in intensity and shifted downfield. A broad, D_2O exchangeable peak, appeared between δ 3.3 and 5.38 ppm.

The degraded material *C* can be identified as IIa based on co-chromatography and the preparation of the semicarbazone derivative which had the same melting point and IR spectrum as the semicarbazone derivative of authentic IIa. Material *B* appeared to contain two components with structures similar to IIa. The high-resolution MS indicate that these components correspond to IIa with one or two hydrogen atoms replaced by hydroxyl groups. These two components have so far resisted complete characterization.

These results are consistent with literature reports which indicate that in air and light crystalline ergocalciferol decomposes, while storage under vacuum results in increased stability (7–9, 11). The extensive oxidation observed in our studies does not rule out other nonoxidative pathways of degradation, but it does indicate that oxidation is the major pathway of ergocalciferol degradation.

The nucleus of the ergocalciferol molecule undergoes extensive oxidation; however, the side chain appears to remain intact. This may be due to the lesser reactivity of the side-chain olefin and to the crystal packing which promotes oxidation of the ergocalciferol nucleus. Preliminary studies of cholecalciferol (Ib) degradation indicate this compound to be much more stable, confirming earlier reports (14). The greater stability exhibited by cholecalciferol may be due to different crystal packing. Recently, studies of hydrocortisone *tert*-butyl acetate have shown that different crystal forms have different reactivity towards oxygen, presumably because of different crystal packing (15). Crystals of cholecalciferol may also contain fewer defects or sites for potential nucleation, therefore being more stable.

REFERENCES

(1) S. R. Byrn, *J. Pharm. Sci.*, **65,** 1 (1976).

(2) I. C. Paul and D. Y. Curtin, *Science*, **187,** 19 (1975).

(3) S. R. Byrn and C. T. Lin, *J. Am. Chem. Soc.*, **98,** 4004 (1976).

(4) C. T. Lin and S. R. Byrn, *Mol. Cryst. Liq. Crystalogr.*, **50,** 99 (1979).

(5) R. J. Clay, A. M. Knevel, and S. R. Byrn, *J. Pharm. Sci.*, **71,** 1289 (1982).

(6) S. R. Byrn, "Solid State Chemistry of Drugs," Academic, New York, N.Y., 1982.

(7) W. Huber and O. W. Barlow, *J. Biol. Chem.*, **149,** 125 (1943).

(8) T. Kanzawa and S. Kolak, *J. Pharm. Soc. Jpn.*, **73,** 1357 (1953).

(9) L. Fuchs and J. Van Niekirk, *Biochemistry 2*, **277,** 32 (1935).

(10) V. A. Dovyatnin and V. I. Koltanova, *Tr. Vses. Nauch. Issled. Vitamin Inst.*, **6,** 128 (1959); *Chem. Abstr.*, **55,** 14829a (1961).

(11) M. M. Amer, A. K. S. Ahmad, and S. P. Varda, *Zette Seifen Anstrichm.*, **s72,** 1040 (1970).

(12) A. Windaus and W. Grundmann, *Ann. Chemie*, **524,** 295 (1936).

(13) R. M. Wing, A. W. Okamura, A. Rego, M. R. Pirio, and A. W. Norman, *Science*, **186,** 939 (1974).

(14) L. T. Grady and K. D. Thakker, *J. Pharm. Sci.*, **69,** 1099 (1980).

(15) C. T. Lin, P. Perrier G. G. Clay, P. A. Sutton, and S. R. Byrn, *J. Org. Chem.*, **47,** 2978 (1982).

ACKNOWLEDGMENTS

This research was supported by NIH Grant GM21174.

Instrumentation of a Tablet Breaking-Strength Tester

RALPH E. BERTERMANN ˣ, MARK E. ADAMS, JOHN WARNER, and MERRIL SINGLETERRY

Received May 16, 1983, from the *Searle Research and Development Division, G. D. Searle & Co., 4901 Searle Parkway, Skokie, IL 60077.* Accepted for publication August 18, 1983.

Abstract □ The instrumentation of a tablet breaking-strength tester, for the automatic recording of hardness values, is described. A comparison is made between a computerized hardness tester and another identical model hardness tester from the same manufacturer ("standard"). Three lots of placebo tablets at different hardness values were compared. No significant difference was observed between the computerized unit compared with the "standard" unit.

Keyphrases □ Tablet-hardness tester—computerized *versus* unaltered models □ Breaking strength—tablets, computerized *versus* unaltered hardness values

The measurement and recording of tablet-hardness values is an important and necessary measurement during the processing of tablets. This project was initiated with the purpose of automating the measurement process in order to allow more measurements to be taken in a given period of time, to eliminate the chances of operator error and bias, and to incorporate the data automatically in a data base for long term storage and statistical treatment.

EXPERIMENTAL SECTION

The hardness tester[1] (Fig. 1), consists of the following: a rotary shaft encoder[2], a tablet-break signal, filters and a gate, and a microcomputer[3]. A table of values was programmed into the computer relating input counts to hardness values. The test button on the hardness tester was pushed to start the hardness measurement cycle. This opened a gate which allowed pulses from the rotary shaft encoder attached to the counterweight shaft, to enter the microcomputer. When the tablet broke, the signal generated by the hardness tester was to turn off the shaft encoder gate. The hardness value of the tablet was then locally displayed and sent to a terminal or computer.

Placebo tablet hardness values obtained over the working range of the instrument were: 5 kiloponds (kp) for round tablets, 10 kp for oval tablets, and 15 kp for capsule-shaped tablets. These tablets were used to validate the computerized tablet-hardness tester. Prior to these tests, each hardness tester had been modified and calibrated according to procedures previously described (1).

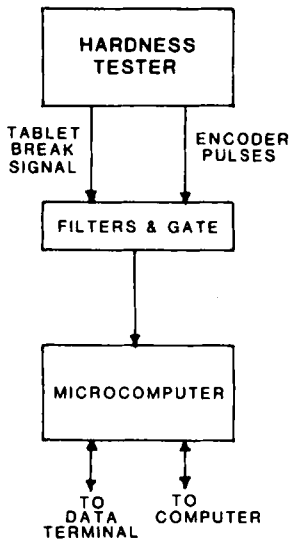

Figure 1—*Computerized hardness-tester block diagram.*

Twenty-five tablets of each hardness value were tested on both the computerized tablet-hardness tester and another identical model tablet-hardness tester, from the same manufacturer ("standard"). The scale reading and digital reading were taken from the computerized instrument after each of the 25 tablets were tested. Also, the scale reading was recorded from the "standard" tablet-hardness tester after another 25 tablets were tested. Tablets

Table I—Tablet-Hardness Values, 5 kp

"Standard" Tester	Computerized Tester	
C1	C2	C3
5.40	5.20	5.10
5.20	6.60	6.36
5.50	5.20	5.38
5.30	5.50	5.60
5.80	5.45	5.47
5.60	6.05	6.10
5.80	5.65	5.38
5.20	5.50	5.75
5.60	5.30	5.38
5.60	5.30	5.38
5.60	5.85	5.99
5.70	5.80	6.10
5.60	5.20	5.38
5.50	5.90	6.10
5.70	4.90	5.00
5.60	6.05	5.99
5.70	5.50	5.75
5.60	5.30	5.47
5.70	5.40	5.38
5.40	5.50	5.60
5.40	5.30	5.47
5.40	5.00	5.10
5.00	5.35	5.47
5.80	5.40	5.47
5.40	5.50	5.85

Table II—Tablet-Hardness Values, 10 kp

"Standard" Tester	Computerized Tester	
C1	C2	C3
10.40	10.00	10.31
10.80	9.80	9.90
9.50	9.80	10.05
10.10	10.60	10.70
9.20	9.40	9.52
9.00	9.40	9.52
10.00	9.20	9.23
9.50	10.60	10.70
9.20	10.20	10.05
9.70	10.00	10.20
10.00	10.20	10.42
9.60	9.40	9.39
10.20	9.05	9.00
9.20	10.40	10.55
10.40	9.00	9.23
10.00	8.90	8.90
9.70	10.20	10.42
9.80	9.80	9.90
9.80	9.60	9.77
9.90	9.30	9.39
9.90	8.80	8.90
10.10	8.90	8.90
10.30	9.40	9.39
9.80	9.85	9.90
10.40	10.40	10.42

[1] Model 2E; Dr. K. Schleuniger & Co., Zurich, Switzerland.
[2] Model ME20-1000; Elm Systems, Wauconda, Ill.
[3] Model 8085; Intel, Santa Clara, Calif.

0022-3549/84/0900-1324$01.00/0
© 1984, American Pharmaceutical Association

Table III—Tablet-Hardness Values, 15 kp

"Standard" Tester	Computerized Tester	
C1	C2	C3
14.90	14.55	14.38
15.70	14.70	14.61
14.80	15.40	15.60
14.90	15.50	15.42
15.60	14.20	14.38
17.50	16.00	15.90
15.80	15.10	15.32
16.00	15.50	15.72
15.10	14.20	14.21
15.00	14.10	14.21
14.10	16.50	16.70
14.20	15.95	15.90
15.30	14.70	14.95
16.00	14.50	14.38
14.20	13.30	13.25
15.20	15.50	15.60
16.60	14.50	14.50
14.50	15.20	15.18
16.40	14.45	14.50
13.50	14.85	15.04
15.30	14.05	14.21
15.40	14.20	14.38
15.40	15.75	15.72
15.30	14.90	14.76
15.10	15.80	16.00

tested on both tablet-hardness instruments, for each hardness group, were from the same lot of tablets. One operator ran the tablets on the computerized tablet-hardness tester and recorded the scale readings; the digital results were recorded on a digital printer. Tablets for the "standard" unit were tested, and scale readings were recorded by a second operator.

RESULTS AND DISCUSSION

Tables I, II, and III show the results of the approximate 5, 10, and 15 kp placebo tablets tested on both the computerized and the "standard" tablet-hardness testers. Column C1 contains the analog data from the "standard" tester, while columns C2 and C3 contain data from the computerized unit. Column C2 data are the analog readings and column C3 data are the readings from the printer. The data were analyzed by the AOVONEWAY, program for the one-way analysis of variance. To compare the means of these populations, a random sample with a normal and independent distribution and equal variance was assumed for each population. The analyses of data from Tables I, II, and III, by the MINITAB B program (2) are listed in the *Appendix*.

Therefore, we questioned whether all of the populations had the same mean. To answer this question, a null hypothesis, that the variation between the tablet-hardness testers is not greater than the variation due to random error, was established.

The F ratio is a useful statistic when determining whether the variation between the computerized tablet-hardness tester and the "standard" tablet-hardness tester is greater than the variation due to random error (3). The corresponding value from an F table for all sets of data for the F ratio to be checked against is 3.1. The F ratios were 0.74, 0.66, and 1.25 for placebo tablets of 5, 10, and 15 kp, respectively. Since all of the F ratio values are <3.1, we accept the null hypothesis and conclude that there is no significant difference between the tablet-hardness testers.

APPENDIX

AOVONEWAY Analysis of 5 kp Data:

		All Data	C1	C2	C3
	−	1		1	
6.4	+	1			1
	−				
	−	5		2	3
	−	5		2	3
	−	9	6	1	2
5.60	+	10	7	1	2
	−	26	7	8	11
	−	6	1	5	
	−	8	3	3	2
	−	4	1	2	1

Analysis and Variance

Due to	DF	SS	MS = SS/DF	F-Ratio
Factor	2	0.150	0.075	0.74
Error	72	7.337	0.102	
Total	74	7.487		
Level	N	Mean	SD	
C1	25	5.504	0.211	
C2	25	5.508	0.370	
C3	25	5.601	0.352	

Pooled SD = 0.319

AOVONEWAY Analysis of 10 kp Data:

		All Data	C1	C2	C3
10.80	+	1	1		
	−	5		2	3
	−	8	3	2	3
	−	7	2	3	2
	−	9	5	2	2
9.90	+	6	2	1	3
	−	9	5	3	1
	−	6	3	1	2
	−	8		5	3
	−	6	3	1	2
9.00	+	4	1	2	1
	−	6		3	3

Analysis of Variance

Due to	DF	SS	MS = SS/DF	F-Ratio
Factor	2	0.372	0.186	0.66
Error	72	20.329	0.282	
Total	74	20.702		
Level	N	Mean	SD	
C1	25	9.860	0.442	
C2	25	9.688	0.554	
C3	25	9.786	0.588	

Pooled SD = 0.531

AOVONEWAY Analysis of 15 kp Data:

		All Data	C1	C2	C3
	−	1	1		
	−				
	−	2	1		1
	−	2	1	1	
16.0	+	9	3	3	3
	−	14	4	5	5
	−	12	7	2	3
	−	10	3	4	3
	−	19	3	7	9
14.0	+	3	1	2	
	−	1	1		
	−	2		1	1

Analysis of Variance

Due to	DF	SS	MS = SS/DF	F-Ratio
Factor	2	1.617	0.809	1.25
Error	72	46.426	0.645	
Total	74	48.043		
Level	N	Mean	SD	
C1	25	15.272	0.859	
C2	25	14.936	0.762	
C3	25	14.993	0.784	

Pooled SD = 0.803

REFERENCES

(1) F. W. Goodhart, J. R. Draper, M. J. Killeen, and F. C. Ninger, *J. Pharm. Sci.*, **65,** 1072 (1976).

(2) T. A. Ryan, B. L. Joiner, and B. F. Ryan, "MINITAB B student Handbook," Wadswoth Publishing Co., **1976.**

(3) J. S. Hunter, "Design of Experiments Course," Westinghouse, **1968.**

ACKNOWLEDGMENTS

The statistical assistance of Robert Dillard is gratefully acknowledged.

The Effects of Salicylate on the Rectal Absorption of Phenylalanine and Some Peptides, and the Effects of These Peptides on the Rectal Absorption of Cefoxitin and Cefmetazole

TOSHIAKI NISHIHATA, CHIA-SHUN LEE, MIDORI YAMAMOTO, J. HOWARD RYTTING ˣ, and TAKERU HIGUCHI *

Received June 8, 1983 from the *Department of Pharmaceutical Chemistry, The University of Kansas, Lawrence, KS 66045.* Accepted for publication October 13, 1983. *Also affiliated with: INTER$_x$, Merck Sharp and Dohme Research Laboratories, Lawrence, KS 66044.

Abstract □ The disappearance of phenylalanine and phenylalanylglycine from a perfusate circulated across rat rectal tissue was enhanced significantly in the presence of salicylate or 5-methoxysalicylate at pH 4.5, 7.4, and 8.5. The disappearance of di-, tri-, and tetraphenylalanine from a perfusate at pH 7.4, although facilitated by the presence of salicylate and 5-methoxysalicylate, was also fairly substantial when no adjuvant was present. These peptide analogues of phenylalanine also enhanced the rectal absorption of cefoxitin and cefmetazole, two highly water soluble antibiotics. Phenylalanine and phenylalanylglycine, both poorly absorbed across the rectal membrane when administered alone, did not enhance the rectal absorption of either antibiotic.

Keyphrases □ Rectal absorption—phenylalanine and peptide analogues □ Adjuvant action—salicylate, 5-methoxysalicylate, and peptides □ Absorption study—*in situ* perfusion method, *in vivo* experiments using a microenema technique

Many peptide drugs have been developed for clinical therapy. However, their administration is generally limited to intramuscular, subcutaneous, or intravenous injection. Parenteral administration has inherent disadvantages for some patients such as small children, elderly persons, or those receiving frequent drug administration (*e.g.*, insulin).

Recently, there have been reports of attempts to develop new dosage forms which do not involve parenteral administration, *e.g.*, insulin suppositories (1-3). Our laboratory has been studying several novel nonsurfactant adjuvants that enhance rectal or small intestinal absorption of water-soluble drugs (4, 5) as well as high molecular weight drugs such as insulin, heparin (6, 7), and gastrin (8).

The rectal absorption of phenylalanine and di-, tri-, and tetraphenylalanine has been studied and the effects of adjuvants on their absorption have been examined and are reported here. In addition, these peptides were found to exert an enhancing effect of their own.

EXPERIMENTAL SECTION

Materials—Cefmetazole[1], cefoxitin[2], phenylalanine[3], and di-, tri-, and tetraphenylalanine[3] were used as obtained from the manufacturer. All other chemicals used were at least reagent grade.

Animals—Sprague-Dawley male rats, 224–250 g, were fasted for 16 h prior to the experiments. During the experiments, rats were anesthetized with sodium pentobarbital (60 mg/kg) and kept on a 38°C surface.

***In Situ* Perfusion of Rat Rectum**—The perfusion experiments were carried out by a method similar to one described previously (4). The rectum was exposed by an abdominal incision and a glass cannula was inserted in the distal direction and tied firmly to keep it in position. A second cannula was inserted through the anus and secured by ligation, thus exposing ~5 cm of the rectal compartment (rectum and lower colon) to the perfusate. The perfusate (5 mL) consisting of a phosphate buffer (0.067 M) was circulated at a rate of 1 mL/min at 38°C; 0.1 M HCl was employed to maintain the perfusate pH at 5.0. The ionic strength was maintained at 0.45 with sodium chloride.

***In Situ* Loop Technique of Rectal and Jejunal Compartments**—For this study, a 5-cm section of the rectal compartment, described above, or the upper jejunum were used by ligating at both ends. A 3.0-mL microenema prepared with a 0.067 M phosphate buffer solution was administered. At a designated time following administration, the rectal and jejunal loops were removed from the body and the amount of compound remaining was measured.

***In Vitro* Rectal Everted Sac Studies**—In these studies about 4 cm of the rectum, including the lower colon, were removed from the body and everted. Following the addition of 0.5 mL of buffer solution into the everted sac, the sac was ligated at both ends. The sac was then immersed in 5 mL of a buffer solution containing the test compounds and maintained for 1 h at 37°C while bubbling a mixture of 95% O_2 and 5% CO_2 through the solution. The concentration of the test compound inside the everted sac was measured, and the permeation percent was calculated from the ratio of the test compound in the inside solution to the initial concentration in the outside solution, *i.e.*:

$$\frac{\text{(concentration inside after 1 h)} \times 100}{\text{initial concentration outside}} = \%\ \text{permeation}$$

***In Vivo* Absorption Studies**—A microenema (1.0 mL/kg) was administered into the anus through a polyethylene tube inserted at a depth of 1 cm. The anus was ligated with thread to prevent leakage of the drug solution. After administration, blood samples were collected from the jugular vein as a function of time.

Assay Method—Cefoxitin and cefmetazole concentrations in the plasma or in the perfusate were measured by HPLC (9). Phenylalanine and its peptides were assayed by HPLC under the following conditions: RP-18 column material with a column length of 15 cm (4.6 mm i.d.); the mobile phase for phenylalanine (I) consisted of methanol and 0.05 M citrate phosphate buffer at pH 3.4 (15:85); the mobile phase for diphenylalanine (II) consisted of methanol-acetonitrile-0.05 M ammonium acetate (28:12:60); the mobile phase for triphenylalanine (III) consisted of methanol-acetonitrile-0.05 M ammonium acetate (25:20:55); and the mobile phase for tetraphenylalanine (IV) consisted of methanol-acetonitrile-0.05 M ammonium acetate (25:25:50). The flow rate was 1.0 mL/min, and a spectrophotometric detector at 254 nm was used.

RESULTS AND DISCUSSION

The absorption of amino acids from the upper digestive tract usually occurs by active transport. In fact, absorption of L-phenylalanine (I) from the jejunum using the *in situ* loop technique was significantly greater than that from the rectal compartment. In the absence of sodium salicylate, 10 ± 1% of a 15-mg/mL dose of phenylalanine disappeared from a rectal loop compared with 79 ± 6% from a jejunal loop after 60 min. In the presence of 60 mg/mL of sodium salicylate, 62 ± 9% of the phenylalanine was lost from the rectal loop while 84 ± 5% was lost from the jejunal loop. As shown in Table I, there was no absorption of phenylalanine from the rectal perfusate at pH 4.8 and only slight absorption at pH 7.4 and 8.5 in the absence of salicylate.

In previous papers (4-6), it has been reported that salicylate and 5-methoxysalicylate enhanced the absorption of many kinds of water-soluble drugs from the rat rectum. The present study indicates that the rectal absorption of amino acids is also facilitated by the presence of salicylate and 5-methoxysalicylate. The presence of 1.0% sodium salicylate or sodium 5-methoxysalicylate in the rat rectal perfusate caused a significant disappearance of I from the perfusate (Table I).

As described above, studies using the *in situ* loop technique also showed that coadministration of 60-mg sodium salicylate/kg significantly enhanced the absorption of I from the rectal compartment and slightly facilitated the

[1] Sankyo Co., Tokyo, Japan.
[2] Merck, Rahway, N.J.
[3] Sigma Chemical Co., St. Louis, Mo.

0022-3549/84/0900-1326$01.00/0
© 1984, American Pharmaceutical Association

Table I—Disappearance of Phenylalanine or Its Peptides from the Rat Rectal Perfusate at 30 min after Circulation [a]

Compound	pH in Perfusate	Amount Lost from Perfusate with Additives, %		
		0.4% Sodium Chloride	1% Sodium Salicylate	1% Sodium 5-Methoxysalicylate
Phenylalanine	4.8	<1.0 (n = 6)	12.4 ± 0.8[b] (n = 6)	—
	7.4	4.8 ± 0.7 (n = 10)	18.6 ± 0.6[b] (n = 10)	28.3 ± 2.0[b] (n = 10)
	8.5	2.8 ± 0.5 (n = 10)	23.1 ± 1.0[b] (n = 10)	—
Diphenylalanine	7.4	23.5 ± 2.2 (n = 6)	39.5 ± 1.7[b] (n = 6)	43.6 ± 2.5[b] (n = 6)
Triphenylalanine	7.4	14.8 ± 1.3 (n = 6)	39.4 ± 3.0[b] (n = 6)	36.8 ± 2.8[b] (n = 6)
Tetraphenylalanine	7.4	20.4 ± 3.2 (n = 4)	44.6 ± 3.2[b] (n = 4)	39.7 ± 4.4[b] (n = 4)

[a] Uncertainties are expressed as *SEM*. [b] $p < 0.001$ compared with the control not containing adjuvant (using a Student's t test).

absorption of I from the jejunum. The significant enhancement of the rectal absorption of peptides with nonsurfactant adjuvants has had limited examination, except for reports by Nishihata *et al.* (4-7, 10-14) on facilitated rectal and intestinal absorption of insulin in the presence of adjuvants.

To further study facilitated peptide absorption, II, III, and IV were examined. As seen in Table I, the disappearance of these peptides from rat rectal perfusate at pH 7.4 was significantly facilitated by the presence of salicylate and 5-methoxysalicylate. This result indicates that rectal administration can offer an effective alternative route for peptide drug delivery.

Matthews (15) has reported that uptake of dipeptides from the small intestine is more rapid than that of comparable equimolar concentrations of the constituent amino acids. The present study shows that absorption of II is faster than that of I even from the rectum. Shoof *et al.* (16) have reported that the uptake of II into the brush-border membrane prepared from the small intestine occurred significantly, and hydrolysis of II occurs at a point on the cytosol side of a diffusion barrier located in the membrane. It has been demonstrated (17) that salicylate at pH 7.4 was taken up into the brush-border membrane vesicles prepared from the rat rectal compartment, including the rectum and lower colon. These findings may explain why II is substantially absorbed from the perfusate even when no adjuvant is present. That is, rectal absorption of II by itself occurs *via* the microvillus membrane in the rectal compartment as well as in the small intestine.

In the study using the *in vitro* rat rectal everted sac technique described above, the percents of the compounds permeating the everted sac membrane after 1 h were 12.4 ± 3.5, 29.6 ± 4.3, 18.3 ± 4.6, and 16.7 ± 3.1% for L-phenylalanine, II, III, and IV, respectively. When the outside solution initially contained 1% sodium salicylate along with 500 μg/mL of the test compound (I, II, III, or IV), the percents of drug permeating the sac increased to 34.6 ± 6.2 ($p < 0.001$ compared with the solution of the drug without salicylate, n = 4), 41.7 ± 6.4 ($p < 0.01$, n = 3), 36.7 ± 5.8 ($p < 0.001$, n = 4), and 30.6 ± 5.4% ($p < 0.001$, n = 3), for I, II, III, and IV, respectively. These results are an additional indication that the losses of phenylalanine, II, III, and IV from the perfusion studies described earlier involved permeation through the rectal membrane.

Nishihata and Higuchi (17) reported that the enhancing action of salicylate on the absorption of cefoxitin and I into the brush-border membrane vesicles appeared to involve the simultaneous uptake of salicylate into the vesicles. This observation raised the question as to whether II, also significantly absorbed by itself, may act as an adjuvant. Subsequent experiments indicated that the presence of 500 μg of II/mL, in a perfusate containing 500 μg of cefoxitin at pH 7.4, did in fact facilitate the disappearance of cefoxitin, raising the drug bioavailability to 27 ± 2% ($p < 0.001$, Student's t test, n = 6), compared with 4 ± 1% (n = 6) in the absence of II.

The adjuvant effects of III and IV were also studied. The disappearance of cefoxitin from rat rectal perfusate was slightly facilitated by the presence of III (16 ± 3% at a dose of 500 μg of III/mL) or IV (15 ± 2%, n = 6 at a dose of 200 μg of IV/mL). This result appears to indicate that the adjuvant effect of the peptides II, III, or IV on rectal drug absorption is contingent upon the simultaneous absorption of the peptides themselves. Their uptake into the microvillus membrane may alter the nature of the membrane barrier. The

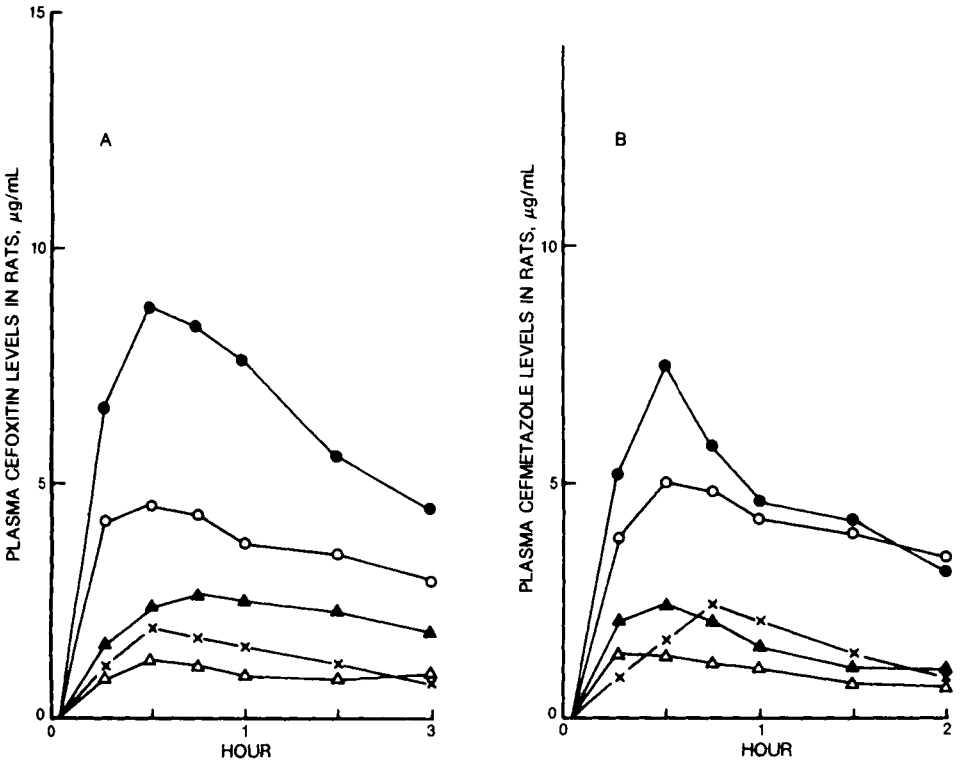

Figure 1 - *(A) Plasma cefoxitin and (B) plasma cefmetazole levels after rectal administration of a microenema containing either 20 mg of cefoxitin/kg or 30 mg of cefmetazole/kg and one of the following: 1 mg of II/mL/kg (△); 27 mg of NaCl/mL/kg (×); 5 mg of II and 27 mg of NaCl/mL/kg (●); 5 mg of II/mL/kg (▲); 1 mg of II and 27 mg of NaCl/mL/kg (○). Rectal administration of cefoxitin or cefmetazole in a microenema without II and/or NaCl produced a plasma cefoxitin level of <0.4 μg/mL and a plasma cefmetazole level of <0.2 μg/mL at peak heights.*

enhancing effect of II was further studied in *in vivo* experiments using a microenema technique. Plasma cefoxitin levels in the rat after rectal administration of a microenema containing 20 mg of cefoxitin and 1–5 mg of II increased significantly over drug levels obtained in the absence of II (Fig. 1). The higher the concentration of II in the microenema, the higher the plasma cefoxitin level. Increasing the ionic strength with NaCl resulted in an even greater increase in the plasma drug levels. These results seem to indicate that rectal absorption of cefoxitin by itself, and enhanced by II, shows some Na^+ dependency. As shown in Fig. 1, rectal absorption of cefmetazole was also enhanced by the presence of II in the microenema.

As shown above and in earlier reports (5, 8), the promotion of the absorption of these antibiotics appears to require the simultaneous absorption of the adjuvant, which alters the nature of the membrane barrier, increasing its permeability.

REFERENCES

(1) E. Touitou, M. Donbrow, and E. Azaz, *J. Pharm. Pharmacol.*, **30,** 662 (1978).

(2) M. Shichiri, Y. Yamasaki, R. Kawamori, M. Kikuchi, N. Hakui, and H. Abe, *J. Pharm. Pharmacol.*, **30,** 806 (1978).

(3) K. Ichikawa, I. Ohato, M. Mitomi, S. Kawamura, H. Maeno, and H. Kawata, *J. Pharm. Pharmacol.*, **32,** 314 (1980).

(4) T. Nishihata, J. H. Rytting, and T. Higuchi, *J. Pharm. Sci.*, **71,** 865 (1982).

(5) T. Nishihata, J. H. Rytting, and T. Higuchi, *J. Pharm. Sci.*, **71,** 869 (1982).

(6) T. Nishihata, J. H. Rytting, T. Higuchi, and L. Caldwell, *J. Pharm. Pharmacol.*, **33,** 334 (1981).

(7) T. Nishihata, G. Liversidge, and T. Higuchi, *J. Pharm. Pharmacol.*, **35,** 616 (1983).

(8) T. Nishihata, J. H. Rytting, L. Caldwell, S. Yoshioka, and T. Higuchi, in "Optimization of Drug Delivery," Alfred Benzon Symposium 17, H. Bundgaard, A. B. Hansen, and H. Kofod, Eds., Munksgaard, Copenhagen, 1982, p. 17.

(9) T. Nishihata, H. Takahagi, M. Yamomoto, H. Tomida, J. H. Rytting, and T. Higuchi, *J. Pharm. Sci.*, **73,** 109 (1984).

(10) T. Nishihata, J. H. Rytting, A. Kamada, and T. Higuchi, *Diabetes*, **30,** 1065 (1981).

(11) T. Nishihata, H. Takahagi, and T. Higuchi, *J. Pharm. Pharmacol.*, **35,** 124 (1983).

(12) A. Kamada, T. Nishihata, S. Kim, M. Yamamoto, and N. Yata, *Chem. Pharm. Bull.*, **29,** 2012 (1981).

(13) T. Nishihata, S. Kim, S. Morishita, A. Kamada, N. Yata, and T. Higuchi, *J. Pharm. Sci.*, **72,** 280 (1983).

(14) S. Kim, A. Kamada, T. Higuchi, and T. Nishihata, *J. Pharm. Pharmacol.*, in press.

(15) D. M. Matthew, *Physiol Rev.*, **55,** 537 (1975).

(16) C. R. Shoaf, W. D. Heizer, and M. Caplow, *Biochim. Biophys. Acta*, **600,** 939 (1980).

(17) T. Nishihata and T. Higuchi, *Life Sci.*, **34,** 419 (1984).

ACKNOWLEDGMENTS

This work was supported in part by grants from $INTER_X$, Merck, Sharp & Dohme Research Laboratories, and the Eagle's Max Baer Heart Fund. The authors also acknowledge the support provided by the Center for Biomedical Research, The University of Kansas.

High-Performance Liquid Chromatographic–Ultraviolet Determination of Primaquine and Its Metabolites in Human Plasma and Urine

GEORGE W. PARKHURST ˣ, MARIS V. NORA, RUSSEL W. THOMAS, and PAUL E. CARSON

Received August 1, 1983, from the *Department of Pharmacology, Rush Medical College, Chicago, IL 60612.* Accepted for publication October 20, 1983.

Abstract □ A high-performance liquid chromatographic method was developed for the simultaneous determination of primaquine and its metabolites from plasma and urine samples obtained after oral administration of primaquine diphosphate. Following partial deproteinization with acetonitrile, samples were chromatographed by direct injection onto a cyano column with UV detection at 254 nm. Levels as low as 100 ng/mL per 20-μL injection were quantitated. Preliminary pharmacokinetic analysis is reported for two human volunteers after oral doses of 60 mg and 90 mg. Two apparent plasma metabolites and two possible urinary metabolites of primaquine are also reported.

Keyphrases □ Primaquine—liquid chromatographic analysis, human plasma and urine, pharmacokinetics □ Liquid chromatography—primaquine, human plasma and urine, pharmacokinetics

Primaquine, 8-[(4-amino-1-methylbutyl)amino]-6-methoxyquinoline (I), is well tolerated in the therapeutic range except in individuals with glucose-6-phosphate dehydrogenase deficiency in whom it causes hemolytic anemia (1). The severity of hemolysis is thought to be related to either the concentration of primaquine or primaquine metabolite(s) and the duration of exposure (2). Nevertheless, primaquine is a true tissue schizonticide and is not only the drug of choice for radical cure of vivax malaria but also is a causal prophylactic agent against falciparum and vivax malaria. Early attempts to correlate primaquine blood levels with either antimalarial effects or toxicity, using a diazotization procedure, were unsuccessful (3).

Recently, several different techniques have been developed which are potentially selective and sensitive enough to measure human primaquine blood concentrations and to quantitate blood concentrations of human metabolites (4–6). The primary objective of this report is to describe the development of a high-performance liquid chromatographic (HPLC) method sensitive enough to measure primaquine concentrations in plasma from human subjects after a single oral dose of primaquine diphosphate. In addition, we report a preliminary pharmacokinetic analysis of human blood level curves, the probable identification of one of the two plasma metabolites, and two unidentified urinary metabolites.

EXPERIMENTAL SECTION

Reagents and Materials—The standards used in this assay were primaquine diphosphate (>99% pure)[1], 6-methoxy-8-aminoquinoline (II)[2], and 8-(3-carboxy-1-methyl propylamino)-6-methoxyquinoline (III)[3]. The chemicals used in the preparation of the mobile phase buffer were reagent-grade ammonium formate and formic acid (88% pure)[4]. Acetonitrile and methanol were UV grade[5]. All solutions containing I, II, and III were placed in amber glassware and refrigerated.

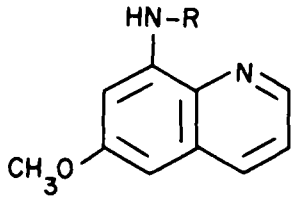

I, R = $-CH(CH_3)CH_2CH_2CH_2NH_2$
II, R = $-H$
III, R = $-CH(CH_3)CH_2CH_2COOH$

HPLC Conditions—The HPLC system consisted of a pump and a fixed-absorbance detector equipped with a 254-nm filter[6]. Samples were either injected manually using an injector with a manual signal recorder[7] or an automated injector[8] and integrator[9,10]. The separations were accomplished using a reverse-phase cyano column (30 × 0.39 cm i.d.; particle size 10 μm)[11]. The mobile phase consisted of a mixture of 0.1 M ammonium formate adjusted to pH 3.85 with formic acid and acetonitrile (89:11). It was filtered through a 0.45-μm filter[12] and deaerated under a house vacuum for 10 min. The flow rate of the mobile phase was 2 mL/min at ambient temperature. Deionized water was used in the final rinsing of glassware and in the preparation of the buffer and the standards[13].

Analytical Procedure—Blood samples were collected in EDTA containers[14] and centrifuged at 1900×*g* for 10 min to separate the plasma. The plasma was kept in aluminum foil covered glass tubes at 4°C until analysis.

The plasma (0.2 mL) was diluted 1:1 with acetonitrile and mixed well. The solution was incubated in the dark for 1 h and centrifuged at 1900×*g* for 10 min. Analyses by HPLC were carried out on 20-μL samples of the resulting supernatant.

Urine was collected in plastic urine specimen jars. The jars were capped and kept at 4°C in the dark until preparation for analysis. Urine was extracted by a modification of the method published by Baty *et al.* (4). Ten grams of resin[15] was suspended in methanol and put in a 1.8 × 25-cm column and washed with 100 mL of methanol followed by 200 mL of deionized water. Up to 100 mL of the urine was passed through the column at a rate of ~5 mL/min. The column was then washed with 100 mL of water. Primaquine and its metabolites were eluted from the column by 75–100 mL of methanol and then quantified by HPLC assay using 10-μL injections. The column was regenerated by washing with 100 mL of water, and then a new sample of urine was passed through the column and the process repeated.

Recovery Studies—Plasma standards containing known amounts of each of the three compounds were compared with standards in distilled water. The plasma standards were treated as in the analytical procedure and the water standards were injected directly. Other deproteinizing agents, *i.e.*, 15% trichloroacetic acid, 5% metaphosphoric acid, 6% perchloric acid, and copper sulfate–sodium tungstate, were also tested for recovery. Additionally, solutions of I and II in plasma and water were placed in membrane cones[16] and centrifuged at 12,000×*g* for 1 h. The concentrations of each compound were then determined for the plasma and water filtrates.

The recoveries were determined for urinary primaquine samples by passing a standard solution of primaquine through the column and analyzing the

[1] Aldrich Chemical Co., Inc., Milwaukee, Wis.
[2] ICN Pharmaceuticals, Plainview, N.Y. (no longer available).
[3] PQC was a gift from Dr. James D. McChesney, School of Pharmacy, University of Mississippi.
[4] Fisher Scientific, Fair Lawn, N.J.
[5] Burdick and Jackson, Muskegon, Mich.
[6] Model 6000A, Model 440; Waters Associates, Milford, Mass.
[7] Model U6K; Houston Instruments, Austin, Tex.
[8] WISP 710B; Waters Associates, Milford, Mass.
[9] Data module; Waters Associates, Milford, Mass.
[10] LC 9540; IBM Instruments, Danbury, Conn.
[11] Waters Associates, Milford, Mass.
[12] Type FG; Millipore Corp., Bedford, Mass.
[13] Milli-RO and Milli-Q deionizing system; Millipore.
[14] Becton, Dickinson & Co., Rutherford, N.J.
[15] Amberlite XAD2; Mallinckrodt, Paris, Ky.
[16] Centriflow membranes, 50,000 mol. wt. cut off; Amicon, Lexington, Mass.

0022-3549/84/0900-1329$01.00/0
© 1984, American Pharmaceutical Association

Table I—Recovery Values from Plasma Using Several Precipitating Agents

	Aceto-nitrile	15% Trichloro-acetic Acid	5% Meta-phospho-ric Acid	6% Perchlo-ric Acid	Copper Sulfate Sodium Tungstate
I (0.78 μg/mL)	98%	38%	38%	46%	0
II (0.34 μg/mL)	97%	30%	33%	53%	0
III (0.6 μg/mL)	98%	—		—	—

eluant for primaquine content. Recoveries of urine metabolites were determined by dividing urine samples into two parts. One part was passed through the column, eluted with methanol, and quantitated by HPLC. Four hundred microliters of the other part was added to an equal volume of acetonitrile, vortex mixed, and left for ≥30 min before being centrifuged. An aliquot of the supernatant was chromatographed, and the two chromatograms were then compared.

Calibration Curves—Calibration standards were prepared by adding known amounts of I and III (0.1 μg/mL–20 μg/mL and 0.23 μg/mL–0.96 μg/mL, respectively) to control plasma and urine samples. Solutions were then assayed by following the analytical procedure. The calibration curves for the quantitation of I and III were obtained by plotting peak height against concentration for each of the standard solutions. (Note: Aqueous solutions of primaquine are light sensitive and will begin to degrade within 30 min. Light protected, aqueous solutions showed no detectable changes after 1 week at −20°C and only slight changes after 1 month.)

Dosing and Sampling Procedure—After Institutional Review Board approval, 60 mg and 90 mg of primaquine diphosphate (calculated as the base) were administered with 118 mL of water to two healthy male volunteers. Three hours after the dose, volunteers were allowed to eat and drink *ad libitum*.

Venous blood was collected at 0, 0.5, 1, 2, 2.5, 3, 4, 5, 6, 7, 8, and 10 h for each subject. Urine was collected at time zero and at each void for up to 72 h.

RESULTS AND DISCUSSION

Assay—To obtain suitable sample preparation from plasma samples for HPLC analysis with UV detection in the nanogram range, various deproteinization techniques were examined on the basis of a previous report (7). The inorganic agents and trichloroacetic acid resulted in nonquantitative and variable recoveries of I and II, Table I. Treatment with acetonitrile (1:1) yielded 98 + 2% recovery of I, II, and III from spiked plasma. Extensive protein binding of primaquine probably accounts for poor recovery with many agents. When solutions containing I and III in plasma and water were filtered through membrane cones, 99% of the compounds were recovered in the water filtrate, while neither compound was detectable in the plasma filtrate[17].

The mobile phase was chosen to achieve separation between I and III and still maintain desirable retention times. Under the HPLC conditions given, I, II, and III had retention times of 6.3 min (K', −4.2), 4.4 min (K', −2.8), and 10.9 min (K', −7.8), respectively.

Calibration curves were constructed for each compound in time zero plasma and urine specimens. In the range of concentrations tested, responses were linear and had coefficients of determination (r^2) >0.99. The detection limit using 20-μL injections was 100 ng/mL of primaquine, 500 ng/mL of III, and 50 ng/mL of II using a signal to noise ratio >3 in plasma and 100 ng/mL of primaquine in urine. Reproducibility of this method at the above detection limits was 98 ± 3.8% for primaquine (n = 10), 98 ± 4.2% for III (n = 10), and 97 ± 1.4% for II (n = 10), using separate determinations. Figure 1 shows

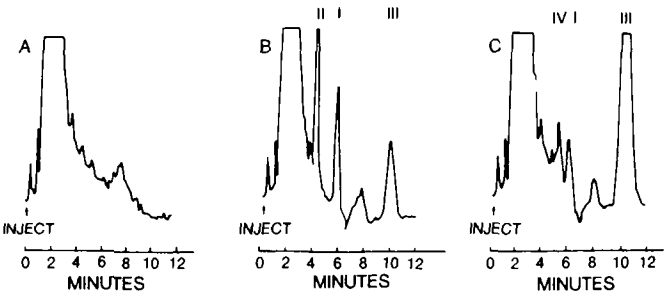

Figure 1—*Chromatograms of (A) time zero plasma; (B) time zero spiked plasma containing 200 ng/mL of 6-methoxy-8-aminoquinoline (II), 450 ng/mL of primaquine (I), and 1.2 μg/mL of primaquine metabolite (III); (C) plasma 2.5 h after a 90-mg oral dose of primaquine diphosphate (I) where IV is the more polar metabolite.*

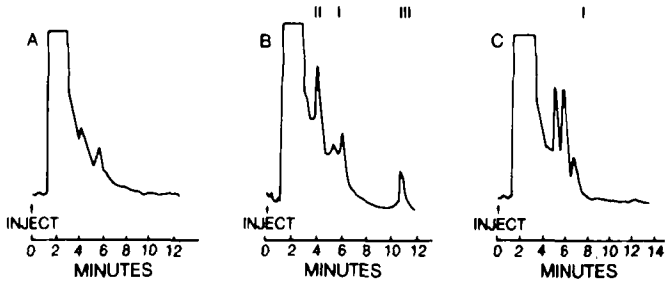

Figure 2—*Chromatograms of (A) time zero urine; (B) time zero spiked urine containing 1.0 μg/mL of 6-methoxy-8-aminoquinoline (II), 1.0 μg/mL of primaquine (I), and 2.0 μg/mL of primaquine metabolite (III); (C) urine 4 h after a 90-mg oral dose of primaquine diphosphate.*

chromatograms of plasma before and 2.5 h after primaquine administration. In addition, a time zero plasma sample spiked with primaquine, II, and III is shown in Fig. 1B. Chromatograms of urine samples taken at time zero, 4 h post primaquine administration, and time zero spiked with I, II, and III are shown in Fig. 2.

Metabolism and Pharmacokinetics—To demonstrate the utility of the present method, it was applied to plasma and urine samples obtained from the two volunteers who were part of an ongoing study (8). These data were fitted to an open one-compartment pharmacokinetic model (9) using a nonlinear least-squares regression program (NONLIN) (10). Oral absorption lag time was incorporated into the model. The unavailability of intravenous data precluded the individual estimation of volume of distribution and bioavailability; therefore, the ratio F/V was inserted in the model:

$$C = \frac{k_a \frac{F}{V} X_o}{(k_a - K)} (e^{-K(t-t_L)} - e^{-k_a(t-t_L)})$$

where t_L is the lag time.

Figure 3 shows the results of the analysis of 11 plasma samples from each volunteer and the fitted curves obtained from these results. As would be expected, there appeared to be a considerable difference in absorption rates between the two subjects; however, the elimination rates were similar for both. Estimated pharmacokinetic parameters are summarized in Table II. Visual analysis of the chromatograms of plasma at the several sampling times after the ingestion of primaquine suggested the presence of primaquine metabolites. However, II, a human metabolite of primaquine metabolism reported by Baty *et al.* (4), was not observed to be present either by comparison of retention times or by addition of II to volunteer samples containing the presumed metabolites. Using our HPLC system, the presumed plasma metabolites were labeled as either more polar than primaquine or less polar than primaquine. They can be detected very shortly after primaquine ingestion and are detectable long after the primaquine concentration falls below detectable levels, Fig. 4. Authentic samples of III[18] (5) have the same retention time as the less polar metabolite in our HPLC system. In addition, in the samples from the two volunteers, the less polar metabolite was subsequently identified as III by mass spectrometry[19]. We conclude that the major primaquine plasma metabolite in humans is the same as that found in rats.

Analysis of the urinary data from the two volunteers indicated that only a small percent of primaquine was excreted unchanged. Values were 4.2% (subject 1) and 2.2% (subject 2) of the oral primaquine dose in 24 h. Chromatograms indicated the presence of two possible primaquine urinary me-

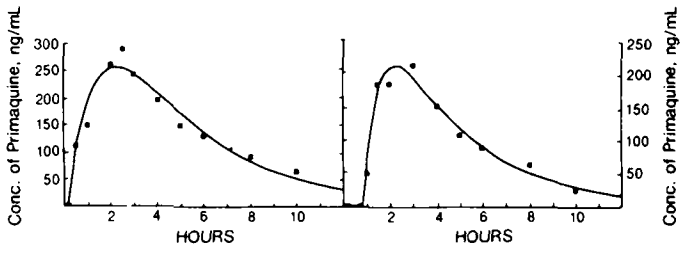

Figure 3—*Fitted blood level curves from two volunteers using a nonlinear least-squares regression program.*

[17] Unpublished results.

[18] Microbiological origin; provided by Dr. J. D. McChesney, School of Pharmacy, University of Mississippi, Oxford, Miss.

[19] Personal communication; Dr. J. D. McChesney.

Table II—Estimated Pharmacokinetic Parameters of Primaquine

	k_a, h^{-1}	Absorption Half-Life, h	k_e, h^{-1}	Elimination Half-Life, h	Lag Time, h	Ratio[a]	r^2
Subject 1[b]	0.81	0.85	0.257	2.7	0.18	7.3	0.946
Subject 2[c]	1.47	0.47	0.287	2.41	0.87	3.5	0.976

[a] Ratio of bioavailability/Vd. [b] After oral administration of 90 mg of primaquine diphosphate. [c] After oral administration of 60 mg of primaquine diphosphate.

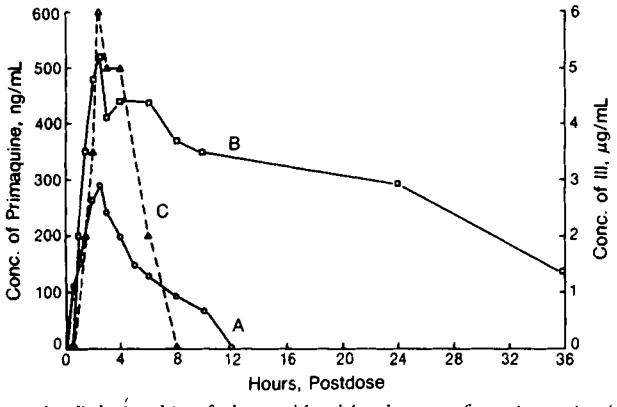

Figure 4—*Relationship of plasma blood level curves for primaquine (A), primaquine metabolite (B), and the more polar metabolite (C), reported as peak height in centimeters.*

tabolites, Fig. 2C. Both of these presumed urinary metabolite compounds are more polar than primaquine in our HPLC system. Neither urinary metabolite appeared to be II or III, but one appears to have a retention time which was the same as that of the more polar plasma metabolite.

The present method utilizing HPLC with UV detection for the simultaneous determination of primaquine and its carboxy metabolite (III), is rapid and precise. The use of this method for plasma and urine samples of volunteers after oral administration of primaquine diphosphate indicates that absorption and metabolism is rapid, that there appear to be at least two plasma metabolites (one identified as an oxidative-deamination product of primaquine, III), and that there appear to be two as yet unidentified urinary metabolites of primaquine.

REFERENCES

(1) P. E. Carson, C. L. Flanagan, C. E. Ickes, and A. S. Alving, *Science*, **124**, 484 (1952).

(2) A. R. Tarlov, G. I. Brewer, P. E. Carson, and A. S. Alving, *Arch. Int. Med.*, **109**, 209 (1962).

(3) "Handbook of Experimental Pharmacology: Antimalarial Drugs," W. Peters and W. H. G. Richards, Eds., Springer-Verlag, New York, NY, 1984, chap. 3.

(4) J. D. Baty, D. A. Price-Evans, and P. A. Robins, *Biomed. Mass Spectrom.*, **2**, 304 (1975).

(5) J. K. Baker, J. D. McChesney, C. D. Hufford, and A. M. Clark, *J. Chromatogr.*, **230**, 69 (1982).

(6) T. G. Rajagopalan, B. Anjaneyulu, V. D. Shanbag, and R. S. Grewal, *J. Chromatogr.*, **224**, 265 (1981).

(7) J. Blanchard, *J. Chromatogr.*, **226**, 455 (1981).

(8) P. E. Carson, R. Hohl, M. V. Nora, G. W. Parkhurst, T. Ahmad, S. Scanlan, and H. Frischer, *Bull WHO*, **59** 427 (1981).

(9) M. Gibaldi and D. Perrier, "Pharmacokinetics," Marcel Dekker, Inc., New York, N.Y., 1975, p. 36.

(10) C. M. Metzler, G. L. Elfring, and A. J. McEwen, *Biometrics*, **30**, 3 (1974).

ACKNOWLEDGMENTS

This investigation received the financial support of the UNDP/World Bank/WHO Special Program for Research Training in Tropical Disease and, in part, by intramural grants and funds from the BRSG to the college of Health Sciences, Rush University.

Quantitation of Metronidazole in Pharmaceutical Dosage Forms Using High-Performance Liquid Chromatography

V. DAS GUPTA

Received June 6, 1983, from the *Department of Pharmaceutics, University of Houston, Houston, TX 77030.* Accepted for publication September 26, 1983.

Abstract □ A high-performance liquid chromatographic (HPLC) method for the quantitation of metronidazole in pharmaceutical dosage forms has been developed. The method is accurate and precise with an *RSD* of 0.68%, based on six readings. The excipients present in various dosage forms did not interfere with the assay procedure. A solution of metronidazole decomposed using heat showed 0% potency.

Keyphrases □ Metronidazole—HPLC, pharmaceutical dosage forms □ HPLC—pharmaceutical dosage forms of metronidazole

Metronidazole is extensively used in medicine as an antiprotozoal agent. The USP-NF method (1) for the quantitation of metronidazole in tablets is based on titration with perchloric acid, which requires a tedious extraction-purification procedure; moreover, other weak bases, impurities, and products of decomposition usually interfere with this type of volumetric titration. The quantitation of metronidazole in biological fluids was reviewed by Wood (2). The purpose of these investigations was to develop a stability-indicating assay procedure for the quantitation of metronidazole in pharmaceutical dosage forms based on HPLC.

EXPERIMENTAL SECTION

Chemicals and Reagents—All the chemicals and reagents were USP, NF, or ACS quality and were used without further purification. The USP quality powder of metronidazole[1] (2-methyl-5-nitroimidazole-1-ethanol; I) was used as received.

Apparatus—The high-performance liquid chromatograph[2] (HPLC) was equipped with a multiple-wavelength detector[3] and a recorder[4]. A semipolar column[5] (30 cm × 4 mm i.d.) was used. The average size of the particles was 10 μm.

[1] G. D. Searle & Co., Chicago, Ill.

[2] ALC202 equipped with U6K universal injector; Waters Associates, Milford, Mass.

[3] Spectroflow monitor SF770; Schoeffel Instruments Corp., Ramsey, N.J.

[4] Omniscribe 5213-12; Houston Instruments, Austin, Tex.

[5] μ-Bondapak phenyl; Waters Associates, Milford, Mass.

0022-3549/84/0900-1331$01.00/0

© 1984, American Pharmaceutical Association

Table II—Estimated Pharmacokinetic Parameters of Primaquine

	k_a, h^{-1}	Absorption Half-Life, h	k_e, h^{-1}	Elimination Half-Life, h	Lag Time, h	Ratio[a]	r^2
Subject 1[b]	0.81	0.85	0.257	2.7	0.18	7.3	0.946
Subject 2[c]	1.47	0.47	0.287	2.41	0.87	3.5	0.976

[a] Ratio of bioavailability/Vd. [b] After oral administration of 90 mg of primaquine diphosphate. [c] After oral administration of 60 mg of primaquine diphosphate.

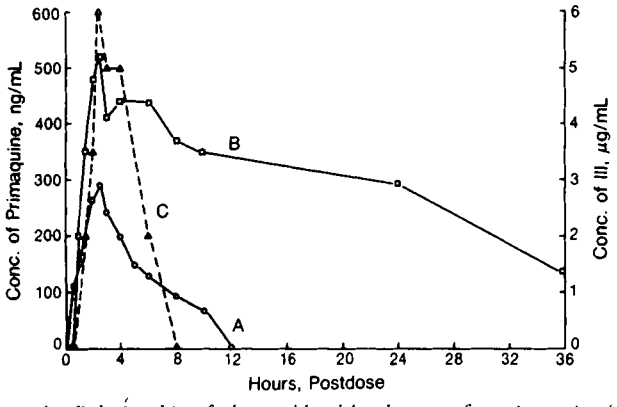

Figure 4—*Relationship of plasma blood level curves for primaquine (A), primaquine metabolite (B), and the more polar metabolite (C), reported as peak height in centimeters.*

tabolites, Fig. 2C. Both of these presumed urinary metabolite compounds are more polar than primaquine in our HPLC system. Neither urinary metabolite appeared to be II or III, but one appears to have a retention time which was the same as that of the more polar plasma metabolite.

The present method utilizing HPLC with UV detection for the simultaneous determination of primaquine and its carboxy metabolite (III), is rapid and precise. The use of this method for plasma and urine samples of volunteers after oral administration of primaquine diphosphate indicates that absorption and metabolism is rapid, that there appear to be at least two plasma metabolites (one identified as an oxidative-deamination product of primaquine, III), and that there appear to be two as yet unidentified urinary metabolites of primaquine.

REFERENCES

(1) P. E. Carson, C. L. Flanagan, C. E. Ickes, and A. S. Alving, *Science*, **124**, 484 (1952).

(2) A. R. Tarlov, G. I. Brewer, P. E. Carson, and A. S. Alving, *Arch. Int. Med.*, **109**, 209 (1962).

(3) "Handbook of Experimental Pharmacology: Antimalarial Drugs," W. Peters and W. H. G. Richards, Eds., Springer-Verlag, New York, NY, 1984, chap. 3.

(4) J. D. Baty, D. A. Price-Evans, and P. A. Robins, *Biomed. Mass Spectrom.*, **2**, 304 (1975).

(5) J. K. Baker, J. D. McChesney, C. D. Hufford, and A. M. Clark, *J. Chromatogr.*, **230**, 69 (1982).

(6) T. G. Rajagopalan, B. Anjaneyulu, V. D. Shanbag, and R. S. Grewal, *J. Chromatogr.*, **224**, 265 (1981).

(7) J. Blanchard, *J. Chromatogr.*, **226**, 455 (1981).

(8) P. E. Carson, R. Hohl, M. V. Nora, G. W. Parkhurst, T. Ahmad, S. Scanlan, and H. Frischer, *Bull WHO*, **59** 427 (1981).

(9) M. Gibaldi and D. Perrier, "Pharmacokinetics," Marcel Dekker, Inc., New York, N.Y., 1975, p. 36.

(10) C. M. Metzler, G. L. Elfring, and A. J. McEwen, *Biometrics*, **30**, 3 (1974).

ACKNOWLEDGMENTS

This investigation received the financial support of the UNDP/World Bank/WHO Special Program for Research Training in Tropical Disease and, in part, by intramural grants and funds from the BRSG to the college of Health Sciences, Rush University.

Quantitation of Metronidazole in Pharmaceutical Dosage Forms Using High-Performance Liquid Chromatography

V. DAS GUPTA

Received June 6, 1983, from the *Department of Pharmaceutics, University of Houston, Houston, TX 77030.* Accepted for publication September 26, 1983.

Abstract □ A high-performance liquid chromatographic (HPLC) method for the quantitation of metronidazole in pharmaceutical dosage forms has been developed. The method is accurate and precise with an *RSD* of 0.68%, based on six readings. The excipients present in various dosage forms did not interfere with the assay procedure. A solution of metronidazole decomposed using heat showed 0% potency.

Keyphrases □ Metronidazole—HPLC, pharmaceutical dosage forms □ HPLC—pharmaceutical dosage forms of metronidazole

Metronidazole is extensively used in medicine as an antiprotozoal agent. The USP-NF method (1) for the quantitation of metronidazole in tablets is based on titration with perchloric acid, which requires a tedious extraction-purification procedure; moreover, other weak bases, impurities, and products of decomposition usually interfere with this type of volumetric titration. The quantitation of metronidazole in biological fluids was reviewed by Wood (2). The purpose of these investigations was to develop a stability-indicating assay procedure for the quantitation of metronidazole in pharmaceutical dosage forms based on HPLC.

EXPERIMENTAL SECTION

Chemicals and Reagents—All the chemicals and reagents were USP, NF, or ACS quality and were used without further purification. The USP quality powder of metronidazole[1] (2-methyl-5-nitroimidazole-1-ethanol; I) was used as received.

Apparatus—The high-performance liquid chromatograph[2] (HPLC) was equipped with a multiple-wavelength detector[3] and a recorder[4]. A semipolar column[5] (30 cm × 4 mm i.d.) was used. The average size of the particles was 10 μm.

[1] G. D. Searle & Co., Chicago, Ill.

[2] ALC202 equipped with U6K universal injector; Waters Associates, Milford, Mass.

[3] Spectroflow monitor SF770; Schoeffel Instruments Corp., Ramsey, N.J.

[4] Omniscribe 5213-12; Houston Instruments, Austin, Tex.

[5] μ-Bondapak phenyl; Waters Associates, Milford, Mass.

0022-3549/84/0900-1331$01.00/0

© 1984, American Pharmaceutical Association

Table I—Assay Results

Dosage Form	Metronidazole, mg/mL or mg/tablet	Other Ingredients, (mg/mL)	Percent of Label Claim Found: Using USP-NF Method (*RSD*, %)	Percent of Label Claim Found: Using HPLC Method (*RSD*, %)
		Recovery Data from Commercial Formulations		
Commercial solution 1[d]	5.0	Sodium Phosphate 4.8, Citric Acid 2.3, and Sodium Chloride 7.9	—[a]	99.2 (0.68)
Commercial solution 2[e]	5.0	Sodium Phosphate 4.8, Citric Acid 2.3, and Sodium Chloride 7.9	—[a]	99.8 (0.66)
Commercial solution 3[f]	5.0	Sodium Phosphate 4.8, Citric Acid, 2.3, and Sodium Chloride 7.9	—[a]	99.8 (0.67)
Commercial vial Powder 1[g]	500 mg/vial of metronidazole as HCl salt	Mannitol, 415	—[a]	104.9 (0.69)
Commercial vial Powder 2[h]	500 mg/vial of metronidazole as HCl salt	Mannitol, 415	—[a]	102.8 (0.69)
Tablets, lot 1[i]	250	Blue Coloring Matter and Excipients	99.5 (0.76)	99.2 (0.70)
Tablets, lot 2[j]	250	Blue Coloring Matter and Excipients	99.3 (0.78)	99.6 (0.68)
Tablet 1[k]	250	Blue Coloring Matter and Excipients	—[b]	100.5 (—[c])
Tablet 2[k]	250	Blue Coloring Matter and Excipients	—[b]	98.3 (—[c])
Tablet 3[k]	250	Blue Coloring Matter and Excipients	—[b]	99.2 (—[c])
Tablet 4[k]	250	Blue Coloring Matter and Excipients	—[b]	101.5 (—[c])
Tablet 5[k]	250	Blue Coloring Matter and Excipients	—[b]	97.8 (—[c])
Tablet 6[k]	250	Blue Coloring Matter and Excipients	98.2(—[c])	98.2 (—[c])
Tablet 7[k]	250	Blue Coloring Matter and Excipients	100.3 (—[c])	100.1 (—[c])
		Recovery Data From Synthetic Mixtures		
Synthetic powder 1	160	Mannitol, 160		99.9 (0.68)
Synthetic powder 2	160	Mannitol, 160		100.4 (0.69)
Synthetic solution 1	2.5	Sodium Phosphate 2.5, Citric Acid 1.5, and Sodium Chloride 4.0	—[a]	100.0 (0.69)
Synthetic solution 2	5.0	Sodium Phosphate 5, Citric Acid 2.5, and Sodium Chloride 8	—[a]	100.2 (0.68)
Synthetic solution 3	2.5	Mannitol 2.5	—[a]	100.2 (0.67)

[a] USP-NF method not specified for solutions and not applicable to metronidazole hydrochloride powder. [b] These single tablets were not assayed using the USP-NF method. [c] Not determined for single-tablet assay. [d] All commercial solutions were obtained from G. D. Searle & Co.; solution no. 1 from lot 52V054N4. [e] Lot ZH 104. [f] Lot 3L 011. [g] Lot 1181-166. [h] Lot 483-174. [i] Lot 782-008; average of 10 tablets, one determination. [j] Lot 683-048; average of four tablets, one determination. [k] Lot 782-008.

Chromatographic Conditions—The mobile phase was an aqueous solution of 0.02 M KH_2PO_4 (pH ~4.2). The flow rate was 2.5 mL/min, and the temperature was ambient. The sensitivity was set at 0.04 (254 nm) and the chart speed was 30.5 cm/h.

Solution Preparation—The stock solutions of metronidazole (1.60 mg/mL) and phenylpropanolamine hydrochloride (10.0 mg/mL) in water were prepared fresh daily. Metronidazole was dissolved in water with the aid of gentle heat (≤60°C) to hasten dissolution. Preliminary investigations indicated that there was no decomposition with gentle heat. A stock solution of acetaminophen (0.40 mg/mL) was prepared by dissolving 40.0 mg of acetaminophen in 1 mL of methanol and then bringing it to volume (100.0 mL) with water. The standard solutions were prepared as needed by diluting the stock solutions with water. For assays, the concentrations (in μg/mL) of metronidazole, phenylpropanolamine hydrochloride, and acetaminophen were 200, 1400 and 40, respectively.

The assay solutions were prepared by mixing a solution (from ready-to-use bags or vials) representing 20.0 mg of metronidazole with 14.0 mL of the stock solution of phenylpropanolamine hydrochloride (the internal standard) and then bringing it to volume (100.0 mL) with water. To assay the contents of the vials containing powder (metronidazole hydrochloride ≅500 mg of metronidazole), the contents were dissolved in water and brought to volume (100.0 mL) with water. Four milliliters of the mixture were combined with 14.0 mL of the stock solution of phenylpropanolamine hydrochloride and brought to volume (100.0 mL) with water.

Extraction Procedure for Tablets—Ten tablets were accurately weighed and ground to a fine powder. (When content uniformity was to be determined, a single tablet was ground to a fine powder.) Powder representing 80.0 mg of metronidazole was added to ~90 mL of water in a 150-mL beaker. The solution was gently heated (with stirring) to 60°C on a hot plate and then allowed to cool to room temperature. The solution was transferred to a 100-mL volumetric flask, brought to volume with water, and filtered[6]. The first 20 mL of the filtrate was rejected; the rest was further diluted. Then, 12.5 mL of the solution was mixed with 7.0 mL of the stock solution of phenylpropanolamine hydrochloride and brought to volume (50.0 mL) with water.

Assay Sample of Decomposed Ready-to-Use Solution (5.0 mg/mL)—Ten milliliters of the solution was mixed with ~4 mL of ~1 M NaOH solution in a 150-mL beaker and then heated to boiling on a hot plate for ~25 min (water was replaced as necessary). The mixture was cooled, the pH adjusted to ~6 using ~0.5 M HCl, and brought to volume (250.0 mL) with water.

Chromatographic Procedure—A 20-μL aliquot of the assay solution was injected into the chromatograph under the conditions described above. For comparison, a 20-μL aliquot of the standard solution containing identical concentrations of metronidazole and phenylpropanolamine hydrochloride was injected after the assay was eluted.

Calculations—Since preliminary investigations indicated that the ratio of the peak heights of metronidazole and phenylpropanolamine hydrochloride were directly related to the concentration of metronidazole (range tested 2–6 μg), the results were calculated using the equation:

$$\frac{R_{pha}}{R_{phs}} \times 100 = \text{percent of label claim found}$$

where R_{pha} is the ratio of the peak heights of drug–internal standard of the

[6] Whatman # 1 filter paper.

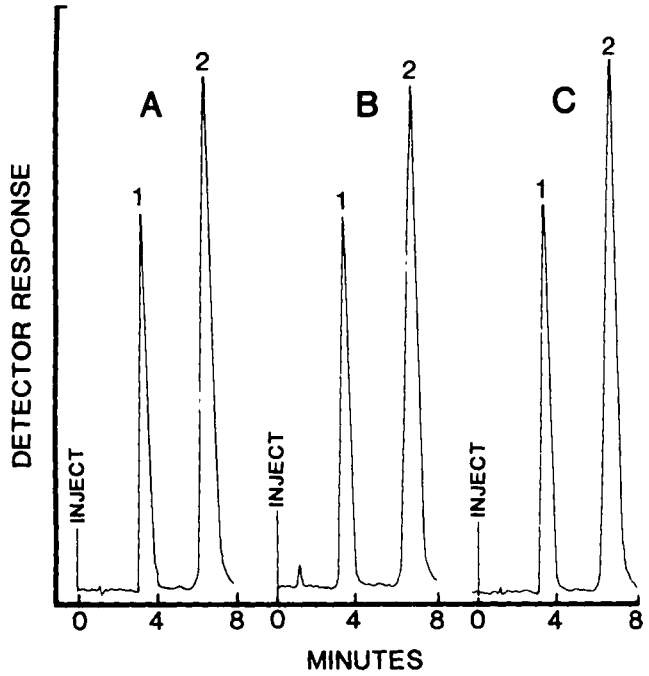

Figure 1—*Typical chromatograms; peaks 1 and 2 are from phenylpropanolamine and metronidazole, respectively. Chromatograms A–C are from a standard solution, a ready-to-use solution (No. 1, Table I), and from tablets, respectively.*

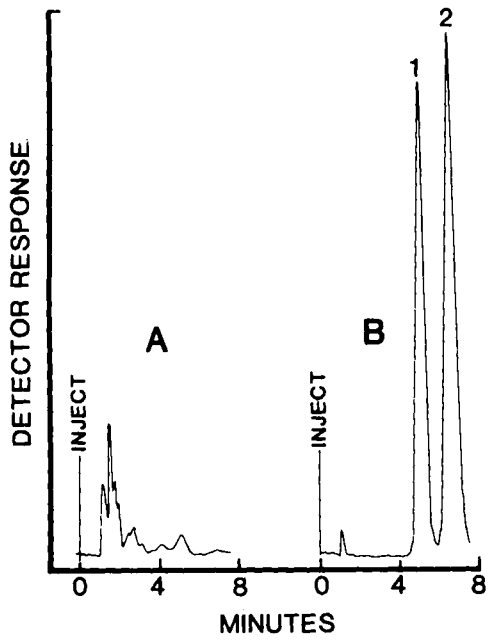

Figure 2—*Typical chromatograms; chromatogram A is from a decomposed solution (see text). All the peaks are from the decomposition products; no internal standard was added to this solution. Chromatogram B is from a standard solution with acetominophen (peak 1) as the internal standard and metronidazole (peak 2).*

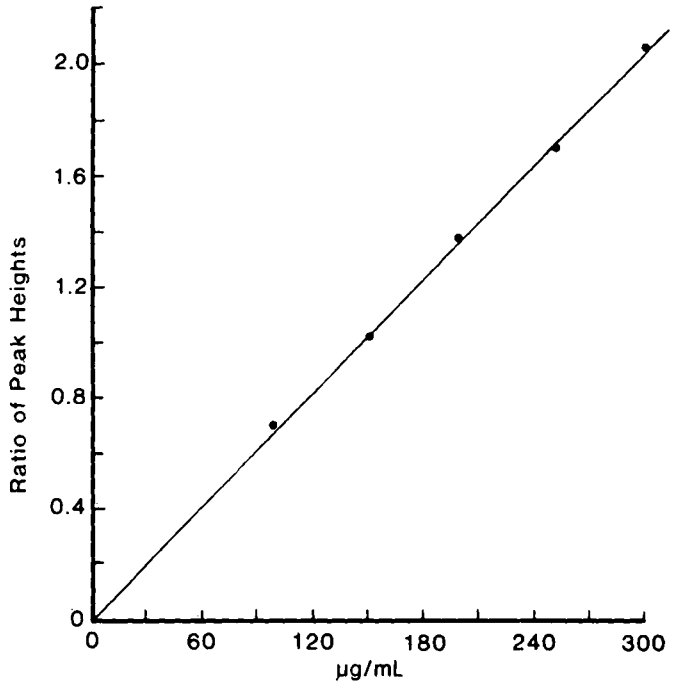

Figure 3—*A calibration curve of the ratio of the peak heights (metronidazole–phenylpropanolamine) and concentration of metronidazole. An average* RSD *based on six injections, was 0.68%.*

assay solution, and R_{phs} is the ratio of the peak heights of drug–standard solution. Alternatively, the results may be calculated using the standard curve.

RESULTS AND DISCUSSION

The assay results (Table I) indicate that the developed HPLC method for the quantitation of metronidazole in pharmaceutical dosage forms can be adopted. It is accurate and precise with an *RSD* of 0.68%, based on six injections. Before developing phenylpropanolamine hydrochloride as the internal standard (Fig. 1), acetaminophen was tried (Fig. 2). Acetaminophen can be used as an internal standard if some active or inactive products of decomposition interfere with the phenylpropanolamine peak. The concentrations were directly related to the ratio of peak heights between a range of 2–6 μg (Fig. 3). No preliminary extraction procedure was required to assay the ready-to-use solutions or the powders, which contained 415 mg of mannitol for each 500 mg of metronidazole. The presence of sodium phosphate, citric acid, and sodium chloride in the ready-to-use solutions, and mannitol in the powders, did not interfere with the assay procedure.

A very simple preliminary extraction procedure was required to assay the tablets. The coloring matter and the excipients present in the tablets did not interfere with the assay procedure. The method is stability indicating since a sample decomposed by using heat (see *Experimental Section*) showed almost 0% potency and a number of new peaks in the chromatogram (Fig. 2A). The developed method can be used to assay metronidazole in various dosage forms and also can be used to test content uniformity of the tablet formulations.

REFERENCES

(1) The United States Pharmacopeia," 20th rev., U.S. Pharmacopeial Convention, Inc., Rockville, Md., 1980, p. 531.

(2) N. F. Wood, *J. Pharm. Sci.*, **64**, 1048 (1975).

A Reply to "Problems Involved with Developing a Suitable Model for Evaluating Exposure to Bis(2-ethylhexyl) Phthalate from Medical Devices"

In February of this year, we reported a study in rats which indicated that chronic oral administration of the phthalate plasticizer, bis(2-ethylhexyl) phthalate (I), can result in induction of antipyrine metabolism[1]. Based on this observation, we hypothesized that the apparent stimulation of antipyrine clearance reported in earlier clinical studies in chronic renal failure patients could be the result of inadvertent exposure to I during hemodialysis treatment. In a subsequent commentary[2], which appeared in the June issue of this journal, Lawrence and Autian questioned the validity of our hypothesis on the grounds that the metabolism of I may differ between parenteral and peroral routes of administration. They cited various literature reports[3-5] which showed that I can be readily hydrolyzed to form mono(2-ethylhexyl) phthalate (II) in various tissues and biological fluids. The rates of hydrolysis were notably rapid in intestinal tissues and the gut contents[5]. Authors of several of these cited articles had stated that orally administered I *would probably* be absorbed from the GI tract primarily as the monoester. Apparently based on these statements, Lawrence and Autian drew the conclusion that II is formed much more extensively (or even exclusively) after oral administration as compared with after parenteral administration. Since there are data indicating differences in biological activities between I and II[6-9], Lawrence and Autian suggested that parenteral studies with I (which presumably better mimic the introduction of I into patients during hemodialysis) should be performed before our results on antipyrine disposition can be accepted as being valid.

There is no disagreement that hydrolysis of I to II can occur in the gut and/or liver after oral administration. However, we would caution that all of the literature articles cited by Lawrence and Autian were reports of *in vitro* studies on the hydrolysis of I by blood and tissue lipases. It is not possible to draw definite conclusions in regards to the *extent* of oral "first-pass" mono-deesterification of I in the various animal species studied. In fact at the time of our study (*ca.* 1981), detailed *in vivo* pharmacokinetic studies of I and its derived monoester were not available. Furthermore, it was not possible to rule out the existence of a significant degree of mono-deesterification following systemic introduction of I (such that the *overall* extent of formation of II would be comparable between enteral and parenteral administration). For example, it is conceivable that the diester can be excreted in the bile and be subjected to hydrolysis during transit through the intestinal tract. Also, extensive systemic hydrolysis of I certainly can occur.

We were aware of the literature on *in vitro* enzymatic hydrolysis of I (and the lack of quantitative information) at the outset of our study. More importantly, it was recognized that further *in vivo* studies were needed to address the unanswered metabolic and pharmacokinetic questions. We have, over the last 2 years, undertaken a series of studies in rats and in hemodialysis patients which provided much greater insights into the relative pharmacokinetic and pharmacological importance of I and its derived monoester. The results of these studies are currently under review for publication. We believe a brief summary of the relevant data will clarify the question concerning the factor of route of administration in the effect of I on antipyrine metabolism and will illustrate the complexities of the issue.

Our first follow-up study was aimed at elucidating the pharmacokinetics of I and derived II following a single intra-arterial (100 mg/kg), intraperitoneal (4 g/kg), or peroral dose (2 g/kg) of the diester. The key finding from this acute dosing study was a striking difference in the relative concentrations of the monoester metabolite to the parent diester between the parenteral and peroral routes of administration. The area under the plasma concentration–time curve (AUC) ratios of II to I were 0.050 ± 0.024, 0.35 ± 0.27, and 6.90 ± 1.75, respectively. A similar difference in AUC ratios between intraperitoneal and oral routes was found during repetitive administration of I. Using the pharmacokinetic methodologies proposed by Pang and Kwan[10] together with AUC data obtained after direct administration of II, we estimated that ~80% of an oral dose of I was hydrolyzed to II during first passage through the GI tract whereas <2% of the intra-arterial or intraperitoneal dose was mono-deesterified in the liver and other systemic tissues.

Our next step was to compare the effect of I on antipyrine clearance following repetitive intraperitoneal and oral administrations of I in the rat. The observed route dependency in the deesterification of I did indeed result in a difference in the effect of the phthalate plasticizer on antipyrine metabolism, although the results were much more complex than were anticipated. The complicating factor (which was alluded to in our earlier publication) was the elapsed time between the last dose of I and the administration of the antipyrine test. Consistent with our earlier study, a marked degree of induction in antipyrine clearance (an approximately twofold increase) was observed at both 4 and 48 h after the last oral dose of the phthalate ester. On the other hand, the effect after intraperitoneal treatment with I was variable depending on the time at which the antipyrine test was performed. At 48 h postadministration of I, a small degree of *inductive* effect (an ~25% increase in antipyrine clearance) was observed. At the earlier time point (*i.e.*, 4 h), either *no effect* or an apparently *inhibitory* effect was observed. The most likely explanation, which would take into account both the route- and time-dependency in the metabolic effects, is that induction is largely associated with the monoester and that the diester exerts an opposing effect, *i.e.*, inhibition of antipyrine metabolism. Indeed, we were able to demonstrate pronounced inhibition of antipyrine clearance after an acute dose of the diester given either intraperitoneally or orally.

Although our new findings in the rat seem to support the contention of Lawrence and Autian that the study on antipyrine metabolism should have been conducted after parenteral pretreatment of I, we have further data in hemodialysis patients which suggest that neither oral nor intraperitoneal administration of I in the rat exactly mimic the situation during clinical exposure. Studies in a group of renal failure patients on maintenance hemodialysis showed that the circulating concentrations of derived II were comparable to the parent diester during a 4-h dialysis session (AUC ratio of 2.42 ± 0.66). This suggests that mono-deesterification of I in the systemic circulation occurs much more readily in humans than in rats. Alternatively, II may be eliminated much more slowly (relative to the parent compound) in humans than in rats.

In summary, we believe the oral bis(2-ethylhexyl) phthalate study in the rat was a reasonable first step in elucidating the potential *in vivo* effects of I on hepatic drug metabolism during human exposure. The results generated from that study are still indicative, albeit in a qualitative fashion, of the probable influence of I on antipyrine disposition in renal failure patients. However, given the differences in the pharmacokinetic and metabolic characteristics of I between the rat and human, we now conclude that further investigations in other animal species are needed to establish a valid experimental model for assessing the biological effects of I.

D. D. Shen[x]
Department of Pharmaceutics, BG-20
School of Pharmacy
University of Washington
Seattle, WA 98195

G. M. Pollack
Division of Pharmaceutics
School of Pharmacy
University of North Carolina
at Chapel Hill
Chapel Hill, NC 27514

Received July 23, 1984.

[1] G. M. Pollack and D. D. Shen, *J. Pharm. Sci.*, **73**, 29 (1984).
[2] W. H. Lawrence and J. Autian, *J. Pharm. Sci.*, **73**, 861 (1984).
[3] P. W. Albro and R. O. Thomas, *Biochem. Biophys. Acta*, **360**, 380 (1973).
[4] I. R. Rowland, *Food Cosmet. Toxicol.*, **12**, 293 (1974).
[5] B. G. Lake, J. C. Phillips, J. C. Linnell, and S. D. Gangolli, *Toxicol. Appl. Pharmacol.*, **39**, 239 (1977).
[6] J. A. Thomas, T. D. Darby, R. F. Wallin, P. J. Garvin, and L. Martis, *Toxicol. Appl. Pharmacol.*, **45**, 1 (1978).
[7] I. Tomita, Y. Nakamura, N. Aoki, and N. Inui, *Environ. Health Perspect.*, **45**, 119 (1982).
[8] D. K. Agarwal, S. Agarwal, and P. K. Seth, *Drug Metab. Dispos.*, **10**, 77 (1982).
[9] T. Takahashi, *Biochem. Pharmacol.*, **26**, 19 (1977).
[10] K. S. Pang and K. C. Kwan, *Drug Metab. Dispos.* **11**, 79 (1983).

The Need for Information on Product Formulations

I thoroughly enjoyed your editorial "Putting An End to Secret Formulations." [1] Over the years I've had numerous debates with manufacturers over the issue of "trade secrets" (Boloney!) *versus* the health professionals' need for information on product formulations.

As you pointed out, any competitors' laboratory worth their salt will rapidly crack such "secret formulations." Therefore, the only ones kept in the dark are the physician prescribers and pharmacist dispensers of these pharmaceuticals.

Although you state that "manufacturers are required by law and regulation to make known the identity and quantity of the medicinally active ingredients in their products," even this is not always the case. For example, in many artificial tear solutions and contact lens solutions, the functionally active components may only be identified as "a water-soluble polymeric system" or "an anionic surface-active agent."

If health care professionals are to make informed product selection decisions, the industry must provide this needed information. Although regulatory remedies may be necessary, industry leaders with vision might see that voluntary cooperation would result in benefits to all concerned.

Must we have mandatory CE before pharmacists accept their obligation to maintain their competence? Must we have mandatory relabeling requirements before the industry responds to the information needs of the public? Must we always have an expensive, legislative, regulated, bureaucratized solution to every problem?

The PMA has taken a significant first step in stating "the medical justification for disclosure . . . warrants release of that information . . ." Let's hope that individual manufacturers respond to your call for "putting an end to secret formulations."

James R. Boyd
Editor-in-Chief
"Facts and Comparisons"
St. Louis, MO 63146

[1] Edward G. Feldmann, *J. Pharm. Sci.*, **73**, 577 (1984).

BOOKS

Instrumental Data for Drug Analysis. Vol. 2. (Elsevier Series in Forensic and Police Science.) By TERRY MILLS III, WILLIAM N. PRICE, and J. CONRAD ROBERTSON. Elsevier Science Publishing Co., Inc. 52 Vanderbilt Ave., New York, NY 10017. 1983. pp. 662-1358. 22 × 28.5 cm. Price $95.00.

This second volume contains data on an additional 300 drug substances bringing the total compounds covered in both volumes to 600.

Each drug substance is allotted two pages on which ultraviolet, electron impact mass, proton nuclear magnetic resonance, and Fourier transform infrared spectra are presented. All spectra are of exceptional quality. Also given are molecular formulas and weights, synonyms, trade names, therapeutic categories and, in shorthand style, HPLC and GC data where applicable. There are also four appendices containing standard KBr infrared spectra and, in tabular form, Kovats retention indices for gas chromatography, the ultraviolet absorption maxima in acid, basic and ethanol solution, and mass spectral indices for base peaks and prominent ions.

The atlas has been compiled by forensic scientists of the Georgia State Crime Laboratory and should be useful for the identification of drugs. Thus, the compilation serves as a supplement to the *Merck Index* which does not present spectra. The two volumes compete with two *CRC Handbooks of Mass Spectra and Spectrophotometric Data of Drugs* which together sell for about the same price. I prefer the volumes under review for better organization, clearer spectra and coverage of more drugs. One can quibble that the shorthand data on HPLC and GC are of questionable value. It also would have been useful to identify for each drug the source of the sample, particularly whether the drug was a USP reference standard.

All efforts to provide comprehensive information on drugs are welcome. Therefore, the authors should be congratulated and encouraged to continue the series.

Reviewed by Klaus G. Florey
The Squibb Institute for Medical Research
P.O. Box 191
New Brunswick, NJ 08903

Applied Therapeutics: The Clinical Use of Drugs, 3rd Ed. Edited by BRIAN S. KATCHER, LLOYD YEE YOUNG, and MARY ANNE KODA-KIMBLE. Applied Therapeutics, Inc., P.O. Box 1903, Spokane, WA 99210-1903. 1983. 1,619 pp. 19.5 × 24 cm. Price $54.00.

The editors and authors of *Applied Therapeutics: The Clinical Use of Drugs*, 3rd edition, have refined and expanded the book previously titled, *Applied Therapeutics for Clinical Pharmacists*. It is appropriate that the title has been changed because the book can be of great value to any health professional involved in treating and monitoring patients receiving drug therapy.

Applied Therapeutics: The Clinical Use of Drugs is relatively comprehensive. The book consists of 61 chapters, 1619 pages with numerous tables and figures. The more commonly occurring chronic and acute diseases are presented with heavy emphasis being placed on drug therapy management. This book is not a substitute for a standard textbook of medicine in terms of understanding pathophysiology and diagnosis of various disease entities. It is an essential companion textbook to a medical textbook, however, and is evolving as the premier book in the field of drug therapy management of disease processes.

The book is well written and referenced. The question and answer format and utilization of case studies is particularly effective in demonstrating appropriate application of pharmacotherapeutic information in specific clinical situations. The book fosters the development of a rational approach to drug therapy management.

There is nothing esoteric about this book. It is a practical guide to optimal drug therapy. It is an excellent manual for the clinician. All health care professionals involved in primary medical care, particularly pharmacists, physicians, and nurse practitioners, would be well served by this book.

Reviewed by Tim R. Covington
Professor and Chairman
School of Pharmacy
West Virginia University
Medical Center
Morgantown, WVA 26506-6303

The Need for Information on Product Formulations

I thoroughly enjoyed your editorial "Putting An End to Secret Formulations." [1] Over the years I've had numerous debates with manufacturers over the issue of "trade secrets" (Boloney!) *versus* the health professionals' need for information on product formulations.

As you pointed out, any competitors' laboratory worth their salt will rapidly crack such "secret formulations." Therefore, the only ones kept in the dark are the physician prescribers and pharmacist dispensers of these pharmaceuticals.

Although you state that "manufacturers are required by law and regulation to make known the identity and quantity of the medicinally active ingredients in their products," even this is not always the case. For example, in many artificial tear solutions and contact lens solutions, the functionally active components may only be identified as "a water-soluble polymeric system" or "an anionic surface-active agent."

If health care professionals are to make informed product selection decisions, the industry must provide this needed information. Although regulatory remedies may be necessary, industry leaders with vision might see that voluntary cooperation would result in benefits to all concerned.

Must we have mandatory CE before pharmacists accept their obligation to maintain their competence? Must we have mandatory relabeling requirements before the industry responds to the information needs of the public? Must we always have an expensive, legislative, regulated, bureaucratized solution to every problem?

The PMA has taken a significant first step in stating "the medical justification for disclosure . . . warrants release of that information . . ." Let's hope that individual manufacturers respond to your call for "putting an end to secret formulations."

James R. Boyd
Editor-in-Chief
"Facts and Comparisons"
St. Louis, MO 63146

[1] Edward G. Feldmann, *J. Pharm. Sci.*, **73**, 577 (1984).

BOOKS

Instrumental Data for Drug Analysis. Vol. 2. (Elsevier Series in Forensic and Police Science.) By TERRY MILLS III, WILLIAM N. PRICE, and J. CONRAD ROBERTSON. Elsevier Science Publishing Co., Inc. 52 Vanderbilt Ave., New York, NY 10017. 1983. pp. 662-1358. 22 × 28.5 cm. Price $95.00.

This second volume contains data on an additional 300 drug substances bringing the total compounds covered in both volumes to 600.

Each drug substance is allotted two pages on which ultraviolet, electron impact mass, proton nuclear magnetic resonance, and Fourier transform infrared spectra are presented. All spectra are of exceptional quality. Also given are molecular formulas and weights, synonyms, trade names, therapeutic categories and, in shorthand style, HPLC and GC data where applicable. There are also four appendices containing standard KBr infrared spectra and, in tabular form, Kovats retention indices for gas chromatography, the ultraviolet absorption maxima in acid, basic and ethanol solution, and mass spectral indices for base peaks and prominent ions.

The atlas has been compiled by forensic scientists of the Georgia State Crime Laboratory and should be useful for the identification of drugs. Thus, the compilation serves as a supplement to the *Merck Index* which does not present spectra. The two volumes compete with two *CRC Handbooks of Mass Spectra and Spectrophotometric Data of Drugs* which together sell for about the same price. I prefer the volumes under review for better organization, clearer spectra and coverage of more drugs. One can quibble that the shorthand data on HPLC and GC are of questionable value. It also would have been useful to identify for each drug the source of the sample, particularly whether the drug was a USP reference standard.

All efforts to provide comprehensive information on drugs are welcome. Therefore, the authors should be congratulated and encouraged to continue the series.

Reviewed by Klaus G. Florey
The Squibb Institute for Medical Research
P.O. Box 191
New Brunswick, NJ 08903

Applied Therapeutics: The Clinical Use of Drugs, 3rd Ed. Edited by BRIAN S. KATCHER, LLOYD YEE YOUNG, and MARY ANNE KODA-KIMBLE. Applied Therapeutics, Inc., P.O. Box 1903, Spokane, WA 99210-1903. 1983. 1,619 pp. 19.5 × 24 cm. Price $54.00.

The editors and authors of *Applied Therapeutics: The Clinical Use of Drugs*, 3rd edition, have refined and expanded the book previously titled, *Applied Therapeutics for Clinical Pharmacists*. It is appropriate that the title has been changed because the book can be of great value to any health professional involved in treating and monitoring patients receiving drug therapy.

Applied Therapeutics: The Clinical Use of Drugs is relatively comprehensive. The book consists of 61 chapters, 1619 pages with numerous tables and figures. The more commonly occurring chronic and acute diseases are presented with heavy emphasis being placed on drug therapy management. This book is not a substitute for a standard textbook of medicine in terms of understanding pathophysiology and diagnosis of various disease entities. It is an essential companion textbook to a medical textbook, however, and is evolving as the premier book in the field of drug therapy management of disease processes.

The book is well written and referenced. The question and answer format and utilization of case studies is particularly effective in demonstrating appropriate application of pharmacotherapeutic information in specific clinical situations. The book fosters the development of a rational approach to drug therapy management.

There is nothing esoteric about this book. It is a practical guide to optimal drug therapy. It is an excellent manual for the clinician. All health care professionals involved in primary medical care, particularly pharmacists, physicians, and nurse practitioners, would be well served by this book.

Reviewed by Tim R. Covington
Professor and Chairman
School of Pharmacy
West Virginia University
Medical Center
Morgantown, WVA 26506-6303

The Need for Information on Product Formulations

I thoroughly enjoyed your editorial "Putting An End to Secret Formulations." [1] Over the years I've had numerous debates with manufacturers over the issue of "trade secrets" (Boloney!) *versus* the health professionals' need for information on product formulations.

As you pointed out, any competitors' laboratory worth their salt will rapidly crack such "secret formulations." Therefore, the only ones kept in the dark are the physician prescribers and pharmacist dispensers of these pharmaceuticals.

Although you state that "manufacturers are required by law and regulation to make known the identity and quantity of the medicinally active ingredients in their products," even this is not always the case. For example, in many artificial tear solutions and contact lens solutions, the functionally active components may only be identified as "a water-soluble polymeric system" or "an anionic surface-active agent."

If health care professionals are to make informed product selection decisions, the industry must provide this needed information. Although regulatory remedies may be necessary, industry leaders with vision might see that voluntary cooperation would result in benefits to all concerned.

Must we have mandatory CE before pharmacists accept their obligation to maintain their competence? Must we have mandatory relabeling requirements before the industry responds to the information needs of the public? Must we always have an expensive, legislative, regulated, bureaucratized solution to every problem?

The PMA has taken a significant first step in stating "the medical justification for disclosure . . . warrants release of that information . . ." Let's hope that individual manufacturers respond to your call for "putting an end to secret formulations."

James R. Boyd
Editor-in-Chief
"Facts and Comparisons"
St. Louis, MO 63146

[1] Edward G. Feldmann, *J. Pharm. Sci.*, **73**, 577 (1984).

BOOKS

Instrumental Data for Drug Analysis. Vol. 2. (Elsevier Series in Forensic and Police Science.) By TERRY MILLS III, WILLIAM N. PRICE, and J. CONRAD ROBERTSON. Elsevier Science Publishing Co., Inc. 52 Vanderbilt Ave., New York, NY 10017. 1983. pp. 662-1358. 22 × 28.5 cm. Price $95.00.

This second volume contains data on an additional 300 drug substances bringing the total compounds covered in both volumes to 600.

Each drug substance is allotted two pages on which ultraviolet, electron impact mass, proton nuclear magnetic resonance, and Fourier transform infrared spectra are presented. All spectra are of exceptional quality. Also given are molecular formulas and weights, synonyms, trade names, therapeutic categories and, in shorthand style, HPLC and GC data where applicable. There are also four appendices containing standard KBr infrared spectra and, in tabular form, Kovats retention indices for gas chromatography, the ultraviolet absorption maxima in acid, basic and ethanol solution, and mass spectral indices for base peaks and prominent ions.

The atlas has been compiled by forensic scientists of the Georgia State Crime Laboratory and should be useful for the identification of drugs. Thus, the compilation serves as a supplement to the *Merck Index* which does not present spectra. The two volumes compete with two *CRC Handbooks of Mass Spectra and Spectrophotometric Data of Drugs* which together sell for about the same price. I prefer the volumes under review for better organization, clearer spectra and coverage of more drugs. One can quibble that the shorthand data on HPLC and GC are of questionable value. It also would have been useful to identify for each drug the source of the sample, particularly whether the drug was a USP reference standard.

All efforts to provide comprehensive information on drugs are welcome. Therefore, the authors should be congratulated and encouraged to continue the series.

Reviewed by Klaus G. Florey
The Squibb Institute for Medical Research
P.O. Box 191
New Brunswick, NJ 08903

Applied Therapeutics: The Clinical Use of Drugs, 3rd Ed. Edited by BRIAN S. KATCHER, LLOYD YEE YOUNG, and MARY ANNE KODA-KIMBLE. Applied Therapeutics, Inc., P.O. Box 1903, Spokane, WA 99210-1903. 1983. 1,619 pp. 19.5 × 24 cm. Price $54.00.

The editors and authors of *Applied Therapeutics: The Clinical Use of Drugs*, 3rd edition, have refined and expanded the book previously titled, *Applied Therapeutics for Clinical Pharmacists*. It is appropriate that the title has been changed because the book can be of great value to any health professional involved in treating and monitoring patients receiving drug therapy.

Applied Therapeutics: The Clinical Use of Drugs is relatively comprehensive. The book consists of 61 chapters, 1619 pages with numerous tables and figures. The more commonly occurring chronic and acute diseases are presented with heavy emphasis being placed on drug therapy management. This book is not a substitute for a standard textbook of medicine in terms of understanding pathophysiology and diagnosis of various disease entities. It is an essential companion textbook to a medical textbook, however, and is evolving as the premier book in the field of drug therapy management of disease processes.

The book is well written and referenced. The question and answer format and utilization of case studies is particularly effective in demonstrating appropriate application of pharmacotherapeutic information in specific clinical situations. The book fosters the development of a rational approach to drug therapy management.

There is nothing esoteric about this book. It is a practical guide to optimal drug therapy. It is an excellent manual for the clinician. All health care professionals involved in primary medical care, particularly pharmacists, physicians, and nurse practitioners, would be well served by this book.

Reviewed by Tim R. Covington
Professor and Chairman
School of Pharmacy
West Virginia University
Medical Center
Morgantown, WVA 26506-6303

Advances in Chromatography, Vol. 22. Edited by J. CALVIN GIDDINGS, ELI GRUSHKA, JACK CAZES, and PHYLLIS R. BROWN. Marcel Dekker, 270 Madison Avenue, New York, NY 10016. 1983. 344 pp. 15.5 × 23.4 cm. Price $49.75.

The latest volume maintains the high quality that chromatographers have come to expect from this invaluable series. Eleven authors present reviews of seven contemporary topical areas in liquid chromatography.

This volume is comprised of chapters dealing with HPLC and mass spectrometry of neuropeptides, HPLC of amino acids, chromatographic resolution of racemates, HPLC of metal complexes, chromatography of carotenoids and retinoids, HPLC of porphyrins, and small bore columns in liquid chromatography. Without exception, these reviews are authored by individuals actively working and publishing in their respective fields and all are authoritative and well written. There is also reasonable uniformity of organization of the first six chapters, indicative of active editorial involvement in the final publication. The final chapter focuses on the theoretical and practical application of a technology (small bore columns) rather than on a specific class of compounds, and is also well written, albeit organized along different lines.

Following a brief introduction, each chapter presents a critical review of the specific analytical problem using detailed examples. The summary sections, in which the authors' views toward the direction that important developments will likely take, separates this treatment from a bland, noncritical review of a multitude of published articles. The chapters are well referenced and generally encompass the literature well into 1982, making this a reasonably up-to-date volume in this rapidly changing field.

Like previous volumes in this series, this book is more useful as a reference for scientists from many disciplines involved with separation problems than as a textbook in a specific graduate course. Because of its obvious emphasis on biologically important molecules (neuropeptides, amino acids, retinoids, and porphyrins), it is particularly recommended to biochemists and clinical/analytical chemists involved with these separation problems. Its treatment, however, is sufficiently broad so that many other researchers who utilize HPLC should consider adding this to their personal libraries.

Reviewed by Jordan L. Cohen
University of Southern California
School of Pharmacy
Los Angeles, CA 90033

Information Theoretic Indices for Characterization of Chemical Structures. By DANAIL BONCHEV. Research Studies Press. John Wiley & Sons, Inc. One Wiley Dr., Somerset, NJ 08873. 1983. 249 pp. 15.5 × 23.5 cm. Price $54.95

This book is a presentation of information theory as it is applied to chemical structures. Regretably, the author devotes only eight pages to the basic Shannon equation—its meaning and broad implications in science. Much of the work presented in this book is based on Bonchev's studies. Chapters 3 and 4 deal with atomic and molecular information, respectively. Under the discussion of molecules, the author briefly reviews graph theory and some of the topological indices such as molecular connectivity. These are not based upon probabilities, as is the Shannon equation, and so should not be classed with indices based upon information theory. A large number of indices are reviewed in Chapter 4 based upon various attributes of molecular structure or their graphic representations. It is apparent that there is a rich potential here for structure quantitation; however, practically no examples are presented where correlations with real physical properties are achieved. Only 30 pages at the end of the book are devoted to applications of any of the indices to chemical or biological problems.

Much of the work presented in this book has yet to bear real fruit in terms of structure quantitation influencing physical or biological properties. Perhaps within a decade much will have been published using this approach in QSAR studies and then this book may be regarded as a classic work. On that basis it is valuable to the scientist with a creative and pioneering spirit. I'm glad I've got a copy.

Reviewed by Lemont B. Kier
Department of Medicinal Chemistry
School of Pharmacy
Virginia Commonwealth University
Richmond, VA

The Clinical Research Process in the Pharmaceutical Industry. (Drugs and the Pharmaceutical Sciences, Vol. 19). Edited by GARY M. MATOREN. Marcel Dekker, Inc., 270 Madison Ave., New York NY 10016. 1984. 549 pp. 16 × 23.5 cm. Price $59.75.

The first edition of this comprehensive reference covers all of the pertinent aspects of industrial pharmaceutical research and development. It represents a major step forward in the identification and description of the critical aspects of new drug development, which the book terms "pharmogenology."

The 27 chapters in this book have been written by a truly distinguished group of academicians, industrial scientists, and regulatory experts. Each chapter represents a step in the critical path through which each new drug must pass on its way towards an N.D.A. submission. In addition, there are a number of specialized chapters in this book dealing with critical aspects that form the background for the drug development process. In these chapters, the following topics are covered: Legal and Ethical Problems in Clinical Research; The Monitoring Process; Research Quality Assurance; The Role of Contract Research Organizations; The Impact of the Pharmaceutical Industry on Health Care; and Career Opportunities in Industrial Clinical Research.

The Clinical Research Process in the Pharmaceutical Industry is an indispensable reference for R&D managers in the pharmaceutical industry, for clinical pharmacists in medical center hospitals, and for academicians and students in clinical research and drug regulatory affairs.

Reviewed by Jack W. Reich
Assistant Dean for Research and Development
Creighton University
School of Pharmacy
Omaha, NE 68178

Drug Dosage and Administration—Modern Theory and Practice. By JOSEPH WARTAK. University Park Press, 300 North Charles Street, Baltimore, MD 21201. 1983. 173 pp. 18 × 26 cm. Price $32.50.

This volume is authored by a research cardiologist from Canada who claims it is "intended for medical students and physicians." The book is divided into five parts dealing with "Dosage of Drugs," "Drug Concentrations in Blood," "Presentation of Drugs," "Administration of Drugs," and "Rational Use of Drugs." Each part is further divided into five or more chapters. In addition, a slide rule is provided for dosage adjustment and calculations. The current volume appears to be closely related to another book, by the same author, entitled "Clinical Pharmacokinetics: A Modern Approach to Individualized Drug Therapy," published by Praeger Scientific.

Part I presents very basic information on drug dosage scales; concepts of minimal, maximal, and average doses; and individualization of drug dosage and dosage adjustment in children and in patients with renal impairment. Use of the slide rule is included in the illustrations.

Part II deals with elementary pharmacokinetic principles presented in a manner that assumes that the reader is completely unfamiliar with any of these concepts. A few comments on the dose-response relationship are also included. Drug dosage forms including basic information on solid, semi-solid, liquid, long-acting, and sustained release dosage forms are presented in Part III.

Part IV contains information on different modes of drug administration including enteral administration, intravenous injection and infusion, pulmonary and local administration, and a few sentences on transdermal drug delivery systems. Planning a treatment program, choice of drugs and the outcome of drug treatment are discussed in Part V. A bibliography of 52 references is presented at the end of the book.

This book is a very superficial presentation of the many concepts embodied in the disciplines of pharmacokinetics and biopharmacokinetics and their application to drug therapy. These concepts are presented in such a simplistic fashion that the text can easily be read by a lay person. The book cannot be recommended for anyone other than the junior medical student, nursing staff, or other paramedical personnel. It is of very limited value for the pharmacist, pharmacy student, academic physician, or pharmaceutical scientist. Its purchase, therefore, cannot be recommended.

Reviewed by Iqbal Ramzan
School of Pharmacy
Department of Pharmaceutics
State University of New York at Buffalo
Buffalo, NY 14260

Advances in Chromatography, Vol. 22. Edited by J. CALVIN GIDDINGS, ELI GRUSHKA, JACK CAZES, and PHYLLIS R. BROWN. Marcel Dekker, 270 Madison Avenue, New York, NY 10016. 1983. 344 pp. 15.5 × 23.4 cm. Price $49.75.

The latest volume maintains the high quality that chromatographers have come to expect from this invaluable series. Eleven authors present reviews of seven contemporary topical areas in liquid chromatography.

This volume is comprised of chapters dealing with HPLC and mass spectrometry of neuropeptides, HPLC of amino acids, chromatographic resolution of racemates, HPLC of metal complexes, chromatography of carotenoids and retinoids, HPLC of porphyrins, and small bore columns in liquid chromatography. Without exception, these reviews are authored by individuals actively working and publishing in their respective fields and all are authoritative and well written. There is also reasonable uniformity of organization of the first six chapters, indicative of active editorial involvement in the final publication. The final chapter focuses on the theoretical and practical application of a technology (small bore columns) rather than on a specific class of compounds, and is also well written, albeit organized along different lines.

Following a brief introduction, each chapter presents a critical review of the specific analytical problem using detailed examples. The summary sections, in which the authors' views toward the direction that important developments will likely take, separates this treatment from a bland, noncritical review of a multitude of published articles. The chapters are well referenced and generally encompass the literature well into 1982, making this a reasonably up-to-date volume in this rapidly changing field.

Like previous volumes in this series, this book is more useful as a reference for scientists from many disciplines involved with separation problems than as a textbook in a specific graduate course. Because of its obvious emphasis on biologically important molecules (neuropeptides, amino acids, retinoids, and porphyrins), it is particularly recommended to biochemists and clinical/analytical chemists involved with these separation problems. Its treatment, however, is sufficiently broad so that many other researchers who utilize HPLC should consider adding this to their personal libraries.

Reviewed by Jordan L. Cohen
University of Southern California
School of Pharmacy
Los Angeles, CA 90033

Information Theoretic Indices for Characterization of Chemical Structures. By DANAIL BONCHEV. Research Studies Press. John Wiley & Sons, Inc. One Wiley Dr., Somerset, NJ 08873. 1983. 249 pp. 15.5 × 23.5 cm. Price $54.95

This book is a presentation of information theory as it is applied to chemical structures. Regretably, the author devotes only eight pages to the basic Shannon equation—its meaning and broad implications in science. Much of the work presented in this book is based on Bonchev's studies. Chapters 3 and 4 deal with atomic and molecular information, respectively. Under the discussion of molecules, the author briefly reviews graph theory and some of the topological indices such as molecular connectivity. These are not based upon probabilities, as is the Shannon equation, and so should not be classed with indices based upon information theory. A large number of indices are reviewed in Chapter 4 based upon various attributes of molecular structure or their graphic representations. It is apparent that there is a rich potential here for structure quantitation; however, practically no examples are presented where correlations with real physical properties are achieved. Only 30 pages at the end of the book are devoted to applications of any of the indices to chemical or biological problems.

Much of the work presented in this book has yet to bear real fruit in terms of structure quantitation influencing physical or biological properties. Perhaps within a decade much will have been published using this approach in QSAR studies and then this book may be regarded as a classic work. On that basis it is valuable to the scientist with a creative and pioneering spirit. I'm glad I've got a copy.

Reviewed by Lemont B. Kier
Department of Medicinal Chemistry
School of Pharmacy
Virginia Commonwealth University
Richmond, VA

The Clinical Research Process in the Pharmaceutical Industry. (Drugs and the Pharmaceutical Sciences, Vol. 19). Edited by GARY M. MATOREN. Marcel Dekker, Inc., 270 Madison Ave., New York NY 10016. 1984. 549 pp. 16 × 23.5 cm. Price $59.75.

The first edition of this comprehensive reference covers all of the pertinent aspects of industrial pharmaceutical research and development. It represents a major step forward in the identification and description of the critical aspects of new drug development, which the book terms "pharmogenology."

The 27 chapters in this book have been written by a truly distinguished group of academicians, industrial scientists, and regulatory experts. Each chapter represents a step in the critical path through which each new drug must pass on its way towards an N.D.A. submission. In addition, there are a number of specialized chapters in this book dealing with critical aspects that form the background for the drug development process. In these chapters, the following topics are covered: Legal and Ethical Problems in Clinical Research; The Monitoring Process; Research Quality Assurance; The Role of Contract Research Organizations; The Impact of the Pharmaceutical Industry on Health Care; and Career Opportunities in Industrial Clinical Research.

The Clinical Research Process in the Pharmaceutical Industry is an indispensable reference for R&D managers in the pharmaceutical industry, for clinical pharmacists in medical center hospitals, and for academicians and students in clinical research and drug regulatory affairs.

Reviewed by Jack W. Reich
Assistant Dean for Research and Development
Creighton University
School of Pharmacy
Omaha, NE 68178

Drug Dosage and Administration—Modern Theory and Practice. By JOSEPH WARTAK. University Park Press, 300 North Charles Street, Baltimore, MD 21201. 1983. 173 pp. 18 × 26 cm. Price $32.50.

This volume is authored by a research cardiologist from Canada who claims it is "intended for medical students and physicians." The book is divided into five parts dealing with "Dosage of Drugs," "Drug Concentrations in Blood," "Presentation of Drugs," "Administration of Drugs," and "Rational Use of Drugs." Each part is further divided into five or more chapters. In addition, a slide rule is provided for dosage adjustment and calculations. The current volume appears to be closely related to another book, by the same author, entitled "Clinical Pharmacokinetics: A Modern Approach to Individualized Drug Therapy," published by Praeger Scientific.

Part I presents very basic information on drug dosage scales; concepts of minimal, maximal, and average doses; and individualization of drug dosage and dosage adjustment in children and in patients with renal impairment. Use of the slide rule is included in the illustrations.

Part II deals with elementary pharmacokinetic principles presented in a manner that assumes that the reader is completely unfamiliar with any of these concepts. A few comments on the dose-response relationship are also included. Drug dosage forms including basic information on solid, semi-solid, liquid, long-acting, and sustained release dosage forms are presented in Part III.

Part IV contains information on different modes of drug administration including enteral administration, intravenous injection and infusion, pulmonary and local administration, and a few sentences on transdermal drug delivery systems. Planning a treatment program, choice of drugs and the outcome of drug treatment are discussed in Part V. A bibliography of 52 references is presented at the end of the book.

This book is a very superficial presentation of the many concepts embodied in the disciplines of pharmacokinetics and biopharmacokinetics and their application to drug therapy. These concepts are presented in such a simplistic fashion that the text can easily be read by a lay person. The book cannot be recommended for anyone other than the junior medical student, nursing staff, or other paramedical personnel. It is of very limited value for the pharmacist, pharmacy student, academic physician, or pharmaceutical scientist. Its purchase, therefore, cannot be recommended.

Reviewed by Iqbal Ramzan
School of Pharmacy
Department of Pharmaceutics
State University of New York at Buffalo
Buffalo, NY 14260

Advances in Chromatography, Vol. 22. Edited by J. CALVIN GIDDINGS, ELI GRUSHKA, JACK CAZES, and PHYLLIS R. BROWN. Marcel Dekker, 270 Madison Avenue, New York, NY 10016. 1983. 344 pp. 15.5 × 23.4 cm. Price $49.75.

The latest volume maintains the high quality that chromatographers have come to expect from this invaluable series. Eleven authors present reviews of seven contemporary topical areas in liquid chromatography.

This volume is comprised of chapters dealing with HPLC and mass spectrometry of neuropeptides, HPLC of amino acids, chromatographic resolution of racemates, HPLC of metal complexes, chromatography of carotenoids and retinoids, HPLC of porphyrins, and small bore columns in liquid chromatography. Without exception, these reviews are authored by individuals actively working and publishing in their respective fields and all are authoritative and well written. There is also reasonable uniformity of organization of the first six chapters, indicative of active editorial involvement in the final publication. The final chapter focuses on the theoretical and practical application of a technology (small bore columns) rather than on a specific class of compounds, and is also well written, albeit organized along different lines.

Following a brief introduction, each chapter presents a critical review of the specific analytical problem using detailed examples. The summary sections, in which the authors' views toward the direction that important developments will likely take, separates this treatment from a bland, noncritical review of a multitude of published articles. The chapters are well referenced and generally encompass the literature well into 1982, making this a reasonably up-to-date volume in this rapidly changing field.

Like previous volumes in this series, this book is more useful as a reference for scientists from many disciplines involved with separation problems than as a textbook in a specific graduate course. Because of its obvious emphasis on biologically important molecules (neuropeptides, amino acids, retinoids, and porphyrins), it is particularly recommended to biochemists and clinical/analytical chemists involved with these separation problems. Its treatment, however, is sufficiently broad so that many other researchers who utilize HPLC should consider adding this to their personal libraries.

Reviewed by Jordan L. Cohen
University of Southern California
School of Pharmacy
Los Angeles, CA 90033

Information Theoretic Indices for Characterization of Chemical Structures. By DANAIL BONCHEV. Research Studies Press. John Wiley & Sons, Inc. One Wiley Dr., Somerset, NJ 08873. 1983. 249 pp. 15.5 × 23.5 cm. Price $54.95

This book is a presentation of information theory as it is applied to chemical structures. Regretably, the author devotes only eight pages to the basic Shannon equation—its meaning and broad implications in science. Much of the work presented in this book is based on Bonchev's studies. Chapters 3 and 4 deal with atomic and molecular information, respectively. Under the discussion of molecules, the author briefly reviews graph theory and some of the topological indices such as molecular connectivity. These are not based upon probabilities, as is the Shannon equation, and so should not be classed with indices based upon information theory. A large number of indices are reviewed in Chapter 4 based upon various attributes of molecular structure or their graphic representations. It is apparent that there is a rich potential here for structure quantitation; however, practically no examples are presented where correlations with real physical properties are achieved. Only 30 pages at the end of the book are devoted to applications of any of the indices to chemical or biological problems.

Much of the work presented in this book has yet to bear real fruit in terms of structure quantitation influencing physical or biological properties. Perhaps within a decade much will have been published using this approach in QSAR studies and then this book may be regarded as a classic work. On that basis it is valuable to the scientist with a creative and pioneering spirit. I'm glad I've got a copy.

Reviewed by Lemont B. Kier
Department of Medicinal Chemistry
School of Pharmacy
Virginia Commonwealth University
Richmond, VA

The Clinical Research Process in the Pharmaceutical Industry. (Drugs and the Pharmaceutical Sciences, Vol. 19). Edited by GARY M. MATOREN. Marcel Dekker, Inc., 270 Madison Ave., New York NY 10016. 1984. 549 pp. 16 × 23.5 cm. Price $59.75.

The first edition of this comprehensive reference covers all of the pertinent aspects of industrial pharmaceutical research and development. It represents a major step forward in the identification and description of the critical aspects of new drug development, which the book terms "pharmogenology."

The 27 chapters in this book have been written by a truly distinguished group of academicians, industrial scientists, and regulatory experts. Each chapter represents a step in the critical path through which each new drug must pass on its way towards an N.D.A. submission. In addition, there are a number of specialized chapters in this book dealing with critical aspects that form the background for the drug development process. In these chapters, the following topics are covered: Legal and Ethical Problems in Clinical Research; The Monitoring Process; Research Quality Assurance; The Role of Contract Research Organizations; The Impact of the Pharmaceutical Industry on Health Care; and Career Opportunities in Industrial Clinical Research.

The Clinical Research Process in the Pharmaceutical Industry is an indispensable reference for R&D managers in the pharmaceutical industry, for clinical pharmacists in medical center hospitals, and for academicians and students in clinical research and drug regulatory affairs.

Reviewed by Jack W. Reich
Assistant Dean for Research and Development
Creighton University
School of Pharmacy
Omaha, NE 68178

Drug Dosage and Administration—Modern Theory and Practice. By JOSEPH WARTAK. University Park Press, 300 North Charles Street, Baltimore, MD 21201. 1983. 173 pp. 18 × 26 cm. Price $32.50.

This volume is authored by a research cardiologist from Canada who claims it is "intended for medical students and physicians." The book is divided into five parts dealing with "Dosage of Drugs," "Drug Concentrations in Blood," "Presentation of Drugs," "Administration of Drugs," and "Rational Use of Drugs." Each part is further divided into five or more chapters. In addition, a slide rule is provided for dosage adjustment and calculations. The current volume appears to be closely related to another book, by the same author, entitled "Clinical Pharmacokinetics: A Modern Approach to Individualized Drug Therapy," published by Praeger Scientific.

Part I presents very basic information on drug dosage scales; concepts of minimal, maximal, and average doses; and individualization of drug dosage and dosage adjustment in children and in patients with renal impairment. Use of the slide rule is included in the illustrations.

Part II deals with elementary pharmacokinetic principles presented in a manner that assumes that the reader is completely unfamiliar with any of these concepts. A few comments on the dose-response relationship are also included. Drug dosage forms including basic information on solid, semi-solid, liquid, long-acting, and sustained release dosage forms are presented in Part III.

Part IV contains information on different modes of drug administration including enteral administration, intravenous injection and infusion, pulmonary and local administration, and a few sentences on transdermal drug delivery systems. Planning a treatment program, choice of drugs and the outcome of drug treatment are discussed in Part V. A bibliography of 52 references is presented at the end of the book.

This book is a very superficial presentation of the many concepts embodied in the disciplines of pharmacokinetics and biopharmacokinetics and their application to drug therapy. These concepts are presented in such a simplistic fashion that the text can easily be read by a lay person. The book cannot be recommended for anyone other than the junior medical student, nursing staff, or other paramedical personnel. It is of very limited value for the pharmacist, pharmacy student, academic physician, or pharmaceutical scientist. Its purchase, therefore, cannot be recommended.

Reviewed by Iqbal Ramzan
School of Pharmacy
Department of Pharmaceutics
State University of New York at Buffalo
Buffalo, NY 14260

Advances in Chromatography, Vol. 22. Edited by J. CALVIN GIDDINGS, ELI GRUSHKA, JACK CAZES, and PHYLLIS R. BROWN. Marcel Dekker, 270 Madison Avenue, New York, NY 10016. 1983. 344 pp. 15.5 × 23.4 cm. Price $49.75.

The latest volume maintains the high quality that chromatographers have come to expect from this invaluable series. Eleven authors present reviews of seven contemporary topical areas in liquid chromatography.

This volume is comprised of chapters dealing with HPLC and mass spectrometry of neuropeptides, HPLC of amino acids, chromatographic resolution of racemates, HPLC of metal complexes, chromatography of carotenoids and retinoids, HPLC of porphyrins, and small bore columns in liquid chromatography. Without exception, these reviews are authored by individuals actively working and publishing in their respective fields and all are authoritative and well written. There is also reasonable uniformity of organization of the first six chapters, indicative of active editorial involvement in the final publication. The final chapter focuses on the theoretical and practical application of a technology (small bore columns) rather than on a specific class of compounds, and is also well written, albeit organized along different lines.

Following a brief introduction, each chapter presents a critical review of the specific analytical problem using detailed examples. The summary sections, in which the authors' views toward the direction that important developments will likely take, separates this treatment from a bland, noncritical review of a multitude of published articles. The chapters are well referenced and generally encompass the literature well into 1982, making this a reasonably up-to-date volume in this rapidly changing field.

Like previous volumes in this series, this book is more useful as a reference for scientists from many disciplines involved with separation problems than as a textbook in a specific graduate course. Because of its obvious emphasis on biologically important molecules (neuropeptides, amino acids, retinoids, and porphyrins), it is particularly recommended to biochemists and clinical/analytical chemists involved with these separation problems. Its treatment, however, is sufficiently broad so that many other researchers who utilize HPLC should consider adding this to their personal libraries.

Reviewed by Jordan L. Cohen
University of Southern California
School of Pharmacy
Los Angeles, CA 90033

Information Theoretic Indices for Characterization of Chemical Structures. By DANAIL BONCHEV. Research Studies Press. John Wiley & Sons, Inc. One Wiley Dr., Somerset, NJ 08873. 1983. 249 pp. 15.5 × 23.5 cm. Price $54.95

This book is a presentation of information theory as it is applied to chemical structures. Regretably, the author devotes only eight pages to the basic Shannon equation—its meaning and broad implications in science. Much of the work presented in this book is based on Bonchev's studies. Chapters 3 and 4 deal with atomic and molecular information, respectively. Under the discussion of molecules, the author briefly reviews graph theory and some of the topological indices such as molecular connectivity. These are not based upon probabilities, as is the Shannon equation, and so should not be classed with indices based upon information theory. A large number of indices are reviewed in Chapter 4 based upon various attributes of molecular structure or their graphic representations. It is apparent that there is a rich potential here for structure quantitation; however, practically no examples are presented where correlations with real physical properties are achieved. Only 30 pages at the end of the book are devoted to applications of any of the indices to chemical or biological problems.

Much of the work presented in this book has yet to bear real fruit in terms of structure quantitation influencing physical or biological properties. Perhaps within a decade much will have been published using this approach in QSAR studies and then this book may be regarded as a classic work. On that basis it is valuable to the scientist with a creative and pioneering spirit. I'm glad I've got a copy.

Reviewed by Lemont B. Kier
Department of Medicinal Chemistry
School of Pharmacy
Virginia Commonwealth University
Richmond, VA

The Clinical Research Process in the Pharmaceutical Industry. (Drugs and the Pharmaceutical Sciences, Vol. 19). Edited by GARY M. MATOREN. Marcel Dekker, Inc., 270 Madison Ave., New York NY 10016. 1984. 549 pp. 16 × 23.5 cm. Price $59.75.

The first edition of this comprehensive reference covers all of the pertinent aspects of industrial pharmaceutical research and development. It represents a major step forward in the identification and description of the critical aspects of new drug development, which the book terms "pharmogenology."

The 27 chapters in this book have been written by a truly distinguished group of academicians, industrial scientists, and regulatory experts. Each chapter represents a step in the critical path through which each new drug must pass on its way towards an N.D.A. submission. In addition, there are a number of specialized chapters in this book dealing with critical aspects that form the background for the drug development process. In these chapters, the following topics are covered: Legal and Ethical Problems in Clinical Research; The Monitoring Process; Research Quality Assurance; The Role of Contract Research Organizations; The Impact of the Pharmaceutical Industry on Health Care; and Career Opportunities in Industrial Clinical Research.

The Clinical Research Process in the Pharmaceutical Industry is an indispensable reference for R&D managers in the pharmaceutical industry, for clinical pharmacists in medical center hospitals, and for academicians and students in clinical research and drug regulatory affairs.

Reviewed by Jack W. Reich
Assistant Dean for Research and Development
Creighton University
School of Pharmacy
Omaha, NE 68178

Drug Dosage and Administration—Modern Theory and Practice. By JOSEPH WARTAK. University Park Press, 300 North Charles Street, Baltimore, MD 21201. 1983. 173 pp. 18 × 26 cm. Price $32.50.

This volume is authored by a research cardiologist from Canada who claims it is "intended for medical students and physicians." The book is divided into five parts dealing with "Dosage of Drugs," "Drug Concentrations in Blood," "Presentation of Drugs," "Administration of Drugs," and "Rational Use of Drugs." Each part is further divided into five or more chapters. In addition, a slide rule is provided for dosage adjustment and calculations. The current volume appears to be closely related to another book, by the same author, entitled "Clinical Pharmacokinetics: A Modern Approach to Individualized Drug Therapy," published by Praeger Scientific.

Part I presents very basic information on drug dosage scales; concepts of minimal, maximal, and average doses; and individualization of drug dosage and dosage adjustment in children and in patients with renal impairment. Use of the slide rule is included in the illustrations.

Part II deals with elementary pharmacokinetic principles presented in a manner that assumes that the reader is completely unfamiliar with any of these concepts. A few comments on the dose-response relationship are also included. Drug dosage forms including basic information on solid, semi-solid, liquid, long-acting, and sustained release dosage forms are presented in Part III.

Part IV contains information on different modes of drug administration including enteral administration, intravenous injection and infusion, pulmonary and local administration, and a few sentences on transdermal drug delivery systems. Planning a treatment program, choice of drugs and the outcome of drug treatment are discussed in Part V. A bibliography of 52 references is presented at the end of the book.

This book is a very superficial presentation of the many concepts embodied in the disciplines of pharmacokinetics and biopharmacokinetics and their application to drug therapy. These concepts are presented in such a simplistic fashion that the text can easily be read by a lay person. The book cannot be recommended for anyone other than the junior medical student, nursing staff, or other paramedical personnel. It is of very limited value for the pharmacist, pharmacy student, academic physician, or pharmaceutical scientist. Its purchase, therefore, cannot be recommended.

Reviewed by Iqbal Ramzan
School of Pharmacy
Department of Pharmaceutics
State University of New York at Buffalo
Buffalo, NY 14260

A publication of the
American Pharmaceutical Association—
the National Professional Society
of Pharmacists

JOURNAL OF PHARMACEUTICAL SCIENCES

Volume 73, 1984

JPMSAE 73(1-12) 1-1910 (1984)
ISSN 0022-3549

Sharon G. Boots
Editor

Sue A. Kruger
Production Editor

Margaret M. Madeleine
Assistant Production Editor

Karen A. Blakney
Copy Editor

Edward G. Feldmann
Contributing Editor

Samuel W. Goldstein
Contributing Editor

Patricia A. Evich
Editorial Secretary

Editorial Advisory Board

Jordan L. Cohen
Kenneth A. Connors
Louis Diamond
Ho-Leung Fung
Milo Gibaldi
Everett N. Hiestand
W. Homer Lawrence
Ian W. Mathison
Carl M. Metzler
Robert E. Notari
Paul L. Schiff, Jr.
Jane E. Shaw

Published monthly under the supervision of the Board of Trustees

"Scientific Proof"—An Elusive Goal

Every two to three years since 1965, we have witnessed the appointment and installation of a new Commissioner to head the U.S. Food and Drug Administration. And, although their respective interests, expertise, and styles of operation have varied, we can honestly say that each performed capably and with distinction. Each of them was a credit to the Agency, to the health care professions, and to the nation.

We have often used the occasion of a new Commissioner's appointment to devote our editorial to welcoming him to Washington and to his new position. But the "welcome" was only an incidental message packaged in with some other key point that appeared to us to be pertinent and timely.

For example, when Commissioner Arthur Hull Hayes assumed office we noted the prevailing change in the national regulatory climate ("FDA Takes a Turn in the Road"). With Commissioner Jere Goyan we addressed his philosophic approach to education *versus* regulation ("FDA: Policeman or Teacher?"). The Alexander M. Schmidt to Donald Kennedy transition prompted us to comment on how each Commissioner has left his own individual imprint on the Agency ("Passing the Baton at FDA"). And, in addition to welcoming the new Commissioner, we have also expressed concern that the frequent rate of turn-over in that office has had a damaging effect on the FDA and the morale of its staff ("A Plea for FDA Stability").

The opening two paragraphs from that latter editorial, in July 1979, are again all too relevant and seem to merit repeating:

"Kings, popes, and presidents come and go with the passing of time. It should not be strange, therefore, that the same is true of Food and Drug Commissioners.

"Nevertheless, the departure of the last several FDA Commissioners has seemed to have come too soon, too abruptly, and all too unexpectedly. Indeed, each of them seems to have little more than arrived, got settled in office, established an operating style, developed a rapport with the health professions and the regulated industry, when 'poof!'—they were gone from office!"

With that lamentation regarding all-too-brief tenure now aside, it is our pleasure to welcome the latest resident to the "hot seat" of the Parklawn Building where FDA is headquartered.

Frank E. Young, M.D., Ph.D., comes to the Agency with little previous FDA or regulatory background, but with a solid reputation as a microbiological scientist. He is noted for his work in genetics and recombinant DNA—an area that is soon going to require some landmark FDA attention and regulation. Consequently, we may again see a fortuitous situation at FDA in that the right person was in the job at just the right time to handle the chief problem or problems of the period.

But the key observation that we would like to bring out in this editorial relates to the increasing complexity of the decisions that the FDA Commissioner is required to make as technology advances and life in general becomes more and more complicated.

Consider, for example, one of the items that Commissioner Young found near the top of his "in box" when he assumed office: namely, the Pandora's Box of artificial sweeteners.

At various times, FDA has approved three artificial sweetening agents: saccharin, cyclamate, and aspartame. Subsequently, it rescinded its approval of cyclamate and that agent is currently off the market in the U.S. (but continues to be available in Canada and some other countries). Later, it acted to rescind its approval of saccharin, but Congress stepped in and, *via* legislation, applied a year-by-year staying action on that ban. And, although it has yet to respond officially (as of this writing), FDA is now the object of a request to Congress by the consumer-oriented lobbying group Common Cause to investigate the merit and justification for FDA's approval of aspartame. Common Cause has been joined by a second organization, the Community Nutrition Institute, which has also mounted a legal challenge to the approval of aspartame.

The basic problem common to all three of these regulatory actions dealing with the artificial sweeteners is the Delany Amendment to the Federal Food, Drug, and Cosmetic Act. That clause prohibits the marketing of any food additive that, under virtually any conditions of use or testing, has been shown to cause cancer. The specific wording reads: "no (food) additive shall be deemed to be safe if it is found to induce cancer when ingested by man or animal."

Deceptively simple sounding, this provision leads to incredible complications. In animal studies, for example, animals have been tested for their full life-time with daily dose-levels at thousands of times what would normally be ingested; then perhaps only a few animals developed tumors—but at just slightly higher levels than the control group. Under these circumstances, how does a scientist make a judgment that the agent induced cancer or not?

Dr. Young will soon find that even the legendary wisdom of Solomon would be sorely tested in deciding upon the artificial sweetner question. Specifically, in addition to the above mentioned brouhaha over aspartame, the Congressional stay on the saccharin ban will expire in April 1985 and, if the stay is not extended, FDA will need to take some action. But perhaps even more significant is the reconsideration now being given to cyclamate.

The FDA's cancer assessment committee concluded in April that cyclamate is not a carcinogen after all, and the National Research Council (NRC) has been commissioned to issue an independent judgment.

The NRC's Commission on Life Sciences reported on its acceptance of this study assignment in that organization's Summer 1984 *newsletter*. In the lead article, entitled "Cyclamates Revisited," the NRC reporter begins with a quote from the September 16, 1980, issue of the *Federal Register:* "Cyclamate has not been shown not to cause cancer; and . . . cyclamate has not been shown not to cause heritable genetic damage." The reader is literally tied in knots by the double negatives!

The difficult position of the FDA Commissioner was further emphasized to us recently in a private conversation with a past Commissioner in which he told us that he saw no proof that saccharin was carcinogenic; but he also saw no absolute proof that it wasn't carcinogenic either. Hence, he felt that the law obligated him to recommend it be banned—demonstration of safety being a prerequisite of marketing approval.

But how can safety be proven? Especially absolute safety, and proven in terms that satisfy scientists, the public, and the Congress?

Commissioner Young will probably be forced "to bite the bullet" in this issue, to a far greater degree than any of his predecessors. It will be a most difficult decision. For his own sake, as well as that of science, the FDA, and the public at large, we hope that he has the scientific wisdom—as well as the scientific knowledge—to make the right choice.

—EDWARD G. FELDMANN
American Pharmaceutical Association
2215 Constitution Avenue, N.W.
Washington, DC 20037

Editor's Note: Dr. Feldmann's editorials are an expression of personal opinion and do not necessarily reflect views or policies of APhA. The editorials are intended to be provocative and to stimulate thinking. Readers having reactions, either pro or con, are invited to submit them for publication in the *Open Forum* section.

0022-3549/84/1000-1337$01.00/0
© 1984, American Pharmaceutical Association

JOURNAL OF PHARMACEUTICAL SCIENCES

OCTOBER 1984
VOLUME 73 NUMBER 10

RESEARCH ARTICLES

Triprolidine Radioimmunoassay: Disposition in Animals and Humans

JOHN W. A. FINDLAY *x, ROBERT F. BUTZ *, GEOFFREY G. COKER ‡, RICHARD L. DEANGELIS *, and RICHARD M. WELCH *

Received August 11, 1983, from the *Department of Medicinal Biochemistry, The Wellcome Research Laboratories, Research Triangle Park, NC 27709, and the ‡ Department of Therapeutic Chemistry, The Wellcome Research Laboratories, Beckenham, Kent, United Kingdom. Accepted for publication December 6, 1983.

Abstract □ A hapten derivative of triprolidine, bearing an acrylic acid side chain *ortho* to the pyridine ring nitrogen atom, was synthesized and coupled to bovine serum albumin. Immunization of New Zealand White rabbits with the resulting drug-protein conjugate resulted in the production of antisera capable of binding a radioiodinated tyramine conjugate of the triprolidine hapten derivative at high antiserum dilutions (1:70,000–1:150,000). These antisera were used to develop a radioimmunoassay (RIA) for triprolidine in human plasma with a sensitivity limit of 0.1 ng/mL (0.01 ng of actual mass). The known hydroxymethyl and carboxyl metabolites of triprolidine cross-reacted weakly (<2 and <0.05%, respectively) with this antiserum. The RIA could be used for the direct analysis of triprolidine in human and rabbit plasma, but not for rat or dog plasma, presumably due to the presence of other interfering substances (possibly metabolites). The validity of the RIA procedure in human plasma was demonstrated by comparative analysis of a number of samples by quantitative TLC (r = 0.985, slope = 1.076). The assay was employed to describe the pharmacokinetics of triprolidine in the rabbit ($t_{1/2,\beta}$ = 1.7 h). The assay had adequate sensitivity to detect low circulating drug concentrations in humans after therapeutic oral doses and also substantiated previous disposition experiments with triprolidine in humans ($t_{1/2,\beta}$ = 2.27 h). TLC analysis demonstrated that the absolute oral bioavailability of triprolidine (1-mg/kg dose) in the dog was low (4%). A comparison of triprolidine pharmacokinetic parameters in dogs, rabbits, rats, and humans revealed considerable similarity in elimination characteristics in these species.

Keyphrases □ Triprolidine—bovine serum albumin conjugate, pharmacokinetics, animal-human comparisons, RIA compared with TLC and GC □ Radioimmunoassay—triprolidine in animals and humans, comparisons with GC and TLC

Triprolidine hydrochloride {(*E*)-2-[3-(1-pyrrolidinyl)-1-*p*-tolylpropenyl]pyridine monohydrochloride monohydrate} has been shown to have potent antihistaminic activity in animals (1–3) and to be clinically efficacious in humans (4–8). However, no detailed reports have appeared on the disposition of this drug, although [^{14}C]triprolidine was shown to be metabolized extensively *in vitro* by the guinea pig liver (9).

Circulating concentrations of triprolidine in human plasma following administration of oral therapeutic doses are very low and quite variable (10), necessitating the use of highly sensitive analytical techniques for their determination. Although TLC (11) and GC (12) procedures have been described for triprolidine, no data on the disposition of the drug were derived from these studies. A sensitive, quantitative TLC method for triprolidine was recently described by DeAngelis and coworkers (10), and the method was used to study some aspects of the disposition of this drug in rats and humans.

In this paper we present details of a specific radioimmunoassay (RIA) procedure for triprolidine which is capable of detecting 0.1 ng/mL of drug in plasma. This assay employs a gamma-emitting ^{125}I-radioligand, and thus is convenient for the analysis of large-scale triprolidine disposition studies. In the course of validating this method for human plasma analysis, the absolute oral bioavailability of triprolidine in the dog was determined by quantitative TLC, and some pharmacokinetic comparisons were made between rats, dogs, rabbits, and humans.

EXPERIMENTAL SECTION

The assay buffer used was 0.05 M Na_2HPO_4/NaH_2PO_4–0.15 M NaCl–0.01 M EDTA·Na_2–0.1% gelatin, pH 7.0. For separation of antibody-bound from free radiolabel, a dextran-coated charcoal suspension was prepared by dissolving 0.5 g of dextran[1] in 200 mL of ice-cold assay buffer, and adding 2 g of RIA-grade charcoal[2] to this solution. This suspension was stirred for at least 30 min at 0°C before use.

Hapten Synthesis—*2-Bromo-6-(4-toluoyl)pyridine* (*I*)—Butyllithium (50 mL, 1.65 M in hexane) was added under nitrogen to a stirred suspension of 2,6-dibromopyridine (19.5 g) in dry ether (200 mL) at −50°C. After 0.75 h a solution of 4-tolunitrile (10 g) in ether (50 mL) was added; stirring was continued at −50°C for 3 h. The mixture was allowed to warm to −30°C and

[1] T-70; Pharmacia Fine Chemicals, Piscataway, N.J.
[2] Schwarz-Mann, Orangeburg, N.Y.

0022-3549/84/1000-1339$01.00/0
© 1984, American Pharmaceutical Association

Table I—Structures and Cross-reactivities of Triprolidine and Related Compounds

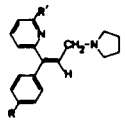

IV and X

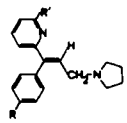

V-IX, XI and XII

Compound	R	R′	IC_{50}, ng/mL	Cross-reactivity, %[a]
IV	CH_3	$CH{=}CHCO_2H$	162.0	0.3
V	CH_3	$CH{=}CHCO_2H$	0.7	83.0
VI	CH_3	H	0.6	100.0
VII	CH_2OH	H	34.0	1.9
VIII	CO_2H	H	>1000.0	<0.05
IX	CF_3	H	1.12	49.1
X	CF_3	H	26.0	2.1
XI	CH_3	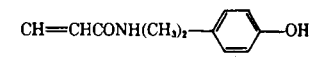	—	—
XII	CH_3	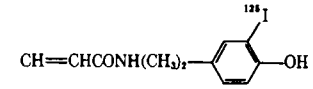	—	—

[a] Cross-reactivity of compound = (IC_{50} of triprolidine)/(IC_{50} of compound) × 100.

treated with HCl (200 mL, 2 M). The precipitated solid was collected, washed with water, and recrystallized from aqueous ethanol. The ketone formed colorless needles (12.2 g), mp 97–98°C. IR (KBr disk): 1660 cm^{-1} (aromatic ketone); ^{1}H-NMR ($CDCl_3$): δ 8.1–7.2 (m, 7, ArH) and 2.4 ppm (s, 3, Ar-CH_3).

Anal.—Calc. for $C_{23}H_{10}BrNO$: C, 56.52; H, 3.65; N, 5.07; Br, 29.0. Found: C, 56.48; H, 3.67; N, 4.93; Br, 28.53.

2-(6-Bromo-2-pyridyl)-2-(4-tolyl)-1,3-dioxolan (II)—A mixture of the above ketone (31 g), toluene (150 mL), ethylene glycol (10 mL), and *p*-toluenesulfonic acid (4 g) was heated at reflux for 6 h using a Dean–Stark trap. After cooling, the toluene solution was washed with excess ice-cold sodium bicarbonate solution, dried, and evaporated to 50 mL. Addition of petroleum ether to the warm solution induced crystallization of the dioxolan. From cyclohexane this formed colorless prisms (24.3 g), mp 110–112°C. ^{1}H-NMR ($CDCl_3$): δ 7.8–7.0 (m, 7, ArH), 4.1 (s, 4, $-CH_2-O-$), and 2.35 ppm (s, 3, Ar-CH_3).

Anal.—Calc. for $C_{15}H_{14}BrNO_2$: C, 56.25; H, 4.45; N, 4.4. Found: C, 56.48; H, 4.26; N, 4.29.

Ethyl (E)-3-[6-[(4-methylphenyl)carbonyl]-2-pyridinyl]propenoate (III)—A solution of II (3.5 g) in ether (100 mL) was cooled to −40°C and treated under nitrogen with butyllithium (10 mL, 1.64 M in hexane). After stirring at −50°C for 2 h, dimethylformamide (2 mL) was added. Two hours later the mixture was warmed to −30°C and treated with HCl (20 mL, 2 M). The organic phase was separated, washed with sodium bicarbonate solution, dried, and evaporated under reduced pressure. The residual aldehyde (2.5 g) was dissolved in 1,2-dimethoxyethane (10 mL) and added to a solution of the phosphonate carbanion produced from triethyl phosphonoacetate (2 g) and sodium hydride (0.22 g) in the same solvent. The mixture was stirred for 2 h, diluted with ether (25 mL), and treated with HCl (5 mL, 2 M). The organic phase was separated, washed with water, dried, and evaporated. The resulting oil was dissolved in ethanol (20 mL) containing concentrated HCl (3 mL) and water (3 mL). After heating on a steam bath for 10 min, the solution was diluted with ice water, rendered alkaline with sodium bicarbonate solution, and extracted with ether. After evaporation the residue was crystallized from cyclohexane as colorless platelets (1 g), mp 108–111°C. ^{1}H-NMR ($CDCl_3$): δ 7.65 (d, 1, J = 16 Hz, olefinic protons) and 6.85 ppm (d, 1, J = 16 Hz), implying *E* configuration.

Anal.—Calc. for $C_{18}H_{17}NO_3$: C, 73.2; H, 5.8; N, 4.75. Found: C, 72.7; H, 5.7; N, 4.59.

(E)-6-[(E)-3-(1-pyrrolinyl)-1-p-tolylpropenyl]-2-pyridineacrylic acid (V)—Butyllithium (10 mL, 1.64 M in hexane) was added under nitrogen to a stirred suspension of triphenyl-2-pyrrolidinoethylphosphonium bromide (13) (7.2 g) in dry toluene (75 mL). After 0.5 h, III (4.8 g) in toluene (50 mL) was added. The suspension, initially orange, became deep purple, then slowly faded to yellow during 2 h heating at 75°C. The cooled solution was diluted with ether (150 mL) and treated with HCl (50 mL, 2 M). The aqueous phase was separated, washed with ether, and basified with potassium carbonate (ice). Basic products were extracted into ether and immediately converted to oxalates by addition of oxalic acid (2.5 g) in ethanol (10 mL). The crude salts (5.1 g) melted at 148–155°C; it was shown by NMR that the new double bond had formed in the ratio 2:1, *Z*:*E*. The mixture of oxalates (3.7 g) was decomposed with sodium bicarbonate solution–ether. A solution of the bases in ethanol (100 mL) containing sodium hydroxide (20 mL, 1 M) was heated on the steam

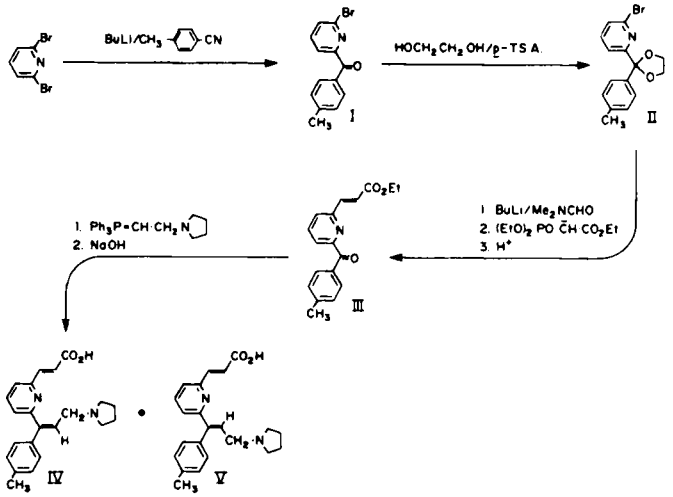

Scheme I—Preparation of triprolidine hapten derivative.

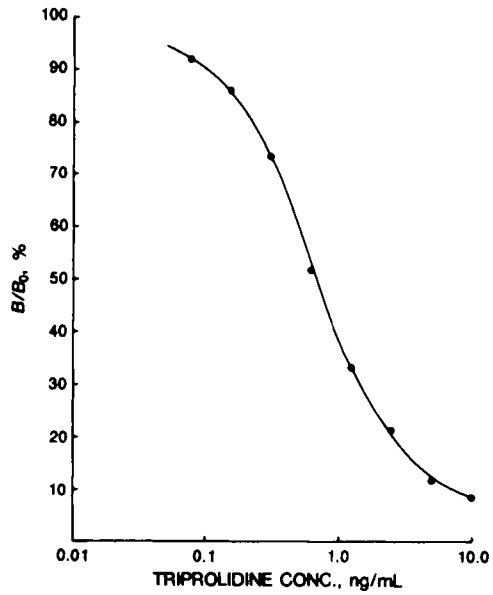

Figure 1—*Typical standard curve for triprolidine RIA in human plasma. Triprolidine was added to blank human plasma.*

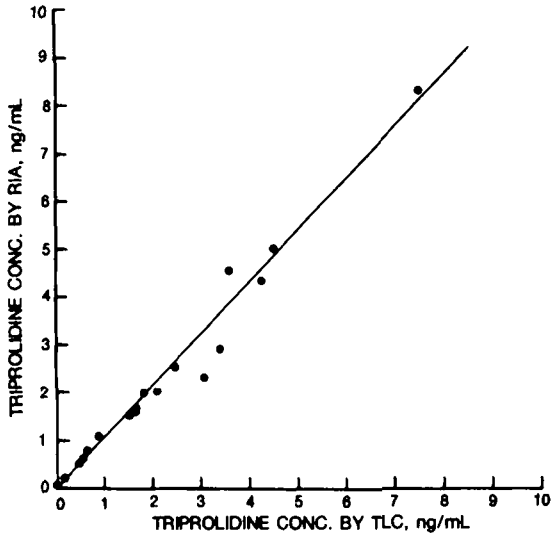

Figure 2—*Correlation of TLC and RIA analysis of triprolidine in human plasma samples.*

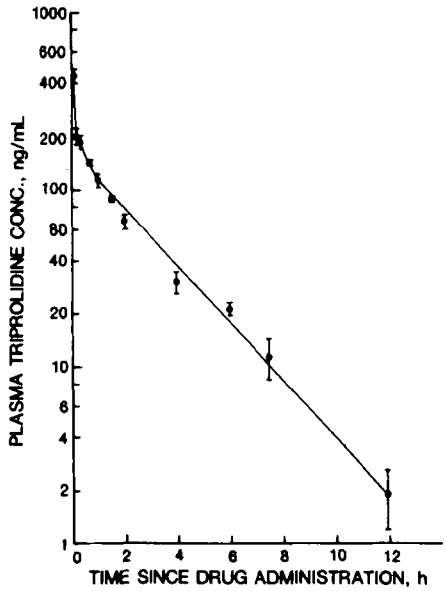

Figure 3—*Plasma disposition of triprolidine in male New Zealand White rabbits after an intravenous dose of 1 mg/kg of triprolidine hydrochloride. Triprolidine plasma concentrations are mean* ± SEM.

bath under reduced pressure for 5 min, neutralized with sulfuric acid (20 mL, 0.5 M), and finally evaporated to dryness. The solid residue was extracted with hot isopropyl alcohol (3 × 50 mL), and the combined filtrates were evaporated to dryness. The pinkish solid residue (2.5 g) was dissolved in hot ethyl acetate. Crystals (1.5 g), mp 160–162°C, were deposited on cooling; recrystallization from ethyl acetate gave the *E,Z*-isomer IV, mp 173–174°C (0.8 g). ^{1}H-NMR ($CDCl_3$) isolated olefinic proton at δ 6.35 ppm (t, 1). Concentration of the mother liquors afforded a second crop of crystals, mp 215–220°C (0.65 g), raised to 220–222°C (dec.) by recrystallization from isopropyl alcohol (0.55 g). ^{1}H-NMR ($CDCl_3$) isolated olefinic proton at δ 7.58 (t, 1), confirming that this was the *E,E*-isomer V.

Anal.—Calc. for $C_{22}H_{24}N_2O_2$: C, 75.86; H, 6.95; N, 8.05. Found: C, 75.57; H, 7.10; N, 8.03.

Conjugation of Acid V with Bovine Serum Albumin—Compound V (30 mg, 0.086 mM) was dissolved in ethanol (3 mL), and water (12 mL) was added. Bovine serum albumin (40 mg, 0.0057 mM) was added, the pH of the solution was adjusted to 5.5, and 1-ethyl-3-(3-dimethylaminoethyl)-carbodiimide hydrochloride[3] (25 mg, 0.161 mM) was added. This final solution was stirred overnight at room temperature, then was subjected to ultrafiltration[4] with water as eluant. After UV absorbance in the dialysate had returned to baseline levels, the solution of protein conjugate in the cell was lyophilized to give the drug–bovine serum albumin conjugate as a fluffy white solid (34 mg).

(E,E)-N-[2-(4-hydroxy-3-^{125}I-phenyl)ethyl]-3-[6-[1-(4-methylphenyl)-3-(1-pyrrolidinyl)-1-propenyl]-2-pyridinyl]propenamide (XII)—Compound V (30 mg, 0.086 mM) was dissolved in dimethylformamide (3 mL), and to this solution triethylamine (20 μL, 0.129 mM) was added. The solution was cooled in an ice bath, isobutyl chloroformate (15 μL, 0.108 mM) was added, and the reaction mixture was stirred at 0°C for 30 min. Tyramine (13 mg, 0.095 mM) in dimethylformamide (1 mL) was added, and the pH was adjusted to 8 with 1 M NaOH. The mixture was stirred overnight at 4°C; the addition of tyramine changed the initial pink/purple color to brown/orange. Solvents were removed under reduced pressure, and the residue was purified by preparative TLC on silica gel plates[5] developed in $CHCl_3$–CH_3OH–NH_4OH (70:30:1). The UV-absorbing band at R_f 0.73, which gave a slowly developing blue color when sprayed with ferric chloride–potassium ferricyanide, yielded the amide XI as an oil (13.6 mg) on elution with 10% CH_3OH–$CHCl_3$.

Amide XI was iodinated in the phenolic moiety by the method of Hunter and Greenwood (14). Compound XI (2 μg) in ethanol (10 μL) was mixed with 0.5 M Na_2HPO_4–NaH_2PO_4, pH 7.4 (25 μL). To this solution was added carrier-free [^{125}I]NaI[6] (1 mCi in 10 μL of NaOH solution) followed by chloramine-T hydrate (10 μg in 10 μL of 0.05 M phosphate buffer). The mixture was stirred for 30 s at room temperature, then sodium metabisulfite (25 μg in 25 μL of 0.05 M phosphate buffer) was added to stop the reaction. Preparative TLC of the reaction mixture on silica gel[5], as above, gave one major radioactive band at R_f 0.77 when radioscanned[7]. The iodinated compound was eluted from the silica with ethanol (13 mL), and the resulting solution was stored at −20°C until required. The approximate yield of iodinated amide XII was 420 μCi.

Immunization Procedure—Male New Zealand White rabbits received a primary immunization of 1 mg of bovine serum albumin-drug conjugate in 1 mL of 0.9% NaCl emulsified with 1 mL of Freund's complete adjuvant[8]. This dose was administered as two intramuscular (vastus lateralis) and eight subcutaneous (along the sides of the dorsal column) injections of 0.2 mL each. At intervals of 2, 4, and 6 weeks following the primary immunization, and at monthly intervals thereafter, booster immunizations of 0.5 mg of immunogen in 0.5 mL of saline, emulsified with 0.5 mL of Freund's complete adjuvant, were administered at multiple subcutaneous sites. Following the second and all subsequent booster immunizations, blood samples were collected from the central ear artery, and serum was collected and stored at −20°C until checked for the presence of antibodies. The antiserum used for the work described in this paper was obtained after 3 months of immunization.

Radioimmunoassay Procedures—All assay points were determined in duplicate; the results were then averaged. All assays were established in 12 × 75-mm polystyrene tubes[9].

Antiserum Titer Determinations—Various dilutions of rabbit antiserum in assay buffer (0.7 mL) were incubated with ^{125}I-triprolidine (50,000 cpm when freshly prepared, in 0.2 mL of assay buffer) and additional assay buffer (0.1 mL) in polystyrene tubes (12 × 75 mm) at 0°C for 2 h. Tubes containing only ^{125}I-triprolidine (0.2 mL) and buffer (0.8 mL) served as total count and nonspecific binding (background tubes). After 2 h, a dextran-coated charcoal suspension (0.5 mL) was added to all assay tubes, except total count tubes, and the contents were vortex-mixed and incubated at 0°C for 5 min. All charcoal-treated tubes were centrifuged at 4°C (≥1000×*g* for 10 min); the supernatants, containing the antibody-bound ^{125}I-triprolidine were decanted into clean polystyrene tubes, and the radioactivity was quantitated in a gamma[10] counter. Radioactivity bound by each antiserum dilution was expressed as percentage of total counts added to each assay tube. The antiserum titer was defined as that dilution which bound 40% of added radioligand.

Radioimmunoassay of Plasma Samples—Plasma samples from the various species were assayed directly, *i.e.*, without any prior extraction from the plasma. This procedure was similar to that given above, except that the assay incubation mixtures consisted of ^{125}I-triprolidine (0.2 mL) antiserum at the appropriate dilution (0.7 mL), and triprolidine standard solutions (0.1 mL) in blank plasma covering the range 0.078–10.0 ng/mL (7.8–1000 pg actual mass per tube). In addition to total count and nonspecific binding tubes, tubes containing antiserum (0.7 mL), ^{125}I-triprolidine (0.2 mL), and assay buffer (0.1 mL) served as maximum binding (B_0) tubes. Incubation and work-up procedures were as above. After quantitation of radioactivity, standard curves were expressed as percent B/B_0 against standard concentration on linear-log

[3] Sigma Chemical Co., St. Louis, Mo.
[4] Amicon cell with PM 10 membranes; Amicon Corp., Danvers, Mass.
[5] Merck silica gel GF_{254} 0.25 mm; E. Merck and Co., Elmsford, N.Y.
[6] Amersham Corp., Arlington Heights, Ill.
[7] Berthold, Model 2760; Beta Analytical Inc., Coraopolis, Pa.
[8] Difco Laboratories, Detroit, Mich.
[9] Walter Sarstedt Inc., Princeton, N.J.
[10] Model 5260 Autogamma Counter; Packard Instrument Co. Inc., Downers Grove, Ill.

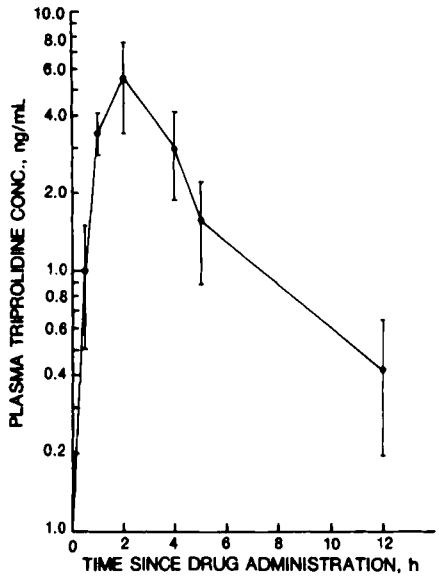

Figure 4—*Plasma triprolidine concentration–time curves in three normal human subjects after a single oral dose of 2.5 mg of triprolidine hydrochloride. Triprolidine concentrations are mean ± SEM.*

scales, where B is the antibody-bound radioactivity in the presence of a given standard concentration.

Cross-reactivity Studies—These studies were carried out as for the RIA except that in addition to the triprolidine standard curve, curves were established with the triprolidine metabolites and related compounds (IV–XI) shown in Fig. 2, and with some structurally unrelated compounds which might be administered concomitantly as medications (pseudoephedrine, guaifenesin, codeine, dextrorphan, aspirin, and acetaminophen). Percentage cross-reactivities were expressed as:

$$(IC_{50} - \text{Compound})/(IC_{50} - \text{triprolidine}) \times 100$$

where IC_{50} is the concentration required to inhibit binding of radioligand to antiserum by 50% (15).

Quantitative Thin-Layer Chromatographic Analysis of Triprolidine—This analytical method was used as published (10) with some modifications. Briefly, the drug was extracted into benzene, the organic layer was separated by centrifugation, and a portion was concentrated by evaporation. The residue was dissolved in chloroform–methanol (85:15, 80 μL) and the entire volume was spotted on a silica gel plate. The plate was developed in chloroform–methanol–ammonium hydroxide (91:8:1) to a height of 11 cm. After spraying with 2 M ammonium bisulfate, the induced fluorescence of the drug was quantitated at an excitation wavelength of 300 nm (cut-off filter 400 nm). The recovery of the drug from plasma across a 1–8-ng/mL concentration range was 95%.

Human Disposition Studies—Three healthy volunteers (2 male, 1 female; mean weight, 68.0 kg) who were not receiving any drug therapy, fasted overnight (12 h) and, at 8 a.m., the next morning, ingested a tablet containing 2.5 mg of triprolidine hydrochloride[11]. No food was consumed until 2 h after drug administration. Plasma was harvested and stored as above. After 1 week, each dog received the same dose of drug by the alternate route of administration, and blood samples were collected in the same manner.
stored at −20°C until analyzed for triprolidine by RIA or TLC.

Animal Disposition Studies—*Dogs*—Two male beagles were fasted overnight. The next morning, both dogs received 1-mg/kg doses of triprolidine hydrochloride, one as an oral dose (gelatin capsule) and the other as intravenous injection (saphenous vein) in isotonic saline (2 mL). Blood samples were collected into EDTA-containing evacuated tubes[12] prior to drug administration and at 0.08, 0.17, 0.33, 0.5, 0.66, 1, 1.5, 2, 4, 6, 8, 12, and 24 h after drug administration. Plasma was harvested and stored as above. After 1 week, each dog received the same dose of drug by the alternate route of administration, and blood samples were collected in the same manner.

Rabbits—Three male New Zealand White rabbits were fasted overnight before intravenous administration of triprolidine hydrochloride (1 mg/kg) in isotonic saline (2 mL) into the marginal ear vein. Blood samples were collected from the contralateral marginal ear veins prior to and at 0.03, 0.17, 0.33, 0.67, 1, 1.5, 2, 4, 6, 7.5, and 12 h after drug administration. Blood samples were processed as described above for dogs.

[11] Actidil; Burroughs Wellcome Co., Greenville, N.C.
[12] Vacutainer; Becton, Dickinson & Co., Rutherford, N.J.

Table II—Intravenous and Oral Administration of Triprolidine (1 mg/kg) to Beagle Dogs

Time, h	Plasma Concentration, ng/mL			
	Dog 46579		Dog 46965	
	Intravenous	Oral	Intravenous	Oral
0.08	184.8	0	290.5	0
0.16	146.1	1.7	225.9	0
0.33	117.6	2.5	211.5	2.0
0.50	94.3	3.5	173.4	6.6
0.67	86.0	4.3	118.2	5.7
1	55.8	4.8	100.1	4.3
1.5	32.6	3.2	50.2	2.8
2	28.4	2.4	35.7	2.2
4	10.4	1.6	10.4	0.9
6	3.8	0.6	3.6	0.3
8	2.7	0	1.9	0
12	1.0	0	0.7	0
AUC_0^{12}, ng·h/mL	211.7	8.7	305.1	11.2
Bioavailability, %		4.1		3.7

Pharmacokinetic Analysis—The mean plasma concentration–time data from the present human and rabbit experiments and a previous rat study (10), and the individual data sets from the dog experiments were analyzed pharmacokinetically by the computer program NONLIN (16), which iteratively minimizes the sum of the squared deviations between observed and computed plasma concentrations at the time points following drug administration. The volume of distribution, Vd_β, was calculated from the intravenous data using the equation $Vd_\beta = \text{Dose}/\text{AUC} \times \beta$, where AUC is the area under the plasma concentration–time curve from time zero to the last plasma sampling time, and β is the rate constant describing the terminal exponential phase of drug elimination from the plasma. Absolute bioavailability was determined from the ratio of the AUC values following oral and intravenous drug administrations.

RESULTS AND DISCUSSION

Synthesis of Hapten and Radioligand—Drug molecules are normally not immunogenic *per se*, and require prior coupling to a macromolecular carrier in order to elicit antibody production in animals (17, 18). A hapten derivative of triprolidine, suitable for coupling to protein, was prepared as shown in Scheme I. Starting from 2,6-dibromopyridine (I), the toluoyl derivative (II) was readily prepared and protected as the dioxolan (III), while the remaining bromine atom was replaced in a three-step procedure leading to the ethyl acrylate derivative (III). A Wittig reaction on the ketone moiety, followed by hydrolysis gave the acryloyl analogue of triprolidine (V, *E,E*-isomer) along with a larger amount of the *E,Z*-isomer (IV). These isomers were readily separated and purified by fractional crystallization. The triprolidine analogue (V) was successfully conjugated to bovine serum albumin by carbodiimide-mediated peptide bond formation, and the resulting drug–protein conjugate, after purification by ultrafiltration, was used for rabbit immunization experiments.

A convenient, gamma-labeled radioligand was prepared by coupling of tyramine to the acryloyl-triprolidine derivative (V) by the mixed anhydride method, followed by iodination of the phenolic moiety of the resulting amide XI with [^{125}I]NaI by the chloramine-T method of Hunter and Greenwood (14). This compound (XII, ^{125}I-triprolidine) was well-recognized by the antiserum, with >80% of 50,000 cpm of freshly prepared radioligand being bound by excess antiserum.

Antiserum Production—All three rabbits immunized with the bovine serum albumin–triprolidine conjugate produced antisera capable of binding ^{125}I-triprolidine after 2–4 months of the immunization program. The titer of these sera was sensitive to the presence of heterologous animal serum added to the incubation mixture. Thus, serum 830/2, which was employed for all of the work reported in this paper, exhibited apparent titers (40% total ^{125}I-triprolidine bound) of 1:140,000, 1:70,000, and 1:50,000 in the presence of human, dog, and rat (Long-Evans and Sprague-Dawley) plasma, respectively. The possibilities that these differences may be due to species variations in plasma proteins or to the presence of endogenous substances which are recognized by the triprolidine antiserum, have not been explored.

Assay Sensitivity, Accuracy, and Precision—Figure 1 is a typical triprolidine RIA standard curve for the assay in human plasma. The sensitivity of this system, defined as the concentration of triprolidine required to inhibit binding of radiotracer to antiserum by 10%, is ~0.1 ng/mL (0.01 ng actual weight). Clearly, this sensitivity could be increased by manipulation of the weight of radioligand and titer of antiserum used in the assay. Multiple analyses (on

different days) were conducted using a series of control triprolidine samples, prepared by addition of the hydrochloride salt to pooled blank human plasma to give various free base concentrations. The concentrations added were 0.2 (n = 25), 2.0 (n = 26), and 20.0 (n = 24) ng/mL; mean concentrations ($\pm SD$) measured were 0.21 (±0.05), 2.15 (±0.23), and 20.35 (±1.81), respectively. The highest control (20 ng/mL) was diluted 1:10 with blank plasma before analysis. These values therefore reflect interassay accuracy and precision data from averaged pairs of data points. The close agreement of the mean measured triprolidine concentrations with those actually added indicates the accuracy of the method. Standard deviations on the 2- and 20-ng/mL control samples indicate roughly 10% CV, while this value rises above 20% for the 0.2-ng/mL sample. Thus, at concentrations clearly above the sensitivity limit of the procedure, the assay method has good precision.

Assay Specificity—The specificity of the antiserum was examined by studying the relative abilities of triprolidine and a series of its metabolites and some related compounds to displace ^{125}I-triprolidine from the antiserum (Table I). The hapten derivative (V), which was coupled to bovine serum albumin to provide the immunogen, is almost as effective as triprolidine in displacing the radiolabel, but the *cis* isomer (IV) is almost 28-fold less effective. Although the *cis* isomer of triprolidine itself was not available for study, the ability of the antiserum to distinguish stereoisomers about the central double bond of the triprolidine parent structure was confirmed by examination of the cross-reactivities of the trifluoromethyl analogues (IX and X). The direct trifluoromethyl analogue of triprolidine (IX) cross-reacted extensively with the antiserum (49%), which indicates that the trifluoromethyl substituent is quite similar, antigenically, to the methyl substituent in triprolidine. However, the *cis*-trifluoromethyl isomer (X) cross-reacted ~25-fold less (2%), again confirming the recognition of stereochemistry around the central double bond. Several other stereospecific drug antisera have been developed recently (19-21), emphasizing that the specific properties of antisera extend beyond recognition of gross stereoelectronic changes to that of relatively fine differences in stereochemistry.

The aromatic acid (VIII), which has been identified as a major metabolite of triprolidine in animals and humans (9), exhibited only 15% inhibition of binding at 1000 ng/mL, indicating very low cross-reactivity (≪0.5%). The structural change in the benzylic alcohol (VII), also a metabolite of triprolidine, was also well-recognized, leading to a relatively low cross-reactivity value of 1.9% relative to triprolidine. A number of compounds which were not structurally related to triprolidine, but which may be coadministered as medications with the drug, were also examined. Codeine, pseudoephedrine, aspirin, acetaminophen chlorpheniramine, guaifenesin, and dextrorphan all showed little inhibition of binding (2–8%) at a concentration of 10 μg/mL. Surprisingly, chlorpheniramine did have weak (2.5%), but measurable, cross-reactivity in the triprolidine radioimmunoassay.

Assay Validation—The RIA procedure for triprolidine in human plasma was validated by comparative analysis of a group of human plasma samples by RIA and by a previously published quantitative TLC method (10). The samples were collected from volunteers at various times after the ingestion of a single dose (2.5 mg) of triprolidine hydrochloride (Fig. 2). The regression equation obtained was, RIA = 1.076 × TLC − 0.071. An excellent correlation (r = 0.985) and good agreement (slope = 1.076) was found for these two analytical methods, confirming the validity of the RIA procedure for triprolidine analysis in human plasma.

To illustrate the utility of the assay procedure, several experiments involving the oral administration of triprolidine hydrochloride to dogs, rats, guinea pigs, rabbits, and humans were established. In the case of dogs and rats, direct analysis of triprolidine by RIA without extraction was unsuccessful due to the failure of plasma samples to dilute in a manner parallel to the triprolidine assay standard curve. Markedly increased apparent triprolidine concentrations were obtained on each dilution, perhaps as a result of cross-reaction from an unknown metabolite that may have a displacement curve nonparallel to that of triprolidine. These samples could be analyzed readily by RIA after a preliminary benzene extraction of triprolidine from the plasma (10). Plasma samples from guinea pigs, rabbits, and humans could be analyzed without prior extraction at dilutions which placed them clearly in the linear portion of the RIA standard curve.

The disposition of triprolidine in three male New Zealand White rabbits, following intravenous injection of 1 mg/kg of triprolidine hydrochloride, was determined by the present RIA procedure (Fig. 3). The plasma concentration–time data, as analyzed by the NONLIN computer program (16), fitted well to a two-compartment open model of drug disposition. The rapid disposition phase was characterized by a rate constant, α = 12.3 h^{-1} ($t_{1/2,\alpha}$ = 0.06 h), while the terminal elimination phase was described by the rate constant, β = 0.41 h^{-1} ($t_{1/2,\beta}$ = 1.68 h). Tissue distribution in the rabbit appeared to be extensive, as indicated by the relatively large volume of distribution (Vd_β = 4.66 L/kg). The $t_{1/2,\beta}$ value for triprolidine in the rabbit (1.68 h) is comparable to the $t_{1/2}$ in humans (10).

Table III—Species Comparison of Kinetic Parameters

Parameter	Rabbit[a]	Human[b]	Dog[a]	Rat[a,c]
α, h^{-1}	12.3	—	1.3	6.0
β, h^{-1}	0.41	0.31	0.45	0.79
$t_{1/2,\alpha}$, h	0.06	—	0.40	0.12
$t_{1/2,\beta}$, h	1.68	2.27	1.5	0.88
Vd_β, L/kg[c]	4.7	2.6	9.3	9.6
AUC, ng·h/mL	462.0	39	259	134

[a] Intravenous 1-mg/kg injections of triprolidine hydrochloride. [b] Total oral dose of 2.5 mg of triprolidine hydrochloride; Vd_β term is actually Vd_β/F. [c] Parameters derived from data in Ref. 10.

The disposition of triprolidine in the plasma of three healthy subjects (two males and one female) following ingestion of 2.5 mg of triprolidine hydrochloride in a proprietary tablet preparation was examined, using RIA for analysis of plasma drug concentrations. The mean plasma concentration–time data are plotted in Fig. 4. In these three subjects, peak triprolidine concentrations ranged from 3.1 to 9.4 ng/mL at 1–2 h after drug administration. Triprolidine could still be detected in the plasma by RIA 24 h after drug ingestion, but levels at that time were close to the sensitivity limit of the method. The concentration–time data gave a good fit to a one-compartment open model of drug disposition, with first-order absorption. The apparent elimination half-life of 2.3 h in these subjects was similar to previously reported values for triprolidine in humans (10). The value for Vd_β/F is large (2.6 L/kg), also implying extensive tissue distribution or drug metabolism, although knowledge of the value of F (fraction of dose bioavailable) is necessary before the true volume of distribution can be calculated.

Although triprolidine could not be determined in dog plasma by the direct RIA procedure, TLC analysis provided data on the disposition of triprolidine in the dog for comparison with other species. Plasma concentrations of triprolidine in two beagles following separate oral and intravenous administrations of 1-mg/kg doses are presented in Table II. Observed peak plasma levels following oral administration (4.8 and 6.6 ng/mL) were 12–26-fold lower than concentrations at the same time after intravenous drug administration. The trapezoidal rule (22) was used to determine the area under the plasma concentration–time curves (AUC), and the absolute bioavailability of the oral dose was expressed as the percentage ratio of AUC values following oral and intravenous drug administrations (23). The bioavailability of triprolidine in these dogs was very low (3.7 and 4.1%), suggesting extensive first-pass metabolism of the drug in the liver and/or gut after oral administration. However, the data available on triprolidine, both from the present study and in general, do not exclude the possibility that this drug is poorly absorbed by the dog after oral administration, which could also result in low oral bioavailability. The intravenous data fitted well to a two-compartment open model of drug disposition and the kinetic parameters emanating from this analysis are presented in Table III. The mean $t_{1/2,\beta}$ and Vd_β values of 1.5 h and 9.2 L/kg, respectively, are comparable with similarly derived parameters in the rabbit in this study and the rat (10) in a previous study (Table III).

In this paper we have described a new RIA procedure for triprolidine, which is sufficiently sensitive and specific for use in the analysis of the drug in human plasma samples up to 24 h after ingestion of therapeutic oral doses. The method has also been used to provide pharmacokinetic data for triprolidine in humans and rabbits for comparison with similar data in dogs and rats. This procedure is currently being used in studies of the pharmacokinetics of triprolidine in humans after oral administration of immediate- and sustained-release drug formulations.

REFERENCES

(1) P. Armitage, H. Herxheimer, and L. Rosa, *Br. J. Pharmacol.*, **7**, 625 (1952).

(2) A. F. Green, *Br. J. Pharmacol.*, **8**, 171 (1953).

(3) E. L. Becker, I. Mota, and D. Wang, *Br. J. Pharmacol.*, **34**, 330 (1968).

(4) R. P. Warm, *Br. Med. J.*, **1**, 1066 (1954).

(5) F. Glassow, *Br. Med. J.*, **1**, 217 (1970).

(6) I. G. Popescu, V. Stroescu, and O. Benescu, *Rev. Roum. Med. Interne.*, **6**, 291, (1969).

(7) H. P. Wassermann, *Dermatologica*, **130**, 201 (1965).

(8) A. S. E. Fowle, D. T. D. Hughes, and S. J. Knight, *Eur. J. Clin. Pharmacol.*, **3**, 215 (1971).

(9) R. Kuntzman, E. Sernatinger, I. Tsai, and A. Klutch, in "Importance of Fundamental Principles in Drug Evaluation," D. Tedeschi and R. Tedeschi, Eds., Raven, New York, N.Y., 1968, p. 87.

(10) R. L. DeAngelis, M. F. Kearney, and R. M. Welch, *J. Pharm. Sci.*, **66**, 841 (1977).

(11) W. W. Fike and I. Sunshine, *Anal. Chem.*, **37**, 127 (1965).
(12) C. R. Fontan, W. C. Smith, and P. L. Kirk, *Anal. Chem.*, **35**, 591 (1963).
(13) F. C. Copp, Br. Pat. No., 1,161,201 (1969).
(14) W. M. Hunter and F. C. Greenwood, *Nature*, **194**, 495 (1962).
(15) G. E. Abraham, *J. Clin. Endocrinol. Metab.*, **29**, 866 (1969).
(16) C. M. Metzler, G. L. Elfring, and A. J. McEwen, *Biometrics*, **30**, 562 (1974).
(17) J. Landon and A. C. Moffat, *Analyst*, **101**, 225 (1976).
(18) V. P. Butler, *Pharmacol. Rev.*, **29**, 103 (1978).
(19) J. W. A. Findlay, J. T. Warner, J. A. Hill, and R. M. Welch, *J. Pharm. Sci.*, **70**, 624 (1981).
(20) C. E. Cook, N. H. Ballentine, T. B. Seltzman, and C. R. Tallent, *J. Pharmacol. Exp. Ther.*, **210**, 391 (1979).
(21) K. Kawashima, A. Levy, and S. Spector, *J. Pharmacol. Exp. Ther.*, **196**, 517 (1976).
(22) M. Gibaldi and D. Perrier, "Pharmacokinetics," Dekker, New York, N.Y., 1975, p. 146.
(23) M. Gibaldi and D. Perrier, "Pharmacokinetics," Dekker, New York, N.Y., 1975, p. 293.

Novel Approach to Zero-order Drug Delivery *Via* Immobilized Nonuniform Drug Distribution in Glassy Hydrogels

PING I. LEE

Received July 25, 1983, from the *Central Research, Ciba-Geigy Corporation, Ardsley, NY 10502.* Accepted for publication October 11, 1983. Present address: Menley & James Laboratories, Philadelphia, PA 19101.

Abstract □ A novel approach to zero-order drug delivery from glassy hydrogel matrices *via* an immobilized, sigmoidal, initial drug distribution has been developed. The method utilizes a controlled-extraction process on initially dry, drug-loaded hydrogels to generate an inflection-point-containing drug concentration profile followed by a vacuum freeze-drying step to rapidly remove the swelling solvent and immobilize *in situ* a nonuniform drug distribution. The drug release from such a system generally exhibits typical zero-order characteristics similar to that of a membrane-reservoir device. However, a saturated reservoir of active ingredient as in the membrane-reservoir device is not required because the constant release is achieved *via* an initially nonuniform concentration distribution instead of the constant activity in a reservoir. The applicability of the present concept and process has been demonstrated experimentally with the release of oxprenolol hydrochloride from hydrogel beads based on 2-hydroxyethyl methacrylate polymerized with a polymeric cross-linking agent.

Keyphrases □ Glassy hydrogels, oxprenolol hydrochloride—nonuniform drug distribution □ Oxprenolol hydrochloride—glassy hydrogels, nonuniform drug distribution □ Drug delivery systems—oxprenolol hydrochloride, glassy hydrogels

Diffusion-controlled polymeric delivery systems are finding increasing applications in the area of controlled release of pharmaceuticals (1–3). To achieve optimal therapeutic effects, especially for drugs with short physiological half-lives, it is often desirable to have a zero-order (or constant-rate) drug delivery (4). Unlike membrane-reservoir devices, monolithic systems where the drug is uniformly dissolved or dispersed in a polymer matrix generally do not exhibit zero-order release behavior. Instead, a release rate that continuously diminishes with time is observed (5, 6). This is a consequence of the increased diffusional distance and decreased area at the penetrating diffusion front. In addition to geometry factors (7), methods that approach zero-order release from monolithic matrices generally involve the introduction of either a constant rate of surface erosion much larger than the drug diffusion rate in the polymer matrix (8–10) or a constant rate of solvent front penetration (the so-called case II swelling) much smaller than the drug diffusion rate in the swollen region (11, 12). The applicability of these systems may be further limited by the need to maintain a constant surface area at the erosion or penetrating solvent front.

An important concept which has not been explored is the approach to zero-order drug release from a glassy polymer matrix having a specific nonuniform initial drug concentration distribution. Hydrogel polymers are unique for this application in that they are glassy in the dry state and capable of immobilizing any nonuniform drug distribution introduced prior to the dehydration step. In the presence of water, hydrogels can absorb a significant amount of water to form an elastic gel and, at the same time, release the dissolved drug by diffusion through the swollen region (13, 14).

This paper reports a method for immobilizing such a nonuniform drug concentration distribution in glassy hydrogel beads and the resulting zero-order drug release behavior. A

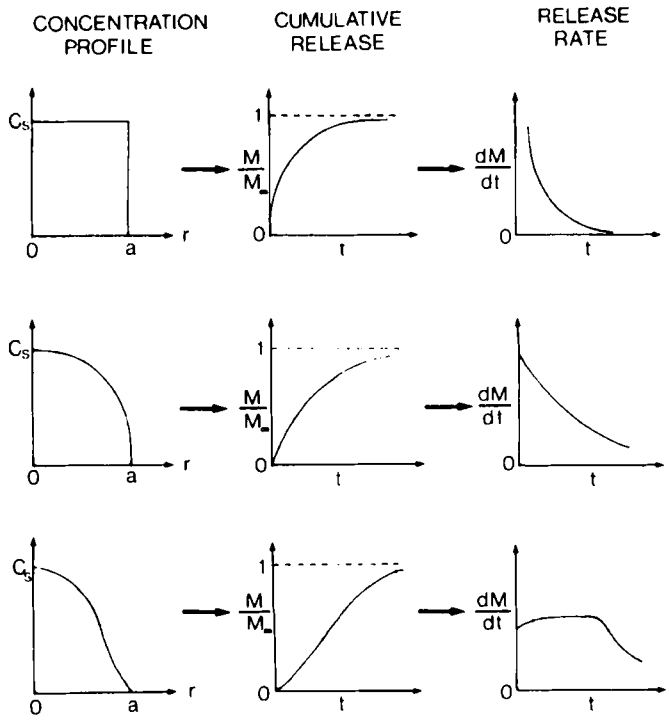

Figure 1—*Theoretical profiles illustrating the characteristics of drug release from spherical matrices as a function of the initial drug concentration distribution.*

0022-3549/84/1000-1344$01.00/0
© 1984, American Pharmaceutical Association

(11) W. W. Fike and I. Sunshine, *Anal. Chem.*, **37**, 127 (1965).
(12) C. R. Fontan, W. C. Smith, and P. L. Kirk, *Anal. Chem.*, **35**, 591 (1963).
(13) F. C. Copp, Br. Pat. No., 1,161,201 (1969).
(14) W. M. Hunter and F. C. Greenwood, *Nature*, **194**, 495 (1962).
(15) G. E. Abraham, *J. Clin. Endocrinol. Metab.*, **29**, 866 (1969).
(16) C. M. Metzler, G. L. Elfring, and A. J. McEwen, *Biometrics*, **30**, 562 (1974).
(17) J. Landon and A. C. Moffat, *Analyst*, **101**, 225 (1976).
(18) V. P. Butler, *Pharmacol. Rev.*, **29**, 103 (1978).
(19) J. W. A. Findlay, J. T. Warner, J. A. Hill, and R. M. Welch, *J. Pharm. Sci.*, **70**, 624 (1981).
(20) C. E. Cook, N. H. Ballentine, T. B. Seltzman, and C. R. Tallent, *J. Pharmacol. Exp. Ther.*, **210**, 391 (1979).
(21) K. Kawashima, A. Levy, and S. Spector, *J. Pharmacol. Exp. Ther.*, **196**, 517 (1976).
(22) M. Gibaldi and D. Perrier, "Pharmacokinetics," Dekker, New York, N.Y., 1975, p. 146.
(23) M. Gibaldi and D. Perrier, "Pharmacokinetics," Dekker, New York, N.Y., 1975, p. 293.

Novel Approach to Zero-order Drug Delivery *Via* Immobilized Nonuniform Drug Distribution in Glassy Hydrogels

PING I. LEE

Received July 25, 1983, from the *Central Research, Ciba-Geigy Corporation, Ardsley, NY 10502.* Accepted for publication October 11, 1983. Present address: Menley & James Laboratories, Philadelphia, PA 19101.

Abstract □ A novel approach to zero-order drug delivery from glassy hydrogel matrices *via* an immobilized, sigmoidal, initial drug distribution has been developed. The method utilizes a controlled-extraction process on initially dry, drug-loaded hydrogels to generate an inflection-point-containing drug concentration profile followed by a vacuum freeze-drying step to rapidly remove the swelling solvent and immobilize *in situ* a nonuniform drug distribution. The drug release from such a system generally exhibits typical zero-order characteristics similar to that of a membrane-reservoir device. However, a saturated reservoir of active ingredient as in the membrane-reservoir device is not required because the constant release is achieved *via* an initially nonuniform concentration distribution instead of the constant activity in a reservoir. The applicability of the present concept and process has been demonstrated experimentally with the release of oxprenolol hydrochloride from hydrogel beads based on 2-hydroxyethyl methacrylate polymerized with a polymeric cross-linking agent.

Keyphrases □ Glassy hydrogels, oxprenolol hydrochloride—nonuniform drug distribution □ Oxprenolol hydrochloride—glassy hydrogels, nonuniform drug distribution □ Drug delivery systems—oxprenolol hydrochloride, glassy hydrogels

Diffusion-controlled polymeric delivery systems are finding increasing applications in the area of controlled release of pharmaceuticals (1–3). To achieve optimal therapeutic effects, especially for drugs with short physiological half-lives, it is often desirable to have a zero-order (or constant-rate) drug delivery (4). Unlike membrane-reservoir devices, monolithic systems where the drug is uniformly dissolved or dispersed in a polymer matrix generally do not exhibit zero-order release behavior. Instead, a release rate that continuously diminishes with time is observed (5, 6). This is a consequence of the increased diffusional distance and decreased area at the penetrating diffusion front. In addition to geometry factors (7), methods that approach zero-order release from monolithic matrices generally involve the introduction of either a constant rate of surface erosion much larger than the drug diffusion rate in the polymer matrix (8–10) or a constant rate of solvent front penetration (the so-called case II swelling) much smaller than the drug diffusion rate in the swollen region (11, 12). The applicability of these systems may be further limited by the need to maintain a constant surface area at the erosion or penetrating solvent front.

An important concept which has not been explored is the approach to zero-order drug release from a glassy polymer matrix having a specific nonuniform initial drug concentration distribution. Hydrogel polymers are unique for this application in that they are glassy in the dry state and capable of immobilizing any nonuniform drug distribution introduced prior to the dehydration step. In the presence of water, hydrogels can absorb a significant amount of water to form an elastic gel and, at the same time, release the dissolved drug by diffusion through the swollen region (13, 14).

This paper reports a method for immobilizing such a nonuniform drug concentration distribution in glassy hydrogel beads and the resulting zero-order drug release behavior. A

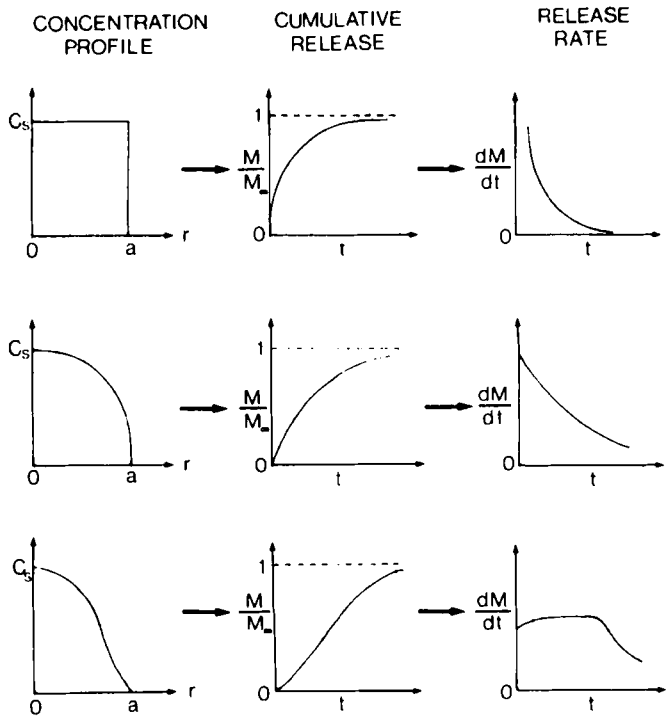

Figure 1—*Theoretical profiles illustrating the characteristics of drug release from spherical matrices as a function of the initial drug concentration distribution.*

0022-3549/84/1000-1344$01.00/0
© 1984, American Pharmaceutical Association

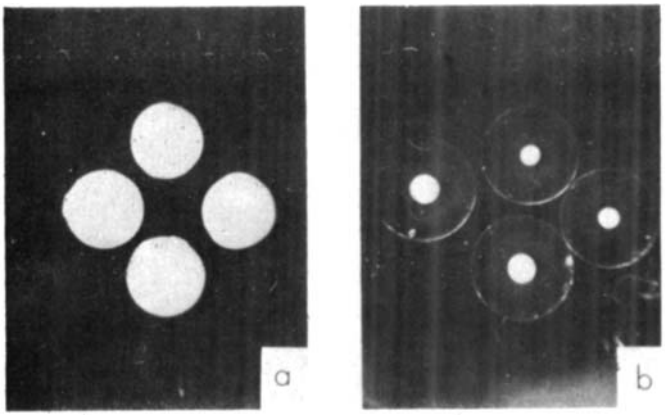

Figure 2—*Photographs showing typical solvent penetration behavior in drug loaded glassy hydrogel beads. Key: (a) original; (b) solvent penetrqted.*

detailed kinetic study of such release systems will be published elsewhere[1].

EXPERIMENTAL SECTION

Spherical hydrogel beads containing purified 2-hydroxyethyl methacrylate[2] (70%) and a polymeric cross-linking agent (30%), which was derived from poly-*n*-butyleneoxide (mol. wt. 2000)[3] by end-capping with 3-isocyanatomethyl-3,5,5-trimethylcyclohexyl-isocyanate[4] followed by reaction with excess 2-hydroxyethyl methacrylate, were synthesized by free-radical suspension polymerization in a saturated salt solution using 0.1% *tert*-butyl peroxy-2-hexanoate[5] as the initiator (15). The fraction of beads with a mean dry diameter of 0.115 cm and a mean swollen diameter of 0.13 cm was used for the release study. These hydrogel beads exhibit a major glass transition temperature (T_g) of ~110°C (as determined by differential scanning calorimetry[6]), an equilibrium ethanol swelling of 49%, and an equilibrium water swelling of 25%.

Oxprenolol hydrochloride[7], a β-blocker with water solubility as high as 77% at room temperature, was used as the model drug. A drug loading of 34.4% was achieved by equilibrating the hydrogel beads in an excess amount (5:1 ratio) of a 50% oxprenolol hydrochloride solution prepared in ethanol–water (60:40). After filtration and a brief rinse, the swollen loaded beads were dried at 50°C in a vacuum oven. These dry, loaded beads were then divided into several portions and subjected to a controlled-extraction process in an excess volume of water under vigorous stirring at 23°C for 5, 15, 20, and 30 min, respectively. The extraction process was controlled so that the extraction time was shorter than the time required for the penetrating solvent fronts to meet at the center to ensure that there would always be an inner glassy core surrounded by a swollen, partially extracted region. Immediately after separation of the extracting solvent, the controlled-extracted beads were freeze-dried under reduced pressure (0.025 mm Hg) for 15 h to rapidly remove the swelling solvent and to immobilize the drug, which was distributed in a nonuniform sigmoidal manner, decreasing from the core to the surface.

The oxprenolol hydrochloride release (under perfect sink diffusion conditions at 37.5°C) was followed continuously on a spectrophotometer[8] at 272 nm using a flow-through cell. The storage stability tests were conducted in capped vials under room conditions.

RESULTS AND DISCUSSION

The release characteristics of matrix devices containing uniformly dissolved or dispersed drug are well known (10, 16–18). However, the effect of nonuniform initial drug distribution on the release behavior has not been reported in the literature. Figure 1 illustrates the characteristics of drug release from spherical matrices as a function of the initial drug distribution[1]. Based on solutions to the diffusion equation, these theoretical curves show that both the uniform and parabolic initial concentration distributions result in an initially high rate of release followed by a rapid decline; the latter distribution exhibits a reduced initial rate of release compared with the former. In contrast, a sigmoidal initial drug distribution is capable of introducing a characteristic inflection point and, therefore, considerable linearity into the cumulative release curve. The duration of the constant-rate release region in such systems generally depends on the slope at the inflection point in the concentration distribution. Although Fig. 1 describes the drug release from spherical matrices, similar results are expected for planar and cylindrical geometries.

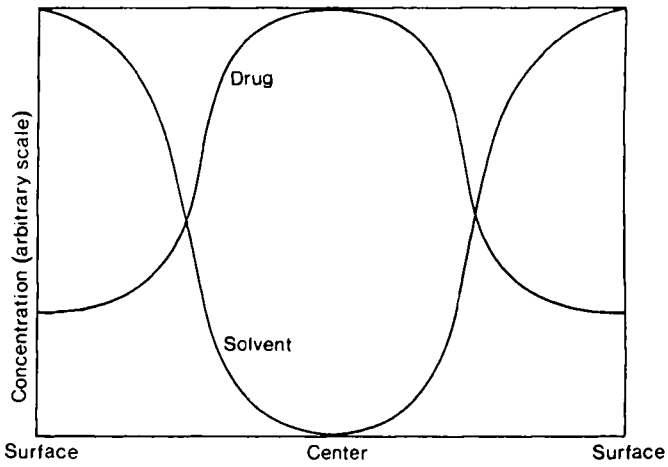

Figure 3—*Idealized solvent and drug distributions during solvent penetration in a drug-loaded glassy hydrogel matrix.*

The parabolic type of concentration distribution described above is characteristic of Fickian diffusion in rubbery polymers (19, 20), whereas the sigmoidal distribution is characteristic of glassy polymers partially penetrated by a swelling solvent undergoing non-Fickian diffusion. As a swelling solvent (in this case, water) penetrates a glassy hydrogel matrix having uniform drug loading, a clear discernible boundary separating an outer, rubbery, swollen region from an unpenetrated glassy core is usually observed (Fig. 2) (14). Such penetration and swelling generally do not follow Fickian diffusion. The existence of some molecular relaxation process in addition to diffusion is believed to be responsible for the observed non-Fickian behavior (12, 21). As a result, an inflection point is built into both the concentration profile of the penetrating solvent and the corresponding drug distribution, as shown in Fig. 3. This is similar to the solvent profiles reported for the partial penetration of organic swelling solvent in glassy polymers (22–24). The physical situation depicted in Fig. 3 is believed to reflect the solvent and drug distributions generated by the controlled-extraction process described in the *Experimental Section*. The subsequent vacuum freeze-drying step is intended to reduce the polymer segmental mobility by lowering the temperature and, at the same time, rapidly remove the swelling solvent to immobilize the drug *in situ* in a sigmoidal distribution in the hydrogel matrix.

As shown in Figs. 4A and B, scanning electron microscopy[9] X-ray microprobe chlorine scans for oxprenolol hydrochloride across the cross sections of the hydrogel beads confirm that the combination of controlled-extraction and freeze-drying steps has immobilized the drug *in situ* with a sigmoidal concentration profile in the 20-min extracted sample compared with the uniform concentration distribution in the unextracted control. The corresponding *in vitro* release of oxprenolol hydrochloride from the controlled-extracted beads is compared with that of the unextracted control in Fig. 5. It is evident that an inflection point and a zero-order release region of up to 60% of the total are introduced by the present process. With the increase in controlled-extraction time, the constant-rate release region extends, and the release half-life more than doubles. The constant-release region also shows a progressively decreasing slope with increased controlled-extraction time. In addition, release time-lags similar to that of membrane-reservoir devices are developed. Inevitably, a certain amount of drug will be lost during the controlled-extraction process. However, as shown in Fig. 6, where the oxprenolol hydrochloride loading is plotted as a function of controlled-extraction time in water, only ~10% of the drug is removed with an extraction time of 30 min.

In the absence of moisture, the sigmoidal drug concentration distribution generated by the present process can be preserved indefinitely in the glassy hydrogel matrix. The release of the entrapped drug should not occur until the hydrogel matrix is swollen at the time of usage. This is illustrated by a comparison of oxprenolol hydrochloride release rates from both the unextracted control and controlled-extracted beads at 0 and 59 d of storage as shown in

[1] Submitted to *Polymer*.
[2] White Chemical Co., Bayonne, N.J.
[3] Polymeg 2000; Quaker Chemical Co., Chicago, Ill.
[4] Veba Chemie, Gelsenkirchen-Buer, West Germany.
[5] Pennwalt Co., Philadelphia, Pa.
[6] DuPont Model 910 differential scanning calorimeter.
[7] Ciba-Geigy Co., Summit, N.J.
[8] ACTA C-III UV-visible; Beckman Instruments, Fullerton, Calif.
[9] Cambridge Stereoscan 180 scanning electron microscope.

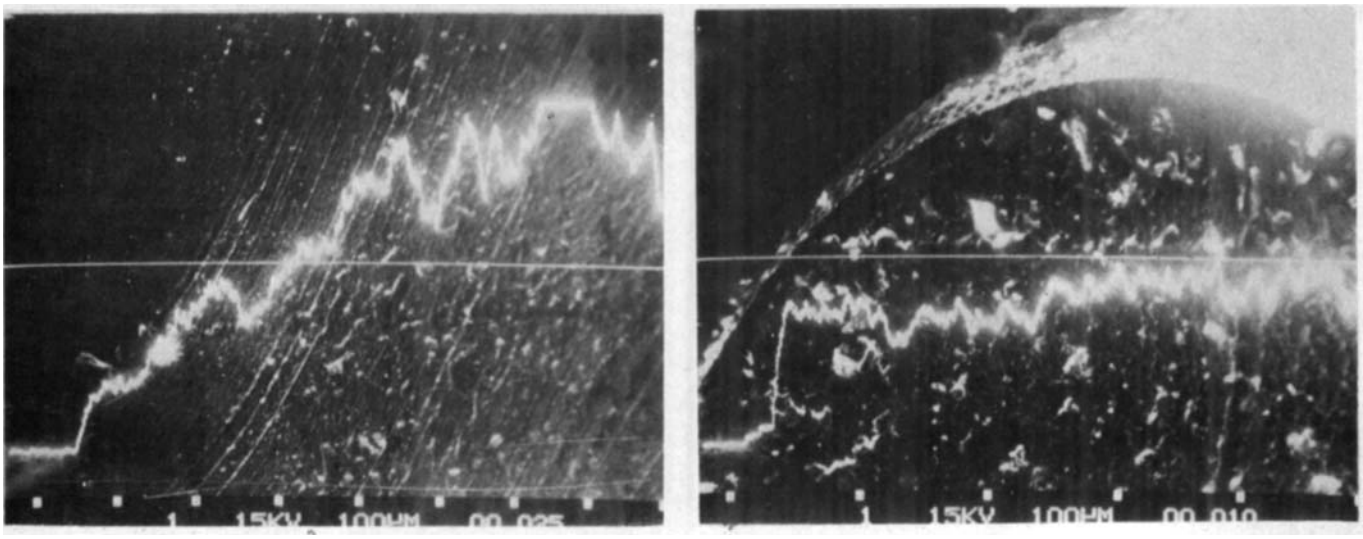

Figure 4—*Scanning electron microscope X-ray microprobe chlorine scans for oxprenolol hydrochloride on the cross section of hydrogel beads. Key: (A) controlled-extracted in water for 20 min; (B) unextracted control.*

Figs. 7A and B. In addition to the specific feature of prolonged zero-order release from controlled-extracted samples compared with the rapid decay of release rate in the unextracted control, there is very little change in the release rates after nearly 2 months of storage.

In summary, a novel appraoch to zero-order drug delivery from glassy hydrogel beads *via* an immobilized sigmoidal drug distribution is described. The combination of controlled-extraction and freeze-drying process is critical in the *in situ* immobilization of such a nonuniform concentration distribution.

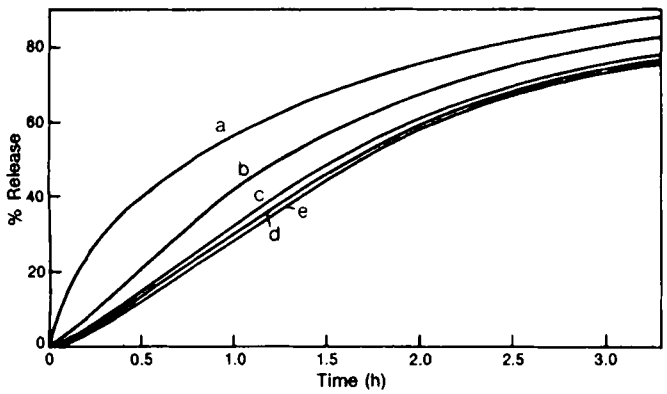

Figure 5—*Effect of controlled-extraction time in water on the* in vitro *release of oxprenolol hydrochloride. Key: (a) control; (b) 5 min; (c) 15 min; (d) 20 min; (e) 30 min.*

The evidence indicates that when the extraction process is carried out on drug-loaded beads in the fully swollen state instead of the dry glassy state, or when the drying is done at an elevated temperature instead of freeze-drying, no inflection point or constant-release region will be observed in the cumulative drug release profiles. Apparently, a parabolic type of drug concentration distribution, characteristic of Fickian diffusion in the rubbery state, does not lead to a zero-order release (Fig. 1). Other parameters such as the hydrogel composition and the extracting solvent also play important roles in determining the resulting release characteristics.

The concept and process described here have several distinct advantages

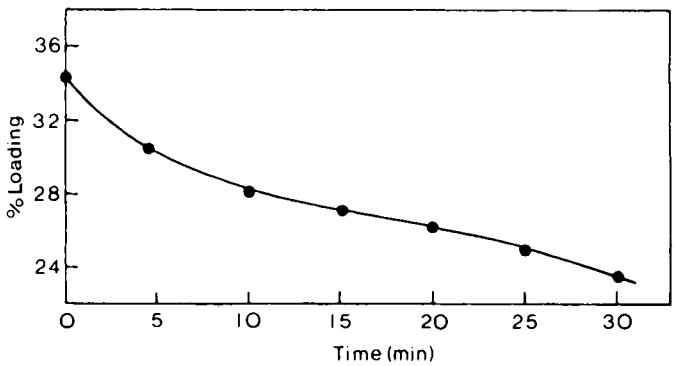

Figure 6—*Oxprenolol hydrochloride loading as a function of controlled-extraction time in water.*

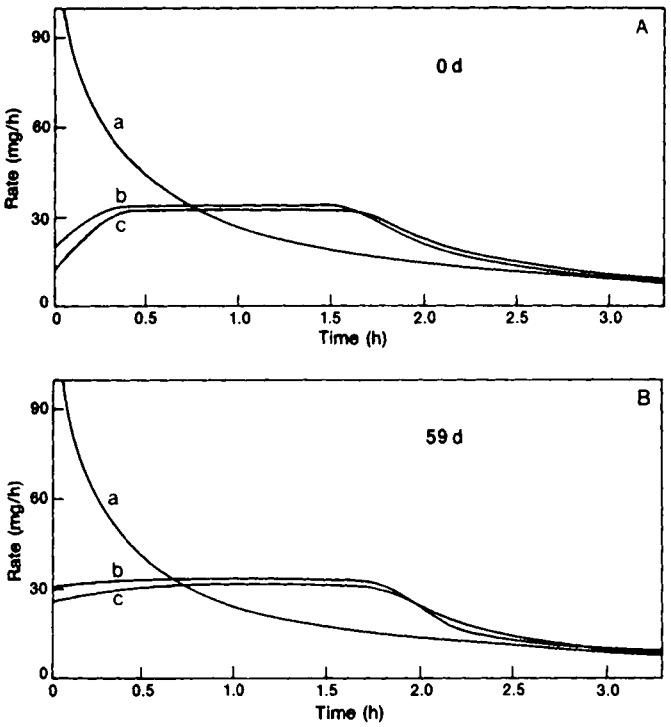

Figure 7—*Effect of storage time on the rate of oxprenolol hydrochloride release. Key: (A) 0 d; (B) 59 d; (a) loaded control; (b) controlled-extracted in water for 20 min; (c) controlled-extracted in water for 30 min.*

in addition to the zero-order release characteristics: (*a*) it is applicable to glassy hydrogels of any geometry including granules, beads, and sheets; (*b*) the burst-effect generally associated with membrane-reservoir devices is eliminated; and (*c*) a saturated reservoir of active ingredient (as in the membrane-reservoir device) is not required because the constant release is achieved by a nonuniform concentration distribution instead of the constant activity in a reservoir. This is particularly suitable for drugs with high water solubility.

REFERENCES

(1) A. F. Kydonieus, Ed., "Controlled Release Technologies: Methods, Theory, and Applications," Vols. I and II, CRC Press, Boca Raton, Fla., 1980.

(2) R. Juniper, Ed., "Pharmaceutical Applications of Polymers," Rubber and Plastic Research Association of Great Britain, Shawbury, England, 1981.

(3) T. J. Roseman and S. Z. Mansdorf, Eds., "Controlled Release Delivery Systems," Dekker, New York, N.Y., 1983.

(4) J. D. Rogers and K. C. Kwan, in "Controlled-Release Pharmaceuticals," J. Urquhart, Ed., American Pharmaceutical Association, Washington, D.C., 1981, p. 95.

(5) T. J. Roseman and W. I. Higuchi, *J. Pharm. Sci.*, **59,** 353 (1970).

(6) J. B. Schwartz, A. P. Simonelli, and W. I. Higuchi, *J. Pharm. Sci.*, **57,** 274 (1968).

(7) D. S. T. Hsieh, W. D. Rhine, and R. Langer, *J. Pharm. Sci.*, **72,** 17 (1983).

(8) P. I. Lee, in "Controlled Release of Pesticides and Pharmaceuticals," D. H. Lewis, Ed., Plenum, New York, N.Y., 1981, p. 39.

(9) J. Heller, *Biomaterials*, **1,** 51 (1980).

(10) P. I. Lee, *J. Membrane Sci.*, **7,** 255 (1980).

(11) H. B. Hopfenberg and K. C. Hsu, *Polym. Eng. Sci.*, **18,** 1186 (1978).

(12) R. W. Korsmeyer and N. A. Peppas, in "Controlled Release Delivery Systems," T. J. Roseman and S. Z. Mansdorf, Eds., Dekker, New York, N.Y., 1983, p. 77.

(13) W. R. Good, in "Polymeric Delivery Systems," R. Kastelnik, Ed., Gordon and Breach, New York, N.Y., 1976, p. 139.

(14) P. I. Lee, *Polym. Commun.*, **24,** 45 (1983).

(15) K. F. Mueller, S. Heiber, and W. Plankl, U.S. Pat. No. 4,224,427 (1978).

(16) T. Higuchi, *J. Pharm. Sci.*, **50,** 874 (1961).

(17) T. Higuchi, *J. Pharm. Sci.*, **52,** 1145 (1963).

(18) R. W. Baker and H. K. Lonsdale, in "Controlled Release of Biologically Active Agents," Vol. 47 of Advances in Experimental Medicine and Biology, A. C. Tanquary and R. E. Lacey, Eds., Plenum, New York, N.Y., 1974, p. 15.

(19) J. Crank, "Mathematics of Diffusion," 2nd ed., Clarendon Press, Oxford, England, 1975.

(20) J. Crank and G. S. Park, Eds., "Diffusion in Polymers," Academic, London, 1968.

(21) N. L. Thomas and A. H. Windle, *Polymer*, **23,** 529 (1982).

(22) R. A. Ware and C. Cohen, *J. Appl. Polym. Sci.*, **25,** 717 (1980).

(23) F. B. Rudolph, *J. Polym. Sci. Polym. Phys. Ed.*, **18,** 2323 (1980).

(24) H. G. Zachmann, *Faserforsch. Textiltech.*, **18,** 95 (1967).

ACKNOWLEDGMENTS

Presented in part at the APS Symposium on Controlled Release Drug Delivery Systems, 130th APhA Annual Meeting in New Orleans, La., April 1983. The author wishes to thank Ms. Kathleen Shields for her contributions in the release experiments.

Kinetics of Drug Action in Disease States III: Effect of Pregnancy on the Relationship Between Phenytoin Concentration and Antiseizure Activity in Rats

RUBY C. CHOU and GERHARD LEVY[x]

Received July 8, 1983, from the *Department of Pharmaceutics, School of Pharmacy, State University of New York at Buffalo, Amherst, NY 14260.* Accepted for publication November 16, 1983.

Abstract □ The purposes of this investigation were to determine the effect of pregnancy on the susceptibility of female rats to experimentally induced seizures and on the relationship between serum phenytoin concentration and antiseizure activity. Pregnant rats (on the 18th day of gestation) were more susceptible than nonpregnant female rats to seizures produced by maximal electroshock or by a body-weight-based dose of pentylenetetrazol. There was no apparent difference between pregnant (20th day of gestation) and nonpregnant rats in the relationship between seizure protection (percent of animals protected) and the serum concentration of total (free plus protein-bound) phenytoin. The relationship between concentration and effect was essentially the same 20 min after an injection of phenytoin and 2 h after the start of a constant-rate infusion preceded by a loading dose of the drug. Since the protein binding of phenytoin is appreciably decreased in late pregnancy, the serum concentration of free phenytoin required for seizure protection tended to be higher in pregnant than in nonpregnant rats. This may be due to the increased susceptibility of pregnant rats to seizure stimuli.

Keyphrases □ Phenytoin—antiseizure activity, effect of pregnancy, maximal electroshock seizure test □ Pregnancy—effect on antiseizure activity, phenytoin, maximal electroshock seizure test

Treatment of epileptic women with phenytoin often requires adjustment of drug dosage during pregnancy for adequate seizure control (1, 2). This appears to be due in part to pregnancy-associated alterations in the pharmacokinetics (3, 4) and possibly in the bioavailability (5) of the drug, and perhaps also to decreased compliance (6). However, the physiological changes associated with pregnancy, including water retention, electrolyte concentration and pH shifts, and altered hormonal concentrations, may provoke seizures in epileptic patients (7–9). It is possible, therefore, that the relationship between phenytoin concentration and antiseizure activity is altered during pregnancy. Such an effect would be in addition to the well-established change in the plasma protein binding of phenytoin in pregnancy (10), which makes it desirable that phenytoin plasma concentration monitoring during pregnancy be based on the concentrations of free rather than total drug.

The purpose of this investigation was to determine the effect of pregnancy on the relationship between serum phenytoin concentration and antiseizure activity in an animal model of experimentally induced seizures. The studies were designed to compare the response of nonmedicated pregnant and nonpregnant female rats to two types of seizure stimuli (electrical and chemical), to relate the antiseizure effect of phenytoin to the serum concentration of both total and free drug, and to compare the concentration–effect relationship after intravenous injection of phenytoin with the corresponding relationship at steady state during intravenous infusion of the drug. Information was also obtained concerning the effect of pregnancy on the distribution of phenytoin between plasma, brain, and cerebrospinal fluid (CSF).

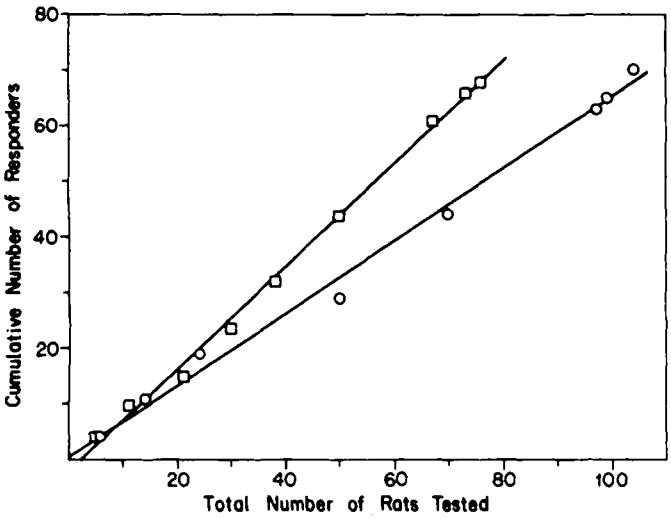

Figure 1—*Seizure response of pregnant (18th day of gestation) (□) and nonpregnant female (○) rats to a maximum electroshock (MES) stimulus. The cumulative number of animals in each group that responded to MES by tonic hind limb extension is plotted against the cumulative number of animals subjected to MES in the course of this investigation. The percentage of pregnant rats responding was 90%; 67% of the nonpregnant female rats responded. The slopes of the regression lines are significantly different,* $p < 0.001$.

EXPERIMENTAL SECTION

Methods—Inbred female Lewis rats, weighing 175–200 g on receipt, were used in this investigation. Some were mated (3) while others were designated as nonpregnant controls. On the 18th day of gestation, the pregnant animals and their concurrent controls were screened by subjecting them to maximal electroshock (MES), using an apparatus that was adjusted to deliver ~ 150 mA for 0.35 s *via* corneal electrodes (11). Only rats that responded to the stimulus by exhibiting the tonic hind limb extensor component of MES seizure were used in the subsequent experiment. The animals had access to food and water at all times except during the hour of testing to avoid possible alterations in their susceptibility to MES due to starvation or dehydration (11).

One day after the MES screening, the rats had a cannula implanted in the right jugular vein under light ether anesthesia (12). This procedure is known to not alter their seizure pattern (13). On the following day, *i.e.*, on the 20th day of gestation of the pregnant animals, the rats received an intravenous injection of phenytoin, 2–12.5 mg/kg, through the cannula (which was then flushed with saline solution). The drug was dissolved in 10% ethanol–normal saline in various concentrations and 1 mL/kg of the solution was injected over 1 min. The solutions were coded so that the experimenter did not know the

Table I—Effect of Pregnancy on the Tonic-Seizure Response of Rats to Pentylenetetrazol Injection [a]

Type of Rats	Body Weight, g	Number Responding/ Total Number
Nonpregnant female	201 ± 8	5/14
Pregnant 18th day of gestation		
Dosed per actual body weight	263 ± 16	8/9
Dosed per average weight of nonpregnant controls	261 ± 11	3/8

[a] Dose of pentylenetetrazol was 26 mg/kg iv.

0022-3549/84/1000-1348$01.00/0
© 1984, American Pharmaceutical Association

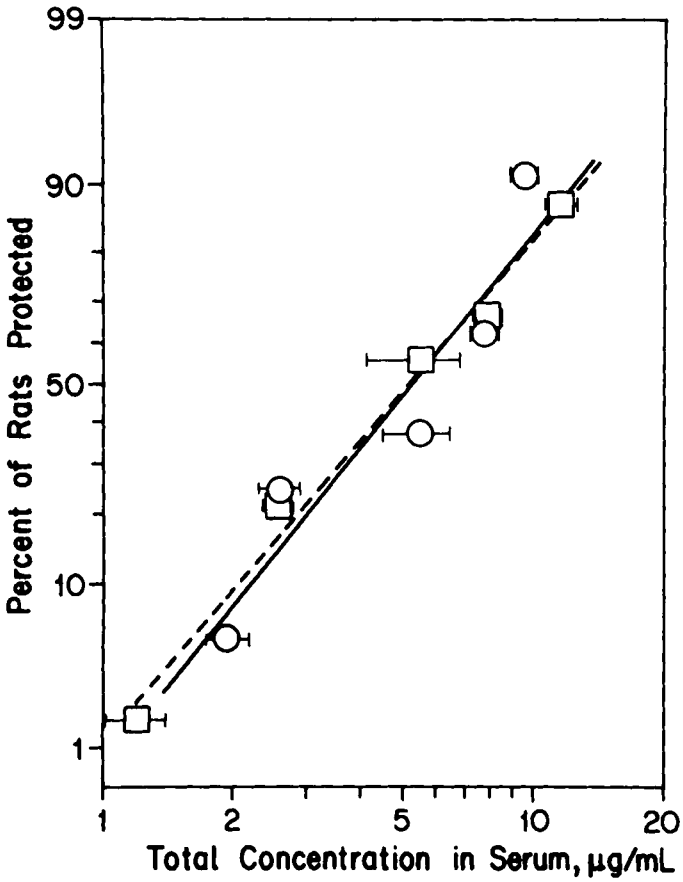

Figure 2—*Relationship between the percent of rats protected from MES-induced tonic seizures (both forelimb and hind limb extension) and serum concentration of phenytoin in pregnant rats at the 20th day of gestation (□) and nonpregnant female (○) rats. The determinations were made 20 min after a rapid intravenous injection of phenytoin, 2–12.5 mg/kg. The data points are based on results from 7–9 rats per point. The horizontal bars represent ± one* SD *of the concentration. The lowest square and the lowest and highest circles represent corrected values for 0 and 100% protection according to Litchfield and Wilcoxon (17). The regression lines and correlation coefficients ($r = 0.993$, $p < 0.001$ for the pregnant rats and $r = 0.940$, $p < 0.02$ for the nonpregnant rats) are based on the probit values for protection and on logarithmic values for serum concentration.*

dose administered. Twenty minutes after the injection, the rats were subjected to MES and the response was recorded. Complete protection was defined as the prevention of tonic seizure, *i.e.*, absence of both forelimb and hind limb extension (14, 15). A blood sample was then obtained through the cannula, and the serum was separated and assayed for phenytoin by HPLC (16).

In another part of the investigation, pregnant (20th day of gestation) and nonpregnant female rats received an intravenous injection of phenytoin solution, 0.340 mL/min for 1 min, followed immediately by a constant-rate infusion of 0.0136 mL/min for 2 h. The phenytoin concentrations of the solutions ranged from 0.874 to 2.46 mg/mL. At 2 h, the rats were subjected to MES and blood sampling.

Other pregnant (18th day of gestation) and nonpregnant female rats, with a jugular vein cannula implanted 1 d earlier, received a rapid injection of pentylenetetrazol, 26 mg/kg, as a 52-mg/mL aqueous solution. The syringe and cannula were then flushed immediately by withdrawal and reinjection of blood. Some of the pregnant rats received the dose based on their actual body weight while others received a dose based on the average body weight of the nonpregnant controls. Tonic seizures, when present, occurred within a few seconds after the injection and were recorded. The pharmacological activity data were analyzed according to Litchfield and Wilcoxon (17).

Also reported here is a summary of phenytoin distribution data derived from various experiments performed over ~1 year. Briefly, pregnant rats at the 20th day of gestation and nonpregnant female rats received a 14.7-mg/kg injection of phenytoin followed immediately by an infusion of 195 μg/min/kg for 2 h, through a jugular vein cannula. At the end of the infusion, samples of CSF and blood (using EDTA as the anticoagulant for separation of plasma) were obtained and the brain was removed. These fluids and one hemisphere of the

Table II—Effect of Pregnancy on the Median Effective Serum Concentrations of Total and Free Phenytoin for Protection Against Maximal Electroshock-Induced Tonic Seizures

Median Conc., μg/mL	Pregnant Female, Day 20 of Gestation	Nonpregnant Female
Total	5.20 3.58–7.55[a]	5.20 3.55–7.62[a]
Free[b]	1.03 0.710–1.49[a]	0.680 0.464–0.997[a]

[a] 95% Confidence limit. [b] Based on free fraction values obtained in studies on other rats (Table III).

brain were assayed for phenytoin by HPLC (16). The average CSF/plasma concentration ratios of phenytoin in pregnant and nonpregnant rats obtained in these studies were used to estimate the plasma concentrations of free phenytoin in the experiment in which the relationship between total phenytoin plasma concentration and antiseizure activity was determined. This had to be done because of the great difficulty in obtaining CSF from rats after MES.

RESULTS

The results of the screening study are summarized in Fig. 1. The data are plotted cumulatively and reflect the results obtained on successive groups of rats that were screened over approximately 6 months. Sixty-seven percent of the nonpregnant female rats and 90% of the pregnant rats exhibited tonic seizures (with hind limb extension) in response to MES, a significant difference in response rate ($p < 0.001$).

To determine if the apparent difference in the susceptibility of pregnant and nonpregnant rats to MES is limited to the electric stimulus only, other groups of nonmedicated animals were subjected to a chemical stimulus, *i.e.*, pentylenetetrazol injection. The seizure response rate of the pregnant rats was significantly higher than that of the nonpregnant controls [$p < 0.02$ when tested by a statistic comparing two success probabilities (18)] on injection

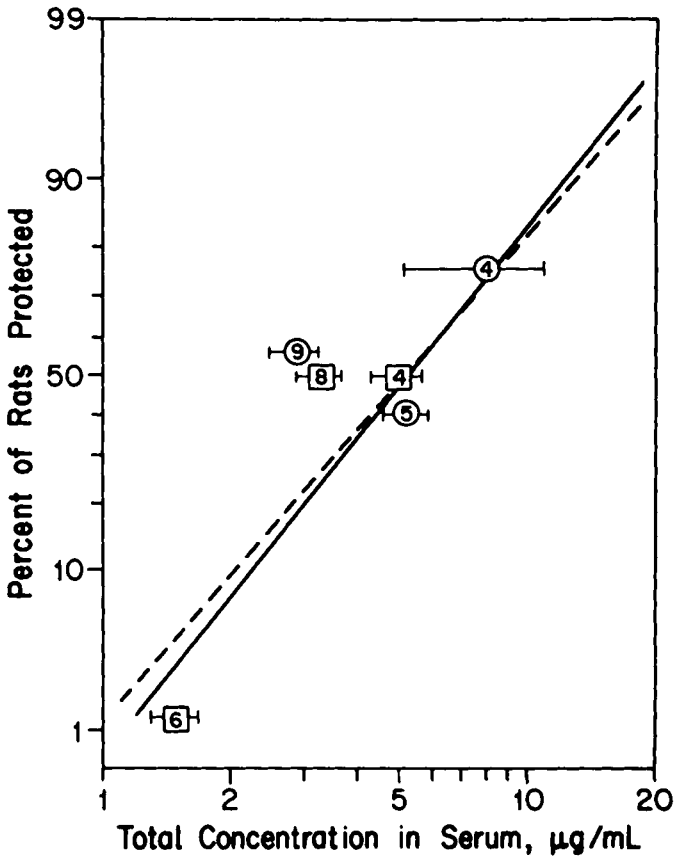

Figure 3—*A plot similar to Fig. 2, except that the results shown here were obtained after a 2-h intravenous infusion of phenytoin. The number of rats per groups are indicated by the number in the symbols. The regression lines are those obtained in the experiment shown in Fig. 2. The lowest square is a corrected value.*

Table III—Effect of Pregnancy on the Distribution of Phenytoin Between Plasma, Cerebrospinal Fluid, and Brain in Rats [a]

Variable	Pregnant Female, Day 20 of Gestation		Nonpregnant Female
Number of animals	22		19
Phenytoin conc., μg/mL or g			
Plasma	14.5 ± 2.4	N.S.	14.0 ± 3.7
CSF	2.78 ± 0.47	$p < 0.001$	1.78 ± 0.42
Brain	26.7 ± 7.3	$p < 0.005$	19.8 ± 5.0
Concentration ratio [b]			
CSF/Plasma	0.193 ± 0.027	$p < 0.001$	0.130 ± 0.019
Brain/Plasma	1.83 ± 0.36	$p < 0.001$	1.43 ± 0.19
Brain/CSF	9.51 ± 1.58	$p < 0.001$	11.1 ± 1.0

[a] Results (mean ± *SD*) obtained after intravenous injection of phenytoin, 14.7 mg/kg, followed by an intravenous infusion of 195 μg/min/kg for 2 h. [b] None of the ratios are significantly correlated with the plasma phenytoin concentration.

of both groups with the same relative (mg/kg) dose (Table I). On the other hand, pregnant rats injected with the convulsant in a dose based on the average weight of the nonpregnant controls exhibited essentially the same seizure response rate as the control animals.

The results of the experiments to determine the relationship between serum concentration of total phenytoin and seizure protection are shown in Fig. 2. The determinations were made 20 min after the intravenous injection of phenytoin. Essentially identical results were obtained with pregnant and nonpregnant rats (Table II).

The results of a more-limited series of experiments, performed under steady-state conditions (constant rate intravenous infusion of phenytoin), are summarized in Fig. 3. For both pregnant and nonpregnant rats the average concentration–response data at two of three phenytoin concentrations were essentially identical to those obtained when phenytoin was administered by rapid injection.

The steady-state distribution of phenytoin between brain and CSF was significantly altered during pregnancy (Table III). The decreased brain/CSF concentration ratio and the increased CSF/plasma concentration ratio of phenytoin in the pregnant rats are consistent with decreased binding of the drug in the brain and plasma, respectively.

The steady-state concentration ratio of phenytoin, CSF/plasma, is a measure of the free fraction of the drug in plasma under *in vivo* conditions (16). The average free fraction value of phenytoin, which is independent of concentration over a wide range (19), was substantially higher in pregnant than in nonpregnant rats (Table III). Using these free fraction values, the experimental concentration data summarized in Fig. 2 were converted to free phenytoin concentrations to determine the relationship between serum concentration of free phenytoin and seizure protection (Fig. 4). The thus estimated median effective serum concentration of free phenytoin was 1.03 μg/mL in the pregnant rats and only 0.680 μg/mL in the nonpregnant animals, while the median effective serum concentration of total (free plus protein-bound) drug was identical in both groups (Table II).

DISCUSSION

Pregnancy is obviously not a disease, but, like many diseases, it is associated with profound changes in physiological status. Thus, an investigation of the effect of pregnancy on the relationship between drug concentration and pharmacological activity is appropriate for inclusion in this series of reports concerning the kinetics of drug action in disease states.

Some women experience epileptic fits only during pregnancy. This condition, known as true gestational epilepsy (7), reflects an increased susceptibility of at least some individuals to the altered physiological conditions associated with pregnancy. Consistent with these observations, there is an increased incidence of electroencephalograms classified as slow or high-voltage fast in pregnant women, reflecting a type of cortical activity that is known to occur more frequently in conditions in which the incidence of convulsions is higher than in the general population (20).

In the present study, a greater percentage of pregnant than nonpregnant rats responded with seizures to an electroshock stimulus. To determine if this difference also occurs in rats after exposure to a chemical stimulus, other groups of animals were given a pentylenetetrazol injection. The design of such a study raises the problem of proper normalization of dosage (3, 21): should the pregnant animals receive the same absolute (mg) or relative (mg/kg) dose of the convulsant drug? Pharmacokinetic evidence suggests that pentylenetetrazol distributes in body water (22). However, animals have seizures within seconds after intravenous injection, *i.e.*, possibly before the distribution of pentylenetetrazol from blood to the total body water space is complete. Significantly, the *relative* volumes of both body water and blood remain essentially constant during pregnancy in rats (23, 24). These considerations suggest that the dose of pentylenetetrazol for pregnant rats should be based on their actual body weight. Under these conditions, the relative number of pregnant rats with tonic seizures after pentylenetetrazol injection was significantly higher than that of nonpregnant controls. No such difference was found when pregnant and nonpregnant rats received the same absolute dose of the convulsant. Thus, while the results of this experiment appear to be consistent with those of the electroshock study, *i.e.*, increased susceptibility to seizures during pregnancy, definitive studies with pentylenetetrazol require determination of effective concentrations of the convulsant in the brain, CSF, or plasma. Such studies are now in progress.

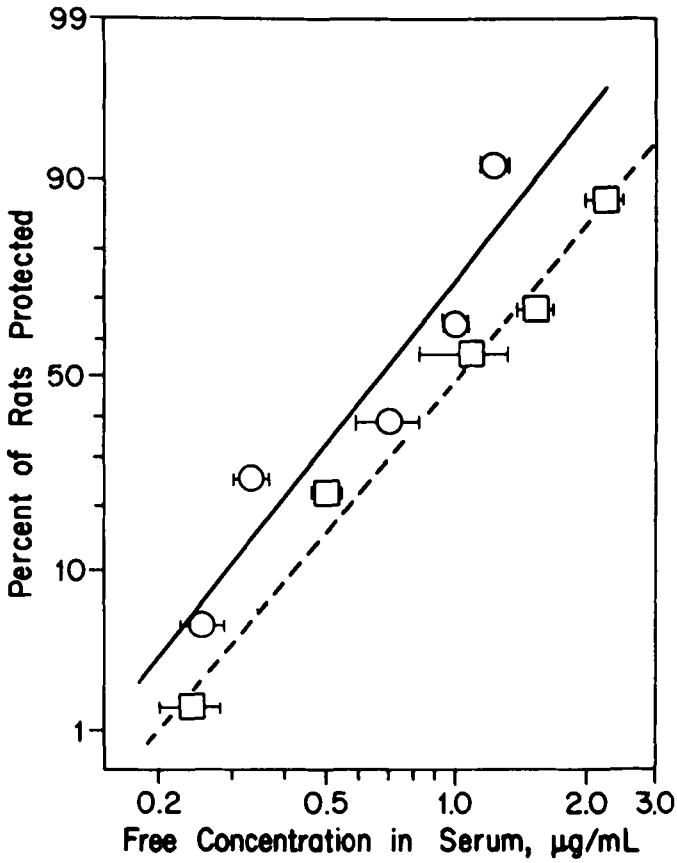

Figure 4—*A plot of the data in Fig. 2, except that serum phenytoin concentrations are corrected for protein binding (determined in other rats) to show the relationship between protection from MES-induced tonic seizures and the estimated serum concentration of free (unbound) phenytoin.*

The entry of phenytoin into the central nervous system (CNS) is rapid and may be blood-flow limited (8, 13, 25–27). Once in the CNS, the drug acts without any apparent delay (13). The major metabolites of phenytoin are pharmacologically inactive (28, 29). Under postdistribution conditions, phenytoin concentrations in plasma ultrafiltrate, brain ultrafiltrate, and CSF are essentially equal (25), and the anticonvulsant effect of the drug is, therefore better correlated with the plasma concentrations of free rather than total (free plus bound) phenytoin (30).

Pregnancy had no apparent effect on the relationship between the serum concentration of total phenytoin and antiseizure activity in rats subjected to maximal electroshock (Fig. 1). However, since the plasma or serum protein binding of phenytoin is significantly decreased during pregnancy in rats (3, 19), pregnant animals apparently require higher serum concentrations of free phenytoin than do nonpregnant controls for equivalent protection against MES-induced seizures.

The original design of this study included determination of phenytoin protein binding in the serum of every phenytoin-treated animal tested for protection against MES seizure. The protein binding determinations were made by equilibrium dialysis before it was found that the results thus obtained were of questionable value due to extensive *in vitro* lipolysis in plasma from pregnant rats (31, 32). Since it is difficult to obtain CSF from rats after application of MES, *in vivo* phenytoin free fraction values (*i.e.*, the ratio of phenytoin concentrations in CSF and plasma) were determined in separate groups of animals from the same source. It should be noted that the CSF-

plasma concentration ratios of phenytoin were obtained in a relatively large number of pregnant and nonpregnant rats (Table III), that the interindividual varition of these values is quite small, and that the free fraction value of phenytoin is independent of concentration over a wide range (19). As is evident in Fig. 4 and Table II, the serum concentrations of free phenytoin required for seizure protection tended to be higher in pregnant than in nonpregnant rats. While a statistical analysis of these hybrid data is not considered appropriate, we state for the record that the median effective concentrations of free drug in the serum of pregnant and nonpregnant animals were not statistically significantly different.

The phenytoin concentration–antiseizure effect relationship was also determined, in a more limited study, in rats that were infused with phenytoin to steady state. The data thus obtained are generally quite similar to those obtained 20 min after a rapid injection of phenytoin (Fig. 4), consistent with the rapid entry of phenytoin into the CNS and with the lack of pharmacological activity of phenytoin metabolites.

As already shown by other investigators (8, 25, 33, 34), it was found in this investigation that the total concentrations of phenytoin are higher in the brain than in the plasma (Table III). This appears to be due to extensive protein binding of the drug in the brain rather than to partitioning into brain lipids (35). The results of the present investigation are also consistent with previous findings of an increased brain–blood phenytoin concentration ratio during pregnancy (34). The reason for this change in drug distribution becomes apparent on examining the concentration ratios relative to CSF determined in this investigation. Since the concentration of proteins in normal CSF is very low, phenytoin in CSF exists almost totally in the unbound form. The increased CSF–plasma phenytoin concentration ratio during pregnancy reflects the decreased plasma protein binding of the drug. By the same reasoning, the decreased brain–CSF phenytoin concentration ratio during pregnancy indicates decreased protein binding of phenytoin in the brain. It appears that the decreased plasma protein binding of the drug is due to lower albumin concentrations and the presence of circulating endogenous binding inhibitors during pregnancy (19, 32); endogenous inhibitors may be responsible also for the decreased binding of phenytoin in the brain.

In an earlier study on Sprague–Dawley rats treated chronically with phenytoin, it was found that pregnant animals had increased serum concentrations of total phenytoin and exhibited increased protection against MES-induced convulsions (36). The present investigation has shown that the relationship between *total* phenytoin serum concentration and seizure protection is essentially the same in pregnant (20th day of gestation) and nonpregnant inbred Lewis rats. Since the protein binding of phenytoin in plasma or serum is appreciably decreased during pregnancy, this suggests that pregnant rats require higher serum concentrations of free phenytoin (the pharmacologically active form of the drug) than do nonpregnant animals for the same degree of seizure protection. This apparent difference may be related to the observed increased susceptibility of unmedicated rats to an experimental seizure stimulus during late pregnancy.

REFERENCES

(1) M. J. Eadie, C. M. Lander, and J. H. Tyrer, *Clin Pharmacokinet.*, **2,** 427 (1977).

(2) N. K. Kochenour, M. G. Emery, and R. J. Sawchuk, *Obstet. Gynecol.*, **56,** 577 (1980).

(3) R. C. Chou and G. Levy, *J. Pharmacol. Exp. Ther.* **229,** 351 (1984).

(4) S.-S. Chen, E. Perucca, J.-N. Lee, and A. Richens, *Br. J. Clin. Pharmacol.*, **13,** 547 (1982).

(5) R. E. Ramsay, R. G. Strauss, B. J. Wilder, and L. J. Willmore, *Neurology*, **28,** 85 (1978).

(6) S. Koch, I. Göpfert-Geyer, E. Jäger-Roman, D. Rating, R. Steldinger, and H. Helge, in "Obstetric Complications in Pregnancies of Epileptic Mothers and their Obstetric Histories," D. Janz, M. Dam, A. Richens, L. Bossi, H. Helge, and D. Schmidt, Eds., Raven, New York, N.Y., 1982, pp. 91–97.

(7) A. H. Knight and E. G. Rhind, *Epilepsia*, **16,** 99 (1975).

(8) D. M. Woodbury, *Epilepsia*, **10,** 121 (1969).

(9) F. Hytten and G. Chamberlain, Eds., "Clinical Physiology in Obstetrics," Blackwell Scientific Publication, Boston, Mass., 1980.

(10) M. Dean, B. Stock, R. J. Patterson, and G. Levy, *Clin Pharmacol. Ther.*, **28,** 253 (1980).

(11) L. A. Woodbury and V. D. Davenport, *Arch. Int. Pharmacodyn. Ther.*, **92,** 97 (1952).

(12) J. R. Weeks and J. D. Davis, *J. Appl. Physiol.*, **19,** 540 (1964).

(13) I. E. Leppik and A. L. Sherwin, *Epilepsia*, **20,** 201 (1979).

(14) Y. Masuda, Y. Shiraishi, T. Karasawa, K. Yoshida, and M. Shimizu, *J. Pharmacol. Dyn.*, **3,** 526 (1980).

(15) J. E. P. Toman, E. A. Swinyard, and L. S. Goodman, *J. Neurophysiol.*, **9,** 231 (1946).

(16) R. C. Chou and G. Levy, *J. Pharmacol. Exp. Ther.*, **219,** 42 (1981).

(17) J. T. Litchfield, Jr. and F. Wilcoxon, *J. Pharmacol. Exp. Ther.*, **96,** 99 (1949).

(18) B. W. Brown, Jr. and M. Hollander, "Statistics, a Biomedical Introduction," Wiley, New York, N.Y., 1977, pp. 173–193.

(19) B. Stock, M. Dean, and G. Levy, *J. Pharmacol. Exp. Ther.*, **212,** 264 (1980).

(20) F. A. Gibbs and D. E. Reid, *Am. J. Obstet. Gynecol.*, **44,** 672 (1942).

(21) J. H. Lin and G. Levy, *J. Pharmacol. Exp. Ther.*, **225,** 653 (1983).

(22) H. W. Jun, *J. Pharm. Sci.*, **65,** 1038 (1976).

(23) M. Dean, L. O'Donnell, S. Penglis, and B. Stock, *Drug Metab. Dispos.*, **8,** 265 (1980).

(24) P. P. L. Tam and S. T. H. Chan, *J. Reprod. Fertil.*, **51,** 41 (1977).

(25) H. Firemark, C. F. Barlow, and L. J. Roth, *Int. J. Neuropharmacol.*, **2,** 25 (1963).

(26) B. J. Wilder, R. E. Ramsay, L. J. Willmore, G. F. Feussner, R. J. Perchalski, and J. B. Shumate, Jr., *Ann. Neurol.* **1,** 511 (1977).

(27) R. E. Ramsay, E. J. Hammond, R. J. Perchalski, and B. J. Wilder, *Arch. Neurol.*, **36,** 535 (1979).

(28) K. Nakamura, Y. Masuda, K. Nakatsuji, and T. Hiroka, *Naunyn-Schmiedeberg Arch. Pharmakol. Exp. Pathol.*, **254,** 406 (1966).

(29) T. Chang, A. Savory, and A. J. Glazko, *Biochem. Biophys. Res. Commun.*, **38,** 444 (1970).

(30). D. W. Shoeman and D. L. Azarnoff, *J. Pharmacol. Exp. Ther.*, **195,** 84 (1975).

(31) R. C. Chou and G. Levy, *J. Pharm. Sci.*, **71,** 471 (1982).

(32) R. C. Chou and G. Levy, *J. Pharm. Sci.*, in press.

(33) E. L. Noach, D. M. Woodbury, and L. S. Goodman, *J. Pharmacol. Exp. Ther.*, **122,** 301 (1958).

(34) B. Westmoreland and N. H. Bass, *Arch. Neurol.*, **24,** 158 (1971).

(35) A. J. Wilensky, in "Epilepsy, a Window to Brain Mechanism," J. S. Lockard and A. A. Ward, Jr., Eds., Raven, New York, N.Y., 1980, pp. 201–213.

(36) G. R. DeVore and D. M. Woodbury, *Epilepsia*, **18,** 387 (1977).

ACKNOWLEDGMENTS

Supported in part by Grant GM 20852 from the National Institute of General Medical Sciences, National Institutes of Health. Mr. David M. Soda provided competent technical assistance.

The preceding publication in this series is M. Danhof, M. Hisaoka, and G. Levy, "Kinetics of Drug Action in Disease States II: Effect of Experimental Renal Dysfunction on Phenobarbital Concentrations in Rats at Outset of Loss of Righting Reflex," *J. Pharmacol. Exp. Ther.*, **230,** 1 (1984).

Drug Permeation Through Human Skin II: Permeability of Ionizable Compounds

JAMES SWARBRICK *x, GEOFFREY LEE *, JEFFREY BROM *, and NIGEL P. GENSMANTEL ‡

Received March 2, 1983, from the *School of Pharmacy, University of North Carolina, Chapel Hill, NC 27514 and ‡Fisons plc, Pharmaceutical Division, Loughborough, LE11 OQY England. Accepted for publication October 13, 1983.

Abstract □ The aim of this study was to establish whether ionized as well as un-ionized forms of certain 4-oxo-4*H*-1-benzopyran-2-carboxylic acids (chromone-2-carboxylic acids) with pK_a values <2 permeated through excised human skin and, if so, to determine the permeability coefficients of the permeating species. The permeation properties of four carboxylic acids were studied as a function of concentration over the pH range 5–7 at 37°C with plexiglass diffusion cells. Plots of J/C^{A^-} (the total flux due to un-ionized and ionized species obtained under steady-state conditions per unit concentration of ionized drug in the donor compartment) against $C^{H_3O^+}$ resulted in straight-line relationships. The intercepts of these plots were shown to equal P^{A^-}, whereas the slopes multiplied by the K_a values of the compounds equalled P^{HA}, the permeability coefficients of the ionized and un-ionized species, respectively. With all four compounds, both species were found to permeate skin, although the permeability coefficients of the un-ionized species were ~10^4 greater than those for the ionized species. It was demonstrated that the relative contributions of the ionized and un-ionized species to the total flux, as well as the total flux, vary significantly, depending on the pH of the drug solution in the donor cell. This may provide a means of controlling the flux of these and similar compounds through human skin.

Keyphrases □ Permeation—permeability of ionizable compounds through human skin, 4-oxo-4*H*-1-benzopyran-2-carboxylic acids □ 4-Oxo-4*H*-1-benzopyran-2-carboxylic acids—ionizable compounds, permeability through human skin □ Absorption—percutaneous, permeability of ionizable compounds through human skin

Many compounds evaluated for their ability to undergo percutaneous absorption following application to the skin are weak to moderately strong electrolytes. Depending on the pK_a of the compound and the pH of the vehicle, such compounds exist as an equilibrium mixture of ionized and un-ionized species in the immediate vicinity of the skin. To control properly the rate at which such electrolytes permeate human skin, it is necessary to determine the permeability coefficients of both forms of the drug. However, much of the theoretical background to percutaneous absorption has been developed through studies of nonelectrolytic permeating species (1, 2), and there is little information available regarding the effect of pH and pK_a on the permeation of ionizable drugs through skin (3, 4).

According to the simple pH-partition hypothesis, only the un-ionized forms of drugs are able to pass through lipoidal membranes in significant amounts (5). If correct, then membrane permeability should be related to the amount of un-ionized drug present, as well as being strongly pH dependent. However, in studies on isolated intestinal membranes (6), it has been indicated that ionized as well as un-ionized sulfonamides can pass through such a barrier. By using rat gastrointestinal segments *in vivo*, the rate constants for absorption of the ionized forms of sulfaethidole and barbital were found to be only three to five times less than those for the un-ionized material (7). With excised human skin, the permeabilities of the ionized forms of ephedrine and scopolamine were calculated to be ~1/20th of those for their un-ionized forms (3). The permeation of ionized drug molecules through skin thus is possible and cannot be assumed to be negligible, especially at pH values at which large numbers of ionized molecules are present. Such conditions would exist with compounds with low pK_a values present on the surface of normal skin.

Human skin is composed of three distinct layers—the stratum corneum, the epidermis, and the underlying dermis. The passage of molecules across the skin and into the capillaries present in the dermis occurs by passive diffusion. The resistance to diffusion is high in the stratum corneum; in contrast, the epidermis and dermis are relatively permeable (8). The steady-state flux (J) (in mol·cm^{-2}·h^{-1}) is given by (2):

$$J = P \cdot C = \frac{C \cdot K^{SC/V} D^{SC}}{\delta} \qquad \text{(Eq. 1)}$$

where P is the permeability coefficient, and C is the concentration of the permeating species in the vehicle. The terms $K^{SC/V}$ and D^{SC} refer, respectively, to the stratum corneum–vehicle partition coefficient and diffusion coefficient of the permeating species within the stratum corneum, which has a thickness of δ.

Assuming that both ionized (A^-) and unionized (HA) species contribute to the total steady-state flux of a permeating electrolyte (here considered to be a monoprotic acid), then:

$$J = J^{HA} + J^{A^-} = (P^{HA} \cdot C^{HA}) + (P^{A^-} \cdot C^{A^-}) \qquad \text{(Eq. 2)}$$

Since the relative concentrations of ionized and un-ionized species for such an acid are expressed as:

$$K_a = \frac{C^{H_3O^+} \cdot C^{A^-}}{C^{HA}} \qquad \text{(Eq. 3)}$$

then Eqs. 2 and 3 can be combined to give:

$$\frac{J}{C^{A^-}} = \left(\frac{P^{HA}}{K_a}\right) C^{H_3O^+} + P^{A^-} \qquad \text{(Eq. 4)}$$

Having determined the total steady-state flux as a function of chromone acid concentration and pH, a plot of J/C^{A^-} *versus* $C^{H_3O^+}$ should be a straight line with a slope of P^{HA}/K_a and an intercept of P^{A^-}. Equation 4 therefore allows estimation of the permeability coefficients of both un-ionized and ionized species. If the latter is zero, then the intercept will also be zero. Such an approach does not appear to have been used before in the determination of percutaneous absorption.

In the present study, the permeation properties of four related 4-oxo-4*H*-1-benzopyran-2-carboxylic acids (chromone-2-carboxylic acids) were investigated over a range of pH

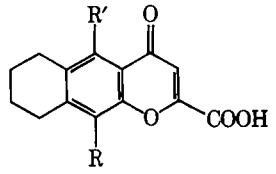

I, R = $-CH_2CH_2CH_3$, R' = OH
II, R = $-CH_2CH_2CH_3$, R' = H
III, R = R' = H

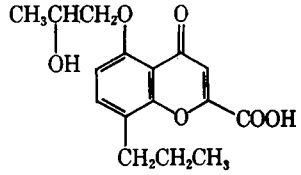

IV

0022-3549/84/1000-1352$01.00/0
© 1984, American Pharmaceutical Association

Table I—Data Derived from Steady-State Flux Determinations of Chromone-2-Carboxylic Acids as a Function of pH and Concentration

Compound	$C^{H_3O^+}$, mol·L^{-1} × 10^7	J/C^{A^-} Mean ± SD, cm/h^{-1} × 10^5	J/C^{A^-} Range	n	$J/C^{A^-} = (P^{HA}/K_a)C^{H_3O^+} + P^{A^-}$ [a]	n
I	100.0	158.0 ± 28.6	100.7–202.7	9	$= (139.0 \pm 21.1)C^{H_3O^+} + (20.2 \pm 12.5)10^{-5}$	26
	10.0	48.0 ± 20.2	15.0–86.4	9		
	1.0	7.3 ± 6.3	0.7–17.9	8		
II	100.0	53.7 ± 9.3	45.7–70.6	10	$= (48.8 \pm 5.8)C^{H_3O^+} + (4.85 \pm 3.7)10^{-5}$	23
	10.0	11.4 ± 2.4	8.0–14.8	8		
	1.0	2.9 ± 0.9	1.4–3.4	5		
III	100.0	7.11 ± 2.87	2.85–12.34	13	$= (4.99 \pm 1.52)C^{H_3O^+} + (2.51 \pm 0.93)10^{-5}$	35
	10.0	3.64 ± 1.80	1.10–6.36	12		
	1.0	1.86 ± 1.10	0.45–4.18	10		
IV	100.0	4.54 ● 3.93	0.86–10.06	11	$= (4.04 \pm 2.40)C^{H_3O^+} + (0.51 \pm 1.63)10^{-5}$	24
	10.0	1.03 ± 0.40	0.61–1.66	7		
	1.0	0.42 ± 0.25	0.13–0.77	6		

[a] Equation derived from plot of individual values of J/C^{A^-} *versus* $C^{H_3O^+}$.

values and concentrations. Equation 4 was then used to determine the permeability coefficients of the un-ionized and ionized species and to evaluate the effect of pH on the total steady-state flux observed and the relative contribution to this flux by the two species.

EXPERIMENTAL SECTION

Skin Samples—As previously reported (9), samples of whole skin were removed from the inner thighs of cadavers within 48 h postmortem. The stratum corneum plus attached epidermis (SCE) was removed from the dermis as an intact sheet of tissue. These SCE samples were dried overnight in a desiccator at 25% relative humidity and then stored at 1 ± 0.5°C. Samples were rehydrated before use in the permeation studies. Because of the large number of studies conducted (>100), it was necessary to use skin samples from at least 10 different cadavers during the total series of experiments.

Materials—Buffer capsules[1] were used to prepare buffers at pH 5, 6, and 7. The pH 7.4 buffer and the solvents used in the HPLC assay of the chromone-2-carboxylic acids have been reported previously (9). A triglyceride of fractionated coconut oil fatty acids[2] (principally caprylic and capric), was used as received.

Permeation Determinations—Plexiglass diffusion cells were used to measure the permeation of the chromone-2-carboxylic acids across samples of SCE at 37 ± 0.5°C. Their design has been described previously (9). Solutions of each chromone acid were prepared in aqueous buffer at pH 5, 6, and 7. At least three different concentrations of chromone acid were used to cover the range of solubilities at a particular pH up to saturation. These solutions were placed in the donor compartments of the cells, whereas pH 7.4 buffer was placed in the stirred receptor compartments. Samples of known volume ranging from 25 to 100 μL were removed from the receptor compartments at known time intervals of ~2 h and immediately replaced with an equal volume of pH 7.4 buffer. The diluting effect of this replacement was taken into account when the total amount of chromone acid that had permeated the SCE at any one time was calculated. The removed samples were analyzed by HPLC (see below), and the permeation study was continued until it became clear that steady-state conditions were achieved (generally, 48–60 h). Values of the steady-state total flux of carboxylic acid were calculated and expressed as moles per square centimeter of skin per hour.

Analysis—Samples were analyzed by HPLC[3] immediately after they were removed from the receptor compartment. The following retention times were observed: compound I, 4.3 min (7:3 MeOH–H_2O, 0.5% NH_4OAc); compound II, 2.9 min (7:3 MeOH–H_2O, 0.5% NH_4OAc); compound III, 5.2 min (1:1 MeOH–H_2O, 0.5% NH_4OAc); compound IV, 4.5 min (1:1 MeOH–H_2O, 0.5% NH_4OAc). The solvent flow rate was 2.0 mL/min, and detection was by UV absorbance at 254 nm. Under these conditions, baseline separation was achieved between the single chromone acid peak and that due to unknown components leached from the skin. All four chromone acids were shown to be stable under the experimental conditions used and for at least the duration of a permeation run. Standard solutions were injected at each time interval when samples were withdrawn and assayed. The coefficients of variation ranged from 3.2 to 5.6% for the four compounds studied. In all cases, the limit of detection was 1–2 ng of chromone acid following the injections of a 100-μL sample.

[1] pHydrion; Micro Essential Labs, Brooklyn, N.Y.
[2] Miglyol 812; Kay-Fries Inc., Montvale, N.J.
[3] Model 440 absorbance detector with model 6000-A pumps, U6K injector, and model 660 solvent programmer; Waters Associates, Milford, Mass.

Solubility Determination—The aqueous solubilities of the chromone-2-carboxylic acids at 37°C were measured by adding excess compound to pH 5.0 buffer. The pH was readjusted to 5.0 with 0.1 M sodium hydroxide solution when necessary. After equilibration overnight, the mixtures were filtered and assayed by HPLC.

Partition Coefficients—Known weights of the four chromone-2-carboxylic acids were equilibrated between equal volumes of mutually saturated triglyceride[2] and the appropriate buffer solution at 37°C. The systems were gently shaken at frequent intervals over a period of 48 h, at which time samples of each phase were assayed by UV spectrophotometry. The apparent partition (distribution) coefficient D was calculated as the ratio of the total amount of drug in each of the two phases and subsequently converted into the true (*i.e.*, un-ionized) partition coefficient K by:

$$D = K(1 - \alpha) \qquad \text{(Eq. 5)}$$

where $(1 - \alpha)$ is the fraction of un-ionized drug and $\alpha = 1/[1 + \text{antilog}(pK_a - pH)]$.

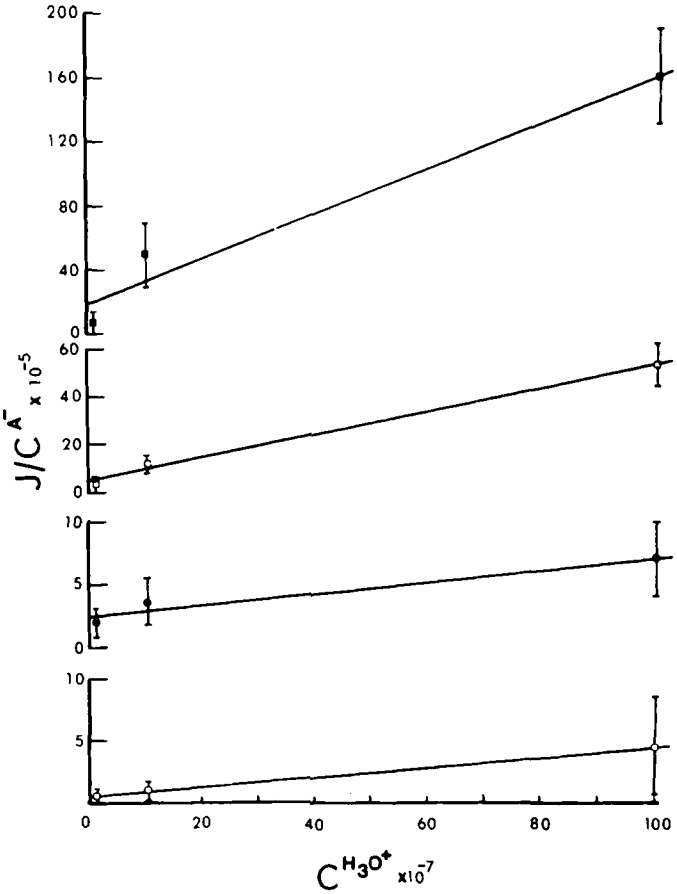

Figure 1—*Plot of* J/C^{A^-} versus $C^{H_3O^+}$ *for the four chromone-2-carboxylic acids studied. Key: (■) I; (□) II; (●) III; (○) IV. Points and vertical bars represent the means and* SD, *respectively, of the individual values of* J/C^{A^-} *at each pH (Table I).*

Table II—Summary of Experimental Results

Compound	S_5, mol·L^{-1} × 10^3	log $K^{M/W}$	$K^{M/W}$·S_5, mol L^{-1}	P^{HA}, cm·h^{-1}	P^{A^-}, cm·h^{-1} × 10^5	D, cm^2·s^{-1} × 10^{10}
I	2.09	4.39	51.3	1.63 ± 0.25[a]	20.2 ± 12.5[a]	0.18
II	12.6	3.35	28.2	0.66 ± 0.08	4.85 ± 3.73	0.82
III	89.2	2.22	14.8	0.09 ± 0.03	2.51 ± 0.93	1.51
IV	187	1.78	11.3	0.15 ± 0.09	0.51 ± 1.63	6.91

[a] 95% Confidence limits.

Ionization Constants—Two methods were used to determine the ionization constants. In the first, a conductometric method (10), all measurements were made at 25°C with a conductivity meter[4]. In the second, a partition–distribution method (11), a biphasic solvent system of dichloroethane–hexane–water was chosen to minimize ion-pair extraction. Large partition coefficients (K) were determined by the interchange technique (12). Distribution coefficients (D) were obtained at various pH values, and the ionization constant was calculated by using a rearranged form of Eq. 5, namely:

$$\log\left(\frac{K}{D} - 1\right) = \text{pH} - \text{p}K_a \qquad \text{(Eq. 6)}$$

RESULTS AND DISCUSSION

The pK_a values of the four chromone-2-carboxylic acids determined in aqueous solution are: 1.93 ± 0.06 (not as previously reported in Ref. 9), 1.87 ± 0.06, 1.75 ± 0.05, and 1.44 ± 0.05 for I, II, III, and IV, respectively. The values for III and IV were obtained by the partition as well as the conductance methods and were consistent with each other. Only the partition method was used with I and II, as the solubility of the undissociated forms were too low to allow use of the conductance method.

Plots of the number of moles of chromone-2-carboxylic acid permeated per square centimeter of SCE *versus* time showed an initial lag phase, followed by a linear steady-state phase 24 to 48 h after initiation of the permeation run. The steady-state total flux of the permeating species (J; in mol/cm^2/h) was calculated from the slope of the linear portion of each plot, and a value of J/C^{A^-} was calculated for each individual determination. The mean, SD, range, and numbers of individual determinations are shown in Table I for the four compounds studied at each of the three pH values. Considering that over the course of the series of experiments it was necessary to use skin from at least 10 different cadavers, the SD values observed are acceptable. Regression analysis of the individual values of J/C^{A^-} *versus* $C^{H_3O^+}$ for each compound was used to compute the relationship expressed in Eq. 4. These results, together with the respective 95% confidence intervals, are also shown in Table I. In Fig. 1, the mean values of J/C^{A^-} listed in Table I plotted against $C^{H_3O^+}$ for the four compounds are shown. The vertical bars represent the SD values.

Utilization of the appropriate pK_a value yields the values of P^{HA} and P^{A^-} listed in Table II. The data show positive, but small, intercepts, indicating that the chromone-2-carboxylate ions have finite permeabilities, although those for IV are not significantly different from zero. In all instances, the permeability of the un-ionized form is ~10^4 times greater than the permeability of the ionized form. In Table II are also presented the solubilities of the compounds in pH 5.0 buffer (S_5) and the triglyceride[2]–water partition coefficients ($K^{M/W}$), calculated as described above.

The triglyceride[2] was chosen as the oil phase in the partition system because preliminary studies (13) over a range of pH values have shown this system to conform closely to the expected theoretical relationship between log D and pH, thereby allowing calculation of log K correctly from observed values of D. In contrast, partition data for I between SCE and water and stratum corneum and water as a function of pH showed a significant deviation from ideality (13). Accordingly, $K^{M/W}$ was used in the present study rather than $K^{SCE/W}$ or $K^{SC/W}$, as this parameter provides a more accurate index of the relative partitioning abilities of the four compounds studied.

By assuming a constant diffusion coefficient and stratum corneum thick-

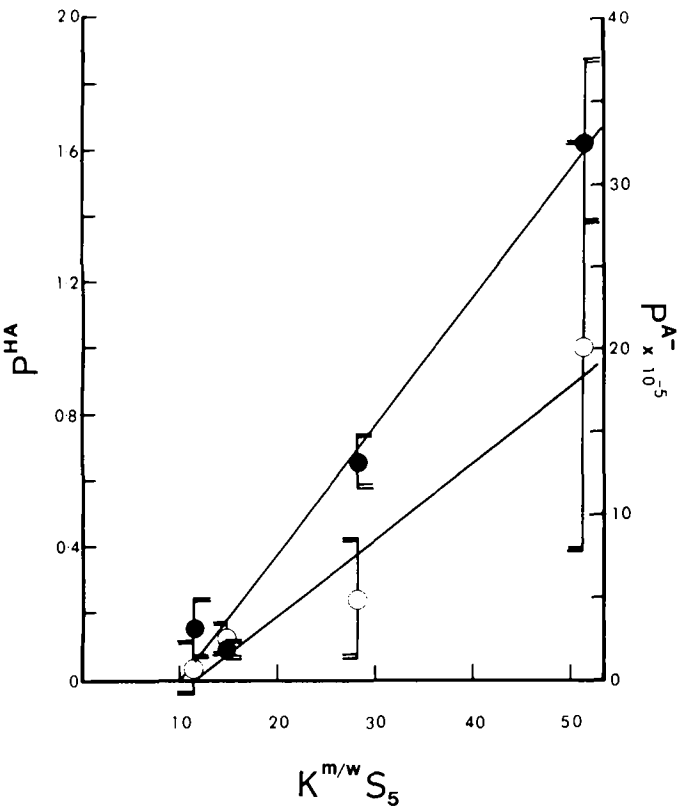

Figure 2—*Relationship between* $K^{M/W}$·S_5 *and* P^{HA} *and* P^{A^-}. *Data are from Table II; vertical bars indicate 95% confidence intervals for each compound.*

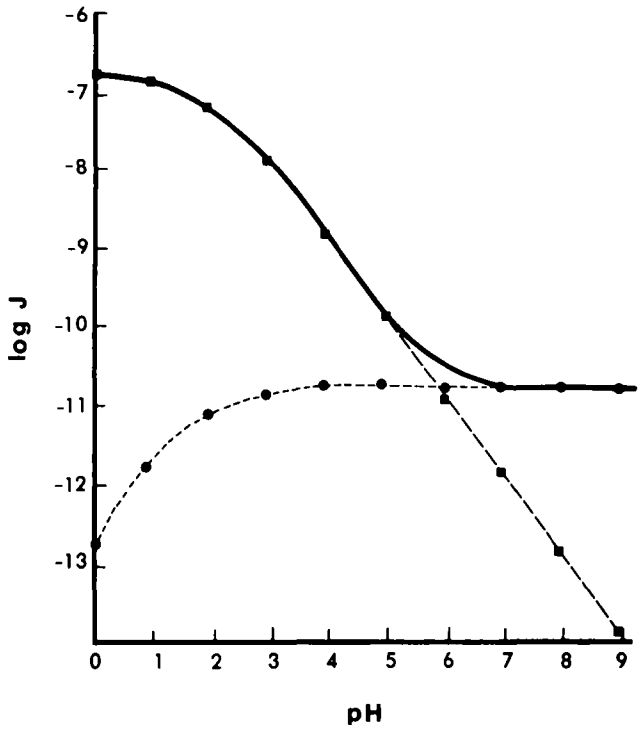

Figure 3—*Theoretical plot of the effect of pH on the total flux* J *and its components* J^{HA} *and* J^{A^-} *for I. Concentration of I is equal to* 10^{-7} *mol·cm*$^{-3}$; pK_a *is equal to 1.93;* P^{HA} *is equal to 1.63 cm·h*$^{-1}$; P^{A^-} *is equal to 2.02* × 10^{-4} *cm·h*$^{-1}$. *Note that the flux (in mol·cm*$^{-2}$·*h*$^{-1}$) *is drawn on a log scale. Key: (■)* J^{HA}; *(●),* J^{A^-}; *(—)* J.

[4] Model B642; Wayne Kerr, Chicago, Il.

ness, it is predicted by Eqs. 1 and 2 that the steady-state total flux is proportional to the product of the partition coefficient of the drug between the stratum corneum and the vehicle and its solubility in the vehicle. Although realizing that $K^{M/W}$ was used in the present study rather than $K^{SC/W}$, such a trend nevertheless appears evident since as $K^{M/W} \cdot S_5$ decreases, so does P^{HA} and P^{A^-} (Fig. 2). This suggests the use of this parameter as a relative indicator of permeability when examining a series of analogues for their ability to penetrate human skin, without recourse to actual permeation studies. The data imply that $K^{M/W} \cdot S_5$ must exceed 10–11 mol $\cdot$ L^{-1} before permeation of the chromone-2-carboxylic acids can be detected.

The values of P^{HA} and P^{A^-} obtained from these experiments can be used to determine how the relative permeation rates of the un-ionized and ionized species change with pH and how this affects the total steady-state flux, *i.e.*, $J^{HA} + J^{A^-}$. This is illustrated for I in Fig. 3, where it should be noted that the flux axis is given in log units. As the pH is increased above the pK_a of 1.93, the concentration of the un-ionized species falls. This leads to a continuous reduction in flux due to the un-ionized species, J^{HA}, since the product $P^{HA} \cdot C^{HA}$ is also falling. At the same time, the concentration of the ionized species rises with increasing pH and then remains constant at a pH value 2 or more units above the pK_a. The net effect is a continuous decline in the total flux as the pH of the solution is increased; in the case of I, this increase is to pH 7. Above this pH, the permeation of chromone ions constitutes the major portion of the total flux, although it is important to remember that the magnitude of the total flux falls dramatically as the pH is raised above the pK_a. Thus, for monoprotic acids in which un-ionized and ionized species have widely separated permeability coefficients (*e.g.*, the chromone-2-carboxylic acids in which the difference between P^{HA} and P^{A^-} is $\sim 10^4$), the pH should be held to as low a value as possible when seeking to maximize the total flux through the skin. The optimal value is at least 1 pH unit below the pK_a, assuming satisfactory tolerance by the skin to such a pH. Minimal flux in the example described here occurs at a pH that is ~5 units or more above the pK_a.

Diffusion coefficients (D) for the four compounds are calculated from Eq. 1 by using the values for $K^{M/W}$ given in Table II and a measured stratum corneum thickness of 10 μm. Since P^{HA} is much greater than P^{A^-}, P was taken to be equal to P^{HA}. The values presented in Table II lie within the range normally found for compounds of this size when they are diffused through the stratum corneum (2).

In summary, the results of this study indicate that chromone-2-carboxylic acids permeate human skin both as un-ionized and ionized species, although the former are $\sim 10^4$ times more permeable. Because of the effect of pH on the relative concentrations of un-ionized and ionized species, it would appear to be possible to control the total flux of these compounds by varying the pH of the drug-containing vehicle applied to the skin.

REFERENCES

(1) B. Idson, *J. Pharm. Sci.*, **64**, 901 (1975).

(2) R. T. Scheuplein and I. H. Blank, *Physiol. Rev.*, **51**, 702 (1971).

(3) A. S. Michaels, S. K. Chandrasekaran, and J. E. Shaw, *AIChE J.*, **21**, 985 (1975).

(4) S. M. Wallace and G. Barnett, *J. Pharmacokinet. Biopharm.*, **6**, 315 (1978).

(5) L. S. Schanker, P. A. Shore, B. B. Brodie, and C. A. M. Hogben, *J. Pharmacol. Exp. Ther.*, **120**, 528 (1957).

(6) H. Nogami, M. Hanano, and J. Watanabe, *Chem. Pharm. Bull.*, **10**, 1161 (1962).

(7) W. G. Crouthamel, G. H. Tan, L. W. Dittert, and J. T. Doluisio, *J. Pharm. Sci.*, **60**, 1160 (1971).

(8) R. T. Scheuplein, *J. Invest. Dermatol.*, **67**, 31 (1976).

(9) J. Swarbrick, G. Lee, and J. Brom, *J. Invest. Dermatol.*, **78**, 63 (1982).

(10) D. J. G. Ives, *J. Chem. Soc.*, **1933**, 731.

(11) J. Kaufman, N. Semo, and W. Koski, *J. Med. Chem.*, **18**, 647 (1975).

(12) C. Golumbic and S. Weller, *Anal. Chem.*, **22**, 1418 (1950).

(13) G. Lee, J. Swarbrick, G. Kiyohara, and D. Payling, *Int. J. Pharm.*, in press.

ACKNOWLEDGMENTS

We thank Fisons plc, Pharmaceutical Division, Loughborough, England, for their generous support of this work and for providing a fellowship to one of us (G.L.).

Adsorption of Phosphate by Aluminum Hydroxycarbonate

JUE-CHEN LIU *§, JOSEPH R. FELDKAMP ‡, JOE L. WHITE ‡, and STANLEY L. HEM *x

Received July 7, 1983, from the **Departments of Industrial and Physical Pharmacy and* ‡*Agronomy, Purdue University, West Lafayette, IN 47907.* Accepted for publication, October 27, 1983. §Present address: College of Pharmacy, Rutgers University, Piscataway, NJ 08854.

Abstract □ Phosphate is specifically adsorbed by aluminum hydroxycarbonate by anion ligand exchange. IR analysis indicated that phosphate exchanged with specifically adsorbed carbonate. Adsorption is favored by low pH and is inversely related to particle size. Adsorption of phosphate decreases the rate of acid neutralization of aluminum hydroxycarbonate. The results are applied to the treatment of hyperphosphatemia and hypophosphatemia.

Keyphrases □ Adsorption—phosphate by aluminum hydroxycarbonate □ Aluminum hydroxycarbonate— adsorption of phosphate

The adsorption of phosphate species by aluminum hydroxide is important, as aluminum hydroxide-containing antacids have been implicated in hypophosphatemia. In contrast, aluminum hydroxide is used as a phosphorus-binding agent in hyperphosphatemia. The interaction of phosphate species with crystalline forms of aluminum hydroxide has been extensively studied due to the wide occurrence of aluminum hydroxide in the soil and the extensive use of phosphorus-containing fertilizers. However, little is known about the interaction of phosphate species with amorphous aluminum hydroxycarbonate, the acid-reactive form of aluminum hydroxide containing specifically adsorbed carbonate which is used in antacids. The purpose of this study was to determine the mechanism of adsorption of phosphate species by aluminum hydroxycarbonate, with emphasis on possible adsorption of phosphate on surface carbonate sites.

BACKGROUND

The binding of phosphorus by aluminum hydroxide in the gastrointestinal tract during antacid therapy was first noted 40 years ago (1, 2). Since that time, it has been confirmed in numerous studies that aluminum hydroxide may reduce the intestinal absorption of phosphate (3–13). Clinical symptoms of phosphorus depletion syndrome parallel serum phosphorus levels and are most likely to be observed in patients who combine aluminum hydroxide antacid therapy with a low dietary phosphorus intake (14, 15). This observation is especially pertinent to critically ill patients who receive only parenteral nutrition and who also require antacid therapy to prevent upper GI bleeding (16).

0022-3549/84/1000-1355$01.00/0

© 1984, American Pharmaceutical Association

ness, it is predicted by Eqs. 1 and 2 that the steady-state total flux is proportional to the product of the partition coefficient of the drug between the stratum corneum and the vehicle and its solubility in the vehicle. Although realizing that $K^{M/W}$ was used in the present study rather than $K^{SC/W}$, such a trend nevertheless appears evident since as $K^{M/W} \cdot S_5$ decreases, so does P^{HA} and P^{A^-} (Fig. 2). This suggests the use of this parameter as a relative indicator of permeability when examining a series of analogues for their ability to penetrate human skin, without recourse to actual permeation studies. The data imply that $K^{M/W} \cdot S_5$ must exceed 10–11 mol $\cdot$ L^{-1} before permeation of the chromone-2-carboxylic acids can be detected.

The values of P^{HA} and P^{A^-} obtained from these experiments can be used to determine how the relative permeation rates of the un-ionized and ionized species change with pH and how this affects the total steady-state flux, *i.e.*, $J^{HA} + J^{A^-}$. This is illustrated for I in Fig. 3, where it should be noted that the flux axis is given in log units. As the pH is increased above the pK_a of 1.93, the concentration of the un-ionized species falls. This leads to a continuous reduction in flux due to the un-ionized species, J^{HA}, since the product $P^{HA} \cdot C^{HA}$ is also falling. At the same time, the concentration of the ionized species rises with increasing pH and then remains constant at a pH value 2 or more units above the pK_a. The net effect is a continuous decline in the total flux as the pH of the solution is increased; in the case of I, this increase is to pH 7. Above this pH, the permeation of chromone ions constitutes the major portion of the total flux, although it is important to remember that the magnitude of the total flux falls dramatically as the pH is raised above the pK_a. Thus, for monoprotic acids in which un-ionized and ionized species have widely separated permeability coefficients (*e.g.*, the chromone-2-carboxylic acids in which the difference between P^{HA} and P^{A^-} is $\sim 10^4$), the pH should be held to as low a value as possible when seeking to maximize the total flux through the skin. The optimal value is at least 1 pH unit below the pK_a, assuming satisfactory tolerance by the skin to such a pH. Minimal flux in the example described here occurs at a pH that is ~5 units or more above the pK_a.

Diffusion coefficients (D) for the four compounds are calculated from Eq. 1 by using the values for $K^{M/W}$ given in Table II and a measured stratum corneum thickness of 10 μm. Since P^{HA} is much greater than P^{A^-}, P was taken to be equal to P^{HA}. The values presented in Table II lie within the range normally found for compounds of this size when they are diffused through the stratum corneum (2).

In summary, the results of this study indicate that chromone-2-carboxylic acids permeate human skin both as un-ionized and ionized species, although the former are $\sim 10^4$ times more permeable. Because of the effect of pH on the relative concentrations of un-ionized and ionized species, it would appear to be possible to control the total flux of these compounds by varying the pH of the drug-containing vehicle applied to the skin.

REFERENCES

(1) B. Idson, *J. Pharm. Sci.*, **64**, 901 (1975).

(2) R. T. Scheuplein and I. H. Blank, *Physiol. Rev.*, **51**, 702 (1971).

(3) A. S. Michaels, S. K. Chandrasekaran, and J. E. Shaw, *AIChE J.*, **21**, 985 (1975).

(4) S. M. Wallace and G. Barnett, *J. Pharmacokinet. Biopharm.*, **6**, 315 (1978).

(5) L. S. Schanker, P. A. Shore, B. B. Brodie, and C. A. M. Hogben, *J. Pharmacol. Exp. Ther.*, **120**, 528 (1957).

(6) H. Nogami, M. Hanano, and J. Watanabe, *Chem. Pharm. Bull.*, **10**, 1161 (1962).

(7) W. G. Crouthamel, G. H. Tan, L. W. Dittert, and J. T. Doluisio, *J. Pharm. Sci.*, **60**, 1160 (1971).

(8) R. T. Scheuplein, *J. Invest. Dermatol.*, **67**, 31 (1976).

(9) J. Swarbrick, G. Lee, and J. Brom, *J. Invest. Dermatol.*, **78**, 63 (1982).

(10) D. J. G. Ives, *J. Chem. Soc.*, **1933**, 731.

(11) J. Kaufman, N. Semo, and W. Koski, *J. Med. Chem.*, **18**, 647 (1975).

(12) C. Golumbic and S. Weller, *Anal. Chem.*, **22**, 1418 (1950).

(13) G. Lee, J. Swarbrick, G. Kiyohara, and D. Payling, *Int. J. Pharm.*, in press.

ACKNOWLEDGMENTS

We thank Fisons plc, Pharmaceutical Division, Loughborough, England, for their generous support of this work and for providing a fellowship to one of us (G.L.).

Adsorption of Phosphate by Aluminum Hydroxycarbonate

JUE-CHEN LIU *§, JOSEPH R. FELDKAMP ‡, JOE L. WHITE ‡, and STANLEY L. HEM *x

Received July 7, 1983, from the **Departments of Industrial and Physical Pharmacy and* ‡*Agronomy, Purdue University, West Lafayette, IN 47907.* Accepted for publication, October 27, 1983. §Present address: College of Pharmacy, Rutgers University, Piscataway, NJ 08854.

Abstract □ Phosphate is specifically adsorbed by aluminum hydroxycarbonate by anion ligand exchange. IR analysis indicated that phosphate exchanged with specifically adsorbed carbonate. Adsorption is favored by low pH and is inversely related to particle size. Adsorption of phosphate decreases the rate of acid neutralization of aluminum hydroxycarbonate. The results are applied to the treatment of hyperphosphatemia and hypophosphatemia.

Keyphrases □ Adsorption—phosphate by aluminum hydroxycarbonate □ Aluminum hydroxycarbonate— adsorption of phosphate

The adsorption of phosphate species by aluminum hydroxide is important, as aluminum hydroxide-containing antacids have been implicated in hypophosphatemia. In contrast, aluminum hydroxide is used as a phosphorus-binding agent in hyperphosphatemia. The interaction of phosphate species with crystalline forms of aluminum hydroxide has been extensively studied due to the wide occurrence of aluminum hydroxide in the soil and the extensive use of phosphorus-containing fertilizers. However, little is known about the interaction of phosphate species with amorphous aluminum hydroxycarbonate, the acid-reactive form of aluminum hydroxide containing specifically adsorbed carbonate which is used in antacids. The purpose of this study was to determine the mechanism of adsorption of phosphate species by aluminum hydroxycarbonate, with emphasis on possible adsorption of phosphate on surface carbonate sites.

BACKGROUND

The binding of phosphorus by aluminum hydroxide in the gastrointestinal tract during antacid therapy was first noted 40 years ago (1, 2). Since that time, it has been confirmed in numerous studies that aluminum hydroxide may reduce the intestinal absorption of phosphate (3–13). Clinical symptoms of phosphorus depletion syndrome parallel serum phosphorus levels and are most likely to be observed in patients who combine aluminum hydroxide antacid therapy with a low dietary phosphorus intake (14, 15). This observation is especially pertinent to critically ill patients who receive only parenteral nutrition and who also require antacid therapy to prevent upper GI bleeding (16).

0022-3549/84/1000-1355$01.00/0

© 1984, American Pharmaceutical Association

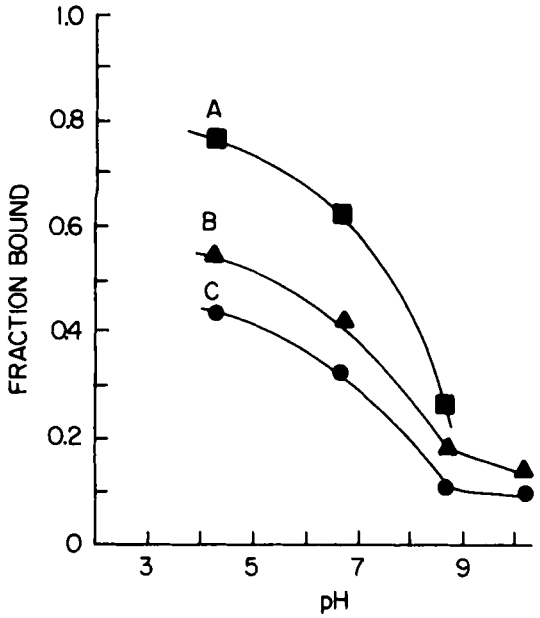

Figure 1—*Effect of pH on the fraction of phosphorus bound by AHCG 1 (A), aluminum hydroxide gel (B), and AHCG 2 (C).*

In two recent studies, slightly different conclusions were reached regarding the effect of aluminum hydroxide on serum phosphorus levels and phosphorus excretion, perhaps due to differences in dosage and duration of therapy. In the first study, seven daily doses containing 525 mg of equivalent aluminum oxide (15.4 mEq) per dose were administered for 28 d to 12 healthy subjects (15). No statistically significant change in serum phosphorus levels occurred, but a statistically significant decrease in phosphorus excretion led to values below the normal phosphorus excretion range. No clinical symptoms were observed in any subject. Because of the change in phosphate excretion, the subjects were described as exhibiting incomplete phosphorus depletion. In a second study, 15 healthy subjects were administered four daily doses containing 450 mg of equivalent aluminum oxide (13.2 mEq) per dose for 12 d (17). Serum phosphorus levels did not change significantly, and no clinical symptoms were observed, although a statistically significant decrease in phosphorus excretion was noted. However, in contrast to the first study, the phosphorus excretion values remained within the normal physiological limits. Therefore, it was concluded that aluminum hydroxide was tolerated by the subjects.

Hyperphosphatemia is most commonly encountered during renal failure. Therapy usually involves reduction in the uptake and absorption of exogenous phosphorus through a low phosphorus diet and the use of phosphorus-binding agents (18–23). Presently, aluminum hydroxycarbonate gel is the chief agent used to treat hyperphosphatemia.

Phosphate species are specifically adsorbed by hydrous metal oxides through anionic ligand exchange, displacing surface hydroxyl or water groups (24).

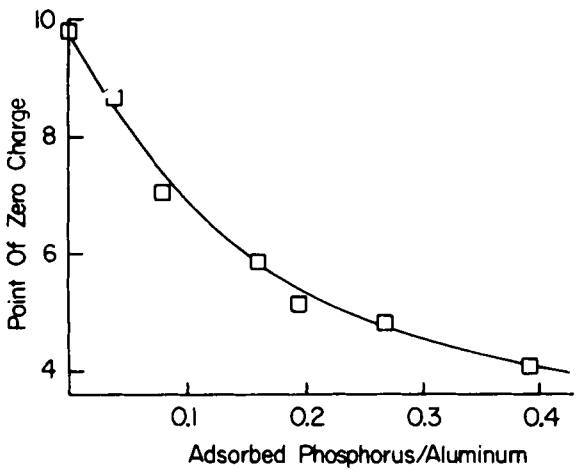

Figure 2—*Effect of phosphate adsorption on PZC of aluminum hydroxide gel.*

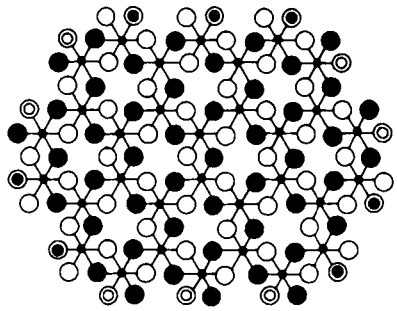

Figure 3—*Schematic of the unit layer of aluminum hydroxide showing the surface hydroxyl and aquo groups. Key: (⊛) upper OH; (○) upper OH_2; (●) lower OH; (⊛) lower OH_2.*

The affinity of anions for aluminum hydroxide at moderate pH conditions follows the order phosphate > arsenate > sulfate > chloride (25). The adsorption of phosphate shifts the point of zero charge (PZC) to lower values and thus alters the surface characteristics (24, 26). This must occur by entering the inner Helmholtz layer, *i.e.*, the first coordination sphere of the aluminum ions on the aluminum hydroxide surface, through the displacement of coordinated hydroxyl and aquo ions by a ligand exchange reaction.

The extent of phosphate adsorption depends on pH, time, concentration, surface area, temperature, and the nature of the adsorbent (26–28).

EXPERIMENTAL SECTION

Materials—Two aluminum hydroxycarbonate gels were obtained commercially and were identified as AHCG 1[1] and AHCG 2[2]. An aluminum hydroxide gel which was free of carbonate was precipitated by adding sufficient 3 M KOH to 2 L of 1 M $AlCl_3$ to reach pH 9.5. Immediately after washing with three volumes of distilled water, 68 g of sorbitol was dissolved in distilled water and added to the aluminum hydroxide gel. The final volume was then adjusted to 4 L by the addition of distilled water. Sorbitol was added to reduce the rate of polymerization (29) and thereby maintain the maximum surface area.

Analytical Procedures—The equivalent aluminum oxide content was determined by chelatometric titration (30). The carbonate content was determined by gasometric displacement (31). The PZC was determined by a potentiometric titration procedure (32). The rate of acid neutralization was determined by automated pH-stat titration[3] at pH 3 and 25°C (33). The amount of phosphorus in solution was determined by the heteropoly blue method (34). The mean hydrodynamic radius was determined by fiber optic Doppler anemometry[4] (35).

The fraction of phosphate species adsorbed at different pH conditions was determined by first adjusting portions of the aluminum hydroxycarbonate or aluminum hydroxide gel containing 15.5 mM of aluminum and 10 mM of KCl to the desired pH with a pH-stat titrator[3]. After the pH adjustment, 25 mL of 1 M NaH_2PO_4 was added, and the volume was adjusted to 100 mL with distilled water. The pH was maintained at the desired level for 1 h at 25°C with constant stirring with the pH-stat titrator[3]. The sample was centrifuged at 15,000 rpm (27,000×*g*) for 30 min, and the supernatant was analyzed for phosphorus. The quantity of phosphate adsorbed was determined by difference.

IR spectra[5] were obtained by air drying the sample and preparing a com-

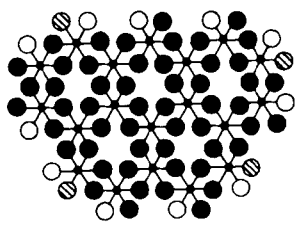

Figure 4—*Schematic of the unit layer of aluminum hydroxycarbonate showing the surface hydroxyl, aquo, and carbonate groups. Key: (●) OH; (○) OH_2; (⊘) CO_3.*

[1] Chattem Chemical Co., Chattanooga, Tenn.
[2] Reheis Chemical Co., Phoenix, Ariz.
[3] PAM 62, TTT 60, ABU 12, TTA 60, REA 160; Radiometer, Copenhagen, Denmark.
[4] SIRA Institute, Ltd., Kent, England.
[5] Model 180; Perkin-Elmer Corp., Norwalk, Conn.

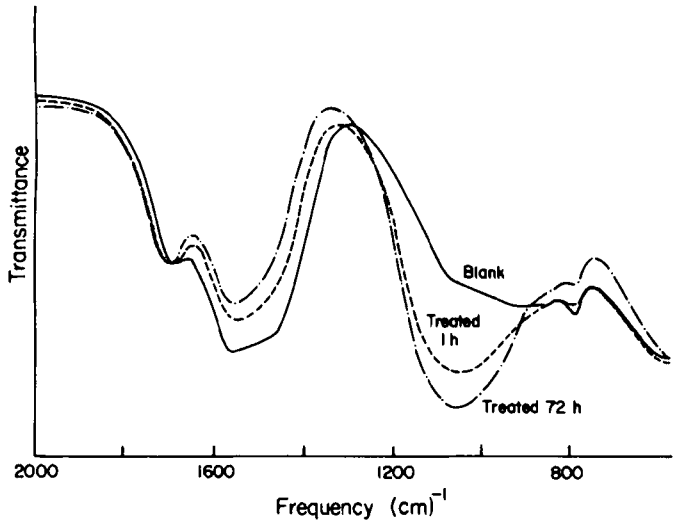

Figure 5—*Change in the IR spectrum of AHCG 2 as a result of phosphate adsorption. Key: (—) blank; (- -) treated for 1 h; (— • —), treated for 72 h.*

pressed disk (1 mg of sample/300 mg of KBr). A sample of AHCG 2 containing 25 mM of equivalent aluminum oxide was diluted to 100 mL with distilled water and adjusted to pH 6.6. Five milliliters of 0.25 M NaH_2PO_4 was added. The sample was shaken at 25°C. Portions were removed and air dried after 1 and 72 h.

The exchange of phosphate species for specifically adsorbed carbonate in aluminum hydroxycarbonate was determined by adding 26.9 mM NaH_2PO_4 to a sample of AHCG 2 containing 15.5 mM equivalent aluminum oxide at pH 6.6 and 25°C. The pH was maintained with a pH-stat titrator[3]. Samples were taken after 30, 60, 120, or 240 min of reaction time and analyzed for total carbonate content and phosphorus in solution.

RESULTS AND DISCUSSION

Phosphate is adsorbed by both aluminum hydroxide and aluminum hydroxycarbonate (Fig. 1). The three adsorbents differed substantially in the amount of phosphate adsorbed. However, this difference does not appear to be related to the presence of carbonate surface groups, in addition to hydroxyl and aquo surface groups, as the fraction of phosphate bound by the sample of aluminum hydroxide (Fig. 1B) was intermediate between the two aluminum hydroxycarbonate gels (Fig. 1A and C). Particle size analysis showed that phosphate adsorption was directly related to surface area, as the mean hydrodynamic radii of aluminum hydroxycarbonate gel 1 (AHCG 1), aluminum hydroxide, and aluminum hydroxycarbonate gel 2 (AHCG 2) were 0.21, 0.28, and 0.51 μm, respectively.

The results shown in Fig. 1 also indicate that phosphate adsorption is dependent on pH, with all three adsorbents exhibiting a similar pH profile. However, the PZC varies from 9.8 for aluminum hydroxide to 7.6 and 6.5 for aluminum hydroxycarbonate 1 and 2, respectively. Thus, phosphate adsorption cannot be explained simply by electrostatic attraction, as the pH profile is not related to the PZC of the adsorbents. The fact that phosphate adsorption is independent of the PZC, *i.e.*, adsorption decreased at pH ~7 for all three adsorbents, indicates that phosphate is specifically adsorbed at the inner Helmholtz layer by a ligand-exchange reaction (24) which is independent of surface potential.

The nature of the surface and the ionic form of the adsorbate are influenced by pH. At low pH conditions, the surface is positive and aquo groups are the predominant sites on the surface. As the pH increases, the surface potential decreases and more hydroxyl sites occur on the surface as the hydroxide concentration in solution increases. Therefore, the phosphate species must compete with hydroxide ions for the hydroxyl sites on the increasingly negative surface. Thus, the high adsorption of phosphate species at low pH can be attributed to the high positive charge of the surface and the weaker competition of hydroxide ions. This behavior is in agreement with the results of a previous study by Huang (27), who concluded that surface acidity and the acid–base behavior of the adsorbed anions are the most important factors controlling the adsorption density.

The conclusion that phosphate is specifically adsorbed by aluminum hydroxide and aluminum hydroxycarbonate is further supported by the depression of the PZC of aluminum hydroxide following phosphate adsorption (Fig. 2). The PZC decreased from 9.8 to 4.1 as the adsorbed phosphate-to-aluminum molar ratio increased from 0 to 0.39. The decrease in PZC can be attributed to the negative charge introduced by the specifically adsorbed phosphate (27).

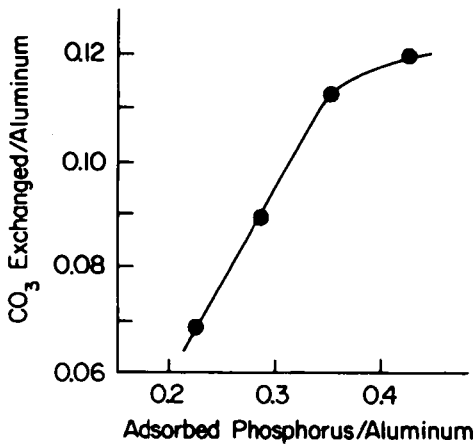

Figure 6—*Exchange of phosphate species for specifically adsorbed carbonate in AHCG 2 at pH 6.6 and 25°C.*

The potential exchangeable sites for aluminum hydroxide are illustrated in Fig. 3. The molecular structure is composed of two fundamental units: two planes of closely packed hydroxyl ions with aluminum sandwiched between them as fused, six-membered rings of octahedrally coordinated aluminum atoms joined by double hydroxide bridges (36). At the surface, the terminal aluminum atoms are coordinated with hydroxyl and aquo groups. The proportion of hydroxyl and aquo surface groups is controlled by the pH–PZC relationship (37) by[6]:

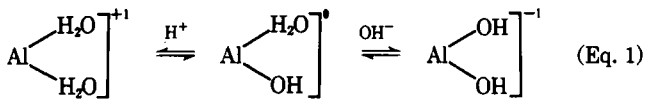

(Eq. 1)

Rajan *et al.* (38) have shown that aquo groups are the predominant adsorption site at low pH conditions and that exchange with surface hydroxyl groups predominates above pH 6.7.

Aluminum hydroxycarbonate has the same basic structure as aluminum hydroxide, except that carbonate groups are present at the surface in addition

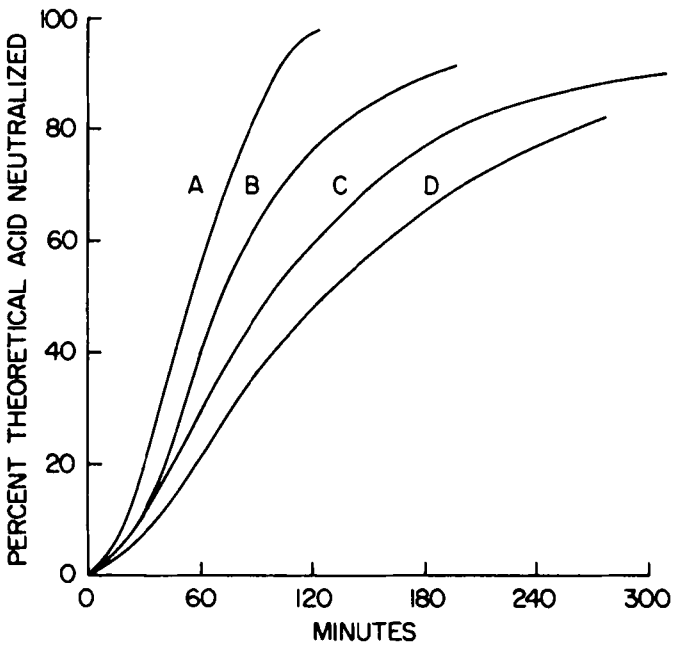

Figure 7—*Effect of phosphate adsorption on the rate of acid neutralization of AHCG 2 at various adsorbed phosphate-to-aluminum molar ratios. Key: (A) 0; (B) 0.016; (C) 0.032; (D) 0.066.*

[6] For clarity, only the bonds associated with the surface sites are shown, even though aluminum is in sixfold coordination in each structure.

to hydroxyl and aquo groups (39) (Fig. 4). The possibility of exchange of phosphate for surface carbonate sites was studied by IR spectroscopy (Fig. 5). The IR spectrum of aluminum hydroxycarbonate exhibits absorption bands between 1400 and 1500 cm^{-1} which have been assigned to specifically adsorbed carbonate (40). After interacting with phosphate for 1 h, the carbonate bands were diminished, and a band at 1080 cm^{-1}, corresponding to P—O stretching (41), was evident. The P—O stretching band increased in intensity with adsorption time while a concomitant decrease in the intensity of the carbonate band occurred. The exchange of phosphate species for carbonate was confirmed by the loss of carbonate which accompanied adsorption of phosphate by AHCG 2 at pH 6.6 (Fig. 6). At low phosphate levels, the ratio of phosphate adsorbed to carbonate exchanged was ~3, indicating that phosphate adsorption by aluminum hydroxycarbonate gel involves exchange with surface carbonate sites as well as hydroxyl and aquo sites.

The effect of phosphate adsorption on the rate of acid neutralization of aluminum hydroxycarbonate was investigated by pH-stat titration at pH 3 and 25°C (Fig. 7). The rate of acid neutralization decreased in response to adsorption of even small amounts of phosphate. For example, the time to neutralize 50% of the sample increased from 57 min, in the absence of phosphate, to 75 min when the adsorbed phosphate-to-aluminum molar ratio was only 0.016. The mechanism for this effect is believed to be related to the difference in solubility between $AlPO_4$, known mineralogically as berlinite, and amorphous aluminum hydroxide. The acid neutralization reactions of $AlPO_4$ and $Al(OH)_3$ are shown by:

$$AlPO_4 + 3H^+ \overset{K_1}{\rightleftharpoons} Al^{3+} + H_3PO_4 \qquad \text{(Eq. 2)}$$

$$Al(OH)_3 + 3H^+ \overset{K_2}{\rightleftharpoons} Al^{3+} + 3H_2O \qquad \text{(Eq. 3)}$$

The logarithims of the equilibrium constants for Eqs. 2 and 3 are 0.5 and 9.66, respectivcly (42). Thus, the Al—O—PO_3 bond is much more resistant to proton attack than the Al—O—H bond.

Adsorption of phosphate species occurs as readily by aluminum hydroxycarbonate as by aluminum hydroxide because phosphate can exchange with specifically adsorbed carbonate. Adsorption is favored by low pH and small particle size. In patients with hypophosphatemia, the depletion of phosphorus will be the greatest for those aluminum hydroxycarbonate gels with the smallest particle size, *i.e.*, those exhibiting the best antacid properties. Thus, an adequate dietary intake of phosphorus is essential of antacid therapy is required. Alternate steps, such as the use of aluminum phosphate gel as an antacid, are not satisfactory because of the poor antacid properties of aluminum phosphate. On the other hand, an aluminum hydroxide gel with the maximum surface area appears to be desirable to treat hyperphosphatemia. The aluminum hydroxide gel used in this study, which was stabilized by adding sorbitol immediately after precipitation (Fig. 1B), would be a good candidate, as it requires 270 min to neutralize 10% of its theoretical acid-neutralizing capacity at pH 3 and 25°C. Thus, this aluminum hydroxide gel will not undergo appreciable acid dissolution during the gastric residence time and will be present throughout the GI tract as a relatively high-surface-area colloidal solid capable of adsorbing phosphate species.

REFERENCES

(1) G. B. Fauley, S. Freeman, A. C. Ivy, A. J. Atkinson, and H. S. Wigodsky, *Arch. Intern. Med.*, **67**, 563 (1941).

(2) L. B. Kirsner, *J. Clin. Invest.*, **22**, 47 (1943).

(3) W. L. Bloom and D. Flinchum, *J. Am. Med. Assoc.*, **174**, 1327 (1960).

(4) A. Ansari, *Minn. Med.*, **53**, 837 (1970).

(5) P. A. Boelens, W. Norwood, C. Kjellstraud, and D. M. Brown, *Am. J. Dis. Child.*, **120**, 350 (1970).

(6) J. S. Fordtran, in "Gastrointestinal Disease," M. H. Sleisenger, Ed., W. B. Saunders, Philadelphia, Pa. 1973, pp. 731–732.

(7) D. E. Abrams, R. B. Silcott, and R. Terry, *West. J. Med.*, **120**, 157 (1974).

(8) L. R. Baker, P. Ackrill, W. R. Cattell, T. C. B. Stamp, and L. Watson, *Br. Med. J.*, **3**, 150 (1974).

(9) C. E. Dent and C. S. Winter, *Br. Med. J.*, **1**, 551 (1974).

(10) J. R. Morrissey and R. F. Basseras, *N. Engl. J. Med.*, **290**, 550 (1974).

(11) A. Littman and B. H. Pine, *Ann. Intern. Med.*, **82**, 544 (1975).

(12) M. Ravid and M. Robson, *J. Am. Med. Assoc.*, **236**, 1380 (1976).

(13) M. Goodman, C. C. Solomons, and P. D. Miller, *Am. J. Med.*, **65**, 868 (1978).

(14) H. Shields, *Gastroenterology*, **75**, 1137 (1978).

(15) P. Herzog, K. F. Schmitt, T. Grendahl, J. van der Linder, Jr., and K. H. Holtermuller, in "Antacids in the Eighties," F. Halter, Ed., Urban and Schwarzenberg, Baltimore, Md., 1982, pp. 123–135.

(16) S. E. Silvis and P. D. Paragas, *Gastroenterology*, **62**, 513 (1972).

(17) V. G. Grunzig, P. W. Lucker, and J. Schnitker, *Drug Res.*, **33**, 258 (1983).

(18) R. S. Goldsmith, J. Furszyfer, W. J. Johnson, A. E. Fournier, and C. D. Arnaud, *Am J. Med.*, **50**, 692 (1971).

(19) E. M. Clarkson, V. A. Luck, and W. V. Hynson, *Clin. Sci.*, **43**, 519 (1972).

(20) W. J. Johnson, R. S. Goldsmith, and C. D. Arnaud, *Med. Clin. North Am.*, **56**, 961 (1972).

(21) W. F. Pinggera and M. M. Popovtzer, *J. Am. Med. Assoc.*, **222**, 1640 (1972).

(22) W. M. Vosik, C. F. Anderson, and W. P. Steffee, *Mayo Clin. Proc.*, **47**, 110 (1972).

(23) M. M. Popovtzer, W. F. Pinggera, and J. B. Robinette, *J. Am. Med. Assoc.*, **231**, 960 (1975).

(24) F. J. Hingston, R. J. Atkinson, and J. P. Quirk, *Nature (London)*, **215**, 1459 (1967).

(25) R. L. Parfitt, *Adv. Agron.*, **30**, 1 (1978).

(26) J. W. Bowden, S. Nagarajah, N. J. Barrow, A. M. Posner, and J. P. Quirk, *Aust. J. Soil Res.*, **18**, 49 (1980).

(27) C. P. Huang, *J. Colloid Interface Sci.*, **53**, 180 (1975).

(28) S. H. Chien, N. K. Savant, and U. Mokwunye, *Soil Sci.*, **133**, 160 (1982).

(29) S. L. Nail, J. L. White, and S. L. Hem, *J. Pharm. Sci.*, **65**, 1195 (1976).

(30) "The United States Pharmacopeia," 20th rev., United States Pharmacopeial Convention, Rockville, Md., 1980, p. 25.

(31) "Official Methods of Analysis of the Association of Official Analytical Chemists," 12th ed., W. Horwitz, Ed., Association of Official Analytical Chemists, Washington, D.C., 1975, p. 147.

(32) J. R. Feldkamp, D. N. Shah, S. L. Meyer, J. L. White, and S. L. Hem, *J. Pharm. Sci.*, **70**, 638 (1981).

(33) N. J. Kerkhof, R. K. Vanderlaan, J. L. White, and S. L. Hem, *J. Pharm. Sci.*, **66**, 1528 (1977).

(34) M. Halmann, in "Analytical Chemistry of Phosphorus Compounds," Wiley, New York, N.Y., 1972, p. 31.

(35) D. A. Ross, H. S. Dhadwal, and R. B. Dyott, *J. Colloid Interface Sci.*, **64**, 533 (1978).

(36) P. H. Hsu, in "Minerals in Soil Environments," J. B. Dixon and S. B. Weed, Eds., Soil Science Society of America, Madison, Wis., 1977, p. 99.

(37) G. A. Park, *Chem. Rev.*, **65**, 177 (1965).

(38) S. S. S. Rajan, K. W. Perrott, and W. M. H. Saunders, *J. Soil Sci.*, **25**, 438 (1974).

(39) E. C. Scholtz, J. R. Feldkamp, J. L. White, and S. L. Hem, *J. Pharm. Sci.*, **73**, 209 (1984).

(40) J. L. White and S. L. Hem, *J. Pharm. Sci.*, **64**, 468 (1975).

(41) K. Nakamoto, in "Infrared Spectra of Inorganic and Coordination Compounds," 2nd ed., Wiley, New York, N.Y., 1970, pp. 117, 176.

(42) W. L. Lindsay, in "Chemical Equilibria in Soils," Wiley, New York, N.Y., 1979, pp. 36, 41, 164.

ACKNOWLEDGMENTS

This report is journal paper 9494, Purdue University Agricultural Experiment Station, West Lafayette, IN 47907. This study was supported in part by William H. Rorer, Inc.

Pharmacokinetic Study on the Mechanism of Tissue Distribution of Doxorubicin: Interorgan and Interspecies Variation of Tissue-to-Plasma Partition Coefficients in Rats, Rabbits, and Guinea Pigs

TETSUYA TERASAKI, TATSUJI IGA ˣ, YUICHI SUGIYAMA, and MANABU HANANO

Received May 18, 1982, from the *Faculty of Pharmaceutical Sciences, University of Tokyo, Hongo, Bunkyo-ku, Tokyo 113, Japan.* Accepted for publication September 9, 1983.

Abstract □ The mechanism of interorgan and interspecies variations in the tissue distribution of doxorubicin was studied in rats, rabbits, and guinea pigs. The permeation properties of doxorubicin were investigated by using isolated rat erythrocytes as a model membrane. A significant dependency of the uptake rate constant on medium pH was observed, suggesting that only un-ionized doxorubicin is diffusible through the plasma membrane. The values of plasma unbound fraction (f_p) of doxorubicin were 0.344 for rats, 0.415 for rabbits, and 0.529 for guinea pigs. The tissue DNA concentrations of rats were larger than those of rabbits and smaller than those of guinea pigs in corresponding organs or tissues. An *in vitro* organ model that described the distribution behavior of doxorubicin in the whole body was constructed, and an equation was derived to estimate the tissue-to-plasma partition coefficients, (K_p) from *in vitro* experiments. The *in vitro* K_p values showed comparatively good agreement with the *in vivo* K_p values for the various organs or tissues in all three species. Doxorubicin is exclusively bound to the nuclei in the cells. The variation of the K_p values in different organs depended on the amount of nuclei per gram of tissue. The primary determinant of the interspecies variation in the K_p values was the difference in tissue DNA concentrations among rats, rabbits, and guinea pigs, and a secondary determinant was the difference in f_p values.

Keyphrases □ Doxorubicin—pharmacokinetics, mechanism of tissue distribution, tissue-to-plasma partition coefficient □ Pharmacokinetics—doxorubicin, mechanism of distribution, tissue-to-plasma partition coefficients □ Partition coefficients—tissue to plasma, mechanism of distribution of doxorubicin

The tissue distribution of doxorubicin has been studied in several animal species (1–5). The characteristic feature of the tissue distribution of doxorubicin is that the tissue-to-plasma partition coefficient (K_p), a commonly used physiological pharmacokinetic parameter, is extraordinarily large and shows clear differences among tissues. Although it has been demonstrated that doxorubicin and its derivatives interact with DNA, chromatin, and nuclei (6–8), the mechanism of tissue distribution of doxorubicin has not been quantitatively elucidated.

In general, the physiological distribution of most drugs is governed by two factors: (*a*) their reversible binding equilibrium with proteins and/or other constituents in blood and tissues and (*b*) the concentration difference of unbound drug, which depends on the membrane permeability (9). Therefore, much has been done on the changes in plasma protein binding as a possible determining factor of interspecies, individual, or disease-state differences in drug distribution (10–12). However, it has not yet been possible to explain organ and interspecies differences in drug distribution in terms of the K_p values for any drug, despite various studies of drug interactions with intracellular organelles, e.g., nuclei, mitochondria, and microsomes.

In previous studies (13, 14), a comparatively good correlation was found between the K_p value of doxorubicin and the tissue DNA concentration, *i.e.*, the amount of nuclei per gram of tissue in rats and rabbits, and there was no significant difference in the characteristics of doxorubicin binding to the nuclei isolated from the rat liver and kidney tissues. The purpose of this study was to elucidate the mechanism of organ and interspecies variation in the tissue distribution of doxorubicin by means of measurements of tissue DNA concentrations and *in vitro* binding studies with plasma and nuclei.

THEORETICAL SECTION

Organ Model—A diagrammatic representation of an anatomical compartment in an organism is presented in Fig. 1. In estimating the K_p value of doxorubicin in the compartment from the results of *in vitro* experiments, the following assumptions were made:

1. The nucleus is the dominant organelle in tissue binding.
2. The variations in tissue distribution depend on the amount of nuclei per gram of tissue, *i.e.*, tissue DNA concentration, and the differences in nuclear binding parameters among tissues and species are negligible.
3. Only the un-ionized form which is free from plasma and nuclear binding can diffuse through the plasma membrane.

It has been reported on the basis of fluorescence microscopy in hamsters (15) that anthracycline antibiotics are localized in the cell nucleus. Furthermore, >85% of doxorubicin was also localized in the 600×*g* subcellular fraction of each tissue after intravenous administration of 10 mg/kg in rats[1]. In a previous study (13), a good correlation was found between *in vivo* K_p value and the tissue DNA concentration. Therefore, it was suggested that the dominant factor in organ differences in the tissue distribution is the amount of nuclei per gram of tissue. Moreover, there was no difference in tissue nuclear binding characteristics of doxorubicin between the liver and kidney (14). Although it was reported that a resistant type of tumor cell has a carrier-mediated influx system and active efflux mechanisms (16, 17), there is little information regarding the permeation of doxorubicin through the plasma membrane into the normal cell. Therefore, the membrane permeability to doxorubicin was examined by using isolated rat erythrocytes as a model membrane in the present study.

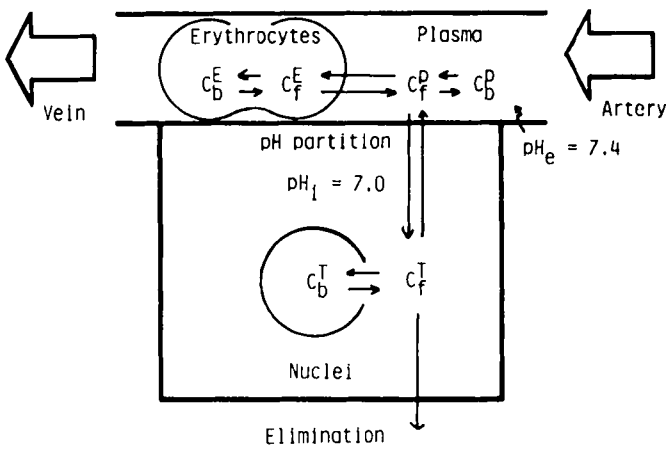

Figure 1—*Diagrammatic representation of the organ model.*

[1] Unpublished results.

0022-3549/84/1000-1359$01.00/0
© 1984, American Pharmaceutical Association

Table I—Comparison of Tissue DNA Concentrations Among Three Species

Tissue	Tissue DNA Concentration[a]		
	Rat, M[b]	Rabbit, M[b]	Guinea Pig, M
Adipose tissue	$1.35 \times 10^{-3} \pm 0.15 \times 10^{-3}$	$4.89 \times 10^{-4} \pm 0.88 \times 10^{-4}$	$1.74 \times 10^{-3} \pm 0.22 \times 10^{-3}$
Muscle	$9.15 \times 10^{-4} \pm 1.59 \times 10^{-4}$	$2.60 \times 10^{-4} \pm 0.53 \times 10^{-4}$	$8.23 \times 10^{-4} \pm 0.52 \times 10^{-4}$
Liver	$6.43 \times 10^{-3} \pm 0.38 \times 10^{-3}$	$3.81 \times 10^{-3} \pm 0.51 \times 10^{-3}$	$8.43 \times 10^{-3} \pm 0.62 \times 10^{-3}$
Gut	$2.05 \times 10^{-2} \pm 0.08 \times 10^{-2}$	$1.77 \times 10^{-2} \pm 0.10 \times 10^{-2}$	$2.57 \times 10^{-2} \pm 0.25 \times 10^{-2}$
Heart	$4.59 \times 10^{-3} \pm 0.38 \times 10^{-3}$	$2.24 \times 10^{-3} \pm 0.08 \times 10^{-3}$	$5.96 \times 10^{-3} \pm 0.37 \times 10^{-2}$
Stomach	$1.11 \times 10^{-2} \pm 0.04 \times 10^{-2}$	$7.77 \times 10^{-3} \pm 0.47 \times 10^{-3}$	$1.81 \times 10^{-2} \pm 0.05 \times 10^{-2}$
Kidney	$1.25 \times 10^{-2} \pm 0.09 \times 10^{-2}$	$1.28 \times 10^{-2} \pm 0.12 \times 10^{-2}$	$1.71 \times 10^{-2} \pm 0.06 \times 10^{-2}$
Lung	$2.35 \times 10^{-2} \pm 0.04 \times 10^{-2}$	$2.00 \times 10^{-2} \pm 0.08 \times 10^{-2}$	$3.25 \times 10^{-2} \pm 0.09 \times 10^{-2}$
Spleen	$5.41 \times 10^{-2} \pm 0.38 \times 10^{-2}$	$5.13 \times 10^{-2} \pm 0.27 \times 10^{-2}$	$5.99 \times 10^{-2} \pm 0.13 \times 10^{-2}$

[a] Mean ± *SE* of each experiment; $n = 3$–7. Calculated with calf thymus DNA (mol. wt. 330.9 per unit nucleotide as sodium salt) as the standard. [b] Obtained from a previous report (13).

From the aforementioned assumptions regarding the distribution of doxorubicin in the organs, an equation can be derived to estimate the K_p value as follows. K_p is defined as the ratio of the tissue concentration to the concentration in the leaving venous plasma, *i.e.*:

$$K_p = \frac{C_f^T + C_b^T}{C_f^P + C_b^P} \quad \text{(Eq. 1)}$$

where C^T and C^P are the drug concentrations in the tissue and venous plasma, respectively, and the subscripts f and b denote the unbound and bound drug species, respectively. Appropriate rearrangement of Eq. 1 gives:

$$K_p = \frac{C_f^T}{C_f^P} \times \frac{C_f^P}{C_f^P + C_b^P} \times \left(1 + \frac{C_b^T}{C_f^T}\right) \quad \text{(Eq. 2)}$$

It has been reported by several investigators that the intracellular pH is slightly lower than that in the extracellular fluid and the blood plasma (18). Since doxorubicin is a basic drug which is more highly ionized at lower than higher pH values, the antibiotic diffuses out less rapidly than it enters, and the concentration of unbound doxorubicin may be somewhat higher inside than outside the tissue cells. Therefore, the ratio of the unbound drug in the tissue to that in plasma can be expressed by:

$$\frac{C_f^T}{C_f^P} = \frac{1 + 10^{pK_a - pH_i}}{1 + 10^{pK_a - pH_e}} \quad \text{(Eq. 3)}$$

The concentration ratio of unbound to bound doxorubicin in the tissue can be described by a Langmuir-type equation:

$$\frac{C_b^T}{C_f^T} = \frac{nK_aC_N}{1 + K_aC_f^T} \quad \text{(Eq. 4)}$$

where n and K_a are the number of binding sites and the affinity constant to nuclei, respectively, and C_N is the tissue DNA concentration. If the relation $K_aC_f^T \ll 1$ holds, Eq. 5 is obtained:

$$\frac{C_b^T}{C_f^T} = nK_aC_N \quad \text{(Eq. 5)}$$

Substituting Eqs. 3 and 5 into Eq. 2 gives:

$$K_p = \frac{1 + 10^{pK_a - pH_i}}{1 + 10^{pK_a - pH_e}} \cdot f_p \cdot (1 + nK_aC_N) \quad \text{(Eq. 6)}$$

where f_p is the unbound fraction in plasma, and pH_i and pH_e are the intra- and extracellular pH values, respectively. The value used for f_p (0.344) was determined in the present study, whereas those for n and K_a were obtained from previously reported data (14) and are 6.70×10^{-2} and 4.85×10^5 M^{-1}, respectively. The values used for C_N were also obtained from previously reported data (13) and are listed in Table I. The values for pK_a, pH_e, and pH_i were obtained from the literature, and are 8.15 (8), 7.4 (18), and 7.0 (18), respectively.

Table II—Physiological Constants for Doxorubicin Tissue Distribution Modeling and the Apparent Tissue-to-Plasma Concentration Ratios at the Terminal Phase after Bolus Intravenous-Injections to Guinea Pigs[a]

Tissue	Volume, mL[b]	Blood flow, mL/min[c]	$K_{p,app}$[d]
Arterial blood	7.6	35.3	—
Adipose tissue	11.6	0.5	64 ± 6
Muscle	145.0	10.2	178 ± 24
Liver	11.6	13.5	273 ± 12
Gut	9.0	9.2	351 ± 60
Heart	0.9	2.7	585 ± 50
Stomach	2.4	3.0	436 ± 43
Kidney	2.1	8.4	595 ± 41
Lung	2.7	35.3	656 ± 91
Spleen	0.3	0.8	1964 ± 311

[a] Body weight, 290 ± 4 g ($n = 4$). [b] Determined experimentally from the wet tissue weight by assuming a density of 1.0 for each tissue except for muscle and arterial blood volume. The muscle volume was assumed to be one-half the body weight, as in rats (22), and the arterial blood volume was calculated from the body weight by previously reported methods (23). [c] Obtained from previously reported data (24, 25). [d] Mean ± *SE* of four guinea pigs.

EXPERIMENTAL SECTION

Materials—Doxorubicin hydrochloride[2] was used. The antibiotic was kept in the dark in a desiccator at 4°C. Solutions of doxorubicin (2×10^{-6}–5×10^{-4} M in 405 mM sucrose) were freshly prepared before use. All other reagents were commercial products of analytical grade.

Animals—Male Wistar rats[3] (weight, 250–270 g), male albino rabbits[4] (weight, 2.6–2.8 kg), and male Hartley guinea pigs[3] (weight, 280–300 g) were used.

Blood-to-Plasma Concentration Ratio—The blood-to-plasma concentration ratio (R_B) was determined as described previously (13).

***In Vivo* Apparent Tissue-to-Plasma Concentration Ratio ($K_{p,app}$) in Guinea Pigs**—Doxorubicin was dissolved in saline and administered to guinea pigs *via* a jugular vein at a dose of 10 mg/kg 2 h after the operation. Food and water were given *ad libitum*. At 6, 12, 24, and 48 h after administration, blood samples were collected *via* a jugular artery, and then the guinea pig was killed by exsanguination. Each tissue was immediately excised, rinsed with saline, and stored at −40°C until use. Doxorubicin contents in plasma and tissues were determined by a TLC scanning method as described previously (13).

Hepatic and Renal Clearances in Guinea Pigs—The urinary excretion of doxorubicin was determined from the total amount excreted through the urinary bladder until 48 h after injection of 10 mg/kg iv. The apparent renal blood clearance ($CL_{B,app}^{KD}$) and the apparent hepatic blood clearance ($CL_{B,app}^{LV}$) were determined, and then the organ intrinsic clearance (CL_{int}) was calculated by:

$$f_p \cdot CL_{int} = \frac{CL_{B,app} \cdot Q_B \cdot R_B}{Q_B - CL_{B,app}} \quad \text{(Eq. 7)}$$

where Q_B is the organ blood flow rate.

***In Vivo* K_p Value**—The K_p value for guinea pigs was calculated from $K_{p,app}$ by a previously described method (13).

Plasma Binding Experiment—The rat plasma was first dialyzed for 16 h at 4°C with a semipermeable membrane[5] against pH 7.4 isotonic buffer (30 mM Tris, 131 mM NaCl, 5.2 mM KCl, 0.9 mM $MgSO_4$, and 1.0 mM $CaCl_2$). The plasma unbound fraction was determined by equilibrium dialysis at 37°C for 15 h against the same buffer as used for predialysis in semimicro cells[6]. No denaturation of proteins after dialysis was observed by polarization analysis (19) with 1-anilino-8-naphthalenesulfonate, as reported previously (20). The degradation of doxorubicin during the equilibrium dialysis and the adsorption of doxorubicin on the dialysis membrane (~30% of the initial content) were corrected for in the calculation of the binding parameters. The concentrations of doxorubicin in both plasma and buffer were determined by a fluorospectrometric TLC scanning method (13).

Tissue DNA Concentration—The tissue DNA concentration of guinea pigs was determined by a previously described method (13). The molecular weight of the DNA used was 330.9 (per unit of nucleotide as the sodium salt).

Preparation of Rat Erythrocytes—After injection of heparin at a dose of 0.1 mL/100 g of body weight (100 U), whole blood was collected *via* a jugular

[2] Adriamycin; Kyowa Hakko Kogyo Co., Ltd., Tokyo.
[3] Nihon Ikagaku Dobutsu Co., Tokyo.
[4] Ichikawaya, Tokyo.
[5] Type 36/32; Visking Co., Chicago, Ill.
[6] Kokugogomu Co., Tokyo.

Table III—Pharmacokinetic Parameters of Doxorubicin in Guinea Pigs [a]

Parameter[b]	Value[c]
Dose, μg	$2.88 \times 10^3 \pm 0.001 \times 10^3$
AUC_p, $\mu g \cdot min/mL$	$2.24 \times 10^2 \pm 0.55 \times 10^2$
$CL^{tot}_{B,app}$, mL/min	5.35 ± 0.73
X_u, μg	$6.52 \times 10^2 \pm 0.35 \times 10^2$
$CL^{KD}_{B,app}$, mL/min	1.22 ± 0.19
$CL^{LV}_{B,app}$, mL/min	4.13 ± 0.57
$f_p CL^{KD}_{int}$, mL/min	3.42 ± 0.37
$f_p CL^{LV}_{int}$, mL/min	$1.43 \times 10 \pm 0.10 \times 10$
β, min^{-1}	$2.94 \times 10^{-4} \pm 1.61 \times 10^{-4}$

[a] Body weight, 290 ± 4 g (n = 4), except for X_u and $CL^{KD}_{B,app}$ (300 g; n = 2). [b] AUC_p, area under the plasma concentration *versus* time curve; $CL^{tot}_{B,app}$, apparent total blood clearance; $CL^{KD}_{B,app}$, apparent renal blood clearance; $CL^{KD}_{B,app}$, apparent hepatic blood clearance; X_u, amount excreted in urine; f_p, plasma unbound fraction; CL_{int}, renal intrinsic clearance; CL^{LV}_{int}, hepatic intrinsic clearance; β, slope of the plasma concentration—time curve at the terminal phase. [c] Mean ± *SE* of four guinea pigs.

artery at 30 min. Erythrocytes were prepared essentially by the procedure of Horie *et al.* (21), except that buffer (pH 7.4) containing 131 mM NaCl, 5.2 mM KCl, 0.9 mM $MgSO_4$, 0.12 mM $CaCl_2$, 3 mM dibasic sodium phosphate, and 10 mM Tris was used in the preparation.

Uptake Experiment—To determine the initial velocity of uptake of doxorubicin, 1.5 mL of the erythrocyte suspension (10% v/v) was incubated in medium containing 20 mM Tris, 131 mM NaCl, 5.2 mM KCl, 0.9 mM $MgSO_4$, 1.12 mM $CaCl_2$, 3 mM dibasic sodium phosphate, and 5 mM glucose. After preincubation for 3 min with shaking (2 Hz) at 37°C, 0.01 mL of an isotonic solution containing various amounts of doxorubicin (1.81–2.59 μg) was added. Triplicate samples of 1.0 mL of the medium were removed and layered on 200 μL of silicone oil with a density of 1.05[7] in a 2.0-mL polyethylene tube[8]. The samples were then centrifuged for 30 s in a tabletop microcentrifuge[8]. The supernatant was discarded, the oil surface was washed with 0.6 mL of distilled water, 0.6 mL of distilled water was again added, and the erythrocytes were completely hemolyzed with vigorous mixing. Then 0.6 mL of 50 mM Tris-HCl buffer (pH 7.4) was added, and the polyethylene tube was centrifuged for 30 s in a tabletop microcentrifuge[8]. To determine the amount of doxorubicin taken into the erythrocytes, doxorubicin in the supernatant was determined by fluorospectrometric TLC scanning method (13).

RESULTS

Distribution to Erythrocytes, Plasma Protein Binding, and Tissue DNA Concentration—No concentration dependency in doxorubicin distribution into erythrocytes in guinea pigs was observed over the tested plasma concentration range of doxorubicin (0.00947–1.549 μg/mL), which corresponded to the *in vivo* plasma concentration range after injection of 10 mg/kg iv. The value of the blood-to-plasma concentration ratio (R_B) was 2.40 ± 0.09 (n = 12).

Furthermore, no concentration dependency of plasma protein binding of doxorubicin was observed over the *in vivo* plasma concentration range of doxorubicin (0.0131–1.884 μg/mL for rats, 0.0108–1.992 μg/mL for rabbits, and 0.00733–2.183 μg/mL for guinea pigs). The values of plasma unbound fraction were 0.344 ± 0.014 (n = 15) for rats, 0.415 ± 0.019 (n = 11) for rabbits, and 0.529 ± 0.021 (n = 12) for guinea pigs. The tissue DNA concentrations in various tissues of guinea pigs are listed in Table I, along with those of rats and rabbits [determined previously (13)].

***In vivo* K_p Value**—The physiological parameters for guinea pigs and the $K_{p,app}$ at the terminal phase after bolus intravenous injection of doxorubicin are summarized in Table II. The pharmacokinetic parameters determined in guinea pigs are listed in Table III. By using the values listed in Tables II and III, the *in vivo* K_p values of doxorubicin of guinea pigs were calculated and are summarized inTable IV, along with those of rats [determined previously (13)] and rabbits [estimated from the literature values (3)].

Membrane Permeability—The uptake of doxorubicin into isolated erythrocytes was measured at pH 7.05, 7.42, 7.85, and 8.07. The plots of cell-to-medium ratio (C/M ratio) *versus* time were linear for 80 s at all pH values studied. When extrapolated, these lines passed through the origin, which suggested that there was no adsorption of doxorubicin on the cell surface. The slope of each line, which represents the uptake rate constant, k (min^{-1}), was plotted against the pH value of the medium (Fig. 2). The good correspondence

[7] Aldrich Chemical Co., Milwaukee, Wis.
[8] Beckman Instrument Co., Felton, Calif.

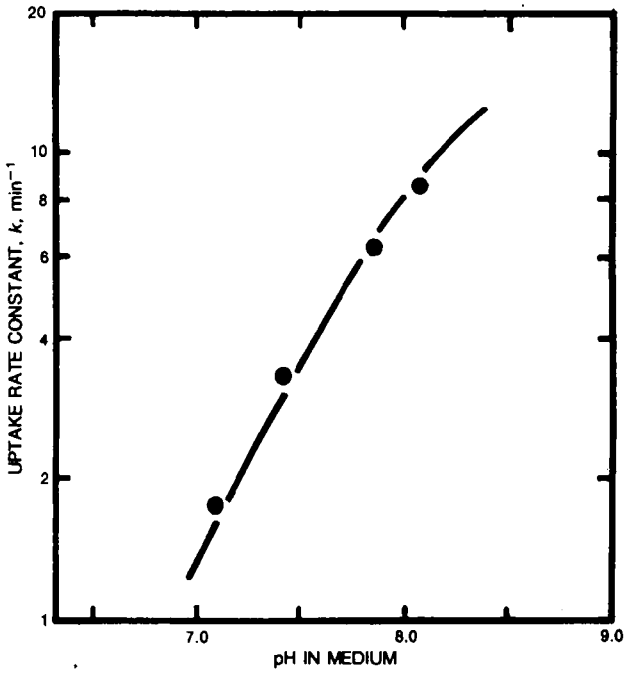

Figure 2—*Log* k-*pH profile for the uptake of doxorubicin into rat erythrocytes. The theoretical curve was calculated by a nonlinear iterative least-squares method (26) with a digital computer by* $k_{pH} = k_0(1/1 + 10^{pK_a - pH})$, *where* k_{pH} *and* k_0 *are the apparent uptake rate constant and the uptake rate constant of undissociated species, respectively;* $k_0 = 2.065 \times 10\ min^{-1}$; $pK_a = 8.15$. *Key: (●) observed values; (—) calculated curve.*

between the calculated and observed values suggests that only un-ionized doxorubicin can permeate through the cell membrane.

Estimation of the K_p value from *In Vitro* Experiments—*In vitro* K_p values for rats, rabbits, and guinea pigs were calculated by Eq. 6 and are listed in Table IV with the *in vivo* K_p values. The *in vivo* and *in vitro* K_p values for rats, rabbits, and guinea pigs are compared in Fig. 3.

DISCUSSION

In this study, the mechanism of *in vivo* tissue distribution of doxorubicin was examined in rats, rabbits, and guinea pigs. The goal of the study was to elucidate the characteristic tissue distribution mechanism to account for interorgan and interspecies variation in drug levels and to determine whether the K_p values obtained from *in vitro* studies coincide with those obtained from *in vivo* studies. The *in vivo* K_p values were characteristically large, and there were fairly large differences among tissues and animal species (Table IV). The K_p values of doxorubicin were also determined from the *in vitro* organ model (Fig. 1), on the basis of the three assumptions described in the *Theoretical Section*, for comparison with *in vivo* values to check the validity of the model. As far as we are aware, the mechanism of tissue distribution of a drug has never been elucidated in detail.

Since there was insufficient information on the plasma membrane permeability of doxorubicin in normal cells, we examined this permeability in isolated intact cells. In a preliminary study, the uptake of doxorubicin into isolated rat hepatocytes, prepared by the method of Berry and Friend (27) as modified by Bauer *et al.* (28), was examined, but the uptake rate of doxorubicin could not be exactly determined due to the rapid metabolism at the incubation temperature of 37°C. Therefore, rat erythrocytes, which can be easily prepared, were utilized as a model membrane. Since it appeared that only the un-ionized molecule could permeate through plasma membranes (Fig. 2), assumption 3 (see *Theoretical Section*) may be applicable to the tissue distribution of doxorubicin. The number of binding sites and the affinity constant for isolated nuclei, which were used for the calculation of the *in vitro* K_p values, were determined previously in quasi-physiological buffer (pH 7.0) containing 135 mM sucrose, 20 mM Tris, 50 mM NaCl, 100 mM KCl, 1 mM $MgSO_4$, and 1 mM $CaCl_2$ at 37°C, and values of $n = 6.70 \times 10^{-2}$ and $K_a = 4.85 \times 10^5\ M^{-1}$ were obtained for rat liver nuclei (14). Since the conditions used for measuring doxorubicin binding were considered to be close to physiological on the basis of both morphological examination of isolated nuclei and the concentrations of the intracellular metal ions (29, 30), the parameters of nuclear binding determined in the *in vitro* studies might be comparable with those determined for the *in vivo* tissue distribution of doxorubicin.

Table IV—*In Vivo* and *In Vitro* K_p Values in Three Species[a]

Tissue	Rat		Rabbit		Guinea Pig	
	In Vivo[b]	*In Vitro*	*In Vivo*[c]	*In Vitro*	*In Vivo*	*In Vitro*
Adipose tissue	33 ± 4.4	36 ± 1.7	19 ± 3.5	16 ± 1.0	54 ± 4.3	70 ± 3.4
Muscle	54 ± 4.2	24 ± 1.9	27 ± 3.9	9 ± 0.6	135 ± 14	34 ± 1.2
Liver	243 ± 39	166 ± 6.4	56 ± 10.3	119 ± 6.2	365 ± 16	335 ± 12
Gut	161 ± 23	528 ± 18	50 ± 7.5	551 ± 20	336 ± 55	1019 ± 43
Heart	230 ± 17	119 ± 5.4	57 ± 5.0	71 ± 2.4	571 ± 48	237 ± 8.4
Stomach	258 ± 29	286 ± 9.6	—	242 ± 9.1	417 ± 40	718 ± 22
Kidney	349 ± 27	322 ± 13	494 ± 43	399 ± 17	684 ± 47	679 ± 22
Lung	354 ± 54	605 ± 19	155 ± 24	623 ± 22	656 ± 91	1289 ± 40
Spleen	404 ± 72	1391 ± 56	746 ± 82	1596 ± 58	1795 ± 259	2374 ± 73

[a] Mean ± *SE* of each experiment. [b] Data obtained from a previous report (13). [c] Values of $K_{p,app}$, except for the spleen, were obtained from previously published data (3), K_p values were then calculated by assuming that R_B was equal to the R_B of the rat, determined previously (13). The value of $K_{p,app}$ for spleens was estimated from the observed values (at 8, 24, and 48 h) in Fig. 6 of Ref. 3, and then the K_p was calculated.

Since. Eq. 6 holds under the condition $K_a C_f^T \ll 1$, its applicability was examined as follows. The plasma concentrations of doxorubicin at the terminal phase after intravenous administration were $<2 \times 10^{-7}$, 8.2×10^{-8}, 1.3×10^{-7}, and 1.2×10^{-7} M for rats, rabbits, guinea pigs, and humans, respectively. Based on the assumption of pH partition, the value of C_f^T was estimated by:

$$C_f^T = \frac{1 + 10^{pK_a - pH_i}}{1 + 10^{pK_a - pH_e}} \cdot f_p C_p \qquad \text{(Eq. 8)}$$

Values for pK_a (8.15), pH_i (7.0), pH_e (7.4), K_a (4.85×10^5 M^{-1}), and f_p (0.344 for rats, 0.415 for rabbits, 0.529 for guinea pigs, and 0.5 for humans) were substituted into the equation; the f_p value for humans was obtained from the study of Chan *et al.* (4). The values of $K_a C_f^T$ were 7.8×10^{-2}, 4.0×10^{-2}, 6.1×10^{-2}, and 5.7×10^{-2} for rats, rabbits, guinea pigs, and humans, respectively. Therefore, Eq. 6 should be applicable to these four species.

To account for interorgan variations of tissue distribution of doxorubicin, four possibilities can be considered: (*a*) organ or tissue difference in the amount of nuclei per organ or tissue wet weight (C_N), (*b*) organ or tissue difference in binding parameters to nuclei (n and K_a), (*c*) larger binding capacity of doxorubicin to other organ or tissue constituents than to nuclei, and (*d*) a specific membrane transport mechanism. In view of the results that doxorubicin was exclusively localized in the cell nucleus (15) and that there was little difference of tissue nuclear binding parameters between liver and kidney (14), but a good correlation between the *in vivo* K_p values and the tissue DNA concentrations was observed (13), the first possibility might primarily account for the differences in doxorubicin distribution among tissues, although the evidence is insufficient to rule out some contribution of the other mechanisms, if they operate. On the assumption that there is no difference in nuclear drug-binding parameters of various tissues among rats, rabbits, and guinea pigs the *in vitro* K_p values were estimated. In Figs. 3A–C, the *in vitro* and *in vivo* K_p values for rats, rabbits, and guinea pigs listed in Table IV, respectively, are compared; comparatively good agreements can be seen. These results suggest that Eq. 6 is applicable to describe the tissue distribution of doxorubicin in rabbits and guinea pigs as well as in rats. Although slight discrepancies are apparent, the *in vitro* K_p values show a relatively good correlation with *in vivo* K_p values. The reason for the discrepancies are probably (*a*) a shift of the intracellular pH from 7.0, (*b*) operation of a specific transport system, (*c*) involvement of other tissue constituents which affect the intracellular binding, and (*d*) slight differences in the nuclear binding parameters among tissues.

Furthermore, the following factors may be involved in the interspecies variations in K_p values: (*a*) differences in tissue DNA concentrations (C_N), (*b*) differences in plasma unbound fraction (f_p), (*c*) differences in nuclear binding parameters (n and K_a), and (*d*) differences in the rate of specific transport. The tissue DNA concentrations of rabbits were smaller than those of rats in all tissues studied, except the kidney and spleen, and those of guinea pigs were larger than those of rats in most tissues except the muscle (Table I). These differences in tissue DNA concentration among rats, rabbits, and guinea pigs are similar to those among the *in vivo* K_p values for these animal species (Table IV). Thus, it was suggested that differences in tissue DNA concentration are an important factor in the interspecies variation in K_p values. Based on the results of plasma protein binding, the difference in f_p values between rats ($f_p = 0.344$) and guinea pigs ($f_p = 0.529$) may be one of the important factors in the variation of *in vivo* K_p values between rats and guinea pigs. However, the difference in f_p values between rabbits ($f_p = 0.415$) and rats ($f_p = 0.344$) may not be a determinant of the variation in K_p values between these two animal species, since the f_p value of rabbits was larger than that of rats, whereas the *in vivo* K_p values of rabbits were smaller than those of rats in most tissues (Table IV). Consequently, it was concluded that the primary determinant of the interspecies variation in K_p values among rats, rabbits, and guinea pigs is the interspecies differences in tissue DNA concentration and that the difference in f_p values is a secondary determinant.

Plasma binding, tissue binding, and membrane permeability have been considered to be factors that affect the tissue distribution of drugs (10), but little quantitative evidence has been obtained up to the present regarding interorgan and/or interspecies variation in the tissue distribution of drugs. To obtain the *in vitro* K_p value, it is important to estimate accurately the *in vitro* tissue binding under physiological conditions. A usual method is to use tissue homogenates, but this leads to several experimental problems such as disruption and degeneration of drug-binding components, requirement for binding cofactors, and drug metabolism. Moreover, the actual drug-binding component often cannot be distinguished from other intracellular constituents. A useful method for physiological estimation of the tissue binding would be to determine the drug binding by using isolated organelles or macromolecules known to be the primary drug binder in the tissues, as shown in the present study with doxorubicin in rats.

In conclusion, the mechanism of the organ or tissue distribution of doxorubicin in rats, rabbits, and guinea pigs may be summarized as follows. Doxorubicin is strongly and exclusively bound to the nuclei in the cells. The variations in the organ or tissue distribution of doxorubicin are due to dif-

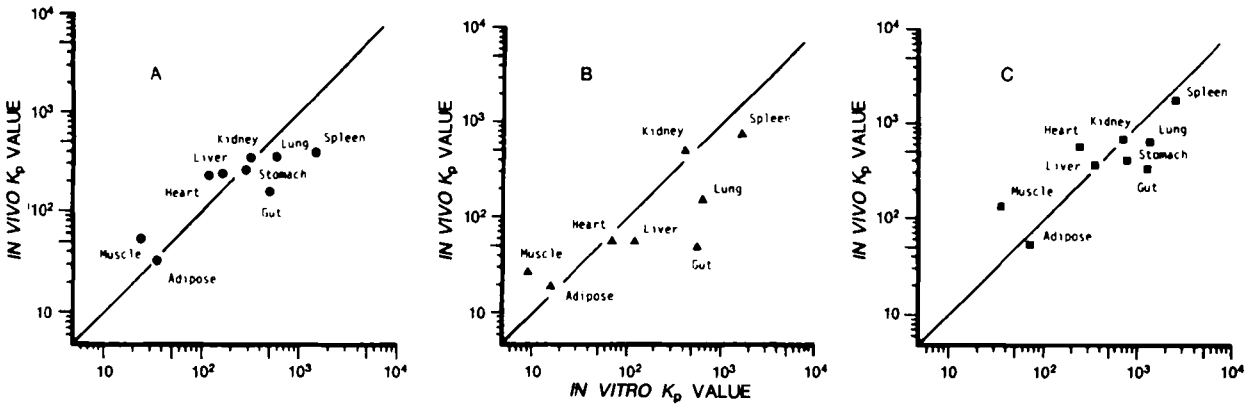

Figure 3—*Comparison between* in vivo *and* in vitro *tissue-to-plasma partition coefficients (K_p values) in rats (A), rabbits (B), and guinea pigs (C). Solid lines represent a 1:1 relationship.*

ferences in the amount of nuclei per gram of organ or tissue. The unbound concentration of doxorubicin in the cytosol must be ~2.3 times higher than that in plasma according to the pH partition hypothesis.

REFERENCES

(1) D. W. Yesair, E. Schwartzbach, D. Schuck, E. P. Denine, and M. A. Asbell, *Cancer Res.*, **32**, 1177 (1972).

(2) N. R. Bachur, R. C. Hildebrand, and R. S. Jaenke, *J. Pharmacol. Exp. Ther.*, **191**, 331 (1974).

(3) P. A. Harris and J. F. Gross, *Cancer Chemother. Rep.*, Part 1, **59**, 819 (1975).

(4) K. K. Chan, J. L. Cohen, J. F. Gross, K. J. Himmelstein, J. R. Bateman, Y. T. Lee, and A. S. Marlis, *Cancer Treat. Rep.* **62**, 1161 (1978).

(5) N. Tavoloni and A. M. Guarino, *Pharmacology*, **21**, 244 (1980).

(6) G. Sabeur, D. Genest, and G. A. Sadron, *Biochem. Biophys. Res. Commun.*, **88**, 722 (1979).

(7) F. Zunino, A. D. Marco, A. Zaccara, and R. A. Gambetta, *Biochim. Biophys. Acta*, **607**, 206 (1980).

(8) T. Skovsgaard, *Biochem. Pharmacol.*, **26**, 215 (1977).

(9) J. R. Gillette, in "Handbook of Experimental Pharmacology," part 3 (J. R. Gillette and J. R. Mitchell, Eds.), Springer-Verlag, New York, N.Y., 1975, p. 35.

(10) J. R. Gillette, *J. Pharmacokinet. Biopharm.*, **1**, 497 (1973).

(11) A. Yacobi, C. M. Lai, and G. Levy, *J. Pharm. Sci.*, **64**, 1995 (1975).

(12) A. P. van Peer, F. M. Berpaire, M. T. Rosseel, and M. G. Bogaert, *Pharmacology*, **22**, 139 (1981).

(13) T. Terasaki, T. Iga, Y. Sugiyama, and M. Hanano, *J. Pharm. Pharmacol.*, **34**, 597 (1982).

(14) T. Terasaki, T. Iga, Y. Sugiyama, and M. Hanano, *J. Pharm. Sci.*, **73**, 524 (1984).

(15) M. J. Egorin, R. C. Hildebrand, E. F. Cimino, and N. R. Bachur, *Cancer Res.*, **34**, 2243 (1974).

(16) T. Skovsgaard, *Biochem. Pharmacol.*, **27**, 1221 (1978).

(17) T. Skovsgaard, *Cancer Res.*, **38**, 1785 (1978).

(18) A. Roos and W. F. Boron, *Physiol. Rev.*, **61**, 296 (1981).

(19) S. K. Chakrabarti, *Biochem. Pharmacol.* **27**, 739 (1978).

(20) H. Y. Yu, Y. Sawada, Y. Sugiyama, T. Iga, and M. Hanano, *J. Pharm. Sci.*, **70**, 323 (1981).

(21) T. Horie, Y. Sugiyama, S. Awazu, and M. Hanano, *J. Pharm. Dyn.*, **4**, 116 (1981).

(22) R. L. Dedrick, D. S. Zaharko, and R. J. Lutz, *J. Pharm. Sci.*, **62**, 822 (1973).

(23) K. B. Bischoff, R. L. Dedrick, D. S. Zaharko, and J. A. Longstreth, *J. Pharm. Sci.*, **60**, 1128 (1971).

(24) P. O. B. Sjoquist, L. Bjellin, and A. M. Carter, *Acta Pharmacol. Toxicol.*, **40**, 369 (1977).

(25) L. L. Peeters, G. Grutters, and C. B. Martin, Jr., *Am. J. Obstet. Gynecol.*, **138**, 1177 (1980).

(26) T. Nakagawa, Y. Koyanagi, and H. Togawa, in "SALS, a Computer Program for Statistical Analysis with Least Squares Fitting," Library Program of the University of Tokyo Computer Center, Tokyo, Japan, 1978.

(27) M. N. Berry and D. S. Friend, *J. Cell Biol.*, **43**, 506 (1969).

(28) H. Bauer, S. Kasperek, and E. Pfaff, *Hoppe-Seyler's Z. Physiol. Chem.* **356**, 827 (1975).

(29) A. I. Lishanskaya and M. I. Mosevitsky, *Biochem. Biophys. Res. Commun.*, **62**, 822 (1975).

(30) D. Veloso, R. W. Guynn, M. Oskarsson, and R. L. Veech, *J. Biol. Chem.*, **248**, 4811 (1973).

ACKNOWLEDGMENTS

This work was taken in part from a dissertation submitted by T. Terasaki to the Graduate School, Division of Pharmaceutical Sciences, University of Tokyo, Tokyo, Japan, in partial fulfilment of the Doctor of Philosophy degree requirements.

The authors are grateful to Kyowa Hakko Kogyo Co., Ltd., for the gift of doxorubicin hydrochloride.

Preparation and Biodistribution of ^{99m}Tc-Labeled Tyramine Iminodiacetic Acid

FAROUK M. ALI *, RAUF SARPER, EUGENE J. MALVEAUX, and BAHJAT A. FARAJ ˣ

Received February 8, 1983, from the *Department of Radiology, Division of Nuclear Medicine, Emory University School of Medicine, Atlanta, GA 30322.* Accepted for publication August 22, 1983. *Present address: King Abdulaziz University, College of Medicine and Allied Sciences, Jeddah, Saudi Arabia.

Abstract □ The synthesis and biodistribution properties of ^{99m}Tc-labeled *N*-substituted tyramine, [*N*-(4-hydroxyphenethyl)iminodiacetic acid] are described. Tissue distribution studies in rats were indicative of high hepatic and kidney extraction, accompanied by rapid plasma and urinary clearance and minimal biliary excretion. These findings were substantiated by organ image analysis. The preliminary data indicate that this labeled material may represent a new class of radiopharmaceuticals for the evaluation of hepatic and renal functions.

Keyphrases □ Biodistribution—^{99m}Tc-labeled tyramine iminodiacetic acid, preparation □ Tyramine iminodiacetic acid—biodistribution and preparation □ Radiopharmaceuticals—preparation and biodistribution of ^{99m}Tc-labeled tyramine iminodiacetic acid

Tyramine (I), a noncatecholic phenethylamine found in a variety of plants and animal tissues (1), is produced by decarboxylation of its parent amino acid tyrosine (2). Normally, the physiological effects of tyramine are minimal because >90% of the tyramine is rendered metabolically inactive by mitochondrial monoamine oxidase during its first passage through the liver after absorption (3, 4). The rapid rate of elimination and its inability to cross the blood–brain barrier (5) protect the body from the adverse peripheral and neurotoxic effects of tyramine.

Abnormal metabolism of tyramine has been implicated in a variety of clinical disorders. Abnormal urinary excretion of the amine occurs in patients suffering from Parkinson's disease (6), schizophrenia, induced hypertensive crisis (7), cystic fibrosis (8), epilepsy (9), hypertyrosinemia (10), depression, and migration (11). We have recently demonstrated that the tyramine concentration is abnormally elevated in the plasma and urine of patients with cirrhosis (12, 13), hepatitis (14), and Reye's syndrome (15), as well as in experimental animals with hepatic insufficiency or portacaval shunt (16).

In view of its clinical importance, we have taken the initiative to develop a radiopharmaceutical from tyramine. In this report, we describe the synthesis, biological distribution, and image characteristics of ^{99m}Tc-labeled *N*-(4-hydroxyphen-

0022-3549/84/1000-1363$01.00/0

© 1984, American Pharmaceutical Association

ferences in the amount of nuclei per gram of organ or tissue. The unbound concentration of doxorubicin in the cytosol must be ~2.3 times higher than that in plasma according to the pH partition hypothesis.

REFERENCES

(1) D. W. Yesair, E. Schwartzbach, D. Schuck, E. P. Denine, and M. A. Asbell, *Cancer Res.*, **32**, 1177 (1972).

(2) N. R. Bachur, R. C. Hildebrand, and R. S. Jaenke, *J. Pharmacol. Exp. Ther.*, **191**, 331 (1974).

(3) P. A. Harris and J. F. Gross, *Cancer Chemother. Rep.*, Part 1, **59**, 819 (1975).

(4) K. K. Chan, J. L. Cohen, J. F. Gross, K. J. Himmelstein, J. R. Bateman, Y. T. Lee, and A. S. Marlis, *Cancer Treat. Rep.* **62**, 1161 (1978).

(5) N. Tavoloni and A. M. Guarino, *Pharmacology*, **21**, 244 (1980).

(6) G. Sabeur, D. Genest, and G. A. Sadron, *Biochem. Biophys. Res. Commun.*, **88**, 722 (1979).

(7) F. Zunino, A. D. Marco, A. Zaccara, and R. A. Gambetta, *Biochim. Biophys. Acta*, **607**, 206 (1980).

(8) T. Skovsgaard, *Biochem. Pharmacol.*, **26**, 215 (1977).

(9) J. R. Gillette, in "Handbook of Experimental Pharmacology," part 3 (J. R. Gillette and J. R. Mitchell, Eds.), Springer-Verlag, New York, N.Y., 1975, p. 35.

(10) J. R. Gillette, *J. Pharmacokinet. Biopharm.*, **1**, 497 (1973).

(11) A. Yacobi, C. M. Lai, and G. Levy, *J. Pharm. Sci.*, **64**, 1995 (1975).

(12) A. P. van Peer, F. M. Berpaire, M. T. Rosseel, and M. G. Bogaert, *Pharmacology*, **22**, 139 (1981).

(13) T. Terasaki, T. Iga, Y. Sugiyama, and M. Hanano, *J. Pharm. Pharmacol.*, **34**, 597 (1982).

(14) T. Terasaki, T. Iga, Y. Sugiyama, and M. Hanano, *J. Pharm. Sci.*, **73**, 524 (1984).

(15) M. J. Egorin, R. C. Hildebrand, E. F. Cimino, and N. R. Bachur, *Cancer Res.*, **34**, 2243 (1974).

(16) T. Skovsgaard, *Biochem. Pharmacol.*, **27**, 1221 (1978).

(17) T. Skovsgaard, *Cancer Res.*, **38**, 1785 (1978).

(18) A. Roos and W. F. Boron, *Physiol. Rev.*, **61**, 296 (1981).

(19) S. K. Chakrabarti, *Biochem. Pharmacol.* **27**, 739 (1978).

(20) H. Y. Yu, Y. Sawada, Y. Sugiyama, T. Iga, and M. Hanano, *J. Pharm. Sci.*, **70**, 323 (1981).

(21) T. Horie, Y. Sugiyama, S. Awazu, and M. Hanano, *J. Pharm. Dyn.*, **4**, 116 (1981).

(22) R. L. Dedrick, D. S. Zaharko, and R. J. Lutz, *J. Pharm. Sci.*, **62**, 822 (1973).

(23) K. B. Bischoff, R. L. Dedrick, D. S. Zaharko, and J. A. Longstreth, *J. Pharm. Sci.*, **60**, 1128 (1971).

(24) P. O. B. Sjoquist, L. Bjellin, and A. M. Carter, *Acta Pharmacol. Toxicol.*, **40**, 369 (1977).

(25) L. L. Peeters, G. Grutters, and C. B. Martin, Jr., *Am. J. Obstet. Gynecol.*, **138**, 1177 (1980).

(26) T. Nakagawa, Y. Koyanagi, and H. Togawa, in "SALS, a Computer Program for Statistical Analysis with Least Squares Fitting," Library Program of the University of Tokyo Computer Center, Tokyo, Japan, 1978.

(27) M. N. Berry and D. S. Friend, *J. Cell Biol.*, **43**, 506 (1969).

(28) H. Bauer, S. Kasperek, and E. Pfaff, *Hoppe-Seyler's Z. Physiol. Chem.* **356**, 827 (1975).

(29) A. I. Lishanskaya and M. I. Mosevitsky, *Biochem. Biophys. Res. Commun.*, **62**, 822 (1975).

(30) D. Veloso, R. W. Guynn, M. Oskarsson, and R. L. Veech, *J. Biol. Chem.*, **248**, 4811 (1973).

ACKNOWLEDGMENTS

This work was taken in part from a dissertation submitted by T. Terasaki to the Graduate School, Division of Pharmaceutical Sciences, University of Tokyo, Tokyo, Japan, in partial fulfilment of the Doctor of Philosophy degree requirements.

The authors are grateful to Kyowa Hakko Kogyo Co., Ltd., for the gift of doxorubicin hydrochloride.

Preparation and Biodistribution of ^{99m}Tc-Labeled Tyramine Iminodiacetic Acid

FAROUK M. ALI *, RAUF SARPER, EUGENE J. MALVEAUX, and BAHJAT A. FARAJ ˣ

Received February 8, 1983, from the *Department of Radiology, Division of Nuclear Medicine, Emory University School of Medicine, Atlanta, GA 30322.* Accepted for publication August 22, 1983. *Present address: King Abdulaziz University, College of Medicine and Allied Sciences, Jeddah, Saudi Arabia.

Abstract □ The synthesis and biodistribution properties of ^{99m}Tc-labeled *N*-substituted tyramine, [*N*-(4-hydroxyphenethyl)iminodiacetic acid] are described. Tissue distribution studies in rats were indicative of high hepatic and kidney extraction, accompanied by rapid plasma and urinary clearance and minimal biliary excretion. These findings were substantiated by organ image analysis. The preliminary data indicate that this labeled material may represent a new class of radiopharmaceuticals for the evaluation of hepatic and renal functions.

Keyphrases □ Biodistribution—^{99m}Tc-labeled tyramine iminodiacetic acid, preparation □ Tyramine iminodiacetic acid—biodistribution and preparation □ Radiopharmaceuticals—preparation and biodistribution of ^{99m}Tc-labeled tyramine iminodiacetic acid

Tyramine (I), a noncatecholic phenethylamine found in a variety of plants and animal tissues (1), is produced by decarboxylation of its parent amino acid tyrosine (2). Normally, the physiological effects of tyramine are minimal because >90% of the tyramine is rendered metabolically inactive by mitochondrial monoamine oxidase during its first passage through the liver after absorption (3, 4). The rapid rate of elimination and its inability to cross the blood–brain barrier (5) protect the body from the adverse peripheral and neurotoxic effects of tyramine.

Abnormal metabolism of tyramine has been implicated in a variety of clinical disorders. Abnormal urinary excretion of the amine occurs in patients suffering from Parkinson's disease (6), schizophrenia, induced hypertensive crisis (7), cystic fibrosis (8), epilepsy (9), hypertyrosinemia (10), depression, and migration (11). We have recently demonstrated that the tyramine concentration is abnormally elevated in the plasma and urine of patients with cirrhosis (12, 13), hepatitis (14), and Reye's syndrome (15), as well as in experimental animals with hepatic insufficiency or portacaval shunt (16).

In view of its clinical importance, we have taken the initiative to develop a radiopharmaceutical from tyramine. In this report, we describe the synthesis, biological distribution, and image characteristics of ^{99m}Tc-labeled *N*-(4-hydroxyphen-

0022-3549/84/1000-1363$01.00/0

© 1984, American Pharmaceutical Association

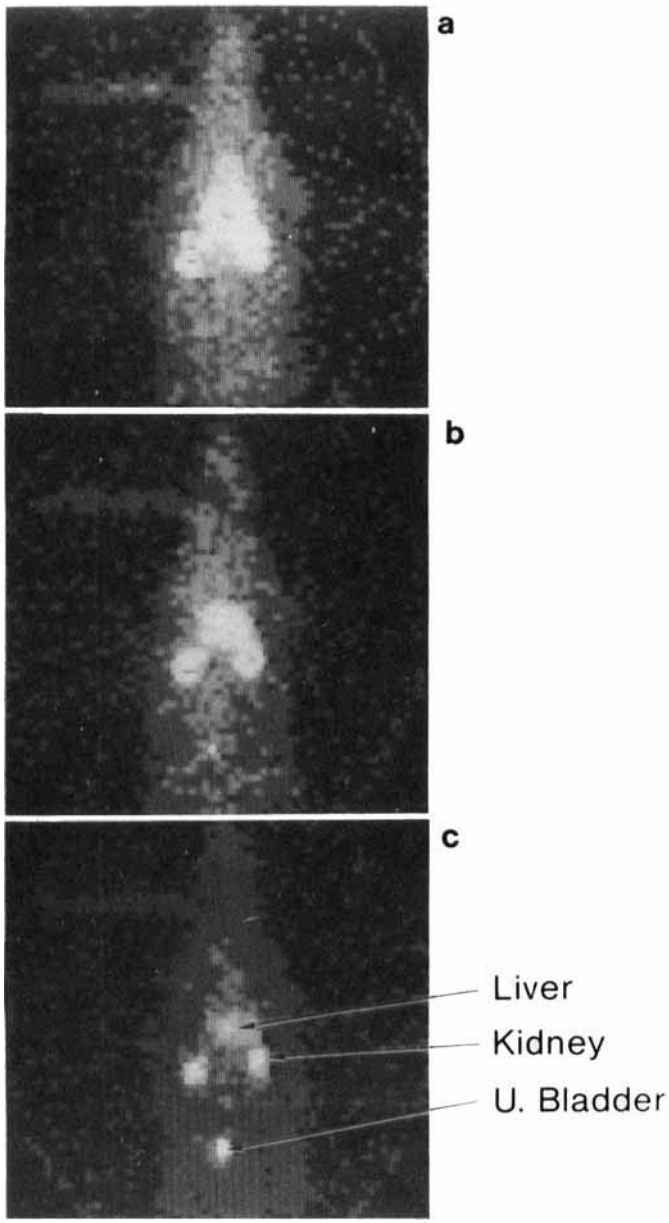

Figure 1—*Scintograms of rats obtained at 2 (a), 5 (b), and 10 (c) min after the intravenous injection of 0.5 mCi/kg of ^{99m}Tc-labeled tyramine diacetic acid.*

ethyl)iminodiacetic acid (II) an iminodiacetic acid-containing radiopharmaceutical which is structurally related to tyramine.

EXPERIMENTAL SECTION

Chemistry—*N*-(4-Hydroxyphenethyl)iminodiacetic acid (II) was prepared by a modified procedure of Callery *et al.* (17). A solution of tyramine[1] (1.37 g, 10 mmol) in 95% ethanol (100 mL) was added dropwise to a stirred solution of chloroacetic acid (1.9 g, 20 mmol) in 95% ethanol (50 mL). During the addition, the mixture was maintained at pH >7 with 5 M NaOH. The resulting mixture was heated under reflux for 48 h, was allowed to cool, and the resulting white precipitate was removed by filtration. This material was

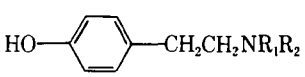

I: $R_1 = R_2 = H$
II: $R_1 = R_2 = -CH_2CO_2H$

washed with 95% ethanol, recrystallized (80% ethanol) and dried under reduced pressure at 50°C, to give 1.0 g (40% yield). The resulting salt was dissolved in water, acidified to pH 3 by the dropwise addition of 6 M HCl, and the resulting precipitate was collected and recrystallized from methanol–water to yield white crystals, mp 284–287°C; IR (Nujol) 3200–2800, 1650, 900, 800, and 700 cm^{-1}; ^{1}H-NMR (D_2O): δ 2.5–3.2 (m, 4, CH_2CH_2), 3.4 (s, 4, CH_2COO), and 6.5–7.0 ppm (m, ArH). TLC on silica gel GF revealed one spot with R_f values of 0 in solvent system A (*tert*-amyl alcohol–benzene–40% methylamine; 24:8:12) and 0.4 in solvent system B (1-butanol–acetic acid–water; 25:4:10). Tyramine had R_f values of 0.75 and 0.65 in solvent systems A and B, respectively.

Anal.—Calc. for $C_{12}H_{15}NO_5$: C, 56.91; H, 5.93; N, 5.33. Found: C, 57.50; H, 6.18; N, 5.65.

Labeling with Technetium-99m—The iminodiacetic acid derivative of tyramine was labeled by stannous chloride reduction of sodium [^{99m}Tc]pertechnetate eluate from a molybdenum-99–technetium-99m generator in aqueous solution.

A solution of the derivative (5 mg, 0.043 mmol) in 1 mL of distilled water (pH 5–6) was prepared in an evacuated glass tube. To this was added 0.2 mL (0.25 mg, 0.0011 mmol) of a solution of stannous chloride prepared by the procedure of Mock (18). The mixture was vortex-mixed for 30 s. Labeling with technetium-99m was accomplished over a period of 5 min by the addition of the pertechnetate (5 mCi).

Radiochemical Purity—The radiochemical purity of ^{99m}Tc-labeled material was examined by silica gel (glass fiber support) and cellulose (plastic sheet support) ascending TLC, with normal saline, 1-butanol–acetic acid–water (4:1:7), and acetonitrile–water (3:1) as solvents. The radiochromatograms of imaging agent were compared with those obtained for both pertechnetate anion and for technetium-99m–tin colloid, which was prepared by the method used for the preparation of the ^{99m}Tc-labeled iminodiacetic acid. Gel permeation chromatography was used to assess the stability of the chemical bond between technetium-99m and tyramine diacetic acid. Prepacked (1 × 10-cm) disposable columns containing Sephadex G-25 medium[2] (10-mL volume) were used. The imaging agent (1 μCi) in 0.2 mL of normal saline was applied to the column and eluted with 50 mL of normal saline. Fractions (1 mL each) were collected and counted. The elution pattern of the ^{99m}Tc-labeled iminodiacetic acid was compared with that of pertechnetate and the technetium-99m–tin colloid.

Biodistribution Studies—The biodistribution studies were carried out in male Sprague–Dawley rats (200–300 g) that were fasted overnight. The rats were anesthetized with sodium pentobarbital (25 mg/kg). A catheter[3] (i.d., 0.58 mm; o.d., 0.965 mm) was inserted into the jugular vein for the administration of imaging agent; another one was placed in the carotid artery for blood sampling. A third catheter was inserted into the common bile duct, retrograde to the liver, for collection of bile. The mixture of the radiopharmaceutical preparation was administered intravenously (0.5 mCi/kg) as a bolus injection. Heparinized blood samples (1 mL) were drawn at predetermined intervals. The rats were then sacrificed serially at intervals to 180 min after injection. At the time of death, the wet weights of the liver, kidney, heart, intestine, brain, spleen, stomach, lung, and muscle were determined. The tissue samples were homogenized[4] in a 4:1 water–organ mixture, and 0.5-mL aliquots were counted. The radioactivity in plasma, bile, and tissue samples was expressed as a percentage of the injected dose per gram of sample. The urine (0.1 mL, 1:100 dilution) from the urinary bladder was also counted.

Image Analysis—Ten rats were evaluated. The imaging system consisted of a mobile camera[5] interfaced with a computer[6]. The study began with an anesthetized rat placed supine on a table under the detector of a portable gamma scintillation camera. The detector was positioned so that the field of view included the liver, lung bases, kidneys, and bladder. The imaging agent (0.5 mCi/mg) was injected intravenously into the jugular vein. Data acquisition by the computer started simultaneously with the injection. Serial images of the whole rat were taken and recorded at predetermined intervals over a period of 3 h.

RESULTS

Radiochemical Analysis—Chemical purity of the tyramine diacetic acid was established by elemental, spectral, and chromatographic analyses. The radiochemical purity and labeling yield of the imaging agent were determined by radiochromatographic analysis. The iminodiacetic acid was labeled with technetium-99m in yields >95% as assessed by silica gel and cellulose TLC

[1] Sigma Chemical Co., St. Louis, Mo.

[2] PD-10; Pharmacia Fine Chemicals.
[3] PE-50; Clay Adams, Parsippany, N.J.
[4] Polytron; Brinkman Instruments, Westbury, N.J.
[5] Picker Dynamo.
[6] Muga Cart Medical Data System.

Table I—Average [a] Percent Injected Radioactivity in Tissues and Plasma of Rats after Intravenous Administration of ^{99m}Tc-Labeled Tyramine Diacetic Acid

Tissue	Radioactivity, % of Dose/g of Tissue					
	5 min	10 min	30 min	60 min	120 min	180 min
Liver	5.2	3.2	2.3	1.4	1.0	0.75
Kidney	8.5	5.21	3.0	2.2	1.8	1.0
Brain	0.3	0.01	0.008	0.007	0.007	0.0051
Heart	0.20	0.16	0.13	0.072	0.072	0.060
Intestine	0.30	0.15	0.11	0.067	0.067	0.0051
Plasma	4.1	1.7	0.85	0.65	0.47	0.28

[a] The range was <10% of each value; $n = 6$ rats per group.

in three solvent systems. On silica gel, the ^{99m}Tc-labeled material exhibited an R_f value of 1.0 in each of the solvents [0.9% NaCl, 1-butanol–acetic acid–water (4:1:1), and acetonitrile–water (3:1)], whereas pertechnetate and technetium-99m–tin colloid gave R_f values of 1 and 0, respectively, in these systems. On cellulose, the labeled iminodiacetic acid migrated with R_f values of 0, 0.8, and 0; the colloid remained at the origin and pertechnetate migrated with R_f values of 1.0, 0.4, and 1.0 in these solvent systems. In all cases, ^{99m}Tc-labeled tyramine diacetic acid yielded a well-defined chromatographic spot. The results of Sephadex G-25 chromatographic analysis revealed that >95% of the labeled material was eluted from the column as compared with 1% of labeled colloid. This was an indication that the iminodiacetic acid is a strong chelating agent. Increased dilution and prolonged standing at room temperature had minimal effect on the radiochemical purity of labeled material, providing further evidence of the stability of this ^{99m}Tc-labeled radiopharmaceutical.

***In Vivo* Studies in Rats**—*Tissue Distribution, Plasma, Urine, and Bile Analyses*—The data in Table I represent the activity in various tissues at 5, 10, 30, 60, 120, and 180 min after the intravenous injection of the imaging agent. Data are expressed as the percentage of administered dose per gram of tissue (wet weight). The tissue distribution data indicate a selective accumulation of the ^{99m}Tc-labeled material by the liver and kidney. There was an ~100-fold increase in the concentration of this agent in the liver and kidney as compared with the brain, intestine, and heart at 5 min postinjection. This was followed by a rapid clearance, since 50% of the activity was eliminated from the liver and kidney by 30 min.

The main elimination pathway of radioactivity after administration of the imaging agent was *via* the kidney. At 180 min, ~50–60% of the radioactive dose was accounted for in the urine. Less than 5% of the dose appeared in the bile at 180 min. Radiochromatographic analysis indicated that most of the activity in plasma, urine, and bile was in the form of the injected ^{99m}Tc-labeled material.

Image Analysis—Imaging studies substantiated the tissue distribution data. In Fig. 1 are shown whole rat body scans obtained at 2, 5, and 10 min after intravenous injection of 0.5 mCi/kg of ^{99m}Tc-labeled tyramine diacetic acid. The scans indicate high and selective uptake followed by a rapid wash-out of the radiopharmaceutical from the liver and kidney with concomitant accumulation of the radioactivity in the urinary bladder.

DISCUSSION

In the present study it has been demonstrated that substitution of the terminal amino group of tyramine with the chelating moiety iminodiacetic acid produced a tyramine derivative which was capable of complexing with technetium-99m in quantitative yield. By utilizing silica gel or cellulose TLC in several solvent systems, the labeled material exhibited a single distinct sharp peak and the absence of a radioactive band associated with pertechnetate or technetium-99m–tin colloid. The stability of the chelate in this radiopharmaceutical was indicated when increased dilution, prolonged storage (up to 4 h), and incubation at 37°C for 1 h had a minimal effect on its radiochemical composition.

Biodistribution studies in rats indicated avid extraction of the labeled material by the liver and kidney with minimal accumulation in the brain, heart, and intestine after intravenous administration. The plasma elimination pattern of ^{99m}Tc-labeled tyramine diacetic acid is indicative of the plasma clearance of endogenous and exogenous amines with high first-pass hepatic extraction (19, 20). The main elimination pathway of radioactivity after administration of the imaging agent was *via* the kidneys, which is similar to that of tyramine (3, 21). Biliary excretion was minimal since <5% of the injected dose appeared in the bile at 3 h postinjection.

Furthermore, evidence supporting the fact that extensive dissociation *in vivo* of ^{99m}Tc-labeled material to colloidal technetium or pertechnetate did not occur was obtained when radiochromatographic analysis of plasma, bile, and urine contents produced a chromatogram identical to that of the imaging agent before injection. This suggests that the ^{99m}Tc-labeled iminodiacetic acid chelate remains intact *in vivo* and is eliminated in an unchanged form.

These preliminary results indicate that ^{99m}Tc-labeled tyramine diacetic acid may represent a new class of radiopharmaceuticals for the evaluation of hepatorenal function independent of the hepatobiliary system.

REFERENCES

(1) A. D. Mosnaim, M. E. Wolf, and O. H. Callaghan, in "Noncatecholic Phenethylamines," part 2, A. D. Mosnaim and M. E. Wolf, Eds., Dekker, New York, N.Y., 1980, p. 201.

(2) J. D. David, W. Dairman, and S. Udenfriend, *Proc. Natl. Acad. Sci. U.S.A.*, **71**, 1771 (1974).

(3) B. A. Faraj, R. A. Carrano, F. M. Ali, E. J. Malveaux, and W. M. Stacciarini, *J. Pharmacol. Exp. Ther.*, **218**, 750 (1981).

(4) K. F. Ilett, C. F. George, and D. S. Davies, *Biochem. Pharmacol.*, **29**, 2551 (1980).

(5) W. H. Oldendorff, *Am. J. Physiol.*, **221**, 1629 (1971).

(6) I. Smith and A. H. Kellow, *Nature (London)*, **221**, 126 (1969).

(7) B. E. Blackwell, E. Marley, and J. Price, *Br. J. Psychiatry*, **113**, 349 (1967).

(8) L. R. Gjessing and R. Lindman, *Lancet*, **ii**, 47 (1967).

(9) M. Swash, A. M. Moffet, and D. R. Scott, *Nature (London)*, **258**, 749 (1975).

(10) H. J. Bremer, U. Jaenicke, and D. Leupold, *Clin. Chim. Acta*, **23**, 244 (1969).

(11) I. Smith, A. H. Kellow, and P. E. Mullen, *Nature (London)*, **230**, 246 (1971).

(12) B. A. Faraj, P. A. Bowen, J. W. Isaacs, and D. Rudman, *N. Engl. J. Med.*, **294**, 1360 (1976).

(13) B. A. Faraj, J. T. Fulenwider, E. B. Rypins, B. Nordlinger, G. L. Ivey, R. D. Jansen, F. M. Ali, V. M. Camp, M. Kutner, F. Schmidt, and D. Rudman, *J. Clin. Invest.*, **64**, 413 (1979).

(14) B. A. Faraj, R. B. Bethel, F. M. Ali, D. Rudman, and J. Galambos, in "Noncatecholic Phenethylamines," part 2, A. D. Mosnaim and M. E. Wolf, Eds., Dekker, New York, N.Y., 1980, p. 81.

(15) B. A. Faraj, S. L. Newman, D. B. Caplan, F. M. Ali, V. M. Camp, and P. A. Ahmann, *Pediatrics*, **64**, 76 (1979).

(16) B. A. Faraj, V. M. Camp, J. Ansley, F. M. Ali, and E. J. Malveaux, *Biochem. Pharmacol.* **29**, 2831 (1980).

(17) P. S. Callery, W. C. Faith, M. D. Loberg, A. T. Fields, and E. B. Harvey, *J. Med. Chem.*, **19**, 962 (1976).

(18) B. H. Mock, *J. Nucl. Med.*, **21**, 78 (1980).

(19) R. L. Wilhams and R. D. Mamelok, *Clin. Pharmacokinet.*, **5**, 528 (1980).

(20) A. S. Nies and D. G. Shand, *Circulation*, **52**, 6 (1975).

(21) B. A. Faraj, P. G. Dayton, V. M. Camp, J. P. Wilson, E. J. Malveaux, and R. C. Schlant, *J. Pharmacol. Exp. Ther.*, **200**, 384 (1977).

ACKNOWLEDGMENTS

This work was supported in part by an Emory University School of Medicine Biomedical Research Grant. Presented in part at the 66th Annual Meeting of the Federation of American Societies for Experimental Biology [*Fed. Proc., Fed. Am. Soc. Exp. Biol.*, **41**, 1567 (1982)].

Enhanced Rectal Absorption of [Asu^{1,7}]-eel Calcitonin in Rats Using Polyacrylic Acid Aqueous Gel Base

KAZUHIRO MORIMOTO *×, HIROAKI AKATSUCHI *, RENJI AIKAWA *, MASATAKA MORISHITA ‡, and KATSUAKI MORISAKA *

Received March 17, 1983, from the *Institute of Pharmaceutical Science, Osaka College of Pharmacy, Osaka, 580, Japan, and from the ‡Toyo Jozo Research Laboratories, Shizuoka, 410-23, Japan. Accepted for publication October 6, 1983.

Abstract □ The effects of polyacrylic acid aqueous gel on the absorption of rectally administered [Asu^{1,7}]-eel calcitonin, a calcitonin analogue, were investigated in rats. The [Asu^{1,7}]-eel calcitonin (1 U/kg) was given into the rectal loop in gel bases at various pH (5.5–8.5) and polyacrylic acid concentrations (0.01–1.0% w/v). The maximum hypocalcemic effect was obtained in ~30 min after administration of the analogue in a 0.1% w/v polyacrylic acid gel base at pH 5.5. The plasma calcium level decreased by ~18% from the initial level. Rectal administration in vehicles such as polyethylene glycol 1000, triglyceride fatty acid mixture base, or saline solution had little or no hypocalcemic effect at a dose of 5 U/kg. The results indicated that a polyacrylic acid aqueous gel base significantly improved the absorption of this analogue. Furthermore, rectal administration in a polyacrylic acid gel base (0.1% w/v; pH 5.5) required a dose 35 times greater than an intravenously administered dose to achieve an equivalent hypocalcemic effect.

Keyphrases □ Calcitonin—enhanced rectal absorption using polyacrylic acid aqueous gel base, rats, bioavailability □ Rectal absorption—Calcitonin, polyacrylic acid aqueous gel base, bioavailability, rats

Calcitonin, a hypocalcemic peptide hormone, has been isolated from the thyroid of mammals and ultimobranchials and has been used for the treatment of Paget's disease as well as certain types of osteoporosis (1). Peptides, such as calcitonin, can be given effectively only by injection because, when taken orally, they are digested by the proteolytic enzymes in the GI tract and metabolized by the liver. This is a problem for patients who are unable to have injections or are in need of long-term therapy.

Rectal administration would be favorable as a dosage route for several classes of drugs because the "first-pass elimination" of high clearance drugs may be partly avoided (2, 3). However, when comparing rectal and oral administration of absorbable drugs, the former dosage requires two or three times the drug concentration of the latter dosage because the absorption surface area of the rectum is smaller than that of the duodenum (1/10,000 the surface arera of small intestine). The bioavailability of poorly absorbable drugs such as calcitonin, a relatively high molecular weight compound, needs to be enhanced by pharmaceutical modification for rectal administration. The aqueous gel bases of polyacrylic acid, which are a group of carboxyvinyl polymers cross-linked with allyl sucrose, have been shown previously to significantly improve the absorption of insulin from the rectum (4, 5) and vagina (6). The present study was designed to evaluate the feasibility of rectally administering a calcitonin analogue using a polyacrylic acid aqueous gel base as an absorption promoter.

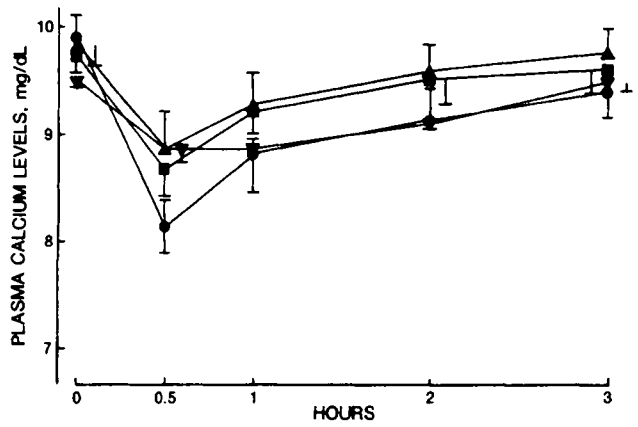

Figure 1—*Effects of the pH of polyacrylic acid gel base (0.01% w/v) on changes in plasma calcium levels following rectal administration of [Asu^{1,7}]-eel calcitonin in rats. The dose of [Asu^{1,7}]-eel calcitonin is 1 U/kg. Each point represents a mean ± SEM of five animals. Key: (●) pH 5.5; (■) pH 6.5; (▲) pH 7.5; (▼) pH 8.5 polyacrylic acid gel.*

EXPERIMENTAL SECTION

Materials—[Asu^{1,7}]-eel calcitonin[1] a synthetic analogue of eel calcitonin in which the disulfide bridge between the first and seventh amino acids in the eel-calcitonin molecule is replaced by a $-CH_2CH_2-$ bridge (7) was used in this study. A polyacrylic acid aqueous gel base[2] of molecular weight 1,250,000 was used as obtained from the manufacturers. All reagents were of analytical or reagent grade.

Preparations—Polyacrylic acid aqueous gel base was prepared by presoaking in distilled water for 15 h at room temperature and adding 10% NaOH solution to adjust each pH and each concentration, as previously described (4). The concentrations of polyacrylic acid in the gel bases were 0.01, 0.05, 0.1, and 1.0% w/v. The pH values selected for the study were 5.5, 6.5, 7.5, and 8.5. [Asu^{1,7}]-eel calcitonin was dissolved in each gel base. If the mixing process trapped air in the gel preparation, the air was removed by centrifugation for 10 min at 3000 rpm. The viscosity of the gel preparation was measured with

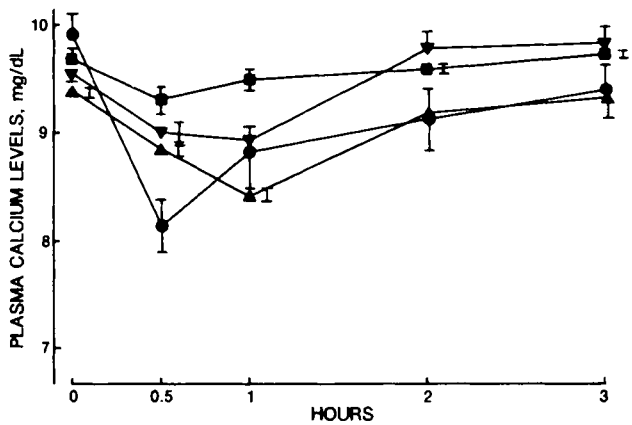

Figure 2—*Effects of the concentration of polyacrylic acid gel base (pH 5.5) on changes in plasma calcium levels following rectal administration of [Asu^{1,7}]-eel calcitonin in rats. The dose of [Asu^{1,7}]-eel calcitonin is 1 U/kg. Each point represents a mean ± SEM of five animals. Key: (▼) 0.01% w/v; (▲) 0.05% w/v; (●) 0.1% w/v; (■) 1.0% w/v polyacrylic acid gel.*

[1] Toyo Jozo Co., Ltd., Shizuoka, Japan.
[2] Carbpol 941; B.F. Goodrich Chemical Co, Cleveland, Ohio.

0022-3549/84/1000-1366$01.00/0
© 1984, American Pharmaceutical Association

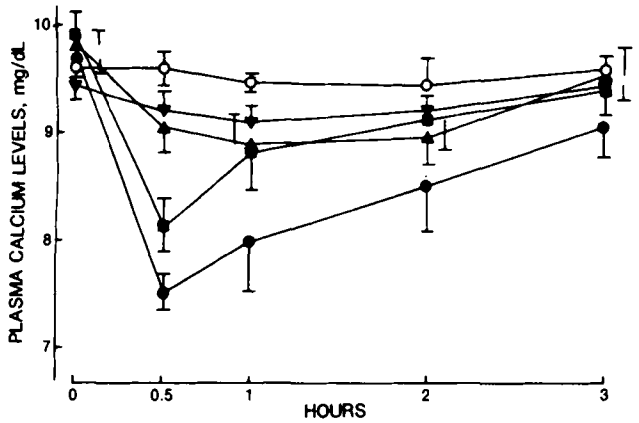

Figure 3—*Dose dependency of plasma calcium levels following rectal administration of [Asu^{1,7}]-eel calcitonin in polyacrylic acid gel base (0.1% w/v; pH 5.5) in rats. Each point represents a mean ± SEM of five animals. Key: (○) 0 U/kg; (▼) 0.1 U/kg; (▲) 0.5 U/kg; (■) 1 U/kg; (●) 5 U/kg.*

a cone and plate viscometer[3] at 37°C, and its osmolarity determined by a freezing-point osmometer[4]. The gel preparations were stored in the dark at 6°C.

Rectal Absorption—Young Wistar strain male rats (4 weeks old) weighing 80–100 g were selected as the experimental animals. The animals were fasted for 20 h prior to the experiments, but water was given freely. During the experiment, the rats were anesthetized with pentobarbital (50 mg/kg). The gel preparations were warmed to 30°C and quantities of 0.25 mL/100 g body weight were injected into the rectal loop (2.5 cm above the anus), which was isolated by ligation with thread. In comparative studies, the analogue was also formulated and administered rectally to separate groups of rats as a saline solution, in a triglyceride fatty acid mixture base[5], and in polyethylene glycol 1000. A fourth group of rats was given the material intramuscularly. Blood samples (0.3 mL) were obtained with a heparinized syringe from the femoral vein 10 min before and at 30 min and 1, 2, and 3 h postdose. The plasma was separated by centrifugation at 3000 rpm. The plasma calcium levels were determined by the *o*-cresolphthalein complexone method as described by Morin (8). The plasma concentration of calcitonin was measured by an enzyme immunoassay described earlier (9).

Protein and Calcium Release from the Rectal Mucosa—Release of protein and calcium from the rectal mucosa caused by the polyacrylic acid gel was determined by the *in situ* recirculation technique. Wistar strain male rats, weighing 260–300 g, were fasted for 20 h prior to the experiments. During the experiments, the animals were anesthetized with pentobarbital (60 mg/kg). The perfusate (20 mL) was recirculated at the rate of 2 mL/min at 37°C for 1 h in the colon and rectum (5 cm above the anus). The amount of protein was determined by Lowry's method (10) and that of calcium by atomic absorption spectroscopy.

RESULTS

Rheological Characteristics of Polyacrylic Acid Aqueous Gel—Polyacrylic acid aqueous gel behaves like a non-Newtonian liquid, and the viscosity is unchanged over a wide range of pH 4.5–12. The apparent viscosities of gel bases at concentrations of 0.01, 0.05, 0.1, and 1.0% w/v were observed to be 24, 177, 285, and 1515 cps, respectively. The values were obtained with a cone and plate viscometer at 37°C and a shear rate of 38.4 s^{-1}. As may be readily seen, the viscosity of the gel base increased with the increase in the concentration of polyacrylic acid. The viscosity of the gel preparation did not change when the calcitonin analogue was dissolved in the gel base.

Rectal Administration of [Asu^{1,7}]-eel Calcitonin—The effects of the pH of gel bases (0.1% w/v) on absorption following the rectal administration at the dose of 1 U/kg in young rats are shown in Fig. 1. The absorption increased with the lowering of the pH of the gel preparation. The hypocalcemic effects were in the following order of strength: pH 5.5 > pH 6.5 > pH 7.5 > pH 8.5 of the gel bases. The peaks of hypocalcemic effects were obtained at 30 min after administration, except with the pH 8.5 gel base. The plasma calcium values, which decreased by ~18% from their original levels, recovered after 1 h.

[3] Type E; Tokyo Keiki Co., Ltd., Tokyo, Japan.
[4] Fiske OS Osmometer; Uxbridge, Mass.
[5] Witepsol H-15; Dynamit Nobel Chemicals, Witten, West Germany.

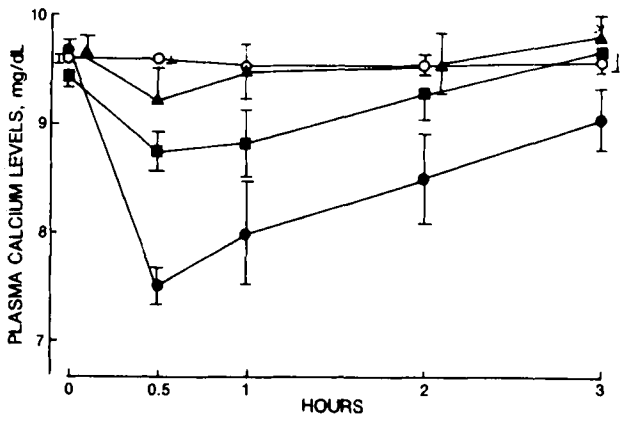

Figure 4—*Changes in plasma calcium levels following rectal administration of [Asu^{1,7}]-eel calcitonin in various bases in rats. The dose of [Asu^{1,7}]-eel calcitonin is 5 U/kg. Each point represents a mean ± SEM of five animals. Key: (○) saline solution; (▲) triglyceride fatty acid mixture base; (■) polyethylene glycol 1000; (●) 0.1% w/v polyacrylic acid gel (pH 5.5).*

The effects of the various concentrations of polyacrylic acid in the gel base (pH 5.5) on calcium levels after the rectal administration in the gel base to young rats are shown in Fig. 2. The time course of the hypocalcemic effects showed varying patterns with different concentrations of the gel after rectal administration. With the 0.1% w/v gel base, the plasma calcium level decreased rapidly for 30 min, at which time the maximum of the hypocalcemic effect was obtained. With the 0.05% w/v gel base, the plasma calcium level decreased slowly and the maximum hypocalcemic effect was found at 1 h. The 0.01% w/v and 1.0% w/v gel bases produced little hypocalcemic action; thus, the maximum hypocalcemic effect was obtained with the gel base at pH 5.5 and 0.1% w/v.

The dose response curves of plasma calcium levels following the rectal administration with the gel base (0.1% w/v; pH 5.5) are shown in Fig. 3. The rapid decrease of the plasma calcium level was observed at doses of 1 and 5 U/kg but, at doses of 0.1 and 0.5 U/kg slight hypocalcemic effects were seen from 30 min to 2 h.

In the experiment shown in Fig. 4, the hypocalcemic effect following rectal administration in polyacrylic acid gel base (0.1% w/v; pH 5.5) was compared with that obtained following administration in a triglyceride fatty acid mixture base, polyethylene glycol 1000, or saline solution at doses of 5 U/kg. The saline solution produced no hypocalcemic effect whereas the triglyceride fatty acid mixture preparation produced little hypocalcemic effect. The polyethylene glycol 1000 preparation produced a slight hypocalcemic effect; the minimum calcium level observed at 30 min after administration of [Asu^{1,7}]-eel calcitonin was ~93% of the initial level. Figure 5 compares the hypocalcemic effect produced by rectally administered material in the polyacrylic acid gel base (0.1% w/v; pH 5.5) with that administered intravenously. The plasma [Asu^{1,7}]-eel calcitonin levels obtained with rectal administration were compared with those with intramuscular administration. An enzyme immunoassay method was used to determine the [Asu^{1,7}]-eel calcitonin levels (Table I).

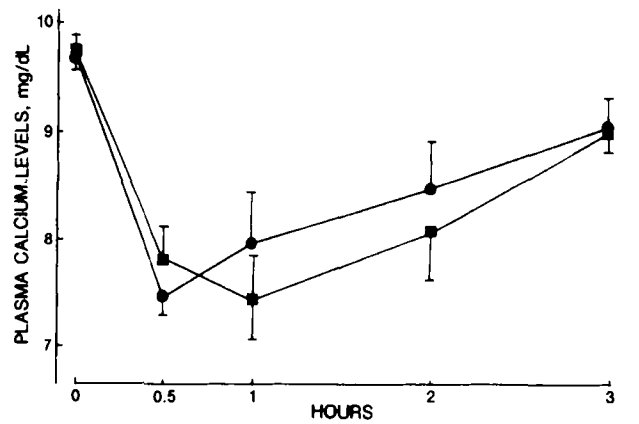

Figure 5—*Changes in plasma calcium levels following rectal administration in 0.1% w/v polyacrylic gel base (pH 5.5) and intravenous administration of [Asu^{1,7}]-eel calcitonin. Each point represents a mean ± SEM of five animals. Key (●) rectal administration (5 U/kg); (■) intravenous administration (0.15 U/kg).*

Table I—Bioavailability of [Asu[1,7]]-eel Calcitonin with Different Routes of Administration [a]

	Dose, U/kg	n	Peak Plasma Conc., mU/mL	AUC_0^{90}, mU·h/mL[b]	Apparent Bioavailability, %
Intramuscular	40	5	57.5 ± 6.1	57.3 ± 13.3	100
Rectal[c]	400	3	8.6 ± 2.1	4.3 ± 0.5	0.8 ± 0.2

[a] Each value is a mean ± *SEM*. [b] Area under plasma concentration *versus* time curve. [c] Gel base; 0.1% w/v, pH 5.5

Table II—Effects of Polyacrylic Acid Aqueous Gel Bases on Protein and Calcium Release from the Rectal Mucosa of Rats [a]

	n	Released Protein, mg	Released Ca^{+2} (mEq × 10^{-4})
Saline Solution	5	0.331 ± 0.018	6.01 ± 0.23
0.1% NaCl Solution	2	0.776 ± 0.155[b]	12.56 ± 0.94[b]
0.01% Gel Base (pH 5.5)	4	0.761 ± 0.041[b]	12.88 ± 0.50[b]
0.1% Gel Base (pH 5.5)	4	0.765 ± 0.070[b]	15.94 ± 1.01[b]
0.1% Gel Base (pH 5.5) containing 0.9% NaCl	4	0.312 ± 0.026	5.84 ± 0.66
0.1% Gel Base (pH 6.5) containing 0.9% NaCl	3	0.388 ± 0.043	6.01 ± 0.21
0.1% Gel Base (pH 7.5) containing 0.9% NaCl	3	0.347 ± 0.022	6.85 ± 0.60

[a] Each value is a mean ± *SEM*. [b] $p < 0.05$ when compared to saline using student's t test.

Rectal administration in a polyacrylic acid gel base (0.1% w/v; pH 5.5) required a dose 35 times greater than an intravenously administered dose to achieve an equivalent hypocalcemic effect (Fig. 5). When the calcitonin analogue was given rectally in the polyacrylic acid gel base, the apparent bioavailability was found to be ~0.80% (Table I) of a comparable intramuscular administration.

Protein and Calcium Releases from the Rectal Mucosa—In order to examine the effect of polyacrylic acid aqueous gel base on rectal mucosa, protein and calcium releasing effects were investigated. Table II shows the amounts of protein calcium released from the rectal mucosa. The protein and calcium releasing effects of 0.01 and 0.1% w/v polyacrylic acid gel base were increased by ~2 times that of saline. However, isotonic gel bases (at pH 5.5, pH 6.5, and pH 7.5 containing 0.9% NaCl) did not show the calcium and protein releasing effect.

DISCUSSION

It has been generally considered difficult for a peptide hormone such as [Asu[1,7]]-eel calcitonin to be absorbed through the intestinal mucosa. In this study, the rectal administration of [Asu[1,7]]-eel calcitonin in a saline solution at a dose of 5 U/kg did not lower the plasma calcium levels (Fig. 4). However, absorption from the rectum was significantly facilitated by a polyacrylic acid gel base. The pH of the gel and the concentration of polyacrylic acid in the gel base affected the rectal absorption. The rectal absorption increased with decreasing pH of the gel base in the range of pH 5.5–8.5 (Fig. 1). In the experiment where the concentrations of the polyacrylic acid in the gel base were varied, the increased absorption was in the following order of strength: 0.1% w/v > 0.05% w/v > 0.01% w/v > 1.0% w/v. The enhanced absorption (as noted by lowering of plasma calcium levels) was concentration dependent in the range of 0.01–0.1% w/v polyacrylic acid. The insignificant plasma calcium lowering effect noted with 1% w/v polyacrylic acid gel might have been due to the high viscosity of the gel and/or the interaction of the calcitonin analogue with the polyacrylic acid in the gel base.

When 1 U/kg was rectally administered in polyacrylic acid gel bases that were either isotonic (293 mOsm/kg) or hypertonic (865 mOsm/kg)—0.1% w/v; polyacrylic acid gel pH 5.5 containing 0.9% w/v and 3% w/v NaCl, respectively—the hypocalcemic effects were little or none (data not shown). Perhaps, the permeability of the calcitonin analogue through the rectal mucosal membrane in isotonic and hypertonic conditions was supressed by the exudation of fluids.

In order to clarify the mechanism of the promoting effect of the polyacrylic acid gel base, the authors studied the release of protein and calcium from the rectal mucosa. The 0.01% w/v and 0.1% w/v gel bases containing no additional sodium chloride (*viz* hypotonic) increased the release of protein and calcium from the rectum. However, the 0.1% w/v gel base containing 0.9% w/v NaCl did not show any such releasing effect. Further, microscopic examination of histological samples revealed that the polyacrylic acid gel base caused no damage to the surface of the rectal mucosa, as shown in a preliminary experiment (4). The amount of protein released by this gel base from the rectal mucosa was negligible compared with that by sodium deoxycholate and sodium lauryl sulfate (11).

The sequestering of calcium ions to polyacrylic acid was previously reported by Murata and Arai (12) and Robb and Sharples (13). These authors found that the polyacrylic acid gel base had chelating properties towards calcium. In the present study, the amount of calcium released by a hypotonic polyacrylic acid gel base from the rectal mucosa was also higher than that with a saline solution. Thus, the polyacrylic acid gel base may have altered the rectal epithelial barrier by depleting calcium ions at the mucosal membrane. Calcium ions are important for preserving a tight intercellular structure.

The comparative bioavailability of the calcitonin analogue following rectal and intramuscular administration showed that ~35 times as much drug was needed in a gel base (0.1% w/v; pH 5.5) given rectally to produce an equivalent hypocalcemic effect. The mechanism of enhancement of rectal absorption by the polyacrylic acid gel is unclear. Its major absorption pathway, perhaps, is *via* a paracellular route through the intercellular channels rather than *via* a transcellular route through the epithelial cells.

This study showed that polyacrylic acid aqueous gel base might be used to promote the rectal absorption of polypeptide drugs, such as [Asu[1,7]]-eel calcitonin.

REFERENCES

(1) J. C. Stevenson and I. M. A. Evans, *Drugs*, **21**, 257 (1981).

(2) A. G. de Boer, F. Moolenaar, L. G. J. de Leede, and D. D. Breimer, *Clin. Pharmacokinet.*, **7**, 285 (1982).

(3) A. G. de Boer, D. D. Breimer, J. Pronk, and J. M. G. Stibbe, *J. Pharm. Sci.*, **69**, 804 (1980).

(4) K. Morimoto, I. Hama, Y. Nakamoto, T. Takeeda, E. Hirano, and K. Morisaka, *J. Pharm. Dyn.*, **3**, 24 (1980).

(5) K. Morimoto, E. Kamiya, T. Takeeda, Y. Nakamoto, and K. Morisaka, *Int. J. Pharm.*, **14**, 149 (1983).

(6) K. Morimoto, T. Takeeda, Y. Nakamoto, and K. Morisaka, *Int. J. Pharm.*, **12**, 107 (1982).

(7) H. Yamauchi, M. Shiraki, T. Ohyama, M. Otani, M. Matsuo, and H. Orimo, *Endocrinol. Jpn.*, **24**, 245 (1977).

(8) L. G. Morin, *Am. J. Clin. Pathol.*, **61**, 114 (1974).

(9) R. Aikawa, E. Mori, K. Hiranaka, M. Miyake, and M. Morishita, *J. Pharm. Sci.*, in press.

(10) E. F. Hartee, *Anal. Biochem.*, **48**, 422 (1972).

(11) K. Nakanishi, S. Miyasaki, M. Masada, and T. Nadai, *Yakugaku Zasshi*, **102**, 1133 (1982).

(12) M. Murata and H. Arai., *Nippon Kagaku Kaishi*, **9**, 1724 (1974).

(13) I. D. Robb and M. Sharples, *J. Colloid Interface Sci.*, **89**, 301 (1982).

ACKNOWLEDGMENTS

The authors would like to express grateful acknowledgment to Professor A. Kamada, Osaka University, for his helpful suggestions.

Percutaneous Absorption and Disposition of Iodochlorhydroxyquin in Dogs

FIKRAT W. EZZEDEEN, SIDNEY J. STOHS ˣ, KAREN L. KILZER, MICHAEL C. MAKOID, and NIHAD W. EZZEDEEN

Received September 12, 1983, from the *Department of Biomedicinal Chemistry, University of Nebraska Medical Center, Omaha, NE 68105.* Accepted for publication October 18, 1983.

Abstract □ The percutaneous absorption and disposition of iodochlorhydroxyquin (5-chloro-7-iodo-8-quinolinol; I) from a 3% cream were studied in five dogs over a 28-d topical treatment period. Plasma levels, determined by HPLC, were 0.275–0.525 μg/mL. The steady-state elimination rate of total I in urine was 2.4–3.0 mg/d. The apparent elimination rate constant and half-life were 0.25 ± 0.05 d^{-1} and 3.1 ± 0.5 d, respectively. Greater than 50% of topically applied I was absorbed over 16 h. Occlusion of the skin without the drug indicated that the skin acted as a reservoir for the drug. Feces analysis for iodochlorhydroxyquin from one dog showed that 27.1 ± 8.5 mg/d was eliminated *via* this route. Tissue levels of I 15 d after the 28-d topical treatment were 0.7 μg/g of liver, 0.2 μg/g of kidney, and 0.8 μg/g of mesenteric fat. The apparent rate constants of plasma level decline after a 100-mg iv bolus dose of I were $\alpha = 3.9\ h^{-1}$ and $\beta = 0.6\ h^{-1}$. The urinary elimination after intravenous administration was biphasic. The rate constant for the slow elimination phase was 0.4 ± 0.1 d^{-1}, and the half-life was 2.0 ± 0.5 d. The primary neurological symptoms observed during topical treatment were ataxia and hind limb paralysis. Microscopic examination revealed liver necrosis. A weight loss of 15.3 ± 2.7% was also observed over the 28-d topical treatment period. The results indicate that significant percutaneous absorption of I occurs, and that chronic high-dose topical treatment may lead to toxicity.

Keyphrases □ Iodochlorhydroxyquin—percutaneous absorption and disposition in dogs □ Absorption—percutaneous, disposition of iodochlorhydroxyquin in dogs □ Neurotoxicity—percutaneous absorption and disposition of iodochlorhydroxyquin in dogs

Iodochlorhydroxyquin (5-chloro-7-iodo-8-quinolinol; I), also known as clioquinol, is a dihalogenated derivative of 8-hydroxyquinoline. It is used widely as an amebicidal agent, and as an antibacterial and antifungal agent for the treatment of various dermatological disorders. Due to its neurotoxicity, the drug is no longer given orally in the United States and Japan, but it is still used orally in many countries (1, 2). Iodochlorhydroxyquin is still used topically for diaper rash and other skin disorders and is presumed to undergo little or no percutaneous absorption. Tateishi and Otsuki (3) first reported that oral administration to dogs, cats, and monkeys resulted in the occurrence of a myelo-opticneuropathy. The neurological symptoms seen in these animals were comparable with those seen in patients suffering from subacute myelo-opticneuropathy (3).

Worden and Heywood (4) have reported hind limb and proprioceptive reflexes and yellow staining of the fur when dogs were treated orally with 250–400 mg of I per kg of body weight daily for 25 weeks. The minimum serum levels of I at the beginning of intoxication during chronic studies in adult dogs were 6–22.6 μg/mL when given 100 mg/kg/d orally (5).

Hansson (6) has studied the oral absorption of the drug in normal humans and reported that 3–5% of a given oral dose was recovered in the urine. Berggren and Hansson (7) have observed that the proportion of an oral dose of halogenated hydroxyquinoline which is absorbed was as high as 46%.

Iodochlorhydroxyquin is believed to undergo limited absorption through the skin, although few data are available on the extent of this absorption. A child with generalized psoriasis treated with ointment containing I was reported to have 18.1 mg/100 mL of the conjugated drug in the urine (8). Fischer and Hartvig (9) treated four patients with widespread dermatitis of an unstated type with an ointment containing 3% I, and serum levels of I were estimated by electron-capture GC to be 0.8–1.2 μg/mL. In this study, we examined the percutaneous absorption and excretion of iodochlorhydroxyquin in dogs.

EXPERIMENTAL SECTION

Animals and Procedure—Five male mongrel dogs (weight, 16.5–19 kg) were used. The dogs were fed a solid diet[1] and had free access to water. All dogs were treated for parasites and vaccinated against hepatitis. The animals were maintained for at least 1 week before initiating the studies. Five grams of 3% iodochlorhydroxyquin cream[2] was applied topically twice daily at 8 a.m. and 4 p.m. for 28 d over a 200-cm^2 area on the back of each dog after the area was shaved. The area was occluded with plastic wrap[3] and gauze. Before application of each new dose of I, the skin was cleansed with water and dried. Blood samples were drawn at the following times during treatment: 0, 1, 2, 4, 6, 8, 10, 12, and 24 h and 2, 3, 4, 7, 14, 21, and 28 d. Blood samples were obtained during the first week through an indwelling catheter placed in the jugular vein. The tubing was tunneled under the skin from the jugular vein to the back behind the head and exteriorized. The exposed end of the catheter was covered with a padded collar around the neck to prevent damage to the catheter by the dog. Each dog was also inserted into an elastic stockinette which enclosed the collar, neck, and thorax and prevented scratching of the jacketed area. The patency of the catheter was maintained by flushing with normal saline and filling with heparin sodium (1000 USP U/mL) every day. A blood sample was withdrawn and discarded, and a 3-mL sample of blood was then withdrawn for analysis.

At the end of the first week of treatment, the catheter was closed. For the subsequent time intervals, blood samples were drawn from a foreleg using heparin as the anticoagulant. Plasma was separated by centrifugation at 3000×*g* for 10 min and refrigerated or frozen if the samples were not analyzed immediately. No plasma sample was kept for more than 3 days before analysis. Urine samples taken every 24 h were collected at the following times during treatment by using metabolism cages: 1, 2, 3, 4, 5, 6, 7, 10, 14, 21, and 28 d. Feces were collected every 24 h from one dog during the 28-d treatment on days 0, 1, 7, 14, 21, and 28.

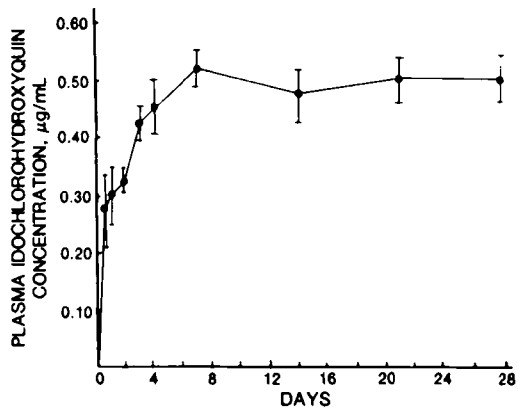

Figure 1—*Mean plasma level ± SD of nonconjugated iodochlorhydroxyquin in five dogs after topical treatment.*

[1] Kasco Dog Chow; Con-Agra Pet Food Division.
[2] Ciba Pharmaceuticals, Summit, N.J.
[3] Saran Wrap; Dow Chemical Co., Midland, Mich.

0022-3549/84/1000-1369$01.00/0
© 1984, American Pharmaceutical Association

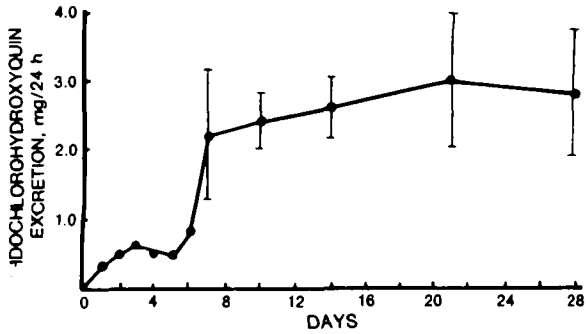

Figure 2—*Mean rate of excretion ± SD of total iodochlorhydroxyquin with time over 28 d of topical treatment of five dogs.*

After the 28-d topical treatment, blood and urine samples were collected at 2, 3, 4, 6, 8, 10, and 12 d posttreatment. Following this 12-d posttreatment interval, the backs of the dogs were again occluded with plastic wrap and gauze without drug, and blood and urine samples were obtained for an additional 6 d. The general condition of the dogs was examined daily, and the animals were weighed weekly.

Two months after topical treatment with I, three dogs were given a single bolus dose of 100 mg of I intravenously dissolved in 2.0 mL of dimethyl sulfoxide and 0.50 mL of ethanol. Blood samples were drawn at 15, 30, 45, 60, 120, and 180 min, and urine samples were collected each 24 h for 6 d.

Microscopic Examinations—The optic nerve from one dog that was killed after 28 d of topical treatment with I was isolated and fixed with glutaraldehyde and examined by electron microscopy. Kidney and liver tissues obtained from the dogs following sacrifice (after the intravenous treatment with I) were examined microscopically. Formalin (10%) was used to fix the tissues. Liver and kidney sections were also fixed and examined from one dog which died 15 d posttreatment.

Sample Analysis—The plasma concentration of nonconjugated iodochlorhydroxyquin was determined by HPLC after ether extraction by using a C_{18} reverse-phase column (10). The total urinary excretion of I after hydrolysis of conjugated metabolites according to Chen *et al.* (11) was assayed by a previously described HPLC procedure (12). The nonabsorbed I remaining on the backs of the dogs after topical treatment was also analyzed by HPLC as previously reported (13).

RESULTS AND DISCUSSION

Iodochlorhydroxyquin (I) cream was applied twice daily for 28 d, and the mean plasma level of nonconjugated I from five dogs were determined and plotted against time (Fig. 1). A steady-state plasma level was achieved in 4–5 d at ~0.5 μg/mL. Our results demonstrated that the drug is readily absorbed through the skin and presumably passes directly into the systemic circulation where easily measurable levels of the nonconjugated form occur after topical treatment (Fig. 1). Plasma levels could be detected 12 h after initial application, and accumulation of the drug in plasma did not occur.

During topical treatment, 24-h urine samples were collected, and the mean rate of elimination was plotted against time (Fig. 2). After day 7, the elimination rate reached steady state and ranged from 2.4 to 3.0 mg/24 h. In previous studies, it has been shown that >90% of the drug excreted in the urine

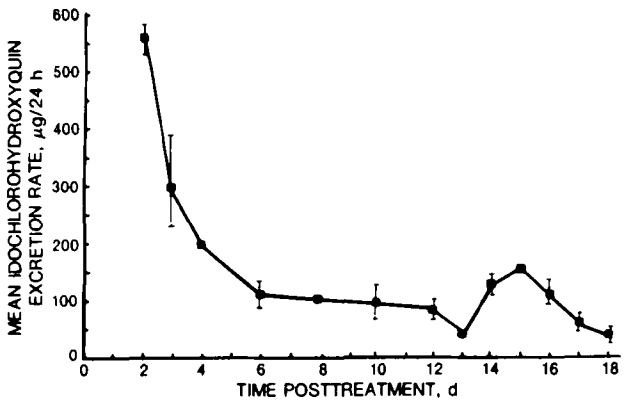

Figure 3—*Mean ± SD of total iodochlorhydroxyquin excreted with time after topical treatment and after again occluding the backs of the dogs with plastic wrap.*

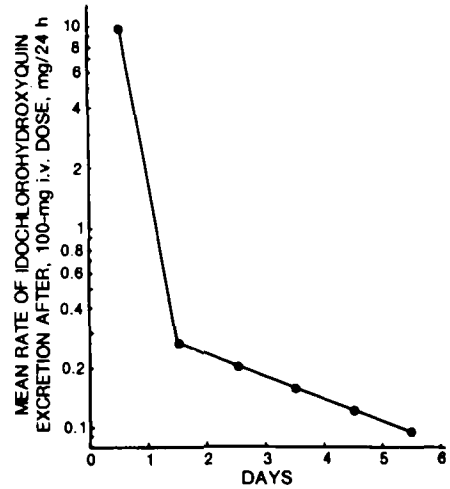

Figure 4—*Logarithmic plot of the mean excretion rate of iodochlorhydroxyquin with time after discontinuation of topical treatment in four dogs.*

is in the conjugated form, either as the glucuronide or sulfate (5). Therefore, the total amount of the drug eliminated in the urine during topical application was determined after hydrolysis of the conjugates. In spite of continuing topical treatment, the plasma levels and urine excretion rates remained constant, suggesting that the drug was being eliminated *via* another route and/or being stored in various tissues of the dogs. Therefore, feces from one dog were collected and analyzed over 28 d of topical treatment. The average total excreted in the feces was 27.1 ± 8.5 mg/24 h, indicating that the drug was being excreted largely by the fecal route as compared with urinary elimination. Previous studies have also shown excretion in the feces. Tamura (2) has reported that most of the iodochlorhydroxyquin conjugates are concentrated in the bile and are excreted into the intestinal lumen. A greenish-colored stool has also been seen in experimental dogs suffering from subacute myelo-opticneuropathy (3) and is due to the formation of an iron chelate of the drug.

After topical treatment for 28 d, the plasma levels and urinary excretion of the drug were followed for an additional 12 d. The elimination rate was plotted against time (Fig. 3). The 24-h rate of total elimination decreased from 568 ± 31 μg at 48 h posttreatment to 78 ± 26 μg after 12 d. The plasma concentration fell under the detection limit of our assay method 1 d after discontinuation of treatment. The rate constant of decline of elimination and the apparent half-life ($t_{1/2}$), were calculated from the slope of a plot of the logarithmic rate of elimination against time (Fig. 4) and Eq. 3 (see below). These values are 0.25 ± 0.05 d^{-1} and 3.0 ± 0.5 d, respectively.

The percentage of the drug absorbed was determined by measuring the amount of drug which remained on the back of each dog (14). Sixteen hours after a single 5-g application of 3% iodochlorhydroxyquin cream, 52.5 ± 4.5% of the drug was absorbed. This value is the mean of 10 determinations.

To determine whether the skin was simply acting as a permeable membrane or as a reservoir for the drug, the areas of application on the dogs were again occluded with plastic wrap and gauze without application of the drug, and the plasma levels and urinary elimination were followed for an additional 6

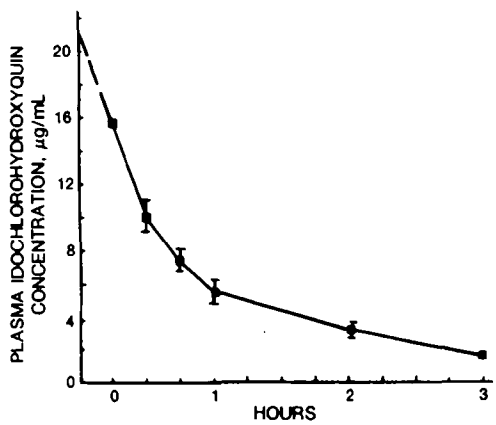

Figure 5—*Nonconjugated plasma concentration plotted with time after intravenous administration of a 100-mg iodochlorhydroxyquin dose in three dogs.*

Table I—Kinetic Parameters Calculated from 100-mg iv Bolus Injection of Iodochlorhydroxyquin in Three Dogs

α	3.9 h^{-1}
β	0.6 h^{-1}
Apparent $t_{1/2}$	1.16 h
A	20 ± 4 μg/mL
B	10 ± 2μg/mL
C_0	20.8 ± 2.6 μg/mL
Apparent Vd	4.91 ± 0.56 L
Apparent V_c	3.45 ± 0.46 L

d. Iodochorhydroxyquin was not detectable in the plasma, whereas the urinary excretion rate increased and, after 3 d of occlusion, again began to decline (Fig. 3). The elimination rate of total iodochlorhydroxyquin was 78 ± 26 μg/24 h at 12 d posttreatment, whereas the rate increased to 153 ± 8 μg/24 h during the third day of occlusion of the application site. These observations suggest that the skin acts as a reservoir for this drug, providing a slow release of I. Occlusion has been previously reported to increase the absorption and penetration of many drugs through the skin due to increased hydration of the stratum corneum and increased skin temperature (14, 15). This mechanism may explain the increase in the elimination of the drug when the site of application was again occluded without drug application.

A single intravenous administration study was conducted to obtain more kinetic data and to observe the effects of placing iodochlorhydroxyquin directly into the systemic circulation. Plasma and urine levels were monitored for 6 d. Three dogs were given 100 mg of I intravenously, and mean plasma concentrations of nonconjugated drug were plotted against time (Fig. 5). The kinetic data were calculated from the slope and intercept of a plot of the log plasma concentration with time (Fig. 6) by:

$$Vd = \frac{\text{dose}}{C_0} \quad \text{(Eq. 1)}$$

$$V_c = \frac{\text{dose}}{A + B} \quad \text{(Eq. 2)}$$

$$t_{1/2} = \frac{0.693}{k} \quad \text{(Eq. 3)}$$

where Vd is the apparent volume of distribution, V_c is the volume of the central compartment, $t_{1/2}$ is the apparent half-life, C_0 is the initial plasma concentration, A and B are the intercepts from the plot of log C against time, and, k is the apparent rate constant. The data are presented in Table I. The apparent rate constant (β) of the slow elimination phase was calculated from the slope of the plot, whereas apparent rate constant (α) for the rapid decline was calculated by the feathering method (16). A biphasic decline in the plasma levels of I was observed (Fig. 6), which may reflect in part the limited aqueous solubility of the drug (2). Furthermore, the rapid disappearance of the drug from plasma may be due to rapid metabolism as well as rapid tissue distribution as a result of the high lipid solubility of the drug.

Urine samples were also collected at various intervals after intravenous administration of I, and the mean rate of elimination with time is presented in Fig. 7. The urinary elimination of total I is biphasic, with an initial rapid elimination phase followed by a slow elimination phase, reflecting changes seen in plasma levels of the drug. The rate constant for the slow phase was determined from the slope, and the apparent $t_{1/2}$ was calculated by Eq. 3. The values are 0.4 ± 0.1 d^{-1} and 2.0 ± 0.5 d, respectively. The results shown in Figs. 6 and 7 suggest that a rapid distribution of I occurs from blood to tissue,

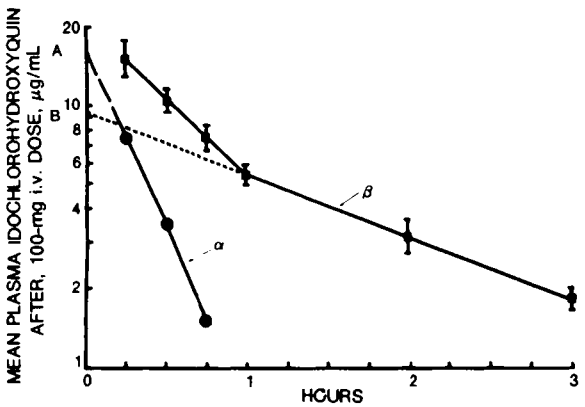

Figure 6—*Mean concentration* ± SD *of nonconjugated iodochlorhydroxyquin in plasma after a 100-mg iv bolus injection in three dogs.*

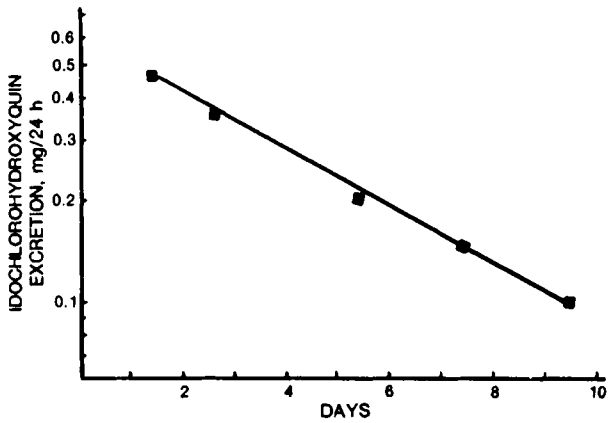

Figure 7—*Excretion rate of total iodochlorhydroxyquin after a 100-mg iv bolus dose.*

followed by a slow elimination of the drug due to the high lipid solubility of iodochlorhydroxyquin.

Liver, kidney, and mesenteric adipose tissue levels of I were analyzed from three dogs. The dogs were killed 2 weeks after intravenous treatment, and the following tissue levels were obtained: liver, 1.22 ± 0.23 μg/g; kidney, 0.83 ± 0.24 μg/g; mesenteric fat, 0.88 ± 0.14 μg/g. In addition, one dog died 15 d after topical treatment of I. The amounts of iodochlorhydroxyquin in the liver, kidney, and mesenteric adipose tissue were 0.74, 0.23, and 0.85 μg/g, respectively. Tissue retention of I has previously been reported. Tamura (2) has found 0.5, 0.3, and 0.1 μg of unconjugated I per gram of fresh liver, mesenteric adipose tissue, and sciatic nerve, respectively, in patients suffering from subacute myelo-opticneuropathy 9 months after oral treatment with I had ceased.

Weight loss occurred in all animals during topical treatment. An average loss of 15.3 ± 2.76% over 28 d was observed, while no weight loss occurred in control animals. Various neurological side effects have been reported after oral administration of iodochlorhydroxyquin (1, 17, 18). No toxicity has been reported after topical application because, in part, long-term studies have not been previously conducted; it has generally been assumed that I is not appreciably absorbed through the skin. During this 28-d study, all dogs became lethargic and less responsive to stimuli. In one of the dogs, partial hind limb paralysis was seen which was identical to that reported by Tateichi and Otsuki (3) after oral administration of iodochlorhydroxyquin. Three of the dogs developed rashes and inflammation of the treated areas. An optic nerve was removed from a dog which was sacrificed after 28 d of topical treatment and examined by electron microscopy. No damage or demyelination was observed. Optic nerve damage after long-term oral use of I has been reported (2). Either the concentrations of I achieved by topical application or the length of time the drug was applied were insufficient to produce optic nerve damage.

One of the dogs died 15 d after topical treatment. The liver was green-gray in color, suggesting hepatocellular toxicity. Microscopic examination of the liver demonstrated diffuse centrilobular and mid-zonal cell necrosis associated with marked dilation and congestion of the sinusoids, as well as the central lobular vein. No significant histological alterations were observed in the kidneys. Three other dogs were sacrificed after completion of the absorption and distribution studies. Histological examination of the kidneys indicated no renal toxicity[4]. However, examination of the livers in each case revealed centrilobular and mid-zonal vacuolization and necrosis with sinusoidal dilation and congestion[4]. The livers of control dogs did not demonstrate these changes. The results suggest that long-term topical application by an occlusion technique, as might be experienced with diaper dermatitis, can result in sufficient absorption to produce hepatotoxicity. Liver and kidney damage after oral treatment is well known and has been previously reported (19, 20).

The achievement of steady-state levels in plasma during topical treatment indicates that accumulation in plasma does not occur. Iodochlorhydroxyquin is rapidly absorbed through the skin. The liver is the main site of metabolism, primarily converting the drug to glucuronide and sulfate conjugates (2). Nonconjugated drug in plasma is transferred to the tissues due to its high lipid solubility (2). As a consequence, prolonged excretion of the drug occurs.

Nonconjugated iodochlorhydroxyquin is neurotoxic (5). Investigations by tissue culture techniques have shown direct toxic effects of the drug on nerves, whereas the glucuronide conjugate produced no cellular toxicity (21).

The results of this study indicate that it is important to use iodochlorhydroxyquin cautiously when topical application is required, particularly when

[4] Unpublished results.

it is used for a prolonged period of time and over a large body surface area, due to the extensive percutaneous absorption and the well-recognized toxicity of the drug.

REFERENCES

(1) Y. Toyokura and T. Takasu, *Jpn. J. Med. Sci. Biol.*, **28**, 87 (1975).

(2) Z. Tamura, *Jpn. J. Med. Sci. Biol.*, **28**, 69 (1975).

(3) J. Tateishi and S. Otsuki, *Jpn. J. Med. Sci. Biol.*, **28**, 165 (1975).

(4) A. N. Worden and R. Heywood, *Lancet*, **i**, 212 (1978).

(5) C. T. Chen, H. Kobama, Y. Egashira, K. Samejima, T. Imanari, and Z. Tamura, *Chem. Pharm. Bull.*, **24**, 2007 (1976).

(6) O. Hansson, *Acta Derm. Venereal.*, **43**, 465 (1963).

(7) L. Berggren and O. Hansson, *Clin. Pharmacol. Ther.*, **9**, 67 (1968).

(8) O. Hansson, *Pediatrics*, **60**, 769 (1977).

(9) T. Fischer and P. Hartvig, *Lancet* **i**, 603, (1977).

(10) F. W. Ezzedeen, A. N. Masoud, S. J. Stohs, and S. J. Lerman, *J. Pharm. Sci.*, **70**, 889 (1981).

(11) C. T. Chen, K. Samejima, and Z. Tamura, *Chem. Pharm. Bull.*, **24**, 97 (1976).

(12) F. W. Ezzedeen, S. J. Stohs, and M. Stublar, *J. Chromatogr.*, **276**, 121 (1983).

(13) F. W. Ezzedeen, S. J. Stohs, and A. N. Masoud, *J. Pharm. Sci.*, **72**, 1036 (1983).

(14) M. Barr, *J. Pharm. Sci.*, **51**, 395 (1962).

(15) J. Wepierri and J. P. Marty, *Trends Pharm. Sci.*, **I**, 23, (1979).

(16) M. Gibaldi and D. Perrier, in "Pharmacokinetics," Dekker, New York, N.Y., 1975, p. 281.

(17) N. H. Wadia, *J. Neurol. Neurosurg. Psych.*, **40**, 268 (1977).

(18) R. S. Hanakago and M. Uono, *Clin. Toxicol.*, **18**, 1427 (1981).

(19) A. N. Worden, R. Heywood, D. E. Prentice, H. Chesterman, K. Skerrett, and P. E. Thomann, *Toxicology*, **9**, 227 (1978).

(20) R. Heywood, H. Chesterman, and A. N. Worden, *Toxicology*, **6**, 41 (1976).

(21) N. Yamaneka, T. Tmanari, Z. Tamura, and K. Yagi, *J. Biochem.*, **73**, 993 (1973).

ACKNOWLEDGMENTS

This research was supported in part by a grant from the Ministry of Higher Education of Iraq.

The authors thank Mrs. Judy Williams and Mrs. Mary Beth Reynolds for technical assistance, Dr. Robert Shuman for electron microscopic examination of the optic nerve, and Dr. S. Salmasi for histological examination of the liver and kidneys.

In Vitro Adsorption–Desorption of Phenethylamines and Phenylimidazoles by a Bentonite and a Resin

M. S. STUL, D. P. VLIERS ˣ, and J. B. UYTTERHOVEN

Received June 17, 1982, from the *Katholieke Universiteit Leuven, Laboratorium voor Oppervlaktechemie, Kardinaal Mercierlaan 92, B-3030 Leuven (Heverlee), Belgium.* Accepted for publication August 4, 1983.

Abstract □ The adsorption of phenethylamines (dextroamphetamine, phentermine, mephentermine, diethylpropion), choline, and phenylimidazoles (levamisole and imazalil) was examined *in vitro* in aqueous solutions on bentonite and on lewatite at 25°C. An ion-exchange mechanism prevails for lewatite and for bentonite up to 0.8 mEq·g^{-1}. The organic cations are more strongly adsorbed on bentonite than on lewatite. On bentonite, the selectivity of adsorption follows the order: primary < secondary < tertiary phenethylamines. An interlamellar monolayer is formed. All drugs, except choline and imazalil, are adsorbed in excess of the cation exchange capacity of bentonite without observable Cl^- adsorption and pH changes. Desorption is reversible for lewatite and partially irreversible for bentonite.

Keyphrases □ Phenethylamines—*in vitro* adsorption-desorption by a bentonite and a resin □ Phenylimidazoles—*in vitro* adsorption-desorption by a bentonite and a resin

The prolonged action of drugs in the GI tract with a peak-and-valley pattern of the drug in the blood (1) is realized by binding, *e.g.*, phenethylamines as diethylpropion, to an ion-exchange resin. The same effect was also observed for an oral dose of a mixture of clay-drug compared to the pure drug [*e.g.*, amphetamine, (2)]. Clindamycine, tetracycline (3), and chlorpheniramine (4) are adsorbed by cation exchange under pH conditions favoring the cationic form of the drugs, and they penetrate into the interlayer spaces of montmorillonite, producing an increase in the basal distance.

There are many important clay-organic interactions, *i.e.*, some animal feed additives are adsorbed on vegetable carriers such as maize or soy starch or on resins; bentonites are used as binder and caloric extender for poultry (5); fungicides such as imazalil, used in the foliar treatment of bananas, contaminate the soil. Clay minerals constitute an interesting commercial alternative to resin. Therefore, the adsorption of phenethylamines, choline, a quaternary amine, and two imidazoles on bentonite and lewatite were investigated as model *in vitro* systems. Desorption behavior was tested with simulated gastric and intestinal fluids.

EXPERIMENTAL SECTION

The macroporous (100–200 mesh) sodium lewatite[1] and bentonite[2] were used as adsorbents. Air-dried resin was equilibrated for 2 weeks with an at-

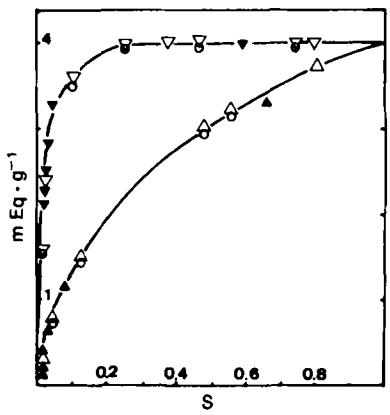

Figure 1—*Adsorption of diethylpropion (△) and imazalil (▽), and sodium desorption (○) on lewatite at pH 4 and 25°C* versus *S, the equivalent fraction of the organic cation in the equilibrium solution. Filled symbols refer to the desorption of the organic cation with a simulated gastric fluid (0.1 M NaCl, pH 2).*

[1] Resin SP 1080 (analytical grade); Merck, F.R.G.
[2] Wyoming bentonite (Volclay); American Colloid Co., U.S.A.

0022-3549/84/1000-1372$01.00/0

© 1984, American Pharmaceutical Association

it is used for a prolonged period of time and over a large body surface area, due to the extensive percutaneous absorption and the well-recognized toxicity of the drug.

REFERENCES

(1) Y. Toyokura and T. Takasu, *Jpn. J. Med. Sci. Biol.*, **28**, 87 (1975).

(2) Z. Tamura, *Jpn. J. Med. Sci. Biol.*, **28**, 69 (1975).

(3) J. Tateishi and S. Otsuki, *Jpn. J. Med. Sci. Biol.*, **28**, 165 (1975).

(4) A. N. Worden and R. Heywood, *Lancet*, **i**, 212 (1978).

(5) C. T. Chen, H. Kobama, Y. Egashira, K. Samejima, T. Imanari, and Z. Tamura, *Chem. Pharm. Bull.*, **24**, 2007 (1976).

(6) O. Hansson, *Acta Derm. Venereal.*, **43**, 465 (1963).

(7) L. Berggren and O. Hansson, *Clin. Pharmacol. Ther.*, **9**, 67 (1968).

(8) O. Hansson, *Pediatrics*, **60**, 769 (1977).

(9) T. Fischer and P. Hartvig, *Lancet* **i**, 603, (1977).

(10) F. W. Ezzedeen, A. N. Masoud, S. J. Stohs, and S. J. Lerman, *J. Pharm. Sci.*, **70**, 889 (1981).

(11) C. T. Chen, K. Samejima, and Z. Tamura, *Chem. Pharm. Bull.*, **24**, 97 (1976).

(12) F. W. Ezzedeen, S. J. Stohs, and M. Stublar, *J. Chromatogr.*, **276**, 121 (1983).

(13) F. W. Ezzedeen, S. J. Stohs, and A. N. Masoud, *J. Pharm. Sci.*, **72**, 1036 (1983).

(14) M. Barr, *J. Pharm. Sci.*, **51**, 395 (1962).

(15) J. Wepierri and J. P. Marty, *Trends Pharm. Sci.*, **I**, 23, (1979).

(16) M. Gibaldi and D. Perrier, in "Pharmacokinetics," Dekker, New York, N.Y., 1975, p. 281.

(17) N. H. Wadia, *J. Neurol. Neurosurg. Psych.*, **40**, 268 (1977).

(18) R. S. Hanakago and M. Uono, *Clin. Toxicol.*, **18**, 1427 (1981).

(19) A. N. Worden, R. Heywood, D. E. Prentice, H. Chesterman, K. Skerrett, and P. E. Thomann, *Toxicology*, **9**, 227 (1978).

(20) R. Heywood, H. Chesterman, and A. N. Worden, *Toxicology*, **6**, 41 (1976).

(21) N. Yamaneka, T. Tmanari, Z. Tamura, and K. Yagi, *J. Biochem.*, **73**, 993 (1973).

ACKNOWLEDGMENTS

This research was supported in part by a grant from the Ministry of Higher Education of Iraq.

The authors thank Mrs. Judy Williams and Mrs. Mary Beth Reynolds for technical assistance, Dr. Robert Shuman for electron microscopic examination of the optic nerve, and Dr. S. Salmasi for histological examination of the liver and kidneys.

In Vitro Adsorption–Desorption of Phenethylamines and Phenylimidazoles by a Bentonite and a Resin

M. S. STUL, D. P. VLIERS ˣ, and J. B. UYTTERHOVEN

Received June 17, 1982, from the *Katholieke Universiteit Leuven, Laboratorium voor Oppervlaktechemie, Kardinaal Mercierlaan 92, B-3030 Leuven (Heverlee), Belgium.* Accepted for publication August 4, 1983.

Abstract □ The adsorption of phenethylamines (dextroamphetamine, phentermine, mephentermine, diethylpropion), choline, and phenylimidazoles (levamisole and imazalil) was examined *in vitro* in aqueous solutions on bentonite and on lewatite at 25°C. An ion-exchange mechanism prevails for lewatite and for bentonite up to 0.8 mEq·g^{-1}. The organic cations are more strongly adsorbed on bentonite than on lewatite. On bentonite, the selectivity of adsorption follows the order: primary < secondary < tertiary phenethylamines. An interlamellar monolayer is formed. All drugs, except choline and imazalil, are adsorbed in excess of the cation exchange capacity of bentonite without observable Cl^- adsorption and pH changes. Desorption is reversible for lewatite and partially irreversible for bentonite.

Keyphrases □ Phenethylamines—*in vitro* adsorption-desorption by a bentonite and a resin □ Phenylimidazoles—*in vitro* adsorption-desorption by a bentonite and a resin

The prolonged action of drugs in the GI tract with a peak-and-valley pattern of the drug in the blood (1) is realized by binding, *e.g.*, phenethylamines as diethylpropion, to an ion-exchange resin. The same effect was also observed for an oral dose of a mixture of clay-drug compared to the pure drug [*e.g.*, amphetamine, (2)]. Clindamycine, tetracycline (3), and chlorpheniramine (4) are adsorbed by cation exchange under pH conditions favoring the cationic form of the drugs, and they penetrate into the interlayer spaces of montmorillonite, producing an increase in the basal distance.

There are many important clay-organic interactions, *i.e.*, some animal feed additives are adsorbed on vegetable carriers such as maize or soy starch or on resins; bentonites are used as binder and caloric extender for poultry (5); fungicides such as imazalil, used in the foliar treatment of bananas, contaminate the soil. Clay minerals constitute an interesting commercial alternative to resin. Therefore, the adsorption of phenethylamines, choline, a quaternary amine, and two imidazoles on bentonite and lewatite were investigated as model *in vitro* systems. Desorption behavior was tested with simulated gastric and intestinal fluids.

EXPERIMENTAL SECTION

The macroporous (100–200 mesh) sodium lewatite[1] and bentonite[2] were used as adsorbents. Air-dried resin was equilibrated for 2 weeks with an at-

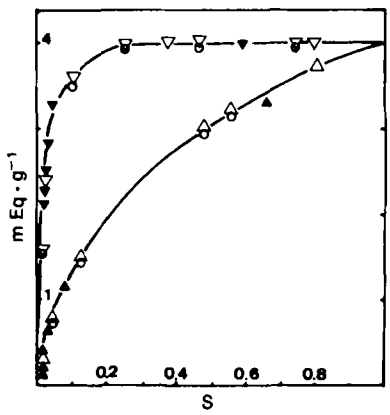

Figure 1—*Adsorption of diethylpropion (△) and imazalil (▽), and sodium desorption (○) on lewatite at pH 4 and 25°C versus S, the equivalent fraction of the organic cation in the equilibrium solution. Filled symbols refer to the desorption of the organic cation with a simulated gastric fluid (0.1 M NaCl, pH 2).*

[1] Resin SP 1080 (analytical grade); Merck, F.R.G.
[2] Wyoming bentonite (Volclay); American Colloid Co., U.S.A.

0022-3549/84/1000-1372$01.00/0

© 1984, American Pharmaceutical Association

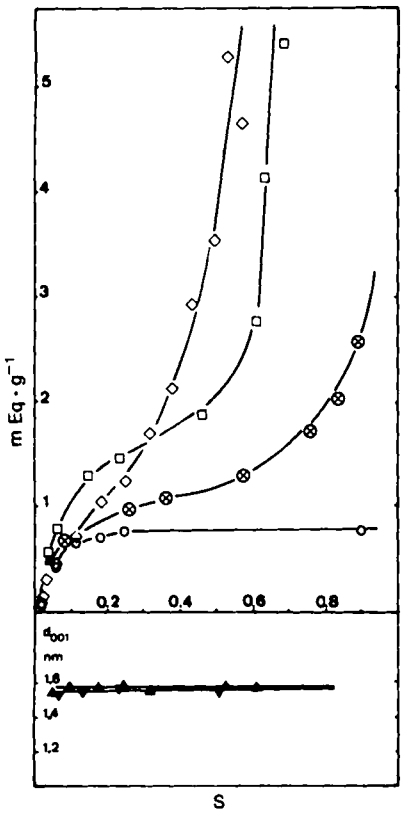

Figure 2—*Adsorption of amphetamine (◇), phentermine (□), and mephentermine (⊗) and sodium desorption (○) on bentonite at pH 5. Basal distances of the amphetamine-bentonite complexes in solution (▲) or dried in 1.333 × 10⁻⁴ Pa vacuum for 1 d at 25°C (▼). S is the equivalent fraction of the organic cation in the equilibrium solution.*

mosphere of 40% relative humidity. The cation exchange capacity (CEC), measured by isotopic dilution of ^{22}Na, was 4 mEq·g^{-1} dry resin. The bentonite fraction, under 0.5 μm, was separated by centrifugation, washed with acidified (pH = 3.5) and neutral NaCl (1 M) solutions for removal of hydroxy-aluminum compounds, and stored in the dark as a 1% suspension. The CEC of the bentonite was 0.7 and 0.8 mEq·g^{-1} clay at pH 4 and 5, respectively.

The adsorbates were the organic cations dextroamphetamine[3], phentermine[4], mephentermine[5], diethylpropion[6], choline[7], levamisole[7], and imazalil[7]. All of these have Cl^- as the anion, except for mephentermine which was purchased as the sulfate. Amphetamine and imazalil were obtained as bases and titrated to the equivalence point with HCl.

Exchanges were carried out in polyethylene tubes by end-over-end shaking for 48 h at 25°C and 0.01 M. For lewatite, 30–50 mg of resin were equilibrated with 30–40 mL of mixed Na-organic cation solutions containing different proportions of the two ions. The lewatite was separated by centrifuging for 5 min at 14,000 rpm. In the case of bentonite, 10-mL portions of a 1% clay suspension, enclosed in dialysis tubing, were equilibrated with 20 mL of mixed Na-organic cation solution.

All adsorptions were carried out at pH 5, except for imazalil and diethylpropion, in order to minimize hydrolysis of the clay. The low pK_a of 6.53 for imazalil necessitated experiments carried out at pH 4 to ascertain the presence of the cation. In the case of diethylpropion, the decomposition of the molecule was minimized by exchange at pH 4. The extent of adsorption was determined by radiometric analyses using: ^{14}C-labeled amphetamine[8], choline[8], and diethylpropion[9]; ^{3}H-labeled imazalil[7] and levamisole[8]; ^{22}Na; ^{36}Cl[10]. Countings were performed on 5-mL aliquots of the supernatant solutions, using a liquid-scintillation counter[11] and a γ-scintillation counter[12]. The concentrations

[3] C.E.R.T.A., 5050 Eghezée, Belgium.
[4] Troponwerke, 5000 Köln 80, F.R.G.
[5] Wyeth, Taflon, Maidenhead, U.K.
[6] Trenker, 1180 Brussels, Belgium.
[7] Janssen Pharmaceutica, 2340 Beerse, Belgium.
[8] C.E.A. Saclay; 91190 Gif-sur-Yvette, France.
[9] Laboratory of Medical Chemistry and Toxicology, University of Liège, Belgium.
[10] I.R.E., 6220 Fleurus, Belgium.
[11] Tricarb 460 C; Packard.
[12] PDG Auto-gamma; Packard.

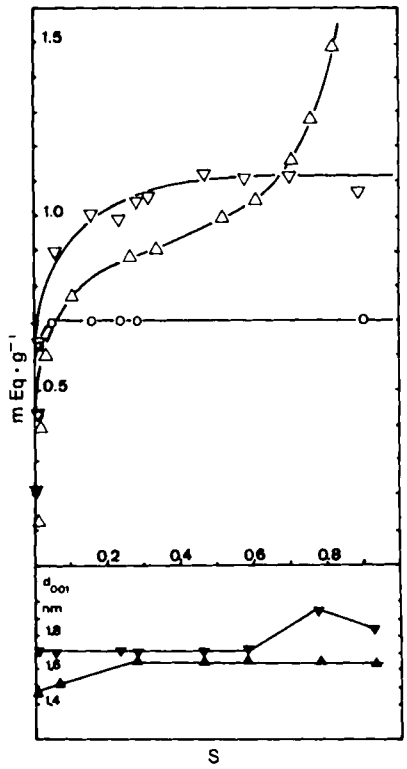

Figure 3—*Adsorption of imazalil (▽) and sodium desorption (○), adsorption of diethylpropion (△) on bentonite at pH 4. Basal distances of the imazalil-bentonite complexes in solution (▼) or dried in 1.333 × 10⁻⁴ Pa vacuum for 1 d at 25°C (▲). S is the equivalent fraction of the organic cation in the equilibrium solution.*

of phentermine and mephentermine were determined by UV absorption at 252 nm[13].

The swelling of the clay was studied by X-ray diffraction. For this purpose the sediment, obtained after centrifuging for 5 min at 14,000 rpm, was transferred into a Lindemann capillary, which was sealed, transferred to a Debye-Scherrer camera, and irradiated with CuK_α. The remainder of the sediment was rinsed with distilled H_2O, centrifuged, air-dried, and dried under high vacuum for 1 d at 25°C before X-ray measurement.

Desorption experiments were carried out on the fully exchanged resins, prepared by mixing 50-mg resin and 40-mL (0.01 M) organic cation. In the case of the clay, the desorption was studied on samples containing a low and a high organic cation content. These were obtained by equilibrating 10 mL

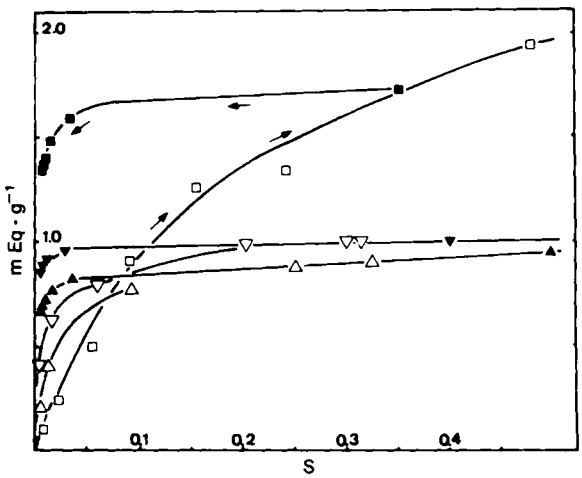

Figure 4—*Release pattern* in vitro *at 25°C by a simulated gastric fluid (0.1 M NaCl, pH 2) from bentonite of phentermine (■), diethylpropion (▲), and imazalil (▼). Open symbols refer to the adsorption isotherm. S is the equivalent fraction of the organic cation in the equilibrium solution.*

[13] Shimadzu QV-50 Spectrophotometer; Kyoto, Japan.

Table I—Natural Log of the Mean Selectivity Coefficient for the Exchange of Na by the Organic Cation on Lewatite and Bentonite at 298 K

	pK_a	Formula	$\ln \overline{K}_c$ (lewatite)	$\ln \overline{K}_c$ (bentonite)
Amphetamine	9.6	$PhCH_2CH(CH_3)NH_3^+$	—	3.35
Phentermine	9.84	$PhCH_2C(CH_3)_2NH_3^+$	1.67	3.39
Mephentermine	10.11	$PhCH_2C(CH_3)_2NH_2CH_3^+$	—	4.63
Diethylpropion	8.78	$PhCOCH(CH_3)NH(C_2H_5)_2^+$	1.45	5.40
Choline		$HO—CH_2—CH_2—N(CH_3)_3^+$	—	3.26
Levamisole	8.00	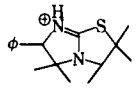	—	6.39
Imazalil	6.53	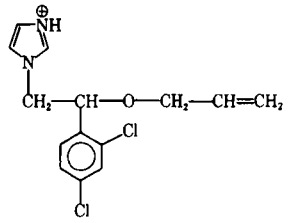	3.9	7.56

of a 1% clay suspension with 30 mL 0.01 M and 30 mL 0.025 M solutions of the organic cation, respectively. The desorption procedure was as follows: after 5 min of centrifugation at 14,000 rpm, 30 mL of the supernatant was removed and used for radioassay. The addition and removal of 20-mL portions of the supernatant was performed every hour thereafter. The amount desorbed was obtained from the radioassay of the successive supernatants and was expressed as a fraction of the initially adsorbed amount. The desorbing agent used was part of a simulated gastric fluid (NaCl 0.1 M, pH 2). The drug release pattern, as a function of time, was followed for a simulated intestinal fluid [122 mmol NaCl, 5 mmol KCl, 1 mmol KH_2PO_4, and 26 mmol $NaHCO_3$/L, *i.e.*, a buffer solution of pH 8, (6)].

RESULTS

Figure 1 shows the adsorption isotherms for diethylpropion and imazalil on lewatite; phentermine follows the same pattern as diethylpropion. In all cases the maximum loading equals the CEC. The adsorption occurs by ion exchange because, at every loading, the Na^+ ion release equals the amount of adsorbed organic cation.

The adsorption isotherms for amphetamine, phentermine, mephentermine, diethylpropion, and imazalil on bentonite, together with basal spacings, are presented in Figs. 2 and 3, respectively. They have two characteristic features: (*a*) a stoichiometric ion-exchange process wherein the Na^+ ion release equals the amount of adsorbed organic cation, and (*b*) adsorption in excess of the CEC. The latter is more pronounced for amphetamine followed by phentermine, mephentermine, and diethylpropion. The excess adsorption is not accompanied by simultaneous adsorption of Cl^- or by pH changes.

The basal spacing of 1.56 nm is independent of the loading and of the type of phenethylammonium cation. For choline and imazalil they are 1.50 and 1.72, respectively. The thickness of a clay plate was 0.96 nm. The differences

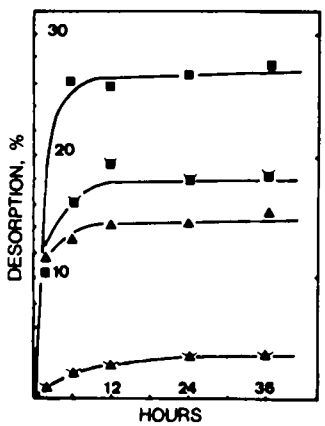

Figure 5—*Kinetic desorption profile with a buffer solution at pH 8 of: (■) phentermine-bentonite (1.06 mEq·g^{-1}), (▣) phentermine-bentonite (2.95 mEq·g^{-1}), (▲) diethylpropion-bentonite (1.14 mEq·g^{-1}), and (▲) diethylpropion-bentonite (1.78 mEq·g^{-1}).*

(*e.g.*, 1.56 − 0.96 nm = 0.60 nm) were indicative of a monolayer of organic cations on the surface.

Lewatite desorption of diethylpropion and imazalil was the reverse of the ion-exchange reaction as verified by the overlap of desorption and adsorption isotherms (Fig. 1). This is also the case for bentonite up to a loading with organic cations of ~0.7 mEq·g^{-1}. It should, however, be mentioned that since the H^+ concentration is much higher during desorption (but still 10 times smaller than the Na concentration), adsorption and desorption isotherms are not fully comparable.

When the loading on bentonite exceeds the CEC, adsorption and desorption curves are not superimposed, Fig. 4. The desorption experiments at pH 8 are presented in Fig. 5; 12 h were required to reach equilibrium. A smaller relative amount was desorbed for high loadings of organic cations as illustrated for phentermine and diethylpropion. Imazalil could not be desorbed at pH 8 because of the pK_a value and the limited solubility of the base (0.3 g·L^{-1}).

DISCUSSION

For lewatite, ion exchange was the only adsorption mechanism, whereas, for bentonite, ion exchange was followed by an excess adsorption process of the organic cations. From molecular models we estimated that 1.49 mEq·g^{-1} amphetamine and 0.9 mEq·g^{-1} diethylpropion can be adsorbed as monolayers in the interlamellar space of bentonite (700 m^2·g^{-1}) (7). Therefore, excess adsorption occurs to a large extent on the external surface, but the mechanism of adsorption is unclear.

For the exchange reaction between a solid exchanger (z) and a solution (s):

$$Na_z + B_s^+ \rightleftharpoons B_z + Na_s^+ \qquad \text{(Eq. 1)}$$

The selectivity coefficient, K_c, is defined as:

$${}^{B}_{Na}K_c = \frac{Z_B \cdot M_{Na}}{Z_{Na} \cdot M_B} \qquad \text{(Eq. 2)}$$

where Z and M refer to the equivalent fraction for the surface phase and the molality for the solution phase concentration. The latter can also be expressed in S units, *i.e.*, the equivalent fraction of the ion under consideration in the equilibrium solutions (8). The dependency of the selectivity coefficient on the organic loading is shown in Fig. 6. The mean $\overline{K}_c$ value is:

$$\ln {}^{B}_{Na}\overline{K}_c = \frac{1}{x_2 - x_1} \int_{x_1}^{x_2} \ln K_c dZ_B \qquad \text{(Eq. 3)}$$

Table II—Total Charge and Charge Density of the Ammonium Group of the Organic Cations [a]

	$-NH_xR_{(3-x)}$	$\sum_i$ (Charge/Volume)$_i$
$PhCH_2CH(CH_3)NH_3^+$	0.6239	0.1166
$PhCH_2C(CH_3)_2NH_3^+$	0.5994	0.1127
$PhCH_2C(CH_3)_2NH_2CH_3^+$	0.6300	0.0765
$PhCOCH(CH_3)NH(C_2H_5)_2^+$	0.7217	0.0494
$HO—CH_2—CH_2—N(CH_3)_3^+$	0.7506	0.0252

[a] Obtained from CNDO/2 calculations.

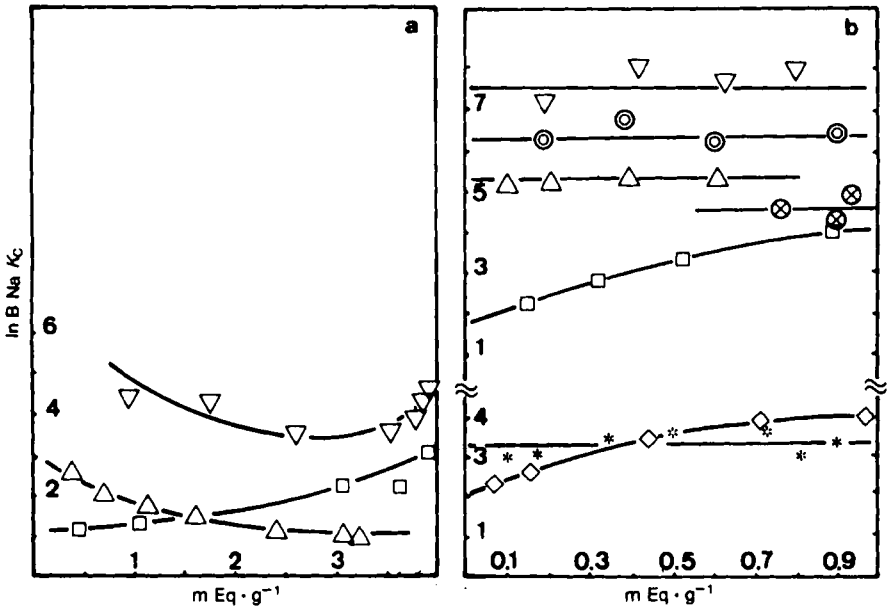

Figure 6—*Surface composition dependence of the selectivity coefficient for the exchange of Na by organic cation B at 25°C on (a) lewatite: phentermine (□), diethylpropion (△), and imazalil (▽) and, (b) bentonite: choline (*), d-amphetamine (◇), phentermine (□); mephentermine (⊗), diethylpropion (△), levamisole (◎), and imazalil (▽).*

The lower limit is necessary for the inaccuracy of the measurements at very small loadings, and the upper limit eliminates the excess adsorption. The mean selectivity coefficients are given in Table I. The data show that the organic cations are more strongly adsorbed on bentonite than on lewatite.

The selectivity order on bentonite was found to be: choline < amphetamine < phentermine < mephentermine < diethylpropion < levamisole < imazalil. This selectivity order is explained by the charge delocalization principle, which is also operative in the case of alkylammonium ions (9–11), histammonium, and ethyldiammonium ions (12). This principle states that selectivity increases with the increasing delocalization of the positive charge over a molecule.

We have calculated the charge on the N and the groups directly attached to it by CNDO/2 (13). This charge divided by the van der Waals volume is a measure of the charge density, as shown in Table II. Figure 7 shows that there is a linear correlation between the charge density and the average exchange selectivity coefficient of the organic cations investigated. There is a deviation for choline, but this is probably due to the absence of a phenyl ring.

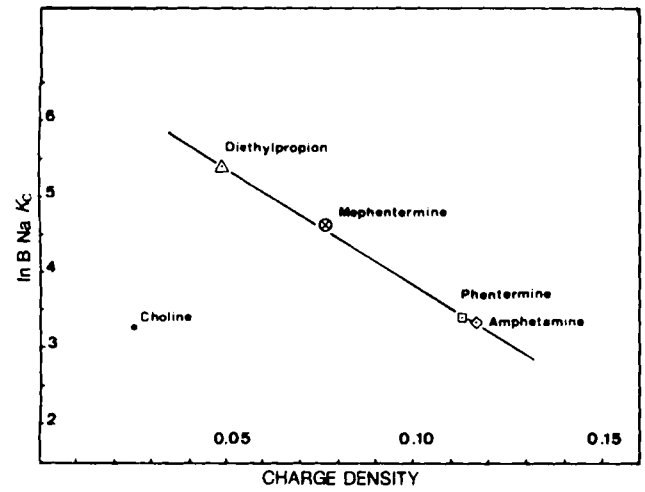

Figure 7—*The selectivity coefficient of exchange as a function of the charge density of the ammonium group.*

REFERENCES

(1) R. E. Notari, "Biopharmaceutics and Pharmokinetics," 2nd ed., Dekker, New York, N.Y., 1975, p. 276.

(2) J. W. McGinity and J. L. Lach, *J. Pharm. Sci.*, **66**, 63 (1977).

(3) L. S. Porubcan, C. J. Serna, J. L. White, and S. L. Hem, *J. Pharm. Sci.*, **67**, 1081 (1978).

(4) M. Sanchez Camazano, M. J. Sanchez, M. T. Vicente, and A. Dominguez-Gil, *J. Pharm. Sci.*, **69**, 1142 (1980).

(5) J. H. Quisenberry, *Clays and Clay Miner.*, **16**, 267 (1968).

(6) L. G. J. De Leede, R. J. V. D. Broek, M. F. H. Zee, and C. J. De Blaey, *Pharm. Weekbl., Sci. Ed., I* **114**, 196 (1979).

(7) R. E. Grimm, "Clay Mineralogy," McGraw-Hill, New York, N.Y , 1968, p. 596.

(8) G. L. Gaines and H. C. Thomas, *J. Chem. Phys.*, **21**, 714 (1953).

(9) A. Maes, L. Van Leemput, A. Cremers, and J. B. Uytterhoeven, *J. Colloid and Interface Sci.*, **77**, 14 (1980).

(10) B. K. G. Theng, D. J. Greenland, and J. P. Quirk, *Clay Miner.*, **7**, 1 (1967).

(11) E. F. Vansant and J. B. Uytterhoeven, *Clays and Clay Miner.*, **20**, 47 (1972).

(12) A. Maes, P. Marijnen, and A. Cremers, *Progr. Colloid and Polymer Sci.*, **65**, 245 (1978).

(13) J. A. Pople and D. L. Beveridge, "Approximate Molecular Orbital Theory," McGraw-Hill, New York, N.Y. 1970, p. 214.

ACKNOWLEDGMENTS

The authors are indebted to the Belgian Government (Programmatie van het Wetenschapsbeleid) for financial support. Discussions with Prof. R. Kinget, Dr. A. Maes, W. Mortier (K. U. Leuven), G. Logghe (State University Ghent), and technical assistance from Mrs. L. Leplat, are appreciated.

Pharmacokinetics and Bioavailability of Ranitidine in Humans

RAYMOND MILLER

Received March 4, 1983, from the *Department of Pharmacology, University of Potchefstroom for CHE, Potchefstroom 2520, South Africa.* Accepted for publication October 5, 1983. Present address: Department of Pharmacology, University of Durban-Westville, Private Bag X54001, Durban 4000, South Africa.

Abstract □ Ranitidine produces a blood concentration curve with a pronounced secondary peak when administered orally and parenterally. A pharmacokinetic model is proposed to describe this reabsorption phenomenon. The choice of a discontinuous cyclic transfer was justified on the basis of physiological considerations and the good agreement with data from oral and intravenous administration. It is proposed that ranitidine accumulates mainly from the systemic circulation into a depot from which drug and bioreversible drug are spontaneously released in response to food intake. The evaluation of the extent of the first-pass effect and the evaluation of bioequivalency are complicated by the model-independent AUC approach because the area under the concentration *versus* time curve (AUC) is dependent on the extent of recycling and thus does not properly reflect the extent of primary absorption. By using intravenous administration as a reference dosage form and the integrated form of the regression equations to calculate the AUC values, the bioavailability of the oral dose was found to be 0.56, which corresponds well with the value of 0.58 obtained by linear-log-linear integration. The least-squares parameter estimate of the primary absorption is 0.43.

Keyphrases □ Pharmacokinetics—bioavailability, ranitidine, humans □ Bioavailability—pharmacokinetics of ranitidine, humans □ Ranitidine—pharmacokinetics, bioavailability, humans

Evidence suggests that ranitidine, a new H_2-receptor antagonist, is at least five times more potent (on a molar basis) than cimetidine in inhibiting gastric acid secretion (1–3). Ranitidine shows unusual pharmacokinetic behavior by producing a significant secondary peak in the drug concentration profile after both oral dosing on a fasting stomach and intravenous administration (4). Cimetidine displays similar pharmacokinetic behavior after oral dosing on a fasting stomach but not after intravenous administration (5–7). Previous workers have concluded that a model requiring two exponential terms did not adequately describe ranitidine plasma level data after oral or intravenous administration (4). It is the purpose of this study to evaluate the pharmacokinetics of ranitidine with the data of Woodings *et al.* (4)[1]. It is proposed that ranitidine pharmacokinetics can be described by a two-compartment model and that the secondary peaks observed in the plasma level data can be described best in terms of discontinuous reabsorption.

EXPERIMENTAL SECTION

Theory—The proposed model (Scheme I) encompasses the kinetics of ranitidine after oral and intravenous administration (8). After oral administration, the drug is presented into the gut, the absorption compartment (G), from which a fraction (F_{G1}) of the dose (D) is absorbed by a first-order process into the central compartment (1) from which samples may be obtained. The remaining fraction ($1 - F_{G1}$) of the drug passes into compartment B in the first-pass transfer process. No assumptions are made about the type of transfer process from G to B because the kinetic behavior of the system does not depend on the rate of input into B but only on the amount of drug in B at the time that recycling takes place. At this time (t_B), a fraction (F_B) of the drug accumulated in B is spontaneously released into the absorption compartment. The drug is eliminated from the central compartment and transferred into compartment B and a peripheral compartment (2) by first-order processes. After intravenous administration, the same model applies, except that the input is a bolus input into the central compartment.

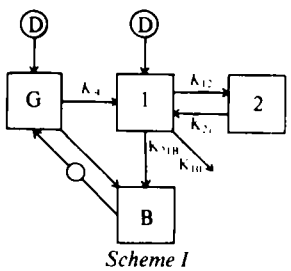

Scheme I

The choice of a discontinuous cyclic transfer process in the model is based on theoretical as well as simulation studies, which indicate that secondary peaks cannot be obtained from linear compartmental systems with continuous cyclic transfer processes (9, 10).

Data Treatment—By using the nonlinear regression program NONLIN (11), the equations describing this model (8) were fitted simultaneously by nonlinear least-squares regression to the intravenous and oral data for each of the six subjects at each dosage level. The data set for subject 1 (dose, 80 mg) was excluded from analysis since intravenous data were not available. The blood sample obtained 2 min after intravenous administration was excluded

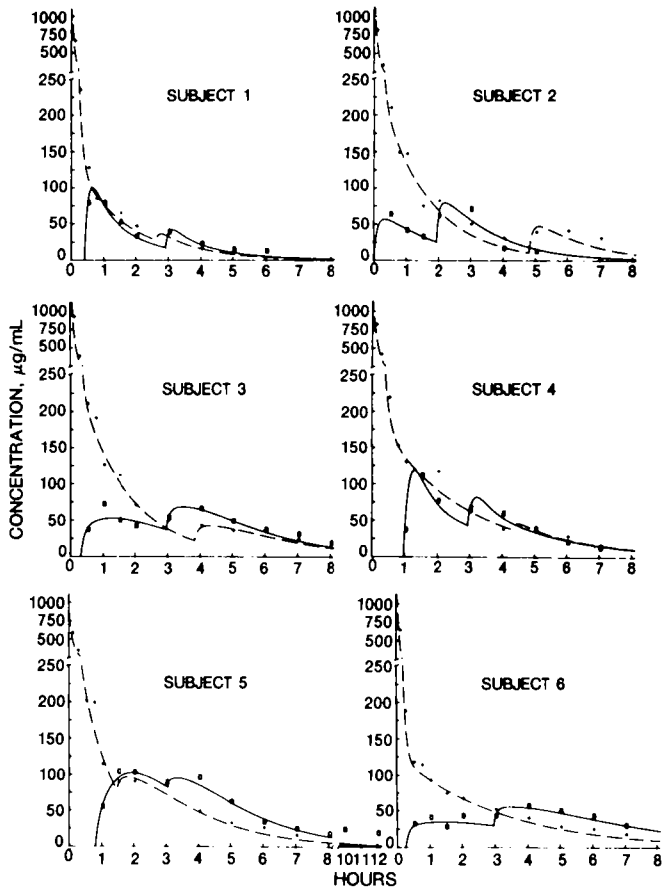

Figure 1—*Simultaneous least-squares fit of appropriate equations (8) for the pharmacokinetic model* (Scheme I) *to ranitidine data from oral (——) and intravenous (- - -) administrations of 20 mg of ranitidine.*

[1] Glaxo-Allenbury's Research (Ware) Ltd., personal communication.

0022-3549/84/1000-1376$01.00/0
© 1984, American Pharmaceutical Association

Table I—Least-Squares Parameter Estimates

Parameter	Subject (Dose, mg)																		
	1(20)	1(40)	2(20)	2(40)	2(80)	3(20)	3(40)	3(80)	4(20)	4(40)	4(80)	5(20)	5(40)	5(80)	6(20)	6(40)	6(80)	Mean	*CV*, %
t_L, h	0.40	0.98	0.00	0.00	0.00	0.31	0.38	0.40	0.97	0.33	0.41	0.81	0.00	0.00	0.27	0.00	0.49	0.34	98
t_B (i.v.), h	2.61	3.90	4.80	2.72	3.81	3.82	3.03	1.30	4.27	0.52	1.36	1.46	1.55	3.95	0.37	1.92	0.50	2.46	59
t_B (p.o.), h	2.91	3.00	1.93	3.98	1.49	2.94	2.67	2.03	2.93	1.32	1.48	2.98	1.26	1.45	2.96	2.88	2.86	2.42	33
k_A, h^{-1}	2.44	1.76	1.82	0.64	1.00	0.65	0.52	0.33	2.45	0.59	0.38	0.56	0.95	2.99	0.61	0.35	0.38	1.08	80
k_{12}, h^{-1}	4.45	6.01	5.82	2.95	4.29	5.54	8.88	2.93	3.54	18.75	5.70	4.22	2.07	5.89	8.13	3.17	6.66	5.82	65
k_{21}, h^{-1}	1.62	2.13	2.31	1.57	1.18	2.18	1.53	2.22	1.35	2.89	4.12	4.63	1.58	1.91	1.37	1.21	2.58	2.14	46
k_{1B}, h^{-1}	3.49	1.40	1.68	2.14	4.81	2.56	1.65	11.32	0.92	21.46	14.62	11.94	3.70	4.30	0.20	20.30	13.31	7.05	99
k_{el}, h^{-1}	3.45	2.57	2.99	2.16	2.90	3.09	3.22	2.57	1.80	11.10	4.28	2.24	1.09	2.02	2.91	3.01	3.25	3.21	67
F_{GI}	0.43	0.40	0.23	0.77	0.16	0.36	0.26	0.42	0.38	0.28	0.65	0.93	0.42	0.32	0.39	0.33	0.62	0.43	46
F_B (i.v.)	0.06	0.23	0.29	0.25	0.04	0.25	0.27	0.20	0.08	0.39	0.19	0.12	0.01	0.17	0.01	0.04	0.39	0.18	71
F_B (p.o.)	0.13	0.25	0.28	0.27	0.20	0.33	0.21	0.16	0.19	0.25	0.63	0.10	0.54	0.21	0.55	0.29	0.26	0.29	53
V, L	16.8	19.2	12.9	29.2	12.9	11.5	8.9	20.1	16.4	3.3	11.7	22.4	36.2	22.0	13.6	20.2	18.4	17.4	44

from data analysis since at this time the drug was apparently not completely mixed in the blood. The intravenous data were, therefore, treated as a bolus administration with plasma concentrations obtained after 5 min.

RESULTS

All estimated microparameters are common for the functions describing the intravenous and oral data except for the time t_B and the fraction F_{BI} of drug release from B (Table I). The results are summarized in Tables I and II and Figs. 1–3. The conventional two-compartment model (12) fitted to the data in the same way as described above performed consistently poorer, as judged by the information criterion of Akaike (13).

The secondary peak in the plasma concentration–time curves after ranitidine administration (Figs. 1–3) appears to be due to a rapid release of ranitidine from a drug depot. The bile and hepatic parenchymal tissues are the most likely primary storage areas (14–16). The time for the release appears to coincide with the intake of food in most cases and is intermediate between the time when free fluids were permitted, 2 h after administration of ranitidine, and the time when a light lunch was provided, 3 h after administration[1]. The mean value of t_B after intravenous administration is 2.5 h, and after oral administration is 2.4 h (Table I).

The transfer of drug into the depot occurs after both oral and intravenous administration of ranitidine since a pronounced secondary peak can be observed after either form of administration. Cimetidine, on the other hand, shows a pronounced secondary peak only after oral administration (5–7). The transfer rate of cimetidine into the depot from the systemic circulation is slow compared with the first-pass transfer (8). The transfer of ranitidine into the depot, however, appears to be mainly from the systemic circulation. The mean transfer of ranitidine from the systemic circulation into the depot is 7.05 h^{-1} (Table I), which is 19 times more rapid than that of cimetidine (0.37 h^{-1}), as determined in a different group of subjects using the same model as in Scheme I (8). The area under the concentration *versus* time curve (AUC) due to ranitidine recycling was calculated by integrating the second half of the regression equations (8). The mean AUC due to recycling, normalized for dose, after intravenous and oral administration is 5.33 $ng \cdot mL^{-1} \cdot h^{-1} \cdot mg^{-1}$ (*CV* 86%) and 6.03 $ng \cdot mL^{-1} \cdot h^{-1} \cdot mg^{-1}$ (*CV*, 44%), respectively. The larger AUC after oral administration may indicate that a certain amount of ranitidine is transferred to the depot during the first-pass transfer. The difference, however, is not statistically significant.

DISCUSSION

The pharmacokinetic model proposed (Scheme I) is a highly simplified functional model constructed according to the given interpretation. The B compartment represents the depot of the drug that is partly released, (F_B) at some time (t_B) soon after or during a meal or spontaneously before a meal. Spontaneous contractions of the gallbladder have been shown to occur in the fasting stage (17). The secondary peak in the plasma concentration–time curves after ranitidine administration (Figs. 1–3) could be explained by enterohepatic circulation of ranitidine, but no information with respect to concentrations of ranitidine in bile is presently available in humans. Biliary accumulation studies in anesthetized rats showed that, in this species, up to 17% of an intravenous dose was excreted in the bile during 4–5 h (14). The model appears to agree well with the data (Figs. 1–3) and shows that the transfer of the drug into compartment B from systemic circulation (1 to B) is primarily responsible for the accumulation of the drug in B, whereas the transfer of the drug into B in the first pass (G to B) only plays a minor role (Figs. 1–3, Table I). Secondary peaks are evident but not pronounced if ranitidine is taken with food (18). The excretion of bile in response to food may play a role if the smaller amount of bile in the hepatic system reduces the uptake rate or capacity of the system.

An interesting aspect of the recycling phenomenon is its influence on the AUC values and the interpretation of bioavailability. The ratio between AUC values cannot be used as a relative measure of the extent of the drug absorption since the AUC is dependent on the extent of recycling. The AUC, therefore, does not properly reflect the extent of primary absorption (F_{GI}). By using the intravenous administration as a reference dosage form and the integrated form of the regression equations to calculate the AUC values, the bioavailability (F) of the oral dosage was 0.56 (Table II). The value obtained by linear trapezoidal integration is 0.49 (4). The linear trapezoidal method is particularly suitable when area estimates are to be compared among data which have similar shapes and sampling schemes; however, in cases in which changes in curvature between data points are excessive or there are long intervals between data points, large algorithm errors are known to occur (11, 19). No single numerical integration procedure presently available can be used to achieve maximal accuracy over all regions of the plasma concentration *versus* time curve. The best approach at present appears to be the use of the spline method during the absorption phase followed by the log-linear trapezoidal method

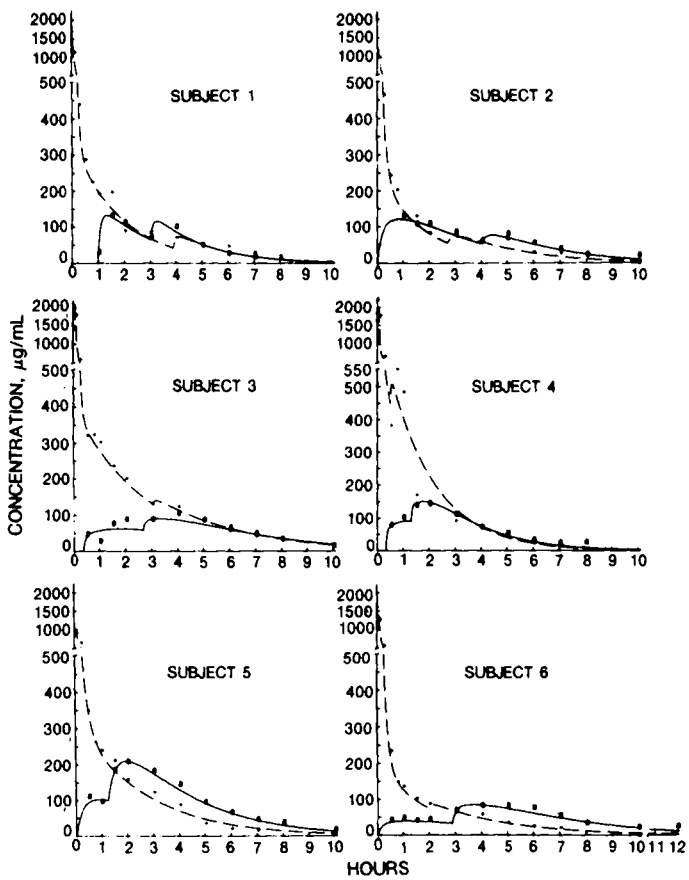

Figure 2—*Simultaneus least-squares fit of appropriate equations (8) for the pharmacokineteic model* (Scheme I) *to ranitidine data from oral (——) and intravenous (- - -) administrations of 40 mg of ranitidine.*

Table II—Pharmacokinetic Parameters

Parameter	Subject (Dose, mg)																	Mean	*CV*, %
	1(20)	1(40)	2(20)	2(40)	2(80)	3(20)	3(40)	3(80)	4(20)	4(40)	4(80)	5(20)	5(40)	5(80)	6(20)	6(40)	6(80)		
$t_{1/2}$, h	1.1	1.29	1.05	1.26	1.61	1.05	1.87	0.83	1.82	0.69	0.50	0.67	1.73	1.69	2.1	1.3	0.98	1.27	37
Vd_{ss}, L	63.2	73.7	45.5	84.0	59.7	40.7	60.4	46.5	59.6	24.7	27.8	42.7	83.7	89.9	94.2	73.1	66.0	60.9	34
AUC (i.v.), ng·h/mL	361.6	897.5	598.9	763.5	2274.7	674.6	1538.6	2608.6	701.0	1591.4	2267.7	610.1	1030.1	2332.6	505.7	782.6	2323.0	—[c]	—[c]
AUC (po), ng·h/mL	188.8	471.8	243.8	627.3	747.6	358.6	603.8	907.8	353.8	548.2	1686.2	478.9	948.0	948.6	369.8	543.8	1305.4	—[c]	—[c]
D (i.v.)/AUC (i.v.), L/h	55.3	44.6	33.4	52.4	35.2	29.6	26.0	30.7	28.5	25.1	35.2	32.8	38.8	34.3	39.5	51.1	34.4	36.9	25
D (i.v.)/AUC$_t$, L/L[a]	58.1	49.6	38.7	63.2	37.3	35.4	28.6	51.4	29.5	36.6	53.9	50.0	39.4	44.5	39.6	60.7	59.9	45.7	24
D_t/AUC (po), L/h[b]	58.2	49.5	38.5	62.9	37.4	35.1	28.1	51.8	29.3	36.1	54.2	49.6	39.2	44.7	39.6	60.4	60.2	45.6	25
Vk_{et}, L/h	58.0	49.3	38.6	63.1	37.4	35.5	28.7	51.7	29.5	36.6	50.1	50.2	39.5	44.4	39.6	60.8	59.8	45.5	24
AUC (po)/AUC (i.v.)	0.52	0.53	0.41	0.82	0.33	0.53	0.39	0.35	0.50	0.34	0.74	0.78	0.92	0.41	0.73	0.69	0.56	0.56	33
D_t/D (po)[b]	0.55	0.58	0.47	0.99	0.35	0.63	0.42	0.59	0.52	0.49	1.14	1.19	0.93	0.53	0.73	0.82	0.98	0.70	37

[a] AUC_t = AUC (i.v.) − $AUC_{(B)}$ where $AUC_{(B)}$ = area under curve resulting from recycling. [b] $D_t = FD(po) + F_BD_B(po)$. [c] The mean value is only applicable if normalized for dose.

during the elimination phase (20). However, since the computer program for the spline method is not generally available, the use of the linear trapezoidal method during the absorption phase and the log-linear trapezoidal method in the postabsorption phase is the most logical general approach. The linear-log-linear trapezoidal combination has the advantage that it is simple to apply and yields very acceptable results (21).

The AUC after intravenous and oral administration was calculated by the linear trapezoidal method for the ascending portions of the curve, whereas the log-linear trapezoidal method was used during the descending parts of the curve. The AUC was extrapolated to infinity by using the least-squares-fitted terminal log-linear slope. The model-independent bioavailability of 0.58 (*CV* 35%) thus calculated corresponds very well to the value of 0.56 calculated from the model-dependent integrated form of the regression equations (Table II).

It is evident that in the presence of recycling it is not possible to calculate F_{G1} by a model-independent approach. With the present model, F_{G1} can be determined by the nonlinear least-squares regression to the intravenous and oral data. The mean value of 0.43 (Table I) corresponds well with the extent of cimetidine primary absorption of 0.45 (8). The AUC is still a useful parameter since, physiologically and pharmacologically, it is a more meaningful parameter than one which measures the extent of primary absorption. The extent of recycled drug, however, plays a large and varying role in the determination of total bioavailability. Those times at which accumulation of drug in the recycling compartment is mainly due to the first-pass effect the secondary peak would usually be observed mainly after oral administration, as is the case for cimetidine (4). Bioavailability calculated by using the AUC after intravenous administration as a reference, therefore, varies, depending on the extent of recycling after intravenous and oral administration. F may appear to be smaller than F_{G1} if recycling after intravenous administration is greater, similar to F_{G1} if the extent of recycling is similar after intravenous and oral administration, and greater than F_{G1} if the extent of recycling after oral administration is greater. This phenomenon can be illustrated by comparing F (Table II) and F_{G1} (Table I) in subject 5. After the 40-mg dose, the secondary peak was negligible after intravenous administration and relatively large after oral administration (Fig. 2). This is reflected by a relatively large F of 0.92, as compared with the F_{G1} of 0.42. After the 80-mg dose, the secondary peaks appear to be equally large after intravenous and oral administration (Fig. 3). This is reflected by a value for F of 0.41 which is still larger than but very similar to the F_{G1} of 0.32. After the 20-mg dose, the secondary peaks after intravenous and oral administration are not very extensive and appear to be similar. The value of 0.78 for F, however, is now smaller than 0.93 for F_{G1}, which reflects more extensive recycling after intravenous administration. For ranitidine, F is generally larger than F_{G1}, except for subject 3 (80-mg dose), subject 5 (20-mg dose), and subject 6 (80-mg dose) in which the opposite is true (Tables I and II). The bioavailability of ranitidine (0.56) is lower than that of cimetidine (0.61), although the extent of primary absorption is very similar (8). This may simply be an artifact of the method of calculating bioavailability, since the greater AUC after intravenous administration of ranitidine due to recycling may artificially reduce this value.

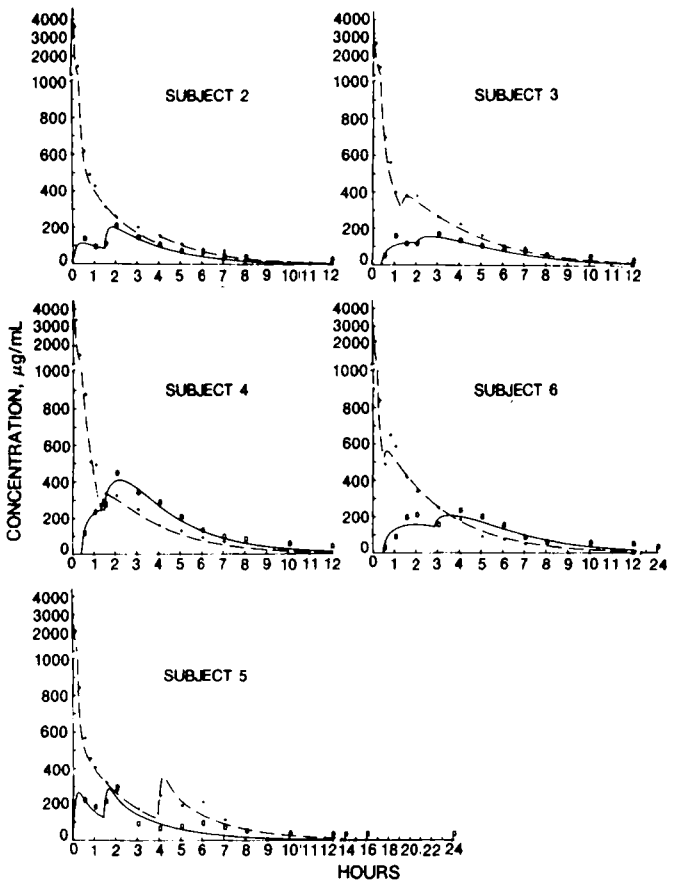

Figure 3—*Simultaneous least-squares fit of appropriate equations (8) for the pharmacokinetic model* (Scheme I) *to ranitidine data from oral (——) and intravenous (- - -) administrations of 80 mg of ranitidine.*

Ranitidine clearance, calculated as the ratio of the dose to AUC after intravenous administration, is 36.9 L/h (Table II), which is similar to cimetidine clearance, which is 35.5 L/h (8). If the AUC is corrected for recycling, the clearance of ranitidine is 45.7 L/h (Table II). Recycling of ranitidine, therefore, apparently decreases the clearance of ranitidine by ~20%. The lower clearance parameter is pharmacokinetically more meaningful and relates to the average plasma concentration attained with any particular dose.

The major difference in the pharmacokinetics of ranitidine and cimetidine appears to be that recycled ranitidine is accumulated mainly from the systemic circulation, whereas accumulation of cimetidine takes place mainly during first-pass transfer. This may be due to high affinity of ranitidine from the systemic circulation for bile. The secondary peak, however, does not seem to be present when cimetidine is taken orally with food (22), and the same phenomenon may occur after intravenous administration. The excretion of bile in response to food may play a role if the smaller amount of bile in the hepatic system reduces the uptake rate or capacity of the system. In this case, neglecting to adhere strictly to the oral administration fasting protocol when administering the drug intravenously could result in secondary peaks that are greatly reduced or absent. Under these circumstances, the assumption that cimetidine is accumulated mainly during the first-pass transfer would not be valid. To avoid any ambiguity, the identical protocol should be followed when the drug is administered extravascularly and intravascularly. In any event, this difference, whether real or spurious, would probably not account for the large difference in potency.

GLOSSARY

AUC = $\int_0^\infty C dt$

B = drug depot compartment

C = blood cimetidine concentration

D = dose
$D_B = X_B + (1 - F_{G1})D$
$D_T = F_{G1}D + F_BD_B$, the apparent amount of the dose absorbed
F = AUC_{po}/AUC_{iv}, the apparent fraction of the dose absorbed
F_B = fraction of drug accumulated in B that is released to G at time $t = t_B$
F_{G1} = fraction of D absorbed by first-order absorption into the central compartment
$1 - F_{G1}$ = fraction of D transferred from G to B
G = compartment from which absorption takes place
K_{ZZ} = first-order transfer rate constants
t = time
t_L = lag time
t_B = time when a part (F_BD_B) of the drug accumulated in B is released to G
Vd = volume of distribution
X_B = amount of drug transferred from compartment 1 to compartment B at time $t = t_B$

REFERENCES

(1) T. Bohman, J. Myren, O. Flaten, and E. Schrumpf, *Scand. J. Gastroenterol.*, **15**, 177 (1980).

(2) T. Bohman, J. Myren, and S. Larsen, *Scand. J. Gastroenterol.*, **15**, 183 (1980).

(3) N. R. Peden, J. H. B. Saunders, and K. G. Wormsley, *Lancet*, **i**, 690 (1979).

(4) E. F. Woodings, G. T. Dixon, C. Harrison, P. Carey, and D. A. Richards, *Gut*, **21**, 187 (1980).

(5) R. Griffiths, R. M. Lee, and D. C. Taylor, in "Proceedings of the Second and International Symposium on Histamine H_2-Receptor Antagonists," Excerpta Medica, Amsterdam, The Netherlands, 1977, p. 38.

(6) R. H. Henn, J. I. Isenberg, V. Maxwell, and R. A. L. Sturdevant, *N. Engl. J. Med.*, **293**, 371 (1975).

(7) S. S. Walkenstein, J. W. Dubb, W. C. Randolph, W. J. Westlake, R. M. Stote, and A. P. Intoccia, *Gastroenterology*, **74**, 360 (1978).

(8) P. Veng-Pedersen and R. Miller, *J. Pharm. Sci.*, **69**, 394 (1980).

(9) C. D. Theron, *Bull. Math. Biophys.*, **34**, 277 (1972).

(10) P. Veng-Pedersen and R. Miller, *J. Pharm. Sci.*, **69**, 204 (1980).

(11) C. M. Metzler, G. L. Elfring, and A. J. McEwan, "A Users Manual for NONLIN and Associated Programs," The Upjohn Co., Kalamazoo, Mich., 1974.

(12) J. G. Wagner, "Fundamentals of Clinical Pharmacokinetics," Hamilton Press, Inc., Hamilton, Ill., 1975, p. 82.

(13) H. Akaike, *Math. Sci.*, **14**, 5 (1976).

(14) J. A. Bell, F. A. A. Dallas, W. N. Jenner, and L. E. Martin, *Biochem. Soc. Trans.*, **8**, 93 (1980).

(15) R. Bine, M. Friedman, S. O. Byers, and C. Bland, *Circulation*, **4**, 105 (1951).

(16) R. W. Brauer and R. L. Pesotti, *Am. J. Physiol.*, **162**, 565 (1950).

(17) E. A. Boyden, *Anat. Rec.*, **40**, 147 (1928).

(18) M. L. McFadyen, P. I. Folb, I. N. Marks, J. P. Wright, and W. Lucke, *Scand. J. Gastroenterol.*, **69** (Suppl.) 109 (1981).

(19) W. L. Chiou, *J. Pharmacokinet. Biopharm.*, **6**, 539 (1978).

(20) K. C. Yeh and K. C. Kwan, *J. Pharmacokinet. Biopharm.*, **6**, 79 (1978).

(21) R. A. Upton, J.-F. Thiercelin, T. W. Guentert, L. Sansom, J. R. Powell, P. E. Coates, and S. Riegelman, *J. Pharmacokinet. Biopharm.*, **8**, 131 (1980).

(22) G. Bodemar, B. Norlander, L. Fransson, and A. Walan, *Br. J. Clin. Pharmacol.*, **7**, 22 (1979).

ACKNOWLEDGMENTS

This work was supported by the South African Research Council.

Dose-Dependent Pharmacokinetic Study of Pefloxacin, A New Antibacterial Agent, in Humans

J. BARRE, G. HOUIN, and J. P. TILLEMENT ˣ

Received June 29, 1983 from the *Laboratoire de Biochimie I et de Pharmacologie, Centre Hospitalier Intercommunal de Créteil, 94010 Créteil Cedex, France.* Accepted for publication September 26, 1983.

Abstract □ A dose-dependent pharmacokinetic study of pefloxacin was performed after four intravenous infusions and four orally administered doses. After intravenous infusion, the pharmacokinetic profiles of the plasma concentrations showed a biphasic decline, with half-lives (mean ± *SD*) of 8.55 ± 4.20 min and 11.50 ± 1.75 h, respectively. Intravenous infusion and oral administration yielded similar results. The pharmacokinetic parameters remained constant in the dose range of 200–800 mg from the plasma and urine data.

Keyphrases □ Pharmacokinetics—dose-dependent, pefloxacin, new antibacterial agent □ Pefloxacin—new antibacterial agent, dose-dependent pharmacokinetics □ Antibacterial agent—dose-dependent pharmacokinetics of pefloxacin

Pefloxacin[1], 1-ethyl-6-fluoro-1,4-dihydro-7-(4-methyl-1-piperazinyl)-4-oxo-3-quinolinecarboxylic acid (I), is a new antibacterial compound shown to be highly active against both Gram-negative and Gram-positive bacteria (1, 2). A large percentage (85%) of the drug administered is transformed into several metabolites, the *N*-oxide, the demethyl, and the oxodemethyl analogues (3). Since the pharmacokinetic data for this drug have not been reported in humans, a preliminary study was performed to investigate the plasma and urine profiles of pefloxacin in a dose-dependency study in humans.

EXPERIMENTAL SECTION

Materials—Pefloxacin and its 6-chloro analogue[1] (II) (the internal standard) showed no impurities in two different TLC systems. All reagents were commercially available analytical grades and used without further purification.

Pefloxacin Analysis—Unchanged pefloxacin in plasma or urine was measured by HPLC (3) using a liquid chromatograph[2] equipped with a UV spectrophotometer (280 nm) and a continuous flow cell with an 8-μL capacity. A 200-mm steel column was used, packed with a monomolecular layer of octadecyltrichlorosilane chemically bonded to silica beads with an average particle size of 7 μm[3].

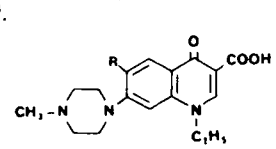

I: R = F
II: R = Cl

[1] Roger Bellon Laboratories, Alfortville, France.

[2] Waters Associates, Paris, France.

[3] Lichrosorb RP-18; Merck, Paris, France.

0022-3549/84/1000-1379$01.00/0

© 1984, American Pharmaceutical Association

D = dose
$D_B = X_B + (1 - F_{G1})D$
$D_T = F_{G1}D + F_BD_B$, the apparent amount of the dose absorbed
F = AUC_{po}/AUC_{iv}, the apparent fraction of the dose absorbed
F_B = fraction of drug accumulated in B that is released to G at time $t = t_B$
F_{G1} = fraction of D absorbed by first-order absorption into the central compartment
$1 - F_{G1}$ = fraction of D transferred from G to B
G = compartment from which absorption takes place
K_{ZZ} = first-order transfer rate constants
t = time
t_L = lag time
t_B = time when a part (F_BD_B) of the drug accumulated in B is released to G
Vd = volume of distribution
X_B = amount of drug transferred from compartment 1 to compartment B at time $t = t_B$

REFERENCES

(1) T. Bohman, J. Myren, O. Flaten, and E. Schrumpf, *Scand. J. Gastroenterol.*, **15**, 177 (1980).

(2) T. Bohman, J. Myren, and S. Larsen, *Scand. J. Gastroenterol.*, **15**, 183 (1980).

(3) N. R. Peden, J. H. B. Saunders, and K. G. Wormsley, *Lancet*, **i**, 690 (1979).

(4) E. F. Woodings, G. T. Dixon, C. Harrison, P. Carey, and D. A. Richards, *Gut*, **21**, 187 (1980).

(5) R. Griffiths, R. M. Lee, and D. C. Taylor, in "Proceedings of the Second and International Symposium on Histamine H_2-Receptor Antagonists," Excerpta Medica, Amsterdam, The Netherlands, 1977, p. 38.

(6) R. H. Henn, J. I. Isenberg, V. Maxwell, and R. A. L. Sturdevant, *N. Engl. J. Med.*, **293**, 371 (1975).

(7) S. S. Walkenstein, J. W. Dubb, W. C. Randolph, W. J. Westlake, R. M. Stote, and A. P. Intoccia, *Gastroenterology*, **74**, 360 (1978).

(8) P. Veng-Pedersen and R. Miller, *J. Pharm. Sci.*, **69**, 394 (1980).

(9) C. D. Theron, *Bull. Math. Biophys.*, **34**, 277 (1972).

(10) P. Veng-Pedersen and R. Miller, *J. Pharm. Sci.*, **69**, 204 (1980).

(11) C. M. Metzler, G. L. Elfring, and A. J. McEwan, "A Users Manual for NONLIN and Associated Programs," The Upjohn Co., Kalamazoo, Mich., 1974.

(12) J. G. Wagner, "Fundamentals of Clinical Pharmacokinetics," Hamilton Press, Inc., Hamilton, Ill., 1975, p. 82.

(13) H. Akaike, *Math. Sci.*, **14**, 5 (1976).

(14) J. A. Bell, F. A. A. Dallas, W. N. Jenner, and L. E. Martin, *Biochem. Soc. Trans.*, **8**, 93 (1980).

(15) R. Bine, M. Friedman, S. O. Byers, and C. Bland, *Circulation*, **4**, 105 (1951).

(16) R. W. Brauer and R. L. Pesotti, *Am. J. Physiol.*, **162**, 565 (1950).

(17) E. A. Boyden, *Anat. Rec.*, **40**, 147 (1928).

(18) M. L. McFadyen, P. I. Folb, I. N. Marks, J. P. Wright, and W. Lucke, *Scand. J. Gastroenterol.*, **69** (Suppl.) 109 (1981).

(19) W. L. Chiou, *J. Pharmacokinet. Biopharm.*, **6**, 539 (1978).

(20) K. C. Yeh and K. C. Kwan, *J. Pharmacokinet. Biopharm.*, **6**, 79 (1978).

(21) R. A. Upton, J.-F. Thiercelin, T. W. Guentert, L. Sansom, J. R. Powell, P. E. Coates, and S. Riegelman, *J. Pharmacokinet. Biopharm.*, **8**, 131 (1980).

(22) G. Bodemar, B. Norlander, L. Fransson, and A. Walan, *Br. J. Clin. Pharmacol.*, **7**, 22 (1979).

ACKNOWLEDGMENTS

This work was supported by the South African Research Council.

Dose-Dependent Pharmacokinetic Study of Pefloxacin, A New Antibacterial Agent, in Humans

J. BARRE, G. HOUIN, and J. P. TILLEMENT ˣ

Received June 29, 1983 from the *Laboratoire de Biochimie I et de Pharmacologie, Centre Hospitalier Intercommunal de Créteil, 94010 Créteil Cedex, France.* Accepted for publication September 26, 1983.

Abstract □ A dose-dependent pharmacokinetic study of pefloxacin was performed after four intravenous infusions and four orally administered doses. After intravenous infusion, the pharmacokinetic profiles of the plasma concentrations showed a biphasic decline, with half-lives (mean ± *SD*) of 8.55 ± 4.20 min and 11.50 ± 1.75 h, respectively. Intravenous infusion and oral administration yielded similar results. The pharmacokinetic parameters remained constant in the dose range of 200–800 mg from the plasma and urine data.

Keyphrases □ Pharmacokinetics—dose-dependent, pefloxacin, new antibacterial agent □ Pefloxacin—new antibacterial agent, dose-dependent pharmacokinetics □ Antibacterial agent—dose-dependent pharmacokinetics of pefloxacin

Pefloxacin[1], 1-ethyl-6-fluoro-1,4-dihydro-7-(4-methyl-1-piperazinyl)-4-oxo-3-quinolinecarboxylic acid (I), is a new antibacterial compound shown to be highly active against both Gram-negative and Gram-positive bacteria (1, 2). A large percentage (85%) of the drug administered is transformed into several metabolites, the *N*-oxide, the demethyl, and the oxodemethyl analogues (3). Since the pharmacokinetic data for this drug have not been reported in humans, a preliminary study was performed to investigate the plasma and urine profiles of pefloxacin in a dose-dependency study in humans.

EXPERIMENTAL SECTION

Materials—Pefloxacin and its 6-chloro analogue[1] (II) (the internal standard) showed no impurities in two different TLC systems. All reagents were commercially available analytical grades and used without further purification.

Pefloxacin Analysis—Unchanged pefloxacin in plasma or urine was measured by HPLC (3) using a liquid chromatograph[2] equipped with a UV spectrophotometer (280 nm) and a continuous flow cell with an 8-μL capacity. A 200-mm steel column was used, packed with a monomolecular layer of octadecyltrichlorosilane chemically bonded to silica beads with an average particle size of 7 μm[3].

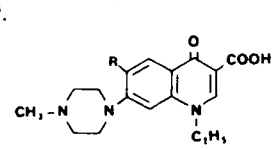

I: R = F
II: R = Cl

[1] Roger Bellon Laboratories, Alfortville, France.

[2] Waters Associates, Paris, France.

[3] Lichrosorb RP-18; Merck, Paris, France.

0022-3549/84/1000-1379$01.00/0

© 1984, American Pharmaceutical Association

Table I—Pharmacokinetic Parameters (Mean ± *SD*) Obtained after Intravenous Infusion of Pefloxacin

Parameter	Dose, mg			
	200	400	600	800
$t_{\alpha,1/2}$, h	0.10 ± 0.05	0.13 ± 0.06	0.09 ± 0.03	0.25 ± 0.07
$t_{\beta,1/2}$, h	9.7 ± 2.1	10.7 ± 1.4	11.8 ± 2.3	13.8 ± 2.7
k_{13}, h^{-1}	0.686 ± 0.675	0.160 ± 0.030	0.170 ± 0.125	0.130 ± 0.064
k_{12}, h^{-1}	7.35 ± 5.54	3.46 ± 1.55	5.63 ± 2.66	3.087 ± 3.582
k_{21}, h^{-1}	1.149 ± 0.094	2.422 ± 0.861	2.12 ± 0.27	1.661 ± 0.709
Vd_1, L	23.2 ± 19.1	46.9 ± 8.7	68.2 ± 20.0	54.6 ± 21.8
Vd_2, L	100.9 ± 40.9	64.8 ± 4.1	83.5 ± 14.7	65.3 ± 30.9
AUC, mg·h/L	23.4 ± 9.3	54.3 ± 4.1	82.2 ± 22.5	130.9 ± 23.7
CL, mL/min	156.4 ± 53.7	123.1 ± 9.8	27.2 ± 31.0	104.8 ± 19.3
U_∞, mg	27.4 ± 13.1	—	76.2 ± 37.1	84.8 ± 19.3
U_∞, %	13.7 ± 6.5	—	12.5 ± 6.6	10.8 ± 2.1
CL_R, mL/min	19.6 ± 5.6	—	15.2 ± 6.6	12.0 ± 0.3

Table II—Pharmacokinetic Parameters (Mean ± *SD*) Obtained after Oral Administration of Pefloxacin

Parameter	Dose, mg			
	200	400	600	800
Lag time, h	0.32 ± 0.14	0.48 ± 0.23	0.26 ± 0.11	0.28 ± 0.22
k_r, h^{-1}	2.11 ± 0.25	1.59 ± 0.71	2.73 ± 2.12	4.01 ± 2.28
$t_{1/2,r}$, h	0.33 ± 0.04	0.46 ± 0.27	0.35 ± 0.19	0.25 ± 0.20
$t_{1/2,el}$, h	11.7 ± 3.6	10.5 ± 2.0	11.3 ± 1.1	12.6 ± 2.5
Vd, L	132.2 ± 26.9	112.0 ± 20.5	109.9 ± 17.7	137.9 ± 2.1
AUC, mg·h/L	25.7 ± 6.3	54.5 ± 11.2	87.9 ± 8.9	105.0 ± 20.7
CL_T, mL/min	135.3 ± 35.5	125.7 ± 25.7	111.3 ± 7.0	130.6 ± 28.6
U_∞, mg	23.6 ± 8.0	44.3 ± 17.3	84.1 ± 23.5	136.4 ± 26.7
U_∞, %	11.8 ± 4.0	11.1 ± 4.3	14.0 ± 3.9	17.0 ± 3.3
CL_R, mL/min	15.3 ± 3.8	12.9 ± 2.6	14.7 ± 3.6	21.9 ± 4.8

The detection limit of the technique was 0.05 μg/mL in plasma and 0.5 μg/mL in urine, with an overall recovery of 90% from both plasma and urine. Standard curves showed good linearity from 0.125 μg/mL to 10 μg/mL, $r > 0.995$.

Human Experiments—Three subjects gave informed consent to participate in the study. They were found to be free from cardiac, renal, hepatic, respiratory, and allergic diseases by clinical and biological examinations. None of the subjects received any drugs for at least 15 d prior to the study. Each subject received four doses (200, 400, 600, and 800 mg) at weekly intervals both by intravenous infusion over 1 h and orally in 200-mg tablet form. Oral administrations were given after a 15-d wash-out period.

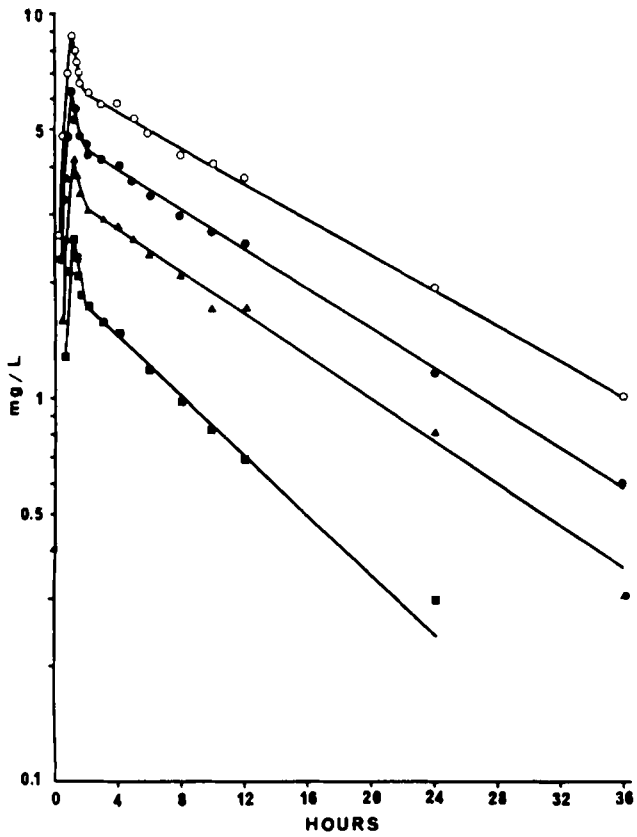

Figure 1—*Plots of mean plasma concentrations of pefloxacin* versus *time obtained in three subjects for each infused dose. The lines were generated from the best-fit pharmacokinetic parameters. Key: (■) 200 mg; (▲) 400 mg; (●) 600 mg; (○) 800 mg.*

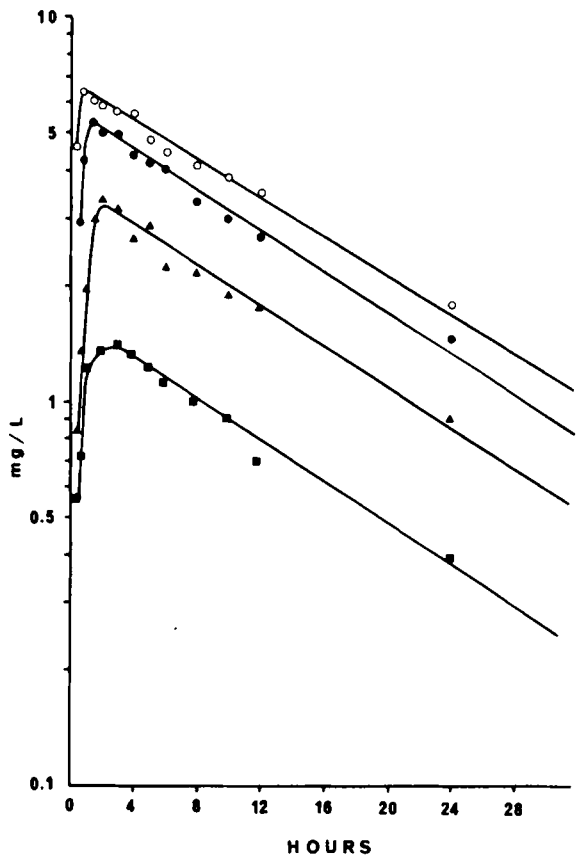

Figure 2—*Plots of mean plasma concentrations of pefloxacin* versus *time obtained in three subjects for each orally administered dose. The lines were generated from the best-fit pharmacokinetic parameters. Key: (■) 200 mg; (▲) 400 mg; (●) 600 mg; (○) 800 mg.*

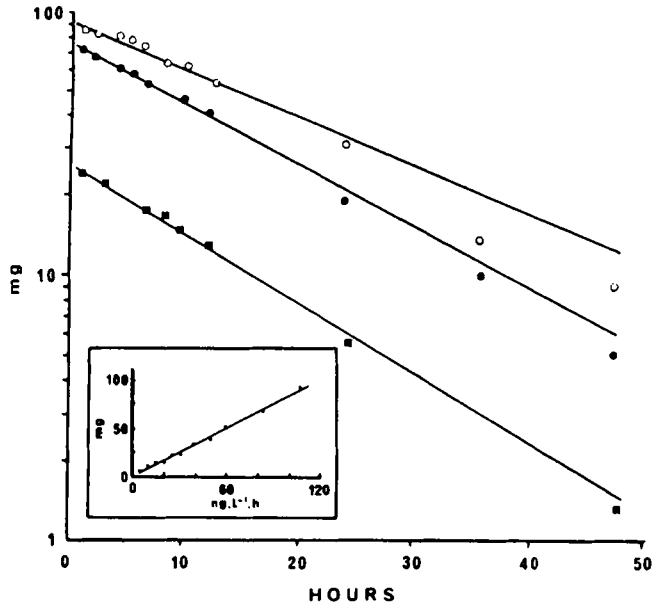

Figure 3—*Semilogarithmic plots of the amounts remaining to be excreted* versus *time in three subjects after an infused dose. Key: (■) 200 mg; (●) 600 mg; (○) 800 mg. Inset: An example of a clearance plot obtained in subject A after an infused dose of 800 mg.*

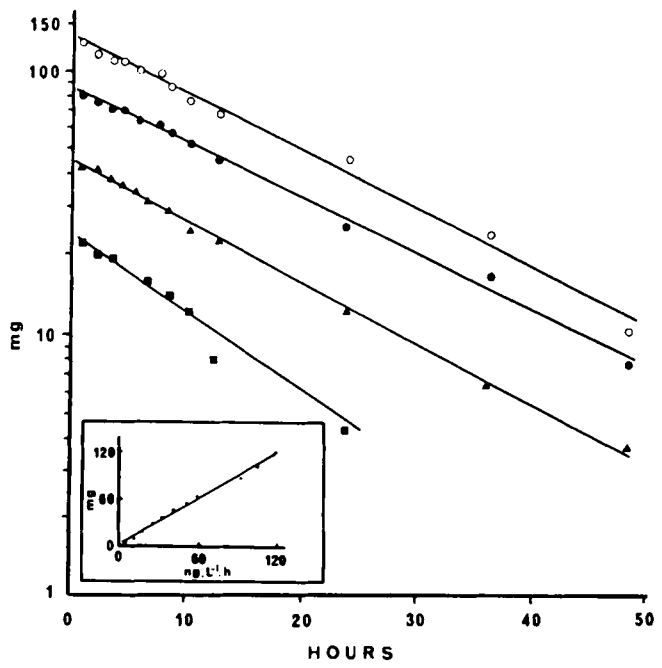

Figure 4—*Semilogarithmic plots of the amounts remaining to be excreted* versus *time in three subjects after an orally administered dose. Key: (■) 200 mg; (▲) 400 mg; (●) 600 mg; (○) 800 mg. Inset: An example of a clearance plot obtained in subject A after the orally administered dose of 800 mg.*

A 7-mL heparinized blood sample was drawn at 0, 0.25, 0.5, 0.75, and 1 h during the infusion and at 10, 15, 30, and 45 min, 1, 1.5, 2, 2.5, 3, 4, 6, 8, 10, 24, 36, and 48 h after the cessation of the infusion. After oral administration, sampling took place at 0, 0.25, 0.5, 0.75, 1, 1.5, 2, 2.5, 3, 4, 5, 6, 8, 10, 12, 24, 36, and 38 h. When variations of the infusion period or the sampling times occurred, the actual times were noted.

Urine samples were collected every hour during the first 6 h, every 2 h during the next 6 h, and every 12 h for the next 3 d.

Calculations—Statistical and pharmacokinetic calculations were performed with a table computer[4] using programs developed previously (4).

RESULTS AND DISCUSSION

Blood Sample Analysis—*Intravenous Infusion*—The mean pefloxacin plasma concentrations obtained from the three subjects receiving intravenous doses are shown in Fig. 1. Individual concentrations were systematically interpreted according to three different pharmacokinetic models, *i.e.*, one-, two-, or three-compartment open models using a Gauss–Newton algorithmic method. When pefloxacin was infused, the rate of input of the drug into the compartmental model was treated as a zero-order process; however, it was a one-order process when given orally.

At each step, the benefit of increasing the number of compartments was evaluated with a statistical Fischer test using the least-squares criterion. It showed that the two-compartment open model was the most suitable. The mean pharmacokinetic parameters (mean ± *SD*) are listed in Table I. It shows a rapid distribution phase corresponding to a 0.146 ± 0.04 h half-life (range: 0.084–0.477) and an elimination phase with an 11.5 ± 2.5 h mean half-life (range: 7.3–15.5). The volumes of distribution are large with a mean of 40.1 ± 19.1 L (range: 6.9–66.7 L) for the central compartment and 78.2 ± 28.5 L (range: 46.2–101.0 L) for the peripheral compartment.

Oral Administration—Mean pefloxacin concentrations obtained from the three subjects receiving oral doses are shown in Fig. 2. With this route of administration, the best fit was obtained with the one-compartment open model and first-order absorption. The mean pharmacokinetic parameters are presented in Table II. All parameters are in the same range as those obtained after intravenous infusion. The apparent elimination half-lives and the areas under the plasma concentration curves are essentially identical. From this last observation, it can be stated that the absolute availability of the tablets was complete, in these subjects, at each dose so that apparent volumes of distribution and total elimination clearances need not be corrected after oral administration of the drug. The distribution phase does not appear after oral administration, being masked by the absorption phenomenon from the GI tract.

Urine Sample Analysis—*Intravenous Infusion*—The rate of unchanged pefloxacin elimination was plotted against the plasma concentration at the corresponding mid-point time of urine collection. It showed a roughly linear renal clearance in each subject for all doses administered ($r > 0.85$). If the renal clearance is constant as a function of time and drug concentration, it is then possible to compute concomitantly the plasma concentrations and the rate of urinary elimination according to the general relation:

$$\frac{dU}{dt} = CL_R \cdot C \cdot dt$$

In each case, a single set of exponential terms adequately described both the plasma concentrations and the urinary elimination of the drug ($r > 0.95$ between observed and calculated values). The total amount excreted in the urine and the estimated renal clearance were added up and are presented in Table I. Furthermore, this concomitant analysis of plasma and urine data clearly show that the renal clearance was independent of the plasma drug concentrations. The urinary data, shown in Fig. 3, are plotted as the semilogarithmic amounts remaining to be excreted *versus* time. As one urine sample could not be collected after the intravenous infusion of the 400-mg dose, the corresponding plot was not drawn.

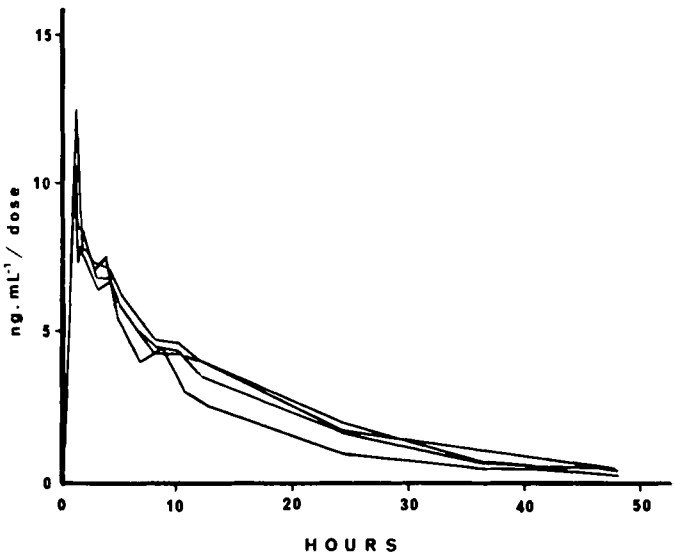

Figure 5—*Superposition of the plasma concentration curve divided by the intravenously administered dose as a function of time, in subject M.*

[4] Model 4052; Tektronix, Paris, France.

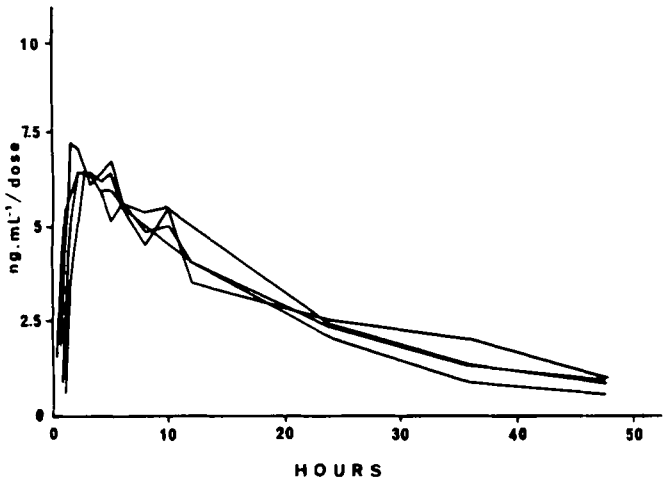

Figure 6—*Superposition of the plasma concentration curve divided by the orally administered dose as a function of time, in subject A.*

The examination of the cumulative excretion curves showed that the time of urinary collection, 4 d, was enough to have a good approximation of the total amount of the drug excreted at infinity. This result was in good accordance with a mean apparent elimination half-life of 12 h. It showed that the urinary excretion of unchanged drug accounted for 14.5 ± 6.5% of the infused drug, which was close to the results obtained in one subject in a preliminary study (3).

Oral Administration—The same pharmacokinetic analysis was performed with the data obtained after oral pefloxacin administration. The urinary data are shown in Fig. 4. The overall recovery of unchanged drug was 13.5 ± 4.1% of administered dose, similar to that observed after intravenous infusion. From this result, a high availability (close to 100% of the dose) could again be expected.

Analysis for Dose-Dependent Kinetics—The phamacokinetic analysis showed that urinary elimination, namely the renal clearance, was independent of the administered dose and plasma concentrations. Since this urinary elimination of the parent drug accounted for only 14.5% of the dose administered, 85.5% of the dose was likely to be eliminated by metabolic routes. Therefore, it was necessary to check the dose independency with parameters which took into account the overall mechanisms of drug elimination. Three methods were used to check the dose dependency from plasma results. Examples of the superposition method are shown in Figs. 5 and 6. The plasma concentrations divided by the administered dose as a function of time show a reasonable superposition for the four doses tested, either after intravenous infusion or oral administration.

According to Dost's law (5), if pharmacokinetic parameters are independent of the dose, the area under the plasma concentration curve must be linearly related to the injected dose. The mean correlation coefficients were 0.956, 0.990, and 0.998 for each subject after infusion and 0.994, 0.993, and 0.919 after oral administration. Despite the good correlation observed, there was little confidence in these results due to limited data available for a linear regression analysis. Accordingly, an analysis of variance (ANOVA) (6) was performed on the area under the curve divided by the administered dose, with the total data available, obtained after either intravenous or oral administration. It failed to show a significant difference at the 5% level between the administered doses (${}_{16}{}^{3}F = 0.46$), route of drug administration (${}_{16}{}^{1}F = 0.02$), and among the subjects (${}_{16}{}^{2}F = 0.68$). Similarly, the same ANOVA failed to show any difference between administered doses (${}_{16}{}^{3}F = 0.51$) and dosage forms (${}_{16}{}^{1}F = 0.26$) when considering urinary unchanged pefloxacin percentages. For this parameter, the analysis showed significant differences among individuals ($p < 0.05$).

Therefore, from all statistical calculations performed, it can be concluded that, within the range of the doses administered, the pharmacokinetic parameters of pefloxacin are not sensitive to dose variations. This includes both systemic and presystemic drug elimination because dose independency is observed after both intravenous and oral administration. The availability of the tablet form can be expected to be complete.

REFERENCES

(1) Y. Goueffon, G. Montay, F. Roquet, and M. Pesson, *C. R. Hebd. Seances Acad. Sci.*, **III,** 292 (1981).

(2) M. Thibault, B. Koumare, C. J. Soussy, and J. Duval, *Ann. Microbiol. (Paris)*, **1981,** 132 A.

(3) G. Montay, Y. Blain, F. Roquet, and A. Le Hir, *J. Chromatogr.*, **172,** 359 (1983).

(4) G. Houin, F. Bree, N. Lerumeur, and J. P. Tillement, *J. Pharm. Sci.*, **72,** 71 (1983).

(5) F. D. Dost, "Grundlagen der Pharmakokinetik," 2nd ed., Gearg Thieme Verlag, Stuttgart, 1968, pp. 156–158.

(6) J. G. Wagner, "Fundamentals of Clinical Pharmacokinetics," Drug Intelligence Publications, Hamilton, Ill., 1975.

ACKNOWLEDGMENTS

The authors gratefully acknowledge Dr. Arunkumar Shastri for his critical revision of the manuscript.

Radioimmunoassay for the Sulfoxide Metabolite of Trifluoperazine and Its Application to a Kinetic Study in Humans

M. ARAVAGIRI, E. M. HAWES, and K. K. MIDHA ˣ

Received June 2, 1983, from the *College of Pharmacy, University of Saskatchewan, Saskatoon, Saskatchewan S7N 0W0 Canada.* Accepted for publication September 8, 1983.

Abstract □ Antibodies were produced in rabbits immunized with 10-[[3-[4-(2-carboxyethyl)-1-piperazinyl]-propyl]]-2-trifluoromethyl-10*H*-phenothiazine sulfoxide–bovine serum albumin conjugate. The subsequently developed radioimmunoassay (RIA) procedure enables, for the first time, the quantitation of the sulfoxide metabolite of trifluoperazine in the plasma of humans after administration of therapeutic doses of trifluoperazine, in which 60 pg of the sulfoxide metabolite in 200 μL of plasma can be measured with a *CV* of <3%. Similar results were obtained by this assay with or without a benzene extraction step and also in the presence or absence of a large excess of trifluoperazine and suspected major metabolites of trifluoperazine. This RIA procedure, together with a previously developed RIA for trifluoperazine was used to directly determine plasma concentrations of trifluoperazine and its sulfoxide metabolite after administration of a single, low, oral dose of trifluoperazine to five healthy volunteers. The rapidly appearing, relatively high concentrations of the sulfoxide metabolite are indicative of presystemic sulfoxidation. The mean plasma elimination half-life for the sulfoxide metabolite of trifluoperazine was 5.8 ± 1.3 h.

Keyphrases □ Pharmacokinetics—trifluoperazine and its sulfoxide metabolite, quantitation by radioimmunoassay □ Radioimmunoassay—trifluoperazine and its sulfoxide metabolite, humans □ Trifluoperazine—pharmacokinetics, radioimmunoassay, sulfoxide metabolite

Phenothiazine antipsychotic agents are extensively metabolized into numerous metabolites, some of which may be of importance with regard to the therapeutic and/or toxic effects of drug treatment. For example, in the case of the sulfoxide metabolite of chlorpromazine, high plasma levels of the drug, which is reputed to be inactive, are associated with poor clinical response in schizophrenic patients under chronic treatment with chlorpromazine. Also, in the case of chlorpromazine, some workers have demonstrated that clinical response correlates better with plasma level ratios involving active drug–inactive drug (such as the 7-hydroxylated material plus chlorpromazine–sulfoxide metabolite) rather than with the steady-state levels of chlorpromazine (1–3). With the piperazine-type, phenothiazine, antipsychotic agent trifluoperazine (I; Scheme I), the importance in clinical therapy of the presumed major metabolites of this drug, including the sulfoxide which is reputed to be inactive, is unknown. The major reason for this is that suitable, sensitive, and specific analytical methods have not been available to measure metabolite concentrations in the plasma of patients under treatment. This slow development of analytical methods can be largely attributed to the reputed instability and adsorptive loss of phenothiazines in all stages of sample handling for analysis and the low plasma levels encountered due to the low doses of trifluoperazine given to patients. In fact, only recently were ultrasensitive analytical methods such as GC–MS (4, 5) and radioimmunoassay (RIA) (6, 7) reported for the quantitation of trifluoperazine in plasma. By these methods, trifluoperazine concentrations were quantitated in plasma after administration of low, single, oral doses of this drug. On the other hand, less sensitive techniques may not be adequate for trifluoperazine plasma level monitoring in most patients; for example, by a method based on HPLC with UV detection, measurement of trifluoperazine in plasma was obtained only while the patient was under chronic treatment with doses of trifluoperazine well above the recommended therapeutic dose (8).

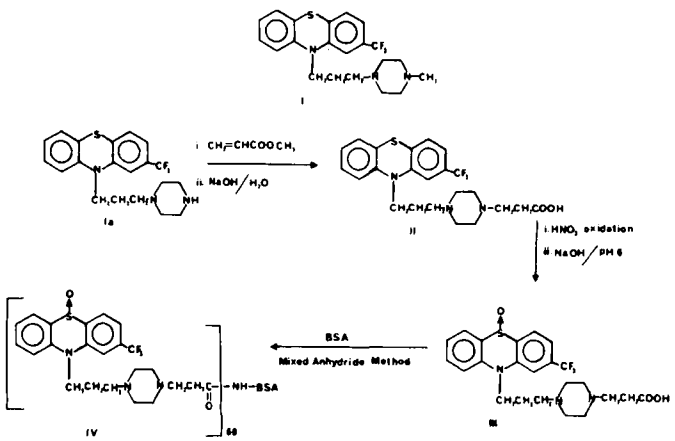

Scheme I

The ultrasensitive biological method of RIA has the advantage over chemical methods of analysis such as GC–MS in that extraction of the biological sample may not be necessary and such methods are more amenable to routine clinical monitoring. In this report, a rapid, sensitive, and specific RIA for the sulfoxide metabolite of trifluoperazine is described. By using this method and a previously reported RIA for trifluoperazine (6), the concentrations of trifluoperazine and the sulfoxide metabolite were determined in plasma samples up to 24 h after the administration of a single 5-mg oral dose of trifluoperazine to five healthy volunteers.

EXPERIMENTAL SECTION

Materials—The sulfoxide, *N*-demethyl, and 7-hydroxy metabolites of trifluoperazine were synthesized in this laboratory by modified literature

Table I—Cross-Reactions [a] of Antiserum Against the Sulfoxide Metabolite of Trifluoperazine

Compound Tested	Cross-Reaction, %
Sulfoxide metabolite of trifluoperazine	100
Trifluoperazine	<1
Sulfone metabolite of trifluoperazine	8
N-Oxide metabolite of trifluoperazine	<1
7-Hydroxy metabolite of trifluoperazine	<1
N-Demethyl metabolite of trifluoperazine	<1
Ethylenediamine metabolite of trifluoperazine	<1
Sulfoxide metabolite of prochlorperazine	39
Sulfoxide metabolite of fluphenazine	62
Sulfoxide metabolite of perphenazine	77
Sulfoxide metabolite of chlorpromazine	<1
Ring sulfoxide metabolite of thioridazine	<1
Prochlorperazine	<1
N-Demethyl sulfoxide metabolite of trifluoperazine	55

[a] Cross-reactions were assessed by the criteria of Abraham (15).

0022-3549/84/1000-1383$01.00/0
© 1984, American Pharmaceutical Association

Table II—Determination by Direct Radioimmunoassay of the Sulfoxide Metabolite in Plasma Samples Spiked with a Fivefold Excess of Trifluoperazine or one of Its Metabolites [a]

Compound Added	Plasma Conc. of the Sulfoxide Metabolite of Trifluoperazine, ng/mL ± SD				
	n	1	2	3	5
Trifluoperazine	5	0.9 ± 0.3	1.8 ± 0.2	2.8 ± 0.2	5.1 ± 0.4
7-Hydroxy metabolite of trifluoperazine	3	1.2 ± 0.4	2.1 ± 0.2	2.9 ± 0.1	4.7 ± 0.1
N-Oxide metabolite of trifluoperazine	3	1.0 ± 0.3	2.1 ± 0.3	3.3 ± 0.1	5.0 ± 0.3
N-Demethyl metabolite of trifluoperazine	3	1.0 ± 0.1	2.0 ± 0.1	2.9 ± 0.3	4.9 ± 0.2

[a] At each standard curve concentration, none of the mean values found for samples containing added trifluoperazine or metabolites differed significantly ($p > 0.05$) from the standards containing the sulfoxide metabolite only determined in the same experiment.

Table III—Intra- and Interassay Variance of the Radioimmunoassay for Trifluoperazine

	Plasma Conc. of the Sulfoxide Metabolite of Trifluoperazine, ng/mL							
	10	7.5	5	3	2	1	0.5	0.3
Intra-assay variance[a]								
SD (B/B_0, %)	0.83	0.89	0.86	1.13	1.73	1.07	0.90	0.48
n	4	4	4	4	4	4	4	4
CV, %	2.5	2.3	1.8	1.9	2.5	1.3	1.0	0.5
Interassay variance[b]								
SD (B/B_0, %)	0.97	0.90	0.69	1.31	2.01	2.27	1.49	0.82
n	7	7	7	7	7	7	7	7
CV, %	3.0	2.3	1.4	2.1	2.7	2.7	1.6	0.8

[a] Intra-assay variance was calculated from assay readings of plasma standards obtained on a single day of analysis. [b] Interassay variance was calculated from assay readings of plasma standards obtained on four different days of analysis.

procedures (9, 10), whereas trifluoperazine dihydrochloride[1] and the other phenothiazines and their metabolites[2] were donated. Aromatic ring-labeled, tritiated trifluoperazine (12.8 Ci/mmol) was procured from a commercial source[3].

Liquid scintillation counting, in which a commercial cocktail was used[4], was performed in a counter equipped with automatic quench compensation[5]. All solvents were analytical grade. The dextran-coated charcoal suspension and the various buffers were prepared in this laboratory. TLC sheets precoated with silica gel without fluorescence indicator (250-xx thickness), used for tracer isolation, were obtained commercially[6]. All experimental procedures were carried out under subdued lighting.

Synthesis of the Immunogen (IV)[7]—To an aqueous solution (10 mL) of 10-[[3-[4-(2-carboxyethyl)-1-piperazinyl]-propyl]]-2-trifluoromethyl-10*H*-phenothiazine sulfoxide dihydrochloride (II) (1.1 g, 2 mmol) (11), was added concentrated HNO_3 in a dropwise manner. The mixture was left in the dark at room temperature for 2 h. During this time the mixture changed from a reddish-brown precipitate to a clear pale-yellow solution. The mixture was adjusted to pH 6.0 with 1 M NaOH solution and subsequently saturated with NaCl. The product was extracted into dichloromethane (5 × 20 mL) and dried over anhydrous sodium sulfate to give the desired hapten III (0.82 g, 80% yield) as pale-yellow flakes, mp 98–102°C, which showed one spot on TLC: R_f 0.15 (benzene–methanol–diethylamine) (100:5:5) (II, R_f 0.25); IR: 1025 cm^{-1} (S → O); ^{1}H-NMR ($CDCl_3$): δ 2.1 (t, 2, J = 6.0 Hz, propyl central CH_2), 2.5 (m, 14, piperazine methylene, CH_2-piperazine, and CH_2CH_2—COOH), 4.2 (t, 2, J = 6.0 Hz, CH_2-phenothiazine), 7.8 (m, 7, ArH), and 10.0 ppm (s, 1, COOH); MS (ammonia CI): quasi-molecular ion $(M + H)^+$ at *m/z* 482 for III and *m/z* 496 for the methyl ester of III.

Anal.—Calc. for $C_{23}H_{26}F_3N_3O_3S$: C, 57.38; H, 5.41; N, 8.73. Found: C, 58.00; H, 5.57; N, 8.66.

The hapten III (0.130 g) was coupled to bovine serum albumin[8] (0.19 g) in dioxane by using a modified mixed-anhydride method (12, 13). This was followed by dialysis first against bicarbonate buffer (0.1 M; pH 8), then against acetate buffer (0.1 M; pH 5.2), and finally against distilled water. During the dialysis against acetate buffer, there was some precipitation, which disappeared when dialyzed again with bicarbonate buffer. After lyophilization, the immunogen IV was obtained as a white crystalline solid (0.27 g). A blank was prepared by subjecting the bovine serum albumin to the coupling conditions, but without the hapten. The number of hapten residues coupled per mole of bovine serum albumin conjugate was determined by the UV[9] method (12, 13) to be 60.

Synthsis of the Sulfoxide Metabolite of [^{3}H]Trifluoperazine—To a solution of [^{3}H]trifluoperazine[3] in ethanol (200 μL, 1 mCi/mL) was added 20 μL of concentrated HNO_3 (11 M). The reaction mixture was left in the dark at room temperature for 3 h and subsequently diluted with water (5 mL), basified with 0.2 mL of saturated sodium carbonate, and extracted with benzene (5 × 3 mL). The benzene was evaporated under a stream of nitrogen at 65°C[10]. The residue, which was reconstituted with 0.2 mL of methanol, was injected into the HPLC system[11], which was operated at ambient temperature with a flow rate of 3 mL/min. The eluted peak corresponding to the sulfoxide metabolite (2.5–3 min) was collected.

To determine the specific activity of the tracer, aliquots of the collected fraction were injected into the HPLC system. The amount of tritiated sulfoxide metabolite was determined by comparing the peak height of the sulfoxide metabolite of [^{3}H]trifluoperazine to that obtained from injections of known amounts of unlabeled metabolite. The tritiated sulfoxide metabolite peak was collected and counted by a liquid scintillation technique. The specific activity of the tritiated sulfoxide metabolite was calculated to be ~12.2 Ci/mmol. The chemical yield was found to be 50.5% by comparing the ratio of the radioactivity of the tritiated sulfoxide product with that of the [^{3}H]trifluoperazine used in the reaction.

The purity of tracer, when required for RIA, was checked by TLC: R_f 0.2 (benzene–methanol–diethylamine; 100:5:5). The purity was always >95%. The working solution of the tritiated sulfoxide metabolite was prepared on the day of assay by diluting the required quantity of the metabolite, freshly collected from the HPLC system, with 0.01 M HCl such that the diluted solution contained 2000–2500 cpm/μL.

Pilot synthesis experiments with unlabeled trifluoperazine using the oxidation procedure and isolation techniques described above gave the sulfoxide metabolite of trifluoperazine as white crystals, uncorrected mp 139–140°C [lit. (9) mp 140–141°C], which gave satisfactory C, H, and N analytical data.

Immunization—Four New Zealand White rabbits[12] (age, 4 months) were each given an intradermal injection of 1 mg of the immunogen emulsified with 0.5 mL of Freund's complete adjuvant–0.5 mL of isotonic saline. Thereafter, rabbits were reimmunized by intradermal injection at 2-week intervals with the same amount of immunogen emulsified with Freund's incomplete adjuvant. After five intradermal injections, the sera of three rabbits showed binding activity to the sulfoxide metabolite of [^{3}H]trifluoperazine. After administration of four intravenous booster doses of 1 mg of the immunogen in 0.25 mL of isotonic saline, which were given *via* the ear vein at 2-week intervals, the three rabbits produced antisera of adequate titer (1:1300 w/v). These rabbits were then sacrificed, and the antisera of each of the rabbits was lyophilized and stored at −20°C. The lyophilized antiserum of one of the rabbits was used for the RIA of trifluoperazine sulfoxide.

Direct Radioimmunoassay Procedure—An aqueous solution of the sulfoxide metabolite of trifluoperazine was prepared by dissolving the sulfoxide in 0.01 M HCl whenever required. Subsequently, standard solutions containing 0.3, 0.5, 1, 2, 3, 5, 7.5, and 10 ng of the sulfoxide/mL were prepared in pooled plasma[13]. The working antiserum solution was prepared by dissolving the lyophilized antiserum in phosphate buffer (0.2 M, pH 7.2). Of this solution, 100 μL was used in each assay tube.

To each polystyrene tube (12 × 75 mm), containing a 200-μL plasma

[1] A gift from Smith, Kline and French Laboratories, Philadelphia, Pa.
[2] Rhône-Poulenc Pharma Inc., Montreal, Quebec, Canada.
[3] Nuclear Research Centre-Negev, Beer-Sheva, Israel.
[4] Ready Solve-MP; Beckman Instruments Inc., Fullerton, Calif.
[5] LKB RackBeta, model 415; Fisher Scientific Co., Toronto, Ontario, Canada.
[6] Terochem Laboratories Ltd., Toronto, Ontario, Canada.
[7] Melting points were determined with a Gallenkamp melting point apparatus and are uncorrected. TLC was performed with Eastman chromatogram sheets, type 13254 (silica gel with fluorescent indicator); spots were observed under shortwave UV light. ^{1}H-NMR spectra were determined in $CDCl_3$ or Me_2SO-d_6 on a Varian T-60 instrument with tetramethylsilane as the internal reference. Low-resolution electron-impact (EI) and chemical-ionization (CI) mass spectra were recorded on a VG Micromass MM16F instrument at 70 eV equipped with a VG 2025 data system. IR spectra were recorded on a Perkin-Elmer 297 instrument (KBr pellets). All EI, CI, ^{1}H-NMR, and IR spectra of synthesized compounds were consistent with assigned structures. Microanalyses for samples dried over phosphorus pentoxide at 60°C under reduced pressure were performed by Mr. R. E. Teed, Department of Chemistry, University of Saskatchewan. All reagents were purchased from Aldrich Chemical Co., Montreal, Quebec, Canada.
[8] Sigma Chemical Co., St. Louis, Mo.
[9] Pye Unicam SP 1700 spectrophotometer.
[10] Thermolyne Dri-Bath; Fisher Scientific Co., Edmonton, Alberta, Canada.
[11] Solvent delivery system (M45; Waters Associates, Milford, Mass.), a valve loop injector fitted with a 1-mL loop (model 7120; Rheodyne, Berkley, Calif.), a radial compression separation system (Z module; Waters Associates), mobile phase composed of 10% sodium acetate buffer (0.1 M; pH 6) in methanol, and a variable-wavelength UV detector (Lambda Max model 480; Waters Associates) fixed at 254 nm.
[12] Mr. Avaldermeer, Sherwood Park, Alberta, Canada.
[13] Canadian Red Cross.

Table IV—Pharmacokinetic Parameters of Trifluoperazine and Its Sulfoxide Metabolite [a]

Subject	Age, years	Weight, kg	T_{max}, h		C_{max}, ng/mL		AUC_{0-24}, ng·h/mL [b]		AUC_{0-24} Metabolite/ AUC_{0-24} Drug, %	$t_{1/2}$, h	
			Metabolite	Drug	Metabolite	Drug	Metabolite	Drug		Metabolite [c]	Drug [d]
1	40	67	4.5	4.5	2.9	1.9	36.3	17.3	210	7.2	10.8
2	40	80	6	3	3.3	3.2	33.9	29.4	115	5.4	7.8
3	22	88	4.5	4.5	3.1	2.5	34.9	22.0	159	6.4	2.5
4	32	74	3	3	2.5	1.1	36.8	9.1	404	6.2	15.2
5	21	94	4.5	3	4.5	1.0	56.9	8.0	711	3.7	8.1
Mean ± *SD*	31 ± 9.2	80.6 ± 10.8	4.5 ± 1.1	3.6 ± 0.8	3.3 ± 0.7	1.9 ± 0.9	39.8 ± 9.6	17.2 ± 8.9	320 ± 245	5.8 ± 1.3	8.9 ± 4.6

[a] Pharmacokinetic parameters of trifluoperazine and its sulfoxide metabolite in the plasma of five healthy volunteers after a 5-mg oral dose of trifluoperazine. [b] AUC_{0-24} was calculated by the trapezoidal rule. [c] Plasma half-life was calculated by the equation $t_{1/2} = 0.693\ k_{el}$, where k_{el} was estimated by using the plasma concentrations between 6 and 24 h. In the case of volunteer 4, the 24-h plasma concentration was estimated, since there was found to be <0.3 ng/mL of the sulfide metabolite present. [d] Plasma half-life was calculated by the equation $t_{1/2} = 0.693/k_{el}$, where k_{el} was estimated by the plasma concentration between 4.5 and 24 h for subjects 1 and 2 and between 4.5 and 12 h for subjects 3–5.

sample (standard or from a volunteer), was added 200 μL of phosphate buffer (0.2 M; pH 7.2) and 5 μL of the sulfoxide metabolite of [^{3}H]trifluoperazine solution (10,000–12,500 cpm). The contents of the tube were mixed[14] for 10 s, and 100 μL of antiserum solution (1:1300 w/v) was added. All of the additions were carried out in an ice bath. The solution was mixed[14] well for 10 s and incubated at 37°C for 80 min. The tubes were then cooled to 4°C in an ice bath, and cold dextran-coated charcoal suspension (1 mL) was added. Each tube was again mixed[14] for 10 s and subsequently incubated for 10 min at 4°C. The samples were then centrifuged (1720×*g* for 10 min at 4°C). The supernatant solution was decanted by a standardized procedure into a scintillation vial containing 10 mL of scintillation cocktail, mixed well, and counted for 5 min. Each plasma sample, standard or unknown, was assayed in triplicate.

The calibration curve was constructed by plotting the logit values of B/B_0 on the *y*-axis and the log values of the sulfoxide metabolite concentrations on the *x*-axis, where B and B_0 are the antibody-bound radioactivity in the presence and absence of the sulfoxide metabolite, respectively. Logit B/B_0 is defined as:

$$\text{Logit } B/B_0 = \text{Log}_e \frac{B/B_0}{1 - B/B_0}$$

Extraction Radioimmunoassay Procedure—Each 1-mL plasma sample (standard or from a volunteer) was basified (pH 12) with saturated Na_2CO_3 (1 mL) and extracted with benzene (2 × 3 mL). The resultant extract was evaporated to dryness under a stream of nitrogen at 65°C, and the residue was reconstituted with 1 mL of phosphate buffer (0.2 M; pH 7.2). Subsequently, the RIA procedure described above was followed, in which 200 μL of 7% aqueous bovine serum albumin solution and 200 μL of reconstituted extract were used in the place of plasma and phosphate buffer, respectively.

The efficiency of the benzene extraction of the sulfoxide metabolite of trifluoperazine was checked by repeating the extraction procedure with spiked plasma samples containing known amounts of the tritiated sulfoxide. Of the total radioactivity added, 98% was found to be extracted from samples containing 0.3–10 ng/mL of the sulfoxide metabolite of trifluoperazine.

Plasma Samples—A 5-mg dose of trifluoperazine[15] was given orally with 50 mL of water to each of five healthy male volunteers, who fasted overnight[16]. Blood samples were withdrawn by venipuncture using evacuated heparinized tubes[17], and contact between blood and the rubber stopper was carefully avoided, as spurious results have been found in the RIA determination of trifluoperazine when blood has been allowed to touch the rubber stopper of these evacuated tubes (14). Blood samples were taken at 0 (predose), 0.5, 1, 1.5, 2, 3, 4.5, 6, 8, 12, and 24 h postdose. The plasma was immediately separated and stored at −20°C until analysis by the procedures described above for the sulfoxide metabolite and by the previously reported RIA method for trifluoperazine (6).

RESULTS

Sensitivity and Specificity of the Radioimmunoassay for the Sulfoxide Metabolite of Trifluoperazine—The amount bound at a zero concentration of the sulfoxide metabolite was determined at 30, 60, 80, 120, and 180 min and at temperatures of 4°C, 22°C (room temperature), and 37°C for the first incubation step in the assay procedure. From the results of these experiments, the optimal conditions for the assay were found to be an incubation time of 80 min at 37°C, where the B_0 was ~30%.

When 200-μL plasma samples are used, as low as 60 pg of the sulfoxide can be measured by the RIA. Under the assay conditions described above, the standard curve was linear from 0.3 to 10 ng/mL; a typical calibration curve can be defined by: logit $y = -2.27 \cdot \log_{10} x + 1.496$ ($r^2 = 0.999$). This range was adequate for the determination of all but one of the unknown concentrations of the sulfoxide metabolite in the plasma samples obtained after administration of a single oral dose of 5 mg of trifluoperazine. These concentrations were determined by running a calibration curve with each set of unknown samples. Concentrations of the sulfoxide metabolite of <0.3 ng/mL, reported for one plasma sample in the present study, were estimated.

The specificity of the antiserum was assessed by the criteria of Abraham (15). The antiserum did not cross-react markedly with trifluoperazine or the available, supposed, major metabolites of trifluoperazine; however, the cross-reactivity of the *N*-demethyl sulfoxide metabolite of trifluoperazine as well as the sulfoxide metabolites of other piperazine-type phenothiazines is understandable (Table I). Interestingly, the sulfoxide of the aliphatic phenothiazine, chlorpromazine, did not cross-react.

Also, to check cross-reactivities, plasma samples containing the sulfoxide metabolite of trifluoperazine over the standard curve range were additionally spiked with trifluoperazine at five times the sulfoxide concentrations, and the sulfoxide concentrations were subsequently determined by the direct RIA procedure. These experiments were repeated an additional four times, and the values obtained were compared with those for the sulfoxide metabolite standard curve samples prepared at the same time in the usual manner. There were no significant differences ($p > 0.05$) in the values obtained for the sulfoxide metabolite among samples of the same sulfoxide concentrations with or without trifluoperazine. Similar results were obtained when the 7-hydroxy, *N*-oxide, and *N*-demethyl metabolites were each separately added at five times the sulfoxide concentrations to plasma samples containing the sulfoxide over the concentration range of the standard curve (Table II).

Intra- and Interassay Variations—Both intra- and interassay variations were determined with plasma standards prepared in accordance with the described procedure. Intra-assay variations were determined from assay readings obtained from a single day, whereas interassay variations were calculated from the assay data obtained on four separate days of analysis (Table III). The *CV* was <4% for both intra- and interassay determinations at all the sulfoxide concentrations studied.

Plasma Concentrations of the Sulfoxide Metabolite of Trifluoperazine and Trifluoperazine—The plasma concentration–time profiles (Fig. 1) obtained by direct RIA after administration of a single 5-mg oral dose of trifluoperazine to five healthy volunteers showed considerable intersubject variations in the plasma concentration of the sulfoxide metabolite and trifluoperazine. The sulfoxide metabolite was present in detectable concentrations at all sampling times. However, in three volunteers (subjects 3–5), no trifluoperazine was detected in the 24-h plasma sample.

The areas under the plasma concentration–time curve from 0 to 24 h (AUC_{0-24}) were calculated by the trapezoidal rule and ranged from 33.9 to 56.9 ng·h/mL for the sulfoxide metabolite and 8.0 to 29.4 ng·h/mL for trifluoperazine. The values of $AUC_{0\ 24}$ for the sulfoxide metabolite were, on the average, 320% of those of trifluoperazine (range, 115–710%). The time required to reach the peak concentrations (t_{max}) in plasma were similar for the sulfoxide metabolite and trifluoperazine and ranged from 3 to 4.5 h, except in one volunteer (subject 2), for whom the t_{max} for the sulfoxide was 6 h. The peak concentrations (C_{max}) ranged from 2.5 to 4.5 ng/mL for the sulfoxide metabolite and from 1.0 to 3.2 ng/mL for trifluoperazine (Table IV).

After reaching these C_{max} values, plasma concentrations declined rapidly in all subjects, so that for the sulfoxide metabolite, the elimination half-life ($t_{1/2}$) from 6 to 24 h was calculated to range from 3.7 to 7.2 h in the five subjects, whereas for trifluoperazine the $t_{1/2}$ was in the range of 2.5–15.2 h. In the latter case, $t_{1/2}$ (4.5–24 h) was calculated for the only two subjects, in

[14] Vortex Genie; Fisher Scientific Co.
[15] Stelazine; Smith, Kline and French Laboratories.
[16] Protocol was approved by the local Ethics Committee on Human Experimentation.
[17] Vacutainer; Becton and Dickinson, Co., Mississauga, Ontario, Canada.

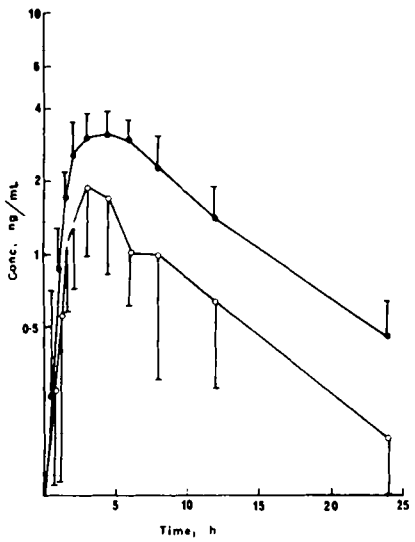

Figure 1—*Mean plasma trifluoperazine (○) and sulfoxide metabolite (●) concentrations in five healthy volunteers after single 5-mg oral doses of trifluoperazine dihydrochloride. Each point represents mean ± SD.*

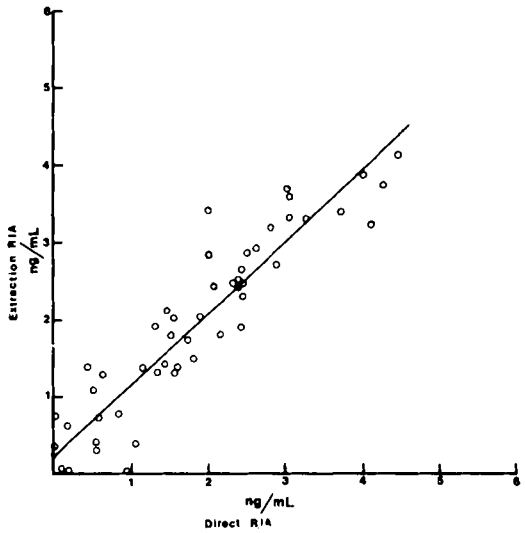

Figure 2—*Comparison of plasma concentrations of the sulfoxide metabolite of trifluoperazine determined for five volunteers after ingestion of 5 mg of trifluoperazine and analyzed by the extraction RIA and the direct RIA procedures (n = 50, r^2 = 0.92, slope = 0.89).*

whom the trifluoperazine plasma concentrations at 24 h could be determined by RIA, whereas for the other three volunteers, $t_{1/2}$ was calculated from the concentration time points at 4.5–12 h. Closer inspection of the data indicated that in the case of one volunteer (subject 2), plasma concentrations of trifluoperazine and the sulfoxide metabolite declined biexponentially after the C_{max} was reached. For this subject, the ($t_{1/2,\alpha}$) and ($t_{1/2,\beta}$) values were calculated as 1.9 and 12.8 h, respectively, for the sulfoxide, whereas the analogous values for trifluoperazine were 1.4 and 16.4 h. All plasma half-lives were estimated from the raw data using the equation $t_{1/2} = 0.693/k_{el}$, where k_{el} is the calculated rate constant of elimination.

The plasma concentrations of the sulfoxide metabolite of trifluoperazine for all plasma samples obtained from the five volunteers were also determined by the extraction RIA procedure. The values obtained were plotted *versus* those obtained by the direct RIA (Fig. 2). The slope of the regression line for this comparison had a value of 0.89, with r^2 = 0.92. The 95% confidence bounds (±0.179) of the slope of this regression line were calculated, and thus, the slope is not significantly different statistically from 1.0. Also, when both techniques were performed on three separate occasions for one of the volunteers (subject 5) and the mean of the extraction technique values were plotted *versus* the mean of the direct RIA technique, the correlation coefficient was determined to be 0.98, and the slope of the regression line was 0.80. These results indicate that the two methods compare favorably.

DISCUSSION

The previously reported trifluoperazine hapten (II) was the starting material used for the synthesis of the desired sulfoxide hapten (III). This starting material (II) was prepared as previously described (11) or by an equally successful alternate routine (Scheme I), in which the *N*-demethylmetabolite of trifluoperazine (Ia) was treated successively with methyl acrylate and base. Subsequent nitric acid oxidation of II gave the desired hapten (III) in good yield, although the relatively high water solubility of this compound necessitated saturation of the reaction mixture with sodium chloride so that organic solvent extraction of the product was feasible. A similar nitric acid treatment procedure was adopted to obtain the tracer required for the RIA of the sulfoxide metabolite of trifluoperazine in which the commercially available ethanolic solution of [^{3}H]trifluoperazine was directly oxidized: The tritiated sulfoxide product was identified by its chromatographic properties (TLC and HPLC), as well as by indirect pilot experiments in which unlabeled trifluoperazine was treated by the same nitric acid procedure and the product was examined by qualitative spectral analysis (CI-MS, EI-MS, IR, ^{1}H-NMR), as well as by elemental analysis.

The development of the present RIA was based on the most successful of the approaches taken in order to develop an RIA for trifluoperazine, in which the drug molecule was linked to bovine serum albumin *via* a two-carbon bridge attached through the N-10 side chain of the trifluoperazine structure (11). The antisera raised to such an immunogen should be specific to the ring portion of the drug molecule, and indeed, the sulfoxide antisera reported here did not cross-react with trifluoperazine, whereas there was significant cross-reactivity with the sulfoxide metabolites of the other available marketed piperazine-type phenothiazines, *i.e.*, fluphenazine, perphenazine, and prochlorperazine. Thus the antisera can be used for the quantitative RIA analysis of the sulfoxide metabolites in plasma. Antibody recognition was not dramatically affected when the 2-trifluoromethyl ring substituent of the sulfoxide metabolite of trifluoperazine was altered to a 2-chloro substituent, as with the sulfoxide metabolite of perphenazine, yet the 2-thioether, a thioridazine ring sulfoxide which has a piperidine side chain, was not recognized by the antibody. Also, regarding other ring-substituted compounds, there was no measured cross-reactivity with the 7-hydroxy metabolite of trifluoperazine, whereas the sulfone metabolite of trifluoperazine demonstrated low binding activity.

This is the first report of a suitable analytical method for the quantitation of the sulfoxide metabolite of trifluoperazine in plasma. This RIA procedure can measure 60 pg of the sulfoxide metabolite in a 200-μL plasma sample, thus obviating the need for large blood samples. Also, similar results were obtained for the assay irrespective of whether the procedure was carried out directly on plasma or on plasma extracts. Thus, a plot of the B/B_0 values obtained in the direct RIA for various plasma standards, covering the range 0.3–10 ng of the sulfoxide per mL, *versus* those obtained in the extraction RIA procedure for the same plasma standards, gave an r^2 value of 0.998.

Regarding the specificity of the antiserum (Tables I and II), there were no significant changes in binding when plasma standards of the sulfoxide metabolite over the standard curve concentration range were spiked with trifluoperazine at concentrations five times those of the sulfoxide. Therefore, it is unlikely that trifluoperazine will interfere with sulfoxide plasma concentration determinations in samples from healthy volunteers or patients treated with trifluoperazine. Also, the available suspected major metabolites of trifluoperazine in humans (the 7-hydroxy, *N*-oxide, and *N*-demethyl compounds) failed to demonstrate cross-reactivity either by the criteria of Abraham (15) or when added to spiked samples of the sulfoxide metabolite at five times the concentration of the sulfoxide. However, as expected, the *N*-demethyl sulfoxide metabolite cross-reacts appreciably with the antiserum. Whether or not the concentrations of the *N*-demethyl sulfoxide metabolite in plasma samples from patients or healthy volunteers are high enough to interfere in the determination of the sulfoxide concentrations awaits study of the levels of this metabolite in humans after single-dose and chronic administration of trifluoperazine. Additional proof for the specificity of the RIA procedure for the sulfoxide metabolite was obtained by comparison of the data for extraction RIA with that for direct RIA determined for the plasma samples from the volunteers dosed with a single 5-mg oral dose of trifluoperazine. Similar results were obtained irrespective of whether the procedure was carried out directly on plasma or on plasma extracts, indicating that physiological material and metabolites nonextractable in benzene do not dramatically interfere in the sulfoxide determinations.

Plasma concentration–time profiles for trifluoperazine after administration of low, single, oral doses of trifluoperazine, in which trifluoperazine plasma concentrations were determined by RIA, have been previously reported (16). The mean values for this previous study with 24 healthy male volunteers, in which the t_{max}, C_{max}, $AUC_{0\text{-}24}$, and $t_{1/2}$ values for one of the tested 5-mg trifluoperazine formulations were 4.0 ± 1 h, 1.9 ± 0.9 ng/mL, 19.3 ± 11

ng·h/mL, and 9.3 ± 7 h, respectively, are in agreement with the values reported here of 3.6 ± 0.8 h, 1.9 ± 0.9 ng/mL, 17.2 ± 9 ng·h/mL, and 8.9 ± 5 h, respectively, for the five volunteers given a single 5-mg oral dose of trifluoperazine. On the other hand, pharmacokinetic parameters in humans for the sulfoxide metabolite of trifluoperazine have not been previously reported. The mean sulfoxide concentrations were of the same order as the mean trifluoperazine concentrations at the first (0.5 h) time point and thereafter were greater (Fig. 1). The presence of significant amounts of the sulfoxide (98% of trifluoperazine) at the 0.5-h sampling point and the fact that the plasma sulfoxide concentrations peaked at about the same time as the plasma trifluoperazine concentrations indicates that a significant proportion of trifluoperazine is metabolized to the sulfoxide metabolite during presystemic absorption. Also, in all volunteers the percent AUC_{0-24} sulfoxide-AUC_{0-24} trifluoperazine ratio was >100%. The 115–710% range for this value in the five volunteers is indicative of large interindividual variation resulting from presystemic metabolism of trifluoperazine by routes such as sulfoxidation.

For four of the five subjects, the terminal elimination half-life of trifluoperazine was longer than that of the more polar sulfoxide metabolite, which suggests a generally faster elimination of the sulfoxide. A similar phenomenon has been reported on comparison of the sulfoxide metabolite of chlorpromazine and chlorpromazine terminal elimination half-lives after administration of low, single, oral doses of chlorpromazine to healthy male volunteers (17). However, pharmacokinetic data obtained from the RIA measurement of plasma concentrations should be viewed with suspicion. Indeed, the RIA antisera used here for trifluoperazine plasma concentration determinations cross-reacts with the *N*-demethyl and 7-hydroxy metabolites of trifluoperazine to the extent of 26 and 24%, respectively (6). When these antisera were used to determine plasma concentrations in an oral single-dose bioequivalency study of two trifluoperazine tablet formulations in five healthy volunteers, a longer mean elimination half-life (11.5 ± 3.7 compared with 8.3 ± 2.4 h for one of the formulations) was found than when the plasma concentrations were determined for the same plasma samples by a specific GC–MS method (18). The RIA method for the sulfoxide metabolite needs to be compared with a sensitive and specific chemical method for the determination of the sulfoxide in plasma to validate the pharmacokinetic data reported here. Due to such reasons as the demonstrated heat sensitivity of the sulfoxide metabolite of trifluoperazine (19) and the low concentrations encountered after administration of this highly potent antipsychotic agent, such development will not be easy. In the meantime, due to the specificity demonstrated in this report, the RIA for the sulfoxide metabolite can be investigated as to its suitability to compare measured sulfoxide concentrations in responding and nonresponding patients under chronic treatment with trifluoperazine. The resultant data will assist in establishing the relationship, if any, between plasma concentrations of the sulfoxide metabolites of trifluoperazine, therapeutic response, and/or adverse drug reactions.

REFERENCES

(1) A. V. P. McKay, A. F. Healey, and J. Baker, *Br. J. Clin. Pharmacol.*, **1**, 425 (1974).

(2) G. Sakalis, T. L. Chan, G. Sathananthan, N. Schooler, S. Goldsberg, and S. Gershon, *Commun. Psychopharmacol.*, **1**, 157 (1977).

(3) Y. Sakurai, R. Takahashi, T. Nakahara, and H. Ikenaga, *Arch. Gen. Psychiatry*, **37**, 1057 (1980).

(4) K. K. Midha, R. M. H. Roscoe, K. Hall, E. M. Hawes, J. K. Cooper, G. McKay, and H. U. Shetty, *Biomed. Mass. Spectrom.*, **9**, 186 (1982).

(5) R. Whelpton, S. H. Curry, and G. M. Watkins, *J. Chromatogr.*, **228**, 321 (1982).

(6) K. K. Midha, J. W. Hubbard, J. K. Cooper, E. M. Hawes, S. Fournier, and P. Yeung, *Br. J. Clin. Pharmacol.*, **12**, 189 (1981).

(7) K. K. Midha, E. M. Hawes, G. Rauw, G. McKay, J. K. Cooper, and H. U. Shetty, *J. Pharmacol. Methods*, **9**, 283 (1983).

(8) S. H. Curry, R. B. Stewart, P. K. Springer, and J. E. Pope, *Lancet*, **i**, 395 (1981).

(9) U. Breyer and G. Schmalzing, *Drug Metab. Dispos.*, **5**, 97 (1977).

(10) E. A. Nodiff, H. L. Sharma, P. C. Taunk, A. P. Shukla, M. D. Sadhnani, S. B. Tambi, and R. L. Mital, *J. Heterocycl. Chem.*, **18**, 1529 (1981).

(11) E. M. Hawes, H. U. Shetty, J. K. Cooper, G. Rauw, G. McKay, and K. K. Midha, *J. Pharm. Sci.*, **73**, 247 (1984).

(12) B. F. Erlanger, F. Borek, S. M. Beiser, and S. Lieberman, *J. Biol. Chem.*, **228**, 713 (1957).

(13) B. F. Erlanger, F. Borek, S. M. Beiser, and S. Lieberman, *J. Biol. Chem.*, **234**, 1090 (1959).

(14) K. K. Midha, J. K. Cooper, Y. D. Lapierre, and J. W. Hubbard, *Can. Med. Assoc. J.*, **124**, 263 (1981).

(15) G. E. Abraham, *J. Clin. Endocrinol. Metab.*, **29**, 866 (1969).

(16) K. K. Midha, E. D. Krochinski, R. M. H. Roscoe, E. M. Hawes, J. K. Cooper, and G. McKay, *J. Pharm. Sci.*, **73**, 261 (1984).

(17) P. K. F. Yeung, J. W. Hubbard, J. K. Cooper, and K. K. Midha, *J. Pharmacol. Exp. Ther.*, **226**, 833 (1983).

(18) K. K. Midha, E. M. Hawes, E. D. Korchinski, J. W. Hubbard, G. McKay, J. K. Cooper, and R. M. H. Roscoe, *Biopharm. Drug Dispos.*, **5**, 215 (1984).

(19) K. Hall, P. K. F. Yeung, and K. K. Midha, *J. Chromatogr.*, **231**, 200 (1982).

ACKNOWLEDGMENTS

The Medical Research Council of Canada Operating Grant (MT-7838) is gratefully acknowledged. We are thankful to Mr. K. Hall for running the mass spectra.

Evaluation of Diethyl Malonate as a Simulant for 1,2,2-Trimethylpropyl Methylphosphonofluoridate (Soman) in Shower Decontamination of the Skin

WILLIAM G. REIFENRATH *x, MILLARD M. MERSHON ‡, FLOYD B. BRINKLEY ‡, GEORGE A. MIURA ‡, CLARENCE A. BROOMFIELD ‡, and H. BRUCE CRANFORD §¶

Received August 16, 1983, from the **Division of Cutaneous Hazards, Letterman Army Institute of Research, The Presidio, San Francisco, CA 94129*, ‡*U.S. Army Medical Research Institute of Chemical Defense, Aberdeen Proving Ground, MD 21010*, and the §*U.S. Army Medical Bioengineering R&D Laboratory, Fort Detrick, Frederick, MD 21701.* Accepted for publication October 20, 1983. ¶ Present address: U.S. Department of Energy, Office of Industrial Programs, Washington, DC 20585.

Abstract □ A shower decontamination bench model has been used to assess quantitatively the importance of several variables (water pressure and temperature, surfactant concentration in the decontamination fluid, nozzle type, and shower time) on decontamination of nontoxic chemical warfare-agent simulants diethyl malonate and thickened diethyl malonate from pig skin *in vitro*. Diethyl malonate was validated as a simulant for 1,2,2-trimethylpropyl methylphosphonofluoridate (soman) by comparison of the skin penetration and decontamination of radiolabeled diethyl malonate to the radiolabeled phosphonofluoridate in shower decontamination trials of pig skin *in vitro*. Percutaneous penetration of diethyl malonate was significantly greater than that of the phosphonofluoridate during the 15-min period after application. However, both were <0.1% of the applied dose. Showering or thickener had no significant effect on the percutaneous penetration of diethyl malonate or the phosphonofluoridate. Most of the phosphonofluoridate removed by showering or scrubbing the skin was inactivated. The quantity of intact 1,2,2-trimethylpropyl methylphosphonofluoridate that penetrated through the skin was below the detection limit of the enzymatic analysis. There was no statistically significant difference between the phosphonofluoridate and diethyl malonate in efficacy of shower decontamination. The presence of thickener did not have a significant effect on decontamination efficacy.

Keyphrases □ Shower decontamination—percutaneous absorption, pig skin □ Diethyl malonate—percutaneous absorption, pig skin □ 1,2,2-Trimethylpropyl methylphosphonofluoridate—percutaneous absorption, pig skin

In the event of skin exposure to toxic chemicals, involved armed forces and civilian groups will need to decontaminate nonambulatory chemically contaminated casualties before they receive medical treatment for wounds. Besides decontamination of the patient, another purpose of decontamination is to protect medical personnel and prevent their exposure to detrimental levels of toxic chemicals. It is generally not possible for medical personnel in protective clothing to provide necessary medical treatment to patients. Consequently, medical personnel must operate in a shirt-sleeve environment.

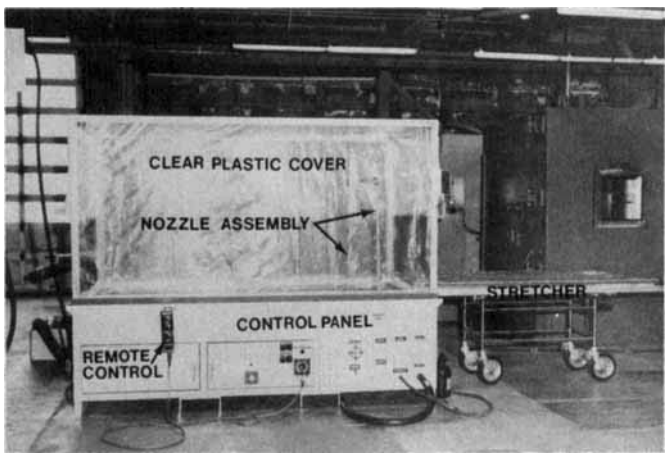

Figure 1—*United States Air Force litter patient decontamination shower (breadboard model).*

Equipment designers do not have sufficient information on nonambulatory casualty decontamination to construct a prototype device for deployment and installation in fixed facilities. To obtain the necessary information, a breadboard model (an experimental item of hardware fabricated during the conceptual phase to reduce technological uncertainty, prove feasibility, and provide realistic cost estimates) of a decontamination device has been fabricated by the U.S. Army Medical Bioengineering Research and Development Laboratory (Fig. 1). The decontamination device is conceived to work as follows. The chemically contaminated patient is placed on a stretcher where all clothes, dressings, *etc.* are removed and the patient is rolled into the decontamination device. (During the entire process, the gas mask will remain on the patient.) The device is surrounded by a clear plastic cover which allows observation of the patient, permits easy access to the patient, and prevents escape of contaminated water. The device, activated and controlled by an operator, can apply soap and water (or other chemicals) to the entire body, except the area under the mask. With the patient stationary, the nozzle assembly cycles back and forth, applying water, soap, and rinse water for a predetermined time. When decontamination is considered complete, the clean side of the machine is opened and the stretcher with patient is removed. Additional background information on the Litter Patient Decontamination Shower is available (1).

In a previous study (1), an assessment was made of the effect of variables functioning in the breadboard device (water pressure, surfactant concentration, water temperature, nozzle

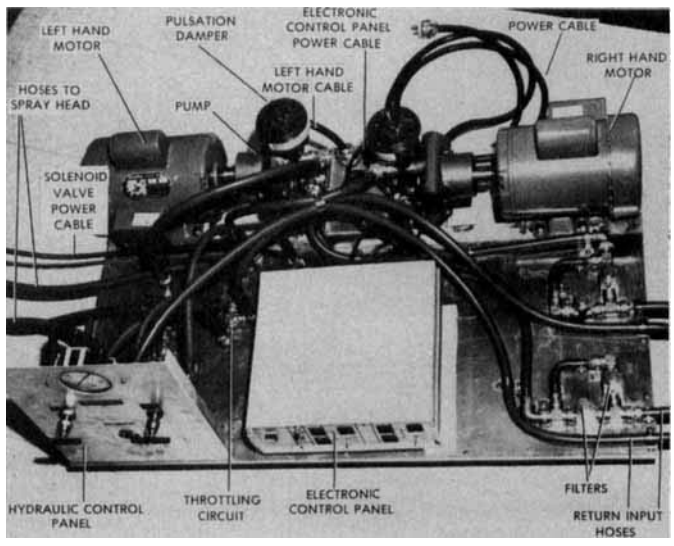

Figure 2—*Litter patient decontamination unit, bench model; top view showing dual water circuits.*

0022-3549/84/1000-1388$01.00/0
© 1984, American Pharmaceutical Association

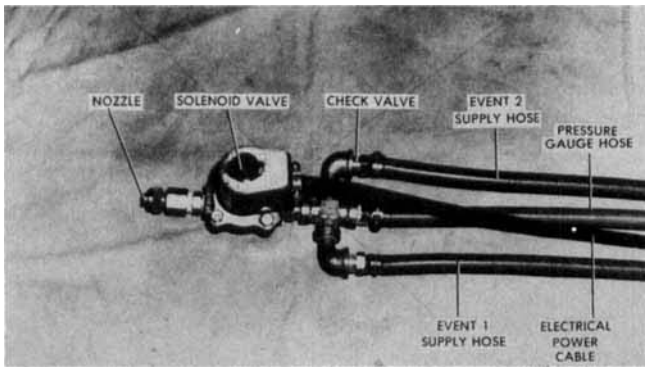

Figure 3—*Litter patient decontamination unit, bench model; shower head and connections are shown.*

type, and shower time) on removal of nontoxic chemical warfare agent simulants from the surface of excised pig skin. Diethyl malonate was used as a simulant for the nerve agent 1,2,2-trimethylpropyl methylphosphonofluoridate (soman), and diethyl malonate thickened with acrylate polymer was used as a simulant for the thickened phosphonofluoridate. Diethyl malonate was chosen because its physical properties (vapor pressure, water solubility, and surface tension) are similar to those of the phosphonofluoridate (1). A decontamination bench model (Figs. 2 and 3) was used to simulate the function of the breadboard decontamination device. The bench model is a single stationary nozzle model of the breadboard device. In the previous report (1), it was found that the force per unit area exerted by the shower water on the skin surface was the major variable responsible for differences in decontamination efficiency. Compared with trials where no showering was done, showering always increased the mean percutaneous penetration of simulant. However, the significance of these results was in question since the effect was small and varied in magnitude and the ability of diethyl malonate to simulate the percutaneous penetration of the phosphonofluoridate was unknown. Therefore, the present study was conducted to compare the percutaneous penetration of radiolabeled diethyl malonate and radiolabeled 1,2,2-trimethylpropyl methylphosphonofluoridate (both unaltered and in the thickened state) in shower decontamination trials of pig skin *in vitro*.

EXPERIMENTAL SECTION

Radiolabeled and Thickened Radiolabeled Diethyl Malonate—Diethyl [2-^{14}C]malonate[1] had a radiochemical purity of 98%; diethyl malonate[2] had a purity of 99%. Radiolabeled diethyl malonate was diluted with unlabeled diethyl malonate to give a specific activity of 5 μCi/mg. Applying 0.27 μL of this dilution to a skin area of 2.85 cm^2 gave a chemical dose of 0.1 mg/cm^2 and a radioactive dose of 1.35 μCi. A sample of thickened radiolabeled diethyl malonate was prepared by adding 20 mg of radiolabeled diethyl malonate to 100 μL of a mixture of acrylate polymer[3] in unlabeled diethyl malonate with a viscosity of 1000 centistokes at 25°C to give a final viscosity of ~200 centistokes at 25°C. Applying 0.28 μL of this mixture to a skin target area of 2.85 cm^2 gave a chemical dose of 0.1 mg/cm^2 and a radioactive dose of 1.76 μCi.

Preparation of Radiolabeled and Thickened Radiolabeled 1,2,2-Trimethylpropyl Methylphospbonofluoridate—Into a 12-mL capped centrifuge tube equipped with a triangular stirring bar was placed 30 μL of triethylamine, 1 mmol (~125 μL) of [1-methyl-^{14}C]3,3-dimethyl-2- butanol[4], and an excess

[1] Batch no. 53, specific activity 4.9 mCi/mmol; Amersham Radiochemicals, Arlington Heights, Ill.
[2] Lot no. 47C-0374; Sigma Chemical Co., St. Louis, Mo.
[3] Polymer K125EA, a polymer made from the following monomers: methyl methacrylate, ethyl acrylate, and butyl acrylate; Rohm and Haas Co., Philadelphia, Pa.
[4] Lot no. 710674, specific activity 5 mCi/mmol; ICN, Chemical and Radioisotope Division, Irvine, Calif.

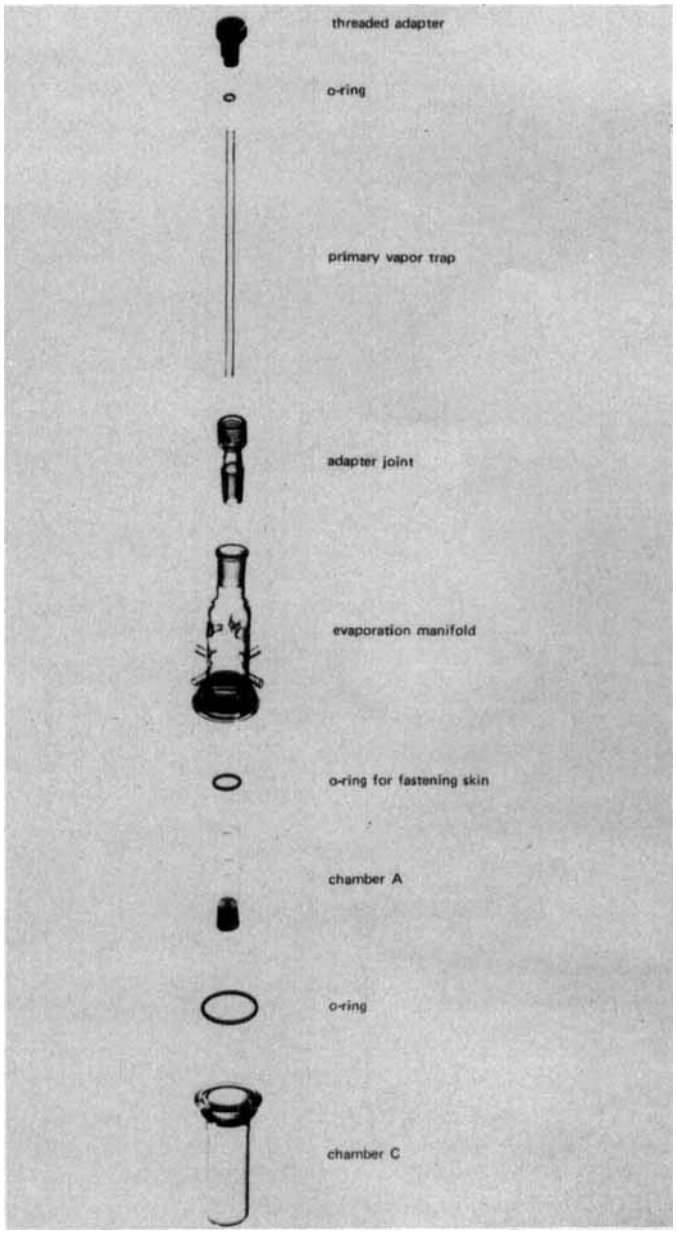

Figure 4—*Apparatus for collection of diethyl malonate and phosphonofluoridate evaporation.*

(~200 μL, 2 mmol) of methylphosphonic difluoride, of which 100 μL was used to rinse the residual pinacolyl alcohol from the vial before it was added to the centrifuge tube. The resultant mixture was allowed to stand at room temperature overnight. One milliliter each of distilled water and $CDCl_3$ were added, the mixture was shaken vigorously, and then centrifuged in a clinical centrifuge[5] at one-half speed for 2 min. The aqueous layer was carefully removed with a pipet, and another 1 mL of distilled water was added. The mixture was shaken and centrifuged as before, the top layer was again carefully removed, and the organic layer was transferred to a flask with molecular sieves. After drying overnight the solution was transferred to an NMR tube for analysis. By ^{1}H- and ^{31}P-NMR, the sample contained 75–82% of the phosphonofluoridate; the remainder was 3,3-dimethyl-2-butanol. The sample was distilled to yield a homogeneous sample by TLC[6] (5% methanol–chloroform) with single spot at R_f 0.82; all of the radioactivity was associated with this single spot.

The radiolabeled phosphonofluoridate was diluted with unlabeled compound so that when 0.27 μL was applied to a 2.85 cm^2 skin area, a chemical dose of 0.1 mg/cm^2 and a radioactive dose of 0.9 μCi were given. A sample of the thickened radiolabeled phosphonofluoridate was prepared by adding 20 mg of radiolabeled compound to 100 μL of a mixture of acrylate polymer

[5] International Equipment Company, Needham Heights, Mass.
[6] Silica gel sheet no. 6061; Eastman Organic Chemicals, Rochester, N.Y.

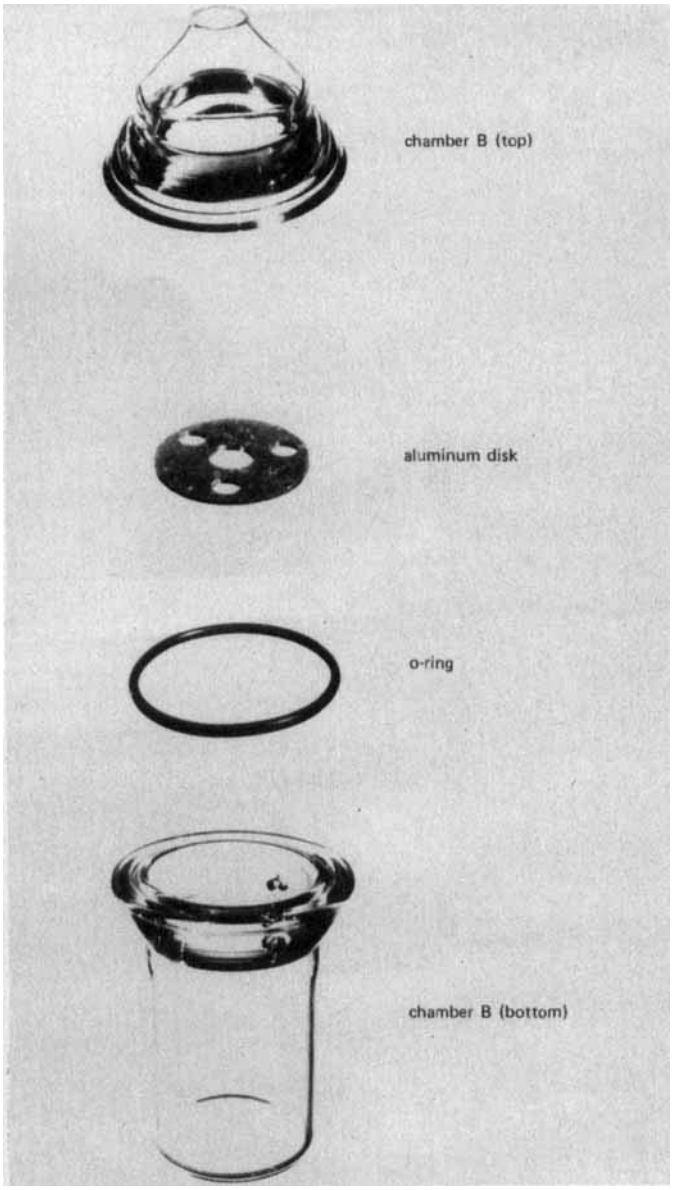

Figure 5—*Apparatus for collection of shower water.*

and unlabeled phosphonofluoridate (1000 centistoke at 25°C) to give a final viscosity of ~200 centistokes at 25°C. Applying 0.28 μL of this mixture to a 2.85 cm^2 skin area gave a chemical dose of 0.1 mg/cm^2 and a radioactive dose of 1.6 μCi.

Acetylcholinesterase Inhibition Assay[7]—Inhibition of acetylcholinesterase activity served as the basis for the enzymatic assay of the ^{14}C-labeled phosphonofluoridate. Enzyme activity was measured by the radiometric method of Siakotos *et al.* (2).

Acetylcholinesterase Stock Solution For Enzymatic Assay of the Phosphonofluoridate—Ten milligrams of eel acetylcholinesterase and 500 mg of bovine plasma albumin were dissolved in 500 mL of 10 mM potassium phosphate buffer, pH 7.0. Aliquots were stored at −20°C. Prior to use, an aliquot of enzyme solution was thawed, and $MgCl_2$ and NaCl were added to a final concentration of 10 mM and 100 mM, respectively.

Preparation of Dilutions and Determination of the Standard Curve—1,2,2-Trimethylpropyl methylphosphonofluoridate (20 mg) was dissolved in 100 mL of normal saline. The initial dilution was made by adding 100 μL of a 1.1 mM stock solution of the phosphonofluoridate to 0.90 g of ice-cold glass-distilled water in ~1.9-mL screw-top vials. Stock solutions (1.1×10^{-8} and 2.2×10^{-8} M) were prepared by serial dilution and kept on ice. Fresh

[7] [^{14}C]Acetyl-β-methylcholine and aqueous scintillation counting fluid (Aquasol) were purchased from New England Nuclear Corp., Boston, Mass. Eel AchE, type VI, was a product of Sigma Chemical Co., St. Louis, Mo. Amberlite CG-120 resin (sodium form, 200–400 mesh) was obtained from Mallinckrodt Co., St. Louis, Mo. Bovine plasma albumin was obtained from Armour Laboratory, Chicago, Ill.

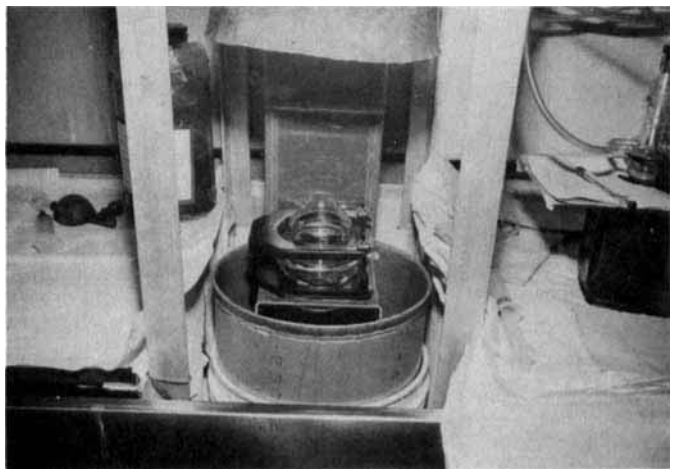

Figure 6—*Shower target assembly mounted in a hood.*

dilutions were prepared daily, and the standard curve was determined immediately after serial dilution. Assays were performed in 12-mL graduated centrifuge tubes. Four replicates were prepared for each concentration of the phosphonofluoridate. The reaction mixture contained 20 μL of 0.5 M potassium phosphate buffer (pH 7.4), 100 μL of eel acetylcholinesterase stock solution, 10 μL of 300 mM $MgCl_2$, the phosphonofluoridate solution, and enough glass-distilled water to make 210 μL. The mixture was incubated for 15 min at 37°C. To this mixture was added 100 μL of 3 mM [^{14}C]acetyl-β-methylcholine (0.1 μCi/100 μL), and the final mixture was incubated for 3 min at 37°C. The reaction was stopped by the addition of 5 mL of 20% (w/v) resin suspension in dioxane. The volume of each stopped-reaction mixture was adjusted to 10 mL with dioxane. After centrifugation, a 5-mL aliquot of dioxane supernatant (containing [^{14}C]acetate) was added to 10 mL of aqueous counting solution. Radioactivity was determined using a scintillation counter[8] which corrected for quenching. Radioactivity from controls, which were incubated with 100 μL of water in place of acetylcholinesterase, was subtracted from all assays to correct for nonenzymatic hydrolysis of the substrate. Inhibition of enzyme activity was expressed as the percentage of control which was not treated with the phosphonofluoridate.

Dilution of Radiolabeled Phosphonofluoridate Samples for Quantitative Enzyme Determination—Samples of solutions of the labeled phosphonofluoridate were kept on ice and diluted serially when necessary with ice-cold glass-distilled water so that appropriate aliquots inhibited the acetylcholinesterase at levels on the linear portion of the standard curve. Assays of the samples were carried out immediately. The procedures described above for the standard curve were followed for the label phosphonofluoridate samples. Stability of the radiolabeled compound was assessed before, during, and after the completion of the study by the enzymatic procedure. Initial and midpoint purities were essentially 100%. Purity was 70% when determined after the completion of the experiments.

Skin Samples—Skin was harvested from each of three female weanling Yorkshire pigs (~25 kg)[9]. After the pigs were sacrificed, hair was clipped from the animals with electric clippers[10]. An incision (~30 cm) was made down the midline of the back. At the 0-, 15-, and 30-cm points along the midline incision, perpendicular incisions (~15 cm) were made on the left side of the animal. A final incision was made parallel to the initial midline incision so that two square sections (15 cm × 15 cm) were formed. A notch was cut in the anterior edge of each section to preserve orientation. Whole-skin sections were removed from the animal and subcutaneous fat was removed by scraping. A small piece of skin from each animal was submitted for histopathological examination, which verified that the skin was normal tissue. The skin was cut into 3.2-cm diameter circles by using a punch. Each skin sample was coded by location. Skin was stored at −60°C for ~1 month prior to use.

Apparatus—Special glassware (Figs. 4 and 5) used in the study was custom-fabricated[11]. The bench-model decontamination unit was fabricated at the U.S. Army Medical Bioengineering R & D Laboratory, Fort Detrick, Frederick, Md. Details of the bench pump design can be found elsewhere (1). An assembly was constructed inside a hood (minimum linear air velocity of 45.8 m/min) to position the shower head of the bench model 30.5 cm above the skin surface when the skin was mounted on chamber A and inside chamber

[8] Model 2660; Packard Instrument Co., Des Plaines, Ill.
[9] Boswell Laboratory Animals, Corcoran, Calif.
[10] Model no. A2 small clipper; Oster Corp., Milwaukee, Wis.
[11] Laboratory Glass Apparatus, Berkeley, Calif.

Table I—Disposition of Radioactivity Following Application of Radiolabeled Diethyl Malonate and 1,2,2-Trimethylpropyl Methylphosphonofluoridate and Thickened Radiolabeled Compounds to Pig Skin

Chemical	Condition[b]	Applied Radioactive Dose, %[a]				
		Evaporation[c]	Decontamination[d]	Scrub[e]	In Skin[f]	Penetration[g]
Diethyl malonate	No shower	63.1 ± 3.6	—	13.8 ± 2.0	2.4 ± 0.7	0.09 ± 0.03
Phosphonofluoridate	No shower	61.0 ± 7.1	—	5.3 ± 1.1	1.1 ± 0.3	0.03 ± 0.02
Diethyl malonate	Shower	54.9 ± 13.7	13.6 ± 3.2	2.1 ± 0.8	2.3 ± 0.5	0.10 ± 0.05
Phosphonofluoridate	Shower	58.0 ± 12.8	4.6 ± 2.2	1.1 ± 0.5	0.6 ± 0.2	0.03 ± 0.02
Thickened diethyl malonate	No shower	53.9 ± 7.8	—	10.3 ± 1.1	2.2 ± 1.4	0.08 ± 0.05
Thickened phosphonofluoridate	No shower	60.4 ± 8.8	—	5.7 ± 2.6	0.8 ± 0.2	0.03 ± 0.02
Thickened diethyl malonate	Shower	52.1 ± 10.4	9.6 ± 1.7	1.9 ± 1.0	1.9 ± 1.0	0.06 ± 0.04
Thickened phosphonofluoridate	Shower	60.4 ± 4.9	5.0 ± 2.2	1.6 ± 0.5	0.9 ± 0.5	0.01 ± 0.01

[a] Data expressed as mean ± *SD* for six replicate determinations. [b] Shower conditions consist of two 1-s bursts of water at a theoretical force per unit area of 0.054 kg/6.45 cm^2 on the skin surface. [c] Radioactivity recovered from the primary vapor trap. [d] Radioactivity removed from the skin by showering. [e] Radioactivity removed from the skin by scrubbing and rinsing the skin surface with 1% aqueous surfactant solution. [f] Radioactivity recovered by oxidation of the skin sample. [g] Radioactivity recovered from chamber A.

B (Fig. 6). The entire shower target assembly was surrounded by a movable shield to control water spray.

Shower Decontamination Trials—The skin disposition of diethyl malonate was compared with that of the phosphonofluoridate, and the skin disposition of thickened diethyl malonate was compared with that of the thickened phosphonofluoridate in shower decontamination trials. These experiments were compared with experiments where procedures remained the same except that no showering was done. Eight combinations of variables, which represented all possibilities, were compared on 6 separate days (48 total trials). The order in which the eight combinations were tested on a given day was randomized. Skin samples from the two sites on each of the three pigs were allocated to the experimental trials in a random fashion, with the restriction that an equal number of samples came from each of the three pigs.

Skin samples were removed from the −60°C freezer to a −8°C freezer the night before trials were made. The skin was placed in a glass vial in a 37°C water bath and allowed to thaw (15–20 min); the weight of the skin and location code were recorded. The thawed skin was attached to chamber A (Fig. 4) with a rubber O-ring. Chamber A was filled with Ringer's lactate, prewarmed to 37°C, and stoppered. Chamber A was placed inside chamber C, both within a water bath at 37°C. After the skin surface temperature reached 25–27°C, the skin surface was dosed with the appropriate chemical by streaking it across the skin surface (2.85 cm^2) with the blunt tip of a 1-μL syringe[12]. Immediately following application, the evaporation manifold was clamped to chamber C with chamber C remaining in the 37°C water bath. A peristaltic pump[13] was connected to the primary vapor trap (a tube containing 200 mg of absorbent powder[14]). The pump pulled air at 60 mL/min, causing air to flow into the inlet tubes of the evaporation manifold, over the skin surface, and into the primary vapor trap. Any radiolabeled chemical that evaporated from the skin surface was absorbed by the primary trap. A secondary safety bubbler trap was connected between the pump and the primary vapor trap.

After 14 min, chamber A was removed and mounted into chamber B (Fig. 5). Fifteen minutes after application of chemical, the skin was showered. The bench model was designed to shower the skin with a decontamination fluid followed by a water rinse. However, in a previous comparison (1) involving removal of thickened and unthickened diethyl malonate from skin, no difference was found between cycles with a 1% aqueous surfactant solution and with plain water. Therefore, distilled water was used in both shower cycles of this study. A total shower time of 2 s was used, 1 s/cycle. The water temperature was 20°C, and the pH was 6.8. After showering, chamber A was removed from chamber B. The sides of chamber A were rinsed into a tared beaker along with the contents and several rinses of chamber B. While tilting chamber A downward, the skin surface was scrubbed with a cotton ball containing 1% aqueous surfactant[15] and rinsed with 1 mL of the 1% aqueous surfactant (pH 6.7). The skin rinse and cotton ball were collected in a counting vial and assayed for radioactivity. The contents and rinses of the interior of chamber A were collected in a tared beaker and assayed for radioactivity (percutaneous penetration). The skin was removed from chamber A and cut into seven approximately equal portions. These were later assayed for radioactivity by combusting the samples[16], trapping the liberated $^{14}CO_2$[17], and counting the radioactivity on a scintillation counter. The primary vapor trap was removed from the evaporation mainfold and the contents (chemical trapped on absorbant powder) were flushed with aqueous (scintillation) counting fluid rinses (~15 mL each) into a counting vial. The content of this counting vial was then divided into six additional counting vials for more accurate counting. For each day, the volume of substance applied to the skin was placed in each of three volumetric flasks to serve as a control; an aliquot was taken from each for radioactivity assay.

When samples of the radiolabeled and thickened radiolabeled phosphonofluoridate were used, aliquots of residues recovered by scrubbing the skin surface, and from chamber A and chamber B, were subjected to the enzymatic assay.

RESULTS AND DISCUSSION

The disposition of radioactivity applied to the skin under the various conditions of the study is given in Table I. Overall recovery of the radioactive dose in these trials was ~70%, with the major portion recovered after evaporation from skin. The balance of the radioactive dose was probably lost by evaporation during the skin application process, before the evaporation manifold was in place. The amounts of evaporated diethyl malonate and 1,2,2-trimethylpropyl methylphosphonofluoridate, as measured by the amount of radioactivity recovered from the primary vapor trap, were very similar. This result was not changed by the presence of thickener.

A higher percentage of the radioactive dose of diethyl malonate than the phosphonofluoridate was recovered from the skin surface (by scrubbing) and from residues in the skin (by oxidation) at the end of 15 min following application without showering. However, showering removed a correspondingly larger percent of the applied radioactive dose of diethyl malonate than phosphonofluoridate so that residues left on the skin surface were similar (1–2%). Again, the presence of thickener did not change this outcome.

The efficiency of shower decontamination (calculated by dividing the percentage in the "Decontamination" column in Table I by the sum of percentages in the last four columns and multiplying by 100) showed little difference between the four test substances as evidenced by the following values (mean ± *SD*): diethyl malonate, 75 ± 7; phosphonofluoridate, 69 ± 14; thickened diethyl malonate, 72 ± 21; thickened phosphonofluoridate, 65 ± 13.

In a previous study (1), it was found that the force per unit area exerted by the shower on the surface of pig skin was the major variable responsible for differences in decontamination efficiency of diethyl malonate and thickened diethyl malonate. Varying the temperature of water from 23°C to 37°C or adding surfactant to the water had little effect on the decontamination efficiency (1). These results, together with the findings that all four test substances were decontaminated equally by the shower, suggest that the mechanism of shower cleaning is mechanical rather than chemical. Apparently, the shower cleans the skin by removing the upper layers of the stratum corneum so that contaminants residing in these upper layers are removed. The velocity of the water droplets in the shower could also contribute to mechanical removal of contaminants not in direct contact with the skin.

During the 15-min period immediately following application the percutaneous penetration of diethyl malonate, as measured by radioactivity appearing in chamber A, was significantly greater than the percutaneous penetration of the phosphonofluoridate (Table I). However, both were <0.1% of the applied dose. An analysis of variance revealed that showering or thickener had no significant influence on the percutaneous penetration of diethyl malonate or the phosphonofluoridate.

Enzymatic analysis showed inactivation of most of the phosphonofluoridate represented by carbon-14 removed from skin by showering or scrubbing (Table II). Any phosphonofluoridate that had penetrated through the skin was below the detection limit of the enzymatic analysis. The purity of the stock samples of the radiolabeled phosphonofluoridate was checked initially, during the

[12] No. 7101; Hamilton Co., Reno, Nev.
[13] Masterflex, with Model 7014 head; Cole Parmer Instrument Co., Chicago, Ill.
[14] Tenax GC; Alltech Associates, Arlington Heights, Ill.
[15] Triton X-100; Rohm and Haas Co.
[16] Model 306 sample oxidizer; Packard Instruments.
[17] Carbosorb; Packard Instruments.

Table II—Enzymatic Analysis of Skin Decontamination Water and Skin Scrub Solution

Chemical	Condition	Active Agent, %[a] Decontamination Water[b]	Active Agent, %[a] Scrub Solution[c]
Phosphonofluoridate	No shower	—	13 ± 12
	Shower	15 ± 6	17 ± 6
Thickened phosphonofluoridate	No shower	—	8 ± 7
	Shower	16 ± 13	15 ± 15

[a] Percent of recovered radioactivity associated with active agent as determined by enzymatic assays. Numbers are mean ± *SD*. [b] Water collected in chamber B after shower decontamination of the skin. [c] One percent aqueous surfactant solution used to scrub and rinse the skin.

course of the study, and after the completion of the experiments. Purity was essentially 100% at the initial and midpoint, but fell to 70% after the completion of the experiments. However, no significant differences were found between results from initial and final samples.

The inactivation of 1,2,2-trimethylpropyl methylphosphonofluoridate in contact with skin is consistent with the observations of Fredricksson (3) who demonstrated the presence of organophosphate ester hydrolases in the skin of rats. Other investigators (4) who compared skin penetration of the phosphonofluoridate activity with radiolabel penetration reported that human skin decomposed at least 80% of the applied phosphonofluoridate as contrasted with 30% inactivation of its penetration of guinea pig skin.

Diethyl malonate was selected as a simulant for the phosphonofluoridate in skin-surface removal studies on the basis of similar physical properties. For both compounds, the majority of the applied dose evaporated. After 15 min, most of the radiolabel that remained (Table I) was recovered from the skin surface (by showering or scrubbing). The lack of agreement between radioactivity and enzyme inhibition assays of the shower and scrub water would suggest that some of the phosphonofluoridate hydrolyzed after it contacted the skin. In the case of diethyl malonate, hydrolysis on the skin is certainly possible. It is, therefore, possible that the shower removed a mixture of the original compounds as well as hydrolysis products, and it is no longer clear what is being compared. Presumably, the intact compound would have a different affinity for the skin than its hydrolysis products. The fact that similar skin decontamination efficiencies (as judged by the percent removal of radioactivity still on the skin after evaporation) were obtained by showering after application of the radiolabeled diethyl malonate and phosphonofluoridate may be fortuitous. However, if the shower removed the upper layers of skin, and thus removed contaminants in these layers indirectly, decontamination of surface residues would be independent of chemical structure, and similar decontamination efficiencies would be obtained as in this study.

Under the conditions of this study, skin penetration of 1,2,2-trimethylpropyl methylphosphonofluoridate and diethyl malonate was limited by the dose, short interval between application and decontamination, and the free evaporation of the chemicals during this interval. The skin penetration of the phosphonofluoridate is complicated by the possibilities of chemical degradation during its passage through the skin. Attempts to compare the percutaneous penetration of this phosphonofluoridate (and other highly toxic organophosphorous compounds) to analogues or simulants must await knowledge of the fate and distribution of these compounds in skin.

REFERENCES

(1) W. G. Reifenrath, Report No. 86, Letterman Army Institute of Research, The Presidio, San Francisco, Calif., 1980.

(2) A. N. Siakotos, M. Filbert, and R. Hester, *Biochem. Med.*, **3**, 1 (1969).

(3) T. Fredricksson, *Acta Derm-Venereol.*, **1969**, 49.

(4) C. van Hooidonk, B. I. Eullen, H. Kienhuis, and J. Bock, Second International Congress of Toxicology, Brussels, July 1982.

ACKNOWLEDGMENTS

This study was supported, in part, by the Life Support System Program Office, United States Air Force, Wright Patterson Air Force Base, Ohio and was conducted at the U.S. Army Medical Research Institute for Chemical Defense and Chemical Systems Laboratory, Aberdeen Proving Ground, Md. In conducting the research described in this report, the investigators adhered to the "Guide for the Care and Use of Laboratory Animals," as promulgated by the Committee on Revision of the Guide for Laboratory Animal Facilities and Care of the Institute of Laboratory Animal Resources, National Research Council.

The authors wish to acknowledge Don Headley Ph.D., Project Officer, U.S. Army Medical Research Institute of Chemical Defense, for his scientific and administrative contributions to the study; Virginia Gildengorin Ph.D., Letterman Army Institute of Research, for statistical analysis; and Mr. Donald Fielder, Chemical Systems Laboratory, for preparing thickened diethyl malonate and thickened soman.

Stereospecific Fluorescence High-Performance Liquid Chromatographic Analysis of Warfarin and Its Metabolites in Plasma and Urine

CHRISTOPHER BANFIELD and MALCOLM ROWLAND ˣ

Received April 18, 1983, from the *Department of Pharmacy, University of Manchester, Manchester M13 9PL, England.* Accepted for publication August 19, 1983.

Abstract □ A stereospecific assay for the simultaneous determination of the enantiomers of warfarin and its major metabolites, 6- and 7-hydroxywarfarin and warfarin alcohols, in plasma and urine was developed. Involved in this determination was the formation of diastereoisomeric esters with carbobenzyloxy-L-proline, separation by normal-phase high-performance liquid chromatography, and detection by fluorescence after postcolumn aminolysis with *n*-butylamine. The determination limit for any enantiomer is in the order of 50–100 ng. The method was applied to the analysis of the enantiomers of warfarin and metabolites in plasma and urine of human subjects receiving racemic drug. The results for warfarin enantiomers are comparable with those obtained by an MS method, involving administration of a synthetic pseudoracemate [$^{12}C(R)$,$^{13}C(S)$]warfarin. In addition to all known metabolites, the detection of 7-*R*-hydroxywarfarin indicates that 7-hydroxylation is stereoselective rather than stereospecific.

Keyphrases □ Fluorescence, HPLC—stereospecific analysis of warfarin and its metabolites □ Warfarin—stereospecific fluorescence HPLC, metabolites □ Isomers—stereospecific fluorescence HPLC, warfarin and its metabolites

Warfarin [3-(α-acetonylbenzyl)-4-hydroxycoumarin] contains an asymmetric center. In humans, the *R*- and *S*-isomers show differences in pharmacological activity (1), hepatic clearance, and metabolism (2–4). Drugs have been shown to interact differently with the isomers; for example, when coadministered with phenylbutazone, the hepatic clearance

0022-3549/84/1000-1392$01.00/0

© 1984, American Pharmaceutical Association

Table II—Enzymatic Analysis of Skin Decontamination Water and Skin Scrub Solution

Chemical	Condition	Active Agent, %[a] Decontamination Water[b]	Active Agent, %[a] Scrub Solution[c]
Phosphonofluoridate	No shower	—	13 ± 12
	Shower	15 ± 6	17 ± 6
Thickened phosphonofluoridate	No shower	—	8 ± 7
	Shower	16 ± 13	15 ± 15

[a] Percent of recovered radioactivity associated with active agent as determined by enzymatic assays. Numbers are mean ± *SD*. [b] Water collected in chamber B after shower decontamination of the skin. [c] One percent aqueous surfactant solution used to scrub and rinse the skin.

course of the study, and after the completion of the experiments. Purity was essentially 100% at the initial and midpoint, but fell to 70% after the completion of the experiments. However, no significant differences were found between results from initial and final samples.

The inactivation of 1,2,2-trimethylpropyl methylphosphonofluoridate in contact with skin is consistent with the observations of Fredricksson (3) who demonstrated the presence of organophosphate ester hydrolases in the skin of rats. Other investigators (4) who compared skin penetration of the phosphonofluoridate activity with radiolabel penetration reported that human skin decomposed at least 80% of the applied phosphonofluoridate as contrasted with 30% inactivation of its penetration of guinea pig skin.

Diethyl malonate was selected as a simulant for the phosphonofluoridate in skin-surface removal studies on the basis of similar physical properties. For both compounds, the majority of the applied dose evaporated. After 15 min, most of the radiolabel that remained (Table I) was recovered from the skin surface (by showering or scrubbing). The lack of agreement between radioactivity and enzyme inhibition assays of the shower and scrub water would suggest that some of the phosphonofluoridate hydrolyzed after it contacted the skin. In the case of diethyl malonate, hydrolysis on the skin is certainly possible. It is, therefore, possible that the shower removed a mixture of the original compounds as well as hydrolysis products, and it is no longer clear what is being compared. Presumably, the intact compound would have a different affinity for the skin than its hydrolysis products. The fact that similar skin decontamination efficiencies (as judged by the percent removal of radioactivity still on the skin after evaporation) were obtained by showering after application of the radiolabeled diethyl malonate and phosphonofluoridate may be fortuitous. However, if the shower removed the upper layers of skin, and thus removed contaminants in these layers indirectly, decontamination of surface residues would be independent of chemical structure, and similar decontamination efficiencies would be obtained as in this study.

Under the conditions of this study, skin penetration of 1,2,2-trimethylpropyl methylphosphonofluoridate and diethyl malonate was limited by the dose, short interval between application and decontamination, and the free evaporation of the chemicals during this interval. The skin penetration of the phosphonofluoridate is complicated by the possibilities of chemical degradation during its passage through the skin. Attempts to compare the percutaneous penetration of this phosphonofluoridate (and other highly toxic organophosphorous compounds) to analogues or simulants must await knowledge of the fate and distribution of these compounds in skin.

REFERENCES

(1) W. G. Reifenrath, Report No. 86, Letterman Army Institute of Research, The Presidio, San Francisco, Calif., 1980.

(2) A. N. Siakotos, M. Filbert, and R. Hester, *Biochem. Med.*, **3**, 1 (1969).

(3) T. Fredricksson, *Acta Derm-Venereol.*, **1969**, 49.

(4) C. van Hooidonk, B. I. Eullen, H. Kienhuis, and J. Bock, Second International Congress of Toxicology, Brussels, July 1982.

ACKNOWLEDGMENTS

This study was supported, in part, by the Life Support System Program Office, United States Air Force, Wright Patterson Air Force Base, Ohio and was conducted at the U.S. Army Medical Research Institute for Chemical Defense and Chemical Systems Laboratory, Aberdeen Proving Ground, Md. In conducting the research described in this report, the investigators adhered to the "Guide for the Care and Use of Laboratory Animals," as promulgated by the Committee on Revision of the Guide for Laboratory Animal Facilities and Care of the Institute of Laboratory Animal Resources, National Research Council.

The authors wish to acknowledge Don Headley Ph.D., Project Officer, U.S. Army Medical Research Institute of Chemical Defense, for his scientific and administrative contributions to the study; Virginia Gildengorin Ph.D., Letterman Army Institute of Research, for statistical analysis; and Mr. Donald Fielder, Chemical Systems Laboratory, for preparing thickened diethyl malonate and thickened soman.

Stereospecific Fluorescence High-Performance Liquid Chromatographic Analysis of Warfarin and Its Metabolites in Plasma and Urine

CHRISTOPHER BANFIELD and MALCOLM ROWLAND ˣ

Received April 18, 1983, from the *Department of Pharmacy, University of Manchester, Manchester M13 9PL, England.* Accepted for publication August 19, 1983.

Abstract □ A stereospecific assay for the simultaneous determination of the enantiomers of warfarin and its major metabolites, 6- and 7-hydroxywarfarin and warfarin alcohols, in plasma and urine was developed. Involved in this determination was the formation of diastereoisomeric esters with carbobenzyloxy-L-proline, separation by normal-phase high-performance liquid chromatography, and detection by fluorescence after postcolumn aminolysis with *n*-butylamine. The determination limit for any enantiomer is in the order of 50–100 ng. The method was applied to the analysis of the enantiomers of warfarin and metabolites in plasma and urine of human subjects receiving racemic drug. The results for warfarin enantiomers are comparable with those obtained by an MS method, involving administration of a synthetic pseudoracemate [$^{12}C(R)$,$^{13}C(S)$]warfarin. In addition to all known metabolites, the detection of 7-*R*-hydroxywarfarin indicates that 7-hydroxylation is stereoselective rather than stereospecific.

Keyphrases □ Fluorescence, HPLC—stereospecific analysis of warfarin and its metabolites □ Warfarin—stereospecific fluorescence HPLC, metabolites □ Isomers—stereospecific fluorescence HPLC, warfarin and its metabolites

Warfarin [3-(α-acetonylbenzyl)-4-hydroxycoumarin] contains an asymmetric center. In humans, the *R*- and *S*-isomers show differences in pharmacological activity (1), hepatic clearance, and metabolism (2–4). Drugs have been shown to interact differently with the isomers; for example, when coadministered with phenylbutazone, the hepatic clearance

0022-3549/84/1000-1392$01.00/0

© 1984, American Pharmaceutical Association

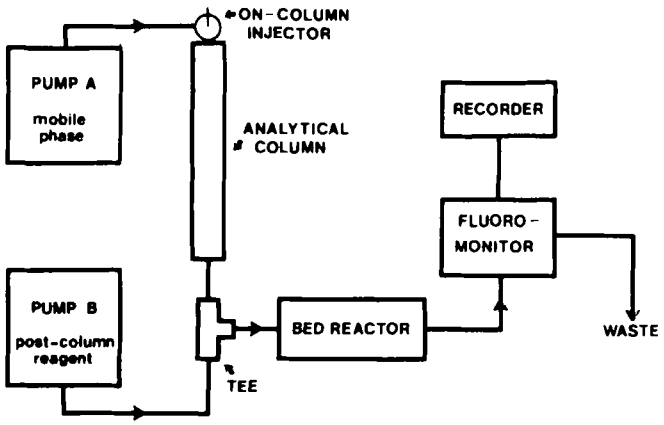

Figure 1—*Flow diagram of HPLC system used for separation and fluorescence detection of warfarin isomers and metabolites.*

of the *S*-isomer is decreased, whereas that of the *R*-isomer is, if anything, hastened (3, 5).

To explore the pharmacokinetics of the individual isomers and drug interactions with warfarin, several stereospecific assays were developed for the determination of warfarin enantiomers in plasma. One assay involved the synthesis of a stable isotope of one of the enantiomers, administration of a pseudoracemate, [^{12}C(*R*),^{13}C(*S*)]warfarin, and determination of the isomers in plasma by MS (6, 7). Another assay used was a stereospecific radioimmunoassay (8). Recently, we reported a high-performance liquid chromatographic (HPLC) technique involving UV detection (9). We now report an extension of the HPLC technique for determination of not only the enantiomers of warfarin, but also its enantiomeric metabolites in plasma and urine after administration of *RS*-warfarin to humans. The method is more sensitive and specific than the UV method.

EXPERIMENTAL SECTION

Reagents and Materials—Racemic warfarin was obtained from its sodium salt[1] by precipitation with 0.1 M HCl. The dried material was recrystallized from absolute ethanol. *R*(+)- and *S*(−)-warfarin[2]; warfarin metabolites[3] [6-hydroxywarfarin, 7-hydroxywarfarin, alcohol 1 (*RS* and *SR* alcohols)]; the selected internal standard[4], 3-α-[(4′-fluorophenyl)-β-acetylethyl]-4-hydroxycoumarin and 4′-fluorowarfarin; imidazole[5]; dicyclohexylcarbodiimide[6]; carbobenzyloxy-L-proline[6]; *n*-butylamine[6]; hexane (HPLC grade)[7]; methanol[8]; and ethyl acetate (HPLC grade)[7] were used as supplied. Peroxide-free ether[9] was prepared by passage through a column of activated alumina[10] (45 g).

Extraction from Plasma—To culture tubes[11] containing citrated plasma were added the internal standard (4′-fluorowarfarin), ranging from 0.85 to 6.8 μg/100 μL of water, sodium hydroxide (0.2 mL), and peroxide-free ether (4 mL). The mixture was shaken mechanically for 5 min and centrifuged[12] at 3000 rpm for 5 min; the organic phase was removed by aspiration. The aqueous phase was then acidified with 3 M HCl (0.5 mL), shaken with peroxide-free ether (8 mL) for 2 min, and centrifuged at 3000 rpm for 10 min; the ethereal layer was transferred to a clean culture tube. The ether was washed free of any citrate by shaking with pH 4 phosphate buffer (5 mL) for 5 min. (If the anticoagulant used is heparin, the pH 4 phosphate buffer

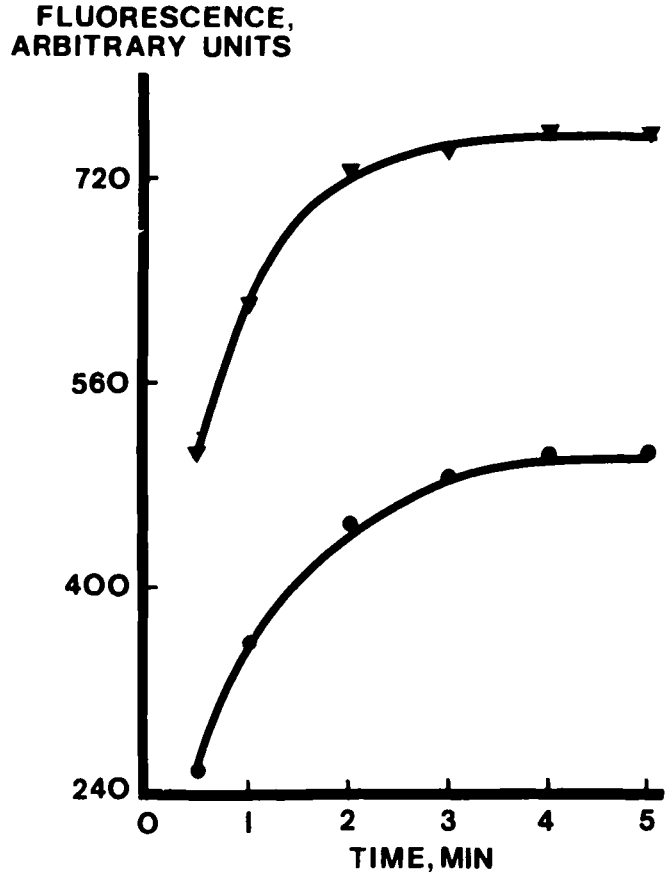

Figure 2—*Fluorescence intensity on incubation of the carbobenzyloxy-L-prolyldiastereoisomeric esters of* RS*-warfarin with* n*-butylamine (●) and 1,3-diaminopropane (▼).*

washing step can be omitted from the procedure.) After allowing the phases to separate, the ethereal layer was dried over calcium chloride (~1 g), centrifuged (3000 rpm for 3 min), and transferred to a culture tube, the tip of which was drawn out to a capacity of 0.2 mL. An antibumping granule was added to each tube, and the ether was evaporated on a heating block at 45°C under a stream of nitrogen. The tubes were washed three times with small volumes of ether, with evaporation of the ether carried out between each addition. Finally, a small volume of ether (100 μL) was added, vortexed, and evaporated to dryness.

Extraction from Urine—To silanized culture tubes containing internal standard (0.8–7 μg of 4′-fluorowarfarin in 100 μL of water) were added a urine sample (0.5 mL), 3 M HCl (0.5 mL), and chloroform (8 mL). The tubes were capped with screw-caps with polytef liners; the mixture was shaken for ~45 min by rotating gently and centrifuged at 3000 rpm for 10 min. The aqueous layer was removed by aspiration, and to the organic phase was added 0.1 M NaOH (1.7 mL). The process of extraction and phase separation was then repeated. The sodium hydroxide layer was transferred to a clean culture tube, acidified with 3 M HCl (0.5 mL), and shaken with chloroform (8 mL) for ~45 min. After centrifugation (10 min), the aqueous layer was removed by aspiration, and the chloroform layer was dried by vortexing for ~10 s over calcium chloride (~1 g/tube), followed by centrifugation at 3000 rpm for 5 min. As much as possible of the chloroform layer was then transferred to a culture tube, the tip of which was drawn out to a capacity of 0.2 mL and evaporated to dryness with a heating block at 65°C under a stream of nitrogen.

Derivatization—To the extracts in the tapered culture tubes were added carbobenzyloxy-L-proline (200 mg/mL of acetonitrile; 10 μL), imidazole (1 mg/ml of acetonitrile; 10 μL), and dicyclohexylcarbodiimine (200 mg/mL of acetonitrile; 10 μL), and the mixture was vortexed for ~10 s. After 2 h at ambient temperature a small volume of ethyl acetate (10 μL) was added to the mixture, and aliquots were analyzed by HPLC.

High-Performance Liquid Chromatography—A flow diagram of the HPLC system used for separation and fluorescence detection of the diastereoisomeric esters after aminolysis is shown in Fig. 1. The mobile phase [ethyl acetate-hexane-methanol-acetic acid (25:74.75:0.25:0.3)] was pumped[13] at a flow

[1] Sorex, U.K.
[2] Gifts from Endo Laboratories, Inc.
[3] Gifts from Dr. William Trager, School of Pharmacy, University of Washington, Seattle, Wash.
[4] Gifts from Ciba Geigy Ltd., Switzerland.
[5] Sigma Chemical Co.
[6] Aldrich Chemical Co.
[7] Rathburn, Scotland.
[8] Analar grade; Fisons, U.K.
[9] May and Baker, Dagenham, U.K.
[10] Alkaline, Brokman type 1; B.D.H., U.K.
[11] Corning Glass Works.
[12] Super Minor Centrifuge, no. 533A; MSE, U.K.
[13] Model 100A; Altex, Anachem Ltd., U.K.

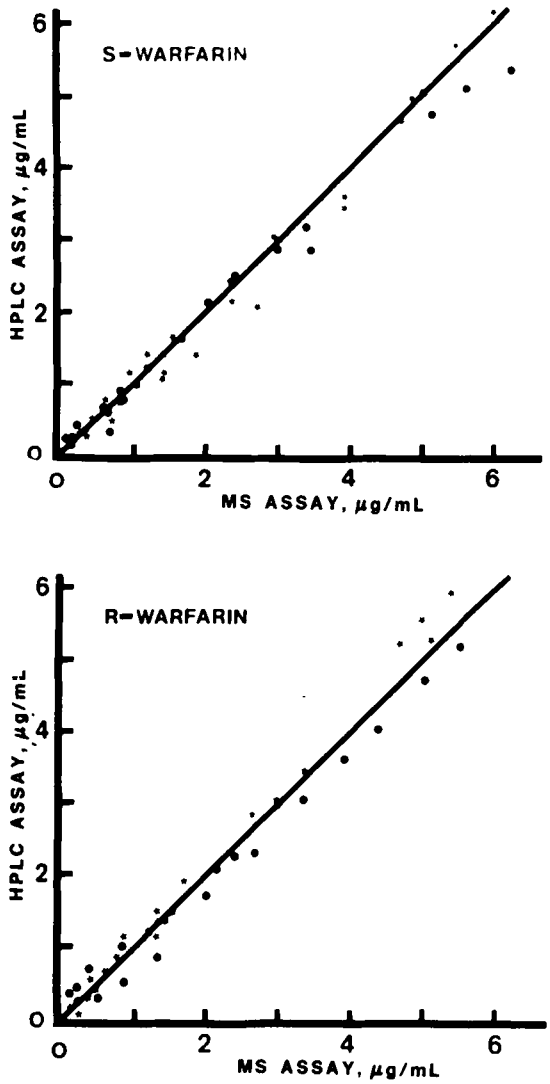

Figure 3—*Comparison between the HPLC assay carried out in this study and an MS assay (16) for the determination of warfarin enantiomers in plasma in subjects receiving racemic warfarin either alone (●) or during phenylbutazone administration (★).*

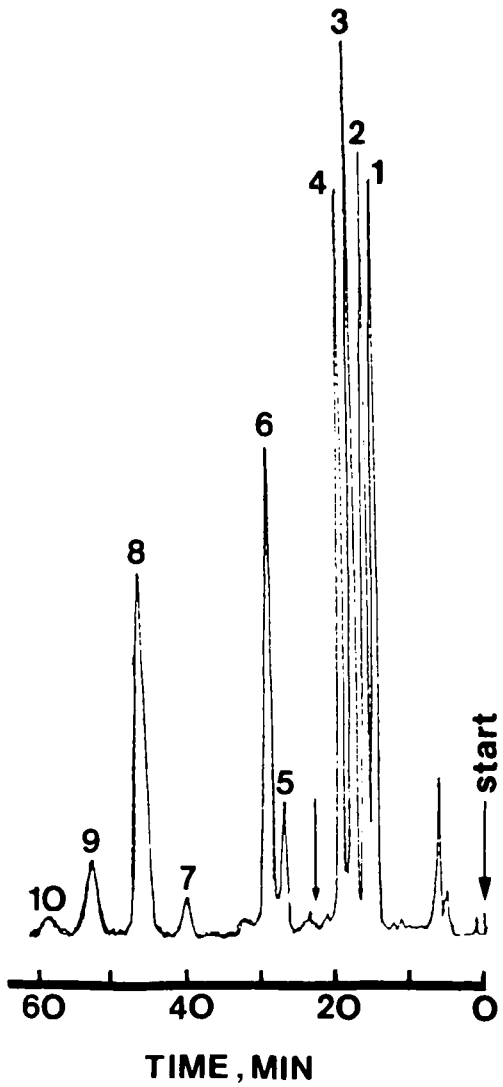

Figure 4—*Chromatogram resulting from extraction and derivatization with carbobenzyloxy-L-proline with subsequent postcolumn aminolysis of plasma (1 mL) obtained from a subject 24 h after oral administration of* RS-*warfarin (1.5 mg/kg). Key: (1)* S-*warfarin (3.2 μg/mL); (2) first eluting peak of internal standard (0.42 μg); (3)* R-*warfarin (4.0 μg/mL); (4) second eluting peak of internal standard (0.42 μg); (5)* SS-*alcohol (not quantitated); (6)* RS-*alcohol (0.53 μg/mL); (7) 6-*S-*hydroxywarfarin (0.11 μg/mL); (8) 7-*S-*hydroxywarfarin (0.77 μg/mL); (9) 6-*R-*hydroxywarfarin (0.18 μg/mL); (10) 7-*R-*hydroxywarfarin (not quantitated). Arrow indicates a change of sensitivity setting from 1 to 0.2 μA.*

rate of 0.8 mL/min through a stainless steel column (250 mm × 5 mm i.d.) packed with silica[14]. The analytical column outlet was fitted through the shortest possible length of polytef tubing (0.030 mm i.d.) to a stainless steel tee[15] (~0.16 cm i.d.), through which the postcolumn reagent [*n*-butylamine–methanol (1:1), pumped[16] at a flow rate 0.4 mL/min] was mixed with the mobile phase. The outlet of the tee was connected to a bed reactor (stainless steel column 3.0 mm i.d. × 25 cm) packed with glass beads[17] (40 μm). The entire system was at ambient temperature. The effluent from the bed reactor was analyzed fluorometrically with excitation at 313 nm, and the emission was measured in the presence of a filter[18] with a sensitivity setting of 6.16 and a time constant of 6 s. For the simultaneous determination of warfarin and metabolites, a range setting of 1 μA was used for between 5 and 1.0 μg per isomer of warfarin. When either the last internal standard ester or *SR*-alcohol had eluted, the range was switched to 0.2 μA to quantitate the other metabolites. At 0.2 μg per isomer of warfarin, the range setting was constant at 0.2 μA throughout the analysis.

The concentrations of enantiomers of warfarin and its oxidation products (6-hydroxywarfarin, 7-hydroxywarfarin) and reduction products (warfarin alcohols) in the unknown samples of plasma and urine were calculated by reference to appropriate calibration curves. These curves were constructed by taking known quantities of the reference materials in warfarin-free plasma and urine through the assay procedure and plotting the peak height ratios obtained, using either isomer of the internal standard, *versus* the known amount of isomeric material per sample.

Elution Order of Warfarin and Metabolites—The individual isomer elution order was established from the administration of either the *R*- or the *S*-warfarin in an isolated perfused rat liver system in a manner similar to that described by Pang and Rowland (10). *R*(+)- or *S*(−)-warfarin (20 μg/mL in Kreb's bicarbonate buffer) was added to the perfusate in a recirculating experiment. After 90 min, the experiment was stopped, and a sample of the reservoir was subjected to analysis for warfarin and metabolites as described above.

RESULTS AND DISCUSSION

Previously, we successfully developed a stereospecific HPLC method for the determination of *R*(+)- and *S*(−)-warfarin in plasma (9). The method involves the reaction of the 4-hydroxy group with carbobenzyloxy-L-proline with formation of diastereoisomeric esters, separation of the esters on silica as the stationary phase, and UV detection at 313 nm. The method has sufficient sensitivity (~0.1 μg per isomer) to measure the plasma concentrations of warfarin enantiomers after chronic maintenance therapy with racemic war-

[14] Si 5-μm; Spherisorb, Phase Separation, U.K.
[15] HETP, U.K.
[16] Model 600DA; Waters Associates.
[17] Whatman 4338-015; Whatman, Inc.
[18] No. 370.

farin and for up to 5 d after a large single oral dose (1.5 mg/kg) of the racemic drug. However, the method is insufficiently sensitive to measure in detail the pharmacokinetics after lower single doses and to measure the concentration of the warfarin metabolites (6-hydroxywarfarin, 7-hydroxywarfarin, warfarin alcohols), which are generally much lower than that of the parent drug (3). These limitations prompted us to develop a more sensitive stereospecific analytical procedure which was still based on the formation of diastereoisomeric esters with carbobenzyloxy-L-proline. Preliminary work showed that this reaction can readily be extended to warfarin metabolites. Use was made of the native fluorescence of warfarin and its metabolites (3).

Postcolumn Aminolysis—Fluorescence techniques often offer greater specificity, as well as enhanced sensitivity, over UV methods. However, by forming an ester at the 4-hydroxyl function, the fluorescent property of warfarin and its metabolites is lost, since only the ionized form of these species fluoresces (3). Therefore, to produce a fluorescent species, the chromatographed esters must be cleaved post column.

The optimal HPLC conditions for separation of the diastereoisomeric esters is the normal-phase mode, with silica used as the stationary phase. The mobile phase [ethylacetate–hexane–methanol–acetic acid (25:74.75:0.25:0.3)] is immiscible with water, so the frequently employed aqueous alkaline hydrolysis of esters could not be employed. The possibility of nonaqueous aminolysis of the carbobenzyloxy-L-proline esters of warfarin enantiomers with organic amines was explored by monitoring the liberated warfarin fluorometrically.

Successful nonaqueous aminolysis and development of a fluorescent species was achieved with *n*-butylamine and 1,3-diaminopropane in methanol. Triethylamine, *N*,*N*-dimethylaniline, and *N*,*N*,*N*′,*N*′-tetramethylethylenediamine were also investigated. However, not only did the warfarin carbobenzyloxy-L-prolyl esters aminolyze more slowly with these organic bases, but fluorescence of the liberated warfarin was also markedly reduced in the presence of these amines, as compared with that achieved in the presence of either *n*-butylamine or 1,3-diaminopropane. TLC analysis [ethyl acetate–hexane–acetic acid (30:70:0.2), silica gel] of the butylamine reaction mixture at the end of the reaction, as judged by the maximum fluorescence reading, confirmed that aminolysis was complete. In place of the two diastereoisomeric esters (R_f 0.27 and 0.32) there was now only one spot corresponding to warfarin (R_f 0.35). Phenyl acetate undergoes aminolysis by *n*-butylamine to form *n*-butylacetamide (11) and, probably, the warfarin esters react similarly. A factor favoring butylamine and 1,3-diaminopropane is that alone, neither reagent produces significant fluorescence.

The fluorescent intensity of a methanolic solution containing the warfarin esters, in the presence of 16.7% base, reached an asymptote within ~4 min (Fig. 2). The data could be described by the first-order expression:

$$\ln (F_{max} - F_t) = \ln F_{max} - kt$$

where F_{max} is the asymptotic value of the fluorescent intensity, F_t is the fluorescent intensity at time t, and k is the first-order rate constant. From such a plot of the data, rate constants of 1.0 ($r^2 > 0.99$) and 1.3 min^{-1} ($r^2 > 0.99$), corresponding to half-lives of 42 and 32 s were obtained for the *n*-butylamine- and 1,3-diaminopropane-catalyzed reactions, respectively. These very short half-lives indicate that the kinetics of aminolysis and production of a fluorescent species is sufficiently rapid for use in an analytical procedure involving a postcolumn reaction step.

Careful selection of the design of the postcolumn reactor is required if chromatographic resolution is to be maintained. Open tubes do not allow effective mixing of the mobile phase and reagent (12). For reaction times greater than 1 min, the long tube required to create sufficient residence time leads to considerable dispersion of sample (13) with resultant loss of resolution and sensitivity. In addition, open-tube reactors are sensitive to changes in flow rate [decreasing flow rate leads to increased residence time resulting in decreased peak height (12)]. In contrast, bed reactors (tubes packed with large-diameter glass beads) provide micromixing of sample and reagents by increasing radial dispersion (14); they are suitable for reactions of up to ~5 min and are less sensitive than open-tube reactors to changes in the flow rate (13). Therefore, based on the reported better performance of bed reactors over tube reactors and the relatively rapid kinetics of aminolysis and development of a fluorescent species, this system was employed in the fluorometric assay (Fig. 1). The residence time in the bed reactor was ~1.5 min (given by the difference in retention of the unretained solute in the presence and absence of the bed reactor). Although it is not critical that the reaction goes to completion, as long as it is reproducible, the less complete the reaction the lower is the overall sensitivity of the assay. Therefore, with the postcolumn reagent [*n*-butylamine–methanol (1:1)] in the HPLC system, which was used at an identical dilution to that in the kinetic study (16.7%), the estimate of half-life computed from the kinetic study was used in conjunction with the residence time in the bed reactor to estimate the percentage of maximum aminolysis

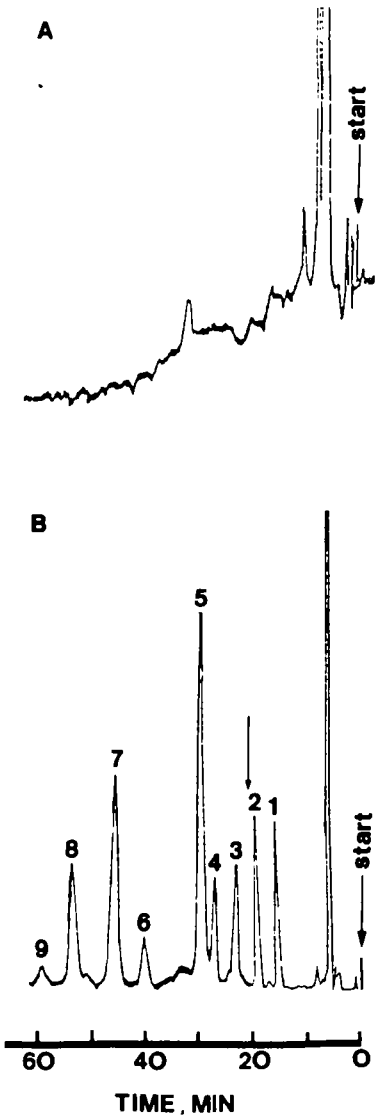

Figure 5—*Chromatogram resulting from extraction and derivatization with carbobenzyloxy-L-proline of a control urine sample (A) and a urine sample (0.5 mL) obtained from a subject between 4 and 5 d after oral administration of* RS-*warfarin (1.5 mg/kg) (B). Key: (1) first eluting peak of internal standard (0.42 μg); (2) second eluting peak of internal standard (0.42 μg); (3)* SR-*alcohol?; (4)* SS-*alcohol (not quantitated); (5)* RS-*alcohol (0.8 μg/mL); (6) 6-*S-*hydroxywarfarin (0.28 μg/mL); (7) 7-*S-*hydroxywarfarin (1.1 μg/mL); (8) 6-*R-*hydroxywarfarin (0.92 μg/mL); (9) 7-*R-*hydroxywarfarin (0.15 μg/mL). For (A), a sensitivity setting of 0.2 μA was used throughout; for (B), the arrow indicates a change of sensitivity setting from 1 to 0.2 μA.*

and fluorescence developed. Under these conditions, at least 78% of the maximum value is obtained. Although 1,3-diaminopropane gives superior results to those of *n*-butylamine, its choice for further investigation was rejected because of the greater toxicity of diamines.

The use of a racemic internal standard which forms diastereoisomeric esters requires a chromatographic system with high resolution to separate the internal standard esters from those of warfarin. Our situation was acute since under optimal chromatographic conditions, the ester of *S*(−)-warfarin elution was followed by the first eluting ester of the racemic internal standard, which preceded the ester of *R*(+)-warfarin. The lack of significant band broadening of the peaks when the postcolumn reactor was used (Fig. 1) is an important feature of the assay technique.

Elution Order of Warfarin and Metabolites—By using the isolated perfused rat liver preparation as a metabolite generator, in all cases, the metabolite derived from the parent molecule with the *S*(−)-configuration eluted first. Thus, 7-*S*-hydroxywarfarin eluted before 7-*R*-hydroxywarfarin, and 6-*S*-hydroxywarfarin eluted before the corresponding *R*-isomer. With the alcohols, the availability of (*R* and *S*)-alcohols (a mixture of all four alcohols), alcohol

1 (*SR* and *RS*), and pure *RS*-alcohol, permitted assignment of the order of elution as *SR*-, *SS*-, *RR*-, and *RS*-alcohol.

Analysis of Plasma—By varying both the concentration of the internal standard (0.85–6.8 μg) and the sensitivity setting on the fluorescence detector, warfarin and its major metabolites can be simultaneously quantitated from plasma (1 mL). The complete analysis time for warfarin and metabolites is 1 h. No major peaks occurred in the chromatogram of control citrated plasma obtained from a healthy volunteer. Similar results were observed for plasma obtained from other subjects. Warfarin and its metabolites had to be separated from citric acid with pH 4 phosphate buffer. In high concentration in citrated plasma, this acid consumes the activating reagent (*N,N*-dicyclohexylcarbodiimide) and also forms esters in place of carbobenzyloxy-L-proline with warfarin and metabolites, leading to nonreproducible results. There were no such problems with heparin, so the pH 4 phosphate buffer wash is not needed when this anticoagulant is used.

Calibration plots for racemic warfarin and the separate metabolites (*RS*-alcohol, 7-*S*- and 7-*R*-hydroxywarfarin, and 6-*S*- and 6-*R*-hydroxywarfarin) in plasma are linear ($r^2 > 0.99$), as are the corresponding plots when these species are analyzed as a multicomponent mixture. Once formed, the respective carbobenzyloxy-L-propyl esters are stable for at least 24 h. The *RSD* over the range 0.1 to 1.0 μg per isomer for the *S*- and *R*-warfarin isomers varied between 8.7 and 1.7% (first eluting esters of the internal standard). By using the second eluting peak of the internal standard, the *CV* ranged between 8.7 and 2.6%. By varying both the concentration of the internal standard (0.85–6.8 μg) and the sensitivity setting on the fluorescence detector, warfarin and its major metabolites could be simultaneously quantitated from plasma (1 mL). The determination limit (with a 10% *CV*) of the metabolites in plasma varied from 0.045 μg for 7-*R*-hydroxywarfarin to 0.15 μg for 6-*R*-hydroxywarfarin, when the first eluting ester of the internal standard was used to compute the peak height ratios. Similar results were obtained when the more slowly eluting ester of the internal standard was used. The noise level of the fluorescence detector was one of the major factors limiting sensitivity.

Analysis from Urine—Preliminary investigations of metabolite extraction from urine by the assay procedure for plasma and detection by the UV (313 nm) procedure were discouraging, because compounds present in metabolite-free urine were UV absorbent and chromatographed with retention times similar to those for the internal standard and the warfarin alcohols.

In contrast, fewer interferences were seen in chromatograms when the extraction procedure described above was used and when fluorescence was the mode of detection. Linear calibration plots were obtained for all the metabolites over their respective ranges (*RS*-alcohol, 0.106–0.85 μg; 7-*R*- and 7-*S*-hydroxywarfarin, 0.1–1.0 μg; 6-*R*- and 6-*S*-hydroxywarfarin, 0.14–1.1 μg). Owing to the lack of a good analytical standard for *SS*-alcohol (alcohol 2), no calibration plots were obtained. The determination limit (with a 10% *CV*) of the metabolites in urine were similar to those in plasma, ranging from 0.042 μg for the 7-*R*-hydroxywarfarin to 0.17 μg for 6-*S*-hydroxywarfarin.

Comparison with a Mass Spectroscopic Assay—As part of a collaborative program, plasma samples[19] from subjects who had participated in a phenylbutazone–warfarin study 2 years previously were received for analysis of *R*(+)- and *S*(−)-warfarin. In the study, subjects received a pseudoracemate of warfarin [^{12}C(*R*),^{13}C(*S*)]warfarin before and during administration of phenylbutazone, and the concentration of the individual enantiomers was determined by an MS method (15). The samples were stored frozen until they were analyzed by us, and the results of the previous analysis were not made available to the analyst until after the results by the present fluorescence method were obtained.

Rigorous statistical evaluation of the performance of the HPLC and the MS methods cannot be shown since both assays were not performed by the same laboratory. The concentrations of the isomers when *RS*-warfarin was administered alone or with phenylbutazone are presented in Fig. 3. The slopes of the warfarin concentrations in the absence or during phenylbutazone treatment are close to 1, suggesting that the two methods give comparable results. These graphs also illustrate both the good stability of warfarin in plasma, since these analyses were performed ~2 years apart, and the lack of interference of phenylbutazone and its metabolites in the analysis of warfarin. This lack of interference in the fluorescence assay was further demonstrated by the absence of interfering peaks and identity of the slopes of the calibration curves for the enantiomers of warfarin when assayed from plasma that was spiked with therapeutic concentrations of phenylbutazone and its major oxidation metabolites, oxyphenbutazone and γ-hydroxyphenylbutazone (16).

Presence of Other Drugs—Interference in the plasma or urine assay by other drug substances such as cimetidine and salicylate drugs that may be administered concomitantly with warfarin was also studied. Cimetidine produced no spurious peaks in the chromatograms in the presence or absence of *RS*-warfarin. As an imidazole, it is a base and presumably was extracted by the acid–base extraction step.

A large peak in the chromatogram, which interferes with the analysis of warfarin metabolites, was observed when urine spiked with salicylate was taken through the assay procedure. Salicylate fluoresces at the maximum wavelength of excitation of warfarin, is activated by dicyclohexylcarbodiimide, and forms an ester with warfarin or consumes the chiral reagent by formation of an ester at the phenolic group. Hence, the quantitation of the metabolites of warfarin in urine in the presence of salicylate is likely to be severely limited by some or all of the factors described above.

***In Vivo* Study**—Figure 4 shows a chromatogram of a plasma sample obtained 24 h after the administration of *RS*-warfarin (1.5 mg/kg) to a healthy volunteer. The metabolic pattern observed is consistent with the stereoselectivity of metabolism shown by other workers after the administration of the individual isomers (3, 4). In addition, a small quantity of 7-*R*-hydroxywarfarin was seen. A similar metabolic pattern can be seen in urine 123 h after ingestion of *RS*-warfarin (1.5 mg/kg) (Fig. 5). In addition, there is a peak which chromatographs with a retention time similar to that of the *SR*-alcohol. This peak is absent in a metabolite-free urine sample taken from the same subject. The presence of this peak suggests that the reduction of the *S*-isomer may not be stereospecific for the *S*-configuration.

[19] Kindly supplied by Dr. R. O'Reilly, Santa Clara Valley Medical Center, San Jose, Calif.

REFERENCES

(1) A. Breckenridge, M. Orme, H. Wesseling, R. J. Lewis, and R. Gibbons, *Clin. Pharmacol. Ther.*, **15**, 424 (1974).

(2) R. A. O'Reilly, *Clin. Pharmacol. Ther.*, **16**, 384 (1974).

(3) R. J. Lewis, W. F. Trager, K. K. Chan, A. Breckenridge, M. Orme, M. Rowland, and W. Schary, *J. Clin. Invest.*, **53**, 1607 (1974).

(4) D. S. Hewick and J. McEwen, *J. Pharm. Pharmacol.*, **25**, 458 (1973).

(5) R. A. O'Reilly, W. F. Trager, C. H. Motley, and W. N. Howald, *J. Clin. Invest.*, **65**, 746 (1980).

(6) W. N. Howald, E. D. Busch, W. F. Trager, R. A. O'Reilly, and C. H. Motely, *Biomed. Mass Spectrom.*, **7**, 35 (1980).

(7) C. Hignite, J. Utrecht, C. Tschanz, and D. Arzarnoff, *Clin. Pharmacol. Ther.*, **28**, 99 (1980).

(8) C. E. Cooke, N. H. Ballentine, T. B. Saltzman, and C. R. Tallent, *J. Pharmacol. Exp. Ther.*, **210**, 391 (1979).

(9) C. R. Banfield and M. Rowland, *J. Pharm. Sci.*, **72**, 921 (1983).

(10) K. S. Pang and M. Rowland, *J. Pharmacokinet. Biopharm.*, **5**, 655 (1977).

(11) W. P. Jenks and J. Carrinolo, *J. Am. Chem. Soc.*, **83**, 675 (1960).

(12) J. M. Reijn, W. E. van der Linden, and H. Poppe, *Anal. Chim. Acta*, **123**, 224 (1981).

(13) R. W. Frei, in "8th Technicon International Congress," London, December 12–14, 1978.

(14) J. F. K. Huber, K. M. Jonker, and H. Poppe, *Anal. Chem.*, **52**, 2 (1980).

(15) W. N. Howald, E. D. Busch, W. F. Trager, R. A. O'Reilly, and C. H. Motely, *Biomed. Mass Spectrom.*, **7**, 35 (1980).

(16) C. Higham, L. Aarons, P. J. L. Holt, M. Lynch, and M. Rowland, *Br. J. Clin. Pharmacol.*, **12**, 123 (1981).

ACKNOWLEDGMENTS

This study was supported by Grant G977/249 from the British Medical Research Council.

Bioavailability of Digoxin Capsules and Tablets: Effect of Coadministered Fluid Volume

JAMES A. BUSTRACK *‡ˣ, JEFFREY D. KATZ §, J. HEYWARD HULL *‡, JAMES R. FOSTER §, JOHN E. HAMMOND ¶‖, and ROBERT H. CHRISTENSON ¶△

Received June 13, 1983, from the *Department of Clinical Research, Burroughs Wellcome Co., Research Triangle Park, NC 27709, ‡Division of Pharmacy Practice, School of Pharmacy, §Department of Medicine, ¶Department of Hospital Laboratories, and ‖Departments of Pathology, Medicine, and Biochemistry, School of Medicine, University of North Carolina, Chapel Hill, NC 27514. Accepted for publication November 18, 1983. △Present address: Departments of Laboratory Services and Pathology, Durham Veterans Administration and Duke University Medical Centers, Durham, NC 27705.

Abstract □ The effect of different coadministered fluid (water) volumes on the consistency of digoxin absorption was studied in 16 male volunteers. Each volunteer received four single-dose treatments (two 0.25-mg digoxin tablets with 30- and 240-mL of water and two 0.2-mg digoxin capsules with 30- and 240-mL of water). Digoxin present in serum and urine samples collected for 48 h after dosing was quantified by RIA. Treatments were compared by evaluating the following model-independent pharmacokinetic parameters: maximum serum concentration (C_{max}); time of maximum serum concentration (t_{max}); area under the serum concentration-time curve for 0–12 h (AUC_{0-12}); cumulative urinary excretion for 0–48 h (CUE_{48}). No significant differences were found between dosage form (tablets *versus* capsules) and coadministered water volume (30 mL *versus* 240 mL) for any of the parameters. For both fluid volumes the AUC_{0-12} and C_{max} were significantly larger ($p < 0.01$) and the t_{max} significantly shorter ($p < 0.01$) for the capsules than for the tablets. The volume of coadministered water had no effect on the amount of digoxin absorbed from either dosage form.

Keyphrases □ Digoxin—bioavailability, coadministered fluid volume □ Fluid volume—bioavailability of digoxin

The bioavailability of orally administered drugs may be affected by a number of factors, including dosage form, physicochemical properties of the drug, first-pass extraction by the liver, interactions prior to absorption between the drug and substances in the GI tract, and certain diseases involving the GI tract. One factor which may affect oral bioavailability, that has received little attention, is the potential influence of coadministered fluid volume on drug absorption. In fact, a commonly accepted notion is that drugs are absorbed more rapidly from concentrated than from dilute solutions (1). However, some studies in experimental animals and humans dispute this point. Ferguson (2) studied the toxicity of a variety of organic and inorganic compounds following oral doses to fasted rats. Equal doses of dissolved compounds were given in increasing water volumes equivalent to 1.25, 2.5, and 5.0% of body weight. The toxicity of all compounds, expressed in terms of median lethal dose (LD_{50}), increased with increasing dilution, indicating that absorption was more rapid and/or more complete from dilute solutions. General mechanisms that have been suggested for increased drug absorption from dilute oral solutions are (*a*) more rapid stomach emptying due to the greater volume and (*b*) relative hypotonicity of the solutions, with consequent exposure of the solute to a greater intestinal surface area (3).

The influence of fluid volume on bioavailability of drugs in humans has been studied with erythromycin stearate (4), ampicillin trihydrate (5), amoxicillin trihydrate (5), theophylline (6), doxycycline hyclate (7), tetracycline hydrochloride (7), and propoxyphene hydrochloride (8). In general, these studies of passively absorbed drugs indicate that the volume of fluid coadministered with a drug of poor water solubility may significantly affect the rate and/or extent of its absorption. The bioavailability of drugs with good water solubility, on the other hand, is relatively unaffected by a change in fluid volume.

Digoxin is a compound that is poorly soluble in water [0.095 mg/mL (9)]. Because of this, concern has been expressed that absorption from a tablet may be affected by administration

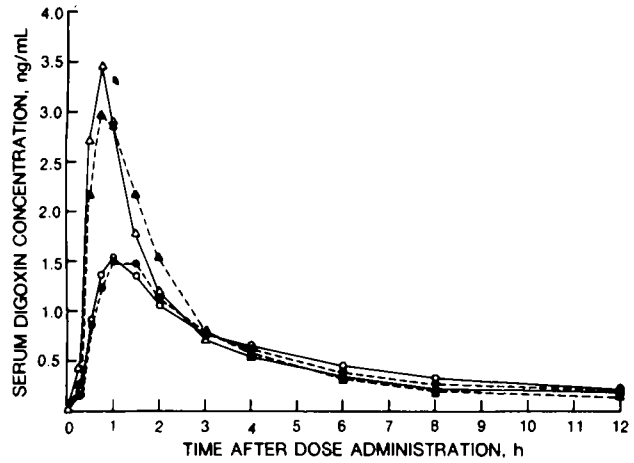

Figure 1—*Mean serum digoxin concentration–time curves during the first 12 h following oral administration. Key: (●) tablets + 30 mL; (○) tablets + 240 mL; (▲) capsules + 30 mL; (△) capsules + 240 mL.*

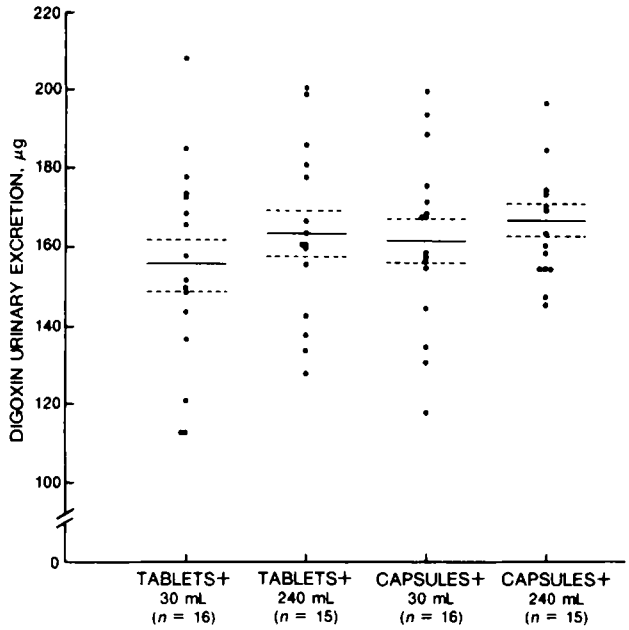

Figure 2—*Cumulative urinary excretion of digoxin during the first 48 h following digoxin administration. Key: (—) mean; (- - -) ± SE.*

0022-3549/84/1000-1397$01.00/0
© 1984, American Pharmaceutical Association

Table I—Area Under the Serum Concentration–Time Curves 0–12 h (ng·h/mL)

Volunteer	Tablets + 30 mL	Tablets + 240 mL	Capsules + 30 mL	Capsules + 240 mL
1	3.34	6.29	5.92	5.72
2	2.86	4.73	6.93	8.02
3	5.61	6.45	8.05	6.25
4	10.96	6.91	10.58	10.35
5	6.02	7.43	7.82	8.26
6	7.25	6.85	8.25	8.27
7	5.97	5.67	10.14	5.02
8	3.83	5.53	5.74	7.48
9	5.73	10.98	9.25	11.51
10	8.75	6.06	9.94	10.58
11	4.76	4.34	8.77	8.21
12	5.75	7.93	5.69	6.07
13	6.39	6.86	5.86	4.64
14	7.71	6.49	8.61	10.14
15	10.31	9.79	8.00	9.07
16	5.60	5.45	7.37	6.54
Mean	6.30	6.74	7.93	7.88
SD	2.27	1.71	1.60	2.08

with different fluid (water) volumes. If this concern was justified, differences in fluid volumes may have had a significant influence on the results of previously published bioavailability studies. Also, many patients take their medications with varying amounts of fluid, ranging from a small ("gulp") to a glassful of water. The difference in patterns of administration could be associated with inconsistency in the amount of digoxin absorbed from tablets during clinical use.

A solid dosage form (capsule) in which the digoxin is already in solution is now available. Theoretically, absorption from this capsule should not be affected by different water volumes and may be more consistent than tablet doses. Thus, a study was conducted to compare the influence of fluid volume on the consistency of digoxin absorption from these two dosage forms when given in bioequivalent doses[1]. This was accomplished by administering digoxin tablets and a digoxin formulation as a solution in soft gelatin capsules [90–100% absorbed (10–12)] with 30 mL and 240 mL of water to healthy volunteers in a crossover study.

EXPERIMENTAL SECTION

Clinical Study—Sixteen healthy male volunteers [23–33 years old (mean 25.1) and 61.2–83.0 kg (mean 72.2)] entered and completed the study. All volunteers were in good health (physical examination, clinical laboratory studies, and an electrocardiogram). Information about the purpose of the study and the procedures to be performed was provided to each volunteer. Each signed an informed consent form (approved by the Institutional Review Board) and participated in the study for approximately 8 weeks.

The volunteers fasted from midnight prior to dosing until 4 h following treatment administration. Volunteers were given 120 mL of water at least 1 h before dosing on the morning of each test day to provide adequate hydration after overnight fluid restriction.

Dosing for each treatment occurred at 8 a.m., and blood and urine collections were made over the next 48 h. Blood samples (5 mL) were obtained by standard venipuncture techniques in vacuum tubes without additives at the following times: just prior to dosing (0 h), 0.25, 0.5, 0.75, 1, 1.5, 2, 3, 4, 6, 8, 12, 24, and 48 h after dose administration. These samples were allowed to clot and immediately centrifuged; the serum was separated and stored at −20°C until the time of analysis.

Urine was collected prior to drug administration (blank specimen), 0–24 h, and 24–48 h after drug administration. At the end of each interval the samples were thoroughly mixed, the volumes measured and recorded, and aliquots were removed and frozen until analysis.

Following dose administration the volunteers were ambulatory; however, no strenuous or abnormal physical activity was permitted. A standardized light lunch was served 4 h after dosing.

[1] Lanoxicaps package insert; Burroughs Wellcome Co., Research Triangle Park, N.C., June 1982.

Table II—Cumulative Urinary Digoxin Excretion (μg/48 h)

Volunteer	Tablets + 30 mL	Tablets + 240 mL	Capsules + 30 mL	Capsules + 240 mL
1	143.0	—[a]	167.0	159.0
2	148.5	200.0	199.5	163.0
3	207.5	160.0	167.5	154.5
4	173.5	178.0	154.5	146.0
5	151.5	199.0	157.5	196.5
6	172.5	127.5	145.0	155.0
7	177.5	160.0	194.0	195.5
8	168.0	167.0	188.5	184.5
9	120.5	160.5	117.5	173.5
10	149.0	163.5	158.0	170.0
11	112.5	137.5	131.0	160.5
12	136.5	133.0	156.5	147.0
13	165.5	185.5	176.0	170.0
14	185.0	180.0	172.0	174.5
15	157.5	155.5	169.0	154.5
16	113.0	142.5	135.0	—[a]
Mean	155.1	163.3	161.8	166.9
SD	26.4	22.4	22.5	15.9

[a] Incomplete urine collection.

Study Design—The treatments listed below were administered using an open, single-dose, four-way complete crossover (Latin square) design:

1. Two 0.25-mg digoxin tablets[2] with 30 mL of water (tablets + 30 mL).
2. Two 0.25-mg digoxin tablets[2] with 240 mL of water (tablets + 240 mL).
3. Two 0.2-mg capsules[3] of digoxin solution with 30 mL of water (capsules + 30 mL).
4. Two 0.2-mg capsules[3] of digoxin solution with 240 mL of water (capsules + 240 mL).

The sixteen volunteers were randomly assigned to four groups for treatment administration. A 2-week washout period followed each treatment.

Sample Analysis—Digoxin concentration in each serum sample was quantified in duplicate by RIA using a double-antibody slurry and ^{125}I-digoxin (available in kit form)[4]. The procedure was identical to that outlined[4] except that the order of double antibody and ^{125}I-digoxin was reversed. Urine samples were also determined in duplicate by RIA (13). The sensitivities of the serum and urine assays were both 0.1 ng/mL.

Pharmacokinetic and Statistical Analyses—The following parameters were determined from the serum concentration–time curves for each volunteer for each treatment: observed maximum serum concentration (C_{max}), time of observed maximum serum concentration (t_{max}), and the area under the serum concentration–time curve (AUC). Additionally, the cumulative urinary excretions of digoxin during the first 48 h after dose were determined (CUE_{48}). These parameters were analyzed using an ANOVA for a crossover design[5]. Individual contrasts were made using the least significant difference.

RESULTS

The doses of digoxin tablets and capsules used in this study are recognized as bioequivalent in both the official product labeling[1] and elsewhere (14, 15). Thus, all comparisons were made without adjusting for the actual differences in the doses administered (0.5 mg for tablets *versus* 0.4 mg for capsules).

Figure 1 graphically presents the serum digoxin concentration–time profiles (0–12 h) for the four treatments, and Fig. 2 presents the cumulative urinary excretions for the first 48 h after dose administration. For purposes of comparing relative bioavailability, the CUE_{48} was used. The AUC_{0-12}, C_{max}, and t_{max} were used for additional descriptive and clinical comparisons. AUC_{0-12} was used instead of AUC_{0-48} because the majority of the serum concentrations after 12 h following single-dose administration were below the level of assay sensitivity.

Tables I and II list the individual values for area under the serum concentration–time curves (ng · h/mL) and cumulative urinary digoxin excretions (μg/48 h). During the study, two urine collections were reported as incomplete by the respective volunteers. Table III gives the summary statistics for the pharmacokinetic parameters (*i.e.*, AUC_{0-12}, C_{max}, t_{max}, and CUE_{48}) determined in this study. Table IV summarizes the statistical analyses (ANOVA) of pharmacokinetic parameters based on the means of serum digoxin concentration and cumulative urinary excretion data.

[2] Lanoxin tablets 0.25 mg, Lot 0G2780 (dissolution rate of 80.9% in 60 min); Burroughs Wellcome Co.

[3] Lanoxicaps 0.2 mg, Lot 0G2778, Burroughs Wellcome Co.

[4] Dac-Cel Digoxin Kit; Wellcome Diagnostics Division, Burroughs Wellcome Co.

[5] User's Guide Statistical Analysis System, 1979; SAS Institute, Cary, N.C.

Table III—Pharmacokinetic Summary Statistics[a] for the Four Treatments

Parameter	Tablets + 30 mL	Tablets + 240 mL	Capsules + 30 mL	Capsules + 240 mL
AUC_{0-12}, ng·h/mL	6.30 ± 2.27	6.74 ± 1.71	7.93 ± 1.60	7.88 ± 2.08
C_{max}, ng/mL	1.84 ± 0.56	1.71 ± 0.37	3.87 ± 1.04	3.67 ± 0.72
t_{max}, h	1.22 ± 0.40	1.00 ± 0.34	0.95 ± 0.45	0.69 ± 0.17
CUE_{48}, μg[c]	155.1 ± 26.4	163.3 ± 22.4[b]	161.8 ± 22.5	166.9 ± 15.9[b]

[a] Mean of 16 values ± *SD*. [b] Mean of 15 values ± *SD*. [c] Cumulative urinary excretion.

Table IV—Pharmacokinetic Parameters and Urinary Excretion Data ANOVA

Comparison	Statistic	AUC_{0-12}, ng·h/mL	C_{max}, ng/mL	t_{max}, h	CUE_{48}, μg[a]
30 mL *versus* 240 mL with Capsules	p[b]	N.S.[d]	N.S.	0.03	N.S.
	Power[c]	0.84	0.78	0.36	1.00
30 mL *versus* 240 mL with Tablets	p	N.S.	N.S.	0.07	N.S.
	Power	0.84	0.78	0.36	1.00
Capsules *versus* Tablets	p	<0.01	<0.01	<0.01	N.S.
	Power	0.99	0.97	0.61	1.00
Dosage Form × Volume Interaction	p	N.S.	N.S.	N.S.	N.S.
	Power	0.55	0.49	0.20	0.95

[a] Cumulative urinary excretion. [b] Two-sided test. [c] Power to detect a difference equal to 20% of the overall mean with $\alpha = 0.05$. [d] Not significant.

Table V—Comparison of Drug Solubilities[a]

Drug	Solubility[b]	Dose Administered	Theoretical Volume of Water Required to Solubilize Dose
Ampicillin trihydrate	6.7 mg/mL (21)	500 mg (5)	74.6 mL
Amoxicillin trihydrate	2.5 mg/mL (21)	500 mg (5)	200.0 mL
Doxycycline hyclate	333.3 mg/mL (21)	200 mg (7)	0.6 mL
Erythromycin stearate	≤0.1 mg/mL (21)	500 mg (4)	≥5000 mL
Propoxyphene hydrochloride	3333.3 mg/mL (21)	130 mg (8)	0.4 mL
Tetracycline hydrochloride	100 mg/mL (21)	500 mg (7)	5.0 mL
Theophylline	8.3 mg/mL (21)	260 mg (6)	31.3 mL
Digoxin	0.095 mg/mL (9)	0.5 mg Tablet[c]	5.3 mL
		0.4 mg Capsule[c]	4.2 mL

[a] For drugs administered in previous studies that evaluated effect of coadministered fluid volume. [b] In water at room temperature. [c] Doses used in present study.

Based on CUE_{48}, there were no significant differences found between dosage form (tablets *versus* capsules) and coadministered water volume (30 mL *versus* 240 mL). Mean CUE_{48} values were 155.1 and 163.3 μg for the tablets with 30 mL and 240 mL of water, respectively. Mean CUE_{48} values for capsules with 30 mL and 240 mL of water were 161.8 and 166.9 μg, respectively. Both fluid volumes showed significantly larger ($p < 0.01$) AUC_{0-12}, and C_{max} values for capsules than tablets. The t_{max} was significantly shorter ($p < 0.01$) for the capsules than for the tablets. Also, capsules administered with 240 mL of water had a significantly shorter t_{max} ($p < 0.05$) than capsules administered with 30 mL of water (0.69 *versus* 0.95 h, respectively). There were no significant interactions between dosage form (tablets *versus* capsules) and coadministered water volume (30 mL *versus* 240 mL) for AUC_{0-12}, C_{max}, t_{max}, and CUE_{48}.

Figure 3 illustrates the between-subject variability in cumulative urinary excretion for the treatments. The *CV* values ranged from 9.5% for capsules administered with 240 mL of water to 17.0% for the tablets administered with 30 mL of water. The two other treatments (capsules + 30 mL and tablets + 240 mL) showed similar *CV* values of 13.9 and 13.7%, respectively.

DISCUSSION

Results of previous studies that evaluated the effect of coadministered fluid volume on bioavailability vary and depend largely on the compound tested. Erythromycin stearate was administered to fasting normal volunteers in single 500-mg doses with 20 mL or 250 mL of water. The results showed that reduction in fluid volume significantly decreased erythromycin serum levels, probably due to the low aqueous solubility of erythromycin stearate (4). Amoxicillin trihydrate (5) and theophylline (6) also show decreased serum levels when administered with smaller fluid volumes.

In some instances, the coadministered fluid volume has minimal or no effect on the bioavailability of the drug tested. Such was the case with doxycycline and tetracycline (water-soluble salts); little effect on the overall serum level-time profiles was seen when each preparation was administered with 25 mL or 250 mL of water (7). Ampicillin trihydrate bioavailability was slightly affected by changes in coadministered fluid volume (5). Although plasma propoxyphene levels have been shown to be lower with a 500 ml volume of water *versus* 250 ml when the drug is given as a capsule, the difference was significant only at the 6-h sampling time (8).

In this study, a comparison of mean CUE_{48} values across both coadministered fluid volume and dosage forms revealed no statistically significant differences. The power to detect a difference of 20% in means for these comparisons with $\alpha = 0.05$ was between 0.95 and 1.00. A comparison of the other pharmacokinetic parameters revealed no significant interactions between dosage form (tablets *versus* capsules) and volume (30 *versus* 240 mL of water). Capsules had significantly larger AUC_{0-12} and C_{max} values and a significantly shorter (earlier) t_{max} than tablets ($p < 0.01$). Interestingly, a significantly shorter t_{max} was observed when the capsules were administered with 240 mL of water than when they were taken with 30 mL of water ($p =$

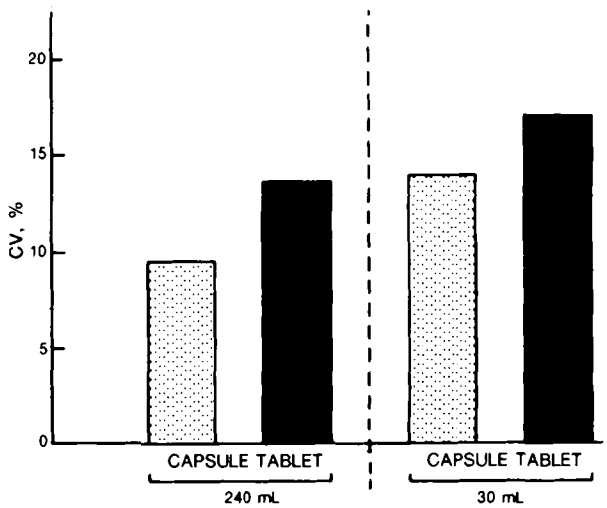

Figure 3—*Between-subject variability in cumulative urinary excretion of digoxin for capsules and tablets (expressed as* CV).

0.03). The larger C_{max} and shorter t_{max} with the capsules *versus* tablets indicate a more rapid absorption rate of the capsule dosage form. Our findings also confirm the results of previous comparative studies, which demonstrate the equivalence of bioavailability of the 0.2-mg capsule and 0.25-mg tablet doses (14, 15).

While no significant differences in the amount of digoxin absorbed were noted based on CUE_{48}, it is interesting to note from Fig. 3 that a smaller *CV* is seen with the capsule than the tablet for both the 240 mL (9.5 *versus* 13.7%) and the 30 mL (13.7 *versus* 17.0%) volumes of water.

Digoxin bioavailability studies (15–20) have used different coadministered volumes of water (100–240 mL). If the results of our study had indicated a difference in bioavailability with different volumes of water, some of the findings of these studies could be questioned. However, since we found no difference in bioavailability with a small *versus* a large amount of fluid, this variable does not have an important influence on digoxin absorption in normal individuals.

A review of drug solubility and volume-related variability in drug absorption is interesting. Table V presents a comparison of the solubilities and doses of drugs that have been administered in previous studies with designs similar to the present study. These data show that concerns over alterations in bioavailability of a drug due to coadministered fluids should not only take into account the solubility of the drug, but also the dose of the respective drug administered. A case in point is digoxin with a solubility of 0.095 mg/mL, one of the lowest values listed. However, because the therapeutic dose is small, only a small volume of water is theoretically required to solubilize the dose in the GI tract.

The results of this study indicate that, in normal volunteers, there are no differences in total digoxin absorption (for either the tablet or capsule forms), when digoxin is administered with relatively small or large volumes of fluid. Such pharmaceutical information is useful in identifying drugs or drug preparations which may or may not be influenced by differences in coadministered fluid volume.

REFERENCES

(1) A. G. Gilman, L. S. Goodman, and A. Gilman, Eds., "The Pharmacological Basis of Therapeutics," 6th ed., Macmillan, New York, N.Y., 1980, p. 5.

(2) H. C. Ferguson, *Toxicol. Appl. Pharmacol.*, **4**, 759 (1962).

(3) J. L. Borowitz, P. F. Moore, G. K. W. Yim, and T. S. Miya, *Toxicol. Appl. Pharmacol.*, **19**, 164 (1971).

(4) P. G. Welling, H. Huang, P. F. Hewitt, and L. L. Lyons, *J. Pharm. Sci.*, **67**, 764 (1978).

(5) P. G. Welling, H. Huang, P. A. Koch, W. A. Craig, and P. O. Madsen, *J. Pharm. Sci.*, **66**, 549 (1977).

(6) P. G. Welling, L. L. Lyons, W. A. Craig, and G. Trochta, *Clin. Pharmacol. Ther.*, **17**, 475 (1975).

(7) P. G. Welling, P. A. Koch, C. C. Lau, and W. A. Craig, *Antimicrob. Agents Chemother.*, **11**, 462 (1977).

(8) P. G. Welling, L. L. Lyons, F. L. S. Tse, and W. A. Craig, *Clin. Pharmacol. Ther.*, **19**, 559 (1976).

(9) Data on file, Burroughs Wellcome Co., Research Triangle Park, N.C.

(10) B. F. Johnson, C. Bye, G. Jones, and G. A. Sabey, *Clin. Pharmacol. Ther.*, **19**, 746 (1976).

(11) P. F. Binnion, *J. Clin. Pharmacol.*, **16**, 461 (1976).

(12) F. I. Marcus, J. Dickerson, S. Pippin, M. Stafford, and R. Bressler, *Clin. Pharmacol. Ther.*, **20**, 253 (1976).

(13) R. H. Christenson, J. E. Hammond, J. H. Hull, and J. A. Bustrack, *Clin. Chim. Acta*, **120**, 13 (1982).

(14) B. F. Johnson, G. Smith, and J. French, *Br. J. Clin. Pharmacol.*, **4**, 209 (1977).

(15) G. I. Mallis, D. H. Schmidt, and J. Lindenbaum, *Clin. Pharmacol. Ther.*, **18**, 761 (1975).

(16) J. Lindenbaum, *Clin. Pharmacol. Ther.*, **17**, 296 (1975).

(17) D. J. Greenblatt, D. W. Duhme, J. Koch-Weser, and T. W. Smith, *N. Engl. J. Med.*, **289**, 651 (1973).

(18) J. Lindenbaum, M. H. Mellow, M. O. Blackstone, and V. P. Butler, Jr., *N. Engl. J. Med.*, **285**, 1344 (1971).

(19) D. H. Huffman, C. V. Manion, and D. L. Azarnoff, *Clin. Pharmacol. Ther.*, **16**, 310 (1974).

(20) J. G. Wagner, M. Christensen, E. Sakmar, D. Blair, J. D. Yates, P. W. Willis, A. J. Sedman, and R. G. Stoll, *J. Am. Med. Assoc.*, **224**, 199 (1973).

(21) J. E. F. Reynolds, Ed., "Martindale—The Extra Pharmacopoeia," 28th ed., Pharmaceutical Press, London, England, 1982, pp. 349, 1006, 1092, 1089, 1155, 1163, 1217.

ACKNOWLEDGMENTS

This paper was presented in preliminary form at the 2nd Annual Meeting of the American College of Clinical Pharmacy, Scottsdale, Arizona, June 1981.

Pharmacokinetics of Fostedil, a New Calcium Antagonist, in Beagle Dogs Following Oral and Intravenous Administration

ELIZABETH W. THOMAS ˣ and BARBARA A. BOPP

Received August 8, 1983, from the *Drug Metabolism Department, Pharmaceutical Products Division, Abbott Laboratories, North Chicago, IL 60064.* Accepted for publication November 28, 1983.

Abstract □ Twelve adult beagle dogs received both an oral and intravenous dose (12 mg/kg) of fostedil in a cross-over design. The plasma levels and urinary excretion of intact fostedil were measured, and the pharmacokinetic parameters of the drug were defined. The results indicate that fostedil was at least 68% bioavailable after an oral dose given as a suspension or solution. The terminal half-life was about 7–8 h. The *in vitro* protein binding, at concentrations of 0.1–100 μg/mL, ranged from 95 to 97%. The binding was not concentration dependent, and saturation of the binding sites was not apparent at concentrations up to 100 μg/mL. Excretion of unchanged drug from the kidneys accounted for only a small percentage of drug clearance.

Keyphrases □ Fostedil—pharmacokinetics, dogs □ Pharmacokinetics—fostedil, dogs □ Blocking agent—calcium entry, fostedil, pharmacokinetics, dogs

Fostedil (I) (diethyl{[4-(2-benzothiazolyl)phenyl]methyl}-phosphonate) is a new calcium entry blocking compound[1] (1–4). This study was designed to determine the pharmacokinetics of fostedil in beagle dogs after intravenous and oral administration.

[1] This compound is being studied under a joint license agreement between Abbott Laboratories, North Chicago, Ill., and Kanebo, Ltd., Japan, and has been reported in the literature as KB-944.

EXPERIMENTAL SECTION

Animals—Five male and seven female adult beagle dogs (8.5–13.0 kg) were randomly divided into three groups of four dogs per group. The groups were dosed at 12 mg/kg, once with an oral solution, an oral suspension, an oral

0022-3549/84/1000-1400$01.00/0

© 1984, American Pharmaceutical Association

0.03). The larger C_{max} and shorter t_{max} with the capsules *versus* tablets indicate a more rapid absorption rate of the capsule dosage form. Our findings also confirm the results of previous comparative studies, which demonstrate the equivalence of bioavailability of the 0.2-mg capsule and 0.25-mg tablet doses (14, 15).

While no significant differences in the amount of digoxin absorbed were noted based on CUE_{48}, it is interesting to note from Fig. 3 that a smaller *CV* is seen with the capsule than the tablet for both the 240 mL (9.5 *versus* 13.7%) and the 30 mL (13.7 *versus* 17.0%) volumes of water.

Digoxin bioavailability studies (15–20) have used different coadministered volumes of water (100–240 mL). If the results of our study had indicated a difference in bioavailability with different volumes of water, some of the findings of these studies could be questioned. However, since we found no difference in bioavailability with a small *versus* a large amount of fluid, this variable does not have an important influence on digoxin absorption in normal individuals.

A review of drug solubility and volume-related variability in drug absorption is interesting. Table V presents a comparison of the solubilities and doses of drugs that have been administered in previous studies with designs similar to the present study. These data show that concerns over alterations in bioavailability of a drug due to coadministered fluids should not only take into account the solubility of the drug, but also the dose of the respective drug administered. A case in point is digoxin with a solubility of 0.095 mg/mL, one of the lowest values listed. However, because the therapeutic dose is small, only a small volume of water is theoretically required to solubilize the dose in the GI tract.

The results of this study indicate that, in normal volunteers, there are no differences in total digoxin absorption (for either the tablet or capsule forms), when digoxin is administered with relatively small or large volumes of fluid. Such pharmaceutical information is useful in identifying drugs or drug preparations which may or may not be influenced by differences in coadministered fluid volume.

REFERENCES

(1) A. G. Gilman, L. S. Goodman, and A. Gilman, Eds., "The Pharmacological Basis of Therapeutics," 6th ed., Macmillan, New York, N.Y., 1980, p. 5.

(2) H. C. Ferguson, *Toxicol. Appl. Pharmacol.*, **4**, 759 (1962).

(3) J. L. Borowitz, P. F. Moore, G. K. W. Yim, and T. S. Miya, *Toxicol. Appl. Pharmacol.*, **19**, 164 (1971).

(4) P. G. Welling, H. Huang, P. F. Hewitt, and L. L. Lyons, *J. Pharm. Sci.*, **67**, 764 (1978).

(5) P. G. Welling, H. Huang, P. A. Koch, W. A. Craig, and P. O. Madsen, *J. Pharm. Sci.*, **66**, 549 (1977).

(6) P. G. Welling, L. L. Lyons, W. A. Craig, and G. Trochta, *Clin. Pharmacol. Ther.*, **17**, 475 (1975).

(7) P. G. Welling, P. A. Koch, C. C. Lau, and W. A. Craig, *Antimicrob. Agents Chemother.*, **11**, 462 (1977).

(8) P. G. Welling, L. L. Lyons, F. L. S. Tse, and W. A. Craig, *Clin. Pharmacol. Ther.*, **19**, 559 (1976).

(9) Data on file, Burroughs Wellcome Co., Research Triangle Park, N.C.

(10) B. F. Johnson, C. Bye, G. Jones, and G. A. Sabey, *Clin. Pharmacol. Ther.*, **19**, 746 (1976).

(11) P. F. Binnion, *J. Clin. Pharmacol.*, **16**, 461 (1976).

(12) F. I. Marcus, J. Dickerson, S. Pippin, M. Stafford, and R. Bressler, *Clin. Pharmacol. Ther.*, **20**, 253 (1976).

(13) R. H. Christenson, J. E. Hammond, J. H. Hull, and J. A. Bustrack, *Clin. Chim. Acta*, **120**, 13 (1982).

(14) B. F. Johnson, G. Smith, and J. French, *Br. J. Clin. Pharmacol.*, **4**, 209 (1977).

(15) G. I. Mallis, D. H. Schmidt, and J. Lindenbaum, *Clin. Pharmacol. Ther.*, **18**, 761 (1975).

(16) J. Lindenbaum, *Clin. Pharmacol. Ther.*, **17**, 296 (1975).

(17) D. J. Greenblatt, D. W. Duhme, J. Koch-Weser, and T. W. Smith, *N. Engl. J. Med.*, **289**, 651 (1973).

(18) J. Lindenbaum, M. H. Mellow, M. O. Blackstone, and V. P. Butler, Jr., *N. Engl. J. Med.*, **285**, 1344 (1971).

(19) D. H. Huffman, C. V. Manion, and D. L. Azarnoff, *Clin. Pharmacol. Ther.*, **16**, 310 (1974).

(20) J. G. Wagner, M. Christensen, E. Sakmar, D. Blair, J. D. Yates, P. W. Willis, A. J. Sedman, and R. G. Stoll, *J. Am. Med. Assoc.*, **224**, 199 (1973).

(21) J. E. F. Reynolds, Ed., "Martindale—The Extra Pharmacopoeia," 28th ed., Pharmaceutical Press, London, England, 1982, pp. 349, 1006, 1092, 1089, 1155, 1163, 1217.

ACKNOWLEDGMENTS

This paper was presented in preliminary form at the 2nd Annual Meeting of the American College of Clinical Pharmacy, Scottsdale, Arizona, June 1981.

Pharmacokinetics of Fostedil, a New Calcium Antagonist, in Beagle Dogs Following Oral and Intravenous Administration

ELIZABETH W. THOMAS ˣ and BARBARA A. BOPP

Received August 8, 1983, from the *Drug Metabolism Department, Pharmaceutical Products Division, Abbott Laboratories, North Chicago, IL 60064.* Accepted for publication November 28, 1983.

Abstract □ Twelve adult beagle dogs received both an oral and intravenous dose (12 mg/kg) of fostedil in a cross-over design. The plasma levels and urinary excretion of intact fostedil were measured, and the pharmacokinetic parameters of the drug were defined. The results indicate that fostedil was at least 68% bioavailable after an oral dose given as a suspension or solution. The terminal half-life was about 7–8 h. The *in vitro* protein binding, at concentrations of 0.1–100 μg/mL, ranged from 95 to 97%. The binding was not concentration dependent, and saturation of the binding sites was not apparent at concentrations up to 100 μg/mL. Excretion of unchanged drug from the kidneys accounted for only a small percentage of drug clearance.

Keyphrases □ Fostedil—pharmacokinetics, dogs □ Pharmacokinetics—fostedil, dogs □ Blocking agent—calcium entry, fostedil, pharmacokinetics, dogs

Fostedil (I) (diethyl{[4-(2-benzothiazolyl)phenyl]methyl}-phosphonate) is a new calcium entry blocking compound[1] (1–4). This study was designed to determine the pharmacokinetics of fostedil in beagle dogs after intravenous and oral administration.

[1] This compound is being studied under a joint license agreement between Abbott Laboratories, North Chicago, Ill., and Kanebo, Ltd., Japan, and has been reported in the literature as KB-944.

EXPERIMENTAL SECTION

Animals—Five male and seven female adult beagle dogs (8.5–13.0 kg) were randomly divided into three groups of four dogs per group. The groups were dosed at 12 mg/kg, once with an oral solution, an oral suspension, an oral

0022-3549/84/1000-1400$01.00/0

© 1984, American Pharmaceutical Association

Table I—Pharmacokinetics of Fostedil in Beagle Dogs Following Intravenous Administration (12 mg/kg)

Dog No.	K_{21}, h^{-1}	K_{12}, h^{-1}	K_{net}, h^{-1}	Beta, h^{-1}	Half-life, h	Vd_1, L/kg	AUC, μg·h/mL	CL_t, L/h/kg
81121	0.291	0.267	0.412	0.145	4.78	1.28	22.80	0.53
81122	0.455	0.597	0.224	0.086	8.06	3.47	15.44	0.78
81128	0.193	0.381	0.386	0.085	8.15	0.76	40.92	0.29
81147	0.454	1.139	0.617	0.135	5.13	0.62	31.26	0.38
81167	0.252	0.519	0.308	0.078	8.88	1.04	37.42	0.32
81170	0.224	0.296	0.430	0.115	6.03	1.17	23.82	0.82
81174	0.302	0.697	0.420	0.096	7.22	1.57	18.24	0.66
81176	0.281	2.332	1.978	0.125	5.54	0.18	34.53	0.36
81179	0.306	0.454	0.501	0.136	5.10	1.13	21.31	0.57
81184	0.214	0.339	0.539	0.118	5.87	0.99	22.54	0.53
82505	0.174	0.213	0.307	0.088	7.88	1.82	21.52	0.56
82506	0.125	0.110	0.370	0.090	7.70	1.56	20.79	0.58
Mean	0.273	0.612	0.541	0.108	6.42[a]	1.30	25.88	0.53
SD	0.101	0.606	0.456	0.024		0.82	8.10	0.17

[a] Calculated from the mean beta rate constant.

Table II—Pharmacokinetics of Fostedil in Beagle Dogs Following Oral Solution Administration (12 mg/kg)

Dog No.	K_a, h^{-1}	Beta, h^{-1}	Half-life, h	AUC, μg·h/mL	F, %	T_{max}, h	C_{max}, μg/mL
81121	4.22	0.033	21.00	21.42	94.0	0.99	1.81
81122	2.83	0.097	7.14	15.16	98.2	0.95	2.21
81128	2.22	0.054	12.83	21.20	51.8	1.10	2.41
81147	1.58	0.155	4.47	13.05	41.8	1.10	2.45
81167	0.91	0.061	11.36	22.50	60.1	1.67	2.13
81170	18.12	0.067	10.34	18.35	77.0	0.25	3.20
81174	1.27	0.075	9.24	15.03	82.4	1.00	2.06
81176	0.68	0.065	10.66	15.43	44.7	1.82	1.83
81179	1.85	0.092	7.53	20.92	98.2	0.87	3.29
81184	17.68	0.073	9.49	13.36	59.3	0.23	2.72
82505	2.12	0.113	6.13	14.20	66.0	0.64	2.14
82506	0.36	0.104	6.66	17.40	83.7	3.05	1.74
Mean	4.49	0.082	8.45[a]	17.33	71.4	1.14	2.33
SD	6.35	0.032		3.44	20.3	0.76	0.51

[a] Calculated from the mean beta rate constant.

capsule, and an intravenous formulation. At ~2-week intervals, the three groups were crossed-over until each group had received each treatment once. The dogs were fasted for at least 12 h prior to dosing and for at least 5 h following dosing. They were housed individually in stainless steel metabolism cages and given water *ad libitum*.

Treatment—The oral and intravenous solution formulations were prepared as 24 mg of fostedil per mL in ethanol–propylene glycol–water (10:60:30, v/v/v). The suspension formulation was prepared as 24 mg/mL in 0.2% hydroxypropyl methylcellulose–water. The oral solution and suspension were administered by gavage, 0.5 mL/kg to each animal. The intravenous solution was administered intravenously as a bolus (0.5 mL/kg) into the right cephalic vein to provide a dose of 12 mg/kg. For the capsule dosing, the drug was weighed into clear gelatin capsules[2] and administered orally with 10 mL of water.

Heparinized blood samples (2–5 mL) were collected from the jugular vein at 0, 0.1 (intravenous route only), 0.25, 0.5, 1, 2, 3, 4, 6, 8, 10, 12, 24, 26, 28, and 32 h postdose. The plasma was harvested and stored frozen. If possible, urine was collected over the following intervals: 0–4, 4–8, 8–12, 12–24, 24–28, and 28–32 h postdose. The volumes were measured and recorded, and a 5-mL aliquot was stored frozen.

Assay of Fostedil in Plasma and Urine—Measurement of plasma and urine concentrations of fostedil was performed by using an HPLC fluorescence assay (5). The procedure was shown to be sensitive (5 ng/mL) and specific for the intact drug.

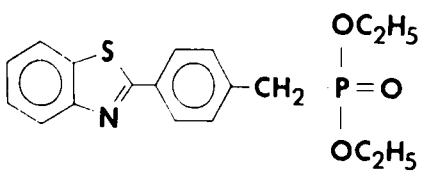

I

[2] No. 0.

Pharmacokinetic Analysis—The individual and mean plasma concentrations *versus* time data were subjected to sequential polyexponential regression analyses using STRIP, a slightly modified version of the computer program CSTRIP (6). Based on the criteria outlined by Sedman and Wagner (7), a triexponential model (*e.g.*, a two-compartment open model) was deemed more appropriate for the intravenous, suspension, and oral solution data. A biexponential model (*e.g.*, a one-compartment open model) was chosen for the capsule dosing data.

The data were fitted with NONLIN (8), using appropriate DFUNC subroutines. For the one-compartment model, the parameters on which iterations were performed included: K_a (apparent input rate constant), K_{net} (apparent net elimination rate constant), Vd (volume of distribution), and the absorption lag time. For the two-compartment model, the estimated preexponential and exponential terms were used to calculate the initial estimates of the microscopic rate constants by using the assumptions and equation described by Gibaldi and Perrier (9). Iterations by NONLIN were then performed on the following parameters: K_a, K_{net}, K_{12}, K_{21}, and Vd_1. During the fitting process, the data were weighted by reciprocal squared concentrations ($1/C^2$) (10).

Protein Binding—Fostedil, labeled with carbon-14 in the 2-position of the benzothiazolyl ring, was used in the *in vitro* protein binding studies. The binding of fostedil (concentrations, 0.1–100 μg/mL) was determined in the plasma of male and female beagle dogs by the ultrafiltration technique described by Rolinson and Sutherland (11). The ultrafiltrates and plasma were oxidized, assayed to determine levels of radioactivity, and corrected for quenching by automatic external standardization.

RESULTS AND DISCUSSION

Single-Dose Intravenous Study—A summary of the pharmacokinetic parameters as derived by NONLIN from the intravenous data is presented in Table I. The total body clearance ranged from 0.5 to 0.8 L/h/kg, with a mean value of 0.53 L/h/kg. The beta half-life ranged from 4.8 to 8.9 h, with a mean value of 6.4 h.

Single-Dose Oral Studies—The calculated pharmacokinetic parameters derived by NONLIN for the oral solution, suspension, and capsule dosing data

Table III—Pharmacokinetics of Fostedil in Beagle Dogs Following Suspension Administration (12 mg/kg)

Dog No.	K_a, h^{-1}	Beta, h^{-1}	Half-life, h	AUC, μg·h/mL	F, %	T_{max}, h	C_{max}, μg/mL
81121	2.79	0.137	5.06	13.41	58.8	1.15	1.57
81122	1.45	0.081	8.56	13.45	87.1	1.82	1.58
81128	1.16	0.031	22.35	27.00	66.0	1.18	1.42
81147	1.57	0.088	7.88	17.50	56.0	1.43	2.16
81167	0.54	0.059	11.75	25.58	68.4	2.25	2.24
81170	1.65	0.024	28.88	19.95	83.8	1.60	2.18
81174	3.24	0.095	7.29	12.03	66.0	1.05	1.25
81176	2.93	0.020	34.65	22.06	63.9	1.07	1.98
81179	2.12	0.120	5.78	12.95	60.8	1.47	1.31
81184	1.29	0.083	8.35	13.84	61.4	1.42	1.77
82505	0.54	0.104	6.66	10.10	46.9	2.68	1.11
82506	2.79	0.110	6.30	9.27	44.6	1.30	1.10
Mean	1.84	0.079	8.77[a]	16.43	63.6	1.53	1.64
SD	0.93	0.038		5.94	12.5	0.50	0.42

[a] Calculated from the mean beta rate constant.

Table IV—Pharmacokinetics of Fostedil in Beagle Dogs Following Capsule Administration (12 mg/kg)

Dog No.	K_a, h^{-1}	K_{net}, h^{-1}	Half-life, h	AUC, μg·h/mL	F, %	T_{max}, h	C_{max}, μg/mL
81121	0.70	0.088	7.88	14.08	61.8	3.62	0.92
81122	1.46	0.136	5.10	6.14	39.8	2.03	0.66
81128	0.13	0.138	5.02	5.89	14.4	7.70	0.29
81147	1.10	0.095	7.29	9.56	30.6	2.68	0.72
81167	10.59	0.099	7.00	11.48	30.7	0.91	1.09
81170	0.60	0.121	5.73	9.86	41.4	3.77	0.80
81174	1.76	0.091	7.62	14.16	77.6	1.78	1.09
81176	1.36	0.076	9.12	10.76	31.2	2.48	0.69
81179	0.16	0.161	4.30	8.10	38.0	6.42	0.48
81184	0.79	0.076	9.12	8.46	37.5	3.49	0.50
82505	0.72	0.122	5.68	15.15	70.4	3.17	1.29
82506	3.08	0.138	5.02	6.98	33.6	1.29	0.84
Mean	1.87	0.112	6.19[a]	10.05	42.24	3.28	0.78
SD	2.86	0.028		3.17	18.4	2.00	0.29

[a] Calculated from the mean K_{net} rate constant.

are listed Tables II–IV, respectively. Figure 1 is a semilogarithmic concentration-time plot of the mean data for each oral and intravenous formulation with the NONLIN generated best-fit curve. As expected for a compound with limited water solubility like fostedil, the absorption kinetics became more complex in progressing from an oral solution to a capsule formulation. Figure 1 illustrates this change, as the two-compartment model disposition kinetics, so distinct after intravenous administration, became less pronounced after oral administration. Indeed, following capsule dosing the data were best described by a one-compartment model, since the distribution phase was completely masked by the complex absorption phase. In the fits for some of the animals, the calculated apparent K_a value approached that of alpha as determined after intravenous administration. Thus, it was impossible to accurately determine the true absorption rate constant. Only an estimated apparent absorption half-life of ~15 min is reported.

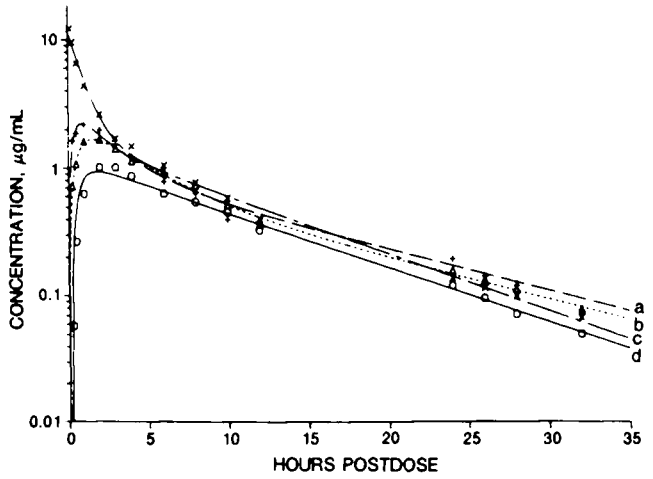

Figure 1—*Mean postdose fostedil concentration* versus *time. Key: (a) oral solution; (b) suspension; (c) intravenous administration; (d) capsule administration of fostedil (12 mg/kg) with NONLIN-generated best-fit curves.*

Studies with radiolabeled drug in rats and dogs have demonstrated the presence of extensive biliary secretion of fostedil and/or its metabolites, suggesting possible enterohepatic circulation[3]. Meal-related secondary peaks in the plasma profiles were observed for many animals in this study. This, in some cases, adversely affected the kinetic analyses. For two of the oral formulations, the mean elimination rate constants were found to be statistically significantly different ($p = 0.015$). However, these differences were considered to be of minor practical importance since the differences could be traced to data from animals displaying unusual plasma drug level profiles. In these cases, the model was inadequate to describe the possible enterohepatic circulation and the complex absorption phenomenon. Thus, the average beta half-life following oral dosing was 7.6 h.

The mean calculated C_{max} values for the oral formulations were: capsule, 0.78 μg/mL; suspension, 1.64 μg/mL, and oral solution, 2.33 μg/mL. An analysis of variance and the Duncan Multiple Range test showed all values to be significantly different from one another.

Since the same dose (12 mg/kg) was administered both orally and intravenously, the systemic availability (F) was calculated as the percent ratio of $(AUC_{0-\infty})$ oral/$(AUC_{0-\infty})$ intravenous (12). The individual F values for these animals following oral dosing are given in Tables II–IV. The mean F values were: oral solution, 71.4%; suspension, 63.6%; capsule, 42.2%. The $AUC_{0-\infty}$ values for the oral solution and suspension formulations were not statistically different ($p = 0.23$) but were greater than those for the capsule dosing. However, the results of another study in this laboratory have suggested that the low bioavailability might have been due to the type of capsule used[4].

Urinary excretion of unchanged drug for both the oral and intravenous dosings was less than 1% of the administered dose over the 32-h collection period.

Protein Binding Studies—The *in vitro* protein binding of [^{14}C]fostedil at

[3] B. A. Bopp, unpublished results.

[4] E. W. Thomas, unpublished results.

concentrations of 0.1–100 μg/mL ranged from 95–97% in dog plasma, and the binding appeared to be similar in the plasma from the male and the female dogs. The binding was not concentration dependent, and saturation of the binding sites was not apparent at concentrations up to 100 μg/mL.

REFERENCES

(1) T. Morita, K. Ito, and T. Nose, *Arzneim.-Forsch. Drug Res.*, **32**, 1053 (1982).

(2) T. Morita, T. Kanazawa, K. Ito, and T. Nose, *Arzneim.-Forsch. Drug Res.*, **32**, 1047 (1982).

(3) T. Morita, T. Kanazawa, K. Ito, and T. Nose, *Arzneim.-Forsch. Drug Res.*, **32**, 1043 (1982).

(4) N. Taira, M. Kawada, and K. Satoh, *J. Cardiovasc. Pharmacol.*, **5**, 349 (1983).

(5) E. W. Thomas, *J. Chromatogr.*, **305**, 233 (1984).

(6) A. J. Sedman and J. G. Wagner, *J. Pharm. Sci.*, **65**, 1006 (1976).

(7) A. J. Sedman and J. G. Wagner, "AUTOAN—A Decision-Making Computer Program," Publication Distribution Service, Ann Arbor, Mich., 1974.

(8) C. M. Metzler, G. L. Elfring, and A. J. McEwen, *Biometrics*, **30**, 562 (1974).

(9) M. Gibaldi and D. Perrier, in "Pharmacokinetics," Marcel Dekker, New York, N.Y., 1975, pp. 69–80.

(10) H. G. Boxenbaum, S. Riegelman, R. M. Elashoff, *J. Pharmacokinet. Biopharm.*, **2**, 123 (1974).

(11) G. N. Rolinson and R. Sutherland, *Br. J. Pharmacol.*, **25**, 638 (1965).

(12) M. Gibaldi and D. Perrier, in "Pharmacokinetics," Marcel Dekker, New York, N.Y., 1975, p. 146.

ACKNOWLEDGMENTS

The authors thank Ms. Sheila T. Bunnell, Mr. Curt J. Contreras, Ms. Marianne K. Johnson, Mr. Lajos L. Varga, and Mr. David S. Wilson for their excellent technical assistance.

Inhibition of Human Polymorphonuclear Leukocyte Cell Responses by Ibuprofen

EUFRONIO G. MADERAZO ˣ, STEVEN P. BREAUX, and CHARLES L. WORONICK

Received September 12, 1983, from the *Medical Research Laboratory, Department of Medicine, Hartford Hospital, Hartford, CT 06115.* Accepted for publication November 19, 1983.

Abstract □ The stimulation of cell swelling, cell aggregation, polymorphonuclear leukocyte locomotion, and lysosomal enzyme release in response to chemoattractant were all inhibited by ibuprofen, a nonsteroidal anti-inflammatory agent. The dosages needed to induce 50% inhibition (ID_{50}) were 5.9, 7.6, 60, and 95 μg/mL, respectively. Aside from the differences in ID_{50}, there was also a difference in the degree of maximum inhibition (I_{max}) of the complement C5a-stimulated responses observed, so that at achievable serum drug concentrations of 20–50 μg/mL, inhibition of 67–78% for cell swelling, 69–82% for cell aggregation, 20–35% for migration response, and 17–38% for lysosomal enzyme release were demonstrated. Also observed were a minor stimulatory effect on nitroblue tetrazolium reduction and an inhibitory effect on the ability to kill *Staphylococcus aureus*, but only at very high concentrations (~2 mg/mL).

Keyphrases □ Ibuprofen—inhibition of polymorphonuclear leukocyte cell responses □ Polymorphonuclear leukocytes—inhibition of response, ibuprofen □ Anti-inflammatory agents—ibuprofen, inhibition of polymorphonuclear leukocytes

Although the acute inflammatory reaction is usually the combined result of vascular, humoral, and cellular responses, there is considerable evidence that the contribution of the polymorphonuclear leukocyte[1] is indispensable (1). This is derived from studies showing inhibition of experimental inflammatory response in PMN-depleted animals, the presence of lysosomal enzymes in inflammatory exudates in humans, and the production of tissue damage in experimental animals by PMN lysosomal lysates. Moreover, one mechanism of action of the effects of a variety of anti-inflammatory drugs, which includes corticosteroids and colchicine, is their ability to inhibit the release of lysosomal enzymes from PMN. Consequently, it is important to determine whether nonsteroidal anti-inflammatory agents, in addition to their inhibitory activity on prostaglandin synthesis (2), also have direct inhibitory effects on PMN function. Although the inhibitory effect of these drugs on PMN migration has been shown previously (3–5), a systematic study to quantitate the effects on this and other PMN responses is lacking. Therefore, we studied and quantitated the effects of the anti-inflammatory drug ibuprofen on PMN responses.

EXPERIMENTAL SECTION

Preparation of Leukocytes and Serum—Blood for these studies was obtained from healthy male and female laboratory and hospital personnel. Polymorphonuclear cells were prepared from heparinized (50 U of preservative-free sodium heparin per mL of blood) whole blood by sedimenting erythrocytes with 6% hetastarch–whole blood at a ratio of 1:5. The leukocyte-rich plasma was washed once with a commercially obtained medium[2] at pH 7.4 and centrifuged at 500×*g*. The cell pellet was resuspended in the same medium, and the PMN concentration was adjusted to 5×10^6 PMNs/mL. This preparation was used for PMN locomotion and bactericidal assays. For leukocyte aggregation, swelling, and lysosomal enzyme release assays, the leukocyte pellet was prepared with Hank's balanced salt solution[1]. To lyse contaminating erythrocytes, the cells were resuspended in ice-cold 0.15 M NH_4Cl (pH 7.5) for 10 min, with five 2-min interval inversions, followed by another wash with HBSS. The final cell pellet was resuspended in HBSS to a cell concentration of 10^7 PMNs/mL. Serum was prepared from clotted whole blood.

Chemotactic Factor—The chemotactic factor used in PMN locomotion studies was derived from zymosan-activated serum prepared by incubation of 5 mg of zymosan with 1 mL of serum at 37°C for 30 min. A 3% solution of this material in the medium[2] was used in the lower compartment.

Partially purified complement C5a fragments were used as the chemotactic factor in leukocyte aggregation, swelling, and lysosomal enzyme release studies. C5a was derived by the activation of normal serum with zymosan in the presence of 1 M ε-aminocaproic acid[3] and purified by gel filtration[4] (6). Active fractions were identified by the lysosomal enzyme release assay, lyophilized, and then dialyzed against 0.1 M phosphate buffer (pH 7.4), and

[1] Polymorphonuclear leukocyte will be abbreviated throughout the text as PMN; Hank's balanced salt solution will be abbreviated as HBSS.

[2] Medium 199; Difco Laboratories, Detroit, Mich.

[3] Sigma Chemical Co., St. Louis, Mo.

[4] Sephadex G-100; Pharmacia Fine Chemicals, Piscataway, N.J.

0022-3549/84/1000-1403$01.00/0

© 1984, American Pharmaceutical Association

concentrations of 0.1–100 μg/mL ranged from 95–97% in dog plasma, and the binding appeared to be similar in the plasma from the male and the female dogs. The binding was not concentration dependent, and saturation of the binding sites was not apparent at concentrations up to 100 μg/mL.

REFERENCES

(1) T. Morita, K. Ito, and T. Nose, *Arzneim.-Forsch. Drug Res.*, **32**, 1053 (1982).

(2) T. Morita, T. Kanazawa, K. Ito, and T. Nose, *Arzneim.-Forsch. Drug Res.*, **32**, 1047 (1982).

(3) T. Morita, T. Kanazawa, K. Ito, and T. Nose, *Arzneim.-Forsch. Drug Res.*, **32**, 1043 (1982).

(4) N. Taira, M. Kawada, and K. Satoh, *J. Cardiovasc. Pharmacol.*, **5**, 349 (1983).

(5) E. W. Thomas, *J. Chromatogr.*, **305**, 233 (1984).

(6) A. J. Sedman and J. G. Wagner, *J. Pharm. Sci.*, **65**, 1006 (1976).

(7) A. J. Sedman and J. G. Wagner, "AUTOAN—A Decision-Making Computer Program," Publication Distribution Service, Ann Arbor, Mich., 1974.

(8) C. M. Metzler, G. L. Elfring, and A. J. McEwen, *Biometrics*, **30**, 562 (1974).

(9) M. Gibaldi and D. Perrier, in "Pharmacokinetics," Marcel Dekker, New York, N.Y., 1975, pp. 69–80.

(10) H. G. Boxenbaum, S. Riegelman, R. M. Elashoff, *J. Pharmacokinet. Biopharm.*, **2**, 123 (1974).

(11) G. N. Rolinson and R. Sutherland, *Br. J. Pharmacol.*, **25**, 638 (1965).

(12) M. Gibaldi and D. Perrier, in "Pharmacokinetics," Marcel Dekker, New York, N.Y., 1975, p. 146.

ACKNOWLEDGMENTS

The authors thank Ms. Sheila T. Bunnell, Mr. Curt J. Contreras, Ms. Marianne K. Johnson, Mr. Lajos L. Varga, and Mr. David S. Wilson for their excellent technical assistance.

Inhibition of Human Polymorphonuclear Leukocyte Cell Responses by Ibuprofen

EUFRONIO G. MADERAZO ˣ, STEVEN P. BREAUX, and CHARLES L. WORONICK

Received September 12, 1983, from the *Medical Research Laboratory, Department of Medicine, Hartford Hospital, Hartford, CT 06115.* Accepted for publication November 19, 1983.

Abstract □ The stimulation of cell swelling, cell aggregation, polymorphonuclear leukocyte locomotion, and lysosomal enzyme release in response to chemoattractant were all inhibited by ibuprofen, a nonsteroidal anti-inflammatory agent. The dosages needed to induce 50% inhibition (ID_{50}) were 5.9, 7.6, 60, and 95 μg/mL, respectively. Aside from the differences in ID_{50}, there was also a difference in the degree of maximum inhibition (I_{max}) of the complement C5a-stimulated responses observed, so that at achievable serum drug concentrations of 20–50 μg/mL, inhibition of 67–78% for cell swelling, 69–82% for cell aggregation, 20–35% for migration response, and 17–38% for lysosomal enzyme release were demonstrated. Also observed were a minor stimulatory effect on nitroblue tetrazolium reduction and an inhibitory effect on the ability to kill *Staphylococcus aureus*, but only at very high concentrations (~2 mg/mL).

Keyphrases □ Ibuprofen—inhibition of polymorphonuclear leukocyte cell responses □ Polymorphonuclear leukocytes—inhibition of response, ibuprofen □ Anti-inflammatory agents—ibuprofen, inhibition of polymorphonuclear leukocytes

Although the acute inflammatory reaction is usually the combined result of vascular, humoral, and cellular responses, there is considerable evidence that the contribution of the polymorphonuclear leukocyte[1] is indispensable (1). This is derived from studies showing inhibition of experimental inflammatory response in PMN-depleted animals, the presence of lysosomal enzymes in inflammatory exudates in humans, and the production of tissue damage in experimental animals by PMN lysosomal lysates. Moreover, one mechanism of action of the effects of a variety of anti-inflammatory drugs, which includes corticosteroids and colchicine, is their ability to inhibit the release of lysosomal enzymes from PMN. Consequently, it is important to determine whether nonsteroidal anti-inflammatory agents, in addition to their inhibitory activity on prostaglandin synthesis (2), also have direct inhibitory effects on PMN function. Although the inhibitory effect of these drugs on PMN migration has been shown previously (3–5), a systematic study to quantitate the effects on this and other PMN responses is lacking. Therefore, we studied and quantitated the effects of the anti-inflammatory drug ibuprofen on PMN responses.

EXPERIMENTAL SECTION

Preparation of Leukocytes and Serum—Blood for these studies was obtained from healthy male and female laboratory and hospital personnel. Polymorphonuclear cells were prepared from heparinized (50 U of preservative-free sodium heparin per mL of blood) whole blood by sedimenting erythrocytes with 6% hetastarch–whole blood at a ratio of 1:5. The leukocyte-rich plasma was washed once with a commercially obtained medium[2] at pH 7.4 and centrifuged at 500×*g*. The cell pellet was resuspended in the same medium, and the PMN concentration was adjusted to 5×10^6 PMNs/mL. This preparation was used for PMN locomotion and bactericidal assays. For leukocyte aggregation, swelling, and lysosomal enzyme release assays, the leukocyte pellet was prepared with Hank's balanced salt solution[1]. To lyse contaminating erythrocytes, the cells were resuspended in ice-cold 0.15 M NH_4Cl (pH 7.5) for 10 min, with five 2-min interval inversions, followed by another wash with HBSS. The final cell pellet was resuspended in HBSS to a cell concentration of 10^7 PMNs/mL. Serum was prepared from clotted whole blood.

Chemotactic Factor—The chemotactic factor used in PMN locomotion studies was derived from zymosan-activated serum prepared by incubation of 5 mg of zymosan with 1 mL of serum at 37°C for 30 min. A 3% solution of this material in the medium[2] was used in the lower compartment.

Partially purified complement C5a fragments were used as the chemotactic factor in leukocyte aggregation, swelling, and lysosomal enzyme release studies. C5a was derived by the activation of normal serum with zymosan in the presence of 1 M ε-aminocaproic acid[3] and purified by gel filtration[4] (6). Active fractions were identified by the lysosomal enzyme release assay, lyophilized, and then dialyzed against 0.1 M phosphate buffer (pH 7.4), and

[1] Polymorphonuclear leukocyte will be abbreviated throughout the text as PMN; Hank's balanced salt solution will be abbreviated as HBSS.

[2] Medium 199; Difco Laboratories, Detroit, Mich.

[3] Sigma Chemical Co., St. Louis, Mo.

[4] Sephadex G-100; Pharmacia Fine Chemicals, Piscataway, N.J.

0022-3549/84/1000-1403$01.00/0

© 1984, American Pharmaceutical Association

Table I—Effect of Ibuprofen on Various Chemotactic Factor (CF)-Stimulated Leukocyte Functions

Function	n	ID_{50}, μg/mL	Maximum Reversal of CF Effects (I_{max}, %)	Reversal of CF Effects at 20–50 μg/mL, %
PMN swelling	2	5.9	87	67–78
PMN aggregation	2	7.6	95	69–82
Chemotaxis	3	60	78	20–35
Lysosomal enzyme release				
Glucosaminidase	3	94	110	19–38
Elastase	3	95	100	17–34

stored at −90°C in small aliquots until use. Each preparation was standardized by dose–response studies to calculate maximum enzyme release (V_{max}) and the concentration of C5a needed to induce 50% of the maximum response (K_m) in PMNs. Three times this value ($K_m \times 3$) was then used in the experiments.

Ibuprofen Preparation—Ibuprofen[5] was prepared by dissolving 16.7 mg of the drug in 1 mL of 0.1 M Tris-HCl buffer, pH 8 (high pH values allowed solubilization of ibuprofen). The mixture was readjusted to pH 7.5, mixed thoroughly, and diluted to 8.35 mL with Tris buffer. The ibuprofen concentration at this point was 2 mg/mL and had an absorbance of 0.176 at 280 nm.

Leukocyte Locomotion Assay—Assays were performed in duplicate by using modified transparent acrylic Boyden chambers[6] and 13-mm diameter, 5-μm pore-size cellulose nitrate filters[7]. The modifications of the Boyden technique, as well as the methods used for calculating the locomotion index (LI) have been previously reported in detail (7).

To test the effect of ibuprofen on PMN locomotion, various concentrations of the drug were added to 5×10^5 PMNs in the upper compartment (total volume of 0.7 mL in the medium[2]). The chemotactic attractant, 3% zymosan-activated normal serum, was introduced into the lower compartment. The prepared chambers were incubated at 37°C in a humidified, 5% CO_2 atmosphere for 90 min. After incubation, the filters were removed, fixed, stained, cleared, and mounted as described previously (7).

The effects of the drug on both the number of PMNs migrating and the locomotion index (distance migrated) were quantitated. To assess the total number of PMNs migrating into the filter, the number of cells was counted at a magnification of ×400. The counting was started at 20 μm below the cell monolayer (proximal filter surface) and continued at 10-μm intervals throughout the thickness of the filter. The locomotion index (LI_{20}), the average distance migrated by PMNs that migrated beyond the 20-μm level, was calculated as described previously (7). The chemotactic responses in the presence of ibuprofen were expressed as change from the control value measured in the absence of the drug.

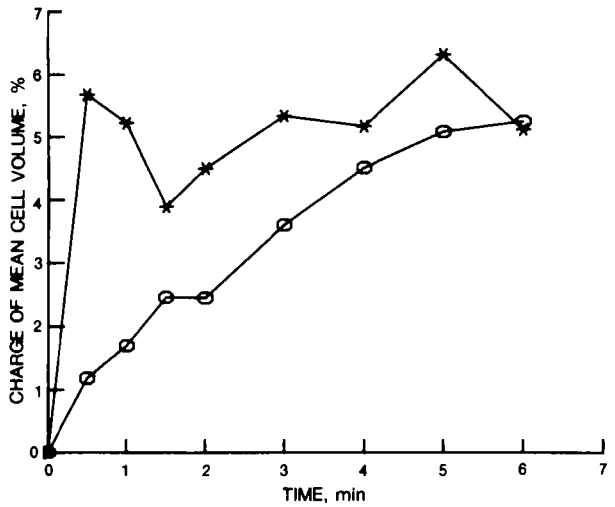

Figure 1—*Effect of ibuprofen on C5a-stimulated PMN swelling. For these experiments, 2×10^6 PMNs were exposed to 2.8 mg of ibuprofen per mL (total volume, 250 μL) for 2 min at 37°C, after which 100 μL of C5a solution ($K_m \times 3$) was added, and incubation was continued for an additional minute. An 80-μL aliquot was added to 20 mL of diluent, and the mean cell volume was determined at the times indicated. Key: (○) with ibuprofen; (✱) no ibuprofen.*

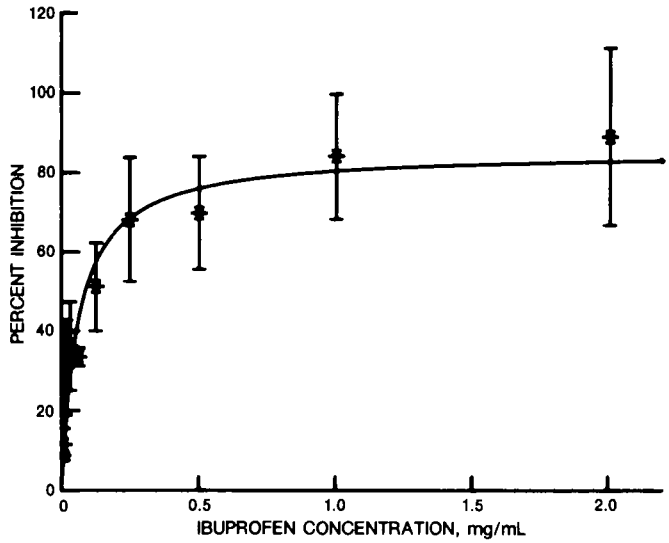

Figure 2—*Effect of ibuprofen on PMN locomotion (LI_{20}) toward activated normal serum as the chemoattractant. The results of three experiments are presented, with the bars representing* SD. *The ID_{50} was calculated to be 60 μg/mL, and the maximum inhibition was 78%.*

Lysosomal Enzyme Release Assay—Lysosomal enzyme release from PMNs was assessed by a method similar to that described by Fantone *et al.* (8). Reaction mixtures containing various concentrations of ibuprofen in the presence of cytochalasin B-treated PMNs (10^7 cells per mL) were preincubated at 37°C for 5 min. To these mixtures, 150 μL (K_m = 50 μL) of C5a was added. The mixtures were incubated at 37°C for 5 min and centrifuged at 200×*g* for 5 min at 4°C. The supernatant solutions were assayed for *N*-acetyl-β-D-glucosaminidase (8) and elastase (9).

Separation of C5a and Ibuprofen—In the study to determine whether ibuprofen has a direct effect on C5a, 2 mL of C5a was incubated with 2 mg of drug for 1 min at 37°C. The drug was then removed by using gel filtration columns[8]. An elution volume between 3.5 and 4.8 mL contained the highest concentration of C5a without the drug.

PMN Aggregation and Swelling—PMN aggregation and cell volume assays were performed by a technique described previously (6). We used a particle counter equipped with a size-distribution analyzer[9]. Reaction mixtures containing various concentrations of ibuprofen were incubated for 2 min at 37°C with 100 μL of PMNs (containing 2×10^6 PMNs). After incubation, 150 μL of C5a was added, and the mixtures were incubated for 60 s at 37°C. Aliquots of 80 μL from these reaction mixtures were added to 20 mL of isotonic solution[10] and immediately analyzed with a particle counter and size analyzer. The first determination of cell number and mean cell volume was obtained 15–30 s after contact of the PMNs with C5a. Subsequent readings were taken in the same vial which was intermittently shaken between readings. Cell number and mean cell volume were calculated for each drug concentration at all time intervals. A decrease in cell number was indicative of cell aggregation.

PMN Nitro Blue Tetrazolium Reduction and Bactericidal Assay—The methods of quantitating nitro blue tetrazolium reduction and bacterial killing by PMNs have been described previously (7). The only modification used for these assay procedures involved the preincubation of PMNs with various concentrations of ibuprofen for 30 min at 37°C.

Analysis of Results—To quantitate the inhibitory effects of ibuprofen, dose–response studies were performed to determine the degree of inhibition as a function of ibuprofen concentration. The percent inhibition (%I) was calculated from:

$$\%I = \left[\frac{R_D - R_{Neg}}{R_{C5a} - R_{Neg}} - 1\right]100$$

where the responses (R) are: R_D, in the presence of ibuprofen plus C5a fragments; R_{C5a}, in the presence of C5a fragments alone; R_{Neg}, in the presence

[5] Motrin; donated by the Upjohn Co., Kalamazoo, Mich.
[6] Ahlco Corp., Meriden, Conn.
[7] Sartorius Filters, Hayward, Calif.
[8] Column PD-10; Pharmacia Fine Chemicals.
[9] Model ZBI particle counter equipped with a model C-1000 Channelyzer; Coulter Electronics, Hialeah, Fla.
[10] Hematall; Fisher Scientific Co., Pittsburgh, Pa.

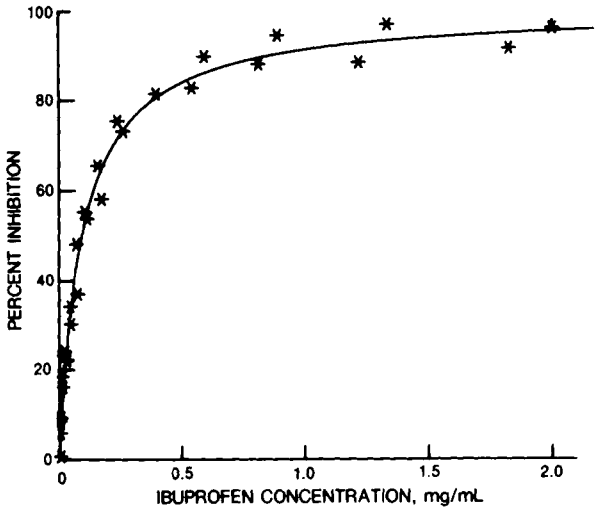

Figure 3—*Effect of ibuprofen on the C5a-stimulated release of the lysosomal enzyme elastase from PMNs. The results of three separate experiments are presented. The ID_{50} was calculated to be 95 μg/mL, and the maximum inhibition of enzyme release was 100%.*

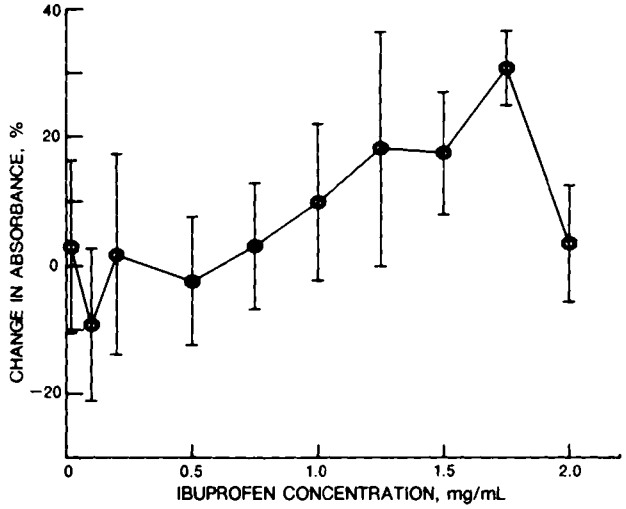

Figure 4—*Effect of ibuprofen on the reduction of nitroblue tetrazolium by PMNs. The percent change in absorbance at 550 nm as a function of ibuprofen concentration is presented for four separate experiments, with the bars representing the* SD. *Change in the positive direction indicates stimulation of nitro blue tetrazolium reduction.*

of neither. We found that the data conformed to a rectangular hyperbola of the form:

$$\%I = \frac{I_{max}\,[\text{ibuprofen}]}{ID_{50} + [\text{ibuprofen}]}$$

where I_{max} is the maximum reversal of chemoattractant effect expected when the ibuprofen concentration is extrapolated to infinite concentration, and ID_{50} is the concentration of ibuprofen that will produce $0.5 \times I_{max}$. The data were analyzed by nonlinear regression (10).

RESULTS

Ibuprofen inhibited all PMN responses to the chemoattractant. These included the locomotory chemotactic response (as measured by the micropore filter technique), lysosomal enzyme release, cell aggregation (as measured by a transient decrease in the number of PMN cells occurring within 30 s from contact with the chemoattractant), and cell swelling. These effects were directed against the cells and not against the chemoattractant, since treatment of C5a with ibuprofen and subsequent removal of the drug by gel filtration[8] did not impair subsequent C5a activity on release of the lysosomal enzyme elastase. The ID_{50} and I_{max} values with ibuprofen varied according to the response tested. A summary of these effects is shown in Table I. Cell swelling and cell aggregation had the lowest ID_{50} values, whereas these values were high for locomotory response and lysosomal enzyme release.

Of additional interest is the effect of ibuprofen on PMN cell swelling. Although it inhibited the rapid cell swelling that occurred 30 s after PMN contact with C5a, the drug itself produced a relatively slower swelling of cells (Fig. 1). The delayed swelling caused by ibuprofen, which eventually exceeded that produced by C5a, occurred with or without the presence of C5a. Six determinations of the effect of ibuprofen on PMN swelling and aggregation were made at an ibuprofen concentration of 1.75 mg/mL. We found that the inhibition of swelling was 90% (calculated value = 87%) and inhibition of aggregation was 96% (calculated value = 95%).

The locomotory index (distance migrated per cell) was inhibited, with an I_{max} value of 78% (Fig. 2), but the number of PMNs migrating did not diminish, except at very high concentrations (40% inhibition at 1.5–2.0 mg/mL) of the drug. Thus, the PMNs are affected in two distinctly different ways, depending on drug concentration. The reduced number of migrating PMNs at high concentrations of ibuprofen was not related to cell death or loss of viability since, in the trypan blue dye exclusion study, 98% of PMNs exposed to 2 mg of drug per mL excluded trypan blue dye, as compared with 94% of control cells. Also shown in the trypan blue dye study is that 55% of control cells had the triangular active morphology and were moving, whereas in the drug-treated PMNs only 12% assumed this active form. This is consistent with inhibition of locomotory response observed by the micropore filter assay.

Lysosomal enzyme release, particularly that of elastase, can be completely inhibited (I_{max} = 100%) by high concentrations of ibuprofen (Fig. 3). The reduced lysosomal enzyme activity observed in the presence of ibuprofen was due to reduced release of enzymes and not direct inhibition of the enzyme by the drug, since addition of ibuprofen after the enzyme release step of the assay, using control PMNs not previously treated with the drug, did not produce any change in the quantity of enzyme activity. There is a suggestion of individual variability in the ibuprofen response of PMNs. A donor with a low PMN locomotory response was found to have ID_{50} values of 191 μg/mL for glucosaminidase and 113 μg/mL for elastase release and I_{max} values of 111 and 113%.

Nitro blue tetrazolium reduction by PMNs was not affected, except at high concentrations of the drug. There was a linear increase ($p < 0.001$) in nitro blue tetrazolium reduction in the presence of 0.5–1.75 mg of the drug per mL and a sharp drop in activity thereafter (Fig. 4). Bactericidal activity against *Staphylococcus aureus* was also not affected by ibuprofen, except at a concentration of 2 mg/mL, at which a discernible inhibition was found (Fig. 5).

Perhaps of greater clinical relevance than the I_{max} values are the estimates of inhibition of the responses at drug concentrations of 20–50 μg/mL, since these are achievable in plasma. These estimates (Table I) indicate that PMN swelling and aggregation induced by C5a are most inhibited by these levels of ibuprofen. The chemotactic (locomotory) response to zymosan-activated normal serum is reduced by 20–35%, and the stimulation of lysosomal enzyme release by C5a is reduced by 17–38% (Table I).

DISCUSSION

The results of these studies indicate that ibuprofen may indeed exert its anti-inflammatory action on multiple sites. Besides its well-known effect on prostaglandin synthesis resulting from its potent inhibitory activity against the enzyme cyclo-oxygenase (11), it has easily demonstrable inhibitory effects on PMN responses to chemoattractant. By comparison, however, ibuprofen is much more active against cyclo-oxygenase than against PMN responses since the ID_{50} to platelet and endothelial cell prostaglandin synthesis was found to be 1 μg/mL [calculated from the data of Parks *et al.* (12)]. Relatively minimal effects on bactericidal function against *S. aureus* and on nitroblue tetrazolium reduction were also demonstrable at very high concentrations. Quantitative assessment of these effects indicates evidence of selectivity. For example, cell aggregation and swelling were inhibited by low concentrations of the drug that are easily achievable in serum with the usual oral doses, whereas lysosomal enzyme release and chemotactic (locomotory) responses required much higher concentrations. From these results, particularly with the effect of ibuprofen on chemotactic response, it is difficult to explain why the use of ibuprofen is not associated with a clinically obvious impairment of antimicrobial host defenses. It is likely that the combined effects on PMN responses and prostaglandin synthesis, but not separately, result in a predominantly anti-inflammatory effect. From these studies, it can be concluded that it is also likely that antimicrobial defenses may suffer at very high concentrations.

Because of its effect on PMN aggregation, it is possible that this drug and other nonsteroidal anti-inflammatory drugs may be useful in the prevention of disorders that result from vascular leukocytic stasis of intravascularly stimulated PMNs, such as adult respiratory distress syndrome related to open heart surgery, filtration leukapheresis, systemic infections, and hemodialysis

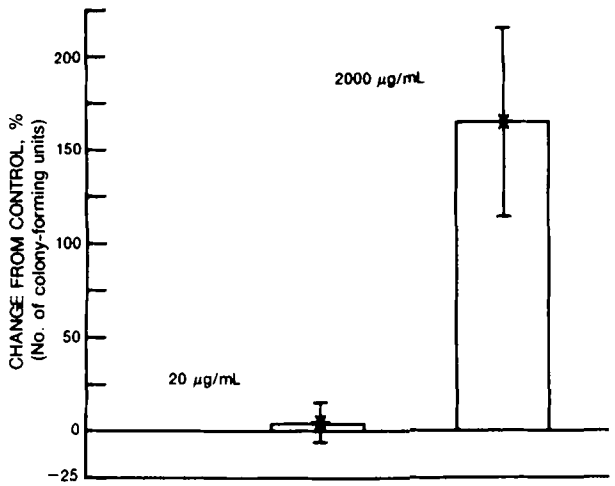

Figure 5—*Effect of ibuprofen on the bactericidal activity of PMNs against* S. aureus. *The percent change from the control is based on the number of colony-forming units remaining. Change in the positive direction indicates inhibition of the bactericidal activity of the cells.*

(13). Moreover, ibuprofen may be a useful agent to prevent the pulmonary complications of bleomycin, since new evidence indicates that this antineoplastic drug concentrates in PMNs and may be delivered at high concentrations to the lungs when conditions for the occurrence of pulmonary vascular leukocytic stasis are present (14).

The mechanism to explain the inhibitory effects of ibuprofen on PMNs is not known. Since aggregation, chemotaxis, and lysosomal enzyme release were inhibited almost to a similar degree by the drug, it is likely that the mechanism involves a pathway common to all three responses. These common pathways include the cell membranes and the cellular messengers, such as cell receptors, calcium, cyclic neucleotides, and arachidonic acid metabolites, particularly of the lipoxygenase pathway. Although the lysosomal membrane was "stabilized" by ibuprofen and other nonsteriodal anti-inflammatory drugs, as reported by this study and others (15), there is yet little direct evidence of cell membrane inhibitory effects by these drugs. Recent evidence points to a regulatory influence of prostaglandins on cyclic neucleotides and calcium (16). Although the effects of specific postaglandins on cyclic nucleotides may be known, it is not possible to predict what effects the inhibition of prostaglandin synthesis would have. This is because prostaglandin effects are concentration-dependent (a low concentration of PGE lowers, while a high cocentration raises, cAMP cellular levels), and also dependent upon the specific compound (*i.e.*, PGF_{2a} increases cGMP; PGE and PGD increases cAMP) (17, 18). Moreover, the effects of the early unstable metabolites (endoperoxides and thromboxane) differ from that of the stable prostaglandins (19).

REFERENCES

(1) I. M. Goldstein, in "Mediators of Inflammation," G. Weissmann, Ed., Plenum, New York, N.Y., 1974, p. 51.

(2) J. R. Vane, *Nature (London) New Biol.*, **231,** 232 (1971).

(3) E. Magluilo, R. Genzi-Cipelli, A. Lago, M. Azzini, E. Mogin, and S. Gallico, *Int. J. Clin. Pharmacol.*, **15,** 417 (1977).

(4) S. Spisani, G. Vanzini, and S. Tramiello, *Experientia*, **35,** 803 (1979).

(5) G. A. Higgs, K. E. Eakins, K. G. Mugridge, S. Moncada, and J. R. Vane, *Eur. J. Pharmacol.*, **66,** 81 (1980).

(6) J. T. O'Flaherty, D. L. Kreutzer, and P. A. Ward, *J. Immunol.*, **119,** 232 (1977).

(7) E. G. Maderazo and P. A. Ward, in "Todd-Sanford-Davidsohn Clinical Diagnosis by Laboratory Methods," Vol. 2, 16th ed., J. B. Henry, Ed., W. B. Saunders Co., Philadelphia, Pa., 1979, p. 1335.

(8) J. Fantone, R. M. Senior, D. L. Kreutzer, M. Jones, and P. A. Ward, *J. Lab. Clin. Med.*, **93,** 17 (1979).

(9) M. J. Castillo, K. Nakajima, M. Zimmerman, and J. C. Powers, *Anal. Biochem.* **99,** 53, (1979).

(10) C. L. Woronick, J. Malnick, and E. G. Maderazo, *J. Lab. Clin. Med.*, **98,** 58 (1981).

(11) T. G. Kantor, *Ann. Intern. Med.*, **91,** 887 (1979).

(12) W. M. Parks, J. C. Hoak, and R. L. Czervoike, *J. Pharmacol. Exp. Ther.*, **219,** 415, (1981).

(13) D. E. Hammerschmidt, L. J. Weaver, L. D. Hudson, P. R. Craddock, and H. S. Jacob, *Lancet*, **i,** 947, (1980).

(14) J. T. Noble, K. Ramberg-Laskaris, and M. S. Klempner, Program Abstracts of the 22nd Interscience Conference on Antimicrobial Agents and Chemotherapy (abstract No. 41), 1982, p. 72.

(15) R. J. Smith, *J. Pharmacol. Exp. Ther.*, **207,** 618 (1978).

(16) D. F. Horrobin, "Prostaglandins. Physiology, Pharmacology and Clinical Significance," Eden Press, Montreal, Canada, 1978, p. 151.

(17) H. R. Hill, in "Leukocyte Chemotaxis. Methods, Physiology and Clinical Implications," J. I. Gallin and P. G. Quie, Eds., Raven, New York, N.Y., 1978, p. 179.

(18) C. J. Dunn, D. A. Willoughby, J. P. Giroud, and S. Yamamoto, *Biomedicine*, **24,** 214, (1976).

(19) G. Weissmann, "Prostaglandins in Acute Inflammation. Current Concepts," monograph published by Upjohn Co., Kalamazoo, Mich., 1980.

ACKNOWLEDGMENTS

This work was supported, in part, by The Upjohn Co.

Preparation of Spherically Agglomerated Crystals of Aminophylline

Y. KAWASHIMA ˣ, S. AOKI, H. TAKENAKA, and Y. MIYAKE *

Received April 21, 1983, from the *Gifu Pharmaceutical University, 5-6-1, Mitahora-higashi, Gifu 502, Japan* and **Eisai Co., Kawashimachyo, Hashimagun, Gifu 483, Japan.* Accepted for publication August 16, 1983.

Abstract □ The spherically agglomerated crystals of aminophylline (theophylline-ethylenediamine complex) can be compounded directly into pharmaceutical formulations without further processing, *e.g.*, granulation. Such crystals were prepared by mixing theophylline and ethylenediamine in a partially miscible solvent system, *i.e.*, organic solvent-ethanol-water. The organic solvents used were chloroform, 1-hexanol, isopropyl acetate, isobutyl acetate, isoamyl acetate, benzene, toluene, *n*-hexane, or *n*-heptane. Spherical crystallization depended upon the solubility of theophylline in the solvent mixture. The resultant agglomerated crystals were identical with the theophylline-ethylenediamine complex by IR, X-ray, and differential scanning calorimetry analyses, and was the α-, β-, or γ-form when the water of crystallization was ≤0.5, 1.0, and 2.5 mol, respectively. When the amount of ethylenediamine used was <1.1 mL (0.0165 mol), the resultant agglomerated crystals were converted to anhydrous theophylline by washing with ethanol. When water was added to the system (≥0.3 mL, *i.e.*, 0.0167 mol), water was occluded in the resultant agglomerates as water of crystallization. Ethylenediamine content in the agglomerated crystals could be controlled by changing the amount of ethylenediamine added in the crystallization solvent.

Keyphrases □ Aminophylline—preparation from spherically agglomerated crystals of theophylline and ethylenediamine □ Spherical crystallization—aminophylline, theophylline, ethylenediamine

In previous papers (1-3), we described a method for the direct agglomeration of crystals during the crystallization process. In this process, a partially miscible mixture, *e.g.*, water-ethanol-chloroform, was used as the crystallization solvent. By selecting the proper ratio, a small amount of water or chloroform was liberated which acted as the collecting liquid and preferentially wetted the resulting crystals and transformed them into a spherical shape. This technique was termed "spherical crystallization" (1) due to the spherical form of the resultant crystals. Sodium theophylline monohydrate crystals, produced by salting out, were directly agglomerated into spheres in a mixture of an ethylenediamine solution of theophylline, an aqueous sodium chloride solution, ethanol, and chloroform (2, 3). Needle-like salicylic acid crystals simultaneously formed and agglomerated into spheres in a mixture of water, ethanol, and chloroform (1).

The present study describes the preparation of spherically agglomerated crystals of the theophylline-ethylenediamine complex (aminophylline) by the spherical crystallization technique, and also describes the crystallization behavior and the physicochemical properties of the resultant agglomerated crystals.

EXPERIMENTAL SECTION

Spherical crystallization process—*Method 1*—A mixture of organic solvent (60 mL), ethanol (12 mL), and water (0.13-10 mL) was used as the crystallization solvent. The amount of water added to the solvent was adjusted so that the resulting spherically agglomerated crystals were ~1 mm in diameter. The organic solvents used were chloroform, 1-hexanol, isopropyl acetate, isobutyl acetate, isoamyl acetate, benzene, toluene, *n*-hexane, or *n*-heptane. All organic solvents were reagent grade and were used as received. Ethylenediamine[1] (3.0 mL) and theophylline[1] (6.0 g) were dissolved in the mixture and agitated at 500 rpm with a paddle type agitator with four blades. Fine white crystals formed and agglomerated simultaneously into spheres. After 2 h, the agglomerated crystals were separated and dried. When using 1-hexanol and isopropyl acetate, 6-7 h of agitation were required.

Method 2—Spherical crystallization was carried out using the crystallization solvent with various amounts of ethylenediamine (1.0-3.5 mL) and water (0.15-0.9 mL), added to alter the ethylenediamine content in the resultant agglomerated crystals. The crystallization solvent, without water, was also used. The aforementioned experimental procedure was followed.

For reference, the theophylline-ethylenediamine complex (aminophylline), without agglomeration, was prepared by a conventional method, referred to as JP(X) (4). To a solution of absolute ethanol (100 mL) and ethylenediamine (9.2 mL) was added theophylline (24.7 g). The mixture was stirred vigorously for 5-6 h, during which time white crystals formed. These were washed with ethanol and dried.

Liberation Test of the Aqueous Phase from the Crystallization Solvent—To a solution of *n*-hexane (10 mL) and ethanol (2 mL), ethylenediamine (0-6 mL) and water (0-0.9 mL) were added to give two phases.

Measurement of the Physicochemical Properties of the Agglomerated Crystals—The spherically agglomerated crystals and the aminophylline crystals, prepared by the conventional method, were photographed through an optical microscope[2] and a scanning electron microscope[3], respectively. The particle size of the agglomerated crystals was measured by sieve analysis, and the crystalline forms of the agglomerated crystals were analyzed by an X-ray diffractometer[4] and an infrared spectrophotometer[5]. The thermal degradation behavior of the agglomerated and conventional crystals was investigated with a differential scanning calorimeter with heating at a rate of 10°C/min. The contents of theophylline and ethylenediamine in the agglomerated crystals were measured spectrophotometrically at 275 nm and by a neutralization titration method with 0.1 M HCl, respectively. The water content was measured by the Karl Fischer method[6].

RESULTS AND DISCUSSION

Spherical Crystallization Behavior of Method 1—It was found that spherical crystallization was dependent upon the solubility of theophylline in the solvent mixture. When chloroform or 1-hexanol were used as the organic solvents, theophylline completely dissolved. When chloroform was used, the fine crystals changed into the spherically agglomerated crystals within a 1-2 h period. With 1-hexanol, 7 h were required to obtain acceptable spherically agglomerated crystals. The solubility of water in 1-hexanol (5) is relatively high when

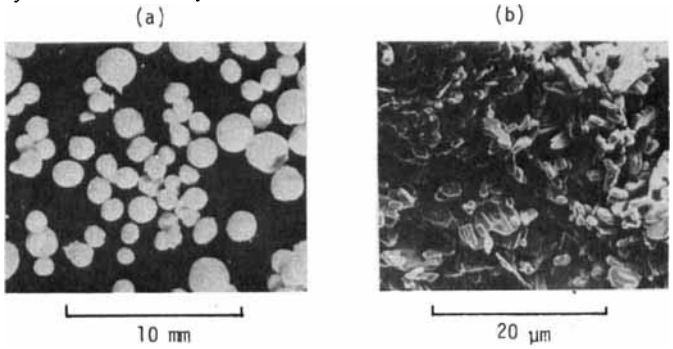

Figure 1—*Photographs of the agglomerated crystals and aminophylline crystals. (a) The spherical agglomerated crystals prepared in a mixture of chloroform-ethanol-water. (b) Aminophylline crystals prepared by a conventional method (4).*

[1] Nakarai Chemical Ltd., Japan.

[2] Olympas Optical Co., Ltd., JM, Japan.
[3] Nihon Denshi, JMS-SI, Japan.
[4] Nihon Denshi, JOX, Japan.
[5] Rigaku CN80852, Japan.
[6] Kyoto Electronics Manufacturing Co., Japan.

0022-3549/84/1000-1407$01.00/0
© 1984, American Pharmaceutical Association

Table I—Effect of Organic Solvents used on Spherical Crystallization

Organic Solvent	Water in the System, mL	Drug and Water Contents in the Agglomerate, %			Average Diameter of Agglomerate, mm	Solubility of Water[a]
		Theophylline	Ethylene-diamine	Water		
1-Hexanol	10.00	84.86	15.15	0.48	0.86	5.85
Isopropyl Acetate	3.75	82.82	16.43	5.78	1.55	1.66
Isobutyl Acetate	3.25	81.38	17.19	6.32	1.45	1.44
Isoamyl Acetate	2.25	84.30	15.74	5.28	1.30	—
Benzene	1.95	83.78	15.79	4.98	0.81	0.0385
Toluene	1.60	83.65	16.27	5.31	0.90	0.0373
n-Hexane	0.25	82.04	17.46	6.19	1.40	0.0073
n-Heptane	0.13	83.17	16.77	5.57	1.35	0.00897
Chloroform	4.00	85.13	15.47	8.31	1.35	0.0118[b]
Aminophylline[c]	—	83.39	14.39	4.21	5.52(μm)[d]	—

[a] Solubility in the organic solvent (v/v %) at 20°C. [b] Solubility at 22°C. [c] Prepared by a conventional method (4). [d] Measured by a photographic counting method.

compared with the solubility of chloroform and the other solvents (Table I). Therefore, the liberation of the aqueous solution, which acted as the collecting liquid for the crystals, appeared to occur less readily from 1-hexanol than chloroform. When a small amount of additional water (*e.g.*, 0.05 mL) was added to the 1-hexanol mixture during crystallization, (*e.g.*, at 2 h) the crystals agglomerated within several minutes.

When isopropyl acetate, isobutyl acetate, isoamyl acetate, benzene, or toluene were used, a part of the theophylline crystals remained undissolved. Since only dissolved theophylline presumably complexes with ethylenediamine, it is assumed that the undissolved theophylline dissolves as the complex precipitates. When using isopropyl acetate, 5 h were required.

When *n*-hexane or *n*-heptane were used, the spherically agglomerated crystals of theophylline formed immediately: the resultant crystals disintegrated into dispersed particles, and the spherically agglomerated crystals of the complex formed.

Physicochemical Properties of Spherically Agglomerated Crystals Prepared by Method 1—The representative photographs of the spherically agglomerated crystals and the theophylline-ethylenediamine complex (aminophylline) crystals, prepared in the conventional manner, are seen in Fig. 1.

The X-ray diffraction patterns of the agglomerated crystals, shown in Fig. 2, indicate that the agglomerates have three different crystalline forms, described here as the α-, β-, and γ-forms. The β-form was identical with aminophylline, while the patterns of the α- and γ-forms were different. The IR spectra of all the agglomerates were identical with that of aminophylline. The above IR and X-ray diffraction analyses suggested that the α- and γ-form of the agglomerated crystals were theophylline-ethylenediamine complexes with different crystalline forms.

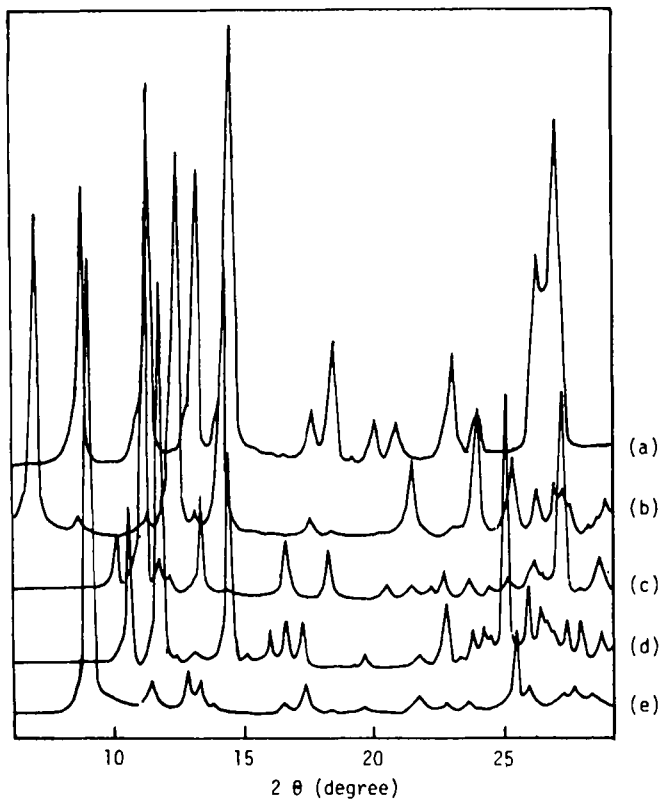

Figure 2—*X-ray powder diffraction patterns of agglomerates, anhydrous theophylline, theophylline monohydrate, and aminophylline. Key: (a) theophylline monohydrate; (b) anhydrous theophylline; (c) α-form of agglomerates; (d) β-form of agglomerates, aminophylline; (e) γ-form of agglomerates.*

The theophylline, ethylenediamine, and water content in the agglomerated crystals is tabulated in Table I. The water content in the agglomerates was classified in the following way: <0.5, 5-6, and 8-10%. Irrespective of the water content, the ratio of theophylline and ethylenediamine remained essentially the same. The water content of 4-6 and 8-10% correspond with ~1 and 2.5 mol of the water of crystallization, respectively, suggesting that the β- and γ-forms of the agglomerated crystals contained 1 and 2.5 mol of water of crystallization, respectively.

Differential scanning calorimetry (DSC) thermograms of the agglomerated crystals are shown in Fig. 3. The endothermic peak due to the release of 1 mol of ethylenediamine appeared at ~120°C and was detected by thermal gravimetry. The water of crystallization in the agglomerated crystals was released in a different way, depending on the crystalline form of the agglomerated crystals. In Table I, the amount of water required for obtaining the acceptable crystals having an average diameter of 0.81-1.55 mm are listed for the various organic solvents used. It was found that decreasing the solubility of water in the solvent decreased the amount of water required for the agglomeration, except for chloroform. This was explained by the fact that the agglomerates prepared using chloroform had higher amounts of water of crystallization (2.5 mol) than the other agglomerated crystals.

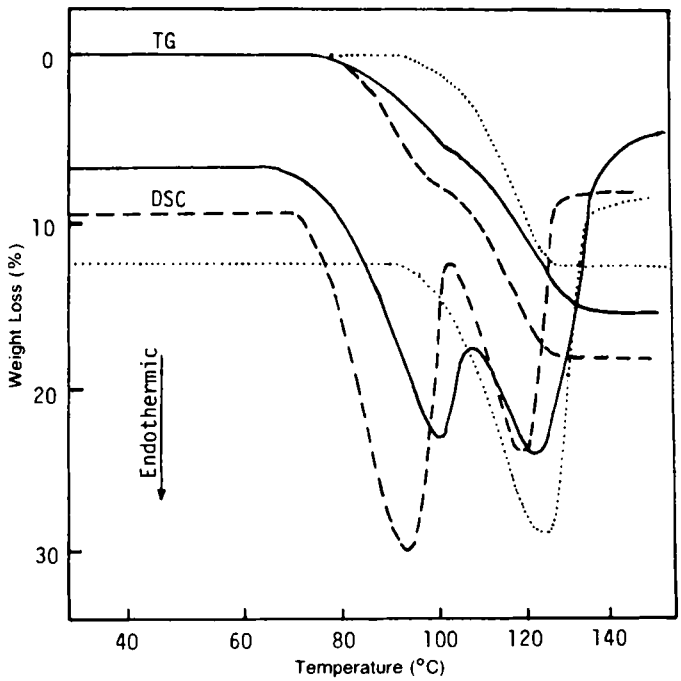

Figure 3—*DSC-TG thermograms of agglomerates and aminophylline. Key: (·····) α-form of agglomerates; (——) β-form of agglomerates, aminophylline; (- - -) γ-form of agglomerates.*

Table II—Effect of the Amounts of Ethylenediamine and Water on Theophylline and Ethylenediamine Contents in the Product

Ethylenediamine in the System, mL	Water in the System, mL	Drug and Water Contents in the Agglomerate, %			Average Diameter of Agglomerate, mm
		Theophylline	Ethylene-diamine	Water	
1.0	0.90	87.43	12.71	4.18	2.20
1.5	0.70	84.51	15.37	3.72	1.20
2.0	0.65	85.42	15.36	4.02	1.10
2.5	0.30	83.63	17.10	4.30	1.35
3.0	0.25	80.53	19.43	5.42	0.90
3.5	0.15	78.47	21.65	3.85	1.10

The theophylline and ethylenediamine content in the agglomerated crystals prepared using *n*-hexane, *n*-heptane, etc., in Table I, did not meet the specified values in JP(X), *i.e.*, 84–86% for theophylline and 14–15% for ethylenediamine. However, the theophylline and ethylenediamine contents in the resultant agglomerated crystals could be adjusted to the specified values in JP(X) by changing the amount of ethylenediamine used for the crystallization, as described below.

Spherical Crystallization Behavior of Method 2—To adjust the theophylline and ethylenediamine contents in the resultant agglomerated crystals to those specified in JP(X), the spherical crystallization was carried out by changing the amount of ethylenediamine (1.0–3.5 mL) and water (0.15–0.9 mL) in the mixture of *n*-hexane (60 mL) and ethanol (12 mL) used as the solvent. It was found that >1.1 mL (0.0165 mol) of ethylenediamine was required to obtain the theophylline-ethylenediamine complex. This critical amount of ethylenediamine corresponded to the amount required to obtain the molecular complex with 6 g of theophylline (0.0333 mol). When the amount of ethylenediamine used was <1.1 mL, the resultant agglomerated crystals were converted to anhydrous theophylline by washing with ethanol. This indicated that ethylenediamine was adsorbed physically on the theophylline crystals. When the ethylenediamine used was >1.1 mL, less water was required to obtain the spherically agglomerated crystals with a 1–2 mm diameter. The excess of ethylenediamine, >1.1 mL, was consumed as the collecting liquid for the crystals and was occluded physically in the agglomerates. The action of ethylenediamine as the collecting liquid was proved by the fact that the agglomerated crystals were prepared in the *n*-hexane (or *n*-heptane) and ethanol mixture with theophylline by adding ethylenediamine alone to the system without water. When the amount of water was <0.3 mL (0.0167 mol of water of crystallization) for 6 g theophylline (0.0333 mol), the water acted only as the collecting liquid for the crystals. When >0.3 mL of water was used, the water was occluded as water of crystallization (1 mol) and acted as the collecting liquid in the agglomerated crystals.

The amounts of ethylenediamine and water required to obtain the acceptable agglomerated crystals for practical use are plotted in Fig. 4. The straight line in Fig. 4 represents a phase separation line. In the region below the line, the solvents were miscible, and no agglomerates formed; whereas, in the region above the line, phase separation occurred and an aqueous solution of ethylenediamine was liberated, which collected the crystals to form the agglomerated crystals. The corrected points, obtained by subtracting the amount of ethylenediamine (1.1 mL, *i.e.*, 0.0165 mol) required to form the complex with theophylline (6 g, *i.e.*, 0.0333 mol) from that of ethylenediamine actually added to the system, lay on the phase separation line when the amount of water used was <0.3 mL. When the amount of water used was >0.3 mL, the corrected points deviated from the phase separation line. This indicated that the water was occluded as the collecting liquid as well as water of crystallization in the agglomerated crystals.

The ethylenediamine and theophylline contents in the agglomerated crystals, prepared using various amounts of ethylenediamine and water, are tabulated in Table II. The average diameter of the resultant agglomerates are also shown in Table II. The water contents in the agglomerates were almost constant, irrespective of the amount of water in the solvent mixture. The ethylenediamine content in the agglomerates increased with increases in the amount of ethylenediamine used. A linear relationship was found between the ethylenediamine content in the agglomerates and the amount of ethylenediamine used, as shown in Fig. 5. This indicated that the ethylenediamine contents in the agglomerated crystals could be adjusted to that of aminophylline specified in JP(X) by changing the amount of ethylenediamine used. The ethylenediamine >14.3% in the agglomerated crystals (corresponding to 1 mol of ethylenediamine included in aminophylline) was released by drastic desiccation, since it was adsorbed only physically.

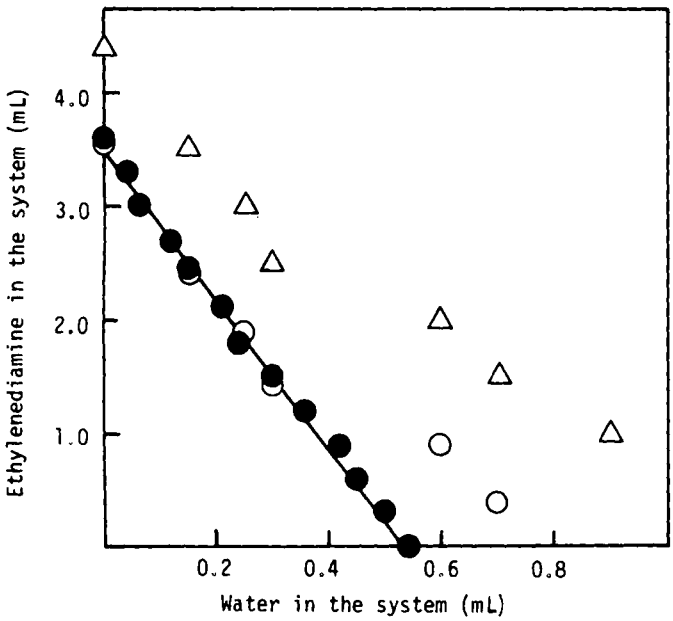

Figure 4—*Relationship between ethylenediamine and water in the system required for agglomeration and phase separation. Key: (△) agglomeration point; (●) phase separation point; (○) corrected point.*

REFERENCES

(1) Y. Kawashima, M. Okumura, and H. Takenaka, *Science*, **216**, 1127 (1982).

(2) Y. Kawashima, S. Y. Lin, M. Naito, and H. Takenaka, *Chem. Pharm. Bull.*, **30**, 1837 (1982).

(3) Y. Kawashima, M. Naito, S. Y. Lin, and H. Takenaka, *Powder Technol.*, **34**, 255 (1983).

(4) "The Japanese Pharmacopeia X," Ministry of Health and Welfare, Tokyo, Japan, 1981, p. 59.

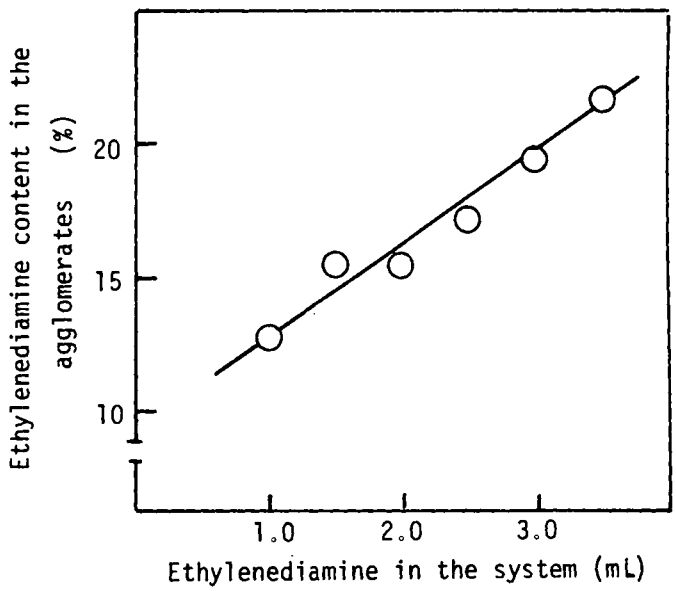

Figure 5—*Effect of the amount of ethylenediamine in the system on ethylenediamine content in the agglomerates.*

(5) "Organic Solvents Hand Book," 1st ed., Organic Synthesis Chemistry Association Japan, Ohm Co., Tokyo, 1981, p. 294.

ACKNOWLEDGMENTS

The authors thank Prof. A. Otsuka, Meijo University, Nagoya, Japan, for the use of the X-ray diffractometer. This paper is part VII of a series on spherical crystallization.

A part of this research was supported by a grant-in-aid (Project No. 59490023) for scientific research, Ministry of Education, Culture and Science, Japan.

Determination of the Ionization Constants of Compounds which Precipitate During Potentiometric Titration Using Extrapolation Techniques

WILLIAM H. STRENG ˣ and M. A. ZOGLIO

Received December 12, 1982, from the *Merrell Dow Research Institute, Merrell Dow Pharmaceuticals, Inc., Subsidiary of The Dow Chemical Co., Cincinnati, OH 45215.* Accepted for publication October 11, 1983.

Abstract □ It is shown that the ionization constants of diacidic compounds can be determined by utilizing potentiometric titration data, even when a precipitate forms during the titration. The two methods presented are particularly useful for compounds for which the pK_a values are close together. A third method is presented which can be used with monoacidic compounds or compounds for which the pK_a values are far apart and form a precipitate during the titration. Four symmetrical diacidic compounds were studied which had similar pK_a values, and one compound was studied which had pK_a values that were far apart. Comparison of the second pK_a of the latter compound with that previously reported determined by a spectrophotometric procedure showed excellent correlation.

Keyphrases □ Ionization constants—determination, compounds which precipitate during potentiometric titration □ Potentiometric titration—determination of ionization constants

A method for determining the microionization constants of zwitterionic compounds is described in which potentiometric data are combined with spectrophotometric data (1). This method should be restricted, however, to well-behaved systems, *i.e.*, those which do not form precipitates or degrade during the course of the experiment. For sparingly soluble compounds, Maulding and Zoglio (2) and Levy and Rowland (3) have presented two techniques. Weak complexing agents were used by Maulding and Zoglio, whereas the method of Levy and Rowland required determining the solubility of the sparingly soluble component. In addition, these methods were only developed for monoprotic compounds or those polyprotic compounds for which pK_a values were sufficiently far apart (about 4 pK_a units) to be considered monoprotic. This study describes a method to determine the macroionization constants of compounds which precipitate during titration and which have similar pK_a values. The type of compounds considered form diacid salts, *i.e.*, there are two nitrogen atoms which can be protonated on each molecule and which undergo the equilibrium shown in Scheme I.

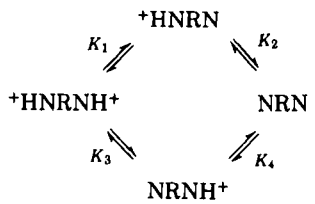

Scheme I

The microionization constants K_1, K_2, K_3, and K_4 are related to the macroionization constants by:

$$K_{13} = K_1 + K_3 \qquad \text{(Eq. 1)}$$

$$\frac{1}{K_{24}} = \frac{1}{K_2} + \frac{1}{K_4} \qquad \text{(Eq. 2)}$$

Utilizing potentiometric titration data, the macroionization constants K_{13} and K_{24} were determined for diprotic compounds in which species solubilities were exceeded and, therefore, which precipitated during the titration. This was accomplished by preparing the appropriate plots, as discussed below.

Measurements were made on four diacid salts in which the pK_a values were similar: 1,1′-(9*H*-fluorene-2,7-diyl)bis[2-diethylamino)ethanone]dihydrochloride (I); 1,1′-(2,8-dibenzofurandiyl)bis[2-(dimethylamino)-1-ethanone]dihydrochloride (II); 1,1′-(2,8-dibenzothiophendiyl)bis[2-(dimethylamino)-1-ethanone]dihydrochloride (III); 2,7-bis[2-(diethylamino)ethoxy]fluoren-9-one dihydrochloride (IV). Measurements were also made on one diacid salt for which the pK_a values were far apart: 10,11-dihydro-*N*-methyl-5*H*-dibenz[b,f]azepine-5-propanamine hydrochloride (V) (desipramine).

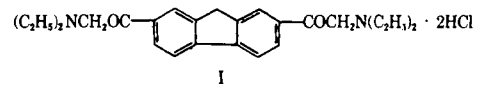

I

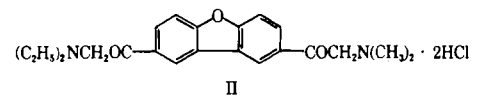

II

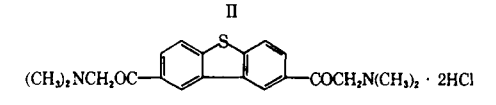

III

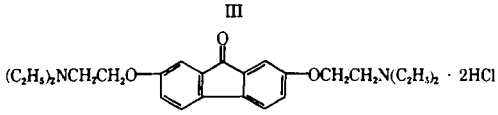

IV

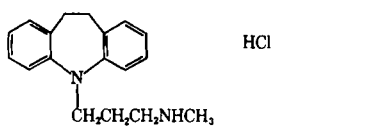

V

0022-3549/84/1000-1410$01.00/0
© 1984, American Pharmaceutical Association

(5) "Organic Solvents Hand Book," 1st ed., Organic Synthesis Chemistry Association Japan, Ohm Co., Tokyo, 1981, p. 294.

ACKNOWLEDGMENTS

The authors thank Prof. A. Otsuka, Meijo University, Nagoya, Japan, for the use of the X-ray diffractometer. This paper is part VII of a series on spherical crystallization.

A part of this research was supported by a grant-in-aid (Project No. 59490023) for scientific research, Ministry of Education, Culture and Science, Japan.

Determination of the Ionization Constants of Compounds which Precipitate During Potentiometric Titration Using Extrapolation Techniques

WILLIAM H. STRENG ˣ and M. A. ZOGLIO

Received December 12, 1982, from the *Merrell Dow Research Institute, Merrell Dow Pharmaceuticals, Inc., Subsidiary of The Dow Chemical Co., Cincinnati, OH 45215.* Accepted for publication October 11, 1983.

Abstract □ It is shown that the ionization constants of diacidic compounds can be determined by utilizing potentiometric titration data, even when a precipitate forms during the titration. The two methods presented are particularly useful for compounds for which the pK_a values are close together. A third method is presented which can be used with monoacidic compounds or compounds for which the pK_a values are far apart and form a precipitate during the titration. Four symmetrical diacidic compounds were studied which had similar pK_a values, and one compound was studied which had pK_a values that were far apart. Comparison of the second pK_a of the latter compound with that previously reported determined by a spectrophotometric procedure showed excellent correlation.

Keyphrases □ Ionization constants—determination, compounds which precipitate during potentiometric titration □ Potentiometric titration—determination of ionization constants

A method for determining the microionization constants of zwitterionic compounds is described in which potentiometric data are combined with spectrophotometric data (1). This method should be restricted, however, to well-behaved systems, *i.e.*, those which do not form precipitates or degrade during the course of the experiment. For sparingly soluble compounds, Maulding and Zoglio (2) and Levy and Rowland (3) have presented two techniques. Weak complexing agents were used by Maulding and Zoglio, whereas the method of Levy and Rowland required determining the solubility of the sparingly soluble component. In addition, these methods were only developed for monoprotic compounds or those polyprotic compounds for which pK_a values were sufficiently far apart (about 4 pK_a units) to be considered monoprotic. This study describes a method to determine the macroionization constants of compounds which precipitate during titration and which have similar pK_a values. The type of compounds considered form diacid salts, *i.e.*, there are two nitrogen atoms which can be protonated on each molecule and which undergo the equilibrium shown in Scheme I.

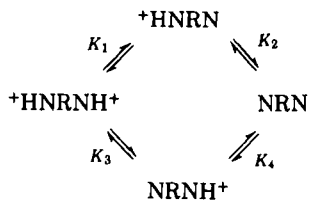

Scheme I

The microionization constants K_1, K_2, K_3, and K_4 are related to the macroionization constants by:

$$K_{13} = K_1 + K_3 \qquad \text{(Eq. 1)}$$

$$\frac{1}{K_{24}} = \frac{1}{K_2} + \frac{1}{K_4} \qquad \text{(Eq. 2)}$$

Utilizing potentiometric titration data, the macroionization constants K_{13} and K_{24} were determined for diprotic compounds in which species solubilities were exceeded and, therefore, which precipitated during the titration. This was accomplished by preparing the appropriate plots, as discussed below.

Measurements were made on four diacid salts in which the pK_a values were similar: 1,1′-(9*H*-fluorene-2,7-diyl)bis[2-diethylamino)ethanone]dihydrochloride (I); 1,1′-(2,8-dibenzofurandiyl)bis[2-(dimethylamino)-1-ethanone]dihydrochloride (II); 1,1′-(2,8-dibenzothiophendiyl)bis[2-(dimethylamino)-1-ethanone]dihydrochloride (III); 2,7-bis[2-(diethylamino)ethoxy]fluoren-9-one dihydrochloride (IV). Measurements were also made on one diacid salt for which the pK_a values were far apart: 10,11-dihydro-*N*-methyl-5*H*-dibenz[b,f]azepine-5-propanamine hydrochloride (V) (desipramine).

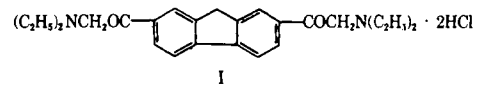

I

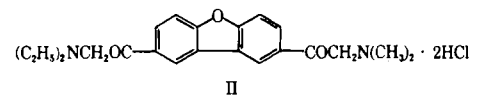

II

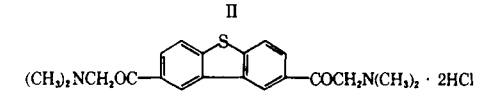

III

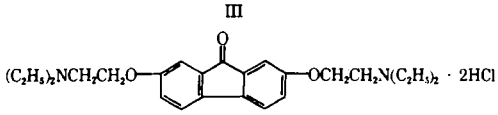

IV

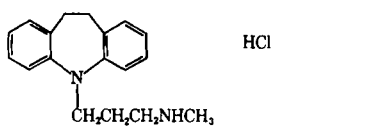

V

0022-3549/84/1000-1410$01.00/0
© 1984, American Pharmaceutical Association

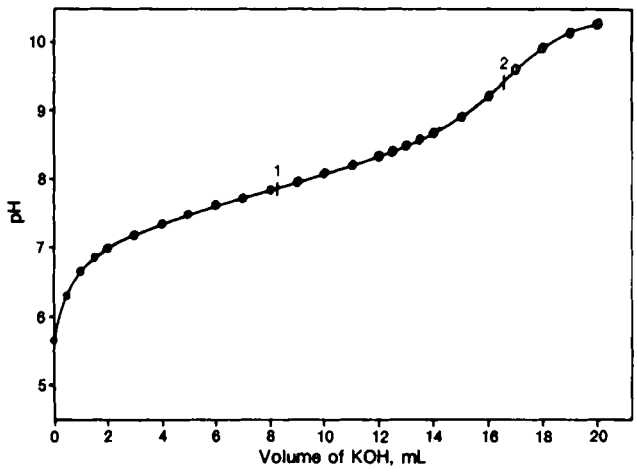

Figure 1—*Titration curve for compound II. Key: (1) first equivalence point; (2) second equivalence point.*

EXPERIMENTAL SECTION

Apparatus and Equipment—Potentiometric measurements were made with the apparatus previously described (1). For compounds I–IV, the apparatus was placed in a constant temperature bath and maintained at 25 ± 0.05°C, whereas the titration of V was done at room temperature (~24°C). Instead of the 50-mL buret used for I–IV, a syringe microburet was used for V.

Solution Preparation—Solutions of I–IV were prepared in the concentration range 3×10^{-4}–19×10^{-4} M. These solutions were titrated with 0.01 M potassium hydroxide, which was standardized with potassium acid phthalate. A solution of V with a concentration of 7×10^{-3} M was prepared, and an excess of 0.10 M hydrochloric acid standardized with potassium hydroxide was added to protonate both nitrogen atoms. This solution was titrated with 0.16 M potassium hydroxide standardized with potassium acid phthalate. All solutions were made with distilled water, boiled to remove oxygen and carbon dioxide, and saturated with nitrogen.

Table I—pK_{13} and pK_{24} Values for Compounds I–V

Compound	pK_{13}	pK_{24}
I[a]	8.16	8.89
II[b]	7.54	8.27
II[a]	7.54	8.24
III[a]	7.42	8.15
IV[a]	8.73	9.35
V[b,c]	1.51	10.24
V[c,d]	—	10.2

[a] Obtained by Method II. [b] Obtained by Method I. [c] The value of S_0 for compound V, obtained in this study was 60.8 μg/mL; the value obtained by Green (9) was 58.6 μg/mL. [d] Spectrophotometric method of Green (9).

THEORETICAL SECTION

In the following equations, { }, [ ], Y, and K represent activity, concentration, activity coefficient, and equilibrium constants on a molar scale, respectively. The total concentration of base added as titrant, halide, and acid being titrated are represented by $[B]$, $[X]$, and $[A]$, respectively.

The equilibria to be considered are not those for the microionization constants given by Scheme I, but rather the equilibria for the macroionization constants given by:

$$(NRN)H_2^{2+} \overset{K_{13}}{\rightleftharpoons} (NRN)H^+ + H^+ \qquad \text{(Eq. 3)}$$

$$(NRN)H^+ \overset{K_{24}}{\rightleftharpoons} NRN + H^+ \qquad \text{(Eq. 4)}$$

for which

$$K_{13} = \frac{\{(NRN)H^+\}\{H^+\}}{\{(NRN)H_2^{2+}\}} \qquad \text{(Eq. 5)}$$

$$K_{24} = \frac{\{NRN\}\{H^+\}}{\{(NRN)H^+\}} \qquad \text{(Eq. 6)}$$

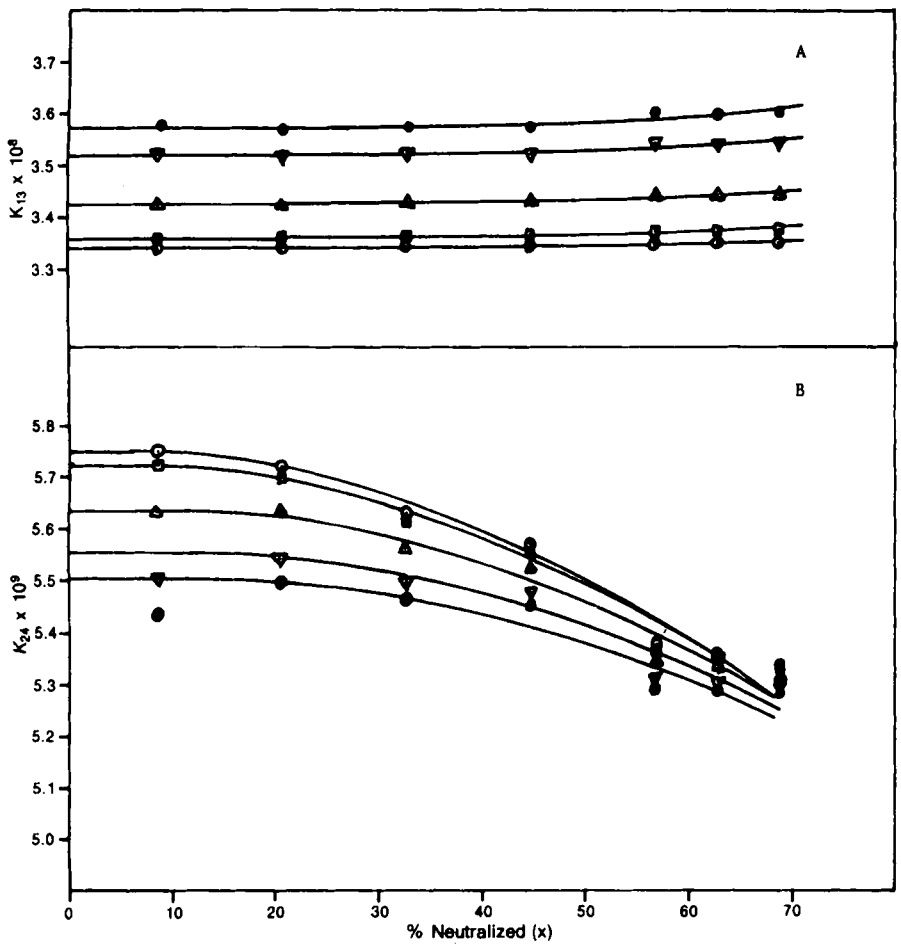

Figure 2—*(A)* K(*n,x*) versus *percent neutralized (x) for* K_{13} *of compound II. Key: the percent neutralized n is (⊙) 12; (⊡) 18; (▲) 24; (▼) 36; (●) 48. (B)* K(*n,x*) versus *percent neutralized (x) for* K_{24} *of compound II.*

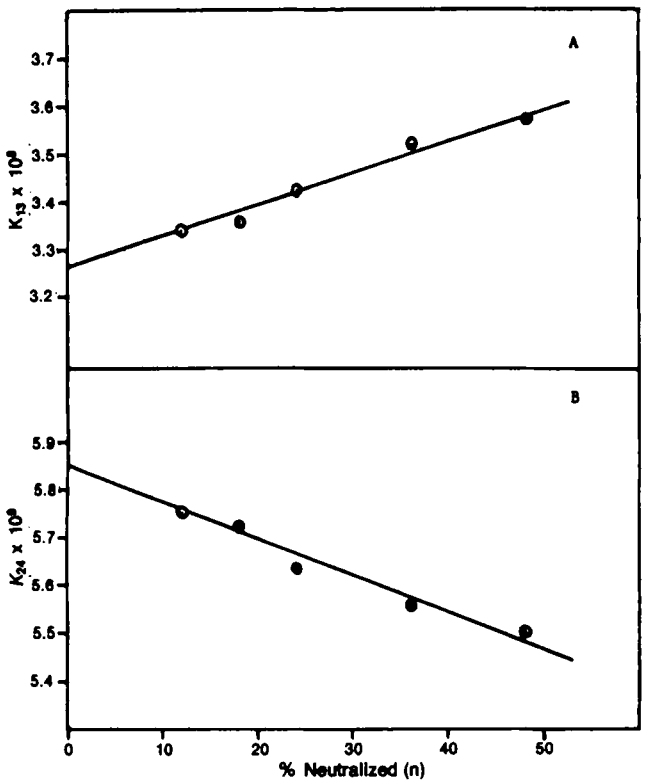

Figure 3—K(*n*,E) versus *percent neutralized (n) for* K_{13} *of compound II. (B)* K(*n*,E) versus *percent neutralized (n) for* K_{24} *of compound II.*

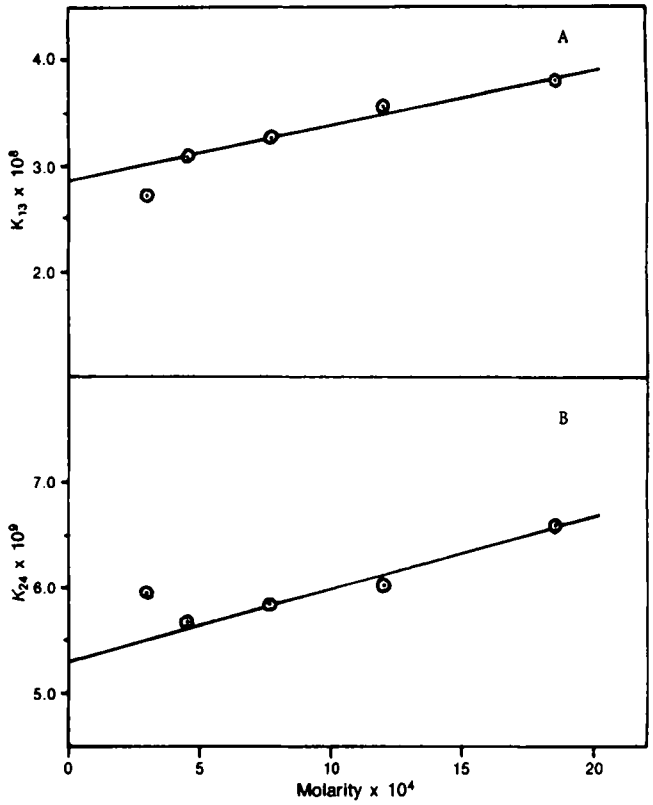

Figure 4—K(*0*,E) versus *molarity for* K_{13} *of compound II. (B)* K(*0*,E) versus *molarity for* K_{24} *of compound II.*

The equations used to determine the equilibrium constants in Eqs. 5 and 6 have been reported by many authors since the late 1800s (4–7) and will not be derived here. The derivation results in:

$$\alpha = \beta K_{13} + \gamma K_{13} K_{24} \qquad \text{(Eq. 7)}$$

where:

$$\alpha = [B]\{H^+\}^3 + \frac{\{H^+\}^4}{Y_{H^+}} - \frac{K_w\{H^+\}^2}{Y_{OH^-}} \qquad \text{(Eq. 8)}$$

$$\beta = \frac{Y_{(NRN)H^+}}{Y_{(NRN)H^+}}\left([A]\{H^+\}^2 - [B]\{H^+\}^2 - \frac{\{H^+\}^3}{Y_{H^+}} + \frac{K_w\{H^+\}}{Y_{OH^-}}\right) \qquad \text{(Eq. 9)}$$

$$\gamma = \frac{Y_{(NRN)H^+}}{Y_{NRN}}\left(2[A]\{H^+\} - [B]\{H^+\} - \frac{\{H^+\}^2}{Y_{H^+}} + \frac{K_w}{Y_{OH^-}}\right) \qquad \text{(Eq. 10)}$$

$$K_w = \{H^+\}\{OH^-\} \qquad \text{(Eq. 11)}$$

Conventional methods (4–7) can be used to determine K_{13} and K_{24} for well-behaved systems. Either of the two sets of experimental data can be combined according to Eqs. 12 and 13, or a plot of α/γ *versus* β/γ can be prepared, and the values for K_{13} and K_{24} determined from the slope and intercept:

$$K_{13} = \frac{\alpha_n\gamma_x - \alpha_x\gamma_n}{\beta_n\gamma_x - \beta_x\gamma_n} \qquad \text{(Eq. 12)}$$

$$K_{24} = \frac{\alpha_x\beta_n - \alpha_n\beta_x}{\alpha_n\gamma_x - \alpha_x\gamma_n} \qquad \text{(Eq. 13)}$$

where the subscripts n and x refer to two different sets of data. Modifications of these approaches can be made to determine the constants in systems in which precipitates are formed.

Method I—To use Eqs. 12 and 13, one set of data should be obtained before the first equivalence point and one should be obtained after. In well-behaved systems, the constants calculated will be independent of the sets of data used. For those systems that are not well behaved, *e.g.*, due to the formation of a precipitate, the values calculated for K_{13} and K_{24} will be incorrect. Those equilibrium constants calculated with data obtained after precipitation started will not be the same. They will, however, change in a systematic manner. Extrapolation of the calculated values to regions in which there is no precipitation should result in the correct value. This procedure can be expressed by:

$$K_T = \lim_{C\to 0}(\lim_{n\to 0}[\lim_{x\to E}[K_c(n,x)]]) \qquad \text{(Eq. 14)}$$

where K_c is the calculated equilibrium constant, C is the concentration, and K_T is the thermodynamic equilibrium constant. In this equation, n and x are two data sets: x is taken between the first and second equivalence points, and n is taken up to the first equivalence point. The limits used are E, the first equivalence point, for data set x; zero base addition for data set n; and infinite dilution for C. Each data set is comprised of a volume of base added and the measured pH. By knowing the concentration of strong base and the number of moles of weak acid initially, the volume of strong base can be expressed as a percentage of the weak acid neutralized.

Values for K_c are calculated by using two sets of data. For each n, there will be a set of K_c values determined with a different value for x. A plot is then prepared of the calculated K_c values *versus* the percentage of the second equivalent neutralized (x) for each n. Each value of n will result in a separate curve. The extrapolated values of K_c at x = 0 are then plotted *versus* the percentage of the first equivalent neutralized (n). The extrapolated value of K_c at n = 0 should equal the correct value, excluding activity effects. A third

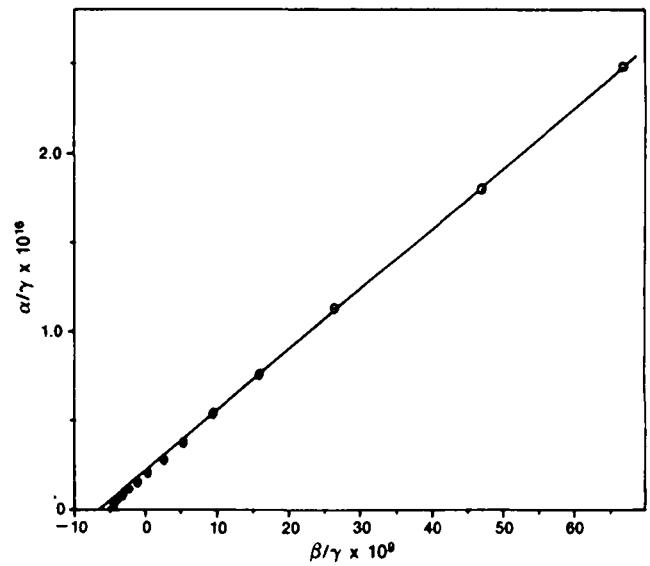

Figure 5—α/γ versus β/γ *for compound II.*

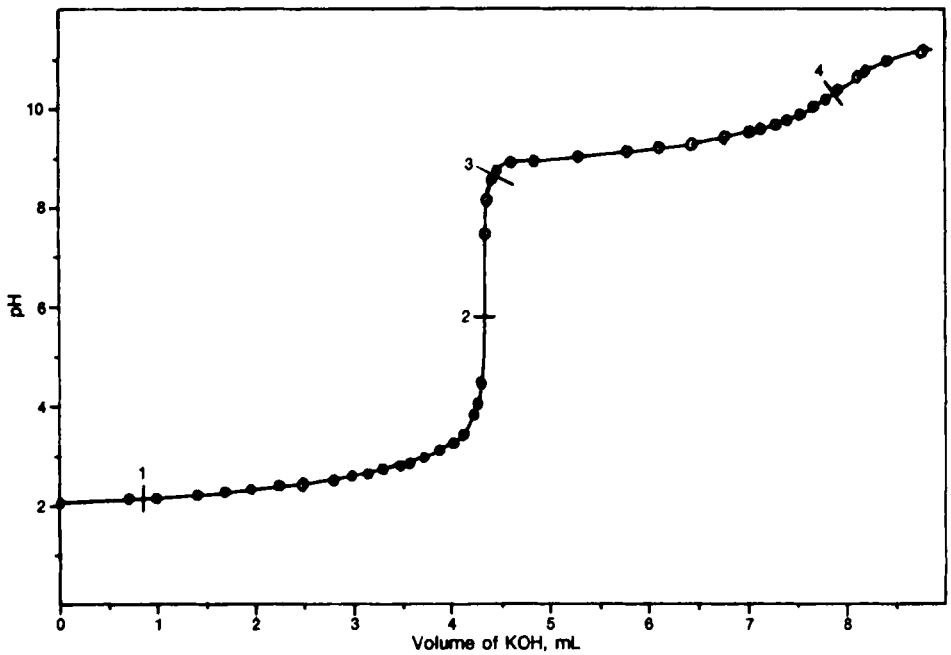

Figure 6—*Titration curve for compound V. Key: (1) starting point; (2) first equivalence point; (3) precipitate formed; (4) second equivalence point.*

plot of K_c *versus* concentration of weak acid will result in the thermodynamic value at infinite dilution.

Method II—A plot of α/γ *versus* β/γ from Eq. 7 will be linear until there is precipitation. Therefore, the determination of the slope of the linear segment and the linear extrapolation of this segment to the intercepts at α/γ and β/γ equal to zero enable the calculation of the equilibrium constants. The thermodynamic constants can be obtained from the infinite dilution value as described in method I.

RESULTS AND DISCUSSION

Figure 1 shows a typical titration curve for compounds I–IV. A precipitate formed during each titration, some of which formed prior to the first equivalence point. The data were treated by method I and/or method II. Approximations to the single ion activity coefficients were made by using the Davies equation (8):

$$-\log Y_i = AZ_i^2\left\{\frac{\sqrt{I}}{1+\sqrt{I}} - 0.2I\right\} \qquad \text{(Eq. 15)}$$

where Y_i is the single ion activity coefficient, A is a parameter for which the value at 25°C is 0.5092 on a molar scale, Z_i is the charge of ion i, and I is the molar ionic strength. The activity coefficients of the uncharged species were assumed to have a value of one.

According to method I, equilibrium constants were calculated with pairs of data; one set of data was from the region prior to the first equivalence point and the second set of data was from the region following the first equivalence point. These constants are written as K(n,x). For each data point designated by n, there was a set of equilibrium constants differentiated by the second data point used in the calculation and designated by x. The calculated values for K(n,x) can therefore be plotted *versus* x, and a separate curve can be obtained for each value of n. Typical plots of this type are shown in Figs. 2A and B for compound II. It can be seen that there is a separate curve for each data set n and that each curve approaches a constant value at x which corresponds to the first equivalence point. These values for K(n,E) are plotted *versus* n (Figs. 3A and B), and the curves obtained were extrapolated to an n value of zero. This value of n corresponds to zero base addition. There is a concentration dependency with these values of K(0,E) (Figs. 4A and B), and extrapolation of these curves to zero concentration will result in thermodynamic values. In Table I, the values obtained by this method for compound II are given.

By using method II, plots similar to those shown in Fig. 5 are obtained in which the deviation from linearity can be either negative or positive. This nonlinearity is due to either the formation of a precipitate during the titration and/or degradation. According to Eq. 7, the slope of the line from the linear segment will equal K_{13}, whereas the value of α/γ at the intercept at which

Table II—Microionization Constants for Compounds I–IV

Compound	$pK_1 = pK_3$	$pK_2 = pK_4$	K_{13}/K_{24}	K_1/K_2
I	8.46	8.59	5.37	1.35
II	7.84	7.94	5.01	1.26
III	7.72	7.85	5.37	1.35
IV	9.03	9.05	4.17	1.05

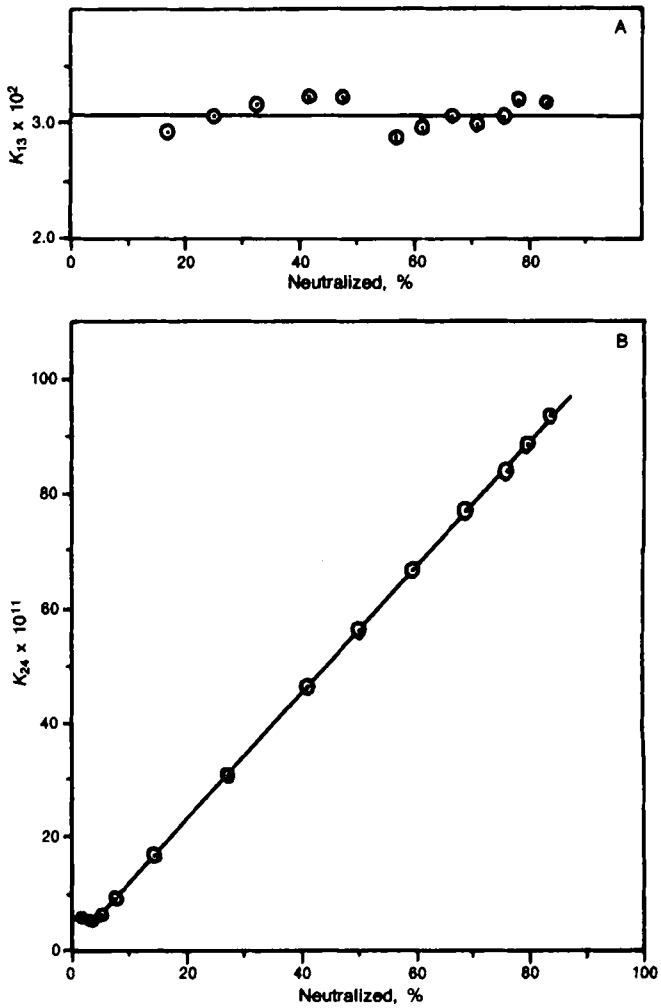

Figure 7—*(A)* K_{13} versus *percent neutralized for compound V. (B)* K_{24} versus *percent neutralized for compound V.*

$\beta/\gamma = 0$ is $K_{13}K_{24}$, and the value of β/γ at the intercept at which $\alpha/\gamma = 0$ is $-K_{24}$. These values of K_{13} and K_{24} have been found to be concentration dependent; therefore, plots similar to those shown in Figs. 4A and B were made to obtain the thermodynamic values. In Table I, the results of these calculations for compounds I–IV are given.

A modification of method I was used to obtain the values of K_{13} and K_{24} of compound V. Since the two pK_a values are far apart, the equilibria were assumed not to interact with each other; therefore, the equilibrium constants were determined by using the following expression for monoprotic compounds:

$$K_n = Z\frac{[H^+]([H^+] + [B] - [OH^-])}{[OH^-] + [A] - [H^+] - [B]} \qquad \text{(Eq. 16)}$$

where Z is the activity coefficient ratio $Y_{(NRN)H^+}/Y_{(NRN)H_2^{2+}}$ for K_{13} and $Y_{(NRN)}/Y_{(NRN)H^+}$ for K_{24}.

Figure 6 shows the titration curve obtained for compound V, and Figures 7A and B show the results of the calculated equilibrium constants *versus* percent neutralized. Precipitation was observed after the first equivalence point (Fig. 6), and therefore, consistent values should be obtained for K_{13} (Fig. 7A). Conversely, a change in the calculated value for K_{24} with respect to percent neutralized would be expected (Fig. 7B). The break in this latter curve at ~5% neutralization is due to the formation of a precipitate. The curve prior to precipitation should have a slope of zero (as in Fig. 7A), whereas the curve after precipitation will not necessarily be linear.

By knowing the value for K_{24} and the pH at which precipitation occurs, the solubility of the base (uncharged) species of compound V was determined by:

$$[NRN]_s = \frac{[A]K_{24}}{[H] + K_{24}} \qquad \text{(Eq. 17)}$$

In Table I, the results of the calculations for compound V are given, along with those values for K_{24} and $[NRN]_s$, as reported by Green (9) and determined by a spectrophotometric procedure. It can be seen there is excellent agreement among these data.

Since compounds I–IV are symmetrical molecules, it should be possible to calculate the microionization constants K_1, K_2, K_3, and K_4 of Scheme I. This is because K_1 should equal K_3, and K_2 should equal K_4. Furthermore, since the protonation sites are separated by large distances, it would be expected the K_2 and K_4 would be the same or only very slightly smaller than K_1 and K_3. The microionization constants were therefore calculated from Eqs. 1 and 2 and gave the results listed in Table II. It can be seen that there is very little difference in the calculated values, with K_2 and K_4 being slightly smaller.

For diprotic compounds with completely independent, equivalent sites of protonation, the ratio K_{13}/K_{24} will equal 4, and K_1/K_2 will equal 1. From these ratios (Table II), it can be seen that the values are very close to the theoretical values.

From these results, it can be concluded that the equilibrium constants of slightly soluble compounds can be determined potentiometrically by extrapolation procedures and give results which are consistent with those reported in the literature. It would be expected that method II would be better to use with those compounds that have equilibrium constants close together, whereas method I would be better to use with those compounds that have equilibrium constants farther apart.

REFERENCES

(1) W. H. Streng, H. E. Huber, J. L. DeYoung, and M. A. Zoglio, *J. Pharm. Sci.*, **65**, 1034 (1976).

(2) H. V. Maulding and M. A. Zoglio, *J. Pharm. Sci.*, **60**, 309 (1971).

(3) R. H. Levy and M. Rowland, *J. Pharm. Sci.*, **60**, 1155 (1971).

(4) A. A. Noyes, *Z. Physik. Chem.*, **11**, 495 (1893).

(5) C. Morton, *Trans. Faraday Soc.*, **24**, 14 (1928).

(6) W. R. Maxwell and J. R. Partington, *Trans. Faraday Soc.*, **31**, 922 (1935).

(7) J. C. Speakman, *J. Chem. Soc.*, 855 (1940).

(8) J. N. Butler, "Ionic Equilibrium a Mathematical Approach," Addison-Wesley Publishing Co., 1964, p. 437.

(9) A. L. Green, *J. Pharm. Pharmacol.*, **19**, 10 (1967).

Degradation of Fenprostalene in Polyethylene Glycol 400 Solution

DAVID M. JOHNSON ˣ **and WILLIAM F. TAYLOR**

Received March 14, 1983, from the *Institute of Pharmaceutical Sciences, Syntex Research, Palo Alto, CA 94304.* Accepted for publiction October 26, 1983.

Abstract □ The kinetics of degradation of fenprostalene (I) in polyethylene glycol 400 solution was examined using HPLC. The degradation of I at 80°C was shown to depend on the presence of oxygen and a large number of polar products were produced, as evidenced by using ^3H-labeled I. Evidence that autoxidation of the polyethylene glycol 400 was concurrent with degradation of I was found from a drop in the apparent pH. Antioxidants were very effective in retarding the rate of degradation in the presence of oxygen. Degradation of I in polyethylene glycol 400 appears to arise from a reaction between the drug and reactive peroxide intermediates formed through air-oxidation of polyethylene glycol 400. This is supported by the finding that I reacts exclusively by a slow transesterification reaction in diethylene glycol, a solvent that is stable to autoxidation.

Keyphrases □ Degradation—fenprostalene in polyethylene glycol 400 □ Fenprostalene—autoxidation, degradation, kinetics □ Kinetics—fenprostalene in polyethylene glycol 400

Fenprostalene[1] (I), a PGF-type prostaglandin containing an aryloxy group at C-16 and an allene functionality at C-5 (1), is used as an abortifacient and for estrus synchronization in cattle (2). We have previously shown that in aqueous solution, I degrades exclusively through hydrolysis of the C-1 methyl ester under both acidic and basic conditions (3). No information is available, however, on the degradation of this family of prostaglandins in nonaqueous environments. Since an injectable formulation of fenprostalene (I) in polyethylene glycol 400 was chosen for development (4), we have investigated the chemical reactivity and degradation products of I in this solvent.

EXPERIMENTAL SECTION

Materials—The fenprostalene[1] (I) used was 99% pure (HPLC). The radiochemical purity of fenprostalene labeled with tritium at C-13 and C-14 was 98%. The acetonitrile used was glass-distilled HPLC-grade, and the water

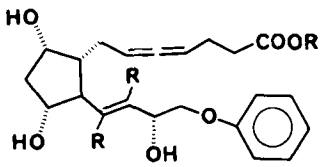

I, R = H, R′ = CH_3
[^3H]I, R = ^3H, R′ = CH_3
II, R = H, R′ = $CH_2CH_2OCH_2CH_2OH$
III, R = R′ = H

[1] Fenprostalene is the generic name for methyl 7-[3,5-dihydroxy-2-(3-hydroxy-4-phenoxy-1-butenyl)cyclopentyl]-4,5-heptadienoate. Obtained from the Institute of Organic Chemistry, Syntex Research, Palo Alto, Calif. The synthesis of I is described in Ref. 1.

0022-3549/84/1000-1414$01.00/0

© 1984, American Pharmaceutical Association

$\beta/\gamma = 0$ is $K_{13}K_{24}$, and the value of β/γ at the intercept at which $\alpha/\gamma = 0$ is $-K_{24}$. These values of K_{13} and K_{24} have been found to be concentration dependent; therefore, plots similar to those shown in Figs. 4A and B were made to obtain the thermodynamic values. In Table I, the results of these calculations for compounds I–IV are given.

A modification of method I was used to obtain the values of K_{13} and K_{24} of compound V. Since the two pK_a values are far apart, the equilibria were assumed not to interact with each other; therefore, the equilibrium constants were determined by using the following expression for monoprotic compounds:

$$K_n = Z\frac{[H^+]([H^+] + [B] - [OH^-])}{[OH^-] + [A] - [H^+] - [B]} \qquad \text{(Eq. 16)}$$

where Z is the activity coefficient ratio $Y_{(NRN)H^+}/Y_{(NRN)H_2^{2+}}$ for K_{13} and $Y_{(NRN)}/Y_{(NRN)H^+}$ for K_{24}.

Figure 6 shows the titration curve obtained for compound V, and Figures 7A and B show the results of the calculated equilibrium constants *versus* percent neutralized. Precipitation was observed after the first equivalence point (Fig. 6), and therefore, consistent values should be obtained for K_{13} (Fig. 7A). Conversely, a change in the calculated value for K_{24} with respect to percent neutralized would be expected (Fig. 7B). The break in this latter curve at ~5% neutralization is due to the formation of a precipitate. The curve prior to precipitation should have a slope of zero (as in Fig. 7A), whereas the curve after precipitation will not necessarily be linear.

By knowing the value for K_{24} and the pH at which precipitation occurs, the solubility of the base (uncharged) species of compound V was determined by:

$$[NRN]_s = \frac{[A]K_{24}}{[H] + K_{24}} \qquad \text{(Eq. 17)}$$

In Table I, the results of the calculations for compound V are given, along with those values for K_{24} and $[NRN]_s$, as reported by Green (9) and determined by a spectrophotometric procedure. It can be seen there is excellent agreement among these data.

Since compounds I–IV are symmetrical molecules, it should be possible to calculate the microionization constants K_1, K_2, K_3, and K_4 of Scheme I. This is because K_1 should equal K_3, and K_2 should equal K_4. Furthermore, since the protonation sites are separated by large distances, it would be expected the K_2 and K_4 would be the same or only very slightly smaller than K_1 and K_3. The microionization constants were therefore calculated from Eqs. 1 and 2 and gave the results listed in Table II. It can be seen that there is very little difference in the calculated values, with K_2 and K_4 being slightly smaller.

For diprotic compounds with completely independent, equivalent sites of protonation, the ratio K_{13}/K_{24} will equal 4, and K_1/K_2 will equal 1. From these ratios (Table II), it can be seen that the values are very close to the theoretical values.

From these results, it can be concluded that the equilibrium constants of slightly soluble compounds can be determined potentiometrically by extrapolation procedures and give results which are consistent with those reported in the literature. It would be expected that method II would be better to use with those compounds that have equilibrium constants close together, whereas method I would be better to use with those compounds that have equilibrium constants farther apart.

REFERENCES

(1) W. H. Streng, H. E. Huber, J. L. DeYoung, and M. A. Zoglio, *J. Pharm. Sci.*, **65**, 1034 (1976).

(2) H. V. Maulding and M. A. Zoglio, *J. Pharm. Sci.*, **60**, 309 (1971).

(3) R. H. Levy and M. Rowland, *J. Pharm. Sci.*, **60**, 1155 (1971).

(4) A. A. Noyes, *Z. Physik. Chem.*, **11**, 495 (1893).

(5) C. Morton, *Trans. Faraday Soc.*, **24**, 14 (1928).

(6) W. R. Maxwell and J. R. Partington, *Trans. Faraday Soc.*, **31**, 922 (1935).

(7) J. C. Speakman, *J. Chem. Soc.*, 855 (1940).

(8) J. N. Butler, "Ionic Equilibrium a Mathematical Approach," Addison-Wesley Publishing Co., 1964, p. 437.

(9) A. L. Green, *J. Pharm. Pharmacol.*, **19**, 10 (1967).

Degradation of Fenprostalene in Polyethylene Glycol 400 Solution

DAVID M. JOHNSON ˣ **and WILLIAM F. TAYLOR**

Received March 14, 1983, from the *Institute of Pharmaceutical Sciences, Syntex Research, Palo Alto, CA 94304.* Accepted for publiction October 26, 1983.

Abstract □ The kinetics of degradation of fenprostalene (I) in polyethylene glycol 400 solution was examined using HPLC. The degradation of I at 80°C was shown to depend on the presence of oxygen and a large number of polar products were produced, as evidenced by using ^3H-labeled I. Evidence that autoxidation of the polyethylene glycol 400 was concurrent with degradation of I was found from a drop in the apparent pH. Antioxidants were very effective in retarding the rate of degradation in the presence of oxygen. Degradation of I in polyethylene glycol 400 appears to arise from a reaction between the drug and reactive peroxide intermediates formed through air-oxidation of polyethylene glycol 400. This is supported by the finding that I reacts exclusively by a slow transesterification reaction in diethylene glycol, a solvent that is stable to autoxidation.

Keyphrases □ Degradation—fenprostalene in polyethylene glycol 400 □ Fenprostalene—autoxidation, degradation, kinetics □ Kinetics—fenprostalene in polyethylene glycol 400

Fenprostalene[1] (I), a PGF-type prostaglandin containing an aryloxy group at C-16 and an allene functionality at C-5 (1), is used as an abortifacient and for estrus synchronization in cattle (2). We have previously shown that in aqueous solution, I degrades exclusively through hydrolysis of the C-1 methyl ester under both acidic and basic conditions (3). No information is available, however, on the degradation of this family of prostaglandins in nonaqueous environments. Since an injectable formulation of fenprostalene (I) in polyethylene glycol 400 was chosen for development (4), we have investigated the chemical reactivity and degradation products of I in this solvent.

EXPERIMENTAL SECTION

Materials—The fenprostalene[1] (I) used was 99% pure (HPLC). The radiochemical purity of fenprostalene labeled with tritium at C-13 and C-14 was 98%. The acetonitrile used was glass-distilled HPLC-grade, and the water

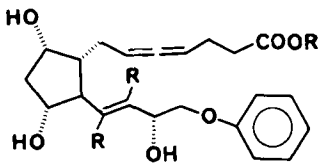

I, R = H, R′ = CH_3
[^3H]I, R = ^3H, R′ = CH_3
II, R = H, R′ = $CH_2CH_2OCH_2CH_2OH$
III, R = R′ = H

[1] Fenprostalene is the generic name for methyl 7-[3,5-dihydroxy-2-(3-hydroxy-4-phenoxy-1-butenyl)cyclopentyl]-4,5-heptadienoate. Obtained from the Institute of Organic Chemistry, Syntex Research, Palo Alto, Calif. The synthesis of I is described in Ref. 1.

0022-3549/84/1000-1414$01.00/0

© 1984, American Pharmaceutical Association

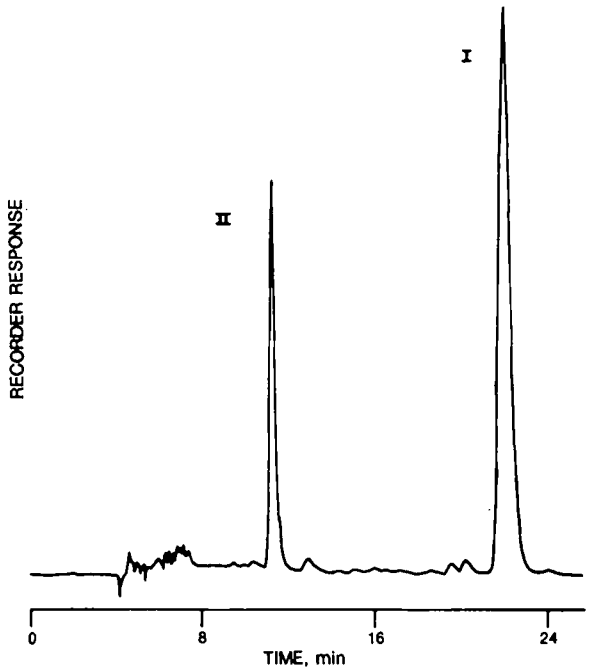

Figure 1—*Chromatogram of a solution of I after partial transesterification to II in diethylene glycol at 80°C.*

was purified through an ion-exchange and filtration system[2]. *dl*-α-Tocopherol was NF grade, propyl gallate and polyethylene glycol 400 were practical grade. All other chemicals were reagent grade.

Kinetic Methods—A mixture of 25 mg of I in 250 mL of polyethylene glycol 400 was stirred for 2 h and then filtered through a 0.7-μm glass membrane. This solution was used to prepare two other solutions, one containing 0.10% *dl*-α-tocopherol and another containing 0.006 M formic acid. The solutions were stored in either 10-mL ampules (5 mL of solution) or in 20-mL test tubes fitted with polytef-faced screw caps. These solutions were maintained at 80°C, 45°C, or 25°C. The samples stored in test tubes at 80°C were cooled, and the caps were removed for a few minutes each day to provide a relatively constant supply of oxygen to the solutions.

Solutions kept at 80°C were assayed by HPLC and compared with a control sample maintained at 4°C. The 45°C and 25°C samples were assayed by HPLC, and the chromatograms were compared to a freshly-prepared external standard of I. The polyethylene glycol 400 solutions of I were diluted 10-fold with water prior to HPLC analysis and 20-fold prior to pH measurements[3]. Diethylene glycol solutions of I were prepared and analyzed exactly as described above for the polyethylene glycol 400 solutions.

Hydrolysis of Degradation Products—A solution of I in polyethylene glycol 400 (100 μg/mL) was allowed to stand for 28 d at 80°C under air. After this period, HPLC assay showed 0.6% of I remaining. Concentrated HCl (41.5 μL) was added to a 5-mL aliquot of this solution and to a control solution of I. Both solutions were heated at 80°C for 3 h. Analysis of these solutions by HPLC showed that quantitative hydrolysis of I in the control solution occurred to give the free acid (III). None of this acid was found in the sample that had previously been degraded in polyethylene glycol 400.

Liquid Chromatographic Method—An HPLC system consisting of a pump[4], a variable-wavelength detector[5], and a 100-μL fixed-loop injector[6] was used. Separations were performed on columns packed with microparticulate bonded octyl material[7]. For analysis of I, a mobile phase of 35–45% acetonitrile in water was used. The eluant was monitored at 219 nm. Quantitation by integration of peak areas gave excellent linearity for I over the range of concentrations investigated in the kinetic studies. The presence of 10% polyethylene glycol 400 in the samples affected the quantitation of I when compared with an injection of a completely aqueous solution of I. The origin of this effect is unknown. To avoid this problem, standards of I were prepared in an aqueous solution containing 10% polyethylene glycol 400.

[2] Barnstead Nanopure System.

[3] Measurements of apparent pH were made on a Radiometer PHM 64 pH meter using a Radiometer combination electrode, type GK2401C. The polyethylene glycol 400 solutions were diluted with 0.01 M KCl solution.

[4] Altex model 110 A.

[5] Cecil model CE 212.

[6] Rheodyne model 70-10.

[7] For *analytical* use, an Ultrasphere 5-μm octyl 250 × 4.6-mm column by Altex was used. For semipreparative isolation of II, a 250 × 10-mm Ultrasphere 5-μm octyl column by Altex was used.

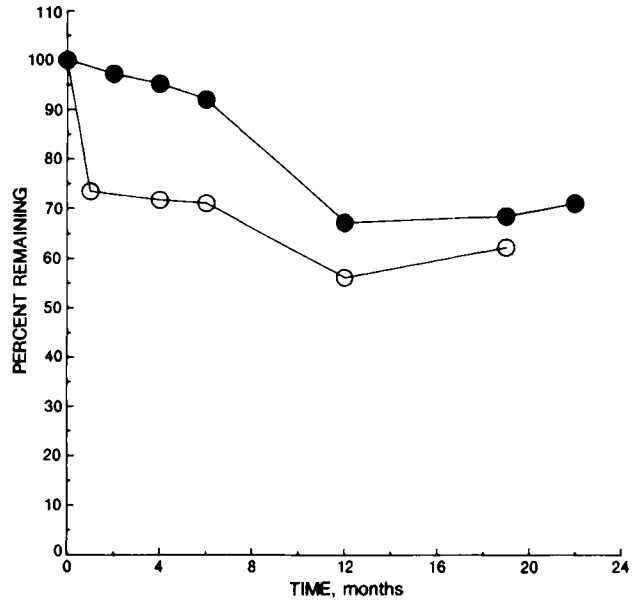

Figure 2—*Degradation rate of I in polyethylene glycol 400 at 25°C (●) and at 45°C (○). The solutions were sealed in ampules under air.*

Coincidentally, the diethylene glycol ester (II) and free acid (III) of fenprostalene (I) gave nearly the same retention time with the unbuffered mobile phase described above. Thus analysis of II in the presence of III was accomplished using a mobile phase of 35:65 acetonitrile–0.01 M aqueous phosphate buffer (pH 6). Under these conditions, III elutes near the solvent front while the retention of II is essentially unaffected by the pH change.

Formation of II in Diethylene Glycol—A solution containing 100 mg of I in 8 mL of diethylene glycol was prepared and sealed in a 10-mL ampule. The solution was allowed to stand at 80°C for 2 months and then was diluted fourfold with water and injected onto the semipreparative reverse-phase HPLC column. The fraction corresponding to the major degradation peak (Fig. 1) was collected and the mobile phase was removed by rotary evaporation to give a clear oil that was 98% pure (HPLC). ^{1}H-NMR ($CDCl_3$)[8]: δ 1.62 (m, 1, CH-8β), 1.79 (m, 1, CH-10α), 2.1–2.4 (m, 6, CH_2-3,7, CH-10β,12α), 2.48 (m, 2, CH_2-2), 3.60 (t, 2, J = 4.8 Hz, CH_2-4′), 3.74 (m, 3, CH-11β, CH_2-16), 4.28 (m, 3, CH-9β, CH_2-1′), 4.54 (m, 1, CH-15β), 5.1–5.2 (m, 2, allene CH),

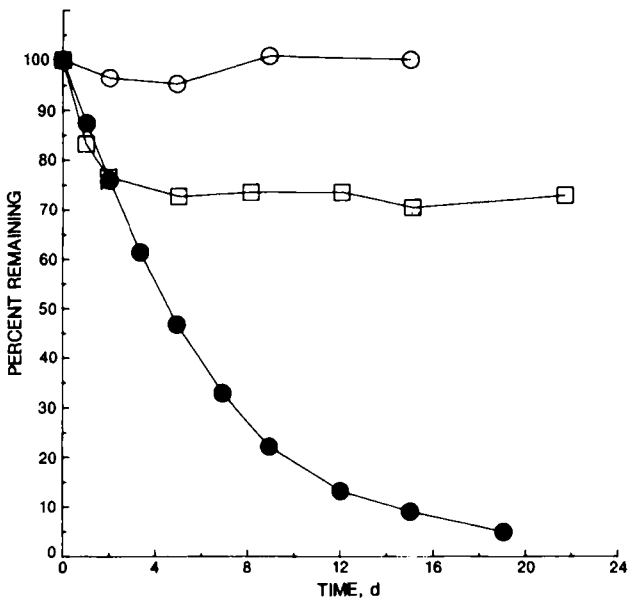

Figure 3—*Degradation rate of I in polyethylene glycol 400 at 80°C under various storage conditions. Key: (○) under nitrogen in a sealed ampule; (□) under air in a sealed ampule; (●) in a test tube exposed to air.*

[8] The NMR spectrum was determined at 300 MHz on a Bruker WM 300 FT spectrometer.

[9] The mass spectrum was obtained in the direct-inlet mode on a Varian MAT 112S system equipped with an SS-200 data system.

Table I—Apparent pH of Fenprostalene (I) Solutions

Solvent	Additive	Initial pH	Apparent pH[a]
Polyethylene Glycol 400	—	5.2	3.5
	N_2	5.2	5.0
	dl-α-tocopherol	5.2	4.5
	formic acid	3.9	3.5
Diethylene Glycol	—	5.8	5.2

[a] pH measured after a 20-fold dilution of the solution with 0.01 M KCl after 15 d at 80°C. [b] All solutions were stored in test tubes with a relatively constant supply of air except the sample stored under nitrogen, which was in a sealed ampule.

5.68 (m, 2, vinyl CH), and 6.9–7.3 ppm (m, 5, ArH). The mass spectrum was run at 90 eV in the CI mode with ammonia as the reagent gas[9]. The peak at *m/z* 476 was attributed to the $M\text{-}NH_4 - H_2O$ ion and a peak at *m/z* 459 to the $MH - H_2O$ ion. Other major peaks were at *m/z* 388, 259, and 241. The CI mass spectrum of the trimethylsilyl ether derivative gave an MNH_4^+ peak at *m/z* 782 with other prominent peaks at *m/z* 675, 581, 491, and 401.

Anal.—Calc. for $C_{26}H_{36}O_8$: C, 65.53; H, 7.62. Found: C, 65.70; H, 7.42.

Additional support for the structural assignment comes from observing that in 0.1 M HCl at 60°C, this diethylene glycol ester (II) hydrolyzes to give the free acid of I with a half-life of ~1 h. This rate is similar to that found for hydrolysis of fenprostalene under the same conditions (3).

Degradation of ^{3}H-Labeled I—A polyethylene glycol 400 solution (1 mL) was prepared containing 500 μg/mL of I with a specific activity of ~130 μCi/mg [^{3}H]I. After an aliquot was removed, the solution was sealed in a glass ampule and stored for 64 h at 80°C. The polyethylene glycol 400 solution containing [^{3}H]I was analyzed by collecting and counting fractions from the reverse-phase HPLC method described above. A 0.040-g sample was accurately weighed and diluted to 1 mL with water. On injection of 108 μL[10] of this solution, fractions of the eluant were collected. A 100-μL aliquot of each fraction was mixed with 15 mL of scintillation fluid[11] and counted in a liquid scintillation counter[12]. A volume of sample equal to the loop volume (108 μL) was also diluted with 15 mL of scintillation fluid and counted[13].

Incorporation of Tritium Into Polyethylene Glycol 400—A 0.4-mL aliquot of the degraded polyethylene glycol 400 solution of [^{3}H]I was added to 5 mL of methanol in a flask equipped with a serum cap containing a needle attached to a source of nitrogen. The other neck was connected to a pear-shaped receiving flask through a vacuum adapter. The round-bottom flask was warmed to 45°C, and a stream of nitrogen was used to transfer the methanol to the receiving flask which was cooled to −78°C. The stream of nitrogen leaving the apparatus was scrubbed with water prior to its escape into the environment. A second 5-mL portion of methanol was added to the residue in the flask, and the procedure was repeated. An aliquot of the resulting methanol solution was diluted with scintillation fluid and the counts per minute were compared with that of the degraded polyethylene glycol 400 solution prior to methanol exchange.

RESULTS AND DISCUSSION

The kinetics of the degradation of I in polyethylene glycol 400 in sealed ampules under air was followed by reverse-phase HPLC. Plots of percent remaining of I *versus* time for the degradation reactions at 25°C and 45°C are shown in Fig. 2. At 25°C a shelf-life of <8 months was observed. At 45°C the initial degradation rate is much faster than at 25°C, but surprisingly, the reaction abruptly stopped with ~60–70% of I remaining. The degradation at 25°C also shows a plateau in the rate profile, but more than 1 year is required for it to become apparent.

To evaluate the role oxygen plays in the above reaction, solutions of I in polyethylene glycol 400 were degraded at 80°C in sealed ampules containing either air or nitrogen in the head space and also in screw-capped test tubes that were opened each day to provide a relatively constant supply of oxygen. Figure 3 shows the dramatic differences observed under the three conditions. As was found at 25°C and 45°C, the degradation reaction at 80°C stopped with ~70% of I remaining unreacted in the ampules with air in the head space. When a constant supply of oxygen was permitted, however, the degradation reaction followed the first-order rate law[14] and nearly went to completion.

[10] The volume of the loop was calibrated using ^{3}H-labeled water.
[11] Oxifluor by New England Nuclear.
[12] Beckman model LS 8100.
[13] The slight difference in final solvent compositions after dilution of 100 μL of either mobile phase or the 4% polyethylene glycol 400–water solution into 15 mL of scintillation fluid had no significant effect on the counting efficiency of [^{3}H]I.
[14] When the data for samples exposed to air (solid circles shown in Fig. 3) is plotted as log percent remaining *versus* time, excellent linearity through >3 half-lives is obtained.

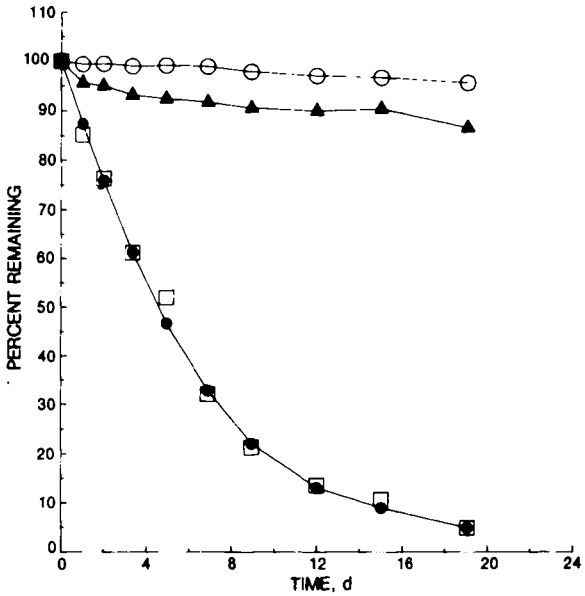

Figure 4—*Degradation rate of I at 80°C in diethylene glycol (▲) and in polyethylene glycol 400 solutions containing no additive (●), formic acid (□), and* dl*-α-tocopherol (○). All solutions were stored in test tubes exposed to air.*

Figure 3 also shows that no degradation of I was observed at 80°C when the solution was kept in an ampule containing nitrogen in the head space.

These results demonstrate that oxygen is required for the degradation of I in polyethylene glycol 400. The role oxygen plays in the degradation of I could be through direct reaction with the prostaglandin or through a reaction with the solvent, polyethylene glycol 400. The latter autoxidation reaction is known to produce peroxides and carboxylic acids (5–8). The highly reactive peroxide intermediates have been implicated in the degradation of several drugs in formulations containing polyethylene glycols (7, 8). Autoxidation of the solvent appears to occur during the degradation of I, which can be seen from the drop in apparent pH from 5.2 to 3.5 in the solution that contained a constant supply of air (Table I)[15]. The solution stored under nitrogen showed almost no pH change under the same conditions. When the initial pH of the solution exposed to air was lowered to 3.9 with formic acid, the rate of disappearance of I was identical to that of the pH 5.2 solution, as shown in Fig. 4. Thus, the pH drift in the solution has no apparent effect on the rate of degradation of I.

Autoxidation of the polyethylene glycol 400 provides a likely explanation for the incomplete reaction of I in sealed ampules containing air (Fig. 3). The autoxidation reaction consumes large amounts of oxygen resulting in the depletion of oxygen from solution; consequently, low peroxide levels are likely to occur as well.

The effect of 0.1% *dl*-α-tocopherol on the rate of degradation of I in polyethylene glycol 400 at 80°C is shown in Fig. 4. Although a constant supply of oxygen was present, the antioxidant prevented degradation of the prostaglandin under the reaction conditions[16]. The higher apparent pH of the solution after 15 d at 80°C compared with the solution without antioxidant (Table I) indicates that *dl*-α-tocopherol also appeared to prevent degradation of the solvent, thus reducing peroxide levels. Stabilization of fenprostalene (I) by the antioxidant is, in fact, likely to be a direct result of preventing peroxide accumulation in polyethylene glycol 400. One cannot, however, rule out the possibility that the antioxidant acts to inhibit reaction of I with oxygen directly.

The reverse-phase HPLC method used to follow the disappearance of I in polyethylene glycol 400 solutions under air did not provide any evidence of the formation of major degradation products. The only change noticed was an increase in the size of the already large solvent front. To unambiguously determine where the major degradation products of I eluted on reverse-phase HPLC, a solution of fenprostalene labeled with tritium at C-13 and C-14 in polyethylene glycol 400 was stored at 80°C for 64 h and analyzed. Fractions

[15] Addition of formic acid to polyethylene glycol 400 resulted in an apparent pH of 3.9 (Table I). This value is higher than that found for the degraded solution even though the concentration of formic acid (6×10^{-3} M) was 20-fold higher than the initial concentration of I (2.5×10^{-4} M). Thus, the pH drop in the degraded solution was due to formation of acidic decomposition products of polyethylene glycol 400, not fenprostalene (I).
[16] A similar effect was observed with 0.05% propyl gallate or 0.5% ascorbic acid as antioxidants.

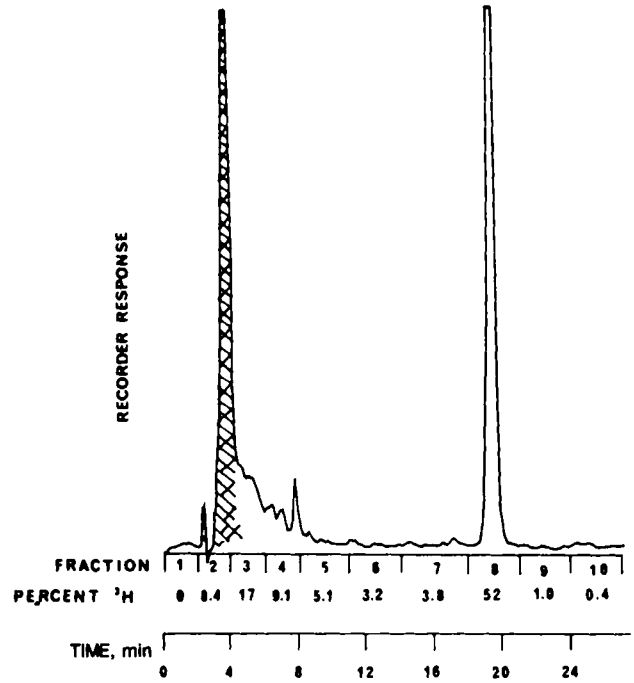

Figure 5—*Chromatogram of a partially degraded solution of [³H]I in polyethylene glycol 400. The percent of total radioactivity is shown for the 10 fractions collected. The hatched area in fraction 2 approximates the response due to the solvent front.*

of the HPLC eluant were collected and counted. The total cpm for all the fractions was 106% of the cpm determined directly by counting an aliquot of the degraded solution equal to the amount injected. Thus, no significant amount of radioactive material was bound to the column.

Both the analogue UV trace and the percent total radioactivity found in each fraction collected are presented in the chromatogram shown in Fig. 5. The peak area of each fraction appears to roughly correlate with the percent of total radioactivity found in that fraction, if the hatched area in fraction 2 is ignored. The large absorbance in fraction 2 is due predominantly to the solvent front. Most of the absorbance and counts in the chromatogram due to degradation products occurred near the solvent front, indicating that the products may be relatively polar compared with I[17]. Many peaks appear to be fused into aggregates, implying that many products are formed. The only evidence we have of their nature is that they are not due to transesterification with the solvent[18]. This was shown by treating a highly degraded (<1% of I remaining) solution of I in polyethylene glycol 400 with concentrated HCl at 80°C. No formation of the free acid (III) occurred under conditions which are known to completely hydrolyze fenprostalene.

The most likely reaction responsible for degradation of fenprostalene (I) in polyethylene glycol 400 is oxidation by reactive peroxides formed as a result of solvent autoxidation. However, the kinetic data described above does not exclude the possibility that oxygen reacts directly with the prostaglandin (as well as with the solvent) to account for at least part of the degradation reaction. Evidence that this pathway is not operating can be seen from the reaction of I in diethylene glycol under air at 80°C. Under conditions identical to those which result in rapid degradation of I in polyethylene glycol 400, the prostaglandin remains relatively stable in diethylene glycol (Fig. 4). The solvent also appears to be stable to autoxidation as evidenced by the small pH change after 15 d at 80°C (Table I)[19].

The slow degradation of I in diethylene glycol shown in Fig. 4 was not found to occur by oxidation, as suspected for the reaction of I in polyethylene glycol 400. Instead, the degradation product was identified as the diethylene glycol ester II of fenprostalene. Thus, while I undergoes a slow transesterification reaction in diethylene glycol, it undergoes a rapid oxidation reaction in polyethylene glycol 400[20]. This implies that fenprostalene (I) is intrinsically stable toward aerobic oxidation in nonaqueous solutions, but is susceptible to oxidation by peroxide intermediates formed during solvent decomposition. The success demonstrated by the use of antioxidants or nitrogen purging in stabilizing I in polyethylene glycol 400 is, therefore, due exclusively to the ability of these agents to prevent autoxidation of the solvent.

REFERENCES

(1) J. M. Muchowski and J. H. Fried, U.S. Pat. No. 3,985,791 (1976).

(2) B. H. Vickery, G. I. McRae, J. S. Kent, and R. V. Tomlinson, *Prostaglandins and Med.*, **5**, 93 (1980); R. C. Herschler, *Agri-Pract.*, **4**, 28 (1983).

(3) D. M. Johnson, W. F. Taylor, G. F. Thompson, and R. A. Pritchard, *J. Pharm. Sci.*, **72**, 946 (1983).

(4) J. S. Kent, U.S. Pat. No. 4,389,414 (1983).

(5) D. A. McKenzie, Technical Service Report, Union Carbide Corporation, January 1973.

(6) R. Hamburger, E. Azaz, and M. Donbrow, *Pharm. Acta. Helv.*, **50**, 10 (1975).

(7) J. W. McGinity, J. A. Hill, and A. L. LaVia, *J. Pharm. Sci.*, **64**, 356 (1975).

(8) C. W. McGary Jr., *J. Polym. Sci.*, **46**, 51 (1960).

(9) J. W. McGinity, T. R. Patel, A. H. Nagvi, and J. A. Hill, *Drug Dev. Commun.*, **2**, 505 (1976) and references cited therein.

(10) H. W. Jun, C. W. Whitworth, and L. A. Luzzi, *J. Pharm. Sci.*, **61**, 1160 (1972); C. W. Whitworth, H. W. Jun, and L. A. Luzzi, *J. Pharm. Sci.*, **62**, 1184 (1973).

(11) R. Ekman, L. Liponkoski, and P. Kahela, *Acta. Pharm. Suec.*, **19**, 241 (1982).

(12) W. G. Lloyd, *J. Am. Chem. Soc.*, **78**, 72 (1956).

ACKNOWLEDGMENTS

The authors thank Ms. J. Nelson and Dr. M. Maddox for their assistance with the NMR data and Dr. L. Partridge and Ms. S. Graul for the mass spectral work. We also thank Dr. H. Parnes for providing ³H-labeled fenprostalene.

[17] A significant amount of the tritium detected in the chromatogram in Fig. 5 was in or near the solvent front. Since polyethylene glycol 400 is weakly retained, if at all, on reverse-phase HPLC, the question of tritium exchange of I with solvent was examined. A 50-fold molar excess of methanol was added to the degraded polyethylene glycol 400 solution. The methanol was then recovered by evaporation using a cold trap. Any tritium present in the polyethylene glycol 400 as —O³H would be incorporated into the methanol and detected by liquid scintillation counting. Only 1.5% of the total tritium present in the sample was found in the methanol recovered. The tritium detected in and near the solvent front in Fig. 5 must, therefore, be a prostaglandin degradation product and not ³H-labeled polyethylene glycol 400.

[18] Both aspirin (10) and indomethacin (11) are reported to undergo transesterification with polyethylene glycols.

[19] Although diethylene glycol is known to undergo autoxidation, long induction periods have been reported (12) and may explain the apparent lack of degradation observed here. Addition of the free radical initiator 2,2′-azobisisobutyronitrile to a solution of I in diethylene glycol resulted in apparent oxidation of both I and the solvent at 80°C. The reaction rate, however, was very slow compared with that in polyethylene glycol 400. Formation of II was not observed under these conditions.

[20] In the presence of *dl*-α-tocopherol (or nitrogen) a slow transesterification reaction of I with polyethylene glycol 400 might be expected; however, no degradation of I was observed (Fig. 4). Thus, transesterification of I in diethylene glycol, while a slow reaction, was faster than in polyethylene glycol 400.

Microbial Kinetics of β-Lactam Antibiotics against *Escherichia coli*

AKIRA TSUJI *x, **SHOICHIRO HAMANO** *¶, **TETSUO ASANO** *, **EMI NAKASHIMA** *, **TSUKINAKA YAMANA** ‡, **and SUSUMU MITSUHASHI** §

Received December 27, 1982, from the *Faculty of Pharmaceutical Sciences and ‡Hospital Pharmacy, Kanazawa University, Takara-machi, Kanazawa 920, Japan and the §School of Medicine, Gunma University, Showa-machi, Maebashi 372, Japan. Accepted for publication October 24, 1983. ¶Present address: Research Center, Taisho Pharmaceutical Co., Ltd., Yoshino-cho, Omiya 330, Japan.

Abstract □ Microbial kinetics of *Escherichia coli* NIHJ JC-2 and *E. coli* B/r were investigated in the presence of β-lactam antibiotics. To maintain a constant drug concentration during the experiment, a novel technique, using a dialysis membrane tube containing the drug solution, was successfully employed. The drug-affected generation curves of *E. coli* exhibited common features. After the addition of drug, an apparent lag period was noted, followed by a first-order decrease of the sensitive organisms and, 6 h later, by a regrowth of resistant organisms, depending on the antibiotic concentration used. The relationship between the apparent generation rate constant, k_{app}, and the antibiotic concentration was found to be nonlinear. This phenomenon is consistent with a saturable receptor site model for the drug action. A good linear free energy relationship was observed between the microbial kinetic parameter, k_{max}, and the alkaline degradation rate constants, k_{OH}, of the cephalosporins studied.

Keyphrases □ Kinetics—microbial, β-lactam antibiotics against *Escherichia coli* □ β-Lactam antibiotics—microbial kinetics against *Escherichia coli*

In dosage regimens for infectious diseases, plasma levels of antibiotics based on the value of minimum inhibitory concentration (MIC) have been used as convenient indices of pharmacological effectiveness. The MIC is defined as the lowest concentration that results in complete inhibition of microbial generation during prolonged contact with an antimicrobial agent (~20 h). However, the quantitative meaning of the MIC is still obscure, and the value does not give any indication of the kinetic behavior of microbial generation in relation to the concentration of the drug remaining in the body at relatively short times after administration of an antibiotic. To evaluate the potency or efficacy of antibiotics more effectively and to establish more reasonable therapeutic guidelines and dosage regimens, it is necessary to investigate the microbial generation kinetics as a function of antibiotic concentration.

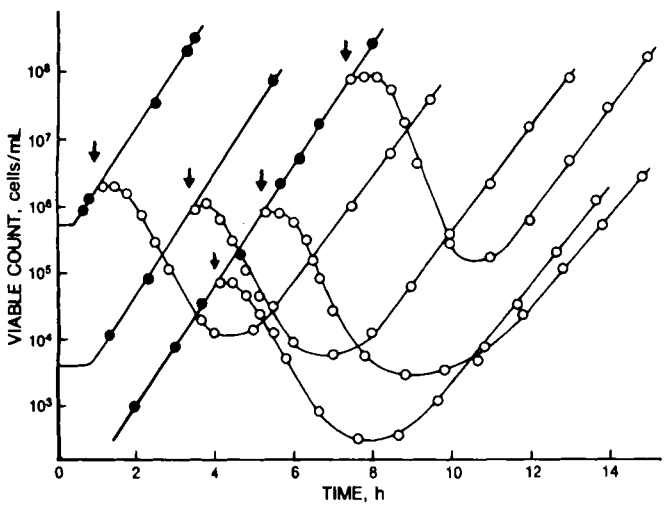

Figure 1—*Effect of organism population at the time of drug addition on the generation curves of* E. coli *B/r in the presence of 0.5 μg of ampicillin/mL and effect of inocula sizes on the generation curves of* E. coli *B/r in antibiotic medium[9] at pH 7.0 and 37°C. The time of drug addition is indicated by the arrow. Key: (●) control generation curves; (○) drug-affected generation curves.*

Several microbial kinetic studies in the presence of antibacterial agents have been reported (1–10); however, there are only a few reports on β-lactam antibiotics (4, 8). Elkhouly and Führer (8) have determined the apparent generation rate constants of *Escherichia coli* in the presence of various concentrations of ampicillin; however, it remains uncertain whether the apparent generation rate constants can be validly expressed as a function of drug concentration under their experimental conditions, because chemical and/or enzymatic degradation of ampicillin may occur under the conditions used in the study. To overcome this possible degradation, we introduced a novel method to keep the drug concentration constant.

The purposes of this study were to establish suitable experimental conditions for the microbial kinetic study of β-lactam antibiotics at constant drug concentrations and to elucidate the kinetic behavior of microbial generation in the presence of β-lactam antibiotics.

EXPERIMENTAL SECTION

Antibiotics—Penicillin G potassium[1] (1600 U/mg), ampicillin sodium[2] (955 μg/mg), methicillin sodium[3] (853 μg/mg), dicloxacillin sodium[2] (900 μg/mg), cefazolin sodium[4] (958 μg/mg), cephalexin monohydrate[5] (925 μg/mg), cefadroxil monohydrate[6] (947 μg/mg), and cephaloridine[5] (971 μg/mg) were used as received. All other chemicals, unless otherwise stated, were of reagent grade and were not further purified.

Organisms—Replicate slants of *E. coli* NIHJ JC-2[7] and *E. coli* B/r[8] [the same strains as used previously (4)] were used in the microbial kinetic study. The slants were prepared from single isolated colonies of the respective organisms and were stored at 4°C.

Culture Medium—Antibiotic medium[9] was rehydrated according to the specifications of the manufacturer and filtered twice through a 0.45-μm membrane filter[10]. This pH 7.0 medium was used for all experiments in the microbial generation studies. The medium was autoclaved at 120°C for 20 min.

Bacterial Generation—An aliquot (5 mL) of culture medium was inoculated from a fresh slant, and the culture was allowed to grow for 15 h at 37°C in an incubator. Samples of this culture were appropriately diluted in several steps to achieve an organism concentration of 10^4 cells/mL.

Two 0.5-mL portions of this culture were finally diluted into 49.5 mL of fresh medium for the control growth and 49.0 mL of fresh medium for the drug-affected growth, respectively. The cultures were maintained at 37°C in a constant-temperature water bath equipped with a shaker.

All pipets and media used were kept at 37°C to protect the organisms from temperature shock.

[1] Meiji Seika Kaisha, Tokyo, Japan.
[2] Takeda Chemical Industries, Osaka, Japan.
[3] Banyu Pharmaceutical Co., Osaka, Japan.
[4] Fujisawa Pharmaceutical Co., Osaka, Japan.
[5] Shionogi Co., Osaka, Japan.
[6] Bristol Meyers Co., Tokyo, Japan.
[7] IFO 12734; Institute for Fermentation, Osaka, Japan.
[8] F-57; Institute for Fermentation.
[9] Antibiotic Medium 3; Difco Laboratories, Detroit, Mich.
[10] Sartorius-Membranfilter GmbH, Göttingen, Federal Republic of Germany.

0022-3549/84/1000-1418$01.00/0
© 1984, American Pharmaceutical Association

Table I—Saturable Kinetic Parameters for *E. coli* NIHJ JC-2 and *E. coli* B/r in Antibiotic Medium [a]

Antibiotic	$10^4 k_{max}$, s^{-1}		S_b, μg/mL		C_{mec}, μg/mL	
	NIHJ JC-2	B/r	NIHJ JC-2	B/r	NIHJ JC-2	B/r
Penicillin G	83.8	28.4	56.6	3.80	4.98	3.06
Ampicillin	60.1	30.4	4.83	0.24	0.41	0.35
Methicillin	—	28.1	—	1.74	—	2.71
Dicloxacillin	—	22.4	—	2.44	—	3.32
Cefazolin	47.7	—	1.68	—	1.30	—
Cephalexin	16.9	—	0.60	—	1.76	—
Cefadroxil	27.9	—	2.56	—	3.69	—
Cephaloridine	87.6	—	9.28	—	0.78	—

[a] At pH 7.0 and 37°C.

Viable Count Method—Samples (0.5 mL) were withdrawn from the cultures and serially diluted into sterilized 0.9% NaCl solution in accordance with a preplanned dilution scheme so that 50–150 colonies per plate would be obtained. From these dilutions, aliquots of 0.5 mL were transferred onto each of three replicate agar plates. The plates were incubated for 20 h at 37°C, and the resulting colonies were counted with an electronic colony counter.

Effect of Shaking Speed on Generation Rates—Four replicate, 49.5-mL volumes of the fresh medium were each inoculated with 0.5 mL of appropriately diluted *E. coli* NIHJ JC-2 culture in the logarithmic growth phase. They were cultured at 37°C and pH 7.0 under four different shaking conditions (0, 82, 130, and 190 strokes/min). The viable counts were determined in samples withdrawn at appropriate time intervals.

Effect of Dialysis Membrane Tube—Fresh solutions of ampicillin of two different concentrations were aseptically prepared for each experiment. They were diluted suitably so that aliquots of 0.5 mL added to replicate 49.5-mL volumes of the *E. coli* NIHJ JC-2 seeded culture yielded final concentrations of 4.0 and 1.25 μg/mL. The solutions were added to the cultures growing at 37°C in the logarithmic phase at an organism concentration of about 10^6 cells/mL. A cellulose tube[11] was knotted at both ends to form a bag (length, 10 cm). The bag, which contained 10 mL of ampicllin solution prepared with fresh culture medium to produce the same concentration as the experimental antibiotic concentration, was placed in the culture medium immediately after the drug was added. The dialysis membrane tube was replaced with a fresh tube every 3 h. At appropriate time intervals, aliquots of 0.5 mL were withdrawn, and the ampicillin concentration was assayed by the usual microbial paper disk method employing *Sarcina lutea*[12] as the test organism.

Effect of Organism Population on Drug-Affected Generation Rates—Three sets of the culture medium, with initial inoculum sizes of 6×10^4, 6×10^5, and 6×10^6 cells/mL, were prepared and used to determine generation curves of the *E. coli* B/r culture in the presence of 0.5 μg of ampicillin/mL at 37°C. The viable counts were obtained at appropriate time intervals.

Effect of Antibiotic Concentrations on Generation Rates—Aliquots (0.5

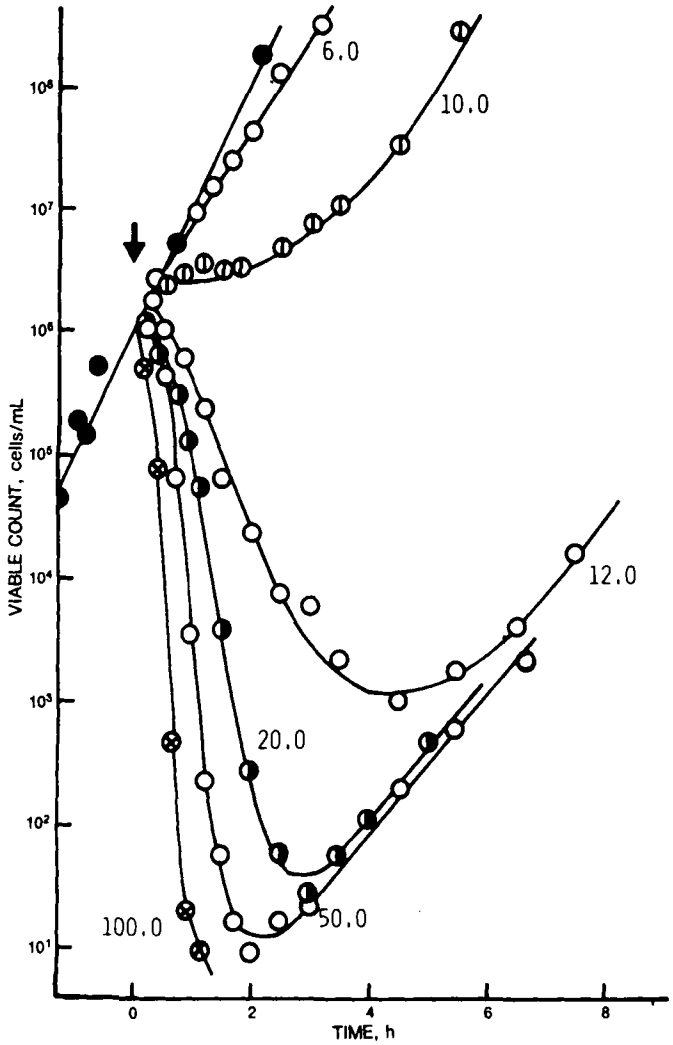

Figure 2—*Generation curves of* E. coli *NIHJ JC-2 in antibiotic medium[9] at pH 7.0 and 37°C in the absence (●) and presence (other symbols) of various concentrations of penicillin G. The numbers inside the figure are drug concentrations in micrograms per milliliter. The time of drug addition is indicated by the arrow.*

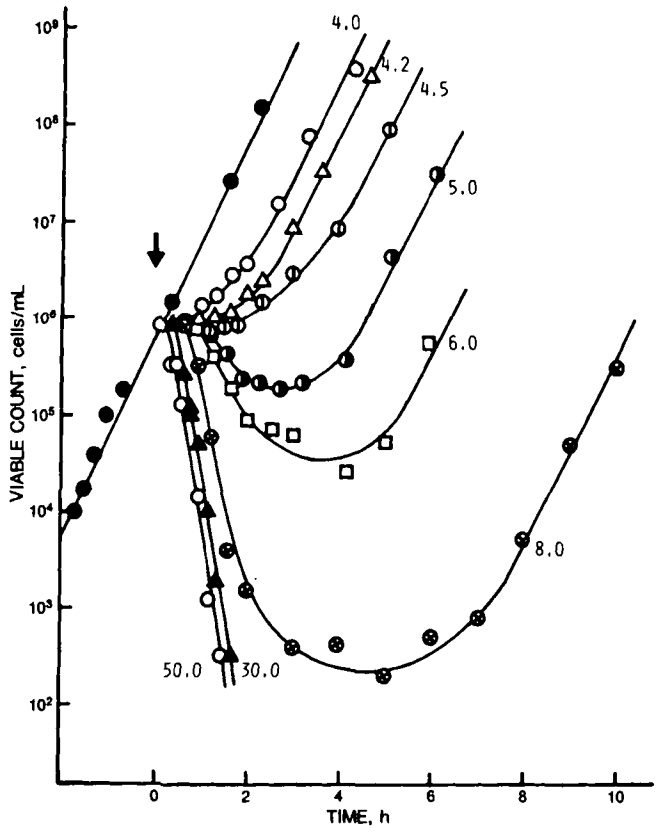

Figure 3—*Generation curves of* E. coli *NIHJ JC-2 in antibiotic medium[9] at pH 7.0 and 37°C in the absence (●) and presence (other symbols) of various concentrations of cefadroxil. The numbers inside the figure are drug concentrations in micrograms per milliliter. The time of the drug addition is indicated by the arrow.*

[11] Visking dialysis membrane, type 20/32; Union Carbide Corp., Chicago, Ill.
[12] IFO 12708; Institute for Fermentation.

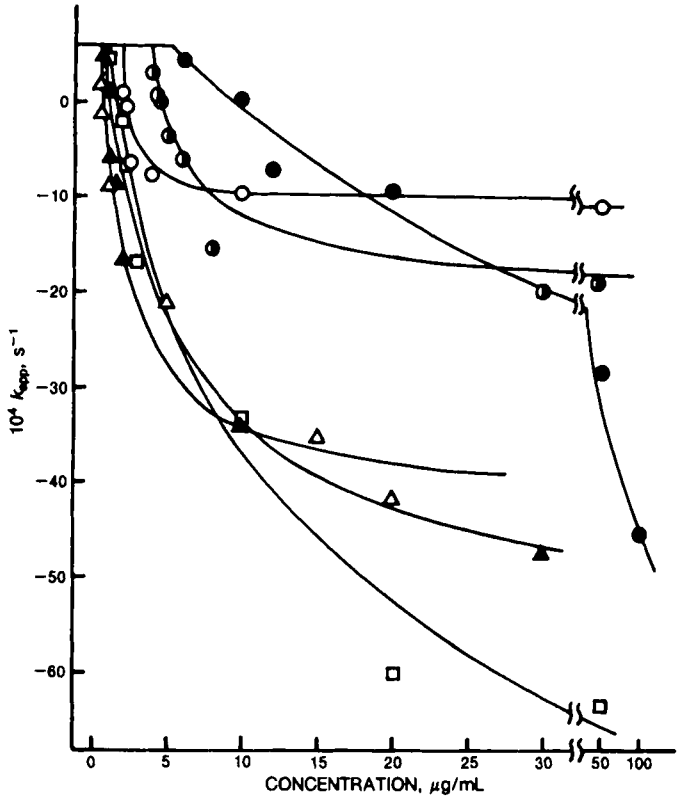

Figure 4—*Dependence of the apparent generation rate constant,* k_{app}, *for* E. coli *NIHJ JC-2 in antibiotic medium*[9] *at pH 7.0 and 37°C on drug concentration. Key: (●) penicillin G; (▲) ampicillin; (○) cephalexin; (△) cefazolin; (◑) cefadroxil; (□) cephaloridine.*

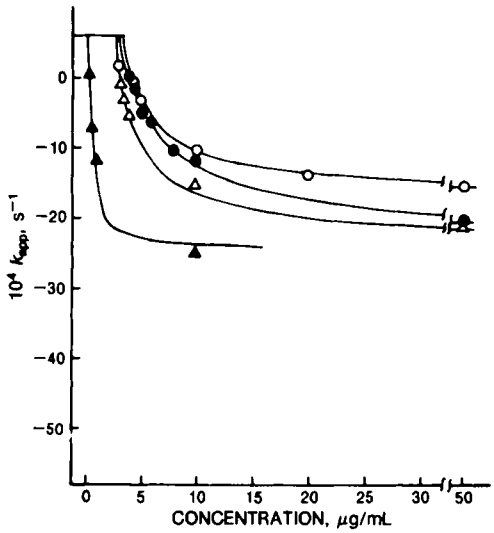

Figure 5—*Dependence of the apparent generation rate constant,* k_{app}, *for* E. coli *B/r in antibiotic medium*[9] *at pH 7.0 and 37°C on drug concentration. Key: (●) penicillin G; (▲) ampicillin; (○) dicloxacillin; (△) methicillin.*

mL) of aqueous solutions of antibiotics were aseptically added to replicate 49.5-mL samples of *E. coli* cultures to yield the desired concentrations. The solutions were added to the cultures growing at 37°C in the logarithmic phase at an organism concentration of 10^6 cells/mL. As soon as the drug solution was added to the culture medium, a dialysis membrane bag containing the drug solution was put into the culture medium, as described above, to keep the drug concentration constant during the experimental period. Samples were withdrawn at appropriate time intervals, and the organism concentrations were determined by the viable count method.

The *E. coli* NIHJ JC-2 culture was carried out in the presence of selected concentrations of penicillin G, ampicillin, cephalexin, cefazolin, cefadroxil, and cephaloridine. The *E. coli* B/r culture was also carried out in the presence of various concentrations of penicillin G, ampicillin, dicloxacillin, and methicillin. As a control, one culture without any drug added was studied in each set of experiments.

RESULTS AND DISCUSSION

Effect of Shaking Speed on Generation Rates—To establish suitable experimental conditions for the kinetic study of antibiotic action on *E. coli*, the bacterial generation rates without antibiotics were determined from the generation time curves obtained at various shaking speeds. The culture of *E. coli* showed an exponential phase which could be expressed as:

$$\ln N = \ln N_0 + k_0 t \qquad \text{(Eq. 1)}$$

where N is the number of organisms per unit volume of broth medium at time t; N_0 is the number of organisms per unit volume of broth medium at the initial time, 0, in the logarithmic generation phase; and k_0 is the apparent generation rate constant for the drug-free culture. The mean generation time, tg, was calculated by:

$$tg = 0.693/k_0 \qquad \text{(Eq. 2)}$$

The generation rate constant, k_0, and the generation time, tg, were calculated by Eqs. 1 and 2. In the absence of agitation, the mean generation time was 22 min (slightly larger than the values obtained for cultures under agitation); however, very similar values of 17–18 min were obtained within the range of 82–190 strokes/min. Therefore, the shaking speed was fixed at 130 strokes/min in this microbial kinetic study.

Table II—Microbial Kinetic Parameter k_{max} of *E. coli* NIHJ JC-2 and Alkaline Degradation Rate, k_{OH}, of Cephalosporins

Cephalosporin	$10^4\ k_{max}, s^{-1}$	$10^2\ k_{OH}, M^{-1}\ s^{-1}$
Cephaloridine	87.6	108[a]
Cefazolin	47.7	31.7[a]
Cephalexin	16.9	7.33[a]
Cefadroxil	27.9	7.06[b]

[a] Reference 17. [b] Reference 18.

Effect of Dialysis Membrane Tube—Ampicillin concentrations in the *E. coli* NIHJ JC-2 culture in the absence or presence of a dialysis membrane tube containing drug solution of the same concentration as that of the culture medium was measured at suitable time intervals.

When the ampicillin concentration was 4.0 μg/mL, the drug concentrations remained nearly constant, both with and without a dialysis membrane tube. On the other hand, at the initial concentration of 1.25 μg/mL in the absence of a dialysis membrane tube, the concentration decreased significantly, with a half-life of ~7 h. However, with replacement of the dialysis membrane tube every 3 h, a constant ampicillin concentration was successfully maintained during the experimental period.

These results indicate the importance of keeping the drug concentration constant during the experiment and demonstrate that the method in which the dialysis membrane tube is utilized is suitable for this purpose. A membrane tube containing antibiotic solution of the appropriate concentration was, therefore, used in all microbial kinetic studies.

Effect of Organism Population on Drug-Affected Generation Rates—Semilogarithmic plots of the viable count *versus* time for *E. coli* B/r cultures treated with 0.5 μg of ampicillin/mL are illustrated in Fig. 1, in which the effects of different initial inoculum sizes and organism populations at the time of drug addition can be seen. No significant effects of the initial inoculum size and organism population at the time of drug addition are apparent.

Effect of Antibiotic Concentrations on Generation Rates—*Shape of Generation Curves*—Typical semilogarithmic plots of viable counts *versus* time for *E. coli* NIHJ JC-2 and *E. coli* B/r cultures in the presence of various concentrations of several β-lactam antibiotics are shown in Figs. 2 and 3 for penicillin G and cefadroxil, respectively.

All antibiotics studied gave very similar generation curves of *E. coli*. After the addition of a drug to the medium, a definite lag period was observed (Figs. 1–3) before the semilogarithmic plots of viable counts decreased linearly with time. As is apparent from the results shown in Figs. 2 and 3, these lag periods tend to become shorter at higher drug concentrations. These periods may depend on the time required for the antibiotic concentration on both sides of the bacterial membrane to reach steady state after drug addition to the broth medium. Garrett and Won (4) have reported similar lag periods in their study on the bactericidal effects of penicillin G, kanamycin, and rifampin against *E. coli* and have suggested that these intervals reflect the drug partitioning process into the bacterial membrane. In this study, however, we were not able to express the lag period as a function of drug concentration.

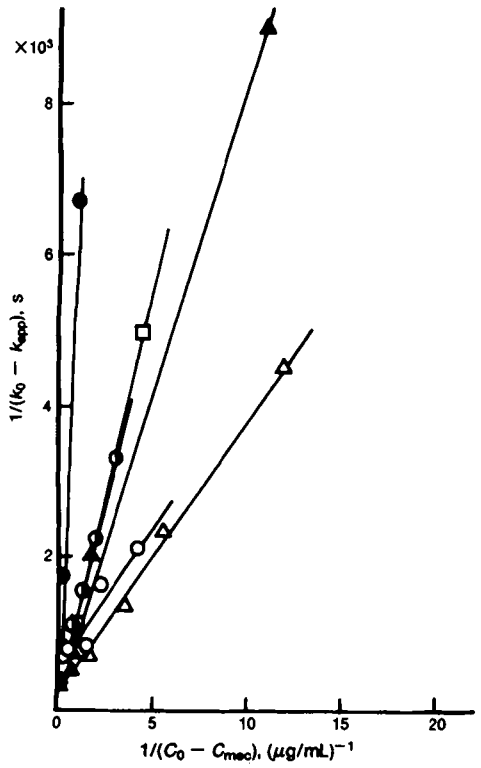

Figure 6—*Applicability of saturation kinetics to the dependency of apparent generation rate constants, k_{app}, of drug-affected* E. coli *NIHJ JC-2 on drug concentration at pH 7.0 and 37°C. Key: (●) penicillin G; (▲) ampicillin; (○) cephalexin; (△) cefazolin; (◑) cefadroxil; (□) cephaloridine.*

At higher drug concentrations, the number of viable cells decreased linearly in the semilogarithmic plots obtained immediately after drug addition. At lower drug concentrations, subsequent to the deviation from the curve of the drug-free culture, a new steady-state generation phase was established.

Apparent generation rate constants, k_{app} (in s^{-1}), of drug-affected cultures were obtained from the slopes of the linear portions of ln N *versus* t plots in accordance with the general rate expression:

$$\ln N = \ln N_0 + k_{app}t \qquad \text{(Eq. 3)}$$

Concentration Dependence of Generation Rate—The apparent generation rate constants, k_{app}, for the drug-affected *E. coli* NIHJ JC-2 and *E. coli* B/r cultures are plotted against antibiotic concentrations in Figs. 4 and 5, respectively. The plots for all antibiotics studied show a marked decrease of k_{app} with an increase in the drug concentration, C, and a tendency to reach maximum rate constants. These nonlinear plots indicate that the apparent generation rates of the drug-affected cultures obey the well-established kinetics of the saturable receptor site model proposed for other antibacterial agents (1, 2, 5–10) and can be expressed by:

$$k_{app} = k_0 - [k_{max} \times (C - C_{mec})]/[S_b + (C - C_{mec})] \qquad \text{(Eq. 4)}$$

where k_{max} and S_b are the proportionality constants relating to drug availability in the cell and drug affinity to receptor or binding sites, and C_{mec} is the minimum effective concentration manifesting antibacterial activity (defined as $C_{mec} = C$ when $k_{app} = k_0$). As suggested previously by Garrett and Won (4), C_{mec} may reflect the binding or removal of effective antibiotic by the components of the medium. The constants of k_{max}, S_b, and C_{mec} were determined by Eq. 4 using the nonlinear regression program NONLIN (11)[13] and are listed in Table I.

When the reciprocal values of the differences between the drug-free generation rate constant, k_0, and the drug-affected generation rate constant, k_{app}, are plotted against the reciprocal of the difference between the drug concentration, C, and the minimum effective concentration, C_{mec}, a good linearity is obtained by:

$$1/(k_0 - k_{max}) = S_b/k_{max}(C - C_{mec}) + 1/k_{max} \qquad \text{(Eq. 5)}$$

The plots are illustrated in Figs. 6 and 7 for *E. coli* NIHJ JC-2 and *E. coli* B/r,

[13] The computer analysis was performed with a FACOM-170F digital computer at the Data Processing Center, Kanazawa University.

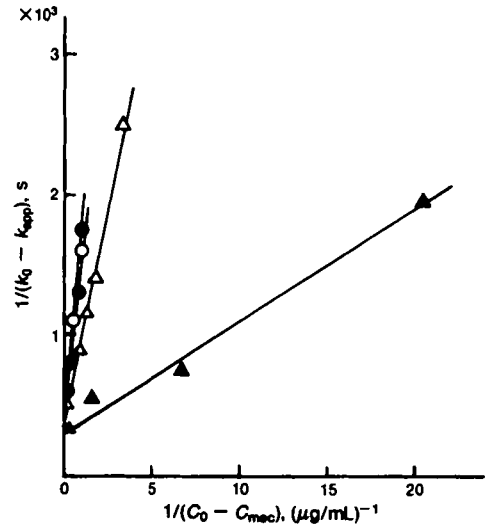

Figure 7—*Applicability of saturation kinetics to the dependency of apparent generation rate constants, k_{app}, of drug-affected* E. coli *B/r on drug concentration at pH 7.0 and 37°C. Key: (●) penicillin G; (▲) ampicillin; (○) dicloxacillin; (△) methicillin.*

respectively. The good agreement of data with Eq. 5 also substantiates the validity of the saturable receptor site model (1, 2, 5–10) for interpretation of the action of β-lactam antibiotics on microbial growth. It is likely that the receptor sites correspond to transpeptidase, which is known to interact with β-lactam antibiotics (12).

The quantitative meaning of the MIC is still unclear, and the magnitude does not always reflect the kinetic behavior of microbial generation in the presence of antibiotics. However, the parameter k_{max} corresponds to the V_{max} in enzyme kinetics and may reflect the intrinsic potency of the antibiotic better than does the MIC.

Structure–Activity Correlation of β-Lactam Antibiotics and Microbial Kinetics—Hermann (13) has suggested that the bactericidal activity of β-lactam antibiotics is parallel to the reactivity of the β-lactam ring, and Indelicato *et al.* (14, 15) and Yamana *et al.* (16, 17) have stated that the alkaline degradation rate, k_{OH}, of cephalosporin parallels antibacterial activity. The mechanism of hydroxide ion-catalyzed degradation of the β-lactam ring in alkaline solution is similar to the mechanism of the acylation of transpeptidase because both reactivities depend on the cleavage energy of the C—O bond of the β-lactam ring. Based on these considerations, a linear free energy relationship can be applied for k_{max} and k_{OH}:

$$G^{\neq}_{k_{max}} = \text{const} \cdot G^{\neq}_{k_{OH}} + \text{const} \qquad \text{(Eq. 6)}$$

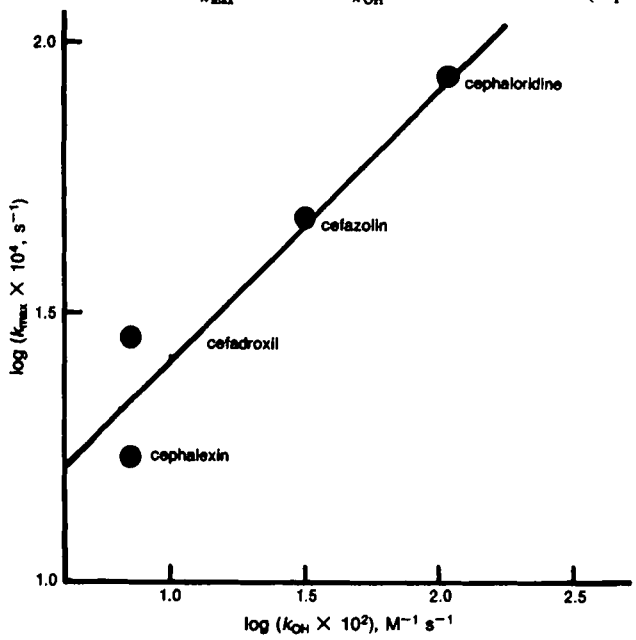

Figure 8—*Relationship between microbial kinetic parameter, k_{max}, of* E. coli *NIHJ JC-2 and alkaline degradation rates, k_{OH}, of cephalosporins.*

and:

$$k_{max} = \text{const} \cdot \exp(-G^{\neq}_{k_{max}}/RT) \quad \text{(Eq. 7)}$$

$$k_{OH} = \text{const} \cdot \exp(-G^{\neq}_{k_{OH}}/RT) \quad \text{(Eq. 8)}$$

where $G^{\neq}_{k_{max}}$ and $G^{\neq}_{k_{OH}}$ are free energies of activation for k_{max} and k_{OH}, respectively, const is a constant, R is the gas constant, and T is the absolute temperature. Taking the common logarithm of both sides of Eqs. 7 and 8 gives:

$$\log k_{max} = \text{const} - G^{\neq}_{k_{max}}/2.303RT \quad \text{(Eq. 9)}$$

$$\log k_{OH} = \text{const} - G^{\neq}_{k_{OH}}/2.303RT \quad \text{(Eq. 10)}$$

Substitution of Eqs. 9 and 10 for $G^{\neq}_{k_{max}}$ and $G^{\neq}_{k_{OH}}$ into Eq. 6, followed by rearrangement, yields:

$$\log k_{max} = \text{const} \cdot \log k_{OH} + \text{const} \quad \text{(Eq. 11)}$$

Equation 11 indicates a linear relationship between log k_{max} and log k_{OH}.

The k_{max} values for *E. coli* NIHJ JC-2 and k_{OH} values for cephalosporins are listed in Table II, and log k_{max} is plotted against log k_{OH} in Fig. 8 (good linearity was obtained). The regression equation obtained is:

$$\log k_{max} = 0.513 \cdot \log k_{OH} + 0.902 \quad \text{(Eq. 12)}$$

with a regression coefficient of 0.951. This relationship suggests that β-lactam antibiotics possessing high reactivity of the C—O bond in alkaline solution will show high bactericidal activity.

Organisms Resistant to Drug Action—Garrett and Won (4) have suggested the following possible explanations in connection with the regrowth of organisms after the first-order decrease of viable cells in drug-affected cultures (Figs. 1–3): (*a*) the consumption or degradation of the drug, (*b*) the production of an inhibitor or inactivator of antibiotic action, and (*c*) the presence of bacteria able to resist the drug action. This study on the microbial kinetics of various β-lactam antibiotics was conducted at constant drug concentrations (achieved by the dialysis membrane tube method); therefore, possibility *a* can be ruled out, but possibilities *b* and *c* still remain.

REFERENCES

(1) E. R. Garrett, G. H. Miller, and R. W. Brown, *J. Pharm. Sci.*, **55**, 593 (1966).

(2) E. R. Garrett, in "Progress in Drug Research," vol. 15, E. Jucker, Ed., Birkhauser Verlag, Basel, Switzerland, 1971, pp. 271–352, and references cited therein.

(3) J. K. Seydel, E. Wempe, G. H. Miller, and L. Miller, *Chemotherapy*, **17**, 217 (1972).

(4) E. R. Garrett and C. M. Won, *J. Pharm. Sci.*, **62**, 1666 (1973).

(5) S. M. Heman-Ackah, *J. Pharm. Sci.*, **63**, 1077 (1974).

(6) S. M. Heman-Ackah, *J. Pharm. Sci.*, **64**, 1612 (1975).

(7) E. R. Garrett, *Scand. J. Infect. Dis.*, **14**, (Suppl.) 54, (1978), and references cited therein.

(8) A. E. Elkhouly and C. Führer, *J. Antibiot.*, **31**, 229 (1978).

(9) K. Boakye-Yiadom and S. M. Heman-Ackah, *J. Pharm. Sci.*, **68**, 1510 (1979).

(10) S. M. Heman-Ackah and E. R. Garrett, *J. Med. Chem.*, **15**, 152 (1972).

(11) C. M. Metzler, "NONLIN, A Computer Program for Parameter Estimation in Nonlinear Systems," Technical Report 7292/69/7292/005, The Upjohn Co., Kalamazoo, Mich.

(12) "Beta-Lactam Antibiotics" S. Mitsuhashi, Ed., Japan Scientific Societies Press, 1981, and references cited therein.

(13) R. B. Hermann, *J. Antibiot.*, **26**, 223 (1972).

(14) J. M. Indelicato and W. L. Wilham, *J. Med. Chem.*, **17**, 528 (1974).

(15) J. M. Indelicato, T. T. Norrilas, R. R. Pfeiffer, W. J. Wheeler, and W. L. Wilham, *J. Med. Chem.*, **17**, 523 (1974).

(16) T. Yamana, A. Tsuji, K. Kanayama, and O. Nakano, *J. Antibiot.*, **27**, 1000 (1974).

(17) T.Yamana and A. Tsuji, *J. Pharm. Sci.*, **65**, 1563 (1976).

(18) A. Tsuji, E. Nakashima, Y. Deguchi, K. Nishide, T. Shimizu, S. Horiuchi, K. Ishikawa, and T. Yamana, *J. Pharm. Sci.*, **70**, 1120 (1981).

ACKNOWLEDGMENTS

The authors wish to acknowledge the gifts of β-lactam antibiotics from Meiji Seika Kaisha, Takeda Chemical Industries, Banyu Pharmaceutical Co., Fujisawa Pharmaceutical Co., Shionogi Co., and Bristol Meyers Co. They also acknowledge the skillful technical assistance of Mr. Y. Deguchi, Miss M. Takeda, and Miss K. Wakiya.

Kinetic Analysis and Characterization of the Bacterial Regrowth after Treatment of *Escherichia coli* with β-Lactam Antibiotics

SHOICHIRO HAMANO *[1], AKIRA TSUJI *[x], TETSUO ASANO *, IKUMI TAMAI *, EMI NAKASHIMA *, TSUKINAKA YAMANA [‡], and SUSUMU MITSUHASHI [§]

Received December 27, 1982, from the **Faculty of Pharmaceutical Sciences* and [‡]*Hospital Pharmacy, Kanazawa University, Takara-machi, Kanazawa 920, Japan* and the [§]*School of Medicine, Gunma University, Showa-machi, Maebashi 372, Japan.* Accepted for publication October 24, 1983. [1]Present address: Research Center, Taisho Pharmaceutical Co., Ltd., Yoshino-cho, Omiya 330, Japan.

Abstract □ The generation curves of *Escherichia coli* B/r and *E. coli* NIHJ JC-2 in the presence of several β-lactam antibiotics were studied from the kinetic point of view. Apparent first-order regrowth of resistant organisms was observed ~6 h after addition of these antibiotics. The time courses of apparent viable counts could be interpreted in terms of the sum of the viable counts of sensitive and resistant organisms. To clarify the nature of the regrowth, experiments involving a second addition of antibiotic, single colonization by subculture, and synchronous cell culture were carried out. Several possible explanations for the results are discussed, including β-lactamase production, selection in terms of membrane permeability, and mutation to acquire drug resistance. A selection process or a modification of membrane permeability caused by contact with the drug seems to be the most probable reason for the regrowth of the organisms.

Keyphrases □ Kinetics—microbial, analysis and characterization of bacterial regrowth after treatment of *Escherichia coli* with β-lactam antibiotics □ β-Lactam antibiotics—kinetic analysis and characterization of bacterial regrowth after treatment of *Escherichia coli*

In the previous paper (1), we described the microbial kinetics of *Escherichia coli* treated with several β-lactam antibiotics. We also mentioned that, once treated with β-lactam antibiotics, the organisms showed an apparent regrowth in spite of the maintenance of a constant drug concentration by the use of a dialysis membrane tube containing the antibiotic solution (1). This regrowth is a well-recognized phenomenon in drug-affected cultures (2–6). Much work has been done on

0022-3549/84/1000-1422$01.00/0

© 1984, American Pharmaceutical Association

and:

$$k_{max} = \text{const} \cdot \exp(-G^{\neq}_{k_{max}}/RT) \quad \text{(Eq. 7)}$$

$$k_{OH} = \text{const} \cdot \exp(-G^{\neq}_{k_{OH}}/RT) \quad \text{(Eq. 8)}$$

where $G^{\neq}_{k_{max}}$ and $G^{\neq}_{k_{OH}}$ are free energies of activation for k_{max} and k_{OH}, respectively, const is a constant, R is the gas constant, and T is the absolute temperature. Taking the common logarithm of both sides of Eqs. 7 and 8 gives:

$$\log k_{max} = \text{const} - G^{\neq}_{k_{max}}/2.303RT \quad \text{(Eq. 9)}$$

$$\log k_{OH} = \text{const} - G^{\neq}_{k_{OH}}/2.303RT \quad \text{(Eq. 10)}$$

Substitution of Eqs. 9 and 10 for $G^{\neq}_{k_{max}}$ and $G^{\neq}_{k_{OH}}$ into Eq. 6, followed by rearrangement, yields:

$$\log k_{max} = \text{const} \cdot \log k_{OH} + \text{const} \quad \text{(Eq. 11)}$$

Equation 11 indicates a linear relationship between log k_{max} and log k_{OH}.

The k_{max} values for *E. coli* NIHJ JC-2 and k_{OH} values for cephalosporins are listed in Table II, and log k_{max} is plotted against log k_{OH} in Fig. 8 (good linearity was obtained). The regression equation obtained is:

$$\log k_{max} = 0.513 \cdot \log k_{OH} + 0.902 \quad \text{(Eq. 12)}$$

with a regression coefficient of 0.951. This relationship suggests that β-lactam antibiotics possessing high reactivity of the C—O bond in alkaline solution will show high bactericidal activity.

Organisms Resistant to Drug Action—Garrett and Won (4) have suggested the following possible explanations in connection with the regrowth of organisms after the first-order decrease of viable cells in drug-affected cultures (Figs. 1–3): (*a*) the consumption or degradation of the drug, (*b*) the production of an inhibitor or inactivator of antibiotic action, and (*c*) the presence of bacteria able to resist the drug action. This study on the microbial kinetics of various β-lactam antibiotics was conducted at constant drug concentrations (achieved by the dialysis membrane tube method); therefore, possibility *a* can be ruled out, but possibilities *b* and *c* still remain.

REFERENCES

(1) E. R. Garrett, G. H. Miller, and R. W. Brown, *J. Pharm. Sci.*, **55**, 593 (1966).

(2) E. R. Garrett, in "Progress in Drug Research," vol. 15, E. Jucker, Ed., Birkhauser Verlag, Basel, Switzerland, 1971, pp. 271–352, and references cited therein.

(3) J. K. Seydel, E. Wempe, G. H. Miller, and L. Miller, *Chemotherapy*, **17**, 217 (1972).

(4) E. R. Garrett and C. M. Won, *J. Pharm. Sci.*, **62**, 1666 (1973).

(5) S. M. Heman-Ackah, *J. Pharm. Sci.*, **63**, 1077 (1974).

(6) S. M. Heman-Ackah, *J. Pharm. Sci.*, **64**, 1612 (1975).

(7) E. R. Garrett, *Scand. J. Infect. Dis.*, **14**, (Suppl.) 54, (1978), and references cited therein.

(8) A. E. Elkhouly and C. Führer, *J. Antibiot.*, **31**, 229 (1978).

(9) K. Boakye-Yiadom and S. M. Heman-Ackah, *J. Pharm. Sci.*, **68**, 1510 (1979).

(10) S. M. Heman-Ackah and E. R. Garrett, *J. Med. Chem.*, **15**, 152 (1972).

(11) C. M. Metzler, "NONLIN, A Computer Program for Parameter Estimation in Nonlinear Systems," Technical Report 7292/69/7292/005, The Upjohn Co., Kalamazoo, Mich.

(12) "Beta-Lactam Antibiotics" S. Mitsuhashi, Ed., Japan Scientific Societies Press, 1981, and references cited therein.

(13) R. B. Hermann, *J. Antibiot.*, **26**, 223 (1972).

(14) J. M. Indelicato and W. L. Wilham, *J. Med. Chem.*, **17**, 528 (1974).

(15) J. M. Indelicato, T. T. Norrilas, R. R. Pfeiffer, W. J. Wheeler, and W. L. Wilham, *J. Med. Chem.*, **17**, 523 (1974).

(16) T. Yamana, A. Tsuji, K. Kanayama, and O. Nakano, *J. Antibiot.*, **27**, 1000 (1974).

(17) T.Yamana and A. Tsuji, *J. Pharm. Sci.*, **65**, 1563 (1976).

(18) A. Tsuji, E. Nakashima, Y. Deguchi, K. Nishide, T. Shimizu, S. Horiuchi, K. Ishikawa, and T. Yamana, *J. Pharm. Sci.*, **70**, 1120 (1981).

ACKNOWLEDGMENTS

The authors wish to acknowledge the gifts of β-lactam antibiotics from Meiji Seika Kaisha, Takeda Chemical Industries, Banyu Pharmaceutical Co., Fujisawa Pharmaceutical Co., Shionogi Co., and Bristol Meyers Co. They also acknowledge the skillful technical assistance of Mr. Y. Deguchi, Miss M. Takeda, and Miss K. Wakiya.

Kinetic Analysis and Characterization of the Bacterial Regrowth after Treatment of *Escherichia coli* with β-Lactam Antibiotics

SHOICHIRO HAMANO *[1], AKIRA TSUJI *[x], TETSUO ASANO *, IKUMI TAMAI *, EMI NAKASHIMA *, TSUKINAKA YAMANA [‡], and SUSUMU MITSUHASHI [§]

Received December 27, 1982, from the **Faculty of Pharmaceutical Sciences* and [‡]*Hospital Pharmacy, Kanazawa University, Takara-machi, Kanazawa 920, Japan* and the [§]*School of Medicine, Gunma University, Showa-machi, Maebashi 372, Japan.* Accepted for publication October 24, 1983. [1]Present address: Research Center, Taisho Pharmaceutical Co., Ltd., Yoshino-cho, Omiya 330, Japan.

Abstract □ The generation curves of *Escherichia coli* B/r and *E. coli* NIHJ JC-2 in the presence of several β-lactam antibiotics were studied from the kinetic point of view. Apparent first-order regrowth of resistant organisms was observed ~6 h after addition of these antibiotics. The time courses of apparent viable counts could be interpreted in terms of the sum of the viable counts of sensitive and resistant organisms. To clarify the nature of the regrowth, experiments involving a second addition of antibiotic, single colonization by subculture, and synchronous cell culture were carried out. Several possible explanations for the results are discussed, including β-lactamase production, selection in terms of membrane permeability, and mutation to acquire drug resistance. A selection process or a modification of membrane permeability caused by contact with the drug seems to be the most probable reason for the regrowth of the organisms.

Keyphrases □ Kinetics—microbial, analysis and characterization of bacterial regrowth after treatment of *Escherichia coli* with β-lactam antibiotics □ β-Lactam antibiotics—kinetic analysis and characterization of bacterial regrowth after treatment of *Escherichia coli*

In the previous paper (1), we described the microbial kinetics of *Escherichia coli* treated with several β-lactam antibiotics. We also mentioned that, once treated with β-lactam antibiotics, the organisms showed an apparent regrowth in spite of the maintenance of a constant drug concentration by the use of a dialysis membrane tube containing the antibiotic solution (1). This regrowth is a well-recognized phenomenon in drug-affected cultures (2–6). Much work has been done on

0022-3549/84/1000-1422$01.00/0

© 1984, American Pharmaceutical Association

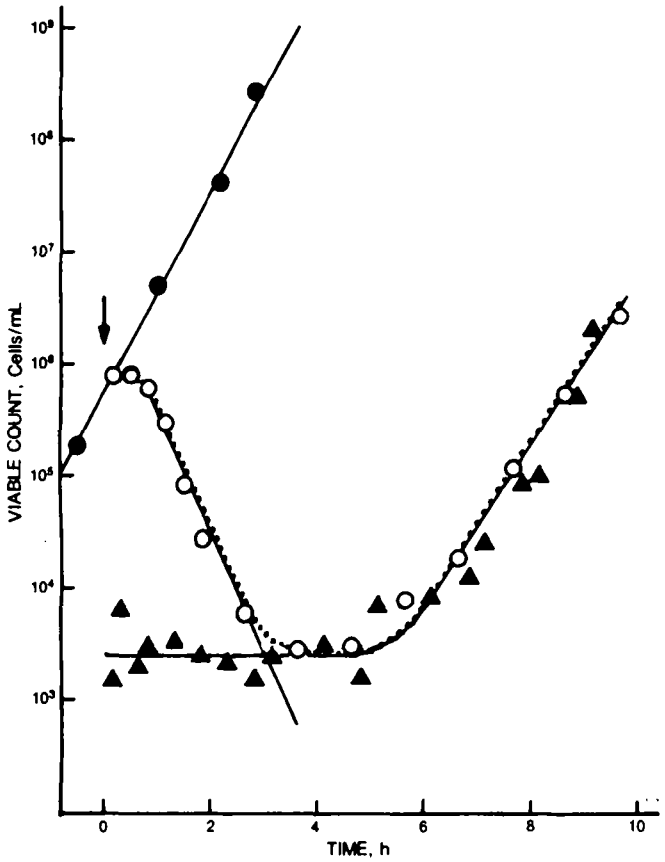

Figure 1—*Generation curves of* E. coli *B/r in antibiotic medium*[3] *at pH 7.0 and 37°C in the absence and presence of 0.5 μg of ampicillin/mL, based on viable counts. Key: (●) control generation curves; (○) drug-affected viable counts in drug-free agar plates; (▲) drug-affected viable counts in drug-containing agar plates. The dotted line was generated from Eqs. 1 and 2 by using the appropriate kinetic parameters (Table I.)*

drug-resistant mechanisms of organisms (7); however, very few reports (2, 6) have focused on the mechanism of regrowth after addition of antibacterial agents to the culture, even though it is very important to prevent the regrowth of organisms in chemotherapy.

The purposes of this study were to establish a mathematical model to describe the entire generation curve of organisms as a function of time and to clarify the nature of regrowth after the bactericidal action of β-lactam antibiotics.

EXPERIMENTAL SECTION

Microorganisms—Replicate slants of *E. coli* NIHJ JC-2[1] and *E. coli* B/r[2] [the same strains as used previously (2)] were used. The slants were prepared from a single isolated colony of the appropriate organism and stored at 4°C.

Culture Medium—Antibiotic medium[3] was rehydrated according to the specifications of the manufacturer and filtered twice through a 0.45-μm filter[4]. The medium was autoclaved at 120°C for 20 min. This pH 7.0 medium was used for all experiments.

Materials—Ampicillin sodium[5] (955 μg/mg), penicillin G potassium[6] (1600 U/mg), and cefazolin sodium[7] (958 μg/mg) were used as received. All other chemicals were of reagent grade and were used without further purification.

[1] IFO 12734; Institute for Fermentation, Osaka, Japan.
[2] F-57; Institute for Fermentation.
[3] Antibiotic Medium 3; Difco Laboratories, Detroit, Mich.
[4] Sartorius-Membranfilter GmbH, Göttingen, Federal Republic of Germany.
[5] Takeda Chemical Industries, Osaka, Japan.
[6] Meiji Seika Kaisha, Tokyo, Japan.
[7] Fujisawa Pharmaceutical Co., Osaka, Japan.

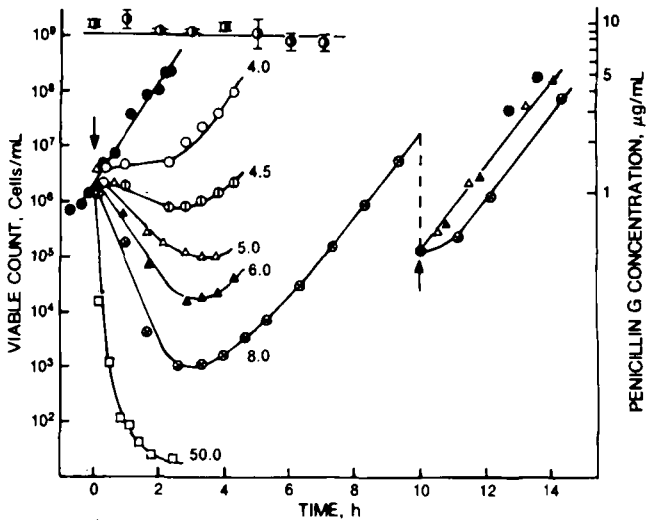

Figure 2—*Generation curves of* E. coli *B/r in antibiotic medium*[3] *at pH 7.0 and 37°C in the absence and presence of various concentrations of penicillin G. The numbers inside the figure are the drug concentrations in micrograms per milliliter. After the first addition (↓) of 8.0 μg of penicillin G/mL, the culture was diluted 100-fold with fresh medium at the second addition (↑). The observed drug concentrations are indicated (○) for 8 μg/mL (nominal) (right-hand axis).*

Bacterial Generation—An aliquot (5 mL) of culture medium was inoculated from a fresh slant and allowed to grow for 15 h at 37°C in an incubator. Samples of this culture were appropriately diluted in several steps to achieve the organism concentration of 10^4 cells/mL.

Two 0.5-mL portions of this cultture were finally diluted into 49.5 mL of fresh medium for control growth and 49.0 mL of fresh medium for drug-affected growth, respectively. The cultures were maintained at 37°C in a constant-temperature water bath equipped with a shaker set at 130 strokes/min. The drug solutions were added to the cultures in the logarithmic growth phase at 37°C. As soon as a drug was added to the cultures, a dialysis membrane tube[8] containing 10 mL of fresh culture medium with the same drug concentration as the organism culture medium was placed in the culture medium and replaced every 3 h with a new one (1). To keep the antibiotic concentration constant during the experiment, a membrane tube was used in all generation studies.

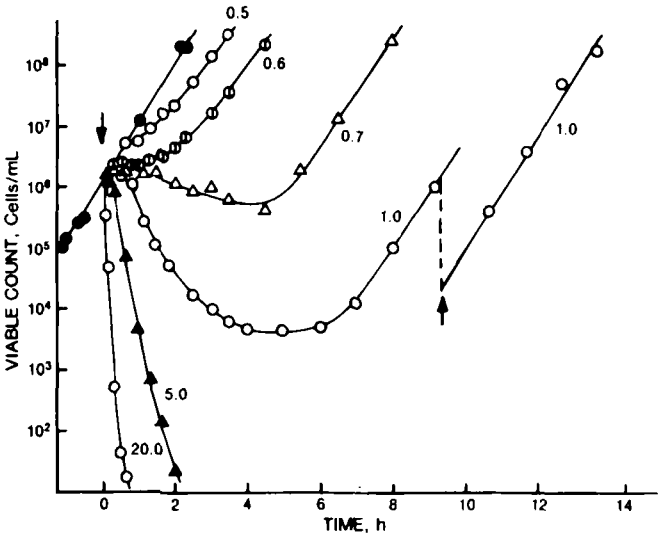

Figure 3—*Generation curves of* E. coli *NIHJ JC-2 in antibiotic medium*[3] *at pH 7.0 and 37°C in the absence and presence of various concentrations of cefazolin. The numbers inside the figure are drug concentrations in micrograms per milliliter. After the first addition (↓) of 1.0 μg of cefazolin/mL, the culture was diluted 100-fold with fresh medium at the second addition (↑).*

[8] Seamless cellulose tubing 20/32; Visking Co.

Table I—Microbial Kinetic Parameters of *E. coli* B/r and *E. coli* NIHJ JC-2 in Antibiotic Medium[3] [a]

Organism	Ns_0, cells/mL	Nr_0, cells/mL	k_{app}, s^{-1}	k_g, s^{-1}	L_1, min	L_2, min
E. coli B/r	8.0×10^5	3.2×10^3	-7.01×10^{-4}	4.67×10^{-4}	53	322
E. coli NIHJ JC-2	1.0×10^6	1.2×10^1	-1.04×10^{-3}	4.95×10^{-4}	55	326

[a] At pH 7.0 and 37°C in the presence of 0.5 and 1.5 μg of ampicillin/mL for *E. coli* B/r and *E. coli* NIHJ JC-2, respectively.

At appropriate time intervals, aliquots (0.5 mL) were withdrawn, and the penicillin G concentration was determined by the usual microbiological paper disk method, employing *Staphylococcus aureus* 209P[9] as the test organism.

Viable Count Method—Samples (0.5 mL) were withdrawn from the cultures and serially diluted into sterilized 0.9% NaCl solution in accordance with a preplanned dilution scheme so that 50–150 colonies per plate would result. From these dilutions, aliquots (0.2 mL) were transferred onto each of three replicate peptone agar plates. The plates were incubated for 20 h at 37°C, and the resulting colonies were counted with an electronic colony counter.

To obtain the viable count of drug-resistant organisms shown in Figs. 1–5, the procedure was the same as that described above, except for the use of peptone agar plates which contained the drug at the desired concentration.

Effect of Second Addition of Antibiotics—Aliquots (0.5 mL) of penicillin G and cefazolin solutions were added to *E. coli* B/r and *E. coli* NIHJ JC-2 cultures, respectively, in the logarithmic growth phase of the culture to give final concentrations of 8.0 μg/mL for penicillin G (culture A) and 1.0 μg/mL for cefazolin (culture B). The drug-affected cultures A and B were allowed to generate for ~10 h at 37°C in an incubator. Portions of these solutions were then diluted 100-fold with fresh medium. Aliquots of the *E. coli* B/r culture were then treated with penicillin G concentrations of 5.0, 6.0, and 8.0 μg/mL, and an aliquot of the *E. coli* NIHJ JC-2 culture was treated with 1.0 μg of cefazolin/mL. One colony of *E. coli* NIHJ JC-2 harvested from culture B in the logarithmic growth phase of regrowth was subcultured, and then the subcultured organism was used as a test organism. The effect of the second addition of cefazolin on this subcultured resistant organism was studied in the same manner as described above.

Population Distribution of Drug-Resistant Organisms—Replicate agar plates containing ampicillin concentrations of 0.1, 0.2, 0.3, 0.4, 0.5, 0.55, 0.6, 0.65, and 0.7 μg/mL were prepared. Samples (0.5 mL) were withdrawn from *E. coli* NIHJ JC-2 culture at an organism concentration of 2×10^6 cells/mL in the logarithmic growth phase and serially diluted. From these dilutions, samples (0.2 mL) were transferred onto the replicate agar plates containing drug. The plates were incubated for 20 h at 37°C, and the number of colonies was counted.

Single Colonization—*E. coli* NIHJ JC-2 obtained from a fresh slant was suspended in 2 mL of 0.9% NaCl. A portion of this solution was transferred onto peptone agar plates with a standard platinum loop and cultured for 20 h at 37°C. One colony from this agar plate was again treated in the same way; the colony that appeared the next day was used as the test organism.

Drug-Affected Growth and Effect of Second Addition—The experimental procedure for drug-affected growth and the effect of the second addition of antibiotic was the same as that described previously (1).

Minimal Inhibitory Concentration of Subcultured Drug-Resistant Organisms—The organism obtained from the regrowth of *E. coli* NIHJ JC-2 after ampicillin treatment (1.5 μg/mL) was purified by single colonization and subcultured up to 29 times on peptone agar plates. The minimal inhibitory concentration (MIC) was determined periodically.

The MIC values were determined by the agar dilution method. Overnight cultures of *E. coli* NIHJ JC-2 were diluted to final concentrations of ~10^6 and 10^8 cells/mL, and 5-μL aliquots of each culture were inoculated and incubated on antibiotic medium[3] agar plates containing serial twofold dilutions of ampicillin. The MIC values were recorded after 18 h of incubation at 37°C.

Effect of Ampicillin Concentrations on Regrowth Rates—Aliquots (0.5 mL) of aqueous solutions of ampicillin were aseptically added to replicate 49.5-mL volumes of *E. coli* NIHJ JC-2 cultures to yield concentrations of 0.55, 0.6, 0.7, and 1.1 μg/mL.

Preparation of Synchronous Cell Cultures—Aliquots (0.5 mL) of phenethyl alcohol solutions were aseptically added to replicate 49.5-mL volumes of *E. coli* NIHJ JC-2 culture in the logarithmic growth phase to yield desired concentrations. The cell concentration at the time of drug addition was ~10^5 cells/mL. A portion of the culture was diluted 1000-fold with fresh medium at 90 min so that the effect of phenethyl alcohol became negligible. A synchronized cell culture was generated from the medium containing 10^5 cells/mL. Aliquots (0.5 mL) of ampicillin solution were added to the synchronized cell culture at an organism concentration of ~2×10^5 cells/mL to achieve final concentrations of 1.25 and 1.5 μg/mL. The viable counts were monitored with an electronic colony counter.

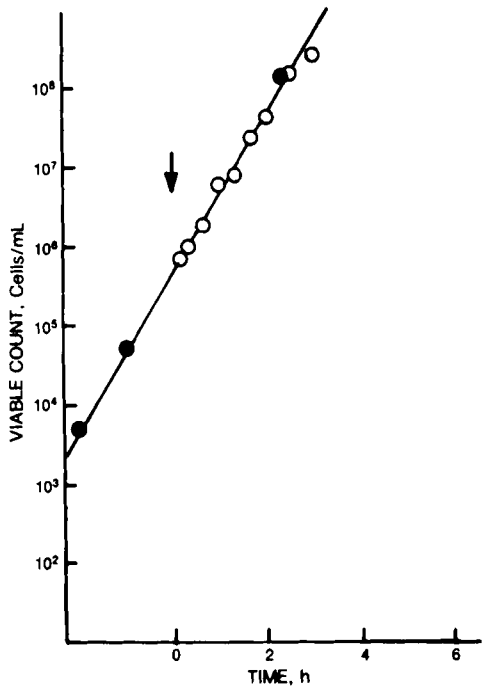

Figure 4—*Semilogarithmic plots of* E. coli *NIHJ JC-2 obtained from the logarithmic regrowth phase after the first addition of cefazolin (1.0 μg/mL) at pH 7.0 and 37°C. The experiment was effected 24 h after development and isolation of resistant organisms.*

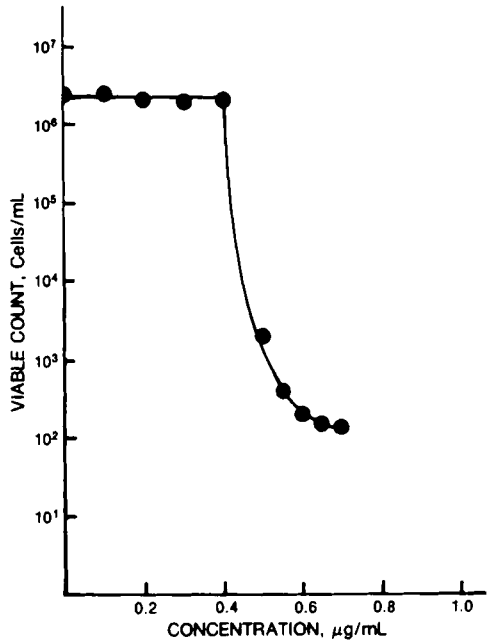

Figure 5—*Population diagram of ampicillin-resistant* E. coli *NIHJ JC-2. The viable counts were performed in agar plates with drug with various ampicillin concentrations after isolation of organisms from drug-free culture.*

[9] IFO 12732; Institute for Fermentation.

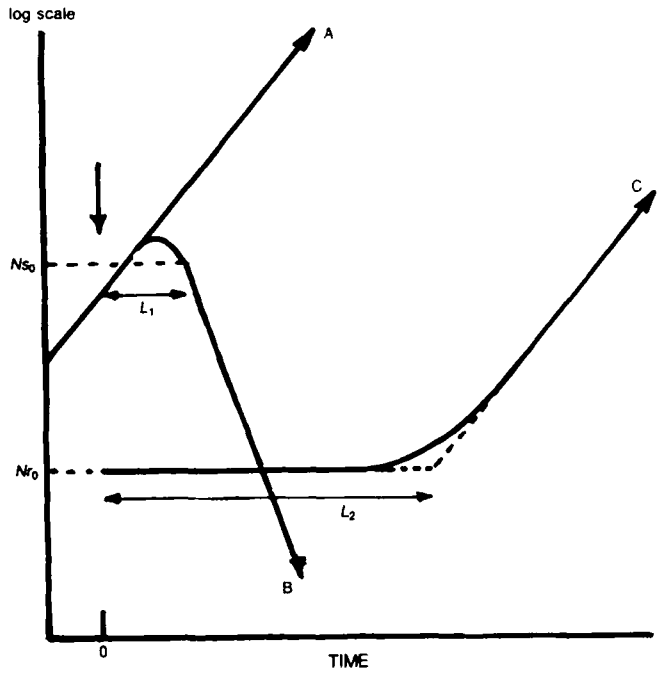

Figure 6—*Generation model for drug-affected organism. Key: (A) control generation curve; (B) generation curve of sensitive organisms; (C) generation curve of resistant organisms; (L_1 and L_2) lag times for sensitive and resistant organisms, respectively; (Ns_0 and Nr_0) initial organism concentrations for sensitive and resistant organisms, respectively; (time 0) time of drug addition.*

Assay of β-Lactamase—Antibiotic medium[3] in a 1.0-L flask was inoculated with 25 mL of an overnight culture of *E. coli* NIHJ JC-2 in the presence of 8 μg of penicillin G/mL at 37°C. After 4 h, the bacteria at a concentration of ~5 × 10^8 cells/mL in the logarithmic growth phase were harvested by centrifugation and washed once with 0.05 M phosphate buffer (pH 7.0). The packed cells were resuspended in 50 mL of 0.05 M phosphate buffer (pH 7.0), and the suspensions were intermittently treated in an ultrasonic disintegrator[10] for 3 min. The disrupted suspensions were centrifuged at 12,000 rpm for 30 min at 5°C to remove broken cells and cell debris; the cell-free extract was retained as the crude enzyme preparation. Activity of β-lactamase was then assayed spectrophotometrically (8) by measuring the decrease in the absorbance at the substrate-specific wavelengths of 233 and 260 nm for penicillin G and cephaloridine, respectively.

RESULTS

Development of Drug-Resistant Organisms—A typical semilogarithmic plot of the viable counts against time is shown (Fig. 1) for the action of 0.5 μg of ampicillin/mL on *E. coli* B/r. After a certain lag period following drug addition, the logarithm of the viable count against time decreased exponentially with time. After a definite period of organism killing, there is a subsequent generation of viable organisms. The slope of the regrowth phase in the presence of drug was found to be very similar to that for the plot in the absence of ampicillin. This result indicates a negligible drug effect in the terminal segments, even though the drug concentration was kept constant by the use of the dialysis membrane tube. A similar result was obtained for the *E. coli* NIHJ JC-2 culture treated with 1.5 μg of ampicillin/mL.

These observations indicate that the apparent generation curves in the presence of drugs (Fig. 1) consist of a first-order decrease of susceptible organisms and a first-order increase of resistant organisms, both of which occur after certain lag times. The lag time is the elapsed time from the time of drug addition to the time at which a decrease or an increase of the viable count begins. Therefore, the apparent generation curves may be expressed by the generation model depicted in Fig. 6, in which t is the time after addition of drug: Ns_0 is the number of susceptible organisms present at time L_1; Nr_0 is the number of resistant organisms at time L_2; L_1 and L_2 are the lag times for the appearances of the first-order decrease of susceptible organisms and the first-order increase of resistant organisms, respectively. This generation

[10] Ultrasonic Disruptor model UR-200P; Tomy Seiko Co. Ltd., Tokyo, Japan.

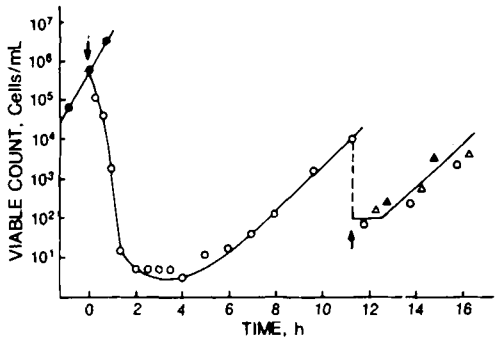

Figure 7—*Generation curves of the purified* E. coli NIHJ JC-2 *in antibiotic medium*[3] *at pH 7.0 and 37°C in the absence and presence of 1.5 μg of ampicillin/mL. After the first addition (↓) of ampicillin, the generating culture was diluted 100-fold with fresh medium at the second additions (▲) of various ampicillin concentrations. Key: (○) 1.5 μg/mL; (△) 1.2 μg/mL; (▲) 1.0 μg/mL.*

model leads to the following equations (see below for the derivation) after a lag period $t > L_1$ (when $L_1 \leqq t \leqq L_2$):

$$N_{app} = Ns_0 \cdot e^{k_{app}(t-L_1)} + Nr_0 \qquad \text{(Eq. 1)}$$

when $t > L_2$:

$$N_{app} = Ns_0 \cdot e^{k_{app}(t-L_1)} + Nr_0 \cdot e^{k_g(t-L_2)} \qquad \text{(Eq. 2)}$$

where N_{app} is the apparent number of organisms present at time t and k_{app} and k_g are the apparent generation rate constants for the susceptible and resistant organisms, respectively. The relationship between the observed number of viable counts and the simulation based on Eqs. 1 and 2 with the appropriate parameters listed in Table I seems to support the model depicted in Fig. 6.

Effect of Second Addition of Antibiotics—The effects of the second addition of penicillin G and cefazolin in the case of resistant organisms are shown in Figs. 2 and 3, respectively. In these experiments, the membrane tube containing the drug solution was used.

In a typical case shown in Fig. 2, a penicillin G concentration of 8 μg/mL

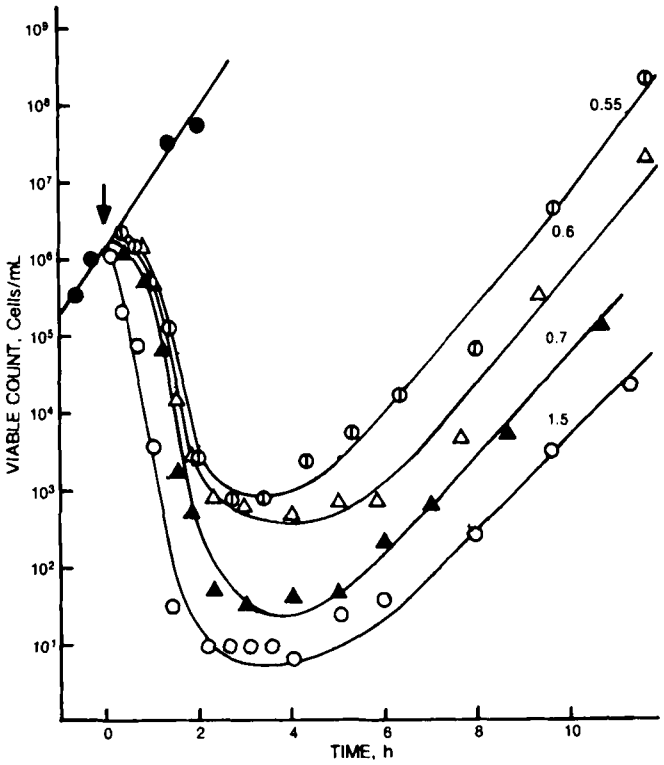

Figure 8—*Generation curves of the purified* E. coli *NIHJ JC-2 in antibiotic medium*[3] *at pH 7.0 and 37°C in the absence and presence of various concentrations of ampicillin. The curves are labeled according to drug concentrations in micrograms per milliliter.*

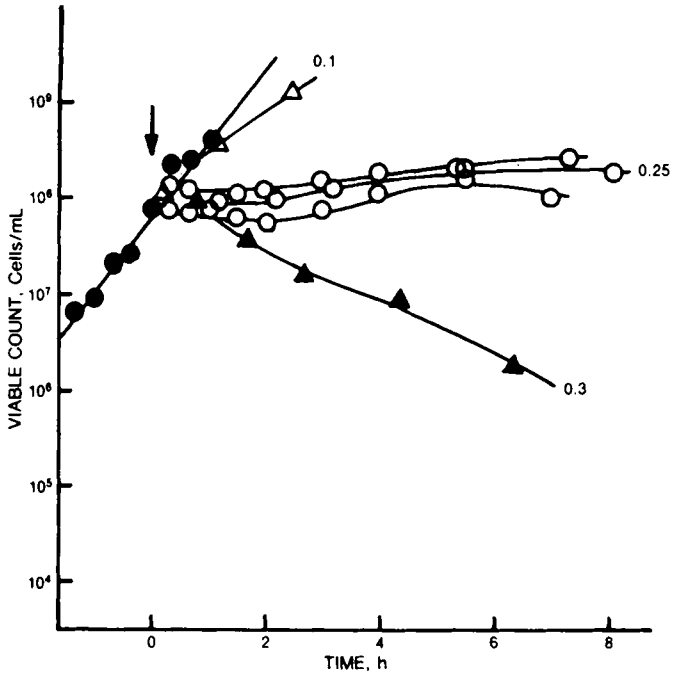

Figure 9—*Generation curves of* E. coli *NIHJ JC-2 in antibiotic medium*[3] *at pH 7.0 and 37°C in the absence and presence of phenethyl alcohol. The curves are labeled according to percent concentrations of phenethyl alcohol.*

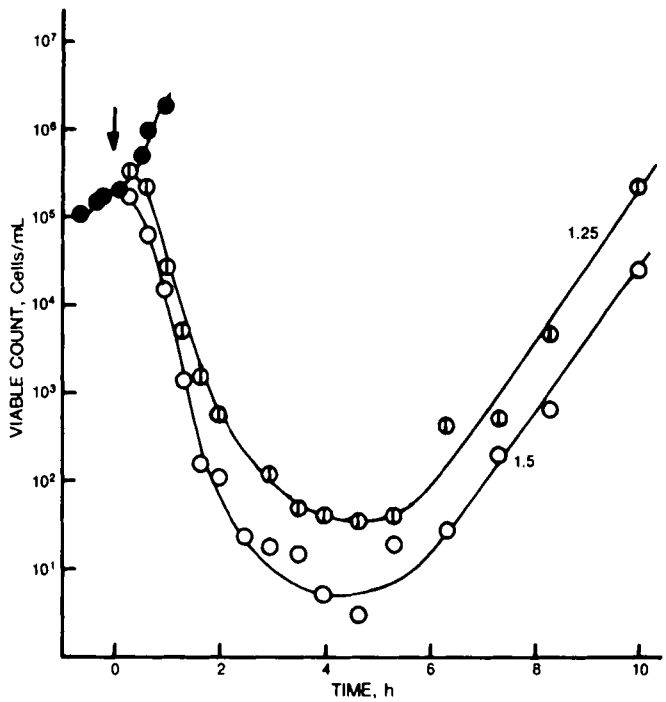

Figure 10—*Generation curves of the synchronized* E. coli *NIHJ JC-2 culture in antibiotic medium*[3] *at pH 7.0 and 37°C in the absence and presence of ampicillin. The curves are labeled according to ampicillin concentrations in micrograms per milliliter.*

was confirmed to be maintained essentially constant. At about 10 h after the first drug addition, when the drug-resistant organisms were in a logarithmic growth phase, the membrane tube was removed, and a 100-fold dilution was made with fresh medium to make the original drug action negligible. The second additions of penicillin G did not greatly affect the generation rate at the concentrations of 5.0 and 6.0 μg/mL (Fig. 2). Even though the first addition of penicillin G at these concentrations markedly reduced the viable counts, the generation rate constants for these concentrations were found to be similar to those of the drug-resistant organism at the first addition, although a slight lag time was observed at 8.0 μg/mL. The result indicates that once the organism has acquired resistance (after the first addition), it is resistant to all drug concentrations lower than that of the first addition. The same result was obtained for cefazolin with *E. coli* NIHJ JC-2 (Fig. 3).

The organism which was made resistant by the addition of 1.0 μg of cefazolin/ml was subcultured and again treated with cefazolin (1.0 μg/mL) on the next day. This drug-affected culture exhibited a generation rate similar to that of the drug-free culture (Fig. 4). This result shows that, once acquired, drug resistance is retained 48 h later.

Population Distribution of Drug-Resistant Organisms—To obtain a population diagram of ampicillin-resistant *E. coli* NIHJ JC-2, viable counts were performed in the agar plates with drug after isolation of organisms from drug-free culture. In Fig. 5 are plotted the resultant viable counts against ampicillin concentrations in the agar plates. A sharp decrease of viable counts was observed when the ampicillin concentration was increased from 0.4 to 0.5 μg/mL. This result suggests that the number of drug-resistant organisms depends on the drug concentration used.

Single Colony Subcultures—*Drug-Affected Generation Curve*—When the organism was purified by repeated subcultures of a single colony and then employed in the drug-affected generation experiment, the drug-resistant organisms increased again after about a 5-h lag period (Fig. 7). This result raises the possibility that some population among the presumably genetically identical organisms may have acquired drug resistance by contact with the drug. If some organisms such as these were originally insensitive to the ampicillin concentration of 1.5 μg/mL, they would not have shown a decrease of viable count after the first addition.

A second addition of antibiotic was also tested. Treatment with concentrations below that of the first addition also did not affect the generation rate of the resistant organisms.

Minimal Inhibitory Concentration for Subcultured Organisms—The MIC of ampicillin for the original strain of *E. coli* NIHJ JC-2 was 3.13 μg/mL at organism concentrations of both 10^6 and 10^8 cells/mL. The resistant organisms obtained after the first addition of ampicillin at 1.5 μg/mL were subcultured serially. The MIC values were in the ranges of 12.5–25 μg/mL at an organism concentration of 10^6 cells/mL and 25–50 μg/mL at 10^8 cells/mL. The MIC values remained essentially unchanged during 29 serial subcultures. This means that the resistance, once acquired, was persistent.

Effect of Drug Concentration on Generation Rate of the Purified Organism—Semilogarithmic plots of viable counts *versus* time for the *E. coli* NIHJ JC-2 culture treated with various concentrations of ampicillin are shown in Fig. 8. The generation curves are clearly concentration dependent, suggesting that the degree of resistance caused by contact with the drug might depend on the drug concentration.

Effect of Cell Cycle at the Time of Drug Addition—*Effect of Phenethyl Alcohol on Bacterial Generation*—The effect of phenethyl alcohol on the generation of *E. coli* NIHJ JC-2 was measured to ascertain the concentration which would effectively retard bacterial generation by the inhibition of DNA synthesis (9). The results (Fig. 9) indicate that 0.25% phenethyl alcohol treatment is suitable for the inhibition of DNA synthesis. Treatment with 0.1% phenethyl alcohol failed to inhibit DNA replication, whereas 0.3% phenethyl alcohol treatment killed the organisms.

Effect of Ampicillin Concentration on Generation Rate—The stationary-phase cells of *E. coli* NIHJ JC-2 were exposed to 0.25% phenethyl alcohol for 90 min. The inhibition was then released by 1000-fold dilution of the inhibitor with fresh medium, so that the effect of phenethyl alcohol became negligible. After this dilution, the synchronous culture started to grow again. Aliquots of ampicillin solution were added to yield concentrations of 1.25 and 1.5 μg/mL when the viable count had doubled. Generation curves similar to that of the nonsynchronous culture were observed (Fig. 10).

DISCUSSION

The apparent drug-affected generation curves for *E. coli* treated with β-lactam antibiotics seem to be the summation of the viable counts for drug-susceptible and drug-resistant organisms (Fig. 1). Based on this hypothesis, a mathematical model for the generation curve is presented in Fig. 6. The apparent number of viable counts can be expressed by:

$$N_{app} = Ns + Nr \qquad \text{(Eq. 3)}$$

where Ns and Nr are the numbers of susceptible and resistant organisms, respectively. When t is in the range of $L_1 \leqq t \leqq L_2$:

$$Ns = Ns_0 \cdot e^{k_{app}(t-L_1)} \qquad \text{(Eq. 4)}$$

$$Nr = Nr_0 \qquad \text{(Eq. 5)}$$

Here, $t = 0$ when the drug is added. Substitution of Eqs. 4 and 5 into Eq. 3 yields Eq. 1 (when t is $t > L_2$):

$$Ns = Ns_0 \cdot e^{k_{app}(t-L_1)} \quad \text{(Eq. 6)}$$

$$Nr = Nr_0 \cdot e^{k_g(t-L_2)} \quad \text{(Eq. 7)}$$

Replacement of Ns and Nr in Eq. 3 by Eqs. 6 and 7 gives Eq. 2.

Although the observed points were scattered around the simulation curve generated from Eq. 1 by incorporating the appropriate parameters (Table I), it appears that the apparent generation curves can be reasonably well described by the present mathematical model.

Garrett and Won (2) have reported the development of penicllin-resistant organisms and proposed the following possible explanation for the regrowth phenomenon: (*a*) the consumption or degradation of drugs, (*b*) production of an inhibitor or inactivator of antibiotic action, (*c*) preexistence of drug-resistant bacteria, and (*d*) acquisition of drug resistance through mutation and/or adaptation by exposure to the drug. Besides these factors, the cell cycle (*e*) may be an important factor in regrowth after the first addition of drug.

In the present study, the drug concentration was kept constant during the experiment by using a dialysis membrane tube containing drug solution. Therefore, possibility *a* is ruled out.

The regrowth pattern appears to depend on the drug concentration (Figs. 2 and 3). The organism, once it acquired resistance after the first drug addition, retained resistance to concentrations below that of the first addition (Figs. 2 and 3), and this persisted for at least 48 h during subculture (Fig. 4). These observations and the population diagram of the resistant organisms (Fig. 5) seem to support the preexistence of insensitive bacteria with different degrees of resistance, although possibilities *b*, *d*, and *e* cannot be excluded completely on the basis of the results shown in Figs. 2–4 and 7.

The subcultured organism from a single colony showed similar apparent regrowth (Fig. 8). The possibility of picking up an organism originally resistant to the ampicillin concentration of 1.5 μg/mL is very small, because the number of organisms which may manifest resistance to 1.5 μg of ampicillin/mL is expected to be <10, judging from the population diagram (Fig. 7).

The possibility of mutation and/or adaptation may be ruled out by the MIC determinations on subcultured organisms. If the resistance was acquired by mutation and/or adaptation, the MIC should increase gradually during repeated subcultures, but in fact it did not change. Furthermore, when the drug was added just at the doubling time (DNA synthesis stage) of the synchronous culture, a similar generation curve was obtained (Fig. 10); so, possibility *e* was ruled out.

The possibility of β-lactamase production still remains; therefore, we assayed β-lactamase activity by using resistant organisms generated with 8 μg of penicillin G/mL, but β-lactamase activity was not detected in the crude preparation. This result excludes the possibility that β-lactamase may have been induced by contact with the drug, leading to the acquisition of resistance.

The remaining and most probable explanation for the bacterial regrowth after the addition of the drug is a selection process and/or change of membrane permeability caused by contact with the drug at various concentrations.

Zimmermann (10) and Sawai *et al.* (11, 12) have reported an indirect method for measuring the outer membrane permeability of β-lactam antibiotics, but it is necessary to use β-lactamase-producing organisms. To confirm the difference in degree of permeability between sensitive and resistant organisms, a direct measurement of membrane permeability is desirable; however, a direct method for such measurement is not available at present.

REFERENCES

(1) A. Tsuji, S. Hamano, T. Asano, E. Nakashima, T. Yamana, and S. Mitsuhashi, *J. Pharm. Sci.*, **73**, 1418 (1984).

(2) E. R. Garrett and C. M. Won, *J. Pharm. Sci.*, **62**, 1666 (1973).

(3) E. R. Garrett and L. K. Lewis, *J. Pharm. Sci.*, **64**, 1936 (1975).

(4) F. Leitner, R. A. Goodhines, R. E. Buck, and K. Price, *J. Antibiot.*, **32**, 718 (1979).

(5) A. E. Elkhouly and C. Führer, *J. Antibiot.*, **31**, 229 (1978).

(6) M. N. Gwynn, Lynn T. Webb, and G. N. Rolinson, *J. Infect. Dis.*, **144**, 263 (1981).

(7) "Beta-Lactam Antibiotics," S. Mitsuhashi, Ed., Japan Scientific Societies Press, 1981.

(8) M. Tajima, S. Masuyoshi, M. Inoue, Y. Takenouchi, S. Sugawara, and S. Mitsuhashi, *J. Gen. Microbiol.*, **126**, 179 (1981).

(9) R. W. Treick and W. A. Konetzka, *J. Bacteriol.*, **88**, 1580 (1964).

(10) W. Zimmermann, *Int. J. Clin. Pharm. Biopharm.*, **17**, 131 (1979).

(11) T. Sawai, K. Matsuba, and S. Yamagishi, *J. Antibiot.*, **30**, 1134 (1977).

(12) T. Sawai, K. Matsuba, A. Tamura, and S. Yamagishi, *J. Antibiot.*, **32**, 59 (1979).

ACKNOWLEDGMENTS

The authors are indebted to Dr. M. Inoue, School of Medicine, Gunma University, Gunma, Japan, for valuable advice on the preparation of synchronous cell cultures. The authors also thank Miss M. Takeda and Miss K. Wakiya for technical assistance.

Spectrofluorometric Determination of Captopril Plus Captopril Disulfide Metabolites in Plasma

EUGENE IVASHKIV

Received January 7, 1983, from *The Squibb Institute for Medical Research, New Brunswick, NJ 08903.* Accepted for publication October 31, 1983.

Abstract □ Captopril disulfides and the drug covalently bound to proteins were reduced with tri-*n*-butylphosphine. After sample purification on an XAD-2 column, captopril was treated with 1-(7-dimethylamino)-4-methyl-2-oxo-2*H*-1-benzopyran-3-yl)-1*H*-pyrrole-2,5-dione to form a fluorescent derivative. After acidification, the fluorescent derivative was extracted into toluene and purified on a C_{18} cartridge. The fluorescence of the dimethylformamide eluate was measured at an excitation wavelength of 380 nm and a fluorescence wavelength of 440 nm.

Keyphrases □ Captopril—spectrofluorometric analysis, plasma □ Angiotensin-converting enzyme inhibitors—captopril, spectrofluorometric analysis, plasma

Captopril (1-[(2*S*)-3-mercapto-2-methylpropionyl]-L-proline; I) a potent, specific, and orally active inhibitor of angiotensin-converting enzyme, has been shown (1) by *in vitro* and *in vivo* metabolism studies to exist in blood as unchanged drug, symmetrical disulfide, captopril–cysteine and captopril–glutathione mixed disulfides, and as captopril covalently bound to plasma albumin by S—S linkages. It has been reported that the plasma proteins and mixed disulfides with endogenous thiol compounds may act as a reservoir from which captopril is liberated over time to exert pharmacological effects (2, 3).

Several methods for determining captopril have been re-

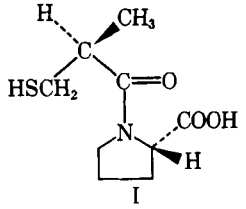

I

0022-3549/84/1000-1427$01.00/0

© 1984, American Pharmaceutical Association

$$Ns = Ns_0 \cdot e^{k_{app}(t-L_1)} \quad \text{(Eq. 6)}$$

$$Nr = Nr_0 \cdot e^{k_g(t-L_2)} \quad \text{(Eq. 7)}$$

Replacement of Ns and Nr in Eq. 3 by Eqs. 6 and 7 gives Eq. 2.

Although the observed points were scattered around the simulation curve generated from Eq. 1 by incorporating the appropriate parameters (Table I), it appears that the apparent generation curves can be reasonably well described by the present mathematical model.

Garrett and Won (2) have reported the development of penicllin-resistant organisms and proposed the following possible explanation for the regrowth phenomenon: (*a*) the consumption or degradation of drugs, (*b*) production of an inhibitor or inactivator of antibiotic action, (*c*) preexistence of drug-resistant bacteria, and (*d*) acquisition of drug resistance through mutation and/or adaptation by exposure to the drug. Besides these factors, the cell cycle (*e*) may be an important factor in regrowth after the first addition of drug.

In the present study, the drug concentration was kept constant during the experiment by using a dialysis membrane tube containing drug solution. Therefore, possibility *a* is ruled out.

The regrowth pattern appears to depend on the drug concentration (Figs. 2 and 3). The organism, once it acquired resistance after the first drug addition, retained resistance to concentrations below that of the first addition (Figs. 2 and 3), and this persisted for at least 48 h during subculture (Fig. 4). These observations and the population diagram of the resistant organisms (Fig. 5) seem to support the preexistence of insensitive bacteria with different degrees of resistance, although possibilities *b*, *d*, and *e* cannot be excluded completely on the basis of the results shown in Figs. 2–4 and 7.

The subcultured organism from a single colony showed similar apparent regrowth (Fig. 8). The possibility of picking up an organism originally resistant to the ampicillin concentration of 1.5 μg/mL is very small, because the number of organisms which may manifest resistance to 1.5 μg of ampicillin/mL is expected to be <10, judging from the population diagram (Fig. 7).

The possibility of mutation and/or adaptation may be ruled out by the MIC determinations on subcultured organisms. If the resistance was acquired by mutation and/or adaptation, the MIC should increase gradually during repeated subcultures, but in fact it did not change. Furthermore, when the drug was added just at the doubling time (DNA synthesis stage) of the synchronous culture, a similar generation curve was obtained (Fig. 10); so, possibility *e* was ruled out.

The possibility of β-lactamase production still remains; therefore, we assayed β-lactamase activity by using resistant organisms generated with 8 μg of penicillin G/mL, but β-lactamase activity was not detected in the crude preparation. This result excludes the possibility that β-lactamase may have been induced by contact with the drug, leading to the acquisition of resistance.

The remaining and most probable explanation for the bacterial regrowth after the addition of the drug is a selection process and/or change of membrane permeability caused by contact with the drug at various concentrations.

Zimmermann (10) and Sawai *et al.* (11, 12) have reported an indirect method for measuring the outer membrane permeability of β-lactam antibiotics, but it is necessary to use β-lactamase-producing organisms. To confirm the difference in degree of permeability between sensitive and resistant organisms, a direct measurement of membrane permeability is desirable; however, a direct method for such measurement is not available at present.

REFERENCES

(1) A. Tsuji, S. Hamano, T. Asano, E. Nakashima, T. Yamana, and S. Mitsuhashi, *J. Pharm. Sci.*, **73**, 1418 (1984).

(2) E. R. Garrett and C. M. Won, *J. Pharm. Sci.*, **62**, 1666 (1973).

(3) E. R. Garrett and L. K. Lewis, *J. Pharm. Sci.*, **64**, 1936 (1975).

(4) F. Leitner, R. A. Goodhines, R. E. Buck, and K. Price, *J. Antibiot.*, **32**, 718 (1979).

(5) A. E. Elkhouly and C. Führer, *J. Antibiot.*, **31**, 229 (1978).

(6) M. N. Gwynn, Lynn T. Webb, and G. N. Rolinson, *J. Infect. Dis.*, **144**, 263 (1981).

(7) "Beta-Lactam Antibiotics," S. Mitsuhashi, Ed., Japan Scientific Societies Press, 1981.

(8) M. Tajima, S. Masuyoshi, M. Inoue, Y. Takenouchi, S. Sugawara, and S. Mitsuhashi, *J. Gen. Microbiol.*, **126**, 179 (1981).

(9) R. W. Treick and W. A. Konetzka, *J. Bacteriol.*, **88**, 1580 (1964).

(10) W. Zimmermann, *Int. J. Clin. Pharm. Biopharm.*, **17**, 131 (1979).

(11) T. Sawai, K. Matsuba, and S. Yamagishi, *J. Antibiot.*, **30**, 1134 (1977).

(12) T. Sawai, K. Matsuba, A. Tamura, and S. Yamagishi, *J. Antibiot.*, **32**, 59 (1979).

ACKNOWLEDGMENTS

The authors are indebted to Dr. M. Inoue, School of Medicine, Gunma University, Gunma, Japan, for valuable advice on the preparation of synchronous cell cultures. The authors also thank Miss M. Takeda and Miss K. Wakiya for technical assistance.

Spectrofluorometric Determination of Captopril Plus Captopril Disulfide Metabolites in Plasma

EUGENE IVASHKIV

Received January 7, 1983, from *The Squibb Institute for Medical Research, New Brunswick, NJ 08903.* Accepted for publication October 31, 1983.

Abstract □ Captopril disulfides and the drug covalently bound to proteins were reduced with tri-*n*-butylphosphine. After sample purification on an XAD-2 column, captopril was treated with 1-(7-dimethylamino)-4-methyl-2-oxo-2*H*-1-benzopyran-3-yl)-1*H*-pyrrole-2,5-dione to form a fluorescent derivative. After acidification, the fluorescent derivative was extracted into toluene and purified on a C_{18} cartridge. The fluorescence of the dimethylformamide eluate was measured at an excitation wavelength of 380 nm and a fluorescence wavelength of 440 nm.

Keyphrases □ Captopril—spectrofluorometric analysis, plasma □ Angiotensin-converting enzyme inhibitors—captopril, spectrofluorometric analysis, plasma

Captopril (1-[(2*S*)-3-mercapto-2-methylpropionyl]-L-proline; I) a potent, specific, and orally active inhibitor of angiotensin-converting enzyme, has been shown (1) by *in vitro* and *in vivo* metabolism studies to exist in blood as unchanged drug, symmetrical disulfide, captopril–cysteine and captopril–glutathione mixed disulfides, and as captopril covalently bound to plasma albumin by S—S linkages. It has been reported that the plasma proteins and mixed disulfides with endogenous thiol compounds may act as a reservoir from which captopril is liberated over time to exert pharmacological effects (2, 3).

Several methods for determining captopril have been re-

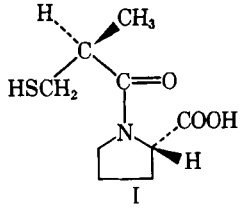

I

0022-3549/84/1000-1427$01.00/0

© 1984, American Pharmaceutical Association

Table I—Fluorescence of Captopril–Reagent as a Function of Concentration

Captopril, μg/mL of Plasma	Fluorescence at 380/440 nm
10.0	110[a]
8.0	88
6.0	64
4.0	46
2.0	22
0	0
1.0	100[b]
0.8	81
0.6	59
0.4	40.5
0.2	20.0
0	0

[a] Sensitivity 1, for concentrations of 0–10 μg/mL. [b] Sensitivity 4, for concentrations of 0–1 μg/mL.

ported, including GC–MS (4), GC (5), and HPLC (6–8). However, total captopril in plasma can be determined only after reduction of captopril disulfides and drug covalently bound to proteins. Tri-*n*-butylphosphine, used for reduction of captopril disulfides in urine (6), is also effective in plasma because it can penetrate the hydrophobic regions of proteins (9).

A rapid and simple analytical method is needed for measuring microgram levels of captopril plus disulfide metabolites in the plasma of patients during prolonged therapy (8), when the drug accumulates. Since all published methods for determination of captopril require expensive instrumentation not available to small hospital laboratories, a fluorometric method for measuring captopril plus disulfide metabolites in plasma has been developed.

EXPERIMENTAL SECTION

Apparatus—Fluorometric measurements were performed on a spectrofluorometer[1]. Samples were shaken on a heavy-duty shaker[2]. A centrifuge[3], 150- and 200-mm test tubes and plastic screw caps with polytef-faced rubber liners[2], 20-mL scintillation vials[2], C_{18} cartridges[4], 10-mL plastic syringes with 21-gauge needles, XAD-2 columns[5], and a water bath[6] set at 50°C were used.

Reagents—Acetone, toluene, hydrochloric acid, phosphoric acid, dimethylformamide, Tris buffer, urea, dibasic sodium phosphate heptahydrate, EDTA, and diethylenetriaminepentaacetic acid were reagent grade. 1-(7 - (Dimethylamino)-4-methyl-2-oxo- 2*H* -1-benzopyran-3-yl)-1*H*-pyrrole-2,5-dione reagent[7] (10 mg dissolved in 10 mL of acetone) was stable in a refrigerator for at least 1 year. A 20% v/v solution of tri-*n*-butylphosphine[8] was prepared in a fume hood by diluting 2 mL of the reagent with 8 mL of acetone.

A 0.1 M, pH 8.2, buffer was made by dissolving 12.1 g of Tris in 980 mL of distilled water; the pH was adjusted with phosphoric acid, and the buffer was diluted to 1 L with distilled water. Urea buffer, for reduction, was prepared daily by dissolving 20 g of urea in 0.1 M, pH 8.2, Tris buffer and diluting to 50 mL. HCl (0.1 M) with EDTA was prepared by adding 100 mg of the disodium salt per liter of acidic solution. A 0.05 M, pH 6.9, phosphate–dimethylformamide buffer was made by dissolving 20 g of dibasic sodium phosphate heptahydrate and 100 mg of diethylenetriaminepentaacetic acid in 650 mL of distilled water and adding 350 mL of dimethylformamide; the pH was adjusted with phosphoric acid. Column activator concentrate[5], 35 mL, was diluted to 500 mL with distilled water and kept in a refrigerator. Plasma was prepared from whole blood using citric acid as anticoagulant. A captopril disulfide[9] standard solution (20 μg/mL) was prepared in methanol and kept in a refrigerator no longer than 3 months.

[1] Model 204; Perkin-Elmer.
[2] Fisher Scientific.
[3] International IEP2741.
[4] SEP-PAK; Waters Associates, Inc.
[5] Brinkmann Instruments.
[6] Organomation Associates, Inc.
[7] Polysciences, Inc.
[8] Strem Chemicals, Inc.
[9] The Squibb Institute for Medical Research.

Table II—Recovery of Captopril and Disulfides from Plasma

Drug or Metabolite	Amount Added, μg/mL	Amount Found, μg/mL	Recovery, %
Captopril	5.0	4.90	98.0
	2.5	2.43	97.2
	1.0	0.98	98.0
	0.5	0.48	96.0
	0.25	0.26	104.0
Captopril Disulfide	5.00	4.96	99.2
	2.5	2.42	96.8
	1.0	0.97	97.0
	0.5	0.49	98.0
	0.25	0.25	100.0
Captopril–Glutathione	12.0	11.70	97.5
	6.0	5.70	95.0
	3.0	2.96	98.7
Captopril–Cysteine	8.0	7.80	97.5
	4.0	3.90	97.5
	2.0	1.93	96.5
Plasma Blank	0	0	—

Preparation of Columns—The protective cotton was removed from an XAD-2 column, and the column was placed on a 200-mm test tube. The diluted column activator (5 mL) was passed through the column, and the column was washed with 5 mL of 0.1 M HCl containing EDTA. Before use, a 21-gauge syringe needle was placed on the tip of the column. Columns were prepared on the day used.

Reduction—Plasma samples and one plasma blank were thawed, and 1.0 mL was transferred to a 20-mL scintillation vial. Urea buffer (5 mL) was added to each vial, followed by 0.1 mL of 20% tri-*n*-butylphosphine solution. Captopril disulfide standard solution (0.10 mL) was added to the plasma blank. The scintillation vials were covered with tin-lined plastic caps, and the samples were mixed on a vortex mixer. The vials were placed in a 50 ± 3°C water bath with the water level at half the height of the vials. The reduction was allowed to take place in the dark for 1 h.

Isolation, Purification, and Derivatization—The samples and standard were removed from the water bath and 5 mL of 0.66 M phosphoric acid was added immediately to each vial. The vials were capped and gently inverted four times to mix the acid. The solutions were decanted onto separate activated XAD-2 columns. Five milliliters of 0.1 M HCl containing EDTA was added to each vial, and the vials were then gently inverted four times.

After each sample passed through a column, the 0.1 M HCl wash was decanted onto the appropriate column. After all the wash had passed through the columns, the syringe needles were removed. The columns were washed with 10 mL and then 20 mL of 0.1 M HCl, placed on 150-mm screw-cap culture tubes, centrifuged at ~1000 rpm for 4 min, and then placed on clean 150-mm screw-cap culture tubes containing 0.1 mL of the reagent. To each column, 10.0 mL of 0.05 M pH 6.9 buffer was added. From time to time, the eluates were gently mixed with the reagent during elution[10]. The reagent blank was prepared in a 150-mm screw-cap culture tube by adding 10 μL of the reagent solution to 1.0 mL of 0.05 M pH 6.9 buffer and mixing.

Extraction of Captopril Derivative—After 10 min, 1.0 mL of each sample and the standard were transferred to 150-mm screw-cap culture tubes. One milliliter of 1.98 M phosphoric acid and 10.0 mL of toluene were added to each sample, standard, and blank. The tubes were shaken on a shaker for 5 min and centrifuged at ~1800 rpm for 5 min.

Purification on C_{18} Cartridges—A C_{18} cartridge was attached to a 10-mL syringe with the plunger removed. The syringe with the cartridge was placed on a 200-mm test tube, and 8.0 mL of toluene extract was transferred to it. The solution passed through the column by gravity; occasionally it was necessary to initiate flow through the cartridge with a plunger. After all the extract passed through the cartridge, 5 mL of toluene was added. At the end of the washing, the remaining toluene was forced out with the plunger and discarded. Each cartridge and syringe was placed on a fresh 200-mm test tube. Dimethylformamide (5.0 mL) was added to each syringe. The solvent was allowed to pass through the column by gravity, and at the end of the elution, the remaining solvent was forced out with the plunger. The eluates were mixed on the vortex mixer.

Fluorescence Measurement and Calculations—Fluorescence of the samples and standard was measured at an excitation wavelength of 380 nm and a fluorescence wavelength of 440 nm using the reagent blank to set the instru-

[10] Sometimes it is necessary to initiate flow through the columns by pressure from the palm of the hand or a rubber bulb.

Table III—Reproducibility of Results [a]

Run	Fluorescence at 380/440 nm
1	54.0
2	53.5
3	53.8
4	55.0
5	56.0
6	54.2
Mean	54.4
SD	0.93
CV	1.7%

[a] Replicate assay of 2 μg of captopril disulfide/mL of plasma.

ment to zero fluorescence. The concentration of captopril per milliliter of plasma was calculated from the concentration and fluorescence of a captopril disulfide standard with the same instrument settings used for the sample and standard measurements.

RESULTS AND DISCUSSION

Captopril has no native fluorescence and a very low absorbance in the UV region. Fluorescence can be obtained by reacting captopril with maleimide derivatives such as *N*-(*p*-2-benzimidazolyl)phenylmaleimide, *N*-(3-pyrene)-maleimide, *N*-[*p*-(2-benzoxozolyl)phenylmaleimide, and 1-(7-(dimethylamino)-4-methyl-2-oxo-2*H*-1-benzopyran-3-yl)-1*H*-pyrrole-2,5-dione which react with the sulfhydryl group. Because of low water solubility, none of these reagents can be used for reaction of captopril in blood.

Among fluorescent-labeling sulfhydryl reagents, 1-(7-(dimethylamino)-4-methyl-2-oxo-2*H*-1-benzopyran-3-yl)-1*H*-pyrrole-2,5-dione was selected for analysis of captopril in serum. It provides good sensitivity and is stable during all steps of the procedure. The synthesis of this reagent was described by Machida *et al.* (10).

Captopril reacts with the reagent on a mole per mole basis. Excess reagent was used to speed up the reaction and to account for some impurities in column eluates, which can consume the reagent. The reaction of captopril with the reagent under the assay conditions was complete in ~15 min. The reaction product is stable in the mixture for at least 1 h. When solutions are acidified and stored in a refrigerator, the product is stable for at least 24 h.

The fluorescent adduct can be extracted from acidified solutions with many water-immiscible solvents such as ethyl acetate, toluene, and dichloromethane. Toluene was chosen because of its selectivity; it extracts very few impurities from aqueous reaction solutions. The captopril–reagent derivative is stable in toluene for at least 24 h, and the adduct can be absorbed quantitatively from toluene onto C_{18} cartridges. The excitation and fluorescence maximum wavelengths of the captopril–reagent adduct vary with the solvent. In dimethylformamide it is 380/440 nm.

Standard curves were prepared in the ranges of 0–1 μg and 0–10 μg of captopril/mL of plasma. Concentrations in the ranges tested produced straight lines that passed through the origin. Data for the standard curves are given in Table I.

The sulfhydryl group of captopril is very reactive. It can react with blood components or be oxidized to captopril disulfide and mixed disulfides. If the sulfhydryl group is not protected immediately after blood is drawn from the patient, the free captopril is oxidized to disulfides. A considerable amount of captopril is covalently bound to plasma proteins.

In vitro experiments show that when ^{14}C-labeled captopril, symmetrical disulfide, and captopril–cysteine mixed disulfide were added to plasma, after 1 week of storage at 5°C, 32% of captopril was covalently bound to plasma proteins and 68% remained as disulfides. In samples stored at −20°C, 68% of the captopril was bound to plasma proteins and 32% remained as disulfides. After 4 weeks of storage, 62% of captopril was bound to plasma proteins at 5°C and 87% at −20°C.

Interchange between the —SH groups of plasma proteins and captopril disulfides can occur. After 4 weeks of storage at 5°C and −20°C, a complete interchange between captopril and captopril–cysteine occurred; 43% of captopril was interchanged for symmetrical captopril disulfide. The *S*-methyl metabolite of captopril is stable in plasma.

To determine total captopril in plasma with the reagent, samples have to be reduced. Tri-*n*-butylphosphine was chosen as the reducing agent because it is a potent agent for the cleavage of captopril disulfide, captopril mixed disulfides, and drug covalently bound to proteins. One mole of tri-*n*-butylphosphine reduces 1 mol of disulfide, and the reaction is relatively rapid and quantitative.

The reduction of disulfides with tri-*n*-butylphosphine is pH and temperature dependent. Almost complete reduction of captopril disulfide is obtained in solutions at pH >8. It takes ~30 min to reduce captopril disulfide with 20 mg of tri-*n*-butylphosphine/mL of plasma at 50°C and ~45 min to reduce captopril bound to proteins. About 96% of the drug is reduced at this concentration. With 2 mg of tri-*n*-butylphosphine/mL of plasma, only 50% reduction is obtained. At room temperature, only ~85% of the plasma sample is reduced. Increasing the temperature to 70°C does not have any effect on the reaction. The volume of urea–Tris buffer up to 10 mL has no effect on the reduction efficiency. However, volumes of plasma >1 mL cause incomplete reduction of captopril disulfides.

Captopril was isolated from the tri-*n*-butylphosphine mixture and purified on XAD-2 resin before it was treated with the reagent. Captopril was retained on XAD-2 resin, while other compounds containing the sulfhydryl group passed through the column. The optimum pH for adsorption of captopril on XAD-2 resin is 0.5–2.5. The adsorptive power of the resin is optimized by the incorporation of a column prewash using an activator solution.

The unimpeded flow rate of the diluted sample through the column would be ~5 mL/min. This is too fast for complete retention of the drug on the resin. The flow rate is reduced to ~1 mL/min with a 21-gauge syringe needle.

Captopril can be quantitatively eluted from XAD resin with dioxane, methanol, ethanol, ethyl acetate, acetonitrile, acetone, isopropyl alcohol, tetrahydrofuran, dichloromethane, chloroform, and other solvents. Some of them elute interfering compounds. However, captopril does not react with fluorescent labels in any of these solvents; it reacts only in aqueous solutions. Removal of organic solvents by evaporation, even under controlled conditions, results in the oxidation of captopril. A 0.05 M phosphate buffer containing dimethylformamide proved to be a suitable eluant. It elutes captopril quantitatively from XAD-2 resin and provides a proper pH and medium for the reaction with the reagent. Up to 35% dimethylformamide does not interfere with the reaction. About 10 mL of dimethylformamide–phosphate buffer, pH 6.9, is needed for complete elution of captopril; ~2 mL of solvent is retained by the column. Therefore, before and after elution, columns must be centrifuged. Captopril is eluted from columns into tubes containing ~100 μg of reagent to prevent reoxidation of the drug. However, if needed, samples can be first eluted, gently mixed by four inversions, and 1 mL of eluate treated with 10 μg of the reagent.

Samples have to be further purified by extraction of the captopril–reagent derivative from the acidic solution with toluene. For complete extraction of the adduct, the ratio of aqueous solution to toluene should be 1:10. Excess reagent and some remaining impurities are removed with C_{18} cartridges. The

Table IV—Total Captopril in Human Plasma Measured by Fluorometric and GC–MS Methods [a]

Patient	Total Captopril, ng/ml		Δ (GC–MS − Fluorometry)	$\frac{\Delta}{\text{Mean}} \times 100$, %
	Fluorometry	GC–MS		
B439 096	769	738	−31	−4.1
100	544	558	+14	+2.5
124	213	217	+4	+1.9
150	523	499	−24	−4.7
201	715	702	−13	−1.8
229	171	157	−14	−8.5
262	539	551	+12	+2.2
301	656	658	+2	+0.3
312	512	505	−7	−1.4
313	650	673	+23	+3.5
338	600	628	+28	+4.6
380	560	554	−6	−1.1
	Mean absolute difference, %			3.05

[a] Patients received 100 mg of captopril orally.

captopril-reagent derivative adsorbs onto the cartridge packing from toluene and can be eluted with dimethylformamide.

A plasma sample with standard captopril disulfide (2 μg/mL) is run along with samples to compensate for incomplete reduction. If high (off scale) fluorescence readings from the sample are obtained, eluates from the cartridges can be diluted to proper concentration with dimethylformamide.

Recovery experiments were carried out by addition of various concentrations of captopril, captopril disulfide, captopril-cysteine disulfide, or captopril-glutathione disulfide to plasma. These were kept at room temperature for 4 h then stored at 5°C overnight. Results are shown in Table II. Recoveries ranged from 95 to 104%.

Reproducibility was checked by performing six assays of a plasma sample spiked with captopril disulfide at 2 μg/mL (Table III). Precision at this concentration is 1.7% (*CV*).

Results obtained by the fluorometric method were compared with those obtained by the GC–MS method (Table IV). The data were correlated by linear regression analysis, which yielded an intercept of 5.6, a slope of 0.9914, and a correlation coefficient of 0.9949. Agreement between the methods is acceptable.

Although the fluorometric method is very sensitive (because as little as 2 ng of a pure captopril standard/mL of dimethylformamide solution can be accurately measured in a 1-cm cell, without HPLC separation), the method can be used for measuring captopril in plasma containing >200 ng of the drug/mL. Therefore, it is suitable for patients who accumulate captopril during extended therapy and have microgram per milliliter levels of captopril plus disulfide metabolites in plasma. It can be especially useful to the small hospital laboratory which does not have expensive instrumentation (such as GC–MS) available.

REFERENCES

(1) H. Shindo, T. Komal, T. Ideka, W. Kawamata, and E. Kameyama, "Proceedings of the 11th Symposium on Drug Metabolism and Action," Nagoya, Japan, November 1979.

(2) B. K. Park, P. S. Grabowski, J. H. K. Yeung, and A. M. Brechenridge, *Biochem. Pharmacol.*, **31**, 1755 (1982).

(3) K. L. Duchin, S. M. Singhvi, D. A. Willard, B. H. Migdalof, and D. N. McKinstry, *Clin. Pharmacol. and Ther.*, **31**, 452 (1982).

(4) P. T. Funke, E. Ivashkiv, M. Malley, and A. I. Cohen, *Anal. Chem.*, **52**, 1086 (1980).

(5) Y. Matsuki, K. Fukuhara, T. Ito, H. Ono, N. Ohara, and T. Yui, *J. Chromatogr.* **188**, 177 (1980).

(6) Y. Kawahara, M. Hisaoka, Y. Yamazaki, A. Inage, and T. Morioka, *Chem. Pharm. Bull.*, **29**, 150 (1981).

(7) B. Jarrott, A. Anderson, R. Hooper, and W. J. Louis, *J. Pharm. Sci.*, **70**, 665 (1981).

(8) K. Onoyama, H. Hirakata, K. Iseki, S. Fujimi, T. Omae, M. Kobayashi, and Y. Kawahara, *Hypertension*, **3**, 456 (1981).

(9) B. J. Sweetman and J. A. Maclaren, *Aust. J. Chem.*, **19**, 2347 (1966).

(10) M. Machida, N. Ushijima, M. I. Machida, and Y. Kanaoka, *Chem. Pharm. Bull.*, **23**, 1385 (1975).

ACKNOWLEDGMENTS

The author thanks A. I. Cohen for his technical advice and the GC–MS correlation results. The author also thanks P. Egli, Drug Metabolism, for a generous supply of radioactive captopril and its disulfides.

Reverse-Phase High-Performance Liquid Chromatographic Determination of Halogenated 8-Hydroxyquinoline Compounds in Pharmaceuticals and Bulk Drugs

EDWARD J. WOJTOWICZ

Received August 23, 1983, from the *Food and Drug Administration, 599 Delaware Avenue, Buffalo, NY 14202.* Accepted for publication December 6, 1983.

Abstract □ A reverse-phase high-performance liquid chromatographic (HPLC) method was developed for determining iodochlorhydroxyquin, 5,7-dichloro-8-hydroxyquinoline, and 5,7-diiodo-8-hydroxyquinoline in creams, ointments, shampoos, tablets, and bulk drugs. A column packed with 10-μm phenyl-silica and a mobile phase of 0.001 M $NiCl_2$ in acetonitrile–methanol–water (30:20:50) was used to separate the nickel complexes of the three drugs, with detection at 273 nm. Analysis of creams, ointments, shampoos, and tablets gave results close to the label declarations. Recovery of standard material added to samples was ≥98%. Linearity of response was shown over a range of 30–150% of label claim for standards of the three drug substances. Multiple analyses of iodochlorhydroxyquin and diiodohydroxyquinoline bulk drugs showed purities of 99.96 and 98.77% with *CV* of 1.17 and 0.73%, respectively. The HPLC method offers an alternative to current USP procedures, which lack stability-indicating and specificity characteristics.

Keyphrases □ HPLC—Halogenated 8-hydroxyquinoline compounds □ 8-Hydroxyquinoline—halogenated, HPLC

The current USP XX IR spectrophotometric procedure (1) for determining iodochlorhydroxyquin (I) in creams and ointments has many deficiencies, as reported by Gruber *et al.* (2), who used GC to determine trimethylsilyl ether derivatives of related halogenated 8-hydroxyquinolines. A colorimetric procedure (3) complexed I with nickel ion. However, other 8-hydroxyquinolines, present as impurities, would interfere to give high results. A normal-phase high-performance liquid chromatographic (HPLC) procedure (4) involved esterification of I using a mixture of pyridine–acetic anhydride, an evaporation step, and a reconstitution of the residue in the mobile phase. Procedures using anion-exchange HPLC (5, 6) and reverse-phase HPLC (7, 8) failed to adequately separate I from other 8-hydroxyquinolines.

In this study, a simple and specific reverse-phase HPLC method was developed to separate and quantitate iodochlorhydroxyquin (I), 5,7-dichloro-8-hydroxyquinoline (II), and 5,7-diiodo-8-hydroxyquinoline (III) as their nickel complexes

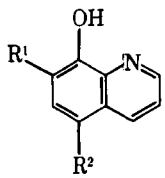

I, $R^1 = I$, $R^2 = Cl$
II, $R^1 = R^2 = Cl$
III, $R^1 = R^2 = I$
IV, $R^1 = H$, $R^2 = Cl$
V, $R^1 = R^2 = H$
I.S., $(C_6H_5)_2NH$

0022-3549/84/1000-1430$01.00/0

© 1984, American Pharmaceutical Association

captopril-reagent derivative adsorbs onto the cartridge packing from toluene and can be eluted with dimethylformamide.

A plasma sample with standard captopril disulfide (2 μg/mL) is run along with samples to compensate for incomplete reduction. If high (off scale) fluorescence readings from the sample are obtained, eluates from the cartridges can be diluted to proper concentration with dimethylformamide.

Recovery experiments were carried out by addition of various concentrations of captopril, captopril disulfide, captopril-cysteine disulfide, or captopril-glutathione disulfide to plasma. These were kept at room temperature for 4 h then stored at 5°C overnight. Results are shown in Table II. Recoveries ranged from 95 to 104%.

Reproducibility was checked by performing six assays of a plasma sample spiked with captopril disulfide at 2 μg/mL (Table III). Precision at this concentration is 1.7% (*CV*).

Results obtained by the fluorometric method were compared with those obtained by the GC–MS method (Table IV). The data were correlated by linear regression analysis, which yielded an intercept of 5.6, a slope of 0.9914, and a correlation coefficient of 0.9949. Agreement between the methods is acceptable.

Although the fluorometric method is very sensitive (because as little as 2 ng of a pure captopril standard/mL of dimethylformamide solution can be accurately measured in a 1-cm cell, without HPLC separation), the method can be used for measuring captopril in plasma containing >200 ng of the drug/mL. Therefore, it is suitable for patients who accumulate captopril during extended therapy and have microgram per milliliter levels of captopril plus disulfide metabolites in plasma. It can be especially useful to the small hospital laboratory which does not have expensive instrumentation (such as GC–MS) available.

REFERENCES

(1) H. Shindo, T. Komal, T. Ideka, W. Kawamata, and E. Kameyama, "Proceedings of the 11th Symposium on Drug Metabolism and Action," Nagoya, Japan, November 1979.

(2) B. K. Park, P. S. Grabowski, J. H. K. Yeung, and A. M. Brechenridge, *Biochem. Pharmacol.*, **31**, 1755 (1982).

(3) K. L. Duchin, S. M. Singhvi, D. A. Willard, B. H. Migdalof, and D. N. McKinstry, *Clin. Pharmacol. and Ther.*, **31**, 452 (1982).

(4) P. T. Funke, E. Ivashkiv, M. Malley, and A. I. Cohen, *Anal. Chem.*, **52**, 1086 (1980).

(5) Y. Matsuki, K. Fukuhara, T. Ito, H. Ono, N. Ohara, and T. Yui, *J. Chromatogr.* **188**, 177 (1980).

(6) Y. Kawahara, M. Hisaoka, Y. Yamazaki, A. Inage, and T. Morioka, *Chem. Pharm. Bull.*, **29**, 150 (1981).

(7) B. Jarrott, A. Anderson, R. Hooper, and W. J. Louis, *J. Pharm. Sci.*, **70**, 665 (1981).

(8) K. Onoyama, H. Hirakata, K. Iseki, S. Fujimi, T. Omae, M. Kobayashi, and Y. Kawahara, *Hypertension*, **3**, 456 (1981).

(9) B. J. Sweetman and J. A. Maclaren, *Aust. J. Chem.*, **19**, 2347 (1966).

(10) M. Machida, N. Ushijima, M. I. Machida, and Y. Kanaoka, *Chem. Pharm. Bull.*, **23**, 1385 (1975).

ACKNOWLEDGMENTS

The author thanks A. I. Cohen for his technical advice and the GC–MS correlation results. The author also thanks P. Egli, Drug Metabolism, for a generous supply of radioactive captopril and its disulfides.

Reverse-Phase High-Performance Liquid Chromatographic Determination of Halogenated 8-Hydroxyquinoline Compounds in Pharmaceuticals and Bulk Drugs

EDWARD J. WOJTOWICZ

Received August 23, 1983, from the *Food and Drug Administration, 599 Delaware Avenue, Buffalo, NY 14202.* Accepted for publication December 6, 1983.

Abstract □ A reverse-phase high-performance liquid chromatographic (HPLC) method was developed for determining iodochlorhydroxyquin, 5,7-dichloro-8-hydroxyquinoline, and 5,7-diiodo-8-hydroxyquinoline in creams, ointments, shampoos, tablets, and bulk drugs. A column packed with 10-μm phenyl-silica and a mobile phase of 0.001 M $NiCl_2$ in acetonitrile–methanol–water (30:20:50) was used to separate the nickel complexes of the three drugs, with detection at 273 nm. Analysis of creams, ointments, shampoos, and tablets gave results close to the label declarations. Recovery of standard material added to samples was ≥98%. Linearity of response was shown over a range of 30–150% of label claim for standards of the three drug substances. Multiple analyses of iodochlorhydroxyquin and diiodohydroxyquinoline bulk drugs showed purities of 99.96 and 98.77% with *CV* of 1.17 and 0.73%, respectively. The HPLC method offers an alternative to current USP procedures, which lack stability-indicating and specificity characteristics.

Keyphrases □ HPLC—Halogenated 8-hydroxyquinoline compounds □ 8-Hydroxyquinoline—halogenated, HPLC

The current USP XX IR spectrophotometric procedure (1) for determining iodochlorhydroxyquin (I) in creams and ointments has many deficiencies, as reported by Gruber *et al.* (2), who used GC to determine trimethylsilyl ether derivatives of related halogenated 8-hydroxyquinolines. A colorimetric procedure (3) complexed I with nickel ion. However, other 8-hydroxyquinolines, present as impurities, would interfere to give high results. A normal-phase high-performance liquid chromatographic (HPLC) procedure (4) involved esterification of I using a mixture of pyridine–acetic anhydride, an evaporation step, and a reconstitution of the residue in the mobile phase. Procedures using anion-exchange HPLC (5, 6) and reverse-phase HPLC (7, 8) failed to adequately separate I from other 8-hydroxyquinolines.

In this study, a simple and specific reverse-phase HPLC method was developed to separate and quantitate iodochlorhydroxyquin (I), 5,7-dichloro-8-hydroxyquinoline (II), and 5,7-diiodo-8-hydroxyquinoline (III) as their nickel complexes

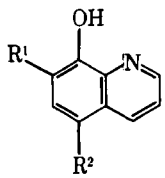

I, $R^1 = I$, $R^2 = Cl$
II, $R^1 = R^2 = Cl$
III, $R^1 = R^2 = I$
IV, $R^1 = H$, $R^2 = Cl$
V, $R^1 = R^2 = H$
I.S., $(C_6H_5)_2NH$

0022-3549/84/1000-1430$01.00/0

© 1984, American Pharmaceutical Association

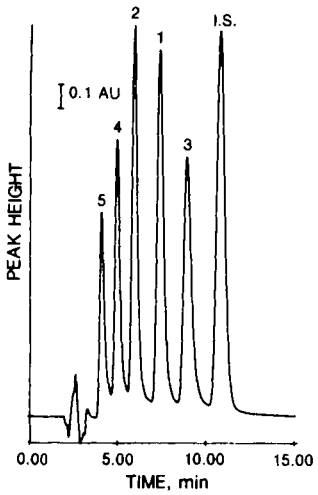

Figure 1—*Chromatogram of a mixture of iodochlorhydroxyquin (1), 5,7-dichloro-8-hydroxyquinoline (2), 5,7-diiodo-8-hydroxyquinoline (3), 5-chloro-8-hydroxyquinoline (4), 8-hydroxyquinoline (5), and diphenylamine (I.S.) determined at a detector setting of 0.1 AU and 273 nm.*

in bulk drug form and in pharmaceuticals. The HPLC system also resolved I, II, and III from 5-chloro-8-hydroxyquinoline (IV) and 8-hydroxyquinoline (V), which are precursors in the syntheses of bulk forms of the drugs.

EXPERIMENTAL SECTION

Materials—Nickel chloride hexahydrate[1], iodochlorhydroxyquin[2], 5,7-dichloro-8-hydroxyquinoline[3], 5,7-diiodo-8-quinolinol[2], 5-chloro-8-hydroxyquinoline[4], 8-hydroxyquinoline[4], and diphenylamine[5] were used as received. Methanol[6], acetonitrile[6], and tetrahydrofuran[6] were distilled in glass.

Chromatographic System—The liquid chromatographic system consisted of a high-pressure pump[7], a variable-wavelength UV detector[8], an integrator-recorder[9], and a phenyl column (10 μm, 30 cm × 3.9 mm)[10]. The mobile phase, 0.001 M $NiCl_2$, was prepared in acetonitrile–methanol–water (30:20:50) and filtered before use. The flow rate of the mobile phase was 1.2 mL/min. The detector was set at 273 nm and at a range of 0.1 AUFS. The integrator-recorder was used at an attenuation setting equal to 8 mV, a threshold value of 3, and a peak width setting of 0.16 in the peak height measuring mode.

Quantitative Procedure for Iodochlorhydroxyquin (I)—Ointment or cream samples containing an equivalent of 30 mg of I were dissolved with heating in 40–50 mL of tetrahydrofuran. The solutions were quantitatively transferred to 100-mL volumetric flasks and diluted to volume with tetrahydrofuran. An accurately weighed 30-mg portion of USP standard I was transferred to a 100-mL volumetric flask and diluted to volume with tetrahydrofuran. Five-milliliter aliquots of sample and standard preparations were transferred to separate 50-mL volumetric flasks. One milliliter of a 10-mg/mL methanolic solution of nickel chloride was added to each flask, and the flasks were shaken to disperse the reagent.

The complex formed between nickel and I produced a yellow solution. An internal standard solution of 80 mg of diphenylamine in 200 mL of methnol was prepared, and 5.0-mL portions were transferred into each 50-mL flask. The petrolatum base in ointments or creams precipitated when the internal standard solution was added. The flasks were diluted to volume with methanol. Injections were made from the final standard and filtered sample solutions. Peak height response relative to the internal standard was used to calculate the amount of I in the samples.

Quantitative Procedure for II—An accurately weighed portion of a shampoo, containing an equivalent of 30 mg of II, was dissolved with heating in 40–50 mL of methanol. The solution was quantitatively transferred to a 100-mL volumetric flask and diluted to volume with methanol. A standard of 30 mg of II was accurately weighed into a 100-mL volumetric flask and diluted to volume with methanol. Two-milliliter aliquots of the sample and standard preparations were transferred into separate 50-mL volumetric flasks. One milliliter of the methanolic nickel chloride reagent and 3.0 mL of the internal standard solution were added to the sample and standard flasks. The solutions were diluted to volume with methanol, and the samples were filtered before HPLC. Peak height response relative to the internal standard was used to quantitate II.

[1] ICN Pharmaceuticals, Inc., Plainview, N.Y.
[2] USP Reference Standard.
[3] Westwood Pharmaceuticals, Buffalo, N.Y.
[4] Pfaltz and Bauer, Stamford, Conn.
[5] Merck and Co, Rahway, N.J.
[6] Burdick and Jackson Laboratories, Muskegon, Mich.
[7] Model 6000A; Waters Associates, Milford, Mass.
[8] Model SF-770; Schoeffel Instruments, Westwood, N.J.
[9] Model 3390A, Hewlett-Packard, Avondale, Pa.
[10] μ-Bondapak; Waters Associates.

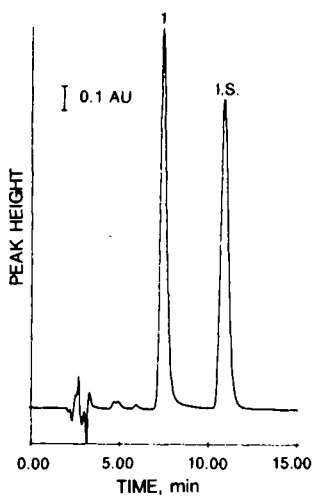

Figure 2—*Chromatogram of ointment preparation of iodochlorohydroxyquin (1) and diphenylamine (I.S.), at a detector setting of 0.1 AU and 273 nm.*

Quantitative Procedure for III—An accurately weighed portion of cream equivalent to 20 mg of III was dissolved with heating in 40–50 mL of tetrahydrofuran. The solution was quantitatively transferred to a 100-mL volumetric flask and diluted to volume with tetrahydrofuran. For the tablet form, 20 tablets were accurately weighed and finely powdered. An accurately weighed portion of the ground composite equivalent to 200 mg of III was transferred to a 250-mL volumetric flask with ~150 mL of tetrahydrofuran. The flask was heated on a steam bath for a few minutes and then shaken for 30 min on a mechanical shaker. After dilution to volume with tetrahydrofuran, a 25-mL aliquot was diluted to volume with tetrahydrofuran in a 100-mL volumetric flask. An accurately weighed 20-mg portion of standard III was diluted to volume with tetrahydrofuran in a 100-mL volumetric flask. Five-milliliter aliquots of the sample and standard preparations were transferred into separate 50-mL volumetric flasks, and 1 mL of the methanolic nickel chloride reagent and 3.0 mL of the internal standard solution were added to each flask. After dilution to volume with methanol, the standard preparation and filtered samples were chromatographed. Peak height response relative to the internal standard was used to quantitate III in the samples.

Quantitation Procedure for Bulk Drugs—Accurately weighed bulk drug

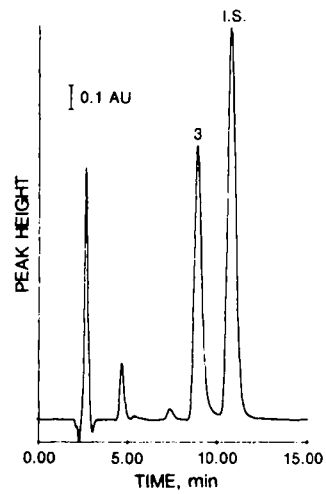

Figure 3—*Chromatogram of cream preparation of 5,7-diiodo-8-hydroxyquinoline (3) and diphenylamine (I.S.), at a detector setting of 0.1 AU and 273 nm.*

Table I—Results of Analyses of Pharmaceutical Formulations

Dosage Form	Active Ingredient	Manufacturer[a]	Found, %[b]
Ointment	3% Iodochlorhydroxyquin	A	3.02, 3.00
Cream	3% Iodochlorhydroxyquin	A	3.00, 3.00
Ointment	3% Iodochlorhydroxyquin plus 0.5% HC[c]	A	3.03, 3.04
Cream	3% Iodochlorhydroxyquin 0.5% HC	A	3.08, 3.04
	3% Iodochlorhydroxyquin plus 1% HC	B	2.92, 2.92
	3% Iodochlorhydroxyquin plus 0.5% HC	C	3.05, 2.98
Shampoo	2% 5,7-dichloro-8-hydroxyquinoline	D	1.98, 1.95
		D	1.96, 1.99
Cream	1% 5,7-diiodo-8-hydroxyquinoline plus 1% HC	E	1.04, 1.02
Tablet	210 mg of 5,7-diiodo-8-hydroxyquinoline tablet	F	208, 209[d]
	650 mg of 5,7-diiodo-8-hydroxyquinoline tablet	F	644, 650[d]

[a] Key: (A) Ciba Pharmaceutical, Summit, N.J.; (B) E. Fougera and Co., Melville, N.Y.; (C) Dome Laboratories, West Haven, Conn.; (D) Westwood Pharmaceuticals, Buffalo, N.Y.; (E) Dermik Laboratories, Fort Washington, Pa.; (F) Vitarine Co., Springfield Gardens, N.Y. for Glenwood Inc., Tenafly, N.J. [b] Each pair of results represents duplicate assays of a different lot of each dosage form. [c] HC = hydrocortisone. [d] mg.

samples were diluted to volume with tetrahydrofuran in 100-mL volumetric flasks and treated similarly to the cream and ointment samples after appropriate dilution.

System Suitability—The HPLC system in this study was suitable when a resolution factor of at least 1.5 was obtained between the sample and internal standard peaks, and a relative *SD* of ≤2% was achieved for the response ratio of the two peaks after five replicate injections.

RESULTS AND DISCUSSION

Early in this study, it was evident that iodochlorhydroxyquin (I) needed to be chemically modified to obtain a satisfactory reverse-phase high-performance liquid chromatogram. This modification had to be quantitative and easy to accomplish for analytical method application.

The formation of chelate complexes of 8-hydroxyquinolates with bivalent inorganic ions was explored. Salts of zinc and bivalent nickel, copper, and cobalt were used as complexing agents for I. Reverse-phase HPLC of methanolic solutions of these complexes, through octadecylsilane columns of 5- and 10-μm particle sizes with mobile phase composed of combinations of methanol, water, acetic acid, and various ion-pairing chemicals, was unsuccessful.

Reverse-phase HPLC has been used with a mobile solvent system containing nickel acetate to determine aniline and its metabolites (9). The use of bivalent metal ion salts in the mobile phase was investigated for the chromatography of chelate complexes of I. When a mobile solvent system of 0.01 M $NiCl_2$ in

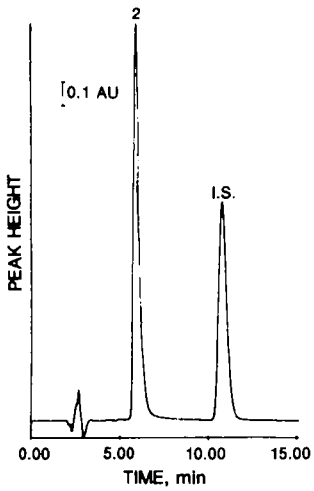

Figure 4—*Chromatogram of shampoo preparation of 5,7-dichloro-8-hydroxyquinoline (2) and diphenylamine (I.S.) at a detector setting of 0.1 AU and 273 nm.*

Table II—Recovery of Added Standards

Product	Standard	Amount Added, mg/g	Amount Found, mg/g	Recovered, %
3% Iodochlorhydroxyquin plus 1% HC[a] cream	I	29.3	29.3	100.0
3% Iodochlorhydroxyquin plus 0.5% HC ointment	I	21.7	21.3	98.2
2% 5,7-dichloro-8-hydroxyquinoline shampoo	II	16.5	16.2	98.2
1% 5,7-diiodo-8-hydroxyquinoline plus 1% HC cream	III	9.7	9.72	100.2
210-mg tablet	III	130.4	129.7	99.5
650-mg tablet	III	126.6	127.0	100.3

[a] HC = hydrocortisone.

methanol–water (75:25) was used, I eluted from a C_{18} column with some tailing.

Substitution of a phenyl-bonded column, addition of acetonitrile to the mobile phase, increase of the water content in the mobile phase to 50%, and reduction of the nickel salt concentration to 0.001 M yielded an HPLC system which separated the nickel complexes of five related standard hydroxyquinolates. This chromatographic system was used to quantitate I, II, and III in pharmaceuticals. Diphenylamine was chosen as the internal standard because it absorbed in the same UV region as the complexes and was adequately separated from the Ni–III complex, which was the last to elute from the column (Fig. 1).

Tetrahydrofuran was chosen as the solvent for petrolatum-based creams or ointments and tablet formulations of I and III. Methanol was used with a shampoo containing II. Warming the samples in the appropriate solvent on a steam bath aided in dispersing the samples and dissolving the active ingredients. Warming the initial standard preparations ensured their complete dissolution.

Addition of the methanolic nickel chloride solution to aliquots of the sample and standard preparations resulted in the immediate formation of the yellow organometallic complex. The metal salt was added in ≥10-fold excess for complete complexation. Addition of the methanolic solution of the internal standard, and dilution with methanol to volume, caused precipitation of the petrolatum in ointment or cream samples and necessitated filtration of these samples before chromatography.

The absorbance maximum for the Ni–I complex was 273 nm; this wavelength was also used in determining the nickel complexes of II and III. The presence of hydrocortisone or formulation excipients in ointments and creams did not interfere with sample analysis. Hydrocortisone eluted in ~4.8 min from the column and had a low absorbance at 273 nm. Figures 2 and 3 are typical chromatograms obtained from ointment and cream preparations of I and III formulated with hydrocortisone. Figure 4 is a chromatogram of a shampoo containing II.

Table I gives the results of duplicate analyses of different lots of preparations containing I, II, and III. Close agreement with label claim is evident. Recoveries for standards added to the prepared samples are listed in Table II. Recoveries of ≥98% were obtained for each added standard.

Linearity of response was tested by preparing a standard curve for five different concentrations of standards of I, II, and III. A correlation coefficient of 0.999 was obtained for each standard over a range of ~30–150% of the label claim, based on sample preparation using the proposed procedure.

Bulk drug samples of I and III were analyzed five times. An average purity of 99.96% with a 1.17% *CV* was obtained for I, while the bulk sample of III had an average purity of 98.77% and a *CV* of 0.73%.

The high selectivity and efficiency achieved by the use of metal ions in mobile solvents for reverse-phase HPLC have been attributed to secondary chemical equilibria (10). These secondary chemical equilibria control retention time and peak symmetry, and, if chromophoric counterions are used, detection will be enhanced. When nickel ion was absent from the mobile phase used in this study, no peaks were detected when a mixture of nickel complexes was injected into the column. Addition of the metal ion and adjustment of acetonitrile content resulted in a well-resolved chromatogram. The solvation effect of the acetonitrile in the mobile phase gave the eluting peaks a symmetry that was lacking in systems of water–methanol solutions of the nickel salt.

The use of metal ion salts in reverse-phase HPLC should find increasing application in research involving biochemical and pharmaceutical substances. The method presented here is stability indicating because possible decomposition products and impurities are separated from the parent compound, and the method is an alternative for the current official USP procedures (1,

11) for assaying and identifying I and III in bulk drug form or pharmaceutical preparations.

REFERENCES

(1) "The United States Pharmacopeia" 20th rev., U.S. Pharmacopeial Convention, Rockville, Md., 1980, pp. 155 and 156.

(2) M. P. Gruber, R. W. Klein, M. E. Foxx, and J. Campisi, *J. Pharm. Sci.*, **61**, 1147 (1972).

(3) R. E. Graham, C. T. Kenner, and E. R. Biehl, *J. Pharm. Sci.*, **64**, 1013 (1975).

(4) E. J. Kubiak and J. W. Munson, *J. Pharm. Sci.*, **71**, 872 (1982).

(5) K. Hayakawa, K. Kitada, M. Hamaki, and M. Miyazaki, *J. Chromatogr.*, **229**, 159 (1982).

(6) K. Miuro, H. Nakamura, H. Tanaka, and Z. Tamura, *J. Chromatogr.* **210**, 536 (1981).

(7) K. W. Phoon and C. Stubley, *J. Chromatogr.*, **246**, 297 (1982).

(8) F. W. Ezzedeen, A. N. Masoud, S. J. Stohs, and S. J. Lerman, *J. Pharm. Sci.*, **70**, 889 (1981).

(9) L. A. Sternson and W. J. DeWitte, *J. Chromatogr.*, **137**, 305 (1977).

(10) B. L. Karger, J. N. LePage, and N. Tanaka, in "High Performance Liquid Chromatography, Advances and Perspectives," vol. 1, C. Horvath, Ed., Academic, New York, N.Y., 1980, pp. 113-206.

(11) "The United States Pharmacopeia," 20th rev., U.S. Pharmacopeial Convention, Rockville, Md., 1980, p. 413.

Distribution and Elimination of Coated Polymethyl [2-^{14}C]Methacrylate Nanoparticles After Intravenous Injection in Rats

DANIEL LEU *§, BARBARA MANTHEY ‡, JORG KREUTER §, PETER SPEISER §, and PATRICK P. DeLUCA *x

Received March 11, 1983, from **The University of Kentucky College of Pharmacy, Lexington, KY 40536* and the §*School of Pharmacy, Swiss Federal Institute of Technology, CH-8603 Schwerzenbach, Switzerland.* Accepted for publication October 28, 1983. ‡Present address: Institute of Toxicology, Swiss Federal Institute of Technology, CH-8092 Zurich, Switzerland.

Abstract □ Surfactant-coated polymethyl [2-^{14}C]methacrylate nanoparticles had significantly different time-course distribution patterns in rats than noncoated and albumin-coated particles. Blood concentrations of poloxamer 188-coated particles were 70-fold higher after 30 min, and the particles persisted at higher levels in the circulation for up to 2 h. The initial and final liver levels were significantly lower (38% after 30 min, 51% after 7 d) and spleen levels were significantly higher (21% after 30 min, 23% after 7 d) than noncoated particles (74% in the liver and 5% in the spleen after 7 d) and the albumin-coated particles (84% in the liver and 5% in the spleen after 7 d). Specific activity was somewhat higher for the surfactant-coated particles in other organs such as the lungs, kidneys, testicles, ovaries, and lymph nodes. The bovine serum albumin sorption behavior of polymethyl methacrylate nanoparticles was followed under various conditions, and adsorption was found to increase with increasing protein concentration and increasing temperature, reaching a maximum at the isoelectric point of pH 4.9 after ~12 h of incubation. The zeta potential of the particles decreased with increasing pH, and the change was more pronounced with the albumin-coated particles.

Keyphrases □ Polymethyl methacrylate—^{14}C-labeled nanoparticles, distribution and elimination in rats, intravenous injection □ Distribution—^{14}C-labeled polymethyl methacrylate nanoparticles, intravenous injection, rats □ Elimination—^{14}C-labeled polymethyl methacrylate nanoparticles, intravenous injection, rats

There is growing interest in polymeric drug-delivery systems for parenteral administration to provide sustained release and action, and to increase the stability of easily metabolized drugs (1, 2). Nanoparticles (10 nm–1 μm) have been suggested as new drug-delivery systems (3–6). The goal is to develop a system to direct potent drug molecules to specific organs or cells, thereby limiting the systemic levels and potential toxicity to healthy or normal tissues and cells.

Polymethyl methacrylate has been used in surgery for over 30 years as a material for artificial bones (7). Implanted methyl methacrylate polymers appear to be well tolerated if the implants are monomer-free and under a certain threshold size (8). However, little is known about the biodegradability and the elimination of polymethyl methacrylate particles from the body. Nanometer-size particles exhibit a much larger surface area than the implants used in previous studies (9, 10) and are expected to degrade much faster. Information on the long-term effects of acrylic polymer particles on the living cell, however, is scarce (11).

It is generally accepted that polymers in the form of nanometer-size particles are mainly taken up by the cells of the reticuloendothelial system, predominantly in the liver and spleen. It was found that 70% of polymethyl [2-^{14}C]methacrylate nanoparticle radioactivity localized in the liver of rats 7 d after intravenous administration in phosphate-buffered saline (12). The clearance of labeled polystyrene divinylbenzene microspheres (3–25 μm) from the blood was size-dependent in beagle dogs (13, 14). Microspheres of ≥8 μm were mechanically filtered and retained in the lungs, while smaller spheres cleared the lungs and localized in the liver and spleen. Although the effect of physicochemical surface properties on distribution has been recently reported (15), the possible long-term effects associated with retention of particulate matter in the body tissues have not been studied.

Emulsifying agents have been found to affect the fractional removal rate of lipid emulsions from the blood stream (16, 17). Since emulsifying agents appear to play a major role in the removal of lipid substances from the blood stream, it was anticipated that adsorbed surfactants also influence the clearance of polymethyl methacrylate nanoparticles from the blood. Other workers have demonstrated the significance of plasma components with respect to the uptake of particulate polymeric matter by cells of the reticuloendothelial system and, accordingly, in the clearance from the blood and subsequent organ distribution (18, 19). Distribution in various organs has been reported to be influenced by the surface charge of the particles. Microspheres with adsorbed positively charged proteins (18) and nonionic surfactant (15) show a decreased uptake by the liver.

0022-3549/84/1000-1433$01.00/0
© 1984, American Pharmaceutical Association

11) for assaying and identifying I and III in bulk drug form or pharmaceutical preparations.

REFERENCES

(1) "The United States Pharmacopeia" 20th rev., U.S. Pharmacopeial Convention, Rockville, Md., 1980, pp. 155 and 156.

(2) M. P. Gruber, R. W. Klein, M. E. Foxx, and J. Campisi, *J. Pharm. Sci.*, **61**, 1147 (1972).

(3) R. E. Graham, C. T. Kenner, and E. R. Biehl, *J. Pharm. Sci.*, **64**, 1013 (1975).

(4) E. J. Kubiak and J. W. Munson, *J. Pharm. Sci.*, **71**, 872 (1982).

(5) K. Hayakawa, K. Kitada, M. Hamaki, and M. Miyazaki, *J. Chromatogr.*, **229**, 159 (1982).

(6) K. Miuro, H. Nakamura, H. Tanaka, and Z. Tamura, *J. Chromatogr.* **210**, 536 (1981).

(7) K. W. Phoon and C. Stubley, *J. Chromatogr.*, **246**, 297 (1982).

(8) F. W. Ezzedeen, A. N. Masoud, S. J. Stohs, and S. J. Lerman, *J. Pharm. Sci.*, **70**, 889 (1981).

(9) L. A. Sternson and W. J. DeWitte, *J. Chromatogr.*, **137**, 305 (1977).

(10) B. L. Karger, J. N. LePage, and N. Tanaka, in "High Performance Liquid Chromatography, Advances and Perspectives," vol. 1, C. Horvath, Ed., Academic, New York, N.Y., 1980, pp. 113-206.

(11) "The United States Pharmacopeia," 20th rev., U.S. Pharmacopeial Convention, Rockville, Md., 1980, p. 413.

Distribution and Elimination of Coated Polymethyl [2-^{14}C]Methacrylate Nanoparticles After Intravenous Injection in Rats

DANIEL LEU *§, BARBARA MANTHEY ‡, JORG KREUTER §, PETER SPEISER §, and PATRICK P. DeLUCA *x

Received March 11, 1983, from **The University of Kentucky College of Pharmacy, Lexington, KY 40536* and the §*School of Pharmacy, Swiss Federal Institute of Technology, CH-8603 Schwerzenbach, Switzerland.* Accepted for publication October 28, 1983. ‡Present address: Institute of Toxicology, Swiss Federal Institute of Technology, CH-8092 Zurich, Switzerland.

Abstract □ Surfactant-coated polymethyl [2-^{14}C]methacrylate nanoparticles had significantly different time-course distribution patterns in rats than noncoated and albumin-coated particles. Blood concentrations of poloxamer 188-coated particles were 70-fold higher after 30 min, and the particles persisted at higher levels in the circulation for up to 2 h. The initial and final liver levels were significantly lower (38% after 30 min, 51% after 7 d) and spleen levels were significantly higher (21% after 30 min, 23% after 7 d) than noncoated particles (74% in the liver and 5% in the spleen after 7 d) and the albumin-coated particles (84% in the liver and 5% in the spleen after 7 d). Specific activity was somewhat higher for the surfactant-coated particles in other organs such as the lungs, kidneys, testicles, ovaries, and lymph nodes. The bovine serum albumin sorption behavior of polymethyl methacrylate nanoparticles was followed under various conditions, and adsorption was found to increase with increasing protein concentration and increasing temperature, reaching a maximum at the isoelectric point of pH 4.9 after ~12 h of incubation. The zeta potential of the particles decreased with increasing pH, and the change was more pronounced with the albumin-coated particles.

Keyphrases □ Polymethyl methacrylate—^{14}C-labeled nanoparticles, distribution and elimination in rats, intravenous injection □ Distribution—^{14}C-labeled polymethyl methacrylate nanoparticles, intravenous injection, rats □ Elimination—^{14}C-labeled polymethyl methacrylate nanoparticles, intravenous injection, rats

There is growing interest in polymeric drug-delivery systems for parenteral administration to provide sustained release and action, and to increase the stability of easily metabolized drugs (1, 2). Nanoparticles (10 nm–1 μm) have been suggested as new drug-delivery systems (3–6). The goal is to develop a system to direct potent drug molecules to specific organs or cells, thereby limiting the systemic levels and potential toxicity to healthy or normal tissues and cells.

Polymethyl methacrylate has been used in surgery for over 30 years as a material for artificial bones (7). Implanted methyl methacrylate polymers appear to be well tolerated if the implants are monomer-free and under a certain threshold size (8). However, little is known about the biodegradability and the elimination of polymethyl methacrylate particles from the body. Nanometer-size particles exhibit a much larger surface area than the implants used in previous studies (9, 10) and are expected to degrade much faster. Information on the long-term effects of acrylic polymer particles on the living cell, however, is scarce (11).

It is generally accepted that polymers in the form of nanometer-size particles are mainly taken up by the cells of the reticuloendothelial system, predominantly in the liver and spleen. It was found that 70% of polymethyl [2-^{14}C]methacrylate nanoparticle radioactivity localized in the liver of rats 7 d after intravenous administration in phosphate-buffered saline (12). The clearance of labeled polystyrene divinylbenzene microspheres (3–25 μm) from the blood was size-dependent in beagle dogs (13, 14). Microspheres of ≥8 μm were mechanically filtered and retained in the lungs, while smaller spheres cleared the lungs and localized in the liver and spleen. Although the effect of physicochemical surface properties on distribution has been recently reported (15), the possible long-term effects associated with retention of particulate matter in the body tissues have not been studied.

Emulsifying agents have been found to affect the fractional removal rate of lipid emulsions from the blood stream (16, 17). Since emulsifying agents appear to play a major role in the removal of lipid substances from the blood stream, it was anticipated that adsorbed surfactants also influence the clearance of polymethyl methacrylate nanoparticles from the blood. Other workers have demonstrated the significance of plasma components with respect to the uptake of particulate polymeric matter by cells of the reticuloendothelial system and, accordingly, in the clearance from the blood and subsequent organ distribution (18, 19). Distribution in various organs has been reported to be influenced by the surface charge of the particles. Microspheres with adsorbed positively charged proteins (18) and nonionic surfactant (15) show a decreased uptake by the liver.

0022-3549/84/1000-1433$01.00/0
© 1984, American Pharmaceutical Association

Table I—Adsorption of Bovine Serum Albumin to Polymethyl Methacrylate Nanoparticles

Parameter Examined	Bovine Serum Albumin Adsorbed[a]	Conditions
Particle conc. (w/v)		
0.1%	3.3 ± 9.1%	pH: 4.9
0.3%	1.2 ± 25%	Incubation time: 4 h
		Albumin conc.: 2% (w/v)
		Temp.: 37°C
Protein conc. (w/v)		
3.0%	32.2 ± 5.0%	pH: 7.4
2.5%	20.0 ± 5.0%	Incubation time: 4 hr
1.5%	11.8 ± 9.3%	Particle conc.: 0.1%
0.5%	9.9 ± 9.1%	Temp.: 37°C
0.2%	4.6 ± 4.3%	
Temperature		
37°C	20.5 ± 7.8%	pH: 4.9
25°C	17.4 ± 8.0%	Incubation time: 4 h
4°C	16.9 ± 10%	Albumin conc.: 2%
		Particle conc.: 0.1%
pH		
3.9	15.8 ± 7.0%	Incubation time: 4 h
4.9	34.8 ± 5.7%	Albumin conc.: 2%
7.4	22.1 ● 5.4%	Particle conc.: 0.1%
		Temp.: 37°C
Time		
1 h	3.1 ± 13%	pH: 4.9
2 h	7.7 ± 9.1%	Albumin conc.: 2%
4 h	19.6 ± 11%	Particle conc.: 0.1%
12 h	24.9 ± 8.0%	Temp.: 37°C
22 h	24.0 ± 8.6%	

[a] Mean of four determinations. The statistical dispersion is given as the *SD* in percent of the mean value. The values are percent of albumin adsorbed from solution, except particle concentration (mg of albumin/mg of particles).

In a previous study, polymethyl methacrylate nanoparticles of ~150 nm were found to accumulate in the lungs in relatively high concentrations 30 min following intravenous administration (12), presumably due to agglomeration of the particles. This paper presents information on the fate of surface-coated polymethyl [2-^{14}C]methacrylate nanoparticles after intravenous injection in rats. Before the animal experiments, the adsorption of the nanoparticles to bovine serum albumin and the resulting surface charge (zeta potential) were determined.

EXPERIMENTAL SECTION

Preparation of ^{14}C-Labeled Nanoparticles—The nanoparticles were prepared as previously described (12) and freeze-dried from a suspension in 0.15 M phosphate-buffered saline. The polymer had a specific activity of 4 mCi/g[1]. The freeze-dried powder contained 56.3% of buffer salts (dibasic sodium phosphate dihydrate-monobasic potassium phosphate-sodium chloride (7.6:1.45:4.8, w/w/w) and 43.7% of polymethyl [2-^{14}C]methacrylate. Particle size determination by photon correlation spectrometry[2] (20) revealed an average diameter of 131 ± 30 nm.

***Preparation of the* Suspension**—*Reference Group*—Nanoparticle-buffer preparation (220 mg) was suspended in 11 mL of distilled water and 33 mL of phosphate-buffered saline, to give a suspension of 2.185 mg of nanoparticles/mL and ultrasonicated for 5 min at 20 kHz in a sonicator cell disrupter with a micro tip[3].

Surfactant Group—The nanoparticle preparation (220 mg) was suspended in 11 mL of 0.5% (w/v) poloxamer 188[4] in water and 33 mL of 0.5% (w/v) poloxamer 188 in phosphate-buffered saline and ultrasonicated.

Protein Group—The nanoparticle preparation (220 mg) was suspended in 76 mL of a 3% (w/v) solution of rat serum albumin[5] in 0.145 M phosphate buffer (pH 4.9), incubated in an end-over-end shaker (22 rpm) at 37°C for 12 h, and then centrifuged at 30,000×g_{ave}[6]. The protein-coated particles were washed twice with 0.145 M phosphate buffer (pH 4.9) and then suspended in 44 mL of phosphate-buffered saline and sonicated. The protein adsorbed was 8.2% from the solution, measured by UV absorbance at 280 nm. This corresponds to 1.92 mg of albumin/mg of nanoparticles. The adsorption of protein was irreversible since protein was not detected in the washings or phosphate-buffered saline suspensions.

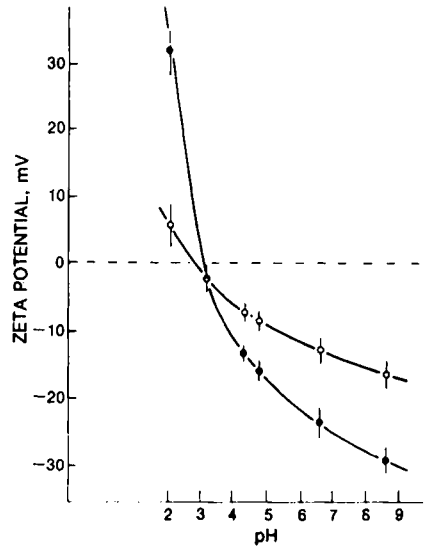

Figure 1—*The influence of pH on the zeta potential of noncoated (○) and protein-coated (●) polymethyl methacrylate nanoparticles. Each value is the mean of 10 measurements; the vertical lines represent* SD.

Specific Activity of the Suspensions—Five 1:1000 dilutions of each suspension and 0.175 mL of a combustion aid[7] were combusted in an oxidizer[8]. The resulting carbon dioxide was absorbed in 7 mL of an absorption medium[9]. This medium was then mixed with 15 mL of scintillation cocktail[10] and the ^{14}C-radioactivity was measured in a liquid scintillation counter[11]. The specific activities of the suspensions were calculated using a quench curve (19) and the following values were obtained: (*a*) reference group: 7.76 ± 0.39 μCi/mL; (*b*) surfactant group: 8.59 ± 0.48 μCi/mL; (*c*) protein group: 6.85 ± 0.16 μCi/mL.

Protein Binding Studies—Experiments were conducted to determine suitable conditions for the adsorption of albumin to the nanoparticles. The parameters assessed were particle concentration, protein concentration, temperature, time of incubation, and pH of the incubation solution. The nanoparticle suspensions were incubated in a solution of bovine serum albumin[12] in 0.145 M phosphate-buffered saline at a constant temperature in glass tubes which were rotated end over end. The suspensions were centrifuged, and the protein concentration in the supernatant was determined by measuring the absorbance at 280 nm. This method was verified by the Lowry test (21).

Surface Charge—The zeta potential of nanoparticle suspensions at different pH values (before and after the adsorption of bovine serum albumin) was calculated after measuring the microelectrophoretic mobility of small particle-agglomerations in a phosphate buffer (ionic strength 0.01 M) with a zeta meter[13]. An optimal particle concentration for tracking in the electrophoretic cell was 25 ppm. Ten particles (or small particle-agglomerations) were counted for each value at a voltage of 100 V. Measurements were not made of particles suspended in different solutions of two surfactants, poloxamer 188 and polysorbate 80[14], because these preparations did not show any agglomerations in a zeta-meter-suitable microscope and, therefore, were not detectable.

Injection—Groups of four (two male and two female) randomly-selected Wistar rats (203–335 g) were used for each suspension and for each time point (0.5, 2, 24 h, and 7 d). The rats were anesthetized with ether and then restrained in a supine position on a hard board. After exposing the femoral vein with sterile instruments, the animal was injected with the nanoparticle suspension using a 26-gauge needle attached to a plastic syringe at a rate of 1 mL/min. Immediately before injection the suspensions were ultrasonicated at 20 kHz for 20 s. The injection dose was 60 μCi/kg of bodyweight (~2

[1] Amersham Radiochemical Centre, Buckinghamshire, U.K.
[2] Model K7025 with 64 channels; Malvern Instruments, Malvern, U.K.
[3] Model W 185 F; Heat Systems Ultrasonic Inc., Plainview, N.Y.
[4] Pluronic F-68; Wyandotte Chemicals, Wyandotte, Mich.
[5] Pel-Freez Biologicals, Rogers, Ark.
[6] Beckman J 2-21, rotor JA 20 (20.000 rpm, 5°C); Beckman Instruments, Palo Alto, Calif.
[7] Packard Instrument Co., Downers Grove, Ill.
[8] Model B 306 Tri-Carb Sample Oxidizer; Packard Instrument Co.
[9] Carbo Sorb; Packard Instrument Co.
[10] Permafluor V; Packard Instrument Co.
[11] Model 3255 Tri-Carb Liquid Scintillation Counter; Packard Instrument Co.
[12] Cohn Fraction V; Sigma, St. Louis, Mo.
[13] Zeta Meter Inc., New York, N.Y.
[14] Tween 80; Atlas Chemie GmbH, Essen, West Germany.

Table II—Distribution of Carbon-14 after Intravenous Administration of Polymethyl [2-^{14}C]Methacrylate Nanoparticles to Rats [a]

Sample	Group[b]	Time after Injection: 30 min Percent of Dose	30 min Specific Activity	2 h Percent of Dose	2 h Specific Activity	24 h Percent of Dose	24 h Specific Activity	7 d Percent of Dose	7 d Specific Activity
Blood	Ref	0.3 ± 32%	0.02	0.1 ± 23%	0.01	0.1 ± 20%	0.00	0.0 ± 36%	0.00
	Sur	20.5 ± 26%	0.12	1.0 ± 34%	0.05	0.1 ± 39%	0.00	0.0 ± 18%	0.00
	RSA	0.3 ± 67%	0.02	0.2 ± 15%	0.01	0.0 ± 40%	0.00	0.0 ± 39%	0.00
Liver	Ref	85.3 ± 4%	7.78	79.2 ± 12%	7.89	80.9 ± 8%	8.07	73.8 ± 6%	6.78
	Sur	37.6 ± 19%	3.16	43.2 ± 14%	3.60	59.8 ± 8%	5.54	51.3 ± 5%	4.84
	RSA	84.7 ± 3%	8.31	83.7 ± 2%	6.81	85.4 ± 1%	7.91	84.2 ± 5%	8.42
Lungs[c]	Ref	1.4 ± 6%	1.16	2.2 ± 0%	2.05	3.3 ± 11%	2.82	0.2 ± 53%	0.18
	Sur	3.8 ± 20%	3.18	3.2 ± 19%	2.63	7.0 ± 32%	6.23	0.6 ± 38%	0.46
	RSA	2.3 ± 28%	2.07	2.9 ± 26%	2.55	2.1 ± 17%	1.90	0.2 ± 15%	0.17
Spleen	Ref	3.7 ± 25%	6.40	2.5 ± 16%	3.37	4.1 ± 6%	6.46	4.6 ± 13%	7.40
	Sur	20.9 ± 7%	34.21	30.6 ± 20%	49.34	13.3 ± 17%	21.45	22.6 ± 14%	32.20
	RSA	3.8 ± 35%	5.91	3.8 ± 15%	6.10	4.6 ± 2%	6.59	4.7 ± 4%	7.72
Kidneys	Ref	0.3 ± 15%	0.14	0.3 ± 48%	0.13	0.1 ± 29%	0.07	0.0 ± 34%	0.01
	Sur	0.9 ± 18%	0.47	0.3 ± 25%	0.13	0.2 ± 27%	0.09	0.0 ± 45%	0.02
	RSA	0.2 ± 27%	0.11	0.2 ± 32%	0.08	0.1 ± 17%	0.07	0.0 ± 19%	0.01
Testicles	Ref	0.01 ± 1%	0.00	0.00 ± 0%	0.00	0.00 ± 9%	0.00	0.00 ± 36%	0.00
	Sur	0.04 ± 11%	0.01	0.01 ± 22%	0.00	0.00 ± 8%	0.00	0.00 ± 44%	0.00
	RSA	0.01 ± 2%	0.00	0.00 ± 47%	0.00	0.00 ± 0%	0.00	0.00 ± 11%	0.00
Ovaries[d]	Ref	0.01 ± 4%	0.10	0.01 ± 0%	0.10	0.01 ± 4%	0.11	0.00 ± 12%	0.03
	Sur	0.10 ± 25%	1.11	0.01 ± 0%	0.73	0.01 ± 4%	0.14	0.01 ± 42%	0.22
	RSA	0.01 ± 0%	0.06	0.01 ± 20%	0.08	0.01 ± 27%	0.08	0.00 ± 35%	0.06
Lymph nodes[e]	Ref	0.02 ± 32%	0.02	0.02 ± 33%	0.02	0.02 ± 16%	0.02	0.02 ± 30%	0.02
	Sur	0.08 ± 21%	0.08	0.04 ± 1%	0.04	0.03 ± 8%	0.03	0.02 ± 22%	0.02
	RSA	0.01 ± 7%	0.01	0.01 ± 38%	0.01	0.01 ± 38%	0.01	0.01 ± 27%	0.01
Total	Ref	91.0 ± 4%	—	84.3 ± 10%	—	92.1 ± 6%	—	84.0 ± 4%	—
	Sur	83.9 ± 9%	—	78.4 ± 9%	—	83.1 ± 6%	—	79.4 ± 4%	—
	RSA	91.3 ± 3%	—	90.8 ± 2%	—	93.0 ± 1%	—	91.4 ± 4%	—

[a] Mean ± *RSD* percent of the administered dose; $n = 4$. The specific activity is the percent of administered dose per gram of tissue (wet weight) or milliliter of blood. The blood volume was assumed to be 64.1 ± 9 mL/kg (24). The 24-h and 7-d values include the elimination by urine and feces (see Table IV). [b] Key: (Ref) untreated particles; (Sur) particles treated with surfactant; (RSA) particles coated with rat serum albumin. [c] Without bronchia. [d] Without tubes. [e] One gram (wet weight).

mL/animal). The incision was sealed with aluminum wound clips and rinsed with an iodine solution.

Organ Distribution and Elimination of ^{14}C-Radioactivity—The animals were anesthetized with ether and injected with an overdose of sodium pentobarbital [100 mg/kg ip of a 2% aqueous solution (22)]. After ~5 min, the abdomen and chest were opened and a blood sample was taken from the vena cava. The vena cava was then cut, and the blood was drained. The liver, lungs, spleen, kidneys, testicles or ovaries, and lymph nodes (from the mesenterium and cervix) were removed. The organs were washed with distilled water, and the connective tissue and fat was removed. The organs were weighed and stored at −20°C for further examination.

After injection, a corresponding group of animals was housed in metabolism cages for 7 d (food and water *ad libitum*). Urine and feces were collected in separate containers and removed every 24 h. Weighed urine and freeze-dried fecal samples were stored at −20°C for further examination.

The organs were homogenized with water (1:10) and an aliquot (0.001–0.5 of an organ, depending on the expected radioactivity) was combusted in an oxidizer. The resulting $^{14}CO_2$ was absorbed in 7 mL of absorption medium, mixed with 15 mL of scintillation cocktail, and analyzed in the liquid scintillation counter. Urine (0.5 mL) was mixed with 15 mL of scintillation cocktail[15] and analyzed in the scintillation counter. Freeze-dried feces was homogenized with water, and a sample of 100 mg was combusted with several drops of a combustion aid. The resulting $^{14}CO_2$ was analyzed in the manner described above for the organs. The percentages of the administered dose of nanoparticles in the organs, blood, and excreta were calculated using the standard values and quench curves (23).

RESULTS

Protein Binding Studies—The adsorption of bovine serum albumin to polymethyl methacrylate nanoparticles as a function of the parameters studied is shown in Table I. From these experiments, the following conditions were selected for protein-coating prior to the zeta potential measurements and the animal studies: concentration of serum albumin, 3.0%; particle concentration, 0.1%; time of incubation, 12 h; buffer, 0.145 M potassium phosphate (pH 4.9); temperature of incubation, 37°C.

Surface Charge—The influence of pH on the zeta potential of noncoated and protein-coated nanoparticles is shown in Fig. 1. The zeta potential decreased with increasing pH for both particle types, but the influence was greater on the coated nanoparticles.

Organ Distribution of ^{14}C-Radioactivity—Table II shows the distribution of ^{14}C-radioactivity in several organs [selected using the findings of Kreuter *et al.* (12)] after intravenous administration of the nanoparticles. The distribution behavior in the reference and protein-coated groups was similar, but, in most of the organs examined, the surfactant group showed a very different accumulation of particles. One fifth of the administered dose of the surfactant

Table III—Comparison of the Distribution of Noncoated and Coated Nanoparticles in Organs [a]

Organ	Comparison	0.5 h	2 h	24 h	7 d
Blood	Ref/Sur	***	**	n.s.	n.s.
	Ref/RSA	n.s.	n.s.	*	n.s.
	Sur/RSA	***	**	n.s.	n.s.
Liver	Ref/Sur	***	***	•	***
	Ref/RSA	n.s.	n.s.	n.s.	*
	Sur/RSA	***	***	***	***
Lungs	Ref/Sur	***	*	*	*
	Ref/RSA	*	n.s.	**	n.s.
	Sur/RSA	*	n.s.	**	*
Spleen	Ref/Sur	***	***	***	***
	Ref/RSA	n.s.	**	*	n.s.
	Sur/RSA	***	***	***	***
Kidneys	Ref/Sur	***	n.s.	n.s.	n.s.
	Ref/RSA	n.s.	n.s.	n.s.	n.s.
	Sur/RSA	***	*	n.s.	*
Testicles	Ref/Sur	**	*	n.s.	n.s.
	Ref/RSA	***	n.s.	*	n.s.
	Sur/RSA	**	n.s.	*	n.s.
Ovaries	Ref/Sur	*	***	n.s.	n.s.
	Ref/RSA	**	n.s.	n.s.	n.s.
	Sur/RSA	*	***	n.s.	n.s.
Lymph nodes	Ref/Sur	***	**	***	n.s.
	Ref/RSA	n.s.	*	n.s.	•
	Sur/RSA	***	***	***	**

[a] Calculated with Student's *t* test. Key: (n.s.) not significant; (*) $p < 0.05$; (**) $p < 0.01$; (***) $p < 0.001$.

[15] Aquasol-2; Packard Instrument Co.

Table IV—Elimination of Carbon-14 after Intravenous Administration of Nanoparticles in Rats [a]

Time	Group[b]	Feces	Urine
Day 0	Ref	0.02 ± 144%	0.96 ± 18%
	Sur	0.02 ± 60%	0.73 ± 13%
	RSA	0.06 ± 0%	—
Day 1	Ref	3.72 ± 3%	0.26 ± 23%
	Sur	2.39 ± 25%	0.34 ± 40%
	RSA	0.68 ± 18%	0.12 ± 9%
Day 2	Ref	0.36 ± 32%	0.04 ± 57%
	Sur	0.83 ± 53%	0.05 ± 32%
	RSA	0.75 ± 7%	0.05 ± 13%
Day 3	Ref	0.15 ± 13%	0.03 ± 67%
	Sur	0.15 ± 21%	0.03 ± 36%
	RSA	0.32 ± 37%	0.03 ± 20%
Day 4	Ref	0.09 ± 68%	0.01 ± 29%
	Sur	0.11 ± 25%	0.01 ± 50%
	RSA	0.15 ± 16%	0.02 ± 29%
Day 5	Ref	0.08 ± 13%	0.01 ± 21%
	Sur	0.08 ± 36%	0.01 ± 50%
	RSA	0.09 ± 7%	0.01 ± 32%
Day 6	Ref	0.05 ± 15%	0.01 ± 31%
	Sur	0.05 ± 24%	0.00 ± 24%
	RSA	0.06 ± 5%	0.01 ± 9%
Day 7	Ref	0.04 ± 18%	0.01 ± 33%
	Sur	0.05 ± 21%	0.00 ± 39%
	RSA	0.06 ± 5%	0.01 ± 17%
Total	Ref	4.06 ± 4%	1.33 ± 14%
	Sur	3.65 ± 24%	1.17 ± 15%
	RSA	2.11 ± 8%	0.25 ± 6%

[a] All values are mean ± *RSD* percent of the administered dose. [b] Key: (Ref) noncoated particles; (Sur) particles treated with surfactant; (RSA) particles coated with rat serum albumin.

group remained in the blood after 0.5 h. This was ~60 times more than that of the other groups. After 2 h, however, the blood level of the surfactant group was of the same order as that of the other groups.

After 0.5 h, 85% of the radioactivity was found in the liver in the reference and the protein groups. This value decreased to ~74% in the reference group but remained constant in the protein group. In the surfactant group, only ~38% was found in the liver after 0.5 h. This value increased to ~60% after 24 h and dropped to 51% after 7 d.

In the lungs, the accumulation after 0.5 h was 1.4% of the administered dose for the reference group. About three times as much was detected in the surfactant group; the value for the protein group was intermediate. The lung radioactivity remained constant for 24 h in the protein group, but it increased almost twofold in the other groups. In all groups, the clearance was essentially complete after 7 d.

In the spleen, the accumulation for the reference and the protein groups showed a similar value of ~4% after 0.5 h, which increased slightly to ~5% after 7 d. In the surfactant group, 21% of the injected dose was localized in the spleen after 0.5 h. This value increased to ~31% after 2 h and dropped to ~23% after 7 d.

In the other organs (kidneys, ovaries, testicles, and lymph nodes) the amount of radioactivity was <1% after 0.5 h, and the values decreased with time. The surfactant group showed a higher accumulation than the reference and protein groups for most values (Tables II and III). Although the absolute quantity in the testicles and ovaries was < 0.1% of the administered dose, higher concentrations of all particle suspensions were found in the ovaries. This higher affinity can be clearly demonstrated using the nanoparticle concentration, given in terms of specific activity, *i.e.*, percent of the dose per gram of organ (wet weight) (Table II). The spleen also showed a very high affinity for the surfactant-treated nanoparticles (3–15 times higher than in the other groups), whereas the affinity of the liver for surfactant-treated particles was significantly lower than the other groups. In all other organs (except the blood after 0.5 h), the specific activity was of the same order of magnitude for all preparations.

Elimination of ^{14}C-Radioactivity—The ^{14}C-elimination in urine and feces was followed for 7 d (Tables IV and V). In all groups, ~1% of the administered dose was excreted in the urine and 2–4% in the feces within 7 d. The majority of the ^{14}C-excretion was found after the first day.

DISCUSSION

It has been suggested that colloidal materials interact with blood components after injection into systemic circulation (13, 25–28). This interaction and coating with blood proteins may influence the subsequent organ distribution of these particles (28, 29). In investigating the sorption behavior of the nanoparticles in aqueous bovine serum albumin solutions, the amount of adsorbed protein was found to be higher with low particle concentrations and with high protein concentrations, as expected. The pH of the incubation medium influenced the adsorption; maximum adsorption was at pH 4.9, the isoelectric point of bovine serum albumin. This finding seems to be a general characteristic of proteinaceous solutions (30). The temperature, in the examined range of 4–37°C, showed only a small influence on the adsorption. Protein adsorption increased with incubation time up to 12 h, when equilibrium apparently occurred.

The greater influence of the pH on the zeta potential of the albumin-coated particles, compared to the noncoated particles, is probably caused by the protonation/deprotonation of the albumin amino groups, but the potential of the noncoated particles is influenced only by surface adsorption of protons or hydroxyl ions. Although a 10-mV difference in zeta potential was observed at pH 7.4, it is not possible to infer that this seemingly insignificant difference would influence body distribution. The effect of charge on distribution warrants further study.

While differences in the organ distribution among the three preparations were observed, the reference group and the protein group show generally the same distribution pattern. The albumin-coating procedure was conducted because albumin has been shown to prevent platelet adhesion and to enhance the biocompatibility of diverse materials (31, 32) and, therefore, was expected to lead to a significant change in the distribution of the particles. However, albumin coating did not alter the organ distribution significantly when compared to the noncoated particles. This suggests that injected noncoated particles soon become coated with serum proteins. Almost 90% of the administered dose in the reference and the protein groups accumulated in the liver and spleen. Since both organs are part of the reticuloendothelial system, this finding suggests that nanoparticles with incorporated or adsorbed antigens hold promise as adjuvants (3, 12). The only difference in the distribution behavior between the reference group and the protein group is that accumulation in the liver remained constant at ~85% in the protein group; in the reference group it decreased from 85% after 30 min to 74% after 7 d.

A distinctively different distribution pattern was obtained in the surfactant group. Only 38% of the administered dose was found in the liver after 30 min, and the accumulation was only 51% after 7 d. This is similar to results reported with poloxamer-coated polystyrene microspheres (15). The apparent loss from the liver between 1 and 7 d indicates some clearance and/or degradation phenomenon. Accumulation was significantly greater in the spleen for the surfactant group (21%) than in the other groups (<4%). After 2 h, the spleen levels increased to 31%, ~12 times higher than the noncoated group and 8 times higher than the protein group. As in the liver, the level of particles in the spleen decreased after 24 h to 13% and increased again to 23% within 7 d. No satisfactory explanation can be given for this oscillation in spleen levels.

Another distinct difference of the surfactant group is an apparent slower

Table V—Comparison of Radioactivity Levels in the Excreta of Rats after Intravenous Administration of Noncoated and Coated Nanoparticles [a]

Comparison	Day 0	Day 1	Day 2	Day 3	Day 4	Day 5	Day 6	Day 7	Total
				Urine					
Ref/Sur	n.s.	n.s.	n.s.	n.s.	n.s.	*	*	n.s.	n.s.
Ref/RSA	—	**	n.s.	n.s.	n.s.	n.s.	n.s.	n.s.	***
Sur/RSA	—	*	n.s.	n.s.	n.s.	*	***	*	***
				Feces					
Ref/Sur	n.s.	*	n.s.	n.s.	n.s.	n.s.	n.s.	n.s.	n.s.
Ref/RSA	n.s.	***	***	*	n.s.	n.s.	n.s.	**	***
Sur/RSA	**	**	n.s.	*	n.s.	n.s.	n.s.	n.s.	**

[a] Calculated with Student's *t* test. Key: (n.s.) not significant; (*) $p < 0.05$; (**) $p < 0.01$; (***) $p < 0.001$.

blood clearance. About 21% of the administered dose still remained in the blood after 30 min, *versus* 0.3% for the other groups. Since nanoparticles may be preferentially taken up by tissues exhibiting enhanced endocytotic activity, such as tumor tissue (33, 34), a longer persistence of the particles in the circulatory system may enhance their potential for accumulation in cancerous tissue. Therefore, surface-treated nanoparticles may possibly be useful as carriers for toxic anticancer drugs.

The accumulation of nanoparticles in the lung was lower than that reported previously (12), in which particles similar to the reference group were used. In that study ~22% of the particles were localized in the lungs after 30 min, a value that decreased continuously to ~13% after 7 d, in this study only 1.4% was detected in the lungs after 30 min. After 24 h and 7 d, 3.3 and 0.2%, respectively, of the administered dose was found in the lungs. The surfactant and the protein groups showed similar lung accumulations of 3.8 and 2.3% after 30 min, respectively, and both values decreased to <1% within 7 d. This finding confirms that if agglomeration occurred, the clusters were small enough to pass through the capillary network in the lungs.

Coagulated particle clusters have been reported to be mechanically trapped by the lung capillaries (13, 14). However, these were clusters of microspheres >3μm in diameter. According to a recent review by Kreuter (28), particles in the submicron range, *i.e.*, 125 nm–1 μm, do not show any major differences in body distribution. It has also been shown that gentle mixing of polymethyl methacrylate nanoparticles with plasma will cause disintegration of particle clusters (20). It is, therefore, believed that the difference in the distribution behavior between surfactant-coated and noncoated particles was due to a difference in surface properties. The difference in the distribution behavior between the noncoated particles in this study and those used previously (12) can be attributed to certain refinements in methodology which minimized agglomeration tendencies. These refinements include sonication by means of a microtip immediately before each injection, as opposed to sonication of the total suspension in a bath-type sonicator ~20 min before the experiment. Additionally, in this study the particles were suspended in 2 mL of phosphate-buffered saline and injected over a period of 2 min into the femoral vein of animals anesthetized with ether; in the earlier experiment the particles were suspended in 0.5 mL and injected over 5–10 s into the tail vein without anesthetization.

The results of this study clearly demonstrate that surfactant-coated nanoparticles result in a slower blood clearance and a significantly different organ distribution after intravenous administration. The targeting of incorporated or adsorbed drugs to specific organs may, therefore, be influenced by pretreatment of the carrier particles with surface-active agents. More experiments with other surfactants are required to gain systematic information about factors that influence the distribution behavior of nanoparticles after intravenous injection. These factors include the surface charge as well as the chemical nature of the surface and, consequently, the agglomeration tendency of the particles. Although scanning electron micrographs of the coated particles did not reveal aggregation, they were not discernibly different from micrographs of noncoated particles. This study has revealed extended residence in the blood and differences in organ distribution patterns with coated nanoparticles. Therefore, physicochemical characterization of the particles, including particle size distribution, is essential to further organ distribution studies.

REFERENCES

(1) T. M. S. Chang, *Enzyme*, **14,** 95 (1972/73).

(2) K. F. O'Driscoll, R. A. Korus, T. Ohnuma, and I. M. Walozack, *J. Pharmacol. Exp. Ther.*, **195,** 382 (1975).

(3) J. Kreuter and P. P. Speiser, *Infect. Immun.*, **13,** 204 (1976).

(4) G. Birrenbach and P. P. Speiser, *J. Pharm. Sci.*, **65,** 1763 (1976).

(5) J. J. Marty, R. C. Oppenheim, and P. P. Speiser, *Pharm. Acta Helv.*, **53,** 17 (1978).

(6) J. Kreuter, *Infect. Immun.*, **53,** 33 (1978).

(7) J. Charnley, "Acrylic Cement in Orthopaedic Surgery," Livingstone, Edinburgh, Scotland, 1970.

(8) F. Bischoff and G. Brynson, *Prog. Exp. Tumor Res.*, **5,** 85 (1964).

(9) B. S. Oppenheimer, E. T. Oppenheimer, I. Danishefsky, A. P. Stout, and F. R. Eirich, *Cancer Res.*, **15,** 333 (1955).

(10) L. Tomatis, *Tumori*, **52,** 165 (1966).

(11) I. Sjöholm and P. Edman, *J. Pharmacol. Exp. Ther.*, **211,** 656 (1979).

(12) J. Kreuter, U. Taeuber, and V. Illi, *J. Pharm. Sci.*, **68,** 1443 (1979).

(13) M. Kanke, G. H. Simmons, D. L. Weiss, B. A. Bivins, and P. P. DeLuca, *J. Pharm. Sci.*, **69,** 755 (1980).

(14) H. G. Schroeder, G. H. Simmons, and P. P. DeLuca, *J. Pharm. Sci.*, **67,** 504 (1978).

(15) L. Illum and S. S. Davis, *J. Pharm. Sci.* **72,** 1086 (1983).

(16) K. M. D'Amico, S. S. Davis, M. Frier, P. Hansrani, J. G. Hardy, and C. G. Wilson, *Br. J. Pharmacol.*, **72,** 83 (1981).

(17) R. Jeppson and S. Roessner, *Acta Pharmacol. Toxicol.*, **37,** 134 (1975).

(18) D. J. Wilkins and P. A. Meyers, *Br. J. Exp. Pathol.*, **47,** 568 (1966).

(19) D. J. Wilkins and P. A. Meyers, in "Surface Chemistry of Biological Systems," N. Blank, Ed., Academic, New York, N.Y., 1970, p. 217.

(20) J. Krueter, *Int. J. Pharm.*, **14,** 43 (1983).

(21) O. H. Lowry, N. J. Rosebrough, A. L. Farr, and R. J. Randall, *J. Biol. Chem.*, **193,** 265 (1951).

(22) C. D. Barnes and L. G. Etherington, "Drug Dosage in Laboratorium Animals," University of California Press, Berkeley, Calif., 1973.

(23) Tri-Carb Sample Oxidizer Operation Manual, Packard Instrument Co., Downers Grove, Ill., 1980.

(24) P. L. Altman and D. S. Dittmer, "Biological Data Book," Fed. Am. Soc. Exp. Biol., Rockville, Md., 1964, p. 264.

(25) M. E. Soderquist and A. G. Walton, *J. Colloid Interface Sci.*, **75,** 386 (1980).

(26) J. Slack, M. Kanke, G. Simmons, and P. P. DeLuca, *J. Pharm. Sci.*, **70,** 660 (1981).

(27) J. Kreuter, *Pharm. Acta. Helv.*, **58,** 217 (1983).

(28) M. Kanke, I. S. Sniecinski, and P. P. DeLuca, *J. Parenteral Sci. Tech.*, **37**(6) (1983).

(29) T. M. Saba, *Arch. Intern. Med.*, **126,** 1031 (1970).

(30) W. Norde and J. Lyklema, *J. Colloid Interface Sci.*, **66,** 257 (1978).

(31) R. E. Baier and R. T. Dutton, *J. Biomed. Mater. Res.*, **3,** 191 (1978).

(32) T. M. S. Chang, "Artificial Cells," Thomas, Springfield, Ill., 1972.

(33) P. Couvreur, P. Tulkens, M. Roland, A. Trouet, and P. P. Speiser, *FEBS Lett.*, **84,** 323 (1977).

(34) F. Brasseur, P. Couvreur, B. Kante, L. Deckers-Passau, M. Roland, C. Deckers, and P. P. Speiser, *Eur. J. Cancer*, **16,** 1441 (1980).

ACKNOWLEDGMENTS

This work was supported in part by NIH-BRSG funds.

The authors are indebted to Dr. R. Yokel, College of Pharmacy, University of Kentucky, Lexington, for his useful instructions concerning the animal experiments.

Oral and Intravenous Pharmacokinetics of Milrinone in Human Volunteers

RONALD M. STROSHANE, RAYMOND F. KOSS, CHARLES E. BIDDLECOME, CAROL LUCZKOWEC, and JEROME EDELSON ˣ

Received May 19, 1983, from the *Department of Drug Metabolism and Disposition, Sterling-Winthrop Research Institute, Rensselaer, NY 12144.* Accepted for publication November 29, 1983.

Abstract □ Thirty-nine healthy men received milrinone either orally or intravenously in two separate double-blind, placebo-controlled studies. The mean bioavailability, based on the area under the plasma concentration *versus* time curves, was 0.92. The plasma data for those subjects in the intravenous study were described by an open two-compartment model with a mean (±*SD*) apparent first-order terminal elimination rate constant (β) of 0.86 (± 0.23) h^{-1}, which corresponds to a half-life of 0.8 h. In the intravenous study, the renal clearance and total body clearance were 21.1 and 25.9 L/h, respectively. The corresponding values in the oral study were 23.8 and 29.7 L/h. Between 79.9 and 84.5% of the total doses were recovered in the urine samples taken at 0–24 h.

Keyphrases □ Milrinone—blood plasma levels, human volunteers, oral and intravenous administration, bioavailability □ Pharmacokinetics—milrinone, an open two-compartment body model □ Cardiotonic agents—milrinone, pharmacokinetics, bioavailability

Milrinone[1] (1,6-dihydro-2-methyl-6-oxo[3,4′-bipyridine]-5-carbonitrile; I), is an experimental cardiotonic agent that is chemically related to amrinone (1). Both compounds, which are neither glycosides nor catechols, have demonstrated positive inotropic effects in animal models (2). In dogs, an intravenous bolus injection of milrinone (0.01–1.0 mg/kg) caused an increase in cardiac contractile force within 1 min, with a duration of action of up to 2 h. The effects could be maintained by intravenous infusion (0.3–10 μg/kg/min) for several hours. Oral activity (0.1–1.0 mg/kg) in dogs was also demonstrated, with an onset of activity within 30 min and a duration of more than 6 h (3).

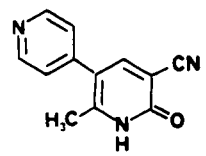

I

Milrinone has been given to patients with severe chronic heart failure (4, 5). Intravenous bolus administration (25–150 μg/kg) resulted in significant increases in the cardiac index. Hemodynamic improvements were maintained with intravenous infusion (0.25–1.0 μg/kg/min) over periods of 24–48 h (5). Thus far, preliminary data disclosed that after intravenous treatment, the oral administration of milrinone (10–20 mg/d divided into three or four doses) maintained the improvement in cardiac function without reported adverse effects (4).

The analytical method for analysis of milrinone in human plasma and urine and the pharmacokinetic parameters following intravenous administration in dogs have been described previously (6). In this report, the results of our investigations into the pharmacokinetics of milrinone in humans following intravenous medication are described, and plasma levels following oral and intravenous administration are compared.

[1] Sterling Drug, Inc., New York, N.Y.

EXPERIMENTAL SECTION

Human Subjects—As part of the safety and pharmacokinetic evaluation of milrinone, 21 normal male volunteers between the ages of 19 and 40 years (mean, 28.5 years) and 18 normal male volunteers between the ages of 18 and 41 years (mean, 28.9 years) were selected to receive milrinone in an intravenous study and an oral study, respectively. Prior to acceptance in a study, each volunteer was examined to ensure that there were no clinical findings indicative of renal, hepatic, or cardiac dysfunction. Appropriate institutional review and approval were obtained prior to initiation of the study, and each volunteer gave informed consent. Subjects were admitted to the clinic the evening before initiation of the study, and all subjects remained in the clinic at least 24 h after receiving medication or placebo.

Study Design—The intravenous and oral studies consisted of six or seven groups of three volunteers each. In the intravenous study, subjects received single injections of 10, 30, 45, 60, 75, 100, or 125 μg of milrinone/kg. Three subjects received each of the seven doses. In the oral study, volunteers received single doses of 1.0, 2.5, 5.0, 7.5, 10.0, or 12.5 mg of either milrinone or placebo; three subjects received each of the six doses. Blood samples (10 mL) were collected in evacuated tubes containing oxalate anticoagulant before medication and at ~2, 5, 10, 15, 30, and 45 min and 1.0, 2.0, 3.0, 4.0, 6.0, 8.0, 12.0, 16.0, and 24.0 h after medication. The blood was centrifuged; plasma was separated and frozen until it was analyzed.

In both studies, urine was collected and measured for total volume, and an aliquot was removed for analysis. Collection times included the following intervals: premedication and 0–4, 4–8, 8–12, and 12–24 h after medication.

Assay Procedure—The analysis of plasma and urine for milrinone concentration followed that described previously (6). The method required extraction of milrinone from plasma or urine with ethyl acetate and back-extraction into acid; the samples were then neutralized and subjected to reverse-phase HPLC. Plasma and urine standards, which were freshly prepared in normal human plasma and urine, were extracted and analyzed with each set of samples from the study subjects. The concentrations of milrinone in plasma were determined by comparison with the regression line of the peak height ratios (drug–internal standard) *versus* milrinone concentration in the standards; the mean (±*SE*) correlation coefficients were 0.9967 (±0.0012) for plasma (n = 19) and 0.9997 (±0.0002) for urine (n = 9). The minimum quantifiable level of milrinone was estimated as that concentration at which the lower 80% confidence limit just encompassed zero (7) and was ~1.9 ng/mL for plasma samples and 19.6 ng/mL for urine samples. The HPLC system used consisted of an automatic injector[2], a pump[3], a precolumn[4], a column[5], and a UV detector[6] which monitored the column effluent at 340 nm. The detector was interfaced with a data processing system[7] for data collection and processing.

Pharmacokinetic Calculations—The data obtained from the analysis of the human plasma samples from the intravenous study were described by an open two-compartment model by a nonlinear regression (NLIN) procedure (8). The concentrations were weighted as the square of their reciprocals. An attempt was made to describe the plasma concentration data obtained from the oral study by either an open one- or two-compartment model with first-order absorption.

The plasma concentration data were also analyzed with respect to the following regression-independent parameters: the maximum observed plasma concentration (C_{max}, oral study only); the time at which C_{max} was observed (t_{max}, oral study only); and the area under the plasma concentration *versus* time curve (AUC_0^∞), which was calculated by using the trapezoidal rule plus

[2] Model 710B WISP; Waters Associates Milford, Mass.
[3] Either model M-45; Waters Associates or mini-pump; Milton-Roy, Riviera Beach, Fla.
[4] Corasil C-18 (37–50 μm); Waters Associates.
[5] Partisil 10/25 ODS-3; Whatman, Clifton, N.J.
[6] Model 440; Waters Associates.
[7] Model 3356 LAS; Hewlett-Packard, Santa Clara, Calif.

0022-3549/84/1000-1438$01.00/0
© 1984, American Pharmaceutical Association

Table I—Pharmacokinetic Parameters in Volunteers after Intravenous Administration of Milrinone

		Regression-Dependent Parameters						Regression-Independent Parameters					
Subject	Dose, μg/kg	α, h^{-1}	β, h^{-1}	A, ng/mL	B, ng/mL	Vd_{ss}, L[a]	Vd_{ss}, L/kg	AUC_0^∞, ng·mL^{-1}·h	AUC_0^∞/ Dose	Vd_{ss}, L/kg[b]	Renal Clearance, L/h	CL_B, L/h	Dose Recovered from Urine, %
1	10	11.5	0.995	79.5	18.1	24.3	0.299	29.6	2.96	0.252	19.6	27.4	71.6
2	10	17.9	1.40	69.7	28.2	21.8	0.253	24.3	2.43	0.170	—[c]	35.4	2.3[c]
3	10	8.85	0.884	38.8	16.0	24.9	0.413	23.5	2.35	0.268	21.3	25.5	83.3
Mean ± *SD*				62.7 ± 21.2	20.8 ± 6.52			25.8 ± 3.3					
4	30	12.0	1.09	244	46.2	26.7	0.311	64.2	2.14	0.222	27.2	40.2	67.8
5	30	10.4	1.04	175	47.8	21.2	0.346	64.7	2.16	0.241	20.3	28.3	71.6
6	30	10.1	0.885	203	54.1	24.9	0.321	87.6	2.92	0.250	21.9	26.4	83.1
Mean ± *SD*				207 ± 34.7	49.4 ± 4.18			72.2 ± 13.4					
7	45	9.62	0.897	336	54.7	26.7	0.349	103	2.29	0.282	25.6	33.2	77.2
8	45	7.95	0.919	491	105	15.6	0.192	182	4.04	0.165	17.6	20.0	87.6
9	45	9.05	0.973	246	59.9	23.5	0.378	93.7	2.08	0.304	24.2	29.8	81.4
Mean ± *SD*				358 ± 124	73.2 ± 27.7			126 ± 48.5					
10	60	10.4	0.910	552	98.0	18.9	0.285	182	3.03	0.197	18.5	21.8	84.8
11	60	10.2	0.939	531	112	19.2	0.269	179	2.98	0.232	20.0	23.8	84.3
12	60	10.2	1.04	628	119	19.3	0.222	182	3.03	0.197	24.0	28.4	84.5
Mean ± *SD*				570 ± 51.0	110 ± 10.7			181 ± 1.7					
13	75	3.36	0.612	297	70.4	22.1	0.383	213	2.84	0.282	18.3	20.0	91.6
14	75	11.2	0.956	792	134	16.8	0.257	223	2.97	0.209	19.9	21.9	90.8
15	75	8.77	0.856	685	140	17.7	0.257	249	3.32	0.213	22.8	20.7	110
Mean ± *SD*				591 ± 260	115 ± 38.6			228 ± 18.6					
16	100	2.80	0.355	442	31.7	34.2	0.499	282	2.82	0.294	18.7	24.1	77.6
17	100	6.45	0.708	600	112	29.8	0.375	272	2.72	0.318	23.6	29.1	81.5
18	100	3.03	0.579	401	88.9	25.3	0.374	306	3.06	0.302	18.5	21.9	84.6
Mean ± *SD*				481 ± 105	77.5 ± 41.3			287 ± 17.5					
19	125	9.14	0.886	923	282	22.1	0.263	436	3.49	0.213	21.7	24.0	89.0
20	125	3.18	0.469	485	50.3	30.3	0.509	286	2.29	0.394	—[c]	25.8	28.5[c]
21	125	2.80	0.707	510	242	17.5	0.248	554	4.43	0.217	16.3	15.8	103
Mean ± *SD*				639 ± 246	191 ± 124			425 ± 134					
Overall mean		8.52	0.862			23.0	0.324		2.87	0.249	21.1	25.9	84.5
± *SD*		3.80	0.230			4.85	0.084		0.61	0.055	2.92	5.69	10.1

[a] $Vd_{ss} = [\text{Dose}(A/\alpha^2 + B/\beta^2)]/(A/\alpha + B/\beta)^2$. [b] $Vd_{ss} = [\text{Dose}(\text{AUMC}_0^\infty)]/(\text{AUC}_0^\infty)^2$. [c] Incomplete urine collection.

Table II—Pharmacokinetic Parameters in Volunteers after Oral Administration of Milrinone

Subject	Dose, mg	Dose, μg/kg	k_e, h^{-1}	AUC_0^∞, ng mL^{-1} h	AUC_0^∞/ Dose	C_{max}, ng/mL	t_{max}, h	Renal Clearance, L/h	CL_B, L/h	Percent Dose Recovered from Urine
22	1.0	12.8	0.72	28.0	2.19	16.7	1.00	11.8[a]	35.7	33.0[a]
23	1.0	13.3	0.78	44.7	3.36	25.4	1.00	17.9	22.4	80.0
24	1.0	13.0	1.20	42.6	3.28	40.9	0.53	8.49[a]	23.5	36.0[a]
Mean ± *SD*				38.4		27.7				
				9.1		12.3				
25	2.5	28.8	1.00	76.4	2.65	50.5	1.50	23.4	32.7	71.6
26	2.5	31.3	0.50	67.3	2.15	32.0	0.48	24.7	37.1	66.4
27	2.5	31.2	0.93	74.5	2.39	41.4	1.00	26.7	33.5	79.6
Mean ± *SD*				72.7		41.3				
				4.8		9.25				
28	5.0	66.9	1.12	121	1.81	105	1.03	36.8	41.3	88.8
29	5.0	74.4	0.62	217	2.92	101	0.50	19.6	23.1	85.2
30	5.0	75.9	1.10	196	2.59	141	1.50	21.3	25.5	83.6
Mean ± *SD*				178		116				
				50.5		22.0				
31	7.5	94.9	0.60	358	3.77	148	1.50	15.4	21.0	79.2
32	7.5	104.5	0.66	286	2.74	125	1.53	19.0	26.2	83.2
33	7.5	90.3	0.67	296	3.27	1184	1.00	2.06[a]	25.3	15.6[a]
Mean ± *SD*				313		152				
				39.0		29.7				
34	10.0	137.6	0.60	392	2.85	231	0.50	20.3	25.5	73.3
35	10.0	148.8	0.74	392	2.64	130	3.00	21.2	25.5	72.7
36	10.0	149.7	0.56	275	1.83	114	1.53	5.68[a]	36.3	8.1[a]
Mean ± *SD*				353		158				
				67.6		63.4				
37	12.5	160.1	0.60	494	3.09	245	1.00	9.09[a]	25.3	35.8[a]
38	12.5	179.3	0.92	382	2.13	334	1.03	35.0	32.7	107
39	12.5	184.6	0.51	297	1.61	123	0.62	28.5	42.1	67.8
Mean ± *SD*				391		234				
				98.8		106				
Overall mean ± *SD*			0.77		2.63		1.13	23.8[b]	29.7	79.9[b]
			0.22		0.60		0.60	6.4[b]	6.7	10.7[b]

[a] Incomplete urine collection. [b] Excluding incomplete collection data.

terminal plasma concentration divided by the terminal elimination rate constant (to correct to infinite time). Total body clearance was determined by dividing the dose by the AUC_0^∞. Other pharmacokinetic parameters were estimated by classical techniques (9).

The data obtained from urine were used to calculate the renal clearance of milrinone by dividing the amount of unchanged milrinone excreted in the urine over a given period by the AUC for that period. The relative bioavailability was determined by dividing the mean normalized AUC_0^∞ for the oral dose by the mean normalized AUC_0^∞ for the intravenous dose.

RESULTS AND DISCUSSION

The concentrations of milrinone in the plasma samples from each volunteer were determined. After intravenous medication, the plasma concentrations declined biexponentially with time, suggesting that a two-compartment model would be appropriate. Pharmacokinetic parameters for each subject in the intravenous study were estimated after computer fitting the data obtained from plasma by an iterative nonlinear least-squares regression technique (8) (Table I).

The mean apparent first-order terminal elimination half-life for milrinone following intravenous medication was ~50 min. The mean apparent volume of distribution at steady state Vd_{ss} was 23.0 L or, dividing by body weight, 0.32 L/kg. The mean value for α (8.52 h^{-1}) corresponded to a distributive-phase half-life of <5 min. The mean regression-independent total body clearance (dose/AUC_0^∞) was 25.9 L/h, whereas the mean regression-independent renal clearance (total intact drug in urine/AUC_0^∞) was 21.1 L/h, which exceeds the glomerular filtration rate and suggests an active excretion mechanism. The values obtained by the trapezoidal rule for the regression-independent AUC_0^∞ were consistently higher than the corresponding regression-dependent AUC_0^∞ ($A/\alpha + B/\beta$). Since the Vd_{ss} values are inversely related to the square of the AUC_0^∞, the regression-independent Vd_{ss} values are consistently lower than the corresponding regression-dependent values. Although there is almost a threefold difference between the highest (subject 4) and lowest (subject 21) clearances, the observed concentration data from the intravenous study were adequately described by the model for both of these subjects; a comparison of the observed and predicted concentrations is shown in Fig. 1. The agreement between the observed values and those predicted by the open two-compartment body model is apparent. The amount of intact milrinone present in the urine over the 24-h period following drug administration was similar in both studies: 84.5% of the dose following intravenous administration and 79.9% of the dose following oral administration. The dosage ratio, oral-intravenous, suggests that the fraction of the oral dose that is bioavailable is ~0.95 (see below).

The plasma concentration data obtained in the oral study were not adequately described by either the open one- or two-compartment model with first-order absorption, although several weighting schemes were tried. Regression-independent parameters were determined for the oral study (Table II). The mean time of maximum plasma concentration was 1.13 h after medication. The renal clearance (23.8 ± 6.4 L/h) was comparable to that found in the intravenous study, as was the total body clearance (29.7 ± 6.7 L/h). The terminal elimination half-life was ~55 min.

Although the same subjects were not used in a crossover manner in the intravenous and oral investigations, an estimate of the absolute bioavailability was obtained by comparing the data from the two independent studies. The mean absolute bioavailability or oral-parenteral ratio, defined as the ratio of the AUC_0^∞/dose for the tablet to the regression-independent AUC_0^∞/dose for the intravenous solution, was 0.92, which is consistent with the urinary excretion data. Analysis of variance indicated that the AUC_0^∞/dose values for medication administered either by the intravenous or oral routes were not significantly different ($p = 0.21$). Furthermore, a statistical analysis of AUC_0^∞/dose against administered dose showed that the AUC_0^∞/dose was not dose dependent ($p = 0.94$).

The mean terminal elimination half-life of milrinone obtained in these human volunteers varied substantially from the value of 3.6-h obtained in dogs at intravenous doses of 5 mg/kg (6). This difference is surprising in light of the relatively good correlation in the amrinone studies between the mean terminal elimination half-life in dogs receiving doses of 5 mg/kg iv (2.37 h) (10) and human volunteers receiving doses of 75 mg iv (3.6 h) (1). Following

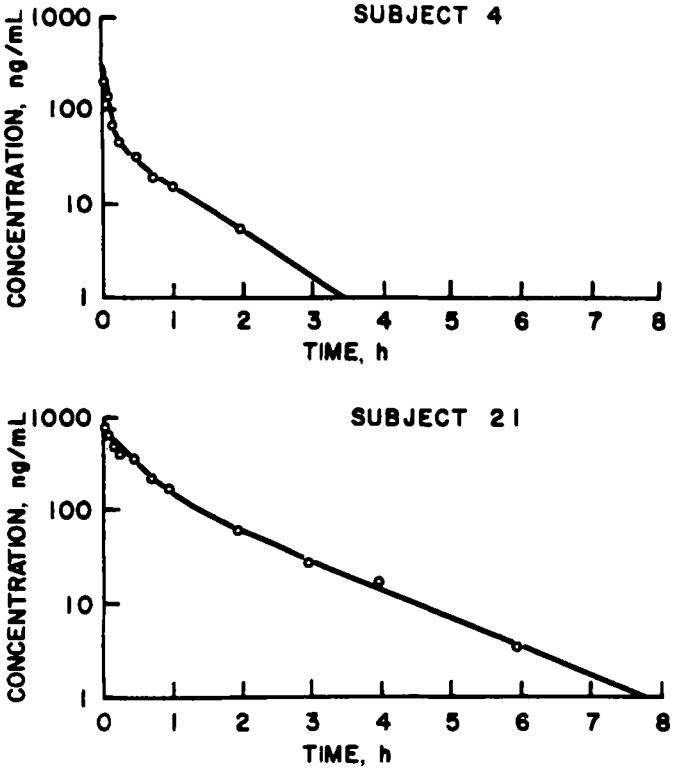

Figure 1—*Plasma concentration of milrinone in human volunteers after intravenous administration. Data points are plasma concentrations observed in two subjects with widely divergent clearance rates and concentrations predicted by the open two-compartment model (solid line).*

oral administration of 75 mg to volunteers, the mean terminal elimination half-life of amrinone was 4.33 h (1).

The mean half-life of amrinone in patients with congestive heart failure was 8.3 h (11), which is more than twice that seen in volunteers with normal cardiac function. We anticipate a similar increase in the terminal elimination half-life of milrinone in patients with congestive heart failure. The decrease in renal and hepatic blood flow in patients with severe cardiac impairment may be responsible for this increase in the duration of the drug in plasma. We are currently studying the pharmacokinetics of milrinone in patients with congestive heart failure as part of clinical efficacy trials. Attempts will be made to correlate the effects of dose on the terminal elimination half-life of milrinone.

REFERENCES

(1) G. B. Park, R. P. Kershner, J. Angellotti, R. L. Williams, L. Z. Benet, and J. Edelson, *J. Pharm. Sci.*, **72**, 817 (1983).

(2) A. A. Alousi, J. M. Canter, M. J. Montenaro, D. J. Fort, and R. A. Ferrari, *J. Cardiovasc. Pharm.*, **5**, 792 (1983).

(3) A. A. Alousi, A. Helstosky, M. J. Montenaro, and F. Cicero, *Fed. Proc.*, **40**(3, part I), no. 2478, March 1, 1981.

(4) C. S. Maskin, E. H. Sonnenblick, and T. H. LeJemtel, *J. Am. Coll. Cardiol.* **1**, 675 (1983).

(5) A. McDowell, D. Baim, J. Cherniles, T. Bekele, E. Braunwald, and W. Grossman, *J. Am. Coll. Cardiol.* **1**, 675 (1983).

(6) J. Edelson, R. F. Koss, J. F. Baker, and G. B. Park, *J. Chromatogr.*, **276**, 456 (1983).

(7) R. W. Ross and H. Stander, in "Some Statistical Problems in Drug Metabolism," Princeton Conference on Applied Statistics, 1975.

(8) J. T. Helwig and K. A. Council, Eds., "SAS User's Guide," SAS Institute, Inc., Raleigh, N.C., 1979, pp. 317-329.

(9) M. Gibaldi and D. Perrier, "Pharmacokinetics," Marcel Dekker, New York, N.Y., 1975.

(10) M. P. Kullberg, B. Dorrbecker, J. Lennon, E. Rowe, and J. Edelson, *J. Chromatogr.*, **187**, 264 (1980).

(11) J. Edelson, T. H. LeJemtel, A. A. Alousi, C. E. Biddlecome, C. S. Maskin, and E. H. Sonnenblick, *Clin. Pharmacol. Ther.*, **29**, 723 (1981).

ACKNOWLEDGMENTS

The contributions of Dr. Kenneth C. Lasseter and his staff at Clinical Pharmacology Associates, Miami, Fla., are gratefully acknowledged. The competent technical assistance of Chester Koblantz, Gerard Palace, and Julie Utter are appreciated. We thank Sibyl Kellman for her help in preparing this manuscript.

Crystallinity and Dissolution Rate of Tolbutamide Solid Dispersions Prepared by the Melt Method

JAMES W. McGINITY *x, PHILIPPE MAINCENT *, and HUGO STEINFINK ‡

Received October 24, 1983, from the **Drug Dynamics Institute, College of Pharmacy and* ‡*Department of Chemical Engineering, University of Texas at Austin, Austin, TX 78712.* Accepted for publication December 21, 1983.

Abstract □ The influence of cooling rate of solid dispersions prepared by the melt method was studied by X-ray diffraction and scanning electron microscopy. Tolbutamide was the model drug investigated, and the carriers included urea and polyethylene glycol 6000. Slow-cooled urea dispersions of tolbutamide demonstrated a complete lack of crystallinity suggesting the formation of an amorphous material. The rapidly cooled dispersion showed peaks for urea and an absence of drug in the X-ray pattern, suggesting that a true molecular dispersion was formed. The X-ray patterns of rapid- and slow-cooled dispersions of tolbutamide and polyethylene glycol 6000 demonstrated that a physical mixture of drug and carrier resulted from both methods of dispersion preparation.

Keyphrases □ Solid dispersions—melt method of preparation, cooling rates and physicochemical properties □ Tolbutamide—solid dispersions with urea and polyethylene glycol 6000 □ X-ray diffraction—tolbutamide, solid dispersions, carriers □ Scanning electron microscopy—solid dispersions □ Dissolution rates—tolbutamide, solid dispersions

The rate-determining step in the absorption process for drugs of low solubility is generally the dissolution rate of such drugs in the GI fluids rather than the rapidity of their diffusion across the gut wall. The formation of solid dispersions of the drug with a water-soluble carrier is one of several techniques that can be used to improve the dissolution properties of poorly soluble or hydrophobic drugs. In 1961, Sekiguchi and Obi (1) became the first researchers to propose the use of solid dis-

0022-3549/84/1000-1441$01.00/0
© 1984, American Pharmaceutical Association

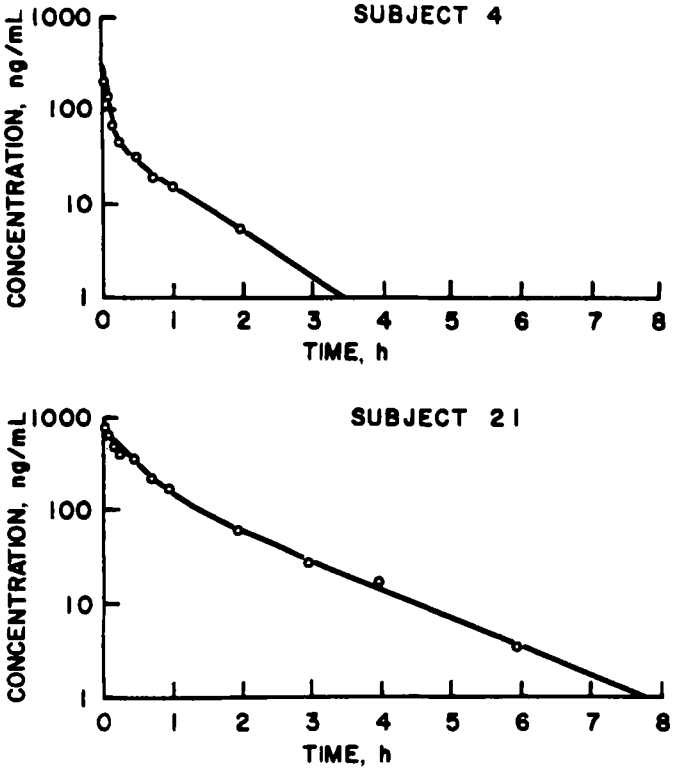

Figure 1—*Plasma concentration of milrinone in human volunteers after intravenous administration. Data points are plasma concentrations observed in two subjects with widely divergent clearance rates and concentrations predicted by the open two-compartment model (solid line).*

oral administration of 75 mg to volunteers, the mean terminal elimination half-life of amrinone was 4.33 h (1).

The mean half-life of amrinone in patients with congestive heart failure was 8.3 h (11), which is more than twice that seen in volunteers with normal cardiac function. We anticipate a similar increase in the terminal elimination half-life of milrinone in patients with congestive heart failure. The decrease in renal and hepatic blood flow in patients with severe cardiac impairment may be responsible for this increase in the duration of the drug in plasma. We are currently studying the pharmacokinetics of milrinone in patients with congestive heart failure as part of clinical efficacy trials. Attempts will be made to correlate the effects of dose on the terminal elimination half-life of milrinone.

REFERENCES

(1) G. B. Park, R. P. Kershner, J. Angellotti, R. L. Williams, L. Z. Benet, and J. Edelson, *J. Pharm. Sci.*, **72**, 817 (1983).

(2) A. A. Alousi, J. M. Canter, M. J. Montenaro, D. J. Fort, and R. A. Ferrari, *J. Cardiovasc. Pharm.*, **5**, 792 (1983).

(3) A. A. Alousi, A. Helstosky, M. J. Montenaro, and F. Cicero, *Fed. Proc.*, **40**(3, part I), no. 2478, March 1, 1981.

(4) C. S. Maskin, E. H. Sonnenblick, and T. H. LeJemtel, *J. Am. Coll. Cardiol.* **1**, 675 (1983).

(5) A. McDowell, D. Baim, J. Cherniles, T. Bekele, E. Braunwald, and W. Grossman, *J. Am. Coll. Cardiol.* **1**, 675 (1983).

(6) J. Edelson, R. F. Koss, J. F. Baker, and G. B. Park, *J. Chromatogr.*, **276**, 456 (1983).

(7) R. W. Ross and H. Stander, in "Some Statistical Problems in Drug Metabolism," Princeton Conference on Applied Statistics, 1975.

(8) J. T. Helwig and K. A. Council, Eds., "SAS User's Guide," SAS Institute, Inc., Raleigh, N.C., 1979, pp. 317-329.

(9) M. Gibaldi and D. Perrier, "Pharmacokinetics," Marcel Dekker, New York, N.Y., 1975.

(10) M. P. Kullberg, B. Dorrbecker, J. Lennon, E. Rowe, and J. Edelson, *J. Chromatogr.*, **187**, 264 (1980).

(11) J. Edelson, T. H. LeJemtel, A. A. Alousi, C. E. Biddlecome, C. S. Maskin, and E. H. Sonnenblick, *Clin. Pharmacol. Ther.*, **29**, 723 (1981).

ACKNOWLEDGMENTS

The contributions of Dr. Kenneth C. Lasseter and his staff at Clinical Pharmacology Associates, Miami, Fla., are gratefully acknowledged. The competent technical assistance of Chester Koblantz, Gerard Palace, and Julie Utter are appreciated. We thank Sibyl Kellman for her help in preparing this manuscript.

Crystallinity and Dissolution Rate of Tolbutamide Solid Dispersions Prepared by the Melt Method

JAMES W. McGINITY *x, PHILIPPE MAINCENT *, and HUGO STEINFINK ‡

Received October 24, 1983, from the **Drug Dynamics Institute, College of Pharmacy and* ‡*Department of Chemical Engineering, University of Texas at Austin, Austin, TX 78712.* Accepted for publication December 21, 1983.

Abstract □ The influence of cooling rate of solid dispersions prepared by the melt method was studied by X-ray diffraction and scanning electron microscopy. Tolbutamide was the model drug investigated, and the carriers included urea and polyethylene glycol 6000. Slow-cooled urea dispersions of tolbutamide demonstrated a complete lack of crystallinity suggesting the formation of an amorphous material. The rapidly cooled dispersion showed peaks for urea and an absence of drug in the X-ray pattern, suggesting that a true molecular dispersion was formed. The X-ray patterns of rapid- and slow-cooled dispersions of tolbutamide and polyethylene glycol 6000 demonstrated that a physical mixture of drug and carrier resulted from both methods of dispersion preparation.

Keyphrases □ Solid dispersions—melt method of preparation, cooling rates and physicochemical properties □ Tolbutamide—solid dispersions with urea and polyethylene glycol 6000 □ X-ray diffraction—tolbutamide, solid dispersions, carriers □ Scanning electron microscopy—solid dispersions □ Dissolution rates—tolbutamide, solid dispersions

The rate-determining step in the absorption process for drugs of low solubility is generally the dissolution rate of such drugs in the GI fluids rather than the rapidity of their diffusion across the gut wall. The formation of solid dispersions of the drug with a water-soluble carrier is one of several techniques that can be used to improve the dissolution properties of poorly soluble or hydrophobic drugs. In 1961, Sekiguchi and Obi (1) became the first researchers to propose the use of solid dis-

0022-3549/84/1000-1441$01.00/0
© 1984, American Pharmaceutical Association

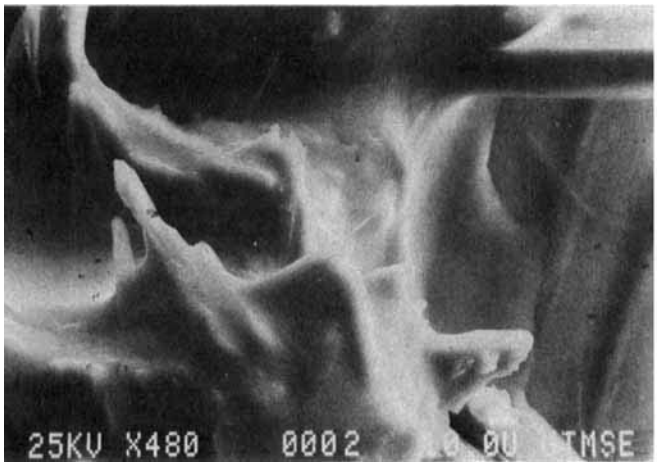

Figure 1—*Scanning electron micrograph of a urea–tolbutamide (2:1) dispersion prepared by process B and aged for 1 d at 25°C.*

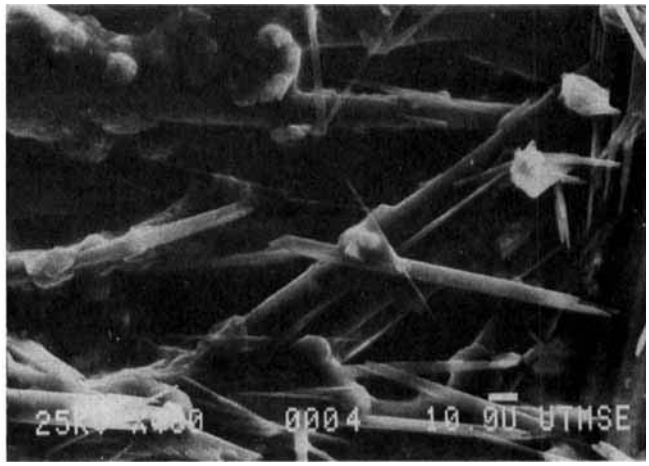

Figure 3—*Scanning electron micrograph of a urea–tolbutamide (2:1) dispersion prepared by process B and aged for 5 months at 25°C.*

persions to increase the dissolution rate and oral absorption of drugs. In recent reports, (2–6), the great variety of drug molecules and water-soluble carriers used to prepare solid dispersions have been reviewed.

Although in previous reports the technology of solid dispersions has been extensively examined, systems in which this technique is utilized have been fraught with problems; thus, few systems have been marketed (3). Since solid dispersions are dynamic systems, further research into the physicochemical properties of these systems is certainly warranted. In recent studies, it has been shown that soluble complexes between drug and carrier may form (7). Kaur and co-workers (5) have studied the phase equilibrium phenomena of solid dispersion systems, whereas Ravis and Chen (4) have compared, by X-ray analysis, the difference in crystallinity between solid dispersions and physical mixtures of drug and carrier. Significant contributions have been made by Ford and Rubinstein (8), who have studied the effect of aging on the dissolution properties of an indomethacin–polyethylene glycol 6000 solid dispersion.

One aspect of solid dispersion technology that has received little attention has been the method of sample preparation. A brief survey of the literature has indicated that there is no uniform method presently used to prepare solid dispersions by the melt method. In several cases, the temperatures to which the carrier and drug were subjected were not reported. Dispersions have been solidified by cooling the melt to room temperature (9, 10). Kaur and co-workers (5, 6) cooled their samples to 4°C, Chiou and Niazi poured the melts onto a stainless steel plate (11), whereas Allen and co-workers (12) rapidly solidified their samples by pouring the melt into an aluminum dish that was placed in a block of dry ice. Other investigators have employed metal pans (2), ice baths (7), and dry ice–acetone baths (13).

The objective of this study was to investigate the influence of cooling conditions on the physicochemical properties of solid dispersions prepared by the melt method. Urea and polyethylene glycol 6000 were the carriers studied, and tolbutamide (1-butyl-3-(*p*-tolylsulfonyl)urea) was the model drug investigated. Some preliminary results were also obtained with salicylic acid and sulfathiazole.

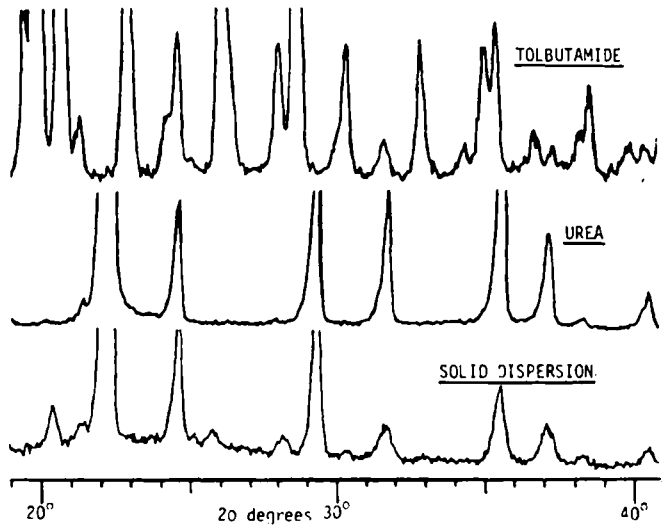

Figure 2—*X-ray patterns of drug, carrier, and rapid-cooled dispersion.*

EXPERIMENTAL SECTION

Materials—Urea[1] (mp 139.7°C), polyethylene glycol 6000[2] (mp 56°C), tolbutamide[3] (mp 125.5°C), salicylic acid[4] (mp 158°C), and sulfathiazole[2] (mp 202°C) were used.

Methods—X-ray diffraction patterns were obtained with an X-ray diffractometer[5] with $CuK_{\alpha 1}$ radiation (0.15405 nm) over a 2θ range of 6–50°. The scanning electron micrographs were recorded on a microscope[6]. Dissolution profiles of drug from dispersion samples were determined with the USP paddle apparatus. For the tolbutamide samples, 900 mL of pH 6.0 buffer were stirred at 50 rpm and maintained at 37°C. The melts were prepared by first heating the carrier in an aluminum dish over an oil bath to 5°C above the melting point of the carrier. The drug was then dissolved into the molten carrier and stirred for 2 min to ensure a homogeneous dispersion. Two methods of cooling were employed. Process A involved the flash cooling of the dispersion by immersion of the aluminum dish containing the molten dispersion in a bath of dry ice and acetone. The preparation of the dispersion by Process B involved the gradual cooling of the oil bath under ambient conditions over a period of several hours. Dispersions from both processes were then passed through a 20-mesh screen, and the 20- to 40-mesh fraction was retained for the dissolution study. Ground samples of the dispersion were employed for the scanning electron microscopic evaluation of the surface crystalline properties. Dispersions in the 60–100 mesh range were used for X-ray analysis. Ratios of carrier to drug, 2:1 w/w, were used for all samples with the exception of the polyethylene glycol 6000–sulfathiazole system, in which a 4:1 ratio was employed. For all these systems, full solution dispersions were obtained prior to the cooling step.

[1] Matheson, Coleman and Bell, Norwood, Ohio.
[2] City Chemical Corp., New York, N.Y.
[3] The Upjohn Co., Kalamazoo, Mich.
[4] Fisher Scientific Co., Fair Lawn, N.J.
[5] Philips.
[6] JEOL JSM35.

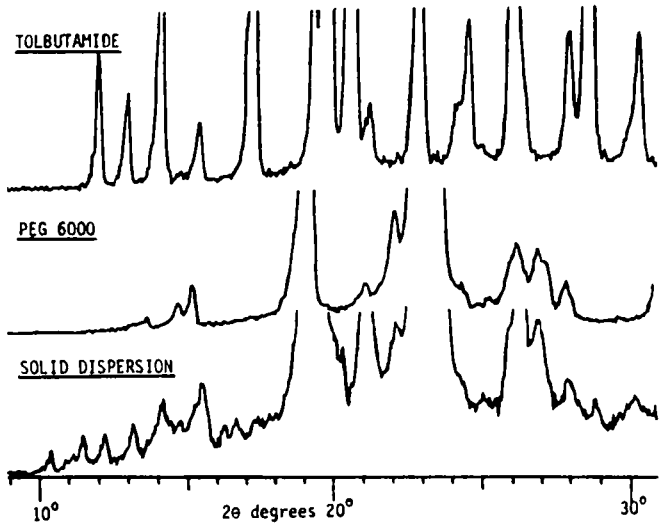

Figure 4—*X-ray patterns of drug, carrier, and rapid-cooled dispersion.*

RESULTS AND DISCUSSION

Powder X-ray diffraction patterns of tolbutamide, urea, and polyethylene glycol 6000 were taken of samples that were both slow and flash cooled. For each material alone, the rate of cooling did not influence the crystallinity since the peak widths of the diffraction profiles remained constant. No additional new diffraction lines were detected, indicating that no degradation or new compound formation had occurred. Minor changes in the intensity of some peaks were seen with samples prepared by either process. However, this was probably due to changes in preferred orientation rather than any alteration in the physicochemical properties of the material. The multitude of peaks obtained with urea and tolbutamide verified the crystalline properties of these solids. The two most intense peaks in the X-ray pattern for polyethylene glycol 6000 were found at 19.2 and 23.4°.

A study of the physical mixture of tolbutamide–urea produced a pattern which was due to the combination of the drug and carrier. Markedly different results were evident with the urea–tolbutamide dispersions prepared by the rapid- and slow-cooled methods. The X-ray patterns for the slow-cooled dispersions demonstrated a complete lack of crystallinity, suggesting the formation of an amorphous material. A scanning electron micrograph of this dispersion is shown in Fig. 1. The X-ray patterns shown in Fig. 2 are those of tolbutamide, urea, and the dispersion prepared by process A (rapid cooled). The complete absence of peaks for the tolbutamide in the dispersion is readily evident. All peaks present from the dispersion sample are those of the carrier. This phenomenon could be due to the formation of a true molecular dispersion of the tolbutamide within the urea matrix, or alternatively, it could mean that tolbutamide is present on the surface of the urea crystals as an amorphous coating.

A similar phenomenon has been reported by Chiou (14) with the griseofulvin–polyethylene glycol 6000 system. Since the peaks for the drug were absent in the X-ray diffraction pattern, Chiou has proposed that an amorphous form of griseofulvin was present in the melt after cooling. However, when X-ray diffraction studies were repeated several days later, major diffraction peaks of griseofulvin were present, indicating crystal formation in the dispersion. This result was obtained for all samples studied with the exception of the 5% drug sample. An examination of the tolbutamide–urea dispersion prepared by process A after storage at 25°C for 45 d indicated that no tolbutamide peaks were present in the X-ray diffraction pattern. These preliminary stability data suggest that some form of molecular interaction may be present between tolbutamide and urea to maintain the drug in the amorphous state. Storage of the slow-cooled dispersion (Fig. 1) at 25°C for 5 months resulted in crystal growth (Fig. 3). The X-ray pattern of this sample was identical to that of the solid dispersion (Fig. 2), indicating that the crystals consisted of urea rather than tolbutamide. X-ray examination of physical mixtures of tolbutamide–urea verified that samples containing as little as 2% drug yield peaks for tolbutamide.

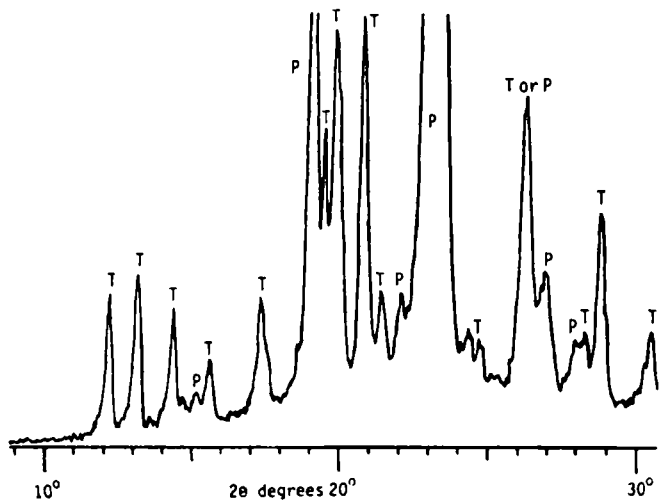

Figure 5—*X-ray pattern of polyethylene glycol 6000–tolbutamide dispersion prepared by process B.*

Table I—Dissolution Characteristics of Polyethylene Glycol 6000–Tolbutamide (2:1) Dispersions [a]

Time, min	Percent Drug Released [b]		
	Rapid Cooled (Process A)	Slow Cooled (Process B)	Physical Mixture
6	36.9 ± 5.3	29.7 ± 2.6	27.8 ± 4.0
10	60.4 ± 3.5	45.8 ± 3.5	44.4 ± 4.2
15	72.3 ± 4.4	57.9 ± 3.5	60.1 ± 1.9
20	78.3 ± 5.4	64.4 ± 1.6	64.2 ± 2.5
25	86.7 ± 4.7	71.5 ± 2.9	70.8 ± 3.4
40	91.0 ± 4.3	75.6 ± 3.5	80.0 ± 2.4
60	96.3 ± 3.0	84.6 ± 1.9	82.8 ± 1.5
100	100.6 ± 1.2	90.5 ± 1.0	87.5 ± 1.8

[a] In 900 mL of pH 6.0 buffer maintained at 37°C and agitated at 50 rpm by the USP paddle method. [b] Mean ± *SD*.

The X-ray patterns of tolbutamide, polyethylene glycol 6000, and the solid dispersion prepared by process A are shown in Fig. 4. Comparison of these patterns indicates that the dispersion is present as a physical mixture of the drug and carrier. The slow-cooled dispersion shown in Fig. 5 had a very similar pattern to the dispersion shown in Fig. 4. The higher intensity of peaks shown in Fig. 5 suggested a greater degree of crystallinity from the slow-cooled samples. This phenomenon was verified by scanning electron microscopy.

The dissolution properties of tolbutamide–polyethylene glycol 6000 dispersions prepared by process A and process B were compared with the dissolution properties of tolbutamide from the physical mixture of the drug and polyethylene glycol 6000 (Table I). Insignificant differences were seen in the dissolution properties of drug from the slow-cooled dispersion and the physical mixture. However, ~15% more drug passed into solution at most time intervals for the dispersion prepared by process A. This phenomenon was probably due to a particle size effect since a smaller drug particle was expected from the flash-cooled dispersion. The lower degree of crystallinity for this dispersion was verified by the X-ray diffraction patterns (Figs. 4 and 5). The greater dissolution rate of dispersions prepared by process A may also be attributed to a greater energy of the drug particles in these dispersions. Less crystalline or more amorphous forms generally possess greater thermodynamic activities than more crystalline forms of the same substance (15).

The peaks for sulfathiazole in the X-ray diffraction patterns of sulfathiazole–urea dispersions were absent for both the slow- and flash-cooled dispersions. This result was similar to that for the tolbutamide–urea dispersions prepared by process A. A physical mixture of both drug and carrier was found with the sulfathiazole–polyethylene glycol 6000 samples. Salicylic acid in urea dispersions produced new peaks in the X-ray diffraction patterns, suggesting that either an interaction occurred or a polymorphic change in either the drug or carrier took place to form a new phase.

In summary, the applications of X-ray diffraction to study the physicochemical properties of solid dispersions have been demonstrated. The rate of cooling of melt dispersions will, in many cases, influence the physical state of both drug and carrier. Other techniques are presently being evaluated for use in conjunction with X-ray diffraction to differentiate and identify polymorphic transitions, degradation product or complex formation, molecular dispersion formation, physical mixtures, and the determination of degrees of crystallinity in the melt dispersions. Future studies will also employ X-ray diffraction to examine changes in the microcrystalline properties of these dispersions as a function of time and temperature.

REFERENCES

(1) K. Sekiguchi and N. Obi, *Chem. Pharm. Bull.*, **9**, 866 (1961).

(2) H. V. Maulding, *J. Pharm. Sci.*, **67**, 391 (1978).
(3) J. W. McGinity, *Pharm. Tech.*, March **1978**, 50.
(4) W. R. Ravis and C. Chen, *J. Pharm. Sci.*, **70**, 1353 (1981).
(5) R. Kaur, D. J. W. Grant, and T. Eaves, *J. Pharm. Sci.*, **69**, 1317 (1980).
(6) R. Kaur, D. J. W. Grant, and T. Eaves, *J. Pharm. Sci.*, **69**, 1321 (1980).
(7) O. I. Corrigan and R. F. Timoney, *Pharm. Acta Helv.*, **51**, 268 (1976).
(8) J. C. Ford and H. Rubinstein, *Pharm. Acta Helv.*, **53**, 93 (1978).
(9) S. A. Said, M. El-Fatatry, and A. S. Geneidi, *Aust. J. Pharm. Sci.*, June **1974**, 42.
(10) D. J. Allen and K. C. Kwan, *J. Pharm. Sci.*, **58**, 1190 (1969).
(11) W. L. Chiou and S. J. Niazi, *J. Pharm. Sci.*, **60**, 1333 (1971).
(12) D. J. Allen, V. A. Yanchick, and D. D. Maness, *J. Pharm. Sci.*, **66**, 494 (1977).
(13) J. W. McGinity, D. D. Maness, and G. J. Yakatan, *Drug Dev. Comm.*, **1**, 369 (1974).
(14) W. L. Chiou, *J. Pharm. Sci.*, **66**, 989 (1977).
(15) J. Mullins and T. Macek, *J. Am. Pharm. Assoc., Sci. Ed.*, **49**, 245 (1960).

ACKNOWLEDGMENTS

The authors thank the Upjohn Co., Kalamazoo, Mich., for the generous supplies of tolbutamide. One of the authors (P. M.) gratefully acknowledges the financial support of the Delegation Generale Recherche Sciences et Techniques (Paris, France).

A High-Performance Liquid Chromatographic Method for The Simultaneous Determination of Nicardipine and Its Pyridine Metabolite II in Plasma

ANNE T. WU ˣ, IAN J. MASSEY, and STANLEY KUSHINSKY

Received September 29, 1983, from the *Department of Analytical and Metabolic Chemistry, Syntex Research, Palo Alto, CA 94304.* Accepted for publication December 5, 1983.

Abstract □ A rapid and specific method in which reverse-phase high-performance liquid chromatography (HPLC) with UV detection was used for the simultaneous determination of nicardipine and its pyridine metabolite II in human plasma is described. Nicardipine, its pyridine metabolite II, and the internal standard were extracted from plasma and partially purified by acid–base partitioning. Final purification and quantitation were achieved by HPLC by using a reverse-phase column and a UV detector (254 nm). The extraction efficiencies for nicardipine and its pyridine metabolite II from 1 mL of plasma were 77.4 and 81.1%, respectively. The sensitivity of the assay was 5 ng/mL for both nicardipine and its pyridine metabolite II, and the linear concentration range of the assay was 5–150 ng/mL for both compounds. The low coefficients of variation (≤5%) for samples spiked with nicardipine and its pyridine metabolite II in this concentration range demonstrate good reliability and reproducibility of the assay. The HPLC procedure has been validated by comparison with a GC–electron-capture detection (ECD) procedure, which gives the combined concentration of nicardipine–its pyridine metabolite II (total) and with an HPLC/GC–ECD procedure, which gives the concentration of its pyridine metabolite II. All three methods, which were developed in our laboratory, were used to analyze nicardipine and its pyridine metabolite II in specimens of plasma from subjects treated with nicardipine hydrochloride. Good correlations were found for concentrations of nicardipine, its pyridine metabolite II, and nicardipine plus the metabolite determined by these three procedures. The HPLC procedure is suitable for use in pharmacokinetic studies following administration of nicardipine hydrochloride to humans.

Keyphrases □ Nicardipine—simultaneous determination with its pyridine metabolite II, reverse-phase HPLC □ HPLC—reverse-phase simultaneous determination of nicardipine and its pyridine metabolite II in human plasma

Nicardipine hydrochloride, 2-(*N*-benzyl-*N*-methylamino)ethyl methyl 1,4-dihydro-2,6-dimethyl-4-(*m*-nitrophenyl)-3,5-pyridinedicarboxylate monohydrochloride (I), is a new calcium entry-blocking agent with potent oral vasodilating activity. The therapeutic efficacy of this compound for the treatment of angina, hypertension, and cerebrovascular disease is under investigation.

Nicardipine hydrochloride, which is effective at relatively low doses, undergoes extensive first-pass metabolism to produce several metabolites (1). Therefore, a sensitive and specific method is required for its determination in human plasma. Various methods have been reported for the determination of nicardipine in plasma. These include gas chromatography (GC) with either electron-capture detection (GC–ECD) (2) or with mass spectrometric detection (GC–MS) (3). However, these methods are relatively nonspecific because they require oxidation of nicardipine prior to GC analysis. Since the product of this oxidation is the pyridine metabolite II of nicardipine, these methods measure the combined concentration of nicardipine plus its pyridine metabolite II (total). Pharmacokinetic analyses of data generated by these methods can be misleading in view of the fact that the vasodilative activity of the pyridine metabolite II is only $^1/_{300}$ that of the parent drug (4). The individual concentrations of nicardipine and its metabolite in human plasma have been investigated recently using a TLC–GC–MS method (5), in which nicardipine was separated from its pyridine metabolite II by TLC prior to analysis by GC–MS. These investigators have found that in healthy volunteers and hypertensive patients, the concentration of nicardipine relative to that of the combined concentrations of nicardipine plus its pyridine metabolite II ranged from 74% to 99% (5). Recently, we developed a method using high-performance liquid chromatography (HPLC) in conjunction with GC–ECD which allowed the individual concentrations of nicardipine and its pyridine metabolite II to be determined[1]. In this HPLC/GC–ECD method, which was developed prior to the availability in our laboratory of a high-sensitivity HPLC detector, HPLC was used to separate nicardipine from the pyridine metabolite II prior to analysis of the latter by GC–ECD. The concentration of nicardipine in a sample of plasma was obtained by subtracting the concentration of the pyridine metabolite II as determined by the HPLC/GC–ECD assay from the combined concentration of nicardipine plus the pyridine metabolite II as determined by the GC–ECD method

[1] Unpublished results (a brief description of this method is given in the text).

0022-3549/84/1000-1444$01.00/0
© 1984, American Pharmaceutical Association

(2) H. V. Maulding, *J. Pharm. Sci.*, **67**, 391 (1978).
(3) J. W. McGinity, *Pharm. Tech.*, March **1978**, 50.
(4) W. R. Ravis and C. Chen, *J. Pharm. Sci.*, **70**, 1353 (1981).
(5) R. Kaur, D. J. W. Grant, and T. Eaves, *J. Pharm. Sci.*, **69**, 1317 (1980).
(6) R. Kaur, D. J. W. Grant, and T. Eaves, *J. Pharm. Sci.*, **69**, 1321 (1980).
(7) O. I. Corrigan and R. F. Timoney, *Pharm. Acta Helv.*, **51**, 268 (1976).
(8) J. C. Ford and H. Rubinstein, *Pharm. Acta Helv.*, **53**, 93 (1978).
(9) S. A. Said, M. El-Fatatry, and A. S. Geneidi, *Aust. J. Pharm. Sci.*, June **1974**, 42.
(10) D. J. Allen and K. C. Kwan, *J. Pharm. Sci.*, **58**, 1190 (1969).
(11) W. L. Chiou and S. J. Niazi, *J. Pharm. Sci.*, **60**, 1333 (1971).
(12) D. J. Allen, V. A. Yanchick, and D. D. Maness, *J. Pharm. Sci.*, **66**, 494 (1977).
(13) J. W. McGinity, D. D. Maness, and G. J. Yakatan, *Drug Dev. Comm.*, **1**, 369 (1974).
(14) W. L. Chiou, *J. Pharm. Sci.*, **66**, 989 (1977).
(15) J. Mullins and T. Macek, *J. Am. Pharm. Assoc., Sci. Ed.*, **49**, 245 (1960).

ACKNOWLEDGMENTS

The authors thank the Upjohn Co., Kalamazoo, Mich., for the generous supplies of tolbutamide. One of the authors (P. M.) gratefully acknowledges the financial support of the Delegation Generale Recherche Sciences et Techniques (Paris, France).

A High-Performance Liquid Chromatographic Method for The Simultaneous Determination of Nicardipine and Its Pyridine Metabolite II in Plasma

ANNE T. WU ˣ, IAN J. MASSEY, and STANLEY KUSHINSKY

Received September 29, 1983, from the *Department of Analytical and Metabolic Chemistry, Syntex Research, Palo Alto, CA 94304.* Accepted for publication December 5, 1983.

Abstract □ A rapid and specific method in which reverse-phase high-performance liquid chromatography (HPLC) with UV detection was used for the simultaneous determination of nicardipine and its pyridine metabolite II in human plasma is described. Nicardipine, its pyridine metabolite II, and the internal standard were extracted from plasma and partially purified by acid–base partitioning. Final purification and quantitation were achieved by HPLC by using a reverse-phase column and a UV detector (254 nm). The extraction efficiencies for nicardipine and its pyridine metabolite II from 1 mL of plasma were 77.4 and 81.1%, respectively. The sensitivity of the assay was 5 ng/mL for both nicardipine and its pyridine metabolite II, and the linear concentration range of the assay was 5–150 ng/mL for both compounds. The low coefficients of variation (≤5%) for samples spiked with nicardipine and its pyridine metabolite II in this concentration range demonstrate good reliability and reproducibility of the assay. The HPLC procedure has been validated by comparison with a GC–electron-capture detection (ECD) procedure, which gives the combined concentration of nicardipine–its pyridine metabolite II (total) and with an HPLC/GC–ECD procedure, which gives the concentration of its pyridine metabolite II. All three methods, which were developed in our laboratory, were used to analyze nicardipine and its pyridine metabolite II in specimens of plasma from subjects treated with nicardipine hydrochloride. Good correlations were found for concentrations of nicardipine, its pyridine metabolite II, and nicardipine plus the metabolite determined by these three procedures. The HPLC procedure is suitable for use in pharmacokinetic studies following administration of nicardipine hydrochloride to humans.

Keyphrases □ Nicardipine—simultaneous determination with its pyridine metabolite II, reverse-phase HPLC □ HPLC—reverse-phase simultaneous determination of nicardipine and its pyridine metabolite II in human plasma

Nicardipine hydrochloride, 2-(*N*-benzyl-*N*-methylamino)ethyl methyl 1,4-dihydro-2,6-dimethyl-4-(*m*-nitrophenyl)-3,5-pyridinedicarboxylate monohydrochloride (I), is a new calcium entry-blocking agent with potent oral vasodilating activity. The therapeutic efficacy of this compound for the treatment of angina, hypertension, and cerebrovascular disease is under investigation.

Nicardipine hydrochloride, which is effective at relatively low doses, undergoes extensive first-pass metabolism to produce several metabolites (1). Therefore, a sensitive and specific method is required for its determination in human plasma. Various methods have been reported for the determination of nicardipine in plasma. These include gas chromatography (GC) with either electron-capture detection (GC–ECD) (2) or with mass spectrometric detection (GC–MS) (3). However, these methods are relatively nonspecific because they require oxidation of nicardipine prior to GC analysis. Since the product of this oxidation is the pyridine metabolite II of nicardipine, these methods measure the combined concentration of nicardipine plus its pyridine metabolite II (total). Pharmacokinetic analyses of data generated by these methods can be misleading in view of the fact that the vasodilative activity of the pyridine metabolite II is only $^1/_{300}$ that of the parent drug (4). The individual concentrations of nicardipine and its metabolite in human plasma have been investigated recently using a TLC–GC–MS method (5), in which nicardipine was separated from its pyridine metabolite II by TLC prior to analysis by GC–MS. These investigators have found that in healthy volunteers and hypertensive patients, the concentration of nicardipine relative to that of the combined concentrations of nicardipine plus its pyridine metabolite II ranged from 74% to 99% (5). Recently, we developed a method using high-performance liquid chromatography (HPLC) in conjunction with GC–ECD which allowed the individual concentrations of nicardipine and its pyridine metabolite II to be determined[1]. In this HPLC/GC–ECD method, which was developed prior to the availability in our laboratory of a high-sensitivity HPLC detector, HPLC was used to separate nicardipine from the pyridine metabolite II prior to analysis of the latter by GC–ECD. The concentration of nicardipine in a sample of plasma was obtained by subtracting the concentration of the pyridine metabolite II as determined by the HPLC/GC–ECD assay from the combined concentration of nicardipine plus the pyridine metabolite II as determined by the GC–ECD method

[1] Unpublished results (a brief description of this method is given in the text).

0022-3549/84/1000-1444$01.00/0
© 1984, American Pharmaceutical Association

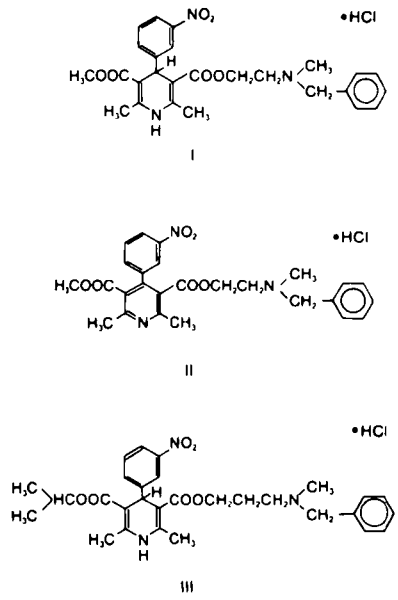

(2). Based on our HPLC/GC-ECD assay, the pyridine metabolite II accounted for 28.58 ± 8.73% (n = 36) of the combined concentration of nicardipine plus the pyridine metabolite II in plasma from subjects treated orally with nicardipine hydrochloride. In view of the presence of varying proportions of nicardipine and its pyridine metabolite II in plasma, a specific method for the determination of the concentrations of nicardipine should be used to provide data for pharmacokinetic analysis. Although the TLC-GC-MS and HPLC/GC-ECD methods have this specificity, they are relatively laborious and do not provide a practical means for the specific determination of nicardipine and its pyridine metabolite II in plasma on a routine basis.

The method described here is a simple HPLC method which allows the simultaneous determination of the individual concentrations of nicardipine and its pyridine metabolite II in human plasma. The assay, which has a sensitivity of 5 ng/mL for nicardipine and the pyridine metabolite II is suitable for the analysis of these compounds in plasma collected from subjects treated orally with nicardipine hydrochloride at doses as low as 20 mg.

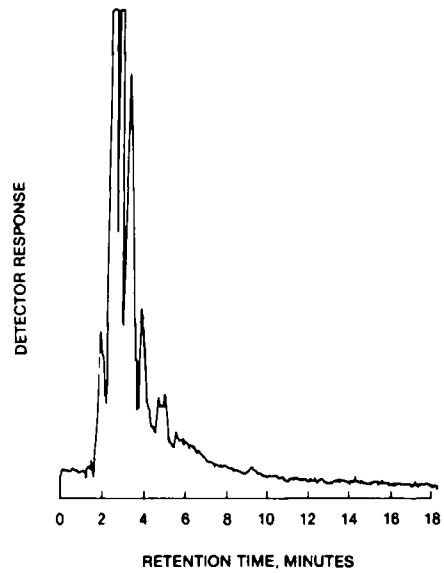

Figure 1—*HPLC chromatogram of a 1-mL blank human plasma sample. Extracted residue was dissolved in 70 μL of mobile phase, and 55 μL was injected onto the liquid chromatograph.*

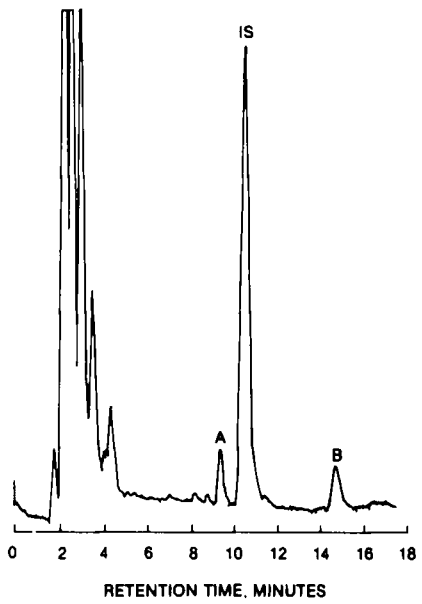

Figure 2—*HPLC chromatogram of a 1-mL blank human plasma sample spiked with nicardipine hydrochloride (A), 5 ng; internal standard (IS), 75 ng; pyridine metabolite II hydrochloride (B), 5 ng. Extracted residue was dissolved in 70 μL of mobile phase, and 55 μL was injected onto the liquid chromatograph.*

EXPERIMENTAL SECTION

Apparatus—A high-performance liquid chromatograph[2] equipped with a fixed UV (254 nm) detector[3] and an automatic injector[4] was used. Separations were performed on a reverse-phase column[5] (250 × 4.6 mm i.d.). A precolumn[6] (70 × 2.1 mm i.d.) was used. Chromatograms were traced on a

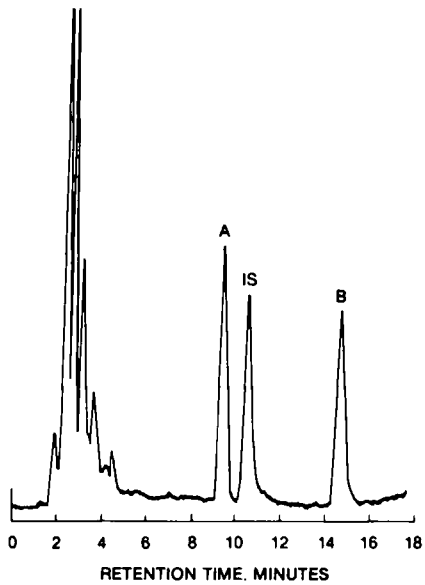

Figure 3—*HPLC chromatogram of a 1-mL blank human plasma spiked with nicardipine hydrochloride (A), 50 ng; internal standard (IS), 75 ng; pyridine metabolite II hydrochloride (B), 50 ng. Extracted residue was dissolved in 70 μL of mobile phase, and 25 μL was injected onto the liquid chromatograph.*

[2] Model 204; Waters Associates, Milford, Mass.
[3] Model 160; Beckman Instruments, Palo Alto, Calif.
[4] Model 710B, Waters Intelligent Sample Processor (WISP); Waters Associates.
[5] Partisil-5, ODS-3, 5 μm; Whatman Inc., Clifton, N.J.
[6] HC pellosil, 30–38 μm; Whatman Inc.

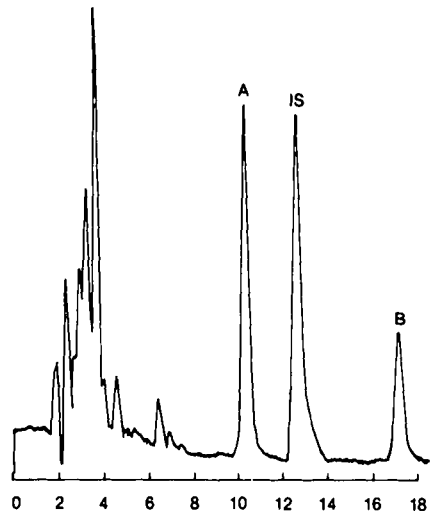

Figure 4—*HPLC chromatogram of a 1-mL sample of plasma collected 40 min after an oral dose of 20 mg of nicardipine hydrochloride. Extracted residue was dissolved in 70 μL of mobile phase, and 40 μL was injected onto the liquid chromatograph.*

strip-chart recorder[7]. The system was operated at ambient temperature, and the detector sensitivity was set at 0.002 AUFS.

Chemicals and Reagents—Nicardipine hydrochloride (I)[8], 2-(*N*-benzyl-*N*-methylamino)ethyl methyl 2,6-dimethyl-4-(*m*-nitrophenyl)-3,5-pyridinedicarboxylate monohydrochloride (II)[9], 2-(*N*-benzyl-*N*-methylamino)-ethyl isopropyl 1,4-dihydro-2,6-dimethyl-4-(*m*-nitrophenyl)-3,5-pyridinedicarboxylate monohydrochloride (III)[8], methanol[10] (HPLC grade), acetonitrile[10] (HPLC grade), absolute ethanol[11], and ether[12] (HPLC grade) were obtained commercially. All other chemicals and reagents were reagent grade.

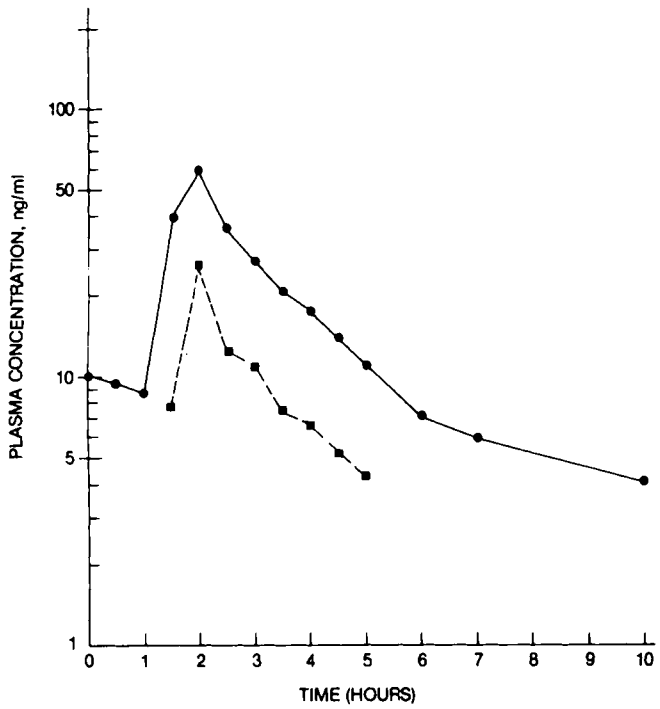

Figure 5—*Semilogarithmic plot of the plasma concentration–time profile for nicardipine (●) and its pyridine metabolite II (■) in one subject following an oral dose of 20 mg of nicardipine hydrochloride on day 4 of a multiple-dose study.*

[7] Model 7130A dual-channel strip chart recorder; Hewlett-Packard, Santa Clara, Calif.
[8] Yamanouchi Pharmaceutical Co. Ltd., Tokyo, Japan.
[9] Syntex Research Center, Edinburgh, Scotland.
[10] J. T. Baker Chemical Co.
[11] U.S. Industrial Chemical Co.
[12] Burdick and Jackson Laboratories.

Table I—Nicardipine Recovery from Spiked Plasma Samples[a]

Nicardipine Hydrochloride Recovered, ng/mL	Nicardipine Hydrochloride Added, ng/mL					
	5	10	20	50	100	150
Mean	4.9	9.2	19.2	51.1	103.4	148.1
SD	0.2	0.5	0.9	2.2	1.1	2.9
CV, %	4.1	5.0	4.5	4.3	1.1	1.9

[a] Total of four assays.

Table II—Pyridine Metabolite II Recovery from Spiked Plasma Samples[a]

Pyridine Metabolite II Hydrochloride Recovered, ng/mL	Pyridine Metabolite II Hydrochloride Added, ng/mL					
	5	10	20	50	100	150
Mean	5.1	9.6	20.3	51.1	98.8	151.3
SD	0.3	0.0	0.3	1.9	0.5	4.2
CV, %	4.9	0.0	1.4	3.7	0.5	2.8

[a] Total of four assays.

The aqueous 2.0 M NaOH solution was washed once with an equal volume of acetonitrile and once with an equal volume of ether before use. Acid buffer was prepared by mixing equal volumes of 0.1 M sodium acetate solution and 0.1 M hydrochloric acid.

Chromatographic Conditions—HPLC was performed by using a mobile phase of acetonitrile–0.02 M KH_2PO_4 (pH 4.8; 53:47 v/v) with a flow rate of 1.5 mL/min (2000 psi).

Standard Solutions—Stock solutions of the internal standard III, nicardipine hydrochloride (I), and the monohydrochloride of its pyridine metabolite II at a concentration of 1 mg/mL were prepared in ethanol. The working solution of internal standard III contained 75 ng/500 μL of 2% ethanolic acid buffer. Spiking solutions, containing 5, 10, 20, 50, 100, and 150 ng of the hydrochloride salts of nicardipine (I) or its pyridine metabolite II per 500 μL of 4% ethanolic acid buffer, were prepared by serial dilution of the stock solutions.

Sample Preparation for the Determination of Nicardipine and Its Pyridine Metabolite II—Human plasma (0.1–1.0 mL) was transferred into a 15-mL culture tube (16 × 125 mm) fitted with a polytef-lined screw cap. The volume was adjusted to 1 mL by the addition of blank human plasma[13]. Ethanolic acid buffer (4%, 1 mL), 500 μL of internal standard solution (III, 75 ng), and 500 μL of 2.0 M NaOH were added to the sample. The mixture was agitated on a vortex mixer for 15 s. The mixture was extracted with 4 mL of ether by shaking on a mechanical shaker for 5 min and centrifuging for 5 min at 5000 rpm. The organic layer was transferred to another 15-mL tube. To the organic phase was added 2 mL of 0.1 M HCl, and the mixture was shaken for 5 min. The mixture was centrifuged, and the organic layer was removed and discarded by using a vacuum aspirator. The aqueous fraction was made alkaline by the addition of 500 μL of 2.0 M NaOH. The mixture was extracted with 4 mL of ether as described previously. After centrifugation, the organic layer was transferred to another 15-mL culture tube, and the solution was evaporated to dryness under a stream of nitrogen in a water bath (45°C). The residue was immediately dissolved in 70 μL of HPLC mobile phase, and the solution was transferred to an autosampler vial[14]. Of this final solution, 20–55 μL was injected onto the liquid chromatograph for analysis.

Quantitation—Concentrations of nicardipine and the pyridine metabolite II in unknown samples were calculated with reference to their corresponding calibration curves, which were generated by using a 1-mL sample of blank plasma spiked with nicardipine hydrochloride and the monohydrochloride of the pyridine metabolite II at levels of 5, 10, 20, 50, 100, and 150 ng/mL. The samples of spiked plasma were processed as described above.

Calibration curves were obtained by plotting the ratio of the peak height for the analyte to that of the internal standard against the amount of analyte added.

HPLC/GC-ECD Assay for the Pyridine Metabolite II—This assay employed as the internal standard the pyridine form[1] of the internal standard III used for the direct HPLC assay described here. Preparation of the samples for HPLC was as described above. HPLC was performed as described above,

[13] Venous blood from four untreated volunteers was drawn into heparinized containers and centrifuged to generate a plasma pool.
[14] 1-Dram vial, 0.4-mL glass insert, compression spring, self-sealing septum, and self-sealing septum assembly; Waters Associates.

Table III—Comparisons of the Concentrations (ng/mL) of Nicardipine, Its Pyridine Metabolite II, and Total [a] in Plasma Determined by Different Methods

Sample	Nicardipine		II		Total	
	GC-ECD + HPLC/GC-ECD (y)	HPLC (x)	HPLC/ GC-ECD (y)	HPLC (x)	GC-ECD (y)	HPLC (x)
1	292.3	287.7	71.7	75.8	364.0	363.5
2	124.2	129.5	40.3	48.9	164.5	178.4
3	98.0	96.2	33.6	27.2	131.6	123.4
4	91.0	80.5	28.5	27.4	119.5	107.9
5	64.6	59.7	19.0	25.9	83.6	85.6
6	33.4	23.6	13.0	14.1	46.4	37.7
7	21.3	20.1	9.3	10.2	30.6	30.3
8	18.9	21.2	9.9	8.7	29.0	29.9
9	18.2	17.3	6.6	7.9	24.8	25.2
10	9.8	8.5	5.4	5.6	15.2	14.1
Correlation equation	$y = 1.0022x + 2.5781$		$y = 0.9168x + 0.6541$		$y = 0.9883x + 2.4848$	
Correlation coefficient	$r = 0.9984$		$r = 0.9825$		$r = 0.9978$	

[a] Total = Nicardipine plus its pyridine metabolite II.

except that a mobile phase of acetonitrile–0.01 M KH_2PO_4 (pH 4.8; 1:1) was employed. Under these conditions, the pyridine metabolite II and the internal standard coeluted and were well separated from nicardipine. The HPLC effluent containing the pyridine metabolite II and the internal standard was collected, made alkaline by the addition of 0.5 mL of 2.0 M NaOH, and extracted with ether (4 mL). The ether extract was evaporated to dryness, and the residue was reconstituted in 50 μL of toluene. A portion of the extract was subjected to GC-ECD analysis (2). The concentration of the pyridine metabolite II in plasma was determined by reference to suitable calibration curves which were constructed by using a procedure analogous to that described above.

RESULTS AND DISCUSSION

The UV absorption maximum of nicardipine was at 237 nm. However, in this assay, the absorption at 254 nm was used for quantitation. Although the use of 254 nm reduces the theoretical sensitivity to some extent, it has the advantage of providing a cleaner chromatogram for blank plasma. A typical chromatogram for 1 mL of blank human plasma processed by this method is shown in Fig. 1. There were no components which eluted with nicardipine, the pyridine metabolite II, or the internal standard. To achieve a clean chromatogram of this type, we found that it was necessary to perform the acid–base partitioning step prior to the HPLC analysis. In addition, we found that the 2.0 M NaOH used in this procedure must be washed once with acetonitrile and once with ether prior to use. If unwashed 2.0 M NaOH is used, potentially interfering components appear in the chromatogram. By using the extraction procedure described above, the extraction efficiencies for nicardipine and its pyridine metabolite II from 1 mL of plasma were 81.1 and 79.6%, respectively.

Representative chromatograms for 1 mL of blank human plasma spiked with nicardipine hydrochloride and the monohydrochloride of the pyridine metabolite II, each at levels of 5 or 50 ng and processed by this procedure, are shown in Figs. 2 and 3, respectively. A typical chromatogram for 1 mL of plasma taken from a subject who received nicardipine hydrochloride is shown in Fig. 4.

A good separation of nicardipine, the pyridine metabolite II, and the internal standard from each other and from other components was obtained. During the HPLC separation, an acidic mobile phase (pH 4.8) with a relatively high buffer concentration (0.02 M KH_2PO_4) was used. The acidic mobile phase causes nicardipine, the pyridine metabolite II, and the internal standard to exist as the corresponding protonated species during chromatography, thereby leading to improved chromatographic peak shapes and reduced retention times. The high buffer concentration was found to be necessary to ensure a good separation between the pyridine metabolite II and the internal standard. At a lower buffer concentration (0.01 M KH_2PO_4), the separation of these three compounds and even their order of elution was found to vary as the column aged. Even with the higher buffer concentration, as the column aged, it was necessary to add a small quantity of methanol to the solvent system [*e.g.*, acetonitrile–0.02 M KH_2PO_4–methanol (43:49:8 v/v/v)], to maintain the elution order and the quality of the separation.

Calibration curves for nicardipine hydrochloride and the monohydrochloride of the pyridine metabolite II showed good linearity. Data for the recovery of nicardipine and the pyridine metabolite II from samples of plasma fortified with these compounds in the range of 5–150 ng/mL are shown in Tables I and II, respectively. The low coefficients of variation (≤5% at all levels) provide evidence of the reproducibility of the method.

The HPLC method was validated against a GC-ECD method which gave the combined concentration of nicardipine plus the pyridine metabolite II and against an HPLC/GC-ECD method, which gave the concentration of the pyridine metabolite II. All three methods were applied to samples of plasma obtained from subjects treated orally with nicardipine hydrochloride (Table III). A comparison of the levels of nicardipine, the pyridine metabolite II, and nicardipine–the pyridine metabolite II determined by the three methods is shown in Table III. The overall agreement between the results obtained by all three methods is good.

A plasma concentration–time profile for nicardipine and the pyridine metabolite II obtained for one subject on day 4 of a multiple-dose study (20 mg, three times per day) is presented in Fig. 5 as evidence of the usefulness of this method for pharmacokinetic analyses.

REFERENCES

(1) S. Higuchi and Y. Shiobara, *Xenobiotica*, **10**, 447 (1980).

(2) S. Higuchi, H. Sasaki, and T. Sado, *J. Chromatogr.*, **110**, 301 (1975).

(3) S. Higuchi and Y. Shiobara, *Biomed. Mass Spectrom.*, **7**, 339 (1980).

(4) S. Higuchi, H. Sasaki, T. Takenaka, T. Ichimura, and T. Sado, "Abstracts of the 95th Annual Meeting of the Pharmaceutical Society of Japan," Nishinomiya, Japan, 1975, vol. 3, p. 229.

(5) S. Higuchi and S. Kawamura, *J. Chromatogr.*, **223**, 341 (1981).

Analysis of *N*-(4-Hydroxyphenyl)retinamide Polymorphic Forms by X-ray Powder Diffraction

F. A. CHRZANOWSKI ˣ, B. J. FEGELY, W. R. SISCO, and M. P. NEWTON

Received December 6, 1982, from the *Department of Chemical and Pharmaceutical Development, McNeil Pharmaceutical, Spring House, PA 19477.* Accepted for publication November 16, 1983.

Abstract □ A quantitative X-ray diffraction method, with zinc oxide used as the internal standard, was developed for the analysis of polymorphic forms I and II of *N*-(4-hydroxyphenyl)retinamide. The standard curve relating peak height ratio to the percentage of form I was linear. The method was precise and accurate to within ±6%.

Keyphrases □ *N*-(4-Hydroxyphenyl)retinamide—X-ray powder diffraction analysis of polymorphic forms □ X-ray powder diffraction—analysis of polymorphic forms of *N*-(4-hydroxyphenyl)retinamide □ Polymorphs—*N*-(4-hydroxyphenyl)retinamide, analysis by X-ray powder diffraction

N-(4-Hydroxyphenyl)retinamide (fenretinide; III), an analogue of vitamin A which was first synthesized by Gander and co-workers (1), has a demonstrated prophylactic effect against mammary tumors in rats. Two polymorphic forms of *N*-(4-hydroxyphenyl)retinamide which occur alone or in combination after recrystallization have been identified by X-ray powder diffraction (Fig. 1).

The polymorphic form of a drug may affect its efficacy. The bioavailability of both chloramphenicol (2) and sulfameter (3) after oral administration in humans is dependent on their polymorphic forms. Studies in animals with polymorphs of indomethacin (4), amobarbital (5), and phenobarbital (6) have demonstrated the nonequivalence of polymorphic forms. To monitor the polymorphic character of *N*-(4-hydroxyphenyl)-retinamide drug substance used in preclinical animal testing and to evaluate the physicochemical properties of the two forms, a quantitative analytical procedure was developed.

X-ray powder diffraction and IR spectroscopy have been used for quantitative analysis of mixtures of polymorphs. Walkling *et al.* (7) have developed an IR spectroscopic method to quantitate difenoxin hydrochloride polymorph mixtures. Aguiar *et al.* (2) have used X-ray powder diffraction to determine the composition of chloramphenicol palmitate polymorph mixtures by calculating the peak height ratio of two peaks, with each peak characteristic of one of the two forms. The calibration line they obtained was curvilinear rather than straight. They found that the amorphous form did not interfere and that they could correct for the amount of a third crystalline form occasionally present. Papariello *et al.* (8) have successfully used X-ray powder diffraction as a nondestructive analytical method for measuring the amount of glutethimide in intact tablets. Black and Lovering (9) have used X-ray powder diffraction to quantitate the crystalline polymorphs in digoxin. X-ray diffraction studies of vitamin A analogues appear to have been limited to single-crystal studies to elucidate their chemical structures (10–14).

In this report is described a quantitative X-ray powder diffraction method which determines the amounts of the polymorphic forms I and II of *N*-(4-hydroxyphenyl)retinamide in samples of *N*-(4-hydroxyphenyl)retinamide drug substance. Zinc oxide was selected as the internal standard since all of its diffraction peaks (Fig. 1) occur at higher reflection angles than those of the two polymorphic forms of *N*-(4-hydroxyphenyl)-retinamide.

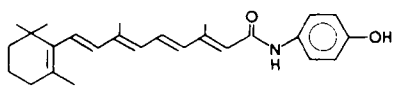

N-(4-hydroxyphenyl)retinamide

EXPERIMENTAL SECTION

Reagents and Materials—Zinc oxide[1] (internal standard), analytical reagent grade, was obtained commercially and was passed through an 80-mesh sieve prior to use. *N*-(4-Hydroxyphenyl)retinamide was ≥99% pure, as determined by an HPLC method in which the 13-*cis* isomer was separated from the all-*trans* isomer, *N*-(4-hydroxyphenyl)retinamide. There was <0.5% 13-*cis* isomer in the test materials. Mixtures of forms I and II gave the same HPLC peak and TLC spot. There were qualitative differences in the IR spectra of forms I and II that were suggestive of polymorphism. The solution NMR spectra were identical, indicating that the two forms were not isomers of each other. The two forms do not interconvert under the conditions described in this report.

Standards—Authentic samples of *N*-(4-hydroxyphenyl)retinamide forms I and II were passed through an 80-mesh sieve. When *N*-(4-hydroxyphenyl)-retinamide was passed through a 200-mesh sieve, the sample could not be used due to the induction of a static electrical charge. The 80-mesh powder samples were used as the 100 and 0% form I standards. The 25, 50, and 75% form I standards were prepared by mixing forms I and II in a mortar.

Assay—A sample (200 mg) of *N*-(4-hydroxyphenyl)retinamide or standard was mixed with 40 mg of zinc oxide in a glass mortar. The *N*-(4-hydroxyphenyl)retinamide–zinc oxide mixture (5:1) was placed into a sample holder, and the powder was pressed into place with a glass slide by moving the slide from side to side, thereby leaving a smooth, lightly compacted surface. The samples were scanned over the 5–37° 2θ range. The peak heights of the sample and internal standard were measured at 19.1° and 31.8° 2θ from a baseline drawn from 11° to 33° 2θ. The ratio $I_{19.1}/I_{31.8}$ was calculated, and the amount of form I was obtained from a standard curve relating $I_{19.1}/I_{31.8}$ *versus* the percentage of form I.

Apparatus—An X-ray diffractometer[2] containing a long fine-focus copper tube X-ray source, diffracted-beam monochromater, theta-compensating slit, and scintillation counter was used. The X-ray tube was operated at 40 kV and 30 mA. The scan speed was 1°/min; range, 5 kcps; time constant, 1. The takeoff angle was 6°.

Reproducibility and Accuracy—A 2.5-g mixture was prepared, as described above, containing 75% form I and 25% form II. The mixture was mixed with zinc oxide (5:1) and analyzed 10 times using a different aliquot for each assay. Nine other mixtures were prepared in which the amount of form I ranged from 19 to 100%. The concentrations of form I were determined for the 10 samples and compared with the known concentrations.

RESULTS AND DISCUSSION

The X-ray powder diffraction patterns for polymorphic forms I and II are shown in Fig. 1. The *d*-spacings and relative intensities of the two polymorphs are tabulated in Table I. It appears that a number of peaks such as 2θ = 19.1°, 25.1°, and 19.8° could be used quantitatively to measure the amounts of forms I and II in samples of drug substance. Since the peaks are sharp and have about the same width at half-height, peak height is a reasonable approximation of the area of the peak. Several peak height and peak height ratio combinations were evaluated. None were sufficiently accurate for determining the composition of known mixtures. The low angle peaks below 11° 2θ, at which

[1] Fisher Scientific Co.
[2] Philips Electronic Instruments, Inc.

0022-3549/84/1000-1448$01.00/0
© 1984, American Pharmaceutical Association

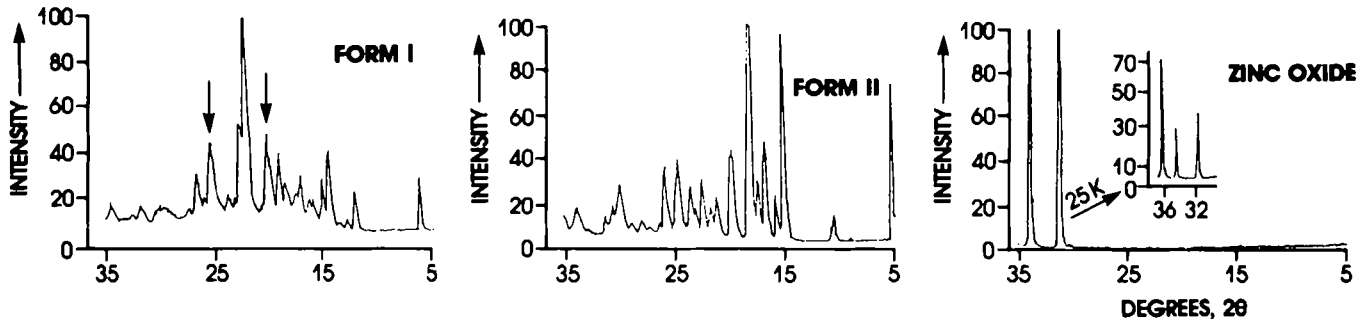

Figure 1—*X-ray diffraction patterns of polymorphic forms I and II and zinc oxide.*

Table I—Tabulated Diffraction Data from *N*-(4-Hydroxyphenyl)retinamide Forms I and II

Form I					Form II				
Line	2θ°	*d*-(nm)	I	I/I_0	Line	2θ°	*d*-(nm)	I	I/I_0
1	5.9	1.4966	30.5	19	1	5.3	1.6658	80.5	45
2	7.3	1.2098	3.5	2	2	9.0	0.9817	3	2
3	11.9	0.7430	22.5	14	3	10.5	0.8417	16	9
4	12.6	0.7019	22	14	4	10.8	0.8184	7	4
5	13.3	0.6651	11.5	7	5	15.1	0.5862	103.5	57
6	14.3	0.6188	68	42	6	15.7	0.5639	22	12
7	14.9	0.5940	71.5	44	7	16.8	0.5272	61	34
8	15.8	0.5604	36.5	23	8	17.4	0.5092	39	22
9	16.2	0.5466	20.5	13	9	18.1	0.4896	180.5	100
10	16.9	0.5241	42.5	26	10	19.7	0.4502	48	27
11	17.2	0.5151	37.5	23	11	19.9	0.4457	51.5	29
12	18.4	0.4817	39.5	24	12	21.1	0.4207	24.5	14
13	19.1	0.4642	80.5	50	13	21.6	0.4110	19	11
14	19.8	0.4480	65.5	40	14	22.5	0.3948	41	23
15	21.9	0.4055	162	100	15	23.0	0.3863	17.5	10
16	22.3	0.3983	72.5	45	16	23.5	0.3782	29	16
17	23.5	0.3782	29.5	18	17	24.6	0.3615	42	23
18	25.1	0.3544	77	48	18	24.8	0.3587	25	14
19	26.4	0.3373	37	23	19	25.9	0.3437	48	27
20	27.2	0.3275	12	7	20	26.4	0.3373	6.5	4
21	29.3	0.3045	12.5	8	21	27.2	0.3275	3	2
22	31.5	0.2837	10.5	6	22	28.0	0.3184	8.5	5
23	34.2	0.2619	11.5	7	23	28.8	0.3097	5	3
					24	29.9	0.2986	24	13
					25	30.6	0.2919	12	7
					26	30.9	0.2891	10	6
					27	31.2	0.2864	8	4
					28	33.9	0.2642	15.5	9

overlap was reduced, would appear to be good candidates for quantitation. Unfortunately, the intensities of the peak heights of each component were not always proportional to the amounts present.

Zinc oxide was selected as the internal standard because of the proximity of its major peak at $2\theta = 31.8°$ (100), 34.5° (002), and 36.3° (101) to the major peaks of the two polymorphic forms of *N*-(4-hydroxyphenyl)retinamide, and a complete absence of zinc oxide peaks in the region below $2\theta = 30°$. Form I has a small peak at $2\theta = 31.5°$ which did not interfere with the measurement of the zinc oxide peak, as evidenced by the good correlation and linearity of the calibration curve. The peak widths at $2\theta = 19.1°$ and 31.8° were between 0.2° and 0.4° when measured at half-height in all tested samples.

The calibration curve, relating the peak height ratio $I_{19.1}/I_{31.8}$ *versus* the percentage form I, was linear ($y = 0.0143 + 0.00259x$; $r = 0.9997$). A *y*-intercept occurred as a result of the method used to establish the baseline and the slight amount of background noise observed at $2\theta = 19.1°$ with 0% form I (100% form II) standards. The excellent correlation and linearity of the calibration curve indicate that the selection of zinc oxide as the internal standard was appropriate. An organic internal standard is usually preferred for the analysis of organic compounds; however, the number of peaks in the X-ray diffraction patterns of the two forms of *N*-(4-hydroxyphenyl)retinamide (Fig. 1) make it unlikely that an organic internal standard would have been suitable.

In Table II are summarized the results obtained from the repetitive testing

Table II—Precision of Analysis of *N*-(4-Hydroxyphenyl)retinamide in a Mixture of Known Composition [a]

Trial	$I_{19.1}/I_{31.8}$	Form I, %
1	0.219	79
2	0.211	76
3	0.215	78
4	0.204	74
5	0.212	76
6	0.206	74
7	0.213	76
8	0.215	78
9	0.220	79
10	0.214	77
	Mean	76.7
	Range	74-79
	Mean Difference	2.1
	SD	1.8
	CV	2.3

[a] 75% form I.

Table III—Analysis of Nine Mixtures

Mixture	Form I Percent Known	$I_{19.1}/I_{31.8}$	Form I Percent Calculated	Difference, %[a]
A	19	0.0564	16	−3
B	60	0.170	60	0
C	53	0.154	54	1
D	80	0.214	77	−3
E	69	0.189	68	−1
F	29	0.084	27	−2
G	90	0.256	93	3
H	100	0.280	106	6
I	40	0.113	38	−2

[a] Mean difference, 2.3%.

of the 75% form I sample. Ten aliquots of this sample were packed and scanned over the range 2θ = 5–37°. The calculated mean was 76.7% form I. All 10 assays were within the 74–79% range. The mean difference was 2.1%, and the *SD* and *CV* were 1.8 and 2.3%, respectively. When zinc oxide was not used as an internal standard and the peak height ratio, $I_{25.1}/I_{19.8}$, was used, the calculated mean percentage of form I for these samples was 55%, and the range was 49–61%. Incorporation of zinc oxide as the internal standard substantially increased the accuracy and precision of the assay method. The uncertainty in the ratios in Table II is ~5%. This value is higher than the *SD* obtained from the repetitive testing of the 75% form I sample (Table II), 1.8%, and may be only a statistical anomaly.

In Table III are summarized the data obtained from the analysis of nine different mixtures of *N*-(4-hydroxyphenyl)retinamide. The mean difference for all nine mixtures was 2.3%. The largest differences between the known and calculated amounts of form I were −3 and +6%.

In summary, this method represents a precise and accurate method, within ±6%, for quantitation of the amount of *N*-(4-hydroxyphenyl)retinamide polymorph I present in samples of drug substance. The amount of form II can be calculated by difference. It appears that zinc oxide merits consideration for use as an internal standard in quantitative X-ray diffraction methods for other organic compounds.

REFERENCES

(1) R. C. Moon, H. J. Thompson, P. J. Becci, C. J. Grubs, R. J. Gander, D. L. Newton, J. M. Smith, S. L. Phillips, W. R. Henderson, L. T. Mullen, C. C. Brown, and M. B. Sporn, *Cancer Res.*, **39**, 1339 (1979).

(2) A. J. Aguiar, J. Krc, A. W. Kinkel, and J. C. Samyn, *J. Pharm. Sci.*, **56**, 847 (1967).

(3) S. A. Khalil, M. A. Moustafa, A. R. Ebian, and M. M. Motawi, *J. Pharm. Sci.*, **61**, 1615 (1972).

(4) T. Y. Yokoyama, T. Umeda, K. Kuroda, T. Nagafuku, T. Yamamoto, and S. Asada, *Yakugaku Zasshi*, **99**, 837 (1979).

(5) Y. Kato and M. Kohketsu, *Chem. Pharm. Bull.*, **29**, 268 (1981).

(6) Y. Kato and F. Watanabe, *Yakugaku Zasshi*, **98**, 639 (1978).

(7) W. D. Walkling, H. Almond, V. Paragamian, N. H. Batuyios, J. A. Meschino, and J. B. Appino, *Int. J. Pharm.* **4**, 39 (1979).

(8) G. J. Papariello, H. Letterman, and R. E. Huettemann, *J. Pharm. Sci.*, **53**, 663 (1964).

(9) D. B. Black and E. G. Lovering, *J. Pharm. Pharmacol.*, **29**, 684 (1977).

(10) W. E. Oberhaansli, H. P. Wagner, and O. Isler, *Acta Crystallogr. Sect. B*, **30**, 161 (1974).

(11) M. M. Thackery and G. Gafner, *Acta Crystallogr. Sect. B*, **31**, 335 (1975).

(12) H. Schenk, *Acta Crystallogr. Sect. B*, **27**, 667 (1971).

(13) M. M. Thackery and G. Gafner, *Acta Crystallogr. Sect. B*, **30**, 1711 (1974).

(14) H. Schenk, R. T. Kops, N. van der Putten, and J. Bode, *Acta Crystallogr. Sect. B*, **34**, 505 (1978).

ACKNOWLEDGMENTS

The authors thank Mr. J. N. Plampin for providing authentic samples of *N*-(4-hydroxyphenyl)retinamide forms I and II, Mr. M. Mutter for providing NMR and IR spectra of the two forms of *N*-(4-hydroxyphenyl)retinamide, and Drs. W. D. Walkling and R. Jenkins for helpful suggestions during the preparation of this manuscript.

This study was presented at the 130th Annual Meeting of the American Pharmaceutical Association, New Orleans, La., April 1983.

Absolute Intramuscular, Oral, and Rectal Bioavailability of Alizapride

G. HOUIN, J. BARRE, and J. P. TILLEMENT ˣ

Received June 29, 1983, from the *Laboratoire de Biochimie I et de Pharmacologie, Centre Hospitalier Intercommunal de Créteil, 94000 Creteil, France.* Accepted for publication October 24, 1983.

Abstract □ A study was designed to estimate the absolute bioavailability of alizapride after intramuscular injection, oral administration as a solution or a tablet, and rectal administration as a suppository compared with that after intravenous injection. A balanced incomplete block-design trial was adopted. The intramuscular injection and the tablet administration showed identical results with those of the intravenous injection. On the contrary, the oral solution and the rectal suppository dosage forms gave lower absorption values, *i.e.*, 75 and 61% of the dose administered was absorbed, respectively.

Keyphrases □ Alizapride—bioavailability, intravenous, intramuscular, oral tablet, oral solution, rectal suppository □ Bioavailability—alizapride, intravenous, intramuscular, oral tablet, oral solution, rectal suppository □ Pharmacokinetics—alizapride, intravenous, intramuscular, oral tablet, oral solution, rectal suppository

Alizapride[1], *N*-[(1-allyl-2-pyrrolidinyl)methyl]-6-methoxy-1*H*-benzotriazole-5-carboxamide (I), is a new drug with antiemetic properties (1–3). It is used mainly in emergencies and is given intravenously in cancer patients (4), the pediatric population (5), and for internal medicine purposes (6). Chronic administration can be continued by intravenous, rectal, or even the oral routes of drug administration if patients are monitored well. For all these pharmaceutical forms, bioavailability results must be known to choose the appropriate dosage regimen for each route of drug administration.

In a previous study (7), it has been shown that the pharmacokinetics of alizapride were independent of the dose administered, in the dosage range of 50–200 mg, either by the intravenous or oral routes. In this report are described the pharmacokinetic results obtained after intramuscular, oral solution or tablets, and rectal administrations compared with those after intravenous injection.

EXPERIMENTAL SECTION

Materials—Alizapride was obtained commercially and showed no impurities in two different TLC systems. All reagents for alizapride analysis in biological materials were of commercially available analytical grade and were used without further purification.

Alizapride Analysis—Alizapride was measured in plasma and urine by using a previously described HPLC method (7).

HPLC involved a single-step extraction, a reverse-phase chromatographic

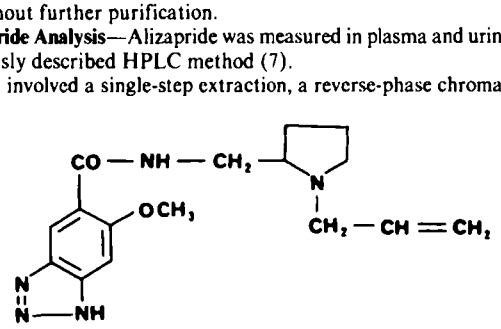

I

[1] Plitican; Delagrange Laboratories, Paris, France.

0022-3549/84/1000-1450$01.00/0

© 1984, American Pharmaceutical Association

of the 75% form I sample. Ten aliquots of this sample were packed and scanned over the range 2θ = 5–37°. The calculated mean was 76.7% form I. All 10 assays were within the 74–79% range. The mean difference was 2.1%, and the *SD* and *CV* were 1.8 and 2.3%, respectively. When zinc oxide was not used as an internal standard and the peak height ratio, $I_{25.1}/I_{19.8}$, was used, the calculated mean percentage of form I for these samples was 55%, and the range was 49–61%. Incorporation of zinc oxide as the internal standard substantially increased the accuracy and precision of the assay method. The uncertainty in the ratios in Table II is ~5%. This value is higher than the *SD* obtained from the repetitive testing of the 75% form I sample (Table II), 1.8%, and may be only a statistical anomaly.

In Table III are summarized the data obtained from the analysis of nine different mixtures of *N*-(4-hydroxyphenyl)retinamide. The mean difference for all nine mixtures was 2.3%. The largest differences between the known and calculated amounts of form I were −3 and +6%.

In summary, this method represents a precise and accurate method, within ±6%, for quantitation of the amount of *N*-(4-hydroxyphenyl)retinamide polymorph I present in samples of drug substance. The amount of form II can be calculated by difference. It appears that zinc oxide merits consideration for use as an internal standard in quantitative X-ray diffraction methods for other organic compounds.

REFERENCES

(1) R. C. Moon, H. J. Thompson, P. J. Becci, C. J. Grubs, R. J. Gander, D. L. Newton, J. M. Smith, S. L. Phillips, W. R. Henderson, L. T. Mullen, C. C. Brown, and M. B. Sporn, *Cancer Res.*, **39**, 1339 (1979).

(2) A. J. Aguiar, J. Krc, A. W. Kinkel, and J. C. Samyn, *J. Pharm. Sci.*, **56**, 847 (1967).

(3) S. A. Khalil, M. A. Moustafa, A. R. Ebian, and M. M. Motawi, *J. Pharm. Sci.*, **61**, 1615 (1972).

(4) T. Y. Yokoyama, T. Umeda, K. Kuroda, T. Nagafuku, T. Yamamoto, and S. Asada, *Yakugaku Zasshi*, **99**, 837 (1979).

(5) Y. Kato and M. Kohketsu, *Chem. Pharm. Bull.*, **29**, 268 (1981).

(6) Y. Kato and F. Watanabe, *Yakugaku Zasshi*, **98**, 639 (1978).

(7) W. D. Walkling, H. Almond, V. Paragamian, N. H. Batuyios, J. A. Meschino, and J. B. Appino, *Int. J. Pharm.* **4**, 39 (1979).

(8) G. J. Papariello, H. Letterman, and R. E. Huettemann, *J. Pharm. Sci.*, **53**, 663 (1964).

(9) D. B. Black and E. G. Lovering, *J. Pharm. Pharmacol.*, **29**, 684 (1977).

(10) W. E. Oberhaansli, H. P. Wagner, and O. Isler, *Acta Crystallogr. Sect. B*, **30**, 161 (1974).

(11) M. M. Thackery and G. Gafner, *Acta Crystallogr. Sect. B*, **31**, 335 (1975).

(12) H. Schenk, *Acta Crystallogr. Sect. B*, **27**, 667 (1971).

(13) M. M. Thackery and G. Gafner, *Acta Crystallogr. Sect. B*, **30**, 1711 (1974).

(14) H. Schenk, R. T. Kops, N. van der Putten, and J. Bode, *Acta Crystallogr. Sect. B*, **34**, 505 (1978).

ACKNOWLEDGMENTS

The authors thank Mr. J. N. Plampin for providing authentic samples of *N*-(4-hydroxyphenyl)retinamide forms I and II, Mr. M. Mutter for providing NMR and IR spectra of the two forms of *N*-(4-hydroxyphenyl)retinamide, and Drs. W. D. Walkling and R. Jenkins for helpful suggestions during the preparation of this manuscript.

This study was presented at the 130th Annual Meeting of the American Pharmaceutical Association, New Orleans, La., April 1983.

Absolute Intramuscular, Oral, and Rectal Bioavailability of Alizapride

G. HOUIN, J. BARRE, and J. P. TILLEMENT ˣ

Received June 29, 1983, from the *Laboratoire de Biochimie I et de Pharmacologie, Centre Hospitalier Intercommunal de Créteil, 94000 Creteil, France.* Accepted for publication October 24, 1983.

Abstract □ A study was designed to estimate the absolute bioavailability of alizapride after intramuscular injection, oral administration as a solution or a tablet, and rectal administration as a suppository compared with that after intravenous injection. A balanced incomplete block-design trial was adopted. The intramuscular injection and the tablet administration showed identical results with those of the intravenous injection. On the contrary, the oral solution and the rectal suppository dosage forms gave lower absorption values, *i.e.*, 75 and 61% of the dose administered was absorbed, respectively.

Keyphrases □ Alizapride—bioavailability, intravenous, intramuscular, oral tablet, oral solution, rectal suppository □ Bioavailability—alizapride, intravenous, intramuscular, oral tablet, oral solution, rectal suppository □ Pharmacokinetics—alizapride, intravenous, intramuscular, oral tablet, oral solution, rectal suppository

Alizapride[1], *N*-[(1-allyl-2-pyrrolidinyl)methyl]-6-methoxy-1*H*-benzotriazole-5-carboxamide (I), is a new drug with antiemetic properties (1–3). It is used mainly in emergencies and is given intravenously in cancer patients (4), the pediatric population (5), and for internal medicine purposes (6). Chronic administration can be continued by intravenous, rectal, or even the oral routes of drug administration if patients are monitored well. For all these pharmaceutical forms, bioavailability results must be known to choose the appropriate dosage regimen for each route of drug administration.

In a previous study (7), it has been shown that the pharmacokinetics of alizapride were independent of the dose administered, in the dosage range of 50–200 mg, either by the intravenous or oral routes. In this report are described the pharmacokinetic results obtained after intramuscular, oral solution or tablets, and rectal administrations compared with those after intravenous injection.

EXPERIMENTAL SECTION

Materials—Alizapride was obtained commercially and showed no impurities in two different TLC systems. All reagents for alizapride analysis in biological materials were of commercially available analytical grade and were used without further purification.

Alizapride Analysis—Alizapride was measured in plasma and urine by using a previously described HPLC method (7).

HPLC involved a single-step extraction, a reverse-phase chromatographic

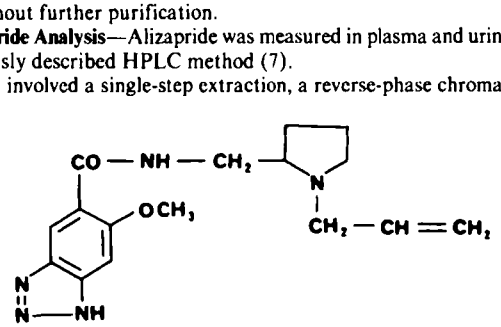

I

[1] Plitican; Delagrange Laboratories, Paris, France.

0022-3549/84/1000-1450$01.00/0

© 1984, American Pharmaceutical Association

Table I—Experimental Design for Alizapride Administration in 10 Subjects [a]

Subject	Form of Administration				
	Intravenous	Intramuscular	Oral Tablet	Oral Solution	Rectal
A	3	1	—	2	—
B	2	3	—	—	1
C	—	3	1	2	—
D	2	1	3	—	
E	—	2	—	1	3
F	3	—	2	—	1
G	1	—	2	3	—
H	—	3	1	—	2
I	1	—	—	2	3
J	—	—	1	3	2

[a] Numbers refer to the order of the forms administered separated by weekly intervals.

separation[2], and fluorometric detection[3]. Under the described conditions, the assay sensitivity was 5 ng/mL in plasma and 0.1 mg/L in urine, with a mean coefficient of variation of 3.9% between 25 and 2000 ng/mL. No endogenous interfering peaks appeared during the assays.

Alizapride Administrations—Because of the five alizapride dosage forms to be tested, a balanced incomplete block design (8) was adopted to avoid a complete block design, which would have led to a very cumbersome protocol. Ten subjects gave informed consent to participate in the study. They were free from cardiac, renal, hepatic, and respiratory diseases and allergies by clinical and biological examinations. None of the subjects received any drugs for at least 15 d prior to the study. Each subject received the same dose of 100 mg in three different forms at intervals separated by 1 week. The order of the pharmaceutical form of drug administration was done in a random, balanced fashion so that each form could be administered at least once. The experimental design for the drug administrations is indicated in Table I, with the numbers indicating the order of drug administration. All drugs were administered after an overnight fast, and oral tablets were administered with 200 mL of water. Subjects were allowed to have a light meal 4 h after drug administration.

Sampling—A 7-mL heparinized blood sample was withdrawn at 0, 5, 10, 15, 20, 30, 45, 60, 90, and 120 min and 3, 4, 6, 8, 10, 12, and 24 h after drug administration. Urine samples were collected every 2 h during the first 12 h, once during the next 12 h, and every 24 h during the next 4 d.

Calculations—Statistical and pharmacokinetic calculations were performed with a table microcomputer[4]. Pharmacokinetic parameters were obtained with previously developed programs (7, 9). The interpretation of drug concentrations as a function of time was systematically performed according to three different pharmacokinetic models, *i.e.*, one-, two-, or three-compartment open models by a Gauss–Newton algorithmic method. At each step, a statistical Fischer test with the least-squares criterion was used to evaluate the benefit of increasing the number of compartments. Pharmacokinetic parameters were then calculated by the equations of Wagner (10). Results were compared for the different pharmaceutical forms using an analysis of variance (ANOVA) adapted to the trial design (11, 12). Furthermore, the symmetrical confidence intervals were estimated for the comparisons of the area under the curves and the amounts excreted unchanged in the urine after each administered form (8, 13).

RESULTS AND DISCUSSIONS

Intravenous Administration—The mean alizapride concentrations obtained from the six subjects receiving the intravenous form are shown in Figs. 1 and 2. The corresponding mean pharmacokinetic parameters estimated from in-

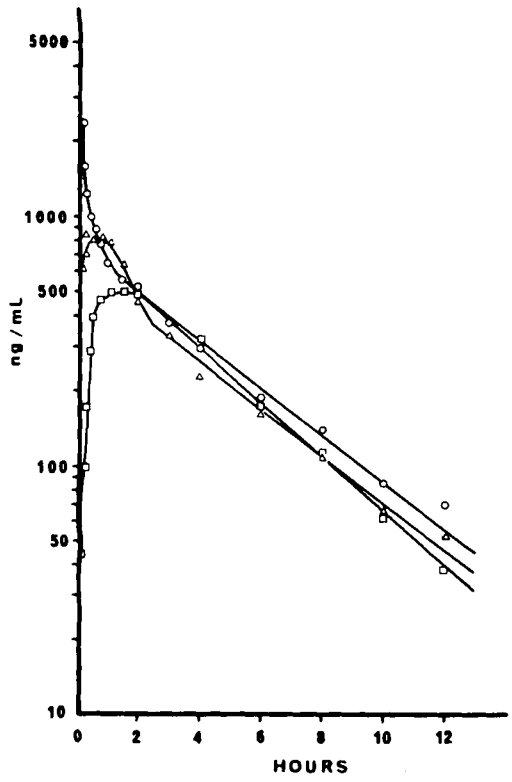

Figure 1—*Mean plasma concentrations of alizapride* versus *time obtained from six subjects after intravenous, intramuscular, or rectal route of administration. Key: (○) intravenous; (△) intramuscular; (□) rectal.*

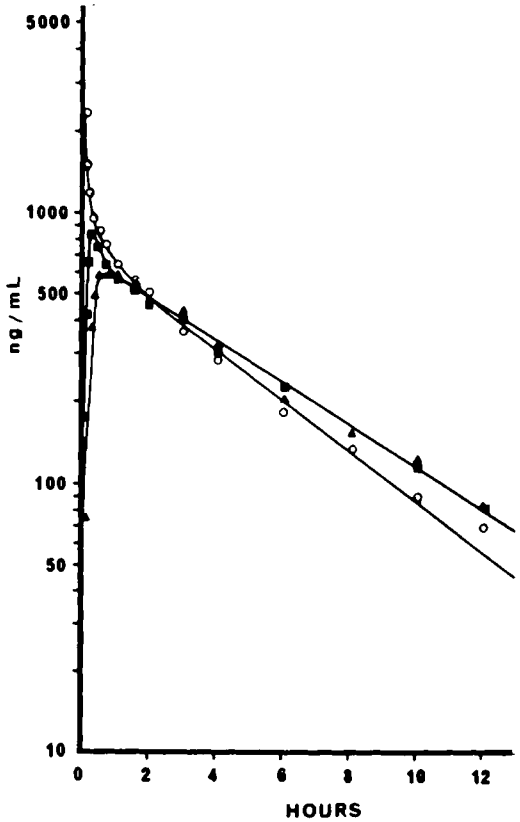

Figure 2—*Mean plasma concentrations of alizapride* versus *time obtained from six subjects after intravenous and oral administration as tablet or solution. Key: (○) intravenous; (▲) tablet; (■) solution.*

[2] Bondapak C_{18}; Water Associates, Paris, France.
[3] JY3; Jobin et Yvon, Paris, France.
[4] Model 4051; Tektronix, Paris, France.

Table II—Mean Values of the Pharmacokinetic Parameters Obtained after Administration of Different Pharmaceutical Forms of Alizapride

Parameter	Alizapride Administration, 100 mg				
	Intravenous	Intramuscular	Oral Tablets	Oral Solutions	Rectal
Lag time, h	—	0.00	0.18 ± 0.15	0.09 ± 0.05	0.17 ± 0.10
K_r, h^{-1}	—	7.13 ± 5.56	6.54 ± 4.82	12.10 ± 10.54	5.21 ± 6.36
$t_{1/2r}$, h	—	0.13 ± 0.06	0.20 ± 0.17	0.13 ± 0.16	0.44 ± 0.48
$t_{1/2\alpha}$, h	0.10 ± 0.05	0.48 ± 0.16	—	0.22 ± 0.07	—
$t_{1/2\beta}$, h	2.75 ± 0.78	2.04 ± 0.51	3.10 ± 0.63	2.68 ± 0.68	2.55 ± 1.24
k_{13}, h^{-1}	0.88 ± 0.54	0.348 ± 0.100	0.234 ± 0.060	0.272 ± 0.063	0.340 ± 0.183
k_{12}, h^{-1}	4.81 ± 2.59	0.66 ± 0.12	—	1.55 ± 0.75	—
k_{21}, h^{-1}	2.14 ± 0.54	0.76 ± 0.64	—	1.41 ± 0.68	—
V_1, L	36.3 ± 22.6	90.4 ± 18.7	112.6 ± 25.4	117.0 ± 59.4	150.3 ± 81.4
V_2, L	61.4 ± 11.3	55.7 ± 31.3	—	65.4 ± 15.2	—
AUC, mg·h/L	3.80 ± 0.62	3.62 ± 1.63	3.53 ± 1.08	2.86 ± 1.24	2.32 ± 0.69
CL, mL/min	461.8 ± 57.3	517.1 ± 160.2	505.6 ± 129.5	585.0 ± 265.0	670.2 ± 161.3
CL_R, mL/min	372.0 ± 58.0	422.5 ± 140.7	397.0 ± 108.8	396.2 ± 142.2	425.0 ± 171.5
U_∞, mg	80.5 ± 5.4	81.4 ± 8.6	78.3 ± 7.3	69.7 ± 7.1	61.8 ± 9.8

dividual results are presented in Table II. The results show a rapid distribution phase corresponding to a half-life of 0.10 ± 0.05 h (range, 0.062–0.15 h) and an elimination phase with a mean half-life of 2.75 ± 0.78 h (range, 1.75–3.99 h). The volumes of distribution were large [36.3 ± 22.6 L (range, 14–68 L) for the central compartment and 61.4 ± 11.3 L (range, 44.1–72.8 L) for the peripheral compartment]. The total clearance of elimination was moderate [461.8 ± 57.3 mL/min (range, 405.5–533 mL/min)]. The mean unchanged drug urinary elimination curves of the six subjects are shown in Fig. 3. The overall urinary elimination of unchanged alizapride (80.51 ± 5.4%) of the dose administered (range, 73.2–88.7%) indicates that urinary excretion is the main route of alizapride elimination. About 20% of the injected dose was not recovered in this study. This cannot be explained by an insufficient amount of urine collected (Fig. 3). So the difference must be accounted for by metabolism or another route of elimination of unchanged drug or its metabolites, such as biliary excretion. It is noteworthy that in a previous study (7) it was shown that the chromatographic method was specific for the unchanged drug, both in urine and plasma, and no extra peak appeared in the chromatograms. Therefore, from the data of alizapride urinary elimination, the renal clearance can be calculated to be 372.0 ± 58.0 mL/min, indicating an active tubular process of alizapride excretion.

Intramuscular Administration—The plot of mean plasma concentrations of alizapride *versus* time is shown in Fig. 1, and the corresponding pharmacokinetic parameters are presented in Table II. The appearance of the drug in plasma is very rapid, corresponding to a rate constant of 7.13 ± 5.56 h^{-1}. Maximum concentrations were 848 ± 193 ng/mL and occurred within 20 min after injection. The calculated parameters were very close to those observed after intravenous injection. It is noteworthy that the area under the plasma concentration curves (AUC) and the amount excreted unchanged in the urine are identical.

Oral Administration—The plot of the mean plasma concentrations of alizapride *versus* time obtained after the oral administration of tablets and solutions are shown in Fig. 2. The corresponding mean pharmacokinetic parameters are listed in Table II. The maximum plasma concentrations were higher after solution administration than after tablet administration (mean, 930 ± 350 ng/mL *versus* 740 ± 90 ng/mL) and occurred slightly sooner after solution administration (0.57 ± 0.34 h *versus* 0.69 ± 0.47 h). Similarly, the lag time observed with the solution dosage form was two times lower than that of the tablet. Compared with the parameters obtained after the intravenous injection, the AUC values were lower (mean, 3.53 ± 1.08 and 2.86 ± 1.24 mg·h/L, respectively, for the tablet and the solution), and the amount excreted unchanged in the urine decreased to 78.3 ± 7.3 and 69.7 ± 7.1 mg for the tablets and solutions, respectively. With these dosage forms, therefore, the bioavailability seemed to decrease, resulting in increased apparent volumes of distribution and total clearances, since these parameters were estimated on the assumption of total absorption. On the contrary, the elimination half-lives and the renal clearances, which are independent of the percentage of the dose administered that was absorbed, are identical with those obtained after intravenous injection.

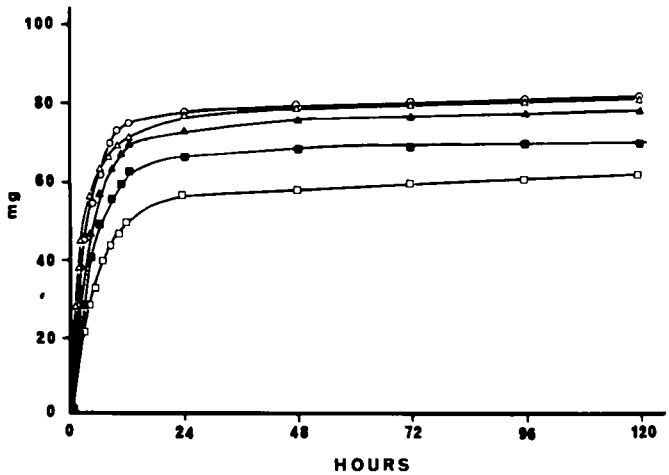

Figure 3—*Mean unchanged alizapride urinary elimination curves obtained from six subjects after each of the different forms was administered. Key: (○) intravenous; (△) intramuscular; (▲) tablet; (■) oral solution; (□) rectal.*

Rectal Administration—The plots of the mean plasma and urine concentrations *versus* time are shown in Figs. 2 and 3, respectively. The corresponding pharmacokinetic parameters are listed in Table II. The maximum plasma concentrations obtained with suppositories were the lowest (630 ± 210 ng/mL) and were seen last at 1.26 ± 1.02 h after administration. The amounts absorbed from this form seemed to be low since the AUC was 2.32 ± 0.69 mg·h/L and the mean urinary elimination was 61.8 ± 9.8 mg. The mean elimination half-lives and renal clearances were identical with those observed after intravenous injection.

Bioavailability Study—The absolute bioavailability of the four dosage forms was estimated from the AUC and the overall amounts of unchanged excreted drug. The ANOVA analyses corresponding to the trial design showed no statistical differences at the 0.05 levels between subjects or time of drug administration for both parameters.

The AUC ANOVA failed to show an overall difference between the dosage forms ($^4_{16}F$ = 2.996, but was very close to the significant value at the 0.05 level, ($^4_{16}F$ = 3.01). However, for the urinary excretion studies, ANOVA showed a significant difference in the tested form at the 0.01 level ($^4_{16}F$ = 5.47). The protected multiple Student t test (11), applied for comparisons of each dosage form against intravenous injections, showed that intramuscular and oral tablet administrations were not significantly different from the intravenous administration (t = 0.9 and 2.25, respectively). However, the oral solution and the rectal suppositories both differed significantly from the intravenous injection at the 0.01 level (t = 10.8 and 18.7, respectively).

The difference observed between the two parameters can be explained by the greater variability observed with the AUC. This is shown by the estimation of the symmetrical confidence interval according to Westlake (8, 13) which yielded 36.9 and 31.2% intervals for the tablet and the intramuscular forms when estimated from AUC and only 13.0 and 13.9% for the same forms, respectively, when estimated from amounts excreted in the urine. Due to this greater variability, the ANOVA was unable to show any difference, although it seemed to occur.

It was surprising to find that the oral solution showed significantly lower bioavailability than did the tablet forms since, in most cases, solutions yielded higher bioavailabilities than did the solid forms. Such an observation has been made with two barbiturates, namely, cyclobarbital (14) and heptabarbital (15). Physiological explanations for such a phenomenen are difficult. Either a precipitation in the stomach and/or the intestinal tract or a delay in the transfer of the drug from the stomach to the intestine can occur (10). The latter was unlikely to have occurred with alizapride since it appeared very rapidly in the blood stream with both oral forms, and the maximum plasma concentrations were obtained very rapidly.

Differences in the rate of absorption of the drug with the extravascular forms were tested by using the nonparametric Kruskal–Wallis test (11) for

the observed plasma maximum concentrations and the time at which they occurred. This test failed to show any difference between the four tested forms with the two chosen parameters. Therefore, the study of the bioavailability of intramuscular, oral solution, tablet, and rectal suppository administration compared with intravenous administration showed that the intramuscular dosage form and oral tablets gave results similar to those obtained by intravenous injection, but the oral solution and the suppositories showed a mean lower bioavailability of 75 and 61%, respectively.

REFERENCES

(1) P. Casanova, *Hepatology*, **16**, 381 (1980).

(2) J. M. Segrestua, J. Gueris, D. Julien, and M. Tiar, *Thérapie*, **34**, 437 (1979).

(3) C. Laville and J. Margarit, *Sem. Hôp. Paris*, **58**, 323 (1982).

(4) E. Pommat, *Sem. Hôp. Paris*, **58**, 363 (1982).

(5) F. Battistelli and H. Lestradet, *Sem. Hôp. Paris*, **58**, 349 (1982).

(6) D. Girard, E. Salles, and A. Bel, *Sem. Hôp. Paris*, **58**, 353 (1982).

(7) G. Houin, F. Bree, N. Lerumeur, and J. P. Tillement, *J. Pharm. Sci.*, **72**, 71 (1983).

(8) W. J. Westlake, in "Principles and Perspectives in Drug Bioavailability," J. Blanchard, R. J. Sawchuk, and B. B. Brodie, Eds., Karger, Basel, 1979, chap. 1.

(9) P. D'Athis, M. O. Richard, D. Delauture, E. Rey, M. Bouvier-d'Yvoire, E. Clément, and G. Olive, *Thérapie*, **36**, 443 (1981).

(10) J. G. Wagner, in "Fundamentals of Clinical Pharmacokinetics," Drug Intelligence, Hamilton, Ill., 1975.

(11) W. G. Cochran and G. M. Cox, in "Experimental Designs," Wiley, New York, N.Y., 1957.

(12) W. J. Westlake, *Biometrics*, **30**, 319 (1974).

(13) W. J. Westlake, *Biometrics*, **32**, 741 (1976).

(14) D. D. Breimer, *J. Pharm. Sci.*, **64**, 1576 (1975).

(15) D. D. Breimer and A. G. de Boer, *Eur. J. Clin. Pharmacol.*, **9**, 169 (1975).

ACKNOWLEDGMENTS

We gratefully acknowledge Dr. Arunkumar Shastri for his critical revision of the manuscript.

Kinetic Study of the Polymorphic Transformations of Phenylbutazone

YOSHIHISA MATSUDA ˣ, ETSUKO TATSUMI, ETSUKO CHIBA, and YUKIE MIWA

Received June 15, 1983, from the *Kobe Women's College of Pharmacy, Higashinada, Kobe 658, Japan.* Accepted for publication December 5, 1983.

Abstract □ The polymorphic transformations of phenylbutazone from metastable forms α and β to stable form δ were studied quantitatively at four temperature and five humidity levels by X-ray powder diffractometry. The transformation of form α conformed with the Avrami-Erofe'ev kinetic model and form β conformed with apparent first-order kinetics. In the two transformation systems, the induction periods depended on the storage conditions and were prolonged with lowering of temperature and humidity. The transformation rate of form α was not affected by humidity, whereas that of form β increased according to a rise in humidity. The temperature dependency of the transformation rate constant was remarkable. The Arrhenius treatment was applicable to the $\beta \rightarrow \delta$ transformation at low temperatures. The overall half-life, including induction period, revealed that form α was more stable than form β under any storage condition. A good linear relationship existed between the induction period and the transformation rate constant, irrespective of the storage conditions. The scanning electron photomicrographs of forms α and β demonstrated that acicular crystals of form δ grew as the transformation progressed. This could be confirmed as the change in particle diameter of the samples.

Keyphrases □ Phenylbutazone—polymorphic transformation, physicochemical stability under different storage conditions □ Polymorphic transformation—phenylbutazone, physicochemical stability under different storage conditions □ Physicochemical stability—phenylbutazone, different storage conditions, polymorphic transformation

The method for improving the bioavailability of a slightly soluble drug is an important problem in the preformulation study of solid dosage forms. Polymorphic transformation is often effective as a technique for increasing solubility. Since the solubility and dissolution rate of a metastable polymorph are usually higher than those of the stable form, the former is more desirable clinically than the latter; however, the former is not always preferable in physicochemical stability. It is well known that, irrespective of temperature, only one crystal form is thermodynamically stable and all other forms convert eventually to the stable one. A metastable form nevertheless may occasionally exhibit sufficient stability to ensure a reasonable shelf life. If a metastable form is used in a formulation because of its excellent dissolution properties, it is prerequisite to demonstrate that the metastable form is never transformed to a more stable form under usual storage conditions.

Although some difficulties are involved in establishing a quantitative method for polymorphic transformation, there are several previous reports on the method (1–8). Due to the complexity of solid-state reaction, the stability-indicating kinetic interpretation has been fully discussed in only a few reports (1, 7, 8). The techniques described here are divided into three groups: IR spectrophotometry based on the quantitative Nujol mull technique (1–3, 6), differential scanning calorimetry (4, 5), and X-ray powder diffractometry (7, 8). Among these, X-ray diffractometry may be the most useful method because heat and liquid relating closely to polymorphic transformation are not involved in the measurement.

In the present investigation, the stability profiles between the two metastable forms of phenylbutazone are comparatively evaluated. The preparation and characterization of the phenylbutazone polymorphism have been described previously (9–16). The polymorphic system has been reported to consist of a stable form (form δ), four metastable forms (forms α, β, γ, and ϵ), and two pseudopolymorphs, among which form ϵ has the highest solubility. For the reasons of high yield and simplicity of preparation, forms α and β were chosen as polymorphic models in this study. The transformations of these forms were measured quantitatively by X-ray powder diffractometry and thoroughly studied over long periods of time under different storage conditions.

0022-3549/84/1000-1453$01.00/0

© 1984, American Pharmaceutical Association

the observed plasma maximum concentrations and the time at which they occurred. This test failed to show any difference between the four tested forms with the two chosen parameters. Therefore, the study of the bioavailability of intramuscular, oral solution, tablet, and rectal suppository administration compared with intravenous administration showed that the intramuscular dosage form and oral tablets gave results similar to those obtained by intravenous injection, but the oral solution and the suppositories showed a mean lower bioavailability of 75 and 61%, respectively.

REFERENCES

(1) P. Casanova, *Hepatology*, **16**, 381 (1980).

(2) J. M. Segrestua, J. Gueris, D. Julien, and M. Tiar, *Thérapie*, **34**, 437 (1979).

(3) C. Laville and J. Margarit, *Sem. Hôp. Paris*, **58**, 323 (1982).

(4) E. Pommat, *Sem. Hôp. Paris*, **58**, 363 (1982).

(5) F. Battistelli and H. Lestradet, *Sem. Hôp. Paris*, **58**, 349 (1982).

(6) D. Girard, E. Salles, and A. Bel, *Sem. Hôp. Paris*, **58**, 353 (1982).

(7) G. Houin, F. Bree, N. Lerumeur, and J. P. Tillement, *J. Pharm. Sci.*, **72**, 71 (1983).

(8) W. J. Westlake, in "Principles and Perspectives in Drug Bioavailability," J. Blanchard, R. J. Sawchuk, and B. B. Brodie, Eds., Karger, Basel, 1979, chap. 1.

(9) P. D'Athis, M. O. Richard, D. Delauture, E. Rey, M. Bouvier-d'Yvoire, E. Clément, and G. Olive, *Thérapie*, **36**, 443 (1981).

(10) J. G. Wagner, in "Fundamentals of Clinical Pharmacokinetics," Drug Intelligence, Hamilton, Ill., 1975.

(11) W. G. Cochran and G. M. Cox, in "Experimental Designs," Wiley, New York, N.Y., 1957.

(12) W. J. Westlake, *Biometrics*, **30**, 319 (1974).

(13) W. J. Westlake, *Biometrics*, **32**, 741 (1976).

(14) D. D. Breimer, *J. Pharm. Sci.*, **64**, 1576 (1975).

(15) D. D. Breimer and A. G. de Boer, *Eur. J. Clin. Pharmacol.*, **9**, 169 (1975).

ACKNOWLEDGMENTS

We gratefully acknowledge Dr. Arunkumar Shastri for his critical revision of the manuscript.

Kinetic Study of the Polymorphic Transformations of Phenylbutazone

YOSHIHISA MATSUDA ˣ, ETSUKO TATSUMI, ETSUKO CHIBA, and YUKIE MIWA

Received June 15, 1983, from the *Kobe Women's College of Pharmacy, Higashinada, Kobe 658, Japan.* Accepted for publication December 5, 1983.

Abstract □ The polymorphic transformations of phenylbutazone from metastable forms α and β to stable form δ were studied quantitatively at four temperature and five humidity levels by X-ray powder diffractometry. The transformation of form α conformed with the Avrami-Erofe'ev kinetic model and form β conformed with apparent first-order kinetics. In the two transformation systems, the induction periods depended on the storage conditions and were prolonged with lowering of temperature and humidity. The transformation rate of form α was not affected by humidity, whereas that of form β increased according to a rise in humidity. The temperature dependency of the transformation rate constant was remarkable. The Arrhenius treatment was applicable to the $\beta \rightarrow \delta$ transformation at low temperatures. The overall half-life, including induction period, revealed that form α was more stable than form β under any storage condition. A good linear relationship existed between the induction period and the transformation rate constant, irrespective of the storage conditions. The scanning electron photomicrographs of forms α and β demonstrated that acicular crystals of form δ grew as the transformation progressed. This could be confirmed as the change in particle diameter of the samples.

Keyphrases □ Phenylbutazone—polymorphic transformation, physicochemical stability under different storage conditions □ Polymorphic transformation—phenylbutazone, physicochemical stability under different storage conditions □ Physicochemical stability—phenylbutazone, different storage conditions, polymorphic transformation

The method for improving the bioavailability of a slightly soluble drug is an important problem in the preformulation study of solid dosage forms. Polymorphic transformation is often effective as a technique for increasing solubility. Since the solubility and dissolution rate of a metastable polymorph are usually higher than those of the stable form, the former is more desirable clinically than the latter; however, the former is not always preferable in physicochemical stability. It is well known that, irrespective of temperature, only one crystal form is thermodynamically stable and all other forms convert eventually to the stable one. A metastable form nevertheless may occasionally exhibit sufficient stability to ensure a reasonable shelf life. If a metastable form is used in a formulation because of its excellent dissolution properties, it is prerequisite to demonstrate that the metastable form is never transformed to a more stable form under usual storage conditions.

Although some difficulties are involved in establishing a quantitative method for polymorphic transformation, there are several previous reports on the method (1–8). Due to the complexity of solid-state reaction, the stability-indicating kinetic interpretation has been fully discussed in only a few reports (1, 7, 8). The techniques described here are divided into three groups: IR spectrophotometry based on the quantitative Nujol mull technique (1–3, 6), differential scanning calorimetry (4, 5), and X-ray powder diffractometry (7, 8). Among these, X-ray diffractometry may be the most useful method because heat and liquid relating closely to polymorphic transformation are not involved in the measurement.

In the present investigation, the stability profiles between the two metastable forms of phenylbutazone are comparatively evaluated. The preparation and characterization of the phenylbutazone polymorphism have been described previously (9–16). The polymorphic system has been reported to consist of a stable form (form δ), four metastable forms (forms α, β, γ, and ϵ), and two pseudopolymorphs, among which form ϵ has the highest solubility. For the reasons of high yield and simplicity of preparation, forms α and β were chosen as polymorphic models in this study. The transformations of these forms were measured quantitatively by X-ray powder diffractometry and thoroughly studied over long periods of time under different storage conditions.

0022-3549/84/1000-1453$01.00/0

© 1984, American Pharmaceutical Association

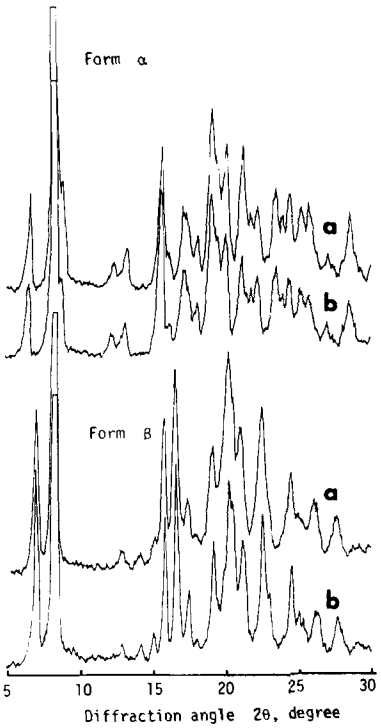

Figure 1—*X-ray diffraction patterns of forms α and β before and after milling. Key: (a) before milling; (b) after milling.*

EXPERIMENTAL SECTION

Preparation and Characterization of Polymorphs—*Form δ*—A single batch of commercial phenylbutazone[1] was used as received. The drug was confirmed to be form δ by X-ray powder diffraction analysis, differential scanning calorimetry (DSC), and IR spectroscopy.

Form α—An acetone solution (20% w/v) of the drug was evaporated to dryness under reduced pressure at 0°C by using a rotary evaporator.

Form β—The same solution as that used for form α was poured into 10 volumes of distilled water and stirred vigorously at room temperature. The separated crystals were removed by filtration through a sintered-glass funnel and dried under reduced pressure. These modifications were also characterized as forms α and β, respectively, according to a previously described method (16).

To expose the maximum surface area to ambient moisture, all modifications were micronized with a pin mill[2] at 26,960 rpm. The specific surface area diameters of the milled forms α and β, measured by an air permeability method (17), were 3.2 and 2.8 μm, respectively. The particle densities of forms α, β, and δ were determined with an air comparison pycnometer[3]. The X-ray powder diffraction patterns and the DSC data of the samples before and after milling indicated that no polymorphic transformation occurred during the milling operation (Figs. 1 and 2).

Determination of Transformation Rate—*Preparation of Calibration Curves by X-ray Powder Diffractometry*—Known quantities of form α or β were thoroughly mixed with form δ in various proportions in a mortar. The mixtures (250 mg each) were subjected to X-ray powder diffraction analysis. The X-ray diffraction pattern was recorded according to a previously described method (16). The instrument was set as follows: (*a*) 35 kV, 7 mA; (*b*) 1° beam slit and 0.2° detector slit; (*c*) count range, 1000 cps; (*d*) time constant, 1 s; (*e*) range of diffraction angle 2θ = 30–5°; (*f*) scanning speed, 4°/min; and (*g*) chart speed, 40 mm/min.

Although the X-ray diffraction pattern of form δ obviously differed from that of forms α and β (16), most of the peaks characterized by these forms in the mixture were not fully separated due to the close vicinity of the diffraction angles. Figure 3 represents the typical X-ray diffraction patterns of various proportions for α–δ and β–δ binary mixtures by weight basis. The changes in peaks (arrows) accompanying various mixing ratios were especially remarkable at the diffraction angles of 6.6°, 7.1°, 19.1°, and 20.1° for the α–δ system and at 15.6°, 16.4°, 20.1°, and 21.0° for the β–δ system. These

[1] Ciba-Geigy (Japan) Ltd.
[2] Contraplex-Labormühle 63C; Alpine AG, Federal Republic of Germany.
[3] Model 930; Beckman-Toshiba Co. Ltd., Tokyo, Japan.

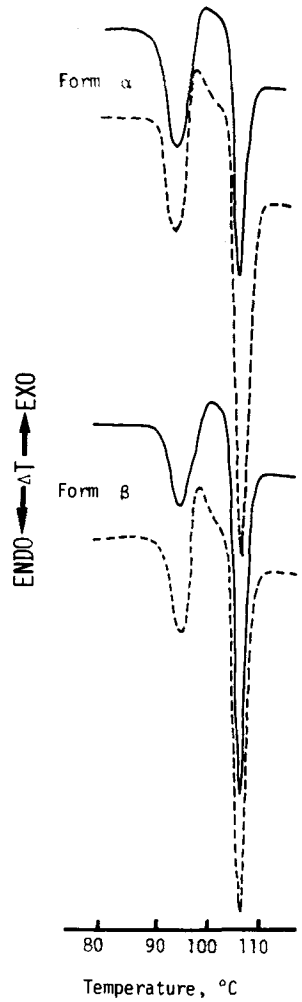

Figure 2—*DSC curves for forms α and β before (—) and after (- - -) milling. Sample weights: 7.30, 9.21, 8.19, and 8.01 mg (from top to bottom); heating rate, 10°C/min; sensitivity, ±20 mJ/s.*

peaks consisted of the individual peak characterizing each form. Thus, the diffraction intensity ratios of the two adjacent diffraction angles were plotted against the weight fraction of each component (Fig. 4). Despite the fluctuation of the individual diffraction intensity, these plots were always reproducible to give a smooth curve for any of the mixing ratios. Since curve a (Fig. 4) for the α–δ system approached infinity at the lower weight fraction of form δ, the reciprocal values of intensity ratios were regressed with curve b (Fig. 4), and their terminal regions were made up for each other (thick line of the left panel, Fig. 4). Although the calibration data for the α–δ and β–δ systems could be obtained as straight lines on the middle part of log-probability and semi-logarithmic scales, respectively, they deviated from these lines on the terminal regions. Therefore, the original calibration curves were used. The conversion rates for the two systems were expressed by the mean of values estimated from the two calibration curves.

The changes in diffraction intensity at these angles are shown for the actual transformation system in Fig. 5. The time course change in relative diffraction intensity was clearly observed, indicating the validity of this method.

Preparation of Calibration Curves by Differential Scanning Calorimetry—For purposes of comparison with the X-ray powder diffractometry method, DSC was employed for determining the conversion rate. Similarly to X-ray powder diffractometry, preparation of an exactly equal amount of mixed samples of varying weight ratios was attempted to accomplish the plotting of DSC data. This was almost impossible from a technical point of view; therefore, the following method was alternatively employed. Different amounts of form α or β were accurately weighed and thermograms of these pure samples were recorded in a closed pan system. The DSC[4] operation conditions were: (*a*) heating rate, 5°C/min; (*b*) sensitivity, ±5 mJ/s; (*c*) chart speed, 40 mm/min; (*d*) flow rate of nitrogen gas, 30 mL/min. Forms α and β exhibited endothermic peaks at 91.0–92.0°C and 95.0–96.5°C, respectively,

[4] DSC-30; Shimadzu Co., Kyoto, Japan.

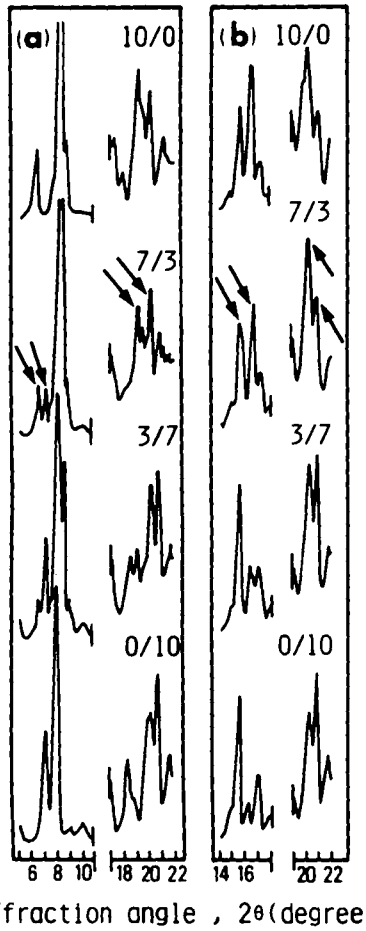

Figure 3—*X-ray diffraction patterns of α–δ and β–δ binary mixtures in various ratios. Key: (a) α–δ system; (b) β–δ system. The fraction in the graph represents the form α (form β)/form δ weight ratio.*

which subsequently underwent polymorphic transformations to show exothermic peaks at 93.0–94.0°C and 96.5–98.0°C, respectively. Two areas consisting of an area surrounded by both an endothermic peak curve and a line connecting the starting point of the endothermic peak with the top of the exothermic peak and another area surrounded by the same curve and the line connecting the same point with the terminal point of the exothermic peak were regarded as areas A and B, respectively (Fig. 6). The areas were measured by a gravimetric technique and were plotted against sample weight. Good straight lines were obtained between both parameters for the two systems. The conversion rate was expressed as the ratio of the mean of the two values estimated with lines A and B to the weight of sample on an aluminum pan.

Storage Conditions and Sampling of Polymorphs—About 1.2 g of a sample was placed in a vial as lightly as possible and stored over saturated solutions of various salts placed in laboratory desiccators. The desiccators were kept in a thermostated cabinet. The samples for thermal analysis were placed on an aluminum pan and stored in the same desiccators. The temperatures and humidities used were 25, 40, 50, and 60°C and 0, 30, 50, 70, and 80% relative humidity, respectively. Phosphorus pentoxide was used to provide a limiting humidity of 0% relative humidity at 60°C. The stored sample was withdrawn from each vial at various time intervals for X-ray powder diffractometry. After the measurement, the sample was returned to the vial for further storage.

Scanning Electron Microscopy—The scanning electron photomicrographs of the samples stored at 60°C and 80% relative humidity were taken with a microscope[5] at magnifications ranging from 600× to 2000×.

RESULTS AND DISCUSSION

Kinetic Interpretation of Transformation Processes—Since the solid-state reaction is essentially a surface phenomenon, the solid–solid transformation of a metastable polymorph may require a long period of time under mild stress condition. The residual percentage was determined by the X-ray powder

[5] Model JSM-U3; JEOL Co. Ltd., Tokyo, Japan.

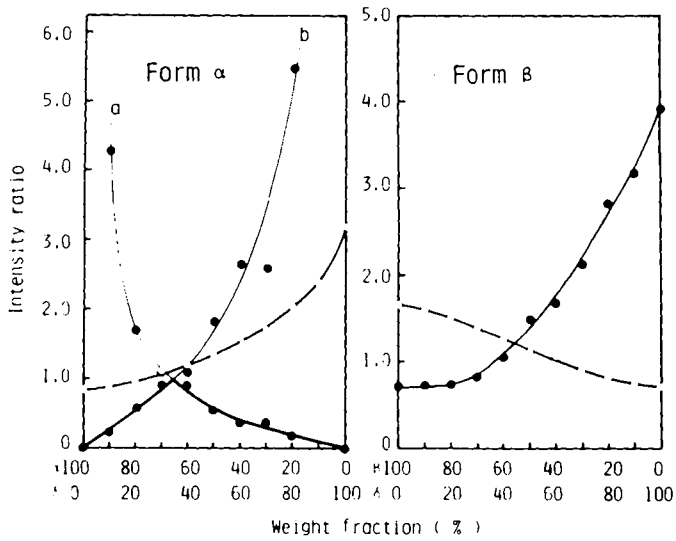

Figure 4—*Calibration curves for forms α and β by X-ray diffractometry Key: (intensity ratio for form α) (○) 20.1°/19.1°; (●) 6.6°/7.1° (a) or 7.1°/6.6° (b); (intensity ratio for form β) (○) 20.1°/21.0°; (●) 15.6°/16.4°.*

diffraction method (Fig. 7). The typical transformation profiles of the forms obtained under the extreme stress condition of 60°C are illustrated. Form β underwent transformation more rapidly than form α at any humidity. A distinct difference on the pattern of curves was seen between forms α and β, suggesting a different mechanism of transformation; the best-fitting curves

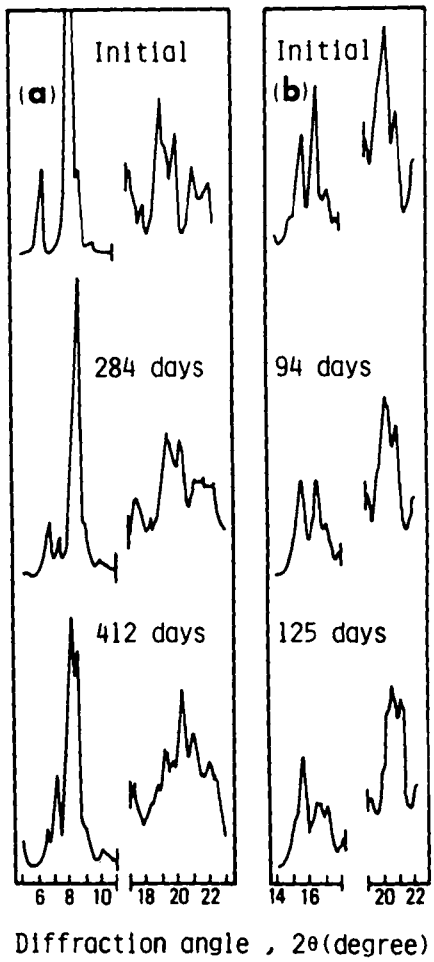

Figure 5—*Changes in X-ray diffraction intensities of forms α and β under polymorphic transformations. Key: (a) α → δ transformation at 40°C and 80% relative humidity. (b) β → δ transformation at 40°C and 30% relative humidity. The number in the graph represents the number of days after storage was begun.*

Table I—Values of m^a for $\alpha \rightarrow \delta$ and $\beta \rightarrow \delta$ Polymorphic Transformation Rate Equations

Transformation System	Temperature, °C	Relative Humidity, %				
		0	30	50	70	80
$\alpha \rightarrow \delta$	25	—[b]	NC[c]	NC	NC	NC
	40	—	NC	NC	2.10	1.93
	50	—	1.91	1.98	1.93	1.76
	60	1.57[d]	—	1.99	2.04	1.89
$\beta \rightarrow \delta$	25	—	0.98	1.03	0.88	1.01
	40	—	0.94	0.84	0.99	0.89
	50	—	1.00	1.01	0.98	0.96
	60	1.02	—	1.02	0.82	0.98

[a] See Eq. 2. [b] Experiment was not carried out. [c] Not calculated; m value could not be calculated because the transformation did not proceed at all or proceeded only to a small extent. [d] Few data were available.

Table II—Correlation Coefficients for the m Values in Table I

Transformation System	Temperature, °C	Relative Humidity, %				
		0	30	50	70	80
$\alpha \rightarrow \delta$	25	—[a]	NC[b]	NC	NC	NC
	40	—	NC	NC	0.952 (6)[c]	0.994 (7)
	50	—	0.998 (5)	0.995 (9)	0.994 (8)	0.998 (8)
	60	1.000 (4)	—	0.987 (6)	0.996 (6)	0.998 (6)
$\beta \rightarrow \delta$	25	—	0.968 (10)	0.986 (10)	0.940 (5)	0.991 (10)
	40	—	0.772 (5)	0.999 (4)	0.990 (5)	0.995 (6)
	50	—	1.000 (5)	0.991 (7)	0.994 (5)	1.000 (5)
	60	0.988 (7)	—	1.000 (4)	0.990 (4)	0.999 (4)

[a] Experiment was not carried out. [b] Not calculated; coefficient of correlation could not be calculated because the transformation did not proceed at all or proceeded only to a small extent. [c] Number of plots are indicated in parentheses.

for form α were all sigmoidal in shape, whereas those for form β were exponential. Similar profiles were obtained for the samples stored under other conditions of temperature and humidity. A common feature was the presence of an induction period similar to that obtained by Moustafa *et al.* (1, 2), which varied depending on the storage condition.

Figure 8 shows the comparison of the residual percentage determined by X-ray diffractometry with that determined by the DSC for the same sample as shown in Fig. 7. Irrespective of the humidity level, a good correspondence was obtained after the middle stage of the $\alpha \rightarrow \delta$ transformation. However, in the earlier stage of the $\alpha \rightarrow \delta$ transformation and throughout the entire process of $\beta \rightarrow \delta$ transformation, such a correspondence could not be established; the DSC resulted in an overestimation of the conversion rate. These results indicate that during the course of heating some further transformation occurred before the transition peak was observed. The DSC thus proved to be inadequate for determining the conversion rate in the present transformation systems; therefore, the subsequent determinations were carried out by the X-ray powder diffractometry method alone.

To confirm the conformance of isothermal kinetic data to theoretical kinetic equations, an interpretation method by Hancock and Sharp (18) was applied to the accompanying Avrami-Erofe'ev equation (19):

$$\ln [-\ln (1 - \alpha)] = m \cdot \ln t + \ln B \qquad \text{(Eq. 1)}$$

where α and t represent a conversion rate of polymorph and storage time, respectively, B is a constant, and m is the constant relating to the mechanism of transformation. In the present transformation systems, Eq. 1 should be modified as:

$$\ln [-\ln (1 - \alpha)] = m \cdot \ln (t - t_i) + \ln B \qquad \text{(Eq. 2)}$$

where t_i is the induction period. Equation 2 indicates that a linear relationship of a gradient m exists between the values of $-\ln (1 - \alpha)$ and $t - t_i$ on the double logarithmic scale. The best-fitting values for m and t_i, which should give the maximum coefficient of correlation, were calculated from the conversion rates to be <80% by the computer-aided least-squares method. The values for m and the correlation coefficients are given in Tables I and II, respectively.

Although several values were somewhat abnormal due to the paucity of data, the integer m values for $\alpha \rightarrow \delta$ and $\beta \rightarrow \delta$ transformations were rounded up to 2 and 1 from their mean values of 1.95 and 0.96, respectively. Equations 3 and 4 are, consequently, derived from Eq. 2:

$$[-\ln (1 - \alpha)]^{1/2} = k_1 (t - t_i) \; (\alpha \rightarrow \delta \text{ transformation}) \qquad \text{(Eq. 3)}$$

$$\ln (1 - \alpha) = -k_2 (t - t_i) \; (\beta \rightarrow \delta \text{ transformation}) \qquad \text{(Eq. 4)}$$

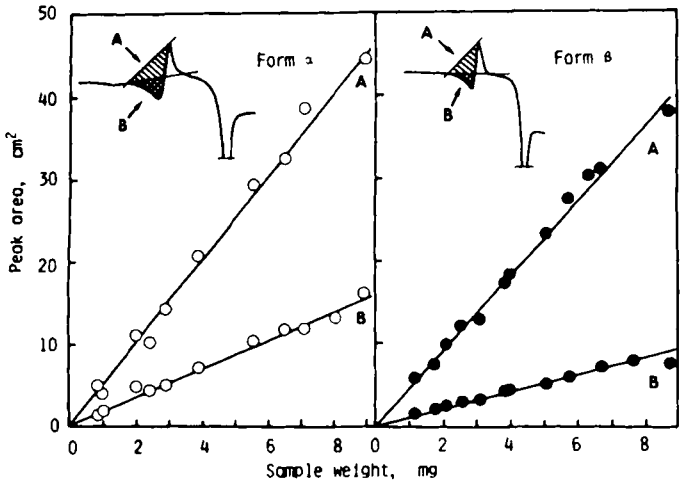

Figure 6—*Calibration curves for forms α and β by DSC. Key: (○) form α; (●) form β. The straight lines A and B indicate the areas A and B, respectively.*

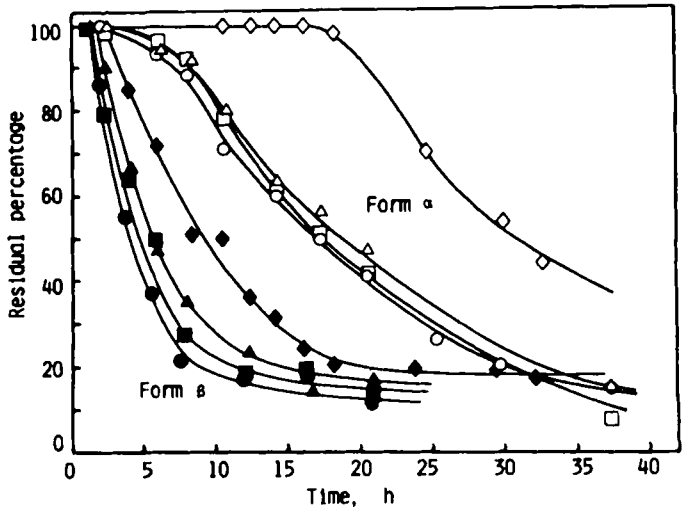

Figure 7—*Time course of $\alpha \rightarrow \delta$ and $\beta \rightarrow \delta$ transformations at 60°C. Key: (◇ ◆) 0%; (△ ▲) 50%; (□ ■) 70%; (○ ●) 80% relative humidity.*

Table III—Correlation Coefficients for Transformation Models[a]

Transformation System	Temperature °C	Relative Humidity, % 0	30	50	70	80
$\alpha \rightarrow \delta$	25	—[b]	NC[c]	NC	NC	NC
	40	—	NC	NC	0.960 (6)[d]	0.992 (7)
	50	—	0.981 (5)	0.995 (9)	0.994 (8)	0.994 (8)
	60	0.986 (4)	—[b]	0.987 (6)	0.993 (6)	0.997 (6)
$\beta \rightarrow \delta$	25	—	−0.969 (10)	−0.967 (10)	−0.966 (5)	−0.944 (10)
	40	—	−0.995 (5)	−0.993 (4)	−0.995 (5)	−0.991 (6)
	50	—	−0.994 (5)	−0.988 (7)	−0.993 (5)	−1.000 (5)
	60	−0.991 (7)	—	−0.999 (4)	−0.976 (4)	−0.998 (4)

[a] See Eqs. 3 and 4 in the text. [b] Experiment was not carried out. [c] Not calculated; coefficient of correlation could not be calculated because the transformation did not proceed at all or proceeded only to a small extent. [d] Number of plots are indicated in parentheses.

Table IV—Overall Half-Lives Under Different Storage Conditions (days)

Transformation System	Temperature °C	Relative Humidity, % 0	30	50	70	80
$\alpha \rightarrow \delta$	25	—[a]	NC[b]	NC	NC	NC
	40	—	NC	NC	411	346
	50	—	165	142	151	125
	60	1.28	—	0.79	0.74	0.74
$\beta \rightarrow \delta$	25	—	456	455	436	360
	40	—	100	98	79	70
	50	—	12.0	9.1	6.3	5.5
	60	0.40	—	0.24	0.21	0.18

[a] Experiment was not carried out. [b] Half-life could not be calculated because the transformation did not proceed at all or proceeded only to a small extent.

where k_1 and k_2 are transformation rate constants. The values for both transformation systems in Fig. 7 were plotted according to Eqs. 3 and 4 (Fig. 9). All values gave straight lines under all storage conditions; hence, the regression analyses were repeated by using Eqs. 3 and 4 to calculate the values of t_i, k_1, and k_2 (Table III).

The m value of 2 suggests that $\alpha \rightarrow \delta$ transformation is controlled by a nucleation-and-growth reaction and that the growth of the stable form may take place by a one- or two-dimensional mechanism (20). According to a reaction model (21) conforming to this kinetic expression (Eq. 3), which described the first formation followed by growth of potential nuclei on the surface of the drug, the nucleation was rapid and complete. Therefore, the growth appeared to be two-dimensional. On the contrary, the result of the $\beta \rightarrow \delta$ transformation conforming to the first-order kinetics suggests that the rate of transformation is controlled by random nucleation (*cf.* instantaneous nucleation for $\alpha \rightarrow \delta$ transformation) in an assemblage of an identical reactant fragment (21).

Effects of Temperature and Humidity on the Induction Period and Transformation Rate Constant—Since the induction period and transformation rate depend on the mobility of constituent atoms or molecules of the solid, they must vary considerably with temperature. The effects of temperature and humidity on the induction period on semilogarithmic scales are illustrated in Fig. 10, in which the relative humidity is converted to absolute humidity to provide a thorough understanding of the water contents. The right terminal point of each regression line represents the limiting absolute humidity corresponding to 100% relative humidity at the designated temperature. Temperature affected the induction period more markedly than did humidity. The two transformation systems showed a common tendency to prolong the induction period with a lowering in temperature and humidity, suggesting the delayed initiation of nucleation of the stable form. It should be emphasized that even under the extreme humidity condition of 0% relative humidity at 60°C the induction period was always a finite value for the two transformation systems. The micronization of samples by milling may cause generation of a large number of point defects or dislocations on the crystal surfaces, resulting in selective heterogeneous nucleation. Judging from the water-absorbing power of phosphorus pentoxide[6], as well as the environmental temperature and atmospheric pressure, complete desorption of water molecules on the sites of potential nuclei formation seems to be difficult under these conditions. Therefore, even though the amount of water is very small, it may serve as a nucleation catalyst.

Moustafa *et al.* (1) interpreted the induction period as the time required for equilibration of the crystal surfaces with water vapor. However, the results that the induction period was a finite value at 0% relative humidity and was prolonged at lower temperatures indicate reasonably that the induction period is defined as the time at which the embryo of a stable form grows to the critical nuclei at the nuclei formation sites.

Figure 11 illustrates the effects of temperature and humidity on the

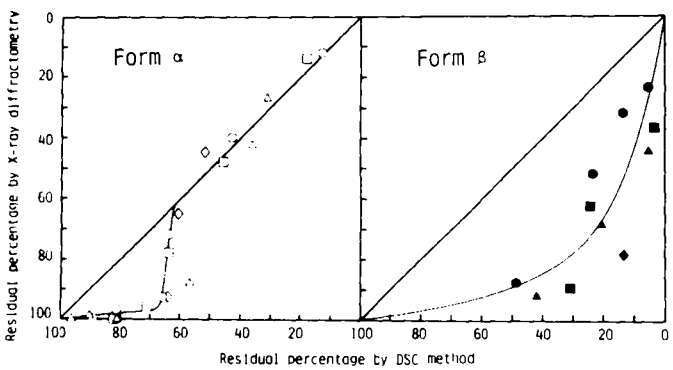

Figure 8—*Relationship between residual percentages of forms α and β at 60°C determined by X-ray diffractometry and those determined by differential scanning calorimetry. Key: (◇ ◆) 0%; (△ ▲) 50%; (□ ■) 70%; (○ ●) 80% relative humidity.*

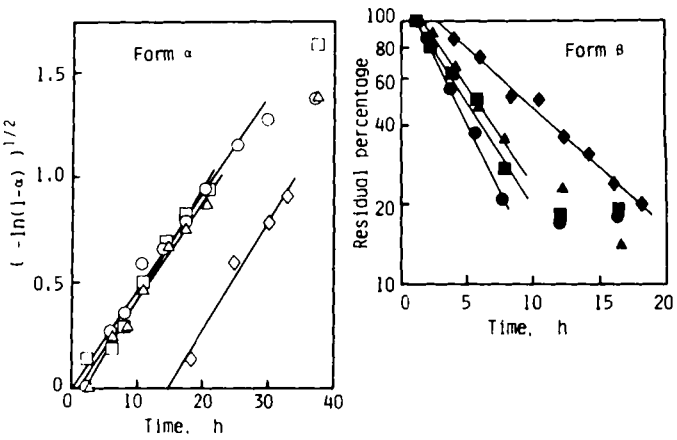

Figure 9—*Applicability of the Avrami-Erofe'ev (19) equation to α → δ transformation and of first-order kinetic model to β → δ transformation at 60°C (see Eqs. 3 and 4). Key: (◇ ◆) 0%; (△ ▲) 50%; (□ ■) 70%; (○ ●) 80% relative humidity.*

[6] The water content remaining in dried air over phosphorus pentoxide in a desiccator is 2.5×10^{-5} mg/L (*cf.* Ref. 22).

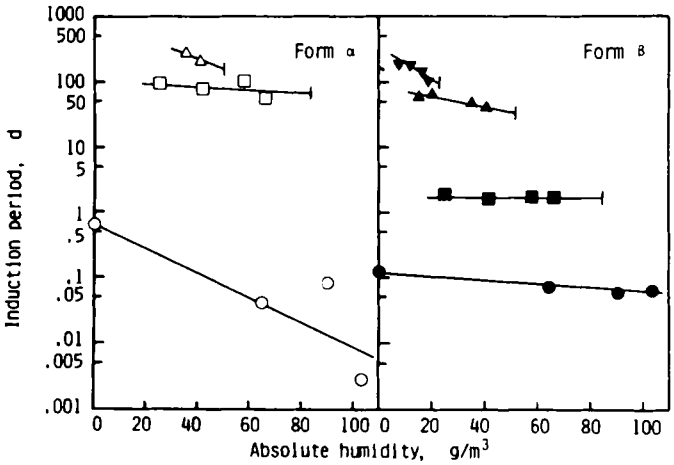

Figure 10—*Effect of absolute humidity on induction periods at different temperatures. Key: (▼) 25°C; (△▲) 40°C; (□■) 50°C; (○●) 60°C. The induction periods for α → δ transformation at 25°C could not be obtained within the time course of this investigation.*

transformation rate constant. The rate constants for forms α and β showed the same dimension of day^{-1}. It was, however, meaningless to use these values for comparison with the rate of transformation, because the mechanisms of transformation differed. The rate constant and the induction period were remarkably affected by temperature, and the rate was increased with a rise in temperature. The difference between the two transformations was distinct: the transformation of form α was not affected by humidity, whereas form β underwent transformation by a complex action of temperature and humidity. Furthermore, the higher the temperature, except for 60°C in the form β transformation, the stronger the dependence on humidity. These data indicate that storage at lower temperature and humidity is essential to inhibit polymorphic transformation.

The estimated half-life, including induction period, was much smaller in form β than in form α under any storage condition, indicating that form β is less stable (Table IV). The order of the thermodynamic instabilities of forms α and β corresponds well to that of superiority in dissolution properties (16).

Figure 12 shows the elevated temperature transformation data plotted by the Arrhenius procedure, in which the logarithmic values for the rate constants obtained by interpolating or extrapolating each regression line of Fig. 11 to the designated absolute humidity are plotted against the reciprocal of absolute temperature. Only one plot was obtainable at each temperature for form α, because the rate constant was not humidity dependent. The rate constant at 25°C was not obtained, because no transformation occurred within the time course of the present investigation. Good linear relationships existed for the β → δ transformation at lower humidities at temperature levels ranging from 25°C to 50°C, indicating that the higher the humidity, the steeper the slope

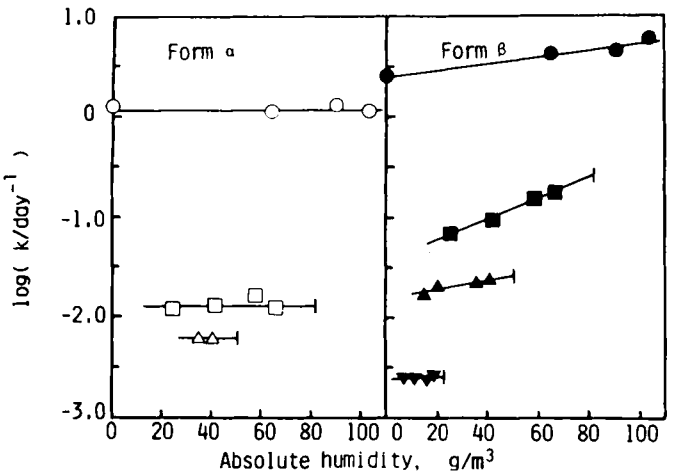

Figure 11—*Effect of absolute humidity on the transformation rate constant at different temperatures. Key: (▼) 25°C; (△▲) 40°C; (□■) 50°C; (○●) 60°C. The transformation rate constants for α → δ transformation at 25°C could not be obtained, because no transformation started within the time course of this investigation.*

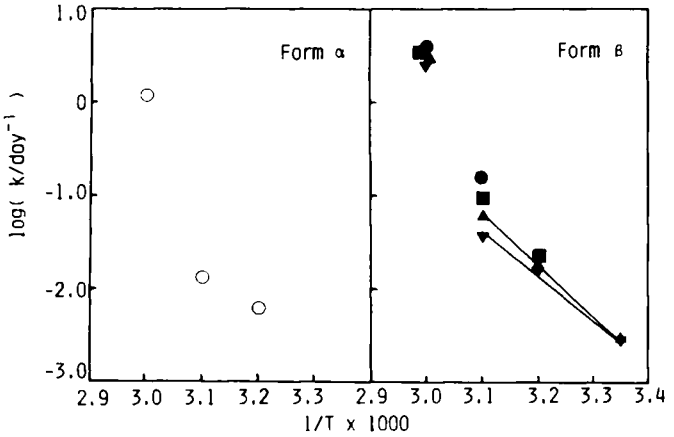

Figure 12—*Arrhenius plot for α → δ and β → δ transformations at different absolute humidities. Key: (○) 0, 20, 40, and 60 g/cm³ for α → δ transformation; (▼) 0 g/cm³, (▲) 20 g/cm³, (■) 40 g/cm³, (●) and 60 g/cm³ for β → δ transformation.*

of the straight line. Although the linearity and/or temperature dependency of the slope at higher humidities were blurry due to insufficient data, the activation energy for transformation was found to increase gradually with an increase in humidity. The dehydration processes from crystals entrapping water of crystallization were also affected by temperature and water vapor pressure (23, 24), *e.g.*, the activation energy for dehydration increases with a rise in water vapor pressure (24). However, the role of water in the present transformation systems fundamentally differed from that in the dehydration reaction. Since the transformation rate is a function of several variables possessing different temperature coefficients, this result is not easily explained.

The activation energies thus determined at absolute humidities of 0 and 20 g/m³ were ~21.7 and 25.1 kcal/mol, respectively. These values were much smaller than the activation energy of ~203 kcal/mol (11) that was determined by the method of Kissinger (25). Weaker intermolecular actions such as van der Waals forces or hydrogen bonds are predominant in polymorphs; therefore, the transformation must not require a higher activation energy. The validity of this suggestion may be supported by the facts that the activation energy for the polymorphic transformation in binaphthyl is ~60 kcal/mol and that for *p*-dichlorobenzene is much smaller (17 kcal/mol) (26). It is also interesting to note that the activation energy for loss of water from cytosine monohydrate is ~25 kcal/mol (26).

The rate constants at 60°C in the two transformation systems were abnormally higher than those estimated by extrapolating the regression lines, suggesting that the activation energies became high at ~60°C. Additional information on other transformation systems is needed to understand why a change in activation energy accompanies a rise in temperature. It has been reported that since not all solid-state reactions conform to the Arrhenius treatment, the activation energy is not necessarily constant with temperature (27, 28).

The kinetic behavior during the induction period and in the transformation rate constant suggest the close relationship between them. The double-logarithmic plotting of both factors gave a good straight line, irrespective of the storage conditions for the two transformation systems (Fig. 13). It was verified

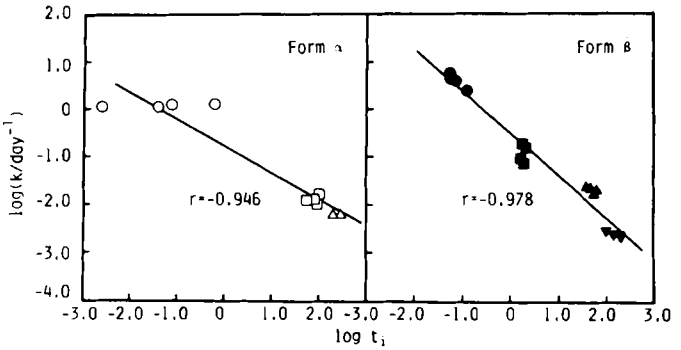

Figure 13—*Relationships between induction period and transformation rate constant for α → δ and β → δ transformations. Key: (▼) 25°C; (△▲) 40°C; (□■) 50°C; (○●) 60°C. The plots for α → δ transformation at 25°C could not be obtained within the time course of this investigation.*

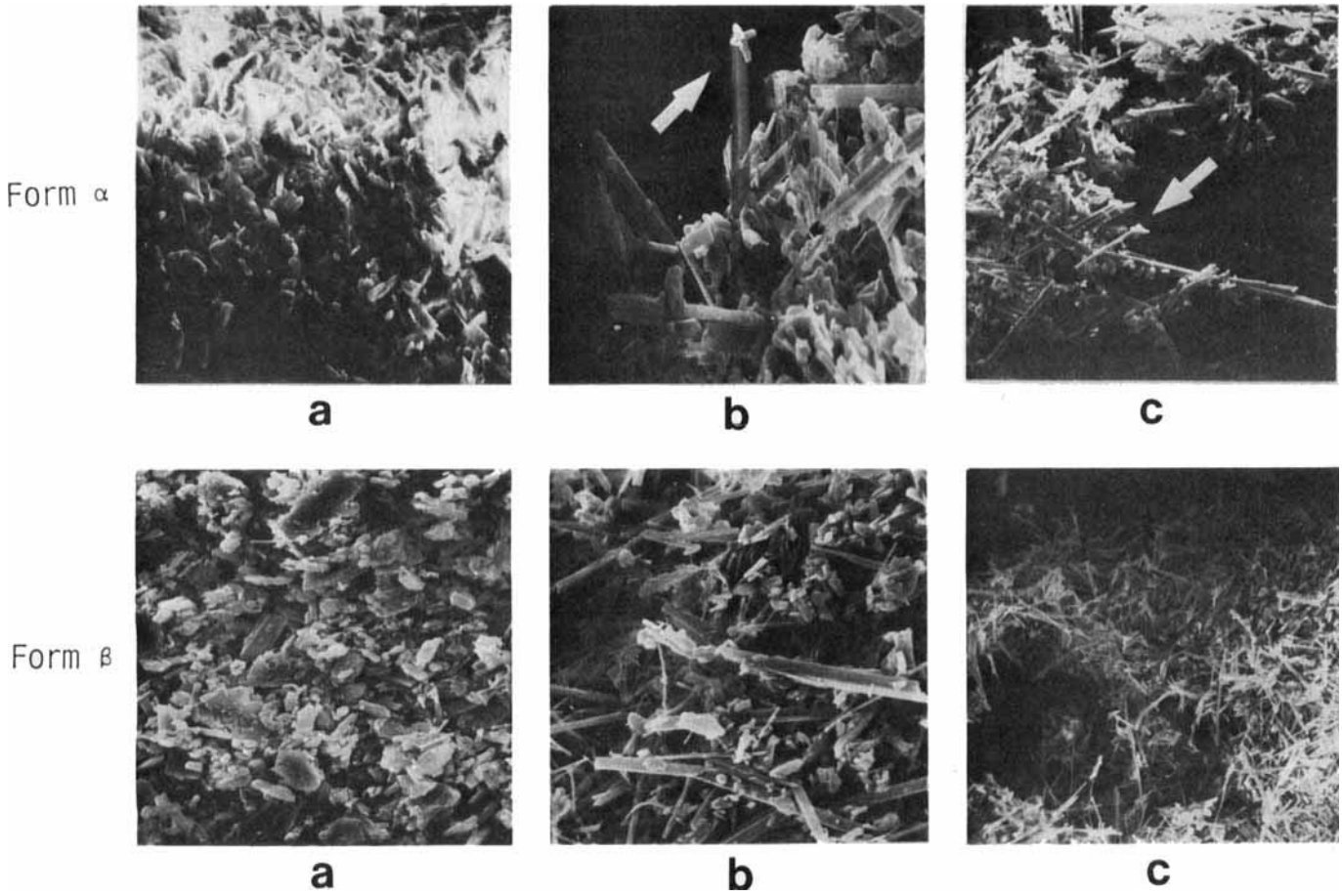

Figure 14—*Scanning electron photomicrographs representing various stages in crystal growth accompanying α → δ and β → δ transformations at 60°C and 80% relative humidity. Key: (a) initial, 2000×, (b) 50% transformed, 2000×; (c) 80% transformed, 600×.*

that prolongation of the induction period led to the subsequent lowering of the rate constant, resulting in further stability. These results indicate that the induction stage is a process that induces control of transformation. The regression analyses showed that these factors were closely correlated with each other at a 5% level of significance. Hence, the following regression equations were obtained:

$$k_1 \times t_i^{0.56} = 0.167 \ (\alpha \rightarrow \delta \text{ transformation}) \qquad \text{(Eq. 5)}$$

$$k_2 \times t_i^{0.88} = 0.319 \ (\beta \rightarrow \delta \text{ transformation}) \qquad \text{(Eq. 6)}$$

It is possible to estimate an approximate induction period for the $\beta \rightarrow \delta$ transformation by substituting the rate constant under a given storage condition (obtained from Fig. 12) into Eq. 6. Assuming that the Arrhenius treatment of the $\alpha \rightarrow \delta$ transformation was applicable in the same temperature range as that of the $\beta \rightarrow \delta$ transformation, the induction period should require not less than ~8.8 years at 25°C.

Microscopic Characterization of Transformation Processes—The morphological changes of the crystal surface in the course of transformation were traced by scanning electron photomicroscopy. Figure 14 shows the photomicrographs of forms α and β which were transformed by 50 and 80% at 60°C and 80% relative humidity in intact samples. Due to minute sizes, any newly born crystal nuclei could not be discriminated in the early stage of transformation. The occurrence and growth of whiskers characterizing form δ were clearly observed during mid and late transformations. The whiskers were thicker and longer in the $\alpha \rightarrow \delta$ transformation than in the $\beta \rightarrow \delta$ transformation. This result may be explained by the fact that the transformation of form α is slower than that of form β, as shown above. Since the transformation rate of form α is independent of moisture, the interface must advance from the nuclei surface into the crystal entity accompanying the growth of the stable form. This view is not contradictory to the previous statement that the growth of the stable phase may be two-dimensional. The knots (arrows in the photos) of sesame seed-sized form α crystals, which are distributed over the surface of acicular crystals of form δ, became thin as the transformation progressed, suggesting their uptake into the crystal entity.

The particle densities of forms α, β, and δ were almost identical, with the measured values being 1.21, 1.21, and 1.19 g/cm^3, respectively. Therefore, it is believed that no visible change in the volume of one crystal occurs during transformation. The fact that acicular crystals much larger than intact crystals in volume are nevertheless growing suggests strongly the sintering of crystals at the potential nuclei formation sites. In this sense, the mechanism of the

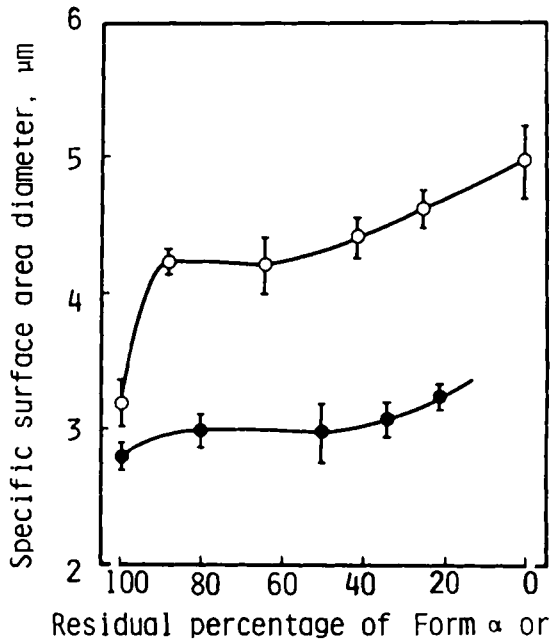

Figure 15—*Changes in particle diameter of samples under transformation. Key: (○) α → δ transformation; (●) β → δ transformation. Each point represents mean ± SD (n = 15).*

present whisker growth is quite different from that of whisker growth on an ethenzamide tablet which is liable to sublimation (29).

The morphological changes were quantitatively confirmed in Fig. 15, in which the specific surface area diameter of the sample was plotted against the percent conversion of form α or β. The growth curves of forms α and β showed a quite similar pattern to the BET-type adsorption isotherm and consisted of three stages: (*a*) a rapidly growing stage up to an ~10% conversion rate; (*b*) a cessation stage without evident increase in particle diameter; (*c*) a regrowing stage of whiskers. The increasing rate of particle diameter of form α at an 80% conversion rate was ~2.8 times as high as that of form β, indicating that a higher increasing rate of the diameter was induced by slower transformation.

In addition to showing the fundamental guideline for solution of a stability problem of polymorphic forms, the practical significance of controlling ambient factors which can maintain the integrity of the selected form has been suggested. A more detailed explanation of the relationship between crystal growth and mechanism of transformation is not available at the present time, and further studies are required to draw definite conclusions.

REFERENCES

(1) M. A. Moustafa, S. A. Khalil, A. R. Ebian, and M. M. Motawi, *J. Pharm. Pharmacol.*, **24,** 921 (1972).

(2) A. R. Ebian, M. A. Moustafa, S. A. Khalil, and M. M. Motawi, *J. Pharm. Pharmacol.*, **25,** 13 (1973).

(3) M. A. Moustafa, S. A. Khalil, A. R. Ebian, and M. M. Motawi, *J. Pharm. Sci.*, **63,** 1103 (1974).

(4) M. A. Moustafa and J. E. Carless, *J. Pharm. Pharmacol.*, **21,** 359 (1969).

(5) E. G. Shami, P. D. Bernardo, E. S. Rattie, and L. J. Ravin, *J. Pharm. Sci.*, **61,** 1318 (1972).

(6) S. Miyazaki, M. Nakano, and T. Arita, *Chem. Pharm. Bull.*, **24,** 1832 (1976).

(7) A. Watanabe, S. Tasaki, Y. Wada, and H. Nakamachi, *Chem. Pharm. Bull.*, **27,** 2751 (1979).

(8) H. Nakamachi, Y. Wada, I. Aoki, Y. Kodama, and K. Kuroda, *Chem. Pharm. Bull.*, **29,** 2956 (1981).

(9) J. Matsunaga, N. Nambu, and T. Nagai, *Chem. Pharm. Bull.*, **24,** 1169 (1976).

(10) H. G. Ibrahim, F. Pisano, and A. Bruno, *J. Pharm. Sci.*, **66,** 669 (1977).

(11) B. W. Müller, *Pharm. Acta Helv.*, **53,** 333 (1978).

(12) A. Chauvet and J. Masse, *Trav. Soc. Pharm. Montpellier*, **38,** 31 (1978).

(13) Y. Matsuda, S. Kawaguchi, H. Kobayashi, and J. Nishijo, *J. Pharm. Pharmacol.*, **32,** 579 (1980).

(14) M. D. Tuladhar, J. E. Carless, and M. P. Summers, *J. Pharm. Pharmacol.*, **35,** 208 (1983).

(15) M. D. Tuladhar, J. E. Carless, and M. P. Summers, *J. Pharm. Pharmacol.*, **35,** 269 (1983).

(16) Y. Matsuda, S. Kawaguchi, H. Kobayashi, and J. Nishijo, *J. Pharm. Sci.*, **73,** 173 (1984).

(17) E. Suito, M. Arakawa, and M. Takahashi, *Kogyokagaku Zasshi*, **59,** 307 (1956).

(18) J. D. Hancock and J. H. Sharp, *J. Am. Ceram. Soc.*, **55,** 74 (1972).

(19 M. Avrami, *J. Chem. Phys.*, **7,** 1103 (1939); B. V. Erofe'ev, *Dokl. Akad. Nauk, SSSR*, **52,** 511 (1946).

(20) H. Schmalzried, in "Solid State Reactions," Verlag Chemie, Weinheim, Federal Republic of Germany, 1981, p. 198.

(21) "Reactions in the Solid State," C. H. Bamford and C. F. H. Tipper, Eds., Elsevier Scientific Publishing Co., Amsterdam, The Netherlands, 1980, pp. 57–86.

(22) "Kagaku Jikken Sohsaho," A. Ogata, T. Koda, and S. Niinobe, Eds., Nankodo Co., Tokyo, 1979, p. 233.

(23) M. C. Ball and L. S. Norwood, *J. Chem. Soc., Ser. A*, **1969,** 1633.

(24) M. C. Ball and R. G. Urie, *J. Chem. Soc., Ser. A*, **1970,** 528.

(25) H. E. Kissinger, *Anal. Chem.*, **29,** 1702 (1957).

(26) S. R. Byrn, in "Solid-State Chemistry of Drugs," Academic, New York, N.Y., 1982, pp. 65–68.

(27) L. F. Jones, D. Dollimore, and T. Nicklin, *Thermochim. Acta*, **13,** 240 (1975).

(28) S. R. Mikhail, D. Dollimore, A. M. Kamel, and N. R. El-Nazer, *J. Appl. Chem. Biotechnol.*, **23,** 419 (1973).

(29) H. Murayama, M. Takahashi, M. Asano, M. Washitake, H. Yuasa, and K. Asahina, *Yakuzaigaku*, **41,** 113 (1981).

ACKNOWLEDGMENTS

This study was presented in part before the 102nd Annual Meeting of the Pharmaceutical Society of Japan, Osaka, April 1982.

The bulk sample of phenylbutazone was generously supplied by Ciba-Geigy (Japan) Ltd. Thanks are also tendered to Dr. H. Nakamachi, Takeda Chemical Industries Ltd., Osaka, for preparation of the scanning electron photomicrographs.

Intravaginal Controlled Administration of Flurogestone Acetate I: Development of a Stability-Indicating Liquid Chromatographic Method and Stability Kinetics of Flurogestone Acetate

MOHAN B. KABADI, KIRTI H. VALIA*, and YIE W. CHIEN ˣ

Received October 3,1983, from the *Controlled Drug Delivery Research Center, College of Pharmacy, Rutgers-The State University of New Jersey, Piscataway, N.J. 08854.* Accepted for publication November 30, 1983. * Present address: Lilly Research Laboratories, Eli Lilly & Co., Indianapolis, IN 46206.

Abstract □ Flurogestone acetate is a synthetic progestin useful for estrus synchronization in sheep. The estrus synchronization is achieved by inserting the drug-impregnated vaginal sponge in the sheep for up to 15 d, during which time flurogestone acetate is administered continuously by intravaginal absorption to suppress estrus and ovulation. The sponge is then withdrawn to regain estrus within 2–4 d. A review of the literature suggests that the analytical methods currently available are not specific, sensitive, and rapid enough. A stability-indicating high-performance liquid chromatographic method was developed, which is capable of characterizing the stability kinetics of flurogestone acetate under various environmental conditions and quantifying the release and absorption profiles of the drug from the vaginal sponges.

Keyphrases □ Flurogestone acetate—stability-indicating HPLC method, stability kinetics □ HPLC—stability-indicating method, flurogestone acetate □ Stability kinetics—flurogestone acetate

Flurogestone acetate (I) is a synthetic progestin used in sheep for estrus synchronization (1). The objective for developing an effective treatment for estrus synchronization is to establish a stage at which estrus can be induced to make the females fertile in a desired season. Estrus synchronization is achieved by prolonged continuous administration of flurogestone acetate-releasing vaginal sponges to the sheep for 15 d; 2–4 d after withdrawal of the sponges most sheep regain their estrus.

Over the years, flurogestone acetate has been assayed by GC (2), gravimetric analysis (2), and radioactive tracers (3). However, these methods lack assay specificity, speed, sensitivity, and/or convenience; therefore, a high-performance liquid chromatographic (HPLC) method was developed to provide a rapid, quantitative, and specific assay for this drug in the presence of its degradation products. This assay was used to study several stability characteristics of flurogestone acetate, including the effects of acid, base, and temperature.

EXPERIMENTAL SECTION

Materials—A high-performance liquid chromatograph equipped with a reciprocating-piston pump[1], injector[2], UV detector (254 nm)[3], and a strip-chart recorder[4] was employed in conjunction with a 10-μm (3.9 mm × 30 cm) C_{18} column[5] for separation.

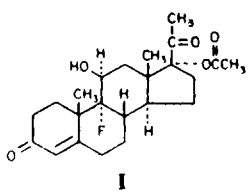

I

All chemicals and reagents were analytical grade unless indicated. Flurogestone acetate[6], testosterone[7], anhydrous dibasic sodium phosphate[8], anhydrous citric acid[8], dibasic potassium phosphate[8], monobasic potassium phosphate[8], and glass-distilled methanol[9] were used as received. Deionized water[10] was freshly prepared and used throughout the study.

Analytical Procedure—A fixed quantity of testosterone was added to each sample as an internal standard to assure injection-to-injection reproducibility. Aliquots were injected into the HPLC column and the peak height ratios of flurogestone acetate to testosterone were then determined and compared with the standard curve for calculation of the flurogestone acetate concentration. Methanol–water (50:50) was used as the mobile phase. The column and the solvent were at ambient temperature. At a solvent flow rate of 2 mL/min, the retention times for flurogestone acetate and testosterone were ~21 and ~32 min, respectively.

Standard Calibration Curve—The standard stock solution of flurogestone acetate and testosterone (internal standard) were prepared in methanol and stored at 4°C. The flurogestone acetate stock solution was diluted as necessary. The standard calibration curves were constructed by plotting peak height ratio *versus* flurogestone acetate concentration. A straight-line fit of the data was made by linear regression analysis, and the correlation coefficient was determined.

Stability Studies—*Effect of pH*—Three methanolic stock solutions (which contained 1.00–1.49 mg/mL of flurogestone acetate) were prepared and then diluted to 71.5, 39.8, and 5.03 μg/mL with 0.1 M HCl (pH 1.0), 0.1 M NaOH (pH 13), and simulated vaginal fluid (pH 7.3), respectively. The simulated vaginal fluid was prepared from 870 mL of 0.4 M Na_2HPO_4 and 130 mL of 0.2 M citric acid made up to 2 L with water. The diluted acidic, basic, and simulated vaginal fluid solutions were placed in well-sealed glass containers and stored at 94°C (by reflux), 30°C, and 38°C (shaken in a water bath[8]), respectively, until the completion of the study. Aliquots (1 mL of the acidic solution or 2 mL of either basic or simulated vaginal fluid solutions) were withdrawn periodically from each flask and assayed for flurogestone acetate

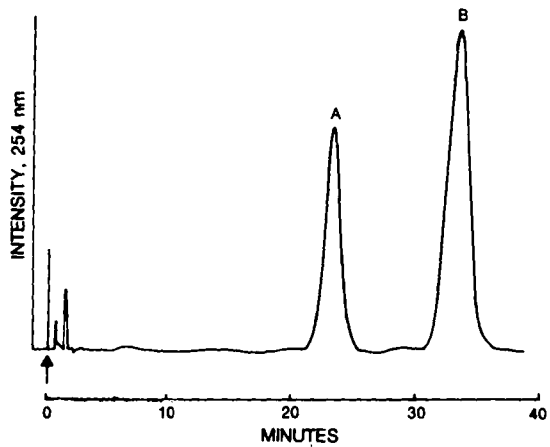

Figure 1—*Representative chromatogram for flurogestone acetate (A) and testosterone (B), as internal standard. Arrow indicates the time of injection.*

[1] Model 6000A; Waters Associates, Milford, Mass.
[2] Model U6K; Waters Associates.
[3] Model 440; Waters Associates.
[4] Omniscribe Recorder; Houston Instruments, Austin, Tex.
[5] μ-Bondapack C_{18}; Waters Associates.
[6] Searle Laboratories, Skokie, Ill.
[7] Sigma Chemical Co., St. Louis, Mo.
[8] Fisher Scientific, Fair Lawn, N.J.
[9] J. T. Baker Chemical Co., Phillipsburg, N.J.
[10] Nanopure; Sybron/Barnstead, Boston, Mass.

0022-3549/84/1000-1461$01.00/0
© 1984, American Pharmaceutical Association

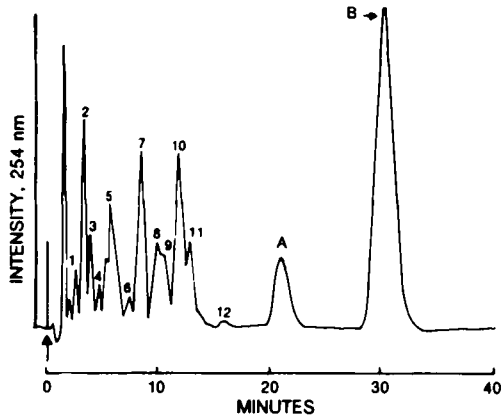

Figure 2—*Chromatogram of flurogestone acetate (A) after 95 h in 0.1 M HCl (pH 1.0) at 94°C. Key: (1–12) degradation products with retention times at 2.02, 3.19, 3.74, 4.71, 5.82, 7.73, 8.81, 9.56, 11.15, 12.61, 13.23, and 15.28 min; (B) testosterone (internal standard).*

and its degradation products. However, the acidic and basic solutions were first neutralized to pH 5.5 and 6.59, respectively, with 1 mL of 0.1 M K_2HPO_4 (pH 9.3) or 2 mL of 0.2 M KH_2PO_4 (pH 4.46); after vortexing, 50 μL of testosterone (0.61 or 0.13 mg/mL) was added to each sample. An aliquot (~100 μL) of each sample was assayed by the HPLC method.

Effect of Temperature—Flurogestone acetate stock solution prepared in simulated vaginal fluid (5.75 μg/mL) was placed in well-sealed glass containers and stored in a shaking water bath at 38°C, 70°C, 80°C, and 90°C. Each experiment was performed in triplicate. An aliquot (2 mL) was withdrawn periodically from each flask and, after cooling, 50 μL of testosterone (0.113 mg/mL) was added. The sample (100 μL) was then assayed by the HPLC method for flurogestone acetate and degradation products.

Treatment of Data—Semilogarithmic plots of the flurogestone acetate concentration as a function of time were constructed to evaluate the kinetics and rates of drug degradation. An Arrhenius plot (4) was then constructed from the kinetic data obtained from the studies with different temperatures. The line of best fit was determined by linear regression analysis.

RESULTS AND DISCUSSION

Chromatographic Data—A typical chromatogram for flurogestone acetate in the presence of testosterone (the internal standard) is shown in Fig. 1. Peaks for flurogestone acetate and testosterone are observed at retention times of 21.2 and 31.5 min, respectively. No interfering peaks were detected in the 40-min run time. The standard curve constructed for flurogestone acetate was linear over the concentration ranges of 0–10 and 10–40 μg/mL ($r > 0.99$) when the peak height ratio of flurogestone acetate to testosterone was used.

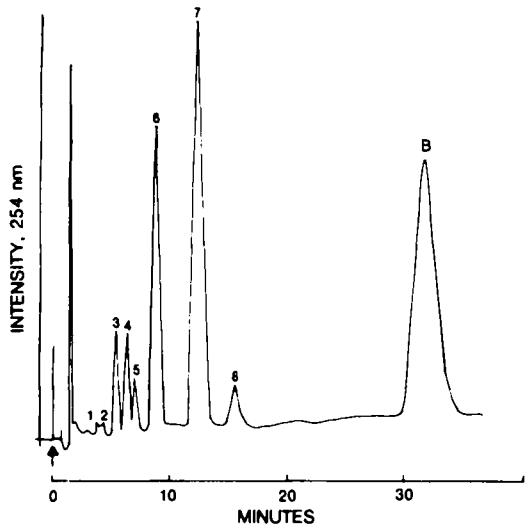

Figure 3—*Chromatogram of flurogestone acetate after 24 h in 0.1 M NaOH (pH 13) at 30°C. Key: (1–8) degradation products with retention times at 3.65, 4.16, 5.08, 6.00, 6.88, 8.34, 11.69, and 14.75 min; (B) testosterone (internal standard).*

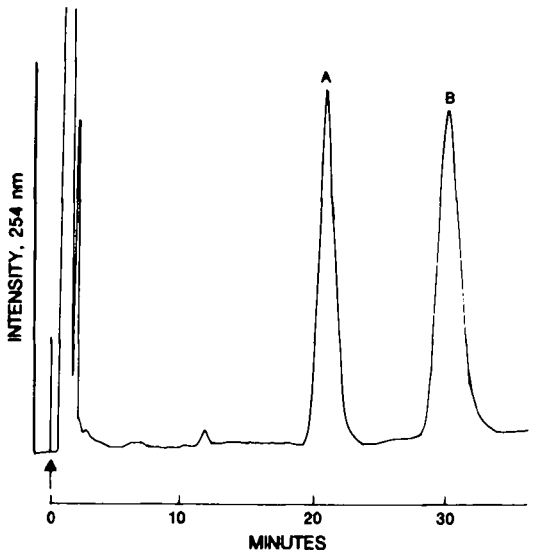

Figure 4—*Chromatogram of flurogestone acetate (A) after 22 d in simulated vaginal fluid (pH 7.3) at 38°C, with testosterone (B) as internal standard. Very little degradation was observed.*

The retention time varied slightly from day to day and with the pH of the injected solution.

The sensitivity of detection for flurogestone acetate at an injection volume of 50 μL was ~ 0.65 μg/mL (at 0.005 AUFS), which was equivalent to the injection of 28 ng of drug into the column. The assay sensitivity can be improved substantially by increasing the injection volume, by using a less-polar mobile phase (by increasing the ratio of methanol to water, *e.g.*, from 50:50 to 70:30), or by changing the detector wavelength from the conventional 254 nm to 236–238 nm, which is the maximum absorbance for flurogestone acetate (ϵ = 17,520) (5).

Solution Stability and Effect of Acid and Base—The HPLC method was used to study the solution stability of flurogestone acetate and to detect the degradation products, if any, under various conditions. Flurogestone acetate solutions in 0.1 M HCl (pH 1), 0.1 M NaOH (pH 13), or simulated vaginal fluid (pH 7.3) were stored at various elevated temperatures for different intervals; samples were taken periodically for chromatographic assay. The samples from 0.1 M HCl solutions at 94°C yielded 12 well-defined peaks of degradation products (Fig. 2); 8 degradation-product peaks formed under alkaline conditions at 30°C (Fig. 3). Under the chromatographic conditions all the degradation peaks appear before 18 min and none interfered with the primary peaks of flurogestone acetate (at 21.2 min) or testosterone (at 31.5 min). The samples from the simulated vaginal fluid (pH 7.3) at 38°C (the vaginal temperature of the sheep) yielded only a very small degradation peak after 22 d (Fig. 4).

A semilogarithmic plot of flurogestone acetate concentrations as a function

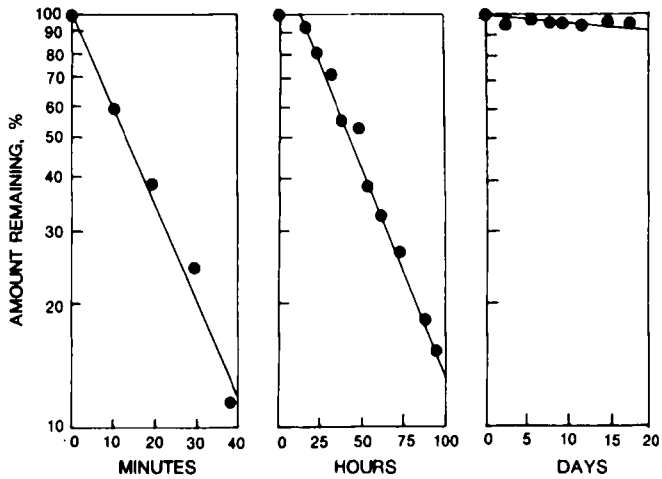

Figure 5—*Degradation profiles of flurogestone acetate in basic (a), acidic (b), and simulated vaginal fluid (c) solutions. Key: (a) pH 13 (30°C), k = 0.053 min^{-1}; (b) pH 1 (94°C), k = 0.023 h^{-1}; (c) pH 7.3 (38°C), k = 0.0018 d^{-1}.*

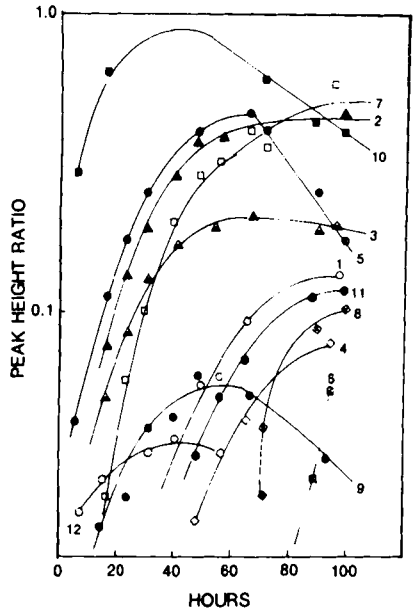

Figure 6—*Time course for the appearance of various degradation products of flurogestone acetate in 0.1 M HCl (pH 1) at 94°C. Key: (1-12) degradation product peaks in Fig. 2.*

of time yields a linear relationship, indicating that the degradation could follow first-order kinetics (Fig. 5). The data in Fig. 5 indicate that the degradation of flurogestone acetate is most rapid at pH 13, intermediate at pH 1, and slowest at pH 7.3. The apparent first-order half-life determined from these first-order kinetic plots is 13 min at pH 13, 30.1 h at pH 1, and ~370 d at pH 7.3, respectively.

Flurogestone acetate degradation, subject to both acid and base catalysis, is minimized at pH 7.3 (the vaginal pH of the sheep). The drug degradation profiles (Figs. 6 and 7) illustrate the time course for the appearance and disappearance of degradation products in acidic (pH 1) and alkaline (pH 13) solutions.

Thermal Stability in Simulated Vaginal Fluid—The thermal stability of flurogestone acetate in simulated vaginal fluid was studied at 70°C, 80°C, and 90°C. The semilogarithmic plot of drug concentration as a function of time was linear at various temperatures (Fig. 8), indicating first-order degradation kinetics. The apparent first-order degradation kinetic constants determined from the slope of these linear plots are 0.0490, 0.1303, and 0.3941 d^{-1} at 70°C, 80°C, and 90°C, respectively. The results suggest that the

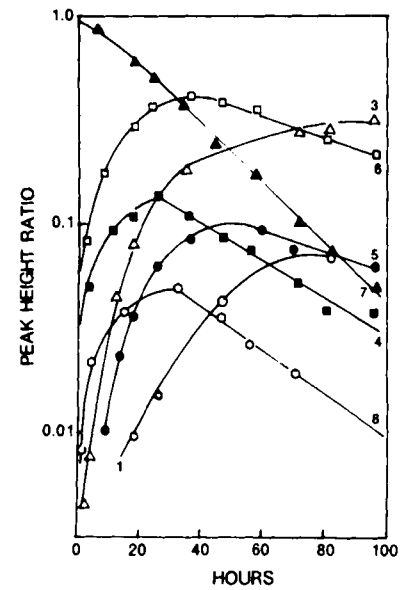

Figure 7—*Time course for the appearance of various degradation products of flurogestone acetate in 0.1 M NaOH (pH 13) at 30°C. Key: (1-8) degradation product peaks in chromatogram in Fig. 3.*

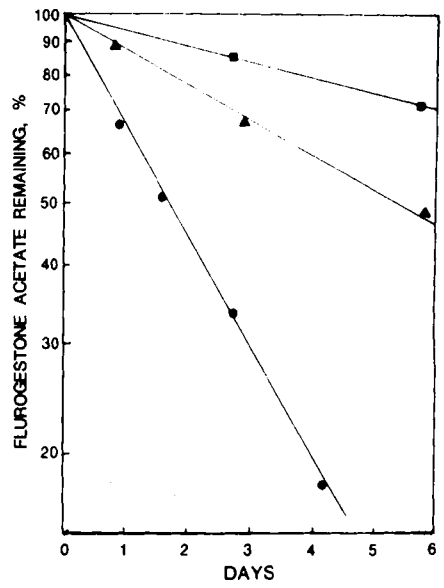

Figure 8—*Thermal stability of flurogestone acetate in the simulated vaginal fluid (pH 7.3) at 70°C (■), 80°C (▲), and 90°C (●). The first-order degradation constants were calculated to be 0.0490 d^{-1} (70°C), 0.1303 d^{-1} (80°C), and 0.3941 d^{-1} (90°C).*

thermal degradation of flurogestone acetate could follow the Arrhenius relationship (4) of:

$$\log k = \log A - \frac{E_a}{2.303R} \cdot \frac{1}{T}$$

where k is the apparent rate constant of degradation obtained from the kinetic plots in Fig. 8, R is the gas constant (1.98 cal/mol·K), T is the absolute temperature (K), E_a is the energy of activation, and A is the frequency factor. The exponential relationship between the apparent first-order rate constants (k) obtained and the reciprocal of the absolute temperature is shown in Fig. 9. Extrapolation of the data obtained at elevated temperatures to the vaginal temperature (38°C) results in a predicted first-order rate of 0.0010 d^{-1}, which compares favorably (95% confidence limit) with the rate constant of 0.0018 d^{-1} obtained experimentally at 38°C. E_a and A values, derived from the slope and intercept, are 25.55 kcal/mol and 9.27×10^{14} d^{-1}, respectively.

The potential utility of the temperature-dependent relationship is determined by the controlling mechanism of degradation (6). Since the E_a value

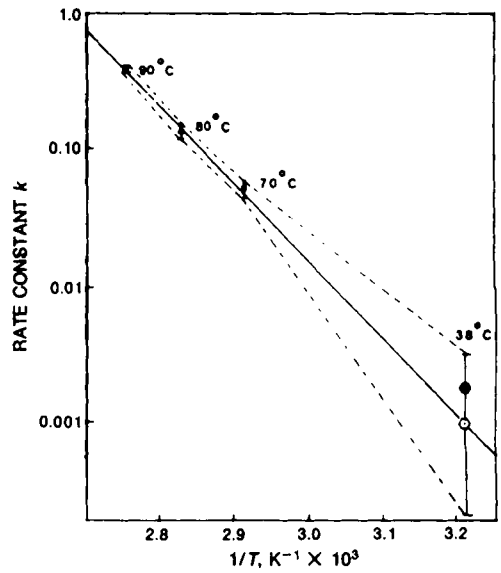

Figure 9—*Arrhenius plot (—) of the thermal degradation rate constants of flurogestone acetate in the simulated vaginal fluid (pH 7.3) with 95% confidence limits (- - -) (7, 8). The filled data points are actual data obtained experimentally; the open data point is the calculated value extrapolated from the Arrhenius plot of the data at elevated temperatures; E_a = 25.55 kcal/mol.*

(25.55 kcal/mol) is rather high, the degradation of flurogestone acetate (in vaginal fluid) could be the result of a solvolytic process, which generally has an energy of activation in the range of 10–30 kcal/mol (6). The higher the value of E_a, the greater the thermal stability of the drug.

CONCLUSIONS

The HPLC method developed is specific and allows a good separation of flurogestone acetate from its degradation products. The degradation is both acid- and base-catalyzed, but is much slower in the simulated vaginal fluid (pH 7.3). Thermodynamic studies indicate that the degradation in simulated vaginal fluid is very slow, as it requires a fairly high energy of activation (25.55 kcal/mol).

This assay should be suitable for determination of the release kinetics of flurogestone acetate from the vaginal sponges and its absorption rate through the vaginal wall. Since it is also a stability-indicating method, the metabolism of flurogestone acetate, if any, in the simulated vaginal fluid or vaginal mucosa could be detected (9).

REFERENCES

(1) "The Control of the Ovarian Cycle in the Sheep," T. J. Robinson, Ed., Sydney University Press, Sydney, Australia, 1967.

(2) J. Morgan, R. Lack, and T. J. Robinson, in "The Control of Ovarian Cycle in the Sheep," T. J. Robinson, Ed., Sydney University Press, Sydney, Australia, 1967, p. 195.

(3) Y. W. Chien, "Novel Drug Delivery Systems," Dekker, New York, N.Y., 1982, chap. 8.

(4) A. N. Martin, J. Swarbrick, and A. Cammarata, "Physical Pharmacy," 2nd ed., Lea and Febiger, Philadelphia, Pa. 1969.

(5) "The Merck Index," 9th ed., Mack Publishing Co., Easton, Pa., 1976, p. 4085.

(6) L. Lachman, H. A. Lieberman, and J. L. Kanig, "The Theory and Practice of Industrial Pharmacy," 2nd ed., Lea and Febiger, Philadelphia, Pa., 1976.

(7) T. Colton, "Statistics in Medicine," Little, Brown and Co., Boston, Mass., 1974.

(8) J. T. Carstensen and K. Su, *Bull. Parenter. Drug Assoc.*, **25**, 287 (1977).

(9) M. B. Kabadi and Y. W. Chien, *J. Pharm. Sci.*, **73**, 1464 (1984).

ACKNOWLEDGMENTS

The authors express their appreciation to Dr. Y. C. Huang for his technical assistance in HPLC method development. This work was extracted in part from the thesis submitted by M. B. Kabadi to the Graduate School of Rutgers–The State University of New Jersey, in partial fulfillment of the Doctor of Philosophy degree requirements.

Intravaginal Controlled Administration of Flurogestone Acetate II: Development of an *In Vitro* System for Studying the Intravaginal Release and Permeation of Flurogestone Acetate

MOHAN B. KABADI and YIE W. CHIEN ˣ

Received October 3, 1983, from the *Controlled Drug Delivery Research Center, College of Pharmacy, Rutgers–The State University of New Jersey, Piscataway, NJ 08854.* Accepted for publication November 30, 1983.

Abstract □ A relatively simple and easily constructed *in vitro* system was developed for studying the mechanism of release and intravaginal absorption of flurogestone acetate from vaginal sponges. The stability-indicating high-performance liquid chromatographic method developed earlier was used to provide a rapid, reproducible, and sensitive assay. The *in vitro* intravaginal release/permeation system developed was capable of determining the rate of flurogestone acetate release from vaginal sponges and, simultaneously, the rate of absorption through the vaginal wall. The design, calibration, and applicability of the system, and the release and absorption profiles of the drug from vaginal sponges in this system are discussed.

Keyphrases □ Drug release—flurogestone acetate, intravaginal, sheep □ Flurogestone acetate—intravaginal release and permeation measurement *in vitro* □ Intravaginal administration—flurogestone acetate, sheep

In 1975, the use of flurogestone acetate-releasing vaginal sponges (Fig. 1) to replace the conventional daily injection of progesterone for estrus synchronization in sheep was introduced (1). On intravaginal administration, the polyurethane sponges release the drug continuously for 15 d, this suppresses estrus and ovulation. Two to four days after removal of the sponges, the sheep reenter estrus and ovulate. During this period, artificial insemination can be performed at a predetermined schedule to promote a specific breeding program (2).

Knowledge of the pattern and rate of drug release is essential for an understanding of the action of flurogestone acetate-impregnated sponges in the vagina (3). Development of a suitable *in vitro* drug release/permeation system is essential to understand the mechanisms of drug release and permeation under *in vivo* conditions (4). Currently, the release profiles are determined by extracting the residual drug content in the vaginal sponges and then assaying it by GC (2) or by radioactivity count (5). However, these *in situ* experiments require the use of large numbers of animals over an extended period of time. Also, the lack of assay sensitivity can jeopardize the

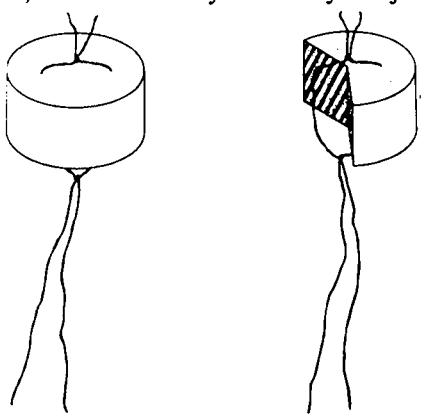

Figure 1—*Diagrammatic illustration of the flurogestone acetate-releasing vaginal sponges*[1].

[1] Synchro-Mate Pessary; G. D. Searle and Co., Chicago, Ill.

0022-3549/84/1000-1464$01.00/0

© 1984, American Pharmaceutical Association

(25.55 kcal/mol) is rather high, the degradation of flurogestone acetate (in vaginal fluid) could be the result of a solvolytic process, which generally has an energy of activation in the range of 10–30 kcal/mol (6). The higher the value of E_a, the greater the thermal stability of the drug.

CONCLUSIONS

The HPLC method developed is specific and allows a good separation of flurogestone acetate from its degradation products. The degradation is both acid- and base-catalyzed, but is much slower in the simulated vaginal fluid (pH 7.3). Thermodynamic studies indicate that the degradation in simulated vaginal fluid is very slow, as it requires a fairly high energy of activation (25.55 kcal/mol).

This assay should be suitable for determination of the release kinetics of flurogestone acetate from the vaginal sponges and its absorption rate through the vaginal wall. Since it is also a stability-indicating method, the metabolism of flurogestone acetate, if any, in the simulated vaginal fluid or vaginal mucosa could be detected (9).

REFERENCES

(1) "The Control of the Ovarian Cycle in the Sheep," T. J. Robinson, Ed., Sydney University Press, Sydney, Australia, 1967.

(2) J. Morgan, R. Lack, and T. J. Robinson, in "The Control of Ovarian Cycle in the Sheep," T. J. Robinson, Ed., Sydney University Press, Sydney, Australia, 1967, p. 195.

(3) Y. W. Chien, "Novel Drug Delivery Systems," Dekker, New York, N.Y., 1982, chap. 8.

(4) A. N. Martin, J. Swarbrick, and A. Cammarata, "Physical Pharmacy," 2nd ed., Lea and Febiger, Philadelphia, Pa. 1969.

(5) "The Merck Index," 9th ed., Mack Publishing Co., Easton, Pa., 1976, p. 4085.

(6) L. Lachman, H. A. Lieberman, and J. L. Kanig, "The Theory and Practice of Industrial Pharmacy," 2nd ed., Lea and Febiger, Philadelphia, Pa., 1976.

(7) T. Colton, "Statistics in Medicine," Little, Brown and Co., Boston, Mass., 1974.

(8) J. T. Carstensen and K. Su, *Bull. Parenter. Drug Assoc.*, **25**, 287 (1977).

(9) M. B. Kabadi and Y. W. Chien, *J. Pharm. Sci.*, **73**, 1464 (1984).

ACKNOWLEDGMENTS

The authors express their appreciation to Dr. Y. C. Huang for his technical assistance in HPLC method development. This work was extracted in part from the thesis submitted by M. B. Kabadi to the Graduate School of Rutgers–The State University of New Jersey, in partial fulfillment of the Doctor of Philosophy degree requirements.

Intravaginal Controlled Administration of Flurogestone Acetate II: Development of an *In Vitro* System for Studying the Intravaginal Release and Permeation of Flurogestone Acetate

MOHAN B. KABADI and YIE W. CHIEN ˣ

Received October 3, 1983, from the *Controlled Drug Delivery Research Center, College of Pharmacy, Rutgers–The State University of New Jersey, Piscataway, NJ 08854.* Accepted for publication November 30, 1983.

Abstract □ A relatively simple and easily constructed *in vitro* system was developed for studying the mechanism of release and intravaginal absorption of flurogestone acetate from vaginal sponges. The stability-indicating high-performance liquid chromatographic method developed earlier was used to provide a rapid, reproducible, and sensitive assay. The *in vitro* intravaginal release/permeation system developed was capable of determining the rate of flurogestone acetate release from vaginal sponges and, simultaneously, the rate of absorption through the vaginal wall. The design, calibration, and applicability of the system, and the release and absorption profiles of the drug from vaginal sponges in this system are discussed.

Keyphrases □ Drug release—flurogestone acetate, intravaginal, sheep □ Flurogestone acetate—intravaginal release and permeation measurement *in vitro* □ Intravaginal administration—flurogestone acetate, sheep

In 1975, the use of flurogestone acetate-releasing vaginal sponges (Fig. 1) to replace the conventional daily injection of progesterone for estrus synchronization in sheep was introduced (1). On intravaginal administration, the polyurethane sponges release the drug continuously for 15 d, this suppresses estrus and ovulation. Two to four days after removal of the sponges, the sheep reenter estrus and ovulate. During this period, artificial insemination can be performed at a predetermined schedule to promote a specific breeding program (2).

Knowledge of the pattern and rate of drug release is essential for an understanding of the action of flurogestone acetate-impregnated sponges in the vagina (3). Development of a suitable *in vitro* drug release/permeation system is essential to understand the mechanisms of drug release and permeation under *in vivo* conditions (4). Currently, the release profiles are determined by extracting the residual drug content in the vaginal sponges and then assaying it by GC (2) or by radioactivity count (5). However, these *in situ* experiments require the use of large numbers of animals over an extended period of time. Also, the lack of assay sensitivity can jeopardize the

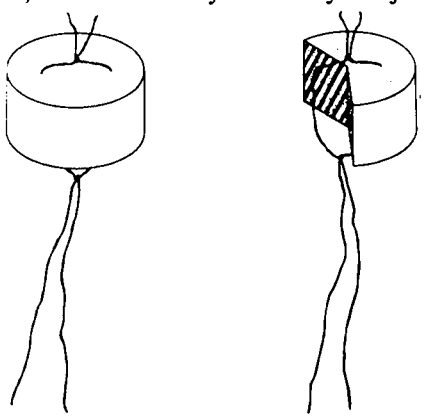

Figure 1—*Diagrammatic illustration of the flurogestone acetate-releasing vaginal sponges*[1].

[1] Synchro-Mate Pessary; G. D. Searle and Co., Chicago, Ill.

0022-3549/84/1000-1464$01.00/0

© 1984, American Pharmaceutical Association

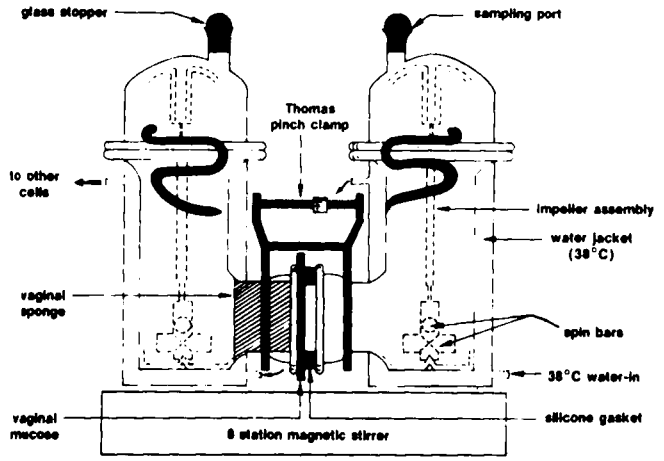

Figure 2—*Intravaginal release/permeation system designed to measure the* in vitro *release of flurogestone acetate from vaginal sponges and vaginal absorption profiles from various solutions of flurogestone acetate.*

accurate determination of the kinetics of the drug-release profile. One prime concern in making release/permeability measurements is determining the rates reliably and in as short a time as possible. The development of such a technique could also make possible the direct measurement of the drug-release flux (6).

With these considerations in mind, a relatively simple and easily constructed *in vitro* intravaginal drug release/permeation system was designed. In conjunction with the HPLC method (7), a reproducible technique for determining the drug release kinetics was developed. The release rates of flurogestone acetate from the vaginal sponges and the permeation rates of the drug through the vaginal mucosa were investigated.

EXPERIMENTAL SECTION

Materials—All chemicals and reagents were analytical grade unless otherwise indicated. Flurogestone acetate[2], testosterone[3], anhydrous dibasic sodium phosphate[4], anhydrous citric acid[4], polyethylene glycol 400 (laboratory grade)[4], and glass-distilled methanol[5] were used as received. Freshly prepared deionized water[6] was used throughout the study.

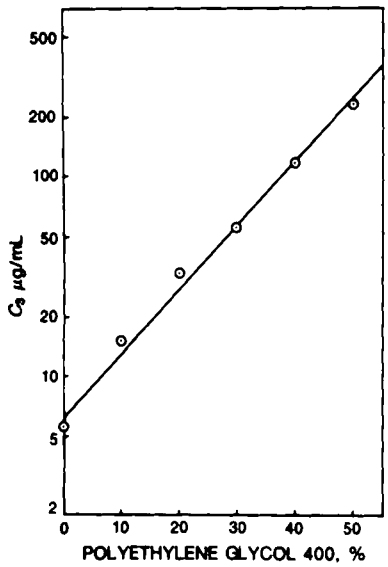

Figure 3—*Exponential relationship between solution solubility (C_s) and the volume fraction (% v/v) of the polyethylene glycol 400 in the simulated vaginal fluid at 38°C.*

[2] Searle Laboratories, Skokie, Ill.
[3] Sigma Chemical Co., St. Louis, Mo.
[4] Fisher Scientific, Fair Lawn, N.J.

Table I—Composition of Elution Media [a] Containing Various Volume Fractions of Polyethylene Glycol 400 in Simulated Vaginal Fluid

Polyethylene Glycol 400 Conc., % v/v	0.02 M Citric Acid, mL	0.04 M Na_2HPO_4, mL	Polyethylene Glycol 400 Volume, mL
0	95	405	0
10	100	400	100
20	135	365	200
30	170	330	300
40	200	300	400
50	235	265	500

[a] The final volume was made up to 1000 mL with distilled water; pH = 7.3.

Drug Release/Permeation System—The system[7] developed for studying the pattern of drug release/permeation is shown schematically in Fig. 2. Each of the donor and receptor cells holds up to 1 L of elution medium which is thermostated at 38°C (the vaginal temperature of the sheep) by a circulating water bath[8]. The impeller assembly can be rotated at a constant speed (30–400 rpm) by a six-station heavy-duty magnetic stirrer (42 × 44 × 12 cm). All six diffusion cells (three pairs) are operated simultaneously at the same speed by a single control.

High-Performance Liquid Chromatography—A chromatograph equipped with a reciprocating-piston pump[9], injector[10], UV detector (at 254 nm)[11], and a strip-chart recorder[12] (1–10 mV) was employed in conjunction with a 5-µm (3.9 mm × 15 cm) C_{18} column[13] for separation. The operating conditions of the HPLC method (7) were slightly modified. A less-polar mobile phase of the methanol–water (65:35) was used. The column and solvent were maintained at ambient temperature. At a solvent flow rate of 1 mL/min, the retention times for flurogestone acetate and testosterone (internal standard) were reduced to ~4 and ~8 min, respectively, to facilitate the assay procedure.

Drug Delivery Device—The vaginal sponges, each containing 40 mg of flurogestone acetate, were commercially available[14]. Each polyurethane sponge was loaded (with hypodermic syringes) with 2 mL of solution containing 20 mg/mL of the drug in acetone–absolute ethanol (1:4). The sponges

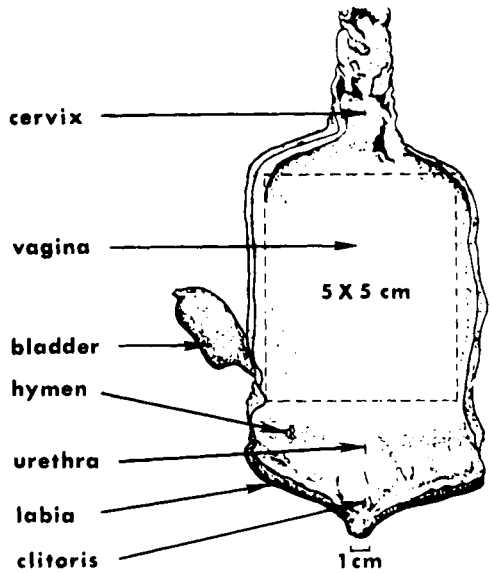

Figure 4—*Sheep vagina that has been cut open vertically. A piece of mucosa (5 × 5 cm), separated from the wall, is sandwiched between diffusion cells for permeation studies.*

[5] Burdick & Jackson Laboratories, Muskegon, Mich.
[6] Nanopure; Sybron/Barnstead, Boston, Mass.
[7] Bellco Glass, Vineland, N.J.
[8] Water Bath Model 80; Fisher Scientific Co., Springfield, N.J.
[9] Model 6000 A; Waters Associates, Milford, Mass.
[10] Model U6K; Waters Associates.
[11] Model 440; Waters Associates.
[12] Omniscribe Recorder; Houston Instruments, Austin, Tex.
[13] 5-µm Spherical C_{18}; Waters Associates.
[14] Chronogest vaginal sponges (40 mg of flurogestone acetate) (800 Grade); Intervet, France.

Table II—Operating Conditions and the Experimentally Obtained Hydrodynamic Parameters

Polyethylene Glycol 400, % v/v	Rotation Speed, rpm	Kinematic Viscosity, cm^2/s	$D \times 10^6$, cm^2/s	$k \times 10^4$, cm/s	Sh_r[a]	$\delta_D \times 10^4$, cm[b]
0	60	0.007	4.47	22.2	995	20.1
	165	0.007	4.47	31.8	1421	14.1
	295	0.007	4.47	52.5	2347	8.5
20	60	0.016	1.96	6.18	631	31.7
	165	0.016	1.96	15.6	1595	12.6
	295	0.016	1.96	26.5	2706	7.4
40	60	0.045	0.695	1.02	294	68.0
	165	0.045	0.695	2.31	664	30.1
	295	0.045	0.695	4.95	1425	14.0

[a] Sherwood number (see text). [b] Calculated from Eq. 2.

were then placed, thread up (Fig. 1), on polyethylene over a wire grid and allowed to dry overnight (8).

Elution Medium—The elution medium was prepared by mixing a given volume of polyethylene glycol 400 with a concentrated solution of simulated vaginal fluid and then diluted to 1 L with distilled water (Table I). The concentrated simulated vaginal fluid was prepared by mixing various quantities of 0.04 M Na_2HPO_4 and 0.02 M citric acid. After the addition of polyethylene glycol 400, the water was added. The pH of the elution medium was 7.3 ± 0.5 (the vaginal pH of sheep).

Determination of Drug Solubility—The solubility of flurogestone acetate at the study temperatures was determined by vigorously mixing an excess of drug particles in 10 mL of elution medium containing various volume fractions of polyethylene glycol 400. At equilibrium (24 h), samples were rapidly filtered through preheated syringes equipped with a filter holder. The clear filtrate was then assayed by HPLC. An exponential relationship between the solubility of the drug and the volume fraction of polyethylene glycol 400 was found (Fig. 3), as expected (9), from the following:

$$\log C_s = \log C_{SVF} + e \cdot f \qquad \text{(Eq. 1)}$$

where, C_s and C_{SVF} denote the solubilities of flurogestone acetate in the polyethylene glycol 400–simulated vaginal fluid and in pure simulated vaginal fluid, respectively; e is the slope of the log solubility *versus* volume fraction profile; and f is the volume fraction of polyethylene glycol 400 (v/v) added. The solubility of the drug (C_{SVF} = 5.4 μg/mL) was enhanced remarkably by the addition of polyethylene glycol 400; the perfect sink condition was thus maintained.

Calibration of the System—*Time to Reach 38°C*—The donor and receptor compartments were maintained at 38°C, and then 600 or 1000 mL of simulated vaginal fluid (at room temperature) was poured into each compartment

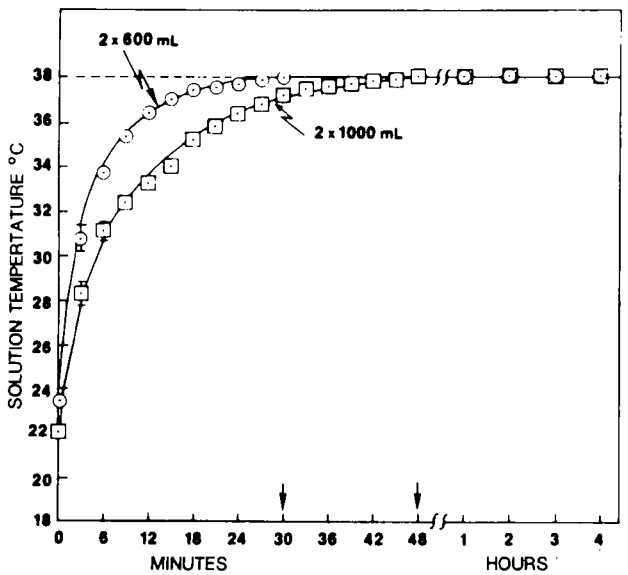

Figure 5—*Time required for the solution temperature in the donor and receptor compartments to reach the equilibrium temperature of 38°C (vaginal temperature of the sheep) from room temperature (n = 3); stirring speed 360 rpm.*

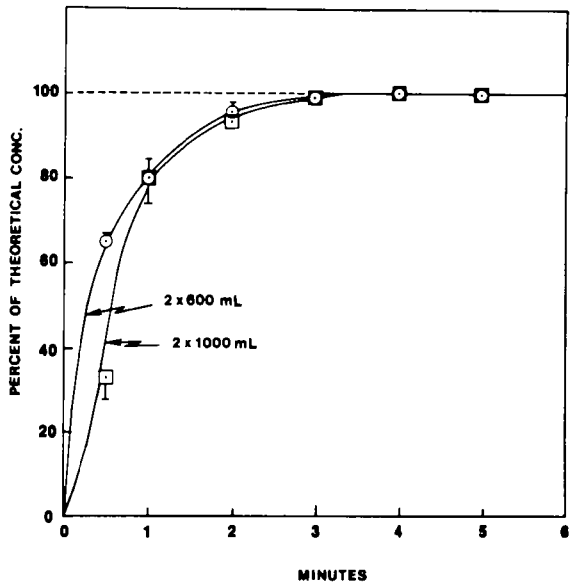

Figure 6—*Time required for the solution in the receptor compartment to reach a theoretical concentration after addition of a known concentration of flurogestone acetate stock solution to the donor solution (n = 3).*

while the stirrer rotated at 330 rpm. Temperature of the elution medium in the receptor compartment was measured[15] every 3 min until the equilibrium temperature of 38°C was reached.

Hydrodynamics of Mixing—After the simulated vaginal fluid solution in each compartment reached 38°C, known concentrations of flurogestone acetate (0.5–1.0 mL) was added to the donor solution, while the stirrer rotated at 330 rpm. Samples were removed from the receptor solution every 30–60 s until the theoretical concentration was reached. Samples were then assayed for the drug by HPLC.

Drug Release Study—A vaginal sponge containing 40 mg of flurogestone acetate was inserted into the flange opening of the donor compartment and an impermeable barrier was sandwiched between the two compartments (Fig. 2). The magnetic stirrer was turned on and adjusted to 330 rpm. Then, 1000 mL of the elution medium containing various volume fractions of polyethylene glycol 400 (preheated to 38°C) was poured into each of the compartments. At scheduled intervals, a 2-mL aliquot of elution medium was withdrawn, but not replaced, from each compartment and assayed for the drug by HPLC.

Drug Permeation Study—The sheep's vagina[16] was cut open vertically (10, 11) and the mucosa was separated from the wall (Fig. 4). The vaginal mucosa was sandwiched between the donor and receptor compartments and clamped. Six hundred milliliters of saturated or unsaturated flurogestone acetate solution (40% polyethylene glycol 400 in simulated vaginal fluid) and 600 mL of drug-free solution (20% polyethylene glycol 400 in simulated vaginal fluid) were added to the donor and receptor compartments, respectively. Samples were removed from the receptor compartment at scheduled intervals for the duration of the experiment. Aliquots were assayed for the drug by HPLC.

Analytical Procedure—The HPLC assay procedure developed earlier (7) was utilized here. A fixed quantity of testosterone was added to each sample as an internal standard to ensure the injection-to-injection reproducibility required. Aliquots were injected into the HPLC column, and the peak height ratios of flurogestone acetate to testosterone were determined and compared with the standard curve for the calculation of flurogestone acetate concentrations.

RESULTS AND DISCUSSION

After assembly, the entire *in vitro* intravaginal release/permeation system (Fig. 2) is totally enclosed so that solvent loss is minimized during a long-term experiment. When a sponge is inserted into the flange opening, the drug-release profile from the sponge can be studied. When the vaginal mucosa is present, permeation can be evaluated. When both are present, release and permeation can be investigated simultaneously.

The impeller assembly of the intravaginal release/permeation system provides excellent stirring (up to 400 rpm), which significantly reduces the thickness of the hydrodynamic diffusion layer on the surface of sponge and

[15] Thermalert Model TH-6D; Baily Instruments, Saddle Brook, N.J.
[16] Dealeman Meats; Warren Township, N.J.

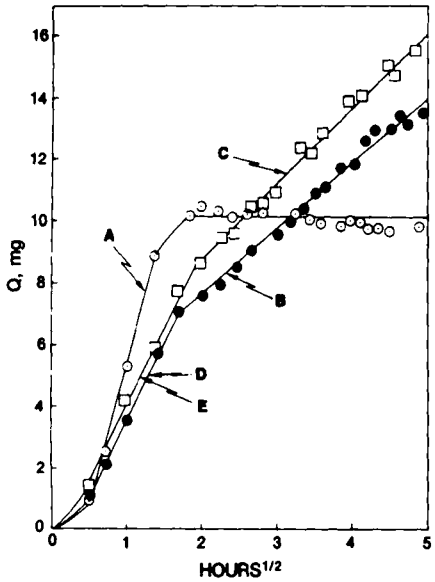

Figure 7—*Linear relationship between the cumulative amount of flurogestone acetate (Q) released from the vaginal sponge (containing 40 mg of the drug) into 1000 mL of elution medium (at nonsink conditions) and the square root of time ($t^{1/2}$). Note the change in the slopes at ~3 h. Key: (A) 0% polyethylene glycol 400, 8.64 mg/h$^{1/2}$; (B) 20% polyethylene glycol 400, 2.14 mg/h$^{1/2}$; (C) 30% polyethylene glycol 400, 2.40 mg/h$^{1/2}$; (D) 4.95 mg/h$^{1/2}$; (E) 4.89 mg/h$^{1/2}$.*

mucosa (Table II). The thickness of the hydrodynamic diffusion layer (δ_D) is related to the Sherwood number (Sh) (12) by the following:

$$\delta_D = \gamma\epsilon/Sh_r = D/k \qquad \text{(Eq. 2)}$$

where γ is the radius of the sponge, ϵ is the porosity of the sponge, Sh_r is the Sherwood number around the radian of the sponge, D is the diffusion coefficient, and k is the mass transfer coefficient. When the Sherwood number is >200, the thickness of the diffusion layer is very small (12); therefore, the effect of solution hydrodynamics on the release of drug from the sponge is negligibly small. This is consistent with the experimental results (Table II).

It is critically important that the magnitude of δ_D be held constant (and as small as possible) so the real mechanisms of drug release and permeation can be obtained and a meaningful comparison between experimental observations can be made. A rotation speed of 330 rpm was used, which maintains a constant thickness of hydrodynamic diffusion layer of $<14 \times 10^{-4}$ cm on the immediate surface of the sponge, and also provides a homogenous drug concentration in the elution medium. Additionally, a drug-stable and water-miscible polymer, *i.e.* polyethylene glycol, was added to the simulated vaginal fluid (elution medium) to enhance the solubility of the drug and to simulate the biological sink. Under these conditions, the cell sensitivity is fairly high, so that hourly measurements of drug release/permeation flux is feasible. The drug release/permeation profile is followed closely by directly assaying the drug concentration in the elution medium. Although the construction of this system is relatively simple, the rate of drug release/permeation can be determined reliably in a short period of time.

The results indicate that it requires 30 and 48 min, respectively, for the elution media (2 × 600 mL and 2 × 1000 mL) to reach the equilibrium temperature of 38°C from room temperature (22°C) (Fig. 5). Therefore, the solutions were always preheated to 38°C before each experiment. For both volumes of solutions (*i.e.*, 2 × 600 mL and 2 × 1000 mL), it took only 3 min

Table III—Effect of Polyethylene Glycol 400 Concentration on Rate of Drug Release from Vaginal Sponges [a]

Polyethylene Glycol 400, % v/v	Kinematic Viscosity, cm^2/s	$Q/t^{1/2}$, mg/h$^{1/2}$ [b]	
		Initial	Steady State
0	0.007	8.64	—
20	0.018	4.95	2.14
30	0.028	4.89	2.40
40	0.044	2.67	2.67
50	0.072	2.55	2.55

[a] Each contains 40 mg of flurogestone acetate. [b] Calculated from Figs. 7 and 8.

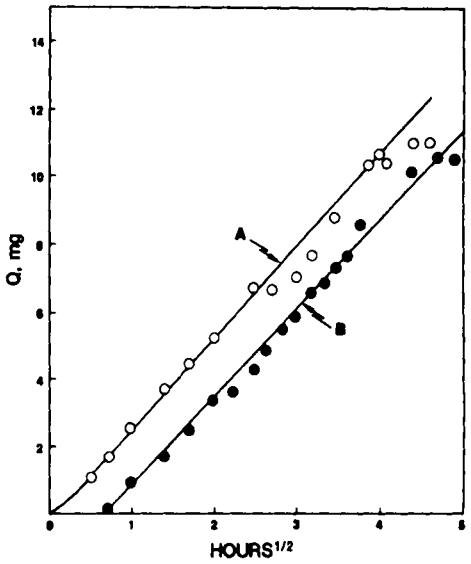

Figure 8—*Linear relationship between the cumulative amount of flurogestone acetate (Q) released from the vaginal sponge (containing 40 mg of the drug) into 1000 mL of elution medium (at sink condition) and square root of time ($t^{1/2}$). Note that there is no change in slope. Key: (A) 50% polyethylene glycol 400, 2.55 mg/h$^{1/2}$; (B) 40% polyethylene glycol 400, 2.67 mg/h$^{1/2}$.*

to reach the theoretical concentration when a rotation speed of 330 rpm was applied (Fig. 6), indicating very rapid mixing even in large volumes.

The release profiles of flurogestone acetate from vaginal sponges into simulated vaginal fluid containing various volume fractions of polyethylene glycol 400 were evaluated. The quantity of drug released was initially high and then decreased. This pattern of a nonlinear drug-release profile was also observed earlier in both *in vitro* (13-17) and *in vivo* (18, 19) studies of matrix-type drug dispersing devices.

Theoretically, when the matrix diffusion is the rate-controlling factor for the drug-release process, the release of drug from an insoluble, inert, polymeric matrix (like the polyurethane sponge in this study) is best described by the following (16):

$$Q = \left[\frac{D\epsilon}{\tau}(2A - \epsilon C_s)C_s t\right]^{1/2} \qquad \text{(Eq. 3)}$$

where Q is the cumulative amount of drug released, D is the diffusivity, ϵ is

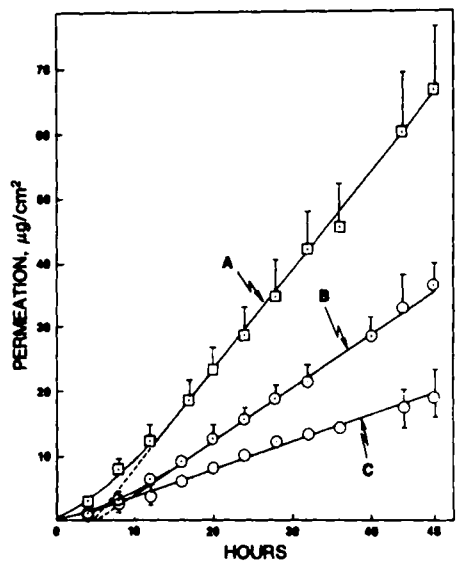

Figure 9—*Linear relationship between the cumulative amount of flurogestone acetate permeating the vaginal mucosa into 600 mL of elution medium and time (t). Note that a zero-order absorption pattern was obtained. The donor solution contained 40% polyethylene glycol 400; the receptor solution contained 20% polyethylene glycol 400. Bars represent* SE. *Key: (A) C_D^s = 116.2 µg/mL (36.48 µg/cm^2/d); (B) $^1/_2C_D^s$ = 66.3 µg/mL (20.68 µg/cm^2/d); (C) $^1/_4C_D^s$ = 30.96 µg/mL (9.98 µg/cm^2/d).*

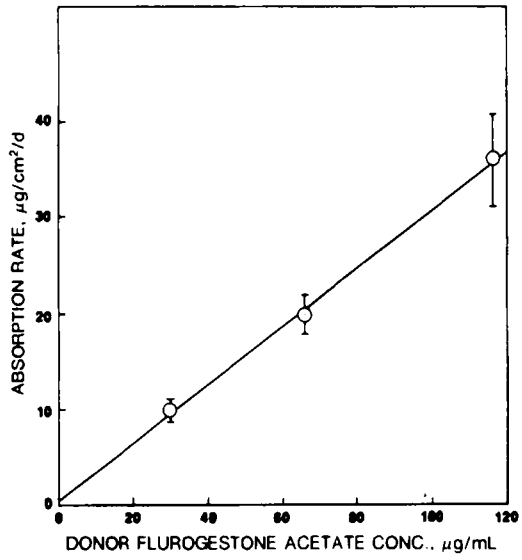

Figure 10—*Linear dependence of the steady-state intravaginal rate of absorption across an isolated vaginal mucosa on the concentration of flurogestone acetate in the donor solution (mucosa side). A P_v value of 0.311 cm/d is obtained from the slope.*

the porosity, and τ is the tortuosity in the sponge matrix; A is the initial loading dose of drug in the sponge; C_s is the solubility of the drug in the elution medium; and t is time. The theoretical model described in Eq. 3 indicates that the cumulative amount of drug released should be a linear function of the square root of time ($t^{1/2}$). Experimentally, this Q *versus* $t^{1/2}$ linearity was achieved (Figs. 7 and 8). There was, however, a break in the slope of the Q *versus* $t^{1/2}$ line when the elution medium was at non-sink conditions (0–30% polyethylene glycol 400–simulated vaginal fluid) (Fig. 7). On the other hand, perfect Q *versus* $t^{1/2}$ linearity was achieved when the elution medium was at sink conditions (40–50% polyethylene glycol 400–simulated vaginal fluid) (Fig. 8).

The results clearly indicate that the release of drug from the vaginal sponge can be divided into two steps: the initial release, which is controlled by the dissolution process of solid drug from the surface of the vaginal sponge, and the steady-state release (which prevails after complete dissolution of the surface drug), in which the drug dispersed inside the sponge matrix is released by the matrix diffusion-controlled mechanism. This is illustrated by comparing the $Q/t^{1/2}$ values generated in various combinations of polyethylene glycol 400 and simulated vaginal fluid (Table III). It has been reported that the initial release rates are remarkably affected by the solution hydrodynamics on the surface of the sponge, depending on both the fluid viscosity and the impeller rotation speed (12). As viscosity of the solution increases (from 0 to 50% polyethylene glycol 400), the initial rate of drug release decreases. On the other hand, the effect of solution hydrodynamics on the steady-state release rates is rather negligible and, therefore, the rates become fairly independent of polyethylene glycol 400 concentration. As polyethylene glycol 400 concentration goes beyond 30%, the steady-state rate of release stays at essentially the same level (2.54 ± 0.14 mg/h$^{1/2}$).

The permeation profiles of flurogestone acetate from the 40% polyethylene glycol 400–simulated vaginal fluid solution (which contains various drug concentrations) through the vaginal mucosa were investigated (Fig. 9). The cumulative amount of drug absorbed (Q) was a linear function of time. As the concentration of flurogestone acetate in the donor compartment decreases (from a 100% to a 25% saturated solution), the rate of drug permeation, $(Q/t)_v$, through the vaginal mucosa was observed to decrease proportionally (Fig. 10). The steady-state permeation rate, $(Q/t)_v$, across the vaginal mucosal barrier is defined by:

$$(Q/t)_v = P_v \cdot \Delta C_v \qquad \text{(Eq. 4)}$$

where P_v and ΔC_v are the permeability coefficient and the concentration gradient across the vaginal barrier, respectively. From the slope of the regression line of $(Q/t)_v$ *versus* ΔC_v, a permeability coefficient of 0.311 cm/d was determined for the intravaginal permeation of flurogestone acetate through the vaginal mucosa of sheep.

CONCLUSIONS

A relatively simple drug release/permeation system was designed for the measurement of *in vitro* drug release and permeation profiles. The system developed is capable of maintaining sink conditions by the use of water-miscible polyethylene glycol 400, which tends to simulate the biological sink. By doing so, it is expected to achieve a better *in vitro–in vivo* correlation. The effect of the diffusion boundary layer on the release and permeation of the drug is minimized by maintaining a thin, but constant, thickness of the hydrodynamic diffusion layer on the surface of the sponge and vaginal mucosa. This was accomplished by constant stirring and maintaining a fixed temperature throughout the experiments. The release of flurogestone acetate from the vaginal sponge followed a surface dissolution-matrix diffusion-type consecutive release. The initial rate was apparently influenced by both the fluid viscosity and impeller rotation speed. The steady-state release, which is described by a linear Q *versus* $t^{1/2}$ profile, was then established. The intravaginal absorption rate of the drug from the solution was observed to be constant and was proportional to the flurogestone acetate concentration in the donor solution. An intravaginal permeability coefficient of 0.311 cm/d was determined. It is surprising to note that the release rate of flurogestone acetate from the sponge is much faster than the rate of absorption (compare Fig. 8 with Fig. 9). An ideal device should deliver the drug at a rate equal to the rate of absorption. This could be achieved by making the device release the drug in zero-order fashion. Since the dose of flurogestone acetate required for estrus synchronization in sheep is only 0.3–0.4 mg/d, a slower release rate than that of the present sponge would be desired. It is apparent that an intravaginal drug delivery system which releases the drug at a slower, but constant, rate should be developed.

REFERENCES

(1) T. J. Robinson, U.S. Pat. No. 3,916,898, November 4, 1975.

(2) Y. W. Chien, "Novel Drug Delivery Systems," Dekker, New York, N.Y., 1982, pp. 413–463.

(3) "The Control of Ovarian Cycle in the Sheep," T. J. Robinson, Ed., Sydney University Press, Sydney, Australia, 1967.

(4) Y. W. Chien, H. J. Lambert, and D. E. Grant, *J. Pharm. Sci.*, **63**, 365 (1974).

(5) L. C. Faulkner and M. L. Hopwood, *J. Anim. Sci.*, **26**, 163 (1967).

(6) J. R. Robinson, "Sustained and Controlled Release Drug Delivery Systems," Dekker, New York, N.Y., 1978, p. 276.

(7) M. B. Kabadi, K. H. Valia, and Y. W. Chien, *J. Pharm Sci.*, **73**, 1461 (1984).

(8) J. Morgan, R. Lack, and T. J. Robinson, in "The Control of the Ovarian Cycle in Sheep," T. J. Robinson, Ed., Sydney University Press, Sydney, Australia, 1967, p. 195.

(9) Y. W. Chien and H. Lambert, *Chem. Pharm. Bull.*, **23**, 1085 (1975).

(10) E. S. E. Hafez, "Reproduction in Farm Animals," 2nd ed., Lea & Febiger, Philadelphia, Pa., 1968.

(11) H. Dellman and E. M. Brown, "Textbook in Histology," Lea & Febiger, Philadelphia, Pa., 1976, p. 345.

(12) K. Tojo, M. Kabadi, and Y. W. Chien, "Effect of Diffusion Boundary Layer on the Rate of Controlled Drug Release," presented at Academy of Pharmaceutical Sciences 35th National Meeting in Miami Beach, Fla., November 1983.

(13) J. Haleblian, R. Runkel, N. Mueller, J. Christopherson, and K. Ng, *J. Pharm. Sci.*, **60**, 541 (1971).

(14) T. J. Roseman and W. I. Higuchi, *J. Pharm. Sci.*, **59**, 353 (1970).

(15) D. R. Kalkwarf, M. R. Skov, L. Smith, and R. Gordon, *Contraception*, **6**, 423 (1972).

(16) T. Higuchi, *J. Pharm. Sci.*, **52**, 1145 (1963).

(17) T. J. Roseman, *J. Pharm. Sci.*, **61**, 46 (1972).

(18) J. C. Cornette and G. W. Duncan, *Contraception*, **1**, 339 (1970).

(19) Y. W. Chien, J. Opperman, B. Nicolova, and H. J. Lambert, *J. Pharm. Sci.*, **71**, 767 (1982).

ACKNOWLEDGMENTS

The authors express their appreciation to Mrs. Elizabeth Skurkay for her assistance in manuscript preparation. This work was extracted in part from the thesis submitted by M. B. Kabadi to the Graduate School of Rutgers–The State University of New Jersey, in partial fulfillment of the Doctor of Philosophy degree requirements.

Quantitation of Flecainide Acetate, A New Antiarrhythmic Agent, in Biological Fluids by Gas Chromatography with Electron-Capture Detection

J. D. JOHNSON, G. L. CARLSON, J. M. FOX, A. M. MILLER, S. F. CHANG ˣ, and G. J. CONARD

Received February 3, 1983, from the *Drug Metabolism Department, Riker Laboratories, Inc., a Subsidiary of 3M, 3M Center, St. Paul, MN 55144.* Accepted for publication November 29, 1983.

Abstract □ A sensitive and selective gas chromatographic (GC) method for the quantitation of flecainide acetate, a new antiarrhythmic agent, was developed. The unchanged drug and internal standard were separated from biological fluids by a sequence of solvent extractions and then the drug was derivatized. The pentafluorobenzamide derivatives were chromatographed on a 3% SP-2250 glass column and detected with a nickel-63 electron-capture detector. By this method, ≥12.5 ng of flecainide/mL can be quantitated in a 1-mL sample of plasma, saliva, or urine. The intraday precision, expressed as the *RSD*, at plasma levels of 12.5, 25, 50, 100, 200, 300, 400, and 600 ng/mL was 3.4, 6.2, 5.3, 6.4, 1.0, 1.6, 2.0, and 0.5%, respectively; the accuracy, expressed as relative error at these levels was −24.6, −6.9, −6.0, +0.6, +3.8, −0.3, +2.4, and −1.4%, respectively. The interday precision at these levels was 13.8, 13.0, 5.7, 7.6, 8.3, 6.1, 9.0, and 5.4%, respectively. Several other antiarrhythmic agents and one β-blocker, which might be administered concurrently with flecainide acetate, do not interfere with the assay.

Keyphrases □ Flecainide acetate—quantitation in biological fluids, GC-ECD □ GC—quantitation of flecainide acetate in biological fluids □ Antiarrythmic agents—flecainide acetate, quantitation in biological fluids, GC-ECD

Flecainide acetate [*N*-(2-piperidylmethyl)-2,5-bis(2,2,2-trifluoroethoxy)benzamide monoacetate] (I) is a new antiarrhythmic agent currently undergoing clinical evaluation worldwide. Pharmacological, pharmacokinetic, and efficacy information have been reported previously (1–9). Sensitive fluorometric methods (10, 11) have also been reported but have suffered from a lack of adequate specificity due to interference. Recently, HPLC methods have been reported (12, 13). In this report, we describe a highly selective and sensitive gas chromatographic (GC) method for the quantitation of the drug in plasma, urine, or saliva following the administration of single or multiple doses.

EXPERIMENTAL SECTION

Reagents—All reagents were analytical reagent grade. Ether was distilled in glass[1]; all other solvents were nanograde[2]. Fresh 0.2 M trimethylamine in benzene was made daily by dilution from a concentrated stock solution stored at −10°C. The derivatization reagent, pentafluorobenzoyl chloride (PFBC)[3], was stored at 4°C. Aqueous solutions of 0.1 M NaOH, 1.0 M NaOH, and 0.5 M HCl were prepared fresh daily in distilled water.

Blank Plasma, Urine, and Saliva—Human plasma, urine, and saliva samples were obtained from volunteers who had not taken any medication during the previous week. Donors were asked to fast for 12 h prior to giving blood. Human saliva was obtained by paraffin stimulation followed by expectoration into a disposable sputum collecting cup.

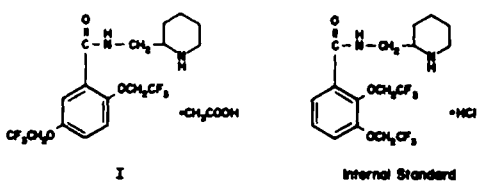

I Internal Standard

Gas Chromatography—A gas chromatograph[4] equipped with an electron-capture detector (15 mCi of nickel-63) and an automatic liquid sampler[5] was used. The glass column (180 cm × 2 mm i.d.) was silanized, packed with 3% SP-2250 on 100–120 mesh Supelcoport[6], and conditioned for 48 h at 275°C. The operating conditions were as follows: injection port temperature, 275°C; detector temperature, 310°C; oven temperature, 268°C (isothermal); carrier gas (5% methane in argon) flow rate, 20 mL/min.

Standard Solutions—All stock solutions of the drug and the internal standard, a positional isomer of flecainide [*N*-(2-piperidylmethyl)-2,3-bis(2,2,2-trifluoroethoxy)benzamide hydrochloride] (14), were made in distilled water. Standard solutions containing 800, 600, 400, 300, 200, 100, 50, 25, and 12.5 ng of flecainide acetate per 0.5 mL were made by diluting a 10-μg/mL primary standard solution. The 10-μg/mL primary standard solution of the internal standard was diluted to give a concentration of 100 ng/0.5 mL. The primary standard solutions of the drug and the internal standard were stored at 4°C.

Extraction—*Plasma*—To glass culture tubes (16 × 150 mm) with polyethylene-lined screw caps, 1-mL aliquots of unknown samples of human plasma and 0.5 mL of distilled water were added. Along with each set of unknown samples, 10 standards in blank human plasma were prepared by adding 0, 12.5, 25, 50, 100, 200, 300, 400, 600, and 800 ng of flecainide acetate in 0.5 mL of distilled water to 1-mL aliquots of blank human plasma. Next, 0.5 mL of internal standard (100 ng) solution, 0.2 mL of 0.2 M trimethylamine (TMA) in benzene, 1 mL of 1 M NaOH, and 10 mL of diethyl ether were added, in that order, to all tubes. The tubes were capped and shaken in a horizontal position for 30 min on a reciprocal mechanical shaker and then centrifuged for 5 min at 700×*g*. Then, 9.0 mL of the organic layer was transferred to a glass tube containing 2 mL of 0.5 M HCl. All tubes were shaken for 15 min and then centrifuged for 3 min. The ether was aspirated and discarded. The remaining aqueous layer was decanted into a 12-mL conical glass centrifuge tube for subsequent derivatization.

Urine—Because of the relatively high concentrations of flecainide in the urine samples, usually less than 1 mL of urine was analyzed. When less than

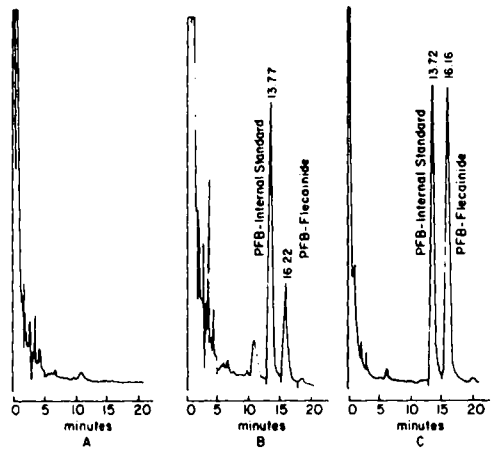

Figure 1—*Chromatograms from human plasma. (A) Blank plasma. (B) Plasma from a human subject dosed with flecainide (I) with the internal standard added (I, 42 ng/mL; internal standard, 100 ng/mL). (C) Mixture of reference pentafluorobenzamide (PFB) derivatives of I and internal standard; amount injected: PFB–I, 1.5 ng; PFB–internal standard, 0.9 ng.*

[1] Burdick-Jackson Laboratories, Inc., Muskegon, Mich.
[2] Mallinkrodt, Inc., St. Louis, Mo.
[3] Aldrich Chemical Co., Milwaukee, Wis.
[4] Model 5840A; Hewlett-Packard, Avondale, Pa.
[5] Model 7671A; Hewlett-Packard.
[6] Supelco, Inc., Bellefonte, Pa.

0022-3549/84/1000-1469$01.00/0
© 1984, American Pharmaceutical Association

Table I—Intraday Precision and Accuracy for Determination of Flecainide (I) in Human Plasma [a]

I Added, ng/mL	I Measured, ng/mL (mean ± *SD*)	*RSD*, %	Relative Error, %
12.5	9.4 ± 0.3	3.4	−24.6
25	23.3 ± 1.4	6.2	−6.9
50	47.0 ± 2.5	5.3	−6.0
100	100.6 ± 6.4	6.4	+0.6
200	207.6 ± 2.0	1.0	+3.8
300	299.1 ± 4.7	1.6	−0.3
400	409.6 ± 8.2	2.0	+2.4
600	591.8 ± 3.1	0.5	−1.4

[a] $n = 5$.

Table II—Interday Precision for Determination of Flecainide (I) in Human Plasma [a]

Sample Concentration, ng/mL	Response Ratio (Mean ± *SD*)	*RSD*, %
12.5	0.32 ± 0.04	13.8
25	0.49 ± 0.06	13.0
50	0.76 ± 0.04	5.7
100	1.32 ± 0.10	7.6
200	2.57 ± 0.21	8.3
300	3.62 ± 0.22	6.1
400	4.93 ± 0.44	9.0
600	6.95 ± 0.37	5.4

[a] $n = 6$.

1 mL of a urine sample was used, blank urine was added to bring the total sample volume to 1 mL. The extraction, derivatization, and analysis procedures were the same as described above for plasma.

Saliva—A saliva sample of 1 mL or less was analyzed in the same manner as described above for plasma; when less than 1 mL was used, distilled water was added to bring the total volume to 1 mL. It was shown that a standard curve (12.5–800 ng/mL) in saliva was the same as that in distilled water; thus, in all subsequent saliva analyses, a flecainide standard curve in distilled water was used for the determination of flecainide concentrations in saliva samples.

Derivatization—For derivatization of both the drug and the internal standard, 2 μL of neat pentafluorobenzoyl chloride was added to each aqueous extract with a 10-μL syringe[7]. Immediately after the addition of pentafluorobenzoyl chloride, the tube was vortexed for 5 s to disperse and suspend the derivatizing reagent. Next, 1 mL of 1 M NaOH was added, and the tube was vortexed for 15 s. Finally, 1 mL of hexane was added and the tube was again vortexed for 15 s. The derivatization sequence was carried out with pairs of tubes.

After the derivatization procedure was completed for all samples, the tubes were capped and centrifuged for 3 min at 700×*g*. Then, ~0.8 mL of each hexane phase was transferred to a clean conical glass tube containing 3 mL of 0.1 M NaOH. The tubes were vortexed for 15 s and centrifuged for 3 min. The hexane phase was then transferred to the glass autosampler vial, and a 5-μL aliquot of each sample was injected into the glass chromatograph.

Calculation—The area ratios (the drug–internal standard) were calculated with an integrating GC terminal[8]. The slope and intercept from the least-squares line of the concentrations of the drug standards *versus* the area ratios of the drug were used to calculate the concentrations in unknown samples.

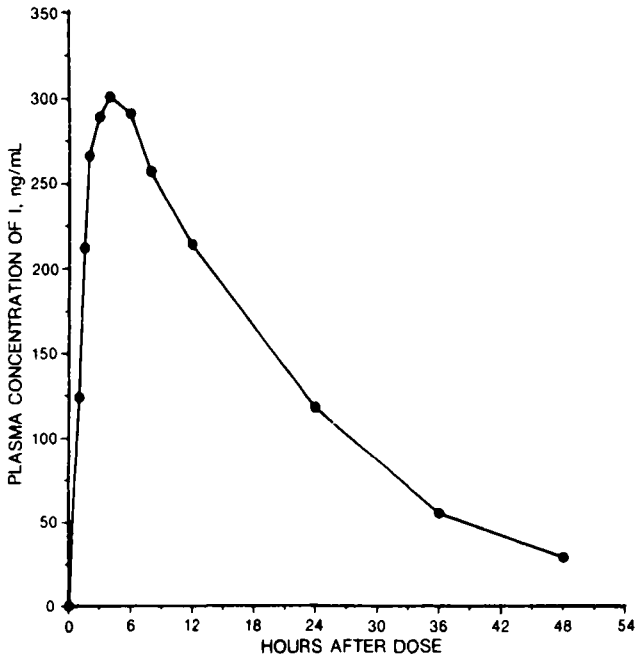

Figure 2—*Plasma concentrations of flecainide (I) in a healthy human subject following a single oral 200-mg dose of I.*

[7] Hamilton.
[8] Model 18850A; Hewlett-Packard.

Radiometric Analysis of Carbon-14—For the extraction recovery, an aqueous solution of ^{14}C-labeled drug (15) was used (9.2 μCi/mg, 10 ng/μL). Aliquots of 0, 5, 10, 40, and 60 μL were added to 1-mL blank human plasma samples in triplicate, and these samples were extracted by standard procedures. After the drug was extracted again into 0.5 M HCl, 1 mL of the aqueous phase was mixed with 0.4 mL of 1 M NaOH and counted in 15 mL of liquid scintillation solution[9]. Triplicate aliquots of the standard solution in 0, 5, 10, 40, and 60 μL were also directly counted in 15 mL of the same liquid scintillation solution. After cold and dark adaptation, carbon-14 was measured in a liquid scintillation counter[10]. Counting data were converted to disintegrations per minute by computer using the BIOAES program[11]. The percent extraction was calculated from the total disintegrations per minute in the aqueous extract compared with the disintegrations per minute in the spiked sample.

Tests for Other Drugs—A 500-ng/0.5 mL deionized water solution was prepared for propranolol hydrochloride, procainamide hydrochloride, disopyramide phosphate, quinidine sulfate, mexiletine hydrochloride, and lidocaine. Of each of these solutions, 0.5 mL was added to 1 mL of human plasma; the mixture was then extracted and derivatized by the procedure described above for flecainide. A positive control, a 600-ng flecainide standard with internal standard added, was run in parallel with the samples described above.

Gas Chromatographic–Mass Spectrometric Analysis—GC–MS analysis was performed on a gas chromatograph–mass spectrometer system which was comprised of a gas chromatograph[12], a magnetic double-focusing mass spectrometer[13], and a data system[14]. A stainless steel column (180 cm × 3.2 mm o.d.) packed with the same material as that for the glass column was used. The operating conditions were as follows: for the gas chromatograph, oven temperature, 245°C; injection port temperature, 230°C; carrier gas flow rate, 25 mL/min (He); for the mass spectrometer, resolving power, 500; source temperature, 250°C; for the data system, acquisition rate, 6 kHz, scan time, 2 s/decade. Unknown samples were extracted and derivatized by standard procedures. Aliquots of the final hexane extract were injected into the GC–MS system. Unknown samples were compared qualitatively with the synthetic pentafluorobenzamide of the drug at *m/z* 195, 278, 301, and 331, which are characteristic of the pentafluorobenzamide derivative of the drug.

RESULTS AND DISCUSSION

Derivatization—Based on the results from earlier studies[15] of ^{14}C-labeled flecainide in animals, it was anticipated that the plasma levels of the drug in humans would be in the low nanogram per milliliter range. Thus, it was decided at the outset that a GC–electron capture detector (GC–ECD) approach would be investigated. Flecainide contains six fluorine atoms which should provide enough ECD sensitivity; however, the material proved to be relatively difficult to chromatograph at the picogram to low nanogram amounts, possibly due to the presence of the piperidyl group. Thus, the piperidyl group was derivatized with pentafluorobenzoyl chloride. Although the perfluorobenzamide derivative, in comparison with its corresponding perfluorobutyramide, has a relatively low vapor pressure, thus requiring a higher column temperature for elution, this disadvantage is counterbalanced by the greater ECD sensitivity of the perfluorobenzamide derivative (16, 17) and the lack of any noticeable interferences.

Chromatography and Peak Separation—Although the drug and the internal

[9] New England Nuclear Corp., Boston, Mass.
[10] Model 3385; Packard Instrument Co., Downers Grove, Ill.
[11] BIOAES: Biological Automatic External Standardization; computer program on file at Riker Laboratories, Inc., St. Paul, Minn.
[12] Model 2740; Varian, Walnut Creek, Calif.
[13] Model 21-491C; Dupont, Wilmington, Del.
[14] Model 21-094; Dupont.
[15] Unpublished results.

standard differ only in the position of the trifluoroethoxy group on the aromatic ring, sufficient separation was achieved by using a 3% SP-2250 column. Under the chromatographic conditions used, there was no interference with the drug or the internal standard by any extractable endogenous materials present in plasma, urine, or saliva. Typical GC tracings of derivatized extracts from blank human plasma, from human plasma of a subject dosed with the drug, and reference flecainide acetate and internal standard derivatives are shown in Fig. 1. The retention times of the pentaflurobenzoyl derivatives of I and internal standard under these experimental conditions are 16.2 and 13.7 min, respectively.

Interference due to excess pentafluorobenzoyl chloride was eliminated by more accurate addition of the 2 μL of this reagent and/or by increasing the amount of NaOH added (from 1.0 to 1.5 mL of 1 M NaOH) to hydrolyze any excess derivatizing reagent. Care must also be taken when transferring the 0.8-mL hexane phase to the tube containing 3 mL of 0.1 M NaOH for the washing step. If any of the aqueous phase is transferred with the hexane, the chromatogram will show a large interfering solvent front.

Adsorption sites on a new column must be saturated by repeated injections of the synthetic derivatives of flecainide and the internal standard. Saturation is adequate when approximately equal peak areas are obtained for several successive injections. Extensive use of a column results in the deterioration of the resolution of flecainide from the internal standard. Repacking the front ~5 cm of the column was found to be necessary after ~800 sample injections.

Extraction Recovery—The extraction recovery of the drug from plasma was determined by carrying ^{14}C-labeled flecainide through the extraction to the derivatization steps and then measuring the total radioactivity recovered. The extraction recovery over the concentration range of 50 to 600 ng/mL was 86 to 91%, with a mean $\pm SD$ of 88 ± 2%.

Selectivity—GC-MS (electron impact) studies of plasma samples from human subjects who received the drug, in comparison with the synthetic pentafluorobenzoyl derivative of the drug, showed identical fragmentation patterns; thus, the pentafluorobenzoyl derivative of the drug is the species actually measured in human plasma samples.

Lidocaine, mexiletine, procainamide, disopyramide, propranolol, and quinidine, drugs which may be present together with flecainide in specimens obtained from patients, were tested for interference under the extraction and derivatization conditions used for the drug and the internal standard. Lidocaine, mexiletine, procainamide, and disopyramide showed no response, whereas propranolol and quinidine showed longer retention times than the pentafluorobenzoyl derivatives of the drug and the internal standard.

Linearity—A total of 9 or 10 single standards (0–800 ng) were run daily with each set of unknown samples. The mathematical expression of the least-squares line from a typical standard curve (0–800 ng) is $y = 0.0096x - 0.0662$. The correlation coefficient is 0.9998, and the coefficient of determination is 0.9996, indicating good linear proportionality between the concentration of flecainide and the detector response. The concentration-response relationship has also been shown to be linear up to a concentration of 1400 ng/mL. However, in most cases a shorter standard curve is used; *e.g.*, for routine analysis of samples after a single dose of flecainide, a 0–600 ng/mL range is used.

Sensitivity—By this method, concentrations as low as 12.5 ng of flecainide/mL of plasma, saliva, or urine can routinely be quantitated. Although not done routinely, under ideal chromatographic conditions, samples containing ≥6 ng of flecainide/mL can be quantitated.

Precision and Accuracy—The intraday precision and accuracy of this method was assessed by carrying five replicate samples at eight concentrations (12.5, 25, 50,100, 200, 300, 400, and 600 ng/mL) through the entire procedure on one analysis day. The intraday precision, expressed as the *RSD*, was 3.4, 6.2, 5.3, 6.4, 1.0, 1.6, 2.0, and 0.5% for the eight concentrations listed above, respectively (Table I). The accuracy of this method, expressed as relative error, at these levels was −24.6, −6.9, −6.0, +0.6, +3.8, −0.3, +2.4, and −1.4%, respectively.

The interday precision, at the concentrations described above, was established by analyzing these standards on 6 separate days over a 1-month period (Table II). The response ratios from 6 separate days for each standard concentration were pooled, and the mean ± *SD* values were calculated. The *RSD* values were 13.8, 13.0, 5.7, 7.6, 8.3, 6.1, 9.0, and 5.4% for concentrations of 12.5, 25, 50, 100, 200, 300, 400, and 600 ng/mL, respectively.

Application—The method has been used to measure plasma, urinary, and salivary levels of flecainide from various metabolic, pharmacological, and therapeutic studies in humans. More than 10,000 samples have been successfully analyzed by this procedure in our laboratory, as well as in several other laboratories worldwide. A typical curve of the plasma concentration of the drug *versus* time following a single oral 200-mg dose of the drug in a healthy human volunteer is shown in Fig. 2.

REFERENCES

(1) J. R. Schmid, B. D. Seebeck, C. L. Henrie, E. H. Banitt, and D. C. Kvam, *Fed. Proc. Fed. Am. Soc. Exp. Biol.*, **34,** 775 (1975).

(2) E. H. Banitt, W. R. Bronn, W. E. Coyne, and J. R. Schmid, *J. Med. Chem.*, **20,** 821 (1977).

(3) G. J. Conard, G. L. Carlson, J. W. Frost, and R. E. Ober, *Clin. Pharmacol. Ther.*, **25,** 218 (1979).

(4) L. Seipel, R. R. Abendroth, and G. Breithhardt, *Z. Kardiol.*, **70,** 524 (1981).

(5) J. L. Anderson, J. R. Stewart, B. A. Perry, D. D. Van Hamersveld, T. A. Johnson, G. J. Conard, S. F. Chang, D. C. Kvam, and B. Pitt, *N. Engl. J. Med.*, **305,** 473 (1981).

(6) H. J. Duff, D. M. Roden, R. J. Maffucci, B. S. Vesper, G. J. Conard, S. B. Higgins, J. A. Oates, R. F. Smith, and R. L. Woosley, *Am. J. Cardiol.*, **48,** 1133 (1981).

(7) M. Hodges, J. Hoback, and E. Graham, *Clin. Pharmacol. Ther.*, **29,** 251 (1981).

(8) G. J. Conard, G. E. Cronheim, and H.-W. Klempt, *Arzneim-Forsch.*, **32,** 155 (1982).

(9) M. Hodges, J. M. Haugland, G. Granrud, G. J. Conard, R. W. Asinger, F. L. Mikell, and J. Krejci, *Circulation*, **65,** 879 (1982).

(10) S. F. Chang, A. M. Miller, M. J. Jernberg, R. E. Ober, and G. J. Conard, *Arzneim-Forsch.*, **33,** 251 (1983).

(11) K. A. Muhiddin and A. Johnston, *Br. J. Clin. Pharmacol.*, **12,** 283p (1981).

(12) S. F. Chang, T. M. Welscher, A. M. Miller, and R. E. Ober, *J. Chromatogr.*, **272,** 341 (1983).

(13) J. W. DeJong, J. A. J. Hegge, E. Harmsen, and P. DeTombe, *J. Chromatogr.*, **229,** 498 (1982).

(14) E. H. Banitt, W. R. Bronn, and W. E. Coyne, *J. Med. Chem.*, **20,** 821 (1977).

(15) E. H. Banitt and G. J. Conard, *J. Label Compounds Radiopharm.*, **18,** 712 (1981).

(16) S. B. Matin and M. Rowland, *J. Pharm. Sci.*, **61,** 1235 (1972).

(17) S. Ahuja, *J. Pharm. Sci.*, **65,** 163 (1976).

ACKNOWLEDGMENTS

The authors thank E. H. Banitt for preparation of the synthetic pentafluorobenzoyl derivatives, W. L. Stebbings, Central Research Laboratories, 3M, for the GC-MS data, and R. E. Ober for his critical review of the manuscript.

Kinetic Steric Factors and Connectivity Indices

JOHN C. SCHUG *, JIMMY W. VIERS *x, and JEFFREY I. SEEMAN ‡

Received June 27, 1983, from the *Department of Chemistry, Virginia Polytechnic Institute and State University, Blacksburg, VA 24061 and ‡Philip Morris Research Center, Richmond, VA 23261. Accepted for publication January 19, 1984.

Abstract □ In this study the relationships between previously reported connectivity indices described by Kier and Hall and steric contributions to the rate constants for several series of reactions are examined. Rate data were examined for four different series of reactions, which were chosen to represent a range of different reaction mechanisms and transition-state structures. For sterically controlled reactions, the relative rates of series of substrates can be correlated either with the connectivity indices of the substrates themselves or with the changes in the indices that accompany formation of transition states. As expected, the significant indices in the correlations are of the cluster and path-cluster types. The connectivity indices should be useful descriptors in helping relate equilibrium properties, chemical reactivities, and pharmacological data to one another.

Keyphrases □ Connectivity indices—relationship with steric contributions to rate constants □ Kinetic steric factors—relationship with connectivity indices to rate constants

The development of structure–activity relationships (SAR) in pharmacology (1, 2) has relied heavily on the use of physicochemical parameters which are based on chemical reactivity relationships, such as Hammett σ-ρ constants and Taft E_s values. Many of the more recent studies, including those in which pattern recognition methods are employed, also make use of other descriptors which reflect substructural information like molecular connectivity and branching characteristics (3). The connectivity indices described by Kier and Hall (4), which were introduced as a generalization of the Randic' branching index (5), have proved to be extremely useful in this regard.

Kier and co-workers and others have been quite successful in obtaining correlations (4, 6–8) of physical, thermodynamic, and pharmacological properties with the connectivity indices, but there has been only one report to date concerned with the relationship between connectivity indices and chemical reactivity (9). There obviously are very close relationships between physicochemical parameters, chemical reactivities, and pharmacological properties, and it is important that these relationships be understood. We have therefore undertaken the present study of correlations between molecular connectivity and chemical reactivity.

It is clear that the connectivity indices described by Kier and Hall carry information about the nature and number of atoms in the molecule, as well as the degree of branching and the amount of folding. The dependence of kinetic steric factors on molecular branching has been well established by the detailed studies of Charton (10), Dubois *et al.* (11), and Ruchardt and Beckhaus (12), among others; therefore, kinetic steric factors may be correlated with connectivity indices. In fact, the link between the two has already been made by Murray (9), who succeeded in finding correlations between the Taft E_s parameters (13) and effective connectivity indices for a series of substituted alkanes.

The connectivity indices are based on hyrogen-suppressed graphs and are defined by:

$$ {}^{m}\chi_t = \sum_{j=1}^{n_m} \left[\prod_{i=1}^{m+1} (\delta_i)^{-1/2} \right]_j \qquad \text{(Eq. 1)} $$

where m is the number of connected edges in the subgraph defined by the atoms whose valencies are denoted by δ_i. The summation is over the entire set of all n_m possible subgraphs of the given order and type. The different types which can occur for $m \geq 3$ are differentiated by t; the designation used is $t = P$ for path, C for cluster, PC for path-cluster, and CH for chain (cycle).

The approach taken by Murray was to correlate kinetic steric factors with χ values for a series of substrates in a particular reaction. This implies that steric factors simply reflect structural features of the ground-state substrate molecules. Although many kinetic data have been successfully correlated with ground-state properties of substrate molecules in the past, it seems that a better approach would be based on the transition-state theory. This would correlate kinetic data with parameters which measure the changes that take place during the activation process for a reaction. In particular, we suggest that a convenient set of parameters can be defined as:

$$ \Delta({}^{m}\chi_t) = {}^{m}\chi_t^{\ddagger} - {}^{m}\chi_t \qquad \text{(Eq. 2)} $$

where ${}^{m}\chi_t^{\ddagger}$ is the connectivity index for transition states and ${}^{m}\chi_t$ is the corresponding quantity for reactant molecules. The utility of $\Delta{}^{m}\chi_t$ to measure kinetic steric factors is suggested by the striking success that Kier and co-workers achieved in correlating molar heats of formation with ${}^{m}\chi_t$. If similar relations hold in the transition state, then it would be expected that the enthalpy of activation and the activation energy will be related to $\Delta{}^{m}\chi_t$.

Our goal was to determine whether correlations could be found between chemical reactivity and connectivity indices (either ${}^{m}\chi_t$ or $\Delta{}^{m}\chi_t$). We considered four different chemical reactions: quaternization of substituted pyridines, bromide exchange reaction of branched alkanes, acid-catalyzed hydrolysis of alkanoic esters, and a nucleophilic substitution process on chlorodinitrobenzene, all of which will be discussed below. In all cases, we have found that both sets of indices do generally correlate with the reactivity data.

Our calculations differed from those of Murray in two respects. First, we calculated ${}^{m}\chi_t$ for the actual full substrate molecules rather than replacing the reactive center with an effective atom that has some arbitrary valence. Second, we treated subgraphs of different types separately, since we expected the cluster or path-cluster terms to be most important. All of our indices were calculated with a FORTRAN program developed along the lines of the algorithm suggested by Kier and Hall (4). We simply employed the list of atomic valencies (δ_i) which they provided, including the empirical values they had found appropriate for halogen atoms[1].

[1] Values of δ used in this study were: $-CH_3$, 1; $-CH_2-$, 2; $-\overset{|}{C}H-$, 3; $-\overset{|}{\underset{|}{C}}-$, 4; $-NH_2$, 3; $\equiv N$, 5; $-N=$(pyridine), 5; $-\overset{|}{\underset{|}{N}}-$ (quaternary), 6; OH, 5; $-O-$, 6; $=O$, 6; $-Br$, 0.254.

0022-3549/84/1000-1472$01.00/0
© 1984, American Pharmaceutical Association

Table I—Standard Heats of Formation in the Gas Phase at 25°C

Compound	ΔH_f°, g/kcal·mol^{-1} Experimental[a]	Calculated (Eq. 2)[b]
Pyridine	34.55	33.96
2-Methylpyridine	23.70	24.79
3-Methylpyridine	25.42	25.01
4-Methylpyridine	24.41	25.01
2,3-Dimethylpyridine	16.32	15.70
2,4-Dimethylpyridine	15.27	15.83
2,5-Dimethylpyridine	15.88	15.83
2,6-Dimethylpyridine	14.03	15.62
3,4-Dimethylpyridine	16.74	15.92
3,5-Dimethylpyridine	17.40	16.05

[a] From Ref. 17. [b] See Table VII for values of $^m\chi_t$.

RESULTS AND DISCUSSION

Substituted Pyridines and Their Quaternization Rates—The alkylation of substituted pyridines is one of the most studied reactions from a structure–reactivity point of view (14–16). Because the steric and branching effects of pyridine alkylation are so well understood, this reaction seemed to be an ideal first candidate for a connectivity index study. Since some of the most striking correlations described by Kier and Hall are for molar heats of formation, we decided to first look at the available data of that type for the alkylpyridines. The only data available were those listed by Cox and Pilcher (17) for the 10 compounds listed in Table I. We found that these values could be described by the simple expression:

$$\Delta H_f^\circ(g)/(\text{kcal}\cdot\text{mol}^{-1}) = -21.80(^1\chi) + 74.27 \qquad \text{(Eq. 3)}$$

where $r = 0.9897$, $RSD = 0.98$, and $n = 10$. The correlation coefficient can be increased to 0.9922 by any of the following:

$$\Delta H_f^\circ(g)/(\text{kcal}\cdot\text{mol}^{-1}) = -32.97(^1\chi) + 10.05(^2\chi) + 84.49 \qquad \text{(Eq. 4)}$$

$$= -24.02(^1\chi) + 4.49(^4\chi_{PC}) + 78.47 \qquad \text{(Eq. 5)}$$

$$= -27.84(^1\chi) + 18.00(^3\chi_C) + 85.28 \qquad \text{(Eq. 6)}$$

Although these findings are not as impressive as the results of Kier and Hall for alkanes, they are significant. The size of the current data set is appreciably smaller than that of Kier and Hall, and the uncertainties in the experimental data are larger. In Fig. 1 are shown the types of subgraphs that contribute to the indices $^2\chi$, $^3\chi_C$, and $^4\chi_{PC}$. It is appropriate that these enter the correlations Eqs. 4–6 since they measure the degree of methylation of the pyridine nucleus; $^4\chi_{PC}$ also contains a measure of the degree of substitution at adjacent pyridine sites.

If one examines the series of rate constants previously reported (14–16) for the methylation of alkylpyridines, it appears that the relative rates are dominated by steric effects and have only subordinate electronic contributions. We have recently published (14, 16) some theoretical studies of this reaction based on the model transition state (TS) corresponding to the activation process shown in Scheme I. We used this model to calculate a set of ($^m\chi_t^\ddagger$) and $\Delta(^m\chi_t)$ for a series of 37 alkyl-substituted pyridines (Table II). The valency of nitrogen in the model transition states was taken to be 6, which is the value suggested by Kier and Hall for quaternized nitrogen (4). This corresponds to the assumption to a fully formed N—CH_3 bond in the TS; in subsequent studies, it may be desirable to use intermediate valencies which correspond to partially formed bonds. For the set of 37 alkylpyridines, in which the relative reaction rates cover four orders of magnitude, the best linear correlation we found was:

$$\ln(k_{rel}) = -10.7\,\Delta^5\chi_{PC} + 2.75 \qquad \text{(Eq. 7)}$$

where $r = 0.8786$, $RSD = 1.28$, $n = 37$, and k_{rel} is the second-order rate constant relative to that of pyridine.

Other powers of the parameters were investigated, and the best correlation obtained was:

$$\ln(k_{rel}) = -10.4(\Delta^5\chi_{PC})^2 - 7.24(\Delta^4\chi_{PC})^2 + 1.30 \qquad \text{(Eq. 8)}$$

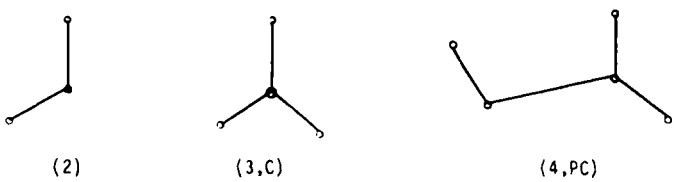

Figure 1—*Illustrative subgraphs of types* $^2\chi$, $^3\chi_C$, $^4\chi_{PC}$.

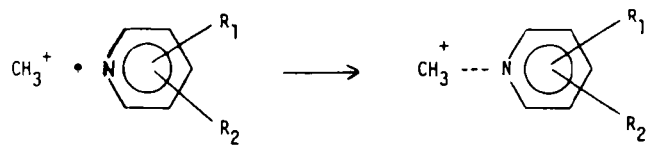

Scheme I

where $r = 0.9092$, $RSD = 1.13$, and $n = 37$. The results of Eq. 8 are compared with the observed values of [ln (k_{rel})] in Table II. In Figure 2 are shown some illustrative subgraphs that contribute to $\Delta^5\chi_{PC}$ and $\Delta^4\chi_{PC}$ for the model transition states. It is easy to see that these terms should constitute measures of steric hindrance in the reaction.

In the case of Eq. 8, as well as for all succeeding correlations involving multiple parameters, statistical tests were applied regarding the utility of the added parameters. Parameters were not added to the correlations unless they were significant at the 90% confidence interval, as indicated by the *F*-test.

Although Eqs. 7 and 8 are quite reasonable, better results might have been expected. Further consideration indicates that there may be a good reason for this discrepancy; although this reaction is dominated by steric factors, there are apparently sizeable electronic contributions in some cases. In fact, Berg *et al.* (18) have studied the iodomethylation of a series of 2-substituted pyridines, using heteroatom substituents as well as alkyl groups, and have arrived at a separation of electronic and steric contributions to the relative rates of reaction. They separated log (k_{rel}) into steric (S°) and electronic (E°) components:

$$\log(k_{rel}) = S^\circ + E^\circ \qquad \text{(Eq. 9)}$$

and, using a Brønsted relation to estimate E°, were able to determine S° and E° for the series of molecules. For the series of 2-alkylpyridines with alkyl groups being methyl, ethyl, isopropyl, and *tert*-butyl, they found values of E°/S° to be −0.59, −0.33, −0.24, and −0.061, respectively. Whether or not their values of S° and E° are precisely correct, it must be concluded that electronic effects are not insignificant in the above series of alkylpyridines and, furthermore, that their fractional contributions vary considerably through the series.

Table II—Relative Rates of Methylation of Substituted Pyridines

Compound	ln (k_{rel}) Observed[a]	Eq. 8[b]
Pyridine	0	0.925
2-Picoline	−0.844	−0.249
3-Picoline	0.531	0.490
4-Picoline	0.742	0.977
2,3-Lutidine	−0.844	−1.395
2,4-Lutidine	−0.083	−0.106
2,5-Lutidine	−0.198	−0.790
2,6-Lutidine	−3.219	−2.657
3,4-Lutidine	1.224	0.644
3,5-Lutidine	0.956	−0.247
2-Ethylpyridine	−1.514	−0.673
2-Isopropylpyridine	−2.590	−2.375
2-*tert*-Butylpyridine	−8.422	−5.570
2-Methyl-3-ethylpyridine	−0.734	−0.823
2-Methyl-3-isopropylpyridine	−0.673	−0.552
2-Methyl-3-*tert*-butylpyridine	−1.109	−0.364
2,6-Diethylpyridine	−5.599	−3.672
2,6-Diisopropylpyridine	−8.805	−9.238
2,4,6-Trimethylpyridine	−2.207	−2.307
2,3,5,6-Tetramethylpyridine	−4.343	−6.629
2,3,4,5,6-Pentamethylpyridine	−4.200	−5.694
3-Ethylpyridine	0.788	0.690
4-Ethylpyridine	0.833	0.971
3-Isopropylpyridine	0.875	0.774
4-Isopropylpyridine	0.788	0.969
3-*tert*-Butylpyridine	1.030	0.875
4-*tert*-Butylpyridine	0.788	0.924
2-Methyl-5-ethylpyridine	0.095	−0.531
2-Methyl-5-isopropylpyridine	0.182	−0.383
2-Methyl-5-*tert*-butylpyridine	0.262	−0.263
2,3-Cyclopentenopyridine	0.642	−0.935
2,3-Cyclohexenopyridine	−1.204	−0.935
2-Ethyl-3-methylpyridine	−1.427	−1.892
2-Ethyl-5-methylpyridine	−0.616	−1.509
2-Ethyl-6-methylpyridine	−5.655	−3.005
2-Isopropyl-3-methylpyridine	−5.776	−3.900
2-Isopropyl-5-methylpyridine	−1.772	−3.644

[a] From Refs. 14–16. [b] See Table VIII for values of $\Delta^m\chi_t$.

Table III—Relative Rates and Steric Factors for the Methylation of 2-Substituted Pyridines

2-Substituent	log (k_{rel})[a]	$S°$ (Experimental)[a]	$S°$ (Eq. 11)[a,b]	$S°$ (Eq. 12)[b]	$S°$ (Eq. 14)[b]
—CH_3	−0.30	−0.73	−0.82	−0.73	−0.80
—C_2H_5	−0.72	−1.08	−1.02	−1.02	−0.94
—Isopropyl	−1.10	−1.44	−1.65	−1.66	−2.07
—*tert*-Butyl	−3.70	−3.44	−4.02	−4.01	−3.78
—CH_2OH	−0.59	−0.67	−0.93	−0.88	−0.84
—CH_2CH_2OH	−0.68	−0.86	−1.20	−1.13	−0.99
—CH_2—Phenyl	−1.05	−1.16	−1.41	−1.29	−1.59
—$CO_2C_2H_5$	−2.14	−1.25	−1.24	−1.42	−1.17
—Phenyl	−2.00	−1.82	−1.62	−1.70	−1.73
—2-Pyridyl	−2.48	−2.35	−1.51	−1.63	−1.56
—NH_2	−0.30	−0.93	−0.89	−0.78	−0.73
—C≡N	−2.70	−0.89	−0.95	−1.00	−0.78
—Br	−2.36	−0.82	−0.67	−0.70	−0.95

[a] From Ref. 18. [b] See Table IX for values of ${}^m\chi_t$ and $\Delta^m\chi_t$.

For the whole set of molecules studied, Berg *et al.* (18) found that the ratio of $E°/S°$ varies from −0.68 to +2.03, so the data cover the range from predominant steric control to predominant electronic control. The values of $S°$ which they obtained for the 2-substituents —CHO and —$COCH_3$ seemed out of line with the rest of their data, so we dropped those compounds from further consideration, leaving a total of 13 compounds to be considered (Table III). No significant correlations could be found for log (k_{rel}); this is consistent with the conclusion that both electronic and steric factors are important in this series (18). The situation was dramatically different when the values of $S°$ were examined. The best single-parameter linear correlation was:

$$S° = -4.43\Delta^6\chi_{PC} + 0.26 \qquad \text{(Eq. 10)}$$

where $r = 0.8739$, $RSD = 0.46$, and $n = 13$. The situation improved dramatically when multiple parameters were permitted. The best linear relation obtained was:

$$S° = -4.11(\Delta^6\chi_{PC}) - 70.1(\Delta^3\chi_C) + 3.00(\Delta^4\chi_P) + 7.27 \qquad \text{(Eq. 11)}$$

where $r = 0.9430$, $RSD = 0.35$, and $n = 13$. When other powers of the parameters were examined, slightly better agreement was found by:

$$S° = -0.584(\Delta^4\chi_{PC})^{-1} - 0.117(\Delta^4\chi_P)^{-1} + 0.338(\Delta^6\chi_{PC})^{-1} + 0.460 \qquad \text{(Eq. 12)}$$

where $r = 0.9585$, $RSD = 0.30$, and $n = 13$. The values of $S°$ calculated from Eqs. 11 and 12 are compared with the experimentally derived values of Berg *et al.* (18) in Table III. These investigators did a credible job of identifying steric contributions to these relative rates. Furthermore, as we expected, Eqs. 10–12 are dominated by path-cluster- and cluster-type terms.

If we correlate $S°$ with the indices of the substrate molecules themselves, the best single-parameter equation is somewhat better than Eq. 10:

$$S° = -3.41({}^5\chi_{PC}) - 0.35 \qquad \text{(Eq. 13)}$$

where $r = 0.9127$, $RSD = 0.47$, and $n = 13$. However, the best multiple-parameter equation is not quite as good as Eqs. 11 or 12:

$$S° = -13.69({}^5\chi_C) - 0.93({}^4\chi_P) - 0.38 \qquad \text{(Eq. 14)}$$

where $r = 0.9270$, $RSD = 0.44$, and $n = 13$. If the calculated values of $S°$ in Table III are examined it is hard to decide whether Eq. 11, 12, or 14 is preferable to the others. The single-parameter correlations behave as expected in that the index occurring in Eq. 10 (${}^6\chi_{PC}$) is of a higher order than that in Eq. 13 (${}^5\chi_{PC}$).

The success of Eqs. 10 and 13 indicates that there should exist a linear relationship between the activation indices ($\Delta^6\chi_{PC}$) and the substrate indices (${}^5\chi_{PC}$). The relation was found to be:

$$\Delta^6\chi_{PC} = 0.712({}^5\chi_{PC}) + 0.154 \qquad \text{(Eq. 15)}$$

where $r = 0.9660$, $RSD = 0.0483$, and $n = 13$. The existence of this relationship is consistent with results of a previous study on the Menschutkin reaction, which has established that relative reactivities of substituted pyridines can be interpreted either in terms of TS calculations or in terms of substrate equilibrium structures with essentially equal success (14–16).

Bromide Exchange Reaction—Another reaction which is generally accepted as being largely sterically controlled is the bromide exchange reaction of alkyl groups:

$$Br^- + RBr \rightarrow BrR + Br^- \qquad \text{(Eq. 16)}$$

which was studied experimentally by de la Mare *et al.* (19). For these reactions, Abraham and co-workers have estimated the nonbonded interactions in a model transition state (Fig. 3) and concluded that steric effects are highly dominant (20). More recently, deTar *et al.* (21) have applied molecular mechanics to the same transition state; they concluded that although steric effects apparently predominate, polar effects must be invoked to interpret the rate constants for the α series of alkyl groups (methyl, ethyl, isopropyl, *tert*-butyl).

We examined the rate constants at 25°C (Table IV) which were listed by deTar *et al.* (21). As before, transition-state valencies were assigned on the basis of fully formed bonds. This included use of the empirical value of 0.254 for bromine.

The best single-parameter correlation was rather poor:

$$\ln(k) = -2.73(\Delta^5\chi_C) - 7.50 \qquad \text{(Eq. 17)}$$

where $r = 0.7269$, $RSD = 3.70$, $n = 7$, and k is in $s^{-1}\ M^{-1}$. With two parameters the results were much better:

$$\ln(k) = -3.70(\Delta^5\chi_C) - 1.30(\Delta^3\chi_C) - 3.44 \qquad \text{(Eq. 18)}$$

where $r = 0.9763$, $RSD = 1.30$, $n = 7$, and k is in $s^{-1}\cdot M^{-1}$.

In this case, the substrate connectivity indices do a slightly better job than do the $\Delta\chi$. In comparison with Eq. 17, we have:

$$\ln(k) = -2.87({}^2\chi) - 2.87 \qquad \text{(Eq. 19)}$$

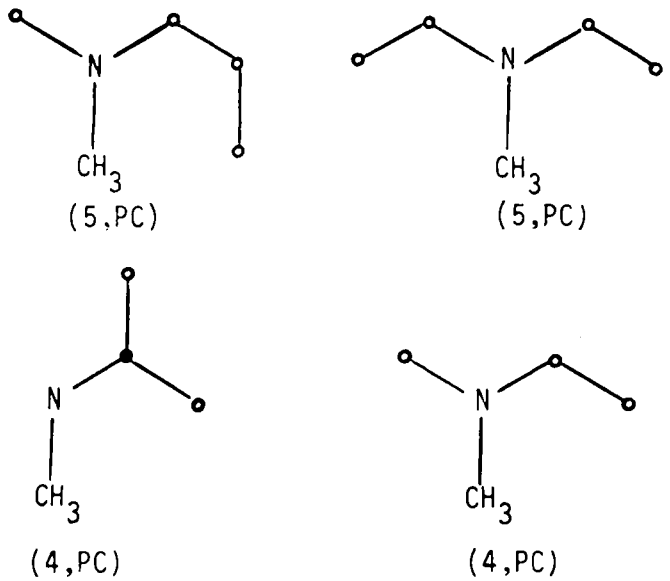

Figure 2—*Illustrative subgraphs contribution to terms in Eq. 8.*

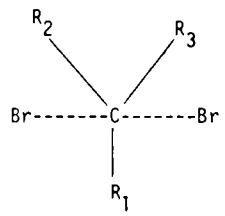

Figure 3—*Transition state for Eq. 16.*

Table IV—Second-Order Rate Constants and Steric Contributions to Activation Energies for Br^- Exchange Reactions [a]

R	ln (k)			$\Delta E^{\ddagger}_{ST}$		
	Observed [b]	Eq. 18 [c]	Eq. 20 [c]	Calc [d]	Eq. 22 [c]	Eq. 23 [c]
Methyl	−2.00	−3.44	−2.81	7.41	7.20	7.50
Ethyl	−6.41	−6.39	−6.08	13.61	12.55	12.95
n-Propyl	−6.81	−5.52	−6.29	13.65	14.40	13.30
Isopropyl	−10.96	−9.63	−9.50	17.77	18.44	18.65
Isobutyl	−9.74	−9.90	−10.42	15.48	16.79	16.07
tert-Butyl	−12.17	−13.27	−13.24	25.38	25.04	24.90
Neopentyl	−17.35	−17.28	−17.08	20.64	19.52	20.57

[a] Rate constants are in seconds^{-1}·Molar^{-1}, activation energies are in kilocalories·moles^{-1}, and the exchange reaction is depicted in Eq. 16. [b] From Ref. 19. [c] See Table X for values of $^{m}\chi_t$ and $\Delta^{m}\chi_t$. [d] From Ref. 21.

where $r = 0.8606$, $RSD = 2.73$, $n = 7$, and k is in $s^{-1}\cdot M^{-1}$. The counterpart of Eq. 18 is:

$$\ln(k) = -2.33(^{2}\chi) - 3.06(^{4}\chi_{PC}) - 2.87 \qquad \text{(Eq. 20)}$$

where $r = 0.9829$, $RSD = 1.10$, $n = 7$, and k is in $s^{-1}\cdot M^{-1}$. Note that Eqs. 19 and 20 contain lower-order indices than do Eqs. 17 and 18. The values of ln (k), as calculated from Eqs. 18 and 20 are compared with the experimental values in Table IV.

We also examined the steric contributions to the activation energies, $\Delta E^{\ddagger}_{st}$, which deTar *et al.* calculated *via* molecular mechanics (21). Correlation of these numbers with the $\Delta\chi$ values yielded the best single- and multiple-parameter correlations:

$$\Delta E^{\ddagger}_{st} = 1.64(\Delta^{3}\chi_C) + 11.96 \qquad \text{(Eq. 21)}$$

where $r = 0.7575$, $RSD = 4.11$, $n = 7$, and $\Delta E^{\ddagger}_{st}$ is in kcal·mol^{-1}, and:

$$\Delta E^{\ddagger}_{st} = 2.35(\Delta^{3}\chi_C) + 2.13(\Delta^{4}\chi_C) + 7.20 \qquad \text{(Eq. 22)}$$

where $r = 0.9865$, $RSD = 1.15$, $n = 7$, and $\Delta E^{\ddagger}_{st}$ is in kcal·mol^{-1}. These are slightly better than Eqs. 17 and 18 involving the rate constants.

When the substrate indices were used, we obtained:

$$\Delta E^{\ddagger}_{st} = 3.89(^{2}\chi) + 7.50 \qquad \text{(Eq. 23)}$$

where $r = 0.9951$, $RSD = 0.62$, $n = 7$, and $\Delta E^{\ddagger}_{st}$ is in kcal·mol^{-1}. In this case no statistically significant second parameter could be added to the correlation. However, Eq. 23 is already superior to Eq. 22. Equations 22 and 23 are compared with the molecular mechanics values of deTar *et al.* in Table IV.

Linear regression of the best single activation index ($\Delta^{3}\chi_C$) against the best single substrate index ($^{2}\chi$), yielded a correlation coefficient of only 0.752. This low value is to be expected in view of the small r associated with Eq. 21.

Whether the substrate connectivity indices ($^{m}\chi_t$) or the changes that occur in them during activation ($\Delta^{m}\chi_t$) are employed, we had slightly better correlations with the steric portion of the activation energy than we did with the rate constants. This tends to support the conclusion of deTar *et al.* (21) that polar effects are not negligible in these reactions.

E_s Values of Taft—The E_s values described by Taft (13) for alkyl groups were derived as steric contributions to the relative rates of hydrolysis reactions:

$$RCOOC_2H_5 + H_3O^+ \rightarrow RCOOH + C_2H_5OH + H^+ \qquad \text{(Eq. 24)}$$

Murray (9) correlated the E_s values with effective connectivity indices obtained for RX molecules, and assigned X an effective valency of 2. We examined these reactions using the model transition state shown in Fig. 4.

By using the $\Delta\chi$ values, the best one-parameter equation obtained was:

$$E_s = -2.48(\Delta^{6}\chi_{PC}) - 0.31 \qquad \text{(Eq. 25)}$$

where $r = 0.9181$, $RSD = 0.58$, and $n = 19$. The use of multiple parameters improved this to:

$$E_s = -2.25(\Delta^{6}\chi_{PC}) - 1.58(\Delta^{4}\chi_{PC}) + 0.08 \qquad \text{(Eq. 26)}$$

where $r = 0.9372$, $RSD = 0.53$, and $n = 19$. When the substrate indices were used for the ethyl esters, we obtained:

$$E_s = -1.57(^{3}\chi_P) + 0.69 \qquad \text{(Eq. 27)}$$

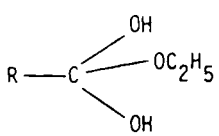

Figure 4—*Transition state for Eq. 24.*

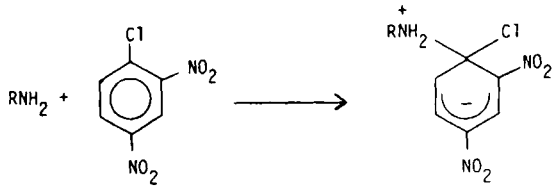

Scheme II

Table V—E_s Values [a]

R	E_s		
	Observed [b]	Eq. 26 [c]	Eq. 27 [c]
CH_3—	0.0	−0.14	0.15
C_2H_5—	−0.07	−0.47	−0.24
$CH_3CH_2CH_2$—	−0.36	−0.48	−0.50
$CH_3CH_2CH_2CH_2$—	−0.39	−0.60	−0.94
$CH_3CH_2CH_2CH_2CH_2$—	−0.40	−0.56	−1.33
$(CH_3)_2CHCH_2CH_2$—	−0.38	−0.85	−1.24
$(CH_3)_2CH$—	−0.47	−1.00	−0.50
$(CH_3)_3C$—	−1.54	−1.67	−0.70
$(CH_3CH_2)_2CH$—	−1.98	−1.28	−1.82
$(CH_3)_3CCH_2$—	−1.74	−1.21	−0.84
$(CH_3CH_2CH_2)_2CH$—	−2.11	−1.55	−2.27
$(CH_3)_3CCH_2C(CH_3)_2$—	−2.57	−2.84	−2.13
$((CH_3)_3C)_2CH$—	−3.18	−3.55	−2.84
$(CH_3)_3CC(CH_3)_2$—	−3.90	−3.83	−3.48
$(CH_3CH_2)_3C$—	−3.80	−2.67	−3.60
$((CH_3)_2CHCH_2)_2CH$—	−2.47	−2.03	−2.65
$((CH_3)_3CCH_2)((CH_3)_3C)(CH_3)C$—	−4.00	−4.62	−4.43

[a] E_s values described by Taft (13). [b] From Ref. 13. [c] See Table XI for values of $^{m}\chi_t$ and $\Delta^{m}\chi_t$.

where $r = 0.9317$, $RSD = 0.53$, and $n = 19$.

In Table V is shown a comparison between Eqs. 26 and 27 with the E_s values given by Taft (13). Equations 25 and 27 are better than the single-parameter correlations described by Murray (9), and Eq. 26 is better than his two-parameter relation.

Here, again, there is a significant correlation between the indices used in Eqs. 25 and 27, *viz.*:

$$\Delta^{6}\chi_{PC} = 0.567(^{3}\chi_P) - 0.303 \qquad \text{(Eq. 28)}$$

where $r = 0.9106$, $RSD = 0.225$, and $n = 19$.

Nucleophilic Substitution of 1-Chloro-2,4-Dinitrobenzene by Alkylamines—As a final example, we chose the nucleophilic substitution of 1-chloro-2,4-dinitrobenzene by an aliphatic amine by the activation process shown in Scheme II. The relative rate constant data were obtained from the experiments of Brady and Cropper (22) (Table VI).

Table VI—Relative Rate Constants for Eq. 28

R	ln (k_{rel}) [a]	Eq. 29 [b]	Eq. 30 [b]
Ethyl	2.219	2.163	2.106
Propyl	2.262	2.269	2.106
Isopropyl	0	0.076	0.796
Butyl	2.303	2.264	2.106
sec-Butyl	−0.094	0.137	1.180
tert-Butyl	−3.270	−3.376	−3.261
Isobutyl	1.917	1.800	0.502
Octyl	2.303	2.307	2.106

[a] From Ref. 22. [b] See Table XII for values of $^{m}\chi_t$ and $\Delta^{m}\chi_t$.

Table VII— $^{m}\chi_t$ Values for Substituted Pyridines [a]

Compound	$^{1}\chi$	$^{2}\chi$	$^{3}\chi_C$	$^{4}\chi_{PC}$
Pyridine	1.850	1.025	0.0	0.0
2-Methylpyridine	2.270	1.471	0.1291	0.1491
3-Methylpyridine	2.260	1.530	0.1667	0.1708
4-Methylpyridine	2.260	1.525	0.1667	0.1925
2,3-Dimethylpyridine	2.687	1.906	0.2561	0.5331
2,4-Dimethylpyridine	2.681	1.975	0.2958	0.3186
2,5-Dimethylpyridine	2.681	1.977	0.2958	0.3198
2,6-Dimethylpyridine	2.691	1.920	0.2582	0.2782
3,4-Dimethylpyridine	2.677	1.960	0.2887	0.6032
3,5-Dimethylpyridine	2.671	2.040	0.3333	0.3157

[a] Equations 3-6.

Table VIII— $\Delta\,^{m}\chi_t$ Values for Substituted Pyridines [a]

Compound	$\Delta^{4}\chi_{PC}$	$\Delta^{5}\chi_{PC}$
Pyridine	0.1571	0.1361
2-Picoline	0.3588	0.2427
3-Picoline	0.1401	0.2525
4-Picoline	0.1571	0.1164
2,3-Lutidine	0.3203	0.4324
2,4-Lutidine	0.3596	0.2114
2,5-Lutidine	0.3432	0.3440
2,6-Lutidine	0.5334	0.4262
3,4-Lutidine	0.1410	0.2209
3,5-Lutidine	0.1231	0.3708
2-Ethylpyridine	0.2856	0.3636
2-Isopropylpyridine	0.2404	0.5585
2-*tert*-Butylpyridine	0.2103	0.7939
2-Methyl-3-ethylpyridine	0.3248	0.3606
2-Methyl-3-isopropylpyridine	0.3268	0.3212
2-Methyl-3-*tert*-butylpyridine	0.3280	0.2908
2,6-Diethylpyridine	0.3958	0.6064
2,6-Diisopropylpyridine	0.3093	0.9714
2,4,6-Trimethylpyridine	0.5352	0.3831
2,3,5,6-Tetramethylpyridine	0.4586	0.7836
2,3,4,5,6-Pentamethylpyridine	0.4616	0.7228
3-Ethylpyridine	0.1420	0.2103
4-Ethylpyridine	0.1571	0.1186
3-Isopropylpyridine	0.1529	0.1842
4-Isopropylpyridine	0.1571	0.1196
3-*tert*-Butylpyridine	0.1434	0.1616
4-*tert*-Butylpyridine	0.1751	0.1202
2-Methyl-5-ethylpyridine	0.3451	0.3043
2-Methyl-5-isopropylpyridine	0.3459	0.2793
2-Methyl--5-*tert*-butylpyridine	0.3464	0.2574
2,3-Cyclopentenopyridine	0.2608	0.4084
2,3-Cyclohexenopyridine	0.2608	0.4084
2-Ethyl-3-methylpyridine	0.2551	0.5104
2-Ethyl-5-methylpyridine	0.2700	0.4673
2-Ethyl-6-methylpyridine	0.4646	0.5125
2-Isopropyl-3-methylpyridine	0.2137	0.6831
2-Isopropyl-5-methylpyridine	0.2208	0.6632

[a] Equations 7 and 8.

An excellent correlation of ln (k_{rel}) was obtained with activation indices:

$$\ln(k_{rel}) = -4.506(\Delta^{5}\chi_{PC}) - 1.087(\Delta^{5}\chi_{P}) + 10.800 \quad \text{(Eq. 29)}$$

where $r = 0.9984$, $RSD = 0.134$, and $n = 8$. The only relation found between ln (k_{rel}) and the substrate alkylamine indices was not nearly as good:

$$\ln(k_{rel}) = -3.929(^{3}\chi_C) + 2.106 \quad \text{(Eq. 30)}$$

where $r = 0.9177$, $RSD = 0.848$, and $n = 8$. The results of Eqs. 29 and 30 were compared with the experimental data (Table VI).

In addition, there is a reasonable linear relation between the indices of Eqs. 29 and 30:

$$^{3}\chi_C = 0.959(\Delta^{5}\chi_{PC}) - 1.559 \quad \text{(Eq. 31)}$$

where $r = 0.9248$, $RSD = 0.191$, and $n = 8$.

CONCLUSIONS

The correlations presented here indicate that the connectivity indices can serve as useful steric parameters in reactivity studies. It appears that they are capable of distinguishing between cases of steric control and electronic control. Either the connectivity indices in the substrate molecules or the changes that occur in formation of the transition state can apparently be used. This ambiguity is consistent with the fact that it is often possible to interpret relative reaction rates for a series of molecules either in terms of transition-state calculations or in terms of substrate-molecule equilibrium properties. For any particular reaction, the activation indices which appear in the correlations are always of higher order than the corresponding substrate indices, and the two sets are generally correlated with one another. We strongly feel that any empirically derived steric parameters must correlate with these indices if they

Table X— $^{m}\chi_t$ Values for Compounds Involved in Bromide Exchange Reactions [a]

R	$^{2}\chi$	$\Delta^{3}\chi_C$	$\Delta^{4}\chi_C$	$^{4}\chi_{PC}$	$\Delta^{5}\chi_C$
Methyl	0.0	0.0	0.0	0.0	0.0
Ethyl	1.403	2.273	0.0	0.0	0.0
n-Propyl	1.492	1.607	0.0	0.0	0.0
Isopropyl	2.868	4.776	1.969	0.0	0.0
Isobutyl	2.204	1.237	0.0	0.8100	1.312
tert-Butyl	4.476	7.577	6.065	0.0	0.0
Neopentyl	3.362	0.9419	−0.0649	2.105	3.410

[a] Equations 17-23.

Table XI— $^{m}\chi_t$ Values for Ethyl Esters Involved in Hydrolysis Reactions [a]

R	$^{3}\chi_P$	$\Delta^{4}\chi_{PC}$	$\Delta^{6}\chi_{PC}$
CH_3—	0.3476	0.0990	0.0289
C_2H_5—	0.5940	0.2194	0.0905
$CH_3CH_2CH_2$	0.7595	0.1781	0.1254
$CH_3CH_2CH_2CH_2$—	1.040	0.1781	0.1796
$CH_3CH_2CH_2CH_2CH_2$—	1.290	0.1781	0.1590
$(CH_3)_2CHCH_2CH_2$—	1.231	0.1781	0.2872
$(CH_3)_2CH$—	0.7580	0.4398	0.1716
$(CH_3)_3C$—	0.8878	0.7275	0.2683
$(CH_3CH_2)_2CH$—	1.606	0.3022	0.3936
$(CH_3)_3CCH_2$—	0.9800	0.1489	0.4704
$(CH_3CH_2CH_2)_2CH$—	1.894	0.3022	0.5126
$(CH_3)_3CCH_2C(CH_3)_2$—	1.800	0.6271	0.8586
$((CH_3)_3C)_2CH$—	2.254	0.2195	0.1461
$(CH_3)_3CC(CH_3)_2$—	2.661	0.5561	0.1348
$(CH_3CH_2)_3C$—	2.739	0.4576	0.8999
$((CH_3)_2CHCH_2)_2CH$—	2.132	0.3022	0.7244
$((CH_3)_3CCH_2)((CH_3)_3C)(CH_3)C$—	3.265	0.4735	0.1754

[a] Equations 25-27.

Table IX— $^{m}\chi_t$ Values for 2-Substituted Pyridines [a]

2-Substituent	$\Delta^{3}\chi_C$	$^{4}\chi_P$	$\Delta^{4}\chi_P$	$\Delta^{4}\chi_{PC}$	$^{5}\chi_C$	$^{5}\chi_{PC}$	$\Delta^{6}\chi_{PC}$
—CH_3	0.1066	0.4481	0.1208	0.3588	0	0.1291	0.2392
—C_2H_5	0.1099	0.6073	0.2591	0.2856	0	0.1967	0.3321
—Isopropyl	0.1114	0.7175	0.3463	0.2404	0.0745	0.4174	0.5240
—*tert*-Butyl	0.1122	0.8064	0.0600	0.2013	0.1937	0.9880	0.8750
—CH_2OH	0.1099	0.4917	0.1837	0.2900	0	0.1384	0.2567
—CH_2CH_2OH	0.1099	0.6606	0.2148	0.2879	0	0.1947	0.3420
—CH_2-phenyl	0.1099	1.308	0.1829	0.2896	0	0.4430	0.3709
—$CO_2C_2H_5$	0.1122	0.6685	0.2000	0.2412	0.0108	0.2283	0.3018
—Phenyl	0.1122	1.142	0.2289	0.2377	0.0215	0.4249	0.4163
—2-Pyridyl	0.1122	1.029	0.2171	0.2392	0.0167	0.3582	0.3802
—NH_2	0.1114	0.3760	0.1235	0.2647	0	0.0745	0.1764
—C≡N	0.1122	0.4289	0.1672	0.2449	0	0.0979	0.2081
—Br	0.0955	0.6162	0.1144	0.5780	0	0.2562	0.3853

[a] Equations 10-14.

Table XII—$\Delta^m\chi_t$ Values for Compounds Undergoing Nucleophilic Substitution [a]

R	$^3\chi_C$	$\Delta^5\chi_P$	$\Delta^5\chi_{PC}$
Ethyl	0.0	0.8533	1.711
Propyl	0.0	1.096	1.629
Isopropyl	0.3333	0.9303	2.156
Butyl	0.0	1.100	1.629
sec-Butyl	0.2357	1.128	2.094
tert-Butyl	0.1366	0.9923	2.907
Isobutyl	0.4082	1.257	1.695
Octyl	0.0	1.061	1.629

[a] Equations 29 and 30.

are at all reasonable. Charton (10) has recently concluded that no one set of steric parameters is suitable for all reactions. Since they take into account the TS structure, the $\Delta^m\chi_t$ values may have sufficient flexibility to be generally useful. This is illustrated by the fact that different indices are important for different reactions.

Within the last year Edward has published two studies in which the molecular basis for the relationship of a number of physical properties and connectivity indices is beginning to be unraveled (7). The inclusion of connectivity indices in recent pattern recognition investigations of pharmacological activities suggests that this type of descriptor variable encodes structural features which influence *in vivo* tests. Our present findings bring together connectivity indices as a descriptor for structural effects in both chemical reactivity and pharmacological activities.

APPENDIX

Tables VII–XII contain the values of $^m\chi_t$ and $\Delta^m\chi_t$ that were employed in all correlations. There is one table for each table in the text. Table VII gives the values employed in Table I, *etc.*

REFERENCES

(1) "Quantitative Structure-Activity Relationships of Analgesics, Narcotic Antagonists and Hallucinogens," G. Barnett, M. Trsic, and R. W. Willette, Eds., NIDA Research Monograph 22, U.S. Dept. of Health, Education, and Welfare, Rockville, Md., 1978.

(2) C. Hansch and A. Leo, "Substituent Constants for Correlation Analysis in Chemistry and Biology," Wiley-Interscience, New York, N.Y., 1979.

(3) A. J. Stuper, W. E. Brugger, and P. C. Jurs, "Computer Assisted Studies of Chemical Structure and Biological Function," Wiley-Interscience, New York, N.Y., 1979.

(4) L. B. Kier and L. H. Hall, "Molecular Connectivity in Chemistry and Drug Research," Academic, New York, N.Y., 1976.

(5) M. Randic', *J. Am. Chem. Soc.*, **97**, 6609 (1975).

(6) L. B. Kier and R. A. Glennon, in "Quantitative Structure-Activity Relationships of Analgesics, Narcotic Antagonists, and Hallucinogens," G. Barnett, M. Trsic, and R. E. Willette, Eds., NIDA Research Monograph 22, U.S. Dept. of Health, Education, and Welfare, Rockville, Md., 1978, p. 159.

(7) J. T. Edward, *Can. J. Chem.*, **60**, 480, 2573 (1982).

(8) A. Sabljic and M. Protic-Sabljic, *Mol. Pharmacol.*, **23**, 213 (1983).

(9) W. J. Murray, *J. Pharm. Sci.*, **66**, 1352 (1977).

(10) M. Charton, *J. Org. Chem.*, **43**, 3995 (1978).

(11) J. E. Dubois, J. A. McPhee, and A. Panaye, *Tetrahedron*, **36**, 919 (1980).

(12) C. Ruchardt and H. D. Beckhaus, *Angew. Chem. Int. Ed. Engl.*, **19**, 429 (1980).

(13) R. W. Taft, Jr., in "Steric Effects in Organic Chemistry," M. S. Newman, Ed., Wiley, New York, N.Y., 1956, p. 556.

(14) J. W. Viers, J. C. Schug, and J. I. Seeman, *J. Am. Chem. Soc.*, **104**, 850 (1982).

(15) J. Schug, J. I. Seeman, and J. W. Viers, *J. Org. Chem.*, **48**, 2399 (1983).

(16) J. I. Seeman, J. W. Viers, J. C. Schug, and M. D. Stovall, *J. Am. Chem. Soc.*, **106**, 143 (1984).

(17) J. D. Cox and G. Pilcher, "Thermochemistry of Organic and Organometallic Compounds," Academic, New York, N.Y., 1970.

(18) U. Berg, R. Gallo, G. Klatte, and J. Metzger, *J. Chem. Soc., Perkin Trans. 2*, **1980**, 1350.

(19) P. B. D. de la Mare, L. Fowden, E. D. Hughes, C. K. Ingold, and J. D. H. Mackie, *J. Chem. Soc.*, **1955**, 3250.

(20) M. H. Abraham, P. L. Grellier, and M. J. Hogarth, *J. Chem. Soc., Perkin Trans. 2*, **1975**, 1365.

(21) D. F. deTar, D. R. McMullen, and N. P. Luthra, *J. Am. Chem. Soc.*, **100**, 2484 (1978).

(22) O. L. Brady and W. H. Cropper, *J. Chem. Soc.*, **1950**, 507.

Relationship between Refractive Index and Dry-Substance Content for Lactulose Syrups

A. DE REIJKE ˣ, P. VAN BEMMEL, and H. W. GELUK

Received November 29, 1982, from the *Duphar B.V., Research Laboratories, 1380 AA Weesp, The Netherlands.* Accepted for publication October 24, 1983.

Abstract □ The relationship between the refractive index and the dry substance content of lactulose syrups of different compositions was investigated. It was found that, for a concentration range of 55–75% of dissolved carbohydrates, the sucrose tables can be used after correction by a factor of 0.97.

Keyphrases □ Lactulose—determination of dry substance, refractive index-dry-substance content relationship □ Refractive index-dry-substance content, lactulose syrups

Lactulose (4-*O*-β-D-galactopyranosyl-D-fructofuranose) is a synthetic disaccharide which is primarily used for the treatment of constipation (1), portal systemic encephalopathy, and hepatic coma (2). The drug, prepared by a base-catalyzed isomerization of lactose, known as the Lobry de Bruyn–Alberda van Ekenstein rearrangement, is commonly marketed as an aqueous syrup. This syrup also contains small amounts of lactose and other carbohydrates formed during the isomerization process (3).

Lactulose, lactose, and galactose can be analyzed by specific chromatographic (4, 5) or enzymatic methods (6); however, suitable methods are not available to determine each of the other sugars. The total weight of the other sugars can be determined from the difference between the amount of the analyzed compounds and the total weight of solid material dissolved in the syrup. Our problem, therefore, was to find a method to determine the amount of carbohydrates present in the lactulose syrup.

Several methods for dry-substance determination of sugars are known and have recently been critically discussed (7). Drying procedures at temperatures of >100°C are not reliable for lactulose syrup because of the possible decomposition of labile carbohydrates and the loss of water by dehydration reactions. Freeze-drying procedures are also unsatisfactory because water is not completely removed from the amorphous or syrupy residue and the remaining water must be determined by a different method. An indirect method for the determination of the dry substance content is by measuring the water content using the Karl Fischer method (8). This method, however, requires special equipment and is time consuming. The dry-substance content of sugar solutions is frequently determined by means of refractometry (9) or densimetry (10). Refractive index measurements, in particular, are easily and accurately accomplished and would be the method of choice provided that the relationship between dry-substance content and refractive index is known. For aqueous sucrose solutions, correlation tables (Brix values) are readily available (9, 11, 12) and are included in the refractive index measuring scale. Refractive index data have also been published for aqueous solutions of other common sugars such as glucose (12), fructose (11), lactose (13, 14), and maltose (9) and for different types of syrups (12, 15–17); however, no data were available for lactulose. Therefore, we have investigated the refractive index-dry-substance relationship for lactulose syrups with different compositions.

Table I—Results for the Solutions of Pure Lactulose in Water

Real Dry Substance, %	°Brix at 20°C	Factor[a]
54.37	55.95	0.972
55.72	57.10	0.976
60.99	62.63	0.974
61.72	63.88	0.966
67.96	70.85	0.959
67.99	70.03	0.971
74.53	76.85	0.970
75.10	77.28	0.972
Mean		0.970

[a] The amount of real dry substance/dry substance from refraction.

Table II—Results for the Solutions of an Artificial Mixture of Pure Lactulose, Lactose, and Galactose

Real Dry Substance, %	°Brix at 20°C	Factor[a]
54.74	56.40	0.971
61.95	63.78	0.971
67.47	69.38	0.972
74.55	76.60	0.973
Mean		0.972

[a] The amount of real dry substance/dry substance from refraction.

EXPERIMENTAL SECTION

Apparatus—Refractive indices were measured on a refractometer[1] thermostated at 20 ± 0.1°C[2]. The water content in the dry substance was determined automatically[3]. For freeze-drying procedures, a self-made laboratory freeze-drier was used. The condenser was cooled with solid carbon dioxide in acetone.

Chemicals—Lactulose, the analytical reference standard, had a purity >99.5% and a water content of 0.23% (recrystalized from methanol). The α-D-lactose monohydrate[4] had a purity of >99.5% and the α-D-galactose[5] had a purity of >99%.

Preparation of Sugar Solutions—Eight solutions of pure lactulose in water were made by weight in the range of 55–75% (Table I). Then, an artificial mixture containing lactulose (89.9%), lactose (4.5%), and galactose (5.6%) was prepared. Four solutions were made by weight in the range of 55–75% by dilution of this mixture with water (Table II).

Another set of sugar solutions was prepared with four samples of lactulose syrup which were freeze-dried. The amorphous residue was kept at 70°C for 2 h. From the residue of each batch, four solutions in water were made by weight in the range of 55–75%. Since it was not possible to obtain a water-free residue, a correction was made for the remaining water determined with the Karl Fischer titration (in the four batches these values were 0.93, 0.98, 0.21, and 0.20%, respectively) (Table III).

[1] Zeiss Opton Abbe refractometer.
[2] Colora Ultra Thermostat K5.
[3] Metrohm Karl Fischer Automat E547.
[4] 0138; Baker.
[5] 1564; Baker.

0022-3549/84/1000-1478$01.00/0
© 1984, American Pharmaceutical Association

Table III—Results for Lactulose Syrups with Known Dry-Substance Content after Freeze-Drying

Real Dry Substance, %	°Brix at 20°C	Factor[a]
Batch 1 54.62	56.40	0.968
Batch 2 54.19	55.80	0.971
Batch 3 54.92	56.53	0.975
Batch 4 54.86	56.18	0.977
Batch 1 61.56	63.53	0.969
Batch 2 61.45	63.58	0.966
Batch 3 62.08	63.60	0.976
Batch 4 61.89	63.38	0.977
Batch 1 67.22	69.53	0.967
Batch 2 67.13	69.25	0.969
Batch 3 67.93	69.73	0.974
Batch 4 68.03	69.63	0.977
Batch 1 74.13	76.60	0.968
Batch 2 74.42	76.83	0.969
Batch 3 74.56	76.10	0.980
Batch 4 74.86	76.38	0.977
Mean[b]		0.973

[a] The amount of real dry substance/dry substance from refraction. [b] Mean of four batches.

Table IV—Mean results for 26 Batches of Lactulose Syrup and 61 Batches of Formulated Product

	Dry Substance, %[a]	°Brix at 20°C	Factor[b]	*SD* of Factor
Lactulose syrup	70.719	72.877	0.970	0.0085
Formulated product	67.072	68.884	0.974	0.010

[a] Using Karl Fischer titration. [b] The amount of real dry substance/dry substance from refraction.

Table V—Correction Factors for Dry-Substance Determination using Sucrose Brix Values for Refractive Index Measurements at 20°C (9, 11, 12)

Product	Correction Factor 30% d.s.	50% d.s.	70% d.s.	Ref.
Lactose	0.969	——[a]	—[a]	13, 14
Maltose	0.979	0.981	—[a]	9
Glucose	1.010	1.015	1.021	12
Fructose	1.013	1.016	1.021	11
HFCS (42)[b]	1.010	1.014	1.018	15-17
CS (42)[c]	0.969	0.970	0.971	12, 15-17
CS (70)[d]	0.988	0.991	0.994	12, 15-17

[a] No data available due to low solubility. [b] High fructose corn syrup, 42% fructose. [c] Corn syrup, acid conversion, 42 D.E. [d] Corn syrup, dual conversion, 70 D.E.

Samples of 26 production batches of lactulose syrup and 61 batches of formulated product[6] were analyzed for dry substance using the Karl Fischer titration and the refractive index (Table IV).

RESULTS AND DISCUSSION

The relationship between the real dry-substance content of lactulose solutions and the dry substance obtained from the refraction and sucrose index (°Brix), is expressed as: real dry substance/dry substance from refraction. From the refractive index-dry-substance relationship, as given for various sugars in the literature, correction factors can be calculated for sucrose dry-substance values.

Table V gives the results for solutions of some common carbohydrates and syrups at three different concentrations. It appears that the factor for the aqueous sugar solutions varies between 0.969 for lactose and 1.021 for glucose and fructose. The mean factor we found in all our experiments was within this range.

It may be concluded from Tables I and II that the factor for pure lactulose, or for lactulose mixed with lactose and galactose, will be ~0.97 for solutions of 55-75% of dry-substance content. Almost the same values were found for lactulose syrups of different compositions. Thus, the presence of other carbohydrates in lactulose syrup does not significantly influence the refractive index. The dry-substance content of lactulose syrups can, therefore, be determined easily and accurately by refractometry using sucrose-dry-substance or Brix values after correction by a factor of 0.97.

[6] Duphalac; the lactulose content is 667 g/L according to the label claim.

REFERENCES

(1) P. Bass and S. Denmis, *J. Clin. Gastroenterol*, **3** (suppl. 1), 23 (1981).

(2) H. O. Conn and M. M. Lieberthal, "The Hepatic Coma Syndromes and Lactulose," Williams and Wilkins, Baltimore, Md. 1979.

(3) A. Olano and I. Martinez-Castro, *Milchwissenschaft*, **36**, 533 (1981).

(4) J. Haverkamp, J. P. Kamerling, and J. F. G. Vliegenthart, *J. Chromatogr.*, **59**, 281 (1971).

(5) F. W. Parrish, K. Hicks, and L. Doner, *J. Dairy Sci.*, **63**, 1809 (1980).

(6) H. Geier and H. Klostermeijer, *Z. Lebensm. Unters. Forsch.*, **171**, 443 (1980).

(7) G. Pollach, L. Wieninger, and H. Berninger, *Z. Zuckerind. Boehm.*, **105**, 451 (1980).

(8) J. Mitchell, Jr. and D. M. Smith, "Aquametry. Part I. A Treatise on Methods for the Determination of Water," 2nd ed., Wiley, New York, N.Y., 1977.

(9) R. C. Weast, "Handbook of Chemistry and Physics," 60th ed., The Chemical Rubber Co., Cleveland, Ohio, pp. E 388-389 (1979-1980).

(10) R. C. Weast, "Handbook of Chemistry and Physics," 60th ed., The Chemical Rubber Co., Cleveland, Ohio, p. D 282 (1979-1980).

(11) F. J. Bates, "Polarimetry, Saccharimetry, and the Sugars," Circ. Nat. Bur. Stand., C440, U.S. Department of Commerce, 1942, p. 670.

(12) H. M. Pancoast and W. R. Junk, "Handbook of Sugars," 2nd ed., AVI Publishing, Westport, Conn., 1980.

(13) E. J. McDonald and A. L. Turcotte, *J. Res. Nat. Bur. Stand.*, **41**, 63 (1948).

(14) F. W. Zerban and J. Martin, *Assoc. Off. Agricult. Chem.*, **32**, 709 (1949).

(15) A. M. Wartman, A. J. Bridges, and M. A. Eliason, *J. Chem. Eng. Data*, **25**, 277 (1980).

(16) A. M. Wartman, C. Hagberg, and M. A. Eliason, *J. Chem. Eng. Data*, **21**, 459 (1976).

(17) F. A. Kurtz and M. A. Eliason, *J. Chem. Eng. Data*, **24**, 44 (1979).

ACKNOWLEDGMENTS

We wish to thank Mr. A. van Rossum for his contribution to this work.

Bare Silica as a Reverse-Phase Stationary Phase: Liquid Chromatographic Separation of Antihistamines with Buffered Aqueous Organic Mobile Phases

HAROLD RICHARDSON ˣ **and BRIAN A. BIDLINGMEYER**

Received October 26, 1982, from *Waters Associates, Milford, MA 01757.* Accepted for publication October 5, 1983.

Abstract □ Unbonded silica gel is an effective support for reverse-phase liquid chromatographic separations of lipophilic amines. Simple buffered aqueous-organic mobile phases provide rapid isocratic separations of antihistamines. Phenylpropanolamine hydrochloride, chlorpheniramine maleate, and dextromethorphan hydrobromide are separated in 8 min on bare silica with a mobile phase of 75% methanol and 25% water which is 0.01 M in $(NH_4)_2HPO_4$. Quantitation is reproducible. A wide variety of additional compounds may be separated using the same mobile phase.

Keyphrases □ Bare silica—reverse-phase stationary phase, liquid chromatography □ Antihistamines—buffered aqueous organic liquid chromatographic mobile phases

The object of this work is to demonstrate that the use of silica in the reverse-phase mode is practical for the liquid chromatographic separation of lipophilic amines. The group of amines used as antihistamines, antitussives, and decongestants are frequently formulated together. When using C_{18}-bonded phase columns, it is necessary to use amine mobile-phase modifiers to ensure good retention and peak shape (1) in the ion-suppression mode. While C_{18}-bonded phases have been reported most often for the separation of these lipophilic amines, recent work (2) suggests that unbonded silica gel, with the maximum concentration of surface silanol groups, is a preferable stationary phase for these compounds.

Using unbonded silica as the stationary phase permits the analyst to separate a wide variety of amine compounds with a simple mobile phase of organic solvent and an aqueous phosphate buffer for pH control. The retention volumes are lower and the peaks are more symmetrical when silica, rather than a C_{18}-bonded support, is used as the stationary phase. However, because this use for unbonded silica is new, it is necessary to demonstrate long-term performance in routine operation.

Table I—Formulations

	Components	Concentration
Syrup		
A	Acetaminophen	625 mg/30 mL
	Phenylpropanolamine hydrochloride	25 mg/30 mL
	Chlorpheniramine maleate	2 mg/30 mL
	Dextromethorphan hydrobromide	20 mg/30 mL
B	Potassium guaiacolsulfonate	100 mg/5 mL
	Pseudoephedrine hydrochloride	30 mg/5 mL
	Chlorpheniramine maleate	2 mg/5 mL
	Dextromethorphan hydrobromide	10 mg/5 mL
E	Phenylpropanolamine hydrochloride	12.5 mg/5 mL
	Chlorpheniramine maleate	2 mg/5 mL
F	Guaifenesin	100 mg/5 mL
	Pseudoephedrine hydrochloride	30 mg/5 mL
	Dextromethorphan hydrobromide	10 mg/5 mL
Tablet		
C	Acetaminophen	325 mg
	Phenylpropanolamine hydrochloride	12.5 mg
	Dextromethorphan hydrobromide	10 mg
D	Pyrilamine maleate	25 mg
G	Theophylline	130 mg
	Ephedrine hydrochloride	24 mg
	Pyrilamine maleate	16.6 mg

This paper demonstrates that practical separations of commercial antihistamine formulations on unbonded silica in the reverse-phase mode result in reproducible analyses and good column life. In addition, the sample preparation is straightforward so that high throughput of samples is attained.

EXPERIMENTAL SECTION[1]

The salts[2], ammonium hydroxide[3], sodium hydroxide[3], hydrochloric acid[3], and phosphoric acid[3] used in this study were obtained commercially. Purified water[4], chromatographic-grade acetonitrile[5], and methanol[5] were used for mobile phase preparation. The mobile phases were filtered through 0.45-μm cellulose acetate filters[6] and deaerated under vacuum in an ultrasonic bath before use.

Seven different over-the-counter pharmaceutical formulations (tablets or syrups) were purchased in a local pharmacy and prepared as samples by dissolving 10 mL, or 1 tablet, in 100 mL of mobile phase and filtering through a 0.5-μm filter[7]. The composition of the various formulations is shown in Table I. A standard solution of formulation A was prepared from pharmaceutical grade materials obtained from a variety of sources. The concentrations of standards were designed to duplicate a 10:1 dilution of label concentration.

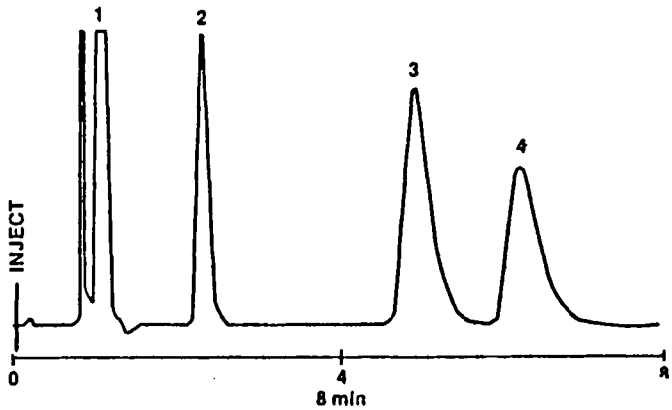

Figure 1—*Separation of a 1:10 solution of syrup A. Operating conditions were: solvent: 75% methanol, 25% H_2O, 0.01 M $(NH_4)_2HPO_4$, pH = 7.8; flow rate: 4 mL/min; 50-μL injection; detection at 254 nm; 0.05 AUFS. Key: (1) acetaminophen; (2) phenylpropanolamine; (3) chlorpheniramine; (4) dextromethorphan.*

[1] The chromatographic system was a Waters Associates, Inc., (Milford, Mass.) Model 244 ALC which included a Model 6000A Solvent Delivery System, Model U6K Injector, Model 480 Variable Wavelength Spectrophotometric Detector, and a Model R401 Refractometer. The column was Radial-PAK μPorasil Silica (8 mm × 10 cm) cartridges which were maintained under radial compression in the Z-Module Radial Compression Separation System (Waters). If excessive back pressure developed, the cartridge was reversed and the tubing to the detector was detached and sent to waste; the cartridge was flushed with mobile phase. When the pressure returned to the original value, the cartridge was returned to the original orientation and the module was reattached to the detector. The analog output of the absorbance (UV) was recorded with a Model 730 Data Module (printer, plotter, and integrator) (Waters) and the quantitation was done at 214 nm. Retention times were converted to retention volumes using the flow rate. Samples were injected automatically using the Model 710B Waters Intelligent Sample Processor (WISP). Automatic control of flow rate, injection, and data documentation was accomplished using the Model 720 System Controller.

[2] Fisher Scientific, Fair Lawn, N.J.

[3] Baker Chemical Co., Phillipsburg, N.J.

[4] Milli-Q System; Millipore Corp., Bedford, Mass.

[5] Waters Associates.

[6] HAWP 04700; Millipore Corp.

[7] Millex Filter; Millipore Corp.

0022-3549/84/1000-1480$01.00/0
© 1984, American Pharmaceutical Association

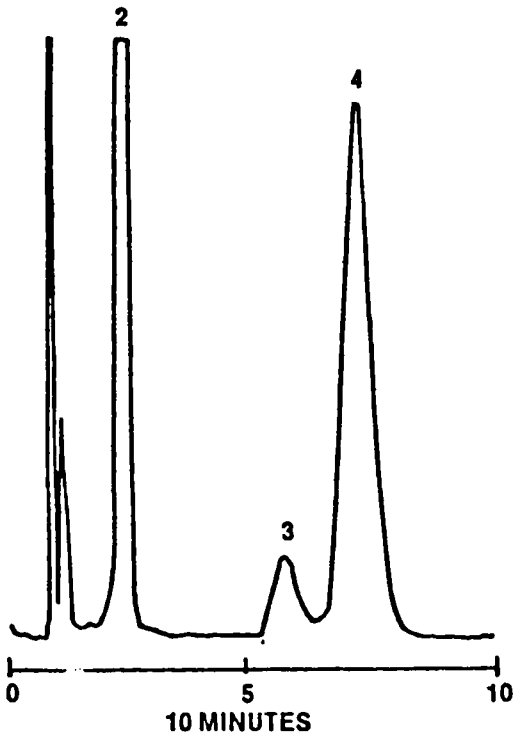

Figure 2—*Chromatogram of the standard solution. Conditions as in Fig. 1, except that detection was at 214 nm and 0.05 AUFS.*

RESULTS AND DISCUSSION

Development of the Separation—Formulation A, which had one nonionic component (acetaminophen) and three amines, was chosen as a demonstration case. The first separations were done with the acetonitrile–aqueous salt eluant described in a previous report (2). This separation resulted in inadequate resolution of chlorpheniramine (10.33 min) and dextromethorphan (11.10 min). Since methanol frequently exhibits different selectivity than acetonitrile (increased α) and weaker solvent strength (increased k'), it was evaluated at various aqueous salt concentrations. Using the organic content of 75% methanol and a salt concentration of 10 mM resulted in the optimized chromatogram shown in Fig. 1. The retention volumes were adequate and the resolution was more than baseline for chlorpheniramine and dextromethorphan. The relationship between the fraction of organic modifier (methanol) and the log retention volume was linear, as shown in a previous report (2).

Determination of Optimum Wavelength of Detection—For the separation shown in Fig. 1, detection was at 254 nm. The absorbance of acetaminophen (molar absorptivity = 13,200 at 248 nm) saturated the detector amplifier and gave a nonlinear response when a sufficient mass of the amines was injected for convenient detection; the amine components are present in much lower concentrations than acetaminophen. Inspection of the UV spectra of the various components indicated that acetaminophen has a minimum absorbance at 217 nm and that a significant improvement of signal strength occurs for phenylpropanolamine at 214 nm. Evaluation at 214 nm indicated that sensitive, reliable quantitation of the lipophilic amines was possible (Fig. 2). At 254 nm, sensitivity for phenylpropanolamine and chlorpheniramine was excellent, while sensitivity for dextromethorphan was not as good. At 214 nm, the relative sensitivity of chlorpheniramine is reduced compared with dextromethorphan and phenylpropanolamine. The quantification is better for all components at 214 nm. Even so, the absorbance of acetaminophen was still too high (from 26 to 350 times as much as the amines) for quantitation. When it was desirable to quantitate acetaminophen, it was necessary to decrease the sample size such that detection of dextromethorphan (254 nm) or chlorpheniramine (214 nm) was very difficult. A different method with greater retention is preferable for acetaminophen.

Table II—Reproducibility of Quantitation with Standard Solution [a]

Compound	Conc., mg/mL	*RSD*, %
Phenylpropanolamine hydrochloride	0.0847	±0.65
Chlorpheniramine maleate	0.00672	±4.53
Dextromethorphan hydrobromide	0.0669	±1.45

[a] n = 30; run completed overnight.

Table III—Linearity of Response with Sample Load

Compound	Slope	Intercept	Coefficient of Correlation
Phenylpropanolamine hydrochloride	0.01952	0.00223	0.9980
Chlorpheniramine maleate	0.02217	0.000038	0.9980
Dextromethorphan hydrobromide	0.01913	0.00239	0.9980

Table IV—Quantitative Analysis of Syrup A

Compound	Conc., mg/mL Found	Label Claim	% of Label Claim
Phenylpropanolamine hydrochloride	0.08008	0.08333	96.1
Chlorpheneramine maleate	0.00629	0.00667	94.3
Dextromethorphan hydrobromide	0.0632	0.06667	94.8

Determination of Reproducibility and Linearity—A standard solution was prepared from pharmaceutical grade materials which duplicated a 10:1 dilution of the label concentrations in Syrup A of phenylpropanolamine, chlorpheniramine, and dextromethorphan. Table II shows that the quantitation of the three bases in the standard solution is excellent: two components had <2% *SD* for a series of 30 injections, and the component present in lowest concentration had a <5% *SD*. The linearity of the system with sample load was evaluated. When plots of sample load in μg *versus* detector response in mg/mL were evaluated, the lines reported in Table III were obtained. The system was linear from 0.002 mg/mL to 0.022 mg/mL. The assay results of a 10:1 dilution of syrup A is shown in Table IV. The concentrations found were ~95% of label for all three components. This method was developed on a single column and several hundred injections were completed with comparable

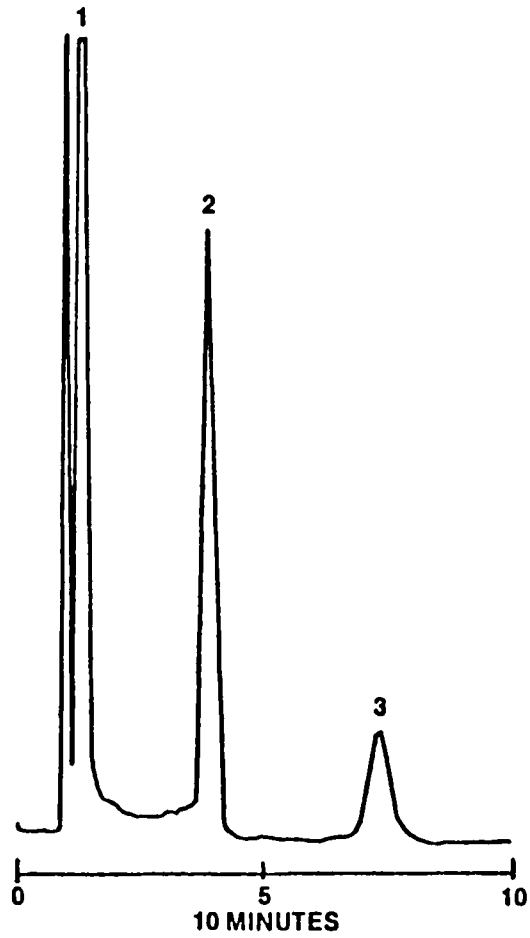

Figure 3—*Chromatogram of over-the-counter cough syrup F. Conditions as in Fig. 2. Key: (1) guaifenesin; (2) pseudoephedrine; (3) dextromethorphan.*

resolution: More than 800 injections were completed on a second column with no change in the separation.

Analysis of Additional Over-the-Counter Pharmaceutical Formulations—The six additional preparations, shown in Table I, were examined to determine whether the silica adsorbent was appropriate for other basic drugs. Chromatograms were obtained using the same mobile phase and detector wavelength as for quantitation of syrup A, and no attempt was made to optimize the separations. For example, Fig. 3 illustrates that other basic drugs are also eluted in this mobile phase system.

CONCLUSIONS

The separation of lipophilic bases on unbonded silica stationary phases in the reverse-phase mode is rapid and convenient. No amine modifiers or gradients are necessary for the separation; only simple buffers are required for pH control. Separations of several samples indicated that a variety of compounds may be separated with this system. Assay of a single sample indicated that linearity, reproducibility, and length of column life are excellent.

REFERENCES

(1) B. A. Bidlingmeyer, *J. Chromatogr. Sci.*, **18**, 525 (1980).

(2) B. A. Bidlingmeyer, J. K. Del Rios, and J. Korpi, *Anal. Chem.*, **54**, 442 (1982).

Hypolipidemic Activity of Phthalimide Derivatives V: Reduced and Hydrolytic Products of Simple Cyclic Imides

JAMES M. CHAPMAN, JR., STEVEN D. WYRICK, P. JOSÉE VOORSTAD, JAMES H. MAGUIRE, GEORGE H. COCOLAS, and IRIS H. HALL ˣ

Received February 24, 1983 from the *School of Pharmacy, University of North Carolina at Chapel Hill, Chapel Hill, North Carolina* 27514. Accepted for publication September 8, 1983.

Abstract □ A series of cyclic imides and related compounds have previously been shown to possess hypolipidemic activity at the low dose level of 20 mg/kg/d. Hydrolytic and reduced products of the cyclic imides were synthesized and examined to discern if possible metabolic products were the active chemical species of these hypolipidemic agents. Phthalimide proved to be the most active cyclic imide tested. Unfortunately, the new products did not, in general, improve hypolipidemic activity in rodents. The exceptions were piperidine which demonstrated improved hypotriglyceridemic activity, and 3,4,5,6-dibenzohomopiperidin-2-one, which demonstrated improved hypocholesterolemic activity compared to phthalimide.

Keyphrases □ Cyclic imides—phthalimide derivatives, reduced and hydrolytic products, hypolipidemic activity □ Phthalimide derivatives—cyclic imides, hypolipidemic activity, reduced and hydrolytic products □ Hypolipidemic activity—phthalimide derivatives, cyclic imides, reduced and hydrolytic products

A series of cyclic imides including phthalimide (I), succinimide, 1,8-naphthalimide, and saccharin have been shown to be potent hypolipidemic agents in rodents (1). After conducting dose response studies on these compounds, the optimum dose appears to be 20 mg/kg/d ip when tested in mice. Thus, we have selected that dose for this structure-activity relationship study. The mode of action of these derivatives is different from standard therapeutic agents on the market in that they do not inhibit the regulating enzyme of cholesterol synthesis, HMG CoA reductase; rather, they regulate mitochondrial citrate exchange and the availability of acetyl CoA, the key intermediate required in the synthesis of fatty acids and cholesterol (1). These agents also decreased cholesterol absorption in the intestine and accelerated cholesterol excretion by the biliary route. The agents had no effect on appetite, organ weights, or body weight, and there was no evidence of organ toxicity or deleterious systemic effects (1). Since these are potentially hypolipidemic agents, we expanded the types of imide rings and examined a series of their reduced and hydrolytic products, which may be potential metabolic products of the parent imide yet retain pharmacological activity.

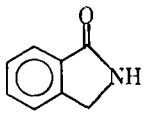

Phthalimidine (II)

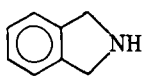

Isoindolin (III)

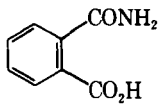

Phthalamic Acid (IV)

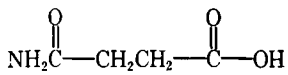

Succinamic Acid (IX)

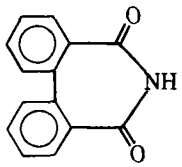

Diphenimide (XVI)

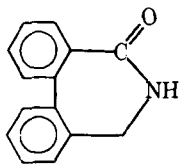

3,4,5,6-Dibenzohomo piperidin-2-one (XVII)

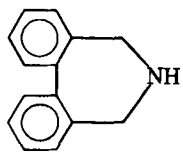

3,4,5,6-Dibenzohomo piperidine (XVIII)

$HO_2C(CH_2)_3CONH_2$

Glutaramic Acid (XIV)

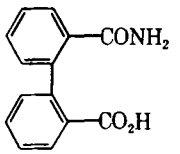

Diphenamic Acid (XIX)

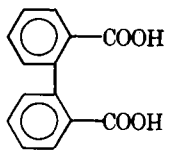

Diphenic Acid (XX)

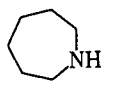

Homopiperidine (XXIII)

$HO_2C(CH_2)_3CONH_2$

Adipamic Acid (XXIV)

0022-3549/84/1000-1482$01.00/0

© 1984, American Pharmaceutical Association

resolution: More than 800 injections were completed on a second column with no change in the separation.

Analysis of Additional Over-the-Counter Pharmaceutical Formulations—The six additional preparations, shown in Table I, were examined to determine whether the silica adsorbent was appropriate for other basic drugs. Chromatograms were obtained using the same mobile phase and detector wavelength as for quantitation of syrup A, and no attempt was made to optimize the separations. For example, Fig. 3 illustrates that other basic drugs are also eluted in this mobile phase system.

CONCLUSIONS

The separation of lipophilic bases on unbonded silica stationary phases in the reverse-phase mode is rapid and convenient. No amine modifiers or gradients are necessary for the separation; only simple buffers are required for pH control. Separations of several samples indicated that a variety of compounds may be separated with this system. Assay of a single sample indicated that linearity, reproducibility, and length of column life are excellent.

REFERENCES

(1) B. A. Bidlingmeyer, *J. Chromatogr. Sci.*, **18**, 525 (1980).

(2) B. A. Bidlingmeyer, J. K. Del Rios, and J. Korpi, *Anal. Chem.*, **54**, 442 (1982).

Hypolipidemic Activity of Phthalimide Derivatives V: Reduced and Hydrolytic Products of Simple Cyclic Imides

JAMES M. CHAPMAN, JR., STEVEN D. WYRICK, P. JOSÉE VOORSTAD, JAMES H. MAGUIRE, GEORGE H. COCOLAS, and IRIS H. HALL ˣ

Received February 24, 1983 from the *School of Pharmacy, University of North Carolina at Chapel Hill, Chapel Hill, North Carolina* 27514. Accepted for publication September 8, 1983.

Abstract □ A series of cyclic imides and related compounds have previously been shown to possess hypolipidemic activity at the low dose level of 20 mg/kg/d. Hydrolytic and reduced products of the cyclic imides were synthesized and examined to discern if possible metabolic products were the active chemical species of these hypolipidemic agents. Phthalimide proved to be the most active cyclic imide tested. Unfortunately, the new products did not, in general, improve hypolipidemic activity in rodents. The exceptions were piperidine which demonstrated improved hypotriglyceridemic activity, and 3,4,5,6-dibenzohomopiperidin-2-one, which demonstrated improved hypocholesterolemic activity compared to phthalimide.

Keyphrases □ Cyclic imides—phthalimide derivatives, reduced and hydrolytic products, hypolipidemic activity □ Phthalimide derivatives—cyclic imides, hypolipidemic activity, reduced and hydrolytic products □ Hypolipidemic activity—phthalimide derivatives, cyclic imides, reduced and hydrolytic products

A series of cyclic imides including phthalimide (I), succinimide, 1,8-naphthalimide, and saccharin have been shown to be potent hypolipidemic agents in rodents (1). After conducting dose response studies on these compounds, the optimum dose appears to be 20 mg/kg/d ip when tested in mice. Thus, we have selected that dose for this structure-activity relationship study. The mode of action of these derivatives is different from standard therapeutic agents on the market in that they do not inhibit the regulating enzyme of cholesterol synthesis, HMG CoA reductase; rather, they regulate mitochondrial citrate exchange and the availability of acetyl CoA, the key intermediate required in the synthesis of fatty acids and cholesterol (1). These agents also decreased cholesterol absorption in the intestine and accelerated cholesterol excretion by the biliary route. The agents had no effect on appetite, organ weights, or body weight, and there was no evidence of organ toxicity or deleterious systemic effects (1). Since these are potentially hypolipidemic agents, we expanded the types of imide rings and examined a series of their reduced and hydrolytic products, which may be potential metabolic products of the parent imide yet retain pharmacological activity.

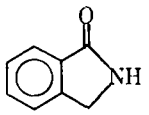

Phthalimidine (II)

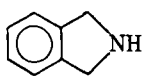

Isoindolin (III)

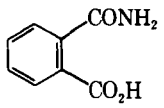

Phthalamic Acid (IV)

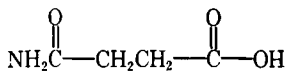

Succinamic Acid (IX)

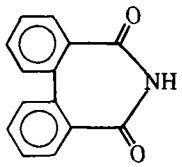

Diphenimide (XVI)

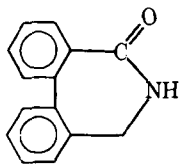

3,4,5,6-Dibenzohomo piperidin-2-one (XVII)

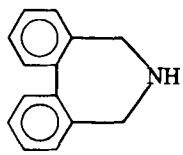

3,4,5,6-Dibenzohomo piperidine (XVIII)

$HO_2C(CH_2)_3CONH_2$

Glutaramic Acid (XIV)

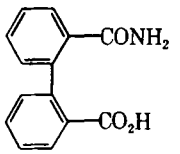

Diphenamic Acid (XIX)

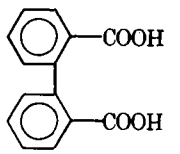

Diphenic Acid (XX)

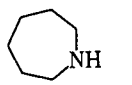

Homopiperidine (XXIII)

$HO_2C(CH_2)_3CONH_2$

Adipamic Acid (XXIV)

0022-3549/84/1000-1482$01.00/0

© 1984, American Pharmaceutical Association

Table I—Hypolipidemic Activity of Reduced and Hydrolytic Products of Cyclic Imides in CF_1 Male Mice at 20 mg/kg/d ip [a]

Compound	Serum Cholesterol, Day 9	Serum Cholesterol, Day 16	Serum Triglyceride, Day 14
I Phthalimide	63 ±8[b]	57 ± 7[b]	44 ± 8[b]
II Phthalimidine	89 ± 6	87 ± 14	78 ± 7[b]
III Isoindoline	86 ± 8	74 ± 5[b]	69 ± 6[b]
IV Phthalamic acid	85 ± 10	52 ± 9[b]	70 ± 4[b]
V Phthalic acid	91 ± 7	78 ± 7[b]	86 ± 4[c]
VI Succinimide	78 ± 9[b]	73 ± 8[b]	68 ± 7[b]
VII 2-Pyrrolidinone	86 ± 7	82 ± 5[b]	80 ± 8[c]
VIII Pyrrolidine	82 ± 7[b]	69 ± 5[b]	93 ± 6
IX Succinamic acid	93 ± 3	87 ± 8	93 ± 7
X Succinic acid	85 ± 6	79 ± 9[c]	94 ± 12
XI Glutarimide	80 ± 4[b]	78 ± 5[b]	77 ± 6[b]
XII Valerolactam	102 ± 4	74 ± 5[b]	94 ± 7
XIII Piperidine	81 ± 6[b]	73 ± 7[b]	34 ± 4[b]
XIV Glutaramic acid	90 ± 7	81 ± 6[b]	58 ± 6[b]
XV Glutaric acid	92 ± 4	74 ± 8[b]	80 ± 4[b]
XVI Diphenimide	81 ± 7[b]	82 ± 4[b]	81 ± 7
XVII 3,4,5,6-Dibenzohomopiperidin-2-one	84 ± 6[b]	49 ± 4[b]	73 ± 5[b]
XVIII 3,4,5,6-Dibenzohomopiperidine	70 ± 6[b]	51 ± 3[b]	52 ± 4[b]
XIX Diphenamic acid	80 ± 7[b]	78 ± 6[b]	56 ± 5[b]
XX Diphenic acid	81 ± 7	82 ± 10	58 ± 2[b]
XXI Adipimide	100 ± 7	76 ± 7[b]	89 ± 5
XXII ϵ-Caprolactam	104 ± 8	75 ± 5[b]	84 ± 7
XXIII Homopiperidine	72 ± 6[b]	71 ± 6[b]	80 ± 8
XXIV Adipamic acid	89 ± 7	79 ± 4[b]	85 ± 6
XXV Adipic acid	73 ± 6[b]	71 ± 7[b]	68 ± 6[b]
1% Carboxymethylcellulose	100 ± 5[b]	100 ± 6[e]	100 ± 6[f]

[a] Expressed as percentages of control (mean ± *SD*). [b] $p < 0.001$. [c] $p < 0.010$. [d] 125 mg%. [e] 122 mg%. [f] 137 mg/dL.

EXPERIMENTAL SECTION

All chemicals used as synthetic intermediates were purchased and used as obtained from the manufacturers[1]. Melting points were obtained on a capillary melting point apparatus[2] and are uncorrected. Column chromatography was performed on silica gel 60 (70–230 mesh)[2]. TLC was performed using precoated silica gel plates with fluorescent indicators[3]. ^{1}H-NMR spectra were obtained on a 60-mHz Fourier transform spectrometer[4]. Elemental analyses for prepared compounds are correct within ±0.4% of theoretical values.

Phthalimidine (II)—Preparation of this compound has been reported previously (1). The yield is 47%; mp 150–152°C.

Isoindoline (III)—The procedure of Bornstein and Shields (2) was used to prepare this compound in 43% yield, bp 98°C/10 mm Hg [lit. (bp) 120°C/30 mmHg]; ^{1}H-NMR ($CDCl_3$): δ 7.2 [s, 4, ArH_4] and 4.19 ppm [s, 4, $(CH_2)_2$].

Phthalamic Acid (IV)—Utilizing the process of Chapman and Stephen (3) 8.0 g (0.0054 mol) of phthalic anhydride was added to 40 mL of concentrated ammonium hydroxide, and the reaction mixture was stirred for 1 h at room temperature. The water was removed under reduced pressure, and the colorless solid residue was dissolved in 80 mL of water. Concentrated hydrochloric acid was added and the mixture was cooled on ice to afford a precipitate, which was removed by filtration to give 1.2 g (13%) of a colorless solid, mp 149–152°C; IR (KBr): 3180 (N—H), 1675, and 1645 (C=O) cm^{-1}.

Anal.—Calc. for $C_8H_7NO_3$ for C, 72.17; H, 5.30. Found: C, 72.38, H, 5.28.

Glutaramic Acid (XIV)—The synthesis of this compound has been reported previously (4).

Diphenimide (XVI)—Utilizing the procedure of Underwood and Kochmann (5), diphenamic acid (25.0 g, 0.10 mol) was added to a solution containing 30 mL of glacial acetic acid and 37 mL of acetic anhydride; the mixture was then stirred under reflux for 7.5 h. On cooling, the crude product which precipitated was removed by filtration and recrystallized from ethanol to afford 10.0 g (43%) of a colorless solid, mp 217–219°C.

Anal.—Calc. for $C_{14}H_9NO_2$: C, 75.33; H, 4.06; N, 6.27. Found: 75.53; H, 4.18; N, 6.28.

3,4,5,6-Dibenzohomopiperidin-2-one (XVIII)—The procedure of Chapman, *et al.* (6) was used to reduce XVI to the lactam. Powdered zinc (5.5 g, 0.085 mol) was stirred for 5 min in a solution of 450 mg of mercuric chloride in 1.5 mL of concentrated hydrochloric acid and 13 mL of water. The supernatant was decanted, and the zinc amalgam was washed with 20 mL of water. Diphenimide (XVI) (1.9 g, 0.0085 mol) was added, followed by 10 mL of water and 15 mL of concentrated hydrochloric acid. The mixture was stirred under reflux for 6 h, and was then filtered hot. The cooled filtrate was extracted with dichloromethane. The organic phase was dried (sodium sulfate) and the solvent evaporated under reduced pressure to afford 2.0 g of crude solid, which was purified by column chromatography[5] to afford 250 mg (13%) of a yellow solid, mp 167–169°C: ^{1}H-NMR ($CDCl_3$): δ 7.04–8.18 [m, 8, $(ArH_4)_2$] and 4.12 ppm (m, 2, CH_2).

Anal.—Calc. for: $C_{14}H_{11}NO$: C, 79.68; H, 4.89; N, 6.22. Found: C, 79.35; H, 5.26; N, 6.49.

3,4,5,6-Dibenzohomopiperidine (XVIII)—The procedure of Uffer and Schletterl (7) for reduction of imides to amines was used. To a 766-mg (0.02-mol) suspension of lithium aluminum hydride in 25 mL of ether was added, in a dropwise manner, a solution of 0.5 g (0.0067 mol) of XVI in 30 mL of dry tetrahydrofuran. The mixture was stirred under reflux for 16 h and the excess hydride was decomposed by dropwise addition of water. The resulting suspension was filtered and the filtrate was extracted with 1.0 M HCl. The aqueous extracts were combined and extracted with ether, made alkaline with sodium hydroxide, and extracted again with ether. The organic extracts were dried (sodium sulfate) and evaporated under reduced pressure to afford 400 mg of a viscous oil which was purified by column chromatography[6] to afford 375 mg (29%) of XVIII as a viscous oil. ^{1}H-NMR ($CDCl_3$): δ 7.42 [m, 8, $(ArH_4)_2$] and 3.64 ppm [s, 4, $(CH_2)_2$].

Anal.—Calc. for $C_{14}H_{13}N$: C, 86.16; H, 6.66; N, 7.17. Found: C, 86.03; H, 6.73; N, 6.97.

Diphenamic Acid (XIX)—Utilizing the procedure of Underwood, *et al.* (5), a 93% yield of product was obtained, mp 189–191°C [lit. (5) mp 187.0–187.5°C].

Adipamic Acid (XXIV)—The synthesis of this compound has been reported previously (4).

RESULTS AND DISCUSSION

Examination of the individual imides, I, VI, XI, XVI, and XXI, for hypolipidemic activity showed that the phthalimide moiety was more active than succinimide, glutarimide, diphenimide, and adipimide (Table I). However, all these imides were more active at 20 mg/kg/d than clofibrate, which is inactive at this dose. Clofibrate requires doses of 150–200 mg/kg to observe a 15% reduction of serum cholesterol levels and a 25% reduction of triglyceride levels. Succinimide, for example, reduced serum triglyceride levels 32% and glutarimide reduced the levels 23%.

Examination of derivatives where the carbonyl groups were reduced demonstrated mixed results. In the phthalimide series, reduced compounds were

[1] Compounds I, V, VI, and X were obtained from Eastman Organic Chemicals; VII, VIII, IX, XI, XII, XV, XX, XXI, XXII, XXIII, and XXV from Aldrich Chemical Company; and XIII from Fisher Scientific Company.

[2] Thomas Hoover Company.

[3] E. M. Reagents.

[4] JEOL, deuterochloroform plus tetramethylsilane.

[5] Dichloromethane:methanol (9:1).

[6] Dichloromethane:ethyl acetate (9:1).

Table II—Hypolipidemic Activity of 3,4,5,6-Dibenzohomopiperidine in Male CF_1 Mice [a]

Dose, mg/kg/d	Serum Cholesterol Day 9	Serum Cholesterol Day 16	Serum Triglyceride Day 14
Control (1% Carboxymethylcellulose)	100 ± 5[c]	100 ± 6[d]	100 ± 6[e]
Compound XVIII			
10	61 ± 5[b]	50 ± 5[b]	48 ± 5[b]
20	68 ± 4[b]	48 ± 4[b]	49 ± 5[b]
40	67 ± 6[b]	54 ± 4[b]	44 ± 6[b]
60	69 ± 5[b]	51 ± 4[b]	55 ± 6[b]

[a] Expressed as percentage of control (mean ± *SD*); $n = 6$. [b] $p < 0.001$. [c] 125 mg%. [d] 122 mg%. [e] 137 mg/dL.

less active than I in both the cholesterol and triglyceride screens; interestingly, the completely reduced compound isoindoline (III) was more active than the partially reduced phthalimidine (II) in both screens. In the succinimide series, the reduced compounds VII and VIII demonstrated less hypotriglyceridemic activity; the partially reduced compound 2-pyrolidinone (VII) demonstrated less hypocholesterolemic activity, but the totally reduced compound, pyrrolidine (VIII) was more active than succinimide in the cholesterol screen, causing 31% reduction. In the glutarimide series, the partially reduced compound, valerolactam (XII), demonstrated approximately the same activity in the cholesterol screen as glutarimide, but it demonstrated less hypotriglyceridemic activity than glutarimide. The fully reduced compound, piperidine (XIII) was more effective in both screens, with a marked reduction, 66%, of serum triglyceride levels. The reduction of diphenimide led to improved hypocholesterolemic activity for both derivatives, lowering serum cholesterol levels 51–49% and the fully reduced derivative serum triglyceride levels 48%. In the adipimide series, the reduction of the carbonyl groups led to little change in hypolipidemic effects in either screen.

Examination of the hydrolytic products of the phthalimide series showed that the half amide, phthalamic acid (IV), afforded approximately the same hypocholesterolemic activity as phthalimide; however, IV produced less effect on lowering triglyceride levels than I. The phthalic acid (V) demonstrated less activity in both screens compared to I. The hydrolytic products of the succinimide series (IX and X), the glutarimide series (XIV and XV), and the adipimide series (X, XXIV, and XXV) demonstrated no improvement in hypolipidemic activity over the parent derivatives. In the diphenimide series, the hydrolytic products XIX and XX demonstrated approximately the same hypocholesterolemic activity as XVI.

In conclusion, there did not appear to be a trend among all of the reduced products of imide analogues with respect to improvement or loss of activity in the hypolipidemic screens in mice. In general, the new compounds examined in this study did not extensively improve the hypocholesterolemic and hypotriglyceridemic activity of the lead compound, phthalimide (I). Piperidine produced improved hypotriglyceridemic activity compared to I, and XVII demonstrated improved hypocholesterolemic activity compared to I. The compound which demonstrated the best activity in both screens, other than I, was XVIII, which was slightly more potent than I in the cholesterolemic screen (6%) and slightly less active in the triglyceridemic screen (8%) in mice (Table II). These differences are probably not significant. Thus, I and XVIII are very similar in hypolipidemic activity. A dose response study with XVIII from 10–60 mg/kg showed that a 20 mg/kg/d dose was optimum for reducing serum cholesterol levels, and a 40 mg/kg/d dose lowered serum triglyceride levels to the level observed for I at 20 mg/kg. Further investigation of these derivatives is warranted since they are more active than commercially available agents, *e.g.*, clofibrate.

REFERENCES

(1) I. H. Hall, P. J. Voorstad, J. M. Chapman, Jr. and G. H. Cocolas, *J. Pharm. Sci.* **72**, 845 (1983).

(2) J. Bornstein and J. E. Shields, *Org. Synth.*, **Coll. Vol. V**, 1064 (1973).

(3) E. Chapman and H. Stephen, *J. Chem. Soc.*, **127**, 1791 (1925).

(4) J. H. Maguire and K. H. Dudley, *Anal. Chem.*, **49**, 292 (1977).

(5) H. W. Underwood and E. L. Kochmann, *J. Am. Chem. Soc.*, **46**, 2072 (1924).

(6) J. M. Chapman, Jr., G. H. Cocolas and I. H. Hall, *J. Med. Chem.* **28**, 243 (1983).

(7) A. Uffer and E. Schlettler, *Helv. Chim. Acta*, **31**, 1397 (1948).

ACKNOWLEDGMENTS

This research was financially supported by NIH Grant 1-R01-HL25680. We also thank Greg Webb and Walter Spivey for technical assistance.

Liquid Crystals as a Potential Ointment Vehicle

SVEN WAHLGREN *, ANNA L. LINDSTROM ‡, and STIG E. FRIBERG §x

Received May 2, 1983, from **The National Corporation of Swedish Pharmacies, Stockholm, Sweden*, ‡*Aco Company, Solna, Sweden*, and the §*Chemistry Department, University of Missouri-Rolla, Rolla, MO 65401.* Accepted for publication October 28, 1983.

Abstract □ A lecithin–water lyotropic liquid crystal was used as an ointment vehicle for a hydrocortisone formulation. The hydrocortisone was soluble in the liquid crystalline phase up to 5% by weight. The diffusion coefficient determined for the hydrocortisone in the liquid crystalline phase was 5.5×10^{-9} $cm \cdot s^{-1}$, which is four magnitudes higher than the corresponding value for skin.

Keyphrases □ Ointments—vehicles, liquid crystals, lecithin–water □ Lecithin—liquid crystals as potential ointment vehicle □ Hydrocortisone—lecithin–water liquid crystals as potential ointment vehicle

The total therapeutic effect of percutaneous preparations depends not only on the action of the drug itself, but also on other factors related to the structure of the vehicle (1, 2). These latter factors may be divided into two main groups.

The first group contains vehicle–barrier interactions, mostly involving changes in the structure of the stratum corneum caused by the vehicle. These interactions may be evaluated *in toto* by use of standardized tests such as the blanching test (3, 4). Stratum corneum structural changes may facilitate or retard the diffusion of the active substance through this layer, as found for the absorption of solvents through skin (5). It has been claimed that some substances enhance penetration of pharmacological agents when topically applied (6).

The second group includes vehicle–drug interactions. Of these, the capacity of the structure to dissolve (solubilize) the active substance, the related chemical potential difference of the drug in the vehicle and in the stratum corneum, and the diffusion rate of the drug through the vehicle are the most important (7). The vehicle is usually a liquid that is immobilized by the presence of polymers or solid particles (1). The factors mentioned above are, therefore, related to the properties of the liquid phase; the immobilization of the bulk has little importance for the drug diffusion.

The possibilities of using colloidal structures as ointment

0022-3549/84/1000-1484$01.00/0

© 1984, American Pharmaceutical Association

Table II—Hypolipidemic Activity of 3,4,5,6-Dibenzohomopiperidine in Male CF_1 Mice [a]

Dose, mg/kg/d	Serum Cholesterol Day 9	Serum Cholesterol Day 16	Serum Triglyceride Day 14
Control (1% Carboxymethylcellulose)	100 ± 5[c]	100 ± 6[d]	100 ± 6[e]
Compound XVIII			
10	61 ± 5[b]	50 ± 5[b]	48 ± 5[b]
20	68 ± 4[b]	48 ± 4[b]	49 ± 5[b]
40	67 ± 6[b]	54 ± 4[b]	44 ± 6[b]
60	69 ± 5[b]	51 ± 4[b]	55 ± 6[b]

[a] Expressed as percentage of control (mean ± *SD*); $n = 6$. [b] $p < 0.001$. [c] 125 mg%. [d] 122 mg%. [e] 137 mg/dL.

less active than I in both the cholesterol and triglyceride screens; interestingly, the completely reduced compound isoindoline (III) was more active than the partially reduced phthalimidine (II) in both screens. In the succinimide series, the reduced compounds VII and VIII demonstrated less hypotriglyceridemic activity; the partially reduced compound 2-pyrolidinone (VII) demonstrated less hypocholesterolemic activity, but the totally reduced compound, pyrrolidine (VIII) was more active than succinimide in the cholesterol screen, causing 31% reduction. In the glutarimide series, the partially reduced compound, valerolactam (XII), demonstrated approximately the same activity in the cholesterol screen as glutarimide, but it demonstrated less hypotriglyceridemic activity than glutarimide. The fully reduced compound, piperidine (XIII) was more effective in both screens, with a marked reduction, 66%, of serum triglyceride levels. The reduction of diphenimide led to improved hypocholesterolemic activity for both derivatives, lowering serum cholesterol levels 51–49% and the fully reduced derivative serum triglyceride levels 48%. In the adipimide series, the reduction of the carbonyl groups led to little change in hypolipidemic effects in either screen.

Examination of the hydrolytic products of the phthalimide series showed that the half amide, phthalamic acid (IV), afforded approximately the same hypocholesterolemic activity as phthalimide; however, IV produced less effect on lowering triglyceride levels than I. The phthalic acid (V) demonstrated less activity in both screens compared to I. The hydrolytic products of the succinimide series (IX and X), the glutarimide series (XIV and XV), and the adipimide series (X, XXIV, and XXV) demonstrated no improvement in hypolipidemic activity over the parent derivatives. In the diphenimide series, the hydrolytic products XIX and XX demonstrated approximately the same hypocholesterolemic activity as XVI.

In conclusion, there did not appear to be a trend among all of the reduced products of imide analogues with respect to improvement or loss of activity in the hypolipidemic screens in mice. In general, the new compounds examined in this study did not extensively improve the hypocholesterolemic and hypotriglyceridemic activity of the lead compound, phthalimide (I). Piperidine produced improved hypotriglyceridemic activity compared to I, and XVII demonstrated improved hypocholesterolemic activity compared to I. The compound which demonstrated the best activity in both screens, other than I, was XVIII, which was slightly more potent than I in the cholesterolemic screen (6%) and slightly less active in the triglyceridemic screen (8%) in mice (Table II). These differences are probably not significant. Thus, I and XVIII are very similar in hypolipidemic activity. A dose response study with XVIII from 10–60 mg/kg showed that a 20 mg/kg/d dose was optimum for reducing serum cholesterol levels, and a 40 mg/kg/d dose lowered serum triglyceride levels to the level observed for I at 20 mg/kg. Further investigation of these derivatives is warranted since they are more active than commercially available agents, *e.g.*, clofibrate.

REFERENCES

(1) I. H. Hall, P. J. Voorstad, J. M. Chapman, Jr. and G. H. Cocolas, *J. Pharm. Sci.* **72**, 845 (1983).

(2) J. Bornstein and J. E. Shields, *Org. Synth.*, **Coll. Vol. V**, 1064 (1973).

(3) E. Chapman and H. Stephen, *J. Chem. Soc.*, **127**, 1791 (1925).

(4) J. H. Maguire and K. H. Dudley, *Anal. Chem.*, **49**, 292 (1977).

(5) H. W. Underwood and E. L. Kochmann, *J. Am. Chem. Soc.*, **46**, 2072 (1924).

(6) J. M. Chapman, Jr., G. H. Cocolas and I. H. Hall, *J. Med. Chem.* **28**, 243 (1983).

(7) A. Uffer and E. Schlettler, *Helv. Chim. Acta*, **31**, 1397 (1948).

ACKNOWLEDGMENTS

This research was financially supported by NIH Grant 1-R01-HL25680. We also thank Greg Webb and Walter Spivey for technical assistance.

Liquid Crystals as a Potential Ointment Vehicle

SVEN WAHLGREN *, ANNA L. LINDSTROM ‡, and STIG E. FRIBERG §x

Received May 2, 1983, from **The National Corporation of Swedish Pharmacies, Stockholm, Sweden*, ‡*Aco Company, Solna, Sweden*, and the §*Chemistry Department, University of Missouri-Rolla, Rolla, MO 65401.* Accepted for publication October 28, 1983.

Abstract □ A lecithin–water lyotropic liquid crystal was used as an ointment vehicle for a hydrocortisone formulation. The hydrocortisone was soluble in the liquid crystalline phase up to 5% by weight. The diffusion coefficient determined for the hydrocortisone in the liquid crystalline phase was 5.5×10^{-9} $cm \cdot s^{-1}$, which is four magnitudes higher than the corresponding value for skin.

Keyphrases □ Ointments—vehicles, liquid crystals, lecithin–water □ Lecithin—liquid crystals as potential ointment vehicle □ Hydrocortisone—lecithin–water liquid crystals as potential ointment vehicle

The total therapeutic effect of percutaneous preparations depends not only on the action of the drug itself, but also on other factors related to the structure of the vehicle (1, 2). These latter factors may be divided into two main groups.

The first group contains vehicle–barrier interactions, mostly involving changes in the structure of the stratum corneum caused by the vehicle. These interactions may be evaluated *in toto* by use of standardized tests such as the blanching test (3, 4). Stratum corneum structural changes may facilitate or retard the diffusion of the active substance through this layer, as found for the absorption of solvents through skin (5). It has been claimed that some substances enhance penetration of pharmacological agents when topically applied (6).

The second group includes vehicle–drug interactions. Of these, the capacity of the structure to dissolve (solubilize) the active substance, the related chemical potential difference of the drug in the vehicle and in the stratum corneum, and the diffusion rate of the drug through the vehicle are the most important (7). The vehicle is usually a liquid that is immobilized by the presence of polymers or solid particles (1). The factors mentioned above are, therefore, related to the properties of the liquid phase; the immobilization of the bulk has little importance for the drug diffusion.

The possibilities of using colloidal structures as ointment

0022-3549/84/1000-1484$01.00/0

© 1984, American Pharmaceutical Association

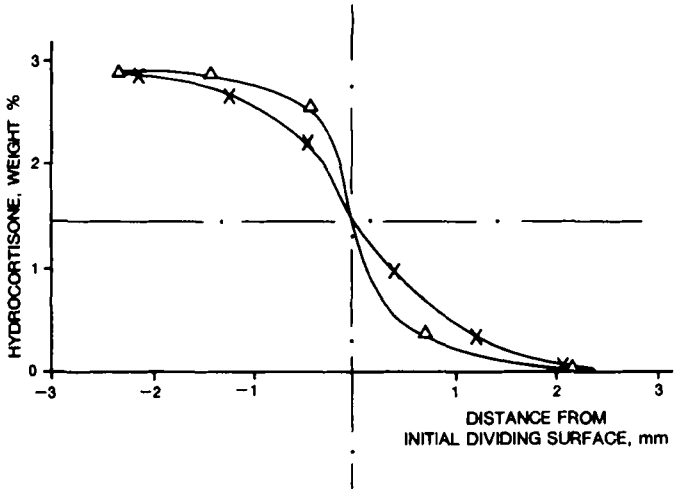

Figure 1—*Concentration profile of hydrocortisone as a function of distance from the initial dividing interface at different times after the start of the experiment. Key: (Δ) 96 h; (×) 192 h; (- - -) $t = \infty$.*

vehicles in a systematic manner have not been utilized in preparations so far, in spite of the interesting solubility properties of these structures (8). This report describes the properties of a lamellar liquid crystal for use as the basic vehicle for an ointment preparation.

The preparation appears to have a series of advantages. It is thermodynamically stable, the solubility in hydrocortisone is considerably higher than in a liquid, and the diffusion of the active substance is higher than is the case for a suspension of solid hydrocortisone, the common preparation form.

EXPERIMENTAL SECTION

Materials—Micronized hydrocortisone[1], and a soy lecithin[2] with 95% phosphatidylcholine were obtained commercially. The purity was checked by TLC. The water was twice distilled.

Preparation—The liquid crystals were prepared by the general technique introduced by Loomis *et al.* (9). The hydrocortisone was dissolved to 1.5% by weight in absolute alcohol, and the lecithin was dissolved to 10% in chloroform. Different volumes of the two solutions to give required hydrocortisone–lecithin ratios were mixed, and the solvent was evaporated at ambient temperature and reduced pressure. The range of volumes were 1–1.95 to give 5% by weight of hydrocortisone in the liquid crystal. Water in a 3:7 weight ratio was added to the hydrocortisone–lecithin mixture and homogenized by a combination of heating to 50°C and vibrational stirring.

The maximum solubility of hydrocortisone was directly detected by visual observation in a microscope with polarized light against the liquid crystalline background. A series of samples with a different percentage of hydrocortisone were examined, and the solubility limit was determined to be the highest hydrocortisone concentration at which no crystals could be observed. The hydrocortisone crystals are a conspicuous feature and easily detected. The presence of crystals was verified from their X-ray diffraction patterns with a camera[3].

Structure Determinations—The liquid crystalline structure was identified from its optical pattern in polarized light, and the spacing ratios in the low-angle X-ray diffraction pattern were obtained with a camera[4].

Diffusion Coefficient—The diffusion rate was determined in the following manner. A glass cylinder (23 mm i.d.) was filled with liquid crystal-containing hydrocortisone. An identical cylinder with the liquid crystal without hydrocortisone was placed on top of the first one with the free surfaces in complete contact. The cylinders were dismantled at different times, and the liquid crystal was pressed from the cylinders, scraped off, and weighed to enable exact calculations of the thickness of removed layers. The cortisone concentration was determined photometrically according to Pharm. Nord. (see *Appendix*).

[1] Upjohn S.A., Lichterstraat, B 2670, Puurs, Belgium.
[2] Epikuron 200; Lucas Meyer, Ausschläger, Elbdeich 21, Hamburg 28, Federal Republic of Germany.
[3] Debye-Scherrer; Seifert & Co., Hamburg, Federal Republic of Germany.
[4] Kiessig; Seifert & Co.

RESULTS

Solubility of Cortisone—The maximum solubility of hydrocortisone in the liquid crystal with 70% lecithin–30% water was 5.0% by weight. This meant a molecular ratio of 1:6 for hydrocortisone–lecithin.

Low-Angle Diffraction—The repeat fraction distance showed a 1:2 spacing ratio, confirming the optical patterns which indicated a lamellar structure. The interlayer spacing for the sample without hydrocortisone was calculated to be 5.3 nm, which is in good agreement with previously reported values (10). A sample with 3% hydrocortisone gave exactly the same interlayer spacing.

Diffusion Rate—The concentration of hydrocortisone *versus* the distance at 96 and 192 h is shown in Fig. 1. The curves show excellent symmetry across the separating surface, which is marked as distance zero on the diagram.

Calculation of Diffusion Coefficient—The second equation of Fick states that:

$$\frac{\partial C}{\partial t} = D\frac{\partial^2 C}{dx^2} \qquad \text{(Eq. 1)}$$

where C is the concentration of diffusing substance, t is time, D is the diffusion coefficient, which is assumed to be constant, and x is the distance along the diffusion axis. From this relation, an explicit expression can be given for the relation between concentration, time, and coordinate for the system in question:

$$C = \frac{C_0^1}{2}[1 - \psi(x/2\sqrt{Dt})] \qquad \text{(Eq. 2)}$$

where $\psi(x/2\sqrt{Dt})$ is the probability integral. The diffusion coefficient is obtained by:

$$D = \frac{x^2}{4t}\left[\frac{1}{\psi^*\left(1 - \frac{2C}{C_0^1}\right)}\right]^2 \qquad \text{(Eq. 3)}$$

where $\psi^*(1 - 2C/C_0^1)$ is the inverse function of the probability integral.

The calculations were made by using the values shown in Fig. 1. The parameter $1 - 2C/C_0^1$ was calculated for a series of points along the curves, and numerical integration was used to obtain $\psi^*(1 - 2C/C_0^1)$. The values obtained gave an average of $D = 5.0 \times 10^{-9} \pm 0.1 \times 10^{-9}$ cm·s^{-1} with a 95% confidence interval.

DISCUSSION

The results of this study show two features of importance for the use of a liquid crystal as an ointment vehicle for percutaneous hydrocortisone preparations. The first feature is the high solubility of hydrocortisone in the lamellar liquid crystalline phase. The value is about four times greater than the corresponding solubility of hydrocortisone in the commonly used ethylene glycol. The reason for this high solubility is not the subject of this report, but the qualitative information may be useful for other applications. According to Israelachvili *et al.* (11), the free energy of a planar layer in a liquid crystal may not be the lowest energy level of an amphiphile–water system. A vesicle with a certain radius may be a more stable configuration for a certain volume of the hydrocarbon chains and a certain cross-sectional area of the polar group. The ratio between the two free energies is $(1 - \alpha)$, in which α depends on the factors mentioned above.

This condition means that the addition of a solute to the structure may in some cases lower the structure-dependent part of the free energy and hence give a higher solubility than can be achieved in an isotropic liquid with a similar chemical composition.

The second feature of importance is the large value of the diffusion coefficient. Its value is distinctly in excess of the one determined for passage through skin. This fact implies a full benefit of the high concentration in the liquid crystal during percutaneous treatment with hydrocortisone. The barrier giving rise to slow release in the commonly used dispersion does not exist in a liquid crystal vehicle. This high diffusion coefficient is related to the location of the hydrocortisone in the structure of the lamellar liquid crystal, and a discussion of the site of the hydrocortisone molecules may be of interest.

The low-angle X-ray diffraction studies showed identical values for the liquid crystal with and without hydrocortisone. This indicates that the hydrocortisone molecules are located between the lecithin molecules in the liquid crystalline structure. A location between the layers would have given a proportional increase of the interlayer spacing. A location between the molecules would facilitate the diffusion of the hydrocortisone molecules.

Such a location and the structure of hydrocortisone make a comparison meaningful with the lecithin–cholesterol–water system (12), which has been

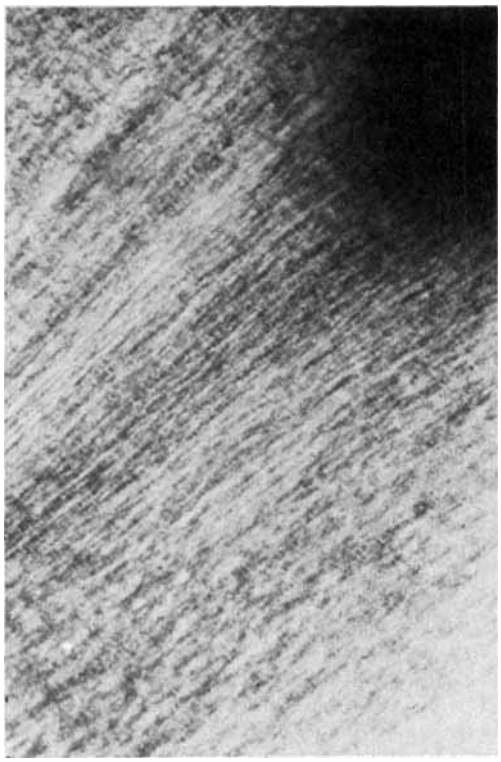

Figure 2—*The optical pattern in polarized light typical of a lamellar structure.*

carefully investigated with regard to its importance for atherosclerotic lesions (13). The influence on the chain order by the presence of cholesterol has been evaluated by McIntosh (14) for the gel state. In all cases the cholesterol molecule is located between the lecithin molecules, and its influence on the interlayer spacing is ascribed to change in tilt and/or order of the hydrocarbon chains. It appears reasonable to assume that the location of the hydrocortisone molecule is between the lecithin molecules and that its diffusion mainly takes place within the constraints of the hydrophobic parts of the lamellar structure.

Diffusion coefficients for the lecithin molecules in liquid crystals with cholesterol have recently been determined by pulsed-spin echo NMR (15). The presence of cholesterol up to 33 mol % counted on lecithin increased the diffusion coefficient for the lecithin by 33%. The amounts of hydrocortisone present in the liquid crystal investigated were less than half the value in the case of cholesterol, and it appears that the presence of hydrocortisone has a relatively minor influence on the diffusion conditions.

The value found for the diffusion coefficient of hydrocortisone was ~10 times less than the one determined previously for lecithin (15) in a lamellar liquid crystal. Two factors contribute to the difference. The values found for lecithin are for the local diffusion parallel to the layers. The values reported for hydrocortisone are bulk volumes for a body of the liquid crystal in which layers have orientations varying in all directions.

A completely statistical distribution of diffusion directions in space would reduce the diffusion coefficient. By assuming equal distribution in all directions and neglecting diffusing perpendicular to the layer plane, the ratio between diffusion as measured by NMR (D_{NMR}) and the total diffusion coefficient measured in this investigation (D_{tot}) would be the average over all angles:

$$D_{tot}/D_{NMR} = \frac{2}{\pi}\int_0^{\pi/2} \sin\theta d\theta = 2/\pi \qquad \text{(Eq. 4)}$$

The ratio between measured values is obviously larger than this, and additional factors must be found to explain the difference.

One such factor originates from the dislocation pattern in a lamellar phase (16). The dislocations are mainly of the focal-conical type or other closed figures. Any part of the total space in the sample in which the layers form a closed figure adds to the total diffusion only to an insignificant amount. A superficial observation of a typical dislocation pattern of a lamellar liquid crystal in this concentration range (Fig. 2) does not rule out a considerable part of the structure consisting of closed figures. The overall diffusion coefficient found in this manner appears to be of reasonable magnitude for a system in which the hydrocortisone molecules are located between the lecithin molecules that diffuse in the hydrophobic layers only. The diffusion coefficient for hydrocortisone in a lamellar liquid crystal was considerably higher than the one for passage through skin; this is a factor of importance for some topical dosage forms.

APPENDIX

Reagents—The following reagents were used for hydrocortisone analysis: absolute ethanol; concentrated acetic acid; a 10% solution of tetramethyl ammonium hydroxide (TMAH)[5], which was kept refrigerated in the dark; 1% TMAH by dilution of 10% TMAH with 9 parts ethanol; 2,3,5-triphenyl tetrazolium chloride (TPTC)[6], which was kept in the refrigerator and dark; 0.5% of TPTC in ethanol, which was prepared immediately before use and protected against light; hydrocortisone standard (50 mg of hydrocortisone standard was dissolved in 100 ml of ethanol; 10.00 mL of this solution was diluted to 100.00 mL with ethanol).

Procedure—Ointment (0.2500 g) was weighed in a 50-mL flask. Ethanol (40 mL) was added, and the mixture was heated to boiling on a water bath with careful stirring. The flask was removed from the water bath and shaken vigorously.

After cooling to room temperature, alcohol was added to 50 mL and the solution was filtered; 5 mL of filtrate and 13 mL of ethanol were added to a 25-mL flask with 2.0 mL of 1% TMAH, and after careful shaking with 2.0 mL of TPTC, 0.5% TPTC was carefully added.

The solution was stored in the dark for 60 min and after 0.05 mL of concentrated acetic acid and ethanol to 25 mL were added, the extinction was determined at 485 nm in a 1-cm cell. As the reference solution was used, 18 mL of ethanol was treated analogously. Calibration was made by using an identical procedure on 5 mL of the hydrocortisone standard and 13 mL of ethanol.

REFERENCES

(1) H. Junginger, H. Heering, C. Führer, and I. Geffers, *Colloid Polym. Sci.*, **259**, 561 (1981).

(2) B. C. Lippold and A. Teubner, *Pharm. Ind.*, **43**, 1123 (1981).

(3) R. Woodford and B. W. Barry, *J. Pharm. Sci.*, **66**, 99 (1977).

(4) B. W. Barry and R. Woodford, *Br. J. Dermatol.*, **97**, 555 (1977).

(5) I. Jacobson, B. Holmberg, and J. E. Wahlberg, *Acta Pharmacol. Toxicol.*, **41**, 497 (1977).

(6) R. B. Stoughton, *Arch. Dermatol.*, **118**, 474 (1982).

(7) H. Schaefer, B. Schroot, and W. Schalla, "Symposium Abstracts Topical Administration of Drugs," Swedish Academy of Pharmaceutical Sciences, 1983, p. 21.

(8) P. Ekwall, in "Advances in Liquid Crystals," vol. 1, G. H. Brown, Ed., Academic, New York, N.Y., 1975, p. 1.

(9) C. R. Loomis, M. J. Janiak, D. M. Small, and G. G. Shipley, *J. Math. Biol.*, **86**, 309 (1974).

(10) N. Moucharafieh and S. E. Friberg, *Mol. Cryst. Liq. Cryst.*, **49**, 201 (1979).

(11) J. N. Israelachvili, D. J. Mitchell, and B. W. Ninham, *J. Chem. Soc. Faraday Trans. II*, **72**, 1525 (1976).

(12) M. Bourgès, D. M. Small, and D. G. Dervichian, *Biochim. Biophys. Acta*, **137**, 157 (1957).

(13) D. M. Small and G. G. Shipley, *Science*, **185**, 222 (1974).

(14) T. J. McIntosh, *Biochim. Biophys. Acta*, **513**, 43 (1978).

(15) G. Lindblom, *Acta Chem. Scand. Sect. B*, **35**, 61 (1981).

(16) M. Kleman, C. E. Williams, M. J. Costello, and T. Gulik-Kozyniski. *Phil. Mag*, **35**, 33 (1977).

[5] Merck 8123.

[6] Merck 8380.

Determination of Ibuprofen in Capillary and Venous Plasma by High-Performance Liquid Chromatography with Ultraviolet Detection

K. S. ALBERT*[x], A. RAABE[‡], M. GARRY[‡], E. J. ANTAL*, and W. R. GILLESPIE*

Received May 9, 1983, from the *The Upjohn Company, Kalamazoo, MI 49001 and [‡]Hazleton Laboratories America, Inc., Madison, Wis. Accepted for publication October 21, 1983.

Abstract □ A high-performance liquid chromatographic (HPLC) method is described which determines ibuprofen in human capillary or venous plasma. Ibuprofen plus the internal standard, flurbiprofen, were extracted from acidified plasma with pentane–ether, back-extracted into base, and then extracted into the pentane–ether solution after acidification of the aqueous phase. A reverse-phase octadecylsilane column with acetonitrile–water–phosphoric acid as mobile phase and UV detection provided a quantifiable peak for 1 μg/mL of ibuprofen in 0.1 mL of plasma. Capillary and venous plasma level curves were virtually superimposable after administration of 400 mg of ibuprofen to four normal volunteers. No ibuprofen was detected in the saliva of the subjects.

Keyphrases □ Ibuprofen—HPLC, small volumes, human plasma and saliva □ Anti-inflammatory agents—ibuprofen, HPLC, capillary and venous plasma, saliva, humans

Ibuprofen, a nonsteroidal phenylpropionic acid derivative possessing potent anti-inflammatory, antipyretic, and analgesic properties (1–3), is used extensively to treat adult rheumatoid arthritis (4–6). In addition, the drug has been shown to be an effective pediatric antipyretic (7). A variety of GC (8–13) and high-performance liquid chromatographic (HPLC) (14–16) methods suitable for measuring ibuprofen in plasma or serum have been reported. With the exception of the electron-capture GC procedure (8), which detects ≥1 μg/mL in 0.1 mL of sample, all methods require >0.5 mL of plasma or serum which limits their use in juvenile or pediatric populations and in multiple-dose studies requiring small sample volumes. The electron-capture procedure (8) is tedious because it involves a TLC step prior to derivatization.

We describe a rapid, specific, and sensitive HPLC method with UV detection for measuring ≥1 μg/mL of ibuprofen in 0.1 mL of plasma or serum. Application of this method to human capillary venous plasma and to saliva is described.

EXPERIMENTAL SECTION

Instrumentation—The high-pressure liquid chromatograph[1] was equipped with a variable-wavelength UV detector[2], an octadecylsilane column[3] (15 cm × 4.6 mm), an automatic injector[4], and a recorder[5]. The flow rate was maintained at 1.5 mL/min (1250 psi) at ambient temperature. The UV detector was set at 195 nm with an attenuation of 0.2 AUFS. The mobile phase was acetonitrile–water–phosphoric acid (550:450:0.5), filtered through a membrane[6] and deaerated before use.

Chemicals and Reagents—Reagents were analytical grade or better. Acetonitrile was distilled in glass[7]. Anhydrous ether was monitored daily for peroxide formation. Stock solutions of ibuprofen[8] (1 mg/mL) and flurbiprofen[8] (1 mg/mL) were prepared in acetonitrile. Appropriate spiking solutions of ibuprofen in acetonitrile and a 10-μg/mL spiking solution of flurbiprofen internal standard in acetonitrile were prepared from the respective stock solutions. The water was deionized[9].

Analytical Method—Standards ranging from 0 to 100 μg/mL were prepared in culture tubes by combining 100 μL each of an appropriate ibuprofen spiking solution, internal standard, and drug-free matrix with 900 μL of deionized water. Samples were prepared by combining 100 μL each of acetonitrile, internal standard, and sample with 900 μL of deionized water. All tubes were vortex-mixed briefly, 0.5 mL of 1 M HCl was added to each, and the tubes were mixed again. The samples were extracted with 10 mL of pentane–ether (80:20, v/v). The upper organic layers were transferred to clean

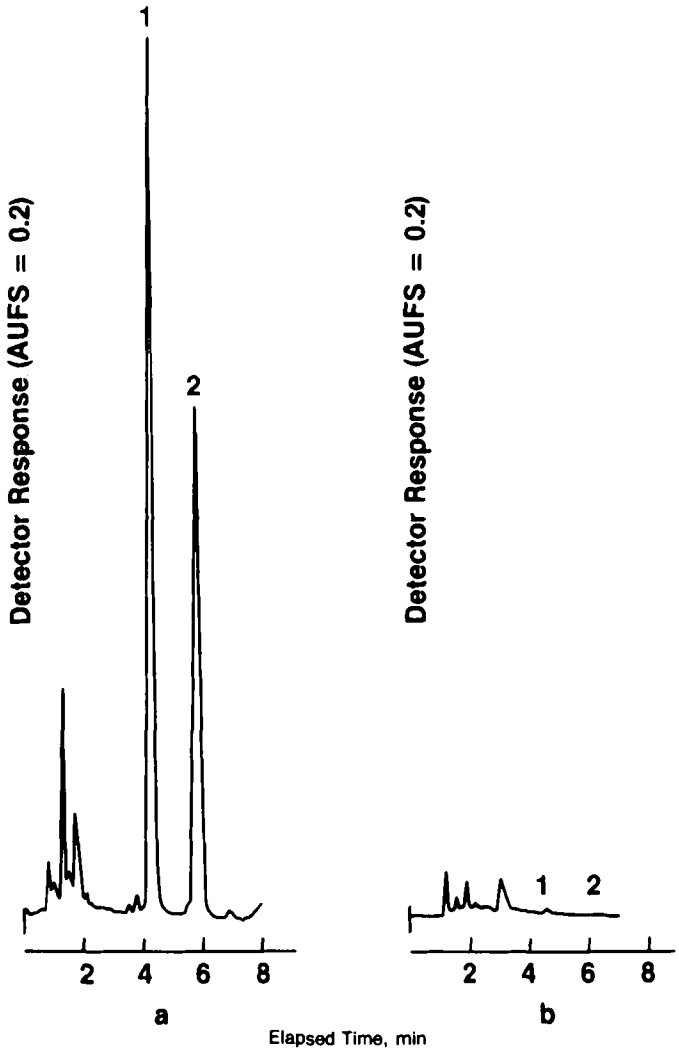

Figure 1—*Typical chromatograms of (a) normal human plasma spiked with 10 μg/mL of internal standard (1) and 6 μg/mL of ibuprofen (2) and (b) unspiked human plasma showing a region where the above peaks would be expected.*

[1] Model 112 pump; Beckman Instruments, Fullerton, Calif.
[2] Spectromonitor III variable-wavelength UV absorbance detector; Laboratory Data Control, Riviera Beach, Fla.
[3] Zorbax ODS; Dupont, Wilmington, Del.
[4] WISP 710B; Waters Associates, Milford, Mass.
[5] Linear Instruments Corp., Reno, Nev.
[6] GS Millipore membrane filtering apparatus; Millipore Corp., Bedford, Mass.
[7] Burdick and Jackson Laboratories, Muskegon, Mich.
[8] The Upjohn Co., Kalamazoo, Mich.
[9] Milli-Q deionized water; Millipore Corp.

0022-3549/84/1000-1487$01.00/0
© 1984, American Pharmaceutical Association

Table I—Sensitivity and Precision of the Assay of Ibuprofen in Plasma

Theoretical Conc., μg/mL	Mean Conc., μg/mL[a]	SD	RSD, %
1.0	1.00	0.116	11.6
3.0	3.01	0.148	4.90
6.0	5.93	0.282	4.75
10.0			
Low curve	10.0	0.191	1.91
High curve	9.39	0.536	5.71
30.0	30.5	0.978	3.20
60.0	60.5	1.43	2.36
100.0	99.5	2.82	2.83

[a] Mean of 14 determinations except for nominal concentration of 60.0 μg/mL, which was the mean of 13 determinations.

culture tubes and extracted with 1.0 mL of 1 M NaOH. After aspirating off the upper organic layer, the pH was adjusted with 2.0 mL of 1 M HCl and the samples were extracted with 10 mL of pentane–ether. The upper organic layer was transferred to clean culture tubes and evaporated to dryness[10]. The residue was dissolved in 0.4 mL of acetonitrile–water (55:45), transferred to vials, and 25 μL was injected onto the HPLC.

Calculations—Calculations were made using baseline-corrected peak height values[11]. Standards were fit to the linear equation, $y = a + bx$, where x corresponds to the concentration of ibuprofen (μg/mL) and y corresponds to the ratio of ibuprofen-to-internal standard peak heights. A split curve was used to calculate the data. The two curves consisted of standards from 1 to 10 μg/mL and from 10 to 100 μg/mL. This was done to prevent negative bias on low-end values caused by variation in the high-end standards. A correlation coefficient was calculated to judge if an adequate curve fit was obtained. Slope and intercept values were also checked to note day-to-day consistencies. Control and sample values were calculated from the appropriate standard curves.

Validation Study—A standard curve with seven data points, a blank plasma control, and two positive plasma controls were assayed in duplicate on each of 3 d. On the fourth day a saliva standard curve, a blank saliva control, and two positive saliva controls were analyzed in duplicate.

To estimate recovery, 100 μL of 10-μg/mL flurbiprofen and ibuprofen spiking solutions were either added to 0.1 mL of plasma and analyzed (matrix standard) or diluted to 0.4 mL with mobile phase and injected directly into the chromatograph (injection standard). Runs were made on four separate occasions and recoveries were determined by comparing matrix-standard peak heights with injection-standard peak heights.

Validation samples were generated by administering ibuprofen to four non-obese volunteers[12] whose average age was 39.5 years (range, 31–47 years) and whose average weight was 69.2 kg (range, 59–77 kg). Each subject fasted

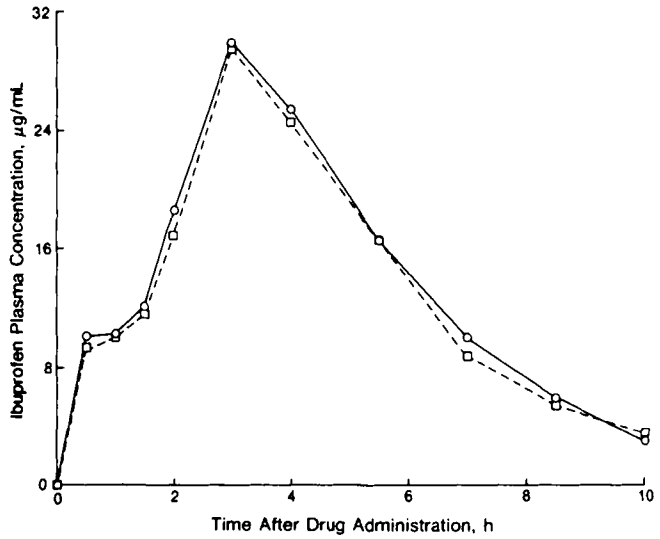

Figure 2—*Average ibuprofen plasma level curves after a single oral 400-mg dose of ibuprofen tablets. Key: (○) capillary plasma; (□) venous plasma.*

[10] N-Evap nitrogen evaporator; Organomation Associates, South Berlin, Mass.
[11] Model 3356 data system integrator; Hewlett-Packard, Avondale, Pa.
[12] Informed written consent was obtained from each subject prior to participation.

Table II—Evaluation of Between- *versus* Within-Day Variation *via* Analysis of Variance

Source	DF[a]	Mean Square	F	p
Low Calibration Curve (1–10 μg/mL)				
Nominal concentration	3	92.8	2546	<0.0001
Day	2	0.0384	1.05	0.37
Error	18	0.0365		
High Calibration Curve (10–100 μg/mL)				
Nominal concentration	3	9166[b]	1593	<0.0001
Day	2	0.0466[b]	0.00811	0.99
Error	17	5.75		

[a] Degrees of freedom. [b] Adjusted for missing day 3, a 60-μg/mL value.

9 h prior to drug administration, then received a 400-mg dose of ibuprofen[13] with 180 mL of water. Food was withheld for an additional 4 h after dosing.

Blood specimens (venous and capillary) were withdrawn at predetermined times over a 10-h period after dosing. Seven milliliters of venous blood was collected at each interval from a forearm vein into evacuated tubes containing sodium heparin[14]. Approximately 0.5 mL of capillary blood was simultaneously collected by fingertip puncture with a sterile blood lancet into heparinized capillary collection tubes[15]. The plasma was harvested and stored frozen until the time of assay.

Saliva samples also were collected at each sampling time and frozen immediately. The production and collection of saliva was facilitated by allowing the subjects to chew on a piece of flexible thermoplastic sheeting[16]. Plasma and saliva samples were assayed using a seven-point standard curve, a blank plasma control, and 5.0- and 50.0-μg/mL positive plasma controls.

RESULTS AND DISCUSSION

A typical chromatogram (Fig. 1) of a plasma extract with and without ibuprofen and the internal standard, flurbiprofen, shows well-resolved sharp peaks free from endogenous interferences. The precision of the assay was assessed by evaluating 14 sets of calibration curve data. Six sets were generated from duplicate curves run on three consecutive days, and eight sets were generated during the analysis of plasma levels of ibuprofen from the four subjects who were administered a 400-mg dose of ibuprofen tablets. The *RSD* ranged from 1.91 to 11.6% (Table I). Excluding the 1-μg/mL concentration, the mean *RSD* was 3.7%. Assay sensitivity was 1 μg/mL for a 0.1-mL sample. The mean correlation coefficient for the low curve was 0.9987, while that for the high curve was 0.9992.

An estimate of within-day *versus* between-day variability was obtained by statistically evaluating the duplicate calibration curve data using a two-way ANOVA with nominal concentrations and days as blocking variables. In this analysis, the mean square associated with days represents between-day variation, while that for the error term represents within-day variation. No significant differences were observed for either the low or high calibration curves (Table II) indicating that between- *versus* within-day variabilities were comparable.

The accuracy of the method was estimated by assaying the two positive plasma controls on 14 separate occasions. The results show that excellent accuracy was obtained at both low and high concentrations; the mean *RSD* was 5.1%. Recoveries were 59.2 and 57.2% for the internal standard and ibuprofen, respectively.

Results from the measurement of ibuprofen in capillary and venous plasma in four normal human volunteers after a single oral 400-mg dose of ibuprofen (tablets) are shown in Fig. 2. Capillary and venous plasma level curves were superimposable. No significant differences between capillary and venous concentrations were observed using the nonparametric Wilcoxon signed-rank test.

In Table III the pharmacokinetic parameters obtained from capillary and venous plasma for the four subjects are compared. Values from the two sampling techniques were virtually identical, demonstrating the utility of capillary sampling for bioavailability/pharmacokinetic studies where small volumes of blood are prerequisites.

Saliva samples were also assayed for ibuprofen; calibration curves, positive controls, and blank (negative) controls were prepared in drug-free saliva rather

[13] Motrin tablets, 400 mg, Lot 270PF; The Upjohn Manufacturing Co., Barceloneta, P.R.
[14] Becton, Dickinson and Co., Rutherford, N.J.
[15] Caraway tubes; Scientific Products, McGaw Park, Ill.
[16] Parafilm M; American Can Co., Greenwich, Conn.

Table III—Comparison of Ibuprofen Pharmacokinetics in Venous and Capillary Plasma Following the Administration of One 400-mg Ibuprofen Tablet to Four Normal Healthy Subjects

Subject	C_{max}, μg/mL		t_{max}, h		AUC_{10}, μg/mL · h		$t_{1/2}$, h	
	Capillary	Venous	Capillary	Venous	Capillary	Venous	Capillary	Venous
1	32.8	32.1	4.0	4.0	180	162	1.65	2.54
2	35.2	31.4	2.0	2.0	151	148	1.95	2.01
3	33.9	32.6	3.0	3.0	107	106	1.50	1.45
4	33.1	32.1	3.0	3.0	138	132	2.49	2.76
Mean	33.7	32.1	3.0	3.0	144	137	1.90	2.19
SD	1.07	0.493	0.816	0.816	30.3	24.0	0.439	0.585

than drug-free plasma[17]. All saliva concentrations were below assay sensitivity, indicating the unsuitability of saliva sampling as a noninvasive alternative to the collection of blood samples.

[17] The precision, sensitivity, and accuracy of the method were comparable whether the biological matrix was plasma or saliva.

REFERENCES

(1) S. S. Adams, K. F. McCullough, and J. S. Nicholson, *Arch. Int. Pharmacodyn. Ther.*, **178**, 115 (1969).

(2) C. D. Brooks, C. A. Schlagel, N. C. Sekhar, and J. T. Sobota, *Curr. Ther. Res. Clin. Exp.*, **15**, 180 (1973).

(3) E. F. Davies and G. S. Avery, *Drugs*, **2**, 416 (1971).

(4) T. G. Kantor, *Ann. Intern. Med.*, **91**, 877 (1979).

(5) M. Thompson, A. W. Craft, M. S. Akyol, and R. Porter, *Curr. Med. Res. Opin.*, **3**, 594 (1975).

(6) F. E. Scheldrake and B. M. Ansell, *Curr. Med. Res. Opin.*, **3**, 604 (1975).

(7) S. Simila, K. Kouvalainen, and S. Keinsnew, *Scand. J. Rheumatol.*, **5**, 81 (1976).

(8) D. G. Kaiser and R. S. Martin, *J. Pharm. Sci.*, **67**, 627 (1978).

(9) L. P. Hackett and L. J. Dusci, *Clin. Chim. Acta*, **87**, 301 (1978).

(10) K. K. Midha, J. K. Cooper, J. W. Hubbard, and I. J. McGilveray, *Can. J. Pharm. Sci.*, **12**, 29 (1977).

(11) D. J. Hoffman, *J. Pharm. Sci.*, **66**, 749 (1977).

(12) G. J. Vangiessen and D. G. Kaiser, *J. Pharm. Sci.*, **64**, 798 (1975).

(13) D. G. Kaiser and G. J. Vangiessen, *J. Pharm. Sci.*, **63**, 219 (1974).

(14) G. L. Kearns and J. T. Wilson, *J. Chromatogr.*, **226**, 183 (1981).

(15) J. L. Shimek, N. G. S. Rao, and S. K. WahbaKhalil, *J. Pharm. Sci.*, **70**, 514 (1981).

(16) D. Pitre and M. Grandi, *J. Chromatogr.*, **170**, 278 (1979).

A New Method for High-Performance Liquid Chromatographic Determination of Drotaverine in Plasma

J. MEZEI ˣ, S. KÜTTEL, P. SZENTMIKLÓSI, S. MARTON, and I. RÁCZ

Received December 7, 1982, from the *Institute of Pharmacy, Semmelweis University of Medicine, Högyes E. 7., 1092. Budapest, Hungary.* Accepted for publication August 30, 1983.

Abstract □ A sensitive, specific high-performance liquid chromatographic procedure was developed for the determination of plasma drotaverine levels. Basic plasma samples were adjusted to pH 1.5 and extracted with chloroform. HPLC [*n*-heptane–dichloromethane–diethylamine (50:25:2)] on a microporous silica column, with a variable-wavelength UV detector set at 302 nm allowed the measurement of drotaverine at the 50-ng/mL level. The utility of this method for determination of drotaverine in dog and rat plasma was demonstrated.

Keyphrases □ Drotaverine—liquid chromatography, plasma □ Liquid chromatography—determination of plasma drotaverine levels

Drotaverine, [1-(3,4-diethoxybenzylidene)-6,7-diethoxy-1,2,3,4-tetrahydroisoquinoline] (I), an effective spasmolytic drug (1), is also marketed as a salt developed with theophylline-7-acetic acid (2).

There are only a few reports in the literature describing the measurement of drotaverine in plasma. ^{14}C-Labeled drotaverine was used to study the pharmacokinetics of the drug in mice (3) and humans (4). The spectrophotometric method (5) and the procedure suggested for the assay of papaverine (6) was found to be neither specific nor sensitive. This paper describes a modification of the high-performance liquid chromatographic method (HPLC) which has been reported for the measurement of papaverine in plasma (7).

EXPERIMENTAL SECTION

Reagents—Drotaverine[1], papaverine hydrochloride[1], drotaveraldine[1] (II), chloroform[2], hydrochloric acid[3], *n*-heptane[4], diethylamine[3], dichloromethane[3], glacial acetic acid[5], and anhydrous sodium sulfate[3] were used without any further purification.

Apparatus—The liquid chromatograph[6] was fitted with a stopped-flow injector[6], a variable-wavelength UV detector[7] (set at 302 nm), and a microporous silica column[8]. The flow rate of the mobile phase was 1.6 mL/min. Chromatograms were recorded[9] at 1 cm/min chart speed.

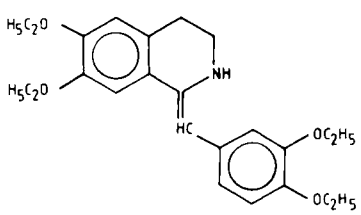

I

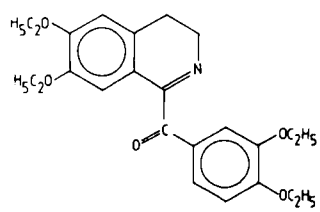

II

[1] Chinoin Chemical Works Ltd., Budapest, Hungary.
[2] Merck, Darmstadt, Federal Republic of Germany.
[3] Reanal Chemical Works, Budapest, Hungary.
[4] Reachim, Soviet Union.
[5] Erdökémia Chemical and Industrial Co., Budapest, Hungary.
[6] Model Liquochrom 307; Labor MIM, Budapest, Hungary.
[7] Model Liquodet 308; Labor MIM, Budapest, Hungary.
[8] Chromspher-Sil 10 μm; 3.9 × 250 mm; Labor MIM, Budapest, Hungary.
[9] NE-230 recorder; EMG, Budapest, Hungary.

0022-3549/84/1000-1489$01.00/0

© 1984, American Pharmaceutical Association

Table III—Comparison of Ibuprofen Pharmacokinetics in Venous and Capillary Plasma Following the Administration of One 400-mg Ibuprofen Tablet to Four Normal Healthy Subjects

Subject	C_{max}, μg/mL		t_{max}, h		AUC_{10}, μg/mL · h		$t_{1/2}$, h	
	Capillary	Venous	Capillary	Venous	Capillary	Venous	Capillary	Venous
1	32.8	32.1	4.0	4.0	180	162	1.65	2.54
2	35.2	31.4	2.0	2.0	151	148	1.95	2.01
3	33.9	32.6	3.0	3.0	107	106	1.50	1.45
4	33.1	32.1	3.0	3.0	138	132	2.49	2.76
Mean	33.7	32.1	3.0	3.0	144	137	1.90	2.19
SD	1.07	0.493	0.816	0.816	30.3	24.0	0.439	0.585

than drug-free plasma[17]. All saliva concentrations were below assay sensitivity, indicating the unsuitability of saliva sampling as a noninvasive alternative to the collection of blood samples.

[17] The precision, sensitivity, and accuracy of the method were comparable whether the biological matrix was plasma or saliva.

REFERENCES

(1) S. S. Adams, K. F. McCullough, and J. S. Nicholson, *Arch. Int. Pharmacodyn. Ther.*, **178**, 115 (1969).

(2) C. D. Brooks, C. A. Schlagel, N. C. Sekhar, and J. T. Sobota, *Curr. Ther. Res. Clin. Exp.*, **15**, 180 (1973).

(3) E. F. Davies and G. S. Avery, *Drugs*, **2**, 416 (1971).

(4) T. G. Kantor, *Ann. Intern. Med.*, **91**, 877 (1979).

(5) M. Thompson, A. W. Craft, M. S. Akyol, and R. Porter, *Curr. Med. Res. Opin.*, **3**, 594 (1975).

(6) F. E. Scheldrake and B. M. Ansell, *Curr. Med. Res. Opin.*, **3**, 604 (1975).

(7) S. Simila, K. Kouvalainen, and S. Keinsnew, *Scand. J. Rheumatol.*, **5**, 81 (1976).

(8) D. G. Kaiser and R. S. Martin, *J. Pharm. Sci.*, **67**, 627 (1978).

(9) L. P. Hackett and L. J. Dusci, *Clin. Chim. Acta*, **87**, 301 (1978).

(10) K. K. Midha, J. K. Cooper, J. W. Hubbard, and I. J. McGilveray, *Can. J. Pharm. Sci.*, **12**, 29 (1977).

(11) D. J. Hoffman, *J. Pharm. Sci.*, **66**, 749 (1977).

(12) G. J. Vangiessen and D. G. Kaiser, *J. Pharm. Sci.*, **64**, 798 (1975).

(13) D. G. Kaiser and G. J. Vangiessen, *J. Pharm. Sci.*, **63**, 219 (1974).

(14) G. L. Kearns and J. T. Wilson, *J. Chromatogr.*, **226**, 183 (1981).

(15) J. L. Shimek, N. G. S. Rao, and S. K. WahbaKhalil, *J. Pharm. Sci.*, **70**, 514 (1981).

(16) D. Pitre and M. Grandi, *J. Chromatogr.*, **170**, 278 (1979).

A New Method for High-Performance Liquid Chromatographic Determination of Drotaverine in Plasma

J. MEZEI ˣ, S. KÜTTEL, P. SZENTMIKLÓSI, S. MARTON, and I. RÁCZ

Received December 7, 1982, from the *Institute of Pharmacy, Semmelweis University of Medicine, Högyes E. 7., 1092. Budapest, Hungary.* Accepted for publication August 30, 1983.

Abstract □ A sensitive, specific high-performance liquid chromatographic procedure was developed for the determination of plasma drotaverine levels. Basic plasma samples were adjusted to pH 1.5 and extracted with chloroform. HPLC [*n*-heptane–dichloromethane–diethylamine (50:25:2)] on a microporous silica column, with a variable-wavelength UV detector set at 302 nm allowed the measurement of drotaverine at the 50-ng/mL level. The utility of this method for determination of drotaverine in dog and rat plasma was demonstrated.

Keyphrases □ Drotaverine—liquid chromatography, plasma □ Liquid chromatography—determination of plasma drotaverine levels

Drotaverine, [1-(3,4-diethoxybenzylidene)-6,7-diethoxy-1,2,3,4-tetrahydroisoquinoline] (I), an effective spasmolytic drug (1), is also marketed as a salt developed with theophylline-7-acetic acid (2).

There are only a few reports in the literature describing the measurement of drotaverine in plasma. ^{14}C-Labeled drotaverine was used to study the pharmacokinetics of the drug in mice (3) and humans (4). The spectrophotometric method (5) and the procedure suggested for the assay of papaverine (6) was found to be neither specific nor sensitive. This paper describes a modification of the high-performance liquid chromatographic method (HPLC) which has been reported for the measurement of papaverine in plasma (7).

EXPERIMENTAL SECTION

Reagents—Drotaverine[1], papaverine hydrochloride[1], drotaveraldine[1] (II), chloroform[2], hydrochloric acid[3], *n*-heptane[4], diethylamine[3], dichloromethane[3], glacial acetic acid[5], and anhydrous sodium sulfate[3] were used without any further purification.

Apparatus—The liquid chromatograph[6] was fitted with a stopped-flow injector[6], a variable-wavelength UV detector[7] (set at 302 nm), and a microporous silica column[8]. The flow rate of the mobile phase was 1.6 mL/min. Chromatograms were recorded[9] at 1 cm/min chart speed.

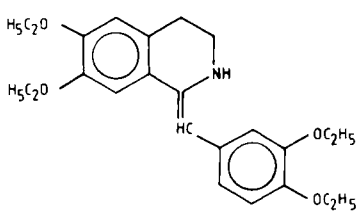

I

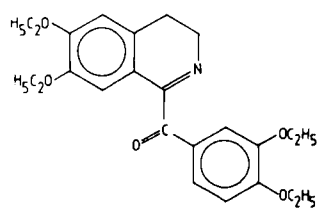

II

[1] Chinoin Chemical Works Ltd., Budapest, Hungary.
[2] Merck, Darmstadt, Federal Republic of Germany.
[3] Reanal Chemical Works, Budapest, Hungary.
[4] Reachim, Soviet Union.
[5] Erdökémia Chemical and Industrial Co., Budapest, Hungary.
[6] Model Liquochrom 307; Labor MIM, Budapest, Hungary.
[7] Model Liquodet 308; Labor MIM, Budapest, Hungary.
[8] Chromspher-Sil 10 μm; 3.9 × 250 mm; Labor MIM, Budapest, Hungary.
[9] NE-230 recorder; EMG, Budapest, Hungary.

0022-3549/84/1000-1489$01.00/0

© 1984, American Pharmaceutical Association

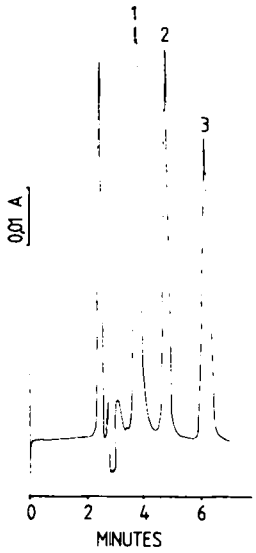

Figure 1—*Chromatograms of a mixed sample of drotaveraldine (0.5 μg), drotaverine (1.0 μg), and papaverine (2.5 μg). Key: (1) drotaveraldine; (2) drotaverine; (3) papaverine.*

A solution containing *n*-heptane–dichloromethane–diethylamine (50:25:2) was filtered[10] and deaerated by refluxing in a water bath. Elution was performed at room temperature. The mobile phase was prepared fresh daily.

Standard Solutions—Solutions of drotaverine hydrochloride in water (25, 50, 100, 150, and 200 μg/mL) were used to spike plasma samples. Papaverine hydrochloride dissolved in chloroform (1000 μg/mL) was used as the internal standard.

Quantitation—Control plasma from rat and dog whole blood was drawn into heparinized tubes, and 10 μL of each standard solution was added to 1.00 mL of the plasma. The spiked plasma samples were adjusted to pH 1.5 using a few drops of 1 M hydrochloric acid. Following the addition of 10.0 mL of chloroform to each tube, the tubes were capped and then shaken on a shaker[11] for 30 min. The mixtures were centrifuged[12] for 10 min, at 4000×*g*. The separated chloroform layers were acidified with 40 μL of glacial acetic acid and then dried with anhydrous sodium sulfate. Eight milliliters of the solution was evaporated to dryness under reduced pressure. Each residue was redissolved in a mixture of 70 μL of chloroform and 10 μL of the internal standard solution. Twenty microliters of the solution was injected onto the column and chromatographed.

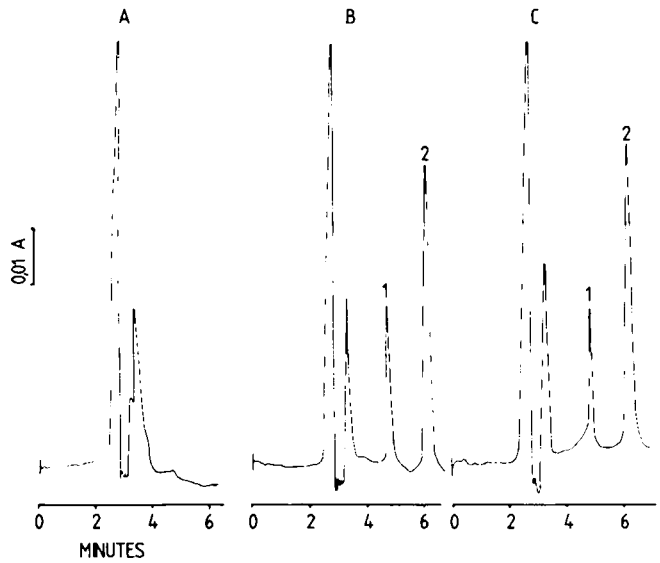

Figure 2—*Chromatograms of extracts from a plasma blank (A), spiked plasma (2.0 μg/mL) (B), and plasma from a rat administered drotaverine (C). Key: (1) drotaverine; (2) papaverine, internal standard.*

[10] G-4 type, 5–15 μm pore size; Schott Jena, Democratic Republic of Germany.
[11] Vibrotherm; Labor MIM, Budapest, Hungary.
[12] Janetzky, Model T-30; Jena, Democratic Republic of Germany.

Table I—Linearity of the Assay Method[a]

Drotaverine Concentration, μg/mL	Peak Height of Drotaverine, mm	Peak Height of Papaverine, mm
0.25	8.3 ± 0.8	103 ± 2.1
0.50	15.0 ± 1.1	108 ± 4.3
1.00	31.3 ± 3.0	103 ± 4.3
1.50	47.5 ± 3.7	108 ± 5.7
2.00	63.1 ± 5.9	108 ± 2.7

[a] Mean ± *SD*; $n = 8$.

A standard curve was prepared by plotting the ratios of peak heights (drotaverine from the extracted plasma samples–internal standard) *versus* the drotaverine concentrations expressed as micrograms per milliliter of plasma. Plasma drotaverine recovery levels were determined by comparing the peak heights of the spiked plasma standards with those of unextracted drotaverine standards (taking into consideration that only 8.0 mL of the original 10.0 mL of chloroform was analyzed).

Sample Preparation and Assay—Drotaverine was orally administered as an aqueous solution of 1.2% to Long Evans rats (200 g) through a gastric tube in doses of 60 mg/kg, and to beagle dogs (10–11 kg) in capsules containing 300 mg of the active substance. Before drug administration, the animals had been fasted overnight with water *ad libitum*. Blood samples were taken prior to dosing and at specified times (0.5, 1, 2, 4, 6, 8, and 24 h) postdose. In the case of rats, three animals at each sampling time were exsanguinated by aortal puncture, and the blood samples were collected separately. For the three beagle dogs, blood samples (2.0 mL) were withdrawn at different time intervals through the saphenous vein. The samples were collected in heparinized, evacuated tubes and centrifuged. One milliliter of each plasma sample was assayed immediately, using the procedure described above for drotaverine-spiked plasma.

Having measured the peak-heights, the ratios (extracted drug–internal standard) were calculated, and the plasma drotaverine levels were read from the calibration curve.

RESULTS AND DISCUSSION

Under the described chromatographic conditions, drotaverine was eluted from the column in 4.7 min and it could be separated from its metabolite, drotaveraldine, which appeared at 3.6 min. The retention time of the internal standard was 6 min (Fig. 1).

After 20–30 samples, the retention time of drotaverine changed gradually to ~4.3 min, due to the decreased retention capacity of the column. To remove impurities from the plasma, the column was washed with methanol[3]; thereafter, the retention capacity was controlled by injecting standard solutions of drotaverine and papaverine onto the column.

Representative chromatograms of blank and spiked plasma extracts and

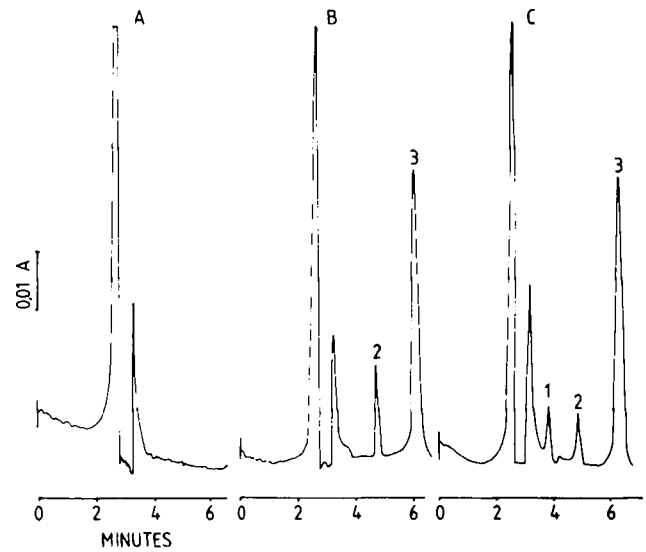

Figure 3—*Chromatograms of extracts from a plasma blank (A), spiked plasma (1.0 μg/mL) (B), and plasma from a dog administered drotaverine (C). Key: (1) drotaveraldine; (2) drotaverine; (3) papaverine, internal standard.*

Table II—Recoveries of Drotaverine from Spiked Rat and Dog Plasma [a]

Drotaverine Concentration, μg/mL	Recovery from Rat Plasma, %	Recovery from Dog Plasma, %
0.25	83.2 ± 4.7	82.8 ± 6.8
0.50	77.0 ± 9.1	84.4 ± 5.2
1.00	82.3 ± 6.5	85.8 ± 8.8
1.50	89.8 ± 6.0	87.9 ± 4.9
2.00	94.3 ± 7.3	88.7 ± 7.1

[a] Mean ± *SD*; $n = 8$.

plasma extracts from a rat given 60 mg/kg of drotaverine, and from a dog given 30 mg/kg of drotaverine, are shown in Figs. 2 and 3.

The drotaverine ultraviolet spectrum has maxima at 242, 302, and 350 nm wavelengths. A variable-wavelength UV detector set at 302 nm was used to eliminate background contributions to the drotaverine peak at 242 nm in blank plasma extracts. The intensity of the maximum at 350 nm is lower than that of the maximum at 302 nm. The detection limit was found to be 50 ng of drotaverine/mL of plasma.

Data in Table I show the linearity of the assay method. A linear regression analysis was performed for the calibration curve prepared from drotaverine-spiked plasma samples. It resulted in the equation $y = 0.2912x + 0.0038$, where y is the ratio of the peak height of the drug divided by the peak height of the internal standard, and x is the drug concentration in the plasma. As evidenced by the experimental data, peak heights were proportional to the drotaverine concentrations for the range examined (from 0.25 to 2 μg of drotaverine/mL of plasma).

Recoveries of drotaverine were nearly quantitative at plasma concentrations of 0.25–2.0 μg/mL, with average recoveries ranging from 77.0 to 94.3% and coefficients of variation ranging from 4.7 to 9.1% (Table II).

REFERENCES

(1) Z. Mészáros, P. Szentmiklósi, and G. Czibula, U.S. Pat. No. 3,337,539, August 22, 1967.

(2) P. Szentmiklósi, Z. Mészáros, *et al.*, U.S. Pat. No. 4,035,366, July 12, 1977.

(3) P. Szentmiklósi and S. Marton, *Acta Pharm. Hung.*, **49**, 50 (1979).

(4) M. H. Rutz-Coudray, L. Balant, C. Revillard, P. Buri, and J. Giust, *Pharm. Acta Helv.*, **51**, 258 (1976).

(5) K. U. Ushbaev and V. A. Katasov, *Gyógyszerészet*, **22**, 424 (1978).

(6) J. Axelrod, R. Schafer, J. K. Inscoe, W. M. King, and A. Sjoerdsma, *J. Pharmacol. Exp. Ther.*, **124**, 9 (1958).

(7) E. Renier, K. Kjeldsen, and M. Pays, *Feuill. Biol.*, **106**, 111 (1979).

Influence of α- and β-Adrenergic Antagonists on Dopamine-Induced Responses in the Isolated Heart of *Mercenaria mercenaria*

DAVID E. MANN, JR. [x] **and RONALD F. GAUTIERI**

Received December 6, 1982, from the *Department of Pharmacology, School of Pharmacy, Temple University, Philadelphia, PA 19140* Accepted for publication September 8, 1983.

Abstract □ Agents with predominantly adrenergic antagonistic properties (the α-blockers, phentolamine and tolazoline, and the β-blocker propranolol), and those with suspected α-blocking capabilities [hydralazine and 3,3′-(4,4′-biphenylene)bis(2,5-diphenyl-2*H*-tetrazolium chloride) (neotetrazolium chloride); I] were added individually to a bath containing an isolated *Mercenaria mercenaria* heart. Two and one-half minutes later, dopamine was added to the bath as the second drug and cardiac responses were noted. Pretreatment with saline controls, followed by dopamine 2.5 min later, produced results that were identical with those which occurred after the administration of dopamine alone, *i.e.*, marked stimulation and cardiac arrest. Pretreatment with phentolamine and I were the only procedures that prevented dopamine-induced cardiac arrest. Phentolamine, tolazoline, and hydralazine generally produced positive inotropic responses when initially added to the bath, whereas propranolol mimicked the effects caused by the addition of dopamine alone or after saline pretreatment. The *M. mercenaria* heart appears to possess an adrenergic receptor of an α-configuration.

Keyphrases □ α- and β-Adrenergic antagonists—dopamine-induced response, heart of *Mercenaria mercenaria* □ Dopamine—α- and β-adrenergic antagonists, effect on heart of *M. mercenaria*, pretreatment controls.

A number of studies have suggested the presence of an adrenergic receptor in the smooth muscle of the heart of *Mercenaria mercenaria*, the hard-shelled clam or quahog. Welsh and Taub (1) administered various drugs to the isolated heart of *M. mercenaria* and noted that epinephrine evoked negative inotropic responses and tachyphylaxis. Fujita and Mann (2) reported similar responses with norepinephrine under comparable experimental conditions. Ciuchta and Mann (3) examined the relative effectiveness of ephedrine isomers in preventing the onset of norepinephrine-induced tachyphylaxis in the *M. mercenaria* heart and found that the *l*-isomer was the most potent, the racemate less potent, and the *d*-isomer least potent. Orzechowski and Mann (4) performed a similar experiment with amphetamine isomers and observed that norepinephrine-induced tachyphylaxis was blocked most effectively by the *d*-isomer, while the *d,l*- and *l*-isomers were equal but less potent. When higher doses of amphetamine isomers were given, norepinephrine elicited positive inotropic responses, suggesting that these agents act upon common receptor sites. It was further speculated that amphetamine, like ephedrine, may block cardiac inhibitory sites on which norepinephrine acts, thus allowing ephedrine to cause stimulation.

Dopamine, which is present in *M. mercenaria* nervous tissue (5), appears to activate excitatory receptors in the clam heart in contrast to epinephrine and norepinephrine, which affect inhibitory receptors. Tachyphylaxis also occurs in the *M. mercenaria* heart after successive, equal doses of dopamine[1].

The purpose of this study was twofold:

1. To determine whether the α-blockers (tolazoline, phentolamine, and hydralazine) and the β-blocker (propranolol) could prevent the excitatory effects of dopamine on the isolated *M. mercenaria* heart, thereby elucidating the nature of its adrenergic receptor;

2. To ascertain whether the hypotensive agent, 3,3′(4,4′-biphenylene)bis(2,5-diphenyl-2*H*-tetrazolium chloride) (neotetrazolium chloride; I), which has both adrenergic α-blocking and gangliolytic actions (6–8), could antagonize

[1] Unpublished results.

0022-3549/84/1000-1491$01.00/0

© 1984, American Pharmaceutical Association

Table II—Recoveries of Drotaverine from Spiked Rat and Dog Plasma [a]

Drotaverine Concentration, μg/mL	Recovery from Rat Plasma, %	Recovery from Dog Plasma, %
0.25	83.2 ± 4.7	82.8 ± 6.8
0.50	77.0 ± 9.1	84.4 ± 5.2
1.00	82.3 ± 6.5	85.8 ± 8.8
1.50	89.8 ± 6.0	87.9 ± 4.9
2.00	94.3 ± 7.3	88.7 ± 7.1

[a] Mean ± *SD*; $n = 8$.

plasma extracts from a rat given 60 mg/kg of drotaverine, and from a dog given 30 mg/kg of drotaverine, are shown in Figs. 2 and 3.

The drotaverine ultraviolet spectrum has maxima at 242, 302, and 350 nm wavelengths. A variable-wavelength UV detector set at 302 nm was used to eliminate background contributions to the drotaverine peak at 242 nm in blank plasma extracts. The intensity of the maximum at 350 nm is lower than that of the maximum at 302 nm. The detection limit was found to be 50 ng of drotaverine/mL of plasma.

Data in Table I show the linearity of the assay method. A linear regression analysis was performed for the calibration curve prepared from drotaverine-spiked plasma samples. It resulted in the equation $y = 0.2912x + 0.0038$, where y is the ratio of the peak height of the drug divided by the peak height of the internal standard, and x is the drug concentration in the plasma. As evidenced by the experimental data, peak heights were proportional to the drotaverine concentrations for the range examined (from 0.25 to 2 μg of drotaverine/mL of plasma).

Recoveries of drotaverine were nearly quantitative at plasma concentrations of 0.25–2.0 μg/mL, with average recoveries ranging from 77.0 to 94.3% and coefficients of variation ranging from 4.7 to 9.1% (Table II).

REFERENCES

(1) Z. Mészáros, P. Szentmiklósi, and G. Czibula, U.S. Pat. No. 3,337,539, August 22, 1967.

(2) P. Szentmiklósi, Z. Mészáros, *et al.*, U.S. Pat. No. 4,035,366, July 12, 1977.

(3) P. Szentmiklósi and S. Marton, *Acta Pharm. Hung.*, **49**, 50 (1979).

(4) M. H. Rutz-Coudray, L. Balant, C. Revillard, P. Buri, and J. Giust, *Pharm. Acta Helv.*, **51**, 258 (1976).

(5) K. U. Ushbaev and V. A. Katasov, *Gyógyszerészet*, **22**, 424 (1978).

(6) J. Axelrod, R. Schafer, J. K. Inscoe, W. M. King, and A. Sjoerdsma, *J. Pharmacol. Exp. Ther.*, **124**, 9 (1958).

(7) E. Renier, K. Kjeldsen, and M. Pays, *Feuill. Biol.*, **106**, 111 (1979).

Influence of α- and β-Adrenergic Antagonists on Dopamine-Induced Responses in the Isolated Heart of *Mercenaria mercenaria*

DAVID E. MANN, JR. [x] **and RONALD F. GAUTIERI**

Received December 6, 1982, from the *Department of Pharmacology, School of Pharmacy, Temple University, Philadelphia, PA 19140* Accepted for publication September 8, 1983.

Abstract □ Agents with predominantly adrenergic antagonistic properties (the α-blockers, phentolamine and tolazoline, and the β-blocker propranolol), and those with suspected α-blocking capabilities [hydralazine and 3,3′-(4,4′-biphenylene)bis(2,5-diphenyl-2*H*-tetrazolium chloride) (neotetrazolium chloride); I] were added individually to a bath containing an isolated *Mercenaria mercenaria* heart. Two and one-half minutes later, dopamine was added to the bath as the second drug and cardiac responses were noted. Pretreatment with saline controls, followed by dopamine 2.5 min later, produced results that were identical with those which occurred after the administration of dopamine alone, *i.e.*, marked stimulation and cardiac arrest. Pretreatment with phentolamine and I were the only procedures that prevented dopamine-induced cardiac arrest. Phentolamine, tolazoline, and hydralazine generally produced positive inotropic responses when initially added to the bath, whereas propranolol mimicked the effects caused by the addition of dopamine alone or after saline pretreatment. The *M. mercenaria* heart appears to possess an adrenergic receptor of an α-configuration.

Keyphrases □ α- and β-Adrenergic antagonists—dopamine-induced response, heart of *Mercenaria mercenaria* □ Dopamine—α- and β-adrenergic antagonists, effect on heart of *M. mercenaria*, pretreatment controls.

A number of studies have suggested the presence of an adrenergic receptor in the smooth muscle of the heart of *Mercenaria mercenaria*, the hard-shelled clam or quahog. Welsh and Taub (1) administered various drugs to the isolated heart of *M. mercenaria* and noted that epinephrine evoked negative inotropic responses and tachyphylaxis. Fujita and Mann (2) reported similar responses with norepinephrine under comparable experimental conditions. Ciuchta and Mann (3) examined the relative effectiveness of ephedrine isomers in preventing the onset of norepinephrine-induced tachyphylaxis in the *M. mercenaria* heart and found that the *l*-isomer was the most potent, the racemate less potent, and the *d*-isomer least potent. Orzechowski and Mann (4) performed a similar experiment with amphetamine isomers and observed that norepinephrine-induced tachyphylaxis was blocked most effectively by the *d*-isomer, while the *d,l*- and *l*-isomers were equal but less potent. When higher doses of amphetamine isomers were given, norepinephrine elicited positive inotropic responses, suggesting that these agents act upon common receptor sites. It was further speculated that amphetamine, like ephedrine, may block cardiac inhibitory sites on which norepinephrine acts, thus allowing ephedrine to cause stimulation.

Dopamine, which is present in *M. mercenaria* nervous tissue (5), appears to activate excitatory receptors in the clam heart in contrast to epinephrine and norepinephrine, which affect inhibitory receptors. Tachyphylaxis also occurs in the *M. mercenaria* heart after successive, equal doses of dopamine[1].

The purpose of this study was twofold:

1. To determine whether the α-blockers (tolazoline, phentolamine, and hydralazine) and the β-blocker (propranolol) could prevent the excitatory effects of dopamine on the isolated *M. mercenaria* heart, thereby elucidating the nature of its adrenergic receptor;

2. To ascertain whether the hypotensive agent, 3,3′(4,4′-biphenylene)bis(2,5-diphenyl-2*H*-tetrazolium chloride) (neotetrazolium chloride; I), which has both adrenergic α-blocking and gangliolytic actions (6–8), could antagonize

[1] Unpublished results.

0022-3549/84/1000-1491$01.00/0

© 1984, American Pharmaceutical Association

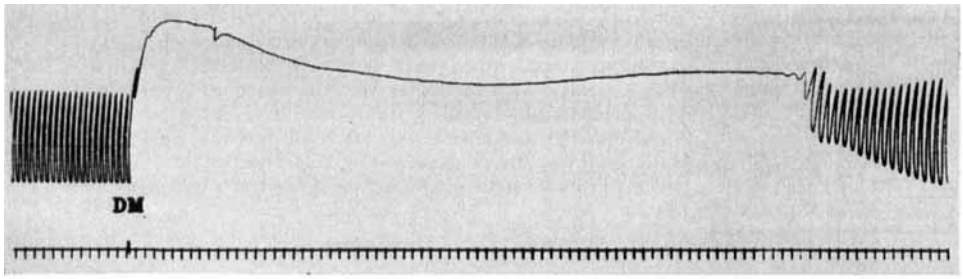

Figure 1—*Effect of dopamine hydrochloride (4 mg) on isolated* M. mercenaria *heart; time interval is 5 s.*

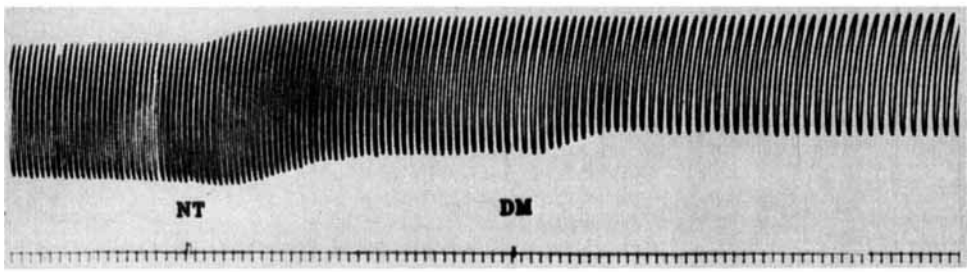

Figure 2—*Preadministration of 3,3′-(4,4′-biphenylene)bis[2,5-diphenyl-2H-tetrazolium chloride] (8 mg) followed by dopamine hydrochloride (4 mg);* $p = <0.05$.

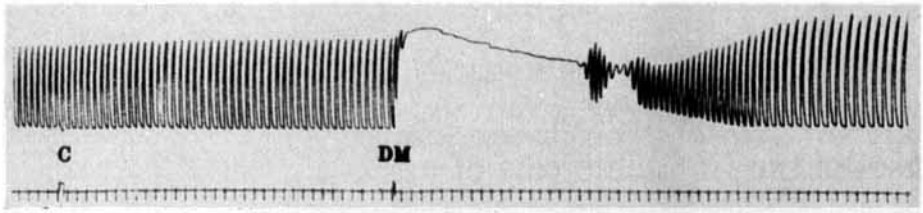

Figure 3—*Preadministration of a vehicle control for 3,3′(4,4′-biphenylene)bis[2,5-diphenyl-2H-tetrazolium chloride] (0.8 mL) followed by dopamine hydrochloride (4 mg);* $p < 0.001$.

Table I—Average Percent Inhibition[a] Within 1 min After Challenging the Isolated *M. mercenaria* Heart with a Test Drug and within 1 min After the Addition of Dopamine Hydrochloride

Compound	*n*	Dose	Average Inhibition after 1 min, % No Challenge	Average Inhibition after 1 min, % Dopamine Hydrochloride Challenge	*p*
Phentolamine mesylate	7	15 mg	36	59	<0.001[b]
Tolazoline hydrochloride	8	15 mg	24	100	—
Propranolol hydrochloride	8	15 mg	100	—[d]	—
Hydralazine hydrochloride	8	15 mg	17	100	—
Saline control	8	2.5	26	100	—
3,3′-(4,4′-Biphenylene)bis(2,5-diphenyl-2*H*-tetrazolium chloride)	15	8	22	32	<0.05[b]
Solvent control	6	0.8 ml	0	100	<0.001[c]

[a] The greatest degree of inhibition within 1 min after drug challenge. [b] Statistically significant compared with saline control. [c] Statistically significant compared with neotetrazolium chloride-treated group. [d] Contractility failed to return after propranolol administration; dopamine administration caused greater spasticity.

the effects of dopamine on the *M. mercenaria* heart. Positive results obtained with I and the other adrenergic α-blockers would presume an adrenergic α-receptor as the site upon which dopamine acts, because the *M. mercenaria* heart is devoid of autonomic ganglia.

EXPERIMENTAL SECTION

Animals—*M. mercenaria*[2] were maintained in a 378.4-L aquarium filled with artificial sea water[3] for at least 2 d prior to use.

Apparatus—The heart was isolated according to the methods of Welsh and Taub (1) and Wait (9). After cracking the shell with a hammer, the heart was removed and attached to a hook embedded in a plastic rod. The rod was then lowered into an aerated[4] glass bathing chamber containing 40 mL of sea water. A thread extending from the apex of the ventricle to a detecting head[5] activated a transducer[6] and physiograph[7] to record contractility.

Materials—When contractions were normal, a glass syringe[8] delivered either 0.8 mL of neotetrazolium chloride[9], 0.8 mL of the vehicle control[9], 2.5 mL of the test drug, or 2.5 mL of a saline control[10], followed 2.5 min later by the addition, using a second syringe[8], of 4 mg (0.1 mL) of dopamine hydrochloride[11]. The test drugs were prepared in the following concentrations: phentolamine mesylate[12], tolazoline hydrochloride[13], and propranolol hydrochloride[14] at 0.6%; hydralazine hydrochloride[15] and I[9] at 1.0%.

Pretreatment Dose Regimen—A 15-mg dose of each agent was administered 2.5 min prior to dopamine challenge (except for I, the dose of which was 8 mg). A 2.5-mL aliquot of the saline control was added to the bath; this volume was equivalent to that of each test drug, except for I. Because the latter compound utilized a vehicle control (5% ethyl alcohol and 20% propylene glycol in distilled water) and a lower dosage than the rest, it has a control volume of only 0.8 mL.

[2] Obtained locally; shell lengths 10–14 cm.

[3] Instant Ocean; Aquarium Supplies, Mentor, Ohio. Maintained at 24–26°C; specific gravity, 1.025.

[4] Oscar's 55 air pump; Berkeley, Calif.

[5] Isotonic myograph, Model 1127; Narco Bio-systems, Inc., Houston, Tex.

[6] Isotonic myograph transducer, MK II; Narco Bio-systems, Inc.

[7] Physiograph Four-B; Narco Bio-systems, Inc.

[8] B-D mL tuberculin syringe with a 1.27-cm, 26-gauge needle; B-D 2-ml Multifit syringe with a 1.27-cm, 26-gauge needle.

[9] I, Cat. No. 102436, Lot No. 1285, ICN Pharmaceuticals, Inc., Life Sciences Group, Cleveland, Ohio. (In distilled water as 1% I, 5% ethyl alcohol (95%), and 20% propylene glycol.) Added to the bath in a volume of 0.8 mL and controlled with equivalent volumes of a distilled water vehicle containing 5% ethyl alcohol and 20% propylene glycol.

[10] Normal saline, 0.9%, Lot No. 94-851-DE-5; Abbott Laboratories, North Chicago, Ill.

[11] Intropin (dopamine hydrochloride), 5 mL ampules containing 40 mg/mL, Lot Nos. A0022, A9158; Arnar-Stone Laboratoris, Inc., McGaw Park, Ill.

[12] Regitine (phentolamine mesylate), Lot. No. B66-R-113; obtained through the courtesy of Ciba Pharmaceutical Co., Div. of Ciba-Geigy Corp., Summit, N.J.

[13] Priscoline (tolazoline hydrochloride), Lot No. A-7856; obtained through the courtesy of Ciba Pharmaceutical Co., Div. of Ciba-Geigy Corp.

[14] Inderal (propranolol hydrochloride), Lot No. R47736A; obtained through the courtesy of Ayerst Laboratories, Inc., New York, N.Y.

[15] Apresoline (hydralazine hydrochloride), Lot No. N-2059; obtained through the courtesy of Ciba Pharmaceutical Co., Div. of Ciba-Geigy Corp.

RESULTS AND DISCUSSION

The typical response elicited by dopamine (4 mg) on the isolated *M. mercenaria* heart bathed in 40 mL of artificial sea water is shown in Fig. 1. The heart stopped contracting at once when dopamine was added to the bath, but recovered its contractility within 6 min. When I (8 mg) was added to the bath, 2.5 min before dopamine challenge, it not only prevented cardiac arrest due to dopamine, but also produced a negative inotropic response that was mimicked by the subsequent addition of dopamine (Fig. 2). By contrast, preadministration of the vehicle control for I, in a volume comparable to that of the test drug (0.8 mL), failed to prevent cardiac arrest caused by dopamine; however, the recovery time for the return of contractility was shortened over that induced by dopamine administration alone (Fig. 3).

The average percent of cardiac inhibition attributed to the test drugs and to dopamine challenge is presented in Table I. The number of animals used in each group ranged from 6 to 15. The percent inhibition was calculated by measuring the amplitude of the peak at the moment of test drug challenge and dopamine challenge, and the lowest amplitude within 1 min after administering each agent; *i.e.*, the response recorded in Fig. 1 after the addition to the bath of dopamine alone represents 100% inhibition.

Although each agent, except the solvent control, caused some degree of cardiac inhibition within 1 min of its administration (Table I), propranolol produced the most dramatic and consistent inhibitory responses. Immediately after the addition of the β-blocker to the bath, the heart lost contractility and became spastic, an excitatory response that was identical with that observed after the administration of dopamine alone (Fig. 1). Two and one-half minutes later, the addition of dopamine produced an even greater response.

Initial administrations of phentolamine, tolazoline, and hydralazine yielded consistently positive inotropic responses during the 2.5-min period prior to the addition of dopamine, whereas I caused variable effects (*i.e.*, positive, negative, or no alteration of the inotropic response) prior to the addition of dopamine. Phentolamine mesylate, an α-adrenergic blocker, and I, an experimental hypotensive agent with presumed α-adrenergic blocking activity, appear to act on an adrenergic receptor of an α-configuration within the *M. mercenaria* heart to block the stimulatory effects of dopamine. Of the two compounds, I is the more potent in this respect.

REFERENCES

(1) J. H. Welsh and R. Taub, *Biol. Bull.*, **95**, 346 (1948).

(2) T. Fujita and D. E. Mann, Jr., *J. Am. Pharm. Assoc., Sci. Ed.*, **47**, 90 (1958).

(3) H. P. Ciuchta and D. E. Mann, Jr., *J. Pharm. Sci.*, **50**, 648 (1961).

(4) R. F. Orzechowski and D. E. Mann, Jr., *J. Pharm. Sci.*, **52**, 337 (1963).

(5) D. Sweeney, *Science*, **139**, 1051 (1963).

(6) W. Antopol and B. W. Zweifach, *Proc. Soc. Exp. Biol. Med.*, **92**, 752 (1956).

(7) E. Nelson, C. Chryssanthou, and W. Antopol, *Fed. Proc., Fed. Am. Soc. Exp. Biol.*, **28**, 738 (1969).

(8) E. Nelson, C. Chryssanthou, F. Teichner, and W. Antopol, *Fed. Proc., Fed. Am. Soc. Exp. Biol.*, **29**, 270 (1970).

(9) R. B. Wait, *Biol. Bull.*, **85**, 79 (1943).

ACKNOWLEDGMENTS

The authors thank the following individuals for their expert assistance in the pursuance of this study: Robert Bonar, Peter Lemke, Scott E. Mann, and Stanley J. Zajkowski.

Identification and Determination of the *S*-Methyl Metabolite of Captopril in Human Plasma by Selected-Ion Monitoring Gas Chromatography–Mass Spectrometry

ALLEN I. COHEN *x, EUGENE IVASHKIV *, TERRENCE McCORMICK *, and DORIS N. McKINSTRY ‡

Received April 14, 1983, from the **Department of Analytical Research, The Squibb Institute for Medical Research, New Brunswick, NJ 08903* and ‡*Department of Clinical Pharmacology, The Squibb Institute for Medical Research, Princeton, NJ 08540.* Accepted for publication November 29, 1983.

Abstract □ The *S*-methyl metabolite of captopril was identified and determined in human plasma by positive chemical ionization selected-ion monitoring gas chromatography–mass spectrometry. After oral administration of 100 mg of captopril to healthy subjects, the maximum plasma level was 60–114 ng/mL. These data for the *S*-methyl metabolite of captopril were correlated to total and unchanged captopril levels.

Keyphrases □ Captopril—identification and determination of the *S*-methyl metabolite in human plasma, gas chromatography-selected-ion monitoring mass spectrometry □ Gas chromatography-selected-ion monitoring mass sepectrometry—determination of the *S*-methyl metabolite of captopril in human plasma after oral administration

Captopril (1-[(2*S*)-3-mercapto-2-methylpropronyl]-L-proline; I) (1, 2) has received considerable attention as an orally active angiotensin-converting inhibitor (3) that is effective in lowering arterial blood pressure (4). The absolute bioavailability and pharmacokinetics of [^{14}C]captopril given orally and intravenously have been reported previously (5). Analysis of the kinetic data suggested that captopril is extensively partitioned into tissue. The interconversion of protein-bound captopril with non-protein-bound mixed disulfides has been suggested as a biotransformation pathway that may extend the pharmacological effects of captopril (5, 6).

Gas chromatography–mass spectrometry (GC–MS) selected-ion monitoring (SIM) methods have been reported for the determination of unchanged captopril in whole blood (7) and total captopril in plasma (8). Total captopril includes unchanged drug, the disulfide dimer of the parent drug, and mixed disulfides with endogenous thiol-containing compounds, *e.g.*, glutathione and cysteine. Recently, the *S*-methyl metabolite of captopril (II) has been identified as a urinary metabolite in humans (9) and rats (6). A GC–MS SIM method was developed to measure the plasma level of the *S*-methyl metabolite (II) after oral administration of captopril. The plasma levels of the metabolite II from samples collected from healthy human subjects after the administration of a single 100-mg tablet of captopril were compared with the free captopril blood levels and total captopril plasma levels determined as IV by GC–MS SIM methods previously reported (7, 8).

0022-3549/84/1000-1493$01.00/0

© 1984, American Pharmaceutical Association

RESULTS AND DISCUSSION

The typical response elicited by dopamine (4 mg) on the isolated *M. mercenaria* heart bathed in 40 mL of artificial sea water is shown in Fig. 1. The heart stopped contracting at once when dopamine was added to the bath, but recovered its contractility within 6 min. When I (8 mg) was added to the bath, 2.5 min before dopamine challenge, it not only prevented cardiac arrest due to dopamine, but also produced a negative inotropic response that was mimicked by the subsequent addition of dopamine (Fig. 2). By contrast, preadministration of the vehicle control for I, in a volume comparable to that of the test drug (0.8 mL), failed to prevent cardiac arrest caused by dopamine; however, the recovery time for the return of contractility was shortened over that induced by dopamine administration alone (Fig. 3).

The average percent of cardiac inhibition attributed to the test drugs and to dopamine challenge is presented in Table I. The number of animals used in each group ranged from 6 to 15. The percent inhibition was calculated by measuring the amplitude of the peak at the moment of test drug challenge and dopamine challenge, and the lowest amplitude within 1 min after administering each agent; *i.e.*, the response recorded in Fig. 1 after the addition to the bath of dopamine alone represents 100% inhibition.

Although each agent, except the solvent control, caused some degree of cardiac inhibition within 1 min of its administration (Table I), propranolol produced the most dramatic and consistent inhibitory responses. Immediately after the addition of the β-blocker to the bath, the heart lost contractility and became spastic, an excitatory response that was identical with that observed after the administration of dopamine alone (Fig. 1). Two and one-half minutes later, the addition of dopamine produced an even greater response.

Initial administrations of phentolamine, tolazoline, and hydralazine yielded consistently positive inotropic responses during the 2.5-min period prior to the addition of dopamine, whereas I caused variable effects (*i.e.*, positive, negative, or no alteration of the inotropic response) prior to the addition of dopamine. Phentolamine mesylate, an α-adrenergic blocker, and I, an experimental hypotensive agent with presumed α-adrenergic blocking activity, appear to act on an adrenergic receptor of an α-configuration within the *M. mercenaria* heart to block the stimulatory effects of dopamine. Of the two compounds, I is the more potent in this respect.

REFERENCES

(1) J. H. Welsh and R. Taub, *Biol. Bull.*, **95**, 346 (1948).

(2) T. Fujita and D. E. Mann, Jr., *J. Am. Pharm. Assoc., Sci. Ed.*, **47**, 90 (1958).

(3) H. P. Ciuchta and D. E. Mann, Jr., *J. Pharm. Sci.*, **50**, 648 (1961).

(4) R. F. Orzechowski and D. E. Mann, Jr., *J. Pharm. Sci.*, **52**, 337 (1963).

(5) D. Sweeney, *Science*, **139**, 1051 (1963).

(6) W. Antopol and B. W. Zweifach, *Proc. Soc. Exp. Biol. Med.*, **92**, 752 (1956).

(7) E. Nelson, C. Chryssanthou, and W. Antopol, *Fed. Proc., Fed. Am. Soc. Exp. Biol.*, **28**, 738 (1969).

(8) E. Nelson, C. Chryssanthou, F. Teichner, and W. Antopol, *Fed. Proc., Fed. Am. Soc. Exp. Biol.*, **29**, 270 (1970).

(9) R. B. Wait, *Biol. Bull.*, **85**, 79 (1943).

ACKNOWLEDGMENTS

The authors thank the following individuals for their expert assistance in the pursuance of this study: Robert Bonar, Peter Lemke, Scott E. Mann, and Stanley J. Zajkowski.

Identification and Determination of the *S*-Methyl Metabolite of Captopril in Human Plasma by Selected-Ion Monitoring Gas Chromatography–Mass Spectrometry

ALLEN I. COHEN *x, EUGENE IVASHKIV *, TERRENCE McCORMICK *, and DORIS N. McKINSTRY ‡

Received April 14, 1983, from the **Department of Analytical Research, The Squibb Institute for Medical Research, New Brunswick, NJ 08903* and ‡*Department of Clinical Pharmacology, The Squibb Institute for Medical Research, Princeton, NJ 08540.* Accepted for publication November 29, 1983.

Abstract □ The *S*-methyl metabolite of captopril was identified and determined in human plasma by positive chemical ionization selected-ion monitoring gas chromatography–mass spectrometry. After oral administration of 100 mg of captopril to healthy subjects, the maximum plasma level was 60–114 ng/mL. These data for the *S*-methyl metabolite of captopril were correlated to total and unchanged captopril levels.

Keyphrases □ Captopril—identification and determination of the *S*-methyl metabolite in human plasma, gas chromatography-selected-ion monitoring mass spectrometry □ Gas chromatography-selected-ion monitoring mass sepectrometry—determination of the *S*-methyl metabolite of captopril in human plasma after oral administration

Captopril (1-[(2*S*)-3-mercapto-2-methylpropronyl]-L-proline; I) (1, 2) has received considerable attention as an orally active angiotensin-converting inhibitor (3) that is effective in lowering arterial blood pressure (4). The absolute bioavailability and pharmacokinetics of [^{14}C]captopril given orally and intravenously have been reported previously (5). Analysis of the kinetic data suggested that captopril is extensively partitioned into tissue. The interconversion of protein-bound captopril with non-protein-bound mixed disulfides has been suggested as a biotransformation pathway that may extend the pharmacological effects of captopril (5, 6).

Gas chromatography–mass spectrometry (GC–MS) selected-ion monitoring (SIM) methods have been reported for the determination of unchanged captopril in whole blood (7) and total captopril in plasma (8). Total captopril includes unchanged drug, the disulfide dimer of the parent drug, and mixed disulfides with endogenous thiol-containing compounds, *e.g.*, glutathione and cysteine. Recently, the *S*-methyl metabolite of captopril (II) has been identified as a urinary metabolite in humans (9) and rats (6). A GC–MS SIM method was developed to measure the plasma level of the *S*-methyl metabolite (II) after oral administration of captopril. The plasma levels of the metabolite II from samples collected from healthy human subjects after the administration of a single 100-mg tablet of captopril were compared with the free captopril blood levels and total captopril plasma levels determined as IV by GC–MS SIM methods previously reported (7, 8).

0022-3549/84/1000-1493$01.00/0

© 1984, American Pharmaceutical Association

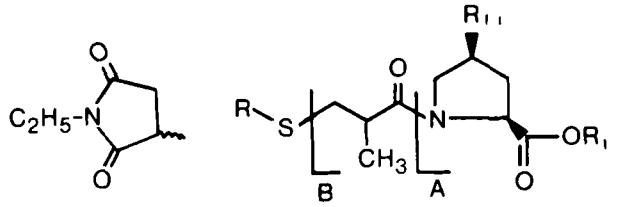

$C_6H_8NO_2$

	R	R_1	R_{11}	MW	MH_+ PCI	A	B
I	H	H	H	217			
II	CH_3	H	H	231			
III	CH_3	H	F	249			
IV	$C_6H_8NO_2$	H	H	342			
V	CH_3	CH_3	H	245	246	128	198
VI	CH_3	CH_3	F	263	264	146	216

EXPERIMENTAL SECTION

Apparatus—A mass spectrometer[1] with a data acquisition system and a GC and interface (7) as well as other equipment and apparatus have been described previously (7, 8).

Reagents—The *S*-methyl metabolite II and its 4-fluoro analogue (III) were pharmaceutical grade materials[2] and were used without additional purification. Redistilled petroleum ether (bp 30–60°C) was first washed with small portions of concentrated sulfuric acid until the discarded sulfuric acid was colorless and then with distilled water prior to distillation. Ammonium hydroxide (3%) was prepared by diluting ammonium hydroxide with distilled water. All other reagents have been previously described; this includes the columns, ethyl acetate, phosphoric acid, methanolic HCl kits, and hydrochloric acid (10).

Extraction of Plasma Samples—The internal reference standard (II) (500 ng) was added to 5 mL of plasma[3] and acidified with 2 mL of 6 M phosphoric acid. The sample was transferred to a 1-g preactivated XAD-2 column (8) by decantation and subsequent rinsing with 0.1 M hydrochloric acid. The washed, vacuum-dried column was eluted with 25 mL of purified ethyl acetate at a rate of 3 mL/min. To the ethyl acetate eluate, collected in a screw-capped tube, (250 × 150 mm), 10 mL of purified petroleum ether and 2 mL of 3% ammonium hydroxide solution were added. The drugs were extracted by shaking into the alkaline aqueous solution. After separation of the layers, the organic phase was removed by aspiration, and 1 mL of 6 M phosphoric acid and 3 g of sodium chloride were added. The solution was washed twice by shaking with 5 mL of ethyl acetate for 5 min and by centrifuging for 5 min. The retained ethyl acetate portions were combined and evaporated to dryness. Compounds II and III were determined as their respective methyl esters, V and VI, by treating the residue with 0.1 mL of 0.8 M methanolic hydrochloric acid solution in a sealed vial at 60°C for 10 min. The solution was evaporated, and the residue was dried in a vacuum desiccator for 1 h. The sample was reconstituted with 20 μL of acetone (10).

Preparation of Standard Curves—Various amounts (0–200 ng of II/mL and 500 ng of III/mL) were added to 5 mL of plasma. A freshly prepared control sample, containing 200 ng of II and 100 ng of III/mL of plasma, was extracted along with each set of samples. These samples were processed by the general scheme described above.

Instrumental Procedure—The combined GC–MS with data system was operated under the SIM mode. In the electron-impact (EI) mode, the unit was tuned from 69 to 502 Da with 1,1,2,2,3,3,4,4,4-nonafluoro-*N*,*N*-bis(nonafluorobutyl)-1-butanamine at an ionization voltage of 70 eV and an emission of 300 μA. The ion source was controlled at a constant temperature of 200°C. Helium was used as the carrier gas at a flow rate of 30 mL/min. For the chromatography in the EI mode, the column was connected through a single-stage jet separator to remove helium from the effluent. Helium, otherwise diverted, was allowed to flow into the ion source from 0.5 min to the end of the acquisition. In positive chemical ionization GC–MS, methane was used as the GC carrier gas and reagent at a flow rate of 15 mL/min. Under these conditions, the source pressure was ~80 Pa. The respective emission and electron energy were 250 μA and 240 V, optimized for the abundance of the *m/z* 219, 414, and 614 ions of 1,1,2,2,3,3,4,4,4-nonafluoro-*N*,*N*-bis(nonafluorobutyl)-1-butanamine.

In both detection modes, the multiplier and electron voltages were only applied during the data collection period. The separator and transfer lines were kept at 275°C, the ion source was maintained at 250°C, and the injector was kept at 290°C. The silanized glass column (80 cm × 2 mm), packed with 3% OV-101[4], was kept at an isothermal temperature of 190°C for 2.5 min until the analytical components were eluted (~1.5 min) and then temperature programmed to 240°C at a rate of 30°C/min to drive off other components.

About 1–2 μL of solution was evaporated on a GC solids injector. Depending on the mode of ionization, the appropriate ion profiles were obtained by SIM. The procedure for measuring the maximum peak heights and processing the data have been reported previously (7).

[1] HP 5985B; Hewlett Packard, Palo Alto, Calif.
[2] E. R. Squibb and Sons, Princeton, N.J.
[3] Serum may be substituted.

Table I—Recovery of the *S*-Methyl Metabolite of Captopril (II) [a]

Storage Temperature, °C	Recovery, ng/mL Initial	1 Week	4 Weeks
5	1630	1580	1590
5	1600	1560	1600
−20	—	1560	1590
−20	—	1610	1590

[a] Plasma (250 mL) was spiked with [^{14}C]II, subdivided, and stored as 5-mL samples; measured in duplicate at each time-temperature condition.

Table II—Recovery of *S*-Methyl Metabolite of Captopril (II)

Set No.[a]	n[b]	Mean (σ), ng/mL	Δ (Taken − Found)
1	4	98.5 (2.8)	
2	3	99.9 (1.5)	
3	4	100.1 (0.9)	
4	3	98.8 (3.2)	
5	5	99.0 (2.0)	
6	3	99.9 (3.1)	
7	4	99.9 (0.1)	
Mean		99.4 (2.25)	0.6
8	4	12.9 (0.7)	−0.4

[a] Sets 1–7 were spiked with 100 ng/mL of plasma. Set 8 was spiked with 12.5 ng/mL of plasma. [b] Replicate measurements of the same sample.

RESULTS AND DISCUSSION

Although the extraction procedure for the metabolite II was patterned after the method developed for the extraction of IV (7), there were several significant differences. The isolation was accomplished by direct adsorption of II from acidified plasma samples onto XAD-2. The back-extraction was performed with 3% ammonium hydroxide. The solubility of II in ethyl acetate was suppressed by the addition of petroleum ether, which resulted in better phase separation. The compounds were then quantitatively extracted into ethyl acetate from aqueous solutions saturated with sodium chloride to remove additional potentially interfering components. Because significantly lower *S*-methyl metabolite II levels were expected, 5 mL of plasma was processed, with a total of 500 ng of III added as the internal reference standard. It was not practical to isolate and measure total captopril and II concurrently because of the great disparity in their levels. It was decided to process individual samples for the metabolite II in plasma, unchanged captopril in whole blood treated with *N*-ethylmaleimide at the time of sampling, and total captopril in plasma (7, 8). The *S*-methyl metabolite II may be stored for at least 4 weeks at either 5°C or −20°C in plasma without decomposition (Table I).

Methylation of the proline carboxylic acid group was chosen because it forms a low-molecular-weight derivative suitable for GC–MS. Both EI and chemical ionization (CI) MS were explored as potential methods, but the greatest sensitivity and specificity was obtained by CI with the MH^+ of esters V and VI. Under these conditions, a linear calibration curve was obtained with a slope of 1.5 and an intercept of 0.001, as determined by linear regression analysis. A correlation coefficient of 0.9981 was obtained from the calibration data. With each set of extracts, a freshly extracted control was measured as a validation of the method. The 26 replicate measurements of the 100-ng/mL extracted control samples showed a mean *SD* of 2.25 ng/mL and an absolute difference of 0.6 ng/mL from the added amount (Table II). A difference of 0.4 ng/mL was found for the four 12.5-ng/mL spiked samples. The *m/z* 128–*m/z* 146 ions, although producing intense EI ions, also had significant interferences from the coeluting background components.

The levels of the *S*-methyl metabolite II were low (Table III) relative to both unchanged and total captopril levels for the same subjects (Table IV). For the comparison, the unchanged captopril blood values were multiplied by two to approximate the plasma levels. The parameter *D* is defined as the

[4] On 80/100 Supelcoport; Bellefonte, Pa.

Table III—*S*-Methyl Metabolite of Captopril Plasma Levels After Oral Administration of Captopril [a]

Time, h	Subject 1	Subject 2	Subject 3	Subject 4	Subject 5	Subject 6	Subject 7	Mean (σ)[b]
0	0.1	0.2	0.2	0.1	0	0.5	0	0.2 (0.2)
0.5	102	7.3	13	36.7	9	43.3	29.7	34.4 (30.5)
1	114	49.4	42.4	73.0	48.6	94.6	84.9	72.4 (25.0)
2	80.2	65.0	62.5	42.1	60.7	78.2	71.7	65.8 (11.9)
3	39.8	46.6	45.2	27.3	35.0	47.5	47.9	41.3 (7.2)
4	27.3	39.4	32.1	21.8	21.2	40.5	37.8	31.4 (7.6)
6	16.2	21.0	15.9	9.9	12.0	17.1	25.3	16.8 (4.8)
8	9.3	14.4	10.0	8.2	9.5	14.2	13.3	11.3 (2.4)
12	5.4	7.4	6.2	3.6	3.8	4.9	8.1	5.6 (1.6)
24	1.4	1.4	1.0	0.4	0.7	1.2	0.7	1.0 (0.4)

[a] Single 100-mg dose. Values are in nanograms per milliliter. [b] *SD*, seven subjects.

Table IV—Mean Values (ng/mL) of Captopril and Metabolites in Plasma Equivalents [a]

Time, h	Total T	2 × Unchanged[b] ($2F$)	Disulfide Metabolites[c] (D)	*S*-Methyl Metabolites[d] (S)	R[e]
0	—	4	—	0.2	—
0.5	1750	1346	404	34.4	0.020
1	3140	1672	1468	72.4	0.023
2	2400	596	1804	65.8	0.027
3	1570	200	1370	41.3	0.026
4	1150	42.7	1107	31.4	0.027
6	680	29.6	650	16.8	0.025
8	460	13.0	447	11.3	0.025
12	270	—	270	5.6	0.021
24	80	—	80	1.0	0.0125[f]

[a] Seven subjects. [b] Assumes plasma is one-half the volume of whole blood. [c] Difference $D = T - 2F$ = disulfide metabolites derived from captopril. [d] Taken from the mean values shown in Table III. [e] $R = S/T$. The mean from samples taken at 0.5–12 h was 0.024; (σ/mean) × 100 = 11. [f] Excluded from determination of the means.

difference between the total captopril level and twice the free captopril level as an expression of the disulfide levels. Uniformly, the individual values followed exactly the mean values (Table IV). Whereas the unchanged captopril levels predominate during the first hour, the disulfides derived from captopril were the significant components after that. Levels of the metabolite II followed most closely the total drug concentrations. The mean ratio between the metabolite II and total captopril, R, was 0.024 for samples taken at 0.5–12 h (Table IV). No zero values of metabolite II were observed in any of the samples taken during the first 12 h, and more than half of the samples collected over 24 h had values of ≥1 ng/mL.

In recent reports, various discussions have been concerned with the concept of interconversion of protein-bound drug to "free" captopril (5) and of a subsequent conversion of captopril or its disulfides to the *S*-methyl metabolite by *S*-methyltransferase (6). The role of *S*-methylation, other than as a metabolic pathway, is not well understood. The discussion following a recent presentation highlights this point (9). This analytical method, combined with the previously reported methods for determining unchanged (7) and total (8) captopril, allows profiling to study the role of *S*-methylation in renal function. Future steady-state studies, combined with pulsed deuterated analogue administration, might help in establishing the role of protein-bound captopril in deep compartments *versus* circulating protein-bound blood components.

REFERENCES

(1) M. A. Ondetti, B. Rubin, and D. W. Cushman, *Science*, **196**, 441 (1977).

(2) D. W. Cushman, H. S. Cheung, E. F. Sabo, and M. A. Ondetti, *Biochemistry*, **16**, 5484 (1977).

(3) R. K. Ferguson, H. R. Brunner, G. A. Turini, H. Gavras, and D. N. McKinstry, *Lancet*, **i**, 775 (1977).

(4) R. C. Heel, R. N. Brogden, T. M. Speight, and G. S. Avery, *Drugs*, **20**, 409 (1980).

(5) K. L. Duchin, S. M. Singhvi, D. A. Willard, B. H. Migdalof, and D. N. McKinstry, *Clin. Pharmacol. Ther.*, **31**, 452 (1982).

(6) B. K. Park, P. S. Grabowski, J. H. K. Young, and A. M. Breckenridge, *Biochem. Pharm.*, **31**, 1755 (1982).

(7) A. I. Cohen, R. G. Devlin, E. Ivashkiv, P. T. Funke, and T. McCormick, *J. Pharm. Sci.*, **71**, 1251 (1982).

(8) E. Ivashkiv, A. I. Cohen, D. N. McKinstry, *J. Pharm. Sci.*, **73**, 1113 (1984).

(9) O. H. Drummer, B. Jarrott, and W. J. Louis, *Clin. Exp. Pharm. Physiol.*, **Suppl. 7**, 81 (1982).

(10) P. T. Funke, E. Ivashkiv, M. F. Malley, and A. I. Cohen, *Anal. Chem.*, **52**, 1086 (1980).

ACKNOWLEDGMENTS

We acknowledge the personal discussions and consultation of W. J. Louis that resulted in this research project.

Relationship of Morphine-Induced Miosis to Plasma Concentration in Normal Subjects

IRA L. FEDDER *, PETER H. VLASSES *, PARVIZ MOJAVERIAN *, MARIO L. ROCCI, JR. ‡, HESCHI H. ROTMENSCH *, BRIAN N. SWANSON *, and ROGER K. FERGUSON *x

Received June 27, 1983, from the *Division of Clinical Pharmacology, Department of Medicine, Jefferson Medical College of Thomas Jefferson University, Philadelphia PA 19107, and the ‡Department of Pharmacy Practice, Philadelphia College of Pharmacy and Science, Philadelphia, PA 19104. Accepted for publication December 6, 1983.

Abstract □ The relationship between morphine plasma concentration and pupil diameter was evaluated 2–10 h following intravenous administration of morphine sulfate (10 mg). Seven healthy male volunteers received 10 mg of morphine intravenously following pretreatment for 4 d with either cimetidine (300 mg po four times a day) or placebo in a single blind, balanced crossover study. Pupil diameters were measured directly from contact prints using calipers and a photographed millimeter scale. Cimetidine pretreatment had no significant effect on pupil size either before or after morphine administration or on morphine pharmacokinetics. The relationship between morphine plasma concentration (2–10 h postdose) and pupil diameter was evaluated from the pooled data from both morphine treatment periods by perpendicular least-squares regression. In each individual, a strong relationship existed between morphine plasma concentrations and pupil diameter ($r = -0.76$ to -0.91; $p < 0.05$). Weaker correlations for both pupil diameter ($r = -0.65$; $p < 0.0001$) and the absolute change in pupil diameter from baseline ($r = 0.72$; $p < 0.0001$) for the grouped data probably reflect intersubject variation in morphine sensitivity. Thus, the miotic response to an intravenous dose of morphine varies in proportion to morphine plasma concentration.

Keyphrases □ Morphine—relationship of morphine-induced miosis and plasma concentration in normal subjects □ Miosis—morphine-induced, relationship to plasma concentration

In the initial 2 h following an intravenous dose of heroin, pupil diameter is directly related to plasma concentration of morphine equivalents in both naive and dependent subjects (1). After oral methadone administration, decreases in pupil diameter appear to follow the same time course as methadone plasma concentration (2). While investigating the effects of oral cimetidine on the disposition of intravenous morphine (3), serial measurements of the extent and duration of morphine-induced miosis were made. In this report are described the relationships observed in individuals between plasma morphine concentrations after an intravenous morphine dose and pupil diameter.

EXPERIMENTAL SECTION

Seven healthy male volunteers (weight, 65–98 kg; age, 20–38 years) participated in a single blind crossover study and were randomly assigned to receive either oral cimetidine (300 mg once every 6 h) or placebo for 4 d. On day four of each treatment period, the volunteers reported for testing after an overnight fast. Each subject received either cimetidine or placebo orally. One hour later, morphine sulfate (10 mg; 8.5 mg of free base) was administered intravenously over 2 min. Plasma was obtained at a series of times postinjection to determine the pharmacokinetics of morphine. Morphine concentrations were determined by radioimmunoassay (4). A 7-d interval separated morphine treatments.

Pupil diameters were measured prior to and at 2, 5, 7, and 10 h after each morphine dose by a photographic technique (5–8). Subjects were placed in a dimly lit room (4 foot candles) and allowed to sit quietly. Black and white photographs of the left eye of each subject were taken with a 35-mm single lens reflex camera[1] with ASA-125 film[2]. The camera was equipped with an electronic flash and a fixed-focus, close-up lens which produced a life size, (*i.e.*, 1:1 magnification) image on the negative. A millimeter scale was photographed under the same magnification. Pupil diameters were measured on the contact prints with calipers and the millimeter scale. A representative example of pupil measurements taken before and after morphine administration is depicted in Fig. 1.

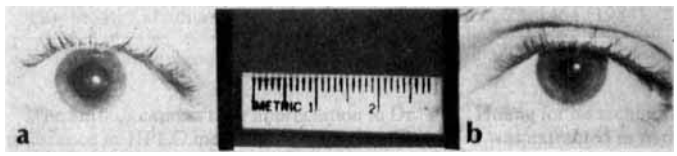

Figure 1—*Pupillary response to intravenously administered morphine sulfate (10 mg) in subject 4. Pupil diameter (5.9 mm) prior to morphine administration (a) is contrasted with pupil diameter 2 h following morphine administration (3.3 mm) (b).*

The relationships within and among individuals between morphine plasma concentration and pupil diameter were evaluated by perpendicular least-squares regression (9). Statistical comparison of pupil diameters as well as the slopes of the regression lines were done by using a paired Student's *t* test (9). All results are expressed as the mean ± *SD*.

RESULTS

Cimetidine pretreatment had no effect on baseline (premorphine) mean pupil diameter (placebo *versus* cimetidine, 6.4 ± 0.7 *versus* 6.3 ± 0.9 mm). A significant correlation existed between morphine plasma concentration and pupil diameter for each treatment period (placebo, $r = -0.69$, $p < 0.0001$; cimetidine, $r = -0.60$, $p < 0.001$). In addition, the mean of the slopes of the regression lines for each individual were not significantly different (placebo = −0.098, cimetidine = −0.110; $p < 0.05$).

Since cimetidine pretreatment appeared to have no effect on morphine pharmacokinetics (3) or on the relationship between morphine plasma concentration and pupil diameter, additional analysis of the combined data was performed. For the combined data, significant correlations were observed between pupil diameter and morphine plasma concentration at corresponding times. A significant correlation existed between the absolute change in pupil diameter from baseline (premorphine) and morphine plasma concentration ($r = 0.72$; $p < 0.0001$). The correlation coefficient for the grouped data (all observations) was −0.65 ($p < 0.0001$), whereas the correlation coefficients for the data from each subject, independent of pretreatment, ranged from −0.76 to −0.91 (Table I). The relationships between pupil diameter (in millimeters) and morphine plasma concentration for the subjects with the highest and lowest correlation coefficients (*i.e.*, subjects 4 and 6, respectively) are shown in Fig. 2.

Table I—Correlation Between Pupil Diameters and Plasma Morphine Concentrations in Healthy Volunteers [a]

Subject	Correlation Coefficient	Slope
1[b]	−0.86[c]	−0.120
2	−0.85[c]	−0.094
3	−0.77[c]	−0.065
4	−0.91[c]	−0.071
5	−0.78[c]	−0.089
6	−0.76[d]	−0.050
7	−0.82[c]	−0.066
Mean ± *SD*	−0.82 ± 0.06	−0.079 ± 0.02

[a] Pupil diameters are in millimeters, and plasma morphine concentrations are in nanograms per milliliter; $n = 10$ after a 10-mg iv infusion of morphine sulfate; data were collected before and at 2, 5, 7, and 10 h after morphine injection and were combined for placebo and cimetidine treatment periods (see text). [b] $n = 9$. [c] $p < 0.01$. [d] $p < 0.05$.

[1] Nikon.
[2] Plus-X.

0022-3549/84/1000-1496$01.00/0
© 1984, American Pharmaceutical Association

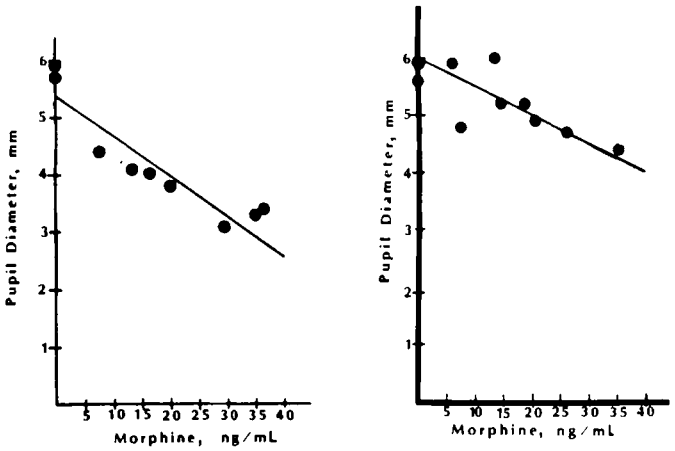

Figure 2—*Regression line derived from the data for subjects 4 and 6. These represent the subjects with the highest and lowest correlation coefficients. For subject 4 (left),* $y = -0.07x + 5.4$, $r = -0.91$, $p < 0.01$; *for subject 6 (right),* $y = -0.05x + 6.0$, $r = -0.76$, $p < 0.05$.

DISCUSSION

Recently, greater emphasis has been placed on evaluating the nature of the relationship between the pharmacokinetics and pharmacodynamics of an agent (10). The data from the present study establish the relationship between the miotic response to morphine and its plasma concentrations in the postdistributive phase. A difference in the magnitude of the correlation coefficients for individuals *versus* the group was observed. This is most probably accounted for by individual variation in pretreatment pupil diameter and sensitivity to morphine; evidence for the latter is the wide range of slopes described in Table I. Cimetidine exhibited no demonstrable effect on pupil diameter prior to or following morphine administration. These findings suggest that H_2-receptors have little role in the regulation of pupil size and are consistent with the lack of effect of cimetidine on morphine pharmacokinetics (3).

These data confirm and extend the previous observations of a relationship between plasma concentration of morphine equivalents following an intravenous dose of heroin and pupil diameter (1, 11). However, correlation coefficients were not reported in those studies, making comparison with the results obtained in this study impossible. Similarly, the time course of methadone-induced miosis appears to parallel methadone plasma concentrations (2).

Photographic pupillometry is an easily performed, readily quantifiable test which may have experimental and clinical utility for monitoring opiate activity. For example, tolerance to the miotic response to morphine has been demonstrated and used in the assessment of opiate dependency (7, 11). Further investigations are warranted to clarify the relationships between the serum concentrations of other opiate analgesics or other ocularly active agents and pupil diameter.

REFERENCES

(1) K. H. Tress and A. A. El-Sobky, *Br. J. Clin. Pharmacol.*, **7,** 213 (1979).

(2) C. E. Inturrisi and K. Verebely, *Clin. Pharmacol. Ther.*, **13,** 923 (1972).

(3) P. Mojaverian, I. L. Fedder, P. H. Vlasses, H. H. Rotmensch, M. L. Rocci, Jr., B. N. Swanson, and R. K. Ferguson, *Br. J. Clin. Pharmacol.*, **14,** 809 (1982).

(4) S. Spector and C. Parker, *Science*, **168,** 1347 (1970).

(5) D. R. Jasinski and W. R. Martin, *Clin. Pharmacol. Ther.*, **8,** 271 (1967).

(6) P. B. Keuhn, A. K. Shawar, W. A. Weigand, and V. F. Smolen, *J Pharm. Sci.*, **65,** 1593 (1976).

(7) E. C. Senay and J. E. Shick, *Drug Alcohol Depend.*, **3,** 133 (1978).

(8) V. F. Smolen, *J. Pharmacokinet. Biopharm.*, **4,** 337 (1976).

(9) D. S. Riggs, J. A. Guarniere, and S. Addelman, *Life Sci.*, **22,** 1305 (1978).

(10) N. H. G. Holford and L. B. Sheiner, *Clin. Pharmacokinet.*, **6,** 429 (1981).

(11) K. H. Tress, A. A. El-Sobky, W. Aherne, and E. Piall, *Br. J. Clin. Pharmacol.*, **5,** 299 (1978).

Evidence Favoring the Venous Equilibrium Model for Hepatic Clearance of (*S*)-(−)-Propranolol

Keyphrases □ Propranolol—hepatic clearance, venous equilibrium model □ Hepatic clearance—propranolol, venous equilibrium model

To the Editor:

Drug clearance is an important pharmacokinetic parameter since it most closely reflects the ability of the body to rid itself of drug. Because the liver is a major site of drug elimination, there is considerable interest in understanding the processes by which drugs are cleared as they pass through this organ. Two physical models for hepatic drug clearance have been proposed. The venous equilibrium or "well-stirred" model assumes that the liver can be viewed as a single homogeneous compartment with the free or unbound drug concentration in hepatic venous blood in equilibrium with that in the liver (1). The sinusoidal model assumes that the liver is composed of a number of parallel tubes with drug-metabolizing enzymes evenly distributed throughout (2). In this model, drug concentration declines continuously as blood traverses the sinusoid. Although the determinants of drug clearance are the same in both models (liver blood flow, unbound fraction of drug in blood, and intrinsic clearance of unbound drug), the equations relating these variables to hepatic clearance differ. For the venous equilibrium model:

$$CL = Q \cdot f_u \cdot CL_{u,int}/(Q + f_u \cdot CL_{u,int}) \quad \text{(Eq. 1)}$$

while for the sinusoidal model:

$$CL = Q(1 - e^{-f_u \cdot CL_{u,int}/Q}) \quad \text{(Eq. 2)}$$

where Q is the liver blood flow, f_u is the fraction of unbound drug in blood, $CL_{u,int}$ is the intrinsic clearance of unbound drug, and CL is the liver clearance.

Despite the difference between these equations, both predict quantitatively similar values for drug clearance under most conditions of varying blood flow, free fraction, or intrinsic clearance. However, an extensive theoretical analysis of the models has suggested that major differences exist in predictions of area under the concentration-time curve (AUC) and systemic availability (F) when highly extracted drugs are administered orally (3). In the venous equilibrium model:

$$F = Q/(Q + f_u \cdot CL_{u,int}) \quad \text{(Eq. 3)}$$

and:

$$\text{AUC} = \text{Dose}/f_u \cdot CL_{u,int} \quad \text{(Eq. 4)}$$

while in the sinusoidal model:

$$F = e^{-f_u \cdot CL_{u,int}/Q} \quad \text{(Eq. 5)}$$

and:

$$\text{AUC} = \text{Dose}(e^{-f_u CL_{u,int}/Q})/Q(1 - e^{-f_u CL_{u,int}/Q}) \quad \text{(Eq. 6)}$$

It is readily appreciated from these equations that changes in blood flow or drug binding will result in approximately linear changes in F and AUC for a highly extracted drug according to the venous equilibrium model, while the sinusoidal model predicts exponential changes.

The venous equilibrium model appears to be much more commonly employed in pharmacokinetic analysis today. However, there is little physiological or experimental evidence to suggest that this model is preferable. Using the isolated perfused rat liver preparation, Pang and Rowland (4) found that the clearance of highly extracted lidocaine was best described by the "well-stirred" model. The hepatic elimination of galactose, however, has been observed to be more consistent with the predictions of the sinusoidal model (5). Both of these investigations were conducted under conditions of perturbed blood flow. Such studies could also be carried out by varying the degree of protein binding (3). Jones *et al.* (6) have recently reported that a sevenfold change in the free fraction of propranolol does not alter effluent unbound propranolol concentration in the perfused rat liver, a finding consistent with venous equilibrium theory. The discovery over the past several years that many highly extracted basic drugs are highly bound to α_1-acid glycoprotein (7) makes this approach feasible not only *in situ* but also in the intact animal, since the concentration of α_1-acid glycoprotein and degree of protein binding may change dramatically and rapidly in a number of conditions and disease states (8–10).

The recently published data of Terao and Shen (11) provides an excellent opportunity to evaluate the relative merits of the proposed models based on *in vivo* observations. These investigators administered oral and intravenous (*S*)-(−)-propranolol to rats 1 and 7 d following implantation of an indwelling jugular venous catheter. The free fraction of (*S*)-(−)-propranolol decreased from an average of 0.169 1 d following catheter insertion to 0.074 7 d later, presumably due to a catheter-stimulated increase in α_1-acid glycoprotein concentration. Bioavailability and AUC were measured following the administration of oral drug on both occasions and are listed in Table I. F was found to increase from 4.1 to 7.8%, while AUC increased from 3.45 to 6.95 μg·min/mL as protein binding increased.

The predicted effect of such a change in binding on these parameters was calculated for both models using Eqs. 3–6. These predictions assume complete absorption of (*S*)-(−)-propranolol, that liver blood flow and intrinsic clearance of unbound drug are the same on both study days and that

Table I—Observed and Predicted Changes in *F* and AUC Secondary to Increased Protein Binding

	$f_u = 0.169$	$f_u = 0.074$	Ratio[b]
Observed F (%)[a]	4.1	7.8	1.90
Predicted			
Venous equilibrium model	—	8.9	2.17
Sinusoidal model	—	24.6	6.00
Observed AUC (μg·min/mL)[a]	3.45	6.95	2.01
Predicted			
Venous equilibrium model	—	7.88	2.28
Sinusoidal model	—	26.32	7.63

[a] Data from Terao and Shen (11). [b] Ratio of value at $f_u = 0.074$ to observed value at $f_u = 0.169$.

0022-3549/84/1000-1498$01.00/0
© 1984, American Pharmaceutical Association

(*S*)-(−)-propranolol is entirely cleared by the liver. The value of $CL_{u,int}$ for each model was estimated from Eqs. 1 and 2 using the (*S*)-(−)-propranolol clearance of 6.61 mL/min/100 g observed following intravenous administration 1 d after catheter insertion. Q was calculated using this value for clearance and an extraction ratio of 0.959. Table I lists the predictions and compares the ratio of predicted or observed values at the time of increased binding to the original observation. As expected, significant differences between the models were observed with the venous equilibrium equations predicting 2.17- and 2.28-fold increases in F and AUC, respectively, given the observed binding change, while the sinusoidal model predicted 6.00- and 7.63-fold increases in these parameters. Clearly, the predictions of the venous equilibrium model more closely approximate the values observed by Terao and Shen (11). In fact, there is remarkably good agreement with only 14.1 and 13.4% error in the predictions of F and AUC, respectively, using this model.

Although this data is limited to observations in one species with a single substrate, it does provide *in vivo* evidence in support of the venous equilibrium model for hepatic clearance. This is important information since there are many clinical situations in which liver blood flow, protein binding, or intrinsic drug clearance may be altered. Knowledge of the appropriate physical model for hepatic clearance allows one to predict with reasonable accuracy the effect of changes in these factors on important pharmacokinetic parameters such as F and AUC. This is particularly crucial when highly extracted compounds are administered orally. Prospective studies examining this issue further with other highly extracted drugs are needed in order to confirm that the venous equilibrium model is indeed the preferred physical model for hepatic drug clearance.

(1) M. Rowland, L. Z. Benet, and G. G. Graham, *J. Pharmacokinet. Biopharm.*, **1**, 123 (1973).

(2). K. Winkler, S. Keiding, and N. Tygstrup, in "The Liver: Quantitative Aspects of Structure and Functions," G. Paumgartner and R. Presig, Eds., Karger, Basel, 1973, pp. 144–155.

(3) K. S. Pang and M. Rowland, *J. Pharmacokinet. Biopharm.*, **5**, 625 (1977).

(4) K. S. Pang and M. Rowland, *J. Pharmacokinet. Biopharm.*, **5**, 655 (1977).

(5) S. Keiding and E. Chiarantini, *J. Pharmacol. Exp. Ther.*, **205**, 465 (1978).

(6) D. B. Jones, D. J. Morgan, G. W. Mihaly, L. K. Webster, and R. A. Smallwood, *J. Pharmacol. Exp. Ther.*, **229**, 522 (1984).

(7) K. M. Piafsky, *Clin. Pharmacokinet.*, **5**, 246 (1980).

(8) B. G. Johansson, C. O. Kindmark, E. Y. Trell, and F. A. Wollheim, *Scand. J. Clin. Lab. Invest.*, **29** (Suppl. 124), 117 (1972).

(9) D. J. Edwards, D. Lalka, F. Cerra, and R. L. Slaughter, *Clin. Pharmacol. Ther.*, **31**, 62 (1982).

(10) K. M. Piafsky, O. Borga, L. Odar-Cederloff, C. Johansson, and F. Sjöquist, *N. Engl. J. Med.*, **299**, 1435 (1978).

(11) N. Terao and D. D. Shen, *J. Pharmacol. Exp. Ther.*, **227**, 369 (1983).

David J. Edwards

Department of Pharmaceutical Sciences
College of Pharmacy and
Allied Health Professions
Wayne State University
Detroit, MI 48202
Pharmacokinetics Laboratory
Department of Pharmacy Services
Detroit Receiving Hospital and
University Health Center
Detroit, MI 48201

Received May 31, 1984.
Accepted for publication August 2, 1984.

Method for Determination of First-Pass Metabolism in Human Skin

Keyphrases □ Metabolism, first-pass—transdermal formulations, human skin □ Transdermal formulations—percutaneous first-pass metabolism, human skin □ Viprostol—transdermal formulations, first-pass metabolism

To the Editor:

The technological advances in drug-delivery systems have allowed increased utilization of transdermal formulations for therapeutic purposes. This route of administration is most suitable for potent drugs possessing short biological half-lives, extensive first-pass metabolism after oral administration, and narrow therapeutic indices. By controlling the rate of delivery and absorption through the skin, it is possible to maintain therapeutic drug concentrations in the blood and/or at the site of action. The systemic blood concentrations of such compounds after transdermal administration in humans is very low and often below the sensitivity levels of specific assay procedures. Nitroglycerin, which undergoes extensive first-pass metabolism when given orally, is one of the most widely used drugs in transdermal systems. To circumvent the assay sensitivity problem and allow for a comparison of dosage forms, Karim (1) has proposed, and effectively implemented, blood sampling from the ipsilateral antecubital forearm veins after application of the topical formulation on the volar surface of the wrist. The purpose of this communication is to describe a similar procedure that can also estimate the percutaneous first-pass metabolism of topically applied compounds, even when extensive biotransformation takes place in the skin.

Drug and/or drug and metabolite (*i.e.*, total) concentrations in samples from the contralateral antecubital forearm will be low and represent the systemic blood concentrations (C_c). The ipsilateral samples will contain higher blood concentrations (C_i), and represent the concentration of the drug absorbed plus C_c at any given time. After correction for C_c, the ipsilateral concentrations will directly reflect the flux of the drug (C_j) through the skin; *i.e.*,

$$C_j = C_i - C_c \qquad \text{(Eq. 1)}$$

where $C_i = C_{p,j} + C_{m,j} + C_{p,c} + C_{m,c}$, $C_c = C_{p,c} + C_{m,c}$, and $C_j = C_{p,j} + C_{m,j}$. In this case C_p is the concentration of the unchanged drug and C_m is the total concentration of metabolites.

In the absence of any metabolism and/or degradation of the drug during the percutaneous absorption process, C_j will consist of the intact drug only, *i.e.*, $C_j = C_{p,j}$. If during the absorption processes the drug undergoes metabolism, C_j will consist of the concentrations of the drug ($C_{p,j}$) and metabolite(s) ($C_{m,j}$) in the ipsilateral samples at any time. In such a situation the magnitude of the first-pass metabolism can be estimated by calculating the fractions of unchanged drug and metabolite(s). Biotransformation and/or binding in the vein from the absorption site (the skin) up to the point of blood sampling would be accounted for but not differentiated from metabolism in the skin. The same is true if degradation processes other than biotransformation were involved.

When the rate of absorption through the skin is constant, and C_j reaches steady-state level, the fraction metabolized in the skin (f_s) can be estimated by:

$$f_s = \frac{C_{m,j}}{C_{p,j} + C_{m,j}} \qquad \text{(Eq. 2)}$$

0022-3549/84/1000-1499$01.00/0

© 1984, American Pharmaceutical Association

(*S*)-(−)-propranolol is entirely cleared by the liver. The value of $CL_{u,int}$ for each model was estimated from Eqs. 1 and 2 using the (*S*)-(−)-propranolol clearance of 6.61 mL/min/100 g observed following intravenous administration 1 d after catheter insertion. Q was calculated using this value for clearance and an extraction ratio of 0.959. Table I lists the predictions and compares the ratio of predicted or observed values at the time of increased binding to the original observation. As expected, significant differences between the models were observed with the venous equilibrium equations predicting 2.17- and 2.28-fold increases in F and AUC, respectively, given the observed binding change, while the sinusoidal model predicted 6.00- and 7.63-fold increases in these parameters. Clearly, the predictions of the venous equilibrium model more closely approximate the values observed by Terao and Shen (11). In fact, there is remarkably good agreement with only 14.1 and 13.4% error in the predictions of F and AUC, respectively, using this model.

Although this data is limited to observations in one species with a single substrate, it does provide *in vivo* evidence in support of the venous equilibrium model for hepatic clearance. This is important information since there are many clinical situations in which liver blood flow, protein binding, or intrinsic drug clearance may be altered. Knowledge of the appropriate physical model for hepatic clearance allows one to predict with reasonable accuracy the effect of changes in these factors on important pharmacokinetic parameters such as F and AUC. This is particularly crucial when highly extracted compounds are administered orally. Prospective studies examining this issue further with other highly extracted drugs are needed in order to confirm that the venous equilibrium model is indeed the preferred physical model for hepatic drug clearance.

(1) M. Rowland, L. Z. Benet, and G. G. Graham, *J. Pharmacokinet. Biopharm.*, **1**, 123 (1973).

(2). K. Winkler, S. Keiding, and N. Tygstrup, in "The Liver: Quantitative Aspects of Structure and Functions," G. Paumgartner and R. Presig, Eds., Karger, Basel, 1973, pp. 144–155.

(3) K. S. Pang and M. Rowland, *J. Pharmacokinet. Biopharm.*, **5**, 625 (1977).

(4) K. S. Pang and M. Rowland, *J. Pharmacokinet. Biopharm.*, **5**, 655 (1977).

(5) S. Keiding and E. Chiarantini, *J. Pharmacol. Exp. Ther.*, **205**, 465 (1978).

(6) D. B. Jones, D. J. Morgan, G. W. Mihaly, L. K. Webster, and R. A. Smallwood, *J. Pharmacol. Exp. Ther.*, **229**, 522 (1984).

(7) K. M. Piafsky, *Clin. Pharmacokinet.*, **5**, 246 (1980).

(8) B. G. Johansson, C. O. Kindmark, E. Y. Trell, and F. A. Wollheim, *Scand. J. Clin. Lab. Invest.*, **29** (Suppl. 124), 117 (1972).

(9) D. J. Edwards, D. Lalka, F. Cerra, and R. L. Slaughter, *Clin. Pharmacol. Ther.*, **31**, 62 (1982).

(10) K. M. Piafsky, O. Borga, L. Odar-Cederloff, C. Johansson, and F. Sjöquist, *N. Engl. J. Med.*, **299**, 1435 (1978).

(11) N. Terao and D. D. Shen, *J. Pharmacol. Exp. Ther.*, **227**, 369 (1983).

David J. Edwards

Department of Pharmaceutical Sciences
College of Pharmacy and
Allied Health Professions
Wayne State University
Detroit, MI 48202
Pharmacokinetics Laboratory
Department of Pharmacy Services
Detroit Receiving Hospital and
University Health Center
Detroit, MI 48201

Received May 31, 1984.
Accepted for publication August 2, 1984.

Method for Determination of First-Pass Metabolism in Human Skin

Keyphrases □ Metabolism, first-pass—transdermal formulations, human skin □ Transdermal formulations—percutaneous first-pass metabolism, human skin □ Viprostol—transdermal formulations, first-pass metabolism

To the Editor:

The technological advances in drug-delivery systems have allowed increased utilization of transdermal formulations for therapeutic purposes. This route of administration is most suitable for potent drugs possessing short biological half-lives, extensive first-pass metabolism after oral administration, and narrow therapeutic indices. By controlling the rate of delivery and absorption through the skin, it is possible to maintain therapeutic drug concentrations in the blood and/or at the site of action. The systemic blood concentrations of such compounds after transdermal administration in humans is very low and often below the sensitivity levels of specific assay procedures. Nitroglycerin, which undergoes extensive first-pass metabolism when given orally, is one of the most widely used drugs in transdermal systems. To circumvent the assay sensitivity problem and allow for a comparison of dosage forms, Karim (1) has proposed, and effectively implemented, blood sampling from the ipsilateral antecubital forearm veins after application of the topical formulation on the volar surface of the wrist. The purpose of this communication is to describe a similar procedure that can also estimate the percutaneous first-pass metabolism of topically applied compounds, even when extensive biotransformation takes place in the skin.

Drug and/or drug and metabolite (*i.e.*, total) concentrations in samples from the contralateral antecubital forearm will be low and represent the systemic blood concentrations (C_c). The ipsilateral samples will contain higher blood concentrations (C_i), and represent the concentration of the drug absorbed plus C_c at any given time. After correction for C_c, the ipsilateral concentrations will directly reflect the flux of the drug (C_j) through the skin; *i.e.*,

$$C_j = C_i - C_c \qquad \text{(Eq. 1)}$$

where $C_i = C_{p,j} + C_{m,j} + C_{p,c} + C_{m,c}$, $C_c = C_{p,c} + C_{m,c}$, and $C_j = C_{p,j} + C_{m,j}$. In this case C_p is the concentration of the unchanged drug and C_m is the total concentration of metabolites.

In the absence of any metabolism and/or degradation of the drug during the percutaneous absorption process, C_j will consist of the intact drug only, *i.e.*, $C_j = C_{p,j}$. If during the absorption processes the drug undergoes metabolism, C_j will consist of the concentrations of the drug ($C_{p,j}$) and metabolite(s) ($C_{m,j}$) in the ipsilateral samples at any time. In such a situation the magnitude of the first-pass metabolism can be estimated by calculating the fractions of unchanged drug and metabolite(s). Biotransformation and/or binding in the vein from the absorption site (the skin) up to the point of blood sampling would be accounted for but not differentiated from metabolism in the skin. The same is true if degradation processes other than biotransformation were involved.

When the rate of absorption through the skin is constant, and C_j reaches steady-state level, the fraction metabolized in the skin (f_s) can be estimated by:

$$f_s = \frac{C_{m,j}}{C_{p,j} + C_{m,j}} \qquad \text{(Eq. 2)}$$

0022-3549/84/1000-1499$01.00/0

© 1984, American Pharmaceutical Association

Table I—Concentrations of II ($C_{p,i}$) and Total Radioactivity in the Ipsilateral (C_i) and Contralateral (C_c) Plasma Samples After Application of a 1.5-mg Dose on the Forearm of Two Male Subjects

Hours of Application	Subject 1 Concentration, ng/mL					Subject 2 Concentration, ng/mL				
	C_c	C_i	$C_{p,i}$	$C_{m,i}$	f_s[a]	C_c	C_i	$C_{p,i}$	$C_{m,i}$	f_s[a]
2	—	18.2	5.8	12.4	0.68	—	2.8	1.2	1.6	0.57
4	0.48	14.7	4.6	10.1	0.69	0.43	4.8	1.4	3.4	0.71
6	0.65[b]	19.3	8.0	11.3	0.59	0.52[b]	11.7	3.7	8.0	0.68
8	0.85	31.5	10.0	21.5	0.68	0.62	11.1	3.2	7.9	0.71
12	0.52	27.8	9.8	18.0	0.65	0.57	14.8	3.2	11.6	0.78
16	—	6.7	2.7	4.0	0.60	—	10.8	2.7	8.1	0.75
Mean					0.65					0.70
CV					6.2%					10%

[a] $f_s = C_{m,j}/C_j$, where $C_j = C_i - C_c$ and $C_{m,j} = C_j - C_{p,j}$. Because $C_{p,i} = C_{p,j} + C_{p,c}$ and the values of $C_{p,c}$ are below the detectable level of 0.05 ng/mL, $C_{p,j}$ was assumed to be essentially the same as $C_{p,i}$ as presented in this table. [b] Interpolated values.

where $C_{p,j}$ and $C_{m,j}$ are concentrations of the drug absorbed either unchanged or as a metabolite(s), respectively. Assuming that (*a*) skin metabolism is much higher than the metabolism in other tissue up to the point of ipsilateral sampling and (*b*) there is no preferential tissue binding of the drug or metabolites, the areas under the plasma concentrations *versus* time profiles of the drug ($AUC_{p,j}$) and metabolite ($AUC_{m,j}$) will be independent of the distribution volume, and the summation of the two values will represent the area under the C_j *versus* time profile (AUC_j). Therefore, f_s can also be calculated by:

$$f_s = \frac{AUC_{m,j}}{AUC_{p,j} + AUC_{m,j}} \quad \text{(Eq. 3)}$$

or:

$$f_s = \frac{AUC_{m,j}}{AUC_j} \quad \text{(Eq. 4)}$$

as by definition $AUC_j = AUC_{p,j} + AUC_{m,j}$.

Methyl (±)-(11α,5*Z*(and 5*E*),13*E*,16*R*(and 16*S*)-16-ethenyl-11,16-dihydroxy-9-oxoprosta-5,13-dien-1-oate (viprostol; I), a prostaglandin analogue, is a topically effective antihypertensive agent (2). In the blood and body it apparently undergoes instantaneous and complete ester hydrolysis to give an equally effective compound, (±)-(11α,5*Z*(and 5*E*), 13*E*,16*R*(and 16*S*))-16-ethenyl-11,16-dihydroxy-9-oxoprosta-5,13-dien-1-oic acid (II). The transdermal administration of [^{14}C]I has shown good absorption in various animal models, as measured by total concentrations of carbon-14 (3). The low systemic concentrations (contralateral) of I or II, require a sophisticated GC–MS technique for quantitation (4). In humans, effective doses of I result in low concentrations of II (not I) in the systemic circulation, often below the sensitivity limit of the GC–MS procedure (76 pg/mL). To study the transdermal absorption, 1.5 mg (specific activity 18.99 μCi/mg) of [^{14}C]I in petrolatum bandages[1] (10 cm^2) was applied to the volar surface of the forearm of normal male subjects, and serial ipsilateral and contralateral blood samples were collected into heparinized tubes. Following centrifugation, the plasma was removed and then stored at −40°C until assay. Total radioactivity in each sample was determined by scintillation counting. The concentration of the unchanged drug (II) in the ipsilateral plasma samples were determined by the specific GC–MS assay procedure (4). Because of the rapid hydrolysis of I to II, it was only possible to measure the concentrations of II by GC–MS, and II is considered to be the unchanged active drug ($C_{p,i}$). Therefore, all calculations were done for II.

[1] Formulation Research Section, Medical Research Division, American Cyanamid Co., Pearl River, N.Y.

Table I summarizes the concentrations of II ($C_{p,i}$) and total radioactivity in the ipsilateral ($C_i = C_{p,i} + C_{m,i}$) and contralateral (C_c) plasma samples after application of a 1.5-mg dose on the forearm of two subjects, randomly selected for this report. In general, C_c was relatively low, <1 ng/mL of which, on the average, <10% (~0.05 ng/mL) was in the form of unchanged II and would not be readily measurable by the GC–MS procedure. C_i, of which 35 and 30% was in the form of unchanged II in subjects 1 and 2, respectively, was quite high. These data indicate that about two-thirds of the dose underwent metabolism during absorption from the topical application site and/or in transit to the point of blood sampling in the same arm. As part of a pharmacokinetic study of topical and intravenous [^{14}C]nitroglycerin, Wester *et al.* were able to measure the absolute bioavailability (57%) and estimate the percutaneous first-pass metabolism (16–21%) in monkeys (5). Basically, the procedure is the same as that used for determination of first-pass metabolism after oral administration, *i.e.*, utilizing the difference between the total radioactivity and unchanged nitroglycerin which reached the systemic circulation. The ipsilateral–contralateral method offers the possibility of determining the percutaneous metabolism after one application in the same subject at the same time.

In summary, the results of this study suggests that this simple procedure may be used for the estimation of percutaneous first-pass metabolism of drugs which are administered transdermally and where the skin is a significant site of biotransformation. It would also be of interest to examine this procedure for percutaneous metabolism of other potent drugs which undergo metabolism in the skin.

(1) A. Karim, *Angiology*, **34**, 11 (1983).
(2) J. E. Birnbaum, P. S. Chan, P. Cervoni, F. Dessy, and L. Van Humbeach, *Prostaglandins*, **23**, 185 (1982).
(3) G. Nicolau, V. K. Batra, S. Gordon, A. Tonelli, W. McWilliams, "5th International Conference on Prostaglandins," Abstracts, p. 506 (1982).
(4) D. B. Cosulich, N. A. Perkinson, V. K. Batra, Academy of Pharmaceutical Sciences, Abstracts, **13**(2), 209 (1983).
(5) R. C. Wester, P. K. Noonan, S. Smeach, and L. Kosobud, *J. Pharm. Sci.*, **72**, 745 (1983).

Avraham Yacobi[x]
Robert A. Baughman
Donna B. Cosulich
Gabriela Nicolau
Pharmacodynamics Department
Medical Research Division
American Cyanamid Company
Pearl River, NY 10965

Received May 3, 1984.
Accepted for publication August 6, 1984.

Area Under Blood Level versus *Time Curves at Steady State for Daily Dosing at Unequal Dosing Intervals*

Most problems that deal with steady-state drug blood levels for multiple dosing assume that doses are administered at equal intervals during a 24-h period, *e.g.*, four tablets every 6 h or three tablets every 8 h. For the one-compartment model, for example, under these circumstances, it is well known that at steady state, the area under the blood level *versus* time curve (AUC) during a 24-h period is (Total Daily Dose)/k_e, where k_e is the first-order elimination rate constant. A question of interest is the value of the AUC at steady state when the doses are not given at equal intervals but where the dosage regimen is regular over some period, in particular, 24 h. This is the more realistic situation, *e.g.*, one tablet at 8 a.m., noon, 4 p.m. and 8 p.m. The following simple proof shows that for the above conditions, at a constant total daily dosage, the AUC at steady state is independent of the dosage time intervals for any input function. The following differential equation describes a one-compartment model, in general:

$$dX_c/dt = f[X(t)] - k_e X_c \qquad \text{(Eq. 1)}$$

where $f[X(t)]$ is in the input function (absorption) and $k_e X_c$ represents first-order elimination.

If $X(t)$ is periodic, so is $f[X(t)]$. (Note that the 24-h dosing schedule does not change.) At steady state, X_c will be periodic with the same period. Here, the period is 24 h for a regular 24-h dosing regimen. Integrating Eq. 1 from t_0 to $t_0 + T$:

$$\int_{t_0}^{t_0+T} (dX_c/dt)dt = \int_{t_0}^{t_0+T} f[X(t)]dt - k_e \int_{t_0}^{t_0+T} X_c dt \qquad \text{(Eq. 2)}$$

$X_c(t_0 + T) - X_c(t_0)$ = (Total dose from t_0 to $t_0 + T$) $- k_e$(AUC) from t_0 to $t_0 + T$. If T is the period (24 h in this example): $X_c(t_0 + T) = X_c(t_0)$, and (Total 24-h dose) = $X_{24} = k_e(\text{AUC})_{24}$, or AUC = $(X_{24})/k_e$. Therefore, the AUC over a 24-h period is dependent on the total dose given during the 24 h, and independent of how it is administered providing that the regimen is periodic.

Using a similar argument, it can be shown that this conclusion holds also for higher-compartment models with any input function, if dosing is periodic during a specific interval.

Sanford Bolton
St. John's University
College of Pharmacy and Allied Health Professions
Jamaica, NY 11439

Received June 25, 1984.

Secret Formulations from the Industry's Perspective

As an individual who has worked in industry some 10 years now, I was most disturbed at some of the comments and implications in Dr. Feldmann's editorial[1] "Putting an End to Secret Formulations." First of all, I take strong exception to his assertion that the reason for industry's reluctance to disclose our formulations is simply to create an illusion of mystery. Those of us in the formulation development end of the business feel very strongly that protection of our formulations is indeed an important issue with respect to competition. While it may be true that another firm could "crack" our formulas if they were willing to invest enough analytical effort (although I question whether it is only a "moderate challenge" for the analyst to completely quantitate any given formula), the very fact that such an effort would have to be made presents a significant barrier to our competition. We have no obligation or desire to give away the substantial investment we have made in developing our formulas without compelling justification. To do otherwise makes no more sense than for GM to provide blueprints of their latest design innovations to Ford and Chrysler on request.

Dr. Feldmann alludes several times to the possibility that (perish the thought!) industry's primary motivation might be to make a profit. Obviously, it *is* the goal of industry as well as the rest of the drug distribution system to make a profit (without which there would be no industry as we know it in the free world, no viable private sector, no pharmaceutical research, and, very likely, no funding for APhA, APS, or this Journal) and we have nothing to apologize for this. A profit is not at all necessarily inconsistent with high ethical standards and a genuine concern for mankind, both of which the U.S. pharmaceutical industry has repeatedly demonstrated. Dr. Feldmann provides no basis for his emotional accusation that somehow industry has been trading "human lives" for profits by not labeling our products with the entire listing of ingredients. Although I am personally unaware of any documented evidence that formulation excipients are causing significant medical problems, there may indeed be a persuasive justification for this information being made available due to substantive safety issues. However, such arguments should be factually presented and weighed against legitimate commercial concerns, not couched in emotional tirades based on highly questionable assumptions.

Beyond these specific concerns, I am disturbed at the hostile tone of this editorial towards industry. I would hope that the Association has matured beyond the simplistic big-business-always-wears-black-hats mentality that was so prevalent in our society in the late 60's and early 70's. The pharmaceutical industry is certainly not above criticism, but the consistently negative portrayals of industry practices and ethics in such editorials are not only inaccurate in my opinion but can hardly be called objective. Such apparent bias and the inevitable polarization it encourages seems highly inappropriate for an organization which claims to represent all of pharmacy.

Douglas W. Mendenhall
Pharmaceutical Products Division
Abbott Laboratories
North Chicago, IL 60064

Received July 27, 1984

[1] E. G. Feldmann, *J. Pharm. Sci.*, **73**, 577 (1984).

Author's Response

I wish to assure Dr. Mendenhall, as well as all our readers, that no "hostile tone" toward industry was intended in my editorial that he cited. Certainly, we can disagree regarding specific policies and still maintain cordial working relationships and feelings of mutual respect.

In fact, the matter of maintaining secrecy regarding drug product ingredients has been an issue of considerable difference of opinion *within* the pharmaceutical industry. In my discussions with industry colleagues over the past several years, many of them have favored full ingredient disclosure for precisely the reasons mentioned in the editorial. And, at the same time, many other industry colleagues felt contrary-minded.

Indeed, it is my understanding that such differences in viewpoint existed not only among industry scientists, but also between various firms. This had prevented PMA as an organization from supporting the concept of complete ingredient disclosure. However, we were happy to learn that 2 months following our editorial, at its meeting on July 9, the PMA Board of Directors voted that its member companies will voluntarily list inactive ingredients in product labeling. According to the PMA announcement, this action "is intended to provide added safety for persons sensitive to an inactive ingredient."

As to the two "specific concerns" voiced by Dr. Mendenhall: (*a*) our readers can make their own judgments as to the relative difficulty that a qualified analytical laboratory would currently encounter in determining the qualitative composition of a typical drug product, and (*b*) each of us in his or her own conscience needs to reconcile the degree that our profit motives will be balanced against our humanitarian and societal concerns.

Edward G. Feldmann
American Pharmaceutical Assoc.
2215 Constitution Avenue, N.W.
Washington, DC 20037

Area Under Blood Level versus *Time Curves at Steady State for Daily Dosing at Unequal Dosing Intervals*

Most problems that deal with steady-state drug blood levels for multiple dosing assume that doses are administered at equal intervals during a 24-h period, *e.g.*, four tablets every 6 h or three tablets every 8 h. For the one-compartment model, for example, under these circumstances, it is well known that at steady state, the area under the blood level *versus* time curve (AUC) during a 24-h period is (Total Daily Dose)/k_e, where k_e is the first-order elimination rate constant. A question of interest is the value of the AUC at steady state when the doses are not given at equal intervals but where the dosage regimen is regular over some period, in particular, 24 h. This is the more realistic situation, *e.g.*, one tablet at 8 a.m., noon, 4 p.m. and 8 p.m. The following simple proof shows that for the above conditions, at a constant total daily dosage, the AUC at steady state is independent of the dosage time intervals for any input function. The following differential equation describes a one-compartment model, in general:

$$dX_c/dt = f[X(t)] - k_e X_c \qquad \text{(Eq. 1)}$$

where $f[X(t)]$ is in the input function (absorption) and $k_e X_c$ represents first-order elimination.

If $X(t)$ is periodic, so is $f[X(t)]$. (Note that the 24-h dosing schedule does not change.) At steady state, X_c will be periodic with the same period. Here, the period is 24 h for a regular 24-h dosing regimen. Integrating Eq. 1 from t_0 to $t_0 + T$:

$$\int_{t_0}^{t_0+T} (dX_c/dt)dt = \int_{t_0}^{t_0+T} f[X(t)]dt - k_e \int_{t_0}^{t_0+T} X_c dt \qquad \text{(Eq. 2)}$$

$X_c(t_0 + T) - X_c(t_0)$ = (Total dose from t_0 to $t_0 + T$) $- k_e$(AUC) from t_0 to $t_0 + T$. If T is the period (24 h in this example): $X_c(t_0 + T) = X_c(t_0)$, and (Total 24-h dose) = $X_{24} = k_e(\text{AUC})_{24}$, or AUC = $(X_{24})/k_e$. Therefore, the AUC over a 24-h period is dependent on the total dose given during the 24 h, and independent of how it is administered providing that the regimen is periodic.

Using a similar argument, it can be shown that this conclusion holds also for higher-compartment models with any input function, if dosing is periodic during a specific interval.

Sanford Bolton
St. John's University
College of Pharmacy and Allied Health Professions
Jamaica, NY 11439

Received June 25, 1984.

Secret Formulations from the Industry's Perspective

As an individual who has worked in industry some 10 years now, I was most disturbed at some of the comments and implications in Dr. Feldmann's editorial[1] "Putting an End to Secret Formulations." First of all, I take strong exception to his assertion that the reason for industry's reluctance to disclose our formulations is simply to create an illusion of mystery. Those of us in the formulation development end of the business feel very strongly that protection of our formulations is indeed an important issue with respect to competition. While it may be true that another firm could "crack" our formulas if they were willing to invest enough analytical effort (although I question whether it is only a "moderate challenge" for the analyst to completely quantitate any given formula), the very fact that such an effort would have to be made presents a significant barrier to our competition. We have no obligation or desire to give away the substantial investment we have made in developing our formulas without compelling justification. To do otherwise makes no more sense than for GM to provide blueprints of their latest design innovations to Ford and Chrysler on request.

Dr. Feldmann alludes several times to the possibility that (perish the thought!) industry's primary motivation might be to make a profit. Obviously, it *is* the goal of industry as well as the rest of the drug distribution system to make a profit (without which there would be no industry as we know it in the free world, no viable private sector, no pharmaceutical research, and, very likely, no funding for APhA, APS, or this Journal) and we have nothing to apologize for this. A profit is not at all necessarily inconsistent with high ethical standards and a genuine concern for mankind, both of which the U.S. pharmaceutical industry has repeatedly demonstrated. Dr. Feldmann provides no basis for his emotional accusation that somehow industry has been trading "human lives" for profits by not labeling our products with the entire listing of ingredients. Although I am personally unaware of any documented evidence that formulation excipients are causing significant medical problems, there may indeed be a persuasive justification for this information being made available due to substantive safety issues. However, such arguments should be factually presented and weighed against legitimate commercial concerns, not couched in emotional tirades based on highly questionable assumptions.

Beyond these specific concerns, I am disturbed at the hostile tone of this editorial towards industry. I would hope that the Association has matured beyond the simplistic big-business-always-wears-black-hats mentality that was so prevalent in our society in the late 60's and early 70's. The pharmaceutical industry is certainly not above criticism, but the consistently negative portrayals of industry practices and ethics in such editorials are not only inaccurate in my opinion but can hardly be called objective. Such apparent bias and the inevitable polarization it encourages seems highly inappropriate for an organization which claims to represent all of pharmacy.

Douglas W. Mendenhall
Pharmaceutical Products Division
Abbott Laboratories
North Chicago, IL 60064

Received July 27, 1984

[1] E. G. Feldmann, *J. Pharm. Sci.*, **73**, 577 (1984).

Author's Response

I wish to assure Dr. Mendenhall, as well as all our readers, that no "hostile tone" toward industry was intended in my editorial that he cited. Certainly, we can disagree regarding specific policies and still maintain cordial working relationships and feelings of mutual respect.

In fact, the matter of maintaining secrecy regarding drug product ingredients has been an issue of considerable difference of opinion *within* the pharmaceutical industry. In my discussions with industry colleagues over the past several years, many of them have favored full ingredient disclosure for precisely the reasons mentioned in the editorial. And, at the same time, many other industry colleagues felt contrary-minded.

Indeed, it is my understanding that such differences in viewpoint existed not only among industry scientists, but also between various firms. This had prevented PMA as an organization from supporting the concept of complete ingredient disclosure. However, we were happy to learn that 2 months following our editorial, at its meeting on July 9, the PMA Board of Directors voted that its member companies will voluntarily list inactive ingredients in product labeling. According to the PMA announcement, this action "is intended to provide added safety for persons sensitive to an inactive ingredient."

As to the two "specific concerns" voiced by Dr. Mendenhall: (*a*) our readers can make their own judgments as to the relative difficulty that a qualified analytical laboratory would currently encounter in determining the qualitative composition of a typical drug product, and (*b*) each of us in his or her own conscience needs to reconcile the degree that our profit motives will be balanced against our humanitarian and societal concerns.

Edward G. Feldmann
American Pharmaceutical Assoc.
2215 Constitution Avenue, N.W.
Washington, DC 20037

Total Synthesis of Natural Products: The 'Chiron' Approach. (Organic Chemistry Series, Vol. 3). By STEPHEN HANESSIAN. Pergamon Press, Inc. Maxwell House, Fairview Park, Elmsford, NY 10523. 1983. 291 pp. 15 × 23 cm. Price: $20.00.

The present generation of organic chemists considers no total synthesis of a natural product to be truly satisfactory unless it also yields an optically pure product. One of the ways of achieving this objective is to begin the synthesis with a substrate drawn from the chiral pool so bountifully provided by nature: amino and hydroxy acids, terpenes, and carbohydrates, many of which are readily available and relatively cheap. In this book, Professor Hanessian, one of the leading practitioners of the art of using carbohydrates as precursors in asymmetric total synthesis, presents both a personal approach to this field and a thorough review, with much informative commentary, of successful syntheses employing carbohydrates as starting materials.

Part 1 of the book describes those features of compounds from the chiral pool—variety in carbon framework, sense of chirality, number of asymmetric centers, functional group sequences—that make them versatile springboards from which to launch asymmetric syntheses. All important, of course, is the designer's perception of the structural and stereochemical relationships between these "chiral templates" and the target structure. Parts 2 and 3 of the book, entitled "Design" and "Discovery" respectively, present guidelines on how to establish the appropriate "visual dialogue" (a functional, if not particularly felicitous, phrase). The central feature of the approach is the identification and selection of "chirons"—suitably functionalized, defunctionalized, or otherwise modified versions of the chiral templates which, after activation, may be assembled to give the target product.

The rest of the book, and by far the largest part, is devoted to "Execution," a detailed discussion of selected carbohydrate-based asymmetric syntheses. These syntheses fall into three main groups: those in which the targets contain reasonably obvious carbohydrate-type symmetry; those in which such symmetry is partially hidden; and those in which only the most hardened fans of the approach would have looked for a carbohydrate precursor in the first place. Each section is further subdivided into chapters according to the types of molecules being synthesized. The relatively straightforward chiral targets (acyclic compounds, tetrahydrofurans, tetrahydropyrans and the like) predominate the earlier chapters and more complex products (*i.e.* prostaglandins, heterocyclic antibiotics, macrolides, and ansa compounds) dominate the later sections. In almost all cases, the syntheses chosen for illustration are of compounds with substantial pharmaceutical significance. The book ends with a brief discussion of a possible role for computers in the visual recognition of chiral templates within target structures.

Not the least virtue of this book is the abundance of flow-sheets (more than 150) for the syntheses discussed. In most cases, the flow sheets show both a retrosynthetic analysis from target via chiron to chiral template, as well as the forward steps, with reagents, of the completed synthesis. It appears that every reference of importance in the field has been included, and the index is reasonably comprehensive. There appear to be very few errors. Those whose chief fascination is the art and philosophy of organic synthesis will certainly read this book with avidity, even if they remain unconvinced that carbohydrates necessarily provide the ideal solution to the problem of introducing asymmetry into a synthetic scheme.

Reviewed by J. P. Michael
Department of Chemistry
University of the Witwatersrand
Johannesburg, South Africa

Molecular Aspects of Anti-Cancer Drug Action. (Topics in Molecular and Structural Biology. 3). Edited by STEPHEN NEIDLE and MICHAEL J. WARING. Verlag Chemie International Inc., 303 N.W. 12th Ave., Deerfield Beach, FL 33441. 1983. 404 pp. 16 × 24 cm. Price: $97.50.

This book, the third in a series on *Topics in Molecular and Structural Biology*, contains eleven chapters dealing largely with Drug-DNA interactions of a number of cancer chemotherapeutic agents currently of high interest. Literature is covered through 1981 with the occasional appearance of a few later citations. Based on a random survey, the book is remarkably free from typographical errors. The text is printed in small (but clear) type. In most cases chemical structures, figures, and tables are easily read; however, in some cases the codes to structural formulae were difficult to read. The selection of topics includes: acridines, three chapters on topics related to anthracycline drugs, quinoxaline antibiotics, bleomycin, platinum compounds, alkylating agents, and methotrexate and analogues. In addition, there are reviews of the chemical and biological damage by certain antitumor drugs.

The chapter on acridines by Denny, Boyuley, Cain, and Waring is an excellent review of the enormous work of the group that was headed by the late Bruce Cain. It culminates in amsacrine and describes the studies (largely by Polish workers) on nitracrine—an active but toxic 1-nitro-acridine derivative—and of the bifunctional acridines. The interactions of daunomycin and adriamycin with nucleic acids is covered in a brief but useful chapter by Neidle and Sanderson; however, this subject has been covered in greater detail in earlier reviews. J. R. Brown presents a timely chapter with much new material on synthetic anthracycline drugs that will be of particular interest to medicinal chemists seeking a rational basis for the synthesis of new agents in this class.

Bifunctional intercalation is again reviewed by Waring and Fox in a chapter dealing with quinoxaline antibiotics. Although this group has not attained clinical significance, the techniques discussed in the study of molecular interactions may be of general use. Another review by Roberts and Pera dealing with the action of platinum antitumor drugs is presented in an authoritative manner. Lown briefly surveys the chemistry of DNA damage by a large number of antitumor agents. This chapter should be of particular value to medicinal chemists.

Molecular Aspects of Anti-Cancer Drug Action will be useful to medicinal chemists seeking rational approaches to the synthesis of antitumor agents. Unfortunately, the high cost of this volume ($97.50) may restrict purchases to technical libraries.

Reviewed by Monroe E. Wall
Research Triangle Institute
P.O. Box 12194
Research Triangle Park, NC 27709

A Guide to the Chemical Basis of Drug Design. By ALFRED BURGER. John Wiley & Sons, Inc., One Wiley Drive, Somerset, NJ 08873. 1983. 300 pp. 16.5 × 23.5 cm. Price: $45.00.

The contributions of Professor Alfred Burger to the discipline of medicinal chemistry, particularly the literature of medicinal chemistry, have long been noted and acknowledged. His current effort attempts to recount those experiences of the medicinal chemist which, in cooperation with biologists and pharmacologists, have resulted in the chemical design of therapeutically useful drug substances. It is the broad scope of this endeavor which accounts for both the success and failure of this latest effort. The success of this overview of drug design resides mainly in those areas in which Professor Burger provides personal insight. This guide, afterall, recounts many ideas and examples which "are results of a lifetime in medicinal chemistry." After a brief introduction in which he traces his early interest in the chemistry of medicinally useful agents, and thus traces the development of medicinal chemistry, the book discusses drug design from three distinct, but oftentimes redundant, viewpoints. Chapter 1 begins as a fascinating discussion of the history of medicinal chemistry but develops into a chapter which lacks direction and depth. Chapter 2 presents areas of research interest with particular emphasis on antihypertensive agents, anti-inflammatory agents, antiviral and antitumor agents, antihistaminics, analgetics and antihyperglycemic agents. It is in this chapter that general aspects of drug design, molecular modifications and quantitative structure-activity relationships are presented. The discussion in each of these areas represents a general overview of the subject and precludes any discussion in depth. For example, in the discussion of recent research in the area of antihypertensive agents the role of presynaptic α_2-adrenoceptors in the action of newer agents such as clonidine is neglected. On the other hand, the discussion of the development of analgetic research is particularly interesting. Chapter 3 is intended as a discussion of selected examples of drug design. Many aspects of drug design of analgetic, anti-inflammatory, anticholinergics and antihistaminic agents discussed in Chapter 2 are repeated in the early part

Total Synthesis of Natural Products: The 'Chiron' Approach. (Organic Chemistry Series, Vol. 3). By STEPHEN HANESSIAN. Pergamon Press, Inc. Maxwell House, Fairview Park, Elmsford, NY 10523. 1983. 291 pp. 15 × 23 cm. Price: $20.00.

The present generation of organic chemists considers no total synthesis of a natural product to be truly satisfactory unless it also yields an optically pure product. One of the ways of achieving this objective is to begin the synthesis with a substrate drawn from the chiral pool so bountifully provided by nature: amino and hydroxy acids, terpenes, and carbohydrates, many of which are readily available and relatively cheap. In this book, Professor Hanessian, one of the leading practitioners of the art of using carbohydrates as precursors in asymmetric total synthesis, presents both a personal approach to this field and a thorough review, with much informative commentary, of successful syntheses employing carbohydrates as starting materials.

Part 1 of the book describes those features of compounds from the chiral pool—variety in carbon framework, sense of chirality, number of asymmetric centers, functional group sequences—that make them versatile springboards from which to launch asymmetric syntheses. All important, of course, is the designer's perception of the structural and stereochemical relationships between these "chiral templates" and the target structure. Parts 2 and 3 of the book, entitled "Design" and "Discovery" respectively, present guidelines on how to establish the appropriate "visual dialogue" (a functional, if not particularly felicitous, phrase). The central feature of the approach is the identification and selection of "chirons"—suitably functionalized, defunctionalized, or otherwise modified versions of the chiral templates which, after activation, may be assembled to give the target product.

The rest of the book, and by far the largest part, is devoted to "Execution," a detailed discussion of selected carbohydrate-based asymmetric syntheses. These syntheses fall into three main groups: those in which the targets contain reasonably obvious carbohydrate-type symmetry; those in which such symmetry is partially hidden; and those in which only the most hardened fans of the approach would have looked for a carbohydrate precursor in the first place. Each section is further subdivided into chapters according to the types of molecules being synthesized. The relatively straightforward chiral targets (acyclic compounds, tetrahydrofurans, tetrahydropyrans and the like) predominate the earlier chapters and more complex products (*i.e.* prostaglandins, heterocyclic antibiotics, macrolides, and ansa compounds) dominate the later sections. In almost all cases, the syntheses chosen for illustration are of compounds with substantial pharmaceutical significance. The book ends with a brief discussion of a possible role for computers in the visual recognition of chiral templates within target structures.

Not the least virtue of this book is the abundance of flow-sheets (more than 150) for the syntheses discussed. In most cases, the flow sheets show both a retrosynthetic analysis from target via chiron to chiral template, as well as the forward steps, with reagents, of the completed synthesis. It appears that every reference of importance in the field has been included, and the index is reasonably comprehensive. There appear to be very few errors. Those whose chief fascination is the art and philosophy of organic synthesis will certainly read this book with avidity, even if they remain unconvinced that carbohydrates necessarily provide the ideal solution to the problem of introducing asymmetry into a synthetic scheme.

Reviewed by J. P. Michael
Department of Chemistry
University of the Witwatersrand
Johannesburg, South Africa

Molecular Aspects of Anti-Cancer Drug Action. (Topics in Molecular and Structural Biology. 3). Edited by STEPHEN NEIDLE and MICHAEL J. WARING. Verlag Chemie International Inc., 303 N.W. 12th Ave., Deerfield Beach, FL 33441. 1983. 404 pp. 16 × 24 cm. Price: $97.50.

This book, the third in a series on *Topics in Molecular and Structural Biology*, contains eleven chapters dealing largely with Drug-DNA interactions of a number of cancer chemotherapeutic agents currently of high interest. Literature is covered through 1981 with the occasional appearance of a few later citations. Based on a random survey, the book is remarkably free from typographical errors. The text is printed in small (but clear) type. In most cases chemical structures, figures, and tables are easily read; however, in some cases the codes to structural formulae were difficult to read. The selection of topics includes: acridines, three chapters on topics related to anthracycline drugs, quinoxaline antibiotics, bleomycin, platinum compounds, alkylating agents, and methotrexate and analogues. In addition, there are reviews of the chemical and biological damage by certain antitumor drugs.

The chapter on acridines by Denny, Boyuley, Cain, and Waring is an excellent review of the enormous work of the group that was headed by the late Bruce Cain. It culminates in amsacrine and describes the studies (largely by Polish workers) on nitracrine—an active but toxic 1-nitro-acridine derivative—and of the bifunctional acridines. The interactions of daunomycin and adriamycin with nucleic acids is covered in a brief but useful chapter by Neidle and Sanderson; however, this subject has been covered in greater detail in earlier reviews. J. R. Brown presents a timely chapter with much new material on synthetic anthracycline drugs that will be of particular interest to medicinal chemists seeking a rational basis for the synthesis of new agents in this class.

Bifunctional intercalation is again reviewed by Waring and Fox in a chapter dealing with quinoxaline antibiotics. Although this group has not attained clinical significance, the techniques discussed in the study of molecular interactions may be of general use. Another review by Roberts and Pera dealing with the action of platinum antitumor drugs is presented in an authoritative manner. Lown briefly surveys the chemistry of DNA damage by a large number of antitumor agents. This chapter should be of particular value to medicinal chemists.

Molecular Aspects of Anti-Cancer Drug Action will be useful to medicinal chemists seeking rational approaches to the synthesis of antitumor agents. Unfortunately, the high cost of this volume ($97.50) may restrict purchases to technical libraries.

Reviewed by Monroe E. Wall
Research Triangle Institute
P.O. Box 12194
Research Triangle Park, NC 27709

A Guide to the Chemical Basis of Drug Design. By ALFRED BURGER. John Wiley & Sons, Inc., One Wiley Drive, Somerset, NJ 08873. 1983. 300 pp. 16.5 × 23.5 cm. Price: $45.00.

The contributions of Professor Alfred Burger to the discipline of medicinal chemistry, particularly the literature of medicinal chemistry, have long been noted and acknowledged. His current effort attempts to recount those experiences of the medicinal chemist which, in cooperation with biologists and pharmacologists, have resulted in the chemical design of therapeutically useful drug substances. It is the broad scope of this endeavor which accounts for both the success and failure of this latest effort. The success of this overview of drug design resides mainly in those areas in which Professor Burger provides personal insight. This guide, afterall, recounts many ideas and examples which "are results of a lifetime in medicinal chemistry." After a brief introduction in which he traces his early interest in the chemistry of medicinally useful agents, and thus traces the development of medicinal chemistry, the book discusses drug design from three distinct, but oftentimes redundant, viewpoints. Chapter 1 begins as a fascinating discussion of the history of medicinal chemistry but develops into a chapter which lacks direction and depth. Chapter 2 presents areas of research interest with particular emphasis on antihypertensive agents, anti-inflammatory agents, antiviral and antitumor agents, antihistaminics, analgetics and antihyperglycemic agents. It is in this chapter that general aspects of drug design, molecular modifications and quantitative structure-activity relationships are presented. The discussion in each of these areas represents a general overview of the subject and precludes any discussion in depth. For example, in the discussion of recent research in the area of antihypertensive agents the role of presynaptic α_2-adrenoceptors in the action of newer agents such as clonidine is neglected. On the other hand, the discussion of the development of analgetic research is particularly interesting. Chapter 3 is intended as a discussion of selected examples of drug design. Many aspects of drug design of analgetic, anti-inflammatory, anticholinergics and antihistaminic agents discussed in Chapter 2 are repeated in the early part

Total Synthesis of Natural Products: The 'Chiron' Approach. (Organic Chemistry Series, Vol. 3). By STEPHEN HANESSIAN. Pergamon Press, Inc. Maxwell House, Fairview Park, Elmsford, NY 10523. 1983. 291 pp. 15 × 23 cm. Price: $20.00.

The present generation of organic chemists considers no total synthesis of a natural product to be truly satisfactory unless it also yields an optically pure product. One of the ways of achieving this objective is to begin the synthesis with a substrate drawn from the chiral pool so bountifully provided by nature: amino and hydroxy acids, terpenes, and carbohydrates, many of which are readily available and relatively cheap. In this book, Professor Hanessian, one of the leading practitioners of the art of using carbohydrates as precursors in asymmetric total synthesis, presents both a personal approach to this field and a thorough review, with much informative commentary, of successful syntheses employing carbohydrates as starting materials.

Part 1 of the book describes those features of compounds from the chiral pool—variety in carbon framework, sense of chirality, number of asymmetric centers, functional group sequences—that make them versatile springboards from which to launch asymmetric syntheses. All important, of course, is the designer's perception of the structural and stereochemical relationships between these "chiral templates" and the target structure. Parts 2 and 3 of the book, entitled "Design" and "Discovery" respectively, present guidelines on how to establish the appropriate "visual dialogue" (a functional, if not particularly felicitous, phrase). The central feature of the approach is the identification and selection of "chirons"—suitably functionalized, defunctionalized, or otherwise modified versions of the chiral templates which, after activation, may be assembled to give the target product.

The rest of the book, and by far the largest part, is devoted to "Execution," a detailed discussion of selected carbohydrate-based asymmetric syntheses. These syntheses fall into three main groups: those in which the targets contain reasonably obvious carbohydrate-type symmetry; those in which such symmetry is partially hidden; and those in which only the most hardened fans of the approach would have looked for a carbohydrate precursor in the first place. Each section is further subdivided into chapters according to the types of molecules being synthesized. The relatively straightforward chiral targets (acyclic compounds, tetrahydrofurans, tetrahydropyrans and the like) predominate the earlier chapters and more complex products (*i.e.* prostaglandins, heterocyclic antibiotics, macrolides, and ansa compounds) dominate the later sections. In almost all cases, the syntheses chosen for illustration are of compounds with substantial pharmaceutical significance. The book ends with a brief discussion of a possible role for computers in the visual recognition of chiral templates within target structures.

Not the least virtue of this book is the abundance of flow-sheets (more than 150) for the syntheses discussed. In most cases, the flow sheets show both a retrosynthetic analysis from target via chiron to chiral template, as well as the forward steps, with reagents, of the completed synthesis. It appears that every reference of importance in the field has been included, and the index is reasonably comprehensive. There appear to be very few errors. Those whose chief fascination is the art and philosophy of organic synthesis will certainly read this book with avidity, even if they remain unconvinced that carbohydrates necessarily provide the ideal solution to the problem of introducing asymmetry into a synthetic scheme.

Reviewed by J. P. Michael
Department of Chemistry
University of the Witwatersrand
Johannesburg, South Africa

Molecular Aspects of Anti-Cancer Drug Action. (Topics in Molecular and Structural Biology. 3). Edited by STEPHEN NEIDLE and MICHAEL J. WARING. Verlag Chemie International Inc., 303 N.W. 12th Ave., Deerfield Beach, FL 33441. 1983. 404 pp. 16 × 24 cm. Price: $97.50.

This book, the third in a series on *Topics in Molecular and Structural Biology*, contains eleven chapters dealing largely with Drug-DNA interactions of a number of cancer chemotherapeutic agents currently of high interest. Literature is covered through 1981 with the occasional appearance of a few later citations. Based on a random survey, the book is remarkably free from typographical errors. The text is printed in small (but clear) type. In most cases chemical structures, figures, and tables are easily read; however, in some cases the codes to structural formulae were difficult to read. The selection of topics includes: acridines, three chapters on topics related to anthracycline drugs, quinoxaline antibiotics, bleomycin, platinum compounds, alkylating agents, and methotrexate and analogues. In addition, there are reviews of the chemical and biological damage by certain antitumor drugs.

The chapter on acridines by Denny, Boyuley, Cain, and Waring is an excellent review of the enormous work of the group that was headed by the late Bruce Cain. It culminates in amsacrine and describes the studies (largely by Polish workers) on nitracrine—an active but toxic 1-nitro-acridine derivative—and of the bifunctional acridines. The interactions of daunomycin and adriamycin with nucleic acids is covered in a brief but useful chapter by Neidle and Sanderson; however, this subject has been covered in greater detail in earlier reviews. J. R. Brown presents a timely chapter with much new material on synthetic anthracycline drugs that will be of particular interest to medicinal chemists seeking a rational basis for the synthesis of new agents in this class.

Bifunctional intercalation is again reviewed by Waring and Fox in a chapter dealing with quinoxaline antibiotics. Although this group has not attained clinical significance, the techniques discussed in the study of molecular interactions may be of general use. Another review by Roberts and Pera dealing with the action of platinum antitumor drugs is presented in an authoritative manner. Lown briefly surveys the chemistry of DNA damage by a large number of antitumor agents. This chapter should be of particular value to medicinal chemists.

Molecular Aspects of Anti-Cancer Drug Action will be useful to medicinal chemists seeking rational approaches to the synthesis of antitumor agents. Unfortunately, the high cost of this volume ($97.50) may restrict purchases to technical libraries.

Reviewed by Monroe E. Wall
Research Triangle Institute
P.O. Box 12194
Research Triangle Park, NC 27709

A Guide to the Chemical Basis of Drug Design. By ALFRED BURGER. John Wiley & Sons, Inc., One Wiley Drive, Somerset, NJ 08873. 1983. 300 pp. 16.5 × 23.5 cm. Price: $45.00.

The contributions of Professor Alfred Burger to the discipline of medicinal chemistry, particularly the literature of medicinal chemistry, have long been noted and acknowledged. His current effort attempts to recount those experiences of the medicinal chemist which, in cooperation with biologists and pharmacologists, have resulted in the chemical design of therapeutically useful drug substances. It is the broad scope of this endeavor which accounts for both the success and failure of this latest effort. The success of this overview of drug design resides mainly in those areas in which Professor Burger provides personal insight. This guide, afterall, recounts many ideas and examples which "are results of a lifetime in medicinal chemistry." After a brief introduction in which he traces his early interest in the chemistry of medicinally useful agents, and thus traces the development of medicinal chemistry, the book discusses drug design from three distinct, but oftentimes redundant, viewpoints. Chapter 1 begins as a fascinating discussion of the history of medicinal chemistry but develops into a chapter which lacks direction and depth. Chapter 2 presents areas of research interest with particular emphasis on antihypertensive agents, anti-inflammatory agents, antiviral and antitumor agents, antihistaminics, analgetics and antihyperglycemic agents. It is in this chapter that general aspects of drug design, molecular modifications and quantitative structure-activity relationships are presented. The discussion in each of these areas represents a general overview of the subject and precludes any discussion in depth. For example, in the discussion of recent research in the area of antihypertensive agents the role of presynaptic α_2-adrenoceptors in the action of newer agents such as clonidine is neglected. On the other hand, the discussion of the development of analgetic research is particularly interesting. Chapter 3 is intended as a discussion of selected examples of drug design. Many aspects of drug design of analgetic, anti-inflammatory, anticholinergics and antihistaminic agents discussed in Chapter 2 are repeated in the early part

of this chapter. The bulk of the chapter is devoted to a discussion of the development and design of chemotherapeutic agents. Again, the major drawback to this chapter, for the most part, is a lack of in-depth discussion of many key areas as exemplified by the brief discussion of antitumor agents.

To offset the problems associated with attempts to cover these broad areas in 300 pages, Professor Burger has extensively documented this coverage by citing 1512 references. Most of these are up to 1980, but several key post-1980 references are included. Unfortunately, several errors appear. For example, isoproterenol is described as the *N*-isopropyl homologue of epinephrine possessing "maximal α-adrenergic properties" (p. 20). Several structures are incorrectly drawn and other seemingly minor, but important, errors occur. For example, chlorisondamine is described as a drug lacking quaternary ammonium groups when, in fact, the opposite is true (p. 33).

Overall, while this project may have been somewhat too ambitious, it does represent another important contribution to the literature of medicinal chemistry by Professor Burger. The book should be of particular interest as background preparation for the organic chemist preparing for a research career in medicinal chemistry.

Reviewed by Ronald F. Borne
School of Pharmacy
The University of Mississippi
University, MS 38677

NOTICES

Acrylonitrile (Environmental Health Criteria 28). World Health Organization, 1211 Geneva 27, Switzerland. 1983. 125 pp. 21 × 14 cm. Price: Sw.fr. 12.

Airborne and Allergenic Pollen of North America. By WALTER H. LEWIS, PRATHIBHA VINAY, and VINCENT E. ZENGER. The Johns Hopkins University Press, Baltimore, MD 21218. 1983. 254 pp. 28.5 × 22 cm. Price: $60.00.

American Drug Index, 28th Ed. Edited by NORMAN F. BILLUPS and SHIRLEY M. BILLUPS, Lippincott, East Washington Square, Philadelphia, PA 19105. 1984. 702 pp. 21 × 14.5 cm. Price: $24.50.

Antimicrobials in Foods (Food Sciences Series, Vol. 10). Edited by ALFRED LARRY BRANEN and P. MICHAEL DAVIDSON. Marcel Dekker, 270 Madison Ave., New York, NY 10016. 1983. 465 pp. 23.5 × 16 cm. Price: $69.75 (20% higher outside the U.S. and Canada).

Aspartame: Physiology and Biochemistry (Food Science and Technology Series, Vol 12). Edited by LEWIS D. STEGINK and L. J. FILER, Jr. Marcel Dekker, 270 Madison Ave., New York, NY 10016. 1984. 670 pp. 24 × 16 cm. Price: $79.75 (20% higher outside the U.S. and Canada).

Azospirillum II: Genetics, Physiology, Ecology. Edited by W. KLINGMULLER. Birkhauser Boston, Inc., 380 Green St., Cambridge, MA 02139. 1984. 194 pp. 24 × 17 cm. Price: $27.95.

Basic Documents, 34th Ed. World Health Organization, 1211 Geneva 27, Switzerland. 1984. 176 pp. 24 × 16 cm. Price: Sw.Fr. 12.

Behavioral Intervention Techniques in Drug Abuse Treatment. (NIDA Research Monograph 46) Edited by JOHN GRABOWSKI, MAXINE L. STITZER, and JACK E. HENNINGFIELD. Department of Health and Human Services, National Institute on Drug Abuse, 5600 Fishers Lane, Rockville, MD 20857. 1984. 163 pp. 23 × 15 cm.

The Biochemistry of the Carotenoids, Vol. II: Animals. By T. W. GOODWIN. Methuen, Inc., 733 Third Ave. New York, NY 10017, 1984. 224 pp. 24 × 16 cm. Price: $50.00.

Cancer Incidence in the USSR. (IARC Scientific Publications No. 48). Edited by N. P. NAPALKOV, G. F. TSERKOVNY, and V. M. MERABISHVILI and in Lyon by D. M. PARKIN, M. SMANS, and C. S. MUIR. International Agency for Research on Cancer, 150 Cours Albert Thomas, 69372 Lyon Cedex 08 France. 1983. 83 pp. 24 × 18.5 cm. Price: $15.00. Sw.Fr. 30.

Chlorine and Hydrogen Chloride (Environmental Health Criteria 21). World Health Organization, 1211 Geneva 27, Switzerland. 1982. 95 pp. 21 × 14 cm. Price: Sw.Fr. 7.

A Clinical Approach to Progress in Infectious Diseases. Edited by W. BRUMFITT and J. M. T. HAMILTON-MILLER. Oxford University Press, 200 Madison Avenue, New York, NY 10016. 1983. 163 pp. 24 × 16 cm. Price: $26.95.

Clinical Management of Prescription Drugs. By JAMES W. LONG. Lippincott, East Washington Square, Philadelphia, PA 19105. 1984. 966 pp. 23.5 × 18.5 cm. Price: $19.50.

Communication in Pharmacy Practice: A Practical Guide for Students and Practitioners. Edited by WILLIAM N. TINDELL, ROBERT S. BEARDSLEY, and FREDERIC R. CURTISS. Sea & Febiger. 600 S. Washington Square, Philadelphia, PA 19106. 182 pp. 21.5 × 14 cm. Price: $11.50 (paper).

Contemporary Research in Pain and Analgesia (NIDA Research Monograph 45, A RAUS Review Report). Edited by ROGER M. BROWN, THEODORE M. PINKERT, and JACQUELINE P. LUDFORD. Department of Health and Human Services, National Institute on Drug Abuse, 5600 Fishers Lane, Rockville, MD 20857. 1983. 81 pp. 23 × 14 cm.

Control of Virus Diseases. Edited by EDOUARD KURSTAK. Marcel Dekker, Inc. 270 Madison Avenue, New York, NY 10016. 1984. 584 pp. 23.5 × 15.5 cm. Price: $115.00 (20% higher outside the U.S. and Canada).

Corporate Crime in the Pharmaceutical Industry. By JOHN BRAITHWAITE. Routledge & Kegan Paul, 9 Park Street, Boston, MA 02108. 1984. 440 pp. 22.5 × 14.5 cm. Price: $45.00.

2,4-Dichlorophenoxyacetic acid (2,4-D) (Environmental Health Criteria 29). World Health Organization, 1211 Geneva 27, Switzerland. 1984. 151 pp. 21 × 14 cm. Price: Sw.Fr. 14.

Directory of Alcohol and Drug Treatment Resources in Ontario, 1984. Addiction Research Foundation, 33 Russell Street, Toronto, Ontario, Canada M5S 2S1. 1984. (Directory and Listing) Price: $29.95.

Drugs, Driving, and Traffic Safety. Edited by ROBERT E. WILLETT and J. MICHAEL WALSH. World Health Organizatin, 1211 Geneva 27, Switzerland. 1983. 57 pp. 21 × 15 cm. Price: Sw.Fr. 5.

Fatty Acids in Cystic Fibrosis (Monographs pediatriiques). By VERA ROGIERS. Editions de l'Université de Bruxelles, Avenue Paul Hégen 26, 1050 Brussels, Belgium. 1983. 106 pp. 24 × 16 cm.

Fourier Transform N. M. R. Spectroscopy, 2nd Ed., Vol. 30 (Studies in Physical and Theoretical Chemistry). By DEREK SHAW. Elsevier Science Publishers. Molenwerfi, PO Box 211, 100 AE Amsterdam, The Netherlands. 1984. 344 pp. 25 × 17 cm. Price: $75.00.

Friedel-Crafts Alkylation Chemistry: A Century of Discovery. By ROYSTON M. ROBERTS and ALI ALI KHALAF. Marcel Dekker, Inc., 270 Madison Avenue, New York, NY 10016. 1984. 790 pp. 26 × 18.5 cm. Price: $165.00 (20% higher outside the U.S. and Canada).

Genotoxicology of N-Nitroso Compounds (Topics in Chemical Mutagenesis, Vol. 1). Edited by T. K. RAO, W. LIJINSKY, and J. L. EPLER. Plenum Publishing Corporation, 233 Spring Street, New York, NY 10013. 1984. 271 pp. 23.5 × 15.5 cm. Price: $39.50.

Guidelines for the Control of Narcotics and Psychotropic Substances. By BROR REXED, K. EDMONDSON, INAYAT KHAN, and ROBERT J. SAMSON. World Health Organization, 1211 Geneva 27, Switzerland. 1984. 141 pp. 24 × 16 cm. Price: Sw.Fr. 17.

Guidelines for Drinking-Water Quality Vol. 1, Recommendations. World Health Organization, 1211 Geneva 27, Switzerland. 1984. 130 pp. 24 × 16 cm. Price: Sw.Fr. 17.

Guidelines on Studies in Environmental Epidemiology (Environmental Health Criteria 27). World Health Organization, 1211 Geneva 27, Switzerland. 1983. 351 pp. 21 × 14 cm. Price: Sw.Fr. 26.

Handbook of Ocular Pharmacology, 3rd Ed. By MARVIN B. SMITH. PSG Publishing Co., Inc., Littleton, MA 01460. 1984. 243 pp. 21 × 15 cm.

Handbook of Psychopharmacology (Drugs, Neurotransmitters, and Behavior, Vol. 18). Edited by LESLIE L. IVERSON, SUSAN D. EVERSON and SOLOMON H. SNYDER. Plenum Publishing Corp., 233 Spring Street, New York, NY 10013. 1984. 532 pp. 25 × 17 cm. Price: $65.00.

The High Nitrogen Compounds. By FREDERIC R. BENSON. John Wiley & Sons, Inc., One Wiley Drive, Somerset, NJ 08873. 1984. 679 pp. 24 × 17 cm. Price: $125.00.

IARC Monographs on the Evaluation of the Carcinogenic Risk of Chemicals to Humans (Vol 31: Some Food Additives and Naturally Occurring Substances). International Agency for Research on Cancer, Lyon, France. Distributed by World Health Organization, 1211 Geneva 27, Switzerland. 1983. 314 pp. 24 × 18 cm. Price: $30.00, Sw.Fr. 60.

IARC Monographs on the Evaluation of the Carcinogenic Risk of Chemicals to Humans (Vol 31: Polynuclear Aromatic Compounds, Part 1, Chemical, Environmental and Experimental Data). International Agency for Re-

of this chapter. The bulk of the chapter is devoted to a discussion of the development and design of chemotherapeutic agents. Again, the major drawback to this chapter, for the most part, is a lack of in-depth discussion of many key areas as exemplified by the brief discussion of antitumor agents.

To offset the problems associated with attempts to cover these broad areas in 300 pages, Professor Burger has extensively documented this coverage by citing 1512 references. Most of these are up to 1980, but several key post-1980 references are included. Unfortunately, several errors appear. For example, isoproterenol is described as the *N*-isopropyl homologue of epinephrine possessing "maximal α-adrenergic properties" (p. 20). Several structures are incorrectly drawn and other seemingly minor, but important, errors occur. For example, chlorisondamine is described as a drug lacking quaternary ammonium groups when, in fact, the opposite is true (p. 33).

Overall, while this project may have been somewhat too ambitious, it does represent another important contribution to the literature of medicinal chemistry by Professor Burger. The book should be of particular interest as background preparation for the organic chemist preparing for a research career in medicinal chemistry.

Reviewed by Ronald F. Borne
School of Pharmacy
The University of Mississippi
University, MS 38677

NOTICES

Acrylonitrile (Environmental Health Criteria 28). World Health Organization, 1211 Geneva 27, Switzerland. 1983. 125 pp. 21 × 14 cm. Price: Sw.fr. 12.

Airborne and Allergenic Pollen of North America. By WALTER H. LEWIS, PRATHIBHA VINAY, and VINCENT E. ZENGER. The Johns Hopkins University Press, Baltimore, MD 21218. 1983. 254 pp. 28.5 × 22 cm. Price: $60.00.

American Drug Index, 28th Ed. Edited by NORMAN F. BILLUPS and SHIRLEY M. BILLUPS, Lippincott, East Washington Square, Philadelphia, PA 19105. 1984. 702 pp. 21 × 14.5 cm. Price: $24.50.

Antimicrobials in Foods (Food Sciences Series, Vol. 10). Edited by ALFRED LARRY BRANEN and P. MICHAEL DAVIDSON. Marcel Dekker, 270 Madison Ave., New York, NY 10016. 1983. 465 pp. 23.5 × 16 cm. Price: $69.75 (20% higher outside the U.S. and Canada).

Aspartame: Physiology and Biochemistry (Food Science and Technology Series, Vol 12). Edited by LEWIS D. STEGINK and L. J. FILER, Jr. Marcel Dekker, 270 Madison Ave., New York, NY 10016. 1984. 670 pp. 24 × 16 cm. Price: $79.75 (20% higher outside the U.S. and Canada).

Azospirillum II: Genetics, Physiology, Ecology. Edited by W. KLINGMULLER. Birkhauser Boston, Inc., 380 Green St., Cambridge, MA 02139. 1984. 194 pp. 24 × 17 cm. Price: $27.95.

Basic Documents, 34th Ed. World Health Organization, 1211 Geneva 27, Switzerland. 1984. 176 pp. 24 × 16 cm. Price: Sw.Fr. 12.

Behavioral Intervention Techniques in Drug Abuse Treatment. (NIDA Research Monograph 46) Edited by JOHN GRABOWSKI, MAXINE L. STITZER, and JACK E. HENNINGFIELD. Department of Health and Human Services, National Institute on Drug Abuse, 5600 Fishers Lane, Rockville, MD 20857. 1984. 163 pp. 23 × 15 cm.

The Biochemistry of the Carotenoids, Vol. II: Animals. By T. W. GOODWIN. Methuen, Inc., 733 Third Ave. New York, NY 10017, 1984. 224 pp. 24 × 16 cm. Price: $50.00.

Cancer Incidence in the USSR. (IARC Scientific Publications No. 48). Edited by N. P. NAPALKOV, G. F. TSERKOVNY, and V. M. MERABISHVILI and in Lyon by D. M. PARKIN, M. SMANS, and C. S. MUIR. International Agency for Research on Cancer, 150 Cours Albert Thomas, 69372 Lyon Cedex 08 France. 1983. 83 pp. 24 × 18.5 cm. Price: $15.00. Sw.Fr. 30.

Chlorine and Hydrogen Chloride (Environmental Health Criteria 21). World Health Organization, 1211 Geneva 27, Switzerland. 1982. 95 pp. 21 × 14 cm. Price: Sw.Fr. 7.

A Clinical Approach to Progress in Infectious Diseases. Edited by W. BRUMFITT and J. M. T. HAMILTON-MILLER. Oxford University Press, 200 Madison Avenue, New York, NY 10016. 1983. 163 pp. 24 × 16 cm. Price: $26.95.

Clinical Management of Prescription Drugs. By JAMES W. LONG. Lippincott, East Washington Square, Philadelphia, PA 19105. 1984. 966 pp. 23.5 × 18.5 cm. Price: $19.50.

Communication in Pharmacy Practice: A Practical Guide for Students and Practitioners. Edited by WILLIAM N. TINDELL, ROBERT S. BEARDSLEY, and FREDERIC R. CURTISS. Sea & Febiger. 600 S. Washington Square, Philadelphia, PA 19106. 182 pp. 21.5 × 14 cm. Price: $11.50 (paper).

Contemporary Research in Pain and Analgesia (NIDA Research Monograph 45, A RAUS Review Report). Edited by ROGER M. BROWN, THEODORE M. PINKERT, and JACQUELINE P. LUDFORD. Department of Health and Human Services, National Institute on Drug Abuse, 5600 Fishers Lane, Rockville, MD 20857. 1983. 81 pp. 23 × 14 cm.

Control of Virus Diseases. Edited by EDOUARD KURSTAK. Marcel Dekker, Inc. 270 Madison Avenue, New York, NY 10016. 1984. 584 pp. 23.5 × 15.5 cm. Price: $115.00 (20% higher outside the U.S. and Canada).

Corporate Crime in the Pharmaceutical Industry. By JOHN BRAITHWAITE. Routledge & Kegan Paul, 9 Park Street, Boston, MA 02108. 1984. 440 pp. 22.5 × 14.5 cm. Price: $45.00.

2,4-Dichlorophenoxyacetic acid (2,4-D) (Environmental Health Criteria 29). World Health Organization, 1211 Geneva 27, Switzerland. 1984. 151 pp. 21 × 14 cm. Price: Sw.Fr. 14.

Directory of Alcohol and Drug Treatment Resources in Ontario, 1984. Addiction Research Foundation, 33 Russell Street, Toronto, Ontario, Canada M5S 2S1. 1984. (Directory and Listing) Price: $29.95.

Drugs, Driving, and Traffic Safety. Edited by ROBERT E. WILLETT and J. MICHAEL WALSH. World Health Organizatin, 1211 Geneva 27, Switzerland. 1983. 57 pp. 21 × 15 cm. Price: Sw.Fr. 5.

Fatty Acids in Cystic Fibrosis (Monographs pediatriiques). By VERA ROGIERS. Editions de l'Université de Bruxelles, Avenue Paul Hégen 26, 1050 Brussels, Belgium. 1983. 106 pp. 24 × 16 cm.

Fourier Transform N. M. R. Spectroscopy, 2nd Ed., Vol. 30 (Studies in Physical and Theoretical Chemistry). By DEREK SHAW. Elsevier Science Publishers. Molenwerfi, PO Box 211, 100 AE Amsterdam, The Netherlands. 1984. 344 pp. 25 × 17 cm. Price: $75.00.

Friedel-Crafts Alkylation Chemistry: A Century of Discovery. By ROYSTON M. ROBERTS and ALI ALI KHALAF. Marcel Dekker, Inc., 270 Madison Avenue, New York, NY 10016. 1984. 790 pp. 26 × 18.5 cm. Price: $165.00 (20% higher outside the U.S. and Canada).

Genotoxicology of N-Nitroso Compounds (Topics in Chemical Mutagenesis, Vol. 1). Edited by T. K. RAO, W. LIJINSKY, and J. L. EPLER. Plenum Publishing Corporation, 233 Spring Street, New York, NY 10013. 1984. 271 pp. 23.5 × 15.5 cm. Price: $39.50.

Guidelines for the Control of Narcotics and Psychotropic Substances. By BROR REXED, K. EDMONDSON, INAYAT KHAN, and ROBERT J. SAMSON. World Health Organization, 1211 Geneva 27, Switzerland. 1984. 141 pp. 24 × 16 cm. Price: Sw.Fr. 17.

Guidelines for Drinking-Water Quality Vol. 1, Recommendations. World Health Organization, 1211 Geneva 27, Switzerland. 1984. 130 pp. 24 × 16 cm. Price: Sw.Fr. 17.

Guidelines on Studies in Environmental Epidemiology (Environmental Health Criteria 27). World Health Organization, 1211 Geneva 27, Switzerland. 1983. 351 pp. 21 × 14 cm. Price: Sw.Fr. 26.

Handbook of Ocular Pharmacology, 3rd Ed. By MARVIN B. SMITH. PSG Publishing Co., Inc., Littleton, MA 01460. 1984. 243 pp. 21 × 15 cm.

Handbook of Psychopharmacology (Drugs, Neurotransmitters, and Behavior, Vol. 18). Edited by LESLIE L. IVERSON, SUSAN D. EVERSON and SOLOMON H. SNYDER. Plenum Publishing Corp., 233 Spring Street, New York, NY 10013. 1984. 532 pp. 25 × 17 cm. Price: $65.00.

The High Nitrogen Compounds. By FREDERIC R. BENSON. John Wiley & Sons, Inc., One Wiley Drive, Somerset, NJ 08873. 1984. 679 pp. 24 × 17 cm. Price: $125.00.

IARC Monographs on the Evaluation of the Carcinogenic Risk of Chemicals to Humans (Vol 31: Some Food Additives and Naturally Occurring Substances). International Agency for Research on Cancer, Lyon, France. Distributed by World Health Organization, 1211 Geneva 27, Switzerland. 1983. 314 pp. 24 × 18 cm. Price: $30.00, Sw.Fr. 60.

IARC Monographs on the Evaluation of the Carcinogenic Risk of Chemicals to Humans (Vol 31: Polynuclear Aromatic Compounds, Part 1, Chemical, Environmental and Experimental Data). International Agency for Re-

search on Cancer, Lyon, France. Distributed by World Health Organization, 1211 Geneva 27, Switzerland. 1983. 477 pp. 24 × 18 cm. Price: $40.00, Sw.Fr. 80.

Iatrogenic Diseases, 2nd Ed. By P. F. D'ARCY and J. P. GRIFFIN. Oxford University Press, 200 Madison Avenue, New York, NY 10016. 1983. 288 pp. 25.3 × 19.5 cm.

Index Nominum 1984, 12th Ed. Edited and Published by the Laboratory of the Swiss Pharmaceutical Society of Zurich, Switzerland. 1984. 1026 pp. 30 × 21 cm. Price: $140.00.

Investigative Microtechniques in Medicine and Biology, Vol. 1. Edited by J. CHAYEN and LUCILLE BITENSKY. Marcel Dekker, Inc., 270 Madison Avenue, New York, NY 10016. 1984. 392 pp. 23.5 × 16 cm. Price: $75.00 (20% higher outside the U.S. and Canada).

Macrophage-Mediated Antibody-Dependent Cellular Cytotoxicity, Immunology Series, Vol. 21. Edited by HILLEL S. KONEN. Marcel Dekker, Inc., 270 Madison Avenue, New York, NY 10016. 1983. 361 pp. 23.5 × 16 cm. Price: $55.00 (20% higher outside the US and Canada).

Management of Pharyngitis in an Era of Declining Rheumatic Fever (Report of the Eighty-Sixth Ross Conference on Pediatric Research). Ross Laboratories, 625 Cleveland Avenue, Columbus, OH 43216. 1984. 140 pp. 21.5 × 14 cm.

Manual of Antibiotics and Infectious Diseases, 5th Ed. Edited by JOHN E. CONTE, JR. and STEVEN L. BARRIERE, Lea & Febiger, 600 Washington Square, Philadelphia, PA 19106. 1984. 351 pp. 20.5 × 15 cm. Price: $18.50 ($23.25 in Canada).

McGraw-Hill Concise Encyclopedia of Science and Technology. Edited by SYBIL P. PARKER, McGraw-Hill, 1211 Avenue of the Americas, New York, NY 10124. 1984. 2065 pp. 28 × 22.5 cm. Price: $89.50.

Measurement in the Analysis and Treatment of Smoking Behavior (National Institute on Drug Abuse Research Monograph Series #48). Edited by JOHN GRABOWSKI and CATHERINE S. BELL, Department of Health and Human Services. Superintendent of Documents, U.S. Government Printing Office, Washington, D.C. 20402. 1983. 121 pp. 23 × 15 cm.

Membrane and Ultrafiltration Technology: Developments Since 1981 (Chemical Technology Review No. 226). Edited by S. TORREY. Noyes Data Corporation, Mill Road at Grand Avenue, Park Ridge, NJ 07656. 1984. 465 pp. 24 × 16 cm. Price: $64.00.

Methods in Organic Synthesis. Edited by The Royal Society of Chemistry. The University, Nottingham, NG7 2RD England. 1984. Price: $133.00.

Modern Liquid Chromatography of Macromolecules (Journal of Chromatography Library). By B. G. BELENKII and I. Z. VILENCHIK. Elsevier Science Publishers, PO Box 330, 1000 AH Amsterdam, The Netherlands. 1984. 432 pp. Price: $110.75 (U.S. and Canada) Dfl. 260.00 (rest of world).

Neurobiology of the Trace Amines: (Analytical, Physiological, Pharmacological, Behavioural, and Clinical Aspects). Edited by ALAN A. BOULTON, GLEN B. BAKER, WILLIAM G. DEWHURST, and MERTON SANDLER. The Human Press, Inc., PO Box 2148, Clifton, NJ 07015. 1984. 624 pp. 23.5 × 15.5 cm. Price: $59.50.

Nomograms for Administration of Critical Care Drugs. By JOHN E. RUETER and PAUL J. MILLER. American Society of Hospital Pharmacists, 4630 Montgomery Avenue, Bethesda, MD 20814. 1984. 46 pp. 19.5 × 17 cm. Price: $15.00.

Nucleic Acids: The Vectors of Life (The Jerusalem Symposia on Quantum Chemistry and Biochemistry, Vol. 16). Edited by BERNARD PULLMAN and JOSHUA JORTNER. D. Reidel Publishing Company. 190 Old Derby Street, Hingham, MA 02043. 1983. 578 pp. 24.5 × 17 cm. Price: $74.00, Dfl. 185.

Nutritional Surveillance. By JOHN B. MASON, JEAN-PIERRE HABICHT, H. TABATABAI, and V. VALVERDE. World Health Organization, 1211 Geneva 27, Switzerland. 1984. 194 pp. 24 × 16 cm. Price: Sw.Fr. 23.

Ozone and Its Reactions with Organic Compounds. By S. D. RAZUMOVSKY and G. E. ZAIKOV. Elsevier Science Publishers, PO Box 3000, 1000 AH Amsterdam, The Netherlands. 1984. 480 pp. Price: $100.00, Dfl. 260.

Parkinson's Disease, A Guide for Patient and Family. By ROGER C. DUVOISIN. Raven Press, 1140 Avenue of the Americas, New York, NY 10036. 1983. 224 pp. Price: $20.50 (cloth), $12.95 (paper).

The Pharmaceutical Quality Control Handbook. By RHYS BRYANT. Aster Publishing Corp., 320 North A Street, Springfield, OR 97477. 1984. 212 pp. 21.5 × 14 cm.

Pharmaceuticals & Health in the Third World. Edited by SURENDRA J. PATEL. Pergamon Press Ltd., Headington Hill Hall, Oxford, OX3 OBW England. 1983. 331 pp. 24.7 × 18.5 cm. Price: $21.00.

Pharmacy and the Law, 2nd Ed. By CARL T. DEMARCO. Aspen Systems Corporation, 1600 Research Blvd., Rockville, MD 20850. 1984. 400 pp. 23 × 16 cm. Price: $39.50.

Proceedings of Working Conference on Parenteral Trace Elements II (Section on Clinical Nutrition). The New York Academy of Medicine, 2 East 103 Street, New York, NY 10029. 1984. 216 pp. 25.5 × 17.5 cm. Price: $7.50.

Prostacyclin in Pregnancy. Edited by PETER J. LEWIS, SALVADOR MONCADA, and JOHN O'GRADY. Raven Press, 1140 Avenue of the Americas, New York, NY 10036. 1983. 230 pp. 25 × 16 cm. Price: $34.00.

Protoplasts 1983. Edited by I. POTRYKUS, C. T. HARMS, A. HINNEN, R. HUTTER, P. J. KING, and R. D. SHILLITO. Birkhauser Boston Inc., 380 Green Street, Cambridge, MA 02139. 1984. 270 pp. 30 × 22 cm. Price: $44.95.

Quality Assurance Principles for Analytical Laboratories. By FREDERICK M. GARFIELD. Association of Official Analytical Chemists, 1111 North 19th Street, Suite 210, Arlington, VA 22209. 1984. 224 pp. Price: $45.50 (softbound).

Styrene (Environmental Health Criteria 26). World Health Organization, 1211 Geneva 27, Switzerland. 1983. 123 pp. 21 × 14 cm. Price: Sw.Fr. 12.

Survey of Drug Research in Immunologic Disease: Vol. 3, Noncondensed Aromatic Derivatives, Part II. Edited by VASSIL ST. GEORGIEV. Karger, PO Box Postfach, CH-4009 Basel, Switzerland. 1983. 582 pp. 25 × 18 cm. Price: $293.50.

Survey of Drug Research in Immunologic Disease: Vol 4, Noncondensed Aromatic Derivatives, Part III. Edited by VASSIL ST. GEORGIEV. Karger. PO Box Postfach, CH-4009 Basel, Switzerland. 1984. 334 pp. 25 × 18 cm. Price: $173.75.

Tetrachloroethylene (Environmental Health Criteria 31). World Health Organization, 1211 Geneva 27, Switzerland. 1984. 48 pp. 21 × 14 cm. Price: Sw.Fr. 7.

Textbook of In Vitro *Practical Pharmacology.* By IAN KITCHEN. Blackwell Scientific Publications, Mosby Book Distributers, 11830 Westline Industrial Drive, St. Louis, MO 63141. 1984. 153 pp. 23.5 × 17.5 cm.

Transport Properties of Dense Plasmas. By W. EBELING, V. E. FORTOV, YU.L. KLIMONTOVICH, N. P. KOVLENKO, W. D. KRAEFT, YU. P. KRASNY, D. KEMP, P. P. KULIK, V. A. RIABY, G. RÖPKE, E. K. ROZANOV, and M. SCHLANGES. Birkhauser Boston Inc., 380 Green Street, Cambridge, MA 02139. 1984. 182 pp. 24 × 17 cm. Price: $29.95.

USP XX/NF XV Supplement 5. The United States Pharmacopeial Convention, Inc., 12601 Twinbrook Parkway, Rockville, MD 20852. 1984. pp. 959–1186.

1984 Year Book of Drug Therapy. Edited by LEO E. HOLLISTER and LOUIS LASAGNA, Year Book Medical Publishers, 35 Wacker Drive, Chicago, IL 60601. 1984. 440 pp. 23.5 × 16 cm. Price: $42.95.

NEW JOURNALS

Alcoholism Treatment Quarterly, (Vol. 1, No. 1). BRUCE CARRUTH, Ed. The Hawthorne Press, Inc., 28 East 22 Street, New York, NY 10010. 1984. 152 pp. 22 × 14 cm. Price: $47.00 for institutions, $63.00 for libraries, and $24.00 for individuals (add 20% for foreign subscriptions).

Journal of Microencapsulation, (Vol. 1, No. 1) J. R. NIXON, Ed. Taylor & Francis Ltd., Rankine Rd., Basingstoke, Hampshire RG24 OPR, UK. 1984. 103 pp. 25 × 17 cm. Price: $54.00.

Natural Product Reports. The Royal Society of Chemistry, Burlington House, Piccadilly, London W1V OBN. 120 pp. Price: $240.00. Six issues a year.

search on Cancer, Lyon, France. Distributed by World Health Organization, 1211 Geneva 27, Switzerland. 1983. 477 pp. 24 × 18 cm. Price: $40.00, Sw.Fr. 80.

Iatrogenic Diseases, 2nd Ed. By P. F. D'ARCY and J. P. GRIFFIN. Oxford University Press, 200 Madison Avenue, New York, NY 10016. 1983. 288 pp. 25.3 × 19.5 cm.

Index Nominum 1984, 12th Ed. Edited and Published by the Laboratory of the Swiss Pharmaceutical Society of Zurich, Switzerland. 1984. 1026 pp. 30 × 21 cm. Price: $140.00.

Investigative Microtechniques in Medicine and Biology, Vol. 1. Edited by J. CHAYEN and LUCILLE BITENSKY. Marcel Dekker, Inc., 270 Madison Avenue, New York, NY 10016. 1984. 392 pp. 23.5 × 16 cm. Price: $75.00 (20% higher outside the U.S. and Canada).

Macrophage-Mediated Antibody-Dependent Cellular Cytotoxicity, Immunology Series, Vol. 21. Edited by HILLEL S. KONEN. Marcel Dekker, Inc., 270 Madison Avenue, New York, NY 10016. 1983. 361 pp. 23.5 × 16 cm. Price: $55.00 (20% higher outside the US and Canada).

Management of Pharyngitis in an Era of Declining Rheumatic Fever (Report of the Eighty-Sixth Ross Conference on Pediatric Research). Ross Laboratories, 625 Cleveland Avenue, Columbus, OH 43216. 1984. 140 pp. 21.5 × 14 cm.

Manual of Antibiotics and Infectious Diseases, 5th Ed. Edited by JOHN E. CONTE, JR. and STEVEN L. BARRIERE, Lea & Febiger, 600 Washington Square, Philadelphia, PA 19106. 1984. 351 pp. 20.5 × 15 cm. Price: $18.50 ($23.25 in Canada).

McGraw-Hill Concise Encyclopedia of Science and Technology. Edited by SYBIL P. PARKER, McGraw-Hill, 1211 Avenue of the Americas, New York, NY 10124. 1984. 2065 pp. 28 × 22.5 cm. Price: $89.50.

Measurement in the Analysis and Treatment of Smoking Behavior (National Institute on Drug Abuse Research Monograph Series #48). Edited by JOHN GRABOWSKI and CATHERINE S. BELL, Department of Health and Human Services. Superintendent of Documents, U.S. Government Printing Office, Washington, D.C. 20402. 1983. 121 pp. 23 × 15 cm.

Membrane and Ultrafiltration Technology: Developments Since 1981 (Chemical Technology Review No. 226). Edited by S. TORREY. Noyes Data Corporation, Mill Road at Grand Avenue, Park Ridge, NJ 07656. 1984. 465 pp. 24 × 16 cm. Price: $64.00.

Methods in Organic Synthesis. Edited by The Royal Society of Chemistry. The University, Nottingham, NG7 2RD England. 1984. Price: $133.00.

Modern Liquid Chromatography of Macromolecules (Journal of Chromatography Library). By B. G. BELENKII and I. Z. VILENCHIK. Elsevier Science Publishers, PO Box 330, 1000 AH Amsterdam, The Netherlands. 1984. 432 pp. Price: $110.75 (U.S. and Canada) Dfl. 260.00 (rest of world).

Neurobiology of the Trace Amines: (Analytical, Physiological, Pharmacological, Behavioural, and Clinical Aspects). Edited by ALAN A. BOULTON, GLEN B. BAKER, WILLIAM G. DEWHURST, and MERTON SANDLER. The Human Press, Inc., PO Box 2148, Clifton, NJ 07015. 1984. 624 pp. 23.5 × 15.5 cm. Price: $59.50.

Nomograms for Administration of Critical Care Drugs. By JOHN E. RUETER and PAUL J. MILLER. American Society of Hospital Pharmacists, 4630 Montgomery Avenue, Bethesda, MD 20814. 1984. 46 pp. 19.5 × 17 cm. Price: $15.00.

Nucleic Acids: The Vectors of Life (The Jerusalem Symposia on Quantum Chemistry and Biochemistry, Vol. 16). Edited by BERNARD PULLMAN and JOSHUA JORTNER. D. Reidel Publishing Company. 190 Old Derby Street, Hingham, MA 02043. 1983. 578 pp. 24.5 × 17 cm. Price: $74.00, Dfl. 185.

Nutritional Surveillance. By JOHN B. MASON, JEAN-PIERRE HABICHT, H. TABATABAI, and V. VALVERDE. World Health Organization, 1211 Geneva 27, Switzerland. 1984. 194 pp. 24 × 16 cm. Price: Sw.Fr. 23.

Ozone and Its Reactions with Organic Compounds. By S. D. RAZUMOVSKY and G. E. ZAIKOV. Elsevier Science Publishers, PO Box 3000, 1000 AH Amsterdam, The Netherlands. 1984. 480 pp. Price: $100.00, Dfl. 260.

Parkinson's Disease, A Guide for Patient and Family. By ROGER C. DUVOISIN. Raven Press, 1140 Avenue of the Americas, New York, NY 10036. 1983. 224 pp. Price: $20.50 (cloth), $12.95 (paper).

The Pharmaceutical Quality Control Handbook. By RHYS BRYANT. Aster Publishing Corp., 320 North A Street, Springfield, OR 97477. 1984. 212 pp. 21.5 × 14 cm.

Pharmaceuticals & Health in the Third World. Edited by SURENDRA J. PATEL. Pergamon Press Ltd., Headington Hill Hall, Oxford, OX3 OBW England. 1983. 331 pp. 24.7 × 18.5 cm. Price: $21.00.

Pharmacy and the Law, 2nd Ed. By CARL T. DEMARCO. Aspen Systems Corporation, 1600 Research Blvd., Rockville, MD 20850. 1984. 400 pp. 23 × 16 cm. Price: $39.50.

Proceedings of Working Conference on Parenteral Trace Elements II (Section on Clinical Nutrition). The New York Academy of Medicine, 2 East 103 Street, New York, NY 10029. 1984. 216 pp. 25.5 × 17.5 cm. Price: $7.50.

Prostacyclin in Pregnancy. Edited by PETER J. LEWIS, SALVADOR MONCADA, and JOHN O'GRADY. Raven Press, 1140 Avenue of the Americas, New York, NY 10036. 1983. 230 pp. 25 × 16 cm. Price: $34.00.

Protoplasts 1983. Edited by I. POTRYKUS, C. T. HARMS, A. HINNEN, R. HUTTER, P. J. KING, and R. D. SHILLITO. Birkhauser Boston Inc., 380 Green Street, Cambridge, MA 02139. 1984. 270 pp. 30 × 22 cm. Price: $44.95.

Quality Assurance Principles for Analytical Laboratories. By FREDERICK M. GARFIELD. Association of Official Analytical Chemists, 1111 North 19th Street, Suite 210, Arlington, VA 22209. 1984. 224 pp. Price: $45.50 (softbound).

Styrene (Environmental Health Criteria 26). World Health Organization, 1211 Geneva 27, Switzerland. 1983. 123 pp. 21 × 14 cm. Price: Sw.Fr. 12.

Survey of Drug Research in Immunologic Disease: Vol. 3, Noncondensed Aromatic Derivatives, Part II. Edited by VASSIL ST. GEORGIEV. Karger, PO Box Postfach, CH-4009 Basel, Switzerland. 1983. 582 pp. 25 × 18 cm. Price: $293.50.

Survey of Drug Research in Immunologic Disease: Vol 4, Noncondensed Aromatic Derivatives, Part III. Edited by VASSIL ST. GEORGIEV. Karger. PO Box Postfach, CH-4009 Basel, Switzerland. 1984. 334 pp. 25 × 18 cm. Price: $173.75.

Tetrachloroethylene (Environmental Health Criteria 31). World Health Organization, 1211 Geneva 27, Switzerland. 1984. 48 pp. 21 × 14 cm. Price: Sw.Fr. 7.

Textbook of In Vitro *Practical Pharmacology.* By IAN KITCHEN. Blackwell Scientific Publications, Mosby Book Distributers, 11830 Westline Industrial Drive, St. Louis, MO 63141. 1984. 153 pp. 23.5 × 17.5 cm.

Transport Properties of Dense Plasmas. By W. EBELING, V. E. FORTOV, YU.L. KLIMONTOVICH, N. P. KOVLENKO, W. D. KRAEFT, YU. P. KRASNY, D. KEMP, P. P. KULIK, V. A. RIABY, G. RÖPKE, E. K. ROZANOV, and M. SCHLANGES. Birkhauser Boston Inc., 380 Green Street, Cambridge, MA 02139. 1984. 182 pp. 24 × 17 cm. Price: $29.95.

USP XX/NF XV Supplement 5. The United States Pharmacopeial Convention, Inc., 12601 Twinbrook Parkway, Rockville, MD 20852. 1984. pp. 959–1186.

1984 Year Book of Drug Therapy. Edited by LEO E. HOLLISTER and LOUIS LASAGNA, Year Book Medical Publishers, 35 Wacker Drive, Chicago, IL 60601. 1984. 440 pp. 23.5 × 16 cm. Price: $42.95.

NEW JOURNALS

Alcoholism Treatment Quarterly, (Vol. 1, No. 1). BRUCE CARRUTH, Ed. The Hawthorne Press, Inc., 28 East 22 Street, New York, NY 10010. 1984. 152 pp. 22 × 14 cm. Price: $47.00 for institutions, $63.00 for libraries, and $24.00 for individuals (add 20% for foreign subscriptions).

Journal of Microencapsulation, (Vol. 1, No. 1) J. R. NIXON, Ed. Taylor & Francis Ltd., Rankine Rd., Basingstoke, Hampshire RG24 OPR, UK. 1984. 103 pp. 25 × 17 cm. Price: $54.00.

Natural Product Reports. The Royal Society of Chemistry, Burlington House, Piccadilly, London W1V OBN. 120 pp. Price: $240.00. Six issues a year.

A publication of the
American Pharmaceutical Association—
the National Professional Society
of Pharmacists

JOURNAL OF PHARMACEUTICAL SCIENCES

Volume 73, 1984

JPMSAE 73(1-12) 1-1910 (1984)
ISSN 0022-3549

Sharon G. Boots
Editor

Sue A. Kruger
Production Editor

Margaret M. Madeleine
Assistant Production Editor

Karen A. Blakney
Copy Editor

Edward G. Feldmann
Contributing Editor

Samuel W. Goldstein
Contributing Editor

Patricia A. Evich
Editorial Secretary

Editorial Advisory Board

Jordan L. Cohen
Kenneth A. Connors
Louis Diamond
Ho-Leung Fung
Milo Gibaldi
Everett N. Hiestand
W. Homer Lawrence
Ian W. Mathison
Carl M. Metzler
Robert E. Notari
Paul L. Schiff, Jr.
Jane E. Shaw

Published monthly under the supervision of the Board of Trustees

Sending Unapproved Drugs Abroad

As this column is being written, legislation is being debated in Congress that would allow United States pharmaceutical manufacturers to export drugs that have not been approved for use in this country.

The issue is a highly controversial one with very vocal opponents, as well as proponents, each stirring up considerable public interest in the issue and support for their respective positions. As just one example, several prominent lay newspapers, including the *New York Times* and the *Washington Post*, have published editorials opposing such legislation.

Those opposed generally make the argument that Americans would create "a double standard"; namely, drugs that have not been shown to be sufficiently safe and effective for marketing in the United States and for use by Americans would be sanctioned for export and use by people living in other lands.

Admittedly, that argument appears appealing and persuasive on purely moral or ethical grounds. Political foes who would wish to cast the United States in a bad light undoubtedly could have a field day playing it to their best advantage. Moreover, there is some unfortunate past history—many, many years ago—when unscrupulous manufacturers did use the export market to "dump" substandard batches of deteriorated or otherwise unsuitable drug products.

However, the legislation that is presently under consideration does seem to have provisions that would adequately safeguard foreign consumers from products of inferior quality. Hence, the basic difference today is not one of manufacturing quality, but rather the degree of proof of safety and effectiveness. Put another way, it revolves around the inherent features of the drug entity rather than characteristics of the dosage form or the drug product. And again even in this regard, the present legislation would only permit export to (*a*) countries having a well-regarded drug regulatory agency that could make a valid judgement as to the suitability of the imported drug for that country's population given the specific circumstances involved or (*b*) other countries only if at least one country having a well-regarded drug regulatory agency has approved the drug. No export would be allowed if any agency throughout the world that is comparable to the U.S. Food and Drug Administration had banned or withdrawn the drug on the grounds of its safety or efficacy.

Unfortunately, in presenting their arguments, the major proponents of the legislation have consistently emphasized only the economic considerations involved. They point out, and correctly so, that under current law American manufacturers can establish plants abroad to produce, sell, and distribute the very drugs that they now are prohibited from producing in their U.S. plants to export for exactly the same purpose. The proponents further note that this serves to send abroad investment capital, jobs, and income that otherwise would benefit the U.S. and its citizens. Jobs are lost, the balance of trade is upset, and technology is drained away.

Editor's Note: Dr. Feldmann's editorials are an expression of personal opinion and do not necessarily reflect views or policies of APhA. The editorials are intended to be provocative and to stimulate thinking. Readers having reactions, either pro or con, are invited to submit them for publication in the *Open Forum* section.

These points are all quite valid. However, they neglect to address what is, in our opinion, the most persuasive argument. Specifically, many drugs needed in other parts of the world are intended to treat conditions for which there is virtually no American market and, hence, there is no reason whatsoever for the drug company to expend the time, effort, and expense of seeking U.S. approval.

For example, in late September, a prominent American pharmaceutical firm presented the results of three clinical studies at a session of the XI International Congress for Tropical Medicine and Malaria in Calgary, Canada. The studies involved clinical investigations that were conducted in close collaboration with the World Health Organization.

Based simply on the news releases prepared for the professional press announcing those reports, the results were dramatic and represent a potential public health breakthrough that would greatly benefit a very significant portion of the world's population—virtually none of whom reside in the U.S.

Specifically, a single oral dose of a new antiparasitic drug (identified as "ivermectin") was found to be a highly promising agent for the treatment of the tropical disease known as onchocerciasis or "river blindness."

An estimated 40 million people in Africa, Central and South America, and Yemen in the Middle East are currently afflicted with this disease. Its victims not only suffer blindness, but a whole host of other seriously debilitating conditions. A tiny blackfly which breeds in fast-moving streams carries the developing larvae of the worm that causes onchocerciasis and is the reason why the disease is referred to as "river blindness."

But, according to all three of the studies reported at the International Congress, a single oral dose of ivermectin reduced to near zero in skin snip samples the numbers of microfilariae or tiny worm larvae which cause the disease. And the drug's side effects or toxicity was nominal at most.

It strikes us as not only ironic, but virtually a social injustice, that current American law prevents the American drug manufacturer—that discovered and developed this drug in its U.S. laboratories—from producing and exporting the drug from its U.S. plants for foreign markets. It is now prohibited from doing so because the drug is not approved in the U.S. and, with no incidence of "river blindness" in the U.S., it is a safe assumption that the drug will not be subjected to the very costly and time-consuming process involved in seeking such approval.

Consequently, recognizing the surface arguments that can be cited in opposing the present legislation to relax the prohibition on exporting of American produced drugs not approved in the U.S., it is our belief that the greater good would be served by passage of such legislation.

—EDWARD G. FELDMANN
American Pharmaceutical Association
2215 Constitution Ave., N.W.
Washington, DC 20037

0022-3549/84/1100-1505$01.00/0
© 1984, American Pharmaceutical Association

JOURNAL OF PHARMACEUTICAL SCIENCES

NOVEMBER 1984
VOLUME 73 NUMBER 11

RESEARCH ARTICLES

Characterization of Polyacryl Starch Microparticles as Carriers for Proteins and Drugs

PER ARTURSSON, PETER EDMAN, TIMO LAAKSO, and INGVAR SJÖHOLM ˣ

Received July 20, 1983, from the *Division of Pharmacy, Department of Drugs, National Board of Health and Welfare, S-751 25 Uppsala, Sweden* and the *Department of Pharmaceutical Biochemistry, Biomedical Center, University of Uppsala, Uppsala, Sweden.* Accepted for publication December 2, 1983.

Abstract □ Biodegradable microparticles of cross-linked starch (maltodextrin) have been designed as carriers of proteins and low molecular weight drugs *in vivo*. Methods are presented for the synthesis of acryloyl starch and its polymerization to microparticles. Macromolecules were immobilized in the microparticles in high yields, *i.e.*, up to 40% of the dry weight consisted of the immobilized protein. The optimal conditions of immobilization were investigated by varying the concentration of starch (D), the concentration of acryloyl groups (T), and the amount of additional cross-linking agent (C). Exclusion of the cross-linking agent gave maximal immobilization of the macromolecules. Enzyme kinetics, release profiles, surface localization, and heat stability of the immobilized macromolecules are also presented. Microparticles based on starch with small amounts of acryloyl groups were completely degraded after incubation with amyloglucosidase. The degradation of microparticles in serum and in the target organelle, the lysosome, was investigated *in vitro*. The polyacrylic starch microspheres (mean diameter, 0.5 μm) constitute an attractive alternative to other drug and enzyme carriers.

Keyphrases □ Drug carrier systems—biodegradable, starch microparticles, lysosomal degradation □ Microspheres—drug carrier system, lysosomal degradation, polyacryl starch

Enzymes have hitherto had relatively limited applications *in vivo* and have essentially been used only for the treatment of blood coagulation disorders. Several problems are associated with the use of enzymes *in vivo*, *e.g.*, the targets of the enzymes are often strictly compartmentalized to specific tissues and cell compartments and administered enzymes cannot readily pass the membranes of these compartments. Furthermore, free enzymes available from human sources are rapidly degraded by proteolytic enzymes. Foreign enzymes, when injected, will induce the formation of antibodies and other immunologic reactions. Systems that will protect the enzymes from degradation and direct them to their specific targets are not yet available. Similarly, suitable carrier systems for low molecular weight drugs are still unavailable for targeting *in vivo*, although several different carriers have been extensively tested (1–4).

Spherical microparticles (<1 μm) made of polyacrylamide or polyacrylic dextran can be used for the immobilization of proteins (5, 6). When the particles are injected intravenously in rats and mice, they are rapidly cleared from the circulatory system by macrophages in the reticuloendothelial system (RES). After uptake, the particles are localized in the lysosomal vacuome (7, 8). This "passive targeting" of microspheres to the RES has been used successfully to treat an artificially induced storage disease in mice (9). However, any system used as an *in vivo* drug carrier must fulfill certain requirements: it must be biocompatible and not induce toxic reactions; it must be biodegradable to avoid accumulation in the tissues; it should be small to avoid respiratory distress after intravenous injection; it must be compartmentalized in such a way that the therapeutic index of the drug or enzyme carried is improved.

This paper describes the preparation and characteristics of biodegradable starch microparticles. The biodegradability of the spheres is investigated *in vitro* with hydrolytic enzymes and an isolated lysosome-enriched rat liver fraction.

EXPERIMENTAL SECTION

Materials—Human serum albumin[1], immunoglobulin G[1], carbonic anhydrase[2], α-amylase[3], amyloglucosidase[2], *N*-acetyl-β-glucoseamidase[2], and lysosyme[4] were used without further purification. *N,N'*-Methylenebisacrylamide[5], 4-methylumbelliferyl-*N*-acetyl-β-D-glucoseamidine[2], *p*-nitrophenyl acetate[2], and the other chemicals used were analytical grade. Hydroxyethyl starch[6] (mol. wt., 400,000; degree of derivatization, 0.7), maltodextrin[7] (mol. wt. 5000), [^{14}C]paraformaldehyde[8], and [^{14}C]starch (prepared from *Nico-*

[1] KABI AB, Stockholm.
[2] Sigma Chemical Co.
[3] Boehringer Mannheim.
[4] Merck Co.
[5] Eastman Kodak Co.
[6] Hydroxyethyl starch was obtained as a gift from Dr. Tony de Belder, Pharmacia, Uppsala, Sweden.
[7] Maltodextrin was obtained as a gift from Dr. Lars Svensson, Stadex AB, Malmö, Sweden.
[8] Amersham, England.

0022-3549/84/1100-1507$01.00/0
© 1984, American Pharmaceutical Association

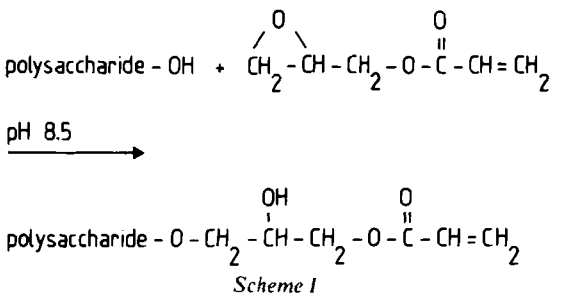

Scheme I

tiana tabacum[9]; mol. wt., 7000–8000) were used without further purification.

Acryloylation of Polysaccharides—Chemical modification of the polysaccharides (Scheme I) with acrylic acid glycidyl ester followed the procedure outlined by Edman *et al.* (7). Maltodextrin or hydroxyethyl starch (10 g) was dissolved in 0.2 M phosphate buffer (pH 8.5) to give a solution of appropriate concentration. Acrylic acid glycidyl ester[10] (10 mL) was added, and the two-phase system was magnetically stirred for up to 15 d. Samples (10 mL) were withdrawn on days 1, 3, 5, 7, 10, and 15 and centrifuged for 15 min at 3000×*g*. Unreacted acrylic acid glycidyl ester was discarded, and the aqueous solution with the derivatized polysaccharide was extracted with 10 parts of toluene to remove remaining unreacted glycidyl ester.

Determination of the Degree of Derivatization of Polysaccharides—The degree of derivatization (acrylic groups/glucose residue) was analyzed by ^{1}H-FT-NMR according to the method of Lepistö *et al.* (10). The measurements were made at 100 MHz on a spectrometer[11] using the water-elimination Fourier transform method. After phase correction of the region containing the acrylic and anomeric proton resonances (δ 4.8–6.7 ppm) the region was integrated. The signals of the anomeric proton (δ 4.8–5.8 ppm) were used as internal standard.

Preparation of Polyacryl Starch Microparticles—Microparticles with or without protein were prepared as described previously (5, 6). Protein and, when applicable, bisacrylamide were dissolved in a solution of acryloylated maltodextrin or in acryloylated hydroxyethyl starch in 0.2 M sodium phosphate buffer, pH 8.5. EDTA (1×10^{-3} M) and ammonium peroxodisulfate were added to the deoxygenated mixture. The water solution (5–10 mL) was homogenized with poloxamer 188[12] in 600 mL of chloroform–toluene (1:4) to produce a water-in-oil emulsion. On addition of *N,N,N′,N′*-tetramethylethylenediamine the water phase droplets were polymerized to microparticles. The microparticles were freed from the organic phase and nonimmobilized protein by repeated washings with buffer.

The microparticle composition is characterized by the D-T-C nomenclature suggested by Hjertén (11), as modified by Edman *et al.* (6). The D-T-C values denote the amounts of the components in the monomer solution used for particle formation: D denotes the concentration of derivatized macromolecules (*i.e.*, acryloylated starch, g/100 mL); T denotes the total concentration of acryloyl groups (g/100 mL); C is the relative amount of the cross-linking agent, bisacrylamide, expressed as the percentage (w/w) of the total amount of acrylic monomers.

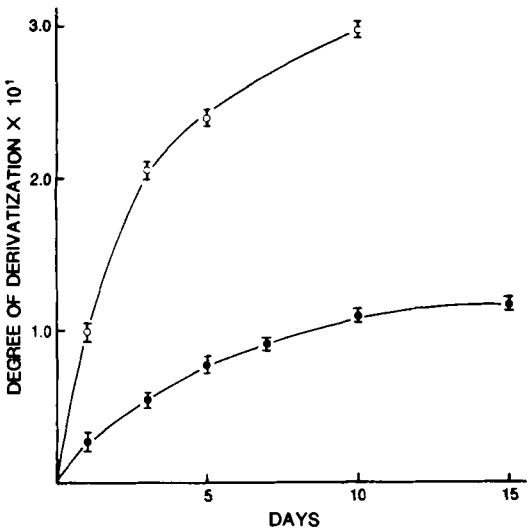

Figure 1—*Derivatization of the polysaccharides. The degree of derivatization (acrylic groups per glucose residue) of maltodextrin (●) and hydroxyethyl starch (○) are expressed as mean values ± SD (n = 5 and 3, respectively).*

[9] New England Nuclear, West Germany.
[10] Fluka AG.
[11] Model JNM-FX 100; JEOL.
[12] Pluronic F68; BASF Wyandotte.

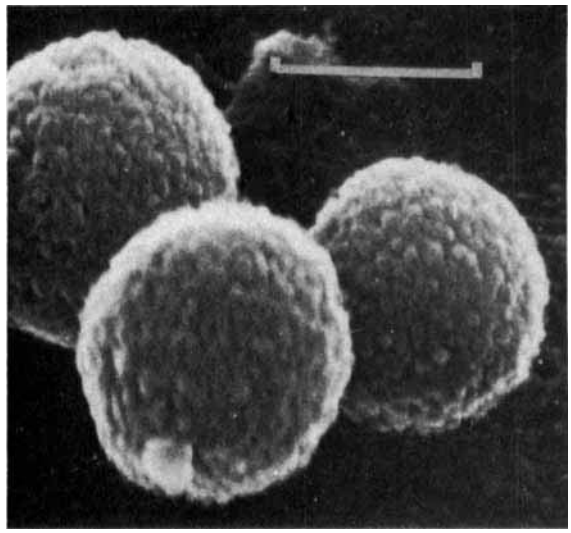

Figure 2—*Scanning electron micrograph (30,000×) of polyacryl starch microparticles (D-T-C 10-0.2-0). The bar indicates 1 μm.*

Radioactive Labeling of Polyacryl Starch Microparticles—Two types of radioactive labels were used. The label was introduced with ^{14}C-labeled *N,N′*-methylenebisacrylamide as the cross-linking agent or with [^{14}C]starch as part of the monomers. In the former case, the labeled derivative was prepared from [^{14}C]paraformaldehyde and acrylamide according to Feuer and Lynch (12) as described by Sjöholm and Edman (7). The radioactive starch was derivatized with acrylic acid glycidyl ester together with the polysaccharides used in the particle preparation.

Protein Determination—The amount of protein incorporated in the microparticles was determined with an automatic amino acid analyzer after hydrolysis in 6 M HCl at 105°C for 20 h. The amount of protein leaking from the microspheres was measured by the method of Lowry *et al.* (13). In each case, the protein studied was used as a standard. In some experiments, ^{125}I-human serum albumin was used to determine the protein content of the microparticles and to follow the leakage of the albumin from the particles.

Determination of Carbonic Anhydrase Activity—The activity of carbonic anhydrase was determined with the chromogenic substrate *p*-nitrophenyl acetate (14). The assay mixture consisted of 4.7 mL of 0.05 M Tris buffer (pH 7.4), 0.25 mL of substrate solution in absolute ethanol at the appropriate concentration, and 0.05 mL of the enzyme (immobilized or in free form) in Tris buffer. The formation of the hydrolysis products was followed spectrophotometrically at 400 nm at room temperature. The velocity of the reaction is the initial increase in absorbance during 1 min. Correction was made for the spontaneous hydrolysis of the substrate in samples that did not contain the enzyme; the particle matrix did not affect the reaction rate (results of control experiments). Furthermore, the particles did not cause light scattering at this wavelength, and no sedimentation was detectable during the time of measurement.

Determination of the Functional Capacity of Immobilized Human Serum Albumin—The functional capacity of immobilized albumin was determined by the method of Kober *et al.* (15). Microparticles containing albumin were incubated with a fixed concentration of [^{14}C]salicylic acid. After centrifugation, the concentration of the free drug was determined by measuring the radioactivity in the supernatant. The amount of salicylic acid bound to albumin was calculated from the percent binding and from a standard curve derived by equilibrium dialysis with different albumin concentrations.

Iodination of Human Serum Albumin—Human serum albumin (10 mg) in 0.5 mL of 0.05 M phosphate buffer (pH 7.3) containing 0.15 M NaCl was labeled with [^{125}I]NaI (1 mCi) in the presence of lactoperoxidase (20 μg) and hydrogen peroxide (0.03% v/v, 20 μL added 3 times at 3-min intervals) according to the method of Phillips and Morrison (16). The reaction was terminated after 10 min by diluting the sample with chilled buffer. The ^{125}I-labeled human serum albumin was isolated from the reaction mixture by gel filtration on a Sephadex G-25 column.

Table I—Characteristics of Microparticles with Immobilized ^{125}I-Human Serum Albumin [a]

Microparticle Composition, D-T-C	Total Yield of Microparticle, %	Total Protein Yield, %	Total Protein Content, mg/mg dry weight	Functional Protein Content, %	Leakage in 6 Weeks, %
		Maltodextrin Particles			
5-0.2-0	7.9	2.2	0.218	41	34
7-0.2-0	5.4	3.4	0.386	—[b]	34
10-0.2-0	28.1	7.3	0.206	44	62
10-0.3-0	58.1	13.8	0.192	75	52
10-0.4-0	46.2	27.5	0.373	58	38
10-0.4-5	44.6	9.8	0.180	40[c]	43
10-0.4-25	19.4	3.8	0.164	47[c]	56
10-1.2-60	55.6	22.4	0.287	74	40
		Hydroxyethyl Starch Particles			
10-0.4-0	31.4	3.8	0.108	79	32
10-0.8-0	70.3	12.7	0.153	58	43
10-1.0-0	93.5	24.7	0.209	42	33
10-1.2-0	87.3	39.4	0.311	63	36
10-1.5-50	69.3	17.0	0.197	95	38

[a] The study was carried out with 100 mg of ^{125}I-labeled human serum albumin/mL of aqueous buffer. The protein content of the particles was determined in a gamma counter. The amount of functionally active protein in the particles was determined by estimating the capacity of the albumin to bind [^{14}C]salicylic acid (15). [b] Not determined. [c] Determined after 50 d.

Determination of Radioactivity, Particle Size, and Density—β-Emitting isotopes were determined in a scintillation counter[13]; the counting efficiency was calculated with an external standard. Iodine-125 was measured in a gamma scintillation counter[14].

The size of the particles was determined from photographs taken with a scanning electron microscope (7). Using this technique, 85% of the microparticles had a diameter of 0.2–1.0 μm; 15% were 1.0–1.6 μm in diameter.

The densities of the microparticles were determined by density gradient centrifugation in colloidal silica coated with polyvinylpyrrolidone[15] (17) utilizing a gradient ranging from 1.02 to 1.10 g/cm^3, obtained with a dual-chamber gradient maker. Density marker beads[16] were used to monitor the gradient according to the manufacturer's specification. The gradient volume was 10 mL. Microparticles (0.5–2.5 mg) in 300 μL of physiological saline were applied to the top of the gradients, which were centrifuged at 400×g for 25 min using a swing-out rotor.

Isolation of a Lysosomal Fraction from Rat Liver Homogenate—The isolation of the lysosomal fraction followed the technique outlined by Beaufay (18). Livers from male Sprague–Dawley rats, which were fasted for 12 h, were removed rapidly and immersed in a beaker containing ice-cold 0.25 M sucrose (pH 5.5). After weighing, the tissue was cut into pieces and homogenized with 3 volumes of the medium in a Potter–Elvehjelm homogenizer. The homogenate was centrifuged at 4°C and 750×g for 10 min. The sediment was redispersed three times and centrifuged. The resulting supernatants were pooled and centrifuged at 12,000×g for 10 min. The supernatant was discarded and the pellet was dissolved in 0.25 M sucrose and centrifuged for 10 min at 6500×g. This step was repeated three times and the supernatants were combined and centrifuged for 15 min at 12,000×g. The resulting sediment was dispersed in water (pH 4.5) and made up to a final volume equal to that of the original tissue. The suspension was frozen and thawed twice before use. The isolated lysosome-enriched fraction was usually preserved with penicillin G. The partition of lysosomes in the different fractions during the preparation was followed by assay of the lysosomal enzyme, N-acetyl-β-glucoseamidase. The enzyme was determined by using 4-methylumbelliferyl-N-acetyl-β-D-glucoseamidine as substrate in 0.15 M acetate buffer, pH 4.2 (19).

Enzymatic Solubilization of Microparticles—α-Amylase (10 U/mL in 0.1 M phosphate buffer, pH 5.5) or amyloglucosidase (0.1–10 U/mL in 0.1 M citrate buffer, pH 4.5) was added to 0.5 mg of radioactive microparticles in the same buffer to give a final volume of 2.0 mL. In other experiments, 1.0 mL of pooled human serum or 1.0 mL of the lysosomal fraction was added to 1.0 mL of radioactive microparticles (0.5 mg dry weight). After incubation at 37°C for 0.5–6 h the particles were centrifuged (3000×g) and the radioactivity in 1.0 mL of the supernatant was measured before or after filtration through a 0.45-μm membrane filter. In some of the experiments, the radioactive degradation products were separated on a Sephadex G-150 column. The degradation products (5 mL) were applied on a 2.6 × 100-cm column. The separation was performed with 0.01 M phosphate buffer (pH 7.4) containing 0.15 M NaCl as the elution medium.

Size Determination of Microparticle Aggregates—Microparticles (100 μL, 50 μg) were suspended in 150 mL of particle-free buffer[17]. The suspensions were used in a particle counter[18], which simultaneously counts particles in 14 size classes. The instrument was fitted with a 50-μm orifice tube. During all measurements the speed and stirrer position were constant. The mean diameters of each size class of suspended microparticles were calculated[19] from the particle distribution.

In some experiments, microparticles containing human serum albumin were incubated with a specific antiserum (*i.e.*, 50 μL of rabbit anti-human serum containing 3.6 mg of immunoglobulin G/mL) in an end-over-end mixer for 45 min prior to the estimation of the mean diameter. In control experiments, the microparticles containing human serum albumin were incubated with 0.15 M NaCl, or empty microparticles were incubated with the corresponding antiserum.

RESULTS

Derivatization of Polysaccharides—The introduction of acryloyl groups into hydroxyethyl starch and maltodextrin with acrylic acid glycidyl ester was followed by NMR for 10 and 15 d, respectively. Hydroxyethyl starch reacted more rapidly and more extensively than maltodextrin (Fig. 1); every 3rd glucose residue was substituted after 10 d compared with every 10th glucose unit for maltodextrin. The higher reaction rate with hydroxyethyl starch can most probably be ascribed to the presence of the hydroxyethyl groups. With maltodextrin, a plateau was reached after ~10 d.

Immobilization of Proteins in Microparticles of Different Composition—Table I summarizes results from the incorporation of ^{125}I-labeled human

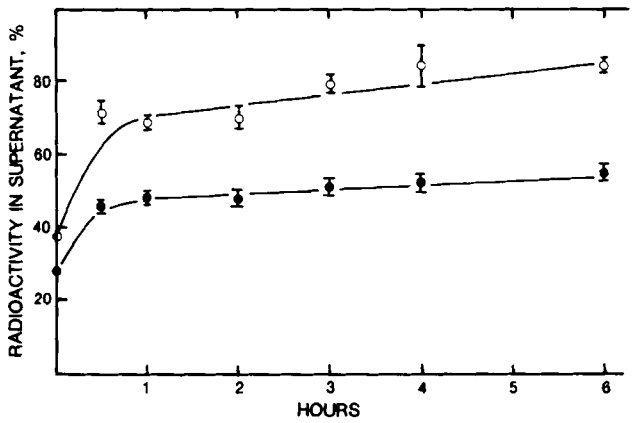

Figure 3—In vitro *digestion of ^{14}C-labeled microparticles in a lysosome-enriched fraction. Maltodextrin particles with D-T-C of 10-0.2-0 (○) and 10-0.4-0 (●) were preincubated in pooled human serum for 1 h prior to incubation with the lysosomal fraction. Mean values* ± SD (n = 3–6).

[13] TriCarb 2405 Spectrometer; Packard.
[14] Auto-Gamma 5110; Packard.
[15] Percoll; Pharmacia AB, Uppsala, Sweden.
[16] Pharmacia AB, Uppsala, Sweden.
[17] Isoton II; Coulter Electronics, England.
[18] Model TAII; Coulter.
[19] Model 9825 computer, Hewlett-Packard.

Table II—Degradation of Maltodextrin Microparticles by Amylogucosidase *In Vitro*

Microparticle Composition, D-T-C	Label	Soluble Radioactivity After 3 h[a]
10-0.2-0	[^{14}C]Starch	103 ± 3
10-0.2-0	[^{125}I-Human serum albumin	100 ± 7
10-0.4-0	[^{14}C]Starch	59 ± 2
10-0.4-25	[^{14}C]Starch	69 ± 2
10-0.4-25	[^{14}C]Bisacrylamide	64 ± 4

[a] Mean in percent of total ± *SD*; $n = 3$.

serum albumin in polyacryl starch microparticles. Three series of experiments were run, varying total concentration of starch (D), total concentration of acrylic groups (T), and degree of cross-linking (C). A decrease of acryloylated starch (D) in the particles decreases the total yield of immobilized protein as well as the yield of particles.

Increase of the concentration of acrylic groups (T) (acryloylated maltodextrin or hydroxyethyl starch) in the aqueous phase resulted in an increase in the amount of albumin immobilized in the particles. The maximal amount of albumin which could be incorporated corresponded to 37% of the dry weight (particles based on maltodextrin and a D-T-C value of 10-0.4-0). The relative amount of cross-linking agent (C) also had an influence on the total protein yield; particle yield and protein content decreased when the cross-linking agent bisacrylamide was introduced into maltodextrin microparticles. The functional capacity of immobilized albumin to bind salicylic acid varied between ~40 and 95%. No systematic trend could be detected; high C values possibly improve the functional capacity.

Microparticle Density, Surface Structure, and Protein Leakage—The density of polysaccharide microparticles was 1.04–1.07 g/mL, which is somewhat lower than that obtained with polyacrylamide particles (5). The density essentially followed the content of acryloyl groups, when both maltodextrin and hydroxyethyl starch were studied. Thus, when T was increased from 0.2 to 0.4, the density of maltodextrin particles increased from 1.04 to 1.06 g/mL. The density was the same when the particles contained up to 30% human serum albumin.

Microparticles based on maltodextrin or hydroxyethyl starch have a surface structure quite different from that of highly cross-linked polyacrylamide particles. The particles have a relatively smooth surface structure with smaller pores (Fig. 2) than polyacrylamide particles with a T-C value of 8-25 (5).

The leakage of ^{125}I-human serum albumin from the microparticles (Table I) was investigated to study the influence of the microparticle composition on the protein fixation within the polymer. Variations in leakage were observed with T and C changes. The maltodextrin microparticles with few acryloyl groups leaked more than particles with higher T values. The hydroxyethyl starch microparticles were generally not as leaky as the maltodextrin spheres; no systematic change was found when T was varied.

When the cross-linking agent *N,N'*-methylenebisacrylamide was added to the maltodextrin microparticles, the leakage of ^{125}I-human serum albumin was accelerated. This is consistent with previous findings that microparticle pore radius increases with the addition of a cross-linking agent (5).

Storage of the microparticles at −20°C was also studied. Maltodextrin microparticles with compositions of 10-0.2-0, 10-0.4-0, and 10-0.4-25 and a batch of hydroxyethyl starch microparticles (10-0.8-0) lost no particle-bound protein when stored at −20°C for 8 weeks.

Table III—Degradation of Maltodextrin Microparticles in Serum and in a Lysosome-Enriched Fraction[a]

Microparticle Composition, D-T-C	Solubilized Radioactivity, %[b] Incubation in Serum, 1 h	Incubation in Lysosomal Fraction, 1 h	Incubation in Lysosomal Fraction, 6 h
	Empty Microparticles		
10-0.2-0	21.8 ± 1.8	44.4 ± 3.2	51.1 ± 3.2
10-0.4-0	12.6 ± 0.8	30.8 ± 1.4	36.4 ± 3.2
10-0.4-20	10.8 ± 2.3	29.2 ± 3.3	53.5 ± 7.8
	Protein-Containing Microparticles[c]		
10-0.2-0	38.0 ± 0.9	68.3 ± 1.4	83.5 ± 2.4
10-0.4-0	28.5 ± 2.3	47.9 ± 3.2	54.3 ± 3.4
10-0.4-20	40.6 ± 1.5	66.5 ± 2.1	73.8 ± 2.4

[a] The [^{14}C]starch-labeled particles were preincubated for 1 h in serum before further incubation in the lysosomal fraction. Mean values ± *SD* for incubation in lysosomes ($n = 3$–6) and incubation in serum ($n = 18$). [b] Cumulative values. [c] Human serum albumin, 100 mg/mL of the aqueous phase.

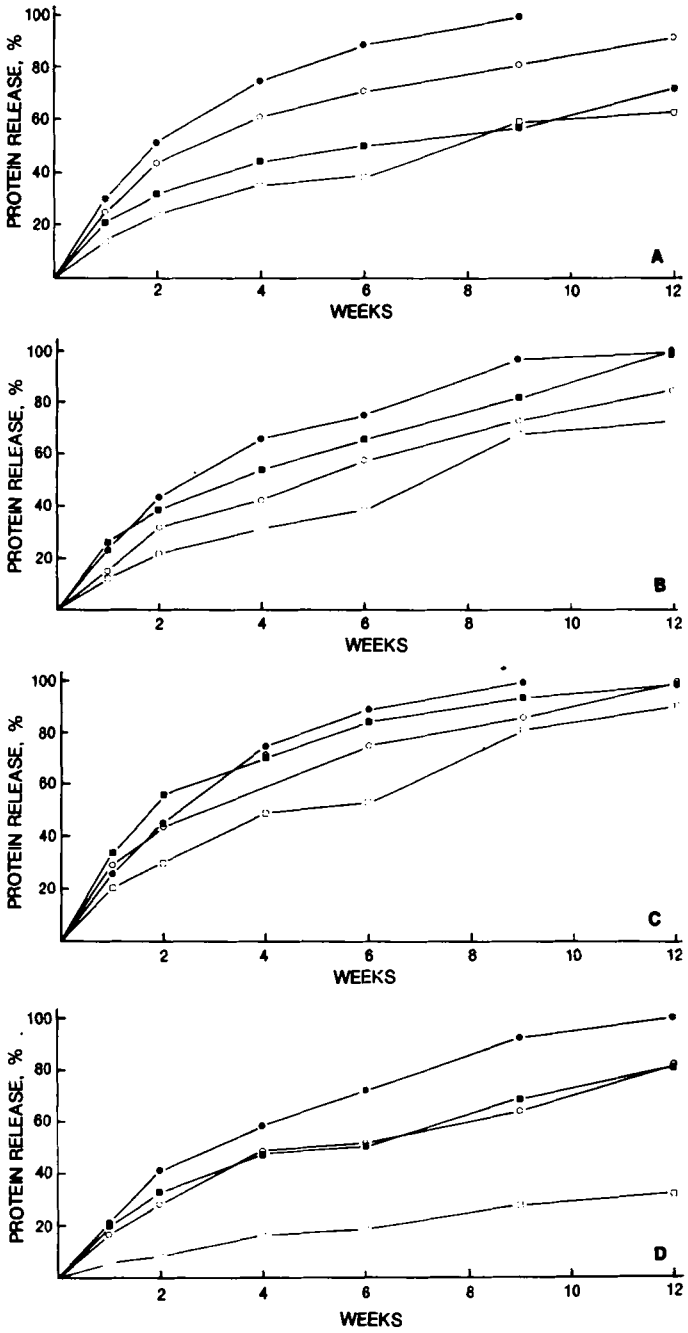

Figure 4—*Release of immobilized proteins during storage at room temperature from microparticles of maltodextrin with D-T-C of 10-0.2-0 (A), 10-0.4-0 (B), and 10-0.4-25 (C) and hydroxyethyl starch with D-T-C of 10-0.8-0 (D). The immobilized proteins were lysozyme (●), human serum albumin (○), carbonic anhydrase (■), and immunoglobulin G (□).*

Enzymatic Degradation of Polyacryl Starch Microparticles—The particles in Table I (0.5 mg dry weight) were incubated with α-amylase, and the release of ^{125}I-human serum albumin was compared with the controls. Maltodextrin microspheres with the D-T-C compositions of 10-0.2-0, 10-0.3-0, and 10-0.4-0 released 27, 24, and 26% of the entrapped radioactivity in 1 h, respectively. Spheres containing bisacrylamide had a lower release, *e.g.*, 15% (D-T-C 10-1.2-60). No significant increase in radioactivity was found in the supernatants when hydroxyethyl starch microspheres were incubated with α-amylase.

The degradation of the starch matrix by amyloglucosidase was investigated for maltodextrin microparticles of different compositions (D-T-C 10-0.2-0, 10-0.4-0, and 10-0.4-25) containing acryloylated ^{14}C-labeled starch and albumin (Table II). The particles were incubated with amyloglucosidase (10 IU/mL) for 3 h at 37°C. Particles with few acrylic groups (D-T-C, 10-0.2-0) were totally solubilized, and all radioactivity was regained in the supernatant

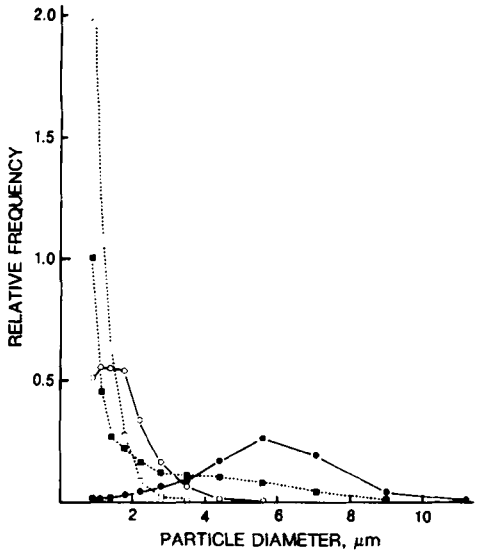

Figure 5—*Size distribution of maltodextrin microparticles (D-T-C 10-0.4-25), including the frequency by weight before (○) and after (●) incubation with specific antiserum and the frequency by number before (□) and after (■) antiserum addition. The relative frequency was obtained by division of the frequency values by the class width.*

after 3 h. When the degradation mixture was gel-filtered on a Sephadex G-150 column, 30% of the radioactivity was obtained in the void volume and 70% in the low molecular weight region. Identical results were obtained when particles with the same composition containing ^{125}I-human serum albumin were incubated with amyloglucosidase. The ^{125}I-albumin-containing microparticles were completely dissolved in 3 h. Spheres containing 0.4% (w/w) acrylic groups (D-T-C 10-0.4-0) or a cross-linking agent (D-T-C 10-0.4-25) were more stable, and 59 and 69%, respectively, of the radioactivity was detected in the supernatant after incubation for 3 h.

The microparticles were also affected by fresh human serum (Table III). Incubation of 0.5 mg of ^{14}C-labeled particles in serum for 1 h at 37°C gave a release of 11-41% of the radioactivity, depending on the particle composition and immobilized protein content. "Empty" spheres and spheres with a high amount of acrylic groups (high T value) were relatively stable in serum, *e.g.*, particles with a D-T-C of 10-0.2-0 containing no protein were 22% digested compared with 38% when albumin was present. Microparticles (D-T-C, 10-0.4-0) containing albumin were solubilized 28% after a 1-h incubation, compared with 38% when spheres with D-T-C 10-0.2-0 were used. However, the rate of degradation was increased when the particles contained protein and a cross-linking agent. The increased rate probably depends on a better penetration of the particles by the enzymes, as both the proteins and increased C may increase the pore radius of the particles. No further degradation was seen when the incubation time was increased to 6 h.

In an attempt to simulate the biological conditions of particles after intravenous injection, the spheres were preincubated in fresh serum for 1 h prior to incubation with isolated rat liver lysosomes for 1 and 6 h (Table III, Fig. 3). Particles with a D-T-C of 10-0.2-0 were highly affected, and ~84% of the radioactivity in the spheres was regained in the supernatant after incubation for 6 h. Particles with larger T, (D-T-C, 10-0.4-0) were more stable; 54% of the spheres were metabolized after 6 h. Corresponding "empty" microspheres were more inert under these conditions. Empty spheres with a D-T-C of 10-0.2-0 were degraded 51% as compared with 84% when the particles contained albumin (Table III).

When the microparticles were incubated directly in the lysosomal fraction, *i.e.*, without preincubation in serum, the amount of solubilized radioactivity after a 6-h incubation was the same as with preincubation. Thus, the metabolism of polyacryl starch microparticles is related to the protein content and the composition of the particle.

Immobilized Proteins in Polyacryl Starch Microparticles—Further studies were performed with three different batches of maltodextrin microparticles and one batch made of hydroxyethyl starch. The maltodextrin microparticles had compositions 10-0.2-0 (I), 10-0.4-0 (II), and 10-0.4-25 (III). The hydroxyethyl starch microspheres (IV) had a composition of 10-0.8-0.

Release Profiles—Microparticles were prepared with proteins of various sizes: lysozyme [mol. wt. 14,400 (20)], carbonic anhydrase [mol. wt. 31,000 (21)], human serum albumin [mol. wt. 66,500 (22)], and human immunoglobulin G [mol. wt. 150,000 (23)]. The spheres were suspended in buffered physiological saline, pH 7.4 with sodium azide (0.1%) added as a preservative.

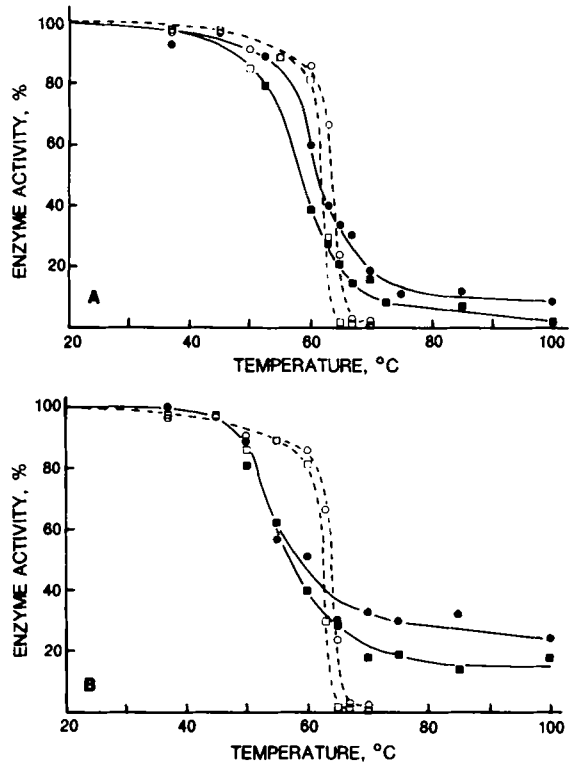

Figure 6—*Thermostability of carbonic anhydrase immobilized in maltodextrin microparticles with D-T-C of 10-0.2-0 (A) and 10-0.4-0 (B) compared with that of the free enzyme. The remaining activity was measured after heating the enzyme for 5 (○, ●) and 30 (□, ■) min. The open symbols represent free enzyme; the solid symbols represent particle-bound enzyme.*

The samples were left at room temperature (22°C) for 1, 2, 4, 6, 9, and 12 weeks. The protein released from the spheres after centrifugation (Fig. 4) was determined by the method of Lowry *et al.* (13).

The most pronounced release, irrespective of particle composition, was obtained when lysozyme was used (Fig. 4A): 100% of the lysozyme was released in 9-12 weeks, depending on the gel composition. Also, release rates generally decrease with increasing molecular weight independent of particle composition. Microparticles containing bisacrylamide as a cross-linking agent (III) (Fig. 4C) released the proteins most rapidly; ~90-100% of the incorporated protein was lost after 12 weeks, irrespective of molecular weight.

Surface Localization—The localization of proteins on the surface of the microparticles can be studied conveniently by adding specific antiserum and following particle aggregation with a Coulter Counter equipped with a computer program. The Coulter Counter cannot detect particles <0.8 μm with the 50-μm orifice tube and does not give an exact measure of the true mean diameter of the microparticles. The results, therefore, cannot be compared with those obtained with the electron microscope, but the method does give a relative measure of the changed size distribution (by number and volume) when the antiserum is added to the microparticles. The mean diameter, based on volume, increased from 2.04 ± 0.82 μm to 5.66 ± 1.65 μm when III microparticles with immobilized human serum albumin were incubated with rabbit anti-albumin serum (Fig. 5). The mean diameter, by number, was also calculated, and a similar increase was noted (Fig. 5). Increases in diameters were also detected for microparticles of other compositions. Empty microparticles did not aggregate after addition of the antiserum.

To further investigate the nature of the surface-localized albumin, the study was repeated after 8 weeks with the same batch of particles. At that time ~50% of the protein had leaked from the spheres (Fig. 4). No significant changes in the aggregation patterns of the washed microparticles could be detected with the Coulter Counter. Obviously, a significant fraction of the immobilized albumin is stably bound on the surface and available for interaction with the antibodies.

Heat Stability—To investigate the effect of immobilization in polyacryl starch microparticles on the stability of proteins, carbonic anhydrase was incorporated into the microparticles. The spheres were exposed to elevated temperatures for 5 or 30 min. After treatment, the spheres were immediately cooled in an ice bath for 5 min. The samples were then incubated at room temperature for 30 min, and the remaining activity was determined. It is apparent that the microspheres protect the enzyme against heat denaturation

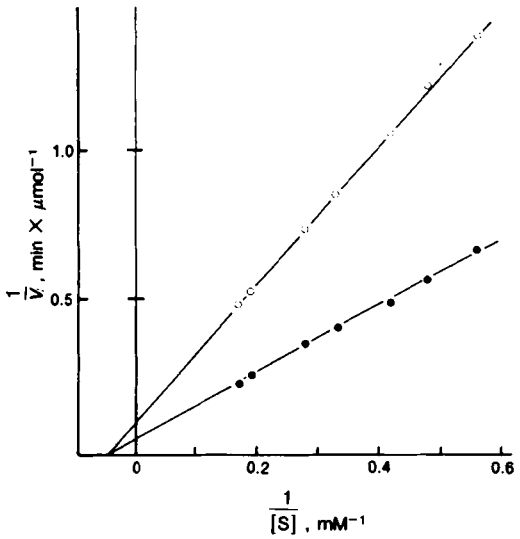

Figure 7—*Lineweaver-Burk plots for the enzymatic activity of carbonic anhydrase in maltodextrin microparticles (D-T-C 10-0.2-0) (○) and free (●) form.*

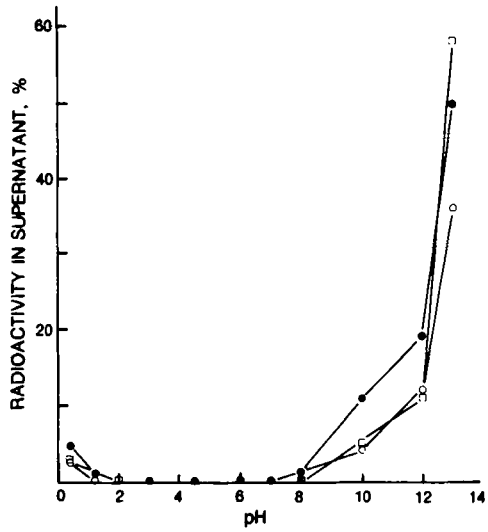

Figure 8—*Stability of ^{14}C-labeled maltodextrin microparticles at different pH. The particles were incubated at 37°C for 12 h. Key to D-T-C values: (●) 10-0.2-0; (○) 10-0.4-0; (□) 10-0.4-25.*

(Fig. 6). Depending on the composition of the spheres, the enzymatic activity after 30 min at 100°C varied between <5 and 20%. Microparticles containing 0.4% acrylic groups (w/w), *i.e.*, II (Fig. 6B), gave better protection against heat than spheres with T = 0.2 (I) (Fig. 6A). The use of a cross-linking agent (III) or hydroxyethyl starch (IV) did not improve the thermal stability of carbonic anhydrase.

Enzymatic Properties of Immobilized Carbonic Anhydrase—To assess the effect of entrapment on the function of the immobilized enzymes, the Michaelis-Menten constant (K_m) of carbonic anhydrase was determined. Regression analysis showed that the Lineweaver-Burk plots for immobilized and soluble enzyme were linear over the entire range of concentrations studied. The calculated K_m for native carbonic anhydrase was 18 mM; for immobilized enzyme, it was 18-24 mM. The increase in K_m by immobilization (irrespective of microsphere composition) is probably due to a limited diffusion rate of substrate and/or reaction products, as observed in other immobilized enzyme systems (24-26).

The maximal reaction rate (v_{max}) of the immobilized enzyme, in I particles, was compared with that of the native enzyme (Fig. 7). The v_{max} of the immobilized enzyme, as calculated from the ordinate intercept, was 58% of that of the free enzyme. Based on amino acid analysis, the amount of enzyme in the two experiments was the same. The enzymatic activity, therefore, is more inhibited in the polyacryl starch particles than in macroporous polyacrylamide microparticles (27).

pH Stability of Polyacryl Starch Microparticles—The pH stability of the polymer matrix was investigated with ^{14}C-labeled starch. The hydroxyethyl starch particles (IV) could not be studied because labeled hydroxyethyl starch is not available and incorporation of ^{14}C-acryloylated starch in these particles would result in inadequate labeling of the particle matrix. The maltodextrin microspheres were incubated at pH 0.4-13 for 12 h at 37°C. Aliquots were withdrawn from the supernatants after centrifugation, and the radioactivity was measured (Fig. 8). The microparticles were stable at pH 2-8. At pH 12, ≤19% of the particles were solubilized; at pH 12.8, ≤58% of the radioactivity was lost from the microparticles. Acidic pH (≥1.2) did not significantly affect the microparticles; at pH 0.5, 5% (at most) was solubilized in 12 h.

DISCUSSION

In our earlier work, small particles were prepared for protein immobilization by polymerization of either acrylic groups in acrylamide and *N,N'*-methylenebisacrylamide to form polyacrylamide microparticles (5) or acrylic groups of acryloyldextran and *N,N'*-methylenebisacrylamide to form polyacryldextran particles (6). These two types of microparticles are only slowly metabolized *in vivo*, with $t_{1/2}$ values of 10-20 weeks (7, 28). The half-life is directly related to the amount of hydrocarbon chains formed during the polymerization (and to some extent to the presence of dextran, which is slowly degraded in the lysosomes). These particles will probably find only limited applications *in vivo*.

In the present paper, a low molecular weight fraction of starch (maltodextrin; mol. wt. 5000) and a preparation of hydroxyethyl starch (mol. wt. 400,000), which are water soluble, were used. The starch compounds were modified with acrylic acid glycidyl ester and polymerized in a water-in-oil emulsion to form small particles; the particle size is essentially determined by the dispersion degree of the emulsion. The cross-links in the microparticles, the hydrocarbon chains, are formed by the acryloyl groups, but their contribution to the matrix structure can be much lower (0.3-0.4% in the polymerization mixture) than in polyacrylamide and polyacryldextran particles. This means that the main part (>95%) of the matrix is composed of maltodextrin or hydroxyethyl starch and will be easily degraded by lysosomal enzymes (maltodextrin particles). The degradation of the maltodextrin microparticles has been followed with ^{14}C-labeled starch from *Nicotiana tabacum* (about the same molecular weight as maltodextrin) included in the microparticles and treated as described for maltodextrin. Unfortunately, no labeled hydroxyethyl starch could be obtained, and consequently, no reliable studies to follow the degradation of hydroxyethyl starch particles have been possible. However, information is available on the metabolism of underivatized hydroxyethyl starch, which is extensively used as a plasma expander in humans. The half-life of hydroxyethyl starch (mol. wt. 450,000; degree of derivatization 0.70) in the spleen and liver of the rat is ~64 and 132 d, respectively (29). It may therefore be concluded that hydroxyethyl starch microparticles are more slowly metabolized than maltodextrin microparticles. Such microparticles are, therefore, the carrier of choice when a prolonged protection of the immobilized material is more essential than a rapid degradation of the particle matrix.

The degradation of the starch particles has been followed *in vitro* in a lysosome-enriched fraction from rat liver prepared by differential centrifugation, in serum, and with isolated enzymes. Maltodextrin particles were relatively rapidly degraded by the lysosomal enzymes; >80% of the radioactivity (originating from the starch matrix) was found in the supernatant after 6 h from particles with a D-T-C of 10-0.2-0, and ~50% from particles with a D-T-C of 10-0.4-0. In serum, with α-amylase, or with amyloglucosidase, the solubilization was faster with the less-modified maltodextrin. When the cross-linking degree was increased by adding *N,N'*-methylenebisacrylamide (yielding particles with a D-T-C of 10-0.4-25) the rate of degradation consistently increased. An increased rate of degradation was also seen when the particles contained immobilized protein. In both of these situations the enzymes could better penetrate the particles and hydrolyze the starch, since both proteins and increased C increase the pore radius (5).

In addition to ^{14}C-labeled starch, the degradation of the different particles was studied with immobilized ^{125}I-human serum albumin or ^{14}C-labeled *N,N'*-methylenebisacrylamide, which gave consistent results. As expected, hydroxyethyl starch particles were resistant to α-amylase and amyloglucosidase treatment. On the other hand, maltodextrin particles (D-T-C 10-0.2-0) were totally solubilized by amyloglucosidase in 3 h, and gel filtration revealed that ~70% of the radioactively labeled starch was regained in the low molecular weight fraction. We thus conclude that the derivatization of starch with acrylic acid glycidyl ester has not profoundly changed the biodegradability; enzymes normally found in animal tissues can dissolve maltodextrin microparticles *in vitro*. Whether the same extensive metabolism of these microparticles can happen *in vivo* and the degradation products can be completely eliminated from the macrophages of the reticuloendothelial system

remains to be seen. Preliminary results[20] indicate that maltodextrin microparticles are metabolized and eliminated *in vivo*, which means that degradation products can also pass the lysosomal membrane.

It is obvious that T (specified essentially by the derivatization degree of the starch) and C (the fraction of added *N,N'*-methylenebisacrylamide) are important factors in the microparticle matrix structure and, therefore, also in biodegradation. The structure will determine the amount of proteins immobilized, their leakage, and the stability of the immobilized proteins towards heat denaturation. The macrostructure of maltodextrin particles, as seen in the electron microscope, is obviously smoother than that of polyacrylamide (T-C 8-25) which exhibits a macroporous structure (5). In the polyacrylamide microparticles, thick bundles of polymer threads are formed, in which the proteins are fixed. The proteins are partly exposed on the surface and can interact with cells (30). Even if biodegradable starch microparticles are not cross-linked to the same extent, proteins obviously can be stably bound on the surface in such a way that they interact with antibodies and form large aggregates.

The pores of polyacryl starch particles are thus smaller than those of highly cross-linked polyacrylamide particles. This means that the initial yield of immobilized proteins will be significantly larger because a larger fraction will be entrapped inside the formed network; the larger the Stokes radius of the protein, the more will be immobilized. Under standard conditions (100 mg of protein/mL of aqueous phase), 35-40% of the dry weight is protein, as shown with human serum albumin. The functional capacity, however, is generally not >40-60%, and ~50% of the protein is released from the particles in 6 weeks. These figures indicate that the fraction of protein trapped inside the particles, and not physically fixed in the polymeric network, is much larger than in the polyacrylamide particles. Moreover, the diffusion of low molecular weight ligands or substrates becomes restricted as the functional binding capacity of human serum albumin is decreased, and the enzymatic activity (K_m, v_{max}) of carbonic anhydrase is impaired. The polymer concentration (T) in the microparticles also influences the thermal stability, which is not greatly increased when T = 0.2%. It is important to note that the polymer concentration in the particles is high enough to guarantee that molecules are localized on the surface and that antibodies can form aggregates with the microparticles. This means that polyacryl starch microparticles could be used for specific targeting within the central compartment *in vivo*. In such a system, specific antibodies may be the instrument to target the microparticles to pathological cells in the circulation (*e.g.*, leukemia cells) or to eliminate circulating macromolecules (*e.g.*, antibodies or immune complexes).

Any drug carrier system designed for injection must be degradable. The metabolism of the polyacryl starch microparticles can be varied within wide limits, and the bulk of the matrix (the maltodextrin fraction) can be completely broken down by endogenous enzymes. The metabolism of the remaining part (the hydrocarbon chains from the acryloyl groups) must be further studied, but in the present system the fraction is small. However, the hydrocarbon chains are the decisive factor in the rate of degradation *in vivo*, which must be chosen according to need in the specific situation. As has been clearly demonstrated, polyacryl starch particles (D-T-C 10-0.4-0 or 10-0.2-0) are degraded in normal serum, and 30-40% of the starch is solubilized in 1 h. The half-life of microparticles in the circulatory system after intravenous injection is also ~1 h (7, 24). It is thus obvious that the derivatization of the starch must be high enough to give a reasonable stability in the circulation to ensure transport of the immobilized material to the target. Our experiments have shown that the leakage of immobilized proteins largely follows the degradation of the microparticles. The composition of the carrier system is thus a compromise: it must persist long enough in the circulatory system and yet must be metabolized rather quickly within the target organ. This principle is valid when the carrier is used for the immobilization of low molecular weight substances (*e.g.*, drugs) or proteins (*e.g.*, enzymes). Moreover, in some situations it is essential to control the release of active material from the carrier within the target cells, *e.g.*, to correlate the rate of release and the rate of denaturation of an enzyme. In such situations, it is important that the metabolism of the carrier can be anticipated and controlled. This is true for the polyacryl starch microparticles.

[20] P. Artursson, T. Laakso, and I. Sjöholm, unpublished results.

REFERENCES

(1) R. C. Oppenheim, *Int. J. Pharm.*, **8,** 217 (1981).

(2) M. Finkelstein and G. Weissman, *J. Lipid Res.*, **19,** 289 (1978).

(3) G. Gregoriadis, *Lancet*, **ii,** 241 (1981).

(4) G. Poste, *Biol. Cell.*, **47,** 19 (1983).

(5) B. Ekman, C. Lofter, and I. Sjöholm, *Biochemistry*, **15,** 5115 (1976).

(6) P. Edman, B. Ekman, and I. Sjöholm, *J. Pharm. Sci.*, **69,** 838 (1980).

(7) I. Sjöholm and P. Edman, *J. Pharmacol. Exp. Ther.*, **211,** 656 (1979).

(8) P. Edman, I. Sjöholm, and U. Brunk, *J. Pharm. Sci.*, **72,** 658 (1983).

(9) P. Edman and I. Sjöholm, *Life Sci.*, **30,** 327 (1982).

(10) M. Lepistö, P. Artursson, P. Edman, T. Laakso, and I. Sjöholm, *Anal. Biochem.*, **133,** 132 (1983).

(11) S. Hjertén, *Arch. Biochem. Biophys.*, **1** Suppl., 147 (1962).

(12) H. Feuer and U. E. Lynch, *J. Am. Chem. Soc.*, **75,** 5027 (1953).

(13) O. H. Lowry, N. I. Rosebrough, A. L. Farr, and R. J. Randal, *J. Biol. Chem.*, **193,** 265 (1951).

(14) Y. Pocker and J. Stone, *J. Am. Chem. Soc.*, **87,** 5497 (1965).

(15) A. Kober, B. Ekman, and I. Sjöholm, *J. Pharm. Sci.*, **67,** 107 (1978).

(16) D. R. Phillips and M. Morrison, *Biochemistry*, **10,** 1766 (1971).

(17) H. Pertoft and T. C. Laurent, in, "Methods of Cell Separation," Vol. 1, N. Catsimpoolas, Ed., Plenum, New York, N.Y., 1977, p. 25.

(18) H. Beaufay, D. S. Bendall, P. Baudhuin, R. Wattiaux, and C. de Duve, *Biochem. J.*, **73,** 628 (1959).

(19) "Lysosomes: A Laboratory Handbook", 2nd ed., I. T. Dingle, Ed., Elsevier/North-Holland, Amsterdam, 1977, p. 118.

(20) P. Jolles, *Angew. Chem. Intern. Ed. Engl.*, **8,** 277 (1969).

(21) S. Lindskog and B. Malmström, *J. Biol. Chem.*, **237,** 1129 (1962).

(22) B. Meloun, L. Morávek, and V. Kostka, *FEBS Lett.*, **58,** 134 (1975).

(23) G. Edelman, B. Cunningham, W. Gall, P. Gottlieb, U. Rutishauser, and M. Waxdal, *Proc. Natl. Acad. Sci. U.S.A.*, **63,** 78 (1969).

(24) L. Goldstein, Y. Levin, and E. Katchalski, *Biochemistry*, **3,** 1913 (1964).

(25) W. E. Hornby, M. D. Lilly, and E. N. Crook, *Biochem. J.*, **98,** 420 (1966).

(26) G. J. H. Melrose, *Rev. Pure Appl. Chem.*, **21,** 83 (1977).

(27) B. Ekman and I. Sjöholm, *J. Pharm. Sci.*, **67,** 693 (1978).

(28) P. Edman and I. Sjöholm, *J. Pharm. Sci.*, **72,** 796 (1983).

(29) "Pharmacology of Hydroxyethyl Starch," J. M. Mishler IV, Ed., Oxford University Press, Oxford, 1982, p. 45.

(30) I. Ljungstedt, B. Ekman, and I. Sjöholm, *Biochem. J.*, **170,** 161 (1978).

ACKNOWLEDGMENTS

This work was supported by the Swedish Medical Research Council, the Swedish Board for Technical Development, and the I. F. Foundation for Pharmaceutical Research. The authors thank Mrs. Elisabeth Tidare, Mr. Erik Thorsell, Mr. Erik Arro, Mr. Matti Lepistö, and Mr. Jan Mazur for technical assistance.

Adsorption of Pepsin by Aluminum Hydroxide I: Adsorption Mechanism

ROBERT J. SEPELYAK *, JOSEPH R. FELDKAMP ‡, TIMOTHY E. MOODY ‡, JOE L. WHITE ‡, and STANLEY L. HEM *x

Received July 18, 1983 from the *Departments of *Industrial and Physical Pharmacy and ‡Agronomy, Purdue University, West Lafayette, IN 47907.* Accepted for publication February 9, 1984.

Abstract □ Adsorption of pepsin by gibbsite and boehmite, non-acid-reactive forms of aluminum hydroxide, was observed and related to the surface area of the adsorbent. Adsorption was pH dependent, with maximum adsorption occurring between pH 2.7–3.3 for gibbsite and pH 2.7–4.3 for boehmite. Electrostatic attraction was an important adsorption mechanism at the pH conditions encountered in the GI tract; the isoelectric point of pepsin was ~1, giving it a negative charge, and the point of zero charge for the adsorbents was >9, giving them a positive charge. However, the pH–adsorption profile can not be fully explained by electrostatic considerations. Desorption studies indicate the importance of specific adsorption because pepsin was not desorbed by washing with acidified water, but was partly desorbed by exchange with phosphate. The IR spectrum of adsorbed pepsin also suggested that specific adsorption of pepsin occurred through anionic ligand exchange involving carboxylate groups of pepsin and surface aluminum ions.

Keyphrases □ Aluminum hydroxide—adsorption, pepsin □ Pepsin—adsorption by aluminum hydroxide □ Adsorption—pepsin by aluminum hydroxide

Aluminum hydroxide is widely used in peptic ulcer therapy. Recent clinical studies, which have shown that aluminum hydroxide-containing antacid products are effective in healing ulcers (1–3), have stimulated interest in the mechanism by which antacids act to heal ulcers. The Food and Drug Administration's OTC Panel on Antacids suggested that the neutralization of gastric acid was the only mechanism of action (4). Because the activity of pepsin is pH dependent, the neutralization of gastric acid will affect the activity of pepsin. Piper and Fenton (5) concluded that one mechanism by which aluminum hydroxide reduced pepsin activity was to raise the pH of the gastric fluid. Kuruvilla (6) concluded that antacids in general reduce pepsin activity by raising the gastric pH. Piper and Fenton (7) also stated that antacids which raise the gastric pH to 4–5, *i.e.*, aluminum hydroxide, only temporarily inhibit pepsin activity while antacids such as sodium bicarbonate, which raise the pH above 8, will denature pepsin and permanently inhibit its activity.

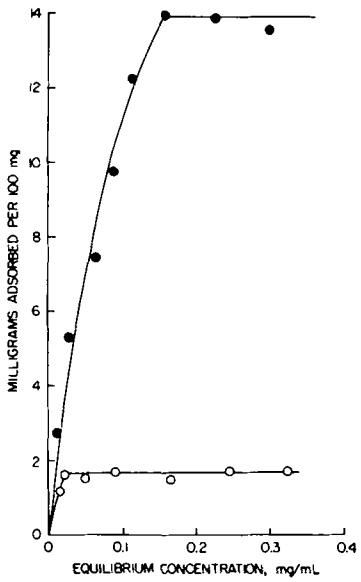

Figure 1—*Adsorption isotherms of pepsin on gibbsite (○) or boehmite (●).*

Other reports have speculated that antacids reduce pepsin activity by precipitating pepsin from solution (8, 9) or by adsorbing pepsin (5, 10–16). The adsorption of bile acids is believed to aid in ulcer therapy (17–19). Earlier studies suggested that antacids act by coating the mucosal lining and protecting it from the digestive action of gastric acid and pepsin (20–22). The reports of ulcer coating by antacids have been contradicted (23, 24), and the recent trend in formulating antacid products has been to incorporate only acid-reactive antacid materials.

This study was undertaken to investigate the interaction of aluminum hydroxide and pepsin with special emphasis on any specific mechanism by which aluminum hydroxide reduces the proteolytic effect of pepsin on the gastrointestinal mucosa.

BACKGROUND

Pepsin, a globular proteolytic enzyme, is secreted by the chief cells of the gastric mucosa as its zymogen, pepsinogen. At ≤pH 5, pepsinogen is converted to pepsin by the cleavage of six peptide segments from the *N*-terminal end of pepsinogen. Pepsin and pepsinogen have molecular weights of ~35,000 and 42,000, respectively (25).

The primary structure of pepsin consists of 327 amino acids including 43 acidic amino acids and 4 basic amino acids (26). The isoelectric point of pepsin is ~1, so pepsin is a negatively charged protein in the GI tract (27). Pepsin is composed of a single polypeptide chain which has folded and packed to form a globular protein. The calculated molecular diameter of pepsin is 4.38 nm (28). The three-dimensional structure is stabilized by three disulfide bonds. Pepsin has only one active site which is believed to include the carboxyl groups from two aspartic acids (29).

The role of pepsin in the body is to digest proteins, and it is most active in hydrolyzing bonds involving phenylalanine, tyrosine, and leucine (30). Bonds involving glutamic acid are hydrolyzed, but to a lesser extent (30). The proteolytic activity of pepsin is dependent on pH. Pepsin A, which has also been termed pepsin III, is the predominant pepsin and exhibits an optimal pH range for activity between 1.5 and 3.0 (31).

The adsorption of pepsin by aluminum hydroxide is well documented, but the mechanism of adsorption has not been elucidated. Pawelczak determined the extent of pepsin adsorption by a number of antacid preparations (32). Wenger and Sundy determined the adsorption of pepsin by various colloidal materials at different pH conditions and suggested that the extent of adsorption was dependent on particle size and the chemical nature of the colloidal material (13). Piper and Fenton determined that aluminum hydroxide and charcoal were the best adsorbers of pepsin among a group of materials (5). Anderson and Harthill found pepsin to be completely adsorbed by an acid-reactive aluminum hydroxide gel as well as by an acid-insoluble aluminum hydroxide gel (14). Liebman also found that pepsin was adsorbed by aluminum hydroxide (15).

EXPERIMENTAL SECTION

Materials—Porcine pepsin[1], gibbsite[2], and boehmite[2] were obtained commercially. The surface area of gibbsite and boehmite was determined by

[1] Worthington Biochemical Corp., Freehold, N.J.
[2] Reynolds Metals Co., Bauxite, Ark.

0022-3549/84/1100-1514$01.00/0
© 1984, American Pharmaceutical Association

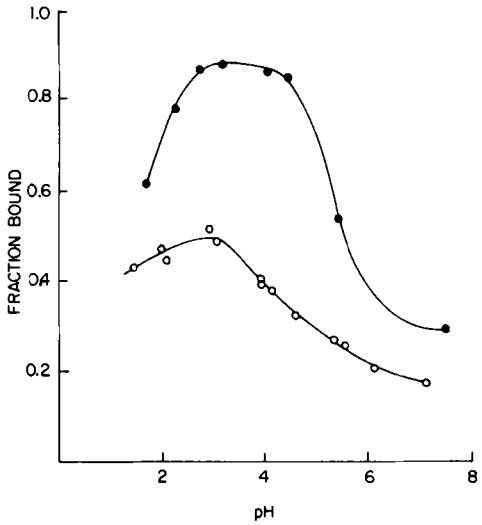

Figure 2—*pH profile of the percent pepsin bound on gibbsite (○) or boehmite (●).*

the triple-point gas adsorption method[3]. The point of zero charge was determined using a continuous titration procedure (33).

Adsorption Isotherms—Adsorption isotherms for pepsin on gibbsite or boehmite were determined at pH 2.3. Pepsin stock solutions were prepared at 2 and 3 mg/mL in 0.01 M HCl for gibbsite and boehmite, respectively. Gibbsite and boehmite stock suspensions (1%) were prepared and sonicated to break up aggregates. Ten milliliters of the stock suspension was transferred into a 25-mL volumetric flask. The suspension was adjusted to pH 2.3 by adding a total of 0.26 or 0.27 mmol of HCl to the gibbsite or boehmite suspensions, respectively. The actual amount of 0.1 M HCl added depended on the amount of pepsin required, since 1 mL of the pepsin solution provided 0.01 mmol of HCl. After the addition of the appropriate amount of 0.1 M HCl, the required amount of pepsin was added. The final volume of the suspension was brought to 25 mL by the addition of distilled water. The suspensions were shaken for a 5-min adsorption period, after which the pH was recorded. The suspensions were centrifuged at 10,000 rpm for 30 min and the supernatants were filtered through a 0.45-μm filter. The absorbance of the supernatants was read at 280 nm (34, 35); the equilibrium pepsin concentration was determined by use of a Beer's law plot, and the amount adsorbed was calculated by difference.

Fraction Bound Study—The percentages of pepsin bound on gibbsite and boehmite were determined at various pH conditions. Pepsin solutions (1 and 2 mg/mL for gibbsite and boehmite, respectively) were prepared in 0.001 M HCl. Gibbsite or boehmite stock suspensions (1%) were prepared and sonicated to break up aggregates. Ten milliliters of the stock suspension was transferred into 25-mL volumetric flasks and adjusted to the desired pH with appropriate quantities of HCl or NaOH. Five milliliters of the appropriate pepsin solution was added, and the final volume was adjusted to 25 mL with distilled water. The suspensions were shaken for 5 min, and the pH was recorded. The suspensions were centrifuged at 10,000 rpm for 25 min, and the supernatants were filtered through a 0.45-μm filter. The absorbance of the supernatants was read at 280 nm. Blanks were prepared and treated in the same manner except that 0.001 M HCl was used instead of the pepsin solution. Also, another pepsin solution was prepared in the absence of gibbsite or boehmite. The percent pepsin bound was calculated by:

$$B = \frac{A_0 - (A_s - A_b)}{A_0} \times 100$$

where B is the percent pepsin bound; A_0 is the absorbance of the pepsin solution without gibbsite or boehmite; A_s is the absorbance of the supernatant from the pepsin-adsorbent suspension; and A_b is the absorbance of the supernatant of the blank.

Desorption by Acid Wash—Pepsin solutions in 0.001 M HCl having a concentration of 1 and 2.5 mg/mL were prepared for gibbsite and boehmite, respectively. Gibbsite and boehmite stock suspensions (1%) were prepared and sonicated to break up aggregates. Ten milliliters of the stock suspension was transferred into 25-mL volumetric flasks and adjusted to pH 2.4 with 0.1 M HCl. The appropriate pepsin solution (5 and 8 mL, respectively) was added to the gibbsite or boehmite suspensions. The suspensions were adjusted to 25 mL with distilled water. A blank was prepared in the same manner, except

[3] Quantasorb; Quantachrome Corp., Greenvale, N.Y.

Table I—Desorption of Pepsin by Washing Pepsin–Adsorbent Complex with Acidified Water (pH 2.4)

Wash	Pepsin Adsorbed, mg/100 mg of Gibbsite	Cumulative Percent Desorbed	Pepsin Adsorbed, mg/100 mg of Boehmite	Cumulative Percent Desorbed
0	1.938		14.413	
1	1.884	2.8	13.137	8.8
2	1.811	6.6	12.977	10.0
3	1.810	6.6	12.926	10.3
4	—		12.861	10.8
5	—		12.829	10.9

0.001 M HCl replaced the pepsin solution. The suspensions were shaken for 5 min, and the pH was recorded. The suspensions were centrifuged at 10,000 rpm for 15 min. The supernatant was decanted, and its volume was recorded. The absorbance of the supernatant was read at 280 nm, and the pepsin concentration determined by use of a Beer's law plot. If the absorbance of the supernatant was >0.001, the solids were washed with acidified water at pH 2.4. The volume of the acidified water added to the solids was the same as the volume of the supernatant that was decanted. The suspension was shaken for 5 min, the pH was recorded, and the procedure was repeated until the absorbance of the supernatant was ≤0.001. The solid phase was resuspended in 25 mL of water at pH 2.4 and lyophilized. The carbon content of the solid phase was determined by microanalysis[4]. The amount of pepsin adsorbed was calculated from the carbon content of pepsin.

Desorption by Exchange with Phosphate—Pepsin solutions having concentrations of 0.5 mg/mL and 2.5 mg/mL in 0.01 M HCl were prepared for gibbsite and boehmite, respectively. Gibbsite and boehmite stock suspensions (1%) were prepared and sonicated to break up aggregates. Ten milliliters of the stock suspension was adjusted to pH 2.4 with 0.01 M HCl. Five milliliters of the appropriate pepsin solution was added, and the volume was adjusted to 20 mL. The suspensions were shaken for 20 min (control). Similar suspensions were prepared, and 5 mL of a 0.12-g/mL phosphate solution was added to 20 mL of suspension after the 20-min shaking period. The control and phosphate-containing suspensions were centrifuged at 10,000 rpm for 15 min, and the supernatants were filtered through a 0.45-μm filter. The absorbance of the supernatants was read at 280 nm; the equilibrium pepsin concentration was determined by use of a Beer's law plot, and the amount adsorbed was calculated by difference.

Infrared Spectroscopy—Samples were lyophilized and prepared as potassium bromide pellets (1 mg of lyophilized sample/300 mg of KBr). The IR spectrum was recorded between 1800–1000 cm^{-1}. The IR spectrophotometer[5] was interfaced with a computer to provide subtraction of different spectra.

RESULTS AND DISCUSSION

Acid-reactive aluminum hydroxide gels, which are known as carbonate-containing aluminum hydroxide or aluminum hydroxycarbonate (36) and which are used in antacid products, usually react completely within 15–20 min at the pH and temperature of the stomach. Although the adsorption of pepsin by acid-reactive aluminum hydroxide has been demonstrated (5, 12–15), elucidation of the mechanism of adsorption requires a stable surface. To obtain a stable aluminum hydroxide surface, gibbsite and boehmite were used as models because they are closely related structurally to acid-reactive aluminum hydroxide, but they react very slowly with acid, *i.e.*, <2% reacts in 90 min at pH 3 and 37°C. Gibbsite is the most stable polymorph of aluminum hydroxide and has the molecular formula $Al(OH)_3$ (37). Boehmite is an aluminum oxyhydroxide which has the molecular formula AlO(OH) (37). Hydroxyl is the only surface group of gibbsite, while hydroxyl and oxide surface groups are present in boehmite. The samples of gibbsite and boehmite had surface areas of 5 and 250 m^2/g, respectively.

The adsorption isotherms of pepsin on gibbsite and boehmite were determined at pH 2.3, the pH of maximum proteolytic activity (31). As seen in Fig. 1, the adsorptive capacity was 1.7 mg of pepsin/100 mg of gibbsite and 13.9 mg of pepsin/100 mg of boehmite. Thus, the adsorptive capacity was related to the surface area of the adsorbent.

The percent pepsin bound by gibbsite and boehmite was determined at various pH values (Fig. 2). Adsorption of pepsin by both gibbsite and boehmite was observed over the pH range of the GI tract. The greater adsorptive capacity of boehmite was again apparent. Maximum pepsin adsorption occurred at pH 2.7–3.3 for gibbsite, while the range was pH 2.7–4.3 for boehmite. The broader range of maximum adsorption observed for boehmite may be due to

[4] Model 240C; Perkin-Elmer Co., Norwalk, Conn.
[5] Model 180; Perkin-Elmer Co., Norwalk, Conn.

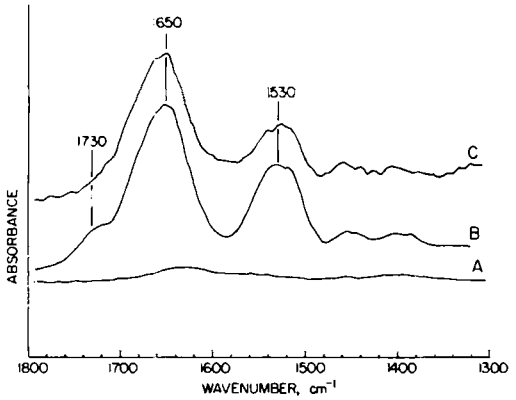

Figure 3—*IR spectrum of boehmite (A), pepsin (B), and pepsin adsorbed on boehmite (C).*

a difference in the pH of maximum adsorption for hydroxyl surface groups when compared with oxide surface groups.

The adsorption of pepsin by gibbsite and boehmite can be partially explained on the basis of electrostatic attraction; the isoelectric point of pepsin was ~1 (38), and the points of zero charge of gibbsite and boehmite were 9.2 and 9.1, respectively. Thus, in the pH region studied, *i.e.*, pH <8, the adsorbent will have a positive surface charge while pepsin will have a negative charge which will decrease as the pH approaches 1. The decreased adsorption at very acidic conditions seen in Fig. 2 may be related to a reduced electrostatic attraction. However, the adsorbent should retain a strong positive charge until the pH was within 1 unit of the point of zero charge, *i.e.*, pH ~8 (39). Thus, the decreased adsorption above pH 3.3 or 4.3 for gibbsite or boehmite, respectively, was not expected based solely on electrostatic attraction.

The pH-adsorption profile seen in Fig. 2 suggests that specific adsorption was also important. Hingston *et al.* (40) and Bowden *et al.* (41) found that anions of incompletely dissociated acids, such as phosphate, are specifically adsorbed by metal oxides and that maximum adsorption occurs when the pH equals the pK_a of the weak acid. The pK_a values of the acidic amino acids in pepsin, such as aspartic acid and glutamic acid, are 3.86 and 4.25, respectively (42), and are in the pH region where maximum adsorption occurred. In addition, the general shape of the pH-adsorption profile is similar to that observed for specific adsorption of anions by metal oxides (40, 41, 43). Bowden *et al.* (41) indicated that the increase in specific adsorption as the pH increases toward the pK_a is due to a more rapid increase in the number of adsorbing species than in the rate of decrease of the positive charge of the surface. The extent of specific adsorption decreases as the pH increases above the pK_a because the surface becomes less positive at a rate greater than the rate of dissociation.

A study of pepsin desorption from gibbsite or boehmite was performed to determine if specific adsorption was an important mechanism. Once pepsin was adsorbed by gibbsite or boehmite at pH 2.4, the pepsin-adsorbent complexes were washed repeatedly with acidified water at pH 2.4. Analysis of the supernatant (Table I) following each wash showed that little pepsin was desorbed by acidic washing. The amount of pepsin adsorbed following five washes was also determined by carbon analysis of the solid phase. The analysis of duplicate samples yielded the following results: 1.80 and 1.74 mg of pepsin adsorbed/100 mg of gibbsite and 12.7 and 13.2 mg of pepsin adsorbed/100 mg of boehmite. It is interesting to note that the adsorptive capacity determined from the plateau of the adsorption isotherm (Fig. 1) also agrees with the results of the desorption experiment. Desorption was expected if the only mechanism of adsorption was electrostatic attraction, as a chloride anion would replace pepsin, or protons would neutralize the negative charge of pepsin, and facilitate pepsin desorption.

Phosphate is specifically adsorbed by aluminum hydroxide by anionic ligand exchange (40, 44). Therefore, washing with phosphate should desorb pepsin if pepsin is also adsorbed by specific adsorption through anionic ligand exchange. The pepsin-gibbsite or pepsin-boehmite complexes were washed with a phosphate solution at 8 times the phosphate concentration of intestinal fluid at pH 2.4. Analysis of the supernatant showed that 95 and 79% of the adsorbed pepsin was desorbed from gibbsite and boehmite, respectively. Since phosphate desorbed pepsin, it was concluded that pepsin was also specifically adsorbed by anion ligand exchange. Phosphate is known to complex with gibbsite by a mono- or bidentate ligand mechanism (40, 44). Desorption studies of monodentate ligands show that binding is reversible, whereas multidentate ligands favor irreversible binding (44). Since phosphate did not totally desorb pepsin, pepsin is believed to form multidentate ligands with gibbsite and boehmite.

The mechanism of adsorption was further investigated by IR spectroscopy. The IR spectrum of pepsin in the 1800–1300-cm^{-1} region is shown in Fig. 3 (line B). The major absorption bands occur at 1530 and 1650 cm^{-1}. The band at 1530 cm^{-1}, known as the amide II band, is due to the N–H deformation vibrations of the main chain of pepsin (45). The band at 1650 cm^{-1}, termed the amide I band, results from the C=O stretching vibrations of the main chain (45). A shoulder present at 1730 cm^{-1} is believed to be due to the C=O stretching vibrations from the undissociated carboxylic acid groups of glutamic and aspartic acids (46).

The IR spectrum of pepsin adsorbed on gibbsite could not be determined because the small amount of adsorbed pepsin could not be detected. However, the degree of adsorption of pepsin on boehmite was sufficient to permit measurement of the IR spectrum of adsorbed pepsin. Boehmite has minimal absorbance in the 1800–1300-cm^{-1} region of the IR spectrum (Fig. 3A). However, to eliminate the contribution of boehmite, the spectrum of the adsorbent was subtracted by computer from the pepsin-boehmite spectrum to produce the IR spectrum of adsorbed pepsin (Fig. 3, line C). The subtraction was performed based on a boehmite band at 1070 cm^{-1}. Before subtracting, a multiplication factor was used on the pepsin-boehmite spectrum to cancel the 1070 cm^{-1} band, *i.e.*, the contribution of boehmite to the spectrum. A multiplication factor of 2.2 was used on the spectrum to produce the same relative absorbance of the amide I band as in pepsin.

As seen in Fig. 3 line C, the amide II band of pepsin at 1530 cm^{-1} was unaffected by adsorption, but the amide I band was shifted to a slightly higher frequency. A slight deformation of structure of pepsin due to adsorption might cause this frequency shift (47). The shoulder at 1730 cm^{-1} was not present in the IR spectrum of adsorbed pepsin, indicating that the carboxyl groups are ionized. The absence of the band at 1730 cm^{-1} supports the ligand exchange adsorption mechanism, since the carboxylic acid groups involved in ligand exchange would have to be in their ionized form to interact by ligand exchange with surface aluminum ions. Thus, ligand exchange would be expected to cause the decrease in absorbance at 1730 cm^{-1} observed for adsorbed pepsin.

Pepsin is adsorbed by aluminum hydroxide in the pH range of the GI tract by specific adsorption involving anionic ligand exchange as well as by electrostatic attraction. Some carboxylate groups of pepsin will displace hydroxyl or water groups from the surface of aluminum hydroxide and covalently bond with surface aluminum. Other carboxylate groups of pepsin which are not physically able to specifically adsorb will interact with the positive surface of aluminum hydroxide by electrostatic attraction. This combination of mechanisms results in strong adsorption which is not reversed by simple washing.

REFERENCES

(1) T. Morris and J. Rhodes, *Gut*, **20**, 538 (1979).

(2) S. K. Lam, K. C. Lam, C. L. Lai, C. K. Yeung, L. Y. C. Yam, and W. S. Wong, *Gastroenterology*, **76**, 315 (1979).

(3) H. J. Priebe, J. J. Skillman, L. S. Bushnell, P. C. Long, and W. Silen, *N. Engl. J. Med.*, **302**, 426 (1980).

(4) *Fed. Regist.*, **39**, 19875 (1974).

(5) D. Piper and B. Fenton, *Am. J. Dig. Dis.*, **NS6**, 134 (1961).

(6) L. Kuruvilla, *Gut*, **12**, 897 (1971).

(7) D. Piper and B. Fenton, *Gut*, **6**, 506 (1965).

(8) M. Schiffrin and S. Komarov, *Am. J. Dig. Dis.*, **8**, 215 (1941).

(9) S. Komarov and O. Komarov, *Am. J. Dig. Dis.*, **7**, 166 (1940).

(10) N. Mutch, *Lancet*, **1**, 859 (1949).

(11) P. Bateson, *J. Pharm. Pharmacol.*, **10**, 123 (1958).

(12) A. Berstad, H. Holm, and E. Kittang, *Scand. J. Gastroenterol.*, **14**, 121 (1979).

(13) J. Wenger and M. Sundy, *J. Clin. Pharmacol.*, **12**, 136 (1972).

(14) W. Anderson and J. Harthill, *J. Pharm. Pharmacol.*, **24**, 166P (1972).

(15) W. Liebman, *IRCS Med. Sci.: Library Compend.*, **8**, 114 (1980).

(16) A. C. Playle, S. R. Gunning, and A. F. Llewellyn, *Pharm. Acta Helv.*, **49**, 298 (1974).

(17) J. Wenger and S. Heymsfield, *J. Clin. Pharmacol.*, **14**, 163 (1974).

(18) J. Wenger and S. Heymsfield, *Gastroenterology*, **64**, 821 (1973).

(19) F. Begeman, V. Schumpelick, and G. Bandomer, *Scand. J. Gastroenterol.*, **16**, 191 (1981).

(20) L. Boyd, W. Russ, and H. Barowsky, *Rev. Gastroenterol.*, **9**, 20 (1942).

(21) G. McHardy and H. Van Rossen, *Curr. Ther. Res. Clin. Exp.*, **4**, 421 (1962).

(22) R. Nelson, *Curr. Ther. Res. Clin. Exp.*, **6**, 83 (1964).

(23) J. Hoon, *Arch. Surg.*, **92**, 467 (1966).

(24) J. Morrissey, T. Honda, Y. Tanaka, and G. Perna, *Arch. Intern. Med.*, **119**, 510 (1967).

(25) W. Taylor, in "Handbook of Physiology," Vol. 5, C. Code, Ed., American Physiology Society, Washington, D.C., 1968, pp. 2568, 2569.
(26) P. Sepulveda, J. Marciniszyn, D. Liu, and J. Tang, *J. Biol. Chem.*, **250**, 5082 (1975).
(27) A. Lehninger, "Biochemistry," 2nd ed., Worth, New York, N.Y., 1975, p. 162.
(28) A. McLaren and G. Peterson, *Nature*, **192**, 960 (1961).
(29) J. Hartsuck and J. Tang, *J. Biol. Chem.*, **247**, 2575 (1972).
(30) W. Taylor, in "Handbook of Physiology," Vol. 5, C. Code, Ed., American Physiology Society, Washington, D.C., 1968, p. 2577.
(31) M. Scijffers, L. Miller, and H. Segal, *Biochemistry*, **3**, 1203 (1964).
(32) M. Pawelczak, *Acta Pol. Pharm.*, **23**, 380 (1966).
(33) J. R. Feldkamp, D. N. Shah, S. L. Meyer, J. L. White, and S. L. Hem, *J. Pharm. Sci.*, **70**, 638 (1981).
(34) A. Lehninger, "Biochemistry," 2nd ed., Worth, New York, N.Y., 1975, p. 83.
(35) J. Tang, *J. Biol. Chem.*, **246**, 4510 (1971).
(36) C. J. Serna, J. L. White, and S. L. Hem, *J. Pharm. Sci.*, **67**, 1144 (1978).
(37) P. H. Hsu, in "Minerals in Soil Environments," J. B. Dixon and S. B. Weed, Eds., Soil Science Society of America, Madison, Wis., 1977, pp. 99-105.
(38) R. Messing, *J. Am. Chem. Soc.*, **91**, 2370 (1969).
(39) D. N. Shah, J. R. Feldkamp, J. L. White, and S. L. Hem, *J. Pharm. Sci.*, **71**, 266 (1982).
(40) F. Hingston, A. Posner, and J. Quirk, *J. Soil Sci.*, **23**, 177 (1972).
(41) J. Bowden, M. Bolland, A. Posner, and J. Quirk, *Nature (London), Phys. Sci.*, **245**, 81 (1973).
(42) A. Lehninger, "Biochemistry," 2nd ed., Worth, New York, N.Y., 1975, p. 79.
(43) F. J. Hingston, R. J. Atkinson, A. M. Posner, and J. P. Quirk, *Nature (London)*, **215**, 1459 (1967).
(44) F. J. Hingston, A. Posner, and J. P. Quirk, *J. Soil Sci.*, **25**, 16 (1974).
(45) F. Parker, "Applications of Infrared Spectroscopy in Biochemistry, Biology and Medicine," Plenum, New York, N.Y., 1971, p. 188.
(46) R. D. B. Fraser and E. Suzuki, in "Physical Principles and Techniques of Protein Chemistry, Part B," S. J. Leach, Ed., Academic, New York, N.Y., 1970, p. 265.
(47) B. Morrissey and R. Stromberg, *J. Colloid Interface Sci.*, **46**, 152 (1974).

ACKNOWLEDGMENTS

Supported in part by the American Foundation for Pharmaceutical Education, through the 1982 AFPE Manufacturing/Industrial Pharmacy Fellowship (R.J.S.), and William H. Rorer, Inc. This report is Journal Paper Number 9490, Purdue University Agricultural Experiment Station, West Lafayette, IN 47907.

Adsorption of Pepsin by Aluminum Hydroxide II: Pepsin Inactivation

ROBERT J. SEPELYAK *, JOSEPH R. FELDKAMP ‡, FRED E. REGNIER §, JOE L. WHITE ‡ and STANLEY L. HEM *x

Received July 18, 1983, from the *Departments of *Industrial and Physical Pharmacy, ‡Agronomy, and §Biochemistry, Purdue University, West Lafayette, IN 47907.* Accepted for publication February 9, 1984.

Abstract □ Pepsin adsorbed on gibbsite or boehmite, non-acid-reactive forms of aluminum hydroxide, had a significantly lower activity than pepsin in solution. IR and desorbed pepsin activity studies showed that the reduced activity of adsorbed pepsin was not due to denaturation of pepsin on adsorption. Steric occlusion of the active site, following pepsin adsorption, was responsible for the lower activity of pepsin adsorbed on gibbsite. The porous morphology of boehmite caused diffusional resistance and steric exclusion, contributing to the decreased activity of adsorbed pepsin. The specific inactivation of pepsin by adsorption on aluminum hydroxide may be important in ulcer therapy.

Keyphrases □ Aluminum hydroxide—adsorption of pepsin, pepsin inactivation □ Pepsin—adsorption by aluminum hydroxide, inactivation □ Adsorption—pepsin adsorption by aluminum hydroxide, pepsin inactivation

The first phase of this study demonstrated that aluminum hydroxide adsorbs pepsin by anionic ligand exchange and electrostatic attractive forces (1). The effect of adsorption on the activity of pepsin and the elucidation of the mechanism responsible for any specific antipepsin effect is the focus of this study.

BACKGROUND

The reduction of pepsin activity by colloidal antacid materials was initially hypothesized to be due to the precipitation of pepsin (2, 3). Berstad (4) has recently concluded that aluminum hydroxide has powerful adsorbent and precipitation effects on pepsin in human gastric juice. Aluminum hydroxide was reported to precipitate pepsin in an inactive form (2). Mutch (5) indicated that pepsin was adsorbed on kaolin, silica gel, calcium phosphate, and magnesium phosphate. Pepsin adsorbed on kaolin or silica gel remained active, but pepsin adsorbed on calcium phosphate or magnesium phosphate was inactive due to denaturation by the high local pH of the surface. Bismuth aluminate, magnesium oxide, and magnesium carbonate were effective in inhibiting pepsin following adsorption (6). Berstad *et al.* (7) assumed that pepsin adsorbed by aluminum hydroxide was inactive. Piper and Fenton (8) stated that the effect of adsorption on pepsin activity was just as important as the pH effect for aluminum hydroxide. Anderson and Harthill (9) found that pepsin adsorbed on an acid-reactive aluminum hydroxide exhibited only 21% of the theoretical activity. Liebman (10) reported that the activity of pepsin was 22% of the control following adsorption on aluminum hydroxide, 29% of the control following adsorption by magnesium hydroxide, and 46% of the control following adsorption by cholestyramine. It was concluded that pepsin was still active while adsorbed because pepsin activity, following dissolution of the three adsorbents, was 88-91% of the control.

EXPERIMENTAL SECTION

Gibbsite[1], boehmite[1], aluminum hydroxycarbonate gel[2], aluminum chlorohydrate[3], porcine pepsin[4], and bovine hemoglobin[4] were obtained commercially. The proteolytic activity of pepsin was determined by either the Anson method (11, 12), using hemoglobin as the substrate, or the dipeptide method (13), which uses the dipeptide *N*-acetyl-L-phenylalanyl-L-3,5-diiodotyrosine as the substrate. The activity of pepsin in the presence of a series of soluble cations was determined using a pepsin solution (20 μg/mL) which was 0.14 mM with respect to the appropriate cation. Likewise, the activity of pepsin in the presence of gibbsite or boehmite was determined using a pepsin solution (20 μg/mL) which contained 0.5 mg/mL of gibbsite or boehmite.

Pepsin solutions (20 μg/mL), or pepsin (20 μg/mL) and gibbsite (0.5 mg/mL) or boehmite (0.5 mg/mL) suspensions, were lyophilized and pre-

[1] Reynolds Metal Co., Bauxite, Ark.
[2] Chattem Chemical Co., Chattanooga, Tenn.
[3] Wicken Products, Huguenot, N.Y.
[4] Worthington Biochemical Corp., Freehold, N.J.

0022-3549/84/1100-1517$01.00/0
© 1984, American Pharmaceutical Association

(25) W. Taylor, in "Handbook of Physiology," Vol. 5, C. Code, Ed., American Physiology Society, Washington, D.C., 1968, pp. 2568, 2569.
(26) P. Sepulveda, J. Marciniszyn, D. Liu, and J. Tang, *J. Biol. Chem.*, **250**, 5082 (1975).
(27) A. Lehninger, "Biochemistry," 2nd ed., Worth, New York, N.Y., 1975, p. 162.
(28) A. McLaren and G. Peterson, *Nature*, **192**, 960 (1961).
(29) J. Hartsuck and J. Tang, *J. Biol. Chem.*, **247**, 2575 (1972).
(30) W. Taylor, in "Handbook of Physiology," Vol. 5, C. Code, Ed., American Physiology Society, Washington, D.C., 1968, p. 2577.
(31) M. Scijffers, L. Miller, and H. Segal, *Biochemistry*, **3**, 1203 (1964).
(32) M. Pawelczak, *Acta Pol. Pharm.*, **23**, 380 (1966).
(33) J. R. Feldkamp, D. N. Shah, S. L. Meyer, J. L. White, and S. L. Hem, *J. Pharm. Sci.*, **70**, 638 (1981).
(34) A. Lehninger, "Biochemistry," 2nd ed., Worth, New York, N.Y., 1975, p. 83.
(35) J. Tang, *J. Biol. Chem.*, **246**, 4510 (1971).
(36) C. J. Serna, J. L. White, and S. L. Hem, *J. Pharm. Sci.*, **67**, 1144 (1978).
(37) P. H. Hsu, in "Minerals in Soil Environments," J. B. Dixon and S. B. Weed, Eds., Soil Science Society of America, Madison, Wis., 1977, pp. 99-105.
(38) R. Messing, *J. Am. Chem. Soc.*, **91**, 2370 (1969).
(39) D. N. Shah, J. R. Feldkamp, J. L. White, and S. L. Hem, *J. Pharm. Sci.*, **71**, 266 (1982).
(40) F. Hingston, A. Posner, and J. Quirk, *J. Soil Sci.*, **23**, 177 (1972).
(41) J. Bowden, M. Bolland, A. Posner, and J. Quirk, *Nature (London), Phys. Sci.*, **245**, 81 (1973).
(42) A. Lehninger, "Biochemistry," 2nd ed., Worth, New York, N.Y., 1975, p. 79.
(43) F. J. Hingston, R. J. Atkinson, A. M. Posner, and J. P. Quirk, *Nature (London)*, **215**, 1459 (1967).
(44) F. J. Hingston, A. Posner, and J. P. Quirk, *J. Soil Sci.*, **25**, 16 (1974).
(45) F. Parker, "Applications of Infrared Spectroscopy in Biochemistry, Biology and Medicine," Plenum, New York, N.Y., 1971, p. 188.
(46) R. D. B. Fraser and E. Suzuki, in "Physical Principles and Techniques of Protein Chemistry, Part B," S. J. Leach, Ed., Academic, New York, N.Y., 1970, p. 265.
(47) B. Morrissey and R. Stromberg, *J. Colloid Interface Sci.*, **46**, 152 (1974).

ACKNOWLEDGMENTS

Supported in part by the American Foundation for Pharmaceutical Education, through the 1982 AFPE Manufacturing/Industrial Pharmacy Fellowship (R.J.S.), and William H. Rorer, Inc. This report is Journal Paper Number 9490, Purdue University Agricultural Experiment Station, West Lafayette, IN 47907.

Adsorption of Pepsin by Aluminum Hydroxide II: Pepsin Inactivation

ROBERT J. SEPELYAK *, JOSEPH R. FELDKAMP ‡, FRED E. REGNIER §, JOE L. WHITE ‡ and STANLEY L. HEM *x

Received July 18, 1983, from the *Departments of *Industrial and Physical Pharmacy, ‡Agronomy, and §Biochemistry, Purdue University, West Lafayette, IN 47907.* Accepted for publication February 9, 1984.

Abstract □ Pepsin adsorbed on gibbsite or boehmite, non-acid-reactive forms of aluminum hydroxide, had a significantly lower activity than pepsin in solution. IR and desorbed pepsin activity studies showed that the reduced activity of adsorbed pepsin was not due to denaturation of pepsin on adsorption. Steric occlusion of the active site, following pepsin adsorption, was responsible for the lower activity of pepsin adsorbed on gibbsite. The porous morphology of boehmite caused diffusional resistance and steric exclusion, contributing to the decreased activity of adsorbed pepsin. The specific inactivation of pepsin by adsorption on aluminum hydroxide may be important in ulcer therapy.

Keyphrases □ Aluminum hydroxide—adsorption of pepsin, pepsin inactivation □ Pepsin—adsorption by aluminum hydroxide, inactivation □ Adsorption—pepsin adsorption by aluminum hydroxide, pepsin inactivation

The first phase of this study demonstrated that aluminum hydroxide adsorbs pepsin by anionic ligand exchange and electrostatic attractive forces (1). The effect of adsorption on the activity of pepsin and the elucidation of the mechanism responsible for any specific antipepsin effect is the focus of this study.

BACKGROUND

The reduction of pepsin activity by colloidal antacid materials was initially hypothesized to be due to the precipitation of pepsin (2, 3). Berstad (4) has recently concluded that aluminum hydroxide has powerful adsorbent and precipitation effects on pepsin in human gastric juice. Aluminum hydroxide was reported to precipitate pepsin in an inactive form (2). Mutch (5) indicated that pepsin was adsorbed on kaolin, silica gel, calcium phosphate, and magnesium phosphate. Pepsin adsorbed on kaolin or silica gel remained active, but pepsin adsorbed on calcium phosphate or magnesium phosphate was inactive due to denaturation by the high local pH of the surface. Bismuth aluminate, magnesium oxide, and magnesium carbonate were effective in inhibiting pepsin following adsorption (6). Berstad *et al.* (7) assumed that pepsin adsorbed by aluminum hydroxide was inactive. Piper and Fenton (8) stated that the effect of adsorption on pepsin activity was just as important as the pH effect for aluminum hydroxide. Anderson and Harthill (9) found that pepsin adsorbed on an acid-reactive aluminum hydroxide exhibited only 21% of the theoretical activity. Liebman (10) reported that the activity of pepsin was 22% of the control following adsorption on aluminum hydroxide, 29% of the control following adsorption by magnesium hydroxide, and 46% of the control following adsorption by cholestyramine. It was concluded that pepsin was still active while adsorbed because pepsin activity, following dissolution of the three adsorbents, was 88-91% of the control.

EXPERIMENTAL SECTION

Gibbsite[1], boehmite[1], aluminum hydroxycarbonate gel[2], aluminum chlorohydrate[3], porcine pepsin[4], and bovine hemoglobin[4] were obtained commercially. The proteolytic activity of pepsin was determined by either the Anson method (11, 12), using hemoglobin as the substrate, or the dipeptide method (13), which uses the dipeptide *N*-acetyl-L-phenylalanyl-L-3,5-diiodotyrosine as the substrate. The activity of pepsin in the presence of a series of soluble cations was determined using a pepsin solution (20 μg/mL) which was 0.14 mM with respect to the appropriate cation. Likewise, the activity of pepsin in the presence of gibbsite or boehmite was determined using a pepsin solution (20 μg/mL) which contained 0.5 mg/mL of gibbsite or boehmite.

Pepsin solutions (20 μg/mL), or pepsin (20 μg/mL) and gibbsite (0.5 mg/mL) or boehmite (0.5 mg/mL) suspensions, were lyophilized and pre-

[1] Reynolds Metal Co., Bauxite, Ark.
[2] Chattem Chemical Co., Chattanooga, Tenn.
[3] Wicken Products, Huguenot, N.Y.
[4] Worthington Biochemical Corp., Freehold, N.J.

0022-3549/84/1100-1517$01.00/0
© 1984, American Pharmaceutical Association

Table I—Pepsin Activity Corrected for the Time Effect

Replicate Number	Elapsed Time to Start Replicate, s	Activity (a), AU	Mean Corrected Activity ($\bar{A}$), AU	Predicted Activity (a_p), AU	Correction Factor, AU	Corrected Activity (A), AU
1	0	3120	3152	3158	−6	3114
2	334	3180	3152	3119	33	3213
3	839	3035	3152	3060	92	3127
4	3685	2740	3152	2726	426	3166
5	4013	2675	3152	2688	464	3139
Mean		2950	—	—	—	3152
SD		±228	—	—	—	±39

pared as potassium bromide disks (1 mg of lyophilized sample/300 mg of KBr) for IR analysis. The pepsin solution was denatured by either adding 1 M NaOH to adjust the pH to 9 (base-denatured pepsin) or by heating the pepsin solution at 90°C for 1 h (heat-denatured pepsin). The denatured pepsin solutions were lyophilized and prepared for IR analysis as above. The IR spectrum was recorded using a spectrophotometer[5] interfaced with a computer. The spectrum of adsorbed pepsin was obtained by subtracting the spectrum of boehmite from the spectrum of pepsin-boehmite based on the 1070 cm^{-1} band of boehmite (1).

Desorbed-pepsin studies were performed by initially interacting pepsin (25 μg/mL) and aluminum hydroxycarbonate gel (1.7 mg equivalent of aluminum oxide/mL) at pH 2.3 in a pH-stat titrator[6]. Preliminary studies indicated immediate adsorption under these conditions. The aluminum hydroxycarbonate was dissolved under pH-stat[6] conditions at pH 2.3 and 5°C. After complete dissolution of the aluminum hydroxycarbonate gel, the activity of pepsin was determined by the modified Anson method.

The activity of desorbed pepsin was also determined by adsorbing pepsin (20 μg/mL) on gibbsite (0.5 mg/mL) or boehmite (0.5 mg/mL) at pH 2.3. After adsorption, a 0.12-g/mL phosphate solution (pH 2.3) was added. The supernatant was analyzed at 280 nm to monitor the desorption of pepsin. The activity of the desorbed pepsin was determined by the modified Anson method.

Samples of gibbsite and boehmite were prepared for scanning electron microscopy[7] by air-drying a sonicated 0.2% suspension. The samples were coated with gold and platinum[8]. A microdrop of a 0.2% sonicated gibbsite or boehmite suspension was placed on a 300-mesh copper grid which was coated with polyvinyl formal[9] and stabilized with evaporated carbon. After air-drying, the sample was examined by transmission electron microscopy[10] at 80 keV.

RESULTS AND DISCUSSION

To improve the precision of the Anson method, which has a *CV* of ~5% (14), five replicates were run rather than three. Pepsin activity tended to decrease with each replicate (Table I). The decrease appeared to be related to time and is believed to be due to the autodigestion of pepsin in the pepsin stock solution. The autodigestion of pepsin was slowed by maintaining the pepsin stock solution at 5°C, but a variation in pepsin activity (a) with time was still observed. A plot of pepsin activity *versus* time for the data in Table I showed that time accounts for the major part of the variation in activity. Equation 1 was used to correct for time to obtain the mean corrected pepsin activity, $\bar{A}$:

$$\bar{A} = r^2 y + (1 - r^2)\bar{a} \qquad \text{(Eq. 1)}$$

where r^2 is obtained from the linear regression analysis and y represents the intercept of the optimal straight line. The experimental mean pepsin activity, $\bar{a}$, is influenced by the time dependence of the replicates. Thus, $\bar{A}$ represents the mean activity that would be observed if autodigestion did not occur. However, if $r^2 = \sim 0$ (indicating only slight time dependence), then $\bar{A} \approx \bar{a}$. If a_p represents the predicted activity at time t, obtained from the optimal straight line, then each individual activity, a, may be corrected to give a corrected pepsin activity, A:

$$A = a + (\bar{A} - a_p) \qquad \text{(Eq. 2)}$$

Thus, the procedure to correct for the effect of time adjusted the mean pepsin activity from 2950 to 3152 activity units and decreased the *SD* from 228 to 39 activity units. The correction for autodigestion of the stock pepsin solution reduced the *CV* ~1%. Perhaps some of the conflicting reports on pepsin inactivation are due to the large *CV* associated with the unmodified Anson method. All results in this study were obtained using the aforementioned modificiation of the Anson method.

The pH-activity profile of pepsin obtained by the modified Anson method is shown in Fig. 1, line A and is similar to previously reported profiles (15, 16). The optimal pH range for pepsin activity is pH 2.2-2.6. Pepsin activity approaches zero at pH 4, which supports one of the goals of peptic ulcer therapy, *i.e.*, to raise the gastric pH to minimize pepsin activity.

The activity of pepsin in the presence of soluble forms of aluminum was determined because numerous investigators have reported an inhibitory effect by aluminum (3, 8, 17, 18). However, Anderson and Harthill (9) reported that aluminum ions had no effect on pepsin activity. Two forms of soluble aluminum (aluminum chloride and aluminum chlorohydrate) were tested for an antipepsin effect at pH 2.4 by the modified Anson method. Aluminum chlorohydrate was chosen because it is an aluminum complex with a +7 charge (19). A concentration ratio of 250 ions per pepsin molecule was chosen to provide a substantial excess of aluminum ions, because pepsin contains ~43 carboxylate groups on the surface. The results (Table II) indicate a slight enhancement of pepsin activity (~4%) by aluminum cation and a slight inhibition (~4%) by aluminum chlorohydrate. These differences are statistically significant at an α level of 0.05. Even though statistically significant differences in pepsin activity were observed in the presence of aluminum ion and aluminum chlorohydrate, these differences are not believed to be large enough to produce any significant *in vivo* effects. Furthermore, aluminum cation did not alter the pH-activity profile of pepsin (Fig. 1, line B).

The first part of this series demonstrated that pepsin was specifically adsorbed by aluminum hydroxide through anionic ligand exchange, involving carboxylate groups of pepsin and surface aluminum ions, and electrostatic attraction (1). Therefore, the effect of adsorption on pepsin activity was examined by determining pepsin activity in the presence of gibbsite or boehmite, non-acid-reactive forms of aluminum hydroxide. Under normal physiological conditions, a 600-mg dose of aluminum hydroxide will produce a pepsin to aluminum hydroxide ratio in the stomach of 0.02:1 to 0.16:1 (20). Thus, a ratio of pepsin to aluminum hydroxide of 0.04:1 was used. The activity of pepsin in the presence of either gibbsite or boehmite was lower than the control (Table

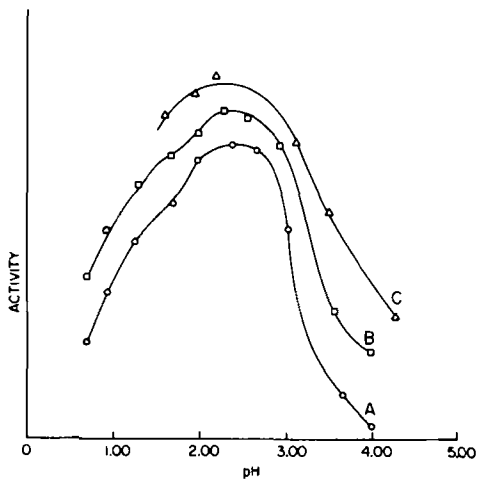

Figure 1—*pH-activity profile. Key: (A) pepsin solution using modified Anson method; (B) pepsin solution in presence of aluminum ion using modified Anson method; (C) pepsin solution using the dipeptide method.*

[5] Model 180; Perkin-Elmer Corp., Norwalk, Conn.
[6] PHM 62, TTT 60, ABU 12, TTA 60, and REA 60; Radiometer, Copenhagen, Denmark.
[7] JSM-U3; Japan Electron Optics Laboratory Co., Ltd., Tokyo, Japan.
[8] Hummer II Sputter Coater; Technics, Alexandria, Va.
[9] Formvar; Ladd Research Industries, Burlington, Vt.
[10] EM-400; Philips, Mahwah, N.J.

Table II—Effect of Soluble Forms of Aluminum on Pepsin Activity

	Aluminum Chloride				Aluminum Chlorohydrate			
	I		II		I		II	
	Treatment	Control	Treatment	Control	Treatment	Control	Treatment	Control
Mean corrected activity, AU	3152	3030	3155	3034	3017	3170	3097	3186
SD	±39	±83	±46	±59	±136	±66	±31	±25
pH	2.26	2.27	2.56	2.58	2.42	2.42	2.37	2.39

Table III—Effect of Gibbsite or Boehmite on Pepsin Activity

	Gibbsite		Boehmite	
	Treatment	Control	Treatment	Control
Mean corrected activity, AU	2518	2999	1571	2753
SD	±100	±148	±40	±79
pH	2.43	2.42	2.64	2.61
Percent Adsorbed	50	—	74	—
Activity of adsorbed pepsin, %	68	—	42	—

III). However, the observed activity of pepsin in the aluminum hydroxide suspensions was not due to adsorbed pepsin alone since not all of the enzyme was adsorbed. Activity due to adsorbed pepsin will be termed immobilized pepsin activity. To calculate the immobilized pepsin activity, the extent of adsorption had to be determined. Also, it was assumed that free pepsin in the aluminum hydroxide suspension had the same activity as pepsin in the control solution. For example, UV analysis of the supernatant from the pepsin–boehmite suspensions indicated that 26% of the pepsin was in solution. Thus, the activity contributed by the free pepsin was calculated to be 716 AU, *i.e.*, 26% of the activity of the control. Since the total activity of the pepsin–boehmite suspension was 1571 AU, the adsorbed pepsin (which comprised 74% of the pepsin in the suspension) had an activity of 855 AU. However, 74% of the activity of the control is 2037 AU. Thus, the adsorbed pepsin exhibited 42% as much activity as unadsorbed pepsin. The adsorbed pepsin in the pepsin–gibbsite suspension was only 68% as active as free pepsin.

The decreased antiproteolytic activity of adsorbed pepsin was directly measured by adsorbing pepsin on gibbsite or boehmite, washing, and separating the solid phase to obtain only immobilized pepsin. Adsorption was strong enough that desorption did not occur when the immobilized pepsin was resuspended (1). Pepsin immobilized on gibbsite was 59–67% as active as free pepsin while pepsin adsorbed on boehmite was only 31–39% as active as the control, as determined by the modified Anson method (Table IV). These results agree with the 68 and 42% activity calculated for pepsin adsorbed on gibbsite and boehmite, respectively, based on the activity of the unwashed suspension (Table III).

Three factors may be involved in the decreased immobilized pepsin activity. A structural change in pepsin may result from adsorption on the aluminum hydroxide surface. The properties of the active site of an enzyme depend on the tertiary structure and any modification of the three-dimensional structure could have an effect on activity. A second factor might involve steric occlusion of the active site due to adsorption. Depending on the orientation of the adsorbed pepsin molecule, the accessibility of the active site may be reduced or blocked altogether. This effect would reduce the rate of proteolysis. A third possible mechanism is the development of a substrate concentration gradient between the bulk solution and the microenvironment of the adsorbed pepsin. The substrate concentration gradient can be due to diffusional resistance of the substrate or steric exclusion of the substrate from reaching the adsorbed pepsin.

The possibility that adsorption produces a structural change in pepsin was investigated by IR spectroscopy and by determining the activity of pepsin which had been desorbed from gibbsite or boehmite. The IR spectra of pepsin, base-denatured pepsin, and heat-denatured pepsin are compared in Fig. 2. The major bands for pepsin occur at 1530 cm^{-1} (amide II) and 1650 cm^{-1} (amide I) (21). The shoulder at 1730 cm^{-1} is due to the C=O stretching vibrations from the carboxylic acid groups of glutamic and aspartic acids (22). The spectra of the base-denatured and heat-denatured pepsin also had bands at 1530 and 1650 cm^{-1}. The base-denatured pepsin had a band at ~1600 cm^{-1} which was due to the strong asymmetric stretching vibrations from the ionized carboxylic acid groups of glutamic and aspartic acids. Since the carboxylic acid groups will be ionized at the pH required for base denaturation, the shoulder at 1730 cm^{-1} was not present in the spectrum of the base-denatured pepsin. Both the base-denatured and the heat-denatured pepsin possess a unique band at 1400 cm^{-1}. This band has not been assigned but is believed to be associated with the denaturation of pepsin.

The IR spectrum of pepsin adsorbed on boehmite was obtained by computer subtraction of the boehmite spectrum from the pepsin–boehmite spectrum and is shown as Fig. 2, line D. The amount of pepsin adsorbed by gibbsite was too low to obtain an IR spectrum. The absence of the band at 1400 cm^{-1} suggests that pepsin was not denatured by adsorption. The amide I band at 1650 cm^{-1} shifted to a slightly higher frequency, possibly due to a slight deformation of the structure of pepsin as a consequence of adsorption. The similarity of the spectra of pepsin and pepsin adsorbed on boehmite suggests that pepsin was still active even when adsorbed on aluminum hydroxide.

Pepsin activity following desorption was determined to further establish whether pepsin was denatured due to adsorption. A dissolution method and an exchange method were used to desorb pepsin. Aluminum hydroxycarbonate gel, the acid-reactive form of aluminum hydroxide, was used as the adsorbent for the dissolution method. A low ratio of pepsin to aluminum hydroxide was used so that the majority of pepsin would be adsorbed. Following dissolution of the aluminum hydroxycarbonate gel, the activity of the desorbed pepsin

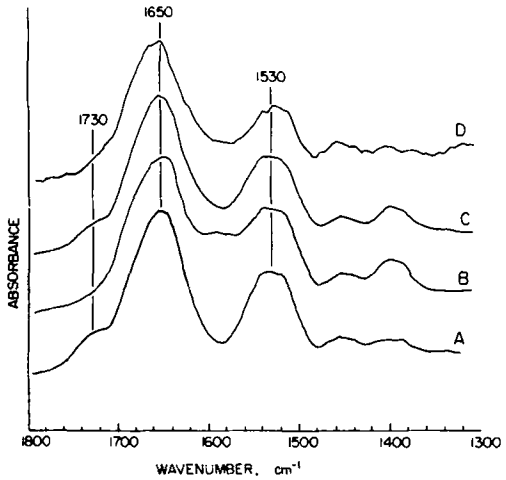

Figure 2—*IR spectra. Key: (A) pepsin; (B) base-denatured pepsin; (C) heat-denatured pepsin; (D) pepsin adsorbed on boehmite.*

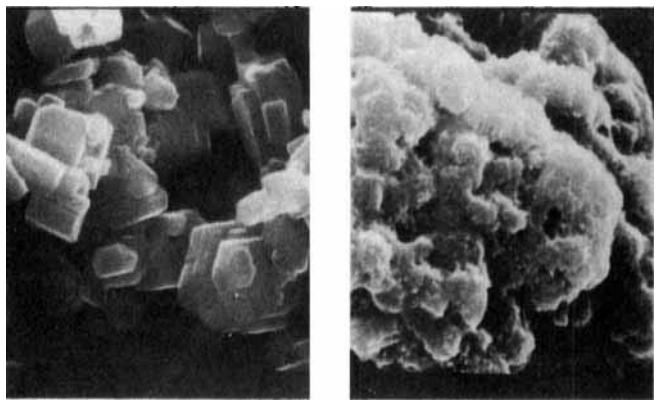

Figure 3—*Scanning electron micrographs of gibbsite (left) and boehmite (right) at 30,000×.*

Table IV—Immobilized Pepsin Activity

	Gibbsite				Boehmite			
	I		II		I		II	
	Treatment	Control	Treatment	Control	Treatment	Control	Treatment	Control
Mean corrected activity, AU	1854	3124	1996	3002	938	3046	1163	2992
SD	±32	±41	±30	±32	±20	±63	±80	±42
pH	2.41	2.42	2.50	2.51	2.48	2.49	2.50	251
Immobilized pepsin activity, %	59.3	—	66.5	—	30.8	—	38.9	—

was determined by the modified Anson method (Table V). The desorbed pepsin was 96% as active as the control indicating that adsorption by aluminum hydroxide did not affect the structure of pepsin enough to alter its activity. This result corresponds well with an earlier study which reported a 94% recovery of activity following dissolution of the adsorbent, aluminum hydroxide (9).

Pepsin was also desorbed from gibbsite or boehmite by exchange with phosphate. As seen in Table VI, almost all of the adsorbed pepsin was desorbed from either gibbsite or boehmite by exchange with phosphate. The activity of the desorbed pepsin, as determined by the modified Anson method, was virtually identical to the controls. However, the mean corrected activity after phosphate exchange includes both desorbed pepsin and pepsin which had not been adsorbed. When Eq. 3 was applied to calculate the activity of only desorbed pepsin, the pepsin desorbed from gibbsite and boehmite was 91 and 96% as active as the control, respectively.

$$D = \frac{\bar{A}_t - \left(\bar{A}_c \frac{F_f}{F_r}\right)}{\bar{A}_c - \left(\bar{A}_c \frac{F_f}{F_r}\right)} \times 100 \qquad \text{(Eq. 3)}$$

where D is the activity of desorbed pepsin, %; $\bar{A}_t$ is the mean corrected activity after phosphate exchange; $\bar{A}_c$ is the mean corrected activity of control; F_f is the fraction of pepsin in the supernatant initially; and F_r is the fraction of pepsin in the supernatant after phosphate exchange. Thus, IR and desorption studies indicate that adsorption of pepsin by aluminum hydroxide does not denature pepsin.

To determine whether steric effects were involved in reducing the activity of adsorbed pepsin, the activity of pepsin against a smaller substrate was studied. Hemoglobin (Hb), the substrate used in the Anson method, is a macromolecule with a mol. wt. of ~35,000 (23). The low-molecular-weight substrate selected was *N*-acetyl-L-phenylalanyl-L-3,5-diiodotyrosine, a dipeptide with a mol. wt. of ~600. The smaller size of the dipeptide should enable it to reach the active site of adsorbed pepsin more easily, and increased activity against the dipeptide should be observed if steric effects are important. The autodigestion of pepsin was observed using the dipeptide, and the mathematical procedure used to correct for the autodigestion of pepsin during the Anson method was also used for the dipeptide method. This method is reported to have a *CV* of 6% (13). When the modifications developed for the Anson method were applied to the dipeptide method, the *CV* was reduced to 2%. The pH–activity profile of pepsin using the dipeptide (Fig. 1, line C) was similar to the pH–activity profile using hemoglobin (Fig. 1, line A).

Table V—Activity of Pepsin Desorbed From Aluminum Hydroxycarbonate Gel by Acid Dissolution

	Treatment	Control
Mean corrected activity, AU	1951	2037
SD	±39	±29
pH	2.63	2.68
Activity of desorbed pepsin, %	96	—

Table VI—Activity of Pepsin Desorbed from Gibbsite and Boehmite by Phosphate Exchange

	Gibbsite		Boehmite	
	Treatment	Control	Treatment	Control
Pepsin in supernatant initially, %	27	—	15	—
Pepsin in supernatant after phosphate exchange, %	96	—	82	—
Mean corrected activity after phosphate exchange, AU	2363	2521	2822	2918
SD	±41	±39	±64	±107
pH	2.49	2.49	2.30	2.30
Activity of desorbed pepsin, %	91	—	96	—

The activity of pepsin adsorbed on gibbsite or boehmite was determined in two separate studies using the modified Anson and the modified dipeptide methods. As seen in Table VII, pepsin adsorbed on gibbsite was less active than the control, but the Student's t test, at an α level of 0.05, showed that the immobilized pepsin activity was statistically the same for both substrates. Thus, both the dipeptide and hemoglobin interacted with the active site of pepsin to the same extent, indicating that both hemoglobin and the dipeptide experienced the same inhibitory steric effect. This steric effect is probably due to steric occlusion of the active site of pepsin resulting from adsorption. Anderson and Harthill (9) also suggested that some active site occlusion occurs when pepsin is adsorbed by aluminum hydroxide.

The immobilized pepsin activity depended on the substrate when pepsin was adsorbed on boehmite (Table VII). Pepsin adsorbed on boehmite was less active than the control, but greater activity occurred with the dipeptide substrate. The t test indicated that the difference in activity against hemoglobin and the dipeptide was statistically significant at an α level of 0.05. These results suggest that a steric factor related to the adsorbent is important, in addition to steric occlusion.

It is possible that the substrate may interact directly with the adsorbent and that the degree of adsorption may differ between hemoglobin and the dipeptide. An adsorption effect occurring between the dipeptide and boehmite can be considered negligible, since the activity of pepsin adsorbed on either boehmite or gibbsite was similar when the dipeptide was used as the substrate. However, hemoglobin may be adsorbed by boehmite since the activity of pepsin adsorbed on boehmite decreased when compared with pepsin adsorbed on gibbsite with hemoglobin as the substrate. This lower activity may be caused by a decrease in hemoglobin concentration in the microenvironment of the adsorbed pepsin due to adsorption of hemoglobin on boehmite. This possibility was discounted when calculation showed that the hemoglobin could form a monomolecular layer 400 times as great as the surface area of the boehmite used in the test. Thus, even if adsorption of a hemoglobin bilayer occurred, the concentration of hemoglobin in solution would not be substantially reduced.

Adsorption of hemoglobin could also affect the activity of adsorbed pepsin if the adsorbed pepsin was "buried" by the adsorption of hemoglobin on the adsorbed pepsin. This mechanism was also discounted because both hemoglobin and the dipeptide were affected equally by pepsin adsorbed on gibbsite.

Diffusional resistance may be partially responsible for the reduced activity of adsorbed pepsin. Hemoglobin has a diffusion coefficient of $6.3\text{–}6.7 \times 10^{-7}$ cm^2/s (24). The diffusion coefficient of the dipeptide has not been determined, but it is expected to be at least 10 times larger than hemoglobin since there is a 58-fold difference in molecular weight. Thus, the dipeptide would be more likely to maintain an equal concentration between the bulk and the mi-

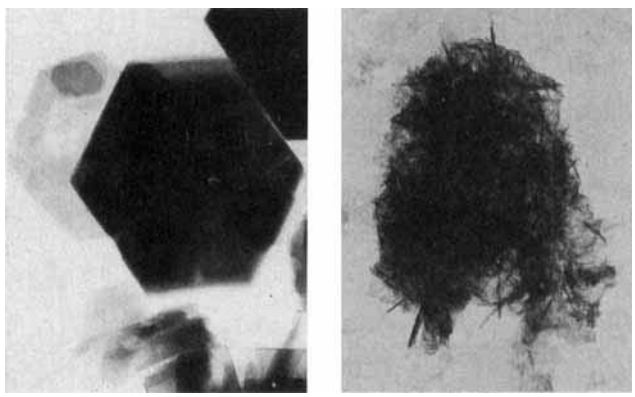

Figure 4—*Transmission electron micrographs of gibbsite (left) and boehmite (right) at 170,000×.*

Table VII—Immobilized Pepsin Activity Using Hemoglobin and Dipeptide Substrates

	Gibbsite								Boehmite							
	I				II				I				II			
	Hemoglobin		Dipeptide		Hemoglobin		Dipeptide		Hemoglobin		Dipeptide		Hemoglobin		Dipeptide	
	T[a]	C[b]	T	C	T	C	T	C	T	C	T	C	T	C	T	C
Mean corrected activity, AU	1854	3124	12.8	24.8	1996	3002	14.0	20.8	938	3046	30.8	66.7	1163	2992	35.9	64.0
SD	±32	±41	±1.2	±1.4	±30	±32	±3.1	±3.3	±20	±63	±1.9	±1.4	±80	±45	±0.8	±1.0
pH	2.41	2.42	2.11	2.11	2.50	2.51	2.16	2.17	2.48	2.49	2.10	2.10	2.50	2.51	2.21	2.22
Immobilized pepsin activity, %	59.3	—	51.6		66.5	—	67.3	—	30.8	—	46.2	—	38.9	—	56.1	—

[a] Treatment. [b] Control.

croenvironment of the adsorbed pepsin. In addition to the size of the diffusing species, the morphology of the surface may be an important factor in diffusional resistance. Scanning electron micrographs of gibbsite and boehmite at 30,000× magnification are shown in Fig. 3. Gibbsite is platy with smooth faces and sharp edges, while boehmite is porous. Because the boehmite particles did not have the well-defined edges of gibbsite, the scanning electron micrographs are not as well resolved.

Transmission electron micrographs (Fig. 4) provide more information on the morphology of the adsorbents. Gibbsite particles again appear to have a well-defined structure with distinct edges. The material is platy which can be seen by close examination of the edges of the hexagonal units. The darker particles are a collection of stacked plates. The individual boehmite particles are shown to be smooth flat plates. The plates tend to roll up and form an aggregate of interpenetrating scrolls. The tubular nature of the boehmite particles was deduced because the cores appear to be less dense. Gibbsite particles and boehmite aggregates are approximately the same size, but the porous nature of the boehmite aggregate results in a larger surface area.

The lower activity against hemoglobin of pepsin adsorbed on boehmite when compared with gibbsite can be explained by the porous nature of the boehmite aggregate. Pepsin adsorbed on gibbsite is similar to adsorption on a smooth flat plate, whereas adsorption on boehmite is similar to adsorption in a long narrow channel (Fig. 5). In the case of pepsin adsorbed on gibbsite, the substrate only has to diffuse to the surface. In this situation, the size of the substrate would not be expected to be a factor. Thus, the observation that pepsin adsorbed on gibbsite was equally active against either hemoglobin or the dipeptide is consistent with the morphology of the gibbsite particle.

The porous boehmite morphology requires that the substrate must diffuse through channels in the porous structure to reach adsorbed pepsin. The dipeptide has a diffusion coefficient high enough to maintain the same concentration throughout the channels as in the bulk solution. The dipeptide is also more likely to reach all of the adsorbed pepsin due to its small size. Thus, the lower activity against hemoglobin of pepsin adsorbed on boehmite can also be related to the morphology of boehmite. The lower diffusion coefficient of hemoglobin would make it difficult to maintain the same concentration of hemoglobin in the channels as in the bulk solution. The continuous digestion of hemoglobin as it diffuses through the channels will also lower the concentration of hemoglobin in the microenvironment of the adsorbed pepsin. Thus, pepsin adsorbed at the opening of a channel will have a faster rate of proteolysis than pepsin adsorbed in the interior of a channel. The large size of hemoglobin may even sterically exclude hemoglobin from narrow pores.

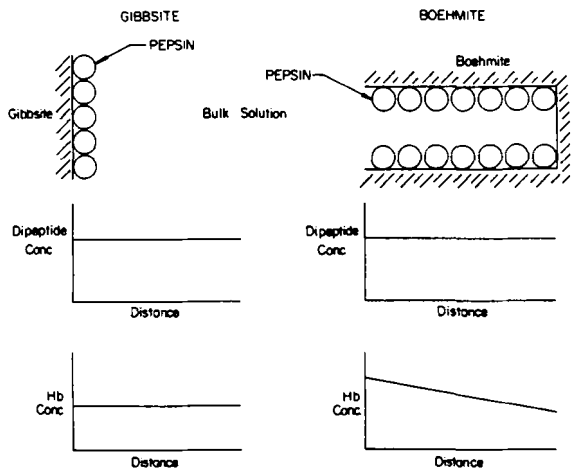

Figure 5—*Schematic diagram of pepsin adsorbed on gibbsite and boehmite.*

The conclusions regarding the importance of the morphology of the adsorbent are consistent with reported differences in activity between low- and high-molecular-weight substrates when an enzyme was adsorbed on a porous material. Immobilized papain on a copolymer had a lower activity using casein than benzoyl-L-arginine ethyl ester as the substrate (25). Pronase adsorbed on a diazotized copolymer had different activities, depending on the molecular weight of the substrate (26). The results were explained on the basis of impedance of substrate access to the catalytic site by the supporting solid matrix. The activity of trypsin adsorbed on aminoethylcellulose also depended on the molecular weight of the substrate (27, 28). It was concluded that the lower activity against the larger substrate was due to the inaccessibility of the adsorbed enzyme.

Thus, pepsin is not denaturerd by adsorption on boehmite or gibbsite. However, the orientation of the adsorbed pepsin results in steric occlusion of the active site, thereby reducing the activity of adsorbed pepsin. In addition to steric occlusion, the activity of pepsin adsorbed on boehmite is also reduced by diffusional resistance and steric exclusion due to the porous morphology of boehmite.

Antacids such as sodium bicarbonate, calcium carbonate, and magnesium hydroxide react very rapidly with acid. pH-Stat titration of these antacid compounds at pH 3 and 37°C showed that the time required to neutralize 50% of the theoretical acid, t_{50}, is <1 min. Therefore, these antacid compounds are expected to be present in the gastric fluid as their soluble ions soon after ingestion. To determine if these antacid compounds exhibit a specific antipepsin effect in addition to the general pH effect, the activity of pepsin in the presence of sodium, calcium, and magnesium ions was determined. Concentrations of ions and pepsin were selected to provide 250 ions per pepsin molecule. As seen in Table VIII, no statistically significant ($\alpha = 0.05$) change in pepsin activity was observed in the presence of sodium, calcium, or magnesium ions.

Aluminum hydroxide reacts more slowly with acid; even amorphous aluminum hydroxycarbonate gel, the acid-reactive form of aluminum hydroxide, does not react as quickly as sodium bicarbonate, calcium carbonate, or magnesium hydroxide. A recent survey of antacid suspensions containing aluminum hydroxide gel and magnesium hydroxide gel showed that the most rapidly reacting product neutralized 96% of the theoretical amount of acid in 15 min at pH 3 and 37°C, while the slowest reacting product neutralized only 31%

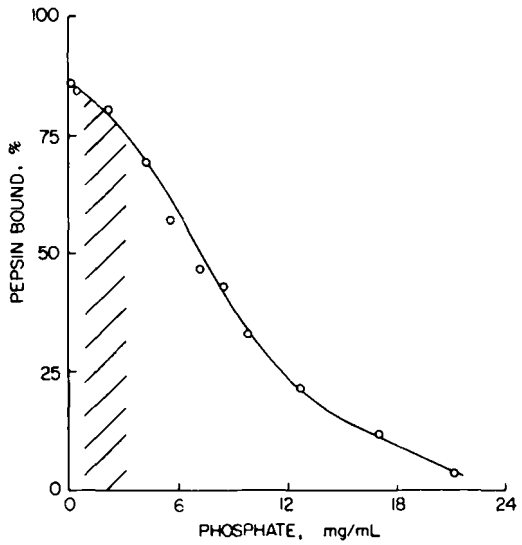

Figure 6—*Effect of phosphate on the fraction of pepsin adsorbed by boehmite. The shaded area indicates the phosphate concentration of gastric fluid.*

Table VIII—Effect of Sodium, Calcium, and Magnesium Ions on Pepsin Activity

	Sodium		Calcium		Magnesium	
	Treatment	Control	Treatment	Control	Treatment	Control
Mean corrected activity, AU	3099	3114	2921	3003	2929	2965
SD	±86	±63	±67	±173	±42	±155
pH	2.43	2.43	2.41	2.41	2.43	2.43

under the same conditions (29). Thus, a solid phase, which can adsorb and inactivate pepsin, will be present in the gastric fluid for a longer time when aluminum hydroxide is used as an antacid in comparison with sodium bicarbonate, calcium carbonate, or magnesium hydroxide.

Before the adsorption and inactivation of pepsin by aluminum hydroxide can be extrapolated to *in vivo* conditions, the possibility that solutes in the gastric fluid (such as phosphate) will compete with pepsin for adsorption by aluminum hydroxide must be considered. Phosphate is also specifically adsorbed by aluminum hydroxide (30, 31). The extent of pepsin adsorption in the presence of phosphate is shown in Fig. 6. The shaded area of the curve indicates the phosphate concentration which is found in gastric fluid (32). Pepsin was 85% bound in the absence of phosphate. The extent of pepsin adsorption gradually decreased with increasing phosphate concentration. Pepsin was 75% bound at the phosphate concentration of the gastric fluid. Therefore, even in the presence of other solutes which are strongly adsorbed by aluminum hydroxide, a major fraction of pepsin would be expected to be adsorbed by aluminum hydroxide.

Non-acid-reactive forms of aluminum hydroxide have been used in ulcer therapy. In 1941 it was reported that non-acid-reactive alumina produced nearly the same symptomatic relief as acid-reactive alumina (33). The effect of non-acid-reactive alumina was attributed to the coating of the gastric mucosa, which provides a physical barrier to gastric acid. Antacid products were marketed that contained a non-acid-reactive aluminum hydroxide. Two gastroscopic studies concluded that non-acid-reactive aluminum hydroxide coated ulcers and acted as an inert physical barrier (34, 35). The results of these studies were contradicted by Hoon (36) who observed no coating, and by Morrissey *et al.* (37) who found approximately one-third of the ulcers completely coated, but the coatings remained for only a short time. Thus, recent thinking has been that acid neutralization is the chief function of antacids. Accordingly, the recent trend in formulating antacid products has been to incorporate only acid-reactive materials. The results of the present study of the adsorption and inactivation of pepsin by gibbsite and boehmite suggest that earlier antacid products containing non-acid-reactive aluminum hydroxide may have promoted ulcer healing by adsorbing and temporarily inactivating pepsin, rather than by coating the ulcers.

Based on this study, it is hypothesized that acid reactive aluminum hydroxycarbonate promotes ulcer healing by neutralizing gastric acid, inactivating pepsin by raising the pH of the gastric contents, and specifically adsorbing and inactivating pepsin. The specific adsorption and inactivation of pepsin by aluminum hydroxide may be responsible for the wide use of aluminum hydroxide in ulcer therapy. The specific adsorption and inactivation of pepsin in ulcer therapy may be enhanced by the use of a non-acid-reactive form of aluminum hydroxide that has a high surface area, such as boehmite.

REFERENCES

(1) R. J. Sepelyak, J. R. Feldkamp, J. L. White, and S. L. Hem, *J. Pharm. Sci.*, **73,** 1514 (1984).

(2) S. Komarov and O. Komarov, *Am. J. Dig. Dis.*, **7,** 166 (1940).

(3) M. Schiffrin and S. Komarov, *Am. J. Dig. Dis.*, **8,** 215 (1941).

(4) A. Berstad, in "Antacids in the Eighties," F. Halter, Ed., Urban & Schwarzenberg, Baltimore, Md., 1982, pp. 17–22.

(5) N. Mutch, *Lancet*, **1,** 859 (1949).

(6) P. Bateson, *J. Pharm. Pharmacol.*, **10,** 123 (1958).

(7) A. Berstad, H. Holm, and E. Kittang, *Scand. J. Gastroenterol.*, **14,** 121 (1979).

(8) D. Piper and B. Fenton, *Am. J. Dig. Dis.*, **NS6,** 134 (1961).

(9) W. Anderson and J. Harthill, *J. Pharm. Pharmacol.*, **24,** 166P (1972).

(10) W. Liebman, *IRCS Med. Sci.: Library Compend.*, **8,** 114 (1980).

(11) M. Anson, *J. Gen. Physiol.*, **22,** 79 (1939).

(12) W. Rick and W. Fritsch, in "Methods of Enzymatic Analysis," 2nd ed., H. Bergmeyer, Ed., Academic, New York, N.Y., 1974, p. 1050.

(13) W. Rick and W. Fritsch, in "Methods of Enzymatic Analysis," 2nd ed., H. Bergmeyer, Ed., Academic, New York, N.Y., 1974, p. 1052.

(14) W. Rick and W. Fritsch, in "Methods of Enzymatic Analysis," 2nd ed., H. Bergmeyer, Ed., Academic, New York, N.Y., 1974, p. 1051.

(15) M. Seijffers, L. Miller, and H. Segal, *Biochemistry*, **3,** 1203 (1964).

(16) A. Berstad, *Scand. J. Gastroenterol.*, **5,** 343 (1970).

(17) K. Persson and B. Bunke, *Acta Pharmacol. Toxicol.*, **19,** 219 (1962).

(18) A. Playle, S. Gunning, and A. Llewellyn, *Pharm. Acta. Helv.*, **49,** 298 (1974).

(19) D. L. Teagarden, J. F. Kozlowski, J. L. White, and S. L. Hem, *J. Pharm. Sci.*, **70,** 758 (1981).

(20) "Scientific Tables," 8th ed., C. Lentner, Ed., Geigy Pharmaceuticals, Ardsley, N.Y., 1982, p. 126.

(21) F. Parker, "Applications of Infrared Spectroscopy in Biochemistry, Biology and Medicine," Plenum, New York, N.Y., 1971, p. 188.

(22) R. D. B. Fraser and E. Suzuki, in "Physical Principles and Techniques of Protein Chemistry, Part B," S. L. Leach, Ed., Academic, New York, N.Y., 1970, p. 265.

(23) W. Taylor, in "Handbook of Physiology," Vol. 5, C. Code, Ed., American Physiology Society, Washington, D.C., 1968, p. 2569.

(24) "Handbook of Biochemistry," 2nd ed., H. Sorber, Ed., The Chemical Rubber Co., Cleveland, Ohio, 1970, pp. C10–C23.

(25) I. Silman, M. Albu-Weissenberg, and E. Katchalski, *Biopolymers*, **4,** 441 (1966).

(26) P. Cresswell and A. Sanderson, *Biochem. J.*, **119,** 447 (1970).

(27) C. Glassmeyer and J. Ogle, *Biochemistry*, **10,** 786 (1971).

(28) R. Haynes and K. Walsh, *Biochem. Biophys. Res. Commun.*, **36,** 235 (1969).

(29) S. L. Hem, J. L. White, J. D. Buehler, J. R. Luber, W. M. Grim, and E. A. Lipka, *Am. J. Hosp. Pharm.*, **39,** 1925 (1982).

(30) F. J. Hingston, A. M. Posner, and J. P. Quirk, *Nature (London)*, **215,** 1459 (1967).

(31) F. J. Hingston, A. M. Posner, and J. P. Quirk, *J. Soil Sci.*, **23,** 179 (1972).

(32) "Scientific Tables," 8th ed., C. Lentner, Ed., Geigy Pharmaceuticals, Ardsley, N.Y., 1982, p. 128.

(33) L. Boyd, W. Russ, and H. Barowsky, *Rev. Gastroenterol.*, **9,** 20 (1942).

(34) G. McHardy and H. Van Rossen, *Curr. Ther. Res. Clin. Exp.*, **4,** 421 (1962).

(35) R. Nelson, *Curr. Ther. Res. Clin. Exp.*, **6,** 83 (1964).

(36) J. Hoon, *Arch. Surg.*, **92,** 467 (1966).

(37) J. Morrissey, T. Honda, Y. Tanaka, and G. Perna, *Arch. Intern. Med.*, **119,** 510 (1967).

ACKNOWLEDGMENTS

Supported in part by the American Foundation for Pharmaceutical Education, through the 1982 AFPE Manufacturing/Industrial Pharmacy Fellowship (R.J.S.), and William H. Rorer, Inc. This report is Journal Paper Number 9491, Purdue University Agricultural Experiment Station, West Lafayette, IN 47907.

Possible Mechanism Behind the Adjuvant Action of Phosphate Derivatives on Rectal Absorption of Cefoxitin in Rats and Dogs

TOSHIAKI NISHIHATA ˣ, CHIA-SHUN LEE, BA THU NGHIEM, and TAKERU HIGUCHI

Received July 18, 1983, from the *Department of Pharmaceutical Chemistry, The University of Kansas, Lawrence, KS 66045.* Accepted for publication January 19, 1984.

Abstract □ The mechanism underlying the ability of phosphate derivatives to act as adjuvants and coadjuvants was examined in *in vivo* and *in situ* preparations in rats and dogs. The adjuvant effect of DL-α-glycerophosphate on the rectal absorption of sodium cefoxitin was greatly augmented by the presence of either sodium phytate or sodium tripolyphosphate. These coadjuvants only slightly enhanced cefoxitin rectal absorption when administered alone. Therefore, enhancement of the permeation of tripolyphosphate and phytate by α-glycerophosphate may be necessary before the coadjuvants can significantly affect cefoxitin absorption. The inhibitory effect of disodium 4,4′-diisothiocyano-2,2′-disulfonate stilbene, which is known to interact with the amino group in the protein fraction, on enhanced cefoxitin absorption suggests the involvement of the protein fraction in transport of cefoxitin across the rectal membrane.

Keyphrases □ Absorption—rectal, cefoxitin, rats and dogs □ Phosphate derivatives—adjuvant or coadjuvant action □ Adjuvants—α-glycerophosphate, enhancement of rectal absorption □ Coadjuvants—phytate, tripolyphosphate, adjuvant action in the presence of α-glycerophosphate □ Bioavailability—cefoxitin, dogs □ Inhibitors—disodium 4,4′-diisothiocyano-2,2′-disulfonate stilbene and calcium chloride

Rectal administration of drugs is becoming more popular due to the convenience of the suppository dosage form. Some anti-inflammatory drugs such as indomethacin (1–3) are currently administered as suppositories in clinical therapy. It has also been suggested (4, 5) that certain drugs which are metabolized by the liver (first-pass effect) after oral administration may have a higher systemic bioavailability when administered rectally.

In our attempt to find novel adjuvants which enhance rectal absorption of drugs poorly absorbed from the rectal compartment due to their high water solubility, we initially examined compounds with chelating activity. The potential link between chelation and adjuvant action was first recognized when the weak chelating agent acetoacetic acid was found to enhance the uptake of sulfadimethoxine into erythrocytes (6). We have since reported that other weak chelating agents such as salicylate analogues (7–9), enamine derivatives of β-diketones (10, 11), and glyceryl derivatives of acetoacetate (12) also effectively enhance drug absorption.

In the present study, we examine the absorption-promoting ability of phosphate derivatives since phosphate is generally known to have chelating ability. Sodium cefoxitin was used as a model water-soluble drug. The adjuvant action of disodium DL-α-glycerophosphate (I), sodium tripolyphosphate, and sodium phytate on the rectal absorption of cefoxitin in rats and dogs is reported. The adjuvant action of glycerol, sodium chloride, and disodium phosphate on rectal absorption of sodium cefoxitin in rats is also described. The ability of several of the compounds described above to act as coadjuvants, agents which promote drug absorption only when their own permeation through the membrane is enhanced by the presence of another absorption-promoting compound, was examined, and speculations concerning the mechanism of adjuvant and coadjuvant action were made.

EXPERIMENTAL SECTION

Materials—Disodium DL-α-glycerophosphate (I)[1], sodium tripolyphosphate[1], and sodium phytate[1] were analytical grade. Sodium cefoxitin[2] was used as obtained from the manufacturer.

Procedures—Sprague-Dawley male rats (weight, 200–225 g) were fasted, with water available, for 16 h prior to experimentation. During the experiments, rats were anesthetized with sodium pentobarbital (60 mg/kg) by intraperitoneal injection and kept on a 38°C surface. Drugs were administered rectally in microenema formulations with dosage volumes of ~ 100 μL/100 g of body weight. The initial pH of the microenema was adjusted to 5.8–6.3 with hydrochloric acid when necessary. To avoid leakage of the solution after administration, the rat anus was ligated with thread. Blood samples were taken from the jugular vein at designated time intervals with a syringe treated with 3% sodium citrate. Plasma samples were collected by centrifugation.

In experiments in which an *in situ* loop was used, the rat rectum was ligated with thread ~4 cm from the anus before administration of a microenema. The *in situ* loop was excised at 1.5 h after microenema administration (wet weight of tissue was 438.4 ± 41.3 mg measured after the experiments). The loop was rinsed with 8 mL of distilled water, and the total volume of the collected rinse solution was adjusted to 10 mL with distilled water. The amount of cefoxitin present in the solution was determined.

Ten male beagle dogs (weight, 9.5–12.0 kg) were also fasted, with water available, for 16 h prior to the experiments (crossover design). Drugs with particle sizes ranging from 72 to 144 μm were administered as 1-g suppositories, prepared with triglyceride suppository base[3] as described previously (12). Blood samples were taken from the jugular vein at designated time intervals.

An *in vitro* study of cefoxitin release from suppositories was carried out at 37°C. One-gram suppositories containing 0.45 mM cefoxitin with I, tripolyphosphate, and/or phytate (see Table II for formulations) were placed in 3 mL of a stirred saline solution. Samples were drawn from the beaker at designated intervals to determine the amount released.

Assays—Assays of cefoxitin were performed by the HPLC method described by Nishihata *et al.* (13).

RESULTS AND DISCUSSION

In a previous study (13), we found that sodium cefoxitin was poorly absorbed by the rat rectum. Plasma cefoxitin levels were undetectable (<0.22 μM) or very low (0.22–0.88 μM) after rectal administration of a microenema containing 44 mM cefoxitin prepared with distilled water. Coadministration of disodium DL-α-glycerophosphate (I) with cefoxitin increased the plasma cefoxitin levels significantly (Table I). A dose-response relationship was apparent since an increase in the concentration of I in the microenema caused an increase in plasma cefoxitin levels.

Glycerol was not as effective in promoting rectal cefoxitin absorption as did I (Table I). For example, 1.09 mmol of glycerol per kg of rat body weight had a similar effect on plasma cefoxitin levels as 103 μmol of I, a 10-fold difference. The sodium ion and phosphate moiety in I may, therefore, be actively involved in the adjuvant effect of the compound.

To investigate the adjuvant activity of the phosphate moiety, the adjuvant action of disodium phosphate, sodium tripolyphosphate, and sodium phytate was studied. Sodium tripolyphosphate and sodium phytate (dose, 0.026

[1] Sigma Chemical Co., St. Louis, Mo.
[2] Merck & Co. Inc., Rahway, N.J.
[3] Witepsol H-15; Chemishe Werk, Witten, Federal Republic of Germany.

0022-3549/84/1100-1523$01.00/0
© 1984, American Pharmaceutical Association

Table I—Effect of α-Glycerophosphate (I), Glycerol (IV), Phosphate (V), Tripolyphosphate (VI), Phytate (VII), and Sodium Chloride (VIII) on Rectal Absorption of Cefoxitin[a]

Dosage Form	Dose of Additive, μmol/kg						Cefoxitin[b]		
	I	IV	V	VI	VII	VIII	Plasma Peak Levels, μM	[AUC], μM·min[c]	Bioavailability, %[d]
Intravenous injection[e]	0	0	0	0	0	0	—	2991 ± 342	100
Microenema	0	0	0	0	0	0	0.31 ± 0.30	61 ± 48	2.0
	0	1090	0	0	0	0	1.36 ± 0.53	122 ± 42	4.1
	103	0	0	0	0	0	2.29 ± 0.62[f]	185 ± 54	6.2
	258	0	0	0	0	0	7.51 ± 1.80[f]	756 ± 113[f]	25.3
	515	0	0	0	0	0	13.43 ± 2.29[f]	1274 ± 196[f]	42.6
	0	0	138	0	0	0	0.58 ± 0.32	96 ± 57	3.2
	0	0	0	54	0	0	2.02 ± 0.49[f]	153 ± 39	5.1
	0	0	0	0	26	0	1.79 ± 0.69[f]	198 ± 26[f]	6.6
	103	0	69	0	0	0	3.51 ± 117[f]	472 ± 93[f,g]	15.8
	103	0	0	27	0	0	15.93 ± 3.69[f,g]	1345 ± 217[f,g]	44.9
	103	0	0	0	13	0	17.60 ± 3.13[f,g]	1618 ± 230[f,g]	54.1
	0	0	0	0	0	520	2.38 ± 0.78[f]	192 ± 65	6.4
	103	0	0	0	0	520	6.64 ± 1.60[f,g]	546 ± 121[f,g]	18.3
	258	0	0	0	0	520	15.20 ± 3.02[f,g]	1548 ± 276[f,g]	51.8

[a] A dose of 33.3 μmol/kg administered as microenemas (100 μL/100 mg) in rats. [b] Values are mean ± *SD*; $n \geq 4$. [c] $[AUC]_{0-240}$ min. [d] [AUC]rectal administration × (dose) intravenous injection × 100/[AUC]intravenous injection × (dose) rectal administration. [e] Intravenous injection of 33.3 μmol/kg administered in saline. [f] $p < 0.001$; Student's *t* test *versus* the results obtained after rectal administration without any additive. [g] $p < 0.001$ *versus* with I alone.

mmol/mL/kg, each contributing 0.27 mmol of sodium to the microenema) weakly enhanced the cefoxitin plasma levels, whereas the presence of disodium phosphate (0.138 mmol/mL/kg; contributing 0.27 mmol of sodium to the microenema) did not enhance cefoxitin absorption (Table I). In a sequential study in which I was coadministered with either sodium tripolyphosphate or sodium phytate in a cefoxitin microenema, the cefoxitin plasma levels were enhanced to a much greater degree than when I was administered alone (Table I). Although the coadministration of disodium phosphate with I only slightly enhanced the plasma cefoxitin level above that obtained with I alone (Table I), this enhancement is worth noticing since disodium phosphate itself had no effect on drug absorption. These results therefore suggest that once the transport of disodium phosphate and particularly sodium tripolyphosphate and sodium phytate through rectal epithelial cells is increased by the presence of I, the adjuvant ability of these phosphate derivatives can be realized.

In male beagle dogs, results were obtained which exhibited a similar trend as observed in the rat studies. The relative bioavailability of cefoxitin [measured by comparing the area under the curve from 0 to 240 min (AUC_{0-240}) of cefoxitin plasma levels after rectal administration to that after intravenous injection] in the absence of any adjuvant in the suppository was <5% (Table II). The presence of I in the suppositories administered to the dogs enhanced the plasma cefoxitin levels (Table II). Administration of either tripolyphosphate or phytate in a suppository containing cefoxitin only slightly enhanced the plasma cefoxitin levels. However, coadministration of I with either tripolyphosphate or phytate in a cefoxitin suppository produced substantially higher cefoxitin plasma levels than when either I or the coadjuvants was administered alone (Table II). Since >95% of the cefoxitin was released from each suppository within 20 min, it is unlikely that the release process was an important factor in this absorption study.

To determine what effect the sodium moiety had in the absorption-promoting ability of I, the adjuvant action of I and sodium chloride was compared in rats. The presence of 0.52 mmol of sodium chloride in a cefoxitin microenema did not have as great an effect on cefoxitin rectal absorption as did 0.258 mmol of I (also contributing 0.52 mmol of sodium/mL) (Table I). The strong adjuvant action of I is therefore not due solely to the sodium content. It is interesting to note that coadministration of sodium chloride with 0.258 mmol of I produced greater cefoxitin plasma levels than those obtained when only 0.258 mmol of I without sodium chloride was administered (Table I). Sodium chloride may, therefore, be effectively acting as a coadjuvant. Studies in which the effect of sodium ion on drug absorption are investigated are currently ongoing in our laboratory.

The exact physicochemical interactions that take place between I and the rectal membrane and that are involved in the enhancement of membrane permeability to cefoxitin and phosphate coadjuvants are not clearly understood. However, the inhibitory effect of disodium 4,4′-diisothiocyano-2,2′-disulfonate stilbene (II) on the enhancing action of I possibly suggests involvement of the membrane protein fraction. Compound II is known to inhibit anion transport through the erythrocyte membrane (14) by interacting with the amino group in the protein fraction (15). The disodium DL-α-glycerophosphate-enhanced disappearance of cefoxitin from the rectal *in situ* loop was suppressed when II was present in the microenema (Table III). Therefore, an interaction may occur between the adjuvant phosphate moiety and the membrane protein fraction, causing a conformational change in the protein. This change in protein structure ensuing from the interaction with I most probably does not result in membrane damage caused by chelation since the adjuvant effect of I on cefoxitin disappearance from a rectal *in situ* loop was only slightly suppressed by calcium chloride (Table III).

When calcium chloride was administered with either sodium tripolyphosphate or sodium phytate without I into a rectal *in situ* loop, the ability of both coadjuvants to enhance the disappearance of cefoxitin was significantly inhibited (Table III). The adjuvant action of these coadjuvants was not affected by coadministration of II (Table III). From these findings, we can speculate that the apparent adjuvant activity of sodium tripolyphosphate and sodium phytate when administered without I may depend primarily on chelating activity. In this study, the enhancing action of phytate was found to be similar to that of EDTA (16). EDTA, a strong chelating agent which has been shown to enhance drug absorption from the small intestine (17) and rectum (16) in rats, has also been found to cause solubilization of protein from erythrocyte ghosts (18). Consequently, the ability of tripolyphosphate and phytate to enhance rectal cefoxitin absorption when administered without I may be a result of membrane damage.

In a previous report by Nishihata *et al.* (12), the difference in the adjuvant action of glyceryl esters of acetoacetate was found to be due, partly, to the

Table II—Effect of α-Glycerophosphate (I), Tripolyphosphate, and Phytate on the Rectal Absorption of Cefoxitin[a]

Dosage Form	Dose of Additives, mmol/body			Cefoxitin, Mean ± *SD*		
	I	Tripolyphosphate	Phytate	Plasma Peak Levels, μM	[AUC], μM·min[b]	Bioavailability, %[c]
Intravenous injection[d]	0	0	0	—	2011 ± 426	100
Suppository	0	0	0	2.0 ± 0.91	291 ± 73	3.6
	1.03	0	0	10.4 ± 2.4[e]	1519 ± 232[e]	19.0
	1.03	0.054	0	21.8 ± 3.2[e]	2458 ± 335[e]	30.6
	1.03	0	0.026	24.3 ± 3.6[e]	2883 ± 437[e]	35.9
	0	0.135	0	3.2 ± 0.80	422 ± 146	5.3
	0	0	0.065	3.9 ± 0.96[e]	519 ± 173[f]	6.5

[a] At a dose of 0.45 mmol/dog administered as 1-g suppositories in dogs; crossover design with $n = 10$. [b] Values are $[AUC]_{0-240}$ min. [c] [AUC]rectal administration × (dose) intravenous injection × 100/[AUC]intravenous injection × (dose) rectal administration. [d] 50 mg of cefoxitin/dog was administered in saline. [e] $p < 0.001$; Student's *t* test, relative to results obtained after administration of suppositories without adjuvant. [f] $p < 0.05$; Student's *t*-test, relative to results obtained after administration of suppositories without adjuvant.

Table III—Effect of 4,4′-Diisothiocyano-2,2′-disulfonate Stilbene (II) and Calcium Chloride (III) on the Enhancement of Plasma Cefoxitin Levels and on Cefoxitin Disappearance from the Rat Rectal *In Situ* Loop by α-Glycerophosphate (I), Sodium Tripolyphosphate, and Sodium Phytate [a]

Adjuvant Concentration	Additive Concentration	Percent Disappearance of Cefoxitin at 1.5 h	$[AUC]_{0-30}$, μM·min
None	None	5.4 ± 5.8	<13 [b]
I (205 mM)	None	38.7 ± 8.1	119 ± 28
	II (1 mg/mL)	16.8 ± 6.3 [b]	52 ± 11 [b]
	III (180 mM)	25.2 ± 5.3	99 ± 18
Tripolyphosphate (108 mM)	None	18.5 ± 4.2	61 ± 11
	II (1 mg/mL)	21.9 ± 7.1	66 ± 9
	III (180 mM)	7.8 ± 3.2 [b]	<13 [b]
Phytate (53 mM)	None	21.8 ± 5.1	67 ± 8
	II (1 mg/mL)	22.5 ± 5.4	77 ± 12
	III (180 mM)	7.6 + 3.9 [b]	<13 [b]

[a] Microenemas contained 15 mg of cefoxitin/mL and had a dosage volume of 100 μL/100 g of rat body weight; $n \geq 3$. [b] $p < 0.001$ *versus* adjuvant without additive.

difference in their ability to permeate the rat rectal tissue. In the present study, we found that the coadjuvants tripolyphosphate and phytate substantially enhanced the absorption of cefoxitin only after their own permeation of the membrane was apparently enhanced by I. Thus, we speculate that adjuvant permeation of the mucosal membrane may be mechanistically necessary before enhanced compound absorption across the rectal membrane can occur.

In conclusion, the enhancing action of I on rectal cefoxitin absorption appears to depend on the affinity of I to the protein fraction in the mucosal membrane. The weak enhancing ability of the phosphate coadjuvants when administered with cefoxitin alone may involve chelating activity and possible damage to the rectal mucosa. However, the large increase in drug absorption after coadministration of I with either chelating agent, tripolyphosphate or phytate, is not just a consequence of the added effect of the enhancing action of I and chelation. These phosphate derivatives apparently have a strong adjuvant efficacy which can be realized only when their own permeation of the mucosal membrane is enhanced by adjuvants such as I.

REFERENCES

(1) K. C. Kwan, G. O. Breault, E. R. Umbenhauer, F. G. McMahon, and D. E. Duggan, *J. Pharmacokinet. Biopharm.*, **4**, 255 (1976).

(2) V. Wright and M. Roberts, *Clin. Med.*, **80**, 12 (1973).

(3) E. C. Huskisson, R. T. Taylor, L. Bureston, P. Chater, and E. D. Hart, *Ann. Rheum. Dis.*, **29**, 393 (1970).

(4) A. G. de Boer, D. D. Breimer, H. Mattie, J. Pronk, and J. M. Gubbens-Stibbe, *Clin. Pharmacol. Ther.*, **20**, 701 (1979).

(5) A. G. de Boer, J. M. Gubbens-Stibbe, and D. D. Breimer, *J. Pharm. Pharmacol.*, **33**, 50 (1981).

(6) T. Nishihata, N. Yata, and A. Kamada, *Chem. Pharm. Bull.*, **27**, 1740 (1979).

(7) T. Nishihata, J. H. Rytting, T. Higuchi, and L. Caldwell, *J. Pharm. Pharmacol.*, **33**, 334 (1981).

(8) T. Nishihata, J. H. Rytting, and T. Higuchi, *J. Pharm. Sci.*, **71**, 865 (1982).

(9) T. Nishihata, J. H. Rytting, and T. Higuchi, *J. Pharm. Sci.*, **71**, 869 (1982).

(10) A. Kamada, T. Nishihata, S. Kim, M. Yamamoto, and N. Yata, *Chem. Pharm. Bull.*, **29**, 2012 (1981).

(11) S. Kim, A. Kamada, T. Higuchi, and T. Nishihata, *J. Pharm. Pharmacol.*, **35**, 100 (1983).

(12) T. Nishihata, S. Kim, S. Morishita, A. Kamada, N. Yata, and T. Higuchi, *J. Pharm. Sci.*, **72**, 280 (1983).

(13) T. Nishihata, H. Takahagi, M. Yamamoto, H. Tomida, J. H. Rytting, and T. Higuchi, *J. Pharm. Sci.*, **73**, 109 (1984).

(14) Z. I. Cabantchik, P. A. Knauf, and A. Rothstein, *Biochim. Biophys. Acta*, **515**, 239 (1978).

(15) J. A. F. op den Kamp, in "Membrane Structure," J. B. Finean and R. H. Michell, Eds., Elsevier/North-Holland, Biomedical Press, Amsterdam, 1981, p. 86.

(16) T. Nishihata, J. H. Rytting, and T. Higuchi, *J. Pharm. Sci.*, **70**, 71 (1981).

(17) H. Kunze, G. Rehbock, and W. Vogt, *Naunyn-Schmiedeberg's Arch. Pharmacol.*, **273**, 331 (1972).

(18) J. A. Reynolds and H. Trayer, *J. Biol. Chem.*, **246**, 7337 (1971).

ACKNOWLEDGMENTS

This work was supported in part by a grant from INTER$_x$, Merck Sharp & Dohme Research Laboratories. The authors also acknowledge support provided by the Center for Biomedical Research, The University of Kansas. The authors thank M. Dillsaver for useful comments and technical assistance.

Physiological Model for Distribution of Sulfathiazole in Swine

JOHN DUDDY ‡§, THOMAS L. HAYDEN ‡, DAVID W. A. BOURNE *¶x, WILLIAM D. FISKE *, IRMA H. BENEDEK *, DOROTHY STANLEY ‡, ALBERTO GONZALEZ ‡, and WILLIAM HEIERMAN ‡

Received August 29, 1983, from the * *College of Pharmacy and the* ‡ *Department of Mathematics, University of Kentucky, Lexington, KY 40506.* Accepted for publication December 19, 1983. Present addresses: §Department of Mathematics, De Paul University, Chicago, IL 60614 and ¶ Department of Pharmacy, University of Queensland, St. Lucia, 4067, Australia.

Abstract □ A physiological flow model was developed for the distribution of sulfathiazole residues in various tissues in swine. The approach was compartmental, in which the compartments and equilibrium constants had physiological meaning. Differential equations were developed, and appropriate parameter values and initial conditions were substituted and solved by a fourth-order Runga-Kutta technique. Simulation values corresponded with the experimentally determined concentration values in plasma and kidney, liver, muscle, fat, and heart tissues.

Keyphrases □ Sulfathiazole—physiological flow model, distribution, swine □ Physiological flow model—sulfathiazole, swine, distribution □ Distribution—physiological model, sulfathiazole, swine

Allergic reaction and increasing bacterial resistance are possible side effects resulting from human consumption of meat derived from animals given antibiotics (1). Consequently, regulations have been promulgated by the Food and Drug Administration setting tolerance levels for antibiotics and other drugs in slaughtered animals (2). Mathematical models which predict the residual amounts of a given drug in various organs at various times after administration are therefore important

© 1984, American Pharmaceutical Association

Table III—Effect of 4,4′-Diisothiocyano-2,2′-disulfonate Stilbene (II) and Calcium Chloride (III) on the Enhancement of Plasma Cefoxitin Levels and on Cefoxitin Disappearance from the Rat Rectal *In Situ* Loop by α-Glycerophosphate (I), Sodium Tripolyphosphate, and Sodium Phytate [a]

Adjuvant Concentration	Additive Concentration	Percent Disappearance of Cefoxitin at 1.5 h	$[AUC]_{0-30}$, μM·min
None	None	5.4 ± 5.8	<13 [b]
I (205 mM)	None	38.7 ± 8.1	119 ± 28
	II (1 mg/mL)	16.8 ± 6.3 [b]	52 ± 11 [b]
	III (180 mM)	25.2 ± 5.3	99 ± 18
Tripolyphosphate (108 mM)	None	18.5 ± 4.2	61 ± 11
	II (1 mg/mL)	21.9 ± 7.1	66 ± 9
	III (180 mM)	7.8 ± 3.2 [b]	<13 [b]
Phytate (53 mM)	None	21.8 ± 5.1	67 ± 8
	II (1 mg/mL)	22.5 ± 5.4	77 ± 12
	III (180 mM)	7.6 + 3.9 [b]	<13 [b]

[a] Microenemas contained 15 mg of cefoxitin/mL and had a dosage volume of 100 μL/100 g of rat body weight; $n \geq 3$. [b] $p < 0.001$ *versus* adjuvant without additive.

difference in their ability to permeate the rat rectal tissue. In the present study, we found that the coadjuvants tripolyphosphate and phytate substantially enhanced the absorption of cefoxitin only after their own permeation of the membrane was apparently enhanced by I. Thus, we speculate that adjuvant permeation of the mucosal membrane may be mechanistically necessary before enhanced compound absorption across the rectal membrane can occur.

In conclusion, the enhancing action of I on rectal cefoxitin absorption appears to depend on the affinity of I to the protein fraction in the mucosal membrane. The weak enhancing ability of the phosphate coadjuvants when administered with cefoxitin alone may involve chelating activity and possible damage to the rectal mucosa. However, the large increase in drug absorption after coadministration of I with either chelating agent, tripolyphosphate or phytate, is not just a consequence of the added effect of the enhancing action of I and chelation. These phosphate derivatives apparently have a strong adjuvant efficacy which can be realized only when their own permeation of the mucosal membrane is enhanced by adjuvants such as I.

REFERENCES

(1) K. C. Kwan, G. O. Breault, E. R. Umbenhauer, F. G. McMahon, and D. E. Duggan, *J. Pharmacokinet. Biopharm.*, **4**, 255 (1976).

(2) V. Wright and M. Roberts, *Clin. Med.*, **80**, 12 (1973).

(3) E. C. Huskisson, R. T. Taylor, L. Bureston, P. Chater, and E. D. Hart, *Ann. Rheum. Dis.*, **29**, 393 (1970).

(4) A. G. de Boer, D. D. Breimer, H. Mattie, J. Pronk, and J. M. Gubbens-Stibbe, *Clin. Pharmacol. Ther.*, **20**, 701 (1979).

(5) A. G. de Boer, J. M. Gubbens-Stibbe, and D. D. Breimer, *J. Pharm. Pharmacol.*, **33**, 50 (1981).

(6) T. Nishihata, N. Yata, and A. Kamada, *Chem. Pharm. Bull.*, **27**, 1740 (1979).

(7) T. Nishihata, J. H. Rytting, T. Higuchi, and L. Caldwell, *J. Pharm. Pharmacol.*, **33**, 334 (1981).

(8) T. Nishihata, J. H. Rytting, and T. Higuchi, *J. Pharm. Sci.*, **71**, 865 (1982).

(9) T. Nishihata, J. H. Rytting, and T. Higuchi, *J. Pharm. Sci.*, **71**, 869 (1982).

(10) A. Kamada, T. Nishihata, S. Kim, M. Yamamoto, and N. Yata, *Chem. Pharm. Bull.*, **29**, 2012 (1981).

(11) S. Kim, A. Kamada, T. Higuchi, and T. Nishihata, *J. Pharm. Pharmacol.*, **35**, 100 (1983).

(12) T. Nishihata, S. Kim, S. Morishita, A. Kamada, N. Yata, and T. Higuchi, *J. Pharm. Sci.*, **72**, 280 (1983).

(13) T. Nishihata, H. Takahagi, M. Yamamoto, H. Tomida, J. H. Rytting, and T. Higuchi, *J. Pharm. Sci.*, **73**, 109 (1984).

(14) Z. I. Cabantchik, P. A. Knauf, and A. Rothstein, *Biochim. Biophys. Acta*, **515**, 239 (1978).

(15) J. A. F. op den Kamp, in "Membrane Structure," J. B. Finean and R. H. Michell, Eds., Elsevier/North-Holland, Biomedical Press, Amsterdam, 1981, p. 86.

(16) T. Nishihata, J. H. Rytting, and T. Higuchi, *J. Pharm. Sci.*, **70**, 71 (1981).

(17) H. Kunze, G. Rehbock, and W. Vogt, *Naunyn-Schmiedeberg's Arch. Pharmacol.*, **273**, 331 (1972).

(18) J. A. Reynolds and H. Trayer, *J. Biol. Chem.*, **246**, 7337 (1971).

ACKNOWLEDGMENTS

This work was supported in part by a grant from INTER$_x$, Merck Sharp & Dohme Research Laboratories. The authors also acknowledge support provided by the Center for Biomedical Research, The University of Kansas. The authors thank M. Dillsaver for useful comments and technical assistance.

Physiological Model for Distribution of Sulfathiazole in Swine

JOHN DUDDY ‡§, THOMAS L. HAYDEN ‡, DAVID W. A. BOURNE *¶x, WILLIAM D. FISKE *, IRMA H. BENEDEK *, DOROTHY STANLEY ‡, ALBERTO GONZALEZ ‡, and WILLIAM HEIERMAN ‡

Received August 29, 1983, from the * *College of Pharmacy and the* ‡ *Department of Mathematics, University of Kentucky, Lexington, KY 40506.* Accepted for publication December 19, 1983. Present addresses: §Department of Mathematics, De Paul University, Chicago, IL 60614 and ¶ Department of Pharmacy, University of Queensland, St. Lucia, 4067, Australia.

Abstract □ A physiological flow model was developed for the distribution of sulfathiazole residues in various tissues in swine. The approach was compartmental, in which the compartments and equilibrium constants had physiological meaning. Differential equations were developed, and appropriate parameter values and initial conditions were substituted and solved by a fourth-order Runga-Kutta technique. Simulation values corresponded with the experimentally determined concentration values in plasma and kidney, liver, muscle, fat, and heart tissues.

Keyphrases □ Sulfathiazole—physiological flow model, distribution, swine □ Physiological flow model—sulfathiazole, swine, distribution □ Distribution—physiological model, sulfathiazole, swine

Allergic reaction and increasing bacterial resistance are possible side effects resulting from human consumption of meat derived from animals given antibiotics (1). Consequently, regulations have been promulgated by the Food and Drug Administration setting tolerance levels for antibiotics and other drugs in slaughtered animals (2). Mathematical models which predict the residual amounts of a given drug in various organs at various times after administration are therefore important

© 1984, American Pharmaceutical Association

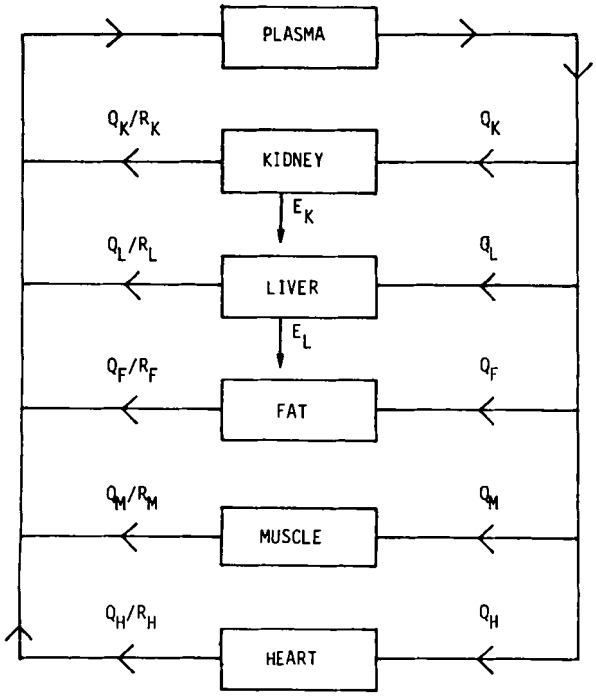

Scheme I—Body compartments in sulfathiazole distribution

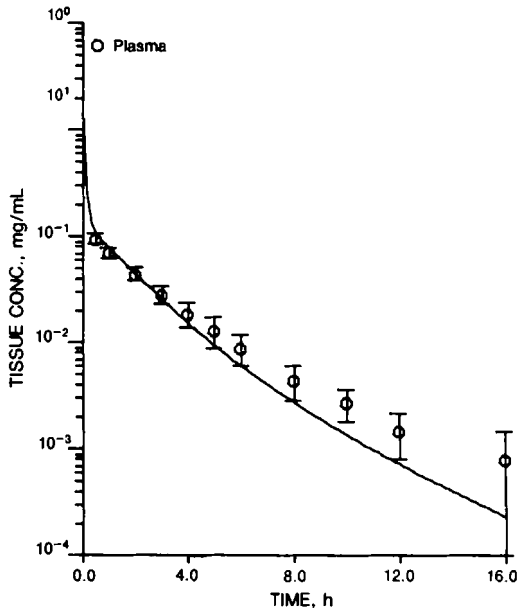

Figure 1—*Semilogarithmic plot of plasma concentration of sulfathiazole (O) versus time after intravenous administration to swine. The points were experimentally determined (SD as error bars), and the line was calculated according to Scheme I with the parameter values from Table I.*

in setting the minimum time until slaughter after administration of the drug. The model must be sensitive to a number of factors, including the characteristic properties of the drug, the species of the animals, and the weight of the animal.

In this report, a model developed for the distribution of sulfathiazole residues in a number of organs in swine is described. Previously, a two-compartment model was used to describe these data (3). This work has been extended by development of a physiologically based model. The additional information obtained and the accuracy of physiological models for drug tissue concentrations has been well recognized in human pharmacokinetic modeling, especially with chemotherapeutic agents. In general, data from a number of organs and knowledge of several physiological parameters are needed. This allows the more detailed physiological model to yield more information than the usual compartmental model, in which the parameters are not directly related to the physiology of the animal. The model developed in this report closely follows the basic ideas developed previously (4, 5) (the Bischoff-Dedrick model). This approach has been applied to pharmacokinetic models in humans for thiopental (5, 6), methotrexate (4, 7, 8), cytarabine (9), and salicylate (10).

Table I—Parameters for Sulfathiazole Distribution in Swine (34 kg)

Plasma Flow to Organs (Q), mL/min	
Q_m	280
Q_f	10
Q_l	460
Q_k	330
Q_h	97
Organ Volumes (V), mL	
V_m	18300
V_f	9610
V_l	790
V_k	165
V_h	200
V_p	1610
Tissue-to-Plasma Equilibrium Constant (R)	
R_m	0.4
R_f	0.2
R_l	1.0
R_k	3.0
R_h	0.55
Tissue Clearance (E), mL/min	
E_k	61.8
E_l	76.8

EXPERIMENTAL SECTION

Theoretical Basis—Like the Bischoff-Dedrick model, the approach described here is a compartmental approach in which the compartments and equilibrium constants have physiological meaning. Scheme I displays the pattern of blood flow through the animal. Since the drug is administered by rapid injection, it was assumed that at the initial time $t = 0$ h the total dose of the drug was homogeneously distributed throughout the plasma compartment.

Compartments corresponding to plasma, kidney, liver, muscle, fat, and heart have been included. Data were available for all of these tissues. In particular,

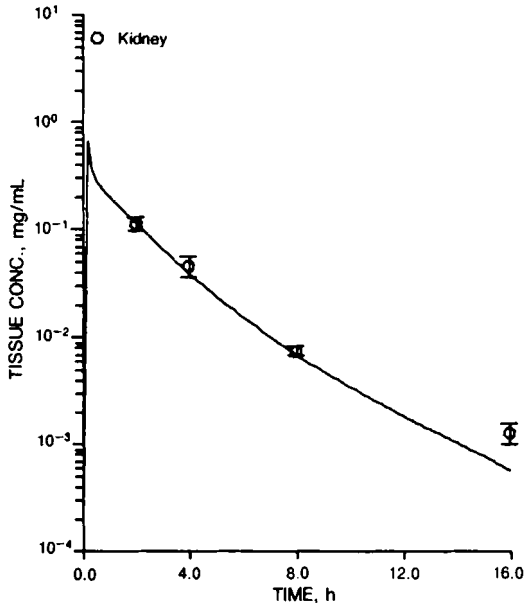

Figure 2—*Semilogarithmic plot of kidney concentration of sulfathiazole (O) versus time after intravenous administration to swine. The points were experimentally determined (SD as error bars), and the line was calculated according to Scheme I with the parameter values from Table I.*

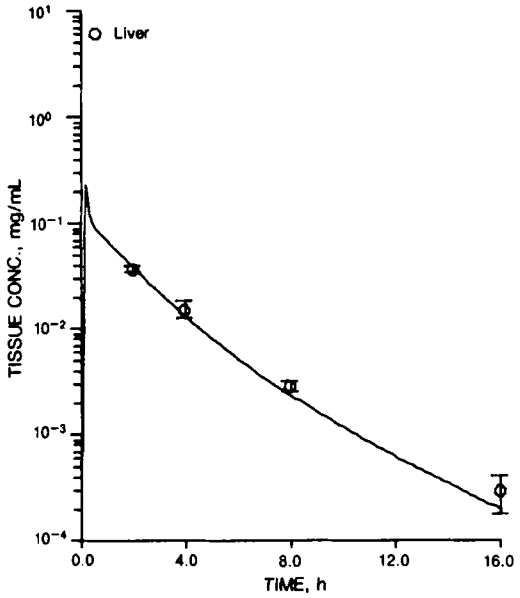

Figure 3—*Semilogarithmic plot of liver concentration of sulfathiazole (O) versus time after intravenous administration to swine. The points were experimentally determined (SD as error bars), and the line was calculated according to Scheme I with the parameter values from Table I.*

small amounts of drug were located in the heart, but it was included in the model as additional verification of the accuracy of the simulation.

From Scheme I a system of ordinary differential equations was derived by using the mass balance approach developed for physiological models (4, 5):

$$Vp \cdot \frac{dC_p}{dt} = \frac{Q_k}{R_k} \cdot C_k + \frac{Q_l}{R_l} \cdot C_l + \frac{Q_f}{R_f} \cdot C_f + \frac{Q_m}{R_m} \cdot C_m + \frac{Q_h}{R_h} \cdot C_h - (Q_k + Q_l + Q_f + Q_m + Q_h) \cdot C_p \quad \text{(Eq. 1)}$$

$$V_k \cdot \frac{dC_k}{dt} = Q_k \cdot C_p - \frac{Q_k}{R_k} \cdot C_k - \frac{E_k}{R_k} \cdot C_k \quad \text{(Eq. 2)}$$

$$V_l \cdot \frac{dC_l}{dt} = Q_l \cdot C_p - \frac{Q_l}{R_l} \cdot C_l - \frac{E_l}{R_l} \cdot C_l \quad \text{(Eq. 3)}$$

$$V_f \cdot \frac{dC_f}{dt} = Q_f \cdot C_p - \frac{Q_f}{R_f} \cdot C_f \quad \text{(Eq. 4)}$$

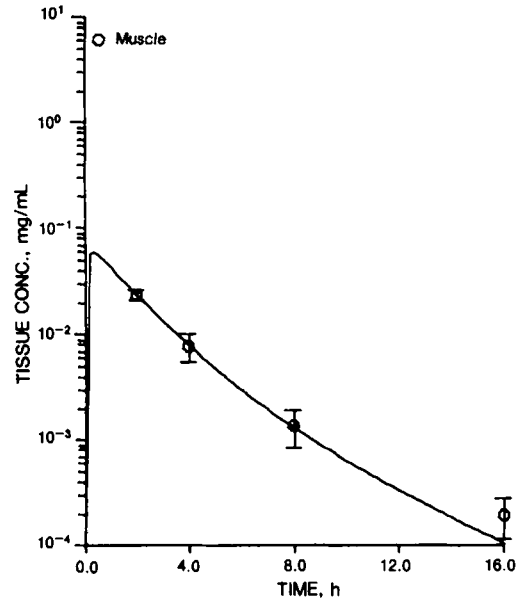

Figure 4—*Semilogarithmic plot of muscle concentration of sulfathiazole (O) versus time after intravenous administration to swine. The points were experimentally determined (SD as error bars), and the line was calculated according to Scheme I with the parameter values from Table I.*

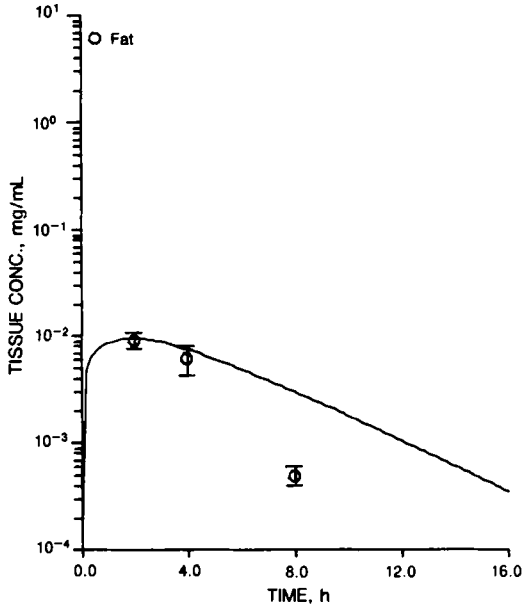

Figure 5—*Semilogarithmic plot of fat concentration of sulfathiazole (O) versus time after intravenous administration to swine. The points were experimentally determined (SD as error bars), and the line was calculated according to Scheme I with the parameter values from Table I.*

$$V_m \cdot \frac{dC_m}{dt} = Q_m \cdot C_p - \frac{Q_m}{R_m} \cdot C_m \quad \text{(Eq. 5)}$$

$$V_h \cdot \frac{dC_h}{dt} = Q_h \cdot C_p - \frac{Q_h}{R_h} \cdot C_h \quad \text{(Eq. 6)}$$

where V is volume, C is concentration, t is time, Q is plasma flow rate, R is the tissue to plasma equilibrium constant, E is the plasma clearance of the organ, and the subscripts represent the various organs: p for plasma, k for kidney, l for liver, f for fat, m for muscle, and h for heart. Hence, Q_m represents the plasma flow rate to the muscle.

The dose of the drug (D) was administered by rapid injection. By assuming it is instantly distributed through the plasma, the following initial conditions apply:

$$C_p(0) = D/V_p \quad \text{(Eq. 7)}$$

$$C_k(0) = C_l(0) = C_f(0) = C_m(0) = C_h(0) = 0 \quad \text{(Eq. 8)}$$

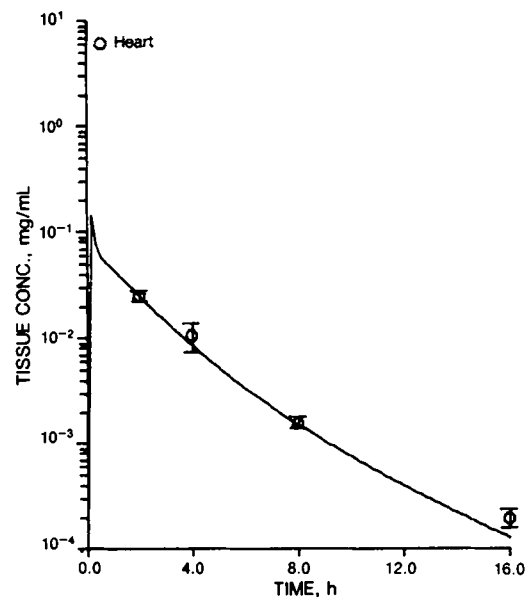

Figure 6—*Semilogarithmic plot of heart concentration of sulfathiazole (O) versus time after intravenous administration to swine. The points were experimentally determined (SD as error bars), and the line was calculated according to Scheme I with the parameter values from Table I.*

On substitution of appropriate parameter values and the initial conditions of Eqs. 7 and 8, Eqs. 1–6 were solved numerically by the fourth-order Runga-Kutta technique.

Parameters—Table I gives the parameters used in the simulation. The volumes for the blood, liver, kidney, and heart were obtained by first computing the organ weight by the method of Adolf (11) and then assuming a tissue density of 1 g/mL. Muscle and fat volumes were calculated from the percentages of body weight found in swine (12) and converted to the corresponding weight in the swine used. The average weight of the experimental swine was 34 kg. The plasma volume was computed as 60% of the whole blood volume. Bischoff *et al.* (13) have indicated that the method of Adolf of calculating blood volume produced a value lower than that reported in humans. Bischoff *et al.* have corrected for this difference by adjusting the Adolf values upward by a factor of 1.43. This adjustment was also made in this study.

Plasma flow rates for kidney, liver, and muscle were obtained from the relationship between plasma flow and body weight reported by Bischoff *et al.* (13). As fat is poorly perfused, it was assumed to have a very low flow rate. The actual value used was determined by perturbation. The heart plasma flow rate (adjusted for weight) was assumed to be the same as that for humans (14).

The total body clearance and renal clearance values were calculated from the data of Bourne *et al.* (3) as $k_{el} \cdot Vd$ and $k_e \cdot Vd$ respectively, where k_{el} is the elimination rate constant, k_e is the excretion into urine rate constant, and Vd is the apparent volume of distribution for a one-compartment pharmacokinetic model. The hepatic clearance term was calculated as the difference between the total body clearance and renal clearance values and represents the formation of an acetyl metabolite and sulfathiazole not recovered in urine.

The initial values for the equilibrium constants (R) were obtained from human autopsy (15) and were perturbed to obtain the simulation values. The dose of sodium sulfathiazole given to each animal was 72 mg/kg of body weight. In the simulation, the dose used was 2290.5 mg/kg of body weight, which was the average amount of sulfathiazole administered.

Experimental Data—The experimental data from Bourne *et al.* (3) were obtained by averaging the concentration of drug in the tissue of the three swine sacrificed at each time point. Sulfathiazole was extracted from tissues, as described by Bevill *et al.* (16), and quantitated by a modified Bratton-Marshall colorimetric method (17). The plasma concentrations (Fig. 1) were calculated as the average of the values obtained from the remaining swine at each time point. Plasma concentrations of sulfathiazole were measured by the modified Bratton-Marshall method of Annino (18).

RESULTS

The experimental data and the simulation for the plasma, kidney, liver, muscle, fat, and heart are shown in Figs. 1–6. The simulation parameters were chosen so that the graphs closely followed the trends indicated by the data. The values of those parameters which were obtained by experimentation or from the literature were not adjusted. The simulation results show a good correlation with the experimental data in all tissues except, possibly, fat. Data were collected from the muscle of the shoulder, loin, and leg. In Fig. 4, the experimental data are the average of these three concentrations in muscle tissue. The results obtained for fat tissue are shown in Fig. 5 (the simulation corresponds with the first two points, whereas the third point may indicate a factor not accountable by the model). The fat tissue included in the simulation is probably more diffuse than the samples taken for the experimental values.

DISCUSSION

A general physiological model has been presented for sulfathiazole in swine. The physiological meaning of each compartment allows the prediction of drug concentrations in those organs. The ability of the model to predict residue levels with reasonable accuracy in many different compartments suggests that the physiological approach is valuable. With this more complete model it should be possible to extrapolate or interpolate tissue concentrations of sulfathiazole in the various important food-providing tissues down to the regulated tolerance levels with more confidence than is possible with the linear compartmental approach. Given suitable estimates of the required parameters, drugs which are likely to give significant residue problems may be identified. Greater reliance on the model can be achieved with parameters specific for the species rather than parameters determined by extrapolation from other species.

REFERENCES

(1) D. W. A. Bourne, *U.S. Pharmacist.* **6,** 58 (1981).

(2) J. R. Markus, *J. Assoc. Off. Anal. Chem.*, **61,** 1285 (1978).

(3) D. W. A. Bourne, L. W. Dittert, G. D. Koritz, and R. F. Bevill, *J. Pharmacokinet. Biopharm.*, **6,** 123 (1978).

(4) R. J. Lutz, R. L. Dedrick, J. A. Straw, M. N. Hart, P. Klubes, and D. S. Zaharko, *J. Pharmacokinet. Biopharm.*, **3,** 77 (1975).

(5) C. N. Chen and J. D. Andrade, *J. Pharm. Sci.*, **65,** 717 (1976).

(6) K. B. Bischoff and R. L. Dedrick, *J. Pharm. Sci.*, **57,** 1346 (1968).

(7) D. S. Zaharko, R. L. Dedrick, K. B. Bischoff, J. A. Longstreth, and V. T. Olivirio, *J. Natl. Cancer Inst.*, **46,** 775 (1971).

(8) R. L. Dedrick, S. C. Zaharko, and R. J. Lutz, *J. Pharm. Sci.*, **62,** 882 (1973).

(9) R. L. Dedrick, D. D. Forrester, J. N. Cannon, S. M. El Dareer, and L. B. Mellet, *Biochem. Pharmacol.*, **22,** 2405 (1973).

(10) C. N. Chen, D. L. Coleman, J. D. Andrade, and A. R. Temple, *J. Pharm. Sci.*, **67,** 38 (1978).

(11) E. F. Adolf, *Science*, **109,** 579 (1949).

(12) "Meat Animals," D. Lister, D. N. Rhodes, V. R. Fowler, and M. F. Fuller, Eds., Plenum, New York, N.Y., 1976, pp. 96 and 122.

(13) K. B. Bischoff, R. L. Dedrick, D. S. Zaharko, and J. A. Longstreth, *J. Pharm. Sci.*, **60,** 1128 (1971).

(14) A. C. Guyton, "Textbook of Medical Physiology," 5th ed., W. B. Saunders, Philadelphia, Pa., 1976, p. 320.

(15) F. Hawking and J. S. Lawrence, "The Sulphonamides," H. K. Lewis and Co. Ltd., 1950, pp. 81 and 84.

(16) R. F. Bevill, R. M. Sharma, S. H. Meechum, S. C. Wozniak, D. W. A. Bourne, and L. W. Dittert, *Am. J. Vet. Res.*, **38,** 973 (1977).

(17) F. Tishler, J. L. Sutter, J. N. Bathish, and H. E. Hagman, *J. Agric. Food Chem.*, **16,** 50 (1968).

(18) J. S. Annino, "Sulfonamides, Standard Methods of Clinical Chemistry," Vol. 3, Academic, New York, N.Y., 1961.

Neutron Activation of Iron Tablets to Evaluate the Effects of Glycine on Iron Absorption

JOHN M. CHRISTENSEN ˣ, MUSA GHANNAM, and JAMES W. AYRES

Received May 2, 1983, from the *School of Pharmacy, Oregon State University, Corvallis, OR 97331.* Accepted for publication December 19, 1983.

Abstract □ Neutron bombardment (neutron flux, 3×10^{12} neutrons/cm^2/s) of prepared iron tablets containing glycine-iron or iron alone was performed to prepare radioactive tablets to assess the effects of glycine on iron absorption from tableted formulations. No interfering isotopes of sufficient quantity were generated during neutron activation of the iron tablets. Cobalt-60 was the major trace mineral detected and accounted for only 1.3% of the total activity. There may have been trace amounts of zinc-65 or chromium-51 present, but they were not detectable above background radioactivity in the final tablet produced. Iron-59 represented >98% of the radioactivity present in the tablets used in the study. Glycine-containing iron tablets produced dramatically higher amounts of iron in blood and tissues of rabbits ($p < 0.05$) than did the same tablet formulations without glycine. The area under the iron blood concentration time curve over 4 h increased by 67% with glycine added to the formulation over control iron tablets. Iron concentrations in tissues 4 h after iron administration was in the order of blood > liver > heart > kidney > muscle.

Keyphrases □ Absorption—iron, effects of glycine, neutron activation of iron tablets □ Neutron activation—iron tablets, effects of glycine on iron absorption □ Formulations—tablets, neutron activation to evaluate the effects of glycine on iron absorption

Several investigators have noted that amino acids may increase iron absorption from the GI tract (1–7). It was proposed that amino acids facilitate increased iron absorption by (*a*) buffering the intestine and delaying the rise in pH toward neutralization at sites where iron is oxidized to insoluble salt forms, (*b*) forming iron-amine chelates that act to enhance iron absorption, and (*c*) stimulating iron transport systems within the animal (6).

In previous studies, it has been shown that glycine enhances iron absorption (6, 7). Also, it has been shown that administration of diets containing glycine compared with diets lacking glycine result in a greater amount of iron absorbed (8). It was the purpose of this study to determine whether glycine added to iron (at a ratio of 2:1, respectively) in a tablet dosage form could increase iron absorption.

To prepare radioactive iron tablets, neutron activation was tested to determine whether this technique offers a viable method of preparing intact tableted dosage forms that can conveniently be made radioactive after formulation. By preparing tableted dosage forms first and then making them radioactive by neutron activation, there is less of a potential for contamination of facilities and there are unique opportunities to use radiolabeled compounds to test some qualities of solid dosage forms.

Table I—Radionuclides Expected To Be Activated in Tablets from Neutron Flux [a]

Element Produced During Neutron Activation	Element Half-Life
^{24}Na	15 h
^{42}K	12.4 h
^{27}Mg	9.5 min
^{56}Mn	2.6 h
^{60}Co	5.26 years
^{51}Cr	27.8 d
^{38}Cl	37.3 min
^{65}Zn	243.6 d
^{59}Fe	45.1 d

[a] Neutron flux, 3×10^{12} neutrons/cm^2/s.

EXPERIMENTAL SECTION

Production of Tablets—Direct compression was used to produce tablets[1]. Two types of tablets were prepared. The first type contained glycine and ferrous chloride. The control tablets did not contain glycine.

Type 1 Tablet—The average weight of each tablet was 0.42 g. The formula for one tablet of type 1 is (in milligrams/percent): granulated sucrose[2] (296.6/71.4), magnesium stearate (29.7/7.1), glycine (39.5/9.5), and ferrous chloride (49.4/11.9).

Type 2 Tablet—The average weight of each tablet was 0.41 g. The formula for one tablet of type 2 is (in milligrams/percent): granulated sucrose[2] (328.1/81), magnesium stearate (28.9/7.1), and ferrous chloride (48.2/11.9).

Disintegration tests were done for both tablet types by using a USP tablet and disintegration tester[3] (9).

Neutron Activation of Tablets—Tablets were put into small scintillation bags[4]. Each bag was sealed by heating and placed in a polyvial[5]. The polyvials were then sealed by heating. Tablet samples were then put in the Oregon State University (OSU) Triga reactor in the Lazy Susan and activated with a neutron flux of 3×10^{12} neutrons/cm^2/s generated by 1 MW of power from the reactor. The irradiation time was 4 h. The tablets were allowed to stand for 1 week after irradiation to allow short-half-life radionuclides to decay.

Neutron Activation Equation—For neutron activation analysis, the following was used:

$$A = N\phi\sigma(1 - e^{-\lambda T})e^{-\lambda t} \qquad \text{(Eq. 1)}$$

where A is the activity at end of irradiation (disintegrations/s), N is the number of atoms, ϕ is the flux (neutrons/cm^2 s), σ is the cross-section (cm^2), λ is the decay constant (s^{-1}), T is the length of irradiation (s), and t is the time elapsed between activation and measurement.

The activity at the time of measurement of radiation depends on the half-life of the isotope of interest and the time that has elapsed between activation and measurements (10, 11). Activation analysis is subject to a variety of errors. These include errors due to flux gradients, self-shielding, and interfering nuclear reactions (10).

The errors due to neutron flux gradients within the reactor can be minimized by rotating or spinning the sample during irradiation (12). The OSU Triga reactor is a circulator reactor, and the samples were rotated around the reactor core during irradiation in the Lazy Susan. For other reactors, the use of an internal standard to determine the flux and to ensure that future samples have the exact orientation and position of irradiation as those of previous samples reduces the necessity to vary flux gradients (12, 13).

The effects of self-shielding can be shown to be a function of the sample mass and length (12). More self-shielding occurs when each of the parameters is larger. With samples of <4 g in mass, very little self-shielding occurs (12, 13). Also, self-shielding is reduced when the sample is homogeneously spread in an inert material (*e.g.*, sucrose) (12). Tablets produced for this study were small (0.41–0.42 g), and the major ingredient in 71–81% of the tablets is granulated sucrose. Both of these factors minimize self-shielding.

Interference in counting iron-59 may occur from cobalt-60 and zinc-65 when counting with a sodium iodide detector in a solid scintillation counting chamber[6]. The 1.099- and 1.292-MeV gamma rays of iron-59 with the 1.173-

[1] Single-punch tablet machine, model TPK-12; Chemical and Pharmaceutical Co., Inc.

[2] Dipac, prepared by co-crystallization of 97% sucrose and 3% dextrin; Armerstone.

[3] New England Nuclear Corp.

[4] Olympic Plastic Co., Los Angeles, Calif.

[5] Tracer Northern TN-1705 MCA 40 cc NAI (T1) detector.

[6] Model No. Gc19ED detector, with Ortec 572 spectroscopy amplifier, Nuclear-Data 600 multichannel analyzer; Princeton Gamma Tech., Princeton, N.J.

0022-3549/84/1100-1529$01.00/0
© 1984, American Pharmaceutical Association

Table II—Sources of Radioactivity in Tablets Used in Animal Study 1 Week after Activation

Sample	^{60}Co, ppm ± 16	^{51}Cr, ppm ± 16	^{65}Zn Upper Limit, %[a]	^{59}Fe, cpm	^{60}Co, cpm
Tablet	0.72 ± 0.04	ND[b]	>0.013	30,176	392
$FeCl_3$	6.8 ± 0.1	11.0 ± 3.0	ND	287,750[c]	3700[c]
Glycine	ND	1.1 ± 0.2	ND	ND	ND
Magnesium stearate	ND	ND	ND	ND	ND
Granulated sucrose[2]	ND	ND	ND	ND	ND

[a] Value represents the upper limit plus 3 standard deviations of the percentage of zinc activity that may be contained in the tablet that was being hidden by background counts. [b] Not detectable. [c] Ratio of count of ^{60}Co-^{59}Fe was equivalent to that of the tablet.

and 1.332-MeV gamma rays of cobalt-60 and the 1.115-MeV gamma rays of zinc-65 would appear as a single peak in a sodium iodide detector. Other radionuclides that produce gamma rays in this range, *i.e.*, nickel, aluminum, copper, manganese, *etc.*, are either not generated to a sufficient extent on bombardment by slow thermal neutrons due to their low cross sections or have half-lives too short to be active at the end of 1 week of storage.

To ensure that the tablets contained only trace amounts of cobalt-60 after activation, all components of the tablet, the powders used for tablet formulations, and the tablets were activated and counted for 100 min in a germanium-lithium [Ge(Li)] detector[7] with a multichannel analyzer. This detector was calibrated at 1 KeV per channel, with the screen having 2048 channels. The samples were analyzed for radioactivity having gamma energys in the range of 80 keV-2.04 MeV, to make certain that the samples to be collected later in the animal study could be reliably counted by the NaI detector as iron-59 counts.

Procedure with Rabbits—The iron-glycine activated tablets, as well as the control activated tablets, were each tested on groups of four rabbits. The tablets were administered to each rabbit before 2 weeks had elapsed from the neutron activation of the tablets. Female rabbits were used (weight, 2.0–3.0 kg each). The ears of each rabbit were shaved with an electric shaver and commercial ointment[8]. The rabbit was then put in a rabbit restrainer with its head out and given orally four tablets with a total activity of 1.1 μCi.

At time periods of 5, 10, 15, 20, 30, 45, 60, 90, 120, 150, 180, 210, and 240 min after tablet administration, 100-μL blood samples were collected from the ears with capillary tubes. Bleeding was initiated by pricking the vein of the ears with a 20-gauge needle. Procaine was used as a local anesthetic. Blood samples were placed into counting vials. The 1.099- and 1.292-MeV gamma rays of 44.6-d iron-59 of each sample were counted for 4000 s in a solid scintillation counter chamber.

At the end of 4 h, the animals were sacrificed by ether administration, and liver, kidney, muscle, and heart samples were taken from the animals, weighed, and then counted as reported previously (7).

RESULTS AND DISCUSSION

When samples are exposed to neutron activation, all elements with atomic numbers greater than 10 are activated. The abundance of the different isotopes of the elements that are to be generated depends on the neutron flux to which they are exposed and whether the isotope of the element has a high or low cross section to the neutron flux to which it is exposed. For example, iron that is subjected to a neutron flux of 3×10^{12} neutrons/cm^2/s produces only iron-59. The other isotopes of iron are not produced to any detectable level because of their low cross sections when exposed to the neutron flux employed.

After the tablets and powders were activated by the OSU Triga reactor in the Lazy Susan, there was too much radioactivity emanating from them to be easily quantitated. The tablets and powders were thus sealed in a lead storage area and kept for 1 week. In Table I is a list of elements that were expected to be generated and suspected to be the cause of the initially high radioactive emissions of the tablets and powders. All elements except iron-59, cobalt-60, zinc-65, and chromium-51 have very short half-lives and would become nonradioactive after 1 week of storage. The tablets and powders were counted in the Ge(Li) detector after 1 week of storage (Table II). Iron-59 accounted for >98% of the radioactivity counted. Cobalt-60 accounted for ~1.3% of the radioactivity present. Only a trace amount of zinc-65 was observed, and no detectable levels of chromium-51 were present in the tablets to be used in the animal study. The ratio of counts of cobalt-60 in the tablet was obtained as:

$$\text{Ratio} = \frac{^{60}\text{Co}_{(\text{cpm})} \times 100}{^{59}\text{Fe}_{(\text{cpm})} + {}^{60}\text{Co}_{(\text{cpm})}} \qquad \text{(Eq. 2)}$$

The majority of the radioactivity contained in the tablets (>98%) originated from one isotope, iron-59. For this reason, the NaI detector could be used to count the samples obtained from the animal study.

The tablets prepared by neutron activation for use in this study were administered to the rabbits before 2 weeks had elapsed from initial activation. Allowing the tablets to stand for longer periods would have caused the cobalt-60/iron-59 ratio to change in the tablets. After 2 months, the cobalt-60 would contribute to >3% of the tablet radioactivity instead of the 1.3% of tablet radioactivity that was measured. The percentage of radioactivity in the tablets due to cobalt-60 would increase the longer the tablets were stored, since iron-59 has a half-life much shorter than that of cobalt-60.

Ferrous chloride was used rather than the more commonly prescribed ferrous sulfate because the tablets were to be activated, and the less radioactive the tablets, the more convenient they are for handling. Sulfur-35, with a half-life of 88 d, is produced when ferrous sulfate is activated. Chlorine-38, with a half-life of 37.3 min, is produced when ferrous chloride is activated (14). Since, chlorine-38 decayed very quickly after the end of bombardment, it was more convenient to use to count the 45-d iron-59.

After the tablets were prepared and before neutron activation, disintegration tests were conducted by using a tablet disintegration apparatus[3]. Tablet hardness averaged 15 kg/in^2 when tested with a tablet hardness tester[9]. Eighteen tablets of each type were tested. Seventeen glycine-iron tablets disintegrated within 18 min, whereas the 18th tablet disintegrated in 23 min. On the other hand, 16 control tablets disintegrated within 15 min, whereas the two others disintegrated within 19 min. Thus, any difference in iron absorption should not be due to differences in tablet disintegration after administration. Dissolution studies, which often correlate more closely with bioavailability, were not conducted.

In Figs. 1 and 2 are shown, respectively, the iron concentration in blood and different tissues following oral administration of glycine-iron and iron control neutron-activated tablets to rabbits. It is evident from these experiments that iron appears more quickly and in greater amounts in blood when the tablets contained glycine. The area under the iron concentration curve for the time during which data were collected increased by 67% when the tablets contained glycine (Fig. 1). From an assessment of the total amount of iron absorbed, the iron-glycine tablets showed a statistically significant increase in the amount of iron absorbed during the first 4 h postdose ($p \leq 0.05$) based on the

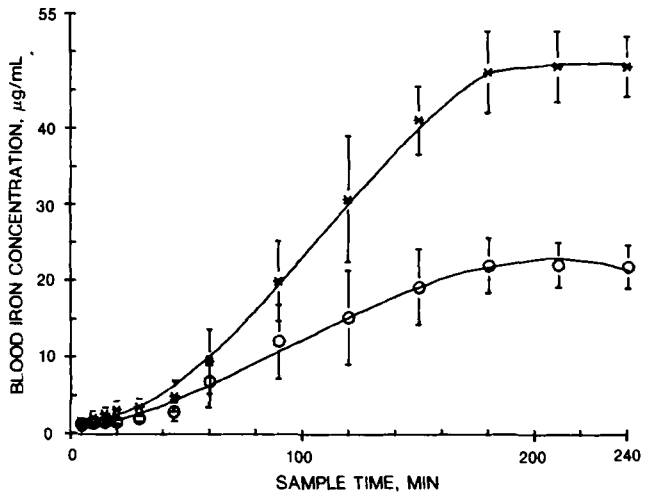

Figure 1—*Blood iron concentration (±SD) versus time curve in rabbits following oral administration of four tablets containing 192.92 mg of ferrous chloride (○) and four tablets containing 197.64 mg of ferrous chloride and 158.12 mg of glycine (*).*

[7] Nair.
[8] Vanderkamp; Van-Kel Industries, Edison, N.J.
[9] Strong Cobb Corp. Inc., Cleveland, Ohio.

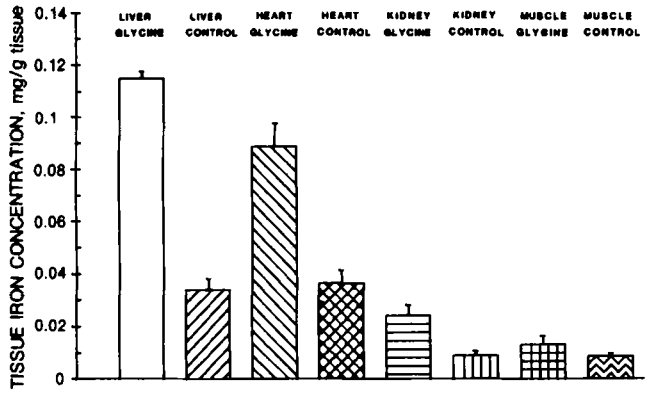

Figure 2—*Iron concentration (±SD) in body tissues 4 h after oral administration of four tablets containing 192.92 mg of ferrous chloride (control) and four tablets containing 197.12 mg of ferrous chloride and 158.12 mg of glycine.*

assumption that the area under the iron concentration–time curve (0–4 h) is an indicator of absorption.

The amount of iron in the different tissues was also consistent with iron levels in the blood. Iron concentration was highest in the tissues of the rabbits that received the glycine–iron tablets (Fig. 2). Iron–glycine tablets generated iron concentrations in tissue that were statistically significantly different from those of control iron tablets ($p < 0.001$ for the tissues of the liver, heart, and kidney; $p < 0.05$ for muscle).

All data were consistent with those from a previous report (7) from our laboratory indicating that glycine increases iron absorption into both blood and tissues. Neutron activation analysis is known to be very useful in analytical problems in which high sensitivity is required (sensitivity can reach 10^{-9} g). It is safe, economical, fast, practical in elemental analysis, and nondestructive (15). Also, thermal neutrons do not activate isotopes with atomic numbers of less than 10; therefore, carbon, hydrogen, oxygen, and nitrogen are not activated.

The data show that neutron activation analysis of final tableted dosage forms of iron can be utilized to investigate the effects of variable formulation factors on the absorption of iron. Further work is needed in the area utilizing multiple dosing, mixed protein hydrolysate, and pure defined amino acid mixtures to optimize tablet formulations for iron absorption. The technique of neutron-activation analysis can be employed for other minerals such as zinc or magnesium and may be used for comparing the rate and extent of absorption of minerals from commercially available vitamin-mineral mixtures (tablets or capsules). This application is currently under investigation in our laboratories.

REFERENCES

(1) D. Kroe, T. D. Kinney, N. Kaufman, and J. V. Klavins, *Blood*, **21**, 546 (1963).

(2) D. Kroe, T. D. Kinney, N. Kaufman, and J. V. Klavins, *Am. J. Physiol.*, **211**, 414 (1966).

(3) D. Van Campen and E. Gross, *J. Nutr.*, **99**, 69 (1969).

(4) D. Van Campen, *J. Nutr.*, **102**, 165 (1972).

(5) D. Van Campen, *J. Nutr.*, **103**, 139 (1973).

(6) W. Forth and W. Rummel, in "International Encyclopedia of Pharmacology and Therapeutics," Vol. II, Pergamon, Great Britain, 1975, pp. 599–746.

(7) J. M. Christensen, M. Ghannam, and J. W. Ayres, *J. Pharm. Sci.* **73**, 1245 (1984).

(8) A. D. A. Moski and F. H. Kratner, *J. Nutr.*, **107**, 24 (1977).

(9) R. E. King, "Remington's Pharmaceutical Sciences," 16th ed., A. Osol, Ed., Mack Publishing Co., Easton, Pa., 1980, p. 1559, chap. 89.

(10) D. DeSoete, R. Gijbels, and J. Hoste, "Neutron Activation Analysis," Wiley-Interscience, New York, N.Y., 1972, p. 50.

(11) C. H. Wang, D. L. Wills, and W. D. Loveland, "Radiotracer Methodology in the Biological, Environmental and Physical Sciences," Oregon State University Press, Corvallis, Ore. 1975, p. 248.

(12) D. Gibbons, "Activation Analysis, Principles and Applications." J. M. A. Lenihan and S. J. Thomson, Eds., Academic, New York, N.Y., 1965, pp. 86 and 87.

(13) S. S. Nargolwalla and E. P. Przybylowicz, "Activation Analysis With Neutron Generators," Wiley, New York, N.Y., 1973, pp. 243–252.

(14) F. E. McKinney, "Isotope Users Guide," Oakridge National Laboratories, Oakridge, Tenn. 1969, p. 69.

(15) K. Bernstein, *Anal. Lab.*, **12**, 151 (1980).

ACKNOWLEDGMENTS

This work was performed as partial fulfillment of an M.S. degree in Pharmacy at Oregon State University, School of Pharmacy. This work was supported in part by a Sigma Xi Scholarship to M.G.

The authors thank Dr. Roman A. Schmitt, Michael R. Conrady, and Terrance V. Anderson, of the Oregon State University Radiation Research Center, for their consultation and technical assistance during the study.

The organization and analysis of the data base associated with this investigation were carried out in part with the PROPHET system, a unique national resource sponsored by the National Institutes of Health. Information about PROPHET, including how to apply for access can be obtained from the Director, Chemical/Biological Information-Handling Program, Division of Research Resources, NIH, Bethesda, MD 20205.

Potential Inhibitors of Tyrosine Hydroxylase and Dopamine-β-Hydroxylase

K. R. SCOTT ˣ, CALVIN J. ALT, MURRAY KEMP, ELISE HAYES, and VASANT G. TELANG

Received June 28, 1983, from *Howard University, College of Pharmacy and Pharmacal Sciences, Department of Medicinal Chemistry, Washington, DC 20059.* Accepted for publication September 26, 1983.

Abstract □ A series of methyl-substituted 1,2,3,4-tetrahydrocarbazoles was synthesized and screened for *in vitro* activity against tyrosine hydroxylase and dopamine-β-hydroxylase. The most potent compounds were evaluated for inhibition of norepinephrine biosynthesis in rats. The results indicated no significant decrease in norepinephrine levels at three dosage levels.

Keyphrases □ Tyrosine hydroxylase—*in vitro* activity, effect of methyl-substituted 1,2,3,4-tetrahydrocarbazoles □ Dopamine-β-hydroxylase—*in vitro* activity, effect of methyl-substituted 1,2,3,4-tetrahydrocarbazoles □ Methyl-substituted 1,2,3,4-tetrahydrocarbazoles—effect on tyrosine hydroxylase and dopamine-β-hydroxylase, *in vitro*

It has been shown that the 1,2,3,4-tetrahydrocarbazole nucleus is an active pharmacophore. Previous studies have shown that the various carbazoles exhibit anti-inflammatory (1–6), antidepressant (7–12), hypoglycemic (13), analgetic (14), cardiotonic (15), anti-infective (16), and anticancer activities (17). It was of interest to extend the initial work of

0022-3549/84/1100-1531$01.00/0
© 1984, American Pharmaceutical Association

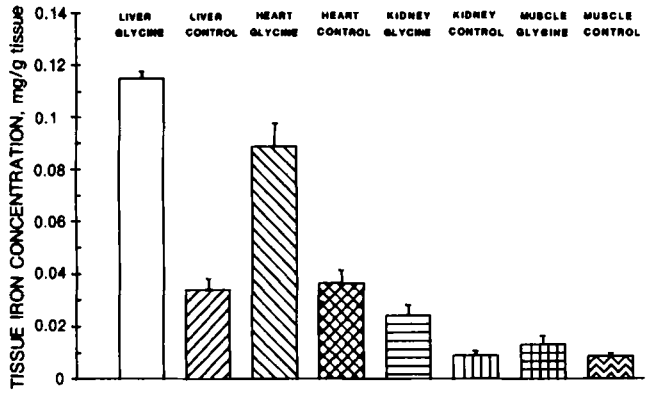

Figure 2—*Iron concentration (±SD) in body tissues 4 h after oral administration of four tablets containing 192.92 mg of ferrous chloride (control) and four tablets containing 197.12 mg of ferrous chloride and 158.12 mg of glycine.*

assumption that the area under the iron concentration–time curve (0–4 h) is an indicator of absorption.

The amount of iron in the different tissues was also consistent with iron levels in the blood. Iron concentration was highest in the tissues of the rabbits that received the glycine–iron tablets (Fig. 2). Iron–glycine tablets generated iron concentrations in tissue that were statistically significantly different from those of control iron tablets ($p < 0.001$ for the tissues of the liver, heart, and kidney; $p < 0.05$ for muscle).

All data were consistent with those from a previous report (7) from our laboratory indicating that glycine increases iron absorption into both blood and tissues. Neutron activation analysis is known to be very useful in analytical problems in which high sensitivity is required (sensitivity can reach 10^{-9} g). It is safe, economical, fast, practical in elemental analysis, and nondestructive (15). Also, thermal neutrons do not activate isotopes with atomic numbers of less than 10; therefore, carbon, hydrogen, oxygen, and nitrogen are not activated.

The data show that neutron activation analysis of final tableted dosage forms of iron can be utilized to investigate the effects of variable formulation factors on the absorption of iron. Further work is needed in the area utilizing multiple dosing, mixed protein hydrolysate, and pure defined amino acid mixtures to optimize tablet formulations for iron absorption. The technique of neutron-activation analysis can be employed for other minerals such as zinc or magnesium and may be used for comparing the rate and extent of absorption of minerals from commercially available vitamin-mineral mixtures (tablets or capsules). This application is currently under investigation in our laboratories.

REFERENCES

(1) D. Kroe, T. D. Kinney, N. Kaufman, and J. V. Klavins, *Blood*, **21**, 546 (1963).

(2) D. Kroe, T. D. Kinney, N. Kaufman, and J. V. Klavins, *Am. J. Physiol.*, **211**, 414 (1966).

(3) D. Van Campen and E. Gross, *J. Nutr.*, **99**, 69 (1969).

(4) D. Van Campen, *J. Nutr.*, **102**, 165 (1972).

(5) D. Van Campen, *J. Nutr.*, **103**, 139 (1973).

(6) W. Forth and W. Rummel, in "International Encyclopedia of Pharmacology and Therapeutics," Vol. II, Pergamon, Great Britain, 1975, pp. 599–746.

(7) J. M. Christensen, M. Ghannam, and J. W. Ayres, *J. Pharm. Sci.* **73**, 1245 (1984).

(8) A. D. A. Moski and F. H. Kratner, *J. Nutr.*, **107**, 24 (1977).

(9) R. E. King, "Remington's Pharmaceutical Sciences," 16th ed., A. Osol, Ed., Mack Publishing Co., Easton, Pa., 1980, p. 1559, chap. 89.

(10) D. DeSoete, R. Gijbels, and J. Hoste, "Neutron Activation Analysis," Wiley-Interscience, New York, N.Y., 1972, p. 50.

(11) C. H. Wang, D. L. Wills, and W. D. Loveland, "Radiotracer Methodology in the Biological, Environmental and Physical Sciences," Oregon State University Press, Corvallis, Ore. 1975, p. 248.

(12) D. Gibbons, "Activation Analysis, Principles and Applications." J. M. A. Lenihan and S. J. Thomson, Eds., Academic, New York, N.Y., 1965, pp. 86 and 87.

(13) S. S. Nargolwalla and E. P. Przybylowicz, "Activation Analysis With Neutron Generators," Wiley, New York, N.Y., 1973, pp. 243–252.

(14) F. E. McKinney, "Isotope Users Guide," Oakridge National Laboratories, Oakridge, Tenn. 1969, p. 69.

(15) K. Bernstein, *Anal. Lab.*, **12**, 151 (1980).

ACKNOWLEDGMENTS

This work was performed as partial fulfillment of an M.S. degree in Pharmacy at Oregon State University, School of Pharmacy. This work was supported in part by a Sigma Xi Scholarship to M.G.

The authors thank Dr. Roman A. Schmitt, Michael R. Conrady, and Terrance V. Anderson, of the Oregon State University Radiation Research Center, for their consultation and technical assistance during the study.

The organization and analysis of the data base associated with this investigation were carried out in part with the PROPHET system, a unique national resource sponsored by the National Institutes of Health. Information about PROPHET, including how to apply for access can be obtained from the Director, Chemical/Biological Information-Handling Program, Division of Research Resources, NIH, Bethesda, MD 20205.

Potential Inhibitors of Tyrosine Hydroxylase and Dopamine-β-Hydroxylase

K. R. SCOTT ˣ, CALVIN J. ALT, MURRAY KEMP, ELISE HAYES, and VASANT G. TELANG

Received June 28, 1983, from *Howard University, College of Pharmacy and Pharmacal Sciences, Department of Medicinal Chemistry, Washington, DC 20059.* Accepted for publication September 26, 1983.

Abstract □ A series of methyl-substituted 1,2,3,4-tetrahydrocarbazoles was synthesized and screened for *in vitro* activity against tyrosine hydroxylase and dopamine-β-hydroxylase. The most potent compounds were evaluated for inhibition of norepinephrine biosynthesis in rats. The results indicated no significant decrease in norepinephrine levels at three dosage levels.

Keyphrases □ Tyrosine hydroxylase—*in vitro* activity, effect of methyl-substituted 1,2,3,4-tetrahydrocarbazoles □ Dopamine-β-hydroxylase—*in vitro* activity, effect of methyl-substituted 1,2,3,4-tetrahydrocarbazoles □ Methyl-substituted 1,2,3,4-tetrahydrocarbazoles—effect on tyrosine hydroxylase and dopamine-β-hydroxylase, *in vitro*

It has been shown that the 1,2,3,4-tetrahydrocarbazole nucleus is an active pharmacophore. Previous studies have shown that the various carbazoles exhibit anti-inflammatory (1–6), antidepressant (7–12), hypoglycemic (13), analgetic (14), cardiotonic (15), anti-infective (16), and anticancer activities (17). It was of interest to extend the initial work of

0022-3549/84/1100-1531$01.00/0
© 1984, American Pharmaceutical Association

Table I—Physical Constants of Methyl-Substituted 1,2,3,4-Tetrahydrocarbazoles

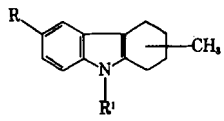

Compound	Formula[a]	CH_3 Position	R	R^1	Melting Point, °C	Boiling Point, °C (mm Hg)
VIII	$C_{13}H_{15}N$	3	H	H	111.0–111.5[b,c]	130–134 (0.8)
IX	$C_{18}H_{26}N_2$	3	H	$(CH_2)_3N(CH_3)_2$	—	154–155[d] (0.35)
X	$C_{20}H_{28}N_2$	3	H	$(CH_2)_2N(CH_2)_5$[e]	70–71[c]	167–174[f] (0.95)
XI	$C_{16}H_{18}N_2$	3	H	$(CH_2)_2CN$	99–100[g]	188–191 (0.7)
XII	$C_{16}H_{19}NO_2$	3	H	$(CH_2)_2COOH$	104–105[h]	195–197 (0.55)
XIII	$C_{14}H_{17}N$	3	H	CH_3	74–75[c]	—
XIV	$C_{18}H_{25}N_3O_2$	3	NO_2	$(CH_2)_3N(CH_3)_2$	102–103[c,i]	—
XVI	$C_{20}H_{28}ClN_3O_2$	3	NO_2	$(CH_2)_2N(CH_2)_5$[e,j]	253.5–254.0[g]	—
XVII	$C_{16}H_{17}N_3O_2$	3	NO_2	$(CH_2)_2CN$	208.0–209.5[g]	—
XVIII	$C_{16}H_{18}NO_4$	3	NO_2	$(CH_2)_2COOH$	216–217[g]	—
XIX	$C_{18}H_{26}N_2$	2	H	$(CH_2)_3N(CH_3)_2$	—	114–116[k] (1.0)
XX	$C_{20}H_{28}N_2$	2	H	$(CH_2)_2N(CH_2)_5$[e]	—	180–184[l] (0.45)
XXI	$C_{16}H_{18}N_2$	2	H	$(CH_2)_2CN$	96–97[c]	184–185 (0.65)
XXII	$C_{16}H_{19}NO_2$	2	H	$(CH_2)_2COOH$	113–114[g]	190–195 (0.6)
XXIII	$C_{18}H_{26}ClN_3O_2$	2	NO_2	$(CH_2)_3N(CH_3)_2$	219–220[g,j]	—
XXIV	$C_{18}H_{26}N_2$	1	H	$(CH_2)_3N(CH_3)_2$	50–51[g,m]	154–159 (0.4)
XXV	$C_{20}H_{28}N_2$	1	H	$(CH_2)_2N(CH_2)_5$[e]	—	184–185[n] (0.30)
XXVI	$C_{16}H_{18}N_2$	1	H	$(CH_2)_2CN$	68[c] (softens); 83–84	104–105 (0.7)
XXVII	$C_{16}H_{19}NO_2$	1	H	$(CH_2)_2COOH$	133–134[c]	—

[a] Compounds IX–XXVII were analyzed for C, H, and N; in addition XVI and XXIII were analyzed for Cl. All values were within ±0.4% of the theoretical value. [b] Lit. (20) mp 108–111°C. [c] Methanol. [d] Maleate, mp 120–121°C. [e] Piperidinoethyl. [f] Hydrochloride, mp 208–209°C. [g] Ethanol. [h] Benzene–methanol. [i] Hydrochloride, mp 226–227°C. [j] Hydrochloride. [k] Hydrochloride, mp 189.5–190.0°C. [l] Maleate, mp 210.5–211.0°C. [m] Maleate, mp 104–105°C. [n] Maleate, mp 111–112°C.

Mooradian *et al.* (15) and to systematically evaluate the following structural modifications of the 1,2,3,4-tetrahydrocarbazole nucleus: the effect of substitution on the aromatic ring; the effect of removal of the proton on the indole nitrogen; and the effect of the addition of an alkyl group to the tetrahydro ring. Representative analogues were evaluated in two *in vitro* systems, tyrosine hydroxylase (18) and dopamine-β-hydroxylase (19) for potential use as antihypertensive agents. The reaction sequence for the synthesis of the methyl-substituted 1,2,3,4-tetrahydrocarbazoles is shown in Scheme I.

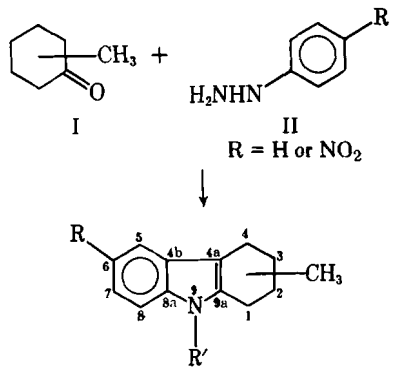

I; II (R = H or NO_2)

III: R′ = H
IV: R′ = CH_3, dialkylaminoalkyl, cycloaminoalkyl, $(CH_2)_2CN$, or $(CH_2)_2COOH$

Scheme I

The methyl-substituted cyclohexanone (I) was treated with the appropriate phenylhydrazine (II) (20, 21) using acetic acid (R = H) or acetic acid and hydrochloric acid (R = NO_2) to give the methyl-1,2,3,4-tetrahydrocarbazoles (III). Treatment of III with the appropriate base, followed either by the addition of methyl iodide, a dialkylaminoalkyl chloride, a cycloaminoalkyl chloride, or acrylonitrile, produced the 9-methyl, 9-dialkylaminoalkyl, 9-cycloaminoalkyl, or 9-(3-cyanopropyl) derivative (IV), respectively. The latter compound was hydrolyzed to the propionic acid derivative with either acid or base. It was shown (22) that 2-methylcyclohexanone undergoes the reactions shown in Scheme II.

These products, 1-methyl-1,2,3,4-tetrahydrocarbazole (V) and 2,3,4,4a-tetrahydro-4a-methyl-1*H*-carbazole (VI), were

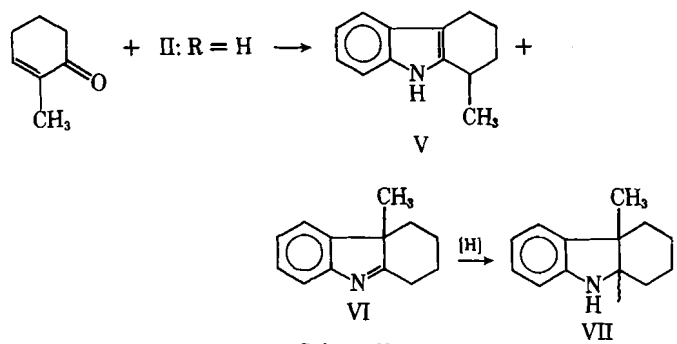

Scheme II

Table II—Physical Constants of 9-Substituted 2,3,4,4a,9,9a-Hexahydro-4a-methyl-1*H*-carbazoles

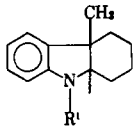

Compound	Formula[a]	R^1	Melting Point, °C	Boiling Point, °C (mm Hg)
XXVIII	$C_{13}H_{17}N$	H	52–53[b]	105–112 (0.6)
XXIX	$C_{18}H_{28}N_2$	$(CH_2)_3N(CH_3)_2$	—	146–154[b,c] (0.6)
XXX	$C_{20}H_{30}N_2$	$(CH_2)_2N(CH_2)_5$[d]	—	165–171[e,f] (0.65)
XXXI	$C_{16}H_{20}N_2$	$(CH_2)_2CN$	70–71[b]	178–180 (0.55)
XXXII	$C_{16}H_{21}NO_2$	$(CH_2)COOH$	91–92[e]	—

[a] Compounds XXVIII–XXXII were analyzed for C, H, and N. All values were within ±0.4% of the theoretical value. [b] Methanol. [c] Maleate, mp 140–141°C. [d] Piperidinoethyl. [e] Ethanol. [f] Maleate, mp 137–138°C.

of interest in view of varying reports (22–24) on the yields as well as investigating a new and related series, 2,3,4,4a,9,9a-hexahydro-4a-methyl-1*H*-carbazole (VII), which occurs on reduction of VI.

Selected compounds from each group were tested for *in vitro* activity against tyrosine hydroxylase and dopamine-β-hydroxylase. The most active compound, X, was tested at three dosage levels for inhibition of norepinephrine biosynthesis in rats.

EXPERIMENTAL SECTION

Instruments—Melting points were obtained using a melting point apparatus[1] and are uncorrected. Observed boiling points were also uncorrected. IR spectra were obtained on a spectrophotometer[2] as KBr pellets or neat. NMR spectra were obtained on a 60-MHz spectrometer[3] with tetramethylsilane as the internal reference. Elemental analyses were also performed[4]. Tritium was assayed on a liquid scintillation counter[5].

Reagents—All ketones[6] and phenylhydrazine[7] were distilled before use. *p*-Nitrophenylhydrazine[8] was recrystallized. L-[3,5-^{3}H]Tyrosine, L-[^{3}H]-epinephrine, [^{3}H]tyramine, *S*-[C^{3}H$_3$]adenosyl-L-methionine, and scintillation fluids[9] were used without further purification. 1,4-Dithiothreitol[10], dopamine, norepinephrine, epinephrine, and *S*-adenosyl-L-methionine[11] were used without further purification. Tyrosine hydroxylase was prepared (25), purified (26), and assayed (27); the protein content was also determined (28). Dopamine-β-hydroxylase (EC 1.14.17.1)[12] was assayed (29); phenylethanolamine-*N*-methyltransferase (EC 2.1.1.28)[12] was also assayed (30).

General Procedure for the Preparation of Methyl-Substituted 1,2,3,4-Tetrahydrocarbazoles (III, R = NO$_2$)—The previous method (21) was modified as follows. One-half mole of 4-methylcyclohexanone and *p*-nitrophenylhydrazine were dissolved in 180 g of glacial acetic acid. The mixture was heated at reflux for 4 h, chilled to 5°C, and filtered. The dried hydrazone was dissolved in 1 L of hydrochloric acid and was heated at reflux for 1 h. The product separated as yellow needles (78% yield), mp 166.5–167.5°C [lit. (31) 165–166°C].

General Procedure for Alkylation of Methyl-Substituted 1,2,3,4-Tetrahydrocarbazoles—*Method A* (*IV*, *R′* = *CH$_3$*)—The previous method (17) was employed using 0.05 mol of 3-methyl-1,2,3,4-tetrahydrocarbazole (VIII) and 0.05 mol of methyl iodide with 3 g of sodium hydride (51%, freed from mineral oil) in 25 mL of dimethylformamide. Chromatography on silica gel afforded 9.2 g (92% yield) of 3,9-dimethyl-1,2,3,4-tetrahydrocarbazole (XIII) as white crystals, mp 74–75°C; ^{1}H-NMR (CDCl$_3$): δ 1.90 (3, d, *J* = 4 Hz, CH$_3$), 3.10 (6, m, CH$_2$), 3.40 (1, m, CH), 3.80 (3, s, CH$_3$—N), and 7.30 ppm (4, m, ArH).

Anal.—Calc. for $C_{14}H_{17}N$: C, 84.23; H, 8.61; N, 7.06. Found: C, 84.46; H, 8.63; N, 7.01.

Table III—1,2,3,4-Tetrahydrocarbazoles and 2,3,4,4a,9,9a-Hexahydrocarbazoles as Inhibitors of Tyrosine Hydroxylase[a]

Compound	IC_{50}, M[b]	±*SEM*, × 10^{-4}	*n*
1,2,3,4-Tetrahydrocarbazole[c]	>4 × 10^{-4}	0.3	3
6-Nitro-1,2,3,4-tetrahydrocarbazole[d]	>4 × 10^{-4}	0.4	3
VIII	>4 × 10^{-4}	0.6	3
IX[e]	>4 × 10^{-4}	0.6	3
X[f]	4 × 10^{-4}	0.3	4
XI	>4 × 10^{-4}	0.3	3
XII	4 × 10^{-4}	0.4	4
XIV[f]	2 × 10^{-4}	0.2	6
XVI[f]	2 × 10^{-4}	0.3	6
XVII	4 × 10^{-4}	0.3	4
XVIII	>4 × 10^{-4}	0.6	3
XIX[f]	>4 × 10^{-4}	0.8	3
XX[e]	>4 × 10^{-4}	0.7	4
XXI	4 × 10^{-4}	0.4	4
XXII	>4 × 10^{-4}	0.6	3
XXIII[f]	4 × 10^{-4}	0.6	4
XXIV[e]	>4 × 10^{-4}	0.8	3
XXV[e]	>4 × 10^{-4}	0.9	3
XXVI	>4 × 10^{-4}	0.7	3
XXVII	>4 × 10^{-4}	0.8	3
XXX[e]	>4 × 10^{-4}	0.4	3
DL-α-Methyltyrosine[g]	2 × 10^{-4}	0.2	6

[a] Each compound was preincubated with the reaction mixture for 5 min before addition of L-tyrosine (5 × 10^{-5} M) as substrate. [b] Data represent a range of 45–55% inhibition; where >4 × 10^{-4} M concentrations are indicated, inhibition was <20% with 4 × 10^{-4} M inhibitor. [c] Data from Ref. 20. [d] Data from Ref. 21. [e] Maleate. [f] Hydrochloride. [g] Data from Ref. 18 gives 2.5 × 10^{-5} M.

Table IV—1,2,3,4-Tetrahydrocarbazoles as Inhibitors of Dopamine-β-Hydroxylase

Compound[a]	*In Vitro* Inhibition, % of Control[b]	±*SEM*	*n*
X[c]	44	1.6	4
XII	72	7.4	4
XIV	68	6.8	6
XVI	55	6.3	4
XVII	76	3.6	4
XXI	59	3.8	6
XXIII	94	1.8	3
O-Benzylhydroxylamine[c]	33	2.2	4

[a] For the salt form, see Table III. [b] Each compound (5 × 10^{-4} M) was preincubated for 15 min before addition of tyramine (5 × 10^{-4} M) as substrate. [c] Significantly different from control, $p < 0.05$.

[1] Thomas-Hoover.
[2] Beckman IR-18A.
[3] Varian EM360A.
[4] Performed by the Schwarzkopf Microanalytical Laboratory, Woodside, N.Y.
[5] Beckman LS-230.
[6] Eastman Chemicals.
[7] Fisher.
[8] Aldrich Chemical Co.
[9] Liquifluor and Econofluor; New England Nuclear.
[10] Schwarz/Mann.
[11] Calbiochem-Behring.
[12] Sigma Chemical Co.

Table V—*In Vivo* Assay Results

Assay		Norepinephrine Level: 1 mg/kg of X	10 mg/kg of X	50 mg/kg of X	α-Methyltyrosine (400 mg/kg)	Saline
I[a]	ng/g of heart tissue	588.6	587.3	594.3	472.5	602.2
	±*SEM*	47.5	75.2	70.8	25.1	97.8
	Decrease, %	2.3	2.5	1.3	21.5	—
II[b]	ng/g of heart tissue	182.0	169.0	163.0	156.0	193.0
	±*SEM*	14.0	13.0	13.0	17.0	24.0
	Decrease, %	5.7	12.4	15.6	19.2	—
III[a]	ng/g of heart tissue	519.9	425.0	487.5	351.6	468.8
	±*SEM*	46.7	28.0	29.7	30.6	29.4
	Decrease, %	—	9.3	—	25.0	—

[a] Data from Ref. 35. [b] Data from Ref. 36.

Method B [*IV*, $R' = (CH_2)_3N(CH_3)_2$]—The previous method (17) was employed using 0.05 mol of 3-methyl-1,2,3,4-tetrahydrocarbazole (VIII) and 0.05 mol of 3-dimethylaminopropyl chloride (17) in dimethylformamide with 3 g of the aforementioned sodium hydride to give 16.7 g (75% yield) of IX, bp 154–155°C (0.35 mm Hg), as a light-yellow oil. ^{1}H-NMR (acetone-d_6): δ 1.82 (3, d, J = 4 Hz, CH_3), 2.05–2.55 (m, CH_2), 2.25 (3, s, CH_3—N), 3.20 (6, m, CH_2), 3.45 (1, m, CH), and 7.22 ppm (4, m, ArH).

Anal.—Calc. for $C_{18}H_{26}N_2$: C, 79.88, H, 9.70, N, 10.41. Found: C, 80.00; H, 9.87; N, 10.46.

Method C [*IV*, $R' = (CH_2)_2CN$]—The previous method (17) was employed using 0.05 mol of 3-methyl-1,2,3,4-tetrahydrocarbazole (VIII) and 0.10 mol of acrylonitrile in benzene containing 1.5 mL of trimethylbenzylammonium hydroxide to give 9.59 g (80% yield) of XI as a white amorphous powder, bp 188–191°C (0.7 mm Hg), mp 99–100°C. IR (KBr): 2250 cm^{-1} (s, C≡N); ^{1}H-NMR (acetone-d_6): δ 1.80 (3, d, J = 4 Hz, CH_3), 2.40 (1, d, J = 17 Hz, CHCN), 2.80 (1, d, J = 17 Hz, CHCN), 2.90 (2, m, —CH_2N), 3.05 (6, m, CH_2), 3.50 (1, m, CH), and 7.20 ppm (4, m, ArH).

Anal.—Calc. for $C_{16}H_{18}N_2$: C, 80.62; H, 7.63; N, 11.76. Found: C, 80.59; H, 7.77; N, 11.55.

3-Methyl-1,2,3,4-tetrahydrocarbazole-9-propionic acid (XII)—Compound XI (0.03 mol) was dissolved in 400 mL of 90% ethanol containing 0.50 mol of potassium hydroxide. The mixture was refluxed for 18 h and then the solvent was evaporated under reduced pressure. The residue was dissolved in water, decolorized, and acidified with hydrochloric acid. The product was extracted with ether, and the organic phase was washed with water and dried (Na_2SO_4). Evaporation of the solvent and distillation of the residue afforded XII, as white crystals, bp 195–197°C (0.55 mm Hg), mp 104–105°C. IR (KBr): 1740 cm^{-1} (s, C=O); ^{1}H-NMR (acetone-d_6): δ 1.75 (3, d, J = 4 Hz, CH_3), 3.00 (6, m, CH_2), 3.45 (1, m, CH), 4.45 (3, t, J = 7 Hz, $NCHCH_2C$), 6.95–7.50 (4, m, ArH), and 10.45 ppm (1, s, COOH).

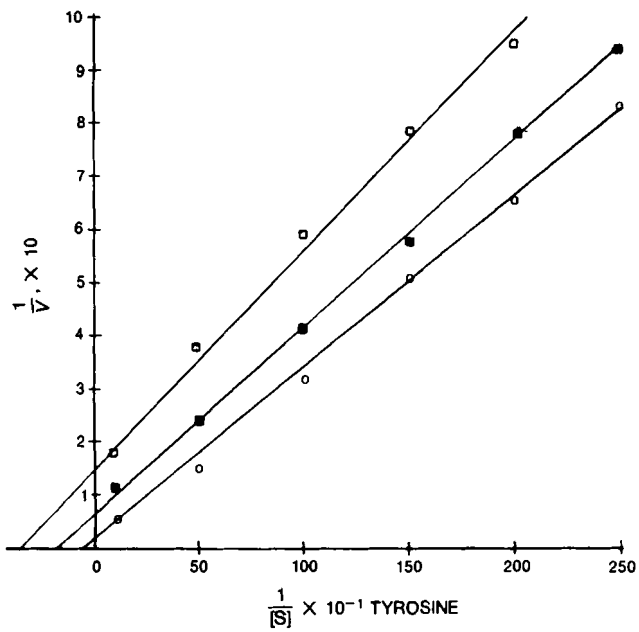

Figure 1—*Effect of X (■) and XIV (□) on the hydroxylation of L-tyrosine. Concentrations of L-tyrosine (substrate) varied from 1 × 10^{-4} to 4 × 10^{-6} M; (○) control.*

Anal.—Calc. for $C_{16}H_{19}NO_2$: C, 74.66; H, 7.46; N, 5.44. Found: C, 74.83; H, 7.62; N, 5.16.

In all alkylation methods when R = NO_2, additional solvent was required.

1-Methyl-1,2,3,4-tetrahydrocarbazole (V)—The previous method for the preparation of III (R = NO_2) was employed. Cyclization was accomplished using dilute sulfuric acid (32). The product was isolated and distilled, bp 121–129°C (0.4 mm Hg), mp 67–68°C as tan crystals [lit. (22) bp 142–146°C (0.3 mm Hg), mp 69°C].

2,3,4,4a-Tetrahydro-4a-methyl-1*H*-carbazole (VI)—The aforementioned hydrazone was cyclized using glacial acetic acid (32) to give a liquid, bp 98–106°C (0.9 mm Hg), picrate 170–171°C as yellow crystals [lit. (33) bp 98–100°C (0.3 mm Hg), picrate 169–171°C]. ^{1}H-NMR ($CDCl_3$): δ 1.26 ppm (3, s, CH_3).

2,3,4,4a,9,9a-Hexahydro-4a-methyl-1*H*-carbazole (VII)—Catalytic hydrogenation of V (0.1 mol) employing platinum oxide in a mixture of hydrochloric acid and alcohol (34) for 8 h gave VII in 82% yield, bp 105–112°C (0.6 mm Hg), mp 52–53°C as white crystals. IR (KBr): 3425 cm^{-1} (s, NH); ^{1}H-NMR ($CDCl_3$): δ 10.2 ppm (1, s, NH).

Anal.—Calc. for $C_{13}H_{17}N$: C, 83.35; H, 9.17; N, 7.48. Found: C, 83.66; H, 9.08; N, 7.48.

Analytical data for the compounds prepared by the above methods are shown in Tables I and II.

Enzyme Inhibition—*Tyrosine Hydroxylase*—Tyrosine hydroxylase inhibitors were screened as previously indicated (27) with the substrate concentration varied from 1 × 10^{-5} to 5 × 10^{-5} M and each potential inhibitor tested at concentrations of 2 × 10^{-4} M and 4 × 10^{-4} M. DL-α-Methyltyrosine[8] was used as a standard inhibitor for this phase. The results are listed in Table III.

Dopamine-β-Hydroxylase—Dopamine-β-hydroxylase inhibitors were screened as previously reported (29). The substrate concentration was 5 × 10^{-4} M. *O*-Benzylhydroxylamine[8] was used as a standard inhibitor in this study. The data are listed in Table IV.

***In Vivo* Determinations**—Thirty male Sprague-Dawley rats, weighing ~200 g, were divided into five groups of six rats each. Each group received an injection of either 1 mg/kg of X, 10 mg/kg of X, or 400 mg/kg of α-methyltyrosine or saline. The intraperitoneal doses were in a volume of 1 mL. After 4 h, the initial dose was repeated and, after an additional 4 h, the animals were sacrificed. The brains, hearts, and blood were taken for analysis (35, 36). Data for each assay are shown in Table V. The experiment was repeated (assay III) with the exceptions that the second dose was repeated after 3 h, the animals were sacrificed 3 h after the last dose, and only the hearts were removed and assayed (35).

RESULTS AND DISCUSSION

From the tyrosine hydroxylase data (Table III), it appears that the active compounds are those that possess a substituent at the 9-position. In the 9-[3-(dimethylamino)propyl] series, the 6-nitro substitution is essential for activity, as IX and XIX were inactive while both XIV and XXIII were active. In the 9-[2-(1-piperidino)ethyl] series, both X (the unsubstituted carbazole) and XVI (the 6-nitro analogue) were active. In the 9-(3-cyanopropyl) series, the initial conclusion reached with the previous analogues held for XI and XVII, but failed with XXI and XXVI due to the extreme insolubility of the latter. In the 9-(3-propionic acid) series, the 6-nitro derivative (XVIII) was inactive, while XII (the unsubstituted analogue) was active. As in the case of the cyanopropyl series, the extreme insolubility of XVIII was a prime factor in the correlation. The hexahydro analogue of X (XXX) was inactive. Inhibition of tyrosine hydroxylase by the tetrahydrocarbazoles was noncompetitive

with tyrosine, as seen in Fig. 1 for X and XIV. Whether this effect is exerted on either tetrahydrofolate or tetrahydropteridine (18) must await further study. All active compounds were assayed for inhibition of dopamine-β-hydroxylase (Table IV). From the data, X was shown to be the most active overall in both systems and was selected for the *in vivo* assay.

In vivo results of X (Table V) are explained on the basis of the assays performed. Assays I and III (35) are paired and show no inhibition. Assay I was repeated due to a high norepinephrine level after α-methyltyrosine treatment. Assay II results indicate significant inhibition; however, the correction for the recovery of norepinephrine from alumina is not included in assay II, while I and III allow for this error[13]. Thus, while X inhibited both tyrosine hydroxylase and dopamine-β-hydroxylase *in vitro*, it was not active *in vivo*. Whether X is metabolized too rapidly and fails to attain the required tissue concentration is not known.

REFERENCES

(1) L. Berger and A. J. Corraz, U.S. Pat. No. 3,868,387 (1975).

(2) Japanese Pat. No. 72-0018 (1972).

(3) H. Baruth and L. O. Randall, *Fed. Proc. Fed. Am. Soc. Exp. Biol.*, **33**, 557 (1974).

(4) A. H. Conney, C. Coutinho, B. Koechlin, R. Swarm, J. A. Cheripko, C. Impellizzeri, and H. Baruth, *Clin. Pharmacol. Ther.*, **16**, 176 (1974).

(5) B. Lacoume, U.S. Pat. No. 3,824,314 (1974).

(6) A. A. Asselin, L. G. Humber, T. A. Dobson, J. Komlossy, and R. R. Martel, *J. Med. Chem.*, **19**, 787 (1976).

(7) Belgian Pat. No. 793,493 (1972).

(8) German Pat. No. 2,240,211 (1973).

(9) D. M. Gallant, M. P. Bishop, and R. Guerrero-Figueroa, *Curr. Ther. Res.*, **14**, 61 (1972).

(10) A. A. Asselin, L. G. Humber, J. Komlossy, and M.-P. Charest, *J. Med. Chem.*, **19**, 792 (1976).

(11) A. Mooradian, P. E. Dupont, A. G. Hlavac, M. D. Accto, and J. Pearl, *J. Med. Chem.*, **20**, 487 (1977).

(12) J. W. Cusic and C. A. Dornfield, U.S. Pat. No. 2,541,211 (1951).

(13) J. McManus, U.S. Pat. No. 3,752,823 (1973).

(14) R. N. Schut, U.S. Pat. No. 3,592,824 (1971).

(15) A. Mooradian, A. G. Hlavac, P. E. Dupont, M. R. Bell, and A. A. Alousi, *J. Med. Chem.*, **18**, 640 (1975).

(16) U. Horlein, German Pat. No. 930,988 (1955).

(17) L. M. Rice and K. R. Scott, *J. Med. Chem.*, **13**, 308 (1970).

(18) S. Udenfriend, P. Saltzman-Nirenberg, and T. Nagatsu, *Biochem. Pharmacol.*, **14**, 837 (1965).

(19) T. Nagatsu and S. Udenfriend, *Clin. Chem.*, **18**, 980 (1972).

(20) C. U. Rogers and B. B. Corson, *J. Am. Chem. Soc.*, **69**, 2910 (1947).

(21) D. S. Deorha and S. S. Joshi, *J. Org. Chem.*, **26**, 3527 (1961).

(22) K. H Pausacker and C. I. Schubert, *J. Chem. Soc.*, **1949**, 1384.

(23) J. McLean, S. McLean, and R. I. Reed, *J. Chem. Soc.*, **1955**, 2519.

(24) I. I. Grandberg, A. N. Kost, and L. S. Yagazhinskii, *J. Gen. Chem. U.S.S.R.*, **30**, 3082 (1960).

(25) T. Nagatsu, M. Levitt, and S. Udenfriend, *J. Biol. Chem.*, **239**, 2910 (1964).

(26) B. N. Lutsky and N. Zenker, *J. Med. Chem.*, **11**, 1241 (1968).

(27) T. Nagatsu, M. Levitt, and S. Udenfriend, *Anal. Biochem.*, **9**, 112 (1964).

(28) O. H. Lowry, N. J. Rosebrough, A. L. Farr, and R. J. Randall, *J. Biol. Chem.*, **193**, 265 (1951).

(29) D. Glick, "Methods of Biochemical Analysis: Analysis of Biogenic Amines and their Related Enzymes," Suppl., Interscience, New York, N.Y., 1971, pp. 164–165.

(30) D. Glick, "Methods of Biochemical Analysis: Analysis of Biogenic Amines and their Related Enzymes," Suppl., Interscience, New York, N.Y., 1971, p. 132.

(31) L. M. Rice, E. Hertz, and M. E. Freed, *J. Med. Chem.*, **7**, 313 (1964).

(32) K. H. Pausacker, *J. Chem. Soc.*, **1950**, 621.

(33) G. Plancher and O. Carrasco, *Atti. Accad. Lincei*, (5), **13**, I 632 (1904).

(34) A. Cohen and B. Heath-Brown, *J. Chem. Soc.*, **1965**, 7179.

(35) D. P. Henry, B. J. Starman, D. G. Johnson, and R. H. Williams, *Life Sci.*, **16**, 375 (1975).

(36) A. H. Anton and D. F. Sayre, *J. Pharmacol. Exp. Ther.*, **138**, 360 (1962).

[13] I. J. Kopin, N.I.M.H., Bethesda, Md., personal communication.

ACKNOWLEDGMENTS

Presented in part at the First Annual Undergraduate Research Seminar, University of West Virginia, 1979.

The authors thank the following: Dr. Andre A. Asselin, Ayerst Pharmaceuticals, Montreal, for helpful discussions on the structural assignments; Drs. Steven L. Platt and Andy Evans, Varian Instrument Division, for the use of their NMR spectrometer; Dr. Nicholas Zenker, University of Maryland, for helpful suggestions on the preparation of tyrosine hydroxylase; Dr. Joseph J. Villafranca, Pennsylvania State University, for sharing his pre-publication manuscript on dopamine-β-hydroxylase; and Dr. Irwin Kopin, NIH, who provided the laboratory space, instruments, animals, and encouragement to complete the final phase of the work.

Direct Preparation of Spherically Agglomerated Salicylic Acid Crystals During Crystallization

Y. KAWASHIMA *[x], M. OKUMURA *, H. TAKENAKA *, and A. KOJIMA[‡]

Received August 17, 1983 from the **Gifu Pharmaceutical University, 5-6-1, Mitahora-higashi, Gifu 502, Japan* and the [‡]*Sanwa Chemical Research Laboratory, 1212, Shimojyo, Kasugai 486, Japan.* Accepted for publication October 11, 1983.

Abstract □ Needle-like salicylic acid crystals were transformed into a spherically shaped dense form during crystallization by the spherical crystallization technique. Agitation of a mixture of ethanol–water–chloroform containing salicylic acid yielded spherically agglomerated salicylic acid crystals. The crystallinity of the agglomerated salicylic acid decreased when the amount of ethanol in the solvent mixture was decreased. The wettability of the agglomerated crystals increased when the amount of ethanol in the solvent mixture was decreased, and this enhanced the dissolution rate of the crystals. The remarkable improvements in the flow and packing of the agglomerated crystals enabled the direct compression of the crystals.

Keyphrases □ Salicylic acid—crystallization of spherically agglomerated crystals □ Crystallization—agglomeration of salicylic acid crystals

A novel agglomeration technique to transform a microcrystalline drug into an agglomerated form during the crystallization process was previously described (1). This technique could enable subsequent processes, such as separation, filtration, drying, etc. to be carried out more efficiently. Furthermore, the resultant agglomerated crystals could be easily

0022-3549/84/1100-1535$01.00/0

© 1984, American Pharmaceutical Association

with tyrosine, as seen in Fig. 1 for X and XIV. Whether this effect is exerted on either tetrahydrofolate or tetrahydropteridine (18) must await further study. All active compounds were assayed for inhibition of dopamine-β-hydroxylase (Table IV). From the data, X was shown to be the most active overall in both systems and was selected for the *in vivo* assay.

In vivo results of X (Table V) are explained on the basis of the assays performed. Assays I and III (35) are paired and show no inhibition. Assay I was repeated due to a high norepinephrine level after α-methyltyrosine treatment. Assay II results indicate significant inhibition; however, the correction for the recovery of norepinephrine from alumina is not included in assay II, while I and III allow for this error[13]. Thus, while X inhibited both tyrosine hydroxylase and dopamine-β-hydroxylase *in vitro*, it was not active *in vivo*. Whether X is metabolized too rapidly and fails to attain the required tissue concentration is not known.

REFERENCES

(1) L. Berger and A. J. Corraz, U.S. Pat. No. 3,868,387 (1975).

(2) Japanese Pat. No. 72-0018 (1972).

(3) H. Baruth and L. O. Randall, *Fed. Proc. Fed. Am. Soc. Exp. Biol.*, **33**, 557 (1974).

(4) A. H. Conney, C. Coutinho, B. Koechlin, R. Swarm, J. A. Cheripko, C. Impellizzeri, and H. Baruth, *Clin. Pharmacol. Ther.*, **16**, 176 (1974).

(5) B. Lacoume, U.S. Pat. No. 3,824,314 (1974).

(6) A. A. Asselin, L. G. Humber, T. A. Dobson, J. Komlossy, and R. R. Martel, *J. Med. Chem.*, **19**, 787 (1976).

(7) Belgian Pat. No. 793,493 (1972).

(8) German Pat. No. 2,240,211 (1973).

(9) D. M. Gallant, M. P. Bishop, and R. Guerrero-Figueroa, *Curr. Ther. Res.*, **14**, 61 (1972).

(10) A. A. Asselin, L. G. Humber, J. Komlossy, and M.-P. Charest, *J. Med. Chem.*, **19**, 792 (1976).

(11) A. Mooradian, P. E. Dupont, A. G. Hlavac, M. D. Accto, and J. Pearl, *J. Med. Chem.*, **20**, 487 (1977).

(12) J. W. Cusic and C. A. Dornfield, U.S. Pat. No. 2,541,211 (1951).

(13) J. McManus, U.S. Pat. No. 3,752,823 (1973).

(14) R. N. Schut, U.S. Pat. No. 3,592,824 (1971).

(15) A. Mooradian, A. G. Hlavac, P. E. Dupont, M. R. Bell, and A. A. Alousi, *J. Med. Chem.*, **18**, 640 (1975).

(16) U. Horlein, German Pat. No. 930,988 (1955).

(17) L. M. Rice and K. R. Scott, *J. Med. Chem.*, **13**, 308 (1970).

(18) S. Udenfriend, P. Saltzman-Nirenberg, and T. Nagatsu, *Biochem. Pharmacol.*, **14**, 837 (1965).

(19) T. Nagatsu and S. Udenfriend, *Clin. Chem.*, **18**, 980 (1972).

(20) C. U. Rogers and B. B. Corson, *J. Am. Chem. Soc.*, **69**, 2910 (1947).

(21) D. S. Deorha and S. S. Joshi, *J. Org. Chem.*, **26**, 3527 (1961).

(22) K. H Pausacker and C. I. Schubert, *J. Chem. Soc.*, **1949**, 1384.

(23) J. McLean, S. McLean, and R. I. Reed, *J. Chem. Soc.*, **1955**, 2519.

(24) I. I. Grandberg, A. N. Kost, and L. S. Yagazhinskii, *J. Gen. Chem. U.S.S.R.*, **30**, 3082 (1960).

(25) T. Nagatsu, M. Levitt, and S. Udenfriend, *J. Biol. Chem.*, **239**, 2910 (1964).

(26) B. N. Lutsky and N. Zenker, *J. Med. Chem.*, **11**, 1241 (1968).

(27) T. Nagatsu, M. Levitt, and S. Udenfriend, *Anal. Biochem.*, **9**, 112 (1964).

(28) O. H. Lowry, N. J. Rosebrough, A. L. Farr, and R. J. Randall, *J. Biol. Chem.*, **193**, 265 (1951).

(29) D. Glick, "Methods of Biochemical Analysis: Analysis of Biogenic Amines and their Related Enzymes," Suppl., Interscience, New York, N.Y., 1971, pp. 164–165.

(30) D. Glick, "Methods of Biochemical Analysis: Analysis of Biogenic Amines and their Related Enzymes," Suppl., Interscience, New York, N.Y., 1971, p. 132.

(31) L. M. Rice, E. Hertz, and M. E. Freed, *J. Med. Chem.*, **7**, 313 (1964).

(32) K. H. Pausacker, *J. Chem. Soc.*, **1950**, 621.

(33) G. Plancher and O. Carrasco, *Atti. Accad. Lincei*, (5), **13**, I 632 (1904).

(34) A. Cohen and B. Heath-Brown, *J. Chem. Soc.*, **1965**, 7179.

(35) D. P. Henry, B. J. Starman, D. G. Johnson, and R. H. Williams, *Life Sci.*, **16**, 375 (1975).

(36) A. H. Anton and D. F. Sayre, *J. Pharmacol. Exp. Ther.*, **138**, 360 (1962).

[13] I. J. Kopin, N.I.M.H., Bethesda, Md., personal communication.

ACKNOWLEDGMENTS

Presented in part at the First Annual Undergraduate Research Seminar, University of West Virginia, 1979.

The authors thank the following: Dr. Andre A. Asselin, Ayerst Pharmaceuticals, Montreal, for helpful discussions on the structural assignments; Drs. Steven L. Platt and Andy Evans, Varian Instrument Division, for the use of their NMR spectrometer; Dr. Nicholas Zenker, University of Maryland, for helpful suggestions on the preparation of tyrosine hydroxylase; Dr. Joseph J. Villafranca, Pennsylvania State University, for sharing his pre-publication manuscript on dopamine-β-hydroxylase; and Dr. Irwin Kopin, NIH, who provided the laboratory space, instruments, animals, and encouragement to complete the final phase of the work.

Direct Preparation of Spherically Agglomerated Salicylic Acid Crystals During Crystallization

Y. KAWASHIMA *[x], M. OKUMURA *, H. TAKENAKA *, and A. KOJIMA[‡]

Received August 17, 1983 from the **Gifu Pharmaceutical University, 5-6-1, Mitahora-higashi, Gifu 502, Japan* and the [‡]*Sanwa Chemical Research Laboratory, 1212, Shimojyo, Kasugai 486, Japan.* Accepted for publication October 11, 1983.

Abstract □ Needle-like salicylic acid crystals were transformed into a spherically shaped dense form during crystallization by the spherical crystallization technique. Agitation of a mixture of ethanol–water–chloroform containing salicylic acid yielded spherically agglomerated salicylic acid crystals. The crystallinity of the agglomerated salicylic acid decreased when the amount of ethanol in the solvent mixture was decreased. The wettability of the agglomerated crystals increased when the amount of ethanol in the solvent mixture was decreased, and this enhanced the dissolution rate of the crystals. The remarkable improvements in the flow and packing of the agglomerated crystals enabled the direct compression of the crystals.

Keyphrases □ Salicylic acid—crystallization of spherically agglomerated crystals □ Crystallization—agglomeration of salicylic acid crystals

A novel agglomeration technique to transform a microcrystalline drug into an agglomerated form during the crystallization process was previously described (1). This technique could enable subsequent processes, such as separation, filtration, drying, etc. to be carried out more efficiently. Furthermore, the resultant agglomerated crystals could be easily

0022-3549/84/1100-1535$01.00/0

© 1984, American Pharmaceutical Association

compounded with other pharmaceutical powders due to their spherical form. We refer to this technique as "spherical crystallization."

Spherically agglomerated crystals of aminophylline were prepared directly by agitating a mixture of chloroform, ethanol, and water which contained ethylenediamine and theophylline (2). It was found that sodium theophylline monohydrate crystals, produced by salting out, were simultaneously agglomerated into spherical shapes in a mixture of an ethylenediamine solution of theophylline, an aqueous solution of sodium chloride, ethanol, and chloroform (3).

In the present study, the needle-like salicylic acid crystals simultaneously formed and agglomerated into a spherical shape in a mixture of water, ethanol, and chloroform. The aim of the study was to elucidate the effects of the composition of crystallization solvent on the physicochemical properties of the resultant agglomerated crystals, *e.g.*, crystalline form, crystallinity, wettability, dissolution rate, and micromeritic properties. The agglomeration behavior of the crystals was also investigated by measuring the sedimentation volume of the resultant crystals in liquid.

EXPERIMENTAL SECTION

Spherical Crystallization Process—*Method 1*—Salicylic acid[1,2] (0.5 g) was dissolved in ethanol (1–5 mL) in a test tube thermally controlled at 60°C. After cooling the ethanol solution to room temperature, 10 mL of water was added to the solution to yield the needle-like salicylic acid crystals. The mixture was allowed to stand for 1 h, then chloroform (0.3–0.5 mL) was added and the mixture was shaken horizontally at 200–400 cpm, using a shaker[2], for 10 min. The mixture was transferred to a measuring cylinder (25 mL) to measure the equilibrium sedimentation volume of the agglomerated crystals. The agglomerated crystals were separated and dried.

Method 2—Fifty milliliters of the ethanol solution (containing 12.5 g of salicylic acid maintained at 40°C) was poured into a mixture of chloroform (9 mL) and water (250 mL). The system was thermally controlled at 5°C and was agitated at 600 rpm by a turbine agitator with 6 blades for 1 h. The resultant crystals were separated and dried and their micromeritic properties were measured.

Measurement of Physicochemical Properties—The crystalline form of the agglomerated salicylic acid was determined using an X-ray diffractometer[3] with 0.15418 nm radiation. The relative diffraction intensity of salicylic acid (2θ = 17.1°) to that of sodium chloride (2θ = 31.6°), used as an internal standard, was taken as a measure of the crystallinity of salicylic acid. Sodium chloride particles fractionated into 150–200 mesh were incorporated into the diffraction samples with an agate mortar and pestle. The coefficient of variation of the relative intensities of diffraction peaks, due to the preferred orientation of particles in a powder, was 0.24. Wettability of the agglomerated crystals for water was determined by the contact angle of water to the agglomerated crystals and measured by the method of Lerk *et al.* (4). The agglomerated crystals weighing 2 g were compressed into a tablet (19.9 mm diameter, 5.3–5.8 mm thickness) at 50–60 kg/cm^2. The pressure was applied for 10–15 min to obtain an acceptable tablet without disintegration during the measurement. A large drop of saturated solution of salicylic acid was placed on the tablet surface, and the height of the drop was measured by a cathetometer. The contant angle (θ) was determined by using the following equations:

$$\theta > 90° \qquad \cos\theta = -1 + \sqrt{\frac{2}{3(1-\epsilon)}\left(\frac{2}{Bh^2} - 1\right)} \qquad \text{(Eq. 1)}$$

$$\theta > 90° \qquad \cos\theta = 1 - \sqrt{\frac{Bh^2}{3(1-\epsilon)(1 - Bh^2/2)}} \qquad \text{(Eq. 2)}$$

$$B = \frac{\rho g}{2\gamma} \qquad \text{(Eq. 3)}$$

where h is the height of the drop, ϵ is the porosity of the tablet, and ρ and γ are the density and the surface tension of the liquid drop. The porosity of the tablet was determined by measuring the apparent density of the tablet and the true density of the agglomerated crystals using a helium-air comparison pycnometer[4]. The surface tension of the salicylic acid saturated solution was measured by a surface tensiometer[5]. The dissolution test of the agglomerated crystals was carried out by the rotating basket method specified in USP at 100 rpm and 37°C (5). One hundred milligrams of the agglomerated crystals were dissolved in deaerated distilled water. Two-milliliter aliquots were withdrawn at appropriate intervals and an equal volume of water was replaced to the vessel. Salicylic acid was assayed spectrophotometrically[6] at 530 nm after adding 1% ferric nitrate to the aliquot.

Measurement of Micromeritic Properties of the Agglomerated Crystals—As a measure of the flow of the crystals, the angle of repose of the agglomerated crystals was measured by pouring powder on a plate (10 cm diameter)[7]. The packing ability of the agglomerated crystals was investigated by tapping them into a 50-mL measuring cylinder using a tapping machine[7]. The ability of the crystals to be formed into tablets was tested by using a single punch machine[8]. The average weight and dimension of the tablets were: 0.382 g, 10.05 mm diameter, and 4.14 mm thickness, respectively. The hardness was measured by a moving plate hardness tester[9].

Table I—Solubility and Degree of Supersaturation

	Ethanol Fraction in the Solvent, %	Conc., μg/mL	Degree of Supersaturation
With Agglomeration	8.8	2.39	19.02
	16.0	3.16	13.19
	22.4	4.65	8.27
	28.0	9.05	3.95
	32.7	16.39	2.03
Without Agglomeration	8.8	2.22	20.48
	16.0	2.82	14.78
	22.4	4.00	9.62
	28.0	6.87	5.20
	32.7	14.28	2.33

RESULTS AND DISCUSSION

Agglomeration Behavior of Salicylic Acid Crystals in Liquid—The recovery of the crystals agglomerated by spherical crystallization (method 1) sharply decreased with >25–30% ethanol in the solvent mixture (Fig. 1). With 33% ethanol in the solvent mixture, 28% of the loading was recovered as agglomerated crystals. Without agglomeration, when no chloroform was added to

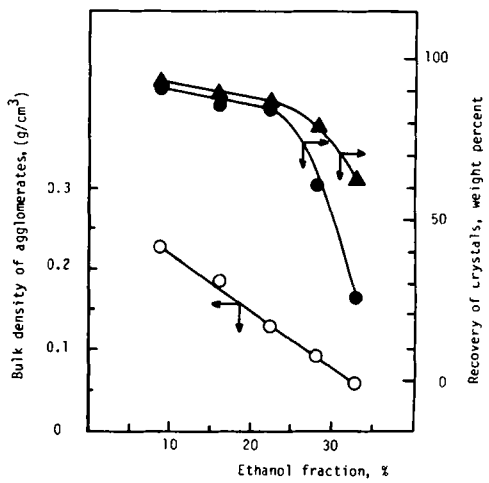

Figure 1—*Recovery and bulk density of agglomerated crystals. Key: (●) recovery of the agglomerated crystals, (▲) recovery of the primary crystals, and (○) bulk density of the agglomerated crystals.*

[1] Nakarai Chemicals, Ltd., Japan.
[2] V-S type; Iwaki Co., Japan.
[3] JDX type; Nihon Denshi, Co., Japan.
[4] Type 1302; Shimadzu Co., Japan.
[5] CBVP-A3 type; Kyowa Co., Japan.
[6] 100-60 type; Hitachi, Ltd., Japan.
[7] Konishi Seisakusho Co., Japan.
[8] Erweka-GmbH, Germany.
[9] Kyowa Seiko Co., Japan.

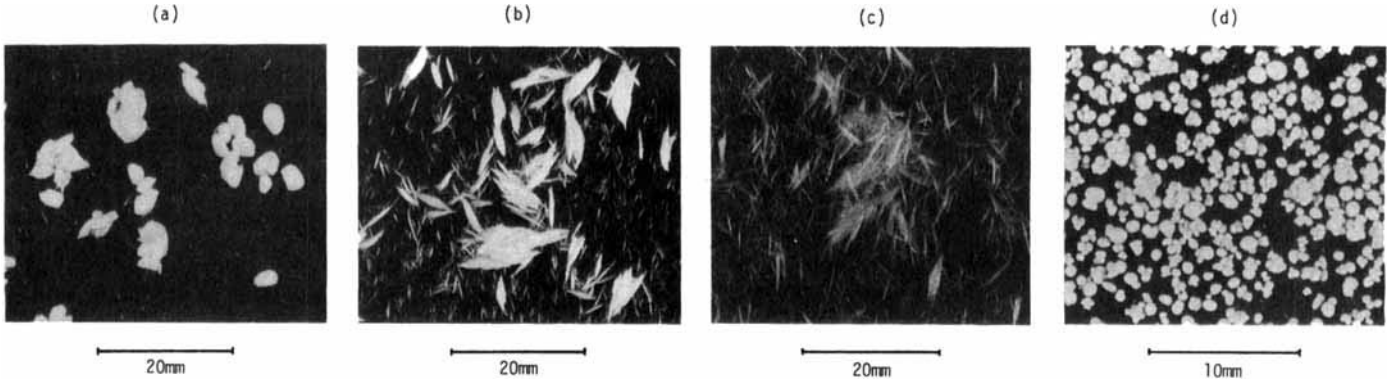

Figure 2—*Photographs of agglomerated crystals prepared with various ethanol fractions by methods 1 and 2: (a), (b), and (c) agglomerated crystals prepared by method 1 (the ethanol fractions in the solvent are 8.8, 22.4, and 28.0%, respectively); (d) spherically agglomerated crystals prepared by method 2.*

the system, the recovery of the crystals was 63%. This finding indicated that the solubility of salicyclic acid in the solvent for spherical crystallization, *i.e.*, ethanol–water–chloroform, was higher than in the ethanol–water mixture without agglomeration, as suggested in Table I.

The sedimentation volume of the agglomerated crystals prepared by spherical crystallization (method 1) was measured to investigate the effect of the composition of the solvent mixture on the agglomeration behavior. Bulk density of the agglomerated crystals, defined as the weight of the crystals recovered divided by the equilibrium sedimentation volume, was plotted against the ethanol fraction of the solvent. The bulk density decreased linearly when the amount of ethanol in the solvent mixture was increased (see Fig. 1). The size of the particles composing the agglomerated crystals decreased with a decrease in the amount of ethanol in the solvent mixture as shown in Fig. 2. Elworthy and Worthington (6) reported that finer sulfadiazine crystals were produced in more highly supersaturated solvents. The degree of supersaturation (Sd) was defined by:

$$Sd = \frac{Co}{Ce} \qquad \text{(Eq. 4)}$$

where Co and Ce are the initial loading and the remaining drug concentrations after crystallization in the solvent, respectively.

As shown in Table I, decreasing the amount of ethanol increased the degree of supersaturation, resulting in fine crystals. The larger agglomerated crystals were loosely compacted and elongated as shown in Fig. 2, resulting in a higher sedimentation volume, *i.e.*, a lower bulk density. The strength of the agglomerated crystals prepared in a solvent mixture with 28.0% ethanol was not enough to hold an agglomerated form after drying. In this study, the solvent mixture with small amount of ethanol afforded the dense, spherically agglomerated crystals.

Physicochemical Properties of the Resultant Crystals—The X-ray diffraction patterns of the agglomerated crystals are shown in Fig. 3; all the patterns coincided with that of the original salicylic acid, and no change in the crystalline form of the basic crystals was found, even after agglomeration. The diffraction intensity varied with the amount of ethanol in the solvent mixture, and may be dependent on the basic crystal size. Increasing the amount of ethanol in the solvent mixture caused the diffraction peaks to increase. The relative diffraction intensities of salicylic acid (17.1°) to that of sodium chloride (31.6°) are shown in Fig. 4 as a function of the amount of ethanol in the solvent mixture. The relative diffraction intensities were assumed as the crystallinity of the elementary crystals composing the agglomerate. As expected, the crystallinity increased when the amount of ethanol in the solvent mixture was increased. The crystallinity of the agglomerated crystals were influenced more strongly by the amount of ethanol in the solvent mixture than the crystals that were not agglomerated. Recrystallization of salicylic acid from chloroform occluded in the agglomerated crystals during drying may have increased the crystallinity of the dried agglomerated crystals, when compared with those that were not agglomerated.

Wettability of the agglomerated crystals by water was investigated by measuring the contact angle of water to the compressed crystals. It was expected that the contact angle would vary with the amount of ethanol in the solvent mixture, since the crystallinity and the elementary crystal size of the agglomerated crystals varied with the amount of ethanol. Gulinkina *et al.* (7) found that a dye crystal with a low crystallinity was more wettable than a dye crystal with a high crystallinity. The contact angles of the agglomerated crystals produced in the solvent with >25% ethanol were higher than those of the crystals that were not agglomerated, as shown in Fig. 5, due to their higher crystallinities. When the amount of ethanol was <25%, the contact angles of the agglomerated crystals became smaller than those of the primary crystals that were not agglomerated. This may be due to the fact that the basic crystal size of the agglomerated material produced in the solvent mixture with small amounts of ethanol was larger than that of the crystals that were not agglomerated.

The differences in the wettability of the crystals suggested that the dissolution behavior of the crystals might vary. The time required for 50% of solute dissolution of the agglomerated crystals prepared from the solvent with 22.4% ethanol (T_{50} = 7 min) was significantly shorter than the others (T_{50} = 20–22 min) at the 1% level, since the crystals were easily wetted, as shown in Fig. 5. Furthermore, their specific surface areas were fairly large, compared with

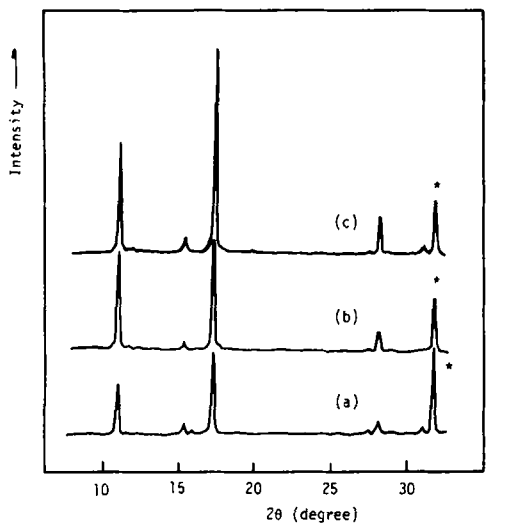

Figure 3—*X-ray powder diffraction patterns of agglomerated salicylic acid crystals. The ethanol fractions for (a), (b), and (c) are 8.8, 22.4, and 28.0%, respectively; (*) denotes the diffraction peak of sodium chloride.*

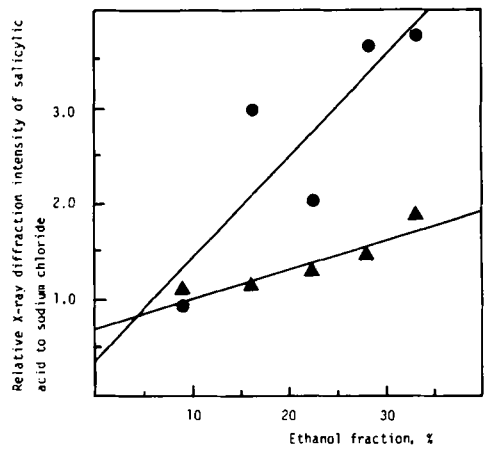

Figure 4—*Effect of ethanol fraction in the solvent on the crystallinity of salicylic acid. Key: (●) agglomerated crystals and (▲) primary crystals.*

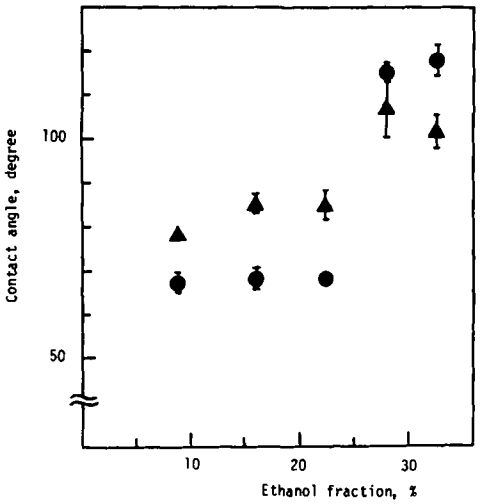

Figure 5—*Contact angles of agglomerated and primary crystals as a function of the ethanol fraction in the solvent. Key: (●) agglomerated crystals and (▲) primary crystals.*

those of the agglomerated crystals prepared with 8.8% ethanol, as suggested in Fig. 2. Although the agglomerated crystals prepared with 28.0% ethanol had large specific surface areas, their poor wettability resulted in a slower dissolution rate (Fig. 6). The dissolution rate of the spherically agglomerated crystals in Fig. 2d did not decrease as much as predicted from their low specific surface areas because of their improved wettability (Fig. 5).

Micromeritic Properties of Agglomerated Salicylic Acid Crystals Prepared by method 2—The agglomerated crystals prepared by method 2 were more compact and more spherical than those prepared by method 1, as shown in Fig. 2. The average diameter of the agglomerated crystals was 930 μm, with a size range from 460 to 1210 μm. The micromeritic properties of the agglomerated crystals were significantly improved compared with those of the crystals that were not agglomerated. The angle of repose of the agglomerated crystal was 36°, while that of the crystals that were not agglomerated was 51°. The packing ability was investigated by tapping the crystals in a measuring cylinder. The data were analyzed by Kawakita and Lüdde (8) and Kuno (9) equations, represented by Eqs. 5 and 6, respectively:

$$\frac{n}{c} = \frac{1}{ab} + \frac{n}{a}$$

$$a = \frac{V_0 - V_\infty}{V_0}, \quad c = \frac{V_0 - V_n}{V_0} \qquad \text{(Eq. 5)}$$

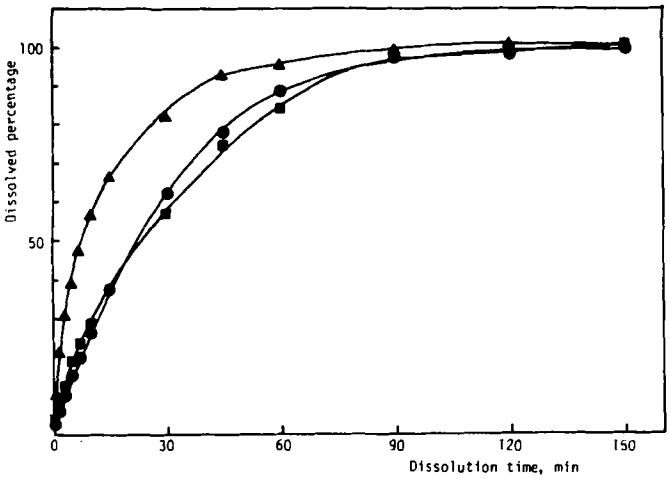

Figure 6—*Dissolution patterns of agglomerated crystals. Key: ethanol fractions of (●) 8.8, (▲) 22.4, and (■) 28.0%.*

Table II—Micromeritic Properties of Primary Crystals and Agglomerates

Micromeritic Properties	Agglomerates	Primary Crystals
Angle of repose	36°	51°
a^a	0.0955	0.3397
b^a	0.0466	0.0295
k^b	0.0049	0.0092
Closest packing density	0.488 g/cm³	0.160 g/cm³
Tablet	Compressible[c]	Not Compressible

[a] Parameter in Eq. 5. [b] Parameter in Eq. 6. [c] Tablet properties: diameter, 10.05 mm; thickness, 4.14 mm; average weight, 0.382 g; weight variation, 2.56% (the maximum percentage difference from the mean weight).

where a and b are the constants, n is the tap number, and V_0, V_n, and V_∞ are the powder bed volumes at initial, nth tapped, and equilibrium state, respectively.

$$\rho_f - \rho_n = (\rho_f - \rho_0) \exp(-kn) \qquad \text{(Eq. 6)}$$

where ρ_f, ρ_n, and ρ_0 are the apparent densities at equilibrium, nth tapped, and initial state, respectively, and k is the constant. All the data satisfied the relationships represented by Eqs. 5 and 6. The packing ability was assessed by comparing the constants a, b, and k in Eqs. 5 and 6, respectively, as shown in Table II. The constant a represents the proportion of consolidation at the closest packing attained. The reciprocals of b and k represent the packing velocity. The constant a for the agglomerated crystals was smaller than that for the crystals that were not agglomerated. This indicated that the agglomerated crystals were easily packed, even without tapping. The larger b value for the agglomerated crystals proved that the packing velocity of the agglomerated crystals by tapping was slower than that of the crystals that were not agglomerated. The smaller k in Eq. 6 for the agglomerated crystals coincided with the above finding. The slow packing velocity corresponded with the proportion of the consolidation of powder bed per tap, which was low. The closest packing density of the agglomerated crystals was larger than that of the crystals that were not agglomerated. Due to the improved flow properties and packing ability of the agglomerated crystals, they were directly compressible; whereas, the crystals that were not agglomerated were not compressible due to their poor flow properties.

REFERENCES

(1) Y. Kawashima, M. Okumura, and H. Takenaka, *Science*, **216**, 1127 (1982).

(2) Y. Kawashima, S. Aoki, and H. Takenaka, *Chem. Pharm. Bull.*, **30**, 1900 (1982).

(3) Y. Kawashima, S. Y. Lin, M. Naito, and H. Takenaka, *Chem. Pharm. Bull.*, **30**, 1837 (1982).

(4) C. F. Lerk, A. J. M. Schoonen, and J. T. Fell, *J. Pharm. Sci.*, **65**, 843 (1976).

(5) "The United States Pharmacopeia" 20th rev., U. S. Pharmacopeial Convention, Rockville, Md., 1980, p. 959.

(6) P. H. Elworthy and H. E. C. Worthington, *J. Pharm. Pharmacol.*, **23**, Suppl. 101S (1971).

(7) I. R. Gulinkina, Z. I. Ezhkova, T. S. Kozlova, L. I. Konysheva, G. M. Makarovskaya, and T. V. Silina, *Zh. Prikl. Khim.*, **53**, 85 (1980); Chem. Abs., Vol. 92, 182549r, (1980).

(8) K. Kawakita and K. H. Lüdde, *Powder Technol.*, **4**, 61 (1970–71).

(9) H. Kuno, "Powder (Theory and Application)," T. Kubo, G. Jimbo, E. Suito, H. Takahashi, and S. Hayakawa, Eds., Maruzen, Tokyo, 1979.

ACKNOWLEDGMENTS

A part of this research was supported by a grant-in-aid (No. 59490023) for Scientific Research Ministry of Education, Culture and Science, Japan.

Effect of Aging on Hydrocortisone–Polyethylene Glycol 4000 and Hydrocortisone–Polyvinylpyrrolidone Dispersions

B. R. HAJRATWALA *x **and D. S. S. HO** ‡§

Received April 19, 1982, from the *Pharmaceutics Division, Wayne State University, Detroit, MI 48202 and the ‡Pharmaceutics Department, University of Otago, Dunedin, New Zealand. Accepted for publication October 14, 1983. §Present address: 121 Jalan Kuala Kangsar, Ipoh, Malaysia.

Abstract □ Dispersions containing 40% hydrocortisone were prepared by the solvent method in polyethylene glycol 4000. Dispersions in polyvinylpyrrolidone were prepared by slow evaporation of solvent (type A) and by fast evaporation of solvent (type B). These dispersions were stored at 25°C for 30 d. Plots of time required for 50% ($t_{50\%}$) and 70% ($t_{70\%}$) of the hydrocortisone dispersion to dissolve (beaker method) *versus* time were obtained. Hydrocortisone–polyethylene glycol showed no apparent significant change in either dissolution rate, X-ray spectra, or scanning electron micrographs. Type A dispersions showed an increase in dissolution rate up to 8 d. Type B dispersions showed an initial decrease followed by an increase in dissolution rate. The initial decrease in dissolution rate of type B dispersions is due to hydrocortisone crystallizing out of the polyvinylpyrrolidone matrix. The increased dissolution for both types of polyvinylpyrrolidone dispersions was not expected and is explained by an increased proportion of the high-energy amorphous component, based on X-ray spectra. Other possibilities such as the presence of polymorphic forms of hydrocortisone and/or reduction in particle aggregation could not be discounted.

Keyphrases □ Hydrocortisone– dispersions with polyethylene glycol 4000 and polyvinylpyrrolidone, effect of aging □ Aging–effect on dispersions, hydrocortisone–polyethylene glycol 4000, hydrocortisone–polyvinylpyrrolidone.

Incorporation of water-soluble carriers with poorly soluble drugs, to increase the dissolution rate of the latter, has been widely studied and extensively reviewed (1, 2). Polyethylene glycol (3–5) and polyvinylpyrrolidone (6–8) have been popular choices as inert carriers for dispersions prepared by solvent or coprecipitation methods.

The effect of aging on solid dispersion systems has not been reported extensively. Aspirin was reported to undergo faster degradation in solid dispersions (9), whereas dissolution profiles for dicumarol–polyethylene glycol tablets did not change appreciably after 1 year of storage (3). Changes in dissolution profiles of other solid dispersions have not been reported. The corticosteroids continue to be of interest due to their poor water solubility and unpredictable dissolution rates (4–7, 10, 11). The present investigation reports the dissolution characteristics of hydrocortisone–polyvinylpyrrolidone dispersions stored at 25°C for 30 d.

EXPERIMENTAL SECTION

Materials—Micronized hydrocortisone[1], polyethylene glycol 4000[2], and polyvinylpyrrolidone[3] (average mol. wt. 30,000–40,000) were used. All other reagents and solvents were of analytical grade.

Sample Preparation and Storage—The solid dispersions of hydrocortisone in polyethylene glycol were prepared by the solvent method (1, 4). Hydrocortisone and varying quantities of carrier were accurately weighed and dissolved in 20 mL of 96% ethanol. The solvent was evaporated under a stream of nitrogen. The resultant solid dispersions were then dried under reduced pressure at 37°C over silica gel for 1 d. The hardened mass was powered and 85/235-mesh (sieve size) particles were used.

The solid dispersions of hydrocortisone–polyvinylpyrrolidone were prepared using the same technique. During an earlier investigation (6) it was found that the rate of evaporation of the solvent had an effect on dispersions. Dispersions were prepared by slow evaporation (type A) and by rapid evaporation (type B) of solvent. All samples were prepared in duplicate and stored in amber bottles in a desiccator over silica gel at 25°C.

Dissolution Studies—Approximately 50 mg of the solid dispersion was introduced directly on the surface of 500 mL of distilled water in a 1-L beaker at 25 ± 0.1°C and stirred at 100 rpm. The dissolution was followed by withdrawing 4-mL samples with a glass syringe fitted with a filter[4] (0.45 μm) to exclude particles. Hydrocortisone was assayed spectrophotometrically at 247.5 nm. Corrections were made for any absorption due to the carrier. The slope of the Beer's law plot was 0.0454 mg^{-1} (SEM = 0.0316, r = 0.9997).

The $t_{50\%}$ and $t_{70\%}$ values were obtained from plots of percent hydrocortisone dissolved *versus* time. All plots were obtained in duplicate. The results were analyzed for significance using the SPSS program for a one-way ANOVA with interval testing and a two-tailed t test.

X-ray Diffraction Studies—Dispersions were spread on glass slides as a thin layer with a small amount of petroleum jelly. CuK radiation was used. Diffraction patterns[5] were obtained by scanning at 1°/min in terms of the 2θ angle.

Thin-Layer Chromatography Studies—Silica gel-coated plates[6] were spotted with solutions containing 10 mg of dispersions in 5 mL of 95% ethanol. The plates were chromatographed using a two-dimensional method. The solvent system used was acetone–benzene (50:50, v/v) followed by dichloroethane–methanol–water (92:8:0.5, v/v/v). The plates were developed with tetrazolium blue (0.05%) and sodium hydroxide (8%) in methanol.

Scanning Electron Microscope Studies—Scanning electron micrographs were obtained from powdered dispersions mounted on stumps with double-sided cellophane tape and coated with gold.

RESULTS AND DISCUSSION

All dispersions contained 40% hydrocortisone; this selection was based on the results of an earlier study (6). At 40% concentration, hydrocortisone–polyvinylpyrrolidone dispersions showed the following changes in dissolution rate. Plots of time required for 50% and 70% of the hydrocortisone in the dispersion to dissolve *versus* percent hydrocortisone yielded zero slopes for dispersions with <40% hydrocortisone and positive slopes for dispersions with >40% hydrocortisone; dispersions with >40% hydrocortisone also exhibited an increased crystalline structure as evidenced by X-ray diffraction spectra (6). A limited study of the effect of aging on 40% hydrocortisone dispersions was therefore undertaken.

Effects of Storage for 30 d on Hydrocortisone–Polyethylene Glycol 4000 Dispersions—The dispersions were white. Thin-layer chromatography detected no decomposition during this study.

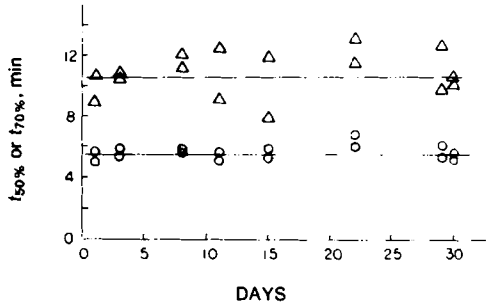

Figure 1—*Plot of* $t_{70\%}$ (△) *and* $t_{50\%}$ (○) *for hydrocortisone in hydrocortisone–polyethylene glycol 4000 dispersions* versus *time.*

[1] Hoechst, Frankfurt, Federal Republic of Germany.
[2] Union Carbide, England.
[3] May and Baker, England.
[4] Millipore Corp., Bedford, Mass.
[5] Phillips X-ray diffractometer; Phillips, Eindhoven, The Netherlands.
[6] Kieselguhr G; Analtech, Newark, Del.

0022-3549/84/1100-1539$01.00/0
© 1984, American Pharmaceutical Association

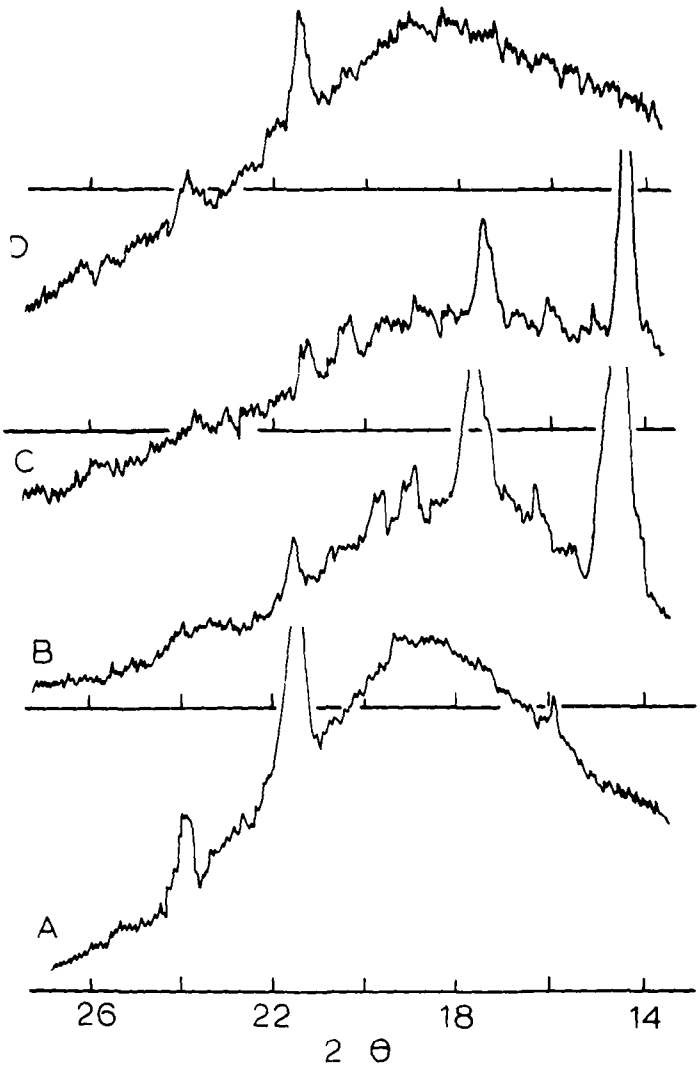

Figure 2—*X-ray diffraction spectra of polyvinylpyrrolidone (A), hydrocortisone (B), hydrocortisone-polyvinylpyrrolidone (type A) dispersion on day 2 (C), and hydrocortisone-polyvinylpyrrolidone (type B) dispersion on day 3 (D).*

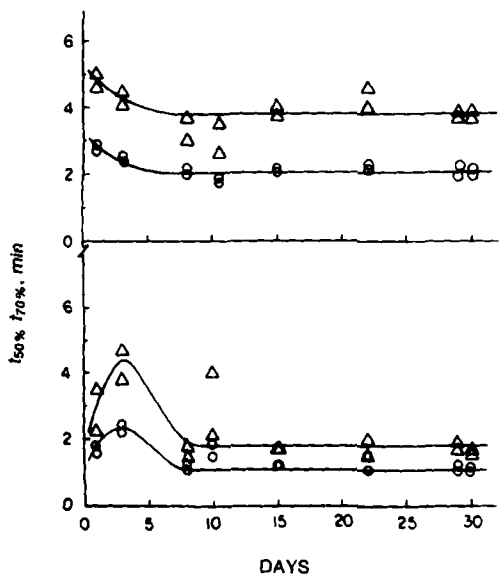

Figure 3—*Plot of* $t_{70\%}$ (△) *and* $t_{50\%}$ (○) *for hydrocortisone-polyvinylpyrrolidone dispersions* versus *time. Dispersions were prepared by the solvent method using a slow rate (upper curve, type A) and a fast rate (lower curve, type B) of evaporation.*

Figure 1 shows a plot of $t_{50\%}$ and $t_{70\%}$ (time required, respectively, for 50% and 70% of the hydrocortisone in the dispersion to dissolve) *versus* time. A one-way ANOVA with interval testing yielded a significant difference between $t_{50\%}$ and $t_{70\%}$ ($p = 0.07$); the two-tailed t test yielded $p < 0.001$. There does not appear to be any change in the dissolution of hydrocortisone over the 30-d storage period. These results are consistent with an earlier study of other polyethylene glycol dispersions (3).

X-ray diffraction spectra showed slight variations in peak heights at different days. These spectra also showed a slight increase in the scattering hump of the dispersions; however, no apparent trend was discernible over the period of this study. Thus, minor changes in X-ray diffraction spectra are not considered significant with respect to the observed dissolution rates. The scanning electron micrographs also did not show any apparent change in these dispersions.

X-ray Diffraction of Polyvinylpyrrolidone and Hydrocortisone—Polyvinylpyrrolidone, a high-molecular-weight polymer, is known to exist in a glass state and to have a relatively high glass-transition temperature of 175°C (12). Physically this polymer is a yellowish, transparent, brittle, glass solid, but the X-ray diffraction pattern (Fig. 2) shows that it is not completely amorphous. Weak diffraction peaks show a degree of order; the ordered portion seems small and the major portion of the solid seems amorphous. This is evident by the presence of the large diffused scattering hump in the spectrum. The diffuse reflection at 18°(2θ) corresponds to a spacing of approximately 0.5 nm, possibly the distance between the polymer chains.

Hydrocortisone is a crystalline compound. A small scattering hump (Fig. 2) is also evident in the diffraction patterns of hydrocortisone and may indicate the presence of a small amount of amorphous hydrocortisone. Such scattering may be caused by the small size of the hydrocortisone crystals.

Effects of Storage for 30 d on Hydrocortisone-Polyvinylpyrrolidone Dispersions—Figure 3 shows plots of $t_{50\%}$ and $t_{70\%}$ *versus* time for type A and B dispersions. For type A dispersions results of a one-way ANOVA with interval testing yielded $p = 0.01$; the two-tailed t test yielded $p < 0.001$. For type B dispersions the first four values in a one-way ANOVA with interval testing resulted in $p = 0.08$; two-tailed t test yielded $p = 0.002$. The last four values in a one-way ANOVA with interval testing resulted in $p = 0.02$; the two-tailed t test yielded $p < 0.001$. For the type A dispersions, $t_{50\%}$ and $t_{70\%}$ initially declined over 10 d and then became constant, indicating an increased dissolution rate in the first 10 d. The type B dispersions show ~50% decrease in dissolution rate in the first 3 d and then a steady increase until about day 10 before leveling off. No attempt was made to develop any mathematical relationship between variables.

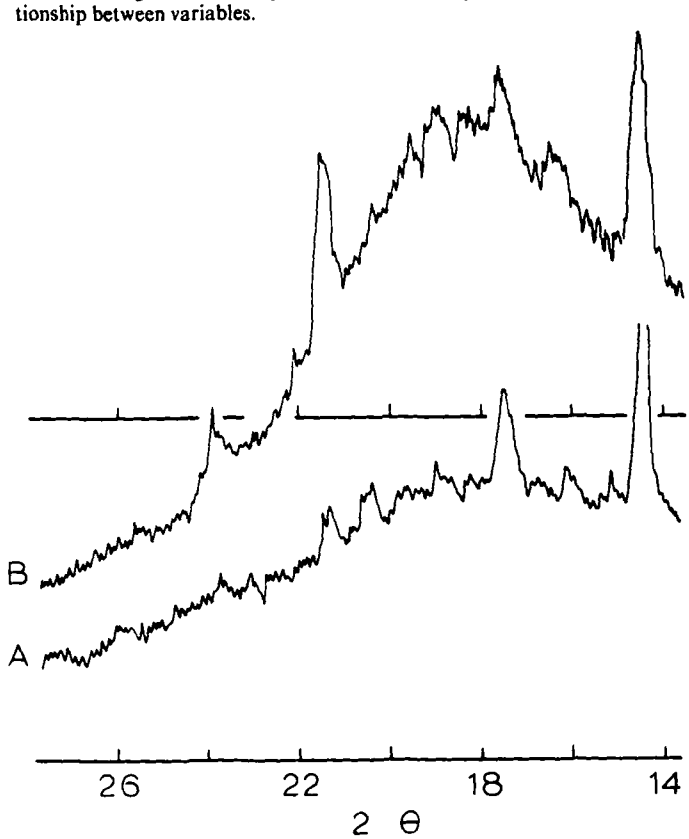

Figure 4—*X-ray diffraction spectra of hydrocortisone-polyvinylpyrrolidone type A dispersions stored at 25°C. Key: (A) after 1 d; (B) after 30 d.*

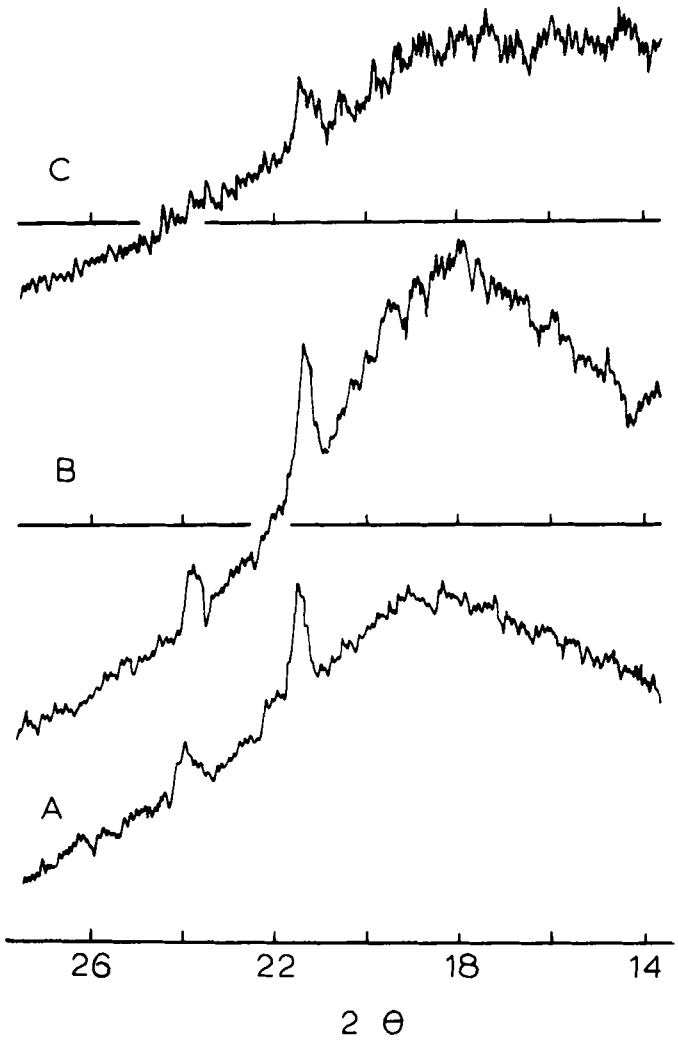

Figure 5—*X-ray diffraction spectra of hydrocortisone-polyvinylpyrrolidone type B dispersions stored at 25°C. Key: (A) after 2 d; (B) after 14 d; (C) after 30 d.*

Figure 2 shows X-ray diffraction spectra for hydrocortisone-polyvinylpyrrolidone dispersions. The X-ray diffraction pattern for type A shows the crystalline structure of hydrocortisone. Type B dispersions show an absence of crystalline structure. Type A dispersions would be expected to show decreased dissolution rates compared with type B. This was observed (Fig. 3) and is consistent with an earlier interpretation (4, 6). However, it is interesting to note that the degree of crystallinity and the resultant modification in dissolution are dependent on the rate of evaporation of solvent during the preparation of these dispersions.

These dispersions are considered to be glassy suspensions of hydrocortisone in polyvinylpyrrolidone. Since such systems are in a metastable state, they may undergo aging transformations yielding stable forms. The rate of the transformations vary with materials and storage conditions. Iopanoic acid and chloramphenicol palmitate were reported to crystallize from a polyvinylpyrrolidone glass solution (1). The initial decrease in the dissolution for type B dispersions (Fig. 3) could be readily explained in terms of hydrocortisone crystallizing out of the polyvinylpyrrolidone matrix.

The increased dissolution rate after an early decrease for type B dispersions and the increased dissolution rate for type A dispersions were unexpected. Figures 4 and 5 show changes in X-ray diffraction spectra for type A and type B dispersions, respectively. Both types of dispersions show increased scattering humps in X-ray diffraction spectra, indicating an increased proportion of an amorphous component. The amorphous forms are high-energy forms and generally possess higher solubility, explaining the increased dissolution. Other possibilities such as the presence of polymorphic form of hydrocortisone in polyvinylpyrrolidone matrix, reduction of particle aggregation, *etc.*, should not be discounted.

REFERENCES

(1) W. L. Chiou and S. Riegelman, *J. Pharm. Sci.*, **60,** 1281 (1971).

(2) B. R. Hajratwala, *Aust. J. Pharm. Sci.*, **NS3,** 101 (1974).

(3) W. R. Ravis and C. Y. Chen, *J. Pharm. Sci.*, **70,** 1353 (1981).

(4) D. S. S. Ho and B. R. Hajratwala, *Aust. J. Pharm. Sci.*, **10,** 65 (1981).

(5) D. S. S. Ho and B. R. Hajratwala, *Proc. Univ. Otago Med. Sch.*, **56,** 13 (1978).

(6) B. R. Hajratwala and D. S. S. Ho, *Aust. J. Pharm. Sci.*, **10,** 70 (1981).

(7) D. S. S. Ho and B. R. Hajratwala, *Proc. Univ. Otago Med. Sch.*, **52,** 43 (1976).

(8) A. Rahman, J. C. Cradock, and J. P. Davignon, *J. Pharm. Sci.*, **67,** 611 (1978).

(9) H. M. El-Banna, N. A. Daabis, and S. A. El-Fattah, *J. Pharm. Sci.*, **67,** 1631 (1978).

(10) L. V. Allen, V. A. Yanchich, and D. D. Maness, *J. Pharm. Sci.*, **66,** 494 (1977).

(11) K. H. Kim and C. I. Jarowski, *J. Pharm. Sci.*, **66,** 1536 (1977).

(12) L. E. Nielsen, "Mechanical Properties of Polymer," Reinhold, New York, N.Y., 1962, p. 15.

ACKNOWLEDGMENTS

Presented in part at the Basic Pharmaceutics Section, APhA Academy of Pharmaceutical Sciences, April 1980 meeting in Washington, D.C. The authors thank Dr. William R. Rivis (School of Pharmacy, Auburn University) for his helpful suggestions and Dr. Patrick L. McKercher (College of Pharmacy, Wayne State University) for assistance with statistical analysis and interpretation.

Liquid Chromatographic Determination and Plasma Concentration Profile of Optical Isomers of Ibuprofen in Humans

EDMUND J. D. LEE *§x, KENNETH M. WILLIAMS *, GARRY G. GRAHAM ‡, RICHARD O. DAY *, and G. DAVID CHAMPION *

Received August 17, 1983, from the *Department of Clinical Pharmacology, St. Vincent's Hospital, Darlinghurst, 2010, Australia and ‡Department of Pharmacology and Physiology, University of New South Wales, Kensington, 2033, Australia. Accepted for publication December 12, 1983.
§Present address: Department of Pharmacology, National University of Singapore, Kent Ridge, Singapore 0511.

Abstract □ A sensitive and specific high-performance liquid chromatographic assay for the optical isomers of ibuprofen in plasma is reported. The isomers were converted to their diastereoisomeric *S*(+)-2-octyl esters and were resolved with two silica columns in series and a mobile phase containing 0.05% isopropyl alcohol in heptane. The lower limit of sensitivity was 0.5 μg/mL. The plasma concentrations of the optical isomers in a normal volunteer following administration of racemic, *S*(+)-, and *R*(−)-ibuprofen are reported. Following administration of *R*(−)-ibuprofen, there was stereoselective inversion of *R*(−)- to *S*(+)-ibuprofen.

Keyphrases □ Optical isomers—liquid chromatography, plasma concentration profiles, ibuprofen, humans □ Ibuprofen—liquid chromatography, plasma concentration profile, optical isomers, humans

The chromatographic resolution of optical isomers is difficult because they have the same physicochemical properties. Methods available for resolution include the use of an optically active stationary phase (1), an optically active mobile phase (2), or, more conventionally, conversion of the optical isomers to diastereoisomers by reaction with an optically active reagent. Separation of isomers of arylpropionic acid derivatives usually can be achieved by the formation of the diastereoisomeric amides with optically active reagents like *R*(+)-α-phenylethylamine (3), *S*(−)-α-methylbenzylamine (4, 5), (*R*)-4-(dimethylamino)-α-methyl-1-naphthalenemethyl-amine (6), and L-leucine (7). Johnson *et al.* (8) have reported a liquid chromatographic assay for the isomers of naproxen based on the formation of diastereoisomeric *S*(+)-2-octyl esters. In this paper is reported the successful modification of the latter method for the quantification of ibuprofen optical isomers in plasma.

Ibuprofen (I) is a nonsteroidal anti-inflammatory agent exhibiting optical isomerism because of a chiral carbon atom on the propionic acid side chain. It is administered clinically as the racemate. In early *in vitro* studies, it has been demonstrated that the *S*(+)-isomer (III) was responsible for the anti-inflammatory activity. However, the *R*(−)-isomer (II) was as active as III *in vivo* (9) because there was stereoselective inversion of II to III *in vivo* (10–13).

There have been few studies in which the pharmacokinetics of II and III in humans have been described because of the difficulty in resolving II and III. Although the inversion of II to III has been inferred from the examination of the urinary metabolites of II and III in humans (10, 11, 13), no data have been presented detailing the time course of the plasma concentrations of each isomer following the administration of II and III. A sensitive and specific high-performance liquid chromatographic (HPLC) assay is described for the determination of II and III in plasma. It was used to follow the concentrations of II and III after oral administration of I (800 mg), II (400 mg), and III (400 mg) and to document the inversion of II to III in humans.

EXPERIMENTAL SECTION

Apparatus—An HPLC pump[1] was attached to an autosampler[2] and a variable-wavelength UV detector[3] set at 220 nm. Two 5-μm silica columns[4] (25 × 0.46 cm) were used in series. The detector signal was recorded and reported as peak areas on a plotter recorder[5]. The whole operation was coordinated by means of a system controller[6].

Reagents—*n*-Hexane and *n*-heptane were HPLC grade[7]; isopropyl alcohol was analytical grade[7]; *S*(+)-2-octanol (>99% pure) was obtained commercially[8]. Hydrogen chloride was bubbled through the octanol. Dichloromethane[7] and methanol[7] were dried over sodium and anhydrous sodium sulfate, respectively.

Standard Solutions—Stock solutions of I[9] were prepared by using dilute sodium hydroxide (solution A, 50 μg/mL; solution B, 500 μg/mL). A stock solution of the internal standard, 4-*n*-pentylphenylacetic acid (IV)[9], was prepared (80 μg/mL). Plasma standard curves for each isomer were constructed (at each run) over the concentration ranges of 0.5–5 and 5–60 μg/mL. In each case, the peak area ratios of each isomer to internal standard were plotted against the concentration of the isomers.

Sample Preparation—Venous blood (10 mL) was collected *via* an indwelling catheter in heparinized tubes[10]. Duplicate plasma samples (1 mL) were then transferred to screw-capped glass tubes (12 mL). Internal standard (100 μL) was added, and the mixture was acidified with 3 M hydrochloric acid (200 μL). Isopropyl alcohol (0.1% v/v) in hexane (10 mL) was added, and the tube was capped and shaken for 5 min. The organic phase was then transferred to a glass tube (20 mL). The extraction was repeated, and the second volume of the organic phase was added to the first volume before being blown to dryness under air at 40°C. The walls of the tube were washed with chloroform (2 mL) which was then transferred to a reaction vial (2 mL). Acidified *S*(+)-2-octanol (25 μL) was added, and the vial was capped and incubated for 1 h at 150°C. On cooling, 0.1% isopropyl alcohol in hexane (2 mL) and saturated sodium bicarbonate (150 μL) were added. The vials were recapped and the mixture vortexed for 30 s and then centrifuged for 5 min. The organic phase was transferred to conical tubes and the solvent evaporated under a stream of air at 40°C. The residue was then reconstituted in mobile phase (100 μL) and transferred to 200-μL sampling vials. An aliquot (4–40 μL) was then injected *via* the autosampler.

To obtain standard curves, either solution A (20–200 μL) or B (20–240 μL) was transferred into screw-capped glass tubes (12 mL). The volume was made up to 1 mL by the addition of blank plasma, and the resultant mixture was treated in a manner similar to that for the unknown samples.

Chromatography—Chromatography was performed at ambient temperature, and resolution of the octyl esters of II, III, and IV was achieved by using two 5-μm silica columns connected in series. The mobile phase was 0.05% v/v isopropyl alcohol in heptane and was pumped at a flow rate of 1 mL/min for 30 min followed by a 20-min washout period at 2 mL/min. The pressure at 1 mL/min was ~800 psi.

[1] Model 6000A; Waters Associates.
[2] WISP 710 B; Waters Associates.
[3] UV-50; Varian Instruments.
[4] Ultrasphere Si 5 μm; Altex.
[5] Data module; Waters Associates.
[6] System controller; Waters Associates.
[7] Ajax Chemicals.
[8] Fluka AG Chemishe Fabrik.
[9] The Boots Co., Nottingham, United Kingdom.
[10] Vacutainer 6484; Becton, Dickinson and Co.

0022-3549/84/1100-1542$01.00/0
© 1984, American Pharmaceutical Association

After every 12 injections there was a 30-min washout period at 2 mL/min. At regular intervals (about 150 injections), the columns were generated by pumping 20 column volumes of dry dichloromethane, 20 column volumes of dry methanol, and then another 20 column volumes of dry dichloromethane through the columns. The columns were reequilibrated with at least 50 column volumes of 0.05% isopropyl alcohol in heptane before use. No attempt was made to dry the isopropyl alcohol–heptane mixture.

The individual peaks were identified by HPLC of the octyl esters of pure II, III, and IV. The eluting fractions representing the octyl esters of II and III were subjected to GC–MS.[11]

To exclude possible interference by other nonsteroidal anti-inflammatory agents, standard solutions of aspirin, carprofen, diflunisal, flurbiprofen, indomethacin, naproxen, and salicylic acid were esterified and chromatographed as described above for I.

Volunteer Study—A normal subject was given I (800 mg)[9], II (400 mg)[9], and III (400 mg)[9] orally on three separate occasions, 1 week apart. Compounds I, II, and III were administered orally in solution. These test solutions were prepared by first dissolving appropriate amounts of pure I, II, or III in dilute sodium hydroxide (0.1 M, 10–20 mL). The volume was then made up to 250 mL with distilled water. Prior to each study, the subject fasted overnight and until 4 h after administration of the drug. Frequent blood samples were collected up to 14 h after administration of the dose.

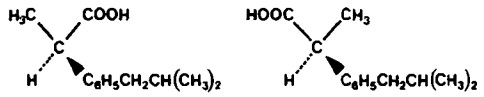

R(–) IBUPROFEN (II) S(+) IBUPROFEN (III)

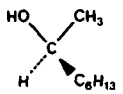

S(+)-2-OCTANOL

RESULTS AND DISCUSSION

Chromatography—The *S*(+)-2-octyl esters of II and III can be separated chromatographically with retention times of ~20 and ~21 min, respectively (Fig. 1). The retention time for the ester of IV was ~26 min. Presence of other anti-inflammatory agents like aspirin, carprofen, diflunisal, flurbiprofen, indomethacin, naproxen, and salicylic acid did not interfere with the assay.

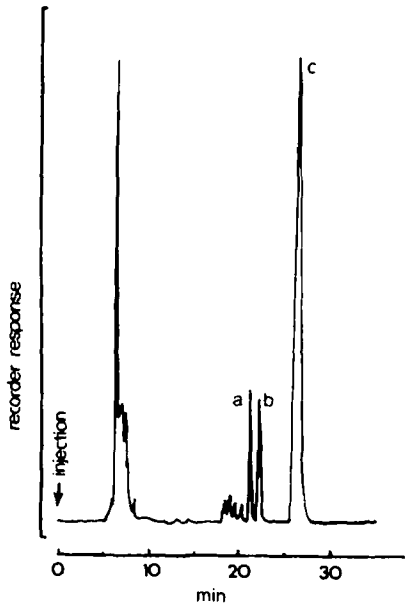

Figure 1—*Typical chromatogram of the S(+)-2-octyl esters of II (0.5 μg/mL of plasma) (a), III (0.5 μg/mL of plasma) (b), and IV (c).*

[11] Model 3200; Finnigan CI-GCMS.

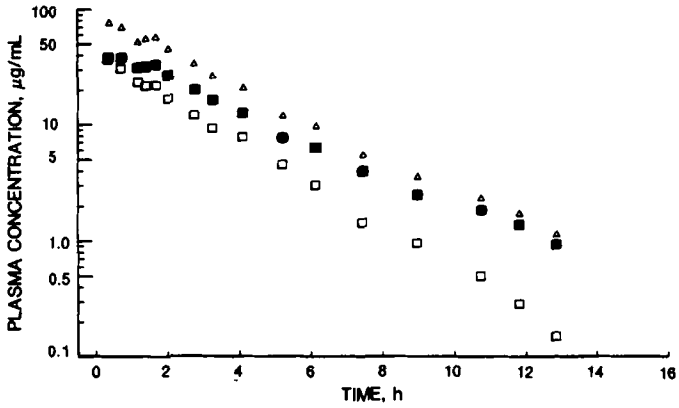

Figure 2—*Plasma levels of I (△), II (□), and III (■) following oral administration of I (800 mg).*

When a sample of II which showed one peak on HPLC was esterified and chromatographed, some III was detected. The amount of III thus detected was small and represented only ~2% of the total amount of II. A similar amount of II was found to be present when a sample of III which showed one peak on HPLC was esterified and chromatographed. These results can be attributed to impurity of the sample, impurity of the octanol, or the possibility of a fractional amount of racemization occurring during sample preparation.

Chromatographic conditions were selected to maintain the retention times described above at which resolution and peak shapes were optimal.

The methane chemical ionization mass spectrum for the esters of II and III were similar and gave the following mass ions: $(M - H)^+$ m/z 317 (28%); $(M - CH_3)^+$ m/z 303 (10%); $(M - C_6H_{11})$ m/z 235 (16%); $(M - C_8H_{15})^+$ m/z (207 (100%); $(M - C_8H_{17}O)$ m/z 189 (8%); $(M - C_8H_{17}OCO)$ m/z 161 (50%).

During development of the assay, four to five peaks, possibly due to contaminants extracted from plasma, were found to elute just prior to that of the octyl ester of II. Significant interference from these peaks occurred at low concentrations of II (<0.5 μg/mL). However, interference could be minimized by maintaining the retention time of II beyond 20 min.

Sample Preparation—Various extraction methods were assessed. In general, more polar solvents extracted greater amounts of plasma contaminants. Extraction with *n*-hexane was found to produce the least interference by contaminants with reasonable recovery of II and III. By using 0.1% isopropyl alcohol in hexane, recovery of II and III was found to be ~64 and 84% after single and double extractions, respectively. Recovering of IV was 74% after two extractions. (Recovery was defined by the ratio of peak areas obtained after treatment of spiked plasma extracts to that obtained after direct esterification of equivalent amounts of II, III, or IV.) Esterification of II and III was complete after 0.5 h at 150°C.

Assay Reproducibility and Sensitivity—It was necessary to construct a standard curve for each of the plasma concentration ranges, 0–10 and 10–60 μg/mL. Typical intercepts and slopes were, respectively, 0.2 and 9.26 for the former and −0.66 and 8.76 for the latter standard curves. The within-run coefficient of variation (*CV*) at plasma concentrations of 2.5 and 50 μg of the octyl ester of II/mL were 4.0 and 5.0%, respectively (n = 5). The corre-

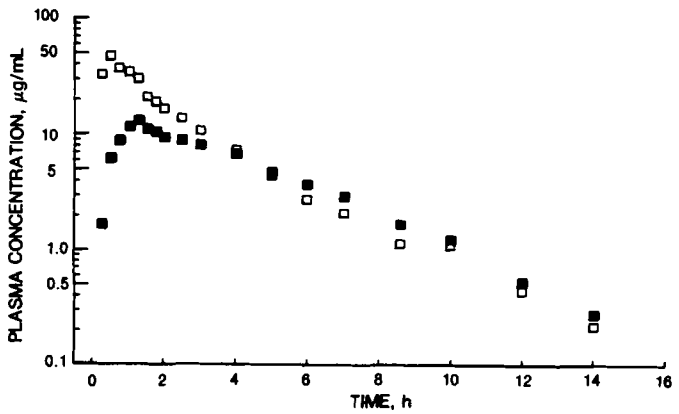

Figure 3—*Plasma levels of II (□) and III (■) following oral administration of II (400 mg).*

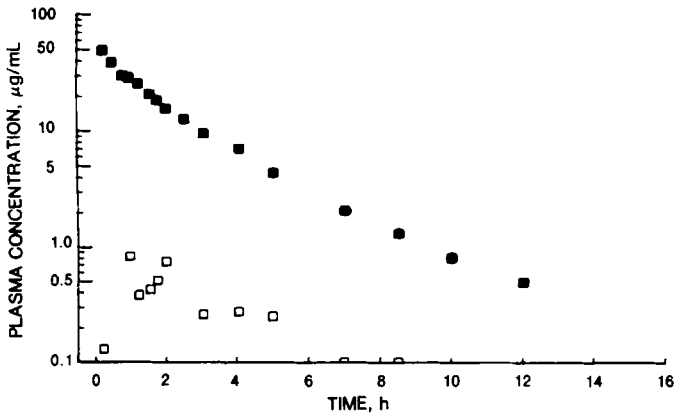

Figure 4—*Plasma levels of II (□) and III (■) following oral administration of III (400 mg).*

sponding *CV* values for the octyl ester of IV were 3.4 and 5.1%. Concentrations of II and III down to 0.5 μg/mL could be measured confidently. Values below this were rejected because of significant interference from the contaminating peaks mentioned above.

Volunteer Study—The applicability of the assay was demonstrated by a preliminary study of the plasma concentration profile of II and III in a normal subject. Absorption after administration of I, II, or III was rapid. Peak levels were attained within 0.5 h (Figs. 2–4). In most of the profiles, a definite biphasic decline could be discerned. Following administration of I, III was apparently eliminated more slowly than II (Fig. 2). This was presumably due to the contribution of the inversion of II to III. Following administration of II, plasma concentrations of III gradually increased and peaked at 1.3 h (Fig. 3). The concentration of III then declined more slowly than that of II. The concentration of III equaled that of II at ~4–5 h and subsequently remained higher than that of II. The peak concentration of III achieved after administrations of II was ~28% of that attained by II.

Only a small amount of II was detected after administration of III (Fig. 4). The low plasma concentrations of II that were observed may be attributed to incomplete optical purity of the *S*(+)-2-octanol and also possibly to some racemization of III during derivatization. However, as the rate of increase of II was slower than that observed for III, it is likely that some inversion of III to II occurs *in vivo*, although this is clearly insignificant compared with the inversion of II to III observed in these studies.

Ibuprofen is cleared almost entirely by metabolism (13). Disposition of the isomers is complicated by the stereoselective inversion of II to III. This metabolic pathway may be common to all the arylpropionic acids, although this area has received little attention (6, 7, 14). The inversion apparently proceeds *via* stereoselective formation of the coenzyme A (CoA) ester of the *R*(−)-arylpropionic acid, with subsequent racemization and release of the *R*(−)- and *S*(+)-enantiomers (15). This mechanism suggests that the "racemase" may be methylmalonyl CoA epimerase. Furthermore, as CoA esters of ibuprofen, fenoprofen, and ketoprofen have been shown to be incorporated into "hybrid triglycerides" (16), we are currently investigating our hypothesis that arylpropionic acids may be stereoselectively sequestered into adipose tissue.

Direct evidence of the stereoselective inversion of II has not been previously demonstrated in humans, and inference of its existence has so far been based on the predominance of dextrorotatory metabolites in urine (10, 11, 13).

This HPLC assay was found to be reproducible and convenient for routine use and has been used to demonstrate unequivocally the *in vivo* inversion of II to III in humans. The method suffers from the drawback of having a long assay time. However, this disadvantage can be overcome by automation of sampling and peak integration. The method was also found to be suitable for analysis of urine and synovial fluid samples and was utilized in formal pharmacokinetic studies. The details of these studies and of the stereospecific uptake of *R*(−)-ibuprofen into adipose tissue will be the subject of later reports.

REFERENCES

(1) W. H. Pirkle, D. W. Honse, and J. M. Finn, *J. Chromatogr.*, **192**, 143 (1980).

(2) J. N. LePage, W. Lindner, G. Davies, D. E. Seitz, and B. L. Karger, *Anal. Chem.*, **51**, 433 (1979).

(3) S. Rendic, V. Sunjic, F. Kajfez, N. Blazevic, and T. Alebic-Kolbah, *Chimia*, **29**, 170 (1975).

(4) G. J. Vangiessen and D. G. Kaiser, *J. Pharm. Sci.*, **64**, 798 (1975).

(5) J. K. Stoltenborg, C. V. Puglisi, F. Rubin, and F. M. Vane, *J. Pharm. Sci.* **70**, 1207 (1981).

(6) J. Goto, N. Goto, and P. Nambara, *J. Chromatogr.*, **239**, 559 (1982).

(7) S. J. Lan, K. J. Kripalani, A. V. Dean, P. Egli, L. T. Difazio, and E. C. Schreiber, *Drug Metab. Dispos.*, **4**, 330 (1976).

(8) D. M. Johnson, A. Reuter, J. M. Collins, and G. F. Thompson, *J. Pharm. Sci.*, **68**, 112 (1979).

(9) S. S. Adams, P. Bresloff, and C. G. Mason, *J. Pharm. Pharmacol.*, **28**, 256 (1976).

(10) W. J. Wechter, D. G. Loughhead, R. J. Reischer, G. J. Vangiesen, and D. G. Kaiser, *Biochem. Biophys. Res. Commun.*, **61**, 833 (1974).

(11) D. G. Kaiser, G. J. Vangiessen, R. J. Reischer, and W. J. Wechter, *J. Pharm. Sci.*, **65**, 269 (1976).

(12) C. A. M. Van Genneken, Ph.D. Thesis, University of Mijmegen, Mijmegen, The Netherlands (1975).

(13) R. F. N. Mills, S. S. Adams, E. E. Cliffe, W. Dickinson, and J. S. Nicholson, *Xenobiotica*, **3**, 589 (1973).

(14) R. J. Bopp, J. F. Nash, A. S. Ridolfo, and E. R. Shepard, *Drug Metab. Dispos.*, **7**, 356 (1979).

(15) Y. Nakamura, T. Yaamaguchi, S. Hashimoto, S. Takahashi, K. Iwatani, and Y. Nakagama, Abstracts of the 12th Symposium on Drug Metabolism and Action, Kanazawa, Japan, 1980.

(16) R. Fears, K. H. Baggaley, R. Alexander, B. Morgan, and R. M. Hindley, *J. Lipids Res.*, **19**, 3 (1978).

ACKNOWLEDGMENTS

The authors are grateful to Dr. A. Duffield for performing the mass spectrometry. This study was supported by an N.H. & M.R.C. grant to K. M. Williams and R. O. Day. In addition, the authors wish to acknowledge the generous assistance from the Boots Co., Australia, and Nottingham, United Kingdom.

Mechanism for the High Bias in the USP Colorimetric Assay for Diazotizable Substances in Hydrochlorothiazide

DAVID H. SIEH ˣ and SOLOMON PERLMAN

Received February 14, 1983, from *The Squibb Institute for Medical Research, E. R. Squibb & Sons, Inc., New Brunswick, NJ 08903.* Accepted for publication October 6, 1983.

Abstract □ The USP XX colorimetric assay for the determination of diazotizable substances in hydrochlorothiazide was studied. Colorimetric assay results of hydrochlorothiazide bulk powder and captopril-hydrochlorothiazide combination tablets were found to have a high bias when compared with HPLC. A kinetic study of the diazotization step in the colorimetric assay and extrapolation of the free amine content, *i.e.*, 4-amino-6-chloro-1,3-benzenedisulfonamide, to time zero provided results which correlated favorably with those obtained by HPLC. The high bias of the colorimetric assay was shown to result from the formation of 4-nitroso derivative of hydrochlorothiazide, which is formed by acid hydrolysis during the diazotization step. Bendroflumethiazide and flumethiazide also showed increasing free amine content when the time of diazotization was increased.

Keyphrases □ Hydrochlorothiazide—bias of USP XX colorimetric assay for diazotizable substances, free amine content □ Colorimetry—high bias in USP XX assay for diazotizable substances, free amine, hydrochlorothiazide

One of the standard compendial assays performed on benzothiadiazines is the colorimetric test for diazotizable substances (free amine). Here, free amine is a general term used to designate any primary aromatic amine present in the material undergoing testing. In this report, free amine specifically refers to the primary aromatic amide decomposition product of hydrochlorothiazide, *i.e.*, 4-amino-6-chloro-1,3-benzenedisulfonamide. In the compendial assays, any free amine is diazotized with nitrous acid, and the resulting diazonium ion reacts with a color reagent such as disodium 4,5-dihydroxynaphthalene-2,7-disulfonate (disodium chromotropate) or *N*-(1-naphthyl)ethylenediamine dihydrochloride (Bratton-Marshall reaction). There is little precedent in the literature regarding problems with this colorimetric assay. In 1970, Turner and co-workers (1) reported difficulty in reproducing the procedure reported in the British Pharmacopoeia (2) for the determination of free amine in bendroflumethazide. They suggested lengthening the time of diazotization to 5 min rather than the recommended 1 min. This modification was incorporated into the procedures of the British and U.S. Pharmacopeias. Currently, the British Pharmacopoeia suggests use of a TLC assay (3), but the U.S. Pharmacopeia suggests the continued use of the colorimetric assay.

HPLC methods have been developed for the determination of free amine in hydrochlorothiazide bulk powder and captopril-hydrochlorothiazide combination tablets (4) and in nadolol-bendroflumethiazide combination tablet formulations (5). The active ingredients have also been assayed by HPLC methods. When compared with HPLC, the colorimetric assay gave results which consistently showed a high bias. Consequently, a kinetic study of the diazotization and extrapolation to time zero is reported, along with a discussion of the source of the anomoly produced in the diazotization step. A mechanism for the production of this artifactual value is also given.

EXPERIMENTAL SECTION

Materials—Hydrochlorothiazide[1] bulk powder and captopril-hydrochlorothiazide combination tablets[2] were used as received. 4-Amino-6-chloro-1,3-benzenedisulfonamide[3] and ACS reagent-grade disodium 4,5-dihydroxynaphthalene-2,7-disulfonate[4], phosphoric acid[4], hydrochloric acid[4], sodium nitrite[4], and ammonium sulfamate[4] were obtained commercially and used without further purification. The *N*-nitroso derivative of hydrochlorothiazide was prepared by the method of Gold and Mirvish (6), mp 155–156°C (dec.) [lit. (6) mp 155–156°C (dec.)].

High-Performance Liquid Chromatography—A prepacked, reverse-phase, medium-polarity column[5] (250 × 4.6 mm i.d.) containing 5-μm particles was used. The mobile phase was double-distilled water–methanol–phosphoric acid (80:20:0.05) at a flow rate of 2.0 mL/min, with detection at 210 nm. Details of the conditions used have been described previously (5).

Kinetic Studies—The USP procedure (7) for the determination of diazotizable substances in hydrochlorothiazide was followed. In a typical study, four weighings of hydrochlorothiazide powder (100 mg each), each with its own blank and standard, were carried through the procedure up to the addition of the sodium nitrite and hydrochloric acid (diazotization). The diazotization was then allowed to proceed for 5, 10, 15, and 30 min, respectively, at ambient temperature. Then, each solution was carried through to the end of the USP procedure.

The kinetic study was repeated exactly as described above with the 4-nitroso derivative of hydrochlorothiazide instead of hydrochlorothiazide. A third experiment was carried out by omitting the addition of sodium nitrite in the diazotization step while carrying the 4-nitroso derivative of hydrochlorothiazide through the procedure.

An extraction procedure[6] was used to prepare the captopril–hydrochlorothiazide combination tablets for free amine analysis. An acidified aqueous tablet extract was washed with chloroform to remove the interfering captopril, and the resulting aqueous phase was carried through the kinetic study as described above.

RESULTS AND DISCUSSION

The free amine content of hydrochlorothiazide bulk powder was determined by the procedure described in USP XX (6). The current USP procedure calls for a 5-min diazotization. A kinetic study of the diazotization step yielded increasing free amine content with increasing reaction time (Fig. 1). Extrapolation of the free amine content to time zero, *i.e.*, *y*-intercept, with linear regression analysis gave results of 0.0004% (r^2 = 0.977) and 0.06% (r^2 = 0.994) for two batches of hydrochlorothiazide. In Table I the data used to calculate these results are shown. Linear regression analysis also gave slopes of 0.0191 ± 0.0021 (11.0%) and 0.0174 ± 0.0019 (10.9%), respectively, for the two batches of hydrochlorothiazide.

In Fig. 1, a similar phenomenon which occurred when captopril-hydrochlorothiazide tablets were assayed for free amine content by the USP procedure is also shown. Once again, a kinetic study of the diazotization step yielded increasing free amine content with increasing reaction time. Extrapolation of the free amine content to zero time, *i.e.*, *y*-intercept with linear regression analysis, gave a result of 0.11% (r^2 = 0.999) for captopril-hydrochlorothiazide tablets which contained 15 mg of hydrochlorothiazide per tablet and 0.13% (r^2 = 0.999) for tablets which contained 25 mg of hydrochlorothiazide per tablet. In Table I, the data used to calculate these results are

[1] Merck.
[2] E. R. Squibb & Sons, Inc.
[3] Fluka AG.
[4] Fisher Scientific Co.
[5] Phenyl; Waters Associates or E. S. Industries.
[6] R. Clay and B. Patel, unpublished results.

0022-3549/84/1100-1545$01.00/0
© 1984, American Pharmaceutical Association

Table I—Free Amine Content of Hydrochlorothiazide Bulk Powder and Captopril-Hydrochlorothiazide Combination Tablets *Versus* Time of Diazotization

	Reaction Time, min[a]	Free Amine Content, %[a]	Reaction Time, min[b]	Free Amine Content, %[b]
Captopril-hydrochlorothiazide Combination tablets	5	0.18	5	0.19
	10	0.26	10	0.26
	15	0.32	15	0.32
	30	0.54	30	0.50
	Lot NX008		Lot NX018	
Hydrochlorothiazide Bulk powder	5	0.11	5	0.16
	10	0.21	10	0.23
	15	0.24	15	0.30
	30	0.59	30	0.59

[a] The tablets contained 15 mg of hydrochlorothiazide. [b] The tablets contained 25 mg of hydrochlorothiazide.

shown. Linear regression analysis also gave slopes of 0.0143 ± 0.0015 (10.5%) and 0.0123 ± 0.0013 (10.6%), respectively, for the combination tablets.

The *RSD* of the slopes was calculated to be 19.5%. This value is surprisingly high in light of the fact that each individual set of data points provided excellent correlation coefficients. One possible factor is that the temperature of the reaction was not strictly controlled, *i.e.*, it was performed at room temperature. An increase in room temperature would be paralleled by an increase in the slope of the line, and a decrease in room temperature would be paralleled by a decrease in the slope of the line.

The extrapolated values are compared with the values obtained from the HPLC assay (Table II). In Table II are also included the values determined by the USP procedure, which has a 5-min diazotization. A high bias exists in the USP method. Since the HPLC assay has a limit of detection of 0.1% and the results of the kinetic study are close to that limit, it is difficult to make a quantitative comparison. Qualitatively, the HPLC assay and the kinetic assay gave results that were substantially lower than those of the USP procedure.

It is tempting to attribute the increase in free amine content to the acid-catalyzed hydrolysis of hydrochlorothiazide. This, however, is not the case. When hydrochlorothiazide was allowed to stand in dilute hydrochloric acid (1:10), no increase in free amine content was observed even after 1 h. The kinetics and rate of decomposition of hydrochlorothiazide in acidic media have been studied by other investigators. For example, Yamana *et al.* (8) have published a report covering the pH-rate profile of hydrochlorothiazide. Mollica *et al.* (9) have published an extensive report on the hydrolysis of benzothiadiazines. They reported the rate constant for hydrolysis of hydrochlorothiazide at pH 1.47 and 45°C to be 1.46×10^{-3} h^{-1}. By using the Arrhenius relationship, the rate constant at 25°C should be $\sim 1.5 \times 10^{-4}$ h^{-1}. This translates into a half-life of 4620 h. Thus, under the acid treatment employed in the colorimetric procedure, a negligible amount of hydrochlorothiazide is hydrolyzed to free amine.

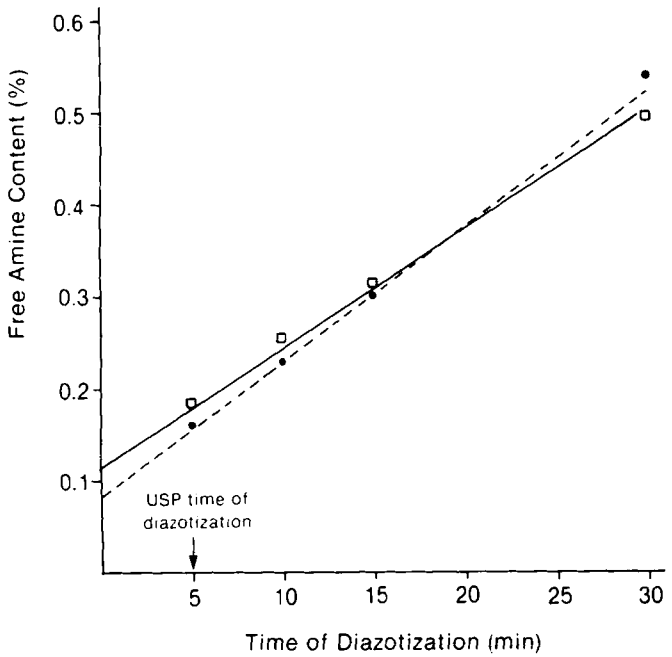

Figure 1—*Free amine content of hydrochlorothiazide bulk powder* (●) *and captopril-hydrochlorothiazide combination tablets* (□) *as a function of time of diazotization.*

Table II—Comparison of HPLC and Kinetic Assays for the Determination of Free Amine Content in Hydrochlorothiazide Bulk Powder and Captopril-Hydrochlorothiazide Combination Tablets

Formulation	Free Amine Content, % HPLC	Colorimetry USP	Colorimetry Kinetic
Captopril-hydrochlorothiazide Combination tablets	≤0.1[a]	0.17[a]	0.11[a]
	≤0.1[b]	0.23[b]	0.13[b]
Hydrochlorothiazide bulk powder	≤0.1[c]	0.11[c]	0.0004[c]
	≤0.1[d]	0.13[d]	0.06[d]

[a] The tablets contained 15 mg of hydrochlorothiazide. [b] Tablets contained 25 mg of hydrochlorothiazide. [c] Lot NX008. [d] NX018.

One of the standard syntheses of *N*-nitrosamines is nitrous acid addition to a secondary amine in which the nitrous acid is generated *in situ* by the addition of sodium nitrite to an aqueous acidic solution of the amine. Depending on the secondary amine, this nitrosation can be very slow (*e.g.*, dimethylamine) or quite rapid (*e.g.*, *N*-methylaniline) (10). In fact, for secondary aromatic amines, the reaction mixture is usually cooled to 0°C to allow nitrosation to take place at a reasonable rate. Since hydrochlorothiazide is a secondary aromatic amine, it would not be surprising that some nitrosamine would be generated in the diazotization reaction. This was found to be the case.

The nitrosation kinetics of hydrochlorothiazide have been reported by Gold and Mirvish (6). They have reported that the reaction was second order and possessed a rate constant of 0.76 M^{-1} s^{-1}. Hydrochlorothiazide was dissolved in 25% aqueous acetic acid, the pH was adjusted to 1.0 with 70% perchloric acid mixed with an aqueous sodium nitrite solution, and the kinetics were followed by measuring the disappearance of the UV maximum and appearance of the λ_{max} of the nitrosamine at 392 nm. The conditions used by Gold and Mirvish are nearly identical to those present in the diazotization reaction in the procedure described in USP XX, *i.e.*, pH 1.0 at 25°C in aqueous media. We can approximate the amount of hydrochlorothiazide nitrosated under these conditions by using the second-order rate equation: $(1/a - x) - (1/a) = kt$, where a is the initial concentration of hydrochlorothiazide (~0.003 M), x is the concentration of the nitrosamine at time t, and k is 0.76 M^{-1} s^{-1}. For example, in 5 and 30 min, 41 and 81% of the hydrochlorothiazide, respectively, was nitrosated.

In Scheme I is depicted the reactions of both hydrochlorothiazide and any

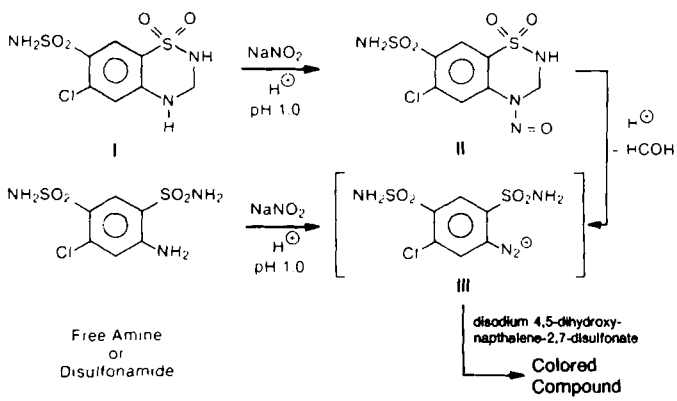

Scheme I

Table III—Acid-Catalyzed Decomposition of the 4-Nitroso Derivative of Hydrochlorothiazide

Time, min	Free Amine Content, %[a]	
	Dilute HCl (1:10)	Sodium Nitrite Dilute HCl
5	0.42	1.07
10	0.55	1.08
15	0.63	1.22
30	1.04	2.09

[a] Procedures described in USP XX for diazotizable substances.

free amine present under nitrosation conditions. The addition of the nitroso group in the 4-position (II) greatly increases the acid lability of the compound compared with hydrochlorothiazide (I). Acid-catalyzed hydrolysis of the 4-nitroso derivative of hydrochlorothiazide could lead to the same intermediate diazonium ion that would be produced by the diazotization of any free amine. This diazonium ion is subsequently reacted with disodium 4,5-dihydroxynaphthalene-2,7-disulfonate, and the resulting colored compound is quantitated by reading at 500 nm.

To prove this hypothesis, the 4-nitroso derivative of hydrochlorothiazide was synthesized by previously reported procedures (6), recrystallized, and then assayed for free amine content by the procedure described in USP XX. The free amine content increased with time just as in the determination of free amine in hydrochlorothiazide (Table III). The nitrosamine was also allowed to react in dilute HCl (1:10) for various periods of time, with no sodium nitrite present. Once again, increasing free amine content with increasing time was observed. Obviously, the nitrosamine is undergoing acid-catalyzed decomposition to the diazonium ion (III, Scheme I), which is subsequently reacting with the color reagent in the assay.

The rate of decomposition of the 4-nitroso derivative of hydrochlorothiazide in nitrous acid was found to be about twice that in dilute HCl (Table III.) This might be due to an equilibrium shift. In addition to the decomposition to the diazonium ion, secondary *N*-nitrosamines can undergo denitrosation back to the secondary amine. This denitrosation is an equilibrium process:

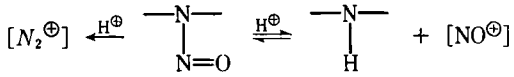

In dilute HCl when $NaNO_2$ is present, the concentration of NO^+ present is increased. Thus, the equilibrium is shifted to the left causing the observed increase in the rate of decomposition.

The results of these experiments indicate conclusively that the diazotization step generates an artifactual interference in the colorimetric assay. Although HPLC is an excellent alternative for the determination of the free amine (disulfonamide) content of hydrochlorothiazide bulk powder and captopril–hydrochlorothiazide combination tablets, it has a limit of detection of ~0.1%. To achieve the sensitivity of the procedure described in USP XX, an alternative colorimetric procedure has been developed[7] which will be discussed in a later report.

All other colorimetric USP XX tests for diazotizable substances in benzothiadiazines in which sodium nitrite in acid media is used have been thrown into doubt as a result of these experiments. In fact, bendroflumethiazide and flumethiazide were shown to yield increasing free amine content with increasing time of diazotization. For example, USP free amine assays gave contents of 0.8% for bendroflumethiazide bulk powder, whereas a value of 0.2% was obtained by HPLC (4).

Numerous *N*-nitrosamines are known carcinogens and mutagens. However, the 4-nitroso derivative of hydrochlorothiazide has been found to be neither carcinogenic nor mutagenic[8] and does not pose any danger in handling. Since the other 4-nitrosobenzothiadiazines have not been tested for carcinogenicity and mutagenicity, care should be exercised when performing the assay for diazotizable substances. In the new colorimetric procedure[7], no *N*-nitrosamines are formed.

REFERENCES

(1) J. C. Turner, A. W. Nicholls, and J. E. Sloman, *Pharm. J.*, **204**, 622 (1970).

(2) "The British Pharmacopoeia," Her Majesty's Stationery Office, London, 1968, p. 90.

(3) "The British Pharmacopoeia," Her Majesty's Stationery Office, London, 1980, p. A61.

(4) J. Kirschbaum and S. Perlman, *J. Pharm. Sci.*, **73**, 686 (1984).

(5) S. Perlman, M. Szyper, and J. Kirschbaum, *J. Pharm. Sci.*, **73**, 259 (1984).

(6) B. Gold and S. Mirvish, *Toxicol. Appl. Pharmacol.*, **40**, 131 (1977).

(7) "United States Pharmacopeia," 20th rev., U.S. Pharmacopeial Convention Inc., Rockville, Md., 1980, p. 379.

(8) T. Yamana, Y. Mizukami, A. Tsuji, and F. Ichimura, *Yakugaki Zasshi*, **89**, 740 (1969); Chem. Abstr., **71**, 53526y.

(9) J. A. Mollica, C. R. Rehm, J. B. Smith, and H. K. Govan, *J. Pharm. Sci.*, **60**, 1380 (1971).

(10) "The Chemistry of the Amino Group," S. Patai, Ed., Wiley-Interscience, New York, N.Y., 1968, and references therein.

ACKNOWLEDGMENTS

The authors thank Sandra Willis for performing many of the assays; Dr. John Dunham, Dr. Glenn Brewer, and Dr. Klaus Florey for help and critical reading of this manuscript; and a special thanks to Dr. Joel Kirschbaum for helpful comments and criticisms. The talents of Jose Alcantara in illustrating and Ruth Lemire in typing this report are gratefully appreciated.

[7] Whigan and P. Stears, unpublished results

[8] R. Kupper and D. Nagel, unpublished results.

α-Phenyl-β-(3,4-dimethoxy)phenethylamines: Novel Inhibitors of Choline Acetyltransferase from *Torpedo* Electric Organ

RAGAB M. SHAFIK *x, RAAFAT SOLIMAN *, SOAD A. EL-HAWASH *, MAHMOUD MORSHEDY ‡, and NABIL A. MANSOUR ‡

Received April 12, 1983, from the **Department of Pharmaceutical Chemistry, Faculty of Pharmacy* and the ‡ *Department of Pesticide Chemistry, Faculty of Agriculture, University of Alexandria, Alexandria, Egypt.* Accepted for publication September 7, 1983.

Abstract □ Some derivatives of α-phenyl-β-(3,4-dimethoxy)phenethylamine that might bear a certain conformational resemblance to choline were prepared. The *in vitro* inhibition of choline acetyltransferase from *Torpedo* electric organ was investigated. These compounds gave variable degrees of inhibition; the most potent inhibitor was, *N,N,N*-trimethyl-α-phenyl-β-(3,4-dimethoxy)phenethylammonium iodide, with an I_{50} of 1.3×10^{-5} M. The inhibition of choline acetyltransferase from *Spodoptera littoralis* larval brains was also determined for comparative study. The aforementioned compound has an I_{50} of 9×10^{-6} M on choline acetyltransferase from this source.

Keyphrases □ α - Phenyl -β- (3,4 - dimethoxy)phenethylamines—synthesis, inhibition of choline acetyltransferase □ Choline acetyltransferase—inhibition, α-phenyl-β-(3,4-dimethoxy)phenethylamines

The phenethylamine (I) skeleton is an integral moiety for many naturally occuring compounds which possess remarkable biological properties, *e.g.*, morphine (1), ephedrine (2), epinephrine (3), norepinephrine (3), and papaverine (4, 5). The structural feature of choline base (II), the β-hydroxy ethylamine derivative, bears some conformational resemblance to I. It has been shown (6) that the most favorable conformation of II, at physiological pH, is the *gauche* disposition (IIa). The latter might be the most suitable conformer for interaction with the choline acetyltransferase (E.C. 2.3.1.6) surface prior to acetylation (7, 8). A bioisosteric *gauche* arrangement (Ia) would be assured by introducing a phenyl group in the α-position. This would also increase lipophilicity. Therefore, we prepared some derivatives (III) of α-phenyl-β-(3,4-dimethoxy)phenethylamine and evaluated them as inhibitors of choline acetyltransferase.

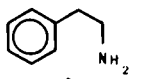

I

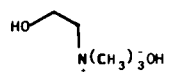

II

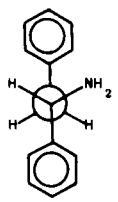

Ia

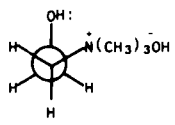

IIa

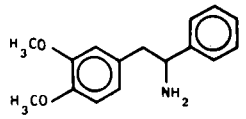

III

Choline acetyltransferase catalyzes the synthesis of acetylcholine, and both O'Brien (9) and Yu and Booth (10) recognized the potential of this enzyme as a target for new drugs and insecticides. For biochemical studies, choline acetyltransferase from *Torpedo* electric organ was used, and the results were compared with those recorded for choline acetyltransferase from *Spodoptera littoralis* larval brains.

Few potent inhibitors of choline acetyltransferase are known, and those that have been tested have not proved useful as insecticides (10). Other reports dealing with mammalian inhibitors of this enzyme have been published, *e.g.*, 5-hydroxy-1,4-naphthalenedione and 4-(1-naphthylvinyl)pyridine (11), halogenoacetylcholines (12), and (2-benzoylethyl)trimethylammonium chloride (13, 14). Most of these compounds are either esters or aromatic ketones which are relatively unstable (12, 14). On the other hand the compounds described here are neither esters nor ketones. Some clear differences existed between the choline acetyltransferases of mites, houseflies, and rats toward their substrate specificity (9). It was also reported that quite marked variation in sensitivity between insect and mouse choline acetyltransferases were displayed when both enzymes were tested against known inhibitors, such as the styrylpyridines (10).

The synthetic approach followed is outlined in Scheme I. 3,4-Dimethoxy-α-nitrostilbene (VI) was prepared using a modification of the method described by Owari (15). α-Phenyl-β-(3,4-dimethoxy)phenethylamine (III) was obtained by reduction of VI with lithium aluminum hydride in ether. The *N*-formyl derivative (VIIa) was obtained from III using the method of Sam *et al.* (16). Treatment of III with ethyl chloroformate in the presence of pyridine afforded the *N*-ethoxycarbonyl derivative (VIIb). The *N*-methyl derivative (VIII) was prepared either from VIIa or VIIb by reduction with lithium aluminum hydride in tetrahydrofuran or ether, respectively. The *N,N*-dimethyl derivative (IX) was obtained by applying an analogous procedure reported by Shafik *et al.* (5) for the preparation of similar compounds. The quaternarization of IX to give the trimethylammonium derivative (X) was carried out by using an excess of methyl iodide in ether.

EXPERIMENTAL SECTION[1]

3,4-Dimethoxy-α-nitrostilbene (VI)—To a solution of 16.6 g (0.1 mol) of veratraldehyde (IV) in 15 mL of methanol was added 13.7 g (0.1 mol) of phenylnitromethane (17) (V) and 0.5 mL of *n*-butylamine. The mixture was kept at room temperature for 72 h, and then the product was removed by filtration, dried, and recrystallized from ethanol to give 10.0 g (35% yield) of yellow needles, mp 105–107°C [lit (18) mp 109°C]; IR ν_{max}: 1365 and 1595 cm^{-1} (C—NO_2).

[1] Melting points were taken in open glass capillaries and are uncorrected. The IR spectra were scanned on a Beckman IR-4210 spectrophotometer with KBr pellets. The ^{1}H-NMR spectra were determined, for solutions in Me_2SO-d_6, on a Varian EM-390 NMR spectrometer, and are reported in δ values (ppm) relative to an internal standard of tetramethylsilane. Analyses were performed by members of the Microanalytical Unit, Faculty of Science, University of Cairo, Egypt.

0022-3549/84/1100-1548$01.00/0
© 1984, American Pharmaceutical Association

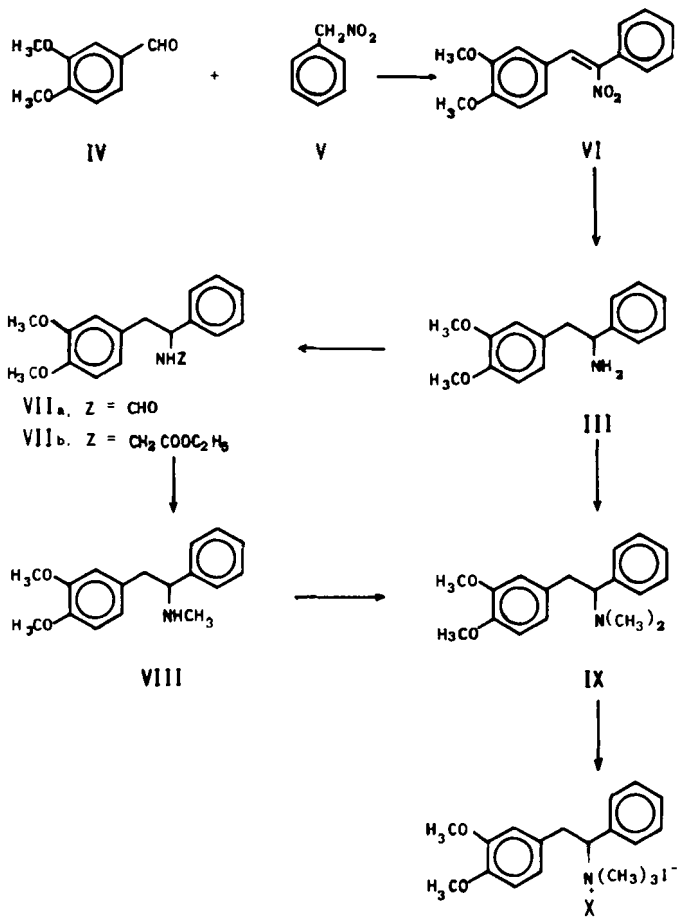

SCHEME I

α-Phenyl-β-(3,4-dimethoxy)phenethylamine (III)—To a stirred mixture of 1.9 g (0.05 mol) of lithium aluminum hydride and 300 mL of ether was added 2.8 g (0.01 mol) of VI. The mixture was refluxed for 72 h, and then chilled. The excess lithium aluminum hydride was destroyed with crushed ice and 20% aqueous NaOH, respectively. The product was isolated by ether extraction and was purified in the usual manner (5) by alternative pH adjustments to give 1.9 g (67% yield) of III as pale-yellow needles, mp 65°C [lit (15) mp 66–67°C]. The hydrochloride salt was obtained by passing dry hydrogen chloride into the ethereal solution of III to give white needles, which were recrystallized from methanol–ether to give 1.9 g (67% yield) of white crystals, mp 176–177°C [lit (19) mp 176–177°C]; IR ν_{max}: 2650 cm^{-1} (NH_3^+); ^{1}H-NMR (Me_2SO-d_6): δ 3.45 (s, 6), 3.55 (d, 2, J = 6 Hz), 4.4 (m, 1), 6.65 (m, 3, ArH), and 7.35 ppm (m, 5, ArH).

N-Formyl-α-phenyl-β-(3,4-dimethoxy)phenethylamine (VIIa)—A solution of 2.6 g (0.01 mol) of III in a mixture of 15 mL of 98% formic acid and 18 mL of acetic anhydride was refluxed for 5 h and then diluted with 100 mL of water. The mixture was extracted with ether and washed with 10% NaOH, then 10% HCl, and water. The ethereal extract was dried (Na_2SO_4), and the solvent was removed under reduced pressure. The oily residue that solidified on standing was recrystallized from benzene–petroleum ether (bp 40–60°C) to give 1.2 g (43% yield) of white crystals, mp 120–121°C; IR ν_{max}: 3400 (NH), 1650, 1550, and 1250 cm^{-1} (amide bands).

Anal.—Calc. for $C_{17}H_{19}NO_3$: C, 71.6; H, 6.6; N, 4.9. Found: C, 71.5; H, 6.2; N, 5.3.

N-Ethoxycarbonyl-α-phenyl-β-(3,4-dimethoxy)phenethylamine (VIIb)—A solution of 2.7 g (0.025 mol) of ethyl chloroformate in 10 mL of benzene was added, dropwise, to a cold, stirred solution of 6.2 g (0.024 mol) of III in 30 mL of pyridine. The mixture was stirred for an additional 3 h and then was refluxed for 4 h. The mixture was poured onto 25 mL of 10% HCl and extracted with benzene. The organic phase was washed with 2 M NaOH and water, and dried (Na_2SO_4). The solvent was removed under reduced pressure to give an oily residue that solidified on standing at room temperature. Recrystallization from benzene–petroleum ether (bp 40–60°C) gave 1.6 g (47% yield) of pale-yellow crystals of VIIb, mp 107°C; IR ν_{max}: 3450 (NH), 1670, 1550, and 1265 cm^{-1} (amide bands).

Anal.—Calc. for $C_{19}H_{23}NO_4$: C, 69.3; H, 7.0; N, 4.3. Found: C, 69.1; H, 7.4; N, 4.3.

N-Methyl-α-phenyl-β-(3,4-dimethoxy)phenethylamine Hydrochloride (VIII)—*Method A*—To a stirred mixture of 1.9 g (0.05 mol) of lithium aluminum hydride and 200 mL of tetrahydrofuran was added 2.8 g (0.01 mol) of VIIa. The mixture was heated at reflux for 16 h, and the solvent was removed under reduced pressure. The residue was chilled to give (as in the preparation of III) the hydrochloride salt, 1.7 g (62% yield) as white crystals, mp 164–165°C.

Anal.—Calc. for $C_{17}H_{22}ClNO_2$: C, 66.3; H, 7.2; Cl, 11.5; N, 4.6. Found: C, 66.5; H, 7.2; Cl, 11.4; N, 4.2.

Method B—To a stirred mixture of 1.9 g (0.05 mol) of lithium aluminum hydride and 300 mL of ether was added 3.3 g (0.01 mol) of VIIb. The mixture was heated at reflux for 14 h. The hydrochloride salt was recrystallized from methanol–ether to give 2.4 g (72% yield) as white crystals, mp 164–165°C. Admixture of the products obtained by both methods (A and B) showed no melting point depression.

N,N-Dimethyl-α-phenyl-β-(3,4-dimethoxy)phenethylamine Hydrochloride (IX)—A mixture of 0.01 mol of the hydrochloride salt of III or VIII, 2.3 g (0.05 mol) of formic acid (98%), and 0.66 g (0.022 mol) of 38% formaldehyde was refluxed for 12 h. The mixture was transferred to an evaporating dish and heated on a water bath until most of the unreacted formic acid and formaldehyde were removed. The syrupy residue was treated with 0.6 mL of formic acid (98%) and 0.2 mL of 38% formaldehyde and allowed to evaporate on the water bath until dryness. The last traces of water were removed by azeotropic distillation with absolute ethanol and benzene. The residual hydrochloride salt was recrystallized from methanol–ether to give 2.0 g (78% yield) as white crystals, mp 218–220°C; IR ν_{max}: 2600 cm^{-1} (NH^+); ^{1}H-NMR (Me_2SO-d_6): δ 2.90 (s, 6), 3.30 (s, 6), 3.80 (d, 2, J = 5 Hz), 4.80 (m, 1), 6.90 (d, 3, J = 9 Hz, ArH), 7.60 ppm (m, 5, ArH).

Anal.—Calc. for $C_{18}H_{24}ClNO_2$: C, 67.2; H, 7.5; Cl, 11.0; N, 4.4. Found: C, 67.4; H, 7.1; Cl, 10.6; N, 4.0.

N,N,N-Trimethyl-α-phenyl-β-(3,4-dimethoxy)phenethylammonium Iodide (X)—To a solution of 2.9 g (0.01 mol) of IX in 100 mL of ether was added 1.7 g (0.012 mol) of methyl iodide. The mixture was allowed to stand at room temperature for 24 h. The crystalline material was removed by filtration and recrystallized from methanol–ether to give 1.8 g (63% yield) of yellow crystals, mp 228–230°C; ^{1}H-NMR (Me_2SO-d_6): δ 3.40 (s, 9), 3.75 (s, 6), 4.50 (m, 2), 6.90 (s, 1), 7.50 (m, 3, ArH), and 7.80 ppm (m, 5, ArH).

Anal.—Calc. for $C_{19}H_{26}INO_2$: C, 53.43; H, 6.1; N, 3.3. Found: C, 53.7; H, 5.9; N, 3.6.

Biochemical Assays—Membranes were prepared from the electric organ of *Torpedo ocellata* (collected near Alexandria, Egypt, and stored frozen at −90°C for up to 6 months) by homogenization (50%, w/v) in ice-cold 10 mM EDTA–20 mM Na_2HPO_4 buffer (pH 7.4). An emulsifier[2] (0.2%, v/v) was added to the homogenate, and the suspension was shaken lightly by hand for few seconds, filtered through cheesecloth, and centrifuged at 100,000×g for 30 min. The supernatant was used as the enzyme source. Head capsules of fourth instar *Spodoptera littoralis* larvae were homogenized in the aforementioned buffer (1 mL/10 head capsules) using a similar procedure. Protein was assayed by the method of Lowry *et al.* (20).

The radiochemical method was used for the determination of choline acetyltransferase activity (21). The incubation mixture contained 0.2 mM [1-^{14}C]acetyl CoA[3] (50 mCi/mmol), 300 mM NaCl, 50 mM Na_2HPO_4 buffer (pH 7.4), 8 mM choline bromide, 20 mM EDTA, and 0.1 mM physostigmine. The labeled acetyl CoA was diluted with the unlabeled compound[4]. In the inhibition studies of choline acetyltransferase activity, the enzyme preparation was incubated with 10 μL of the inhibitor solution for different intervals.

RESULTS AND DISCUSSION

The radioactivity assay was used to find the acetyl CoA concentration in the incubation medium and different protein concentrations for optimal *Torpedo* electric organ choline acetyltransferase activity. A range of 0.1–0.2 mM acetyl CoA was necessary to give near-optimal activities. Such high acetyl CoA concentrations gave linear activity curves over a greater range, maintaining linearity up to 120 μg of enzyme in the incubation mixture. Under these conditions the enzyme-specific activities of six different preparations were 14.60 ± 0.16 (mean ± SD) and 6.64 ± 0.12 λ_{max} 412·mg^{-1} of protein·h^{-1} for *Torpedo* electric organ and *Spodoptera* larval brain preparations, respectively. The differences in membrane binding might be due to differences among the surface charges of choline acetyltransferase from the two species.

As can be seen from the structures of I and II, the quaternary ammonium derivative (X) was the most potent inhibitor in a micromolar range for choline

[2] Triton X-100; Rohm and Haas.
[3] The Radiochemical Center, Amersham, England.
[4] Sigma Chemical Co., St. Louis, Mo.

Table I—*In Vitro* Inhibition of Choline Acetyltransferase Activity from Two Sources by α-Phenyl-β-(3,4-dimethoxy)phenethylamine Derivatives

Compound[a]	Inhibition Constants			
	Torpedo		*Spodoptera*	
	I_{50}, M	K_i, μM	I_{50}, M	K_i, μM
III	7.0×10^{-5}	60	2.7×10^{-5}	40
VIII	5.8×10^{-5}	45	2.5×10^{-5}	32
IX	4.0×10^{-5}	35	1.8×10^{-5}	25
X	1.3×10^{-5}	10	9.0×10^{-6}	6

[a] The I_{50} values were compared with those determined for diisopropylfluorophosphonate ($I_{50} = 5 \times 10^{-4}$ M from both sources). Lit. (10) data reported for diisopropylfluorophosphonate using choline acetyltransferase (house fly or mouse): $I_{50} = 1 \times 10^{-4}$ M.

acetyltransferase from both sources. From the I_{50} and K_i values obtained, the *Spodoptera* larval enzymes were shown to be more sensitive toward the synthesized compounds (III and VIII–X) than the *Torpedo* electric organ enzymes. However, the best *in vitro* choline acetyltransferase inhibitor was the charged compound (X), whereas the uncharged compounds (III, VIII, and IX) were relatively poor inhibitors (Table I).

Several choline analogues ($SCNCH_2CH_2\overset{+}{N}R^1R^2R^3X^-$) were previously tested (22) on rats as possible *in vivo* choline acetyltransferase inhibitors; the data revealed poor correlation between the K_i value and the insecticidal activity of such compounds when tested against several insect species. The most likely explanation was that since the molecule is charged, it would not readily penetrate the nerve cord and reach the cells in which the enzyme is located. The present work was thus directed toward *in vitro* inhibition studies using some uncharged phenethylamines (III, VIII, and IX) to avoid the problems of compound penetration to the target. The quaternary analogue (X) was also investigated.

REFERENCES

(1) H. B. Murphree, in "Drill's Pharmacology in Medicine," J. R. Di Palma, Ed., McGraw-Hill, New York, N.Y., 1965, p. 251.

(2) K. K. Chen and C. F. Schmidt, *J. Pharmacol. Exp. Ther.*, **24**, 339 (1925).

(3) D. J. Triggle, in "Medicinal Chemistry," Part II, A. Burger, Ed., Wiley, New York, N.Y., 1970, p. 1239.

(4) L. S. Goodman and A. Gilman, Eds., "The Pharmacological Basis of Therapeutics," 4th ed., Macmillan, London, England, 1970, pp. 753 and 754.

(5) R. M. Shafik, R. Soliman, and A. M. M. Hassan, *J. Pharm. Sci.*, **67**, 991 (1978).

(6) F. G. Canepa, P. Pauling, and H. Sorum, *Nature (London)*, **210**, 907 (1966).

(7) M. S. Steinberg, N. S. Cohen, and W. W. Weber, *Biochem. Biophys. Acta*, **235**, 89 (1971).

(8) R. Roskoski, Jr., *J. Biol. Chem.*, **249**, 2156 (1974).

(9) R. D. O'Brien, "Insecticides: Action and Metabolism" Academic, New York, N.Y., 1967.

(10) C. C. Yu and G. M. Booth, *Life Sci.*, **10**, 337 (1971).

(11) D. R. Haubrich and P. F. L. Wang, *Biochem. Pharmacol.*, **25**, 669 (1976).

(12) G. I. Henderson and B. V. Rama Sastry, *Biochem. Pharmacol.*, **27**, 1331 (1978).

(13) A. K. Chaturvedi, P. P. Rowell, and B. V. Rama Sastry, *J. Pharm. Sci.*, **67**, 657 (1978).

(14) P. P. Rowell, A. K. Chaturvedi, and B. V. Rama Sastry, *J. Pharmacol. Exp. Ther.*, **205**, 624 (1978).

(15) S. Owari, *Pharm. Bull. (Jpn.)*, **1**, 174 (1953).

(16) J. Sam, R. M. Shafik, and K. Aparajithan, *J. Pharm. Sci.*, **59**, 59 (1970).

(17) A. P. Black and F. H. Babers, in "Organic Syntheses," Coll. Vol. II, A. H. Blatt, Ed., Wiley, London, England, 1947, p. 512.

(18) H. Kauffman, *Chem. Ber.*, **25B**, 1422 (1919).

(19) W. D. McPhee and E. S. Eriskson, Jr., *J. Chem. Soc.*, **68**, 624 (1946).

(20) O. H. Lowry, N. J. Rosebrough, A. L. Farr, and R. J. Randall, *J. Biol. Chem.*, **193**, 265 (1951).

(21) F. Fonnum, *J. Neurochem.*, **20**, 1351 (1975).

(22) C. A. Baillie, J. R. Corbett, J. R. Dowsett, D. B. Sattelle, and J. J. Callec, *Pestic. Sci.*, **6**, 645 (1975).

ACKNOWLEDGMENTS

The authors are grateful to Dr. Shebl M. Sherby, Faculty of Agriculture, University of Alexandria for his kind help, and Dr. Samia El-Dardiry, Faculty of Medicine University of Tanta, for her useful comments dealing with the preparation of this manuscript. This research was supported by the National Science Foundation Grant (INT 78-01468) to the University of Alexandria, Egypt.

Excitatory Amino Acid Receptor Interactions of a Novel α-Phosphinic Acid Analogue of α-Methylaspartic Acid

L. A. CATES *x, V-S. LI *, Z-S. HU *, J. LEHMANN ‡, J. T. COYLE ‡, and J. W. FERKANY ‡

Received October 14, 1983, from the **Department of Medicinal Chemistry, College of Pharmacy, University of Houston, Houston, TX 77004* and the ‡*Departments of Neuroscience, Pharmacology, and Psychiatry, Division of Child Psychiatry, Johns-Hopkins University, School of Medicine, Baltimore, MD 21205.* Accepted for publication November 30, 1983.

Abstract □ An α-phosphino analogue of α-methylaspartate has been synthesized. The compound may not interact with excitatory amino acid receptors directly, as assessed by direct *in vitro* radioreceptor binding methods; however, it possesses weak anticonvulsant activity and exhibits an excitant action *in vitro* that is apparently not mediated by a *N*-methyl-D-aspartate receptor.

Keyphrases □ Excitatory amino acid receptors—*N*-methyl-D-aspartate, glutamate, kainate □ Anticonvulsants—*in vitro*, rats, excitatory amino acids □ Phosphinic acids—excitatory amino acid receptors, anticonvulsant activity

Phosphorus analogues of amino acids have been investigated previously; however, most studies have involved phosphonic acid derivatives such as aminomethanephosphonic acid (I). Only in recent years have aminophosphinic acids with unsubstituted amino groups been prepared. The first, glycine analogue II, was synthesized in 1964 by a procedure which provides only limited types of products (1).

Phosphinic acids possess a hydrogen atom in lieu of one of the two hydroxyl groups found in phosphonic acids and, therefore, are monobasic with less bulk on the phosphorus atom. Phosphinic acids are the closest phosphorus analogues of carboxylic acids and this similarity has led to a limited number of investigations of aminophosphinic acids for biological activity. In 1961, Linfield *et al.* prepared phosphinic acids bearing substituted α-anilino and phenyl groups (III) by the addition of hypophosphorus acid to the appropriate

0022-3549/84/1100-1550$01.00/0

© 1984, American Pharmaceutical Association

Table I—*In Vitro* Inhibition of Choline Acetyltransferase Activity from Two Sources by α-Phenyl-β-(3,4-dimethoxy)phenethylamine Derivatives

Compound[a]	Inhibition Constants			
	Torpedo		*Spodoptera*	
	I_{50}, M	K_i, μM	I_{50}, M	K_i, μM
III	7.0×10^{-5}	60	2.7×10^{-5}	40
VIII	5.8×10^{-5}	45	2.5×10^{-5}	32
IX	4.0×10^{-5}	35	1.8×10^{-5}	25
X	1.3×10^{-5}	10	9.0×10^{-6}	6

[a] The I_{50} values were compared with those determined for diisopropylfluorophosphonate ($I_{50} = 5 \times 10^{-4}$ M from both sources). Lit. (10) data reported for diisopropylfluorophosphonate using choline acetyltransferase (house fly or mouse): $I_{50} = 1 \times 10^{-4}$ M.

acetyltransferase from both sources. From the I_{50} and K_i values obtained, the *Spodoptera* larval enzymes were shown to be more sensitive toward the synthesized compounds (III and VIII–X) than the *Torpedo* electric organ enzymes. However, the best *in vitro* choline acetyltransferase inhibitor was the charged compound (X), whereas the uncharged compounds (III, VIII, and IX) were relatively poor inhibitors (Table I).

Several choline analogues ($SCNCH_2CH_2\overset{+}{N}R^1R^2R^3X^-$) were previously tested (22) on rats as possible *in vivo* choline acetyltransferase inhibitors; the data revealed poor correlation between the K_i value and the insecticidal activity of such compounds when tested against several insect species. The most likely explanation was that since the molecule is charged, it would not readily penetrate the nerve cord and reach the cells in which the enzyme is located. The present work was thus directed toward *in vitro* inhibition studies using some uncharged phenethylamines (III, VIII, and IX) to avoid the problems of compound penetration to the target. The quaternary analogue (X) was also investigated.

REFERENCES

(1) H. B. Murphree, in "Drill's Pharmacology in Medicine," J. R. Di Palma, Ed., McGraw-Hill, New York, N.Y., 1965, p. 251.

(2) K. K. Chen and C. F. Schmidt, *J. Pharmacol. Exp. Ther.*, **24**, 339 (1925).

(3) D. J. Triggle, in "Medicinal Chemistry," Part II, A. Burger, Ed., Wiley, New York, N.Y., 1970, p. 1239.

(4) L. S. Goodman and A. Gilman, Eds., "The Pharmacological Basis of Therapeutics," 4th ed., Macmillan, London, England, 1970, pp. 753 and 754.

(5) R. M. Shafik, R. Soliman, and A. M. M. Hassan, *J. Pharm. Sci.*, **67**, 991 (1978).

(6) F. G. Canepa, P. Pauling, and H. Sorum, *Nature (London)*, **210**, 907 (1966).

(7) M. S. Steinberg, N. S. Cohen, and W. W. Weber, *Biochem. Biophys. Acta*, **235**, 89 (1971).

(8) R. Roskoski, Jr., *J. Biol. Chem.*, **249**, 2156 (1974).

(9) R. D. O'Brien, "Insecticides: Action and Metabolism" Academic, New York, N.Y., 1967.

(10) C. C. Yu and G. M. Booth, *Life Sci.*, **10**, 337 (1971).

(11) D. R. Haubrich and P. F. L. Wang, *Biochem. Pharmacol.*, **25**, 669 (1976).

(12) G. I. Henderson and B. V. Rama Sastry, *Biochem. Pharmacol.*, **27**, 1331 (1978).

(13) A. K. Chaturvedi, P. P. Rowell, and B. V. Rama Sastry, *J. Pharm. Sci.*, **67**, 657 (1978).

(14) P. P. Rowell, A. K. Chaturvedi, and B. V. Rama Sastry, *J. Pharmacol. Exp. Ther.*, **205**, 624 (1978).

(15) S. Owari, *Pharm. Bull. (Jpn.)*, **1**, 174 (1953).

(16) J. Sam, R. M. Shafik, and K. Aparajithan, *J. Pharm. Sci.*, **59**, 59 (1970).

(17) A. P. Black and F. H. Babers, in "Organic Syntheses," Coll. Vol. II, A. H. Blatt, Ed., Wiley, London, England, 1947, p. 512.

(18) H. Kauffman, *Chem. Ber.*, **25B**, 1422 (1919).

(19) W. D. McPhee and E. S. Eriskson, Jr., *J. Chem. Soc.*, **68**, 624 (1946).

(20) O. H. Lowry, N. J. Rosebrough, A. L. Farr, and R. J. Randall, *J. Biol. Chem.*, **193**, 265 (1951).

(21) F. Fonnum, *J. Neurochem.*, **20**, 1351 (1975).

(22) C. A. Baillie, J. R. Corbett, J. R. Dowsett, D. B. Sattelle, and J. J. Callec, *Pestic. Sci.*, **6**, 645 (1975).

ACKNOWLEDGMENTS

The authors are grateful to Dr. Shebl M. Sherby, Faculty of Agriculture, University of Alexandria for his kind help, and Dr. Samia El-Dardiry, Faculty of Medicine University of Tanta, for her useful comments dealing with the preparation of this manuscript. This research was supported by the National Science Foundation Grant (INT 78-01468) to the University of Alexandria, Egypt.

Excitatory Amino Acid Receptor Interactions of a Novel α-Phosphinic Acid Analogue of α-Methylaspartic Acid

L. A. CATES *x, V-S. LI *, Z-S. HU *, J. LEHMANN ‡, J. T. COYLE ‡, and J. W. FERKANY ‡

Received October 14, 1983, from the **Department of Medicinal Chemistry, College of Pharmacy, University of Houston, Houston, TX 77004* and the ‡*Departments of Neuroscience, Pharmacology, and Psychiatry, Division of Child Psychiatry, Johns-Hopkins University, School of Medicine, Baltimore, MD 21205.* Accepted for publication November 30, 1983.

Abstract □ An α-phosphino analogue of α-methylaspartate has been synthesized. The compound may not interact with excitatory amino acid receptors directly, as assessed by direct *in vitro* radioreceptor binding methods; however, it possesses weak anticonvulsant activity and exhibits an excitant action *in vitro* that is apparently not mediated by a *N*-methyl-D-aspartate receptor.

Keyphrases □ Excitatory amino acid receptors—*N*-methyl-D-aspartate, glutamate, kainate □ Anticonvulsants—*in vitro*, rats, excitatory amino acids □ Phosphinic acids—excitatory amino acid receptors, anticonvulsant activity

Phosphorus analogues of amino acids have been investigated previously; however, most studies have involved phosphonic acid derivatives such as aminomethanephosphonic acid (I). Only in recent years have aminophosphinic acids with unsubstituted amino groups been prepared. The first, glycine analogue II, was synthesized in 1964 by a procedure which provides only limited types of products (1).

Phosphinic acids possess a hydrogen atom in lieu of one of the two hydroxyl groups found in phosphonic acids and, therefore, are monobasic with less bulk on the phosphorus atom. Phosphinic acids are the closest phosphorus analogues of carboxylic acids and this similarity has led to a limited number of investigations of aminophosphinic acids for biological activity. In 1961, Linfield *et al.* prepared phosphinic acids bearing substituted α-anilino and phenyl groups (III) by the addition of hypophosphorus acid to the appropriate

0022-3549/84/1100-1550$01.00/0

© 1984, American Pharmaceutical Association

Schiff bases and reported antibacterial properties associated with some of these derivatives (2). Except for II, the only unsubstituted α-aminophosphinic acids reported are those by Khomutov and Osipova (3) and Bayliss *et al.* (4), which were synthesized by the addition of hypophosphorus acid to oximes and diphenylmethylimines, respectively. The amino acid analogues resulting from the latter process were investigated for antibacterial properties with alanine (IV), valine (V), and methionine (VI) derivatives displaying significant activity. In addition, the effect of V was reversed by valine, an indication that a false substrate mechanism was operative.

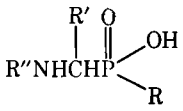

I, R = OH, R′ = R″ = H
II, R = R′ = R″ = H

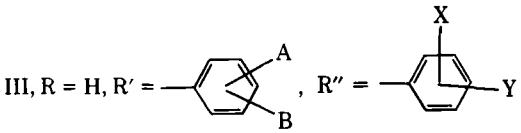

III, R = H, R′ =
IV, R = R″ = H, R′ = CH_3
V, R = R″ = H, R′ = $-CH(CH_3)_2$
VI, R = R″ = H, R′ = $-CH_2CH_2SCH_3$

In this paper we describe the synthesis (*Scheme I*) and biological testing of DL-α-amino-α-methyl-β-carboxyethanephosphinic acid (IX) and two of its precursors (VII and VIII). Compound IX represents the bioisosteric replacement of one carboxyl group of α-methylaspartic acid with a P(O)H(OH) moiety. α-Methylaspartic acid has been investigated for its ability to reduce aspartic acid utilization (5) and for its effect in many enzyme systems such as inhibition of tyrosine aminotransferase (6) and asparaginase (7). Moreover, IX is related to the antagonists of amino acid receptors including 2-amino-4-phosphonobutyric acid and 2-amino-7-phosphonoheptanoic acid.

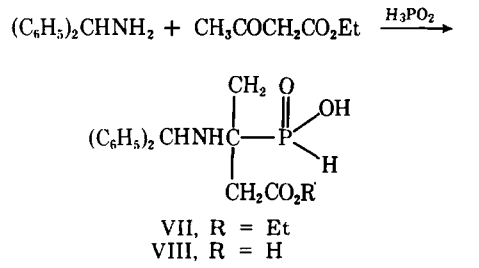

VII, R = Et
VIII, R = H

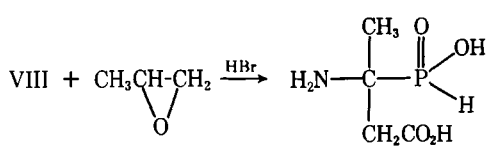

Scheme I

Table I—Effect of VII, VIII, and IX on the Specific Binding of Tritiated Kainic Acid, L-Glutamate, and 2-Amino-7-phosphonoheptanoic Acid to Rat Brain Membranes *In Vitro*[a]

Compound	Specifically Bound Ligand, % Displacement: Tritiated L-Glutamate	Tritiated Kainic Acid	Tritiated 2-Amino-7-phosphoheptanoic Acid
	Tris-Citrate		
VII	14	8	0
VIII	0	7	0
IX	0	11	28
	Tris-HCl		
VII	6	—	—
VIII	8	—	—
IX	8	—	—

[a] Compounds (10^{-4} M) were incubated in the presence of the indicated ligand as described. Reference IC_{50} values for L-glutamate, kainic acid, and 2-amino-7-phosphonoheptanoic acid are 1 μM, 5 nM, and 5 μM, respectively.

Three different types of excitatory amino acid receptors have been proposed to exist (8): (a) "glutamate receptors," which may be preferentially activated by L-glutamic acid or quisqualate, and blocked by glutamate diethyl ester or 2-amino-4-phosphonobutyric acid; (b) "kainate receptors," preferentially activated by kainate and closely related structures, for which there are no known receptor antagonists; (c) "*N*-methyl-D-aspartate receptors," preferentially activated by *N*-methyl-D-aspartate and ibotenic acid, and antagonized by 2-amino-5-phosphonopentanoate and 2-amino-7-phosphonoheptanoate. Excitatory amino acids may be the most common neurotransmitters in the brain. Antagonists of excitatory amino acid receptors are sought for application in controlling seizures and suppressing certain neurodegenerative disorders.

RESULTS AND DISCUSSION

Compounds VII–IX were tested for direct interactions with excitatory amino acid receptors in available *in vitro* excitatory amino acid receptor binding assays (9–11). As shown in Table I, none of the compounds possessed inhibitory activity, with the exception of the marginal effects of IX, at the site labeled by tritiated 2-amino-7-phosphonoheptanoic acid.

The major role of inactivation of synaptically released excitatory amino acid neurotransmitters is high-affinity, sodium-dependent reuptake (5). Compound IX inhibited such uptake by slightly more than 50% at a concentration of 5×10^{-4} M (Table II), which is at least 100-fold less potent than L-glutamate or D- or L-aspartate in this respect (12). Thus, IX is a weak inhibitor of high-affinity excitatory amino acid uptake in the rat brain. These data may suggest that IX itself is transported into synaptosomes by the excitatory amino acid carrier, albeit with low affinity. Compounds VII and VIII demonstrated no interaction with the carrier.

In the [^{3}H]acetylcholine release system, which reflects the neuronal excitation induced by excitatory amino acids acting at *N*-methyl-D-aspartate receptors (13), IX caused an increase in spontaneous [^{3}H]acetylcholine release and tended to enhance *N*-methyl-DL-aspartate-evoked [^{3}H]acetylcholine release (Table III). Compound VIII caused an increase in spontaneous [^{3}H]acetylcholine release (Table III).

Compounds VII–IX were tested *in vivo* for ability to protect against electroshock and subcutaneously administered pentylenetetrazol[1]-induced (scMet) seizures. Compounds VII and IX afforded protection against scMet of 25 and 50%, respectively, at doses of 600 mg/kg. No acute disruption of neurological function was detected in the rotorod test for VII–IX at doses of ≥600 mg/kg.

Of these results, the most striking is the coincidence of the activity of IX in enhancing spontaneous [^{3}H]acetylcholine release and as an anticonvulsant. Because the response to *N*-methyl-D-L-aspartate was not decreased during exposure to IX, it is unlikely that IX interacts directly with *N*-methyl-D-aspartate receptors. Since IX is only weakly active in inhibiting the specific

[1] Metrazol.

Table II—Effect of VII, VIII, and IX on the Uptake of L-[^{3}H]Glutamate, D-[^{3}H]Aspartate, and L-[^{3}H]Aspartate into Synaptosomes Prepared from Rat Corpus Striatum or Cerebellum [a]

Compound	Specific Uptake, % Inhibition		
	L-[^{3}H]Glutamate	D-[^{3}H]Aspartate	L-[^{3}H]Aspartate
	Corpus Striatum		
VII	0	0	0
VIII	0	7	0
IX	53	56	56
	Cerebellum		
VII	2	0	0
VIII	4	0	5
IX	59	57	59

[a] Synaptosomes were incubated in the presence of various ligands with or without the compounds (at a concentration of 5×10^{-4} M). Reference IC_{50} values for L-glutamate, D-aspartate, and L-aspartate are 1–5 μM (12).

Table III—[^{3}H]Acetylcholine Release Studies [a]

		[^{3}H]Acetylcholine Release, % of Control	
		Spontaneous	Evoked [b]
Control	9	100 ± 3.8	100 ± 9.8
VII, 0.3 mM	4	103 ± 5.0	70 ± 6.1
VII, 0.3 mM	4	116 ± 3.8 [d]	108 ± 4.9
IX, 0.3 mM	3	113 ± 1.3 [c]	87 ± 2.4
IX, 1.0 mM	3	166 ± 5.0 [c]	129 ± 39.3

[a] Test substances were added on interval six. Stimulation, a 2-min application of 50 μM *N*-methyl-D-aspartate, was applied at intervals three and nine. The effect of test substances on the parameters S_{pII}/S_{pI} and $S_{II} - S_{pII}/S_I - S_{pI}$ is expressed as percent of control (13). [b] *N*-Methyl-DL-aspartate-evoked release. [c] $p < 0.05$, Mann–Whitney two-tailed U test.

binding of the *N*-methyl-D-aspartate receptor antagonist tritiated 2-amino-7-phosphonoheptanoic acid, interaction of IX with *N*-methyl-D-aspartate receptors is unlikely to be the mechanism of action of this compound. Further biological investigations are required to determine the mechanism of action by which IX exerts its effects in these various biological systems.

DL-α-Benzhydrylamino-α-methyl-β-carbethoxyethanephosphinic Acid (VII)—This compound was prepared using a modification of previously reported procedures (2, 4). A mixture of 23.65 g (0.129 mol) of 1,1-diphenylmethylamine (14) and 16.78 g (0.129 mol) of ethyl acetoacetate in 80 mL of benzene was refluxed for 2 h and then distilled with azeotropic removal of water using a Dean–Stark trap. To the cooled residue was slowly added 8.96 g (0.129 mol) of 95% hypophosphorous acid, which was obtained by evaporation of a commercial 50% aqueous solution at 30–40°C (2 mm) and the mixture was heated at reflux for 2 h. The resultant solid was removed by filtration, washed with benzene, and dried in a vacuum oven at 50°C to yield 16.2 g (35%) of the product as white granules, mp (ethanol) 172–173°C; IR (KBr): 2600 (P—OH), 2350 (P—H), 1740 (C=O), 1600 (C=C), and 1200 (P=O) cm^{-1}; ^{1}H-NMR (D_2O–NaOD): δ 1.08 (d, 3, J = 16 Hz, CH_3), 1.19 (CH_2O), 5.52 (s, 1, CH), 7.23–7.59 (m, 10, ArH), and 3.52 and 9.94 ppm (1:1 d, 1, J = 510 Hz, P—H).

Anal.—Calc. for $C_{19}H_{24}NO_4P$: C, 63.12; H, 6.69; N, 3.87. Found: C, 63.24; H, 6.72; N, 3.84.

DL-α-Benzhydrylamino-α-methyl-β-carboxyethanephosphinic Acid (VIII)—Ten grams of VII in 150 mL of 0.5 M NaOH was heated at 90°C for 4 h. The resultant solution was cooled and treated with concentrated HCl (pH 1). The precipitate thus formed was removed by filtration, washed with water until free of NaCl, and dried in a vacuum oven at 55°C to give 8.4 g (91% yield) of the product as a white powder, mp 190–191°C; IR (KBr): 2500–2700 (P—OH, C—OH), 2300 (P—H), 1700 (C=O), 1600 (C=C), and 1190 (P=O) cm^{-1}; ^{1}H-NMR (D_2O–NaOD): 1.14 (d, 3, J = 14 Hz, CH_3), 2.46 (d, 2, J = 10 Hz, CH_2), 5.56 (s, 1, CH), 7.25–7.63 (m, 10, ArH), and 3.59 and 10.01 ppm (1:1 d, 1, J = 510 Hz, P—H).

Anal.—Calc. for $C_{17}H_{20}NO_4P$: C, 61.26; H, 6.05; N, 4.20. Found: C, 61.17; H, 6.09; N, 4.20.

DL-α-Amino-α-methyl-β-carboxyethanephosphinic Acid (IX)—Using a modification of the method of Dingwall *et al.* (15), 2.6 g of VIII in 40 mL of 48% HBr was heated at 75°C for 4 h. The benzhydryl bromide was extracted with benzene, and the aqueous layer was treated with propylene oxide at pH 3–4. The resulting solution was concentrated under reduced pressure and the resulting solid was removed by filtration, washed with ethanol and ether, and dried in a vacuum oven at 55°C to yield 0.5 g (38%) of IX, mp 214–215°C; IR (KBr): 3240 (NH_3^+), 2700–2500 (P—OH, C—OH), 2380 (P—H), and 1685 (C=O) cm^{-1}; ^{1}H-NMR (D_2O): δ 1.47 (d, 3, J = 14 Hz, CH_3), 2.88, 2.76 (dd, 2, J = 9 Hz, CH_2), and 3.53 and 10.32 ppm (1:1 d, 1, J = 540 Hz, P—H).

Anal.—Calc for $C_4H_{10}NO_4P$: C, 28.93; H, 6.07; N, 8.43. Found: C, 28.85, H, 6.03, N, 8.34.

Biological Testing—*Animals*—For *in vitro* neurochemical studies, adult, male, albino rats[3] weighing 150–200 g were employed. *In vivo* testing for anticonvulsant activity and neurological toxicity of compounds was performed using mice[4].

Anticonvulsant Activity and Neurological Toxicity—Anticonvulsant activity of the compounds was evaluated against both maximal electroshock (MES) and pentylenetetrazol-induced seizures (scMet) by contractors of the Antiepileptic Drug Development Program administered by the National Institute for Neurological and Communicative Disorders and Stroke, Bethesda, Md, according to previously described procedures (16).

Neurochemical Assays—*Excitatory Amino Acid Uptake*—Crude synaptosomal fractions of rat cerebellum or corpus striatum were prepared as previously described (17) and resuspended in 0.32 M sucrose. Two hundred-microliter aliquots (100 μg of protein) of the suspension were added to borosilicate tubes containing 800 μL of Krebs HEPES buffer (pH 7.4) and 0.5 μM of D-[^{3}H]aspartate, L-[^{3}H]aspartate, or L-[^{3}H]glutamate with or without the test substance. Following a 3 min incubation at 30°C, the reaction was terminated by rapid filtration over glass fiber filters[5] maintained under reduced pressure. The filters were washed with 1 × 5 mL of ice-cold buffer, dried, and the radioactivity was determined by liquid scintillation counting. Parallel incubations were performed at 2°C to determine nonspecific uptake.

Receptor Binding Assays—Specific binding of excitatory amino acid analogues to brain membranes was performed, with minor modifications, according to previously published procedures. Briefly, brain membranes were prepared according to the method of Enna and Snyder (18) and stored frozen at −80°C until use. For assay, the membranes were thawed and washed four times by centrifugation, and the final pellet was resuspended in sufficient buffer to yield a protein concentration of 0.15–0.2 mg/mL. Specific binding of [^{3}H]kainic acid (2 nM) was assayed according to the procedure of London and Coyle (9). Specific binding of tritiated 2-amino-7-phosphonoheptanoic acid (50 nM) was assayed as described by Ferkany and Coyle (10). Specific binding of L-[^{3}H]glutamate (100 nM) was assayed by the method of Slevin *et al.* (11), with the exception that the assay was conducted in both Tris-citrate and Tris-HCl buffers (pH 7.1, 37°C, 0.05 M). In all instances, nonspecific binding was defined as that obtained by incubating the membranes in the presence of the indicated ligand and 10^{-3} M L-glutamate. The assays were terminated by centrifugation, and the pellets were rinsed rapidly and superficially with ice-cold buffer and solubilized[6]. Radioactivity was determined by liquid scintillation counting.

[^{3}H]Acetylcholine Release Evoked by *N*-Methyl-D-aspartate Receptor Stimulation—The release of [^{3}H]acetylcholine from the corpus striatum of the brain, evolved by exposure to excitatory amino acid receptor agonists, was measured as previously described (13). Striatal slices were exposed by [^{3}H]choline, which is selectively accumulated by cholinergic interneurons and synthesized into [^{3}H]acetylcholine. The slices were placed in chambers and superfused with Krebs medium, the superfused phase was collected, and the radioactivity released from the tissue into the superfused phase was measured by liquid scintillation counting. Exposure to agonists of *N*-methyl-D-aspartate receptors caused an increase in release while addition of magnesium or *N*-methyl-D-aspartate receptor antagonists, such as 2-amino-5-phosphonopentanoic acid or 2-amino-7-phosphonoheptanoic acid, inhibited release caused by agonists. Agonists or antagonists of other excitatory amino acid receptors (*e.g.*, quisqualate or kainate) have little or no effect in general (13).

The action of test substances in this paradigm were assessed by determining if (*a*) they evoked [^{3}H]acetylcholine release by themselves or (*b*) they inhibited the release of [^{3}H]acetylcholine evoked by *N*-methyl-DL-aspartate (50 μM).

REFERENCES

(1) H. D. F. Toy and E. H. Uhing, U.S. Patent No. 3,160,632 (1964).

(2) W. M. Linfield, E. Jungermann, and A. T. Guttmann, *J. Org. Chem.*, **26**, 4088 (1961).

(3) R. H. Khomutov and T. I. Osipova, *Izv. Akad. Nauk SSSR, Ser. Khim.*, **1978**, 1951; *Chem. Abstr.*, **89**, 197655j (1978).

(4) E. K. Bayliss, C. D. Campbell, J. G. Dingwall, and W. Pickles, in "Phosphorus Chemistry- Proceedings of the 1981 International Conference," ACS Symposium Series 171, L. D. Quin and G. Verkade, Eds., American Chemical Society, Washington, D.C., 1981, p. 183.

(5) E. Roberts and P. F. Hunter, *Proc. Soc. Exp. Biol. Med.*, **83**, 720 (1953).

(6) G. Litwack and J. E. Miller, *J. Biol. Chem.*, **246**, 3234 (1971).

(7) M. I. Lerman and I. V. Vereukina, *Biokhimiya*, **27**, 526 (1962).

(8) J. C. Watkins and R. H. Evans, *Annu. Rev. Pharm.*, **21**, 165 (1981).

(9) E. London and J. T. Coyle, *Mol. Pharmacol.*, **15**, 492 (1979).

(10) J. W. Ferkany and J. T. Coyle, *Life Sci.*, **33**, 1295 (1983).

(11) J. Slevin, J. Collins, K. Lindsley, and J. T. Coyle, *Brain Res.*, **249**, 353 (1982).

(12) M. E. Sandoval, P. Harch, and C. Cotman, *Brain Res.*, **142**, 285 (1978).

(13) J. Lehmann and B. Scatton, *Brain Res.*, **252**, 77 (1982).

(14) A. P. Terent'ev and N. I. Gusar, *J. Gen. Chem. USSR*, **35**, 124 (1965).

(15) J. G. Dingwall, W. K. Bayliss, and C. D. Campbell, *Ger. Offen.*, 2,722,162; Chem. Abstr., **88**, 105559j (1978).

(16) DHEW Publication No. (NIH)76-1093, Bethesda, Md., 1976.

(17) D. A. Redburn, D. Bloome, J. W. Ferkany, and S. J. Enna, *Brain Res.*, **152**, 511 (1978).

(18) S. J. Enna and S. Snyder, *Mol. Pharmacol.*, **13**, 442 (1977).

ACKNOWLEDGMENTS

This work was supported by grants from the Robert A. Welch Foundation, Grant E-920 (L.A.C.), by USPHS grants RSDA Type II MH00125, NS13584, NS18414, and MH26654, and grants from the Surdna Foundation and the McKnight Foundation (J.T.C.), and an individual fellowship, USPHS NS06798 (J.W.F.).

Quantitation of Acetaminophen, Chlorpheniramine Maleate, Dextromethorphan Hydrobromide, and Phenylpropanolamine Hydrochloride in Combination Using High-Performance Liquid Chromatography

V. DAS GUPTA *x and ARUN R. HEBLE ‡

Received July 5, 1983, from the **Department of Pharmaceutics, University of Houston, Houston, TX 77030* and ‡*Ohm Laboratories, New Brunswick, NJ 08902.* Accepted for publication November 22, 1983.

Abstract □ A high-performance liquid chromatographic (HPLC) method has been developed for the quantitation of acetaminophen, chlorpheniramine maleate, dextromethorphan hydrobromide, and phenylpropanolamine hydrochloride in combination in pharmaceutical dosage forms using a single column and three different mobile phases. The method developed is sensitive for the content uniformity test for tablets. No preliminary extraction procedure is required for liquid preparation and a very simple extraction procedure is required for tablets. The method is accurate and precise with *RSD* (based on five injections) of 1.2, 2.4, 1.9, and 1.6% for acetaminophen, chlorpheniramine, dextromethorphan, and phenylpropanolamine, respectively.

Keyphrases □ Acetaminophen—HPLC, content uniformity □ Chlorpheniramine maleate—HPLC, content uniformity □ Dextromethorphan hydrobromide—HPLC, content uniformity □ Phenylpropanolamine hydrochloride—HPLC, content uniformity

One popular commercial product[1] contains an analgesic (acetaminophen), an antihistamine (chlorpheniramine maleate), an antitussive (dextromethorphan hydrobromide), and a decongestant (phenylpropanolamine hydrochloride). The product is extensively used for the relief of symptoms of coughs and colds. The dosage forms also contain excipients, some of which may interfere with the analysis of the active ingredients. The problem of analysis is further complicated by the presence of 325 mg of acetaminophen *versus* only 1 mg of chlorpheniramine maleate per tablet (or per 15 mL of the liquid). The quantities of dextromethorphan hydrobromide and phenylpropanolamine hydrochloride present are 10 and 12.5 mg per tablet (or 15 mL of the liquid), respectively. Acetaminophen has high absorbance in the useful UV range, but that of phenylpropanolamine hydrochloride is very poor. For example, at 256 nm (the wavelength of maximum absorption of phenylpropanolamine hydrochloride) a 1350-μg/mL aqueous solution of phenylpropanolamine hydrochloride has an absorption similar to a 20-μg/mL solution of acetaminophen. No single method is available to determine the active ingredients quantitatively in this combination.

High-performance liquid chromatographic (HPLC) methods for the quantitation of acetaminophen (1–4), chlorpheniramine maleate (5, 6), dextromethorphan hydrobromide (3, 7, 8), and phenylpropanolamine hydrochloride (6, 9–11) have been reported. None of the reported methods is applicable when ingredients are present in this combination.

This paper reports the quantitation of acetaminophen (I), chlorpheniramine maleate (II), dextromethorphan hydrobromide (III), and phenylpropanolamine hydrochloride (IV) in combination, using HPLC. The method requires three different mobile phases for complete analysis.

EXPERIMENTAL SECTION

Materials—All chemicals and reagents were USP, NF, or ACS quality and used without further purification. The sodium salt of 1-heptanesulfonic acid[2] was used as received.

A liquid chromatograph[3] attached to a multiple-wavelength detector[4] and a recorder[5] was used. The column[6] (30 cm × 4 mm i.d.) was purchased and

[1] Comtrex; Bristol-Myers Products, New York, N.Y.

[2] Eastman Kodak Co., Rochester, N.Y.

[3] Waters ALC202 equipped with a U6K Universal injector; Waters Associates, Milford, Mass.

[4] Spectroflow Monitor 770; Schoeffel Instruments, Ramsey, N.J.

[5] Omniscribe 5213-12; Houston Instruments, Austin, Tex.

[6] μ-Bondapak phenyl; Waters Associates, Milford, Mass.

0022-3549/84/1100-1553$01.00/0

© 1984, American Pharmaceutical Association

REFERENCES

(1) H. D. F. Toy and E. H. Uhing, U.S. Patent No. 3,160,632 (1964).

(2) W. M. Linfield, E. Jungermann, and A. T. Guttmann, *J. Org. Chem.*, **26**, 4088 (1961).

(3) R. H. Khomutov and T. I. Osipova, *Izv. Akad. Nauk SSSR, Ser. Khim.*, **1978**, 1951; *Chem. Abstr.*, **89**, 197655j (1978).

(4) E. K. Bayliss, C. D. Campbell, J. G. Dingwall, and W. Pickles, in "Phosphorus Chemistry- Proceedings of the 1981 International Conference," ACS Symposium Series 171, L. D. Quin and G. Verkade, Eds., American Chemical Society, Washington, D.C., 1981, p. 183.

(5) E. Roberts and P. F. Hunter, *Proc. Soc. Exp. Biol. Med.*, **83**, 720 (1953).

(6) G. Litwack and J. E. Miller, *J. Biol. Chem.*, **246**, 3234 (1971).

(7) M. I. Lerman and I. V. Vereukina, *Biokhimiya*, **27**, 526 (1962).

(8) J. C. Watkins and R. H. Evans, *Annu. Rev. Pharm.*, **21**, 165 (1981).

(9) E. London and J. T. Coyle, *Mol. Pharmacol.*, **15**, 492 (1979).

(10) J. W. Ferkany and J. T. Coyle, *Life Sci.*, **33**, 1295 (1983).

(11) J. Slevin, J. Collins, K. Lindsley, and J. T. Coyle, *Brain Res.*, **249**, 353 (1982).

(12) M. E. Sandoval, P. Harch, and C. Cotman, *Brain Res.*, **142**, 285 (1978).

(13) J. Lehmann and B. Scatton, *Brain Res.*, **252**, 77 (1982).

(14) A. P. Terent'ev and N. I. Gusar, *J. Gen. Chem. USSR*, **35**, 124 (1965).

(15) J. G. Dingwall, W. K. Bayliss, and C. D. Campbell, *Ger. Offen.*, 2,722,162; Chem. Abstr., **88**, 105559j (1978).

(16) DHEW Publication No. (NIH)76-1093, Bethesda, Md., 1976.

(17) D. A. Redburn, D. Bloome, J. W. Ferkany, and S. J. Enna, *Brain Res.*, **152**, 511 (1978).

(18) S. J. Enna and S. Snyder, *Mol. Pharmacol.*, **13**, 442 (1977).

ACKNOWLEDGMENTS

This work was supported by grants from the Robert A. Welch Foundation, Grant E-920 (L.A.C.), by USPHS grants RSDA Type II MH00125, NS13584, NS18414, and MH26654, and grants from the Surdna Foundation and the McKnight Foundation (J.T.C.), and an individual fellowship, USPHS NS06798 (J.W.F.).

Quantitation of Acetaminophen, Chlorpheniramine Maleate, Dextromethorphan Hydrobromide, and Phenylpropanolamine Hydrochloride in Combination Using High-Performance Liquid Chromatography

V. DAS GUPTA *x and ARUN R. HEBLE ‡

Received July 5, 1983, from the **Department of Pharmaceutics, University of Houston, Houston, TX 77030* and ‡*Ohm Laboratories, New Brunswick, NJ 08902.* Accepted for publication November 22, 1983.

Abstract □ A high-performance liquid chromatographic (HPLC) method has been developed for the quantitation of acetaminophen, chlorpheniramine maleate, dextromethorphan hydrobromide, and phenylpropanolamine hydrochloride in combination in pharmaceutical dosage forms using a single column and three different mobile phases. The method developed is sensitive for the content uniformity test for tablets. No preliminary extraction procedure is required for liquid preparation and a very simple extraction procedure is required for tablets. The method is accurate and precise with *RSD* (based on five injections) of 1.2, 2.4, 1.9, and 1.6% for acetaminophen, chlorpheniramine, dextromethorphan, and phenylpropanolamine, respectively.

Keyphrases □ Acetaminophen—HPLC, content uniformity □ Chlorpheniramine maleate—HPLC, content uniformity □ Dextromethorphan hydrobromide—HPLC, content uniformity □ Phenylpropanolamine hydrochloride—HPLC, content uniformity

One popular commercial product[1] contains an analgesic (acetaminophen), an antihistamine (chlorpheniramine maleate), an antitussive (dextromethorphan hydrobromide), and a decongestant (phenylpropanolamine hydrochloride). The product is extensively used for the relief of symptoms of coughs and colds. The dosage forms also contain excipients, some of which may interfere with the analysis of the active ingredients. The problem of analysis is further complicated by the presence of 325 mg of acetaminophen *versus* only 1 mg of chlorpheniramine maleate per tablet (or per 15 mL of the liquid). The quantities of dextromethorphan hydrobromide and phenylpropanolamine hydrochloride present are 10 and 12.5 mg per tablet (or 15 mL of the liquid), respectively. Acetaminophen has high absorbance in the useful UV range, but that of phenylpropanolamine hydrochloride is very poor. For example, at 256 nm (the wavelength of maximum absorption of phenylpropanolamine hydrochloride) a 1350-μg/mL aqueous solution of phenylpropanolamine hydrochloride has an absorption similar to a 20-μg/mL solution of acetaminophen. No single method is available to determine the active ingredients quantitatively in this combination.

High-performance liquid chromatographic (HPLC) methods for the quantitation of acetaminophen (1–4), chlorpheniramine maleate (5, 6), dextromethorphan hydrobromide (3, 7, 8), and phenylpropanolamine hydrochloride (6, 9–11) have been reported. None of the reported methods is applicable when ingredients are present in this combination.

This paper reports the quantitation of acetaminophen (I), chlorpheniramine maleate (II), dextromethorphan hydrobromide (III), and phenylpropanolamine hydrochloride (IV) in combination, using HPLC. The method requires three different mobile phases for complete analysis.

EXPERIMENTAL SECTION

Materials—All chemicals and reagents were USP, NF, or ACS quality and used without further purification. The sodium salt of 1-heptanesulfonic acid[2] was used as received.

A liquid chromatograph[3] attached to a multiple-wavelength detector[4] and a recorder[5] was used. The column[6] (30 cm × 4 mm i.d.) was purchased and

[1] Comtrex; Bristol-Myers Products, New York, N.Y.

[2] Eastman Kodak Co., Rochester, N.Y.

[3] Waters ALC202 equipped with a U6K Universal injector; Waters Associates, Milford, Mass.

[4] Spectroflow Monitor 770; Schoeffel Instruments, Ramsey, N.J.

[5] Omniscribe 5213-12; Houston Instruments, Austin, Tex.

[6] μ-Bondapak phenyl; Waters Associates, Milford, Mass.

0022-3549/84/1100-1553$01.00/0

© 1984, American Pharmaceutical Association

Table I—Chromatographic Conditions

Compound	Mobile Phase	Flow Rate, mL/min	Sensitivity	Wavelength, nm
Acetaminophen	1	1.5	0.04	256 (Fig. 1)
Phenylpropanolamine	2	2.5	0.02	256 (Fig. 1)
Chlorpheniramine and dextromethorphan	3	2.0	0.02	262 (Fig. 2)
Dextromethorphan[a]	4	2.0	0.02	279 (Fig. 3)
Chlorpheniramine and dextromethorphan[a]	4	2.3	0.02	262 (Fig. 4)

[a] It was necessary to develop another mobile phase due to interference from the excipients in liquid dosage form.

used as received. The four different mobile phases used were an aqueous buffer (pH ~ 7) containing 0.02 M ammonium acetate and 15% v/v of methanol (mobile phase 1); an aqueous buffer containing 0.02 M KH_2PO_4 with pH adjusted[7] to ~2.6 with an 85% aqueous solution of phosphoric acid (0.4 mL/L) (mobile phase 2); an aqueous buffer (pH ~ 3.3) containing 0.005 M sodium 1-heptanesulfonate, 1% v/v of glacial acetic acid, and 48% v/v of methanol (mobile phase 3); and an aqueous buffer (pH ~ 4.1) containing 1% v/v of ammonium formate buffer (3) and 40% v/v of methanol (mobile phase 4). The temperature was ambient and the chromatograph chart speed was 30.5 cm/h. Other chromatographic conditions are listed in Table I.

Preparation of Stock and Standard Solutions—The stock solution of acetaminophen (1.0 mg/mL) was prepared by dissolving 100 mg of acetaminophen in methanol to make 100 mL of the solution. A stock solution of chlorpheniramine maleate was prepared by dissolving 50 mg in water to make 100 mL. The standard solutions were prepared as follows: for acetaminophen, 2 mL of the stock solution was diluted to 100 mL with water; for phenylpropanolamine hydrochloride, 50 mg of the powder was dissolved in water to make 100 mL; for dextromethorphan hydrobromide, 40 mg of the powder was dissolved in water to make 200 mL; for a mixture of chlorpheniramine maleate and dextromethorphan hydrobromide, dextromethorphan hydrobromide powder (40 mg) was mixed with 8.0 mL of the stock solution of chlorpheniramine maleate and brought to 100 mL with water. Other solutions of different concentrations were prepared as needed.

Sample Preparation—*Commercial Liquid*—For the acetaminophen assay, a 2.3-mL quantity of the commercial liquid was diluted to 50 mL with water. A 2-mL quantity of this solution was mixed with 2 mL of methanol and diluted to 100 mL with water. For all others, 15 mL of the liquid was diluted to 25 mL with water. If dextromethorphan hydrobromide was to be assayed at 279 nm (Table I), then 7.5 mL of the liquid was diluted to 25 mL with water.

Tablets—Ten tablets were accurately weighed and ground to a fine powder. For the acetaminophen assay, enough powder to represent 50 mg of acetaminophen was mixed with ~40 mL of methanol. The mixture was stirred for 2–3 min, brought to volume (50 mL) with methanol, and filtered. The first 10 mL of the filtrate was rejected, and then a portion was collected and diluted (2 mL to 100 mL) with water. For all others, enough powder to represent two tablets was mixed with ~45 mL of water and stirred for 4–5 min. The mixture was brought to volume (50 mL) with water and filtered. The first 10 mL of the filtrate was rejected, and then a portion of the clear filtrate was collected for assay. If dextromethorphan was to be assayed at 279 nm, then powder representing one tablet was used. The rest of the procedure was as described.

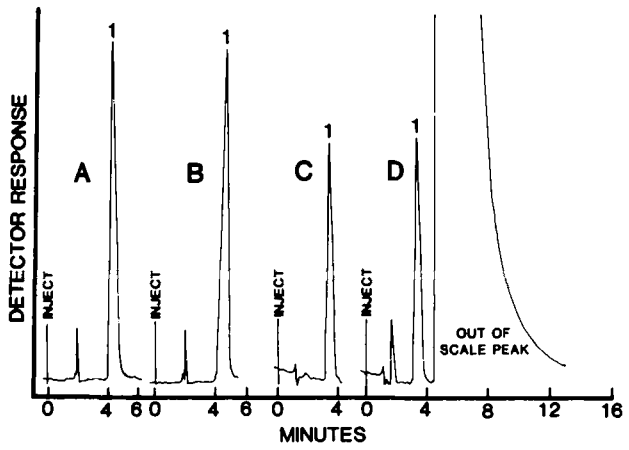

Figure 1—*Sample chromatograms. Key: (A) standard solution of acetaminophen (I); (B) tablet of I; (C) standard solution of phenylpropanolamine hydrochloride (IV); (D) tablet of IV. Peak 1 is the respective drug peak; the out of scale peak in chromatogram D is from acetaminophen.*

[7] Beckman Zeromatic SS-3 pH meter; Beckman Instruments, Fullerton, Calif.

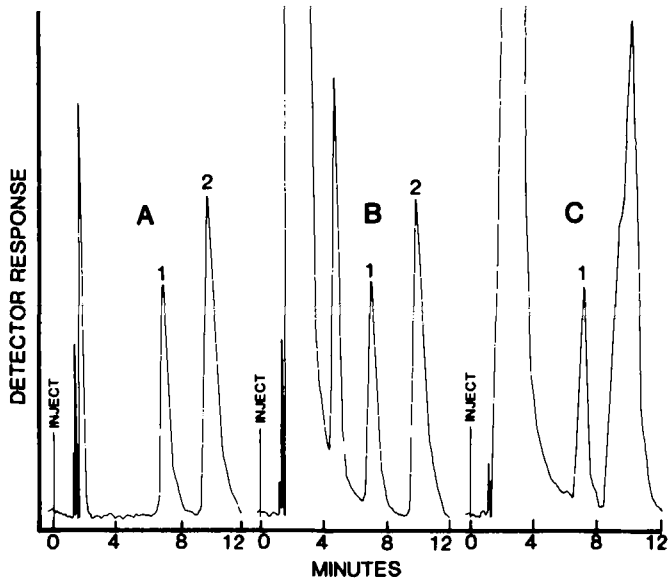

Figure 2—*Sample chromatograms from a standard solution (A), a tablet (B), and a liquid preparation (C) using mobile phase 3 at 262 nm. Key: (1) chlorpheniramine; (2) dextromethorphan. The out of scale peaks in chromatograms B and C are from acetaminophen. The other peak in chromatogram C is from the excipient and dextromethorphan (upper part).*

Content Uniformity of the Tablets (Except Acetaminophen)—A single tablet was ground to a fine powder, mixed with ~23 mL of water, and stirred for 4–5 min. The mixture was brought to volume (25.0 mL) with water and filtered. The first 7 mL of the filtrate was rejected, and then a portion of the clear filtrate was collected for assay. If dextromethorphan hydrobromide was to be assayed at 279 nm, the filtrate was diluted (1:1) with water. It was not considered necessary to determine the content uniformity of acetaminophen (325 mg/tablet) since it represented the bulk of the tablet.

Chromatographic Procedure—The assay sample (20.0 μL) was injected into the chromatograph under the described conditions. For comparison, an identical volume of the standard solution was injected after the assay sample eluted.

Since preliminary investigations indicated that peak heights were directly related to the concentrations (range tested ±50% of the standard solutions), the results were calculated by:

$$\frac{Ph_a}{Ph_s} \times 100 = \text{Percent of the label claim}$$

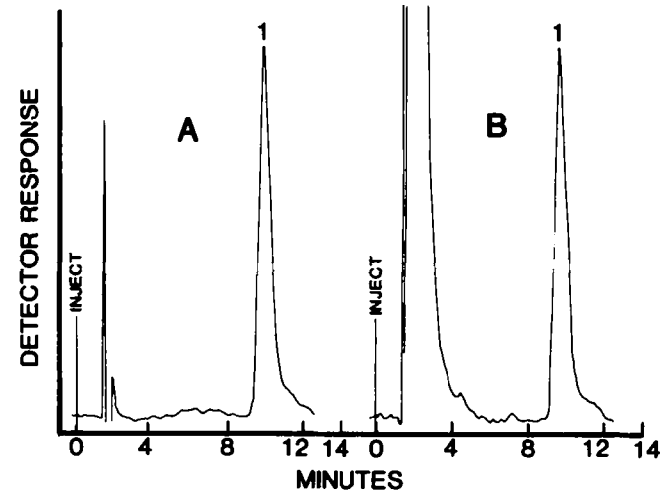

Figure 3—*Sample chromatograms from a standard solution and a liquid dosage form using mobile phase 4 at 279 nm. Key: (1) dextromethorphan. At this wavelength, the peak from chlorpheniramine was very small (peak before peak 1).*

Table II—Assay Results

Dosage Forms	Acetaminophen	Chlorpheniramine	Dextromethorphan	Phenylpropanolamine
		Assay Results, % of the Label Claim[a]		
Commercial Formulations				
Tablet[b]	98.7	99.5[c]	97.1[c]	96.2
Tablet[d]	99.2	99.0[c]	100.2[c]	98.7
Tablets[d] (Different lot)	100.8	99.0[c]	99.4[c]	100.0
Elixir[d]	101.4	99.4[e]	100.5[e]	100.2
Elixir[d] (Different lot)	100.8	99.9[c]	100.5[f]	101.1
Synthetic Mixture[g]	100.8	99.5	100.0	99.2
		Content Uniformity Results		
Tablet 1[b]	—[h]	97.2	99.4	98.1
Tablet 2[b]	—	93.1	100.2	99.7
Tablet 3[b]	—	94.2	97.4	94.4
Tablet 4[b]	—	105.4	103.4	102.5
Tablet 5[b]	—	103.2	101.7	102.1
Tablet 6[d]	—	97.4	96.8	98.5
Tablet 7[d]	—	96.8	97.9	99.1
Tablet 8[d]	—	102.7	102.1	101.8
Tablet 9[d]	—	99.6	99.1	100.0
Tablet 10[d]	—	103.0	102.3	103.1

[a] The label claim per tablet or per 15 mL of the liquid was: acetaminophen, 325 mg; chlorpheniramine maleate, 1 mg; dextromethorphan hydrobromide, 10 mg; phenylpropanolamine hydrochloride, 12.5 mg. [b] Ohm Laboratories; N. Brunswick, N.J. [c] Using mobile phase 3. In tablets of one manufacturer, the excipients interfered with dextromethorphan assay when mobile phase 4 was used. [d] Bristol-Myers; New York, N.Y. [e] Using mobile phase 4 at 262 nm. There was interference with dextromethorphan assay from the excipients when mobile phase 3 was used. [f] Using mobile phase 4 at 279 nm. [g] Contained the same active ingredients as stated under footnote *a* per 500 mg of powder plus 31.5 mg of corn starch and 120 mg of lactose. [h] Not determined.

where Ph_a is the peak height of the assay sample and Ph_s is that of the standard solution, which contained identical concentrations of drugs based on the label claim.

RESULTS AND DISCUSSION

Acetaminophen Assay—The results (Table II) indicate that the developed method can be adopted for the quantitation of acetaminophen in tablets and liquids without any interference from other active ingredients and excipients (Fig. 1A and B). This was expected since the bulk of the tablet was acetaminophen and the liquid contained 325 mg/15 mL. The peak heights were related to the concentrations (range tested, 0.2–0.6 μg) with an *RSD* of 1.2% based on five injections.

Phenylpropanolamine Hydrochloride (IV)—The results (Table II) indicate that the developed method can be used to quantify IV in tablets and liquids. It was tedious to separate phenylpropanolamine from other ingredients, especially from the out of scale peak (Fig. 1D) of acetaminophen. Many different mobile phases were tried, including an aqueous solution buffered with either 0.02 M ammonium acetate or 0.02 M KH_2PO_4, with the pH adjusted to ≥3.2 with acetic acid. In each case, I did not separate from IV, *i.e.*, acetaminophen started eluting before all of the phenylpropanolamine had eluted. It was necessary to decrease the retention time of IV and increase that of I. Initially, the mobile phases had methanol (≤15%) and the pH was >3. Subsequently, only water was used in the mobile phase (to increase the retention time of I), and the pH was adjusted to 2.6 (to decrease the retention time of IV) with phosphoric acid. This mobile phase (Table I), which gave excellent separation (Fig. 1C and D), could be used to analyze IV in tablets and liquids (Table II) and for content uniformity tests. The peak heights were related to the concentrations (range tested, 5–15 μg) with an *RSD* of 1.6% based on five injections.

Chlorpheniramine Maleate (II) and Dextromethorphen Hydrobromide (III)—The assay method can be adapted for the quantitation of chlorpheniramine and dextromethorphan (Table II) in tablets and liquids using mobile phase 3 or 4. Initially, mobile phase 3, similar to one reported in the literature (6), was developed. This mobile phase separated both chlorpheniramine (II) and dextromethorphan (III) from the other tablet ingredients (Fig. 2A and B). In the liquid dosage form, the excipients (probably a preservative not disclosed on the label) interfered (Fig. 2C) with the dextromethorphan assay peak. Therefore, it was necessary to develop another mobile phase for dextromethorphan in the liquid dosage form. Mobile phase 4, similar to that reported previously (3), was used (Fig. 3) to successfully quantify dextromethorphan in the liquid dosage form at 279 nm (wavelength of maximum absorption). By selecting this wavelength, it was possible to increase the sensitivity of the method twofold for the analysis of dextromethorphan. However, mobile phase 4 at 262 nm could also be used to analyze both chlorpheniramine and dextromethorphan (Fig. 4) in the liquid dosage and tablet forms from one manufacturer. In tablets from a different manufacturer, there was interference with the dextromethorphan peak from the excipients (probably the yellow color) not disclosed on the label (Fig. 4C) when mobile phase 4 was used. Although either mobile phase 3 or 4 could be used to analyze II and III for one manufacturer's tablets, only mobile phase 3 could be used to assay the same ingredients in the second manufacturer's tablets. In the liquid dosage form from the second manufacturer, only mobile phase 4 could be used to analyze II and III.

The peak heights were related to concentrations (range tested, 0.4–1.2 μg for II and 4–12 μg for III at 262 nm or 2–6 μg at 279 nm) and the *RSD* values, based on five injections, were 2.4 and 1.9% for II and III, respectively.

The developed method can be adapted for the quantitation of I–IV in pharmaceutical dosage forms using a single column and three different mobile phases. The method can also be used for the determination of the content uniformity of the tablets (Table II). This is important since the quantity of chlorpheniramine maleate was only 1 mg in a >500-mg tablet.

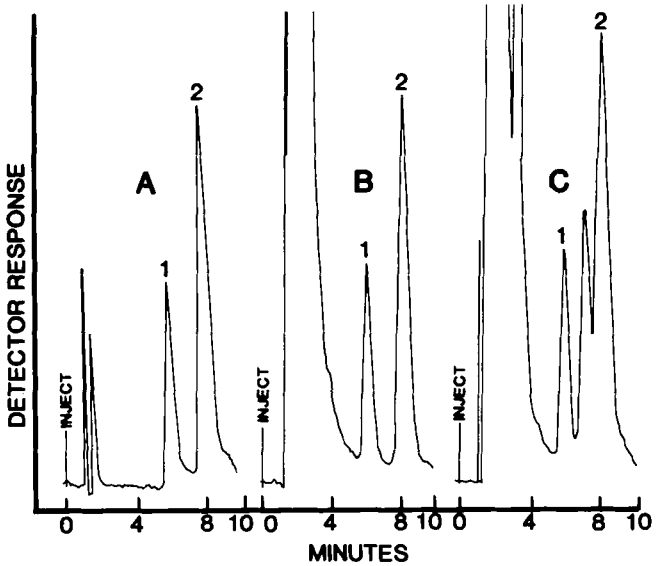

Figure 4—*Sample chromatograms from a standard solution, a liquid dosage form, and a tablet using mobile phase 4 at 262 nm. Key: (1) chlorpheniramine; (2) dextromethorphan. At this wavelength, chlorpheniramine could also be assayed. In chromatogram C, the excipients from the tablet interfered with the peak of dextromethorphan.*

REFERENCES

(1) F. J. Sena, J. T. Piechocki, and K. L. Li, *J. Pharm. Sci.*, **68**, 1465 (1979).

(2) V. D. Gupta, *J. Pharm. Sci.*, **69**, 110 (1980).

(3) W. O. McSharry and I. V. E. Savage, *J. Pharm. Sci.*, **69**, 212 (1980).

(4) L. Carnevale, *J. Pharm. Sci.*, **72**, 196 (1983).

(5) A. G. Ghanekar and V. D. Gupta, *Am. J. Hosp. Pharm.*, **34**, 651 (1977).

(6) J. R. Koziol, J. T. Jacob, and R. G. Achari, *J. Pharm. Sci.*, **68**, 1135 (1979).

(7) M. K. Chao, I. J. Holcomb, and S. A. Fusari, *J. Pharm. Sci.*, **68**, 1463 (1979).

(8) E. J. Kubiak and J. W. Munson, *J. Pharm. Sci.*, **69**, 1380 (1980).

(9) V. D. Gupta and A. G. Ghanekar, *J. Pharm. Sci.*, **66**, 895, (1977).

(10) A. G. Ghenekar and V. D. Gupta, *J. Pharm. Sci.*, **67**, 873 (1978).

(11) D. R. Heidemann, *J. Pharm. Sci.*, **70**, 820 (1981).

ACKNOWLEDGMENTS

The work was supported in part by Ohm Laboratories, North Brunswick, N.J.

Determination of Codeine in Human Plasma by Reverse-Phase High-Performance Liquid Chromatography

V. NITSCHE *x and H. MASCHER

Received January 1, 1983, from the *Pharmakologische Untersuchungsgesellschaft m.b.H., A-1171 Vienna, Austria.* Accepted for publication November 16, 1983. * Present address: Biokinet, A-1080 Vienna, Austria.

Abstract □ A high-performance liquid chromatographic (HPLC) method for the determination of codeine in human plasma is described. The specific, precise, and sensitive method can be used to determine plasma codeine levels after administration of therapeutic doses of codeine. After purification on a C_{18} extraction column, codeine in the form of hydrochloride is eluted. After addition of the internal standard, the codeine is separated on a reverse-phase C_{18} column using a slightly alkaline mobile phase and is then determined by UV detection. The analysis takes 3.5 min per run; the limit of detection is ~3 μg/L for a 50-μL loop and 800 μL of plasma. The absolute recovery is 98.4 ± 6.7% (n = 14) in the 10-300-μg/L range. Within the range, the calibration curve is linear.

Keyphrases □ Bioavailability—codeine, human plasma, HPLC □ Codeine—bioavailability, HPLC □ HPLC—bioavailability of codeine

Numerous methods for the detection of codeine are reported in the literature, including GC (1-5), GC-MS (6-9), TLC (10-12), RIA (3, 13-15), radioactive labeling (16, 17), and several high-performance liquid chromatographic (HPLC) methods. However, with one exception (18), these have not been used to detect codeine in plasma (19-21).

Some of the detection methods are not sufficiently sensitive or selective and others require sophisticated equipment (GC-MS) or specialized techniques (RIA). Our objective was to develop an HPLC method which is well suited for routine determination of codeine in plasma.

EXPERIMENTAL SECTION

Material and Methods—A liquid chromatograph[1] equipped with a UV detector[2] was used. The loop volume was 50 μL, but could be increased to 150 μL without affecting separation performance. Membrane filters[3] (pore size, 0.45 μm) and a 10-μL syringe[4] were also used.

Codeine hydrochloride[5] and diazepam[5] (internal standard) were used as supplied. Methanol[6] and ammonium carbonate[7] were AR grade. The C_{18} extraction columns[6] had a volume of 1 mL. Solutions of 0.1 M HCl, 1 M ammonium hydroxide, methanol-0.1 M ammonium hydroxide (20:80; mixture A), and methanol-0.1 M HCl (50:50; mixture B) were prepared. The internal standard solution was ~200 μg of diazepam/20 mL of methanol.

The buffer (pH 8.9) was made with 80.5 mL of 0.1 M borate solution (1.237 g of boric acid in 10 mL of 0.1 M NaOH) and 19.5 mL of 0.1 M HCl. Distilled water was used throughout.

The mobile phase was methanol-0.1 M ammonium carbonate (70:30). The mixture was used within 2-3 d, because tailing at the codeine peak was sometimes observed with older mixtures.

The chromatographic conditions included a 250 × 4-mm column[8], filled in-house[9] with Polygosil C 18, 7.5 μm; the flow rate was 2.0 mL/min; the column oven temperature was 45°C; the detector wavelength was 220 nm, 0.01 AUFS, time constant 1 min; the injection volume was 50-150 μL by loop; and the recorder advance was 10 mm/min.

Sample Preparation—Plasma (citrate anticoagulant) was filtered through a 0.45-μm membrane filter and 0.8 mL was mixed with 0.3 mL of buffer (pH 8.9). The mixture was quantitatively transferred into a C_{18} extraction column[6] and centrifuged at 500×g for 1-2 min; the plasma passed completely through the tube. To eliminate interfering substances, the extraction column was washed with 1 mL of 0.1 M HCl, 1 mL of mixture A, and 0.3 mL of 0.1 M HCl (each wash was followed by a 1-min centrifugation at 500×g). The eluates were discarded. Codeine was then eluted with 300 μL of mixture B. With commonly used centrifuges, 10-40 extraction columns can be eluted at the same time, which shortens the analysis time. The ammonium hydroxide solution (~30 μL, pH >8) and 5 μL of the internal standard solution were added to the eluate. After thorough mixing, the loop was rinsed and filled with ~100 μL (~180 μL if a 150-μL loop was used) of this solution.

Standard Preparation—Samples (2, 8, 20 and 40 μL) of a solution containing 4 ng of codeine base/μL (weighed as codeine hydrochloride, dissolved in water and diluted accordingly) were added to 0.8-mL plasma blanks. The remainder of the procedure is as described in *Sample Preparation*.

The quotients of the peak areas (codeine-internal standard) of the samples were compared with a calibration curve.

Bioavailability Study—In a randomized crossover study, bioavailability was determined with six healthy male volunteers (mean age, 46.8 ± 15.2; mean weight, 74.1 ± 9.7 kg; and mean height 178.3 ± 6.25 cm). The subjects underwent medical examinations and laboratory tests which showed them to be in good health. All subjects had been informed of the investigation procedures and had expressed their agreement in writing.

The subjects received two different oral codeine-doxycycline preparations on different days. The test preparations were 100 mg of doxycycline with 30 mg of codeine base as the phosphate in diffusion pellets (preparation 1)[10] and 100 mg of doxycycline with 30 mg of codeine base as resinate (preparation 2)[11]; both were sustained-release preparations. The dose was two capsules per

[1] Model 8000; Spectra Physics, Santa Clara, Calif.
[2] Spectromonitor III; Laboratory Data Control, Riviera Beach, Fla.
[3] Sartorius; Göttingen, F.R.G.
[4] Hamilton, Bonaduz, Switzerland.
[5] Gerot Pharmazeutika, Vienna, Austria.
[6] Baker, Deventer, The Netherlands.
[7] Merck.
[8] Hibar RT; Merck.
[9] Machery/Nagel, Düren, F.R.G.
[10] Batch 4PA-222, Doxitussin; Gerot Pharmazeutika.
[11] Batch 810238, Vibratussal; Pfizer, Karlsruhe, F.R.G.

0022-3549/84/1100-1556$01.00/0

© 1984, American Pharmaceutical Association

REFERENCES

(1) F. J. Sena, J. T. Piechocki, and K. L. Li, *J. Pharm. Sci.*, **68**, 1465 (1979).

(2) V. D. Gupta, *J. Pharm. Sci.*, **69**, 110 (1980).

(3) W. O. McSharry and I. V. E. Savage, *J. Pharm. Sci.*, **69**, 212 (1980).

(4) L. Carnevale, *J. Pharm. Sci.*, **72**, 196 (1983).

(5) A. G. Ghanekar and V. D. Gupta, *Am. J. Hosp. Pharm.*, **34**, 651 (1977).

(6) J. R. Koziol, J. T. Jacob, and R. G. Achari, *J. Pharm. Sci.*, **68**, 1135 (1979).

(7) M. K. Chao, I. J. Holcomb, and S. A. Fusari, *J. Pharm. Sci.*, **68**, 1463 (1979).

(8) E. J. Kubiak and J. W. Munson, *J. Pharm. Sci.*, **69**, 1380 (1980).

(9) V. D. Gupta and A. G. Ghanekar, *J. Pharm. Sci.*, **66**, 895, (1977).

(10) A. G. Ghenekar and V. D. Gupta, *J. Pharm. Sci.*, **67**, 873 (1978).

(11) D. R. Heidemann, *J. Pharm. Sci.*, **70**, 820 (1981).

ACKNOWLEDGMENTS

The work was supported in part by Ohm Laboratories, North Brunswick, N.J.

Determination of Codeine in Human Plasma by Reverse-Phase High-Performance Liquid Chromatography

V. NITSCHE *x and H. MASCHER

Received January 1, 1983, from the *Pharmakologische Untersuchungsgesellschaft m.b.H., A-1171 Vienna, Austria.* Accepted for publication November 16, 1983. * Present address: Biokinet, A-1080 Vienna, Austria.

Abstract □ A high-performance liquid chromatographic (HPLC) method for the determination of codeine in human plasma is described. The specific, precise, and sensitive method can be used to determine plasma codeine levels after administration of therapeutic doses of codeine. After purification on a C_{18} extraction column, codeine in the form of hydrochloride is eluted. After addition of the internal standard, the codeine is separated on a reverse-phase C_{18} column using a slightly alkaline mobile phase and is then determined by UV detection. The analysis takes 3.5 min per run; the limit of detection is ~3 μg/L for a 50-μL loop and 800 μL of plasma. The absolute recovery is 98.4 ± 6.7% (n = 14) in the 10-300-μg/L range. Within the range, the calibration curve is linear.

Keyphrases □ Bioavailability—codeine, human plasma, HPLC □ Codeine—bioavailability, HPLC □ HPLC—bioavailability of codeine

Numerous methods for the detection of codeine are reported in the literature, including GC (1-5), GC-MS (6-9), TLC (10-12), RIA (3, 13-15), radioactive labeling (16, 17), and several high-performance liquid chromatographic (HPLC) methods. However, with one exception (18), these have not been used to detect codeine in plasma (19-21).

Some of the detection methods are not sufficiently sensitive or selective and others require sophisticated equipment (GC-MS) or specialized techniques (RIA). Our objective was to develop an HPLC method which is well suited for routine determination of codeine in plasma.

EXPERIMENTAL SECTION

Material and Methods—A liquid chromatograph[1] equipped with a UV detector[2] was used. The loop volume was 50 μL, but could be increased to 150 μL without affecting separation performance. Membrane filters[3] (pore size, 0.45 μm) and a 10-μL syringe[4] were also used.

Codeine hydrochloride[5] and diazepam[5] (internal standard) were used as supplied. Methanol[6] and ammonium carbonate[7] were AR grade. The C_{18} extraction columns[6] had a volume of 1 mL. Solutions of 0.1 M HCl, 1 M ammonium hydroxide, methanol-0.1 M ammonium hydroxide (20:80; mixture A), and methanol-0.1 M HCl (50:50; mixture B) were prepared. The internal standard solution was ~200 μg of diazepam/20 mL of methanol.

The buffer (pH 8.9) was made with 80.5 mL of 0.1 M borate solution (1.237 g of boric acid in 10 mL of 0.1 M NaOH) and 19.5 mL of 0.1 M HCl. Distilled water was used throughout.

The mobile phase was methanol-0.1 M ammonium carbonate (70:30). The mixture was used within 2-3 d, because tailing at the codeine peak was sometimes observed with older mixtures.

The chromatographic conditions included a 250 × 4-mm column[8], filled in-house[9] with Polygosil C 18, 7.5 μm; the flow rate was 2.0 mL/min; the column oven temperature was 45°C; the detector wavelength was 220 nm, 0.01 AUFS, time constant 1 min; the injection volume was 50-150 μL by loop; and the recorder advance was 10 mm/min.

Sample Preparation—Plasma (citrate anticoagulant) was filtered through a 0.45-μm membrane filter and 0.8 mL was mixed with 0.3 mL of buffer (pH 8.9). The mixture was quantitatively transferred into a C_{18} extraction column[6] and centrifuged at 500×g for 1-2 min; the plasma passed completely through the tube. To eliminate interfering substances, the extraction column was washed with 1 mL of 0.1 M HCl, 1 mL of mixture A, and 0.3 mL of 0.1 M HCl (each wash was followed by a 1-min centrifugation at 500×g). The eluates were discarded. Codeine was then eluted with 300 μL of mixture B. With commonly used centrifuges, 10-40 extraction columns can be eluted at the same time, which shortens the analysis time. The ammonium hydroxide solution (~30 μL, pH >8) and 5 μL of the internal standard solution were added to the eluate. After thorough mixing, the loop was rinsed and filled with ~100 μL (~180 μL if a 150-μL loop was used) of this solution.

Standard Preparation—Samples (2, 8, 20 and 40 μL) of a solution containing 4 ng of codeine base/μL (weighed as codeine hydrochloride, dissolved in water and diluted accordingly) were added to 0.8-mL plasma blanks. The remainder of the procedure is as described in *Sample Preparation*.

The quotients of the peak areas (codeine-internal standard) of the samples were compared with a calibration curve.

Bioavailability Study—In a randomized crossover study, bioavailability was determined with six healthy male volunteers (mean age, 46.8 ± 15.2; mean weight, 74.1 ± 9.7 kg; and mean height 178.3 ± 6.25 cm). The subjects underwent medical examinations and laboratory tests which showed them to be in good health. All subjects had been informed of the investigation procedures and had expressed their agreement in writing.

The subjects received two different oral codeine-doxycycline preparations on different days. The test preparations were 100 mg of doxycycline with 30 mg of codeine base as the phosphate in diffusion pellets (preparation 1)[10] and 100 mg of doxycycline with 30 mg of codeine base as resinate (preparation 2)[11]; both were sustained-release preparations. The dose was two capsules per

[1] Model 8000; Spectra Physics, Santa Clara, Calif.
[2] Spectromonitor III; Laboratory Data Control, Riviera Beach, Fla.
[3] Sartorius; Göttingen, F.R.G.
[4] Hamilton, Bonaduz, Switzerland.
[5] Gerot Pharmazeutika, Vienna, Austria.
[6] Baker, Deventer, The Netherlands.
[7] Merck.
[8] Hibar RT; Merck.
[9] Machery/Nagel, Düren, F.R.G.
[10] Batch 4PA-222, Doxitussin; Gerot Pharmazeutika.
[11] Batch 810238, Vibratussal; Pfizer, Karlsruhe, F.R.G.

0022-3549/84/1100-1556$01.00/0

© 1984, American Pharmaceutical Association

Table I—Reproducibility of Codeine Determination in Blank Plasma Spiked with Codeine

Codeine Added, μg/L	Codeine Found, μg/L (mean ± *SD*)
303	304.8 ± 3.70[a]
152	147.3 ± 6.24[b]
19	16.9 ± 1.94[c]

[a] $n = 4$. [b] $n = 5$. [c] $n = 3$.

person (60 mg of codeine). A 1-week wash-out phase passed between the examination days. The subjects ingested the preparations with liquid in the morning after fasting overnight. Two hours after administration they had a light breakfast.

Blood samples were taken at 0, 1, 2, 3, 4, 5, 7, and 24 h after administration. The plasma obtained from the blood samples was frozen until assayed. The samples were analyzed by the method described above. A Student's *t* test for dependent samples was used to statistically compare the areas under the curves (AUC). Concentrations in the plasma after 24 h were usually at the limit of detection and could not be accurately determined; therefore, the values have not been included.

RESULTS

Recovery and Reproducibility—Codeine was added to the plasma and assayed according to specifications. The results were compared with those of codeine added to 300 μL of distilled water (plus internal standard and ammonium hydroxide) directly injected into the chromatograph. The recovery was 98.4 ± 6.6% (mean value ± *SD*; $n = 16$) (Table I).

Extracts of samples from the bioavailability study were injected twice within 15 h. The *SD* was 0.3–5.9 with a *CV* of 0.6–10%. Repeated extraction and injection of several samples (20–155 μg/L of plasma) gave an *SD* of 0.14–11 with a *CV* of 0.8–12.9%.

We found a linear regression ($r = 0.9989$; $n = 14$; $k = 0.0038596$; $d = 0.01646$) of the calibration curve in the 10–300-μg/L range by adding codeine to blank plasma (Table I). The limit of detection with 0.8 mL of plasma and a 50-μL loop is 3 μg/L of plasma. If a 150-μL loop and greater volume of plasma are used, the limit of detection can be reduced to <1 μg/L of plasma. There are no interfering substances present in the chromatogram; the limit is due to UV absorption constraints.

Bioavailability Study—Representative chromatograms of plasma samples are shown in Fig. 1. The individual and mean (±*SD*) values obtained in the bioavailability study are given in Tables II and III and are graphically represented in Fig. 2. The AUC value, a measure of relative bioavailability, and the half-life calculated from each plasma level curve are shown in Table III.

DISCUSSION

The method outlined above offers advantages over GC, GC–MS, and TLC with regard to handling and analysis duration. Moreover, the rate of recovery is extremely high.

The only substantial obstacle encountered in the development of this assay

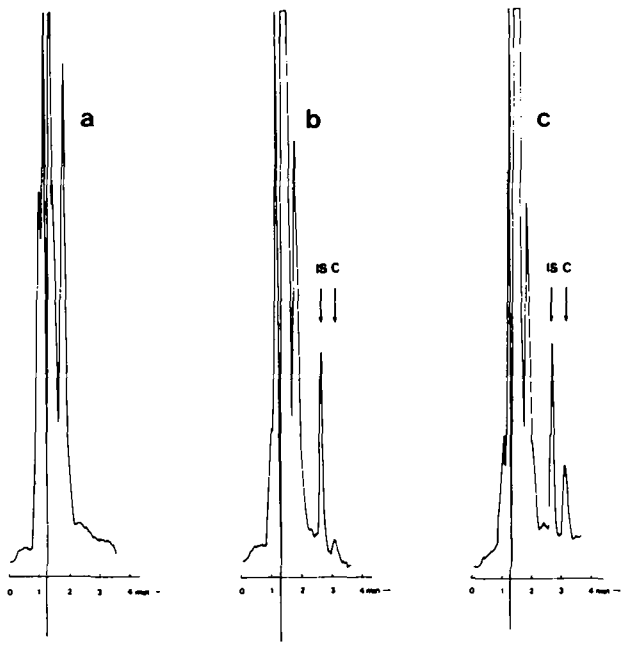

Figure 1—*Chromatograms of blank plasma (a), plasma with 13 μg/L of codeine (b), and plasma with 59 μg/L of codeine (c). Key: (IS) internal standard; (C) codeine.*

method was the multitude of endogenous substances detected in the codeine range at a wavelength of 220 nm. The problem was solved by selective prepurification of the plasma on a C_{18} extraction column[6]. Any neutral substances and acids that could interfere with the determination of codeine in the chromatogram with an alkaline mobile phase were retained by the extraction column or eluted during the washing; codeine was eluted quantitatively in the form of its salt. No interference was found with frequently coadministered drugs, such as benzodiazepines (*e.g.*, oxazepam, diazepam, flurazepam, and nitrazepam), doxycycline, bromhexine, amoxicillin, and ethambutol, using this procedure. The metabolites of codeine, its glucuronide, and some other narcotics do not interfere with codeine (retention times: codeine, 3.1 min; codeine glucuronide, 1.4 min; norcodeine, <1.6 min; morphine, 1.7 min; nalorphin, 1.3 min).

The results of bioavailability studies using this HPLC method agree with results obtained by other methods with similar dosages. After administration of 60 mg of codeine sulfate, a maximum level of 100–120 μg/L and an elimination half-life of 3.0–4.2 h (4) were obtained by GC. After administration of 65 mg of codeine phosphate, a maximum of 117 μg/L and an elimination half-life of 3.60 ± 0.15 ($n = 6$) were found by RIA (12). With a 25-mg dose of labeled codeine phosphate, a maximum level of ~40 μg/L and elimination half-lives of 2.2 h (1.8–2.8; $n = 4$) for tablets and 4.2 h (3.2–5.2; $n = 4$) for slow-release capsules were obtained (14). TLC indicates a maximum level of 90 μg/L after administration of 70 mg of codeine phosphate in the form

Table II—Plasma Concentrations After Oral Administration of 60 mg of Codeine

Subject	Preparation	Plasma Concentration, μg/L[a] 1 h	2 h	3 h	4 h	5 h	7 h
A	1[b]	34.00	55.00	65.00	58.00	52.00	39.00
	2[c]	16.00	59.00	77.00	87.00	76.00	50.00
B	1	59.00	62.00	64.00	66.00	50.00	26.00
	2	10.00	21.00	33.00	60.00	50.00	37.00
C	1	93.00	187.00	155.00	133.00	115.00	88.00
	2	22.00	125.00	181.00	158.00	133.00	77.00
D	1	60.00	109.00	80.00	64.00	49.00	38.00
	2	29.00	108.00	94.00	42.00	30.00	20.00
E	1	38.00	115.00	89.00	82.00	59.00	45.00
	2	14.00	68.00	96.00	100.00	83.00	57.00
F	1	8.00	38.00	87.00	73.00	54.00	34.00
	2	19.00	65.00	71.00	54.00	72.00	42.00
Mean	1	48.67	94.33	90.00	79.33	63.17	45.00
SD		±28.93	±54.76	±33.57	±27.55	±25.64	±21.98
Mean	2	18.33	74.33	92.00	83.50	74.00	47.17
SD		±6.65	±37.17	±49.17	±42.38	±34.88	±19.30

[a] Plasma concentrations measured at 0 and 24 h were 0 μg/L. [b] Doxycycline (100 mg) in 30 mg of codeine base as the phosphate. [c] Doxycycline (100 mg) in 30 mg of codeine base as the resinate.

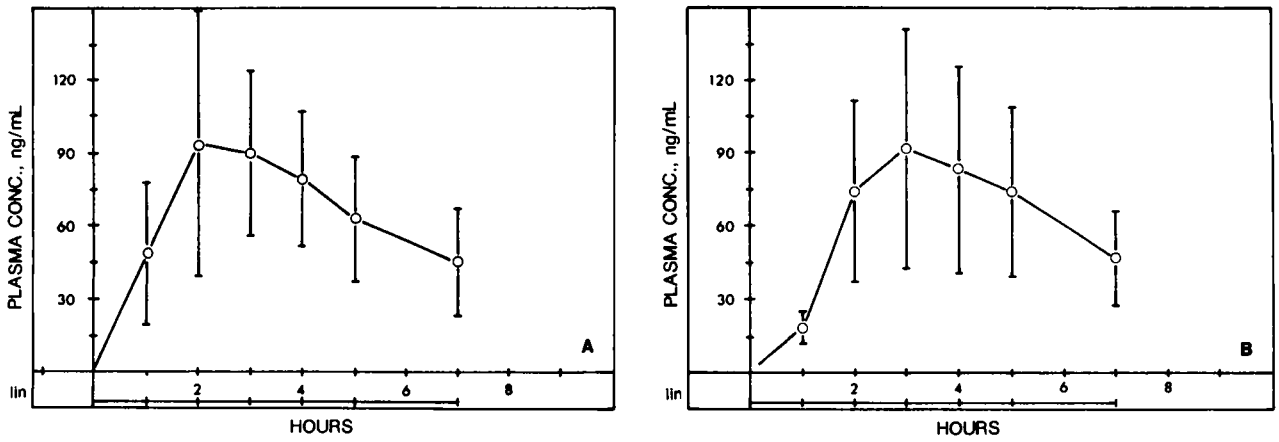

Figure 2—*Mean plasma concentration of six volunteers after ingestion of 60 mg of codeine in two different preparations.*

Table III—Area Under the Curve (AUC) and Half-Life ($t_{1/2}$) After Oral Administration of 60 mg of Codeine

Subject	AUC		$t_{1/2}$	
	Preparation 1[a]	Preparation 2[b]	Preparation 1	Preparation 2
A	329.00	403.00	5.42	3.68
B	352.00	236.00	2.22	4.34
C	828.50	762.50	2.89	3.20
D	424.50	338.00	4.65	1.90
E	457.50	459.50	3.30	3.70
F	321.00	359.00	3.68	—
Mean	452.1	426.3	3.69	3.36
SD	±192.3	±180.7	±1.07	±0.82

[a] Doxycycline (100 mg) in 30 mg of codeine base as the phosphate. [b] Doxycycline (100 mg) in 30 mg of codeine base as the resinate.

of a slow-release preparation, with a maximum level of ~95 μg/L and an elimination half-life of 2.2–3.9 h after administration of 35 mg of codeine phosphate in tablet form (9). This rapid HPLC method is, therefore, well suited for pharmacokinetic and clinical detection of codeine in plasma.

REFERENCES

(1) R. A. Zweidinger, F. M. Weinberg, and R. W. Handy, *J. Pharm. Sci.*, **65,** 427 (1976).

(2) B. Dahlström, L. Paalzow, and P. O. Edlund, *Acta Pharmacol. Toxicol.*, **41,** 273 (1977).

(3)N. J. Jain, T. C. Sneath, W. J. Leung, and R. D. Budd, *J. Pharm. Sci.*, **66,** 66 (1977).

(4) M. K. Brunson and J. F. Nash, *Clin. Chem. (Winston-Salem, N.C.)*, **27,** 1956 (1975).

(5) G. Brugaard and K. E. Rasmussen, *J. Chromatogr.*, **147,** 476 (1978).

(6) G. Lhoest and M. Mercier, *Pharm. Acta Helv.*, **55,** 316 (1980).

(7) D. Pearce, S. Wiersema, M. Kuo, and C. Emery, *Clin. Toxicol.*, **14,** 161 (1979).

(8) E. J. Cone, C. W. Gorodetzky, S. Y. Yeh, W. D. Darwin, and W. F. Buchwald, *J. Chromatogr.*, **230,** 57 (1982).

(9) W. O. R. Ebbighausen, J. H. Mowat, P. Vestergaard, and N. S. Kline, *Adv. Biochem. Psychopharmacol.*, **7,** 135 (1973).

(10) R. D. Budd, D. F. Mathis, and W. J. Leung, *Clin. Toxicol.*, **16,** 61 (1980).

(11) P. Haefelfinger, *J. Chromatogr.*, **124,** 351 (1976).

(12) H. Fischer, H. G. Eulenhöfer, and R. Kraft, *Drug Res.*, **21,** 1692 (1971).

(13) J. A. W. Findlay, R. F. Butz, and R. M. Welch, *Clin. Pharmacol. Ther.*, **22,** 439 (1977).

(14) J. W. A. Findlay, R. F. Butz, and R. M. Welch, *Life Sci.*, **19,** 389 (1976).

(15) J. W. A. Findlay, E. C. Jones, R. F. Butz, and R. M. Welch, *Clin. Pharmacol. Ther.*, **24,** 60 (1978).

(16) W. D. Bechtel and E. Sinterhauf, *Drug Res.*, **28,** 308 (1978).

(17) K. Sinterhauf and W. D. Bechtel, *Drug Res.*, **30,** 1012 (1980).

(18) I. W. Tsina, M. Fass, J. A. Debban, and S. B. Matin, *Clin. Chem. (Winston-Salem, N.C.)*, **25,** 1137 (1982).

(19) C. Olieman, L. Maat, K. Waliszewski, and H. C. Beyerman, *J. Chromatogr.*, **133,** 382 (1977).

(20) C. Y. Wu, and J. J. Wittick, *Anal. Chem.*, **49,** 359 (1977).

(21) J. O. Svensson, A. Rane, J. Säwe, and F. Sjögnvist, *J. Chromatogr.*, **230,** 427 (1982).

ACKNOWLEDGMENTS

The authors thank H. Schütz for technical assistance, Gerot Pharmazeutika for providing the codeine and diazepam, and Dr. Wagner Löffler for filling the HPLC column.

Influence of Lipid Composition and Ionic Strength on the Physical Stability of Liposomes

DAAN J. A. CROMMELIN

Received February 3, 1983, from the *Department of Pharmaceutics, Pharmaceutical Laboratory, University of Utrecht, 3511 GH Utrecht, The Netherlands.* Accepted for publication November 22, 1983.

Abstract □ The effect of including charge-inducing agents (stearylamine or phosphatidylserine) on the zeta potential of phosphatidylcholine-cholesterol-containing liposomes in aqueous media with varying ionic strength (sodium chloride) was investigated. In 150 mM ionic strength solutions, the experimentally obtained zeta potentials were in good agreement with predictions made with the Gouy-Chapman equation, after proper correction for bulk ionic interaction. However, at low ionic strength, substantial deviations occurred which were ascribed to incomplete dissociation of the phosphatidylserine molecules or protonation of the stearylamine molecules due to the large diffuse double layer (Debye length). Predictions were made on the physical stability of the liposomes based on the Derjaguin-Landau-Verwey-Overbeek (DLVO) theory and current knowledge of hydration effects on interparticle interaction. For negatively charged liposomes, both at low and high ionic strength, no increase in particle size was found after storage. For low ionic strength solutions, this agreed with the calculations; for the high ionic strength solutions, aggregate formation in a secondary minimum was expected. For positively charged liposomes, the physical stability predicted from theoretical considerations did not correlate with the experimentally observed stability.

Keyphrases □ Liposomes—phosphatidylcholine-cholesterol, ionic strength, lipid composition physical stability □ Stearylamine—liposomes with phosphatidylcholine and cholesterol, physical stability □ Phosphatidylserine—liposomes with phosphatidylcholine and cholesterol, physical stability

The surface potential is an important parameter influencing liposomal behavior. *In vivo*, the surface charge density has been found to influence the distribution of liposomes (1, 2) and *in vitro*, a high potential might contribute to their physical stability by reducing the rate of aggregation and fusion. Frøkjaer *et al.* (3) reported an increase in physical stability of liposomes (against aggregation or fusion) by decreasing the ionic strength and increasing the surface charge density of liposomes consisting of phosphatidylcholine (I) and phosphatidylserine (II). However, if there is no electrostatic repulsion between two liposomes this will not necessarily result in aggregate formation or fusion of the colliding particles, as many uncharged liposomes are fully stabilized by hydration energies (4, 5).

The influence of the surface charge density and ionic strength on the zeta potential of I and cholesterol-containing liposomes with stearylamine (III) or II was investigated by microelectrophoresis. The zeta potentials obtained experimentally were compared with surface potentials (Ψ_0) predicted by the Gouy-Chapman equation.

Using the Derjaguin-Landau-Verwey-Overbeek (DLVO) theory (6) and information on hydration energies between phospholipid vesicles (4, 5), calculations were made on the physical stability of the liposomes against aggregation or fusion. These predictions were verified by determining the actual size by dynamic light scattering. Because the surface potential cannot be measured by electrophoresis, the zeta potential, instead of Ψ_0, was used for the evaluation of the experimental results.

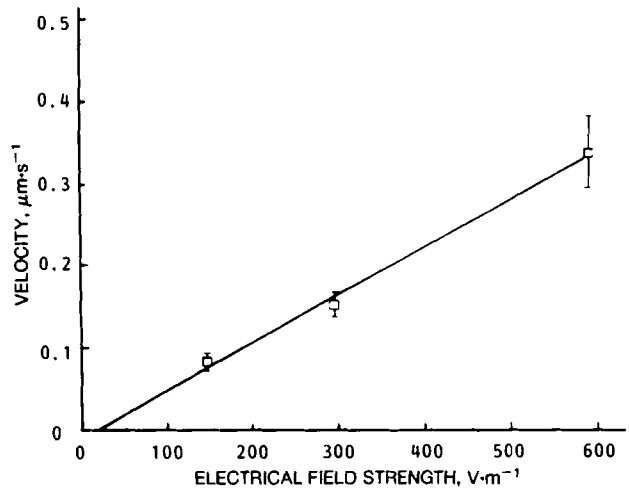

Figure 1—*Dependence of velocity on electrical field strength for liposomes composed of phosphatidylcholine-cholesterol-stearylamine (10:4:2); ionic strength, 2.3 mM. The line represents least-squares fit and the vertical bars are* SD.

EXPERIMENTAL SECTION

Positively and negatively charged multilamellar liposomes were prepared by the "film" method (7). Positive liposomes consisted of phosphatidylcholine (I)[1], cholesterol[2], and stearylamine (III)[3] in the molar ratio 10:4:1, 2, or 3, corresponding to maximum (positive) surface charge densities of 0.019, 0.037, or 0.054 C·m^{-2}, respectively. For negative liposomes, phosphatidylserine (II)[4] was used instead of III. With II, maximum (negative) charge densities of ~0.018, 0.034, or 0.047 C·m^{-2}, respectively, can be reached.

After film formation in pear-shaped flasks in a rotary evaporator at 40–45°C, the film was left under reduced pressure for ≥2 h in a desiccator. It was hydrated with NaCl solution (ionic strength, 2–150 mM). The water was

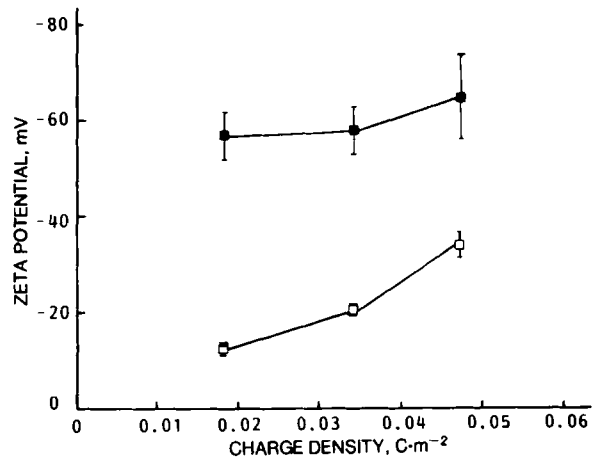

Figure 2—*Zeta potential of negative liposomes as a function of surface charge density for 6.6 mM (■) and 152 mM (□) ionic strengths. Liposome composition: phosphatidylcholine-cholesterol-phosphatidylserine (10:4:1, 2, or 3) with a charge density of 0.018, 0.034, or 0.047 C·m^{-2}, respectively. Vertical bars represent* SD.

[1] Egg yolk, L-α-phosphatidylcholine type V-E; Sigma Chemical Co., St. Louis, Mo.
[2] Sigma Chemical Co.
[3] ICN Pharmaceuticals, Plainview, N.Y.
[4] Bovine brain; Sigma Chemical Co.

0022-3549/84/1100-1559$01.00/0
© 1984, American Pharmaceutical Association

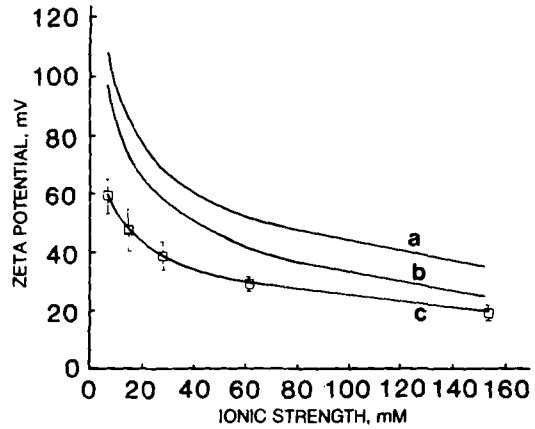

Figure 3—*Effect of ionic strength on the zeta potential for negative liposomes composed of phosphatidylcholine-cholesterol-phosphatidylserine (10:4:2). Key: (a) surface potential calculated according to Eq. 1; (b) surface potential calculated according to Eq. 2 (K = 0.0008 $m^3 \cdot mol^{-1}$), and Eq. 1; (c) experimental zeta potential. Vertical bars represent* SD.

freshly distilled in glass, and nitrogen was passed through the solution for 10 min. The final phospholipid concentration was ~7.5 μmol/mL. Negative liposome dispersions contained 1 mM EDTA. The pH was adjusted to 5.9 ± 0.1 with dilute HCl or NaOH. After pH adjustment, the concentration of NaCl in the dispersion was determined conductometrically[5]. If necessary, corrections for EDTA were applied. After complete dispersion of the film by shaking and vortexing at 40-45°C, the liposomes were stored overnight at 4-6°C and extruded the next day through membrane filters[6] with 400-nm pores (8).

Mobilities of the liposomes were measured in a cylindrical-cell microelectrophoresis apparatus[7] at 25°C. Heat effects were minimized by using currents of <2 mA and short current passage times. The liposome dispersions were diluted with the hydration medium to avoid an overcrowded field of view. To minimize electrode polarization, successive measurements were made in both current directions. At least 20 particles were measured in each direction at the lower and upper stationary levels. Data obtained for both directions of liposome movement did not differ significantly (Student's t test; $p = 0.95$) and were averaged.

Mean diameters of the liposomes were measured with a dynamic light-scattering technique[8] 1 d after extrusion and after 7 and 14 d. A polydispersity index was also obtained[8]. This index ranges from 0 to 9; 0 refers to a monodispersed system, 9 to an extremely polydispersed system. A gold suspension approaching a normal size distribution with a mean diameter of ~50 nm and a CV of 15% has a polydispersity index of 3[9]. The dispersions were stored at

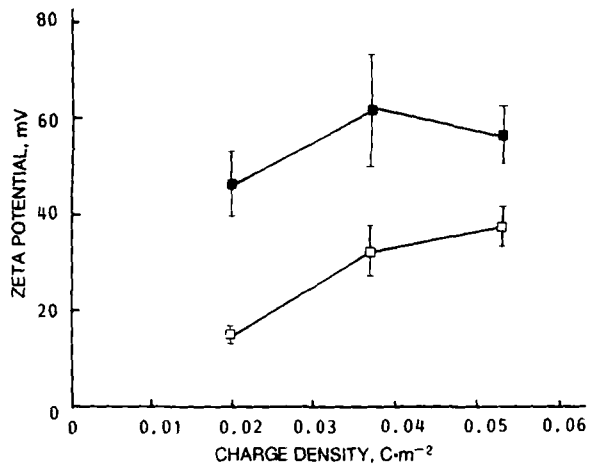

Figure 4—*Zeta potential of positive liposomes as a function of surface charge density for 2.3 (■) and 153 mM (□) ionic strengths. Liposome composition: phosphatidylcholine-cholesterol-stearylamine (10:4:1, 2, or 3) with a charge density of 0.019, 0.037, or 0.054 $C \cdot m^{-2}$, respectively.*

[5] PW 9505; Philips Cambridge, U.K.
[6] Unipore filters; Biorad, Richmond, Calif.
[7] Mark II; Rank Brothers, Bottisham, U.K.
[8] Nanosizer; Coulter Electronics Ltd., Luton, U.K.
[9] J. Leuvering, personal communication.

Table I—Effect of Ionic Strength on the Zeta Potential of Positive Liposomes [a]

Ionic Strength, mM[b]	Zeta Potential, mV	CV, %	Ψ_0, mV[c]
2.3	62	13	133
15.3	57	13	85
150	34	15	38

[a] Composition: phosphatidylcholine-cholesterol-stearylamine (10:4:2); charge density, 0.037 ($C \cdot m^{-2}$). [b] NaCl solutions. [c] Calculated according to the Gouy-Chapman equation (Eq. 1).

4-6°C, protected from light. Before measuring the mean diameter, the dispersions were equilibrated for at least 3 h at room temperature (20-25°C). Appropriate corrections were made for temperature-dependent parameters (*e.g.*, medium viscosity). Before taking the readings, the dispersions were diluted 10-100 times with solutions of the same ionic strength. For these dilute dispersions, the influence of the ionic strength on the particle size measurement is negligible (9).

The influence of dilution on the calculated diameters and polydispersity indices was investigated. In the concentration range covered by the dynamic light-scattering technique, the average size of primary or fused vesicles and the aggregate dimensions did not depend on the phospholipid concentration. The absorption (at 700 nm) per μmol/mL of phospholipid per cm path length was constant after dilution. These findings justify the conversion of the data obtained with the dilute dispersions to the original dispersions.

The purity of I and II was assessed as described by Frøkjaer *et al.* (3). Lysophosphatidylcholine and lysophosphatidylserine were separated from intact phospholipids by TLC [silica gel[10], chloroform-methanol-water (65:35:5)] visualized with iodine vapor. The spots were scraped off, and the compounds were extracted with methanol. The lysophosphatidylcholine and lysophosphatidylserine content was determined by phosphate analysis (10). Before the liposome preparation, <2 and 5% of these compounds were detectable in I- and II-containing vials, respectively. In a comparable system, Kitagawa *et al.* (11) found that the presence of these compounds in these concentrations had a negligible effect on particle size. One week after liposome preparation, no detectable lysophosphatidylcholine and lysophosphatidylserine increase was observed.

RESULTS AND DISCUSSION

A linear relationship between the velocity of liposomes and the electrical field strength is predicted by theory. In our experiment, results agreed with theory (Fig. 1). There was no difference between mobilities at the lower and the upper stationary levels for the same dispersion. All calculated zeta potentials were taken from upper stationary level data. The Helmholtz-Smoluchowski equation was used to calculate the zeta potential from mobility data. In cases of low ionic strength, particles with an estimated diameter >1 μm were selected for mobility measurements to avoid corrections for relaxation (12, 13).

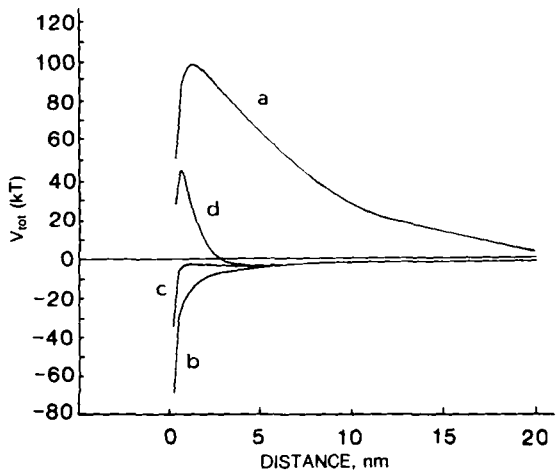

Figure 5—*Calculation of interaction energies (V_{tot}) between two liposomes (radii 200 nm) according to the Derjaguin-Landau-Verwey-Overbeek theory as a function of interparticle distance. The Hamaker constant is 5 × 10^{-21} J, based on data reported by Rand (5). Key [zeta potential (mV)/ionic strength (mM)]: (a) 30/3; (b) 10/150; (c) 20/150; (d) 30/150.*

[10] Precoated silica gel 60 F_{254}; E. Merck, Darmstadt, F.R.G.

Table II—Effect of Changing the Ionic Strength of the Outer Aqueous Medium of Liposome Dispersions on the Zeta Potential [a]

Charge	Initial: Ionic Strength, mM [b]	Initial: Zeta Potential mV [c]	After Changing: Ionic Strength, mM [b]	After Changing: Zeta Potential, mV [c]
+[d]	2.3	62	150	27
+	150	34	3.3	62
−[e]	6.6	59	150	20
−	150	20	—[f]	--

[a] Mobilities were measured at least 2 h after changing the medium. [b] NaCl solutions, for negative liposomes in combination with 1 mM EDTA. [c] Zeta potentials are the mean of duplicate experiments. [d] Composition of positive liposomes: phosphatidylcholine-cholesterol-stearylamine (10:4:2). [e] Negative liposomes: phosphatidylcholine-cholesterol-phosphatidylserine (10:4:2). [f] Not available.

Figure 2 is a plot of the zeta potential *versus* the surface charge density (σ). This parameter was calculated assuming a surface area of 0.70 nm^2 per I or II molecule. Values from 0.67 nm^2 (14) to 0.72 nm^2 (15, 16) were reported for I and 0.70 nm^2 for II (17, 18). The value used for the area covered by one cholesterol molecule was 0.28 nm^2 (7), and for one molecule of III the value used was 0.25 nm^2. For 1:1 bilayer combinations consisting of I and cholesterol, an area of 0.96 nm^2 was found for a unit consisting of one molecule of I and one molecule of cholesterol (5). This indicated that interactions between the different molecular species in the bilayer do not substantially influence the area covered by the individual molecules. The surface charge density could be calculated (19) from these data. It was assumed that the phospholipids and additives spread evenly and laterally over the bilayers (20). For I- and II-containing vesicles with relatively large radii of curvature (like those used in this study), the distribution over the two halves of the bilayer is expected to be fairly symmetrical (20, 21). At the experimental pH, both the deprotonation of II and the protonation of III were almost complete (22, 23). For negative liposomes, zeta potentials were obtained at two ionic strength levels as a function of II content. For an ionic strength of 152 mM, a nearly linear increase of the zeta potential with surface charge density was observed. For low ionic strength data (6.6 mM), this increase was less pronounced.

A comparison was made between the experimentally obtained zeta potentials and surface potentials calculated from the surface charge density. The effect of ionic strength on the zeta potential for the negative liposomes with an intermediate II content (charge density 0.034 $C \cdot m^{-2}$) is shown in Fig. 3. Line a represents the effect on the surface potential as predicted by the Gouy-Chapman equation for a single symmetrical electrolyte (Eq. 1):

$$\sigma = (8 \cdot N \cdot \epsilon_r \cdot \epsilon_0 \cdot kT)^{1/2} \cdot C^{1/2} \cdot \sinh (0.5 \cdot e \cdot \Psi_0/kT) \quad \text{(Eq. 1)}$$

Line b gives the surface potential calculated (with Eq. 1) after correction of the surface-charge density for the sodium ion interaction with II (Eq. 2). This interaction reduces the effective surface charge density (24):

$$\sigma_{corr} = \frac{\sigma}{1 + K \cdot C \cdot \exp\left(\frac{-e \cdot \Psi_0}{kT}\right)} \quad \text{(Eq. 2)}$$

where σ_{corr} and σ are the corrected and uncorrected surface charge density ($C \cdot m^{-2}$), respectively; e is the charge of a proton (C); k is the Boltzmann constant ($J \cdot K^{-1}$); T is absolute temperature (K); K is the intrinsic binding constant (m^3/mol); C is the concentration (mol/m^3); N is Avogadro constant (mol^{-1}); ϵ_0 is the permittivity ($C \cdot V^{-1} \cdot m^{-1}$); and ϵ_r is the relative permittivity (no units).

A value of 0.8×10^{-3} $m^3 \cdot mol^{-1}$ was used (25) for the instrinsic binding constant of the sodium ion to II, and the value for the relative permittivity of water was 78.3 (26). The zeta potential data comply reasonably well with the corrected surface potentials for the dispersions in 61 and 152 mM NaCl. In principle, the surface potential always has to exceed the zeta potential as the hydrodynamic plane of shear does not coincide with the surface, but is positioned at a finite distance from it (27). For the lower NaCl concentrations, the deviation between experimental and theoretical data increased. The influence of the divalence of the $EDTA^{2-}$ ion was neglected in the calculations, as the inclusion of a divalent ion complicated them considerably. This approach was justified because it was found experimentally that for the negative liposomes, under conditions where the influence of the $EDTA^{2-}$ ion is expected to be most pronounced (low II content, low ionic strength), the presence of $EDTA^{2-}$ ion in the aqueous medium did not change the zeta potential significantly [Student's t test, $p = 0.95$]: with EDTA, 58 mV (SD 8 mV, $n = 42$), without EDTA, 55 mV (SD 7.5 mV, $n = 35$).

The correction proposed by Nir and Bentz (24) takes into account interactions of the bilayer II molecules with cations from the bulk. The large deviation from the theoretical predictions at low ionic strength might be caused by a limitation in the ionization of II. In a solution of NaCl with an ionic strength of 5 mM, the Debye length ($1/\kappa$) is 4.4 nm and exceeds the distance between the molecules (2-3 nm, assuming the II molecules to be spread evenly over the bilayer). Therefore, mutual interference cannot be excluded. For a solution of 150 mM ionic strength, the Debye length is only 0.8 nm and no interaction is expected. Hauser *et al.* (20) suggested an analogous mechanism for the incomplete ionization of fatty acids clustering in bilayers.

Table III—Physical Stability of Positive and Negative Liposomes: Particle Size of Liposome Dispersions 1 and 7 d After Extrusion [a]

Ionic Strength, mM	Zeta Potential, mV	Diameter, nm [b]: Day 1	Diameter, nm [b]: Day 7	Stability [c]: Observed	Stability [c]: Predicted [d] ($V_{rep}^{el} + V_{att}$)
Phosphatidylcholine-Cholesterol-Stearylamine (10:4:*N*)					
2.3					
$N = 1$	46	271[e]	270[e]	+	+
$N = 2$	61	522[f]	—[g]	−	+
$N = 3$	57	—[g]	—[g]	−	+
150					
$N = 1$	17	—[g]	—[g]	−	−
$N = 2$	34	571[f]	—[g]	−	+/−
$N = 3$	39	376[e]	300[e]	+	+/−
Phosphatidylcholine-Cholesterol-Phosphatidylserine (10:4:*N*) [h]					
6.6					
$N = 1$	−57	300	309	+	+
$N = 2$	−58	276	267	+	+
$N = 3$	−65	320	311	+	+
150					
$N = 1$	−12	301	285	+	−
$N = 2$	−20	350	346	+	−
$N = 3$	−34	238	234	+	+/−

[a] Protected from light at 4-6°C. [b] Mean of duplicate experiments. CV of sequential readings of the mean diameters of the same dispersion, 3%. [c] (+) stable; (−) unstable; (+/−) secondary minimum over −3 kT at an interparticle distance >2.5 nm. [d] (V_{rep}^{el}) electrostatic repulsive energy; (V_{att}) van der Waals attractive energy (effective Hamaker constant, 5×10^{-21} J). Predictions made using the Derjaguin-Landau-Verwey-Overbeek theory. [e] Polydispersity index 2-3. [f] Polydispersity index 7. [g] Strongly heterodisperse with mean diameters >1000 nm. [h] Polydispersity index 2-3 for all negative liposomes.

The results obtained with positive liposomes at two ionic strength levels are plotted in Fig. 4. For the 150 mM ionic strength series, the zeta potential increase leveled off at charge densities >0.037 $C \cdot m^{-2}$. Little increase of the potential with the surface charge density was found for solutions of 2.3 mM ionic strength.

Table I gives the zeta potentials of the positive liposomes with an intermediate III content over an ionic strength range from 2.3 to 150 mM. The experimental results were compared with the calculated surface potentials (Gouy-Chapman equation) listed in the last column. Here, as with the negative liposomes, for the high ionic strength dispersions a good agreement with theory was found; for low ionic strength, the experimental values for the zeta potentials were too low.

The proposed explanation for the deviation of the experimental zeta potentials from theory implies that changing the outer aqueous medium of the liposome dispersions from low to high ionic strength and *vice versa*, has in principle a reversible impact on the zeta potential. The effect of changes in the ionic strength in the aqueous phase outside the bilayer on the zeta potential was investigated. The positive and negative liposomes with intermediate III and II content, respectively, prepared under low ionic strength conditions, were mixed with at least 100-fold excess of an NaCl solution of high ionic strength (150 mM). After 2 h of equilibration, the mobilities were determined. For the positive liposomes, the reverse was done: dispersions in the high ionic strength medium were diluted with the low ionic strength solution. The results are listed in Table II. Changing the medium resulted in zeta potentials comparable with those existing after preparation of the liposomes at that particular ionic strength. This is an indication that preparing these types of liposomes at low or high ionic strength does not result in structures that differ irreversibly from each other.

The physical stability, on storage at 4°C, was investigated for various types of positively and negatively charged liposomes. Results of particle size measurements 1 d and 7 d after extrusion through 400-nm membrane filters are shown in Table III. Deviations of the reported particle diameter from the pore diameter (400 nm) were ascribed to differences in filtered liposome dispersion volumes. The initial filtrate generally contained smaller-sized liposomes. There was a distinct difference between the behavior of stable and unstable dispersions. For unstable dispersions, the mean particle diameter was at least double the diameter of the membrane pore with a polydispersity index >7 after 1

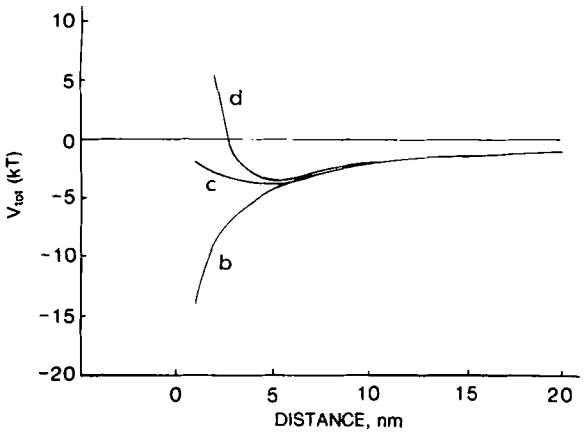

Figure 6—*Magnification of part of Fig. 5 to show occurrence of secondary minima.*

week. Stable dispersions had diameters <400 nm and polydispersity indices of 2–3 both at the day of extrusion and after 1 week. In all cases, changes in particle size occurred independently of phospholipid concentration within the first week of storage. No difference was found in particle diameters of the negative liposomes measured after 7 or 14 d of storage. This was also true for the two stable positive liposome dispersions.

Frøkjaer *et al.* (3) found, for I- and II-containing liposomes, an enhanced stability with decreasing ionic strength and increasing II content. Under the experimental conditions in this study, negative liposomes were stable independent of ionic strength and surface charge density. Positive liposomes had no correlation between the zeta potential and particle size stability; those with low surface charge density were stable at an ionic strength of 2.3 mM. Liposomes with high surface charge density, on the other hand, were stable at an ionic strength of 150 mM. A high positive zeta potential (61 or 57 mV), as was observed with the low ionic strength medium, did not therefore, guarantee a stable dispersion. Whether particle size growth was caused by aggregation or fusion of the particles was not studied.

We investigated whether the experimental results could be predicted by the existing theories on the physical stability of liposome dispersions. The interaction energy between two approaching liposomes was calculated according to the DLVO theory (6) using $V_{tot} = V_{att} + V^{el}_{rep}$, or:

$$V_{tot} = -\frac{aA}{12H} + 2\epsilon_r\epsilon_0\Psi_0^2 a \cdot \ln(1 + e^{-\kappa H}) \qquad \text{(Eq. 3)}$$

where V_{tot}, V^{el}_{rep}, and V_{att} are the total, electrostatic repulsive, and attractive energies, respectively; a is the radius of the liposome; H is the distance between the bilayer surfaces; and A is the effective Hamaker constant. In Eq. 3, V_{att} is calculated with a simplified equation for solid spheres and $H \ll a$. Results obtained with the complete equation for spherical shells, as given by Nir and Bentz (24), differed <5% for $H \leq 20$ nm.

The results suggest that, for low ionic strength (3 mM) dispersions with a zeta potential of >30 mV, a V_{tot} of at least 100 kT can be reached (Fig. 5). This implies that the rate of aggregation of these charged primary particles (compared with uncharged particles) is reduced by at least a factor of 10^9, and that dimer formation is limited to <10% of the primary particles over 2 weeks (6). Therefore, at low ionic strength the dispersions used should be stable (Figs. 2 and 4). Aggregation in the primary or secondary minimum was unlikely as the electrostatic repulsion exceeded the van der Waals attraction. These calculations are estimates because the effective Hamaker constants for the I, cholesterol, and II or III systems are not known precisely. Rand (5) reported a value of 9×10^{-21} J for pure I and 1.2×10^{-21} J for I-cholesterol (1:1) bilayers. We chose 5×10^{-21} J for our calculations. For low ionic strengths, all dispersions were predicted to be stable. However, for the positive liposomes, aggregation or fusion occurred with two of three dispersions.

For the 150 mM ionic strength dispersions, V^{el}_{rep} was not dominant. Secondary minima could be observed by using realistic Ψ_0 values (Fig. 6). The secondary minima are not affected by repulsive hydration energy, as the influence of this energy decreases steeply with increasing interparticle distance and can virtually be neglected for interparticle distances >2.5 nm (5). As far as electrical repulsion is concerned, the dispersions with low III and intermediate II content should behave similarly under 150 mM ionic strength conditions as they have similar zeta potentials (−17 and −20 mV, respectively). Experimentally, the negative liposomes were stable, and the positive liposomes were unstable. Apparently factors other than the electrical repulsion (*e.g.*, V_{att}) control stability. As stated above, the secondary minima shown in Fig. 6 are not affected by the hydration forces. In the case of negatively charged liposomes containing 100% II, aggregation in the secondary minimum is assumed to be a reversible process in the presence of sodium ions (28). In these dispersions, both aggregate formation and dissociation occur. In the dispersions under investigation, an analogous situation is likely. The mass average aggregate size at equilibrium was calculated for a −4-kT secondary minimum for negative liposomes of the compositions used in this study. Diameters of 200 and 400 nm were taken with phospholipid concentrations between 7.5×10^{-3} M (the concentration of the dispersions on storage) and 7.5×10^{-5} M (the minimum concentration used in dynamic light-scattering studies). The equations and boundary conditions for these calculations have been described by Bentz and Nir (28). Under the chosen conditions substantial aggregate formation was predicted, depending on the phospholipid concentration. This could not be confirmed experimentally, as no concentration-dependent mean diameter or polydispersity was observed in this study.

The negatively charged liposome dispersion (predicted to aggregate in the secondary minimum) was stable. If the physical model that was used to predict the stability is correct, the experimental results indicate that V_{att} is overrated for the negatively charged liposomes. This might be ascribed to an overestimation of the value for the Hamaker constant.

It is remarkable that two positively charged liposome dispersions (zeta potentials of 34 and 39 mV) that are both predicted to form aggregates in the secondary minimum (Table III) behave differently. The first one forms aggregates; the second is stable for at least 2 weeks.

CONCLUSIONS

Increasing the charge density from ~0.018 to 0.050 C·m^{-2} resulted in considerably larger zeta potentials for the dispersions with an ionic strength of 150 mM. Almost no increase was found at an ionic strength of ~5 mM. The zeta potentials were larger at low ionic strength, but not as large as predicted by the (corrected) Gouy-Chapman equation. Based on these data for low ionic strength, high electrostatic repulsive energies, and thus stable dispersions, were expected. However, two of the positive liposome dispersions were not stable. Apparently, in these systems particles can form aggregates because of a mechanism interfering with the "classical" DLVO theory (with consideration given to repulsive hydration forces).

On the other hand, for high ionic strength dispersions, DLVO calculations predicted an irreversible aggregation in a primary minimum or a reversible aggregation in the secondary minimum. However, no aggregation at all (negative liposomes and one positive liposome dispersion) or irreversible aggregation was found. This unexpected stability against aggregation in the primary minimum can be ascribed to the hydration forces. However, hydration forces do not extend far enough from the surface of the bilayer to affect the reversible aggregation in the secondary minimum.

REFERENCES

(1) R. L. Juliano, D. Stamp, and N. McCullough, in "Liposomes and Their Uses in Biology and Medicine," D. Papahadjopoulos, Ed., Ann. N.Y. Acad. Sci., Vol. 308, 1978, p. 411.

(2) A. Rahman, A. Kessler, N. More, B. Sikic, G. Rowden, G. Woolley, and P. S. Schein, *Cancer Res.*, **40**, 1532 (1980).

(3) S. Frøkjaer, E. L. Hjorth, and O. Worts, in "Optimization of Drug Delivery," H. Bundgaard, A. Bagger Hansen, and H. Kofod, Eds., Munkgaard, Copenhagen, 1982.

(4) D. M. Leneveu, R. P. Rand, and V. A. Parsegian, *Nature (London)*, **259**, 601 (1976).

(5) R. P. Rand, *Annu. Rev. Biophys. Bioeng.*, **10**, 277 (1981).

(6) E. J. W. Verwey and J. Th. G. Overbeek, "Theory of the Stability of Lyophobic Colloids," Elsevier, Amsterdam, 1948.

(7) F. Szoka and D. Papahadjopoulos, *Annu. Rev. Biophys. Bioeng.*, **9**, 467 (1980).

(8) F. Olson, C. A. Hunt, F. C. Szoka, W. J. Vail, and D. Papahadjopoulos, *Biochim. Biophys. Acta*, **557**, 9 (1979).

(9) J. L. Anderson, F. Rauh, and A. Morales, *J. Phys. Chem.*, **82**, 608 (1978).

(10) C. H. Fiske and Y. Subbarow, *J. Biol. Chem.*, **66**, 375 (1925).

(11) T. Kitagawa, K. Inoue, and S. Nojima, *J. Biochem.*, **79**, 1123 (1976).

(12) P. H. Wiersema, A. L. Loeb, and J. Th. G. Overbeek, *J. Colloid Interface Sci.*, **22**, 78 (1966).

(13) P. C. Hiemenz, "Principles of Colloid and Surface Chemistry," Dekker, New York, N.Y., 1977.

(14) D. Papahadjopoulos and H. K. Kimelberg, in "Progress in Surface Science," S. G. Davison, Ed., Pergamon, Oxford, 1973, p. 141.

(15) D. M. Small, *J. Lipid Res.*, **8**, 551 (1967).
(16) S. M. Johnson, A. D. Bingham, M. W. Hill, and E. D. Korn, *Biochim. Biophys. Acta*, **233**, 820 (1971).
(17) S. Ohki and N. Düzgünes, *Biochim. Biophys. Acta*, **552**, 438 (1979).
(18) H. Hauser, M. C. Phillips, and M. D. Barratt, *Biochim. Biophys. Acta*, **413**, 341 (1975).
(19) M. S. Fernandez, *Biochim. Biophys. Acta*, **646**, 23 (1981).
(20) H. Hauser, W. Guyer, and K. Howell, *Biochemistry*, **18**, 3285 (1979).
(21) J. A. Berden, R. W. Barker, and G. K. Radda, *Biochim. Biophys. Acta*, **375**, 186 (1975).
(22) A. D. Bingham, M. W. Hill, and N. G. A. Miller, in "Methods in Membrane Biology," E. Korn, Ed., Plenum, New York, N.Y., 1974.
(23) M. Ptak, M. Egret-Charlier, A. Sanson, and O. Boulossa, *Biochim. Biophys. Acta*, **600**, 387 (1980).
(24) S. Nir and J. Bentz, *J. Colloid Interface Sci.*, **65**, 399 (1978).
(25) C. Newton, W. Pangborn, S. Nir, and D. Papahadjopoulos, *Biochim. Biophys. Acta*, **506**, 281 (1978).
(26) "Handbook of Chemistry and Physics," 56th ed., C. R. C. Press, Cleveland, Ohio (1975).
(27) M. Eisenberg, T. Gresalfi, T. Riccio, and S. McLaughlin, *Biochemistry*, **18**, 5213 (1979).
(28) J. Bentz and S. Nir, *Proc. Natl. Acad. Sci. (USA)*, **78**, 1634 (1981).

ACKNOWLEDGMENTS

The author acknowledges the helpful discussions with Dr. O. Patmamanoharan (Department of Physical and Colloid Chemistry of the University of Utrecht) and Dr. J. Leuvering (Organon B. V.), and the critical remarks by Dr. P. J. J. M. van Mil during preparation of the manuscript.

Hydrolysis of Some Poly(*ortho*-ester)s in Homogeneous Solutions

TUE HUU NGUYEN *, CHUNG SHIH[§], KENNETH J. HIMMELSTEIN *[§‡x], and TAKERU HIGUCHI *[§]

Received November 14, 1983, from the **Departments of Pharmaceutical Chemistry and* [‡]*Chemical and Petroleum Engineering, The University of Kansas, Lawrence, KS 66045* and [§]*INTER$_x$ Research Corp., Merck Sharp & Dohme Research Laboratories, Lawrence, KS 66044.* Accepted for publication January 13, 1984.

Abstract □ The hydrolysis of poly(*ortho*-ester)s and a monomeric model compound, 3,9-dibenzyloxy-3,9-diethyl-2,4,8,10-tetraoxaspiro[5,5]undecane, was carried out in dioxane-d_8–dioxane and followed by ^{1}H-NMR and HPLC, respectively. Experimental results suggested that the polymer degradation proceeds to a large extent *via* random scission. The hydrolysis was catalyzed by the acid; the catalytic rate constant increased predictably with decreasing aqueous pK_a of the acid. The reaction is first order with respect to the catalyst concentration and the number of *ortho*-ester linkages present, and it is independent of water in the concentration range studied. Strain at the *ortho*-ester bond may be a factor influencing the hydrolysis rate.

Keyphrases □ Hydrolysis—poly(*ortho*-ester)s, homogeneous solutions □ Polymers—hydrolysis of poly(*ortho*-ester)s, homogeneous solutions □ Degradation—polymers, hydrolysis of poly(*ortho*-ester)s, homogeneous solutions □ Poly(*ortho*-ester)s—hydrolysis, homogeneous solutions

Poly(*ortho*-ester)s are a novel class of polymers with potential utility in drug delivery systems. Their use as an erodible matrix for the delivery of a steroid has been demonstrated by Heller *et al.* (1). In these systems, water-soluble salts were incorporated into the polymer, and the release mechanism appeared to be similar in part to that described by Fedors (2). Osmotic imbibition of water induced the swelling of the matrix, which subsequently burst and released the drug.

Poly(*ortho*-ester)s, as with most *ortho*-esters, undergo acid-catalyzed hydrolysis quite readily and are relatively unreactive in neutral or basic media (3, 4). Thus, when exposed to an aqueous environment, the erosion of the polymeric matrix may be induced by the presence of an acidic catalyst. The acid may be external or may be generated *in situ* by an acid-producing agent such as acid anhydride incorporated in the device. Since acid anhydrides are neutral, and therefore noncatalytic, they add to the stability of the device during storage.

Following this rationale Shih *et al.* (5) have demonstrated the use of poly(*ortho*-ester)s delivery systems, achieving zero-order release of timolol maleate. The release rate was effectively controlled by the amount of acid anhydride incorporated into the device and the aqueous pK_a of the corresponding acid. It was proposed that the mechanism of drug release from such a system results from the contribution of several processes, namely, the permeation of water into the polymer matrix, the hydrolysis of the acid anhydride to the corresponding acid, the hydrolysis of the *ortho*-ester linkages, and the dissolution of the drug species into the medium (5).

The present studies were undertaken as part of an effort to understand the various physicochemical processes which govern the release of drugs from poly(*ortho*-ester)s delivery systems. In an attempt to separate the various contributing factors, we report the kinetics of the hydrolysis of poly(*ortho*-ester)s [poly(3,9-dialkyloxy-3,9-diethyl-2,4,8,10-

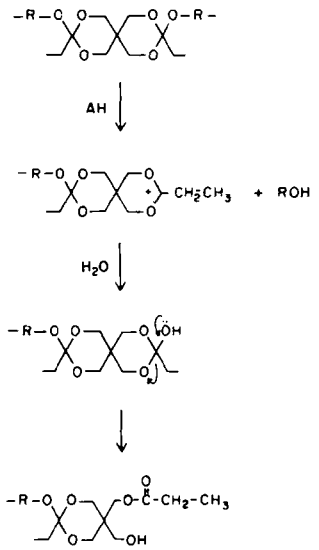

*Scheme I—Acid-catalyzed hydrolysis of poly(*ortho*-ester)s.*

© 1984, American Pharmaceutical Association

(15) D. M. Small, *J. Lipid Res.*, **8**, 551 (1967).
(16) S. M. Johnson, A. D. Bingham, M. W. Hill, and E. D. Korn, *Biochim. Biophys. Acta*, **233**, 820 (1971).
(17) S. Ohki and N. Düzgünes, *Biochim. Biophys. Acta*, **552**, 438 (1979).
(18) H. Hauser, M. C. Phillips, and M. D. Barratt, *Biochim. Biophys. Acta*, **413**, 341 (1975).
(19) M. S. Fernandez, *Biochim. Biophys. Acta*, **646**, 23 (1981).
(20) H. Hauser, W. Guyer, and K. Howell, *Biochemistry*, **18**, 3285 (1979).
(21) J. A. Berden, R. W. Barker, and G. K. Radda, *Biochim. Biophys. Acta*, **375**, 186 (1975).
(22) A. D. Bingham, M. W. Hill, and N. G. A. Miller, in "Methods in Membrane Biology," E. Korn, Ed., Plenum, New York, N.Y., 1974.
(23) M. Ptak, M. Egret-Charlier, A. Sanson, and O. Boulossa, *Biochim. Biophys. Acta*, **600**, 387 (1980).
(24) S. Nir and J. Bentz, *J. Colloid Interface Sci.*, **65**, 399 (1978).
(25) C. Newton, W. Pangborn, S. Nir, and D. Papahadjopoulos, *Biochim. Biophys. Acta*, **506**, 281 (1978).
(26) "Handbook of Chemistry and Physics," 56th ed., C. R. C. Press, Cleveland, Ohio (1975).
(27) M. Eisenberg, T. Gresalfi, T. Riccio, and S. McLaughlin, *Biochemistry*, **18**, 5213 (1979).
(28) J. Bentz and S. Nir, *Proc. Natl. Acad. Sci. (USA)*, **78**, 1634 (1981).

ACKNOWLEDGMENTS

The author acknowledges the helpful discussions with Dr. O. Patmamanoharan (Department of Physical and Colloid Chemistry of the University of Utrecht) and Dr. J. Leuvering (Organon B. V.), and the critical remarks by Dr. P. J. J. M. van Mil during preparation of the manuscript.

Hydrolysis of Some Poly(*ortho*-ester)s in Homogeneous Solutions

TUE HUU NGUYEN *, CHUNG SHIH[§], KENNETH J. HIMMELSTEIN *[§‡x], and TAKERU HIGUCHI *[§]

Received November 14, 1983, from the **Departments of Pharmaceutical Chemistry and* [‡]*Chemical and Petroleum Engineering, The University of Kansas, Lawrence, KS 66045* and [§]*INTER$_x$ Research Corp., Merck Sharp & Dohme Research Laboratories, Lawrence, KS 66044.* Accepted for publication January 13, 1984.

Abstract □ The hydrolysis of poly(*ortho*-ester)s and a monomeric model compound, 3,9-dibenzyloxy-3,9-diethyl-2,4,8,10-tetraoxaspiro[5,5]undecane, was carried out in dioxane-d_8–dioxane and followed by ^{1}H-NMR and HPLC, respectively. Experimental results suggested that the polymer degradation proceeds to a large extent *via* random scission. The hydrolysis was catalyzed by the acid; the catalytic rate constant increased predictably with decreasing aqueous pK_a of the acid. The reaction is first order with respect to the catalyst concentration and the number of *ortho*-ester linkages present, and it is independent of water in the concentration range studied. Strain at the *ortho*-ester bond may be a factor influencing the hydrolysis rate.

Keyphrases □ Hydrolysis—poly(*ortho*-ester)s, homogeneous solutions □ Polymers—hydrolysis of poly(*ortho*-ester)s, homogeneous solutions □ Degradation—polymers, hydrolysis of poly(*ortho*-ester)s, homogeneous solutions □ Poly(*ortho*-ester)s—hydrolysis, homogeneous solutions

Poly(*ortho*-ester)s are a novel class of polymers with potential utility in drug delivery systems. Their use as an erodible matrix for the delivery of a steroid has been demonstrated by Heller *et al.* (1). In these systems, water-soluble salts were incorporated into the polymer, and the release mechanism appeared to be similar in part to that described by Fedors (2). Osmotic imbibition of water induced the swelling of the matrix, which subsequently burst and released the drug.

Poly(*ortho*-ester)s, as with most *ortho*-esters, undergo acid-catalyzed hydrolysis quite readily and are relatively unreactive in neutral or basic media (3, 4). Thus, when exposed to an aqueous environment, the erosion of the polymeric matrix may be induced by the presence of an acidic catalyst. The acid may be external or may be generated *in situ* by an acid-producing agent such as acid anhydride incorporated in the device. Since acid anhydrides are neutral, and therefore noncatalytic, they add to the stability of the device during storage.

Following this rationale Shih *et al.* (5) have demonstrated the use of poly(*ortho*-ester)s delivery systems, achieving zero-order release of timolol maleate. The release rate was effectively controlled by the amount of acid anhydride incorporated into the device and the aqueous pK_a of the corresponding acid. It was proposed that the mechanism of drug release from such a system results from the contribution of several processes, namely, the permeation of water into the polymer matrix, the hydrolysis of the acid anhydride to the corresponding acid, the hydrolysis of the *ortho*-ester linkages, and the dissolution of the drug species into the medium (5).

The present studies were undertaken as part of an effort to understand the various physicochemical processes which govern the release of drugs from poly(*ortho*-ester)s delivery systems. In an attempt to separate the various contributing factors, we report the kinetics of the hydrolysis of poly(*ortho*-ester)s [poly(3,9-dialkyloxy-3,9-diethyl-2,4,8,10-

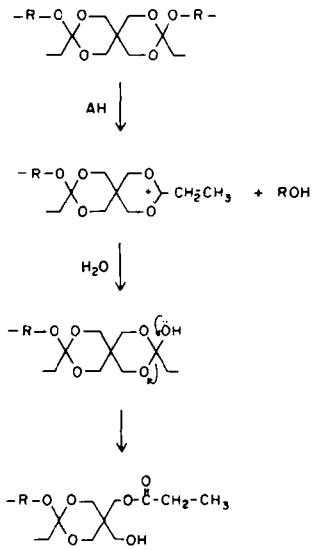

*Scheme I—Acid-catalyzed hydrolysis of poly(*ortho*-ester)s.*

© 1984, American Pharmaceutical Association

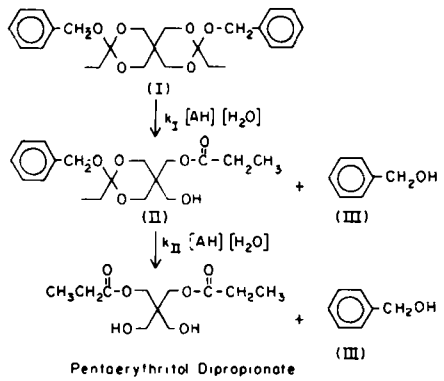

Scheme II—Acid-catalyzed hydrolysis of 3,9-dibenzyloxy-3,9-diethyl-2,4,8,10-tetraoxaspiro[5,5]undecane.

tetraoxaspiro[5,5]undecane)] and a monomeric model compound, 3,9-dibenzyloxy-3,9-diethyl-2,4,8,10-tetraoxaspiro[5,5]undecane (I) in homogeneous solutions. From this experiment, the intrinsic reactivity of the polymers may be independently obtained. The mode of depolymerization, the reaction rate constants, and the sensitivity of the reaction to the nature of the catalysts and to the concentration of water and acid were determined.

Several papers and reviews on *ortho*-ester chemistry have been published (3, 4, 6–11). The acid-catalyzed hydrolyses of *ortho*-esters is now thought to proceed *via* three steps. The first, and generally the rate-determining, step is the generation of a dialkoxycarbonium ion and an alcohol. The carbonium ion hydrates readily in the second step to form an unstable intermediate, the hydrogen *ortho*-ester, which breaks down to give an ester and an alcohol. For cyclic *ortho*-esters, the exocyclic alkoxy group is normally expelled in the first stage (11). Accordingly, the acid-catalyzed hydrolysis of I and poly(*ortho*-ester)s may be described as shown in Schemes I and II. The final products, alcohol and pentaerythritol dipropionate, were isolated and identified by HPLC comparison with authentic samples.

EXPERIMENTAL SECTION

Materials—Compound I and all polymers were used as provided[1]. Compound I was further purified by preparative TLC with precoated silica-gel glass plate[2]. The solvent system was 5% v/v ethyl acetate[3] in hexane[3]. The band at R_f 0.89 was located under short-wavelength UV light, removed from the plate, and extracted with methylene chloride[3]. The solvent was evaporated with a commercial evaporator[4], and the residual solvent was removed under reduced pressure at room temperature for 12 h. Water was distilled in an all-glass apparatus. Dioxane[3] was dried with lithium aluminum hydride[5] and distilled. Acetonitrile[3], HPLC grade, dioxane-d_8[6], trichloroacetic acid[6], dichloroacetic acid[6], monochloroacetic acid[6], formic acid[6], phthalic acid[6], and maleic acid[6] were used as received.

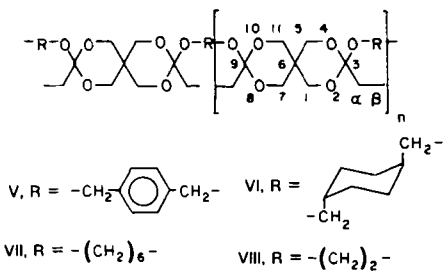

[1] Provided by Dr. J. Heller, SRI International, Menlo Park, Calif.
[2] Precoated silica gel GF 1500-μm glass plate; Analtech, Inc., Newark, Del.
[3] Fisher Scientific Co., Fair Lawn, N.J.
[4] Rotavapor; Brinkman Instruments, Westbury, N.Y.
[5] Alfa Products, Danvers, Mass.
[6] Aldrich Chemical Co., Inc., Milwaukee, Wis.

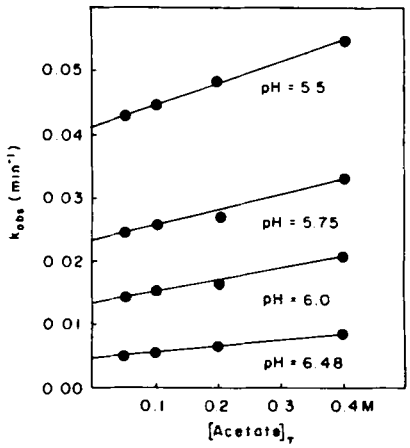

Figure 1—*Buffer-catalyzed hydrolysis of I in dioxane–water (50:50, v/v) at 25°C; μ = 0.5 M with KCl. Plot of the observed rate constant* versus *total buffer concentration.*

Methods—The hydrolysis of I was conducted both in 50% v/v buffered dioxane–water solutions and in pure dioxane. Samples of I were accurately weighed into 5-mL volumetric flasks and dissolved in 4 mL of dioxane. To start the experiment, measured amounts of water and acid stock solution in dioxane were transferred to the flask, and the volumes were brought to 5 mL with dioxane. The initial concentration of I was 0.01 M. In experiments in buffered solutions, 100 μL of a stock solution of I in dioxane was injected directly into 4 mL of buffered solution; the volume was then made up to 5 mL with the same solution resulting in an initial 0.02 M concentration of I. The flasks were stoppered and sealed[7] and then placed in a water bath. The reaction was monitored by following the disappearance of I and the appearance of benzyl alcohol (III) by HPLC. The mobile phase consisted of 20% v/v acetonitrile–water for III and 80% v/v acetonitrile–water for I. The flow rate was 2 mL/min, and the detector was set at 254 nm. The column employed was an ultrasphere-octadecysilane[8].

A series of four poly(*ortho*-ester)s, the structures of which are shown, was chosen for the study. Accurately weighed amounts of polymer were dissolved in dioxane-d_9. A total of 400 μL of the solution was transferred into ^{1}H-NMR sample tubes[9]. Immediately before the experiment, measured quantities of water and stock solution of acid in dioxane-d_8 were injected into the tube. The total volume was brought to 500 μL with dioxane-d_8 and mixed. The resulting concentration of polymer was 8% w/v. The sample tubes were then sealed and placed in a water bath at 37°C. Readings were performed periodically on a ^{1}H-NMR spectrometer[10].

For the condensation copolymer of 3,9-bis(ethylidene)-2,4,8,10-tetraoxaspiro[5,5]undecane (IV) and 1,4-benzenedimethanol (V), monitoring of the disappearance of the peaks at δ = 1.8 ppm corresponding to the α methylene group or the appearance of the methylene group α to the carbonyl carbon of the degraded product at δ = 2.3 ppm gives a direct account of the rate of bond

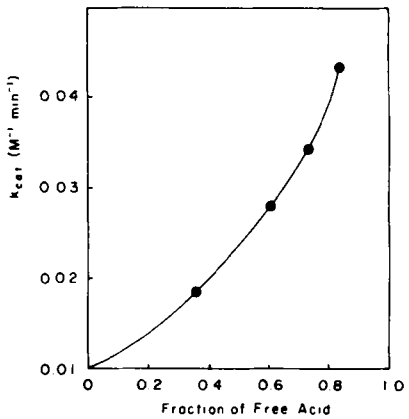

Figure 2—*Buffer-catalyzed hydrolysis of I in dioxane–water (50:50, v/v) at 25°C; μ = 0.5 M with KCl. Plot of the rate constant of the general acid-catalyzed reaction* versus *the fraction of free acetic acid.*

[7] Parafilm.
[8] Altex, Berkeley, Calif.
[9] Kontes Glass Co., Vineland, N.J.
[10] Model T60; Varian Instrument Co., Palo Alto, Calif.

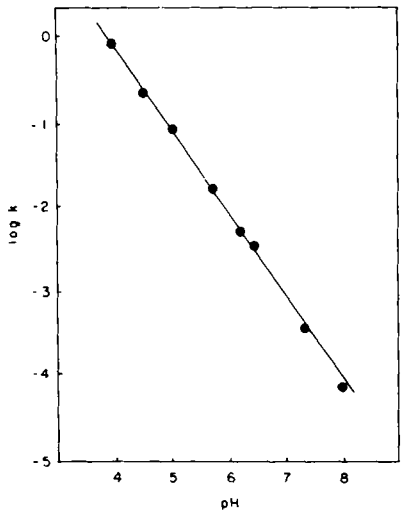

Figure 3—*Hydrolysis of I in dioxane-water (50:50) at 25°C; μ = 0.1 M with KCl. Plot of the logarithm of the observed rate constant at zero buffer concentration* versus *pH.*

cleavage. Only the appearance of the quartet at δ = 2.3 ppm can be used in the cases of the condensation copolymers of IV and diols such as 1,4-*trans*-cyclohexanedimethanol (VI) and 1,6-hexanediol (VII) due to interference of other protons in the system.

RESULTS AND DISCUSSION

pH-Rate Profile—The hydrolysis of I was carried out in 50% v/v buffered dioxane-water solutions at 25°C. The use of mixed solvent rendered the interpretation of the pH determination[11] somewhat difficult. However, when the apparent pH in the 50% v/v dioxane-water solvent system was plotted against the pH of the aqueous buffered solutions, prepared similarly but without dioxane, a straight line was obtained with a zero-intercept and a slope of 1.05. This seems to suggest that the changes in the pH-meter readings were proportional to the changes in the hydronium ion activity in this system. The pH range studied was from 4 to 8. The buffer concentration was varied from 0.4 to 0.005 M, whereas the ionic strength was kept at 0.1 or 0.5 M with KCl. It was assumed that the salts employed were fully ionized. The loss of I was followed by HPLC and found to follow pseudo-first-order kinetics. The effect of acetate buffer concentration on the reaction rate is illustrated in Fig. 1. The observed rate constant seems to increase linearly with buffer concentration. The slope of the lines increases with decreasing pH, suggesting that the free acid is the catalytic species. However, a plot of the rate constants of the general acid-catalyzed reaction against the fraction of free acid (Fig. 2) did not yield a straight line as expected. A change in the activity coefficient of the free acid and the anion at high buffer concentrations may be a possible explanation. The pK_a of acetic acid under the reaction conditions was determined to be 6.22 by pH titration.

The rate constants extrapolated to zero buffer concentration were employed to construct the pH-rate profile. As evident from the linearity of the plot of

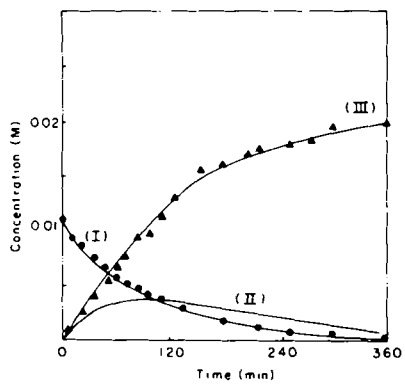

Figure 4—*Hydrolysis of I in dioxane at 37°C; water, 2 M; maleic acid, 1.25 × 10⁻³ M. Plot of the concentration of different species* versus *time. Points are experimental data; solid lines are generated from the kinetic model.*

[11] Accumet model 610A; Fisher Scientific Co.

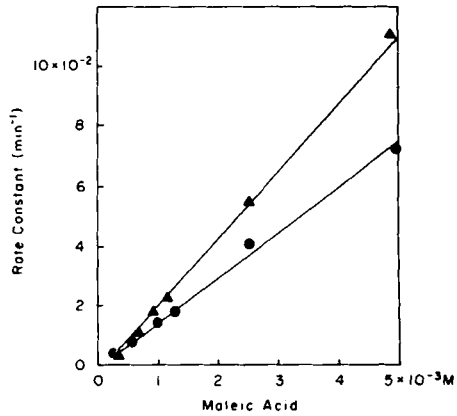

Figure 5—*Hydrolysis of I in dioxane at 37°C; water, 2 M. Plot of the two consecutive rate constants* versus *maleic acid concentration. Key: (▲) k_{II}; (●) k_I.*

the logarithm of the pseudo-first-order rate constant extrapolated to zero buffer concentration *versus* pH with a slope of −1 (Fig. 3), hydronium ions appear to be the catalyst in this pH range. The reaction was also studied at pH 13. No noticeable degradation could be detected. The value for the specific acid-catalyzed reaction (k_{H^+}) was obtained from the intercept of the line with the ordinate. A k_{H^+} value of 1.03×10^4 min^{-1} M^{-1} at μ = 0.1 M was only slightly smaller than the k_{H^+} of 1.09×10^4 min^{-1} M^{-1} at μ = 0.5 M, suggesting that the effect of the salt was not significant.

Mode of Depolymerization—There are two types of linkages involved, the internal linkages and those at the end of the polymer chain. Differentiation of their reactivity directly from the polymer molecules is difficult. However, I has two *ortho*-ester linkages. When they are intact, the bonds are similar to the internal bonds. When one bond is broken, the remaining one resembles the one at the end of the chain. Thus, according to Scheme II, it is possible to determine the relative reactivity of those two types of bonds by comparing the rate of disappearance of I and the monoester (II), its partially degraded product.

The reaction was carried out in dioxane at 37°C. The concentrations of I and water were 0.01 and 2 M, respectively. The maleic acid concentration was varied from 2.5×10^{-4} to 5×10^{-3} M. The loss of I and the formation of III were followed by HPLC.

The differential equations defining the kinetic system are:

$$\frac{-d[I]}{dt} = k_I [I] \qquad \text{(Eq. 1)}$$

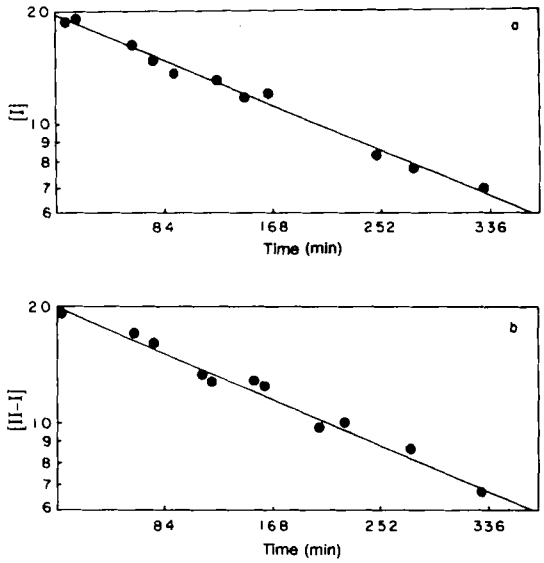

Figure 6—*Hydrolysis of the IV-V copolymer in dioxane-d_8 at 37°C; water, 2 M; trichloroacetic acid, 1.25 × 10⁻³ M. Plot of logarithm of peak integration* versus *time. [I], integration of NMR peaks during the reaction; [II], integration of peaks when the reaction is completed. Key: (a) disappearance of the α-methylene protons in the polymer; (b) appearance of methylene protons α to the carbonyl carbon in the degradation product.*

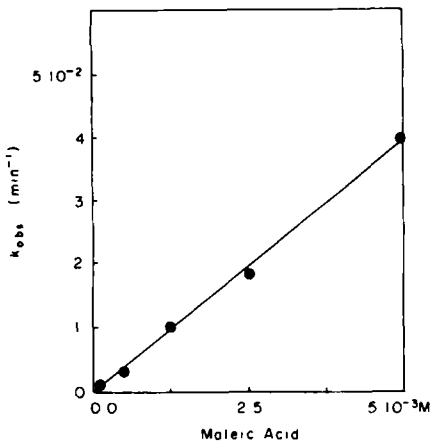

Figure 7—*Hydrolysis of I in dioxane at 37°C; water, 2 M. Plot of the observed rate constant* versus *maleic acid concentration.*

$$\frac{d[II]}{dt} = k_I [I] - k_{II} [II] \quad \text{(Eq. 2)}$$

$$\frac{d[III]}{dt} = k_I [I] + k_{II} [II] \quad \text{(Eq. 3)}$$

At $t = 0$, $[I] = [I]_0$, which is the initial concentration of I, and $[II] = [III] = 0$.

The estimation of k_I and k_{II}, the apparent pseudo-first-order rate constants for the two consecutive steps, respectively, was performed on a computer[12] by a nonlinear regression program based on a pattern-search algorithm. Typical experimental data and the fitted curves generated for the reaction from the kinetic model above are shown in Fig. 4.

The constants k_I and k_{II} obtained for various maleic acid concentrations are plotted in Fig. 5. The slope of the lines was taken to be the second-order rate constant for the reaction. The ratio k_{II}/k_I was ~1.55, suggesting that the bonds at the end of the chain are only slightly more reactive than the internal linkages.

In fig. 6, a semilogarithmic plot of the ^{1}H-NMR peak integration of the IV-V copolymer, as a function of time resulting from the hydrolysis in dioxane-d_8 at 37°C catalyzed by 2.55×10^{-3} M dichloroacetic acid, is shown. The water concentration was 2 M. The concentration of the IV-V copolymer was 8% w/v or ~0.23 M of the monomeric unit. Since each monomer has two *ortho*-ester linkages, the amount of water present was about five times that required for complete hydrolysis of the sample.

The pseudo-first-order rate constants for the disappearance of the methylene group and for the appearance of the methylene group α to the carbonyl carbon are 3.69×10^{-3} min^{-1} and 3.81×10^{-3} min^{-1}, respectively. This seems to validate the analytical procedure. The linear relationship suggests a random scission process in which the majority of the bonds are of equal accessibility

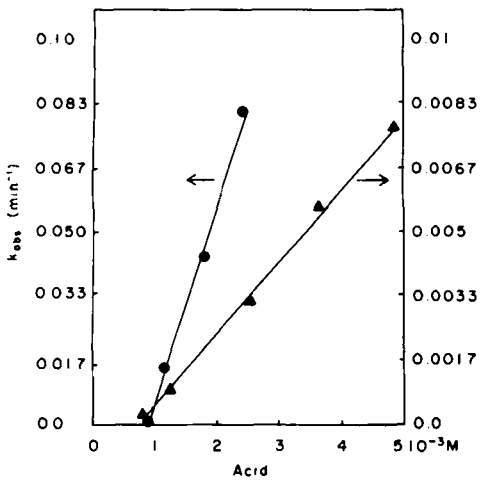

Figure 8—*Hydrolysis of the IV-V copolymer in dioxane-*d_8 *at 37°C; water, 2 M. Plot of the observed rate constant* versus *acid concentration. Key: (●) catalyzed by trichloroacetic acid; (▲) catalyzed by dichloroacetic acid.*

[12] Honeywell.

Table I—Second-Order Rate Constant for the Hydrolysis of I in Dioxane and the IV-V Copolymer in Dioxane-d_8 at 37°C[a]

Acid	Aqueous pK_a	k_2, M^{-1}·min^{-1}	
		I	IV-V Copolymer
Trichloroacetic acid	0.7	116.85	54.17
Dichloroacetic acid	1.48	4.65	1.99
Monochloroacetic acid	2.85	0.09	0.045
Formic acid	3.75		0.006
Maleic acid	1.83, 6.07	7.26	3.73
Phthalic acid	2.89, 5.51	0.47	

[a] The concentration of water was 2 M.

and the rate of scission is first order with respect to the number of *ortho*-ester linkages.

Effect of Acid Concentration and pK_a on the Hydrolysis of Poly(*ortho*-ester)s—The observed rate constant of the hydrolysis of I in dioxane at 37°C was plotted against the maleic acid concentration (Fig. 7). The reaction velocity of the IV-V copolymer in dioxane-d_8 at 37°C in the presence of different amounts of trichloroacetic acid and dichloroacetic acid is shown in Fig. 8. A linear relationship was apparent in all cases in the concentration range studied. The slope of the lines was taken as the second-order rate constant (k_2) of the reaction. The nonzero-intercept seen with the IV-V copolymer can be attributed to the presence of a small amount of alkaline impurities in the polymer.

The second-order rate constants for the hydrolytic reaction catalyzed by different acids are listed in Table I. A straight line can be drawn through the plot (Fig. 9) of log k_2 *versus* acid aqueous pK_a. A positive deviation was observed for the points corresponding to phthalic acid and maleic acid.

The unusually high acidity of the first dissociable proton of maleic acid (pK_{a_1}, 1.83), a diacid with its carboxylic groups in a *cis* position to each other, as compared with that of its *trans*-isomer, fumaric acid (pK_{a_1}, 3.03), was attributed to intramolecular hydrogen bonding which stabilizes the carboxylate monoanion. This interaction is further enhanced in an aprotic environment (12). Thus, it was not unexpected to see the deviation from a linear relationship found with the monoacid. A similar explanation should also hold true for phthalic acid, in which the second carboxyl group is in the *ortho*-position. The k_2 values for the hydrolysis of I are approximately twice that of the IV-V copolymer. The difference is probably due to the analytical methods employed. The degradation of I was monitored by following its disappearance by HPLC. Thus, the scission of one *ortho*-ester linkage results in the loss of one molecule of I. The NMR technique gives a true account of the rate of cleavage of the linkages. Statistically, it is expected that the rate constant of the disappearance of I should be approximately twice as fast as the rate of bond cleavage if the reactivity of the *ortho*-ester bond on the monomer and on the polymers is similar. This was further confirmed when

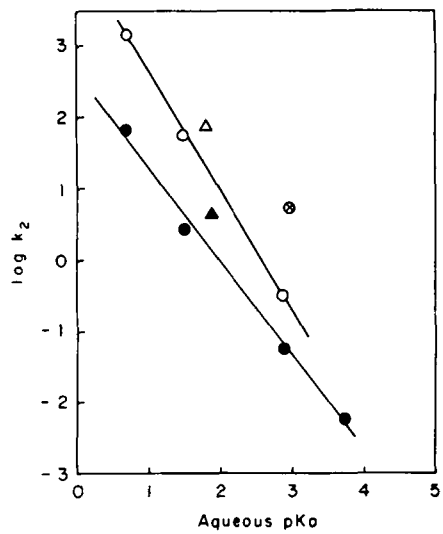

Figure 9—*Plot of the logarithm of the second-order rate constant* versus *aqueous* pK_a; *water, 2 M. The organic acids used were trichloroacetic acid (*pK_a, *0.70), dichloroacetic acid (*pK_a, *1.48), monochloroacetic acid (*pK_a, *2.85), formic acid (*pK_a, *3.75), Maleic acid (*pK_a, *1.83, 6.07) and phthalic acid (*pK_a, *2.89, 5.51). Key: hydrolysis of the IV-V copolymer in dioxane-*d_8 *at 37°C catalyzed by carboxylic monoacid (●), and by maleic acid (▲); hydrolysis of I in dioxane at 37°C catalyzed by carboxylic monoacid (○), by maleic acid (△), and by phthalic acid (⊗).*

Table II—Hydrolysis of I in Dioxane and the IV-V Copolymer in Dioxane-d_8 at 37°C [a]

Water Concentration, M	Dielectric Constant	Observed Rate Constant, min^{-1}	
		I [b]	IV-V Copolymer [c]
0.1	2.86		3.4×10^{-3}
0.5	5.37	1.63×10^{-2}	
1	8.34	1.72×10^{-2}	
2	13.73	1.97×10^{-2}	5.39×10^{-3}
3	18.52	2.23×10^{-2}	5.56×10^{-3}
4	22.80	2.56×10^{-2}	

[a] I, 0.01 M; IV-V copolymer, 8% w/v. [b] Reaction catalyzed by 2.5×10^{-3} M maleic acid. [c] Reaction catalyzed by 3.5×10^{-3} M dichloroacetic acid.

Table III—Hydrolysis of Poly(*ortho*-ester)s in Dioxane-d_8 at 37°C Catalyzed by Dichloroacetic Acid

Polymer	k_2, $M^{-1} \cdot min^{-1}$
IV-VI copolymer	0.87
IV-VII copolymer	1.80
IV-V copolymer	1.96
IV-VIII copolymer	2.81

k_2 values for the hydrolysis of I in dioxane at 37°C in the presence of maleic acid and 2 M water obtained by ^{1}H-NMR were compared with those obtained under the same conditions by HPLC. The ratio of k_2 HPLC-k_2 ^{1}H-NMR was 2.15.

Effect of Water Concentration on the Hydrolysis of Poly(*ortho*-ester)s—A semilogarithmic plot of the degradation of the 8% w/v IV-V copolymer in dioxane-d_8 at 37°C catalyzed by 3.5×10^{-3} M dichloroacetic acid in the presence of 0.1 M water is presented in Fig. 10. As expected, the reaction proceeded until ~25% of the *ortho*-ester linkages were cleaved. The initial slope was employed a the pseudo-first-order rate constant for the reaction. The observed rate constants for the reaction at different water concentrations are listed in Table II, along with the estimated dielectric constant of the dioxane-water system. These are computed from the dielectric constant of water of 78.54 (13) and from the dielectric constant for dioxane of 2.209 (13), assuming that the contribution of each component to the dielectric constant of the system is proportional to its mole fraction. The observed rate constant increases only 1.5-fold for a 30-fold increase in water concentration. A similar observation can be made for the hydrolysis of I in dioxane at 37°C catalyzed by 2.5×10^{-3} M maleic acid. When the rate constants were plotted (Fig. 11) against the solvent dielectric constant, an apparent linear relationship with a nonzero-intercept was observed. Thus, the experimental results suggest that, over the range studied, the reaction proceeds independently of the amount of water present, and the increase in reaction velocity is due to the change in polarity of the reaction medium. This is reasonable since the rate-determining step of the reaction is the formation of the dialkoxy carbonium ion which is independent of the water concentration.

Effect of Polymer Structure on the Hydrolysis Rate—The second-order rate constants for the hydrolysis of four polymers in dioxane-d_8 at 37°C catalyzed by dichloroacetic acid are shown in Table III. The polymers and water concentrations were held constant at 8% w/v and 2 M, respectively. Bunton and DeWolfe (7) have shown that an increase in the basicity of the oxygen atom on the leaving alkoxy group or a stabilization of the forming carbonium ion will result in a more reactive *ortho*-ester. For the polymers under consideration, once the alkoxy groups are cleaved, the resulting carbonium ions are identical; thus, if the observations of Bunton and DeWolfe are applicable, the difference in their reactivity should originate from the difference in the basicity

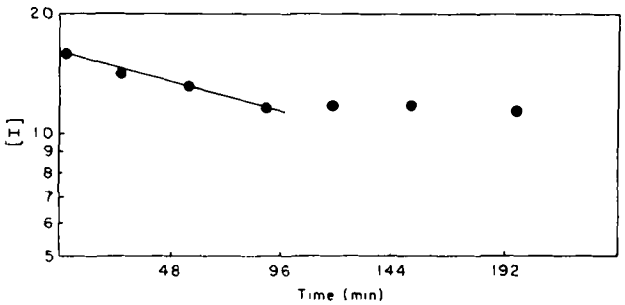

Figure 10—*Hydrolysis of the IV-V copolymer in dioxane-*d_8 *at 37°C; water, 0.1 M; polymer, 8.17% w/v; dichloroacetic acid, 3.5×10^{-3} M. [I], integration of NMR peaks during the reaction.*

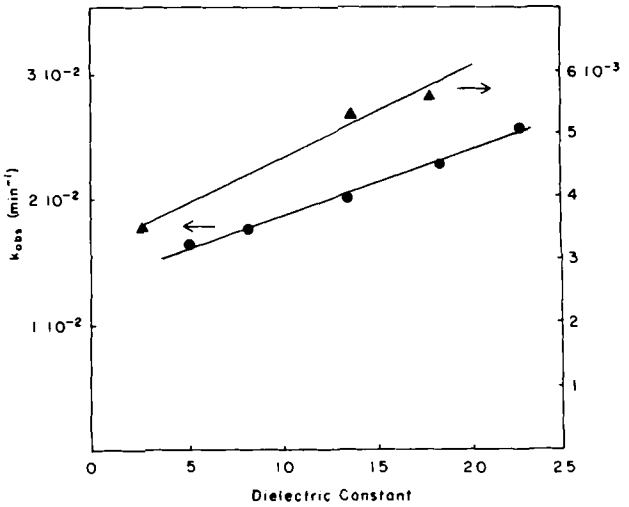

Figure 11—*Plot of the observed rate constant* versus *dielectric constant. Key (▲) hydrolysis of the IV-V copolymer in dioxane-*d_8 *catalyzed by 3.5×10^{-3} M dichloroacetic acid; (●) hydrolysis of I in dioxane at 37°C catalyzed by 2.5×10^{-3} M maleic acid.*

of the diol oxygen atoms. This would predict that IV-V and IV-ethylene glycol (VIII) copolymers are the most stable. The fact that the rank order of the second-order rate constant for the polymers studied cannot be rationalized in terms of the inductive effect of the diol alkyl chain on the basicity of the oxygen atoms at the reaction site implies that another driving force may be more influential. When the rate constants are compared with the molecular size of the diols, an apparent correlation is found. The smaller the diol molecule, the more reactive the polymer, suggesting that strain at the *ortho*-ester bond may be a factor determining the hydrolysis rate.

CONCLUSIONS

The hydrolysis of four poly(*ortho*-ester)s and a monomeric model compound in homogeneous solution was investigated. It appears that the reactivity of the *ortho*-ester linkage in the polymer chain is comparable to that of the linkage in the monomeric model compound. In 50% dioxane-water, the reaction is subject to both specific and general acid catalysis. In dioxane, the hydrolysis reaction is acid catalyzed and independent of the water concentration in the range studied. The rate equation for the hydrolysis of poly(*ortho*-ester)s in dioxane may be written as:

$$\frac{-d[n]}{dt} = k_2 [n] [AH] \qquad \text{(Eq. 4)}$$

where n is the concentration of *ortho*-ester linkage, AH is the concentration of the acid, and k_2 is the second-order rate constant of the reaction. The logarithm of the second-order rate constant is linearly related to the aqueous pK_a of the catalyst. The experimental results suggest that the bonds at the end of the polymer chain may be slightly more reactive than the internal linkages, but overall, the reaction proceeds to a large extent *via* random scission. Strain at the *ortho*-ester linkages may play a role in the determination of its reactivity.

REFERENCES

(1) J. Heller, D. W. Penhale, R. F. Helwing, and B. K. Kritzinger, International Symposium on Controlled Release of Bioactive Materials, Ft. Lauderdale, Fla., 1981, p. 90.

(2) R. F. Fedors, *Polymer*, **21**, 207 (1980).

(3) E. H. Cordes and H. G. Bull, *Chem. Rev.*, **74**, 581 (1974).

(4) E. H. Cordes, in "The Chemistry of Carboxylic Acids and Esters," S. Patai, Ed., 1969.

(5) C. Shih, T. Higuchi, and K. J. Himmelstein, *Biomaterials*, **5**, 237 (1984).

(6) K. Kwart and M. Price, *J. Am. Chem. Soc.*, **82**, 5123 (1960).

(7) C. A. Bunton and R. H. DeWolfe, *J. Org. Chem.*, **30**, 1371 (1965).

(8) M. Price, J. Adams, C. Lagenam, and E. H. Cordes, *J. Org. Chem.*, **34**, 22 (1969).

(9) E. Anderson and T. H. Fife, *J. Org. Chem.*, **37**, 1993 (1972).

(10) M. Ahmad, R. G. Bergstrom, M. J. Cashen, Y. Chiang, A. J. Kresge, R. A. McClelland, and M. F. Powell, *J. Am. Chem. Soc.*, **101**, 2669 (1979).

(11) Y. Chiang, A. J. Kresge, and C. I. Young, *J. Org. Chem.*, **44**, 619 (1979).

(12) M. Maclean Davis, in "The Chemistry of Non-Aqueous Solvents," Vol. II, J. J. Lagowski, Ed., 1970.

(13) Handbook of Chemistry and Physics, 62nd ed., CRC Press Inc., 1982.

ACKNOWLEDGMENTS

All polymers and the model compound were provided by Dr. J. Heller of SRI International, Menlo Park, CA 94304. This work was supported by INTER$_x$ Research Corp., Merck Sharp & Dohme Research Laboratories.

Synthesis and *In Vitro* Antiviral Activity of 3′-*O*-Acyl Derivatives of 5′-Amino-5′-deoxythymidine: Potential Prodrugs for Topical Application

TAI-SHUN LIN

Received April 20, 1983, from the *Department of Pharmacology and Comprehensive Cancer Center, Yale University School of Medicine, New Haven, CT 06510.* Accepted for publication September 19, 1983.

Abstract □ A series of 3′-*O*-acyl derivatives of 5′-amino-5′-deoxythymidine (5′-NH_2-TdR) (IIIa–j) was synthesized by acylation of 5′-azido-5′-deoxythymidine (I). The resulting acetoxy azides were reduced by catalytic hydrogenation to give the corresponding amines. The antiviral activity against herpes simplex virus type 1 (HSV-1) *in vitro*, the aqueous solubilities, and the octanol–water partition coefficients of these compounds were determined. All these derivatives have shown potency against HSV-1 virus similar to the parent compound, except the aromatic and highly branched aliphatic esters, IIIi and IIIj, which are less active. Because of their markedly improved lipophilicity, these compounds are believed to penetrate the biological membranes more easily, and thus, would be more effective for the topical treatment of cutaneous herpes virus infections.

Keyphrases □ 3′-*O*-Acyl derivatives of 5′-amino-5′-deoxythymidine—synthesis, antiviral activity □ Prodrugs—potential, topical application. 3′-*O*-acyl derivatives of 5′-amino-5′-deoxythymidine

The 5′-amino analogue of thymidine (5′-NH_2-TdR) has demonstrated potent antiviral activity against herpes simplex virus type 1 (HSV-1) in the complete absence of toxicity to the uninfected host Vero cells in culture (1, 2). This compound was therapeutically effective in the topical therapy of herpetic keratouveitis in rabbits, and systemic administration into the neonatal mouse revealed no adverse effect *in vivo* or by the histopathological examination (3). Chen *et al.* (4) have recently found that 5-NH_2-TdR was a substrate for the HSV-1-encoded thymidine kinase but was not a substrate for the cellular thymidine kinase. The complete lack of toxicity of 5′-NH_2-TdR to the uninfected Vero cells is probably due to the lack of the herpes simplex virus-induced thymidine kinase which is required for activation (4, 5).

Recently, Baker *et al.* (6) have reported the synthesis of a series of 5′-*O*-acyl derivatives of 9-β-D-arabinofuranosyladenine (vidarabine, ara-A). These compounds were designed as prodrugs for vidarabine and have demonstrated better lipophilicity, and thus, the potential for improved membrane transport over vidarabine. Among these compounds, the 5′-*O*-valeryl derivative has shown a marked increase in both lipophilicity and antiviral activity compared with that of vidarabine.

Recently, Hettinger *et al.* (7) have reported that both 5-iodo-2′-deoxyuridine (idoxuridine, IUdR) and 5-iodo-3′,5′-di-*O*-acetyl-2′-deoxyuridine (Ac_2IDU), an *O*-acetyl derivative of IUdR, were effective against keratitis. However, Ac_2IDU was significantly more effective than the placebo 1 d sooner than was idoxuridine. The greater lipid solubility of the Ac_2IDU that resulted in greater epithelial penetration could account for this difference. Based on these findings, a series of 3′-*O*-acyl derivatives of 5′-NH_2-TdR has been synthesized. Preliminary studies indicated that all these compounds retain the same degree of antiviral activity in comparison with the parent compound, except the 3′-*O*-*tert*-butylacetyl and 3′-*O*-benzoyl esters, IIIi and IIIj, which were found to be less active. The lipophilicities of these derivatives increased

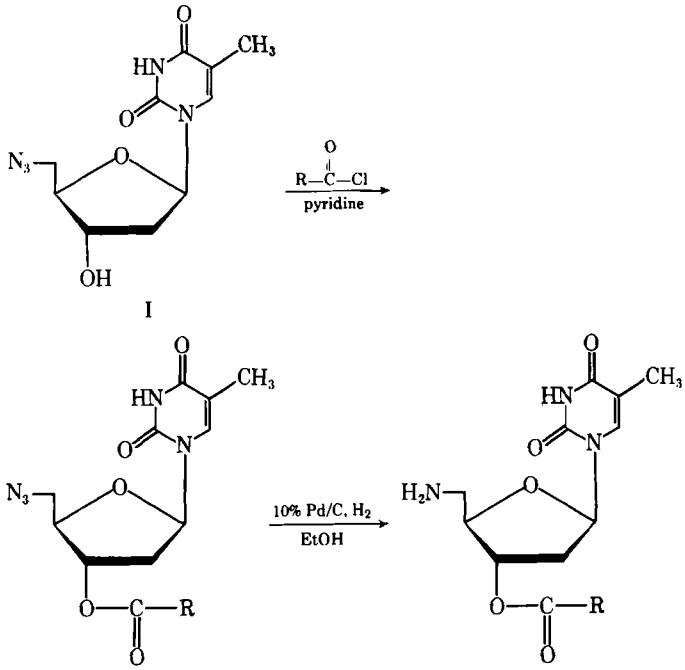

Scheme I

0022-3549/84/1100-1568$01.00/0
© 1984, American Pharmaceutical Association

(10) M. Ahmad, R. G. Bergstrom, M. J. Cashen, Y. Chiang, A. J. Kresge, R. A. McClelland, and M. F. Powell, *J. Am. Chem. Soc.*, **101**, 2669 (1979).

(11) Y. Chiang, A. J. Kresge, and C. I. Young, *J. Org. Chem.*, **44**, 619 (1979).

(12) M. Maclean Davis, in "The Chemistry of Non-Aqueous Solvents," Vol. II, J. J. Lagowski, Ed., 1970.

(13) Handbook of Chemistry and Physics, 62nd ed., CRC Press Inc., 1982.

ACKNOWLEDGMENTS

All polymers and the model compound were provided by Dr. J. Heller of SRI International, Menlo Park, CA 94304. This work was supported by INTER$_x$ Research Corp., Merck Sharp & Dohme Research Laboratories.

Synthesis and *In Vitro* Antiviral Activity of 3′-*O*-Acyl Derivatives of 5′-Amino-5′-deoxythymidine: Potential Prodrugs for Topical Application

TAI-SHUN LIN

Received April 20, 1983, from the *Department of Pharmacology and Comprehensive Cancer Center, Yale University School of Medicine, New Haven, CT 06510.* Accepted for publication September 19, 1983.

Abstract □ A series of 3′-*O*-acyl derivatives of 5′-amino-5′-deoxythymidine (5′-NH_2-TdR) (IIIa–j) was synthesized by acylation of 5′-azido-5′-deoxythymidine (I). The resulting acetoxy azides were reduced by catalytic hydrogenation to give the corresponding amines. The antiviral activity against herpes simplex virus type 1 (HSV-1) *in vitro*, the aqueous solubilities, and the octanol–water partition coefficients of these compounds were determined. All these derivatives have shown potency against HSV-1 virus similar to the parent compound, except the aromatic and highly branched aliphatic esters, IIIi and IIIj, which are less active. Because of their markedly improved lipophilicity, these compounds are believed to penetrate the biological membranes more easily, and thus, would be more effective for the topical treatment of cutaneous herpes virus infections.

Keyphrases □ 3′-*O*-Acyl derivatives of 5′-amino-5′-deoxythymidine—synthesis, antiviral activity □ Prodrugs—potential, topical application. 3′-*O*-acyl derivatives of 5′-amino-5′-deoxythymidine

The 5′-amino analogue of thymidine (5′-NH_2-TdR) has demonstrated potent antiviral activity against herpes simplex virus type 1 (HSV-1) in the complete absence of toxicity to the uninfected host Vero cells in culture (1, 2). This compound was therapeutically effective in the topical therapy of herpetic keratouveitis in rabbits, and systemic administration into the neonatal mouse revealed no adverse effect *in vivo* or by the histopathological examination (3). Chen *et al.* (4) have recently found that 5-NH_2-TdR was a substrate for the HSV-1-encoded thymidine kinase but was not a substrate for the cellular thymidine kinase. The complete lack of toxicity of 5′-NH_2-TdR to the uninfected Vero cells is probably due to the lack of the herpes simplex virus-induced thymidine kinase which is required for activation (4, 5).

Recently, Baker *et al.* (6) have reported the synthesis of a series of 5′-*O*-acyl derivatives of 9-β-D-arabinofuranosyladenine (vidarabine, ara-A). These compounds were designed as prodrugs for vidarabine and have demonstrated better lipophilicity, and thus, the potential for improved membrane transport over vidarabine. Among these compounds, the 5′-*O*-valeryl derivative has shown a marked increase in both lipophilicity and antiviral activity compared with that of vidarabine.

Recently, Hettinger *et al.* (7) have reported that both 5-iodo-2′-deoxyuridine (idoxuridine, IUdR) and 5-iodo-3′,5′-di-*O*-acetyl-2′-deoxyuridine (Ac_2IDU), an *O*-acetyl derivative of IUdR, were effective against keratitis. However, Ac_2IDU was significantly more effective than the placebo 1 d sooner than was idoxuridine. The greater lipid solubility of the Ac_2IDU that resulted in greater epithelial penetration could account for this difference. Based on these findings, a series of 3′-*O*-acyl derivatives of 5′-NH_2-TdR has been synthesized. Preliminary studies indicated that all these compounds retain the same degree of antiviral activity in comparison with the parent compound, except the 3′-*O*-*tert*-butylacetyl and 3′-*O*-benzoyl esters, IIIi and IIIj, which were found to be less active. The lipophilicities of these derivatives increased

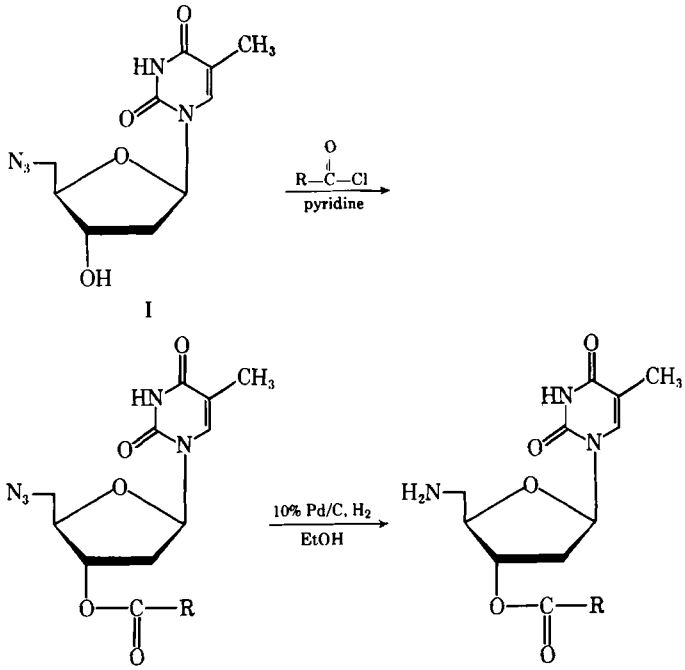

Scheme I

0022-3549/84/1100-1568$01.00/0
© 1984, American Pharmaceutical Association

Table I—Physical Data for 5′-*O*-Acyl Derivatives of 5′-Amino-5′-deoxythymidine

Compound	Solubility, mg/mL[a]	ε Value		Partition Coefficient (P)[d]	log P
		Buffer[b]	1-Octanol[c]		
5′-NH_2-TdR	57.5	10,146	7674	0.00886	−2.05
IIIa	339.1	9,630	8971	0.0319	−1.49
IIIb	88.8	9,504	8154	0.0323	−1.49
IIIc	433.7	8,884	8347	0.0645	−1.19
IIId	17.2	9,629	9036	0.268	−0.57
IIIe	6.9	9,546	9053	0.504	−0.29
IIIf	28.7	8,622	8797	1.87	0.27
IIIg	131.1	8,996	9674	2.21	0.34
IIIh	174.7	8,953	7683	0.148	−0.83
IIIi	407.8	8,994	8742	0.333	−0.48
IIIj	3.0	11,293	8861	0.357	−0.45

[a] Determined in 0.1 M phosphate buffer (pH 7.0). [b] At λ_{max} 265 in 0.1 M phosphate buffer (pH 7.0). [c] At λ_{max} 265 in 1-octanol. [d] P = $[solute]_{1\text{-octanol}}/[solute]_{phosphate\ buffer}$.

markedly with the increase of the carbon-chain length, the 3′-*O*-octanoyl ester IIIg showing the highest lipophilicity. Because of their increased lipophilicity, these prodrugs might penetrate the biological membranes and the lipoidal stratum corneum more readily (8), and therefore, would be more suitable and effective for topical application for treatment of cutaneous virus infections.

RESULTS AND DISCUSSION

Chemistry—A series of 3′-*O*-acyl derivatives of 5′-amino-5′-deoxythymidine (5′-NH_2-TdR) with various chain lengths (IIIa-i) and aromatic substituents (IIIj) were synthesized as outlined in Scheme I. Treatment of 5′-azido-5′-deoxythymidine (I) (2) with the corresponding acyl chloride in pyridine at 4°C for 24 h gave the 5′-azido-3′-*O*-acyl compounds IIa-j. Catalytic (10% palladium on charcoal) hydrogenation of IIa-j in EtOH afforded the desired 5′-amino-3′-*O*-acyl derivatives IIIa-j. These compounds were characterized by ^{1}H-NMR spectroscopy and elemental analysis. The ^{1}H-NMR spectra (Me_2SO-d_6) showed a downfield shift for the 3′-methinyl protons in all of these compounds in comparison with 5′-amino-5′-deoxythymidine, except the highly branched 3′-*O*-*tert*-butylacetyl ester IIIi. The downfield shift probably is caused by the deshielding effect of the 3′-*O*-acyl function. The C-1′, C-2′, C-4′, and C-5′ protons in the sugar moiety, and the C-6 proton in the pyrimidine base ring in IIIi, shifted upfield relative to that of the parent compound. This upfield shift appears to be the result of the shielding effect exerted by the highly branched *tert*-butylacetyl substituent in the 3′-*O*-acyl group.

The water solubility and partition coefficient (P) of IIIa-j were determined by UV spectroscopy (6, 9, 10), and the data are summarized in Table I. The aqueous solubilities of the short-chain (R = 1-3 carbons) esters, IIIa-c, increase 6-, 1.5-, and 7.5-fold, respectively, over that of the parent compound, 5′-amino-5′-deoxythymidine (5′-NH_2-TdR). As the carbon-chain length increases to five-seven carbon atoms (IIId-f), the aqueous solubilities decrease. In this series, the 3′-*O*-hexanoyl derivative IIIe is the least soluble in water, with a solubility of 6.9 mg/mL. Unexpectedly, the water solubility of the eight-carbon chain ester, IIIg, increased to 131.1 mg/mL, which is ~2 times greater than that of the parent compound (57.5 mg/mL). Among these 3′-*O*-acyl derivatives, the 3′-*O*-butyryl ester IIIc and the 3′-*O*-benzoyl ester IIIj possess the highest and the lowest water solubilities, with values of 433.7 mg/mL and 3.0 mg/mL, respectively. The highly branched 3′-*O*-*tert*-butylacetyl ester IIIi, has the second highest water solubility (407.8 mg/mL).

The lipophilicities of these 3′-*O*-acyl derivatives (IIIa-j) were determined *via* a 1-octanol–water (0.1 M phosphate buffer) distribution measured in terms of partition coefficient (P). As expected, the lipophilicities of these compounds increase commensurately with the increase of the carbon-chain length. The 3′-*O*-octanoyl ester IIIg has the greatest lipophilicity, as reflected by the P value which approaches 2.21. Compound IIIg was found to be ~250 times more lipid soluble than the parent compound (5′-NH_2-TdR, P = 0.00886). The highly branched 3′-*O*-*tert*-butylacetyl and the aromatic substituted 3′-*O*-benzoyl derivatives, IIIi and IIIj, are also quite lipid soluble, with P values of 0.333 and 0.357, respectively.

Biological Activity—The antiviral activity of these compounds against herpes simplex virus type 1 (HSV-1) was determined. The effect of these compounds on the replication of the uninfected host Vero cells was also investigated. The results are listed in Table II. At 400 μM, IIIa-h show significant antiviral activity by inhibition of the formation of infectious HSV-1 virions, the inhibition ranging from 95% for IIIa to 99% for IIIe. The aromatic substituted 3′-*O*-benzoyl derivative IIIj is less active than the aliphatic straight-chain esters, and the highly branched *tert*-butylacetyl ester IIIi demonstrates little antiviral activity.

All compounds, except the long-chain esters IIIf and IIIg, show little or no cytotoxicity to the host Vero cells at the test concentrations. However, IIIf and IIIg were found to be somewhat cytotoxic against the Vero cells at 400 and 200 μM, respectively. It is worthwhile to acknowledge that among these compounds the valeryl ester IIId and the hexanoyl ester IIIc have shown significant antiviral activity and favorable lipophilicity with no apparent cytotoxicity to the host.

Table II—Effect of Various 5′-Amino-3′-*O*-acyl-thymidine Derivatives on the Replication of Herpes Simplex Virus Type 1 and Vero Cells *In Vitro*[a]

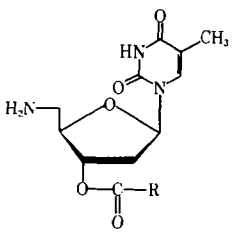

Compound	R	Conc., μM	Percent Inhibition	
			HSV-1	Vero Cells
IIIa	CH_3	400	95	None
IIIb	CH_2CH_3	400	97	None
IIIc	$CH_2CH_2CH_3$	400	97	20
IIId	$CH_2(CH_2)_2CH_3$	400	98	19
IIIe	$CH_2(CH_2)_3CH_3$	200	99	None
		400	99.6	25
IIIf	$CH_2(CH_2)_4CH_3$	400	99.2	66
IIIg	$CH_2(CH_2)_5CH_3$	200	96	83
IIIh	$CH(CH_3)_2$	400	96	40
IIIi	$C(CH_3)_3$	400	19	.....
IIIj	C_6H_5	400	62	–
5′-Amino-5-deoxythymidine		100	92	None
		400	99	None

[a] Assays were carried out in triplicate with appropriate controls. Virus titer in absence of compound was 2.1×10^7 pfu.

EXPERIMENTAL SECTION[1]

General Procedure for the Synthesis of IIIa–j—Compound I (10.0 g, 0.037 mol) was dissolved in 100 mL of pyridine at room temperature. The solution was cooled in an ice-bath, and, with stirring, 0.045 mol of the appropriate acyl chloride was added dropwise *via* an addition funnel. The mixture was stirred at 4°C for 24 h, and then 8 mL of water was added. The solvent was evaporated under reduced pressure below 30°C. The glassy residue was dissolved

[1] Melting points were taken on a Thomas-Hoover Unimelt apparatus and are not corrected. The thin-layer chromatography was performed on EM Silica gel 60 F_{254} sheets (0.2 mm). The UV spectra were recorded on a Beckman-25 spectrophotometer, and the NMR spectra were taken on a Varian T-60 spectrometer at 60 MHz, using Me_4Si as internal reference. The elemental analyses were carried out by Baron Consulting Co., Analytical Services, Orange, Conn. Where analyses are indicated only by symbols of the elements, the analytical results obtained for those elements were within ±0.4% of the theoretical values.

Table III—Characteristics of 5′-*O*-Acyl Derivatives of 5′-Amino-5′-deoxythymidine

Compound	Formula[a]	Description	Yield, %[b]	Melting Point, °C
IIIa	$C_{12}H_{17}N_3O_5$	white powder	62	137–138
IIIb	$C_{13}H_{19}N_3O_5$	white powder	32	141–142
IIIc	$C_{14}H_{21}N_3O_5$	white powder	30	228–231 (dec.)
IIId	$C_{15}H_{23}N_3O_5$	white powder	36	162–163
IIIe	$C_{16}H_{25}N_3O_5$	white powder	28	210–215 (dec.)
IIIf	$C_{17}H_{27}N_3O_5$	white powder	29	213–214 (dec.)
IIIg	$C_{18}H_{29}N_3O_5$	white needles	22	220–221 (dec.)
IIIh	$C_{14}H_{21}N_3O_5$	white needles	20	240–242 (dec.)
IIIi	$C_{16}H_{25}N_3O_5$	white needles	25	235–236 (dec.)
IIIj	$C_{17}H_{19}N_3O_5$	white needles	22	234–235 (dec.)

[a] All compounds were analyzed for C, H, and N; all values were within ±0.4% of the theoretical value. [b] Yield calculations are based on 5′-azido-5′-deoxythymidine (I).

in 200 mL of $CHCl_3$ and the organic phase was washed with H_2O, saturated $NaHCO_3$ solution, and H_2O. The solution was then clarified with amorphous carbon[2], filtered, and dried over anhydrous $MgSO_4$. The solvent was removed under reduced pressure to give the corresponding 5′-azido-3′-*O*-acyl derivatives IIa–j.

Solutions of IIa–j in 100 mL of EtOH were hydrogenated at 50 psi at room temperature in the presence of 10% palladium on charcoal (0.5 g) for 2 h. After filtration, the filtrates were concentrated to afford glassy residues which were crystallized from EtOH–Et_2O to give the 5′-amino-3′-*O*-acyl derivatives IIIa–j. The physical data of these compounds are listed in Tables I and III.

Determination of Solubility for IIIa–j—Each compound (10 mg) was stirred overnight at room temperature (21°C) in 10 mL of 0.1 M phosphate buffer. Excess compound was removed by filtration through a sintered glass funnel, and the concentration of the solute was determined by UV spectroscopy using the epsilon (ϵ) value, which was previously determined in the phosphate buffer.

Determination of Partition Coefficients for IIIa–j—Solutions (10 mL) of each compound in 0.1 M phosphate buffer having a UV absorbance of 1.0–1.7 of the λ_{max} were vigorously stirred at room temperature (21°C) for 2 h with 10 mL of 1-octanol. The solutions were then transferred to a 60-mL separatory funnel, and the layers were separated. The concentration of the solutes in aqueous phosphate buffer and in 1-octanol at equilibrium were determined by the UV spectroscopic technique, and the partition coefficient of each compound was calculated as $P = [\text{solute}]_{\text{1-octanol}}/[\text{solute}]_{\text{water}}$.

^{1}H-NMR Data (Me_2SO-d_6)—*5′-Amino-5′-deoxythymidine*—δ 1.80 (s, 3, 5-CH_3), 2.15 (t, 2, 2′-H), 2.77 (br d, 2, 5′-H), 3.70 (m, 1, 4′-H), 4.25 (m, 1, 3′-H), 4.78 (br s, 2, 5′-NH_2, D_2O exchangeable), 6.17 (t, 1, $J_{1',2'}$ = 7 Hz, 1′-H), and 7.62 ppm (s, 1, 6-H).

Compound IIIa—δ 1.80 (s, 3, 5-CH_3), 2.11 (s, 3, $COCH_3$), 2.21–2.53 (m, 2, 2′-H), 2.83 (br d, 2, 5′-H), 3.88 (m, 1, 4′-H), 4.63 (br s, 2, 5′-NH_2, D_2O exchangeable), 5.26 (m, 1, 3′-H), 6.18 (t, 1, $J_{1',2'}$ = 7 Hz, 1′-H), and 7.78 ppm (s, 1, 6-H).

Compound IIIb—δ 1.02 (t, 3, C—CH_3), 1.79 (s, 3, 5-CH_3), 2.02–2.62 (m, 4, 2′-H and -$COCH_2$-C), 2.77 (br d, 2, 5′-H), 3.82 (m, 1, 4′-H), 4.59 (br s, 2, 5′-NH_2, D_2O exchangeable), 5.22 (m, 1, 3′-H), 6.12 (t, 1, $J_{1',2'}$ = 7 Hz, 1′-H), and 7.72 ppm (s, 1, 6-H).

Compound IIIc—δ 0.92 (t, 3, C—CH_3), 1.62 (m, 2, C-CH_2-C), 1.82 (s, 3, 5-CH_3), 2.11–2.61 (m, 4, 2′-H and -$COCH_2$-C), 3.12 (br d, 2, 5′-H), 4.16 (m, 1, 4′-H), 5.21 (m, 1, 3′-H), 6.16 (t, 1, $J_{1',2'}$ = 7 Hz, 1′-H), 7.68 (s, 1, 6-H), and 8.48 ppm (br s, 2, 5′-NH_2, D_2O exchangeable).

Compound IIId—δ 0.95 (m, 3, C-CH_3), 1.10–1.70 [m, 4, C-$(CH_2)_2$-C], 1.80 (s, 3, 5-CH_3), 2.38 (t, 4, 2′-H and -$COCH_2$-C), 3.14 (br d, 2, 5′-H), 4.12 (m, 1, 4′-H), 5.19 (m, 1, 3′-H), 6.11 (t, 1, $J_{1',2'}$ = 7 Hz, 1′-H), 7.68 (s, 1, 6-H), and 7.90 ppm (br s, 2, 5′-NH_2, D_2O exchangeable).

Compound IIIe—δ 0.90 (m, 3, C-CH_3), 1.04–1.59 [m, 6, C-$(CH_2)_3$-C], 1.74 (s, 3, 5-CH_3), 2.32 (m, 4, 2′-H and -$COCH_2$-C), 2.80 (br d, 2, 5′-H), 3.84 (m, 1, 4′-H), 4.61 (br s, 2, 5′-NH_2, D_2O exchangeable), 5.20 (m, 1, 3′-H), 6.10 (t, 1, $J_{1',2'}$ = 7 Hz, 1′-H), and 7.70 ppm (s, 1, 6-H).

Compound IIIf—δ 0.90 (m, 3, C-CH_3), 1.10–1.68 [m, 8, C-$(CH_2)_4$-C], 1.80 (s, 3, 5-CH_3), 2.39 (br t, 4, 2′-H and -$COCH_2$-C), 3.20 (br d, 2, 5′-H), 4.20 (m, 1, 4′-H), 5.26 (m, 1, 3′-H), 6.09 (t, 1, $J_{1',2'}$ = 6.5 Hz, 1′-H), 7.79 (s, 1, 6-H), and 8.59 ppm (br s, 2, 5′-NH_2, D_2O exchangeable).

Compound IIIg—δ 0.88 (m, 3, C-CH_3), 1.02–1.68 [m, 10, C-$(CH_2)_5$-C], 1.80 (s, 3, 5-CH_3), 2.34 (br t, 4, 2′-H and -$COCH_2$-C), 3.18 (br d, 2, 5′-H), 4.16 (m, 1, 4′-H), 5.22 (m, 1, 3′-H), 6.13 (t, 1, $J_{1',2'}$ = 7.5 Hz, 1′-H), 7.72 (s, 1, 6-H), and 8.52 ppm (br s, 2, 5′-NH_2, D_2O exchangeable).

Compound IIIh—δ 1.05 (s, 3, C-CH_3), 1.17 (s, 3, C-CH_3), 1.83 (s, 3, 5-CH_3), 2.25–3.85 (m, 3, 2′-H and -$COCH<$), 3.17 (br d, 2, 5′-H), 4.18 (m, 1, 4′-H), 5.20 (m, 1, 3′-H), 6.12 (t, 1, $J_{1',2'}$ = 6.5 Hz, 1′-H), 7.70 (s, 1, 6-H), and 8.55 ppm (br s, 2, 5′-NH_2, D_2O exchangeable).

Compound IIIi—δ 0.82 [s, 9, C-$(CH_3)_3$], 1.26 (s, 3, 5-CH_3), 1.02–1.70 (m, 4, 2′-H and -$COCH_2$-C, overlapping with 5-CH_3), 2.20 (br d, 2, 5′-H), 3.20 (m, 1, 4′-H), 4.22 (m, 1, 3′-H), 5.18 (t, 1, $J_{1',2'}$ = 7 Hz, 1′-H), 6.72 (s, 1, 6-H), and 7.48 ppm (br s, 2, 5′-NH_2, D_2O exchangeable).

Compound IIIj—δ 1.84 (s, 3, 5-CH_3), 2.55 (m, 2, 2′-H), 3.32 (m, 2, 5′-H), 4.40 (m, 1, 4′-H), 5.52 (m, 1, 3′-H), 6.30 (t, 1, $J_{1',2'}$ = 7 Hz, 1′-H), 7.32–8.20 (m, 6, 6-H and -C_6H_5), and 8.42 ppm (br s, 2, 5′-NH_2, D_2O exchangeable).

Biological Test Procedures—The antiviral activities of various compounds listed in Table I were determined. Vero cells were grown to confluency in 25-cm^2 flasks using Dulbecco's medium supplemented with 10% fetal calf serum. The cells were then infected with Herpes simplex virus type 1 (CL-101)[3] at a multiplicity of infection (MOI) of 20. After a 1-h absorption period at 37°C, the viral inoculum was removed, and the flask was washed once with phosphate-buffered saline. The test compounds indicated in Table I were dissolved in Dulbecco's medium supplemented with serum and then added to the flask. The infected cultures were incubated at 37°C for 40 h and then frozen until virus titrations were performed. Virus was released by freezing and thawing the media–cell suspension one time. The cell lysates were diluted directly, and the virus yield was assayed by plaque formation on Vero cells. The number of plaque-forming units (pfu) of virus in the drug-treated cultures relative to that found in the drug-free condition was determined and expressed as percent inhibition in Table III.

The cytotoxicity of the various test compounds on the uninfected host Vero cells was determined (Table III). Vero cells in Dulbecco's medium (2.5 mL) supplemented with 10% fetal calf serum were added to eight 25-cm^2 flasks at a concentration equivalent to 0.1 confluency for each compound under assay. After incubation at 37°C in 5% CO_2–95% air for 1 d, the test compound, dissolved in 2.5 mL of the above growth medium, was added and two flasks were harvested immediately by decanting the medium, washing once with 5 mL of buffered saline, and then incubating at 37°C for 15 min with a 5-mL solution of trypsin (0.125%) and EDTA (0.02%). The cells dislodged from the flask by this latter procedure were generally in clumps and were dispersed by repeated forceful pipetting of the suspension against the surface of the flask. To 1 mL of the well-dispersed cell suspension, 0.2 mL of trypan blue solution was added, and the number of cells was counted using a hemocytometer. Each day for the next 3 d, two of the remaining flasks were harvested in the aforementioned manner for determination of cell number.

REFERENCES

(1) T. S. Lin, J. R. Neenan, Y. C. Cheng, W. H. Prusoff, and D. C. Ward, *J. Med. Chem.*, **19**, 495 (1976).

(2) T. S. Lin and W. H. Prusoff, *J. Med. Chem.*, **21**, 109 (1978).

(3) D. Pavan-Langston, N. H. Park, J. Lass, J. Papale, D. M. Albert, T. S. Lin, W. H. Prusoff, and D. H. Percy, *Proc. Soc. Exp. Biol. Med.*, **170**, 1 (1982).

(4) M. S. Chen, G. T. Shiau, and W. H. Prusoff, *Antimicrob. Agents Chemother.*, **18**, 433 (1980).

(5) M. S. Chen, D. C. Ward, and W. H. Prusoff, *J. Biol. Chem.*, **251**, 4833 (1976).

(6) D. C. Baker, T. H. Haskell, and S. R. Putt, *J. Med. Chem.*, **21**, 1218 (1978).

(7) M. E. Hettinger, D. Pavan-Langston, N. H. Park, D. M. Albert, E. DeClercq, and T. S. Lin, *Arch. Ophthalmol.*, **99**, 1618 (1981).

[2] Norit.

[3] Obtained from Dr. Wilma Summers who originally received the virus from Dr. Saul Kit.

(8) C. D. Yu, J. L. Fox, F. H. Ho, and W. I. Higuchi, *J. Pharm. Sci.*, **68**, 1341 (1979).
(9) R. E. Harmon, T. S. Lin, and S. K. Gupta, *J. Med. Chem.*, **16**, 940 (1973).
(10) T. Higuchi and I. H. Pitman, *J. Pharm. Sci.*, **62**, 55 (1973).

ACKNOWLEDGMENT

This research was supported by PHS Grant EY022168 11 and PHS Grant CA-05262 from the National Cancer Institute, Department of Health and Human Services. The author expresses his appreciation to Diane Mozdziesz and J. J. Lee for their excellent technical assistance.

Determination of Orally Coadministered Nadolol and Its Deuterated Analogue in Human Serum and Urine by Gas Chromatography with Selected-Ion Monitoring Mass Spectrometry

ALLEN I. COHEN [§x], RICHARD G. DEVLIN [‡¶], EUGENE IVASHKIV [*§], PHILLIP T. FUNKE [*¶], and TERRENCE McCORMICK [*¶]

Received April 4, 1983, from the *Departments of *Analytical Research and [‡]Clinical Pharmacology, The Squibb Institute for Medical Research, [§]New Brunswick, NJ 08903* and [¶]*Princeton, NJ 08540.* Accepted for publication September 23, 1983.

Abstract □ A cartridge serum and urine extraction procedure of the β-adrenergic antagonist, nadolol, employing a cross-linked styrene-divinyl benzene macroreticular resin is described. Samples were analyzed as the silylated derivative by gas chromatography–mass spectrometry (GC–MS) using selected-ion monitoring. When nadolol was orally coadministered with its deuterated analogue, relative bioavailability could be demonstrated with six or fewer subjects. Employing a base-deactivated GC phase, the limit of detection is 1 ng and 0.5 ng/mL of serum for nadolol and the deuterated analogue, respectively. For levels of <10 ng/mL, the respective coefficients of variation are 4 and 2%. For concentrations of >10 ng/mL, the *CV* is 1% for nadolol and nadolol-d_9.

Keyphrases □ Nadolol—human serum and urine, GC–MS, selected-ion monitoring, nadolol-d_9 □ GC–MS—selected-ion monitoring, nadolol, human serum and urine, nadolol-d_9

Nadolol (I) is a nonselective β-adrenergic antagonist recommended for the treatment of hypertension and angina pectoris (1, 2). Dreyfuss *et al.* have determined bioavailability parameters of orally and intravenously administered [^{14}C]-nadolol (3, 4) in mildly hypertensive humans. Nadolol is partially and variably absorbed (1), like other β blockers, but it is eliminated without metabolism. With oral administration, the pharmacokinetic profile of nadolol is described by an open two-compartment model with respective absorption, distribution, and elimination half-lives of ~1, 1.5, and 17 h (3, 4).

A gas chromatography–selected-ion monitoring mass spectrometry (GC–SIM MS) determination of nadolol serum levels was previously reported (5). Carlin *et al.* (6) have recently presented an elegant application of GC–SIM MS to the measurement of low levels of the β-blocker timolol and its deuterated analogue in a coadministration bioavailability evaluation. Coadministration bioavailability studies for other drug types have been reported by Strong *et al.* (7), Wolen *et al.* (8), d'A. Heck *et al.* (9), Walle and Walle (10), Alkalay *et al.* (11), Murphy and Sullivan (12), and most recently by Cohen *et al.* (13). The extraction and isolation procedure (5) has been simplified for more effective sample processing by GC–SIM MS (13). The bioavailability of two 80-mg formulations of nadolol (I) given to six subjects, administered either as a tablet or solution along with a concomitant 80-mg solution of nonadeuterated nadolol (II) is presented.

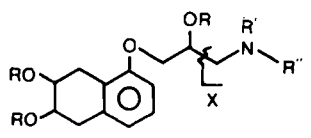

		R	R'	R''	X EI	MH$^+$ PCI
Nadolol	I	H	H	$C(CH_3)_3$		
Deuterated nadolol	II	H	H	$C(CD_3)_3$		
Internal reference	III	H	CH_3	$C(CH_3)_3$		
	IV	$Si(CH_3)_3$	H	$C(CH_3)_3$	86	526
	V	$Si(CH_3)_3$	H	$C(CD_3)_3$	95	535
	VI	$Si(CH_3)_3$	CH_3	$C(CH_3)_3$	100	540

EXPERIMENTAL SECTION

Reagents—Nadolol (I)[1] and its *N*-methyl derivative (III)[1] were characterized, pharmaceutical-grade materials (14). The structures and purity were confirmed by elemental analyses, ^{1}H-NMR, and MS (15) and by GC–MS after silylation. The nonadeuterated nadolol (II) was prepared from the

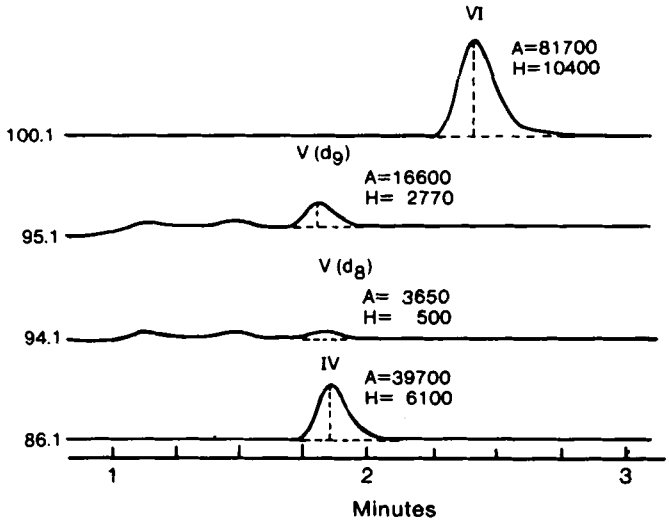

Figure 1—*EI–SIM of a typical processed serum extract containing 133, 83.4, and 250 ng/mL of I, II, and III, respectively, measured as their trimethylsilylated derivatives, IV, V, and VI.*

[1] Nadolol (CAS 42200-33-9), *N*-methyl derivative (CAS 67247-47-6); E. R. Squibb & Sons, Princeton, N.J. Deuterium-labeled *tert*-butylamine; Merck, Sharp and Dohme of Canada.

0022-3549/84/1100-1571$01.00/0
© 1984, American Pharmaceutical Association

(8) C. D. Yu, J. L. Fox, F. H. Ho, and W. I. Higuchi, *J. Pharm. Sci.*, **68**, 1341 (1979).
(9) R. E. Harmon, T. S. Lin, and S. K. Gupta, *J. Med. Chem.*, **16**, 940 (1973).
(10) T. Higuchi and I. H. Pitman, *J. Pharm. Sci.*, **62**, 55 (1973).

ACKNOWLEDGMENT

This research was supported by PHS Grant EY022168 11 and PHS Grant CA-05262 from the National Cancer Institute, Department of Health and Human Services. The author expresses his appreciation to Diane Mozdziesz and J. J. Lee for their excellent technical assistance.

Determination of Orally Coadministered Nadolol and Its Deuterated Analogue in Human Serum and Urine by Gas Chromatography with Selected-Ion Monitoring Mass Spectrometry

ALLEN I. COHEN [§x], RICHARD G. DEVLIN [‡¶], EUGENE IVASHKIV [*§], PHILLIP T. FUNKE [*¶], and TERRENCE McCORMICK [*¶]

Received April 4, 1983, from the *Departments of *Analytical Research and [‡]Clinical Pharmacology, The Squibb Institute for Medical Research, [§]New Brunswick, NJ 08903* and [¶]*Princeton, NJ 08540.* Accepted for publication September 23, 1983.

Abstract □ A cartridge serum and urine extraction procedure of the β-adrenergic antagonist, nadolol, employing a cross-linked styrene-divinyl benzene macroreticular resin is described. Samples were analyzed as the silylated derivative by gas chromatography–mass spectrometry (GC–MS) using selected-ion monitoring. When nadolol was orally coadministered with its deuterated analogue, relative bioavailability could be demonstrated with six or fewer subjects. Employing a base-deactivated GC phase, the limit of detection is 1 ng and 0.5 ng/mL of serum for nadolol and the deuterated analogue, respectively. For levels of <10 ng/mL, the respective coefficients of variation are 4 and 2%. For concentrations of >10 ng/mL, the *CV* is 1% for nadolol and nadolol-d_9.

Keyphrases □ Nadolol—human serum and urine, GC–MS, selected-ion monitoring, nadolol-d_9 □ GC–MS—selected-ion monitoring, nadolol, human serum and urine, nadolol-d_9

Nadolol (I) is a nonselective β-adrenergic antagonist recommended for the treatment of hypertension and angina pectoris (1, 2). Dreyfuss *et al.* have determined bioavailability parameters of orally and intravenously administered [^{14}C]-nadolol (3, 4) in mildly hypertensive humans. Nadolol is partially and variably absorbed (1), like other β blockers, but it is eliminated without metabolism. With oral administration, the pharmacokinetic profile of nadolol is described by an open two-compartment model with respective absorption, distribution, and elimination half-lives of ~1, 1.5, and 17 h (3, 4).

A gas chromatography–selected-ion monitoring mass spectrometry (GC–SIM MS) determination of nadolol serum levels was previously reported (5). Carlin *et al.* (6) have recently presented an elegant application of GC–SIM MS to the measurement of low levels of the β-blocker timolol and its deuterated analogue in a coadministration bioavailability evaluation. Coadministration bioavailability studies for other drug types have been reported by Strong *et al.* (7), Wolen *et al.* (8), d'A. Heck *et al.* (9), Walle and Walle (10), Alkalay *et al.* (11), Murphy and Sullivan (12), and most recently by Cohen *et al.* (13). The extraction and isolation procedure (5) has been simplified for more effective sample processing by GC–SIM MS (13). The bioavailability of two 80-mg formulations of nadolol (I) given to six subjects, administered either as a tablet or solution along with a concomitant 80-mg solution of nonadeuterated nadolol (II) is presented.

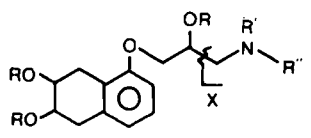

		R	R'	R''	X EI	MH$^+$ PCI
Nadolol	I	H	H	$C(CH_3)_3$		
Deuterated nadolol	II	H	H	$C(CD_3)_3$		
Internal reference	III	H	CH_3	$C(CH_3)_3$		
	IV	$Si(CH_3)_3$	H	$C(CH_3)_3$	86	526
	V	$Si(CH_3)_3$	H	$C(CD_3)_3$	95	535
	VI	$Si(CH_3)_3$	CH_3	$C(CH_3)_3$	100	540

EXPERIMENTAL SECTION

Reagents—Nadolol (I)[1] and its *N*-methyl derivative (III)[1] were characterized, pharmaceutical-grade materials (14). The structures and purity were confirmed by elemental analyses, ^{1}H-NMR, and MS (15) and by GC–MS after silylation. The nonadeuterated nadolol (II) was prepared from the

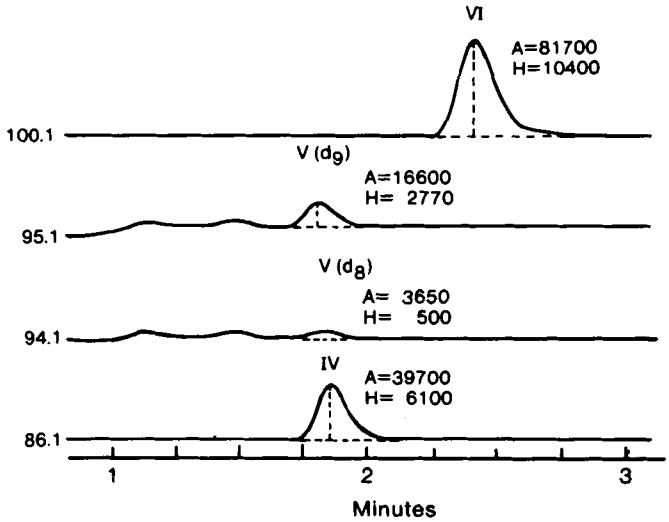

Figure 1—*EI–SIM of a typical processed serum extract containing 133, 83.4, and 250 ng/mL of I, II, and III, respectively, measured as their trimethylsilylated derivatives, IV, V, and VI.*

[1] Nadolol (CAS 42200-33-9), *N*-methyl derivative (CAS 67247-47-6); E. R. Squibb & Sons, Princeton, N.J. Deuterium-labeled *tert*-butylamine; Merck, Sharp and Dohme of Canada.

0022-3549/84/1100-1571$01.00/0
© 1984, American Pharmaceutical Association

Table I—Serum Concentrations of Nadolol for Subjects 1-6 (Solution *versus* Deuterated Solution)

Hours Postdose	Serum Concentration, ng/mL: Deuterated Solution (II) 1	2	3	4	5	6	Solution (I) 1	2	3	4	5	6
1	89.3	39.0	37.5	50.1	29.7	33.0	113.0	46.1	44.7	63.7	31.7	35.6
2	178.0	74.2	33.6	49.6	21.5	26.9	197.0	92.2	39.3	59.5	23.8	30.7
3	118.0	314.0	76.4	70.7	45.3	209.0	136.0	369.0	100.0	86.5	53.6	247.0
4	98.4	282.0	88.8	61.8	127.0	184.0	112.0	314.0	110.0	80.5	122.0	209.0
5	90.5	179.0	65.9	64.9	90.7	83.3	113.0	208.0	82.4	86.0	129.0	97.9
6	55.8	115.0	69.9	67.4	69.8	75.2	68.3	134.0	86.9	68.7	85.4	92.2
8	51.2	113.0	58.5	51.0	68.0	78.0	64.1	131.0	72.0	62.8	71.0	80.2
12	41.9	62.1	32.8	29.0	41.2	47.1	48.8	74.6	40.5	39.8	50.4	59.1
24	22.0	31.5	19.3	20.6	26.8	18.9	27.1	36.1	26.6	24.6	31.3	22.2
48	11.5	6.5	7.9	9.4	2.5	2.2	10.6	8.3	10.7	13.5	4.0	3.0

epoxyketal intermediate (VII) (14) by the reaction with 98 atom-% deuterium-labeled *tert*-butylamine (VIII)[1].

Synthesis of II—A solution of 17 mL of methanol containing 4.9 g (17.7 mmol) of VII and 4.3 g (52.4 mmol) of V was refluxed for 2.5 h using a dry-ice condenser. The volatiles were then distilled into a dry-ice trap at 60–70°C at 20 torr and used again until the remaining VIII was <10% of the original amount. The combined residues were purified by extraction with 100 and 50 mL of 6% w/v aqueous citric acid from 100 mL of ether. The aqueous layer was adjusted to pH 10.8 with 5 M NaOH and then was extracted with 200 mL of ether (4×). The dried residue was dissolved in 60 mL of warm water containing 8 mL concentrated hydrochloric acid, and was allowed to stand for 3 h. The pH of the cooled aqueous solution was adjusted to pH 7.8 with 5 M NaOH, washed with 100 mL of dichloromethane, then made to pH 10.2 with 10 M NaOH, saturated with sodium chloride, and exhaustively extracted with dichloromethane. The pooled extract was then treated with activated charcoal and concentrated under reduced pressure. The crude product was crystallized from 350 mL of warm acetone and then cooled to room temperature. The slurry was cooled in an ice bath, and 350 mL of hexane was gradually added. The crystalline material was collected by filtration, and then the material was washed with 100 mL of cold acetone–hexane (1:1) and dried, to give (70% yield) a crystalline powder, mp 128–130°C; IR (KBr): 2208 cm^{-1} (C—D stretch); 100-MHz ^{1}H-NMR (methanol-d_4): δ 2.5–3 (m, 6, CH_2N, 2 CH_2Ar), 6.5–7.1 (m, 3, ArH), and 3.8–4.1 ppm (m, 5, CH—O) [identical patterns as I except δ 1.12 ppm (s, 9, CH_3) is replaced with a broad weak peak (CD_2H—)]; EI-MS M^+: *m/z* 318, 300 ($M^+ - CD_3$), 274 (rearrangement, $M^+ - C_2H_4O$), and 95 [$CH_2NHC(CD_3)_3$ base ion] (estimated octadeutero analogue 10–15%). EI GC-MS of V M^+: *m/z* 534 (absent), 519 ($M^+ - CH_3$), 516 ($M^+ - CD_3$), 95 (base ion) (*c.f.*, Fig. 1); PCI GC-MS of V MH^+: *m/z* 535 (*c.f.*, Fig. 2) (estimated octadeutero analogue 10–15%).

Anal.—Calc. for $C_{17}H_{18}D_9NO_4$: C, 64.12; D and H, 11.39 (8.55 as H); N, 4.40. Calc. for $C_{17}H_{27}NO_4$: C, 65.99; H, 8.80; N, 4.53. Found: C, 64.10; H, 8.69 (H equivalent to 27 atoms/mol), N, 4.38.

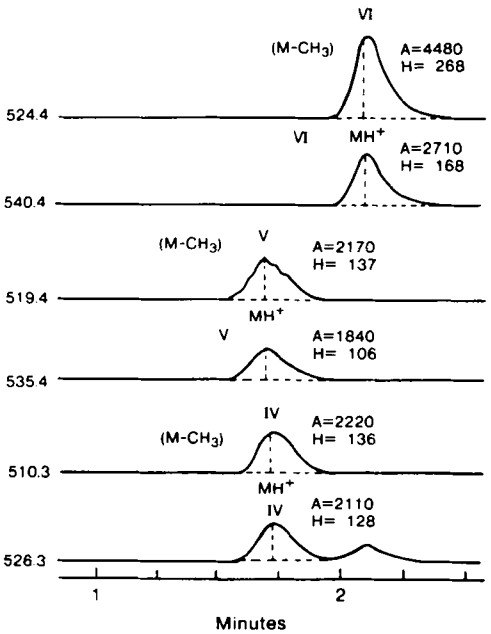

Figure 2—*PCI-SIM of a typical processed serum extract containing 122, 127, and 250 ng/mL of I, II, and III, respectively, measured as their trimethylsilylated derivatives, IV, V, and VI.*

The extraction cartridges[2] were used as received. *N*-(Trimethylsilyl)imidazole in pyridine[3] (1.5 mEq/mL) was obtained in 1-mL sealed ampules.

Standard Solutions—Stock solutions of I, II, and III prepared in 0.1 M HCl were refrigerated and used for at least 6 months. Diluted working solutions were prepared daily in 0.1 M HCl.

Equipment—Various equipment used in the sample preparation include: evaporators[4,5], vortex mixer[6], reaction vials[7], vial seals[8], crimper[9], centrifuge[10], screw-cap culture tubes[11], disposable Pasteur pipets[12], syringes[13], repipet dispenser[14], and dessicators.

Extraction Procedure—*Serum*—Thawed and centrifuged 1-mL serum samples, processed in groups of 35, were transferred to the extraction cartridges[2], placed on 150 mL screw-top culture tubes, and 250 ng of internal reference solution III and 1 mL of distilled water were added to each cartridge. A 1.0-mL blank serum sample containing 500 ng of I, 500 ng of II, and 250 ng of III was processed with each set of samples. A calibration sample curve was prepared using blank serum to which 0–500 ng each of I and II and 250 ng of III were added.

The cartridges were centrifuged at 800 rpm for 30 s. The cartridge caps were removed, and the cartridges were then centrifuged for 5 min at 1000 rpm, and, if required at 1500 rpm until centrifugation was complete. After the addition of 4 mL of water, the cartridge was centrifuged at 1000 rpm for 4 min, followed by 1500 rpm for 1 min. To each cartridge, placed on a scintillation vial, 2 mL of methanol was added, and the cartridges were centrifuged at 1000 rpm for 5 min. The contents of the cartridge was evaporated in a sample concentrator at 65°C, reconstituted in 0.5 mL of methanol, and transferred to a 1-mL reaction vial. A solution of I, II, and III, which constitutes the unextracted control, was evaporated[4]. Each solution was evaporated[5] to dryness under nitrogen at 60°C. After drying under reduced pressure in a desiccator for 30 min, the samples were capped.

Urine—To each cartridge 0.5 or 0.1 mL of thawed urine was added, followed by 0.5 μg of III internal reference solution and 3 mL of H_2O. These samples were then processed in the same manner as serum samples.

Calibration and Preparation of Control Blood and Urine Samples—Varying amounts of I (and an equal amount of II for simultaneous measurements) were added to cartridges containing 1 mL of serum to yield concentrations from 0 to 500 ng/mL. To each cartridge, 250 ng of internal reference III was added. The control sample represents the calibration point equal to 500 ng of I and II and 250 ng of III.

The urine standard curve was prepared from urine samples containing from 0 to 1 μg of I and II and 0.5 μg of III. Only 0.1 mL of urine was needed from samples collected within the first 4 h, and 0.5 mL was required after 4 h. Like the serum control, the control urine represents the 2:1 calibration point. The ratio of the maximum peak heights *versus* the respective nanogram (or microgram) ratio was fitted by linear regression[15] (13). For serum:

$$R_1 = 0.01916 + 1.0654R'_1 \text{ (nadolol)} \qquad \text{(Eq. 1)}$$

$$R_2 = 0.00467 + 0.7969R'_2 \text{ (deuterated nadolol)} \qquad \text{(Eq. 2)}$$

[2] Type W, cross-linked styrene-divinyl benzene macroreticular resin with activators; E. I. DuPont Co., Wilmington, Del.
[3] Tri Sil Z; Pierce Chemical Co., Rockford, Ill.
[4] Model SC248 with scintillation adapter No. 3500750-4; Brinkmann Instruments.
[5] SC-3 concentrator with DB-3 dri-block heating bath; Techne.
[6] Cat. No. 12-812; Fisher Scientific Co.
[7] Cat. No. 3-3123, 1-mL; Supelco, Bellefonte, Pa.
[8] Cat. No. 5080-8713; Hewlett-Packard Co.
[9] Cat. No. 6-406-20; Fisher Scientific Co.
[10] International Centrifuge Co.
[11] Cat. No. 14-930-10J, 25 × 150 mm; Fisher Scientific Co.
[12] Cat. No. 13-678-6B, Pasteur Type, 23-cm long; Fisher Scientific Co.
[13] Size 100A-FN, Cat. No. 2-1536, fine needle 100 μL; Supelco.
[14] 1 mL; Lab Industries.
[15] The BASIC program for the HP 5985B GC–MS is available on request.

Table II—Serum Concentrations of Nadolol for Subjects 1–6 (Tablet *versus* Deuterated Solution)

Hours Postdose	Serum Concentration, ng/mL: Deuterated Solution (II) 1	2	3	4	5	6	Tablet (I) 1	2	3	4	5	6
1	47.8	56.3	18.5	52.9	19.7	13.1	67.4	77.9	8.7	67.1	20.4	14.9
2	54.0	94.7	81.6	73.6	16.9	41.0	68.0	124.0	84.8	92.3	17.8	47.7
3	136.5	234.0	114.0	126.0	29.8	83.4	165.0	269.0	128.0	153.0	38.8	133.0
4	119.0	177.0	132.0	92.9	80.8	85.5	140.0	210.0	143.0	116.0	109.0	144.0
5	121.0	118.0	105.0	68.6	61.6	56.2	111.0	141.0	117.0	85.7	80.8	91.9
6	79.3	107.0	92.4	62.9	43.7	47.1	90.9	128.0	106.0	79.4	61.2	77.4
8	64.9	90.0	86.1	50.9	37.4	42.9	78.0	116.0	100.0	65.1	48.9	69.5
12	51.0	59.3	52.2	30.9	26.7	37.5	48.5	74.9	59.3	39.0	34.8	55.7
24	19.9	23.8	27.0	18.2	9.8	15.1	23.3	28.4	31.8	26.6	13.2	21.2
48	4.4	6.6	7.0	7.5	3.9	2.0	6.1	9.4	7.8	10.7	4.7	4.8

For urine:

$$R_1 = 0.05734 + 0.9781R'_1 \text{ (nadolol)} \quad \text{(Eq. 3)}$$

$$R_2 = 0.04410 + 0.8248R'_2 \text{ (deuterated nadolol)} \quad \text{(Eq. 4)}$$

where R'_1 and R'_2 are concentration ratios and R_1 and R_2 are the measured ratios (13).

Selected-Ion Monitoring—The extracted samples were reconstituted in 40 μL of *N*-(trimethylsilyl)imidazole in pyridine[3] at least 1 h prior to analysis. *N*-(Trimethylsilyl)imidazole (0.25 μL in pyridine) was drawn into a 10-μL syringe, followed by 1 μL of solution. The appropriate ion profiles (*m/z* 86.1, *m/z* 95.2, and *m/z* 100.2) were obtained by selected-ion monitoring (SIM). The maximum peak heights were measured using a program written especially for the batch processing of data (13).

Instrumental Procedure—The combined GC–MS, with the data system[16], was tuned[17] for electron-impact (EI) MS from 69 to 502 D using perfluorobutylamine at an ionization voltage of 70 eV and at an emission of 300 μA. The ion source was controlled at a constant temperature of 200°C. For positive chemical ionization (PCI) MS the source parameters were optimized at an ionization voltage of 300 eV.

A septum guide[18] was attached to the GC injector. The analysis was carried out on an 80-cm × 2-mm i.d. silanized glass column packed with 3% SP-2100DB[19], which was connected through a single-stage jet separator. The transfer line and separator were maintained at 275°C, while the column was kept at an isothermal temperature of 230°C and the injector was heated to 265°C. Typical retention times of 1.9 min for the silylated compounds (IV and V) and 2.5 min for the silylated internal reference (VI) were obtained at a helium flow rate of 30 mL/min (Fig. 1). Helium, otherwise diverted, was allowed to flow into the ion source at 1.3 min after sample injection until the end of the measurement. The multiplier and electron voltages were only applied during the data collection period, from 1.5 min after injection until the termination of the run.

Positive CI GC–MS was obtained with methane as the GC carrier gas, at a flow rate of 20 mL/min, flowing directly into the source to create a 1-torr source pressure (Fig. 2). Otherwise, the chromatographic conditions were identical to that of the EI GC–SIM MS.

Drug Administration—All subjects fasted for 8 h prior to and for 4 h after dosing. Twenty-milliliter blood samples were drawn[20] from an antecubital vein, under sterile conditions. The whole blood was allowed to clot and was then centrifuged. Urine was collected for 0–4, 4–8, 8–12, 12–24, and 24–48 h after dosing. After measurement of the total volume for each collection, a 15-mL aliquot was transferred to a small, labeled plastic container and frozen.

RESULTS AND DISCUSSION

The cartridge extraction procedure (16) is based on a column packed with cross-linked styrene–divinyl benzene macroreticular resin, processed manually with a conventional laboratory centrifuge. Timolol samples were separated on a reverse-phase C_{18} cartridge, supplemented with acid–base extractions (6). Using [^{14}C]nadolol as a tracer, nadolol is quantitatively absorbed on the column from pH 2–13.5 solutions. Washing with distilled water removed potentially interfering serum components without disturbing the absorbed I. Nadolol is quantitatively displaced with methanol, but <80% is displaced by equal amounts of acetone. Lower polarity solvents such as dichloromethane did not displace I at all. On the other hand, solvent mixtures containing ≥25% methanol also produced quantitative elution. The radioactivity was quantitatively recovered with 0.5–2 mL of methanol. The dried eluate was sufficiently pure to be directly silylated for GC–MS analysis. Similarly, processed urine samples yielded excellent recoveries for microgram quantities of I. This isolation procedure directly replaces the fluorometric (17) and MS (5) extraction procedures. It is also likely that other β-adrenergic agents would behave similarly in this extraction system.

The GC–MS SIM processing efficiency was improved by reducing "ghosting" and tailing of the underivatized secondary amine. A glass column containing a specially base-deactivated methyl silicone polymer packed phase[19] was operated isothermally. Background components with interfering ions were minor, although the background at *m/z* 95 was somewhat greater than at the even-mass *m/z* 86 and 100 ions (Fig. 1). Confirmation of the structures of the silylated derivatives was made by PCI GC–MS SIM (Fig. 2). For I the limit of detection is at least 1 ng/mL, and for the deuterated analogue (II) it is ~50% of that value. Nine of twelve time-zero samples were found to have no detectable I, while two contained 0.1 ng and another 0.3 ng per milliliter. All 12 deuterated analogue (II) values were measured as zero. All 48-h serum samples had nonzero values (Tables I–III). The estimated *CV* for measurements at 10 ng/mL are 4% for I and 2% for II, which decreases to 1% for both I and II at greater concentrations.

Urine contained from 0.2 to 24 μg/mL of I and II. As a percentage of the dose, the amounts excreted with time were not necessarily influenced by urine

Table III—Mean Serum Concentrations of Nadolol After Concomitant Administration of Perdeuterated Solution with Either a Tablet or an Oral Solution[a]

Hours Postdose	Mean Serum Concentration, ng/mL: Tablet (I)	Deuterated Solution (II)	Solution (I)	Deuterated Solution (II)
1.0				
Mean	42.7	34.7	55.8	46.4
SEM	12.7	8.0	12.3	9.0
2.0				
Mean	72.4	60.3	73.8	64.0
SEM	15.1	11.7	26.6	24.1
3.0				
Mean	147.8	120.6	165.4	138.9
SEM	30.3	27.6	49.0	42.2
4.0				
Mean	143.7	114.5	157.9	140.3
SEM	14.6	14.9	35.9	33.0
5.0				
Mean	104.6	88.4	119.4	95.7
SEM	9.3	12.1	19.1	17.3
6.0				
Mean	90.5	71.7	89.2	75.5
SEM	9.7	10.3	9.8	8.3
8.0				
Mean	79.6	62.0	80.2	70.0
SEM	10.0	9.1	10.5	9.6
12.0				
Mean	51.7	42.9	52.2	42.4
SEM	6.1	5.3	5.3	4.8
24.0				
Mean	24.1	19.0	28.0	23.2
SEM	2.7	2.5	2.0	2.0
48.0				
Mean	7.2	5.2	8.4	6.7
SEM	1.0	0.9	1.7	1.5

[a] All doses were 80 mg.

[16] Model HP5985B; Hewlett-Packard, Palo Alto, Calif.
[17] AUTOTUNE, Hewlett-Packard.
[18] Cat. No. 2-0839; Supelco.
[19] One 80/100 Supelcoport; Supelco.
[20] Vacutainers; Becton, Dickinson and Co.

Table IV—Urinary Excretion of Nadolol for Subjects 1–6 (Solution *versus* Deuterated Solution)

Hours Postdose	Urinary Excretion, % of Dose[a]											
	Deuterated Solution (II)						Solution (I)					
	1	2	3	4	5	6	1	2	3	4	5	6
0–4	1.58	3.96	1.47	1.36	1.34	1.38	1.29	4.70	1.82	1.68	1.61	1.71
0–8	4.24	8.39	3.88	2.92	3.11	5.27	5.04	9.79	4.78	3.64	3.73	6.57
0–12	5.50	10.30	4.73	3.99	5.11	6.63	6.59	12.04	5.82	5.02	6.20	8.29
0–24	7.87	13.36	5.84	6.28	7.40	7.68	9.46	15.71	7.22	7.82	9.03	9.59
0–48	10.63	17.01	7.72	8.68	8.72	8.75	12.74	20.09	9.50	10.82	10.67	10.91

[a] All doses were 80 mg.

Table V—Urinary Excretion of Nadolol for Subjects 1–6 (Tablet *versus* Deuterated Solution)

Hours Postdose	Urinary Excretion, % of Dose[a]											
	Deuterated Solution (II)						Tablet (I)					
	1	2	3	4	5	6	1	2	3	4	5	6
0–4	1.65	1.53	1.38	2.33	0.81	2.41	2.03	1.82	1.35	2.94	0.88	2.93
0–8	5.12	3.94	2.04	4.31	2.70	5.20	6.02	4.70	2.11	5.42	3.27	7.51
0–12	6.21	5.30	3.06	5.49	5.05	6.26	7.37	6.38	3.30	7.00	6.26	9.12
0–24	8.81	10.27	5.54	7.97	5.57	8.51	10.54	12.42	6.15	10.14	6.94	12.34
0–48	11.44	12.80	7.06	10.52	7.09	9.27	13.75	15.56	7.96	13.37	8.87	13.35

[a] All doses were 80 mg.

volume (Tables IV and V). The amount of drug excreted is directly related to the circulating serum levels just prior to or during the collection period.

Since the deuterated analogue (II) was administered to all subjects, an evaluation of the variation bioavailability can be readily assessed. As a rule, no subject exhibited identical bioavailability for II with respect to maximum concentration levels, time to maximum, and area under the curve. Consequently comparison of intrasubject data is unreliable, which then requires treating the composite data (Table III). With this limited data set of six subjects, sufficient smoothing has occurred to begin to show equivalence between the legs of the administration of the deuterated analogue (Table III).

Table VI—Area Under the Serum Concentration–Time Curve from 0 to 48 h

Subject	AUC_{0-48}, ng·h/mL					
	Tablet (I)	Deuterated Solution (II)	Relative Area (Ratio)	Solution (I)	Deuterated Solution (II)	Relative Area (Ratio)
1	1802	1608	1.12	1971	1681	1.17
2	2585	2092	1.24	2970	2542	1.17
3	2081	1836	1.13	1654	1287	1.28
4	1732	1326	1.31	1591	1267	1.26
5	1078	823	1.31	1716	1465	1.17
6	1641	1074	1.53	1908	1626	1.17
Mean	1820	1460	1.27	1968	1645	1.20
SEM	204	195	0.06	209	192	0.02
	Tablet *versus* Solution[a]					
			Absolute Area			Relative Area
	RSD, %		14.4			11.0
	Number of Subjects Required		7.2 (=8)			4.2 (=6)

[a] No statistically significant differences were observed between tablet and solution or between deuterated solutions.

Table VII—Mean Cumulative Urinary Excretion of Nadolol

Interval	Mean Cumulative Excretion, % of Dose							
	Tablet (I)	Deuterated Solution (II)	Relative Excretion (Ratio)	Solution (I)	Deuterated Solution (II)	Relative Excretion (Ratio)	No. of Subjects Required[a]	
							Absolute	Relative
0–4 h								
Mean	1.99	1.68	1.16	2.24	1.85	1.22	98	2
SEM	0.34	0.25	0.04	0.49	0.42	0.01		
0–8 h								
Mean	4.84	3.88	1.22	5.59	4.63	1.21	54	4
SEM	0.79	0.52	0.05	0.95	0.83	0.01		
0–12 h								
Mean	6.57	5.23	1.24	7.32	6.04	1.22	36	2
SEM	0.78	0.48	0.05	1.04	0.92	0.01		
0–24 h								
Mean	9.76	7.78	1.25	9.80	8.07	1.22	12	2
SEM	1.09	0.77	0.05	1.24	1.11	0.01		
0–48 h								
Mean	12.14	9.70	1.25	12.44	10.25	1.22	10	2
SEM	1.23	0.95	0.04	1.57	1.41	0.01		

[a] No statistically significant differences were observed between tablet and solution or between deuterated solutions.

The urinary excretion patterns of nadolol (I) and nadolol-d_9 (II) are summarized in Tables IV and V. Depending on the drug form, subject, and leg, 8–20% (mean 12%) and 7–17% (mean 10%) of the respective doses of I and II are excreted in 48 h. Although not entirely unexpected, the deuterated solution formulation (II) has lower bioavailability than either the solution or tablet formulations of I. From the statistical criteria applied to absolute bioavailability data, the deuterated solution formulation is marginally bioequivalent, differing by <20% from the nondeuterated tablet and solution formulations. The tablet and solution formulations of I are bioequivalent, on the other hand, and the urinary excretion values also parallel these observations.

The use of the nonadeuterated analogue was based on the availability of intermediates. Apparently extensive deuterium labeling in the side chain resulted in reduced absorption and lower bioavailability. While it might have been more appropriate to have used ^{13}C- and ^{15}N-labeled nadolol to reduce the isotope effects, the deuterated form yielded reliable results which paralleled those of the nonlabeled forms of I.

The mean serum values of the area under the bioavailability curve can be calculated from the absolute areas in the conventional way (18)[21] or from the relative area, defined as absolute area the formulation of I divided by the value for the coadministered II (Table VI). From the absolute area, seven to eight subjects would be required as the minimum number to demonstrate bioequivalence, while only four to five subjects would be required to show the bioequivalence using coadministration[21]. Increasing this number to six ensures staying within the confidence of establishing bioequivalence. The use of the relative parameter is even more striking in the evaluation of the urinary excretion data, which required a minimum of 10 subjects in the normal approach and either 2 or 4 subjects using relative bioavailability (Table VII).

For studies employing analytical methods with reasonable precision, the limitation in bioavailability studies continues to be in the variability of the disposition by the subjects. In these instances, the use of coadministration represents the optimum method of generating a reliable data set with a minimum of subjects. Rapidly processed, an early evaluation of the bioavailability of a new dosage form can be made. It also takes the greatest advantage of the MS selective capability. Finally, the introduction of new low-priced high-performance EI mass selective detectors should result in a wider acceptance of coadministration relative bioavailability and absolute bioavailability MS evaluations.

[21] M. Stern; personal communication.

REFERENCES

(1) R. C. Heel, R. N. Brogden, G. E. Pakes, T. M. Speight, and G. S. Avery, *Drugs*, **20**, 1 (1980).

(2) M. F. Blanford, *Drug Intell. Clin. Pharm.*, **14**, 825 (1980).

(3) J. Dreyfuss, L. J. Brannick, R. A. Vukovich, J. M. Shaw, and D. A. Willard, *J. Clin. Pharmacol.*, **17**, 300 (1977).

(4) J. Dreyfuss, D. L. Griffith, S. M. Singhvi, J. M. Shaw, J. J. Ross, Jr., R. A. Vukovich, and D. A. Willard, *J. Clin. Pharmacol.*, **19**, 712 (1979).

(5) P. T. Funke, M. F. Malley, E. Ivashkiv, and A. I. Cohen, *J. Pharm. Sci.* **67**, 653 (1978).

(6) J. R. Carlin, R. W. Walker, R. O. Davies, R. T. Ferguson, and W. J. A. VandenHeuvel, *J. Pharm. Sci.*, **69**, 1111 (1980).

(7) J. M. Strong, J. S. Dutcher, W.-K. Lee, and A. J. Atkinson, Jr., *Clin. Pharmacol. Ther.*, **18**, 613 (1975).

(8) R. L. Wolen, R. H. Carmichael, A. S. Ridolfo, L. Thompkins, and E. A. Ziege, *Biomed. Mass Spectrom.*, **6**, 173 (1979).

(9) H. d'A. Heck, S. E. Buttrill, Jr., N. W. Flynn, R. L. Dyer, M. Anbar, T. Cairns, S. Dighe, and B. E. Cabana, *J. Pharmacokinet. Biopharm.*, 7, 233 (1979).

(10) T. Walle and U. K. Walle, *Res. Commun. Chem. Pathol. Pharmacol.*, **23**, 453 (1979).

(11) D. Alkalay, W. E. Wagner, Jr., S. Carlsen, L. Khemani, J. Volk, M. E. Barlett, and A. LeSher, *Clin. Pharmacol. Ther.*, **27**, 697 (1980).

(12) P. J. Murphy and H. R. Sullivan, *Annu. Rev. Pharmacol. Toxicol.*, **20**, 609 (1980).

(13) A. I. Cohen, R. G. Devlin, E. Ivashkiv, P. T. Funke, and T. McCormick, *J. Pharm. Sci.*, **71**, 1251 (1982).

(14) M. E. Condon, C. C. Cimarusti, R. Fox, V. L. Narayanan, J. Reid, J. E. Sundeen, and F. P. Hauck, *J. Med. Chem.*, **21**, 913 (1978).

(15) L. Slusarek and K. Florey, in "Analytical Profiles of Drug Substances," Vol. 9, K. Florey, Ed., Academic, New York, N.Y., 1980, p. 455.

(16) R. C. Williams and J. L. Viola, *J. Chromatogr.*, **185**, 505 (1979).

(17) E. Ivashkiv, *J. Pharm. Sci.*, **66**, 1168 (1977).

(18) J. M. Lachin, *Control. Clin. Trials*, **2**, 93 (1981).

ACKNOWLEDGMENTS

The statistical evaluation of the data, provided by M. Stern, and the synthesis of the deuterated analogue and internal reference by Dr. F. Dürsch is gratefully acknowledged.

A New Series of Reductive Amination Derivatives of Daunorubicin: Syntheses, Partition Coefficients, and DNA Binding

SHAU-FONG YEN *, W. DAVID WILSON *x, STEVENS W. PEARCE §, and EDMOND J. GABBAY §†

Received April 19, 1983, from the **Department of Chemistry, Georgia State University, Atlanta, GA 30303* and the §*Department of Chemistry, University of Florida, Gainesville, FL, 32611.* Accepted for publication December 6, 1983. †Deceased.

Abstract □ A series of daunorubicin derivatives were prepared by sodium cyanoborohydride reductive amination of daunorubicin with appropriate amines. All derivatives were found to bind quite strongly to DNA and viscosity increases with linear DNA indicated that each formed an intercalation complex. A range of octanol-aqueous buffer partition coefficients was obtained, around the values of daunorubicin and dauxorubicin hydrochloride, by varying the character of the starting amine. All monoamine derivatives had activity against P388 leukemia in mice which was similar to that of daunorubicin. A diamine derivative had reduced activity against P388. Several anthracyclines administered as DNA complexes had similar activity against P388 but significantly reduced toxicity compared to the uncomplexed compounds. For anthracyclines which bind strongly to DNA, optimum activity against P388 leukemia in mice seems to be centered on compounds with octanol-buffer partition coefficients in the range of 0.5–0.8.

Keyphrases □ Anthracyclines—new derivatives, antineoplastic agents □ Toxicity—reduced cardiotoxicity, anthracyclines

The glycosidic anthracycline antibiotics daunorubicin (I) and dauxorubicin hydrochloride (II), are being clinically used as antineoplastic agents (1–8). Unfortunately, these drugs are severely limited by their dose related cardiotoxicity (1–5). Although the molecular basis of the cardiotoxicity is not clear, two proposed mechanisms are widely accepted. First, the anthracyclines are reduced to semiquinone free radicals and, subsequently, generate oxygen radicals which cause membrane lipid peroxidation and DNA strand scission (9–11). Second, the chemically labile glycosidic bonds of I and II are cleaved by glycosidases to form the respective aglycons during *in vivo* metabolism (1–4, 9, 12). The water insoluble aglycons accu-

0022-3549/84/1100-1575$01.00/0

© 1984, American Pharmaceutical Association

The urinary excretion patterns of nadolol (I) and nadolol-d_9 (II) are summarized in Tables IV and V. Depending on the drug form, subject, and leg, 8–20% (mean 12%) and 7–17% (mean 10%) of the respective doses of I and II are excreted in 48 h. Although not entirely unexpected, the deuterated solution formulation (II) has lower bioavailability than either the solution or tablet formulations of I. From the statistical criteria applied to absolute bioavailability data, the deuterated solution formulation is marginally bioequivalent, differing by <20% from the nondeuterated tablet and solution formulations. The tablet and solution formulations of I are bioequivalent, on the other hand, and the urinary excretion values also parallel these observations.

The use of the nonadeuterated analogue was based on the availability of intermediates. Apparently extensive deuterium labeling in the side chain resulted in reduced absorption and lower bioavailability. While it might have been more appropriate to have used ^{13}C- and ^{15}N-labeled nadolol to reduce the isotope effects, the deuterated form yielded reliable results which paralleled those of the nonlabeled forms of I.

The mean serum values of the area under the bioavailability curve can be calculated from the absolute areas in the conventional way (18)[21] or from the relative area, defined as absolute area the formulation of I divided by the value for the coadministered II (Table VI). From the absolute area, seven to eight subjects would be required as the minimum number to demonstrate bioequivalence, while only four to five subjects would be required to show the bioequivalence using coadministration[21]. Increasing this number to six ensures staying within the confidence of establishing bioequivalence. The use of the relative parameter is even more striking in the evaluation of the urinary excretion data, which required a minimum of 10 subjects in the normal approach and either 2 or 4 subjects using relative bioavailability (Table VII).

For studies employing analytical methods with reasonable precision, the limitation in bioavailability studies continues to be in the variability of the disposition by the subjects. In these instances, the use of coadministration represents the optimum method of generating a reliable data set with a minimum of subjects. Rapidly processed, an early evaluation of the bioavailability of a new dosage form can be made. It also takes the greatest advantage of the MS selective capability. Finally, the introduction of new low-priced high-performance EI mass selective detectors should result in a wider acceptance of coadministration relative bioavailability and absolute bioavailability MS evaluations.

[21] M. Stern; personal communication.

REFERENCES

(1) R. C. Heel, R. N. Brogden, G. E. Pakes, T. M. Speight, and G. S. Avery, *Drugs*, **20**, 1 (1980).

(2) M. F. Blanford, *Drug Intell. Clin. Pharm.*, **14**, 825 (1980).

(3) J. Dreyfuss, L. J. Brannick, R. A. Vukovich, J. M. Shaw, and D. A. Willard, *J. Clin. Pharmacol.*, **17**, 300 (1977).

(4) J. Dreyfuss, D. L. Griffith, S. M. Singhvi, J. M. Shaw, J. J. Ross, Jr., R. A. Vukovich, and D. A. Willard, *J. Clin. Pharmacol.*, **19**, 712 (1979).

(5) P. T. Funke, M. F. Malley, E. Ivashkiv, and A. I. Cohen, *J. Pharm. Sci.* **67**, 653 (1978).

(6) J. R. Carlin, R. W. Walker, R. O. Davies, R. T. Ferguson, and W. J. A. VandenHeuvel, *J. Pharm. Sci.*, **69**, 1111 (1980).

(7) J. M. Strong, J. S. Dutcher, W.-K. Lee, and A. J. Atkinson, Jr., *Clin. Pharmacol. Ther.*, **18**, 613 (1975).

(8) R. L. Wolen, R. H. Carmichael, A. S. Ridolfo, L. Thompkins, and E. A. Ziege, *Biomed. Mass Spectrom.*, **6**, 173 (1979).

(9) H. d'A. Heck, S. E. Buttrill, Jr., N. W. Flynn, R. L. Dyer, M. Anbar, T. Cairns, S. Dighe, and B. E. Cabana, *J. Pharmacokinet. Biopharm.*, 7, 233 (1979).

(10) T. Walle and U. K. Walle, *Res. Commun. Chem. Pathol. Pharmacol.*, **23**, 453 (1979).

(11) D. Alkalay, W. E. Wagner, Jr., S. Carlsen, L. Khemani, J. Volk, M. E. Barlett, and A. LeSher, *Clin. Pharmacol. Ther.*, **27**, 697 (1980).

(12) P. J. Murphy and H. R. Sullivan, *Annu. Rev. Pharmacol. Toxicol.*, **20**, 609 (1980).

(13) A. I. Cohen, R. G. Devlin, E. Ivashkiv, P. T. Funke, and T. McCormick, *J. Pharm. Sci.*, **71**, 1251 (1982).

(14) M. E. Condon, C. C. Cimarusti, R. Fox, V. L. Narayanan, J. Reid, J. E. Sundeen, and F. P. Hauck, *J. Med. Chem.*, **21**, 913 (1978).

(15) L. Slusarek and K. Florey, in "Analytical Profiles of Drug Substances," Vol. 9, K. Florey, Ed., Academic, New York, N.Y., 1980, p. 455.

(16) R. C. Williams and J. L. Viola, *J. Chromatogr.*, **185**, 505 (1979).

(17) E. Ivashkiv, *J. Pharm. Sci.*, **66**, 1168 (1977).

(18) J. M. Lachin, *Control. Clin. Trials*, **2**, 93 (1981).

ACKNOWLEDGMENTS

The statistical evaluation of the data, provided by M. Stern, and the synthesis of the deuterated analogue and internal reference by Dr. F. Dürsch is gratefully acknowledged.

A New Series of Reductive Amination Derivatives of Daunorubicin: Syntheses, Partition Coefficients, and DNA Binding

SHAU-FONG YEN *, W. DAVID WILSON *x, STEVENS W. PEARCE §, and EDMOND J. GABBAY §†

Received April 19, 1983, from the **Department of Chemistry, Georgia State University, Atlanta, GA 30303* and the §*Department of Chemistry, University of Florida, Gainesville, FL, 32611.* Accepted for publication December 6, 1983. †Deceased.

Abstract □ A series of daunorubicin derivatives were prepared by sodium cyanoborohydride reductive amination of daunorubicin with appropriate amines. All derivatives were found to bind quite strongly to DNA and viscosity increases with linear DNA indicated that each formed an intercalation complex. A range of octanol-aqueous buffer partition coefficients was obtained, around the values of daunorubicin and dauxorubicin hydrochloride, by varying the character of the starting amine. All monoamine derivatives had activity against P388 leukemia in mice which was similar to that of daunorubicin. A diamine derivative had reduced activity against P388. Several anthracyclines administered as DNA complexes had similar activity against P388 but significantly reduced toxicity compared to the uncomplexed compounds. For anthracyclines which bind strongly to DNA, optimum activity against P388 leukemia in mice seems to be centered on compounds with octanol-buffer partition coefficients in the range of 0.5–0.8.

Keyphrases □ Anthracyclines—new derivatives, antineoplastic agents □ Toxicity—reduced cardiotoxicity, anthracyclines

The glycosidic anthracycline antibiotics daunorubicin (I) and dauxorubicin hydrochloride (II), are being clinically used as antineoplastic agents (1–8). Unfortunately, these drugs are severely limited by their dose related cardiotoxicity (1–5). Although the molecular basis of the cardiotoxicity is not clear, two proposed mechanisms are widely accepted. First, the anthracyclines are reduced to semiquinone free radicals and, subsequently, generate oxygen radicals which cause membrane lipid peroxidation and DNA strand scission (9–11). Second, the chemically labile glycosidic bonds of I and II are cleaved by glycosidases to form the respective aglycons during *in vivo* metabolism (1–4, 9, 12). The water insoluble aglycons accu-

0022-3549/84/1100-1575$01.00/0

© 1984, American Pharmaceutical Association

mulate in heart tissue. The anthracyclines are no doubt capable of multiple mechanisms of action at several biological sites. Their antitumor activity is believed to be at least partially due to their ability to bind *in vivo* to DNA of nuclear deoxyribonucleoprotein (1-8). The results of X-ray diffraction and model building studies have shown that there is a specific complex formed between the anthracyclines and DNA (7, 8). As part of a continuing effort (13, 14) to prepare derivatives of I and II with higher specificity, reduced toxicity, and also to develop *in vitro* methods for biological activity evaluation, we report the synthesis and biological effects of a new series of anthracycline amine derivatives IV–VII. The results of *in vivo* testing for the DNA complexes with some of the new analogues are also presented.

Since bulky substituents at C-13, such as rubidazone, III, maintain high antineoplastic activity (1), it is reasonable to expect that anthracycline analogues at this position would be active. In an attempt to reduce the accumulation of the aglycons in heart tissue, their water solubility was increased by introducing charged amino derivatives at C-13. It should be noted that these cationic groups could also potentially enhance binding affinity to DNA. In addition, varying the hydrophobic character of the substituents on C-13 was used to vary the partition coefficient of these C-13 derivatives.

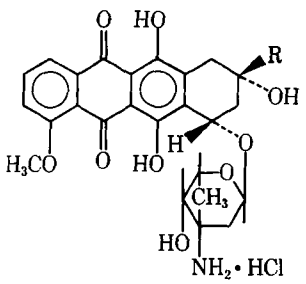

I, R = $COCH_3$ (Daunorubicin)
II, R = $COCH_2OH$ (Dauxorubicin)
III, R = $C(NNHCOC_6H_5)CH_3$ (Rubidazone)
IV, R = $CH(NHCH_3{\cdot}HCl)CH_3$
V, R = $CH(NH(CH_2)_3CH_3{\cdot}HCl)CH_3$
VI, R = $CH(NH(CH_2)_3OH{\cdot}HCl)CH_3$
VII, R = $CH(NH(CH_2)_3NH_2(CH_3)_2{\cdot}2HCl)CH_3$
VIII, R = $CH(OH)CH_3$ (Daunorubicinol)

EXPERIMENTAL SECTION[1]

(7*S*,9*S*)-7-[(3-Amino-2,3,6-trideoxy-α-L-lyxo-hexopyranosyl)oxy]-9-(1-methylaminoethyl)-7,8,9,10-tetrahydro-6,9,11-trihydroxy-4-methoxy-5,12-naphthacenedione Dihydrochloride (C-13-Methylaminohydrodaunorubicin; IV)—Methylamine hydrochloride (2.0 g, 30 mmol) and I (175 mg, 0.3 mmol) were dissolved in 20 mL of methanol. To this was added 0.3 mL of a 1.0 M methanolic solution of NaOH and, after 15 min equilibration, 1.0 mL of a freshly prepared methanolic solution of $NaCNBH_3$ (0.3 mmol/mL). The reaction was carried out at room temperature in a sealed tube for 12 h, at which time TLC of the reaction mixture on silica-gel plates (20% methanol–chloroform) indicated only the presence of IV and a trace amount of VIII. The amount of NaOH added only partially neutralizes the added amine hydrochloride. It was found experimentally that addition of larger amounts of NaOH caused the appearance of numerous unidentified side products (TLC analysis) which were difficult to remove. Addition of less NaOH caused the reaction to proceed quite slowly and allowed the formation of larger amounts of daunorubicinol, VIII. The amount of NaOH added was, thus, chosen to optimize the yield of the desired product. The methanol was evaporated under reduced pressure and then the residue was dissolved in 10 mL of pH 10.4 aqueous borate buffer (0.01 M) and extracted three times with a total of 30 mL of $CHCl_3$. The combined chloroform extracts were washed three times with distilled water, dried over Na_2SO_4, and evaporated under reduced pressure. The solid was dissolved in methanol and acidified with slightly more than two equivalents of aqueous 12 M HCl. The solvent was evaporated under reduced pressure and the residue triturated three times with 1% methanol in chloroform. At this time only IV could be detected by TLC. The dark red solid was recrystallized from ethanol–ethylacetate to give 80 mg (45%) of IV (mp, slowly dec. >179°C); TLC (silica gel, 30% CH_3OH in CH_2Cl_2): R_f 0.19; IR (KBr): 3452 (N—H), 1622, and 1589 cm^{-1} (C=O of C ring); ^{1}H-NMR (free base in $CDCl_3$): δ 8.07 (d, J = 8.0 Hz, H-1), 7.78 (t, J = 1.5 Hz, H-2), 7.37 (d, J = 8.2 Hz, H-3), 5.52 (m, H-1′), 5.28 (m, H-7), 4.06 (s, OCH_3), 4.2–3.8 (br m, OH-9, H-5′, and H-3′), 3.6–2.4 (br m, H-4′, H-10, and H-13), 2.57 (d, J = 2.8 Hz, NCH_3), 2.0–1.3 (br m, H-8 and CH_2-2′), 1.26 (d, J = 7.3 Hz, CH_3-5′), and 1.18 ppm (d, J = 6.5 Hz, CH_3-14).

Anal.—Calc. for $C_{28}H_{36}Cl_2N_2O_9$: C, 53.08; H, 6.04. Found: C, 52.90; H, 6.06.

(7*S*,9*S*)-7-[(3-Amino-2,3,6-trideoxy-α-L-lyxo-hexopyranosyl)oxy]-9-(1-butylaminoethyl)-7,8,9,10-tetrahydro-6,9,11-trihydroxy-4-methoxy-5,12-naphthacenedione Dihydrochloride (C-13-Butylaminohydrodaunorubicin; V)—The reaction of butylamine hydrochloride with I was conducted as for IV, and the product was purified in a similar manner to yield dark red solid V in 67% yield (mp slowly dec. >160°C); TLC (silica gel, 20% CH_3OH in CH_2Cl_2): R_f 0.52; IR (KBr): 3452 (N—H), 1622, and 1581 cm^{-1} (C=O of C ring); ^{1}H-NMR (free base in $CDCl_3$): δ 8.07 (d, J = 8.0 Hz, H-1), 7.76 (t, J = 1.5 Hz, H-2), 7.39 (d, J = 8.0 Hz, H-3), 5.50 (m, H-1′), 5.26 (m, H-7), 4.08 (s, OCH_3), 4.5–3.8 (br m, OH-9, H-5′, and H-3′), 3.5–2.2 (br m, H-4′, H-10, H-13, and CH_2—α-N-butyl), 2.0–1.1 (br m, H-8, CH_2-2′, CH_2—β-N-butyl, CH_2—γ-N-butyl, and CH_2—δ-N-butyl), 1.29 (d, J = 6.4 Hz, CH_3-5′), 1.21 (d, J = 6.4 Hz, CH_3-14), and 0.94 ppm (t, J = 7.4 Hz, CH_3—N-butyl).

Anal.—Calc. for $C_{31}H_{42}Cl_2O_9N_2$: C, 55.11; H, 6.56. Found: C, 55.46; H, 6.30.

(7*S*,9*S*)-7-[(3-Amino-2,3,6-trideoxy-α-L-lyxo-hexopyranosyl)oxy]-9-[1-(3-hydroxypranyl)aminoethyl]-7,8,9,10-tetrahydro-6,9,11-trihydroxy-4-methoxy-5,12-naphthacenedione Dihydrochloride (C-13-1-Propanolaminohydrodaunorubicin; VI)—The reaction of 3-amino-1 propanol hydrochloride with daunorubicin was conducted as for IV and the product was purified to give dark red solid VI in 38% yield (mp slowly dec. >174°C); TLC (silica gel, 20% CH_3OH in CH_2Cl_2): R_f 0.58; IR (KBr): 3443 (N—H), 1622, and 1581 cm^{-1} (C=O of C ring); ^{1}H-NMR (free base in $CDCl_3$): δ 8.05 (d, J = 7.3 Hz, H-1), 7.76 (t, J = 1.0 Hz, H-2), 7.37 (d, J = 8.2 Hz, H-3), 5.52 (m, H-1′), 5.28 (m, H-7), 4.10 (s, OCH_3), 4.5–3.6 (br m, OH-9, H-5′, H-3′), 3.5–2.2 (two m, CH_2—γ-propanol, CH_2—α-propanol, H-4′, H-10, and H-13), 1.9–1.5 (br m, H-8, CH_2-2′ and CH_2—β-propanol), 1.36 (d, J = 6.4 Hz, CH_3-5′), and 1.29 ppm (m, J = 5.5 Hz, CH_3-14).

Anal.—Calc. for $C_{30}H_{40}Cl_2N_2O_{10}$: C, 54.61; H, 5.96. Found: C, 54.71; H, 5.97.

(7*S*,9*S*)-7-[(13-Amino-2,3,6-trideoxy-α-L-lyxo-hexopyranosyl)oxy]-9-[1-(3,3-dimethyl-1,3-diaminoethyl)]-7,8,9,10-tetrahydro-6,9,11-trihydroxy-4-methoxy-5,12-naphthacenedione Trihydrochloride (C-13-*N*,*N*-Dimethyl-1,3-propanediaminohydrodaunorubicin; VII)—The reaction of N,N-dimethyl-1,3-diaminopropane dihydrochloride with I was conducted as for IV and the product was purified to give dark red solid VII in 70% yield (slowly dec. >180°C); TLC (silica gel, 30% CH_3OH in CH_2Cl_2): R_f 0.08; IR (KBr): 3451 (N—H), 1622, and 1589 cm^{-1} (C=O of C ring); ^{1}H-NMR (free base in $CDCl_3$): δ 7.94 (d, J = 7.8 Hz, H-1), 7.72 (t, J = 1.5 Hz, H-2), 7.34 (d, J = 8.0 Hz, H-3), 5.45 (m, H-1′), 5.17 (m, H-7), 4.05 (s, OCH_3), 4.5–3.9 (br m, OH-9, H-5′, and H-3′), 3.5–2.0 (br m, H-4′, H-10, H-13, CH_2—α-N-ethylene, and CH_2—β-N-ethylene), 2.23 (s, NCH_3), 1.8–1.1 (br m, H-8, CH_2-2′), 1.29 (d, J = 7.3 Hz, CH_3-5′) and 1.09 ppm (d, J = 6.5 Hz, CH_3-14).

Anal.—Calc. for $C_{32}H_{46}Cl_3N_3O_9{\cdot}H_2O$: C, 51.86; H, 6.53. Found: C, 51.77; H, 6.53.

Octanol–buffer partition coefficients were determined by standard equilibration methods (15). Extinction coefficients at 480 nm, determined for the two different phases, were used for concentration determinations. Binding constants of the derivatives were determined as previously described (16) using spectrophotometric changes at 480 nm. The results were analyzed using standard methods (16–18). Viscosity measurements were made using a viscometer[2] with electronic timing as previously described (13, 14). The system for determining inhibition of *E. coli* RNA polymerase is the same as previously described for anthracycline derivatives (13). Salmon sperm DNA was used as obtained[3]. Stock solutions of DNA were made in 2 mM [1,4-piperazinebis(ethanesulfonic acid)] buffer (PIPES), pH 7.8, with NaCl added to adjust ionic strength. Anthracycline stock solutions (10 mM) were made in distilled

[1] NMR spectra were recorded from 0–10 ppm on either a JEOL GX270 or on a Varian XL-100 spectrometer. Elemental analyses were performed at Atlantic Microlab, Inc., Atlanta, Georgia. Compounds I–III were obtained from the Drug Development Branch of NCI.

[2] Beckman-Zimm rotating cylinder viscometer.

[3] Worthington Biochemical Corp.

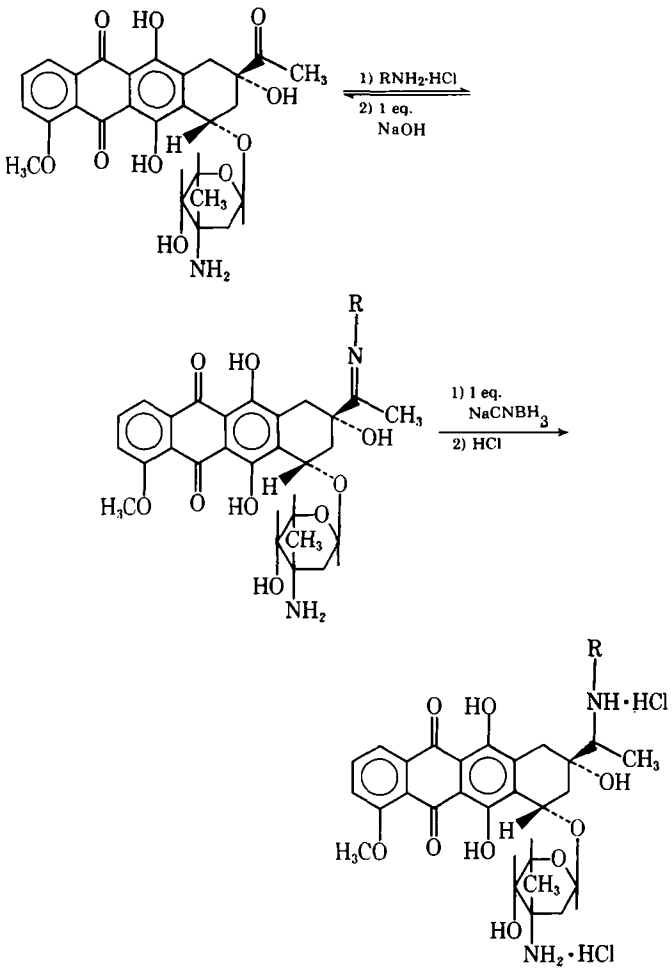

Scheme I—Synthesis of reductive derivatives of daunorubicin, IV-VII.

water and diluted with appropriate buffer as needed.

Anthracycline-DNA complexes for biological testing were prepared by dissolving DNA (5 mM) in 0.1 mM phosphate buffer at pH 7. Anthracyclines were dissolved (0.01 M) in water and added very slowly with vigorous stirring to the DNA solution until a ratio of 1:5 of drug to DNA was obtained. The solution was warmed to 40°C with stirring until all solids had dissolved and then was lyophilized. Volumes were varied depending on the amount of drug desired.

RESULTS

Chemistry—The syntheses of IV-VII were carried out in good yield by treating daunorubicin with appropriate amines and $NaCNBH_3$ (19) as shown in Scheme I. The reactions were monitored by TLC. Typically, four spots of a reaction mixture were observed: (*a*) starting material, I; (*b*) daunorubicinol, VIII, which results from the reduction of I by $NaCNBH_3$; (*c*) a component with high mobility which is presumably the aglycon of I; (*d*) the component which after purification was identified as the desired product and which always had the smallest R_f value. Daunorubicinol, VIII, was identified by treating I with $NaCNBH_3$ directly under mild conditions. Typically, at the end of a reaction, the first three components were present in trace amount and frequently no starting material was detected.

All reactions were performed on a relatively small scale due to the expense of I. In addition to elemental analysis, the authenticity and purity of IV-VII were confirmed as follows: (*a*) NMR of aromatic, sugar, and methoxy peaks of the neutral species in $CDCl_3$ showed no significant change from I; (*b*) the C=O IR stretching vibrations of C-13 at 1712 cm^{-1} disappear after reaction; (*c*) the bands at 1622 and 1581 cm^{-1} of the two carbonyl groups of the C ring remain unchanged, indicating that the quinone is not reduced by $NaCNBH_3$; (*d*) the UV-visible spectra of the derivatives are similar to the parent compound I, indicating that the chromophore is not modified; (*e*) TLC of the purified compounds on silica gel gives only a single spot.

Biological Testing—Compounds IV-VII, along with I and II, were submitted to the National Cancer Institute for antitumor activity testing against lymphocytic leukemia P388 in mice. As shown in Table I, all derivatives are

Table I—Biological Testing Results Against Mouse Lymphocytic Leukemia [a]

Compound	NSC Number	Optimal Dose, mg/kg	Toxic Dose, mg/kg[b]	T/C[c]
I	082151	1.0	2.0	175
II	123127	1.0	3.0	204
IV	257455	8.0	16.0	159
V	263673	5.0	10.0	183
VI	266537	16.0	32.0	188
VII	256466	6.25	20.0	131

[a] All tests were arranged through the Drug Research and Development Program, Division of Cancer Treatment, National Cancer Institute. CDF mice bearing intraperitoneally implanted P388 lymphocytic leukemia (10^6 cells) on day 0 were treated on days 1-9 with the specified intraperitoneal dose of aqueous drug solutions. Detailed protocols are described in Ref. 22. The toxic dose is defined as the dose at which T/C has dropped from its maximum value to 100. [c] T/C is the mean survival time of treated/control animals, in percent, and must be ≥125 for an active result.

Table II—Binding of the Anthracycline Drugs to DNA [a]

Compound	K_0[b] × 10^{-5} (PIPES/51 mM Na^+) [c]	K_0[b] × 10^{-5} (PIPES/201 mM Na^+) [c]
I	9.3	5.8
II	14.6	10.0
IV	10.3	3.0
V	10.5	2.6
VI	5.8	1.6
VII	28.0	10.9

[a] Binding measurements were conducted using spectrophotometric changes at 480 nm as previously described (10, 11, 18). [b] K_0 represents the equilibrium constant for binding of a drug molecule to an isolated site on the DNA double helix. It is determined from the intercept on the vertical axis of a Scatchard plot of binding data. [c] 2 mM PIPES buffer, pH 7.8, with 40 mM NaCl added. [d] 2 mM PIPES buffer, pH 7.8, with 200 mM NaCl added.

active with V and VI showing greater activity than the parent compound I. Relative to I and II, all derivatives require larger amounts of compound (mg/kg) to reach both the optimum and toxic doses (Table I). The ratio of toxic to the optimal dose is approximately two for I and is not significantly increased for any of the derivatives. The activity of V and VI is quite encouraging and we have, therefore, analyzed the interaction of all of these compounds with DNA and have measured their octanol-water partition coefficients to determine how the biological testing results correlate with the binding and the partitioning properties.

Mode of Binding—Since I and II are known to bind to DNA by intercalation, IV through VII might also be expected to intercalate. A consistent indicator of intercalation is the ability of a drug to increase the length of linear DNA (20). All of the derivatives gave large increases in viscosity, as expected for intercalators in the presence of linear DNA[4] (16). The increases, at similar amounts of bound drug, were only ~80% of that obtained with I and II, indicating that replacing the keto function by the amino substituents perturbs the interaction of the anthracycline ring system with the double helix. It seems conclusive that all of the derivatives bind to DNA by intercalation, but the structure of the complex formed could be somewhat different from that for I and II with DNA.

DNA-Induced Absorption Spectral Changes and DNA Binding Studies—The anthracycline chromophore has an intense visible absorption band near 480 nm which exhibits shifts to longer wavelengths and hypochromism on intercalation with DNA. Similar effects are seen for the derivatives IV-VII as for I and II. These spectral changes can be used to calculate equilibrium constants for the interaction of the anthracyclines with DNA (14, 16). Because the binding of these compounds to DNA is complex (17), their interactions with DNA have been compared by determining the intercept on the vertical axis from Scatchard plots of spectrophotometric binding data. This limit should be the apparent equilibrium constant, K_0, for binding of a drug molecule to an isolated binding site in DNA (16). This method has the advantage of giving accurate relative binding strengths for a series of derivatives while not requiring any specific assumption about binding models for the DNA-drug interaction. A similar treatment has been used to compare the binding of antitumor platinum drugs with DNA (18). The results for derivatives IV-VII compared to I are shown in Table II at two different ionic strengths.

Inhibition of *Escherichia coli* RNA Polymerase—If the anthracyclines function in part by binding to DNA, they should exert dramatic effects on the biological as well as the physical properties of DNA. The potential biological inhibition in a standard *E. coli* RNA polymerase assay system (9) was mon-

[4] Unpublished results.

Table III—Relative Inhibition of DNA-Dependent *E. coli* RNA Polymerase[a]

Compound	Enzymatic Activity, %
none (control)	100
I	9
II	9
IV	10
V	13
VI	10
VII	5

[a] The kinetics of incorporation of [^{3}H]UMP into RNA using *E. coli* RNA polymerase was monitored for the compounds indicated. Heterogeneous calf thymus DNA (0.12 mM P/L) was used as the template for nonspecific RNA polymerization. Drugs were added at 0.12 mM concentration and reductions in activity of RNA polymerase monitored as previously described (13).

Table IV—1-Octanol–Buffer Partition Coefficients

Compound	Partition Coefficient[a]
I	2.8
II	0.5
IV	0.3
V	4.3
VI	0.8
VII	0.1

[a] Determined spectrophotometrically between 1-octanol saturated with buffer (2 mM PIPES, pH 7.8, with 20 mM NaCl) and octanol saturated buffer using standard procedures (21).

Table V—Biological Activity of Anthracycline–DNA Complexes[a]

Compound[b]	NSC Number	Optimal Dose, mg/kg[c]	Toxic Dose, mg/kg	T/C, %
I	082151	1.0	2.0	175
I-nDNA	257454	0.83	5.2	217
I-sDNA	257453	1.67	4.5	197
I-dDNA	262198	0.83	3.2	182
V-nDNA	263674	6.7	>50[d]	224
VI-nDNA	266538	>8[d]	>8[d]	173
VII-nDNA	262650	6.7	13	145

[a] Testing results and column headings are as in Table I. [b] All compounds were prepared at a 1:5 ratio of drug to DNA as described in the *Experimental Section*: nDNA is native salmon sperm DNA; sDNA is sonicated; dDNA is denatured. [c] Doses are calculated based on the amount of drug in the DNA–drug complex. The actual dose of the complex was six times greater than that indicated. [d] This indicates the maximum dose administered in the test. The optimum or toxic doses may be greater than this value.

itored and the results are shown in Table III. As with other anthracycline derivatives, the polymerase inhibition results parallel binding interactions (13, 14) and strong inhibition of the polymerase is obtained for IV–VII.

Partition Coefficients—The charged amine function on an already slightly polar parent molecule obviously has the potential for reducing membrane permeability. Octanol–buffer partition coefficients (15) were determined to assess the relative ability of the derivatives to pass through membranes as compared to I and II. The partition coefficients are listed in Table IV and, as expected, show decreases for IV, VI, and a large decrease for VII. The butyl derivative actually partitions better into the organic phase than I.

DNA–Anthracycline Complexes: Biological Testing—It has been proposed that complexes of drugs such as the anthracyclines with suitable biopolymers should be absorbed faster into tumor cells than into normal cells due to the higher potential endocytic activity of tumor cells (21). Since the absorption of drugs through their macromolecular complexes should depend much less on their partition coefficients than absorption of free drugs, complexes of I, II, V, VI, and VII with DNA were prepared. The testing results for these complexes are shown in Table V. As can be seen from the results with I, the physical state of the DNA has some effect on activity, with the native high molecular weight DNA complex giving higher activity than the sonicated or denatured samples. The complex of I with native DNA has higher activity than I alone, has a similar optimum dose (based on the amount of drug in the dose), and has a significantly improved chemotherapeutic index as compared with uncomplexed I. The results with the derivatives indicate similar behavior. The complex with VI could not be thoroughly investigated due to limitations in the amount of material available. The complex with VII was better than the free drug but not as significantly improved as one might expect based on its DNA binding properties. The complex with V shows marked improvement and has the highest activity in this series.

DISCUSSION

All of the derivatives of this study have been shown to bind strongly to DNA through an intercalation complex. The enhanced binding of IV and V relative to I is due to increased sodium ion release by these compounds on complexation with DNA (16). This might also partially account for the greater binding of VII, but the large enhancement for this compound, even at higher ionic strength, indicates some additional favorable interactions with DNA. At the higher ionic strength, which is closer to physiological conditions, only VII binds to DNA better than I. The slightly reduced binding of VI could be due to problems of hydration of the alcohol in the complex *versus* the free solution state.

Compounds IV and V bind quite similarly to DNA (Table II) whereas VII binds much more strongly to DNA than IV or V but partitions poorly (Table IV) and has the lowest activity of all of the compounds of this series. The propanolamine derivative VI has a lower binding constant than the other analogues (although it still binds strongly to DNA), and it has an intermediate partition coefficient. This compound has the highest *in vivo* activity of any of the derivatives and is more active than the parent compound I. Although there are too few compounds here to construct a structure–activity plot, it is interesting to note that dauxorubicin hydrochloride also has high activity coupled with a high DNA binding constant and an intermediate partition coefficient. This suggests that activity for those anthracycline derivatives which bind strongly to DNA and do not have other complicating factors might be found to peak at a partition coefficient of ~0.7. The low dose of II required relative to VI could be due, in part, to the larger DNA binding constant of II (Table II). Further investigation with a series of anthracyclines with partition coefficients of ~0.7 and high DNA binding constants would be of interest.

Because of the high DNA binding constant and low partition coefficient for VII it was expected that a dramatic enhancement in activity against P388 might be obtained for this compound through preparation and administration of a DNA complex. This idea is based on the so called "lysosomotropic" principle, which predicts selective uptake by antineoplastic cells of high molecular weight macromolecule–drug complexes. This delivery system could potentially increase the efficacy of the complexed drug relative to the free species, especially for derivatives such as VII which have low partition coefficients but bind strongly to DNA. As can be seen by comparison of biological testing results on VII in Tables I and V, although activity was increased, the results were not remarkable. All of the compounds analyzed as DNA complexes had similar optimal doses both complexed and uncomplexed. The toxic doses were generally significantly increased in the complexes relative to the uncomplexed derivatives. This suggests that the DNA is acting more to prevent toxicity than enhance activity. Obviously, if toxicity is lowered, the mean survival time for treated/control animals (T/C) at the maximum could rise slightly as the probability of a toxic reaction is shifted to higher dose levels relative to the optimum dose. Metabolic reactions, such as aglycon formation, would also be expected to be slower when an anthracycline is bound to DNA; this may be one of the major advantages of administering these compounds as DNA complexes. The activity of the V–DNA complex is encouraging and this compound and its DNA complex are being further investigated in *in vivo* systems.

REFERENCES

(1) F. Arcamone, "Doxorubicin," Academic, New York, N.Y., 1981.

(2) F. Arcamone in "Topics in Antibiotic Chemistry, Vol. 2," P. G. Sammes, Ed., Halsted Press, New York, N.Y., 1978, pp. 98–239.

(3) D. W. Henry, *ACS Symp. Ser.*, **30,** 15 (1976).

(4) D. W. Yesair and S. McNitt, *Z. Physiol. Chem.* **357,** 1066 (1976).

(5) D. D. Von Hoff, M. Rozencweig, and M. Flavik in "Advances in Pharmacology and Chemotherapy, Vol. 15," F. Garattini, F. Hawking, A. Goldin, and I. J. Kopin, Eds., Academic, New York, N.Y., 1978, pp. 1–50.

(6) M. J. Waring in "The Molecular Basis of Antibiotic Action," 2nd ed., E. F. Gale, E. Cundliffe, P. E. Reynolds, M. H. Richmond, and M. J. Waring, Eds., Wiley, London, pp. 258–401.

(7) S. Neidle in "Topics in Antibiotic Chemistry, Vol. 2," P. G. Sammes, Ed., Halsted Press, New York, N.Y., 1978, pp. 240–278.

(8) W. D. Wilson and R. L. Jones, *Advan. Pharmacol. Chemother.*, **18,** 177 (1981).

(9) N. R. Bachur, S. L. Gordon, M. V. Gee, and H. Kon, *Proc. Natl. Acad. Sci. USA*, **76,** 954 (1979).

(10) J. W. Lown and S. K. Sim, *Com. J. Chem.*, **54,** 2563 (1976).

(11) E. G. Minnaugh, M. A. Trush, and T. E. Gram, *Biochem. Pharm.*, **30,** 2797 (1981).

(12) A. D. Barone, R. F. Atkinson, D. L. Wharry, and T. H. Koch, *J. Am. Chem. Soc.*, **103,** 1606 (1981).

(13) W. D. Wilson, D. Grier, R. Reimer, J. Bauman, J. Preston, and E. J. Gabbay, *J. Med. Chem.*, **19**, 381 (1976).
(14) E. J. Gabbay, D. Grier, R. E. Fingerle, R. Reimer, R. Levy, S. W. Pearce, and W. D. Wilson, *Biochemistry*, **15**, 2062 (1976).
(15) A. Leo, C. Hansch, and D. Elkins, *Chem. Rev.*, **71**, 613 (1971).
(16) W. D. Wilson and I. G. Lopp, *Biopolymers*, **18**, 3025 (1979).
(17) S.-F. Yen, W. Germon, and W. D. Wilson, *J. Am. Chem. Soc.*, **105**, 3717 (1983).
(18) M. Howe-Grant and S. J. Lippard, *Biochemistry*, **18**, 5762 (1979).
(19) R. F. Borch, M. D. Bernstein, and H. D. Durst, *J. Am. Chem. Soc.*, **93**, 2897 (1971).
(20) G. Cohen and H. Eisenberg, *Biopolymers*, **8**, 45 (1969).
(21) A. Trouet, D. Deprez-De Campeneere, A. Zenebergh, and R. Hulkoven in "Adriamycin Review," European Press, Ghent, Belgium, 1975, pp. 62-69.
(22) R. I. Geran, N. H. Greenberg, M. M. MacDonald, A. M. Schumacher, and B. J. Abbott, *Cancer Chemother. Rep. Part 3*, **3**, 9 (1972).

ACKNOWLEDGMENTS

Professor Edmond Gabbay died as the experimental work for this paper was being conducted. His creative ideas and experimental work in organic, medicinal, and biochemistry will stand as a memorial to him, and this paper is dedicated to his memory.

This work was supported by National Institutes of Health Grants GM 30267 (to W.D.W.) and GM 17503 (to E.J.G.).

Liquid Membrane Phenomenon in Diuretics

S. B. BHISE, D. BHATTACHARJEE, and R. C. SRIVASTAVA ˣ

Received March 17, 1983, from the *Birla Institute of Technology and Science, Pilani-333031, India.* Accepted for publication February 24, 1984.

Abstract □ Surface activity and critical micelle concentrations are reported for two diuretic drugs, furosemide and triamterene. The drugs generate a liquid membrane on a supporting membrane. Transport of chloride, sodium, and potassium ions through the liquid membranes generated by the drugs was studied. The data suggest that the phenomenon of liquid membrane formation may contribute to the diuretic action.

Keyphrases □ Diuretics—liquid membrane phenomenon, critical micelle concentrations, chloride, sodium, potassium ion transport, furosemide, triamterene □ Furosemide—liquid membrane phenomenon, anion/cation transport □ Triamterene—liquid membrane phenomenon, anion/cation transport

Drugs known to act by altering the permeability of cell membranes are mostly surface active. Surface-active agents added to an aqueous phase are known to generate a surfactant-layer liquid membrane at the interface which modifies material transport across it (1). It is therefore likely that the liquid membranes generated by surface-active drugs play a role in the mechanism of drug action. A wide category of surface-active drugs have been investigated in this laboratory (2-7), and results indicated that the liquid membranes contribute to the mechanism of drug action.

Most of the high-ceiling diuretics (8) are known to act by altering the reabsorption of cations (*e.g.*, Na^+) and anions (*e.g.*, Cl^-) in the ascending limb of the loop of Henle (8). Although diuretics act by modifying the membrane permeability, their surface activity is not documented in the literature. In the present study, surface activity of these drugs is demonstrated—critical micelle concentrations (CMC) have been determined—and the existence of liquid membranes generated by them at the interface is confirmed. Transport of relevant cations and anions in the presence of the liquid membranes generated by the drugs has been studied. The data indicate that the liquid membranes generated by the diuretic drugs contribute to the mechanism of their action. A cellulose nitrate microfiltration membrane/aqueous interface was chosen as a site for the formation of the liquid membranes to eliminate the possibility of active and specific interaction of the drugs with the constituents of the biological membranes and to highlight the role of passive transport through the liquid membranes. Two structurally dissimilar diuretic drugs (furosemide and triamterene) were chosen for the present study.

EXPERIMENTAL SECTION

Material—Furosemide[1], triamterene[2], sodium chloride[3], potassium chloride[3], and water (glass distilled over potassium permanganate) were used.

Methods—The critical micelle concentration (CMC) of aqueous furosemide and triamterene solutions were determined from the variation in surface tension with concentration at 37 ± 0.1°C. The surface tensions were measured using a tensiometer[4]. To prepare an aqueous solution of furosemide, the drug

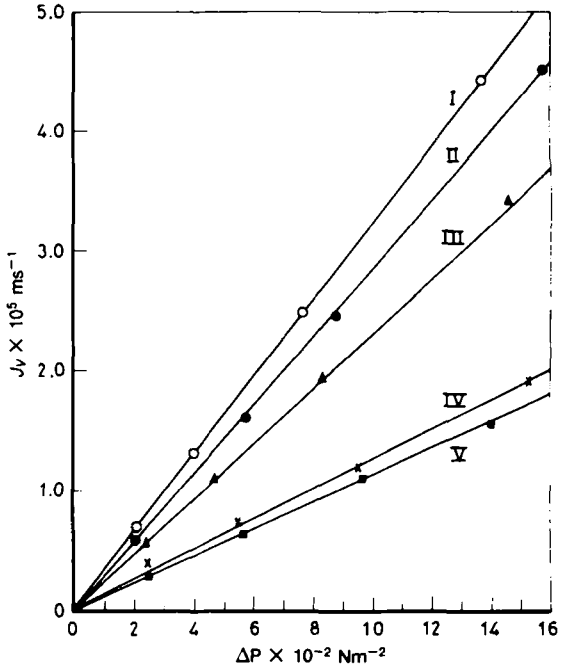

Figure 1—*Hydraulic permeability data. Curves I, II, III, IV, and V are for 0, 2.08 × 10^{-5}, 4.16 × 10^{-5}, 8.3 × 10^{-5}, and 24.9 × 10^{-5} M furosemide concentrations, respectively.*

[1] Hoechst Pharmaceutical, Ltd.
[2] S, K & F Ltd.
[3] Analytical grade.
[4] Model 21 Tensiomat; Fisher.

© 1984, American Pharmaceutical Association

(13) W. D. Wilson, D. Grier, R. Reimer, J. Bauman, J. Preston, and E. J. Gabbay, *J. Med. Chem.*, **19**, 381 (1976).
(14) E. J. Gabbay, D. Grier, R. E. Fingerle, R. Reimer, R. Levy, S. W. Pearce, and W. D. Wilson, *Biochemistry*, **15**, 2062 (1976).
(15) A. Leo, C. Hansch, and D. Elkins, *Chem. Rev.*, **71**, 613 (1971).
(16) W. D. Wilson and I. G. Lopp, *Biopolymers*, **18**, 3025 (1979).
(17) S.-F. Yen, W. Germon, and W. D. Wilson, *J. Am. Chem. Soc.*, **105**, 3717 (1983).
(18) M. Howe-Grant and S. J. Lippard, *Biochemistry*, **18**, 5762 (1979).
(19) R. F. Borch, M. D. Bernstein, and H. D. Durst, *J. Am. Chem. Soc.*, **93**, 2897 (1971).
(20) G. Cohen and H. Eisenberg, *Biopolymers*, **8**, 45 (1969).
(21) A. Trouet, D. Deprez-De Campeneere, A. Zenebergh, and R. Hulkoven in "Adriamycin Review," European Press, Ghent, Belgium, 1975, pp. 62-69.
(22) R. I. Geran, N. H. Greenberg, M. M. MacDonald, A. M. Schumacher, and B. J. Abbott, *Cancer Chemother. Rep. Part 3*, **3**, 9 (1972).

ACKNOWLEDGMENTS

Professor Edmond Gabbay died as the experimental work for this paper was being conducted. His creative ideas and experimental work in organic, medicinal, and biochemistry will stand as a memorial to him, and this paper is dedicated to his memory.

This work was supported by National Institutes of Health Grants GM 30267 (to W.D.W.) and GM 17503 (to E.J.G.).

Liquid Membrane Phenomenon in Diuretics

S. B. BHISE, D. BHATTACHARJEE, and R. C. SRIVASTAVA ˣ

Received March 17, 1983, from the *Birla Institute of Technology and Science, Pilani-333031, India.* Accepted for publication February 24, 1984.

Abstract □ Surface activity and critical micelle concentrations are reported for two diuretic drugs, furosemide and triamterene. The drugs generate a liquid membrane on a supporting membrane. Transport of chloride, sodium, and potassium ions through the liquid membranes generated by the drugs was studied. The data suggest that the phenomenon of liquid membrane formation may contribute to the diuretic action.

Keyphrases □ Diuretics—liquid membrane phenomenon, critical micelle concentrations, chloride, sodium, potassium ion transport, furosemide, triamterene □ Furosemide—liquid membrane phenomenon, anion/cation transport □ Triamterene—liquid membrane phenomenon, anion/cation transport

Drugs known to act by altering the permeability of cell membranes are mostly surface active. Surface-active agents added to an aqueous phase are known to generate a surfactant-layer liquid membrane at the interface which modifies material transport across it (1). It is therefore likely that the liquid membranes generated by surface-active drugs play a role in the mechanism of drug action. A wide category of surface-active drugs have been investigated in this laboratory (2-7), and results indicated that the liquid membranes contribute to the mechanism of drug action.

Most of the high-ceiling diuretics (8) are known to act by altering the reabsorption of cations (*e.g.*, Na^+) and anions (*e.g.*, Cl^-) in the ascending limb of the loop of Henle (8). Although diuretics act by modifying the membrane permeability, their surface activity is not documented in the literature. In the present study, surface activity of these drugs is demonstrated—critical micelle concentrations (CMC) have been determined—and the existence of liquid membranes generated by them at the interface is confirmed. Transport of relevant cations and anions in the presence of the liquid membranes generated by the drugs has been studied. The data indicate that the liquid membranes generated by the diuretic drugs contribute to the mechanism of their action. A cellulose nitrate microfiltration membrane/aqueous interface was chosen as a site for the formation of the liquid membranes to eliminate the possibility of active and specific interaction of the drugs with the constituents of the biological membranes and to highlight the role of passive transport through the liquid membranes. Two structurally dissimilar diuretic drugs (furosemide and triamterene) were chosen for the present study.

EXPERIMENTAL SECTION

Material—Furosemide[1], triamterene[2], sodium chloride[3], potassium chloride[3], and water (glass distilled over potassium permanganate) were used.

Methods—The critical micelle concentration (CMC) of aqueous furosemide and triamterene solutions were determined from the variation in surface tension with concentration at 37 ± 0.1°C. The surface tensions were measured using a tensiometer[4]. To prepare an aqueous solution of furosemide, the drug

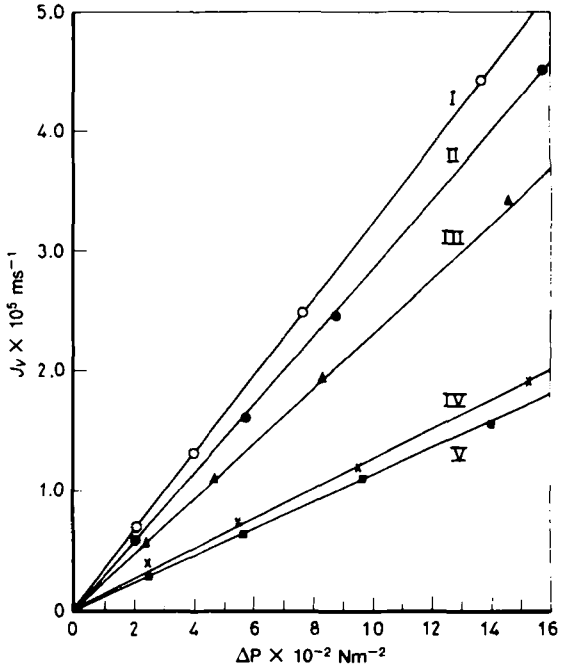

Figure 1—*Hydraulic permeability data. Curves I, II, III, IV, and V are for 0, 2.08 × 10^{-5}, 4.16 × 10^{-5}, 8.3 × 10^{-5}, and 24.9 × 10^{-5} M furosemide concentrations, respectively.*

[1] Hoechst Pharmaceutical, Ltd.
[2] S, K & F Ltd.
[3] Analytical grade.
[4] Model 21 Tensiomat; Fisher.

© 1984, American Pharmaceutical Association

Table I—Values of the Hydraulic Conductivity Coefficient (L)[a] at Various Concentrations of Furosemide and Triamterene

	Furosemide Concentration, × 10^5 M					Triamterene Concentration, × 10^6 M				
	0	2.08 (0.25 CMC)	4.16 (0.5 CMC)	8.3 (CMC)	24.9	0	2.0 (0.2 CMC)	5.0 (0.5 CMC)	10.0 (CMC)	30.0
$L^b \times 10^8$ ($m^3 \cdot s^{-1} \cdot N^{-1}$)	3.56 ± 0.266	2.73 ± 0.105	2.20 ± 0.416	1.11 ± 0.075	1.26 ± 0.058	3.56 ± 0.090	3.06 ± 0.102	1.95 ± 0.088	0.59 ± 0.072	0.56 ± 0.066
$L^c \times 10^8$ ($m^3 \cdot s^{-1} \cdot N^{-1}$)	—	2.94 ± 0.105	2.33 ± 0.416	—	—	—	2.96 ± 0.102	2.08 ± 0.088	—	—

[a] Expressed as mean ± *SD*. [b] Experimental values. [c] Calculated on the basis of the mosaic model.

was dissolved in acetone and added (stirred constantly) to the aqueous phase. The concentration of acetone in all the furosemide solutions was ≤0.4% (v/v). A corresponding control solution with 0.4% (v/v) acetone was used as a blank. For preparing aqueous solutions of triamterene, a 0.12% (v/v) aqueous solution of dioxane was used as a solvent. A corresponding blank solution, without triamterene, was used for comparison of surface tension values. The CMC values for furosemide and triamterene were 8.3×10^{-5} and 1×10^{-5} M, respectively.

The all-glass transport cell previously desribed (2) was used for the transport studies. A cellulose nitrate microfiltration membrane[5], which acted as support for the liquid membrane, separated the cell into two compartments, C and D. The hydraulic permeability data were obtained at concentrations below and above the CMC values of the drugs, using the method previously described (2).

The solute permeability (ω) of chloride ions was measured in the presence of furosemide; that of sodium and potassium ions was measured in the presence of triamterene using (9, 10):

$$\left(\frac{J_s}{\Delta\pi}\right)_{J_V=0} = \omega \qquad \text{(Eq. 1)}$$

where J_s and J_V are, respectively, the solute flux and the volume flux per unit area of the membrane; $\Delta\pi$ is the osmotic pressure difference across the membrane. The method of measurement has been described (2).

Two sets of experiments were performed for solute permeability measurements. In the first set, aqueous solutions of the drugs and the permeating species were kept in one compartment (compartment C of the transport cell, Fig. 1. of Ref. 2) and the other compartment (D) was filled with distilled water. In the second set of experiments, aqueous solutions of the drugs were taken in compartment D while compartment C contained aqueous solutions of the permeating species. No drug was used in the control experiments. Since hydrophobic ends of the surface-active drugs would be preferentially oriented towards the hydrophobic supporting membrane (the cellulose nitrate microfiltration membrane) in the first set of experiments, the permeating species would face the hydrophilic surface of the drug liquid membrane. In the second set of experiments, however, the permeating species would face the hydrophobic surface of the drug liquid membranes.

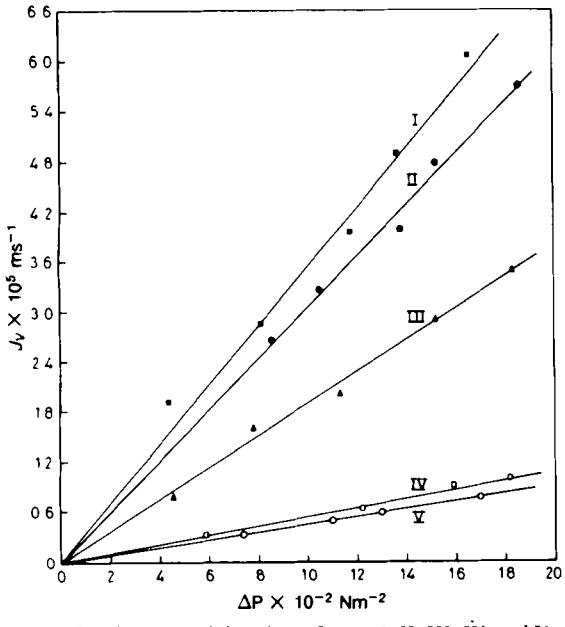

Figure 2—*Hydraulic permeability data. Curves I, II, III, IV, and V are for 0, 2.0×10^{-6}, 5.0×10^{-6}, 1.0×10^{-5}, and 3.0×10^{-5} M triamterene concentrations, respectively.*

[5] Cat. No. 11307; Sartorius (thickness, 1×10^{-4} M; area, 1.794×10^{-5} m^2).

The concentrations of the diuretic drugs used in the solute permeability experiments were always higher than their CMC values to ensure that the supporting membrane was completely covered by the liquid membranes generated by them. The concentration of furosemide was 2.5×10^{-4} M and that of triamterene was 3.0×10^{-5} M. Fifteen replicates were taken for each value of ω. All measurements were made at a constant temperature using a thermostat set at 37 ± 0.1°C.

Assays—The amount of chloride ions transported to the other compartment was measured by the spectrophotometric[6] determination at 540 nm of its product with brucine[3] and potassium persulfate[3] (11). The amounts of sodium and potassium ions transported to the other compartment were measured using a flame photometer[7].

RESULTS AND DISCUSSION

Hydraulic Permeability Data—The hydraulic permeability data at various concentrations of the diuretic drugs, in the case of both furosemide and triamterene, were found to obey the linear relationship (9);

$$J_V = L\Delta P \qquad \text{(Eq. 2)}$$

where J_V represents the volume flux per unit area of the membrane, ΔP is the applied pressure difference, and L is the hydraulic conductivity coefficient. The data for furosemide and triamterene are shown in Figs. 1 and 2, respectively. The values of L, calculated from the slopes of the straight lines in Figs. 1 and 2, show a progressive decrease (Table I) with increase in drug concentration up to the CMC, after which they become more or less constant. This gradation (Table I) is in keeping with the liquid membrane hypothesis (1) and indicates the progressive coverage of the supporting membrane with the liquid membrane with an increase in the concentration of the drug up to its CMC; at this concentration it is completely covered. Analysis of the flow data (Figs. 1 and 2, Table I) in the light of the mosaic membrane model (12–14) furnishes additional support for liquid membrane formation in series with the supporting membrane. The values of L (for both furosemide and triamterene), calculated using the mosaic membrane model at concentrations below the CMC values of the drugs, match the experimentally determined values (Table I) lending support to liquid membrane formation. The method of calculation is described in earlier publications (2–7).

Role of Liquid Membrane Formation in Diuretic Action—The primary action of furosemide is to reduce active absorption of chloride ions (8). The results indicate that the liquid membrane formed by furosemide, even on an inert support, impedes the transport of chloride ions (Table II). Similarly, the liquid membrane generated by triamterene offers resistance to the transport of Na^+ and K^+ ions (Table II). The significance of these observations is enhanced because the concentrations at which the complete liquid membranes are generated in series with the supporting membrane are low (on the order of μM) and compares favorably with the concentrations of these drugs in renal tubules (15, 16).

In the case of triamterene, the data indicate (Table II) that the transport of potassium ions is impeded more than the transport of sodium ions. This agrees with the reported observations on biological cells that triamterene is a potassium-sparing diuretic (17). In spite of the fact that in the present study an inert membrane like cellulose nitrate microfiltration membrane was used as support for the liquid membranes, the trend observed in the permeability of the cations is similar to that expected in biological cells. This strongly indicates that the liquid membranes generated by diuretic drugs, like triamterene, play a significant role in the mechanism of its action.

An examination of Table II reveals that the resistance offered to the transport of chloride ions (in the case of furosemide) and that of potassium ions (in the case of triamterene) is maximal when the liquid membranes generated by these drugs presented a hydrophilic surface to the approaching

[6] Spectronic-20; Bausch & Lomb.

[7] Flame Photometer Type 121; Systronics.

Table II—Solute Permeability (ω) of Ions in the Presence of Furosemide or Triamterene [a]

	ω_1 [b] $\times 10^{12}$ mol · s^{-1} · N^{-1}	ω_2 [c] $\times 10^{12}$ mol · s^{-1} · N^{-1}	ω_3 [d] $\times 10^{12}$ mol · s^{-1} · N^{-1}
	Furosemide [e]		
(Sodium) chloride	250.7 ± 35	189.0 ± 36	419.4 ± 79
	Triamterene [f]		
Potassium (chloride)	168.8 ± 12	91.6 ± 7	359.2 ± 9
Sodium (chloride)	111.2 ± 15	207.4 ± 15	232.5 ± 6

[a] Expressed as mean ± *SD*. [b] The drug in compartment D of the transport cell. [c] The drug in compartment C of the transport cell. [d] Control value; when no drug was used. [e] Concentration, 24.9×10^{-5} M. [f] Concentration, 3.0×10^{-5} M.

permeating species (the first set of experiments). In the light of these observations, it appears likely that the action sites of diuretic drugs like furosemide and triamterene themselves may be hydrophobic so that the hydrophobic ends of these drugs get attached to them leaving the hydrophilic parts to face the permeating species. If the action sites are hydrophobic they should be located within the hydrophobic core of the lipid bilayer of the membranes. To substantiate these conjectures, which appear logical in the light of the trends observed in the present experiments, further investigations are needed.

The permeability of sodium ions is impeded most when the triamterene liquid membrane presents its hydrophobic surface to the cation (Table II). The observation, however, is of limited biological significance because triamterene is known to be a potassium-sparing diuretic (17).

Diuretic drugs are also known to cause reduction in bile flow (18) and to alter ionic fluxes across isolated erythrocytes (19). The phenomenon of liquid membrane formation may be a plausible explanation for these effects. The decrease in reabsorption of water which results in diuresis is considered mainly a consequence of modification in the permeability of ions (8). The present study, however, indicates that the liquid membrane generated by the diuretic drug itself offers resistance to volume flux of water.

Though the observed reduction in permeability of the ions (Table II), due to the liquid membrane generated by the drugs, is passive in nature, it is likely to be accompanied by a consequent decrease in active transport. This would occur because access of the permeating species to the active sites on the biological membrane would be reduced due to the formation of the liquid membranes in series with the biological membrane. Thus, the liquid membranes generated by diuretic drugs may contribute significantly to the mechanism of drug action by impeding transport of ions as well as water.

REFERENCES

(1) R. E. Kesting, W. J. Subcasky, and J. D. Paton, *J. Colloid Interface Sci.*, **28**, 156 (1968).

(2) S. B. Bhise, P. R. Marwadi, S. S. Mathur, and R. C. Srivastava, *J. Pharm. Sci.*, **71**, 526 (1982).

(3) R. C. Srivastava, R. P. S. Jakhar, and S. B. Bhise, *J. Colloid Interface Sci.*, **87**, 56 (1982).

(4) S. B. Bhise, P. R. Marwadi, S. S. Mathur, and R. C. Srivastava, *J. Pharm. Sci.*, **72**, 599 (1983).

(5) S. B. Bhise, P. R. Marwadi, S. S. Mathur, and R. C. Srivastava, *Biophys. Chem.*, **17**, 187 (1983).

(6) R. C. Srivastava, R. K. Sharma, and S. B. Bhise, *J. Colloid Interface Sci.*, **93**, 72 (1983).

(7) R. C. Srivastava, R. K. Sharma, R. Srinivasan, and S. B. Bhise, *J. Colloid Interface Sci.*, **94**, 456 (1983).

(8) G. H. Mudge, in "The Pharmacological Basis of Therapeutics," 6th ed., A. G. Gilman, L. S. Goodman, and A. Gilman, Eds., Macmillan, New York, N.Y., 1980, pp. 903 and 904.

(9) A. Katchalsky and P. F. Curran, "Nonequilibrium Thermodynamics in Biophysics," Harvard University Press, Cambridge, Mass., 1967, pp. 113-116.

(10) A. Katchalsky and O. Kedem, *Biophys. J.*, **2**, 53 (1962).

(11) F. E. Snell and C. T. Snell, "Colorimetric Methods of Analysis," D. Van Nostrand, New York, N.Y., 1959, p. 610.

(12) K. S. Spiegler and O. Kedem, *Desalination*, **1**, 311 (1966).

(13) T. K. Sherwood, P. L. T. Brian, and R. E. Fischer, *Ind. Eng. Chem. Fundam.*, **6**, 2 (1967).

(14) F. L. Harris, G. B. Humphreys, and K. S. Spiegler, in "Membrane Separation Processes," P. Meares, Ed., Elsevier, Amsterdam, The Netherlands, 1976, p. 126.

(15) L. Z. Benet, *J. Pharmacokinet. Biopharm.*, **7**, 1 (1979).

(16) U. Gundert-Remy, D. Van kenne, E. Weber, H. E. Geissler, B. Grebian, and E. Mutschler, *Eur. J. Clin. Pharmacol.*, **16**, 39 (1979).

(17) G. H. Mudge, in "The Pharmacological Basis of Therapeutics," 6th ed., A. G. Gilman, L. S. Goodman, and A. Gilman, Eds., Macmillan, New York, N.Y., 1980, p. 908.

(18) S. Erlinger, D. Dhumeaux, P. Bertholof, and M. Dumont, *Am. J. Physiol.*, **219**, 416 (1970).

(19) M. J. Dunn, in "Modern Diuretic Therapy in the Treatment of Cardiovascular and Renal Disease," A. F. Lant and G. M. Wilson, Eds., Excerpta Medica, Amsterdam, The Netherlands, 1973, p. 196.

ACKNOWLEDGMENTS

The authors thank the Council of Scientific and Industrial Research, New Delhi, for supporting the investigation. Gifts of furosemide and triamterene from Hoechst Pharmaceuticals and S, K & F Ltd., respectively, are gratefully acknowledged. The authors also thank Prof. S. S. Mathur for his active interest in this research.

Difference Spectrophotometric Assay of 1,2-Diphenolic Drugs in Pharmaceutical Formulations II: Germanium Dioxide Reagent

ALEXANDER G. DAVIDSON

Received August 8, 1983, from the *Department of Pharmacy, University of Strathclyde, Glasgow G1 1XW, United Kingdom.* Accepted for publication November 28, 1983.

Abstract □ A rapid, difference UV spectrophotometric assay of formulated drugs containing a 1,2-diphenolic group is described. In this assay are utilized the bathochromic shift of the absorption band of 1,2-diphenolic substances from ~280 to ~287 nm and the concomitant hyperchromic effect induced by the addition of germanium dioxide to an aqueous solution of the drug buffered at pH 6. The absorbance of the solution of the complexed drug relative to that of an equimolar solution of the free drug, which is maximum at ~292 nm, is proportional to the concentration of the drug and is unaffected by the presence of other UV-absorbing substances in the formulations that lack the 1,2-diphenolic moiety. Applications of the assay are described for formulations containing epinephrine, isoetharine, isoproterenol, levodopa, and methyldopa.

Keyphrases □ 1,2-Diphenolic drugs—difference UV assay in formulations □ Difference absorption spectrophotometry—assay of 1,2-diphenolic substances

To avoid the interference that may occur in conventional UV-spectrophotometric procedures for the determination of 1,2-diphenolic drugs [*e.g.*, epinephrine (adrenaline), levodopa, and methyldopa] in formulations due to the presence of coformulated drugs, oxidation products, and formulation excipients, many of the absorption spectrophotometric methods currently employed involve the conversion of the drugs to colored derivatives and the measurement of absorbance in the visible region (1–5). In a previous report (6), a new difference UV-spectrophotometric procedure for drugs containing a 1,2-diphenolic moiety was described, based on the measurement of the difference absorbance (ΔA) at ~292 nm between two equimolar solutions of the drug in pH 7 phosphate buffer, one of which also contains 0.1 M boric acid. The boric acid esters of the drugs form very rapidly and have a longer wavelength of maximum absorption (λ_{max}) and a greater absorptivity than the nonesterified drug. The absorbance of the solution containing boric acid relative to that of the nonesterified drug is proportional to the concentration of the drug and is unaffected by the presence of other UV-absorbing substances in the sample, including monophenols, provided that the absorbance of these substances at the wavelength of measurement is unchanged by the boric acid.

Dihydroxylic and polyhydroxylic substances are known to react with other inorganic acids in addition to boric acid, *e.g.*, arsenious acid (7), orthotelluric acid (8), and germanium dioxide[1] (9, 10). The reaction of germanium dioxide with certain dihydroxylic and polyhydroxylic reagents has been used in both the identification (11) and quantitative determination (12) of trace levels of germanium. In this report, the reagent germanium dioxide is examined for application in the difference spectrophotometric assay of 1,2-diphenolic drugs.

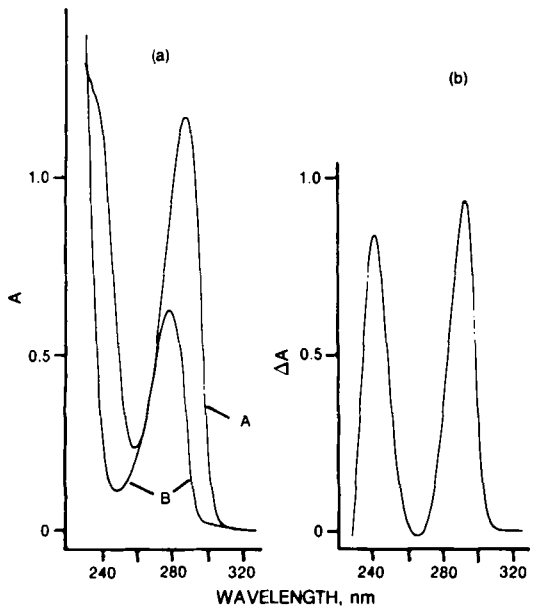

Figure 1—*(a) UV absorption spectra of aqueous solutions of epinephrine bitartrate (2×10^{-4} M) at pH 6 in the presence (A) and absence (B) of germanium dioxide (0.4 mg·mL^{-1}). (b) Difference UV absorption spectrum of epinephrine bitartrate (2×10^{-4} M) (solution A relative to solution B).*

EXPERIMENTAL SECTION

Apparatus—Absorption and difference absorption spectra of solutions in 1-cm silica quartz cells were recorded from 330 to 220 nm with a recording double-beam UV-visible spectrophotometer[2]. The spectral slit width was 1 nm, the scan speed was 1 nm s^{-1}, and the response (time constant) was 0.5 s.

Reagents—Epinephrine bitartrate[3], isoproterenol sulfate[4], isoetharine hydrochloride[5], levodopa[6], and methyldopa[6] were obtained commercially. Stock buffer (pH 6) was prepared by dissolving 9.67 g of citric acid and 22.40 g of anhydrous sodium monohydrogen phosphate in water and diluting to 500.0 mL. The working buffer (pH 6) was prepared by diluting 100.0 mL of stock buffer to 500.0 mL with water. The germanium dioxide reagent was prepared by dissolving, with heat, 500 mg of germanium dioxide[3] in 100.0 mL of stock buffer (pH 6); the solution was allowed to cool and diluted to 500.0 mL with water.

Standard Solutions—Approximately 50 mg of the reference substance was accurately weighed into a 250.0-mL calibrated flask, dissolved in 50 mL of water and 2.5 mL of 0.1 M HCl[7], and diluted to volume with water. A 5.0-mL aliquot was transferred to each of two 25.0-mL calibrated flasks containing 10 mL of pH 6 buffer and 10 mL of germanium dioxide reagent, respectively, and diluted to volume with water. Five minutes later, the absorbance (at the wavelength of maximum difference absorbance, ~292 nm) of the solution containing germanium dioxide in the sample cell was measured relative to that of the free drug in the reference cell. The measured difference in absorbance was corrected only for the blank buffer solutions, which were prepared by diluting the pH 6 buffer and the germanium dioxide reagent (2:3) with water, as described above for the standard solutions.

Sample Solutions—*Aqueous Formulations*—The samples were diluted with water to give a 0.2-mg·mL^{-1} drug concentration based on the declared

[1] Formerly known as germanic acid.
[2] 552 spectrophotometer; Perkin-Elmer Corp.
[3] BDH Chemicals Ltd., Poole, Dorset BH12 4NN, United Kingdom.
[4] Halewood Chemicals Ltd., Staines, Middlesex TW19 6BJ, United Kingdom.
[5] Riker Laboratories, Loughborough, Leicestershire LE11 1EP, United Kingdom.
[6] Merck Sharp & Dohme Research Laboratories, Hoddesdon, Herts. EN11 9BU, United Kingdom.
[7] To prevent oxidation of the drug.

0022-3549/84/1100-1582$01.00/0
© 1984, American Pharmaceutical Association

Table I—Substances Displaying Difference Absorbance at 292 nm

Substance	Phenol Classification	λ_{max} of $\Delta A(GeO_2)$, nm	$\Delta\epsilon_{292}$ (GeO_2)	$\Delta\epsilon_{292}$ (GeO_2)/ϵ_{280} of Free Drug	$\Delta\epsilon_{292}$ (H_3BO_3)/ϵ_{280} of Free Drug
Epinephrine	1,2-Diphenol	291.5	4366	1.64	0.94
Isoetharine	1,2-Diphenol	292.0	4523	1.48	0.89
Isoproterenol	1,2-Diphenol	292.0	4442	1.49	0.88
Levodopa	1,2-Diphenol	292.5	4358	1.56	0.91
Methyldopa	1,2-Diphenol	292.5	4306	1.40	0.85
Carbidopa	1,2-Diphenol	292.5	4216	1.58	0.70
Norepinephrine	1,2-Diphenol	291.5	4211	1.62	0.91
Dopamine	1,2-Diphenol	292.5	4077	1.43	0.82
1,2-Benzenediol	1,2-Diphenol	287.0	2629	—	—
3-Methyl-1,2-benzenediol	1,2-Diphenol	285.0	1631	—	—
Pyrogallol	1,2,3-Triphenol	280.0	93	—	—
n-Propyl Gallate	1,2,3-Triphenol	306.0	6115	—	—
Benserazide	1,2,3-Triphenol	283.0	250	—	—

concentration of the drug in the formulation, and the assay was continued as described above.

Tablets—Twenty tablets were weighed and powdered. Powder containing ~20 mg of drug was shaken mechanically with 80 mL of water and 1 mL of 0.1 M HCl[7] for 30 min and then diluted with water to 100.0 mL in a calibrated flask. The extract was clarified through filter paper[8]. The first 10 mL was discarded, and the assay was continued as described above.

Treatment of the Results—The concentration of drug in the sample solutions, and hence in the sample, was calculated from the proportional relationship that exists between the measured difference absorbance and the concentration of the drug.

RESULTS AND DISCUSSION

Potentiometric investigations have shown that strong chelates are formed between germanium and dihydroxylic and polyhydroxylic compounds with at least two hydroxyl groups in the vicinal position. Germanium-ligand chelates, 1:1 or 1:2, are formed with glycols and polyhydroxylic sugars (13), whereas 1,2-diphenols form chelates with 1:3 ratios (14).

Complexation of 1,2-diphenols with germanium dioxide, like that with boric acid (6), induces a bathochromic shift of their UV-absorption bands (15). The effect is illustrated in Fig. 1a for aqueous solutions of epinephrine at pH 6, where a shift in the λ_{max} from 279 nm to 287 nm and a large increase in absorbance in the presence of germanium dioxide is shown. The maximum ΔA of the solution of epinephrine in the presence of germanium dioxide relative to an equimolar solution of free drug occurs at 291.5 nm, which is almost identical to that of the epinephrine–boric acid product (6). The magnitude of the $\Delta A_{291.5}$ generated by the germanium dioxide reagent was, however, ~75% greater than that given by boric acid (Table I). Other 1,2-diphenolic substances give similar values for the wavelength of maximum ΔA (292 ± 0.5 nm) [except for 1,2-benzenediol (287 nm) and 3-methyl-1,2-benzediol (285 nm)] with a corresponding increase in ΔA values compared with those given by boric acid (Table I).

The pH and the concentration of germanium dioxide were chosen to provide conditions of high sensitivity, reproducible ΔA, and a proportional relationship between the measured ΔA and concentration of drug. The effects of variation of pH and concentration of germanium dioxide on the absorbance at 291.5 nm of equimolar solutions of epinephrine (1.4×10^{-4} M) are shown in Fig. 2. The highest $A_{291.5}$ was obtained with the higher pH values and concentrations of germanium dioxide. Parallel investigations of the assay conditions, however, showed that, although there was a linear relationship significant at the 99% confidence level between the measured $\Delta A_{291.5}$ and the concentration of epinephrine, a small but not insignificant negative intercept was consistently obtained when the solutions were buffered at pH 7. This was not observed with solutions at pH 6. Therefore, pH 6 and a final germanium dioxide concentration of 0.4 mg·mL^{-1} (3.8×10^{-3} M) were chosen for the assay as a compromise which satisfied the requirements of high sensitivity and the proportionality of the measured value with concentration of analyte. The smaller concentration of germanium dioxide necessary for maximum complex formation compared with that of boric acid (0.1 M) is consistent with the observation that the stability constants of 1,2-diphenol–germanium complexes are considerably higher than those of the boric acid esters (15).

Although the 1,2-diphenol–germanium complexes appear to form rapidly, as observed by an almost instantaneous increase in the ΔA_{292} on mixing of the reagents, there is a gradual decrease of ~2% in the A_{292} of the complex during the first 5 min, after which the A_{292} and ΔA_{292} are stable for at least an additional 30 min. Measurement of the ΔA was, therefore, carried out 5 min after the preparation of the solutions.

Validation—All five drugs for which assays of formulations have been developed (Table II) were found to show a proportional relationship between the ΔA at its λ_{max} at ~292 nm and the concentration of the drug in the range of 0–60 μg·mL^{-1} when the solutions were buffered at pH 6. For example, the linear regression equation for epinephrine bitartrate was $y = 0.01307x - 0.0011$, where y is $\Delta A_{291.5}$ and x is the concentration of the drug in micrograms per milliliter ($n = 6$; correlation coefficient = 0.99998). The other four drugs also gave satisfactory linear graphs with intercepts which, being <0.5% of the measured ΔA at the analytical concentration of 40 μg·mL^{-1}, were negligible. For comparison, the linear regression equation for a similar series of solutions of epinephrine bitartrate buffered at pH 7 was $y = 0.01388x - 0.0224$, confirming the slightly greater sensitivity and unsatisfactory proportionality of the measured value and concentration at this pH.

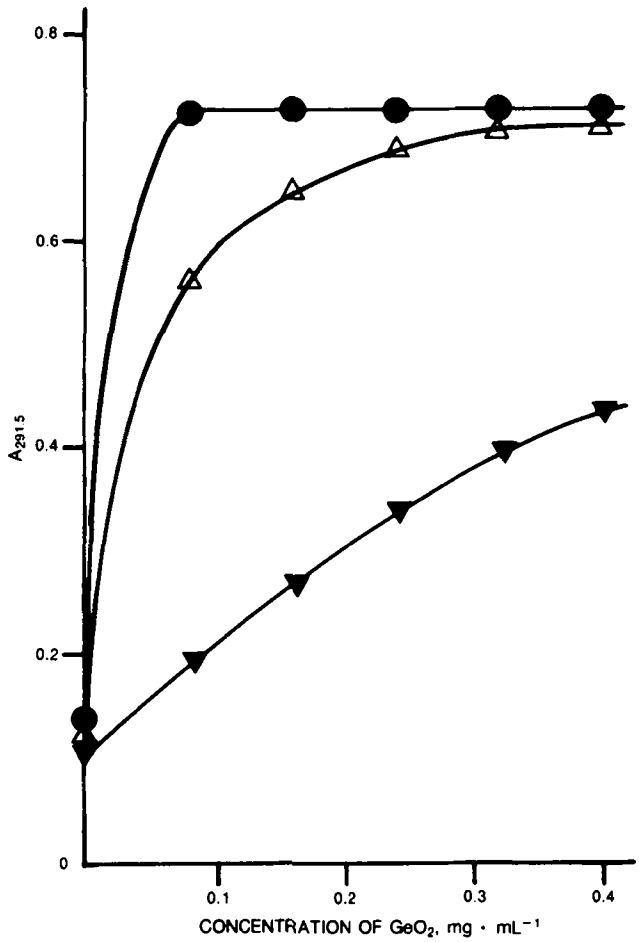

Figure 2—*Effects of variation of pH and concentration of germanium dioxide (GeO_2) on absorbance at 291.5 nm of epinephrine bitartrate (1.4×10^{-4} M). Key: (●) pH 7; (△) pH 6; (▼) pH 5.*

[8] Whatman No. 1.

Table II—Assay Results

Drug	Formulation	Label Claim Amount	Source[a]	Other UV-Absorbing Components[b]	Amount Found, % of Label Claim	
					ΔA Method	Official Method
Epinephrine bitartrate	Injection BP	1.8 mg mL^{-1}	E	—	99.5	98.1[c]
			C[d]	—	99.9	98.6[c]
	Solution BP	1.8 mg mL^{-1}	E	Chlorocresol, 1 mg mL^{-1}	101.2	100.0[c]
			C[e]	Chlorocresol, 1 mg mL^{-1}	97.4	97.1[c]
	Eye-drops with zinc sulfate BP	0.9 mg mL^{-1}	E	—	99.5	99.0
			C[f]	—	99.0	99.0
	Spray, Co. with atropine BPC	8.0 mg mL^{-1}	E	Papaverine HCl, 8 mg mL^{-1}	100.8	99.0
			C[g]	Papaverine HCl, 8 mg mL^{-1}	100.8	98.7
Isoetharine hydrochloride	Tablet	10 mg	C[h]	—	98.1	—
Isoproterenol sulfate	Tablet BP	10 mg	C[i]	—	100.9	100.5
	Spray BPC (1968)	10 mg mL^{-1}	E	—	100.8	99.5
			C[j]	—	100.0	99.6
Levodopa	Tablet BP	500 mg	C[k]	—	98.0	99.0
Methyldopa	Tablet BP	125 mg	C[l]	—	101.7	102.7
	Tablet BP	250 mg	C[m]	—	101.0	101.8
	Tablet	250 mg	C[n]	Hydrochlorothiazide, 15 mg	98.7	—

[a] E, prepared sample; C, commercial sample. [b] Compounds absorbing at λ_{max} of free drug at ~280 nm. [c] Gravimetric stage only; for discussion refer to Ref. 6. [d] Lot 2EP082, Evans. [e] Lot 7H046, Evans. [f] Lot R8208, Macarthys. [g] Lot 4B028, Evans. [h] Lot 2B01G, Riker. [i] Lot 032124C, Charnwood Pharmaceuticals. [j] Lot 98174, Thornton and Ross. [k] Lot 8056, Brocades. [l] Lot 6770B022, Norton. [m] Lot 2432, Cox. [n] Lot 22034, Merck Sharp and Dohme.

In precision studies in which a sample of adrenaline injection BP was assayed 10 times by the described procedure, the mean concentration was found to be 100.7% of the declared amount, and the *RSD* of $\Delta A_{291.5}$ of the sample solutions was 0.27%, indicating that the reproducibility of the measured value was excellent.

To investigate the specificity of the procedure for 1,2-diphenolic substances, a number of monophenols, diphenols, and triphenols were examined for difference absorbance at 292 nm under the conditions of the assay. The results in Table I indicate the $\Delta\epsilon_{292}$ for those substances that contain a 1,2-diphenolic group. Also shown are the ratios of difference absorptivity at 292 nm, using germanium dioxide and boric acid reagents, to the absorptivity of the free drug at its λ_{max} (~280 nm). The results demonstrate that the ΔA generated by germanium dioxide is 40–64% greater than the absorbance of the free drug and that the ΔA procedure using germanium dioxide is more sensitive than both a conventional UV-spectrophotometric assay and the ΔA procedure using boric acid.

Substances containing a 1,2,3-triphenolic group show difference absorbance, also observed for the boric acid reagent (6), although the λ_{max} of the complexes and their $\Delta\epsilon_{292}$ are much less consistent than those given by the 1,2-diphenols.

Monophenols (*o*-, *m*-, and *p*-cresols; *o*-, *m*-, and *p*-aminophenols; 4-methyl-2-nitrophenol; 2-methoxyphenol; 4-chloro-*m*-cresol; *p*-hydroxybenzoic acid; orciprenaline; acetaminophen; 2,7-dihydroxynaphthalene; salicylaldehyde), diphenols (resorcinol and hydroquinone), and a triphenol (phloroglucinol) lacking the 1,2-diphenolic group do not display difference absorbance and do not interfere in the ΔA procedure for 1,2-diphenolic substances. Salicylic acid and salicylamide, which were found to give weak ΔA_{292} values with boric acid (6), gave zero ΔA_{292} values with the germanium dioxide reagent. Papaverine, hydrochlorothiazide, and atropine, which are coformulated drugs in certain formulations of 1,2-diphenolic drugs (Table II), also give zero ΔA_{292} values and do not interfere in the assay. The coincidence of the isosbestic points at ~270 and 263 nm in the difference spectra of the sample solutions and appropriate reference solutions (*i.e.*, wavelengths of zero difference absorbance due to the equal absorptivity of the complexed and free forms of the drug) provide additional evidence of the selectivity of the procedure (6).

Assay Results—The accuracy of the ΔA procedures for formulations was investigated by comparing the results obtained in this study with those given by the official procedures of the British Pharmacopoeia (16, 17) and British Pharmaceutical Codex (18, 19) for preparations containing a 1,2-diphenolic drug, that were either commercial samples purchased locally or samples prepared in the laboratory by compendial formulations.

The results in Table II indicate that good agreement was achieved between the assay values of the ΔA procedure and the official procedures for both the prepared samples and the commercial samples, including those containing UV-absorbing substances that interfere in a conventional UV assay. The excellent recoveries of added drugs in the prepared samples confirm the accuracy of the ΔA method and indicate its application as a rapid and selective procedure for the assay of 1,2-diphenolic drugs in formulations.

REFERENCES

(1) R. Gomez, R. B. Hagel, and E. A. MacMullan, in "Analytical Profiles of Drug Substances," Vol. 5, K. Florey, Ed., Academic, New York, N.Y., 1976, pp. 189–223.

(2) D. H. Szulczewski and W. Hong, in "Analytical Profiles of Drug Substances," Vol. 7, K. Florey, Ed., Academic, New York, N.Y., 1978, pp. 193–229.

(3) N. A. El-Rabbat and N. M. Omar, *J. Pharm. Sci.*, **67**, 779 (1978).

(4) R. B. Salama and H. A. El-Obeid, *Analyst*, **101**, 136 (1976).

(5) T. A. LaRue and E. R. Blakley, *Anal. Chim. Acta*, **31**, 400 (1964).

(6) A. G. Davidson, *J. Pharm. Biomed. Anal.*, **2**, 45 (1984).

(7) P. J. Antikainen and K. Tevanen, *J. Inorg. Nucl. Chem.*, **32**, 1915 (1970).

(8) P. J. Antikainen, *Suomen Kemistilehti*, **B39**, 45 (1957).

(9) A. Tchakirian, *C. R. Acad. Sci.*, **185**, 229 (1928).

(10) P. Bevillard, *C. R. Acad. Sci.*, **235**, 880 (1952).

(11) F. Feigl, "Spot Tests in Inorganic Analysis" 5th ed., Elsevier Publishing Co., Amsterdam, 1958, p. 112.

(12) I. A. Prostak and L. I. Ganago, *Izv. Vyssh. Ucheb. Zaved., Khim. Khim. Technol.*, **17**, 559 (1974); *Chem. Abstr.*, **81**, 44900v (1974).

(13) P. J. Antikainen, *Acta Chem. Scand.*, **13**, 312 (1959).

(14) P. J. Antikainen and H. Oksanen, *Acta Chem. Scand.*, **22**, 2867 (1968).

(15) U. Weser, *Hoppe-Seyler's Z. Physol. Chem.*, **349**, 982 (1968); *Chem. Abstr.*, **69**, 74143v (1968).

(16) "British Pharmacopoeia 1980," Her Majesty's Stationery Office, London, 1980, pp. 570, 580, 711, 720, 781, and 787.

(17) "British Pharmacopoeia 1973," Her Majesty's Stationery Office, London, 1973, p. 257.

(18) "British Pharmaceutical Codex," Pharmaceutical Press, London, 1973, p. 794.

(19) "British Pharmaceutical Codex," Pharmaceutical Press, London, 1968, p. 1260.

ACKNOWLEDGMENTS

The technical assistance of Mrs. Pauline Constable is gratefully acknowledged.

Synthesis and Dopaminergic Activity of 3-(3,4-Dihydroxyphenyl)-1-*n*-propylpyrrolidine Hydrobromide

A. MICHAEL CRIDER *§ˣ, TALAL F. HEMDI *, MOHAMED N. HASSAN ‡, and STANLEY FAHN ‡

Received June 20, 1983, from the *College of Pharmacy, University of Toledo, Toledo, OH 43606 and the ‡Department of Neurology, Columbia University College of Physicians and Surgeons, New York, NY 10032. Accepted for publication December 12, 1983. Present address: §School of Pharmacy, Northeast Louisiana University, Monroe, LA 71209

Abstract □ 3-(3,4-Dihydroxyphenyl)-1-*n*-propylpyrrolidine hydrobromide was synthesized by a six-step reaction sequence and was evaluated, and compared with apomorphine, for central dopaminergic agonist activity. The compound produced behavioral and biochemical changes characteristic of central dopaminergic stimulation. Administration of 3-(3,4-dihydroxyphenyl)-1-*n*-propylpyrrolidine hydrobromide to rats resulted in the reversal of the reserpine syndrome, stereotypic behavior, contralateral turning following 6-hydroxydopamine lesion of the substantia nigra, a decrease in dopamine turnover, and inhibition of prolactin release. These results indicate that 3-(3,4-dihydroxyphenyl)-1-*n*-propylpyrrolidine hydrobromide is a dopaminergic agonist. However, the compound exhibited a lower potency but a slightly longer duration of action than apomorphine.

Keyphrases □ 3-(3,4-Dihydroxyphenyl)-1-*n*-propylpyrrolidine hydrobromide—synthesis, central dopaminergic activity, compared with apomorphine □ Dopaminergic activity—central, apomorphine, 3-(3,4-dihydroxyphenyl)-1-*n*-propylpyrrolidine hydrobromide

In an attempt (1) to prepare compounds with dopaminergic activity, our efforts were directed toward the synthesis of a compound in which the ethylamine chain of dopamine (I) is embodied in a pyrrolidine ring. Specifically, the purpose of this investigation was to synthesize and evaluate the dopaminergic activity of 3-(3,4-dihydroxyphenyl)-1-*n*-propylpyrrolidine (XI). The substitution of an *n*-propyl group on nitrogen has been shown to optimize activity in a variety of dopamine agonists (2, 3). Thus, the *n*-propyl substitution on the pyrrolidine ring nitrogen should maximize dopaminergic activity.

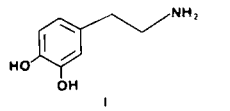

I

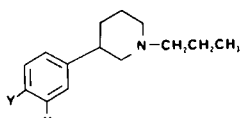

II : X = OH, Y = H
III : X = OH, Y = OH

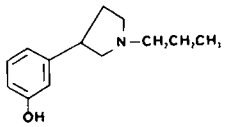

IV

During the course of this investigation, a preliminary report indicated that II was a selectively acting dopamine autoreceptor agonist (4). Further testing of II has shown that this compound is a centrally acting dopamine autoreceptor agonist (5, 6). Structure-activity studies revealed that the pyrrolidine analogue IV of 3-(3-hydroxyphenyl)-1-*n*-propylpiperidine (II) was very weak as a dopamine autoreceptor agonist (7). These workers did not report the synthesis and biological activity of the target compound of their investigation. However, the (3,4-dihydroxyphenyl)piperidine III was prepared and pharmacologically evaluated. Compound III, unlike II, exhibited potent postsynaptic dopaminergic agonism.

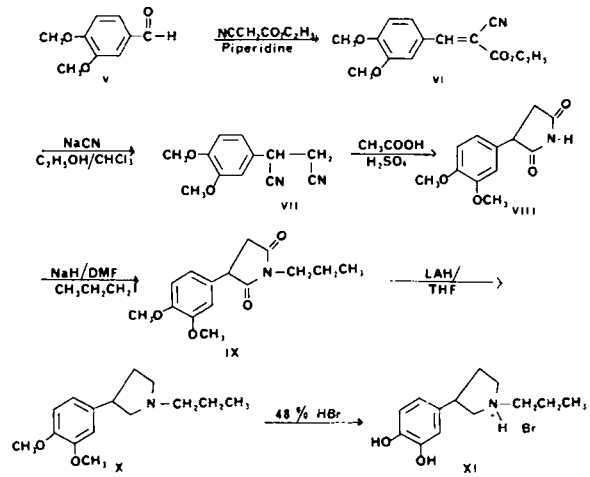

Scheme I

EXPERIMENTAL SECTION[1]

Ethyl α-Cyano-β-(3,4-dimethoxyphenyl)acrylate (VI)—A mixture of 3,4-dimethoxybenzaldehyde (V) (20.0 g, 0.120 mol), ethyl cyanoacetate (12.8 g, 0.120 mol), and piperidine (1.5 mL) in toluene (200 mL) was heated to 110 °C. Water was removed during heating *via* a Dean-Stark trap. The mixture was cooled, and the solvent was removed under reduced pressure to yield 28.4 g (90%) of a light-yellow solid. An analytical sample was prepared by recrystallization from ethanol-chloroform to give VI, mp 156–158 °C [lit. (8) mp 155 °C]; IR (KBr): 2275 (C≡N), 1740 (C=O, ester), and 1610 cm^{-1} (C=C); ^{1}H-NMR ($CDCl_3$): δ 1.40 (t, 3, J = 8 Hz, CH_3), 3.97 (s, 6, OCH_3), 4.33 (q, 2, J = 8 Hz, CH_2), 6.83–7.80 (m, 3, ArH), and 8.17 ppm (s, 1, CH=C).

Anal.—Calc. for $C_{14}H_{15}NO_4$: C, 64.35; H, 5.80; N, 5.36. Found: C, 64.16; H, 5.95; N, 5.24.

(3,4-Dimethoxyphenyl)succinonitrile (VII)—Ethyl α-cyano-β-(3,4-dimethoxyphenyl)acrylate (35.0 g, 0.134 mol) was dissolved in a mixture of chloroform (400 mL) and ethanol (300 mL) and treated dropwise with a solution of sodium cyanide (6.90 g, 0.141 mol) in water (100 mL). The mixture was refluxed for 15 h, cooled, and acidified with concentrated hydrochloric acid. Evaporation of the solvents under reduced pressure gave a light-pink solid that was partitioned between water (300 mL) and chloroform (200 mL). The aqueous phase was extracted with chloroform (2 × 200 mL), and the combined chloroform extracts were dried (sodium sulfate), filtered, and evaporated to afford a light-pink solid. Recrystallization from ethanol afforded 24.4 g (84%) of VII, mp 108–110°C; IR (KBr): 2300 (C≡N), 1620 (ArH), and 1280 cm^{-1} (C—O, ether); ^{1}H-NMR (Me_2SO-d_6): δ 3.33 (d, 2, J = 7 Hz, CH_2CN), 3.80 (s, 6, OCH_3), 4.67 (t, 1, J = 6 Hz, CHCN), and 7.03 ppm (m, 3, ArH).

Anal.—Calc. for $C_{12}H_{12}N_2O_2$: C, 66.64; H, 5.60; N, 12.96. Found: C, 66.24; H, 5.67; N, 12.78.

2-(3,4-Dimethoxyphenyl)succinimide (VIII)—Compound VIII was prepared according to the procedure of Crooks (9) for the preparation of spirosuccini-

[1] Melting points were determined on a Fisher-Johns melting point apparatus and are uncorrected. IR spectra were recorded as potassium bromide pellets with a Perkin-Elmer 137 Spectrophotometer. NMR spectra were recorded on a Varian EM360A spectrometer. Chemical shifts are reported in parts per million (δ) relative to tetramethylsilane (1%) or, in the case of D_2O (1%), sodium 2,2-dimethyl-2-silapentane-5-sulfonate. Analytical data were obtained from Micro-Analysis Inc., Wilmington, DE. Male Sprague-Dawley rats weighing 175–225 g were given free access to food and water and exposed to a 14:10 h light-dark cycle. Drugs were administered by intraperitoneal injections. Drugs and analytical-grade chemicals were purchased from commercial sources. Spiperone was a gift from Janssen Pharmaceutical Company, Inc. (New Brunswick, NJ). The vehicle for XI and apomorphine was 0.01 M sodium bisulfite solution.

0022-3549/84/1100-1585$01.00/0
© 1984, American Pharmaceutical Association

Table I—Behavioral Changes Effected by Apomorphine and XI [a,b]

Treatment	Catalepsy	Stereotypy	Locomotor Activity	Number of Rotations
Control	3	0	250 ± 35	0
Apomorphine	0	3	1825 ± 225	650 ± 125
XI	0	3	1798 ± 206	635 ± 140

[a] Catalepsy, stereotypy, and locomotor activity were assessed in rats ($n = 6$) pretreated with reserpine (5 mg/kg). Catalepsy and stereotypy were scored (see text) before the administration, and at the time of peak effect, of the dopamine agonists. Rotating rats ($n = 9$) were treated with dopamine agonists or vehicle. Results are expressed as mean ± *SEM*. All changes were statistically significant ($p < 0.05$). [b] Apomorphine and compound XI were administered at dosages of 2 and 100 mg/kg ip, respectively.

Table II—Biochemical Effects of Apomorphine and XI [a,b]

Treatment	Dopamine	Dihydroxyphenylacetic Acid	Homovanillic Acid	Prolactin
Control	7.2 ± 0.4	0.75 ± 0.3	0.44 ± 0.4	20.0 ± 4.0
Apomorphine	9.0 ± 0.5	0.50 ± 0.3	0.28 ± 0.4	2.0 ± 1.0
XI	10.1 ± 0.4	0.46 ± 0.5	0.24 ± 0.3	4.5 ± 2.5

[a] Dopamine, dihydroxyphenylacetic acid, and homovanillic acid are expressed as nanogram per milligram of striatal tissue, and prolactin as nanogram per milliliter of serum. The results represent the mean ± *SEM* of $n = 5$. All changes were statistically significant ($p < 0.05$). [b] Apomorphine and XI were administered at doses of 2 and 100 mg/kg ip, respectively.

mides. A mixture of (3,4-dimethoxyphenyl)succinonitrile (25.6 g, 0.118 mol), glacial acetic acid (150 mL), and 78% sulfuric acid (25 mL) was refluxed for 1 h, cooled, and evaporated under reduced pressure. The resulting mass was triturated with water (300 mL), and the solid material was removed by filtration. Recrystallization from ethanol gave 12.9 g (46%) of white crystals, mp 181–183°C; IR (KBr): 1785 (C=O, imide), 1725 (C=O, imide), and 1280 cm^{-1} (C—O, ether); ^{1}H-NMR (Me_2SO-d_6): δ 2.90 (m, 2, ring CH_2), 3.70 (s, 6, OCH_3), 4.03 (m, 1, ring CH), and 6.87 ppm (m, 3, ArH).

Anal.—Calc. for $C_{12}H_{13}NO_4$: C, 61.26; H, 5.58; N, 5.96. Found: C, 61.15; H, 5.60; N, 5.97.

2-(3,4-Dimethoxyphenyl)-*N*-(*n*-propyl)succinimide (IX)—A 50% mineral oil dispersion of sodium hydride (5.28 g, 0.11 mol) was washed with hexane (3 × 30 mL) and suspended in dimethylformamide (100 mL). A solution of 2-(3,4-dimethoxyphenyl)succinimide (25.8 g, 0.11 mol) in dimethylformamide (100 mL) was added to the sodium hydride suspension in a dropwise manner while maintaining a nitrogen atmosphere. After the addition had been completed, the mixture was heated at 80°C for 2 h and cooled to room temperature. A solution of *n*-propyl iodide (18.7 g, 0.11 mol) in dimethylformamide (30 mL) was added dropwise and the mixture was heated at 80°C for 15 h. The mixture was cooled, treated with a few drops of absolute ethanol, filtered, and the solvent was evaporated to give a light-tan solid. Recrystallization from isopropyl alcohol yielded 18.7 g (61%) of a white solid, mp 76–77°C; IR (KBr): 1785 (C=O, imide) and 1725 cm^{-1} (C=O, imide); ^{1}H-NMR ($CDCl_3$): δ 0.90 (t, 3, $J = 6$ Hz, CH_3), 1.33–4.07 (m, 13, including singlet 3.90, OCH_3), and 6.80 ppm (m, 3, ArH).

Anal.—Calc. for $C_{15}H_{19}NO_4$: C, 64.95; H, 6.92; N, 5.05. Found: C, 64.79; H, 7.01; N, 4.93.

3-(3,4-Dimethoxyphenyl)-1-*n*-propylpyrrolidine (X)—A solution of IX (18.0 g, 0.065 mol) in anhydrous tetrahydrofuran (100 mL) was added to a suspension of lithium aluminum hydride (14.8 g, 0.389 mol) in tetrahydrofuran (100 mL). The mixture was refluxed for 19 h, cooled, and the excess lithium aluminum hydride was decomposed by the dropwise addition of water. The resulting sludge was filtered and the inorganic residue was washed with tetrahydrofuran (2 × 50 mL). The combined solvents were evaporated, and the residue was partitioned between chloroform (300 mL) and water (100 mL). The chloroform phase was dried (sodium sulfate), filtered, and the solvent was evaporated to afford a dark-brown oil. Vacuum distillation gave 12.0 g (74%) of a colorless oil, bp 136–138°C (0.7 mm). The hydrochloride of X was prepared and recrystallized from ethanol–ether to yield a white solid, mp 131–133°C; ^{1}H-NMR (D_2O): δ 1.13 (t, 3, $J = 6$ Hz, CH_3), 1.57–3.97 (m, 17, including singlets at 3.93 and 3.97, OCH_3), and 7.03 ppm (m, 3, ArH).

Anal.—Calc. for $C_{15}H_{24}ClNO_2$: C, 63.02; H, 8.48; N, 4.90. Found: C, 63.34; H, 8.35; N, 4.82.

3-(3,4-Dihydroxyphenyl)-1-*n*-propylpyrrolidine Hydrobromide (XI)—A solution of X (3.0 g, 0.012 mol) in 48% aqueous hydrobromic acid (30 mL) was refluxed for 3 h under a nitrogen atmosphere. The solvent was evaporated under reduced pressure, and water was removed from the resulting oil by azeotropic distillation with absolute ethanol several times. Trituration of the oil with ether gave a light-yellow solid. Recrystallization from absolute ethanol ether afforded 2.2 g (60%) of a tan solid, mp 152–154°C; IR (KBr): 3450 cm^{-1} (OH, phenol); ^{1}H-NMR (D_2O): δ 1.03 (t, 3, $J = 6$ Hz, CH_3), 1.30–4.47 (m, 11, aliphatic CH_2, ring CH_2, and ring CH), and 6.90 ppm (m, 3, ArH).

Anal.—Calc. for $C_{13}H_{20}BrNO_2$: C, 51.66; H, 6.68; Br, 26.44; N, 4.46. Found: C, 51.53; H, 6.55; Br, 26.34; N, 4.60.

Locomotor Activity—Rats treated 12–18 h previously with reserpine (5 mg/kg) were given vehicle, apomorphine (0.12–2.0 mg/kg), or XI (10–100 mg/kg) and tested for increases in locomotor activity. Locomotor activity[2] was monitored by the minute in single rats by electronic activity meters[3] with an input to a multichannel recorder. Testing was done every 5–7 d to allow recovery from the drugs.

Catalepsy—This was assessed, using the method of Kolbe *et al.* (10), by the length of time a reserpinized rat maintained an abnormal posture with its front paws over a bar (2 cm diameter) 7 cm from bench level. Catalepsy was scored in control reserpinized rats, and in experimental animals, just prior to drug administration and at the peak of effect of apomorphine or XI as follows: 0–9 s = 0; 10 s–2.5 min = 1; 2.6–5.0 min = 2; 5.1–10 min = 3; 10.1–20 min = 4; >20 min = 5.

Stereotypy—This was scored by the method of Kolbe *et al.* (10) at the peak effect of apomorphine or XI as follows: animals indistinguishable from vehicle-treated controls = 0; discontinuous sniffing and continuous locomotor activity = 1; continuous sniffing and discontinuous locomotor activity = 2; continuous sniffing and discontinuous biting, licking, or gnawing = 3; continuous compulsive biting, licking, or gnawing with no locomotor activity = 4.

Rotational Behavior—The left substantia nigra was lesioned according to the method of Reches *et al.* (11). Coordinates were AP −3.7 mm, L +1.9 mm, and DV −7.3 mm. Two weeks after lesioning, apomorphine (0.12–2.0 mg/kg) or XI (10–100 mg/kg) was administered and the resulting total number of rotations recorded. Rats were allowed 4–5 d between test doses. There was no rotation either spontaneously or in response to vehicle administration.

Effects of Apomorphine and XI on Dopamine Turnover—Rats were treated with vehicle, a single maximal dose of apomorphine (2 mg/kg), or XI (100 mg/kg), and the time courses of changes in striatal dopamine were determined. Dose-dependent changes in striatal dopamine were also obtained with apomorphine (0.12–2.0 mg/kg) and XI (10–100 mg/kg). In this study, rats were sacrificed at the times of peak effect of the dopamine agonists as determined from the time-response studies.

In the above studies, the animals were sacrificed by decapitation and the brains rapidly removed. The corpora striata were dissected on an ice-cold glass plate and immediately frozen on dry ice. Dopamine, dihydroxyphenylacetic acid, and homovanillic acid were measured by HPLC with electrochemical detection as previously described (12).

Effects of Apomorphine and XI on Serum Prolactin—Time and dose-dependent changes in serum prolactin induced by the dopamine agonists were investigated simultaneously with dopamine turnover. Following decapitation, trunk blood was collected and allowed to clot, samples were centrifuged at 5000×*g* for 5 min, and serum was stored at −70°C until assayed. Serum prolactin levels were determined by the double-antibody radioimmunoassay method using the reagents supplied by the NIAMDD rat pituitary hormones program. Results are expressed as nanograms per milliliter.

[^{3}H]Spiperone Binding—Competitive inhibition of [^{3}H]spiperone binding by the dopamine agonists was performed by the method of Seeman *et al.* (13) using fresh striatal membrane preparations. Protein concentrations, as measured by Lowry assay (14), were 250–400 ng/mL. Binding assays were performed in triplicate twice.

RESULTS AND DISCUSSION

Neuroleptic-induced hypomotility and catalepsy in rodents are dependent on the inhibition of dopaminergic function (15). The neuroleptic-induced state is antagonized by levodopa (16), apomorphine, or bromocriptine (17). Reserpine induces experimental parkinsonism because it depletes presynaptic dopamine by inhibiting the ATP-Mg^{2+} facilitated transport mechanism at the membrane of the intracellular storage granules (18). Apomorphine or XI reverses the reserpine syndrome and produces stereotypic behavior in a manner similar to other known dopamine agonists. The behavioral effects of XI and apomorphine in rats are summarized in Table I.

Reserpine-induced catalepsy (mean score = 3) was antagonized by both apomorphine and XI in a dose-related manner. The minimum doses of apomorphine and XI which produced a score of zero were 1.0 and 25 mg/kg, re-

[2] All behavioral observations were made between 08:00 and 14:00 hr.
[3] Columbus Instruments, Columbus, Ohio.

spectively. Apomorphine and XI also produced complete clearing of the reserpine-induced ptosis and hunched posture.

Both apomorphine and XI induced dose-dependent stereotyped behavior. A peak score of three (continuous sniffing with discontinuous licking or gnawing) was seen with apomorphine and XI at doses of 2.0 and 100 mg/kg, respectively. Maximal stereotypy was seen at 15 min following the administration of apomorphine and at 30 min after XI had been administered.

6-Hydroxydopamine destroys the presynaptic nerve terminals of the nigro-striatal pathway, causing postsynaptic denervation supersensitivity on the side of the lesion. Contralateral rotation in this model is indicative of direct stimulation of dopaminergic receptors in the denervated caudate nucleus (19). Apomorphine and XI (Table I) were both effective in producing this type of turning behavior. The minimal effective dose with XI was 10 mg/kg while a dose of 40–50 mg/kg produced 50% of maximal rotation. The time of peak effect was 20 min with a duration of 75–90 min. With apomorphine, the minimal effective dose was 0.25 mg/kg and the dose that produced 50% of maximal rotation was 1.0 mg/kg. Apomorphine exhibited its peak effect at 20 min and caused rotation for a period of 50–60 min. Rotation was apparent by 2–3 min for both XI and apomorphine.

The results of the biochemical studies on 3-(3,4-dihydroxyphenyl)-1-*n*-propylpyrrolidine hydrobromide (XI) and apomorphine are summarized in Table II. Apomorphine (2.0 mg/kg) and XI (100 mg/kg) induced rapid increases in dopamine accumulation. Maximal effect of ~30–35% increases was obtained with both compounds at 15–20 min with a return to the control value at ~90 min. Both apomorphine and XI produced striatal dopamine accumulation in a dose-dependent manner with EC_{50} values of ~0.75 and 40 mg/kg, respectively. Apomorphine and XI also induced dose-related decreases in dihydroxyphenylacetic acid and homovanillic acid.

The administration of XI (100 mg/kg) or apomorphine (2 mg/kg) resulted in rapid decreases in serum prolactin levels. Maximal decreases were obtained 20–45 min after administration of the test compound. In the dose-response study, apomorphine and XI produced dose-dependent decreases in serum prolactin levels with IC_{50} values of 0.5 and 15 mg/kg, respectively.

Compound XI inhibited [^{3}H]spiperone binding to striatal membrane preparations with an IC_{50} of ~10 μM. The IC_{50} value for apomorphine was 200 nM. The time courses of the behavioral and biochemical effects of both apomorphine and XI are generally in close agreement. Compound XI exhibited a much lower affinity for the butyrophenone binding site in the competition binding studies with [^{3}H]spiperone than apomorphine or other known dopamine agonists. However, this low affinity correlates with the potency observed in behavioral and biochemical studies, as apomorphine and XI have similar molecular weights.

3-Phenylpiperidines may exist in a stable conformation in which the β-phenethylamine system assumes a *trans* (antiperiplanar) conformation (20). This conformation is preferred by most dopamine agonists (7). The lack of dopamine autoreceptor activity by the pyrrolidine analogue IV has been attributed to an inability to attain this conformation (7, 20). Thus, XI may not be optimally binding at its receptor sites.

In vivo, apomorphine or bromocriptine produce behavioral and biochemical changes characteristic of central dopaminergic stimulation; these include reversal of the reserpine syndrome, stereotypic behavior, contralateral rotation following unilateral 6-hydroxydopamine lesion of the substantia nigra, reduction in the rate of dopamine turnover, and inhibition of prolactin release. We have compared 3-(3,4-dihydroxyphenyl)-1-*n*-propylpyrrolidine hydrobromide (XI) with apomorphine for these behavioral and biochemical actions. The results reported here show that XI induced typical changes, and it may, therefore, be tentatively concluded that it acts as an effective dopaminergic agonist, with a much lower potency but a slightly longer duration of action, than apomorphine.

Further work is in progress to compare the dopaminergic activity of XI with other known dopamine agonists. Additionally, structure-activity studies are currently being performed with the 3-phenylpyrrolidine series.

REFERENCES

(1) A. M. Crider, R. Grubb, K. A. Bachmann, and A. K. Rawat, *J. Pharm. Sci.*, **70,** 1319 (1981).

(2) A. M. Crider, J. M. Robinson, H. G. Floss, J. M. Cassady, and J. A. Clemens, *J. Med. Chem.*, **20,** 1473 (1977).

(3) D. E. Nichols, in "Dopamine Receptors," C. Kaiser and J. W. Kebabian, Eds., American Chemical Society, Washington, 1983, p. 197.

(4) D. C. Remy and G. E. Martin, *Annu. Rep. Med. Chem.*, **15,** 12 (1980).

(5) S. Hjorth, A. Carlsson, H. Wikstrom, P. Lindberg, D. Sanchez, U. Hacksell, L.-E. Arvidsson, U. Svensson, and J. L. G. Nilsson, *Life Sci.*, **28,** 1225 (1981).

(6) G. M. Martin, D. R. Haubrich, and M. Williams, *Eur. J. Pharmacol.*, **76,** 15 (1981).

(7) U. Hacksell, L.-E. Arvidsson, U. Svensson, J. L. G. Nilsson, D. Sanchez, H. Wikstrom, H. Lindberg, S. Hjorth, and A. Carlsson, *J. Med. Chem.*, **24,** 1475 (1981).

(8) H. Kauffman, *Chem. Ber.*, **52B,** 1422 (1919); through *Chem. Abstr.*, **14,** 1327 (1920).

(9) P. A. Crooks and R. Szyndler, *J. Med. Chem.*, **23,** 679 (1980).

(10) H. Kolbe, A. Clow, P. Jenner, and C. D. Marsden, *Neurology*, **31,** 434 (1981).

(11) A. Reches, L. R. Mielke, and S. Fahn, *Neurology*, **32,** 887 (1982).

(12) A. Reches and S. Fahn, *Ann. Neurol.*, **12,** 267 (1982).

(13) P. Seeman, M. Cahu-Wong, J. Tedesco, and K. Wond, *Proc. Natl. Acad. Sci. U.S.A.*, **72,** 4372 (1975).

(14) O. H. Lowry, N. I. Rosebrough, A. I. Farr, and R. J. Randall, *J. Biol. Chem.*, **193,** 265 (1951).

(15) J. M. van Rossum, *Intl. J. Neurobiol.*, **12,** 207 (1970).

(16) A. Carlsson, M. Lindqvist, and T. Magnusson, *Nature*, **180,** 1200 (1957).

(17) A. M. Johnson, D. M. Loew, and J. M. Vigouret, *Br. J. Pharmacol.*, **56,** 59 (1976).

(18) A. Carlsson, N. A. Hillarp and B. Waldeck, *Acta Physiol. Scan.* **Suppl. 59 215,** 215 (1963).

(19) U. Ungerstedt, *Acta Physiol. Scan.* **Suppl. 82 367,** 69 (1971).

(20) J. G. Cannon, *Annu. Rev. Pharmacol. Toxicol.*, **23,** 103 (1983).

ACKNOWLEDGMENTS

This research was supported in part by a grant from the Parkinson's Disease Foundation, New York, N.Y. Mohamed N. Hassan is a recipient of a Fellowship from the Ontario Ministry of Health, Canada.

Physical Model Approach to Gastrointestinal Absorption of Prostaglandins II: *In Situ* Rat Intestinal Absorption of Dinoprost

J. Y. PARK *[¶], N. F. H. HO *[§x], and W. MOROZOWICH [‡]

Received March 29, 1976, from the *College of Pharmacy, University of Michigan, Ann Arbor, MI 48109 and the [‡]Upjohn Co., Kalamazoo, MI 49001. Accepted for publication November 11, 1976. Present addresses: [§]Upjohn Co., Kalamazoo, MI 49001 and [¶]Boehringer Ingelheim, Ridgefield, CT 06877.

Abstract □ *In situ* absorption studies with dinoprost in the rat jejunum were carried out using a modified Doluisio technique. The absorption rate was first order. There was a sigmoidal decrease in the rate with increasing buffer pH (from 3.5 to 9.5), which strongly indicated the partitioning of weak acid species into the lipoidal membrane. An asymptotic minimum rate was attained from buffer pH 7.5 to 9.5, operationally indicative of transport of anions across aqueous pores. The importance of the aqueous diffusion layer on the mucosal side of the membrane was evident; rates at pH 3.5 and 4.5 were faster at high agitation hydrodynamics in the lumen solution. Preliminary studies showed that there was no metabolism in the lumenal solution and that metabolism occurred within the membrane. The transport mechanism involved simultaneous passive diffusion and bioconversion in the membrane because (*a*) a 1.5 × 10^4-fold range in dinoprost concentration (0.014–210 μM) showed no saturable carrier-mediated tendency on the rate, (*b*) iodoacetic acid and indomethacin did not inhibit the absorption rate, and (*c*) the shape of the absorption-pH profiles was suggestive of passive diffusion. The prostaglandin did not have apparent adverse membrane and vascular effects under the conditions employed. The quantification and factorization of the physically meaningful transport parameters were accomplished using the physical model previously described. The permeability coefficients of the aqueous diffusion layer for the oscillation and static hydrodynamic situations were 0.8 × 10^{-4} and 1.7 × 10^{-4} cm/s, respectively. The effective transport-bioconversion permeability coefficients of the membrane were 2.57 × 10^{-4} cm/s at buffer pH 3.5 and 1.46 × 10^{-4} cm/s at pH 4.5; the effective permeability coefficient of the aqueous pores was 1.5 × 10^{-5} cm/s. Depending upon the buffer pH, 3.5 or 4.5, and the two hydrodynamic situations, the total transport rate was 45–76% aqueous diffusion controlled.

Keyphrases □ Dinoprost—GI absorption, effect of concentration, pH, buffer capacity, and hydrodynamics, rats □ Absorption, GI—dinoprost, effect on concentration, pH, buffer capacity, and hydrodynamics, rats □ Prostaglandins—dinoprost, GI absorption, effect of concentration, pH, buffer capacity, and hydrodynamics, rats

The purpose of this paper is to provide a quantitative insight into some aspects of the absorption process of dinoprost[1] in rat intestines and to identify and assess potential physiological reactions of the membrane and mesenteric circulatory system that may compromise the attainment of an unambiguous physicochemical interpretation of the absorption mechanism. This goal is only part of the larger objectives of a rational biopharmaceutical development of oral delivery systems of the prostaglandins and the molecular design of prostaglandin derivatives and analogues.

To provide the conceptual basis for the biopharmaceutical design, special emphasis is placed on the *in situ* experiments with dinoprost, on the transport processes, and on quantification of the transport and enzymatic kinetic parameters.

Absorption of dinoprost (II), dinoprostone (I), and the methyl ester of the 15-methyl derivative of dinoprost is accompanied by extensive metabolism in the small intestines of the rat (1). Similar results were found in absorption experiments using intact intestinal loops of dogs (2). Using 1-[^{14}C]prostaglandin E_1, Parkinson and Schneider (3) found that only minute amounts of the intact weak acid survived the transport from the mucosal to the serosal fluid of rat jejunum segments *in vitro*. They attributed the loss of the ^{14}C-label to an oxidative process leading to the formation of carbon dioxide. Prostaglandin E_1 is metabolized by homogenates of both rat and dog stomach and jejunum (4). Intestinal absorption of prostaglandin E_1 and dinoprost *via* the lymphatic system appear to be insignificant (2, 5).

The absorption, distribution, excretion, and metabolism of dinoprostone were studied in female rats following oral administration (6). Recently, Bito (7) reviewed the literature and made postulations on the membrane carrier-mediated transport mechanism of the prostaglandins with respect to specific tissues and tissue functionality. Although the transport of dinoprost across the rabbit vagina appears to be a saturable carrier-mediated process, definitive mechanistic studies on intestinal transport in animals are lacking.

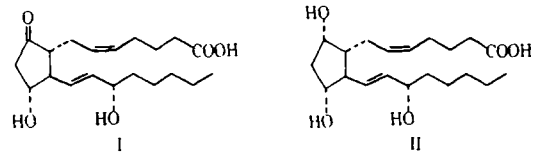

The literature on the chemistry, metabolism, and biology of prostaglandins is extensive and was reviewed previously (8). Prostaglandins are substrates to NAD^+-dependent 15-hydroxyprostaglandin dehydrogenase, Δ^{13}-reductase, β-oxidase, and ω-oxidase (9–11). The bioconversion to the 15-oxo and then the 13,14-dihydro-15-oxo forms is sequential. The pK_a of dinoprost is 4.9, and the solubility of the free acid in water is 1.5 mg/mL. The critical micelle concentration (CMC) increases with pH and is ~4 × 10^{-3} M at pH 3 and ~2 × 10^{-2} M at pH 6.0 (12).

Aqueous solutions of a 5-mg/mL dinoprost equivalent as the tromethamine salt are stable for at least 3 months at room temperature and pH 7–9. No decomposition of 15-mg/mL aqueous solutions at about pH 6.7 was found over 7 d and a 4–47°C temperature range (13). Epimerization to the 15-epi derivative of dinoprost occurs at very low pH, but there are no kinetic data. However, studies in the epimerization kinetics of 15(*R*)- and 15(*S*)-15-methyl derivatives of dinoprost methyl ester serve as a useful guideline (14). When each analogue was incubated in an acidic medium, each epimerized at C-15 to give approximately a 1:1 mixture of the 15(*R*)- and 15(*S*)-forms. About 50% epimerized in 1 h at pH 1.36, and 5% epimerized in 3 h at pH 3.12.

EXPERIMENTAL SECTION

Materials and Apparatus—Dinoprost tromethamine and the 15-oxo and 13,14-dihydro-15-oxo derivatives were used without further purification[2]. [9-^{3}H]Dinoprost(prostaglandin $F_{2\alpha}$)(9.2 Ci/mmol) was obtained from two sources[2,3]. Other radiolabeled chemicals[3] included ^{14}C-labeled 1-butanol (10 mCi/mmol), 1-octanol (10 mCi/mmol), and benzoic acid (5 mCi/mmol). Indomethacin and iodoacetic acid also were used. The isotonic buffers are

[1] Dinoprost is prostaglandin $F_{2\alpha}$; dinoprostone is prostaglandin E_1.

[2] Supplied by The Upjohn Co., Kalamazoo, Mich.

[3] Aquasol, New England Nuclear, Boston, Mass.

0022-3549/84/1100-1588$01.00/0
© 1984, American Pharmaceutical Association

Table I—Standard Isotonic Buffer Solutions

Component[a]	pH 3.5	pH 4.5	pH 6.0[b]	pH 7.5[b]	pH 9.5[b]
Citric acid monohydrate, g	14.75	11.03	—	—	—
Dibasic potassium phosphate, anhydrous, g	10.38	16.53	—	—	—
Potassium sulfate, g	7.0	2.63	11.93	11.93	9.13
Monobasic potassium phosphate, anhydrous, g	—	—	9.07	9.07	—
Boric acid, g	—	—	—	—	10.33
Distilled water[c]	*q.s.*	*q.s.*	*q.s.*	*q.s.*	*q.s.*

[a] Reagent-grade chemicals were used without further purification. All solutions were adjusted to 300–310 mOsm/kg with potassium sulfate. For buffer solutions less than the buffer capacities of the standard preparations, the concentrations of buffer reagents were reduced proportionally and adjusted to isoosmotic conditions with potassium sulfate. [b] The pH was adjusted with 1 M NaOH. [c] The final volume was 1 L.

listed in Table I. A commercial scintillation cocktail[3] was used. A liquid scintillation counter[4], research pH meter[4], osmometer[5], two-directional flow pump[6], and a centrifuge[7] were used.

***In Situ* Absorption Procedures**—Male Sprague–Dawley rats, 220–275 g, fasted for 12–16 h, were anesthetized with 20% urethane solution, 1–2 mg/g ip. An appropriate 22-cm section of the jejunum was selected, washed profusely with normal saline, cannulated, connected to two 5.0-mL syringe barrels and the two-directional pump. The last wash consisted of the buffer intended for the ensuing experiment.

Exactly 2 mL of the radiolabeled solute in isotonic buffer was introduced into the lumen of the jejunum. With the aid of the flow pump, 0.5 mL of solution was pushed up the barrel of one syringe at the rate of 0.075 mL/s, up the other syringe, and finally up the first syringe, whereupon a 20-μL sample was withdrawn with an automatic pipet for assay. This first sample was regarded as the time zero sample, which was 30–35 s after the initial introduction of the 2-mL drug solution into the intestinal lumen.

The initial oscillation of the lumenal solution was done to obtain a uniform mixing of the 2-mL drug solution with the residual solution in the gut lumen from the final wash. The apparent surface area to volume ratio was 11.2[8]. All absorption experiments were carried out at 37°C.

In experiments involving static hydrodynamic conditions, the drug remained in the lumen until, at regular 150-s sampling intervals, 0.5 mL of the lumenal solution was pushed up into the barrel of the syringe with the pump at 0.075 mL/s, and a 20-μL sample was withdrawn. Then the solution was pumped back into the lumen and remained there until the next regular sampling interval. This sampling procedure took no more than 10 s, and at least 75% of the solution volume always remained in the lumen. The regularity of the sampling time interval under these "static" experimental conditions was necessary physicochemically to maintain some constancy in the hydrodynamics of the solution in the gut lumen. This constancy is important when the transport rate is influenced significantly by the permeability of the unstirred aqueous layer.

Chromatography—For TLC, precoated silica gel F-250 plates[9] were developed in ethyl acetate–acetic acid–isooctane–water (90:20:50:100, by volume) (15). Dinoprost and its metabolites were readily observed by spraying with 15% ammonium sulfate. Zones of radioactivity were quantified in the scintillation cocktail with 0.5-cm scrapings. With this TLC system, no impurities in the original [^{3}H]dinoprost solutions were detected.

During the *in situ* intestinal absorption studies, samples from the lumenal solution, blood, and small intestine were taken. Lumenal solution or blood, 0.1 mL, was extracted two to three times with 2 mL of ethyl acetate, concentrated by evaporation with a nitrogen stream, and then spotted. A 1-cm intestinal segment, previously washed with normal saline, was excised, homogenized in the cold, extracted three times with 2 mL of ethyl acetate, concentrated with a nitrogen stream, and spotted.

Qualitative and quantitative analyses of samples from the lumenal solution and the blood (after extraction with ethyl acetate) were performed by HPLC[10]

[4] LS-200 spectrometer; Beckman.
[5] Advanced Instruments, Newton Highlands, Mass.
[6] Model RRP-G-150, Fluid Metering, Oyster Bay, N.Y.
[7] Model SS-3 automatic, Ivan Sorvall, Norwalk, Conn.
[8] The apparent surface area to volume ratio for a 22-cm intestinal segment and 2.2 mL of solution (2.0 mL of isotonic buffer solution of radiolabeled solute and 0.2 mL of residual wash solution in the lumen) is 11.2 This value is calculated by considering the intestinal lumen as a right cylinder:

$$\frac{A}{V} = 2\sqrt{\frac{\pi h}{V}}$$

where A/V is the apparent surface area to volume ratio and h is the length of the intestinal segment.
[9] Analtech, Newark, Del.
[10] Du Pont model A-20 liquid chromatograph.

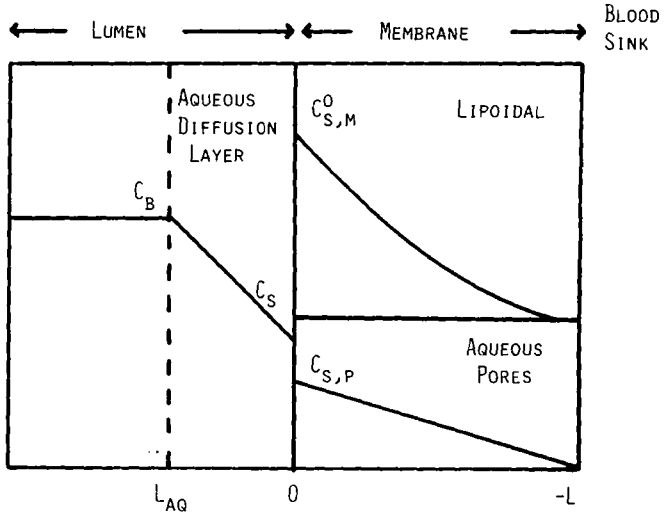

Figure 1—*Physical model for the simultaneous intestinal membrane transport of dinoprost. An aqueous diffusion layer is in series with the membrane consisting of two parallel pathways: the diffusional transport-bioconversion pathway and the aqueous pore pathway. The model depicts the boundary concentrations and distances.*

after conversion of the prostaglandins to the *p*-nitrophenacyl esters as described previously (16).

THEORETICAL SECTION

As will be seen, the following physical model (17) is consistent with the dinoprost absorption in the rat jejunum (Fig. 1). It consists of an aqueous diffusion layer (often referred to as the unstirred aqueous layer) in the lumen in series with the intestinal membrane followed by the blood sink. Operationally, the membrane is comprised of two parallel pathways: the simultaneous diffusional transport-bioconversion pathway in the lipoidal fraction of the membrane and the aqueous pore pathway. It is assumed that the nondissociated and anionic species have equal facility across the aqueous pores. This approach leads to the semilogarithmic expression:

$$\ln C_b = \ln C_b(0) - k_u t \qquad \text{(Eq. 1)}$$

where C_b are the total drug concentration remaining in the lumenal solution at time t, and $C_b(0)$ is the initial concentration. The apparent first-order absorption rate constant, k_u, is given by:

$$k_u = \frac{A}{V} \cdot \frac{1}{\frac{1}{P_{aq}} + \frac{1}{P_{e,m}}} \qquad \text{(Eq. 2)}$$

where A/V is the apparent surface area to solution volume ratio, and P_{aq} and $P_{e,m}$ are the effective permeability coefficients of the aqueous diffusion layer and the membrane, respectively. Furthermore:

$$P_{e,m} = \frac{\alpha K X_s \sqrt{kD}}{\tanh\left(L\sqrt{k/D}\right),} + P_p \qquad \text{(Eq. 3)}$$

where K is the membrane lipoidal biophase–aqueous partition coefficient, X_s is the fraction of nondissociated species at the membrane surface, L is the thickness of the membrane, D is the diffusion coefficient in the membrane, k is the apparent first-order bioconversion rate constant, P_p is the permeability coefficient of the aqueous pores, and α is the volume fraction of the diffusional transport-bioconversion pathway of the lipoidal membrane.

The concentration profile in the diffusional transport-bioconversion pathway is described by:

$$C_m = \frac{C_{m,s} \sinh\left[\sqrt{k/D}(L + x)\right]}{\sinh\left(L\sqrt{k/D}\right)} \qquad (0 \geq x \leq -L) \qquad \text{(Eq. 4)}$$

where $C_{m,s}$ is the concentration of the drug at the surface on the membrane side. Thus, this model assumes that only intracellular metabolism is significant and that cavital and membrane digestion is insignificant (17, 18).

RESULTS AND DISCUSSION

General Absorption Studies—The absorption of [^{3}H]dinoprost at various isotonic buffer values pH and high buffer capacity under the continuous oscillation procedure is shown in Fig. 2. There was a logarithmic change in the concentration remaining in the lumen of the jejunum with time. The slopes decreased with increasing pH. At pH 7.5 and 9.5, the finite rate constants of

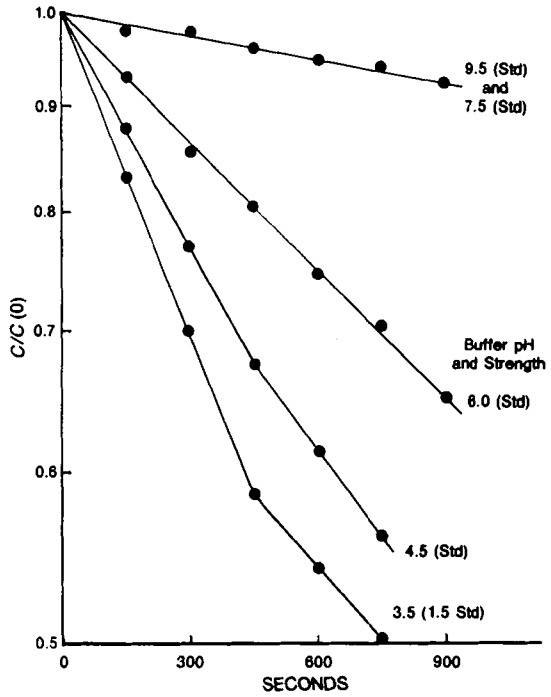

Figure 2—*Semilogarithmic change in the fraction of [^3H]dinoprost remaining in the lumen with time.*

the anionic species were about the same. The absorption at pH 3.5 and 4.5 tended to depart from linearity at later times, most likely due to the flow of intestinal secretions changing the surface and bulk pH with time.

The marked influence of the aqueous diffusion layer on the transport kinetics is observed in the first-order plots in Fig. 3. All other factors being constant, the hydrodynamics produced by the oscillation of the lumenal solution had a larger effect on the slope than the hydrodynamics produced by the static method with 150-s sampling intervals. The higher the degree of agitation, the thinner the aqueous diffusion layer on the mucosal side of the intestinal membrane (19).

Table II is a summary of the absorption experiments at tracer concentrations in the jejunum; the results are also illustrated in Fig. 4. The k_u-pH

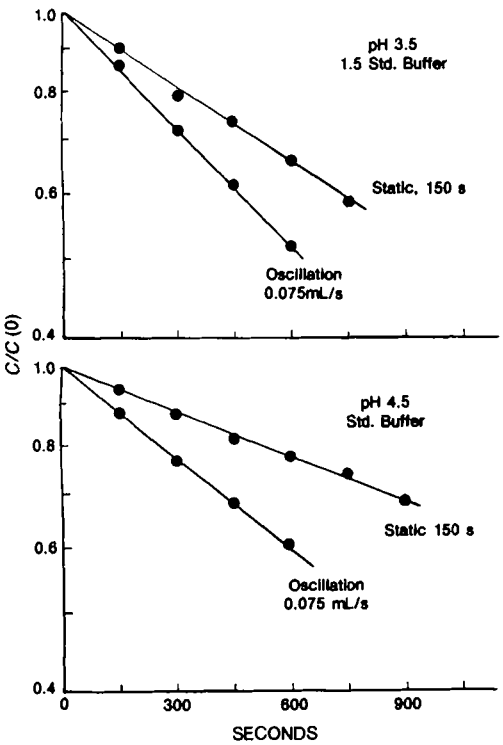

Figure 3—*Comparison of the* in situ *absorption of dinoprost at buffer pH 3.5 and 4.5 under two hydrodynamic conditions.*

Table II—*In Situ* Absorption of Dinoprost (5×10^{-3} μg/mL) in Rat Jejunum at 30°C: Apparent Rate Constants [a]

Hydrodynamic Condition	Buffer pH	Buffer Capacity	Number of Experiments	$k_u \times 10^4$ s^{-1} (± *SD*)
Oscillation 0.075 mL/s	3.5	Standard	3	11.49 (0.05)
		1.5 Standard	1	11.1
	4.5	Standard	4	9.24 (0.70)
	6.0	Standard	5	4.64 (0.14)
	7.5	Standard	3	3.86 (0.18)
		1.5 Standard	3	1.56 (0.15)
	8.5	1.5 Standard	1	1.8
	9.5	Standard	2	1.51 (0.08)
Static, 150-s intervals	3.5	1.5 Standard	2	6.37 (0.35)
	4.5	Standard	2	5.50 (0.22)
	6.0	Standard	1	3.46
	7.5	1.5 Standard	2	1.48 (0.4)

[a] This table is a summary of all experiments with tracer concentrations of [^{3}H]dinoprost.

profiles were similar to those expected for weak acids such as the 1-alkanoic acids (20). At low pH, the absorption under the higher degree of agitation of the solution was greater and less aqueous diffusion controlled than the absorption under less agitation. The differences in the absorption rate constants between the two hydrodynamic conditions became smaller with increasing pH. This result is attributed to the increasing importance of the membrane as the rate-controlling transport barrier. From about pH 7.5 and higher, the k_u-pH profiles for the two hydrodynamic situations converged to an asymptotic minimum. In an operational way, this result is indicative of the rate-limiting transport of the anions across the aqueous pores of the jejunal membrane.

Physiological Effects of Dinoprost on Membrane System—The objectives of the following studies were to identify and to assess potential physiological membrane reactions to dinoprost that may compromise an unambiguous biophysical interpretation and quantification of the absorption mechanism. These objectives were accomplished by following dinoprost absorption at varying concentrations repeatedly within the same intestinal segment of a rat and also between rats and by absorption experiments with selective permeating species in the absence and presence of dinoprost.

Tables III and IV show the results of successive absorption experiments in the same jejunal segment of a rat with various buffer pH combinations and with prostaglandin concentration combinations (up to 10 μg/mL) at pH 6. Taken together, the results indicated that pH and dinoprost did not have adverse effects on the membrane under the experimental conditions. The within-rat variation was small. A 1.5×10^4-fold increase in the concentration, corresponding to 0.014 and 210 mM, respectvely, did not influence the absorption rate constant.

The absorption rates of 1-[^{14}C]butanol in the jejunum in the absence and

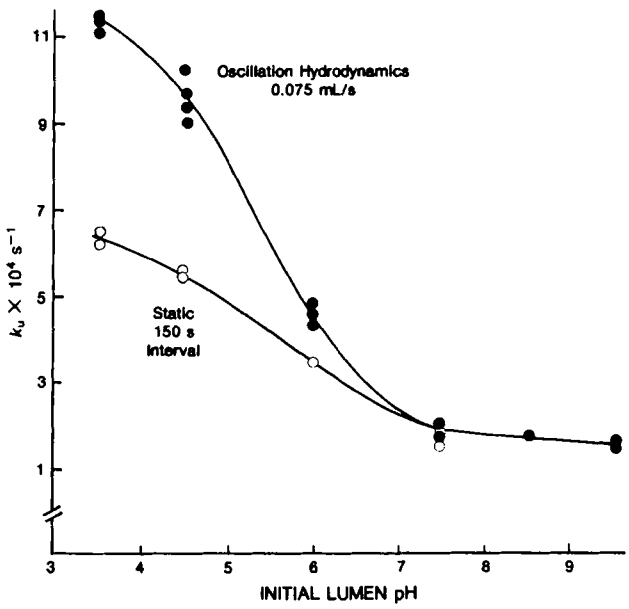

Figure 4—*Apparent first-order rate constants* versus *high buffer capacity pH under two hydrodynamic conditions in the rat jejunum.*

Table III—Successive Absorption Experiments of [^{3}H]Dinoprost in Same Jejunum Segment at Various Buffer-pH Combinations [a]

Order of Experiment	Rat A		Rat B		Rat C	
	Buffer pH	$k_u \times 10^4$ s^{-1}	Buffer pH	$k_u \times 10^4$ s^{-1}	Buffer pH	$k_u \times 10^4$ s^{-1}
1	3.5	11.51	4.5	10.42	7.5	4.08
2	9.5	1.43	7.5	3.65	4.5	9.1
3	3.5	11.43	4.5	8.8	7.5	3.86

[a] All buffers were of standard buffer capacities. The concentration of [^{3}H]dinoprost was 5×10^{-3} μg/mL.

Table IV—Successive Absorption Experiments at pH 6.0 in Same Jejunum Segment at Various Dinoprost Concentration Combinations [a]

Order of Experiment	Rat A		Rat B		Rat C		Rat D	
	Concentration, μg/mL	$k_u \times 10^4$ s^{-1}	Conc., μg/mL	$k_u \times 10^4$ s^{-1}	Conc., μg/mL	$k_u \times 10^4$ s^{-1}	Conc., μg/mL	$k_u \times 10^4$ s^{-1}
1	5×10^{-3}	4.28	1	4.79	10	5.1	100	4.37
2	1	4.57	5×10^{-3}	4.64	10	5.0	100	4.41
3	5×10^{-3}	4.44	1	5.96	—	—	100	4.86

[a] Concentration of 1, 10, and 100 μg/mL refers to dinoprost tromethamine salt. Tracer [^{3}H]dinoprost concentrations of 5×10^{-3} μg/mL were added.

Table V—Absorption of 1-[^{14}C]Butanol in the Jejunum at pH 6.0 in the Absence and Presence of Dinoprost [a]

Concentration of Nonlabeled Dinoprost Tromethamine Salt[b], μg/mL	N	$k_u \times 10^3$ s^{-1} for 1-Butanol
0	4	1.59 (0.16)
10	2	1.51 (0.2)
100	3	1.61 (0.13)

[a] Oscillator (0.075 mL/s) hydrodynamics were used. The 10 and 100 μg/mL are equivalent to 21 and 210 μM, respectively.

presence of dinoprost were not statistically different (Table V), providing further support that there were no significant adverse membrane and vascular effects to transport. There was also no effect on the transport of 1-[^{14}C]octanol at pH 4.5 (Fig. 5). The fact that the absorption of [^{14}C]benzoate anions at pH 8.5 was not influenced by the presence of dinoprost indicated that the prostaglandin did not significantly affect the aqueous pore pathway of the jejunal membrane (Table VI). It is concluded that dinoprost does not have apparent adverse membrane and vascular effects under the experimental conditions employed.

Mechanism of Membrane Transport—It was postulated that the transport of dinoprost in the rat occurs by passive transport across the aqueous diffusion layer and then by the simultaneous passive membrane transport and bioconversion mechanism. The k_u-pH plots in Fig. 4, which are of the kind predicted by the pH-partition-aqueous diffusion layer hypothesis for the passive absorption of weak acids, serve as part of the basis for the postulation of the passive mechanism of the total transport process across the jejunal membrane *per se*. Comparison of the absorption-pH profiles of dinoprost and *n*-butyric acid (Fig. 6) illustrates this point.

The following results provide additional evidence that the absorption does not involve a membrane-saturable process. The rate constant of dinoprost at pH 6 and 7.5 was not concentration dependent with concentrations from 1.4 $\times 10^{-2}$ to 200 μM (a 1.5×10^4-fold range) (Table VII and Fig. 7). Furthermore, the absorption was not affected by iodoacetic acid and indomethacin, substances that inhibit the carrier-mediated transport of natural prosta-

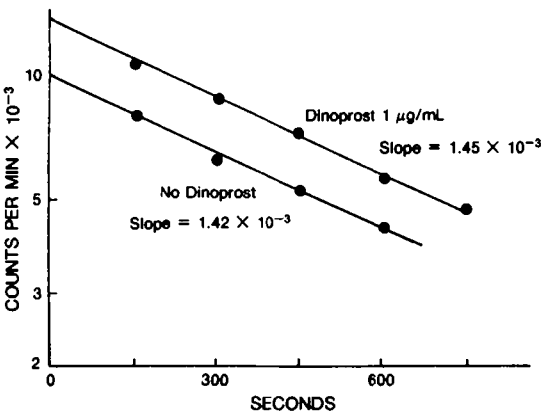

Figure 5—*Semilogarithmic plots of the concentration of 1-[^{14}C]octanol remaining in the lumen of the jejunum with time in the presence and absence of dinoprost under static (150-sec sampling interval) hydrodynamics.*

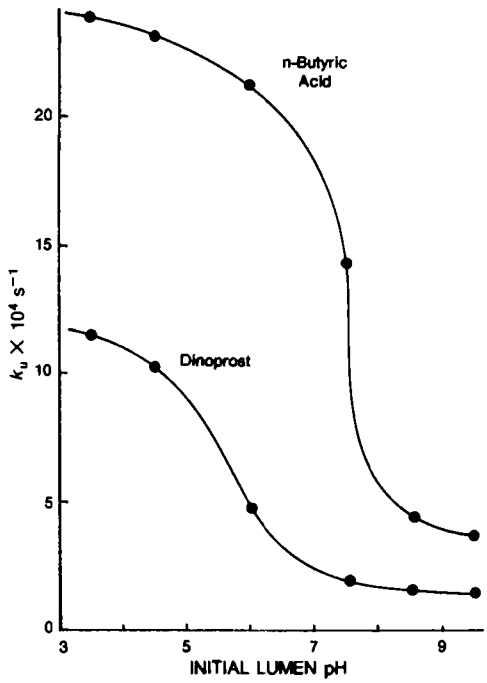

Figure 6—*Comparison of the absorption-pH profiles of dinoprost and* n-*butyric acid under oscillation (0.075 mL/s) hydrodynamics in the rat jejunum. Dinoprost undergoes simultaneous diffusional transport-bioconversion kinetics in the membrane while* n-*butyric acid is passively absorbed.*

Table VI—*In Situ* Absorption of [^{14}C]Benzoate at pH 8.5 in the Absence and Presence of Dinoprost in the Jejunum [a]

Order of Experiment[b]	Rat A		Rat B		Rat C	
	Dinoprost, μg/mL	$k_u \times 10^4$ s^{-1}	Dinoprost, μg/mL	$k_u \times 10^4$ s^{-1}	Dinoprost, μg/mL	$k_u \times 10^4$ s^{-1}
1	0	6.36	0	5.32	1	5.85
2	1	6.80	1	4.74	0	4.22
3	0	6.45	0	5.29	1	5.22

[a] Oscillation (0.075 mL/s) hydrodynamics were employed. The pH 8.5, 1.5 standard buffer capacity, was used. Dinoprost was used as the tromthamine salt. [b] In the same 22-cm jejunal segment.

Table VII—*In Situ* Absorption of [^{3}H]Dinoprost at Various Concentrations and Buffer pH [a]

Buffer pH	Buffer Capacity	Number of Experiments	Dinoprost Concentration, μg/mL	$k_u \times 10^4$ s^{-1} (±*SD*)
6.0	Standard	3	5×10^{-3}	4.45 (0.18)
		2	1	5.11 (0.75)
		2	10	5.05 (0.07)
		3	100	4.61 (0.26)
7.5	1.5 Standard	3	5×10^{-3}	1.56 (0.15)
		3	1	1.81 (0.17)

[a] Oscillation (0.075 mL/s^{-1}) hydrodynamics were employed. The dinoprost concentrations were 1-100 μg/mL of dinoprost tromethamine with 5×10^{-3} μg/mL of [^{3}H]dinoprost added.

Table VIII—Absorption of [^{3}H]Dinoprost in the Absence and Presence of Indomethacin at Buffer pH 7.5 [a]

Order of Experiment	Rat A Indomethacin, M	Rat A $k_u \times 10^4$ s^{-1}	Rat B Indomethacin, M	Rat B $k_u \times 10^4$ s^{-1}
1	0	1.99	10^{-5}	1.71
2	10^{-5}	1.83	0	1.74
3	0	1.71	10^{-5}	1.61

[a] Oscillation (0.075 mL/s) hydrodynamics were employed. The buffer capacity was 1.5 standard. The dinoprost concentration was 1 μg/mL of dinoprost tromethamine with 5×10^{-3} μg/mL of [^{3}H]dinoprost added. The experiments were performed in the same 22-cm jejunal segment.

Table IX—*In Situ* Absorption of [^{3}H]Dinoprost in the Absence and Presence of Iodoacetic Acid at Buffer pH 6.0 [a]

Order of Experiment	Rat A Iodoacetic Acid, mM	Rat A $k_u \times 10^4$ s^{-1}	Rat B Iodoacetic Acid, mM	Rat B $k_u \times 10^4$ s^{-1}	Rat C Iodoacetic Acid, mM	Rat C $k_u \times 10^4$ s^{-1}
1	0	4.50	2	4.83	10	4.64
2	2	4.77	0	4.81	--	—
3	0	4.80	2	4.73	—	—

[a] Oscillation (0.075 mL/s^{-1}) hydrodynamics were employed. The buffer capacity was 1.5 standard. The [^{3}H]dinoprost concentrations were 5×10^{-3} μg/mL for rats A and B and 0.1 μg/mL for rat C.

glandins (21) (Tables VIII and IX). Indomethacin also is a prostaglandin synthetase inhibitor.

Preliminary Metabolism Studies—These studies were carried out to characterize generally dinoprost metabolism in the first 20 min of *in situ* rat intestinal absorption experiments with pH 6.0 buffer. In the first 5 min, <1.0% of the 15-oxo and 13,14-dihydro-15-oxo forms appeared in the lumenal solution (Fig. 8); in 20 min, ~10% of these major metabolites was present. No metabolism occurred *in vitro* in rat blood and the lumenal secretion solution (Fig. 9). However, dinoprost and its two major metabolites were found in the intestinal segments and the blood in the *in situ* absorption studies. If β-oxidation products were present, they could not be detected by the chromatographic techniques employed.

The results of the preliminary *in vitro* and *in situ* studies together indicate

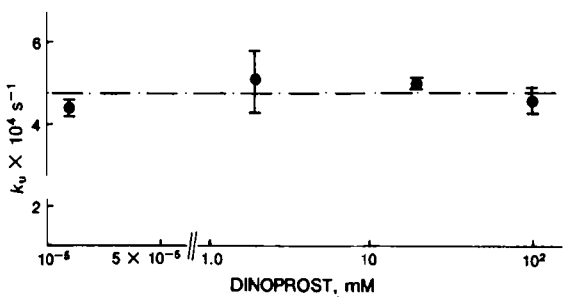

Figure 7—*Effect of dinoprost concentration on the intestinal absorption rate constant at pH 6.0 and oscillation hydrodynamics. The bars represent the standard deviations; the dash line is the mean rate constant for all concentrations, which is equal to 4.8 × 10^{-4} s.*

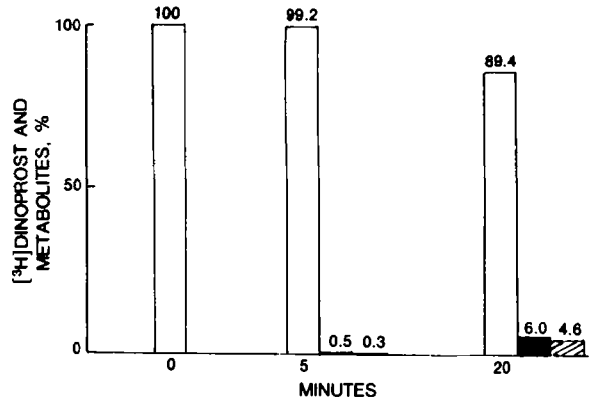

Figure 8—*Percent of radiolabeled dinoprost and metabolites found in the lumen of the rat jejunum* in situ *with time. Key:* □, *dinoprost;* ■, *15-oxo metabolite; and* ▨, *13,14-dihydro-15-oxo metabolite.*

that there is no dinoprost metabolism in the lumen; metabolism by 15-hydroxyprostaglandin dehydrogenase and Δ^{13}-reductase occurs in the membrane and there is a back-diffusion of metabolites into the lumen. The possibility of membrane contact metabolism seems unlikely, since the enzyme systems usually associated with the membrane surface include the carbohydrases, peptidases, lipases, hydrolases, and isoenzymes of alkaline phosphatase (18). Studies are currently directed toward determining, through the use of inhibitors, whether enzymes relevant to prostaglandin metabolism are present at the membrane surface.

Permeability Coefficients—The theoretical physical model described is operationally consistent with the experimental evidence. Consequently, the permeability coefficients of the aqueous diffusion layer, the diffusional transport-bioconversion, and aqueous pore pathways of the jejunal membrane are readily found.

Between two absorption rate constants obtained at the same buffer pH but under different hydrodynamics in the lumen, the following relationships hold:

$$\frac{1}{P_{aq}} + \frac{1}{P_{e,m}} = \frac{A}{Vk_u} \qquad \text{(Eq. 5)}$$

$$\frac{1}{P_{aq}'} + \frac{1}{P_{e,m}} = \frac{A}{vk_u} \qquad \text{(Eq. 6)}$$

$$r^* = P_{aq}'/P_{aq} \qquad \text{(Eq. 7)}$$

The rate constant, k_u, and the permeability coefficient of the aqueous diffusion layer, P_{aq}, are different from k_u' and P_{aq}' because of the differences in the hydrodynamic conditions. In contrast, the effective permeability coefficient, $P_{e,m}$, is independent of the hydrodynamics. The ratio r^* already was determined for a number of hydrodynamic situations in the rat intestinal tract using the 1-alkanol series (19). Between the continuous oscillation (0.075-mL/s) and the static (150-s) sampling interval cases, r^* is 2.12.

As shown in Table X, the permeability coefficients of P_{aq} for the static and oscillation hydrodynamic situations are 0.8×10^{-4} and 1.7×10^{-4} cm/s,

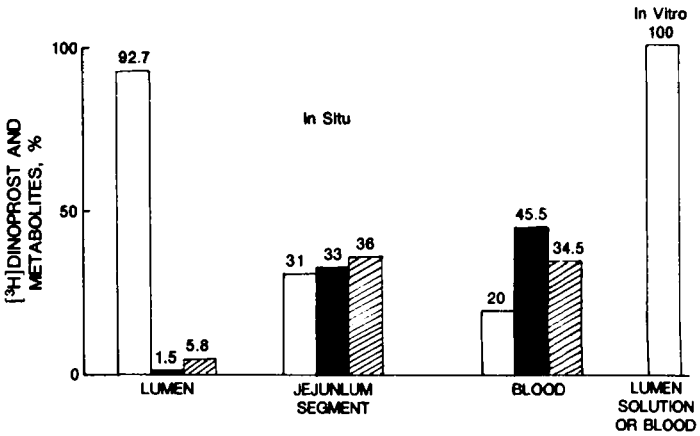

Figure 9—*Percent of radiolabeled dinoprost and metabolites found in the lumenal solution, jejunal gut segment, and blood after 20 min from* in situ *absorption experiments and in the lumenal solution and blood after 20 min exposure from* in vitro *experiments.*

Table X—Permeability Coefficients of the Aqueous Diffusion Layer [a]

Buffer pH	$k_u \times 10^4$ s^{-1} Static, 150 s	$k_u \times 10^4$ s^{-1} Oscillation, 0.075 mL/s	Permeability Coefficient $\times 10^4$ cm/s $P_{aq(static)}$	Permeability Coefficient $\times 10^4$ cm/s $P_{aq(oscillation)}$
3.5	6.61	11.09	0.8	1.64
4.5	5.66	8.65	0.8	1.64

[a] The P_{aq} for the static and oscillation situations and $P_{c,m}$ were calculated from the experimental rate constants with Eqs. 5 and 6. The r^* is 2.12, and A/V is 11.2.

Table XI—Factorization of the Effective Permeability Coefficients of the Jejunum Membrane at Various Buffer pH Values into the Permeability Coefficients of the Aqueous Pores and Principal Membrane Pathway

Buffer pH	Buffer Capacity	Permeability Coefficient $\times 10^4$ cm/s $P_{c,m}$[a]	P_{pore}	$\frac{KX\sqrt{kD}}{\tanh(L\sqrt{k/D})}$
3.5	1.5 Standard	2.59	0.15	2.44
4.5	Standard	1.44	0.15	1.29
6.0	Standard	0.53	0.15	0.38
7.5	1.5 Standard	0.15	0.15	0
9.5	Standard	0.15	0.15	0

[a] Defined by Eq. 3.

respectively. The $P_{c,m}$ values are 2.57×10^{-4} cm/s at buffer pH 3.5 and 1.46×10^{-4} cm/s at pH 4.5. Since the aqueous diffusion coefficient of dinoprost is equal to 5.1×10^{-6} cm^2/s, the effective diffusion layer thickness is 310 μm for the oscillation hydrodynamics and 662 μm for the static situation.

The permeability coefficient of the aqueous pores, P_p, is determined from the experimental data in the limit of the buffer pH $\gg$ pK_a; thus:

$$k_{u,min} = \frac{A/V}{\frac{1}{P_{aq}} + \frac{1}{P_p}} \qquad \text{(Eq. 8)}$$

Using Tables II and X where the average $k_{u,min}$ is 1.51×10^{-4} s^{-1} and P_{aq} (oscillation) is 1.7×10^{-4} cm/s, one finds that P_p is 1.5×10^{-5} cm/s. In perspective (6), the P_p of the salicylate and *p*-aminobenzoate ions in the jejunum is 2.8×10^{-5} cm/s, and that of taurocholate anions is negligible. It is reasonable to assume that the P_p of the nondissociated dinoprost species is at least equal to, if not slightly larger than, the P_p of the anion. Consequently, the effective permeability coefficient of the principal transport-bioconversion pathway of the membrane, which is pH dependent, can be found to complete the factorization of the effective permeability coefficient of the membrane (Table XI).

The extent to which the transport rate is influenced by the aqueous diffusion layer barrier in front of the mucosal membrane is presented in Table XII. As one would expect, the rate constant was more aqueous diffusion controlled at pH 3.5 than at pH 4.5, and the oscillation situation was less aqueous diffusion controlled as compared with the static situation. Although the degree of agitation of the lumenal solution at pH 3.5 produced by rapidly oscillating the solution was high, the rate was 60% diffusion controlled. At higher pH values, the rate was less aqueous diffusion controlled.

General Observations of Buffer Capacity on Absorption—The first-order absorption-time profiles at pH 3.5 and 4.5 tended to depart from linearity with time (Fig. 2). For cases where different buffer capacities at initial pH 3.5 and 7.5 were used, the rate constants varied with buffer capacity (Table II). Because of these observations and other intestinal absorption studies (22), all absorption studies were carried out at sufficiently high buffer capacities such that the initial rate constants at all buffer pH were independent of buffer strength.

To complete the baseline studies, additional experiments were carried out

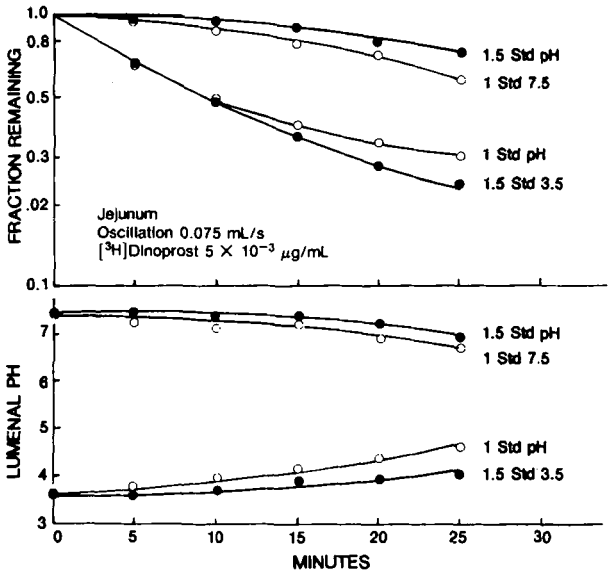

Figure 10—*Semilogarithmic change in the lumenal concentration of dinoprost and bulk pH change with time for pH 3.5 and 7.5 under oscillation hydrodynamics and two buffer strengths.*

wherein both the intestinal absorption and bulk lumenal pH changes with time were simultaneously followed at initial pH 3.5 and 7.5 and two buffer strengths. The first-order absorption curves at pH 3.5 were linear for a short time and then gradually decreased with time, while the bulk lumenal pH increased with time toward pH 6.0 (Fig. 10). These changes occurred more rapidly with the lower of the two buffer strengths. In both cases, the initial slopes in the absorption curves were about the same. In contrast, the increase in the absorption with time at pH 7.5 was accompanied wih a slow decrease in the bulk pH with time. These changes occurred faster at lower buffer capacities.

All of these observations are consistent with the mechanistic studies on the rat intestinal absorption of *n*-butyric acid (19) in which the factors influencing the dynamics of the surface pH, *i.e.*, the pH at the aqueous-membrane interface, were quantitatively assessed. Because the surface pH depends on the net effect of the fluxes of the intestinal buffer secretions and buffer species from the bulk solution, sufficiently high buffer capacity solutions in the lumen must be used to have a baseline control of the surface pH relative to the initial bulk pH.

CONCLUSIONS

The objectives of providing a broad insight into the absorption process and of identifying and assessing potential physiological reactions of the membrane to the prostaglandins that can compromise an unambiguous biophysical interpretation of the absorption mechanism *via* the physical mode approach have been met. *In situ* baseline absorption studies with [^{3}H]dinoprost in the rat jejunum were carried out using a modified Doluisio technique for better control of the hydrodynamics. The experimental variables included a wide range of buffer pH (3.5-9.5), buffer capacity, hydrodynamics, and prostaglandin concentrations. The physical model was applied to the results to obtain quantitative estimates of the permeability coefficients of the aqueous diffusion layer, the aqueous pore pathway, and the effective diffusional transport-bioconversion pathway of the membrane. Studies are in progress to distinguish further the occurrence of metabolism within the membrane from membrane contact metabolism and to obtain the factorization of the apparent *in situ*

Table XII—Influence of the Aqueous Diffusion Layer on the Transport Rate of Dinoprost in the Jejunum

Buffer pH	Hydrodynamic Condition[a]	$k_{u,exp} \times 10^4$ s^{-1}	$k_{u,max} \times 10^4$ s^{-1}	Percent of Rate Constant Aqueous Diffusion Controlled
3.5	Static, 150 s	6.61	8.96	74
	Oscillation	11.09	19.0	58
4.5	Static, 150 s	5.66	8.96	63
	Oscillation	8.65	19.0	46
6.0	Static 150 s	3.56	8.96	40
	Oscillation	4.67	19.0	25
7.5 and 9.5	Oscillation	1.51	19.0	8

[a] Static case: $k_{u,max} = AP_{aq}/V = 11.2 \times 0.8 \times 10^{-4} = 8.96 \times 10^{-4}$. Oscillation: $k_{u,max} = 11.2 \times 1.7 \times 10^{-4} = 19.0 \times 10^{-4}$.

enzyme rate constant from the coupled diffusional transport-bioconversion kinetic constant.

REFERENCES

(1) W. E. Magee, S. B. Armour, and O. V. Miller, *Biochim. Biophys. Acta*, **306**, 270 (1973).

(2) A. Robert, W. E. Magee, O. V. Miller, and J. E. Nezamis, *Biochem. Biophys. Acta*, **348**, 269 (1974).

(3) T. M. Parkinson and J. C. Schneider, *Biochem. Biophys. Acta*, **176**, 78 (1969).

(4) J. Nakano, A. V. Prancan, and N. H. Morsy, *Jpn. J. Pharmacol.*, **23**, 355 (1973).

(5) T. M. Parkinson, J. C. Schneider, J. J. Krake, and W. I. Miller, *Life Sci.*, **7**, 883 (1968).

(6) T. Nishibori, Y. Matsuoka, and T. Matsumoto, *Pharmacometrics (Japan)*, **8**, 797 (1974).

(7) L. Z. Bito, *Prostaglandins*, **9**, 851 (1975).

(8) T. O. Oesterling, W. Morozowich, and T. J. Roseman, *J. Pharm. Sci.*, **61**, 1861 (1972).

(9) F. F. Sun, *Biochim. Biophys. Acta*, **348**, 249 (1974).

(10) J. Nakano, E. Anggard, and B. Samuelsson, *Eur. J. Biochem.*, **11**, 386 (1969).

(11) M. A. Marrazzi and F. M. Matschinsky, *Prostaglandins*, **1**, 373 (1972).

(12) T. J. Roseman and S. H. Yalkowsky, *J. Pharm. Sci.*, **62**, 2933 (1973).

(13) T. J. Roseman, B. Sims, and R. G. Stehle, *Am J. Hosp. Pharm.* **30**, 236 (1973).

(14) A. Robert and E. W. Yankee, *Proc. Soc. Exp. Bil. Med.*, **148**, 1155 (1975).

(15) K. Green and B. Samuelsson, *J. Lipid Res.*, **5**, 117 (1964).

(16) W. Morozowich and S. L. Douglas, *Prostaglandins*, **10**, 19 (1975).

(17) N. F. H. Ho, J. Y. Park, W. Morozowich, and W. I. Higuchi, *J. Theoret. Biol.* **61**, 185 (1976).

(18) A. M. Ugolev, "Physiology and Pathology of Membrane Digestion," Plenum, New York, N.Y., 1968.

(19) K. Desai, Ph.D. thesis, University of Michigan, Ann Arbor, Mich., 1976.

(20) N. F. H. Ho, W. I. Higuchi, and J. S. Turi, *J. Pharm. Sci.*, **61**, 192 (1972).

(21) L. Z. Bito, *Fed. Proc., Fed. Soc. Exp. Biol.*, **33**, 589 (1974).

ACKNOWLEDGMENTS

The authors acknowledge with appreciation the following individuals from The Upjohn Co., Kalamazoo, Mich.: S. L. Douglas for technical assistance in the HPLC analyses, Dr. D. G. Kaiser for a generous supply of ^{3}H-dinoprost, and Dr. T. O. Oesterling for encouragement and support.

Physical Model Approach to Gastrointestinal Absorption of Prostaglandins III: *In Situ* Rat Intestinal Absorption of Dinoprostone

J. D. ROGERS *[¶], N. F. H. HO *[§x], and W. MOROZOWICH [‡]

Received October 18, 1976, from the **College of Pharmacy, University of Michigan, Ann Arbor, MI 48109* and the [‡]*Upjohn Co., Kalamazoo, MI 49001.* Accepted for publication February 16, 1977. Present addresses: [¶]Merck, Sharp & Dohme, West Point, PA 19486 and the [§]Upjohn Co., Kalamazoo, MI 49001.

Abstract □ *In situ* absorption studies with dinoprostone in the rat jejunum were carried out to provide a quantitative mechanistic insight of the absorption process. The variables included buffer pH (3.5-9.5), buffer capacity, hydrodynamics in the lumen, and concentration. The disappearance kinetics from the lumen was first order. The rate decreased with increasing pH in a sigmoidal manner and reached a minimum at about pH 9. These results indicate the effects of the partitioning of nondissociated species in the lipoidal membrane and transport across aqueous pores. The rate was higher with the higher degree of agitation of the lumenal solution. Between two hydrodynamic situations, the differences in the rates were large at pH 4.5 where the transport was largely aqueous diffusion controlled and then tended to become smaller with increasing pH where the transport became effectively membrane controlled. The 15-oxo- and 13,14-dihydro-15-oxo metabolites of dinoprostone were found. The physical model was applied to quantify the permeability coefficients of the aqueous diffusion layer and the aqueous pores of the membrane and the effective membrane transport-bioconversion permeability coefficient at various pH values. The overall absorption process of dinoprostone was similar to that of the less lipophilic dinoprost reported earlier and also more rapid. Hence, baseline absorption studies were completed with two major reference prostaglandins from which estimations of intestinal absorption can be made for their analogues and derivatives.

Keyphrases □ Absorption, GI—dinoprostone, rat jejunum, effect of buffer pH, buffer capacity, lumenal hydrodynamics, and concentration □ Dinoprostone—GI absorption, effect of buffer pH, buffer capacity, lumenal hydrodynamics, and concentration □ Prostaglandins—dinoprostone, GI absorption, effect of buffer pH, buffer capacity, lumenal hydrodynamics, and concentration, rat jejunum □ Oxytocic agents—dinoprostone, GI absorption, effect of buffer pH, buffer capacity, lumenal hydrodynamics, and concentration, rat jejunum

In situ absorption studies in the rat jejunum have been carried out to provide a quantitative mechanistic insight into the intestinal absorption of dinoprostone (I)[1]. These studies were intended to serve as baselines for comparisons between dinoprostone and its analogues and derivatives and other natural prostaglandins such as dinoprost (II).

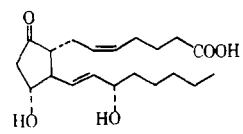

I

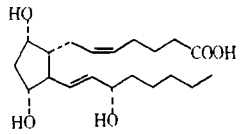

II

Magee *et al.* (1) were the first to study the *in situ* rat intestinal absorption of dinoprostone by the Doluisio *et al.* (2) technique. With the entire small intestines and 0.01 M phosphate buffer (pH 6.4), the disappearance half-life from the intestinal solution was 40 min. The 15-oxo metabolite was found in the lumen. No mechanistic interpretation on the absorption process was made.

Recently, *in situ* absorption studies with dinoprost in the rat jejunum, using a modified Doluisio technique, showed that the absorption rate was first order and was dependent on the pH and hydrodynamics in the intestinal lumen (3). No metabolism involving 15-hydroxyprostaglandin dehydrogenase occurred in the intestinal lumen and at the membrane surface; however, metabolism occurred within the biomembrane. The transport mechanism involved simultaneous passive diffusion and enzymatic bioconversion in the membrane. The quanti-

[1] Dinoprostone is prostaglandin E_2; dinoprost is prostaglandin $F_{2\alpha}$.

0022-3549/84/1100-1594$01.00/0

© 1984, American Pharmaceutical Association

enzyme rate constant from the coupled diffusional transport-bioconversion kinetic constant.

REFERENCES

(1) W. E. Magee, S. B. Armour, and O. V. Miller, *Biochim. Biophys. Acta*, **306**, 270 (1973).

(2) A. Robert, W. E. Magee, O. V. Miller, and J. E. Nezamis, *Biochem. Biophys. Acta*, **348**, 269 (1974).

(3) T. M. Parkinson and J. C. Schneider, *Biochem. Biophys. Acta*, **176**, 78 (1969).

(4) J. Nakano, A. V. Prancan, and N. H. Morsy, *Jpn. J. Pharmacol.*, **23**, 355 (1973).

(5) T. M. Parkinson, J. C. Schneider, J. J. Krake, and W. I. Miller, *Life Sci.*, **7**, 883 (1968).

(6) T. Nishibori, Y. Matsuoka, and T. Matsumoto, *Pharmacometrics (Japan)*, **8**, 797 (1974).

(7) L. Z. Bito, *Prostaglandins*, **9**, 851 (1975).

(8) T. O. Oesterling, W. Morozowich, and T. J. Roseman, *J. Pharm. Sci.*, **61**, 1861 (1972).

(9) F. F. Sun, *Biochim. Biophys. Acta*, **348**, 249 (1974).

(10) J. Nakano, E. Anggard, and B. Samuelsson, *Eur. J. Biochem.*, **11**, 386 (1969).

(11) M. A. Marrazzi and F. M. Matschinsky, *Prostaglandins*, **1**, 373 (1972).

(12) T. J. Roseman and S. H. Yalkowsky, *J. Pharm. Sci.*, **62**, 2933 (1973).

(13) T. J. Roseman, B. Sims, and R. G. Stehle, *Am J. Hosp. Pharm.* **30**, 236 (1973).

(14) A. Robert and E. W. Yankee, *Proc. Soc. Exp. Bil. Med.*, **148**, 1155 (1975).

(15) K. Green and B. Samuelsson, *J. Lipid Res.*, **5**, 117 (1964).

(16) W. Morozowich and S. L. Douglas, *Prostaglandins*, **10**, 19 (1975).

(17) N. F. H. Ho, J. Y. Park, W. Morozowich, and W. I. Higuchi, *J. Theoret. Biol.* **61**, 185 (1976).

(18) A. M. Ugolev, "Physiology and Pathology of Membrane Digestion," Plenum, New York, N.Y., 1968.

(19) K. Desai, Ph.D. thesis, University of Michigan, Ann Arbor, Mich., 1976.

(20) N. F. H. Ho, W. I. Higuchi, and J. S. Turi, *J. Pharm. Sci.*, **61**, 192 (1972).

(21) L. Z. Bito, *Fed. Proc., Fed. Soc. Exp. Biol.*, **33**, 589 (1974).

ACKNOWLEDGMENTS

The authors acknowledge with appreciation the following individuals from The Upjohn Co., Kalamazoo, Mich.: S. L. Douglas for technical assistance in the HPLC analyses, Dr. D. G. Kaiser for a generous supply of ^{3}H-dinoprost, and Dr. T. O. Oesterling for encouragement and support.

Physical Model Approach to Gastrointestinal Absorption of Prostaglandins III: *In Situ* Rat Intestinal Absorption of Dinoprostone

J. D. ROGERS *[¶], N. F. H. HO *[§x], and W. MOROZOWICH [‡]

Received October 18, 1976, from the **College of Pharmacy, University of Michigan, Ann Arbor, MI 48109* and the [‡]*Upjohn Co., Kalamazoo, MI 49001.* Accepted for publication February 16, 1977. Present addresses: [¶]Merck, Sharp & Dohme, West Point, PA 19486 and the [§]Upjohn Co., Kalamazoo, MI 49001.

Abstract □ *In situ* absorption studies with dinoprostone in the rat jejunum were carried out to provide a quantitative mechanistic insight of the absorption process. The variables included buffer pH (3.5-9.5), buffer capacity, hydrodynamics in the lumen, and concentration. The disappearance kinetics from the lumen was first order. The rate decreased with increasing pH in a sigmoidal manner and reached a minimum at about pH 9. These results indicate the effects of the partitioning of nondissociated species in the lipoidal membrane and transport across aqueous pores. The rate was higher with the higher degree of agitation of the lumenal solution. Between two hydrodynamic situations, the differences in the rates were large at pH 4.5 where the transport was largely aqueous diffusion controlled and then tended to become smaller with increasing pH where the transport became effectively membrane controlled. The 15-oxo- and 13,14-dihydro-15-oxo metabolites of dinoprostone were found. The physical model was applied to quantify the permeability coefficients of the aqueous diffusion layer and the aqueous pores of the membrane and the effective membrane transport-bioconversion permeability coefficient at various pH values. The overall absorption process of dinoprostone was similar to that of the less lipophilic dinoprost reported earlier and also more rapid. Hence, baseline absorption studies were completed with two major reference prostaglandins from which estimations of intestinal absorption can be made for their analogues and derivatives.

Keyphrases □ Absorption, GI—dinoprostone, rat jejunum, effect of buffer pH, buffer capacity, lumenal hydrodynamics, and concentration □ Dinoprostone—GI absorption, effect of buffer pH, buffer capacity, lumenal hydrodynamics, and concentration □ Prostaglandins—dinoprostone, GI absorption, effect of buffer pH, buffer capacity, lumenal hydrodynamics, and concentration, rat jejunum □ Oxytocic agents—dinoprostone, GI absorption, effect of buffer pH, buffer capacity, lumenal hydrodynamics, and concentration, rat jejunum

In situ absorption studies in the rat jejunum have been carried out to provide a quantitative mechanistic insight into the intestinal absorption of dinoprostone (I)[1]. These studies were intended to serve as baselines for comparisons between dinoprostone and its analogues and derivatives and other natural prostaglandins such as dinoprost (II).

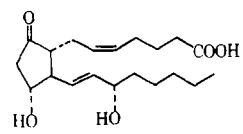

I

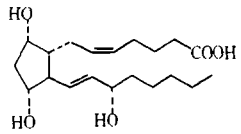

II

Magee *et al.* (1) were the first to study the *in situ* rat intestinal absorption of dinoprostone by the Doluisio *et al.* (2) technique. With the entire small intestines and 0.01 M phosphate buffer (pH 6.4), the disappearance half-life from the intestinal solution was 40 min. The 15-oxo metabolite was found in the lumen. No mechanistic interpretation on the absorption process was made.

Recently, *in situ* absorption studies with dinoprost in the rat jejunum, using a modified Doluisio technique, showed that the absorption rate was first order and was dependent on the pH and hydrodynamics in the intestinal lumen (3). No metabolism involving 15-hydroxyprostaglandin dehydrogenase occurred in the intestinal lumen and at the membrane surface; however, metabolism occurred within the biomembrane. The transport mechanism involved simultaneous passive diffusion and enzymatic bioconversion in the membrane. The quanti-

[1] Dinoprostone is prostaglandin E_2; dinoprost is prostaglandin $F_{2\alpha}$.

0022-3549/84/1100-1594$01.00/0

© 1984, American Pharmaceutical Association

Table I—*In Situ* Absorption of [^{3}H]Dinoprostone in the Rat Jejunum [a]

Hydrodynamic Condition	Buffer pH	Buffer Capacity	Number of Experiments	$k_u \times 10^4$ s^{-1} ±SD
Oscillation, 0.075 mL/s	3.5	Std	5	14.59 (1.50)
		1.5 Std	3	16.60 (0.40)
	4.5	Std	2	9.81 (0.29)
		1.5 Std	9	11.94 (0.58)
	6.0	Std	13	7.63 (0.45)
	6.5	Std	4	6.22 (0.68)
	7.5	Std	2	4.60 (0.21)
		1.5 Std	4	2.98 (0.35)
	8.5	Std	2	2.05 (0.64)
	9.5	Std	4	2.00 (0.77)
Static, 150-s intervals	3.5	Std	3	8.60 (0.77)
		1.5 Std	3	8.78 (0.38)
	4.5	Std	2	6.67 (0.51)
		1.5 Std	6	7.81 (0.72)
	5.0	Std	6	5.44 (0.38)
	6.5	Std	2	4.59 (0.30)
	7.5	Std	2	3.47 (0.06)
		1.5 Std	2	2.70 (0.28)
	8.5	Std	2	2.2 (0.25)
	9.5	Std	2	1.93 (0.25)

[a] Initial concentration of [^{3}H]dinoprostone was 5×10^{-4} mg/mL or 1.7×10^{-6} mg/mL. The k_u is the apparent first-order transport rate constant. Std means standard buffer capacity (see Ref. 3 for buffer formula).

fication and factorization of the permeability coefficients of the aqueous boundary layer in front of the membrane and the passive diffusional-bioconversion and aqueous pore pathways of the membrane were accomplished using the physical model derived previously (4).

EXPERIMENTAL SECTION

In situ absorption studies with dinoprostone in the rat jejunum were carried out by a modified Doluisio technique (4). The experimental variables included a wide range of buffer pH (3.5–9.5), buffer capacity, dinoprostone concentration, and hydrodynamic situations. Dinoprostone[2], [^{3}H]dinoprostone[3], 1-[^{14}C]butanol[3], and *n*-[^{14}C]butyric acid[3] were used without further purification. All buffer and rinsing solutions were isoosmotic.

Male Sprague-Dawley rats, 220–275 g, were used. A 22-cm segment of jejunum was exposed and cannulated. All experiments were conducted at 37°C.

To assess membrane damage, villous immobility, or vasoconstriction caused by concentrations of prostaglandins that might be used in subsequent experiments, the jejunal absorption of 1-[^{14}C]butanol, 1-[^{14}C]octanol, and *p*-[^{14}C]aminobenzoic acid was followed in the presence and absence of experimental concentrations of dinoprostone at constant hydrodynamic conditions. The effect on intestinal secretions was observed by following the absorption of *n*-[^{14}C]butyric acid in the absence and presence of dinoprostone at a constant hydrodynamic condition.

In the *in situ* absorption studies, exactly 2 mL of radiolabeled solute in isotonic buffer was introduced into the lumen of the jejunum by means of the pump. To control the hydrodynamics, the experiments were conducted by the so-called static and oscillation methods. In the oscillation method, the lumenal solution was continuously pumped back and forth at 0.075 mL/s. All sampling points were at 150-s intervals.

At all times, at least 80% of the drug solution remained in the lumenal segment. The initial tracer concentration of [^{3}H]dinoprostone was 0.1 μCi/mL of drug-buffer solution, equivalent to 5×10^{-4} mg/mL. Twenty microliters of lumenal solution was taken at intervals with the aid of an automatic pipet and transferred into 10 mL of a liquid scintillation[4] cocktail[5].

TLC was performed on silica gel plates and developed with the A-IX system (5). Quantitative determinations of radioactivity on the silica gel plates were done from 0.5-cm section scrapings in the scintillation cocktail[5].

THEORETICAL SECTION

Recently, a physical model was derived for the stimultaneous passive transport and bioconversion of dinoprost across the intestinal membrane. It was consistent with the *in situ* absorption studies in the rat jejunum. Because of the similarities of the intestinal absorption of dinoprostone to dinoprost, the identical model is applied here (3, 4).

The disappearance rate in the intestinal lumen follows an apparent first-order transport process:

$$\frac{dC_b}{dt} = -k_u C_b \qquad \text{(Eq. 1)}$$

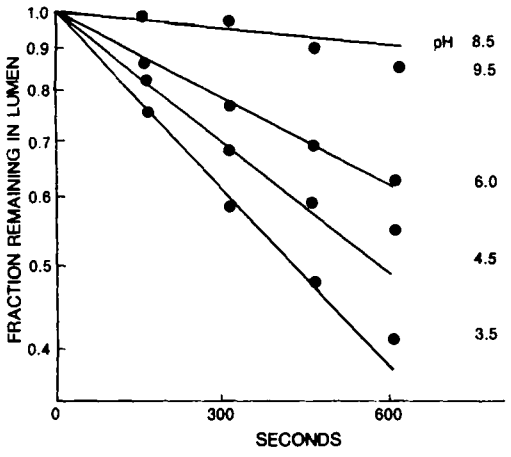

Figure 1—*In situ absorption of dinoprostone at various buffer pH values and high buffer capacity under oscillating (0.075 mL/s) hydrodynamics in the rat jejunum.*

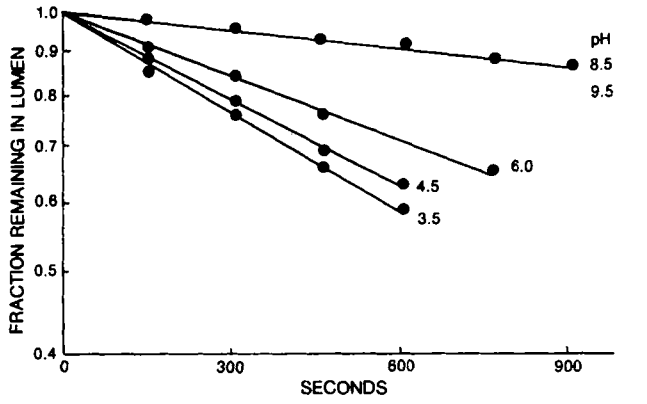

Figure 2—*In situ absorption of dinoprostone at various buffer pH values and high buffer capacity under static conditions (150-s intervals) in the rat jejunum.*

[2] The Upjohn Co.
[3] New England Nuclear Co.
[4] Beckman model LS 200 spectrometer.
[5] Aquasol.

Table II—Assessment of the Presence of Metabolism and Impurity Compounds on the Determination of the Absorption Rate Constant of Dinoprostone in the Rat Jejunum

Buffer pH	Hydrodynamic Condition	$k_u \times 10^4$ s^{-1} Uncorrected	Corrected
3.5	Static	9.1	8.4
	Oscillation	17.0	16.9
4.5	Static	8.9	8.5
	Oscillation	12.0	11.7
6.0	Static	6.2	5.9
	Oscillation	7.4	7.3

and:

$$k_u = \frac{A/V}{\frac{1}{P_{aq}} + \frac{1}{\frac{KX_s\sqrt{kD}}{\tanh(L\sqrt{k/D})} + P_p}} \quad \text{(Eq. 2)}$$

where C_b is the total dinoprostone concentration in the bulk lumenal solution; t is the time in s; k_u is the apparent first-order absorption rate constant in s^{-1}; P_{aq} is the permeability coefficient of aqueous diffusion layer; P_p is the permeability coefficient of the aqueous pores of the membrane; L is the membrane thickness; k is the apparent first-order enzyme rate constant in s^{-1}; D is the diffusion coefficient of dinoprostone in the membrance (cm^2/s); A is the apparent lumenal surface area; X_s is the fraction of nondissociated dinoprostone species at the membrane surface; K is the lipoidal membrane-aqueous partition coefficient of the nondissociated prostaglandin acid; V is the volume of lumenal solution. The integration of Eq. 1 between the limits of the initial total concentration $C_b(0)$ and $C_b(t)$ leads to the semilogarithmic expression:

$$\ln C_b = \ln C_b(0) - k_u t \quad \text{(Eq. 3)}$$

By using Eq. 2, one can readily determine the apparent absorption rate constants under varying pH and hydrodynamic conditions in the lumen. In turn, the permeability coefficients of the aqueous diffusion layer and the membrane itself can be factored out.

The permeability coefficients of the aqueous diffusion layer are found as follows. Under two hydrodynamic conditions at constant buffer pH, two rates of absorption are expected. Accordingly, this situation is described by the following set of linear algebraic equations:

$$\frac{1}{P_{aq}} + \frac{1}{P_{e,m}} = \frac{A/V}{k_u} \quad \text{(Eq. 4)}$$

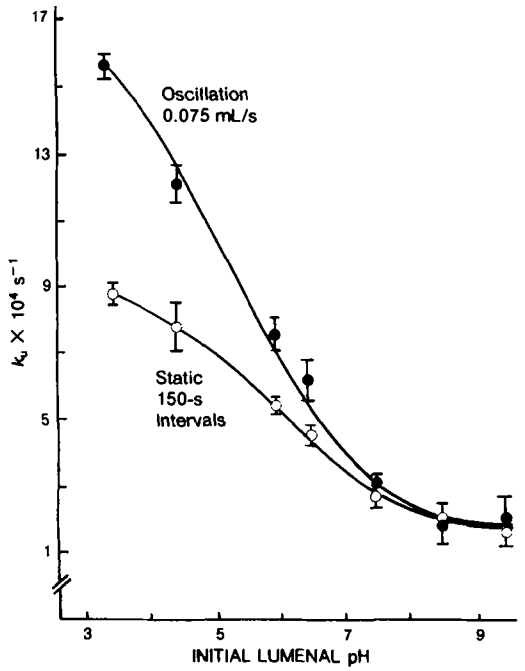

Figure 3—*Apparent absorption rate constants versus high buffer capacity pH under two hydrodynamic conditions for dinoprostone in the rat jejunum.*

Table III—*In Situ* Absorption of 1-[^{14}C]Butanol and 1-[^{14}C]Octanol in the Presence and Absence of Dinoprostone at pH 4.5 and 6.0 under Oscillation (0.075 mL/s) Hydrodynamics; Assessment of Effects on the Aqueous Diffusion Layer, Membrane, and Vascular System

Buffer pH	Rat	Order of Experiment[a]	Dinoprostone, μg/mL	$k_u \times 10^3$ s^{-1}
		1-[^{14}C]Butanol		
4.5	A	1	0	1.9
		2	1.76	1.4
	B	1	1.76	1.8
		2	0	1.6
6.0	C	1	0	1.4
		2	1.76	1.4
	D	1	1.76	1.2
		2	0	1.2
		1-[^{14}C]Octanol		
4.5	A	1	0	2.6
		2	1.76	2.5
	B	1	1.76	2.5
		2	0	2.7
6.0	C	1	0	2.8
		2	1.76	2.7
	D	1	1.76	3.0
		2	0	2.7

[a] In the same jejunal segment.

$$\frac{1}{P_{aq}'} + \frac{1}{P_{e,m}} = \frac{A/V}{k_u'} \quad \text{(Eq. 5)}$$

where the effective permeability coefficient of the membrane, $P_{e,m}$, is:

$$P_{e,m} = \frac{KX_s\sqrt{kD}}{\tanh(L\sqrt{k/D})} + P_p \quad \text{(Eq. 6)}$$

Here it is noted that the first-order rate constant, k_u, and the permeability coefficient of the aqueous diffusion layer, P_{aq}, are different from k_u' and P_{aq}' due to the difference in hydrodynamic conditions but that the effective permeability coefficient of the membrane is not affected by the hydrodynamics in the lumenal solution. Subsequently, if one knows the value of the ratio between P_{aq} and P_{aq}', *i.e.*:

$$\frac{P_{aq}'}{P_{aq}} = r^* \; (P_{aq}' > P_{aq};\; k_u' > k_u) \quad \text{(Eq. 7)}$$

where $r^* \geq 1.0$, it follows that:

$$\frac{1}{P_{aq}} + \frac{1}{P_{e,m}} = \frac{A/V}{k_u} \quad \text{(Eq. 8)}$$

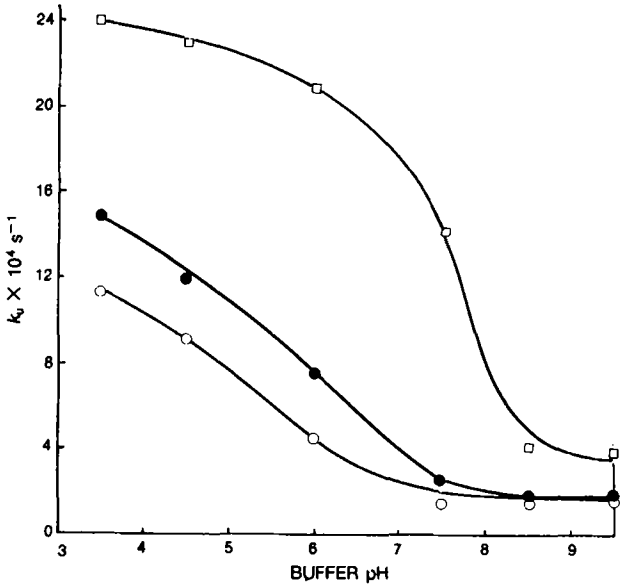

Figure 4—*Comparison of the absorption rate constant-buffer pH profiles of dinoprostone (●), dinoprost (○), and n-butyric acid (□) in the rat jejunum. The pK_a of these acids is 4.9.*

Table IV—*In Situ* Absorption of *n*-[^{14}C]Butyric Acid in the Rat Jejunum in the Presence and Absence of Dinoprostone at Buffer pH 4.5 and 9.5 under Oscillation (0.075 mL/s) Hydrodynamics [a]

pH	Dinoprostone, μg/mL	$k_u \times 10^3$ s^{-1}
4.5	0	3.13
		2.89
	0.5	2.96
		2.63
9.5	0	0.52
		0.52
	0.5	0.5
		0.51

[a] $n = 2$.

$$\frac{1}{r^* P_{aq}} + \frac{1}{P_{e,m}} = \frac{A/V}{k_u'} \qquad \text{(Eq. 9)}$$

Hence, one has a system of two equations in two unknowns, which can be solved in the usual manner. The r^* was determined previously for a number of hydrodynamic situations in the rat intestinal tract using the 1-alkanol series (6).

The permeability coefficient of the aqueous pores of the membrane is determined at buffer pH $\gg$ pK_a. In this situation, X_s approaches zero, causing Eq. 2 to become:

$$k_u = \frac{A}{V} \frac{1}{\frac{1}{P_{aq}} + \frac{1}{P_p}} \qquad \text{(Eq. 10)}$$

RESULTS AND DISCUSSION

General Absorption Experiments—Dinoprostone absorption at various pH values at high buffer capacity and at two hydrodynamic conditions is shown in Figs. 1 and 2. These plots reflect the change in the total radioactivity in the lumenal solution with time. The decrease in rate concomitant with the increase in pH strongly indicates the importance of the partitioning of nondissociated species of dinoprostone (pK_a ~4.9) into the lipoidal diffusion-bioconversion pathway of the membrane as part of the total transport process.

By comparing Figs. 1 and 2, one notices the marked influence of the aqueous diffusion layer on transport kinetics. The hydrodynamics of the oscillation procedure produced a larger effect on the slope than did the hydrodynamics of the static procedure with 150-s sampling intervals; the higher degree of agitation produced a thinner aqueous diffusion layer on the mucosal side of the membrane.

Table I summarizes the absorption experiments using tracer dinoprostone concentrations at various hydrodynamic conditions, buffer pH, and buffer capacities. The buffer capacity effect on the absorption rate constant is evident. For example, at the nominal buffer pH of 4.5, the rate constant was higher at a high buffer capacity than at a lower capacity. This result is attributed to the relative differences in the surface pH and bulk lumenal pH, which depends on the net fluxes of intestinal secretions and bulk buffer species across the aqueous diffusion layer (6). The bulk pH initially at pH 4.5 increased slower with time the higher buffer capacity than with the lower capacity solution. In contrast, in the pH region beyond 6.0–6.5, the bulk pH (*e.g.*, 7.5) tended to decrease slower with time with the high buffer capacity than the lower buffer capacity solution and converged to approximately pH 6.3. These results emphasize the need to have sufficiently high buffer capacity solutions for baseline control of the surface pH relative to the initial bulk pH.

Figure 3 is a plot of k_u *versus* buffer pH at high buffer capacities taken from the results in Table I. The relative differences in the k_u values for the oscillation and static hydrodynamic cases become smaller as the buffer pH increased. At pH 9.5, the rate constants were about the same. These results were expected

Table V—*In Situ* Absorption of *p*-[^{14}C]Aminobenzoic Acid in the Presence and Absence of Dinoprostone at pH 8.5 under Oscillation (0.075 mL/s) Hydrodynamics: Assessment of Effects on the Aqueous Pore Pathway of the Membrane

Order of Experiment [a]	Rat A Dinoprostone, μg/mL	Rat A $k_u \times 10^4$ s^{-1}	Rat B Dinoprostone, μg/mL	Rat B $k_u \times 10^4$ s^{-1}
1	0	3.5	1.76	4.2
2	1.76	3.6	0	3.8

[a] In the same jejunal segment.

Table VI—Effect of Dinoprostone Concentration on the Absorption at pH 6.0 and Oscillation Hydrodynamics

Rat	Order of Experiment [a]	Dinoprostone, mg/mL	$k_u \times 10^4$ s^{-1}
A	1	8.0×10^{-7}	7.3
	2	8.0×10^{-7}	7.9
B	1	1.6×10^{-5}	8.0
	2	1.6×10^{-5}	6.8
C	1	5.0×10^{-4}	7.2
	2	5.0×10^{-4}	7.9
D	1	1.0×10^{-3}	7.1
	2	1.0×10^{-3}	5.1

[a] In the same jejunal segment.

Table VII—Estimation of the Permeability Coefficient of the Aqueous Diffusion Layer (P_{aq}) [a]

Rat	Buffer pH	Hydrodynamic Condition	Average $k_u \times 10^4$ s^{-1}	$P_{aq} \times 10^4$ cm/s Static	$P_{aq} \times 10^4$ cm/s Oscillation
A	6.0	Static	5.44	0.89	1.88
		Oscillation	7.63		
B	6.5	Static	4.59	0.83	1.74
		Oscillation	6.22		

[a] Average $P_{aq(static)} = 0.86 \times 10^{-4}$ cm/s. Average $P_{aq(oscillation)} = 1.82 \times 10^{-4}$ cm/s. The P_{aq} value was calculated with the aid of Eqs. 8 and 9 with $A/V = 11.2$ and $r^* = 2.12$.

since the total transport rate is more aqueous diffusion controlled at low pH and more effectively membrane controlled with increasing pH. The shapes of the profiles are similar in character to those reported earlier for dinoprost (4). These prostaglandins are known to undergo metabolism in the jejunal membrane to, at least, the 15-oxo and 13,14-dihydro-15-oxo metabolites.

In following dinoprostone absorption, there was always some concentration of extraneous tritium-labeled compounds in the intestinal lumen as well as in the original stock solution[6] as determined by quantitative TLC. These concentrations were always about 10% of the total activity at all sampling intervals during the absorption experiments. Furthermore, the back-diffusion of the 15-oxo derivative of dinoprostone from the membrane into the lumen was detected with time. *In vitro* studies in rat intestinal secretions at pH 6.0 indicated that no metabolism was occurring. The rate constants taken from first-order absorption–time plots corrected for nondinoprostone substances were no different from constants from uncorrected plots (Table II).

Assessment of Aqueous Diffusion Layer, Membrane, and Vascular Effects of Dinoprostone on Absorption—The absorption of various selected radiolabeled solutes (1-butanol, 1-octanol, *n*-butyric acid, and *p*-aminobenzoic acid) was carried out under various pH conditions in the presence and absence of dinoprostone to evaluate possible effects of the postaglandin on the aqueous diffusion layer, membrane permeability, and vascularity of the intestines affecting the blood sink. 1-Butanol and *n*-butyric acid were chosen because their absorption rates are known to be membrane controlled; the absorption rate of 1-octanol is controlled by diffusion across the aqueous boundary layer (6). Successive experiments were often performed in the same jejunal segment of each rat since within-rat variations are usually smaller than between-rat variations.

When using 1-[^{14}C]butanol to focus principally on the membrane effects and 1-[^{14}C]octanol to focus on the aqueous diffusion layer and vascular effects,

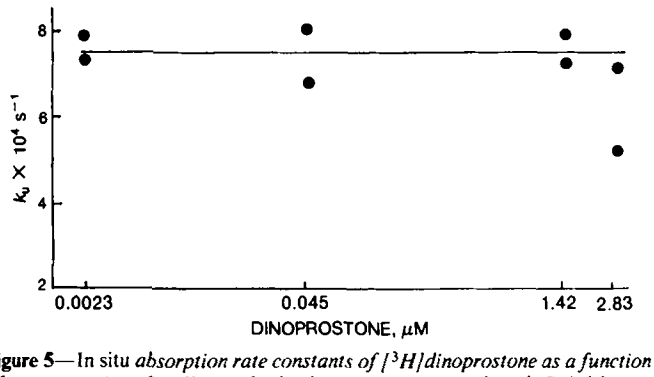

Figure 5—In situ *absorption rate constants of [^{3}H]dinoprostone as a function of concentration. Oscillation hydrodynamics were employed. Solid line is the average rate constant.*

[6] One impurity in the original stock solution had the same R_f as PGA.

Table VIII—Comparison of Diffusional Rates across the Aqueous Layer Barrier in Front of the Mucosal Membrane to the Total Absorption Rates

Hydrodynamic Condition	$P_{aq} \times 10^4$ cm/s	Buffer pH	$k_u \times 10^4$ s^{-1} Experimental	$k_u \times 10^4$ s^{-1} Maximum[a]	Fraction of Absorption Rate Controlled by Aqueous Diffusion Layer
Oscillation, 0.075 mL/s	1.82	3.5	16.6	20.38	0.81
		4.5	11.94	20.38	0.59
		6.0	7.63	20.38	0.37
		7.5	2.98	20.38	0.15
		8.5	2.05	20.38	0.10
		9.5	2.0	20.38	0.10
Static, 150-s interval	0.86	3.5	8.78	9.63	0.91
		4.5	7.81	9.63	0.81
		6.0	5.44	9.63	0.56
		7.5	2.70	9.63	0.28
		8.5	2.2	9.63	0.23
		9.5	1.93	9.63	0.20

[a] $k_{u,max} = \frac{AP_{aq}}{V} = 11.2\,P_{aq}$.

Table IX—Factorization of Effective Permeability Coefficients of the Jejunal Membrane at Various Buffer pH Values into the Permeability Coefficients of the Aqueous Pores and Principal Membrane Pathway

Hydrodynamic Condition	Buffer pH	Average $k_u \times 10^4$ s^{-1}	Permeability Coefficients $\times 10^4$ cm/s P_{aq}	$P_{c,m}$[a]	P_p	P_m[a]
Oscillation 0.075 mL/s	3.5	16.6	1.82	7.98	0.2	7.78
	4.5	11.94	1.82	2.57	0.2	2.37
	6.0	7.63	1.82	1.09	0.2	0.89
	7.5	2.98	1.82	0.31	0.2	0.11
	8.5	2.05	1.82	0.2	0.2	0
	9.5	2.0	1.82	0.2	0.2	0
Static 150-s interval	3.5	8.78	0.86	—	0.2	—
	4.5	7.81	0.86	—	0.2	—
	6.0	5.44	0.86	1.12	0.2	0.92
	7.5	2.70	0.86	0.33	0.2	0.13
	8.5	2.2	0.86	0.2	0.2	0
	9.5	1.93	0.86	0.2	0.2	0

[a] $P_{c,m}$ is defined by Eq. 6, and $P_m = \frac{KX_s\sqrt{kD}}{\tanh(L\sqrt{k/D})}$.

the absorption of these solutes was not affected by 1.76 μg/mL of dinoprostone at pH 4.5 and 6.0 (Table III). These pH conditions were chosen since the absorption is pH dependent (Table I) while the alkanol absorption is pH independent. Furthermore, when using *n*-butyric acid at pH 4.5 to assess the lipoidal and aqueous pore pathways of the membrane and *n*-butyric acid and the larger molecular size *p*-aminobenzoic acid at high pH to assess possible changes in the aqueous pores, a 1.76-μg/mL concentration did not have any apparent effect (Tables IV and V). As will be seen later, absorption was not influenced by concentrations up to 1×10^{-3} mg/mL (equivalent to 2.83 μM). From all of these results together, it is concluded that dinoprostone does not have significant adverse effects on the membrane system so that an unambiguous quantification and interpretation of the membrane permeability coefficients can be made.

Mechanism of Dinoprostone Absorption in Intestines—Since dinoprost is transported across the lipoidal membrane by a simultaneous passive diffusion-bioconversion kinetic process (3, 4), this is good reason to expect that dinoprostone follows the identical mechanism. For comparison, the absorption rate constant *versus* buffer pH plots are shown in Fig. 4 for both prostaglandins. Although *n*-butyric is only passively absorbed (6), it is included here to point out the similarities of the general pH-partition phenomena with *n*-butyric acid to the prostaglandins.

As shown in Fig. 4, the absorption rate constants of dinoprost from pH 3.5 to 7.5 were comparatively less than those of the more lipophilic dinoprostone at comparable pH. They tended to converge at about pH 8.5, as might be expected for the transport of the anions across the aqueous pore pathway. In contrast, the absorption-pH profile of *n*-butyric acid was higher than that for the prostaglandins and was also shifted more to the right. The asymptotic minimum absorption rate of *n*-butyric acid across the aqueous pore at pH 8.5 and higher was faster than the prostaglandins by a factor of two. In summary, the comparative profiles of these three weak acids represent the net interplay of the pH and permeabilities of the aqueous diffusion layer barrier in front of the membrane and the membrane itself.

The possibility of a facilitated transport process is virtually eliminated by the absorption data found in Table VI and Fig. 5. Contrary to the theory of the facilitated mechanism, a relatively constant absorption rate at pH 6.0 was found over a 1.25×10^3-fold range of dinoprostone concentrations (from 8×10^{-4} to 1.0 μg/mL).

Permeability Coefficients—The permeability coefficients of the aqueous diffusion layer, estimated from the pH 6.0 and 6.5 absorption data, were 0.86×10^{-4} cm/s for the static hydrodynamics and 1.82×10^{-4} cm/s for the oscillation case (Table VII). The data at pH 3.5 and 4.5 were not employed, since the absorption rates are highly aqueous diffusion controlled where Eqs. 8 and 9 become insensitive. The coefficients compare well with the 0.8×10^{-4} and 1.7×10^{-4} cm/s found in the dinoprost studies (3). Using the P_{aq} values, one gets estimates on how much the total absorption rate is aqueous diffusion controlled or membrane controlled (Table VIII). At low pH, the absorption is governed by diffusion in front of the membrane, while at higher pH it is controlled more by the membrane.

With the average $k_u = 2.0 \times 10^{-4}$ s^{-1} at high pH and Eq. 10, the permeability coefficient of the aqueous pores for the dinoprostone anions is 2.0×10^{-5} cm/s. In perspective, P_p is 1.5×10^{-5} cm/s for dinoprost. Since the permeability coefficients of the aqueous diffusion layer and the aqueous pores of the membrane are known, the factorization of the effective permeability coefficient for the simultaneous membrane transport and bioconversion of dinoprostone, *i.e.*, $KX_s\sqrt{kD}/\tanh(L\sqrt{k/D})$, is readily attained. Table IX summarizes the quantitative estimates of all of the permeability coefficients.

CONCLUSIONS

Baseline intestinal absorption studies of dinoprostone in the rat were established, and the results were mechanistically consistent with dinoprost. These two important prostaglandins provide the reference compounds from which the *in situ* absorption and metabolism in the intestinal membrane of their respective derivatives and analogues can be studied on a predictive level *via* the physical model approach. Such studies are in progress.

REFERENCES

(1) W. E. Magee, S. B. Armour, and O. V. Miller, *Biochim. Biophys. Acta*, **306**, 270 (1973).

(2) J. T. Doluisio, N. F. Billups, L. W. Dittert, E. T. Sugita, and J. F. Swintosky, *J. Pharm. Sci.*, **58**, 1196 (1969).
(3) J. Y. Park, N. F. H. Ho, and W. Morozowich, *J. Pharm. Sci.*, **73**, 1588.
(4) N. F. H. Ho, J. Park, W. Morozowich, and W. I. Higuchi, *J. Theor. Biol.*, **61**, 185 (1976).
(5) M. Hamberg and B. Samuelsson, *J. Biol. Chem.*, **241**, 257 (1966).
(6) K. Desai, Ph.D. thesis, University of Michigan, Ann Arbor, Mich., 1976.

ACKNOWLEDGMENTS

The authors thank Dr. R. S. Hsi, The Upjohn Co., for the generous supply of [^{3}H]dinoprostone.

Influence of Mode of Intravenous Administration and Blood Sample Collection on Rat Pharmacokinetic Data

FRANCIS L. S. TSE ˣ, TSAILING CHANG, BARBARA FINKELSTEIN, FRANCES BALLARD, and JAMES M. JAFFE

Received June 13, 1983, from the *Drug Metabolism Section, Sandoz, Inc., East Hanover, NJ 07936.* Accepted for publication February 16, 1984.

Abstract □ The influence of the mode of intravenous dosing and blood sample collection on the pharmacokinetics of 4-[(3-methoxyphenyl)-methyl]-2,2,6,6-tetramethyl-1-oxa-4-aza-2,6-disilacyclohexane hydrochloride (I) was studied in the rat. Blood samples obtained from the tail and by exsanguination following injection of the ^{14}C-labeled drug into the caudal vein, the jugular vein, and the heart were analyzed for total radioactivity, and the concentration profiles from the different treatments were compared. Dosing and sampling from the tail vein resulted in significantly different blood levels (and related pharmacokinetic parameters) when compared to other methods, probably attributable to a local depot effect. Intracardiac administration tended to cause higher drug levels in the heart than intravenous doses, although no significant differences were found between the respective blood concentrations. The results showed that caudal vein injection is a simple and adequate method of intravenous administration in rats designated for exsanguinated blood and tissue collection. For serial blood sampling in individual animals, the dose may be given *via* the jugular vein and the blood collected from the cut tail. These methods require little or no surgical preparations and are particularly suitable for prolonged sampling in studies where a relatively large number of animals are involved.

Keyphrases □ Pharmacokinetics—influence of mode of intravenous administration and blood sample collection, rat □ Dosing—pharmacokinetics, mode of intravenous administration, blood sample collection

During the developmental process of a potential therapeutic agent, pharmacokinetic studies are often conducted at the same time as toxicity trials. While the oral route of administration is invariably used in these studies in order to be consistent with the toxicity tests, additional experiments employing intravenous doses are usually performed so that important pharmacokinetic parameters such as the volume of distribution and absolute oral bioavailability or absorption can be determined. In the rat, the caudal vein is often used as the site of injection. In contrast, injection *via* the jugular or femoral vein requires surgical exposure of the vein (1) and can be cumbersome in studies involving a large number of animals. Drugs are also administered by simple cardiac puncture, but the results may not be truly representative of an intravenous dose. Potential complications such as embolization and excessive local drug toxicity are further limitations of the intracardiac route. Intraperitoneal injection, commonly used for the administration of compounds to small animals, is different from intravenous dosing in that drug absorption from the peritoneal cavity is slower (2) and entails passage into the portal circulation, resulting in incomplete systemic bioavailability (3).

In recent years, numerous sensitive analytical methods that require only microsamples of blood have been developed, and pharmacokinetic data from individual rats or similar small animals can be obtained by serial sample collection. Several methods using a chronic indwelling catheter to facilitate repeated blood collection have been described (4–6), but the animal preparation procedures are elaborate and tedious and are incompatible with prolonged sampling periods in studies involving a large number of animals. Other methods of vascular access and their potential complications have been described in a recent review (7). A simple alternative to cannulation is the nonsurgical method of bleeding the rat from the cut end of its tail. However, due to the relatively low regional blood flow (8, 9), which could result in delayed mixing of the administered drug, the validity of tail concentration data remains unclear.

Using a new skeletal muscle relaxant, 4-[(3-methoxyphenyl)-methyl]-2,2,6,6-tetramethyl-1-oxa-4-aza-2,6-disilacyclohexane hydrochloride[1] (I), as a test compound, the present study was undertaken to examine the effect of the mode of intravenous dosing and blood sample collection on pharmacokinetic data in the rat. Blood was obtained from the tail and by exsanguination following injection of the ^{14}C-labeled drug into the caudal vein, the jugular vein, and the heart. Radioactivity concentration in the heart tissue after intracardiac administration was also measured for comparison with existing intravenous data.

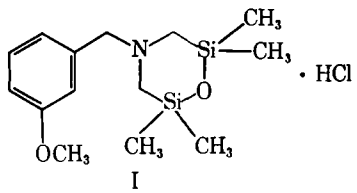

I

EXPERIMENTAL SECTION

Dose Administration and Sample Collection—Male Sprague–Dawley rats, average weight 250 g, were used. They were housed individually in standard cages and had free access to food and water at all times. The rats were divided randomly into three groups of 24 each for drug administration *via* the caudal vein, the jugular vein, and the heart.

Radioactive I was labeled with carbon-14 at the methylene group of the

[1] Compound 58-112 hydrochloride; Sandoz, Inc., East Hanover, N.J.

0022-3549/84/1100-1599$01.00/0
© 1984, American Pharmaceutical Association

(2) J. T. Doluisio, N. F. Billups, L. W. Dittert, E. T. Sugita, and J. F. Swintosky, *J. Pharm. Sci.*, **58**, 1196 (1969).
(3) J. Y. Park, N. F. H. Ho, and W. Morozowich, *J. Pharm. Sci.*, **73**, 1588.
(4) N. F. H. Ho, J. Park, W. Morozowich, and W. I. Higuchi, *J. Theor. Biol.*, **61**, 185 (1976).
(5) M. Hamberg and B. Samuelsson, *J. Biol. Chem.*, **241**, 257 (1966).
(6) K. Desai, Ph.D. thesis, University of Michigan, Ann Arbor, Mich., 1976.

ACKNOWLEDGMENTS

The authors thank Dr. R. S. Hsi, The Upjohn Co., for the generous supply of [^{3}H]dinoprostone.

Influence of Mode of Intravenous Administration and Blood Sample Collection on Rat Pharmacokinetic Data

FRANCIS L. S. TSE ˣ, TSAILING CHANG, BARBARA FINKELSTEIN, FRANCES BALLARD, and JAMES M. JAFFE

Received June 13, 1983, from the *Drug Metabolism Section, Sandoz, Inc., East Hanover, NJ 07936.* Accepted for publication February 16, 1984.

Abstract □ The influence of the mode of intravenous dosing and blood sample collection on the pharmacokinetics of 4-[(3-methoxyphenyl)-methyl]-2,2,6,6-tetramethyl-1-oxa-4-aza-2,6-disilacyclohexane hydrochloride (I) was studied in the rat. Blood samples obtained from the tail and by exsanguination following injection of the ^{14}C-labeled drug into the caudal vein, the jugular vein, and the heart were analyzed for total radioactivity, and the concentration profiles from the different treatments were compared. Dosing and sampling from the tail vein resulted in significantly different blood levels (and related pharmacokinetic parameters) when compared to other methods, probably attributable to a local depot effect. Intracardiac administration tended to cause higher drug levels in the heart than intravenous doses, although no significant differences were found between the respective blood concentrations. The results showed that caudal vein injection is a simple and adequate method of intravenous administration in rats designated for exsanguinated blood and tissue collection. For serial blood sampling in individual animals, the dose may be given *via* the jugular vein and the blood collected from the cut tail. These methods require little or no surgical preparations and are particularly suitable for prolonged sampling in studies where a relatively large number of animals are involved.

Keyphrases □ Pharmacokinetics—influence of mode of intravenous administration and blood sample collection, rat □ Dosing—pharmacokinetics, mode of intravenous administration, blood sample collection

During the developmental process of a potential therapeutic agent, pharmacokinetic studies are often conducted at the same time as toxicity trials. While the oral route of administration is invariably used in these studies in order to be consistent with the toxicity tests, additional experiments employing intravenous doses are usually performed so that important pharmacokinetic parameters such as the volume of distribution and absolute oral bioavailability or absorption can be determined. In the rat, the caudal vein is often used as the site of injection. In contrast, injection *via* the jugular or femoral vein requires surgical exposure of the vein (1) and can be cumbersome in studies involving a large number of animals. Drugs are also administered by simple cardiac puncture, but the results may not be truly representative of an intravenous dose. Potential complications such as embolization and excessive local drug toxicity are further limitations of the intracardiac route. Intraperitoneal injection, commonly used for the administration of compounds to small animals, is different from intravenous dosing in that drug absorption from the peritoneal cavity is slower (2) and entails passage into the portal circulation, resulting in incomplete systemic bioavailability (3).

In recent years, numerous sensitive analytical methods that require only microsamples of blood have been developed, and pharmacokinetic data from individual rats or similar small animals can be obtained by serial sample collection. Several methods using a chronic indwelling catheter to facilitate repeated blood collection have been described (4–6), but the animal preparation procedures are elaborate and tedious and are incompatible with prolonged sampling periods in studies involving a large number of animals. Other methods of vascular access and their potential complications have been described in a recent review (7). A simple alternative to cannulation is the nonsurgical method of bleeding the rat from the cut end of its tail. However, due to the relatively low regional blood flow (8, 9), which could result in delayed mixing of the administered drug, the validity of tail concentration data remains unclear.

Using a new skeletal muscle relaxant, 4-[(3-methoxyphenyl)-methyl]-2,2,6,6-tetramethyl-1-oxa-4-aza-2,6-disilacyclohexane hydrochloride[1] (I), as a test compound, the present study was undertaken to examine the effect of the mode of intravenous dosing and blood sample collection on pharmacokinetic data in the rat. Blood was obtained from the tail and by exsanguination following injection of the ^{14}C-labeled drug into the caudal vein, the jugular vein, and the heart. Radioactivity concentration in the heart tissue after intracardiac administration was also measured for comparison with existing intravenous data.

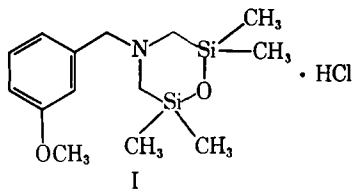

I

EXPERIMENTAL SECTION

Dose Administration and Sample Collection—Male Sprague–Dawley rats, average weight 250 g, were used. They were housed individually in standard cages and had free access to food and water at all times. The rats were divided randomly into three groups of 24 each for drug administration *via* the caudal vein, the jugular vein, and the heart.

Radioactive I was labeled with carbon-14 at the methylene group of the

[1] Compound 58-112 hydrochloride; Sandoz, Inc., East Hanover, N.J.

0022-3549/84/1100-1599$01.00/0
© 1984, American Pharmaceutical Association

Table I—Summary of Treatments

Treatment	Route of Dosing/Sampling	Dose, mg/kg	No. of Rats
1	Caudal Vein/Tail	10	3
2	Caudal Vein/Vena Cava	10	3/time point
3	Jugular Vein/Tail	10	3
4	Jugular Vein/Vena Cava	10	3/time point
5	Intracardiac/Tail	5	3
6	Intracardiac/Vena Cava	5	3/time point

benzyl moiety. The radiochemical purity of the product was established by the inverse isotope dilution method to be >95%, and the specific activity was 3.25 μCi/mg. The dose was prepared as a 10 mg/mL solution in water. For the intravenous doses (10 mg/kg), each rat received 1 mL of the solution/kg body weight. For injection into the caudal vein, the tail was first immersed for 1–2 min in warm water; for jugular vein dosing, the rats were maintained under light ether anesthesia and the vein was exposed by a small skin incision made in the neck to one side of midline. For intracardiac administration, the dose was reduced from 10 to 5 mg/kg due to frequent deaths at the high dose level. Thus, each rat received 1 mL/kg of the solution (5 mg/mL in normal saline) *via* a single cardiac puncture.

Serial blood samples (250 μL) were collected in heparinized micropipettes[2] from three rats in each dose group *via* the cut tail immediately before and at 5, 15, and 30 min and 1, 3, 5, and 8 h postdose. Of the remaining 21 rats three each were sacrificed at 5, 15, and 30 min and 1, 3, 5, and 8 h postdose. Blood (~5 mL) was collected *via* the vena cava. The heart of each sacrificed rat receiving the intracardiac dose was collected (Table I).

Analysis of Radioactivity—Aliquots of dose preparations, blood, and heart tissue homogenates were air dried and combusted in a sample oxidizer[3] using 9 mL of absorption medium[4] and 12 mL of scintillation cocktail[5]. Radioactivity was measured in a liquid scintillation counter[6]. The quench correction and efficiency of the counter were determined from a standard curve constructed using ^{14}C-labeled hexadecane[7] of known specific activity. The limit of sensitivity of the assay was defined as twice the mean background count. Gross sample counts below this level were considered to be not significantly different from zero. Blood and tissue concentrations of radioactivity were calculated as nanogram equivalents of I per milliliter or gram.

Treatment of Data—The dose-normalized blood levels of radioactivity at each sampling time were examined by analysis of variance. Because of the observed differences in data variance between groups, the statistical tests were performed on log-transformed data (10). If differences ($p < 0.05$) due to treatments were observed, results from individual treatments were compared by the Student's t test.

Since, in half of the experiments, blood at each sampling time was collected from different (sacrificed) rats, only mean concentration data were available for pharmacokinetic analysis. For consistency, only mean blood levels from the serially bled animals were used for this purpose. The blood concentration data were fitted to a biexponential function of the form:

$$C = Ae^{-\alpha t} + Be^{-\beta t} \quad (\alpha > \beta) \qquad \text{(Eq. 1)}$$

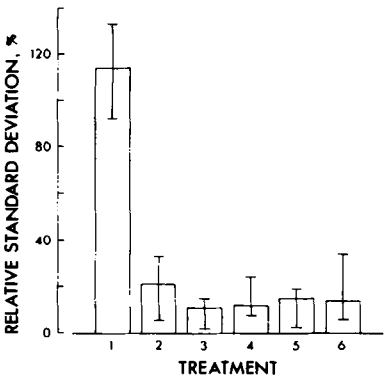

Figure 1—RSD *in blood radioactivity levels following all treatments. Each bar represents the median and range of seven time point observations.*

[2] Microcaps; Drummond Scientific Co., Broomall, Pa.
[3] Model 306; Packard Instrument Co., Downers Grove, Ill.
[4] Carbosorb II; Packard Instrument Co.,
[5] Permafluor V; Packard Instrument Co.
[6] Packard Tri-Carb 460; Packard Instrument Co.
[7] Packard Instrument Co.

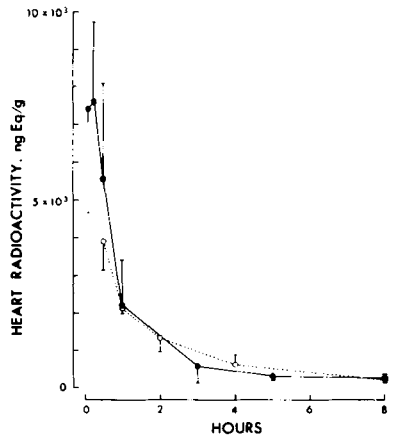

Figure 2—*Mean concentrations of radioactivity in the heart following caudal vein (○) 10 mg/kg, and intracardiac (●), 5 mg/kg injections. Each bar represents one* SD. *The data for caudal vein injection are adapted from Bhuta*[9].

where C is the blood concentration of radioactivity at time, t, A and B are constants, and α and β are composite first-order rate constants. Attempts to fit the data to a triexponential function resulted in greater errors in parameter values with no increase in coefficients of determination. Initial estimates of pharmacokinetic parameters were obtained by standard graphic methods (11) while improved parameter estimates together with statistical analysis were obtained using the iterative nonlinear regression program NONLIN (12) on a computer[8]. The blood level data were weighted by their reciprocals in the regression analysis.

RESULTS

Mean blood levels of radioactivity, together with statistical analyses, are given in Table II. Results of pharmacokinetic analyses are given in Table III. The goodness of fit of the data to Eq. 1 was demonstrated by correlation coefficients of 0.97–1.00.

Comparison of the blood radioactivity levels showed that dosing and sampling, both from the tail vein (treatment 1), resulted in elevated blood level measurements throughout the 8 h sampling period, although the differences were statistically significant only at 0.083, 0.25, and 8 h. Treatment 1 also had a greater interanimal variability in blood levels, as indicated by the large *RSD* values (coefficients of variation) illustrated in Fig. 1. Comparison of the results from treatments 3 *versus* 4 and treatments 5 *versus* 6 also suggested that blood sampling near the site of drug administration yielded higher initial concentrations than at a more distal sampling site, although the differences were not statistically significant.

From Table III, analysis of blood level data obtained from all six treatments yielded similar distribution half-lives of 15–30 min. The elimination half-lives for treatments 2–5 were ~5 h, identical with those observed in previous experiments in which the drug was administered *via* the tail vein and blood was collected from the vena cava for 24 h (~5 half-lives)[9]. Thus, the 8-h sampling period employed in the present study was sufficient to describe the terminal linear phase. For treatments 1 and 6, the half-lives appeared longer. Because of the higher tail blood concentrations obtained following the caudal vein dose (treatment 1), the area under the curve value was almost 10 times greater than those observed for the other treatments. Accordingly, treatment 1 also resulted in markedly reduced plasma clearance and volumes of distribution.

During the intracardiac dosing experiments, it was necessary to reduce the dose from 10 to 5 mg/kg because of frequent deaths occurring at the high dose level, apparently due to elevated initial drug concentrations in the heart. This was confirmed by comparing the heart radioactivity concentration obtained following the intracardiac injection to existing data[9] measured after dosing *via* the caudal vein (Fig. 2). Despite a twofold difference in dose level, the 10-mg/kg caudal vein dose and the 5-mg/kg intracardiac dose gave similar radioactivity concentration in the heart at all times.

DISCUSSION

Assuming equal metabolic fate for the drug administered *via* the caudal vein, the jugular vein, and the heart, the blood concentration data of total radioactivity alone would generate sufficient information to answer the

[8] 4341; IBM.
[9] S. I. Bhuta, unpublished results.

Table II—Blood Levels of Radioactivity Obtained from All Treatments, Mean ± *SD*

Treatment	Dose, mg/kg[a]	Blood Concentration of I Equivalents, ng Eq/mL						
		0.083 h	0.25 h	0.5 h	1 h	3 h	5 h	8 h
1	10	23370 ± 21590	23140 ± 29250	12710 ± 16850	5020 ± 5380	4460 ± 5550	3060 ± 3490	2010 ± 2100
2	10	2310 ± 430	1860 ± 380	1160 ± 380	990 ± 210	540 ± 30	440 ± 100	310 ± 90
3	10	1780 ± 340	1420 ± 90	1150 ± 20	980 ± 50	510 ± 70	420 ± 50	280 ± 30
4	10	2260 ± 170	1940 ± 190	1420 ± 140	890 ± 110	500 ± 100	340 ± 80	200 ± 40
5	5	970 ± 160	880 ± 130	665 ± 125	570 ± 65	360 ± 25	285 ± 45	205 ± 5
6	5	1590 ± 95	1785 ± 610	1235 ± 170	625 ± 60	320 ± 85	290 ± 60	175 ± 15
t test among treatments[b]		1 > 2-6	1 > 2-5	NSD[c]	NSD[c]	NSD[c]	NSD[c]	1 > 2-6

[a] For statistical comparisons only, the raw data were dose-normalized and log-transformed. [b] Significant at $p < 0.05$. [c] No significant differences by analysis of variance.

Table III—Pharmacokinetic Parameters Obtained from All Treatments

Parameter[a]	Treatment					
	1	2	3	4	5[b]	6[b]
D, mg/kg	10	10	10	10	5	5
α, h^{-1}	2.4	2.8	1.6	2.0	1.8	1.5
	(−0.81 − 5.6)[c]	(0.11 − 5.5)	(0.012 − 3.2)	(1.2 − 2.8)	(0.29 − 3.3)	(−0.61 − 3.5)
β, h^{-1}	0.086	0.14	0.13	0.17	0.12	0.091
	(−0.32 − 0.50)	(0.22 − 0.27)	(0.011 − 0.25)	(0.093 − 0.25)	(0.042 − 0.19)	(−0.31 − 0.49)
$t_{1/2,\alpha}$, h	0.29	0.25	0.43	0.35	0.38	0.48
$t_{1/2,\beta}$, h	8.1	5.0	5.3	4.1	5.8	7.6
AUC, ng Eq·h/mL	62812	6925	6658	5622	4577	5416
CL_p, L/h/kg	0.16	1.4	1.5	1.8	1.1	0.92
Vd_1, L/kg	0.33	3.7	5.4	3.9	4.7	2.5
Vd_β, L/kg	1.9	10	12	11	9.1	10

[a] D, dose of I; α and β, composite first-order rate constants; $t_{1/2,\alpha}$, half-life of distribution = $0.693/\alpha$; $t_{1/2,\beta}$, half-life of elimination = $0.693/\beta$; AUC, area under concentration *versus* time curve = $A/\alpha + B/\beta$; CL_p, plasma clearance = D/AUC; Vd_1, apparent distribution volume of the central compartment in a two-compartment model = $D/(A + B)$; Vd_β, apparent overall distribution volume = CL_p/β. [b] For comparison between treatments, the data must be dose-normalized by doubling the values of D and AUC for treatments 5 and 6. [c] 95% Confidence interval.

questions outlined in the present study. By comparing treatment 1 *versus* 2, treatment 3 *versus* 4, and treatment 5 *versus* 6, the data seem to indicate that blood sampling near the site of drug administration yielded higher initial concentrations than at a more distal sampling site. Nonetheless, tail blood sampling after caudal vein administration (treatment 1) is the only treatment in this study that gave significantly different blood radioactivity levels and related pharmacokinetic parameters. Evidently, dosing *via* the caudal vein results in some residual drug at and/or near the injection site, so that sampling from the same location leads to elevated drug concentrations which are artifacts and which probably do not represent the circulating concentrations in blood. This phenomenon occurred despite the choice of a compound for this study with relatively high aqueous solubility. Furthermore, because it is technically difficult to uniformly dose *via* the tail vein (1), the magnitude of this depot effect can be quite variable, as demonstrated by the large interanimal differences in the blood levels measured for this group (Fig. 1).

However, the artifact which results from high concentrations after caudal vein dosing can be avoided if blood samples are obtained from an appropriate vein such as the vena cava, since the residual drug at the injection site probably represents a minute portion of the dose. Conversely, if the dose is administered *via* a different (*e.g.*, jugular) vein, the tail blood data seem to reflect true kinetics in the rat. These deductions are based on the close similarities in blood levels as well as pharmacokinetic parameters between treatments 2 and 3 and treatment 4. Treatment 4 concerns blood collected from the vena cava following drug administration *via* a major (jugular) vein and, therefore, is believed to provide data which most accurately describe the pharmacokinetics of the drug. From the results of treatments 2 and 4, it can also be deduced that the application of brief ether anesthesia in the jugular vein dosing procedure has no effect on the blood levels and pharmacokinetic parameters of the drug. Previous investigators (13) have reported that ether may interfere with hepatic drug metabolism and should not be used as an anesthetic in kinetic studies of drugs with short elimination half-lives (~15 min), but may be used for drugs with longer half-lives (>1.2 h).

The results of this study also demonstrate the potential differences between intravenous and intracardiac drug administration. After intracardiac dosing, substantial tissue uptake of drug occurred in the heart, resulting in excessive local drug toxicity at the 10-mg/kg dose level. However, the overall amount of drug reaching the systemic circulation appears comparable to that after the intravenous doses, as indicated by the similar blood radioactivity profiles obtained from treatments 2–4, and treatments 5 and 6, after normalizing by the doses.

In summary, dosing and subsequent sampling from the tail vein results in artifactual and variable blood concentration data due probably to a local depot effect. Although intracardiac injection appears to give blood levels similar to those obtained from true intravenous doses, the former tends to cause substantial tissue uptake of drug in the heart and should not be used in tissue distribution studies. For experiments employing a relatively large number of rats designated for exsanguinated blood and tissue collection, caudal vein injection is a convenient and appropriate method of intravenous dosing. On the other hand, if serial blood samples are needed to establish pharmacokinetic profiles in individual animals, they can be obtained simply from the cut tail after administering the dose *via* the jugular vein. Although injection *via* the jugular vein requires surgical preparation of the rat, it appears to be one of the more reliable methods for intravenous drug administration and, unlike most cannulation techiques, imposes no stress which may affect at least some aspects of normal physiology resulting in altered drug kinetics (7, 9, 14, 15).

Although these findings are probably applicable to a variety of drugs, the magnitude of the observed differences could be dependent upon the physicochemical properties of the individual compounds. Thus, further studies using additional compounds with significantly different chemical properties are warranted in order to evaluate the general applicability of these results.

REFERENCES

(1) H. B. Waynforth, "Experimental and Surgical Technique in the Rat," Academic, London, 1980, pp. 39–42.

(2) F. L. S. Tse and P. G. Welling, *J. Parenteral Drug Assoc.*, **34,** 484 (1980).

(3) G. Lukas, S. D. Brindle, and P. Greengard, *J. Pharmacol. Exp. Ther.*, **178,** 562 (1971).

(4) R. S. Pope, *J. Appl. Physiol.*, **24,** 276 (1968).

(5) B. Scharschmidt and P. D. Berk, *Proc. Soc. Exp. Biol. Med.*, **143,** 364 (1973).

(6) R. A. Upton, *J. Pharm. Sci.*, **64,** 112 (1975).

(7) D. M. Cocchetto and T. D. Bjornsson, *J. Pharm. Sci.*, **72,** 465 (1983).

(8) R. P. Rand, A. C. Burton, and T. Ing, *Can. J. Physiol. Pharmacol.*, **43,** 257 (1965).

(9) W. M. Johannessen, I. M. Tyssebotn, and J. Aarbakke, *J. Pharm. Sci.*, **71,** 1352 (1982).

(10) B. J. Winer, "Statistical Principles in Experimental Design," McGraw-Hill, New York, N.Y., 1971, p. 397.

(11) J. G. Wagner, "Fundamentals of Clinical Pharmacokinetics," 1st ed., Drug Intelligence, Hamilton, Ill., 1975, pp. 59–63.

(12) C. M. Metzler, G. L. Elfring, and A. J. McEwen, *Biometrics*, **30,** 562 (1974).

(13) W. Johannessen, G. Gadeholt, and J. Aarbakke, *J. Pharm. Pharmacol.*, **33,** 365 (1981).

(14) W. F. Bousquet, B. D. Rupe, and T. S. Miya, *J. Pharmacol. Exp. Ther.*, **147**, 376 (1965).
(15) R. E. Stitzel and R. L. Furner, *Biochem. Pharmacol.*, **16**, 1489 (1967).

ACKNOWLEDGMENTS

The authors thank Mr. Kenrick Talbot for preparing the radioactive drug, Ms. Constance Farley for technical assistance, and Mr. Edward Barry for helpful discussions.

Nonaqueous Cephalosporin Suspension for Parenteral Administration: Cefazolin Sodium

KENNETH S. E. SU ˣ, JOHN F. QUAY, KRISTINA M. CAMPANALE, and JOHN F. STUCKY

Received December 16, 1983, from *Lilly Research Laboratories, Eli Lilly and Company, Indianapolis, IN 46285.* Accepted for publication February 24, 1984.

Abstract □ The flocculation-deflocculation behavior of cefazolin sodium (I) in nonaqueous media and the effect of surfactants as measured by zeta potential, sedimentation, and porosity were studied. A significant difference in zeta potential was observed when the particles were suspended in different nonaqueous media. The addition of surfactant produced a deflocculated state. The surfactant deflocculated the particles by a process of supersaturation and crystallization involving a surfactant-cefazolin complex. The shielding effect of the surfactant on the surface of the particles also apparently affected their electrophoretic properties. Kinetic studies on the stability of the drug as a function of temperature were conducted; it appears that the chemical stability in ethyl oleate at room temperature is adequate for a reasonable shelf life. The efficiency of absorption of the drug from the ethyl oleate suspension was evaluated after intramuscular administration in dogs. The area under the plasma concentration *versus* time curve and urinary recovery indicated that cefazolin was 100% bioavailable from this nonaqueous preparation.

Keyphrases □ Cefazolin sodium—surfactants, stability, bioavailability □ Cephalosporin—nonaqueous suspension, stability, bioavailability

Parenteral pharmaceutical suspensions have been used for a long time (1–4). In general, this dosage form is comprised of a physiologically active agent and a vehicle. The vehicle is typically comprised of a suspending liquid, an emulsifying agent, a surfactant, density- and viscosity-adjusting substances, and preservatives. While water is generally the preferred suspending liquid, some physiologically active agents such as the cephalosporin antibiotics are not chemically stable in water-based parenteral pharmaceutical suspensions. Therefore, to achieve a ready-to-use cephalosporin preparation which can be stored at room temperature, it is desirable to develop a satisfactory suspension utilizing a nonaqueous liquid as the suspending medium. This paper describes the preparation of a unique, simple flocculated ready-to-use cefazolin sodium suspension which is dispersed in a nonaqueous medium. The efficiency of absorption of cefazolin from the nonaqueous system administered intramuscularly in dogs is also reported.

Table I—Flocculation-Deflocculation Behavior of Cefazolin Sodium in Peanut Oil [a]

Conc. of Polysorbate 80, %	Sedimentation Volume, H_u/H_o %[b]	Number of Turns to Redisperse
0	48	268
0.17	87	>3500
0.50	82	∞
3.30	63	∞

[a] In the presence of polysorbate 80. [b] Ultimate settled height (H_u) is based on the sedimentation height on day 33.

EXPERIMENTAL SECTION

The following chemicals were used: sterile micronized cefazolin sodium[1]; polysorbate 80, commercial grade[2]; lecithin[3]; ethyl oleate[4]; peanut oil[5]; cefazolin sodium[6]. For *in vivo* studies, sterile micronized cefazolin sodium and ethyl oleate were prepared under sterile conditions. The sterile cefazolin sodium was aseptically micronized[7] and ethyl oleate was sterilized in a preheated oven at 155°C for 5 h. For *in vitro* studies, the materials were used without further sterilization.

Particle Size Distribution—The determination of particle size distribution was conducted by the sedimentation method using a micromerograph[8]. The mean particle size diameter of the micronized material was 7 μm.

Preparation of Suspensions—For *in vitro* studies, suspensions were prepared using an electric mixer[9] to disperse 12.5 g of micronized cefazolin sodium in 50 mL of peanut oil in the presence of various amounts of polysorbate 80 [*i.e.*, 0, 0.17, 0.50, and 3.3% (w/v), respectively]. Suspensions containing lecithin in ethyl oleate were prepared in the same manner. However, the concentration of lecithin added was 0, 0.2, 0.4, 0.6, 0.8, and 1.0% (w/v). For *in vivo* studies, the suspension was aseptically prepared by dispersing 1 g-equivalent activity of sterile micronized cefazolin sodium in 3.0 mL of sterile ethyl oleate with an electric mixer. The suspension was then passed through a 150-mesh sterile stainless steel screen and mixed until uniform. For *in vivo* control studies, aqueous solutions of cefazolin sodium were prepared for intravenous and intramuscular administration by dissolving the sodium salt[6] in isotonic saline to a final concentration of 100 mg/mL as cefazolin.

Sedimentation Volume—The sedimentation volumes were recorded in terms of the ultimate settled height, H_u, to the original height, H_o, as described in the literature (5, 6):

$$\text{Sedimentation Volume} = H_u/H_o \qquad \text{(Eq. 1)}$$

Redispersibility—The number of revolutions necessary to restore the suspension to homogeneity was recorded by means of a multi-purpose rotator[10] with the modification described by Matthews and Rhodes (7).

Turbidity—The turbidity of the supernatant of the suspensions was measured by an analytical nephelometer[11] after cefazolin sodium suspensions had been kept at 25°C for 1 month. The procedure was carried out as described by the manufacturer (8).

Crystal Growth—Crystal size changes with time were microscopically examined. Cefazolin sodium (I) in the dry state was compared with I in a suspension at initial time, and in a suspension stored for 3 months at 25°C.

Viscosity—The viscosities of ethyl oleate and peanut oil were measured with a viscometer[12].

Porosity—The porosity of a sedimentation bed was determined by the method of Kaneniwa and Takamura (9).

[1] Lilly Research Laboratories, Indianapolis, Ind.
[2] Tween 80; ICI America Inc., Wilmington, Del.
[3] American Lecithin Company, Atlanta, Ga.
[4] Pfaltz and Bauer, Inc., Stamford, Conn.
[5] Sessions Oil Mills, Interprise, Ala.
[6] KEFZOL; Eli Lilly and Company, Indianapolis, Ind.
[7] Sturtvant Mill; Sturtvant Mill Company, Boston, Mass.
[8] Sharples, Pennwalt Corp., Warminster, Pa.
[9] Lightnin' Mixing Equipment Co., Inc., Rochester, N.Y.
[10] Scientific Industries, Inc., Bohemia, N.Y.
[11] Hach Chemical Company, Ames, Iowa.
[12] Brookfield Engineering Laboratories, Inc., Stoughton, Mass.

0022-3549/84/1100-1602$01.00/0
© 1984, American Pharmaceutical Association

(14) W. F. Bousquet, B. D. Rupe, and T. S. Miya, *J. Pharmacol. Exp. Ther.*, **147**, 376 (1965).
(15) R. E. Stitzel and R. L. Furner, *Biochem. Pharmacol.*, **16**, 1489 (1967).

ACKNOWLEDGMENTS

The authors thank Mr. Kenrick Talbot for preparing the radioactive drug, Ms. Constance Farley for technical assistance, and Mr. Edward Barry for helpful discussions.

Nonaqueous Cephalosporin Suspension for Parenteral Administration: Cefazolin Sodium

KENNETH S. E. SU ˣ, JOHN F. QUAY, KRISTINA M. CAMPANALE, and JOHN F. STUCKY

Received December 16, 1983, from *Lilly Research Laboratories, Eli Lilly and Company, Indianapolis, IN 46285.* Accepted for publication February 24, 1984.

Abstract □ The flocculation-deflocculation behavior of cefazolin sodium (I) in nonaqueous media and the effect of surfactants as measured by zeta potential, sedimentation, and porosity were studied. A significant difference in zeta potential was observed when the particles were suspended in different nonaqueous media. The addition of surfactant produced a deflocculated state. The surfactant deflocculated the particles by a process of supersaturation and crystallization involving a surfactant-cefazolin complex. The shielding effect of the surfactant on the surface of the particles also apparently affected their electrophoretic properties. Kinetic studies on the stability of the drug as a function of temperature were conducted; it appears that the chemical stability in ethyl oleate at room temperature is adequate for a reasonable shelf life. The efficiency of absorption of the drug from the ethyl oleate suspension was evaluated after intramuscular administration in dogs. The area under the plasma concentration *versus* time curve and urinary recovery indicated that cefazolin was 100% bioavailable from this nonaqueous preparation.

Keyphrases □ Cefazolin sodium—surfactants, stability, bioavailability □ Cephalosporin—nonaqueous suspension, stability, bioavailability

Parenteral pharmaceutical suspensions have been used for a long time (1–4). In general, this dosage form is comprised of a physiologically active agent and a vehicle. The vehicle is typically comprised of a suspending liquid, an emulsifying agent, a surfactant, density- and viscosity-adjusting substances, and preservatives. While water is generally the preferred suspending liquid, some physiologically active agents such as the cephalosporin antibiotics are not chemically stable in water-based parenteral pharmaceutical suspensions. Therefore, to achieve a ready-to-use cephalosporin preparation which can be stored at room temperature, it is desirable to develop a satisfactory suspension utilizing a nonaqueous liquid as the suspending medium. This paper describes the preparation of a unique, simple flocculated ready-to-use cefazolin sodium suspension which is dispersed in a nonaqueous medium. The efficiency of absorption of cefazolin from the nonaqueous system administered intramuscularly in dogs is also reported.

Table I—Flocculation-Deflocculation Behavior of Cefazolin Sodium in Peanut Oil [a]

Conc. of Polysorbate 80, %	Sedimentation Volume, H_u/H_o %[b]	Number of Turns to Redisperse
0	48	268
0.17	87	>3500
0.50	82	∞
3.30	63	∞

[a] In the presence of polysorbate 80. [b] Ultimate settled height (H_u) is based on the sedimentation height on day 33.

EXPERIMENTAL SECTION

The following chemicals were used: sterile micronized cefazolin sodium[1]; polysorbate 80, commercial grade[2]; lecithin[3]; ethyl oleate[4]; peanut oil[5]; cefazolin sodium[6]. For *in vivo* studies, sterile micronized cefazolin sodium and ethyl oleate were prepared under sterile conditions. The sterile cefazolin sodium was aseptically micronized[7] and ethyl oleate was sterilized in a preheated oven at 155°C for 5 h. For *in vitro* studies, the materials were used without further sterilization.

Particle Size Distribution—The determination of particle size distribution was conducted by the sedimentation method using a micromerograph[8]. The mean particle size diameter of the micronized material was 7 μm.

Preparation of Suspensions—For *in vitro* studies, suspensions were prepared using an electric mixer[9] to disperse 12.5 g of micronized cefazolin sodium in 50 mL of peanut oil in the presence of various amounts of polysorbate 80 [*i.e.*, 0, 0.17, 0.50, and 3.3% (w/v), respectively]. Suspensions containing lecithin in ethyl oleate were prepared in the same manner. However, the concentration of lecithin added was 0, 0.2, 0.4, 0.6, 0.8, and 1.0% (w/v). For *in vivo* studies, the suspension was aseptically prepared by dispersing 1 g-equivalent activity of sterile micronized cefazolin sodium in 3.0 mL of sterile ethyl oleate with an electric mixer. The suspension was then passed through a 150-mesh sterile stainless steel screen and mixed until uniform. For *in vivo* control studies, aqueous solutions of cefazolin sodium were prepared for intravenous and intramuscular administration by dissolving the sodium salt[6] in isotonic saline to a final concentration of 100 mg/mL as cefazolin.

Sedimentation Volume—The sedimentation volumes were recorded in terms of the ultimate settled height, H_u, to the original height, H_o, as described in the literature (5, 6):

$$\text{Sedimentation Volume} = H_u/H_o \qquad \text{(Eq. 1)}$$

Redispersibility—The number of revolutions necessary to restore the suspension to homogeneity was recorded by means of a multi-purpose rotator[10] with the modification described by Matthews and Rhodes (7).

Turbidity—The turbidity of the supernatant of the suspensions was measured by an analytical nephelometer[11] after cefazolin sodium suspensions had been kept at 25°C for 1 month. The procedure was carried out as described by the manufacturer (8).

Crystal Growth—Crystal size changes with time were microscopically examined. Cefazolin sodium (I) in the dry state was compared with I in a suspension at initial time, and in a suspension stored for 3 months at 25°C.

Viscosity—The viscosities of ethyl oleate and peanut oil were measured with a viscometer[12].

Porosity—The porosity of a sedimentation bed was determined by the method of Kaneniwa and Takamura (9).

[1] Lilly Research Laboratories, Indianapolis, Ind.
[2] Tween 80; ICI America Inc., Wilmington, Del.
[3] American Lecithin Company, Atlanta, Ga.
[4] Pfaltz and Bauer, Inc., Stamford, Conn.
[5] Sessions Oil Mills, Interprise, Ala.
[6] KEFZOL; Eli Lilly and Company, Indianapolis, Ind.
[7] Sturtvant Mill; Sturtvant Mill Company, Boston, Mass.
[8] Sharples, Pennwalt Corp., Warminster, Pa.
[9] Lightnin' Mixing Equipment Co., Inc., Rochester, N.Y.
[10] Scientific Industries, Inc., Bohemia, N.Y.
[11] Hach Chemical Company, Ames, Iowa.
[12] Brookfield Engineering Laboratories, Inc., Stoughton, Mass.

0022-3549/84/1100-1602$01.00/0
© 1984, American Pharmaceutical Association

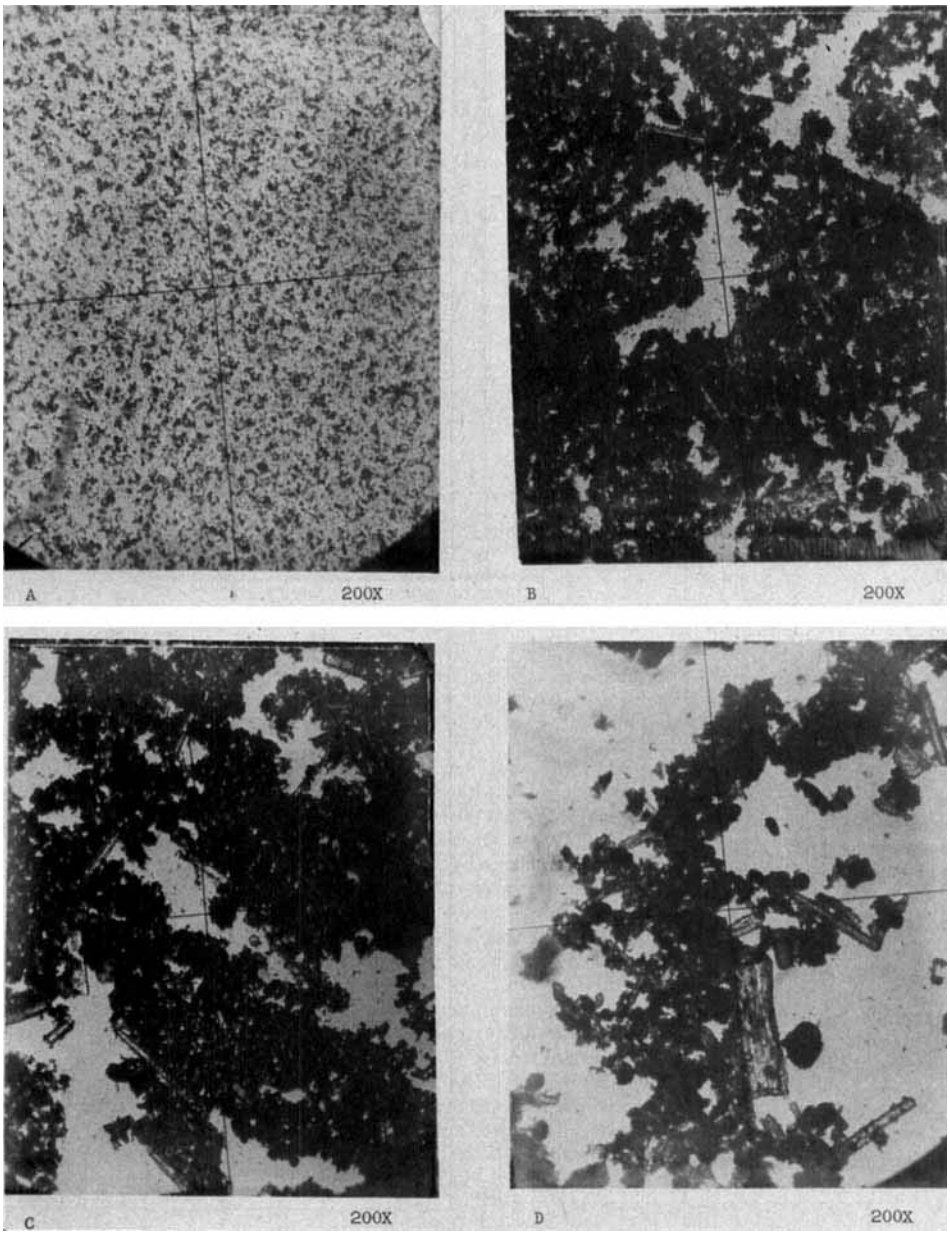

Figure 1—*Microscopic examination of agglomeration and crystal growth of cefazolin sodium suspension in the presence of 0% (A), 0.17% (B), 0.5% (C), and 3.3% (D) polysorbate 80.*

Electrophoretic Mobility—Electrophoretic mobility was measured with a zeta meter[13] equipped with a high voltage power booster[13]. The measurement procedure is described in the literature (10). Zeta potential (ZP) was calculated from the Helmholtz-Smoluchowski equation:

$$ZP = \frac{4\eta}{D} EM \qquad \text{(Eq. 2)}$$

where, at a fixed temperature, η is the viscosity of the suspensing medium in equilibrium, D is the dielectric constant of the suspending medium, EM is the electrophoretic mobility in cm/s per electrostatic volts (esu)/cm, and ZP is the zeta potential of the suspended particle in esu. Since the ZP is always <1 (practical) volt, it is more conveniently expressed in millivolts. Equation 2 then becomes:

$$ZP = 113{,}000 \frac{\eta}{D} EM \qquad \text{(Eq. 3)}$$

where ZP is in the unit of millivolts (mV) and EM is expressed in μm/s per V/cm. The dielectric constants of ethyl oleate and peanut oil have been described (11).

Kinetic Study on Stability of Cefazolin Sodium Suspension—Stability studies were conducted at 57°C, 60°C, 80°C, and 90°C as a function of time. Samples were assayed microbiologically according to CFR§436.105 (*i.e.*, Certified Federation Registration) with *Bacillus subtilis* ATCC 6633 substituted as the assay organism. The kinetic treatment of the data has been previously described (12, 13).

***In Vivo* Bioavailability Evaluation**—Female mongrel dogs (weight 13–20 kg) were fasted overnight with access to water. On the day of the experiment, they were transferred to stocks in which they could stand or sit comfortably for the duration of the test. A retention catheter[14] was inserted into the urinary bladder of each dog for collection of all urine produced during the test period.

Cefazolin sodium (I) was administered as a single 15-mg/kg bolus dose *via* acephalic vein (intravenous) or the biceps femoris muscle (intramuscular). At specified time intervals, samples of urine were collected, chilled in an ice bath, and then frozen until analyzed. At the same time, a blood sample was withdrawn from one cephalic vein into a heparinized evacuated tube[15]. After centrifugation, a plasma sample was removed, chilled, frozen, and analyzed in the following manner. On the day of the assay, the plasma and urine samples were thawed. Urine samples were diluted, as required, in isotonic 0.1 M phosphate buffer (pH 6.0). The antibacterial activity of the diluted samples was assayed in a disk plate agar diffusion test with *B. subtilis* against standard solutions of cefazolin in the same buffer. Plasma samples were diluted with dog serum and assayed in the same way against standard solutions of cefazolin in dog serum.

[13] Zeta-Meter Inc., New York, N.Y.

[14] French No. 14; Foley.

[15] Vacutainer; Becton, Dickinson and Co.

Table II—Chemical Stability of Cefazolin Sodium Suspended in Ethyl Oleate

Lot No.	Age and Storage Condition	Experimental Value[a], % of Initial	Predicted Value, % of Initial
P35294	3 months, 25°C	103.8	99.6
G43061	1 month, 25°C	98.9	99.9
G43060	1 month, 37°C	101.5	99.3
G43046	1.5 months, 40°C	104.1	97.1
G43034	2 weeks, 60°C	90.4	90.8

[a] Mean of three determinations.

RESULTS AND DISCUSSION

During the entire study, cefazolin sodium particles were well suspended in ethyl oleate; a good flocculated system resulted. In contrast, caking was observed in the peanut oil suspensions. A significant difference in zeta potential was observed between cefazolin sodium particles suspended in peanut oil and ethyl oleate (*i.e.*, −2.57 mV ± 0.09 mV *versus* −27.1 mV ± 1.03 mV, respectively). These results are consistent with reported data that the ability to be suspended is correlated with the zeta potential (7, 14).

Effect of a wetting agent on the physical stability of a nonaqueous suspension was evaluated. Surfactants are widely used in pharmaceutical formulations as wetting agents. In the cefazolin sodium suspension in peanut oil, the addition of various amounts of polysorbate 80 produced a deflocculated state. This change was indicated by the difficulty of redispersibility, evidenced by the number of revolutions of the redispersing apparatus required to return the system to a homogenous state (Table I). There was an increase in sedimentation volume by adding 0.17% of polysorbate 80. However, an increase in concentration of polysorbate 80 above this concentration produced a reduction in sedimentation volume. In general, in an aqueous suspension system, a progressive rise in sedimentation volume is accompanied by an increase in the ease of redispersibility (15). In contrast to the conventional aqueous system, no correlation between the redispersibility of the sedimentation bed and the sedimentation volume was found in this nonaqueous system. Considering the interaction of polysorbate 80 with cefazolin sodium, it is possible that cefazolin sodium particles were deflocculated by a process of supersaturating and crystallizing effects produced by the solubilization of the polysorbate 80–cefazolin sodium complex. As shown in Fig. 1, microscopic examination indicated that extensive agglomeration and crystal growth did indeed occur.

An emulsifying agent is commonly included in the formulation of parenteral preparations. Because the agent lowers interfacial tension, the drainage property of a parenteral suspension from the vial can be remarkably improved. In this study, lecithin was chosen as an emulsifying agent and the effect of lecithin on the stability of cefazolin sodium dispersed in ethyl oleate was evaluated. Unlike the peanut oil system, cefazolin sodium in the ethyl oleate suspension in the presence of lecithin produced a deflocculated state accompanied by a decrease in sedimentation volume. The zeta potential of cefazolin sodium decreased with the addition of lecithin and remained essentially constant throughout the concentration range studied (Fig. 2). Furthermore, the effect of increasing lecithin concentration on the zeta potential of cefazolin sodium was paralleled by the effect of lecithin concentration on redispersibility. The data on the porosity of the sedimentation bed correlated well with the data on the sedimentation volume ratio. As shown in Fig. 3, the porosity of the sedimentation bed decreased with the addition of lecithin and the suspension resulted in a deflocculated state which correlates to ability to be suspended.

It is also of interest to compare the appearance of the supernatants of the suspensions relative to their physical stability. As shown in Fig. 4, the turbidity was minimum at 0 and 1.0% of lecithin in the formulation. No correlation was found between the degree of turbidity in the supernatant and the degree of flocculation. These data suggest that the cefazolin sodium particles might be initially well dispersed due to an electrical repulsive force between particles. In the presence of lecithin, however, the contribution of electrical repulsive

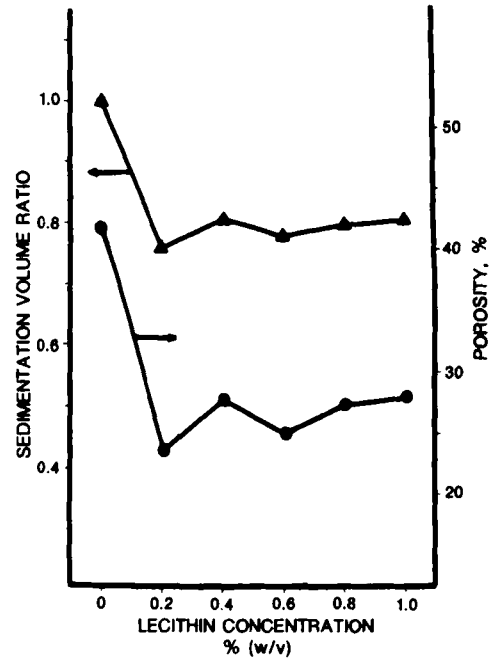

Figure 3—*Influence of lecithin concentrations on sedimentation volume of cefazolin sodium suspensions in ethyl oleate and on porosity of its sedimentation bed.*

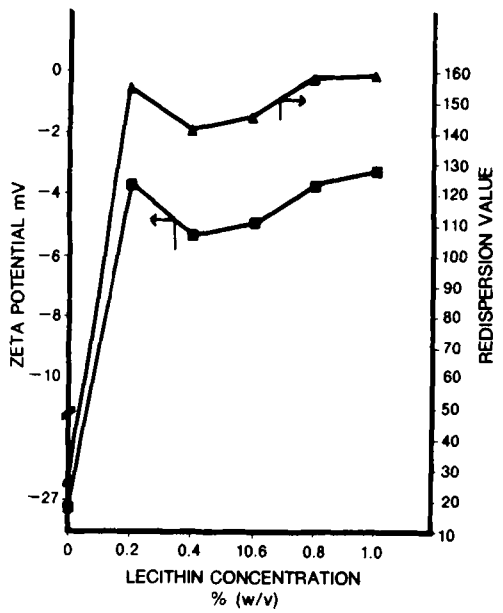

Figure 2—*Influence of lecithin concentrations on zeta potential and redispersibility of cefazolin sodium suspensions in ethyl oleate.*

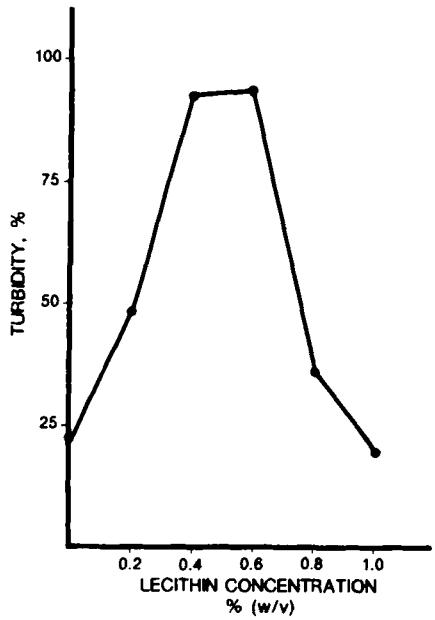

Figure 4—*Influence of lecithin concentrations on turbidities of cefazolin sodium suspensions in ethyl oleate.*

Table III—Comparison of the Performance of Aqueous and Nonaqueous Formulations of Cefazolin in Female Mongrel Dogs

Cefazolin Sodium Formulation	Time of Peak Mean Plasma Concentration, min	Peak Mean Plasma Concentration, μg/mL	Urinary Recovery, % of Dose	AUC[b], μg·min/mL
Solution				
Intravenous	1.0	134 ± 15	89.1 ± 2.4	4609 ± 363
Intramuscular	40	32.4 ± 2.4	79.8 ± 2.4	4319 ± 341
Suspension in Ethyl Oleate				
Intramuscular	40	28.1 ± 4.0	94.1 ± 8.0	4512 ± 256

[a] Cumulative (24-h) recovery of antibacterial activity in urine. [b] Area under the plasma concentration *versus* time curve.

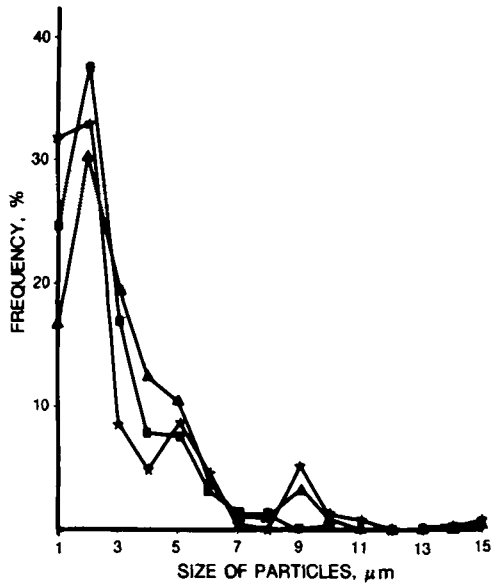

Figure 5—*Particle size frequency distribution curve of cefazolin sodium suspension in ethyl oleate. Key: (■) cefazolin sodium in dry state; (*) cefazolin sodium suspension at initial time; (▲) cefazolin sodium suspension aged 3 months at 25°C.*

force was diminished by a shielding effect on the surface of cefazolin particles as reflected in their electrophoretic properties.

Figure 5 shows the results of the evaluation of crystal growth. Measurement of changing particle size distribution as a function of time under three different storage conditions showed no significant crystal growth.

The potency of cefazolin sodium in ethyl oleate was studied at high temperatures. An Arrhenius plot (with 95% confidence limits) of degradation constants of cefazolin sodium suspension as a function of temperature is shown

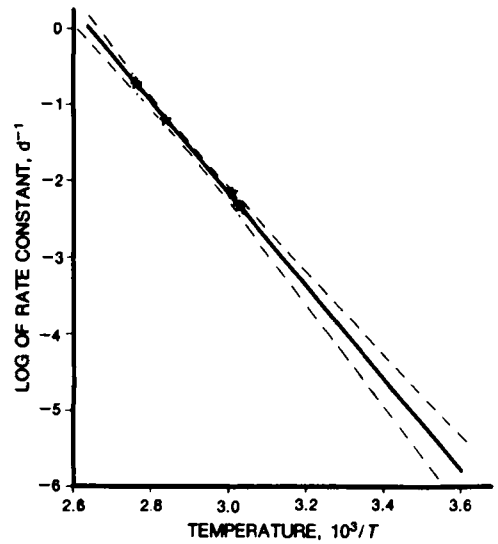

Figure 6—*Arrhenius plot with 95% confidence limits of degradation constants of cefazolin sodium suspension in ethyl oleate:* y = −5.916x + 15.556; r = 0.998.

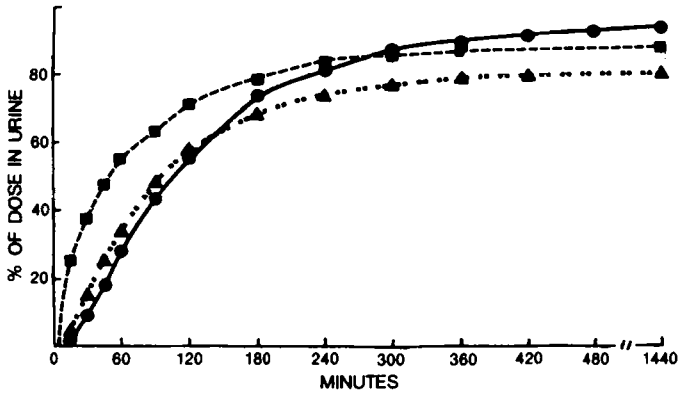

Figure 7—*Mean recovery of antibacterial activity in the urine of female mongrel dogs after administration of 15 mg/kg of cefazolin. Key: (■) aqueous solution administered intravenously; (▲) aqueous solution administered intramuscularly; (●) ethyl oleate suspension administered intramuscularly.*

in Fig. 6 ($y = -5.916x + 15.556$, $r = 0.998$). By extrapolation from the Arrhenius plot, it appears that the chemical stability of cefazolin sodium in ethyl oleate would be adequate for satisfactory shelf life at room temperature. As shown in Table II, the experimental values are well correlated with the predicted values.

In Table III, the performance of one intravenous and two different intramuscular formulations of cefazolin sodium in female mongrel dogs are compared. Based on the results of an analysis of variance, there are no statistically significant differences between the mean values for the area under the plasma concentration *versus* time curves for any of the three treatments ($p > 0.1$). By the same criterion, there are also no differences between the amounts of antibacterial activity recovered in urine by 24 h for the three treatments. The time course of the appearance of antibacterial activity in urine (Fig. 7) suggests that, as expected, cefazolin is more rapidly excreted in the urine following intravenous administration than following intramuscular administration.

The mean peak plasma concentration obtained following intravenous administration of cefazolin was significantly higher than that obtained with the intramuscular preparations, but the mean peak plasma concentrations obtained with the two intramuscular preparations were not different ($p > 0.1$). From these comparisons, it is concluded that in dogs administered 15 mg/kg intramuscularly, the total availability of cefazolin sodium suspended in ethyl oleate is not significantly different from that in aqueous solution. Furthermore, judged by the area under the plasma concentration *versus* time curve and the urinary recovery of antibacterial activity, the bioavailability of cefazolin sodium from this nonaqueous preparation approaches 100%.

In summary, it is known that physical stability is one of the most challenging problems when developing an acceptable suspension. This study demonstrates that by application of fundamental physical parameters, including sedimentation height, sedimentation rate, porosity of sedimentation bed, redispersibility, zeta potential, and turbidity, a good understanding of the physical stability of a nonaqueous cephalosporin suspension can be reached and potential problems relating to physical stability can be identified in the early stages of product development.

REFERENCES

(1) J. M. Robinson, *J. Mich. State Med. Soc.*, **48**, 337 (1949).

(2) T. Savolainnen and V. Tommila, *Ann. Med. Exp. Biol. Fenn.*, **33**, 345 (1955).

(3) W. M. Lukash and P. R. Frank, *Am. J. Med Sci.*, **246**, 429 (1963).

(4) J. P. Remington, "Remington's Pharmaceutical Sciences" 14th ed., Mack, Easton, Pa., 1970, p. 1723.
(5) C. S. Robinson, *Ind. Eng. Chem.*, **18**, 869 (1926).
(6) H. T. Ward and K. Kammermeyer, *Ind. Eng. Chem.*, **32**, 622 (1940).
(7) B. A. Matthews and C. T. Rhodes, *J. Pharm. Sci.*, **57**, 569 (1968).
(8) "The Manual of Hach Analytical Nephelometer Model 2424", Hach Chemical Company, Ames, Iowa, 1974, pp. 5-11.
(9) N. Kaneniwa and K. Takamura, *Yakugaku Zasshi*, **94**, 280 (1974).
(10) "Zeta-Meter Manual", Zeta-Meter Inc., New York, N.Y., 1968, pp. 108-125.
(11) N. A. Lange, "Lange's Handbook of Chemistry", 11th ed., McGraw-Hill, New York, N.Y. 1973, pp. 10-149.
(12) J. T. Carstensen, K. S. E. Su, P. Maddrell, J. B. Johnson, and H. N. Newmark, *Bull. Parenter. Drug Assoc.*, **25**, 193 (1971).
(13) J. T. Carstensen and K. S. E. Su, *Bull. Parenter. Drug Assoc.*, **25**, 287 (1971).
(14) B. A. Haines, Jr. and A. N. Martin, *J. Pharm. Sci.*, **50**, 228 (1961).
(15) R. D. C. Jones, B. A. Matthews, and C. T. Rhodes, *J. Pharm. Sci.*, **59**, 518 (1970).

ACKNOWLEDGMENTS

This paper was presented in part to the Basic Pharmaceutics Section, Academy of Pharmaceutical Sciences, 33rd National Meeting, San Diego, Calif., November 1982. The authors thank Drs. R. F. Bergstrom and C. W. McKeehan, and Messrs. R. L. Robison, W. K. Agan, W. R. Brown, and M. O. Clarkson for their technical assistance and helpful discussions, and Mrs. C. Lammers for her assistance in preparing the manuscript.

Liquid Chromatographic Assay for Diflorasone Diacetate in Cream and Ointment Formulations

M. C. SHAW and A. J. VANDERWIELEN[x]

Received October 3, 1983, from *Product Control I, The Upjohn Company, Kalamazoo, MI 49001.* Accepted for publication February 29, 1984.

Abstract □ A high-performance liquid chromatographic assay for quantitating diflorasone diacetate (I) in cream and ointment formulations and in bulk form is described. Isoflupredone acetate (II) was used as the internal standard and a 3-μm silica gel column with a mobile phase comprised of water-saturated butyl chloride–water-saturated methylene chloride–tetrahydrofuran–acetic acid (350:125:10:15) led to an efficient separation. The method gave accurate results for four formulations, two creams and two ointments, as well as the bulk drug. The assay has an *RSD* of ~1.8% for the cream formulations, 1.3% for the ointment formulations, and 1.0% for the bulk drug. The method is specific for I and capable of resolving structurally related compounds.

Keyphrases □ Diflorasone diacetate - HPLC, cream, ointment, bulk drug □ HPLC—diflorasone diacetate, cream, ointment, bulk drug

Diflorasone diacetate (I) in topical formulations is indicated for the relief of inflammatory manifestations of acute and chronic corticosteroid-responsive dermatoses (1). It is available as a 0.05% cream- or ointment-based topically applied product[1]. The high-performance liquid chromatographic (HPLC) analysis of similar topical anti-inflammatory steroids has appeared (2). This report describes a new normal-phase HPLC assay that is specific for diflorasone diacetate in two cream and two ointment formulations. The assay is also capable of separating several structurally related compounds: the 9,11-epoxide (III), 6β-fluoro analogue (IV), 6-defluoro analogue (V), the 17-OH,21-OAc analogue (VI), and the 17-OAc,21-OH analogue (VII) of I.

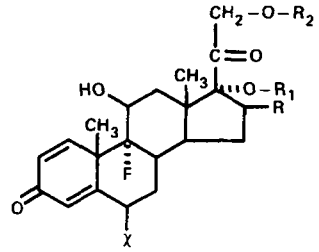

I R=CH_3, R_1=Ac, R_2=Ac, X=α-F
II R=H, R_1=H, R_2=Ac, X=H
IV R=CH_3, R_1=Ac, R_2=Ac, X=β-F
V R=CH_3, R_1=Ac, R_2=Ac, X=H
VI R=CH_3, R_1=H, R_2=Ac, X=α-F
VII R=CH_3, R_1=Ac, R_2=H, X=α-F

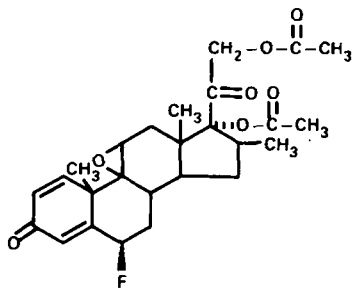

III

EXPERIMENTAL SECTION

Materials—Diflorasone diacetate[2] (I), isoflupredone acetate[2] (II), and the related compounds III–VII[2] (3–7) were obtained in pure form and dissolved in water-saturated chloroform for chromatography and spectroscopy. Solvents and reagents were commercial analytical grade. Placebo materials were obtained in-house[2].

Chromatographic Conditions—A modular liquid chromatograph including pump[3], fixed-loop injector[4], fixed-wavelength detector[5] (254 nm), and a minicomputer[6] were used. Commercial 3-μm[7] silica gel columns (10 cm × 4.6 mm i.d.) were used at ambient temperature. The mobile phase, deaerated under vacuum sonication prior to use, consisted of water-saturated butyl

[1] Florone Cream, Florone Ointment; The Upjohn Company, Kalamazoo, Mich.
[2] The Upjohn Company.
[3] Model 110A; Altex Scientific Inc., Berkeley, Calif.
[4] Model AH60 equipped with a 10-μL fixed volume loop; Valco Instruments Co., Houston, Tex.
[5] Model 1203; LDC Corp., Riviera Beach, Fla.
[6] PDP 11-40; Digital Equipment Corp., Marlborough, Mass.
[7] Part #0258-1500; Perkin-Elmer Corp., Norwalk, Conn.

0022-3549/84/1100-1606$01.00/0
© 1984, American Pharmaceutical Association

(4) J. P. Remington, "Remington's Pharmaceutical Sciences" 14th ed., Mack, Easton, Pa., 1970, p. 1723.
(5) C. S. Robinson, *Ind. Eng. Chem.*, **18**, 869 (1926).
(6) H. T. Ward and K. Kammermeyer, *Ind. Eng. Chem.*, **32**, 622 (1940).
(7) B. A. Matthews and C. T. Rhodes, *J. Pharm. Sci.*, **57**, 569 (1968).
(8) "The Manual of Hach Analytical Nephelometer Model 2424", Hach Chemical Company, Ames, Iowa, 1974, pp. 5-11.
(9) N. Kaneniwa and K. Takamura, *Yakugaku Zasshi*, **94**, 280 (1974).
(10) "Zeta-Meter Manual", Zeta-Meter Inc., New York, N.Y., 1968, pp. 108-125.
(11) N. A. Lange, "Lange's Handbook of Chemistry", 11th ed., McGraw-Hill, New York, N.Y. 1973, pp. 10-149.
(12) J. T. Carstensen, K. S. E. Su, P. Maddrell, J. B. Johnson, and H. N. Newmark, *Bull. Parenter. Drug Assoc.*, **25**, 193 (1971).
(13) J. T. Carstensen and K. S. E. Su, *Bull. Parenter. Drug Assoc.*, **25**, 287 (1971).
(14) B. A. Haines, Jr. and A. N. Martin, *J. Pharm. Sci.*, **50**, 228 (1961).
(15) R. D. C. Jones, B. A. Matthews, and C. T. Rhodes, *J. Pharm. Sci.*, **59**, 518 (1970).

ACKNOWLEDGMENTS

This paper was presented in part to the Basic Pharmaceutics Section, Academy of Pharmaceutical Sciences, 33rd National Meeting, San Diego, Calif., November 1982. The authors thank Drs. R. F. Bergstrom and C. W. McKeehan, and Messrs. R. L. Robison, W. K. Agan, W. R. Brown, and M. O. Clarkson for their technical assistance and helpful discussions, and Mrs. C. Lammers for her assistance in preparing the manuscript.

Liquid Chromatographic Assay for Diflorasone Diacetate in Cream and Ointment Formulations

M. C. SHAW and A. J. VANDERWIELEN[x]

Received October 3, 1983, from *Product Control I, The Upjohn Company, Kalamazoo, MI 49001.* Accepted for publication February 29, 1984.

Abstract □ A high-performance liquid chromatographic assay for quantitating diflorasone diacetate (I) in cream and ointment formulations and in bulk form is described. Isoflupredone acetate (II) was used as the internal standard and a 3-μm silica gel column with a mobile phase comprised of water-saturated butyl chloride–water-saturated methylene chloride–tetrahydrofuran–acetic acid (350:125:10:15) led to an efficient separation. The method gave accurate results for four formulations, two creams and two ointments, as well as the bulk drug. The assay has an *RSD* of ~1.8% for the cream formulations, 1.3% for the ointment formulations, and 1.0% for the bulk drug. The method is specific for I and capable of resolving structurally related compounds.

Keyphrases □ Diflorasone diacetate - HPLC, cream, ointment, bulk drug □ HPLC—diflorasone diacetate, cream, ointment, bulk drug

Diflorasone diacetate (I) in topical formulations is indicated for the relief of inflammatory manifestations of acute and chronic corticosteroid-responsive dermatoses (1). It is available as a 0.05% cream- or ointment-based topically applied product[1]. The high-performance liquid chromatographic (HPLC) analysis of similar topical anti-inflammatory steroids has appeared (2). This report describes a new normal-phase HPLC assay that is specific for diflorasone diacetate in two cream and two ointment formulations. The assay is also capable of separating several structurally related compounds: the 9,11-epoxide (III), 6β-fluoro analogue (IV), 6-defluoro analogue (V), the 17-OH,21-OAc analogue (VI), and the 17-OAc,21-OH analogue (VII) of I.

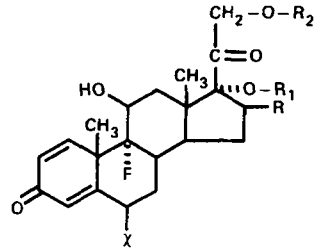

I R=CH_3, R_1=Ac, R_2=Ac, X=α-F
II R=H, R_1=H, R_2=Ac, X=H
IV R=CH_3, R_1=Ac, R_2=Ac, X=β-F
V R=CH_3, R_1=Ac, R_2=Ac, X=H
VI R=CH_3, R_1=H, R_2=Ac, X=α-F
VII R=CH_3, R_1=Ac, R_2=H, X=α-F

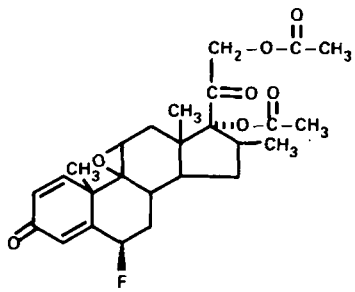

III

EXPERIMENTAL SECTION

Materials—Diflorasone diacetate[2] (I), isoflupredone acetate[2] (II), and the related compounds III–VII[2] (3–7) were obtained in pure form and dissolved in water-saturated chloroform for chromatography and spectroscopy. Solvents and reagents were commercial analytical grade. Placebo materials were obtained in-house[2].

Chromatographic Conditions—A modular liquid chromatograph including pump[3], fixed-loop injector[4], fixed-wavelength detector[5] (254 nm), and a minicomputer[6] were used. Commercial 3-μm[7] silica gel columns (10 cm × 4.6 mm i.d.) were used at ambient temperature. The mobile phase, deaerated under vacuum sonication prior to use, consisted of water-saturated butyl

[1] Florone Cream, Florone Ointment; The Upjohn Company, Kalamazoo, Mich.
[2] The Upjohn Company.
[3] Model 110A; Altex Scientific Inc., Berkeley, Calif.
[4] Model AH60 equipped with a 10-μL fixed volume loop; Valco Instruments Co., Houston, Tex.
[5] Model 1203; LDC Corp., Riviera Beach, Fla.
[6] PDP 11-40; Digital Equipment Corp., Marlborough, Mass.
[7] Part #0258-1500; Perkin-Elmer Corp., Norwalk, Conn.

0022-3549/84/1100-1606$01.00/0
© 1984, American Pharmaceutical Association

Table I—Response Factors for Related Compounds

Compound	Mean Response Factor[a]
I	1.00
III	1.64
IV	1.04
V	1.23
VI	1.04
VII	0.96

[a] Mean of nine determinations, peak area response. Results calculated as in the *Experimental Section.*

chloride-water-saturated methylene chloride-tetrahydrofuran-acetic acid (350:125:10:15). The flow rate was adjusted to 2.5 mL/min.

Internal Standard—A solution of water-saturated chloroform containing 0.04 mg/mL of isoflupredone acetate (II) was used. About 3 mg of diflorasone diacetate (I) reference standard[2] was weighed accurately and 100.0 mL of internal standard solution was added.

Sample Preparations—*Creams*—Cream containing 1 mg of diflorasone diacetate was accurately weighed into a 35-mL screw-cap disposable vial[8], 30.0 mL of internal standard solution was added, and the solution was shaken for 30 min. The vial was then centrifuged at 2000 rpm for 15 min. The top layer (excipient) was then removed by aspiration leaving a clear lower chloroform layer.

Ointments—Ointment containing 0.5 mg diflorasone diacetate was accurately weighed into a 35-mL screw-cap disposable vial[8], 15.0 mL of internal standard solution was added, and the sample treated as in the cream assay.

Bulk Drug—About 1.5 mg of diflorasone diacetate was dissolved in 50.0 mL of internal standard solution.

Procedure—Aliquots of sample or standard preparation were injected using a 10-μL fixed-loop injector. The resulting chromatograms were recorded and analyzed by computer integration. Two reference standard weighings, weight normalized for response, were run at the beginning and end of the run and at every 6-8 samples. The detector attenuation was set at 0.032 absorbance units.

The diflorasone diacetate (I) content, expressed in milligrams per gram for creams and ointments and in percent for bulk drug, was calculated using the internal standard method and peak area response(8).

Recovery studies were performed by adding 50-150% of the labeled amount of diflorasone diacetate (I) to each of the two types of cream and ointment placebos. The samples were then treated as described under *Sample Preparations.*

The relative response of the structurally related compounds III-VII were determined by comparing the weight-normalized response for accurately prepared water-saturated chloroform solutions of each (~0.05 mg/mL) with a similar preparation of diflorasone diacetate (I). The response factors were calculated using peak area response (Table I).

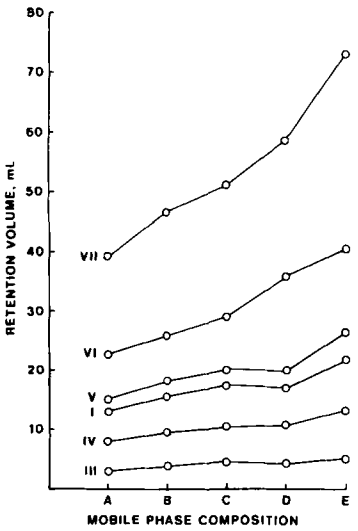

Figure 1—*Plot of retention volume* versus *mobile phase composition of water-saturated butyl chloride-water-saturated methylene chloride-tetrahydrofuran-acetic acid in a ratio of 325:150:10:15 (A), 350:125:10:15 (B), 375:100:10:15 (C), 350:125:5:15 (D), and 350:125:10:5 (E).*

[8] Part #225290; Wheaton Laboratory Products, Millville, N.J.

Table II—Diflorasone Diacetate Recovery from Placebo Cream and Ointment Formulations Using Peak Area Ratio Response

Formulation	Average Recovery, %[a]	*RSD*, %
Cream		
A	99.4	1.5
B	100.1	0.6
Ointment		
C	100.2	0.6
D	100.8	0.9

[a] Six point recovery curve from 50-150% of recommended assay concentration.

RESULTS

Chromatography and Specificity—The selectivity of the chromatographic conditions for I is demonstrated by its ability to resolve compound IV, which differs only in the spatial orientation of the fluorine atom at the 6-position. In addition compound V, which lacks a fluorine atom at the 6-position, is also resolved from I.

The development of chromatographic conditions appropriate for the analysis of I in bulk form and in cream and ointment formulations was based in part on the work of Beyer (9). In addition to the microparticulate column[9] described by Beyer, other 5- and 10-μm silica columns[10] were tried, but with limited success.

Experimentation with mobile phases containing butyl chloride and methylene chloride in addition to polar modifiers (tetrahydrofuran, methanol, acetic acid) revealed that the proportion of methylene chloride was important in column selectivity. Figure 1 depicts the effect on retention volume of selective changes in a mobile phase containing water-saturated methylene chloride. These data were obtained using a small-particle short silica column offering resolution of all peaks of interest, a reasonable analysis time, reproducible chromatography, and lack of placebo interference[7]. The final mobile phase condition chosen (Fig. 1, condition B) was judged to offer the most satisfactory results from the standpoint of resolution and analysis time. The chromatographic separation of compounds I-VII, using condition B, is shown in Fig. 2.

Recovery and Linearity—Recovery of I from either cream- or ointment-spiked placebos was tested by adding 50-150% of the labeled amount of I (0.5 mg of I/g) to each of the cream or ointment placebo formulations. The average recovery of I, calculated using peak area response, for the two cream formulations, "A" and "B," and ointment formulations, "C" and "D," are shown in Table II. A plot of the amount of I added *versus* the amount of I recovered indicated that the slope was within experimental error of the expected slope of I, and the *y*-intercept was 0 for all the formulations tested. The coefficients of correlation, *r*, for the recovery plots were >0.999, indicating that the assay is linear for the cream or ointment formulations tested (50-150% of labeled amount of I, 0.5 mg of I/g).

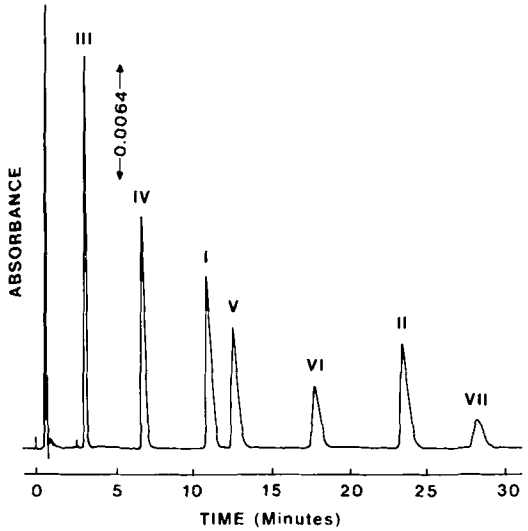

Figure 2—*Chromatogram of diflorasone diacetate and related compounds.*

[9] Part #27477; Waters Associates, Millford, Mass.

[10] Part #850952-701; E.I. DuPont, Wilmington, Del. and Part 8634989; IBM Instruments, Danbury, Conn.

Table III—Diflorasone Diacetate (I) Assay Results for Cream and Ointment Formulations Using Peak Area Ratio Response

Formulation[a]	I Found, mg/g[b]	Percent of Label, %
Cream		
A	0.494–0.505	98.8–101.0
B	0.483 0.510	96.6–102.0
Ointment		
C	0.488–0.498	97.6–99.6
D	0.451–0.485	90.2–97.0

[a] Product (A and C) and experimental (B and D) formulations. [b] Range of assay results obtained after assaying four lots per formulation.

Quantitation of III–VII was examined to determine if the responses of these structurally related compounds were linear over the 0.1–1.0% (w/w) range. These data were obtained to test the applicability of the method for potential impurities. The individual slopes for the calibration curves using peak area percent for III–VII were all 0.96–1.00 and the y-intercepts were not significantly different from zero. The coefficients of correlation, r, for plots of related compounds added *versus* amount found were all >0.999.

DISCUSSION

Presented in Table III are the range of results obtained using the procedure for cream and ointment product formulations A and C and cream and ointment experimental formulations B and D. The precision of the method was determined by replicate analyses of lots from each formulation. The day-to-day assay precision, expressed as *RSD*, was ~1.8% for cream formulations A and B and ~1.3% for ointment formulations C and D.

In addition to the determination of I in cream and ointment formulations, three lots of bulk drug were assayed for purity on the "as is" basis (Table IV). The *RSD* for the purity determination of I was ~1.0% using peak area ratio response.

The chromatographic method described is an accurate and precise method for the determination of diflorasone diacetate (I) in creams, ointments, and bulk drug. The method was found to be reproducible as well as rugged, making it suitable for use as a routine assay. The ability of the method to separate structurally related compounds makes the method useful for monitoring bulk drug and product stability.

Table IV—Diflorasone Diacetate Assay Results for Bulk Drug Using Peak Area Ratio Response

Lot	Assay[a] %	RSD, %
I1	99.3	1.1
I2	99.2	0.9
I3	99.7	0.7

[a] Calculated on the "as is" basis; the results are averages of six determinations over 2 d.

REFERENCES

(1) "Physician's Desk Reference," 35th ed., 1981, p. 1823.

(2) J. Kirschbaum, R. Poet, K. Bush, and G. Petrie, *J. Chromatogr.* **190**, 481 (1980).

(3) U.S. Patent No. 4,340,538 (Col. 5, line 50ff).

(4) U.S. Patent No. 4,340,538 (Structure IV).

(5) U.S. Patent No. 3,312,590 (Formula III).

(6) U.S. Patent No. 3,557,158 (Formula XVI).

(7) U.S. Patent No. 3,980,778 (Formula 12).

(8) L. R. Snyder and J. J. Kirkland, "Introduction to Modern Liquid Chromatography," 2nd ed., Wiley-Interscience, New York, N.Y., 1979, pp. 552–556.

(9) W. F. Beyer, *Pharmacopeial Forum*, July–August, 2232 (1982).

ACKNOWLEDGMENTS

The authors thank W. F. Beyer, K. P. Shephard, and J. D. Stodola for helpful discussions during the experimental work.

Effect of Nitroglycerin-Soluble Additives on the Stability of Molded Nitroglycerin Tablets

M. J. PIKAL ˣ, A. L. LUKES, and J. W. CONINE

Received June 22, 1983, from *Eli Lilly and Company, Indianapolis, IN 46285.* Accepted for publication February 1, 1984.

Abstract □ Nitroglycerin vapor pressures at 25°C were determined for additive–nitroglycerin systems over the additive–nitroglycerin weight ratio range of 0.5 to 3.0 for 16 additives exhibiting solubility in nitroglycerin. The effects of the additives on nitroglycerin chemical stability at 25°C and 50°C were also studied. Tablet stability characteristics, *i.e.*, content uniformity, open-dish stability, and chemical decomposition were evaluated for selected tablet formulations. Most additives lowered the vapor pressure of nitroglycerin sufficiently to stabilize content uniformity when used at additive–nitroglycerin weight ratios near 1. Higher additive levels are needed for significant potency stabilization in open-dish stability tests, but these levels normally decrease the chemical stability of nitroglycerin. However, stabilization of content uniformity, a twofold reduction of potency loss in an open-dish stability test, and chemical stability are possible with at least three of the additives studied.

Keyphrases □ Nitroglycerin—vapor pressure in sublingual molded tablets, intertablet migration, effect of additives □ Tablet stability—nitroglycerin sublingual molded tablets, vapor pressure, intertablet migration, effect of additives

A number of workers have emphasized both the physical instability of molded nitroglycerin tablets arising from vaporization, and subsequent migration of nitroglycerin, and the improvement in stability obtained by incorporating a nitroglycerin-soluble additive in the formulation (1–7). The additive lowers the vapor pressure of nitroglycerin which results in: (*a*) a reduction of the evaporation rate of nitroglycerin from tablets exposed to ambient air currents (1); (*b*) a marked decrease in losses due to absorption in packaging material (7); (*c*) stabilized content uniformity, in that most of the intertablet nitroglycerin migration which occurs in conventional (unstabilized) tablets is thermodynamically impossible in a closed system of stabilized tablets (4). A modest vapor pressure reduction is sufficient to stabilize the content uniformity within a sample of tablets (4). However, both evaporation rate and package absorption are least for the formulation of lowest vapor pressure.

Although there have been several reports of chemical instability in nitroglycerin tablets (8, 9), chemical decomposition is normally not a problem in conventional nitroglycerin tablets. However, the agent employed to stabilize content uniformity may have an adverse effect on chemical stability. Several studies (7, 8, 10) suggest that both povidone (7) and polyeth-

0022-3549/84/1100-1608$01.00/0

© 1984, American Pharmaceutical Association

Table III—Diflorasone Diacetate (I) Assay Results for Cream and Ointment Formulations Using Peak Area Ratio Response

Formulation[a]	I Found, mg/g[b]	Percent of Label, %
Cream		
A	0.494–0.505	98.8–101.0
B	0.483 0.510	96.6–102.0
Ointment		
C	0.488–0.498	97.6–99.6
D	0.451–0.485	90.2–97.0

[a] Product (A and C) and experimental (B and D) formulations. [b] Range of assay results obtained after assaying four lots per formulation.

Quantitation of III–VII was examined to determine if the responses of these structurally related compounds were linear over the 0.1–1.0% (w/w) range. These data were obtained to test the applicability of the method for potential impurities. The individual slopes for the calibration curves using peak area percent for III–VII were all 0.96–1.00 and the y-intercepts were not significantly different from zero. The coefficients of correlation, r, for plots of related compounds added *versus* amount found were all >0.999.

DISCUSSION

Presented in Table III are the range of results obtained using the procedure for cream and ointment product formulations A and C and cream and ointment experimental formulations B and D. The precision of the method was determined by replicate analyses of lots from each formulation. The day-to-day assay precision, expressed as *RSD*, was ~1.8% for cream formulations A and B and ~1.3% for ointment formulations C and D.

In addition to the determination of I in cream and ointment formulations, three lots of bulk drug were assayed for purity on the "as is" basis (Table IV). The *RSD* for the purity determination of I was ~1.0% using peak area ratio response.

The chromatographic method described is an accurate and precise method for the determination of diflorasone diacetate (I) in creams, ointments, and bulk drug. The method was found to be reproducible as well as rugged, making it suitable for use as a routine assay. The ability of the method to separate structurally related compounds makes the method useful for monitoring bulk drug and product stability.

Table IV—Diflorasone Diacetate Assay Results for Bulk Drug Using Peak Area Ratio Response

Lot	Assay[a] %	RSD, %
I1	99.3	1.1
I2	99.2	0.9
I3	99.7	0.7

[a] Calculated on the "as is" basis; the results are averages of six determinations over 2 d.

REFERENCES

(1) "Physician's Desk Reference," 35th ed., 1981, p. 1823.

(2) J. Kirschbaum, R. Poet, K. Bush, and G. Petrie, *J. Chromatogr.* **190**, 481 (1980).

(3) U.S. Patent No. 4,340,538 (Col. 5, line 50ff).

(4) U.S. Patent No. 4,340,538 (Structure IV).

(5) U.S. Patent No. 3,312,590 (Formula III).

(6) U.S. Patent No. 3,557,158 (Formula XVI).

(7) U.S. Patent No. 3,980,778 (Formula 12).

(8) L. R. Snyder and J. J. Kirkland, "Introduction to Modern Liquid Chromatography," 2nd ed., Wiley-Interscience, New York, N.Y., 1979, pp. 552–556.

(9) W. F. Beyer, *Pharmacopeial Forum*, July–August, 2232 (1982).

ACKNOWLEDGMENTS

The authors thank W. F. Beyer, K. P. Shephard, and J. D. Stodola for helpful discussions during the experimental work.

Effect of Nitroglycerin-Soluble Additives on the Stability of Molded Nitroglycerin Tablets

M. J. PIKAL ˣ, A. L. LUKES, and J. W. CONINE

Received June 22, 1983, from *Eli Lilly and Company, Indianapolis, IN 46285.* Accepted for publication February 1, 1984.

Abstract □ Nitroglycerin vapor pressures at 25°C were determined for additive–nitroglycerin systems over the additive–nitroglycerin weight ratio range of 0.5 to 3.0 for 16 additives exhibiting solubility in nitroglycerin. The effects of the additives on nitroglycerin chemical stability at 25°C and 50°C were also studied. Tablet stability characteristics, *i.e.*, content uniformity, open-dish stability, and chemical decomposition were evaluated for selected tablet formulations. Most additives lowered the vapor pressure of nitroglycerin sufficiently to stabilize content uniformity when used at additive–nitroglycerin weight ratios near 1. Higher additive levels are needed for significant potency stabilization in open-dish stability tests, but these levels normally decrease the chemical stability of nitroglycerin. However, stabilization of content uniformity, a twofold reduction of potency loss in an open-dish stability test, and chemical stability are possible with at least three of the additives studied.

Keyphrases □ Nitroglycerin—vapor pressure in sublingual molded tablets, intertablet migration, effect of additives □ Tablet stability—nitroglycerin sublingual molded tablets, vapor pressure, intertablet migration, effect of additives

A number of workers have emphasized both the physical instability of molded nitroglycerin tablets arising from vaporization, and subsequent migration of nitroglycerin, and the improvement in stability obtained by incorporating a nitroglycerin-soluble additive in the formulation (1–7). The additive lowers the vapor pressure of nitroglycerin which results in: (*a*) a reduction of the evaporation rate of nitroglycerin from tablets exposed to ambient air currents (1); (*b*) a marked decrease in losses due to absorption in packaging material (7); (*c*) stabilized content uniformity, in that most of the intertablet nitroglycerin migration which occurs in conventional (unstabilized) tablets is thermodynamically impossible in a closed system of stabilized tablets (4). A modest vapor pressure reduction is sufficient to stabilize the content uniformity within a sample of tablets (4). However, both evaporation rate and package absorption are least for the formulation of lowest vapor pressure.

Although there have been several reports of chemical instability in nitroglycerin tablets (8, 9), chemical decomposition is normally not a problem in conventional nitroglycerin tablets. However, the agent employed to stabilize content uniformity may have an adverse effect on chemical stability. Several studies (7, 8, 10) suggest that both povidone (7) and polyeth-

0022-3549/84/1100-1608$01.00/0

© 1984, American Pharmaceutical Association

Table I—Reduction of Nitroglycerin Vapor Pressure at 25°C by Additives[a]

Additive	Density	Mol. Wt.	Eq. 1 Parameters			P/P_0		$(\partial \ln P/\partial \ln N)_A$	
			χ_0	n	b	R = 1.0	R = 2.0	R = 1.0	R = 2.0
I Povidone	1.10	35,000	+0.174	4	−12.5	0.46	0.07	1.6	3.8
II Polyethylene glycol 400	1.11	400	+3.89	1	−6.77	0.56	0.22	1.0	1.7
III Polyethylene glycol 4000	1.11	4,000	+0.50	2	−3.56	0.62[b]	0.62	0[b]	0[b]
IV Polyethylene glycol 20,000	1.10	20,000	+0.343	4	−14.7	0.58[b]	0.58	0[b]	0[b]
V Polyoxyl 40 stearate	1.08	2,060	−0.082	2	−1.216	0.58	0.33	0.65	1.0
VI Polyoxyethylene(23) lauryl ether	1.06	1,200	+0.885	2	−2.438	0.67	0.36	0.65	1.1
VII Octoxynol	1.065	692	+0.576	2	−1.192	0.67	0.42	0.49	0.82
VIII Polysorbate 20	1.08	1,226	−0.24	2	−0.580	0.58	0.35	0.57	0.83
IX Polysorbate 60	1.06	1,310	+0.528	4	−3.14	0.71	0.37	0.59	1.3
X Polysorbate 80	1.06	1,308	+0.242	4	−2.07	0.67	0.38	0.56	1.1
XI Ethylenediamine tetra [polyoxyethylene (52) polyoxypropylene (12)]	1.08	12,000	−0.166	2	−1.213	0.59	0.33	0.66	1.0
XII Ethylenediamine tetra [polyoxyethylene (132) polyoxypropylene (16)]	1.08	27,000	+0.019	2	−2.43	0.63[c]	0.63	0[c]	0[c]
XIII Polaxamer 188	1.08	8,350	−0.888	2	−0.233	0.51	0.47[d]	0.66	0.0[d]
XIV 50% Acetylated monoglycerides	0.94	400	—	—	—	0.94[e]	0.85	≃0.09	—
XV 100% Acetylated monoglycerides	0.99	440	1.253	2	−1.105	0.79	0.56	0.34	0.65
XVI Bis(2-ethylhexyl)phthalate	0.980	390	1.568	4	−1.263	0.96	0.74	0.17	0.58

[a] At selected R values (R is additive-nitroglycerin weight ratio). [b] Equilibrium solubility is R = 0.9. [c] Equilibrium solubility is R = 0.8. [d] Equilibrium solubility is R = 1.1. [e] Incomplete solubility even at R = 0.5. A small fraction of the sample appears to be essentially insoluble in nitroglycerin.

ylene glycol (8, 10) may accelerate the hydrolysis of nitroglycerin to a point where, at high temperature, decomposition becomes a significant factor in tablet stability. This study was initiated to investigate the effects of selected nitroglycerin-soluble materials on nitroglycerin vapor pressure and on tablet stability as part of an effort to develop tablet formulations which would stabilize content uniformity without adversely affecting chemical stability.

EXPERIMENTAL SECTION

Materials and Assay Procedure—The nitroglycerin and povidone were described previously (4). The other additives were obtained from commercial sources[1] and were used as supplied except for vacuum drying to remove volatiles. Nitroglycerin-additive samples were prepared as previously described (4). Samples denoted "powder" are nitroglycerin-additive-β-lactose systems in powder form containing ~1.5% nitroglycerin.

Nitroglycerin was assayed as described previously (7) while dinitroglycerin and mononitroglycerin were assayed semiquantitatively by TLC (11) and quantitatively by HPLC. The HPLC method[2] employed a partisil ODS column[3] and a 230 nm UV detector[3]. The solvent was 70:30 (v/v) water-acetonitrile at a flow rate of 3 mL/min. Four peaks were observed with partially decomposed nitroglycerin with retention times (1–5 min) in the following order: nitric acid with glycerol, mononitroglycerin (both isomers), dinitroglycerin (both isomers), and nitroglycerin. High levels of povidone yielded a small peak at the dinitroglycerin retention time, making a small povidone correction necessary. This peak appeared to be due to unreacted monomer. Variation in the solvent composition between the sample and the elution medium resulted in small positive or negative peaks at the mononitroglycerin retention time. Probably because of this interference, the mononitroglycerin assay data are much less precise than the corresponding data for the di- and tri-esters.

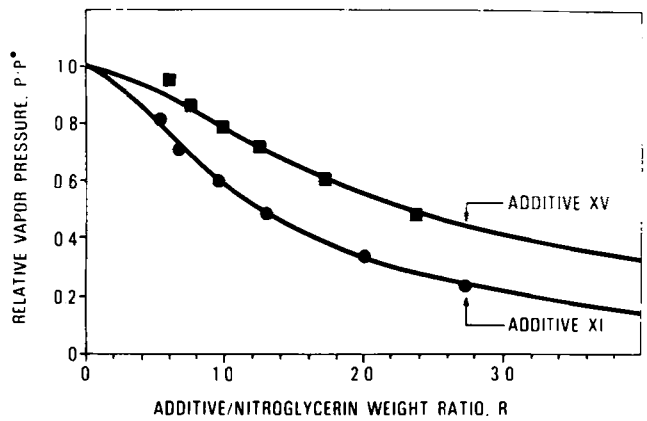

Figure 1—*Vapor pressure of nitroglycerin at 25°C in solutions of nitroglycerin and additive XV (■) and additive XI (●). The lines represent* P/P_0 *calculated from Eq. 1.*

Vapor-Pressure Measurements—Vapor pressures were measured by the modified Knudsen effusion method (4, 12). Powder systems of nominal additive-nitroglycerin weight ratios of 0.5, 1.0, and 2.0 were studied. Differential measurements (4, 12) were made on each sample. Continuous measurements of vapor pressure were made (4) on samples of additive-nitroglycerin weight ratios of 0.5. Replicate measurements were carried out (4).

RESULTS

Vapor-Pressure Reduction—Vapor-pressure results are summarized in Table I. Density data are either measured in this laboratory or were given by the supplier of the additive. The additive molecular weight was calculated from the average chemical formula or was taken directly from information provided by the supplier.

Vapor pressure raw data were found to be well represented by the equation (13):

$$\ln P/P_0 = \ln(1-\phi_2) + \left(1 - \frac{V_1}{V_2}\right)\phi_2 + \chi\phi_2 \qquad \text{(Eq. 1)}$$

where P is the vapor pressure of the additive-nitroglycerin solution, P_0 is the vapor pressure of pure nitroglycerin, ϕ_2 is volume fraction of additive in the

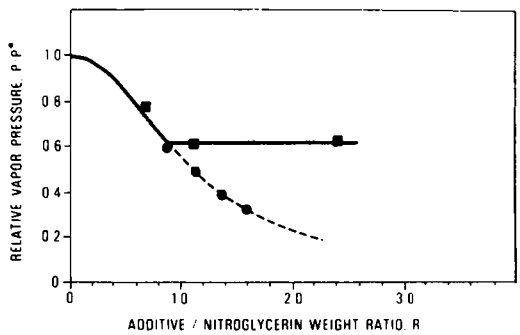

Figure 2—*Vapor pressure of nitroglycerin at 25°C in a nitroglycerin-additive system exhibiting incomplete miscibility (polyethylene glycol 400). Key: (■) equilibrium (time zero) data; (●) dynamic (real time) data in a supersaturated system.*

[1] The sources of the additives (Table I) were: II, III, IV, Baker Chemical Co.; V (Myrj 52), VI (Brig 35), VIII (Tween 20), IX (Tween 60), X (Tween 80), ICI, Atlas Chemical Co.; XI (Tetronic 707), XII (Tetronic 904), XIII (Pluronic F68), BASF Wyandote Chemical Co.; XIV (Myvacet 5-07), XV (Myvacet 9-40).

[2] J. W. Becker and J. A. Sefranka, unpublished results.

[3] Waters Associates, Milford, Mass.

Table II—Water Absorption and Chemical Stability of Additive–Nitroglycerin Powder Systems

	Additive	R	Water Content of Powder, % (w/w) at 87% Rel. Humidity[a]	Decomposition, % after 2 months at 50°C (Dinitroglycerin Content)[b]	
				Dried	87% Rel. Humidity
	None	0	1.3	1 (N)	0 (N)
I	Povidone	1	2.1	38 (M)	33 (M)
		2	3.1	—	45 (M)
II	Polyethylene glycol 400	1	2.7	10 (T)	15 (M)
		2	3.8	—	13 (T)
V	Polyoxyl 40 stearate	1	1.5	0 (N)	7 (M)
		2	2.4	—	15 (M)
VI	Polyoxyethylene (23) lauryl ether	1	1.6	4 (T)	6 (T)
		2	2.2	—	15 (M)
VII	Octoxynol	1	1.4	0 (N)	1 (N)
		2	1.6	—	1 (N)
VIII	Polysorbate 20	1	1.7	5 (T)	7 (T)
		2	2.1	—	15 (M)
IX	Polysorbate 60	1	1.6	2 (T)	6 (M)
		2	2.1	—	12 (M)
X	Polysorbate 80	1	1.4	14 (M)	10 (M)
		2	1.8	—	— (M)
XI	Ethylenediamine tetra [polyoxyethylene(52)polyoxypropylene (12)]	1	1.4	3 (T)	11 (M)
		2	2.1	—	22 (M)
XV	100% Acetylated monoglycerides	1	1.2	0 (N)	2 (N)
		2	1.4	—	3 (N)

[a] The water contents of the dried powders were all in the range 0.45–0.58% (w/w). [b] Storage in closed glass bottles. Dinitroglycerin content determined by TLC; N = none detected; T = trace observed (~2–5%); M = moderate level observed.

nitroglycerin phase, V_1 and V_2 are the molar volumes of nitroglycerin and additive, respectively, and χ is the interaction parameter which was arbitrarily assumed to have the form:

$$\chi = \chi_0 + b\phi_2^n \qquad \text{(Eq. 2)}$$

where χ_0, b, and n are constants evaluated from the data. An integer value of n was chosen to give the best linear least-squares fit of χ as a function of ϕ_2^n. Additivity of volume was assumed so ϕ_2 may be calculated from the additive-to-nitroglycerin weight ratio, R, according to:

$$\phi_2 = \frac{R}{R + \rho_2/\rho_1} \qquad \text{(Eq. 3)}$$

where ρ_2 and ρ_1 are the densities of additive (Table I) and nitroglycerin (14), respectively.

Data representative of systems exhibiting complete miscibility of nitroglycerin and additive over the composition range studied are shown in Fig. 1. The solid line represents P/P_0 calculated from Eq. 1 while the squares and circles are experimental points obtained by averaging at least four independent measurements. With some additives (III, IV, XII, XIII), miscibility is observed only at lower R values. Consequently, the vapor pressure of these systems at equilibrium is independent of composition at R values larger than the solubility limit (Fig. 2, square symbols). However, during the vapor pressure measurement, R increases as effusion proceeds and normally a supersaturated solution of additive in nitroglycerin is formed. The data represented by circles (Fig. 2) were obtained from supersaturated solutions formed during the effusion measurement.

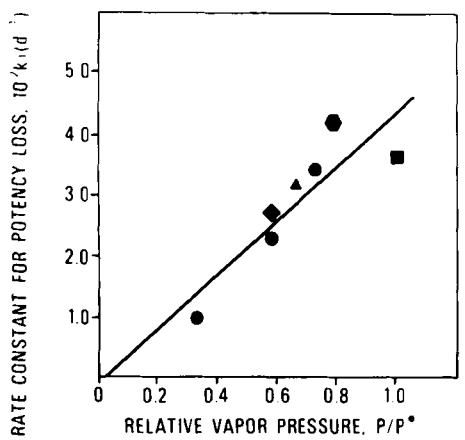

Figure 3—*Correlation between potency losses in open-dish stability tests and nitroglycerin vapor pressures. Key: (■) no additive; (●) additive V; (▲) additive VII; (◆) additive VIII; (●) additive XV.*

Smoothed values of relative vapor pressures, P/P_0, and values of the partial derivative $(\partial \ln P/\partial \ln N)_A$, were calculated from Eq. 1 (Table I). Here, A and N are the masses of additive and nitroglycerin, respectively. A large value of this derivative indicates that evaporation of a small amount of nitroglycerin from the sample produces a large reduction in vapor pressure.

Stability—*Chemical Stability of Powders*—The chemical stability of nitroglycerin in additive–nitroglycerin phases was studied for both dried powders[4] and for powders equilibrated with 87% relative humidity prior to storage (Table II). The systems studied were ~98% lactose powder with the additive–nitroglycerin phase coated on the lactose crystals.

Tablet Stability in Closed Bottles—The effects of selected additives on chemical stability and content uniformity stability were investigated for tablet samples sealed in glass bottles (Table III). As an index of chemical stability at ambient temperature, dinitroglycerin content (HPLC assay) after 2 years storage at 25°C are listed.

Potency losses after 2 years at 25°C averaged 12% for the tablets containing povidone (with no apparent correlation with level of povidone), ~9% for tablet Lot N, an average of 6% for the tablets without an additive, and 2–5% for other tablets. As a measure of chemical stability at high temperature, potency losses after 6 months at 50°C were determined for selected tablet lots (Table III). Potency loss data are uncertain within ~±3%, so except for the greater potency losses shown by lot K, lot N, and the povidone containing lots, all lots are essentially equivalent. Content uniformity (Table III) is expressed as the relative standard deviation for single tablet nitroglycerin assay (weight nitroglycerin per unit tablet weight) of thirty tablets.

Tablet Stability in an Open-Dish Test—Tablets were stored at 25°C in open petri dishes exposed to ambient air currents. Thirty tablet samples were taken for single tablet assay at day six and day twelve. The observed changes in potency and content uniformity are tabulated (Table IV).

DISCUSSION

Vapor Pressure and Open-Dish Stability—The loss in tablet potency during open-dish storage is undoubtedly due to evaporation of nitroglycerin, and therefore the rate of loss should correlate with the nitroglycerin vapor pressure. To provide rate data suitable for correlation with the tablet vapor pressure, effective first-order rate constants for potency loss were determined from the data in Table IV[5]. The resulting rate constants are plotted as a function of relative vapor pressure of nitroglycerin (from Table I) in Fig. 3. The line is the linear regression line ($r = 0.88$). Considering the difficulty in obtaining

[4] The dried samples were air dried in a forced-air oven at 43°C. Relative humidity decreases in ambient air (25°C; relative humidity, ~55%) ~three-fold when heated to 43°C by the drying oven. Thus, the dried samples were equilibrated with ~18% relative humidity at 43°C.

[5] The data were consistent with first-order loss of nitroglycerin, *i.e.*, linear semilogarithmic plots of potency *versus* time. However, insufficient data were available to reveal subtle variations from first-order behavior.

Table III—Stability of 0.3-mg Nitroglycerin Tablets in Closed Bottles

Tablet Lot[a]	Additive	R	Chemical Stability: Dinitroglycerin, % (2 years at 25°C)	Chemical Stability: Potency Loss, % (6 months at 50°C)	Content Uniformity, σ (w/w)[b]: Initial	6 months at 25°C	2 years at 25°C
A	None	0	1.0	4	5	9	10
B	None	0	0.4	—	7	—	13
C	None	0	0.7	—	4	—	16
D	I	1	7.6	—	3	—	3
E	I	1	8.2	92	2	—	4
F	I	1	8.6	—	2	—	5
G	I	2	4.3	—	1	—	2
H	I	3	1.5	—	1	—	2
I	V	0.6	1.5	5	4	4	5
J	V	1	1.8	6	2	4	4
K	V	2	4.4	40	3	6	6
L	VII	1	1.2	6	3	3	4
M	VIII	1	2.1	6	2	3	5
N	X	1	6.8	29	3	—	7
O	XV	1	1[c]	8	5	5	5

[a] All lots were experimental lots prepared for this study. [b] *RSD* for assay of 30 tablets in weight of nitroglycerin per unit weight of tablet. [c] Semi-quantitative TLC result.

Table IV—Stability of Nitroglycerin Tablets Exposed to Ambient Air (Open-Dish Evaporation Test)

Tablet Lot	Additive	R	Potency, μg/Tablet: Initial	6 d	12 d	Content Uniformity, σ (w/w): Initial	6 d	12 d
A	None	0	344	292	222	5	9	15
I	Polyoxyl 40 stearate	0.66	351	295	233	4	2	1
J	Polyoxyl 40 stearate	1.0	361	316	275	2	2	2
K	Polyoxyl 40 stearate	2.0	352	327	314	3	3	3
L	Octoxynol	1.0	364	308	249	3	3	3
M	Polysorbate 20	1.0	368	308	266	2	3	2
O	100% Acetylated monoglycerides	1.0	351	296	212	5	4	2

reproducible potency loss data on samples stored in an open dish[6], the correlation is very good. The rate of potency loss is essentially proportional to the initial vapor pressure of nitroglycerin in the tablet formulation.

Content Uniformity of Tablets—Poor content uniformity at the time of manufacture may arise from causes unrelated to the volatility of nitroglycerin, *i.e.*, poor mixing, solution migration during drying and subsequent tablet surface erosion, *etc.* However, a decrease in content uniformity on aging in closed bottles is due to migration of nitroglycerin, largely intertablet migration (2-4).

An additive will be effective in preventing intertablet nitroglycerin migration if two criteria are met (4): (*a*) the additive lowers the vapor pressure of nitroglycerin by more than ~15%; (*b*) Evaporation of nitroglycerin from the additive-nitroglycerin phase results in significant further reduction of vapor pressure [*i.e.*, the quantity $(\partial \ln P/\partial \ln N)_A$ (Table I) should be large[7]].

If criterion *a* is met, condensation of nitroglycerin in empty tablet pores is prevented, while meeting criterion *b* minimizes condensation in tablet pores that are partially filled with nitroglycerin-additive phase (4). Thus, the relative importance of criteria *a* and *b* depends on whether the small pores (condensation sites) in fresh tablets are empty or are partially filled with nitroglycerin-additive phase. This detailed information is not available. However, if both criteria are met, the additive should be effective in preventing significant intertablet transfer of nitroglycerin.

On this basis, all additives studied, with the exception of additive XIV, should stabilize content uniformity if used at the proper level. Additives III, IV, XII, and XIII are soluble in nitroglycerin only at lower R values, and therefore to meet criterion *b*, these additives must be used at levels below the solubility limit. However, in each of these cases, a value of R may be chosen to give both large $(\partial \ln P/\partial \ln N)_A$ and $P/P_0 < 0.85$.

The lower effective limit for $(\partial \ln P/\partial \ln N)_A$ in a formulation is not known. However, content uniformity data (Tables III and IV) suggest that $(\partial \ln P/\partial \ln N)_A > 0.3$ is sufficient. The formulation for tablet lot O (additive XV at R = 1) yields a stabilized tablet with respect to content uniformity with $P/P_0 = 0.79$ and $(\partial \ln P/\partial \ln N)_A = 0.34$. All other tablet formulations with additives produced greater reductions of vapor pressure and larger values $(\partial \ln P/\partial \ln N)_A$ without any obvious improvement in content uniformity stability.

Chemical Decomposition—Except for XV and VII, the additives accelerate the decomposition of nitroglycerin. In general, the effect of the additive on stability is minimal at R = 1 but becomes significant at R = 2. A particularly good example of this behavior is shown by tablets (Table III) and dried powders (Table II) containing additive V. Samples at R = 0.66 and R = 1.0 are essentially stable, while samples at R = 2 are unstable.

Samples containing I, II and X (Tables II and III) appear to be unstable at 50°C, even at R = 1, but at least for I and II, the high temperature stability is not particularly sensitive to additive levels above R = 1. Potency loss data (*Results* section) suggest the same conclusion at 25°C for I, although the dinitroglycerin content decreases as R increases (Table III). However, at 25°C the stability of nitroglycerin is sensitive to the level of soluble polyethylene glycol[8]. Samples with R = 1 apparently are stable, but the 25°C-stability of nitroglycerin in a phase containing a high level of polyethylene glycol (R = 2) is poor[8].

Since hydrolysis is a major reaction pathway for decomposition of nitroglycerin in tablets, water content and alkalinity of the nitroglycerin phase should be important variables. Although the water content of the nitroglycerin phase could not be measured (15), the water content of the powder system as a whole was determined (Table II). The water content of all dried samples was 0.45-0.58% (w/w). As expected, the data generally show greater decomposition for the sample equilibrated at high humidity (I and X are exceptions) than for the corresponding dried sample.

The alkalinity was characterized by measuring the pH of a 10% aqueous solution (or dispersion) of the additive in water[9]. The hydrolysis rate would be expected to be at a minimum in a weak acid (16, 17). The exact relationship between pH of a 10% aqueous solution of additive and acid- or base-catalysis in a nitroglycerin-additive phase is not clear. However, if acidic or basic impurities in the additives used were the dominant factor in stability, one would expect a good correlation (nonlinear) between pH and stability; good correlation was not observed[9].

Disintegration Time—While a detailed discussion of disintegration time is beyond the scope of this study, the effect of the additive on disintegration time merits comment. An additive may function as an additional binder re-

[6] Variations in air currents with storage location and presence of materials which may absorb nitroglycerin near the storage location limit reproducibility of open-dish stability data.

[7] Lilly 0.6-mg tablets are stabilized with Povidone at R = 0.6 which results in $(\partial \ln P/\partial \ln N)_A = 0.59$. Other established stabilized formulations (Lilly 0.3- and 0.4-mg tablets and Parke Davis Nitrostat) yield larger values of this derivative.

[8] Dried powders (lactose-nitroglycerin-additive) were aged 2 years at 25°C. Polyethylene glycol 400 and polyethylene glycol 1000 systems at R = 0.62 showed only trace levels of dinitroglycerin, but at R = 2.2, the ratio of dinitroglycerin species to trinitroglycerin was ~0.6. Potency loss for the polyethylene glycol 400 sample was 52%. Polyethylene glycol 4000 at R = 2.2, which is soluble only to R = 0.9, showed only trace levels of dinitroglycerin. Even at R = 2, potency losses and dinitroglycerin contents (as percentage of total nitroglycerin compounds) were only several percent for additives V, VII, and XV and were <15% for other additives studied (VI, VIII, IX, X, and XI).

[9] The measured pH values for the indicated additives were: I (3.5), II (6.0), V (4.6), VI (2.4), VII (3.5), VIII (3.9), IX (3.9), X (3.8), XI (7.8), and XV (5.8). These additives were all vacuum dried before use.

sulting in an increase in disintegration time, the effect increasing as the additive content of the tablet increases. For example, conventional tablets (Table III) typically disintegrate within ~10 s, but tablets with additives present at 1% of the tablet weight require 20–30 s for all additives except povidone. Tablets formulated with 2% of either additive V or additive VIII require ~100 s for disintegration. These times refer to tablets aged 2 years at 25°C. While 100 s is near the UPS limit for 2 min, a reduction in tablet density will significantly reduce the disintegration time. The data quoted above refer to a fixed tablet density (1.16 g/mL). Thus, it may be possible to reduce the tablet density by using less lactose, thereby reducing the disintegration time to a more acceptable level.

With the exception of tablets containing additive I (povidone), the disintegration times for fresh tablets are essentially the same as for aged tablets. Fresh tablets containing 1% povidone typically disintegrate within 20 s, but after prolonged aging (more than 2 years at 25°C) they may require 1–2 min for disintegration. Evidently the povidone cross-links to some extent which retards disintegration. When these tablets are left undisturbed in water for some time, a "ghost" of insoluble material in the shape of the tablet remains. Thus, with the exception of severely aged povidone-containing tablets, excessive disintegration time is not a problem for the tablet systems studied (Table III), at least for ≤1% additive.

CONCLUSIONS

A number of nitroglycerin-soluble additives sufficiently lower the vapor pressure of nitroglycerin to stabilize the content uniformity of molded nitroglycerin tablets. In general, an additive–nitroglycerin weight ratio, R, of 1 is adequate for this purpose. Tablet potency losses in open-dish evaporation tests are roughly proportional to the vapor pressure of nitroglycerin in the tablet, and higher levels of additive (R = 2) are normally needed to achieve a significant improvement in open-dish stability. However, with few exceptions (VII and XV) high additive levels lead to reduced chemical stability, particularly at high temperature, and a compromise must be made between chemical stability and open-dish stability. For packaging in sealed glass bottles, open-dish potency loss is of little importance, and a compromise of chemical stability is not necessary. For example, additives VII and XV stabilize content uniformity with no measurable loss of chemical stability and several other additives (V in particular) do not seriously affect chemical stability when used at R = 1[10].

REFERENCES

(1) R. R. Shangraw and A. M. Contractor, *J. Am. Pharm. Assoc.*, **N512,** 633 (1972).

(2) S. Fusari, *J. Pharm. Sci.*, **62,** 122 (1973).

(3) S. Fusari, *J. Pharm. Sci.*, **62,** 2012 (1973).

(4) M. J. Pikal, A. L. Lukes, and L. F. Ellis, *J. Pharm. Sci.*, **65,** 1278 (1976).

(5) F. W. Goodhart, H. Gucluyildiz, R. E. Daly, L. Chafetz, and F. C. Ninger, *J. Pharm. Sci.*, **65,** 1466 (1976).

(6) H. Gucluyildiz, F. W. Goodhart, and F. C. Ninger, *J. Pharm. Sci.*, **66,** 265 (1977).

(7) M. J. Pikal, D. A. Bibler, and B. Rutherford, *J. Pharm. Sci.*, **66,** 1293 (1977).

(8) D. Stephenson and J. F. Humphreys-Jones, *J. Pharm. Pharmacol.*, **3,** 767 (1951).

(9) W. Kross and H. Roth, *Pharm. Ztg.*, **120,** 1490 (1975); *Chem. Abstr.*, **84,** 22035b (1976).

(10) P. Suphajettra, J. Lim, and J. Strohl, Abstracts of 124th APhA Annual Meeting, APhA Academy of Pharmaceutical Sciences, May 1977.

(11) D. P. Page, N. A. Carson, C. A. Buhr, P. E. Flinn, C. E. Wells, and M. T. Randall, *J. Pharm. Sci.*, **64,** 141 (1975).

(12) M. J. Pikal and A. L. Lukes, *J. Pharm. Sci.*, **65,** 1269 (1976).

(13) G. N. Lewis and M. Randall, "Thermodynamics," 2nd ed., revised by K. S. Pitzer and L. Brewer, McGraw Hill Co., New York, N.Y., 1961, p. 294.

(14) "Handbook of Chemistry and Physics," 38th ed., Chemical Rubber Publishing Co., Cleveland, Ohio, 1956.

(15) V. V Gorbunov, *Teor. Vzryvchatykh Veshchestv*, **1963,** 219; *Chem. Abstr.*, **59,** 9728b (1963).

(16) R. C. Farmer, *J. Chem. Soc.*, **117,** 806 (1920).

(17) M. C. Crew and F. J. Dicarlo, *J. Chromatogr.*, **35,** 506 (1968).

[10] Only two stabilized nitroglycerin tablet products are available in the U.S. market. Parke-Davis' formulation uses polyethylene glycol 4000 as the additive while the Lilly formulation currently uses povidone.

γ-Aminobutyric Acid Uptake Inhibition and Anticonvulsant Activity of Nipecotic Acid Esters

A. MICHAEL CRIDER *§x, J. D. WOOD ‡, KATHRYN D. TSCHAPPAT *, CHRISTINE N. HINKO *, and KAREN SEIBERT *

Received May 16, 1983, from the **College of Pharmacy, The University of Toledo, Toledo, OH 43606* and the ‡*Department of Biochemistry, University of Saskatchewan, Saskatoon, Saskatchewan, Canada.* Accepted for publication October 5, 1983. Present address: § School of Pharmacy, Northeast Louisiana University, Monroe, LA 71209.

Abstract □ *n*-Alkyl esters of nipecotic acid were prepared by Fischer esterification, and the esters were evaluated against bicuculline-induced seizures in mice. Evaluation of the alkyl esters for inhibition of γ-aminobutyric acid uptake into mouse whole brain mini-slices revealed that the order of potency was proportional to chain length. The octyl ester inhibited γ-aminobutyric acid and β-alanine uptakes by apparently nonspecific mechanisms. A variety of phenyl esters of nipecotic acid were also synthesized utilizing either dicyclohexylcarbodiimide or 1,1′-carbonyldiimidazole as the condensing agent. Most of the phenyl esters were potent inhibitors of γ-aminobutyric acid uptake. The uptake inhibition appeared to involve specific and nonspecific (detergent-like) mechanisms. The *m*-nitrophenyl and *p*-nitrophenyl esters were particularly potent against bicuculline-induced seizures in mice.

Keyphrases □ Nipecotic acid esters—synthesis, anticonvulsant activity □ Anticonvulsant agents—potential, nipecotic acid esters, synthesis

γ-Aminobutyric acid appears to act as a major inhibitory neurotransmitter in the central nervous system (1–3). Impairment in γ-aminobutyric acid neurotransmission may contribute to the symptoms of Huntington's disease, Parkinsonism, and epilepsy (4). Thus, compounds that potentiate γ-aminobutyric acid neurotransmission have considerable therapeutic potential.

(±)-Nipecotic acid (I) has been found to be a potent inhibitor of γ-aminobutyric acid uptake into rat cerebral cortex (5) and mouse whole brain mini-slices (6). The *R*-(−) enantiomer of nipecotic acid (I) has approximately five times greater affinity for the γ-aminobutyric acid uptake carrier than the *S*-(+) enantiomer (7).

As with several other compounds (8) having the potential of interacting with the γ-aminobutyric acid system, (±)-nipecotic acid (I) does not readily penetrate the blood–brain barrier (9). However, prodrug esters of nipecotic acid (I) that pass into the central nervous system have been evaluated for anticonvulsant activity (10–13) and γ-aminobutyric acid uptake inhibition (13, 14).

0022-3549/84/1100-1612$01.00/0

© 1984, American Pharmaceutical Association

sulting in an increase in disintegration time, the effect increasing as the additive content of the tablet increases. For example, conventional tablets (Table III) typically disintegrate within ~10 s, but tablets with additives present at 1% of the tablet weight require 20–30 s for all additives except povidone. Tablets formulated with 2% of either additive V or additive VIII require ~100 s for disintegration. These times refer to tablets aged 2 years at 25°C. While 100 s is near the UPS limit for 2 min, a reduction in tablet density will significantly reduce the disintegration time. The data quoted above refer to a fixed tablet density (1.16 g/mL). Thus, it may be possible to reduce the tablet density by using less lactose, thereby reducing the disintegration time to a more acceptable level.

With the exception of tablets containing additive I (povidone), the disintegration times for fresh tablets are essentially the same as for aged tablets. Fresh tablets containing 1% povidone typically disintegrate within 20 s, but after prolonged aging (more than 2 years at 25°C) they may require 1–2 min for disintegration. Evidently the povidone cross-links to some extent which retards disintegration. When these tablets are left undisturbed in water for some time, a "ghost" of insoluble material in the shape of the tablet remains. Thus, with the exception of severely aged povidone-containing tablets, excessive disintegration time is not a problem for the tablet systems studied (Table III), at least for ≤1% additive.

CONCLUSIONS

A number of nitroglycerin-soluble additives sufficiently lower the vapor pressure of nitroglycerin to stabilize the content uniformity of molded nitroglycerin tablets. In general, an additive–nitroglycerin weight ratio, R, of 1 is adequate for this purpose. Tablet potency losses in open-dish evaporation tests are roughly proportional to the vapor pressure of nitroglycerin in the tablet, and higher levels of additive (R = 2) are normally needed to achieve a significant improvement in open-dish stability. However, with few exceptions (VII and XV) high additive levels lead to reduced chemical stability, particularly at high temperature, and a compromise must be made between chemical stability and open-dish stability. For packaging in sealed glass bottles, open-dish potency loss is of little importance, and a compromise of chemical stability is not necessary. For example, additives VII and XV stabilize content uniformity with no measurable loss of chemical stability and several other additives (V in particular) do not seriously affect chemical stability when used at R = 1[10].

REFERENCES

(1) R. R. Shangraw and A. M. Contractor, *J. Am. Pharm. Assoc.*, **N512,** 633 (1972).

(2) S. Fusari, *J. Pharm. Sci.*, **62,** 122 (1973).

(3) S. Fusari, *J. Pharm. Sci.*, **62,** 2012 (1973).

(4) M. J. Pikal, A. L. Lukes, and L. F. Ellis, *J. Pharm. Sci.*, **65,** 1278 (1976).

(5) F. W. Goodhart, H. Gucluyildiz, R. E. Daly, L. Chafetz, and F. C. Ninger, *J. Pharm. Sci.*, **65,** 1466 (1976).

(6) H. Gucluyildiz, F. W. Goodhart, and F. C. Ninger, *J. Pharm. Sci.*, **66,** 265 (1977).

(7) M. J. Pikal, D. A. Bibler, and B. Rutherford, *J. Pharm. Sci.*, **66,** 1293 (1977).

(8) D. Stephenson and J. F. Humphreys-Jones, *J. Pharm. Pharmacol.*, **3,** 767 (1951).

(9) W. Kross and H. Roth, *Pharm. Ztg.*, **120,** 1490 (1975); *Chem. Abstr.*, **84,** 22035b (1976).

(10) P. Suphajettra, J. Lim, and J. Strohl, Abstracts of 124th APhA Annual Meeting, APhA Academy of Pharmaceutical Sciences, May 1977.

(11) D. P. Page, N. A. Carson, C. A. Buhr, P. E. Flinn, C. E. Wells, and M. T. Randall, *J. Pharm. Sci.*, **64,** 141 (1975).

(12) M. J. Pikal and A. L. Lukes, *J. Pharm. Sci.*, **65,** 1269 (1976).

(13) G. N. Lewis and M. Randall, "Thermodynamics," 2nd ed., revised by K. S. Pitzer and L. Brewer, McGraw Hill Co., New York, N.Y., 1961, p. 294.

(14) "Handbook of Chemistry and Physics," 38th ed., Chemical Rubber Publishing Co., Cleveland, Ohio, 1956.

(15) V. V Gorbunov, *Teor. Vzryvchatykh Veshchestv*, **1963,** 219; *Chem. Abstr.*, **59,** 9728b (1963).

(16) R. C. Farmer, *J. Chem. Soc.*, **117,** 806 (1920).

(17) M. C. Crew and F. J. Dicarlo, *J. Chromatogr.*, **35,** 506 (1968).

[10] Only two stabilized nitroglycerin tablet products are available in the U.S. market. Parke-Davis' formulation uses polyethylene glycol 4000 as the additive while the Lilly formulation currently uses povidone.

γ-Aminobutyric Acid Uptake Inhibition and Anticonvulsant Activity of Nipecotic Acid Esters

A. MICHAEL CRIDER *§x, J. D. WOOD ‡, KATHRYN D. TSCHAPPAT *, CHRISTINE N. HINKO *, and KAREN SEIBERT *

Received May 16, 1983, from the **College of Pharmacy, The University of Toledo, Toledo, OH 43606* and the ‡*Department of Biochemistry, University of Saskatchewan, Saskatoon, Saskatchewan, Canada.* Accepted for publication October 5, 1983. Present address: § School of Pharmacy, Northeast Louisiana University, Monroe, LA 71209.

Abstract □ *n*-Alkyl esters of nipecotic acid were prepared by Fischer esterification, and the esters were evaluated against bicuculline-induced seizures in mice. Evaluation of the alkyl esters for inhibition of γ-aminobutyric acid uptake into mouse whole brain mini-slices revealed that the order of potency was proportional to chain length. The octyl ester inhibited γ-aminobutyric acid and β-alanine uptakes by apparently nonspecific mechanisms. A variety of phenyl esters of nipecotic acid were also synthesized utilizing either dicyclohexylcarbodiimide or 1,1′-carbonyldiimidazole as the condensing agent. Most of the phenyl esters were potent inhibitors of γ-aminobutyric acid uptake. The uptake inhibition appeared to involve specific and nonspecific (detergent-like) mechanisms. The *m*-nitrophenyl and *p*-nitrophenyl esters were particularly potent against bicuculline-induced seizures in mice.

Keyphrases □ Nipecotic acid esters—synthesis, anticonvulsant activity □ Anticonvulsant agents—potential, nipecotic acid esters, synthesis

γ-Aminobutyric acid appears to act as a major inhibitory neurotransmitter in the central nervous system (1–3). Impairment in γ-aminobutyric acid neurotransmission may contribute to the symptoms of Huntington's disease, Parkinsonism, and epilepsy (4). Thus, compounds that potentiate γ-aminobutyric acid neurotransmission have considerable therapeutic potential.

(±)-Nipecotic acid (I) has been found to be a potent inhibitor of γ-aminobutyric acid uptake into rat cerebral cortex (5) and mouse whole brain mini-slices (6). The *R*-(−) enantiomer of nipecotic acid (I) has approximately five times greater affinity for the γ-aminobutyric acid uptake carrier than the *S*-(+) enantiomer (7).

As with several other compounds (8) having the potential of interacting with the γ-aminobutyric acid system, (±)-nipecotic acid (I) does not readily penetrate the blood–brain barrier (9). However, prodrug esters of nipecotic acid (I) that pass into the central nervous system have been evaluated for anticonvulsant activity (10–13) and γ-aminobutyric acid uptake inhibition (13, 14).

0022-3549/84/1100-1612$01.00/0

© 1984, American Pharmaceutical Association

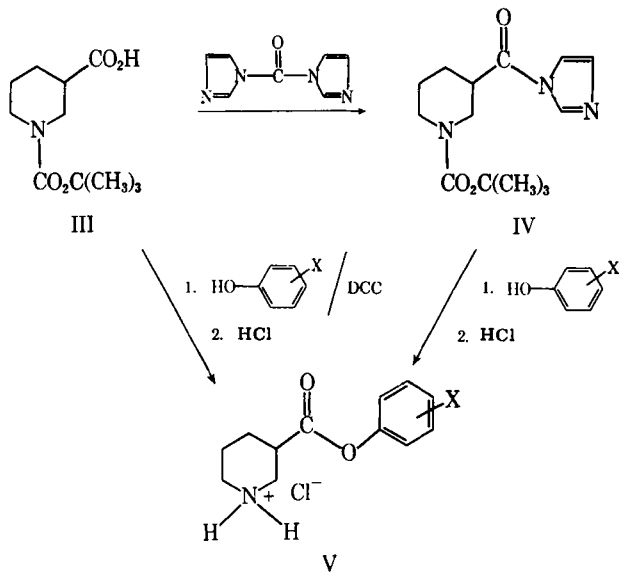

Scheme I

In a previous report, the *p*-nitrophenyl ester Vc was found to exhibit potent anticonvulsant activity and γ-aminobutyric acid uptake inhibition. The octyl ester IIc was also a strong inhibitor of γ-aminobutyric acid uptake (13). The results of this preliminary study indicated that Vc inhibited γ-aminobutyric acid uptake into mouse whole brain mini-slices by a combination of specific and nonspecific (detergent-like) effects. The specific effect is due to the hydrolysis product, nipecotic acid (I), while the nonspecific effect is caused by the intact ester. The octyl ester IIc apparently is not hydrolyzed under the assay conditions of the γ-aminobutyric acid uptake and the inhibition is entirely due to the intact ester.

Based on the activity of Vc, it was of interest to examine the structure-activity relationships of substituted-phenyl esters of I. Specifically, the lipophilicity and the electronic character of the phenyl substituent were varied in order to determine the effect on anticonvulsant activity and γ-aminobutyric acid uptake inhibition. An additional objective of this study was to evaluate the γ-aminobutyric acid uptake inhibition of the heptyl IIb and nonyl IId esters to determine if their action was nonspecific, as was the case with IIc.

RESULTS AND DISCUSSION

The alkyl esters (IIa-d) were synthesized by Fischer esterification of I with an appropriate alcohol in the presence of dry hydrogen chloride (13). Phenyl esters (Va-q) of nipecotic acid were prepared by utilizing either dicyclohexylcarbodiimide or 1,1′-carbonyldiimidazole as the condensing agent (Scheme I); the physical properties of these compounds are given in Table I.

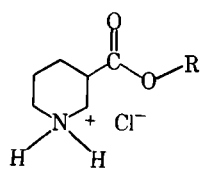

IIa, R = C_6H_{13}
IIb, R = C_7H_{15}
IIc, R = C_8H_{17}
IId, R = C_9H_{19}

Termination of γ-aminobutyric acid with its postsynaptic receptor is brought about by high-affinity uptake systems in nerve terminals and glial cells (3). These carriers exhibit different substrate specificities for γ-aminobutyric acid and its derivatives (15, 16). The results of Breckenridge *et al.* (16) have confirmed that both neuronal and glial uptake processes prefer a folded conformation in the molecule. These same workers found that neuronal γ-aminobutyric acid uptake is markedly influenced by compounds having long alkyl chains. In contrast, inhibition of β-alanine uptake was more strongly affected by compounds having shorter alkyl chains. The speculation was that the glial uptake carrier has a more shallow hydrophobic bonding site.

Based on the work by Breckenridge and co-workers (16), we were interested in evaluating homologues of IIc for γ-aminobutyric acid uptake inhibition. The nonyl ester IId completely inhibited γ-aminobutyric acid uptake, while the heptyl ester IIb and hexyl ester IIa were less potent uptake inhibitors (85 and 53%, respectively). The results of IIc on β-[^{3}H]alanine uptake, a measure of glial uptake inhibition (16), are given in Table II. Since 1 mM nipecotic acid (I) only inhibits β-alanine uptake by 85%, the 100% uptake inhibition by IIc strongly suggests a nonspecific cationic detergent effect. Such a mechanism is further supported by the fact that IIc more potently inhibits γ-aminobutyric acid (100 *versus* 96%) and L-proline (13) (99 *versus* 21%) uptake than the parent amino acid I. Although IIc apparently inhibits both γ-aminobutyric acid and β-alanine by nonspecific mechanisms, it is rather difficult to explain the differences in uptake inhibition of γ-aminobutyric acid and β-alanine on dilution of the inhibitor (16 *versus* 50%) at 0.5 mM, respectively.

All of the phenyl esters, with the exception of Vd, were potent inhibitors of γ-aminobutyric acid uptake (Table III). As was the case with *p*-nitrophenyl ester Vc (13), these derivatives probably inhibit γ-aminobutyric acid uptake by a combination of specific and nonspecific effects. The phenyl substituents vary considerably in terms of lipophilic and electronic character. However, no readily apparent correlation exists between these parameters and either γ-aminobutyric acid uptake inhibition or anticonvulsant activity.

The esters were also evaluated for their ability to protect against bicuculline-induced seizures (Table IV). A single dose (150 mg/kg sc) of each compound was tested, with this dose being administered 60 min prior to bicuculline challenge. The dose and pretreatment time were chosen on the basis of preliminary testing of other compounds in the series (13). A subcutaneous route of injection was used to reduce peripheral hydrolysis. Currently, individual compounds are being evaluated at a variety of doses and pretreatment times in an effort to calculate specific ED_{50} values and times of peak effect.

As indicated in Table IV, all compounds (with the exception of Vd and Vn) demonstrated a significant degree of protection against clonic convulsions, tonic convulsions, or death induced by bicuculline. Although complete protection from clonic spasms was not observed with any of the compounds tested at this dose, IIb, IId, and Vb provided protection from clonic convulsions in seven of eight mice and IIb, Vc, and Ve protected all eight animals in each group from tonic convulsions and death. In addition, IIc, IId, Vb, Vk, Vp, and Vq prevented tonic convulsions and death in at least seven of eight animals. Antagonism of convulsions induced by bicuculline, a putative γ-aminobutyric acid receptor antagonist, suggests that these nipecotic acid esters may be producing their effects by interaction with the γ-aminobutyric acid system.

EXPERIMENTAL SECTION[1]

***n*-Heptyl 3-Piperidinecarboxylate Hydrochloride (IIb)**—This compound was prepared according to conditions previously described (13) in 21% yield, mp 74-75°C; IR (KBr): 2500 (NH_2^+), 1760 (C=O), and 1225 cm^{-1} (C—O); ^{1}H-NMR ($CDCl_3$): δ 0.90 (t, 3, CH_3), 1.07-3.80 (m, 19, aliphatic CH_2, ring CH, and ring CH_2), 4.10 (t, 2, OCH_2), and 9.45 ppm (br s, 2, NH_2^+).

Anal.—Calc. for $C_{13}H_{26}ClNO_2$: C, 59.17; H, 9.95; N, 5.31. Found: C, 59.43; H, 9.87; N, 5.01.

***n*-Nonyl 3-Piperidinecarboxylate Hydrochloride (IId)**—Compound IId was synthesized following the general method (13) in 51% yield, mp 85-86°C; IR (KBr): 2500 (NH_2^+), 1760 (C=O), and 1225 cm^{-1} (C—O); ^{1}H-NMR ($CDCl_3$): δ 0.87 (t, 3, CH_3), 1.03-3.77 (m, 23, aliphatic CH_2, ring CH, and ring CH_2), 4.07 (t, 2, OCH_2), and 9.43 ppm (br s, 2, NH_2^+).

Anal.—Calc. for $C_{15}H_{30}ClNO_2$: C, 61.71; H, 10.38; N, 4.80. Found: C, 61.79; H, 10.27; N, 5.02.

1-(1-*tert*-Butyloxcarbonyl-3-piperidinocarbonyl)imidazole (IV)—A mixture of III (13) (3.00 g, 0.013 mol) and 1,1′-carbonyldiimidazole (2.10 g, 0.013 mol) in 150 mL of tetrahydrofuran was heated at reflux overnight. Removal of the solvent gave a yellow oil, which was dissolved in 50 mL of chloroform

[1] Melting points were determined on a Fisher-Johns melting point apparatus and are uncorrected. IR spectra were recorded as potassium bromide pellets with a Perkin-Elmer spectrophotometer. ^{1}H-NMR spectra were recorded on a Varian EM 360A spectrometer. Chemical shifts are reported in parts per million (δ) relative to tetramethylsilane (1%) or, in the case of D_2O (1%), sodium 2,2-dimethyl-2-silapentane-5-sulfonate. Analytical data were obtained from Micro-Analysis Inc., Wilmington, Del.

Table I—Physical Properties of Phenyl 3-Piperidinecarboxylate Hydrochlorides (V)

Compound	X	Method	Melting Point, °C	Yield, %	Formula[a]	IR, cm^{-1}	^1H-NMR[b]
Va	—H	B[c]	161–163	46[k]	$C_{12}H_{16}ClNO_2$	1785 (C=O)	δ 1.97 (m, 4, CH_2CH_2CH), 3.33 (m, 5, $CH_2NH_2^+CH_2CH$), 6.93–7.40 (m, 5, ArH), 9.67 ppm (br s, 2, NH_2^+)
Vb	—*m*-NO_2	A[d]	190–192	44[j]	$C_{12}H_{15}ClN_2O_4$		
Vc	—*p*-NO_2[e]	A[d]	160–162	60[j]	$C_{12}H_{15}ClN_2O_4$	1780 (C=O)	2.0 (m, 4, CH_2CH_2CH), 3.1–3.5 (br m, 5, $CH_2NH_2^+CH_2CH$), 7.3–8.2 ppm (m, 4, ArH)
Vd	—*m*-CN	B[c]	149.5–151.5	14[i]	$C_{13}H_{15}ClN_2O_2$	1750 (C=O)	2.03 (m, 4, CH_2CH_2CH) 2.63–3.80 (m, 5, $CH_2NH_2^+CH_2CH$), 7.60 ppm (m, 4, ArH)
Ve	—*p*-CN	A[c]	148.5–150.0	20[k]	$C_{13}H_{15}ClN_2O_2$	1785 (C=O)	2.13 (m, 4, CH_2CH_2CH), 2.73–4.07 (m, 5, $CH_2NH_2^+CH_2CH$), 7.33 (d, 2, J = 8 Hz, ArH), 7.87 ppm (d, 2, J = 8 Hz, ArH)
Vf	—*o*-CN	B[c]	142–143	36[k]	$C_{13}H_{15}ClN_2O_2$	2270 (C≡N), 1795 (C=O)	2.03 (m, 4, CH_2CH_2CH), 2.60–4.83 (m, 5, $CH_2NH_2^+CH_2CH$), 7.23–8.03 ppm (m, 4, ArH)
Vg	—*m*-CF_3	B[c]	111–113	35[k]	$C_{13}H_{15}ClF_3NO_2$	1810 (C=O)	2.20 (m, 4, CH_2CH_2CH), 3.57 (m, 5, $CH_2NH_2^+CH_2CH$), 7.70 ppm (s, 4, ArH)
Vh	—*p*-CF_3	B[f]	183–184	30[k]	$C_{13}H_{15}ClF_3NO_2$	1800 (C=O)	2.17 (m, 4, CH_2CH_2CH), 2.70–4.07 (m, 5, $CH_2NH_2^+CH_2CH$), 7.43 (d, 2, J = 8 Hz, ArH), 7.83 ppm (d, 2, J = 8 Hz, ArH)
Vi	—*m*-F	B[c]	124–126	48[k]	$C_{12}H_{15}ClFNO_2$		
Vj	—*p*-Cl	B[c]	174.5–175.0	28[k]	$C_{12}H_{15}Cl_2NO_2$	1785 (C=O)	2.07 (m, 4, CH_2CH_2CH), 3.67–3.87 (m, 5, $CH_2NH_2^+CH_2CH$), 7.20 (d, 2, J = 8 Hz, ArH), 7.50 ppm (d, 2, J = 8 Hz, ArH)
Vk	—*p*-Br	B[d]	225.0–226.5	50[l]	$C_{12}H_{15}BrClNO_2$	1750 (C=O)	1.87 (m, 4, CH_2CH_2CH), 2.67–3.57 (m, 5, $CH_2NH_2^+CH_2CH$), 7.17 (d, 2, J = 8 Hz, ArH), 7.67 (d, 2, J = 8 Hz, ArH), 9.50 ppm (br s, 2, NH_2^+)
Vl	—*p*-I	B[g]	255–256	69[k]	$C_{12}H_{15}ClINO_2$	1785 (C=O)	1.90 (m, 4, CH_2CH_2CH), 3.20 (m, 5, $CH_2NH_2^+CH_2CH$), 7.07 (d, 2, J = 8 Hz, ArH), 7.80 (d, 2, J = 8 Hz, ArH), 9.47 ppm (br s, 2, NH_2^+)
Vm	—*p*-$C(CH_3)_3$	B[c]	178–179	31[k]	$C_{16}H_{24}ClNO_2$	1750 (C=O)	1.30 [s, 9, $C(CH_3)_3$], 1.47–3.87 (m, 8, ring CH_2), 4.13 (m, 1, ring CH), 6.97 (d, 2, J = 8 Hz, ArH), 7.36 (d, 2, J = 8 Hz, ArH), 9.70 ppm (br s, 2, NH_2^+)
Vn	—*p*-OCH_3	B[d]	190.0–190.5	57[k]	$C_{13}H_{18}ClNO_3$	1785 (C=O)	2.00 (m, 4, CH_2CH_2CH), 2.67–3.90 (m, 8, including singlet at 3.90, OCH_3), 7.13 ppm (br s, 4, ArH)
Vo	—*p*-$COCH_3$	A[c]	171.5–172.5	30[k]	$C_{14}H_{18}ClNO_3$	1785 (C=O, ester), 1710 (C=O, ketone)	2.03 (m, 4, CH_2CH_2CH), 2.67 (s, 3, $COCH_3$), 2.70–3.83 (m, 5, $CH_2NH_2^+CH_2CH$), 7.20 (d, 2, J = 8 Hz, ArH), 7.93 (d, 2, J = 8 Hz, ArH)
Vp	—*p*-CO_2CH_3	A[h]	186.0–187.5	33[k]	$C_{14}H_{18}ClNO_4$	1800 (C=O, ester), 1755 (CO_2CH_3)	1.40–3.80 (m, 9, ring CH and CH_2), 3.97 (s, 3, $COOCH_3$), 7.27 (d, 2, J = 8 Hz, ArH), 8.07 ppm (d, 2, J = 8 Hz, ArH)
Vq	—*p*-$CO_2C_2H_5$	B[d]	186.0–186.5	46[k]	$C_{15}H_{20}ClNO_4$	1820 (C=O, ester) 1750 ($CO_2C_2H_5$)	1.33 (t, 3, J = 6 Hz, CH_3), 1.90 (m, 4, CH_2CH_2CH), 3.40 (m, 5, $CH_2NH_2^+CH_2CH$), 4.33 (q, 2, J = 6 Hz, CH_2CH_3) 7.40 (d, 2, J = 8 Hz, ArH), 8.07 (d, 2, J = 8 Hz, ArH), 9.60 ppm (br s, 2, NH_2^+)

[a] Compounds Va, Vb, and Vd–q were analyzed for C, H, and N; all values were within ±0.4% of the theoretical value. [b] Compounds Va and Vn were run in Unisol-*d*; Vc–j and Vn–p were run in D_2O; Vd, Vl, and Vq were run in Me_2SO-d_6. [c] Recrystallized from ethanol–ether. [d] Recrystallized from ethanol. [e] Reported in the literature (13). [f] Recrystallized from 95% ethanol–ether. [g] Recrystallized from 95% ethanol. [h] Recrystallized from methanol–ether. [i] Pale-pink crystals. [j] Pale-yellow crystals. [k] White crystals. [l] Brown crystals.

and washed three times with 25-mL portions of water. The organic phase was separated, dried (sodium sulfate), and evaporated to yield an almost colorless oil. Trituration of the oil with hexane gave, after drying, 2.88 g (79%) of a white solid, mp 95–99°C. An analytical sample was prepared by recrystallization from petroleum ether (bp 39–55°C) to yield pure product, mp 105–106°C; IR (KBr): 1735 (C=O, imidazolide) and 1700 cm^{-1} (C=O, carbamate); ^1H-NMR ($CDCl_3$): δ 1.50–4.47 [m, 18, ring CH, ring CH_2, and $C(CH_3)_3$ at 1.50], 7.10 (s, 1, —N—CH=N—CH=CH), 7.50 (s, 1,

Table II—Effect of IIc on the Uptakes of γ-Aminobutyric Acid and β-Alanine [a]

Conc. of Inhibitor, mM	β-Alanine Uptake, % Inhibition		γ-Aminobutyric Acid Uptake, % Inhibition	
	IIc	Nipecotic Acid	IIc	Nipecotic Acid
1.0	100 ± 0	85 ± 1	100 ± 1	96 ± 1
0.2	92 ± 1	71 ± 2	48 ± 3	89 ± 1
0.05	50 ± 2	47 ± 4	16 ± 2	75 ± 1

[a] All values are mean ± *SEM* for six samples.

Table III—Inhibition of γ-Aminobutyric Acid Uptake by Nipecotic Acid Esters [a]

Inhibitor[b]	Inhibition of Uptake, %[c]
I	96.3 ± 0.2
Va	81.2 ± 0.6
Vb	97.5 ± 0.5
Vc	99.0 ± 0.1
Vd	33.4 ± 2.2
Ve	94.4 ± 0.2
Vf	98.0 ± 0.3
Vg	95.1 ± 0.5
Vh	97.3 ± 0.3
Vi	92.0 ± 0.3
Vj	94.2 ± 0.4
Vk	95.8 ± 0.4
Vl	98.2 ± 0.1
Vm	97.5 ± 0.3
Vn	82.5 ± 0.5
Vo	90.9 ± 0.5
Vp	92.4 ± 0.1
Vq	95.5 ± 0.3
IIa	52.7 ± 1.6
IIb	84.9 ± 1.4
IIc	99.7 ± 0.1
IId	99.8 ± 0.1

[a] Uptake measured into mouse whole brain mini-slices. [b] Inhibitor concentration = 1 mM. [c] All values are mean ± *SEM* for six samples.

$-\overline{N-CH=N-CH=C}H$), and 8.23 ppm (s, 1, $-\overline{NCH=N-CH=CH}$).

Anal.—Calc. for $C_{14}H_{21}N_3O_3$: C, 60.18; H, 7.59; N, 15.04. Found: C, 60.06; H, 7.58; N, 14.87.

Representative Procedures for the Synthesis of the Phenyl 3-Piperidinecarboxylate Hydrochlorides (V)—*Method A*—The synthesis of *m*-nitrophenyl 3-piperidinecarboxylate hydrochloride (Vb) is representative of the general procedure. A solution of III (3.00 g, 0.013 mol) and *m*-nitrophenol (1.82 g, 0.013 mol) in acetonitrile (150 mL) was treated in one portion with dicyclohexylcarbodiimide (2.70 g, 0.013 mol). A white precipitate of dicyclohexylurea formed immediately. Stirring was continued for 48 h, the dicyclohexylurea was removed by filtration, and the filtrate was saturated with hydrogen chloride at 0–5°C. The solvent was evaporated under reduced pressure and the resulting solid was recrystallized from absolute ethanol to yield 1.65 g (44%) of light-yellow crystals, mp 190–192°C; IR (KBr): 1785 cm^{-1} (C=O, ester); ^{1}H-NMR (D_2O): δ 1.65–4.00 (m, 9, ring CH and CH_2) and 7.55–8.45 ppm (m, 4, ArH).

Anal.—Calc. for $C_{12}H_{15}ClN_2O_4$: C, 50.26; H, 5.28; N, 9.77. Found: C, 50.49; H, 5.42; N, 9.63.

Method B—The synthesis of *m*-fluorophenyl 3-piperidinecarboxylate hydrochloride (Vi) is representative of the general method. A solution of IV (2.90 g, 0.010 mol) and *m*-fluorophenol (1.17 g, 0.010 mol) in acetonitrile (200 mL) was heated at reflux for 48 h, and the solvent was removed under reduced pressure. The resulting oil was dissolved in chloroform (200 mL) and washed three times with 25-mL portions of water. The organic phase was dried (sodium sulfate) and saturated with dry hydrogen chloride at 0–5°C. Evaporation of the solvent gave a light-yellow oil which solidified after trituration with ether. Recrystallization from ethanol–ether gave 1.30 g (48%) of analytically pure product, mp 124–126°C; IR (KBr): 1785 cm^{-1} (C=O, ester); ^{1}H-NMR (D_2O): δ 1.67–4.00 (m, 9, ring CH and CH_2) and 6.90–7.80 ppm (m, 4, ArH).

Anal.—Calc. for $C_{12}H_{15}ClFNO_2$: C, 55.49; H, 5.83; N, 5.39. Found: C, 55.76; H, 5.83; N, 5.53.

Table IV—Antagonism of Bicuculline-Induced Convulsions by Esters of Nipecotic Acid

Pretreatment[a]	Number Mice Protected/Total Number Mice[b]		
	Clonic Convulsions	Tonic Convulsions	Death
Saline	0/116	0/116	0/116
IIa	3/8[e]	4/8	5/8
IIb	7/8	8/8	8/8
IIc	6/8	7/8	7/8
IId	7/8	7/8	7/8
Vb	7/8	8/8	7/8
Vc[c]	4/8	8/8	8/8
Vd	0/8[d]	1/8[d]	0/8[d]
Ve	6/8	8/8	8/8
Vf	4/8	6/8	6/8
Vg	3/8[e]	6/8	6/8
Vi	1/7[d]	3/7[e]	2/7[d]
Vj	2/8[d]	4/8	4/8
Vk	5/8	7/8	7/8
Vm	6/8	6/8	6/8
Vn	0/8[d]	0/8[d]	0/8[d]
Vo	1/8[d]	5/8	7/8
Vp	4/8	7/8	7/8
Vq	3/8[e]	7/8	7/8

[a] Compounds (150 mg/kg sc) were administered 60 min prior to bicuculline (3.00 or 3.75 mg/kg sc). Compounds Vh and Vl were also tested but limited solubility and stability of the compounds prevents the reporting of reproducible data. [b] The animal was considered protected from clonic convulsions if it failed to exhibit an episode of clonic spasms for at least 5 s. The animal was considered protected from tonic convulsions if it failed to exhibit hind limb extension. [c] Previously reported (13). [d] Not significantly different from saline controls. [e] Significantly different from saline controls ($p < 0.05$). All other values in the table are significantly different from saline controls ($p < 0.01$).

Biological Testing—Male Sprague-Dawley mice[2] received an injection of 3.0 or 3.75 mg/kg sc of bicuculline in a volume of 0.01 mL/g. The bicuculline was prepared by dissolving the solid in 0.1 M HCl and adjusting to pH 5 with 0.1 M NaOH (13). Each compound was evaluated for its ability to protect against bicuculline-induced seizures at a dose of 150 mg/kg sc injected 1 h prior to bicuculline administration. Groups of eight mice per compound were tested. Groups of four control mice were pretreated with 0.9% NaCl and tested before and after each experimental group to ensure maximal convulsant potency of the bicuculline.

The incidence and onset of clonic and tonic convulsions and fatality induced by bicuculline were recorded for each of the animals. A clonic convulsion was defined as a single episode of clonic spasms of at least a 5-s duration. A tonic seizure was defined as a brief period of hind limb flexion followed by a prolonged period of hind limb extension. The animals were observed for at least 45 min after the injection of bicuculline. The uptakes of γ-[^{3}H]aminobutyric acid and tritiated β-alanine were carried out following reported procedures (6, 17).

REFERENCES

(1) J. K. Saelens and F. J. Vinick, in "Annual Reports in Medicinal Chemistry," Vol. 13, F. H. Clarke, Ed., Academic, New York, N.Y., 1978, p. 31.

(2) D. R. Curtis, in "GABA-Neurotransmitters, Pharmacochemical, Biochemical and Pharmacological Aspects," P. Krogsgaard-Larsen, J. Scheel-Krüger, and H. Kofod, Eds., Academic, New York, N.Y., 1979, p. 18.

(3) A. Schousboe, L. Hertz, O. M. Larsson, and P. Krogsgaard-Larsen, *Brain Res. Bull. Suppl.*, **2**, 403 (1980).

(4) S. J. Enna, *Biochem. Pharmacol.*, **30**, 907 (1981).

(5) P. Krogsgaard-Larsen and G. A. R. Johnston, *J. Neurochem.*, **25**, 797 (1975).

(6) J. D. Wood, D. Tsui, and J. W. Phillis, *Can. J. Physiol. Pharmacol.*, **57**, 581 (1979).

(7) G. A. R. Johnston, P. Krogsgaard-Larsen, A. L. Stephanson, and B. Twitchin, *J. Neurochem.*, **26**, 1029 (1976).

(8) P. S. Callery, L. A. Geelhaar, M. S. B. Nayar, M. Stogniew, and K. G. Rao, *J. Neurochem.*, **38**, 1063 (1982).

(9) D. Lodge, G. A. R. Johnston, D. R. Curtis, and S. J. Brand, *Brain Res.*, **136**, 513 (1977).

(10) R. W. Horton, J. F. Collins, G. M. Anlezark, and B. S. Meldrum, *Eur. J. Pharmacol.*, **59**, 75 (1979).

[2] Harlan Sprague-Dawley, Madison, Wis.

(11) H. H. Frey, C. Popp, and W. Löscher, *Neuropharmacology*, **18**, 581 (1979).
(12) C. G. Wermuth, A. Zinoune, J. J. Bourguignon, and J. P. Chambon, in "The Chemical Regulation of Biological Mechanisms," A. M. Creighton and S. Turner, Eds., The Royal Society of Chemistry, London, 1982. p. 112.
(13) A. M. Crider, T. T. Tita, J. D. Wood, and C. N. Hinko, *J. Pharm. Sci.*, **71**, 1214 (1982).
(14) J. D. Wood, A. Schousboe, and P. Krogsgaard-Larsen, *Neuropharmacology*, **19**, 1149 (1980).
(15) S. L. Earley, E. K. Michaelis, and M. P. Mertes, *Biochem. Pharmacol.*, **30**, 1105 (1981).
(16) R. J. Breckenridge, S. H. Nicolson, A. J. Nicol, C. J. Suckling, B. Leigh, and L. Iversen, *Biochem. Pharmacol.*, **30**, 3045 (1981).
(17) L. L. Iversen and M. J. Neal, *J. Neurochem.*, **15**, 1141 (1968).

ACKNOWLEDGMENTS

A portion of this work was presented at the 14th Central Regional Meeting of The American Chemical Society, Midland, Michigan, June 1982. This investigation was funded by research grants from the Epilepsy Foundation of America, The Upjohn Company, the University of Toledo Faculty Research Awards and Fellowships Program, and the Medical Research Council of Canada. The authors thank David L. Miskell and Eugen Kurylo for their technical assistance.

Accurate, Wide-Range, Automated, High-Performance Liquid Chromatographic Method for the Estimation of Octanol/Water Partition Coefficients I: Effect of Chromatographic Conditions and Procedure Variables on Accuracy and Reproducibility of the Method

J. E. GARST ˣ and W. C. WILSON

Received March 7, 1983, from the *Department of Animal Science, University of Illinois, 126 Animal Sciences Laboratory, 1207 West Gregory Drive, Urbana, IL 61801.* Accepted for publication November 29, 1983.

Abstract □ A high-performance liquid-chromatographic (HPLC) procedure is reported for estimation of the logarithm of the octanol/water partition coefficient, log P(o/w). This automated log P(o/w) measurement (ALPM) circumvents many inherent difficulties with the shake-flask method, yet gives high reproducibility and excellent overall correlation with shake-flask results. Partition coefficients for numerous structurally diverse chemicals, ranging from ~0 to ~8 log P(o/w) units, can be determined; however, values for zwitterionic compounds cannot be obtained. Additional advantages of ALPM include lower cost and greater safety when compared with other HPLC or shake-flask procedures. Chromatographic conditions (*i.e.*, flow rate and temperature) and variables (*i.e*, column length and solvent composition) affecting this method are discussed in detail. ALPM may also find application in quality control of HPLC columns, qualitative-quantitative analysis, and in computer-controlled method development and analysis.

Keyphrases ◻ HPLC-octanol/water partition coefficients □ Partition coefficients-octanol/water, HPLC

The logarithm of the octanol/water partition coefficient of a compound, log P(o/w), often parallels the biological effects of that substance (1, 2). Although log P(o/w) correlations are commonly used to optimize a specific biological response, they can also be a valuable predictor of adverse effects from chemical agents (3, 4). Consideration of this parameter in structure-toxicity as well as structure-activity studies might substantially reduce drug development costs (1). Furthermore, the increasing cost of animals and animal care, combined with growing public discontent over the use of animals in scientific research, will inevitably make prediction of toxicological responses much more important (5, 6).

Ideally, determination of the partition coefficient, P(o/w), requires measurement of the equilibrium ratio of the concentrations of a single component, X, dissolved in nonpolar and polar layers using simple separatory funnel shake-flask procedures (2):

$$P(o/w) = [X]_{octanol}/[X]_{water} \qquad \text{(Eq. 1)}$$

Although the polar phase is nearly always water, the choice of nonpolar phase is arbitrary; chloroform, hexane, and other solvents have been used, but octanol is the most common choice (2). There is, however, nothing unique about biological correlations using octanol/water as opposed to another solvent/water system. In 1954, Collander showed that partition data can be converted between solvent/water systems by least-squares regression (7), but Leo has described limitations in the use of this relationship (8).

Many economic and scientific problems occur with shake-flask log P(o/w) measurements. Since analytical procedures differ with each compound, the traditional method is time consuming and expensive (3). Log P(o/w) measurements may have only limited reproducibility among laboratories. For example, the seven reported shake-flask log P(o/w) values for naphthalene range from 3.01 to 3.59 (2). Analysis error is always a concern, but microemulsions can also alter distribution of the compound between the two phases (9). Formation of other components in the shake-flask could also alter phase equilibrium. The physical difficulties of measurement may be minimized by improved analytical techniques and sample centrifugation, but chemical interactions (changing the number of components) could affect the accuracy of even reproducibly obtained partition coefficients.

While measurement is always preferred, approximate values can be obtained by calculations based on the concept that the overall log P(o/w) reflects the summation of hydrophobic contributions from each constitutive group (π-approach) or fragment (f-approach) (2, 10, 11). Although calculated values often afford good estimates of log P(o/w), additivity of such constants may not always be observed (3). Problems of reproducibly and accurately measuring the shake-flask log P(o/w), knowledge of the increment for a particular molecular unit, and limitations in the additivity of such groups often re-

0022-3549/84/1100-1616$01.00/0
© 1984, American Pharmaceutical Association

(11) H. H. Frey, C. Popp, and W. Löscher, *Neuropharmacology*, **18**, 581 (1979).
(12) C. G. Wermuth, A. Zinoune, J. J. Bourguignon, and J. P. Chambon, in "The Chemical Regulation of Biological Mechanisms," A. M. Creighton and S. Turner, Eds., The Royal Society of Chemistry, London, 1982. p. 112.
(13) A. M. Crider, T. T. Tita, J. D. Wood, and C. N. Hinko, *J. Pharm. Sci.*, **71**, 1214 (1982).
(14) J. D. Wood, A. Schousboe, and P. Krogsgaard-Larsen, *Neuropharmacology*, **19**, 1149 (1980).
(15) S. L. Earley, E. K. Michaelis, and M. P. Mertes, *Biochem. Pharmacol.*, **30**, 1105 (1981).
(16) R. J. Breckenridge, S. H. Nicolson, A. J. Nicol, C. J. Suckling, B. Leigh, and L. Iversen, *Biochem. Pharmacol.*, **30**, 3045 (1981).
(17) L. L. Iversen and M. J. Neal, *J. Neurochem.*, **15**, 1141 (1968).

ACKNOWLEDGMENTS

A portion of this work was presented at the 14th Central Regional Meeting of The American Chemical Society, Midland, Michigan, June 1982. This investigation was funded by research grants from the Epilepsy Foundation of America, The Upjohn Company, the University of Toledo Faculty Research Awards and Fellowships Program, and the Medical Research Council of Canada. The authors thank David L. Miskell and Eugen Kurylo for their technical assistance.

Accurate, Wide-Range, Automated, High-Performance Liquid Chromatographic Method for the Estimation of Octanol/Water Partition Coefficients I: Effect of Chromatographic Conditions and Procedure Variables on Accuracy and Reproducibility of the Method

J. E. GARST ˣ and W. C. WILSON

Received March 7, 1983, from the *Department of Animal Science, University of Illinois, 126 Animal Sciences Laboratory, 1207 West Gregory Drive, Urbana, IL 61801.* Accepted for publication November 29, 1983.

Abstract □ A high-performance liquid-chromatographic (HPLC) procedure is reported for estimation of the logarithm of the octanol/water partition coefficient, log P(o/w). This automated log P(o/w) measurement (ALPM) circumvents many inherent difficulties with the shake-flask method, yet gives high reproducibility and excellent overall correlation with shake-flask results. Partition coefficients for numerous structurally diverse chemicals, ranging from ~0 to ~8 log P(o/w) units, can be determined; however, values for zwitterionic compounds cannot be obtained. Additional advantages of ALPM include lower cost and greater safety when compared with other HPLC or shake-flask procedures. Chromatographic conditions (*i.e.*, flow rate and temperature) and variables (*i.e*, column length and solvent composition) affecting this method are discussed in detail. ALPM may also find application in quality control of HPLC columns, qualitative-quantitative analysis, and in computer-controlled method development and analysis.

Keyphrases ◻ HPLC-octanol/water partition coefficients □ Partition coefficients-octanol/water, HPLC

The logarithm of the octanol/water partition coefficient of a compound, log P(o/w), often parallels the biological effects of that substance (1, 2). Although log P(o/w) correlations are commonly used to optimize a specific biological response, they can also be a valuable predictor of adverse effects from chemical agents (3, 4). Consideration of this parameter in structure-toxicity as well as structure-activity studies might substantially reduce drug development costs (1). Furthermore, the increasing cost of animals and animal care, combined with growing public discontent over the use of animals in scientific research, will inevitably make prediction of toxicological responses much more important (5, 6).

Ideally, determination of the partition coefficient, P(o/w), requires measurement of the equilibrium ratio of the concentrations of a single component, X, dissolved in nonpolar and polar layers using simple separatory funnel shake-flask procedures (2):

$$P(o/w) = [X]_{octanol}/[X]_{water} \qquad \text{(Eq. 1)}$$

Although the polar phase is nearly always water, the choice of nonpolar phase is arbitrary; chloroform, hexane, and other solvents have been used, but octanol is the most common choice (2). There is, however, nothing unique about biological correlations using octanol/water as opposed to another solvent/water system. In 1954, Collander showed that partition data can be converted between solvent/water systems by least-squares regression (7), but Leo has described limitations in the use of this relationship (8).

Many economic and scientific problems occur with shake-flask log P(o/w) measurements. Since analytical procedures differ with each compound, the traditional method is time consuming and expensive (3). Log P(o/w) measurements may have only limited reproducibility among laboratories. For example, the seven reported shake-flask log P(o/w) values for naphthalene range from 3.01 to 3.59 (2). Analysis error is always a concern, but microemulsions can also alter distribution of the compound between the two phases (9). Formation of other components in the shake-flask could also alter phase equilibrium. The physical difficulties of measurement may be minimized by improved analytical techniques and sample centrifugation, but chemical interactions (changing the number of components) could affect the accuracy of even reproducibly obtained partition coefficients.

While measurement is always preferred, approximate values can be obtained by calculations based on the concept that the overall log P(o/w) reflects the summation of hydrophobic contributions from each constitutive group (π-approach) or fragment (f-approach) (2, 10, 11). Although calculated values often afford good estimates of log P(o/w), additivity of such constants may not always be observed (3). Problems of reproducibly and accurately measuring the shake-flask log P(o/w), knowledge of the increment for a particular molecular unit, and limitations in the additivity of such groups often re-

0022-3549/84/1100-1616$01.00/0
© 1984, American Pharmaceutical Association

strict correlation analysis to academic research or the most rewarding industrial compounds.

There have been numerous attempts to employ high-performance liquid chromatography (HPLC) to estimate log P(o/w). Mirrlees *et al.* described the theory behind these efforts, most of which utilize the linear relationship between log P(o/w) and the logarithm of the capacity factor, log k', where $k' = [(t - t_0/t_0)]$ and t and t_0 refer to the elution times of compound and void volume marker, respectively (12):

$$\log P(o/w) = (m \times \log k') + b \qquad \text{(Eq. 2)}$$

Henry *et al.* modified Eq. 2 so that higher log P(o/w) values could be determined by defining log V_r, the logarithm of the retention volume, as a function of the flow rate, FR, according to (13):

$$\log V_r = \log [(t - t_0) \times FR] \qquad \text{(Eq. 3)}$$

They argued that since $\log k' = \log [(t - t_0/t_0)] = \log (t - t_0) - \log t_0$, the log t_0 term could be incorporated into the constant b. Since this value differs from column to column, the separate constant, c, is justified:

$$\log P(o/w) = (m \times \log V_r) + b + c \qquad \text{(Eq. 4)}$$

Equation 4 describes a proportionality between the retention volume of a compound and its partitioning between mobile and stationary phases. The constants m, b, and c reflect the chromatographic process, the conversion from stationary/mobile phase to octanol/water phase partitioning, and the difference between columns.

Despite problems with HPLC measurement of log P(o/w), Baker *et al.* and Henry *et al.* suggested that HPLC retention data may prove to be a better correlate of biological activity than the octanol/water partition coefficient (9, 13). In this paper, an automated log P(o/w) measurement (ALPM), based on further modification of Eqs. 3 and 4 is reported; it allows variable flow rates, temperatures, and column lengths, and compensates for column changes over time. This alteration affords a corrected retention volume proportional to log P(o/w) and enables estimation of the latter from 0 to nearly 8 units. The ALPM log P(o/w) displays high reproducibility and excellent general correlation with the shake-flask result. The subsequent paper of this series demonstrates the value of ALPM in predicting biological activities (14).

EXPERIMENTAL SECTION

Definitions—The procedure utilizes a temperature- and column-length-corrected retention volume, V_{cr}, in analogy to the definition of the retention volume (V_r) by Henry *et al.* (13). Specifically, the term $(t - t_0)$ in Eq. 3 is replaced by the value from Eq. 6, which is obtained from extrapolated measurements of percent alcohol (as the abscissa) *versus* log $(t - t_0)$ when the percent alcohol is 0, by taking the antilog of the linear relationship in Eq. 5:

$$\log (t - t_0) = [(\text{slope} \times \text{percent alcohol}) + \text{tci}] \qquad \text{(Eq. 5)}$$

$$(t - t_0) = 10^{[(\text{slope} \times \text{percent alcohol}) + \text{tci}]} \qquad \text{(Eq. 6)}$$

where: $t - t_0$ is the elution time of compound minus the elution time of the void volume marker (min); the percent alcohol is 0 (for 100% aqueous buffer); slope is the slope of log $(t - t_0)$ *versus* percent alcohol plot; tci represents the temperature-corrected intercept, i + [(CT − RT) × 0.015 per degree] where i is the intercept (0% alcohol); CT represents the column temperature; RT represents the reference temperature (for this work, RT = 25°C). Correction for different column lengths involves referencing the results to a 25-cm column. Since a shorter column would proportionally reduce V_{cr}, multiplication by the ratio (25/CL) restores V_{cr} to a constant value. Thus:

$$V_{cr} = \frac{10^{[(\text{slope} \times \text{percent alcohol}) + \text{tci}]} FR\ (25\ \text{cm})}{CL} \qquad \text{(Eq. 7)}$$

where CL is the column length (cm) and FR is the flow rate (mL/min)[1].

Log P(o/w) can be determined from Eq. 8 using the corrected retention volume, V_{cr}, from Eq. 7 and C_{cf}, a column correction factor measured in log P(o/w) units, which replaces c in Eq. 4:

$$\log P(o/w) = (m \times \log V_{cr}) + b + C_{cf} \qquad \text{(Eq. 8)}$$

Column changes are compensated by the column correction factor, C_{cf} (measurement is described below). With methanol as the alcoholic cosolvent and using a reference temperature of 25°C, two sets of constants are reported in Eqs. 9 and 10[2]. For 0.004 M trifluoroacetic acid and 0.035 M triethylamine[2]:

$$m = 1.118(\pm 0.010);\ b = -0.588(\pm 0.019);\ r^2 = 0.9988;\ SE = 0.0409 \qquad \text{(Eq. 9)}$$

For 0.015 M triethylamine[2]:

$$m = 1.169(\pm 0.032);\ b = -0.946(\pm 0.092);\ r^2 = 0.9993;\ SE = 0.0578 \qquad \text{(Eq. 10)}$$

Log V_{ccr} is defined as the C_{cf} and column-corrected equivalent to log V_{cr}:

$$\log V_{ccr} = \log V_{cr} + (C_{cf}/m) \qquad \text{(Eq. 11)}$$

Replacement of log V_{cr} in Eq. 8 by $[\log V_{ccr} - (C_{cf}/m)]$ from Eq. 11 affords a column-independent definition of chemical hydrophobicity, which can be related to log P(o/w) as in Eq. 12 with the same constants, m and b:

$$\log P(o/w) = (m \times \log V_{ccr} + b) \qquad \text{(Eq. 12)}$$

Instrumentation and Columns—All experiments were performed on a liquid chromatograph equipped with column-temperature control, automatic injector, automatic sample changer, and serial computer interface[3]. HPLC peaks were detected using either the fixed-wavelength detector at 254 nm or the variable-wavelength detector at 190–600 nm, as necessary. Retention times, computed by the HPLC hardware are independent of the volume and concentration injected from 1 to at least 30 μL for benzyl alcohol and quinoline using a 1-mg/mL solution[4]. Columns of 1, 3, 10, and 25 cm, packed with 10-μm, C_8-alkylated adsorbant, were used without modification[5].

Chemicals—HPLC-grade methanol[6] and deionized[7], distilled water were used as HPLC solvents. Nicotinic hydrazide *N*-oxide[8], pyridine *N*-oxide[8], triethylamine[8], trifluoroacetic acid[8], and tetrahydrofuran[8] were obtained commercially. The triethylamine or trifluoracetic acid, used as buffers, must be present only in the aqueous solvent reservoir to prevent rapid destruction of the HPLC ball valves. Although Mirrlees *et al.* chose pyridine *N*-oxide as the void volume marker, nicotinic hydrazide *N*-oxide elutes earlier under our conditions and is preferred (12). Chemicals were obtained from various sources[8,9] or were synthesized (15).

Procedures—Several milligrams of nicotinic hydrazide *N*-oxide and the compound to be measured were diluted to 1–2 mL with methanol. (To improve the solubility of agents with log P(o/w) values of >4.5, several microliters of saturated aqueous nicotinic hydrazide *N*-oxide can be substituted for the solid nicotinic hydrazide *N*-oxide and tetrahydrofuran can replace methanol in the injection solution.) Several microliters of the solution were injected for each analysis. The choice of organic injection solvent had no detectable effect on the log V_{cr}. Routine data analysis utilized a minicomputer and software written

[1] Although percent alcohol is zero for the determination of V_{cr} in Eq. 7, prior ALPM determinations of the log P(o/w) and the slope, and knowledge of the current value of t_0 enable Eqs. 7 and 8 to be solved for the theoretical elution time for that compound at any percent of the appropriate solvent where equilibrium conditions are maintained.

[2] Values for the constants m, b, and C_{cf} (Eq. 8) are valid only under the conditions stated here and only with Hewlett-Packard Model 1084B HPLC instruments manufactured before the June 1982 reduction in the injector system volume for narrower bore columns. Use of this procedure under the conditions stated, but with other HPLC instruments, will require the determination of new values for these constants.

[3] Model 1084B; Hewlett-Packard.

[4] Unpublished results.

[5] RP-8 Merck brand reverse-phase, silica columns; Brownlee Laboratories, Santa Clara, Calif. The RP-8 packing material used herein has been changed since this work was completed. As a result, identical columns are no longer available; but more efficient and pH-resistant C_8 types of packing could afford better results using these procedures. New regression constants must be determined, however.

[6] MCB Manufacturing Chemists Inc., Cincinnati, Ohio.

[7] Milli-Q system; Millipore Corp., Bedford, Mass.

[8] Aldrich Chemical Co., Milwaukee, Wis. Nicotinic hydrazide *N*-oxide was obtained from the Alfred Bader group of Aldrich.

[9] Chem Service Inc., West Chester, Pa.; Pfaltz and Bauer, Stamford, Conn.; K and K Laboratories, Plainview, N.Y.

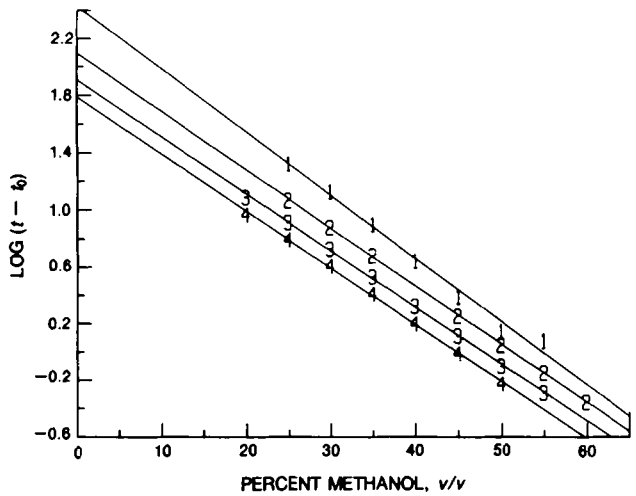

Figure 1—*Log* (t − t_0) versus *percent methanol for different flow rates. A parallel, linear relationship is apparent for all flow rates examined although statistical scatter increases using 1 mL/min for 1-(3-furyl)-4-methylpentan-1-one. Key: (1) 1 mL/min; (2) 2 mL/min; (3) 3 mL/min; (4) 4 mL/min.*

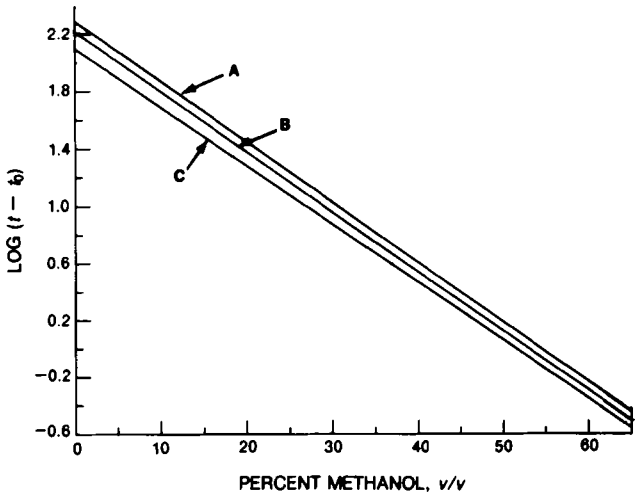

Figure 2—*Log* (t − t_0) versus *percent methanol for different temperatures. A parallel, linear relationship is apparent for temperatures from 17°C to 37°C for 1-(3-furyl)-4-methylpentan-1-one. Key: (A) 17°C; (B) 27°C; (C) 37°C.*

for this purpose[10]. When used, automatic data processing involved computer control of the chromatograph, data entry, and analysis steps[10].

Interpretation of Summary Data Tables—ALPM can produce considerable information that is helpful in evaluating the log P(o/w) results obtained for each compound. For example, some indication of HPLC equilibrium status, as discussed elsewhere, is given by these data (14)[11]. Equal values for n_0 and n indicate that all measured values were used in the linear regression process (*e.g.*, significant deviation from linearity over the measured range was not encountered). The greater the difference between n_0 and n, the more likely that curvilinearity, rather than simple statistical scatter, accounts for points being deleted from the linear regression (14). Where F_{calc} exceeds F_{set}, the data are indeed curved, but the low SE often suggests that the curve was randomly generated and need not be considered further. Increasing caution in accepting the data is urged when the SE exceeds 0.01 and/or the correlation coefficient falls below 0.999. However, the log P(o/w) may still be quite close to the literature value when high SE values and/or low correlations occur.

RESULTS

Figures 1 and 2 for 1-(3-furyl)-4-methylpentan-1-one typify log ($t - t_0$) *versus* percent methanol for different flow rates and column temperatures. The extrapolated intercept at 100% aqueous buffer was determined, corrected for measurement conditions by Eq. 7, and then converted to log P(o/w) according to Eq. 8, using the appropriate constants. The second paper in this series discusses the meaning of flow plot linearity and the extrapolation concept in greater detail (14).

Variable Flow Rates—Flow rates of 1-4 mL/min are statistically parallel for 1-(3-furyl)-4-methylpentan-1-one (Fig. 1). This is expected since flow rate and elution time are inversely related (16). All commercial HPLC instruments have some limitations. The HPLC used for these studies requires check valves to regulate the pumping process and requires at least a 10-bar column pressure to ensure correct seating of these values. The increased scatter and inaccuracy apparent at 1-mL/min flow rates for 1-(3-furyl)-4-methylpentan-1-one and naphthalene (*cf.*, Fig. 1, Table I) may arise from the low pressure generated with small columns by this low flow rate. Unrecognized instrumental limitations of this and/or other types may have contributed to past difficulties with other HPLC log P(o/w) determinations.

Temperature Variations—While temperature variations are probably not a major factor during a single run, they can affect the log V_{ccr} measurement and log P(o/w) reproducibility (Fig. 2, Table I). Data for several compounds suggest a consistent decrease in the intercept and a slight, but generally insignificant change in the slope as the temperature increases. As a result, an empirical intercept correction term, to restore the intercept to that expected at 25°C, is included in Eq. 6 and is supported by data in Table I. Column temperatures near 35°C are favored because temperature correction is empirical and valid only over a narrow range, elution times are faster, column pressures are lower, and the results are more reproducible. Once obtained, however, these data are referenced to 25°C for comparison with literature values; other reference temperatures could be used, but a new correction formula and regression constants would be needed.

Mobile Phase—The aforementioned findings have clarified the role of HPLC instrumental variables on the determination of log P(o/w), but the choice of mobile phase and column variables is also critical. The partition coefficient of most value in correlation work is that of the uncharged, neutral form, since this can exceed the ionized form by 1000-fold (2). To maintain the chemical in that form, dilute acid or base is required for acids or bases, respectively. Since halogen salts should be avoided when using stainless steel and concentrated salt solutions can ooze and block the very small-diameter tubing, miscible volatile organic acids and bases are preferred.

Although the log V_{cr} values for carboxylic acids and phenols were unaffected by concentrations of >0.004 M trifluoroacetic acid[4], base concentrations of ≫0.004 M were required. Elution of pyridine with 0.02 M Tris, trimethylamine, and triethylamine indicated that the strongest base gave the lowest log V_{ccr} measurement (*i.e.*, reduced tailing) ($r > 0.99$, Table II). As triethylamine elutes pyridine more quickly than the organic bases, it was chosen as the base modifier. Triethylammonium siloxide ion-pair formation was supported by the fact that the strongest base, NaOH, eluted pyridine slower than any of the organic bases. If a simple base interaction were involved, NaOH should have eluted pyridine before the organic bases. However, the determination with NaOH affected subsequent column performance.

The high pH of the triethylamine solution might have caused serious column degradation and only 0.015 M was used initially. However, column deterioration was less of a problem than anticipated, and the optimal concentration was determined. Triethylamine concentration *versus* log V_{cr} for pyridine (a compound very sensitive to base concentration) is shown in Fig. 3. It appears that concentrations at or somewhat above 0.06 M afford log V_{cr} values totally independent of base concentration; 0.035 M triethylamine affords greater independence of log V_{cr} from base concentration than does 0.015 M. However, the use of 0.035 M triethylamine probably offers increased column life. Although changes do occur as a result of base degradation, some columns have been used for many months by taking advantage of an external standard column factor (described below).

[10] Hewlett-Packard Model 9845B desktop computer with 187 Kbytes internal memory, internal printer, I/O-, Graphics-, Advanced Programming-, and Structured Programming ROMS, and the necessary instrument interfaces were used for data acquisition and/or analysis. A more complete description of this copyrighted ALPM software, enabling multicomputer-controlled log P(o/w) determination, computation, and comparative analysis, complete with an example, is in preparation.

[11] Condition numbers 1-4 refer to organic solvents methanol, absolute ethanol, isopropyl alcohol, or acetonitrile, respectively. n_0 and n refer to the numbers of data points actually measured and those used in the linear regression. Low, high, intercept, slope, and r relate the lowest and highest solvent percentage measurements used in the regression line, its intercept, slope, and correlation coefficient r, respectively. F_{set} indicates that table F value above which a quadratic fit is indicated (or below which the points are accepted as statistically linear). F_{calc} represents the computed F value required for a linear fit of the measured number of points, all at the 96.9% confidence level. If F_{calc} is below F_{set}, the data are not statistically curved. Choice of the unusual 96.9% confidence level for a linear relationship was based on deviations encountered with benzene (14). SE refers to the standard error of estimate of log ($t - t_0$) by linear regression on percent methanol. V_{ccr} and C_{cf} are defined as the corrected column retention volume and the column correction factor, respectively. ALPM log P and log P range refer to the octanol/water partition coefficient as measured by ALPM and the range of shake-flask log P(o/w) literature values when present. Likewise, when present, Best indicates the single literature value closest to ALPM.

Table I—Flow Rate and Temperature Comparisons with Methanol as Organic Cosolvent

Compound	Obs.	n_0	Flow Rate, mL/min	Column Length, cm	Column Serial No.	Condition	Oven Temp, °C	Intercept	Slope	Solvent Percentage Low	Solvent Percentage High	n	r	F_{set}	F_{calc}	SE	log V_{cor}	C_{cf}	ALPM log P	Best
4-Bromophenol	1	10	2	10	1349	1	27	2.055 ± 0.050	−0.038 ± 0.001	40	55	8	0.9996	8.847	4.857	0.0065	+2.78 ± 0.05	+0.00	+2.56 ± 0.06	+2.59
	2	10	2	10	1349	1	32	1.963 ± 0.049	−0.037 ± 0.001	40	55	8	0.9996	8.847	4.450	0.0064	+2.77 ± 0.05	+0.00	+2.54 ± 0.06	+2.59
	3	10	2	10	1349	1	37	1.820 ± 0.051	−0.035 ± 0.001	35	55	10	0.9993	7.246	0.459	0.0105	+2.70 ± 0.05	+0.00	+2.46 ± 0.06	+2.59
	4	10	2	10	1349	1	42	1.750 ± 0.012	−0.035 ± 0.000	40	55	8	1.000	8.847	0.244	0.0016	+2.70 ± 0.01	+0.00	+2.47 ± 0.01	+2.59
1-(3-Furyl)-4-methylpentan-1-one	5	7	1	3	0000	2	37	2.432 ± 0.236	−0.044 ± 0.006	25	55	7	0.9942	10.646	1.296	0.0570	+3.53 ± 0.24	+0.00	+3.17 ± 0.28	—
	6	8	2	3	0000	2	17	2.289 ± 0.043	−0.042 ± 0.001	25	60	8	0.9997	8.847	1.172	0.0126	+3.39 ± 0.04	+0.00	+3.00 ± 0.05	—
	7	7	2	3	0000	2	27	2.207 ± 0.037	−0.042 ± 0.001	25	60	7	0.9999	10.646	0.272	0.0101	+3.46 ± 0.04	+0.00	+3.08 ± 0.04	—
	8	7	2	3	0000	2	37	2.097 ± 0.032	−0.041 ± 0.001	25	60	7	0.9999	10.646	0.143	0.0087	+3.50 ± 0.03	+0.00	+3.13 ± 0.04	—
	9	8	3	3	0000	2	37	1.911 ± 0.046	−0.040 ± 0.001	20	55	8	0.9996	8.847	8.318	0.0149	+3.49 ± 0.05	+0.00	+3.12 ± 0.05	—
	10	9	3	3	0000	2	37	1.920 ± 0.035	−0.040 ± 0.001	20	60	9	0.9997	7.862	7.139	0.0134	+3.50 ± 0.04	+0.00	+3.13 ± 0.04	—
	11	7	4	3	0000	2	37	1.896 ± 0.024	−0.043 ± 0.001	35	55	5	1.0000	30.766	7.868	0.0025	+3.60 ± 0.02	+0.00	+3.25 ± 0.03	—
Naphthalene	12	12	1	3	0001	3	35	2.334 ± 0.020	−0.037 ± 0.000	30	55	12	0.9999	6.522	5.607	0.0059	+3.45 ± 0.02	+0.05	+3.30 ± 0.02	+3.45
	13	12	2	3	0001	3	35	2.113 ± 0.017	−0.038 ± 0.000	30	55	12	0.9999	6.522	2.821	0.0051	+3.53 ± 0.02	+0.05	+3.38 ± 0.02	+3.45
	14	10	3	1	0101	3	35	1.558 ± 0.020	−0.038 ± 0.000	30	50	10	0.9999	7.246	3.275	0.0047	+3.58 ± 0.02	+0.00	+3.44 ± 0.02	+3.45
	15	14	3	1	0102	3	35	1.589 ± 0.017	−0.039 ± 0.000	30	50	10	0.9999	7.246	4.082	0.0040	+3.58 ± 0.02	−0.04	+3.44 ± 0.02	+3.45
	16	12	3	3	0001	3	35	1.976 ± 0.019	−0.039 ± 0.000	30	55	12	0.9999	6.522	0.713	0.0056	+3.57 ± 0.02	+0.05	+3.43 ± 0.02	+3.45
	17	9	4	3	0001	3	15	2.236 ± 0.032	−0.042 ± 0.001	30	55	8	0.9998	8.847	5.745	0.0066	+3.61 ± 0.03	+0.00	+3.47 ± 0.04	+3.45
	18	12	4	3	0001	3	25	2.078 ± 0.023	−0.041 ± 0.001	30	55	12	0.9998	6.522	0.738	0.0068	+3.60 ± 0.02	+0.00	+3.46 ± 0.03	+3.45
	19	12	4	3	0001	3	35	1.896 ± 0.019	−0.039 ± 0.000	30	55	12	0.9999	6.522	2.685	0.0056	+3.57 ± 0.02	+0.00	+3.43 ± 0.02	+3.45
	20	12	4	3	0001	3	45	1.776 ± 0.025	−0.038 ± 0.001	30	55	12	0.9998	6.522	4.740	0.0075	+3.60 ± 0.03	+0.00	+3.46 ± 0.03	+3.45

[a] See footnote 11 (in text) for definitions.

Table II—Log V_{ccr} of Pyridine *versus* 0.02 M Base

Base	Log V_{ccr}	pK_b
Organic		
Tris	1.69	5.92
Trimethylamine	1.38	4.13
Triethylamine	1.22	2.99
Inorganic		
Sodium hydroxide	1.83	~0

When 0.035 M triethylamine is used for bases and neutral compounds and 0.004 M trifluoroacetic acid is used for acidic compounds, the acid and base least-squares linear correlation equations become statistically indistinguishable in the range of 0.3–6 log P(o/w) units, and probably higher. This effect is dramatically exemplified by the relationship between log V_{ccr} and log P(o/w) (Fig. 4). The upper line in Fig. 4 represents the acidic and numerous basic or neutral compounds; the lower line depicts basic or neutral compounds measured in 0.015 M triethylamine. As triethylamine levels increase, the lower line in Fig. 4 merges with the upper line. Triethylamine at 0.06 M may prove statistically valuable for the most accurate determinations below 0.3 log P(o/w) units (Fig. 3). This is also evidenced by the very slight deviation of the overall column-corrected log P(o/w) *versus* literature correlation from a zero intercept as indicated in Fig. 5. Equations 8–12 describe the regression equations relating log P(o/w) and/or log V_{cr} for the different acid and base concentrations.

Several nonaqueous mobile phases were also studied. Figure 6 is a plot of percent cosolvent *versus* log $(t - t_0)$ using four different organic solvents and 0.015 M triethylamine to elute 1-(3-furyl)-4-methylpentan-1-one. Note that different slopes and extrapolated intercepts are obtained for these lines; this suggests that a solvent-strength-related intercept conversion factor could allow measurement of higher log P(o/w) values in other alcohols. Although methanol was chosen as the organic mobile phase for economic reasons, isopropyl alcohol may facilitate determination of even higher values, despite increased slopes and the resultant increase in the log P(o/w) error. Nonalcoholic solvents, such as acetonitrile, may distort the linear response of log $(t - t_0)$ *versus* percent solvent and complicate the conversion process (14).

Column Variables—The HPLC column is also critical to ALPM. The following column lengths afford an optimum elution time for the various log P(o/w) ranges: 0–~0.8, 50 cm; ~0.3–~1.5, 25 cm; ~1–~3, 10 cm; ~2.2–~5, 3 cm; and >~5, 1 cm. However, compounds run on different columns or the next longer or shorter column length give statistically the same results (Table I: obs. 15 and 16; Table III: obs. 22 and 23, 25 and 26, 39 and 40, and 62 and 63). These data indicate that only two or three column lengths are required. Despite the fact that ALPM has enabled measurements as high as 7.8 for hexabromobiphenyl (14), existing shake-flask methods cannot ensure that values of >6 log P(o/w) units are not low; therefore, some uncertainty does exist in fitting very high ALPM values (17). Although ALPM values for anthracene, 1,1,1-trichloro-2,2-bis(*p*-chlorophenyl)ethane (DDT), and diethylstilbesterol are only slightly higher than the shake-flask result, ALPM values for phenylphosphonothioic acid *O*-ethyl *O*-*p*-nitrophenyl ester (EPN), [2.2]paracyclophane, and progesterone are considerably higher (*cf.* Table V of Ref. 14).

Column-length differences are readily corrected by Eq. 7, except when using a 1-cm column or when the column has deteriorated. A packing error of 0.1 mm becomes important with a 1-cm column and requires the use of the column

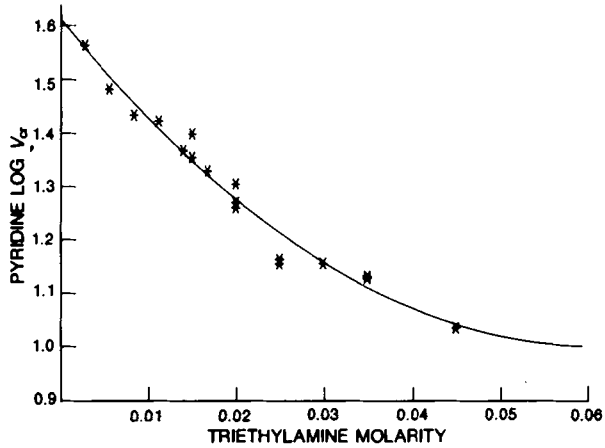

Figure 3—*Log* V_{cr} versus *triethylamine concentration. Dependence of pyridine log* V_{cr} *on triethylamine concentration becomes insignificant at* $\geq 0.06 M$.

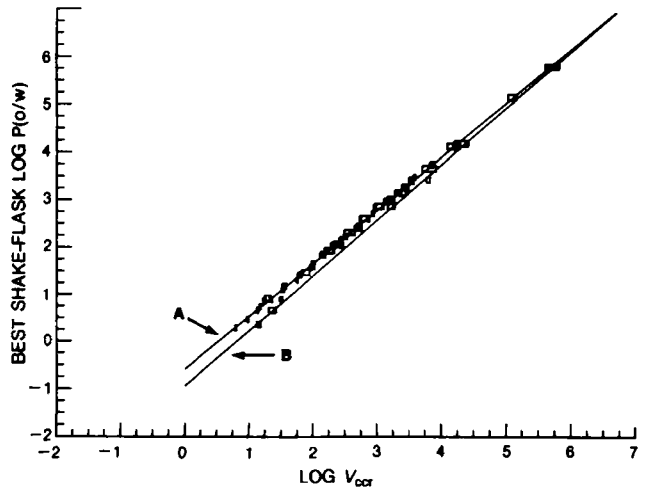

Figure 4—*Correlation between shake-flask log P(o/w) and ALPM log V_{ccr}. Although the correlation of acids is independent of concentration, the correlation of bases and neutral agents is dependent on triethylamine concentration. The boxes represent the 95% confidence limits (±2 SD) in ALPM log V_{ccr} (mean SE = ±0.049) and the mean 67% confidence limit (±SD) in log P(o/w). Key: (A) acidic compounds in 0.004 M trifluoroacetic acid; basic compounds in 0.035 M triethylamine (n = 58, r = 0.9994); (B) basic and neutral compounds in 0.015 M triethylamine (n = 8, r = 0.9996).*

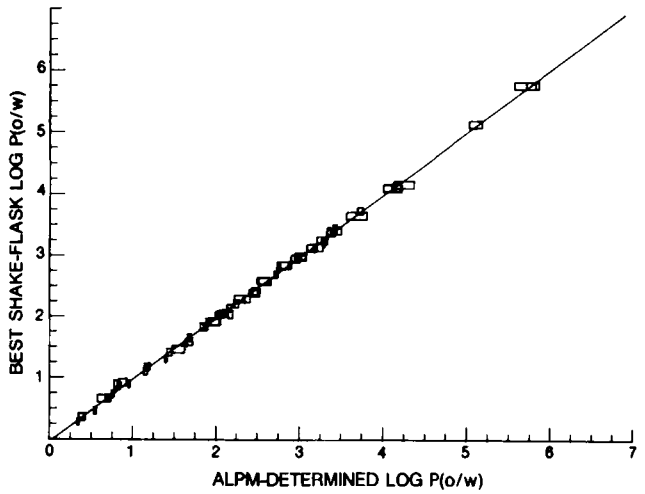

Figure 5—*Correlation between shake-flask and ALPM log P(o/w). Error boxes indicate the variable 95% confidence limits (±SD) (mean = 0.044) in shake-flask log P(o/w) as determined from the compounds shown in Table IV (n = 66, r = 0.9994). The SE of the estimate is 0.045.*

correction factor, C_{cf}. C_{cf} is determined by measuring the log P(o/w) of several agents with otherwise reproducible values. With these agents, any consistent error in log P(o/w) measured at essentially the same time is assigned to C_{cf}. Records normally include the time of C_{cf} assignment, which is checked and updated frequently. Column correction appears to be a valid technique as long as double peaks do not complicate the computation of retention times.

In early work, column deterioration frequently occurred when changing acid-base conditions. Although changing from organic acid to organic base posed few problems, changing from organic base to organic acid consistently destroyed columns. Hypothetically, changing from ion-paired triethylamine to trifluoroacetic acid could result in chemical reactions and/or heat liberation disrupting the column packing. Prior thorough washing with distilled, deionized water failed to prevent column deterioration. Therefore, columns of each length should be dedicated to each acid or base condition to maximize column life.

Changes in column C_{cf} values occur most under basic conditions. The greatest alterations occur when switching to a column that has not been used for an extended period, suggesting that base degradation may be a slow, continuous process. Nevertheless, such changes can be corrected using the C_{cf}; but, in contrast to the 1-cm columns, the C_{cf} for longer columns generally should not be negative, because overpacking is not a problem[12].

DISCUSSION

The value of the partition coefficient to pharmacology and toxicology arises from the dependence of Fick's permeability constant on the partition coefficient (18). As a result, the partition coefficient [*i.e.*, log P(o/w)] governs the absorption, distribution, metabolism, and excretion of chemicals (18-20). Many HPLC procedures that measure log P(o/w) have distinct advantages over shake-flask methods. HPLC procedures provide a continuous scale for measurement of both low and high partition coefficients and offer greater assurance that spectroscopic detection monitors component X, rather than highly absorbent trace impurities (9). In addition, HPLC measurement of elution times can be relatively fast and the conditions carefully controlled (12). HPLC procedures utilize lower concentrations of the agent of interest and may better avoid disequilibria (*e.g.*, multiple components), but HPLC elution time measurements, made as a function of solvent composition, may identify such disequilibria should they occur. The same assurance for shake-flask studies requires, at minimum, the repetition of log P(o/w) measurements at different concentrations and extrapolation to infinite dilution. HPLC methods can also enable partition coefficient determination when compounds are sufficiently unstable as to prevent their determination by conventional shake-flask techniques (21).

Despite these advantages, most available HPLC methods rarely cover much more than 3-3.5 log P(o/w) units (12, 13, 22, 23). Previous HPLC log P(o/w) methods have made use of C_{18} reverse-phase silica columns (9, 22) and/or packing materials coated with octanol to make the columns more "octanol-like" (12, 13, 23, 24). Some still gave poor correlations between elution data and literature or measured log P(o/w) values (13, 25). A relatively recent HPLC method by Veith *et al.* affords a large range of log P(o/w) (26). It uses a curvilinear fit between log P(o/w) and an elution parameter obtained from a programmed nonlinear increase in HPLC flow rate, but even this method gives substantial unexplained deviations from a smooth curve.

ALPM differs in several respects from the other HPLC procedures. ALPM uses C_8 reverse-phase columns, which contain greater hydrocarbon surface areas than either the equivalent C_2 or C_{18} packings (27). Besides using a different alkyl group length, ALPM gives greater assurance than shake-flask or other HPLC methods that the partitioning process achieves the equilibrium so essential to accurate determinations (14). Judicious choices of flow rate, column temperatures, and column lengths allow compounds of widely differing lipophilicities to elute within 10 min. Previously, only Henry *et al.* and Veith *et al.* utilized variable flow rates to expedite the elution process (13, 26). Rapid elution of peaks by ALPM retains excellent peak shapes, which facilitate accurate elution times.

The logarithm of the corrected retention volume (V_{cr}) first obtained by ALPM is converted by linear regression to log P(o/w) values based on the shake-flask procedure. The discovery that two distinct lines (*e.g.*, Fig. 4)

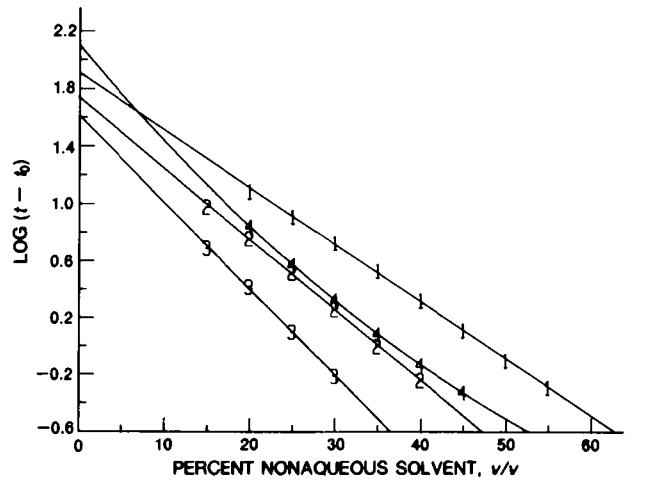

Figure 6—*Log $(t - t_0)$ versus cosolvent. Alcohols afford a linear relationship, although the slopes differ considerably for 1-(3-furyl)-4-methylpentan-1-one. Nonalcoholic solvents, however, do not always give a linear relationship. Key: (1) methanol; (2) absolute ethanol; (3) isopropyl alcohol; (4) acetonitrile.*

[12] Using one 10-cm column, however, it became apparent from several prior determinations using several different compounds, that the column C_{cf} had changed substantially from a positive (*i.e.*, needing a correction) to a negative (*i.e.*, being overcorrected) value. An explanation of this C_{cf} reversal is unclear, but its occurrence is noteworthy.

Table III—HPLC Log P(o/w) Standards using Methanol as Cosolvent [a]

Compound	Obs	n_0	Flow Rate, mL/min	Column Length, cm	Column Serial Number	Condition	Oven Temp., °C	n	r	log V_{ccr}	C_{cf}	ALPM log P	log P Range	Best
Acetanilide	1	19	2	10	1516	3	35	14	0.9998	+1.54 ± 0.01	+0.00	+1.18 ± 0.01	+1.16 to +1.36	+1.17
	2	9	2	10	7172	3	32	9	0.9993	+1.53 ± 0.02	+0.09	+1.17 ± 0.03	+1.16 to +1.36	+1.17
	3	8	2	10	9412	3	34	8	0.9998	+1.55 ± 0.02	+0.00	+1.19 ± 0.02	+1.16 to +1.36	+1.17
Acetophenone	4	10	2	10	1361	3	37	10	0.9998	+1.99 ± 0.02	+0.10	+1.68 ± 0.02	+1.58 to +1.73	+1.65
Acridine	5	14	2	1	0102	3	35	12	0.9999	+3.50 ± 0.02	−0.04	+3.35 ± 0.02	+3.40	+3.40
	6	7	4	3	0000	2	37	7	0.9999	+3.79 ± 0.03	+0.00	+3.47 ± 0.03	+3.40	+3.40
4-Aminopyridine	7	11	2	25	8390	3	35	11	0.9971	+0.79 ± 0.01	+0.00	+0.34 ± 0.01	+0.28	+0.28
Aniline	8	6	2	25	0000	2	37	6	0.9999	+1.49 ± 0.02	+0.00	+0.79 ± 0.02	+0.85 to +0.98	+0.89
	9	7	4	25	8390	3	35	7	0.9999	+1.35 ± 0.00	+0.00	+0.96 ± 0.01	+0.85 to +0.98	+0.89
Anisole	10	7	3	10	1516	3	35	6	0.9996	+2.34 ± 0.04	+0.00	+2.06 ± 0.04	+2.04 to +2.11	+2.04
Benzoic acid	11	6	3	10	1516	1	37	6	0.9999	+2.44 ± 0.03	+0.00	+2.18 ± 0.03	+1.87 to +2.03	+2.03
Benzonitrile	12	12	2	10	1361	3	37	12	0.9999	+1.96 ± 0.01	+0.10	+1.65 ± 0.01	+1.56	+1.56
Benzyl alcohol	13	7	2	10	9412	3	37	7	0.9997	+1.52 ± 0.02	+0.10	+1.16 ± 0.02	+1.10	+1.10
Biphenyl	14	6	4	3	0001	3	35	6	0.9997	+4.18 ± 0.10	+0.00	+4.11 ± 0.11	+3.16 to +4.17	+4.09
4-Bromoacetanilide	15	10	3	10	1346	3	37	9	0.9997	+2.62 ± 0.03	+0.22	+2.37 ± 0.04	+2.29	+2.29
	16	10	3	10	1361	3	37	8	0.9993	+2.54 ± 0.06	+0.00	+2.29 ± 0.06	+2.29	+2.29
4-Bromoaniline	17	12	3	10	1346	3	37	10	0.9998	+2.36 ± 0.02	+0.00	+2.09 ± 0.02	+2.05 to +2.26	+2.05
	18	12	3	10	9412	3	37	10	0.9994	+2.37 ± 0.04	+0.10	+2.10 ± 0.04	+2.05 to +2.26	+2.05
Bromobenzene	19	8	3	3	0001	3	35	6	0.9997	+3.19 + 0.05	+0.00	+3.01 ± 0.06	+2.99	+2.99
4-Bromophenol	20	12	3	10	1349	1	37	8	0.9995	+2.79 ± 0.06	+0.00	+2.56 ± 0.07	+2.59 to +2.74	+2.59
4-Chloroaniline	21	10	2	10	1346	3	37	10	0.9998	+2.17 + 0.02	+0.22	+1.88 ± 0.02	+1.83	+1.83
Chlorobenzene	22	12	4	3	0001	3	35	10	0.9989	+3.04 ± 0.06	+0.00	+2.84 ± 0.06	+2.18 to +2.84	+2.84
	23	5	4	10	1516	3	35	5	0.9996	+3.01 ± 0.07	+0.00	+2.81 ± 0.08	+2.18 to +2.84	+2.84
4-Chlorophenol	24	8	2	10	9412	1	37	7	0.9995	+2.70 ± 0.06	+0.10	+2.46 ± 0.06	+2.35 to +2.53	+2.39
3-Cyanopyridine	25	8	2	25	0000	2	37	7	0.9995	+1.14 ± 0.03	+0.00	+0.38 ± 0.03	+0.36	+0.36
	26	6	2	50	0000	2	37	6	0.9995	+1.15 ± 0.03	+0.00	+0.39 ± 0.04	+0.36	+0.36
4-Cyanopyridine	27	7	2	25	8390	3	35	7	0.9996	+0.97 ± 0.01	+0.00	+0.55 ± 0.02	+0.46	+0.46
1,2-Dibromobenzene	28	5	4	3	0001	3	35	4	0.9999	+3.80 ± 0.11	+0.00	+3.68 ± 0.12	+3.64	+3.64
1,4-Dichlorobenzene	29	9	4	3	0001	3	35	9	0.9996	+3.52 ± 0.04	+0.00	+3.37 ± 0.05	+3.37 to +3.38	+3.37
1,2-Dihydroxybenzene	30	8	2	25	9154	1	35	8	0.9987	+1.28 ± 0.04	+0.00	+0.88 ± 0.04	+0.84 to +1.01	+0.92
2,4-Dimethylphenol	31	10	3	10	1349	1	37	10	0.9997	+2.70 ± 0.03	+0.00	+2.47 ± 0.04	+2.30 to +2.42	+2.42
Diphenylamine	32	12	4	3	0001	3	35	11	0.9998	+3.84 ± 0.03	+0.05	+3.72 ± 0.03	+3.22 to +3.72	+3.72
Diphenylnitrosamine	33	10	4	10	1361	3	37	6	0.9996	+3.35 ± 0.08	+0.10	+3.18 ± 0.09	+3.13	+3.13
4-Ethylphenol	34	10	2	10	1349	1	37	7	0.9995	+2.81 ± 0.07	+0.00	+2.59 ± 0.07	+2.26 to 2.58	+2.58
3-Fluoroaniline	35	12	2	10	1361	3	37	12	0.9998	+1.74 ± 0.01	+0.10	+1.40 ± 0.01	+1.30	+1.30
Hexachlorobenzene	36	5	4	3	0000	2	37	5	0.9999	+5.70 ± 0.11	+0.00	+5.70 ± 0.12	+5.75	+5.75
	37	4	4	3	0001	3	35	4	1.0000	+5.70 ± 0.07	+0.00	+5.79 ± 0.07	+5.75	+5.75
Indole	38	10	3	10	1346	3	37	10	0.9997	+2.43 ± 0.02	+0.22	+2.16 ± 0.03	+2.00 to 2.25	+2.14
Iodobenzene	39	13	3	1	0101	3	35	9	0.9999	+3.44 ± 0.02	−0.10	+3.29 ± 0.03	+3.25	+3.25
	40	6	3	3	0001	3	35	6	0.9996	+3.43 ± 0.06	+0.00	+3.27 ± 0.06	+3.25	+3.25
4-Methoxyaniline	41	8	2	25	8390	3	37	8	0.9995	+1.23 ± 0.02	+0.00	+0.83 ± 0.02	+0.78 to 0.95	+0.86
3-Methoxyphenol	42	10	2	10	1349	1	37	10	0.9994	+1.99 ± 0.03	+0.00	+1.68 ± 0.04	+1.58	+1.58
4-Methylaniline	43	10	2	10	1361	3	37	8	0.9995	+1.78 ± 0.03	+0.10	+1.44 ± 0.03	+1.39 to +1.41	+1.41
4-Methylphenol	44	10	2	10	1349	1	37	8	0.9991	+2.27 ± 0.06	+0.00	+1.98 ± 0.07	+1.92 to +1.99	+1.92
Naphthalene	45	12	3	3	0001	3	35	12	0.9999	+3.57 ± 0.02	+0.05	+3.43 ± 0.02	+3.01 to +3.59	+3.45
1-Naphthol	46	4	4	10	1516	1	37	4	1.0000	+3.22 ± 0.04	+0.00	+3.04 ± 0.04	+2.31 to +2.98	+2.98
	47	8	4	10	9412	1	37	6	0.9999	+3.16 ± 0.03	+0.10	+2.98 ± 0.03	+2.31 to +2.98	+2.98
Nitrobenzene	48	10	2	10	1346	3	37	10	0.9998	+2.13 ± 0.02	+0.22	+1.83 ± 0.02	+1.79 to +1.88	+1.83
4-Nitrophenol	49	12	2	10	1349	1	37	8	0.9989	+2.24 ± 0.07	+0.00	+1.96 ± 0.08	+1.38 to +2.08	+1.91
Pentachlorophenol	50	8	4	3	0001	1	40	8	0.9997	+5.08 ± 0.07	+0.00	+5.11 ± 0.07	+5.01 to +5.12	+5.12
Phenazine	51	5	2	3	0000	2	30	5	0.9998	+3.22 ± 0.05	+0.00	+2.80 ± 0.06	+2.84	+2.84
Phenol	52	5	2	10	1516	1	37	5	0.9995	+1.88 ± 0.07	+0.00	+1.55 ± 0.07	+1.46 to +1.51	+1.46
Phenothiazine	53	10	4	3	0001	3	35	7	0.9993	+4.30 ± 0.11	+0.05	+4.24 ± 0.12	+3.78 to +4.15	+4.15
Phenylthiourea	54	12	3	25	8390	3	35	10	0.9997	+1.16 ± 0.01	+0.00	+0.76 ± 0.02	+0.73	+0.73
Pyridine	55	7	3	25	0000	2	37	5	0.9993	+1.36 ± 0.05	+0.00	+0.63 ± 0.06	+0.64 to +0.66	+0.66
	56	12	3	25	8390	3	37	12	0.9991	+1.13 ± 0.01	+0.00	+0.72 ± 0.02	+0.64 to +0.66	+0.66
	57	4	4	25	0000	2	37	4	1.0000	+1.40 ± 0.02	+0.00	+0.68 ± 0.02	+0.64 to +0.66	+0.66
	58	6	4	25	8390	3	35	6	0.9998	+1.13 ± 0.01	+0.00	+0.72 ± 0.02	+0.64 to +0.66	+0.66
Quinoline	59	12	3	10	1346	3	37	11	0.9998	+2.29 ± 0.02	+0.00	+2.01 ± 0.02	+2.02 to +2.06	+2.02
Salicylic acid	60	5	3	10	1516	1	37	5	0.9999	+2.51 ± 0.03	+0.00	+2.25 ± 0.03	+2.21 to +2.26	+2.21
Toluene	61	12	4	10	1346	3	37	12	0.9998	+2.93 ± 0.02	+0.22	+2.72 + 0.02	+2.11 to +2.80	+2.69
2,4,6-Tribromophenol	62	10	3	1	0201	1	37	10	0.9996	+4.13 ± 0.05	+0.00	+4.05 ± 0.05	+3.96 to +4.23	+4.10
	63	5	4	3	0000	1	37	4	1.0000	+4.23 ± 0.05	+0.00	+4.16 ± 0.05	+3.96 to +4.23	+4.10
3-Trifluoromethylphenol	64	10	3	10	1349	1	37	8	0.9997	+3.14 ± 0.05	+0.00	+2.95 ± 0.05	+2.95 to +3.17	+2.95
2-Xylene	65	9	3	3	0002	3	37	9	0.9999	+3.35 ± 0.02	+0.00	+3.18 ± 0.02	+2.77 to +3.12	+3.12
3-Xylene	66	10	3	3	0002	3	37	10	1.0000	+3.44 ± 0.01	+0.00	+3.28 ± 0.01	+3.20	+3.20

[a] See footnote 11 (in text) for definitions.

correlate acidic and basic chemicals has been previously reported (24, 25). However, conditions, in which reverse-phase columns offer a single linear correlation between log P(o/w) and HPLC data have not yet been elucidated. Hexabromobiphenyl afforded an ALPM log P(o/w) value of 7.8, the highest value yet measured (14). For neutral compounds, log P(o/w) measurement could be made under either acid- or base-elution conditions. Comparison of acid and base conditions for several neutral chemicals suggests occasional differences can occur (14). Base conditions seem favored for the measurement of the log P(o/w) of neutral compounds due to the substantial linearity already observed under these conditions, but this is currently under investigation.

ALPM reproducibility averages 1.06 ± 0.46% (*SD*) of the average HPLC measured value over 54 runs (Table IV). Errors in these measurements appear related to the slope of the individual log $(t - t_0)$ *versus* percent methanol lines. Although they increase as the log P(o/w) increases, they change little as a percentage of the log P(o/w) value. Reproducibility of the literature shake-flask values for virtually the same compounds averages 6.13 ± 2.76% (*SD*)

Table IV—Reproducibility of Log P(o/w) Measurements [a]

Compound	Runs	ALPM Average ± SD	Measurements	Shake-Flask Average ± SD
Acetanilide	15	1.18 ± 0.01	3	1.23 ± 0.11
Acetophenone	2	1.67 ± 0.01	2	1.66 ± 0.08
Biphenyl	2	4.12 ± 0.01	2	3.88 ± 0.41
4-Bromoaniline	8	2.07 ± 0.02	8	2.15 ± 0.15
4-Bromophenol	7	2.52 ± 0.04	7	2.60 ± 0.13
3-Chlorophenol	3	2.37 ± 0.02	3	2.49 ± 0.02
4-Chlorophenol	3	2.39 ± 0.06	3	2.42 ± 0.07
Naphthalene	9	3.42 ± 0.03	9	3.35 ± 0.19
1-Naphthol	2	3.01 ± 0.04	2	2.71 ± 0.35
Pentachlorobenzene	3	5.18 ± 0.06	3	4.94[b] —
Pentachlorophenol	1	5.11[b] —	1	5.33 ± 0.46
ALPM log P(o/w)		average error = 1.06% (±0.46%) for 54 values		
Shake-flask log P(o/w)		average error = 6.13% (±2.76%) for 40 values		

[a] The error in ALPM increases as the slope of log $(t - t_0)$ *versus* percent methanol becomes more negative. The average error is expressed as a percent of the log P(o/w) value for both the ALPM and shake-flask results. The shake-flask data are from Refs. 2, 3, and 26. [b] Not included in error determination.

of the measured value. Table III summarizes typical information obtained by ALPM for the standards used in Figs. 4 and 5.

In addition to high accuracy and excellent reproducibility, measurement of log P(o/w) by this procedure is less expensive and safer than by other methods. The shorter columns required for the majority of agents are 10–50% as expensive as 25-cm columns and generate much lower back-pressures. Neglecting the instrumentation cost, samples can be processed for ~$10.00 (which compares well with the cost of calculated values), yet the results provide as good or better a correlation with biological data (14). Even differences between isomers can be determined. All HPLC methods avoid the cumbersome use of often leaky separatory funnels and traditional UV-visible spectrophotometric analysis, with its manipulation of standards and analysis solutions; but ALPM also avoids exposure to toxicants. Samples can be prepared in a glove box and automatically injected under computer control, with wastes delivered directly into approved waste containers.

For maximal statistical validity and accuracy, ALPM requires numerous elution-time measurements. The error in ALPM log P(o/w) generally decreases as the number of measurements increase, so the needed number of determinations must be based on user requirements. An entire computer-operated run can generally be completed within 1 h for six measurements from ~55 to 30% methanol (5% increments) in descending order or within ~1.5 h for duplicate data measured first in descending, and then ascending, order. Facts pertinent to the choice of the methanol percentage range are presented in the following paper (14). Although somewhat more time is required for ALPM than for single-measurement HPLC procedures, labor expenses can be virtually eliminated by this computer-controlled analysis; it can automatically process up to 24 single or 12 duplicate runs while operating day and night.

The chemical need not be pure to use computer-data acquisition, but other components must provide smaller peak areas than either the void volume marker or the compound of interest. This purity limitation involves only the computer assignment of t and t_0. If the compound does not meet that requirement, log P(o/w) may still be measured, provided that the component peaks and times can be manually identified, but elution times must be entered into the computer *via* the keyboard. Less-obvious advantages of this desk-top-computer control include: routines for the unattended monitoring and response to HPLC-operational problems; recovery from power outages; versatile alphabetical data file listing (*e.g.* Table I); and a data format usable with commercial statistical and graphics packages.

Greater detection selectivity can be achieved for certain chemical by using variable-wavelength or fluorescence detectors. Refractive index (RI) or conductivity detectors should work, but as they measure changes instead of actual values, a given peak can be positive or negative. As a result, automated computer-data acquisition can become troublesome. Moreover, because of their enhanced sensitivity, these detectors also raise more questions about the identity of the eluting agent than do variable-wavelength detectors.

ALPM represents a major improvement in log P(o/w) measurement technology, especially for those requiring values for many compounds. It is not, however, without some problems. Other than the obvious requirements that the substance be stable in the injection solvent under the measurement conditions for the period of detection, only log P(o/w) values above zero may be measured currently. Second, log P(o/w) standards must be run externally before and/or after the compound of interest because no method is available to elucidate the peak of interest or a simultaneously measured standard. Third, ALPM fails for zwitterionic compounds which elute immediately in either acid or base and could afford incorrect values for compounds with complex, multiple pK values. Fourth, HPLC measurement of log P(o/w) values >~8 units becomes increasingly difficult. These compounds often have poor solubility even in tetrahydrofuran, and the high negative slopes encountered with these agents leads to peak broadening when higher percentages of aqueous buffer are used. This broadening diminishes the accuracy of HPLC-computed elution times and can even affect peak detection. As a result, high log P(o/w) compounds limit the range of percentages over which good data can be obtained and raise the absolute log P(o/w) error accordingly. The necessary use of the shortest columns and high flow rates for compounds with high log P(o/w) values also hastens elution of the void volume marker peak. This can cause computer-processing difficulties if that critical peak is missed or incorrectly assigned. Such problems are readily evident and, since the HPLC output is available, the data can be manually corrected often with no loss of information.

During the course of this study, several alternative uses of ALPM became apparent. Because elution times of organic acids are essentially independent of acid concentration, and 0.004 M trifluoroacetic acid has minimal effect on column life, this procedure should provide an excellent, reproducible, and automated method for quality control of RP-8, and likely all reverse-phase HPLC columns, once the necessary constants m, b, and C_{cf} are determined.

ALPM may also become a valuable addition to qualitative-quantitative analysis and structure assignment. For example, reaction of phenylmagnesium bromide with 3-cyanofuran gave two products after acid hydrolysis, which were not separable by simple vacuum distillation. We have found that treatment of other simple Grignard reagents with 3-cyanofuran gives no such problem. ALPM log P(o/w) analysis confirmed the suspected identity of the unwanted component as biphenyl, a well-known phenylmagnesium bromide degradation product.

Yet another use of ALPM technology may be automated method development and analysis. Specifically, overlap plotting of individual log $(t - t_0)$ *versus* percent solvent data for each compound can indicate the single percentage of solvent that allows easy separation of the compounds. Furthermore, once the log P(o/w) of a compound, the elution time (t_0) of the void volume marker, and the column correction factor (C_{cf}) are known, the elution time for a given agent may be computed for various aqueous-buffer methanol compositions.

REFERENCES

(1) C. Hansch, in "Correlation Analysis in Chemistry and Biology," N. B. Chapman and J. Shorter, Eds., Plenum, New York, N.Y., 1978.

(2) C. Hansch and A. Leo, "Substituent Constants for Correlation in Chemistry and Biology," Wiley, New York, N.Y., 1979.

(3) G. D. Veith, K. J. Macek, S. R. Petrocelli, and J. Carroll, in "Aquatic Toxicology," J. G. Eaton, P. R. Parrish, and A. C. Hendricks, Eds., American Society for Testing and Materials, STP 707, Philadelphia, Pa., 1980, p. 116.

(4) J. E. Garst and B. J. Wilson, in "Oxygen and Oxy-Radicals in Chemistry and Biology," M. A. J. Rodgers and E. L. Powers, Eds., Academic, New York, N.Y., 1981, p. 507.

(5) A. N. Rowan, *Pharm. Technol.*, **4**, 10 (1980); A. N. Rowan, *Pharm. Technol.*, **5**, 64 (1981).

(6) R. Dagani, *Chem. Eng. News.* **61**, 7 (1983).

(7) R. Collander, *Acta Chem. Scand.*, **5**, 774 (1954).

(8) A. J. Leo, in "Drug Design," Vol. 1, E. Ariens, Ed., Academic, New York, N.Y. 1972, p. 271.

(9) J. K. Baker, D. O. Rauls, and R. F. Borne, *J. Med. Chem.*, **22**, 1301 (1979).

(10) R. F. Rekker, "The Hydrophobicity Fragmental Constant," Elsevier, New York, N.Y., 1977.

(11) J. T. Chou and P. C. Jurs, *J. Chem. Inf. Comput. Sci.*, **19**, 172 (1979).

(12) M. S. Mirrlees, S. J. Moulton, C. T. Murphy, and P. J. Taylor, *J. Med. Chem.*, **19**, 615 (1976).

(13) D. Henry, J. H. Bock, J. L. Anderson, and G. R. Carlson, *J. Med. Chem.*, **19**, 619 (1976).

(14) J. E. Garst, *J. Pharm. Sci.*, **73**, 1623 (1984).

(15) J. E. Garst and B. J. Wilson, *J. Agric. Food Chem.*, **32**, 1083 (1984).

(16) E. L. Johnson and R. Stevenson, "Basic Liquid Chromatography," Varian Associates, Palo Alto, Calif., 1978, p. 33.

(17) J. A. Katzenellenbogen, K. E. Carlson, D. F. Heiman, and J. E. Lloyd, in "Radiopharmaceuticals: Structure-Activity Relationships," R. P. Spencer, Ed., Grune and Stratton, New York, N.Y., 1981, p. 23.

(18) D. H. K. Lee, in "Handbook of Physiology," H. L. Faith, S. D. Murphey, and S. R. Geiger, Eds., American Physiology Society, Bethesda, Md., 1977, p. 303.
(19) P. J. Little and A. J. Ryan, *J. Med. Chem.*, **25**, 622 (1982).
(20) E. J. Lien, *Annu. Rev. Pharmacol. Toxicol.*, **21**, 31 (1981).
(21) C. L. K. Lins, J. H. Block, R. F. Doerge, and G. J. Barnes, *J. Pharm. Sci.*, **71**, 614 (1982).
(22) T. Yamana, A. Tsuji, E. Miyamota, and O. Kubo, *J. Pharm. Sci.*, **66**, 747 (1977).
(23) S. H. Unger, J. R. Cook, and J. S. Hollenberg, *J. Pharm. Sci.*, **67**, 1364 (1978).
(24) K. Miyake and H. Terada, *J. Chromatogr.*, **157**, 396 (1978).
(25) R. M. Carlson, R. E. Carlson, and H. L. Kopperman, *J. Chromatogr.*, **107**, 219 (1975).
(26) G. D. Veith, N. M. Austin, and R. T. Morris, *Water Res.*, **13**, 43 (1979).
(27) "Technical Notes on Reverse Phase Chromatography," (Bulletin TN 910), Brownlee Laboratories, Santa Clara, Calif., October 1977.

ACKNOWLEDGMENTS

This work was described at the February 1982 meeting of the Society of Toxicology in Boston, Mass. and the March 1984 Pittsburgh Conference in Atlantic City, N.J.

The authors appreciate financial support by the University of Illinois Research Board, the Biomedical Support Group (BRSG-207-RR07038), and the U.S. Government (Hatch 20-323 and NIEHS 02193). Statistical assistance by D. Gianola and the late H. W. Norton is also appreciated.

Accurate, Wide-Range, Automated, High-Performance Liquid Chromatographic Method for the Estimation of Octanol/Water Partition Coefficients II: Equilibrium in Partition Coefficient Measurements, Additivity of Substituent Constants, and Correlation of Biological Data

J. E. GARST

Received March 7, 1983, from the *Department of Animal Science, University of Illinois, 126 Animal Sciences Laboratory, 1207 West Gregory Drive, Urbana, IL 61801.* Accepted for publication November 29, 1983.

Abstract □ Occasionally, results from the highly reproducible automated log P(o/w) measurement (ALPM) differ from those determined by shake-flask methods. Several specific examples affording different values are presented. One source of these differences may be curvilinearity in plots of log $(t - t_0)$ *versus* percent methanol, which complicate accurate intercept determinations and, thus, estimates of log P(o/w). Other sources of these differences are presented and discussed, although their cause remains unclear. Equilibrium ALPM log P(o/w) measurements of various phenyl-, methyl-, fluoro-, chloro-, and bromobenzenes, suggest substituent constants are not strictly additive. Moreover, the higher values indicate that calculated values may not be accurate for those compounds having multiple substituents or high log P(o/w) values. ALPM gives better predictability of the *in vivo* concentration process of 8 or 12 toxicants in fish than the shake-flask method, another HPLC method, or even calculated log P(o/w) values. However, it equally correlates the binding to bovine serum albumin by 34 chemicals as predicted by a combination of shake-flask and calculated log P(o/w) values reported elsewhere.

Keyphrases □ HPLC—octanol/water partition coefficient, equilibrium □ Partition coefficients—octanol/water, HPLC, equilibrium, biological correlation

An automated log P(o/w) measurement (ALPM) has been developed that utilizes high-performance liquid chromatography (HPLC) to accurately and reproducibly estimate the logarithm of the octanol/water partition coefficient at costs comparable with computation (1). ALPM differs from earlier HPLC procedures in that variable column lengths, flow rates, and temperatures have enabled determinations over the 0–8 log P(o/w) range (1). Most previous HPLC log P(o/w) procedures have involved measurement of the capacity factor, k', using a single determination at a fixed composition of water, buffer, or a low percentage of alcohol in water or buffer (2, 3):

$$k' = (t - t_0)/t_0 \qquad \text{(Eq. 1)}$$

where t and t_0 refer to the elution time of the compound of interest and void volume marker, respectively. From that data log P(o/w) has been calculated by:

$$\log P(o/w) = (m \times \log k') + b \qquad \text{(Eq. 2)}$$

Determination of log P(o/w) by shake-flask techniques requires that equilibrium be established between the aqueous and octanol phases for the single component being measured (1). Equilibrium is essential even when partitioning occurs between HPLC phases. To date, no HPLC log P(o/w) method has provided solid evidence that equilibrium is attained during the elution process. Theoretically, if HPLC equilibrium is attained at each percentage of mobile phase during such measurements, a linear relationship between percent mobile phase and log k' or log $(t - t_0)$ should be apparent. Yamana *et al.* did demonstrate a linear dependence of log k' on the percentage of methanol used for elution (3). However, despite lower error and a better correlation using the extrapolated intercept at 0% methanol, they opted to use data measured at 30% methanol for procedural uniformity. Unfortunately, they failed to consider fully the significance of linearity. Deviations from linearity suggest a departure from HPLC equilibrium caused by changing interactions between the chemical and either the mobile or stationary phase. Although linearity of such plots over a limited solvent range can not prove that HPLC equilibrium is attained, curvilinearity is contrary evidence.

Unlike most procedures, ALPM utilizes the extrapolated linear intercept from computer-assisted log $(t - t_0)$ *versus* solvent composition measurements. As such, ALPM not only makes many more measurements, but in doing so better establishes equilibrium HPLC behavior for the agent being

0022-3549/84/1100-1623$01.00/0
© 1984, American Pharmaceutical Association

(18) D. H. K. Lee, in "Handbook of Physiology," H. L. Faith, S. D. Murphey, and S. R. Geiger, Eds., American Physiology Society, Bethesda, Md., 1977, p. 303.
(19) P. J. Little and A. J. Ryan, *J. Med. Chem.*, **25**, 622 (1982).
(20) E. J. Lien, *Annu. Rev. Pharmacol. Toxicol.*, **21**, 31 (1981).
(21) C. L. K. Lins, J. H. Block, R. F. Doerge, and G. J. Barnes, *J. Pharm. Sci.*, **71**, 614 (1982).
(22) T. Yamana, A. Tsuji, E. Miyamota, and O. Kubo, *J. Pharm. Sci.*, **66**, 747 (1977).
(23) S. H. Unger, J. R. Cook, and J. S. Hollenberg, *J. Pharm. Sci.*, **67**, 1364 (1978).
(24) K. Miyake and H. Terada, *J. Chromatogr.*, **157**, 396 (1978).
(25) R. M. Carlson, R. E. Carlson, and H. L. Kopperman, *J. Chromatogr.*, **107**, 219 (1975).
(26) G. D. Veith, N. M. Austin, and R. T. Morris, *Water Res.*, **13**, 43 (1979).
(27) "Technical Notes on Reverse Phase Chromatography," (Bulletin TN 910), Brownlee Laboratories, Santa Clara, Calif., October 1977.

ACKNOWLEDGMENTS

This work was described at the February 1982 meeting of the Society of Toxicology in Boston, Mass. and the March 1984 Pittsburgh Conference in Atlantic City, N.J.

The authors appreciate financial support by the University of Illinois Research Board, the Biomedical Support Group (BRSG-207-RR07038), and the U.S. Government (Hatch 20-323 and NIEHS 02193). Statistical assistance by D. Gianola and the late H. W. Norton is also appreciated.

Accurate, Wide-Range, Automated, High-Performance Liquid Chromatographic Method for the Estimation of Octanol/Water Partition Coefficients II: Equilibrium in Partition Coefficient Measurements, Additivity of Substituent Constants, and Correlation of Biological Data

J. E. GARST

Received March 7, 1983, from the *Department of Animal Science, University of Illinois, 126 Animal Sciences Laboratory, 1207 West Gregory Drive, Urbana, IL 61801.* Accepted for publication November 29, 1983.

Abstract □ Occasionally, results from the highly reproducible automated log P(o/w) measurement (ALPM) differ from those determined by shake-flask methods. Several specific examples affording different values are presented. One source of these differences may be curvilinearity in plots of log $(t - t_0)$ *versus* percent methanol, which complicate accurate intercept determinations and, thus, estimates of log P(o/w). Other sources of these differences are presented and discussed, although their cause remains unclear. Equilibrium ALPM log P(o/w) measurements of various phenyl-, methyl-, fluoro-, chloro-, and bromobenzenes, suggest substituent constants are not strictly additive. Moreover, the higher values indicate that calculated values may not be accurate for those compounds having multiple substituents or high log P(o/w) values. ALPM gives better predictability of the *in vivo* concentration process of 8 or 12 toxicants in fish than the shake-flask method, another HPLC method, or even calculated log P(o/w) values. However, it equally correlates the binding to bovine serum albumin by 34 chemicals as predicted by a combination of shake-flask and calculated log P(o/w) values reported elsewhere.

Keyphrases □ HPLC—octanol/water partition coefficient, equilibrium □ Partition coefficients—octanol/water, HPLC, equilibrium, biological correlation

An automated log P(o/w) measurement (ALPM) has been developed that utilizes high-performance liquid chromatography (HPLC) to accurately and reproducibly estimate the logarithm of the octanol/water partition coefficient at costs comparable with computation (1). ALPM differs from earlier HPLC procedures in that variable column lengths, flow rates, and temperatures have enabled determinations over the 0–8 log P(o/w) range (1). Most previous HPLC log P(o/w) procedures have involved measurement of the capacity factor, k', using a single determination at a fixed composition of water, buffer, or a low percentage of alcohol in water or buffer (2, 3):

$$k' = (t - t_0)/t_0 \qquad \text{(Eq. 1)}$$

where t and t_0 refer to the elution time of the compound of interest and void volume marker, respectively. From that data log P(o/w) has been calculated by:

$$\log P(o/w) = (m \times \log k') + b \qquad \text{(Eq. 2)}$$

Determination of log P(o/w) by shake-flask techniques requires that equilibrium be established between the aqueous and octanol phases for the single component being measured (1). Equilibrium is essential even when partitioning occurs between HPLC phases. To date, no HPLC log P(o/w) method has provided solid evidence that equilibrium is attained during the elution process. Theoretically, if HPLC equilibrium is attained at each percentage of mobile phase during such measurements, a linear relationship between percent mobile phase and log k' or log $(t - t_0)$ should be apparent. Yamana *et al.* did demonstrate a linear dependence of log k' on the percentage of methanol used for elution (3). However, despite lower error and a better correlation using the extrapolated intercept at 0% methanol, they opted to use data measured at 30% methanol for procedural uniformity. Unfortunately, they failed to consider fully the significance of linearity. Deviations from linearity suggest a departure from HPLC equilibrium caused by changing interactions between the chemical and either the mobile or stationary phase. Although linearity of such plots over a limited solvent range can not prove that HPLC equilibrium is attained, curvilinearity is contrary evidence.

Unlike most procedures, ALPM utilizes the extrapolated linear intercept from computer-assisted log $(t - t_0)$ *versus* solvent composition measurements. As such, ALPM not only makes many more measurements, but in doing so better establishes equilibrium HPLC behavior for the agent being

0022-3549/84/1100-1623$01.00/0
© 1984, American Pharmaceutical Association

Table I—Acid–Base Dependency of Certain ALPM Results with Methanol as the Organic Cosolvent [a]

Compound	Obs.	n_0	Rate, mL/min	Column Length, cm	Column Serial Number	Condition[b] Solvent Percentage	Oven Temp., °C	Solvent Percentage Low	Solvent Percentage High	n	r	C_{cf}[c]	ALPM log P	log P Range
Acetanilide	1	12	2	10	1516	1	35	15	50	12	0.9999	+0.00	+1.56 ± 0.01	+1.16 to +1.36
	2	19	2	10	1516	3	35	10	50	14	0.9998	+0.00	+1.18 ± 0.01	+1.16 to +1.36
	3	9	2	10	7172	3	32	15	55	9	0.9993	+0.09	+1.17 ± 0.03	+1.16 to +1.36
	4	8	2	10	9412	1	37	25	50	7	0.9995	+0.00	+1.66 ± 0.05	+1.16 to +1.36
	5	8	2	10	9412	1	37	30	50	5	0.9996	+0.00	+1.65 ± 0.08	+1.16 to +1.36
	6	8	2	10	9412	3	34	20	55	8	0.9998	+0.00	+1.19 ± 0.02	+1.16 to +1.36
	7	7	2	10	9412	4	37	30	50	5	0.9997	+0.00	+1.67 ± 0.07	+1.16 to +1.36
Benzene	8	17	2	10	1516	1	35	40	60	9	0.9998	+0.00	+2.15 ± 0.03	+1.56 to +2.15
	9	22	2	10	1516	3	35	30	60	10	0.9992	+0.00	+2.01 ± 0.04	+1.56 to + 2.15
	10	16	2	10	7172	3	35	35	60	9	0.9999	+0.09	+2.06 ± 0.02	+1.56 to +2.15
	11	14	3	10	1361	3	35	35	60	12	0.9996	+0.10	+1.93 ± 0.02	+1.56 to +2.15
Iodobenzene	12	13	3	1	0101	3	35	30	50	9	0.9999	−0.10	+3.29 ± 0.03	+3.25
	13	6	3	3	0001	3	35	25	50	6	0.9996	+0.00	+3.27 ± 0.06	+3.26
	14	6	4	3	0000	1	37	30	50	5	0.9997	+0.00	+3.48 ± 0.08	+3.25

[a] See Ref. 1. [b] Key: (1) 0.004 M trifluoroacetic acid; (2) 0.015 M triethylamine; (3) 0.035 M triethylamine; (4) 0.004 M acetic acid. [c] Column correction factor.

measured. The logarithm of the corrected retention volume, log V_{cr}, is converted by linear regression to the ALPM log P(o/w) (1). This paper describes the nature of this linearity and the ALPM linear extrapolation process. Several interesting discrepancies between ALPM and shake-flask log P(o/w) values are reported and discussed, and the ALPM-measured log P(o/w) values for certain phenylated, methylated, and halogenated benzenes are examined. This paper also compares equilibrium ALPM results with shake-flask and calculated log P(o/w) values used by Veith *et al.* to estimate the *in vivo* concentration process of chemicals in fish and by Helmer *et al.* to estimate the binding of chemicals to bovine serum albumin (4, 5).

EXPERIMENTAL SECTION

Definitions of terms, the equations for the calculation of ALPM log P(o/w), and a description of instrumentation, columns, conditions, and procedures are reported in the preceding paper (1).

RESULTS

Figure 1 illustrates that HPLC equilibrium [*i.e.*, linearity of log $(t - t_0)$ *versus* percent methanol] depends on the compound and not necessarily on the mechanical aspects of measurement. For instance, acetanilide, like the majority of compounds, gives a linear relationship between log $(t - t_0)$ and methanol percentage. Unlike acetanilide, but when run simultaneously, benzene seemingly interacts with the mobile phase, as demonstrated by the concave curvilinearity apparent at low percentages of methanol (Fig. 1). This increasingly rapid elution by water is pH independent; measurement using 0.004 M trifluoroacetic acid also affords a concave curvilinearity[1]. The benzene curve from ~60 to 35% MeOH is linear (*i.e.*, statistically, this region is not curved). Between these percentages, HPLC equilibrium is evidently maintained[2]. Extrapolation of the linear segment to 0% methanol and correction for conditions of measurement, as reported in the preceding paper for three separate determinations using 0.035 M triethylamine, indicates that the log P(o/w) for benzene is 2.00 ± 0.06 (*SD*); the relatively high standard deviation probably reflects the error in intercept measurement caused by curvilinearity. Although measurement using 0.004 M trifluoroacetic acid affords a concave curvilinearity, it yields a log P(o/w) of 2.15 ± 0.03 (*SE*), which is statistically identical to the benzene shake-flask value of 2.13. Regardless of the pH difference, either benzene curvilinear (*i.e.*, quadratic) intercept affords a log P(o/w) value substantially lower than that measured by extrapolation of the linear segment. This supports the midrange linear extrapolation approach.

In contrast with benzene, methylisobutylxanthine increasingly interacts with the stationary phase (indicated by the convex curvature in Fig. 1), but the cause for this phenomenon is not clear. Evaluation of this convex relationship is complicated by the unavailability of shake-flask results for methylisobutylxanthine. Future studies may be directed toward understanding these apparent disequilibria. For now, the results indicate that measurement of log $(t - t_0)$, particularly at a single, low alcoholic percentage (as is commonly practiced), could introduce substantial measurement error if HPLC equilibrium (*i.e.*, linearity) is not attained. This may have had considerable bearing on previous attempts to measure log P(o/w) by HPLC methods, regardless of column adsorbent.

While acids or bases can best be determined under acidic or basic conditions, respectively, ALPM measurement of neutral compounds can be performed in either acid or base (1). The data in Table I indicate that the extrapolated intercepts and log P(o/w) results for neutral compounds can be statistically the same (*e.g.*, iodobenzene) or they can differ (*e.g.*, benzene and acetanilide) depending on the measurement pH. These data are grouped primarily by compound name and secondarily by column serial number, but the results indicate column independence.

Figure 2 graphically illustrates results of ALPM log P(o/w) determinations of several benzene derivatives with phenyl, methyl, fluoro, chloro, and bromo substituents. Individual data for these compounds are listed in Table II. Figure 2 demonstrates that substituent additivity is generally invalid. Each substituent group appears to afford a concave relationship, although insufficient data are available for the fluoro and phenyl substituents to justify more than a linear

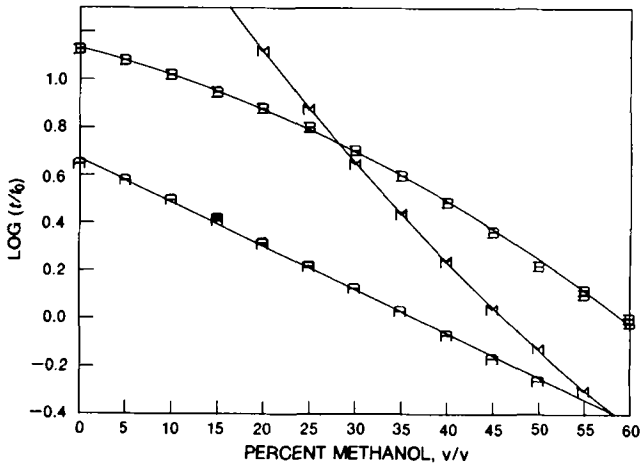

Figure 1—*Linearity of log* $(t - t_0)$ *data. Log* $(t - t_0)$ versus *percent methanol plots for acetanilide (A) and benzene (B) run simultaneously using 0.035 M triethylamine indicate that curvature depends on the compound. Methylisobutylxanthine (M) measured using 0.004 M trifluoroacetic acid gives a curvature opposite to that of benzene.*

[1] Unpublished results.

[2] Generally in ALPM, log $(t - t_0)$ values for methanol percentages of <25–30% are rarely measured. Not only do such measurements substantially increase the determination time, but the data often show greater statistical scatter (*e.g.*, Fig. 1, acetanilide between 8 and 15% methanol) or curvature (*e.g.*, Fig. 1, benzene and methylisobutylxanthine). Either condition requires that these points ultimately be excluded from the linear (*i.e.*, equilibrium) extrapolation. The results in Fig. 1 have been reproduced using several columns. Although not shown, high methanol percentages could also lead to curvature of log $(t - t_0)$. To maintain the greatest accuracy when measuring compounds with high partition coefficients, alcohol percentages of >60–65% should be used cautiously, and preferably with several points at and below 50% alcohol. Actually, use of these high percentages should be restricted to extremely high log P(o/w) compounds for which the lower values are difficult to obtain even on short columns. The difference $(t - t_0)$ should also exceed 0.3 min for greatest accuracy, although this empirical value actually depends on the accuracy of the elution-time measurements.

Table II—Partition Coefficient Summary for Various Substituted Benzenes

Compound	Obs.	ALPM log P	log P Range	Best[a]
Benzene	1	+2.01 ± 0.04	+1.56 to +2.15	+1.99
	2	+2.06 ± 0.02	+1.56 to +2.15	+1.99
	3	+1.93 ± 0.02	+1.56 to +2.15	+1.99
Biphenyl	4	+4.11 ± 0.11	+3.16 to +4.17	+4.09
	5	+4.13 ± 0.07	+3.16 to +4.17	+4.09
Bromobenzene	6	+3.02 ± 0.01	+2.99	+2.99
	7	+3.01 ± 0.02	+2.99	+2.99
	8	+3.06 ± 0.04	+2.99	+2.99
	9	+3.01 ± 0.06	+2.99	+2.99
Chlorobenzene	10	+2.79 ± 0.09	+2.18 to +2.84	+2.84
	11	+2.84 ± 0.06	+2.18 to +2.84	+2.84
	12	+2.81 ± 0.08	+2.18 to +2.84	+2.84
1,2-Dibromobenzene	13	+3.77 ± 0.06	+3.64	+3.64
	14	+3.68 ± 0.12	+3.64	+3.64
	15	+3.78 ± 0.02	+3.64	+3.64
1,2-Dichlorobenzene	16	+3.56 ± 0.07	+3.37 to +3.40	+3.40
1,3-Dichlorobenzene	17	+3.57 ± 0.04	+3.24 to +3.44	+3.44
1,4-Dichlorobenzene	18	+3.37 ± 0.05	+3.37 to +3.38	+3.37
Fluorobenzene	19	+2.14 ± 0.07	+2.27	+2.27
	20	+2.20 ± 0.04	+2.27	+2.27
	21	+2.22 ± 0.05	+2.27	+2.27
	22	+2.20 ± 0.07	+2.27	+2.27
Hexabromobenzene	23	+6.15 ± 0.14	—	—
	24	+6.07 ± 0.22	—	—
Hexachlorobenzene	25	+5.70 ± 0.17	+5.75	+5.75
	26	+5.79 ± 0.08	+5.75	+5.75
Hexafluorobenzene	27	+2.80 ± 0.09	+2.22	+2.22
Hexamethylbenzene	28	+5.00 ± 0.04	+4.31	+4.31
Mesitylene	29	+3.86 ± 0.03	+3.42	+3.42
	30	+3.87 ± 0.02	+3.42	+3.42
	31	+3.86 ± 0.02	+3.42	+3.42
	32	+3.87 ± 0.02	+3.42	+3.42
	33	+3.94 ± 0.01	+3.42	+3.42
Pentachlorobenzene	34	+5.21 ± 0.08	+4.94	+4.94
	35	+5.11 ± 0.06	+4.94	+4.94
	36	+5.21 ± 0.15	+4.94	+4.94
Pentamethylbenzene	37	+4.57 ± 0.02	—	—
	38	+4.55 ± 0.03	—	—
4-Terphenyl	39	+6.03 ± 0.07	—	—
	40	+5.88 ± 0.17	—	—
1,2,4,5-Tetrabromobenzene	41	+5.25 ± 0.05	—	—
1,2,3,5-Tetrachlorobenzene	42	+4.61 ± 0.04	+4.46	+4.46
	43	+4.73 ± 0.02	+4.46	+4.46
1,2,4,5-Tetramethylbenzene	44	+4.24 ± 0.02	—	—
Toluene	45	+2.70 ± 0.04	+2.11 to +2.80	+2.69
	46	+2.72 ± 0.02	+2.11 to +2.80	2.69
	47	+2.66 ± 0.09	+2.11 to +2.80	+2.69
1,3,5-Tribromobenzene	48	+4.60 ± 0.05	—	—
	49	+4.63 ± 0.05	—	—
1,3,5-Trichlorobenzene	50	+4.18 ± 0.03	—	—
1,2,4-Trifluorobenzene	51	+2.52 ± 0.07	—	—
2-Xylene	52	+3.18 ± 0.02	+2.77 to +3.12	+3.12
3-Xylene	53	+3.28 ± 0.01	+3.20	+3.20
4-Xylene	54	+3.29 ± 0.01	+3.15	+3.15

[a] Single literature value closest to ALPM log P.

fit. Table III lists ALPM-derived substituent constants, obtained by two different procedures, and shake-flask literature values (6). If the 0.035 M triethylamine value for benzene is used in the substituent constant calculation, the ALPM-derived constants are higher than those obtained by the octanol/water shake-flask method. These values closely resemble those obtained with the "hyperdiscriminating" solvents benzene or chloroform (7). If the monosubstituted benzene is used instead of benzene for the substituent constant calculation, the ALPM-derived value is lower and is closer to the shake-flask result. However, an average of these ALPM-derived values affords results close to the shake-flask substituent constant.

DISCUSSION

As a result of the potentially high error when using a single capacity factor measurement, many workers have begun to use the logarithm of the extrapolated intercept at 100% aqueous solvent in correlation work. For example, Butte *et al.* extrapolated data measured from 75–90% methanol to 0% methanol in their studies of various phenolic compounds eluting from an 10-μm octadecylsilane LiChrosorb RP-18 column (8). Bieganowska extrapolated values from 60–80% methanol (obtained using a 10-μm RP-18 column) in her investigation of the elution properties of *N*-phenylamides of benzoylacetic acid (9). In more extensive studies, Hafkenscheid and Tomlinson have examined 32 simple, but diverse, compounds over the range from 30 to

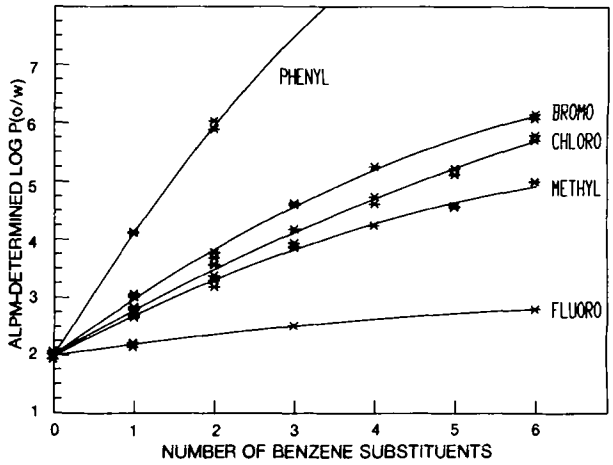

Figure 2—*ALPM log P(o/w)* versus *the benzene substituent number. This plot of ALPM log P(o/w) for various substituted benzenes* versus *the number of groups on the benzene ring reveals that strict substituent additivity is not the rule.*

90% methanol and extrapolated the RP-18 elution results to zero, generally obtaining a correlation coefficient of >0.999 (10). Braumann and Grimme used an extrapolated 0% methanol result obtained from 55 to 80% methanol with pyridazinones eluting over an RP-18 column (11). Close examination of the latter study reveals that correlation coefficients between 0.995 and 0.999 were often obtained, in contrast to the 0.999 minimum for ALPM (1), suggesting that curvature was perhaps unrecognized. Hanai and Hubert used acetonitrile/water from ≥30 to 90% in their study of urinary aromatic acids (12).

Questions arise as to the proper choice of solvent, solvent percentage range, and the extent of log $(t - t_0)$ *versus* percent solvent linearity for obtaining these extrapolated results. In this regard, an understanding of the way these factors can influence the log $(t - t_0)$ *versus* percent solvent relationship is pertinent. Acetonitrile, but not the alcoholic solvents, gave a curved plot of log $(t - t_0)$ as ordinate *versus* the percent of nonaqueous solvent for ALPM work with 1-(3-furyl)-4-methylpentan-1-one (1). The present study reveals, however, that curved plots can be obtained even in methanol. In their detailed studies, Schoenmakers *et al.* examined the elution behavior of 32 compounds from an RP-18 column using methanol, acetonitrile, or tetrahydrofuran; they also found plots of solvent fraction *versus* the logarithm of the capacity factor (as ordinate) were often curved, irrespective of the solvent (13). Although methanol afforded the greatest separation potential, it required such a long time for elution of highly nonpolar agents that it was useless. While other researchers have used higher methanol percentages to solve this problem, ALPM utilizes different column lengths for the less polar agents.

Hanai and Hubert, in their studies using an octadecylsilica column, found that curvature can occur at either high or low acetonitrile levels (12). Results obtained using methanol (Fig. 1) reveal that curvature can be either concave or convex, depending on the compound. A comparison of RP-8 ALPM findings for specific compounds with the results of Schoenmakers *et al.* using RP-18 columns reveals that compounds need not have the same concave or convex curvature; thus, curvature is also column dependent. Overall, HPLC equilibrium can depend on the organic solvent(s), the chemical, and/or the column, among other factors. Indeed, so many factors become important that one wonders if these relationships are ever really linear. In this regard, Schoenmakers *et al.* have theorized that these relationships should actually be qua-

Table III—Aromatic Substituent Constants[a]

Substituent	ALPM Constant: Mono-substituted[b]	ALPM Constant: Di-substituted[c]	ALPM Constant: Mean[d]	Shake-Flask Constant[e]
Phenyl	2.12	1.84	1.98	1.96
Methyl	0.69	0.56	0.63	0.56
Fluoro	0.19	—	—	0.14
Chloro	0.81	0.69	0.75	0.71
Bromo	1.03	0.72	0.88	0.86

[a] All ALPM values determined using 0.035 M triethylamine (1). [b] ALPM constant computed from the difference between ALPM values for the log P(o/w) of the monosubstituted benzene and benzene. [c] ALPM constant computed from the difference between ALPM values for the log P(o/w) of the disubstituted benzene and that of the monosubstituted benzene. [d] Average of mono- and disubstituted values. [e] Derived from octanol/water data (6).

Table IV—"Bioconcentration Factor" (Log BCF) Predicted from Various Log P(o/w) Measurements [a]

	Measured log BCF	Calculated log BCF		
		Other HPLC	ALPM	Calculated
Acenaphthene	2.58	3.18 (4.49)	2.83 (4.02)	3.15 (4.45)
Butyl benzyl phthalate	2.89[b]	3.38 (4.75)	3.64 (5.09)	—
2-Chlorophenol	2.33	0.40 (0.83)	1.53 (2.32)	1.42 (2.17)
1,2-Dichlorobenzene	1.95	2.62 (3.75)	2.47 (3.56)	2.47 (3.55)
1,3-Dichlorobenzene	1.82[b]	2.77 (3.95)	2.48 (3.57)	2.47 (3.55)
1,4-Dichlorobenzene	1.78	2.64 (3.78)	2.33 (3.37)	2.47 (3.55)
Diethyl phthalate	2.07	1.80 (2.67)	2.02 (2.96)	—
Dimethyl phthalate	1.76	—	1.19 (1.87)	0.96 (1.56)
2,4-Dimethylphenol	2.18[b]	1.28 (1.99)	1.64 (2.46)	1.70 (2.54)
N-Nitrosodiphenylamine	2.34[b]	2.47 (3.55)	2.19 (3.18)	—
1,2,3,4-Tetrachlorobenzene	3.26	3.57 (5.00)	3.32 (4.67)	3.55 (4.97)
Pentachlorobenzene	3.53	3.79 (5.29)	3.69 (5.16)	4.09 (5.68)[c]

[a] Numbers in parentheses are log P(o/w) values used to calculate log BCF by the formula of Veith *et al.* (4): log BCF = 0.76 × [log P(o/w)] − 0.23. [b] Measured log BCF was better approximated using "Other HPLC" or "Calculated" values than by "ALPM" log P(o/w) values. [c] Calculated from values determined by this study.

dratic (13). While it is difficult to explain why results are so often linear, it is clear that equilibrium (*i.e.*, state of linearity) must now be considered in HPLC methods for hydrophobicity determination, if more meaningful data are to be obtained.

Unfortunately, it is difficult to know the status of such equilibria without a time-consuming measurement of all significant log $(t - t_0)$ results at incremental percentages from 0 to 100% solvent. Although ALPM software can achieve this, once these data are obtained, they are often of little use[2]. If they are linear, only a few points would be needed, and the time required could be greatly reduced. If they are curved, it may be unclear at which end or over which region the curvature occurs. The only answer is to understand the real cause of this curvilinear behavior. However, the use by ALPM of statistically valid log $(t - t_0)$ *versus* 55–35% methanol percentage data with linearity (or curvilinearity) testing, as for benzene, seems to afford the fastest and, by covering the range of maximum solvent independence, the best assurance of the actual equilibrium condition.

HPLC-determined hydrophobicity is generally considered to be a composite of partition and absorption processes (14). If absorption events could be eliminated from HPLC measurements, then data from the HPLC partition process could be compared with that from the shake-flask method to discern discrepancies. However, absorption processes probably cannot be prevented using octadecylsilane columns because of a structured methanol layer on the column packing surface (14). ALPM utilizes C_8 or octylsilylated columns, which are less likely to bind methanol. In this regard, the high correlations of ALPM data with the shake-flask results over such a wide range, as reported in the first paper (1) and in Table IV herein, suggest absorption processes are of minimal importance. As a result, unexplainable differences between ALPM and shake-flask log P(o/w) results should be rare. However, discrepancies warrant attention. In general, they could signify an absorption process with the ALPM partition column, another ALPM anomaly, or perhaps even shake-flask irregularities. ALPM discrepancies could indicate how the processes unique to individual chemicals alter simple partitioning phenomena. While such deviations could have considerable relevance to predicting biological activities, they affect only that isolated value. On the other hand, shake-flask irregularities could also identify improperly computed substituent constants and errors in calculated values.

One inconsistency between the ALPM and shake-flask log P(o/w) values occurs for benzene, a primary standard for the calculation of log P(o/w). ALPM measurement using the established 0.035 M triethylamine conditions does not give the reproducible and accepted shake-flask value of 2.13, but affords a mean of 2.00 ± 0.06 for three determinations. ALPM measurement in 0.004 M trifluoroacetic acid yields 2.15 ± 0.03, which is statistically the same as the shake-flask result. The data indicate a possible pH dependency of log P(o/w); however, no significant variation of shake-flask log P(o/w) with pH is evident with benzene[3].

ALPM estimates of log P(o/w) reflect the ratio of chemical on the stationary phase (SP) to that in the mobile phase (MP) (Eq. 3). If the ALPM result has the same value as the shake-flask approach, pure partitioning would be indicated. If not, the ALPM result can be evaluated to determine which changes would give the altered ratio (1):

$$\log P(o/w)_{ALPM} = m \times \log ([X]_{SP}/[X]_{MP}) + b \qquad \text{(Eq. 3)}$$

where $[X]_{SP}/[X]_{MP} = V_{ccr}$.

Assuming the ALPM acid result and the reproducible 2.13 literature shake-flask log P(o/w) for benzene are correct, the lower ALPM value in base suggests that benzene is eluting earlier in base than in acid. This could result from a reduced interaction between benzene and the stationary phase or an increased interaction between benzene and the mobile phase. Four facts argue against the former possibility and support the latter: (*a*) excellent correlations are obtained under basic conditions for many agents having higher or lower log P(o/w) values; (*b*) benzene is chemically unlikely to combine with column functionalities; (*c*) it has no substituents to hinder column interactions; (*d*) the log $(t - t_0)$ *versus* percent methanol plot is curved regardless of pH for benzene, but not for acetanilide. The well-known benzene-water azeotrope also supports occurrence of such an interaction.

The lower base log P(o/w) observation has some generality. Base-determined ALPM values for the smaller, more water-soluble, heterocyclic compounds pyrrole, furan, and thiophene, are similarly lower than their shake-flask counterparts (Table V, obs. 21, 45, and 46) (6, 15, 16). Increasing compound size appears to diminish the differences between ALPM and the shake-flask results. The 2.20 average ALPM value for fluorobenzene is lower than the 2.27 shake-flask result. Fluorobenzene, like benzene, affords a curvilinear relationship between log $(t - t_0)$ and percent methanol. However, no curvilinearity or deviation was apparent with chlorobenzene (Table II, obs. 10–12 and 19–22). Similarly, the ALPM value for the larger aromatics naphthalene and anthracene are statistically the same as their shake-flask values.

These data could support the existence of a hydrogen-bonded solvation shell about the smaller aromatic agent. Masking of lipophilic aromatics by a hydrophilic shell could impede their column binding; it would, however, decrease as the size of the aromatic chemical increases. Knowledge of whether the complete log $(t - t_0)$ *versus* percent methanol relationship for these heteroaromatic agents is curvilinear would be useful in evaluating this proposal, but their weak UV absorption (when compared with baseline triethylamine-methanol solutions) has precluded obtaining that information. The lower ALPM value for benzene in base, as opposed to acid, could arise from stronger hydrogen bonding caused by a greater electron density on the hydroxyl ion. Such a solvation shell, if formed, could also reduce penetration of these smaller π-excessive aromatic agents through lipid-like biomembranes, suggesting that the ALPM result may be more relevant than the shake-flask result in predicting biological properties. However, no comparative biological data are presently available to support that suggestion.

Different values for ALPM and shake-flask results can occur even when a linear relationship is evident, regardless of measurement pH. The 1.17 value for acetanilide obtained in base using ALPM is consistent with the pH-independent literature shake-flask result[4], requiring the higher ALPM value obtained in acid to be explained (Table I). The possibility of a fast trifluoroacetylation reaction was discounted by substitution of acetic acid (Table I, obs. 7). Since the acid plot of log $(t - t_0)$ *versus* percent methanol is also linear, the higher value can only be explained by increased column binding by acetanilide under acid conditions. In this regard, reversible Michael addition of a silanol residue to a multisubstituted and benzene-stabilized imine by the process in Scheme I is proposed. While occurrence of this base-catalyzed process in dilute acid may seem strange, the acid could represent a compromise between the needed tautomerization and sorbant-imine-catalyzed Michael reaction. The Michael reaction is a highly reversible process (17); its occurrence would statistically delay departure of the compound from the column. The present data are insufficient to determine that this reaction actually occurs on the column. Theoretically, it would be prevented if no free, unalkylated silanol residues were present. Future studies using spherical, extensively capped packing materials could conceivably eliminate this process. If such a chemical event could also occur with nucleophiles in membranes, the ALPM determi-

[3] J. E. Garst and A. Leo, unpublished results.

[4] Albert Leo, personal communication.

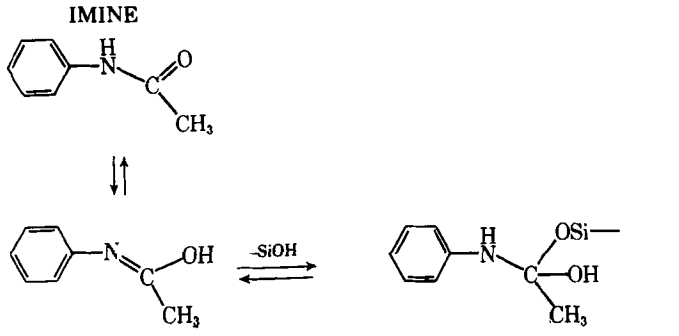

Scheme I

Table V—Partition Coefficients of Miscellaneous Compounds

Compound	Obs.	ALPM log P	log P Range	Best[a]
Acridine	1	+3.31 ± 0.03	+3.40	+3.40
4-Aminopyridine	2	+0.33 ± 0.04	+0.28	+0.28
Anisole	3	+1.97 ± 0.08	+2.04 to +2.11	+2.04
Anthracene	4	+4.66 ± 0.09	+4.45	+4.45
	5	+4.67 ± 0.09	+4.45	+4.45
2-Benzofuroic acid	6	+2.51 ± 0.04	—	—
3-Bromoquinoline	7	+2.90 ± 0.02	+3.03	+3.03
3-Bromothiophene	8	+2.59 ± 0.03	—	—
Caffeine	9	+0.65 ± 0.03	−0.07 to +0.01	−0.07
	10	+0.61 ± 0.04	−0.07 to +0.01	−0.07
3-Cyanopyridine	11	+0.54 ± 0.01	+0.36	+0.36
1,1,1-Trichloro-2,2-bis(*p*-chlorophenyl)-ethane (DDT)	12	+6.40 ± 0.11	+3.98 to +6.19	+6.19
4,4′-Dibromobiphenyl	13	+5.66 ± 0.07	—	—
2,3-Dibromothiophene	14	+3.53 ± 0.06	—	—
Diethylstilbestrol	15	+5.46 ± 0.11	+5.07	+5.07
1,2-Dihydroxybenzene	16	+0.95 ± 0.06	+0.84 to +1.01	+0.92
	17	+0.90 ± 0.11	+0.84 to +1.01	+0.92
2,4-Dinitrophenol	18	+1.79 ± 0.06	+1.50 to +1.54	+1.54
Phenylphosphono-thioic acid *O*-ethyl *O*-*p*-nitrophenyl ester (EPN)	19	+5.34 ± 0.08	+3.49	+3.49
Ferulic acid	20	+2.37 ± 0.03	—	—
Furan	21	+1.13 ± 0.02	+1.34	+1.34
Hexabromobiphenyl	22	+7.80 ± 0.15	—	—
4-Hydroxycinnamic acid	23	+2.20 ± 0.05	—	—
Methylisobutyl-xanthine	24	+2.29 ± 0.08	—	—
	25	+2.24 ± 0.08	—	—
3-Methylindole	26	+2.50 ± 0.09	+2.60	+2.60
3-Methylpyridine	27	+1.18 ± 0.01	+1.20 to +1.24	+1.20
α-Naphthoflavone	28	+4.82 ± 0.12	—	—
β-Naphthoflavone	29	+4.94 ± 0.08	—	—
1-Naphthoic acid	30	+3.36 ± 0.02	+3.10	+3.10
	31	+3.43 ± 0.02	+3.10	+3.10
α-Naphthylthiourea	32	+1.66 ± 0.02	—	—
4-(4-Nitrobenzyl)-pyridine	33	+2.88 ± 0.04	—	—
4-Nitrophenol	34	+1.96 ± 0.08	+1.38 to +2.08	+1.91
Ochratoxin A	35	+4.74 ± 0.11	—	—
[2.2]Paracyclophane	36	+4.47 ± 0.04	+2.33	+2.33
Phenol	37	+1.53 ± 0.09	+1.46 to +1.51	+1.49
Phenylacetic acid	38	+1.95 ± 0.04	+1.41 to +1.51	+1.51
	39	+1.96 ± 0.05	+1.41 to +1.51	+1.51
4-Phenylphenol	40	+3.63 ± 0.03	+3.20	+3.20
	41	+3.54 ± 0.03	+3.20	+3.20
Phenylthiourea	42	+0.77 ± 0.03	+0.73	+0.73
Progesterone	43	+5.01 ± 0.17	+3.70 to +3.87	+3.87
	44	+4.89 ± 0.10	+3.70 to +3.87	+3.87
Pyrrole	45	+0.62 ± 0.04	+0.75	+0.75
Thiophene	46	+1.74 ± 0.02	+1.81	+1.81
4-Toluic acid	47	+2.67 ± 0.02	+2.27	+2.27
	48	+2.66 ± 0.03	+2.27	+2.27
Trifluoromethyl-benzene	49	+3.37 ± 0.02	+2.79 to +3.01	+3.01
	50	+3.35 ± 0.02	+2.79 to +3.01	+3.01
2,4,6-Trinitrophenol	51	+1.46 ± 0.02	+2.03	+2.03
α-Tropolone	52	+1.54 ± 0.04	+0.53 to +0.75	+0.75

[a] Single literature value closest to ALPM log P.

Table VI—Prediction of Log Bovine Serum Albumin Binding (1/*C*)

Compound	log 1/*C*	Calculated log 1/*C*[a] Literature Value	Calculated log 1/*C*[a] ALPM
Phenol	3.32	3.40 (1.46)	3.46 (1.54)
3-Fluorophenol	3.86	3.75 (1.93)	3.71 (1.88)
4-Fluorophenol	3.52	3.63 (1.77)	3.66 (1.81)
3-Chlorophenol	4.30	4.18 (2.50)	4.08 (2.37)
4-Chlorophenol	4.00	4.10 (2.39)	4.12 (2.42)
4-Bromophenol	4.22	4.25 (2.59)	4.20 (2.53)
4-Iodophenol	4.40	4.49 (2.91)	4.38 (2.76)
4-Methylphenol	3.70	3.76 (1.94)	3.79 (1.98)
3-Ethylphenol	4.22	4.10 (2.40)	4.21 (2.54)
3-Trifluoromethylphenol	4.52	4.51 (2.95)	4.49 (2.91)
3-Cyanophenol	3.26	3.22 (1.22)	3.68 (1.84)[c]
3-Hydroxyphenol	3.15	2.90 (0.80)	2.93 (0.84)
3-Methoxyphenol	3.54	3.49 (1.58)	3.57 (1.69)
4-Methoxyphenol	3.40	3.31 (1.34)	3.45 (1.53)
3-Nitrobenzyl alcohol	2.94	3.18 (1.17)	3.34 (1.38)[c]
4-Methoxybenzyl alcohol	2.94	3.13 (1.10)	3.25 (1.27)[c]
Benzonitrile	3.23	3.47 (1.56)	3.53 (1.63)
Acetophenone	3.31	3.49 (1.58)	3.56 (1.67)
Nitrobenzene	3.58	3.69 (1.85)	3.68 (1.83)
4-Bromoacetanilide	4.00	3.94 (2.18)[b]	4.05 (2.33)
4-Nitroanisole	4.00	3.82 (2.03)[b]	3.97 (2.22)
4-Chloronitrobenzene	4.07	4.10 (2.39)	3.97 (2.23)
2,4-Dichloronitrobenzene	4.59	4.50 (2.93)[b]	4.39 (2.78)
Naphthalene	4.91	4.83 (3.37)	4.90 (3.47)
Azobenzene	5.29	5.17 (3.82)	5.61 (4.40)[c]
Anisole	4.00	3.89 (2.11)	3.80 (1.99)
3-Fluoroaniline	3.09	3.28 (1.30)	3.35 (1.41)
4-Chloroaniline	3.68	3.68 (1.83)[b]	3.71 (1.87)
4-Methoxyaniline	2.92	2.89 (0.78)[b]	1.94 (0.85)
4-Bromoaniline	4.06	3.83 (2.03)[b]	3.86 (2.07)
4-Methylaniline	3.30	3.34 (1.39)	3.38 (1.44)
1-Naphthylamine	3.94	3.98 (2.23)[b]	3.87 (2.09)
Indole	4.07	3.91 (2.14)	3.92 (2.15)
Thymol	4.66	4.78 (3.30)	5.00 (3.59)

[a] Determined using the regression constants reported by Helmer *et al.* (5), the value of log P(o/w) given in parentheses, and: log (1/*C*) = 0.751 × log P(o/w) + 2.301. [b] Calculated log P(o/w) used by Helmer *et al.* (5). [c] ALPM log P(o/w) and Helmer *et al.* (5) data differ by more than ±3 *SD* based on the shake-flask error (*i.e.*, 6.13 ± 2.76%) reported in the preceding paper (1).

nation in acid might more adequately reflect biological activities than would either the pure solvent/water partition measurement or the new, improved end-capped, partition column packings.

Several other compounds have also given ALPM estimates of log P(o/w) that differ from the shake-flask result. In principle, if triethylamine (pK_a = 11.01) forms an ion-pair with silanol residues, as suggested in the preceding paper (1), an amine of comparable basicity would do the same, delaying its elution and raising its apparent log P(o/w) value. Amines of lower basicity would not be affected. Thus, little difference between shake-flask and ALPM values has been found for diphenylamine (pK_a = 0.79), 3-bromoquinoline (pK_a = 2.69), 4-bromoaniline (pK_a = 3.86), pyridine (pK_a = 5.25), and acridine (pK_a = 5.58) (1). Although the ALPM value of 4-aminopyridine (pK_a = 9.11) appears unaffected, phenethylamine (pK_a = 9.84) affords an ALPM value of 2.84, ~0.4 units higher than the shake-flask result (6). This discrepancy for phenethylamine could prove advantageous in studies of new column packings. The absence of unalkylated silanol groups on a particular packing should theoretically result in no deviation for this agent and provide an excellent experimental tool to examine silica gel alkylation.

Two other compounds studied appear inconsistent with shake-flask data. Both the reproducible shake-flask method and the octanol-saturated, kieselguhr-packed column of Mirrlees *et al.* indicate that the log P(o/w) for caffeine ranges from −0.07 to 0.01 (2, 6). These values differ considerably from the reproducible ALPM value of ~0.63 (Table V). A base-related explanation for the high ALPM value of caffeine is unlikely; however, literature shake-flask data also suggest inconsistencies in the xanthine series. While the −0.07 value of Anderson, cited by Hansch and Leo, is consistent with the findings of others, his report of −0.02 for theophylline and −0.80 for theobromine, two dimethylated xanthines which should have similar values, complicate evaluation of this matter (6).

ALPM also does not afford a result similar to the shake-flask literature for α-tropolone (Table V). Although some enhanced column-binding process cannot be discounted, the 1.54 ± 0.04 ALPM value is close to the 1.45 shake-flask value of the similar *p*-hydroxyacetophenone (6). Likewise, a value of 1.61, estimated from that of catechol (Table V) and the ALPM substituent constant for a methyl group, is closer to the 1.54 ALPM value than to the

Table VII—Comparison of Results in Table VI

Source	Regression Equations	No. of Compounds
Helmer *et al.* (5)	$\log (1/C) = 0.751\ (\pm 0.070) \times \log P(o/w) + 2.301\ (\pm 0.150)$	42
Helmer *et al.* (5)	$\log (1/C) = 0.785\ (\pm 0.064) \times \log P(o/w) + 2.234\ (\pm 0.138)$	34
ALPM	$\log (1/C) = 0.752\ (\pm 0.092) \times \log P(o/w) + 2.246\ (\pm 0.204)$	34

	Helmer *et al.* (5)	Helmer *et al.* (5)	ALPM
r	0.960	0.976	0.949
SE of estimate	0.159	0.130	0.189
n	42	34	34
Calculated log $(1/C)$ values differ <0.1:		21 of 34 compounds	
Observed log $(1/C)$ values closer to Helmer *et al.* (5):		7 of 13 compounds	
Observed log $(1/C)$ values closer to ALPM:		6 of 13 compounds	

0.53–0.75 range reportedly obtained by shake-flask (6). α-Tropolone shows no evidence of curvilinearity in its log $(t - t_0)$ *versus* percent methanol plot. Furthermore, this deviation occurs at a log P(o/w) value where other compounds give virtually identical shake-flask and ALPM results (Table V). The fact that α-hydroxy ketones in general, and α-tropolone specifically, readily hydrate and dimerize may be relevant to these discrepancies (18). Perhaps biological properties may be better predicted by the higher ALPM result, especially if the higher ALPM log P(o/w) value reflects partitioning of a stable dimer or unhydrated species.

In the course of these determinations various substituted benzenes were examined (Fig. 2). Concave curvature of their ALPM log P(o/w) values continues from 0 to 6 substituents seemingly without regard to the electron-donating or electron-withdrawing character of the substituent. Figure 2 also indicates that values for the various fluorobenzenes deviate the least from linearity when compared to methyl, phenyl, chloro, or bromo substituents. This near linearity for the smaller fluorine groups suggests that spatial rather than electronic factors influence ALPM log P(o/w). Other correlation parameters, such as molar refractivity, are known to have a major spatial component (6). Such factors may also explain results with [2.2]paracyclophane, which has a reported shake-flask log P(o/w) of 2.33 (6). ALPM yields the much higher value of 4.47 (Table V), yet even this value is significantly lower than that expected based on double the 3.29 ALPM value for *p*-xylene (Table II).

Since ALPM affords a continuous, wide-range estimation of log P(o/w) by a column-binding method and since considerable shake-flask data also indicate that these groups are not truly additive (6), perhaps strict additivity is simply fallacious. This would suggest clear limitations on the calculation of log P(o/w) values using various additivity schemes. However, even calculations should afford minimal error when one or two benzene substituents are present. In this case, ALPM often gives values very close to the calculated value (using benzene = 2.13). ALPM gives 3.56 and 3.57 for both the 1,2- and 1,3-dichlorobenzenes, respectively, but only 3.37 for 1,4-dichlorobenzene. The shake-flask procedure gives 3.40 and 3.44 for the 1,2- and 1,3-dichlorobenzenes, respectively, but 3.37 for 1,4-dichlorobenzene. Veith *et al.* reported 3.55 as the calculated value for all the dichlorobenzenes (4). Since ALPM gave that value for 1,2- and 1,3-dichlorobenzenes, but afforded the noticeably lower 3.37 shake-flask value for the *para* isomer, perhaps ALPM can detect real differences between isomers which are not evident in calculations. Occasionally, ALPM better supports the calculated value for compounds with sterically noninteracting substituents. For instance, the shake-flask log P(o/w) of mesitylene is 3.42 (6) and the calculated value is 3.81 (6), yet ALPM yields 3.87.

Attempts to calculate log P(o/w) values using various additivity schemes may lead to inaccurate values for interacting, multiply substituted, and high log P(o/w) compounds; these compounds have log P(o/w) values which are otherwise difficult to measure directly and, in part, prompted development of the additivity concept. Thus, ALPM gives interesting differences between shake-flask and/or calculated values for such compounds as 1,2,3,4-tetrachlorobenzene or pentachlorobenzene (Table IV), and hexamethylbenzene [ALPM, 5.00; shake-flask, 4.31 (6); calculated, 5.49 (6)]. These findings and interesting discrepancies for phenylphosphothioic acid *O*-ethyl *O*-*p*-nitrophenyl ester (EPN) and progesterone in Table V could suggest that the best way to determine log P(o/w) is ALPM measurement.

One clear comparison of method is the prediction of biological data. In this regard, ALPM log P(o/w) values seem to afford equal or better predictions. Table IV compares ALPM log P(o/w) data with those obtained from calculated values and another HPLC method in predicting the measured *in vivo* concentration process of various compounds in bluegill sunfish (4, 19). For 8 of 12 compounds having sufficient UV absorption to allow evaluation with the current detector system, ALPM measurement gave equal or better approximation of the "bioconcentration" factor (as log BCF) than did either the calculated or HPLC-determined values reported by Veith *et al.* (4, 19). Since, *in vivo* measurement of the concentration process may cost from $3000 to $10,000 (depending on the need for radiolabeled agents), this represents a significant savings (4).

Log P(o/w) data for 34 compounds, having sufficient availability and UV absorption to enable ALPM measurement, were compared with the combination of shake-flask and calculated log P(o/w) values reported by Helmer *et al.* with regard to prediction of bovine serum albumin binding (Table VI) (5). Correlation coefficients, standard errors, and other measures of similarity are shown in Table VII. Several major discrepancies occur between shake-flask and ALPM values. Although Helmer *et al.* measured a value of 1.22 (5) and Hansch and Leo cite 1.70 as the shake-flask value of 3-cyanophenol (6), ALPM measured an even higher 1.84. Calculations would suggest a value near 0.89; however, electron-withdrawing groups tend to greatly increase this value. Thus, the ALPM value for 3-cyanophenol is similar to both the ALPM and shake-flask result for 4-nitrophenol (Table V). In view of the measurement error in the binding term, log $(1/C)$, and the wide range of literature shake-flask log P(o/w) values cited for these compounds, these methods are judged indistinguishable.

In summary, any direct HPLC method is quicker and can ensure measurement of the correct component better than shake-flask techniques. But only ALPM, which measures considerable elution data, can easily offer considerable insight into whether equilibrium is obtained between the mobile and stationary HPLC phases. Examination of benzene suggests that if linearity (*i.e.*, equilibrium) is not attained, altered physical interactions between the chemical and the mobile or stationary phases may be responsible for deviations between ALPM and the shake-flask result. If linearity is attained, acetanilide data suggest that altered column-binding interactions may more satisfactorily explain deviations between these measurement methods. Full understanding of chemical-mobile phase and chemical-stationary phase interactions is required to elucidate chemical factors which could change the partition coefficient apparent in biological situations. In addition to providing a computer-operated method to expedite this data acquisition, ALPM estimation of log P(o/w) and of biological activities can offer improved or equal accuracy, a major cost reduction, and a speed greater than existing HPLC and shake-flask log P(o/w) determinations. In the few cases where ALPM and shake-flask results differ, more research is necessary to establish the exact nature of the discrepancy, with biological data affording the ultimate tool to determine the most suitable parameter. Future ALPM developments should further enhance accuracy by enabling the simultaneous measurement of the void volume marker, the compound of interest, and internal log P(o/w) standard, all under computer control.

REFERENCES

(1) J. E. Garst and W. C. Wilson, *J. Pharm. Sci.*, **73**, 1616 (1984).

(2) M. S. Mirrlees, S. J. Moulton, C. T. Murphy, and P. J. Taylor, *J. Med. Chem.*, **19**, 615 (1976).

(3) T. Yamana, A. Tsuji, E. Miyamota, and O. Kubo, *J. Pharm. Sci.*, **66**, 747 (1977).

(4) G. D. Veith, K. J. Macek, S. R. Petrocelli, and J. Carroll, in "Aquatic Toxicology," J. G. Eaton, P. R. Parrish, and A. C. Henricks, Eds., American Society for Testing and Materials, STP 707, Philadelphia, Pa., 1980, p. 116.

(5) F. Helmer, K. Kiehs, and C. Hansch, *Biochemistry*, **7**, 2858 (1968).

(6) C. Hansch and A. Leo, "Substituent Constants for Correlation Analysis in Chemistry and Biology," Wiley, New York, N.Y., 1979.

(7) R. F. Rekker, "The Hydrophobicity Fragmental Constant," Elsevier, New York, N.Y., 1977.
(8) W. Butte, C. Fooken, R. Klussman, and D. Schulle, *J. Chromatogr.*, **214**, 59 (1981).
(9) M. L. Bieganowska, *J. Liq. Chromatogr.*, **5**, 39 (1982).
(10) T. I. Hafkenscheid and E. Tomlinson, *J. Chromatogr.*, **18**, 409 (1981).
(11) T. Braumann and L. H. Grimme, *J. Chromatogr.*, **206**, 7 (1981).
(12) T. Hanai and J. Hubert, *J. Chromatogr.*, **239**, 527 (1982).
(13) P. J. Schoenmakers, H. A. H. Billet, and L. DeGalan, *J. Chromatogr.*, **185**, 179 (1979).
(14) T. L. Hafkenscheid and E. Tomlinson, *Int. J. Pharm.*, **17**, (1983).
(15) "Lange's Handbook of Chemistry," 11th ed., J. A. Dean, Ed., McGraw-Hill, New York, N.Y., 1979.
(16) "Chemistry of Carbon Compounds," Vol. 4, Part A, E. H. Rodd, Ed., Elsevier, New York, N.Y., 1957, p. 145.
(17) E. D. Bergmann, D. Ginsburg, and R. Pappo, *Org. React.*, **10**, 179 (1959).
(18) "Merck Index," 9th ed., M. Windholz, Ed., Merck and Co., Rahway, N.J., 1976, pp. 207 and 368.
(19) G. D. Veith, N. M. Austin, and R. T. Morris, *Water Res.*, **13**, 43 (1979).

ACKNOWLEDGMENTS

The author appreciates financial support by the University of Illinois Research Board, the Biomedical Support Group (BRSG-S07-RR07038), and the U.S. Government (HATCH 20-323 and NIEHS 02193). Statistical assistance by D. Gianola and the late H. W. Norton is also appreciated.

Generic Tolbutamide Tablet Dissolution: Intralot and Interlot Variation

JAMES W. AYRES *[x], HUA-PIN HUANG *, and KENNETH ALBERT[‡]

Received August 8, 1983, from the **School of Pharmacy, Oregon State University, Corvallis, OR 97331* and the [‡] *Medical Bioavailability Unit, The Upjohn Company, Kalamazoo, MI 49001.* Accepted for publication October 26, 1983.

Abstract □ Dissolution profiles for 62 lots of tolbutamide tablets from six manufacturers have been characterized using the USP paddle-stirrer apparatus. Results of paddle-stirrer dissolution for percent drug dissolved at 10, 20, and 30 min correlated well ($r^2 = 0.7444$) with results from the USP rotating-basket test for 39 lots of tolbutamide. Interlot and intralot variability in tolbutamide dissolution was highly dependent on the manufacturer. For one product, the intralot range (for six paddle-stirred tablets) of percent drug dissolved after 30 min was 50–68% while the maximum interlot range for mean dissolution was 58–104%. One lot failed to meet both the rotating-basket and the paddle-stirrer dissolution specifications. Tablet response to aging at 60, 75, and 98% relative humidity over time was also highly manufacturer specific. The innovator's product repeatedly dissolved well when fresh or aged at all humidities. Dissolution from some generic tablets was dramatically depressed by humidity aging, even after only 3 d. Pretreatment of tablets with simulated gastric fluid modified the dissolution profile of one poorly dissolving lot of tablets. Results indicate that manufacturing quality control is highly variable among tolbutamide tablets.

Keyphrases □ Tolbutamide—dissolution, intra- and interlot variation, effect of humidity aging □ Dissolution studies—tolbutamide, intra- and interlot variation, effect of humidity aging

Tolbutamide tablets must meet United States Pharmacopeia (USP) dissolution requirements which are established because ". . . in many cases it is possible to correlate dissolution rates with biological availability of the active ingredient" (1). Dissolution testing is also recognized (2) as useful for quality control purposes.

Tolbutamide exhibits only limited solubility and the United States Food and Drug Administration (FDA) recognizes that tolbutamide products are prone to bioavailability problems. Currently, the FDA lists 12 manufacturers' products as "therapeutically equivalent to each other" (3). Large variations in lot-to-lot dissolution of tolbutamide products indicate variations in quality and possible variations in bioavailability since low tolbutamide bioavailability is sometimes related to poor tolbutamide tablet dissolution (4–6). If such variations occur for different lots of products which have been ruled "therapeutically equivalent" by the FDA, then satisfaction of current FDA regulations may not assure lot-to-lot equivalence of products on the FDA list.

Previous work has shown extensive lot-to-lot variation in dissolution of tolbutamide tablets for six lots of one manufacturer (7), while there was uniformity for the originator's product. Others have demonstrated that humidity "aging" of tolbutamide tablets differentially affected dissolution for two different brands of products (8). Also, the physiological exposure to acid of ingested tablets is not mimicked by the current USP dissolution test although exposure of tolbutamide tablets to gastric acid has been reported to be necessary for disintegration and dissolution of some formulations (9).

Therefore, the purposes of this study were: (*a*) to evaluate the dissolution characteristics of several fresh lots of tolbutamide listed as therapeutically equivalent by the FDA; (*b*) to evaluate many of the same lots after humidity "aging" of the tablets; (*c*) to determine the effect of tablet exposure to gastric acid on tolbutamide dissolution for both fresh and humidity-aged tablets.

EXPERIMENTAL SECTION

Products were obtained commercially, stored in tightly closed, opaque containers in the dark at room temperature for 1–3 months, and tested using the USP rotating-basket (10) or paddle-stirrer dissolution test (1). Samples (3 mL) were collected with a continuous flow (set at 5–10 mL/min) eight-channel peristaltic pump[1] fitted with stainless steel 20–30 μm in-line filters. Samples were collected for 6 tablets for 10, 20, 30, and 45 min for the rotating-basket test (150 rpm) and at 10, 20, and 30 min for the paddle-stirrer test (75 rpm) in order to establish a dissolution *versus* time profile (rather than single time point dissolution values). All samples were replaced with temperature-equilibrated dissolution medium.

Filtered samples were diluted, the UV absorbance was measured at 226 nm (1), and the concentration of tolbutamide was calculated based on a seven point standard curve prepared the same day as unknowns were collected. Standard curves were generated by preparing known concentrations of either USP reference standard or company-provided tolbutamide. The UV spectra from these sources were superimposable and the standard curves considered equivalent as the null hypothesis of equal slopes and intercepts could not be rejected ($\alpha = 0.05$). Standard curves were fit with parabolic regression and had coefficients of variation of <4%. The average inversely estimated percent

[1] Gilson minipuls 2, eight channel peristaltic pump; Gilson Medical Electronics, Middleton, Wis.

0022-3549/84/1100-1629$01.00/0
© 1984, American Pharmaceutical Association

(7) R. F. Rekker, "The Hydrophobicity Fragmental Constant," Elsevier, New York, N.Y., 1977.
(8) W. Butte, C. Fooken, R. Klussman, and D. Schulle, *J. Chromatogr.*, **214**, 59 (1981).
(9) M. L. Bieganowska, *J. Liq. Chromatogr.*, **5**, 39 (1982).
(10) T. I. Hafkenscheid and E. Tomlinson, *J. Chromatogr.*, **18**, 409 (1981).
(11) T. Braumann and L. H. Grimme, *J. Chromatogr.*, **206**, 7 (1981).
(12) T. Hanai and J. Hubert, *J. Chromatogr.*, **239**, 527 (1982).
(13) P. J. Schoenmakers, H. A. H. Billet, and L. DeGalan, *J. Chromatogr.*, **185**, 179 (1979).
(14) T. L. Hafkenscheid and E. Tomlinson, *Int. J. Pharm.*, **17**, (1983).
(15) "Lange's Handbook of Chemistry," 11th ed., J. A. Dean, Ed., McGraw-Hill, New York, N.Y., 1979.
(16) "Chemistry of Carbon Compounds," Vol. 4, Part A, E. H. Rodd, Ed., Elsevier, New York, N.Y., 1957, p. 145.
(17) E. D. Bergmann, D. Ginsburg, and R. Pappo, *Org. React.*, **10**, 179 (1959).
(18) "Merck Index," 9th ed., M. Windholz, Ed., Merck and Co., Rahway, N.J., 1976, pp. 207 and 368.
(19) G. D. Veith, N. M. Austin, and R. T. Morris, *Water Res.*, **13**, 43 (1979).

ACKNOWLEDGMENTS

The author appreciates financial support by the University of Illinois Research Board, the Biomedical Support Group (BRSG-S07-RR07038), and the U.S. Government (HATCH 20-323 and NIEHS 02193). Statistical assistance by D. Gianola and the late H. W. Norton is also appreciated.

Generic Tolbutamide Tablet Dissolution: Intralot and Interlot Variation

JAMES W. AYRES *[x], HUA-PIN HUANG *, and KENNETH ALBERT[‡]

Received August 8, 1983, from the **School of Pharmacy, Oregon State University, Corvallis, OR 97331* and the [‡] *Medical Bioavailability Unit, The Upjohn Company, Kalamazoo, MI 49001.* Accepted for publication October 26, 1983.

Abstract □ Dissolution profiles for 62 lots of tolbutamide tablets from six manufacturers have been characterized using the USP paddle-stirrer apparatus. Results of paddle-stirrer dissolution for percent drug dissolved at 10, 20, and 30 min correlated well ($r^2 = 0.7444$) with results from the USP rotating-basket test for 39 lots of tolbutamide. Interlot and intralot variability in tolbutamide dissolution was highly dependent on the manufacturer. For one product, the intralot range (for six paddle-stirred tablets) of percent drug dissolved after 30 min was 50–68% while the maximum interlot range for mean dissolution was 58–104%. One lot failed to meet both the rotating-basket and the paddle-stirrer dissolution specifications. Tablet response to aging at 60, 75, and 98% relative humidity over time was also highly manufacturer specific. The innovator's product repeatedly dissolved well when fresh or aged at all humidities. Dissolution from some generic tablets was dramatically depressed by humidity aging, even after only 3 d. Pretreatment of tablets with simulated gastric fluid modified the dissolution profile of one poorly dissolving lot of tablets. Results indicate that manufacturing quality control is highly variable among tolbutamide tablets.

Keyphrases □ Tolbutamide—dissolution, intra- and interlot variation, effect of humidity aging □ Dissolution studies—tolbutamide, intra- and interlot variation, effect of humidity aging

Tolbutamide tablets must meet United States Pharmacopeia (USP) dissolution requirements which are established because ". . . in many cases it is possible to correlate dissolution rates with biological availability of the active ingredient" (1). Dissolution testing is also recognized (2) as useful for quality control purposes.

Tolbutamide exhibits only limited solubility and the United States Food and Drug Administration (FDA) recognizes that tolbutamide products are prone to bioavailability problems. Currently, the FDA lists 12 manufacturers' products as "therapeutically equivalent to each other" (3). Large variations in lot-to-lot dissolution of tolbutamide products indicate variations in quality and possible variations in bioavailability since low tolbutamide bioavailability is sometimes related to poor tolbutamide tablet dissolution (4–6). If such variations occur for different lots of products which have been ruled "therapeutically equivalent" by the FDA, then satisfaction of current FDA regulations may not assure lot-to-lot equivalence of products on the FDA list.

Previous work has shown extensive lot-to-lot variation in dissolution of tolbutamide tablets for six lots of one manufacturer (7), while there was uniformity for the originator's product. Others have demonstrated that humidity "aging" of tolbutamide tablets differentially affected dissolution for two different brands of products (8). Also, the physiological exposure to acid of ingested tablets is not mimicked by the current USP dissolution test although exposure of tolbutamide tablets to gastric acid has been reported to be necessary for disintegration and dissolution of some formulations (9).

Therefore, the purposes of this study were: (*a*) to evaluate the dissolution characteristics of several fresh lots of tolbutamide listed as therapeutically equivalent by the FDA; (*b*) to evaluate many of the same lots after humidity "aging" of the tablets; (*c*) to determine the effect of tablet exposure to gastric acid on tolbutamide dissolution for both fresh and humidity-aged tablets.

EXPERIMENTAL SECTION

Products were obtained commercially, stored in tightly closed, opaque containers in the dark at room temperature for 1–3 months, and tested using the USP rotating-basket (10) or paddle-stirrer dissolution test (1). Samples (3 mL) were collected with a continuous flow (set at 5–10 mL/min) eight-channel peristaltic pump[1] fitted with stainless steel 20–30 μm in-line filters. Samples were collected for 6 tablets for 10, 20, 30, and 45 min for the rotating-basket test (150 rpm) and at 10, 20, and 30 min for the paddle-stirrer test (75 rpm) in order to establish a dissolution *versus* time profile (rather than single time point dissolution values). All samples were replaced with temperature-equilibrated dissolution medium.

Filtered samples were diluted, the UV absorbance was measured at 226 nm (1), and the concentration of tolbutamide was calculated based on a seven point standard curve prepared the same day as unknowns were collected. Standard curves were generated by preparing known concentrations of either USP reference standard or company-provided tolbutamide. The UV spectra from these sources were superimposable and the standard curves considered equivalent as the null hypothesis of equal slopes and intercepts could not be rejected ($\alpha = 0.05$). Standard curves were fit with parabolic regression and had coefficients of variation of <4%. The average inversely estimated percent

[1] Gilson minipuls 2, eight channel peristaltic pump; Gilson Medical Electronics, Middleton, Wis.

0022-3549/84/1100-1629$01.00/0
© 1984, American Pharmaceutical Association

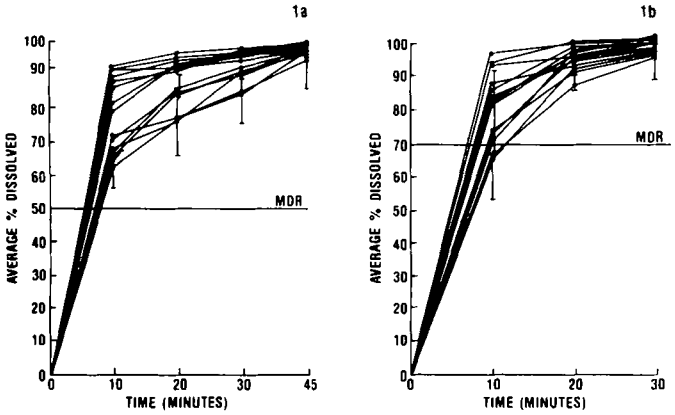

Figure 1—*Average percent of labeled tolbutamide dissolved from 500 mg of U tolbutamide tablets using the rotating-basket test (a) and the paddle-stirrer test (b). MDR is minimum dissolution requirement. Each data point is the average of six tablets and each line is for a different test (Table I). Data variation bars show the range of observed values for the slowest dissolving lots.*

of theory for standard concentrations was 100 ± 0.5% and all individual concentrations were estimated within 3% of theoretical values. The use of UV absorbance as a measure of dissolved tolbutamide was considered appropriate as HPLC analysis (11) of 37 different lots of tolbutamide resulted in only one absorption peak with a retention time equal to that of standard tolbutamide. Content analysis of these lots by HPLC also gave the same results as UV analysis which indicates that the only UV-absorbing material released was tolbutamide.

Humidity aging of tablets was accomplished by manipulating water vapor pressure in closed tanks using saturated salt solutions (12). Standard all-glass aquariums (50 × 26 × 30 cm) with glass covers were used for constant humidity chambers. A saturated solution of potassium sulfate was prepared in deionized, distilled water and placed in the bottom of the tank to a depth of 2–3 cm (~2.6 L) to produce 98% relative humidity (rh). Solutions of sodium dichromate or potassium carbonate were used for 60% rh and sodium chloride was used for 75% rh. A galvanized rack was placed in the tank to hold aluminum foil-lined petri dishes 7 cm above the surface of the liquid. Air circulation was maintained within the tank by a small electrical fan mounted inside the tank. Humidity was monitored daily with a wet and dry bulb hygrometer. No attempt was made to regulate temperature within the chambers as temperature variability within the laboratory was small and temperature dependence of relative humidity using the salt solutions is small (12). The average relative humidity chamber temperature during the experiments was 20.1°C with a maximum range of 1.1°C. The chamber was made airtight by the use of foam strips impregnated with petroleum as a seal between the glass cover and the aquarium.

Tablets were subjected to the aging process by placing four tablets of each lot in aluminum foil-lined petri dishes without covers, taking care that no tablet

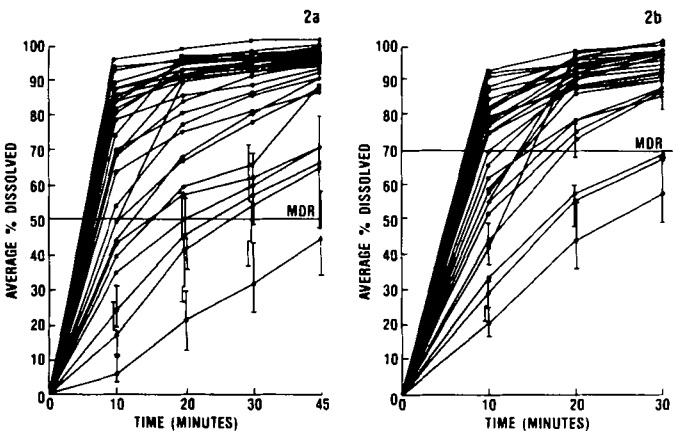

Figure 2—*Average percent of labeled tolbutamide dissolved from 500 mg of P tolbutamide tablets using the rotating-basket method (a) and the paddle-stirrer method (b). Each data point is the average of six tablets and each line is for a different lot, except tablets which failed the test. The lots which failed (2b) are the same lot number of the same manufacturer (P) but distributed under different private labels.*

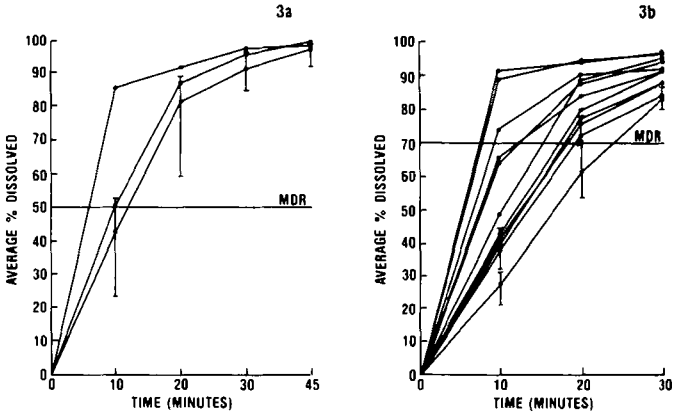

Figure 3—*Average percent of labeled tolbutamide dissolved from 500 mg of M tolbutamide tablets using the rotating-basket test (a) and the paddle-stirrer test (b).*

touched another. The chamber was then sealed and not opened until the end of the aging period.

Dissolution tests wherein the products were exposed to enzyme-free simulated gastric fluid (acid pretreatment) utilized 9.6 mL of concentrated hydrochloric acid per liter of water (pH ~1.1–1.2). Tablets of each product were allowed to separately dissolve, each in 900 mL of the simulated gastric fluid, in a USP rotating-basket apparatus at 150 rpm for 30 min. After 30 min the baskets were raised and allowed to drain. The acid dissolution medium was filtered under vacuum and then the filter paper with any retained solids was placed in a dissolution resin kettle (containing 900 mL of pH 7.4 phosphate buffer) fitted for paddle-stirrer dissolution. The contents of the basket were transferred to the phosphate buffer by gently dipping the basket (using forceps) into the buffer. Then the paddle was lowered and stirred at 75 rpm and samples were collected over time to determine the amount of tolbutamide dissolved.

RESULTS AND DISCUSSION

All lots passed the disintegration, assay, content uniformity, and tablet weight variation tests. However, there was considerable variation in dissolution characteristics among and within some lots.

Figure 1 shows that dissolution of tolbutamide from the innovators' (U) tablets[2] is relatively uniform within and among lots in both the rotating-basket and paddle-stirred apparatus. Figure 2 for the P product[3] shows wide interlot and intralot variation in dissolution. One lot (Fig. 2a) failed the USP rotating-basket test. The same lot number sold under a private label also failed the paddle-stirrer test (Fig. 2b) but passed the rotating-basket test. The cause of this dissolution variation is unknown. This lot is not the one reported earlier which also failed USP requirements (7). Figures 3–4 show dissolution profiles for tolbutamide products of some other manufacturers[4].

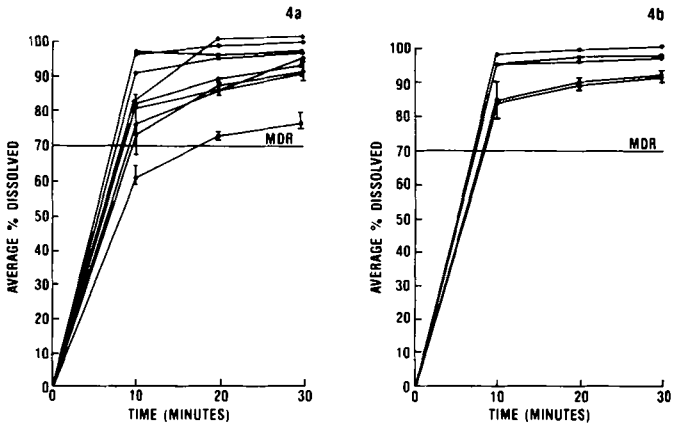

Figure 4—*Average percent of labeled tolbutamide dissolved using paddle-stirrer dissolution from 500 mg of: S, and PH (a); Z (b) tolbutamide tablets.*

[2] Upjohn.
[3] Premo.
[4] Fig. 3, Mylan (M); Fig. 4, Pharmadyne (PH), Smith Kline & French (S), and Zenith (Z).

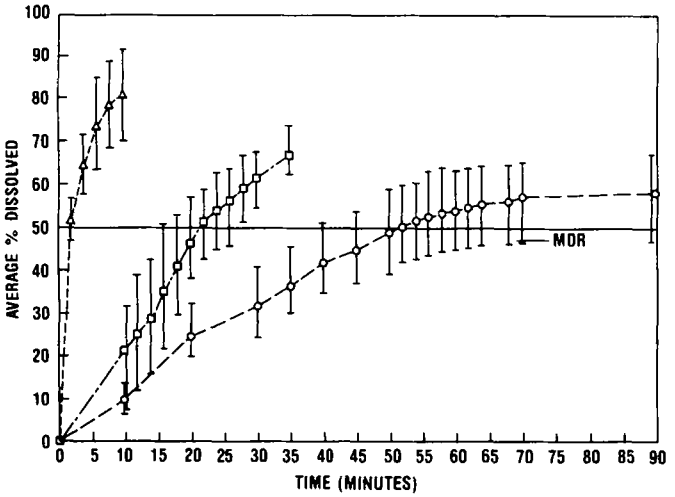

Figure 5—*Percent of labeled amount of tolbutamide dissolved* versus *time using the rotating basket for 6 tablets each of three different lots of product P. Data variation bars are the standard deviation of the mean. These can be compared to ranges shown in Figs. 1 and 2.*

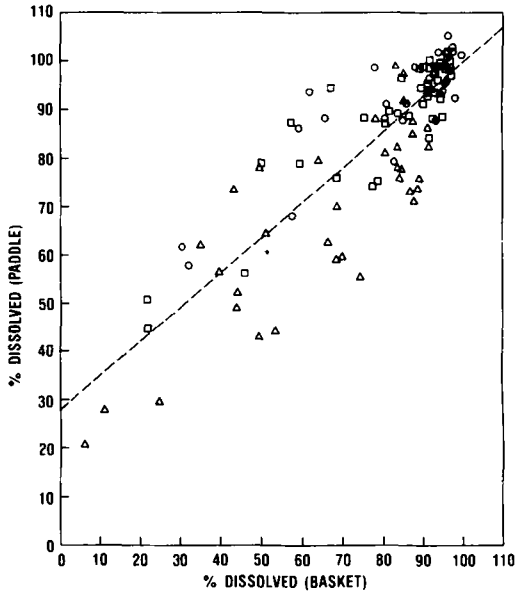

Figure 6—*Comparison of tolbutamide dissolved in paddle stirrer method* versus *rotating basket method. The generated regression line is F(x) = 27.95 + 0.705 x with $r^2 = 0.7444$; r^2 was not improved substantially by fitting to a polynomial of degree two or three. Key: (△) 10 min results; (□) 20 min results; (○) 30 min results.*

It is clear that interlot and intralot variation is manufacturer specific. For example, generic product in Fig. 3b is more variable than product in Fig. 1b, but some of the generic products in Fig. 4 produce dissolution profiles similar to those shown in Fig. 1b. Unfortunately, only a few product lots were available and these were only evaluated according to paddle-stirrer requirements (1). More lots should be tested to fully define the dissolution profiles of these products.

Figure 5 expands the information in Fig. 2a regarding both interlot and intralot variation for product P dissolution. The amount of drug released is highly dependent on the bottle (lot) used and the tablet within a bottle (lot) tested. The time to 50% dissolution was reported by Levy (6) to be related to clinical effectiveness for tolbutamide. The three lots in Fig. 5 required 1.9 min, 21.4 min, and 51.1 min, respectively, to average 50% dissolution in the USP rotating basket test. It must be noted that this test differs from the Levy (6) test, and the 51.1-min dissolution time does not necessarily imply the product will fail clinically. However, slow dissolution with wide intralot and interlot variations in dissolution rate are indicative of degree of quality control (1, 2).

The time to 50% (rotating-basket) and 70% (paddle-stirrer) dissolution for some lots of tolbutamide tested are shown in Table I. Intralot and interlot variability is manufacturer specific. The U product reached 50% and 70% dissolution ~40% faster and with 25–50% of the variation of P and M products. Products U, S, and Z were about equal in time to 70% dissolution, but too few S and Z lots were tested to be conclusive. In general, products dissolving most slowly or most rapidly in the rotating basket also dissolved slowly or rapidly, respectively, in the paddle-stirred test (Table I, Fig. 6) which indicates the two tests are correlated. However, the range of percent dissolved shows more

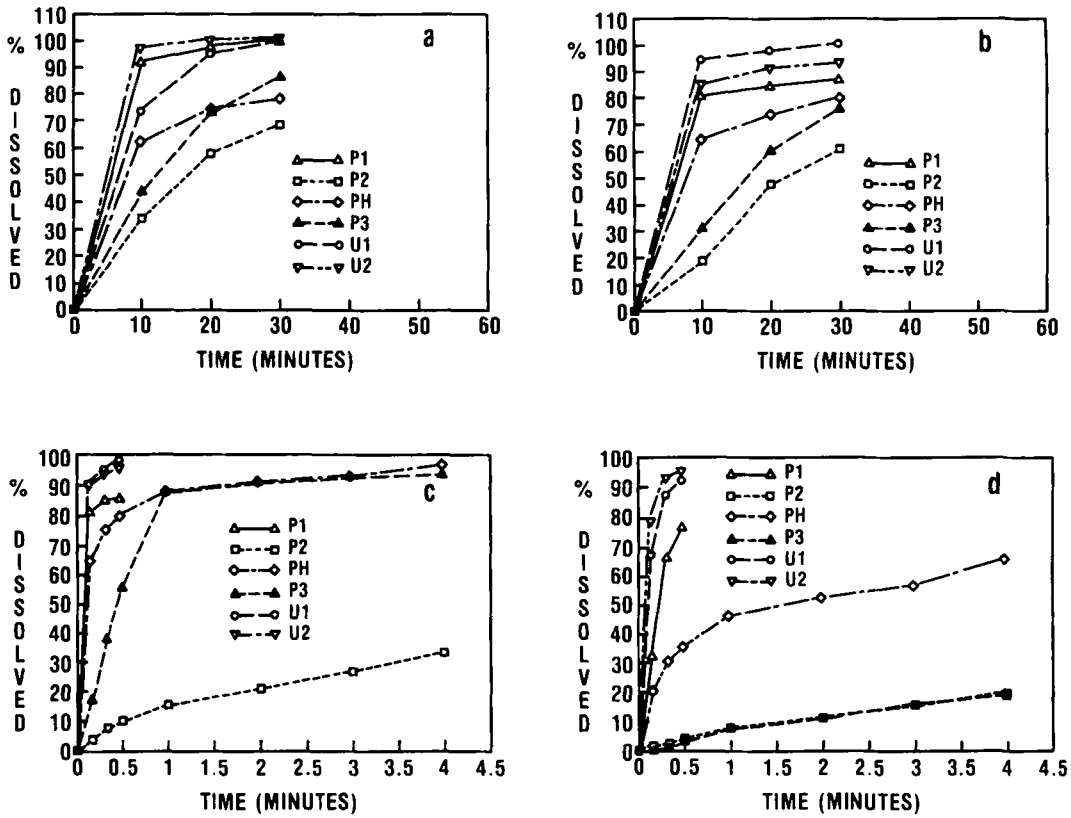

Figure 7—*Effect of 12 weeks of humidity aging on dissolution of P, PH, and U tolbutamide tablets at room humidity and in the closed original container (a), 60% relative humidity (b), 75% relative humidity (c) and 98% relative humidity (d). Key: (△) P1, (□) P2; (◇) PH; (▲) P3; (○) U1; (▽) U2.*

Table I—Time (min) to Reach Compendial Required Dissolution of Labeled Tolbutamide[a]

Product Identification Number[b]	Lot Number	Rotating Basket, 50%[c]	Paddle Stirrer, 70%[d]
U1	495 EP	5.4	7.5
U2	871 FP	5.7	9.9
U3	606 FT	5.6	9.6
U4	461 FU	5.8	7.2
U5	592 FK	5.5	8.2
U6	109 FS	5.5	8.5
U7	740 HR	6.4	8.5
U8	407 HP	6.2	8.4
U9	486 HT	7.6	11.8
U10	926 HY	8.0	7.5
U11	246 JB	7.0	9.4
U12	606 FT	7.3	8.6
U13	461 FU	7.1	8.0
U14	871 FP	7.5	11.6
Mean for U		6.46	8.9
CV, %		14.29	16.06
P1	C80177	6.4	8.0
P2	A80687	5.4	7.2
P3	A80547	15.3	16.3
P4	A80167	20.2	14.8
P5	B80167	14.9	9.5
P6	A90227	6.1	9.6
P7	B90257	7.2	13.9
P8	A80587	23.6	33.5
P9	8111-04	7.8	8.8
P10	B80737	10.3	9.0
P11	A81607	5.9	9.1
P12	B80987	9.4	18.8
P13	810071	10.1	14.9
P14	C81447	5.9	9.2
P15	B80987R	12.4	17.6
P16	810072	6.2	8.8
P17	A80587	26.4	31.9
P17	A80587	54.6	49.7
P18	810073	6.7	13.6
P19	B90367	5.3	7.6
P20	B91517	5.6	9.3
P21	A90737	5.3	7.6
P22	A90787	6.0	8.6
P23	A90757	5.7	8.0
P24	E006D	7.3	13.6
P25	A91157	5.7	8.3
P26	E007D	7.3	10.2
P27	A00258	--	11.6
P28	A00658	—	20.5
Mean Average for P		11.22	14.2
CV, %		92.8	67.35
M1	E011D	5.8	7.6
M2	E010DR	11.6	15.3
M3	E008D	9.8	12.4
M4	G032K	—	12.4
M5	G046D1	—	18.2
M6	E008D	--	17.3
M7	595-215	--	23.8
M8	592-187	—	18.0
M9	607-230	--	9.5
M10	G050D	—	19.3
M11	9M80D	--	7.9
Mean for M		—	14.71
CV, %		—	35.25
PH1	8111-05	7.5	16.2
PH2	8111-06	5.2	8.4
PH3	8111-03	6.0	9.0
Z1	2245-18-1	--	8.3
Z2	2245-18-2	—	8.1
Z3	7181	—	7.2
Z4	2245-03-70	--	7.3
Z5	2245-03-80	—	7.3
S1	BX19409	--	7.3
S2	E060	-	7.7
S3	A29409	—	8.4
S4	A29409	—	8.6
S5	B59409	-	9.6

[a] Estimate based on interpolation between closest time intervals sampled. [b] Product identification: U, Upjohn; P, Premo; M, Mylan; PH, Pharmadyne; Z, Zenith; S, Smith Kline & French. [c] Method requires at least 50% dissolution in 45 min. [d] Method requires at least 70% dissolution in 30 min. Some lots in different-size bottles or received at different times were evaluated twice (U3, U12; U4, U13; U2, U14; M3, M6; S3, S4).

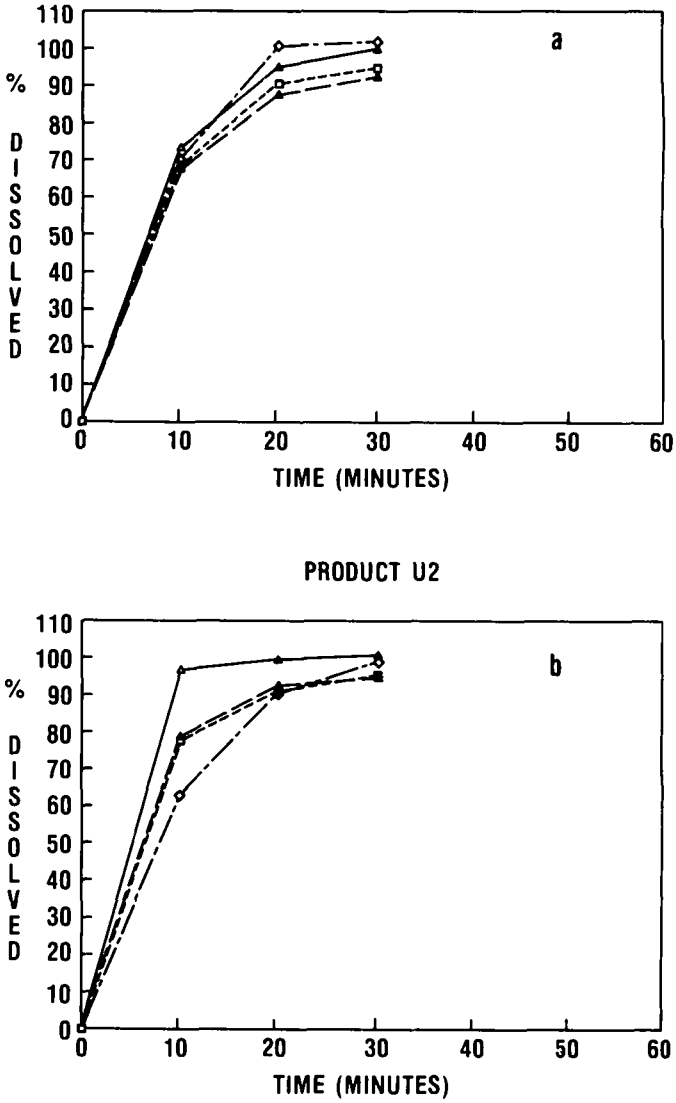

Figure 8—*Effect of aging tolbutamide tablets for various times at 98% relative humidity for two lots (a, b) of U products. Key: (△) fresh; aged (□) 3 weeks, (◇) 6 weeks, (▲) 12 weeks.*

variation in the basket-stirrer tests at each sampling time. This may be because more rapid dissolution occurs with paddle stirring and there is a natural compression of the possible range of percent dissolved drug on the upper end (*i.e.*, 100% is an upper boundary). Thus, one comparative effect is that intralot variation is compressed or more difficult to identify in the paddle-stirring test than in the rotating-basket test.

Khalil *et al.* (8) reported that humidity aging may be used to identify tolbutamide tablets which were not equivalent in their dissolution responses. The effects of humidity aging on tolbutamide lots selected for a paddle-stirrer dissolution study (based on their range of dissolution profiles when fresh) are shown in Fig. 7. Dissolution profiles of U tablets were little affected by aging ≤12 weeks at rh values of 60, 75, or 98%. The other manufacturers' products were not affected by 60% rh, but two lots failed the dissolution test after 75% and three lots failed after 98% rh. Lots P2 and P3 failed to pass the test even after 18 h of dissolution following 12 weeks at 98% rh; these tablets remained intact, or nearly intact.

Figures 8 and 9 show the combined time and rh effects on tablet dissolution. The U products were only slightly affected for all times at 98% rh (Fig. 8b). Lesser effects occurred with 60 and 75% rh. For P and PH products, 98% rh aging variously affected dissolution depending on the lot (Figs. 9). Both 60 and 75% rh affected lot P2 but not lot P1 tablets (Figs. 10). The reason for this lot-specific variable response is unknown. The *CV* for percent tolbutamide dissolved at all rh values is low when the percent of labeled drug dissolved is high (>90%) and sometimes when the percent is low (<10%). Products that are dissolved 20–80% at any given sampling time show differences in both intralot and interlot variation among manufacturers; the same is seen with unaged tablets. Thus, since the innovator's products (U) dissolve quickly

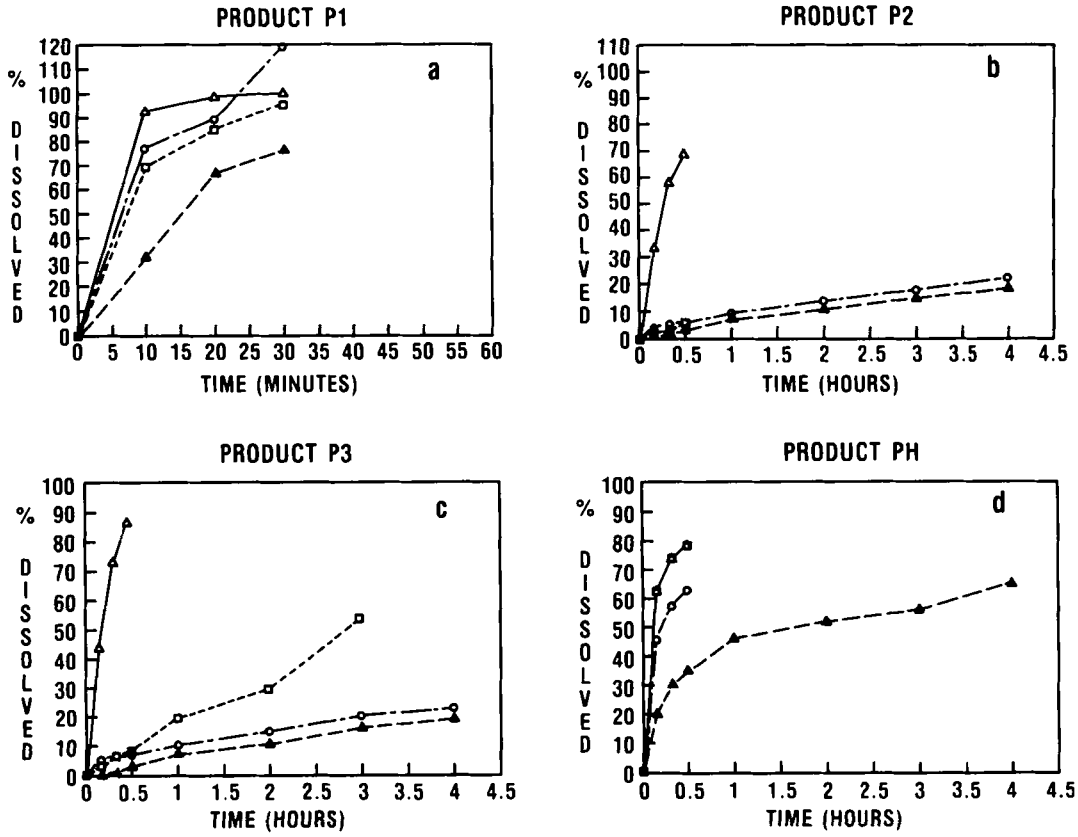

Figure 9—*Effect of aging tolbutamide tablets for various times at 98% relative humidity for P and PH products. P1 (a), P2 (b), and P3 (d) are different lots of P. For PH (d), fresh tablets and tablets aged for 3 weeks aging gave nearly identical values. Key: (△) fresh; aged (□) 3 weeks, (○) 6 weeks, (▲) 12 weeks.*

(>95% after 30 min for fresh and humidity-aged tablets), the dissolution *CV* for U products was generally much lower than for the generic products which dissolved more slowly (for fresh tablets and humidity-aged tablets).

The finding that tolbutamide tablets from different manufacturers and different lots from the same manufacturer did not dissolve equivalently after as little as 3 weeks of aging at different rh values prompted investigation of the effects of shorter exposure. There was no effect on product U (Fig. 11).

Dissolution of P products continued to be variable and effects ranged from marked depression of dissolution (after only 24 h exposure to 98% rh) to virtually no effect, depending on the lot tested. The effects of humidity were lot specific for M (Fig. 12), dramatically depressing dissolution for one lot but not the other. No effect was observed for S products and both lots of Z products were depressed.

One product, reported to fail the USP dissolution test (7), has been evalu-

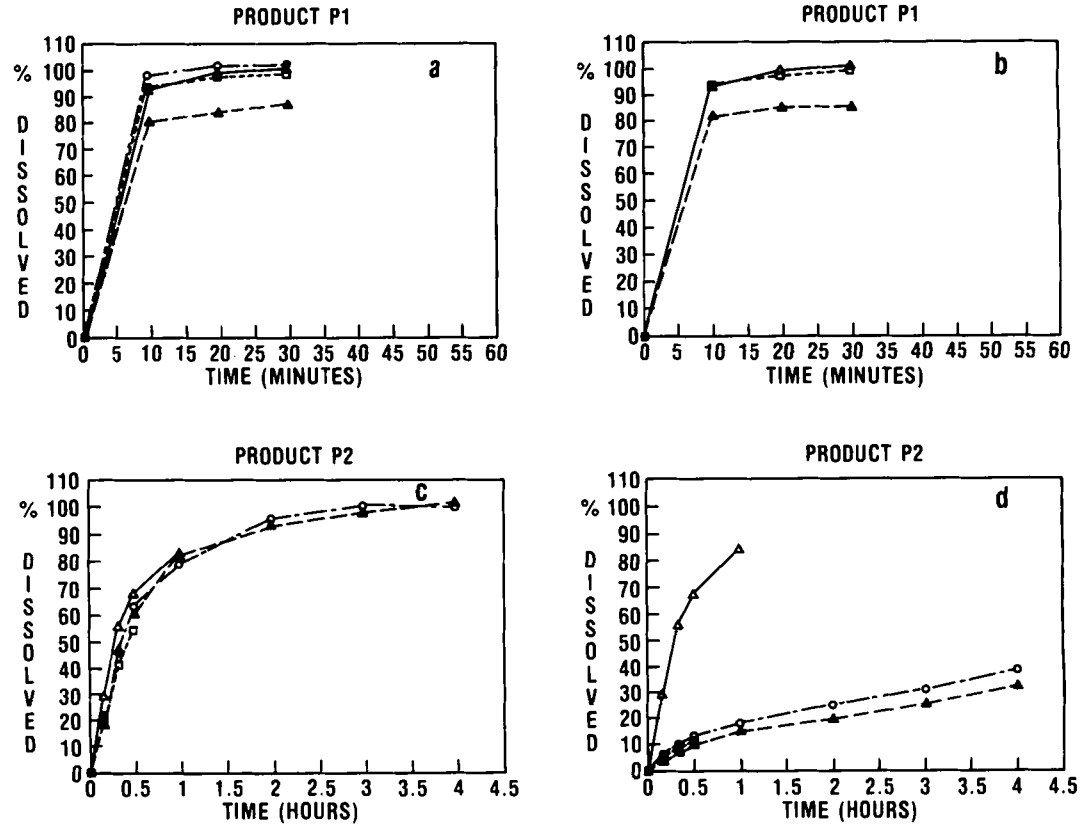

Figure 10—*Dissolution response of two lots of generic product P to 60% (a and c) and 75% (b and d) relative humidity aging for different time periods. Key: see Fig. 9.*

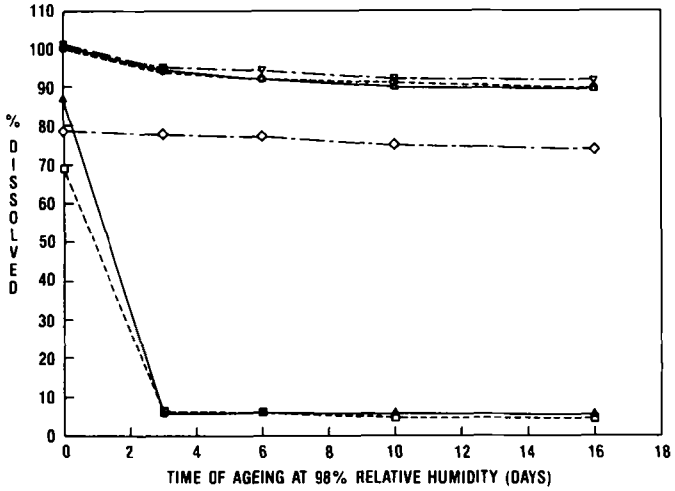

Figure 11—*Effect of short time aging on paddle-stirred dissolved drug at 30 min of different lots of U, P, and PH tolbutamide at 98% relative humidity. Key: (△) P1; (□) P2; (▲) P3; (◇) PH; (○) U1; (▽) U2.*

ated in 4 human subjects (13). The cause of the large *in vivo* variability in such a small study can not be precisely assigned. It may be due to product formulation and variable dissolution or subject variation. The variation observed *in vivo*, although larger for product P than U, was less than one might expect based on the USP dissolution test. That may be because the test does not simulate the normal exposure of tablets to the gastric acid of the stomach followed by exposure to intestinal fluid. Tuttle *et al.* (9) have reported that some tolbutamide tablets require exposure to an acidic environment in order to disintegrate and dissolve. It was proposed that these tablets contain inert formulation ingredients which are pH sensitive. Therefore, some tablets were pretreated in 0.1 M HCl for 30 min and then allowed to dissolve in pH 7.4 phosphate buffer using the USP paddle-stirrer test described in the *Experimental Section.*

Acid pretreatment produced a dramatic effect on dissolution time of P, but

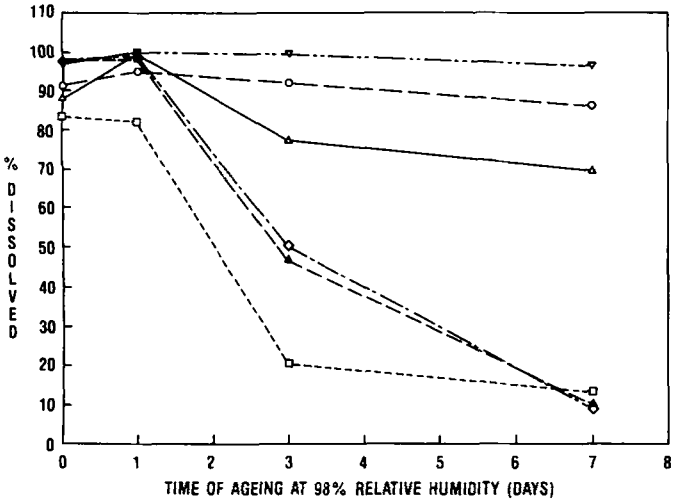

Figure 12—*Variation in paddle-stirred dissolved drug at 30 min of M, S, and Z after short-time aging at 98% relative humidity. Key: (△) M1; (□) M2; (◇) Z1; (▲) Z2; (○) S1; (▽) S2.*

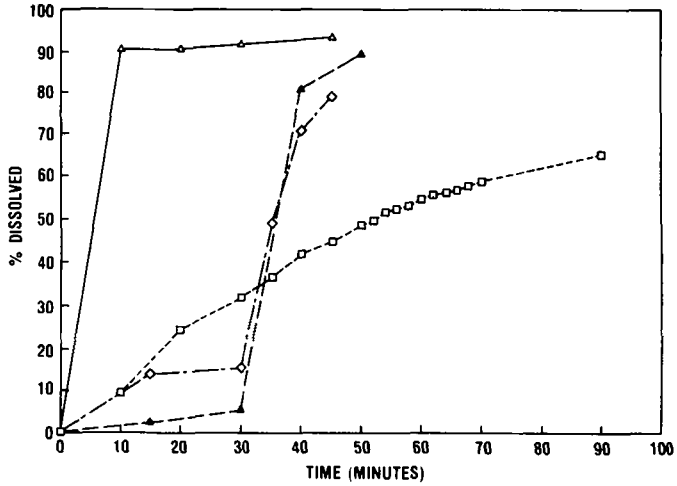

Figure 13—*Effect of pretreatment with simulated gastric fluid on U and P tolbutamide tablet products. The "no pretreatment" dissolution [(△)U; (□)P] was in phosphate buffer (pH 7.4) from time zero. The "acid pretreatment" dissolution [(◇)U; (▲)P] was in acid from time zero to 30 min and then in phosphate buffer from time 30 min to the last data point.*

had practically no effect on U (Fig. 13). That is, after acid pretreatment, both P and U dissolved at about the same rate as U without acid pretreatment. This dependence of the generic product on acid pretreatment may be undesirable (9).

Prolonged contact of tolbutamide with the GI tract, due to poor dissolution, may cause nausea, vomiting, or cramps (14). Constant patient monitoring appears prudent when products with highly variable interlot and intralot rates of dissolution are employed.

REFERENCES

(1) "U.S. Pharmacopeia," 20th rev., U.S. Pharmacopeial Convention, Rockville, Md., 1980, pp. 805 and 1031.

(2) W. A. Hanson, "Handbook of Dissolution Testing," Pharmaceutical Technology Publications, Springfield, Oregon, 1982.

(3) "Approved Prescription Drug Products with Therapeutic Equivalence Evaluations," 3rd ed., U.S. Department of Health and Human Services, Public Health Service, Food and Drug Administration, Bureau of Drugs, Washington, D.C., 1982, pp. 3-171.

(4) A. K. Carter, *Can. Med. Assoc. J.*, **88,** 98 (1963).

(5) S. Caminetsky, *Can. Med. Assoc. J.*, **88,** 950 (1963).

(6) Gerhard Levy, *Can. Med. Assoc. J.*, **90,** 978 (1964).

(7) J. W. Ayres, *Am. J. Hosp. Pharm.*, **37,** 1329 (1980).

(8) S. A. H. Khalil, L. M. M. Ali, and M. M. Khalek, *Pharmazie*, **29,** 38 (1974).

(9) C. B. Tuttle, M. Mayersohn, and G. C. Walker, *Can. J. Pharm. Sci.*, **8,** 31 (1973).

(10) "U.S. Pharmacopeia," 19th rev., U.S. Pharmacopeial Convention, Rockville, Md., 1975, p. 651.

(11) D. J. Weber, *J. Pharm. Sci.*, **65,** 1502 (1976).

(12) "International Critical Tables," Vol I, McGraw-Hill, New York, N.Y., 1926, p. 67.

(13) "Drug Absorption and Disposition: Statistical Considerations," Kenneth S. Albert, Ed., American Pharmaceutical Association Academy of Pharmaceutical Sciences, 1980, pp. 92-93.

(14) S. Niazi, "Textbook of Biopharmaceutics and Clinical Pharmacodynamics," Appleton-Century-Crofts, New York, N.Y., 1979, p. 13.

Liquid Chromatographic Analysis of Sulfaquinoxaline and Its Application to Pharmacokinetic Studies in Rabbits

J. G. EPPEL and J. J. THIESSEN ˣ

Received September 9, 1983, from the *Faculty of Pharmacy, University of Toronto, Toronto, Canada M5S 1A1.* Accepted for publication February 24, 1984.

Abstract □ A specific, sensitive high-performance liquid chromatographic method is described for sulfaquinoxaline (I) and its major metabolite, the N^4-acetyl metabolite (II), in biological fluids. Detection limits for I and II were 0.25 and 0.50 μg/mL in plasma and 0.10 and 0.20 μg/mL in urine, respectively. The pharmacokinetics of sulfaquinoxaline and its metabolite were studied in New Zealand White rabbits after individual doses of 50 mg/kg of sulfaquinoxaline and its metabolite were administered intravenously. Mean (±*SD*) plasma half-lives were 12.7 (8.0) h for sulfaquinoxaline and 15.4 (3.5) h for the metabolite. After administration of the *N*-acetyl metabolite sulfaquinoxaline appeared in the plasma and urine indicating that deacetylation had occurred. The repercussions of this observation are briefly discussed with respect to two rabbits in which plasma analyses and complete urine collections were made. As sulfaquinoxaline is administered prophylactically to rabbits by some breeders, it is recommended that investigators allow a washout period of about one week after receipt of the animals.

Keyphrases □ Sulfaquinoxaline—HPLC, pharmacokinetics, rabbits □ Pharmacokinetics—sulfaquinoxaline, rabbits, HPLC

Laboratory animal breeders frequently use sulfaquinoxaline (I) on a chronic basis in feed or water to prevent outbreaks of coccidiosis in rabbits. Measurable quantities of sulfaquinoxaline or its metabolite may therefore be present in the blood or tissues of these animals after delivery to the laboratory. This report examines the hitherto unreported pharmacokinetics of the drug and its major metabolite, the N^4-acetyl metabolite (II), in rabbits, to determine the washout period needed to avoid incorrect conclusions from pharmacokinetics or pharmacodynamic studies.

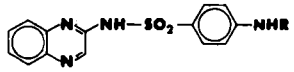

I R·H
II R·COCH$_3$

BACKGROUND

A number of analytical procedures have been used to detect sulfaquinoxaline and related compounds. These include spectrophotometry (1-4), GC (5), TLC and column chromatography (6-10), and high-performance liquid chromatography (HPLC) (11-15). A new HPLC assay has been developed for both sulfaquinoxaline and its major metabolite in order to improve upon the specificity, sensitivity, simplicity, and/or analysis time of available methods, and to explore the pharmacokinetics of the drug and its metabolite in selected species.

Pharmacokinetic studies of sulfaquinoxaline and/or its metabolites have been conducted in a number of species but not, surprisingly, in rabbits. Elimination half-lives for sulfaquinoxaline reportedly range from 6 to 15 h in cattle (16, 17), to ≥1 d in rats (18-20) and dogs (19, 20). This wide range of half-lives obviates a reliable estimate of the washout time required for sulfaquinoxaline or its metabolites in rabbits. This report, therefore, provides information on the pharmacokinetics of sulfaquinoxaline and its N^4-acetyl metabolite in rabbits.

EXPERIMENTAL SECTION

Instrumentation—A high-pressure pump[1], a high-pressure injector[2], a UV detector[3] (252 or 360 nm), and a recorder[4] comprised the chromatographic apparatus. Chromatography was performed on a reverse-phase column[5], using a reverse-phase precolumn[6] to extend column life. The mobile phase, at a flow rate of 1.7 mL/min, consisted of 35 parts methanol[7] and 65 parts 0.2 M KH_2PO_4-Na_2HPO_4 buffer[8] (pH 7). Prior to use, the mobile phase was sonicated for 5 min to remove trapped gas.

Preparation of Standards—An alkaline, aqueous stock solution (pH ~11) was prepared containing 0.2 and 0.4 mg/mL of sulfaquinoxaline[9] and the N^4-acetyl metabolite[9], respectively. Appropriate dilutions with water were prepared to yield standards ranging in concentration from 0.5 to 200 μg/mL for sulfaquinoxaline and 1.0 to 400 μg/mL for the metabolite. At the time of analysis, 50 μL of the standards was added to blank rabbit plasma (100 μL), or 100 μL of the standards was added to blank rabbit urine (500 μL).

Sample Preparation—A fixed plasma volume (100 μL) was used for all samples. Acetone[8] (300 μL) was added slowly, while vortexing, to precipitate proteins. The mixture was centrifuged (1700×*g*) for 4 min, 100 μL of the supernatant was evaporated to dryness at 65°C under a nitrogen stream, and the residue was reconstituted with 200 μL of mobile phase. An appropriate volume (20-100 μL) was injected. Glacial acetic acid-sodium acetate buffer[10] (3 M, pH 6, 500 μL) was added to a fixed volume of urine (500 μL). After mixing, the solution was extracted with methylene chloride[11] (4.0 mL). The organic phase (0.5-1.5 mL) was evaporated to dryness, following which the sample was prepared for chromatography as described above.

Pharmacokinetic Studies in Rabbits—Sulfaquinoxaline or its metabolite (50 mg/kg) was administered as an intravenous bolus dose to male New Zealand White rabbits[12] receiving 150 g of rabbit feed[13] daily and water *ad libitum*. The sulfonamide solution was prepared by dissolving sulfaquinoxaline or its metabolite in a minimum of base and back-titrating with acid to a pH of ~9 and ~10 for the drug or the metabolite, respectively. A portion of the filtered[14] solution was retained for analysis. After dose administration *via* a marginal ear vein, blood was collected from the contralateral vein through a catheter[15]. Harvested plasma from heparinized blood was frozen until analyzed. Complete, quantitative urine collections were accomplished with an indwelling bladder catheter[16] for the first 8 h followed by further recovery from a metabolic cage[17]. The urine samples were carefully mixed, centrifuged, and the supernatant was frozen until analyzed.

Data Analysis—Calibration curves of sulfaquinoxaline or the N^4-acetyl metabolite were based upon absolute peak heights obtained from a fixed HPLC injection volume. Unknown concentrations were obtained by interpolation from these linearized curves. Pharmacokinetic parameters were computed by standard methods (21). Data were analyzed[18] with a nonlinear regression program developed by D'Argenio and Schumitsky (22). The weighting factor throughout was the inverse-square of the observed data. The required number of exponentials was established by the method of Boxenbaum *et al.* (23).

RESULTS AND DISCUSSION

Development of Assay—Figure 1 illustrates chromatograms of sulfaquinoxaline and its metabolite obtained after processing rabbit plasma and urine samples. The drug and its metabolite eluted in a reasonable period of time, were well resolved, and well separated from materials inherently present in biological fluids. A number of compounds, including nine other sulfonamides,

[1] Model 100A; Altex.
[2] Universal Inlet HPLC valve; Valco.
[3] Waters Associates.
[4] Tracor Westronics MT.
[5] Hibar II, C_{18} 10 μm, 250 × 4.6 mm i.d.; E. Merck.
[6] C_{18}, 30-40 μm, 40 × 3.2 mm i.d.; Perisorb.
[7] HPLC grade; Fisher Scientific.
[8] Certified ACS; Fisher Scientific.
[9] Merck Sharp and Dohme.
[10] BDH Analar; J.T. Baker.
[11] Glass distilled; Burdick & Jackson.
[12] Riemans Fur Ranch, Ontario.
[13] Purina.
[14] 0.2 μm, Amicon.
[15] Deseret; Angiocath.
[16] 3mL pediatric; Foley.
[17] Nalgene rabbit cage.
[18] LSI 11/23; Digital Equipment Corp.

0022-3549/84/1100-1635$01.00/0
© 1984, American Pharmaceutical Association

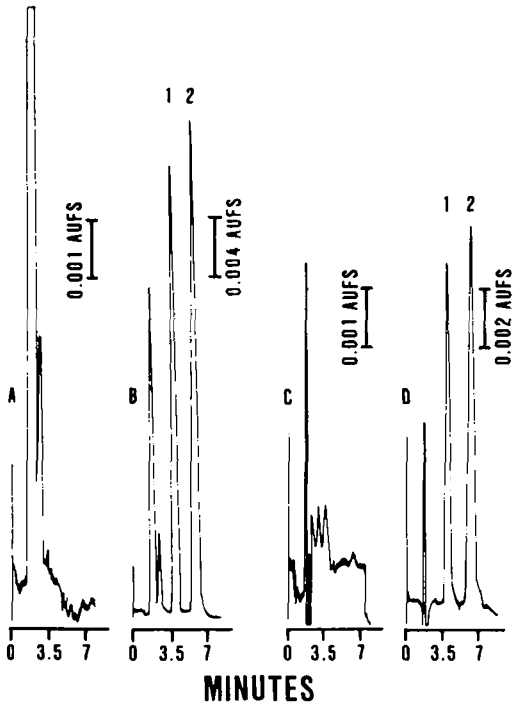

Figure 1—*Chromatograms obtained for sulfaquinoxaline (1) and the* N^4*-acetyl metabolite (2) in rabbit plasma and urine. The mobile phase consisted of 35 parts methanol and 65 parts 0.2 M, pH 7, phosphate buffer flowing at 1.7 mL/min through an* RP_{18} *column (250 × 4.6 mm i.d.). Detection was at 252 nm for plasma and 360 nm for urine. Key: (A) blank rabbit plasma; (B) sulfaquinoxaline (52.25 μg/mL) and the* N^4*-acetyl metabolite (100.5 μg/mL) in blank rabbit plasma; (C) blank rabbit urine; (D) sulfaquinoxaline (39.80 μg/mL) and the* N^4*-acetyl metabolite (83.40 μg/mL) in blank rabbit urine.*

were tested as potential internal standards. Invariably they eluted too quickly or interfered with the quantitation of I and II which exhibited retention times of ~3.6 and 5.5 min, respectively. Since no suitable internal standard was found, a fixed-volume injection method was employed. The absolute limits of detection, expressed as a measurable peak at least three times the baseline noise, were 2.8 and 5.5 ng for I and II, respectively. Using the aforementioned sample preparation methods, the limits became 0.25 and 0.50 μg/mL in plasma and 0.10 and 0.20 μg/mL in urine, respectively.

The composition of the mobile phase was examined and it was found that decreasing the methanol concentration increased the retention times for both compounds. However, the retention time of II increased at a faster rate than I. Buffer strength had little effect on the range from 0.10 to 0.25 M. The pH of the buffer had a pronounced effect on I and II. Increases in pH >4 led to rapid decreases in times, especially for II. The results for sulfaquinoxaline are in keeping with its reported pK_a of ~6 (11, 19). Surprisingly, pH 7 proved to be a good compromise between short times and well-resolved peaks, even though it exceeded the pK_a.

Table I—The Effect of Urine pH Buffered With 3 M Acetate Buffer on the Recovery of Sulfaquinoxaline (I) and the N^4-Acetyl Metabolite (II)

Compound	Buffer-Urine pH	Relative Compound Peak Height[a]	Relative Interference Peak Height[b]
I	4.49	0.91	0.0275
	4.94	0.95	0.0221
	5.42	0.97	0.0176
	5.95	0.89	0.0097
	6.52	0.85	0.0024
II	4.49	0.97	0.0056
	4.94	1.00	0.0069
	5.42	1.00	0.0080
	5.95	0.88	0.0100
	6.52	0.42	0.0123

[a] Ratio of the peak height of the compound, after adjusting for interference peaks, to the height from a standard prepared in water. [b] Ratio of the interference peak height observed in blank urine to the peak height of the compound corrected for the interfering peak; measured at 252 nm.

Table II—Intra-assay Variability in the Analysis of Plasma or Urine Sulfaquinoxaline (I) and the N^4-Acetyl Metabolite (II) Standards[a]

Compound	Conc., μg/mL		CV, %	
	Plasma	Urine	Plasma	Urine
I	0.2662	0.2130	26.04	8.97
	2.662	1.065	2.89	19.04
	26.62	10.65	1.14	1.83
	106.5	42.60	1.35	2.97[b]
II	0.5175	0.4140	20.60	10.48
	5.175	2.070	7.34	7.03
	51.75	20.70	6.85	1.49
	207.0	82.80	1.41	1.36[b]

[a] $n = 5$. [b] $n = 4$.

Acetone, acetonitrile, anhydrous ethanol, methanol, and perchloric acid were examined as plasma protein precipitating agents. Perchloric acid was eliminated because the evaporation step was too time-consuming. Peak heights obtained for the drug and the metabolite after acetone treatment were consistently higher (4–8%) than those seen after treatment with the other agents. Furthermore, acetone provided the finest, most stable precipitate, clearest supernatant after centrifugation, and has been shown to be thorough in removing proteins (24). It was, therefore, the agent of choice.

It was initially anticipated that the plasma assay for sulfaquinoxaline and the N^4-acetyl metabolite could simply be extended to urine analysis. However, it was found that unknown, apparently endogenous components appeared as interfering peaks in the chromatograms. Consequently, various approaches were used with the following observations: (*a*) methylene chloride was chosen as an extracting solvent because solubility tests indicated that the drug and its metabolite were about four times more soluble in this solvent than in acidic water, and this ratio exceeded that observed for ether;. (*b*) because of its high buffering capacity, a strong buffer was needed to acidify the normally alkaline [pH 8–9 (25)] rabbit urine. Phosphate buffer was unsuitable due to solubility problems at concentrations >1 M. Acetate buffer, 3 M, provided the most accurate and predictable buffering of the urine. Table I indicates the degree of recovery of the drug and the metabolite in urine with this buffer; (*c*) a pH of 6 was selected as a compromise between adequate recovery of the sulfonamides and minimal solvent front and interference peak heights. To eliminate the latter, the secondary maximum, 360 nm ($\epsilon = 7.2 \times 10^3$ for the drug and the metabolite), was chosen as the detection wavelength even though 252 nm ($\epsilon = 3.2 \times 10^4$ for the drug and its metabolite), as used for plasma samples, was preferred.

Calibration curves were highly linear ($r > 0.99$) over the concentration ranges in plasma and urine of 0.25–200 μg/mL and 0.10–40 μg/mL, respectively, for sulfaquinoxaline and 0.50–400 μg/mL and 0.20–80 μg/mL, respectively, for the N^4-acetyl metabolite. Intra-assay variability is summarized in Table II and, except for the lowest concentrations, was <10%. Interassay analysis of the calibration curves in plasma provided mean (±*SD*) slopes and intercepts of 0.395 (0.166) and 0.00405 (0.0236), respectively, for sulfaquinoxaline ($n = 9$) and 0.348 (0.0261) and −0.00385 (0.0138), respectively, for the N^4-acetyl metabolite ($n = 4$). Such variability, when based on peak-height analysis without an internal standard, reflects changes in column characteristics. However, this presents no difficulty if calibration curves are generated with each set of samples. As only two calibration curves were prepared for urine samples, interassay results are not available.

Of the reported HPLC assays for sulfaquinoxaline (11–15), none describes the simultaneous measurement of the drug and its N^4-acetyl metabolite. Only one of these assays (14) has been developed to measure sulfaquinoxaline in plasma or tissues, and it employs inconvenient extraction methods and yields

Table III—Mean (±*SD*) Pharmacokinetic Parameters Obtained From Plasma Analysis of Sulfaquinoxaline (I) and the N^4-Acetyl Metabolite (II) After Single Intravenous Doses of I and II, Respectively

Variable	I	II
n	11	4
Dose, mg/kg	49.64 (0.76)	49.94 (1.29)
AUC, μg·h/mL[a]	836.1 (363.6) 737.3 (166.6)[b]	2769.9 (326.6)
TBC, (mL/h/kg)[c]	66.47 (19.75) 70.36 (15.78)[b]	18.18 (1.82)
V_1, mL/kg[d]	210.7 (41.85)	140.2 (59.37)
Terminal Constant, h^{-1}	0.0645 (0.0188)	0.0494 (0.0174)
Terminal Half-Life, h	12.67 (7.99)	15.96 (7.40)

[a] Area under the plasma concentration-time curve from time 0 to infinity. [b] Mean (±*SD*) results excluding Rabbit No. 83 (see text). [c] Total body clearance from plasma. [d] Volume of distribution in the central compartment.

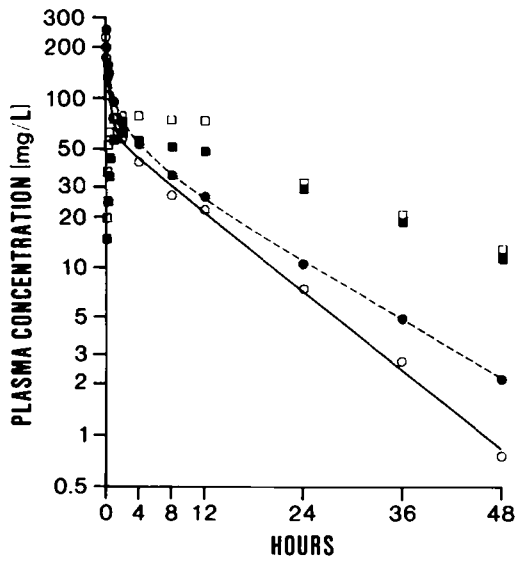

Figure 2—*Plasma sulfaquinoxaline (○) and the* N^4*-acetyl metabolite (□) observed in two rabbits following intravenous sulfaquinoxaline administration. Key: rabbit 143 (○,□) bolus dose was 49.03 mg/kg [(—) indicates the best fit of the data to a biexponential equation]; rabbit 150 (●,■) bolus dose was 49.51 mg/kg [(- - -) indicates the best fit of the data to a triexponential equation].*

a retention time of 13 min. The new method described herein was simple, reproducible, and had the requisite sensitivity to measure the drug and its metabolite in animal tissues or fluids. Also, interference from potential metabolites was not encountered.

Pharmacokinetic Studies in Rabbits—The intravenous administration of I to rabbits provided multiexponential profiles for the drug and the metabolite in plasma. Table III includes the mean (±*SD*) pharmacokinetic parameters for the drug obtained after fitting the data to bi- or triexponential equations. Seven rabbits required three exponentials while four required only two exponentials. Plasma profiles for two of the rabbits are shown in Fig. 2.

One rabbit (No. 83) displayed a total body clearance for the drug that was one-third as great as the mean clearance observed for the remainder of the rabbits. Plasma levels of the drug in this animal were elevated, while plasma levels of the metabolite were reduced. Also, the terminal phase of the metabolite profile was parallel to that of the parent drug. All of the other rabbits displayed nonparallel terminal phases with a mean (±*SD*) metabolite half-life of 15.4 (3.5) h. The data would suggest that rabbit 83 is a slow acetylator, although the clearances of the other animals could not be allocated to definable

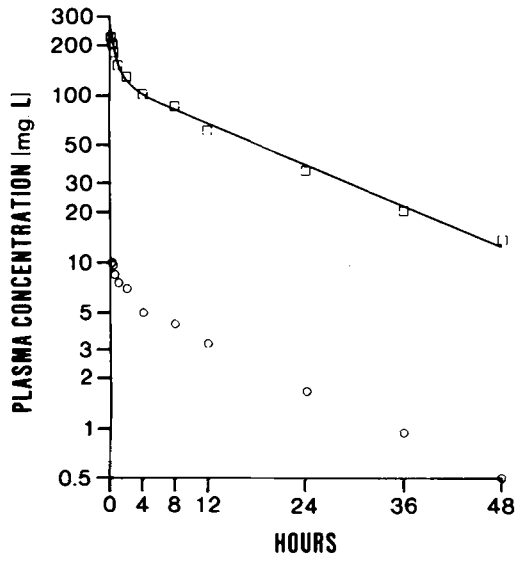

Figure 3—*Plasma sulfaquinoxaline (○) and the* N^4*-acetyl metabolite (□) observed in rabbit 143 after an intravenous bolus dose (51.16 mg/kg) of the acetylated compound. The solid line represents the best fit of the data to a biexponential equation.*

Table IV—Urinary Excretion Data Observed in Two Rabbits Given Both Sulfaquinoxaline (I) and Its Metabolite (II) on Separate Occasions

Rabbit	Compound Administered	Dose, mg/kg	Amount Excreted, mg/kg[a]		Renal Clearance, mL/h/kg[b]	
			I	II	I	II
179	I	48.96	3.172	13.36	5.978	8.054
	II	49.71	5.343	32.06	61.35	10.85
184	I	49.08	3.035	16.47	5.421	8.477
	II	48.21	3.588	31.83	32.06	13.42

[a] 0-96 h. [b] Amount excreted to 48 h/AUC from 0 to 48 h.

groups. While the phenomenon of fast and slow acetylation has been widely reported and reviewed (26), no known studies have used sulfaquinoxaline as a probe.

Rabbits reportedly lack the ability to deacetylate (27) whereas such metabolism has been observed in other species (27–30). The N^4-acetyl metabolite was, therefore, administered intravenously to 4 rabbits. Unexpectedly, a plasma chromatographic peak was observed with a retention time corresponding to sulfaquinoxaline. Initially it was felt that the presence of sulfaquinoxaline reflected contamination of the metabolite dose by the drug. However, HPLC analysis of the filtered metabolite solution administered to the rabbits confirmed the absence of the drug. Figure 3 illustrates the profiles observed in one of the experiments. Table III also includes the mean (±*SD*) pharmacokinetic parameters obtained for the metabolite after its administration to four rabbits. The mean terminal half-life of the metabolite in these experiments agrees well with that observed after sulfaquinoxaline administration. Two animals (Nos. 179 and 184) were studied in greater detail by monitoring both plasma and urine for 96 h after administering the drug and the metabolite on different occasions, two weeks apart. The results in Table IV indicate a sizeable urinary excretion of the drug following administration of the metabolite. The results also demonstrate that urinary recovery of the drug and the metabolite do not account for either administered dose. Perhaps the sulfonamides undergo partial elimination *via* the feces (18) and/or alternate routes of metabolism (17, 19, 31). Finally, the renal clearances of sulfaquinoxaline are notably different when sulfaquinoxaline or the N^4-acetyl metabolite are administered. This anomaly remains to be explored.

From the total body clearance of rabbits 179 and 184 (90.52 and 86.17 mL/h/kg, respectively), one might surmise that the rabbits disposed of the drug in an identical manner and that they might even be identical genetic acetylators. Analysis of the plasma data from these rabbits according to the technique proposed by Wagner *et al.* (32) for prednisone-prednisolone interconversion *in vivo*, provided intriguing results. The method, which permits a calculation of each clearance in the interconversion, pointed to a 40% greater acetylation clearance in rabbit 184 accompanied by a 32% greater deacetylation clearance. The obvious effect of these parallel differences would to be provide an identical total body clearance of the drug in the two rabbits. This preliminary observation has important implications in defining the genetic acetylation characteristics of humans and animals.

The primary purpose in developing an HPLC assay for sulfaquinoxaline and the N^4-acetyl metabolite was to monitor their presence in purchased rabbits. The relatively high single dose of the drug administered in this study required ~4 d to reach plasma levels of the drug and the metabolite, <0.25 and 0.50 μg/mL, respectively. Even though animal breeders undoubtedly use lower chronic daily doses for prophylactic treatment, it would seem prudent for investigators to avoid using rabbits for 1 week after receipt from a supplier.

REFERENCES

(1) S. W. Tyler, R. O. Brooke, and W. S. Baker, *Anal. Chem.*, **21**, 1091 (1949).

(2) J. P. Dux and C. Rosenblum, *Anal. Chem.*, **21**, 1524 (1949).

(3) F. Tishler and J. L. Suttler, *J. Agri. Food Chem.*, **16**, 50 (1968).

(4) C. R. Szalkowski, *J. Assn. Off. Anal. Chem.*, **56**, 758 (1973).

(5) S. Crisp, *Analyst*, **96**, 671 (1971).

(6) L. Lepri, P. G. Desideri, and D. Heimler, *J. Chromatogr.*, **169**, 271 (1979).

(7) S. Klein and B. T. Kho, *J. Pharm. Sci.*, **51**, 966 (1962).

(8) L. R. Alexander and E. R. Stanley, *J. Assn. Off. Anal. Chem.*, **48**, 278 (1965).

(9) J. J. Antkowiak and A. L. Spatorico, *J. Chromatogr.*, **29**, 277 (1967).

(10) P. W. Hammond and R. E. Weston, *Analyst*, **94**, 921 (1969).

(11) S. C. Su, A. V. Hartkope, and B. L. Karger, *J. Chromatogr.*, **119**, 523 (1976).

(12) P. H. Cobb and G. T. Hill, *J. Chromatogr.*, **123**, 444 (1976).
(13) G. B. Cox and K. Sugden, *Analyst*, **102**, 29 (1977).
(14) T. Sakano, S. Masuda, and T. Amano, *Chem. Pharm. Bull.*, **29**, 2290 (1981).
(15) W. A. Trujkillo, *J. Liq. Chromatogr.*, **3**, 1219 (1980).
(16) L. M. Jones and H. A. Smith, *Am. J. Vet. Res.*, **10**, 318 (1949).
(17) C. M. Stowe, D. Pallesen, and W. Hartman, *Am. J. Vet. Res.*, **18**, 511 (1957).
(18) R. H. Silber and I. Clark, *Arch. Biochem.*, **10**, 9 (1946).
(19) A. O. Seeler, C. W. Mushett, O. Graessle, and R. H. Silber, *J. Pharm. Exp. Ther.*, **82**, 357 (1944).
(20) C. W. Mushett and A. O. Seeler, *J. Pharm. Exp. Ther.*, **91**, 84 (1947).
(21) M. Gibaldi and D. Perrier, "Pharmacokinetics," 2nd ed., Dekker, New York, N.Y., 1982.
(22) D. Z. D'Argenio and A. Schumitzky, *Comp. Prog. Biomed.*, **9**, 115 (1979).
(23) H. G. Boxenbaum and S. Riegelman, *J. Pharm. Biopharm.*, **2**, 123 (1974).
(24) J. Blanchard, *J. Chromatogr.*, **226**, 455 (1981).
(25) C. Kozma, W. Macklin, L. M. Cummins, and R. Mauer, in "The Biology of the Laboratory Rabbit," S. H. Weisbroth, R. E. Flatat, and A. L. Kraus, Eds., Academic, New York, N.Y., 1974, p. 63.
(26) P. K. N. Lunde, K. Frislid, and V. Hansteen, *Clin. Pharm.*, **2**, 182 (1977).
(27) W. W. Weber, in "Handbook of Experimental Pharmacology," Vol. 28, part 2, B. B. Brodie and J. R. Gillette, Eds., Springer-Verlag, Berlin, 1971, pp. 547–577.
(28) H. Schroder, *J. Pharm. Pharmacol.*, **25**, 591 (1973).
(29) T. L. Ding, E. T. Lin, and L. Z. Benet, Arzneim.-Forsch., **28**(I), 281 (1978).
(30) G. P. Stec, T. I. Ruo, and J. P. Thenot, *Clin. Pharm. Ther.*, **28**, 659 (1980).
(31) J. V. Scudi, R. H. Silber, *J. Biol. Chem.*, **156**, 343 (1944).
(32) J. G. Wagner, A. R. DiSarto, W. R. Gillespie, and K. S. Albert, *Res. Comm. Chem. Path. Pharmacol.*, **32**, 387 (1981).

ACKNOWLEDGMENTS

Supported in part by the Medical Research Council of Canada. The authors thank Mr. G. Kieltyka, Mrs. B. Cory, and Mrs. S. Selliah for their technical assistance.

Preparation of 7,8-Dimethoxy-3,4-dihydroisoquinoline, Facile Route to 7,8-Dioxygenated-3,4-dihydroisoquinolines

A. M. EL-FISHAWY, D. J. SLATKIN, J. E. KNAPP, and P. L. SCHIFF, JR. ˣ

Received January 17, 1983, from the *Department of Pharmacognosy, School of Pharmacy, University of Pittsburgh, Pittsburgh, PA 15261.* Accepted for publication October 17, 1983.

Abstract □ Oxidation of 7,8-dimethoxy-1,2,3,4-tetrahydroisoquinoline with potassium permanganate in acetone afforded 7,8-dimethoxy-3,4-dihydroisoquinoline as the primary product. Hence, oxidation of the appropriate secondary nonphenolic 7,8-dioxygenated tetrahydroisoquinoline alkaloid is thus a facile method for the generation of the corresponding imine. The imine is not easily prepared *via* the usual synthetic route involving ring closure of β-phenethylamine derivatives.

Keyphrases □ 7,8-Dimethoxy-1,2,3,4-tetrahydroisoquinoline—oxidation with potassium permanganate □ 7,8-Dimethoxy-3,4-dihydroisoquinoline—synthesis, secondary amine, oxidation with potassium permanganate □ 7,8-Dioxygenated-3,4-dihydroisoquinoline—secondary amine, oxidation with potassium permanganate

As a continuation of our studies of the alkaloids of *Tiliacora dinklagei* and of the synthesis of various 7,8-dioxygenated-1,2,3,4-tetrahydroisoquinolines (1), it was considered appropriate to attempt to prepare the isoquinolone analogues of these bases. Thirteen simple isoquinolones have been isolated from higher plants to date with most of these alkaloids possessing 6,7-dioxygenation while a few possess 5,6,7-trioxygenation (2). Although no examples of naturally occurring 7,8-dioxygenated isoquinolone alkaloids could be found in the literature, it was felt that preparation of these bases from their isoquinoline counterparts would provide a ready source of physicochemical and spectral data in anticipation of the possible ultimate isolation of these isoquinolones from natural sources.

Isoquinolones are known to arise in nature *via* the oxidation of benzylisoquinolines or from the *in vivo* oxidation of protoberberines, phthalideisoquinolines, or spirobenzylisoquinolines (2). The use of potassium permanganate as an oxidizing agent in the conversion of isoquinoline-derived alkaloids to isoquinolones is well documented (3–5) and it was thus felt that a facile method for the preparation of 7,8-dimethoxyisoquinolone (1-oxo-7,8-dimethoxy-1,2,3,4-tetrahydroisoquinoline) (I) would be the analogous oxidation of 7,8-dimethoxy-1,2,3,4-tetrahydroisoquinoline (II) with potassium permanganate. In fact, oxidation of isoquinoline II with potassium permanganate in acetone afforded, instead, the imine, 7,8-dimethoxy-3,4-dihydroisoquinoline (III) [as characterized by its physicochemical properties, preparation of the methiodide (IV), and sodium borohydride reduction back to II]. This oxidation was repeated on two additional occasions with the same imine being produced in each case. Although 6,7-dioxygenated imines of this series are easily prepared *via* formylation of the parent β-phenethylamine followed by ring closure (6, 7), this same simple procedure is not possible for the 7,8-dioxygenated series since ring closure always proceeds in a less hindered fashion to afford the 6,7-analogues (6). Hence, oxidation of the appropriate secondary nonphenolic 7,8-dioxygenated alkaloids (7,8-dimethoxy or 7,8-methylenedioxy) with potassium permanganate should be a facile method for generating the corresponding imines. It can be assumed that preparation of phenolic alkaloids of this series would require protection of the phenolic group, *e.g.*, *via* the benzyl ether, to prevent further oxidation during the reaction. Examples of this include the use of sodium hypochlorite in the oxidation of 6,7-dimethoxy-8-benzyloxy-1,2,3,4-tetrahydroisoquinoline to the corresponding imine (8) and mercuric acetate in the oxidation of 2-methyl-7-methoxy-8-benzyloxy-1,2,3,4-tetrahydroisoquinoline to its corresponding quaternary imine (9).

EXPERIMENTAL SECTION[1]

7,8-Dimethoxy-3,4-dihydroisoquinoline (III)—To a stirred solution of 7,8-dimethoxy-1,2,3,4-tetrahydroisoquinoline (II) (145 mg) (1) in acetone (40 mL) was slowly added a solution of potassium permanganate (5%) (10 mL) over a period of 1 h. The reaction was stirred for an additional 48 h after which time TLC [silica gel G; benzene–acetone–methanol–ammonium hydroxide (16:16:4:1)] indicated that all of the starting material II (R_f 0.37) had been oxidized to a second product (R_f 0.63) with no other spots appearing on the chromatogram. Other solvent systems used indicated the same results [chloroform–ethyl acetate–methanol–ammonium hydroxide (20:20:4:0.5)—starting material R_f 0.38 and oxidized product R_f 0.83; chloroform–methanol–ammonium hydroxide (90:10:1)—starting material R_f 0.64 and oxidized product R_f 0.85]. The resulting suspension was filtered and the residue of manganese dioxide washed with hot acetone (20 mL) (4×). The filtrate and washings were combined and evaporated to afford 7,8-dimethoxy-3,4-dihydroisoquinoline (III) as a pale-yellow residue (131 mg; 91% yield). The residue was dissolved in chloroform (2 mL) and passed through a column of silicic acid (10 g). Elution with chloroform (5 mL) followed by chloroform–methanol (95:5) (10 mL) afforded the imine III as the same pale-yellow residue (128 mg) which was crystallized as its methiodide salt. The imine III exhibited the following spectral properties: UV λ_{max} (MeOH) (log ε): 320, (3.34), 262 (3.92), and 227 (4.42) with no bathochromic shift on the addition of 3 drops of 0.1 M methanolic KOH; λ_{max} (MeOH–0.1 M HCl) (log ε): 375 (3.41), 297 (4.04), 237 (sh) (4.10), and 218 (sh) (4.17); IR ν_{max} (KBr): 1625, 1580, 1490, 1455, 1420, 1345, 1295, 1270, 1240, 1085, 1060, 1007, 985, 855, 810, 775, and 750 cm^{-1}; ^{1}H-NMR ($CDCl_3$): δ 2.64 (2 closely overlapping triplets, 4, J = 8 Hz, C-3 and C-4), 3.89 (s, 3, C-7 $ArOCH_3$), 3.93 (s, 3, C-8 $ArOCH_3$), 6.90 (s, 2, C-5 and C-6 ArH), and 8.7

[1] Melting points were determined on a Fisher–Johns hot-stage melting point apparatus and are uncorrected. UV absorption spectra were obtained on a Perkin-Elmer Model 552 UV/VIS spectrophotometer. Infrared absorption spectra were taken on a Perkin-Elmer model 267 Grating Infrared Spectrophotometer. ^{1}H-NMR spectra were recorded on a Hitachi Perkin-Elmer Model R-24 High Resolution Spectrometer with deuterochloroform or deuteromethanol as solvent, and with tetramethylsilane as the internal standard; chemical shifts were reported in δ (ppm) units. ^{13}C-NMR spectra were recorded on a JEOL FX-900 high resolution spectrometer with deuterochloroform as solvent. Low resolution mass spectra were taken on a Finnegan EI Mass Spectrometer (Extranuclear Laboratories, Inc., Spectrel). Silica gel G (Camag) was used for TLC and spots were visualized by spraying with $KMnO_4$ (1%) in Na_2CO_3 (1%). Silicic acid (Mallinckrodt) was used for column chromatography.

0022-3549/84/1100-1639$01.00/0
© 1984, American Pharmaceutical Association

ppm (br s, 1, C-1 ArH); ^{13}C-NMR: 24.5 (C-4), 47.4 (C-3), 56.0 (C-7 OCH_3), 61.8 (C-8 OCH_3) 115.0 (C-6), 121.7 (C-8a), 122.4 (C-5), 129.2 (C-4a), 147.2 (C-7), 151.3 (C-8), and 155.8 ppm (C-1) (10-12); MS M^+: *m/z* 191 (83%) (calc. for $C_{11}H_{13}NO_2$, 191.0946; obs., 191.0947), 176 (65), 161 (66), 146 (70), 133 (35), 116 (79), 105 (26), 89 (49), 77 (86), 62 (47) and 51 (100).

7,8-Dimethoxy-3,4-dihydroisoquinoline Methiodide (IV)—To 7,8-dimethoxy-3,4-dihydroisoquinoline (**III**) (100 mg) in acetone (5 mL) was added methyl iodide (0.25 mL), and the resulting solution was allowed to stand overnight. The resulting yellow crystals were removed by filtration, washed with cold acetone, and recrystallized twice from acetone–methanol to afford IV as yellow needles (112 mg), mp 165–166°C; UV λ_{max} (MeOH) (log ϵ): 375 (3.03), 297 (3.77), and 218 (4.06); IR ν_{max} (KBr): 1668, 1582, 1498, 1270, 1254, 1080, 1033, 954, and 820 cm^{-1}; ^{1}H-NMR (CD_3OD): δ 3.39 (2 closely overlapping poorly defined triplets, 4, J = 8 Hz), 3.86 (s, 3, N-2 N^+CH_3), 3.95 (s, 3, C-7 $ArOCH_3$), 4.10 (s, 3, C-8 $ArOCH_3$), 7.15 (d, 1, J = 8 Hz, C-5 ArH), 7.52 (d, J = 8 Hz, C-6 ArH), and 9.27 ppm (br s, 1, C-1 ArH); MS M^+: *m/z* 191 (100%) ($M^+ - CH_3I$), 142 (52), 127 (57), and 77 (23).

7,8-Dimethoxy-1,2,3,4-tetrahydroisoquinoline (**II**)—To 7,8-dimethoxy-3,4-dihydroisoquinoline (III) (60 mg) in methanol (30 mL) was added, with stirring, sodium borohydride (200 mg) over a period of 30 min. The mixture was stirred for an additional 8 h and was then filtered. The filtrate was evaporated to give a residue which was dissolved in HCl (5%) (20 mL), basified with NH_4OH to pH 8–9, and extracted with chloroform (50 mL) (4×). The chloroform extracts were combined, dried (anhydrous sodium sulfate), filtered, and the filtrate was evaporated to afford a residue (50 mg) which was dissolved in methanolic HCl (5%) (4 mL). The solvent was subsequently removed by evaporation and the resulting residue treated with a mixture of acetone–methanol (12:1) (3 mL) to afford yellowish-white crystals of II HCl, mp 189–191°C, identical with authentic 7,8-dimethoxy-1,2,3,4-tetrahydroisoquinoline hydrochloride by direct comparison [mp, UV, IR (1)].

REFERENCES

(1) D. Dwuma-Badu, J. S. K. Ayim, T. T. Dabra, M. M. El-Azizi, P. L. Schiff, Jr., D. J. Slatkin, and J. E. Knapp, *J. Natl. Prod.*, **46**, 342 (1983).

(2) B. D. Krane and M. Shamma, *J. Natl. Prod.*, **45**, 377 (1982).

(3) W.-N. Wu, J. L. Beal, and R. W. Doskotch, *Tetrahedron*, **33**, 2919 (1977).

(4) Z. F. Ismailov and S. Yu Yunusov, *Khim Prir. Soedin.*, **2**, 43 (1966); *Chem. Abstr.*, **65**, 2320 (1966).

(5) N. M. Mollov and H. B. Dutschewska, *Tetrahedron Lett.*, **32**, 2219 (1964).

(6) R. W. Doskotch, P. L. Schiff, Jr., and J. L. Beal, *Tetrahedron*, **25**, 469 (1969).

(7) M. Shamma, "The Isoquinoline Alkaloids," Academic, New York, N.Y., 1972, p. 7.

(8) A. Brossi, F. Schenker, and W. Leimgruber, *Helv. Chim. Acta*, **47**, 2089 (1964).

(9) G. Grethe, M. Uskokovic, and A. Brossi, *J. Org. Chem.*, **33**, 2500 (1968).

(10) M. Shamma and D. H. Hindenlang, "Carbon-13 NMR Shift Assignments of Amines and Alkaloids," Plenum, New York, N.Y., 1979, pp. 114 and 115.

(11) D. P. Burum and R. R. Ernst, *J. Mag. Res.*, **39**, 163 (1980).

(12) D. M. Doddrell and D. T. Pegg, *J. Am. Chem. Soc.*, **102**, 6388 (1980).

ACKNOWLEDGMENTS

The authors are grateful to Mr. Joseph Bender, School of Pharmacy, University of Pittsburgh for determining the low-resolution mass spectra and to Dr. Alvin Marcus, Department of Chemistry, University of Pittsburgh for determining the high-resolution mass spectrum.

Determination of Heparin Activity by a New Laser Nephelometric Method and Comparison to the USP Method

A. ESCOBAR *x, R. T. MAHER, M. L. COURTNEY ‡, and A. J. VALICENTI

Received March 22, 1982, from the *Travenol Laboratories, Inc., Morton Grove, IL 60053.* Accepted for publication October 21, 1982. Present addresses: *Arner-Stone Labs, Aquadilla, Puerto Rico 00604 and ‡Oregon State University, Corvallis, OR 97333.

Abstract □ A new method for the determination of heparin activity in solutions has been developed, based on the increase in light scattering observed during the clotting of plasma. The recalcification clotting time (RCT) of sheep plasma is measured in the presence of heparin, using a laser nephelometer. The activity of heparin in the sample is determined from a standard curve of the logarithm of RCT *versus* heparin activity. The results indicate that this method is simpler, faster, and more reproducible than the current USP grading method.

Keyphrases □ Heparin—activity, laser nephelometry method, comparison to USP method, recalcification clotting time □ Laser nephelometry—heparin activity, comparison to USP method, recalcification clotting time □ Recalcification clotting time—heparin activity, laser-nephelometry, comparison to USP method

Heparin is an anticoagulant widely used in the treatment of myocardial infarction and thromboembolic disease (1). The anticoagulant effect of the drug cannot be predicted by chemical analysis because it has not been related to any specific functional group or to molecular weight (2). Therefore, the activity of heparin, rather than its concentration, must be measured.

Evaluation of the anticoagulant activity of heparin is based on the ability of the drug to prolong the clotting of recalcified sheep plasma (*i.e.*, sheep plasma to which calcium ions are added to promote coagulation). This ability can be measured instrumentally and visually. Reed *et al.* (3) developed an instrumental method based on measurement of the time needed for a sample of recalcified sheep plasma to reach a pre-established viscosity, *i.e.*, a predetermined degree of clotting. This time is then related to the times needed for a set of standards to reach the same viscosity. The USP method, which does not use instruments, is based on the visual evaluation of the degree of clotting of samples as compared with that of a set of standards.

This work describes the development of a nephelometric method to determine heparin activity and compares this method with the USP procedure. Woziwodzki (4) used nephelometric techniques to study the clotting of plasma. More recently Tanaka (5) used laser nephelometric techniques to study the structure of polyacrylamide gels. Because a clot is essentially a gel composed of a fibrin polymer (1), it was postulated that a laser nephelometer could be used to measure the clotting time.

EXPERIMENTAL SECTION

Apparatus and Reagents—The cuvette compartment of a laser nephelometer[1] was modified to allow external circulation of water, thus maintaining

[1] Hyland PDQ Laser Nephelometer, Northbrook, Ill.

0022-3549/84/1100-1640$01.00/0

© 1984, American Pharmaceutical Association

ppm (br s, 1, C-1 ArH); ^{13}C-NMR: 24.5 (C-4), 47.4 (C-3), 56.0 (C-7 OCH_3), 61.8 (C-8 OCH_3) 115.0 (C-6), 121.7 (C-8a), 122.4 (C-5), 129.2 (C-4a), 147.2 (C-7), 151.3 (C-8), and 155.8 ppm (C-1) (10-12); MS M^+: *m/z* 191 (83%) (calc. for $C_{11}H_{13}NO_2$, 191.0946; obs., 191.0947), 176 (65), 161 (66), 146 (70), 133 (35), 116 (79), 105 (26), 89 (49), 77 (86), 62 (47) and 51 (100).

7,8-Dimethoxy-3,4-dihydroisoquinoline Methiodide (IV)—To 7,8-dimethoxy-3,4-dihydroisoquinoline (**III**) (100 mg) in acetone (5 mL) was added methyl iodide (0.25 mL), and the resulting solution was allowed to stand overnight. The resulting yellow crystals were removed by filtration, washed with cold acetone, and recrystallized twice from acetone–methanol to afford IV as yellow needles (112 mg), mp 165–166°C; UV λ_{max} (MeOH) (log ϵ): 375 (3.03), 297 (3.77), and 218 (4.06); IR ν_{max} (KBr): 1668, 1582, 1498, 1270, 1254, 1080, 1033, 954, and 820 cm^{-1}; ^{1}H-NMR (CD_3OD): δ 3.39 (2 closely overlapping poorly defined triplets, 4, J = 8 Hz), 3.86 (s, 3, N-2 N^+CH_3), 3.95 (s, 3, C-7 $ArOCH_3$), 4.10 (s, 3, C-8 $ArOCH_3$), 7.15 (d, 1, J = 8 Hz, C-5 ArH), 7.52 (d, J = 8 Hz, C-6 ArH), and 9.27 ppm (br s, 1, C-1 ArH); MS M^+: *m/z* 191 (100%) ($M^+ - CH_3I$), 142 (52), 127 (57), and 77 (23).

7,8-Dimethoxy-1,2,3,4-tetrahydroisoquinoline (**II**)—To 7,8-dimethoxy-3,4-dihydroisoquinoline (III) (60 mg) in methanol (30 mL) was added, with stirring, sodium borohydride (200 mg) over a period of 30 min. The mixture was stirred for an additional 8 h and was then filtered. The filtrate was evaporated to give a residue which was dissolved in HCl (5%) (20 mL), basified with NH_4OH to pH 8–9, and extracted with chloroform (50 mL) (4×). The chloroform extracts were combined, dried (anhydrous sodium sulfate), filtered, and the filtrate was evaporated to afford a residue (50 mg) which was dissolved in methanolic HCl (5%) (4 mL). The solvent was subsequently removed by evaporation and the resulting residue treated with a mixture of acetone–methanol (12:1) (3 mL) to afford yellowish-white crystals of II HCl, mp 189–191°C, identical with authentic 7,8-dimethoxy-1,2,3,4-tetrahydroisoquinoline hydrochloride by direct comparison [mp, UV, IR (1)].

REFERENCES

(1) D. Dwuma-Badu, J. S. K. Ayim, T. T. Dabra, M. M. El-Azizi, P. L. Schiff, Jr., D. J. Slatkin, and J. E. Knapp, *J. Natl. Prod.*, **46**, 342 (1983).

(2) B. D. Krane and M. Shamma, *J. Natl. Prod.*, **45**, 377 (1982).

(3) W.-N. Wu, J. L. Beal, and R. W. Doskotch, *Tetrahedron*, **33**, 2919 (1977).

(4) Z. F. Ismailov and S. Yu Yunusov, *Khim Prir. Soedin.*, **2**, 43 (1966); *Chem. Abstr.*, **65**, 2320 (1966).

(5) N. M. Mollov and H. B. Dutschewska, *Tetrahedron Lett.*, **32**, 2219 (1964).

(6) R. W. Doskotch, P. L. Schiff, Jr., and J. L. Beal, *Tetrahedron*, **25**, 469 (1969).

(7) M. Shamma, "The Isoquinoline Alkaloids," Academic, New York, N.Y., 1972, p. 7.

(8) A. Brossi, F. Schenker, and W. Leimgruber, *Helv. Chim. Acta*, **47**, 2089 (1964).

(9) G. Grethe, M. Uskokovic, and A. Brossi, *J. Org. Chem.*, **33**, 2500 (1968).

(10) M. Shamma and D. H. Hindenlang, "Carbon-13 NMR Shift Assignments of Amines and Alkaloids," Plenum, New York, N.Y., 1979, pp. 114 and 115.

(11) D. P. Burum and R. R. Ernst, *J. Mag. Res.*, **39**, 163 (1980).

(12) D. M. Doddrell and D. T. Pegg, *J. Am. Chem. Soc.*, **102**, 6388 (1980).

ACKNOWLEDGMENTS

The authors are grateful to Mr. Joseph Bender, School of Pharmacy, University of Pittsburgh for determining the low-resolution mass spectra and to Dr. Alvin Marcus, Department of Chemistry, University of Pittsburgh for determining the high-resolution mass spectrum.

Determination of Heparin Activity by a New Laser Nephelometric Method and Comparison to the USP Method

A. ESCOBAR *x, R. T. MAHER, M. L. COURTNEY ‡, and A. J. VALICENTI

Received March 22, 1982, from the *Travenol Laboratories, Inc., Morton Grove, IL 60053.* Accepted for publication October 21, 1982. Present addresses: *Arner-Stone Labs, Aquadilla, Puerto Rico 00604 and ‡Oregon State University, Corvallis, OR 97333.

Abstract □ A new method for the determination of heparin activity in solutions has been developed, based on the increase in light scattering observed during the clotting of plasma. The recalcification clotting time (RCT) of sheep plasma is measured in the presence of heparin, using a laser nephelometer. The activity of heparin in the sample is determined from a standard curve of the logarithm of RCT *versus* heparin activity. The results indicate that this method is simpler, faster, and more reproducible than the current USP grading method.

Keyphrases □ Heparin—activity, laser nephelometry method, comparison to USP method, recalcification clotting time □ Laser nephelometry—heparin activity, comparison to USP method, recalcification clotting time □ Recalcification clotting time—heparin activity, laser-nephelometry, comparison to USP method

Heparin is an anticoagulant widely used in the treatment of myocardial infarction and thromboembolic disease (1). The anticoagulant effect of the drug cannot be predicted by chemical analysis because it has not been related to any specific functional group or to molecular weight (2). Therefore, the activity of heparin, rather than its concentration, must be measured.

Evaluation of the anticoagulant activity of heparin is based on the ability of the drug to prolong the clotting of recalcified sheep plasma (*i.e.*, sheep plasma to which calcium ions are added to promote coagulation). This ability can be measured instrumentally and visually. Reed *et al.* (3) developed an instrumental method based on measurement of the time needed for a sample of recalcified sheep plasma to reach a pre-established viscosity, *i.e.*, a predetermined degree of clotting. This time is then related to the times needed for a set of standards to reach the same viscosity. The USP method, which does not use instruments, is based on the visual evaluation of the degree of clotting of samples as compared with that of a set of standards.

This work describes the development of a nephelometric method to determine heparin activity and compares this method with the USP procedure. Woziwodzki (4) used nephelometric techniques to study the clotting of plasma. More recently Tanaka (5) used laser nephelometric techniques to study the structure of polyacrylamide gels. Because a clot is essentially a gel composed of a fibrin polymer (1), it was postulated that a laser nephelometer could be used to measure the clotting time.

EXPERIMENTAL SECTION

Apparatus and Reagents—The cuvette compartment of a laser nephelometer[1] was modified to allow external circulation of water, thus maintaining

[1] Hyland PDQ Laser Nephelometer, Northbrook, Ill.

0022-3549/84/1100-1640$01.00/0

© 1984, American Pharmaceutical Association

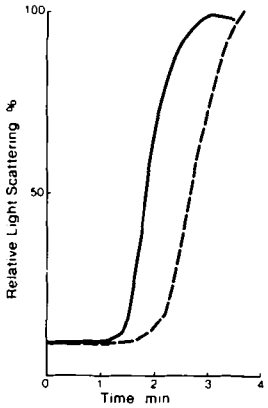

Figure 1—*Strip-chart recording of light scattering during clot formation. Key: (——) 0.88 U of heparin/mL; (- - -) 1.06 U of heparin/mL; 0% is 0.9% NaCl.*

a temperature of 37 ± 0.5°C. The following were used as received from the manufacturers: heparin sodium USP reference standard, sodium chloride[2], calcium chloride[2], and frozen sheep plasma[3].

Standard Preparation—A 3-U/mL (USP units) heparin stock solution in 0.9% NaCl was prepared from a sodium heparin reference standard. The working standards were prepared from this stock solution using 0.9% NaCl as a diluent. Because the activity range of the working standards depends on the lot of sheep plasma used, the range was determined by measuring the clotting times of several working standards having activities between 1 and 3 U/mL. For the plasma used in these studies, the activities ranged between 1.10 and 1.40 U/mL with clotting times between 100 and 200 s. Clotting times higher or lower than this range showed deviations from linearity for the logarithm of clotting time *versus* activity.

Procedure—Samples were diluted with 0.9% NaCl to an activity within the range of the standard curve. The sheep plasma was thawed at room temperature, filtered, and kept in an ice bath during the analysis.

The instrument was standardized by setting zero light scattering with a solution of 1 mL of 0.9% NaCl mixed with 0.5 mL of sheep plasma. Maximum light scattering was set at 190 using a fully clotted sample prepared by incubating a mixture of 0.5 mL of 0.9% NaCl, 0.5 mL of sheep plasma, and 0.5 mL of 0.02 M $CaCl_2$ for 5 min at 37°C.

A 0.5-mL aliquot of the diluted sample was mixed with 0.5 mL of sheep plasma in a 10 × 75-mm test tube and incubated at 37°C for at least 3 min. Immediately after addition of 0.5 mL of 0.02 M $CaCl_2$ (prewarmed to 37°C), a timer was started and the contents of the tube were remixed. The tube was placed in the nephelometer, and the time was recorded when the display reached 100. This is defined as the recalcification clotting time (RCT). Three determinations were made on each solution. The activity of the test solution was determined from a standard curve of the logarithm of mean RCT *versus* heparin activity.

Comparison of the Nephelometric and USP Methods—Three aqueous solutions of sodium heparin[4] buffered with citric acid[5] and sodium monohydrogen phosphate[3], with activities of 45.07, 49.97, and 54.91 U/mL, were prepared. These solutions were analyzed for heparin activity using both the USP XX (6) and nephelometric methods. On each of 3 d, two technicians analyzed each solution using a randomized order, making three determinations on duplicate dilutions of each sample.

RESULTS AND DISCUSSION

Figure 1 illustrates the increase in light scattering during clot formation for two levels of heparin activity. The two curves differ only in the amount of time elapsed before clot formation begins. The midpoint of the clotting curve was chosen as the end point for clotting time because it lies in the linear section of greatest slope, allowing timing instruments to be stopped with the greatest precision.

Reed *et al.* showed that the logarithm of clotting time varies linearly with heparin activity (3). The nephelometric method produced similar results. Good correlation with a straight line at the 95% confidence level was obtained with a standard curve consisting of at least four points. For the comparison study, the average correlation coefficient for the nephelometric standard curves was 0.9901.

The results indicate that the nephelometric assay is more reproducible than the USP assay. The coefficients of variation, calculated at an activity of 50 U/mL, were 2.79% for the nephelometric assay and 5.94% for the USP method. For each method, the total observed variation in assay results was statistically analyzed in terms of each of the underlying sources of assay imprecision. The results of this variance component analysis and the relative contribution of each source of variation are shown in Table I. For the nephelometric assay, determination of clotting time is the largest contributor to variance. This variability is due to normal changes in the clotting response of sheep plasma. The greatest sources of assay imprecision for the USP assay are daily shifts in assay results and technician differences. The technician variance seems to be due to the subjectivity of the grading system, indicating not only differences in the way two technicians grade, but also differences in the way a single technician grades from day to day. This factor seems to be eliminated with the instrumental method.

Table I—Comparison of the Precision of the Nephelometric and USP Methods

Variance Components	Nephelometric Method: Variance Estimate, U/mL²	Nephelometric Method: Relative Contribution to Total Variance, %	USP Method: Variance Estimate, U/mL²	USP Method: Relative Contribution to Total Variance, %
Date	0.000	0.0	4.414	48.6
Concentration * date	0.000	0.0	0.045	0.5
Tech	0.000	0.0	2.292	25.2
Concentration * tech	0.000	0.0	0.000	0.0
Date * tech	0.612	23.5	1.563	17.2
Concentration * date * tech	0.898	34.5	0.259	2.9
Dilution (concentration * date * tech)	0.097	3.7	0.000	0.0
Determination (dilution)	0.998	38.3	0.513	5.6
Total variance	2.60	100.0	9.09	100.0
SD, U/mL	1.39[a]	—	2.97[b]	—
CV[c] at heparin activity of 50 U/mL	2.78	—	5.94	—

[a] Mean of three determinations per dilution. [b] Mean of two determinations per dilution. [c] Calculated using the formula: $CV = (SD/\text{heparin activity}) \times 100$.

Table II—Comparison of the Accuracy of the Nephelometric and USP Methods

Technician	Theoretical Heparin Activity, U/mL	Mean Bias[a]: Nephelometric	Mean Bias[a]: USP	Recovery, %: Nephelometric	Recovery, %: USP
1	45.07	−0.64	−1.25	98.6	97.2
	49.97	−0.83	−2.87	98.3	94.3
	54.92	−0.75	−2.83	98.6	94.9
2	45.07	−0.25	1.43	99.5	103.2
	49.97	−1.91	−0.41	96.4	99.2
	54.92	−1.14	−0.82	97.9	98.5

[a] Difference between theoretical and experimentally determined activity.

The accuracy of each method was evaluated by comparing observed assay values with theoretical heparin activity (Table II). Although both methods demonstrate a negative mean bias at nearly all concentration levels for both technicians, the observed biases were within the precision limits found for each method. This negative bias is most likely a systematic error in the experimental procedure (*e.g.*, preparation of the test solutions) because it was observed in all results except one. The two methods were tested for equivalency by analyzing the ranks of the mean biases. This analysis showed no significant difference between methods ($p > 0.05$).

The nephelometric method has definite advantages over the USP method. It is faster (a single assay can be completed in less than half the time the USP method takes) and simpler (it does not involve the subjective grading, lengthy procedure, and calculations of the USP method). The nephelometric method is also more sensitive. Activities of 1 U/mL of heparin can be detected with the nephelometer *versus* 3 U/mL with the USP assay.

REFERENCES

(1) "The Pharmacological Basis of Therapeutics," 5th ed., L. S. Goodman and A. Gilman, Eds., MacMillan, New York, N.Y., 1975, pp. 1350–1364.

[2] Scientific Products, McGaw Park, Ill.
[3] Irvine Scientific, Santa Ana, Calif.
[4] Diosynth, Inc., Chicago, Ill.

(2) J. Ehrlich and S. S. Stivala, *J. Pharm. Sci.*, **62**, 517 (1973).
(3) M. Reed, G. Wilson, W. Davenport, T. Schmitz, and M. Klamrzynski, *J. Pharm. Sci.*, **63**, 1455 (1974).
(4) G. Woziwodzki, *Z. Med. Labortech.*, **11**, 28 (1970).
(5) T. Tanaka, *Sci. Am.*, **244**(1), 124 (1981).
(6) "The United States Pharmacopeia," 20th rev., U.S. Pharmacopeial Convention, Rockville, Md., 1980, pp. 365 and 366.

ACKNOWLEDGMENTS

Presented at the American Pharmaceutical Association Academy of Pharmaceutical Sciences 31st National Meeting (Pharmaceutical Analysis and Control Section), Orlando, Fla., 1981. The authors would like to thank Alok Krishen for his help in the statistical analysis and Mark Wyzgala for his valuable technical assistance.

Comparative Pharmacokinetics of [^{65}Zn]Zinc Sulfate and [^{65}Zn]Zinc Pantothenate Injected Intravenously in Rabbits

OLIVIER GUILLARD *[x], PHILIPPE COURTOIS [‡], PATRICK MURAI *, DANIEL DUCASSOU [‡], and DANIEL REISS *

Received March 14, 1980, from the **Laboratory of Biochemistry and* [‡]*Pharmacology Jean Bernard Hospital, BP 577, 86021 Poitiers Cedex, France.* Accepted for publication December 12, 1983.

Abstract □ The pharmacokinetics of zinc sulfate were compared with those of a new zinc salt, pantothenate, in rabbits. Each salt was administered at a dosage of 3.3 μCi of zinc-65/kg of body weight. The measured pharmacokinetics of the two compounds responded to a two-compartment open model. The urinary elimination of the two salts was similar, as was their localization in the skin and fur, but zinc pantothenate was fixed by the liver to a lesser extent than was zinc sulfate.

Keyphrases □ [^{65}Zn]Zinc sulfate—intravenous administration to rabbits, pharmacokinetics □ [^{65}Zn]Zinc pantothenate—intravenous administration to rabbits, pharmacokinetics □ Pharmacokinetics—comparison of [^{65}Zn]zinc sulfate and [^{65}Zn]zinc pantothenate injected intravenously, rabbits □ Zinc salts—zinc sulfate and zinc pantothenate, comparative pharmacokinetics, intravenous administration to rabbits

Zinc sulfate is used to treat acrodermatitis enteropathica (1, 2), a condition associated with abnormal zinc metabolism. Zinc pantothenate, which we synthesized in our laboratory, had a much lower toxicity when administered orally to animals than did zinc sulfate and exhibited better gastric tolerance (3). We report here a comparative pharmacokinetic study of the intravenous injection of the two radioactive zinc salts.

EXPERIMENTAL SECTION

Reagents—[^{65}Zn]Zinc pantothenate was prepared as previously described (4). The principle of the reaction is an exchange between calcium pantothenate and [^{65}Zn]zinc sulfate with a specific radioactivity of 3.5 mCi/mg.

Animal Treatment—Six male rabbits (mean weight, 2.5 kg) were isolated in metabolism cages and placed on a water diet 12 h prior to the experiment. The necks of the animals were shaved, and a 0.5% solution of lidocaine was applied as a light topical anesthesia. The jugular vein was freed, and a catheter was inserted. Bleeding was prevented by placing a small sponge imbibed with anesthetic under the suture. The protruding catheter was fixed to the skin with a bandage, thus permitting both injection of the products tested and blood sampling.

Protocol and Analytical Procedures—Each zinc salt was injected into the jugular vein at a dose of 3.3 μCi of zinc-65/kg, and blood samples were taken at 5, 10, 15, 30, and 60 min and 2, 4, and 6 h postinjection. Blood samples (4 mL) were taken at the indicated times in a dry polypropylene tube (5), and serum was separated by centrifugation for 10 min at 3000 rpm. Animals were sacrificed 6.5 h after injection, and various organs or tissue fragments were removed and weighed: liver, kidneys, whole skin with fur, and, after washing with physiological saline, the small intestine.

Radioactivity was determined with a liquid scintillation counter[1]. Serum activity is expressed as disintegration per minute after quench correction (Fig. 1). For urine elimination and tissue and organ samples, the results are expressed as the percentage of the total quantity administered (Table I).

[1] Model 9000 γ; Beckman.

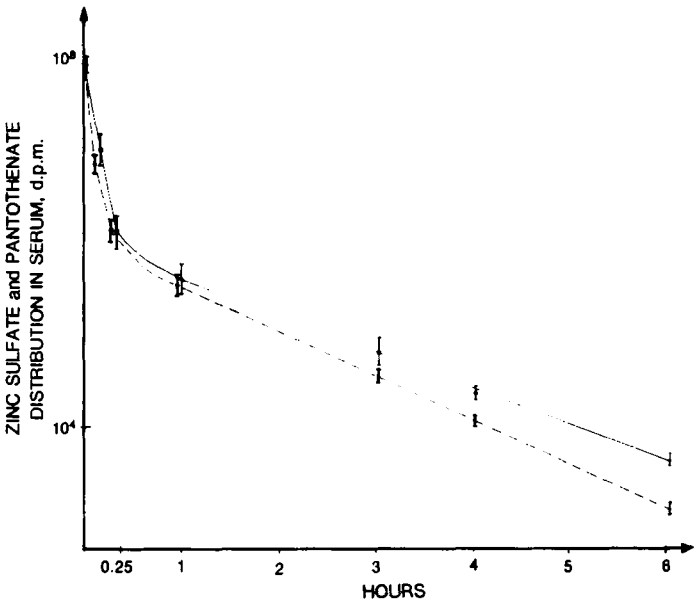

Figure 1—*Kinetics of the blood distribution of [^{65}Zn]zinc sulfate (—) and [^{65}Zn]zinc pantothenate (- -) after intravenous injection to six rabbits. The radioactivity is expressed as disintegrations per minute (d.p.m.). Results are expressed as the mean* ± SE.

RESULTS AND DISCUSSION

The pharmacokinetic data indicate that the distribution half-life (α) of zinc pantothenate is shorter (0.11 h^{-1}) than that of zinc sulfate (0.134 h^{-1}) (Fig. 1). Urinary elimination is very low and does not exceed 1% of the administered dose, which confirms results of previous studies with rats (6) and dogs (7) with zinc sulfate alone.

Both salts exhibit a similar distribution in the kidneys, the small intestine, the skin, and the fur. In the present study, there is a clear difference in hepatic

Table I—Tissue Distribution and Urine Elimination of [^{65}Zn]Zinc Pantothenate and [^{65}Zn]Zinc Sulfate after Intravenous Administration [a]

Tissue or Fluid	Radioactivity, Percentage of Total	
	[^{65}Zn]Zinc Pantothenate	[^{65}Zn]Zinc Sulfate
Liver	8	17
Kidney	2	2
Whole skin and fur	4	2
Small Intestine	1	1
Urine elimination	1	1

[a] Results were obtained 6.5 h after administration to six rabbits; results are expressed as percentage of the total activity.

0022-3549/84/1100-1642$01.00/0
© 1984, American Pharmaceutical Association

(2) J. Ehrlich and S. S. Stivala, *J. Pharm. Sci.*, **62**, 517 (1973).
(3) M. Reed, G. Wilson, W. Davenport, T. Schmitz, and M. Klamrzynski, *J. Pharm. Sci.*, **63**, 1455 (1974).
(4) G. Woziwodzki, *Z. Med. Labortech.*, **11**, 28 (1970).
(5) T. Tanaka, *Sci. Am.*, **244**(1), 124 (1981).
(6) "The United States Pharmacopeia," 20th rev., U.S. Pharmacopeial Convention, Rockville, Md., 1980, pp. 365 and 366.

ACKNOWLEDGMENTS

Presented at the American Pharmaceutical Association Academy of Pharmaceutical Sciences 31st National Meeting (Pharmaceutical Analysis and Control Section), Orlando, Fla., 1981. The authors would like to thank Alok Krishen for his help in the statistical analysis and Mark Wyzgala for his valuable technical assistance.

Comparative Pharmacokinetics of [^{65}Zn]Zinc Sulfate and [^{65}Zn]Zinc Pantothenate Injected Intravenously in Rabbits

OLIVIER GUILLARD *[x], PHILIPPE COURTOIS [‡], PATRICK MURAI *, DANIEL DUCASSOU [‡], and DANIEL REISS *

Received March 14, 1980, from the **Laboratory of Biochemistry and* [‡]*Pharmacology Jean Bernard Hospital, BP 577, 86021 Poitiers Cedex, France.* Accepted for publication December 12, 1983.

Abstract □ The pharmacokinetics of zinc sulfate were compared with those of a new zinc salt, pantothenate, in rabbits. Each salt was administered at a dosage of 3.3 μCi of zinc-65/kg of body weight. The measured pharmacokinetics of the two compounds responded to a two-compartment open model. The urinary elimination of the two salts was similar, as was their localization in the skin and fur, but zinc pantothenate was fixed by the liver to a lesser extent than was zinc sulfate.

Keyphrases □ [^{65}Zn]Zinc sulfate—intravenous administration to rabbits, pharmacokinetics □ [^{65}Zn]Zinc pantothenate—intravenous administration to rabbits, pharmacokinetics □ Pharmacokinetics—comparison of [^{65}Zn]zinc sulfate and [^{65}Zn]zinc pantothenate injected intravenously, rabbits □ Zinc salts—zinc sulfate and zinc pantothenate, comparative pharmacokinetics, intravenous administration to rabbits

Zinc sulfate is used to treat acrodermatitis enteropathica (1, 2), a condition associated with abnormal zinc metabolism. Zinc pantothenate, which we synthesized in our laboratory, had a much lower toxicity when administered orally to animals than did zinc sulfate and exhibited better gastric tolerance (3). We report here a comparative pharmacokinetic study of the intravenous injection of the two radioactive zinc salts.

EXPERIMENTAL SECTION

Reagents—[^{65}Zn]Zinc pantothenate was prepared as previously described (4). The principle of the reaction is an exchange between calcium pantothenate and [^{65}Zn]zinc sulfate with a specific radioactivity of 3.5 mCi/mg.

Animal Treatment—Six male rabbits (mean weight, 2.5 kg) were isolated in metabolism cages and placed on a water diet 12 h prior to the experiment. The necks of the animals were shaved, and a 0.5% solution of lidocaine was applied as a light topical anesthesia. The jugular vein was freed, and a catheter was inserted. Bleeding was prevented by placing a small sponge imbibed with anesthetic under the suture. The protruding catheter was fixed to the skin with a bandage, thus permitting both injection of the products tested and blood sampling.

Protocol and Analytical Procedures—Each zinc salt was injected into the jugular vein at a dose of 3.3 μCi of zinc-65/kg, and blood samples were taken at 5, 10, 15, 30, and 60 min and 2, 4, and 6 h postinjection. Blood samples (4 mL) were taken at the indicated times in a dry polypropylene tube (5), and serum was separated by centrifugation for 10 min at 3000 rpm. Animals were sacrificed 6.5 h after injection, and various organs or tissue fragments were removed and weighed: liver, kidneys, whole skin with fur, and, after washing with physiological saline, the small intestine.

Radioactivity was determined with a liquid scintillation counter[1]. Serum activity is expressed as disintegration per minute after quench correction (Fig. 1). For urine elimination and tissue and organ samples, the results are expressed as the percentage of the total quantity administered (Table I).

[1] Model 9000 γ; Beckman.

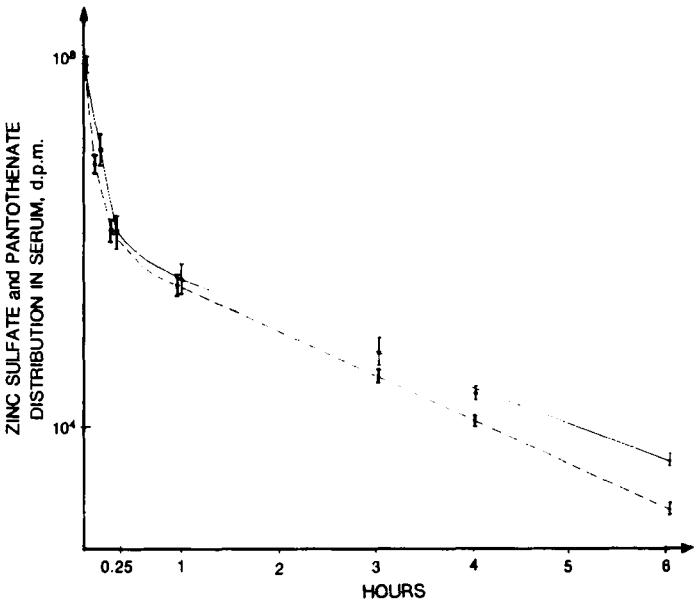

Figure 1—*Kinetics of the blood distribution of [^{65}Zn]zinc sulfate (—) and [^{65}Zn]zinc pantothenate (- -) after intravenous injection to six rabbits. The radioactivity is expressed as disintegrations per minute (d.p.m.). Results are expressed as the mean* ± SE.

RESULTS AND DISCUSSION

The pharmacokinetic data indicate that the distribution half-life (α) of zinc pantothenate is shorter (0.11 h^{-1}) than that of zinc sulfate (0.134 h^{-1}) (Fig. 1). Urinary elimination is very low and does not exceed 1% of the administered dose, which confirms results of previous studies with rats (6) and dogs (7) with zinc sulfate alone.

Both salts exhibit a similar distribution in the kidneys, the small intestine, the skin, and the fur. In the present study, there is a clear difference in hepatic

Table I—Tissue Distribution and Urine Elimination of [^{65}Zn]Zinc Pantothenate and [^{65}Zn]Zinc Sulfate after Intravenous Administration [a]

Tissue or Fluid	Radioactivity, Percentage of Total	
	[^{65}Zn]Zinc Pantothenate	[^{65}Zn]Zinc Sulfate
Liver	8	17
Kidney	2	2
Whole skin and fur	4	2
Small Intestine	1	1
Urine elimination	1	1

[a] Results were obtained 6.5 h after administration to six rabbits; results are expressed as percentage of the total activity.

0022-3549/84/1100-1642$01.00/0
© 1984, American Pharmaceutical Association

binding of the two salts: the zinc sulfate is fixed to a greater extent than is the zinc pantothenate (17 *versus* 8%).

The efficient distribution and diffusion of zinc pantothenate in the skin and the fur, as well as its less important retention in the liver, would suggest a therapeutic use in the treatment of disorders of the skin and scalp.

REFERENCES

(1) E. J. Moynahan, *Lancet*, **i**, 399 (1974).

(2) O. Guillard, A. Piriou, C. Dumas, M. C. Saux, and Ph. Courtois, *J. Pharmacol. (Paris)*, **11**, 33 (1980).

(3) D. Reiss, A. Piriou, M. Boulard, and O. Guillard, *Drug Intell. Clin. Pharm.*, **13**, 611 (1979).

(4) O. Guillard, P. Aumonier, and Ph. Courtois, *Bull. Soc. Pharm. Bordeaux*, **116**, 47 (1977).

(5) O. Guillard, A. Piriou, P. Mura, and D. Reiss, *Clin. Chem.*, **25**, 1867 (1979).

(6) J. P. Okunevick, O. A. Schjeide, E. N. Carlsen, and T. G. Hennessy, *Nature (London)*, **198**, 966 (1963).

(7) G. E. Schelline, I. L. Chaikoff, H. B. Jones, and M. L. Montgomery, *J. Biol. Chem.*, **147**, 409 (1943).

ACKNOWLEDGMENTS

The authors are indebted to Michele Jarossay for typing the manuscript.

Epiandrosterone- and Dehydroepiandrosterone-3β-alkanesulfonates as Inhibitors of Mouse Glucose-6-phosphate Dehydrogenase Activity

MAGID ABOU-GHARBIA *[x], ELAINE N. CHEESEMAN, LAURA PASHKO, ARTHUR SCHWARTZ, and DANIEL SWERN [†]

Received September 15, 1983, from the *Fels Research Institute and Department of Chemistry, Temple University, Philadelphia, PA 19122.* Accepted December 14, 1983. *Present address: Wyeth Laboratories, Philadelphia, PA 19101. [†]Deceased.

Abstract □ 3β-Alkanesulfonates of dehydroepiandrosterone, 16α-bromodehydroepiandrosterone, epiandrosterone, and 16α-bromoepiandrosterone were prepared in 54–95% yield *via* the reaction of long chain alkanesulfonyl chlorides with the corresponding dehydroepiandrosterone, and epiandrosterone analogues. These compounds inhibit mouse glucose-6-phosphate dehydrogenase activity.

Keyphrases □ 3β-Alkanesulfonates—synthesis, screened as glucose-6-phosphate dehydrogenase inhibitors □ Long-chain alkanesulfonyl chlorides—synthesis, antitumor agents

In a series of clinical and epidemiological studies several investigators have found that women with subnormal plasma concentrations of the adrenal steroid dehydroepiandrosterone (Ia) have a high risk of developing breast cancer (1–3). We have found that long-term treatment of various mouse strains with Ia inhibits the development of spontaneous breast cancer (4) and chemically induced lung (5) and colon tumors (6). It also blocks the 12-*O*-tetradecanoylphorbol-13-acetate (tumor promoter) stimulation of DNA synthesis in mouse epidermis (7) and inhibits the rate of [^{3}H]thymidine incorporation in various cell lines in culture (4).

Compound Ia is a potent noncompetitive inhibitor of mammalian glucose-6-phosphate dehydrogenase (G6PDH) (8, 9). Inhibition of this enzyme and the pentose-phosphate shunt, a major source of extramitochondrial NADPH, may account for the reduction in DNA synthesis rate by the steroid (10). Dehydroepiandrosterone in human plasma is largely sulfated. According to Oertel and Hoppe-Seyler, the predominant sulfated form of Ia in human plasma is not dehydroepiandrosterone sulfate (Ib), but an ester of Ib and a diglyceride, known as dehydroepiandrosterone sulfatide (II) (11). The sulfatide was found to be a more potent inhibitor of G6PDH than Ia (9).

We have observed that II is more effective than Ia in inhibiting mouse epidermal G6PDH as well as in blocking 12-*O*-tetradecanoylphorbol-13-acetate stimulation of DNA synthesis in mouse epidermis (7). On the other hand II is a labile material and decomposes readily within a few days, even

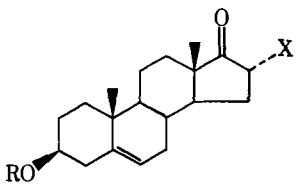

Ia, R = H, X = H
Ib, R = SO_3H
Ic, R = H, X = Br
Id, R = $SO_2(CH_2)_7CH_3$, X = H
Ie, R = $SO_2(CH_2)_7CH_3$, X = Br
If, R = $SO_2(CH_2)_{15}CH_3$, X = H
Ig, R = $SO_2(CH_2)_{15}CH_3$, X = Br

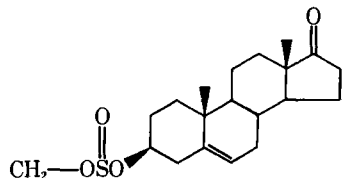

II

when stored at −5°C, to the sulfate Ib, resulting in loss of biological activity. Replacement of the sulfate functionality with sulfonate should lead to more stable analogues. In the search for stable and potent derivatives of II, we decided to incorporate the long chain alkanesulfonates into compounds which have already demonstrated a greater activity as inhibitors of glucose-6-phosphate dehydrogenase such as 16α-bromoepiandrosterone (7). Accordingly, 3β-alkanesulfonates of Ia, 16α-bromodehydroepiandrosterone (Ic), epiandrosterone (IIIa), and 16α-bromoepiandrosterone (IIIb) were prepared.

RESULTS AND DISCUSSION

Chemistry—3β-Alkanesulfonates of dehydroepiandrosterone and epiandrosterone (I and V) were synthesized by the reaction of a long chain alkanesulfonyl chloride IVa–e with the corresponding dehydroepiandrosterone or epiandrosterone analogue in the presence of dry triethylamine (Scheme I).

Long-chain alkanesulfonyl chlorides IVa–e were prepared in 60–85% yields from the corresponding fatty alcohol *via* a modification of the King and Aslam procedure (12) in which the hydroxyl group was replaced by the isothiuronium functionality and then the sulfur moiety was oxidized with chlorine in aqueous medium (Scheme II).

Biological Activity—The compounds listed in Table I were evaluated for their abilities to inhibit mouse epidermal glucose-6-phosphate dehydrogenase (Table II). Among the 3β-alkanesulfonates, compound Vf and its 16α-bromo analogue (Vg), both with the hexadecanesulfonyl side chain attached to the 3β-position of the epiandrosterone molecule, are the most potent inhibitors.

0022-3549/84/1100-1643$01.00/0

© 1984, American Pharmaceutical Association

binding of the two salts: the zinc sulfate is fixed to a greater extent than is the zinc pantothenate (17 *versus* 8%).

The efficient distribution and diffusion of zinc pantothenate in the skin and the fur, as well as its less important retention in the liver, would suggest a therapeutic use in the treatment of disorders of the skin and scalp.

REFERENCES

(1) E. J. Moynahan, *Lancet*, **i**, 399 (1974).

(2) O. Guillard, A. Piriou, C. Dumas, M. C. Saux, and Ph. Courtois, *J. Pharmacol. (Paris)*, **11**, 33 (1980).

(3) D. Reiss, A. Piriou, M. Boulard, and O. Guillard, *Drug Intell. Clin. Pharm.*, **13**, 611 (1979).

(4) O. Guillard, P. Aumonier, and Ph. Courtois, *Bull. Soc. Pharm. Bordeaux*, **116**, 47 (1977).

(5) O. Guillard, A. Piriou, P. Mura, and D. Reiss, *Clin. Chem.*, **25**, 1867 (1979).

(6) J. P. Okunevick, O. A. Schjeide, E. N. Carlsen, and T. G. Hennessy, *Nature (London)*, **198**, 966 (1963).

(7) G. E. Schelline, I. L. Chaikoff, H. B. Jones, and M. L. Montgomery, *J. Biol. Chem.*, **147**, 409 (1943).

ACKNOWLEDGMENTS

The authors are indebted to Michele Jarossay for typing the manuscript.

Epiandrosterone- and Dehydroepiandrosterone-3β-alkanesulfonates as Inhibitors of Mouse Glucose-6-phosphate Dehydrogenase Activity

MAGID ABOU-GHARBIA *[x], ELAINE N. CHEESEMAN, LAURA PASHKO, ARTHUR SCHWARTZ, and DANIEL SWERN [†]

Received September 15, 1983, from the *Fels Research Institute and Department of Chemistry, Temple University, Philadelphia, PA 19122.* Accepted December 14, 1983. *Present address: Wyeth Laboratories, Philadelphia, PA 19101. [†]Deceased.

Abstract □ 3β-Alkanesulfonates of dehydroepiandrosterone, 16α-bromodehydroepiandrosterone, epiandrosterone, and 16α-bromoepiandrosterone were prepared in 54–95% yield *via* the reaction of long chain alkanesulfonyl chlorides with the corresponding dehydroepiandrosterone, and epiandrosterone analogues. These compounds inhibit mouse glucose-6-phosphate dehydrogenase activity.

Keyphrases □ 3β-Alkanesulfonates—synthesis, screened as glucose-6-phosphate dehydrogenase inhibitors □ Long-chain alkanesulfonyl chlorides—synthesis, antitumor agents

In a series of clinical and epidemiological studies several investigators have found that women with subnormal plasma concentrations of the adrenal steroid dehydroepiandrosterone (Ia) have a high risk of developing breast cancer (1–3). We have found that long-term treatment of various mouse strains with Ia inhibits the development of spontaneous breast cancer (4) and chemically induced lung (5) and colon tumors (6). It also blocks the 12-*O*-tetradecanoylphorbol-13-acetate (tumor promoter) stimulation of DNA synthesis in mouse epidermis (7) and inhibits the rate of [^{3}H]thymidine incorporation in various cell lines in culture (4).

Compound Ia is a potent noncompetitive inhibitor of mammalian glucose-6-phosphate dehydrogenase (G6PDH) (8, 9). Inhibition of this enzyme and the pentose-phosphate shunt, a major source of extramitochondrial NADPH, may account for the reduction in DNA synthesis rate by the steroid (10). Dehydroepiandrosterone in human plasma is largely sulfated. According to Oertel and Hoppe-Seyler, the predominant sulfated form of Ia in human plasma is not dehydroepiandrosterone sulfate (Ib), but an ester of Ib and a diglyceride, known as dehydroepiandrosterone sulfatide (II) (11). The sulfatide was found to be a more potent inhibitor of G6PDH than Ia (9).

We have observed that II is more effective than Ia in inhibiting mouse epidermal G6PDH as well as in blocking 12-*O*-tetradecanoylphorbol-13-acetate stimulation of DNA synthesis in mouse epidermis (7). On the other hand II is a labile material and decomposes readily within a few days, even

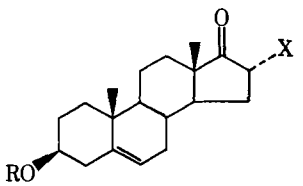

Ia, R = H, X = H
Ib, R = SO_3H
Ic, R = H, X = Br
Id, R = $SO_2(CH_2)_7CH_3$, X = H
Ie, R = $SO_2(CH_2)_7CH_3$, X = Br
If, R = $SO_2(CH_2)_{15}CH_3$, X = H
Ig, R = $SO_2(CH_2)_{15}CH_3$, X = Br

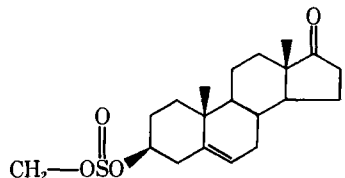

II

when stored at −5°C, to the sulfate Ib, resulting in loss of biological activity. Replacement of the sulfate functionality with sulfonate should lead to more stable analogues. In the search for stable and potent derivatives of II, we decided to incorporate the long chain alkanesulfonates into compounds which have already demonstrated a greater activity as inhibitors of glucose-6-phosphate dehydrogenase such as 16α-bromoepiandrosterone (7). Accordingly, 3β-alkanesulfonates of Ia, 16α-bromodehydroepiandrosterone (Ic), epiandrosterone (IIIa), and 16α-bromoepiandrosterone (IIIb) were prepared.

RESULTS AND DISCUSSION

Chemistry—3β-Alkanesulfonates of dehydroepiandrosterone and epiandrosterone (I and V) were synthesized by the reaction of a long chain alkanesulfonyl chloride IVa–e with the corresponding dehydroepiandrosterone or epiandrosterone analogue in the presence of dry triethylamine (Scheme I).

Long-chain alkanesulfonyl chlorides IVa–e were prepared in 60–85% yields from the corresponding fatty alcohol *via* a modification of the King and Aslam procedure (12) in which the hydroxyl group was replaced by the isothiuronium functionality and then the sulfur moiety was oxidized with chlorine in aqueous medium (Scheme II).

Biological Activity—The compounds listed in Table I were evaluated for their abilities to inhibit mouse epidermal glucose-6-phosphate dehydrogenase (Table II). Among the 3β-alkanesulfonates, compound Vf and its 16α-bromo analogue (Vg), both with the hexadecanesulfonyl side chain attached to the 3β-position of the epiandrosterone molecule, are the most potent inhibitors.

0022-3549/84/1100-1643$01.00/0

© 1984, American Pharmaceutical Association

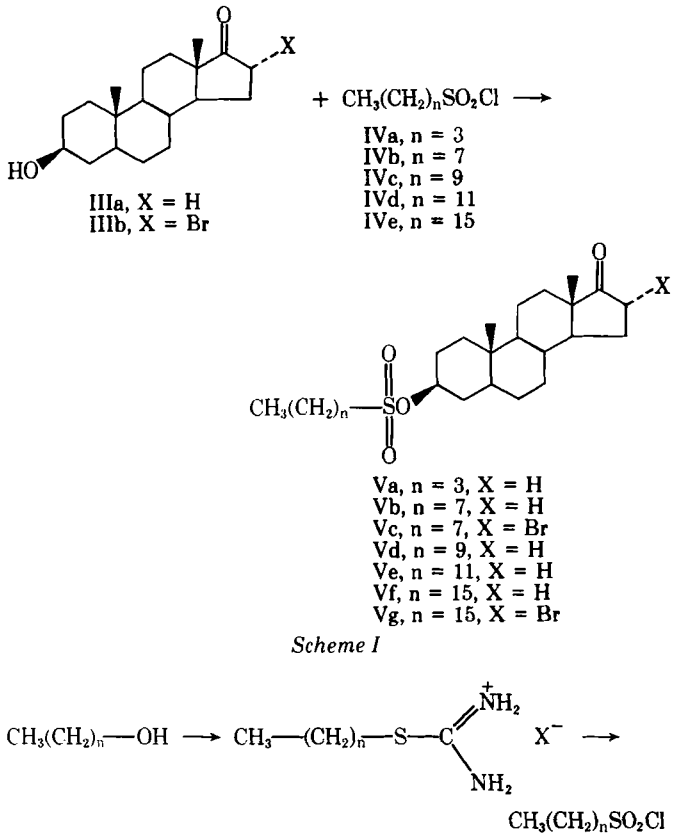

Scheme I

IVa–e (X = halogen)

Scheme II

Compound Vg is twice as active as the parent steroid Ia, showing 88% inhibition compared with the 46% inhibition produced by Ia.

Inhibition of this enzyme will consequently inhibit the pentose-phosphate shunt which generates ribose-phosphate and the bulk of extramitochondrial reduced nicotinamide adenine diphosphate (NADPH) (13), both of which are necessary for deoxyribonucleotide and fatty acid syntheses.

EXPERIMENTAL SECTION

Chemical Syntheses—All melting points were determined on apparatus[1] and are uncorrected. IR spectra were recorded on a spectrophotometer[2]. Elemental analyses were performed by Galbraith Laboratories.

Dehydroepiandrosterone Sulfatide (II)—This compound was prepared in 68% yield from the reaction of Ia-silver sulfate with dipalmitoyl-L-2-iodopropylene glycol following a reported procedure (14).

Alkanesulfonyl Chlorides IVa–d—These compounds were prepared from long-chain fatty alcohols following reported procedures (7). Dodecansulfonyl chloride IVe was similarly prepared in 75% yield, bp 126–130°C at 4 mm Hg.

Anal.—Calc. for $C_{12}H_{25}ClO_2S$: C, 53.60; H, 9.27; Cl 13.18; S, 11.92. Found: C, 53.75; H, 9.42; Cl, 12.90; S, 11.83.

General Procedure for the Preparation of 3β-Alkanesulfonates I, V, and VI—A modified procedure of Tesser and Balvert-Geev (15) was used in which 0.05 mol of the steroid was dissolved in 25 mL of dichloromethane and stirred. To this solution was added 0.65 g of dry triethylamine. The solution was cooled in an ice bath for 15 min and 0.006 mol of the appropriately substituted alkanesulfonyl chloride was added over a period of 10 min. The mixture was stirred for an additional 5 min, then was washed four times with cold water, dried (sodium sulfate), and evaporated under reduced pressure. The white solid formed was recrystallized from a suitable solvent (Table I).

Glucose-6-phosphate Dehydrogenase Assay—Epidermal G6PDH was prepared by a modification of the procedure of Ziboh *et al.* (16). Male ICR mice (6–8 weeks old) in hair resting phase were shaved 2–3 d before use. Only those mice showing no hair regrowth were used. Mice were sacrificed and a depilatory[3] was applied to the shaved area. After 5 min, the depilatory was washed off, the skin was cut out, placed in 55°C water for 30 s and the epidermis was scraped off with a scalpel. The scrapings were frozen and thawed three times in liquid nitrogen and then homogenized in 10 volumes of 0.25 M sucrose. The homogenate was centrifuged at 105,000×*g* for 1 h at 0°C. The supernatant was concentrated to one-fifth of its original volume[4] and the concentrated cytosol was used in the G6PDH assay. Steroid inhibition of G6PDH activity was determined according to the procedure of Oertel and Rebelein (9). Steroids were dissolved in dioxane immediately before testing. The reaction medium consisted of 3 mL of 0.05 M triethanolamine–0.005 M EDTA buffer (pH 7.6), 0.01 M NADP[5] solution, and 0.02 mL of dioxane or steroid in dioxane. The reaction was run at 25°C and was initiated by the addition of 0.005 mL of a 0.03 M glucose-6-phosphate[5] solution. Activity was measured in minutes from changes in absorbance at 366 nm on a recording spectrophotometer[6]. The inhibition produced by the added steroid was expressed as percent of control value. (The inhibition values in Table II were obtained by subtracting the percent control activity from 100.)

[1] Thomas-Hoover Unimelt.
[2] Unicam SP-1000.
[3] Nair.
[4] Sephadex G-25.
[5] Sigma.
[6] Gilford 2400-S.

Table I—3β-Alkanesulfonates of Dehydroepiandrosterone and Epiandrosterone

Compound	mp, °C	Yield, %	IR ν_{max}·cm^{-1} (SO_3, CO)	Formula[e]
Va	132–133[a]	91	1370, 1155, 1735	$C_{23}H_{38}SO_4$[f]
Vb	52–53[b]	80	1350, 1140, 1730	$C_{27}H_{46}SO_4$
Id	97–98[c]	70	1170, 1357, 1747	$C_{27}H_{44}SO_4$
Vc	75–76[c]	54	1172, 1368, 1751	$C_{27}H_{46}BrSO_4$
Ie	145–146[c]	54	1168, 1359, 1751	$C_{27}H_{43}BrSO_4$
Vd	60–61[b]	82	1210, 1400, 1740	$C_{29}H_{50}SO_4$
Ve	33–35[a]	68	1135, 1365, 1735	$C_{31}H_{53}SO_4$
If	88–89[c]	65	1168, 1355, 1748	$C_{35}H_{59}SO_4$
Ig	118–120[c]	61	1162, 1360, 1745	$C_{35}H_{57}BrSO_4$
VI[g]	74–76[c]	71	1167, 1367, 1740	$C_{35}H_{59}SO_5$
Vf	45–48[d]	95	1160, 1375, 1745	$C_{35}H_{61}SO_4$
Vg	68–71[d]	78	1170, 1380, 1735	$C_{35}H_{61}BrSO_4$

[a] Recrystallized from ethanol-hexane. [b] Recrystallized from hexane-petroleum ether. [c] Recrystallized from $CHCl_3$-petroleum ether. [d] Recrystallized from petroleum ether. [e] Compounds Id–Ig, Va–Vg, and VI were analyzed for C, H, and S; in addition, Ie, Ig, Vc, and Vg were analyzed for Br. Unless otherwise indicated, all values were within ±0.4% of the theoretical value. [f] Calc. for Br, 12.49; found, 11.94. [g] The five-membered ring D is expanded to a six-membered ring lactone. The structure of VI is:

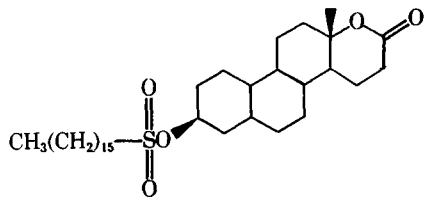

Table II—Inhibition of Mouse Epidermal G6PDH Activity by 3β-Alkanesulfonates of Dehydroepiandrosterone and Epiandrosterone[a]

Steroid	Concentration, M	Percent Inhibition[b]
Ia	10^{-5}	46 ± 2.4
Ia	10^{-7}	10 ± 1.7
II	10^{-5}	54 ± 3.7
II	10^{-7}	36 ± 2.6
Va	10^{-5}	18 ± 1.7
Vb	10^{-5}	23 ± 4.0
Id	10^{-5}	26 ± 4.4
Vc	10^{-5}	7 ± 1.5
Ie	10^{-5}	22 ± 3.0
Vd	10^{-5}	18 ± 1.4
Ve	10^{-5}	34 ± 2.8
If	10^{-5}	28 ± 2.1
Ig	10^{-5}	7 ± 0.7
VI	10^{-5}	12 ± 1.4
Vf	10^{-5}	58 ± 5.0
Vg	10^{-5}	88 ± 0.7

[a] Conditions are as described in the *Experimental Section*. [b] Values are averages of two or more replicates ± *SD*.

REFERENCES

(1) R. D. Bulbrook, J. L. Hayward, and C. C. Spicer, *Lancet*, **ii**, 395 (1971).

(2) D. P. Rose, P. Stauber, A. Thiel, J. J. Crawley, and J. R. Milbrath, *Eur. J. Cancer*, **13**, 43 (1977).

(3) J. H. H. Thijssen, J. Poortman, and F. Schwarta, *J. Steroid Biochem.*, **6**, 729 (1975).

(4) A. Schwartz, G. Hard, L. Pashko, M. Abou-Gharbia, and D. Swern, *Nutr. Cancer*, **3**, 46 (1981).

(5) A. G. Schwartz and R. H. Tannen, *Carcinogenesis*, **2**, 1335 (1981).

(6) J. W. Nyce, P. N. Magee, G. C. Hard, and A. G. Schwartz, in press.

(7) L. Pashko, A. G. Schwartz, M. Abou-Gharbia, and D. Swern, *Carcinogenesis*, **2**, 717 (1981).

(8) P. A. Marks and J. Banks, *Proc. Natl. Acad. Sci., U.S.A.*, **46**, 447 (1960).

(9) G. W. Oertel and I. Rebelein, *Biochim. Biophys. Acta*, **184**, 459 (1969).

(10) C. R. Dworkin, S. D. Gorman, L. L. Pashko, V. J. Cristafalo and A. G. Schwartz, in press.

(11) G. W. Oertel, *Z. Hoppe-Seylers Physiol. Chem.*, **343**, 276 (1966).

(12) J. F. King and M. Aslam, *Synthesis*, **1980**, 285.

(13) J. P. Flatt, *J. Lipid Res.*, **11**, 131 (1970).

(14) M. Abou-Gharbia, L. Pashko, A. Schwartz, and D. Swern, *J. Pharm. Sci.*, **70**, 1154 (1981).

(15) G. I. Tesser and I. C. Balvert-Geev, *J. Peptide Protein Res.*, **7**, 295 (1975).

(16) V. A. Ziboh, M. A. Dreize, and S. L. Hsia, *J. Lipid Res.*, **11**, 346 (1970).

Nalmefene: Radioimmunoassay for a New Opioid Antagonist

ROSS DIXON [¶x], JANE HSIAO [*], WILLIAM TAAFFE [‡], ELLIOTT HAHN [§], and RONALD TUTTLE [¶]

Received December 5, 1983, from [¶]*Key Pharmaceuticals, Inc., Miami, FL 33169*, [*]*Innotech Laboratories, Inc., Ft. Lauderdale, FL 33314*, the [‡]*Institute for Clinical Pharmacology, St. James Hospital, Dublin, Ireland*, and [§]*Rockefeller University, New York, NY 10021.* Accepted for publication February 3, 1984.

Abstract □ A specific radioimmunoassay (RIA) has been developed for the quantitation of a new opioid antagonist, nalmefene, in human plasma. The method employs a rabbit antiserum to an albumin conjugate of naltrexone-6-(*O*-carboxymethyl)oxime and [^{3}H]naltrexone as the radioligand. Assay specificity was achieved by extraction of nalmefene from plasma at pH 9 into ether prior to RIA. The procedure has a limit of sensitivity of 0.2 ng/mL of nalmefene using a 0.5-mL sample of plasma for analysis. The intra- and interassay coefficients of variation did not exceed 5.6 and 11%, respectively. The specificity of the RIA was established by demonstrating excellent agreement (r = 0.99) with a less sensitive and more time consuming HPLC procedure in the analysis of clinical plasma samples. The use of the RIA for the pharmacokinetic evaluation of nalmefene is illustrated with plasma concentration profiles of the drug in humans following intravenous and oral administration.

Keyphrases □ Nalmefene—human plasma, RIA, compared with HPLC □ RIA—compared with HPLC, nalmefene, human plasma

Nalmefene [17-(cyclopropylmethyl)-4,5α-epoxy-6-methylenemorphinan-3,14-diol] is a potent, orally active narcotic antagonist (1) which is undergoing clinical evaluation in humans. The drug is a structural analogue of naltrexone with an exocyclic methylene group in the 6-position. Hahn *et al.* (1) indicated in preliminary pharmacology studies that orally administered nalmefene was about 50 times more potent than naloxone in its ability to antagonize the antinociceptive activity of an ED_{95} dose of morphine in either the mouse hot-plate or tail-clip procedures. Furthermore, nalmefene was 16 times more potent than naloxone in precipitating narcotic withdrawal in morphine-dependent rhesus monkeys. Recently, nalmefene has been shown to decrease the food and water intake and weight gain in obese and lean Zucker rats, lending further support to a possible role for opioids in the control of food intake (2).

The present study was undertaken to develop a simple and specific radioimmunoassay (RIA) for nalmefene which would provide greater sensitivity and ease of operation than a recently reported high-performance liquid chromatographic (HPLC) procedure (3). It was hoped that the RIA might be utilized in a wide variety of human tolerance and pharmacokinetic studies that are under way with nalmefene.

The initial approach taken in the development of the RIA was to produce an antiserum which would cross-react almost equally well with nalmefene and naltrexone. In this way, high specific activity, commercially available [^{3}H]naltrexone could be used as the radioligand for the assay. Furthermore, the hapten which was likely to elicit the production of such an antiserum could be readily prepared from naltrexone in a fashion similar to the recently reported synthesis of naloxone-6-(*O*-carboxymethyl)oxime (4).

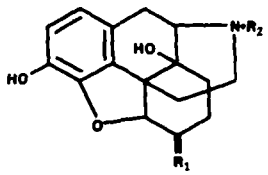

Nalmefene, R_1 = CH_2, R_2 = CH_2—◁
Naltrexone, R_1 = O, R_2 = CH_2—◁
Naloxone, R_1 = O, R_2 = $CH_2CH{=}CH_2$
Hapten, R_1 = N—O—CH_2COOH, R_2 = CH_2—◁

EXPERIMENTAL SECTION

Preparation of Immunogen and Antibody Production—The hapten, naltrexone-6-(*O*-carboxymethyl)oxime[1], was covalently coupled to bovine serum albumin using the mixed anhydride procedure of Erlanger *et al.* (5). The resulting conjugate was dialyzed against 0.05 M $NaHCO_3$, then water, and was then isolated by lyophilization. UV analysis of the immunogen indicated that ~17 moles of hapten were covalently coupled to 1 mol of albumin.

Two New Zealand White rabbits were immunized intradermally and boosted intravenously with the immunogen as previously described by Dixon and Crews (6). The antiserum with the highest titer of antibodies to nalmefene, obtained following the second booster immunization, was used for all subsequent studies. The antiserum was divided into 1-mL aliquots, lyophilized, and stored at −20°C.

Radioimmunoassay Procedure—Plasma samples (0.1–0.5 mL) containing

[1] Synthesized according to the procedure reported for naloxone-6-(*O*-methyl)oxime (4). The NMR, IR, and mass spectra were compatible with the proposed structure.

0022-3549/84/1100-1645$01.00/0

© 1984, American Pharmaceutical Association

REFERENCES

(1) R. D. Bulbrook, J. L. Hayward, and C. C. Spicer, *Lancet*, **ii**, 395 (1971).

(2) D. P. Rose, P. Stauber, A. Thiel, J. J. Crawley, and J. R. Milbrath, *Eur. J. Cancer*, **13**, 43 (1977).

(3) J. H. H. Thijssen, J. Poortman, and F. Schwarta, *J. Steroid Biochem.*, **6**, 729 (1975).

(4) A. Schwartz, G. Hard, L. Pashko, M. Abou-Gharbia, and D. Swern, *Nutr. Cancer*, **3**, 46 (1981).

(5) A. G. Schwartz and R. H. Tannen, *Carcinogenesis*, **2**, 1335 (1981).

(6) J. W. Nyce, P. N. Magee, G. C. Hard, and A. G. Schwartz, in press.

(7) L. Pashko, A. G. Schwartz, M. Abou-Gharbia, and D. Swern, *Carcinogenesis*, **2**, 717 (1981).

(8) P. A. Marks and J. Banks, *Proc. Natl. Acad. Sci., U.S.A.*, **46**, 447 (1960).

(9) G. W. Oertel and I. Rebelein, *Biochim. Biophys. Acta*, **184**, 459 (1969).

(10) C. R. Dworkin, S. D. Gorman, L. L. Pashko, V. J. Cristafalo and A. G. Schwartz, in press.

(11) G. W. Oertel, *Z. Hoppe-Seylers Physiol. Chem.*, **343**, 276 (1966).

(12) J. F. King and M. Aslam, *Synthesis*, **1980**, 285.

(13) J. P. Flatt, *J. Lipid Res.*, **11**, 131 (1970).

(14) M. Abou-Gharbia, L. Pashko, A. Schwartz, and D. Swern, *J. Pharm. Sci.*, **70**, 1154 (1981).

(15) G. I. Tesser and I. C. Balvert-Geev, *J. Peptide Protein Res.*, **7**, 295 (1975).

(16) V. A. Ziboh, M. A. Dreize, and S. L. Hsia, *J. Lipid Res.*, **11**, 346 (1970).

Nalmefene: Radioimmunoassay for a New Opioid Antagonist

ROSS DIXON [¶x], JANE HSIAO [*], WILLIAM TAAFFE [‡], ELLIOTT HAHN [§], and RONALD TUTTLE [¶]

Received December 5, 1983, from [¶]*Key Pharmaceuticals, Inc., Miami, FL 33169*, [*]*Innotech Laboratories, Inc., Ft. Lauderdale, FL 33314*, the [‡]*Institute for Clinical Pharmacology, St. James Hospital, Dublin, Ireland*, and [§]*Rockefeller University, New York, NY 10021.* Accepted for publication February 3, 1984.

Abstract □ A specific radioimmunoassay (RIA) has been developed for the quantitation of a new opioid antagonist, nalmefene, in human plasma. The method employs a rabbit antiserum to an albumin conjugate of naltrexone-6-(*O*-carboxymethyl)oxime and [^{3}H]naltrexone as the radioligand. Assay specificity was achieved by extraction of nalmefene from plasma at pH 9 into ether prior to RIA. The procedure has a limit of sensitivity of 0.2 ng/mL of nalmefene using a 0.5-mL sample of plasma for analysis. The intra- and interassay coefficients of variation did not exceed 5.6 and 11%, respectively. The specificity of the RIA was established by demonstrating excellent agreement (r = 0.99) with a less sensitive and more time consuming HPLC procedure in the analysis of clinical plasma samples. The use of the RIA for the pharmacokinetic evaluation of nalmefene is illustrated with plasma concentration profiles of the drug in humans following intravenous and oral administration.

Keyphrases □ Nalmefene—human plasma, RIA, compared with HPLC □ RIA—compared with HPLC, nalmefene, human plasma

Nalmefene [17-(cyclopropylmethyl)-4,5α-epoxy-6-methylenemorphinan-3,14-diol] is a potent, orally active narcotic antagonist (1) which is undergoing clinical evaluation in humans. The drug is a structural analogue of naltrexone with an exocyclic methylene group in the 6-position. Hahn *et al.* (1) indicated in preliminary pharmacology studies that orally administered nalmefene was about 50 times more potent than naloxone in its ability to antagonize the antinociceptive activity of an ED_{95} dose of morphine in either the mouse hot-plate or tail-clip procedures. Furthermore, nalmefene was 16 times more potent than naloxone in precipitating narcotic withdrawal in morphine-dependent rhesus monkeys. Recently, nalmefene has been shown to decrease the food and water intake and weight gain in obese and lean Zucker rats, lending further support to a possible role for opioids in the control of food intake (2).

The present study was undertaken to develop a simple and specific radioimmunoassay (RIA) for nalmefene which would provide greater sensitivity and ease of operation than a recently reported high-performance liquid chromatographic (HPLC) procedure (3). It was hoped that the RIA might be utilized in a wide variety of human tolerance and pharmacokinetic studies that are under way with nalmefene.

The initial approach taken in the development of the RIA was to produce an antiserum which would cross-react almost equally well with nalmefene and naltrexone. In this way, high specific activity, commercially available [^{3}H]naltrexone could be used as the radioligand for the assay. Furthermore, the hapten which was likely to elicit the production of such an antiserum could be readily prepared from naltrexone in a fashion similar to the recently reported synthesis of naloxone-6-(*O*-carboxymethyl)oxime (4).

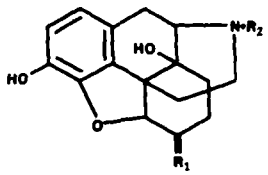

Nalmefene, R_1 = CH_2, R_2 = CH_2—◁
Naltrexone, R_1 = O, R_2 = CH_2—◁
Naloxone, R_1 = O, R_2 = $CH_2CH{=}CH_2$
Hapten, R_1 = N—O—CH_2COOH, R_2 = CH_2—◁

EXPERIMENTAL SECTION

Preparation of Immunogen and Antibody Production—The hapten, naltrexone-6-(*O*-carboxymethyl)oxime[1], was covalently coupled to bovine serum albumin using the mixed anhydride procedure of Erlanger *et al.* (5). The resulting conjugate was dialyzed against 0.05 M $NaHCO_3$, then water, and was then isolated by lyophilization. UV analysis of the immunogen indicated that ~17 moles of hapten were covalently coupled to 1 mol of albumin.

Two New Zealand White rabbits were immunized intradermally and boosted intravenously with the immunogen as previously described by Dixon and Crews (6). The antiserum with the highest titer of antibodies to nalmefene, obtained following the second booster immunization, was used for all subsequent studies. The antiserum was divided into 1-mL aliquots, lyophilized, and stored at −20°C.

Radioimmunoassay Procedure—Plasma samples (0.1–0.5 mL) containing

[1] Synthesized according to the procedure reported for naloxone-6-(*O*-methyl)oxime (4). The NMR, IR, and mass spectra were compatible with the proposed structure.

0022-3549/84/1100-1645$01.00/0

© 1984, American Pharmaceutical Association

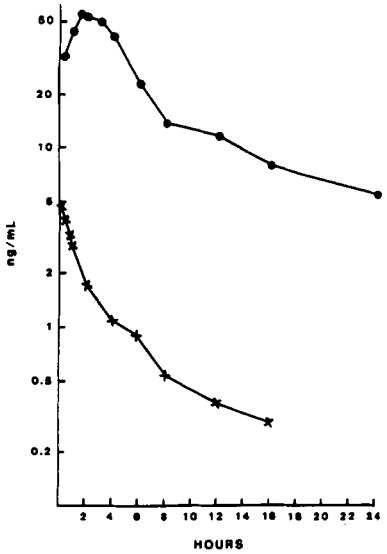

Figure 1—*Plasma concentrations of nalmefene following an intravenous injection (×) of 0.5 mg of nalmefene hydrochloride and an oral dose (●) of 64 mg of nalmefene hydrochloride.*

either known or unknown concentrations of nalmefene were diluted with 0.1 mL of 1 M borate buffer (pH 9) and extracted by vortexing with 2.5 mL of ether in a 12 × 75 mm disposable glass culture tube. Following brief centrifugation, the tubes were immersed in a shallow bath of 2-propanol–dry ice and the aqueous phases were frozen. The organic phase was decanted into a 12 × 75 mm tube and the ether was evaporated using a water bath at 50°C.

Each residue was dissolved in 0.1 mL of methanol and diluted with 0.4 mL of assay buffer[2]. Duplicate 0.2-mL aliquots of each extract were added to 12 × 75 mm tubes followed consecutively by 30,000 dpm of [^{3}H]naltrexone[3] in 0.2 mL of buffer and 0.2 mL of antiserum diluted 1:10,000 with buffer. After incubation at 4°C for 30 min, 0.5 mL of a well stirred suspension of dextran-charcoal[4] at 4°C was added to each tube, the contents were briefly vortexed and then allowed to stand at 4°C for ~10 min. The tubes were centrifuged at 4°C for 10 min at 1200×*g* and each supernatant, containing the antibody-bound radioligand, was decanted into a containing vial. After the addition of 10 mL of scintillation fluid[5], the vial was assayed in a liquid scintillation counter.

A calibration curve was generated using a four-parameter logistic curve-fitting program for a desk-top calculator[6] (7). Both the plasma standards and unknown samples were taken through the entire extraction and RIA procedure.

RESULTS AND DISCUSSION

Radioimmunoassay Characteristics—Depending on the degree of sensitivity required, two different ranges of calibration curves were used. The more sensitive assay ranged from 0.2 to 8 ng/mL using a 0.5-mL sample of plasma for analysis, while the other used a 0.1-mL sample and ranged from 2 to 100 ng/mL. In both instances, the logit-log plots were linear and the interday coefficients of variation ($n = 6$) for both standard curves did not exceed 11% for any individual standard (range, 2.4–11%). Linear regression analysis of the mean concentrations of nalmefene found *versus* the amount of nalmefene present in each plasma standard ($n = 6$) gave correlation coefficients of 0.999 and slopes within 6% of unity for both calibration curves. If necessary, unknown plasma samples with concentrations of nalmefene >100 ng/mL were appropriately diluted to bring the concentrations within the range of the 2–100-ng/mL calibration curve.

Using dextran-charcoal for the separation of antibody-bound and free radioligand, ~50% of the [^{3}H]naltrexone was bound in the presence of diluted antiserum alone while the nonspecific binding (no antiserum) was ~4%. The recovery of nalmefene from plasma using the present extraction procedure was 85 ± 4%; however, since both the standard and unknown plasma samples were handled in an identical fashion, no correction for recovery was necessary.

Assay Specificity—As mentioned previously, nalmefene and naltrexone were expected to cross-react about equally well with the antiserum, thereby allowing the use of commercially available [^{3}H]naltrexone as the radioligand for the quantitation of nalmefene. Cross-reactivity studies confirmed these expectations in that nalmefene exhibited an apparent cross-reactivity of 90% relative to naltrexone. At the same time 6β-naltrexol, the major metabolite of naltrexone found in plasma (8), cross-reacted 40%. The latter observation is not surprising since little antigenic specificity can be expected at the 6 position where the hapten was coupled to albumin. Thus, this antiserum would be of little value for use in a specific RIA for naltrexone due to the extensive cross-reactivity of 6 β-naltrexol. Naloxone, which only differs from naltrexone by having an *N*-allyl function, cross-reacted 20% with the antiserum, an indication that the *N*-cyclopropylmethyl group on the hapten was not a potent antigenic determinant.

During the initial developmental stages of the RIA, the apparent plasma concentrations of nalmefene in clinical samples were considerably higher when the plasma was assayed directly than following the extraction procedure outlined above. This was probably due to high concentrations of nalmefene glucuronide, in the presence of unconjugated nalmefene, cross-reacting to some extent with the antiserum. Therefore, the extraction step became a critical component of the assay procedure since nalmefene glucuronide would not be extracted into ether at alkaline pH.

A definitive and rigorous evaluation of the specificity of the RIA was made by comparing it with a recently established HPLC procedure (3). Clinical plasma samples obtained from four subjects who had received single oral doses of nalmefene hydrochloride (32 or 64 mg) were assayed by both analytical procedures and the joint determinations ($n = 21$) were subjected to linear regression analysis (RIA = y). Over a concentration range of 4–58 ng/mL, the correlation coefficient, regression-line slope, and y-intercept were 0.998, 0.996, and 0.38, respectively, which demonstrated excellent agreement between the two procedures and validated the specificity of the RIA for the quantitation of intact nalmefene in clinical plasma samples.

Nalmefene Plasma Concentrations in Humans—To illustrate the utility of the RIA, some typical plasma concentration profiles of nalmefene in subjects who had received various intravenous and oral doses of the drug are shown in Fig. 1.

Following intravenous administration of 0.5 mg of nalmefene hydrochloride, the plasma concentrations of the intact drug declined rapidly over the first 2 h, followed by a slower elimination phase up to 16 h, at which time the plasma concentration approached the limit of sensitivity of the assay (0.2 ng/mL). For the subject who received a 64-mg dose orally in solution, a peak plasma concentration of 55 ng/mL was reached 1.5 h after dosing and declined to 6 ng/mL after 24 h.

In conclusion, a simple and specific RIA for the quantitation of nalmefene in human plasma has been developed and validated by comparison with an established HPLC procedure. The RIA provides adequate sensitivity to obtain pharmacokinetic profiles of the drug following both intravenous and oral administration to humans. By virtue of its simplicity, the assay can facilitate the analysis of the ever increasing number of plasma samples which are being generated during new drug development studies.

REFERENCES

(1) E. F. Hahn, J. Fishman, and R. D. Heilman, *J. Med. Chem.*, **18**, 259 (1975).

(2) C. L. McLaughlin and C. A. Baile, *Pharmacol. Biochem. Behav.*, **19**, 235 (1983).

(3) R. Dixon and J. Hsiao, *Res. Commun. Chem. Pathol. Pharmacol.*, **42**, 449 (1983).

(4) E. F. Hahn, R. Lahita, M. J. Kreek, C. Duma, and C. E. Inturrisi, *J. Pharm. Pharmacol.*, **35**, 833 (1983).

(5) B. F. Erlanger, F. Borek, S. M. Beiser, and S. Lieberman, *J. Biol. Chem.*, **234**, 1090 (1959).

(6) R. Dixon and T. Crews, *J. Anal. Toxicol.*, **2**, 210 (1978).

(7) M. L. Jaffe, P. J. Munson, and D. Rodbard, "Four Parameter Logistic Curve-Fitting Program for the TI-59 Calculator," National Institute of Child Health, NIH, Bethesda, Md., 1979.

(8) M. E. Wall, D. R. Brine, and M. Perez-Reyes, *Drug Metab. Dispos.*, **9**, 369 (1981).

ACKNOWLEDGMENTS

Elliott Hahn is an Established Fellow of the New York Heart Association. The authors appreciate the assistance of Ms. Debbie LaBrie in the preparation of this manuscript.

[2] Tris buffer (0.05 M) at pH 7.4 containing 0.1% gelatin (Knox) and 0.1% sodium azide.

[3] Naltrexone [15,16-^{3}H], specific activity 34.8 Ci/mM, was purchased from New England Nuclear, Boston, Mass. and stored in methanol at −20°C.

[4] Assay buffer containing 0.05% (w/v) dextran T-70 (Sigma) and 0.5% (w/v) charcoal (Schwartz-Mann) was stored at 4°C.

[5] Aquasol; New England Nuclear.

[6] TI-59; Texas Instruments, Lubbock, Tex.

Determination of the Partition Coefficient and Acid Dissociation Constants of Iodochlorhydroxyquin by an Improved Partition Method

HIROSHI TANAKA ˣ and ZENZO TAMURA

Received January 4, 1983, from the *Faculty of Pharmaceutical Sciences, University of Tokyo, 7-3-1 Hongo, Bunkyo-ku, Tokyo 113, Japan.* Accepted for publication September 29, 1983.

Abstract □ A simple and precise method for determining partition coefficients was developed utilizing a disposable injector. The method was used to determine the partition ratio of iodochlorhydroxyquin between *n*-decane and phosphate-buffered saline, pH 7.4. The partition ratio was found to be 1750 with a coefficient of variation of 3%. Moreover, it was found that iodochlorhydroxyquin did not associate in *n*-decane at a concentration $< 1 \times 10^{-3}$ M. The acid dissociation constants and the partition coefficient of the undissociated species were determined. These values corresponded well with the values obtained from spectrophotometric methods.

Keyphrases □ Iodochlorhydroxyquin—partition coefficients, acid dissociation constants □ Improved partition method—partition coefficients, dissociation constants, iodochlorhydroxyquin

Iodochlorhydroxyquin (5-chloro-7-iodo-8-quinolinol; I), an amphoteric molecule sparingly water soluble at neutral or slightly acidic pH values, has been studied *in vivo* using a radionuclide-labeled compound (1). Repeated administrations of I to beagle dogs led to neurological disorders with concomitant demonstration of I in the central nervous system (CNS) by quantitative GC measurements (2). Intestinal absorption, renal excretion, and the distribution of I to various tissues, especially to the CNS, were thought to be influenced by the concentration of the undissociated species. The acid dissociation constants and partition coefficient of the undissociated species have not been reported, primarily because I is extremely insoluble in water and is strongly adsorbed onto glassware.

Special glassware was used to determine the partition ratio of long-chain fatty acids between *n*-heptane and an aqueous phosphate buffer (3); however, accurate values >1000 were not determined. Using a disposable injector, we have developed a more precise and convenient method for determining large partition ratios. This methodology has been used to determine the partition coefficient of the undissociated species and acid dissociation constants of I.

EXPERIMENTAL SECTION

Syntheses of Tritiated Analogues of 5-Chloro-7-iodo-8-quinolinol—Tritiated I was synthesized according to the method reported by Urakubo and Kido (4) (Scheme I). To a mixture of 2-amino-4-chlorophenol[1] (14.4 mg, 0.1 mmol), 4-chloro-2-nitrophenol[1] (8.8 mg, 0.05 mmol), glycerol[2] (0.11 mmol), and [1(3)-^{3}H]glycerol[3] (1.6 mCi, 2.3 Ci/mmol) was added 21 μL of concentrated sulfuric acid. The mixture was refluxed at 125°C for 2 h, and then the remaining 4-chloro-2-nitrophenol was removed by sublimation (the temperature was increased to 160°C for 15 min). The residual material was extracted twice with 1.5 mL of distilled water and with the same volume of 7% H_2SO_4. The total aqueous phase was adjusted to pH 5 with 30% NaOH, and the resulting precipitate was removed by centrifugation and washed with distilled water to give 5-chloro-8-[2(4)-^{3}H]quinolinol as a gray powder, which was purified by sublimation at 140°C. This afforded 10.7 mg (60% yield) of crystalline material, mp 129°C (a radiochemical yield of 26%). 8-[2(4)-^{3}H]Quinolinol was synthesized in a similar manner (30% yield), mp 76°C.

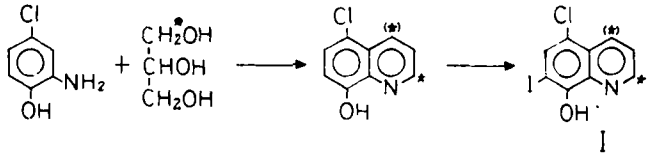

Scheme I

Preparation of 5-Chloro-7-iodo-8-[2(4)-^{3}H]quinolinol—5-Chloro-8-[2(4)-^{3}H]quinolinol (8.6 mg) was dissolved in 3 mL of 60 mM glycine buffer (pH 1.35) and was iodinated with iodine monochloride as described by Hales and Randle (5). The excess reagent was decomposed by adding 0.5 M $Na_2S_2O_3$, the precipitate was washed twice with the buffer, twice with distilled water, and was then dried under reduced pressure over phosphorus pentoxide to give 12.1 mg (83% yield) of 5-chloro-7-iodo-8-[2-(4)-^{3}H]quinolinol as a white solid, mp 173°C (dec.).

The chromatographic behavior (TLC, silica gel) and the melting points of these labeled compounds were identical with those of authentic cold materials (6). The radiochemical purity of tritiated I was determined to be 99.3% by an isotopic recrystallization method.

Other Chemicals—*n*-Decane[1], reagent grade, was purified by shaking several times with concentrated sulfuric acid until the acidic layer became colorless, and was then distilled under reduced pressure. The buffers were 0.02 M, containing 0.13 M NaCl and 5 mM EDTA to prevent the interference of metal ions; pH values of the buffer were adjusted with an accuracy of ±0.01. The scintillation cocktail consisted of 5 g of 2,5-diphenyloxazole (PPO)[4] and 134 mg of 2,2′-*p*-phenylene-*bis*(4-methyl-5-phenyloxazole) (dimethyl POPOP)[5] per liter of toluene[2]. All other chemicals were of the highest purity available.

The General Procedure for the Measurement of Partition Ratios—A glass tube (19 mm i.d. × 37 mm depth) containing 3.5 mL of buffer was covered with a polyethylene cap with two holes (4 mm i.d. and 1 mm i.d., respectively). A 25-gauge disposable needle[6] was inserted into the tube through the larger

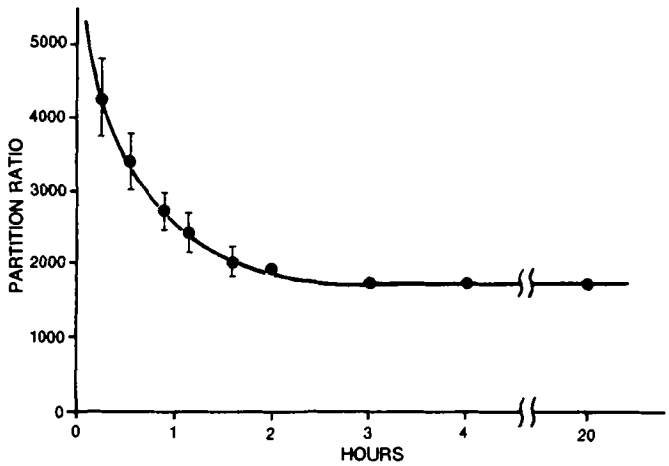

Figure 1—*Time course of partition equilibrium of iodochlorhydroxyquin between n-decane and 0.02 M phosphate-0.13 M NaCl-5 mM EDTA buffer (pH 7.4) at 25°C. [^{3}H]Iodochlorhydroxyquin was initially added to the organic layer.*

[1] Tokyo Kasei, Tokyo.
[2] Kanto Kagaku, Tokyo.
[3] Ethanol solution; Amersham International, Amersham, Buckinghamshire HP 79LL, England.
[4] Nakarai Kagaku, Kyoto.
[5] Eastman Kodak, Rochester, N.Y.
[6] Terumo, Tokyo.

0022-3549/84/1100-1647$01.00/0
© 1984, American Pharmaceutical Association

Table I—Determination of the Dissociation Constants of Iodochlorhydroxyquin at 25°C

In Dilute Hydrochloric Acid					
HCl, M	pH	$\frac{A_{266}}{A_{252.5}}$	$\log \frac{[CF^+]}{[CF]}$	pK_1'	$pK_{1,0}$[a]
0.0117	2.02	1.102	0.180	2.20	2.15
0.0092	2.12	1.100	0.176	2.30	2.25
0.0075	2.21	1.026	0.035	2.25	2.20
0.0057	2.32	0.961	−0.078	2.24	2.20
0.0048	2.39	1.000	−0.011	2.38	2.34
0.0039	2.48	0.913	−0.159	2.32	2.29
0.0028	2.61	0.824	−0.306	2.30	2.28
0.0023	2.70	0.794	−0.357	2.34	2.32
Mean ± *SD*					2.25 ± 0.07
In 1 mM Sodium Carbonate Buffer					
	pH	$\frac{A_{266}}{A_{252.5}}$	$\log \frac{[CF]}{[CF^-]}$	pK_2'	$pK_{2,0}$[b]
	8.10	1.164	0.208	8.31	8.33
	8.20	1.306	0.055	8.26	8.28
	8.29	1.375	−0.022	8.27	8.29
	8.40	1.463	−0.125	8.28	8.30
	8.41	1.426	−0.081	8.33	8.35
	8.50	1.540	−0.224	8.28	8.30
	8.58	1.554	−0.243	8.34	8.36
	8.70	1.594	−0.299	8.40	8.43
Mean ± *SD*					8.33 ± 0.05

[a] $pK_{1,0}$ was calculated from Eq. 9. [b] $pK_{2,0}$ was calculated from Eq. 10.

hole of the cap and fixed so that the tip of the needle almost reached the bottom. A disposable tuberculine syringe (2.5 mL)[6] was connected to the needle. The *n*-decane solution of [^{3}H]iodochlorhydroxyquin (0.2 mL) was gently placed on the aqueous layer with a microsyringe through the smaller hole of the cap. The tubes were gently shaken by a reciprocating shaker[7] 73 times per min for 3 h at 25 ± 0.5°C. After the equilibration, 2 mL of the aqueous layer was removed (with the tuberculine syringe) and the solution was transferred to a weighed scintillation vial. The vial was weighed again to accurately determine the volume of the sample. After removal of the polyethylene cap with the needle, 50 μL of the organic layer was removed and transferred to a weighed scintillation vial. The volume was again determined by weighing the vial. Ten milliliters of the scintillation cocktail was added to each vial and the radioactivity was counted with a liquid scintillation counter[8]. The vial containing the aqueous sample was shaken 100 times before counting.

RESULTS AND DISCUSSION

Determination of the Partition Ratio of I by the Partition Method—The partition ratio is defined as follows:

$$\text{Partition ratio} = \frac{\text{Radioactivity in organic phase}}{\text{Radioactivity in aqueous phase}} \qquad \text{(Eq. 1)}$$

Figure 1 shows that the partition equilibrium was reached after 3 h and was maintained for ≥17 h with a variation of ±3%. As shown in Fig. 2, the partition ratios of I, 8-quinolinol, and 5-chloro-8-quinolinol at pH 7.4 were measured over a wide concentration range. Since the partition ratios remained constant, it appeared that the 8-quinolinols did not associate in a manner similar to the fatty acids (3). The partition ratio of I was 1750, while those of 8-quinolinol and 5-chloro-8-quinolinol were 24.1 and 247, respectively.

Determination of the Dissociation Constants of I by the Partition Method—The partition ratio (Eq. 2) assumes that the ionized forms of I are not found in the organic phase and that un-ionized molecules of I are found in both phases.

$$\text{Partition ratio} = \frac{[CF]_o}{[CF^+]_w + [CF]_w + [CF^-]_w} = \frac{K_p}{\frac{(H^+)_w}{K_1'} + 1 + \frac{K_2'}{(H^+)_w}} = \frac{K_p}{10^{(pK_1'-pH)} + 1 + 10^{(pH-pK_2')}} \qquad \text{(Eq. 2)}$$

[7] BT-21; Yamato Kagaku, Tokyo.
[8] Tri-Carb Model 3255; Packard Instruments, Downers Grove, Ill.

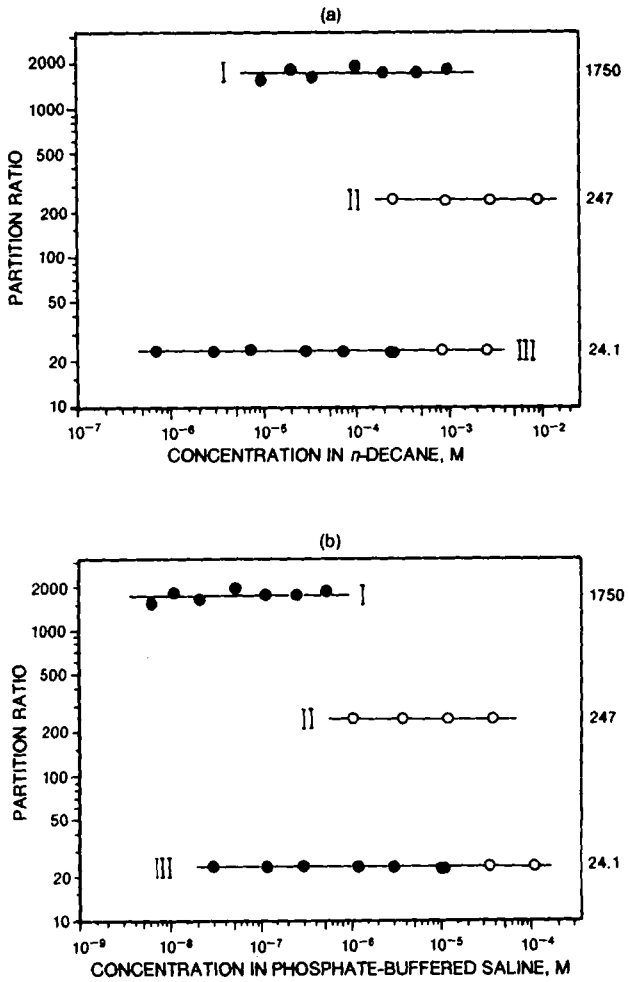

Figure 2—*Effect of concentration on the partition ratio of iodochlorhydroxyquin (I), 5-chloro-8-quinolinol (II), and 8-quinolinol (III) between n-decane and phosphate-buffered saline (pH 7.4) at 25°C. Key: (●) radioisotope method; (○) values from the spectrophotometric measurement.*

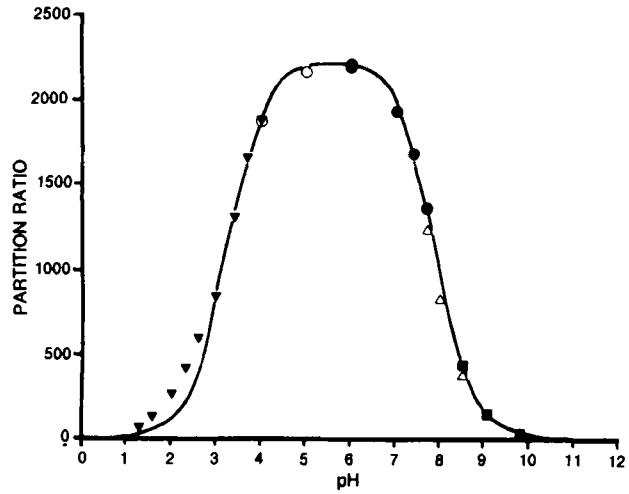

Figure 3—*Effect of pH on the partition ratio of iodochlorhydroxyquin between n-decane and the 0.02 M buffer–0.13 M NaCl–5 mM EDTA system at 25°C. Key: (▼) glycine–hydrochloric acid; (○) acetate; (●) phosphate; (△) Tris-HCl and (■) glycine–sodium hydroxide; (—) hypothetical curve for Eq. 3.*

In Eq. 2, the subscripts o and w indicate the organic and the aqueous phases, respectively. [CF], [CF$^+$], [CF$^-$], and (H$^+$) represent the concentration of the molecular, the cationic, and the anionic forms of I, and the activity of the hydrogen ion, respectively. The partition coefficient, K_p, is expressed as $K_p = [CF]_o/[CF]_w$. The dissociation constants of I in acidic and basic media are expressed as $K_1' = [CF]_w(H^+)/[CF^+]_w$, and $K_2' = [CF^-]_w(H^+)/[CF]_w$, respectively. Accordingly, those constants may be calculated from the pH profile of the partition ratio.

The partition ratio at various pH values (1.2–9.8) was measured using five buffer systems. Figure 3 shows that the pH profile of the partition ratios in I was a bell-shaped curve with a maximum at pH 5.6. The constants, K_p, K_1', and K_2' were estimated from the data in Fig. 3 as follows: $K_p = 2230 \pm 43$ (CV 1.9%), $n = 11$; $K_1' = 5.6 \times 10^{-4}$, $pK_1' = 3.25$; $K_2' = 1.29 \times 10^{-8}$, $pK_2' = 7.89$. Consequently, Eq. 2 can be expressed as:

$$\text{Partition ratio} = \frac{2230}{10^{(3.25-pH)} + 1 + 10^{(pH-7.89)}} \qquad \text{(Eq. 3)}$$

The solid line in Fig. 3 is the hypothetical curve for Eq. 3, and it agrees well with the observed values in the pH range of 3–10.

Inquiry of the Partition Method by a Spectrophotometric Approach—Compound I and its ionized forms show characteristic UV absorption. The dissociation constants of such compounds, in general, can be calculated from the spectral data. The spectrophotometric method is based on the general equation:

$$A = [CF^+]\epsilon^c + [CF]\epsilon^n + [CF^-]\epsilon^a \qquad \text{(Eq. 4)}$$

where A, total absorbance, is the sum of the respective absorbance of each species, and ϵ^n, ϵ^c, and ϵ^a represent the molar extinction coefficients of the un-ionized, cationic, and anionic forms of I, respectively. When the pH value is lower than $pK_2' - 2$ or higher than $pK_1' + 2$, the term [CF$^-$] or [CF$^+$] can be neglected, respectively. In this case, pK_1' and pK_2' are as follows:

$$pK_1' = pH + \log\frac{[CF^+]}{[CF]} \qquad \text{(Eq. 5)}$$

$$pK_2' = pH + \log\frac{[CF]}{[CF^-]} \qquad \text{(Eq. 6)}$$

Both the anionic and cationic forms of I showed an absorption maximum at 266 nm, and the values of ϵ_{266}^a or ϵ_{266}^c, calculated from the spectrophotometric data by dissolving I in 1 mM sodium carbonate buffer or in diluted hydrochloric acid, were 3.81×10^4 and 2.80×10^4, respectively. However, the value of ϵ^n could not be determined because I was sparingly soluble in the neutral aqueous solution. Accordingly, we estimated $\epsilon_{\lambda_{max}}^n$ (252.5 nm) and ϵ_{266}^n as 1.2×10^4 and 0.42×10^4, respectively, by extrapolating the ϵ values measured in the various concentrations of methanol (Fig. 4). $\epsilon_{252.5}^c$ and $\epsilon_{252.5}^a$ were found to be 2.00×10^4 and 1.92×10^4, respectively. Thus, Eqs. 5 and 6 may be expressed as follows:

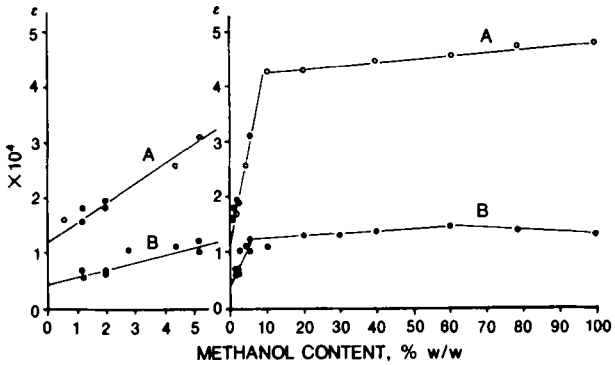

Figure 4—*Effect of methanol content in aqueous solution on the ε of iodochlorhydroxyquin at 252.5 (A) and 266(B) nm.*

$$pK_1' = pH + \frac{1.20 \times A_{266}/A_{252.5} - 0.42}{2.80 - 2.00 \times A_{266}/A_{252.5}} \qquad \text{(Eq. 7)}$$

$$pK_2' = pH + \frac{1.92 \times A_{266}/A_{252.5} - 3.81}{0.42 - 1.20 \times A_{266}/A_{252.5}} \qquad \text{(Eq. 8)}$$

The dissociation constants of I were calculated from the data listed in Table I. Similarly $pK_{1,0}$ and $pK_{2,0}$, calculated from the following Debye-Hückel equations, were 2.25 and 8.33 at 25°C, respectively.

$$pK_1' = pK_{1,0} + 0.509\sqrt{I} \qquad \text{(Eq. 9)}$$

$$pK_2' = pK_{2,0} - 0.509\sqrt{I} \qquad \text{(Eq. 10)}$$

where I represents the ionic strength.

The values pK_1' and pK_2', obtained from the spectrophotometric results at the same temperature and the same ionic strength as the partition method, were 3.17 ± 0.11 and 8.05 ± 0.08 at 25°C, respectively, and agree well with those obtained by the partition method.

REFERENCES

(1) Y. Toyokura, T. Takasu, and O. Matsuoka, *Jpn. J. Med. Sci. Biol.*, **28** (Suppl.), 79 (1975).

(2) K. Hayakawa, T. Imanari, Z. Tamura, S. Kuroda, H. Ikeda, and J. Tateishi, *Chem. Pharm. Bull. (Tokyo)*, **25**, 2013 (1977).

(3) R. B. Simpson, J. D. Ashbrook, E. C. Santos, and A. A. Spector, *J. Lipid Res.*, **15**, 415 (1974).

(4) G. Urakubo and Y. Kido, *Radioisotopes*, **24**, 500 (1975).

(5) C. N. Hales and P. J. Randle, *Biochem. J.*, **88**, 137 (1963).

(6) "The Merck Index," 9th ed., Rahway, NJ., 1976, pp. 276, p 644, 664.

ACKNOWLEDGMENTS

We thank Dr. R. Horikawa for his valuable suggestions. This work was supported in part by a Grant-in-Aid for SMON Research from the Ministry of Health and Welfare of Japan.

Determination of Meclocycline, a Tetracycline Analogue, in Cream Formulations by Liquid Chromatography

ANNELI M. DEPAOLIS *x, THOMAS E. BRITT ‡, ARLENE J. HOLMAN *, EUGENE J. McGONIGLE *, GERALD KAPLAN ‡, and WALTER C. DAVIES ‡

Received May 26, 1983, from the *Research Laboratories, Ortho Pharmaceutical Corp., Raritan, NJ 08869 and ‡Johnson & Johnson Research Center, New Brunswick, NJ 08902. Accepted for publication November 16, 1983.

Abstract □ A rapid and sensitive high-performance liquid chromatographic quantitation of meclocycline (I) in a cream formulation is described. The acidified methanolic extract of the sample was diluted with mobile phase and analyzed on a reverse-phase column by using a mobile phase consisting of EDTA buffer (pH 6.6)-tetrahydrofuran (85:15 v/v). The method gave linear, quantitative, and reproducible results with a detection limit of 0.4 ppm for meclocycline.

Keyphrases □ Meclocycline—tetracycline analogue, cream formulations, HPLC □ Cream formulations—meclocycline, tetracycline analogue, HPLC

Meclocycline sulfosalicylate (I), a 7-chloro-6-methylene-5-hydroxy-derivative of tetracycline, is marketed as a topical antibiotic cream formulation[1] for the treatment of acne. Methods for quantitating meclocycline and its impurities have not been reported. However, high-performance liquid chromatographic (HPLC) methods have been shown to be most effective for separating tetracyclines and their degradation products. These HPLC methods have been extensively reviewed (1). The reverse-phase mode has become the most widely used column packing for tetracyclines with a mobile phase at a low pH range (1.2–2.5), which is generally not recommended for bonded silica columns. In an additional method, a microparticulate phenyl column and single-step gradient elution at pH 2.2 are used (2). These types of systems have been found not to be applicable to the separation of meclocycline and its impurities. It has been preferred to have a system with a less acidic mobile phase, not only to prolong the lifetime of the column but to retard the degradation of tetracyclines known to occur at low pH (3). Among the various reverse-phase packings, Vydac TP C_{18} has been found to be very suitable for use with mobile phases in the near neutral region for the separation of tetracyclines and their degradation products (4). By utilizing this column and a mobile phase of tetrahydrofuran in ammonium EDTA buffer at pH 6.6, a baseline separation of meclocycline, and its potential degradation products and impurities in pharmaceutical cream was achieved. In this report is described a rapid, linear, and reproducible method for the quantitation of meclocycline in a cream formulation.

EXPERIMENTAL SECTION

Materials—Meclocycline sulfosalicylate[2] (I) (4*S*,4a*R*,5*S*,5a*R*,12a*S*)-7-chloro-4-(dimethylamino)-1,4,4a,5,5a,6,11,12a-octahydro-3,5,10,12,12a-pentahydroxy -6- methylene-1,11-dioxo-2-naphthacenecarboxamide, mono(5-sulfosalicylate), was used in all experiments as received. For the cream samples, a 1% w/w formulation of meclocycline sulfosalicylate cream[1] was used. Tetrahydrofuran[3] was HPLC grade; EDTA[4] and all the other chemicals and solvents were analytical reagent grade.

Preparation of Mobile Phase—EDTA (0.6 g) was mixed with 2 mL of methanol and dissolved in 15 mL of concentrated ammonium hydroxide. Approximately 1800 mL of distilled water was added, and the pH was adjusted to precisely 6.6 with glacial acetic acid. The solution was diluted to 2 L with distilled water. The 0.001 M ammonium EDTA buffer solution was filtered through a fluoropore membrane filter (0.5 μm), mixed with tetrahydrofuran in the ratio of 85:15 v/v, and deaerated under vacuum.

Chromatographic System—A liquid chromatograph[5] equipped with an automatic sample injector[6] was used for all HPLC work. The column was packed with octadecylsilane material bonded to microparticulate silica gel (10 μm)[7]. The columns were periodically purged with 95% ethyl alcohol (form III)[8] for optimum resolution. Since the columns were obtained from the manufacturer preserved in denatured alcohol, no column conditioning was necessary. The flow rate was 0.8 mL/min, and a 10-mV strip chart recorder was employed at a chart speed of 0.5 cm/min.

Standard Solution Preparation—A portion (30–50 mg) of the reference standard, meclocycline sulfosalicylate (I) (or 25 mg of USP meclocycline base reference standard) was weighed to the nearest 0.1 mg and dissolved in and diluted to 100 mL with methanol. A 2.0-mL aliquot of the solution described above was diluted to 50.0 mL with mobile phase. The solution was filtered through a Swinney filter with a syringe and used as an external standard. Filters[9] (0.5 μm) were used and stored in methanol prior to use.

Sample Preparation—A portion of the meclocycline sulfosalicylate cream (equivalent to ~8 mg of I or ~5 mg of meclocycline base) was weighed to the nearest 0.1 mg into a 50-mL stoppered centrifuge tube. Equal volumes of methanol (20 mL) and 0.0125 M sulfuric acid (20 mL) were added to the tube. The sample was thoroughly dispersed by a combination of sonication (~60 min) and vortexing (2 min). Inadequate dispersing produced poor recoveries. The dispersed mixture was quantitatively transferred into a 50-mL volumetric flask and diluted to volume with methanol. After centrifugation at ~2000×*g* for 10 min, a 5.0-mL aliquot of the supernatant liquid was diluted to 50.0 mL with the mobile phase. The mixture was filtered through a Swinney filter as described above. The samples should not be stored in the mobile phase solution longer than a day, or loss of meclocycline will be observed.

Analytical Procedure—Chromatograms for all standards and samples were obtained at ambient temperature by injecting 10-μL aliquots at a detector sensitivity of 0.02 AUFS. When the flow rate was 0.8 mL/min, the average retention time of meclocycline was 7 min, although depending on the column condition the retention time can vary between 5.5 and 8.5 min. By small adjustments of tetrahydrofuran in the mobile phase, the retention time may be varied to the desired value. The resolution factors are 3.0 for methacycline and meclocycline and 1.7 for C-4-epimeclocycline and meclocycline, and the tailing factor for meclocycline is 1.0. For quantitation of meclocycline, samples were injected with an automatic sample injector and bracketed with standards in the sequence: STD-1, STD-1, STD-2, STD-2, SAMP-1, SAMP-1, SAMP-2, SAMP-2, STD-1, STD-1, STD-2; STD-2 (where STD is the standard solution and SAMP is the sample solution). A basic program designed for a computer system[10] was used for quantitation of the samples of meclocycline in sequence with the standards as listed above. The percentage of meclocycline base in the cream by weight was calculated by: $(A_{samp} \times W_{std} \times P)/(A_{std} \times W_{samp} \times 50)$. The peak areas and weights, in milligrams, of sample and standard, are A_{samp}, W_{samp}, and A_{std}, W_{std}, respectively. The potency[11] (P) of meclocycline is usually equivalent to not less than 620 μg/mg

[1] Meclan Cream (1%); Ortho Pharmaceutical Corp., Raritan, N.J.
[2] Pfizer Inc., New York, N.Y.
[3] Burdick & Jackson Laboratories, Inc., Muskegon, Mich.
[4] J. T. Baker Chemical Co., Phillipsburg, N.J.
[5] Model 440 244 equipped with a model 6000A pumping system and a model 440 UV detector operated at 340 nm; Waters Associates, Milford, Mass.
[6] WISP 710A; Waters Associates.
[7] Vydac 201 TP reverse phase (25 cm × 3.2 mm i.d.); Separations Group, Hesperia, Calif.
[8] Sargent-Welch Scientific Co. Skokie, Ill.
[9] Fluorophore FHL P04700; Millipore Corp.
[10] HP3356; Hewlett-Packard Co., Palo Alto, Calif.
[11] Meclocycline sulfosalicylate occurs as a monohydrate with a maximum theoretical potency of 669 μg/mg relative to the pure anhydrous base, which has been assigned a potency of 1000 μg/mg.

0022-3549/84/1100-1650$01.00/0
© 1984, American Pharmaceutical Association

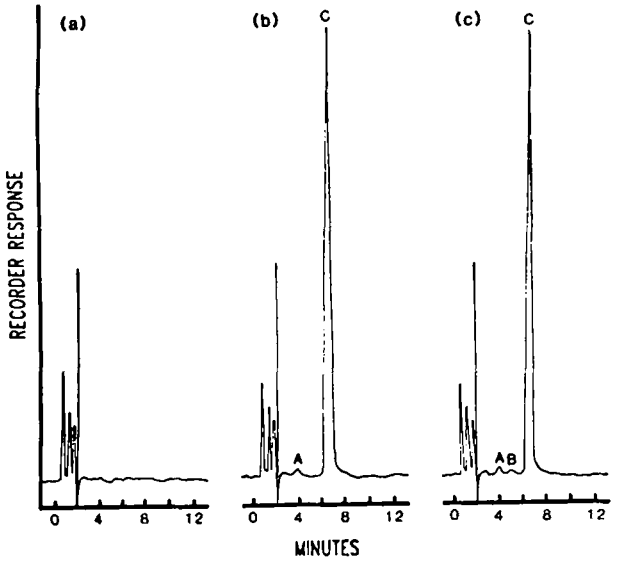

Figure 1—*Typical chromatograms of cream placebo (a), standard I (b), and a 1% cream sample preparation of I (c). Key: (A) methacycline; (B) C-4-epimer of I; (C) I. Conditions: mobile phase, 0.001 M ammonium EDTA buffer (pH 6.6)–tetrahydrofuran (85:15); column, reverse-phase*[7], *25 cm × 3.2 mm i.d.; flow rate, 0.8 mL/min; detector, UV at 340 nm.*

and usually in the area of 665-670 μg/mg[12], and for USP meclocycline base it is 1000 μg/mg.

RESULTS AND DISCUSSION

Typical chromatograms obtained for the cream placebo, standard meclocycline sulfosalicylate (I), and a 1% cream sample preparation of I are shown in Fig. 1. The system gave a baseline separation for meclocycline, methacycline, and the C-4-epimer of meclocycline at ambient temperature. Meclocycline eluted with an average retention time of 7 min. The peak at 4 min corresponded to methacycline, an impurity always present in the raw material but never present at >3% of the total weight. The peak at 5 min was identified to be the C-4-epimer of meclocycline (5). By varying the relative amount of tetrahydrofuran in the mobile phase, the retention times of meclocycline and impurities could easily be shifted. The objective was to keep the retention time of meclocycline in the range of 5.5–8.5 min. The ammonium EDTA buffer in the mobile phase was a crucial ingredient to give well-defined and sharp peaks on HPLC chromatograms. It was also necessary to dilute the sample with the mobile phase in the sample preparation. If only methanol was utilized, leading peaks were observed. The wavelength of 340 nm was selected for maximum sensitivity and for the least amount of interference from UV-absorbing components of cream excipients. The minimum detection for meclocycline was 0.4 ppm at 340 nm.

[12] The potency was determined by a microbiological assay method.

Table I—Recovery of Meclocycline Base from Spiked Cream Placebo [a]

Theoretical Label Claim, %	Percent Recovery[b] Peak Areas	Peak Heights
80	101	100
	97.0	96.2
100	96.0	98.5
	96.8	96.0
120	98.7	98.2
	96.9	97.6
Average	$\bar{X}_6$ = 97.7%	$\bar{X}_6$ = 97.8%
SD	±1.83%	±1.51%
RSD	±1.87%	±1.54%

[a] Representative of 80-120% of theoretical label claim; label claim is 1% w/w meclocycline base. [b] Meclocycline base.

The results of recovery studies performed on cream placebos spiked with I are shown in Table I. The spiking covered the range of 80-120% of the theoretical label claim, which is usually 1% meclocycline base by weight. The recoveries, ranging from 96 to 101%, were comparable whether peak areas or heights were used. The data demonstrate the method to give linear, quantitative, and reproducible results with a minimum of sample handling.

A few other commercially available reverse-phase columns (C_{18}[13,14], ODS[15], and C_8[15]) were tested under the same operating conditions but were found to be not suitable. It seems that meclocycline was bound on these columns and would not elute until purged with methanol. When the solvent system was changed to consist of 1% phosphoric acid–methanol (45:55), the C_{18}[13] reverse-phase column gave a separation of methacycline and meclocycline, but no separation of meclocycline and its C-4-epimer was observed. Since the pH of the latter mobile phase was ~2, meclocycline was assumed to be mainly in the ionic form with a protonated dimethylamino group, which is analogous to other tetracyclines (6). It therefore seems that on reverse-phase columns, the C-4 isomers of meclocycline cannot be separated as ionic species but rather as doubly charged zwitterions, the most likely form of tetracyclines between pH 3.0 and 6.5 reported previously (6).

In conclusion, the described method gives a rapid and reproducible quantitation of meclocycline in the cream formulation of meclocycline sulfosalicylate.

REFERENCES

(1) J. H. Knox and J. Jurand, *J. Chromatogr.*, **186**, 763 (1979).

(2) N. Muhammad and J. A. Bodnar, *J. Pharm. Sci.*, **69**, 928 (1980).

(3) J. R. D. McCormick, S. M. Fox, L. L. Smith, B. A. Bitler, J. Reichenthal, V. E. Origoni, W. H. Muller, R. Winterbottom, and A. P. Doerschuk, *J. Am. Chem. Soc.*, **79**, 2849 (1957).

(4) G. D. Mack and R. B. Ashworth, *J. Chromatogr. Sci.*, **16**, 93 (1978).

(5) A. M. DePaolis, *J. Liq. Chromatogr.*, **7**, 1367 (1984).

(6) C. R. Stephens, K. Murai, K. J. Brunings, and R. B. Woodward, *J. Am. Chem. Soc.*, **78**, 4155 (1956).

[13] Waters Associates.
[14] Alltech Associates, Inc., Deerfield, Ill.
[15] DuPont Co., Wilmington, Del.

Preparation of Alkoxyquinoline Derivatives and Their Evaluation as Potential Central Nervous System Stimulants

M. EL-KERDAWY, A. ABOU-OUF, A. TANTAWY*[x], and I. ABOU EL-DAHAB

Received November 30, 1982, from the *Organic and Pharmaceutical Chemistry Deprtment, Faculty of Pharmacy, University of Mansoura, El-Mansoura, Egypt.* Accepted for publication April 18, 1983. *Present address: Holy Mecca, Ibn Sina Clinic, P.O.B. 1576, Saudi Arabia.

Abstract □ A variety of substituted amides of 6,7-dimethoxy-2-hydroxyquinoline-3-carboxylic acid were synthesized. Three of these compounds, tested as potential central nervous system stimulants, showed no marked biological activity.

Keyphrases □ Alkoxyquinoline derivatives—potential CNS stimulants, synthesis □ Stimulants—CNS, alkoxyquinoline derivatives, synthesis

The analeptic activity of aromatic heterocyclic tetrazoles (1), such as nikethamide, ethamivan, and their *N*-ethylamides (2, 3) is well known. In addition, the *N*,*N*-diethylamides of numerous ring systems (such as pyrazole, thiazole, isoxazole, and the imidazolopyrimidines) as well as some xanthines and pyridines show analeptic activity (2, 4). Some CNS-sympathomimetic drugs such as the benzyl-, morpholinyl-, and piperidyl-*N*-ethylamide derivatives (2, 3) are also employed as psychomotor stimulants to elevate the mood or to improve the sense of well being of patients suffering from certain psychiatric depressions. The biological effects of the aforementioned drugs could be explained by the incorporation of a nitrogen atom in the ring systems (5), possibly providing resistance to enzymatic inactivation by steric protection of the amino groups (6), as in the case of phenmetrazine or methylphenidate. Similarly, *N*-alkyl groups, which are substituted with more bulky groups than methyl, diminished activity; the absence of the aromatic nucleus or its replacement by an alkyl group resulted in compounds of little or no activity (6). On the other hand, iproniazide (7), a monamine oxidase (MAO) inhibitor, appears to reverse the action of reserpine.

Since maximum MAO inhibition and analeptic activity are shown by compounds similar to amphetamine, *e.g.*, phenipraxine and a nitrogenisostere of methamphetamine (8), the present work describes the synthesis of potential CNS-stimulating agents, which have both aminoalkane and heterocyclic structural systems, such as quinoline. A series of substituted amides derived from 2-hydroxy-6,7-dimethoxyquinoline-3-carboxylic acid, which appeared likely to possess a CNS-stimulating effect, were prepared. In addition, the unsubstituted hydrazide derivatives of the compounds were alkylated to overcome the insignificant MAO inhibitory properties of unsubstituted hydrazines (9, 10). In the present investigation, the 6,7-dimethoxyquinoline system was varied to obtain 3-carboxylic acid hydrazides and hydrazones (Scheme I) for evaluation as CNS stimulants.

EXPERIMENTAL SECTION

Chemistry—*6,7-Dimethoxy-2-hydroxyquinoline-3-carboxylic Acid Hydrazide (IX)*—Hydrazine hydrate (0.1 mol) was added to a suspension of 6,7-dimethoxy-3-ethoxycarbonyl-2-hydroxyquinoline (I) (11) (0.02 mol) in ethanol (200 mL). The mixture was heated at reflux for 3 h. The hydrazide was removed by filtration, washed with water, dried, and recrystallized (Table I).

Interaction of 6,7-Dimethoxy-3-ethoxycarbonyl-2-hydroxyquinoline and Phenylhydrazines (X and XI)—Phenylhydrazine or 2,4-dinitrophenylhydrazine (0.02 mol) was added to a suspension of 6,7-dimethoxy-3-ethoxy-

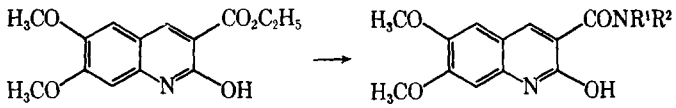

I II–XVI

Scheme I

Table I—Newly Synthesized Alkoxyquinoline Derivatives (II–XVI)

Compound	R^1	R^2	mp, °C	Yield, %	Molecular Formula[a]
I[b]	—	—	275[c]	70	$C_{14}H_{15}NO_5$
II	H	CH_3	300[d]	75	$C_{13}H_{14}N_2O_4$
III	CH_2CH_3	CH_2CH_3	300[d]	80	$C_{16}H_{20}N_2O_4$
IV	H	$CH_2C_6H_5$	300[d]	70	$C_{19}H_{18}N_2O_4$
V	$(CH_2)_5$	$(CH_2)_5$	300[d]	85	$C_{17}N_{20}N_2O_4$
VI	$(CH_2)_2O(CH_2)_2$	$(CH_2)_2O(CH_2)_2$	300[d]	85	$C_{16}H_{18}N_2O_5$
VII	H	$NHCOCH_2CH_2CO_2H$	300[e]	60	$C_{16}H_{17}N_3O_7$
VIII	H	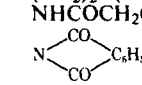	300[f]	80	$C_{20}H_{15}N_3O_6$
IX	H	NH_2	300[g]	80	$C_{12}H_{13}N_3O_4$
X	H	NHC_6H_5	300[h]	80	$C_{18}H_{17}N_3O_4$
XI	H	$NHC_6H_3(3,5\text{-}NO_2)$	300[h]	73	$C_{18}H_{15}N_5O_8$
XII	H	$N{=}CHC_6H_4(p\text{-}OCH_3)$	300[f]	73	$C_{20}H_{19}N_3O_5$
XIII	H	$N{=}CHC_6H_4(o\text{-}NO_2)$	300[f]	80	$C_{19}H_{16}N_4O_6$
XIV	H	$N{=}CHC_6H_4(p\text{-}OH)$	300[f]	75	$C_{19}H_{17}N_3O_5$
XV	H	$N{=}CHC_6H_3(3,4\text{-}OCH_3)$	300[f]	80	$C_{21}H_{21}N_3O_6$
XVI	H	$N{=}CHCH{=}CHC_6H_5$	300[f]	70	$C_{21}H_{19}N_3O_4$

[a] Elemental analyses for C and H were obtained for II–XVI; VII, VIII, X, and XI were also analyzed for N. Unless otherwise indicated, all values were within ± 0.4% of the theoretical value. [b] Calc. for C, 50.31; H, 4.97. Found: C, 50.26; H, 4.80. [c] Recrystallized from methanol (*cf.* Ref. 11). [d] Recrystallized from methanol. [e] Recrystallized from AcOH. [f] Recrystallized from dimethylformamide. [g] Recrystallized from water. [h] Recrystallized from ethanol-water.

0022-3549/84/1100-1652$01.00/0
© 1984, American Pharmaceutical Association

carbonyl-2-hydroxyquinoline (I) (0.01 mol) in ethanol (20 mL). The mixture was heated at reflux for 2 h. The solid was removed by filtration and recrystallized.

6,7-Dimethoxy-2-hydroxyquinoline-3-carboxylic Acid Hydrazones (XII-XVI)—The appropriate aldehyde (0.02 mol) was added to 6,7-dimethoxy-2-hydroxyquinoline-3-carboxylic acid hydrazide (IX) (0.01 mol) in glacial acetic acid. The mixture was heated at reflux for 1 h, and the material was removed by filtration and recrystallized.

Interaction of 6,7-Dimethoxy-2-hydroxyquinoline-3-carboxylic Acid Hydrazide and Acid Anhydrides (VII and VIII)—A mixture of the hydrazide (IX) (0.01 mol) and the appropriate acid anhydride (0.02 mol) in glacial acetic acid (30 mL) was heated at reflux for 3 h. The mixture was allowed to stand overnight. The material was removed by filtration and recrystallized. For VIII ^{1}H-NMR[1] ($CDCl_3$): δ 7.25 (s, 1, OH), 8.1-7.0 (m, 7, ArH), 4.3 (s, 1, NH), and 3.7 ppm (m, 6, 2 OCH_3).

Interaction of 6,7-Dimethoxy-3-ethoxycarbonyl-2-hydroxyquinoline and Different Amines (II-VI)—A mixture of 6,7-dimethoxy-3-ethoxycarbonyl-2-hydroxyquinoline (I) (0.01 mol) and the appropriate amine (0.02 mol) was heated at reflux in methanol (20 mL) for 3 h. Approximately 15 mL of the solvent was removed under reduced pressure, the residue was cooled, and the solid material was removed by filtration and recrystallized from a suitable solvent. For II, ^{1}H-NMR ($CDCl_3$): δ 6.8 (s, 1, OH), 8.1-7.03 (m, 3, ArH), 4.2 (s, 1, NH), 3.8 (m, 6, 2 OCH_3), and 1.5 ppm (s, 3, CH_3). For V [6,7-dimethoxy-3-(piperidinocarbonyl)-2-hydroxyquinoline], MS: *m/z* 316 (M^+), 232 ($M - C_5H_{10}N$), 204 [$M - (C_5H_{10}N + CO)$], 189 [$M - (C_5H_{10}N + CO + CH_3)$], and 173 [$M - (C_5H_{10}N + CO + OCH_3)$].

Biological Screening—Three compounds (III, V, and VII) of this series of alkoxyquinolines were used for preliminary pharmacological screening as CNS stimulants. Each was suspended in distilled water and administered to albino mice by oral intubation and intraperitoneal injection in doses up to 1 g/kg of body weight. The behavior and normal characteristics of the animals (heart rate, locomotor activity, reflexes, *etc.*) were recorded before and for 24 h after administration of the compounds.

RESULTS AND DISCUSSION

The animals given III showed transient increases in respiratory rate (from 198 to 300/min) 5 min after administration and returned to normal values 7 min later. Otherwise, there were no signs of CNS stimulation of the animals at the doses studied. There was no change in animal behavior, activity, and locomotion. None of the animals showed any signs of toxicity or mortality within 24 h after administration of the different compounds in the doses given.

From the biological screening, it is obvious that the tested compounds, although they are structurally related to the well-known carboxamide and *N,N*-alkylated derivatives of heterocyclic types of compounds, do not have a marked MAO inhibitory action. This leads to the conclusion that these bioisostere moieties of the fused heterocyclic systems structurally related to the quinoline series are biologically inactive as CNS stimulants.

REFERENCES

(1) E. G. Gross and R. M. Featherstone, *J. Pharmacol. Exp. Ther.*, **87,** 299 (1964).

(2) M. Hoffer and M. Reinert, *Arch. Int. Pharmacodyn.*, **56,** 211 (1937).

(3) F. Uhlmann, *Ges. Z. Exp. Med.*, **43,** 556 (1924); through *Chem. Abstr.* **13,** 5402 (1925).

(4) W. R. Boon, *J. Chem. Soc.*, **1945** 601, **1947** 307.

(5) I. V. Anonimova, *Med. Lett. Drug. Ther.*, **11,** 47 (1969); through *Chem. Abstr.*, **72,** 20229 (1970).

(6) K. Rickels, *Clin. Pharmacol. Ther.* **11,** 698 (1970).

(7) E. A. Zeller, J. Barsky, J. R. Fouts, W. R. Kirchheiner, and L. S. Varrorden, *Experientia*, **8,** 349 (1952).

(8) J. H. Biel, P. A. Nuhfer, and A. C. Conway, *Ann. N.Y. Acad. Sci.*, **80,** 568 (1959).

(9) P. Zeller, A. Pletscher, K. F. Gey, H. Gutmann, B. Hegedus, and O. Straub, *Ann. N.Y. Acad. Sci.*, **80,** 555 (1959).

(10) A. Pletscher and K. F. Gey, *Helv. Physiol. Pharmacol. Acta*, **16,** 26 (1958).

(11) S. Somasekhara and R. Phadka, *J. Indian Inst. Sci.*, **37,** 120 (1955).

[1] ^{1}H-NMR and MS spectra were determined on Varian spectrometers.

Determination of Phenylbutazone in Tablets by Nuclear Magnetic Resonance Spectrometry

RONA STROMBERG

Received April 18, 1983, from the *Food and Drug Administration, Department of Health and Human Services, New York Regional Laboratory, Brooklyn, NY 11232.* Accepted for publication October 6, 1983.

Abstract □ A method for the quantitative analysis of phenylbutazone in tablets using NMR is reported. The method is both accurate and precise. Using synthetic mixtures, the mean recovery value $\pm SD$ was 100.5 ± 0.86%. The NMR results of commercial preparations are compared with those obtained by the USP XX procedure. The NMR spectrum, in addition, provides a very specific means of identification for phenylbutazone.

Keyphrases □ Phenylbutazone—NMR analysis, comparative analyses □ NMR—phenylbutazone, comparative analyses

Phenylbutazone, 4-butyl-1,2-diphenyl-3,5-pyrazolidinedione (I), a synthetic pyrazolone derivative chemically related to aminopyrine, has anti-inflammatory, antipyretic, analgesic, and mild uricosuric properties (1). Approaches to the quantitative determination of phenylbutazone in tablets have varied. Tomaskova (2) reported a GC method using flame-ionization detection. A quantitative IR spectroscopic method was described by Pawelcyzk and Marciniec (3). Differential spectrophotometry, relying on the differences in absorption between acidic and basic species of phenylbutazone, was employed by Bezakova *et al.* (4). Other assay techniques have included separation on an ion-exchange column followed by titration (5) and acid hydrolysis to form benzidine, which was subsequently oxidized, and determined colorimetrically (6). The method of USP XX for the assay of phenylbutazone in tablets entails an ether-based extraction with a UV spectrophotometric determination (7). All these approaches require either lengthy sample preparations and/or nonspecific determinations. In contrast, nuclear magnetic resonance spectrometry (NMR) offers the advantages of minimal sample preparation, simplicity and specificity for the active ingredient.

NMR studies on phenylbutazone have dealt with its carbon-13 spectrum (8), degradation products (9, 10), and the monitoring of its dissolution kinetics (11). However, this technique has not been applied to the quantitative determination of the drug in pharmaceuticals. This paper describes a method in which a carbon tetrachloride–nitromethane mixture is used as the solvent and hexamethylcyclotrisiloxane

0022-3549/84/1100-1653$01.00/0

© 1984, American Pharmaceutical Association

carbonyl-2-hydroxyquinoline (I) (0.01 mol) in ethanol (20 mL). The mixture was heated at reflux for 2 h. The solid was removed by filtration and recrystallized.

6,7-Dimethoxy-2-hydroxyquinoline-3-carboxylic Acid Hydrazones (XII-XVI)—The appropriate aldehyde (0.02 mol) was added to 6,7-dimethoxy-2-hydroxyquinoline-3-carboxylic acid hydrazide (IX) (0.01 mol) in glacial acetic acid. The mixture was heated at reflux for 1 h, and the material was removed by filtration and recrystallized.

Interaction of 6,7-Dimethoxy-2-hydroxyquinoline-3-carboxylic Acid Hydrazide and Acid Anhydrides (VII and VIII)—A mixture of the hydrazide (IX) (0.01 mol) and the appropriate acid anhydride (0.02 mol) in glacial acetic acid (30 mL) was heated at reflux for 3 h. The mixture was allowed to stand overnight. The material was removed by filtration and recrystallized. For VIII ^{1}H-NMR[1] ($CDCl_3$): δ 7.25 (s, 1, OH), 8.1-7.0 (m, 7, ArH), 4.3 (s, 1, NH), and 3.7 ppm (m, 6, 2 OCH_3).

Interaction of 6,7-Dimethoxy-3-ethoxycarbonyl-2-hydroxyquinoline and Different Amines (II-VI)—A mixture of 6,7-dimethoxy-3-ethoxycarbonyl-2-hydroxyquinoline (I) (0.01 mol) and the appropriate amine (0.02 mol) was heated at reflux in methanol (20 mL) for 3 h. Approximately 15 mL of the solvent was removed under reduced pressure, the residue was cooled, and the solid material was removed by filtration and recrystallized from a suitable solvent. For II, ^{1}H-NMR ($CDCl_3$): δ 6.8 (s, 1, OH), 8.1-7.03 (m, 3, ArH), 4.2 (s, 1, NH), 3.8 (m, 6, 2 OCH_3), and 1.5 ppm (s, 3, CH_3). For V [6,7-dimethoxy-3-(piperidinocarbonyl)-2-hydroxyquinoline], MS: *m/z* 316 (M^+), 232 ($M - C_5H_{10}N$), 204 [$M - (C_5H_{10}N + CO)$], 189 [$M - (C_5H_{10}N + CO + CH_3)$], and 173 [$M - (C_5H_{10}N + CO + OCH_3)$].

Biological Screening—Three compounds (III, V, and VII) of this series of alkoxyquinolines were used for preliminary pharmacological screening as CNS stimulants. Each was suspended in distilled water and administered to albino mice by oral intubation and intraperitoneal injection in doses up to 1 g/kg of body weight. The behavior and normal characteristics of the animals (heart rate, locomotor activity, reflexes, *etc.*) were recorded before and for 24 h after administration of the compounds.

RESULTS AND DISCUSSION

The animals given III showed transient increases in respiratory rate (from 198 to 300/min) 5 min after administration and returned to normal values 7 min later. Otherwise, there were no signs of CNS stimulation of the animals at the doses studied. There was no change in animal behavior, activity, and locomotion. None of the animals showed any signs of toxicity or mortality within 24 h after administration of the different compounds in the doses given.

From the biological screening, it is obvious that the tested compounds, although they are structurally related to the well-known carboxamide and *N,N*-alkylated derivatives of heterocyclic types of compounds, do not have a marked MAO inhibitory action. This leads to the conclusion that these bioisostere moieties of the fused heterocyclic systems structurally related to the quinoline series are biologically inactive as CNS stimulants.

REFERENCES

(1) E. G. Gross and R. M. Featherstone, *J. Pharmacol. Exp. Ther.*, **87,** 299 (1964).

(2) M. Hoffer and M. Reinert, *Arch. Int. Pharmacodyn.*, **56,** 211 (1937).

(3) F. Uhlmann, *Ges. Z. Exp. Med.*, **43,** 556 (1924); through *Chem. Abstr.* **13,** 5402 (1925).

(4) W. R. Boon, *J. Chem. Soc.*, **1945** 601, **1947** 307.

(5) I. V. Anonimova, *Med. Lett. Drug. Ther.*, **11,** 47 (1969); through *Chem. Abstr.*, **72,** 20229 (1970).

(6) K. Rickels, *Clin. Pharmacol. Ther.* **11,** 698 (1970).

(7) E. A. Zeller, J. Barsky, J. R. Fouts, W. R. Kirchheiner, and L. S. Varrorden, *Experientia*, **8,** 349 (1952).

(8) J. H. Biel, P. A. Nuhfer, and A. C. Conway, *Ann. N.Y. Acad. Sci.*, **80,** 568 (1959).

(9) P. Zeller, A. Pletscher, K. F. Gey, H. Gutmann, B. Hegedus, and O. Straub, *Ann. N.Y. Acad. Sci.*, **80,** 555 (1959).

(10) A. Pletscher and K. F. Gey, *Helv. Physiol. Pharmacol. Acta*, **16,** 26 (1958).

(11) S. Somasekhara and R. Phadka, *J. Indian Inst. Sci.*, **37,** 120 (1955).

[1] ^{1}H-NMR and MS spectra were determined on Varian spectrometers.

Determination of Phenylbutazone in Tablets by Nuclear Magnetic Resonance Spectrometry

RONA STROMBERG

Received April 18, 1983, from the *Food and Drug Administration, Department of Health and Human Services, New York Regional Laboratory, Brooklyn, NY 11232.* Accepted for publication October 6, 1983.

Abstract □ A method for the quantitative analysis of phenylbutazone in tablets using NMR is reported. The method is both accurate and precise. Using synthetic mixtures, the mean recovery value $\pm SD$ was 100.5 ± 0.86%. The NMR results of commercial preparations are compared with those obtained by the USP XX procedure. The NMR spectrum, in addition, provides a very specific means of identification for phenylbutazone.

Keyphrases □ Phenylbutazone—NMR analysis, comparative analyses □ NMR—phenylbutazone, comparative analyses

Phenylbutazone, 4-butyl-1,2-diphenyl-3,5-pyrazolidinedione (I), a synthetic pyrazolone derivative chemically related to aminopyrine, has anti-inflammatory, antipyretic, analgesic, and mild uricosuric properties (1). Approaches to the quantitative determination of phenylbutazone in tablets have varied. Tomaskova (2) reported a GC method using flame-ionization detection. A quantitative IR spectroscopic method was described by Pawelcyzk and Marciniec (3). Differential spectrophotometry, relying on the differences in absorption between acidic and basic species of phenylbutazone, was employed by Bezakova *et al.* (4). Other assay techniques have included separation on an ion-exchange column followed by titration (5) and acid hydrolysis to form benzidine, which was subsequently oxidized, and determined colorimetrically (6). The method of USP XX for the assay of phenylbutazone in tablets entails an ether-based extraction with a UV spectrophotometric determination (7). All these approaches require either lengthy sample preparations and/or nonspecific determinations. In contrast, nuclear magnetic resonance spectrometry (NMR) offers the advantages of minimal sample preparation, simplicity and specificity for the active ingredient.

NMR studies on phenylbutazone have dealt with its carbon-13 spectrum (8), degradation products (9, 10), and the monitoring of its dissolution kinetics (11). However, this technique has not been applied to the quantitative determination of the drug in pharmaceuticals. This paper describes a method in which a carbon tetrachloride–nitromethane mixture is used as the solvent and hexamethylcyclotrisiloxane

0022-3549/84/1100-1653$01.00/0

© 1984, American Pharmaceutical Association

is the internal standard. Preparations containing known amounts of phenylbutazone and commercial tablets were analyzed.

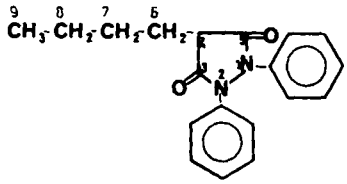

EXPERIMENTAL SECTION

Materials—An NMR spectrometer[1] (90 MHz) with an ambient probe temperature of 41°C was used. Samples were placed in precision-type, 5-mm, NMR tubes[2]. Phenylbutazone[3], hexamethylcyclotrisiloxane[4], tetramethylsilane[5], carbon tetrachloride[6], and nitromethane (>99% pure)[7] were used as obtained. Tablets were obtained from various commercial sources.

Phenylbutazone Analysis—Twenty tablets were weighed and finely powdered. An accurately weighed portion of this powder, containing ~150 mg of phenylbutazone, was transferred into a glass-stoppered centrifuge tube. Hexamethylcyclotrisiloxane (~64 mg) and 2 mL of carbon tetrachloride containing two drops of nitromethane/mL were added, and the mixture was shaken for 2 min. Insoluble excipients were allowed to rise and ~0.5 mL of the bottom layer was transferred to an analytical NMR tube. (For spectrometers which require a deuterium signal for field-frequency lock, approximately three drops of Me_2SO-d_6 should be added). The spin rate was adjusted so that no spinning side bands occurred between 0.4 and 0.6 ppm (hexamethylcyclotrisiloxane region), or between 6.9 and 7.5 ppm (phenyl region of phenylbutazone). The intensity of the spectrum was maximized with the RF power and amplitude setting; care was taken to avoid saturation, particularly in the spectrum of the sharp hexamethylcyclotrisiloxane signal. The delta (δ) scale was used to express magnetic field strength and all peak field positions were referenced to hexamethylcyclotrisiloxane at 0.14 ppm. The resonance signals for phenylbutazone, which appear as a broad resonance peak centered at ~7.25 ppm, and the singlet for hexamethylcyclotrisiloxane, the internal standard, at 0.14 ppm were integrated a minimum of five times, and the results were averaged. The amount of phenylbutazone was calculated as follows: mg/tablet = $(A_p/A_h) \times (EW_p/EW_h) \times$ (mg hexamethylcyclotrisiloxane/mg sample) × mean tablet weight, where A_p is the integral value of the signal representing phenylbutazone, A_h is the integral value of the signal representing the internal standard, EW_p is the equivalent weight of phenylbutazone (formula weight/10 protons = 30.84), and EW_h is the equivalent weight of the internal standard (formula weight/18 protons = 12.35).

RESULTS AND DISCUSSION

The absence of proton resonance signals for carbon tetrachloride makes it an ideal solvent for NMR spectroscopic work. Both phenylbutazone and hexamethylcyclotrisiloxane were soluble in carbon tetrachloride, but in the proposed method, the volume of this solvent was made slightly suboptimal with respect to phenylbutazone to obtain a relatively high concentration of drug and a low instrument noise level. The addition of a few drops of nitromethane, originally intended to serve as the internal standard, improved the solubility of phenylbutazone in the NMR solvent, and compensated for the lower sample volume. The resonance signal for nitromethane appeared at δ 4.10 ppm and was well separated from any other peak. Alternatively, the amount of sample specified in the assay method may be dissolved in 3 mL of carbon tetrachloride, but an adjustment of the attenuation setting is required. The utility of hexamethylcyclotrisiloxane as an internal standard has been demonstrated (12-14). Under the described experimental conditions, its resonance peak appears as a singlet at an extreme upfield position (~δ 0.14 ppm). This combination of solvent system and internal standard provides a specific interference-free means of identification and quantitation of the active ingredient.

The amount of phenylbutazone present in the dosage form is determined by integrating the broad resonance signal pattern centered at ~δ 7.25 ppm, arising from the 10 aromatic protons at positions 1 and 2, and the singlet at ~δ 0.14 ppm, due to the 18 methyl protons of the internal standard.

[1] Model EM-390; Varian Associates, Palo Alto, Calif.
[2] Kontes, Vineland, N.J.
[3] USP Reference Standard; U.S. Pharmacopeial Convention Inc., Rockville, Md.
[4] K & K Laboratories, Plainview, N.Y.
[5] Wilmad Glass Co., Buena, N.J.
[6] Fisher Scientific Co., Fair Lawn, N.J.
[7] Aldrich Chemical Co., Milwaukee, Wis.

Table I—NMR Determination of Phenylbutazone in Standard Mixtures[a]

Standard Mixture	Internal Standard Added, mg	Phenylbutazone Added, mg	Phenylbutazone Found, mg	Phenylbutazone Recovery, %
1	30.0	77.4	77.9	100.6
2	29.7	76.1	75.6	99.4
3	29.8	75.8	75.6	99.7
4	30.7	76.5	77.2	100.9
5	29.5	77.3	77.5	100.3
6	32.1	76.7	77.5	101.0
7	30.4	37.9	38.7	102.0
8	31.8	113.7	113.4	99.7
Mean ± *SD*				100.5 ± 0.9

[a] Half the amount of phenylbutazone specified in the method, dissolved in a similarly decreased volume of solvent, was used in order to conserve sample.

Table II—NMR and Compendial Determinations of Phenylbutazone in Commercial Tablets

Sample	Amount Declared, mg/Tablet	Amount Found, %[a] NMR	Amount Found, %[a] USP XX	Difference, %
1	100	97.9	96.7	1.2
2	100	100.5	97.3	3.2
3	100	103.0	99.7	3.3
4	100	98.7	97.6	1.1
5	100	102.7	100.4	2.3

[a] Since each tablet is declared to contain 100 mg of drug, the quantity found in mg/tablet is identical to the percent of declared values.

In addition to their utility in the quantitative analysis of phenylbutazone in dosage forms, the proton resonance characteristics of this molecule may be used for identification. The coupling of the methine proton at position 4 with the methylene protons at position 6 produces a triplet centered at ~δ 3.18 ppm. The complex splitting patterns seen in the region between δ 0.7 and 2.2 ppm may be assigned consecutively to the methyl protons at position 9 and to the methylene protons on carbons 6-8. The resonance signal pattern centered at ~δ 1.4 ppm arises from the overlapping of the peaks for the protons of the two methylene groups at positions 7 and 8.

The analysis of several known phenylbutazone mixtures is summarized in Table I. The results show that the method is both accurate and precise. The mean recovery value ±*SD* was 100.5 ± 0.9%. The relative proportions of phenylbutazone and hexamethylcyclotrisiloxane, as noted in Table I, had no significant bearing on the accuracy of the determination for the range of proportions shown.

The proposed method was also applied to commercial preparations. Table II summarizes the results of the analysis of five lots of tablets. For comparison purposes, the same composites were analyzed by the USP XX method. The data in Table II show that the results by the official method were 1.1-3.3% lower than those obtained by the NMR method. One of the possible reasons for these discrepancies may be the losses incurred with the official method during the extraction steps. Recovery studies from two commercial preparations, spiked with a known amount of phenylbutazone, gave a mean recovery value of 100.1%.

REFERENCES

(1) "Remington's Pharmaceutical Sciences," 14th ed., Mack Publishing, Easton, Pa., 1965, p. 1138.

(2) V. Tomaskova, *Farm. Obz.*, **49**, 313 (1980); *Chem. Abstr.*, **93**, 245604y (1980).

(3) E. Pawelczyk and B. Marciniec, *Acta Pol. Pharm.*, **35**, 643, (1978).

(4) Z. Bezakova, M. Bachrata, M. Blesova, and L. Knazko, *Farm. Obz.*, **49**, 157 (1980); *Chem. Abstr.*, **93**, 101537f (1980).

(5) J. Jarzebinski and K. Posepna, *Farm. Pol.*, **33**, 77 (1977); *Chem. Abstr.*, **87**, 106775t (1977).

(6) N. S. Simonova, *Farmatsiya*, **27**, 29 (1978); *Chem. Abstr.*, **88**, 197735q (1978).

(7) "The United States Pharmacopeia," 20th rev., U.S. Pharmacopeial Convention, Rockville, Md., 1980, p. 617.

(8) S. P. Singh, S. S. Parmar, V. I. Stenberg, and S. A. Farnum, *J. Heterocycl. Chem.*, **15**, 13 (1978).

(9) F. Matsui, D. L. Robertson, M. A. Poirier, and E. G. Lovering, *J. Pharm. Sci.*, **69**, 469 (1980).

(10) R. Wachowiak, *Arzneim-Forsch.*, **29**, 725 (1979).
(11) K. G. Mooney, M. Rodriguez-Gaxiola, M. Mintun, K. J. Himmelstein, and V. J. Stella, *J. Pharm Sci.*, **70**, 1358 (1981).
(12) J. W. Turczan and B. A. Goldwitz, *J. Pharm. Sci.*, **62**, 1705 (1973).
(13) J. W. Turczan and B. A. Goldwitz, *J. Pharm. Sci.*, **61**, 1309 (1972).
(14) E. B. Sheinin, W. R. Benson, and M. M. Smith, Jr., *J. Assoc. Off. Anal. Chem.*, **56**, 124 (1973).

ACKNOWLEDGMENTS

The author thanks Dr. Cesar Lau-Cam, Science Advisor, FDA, New York Regional Laboratory, and Professor of Pharmacognosy, St. John's University, College of Pharmacy and Allied Health Professions, Jamaica, N.Y., for his help in the preparation of this report; Mr. Richard Muzeni, FDA, New York Regional Laboratory, for analyzing the composite samples by the official method; Mr. John Turczan, FDA, New York Regional Laboratory, for many valuable discussions; and Mr. Richard Klein, FDA, New York Regional Laboratory, for his excellent artwork.

Influence of Food on the Bioavailability of Enalapril

B. N. SWANSON *, P. H. VLASSES *, R. K. FERGUSON *, P. A. BERGQUIST *, A. E. TILL ‡, J. D. IRVIN ‡, and K. HARRIS ‡

Received August 25, 1983, from the **Division of Clinical Pharmacology, Jefferson Medical College of Thomas Jefferson University, Philadelphia, PA 19107* and ‡*Merck Sharp & Dohme Research Laboratories, West Point, PA 19486.* Accepted for publication December 5, 1983.

Abstract □ In a randomized, two-period crossover study in 12 normal volunteers, serum and urine concentrations of the angiotensin-converting enzyme inhibitor enalapril and its active metabolite enalaprilat were determined following administration of a single 40-mg tablet of enalapril maleate administered both in the fasting state and with a standard breakfast. A 7-d interval separated the two treatment periods. Area under the serum concentration-time curves for enalaprilat and urinary recoveries for enalaprilat and total drug did not differ significantly between the fed and fasted conditions. The mean observed maximum serum concentration of enalaprilat was slightly higher for the fasting treatment, but the time to peak concentration was almost identical for the two treatments. Enalapril maleate is unlike the prototype angiotensin-converting enzyme inhibitor captopril in that a standard meal does not appear to influence absorption of this new drug.

Keyphrases □ Enalapril maleate—bioavailability, influence of food □ Enalaprilat—metabolite of enalapril, bioavailability, influence of food □ Angiotensin-converting enzyme—enalapril maleate, bioavailability, influence of food

Food is known to alter the bioavailability of many drugs (1). The presence of food in the GI tract has been shown to reduce, by 30–40%, the absorption of the recently marketed oral angiotensin-converting enzyme (ACE) inhibitor captopril (2). Compromised absorption of captopril could affect the magnitude or duration of the antihypertensive effect of this drug (3). Enalapril maleate is a new ACE inhibitor which, like captopril, has been shown to be effective in the treatment of hypertension and congestive heart failure (4). Enalapril ((*S*)-1-[*N*-[1-(ethoxycarbonyl)-3-phenylpropyl]-L-alanyl]-L-proline; I) is a prodrug which is deesterified to an active diacid form, enalaprilat ((*S*)-1-[*N*-(1-carboxy-3-phenylpropyl)-L-alanyl]-L-proline; II) (4). Since enalapril lacks the sulfhydryl moiety of the chemical structure of captopril, it may have a more favorable benefit-to-risk ratio. Oral absorption of enalapril may also be more complete than captopril since the sulfhydryl group of the latter binds to other thiol groups in food.

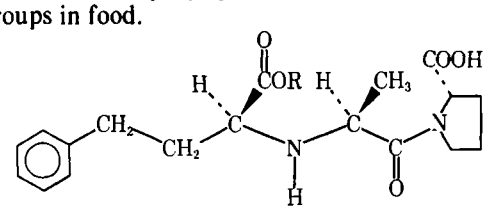

I, R = CH_2CH_3
II, R = H

The purpose of this study was to investigate whether consumption of food alters the rate or extent of absorption of enalapril when a single dose is administered to healthy male volunteers.

EXPERIMENTAL SECTION

Subjects—Twelve healthy, normotensive male subjects (age, 23–37 years) volunteered to participate in this study. They were judged to be in good health on the basis of history, physical examination, routine laboratory data, standard electrocardiogram, and diastolic blood pressure (≤90 mm Hg). All subjects weighed within ±10% of the ideal body weights for their ages and heights. No medications other than enalapril maleate were taken by the subjects from 1 week prior to the study until its completion. The protocol was approved by the Committee on Research of Thomas Jefferson University.

Study Design—This was an open, randomized, two-way crossover study in which enalapril maleate (40 mg) was administered as a single dose in its market image. Subjects fasted from midnight of the previous night. On the first day of each treatment period, subjects received doses of enalapril maleate either in a fasting state or immediately after a standard prescribed breakfast by a randomized design. The breakfast consisted of one egg, two pieces of toast or bread, two strips of bacon or two sausages, 150 mL of low fat milk or 100 mL of orange juice, tea, or coffee. All volunteers resumed their normal diets each day at lunch (4 h after dosing). Treatments were separated by 7 d.

Blood was drawn at 0, 1, 2, 3, 4, 6, 8, 12, 16, 24, 36, 48, 60, and 72 h postdrug administration. Urine was collected at −1–0, 0–2, 2–4, 4–6, 6–8, 8–12, 12–24, 24–36, 36–48, 48–72, 72–96, and 96–120 h after each treatment. Blood pressure and pulse rate were measured in the supine and sitting positions at regular intervals for 24 h postadministration. Adverse effects were monitored throughout the study.

Biochemical Analysis and Statistical Methods—The assay value for the enalapril maleate tablet was 42.02 mg, equivalent to 29.88 mg of enalaprilat per tablet. A radioimmunoassay procedure (5) was used to analyze the serum and urine samples for enalaprilat and for total drug (enalaprilat after enzymatic hydrolysis of enalapril). After mixing and incubation overnight at room temperature, the hydrolysis of enalapril to enalaprilat was virtually complete. The assay was considered to be accurate and reproducible at enalaprilat concentrations >1 ng/mL in serum and 0.5 μg/mL in urine; the interassay coefficient of variation was 8%. Concentrations below these values were not considered detectable and, hence, zero for the purpose of data analysis.

All parameters were analyzed by using an analysis of variance for a two-period crossover design (6). These results were corroborated by a nonparametric method based on ranks of the data (7). The posterior probabilities were calculated by the method of Rodda and Davis (8). The power analysis was based on the *t* test.

RESULTS

The mean serum profiles for enalaprilat after administration of enalapril maleate in the fasting and fed states are depicted in Fig. 1. Profiles for the two treatments are virtually superimposable. Mean urinary excretion rate plots

0022-3549/84/1100-1655$01.00/0
© 1984, American Pharmaceutical Association

(10) R. Wachowiak, *Arzneim-Forsch.*, **29**, 725 (1979).
(11) K. G. Mooney, M. Rodriguez-Gaxiola, M. Mintun, K. J. Himmelstein, and V. J. Stella, *J. Pharm Sci.*, **70**, 1358 (1981).
(12) J. W. Turczan and B. A. Goldwitz, *J. Pharm. Sci.*, **62**, 1705 (1973).
(13) J. W. Turczan and B. A. Goldwitz, *J. Pharm. Sci.*, **61**, 1309 (1972).
(14) E. B. Sheinin, W. R. Benson, and M. M. Smith, Jr., *J. Assoc. Off. Anal. Chem.*, **56**, 124 (1973).

ACKNOWLEDGMENTS

The author thanks Dr. Cesar Lau-Cam, Science Advisor, FDA, New York Regional Laboratory, and Professor of Pharmacognosy, St. John's University, College of Pharmacy and Allied Health Professions, Jamaica, N.Y., for his help in the preparation of this report; Mr. Richard Muzeni, FDA, New York Regional Laboratory, for analyzing the composite samples by the official method; Mr. John Turczan, FDA, New York Regional Laboratory, for many valuable discussions; and Mr. Richard Klein, FDA, New York Regional Laboratory, for his excellent artwork.

Influence of Food on the Bioavailability of Enalapril

B. N. SWANSON *, P. H. VLASSES *, R. K. FERGUSON *, P. A. BERGQUIST *, A. E. TILL ‡, J. D. IRVIN ‡, and K. HARRIS ‡

Received August 25, 1983, from the **Division of Clinical Pharmacology, Jefferson Medical College of Thomas Jefferson University, Philadelphia, PA 19107* and ‡*Merck Sharp & Dohme Research Laboratories, West Point, PA 19486.* Accepted for publication December 5, 1983.

Abstract □ In a randomized, two-period crossover study in 12 normal volunteers, serum and urine concentrations of the angiotensin-converting enzyme inhibitor enalapril and its active metabolite enalaprilat were determined following administration of a single 40-mg tablet of enalapril maleate administered both in the fasting state and with a standard breakfast. A 7-d interval separated the two treatment periods. Area under the serum concentration-time curves for enalaprilat and urinary recoveries for enalaprilat and total drug did not differ significantly between the fed and fasted conditions. The mean observed maximum serum concentration of enalaprilat was slightly higher for the fasting treatment, but the time to peak concentration was almost identical for the two treatments. Enalapril maleate is unlike the prototype angiotensin-converting enzyme inhibitor captopril in that a standard meal does not appear to influence absorption of this new drug.

Keyphrases □ Enalapril maleate—bioavailability, influence of food □ Enalaprilat—metabolite of enalapril, bioavailability, influence of food □ Angiotensin-converting enzyme—enalapril maleate, bioavailability, influence of food

Food is known to alter the bioavailability of many drugs (1). The presence of food in the GI tract has been shown to reduce, by 30–40%, the absorption of the recently marketed oral angiotensin-converting enzyme (ACE) inhibitor captopril (2). Compromised absorption of captopril could affect the magnitude or duration of the antihypertensive effect of this drug (3). Enalapril maleate is a new ACE inhibitor which, like captopril, has been shown to be effective in the treatment of hypertension and congestive heart failure (4). Enalapril ((*S*)-1-[*N*-[1-(ethoxycarbonyl)-3-phenylpropyl]-L-alanyl]-L-proline; I) is a prodrug which is deesterified to an active diacid form, enalaprilat ((*S*)-1-[*N*-(1-carboxy-3-phenylpropyl)-L-alanyl]-L-proline; II) (4). Since enalapril lacks the sulfhydryl moiety of the chemical structure of captopril, it may have a more favorable benefit-to-risk ratio. Oral absorption of enalapril may also be more complete than captopril since the sulfhydryl group of the latter binds to other thiol groups in food.

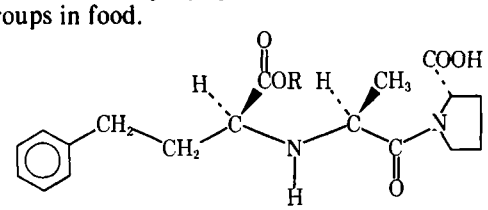

I, R = CH_2CH_3
II, R = H

The purpose of this study was to investigate whether consumption of food alters the rate or extent of absorption of enalapril when a single dose is administered to healthy male volunteers.

EXPERIMENTAL SECTION

Subjects—Twelve healthy, normotensive male subjects (age, 23–37 years) volunteered to participate in this study. They were judged to be in good health on the basis of history, physical examination, routine laboratory data, standard electrocardiogram, and diastolic blood pressure (≤90 mm Hg). All subjects weighed within ±10% of the ideal body weights for their ages and heights. No medications other than enalapril maleate were taken by the subjects from 1 week prior to the study until its completion. The protocol was approved by the Committee on Research of Thomas Jefferson University.

Study Design—This was an open, randomized, two-way crossover study in which enalapril maleate (40 mg) was administered as a single dose in its market image. Subjects fasted from midnight of the previous night. On the first day of each treatment period, subjects received doses of enalapril maleate either in a fasting state or immediately after a standard prescribed breakfast by a randomized design. The breakfast consisted of one egg, two pieces of toast or bread, two strips of bacon or two sausages, 150 mL of low fat milk or 100 mL of orange juice, tea, or coffee. All volunteers resumed their normal diets each day at lunch (4 h after dosing). Treatments were separated by 7 d.

Blood was drawn at 0, 1, 2, 3, 4, 6, 8, 12, 16, 24, 36, 48, 60, and 72 h postdrug administration. Urine was collected at −1–0, 0–2, 2–4, 4–6, 6–8, 8–12, 12–24, 24–36, 36–48, 48–72, 72–96, and 96–120 h after each treatment. Blood pressure and pulse rate were measured in the supine and sitting positions at regular intervals for 24 h postadministration. Adverse effects were monitored throughout the study.

Biochemical Analysis and Statistical Methods—The assay value for the enalapril maleate tablet was 42.02 mg, equivalent to 29.88 mg of enalaprilat per tablet. A radioimmunoassay procedure (5) was used to analyze the serum and urine samples for enalaprilat and for total drug (enalaprilat after enzymatic hydrolysis of enalapril). After mixing and incubation overnight at room temperature, the hydrolysis of enalapril to enalaprilat was virtually complete. The assay was considered to be accurate and reproducible at enalaprilat concentrations >1 ng/mL in serum and 0.5 μg/mL in urine; the interassay coefficient of variation was 8%. Concentrations below these values were not considered detectable and, hence, zero for the purpose of data analysis.

All parameters were analyzed by using an analysis of variance for a two-period crossover design (6). These results were corroborated by a nonparametric method based on ranks of the data (7). The posterior probabilities were calculated by the method of Rodda and Davis (8). The power analysis was based on the *t* test.

RESULTS

The mean serum profiles for enalaprilat after administration of enalapril maleate in the fasting and fed states are depicted in Fig. 1. Profiles for the two treatments are virtually superimposable. Mean urinary excretion rate plots

0022-3549/84/1100-1655$01.00/0
© 1984, American Pharmaceutical Association

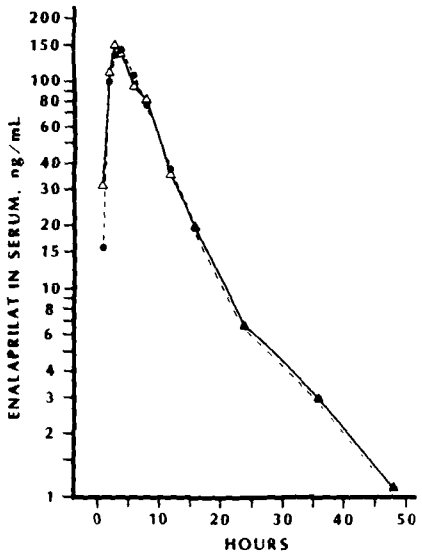

Figure 1—*Mean enalaprilat serum concentrations following administration of an enalapril maleate 40-mg tablet to fasting (●) and fed (△) healthy subjects (n = 12).*

for enalaprilat and total drug (Figs. 2 and 3, respectively) were similar for the fasting and fed states as well. Serum parameters for enalaprilat and urine parameters for enalaprilat and total drug are presented in Table I, as are power analyses and posterior probability results. Mean peak serum concentrations of enalaprilat were 154 and 147 ng/mL for the fasting and nonfasting treatments and were observed at 3.3 and 3.4 h, respectively, after administration of enalapril maleate. Mean serum $AUC_{0\text{-}24}$ values for enalaprilat obtained from the fasting and nonfasting treatments were essentially the same and accounted, on the average, for 93% of the total AUC (from time zero to the time of the lowest detectable serum concentration) for both treatments. For most subjects, the maximum serum concentration for enalapril (obtained as the difference between enalaprilat equivalents before and after sample hydrolysis) was observed at 1 h, the first sampling time, and tended to be slightly higher during the fasting state. In two subjects, the maximum was at 2 h (data not shown).

Mean urinary recoveries (0–48 h) of enalaprilat were 31 and 32% of the dose for the fasting and nonfasting treatments, respectively; recoveries of total drug after hydrolysis of urinary enalapril were 53 and 58% of the dose, respectively. The mean urinary recovery ratio of enalaprilat–total drug was 0.58 for the fasting treatment and 0.54 for the nonfasting treatment. No statistically significant differences were found between treatments for any of the serum or urine parameters considered.

Table I—Mean Serum Parameters for Enalaprilat and Urine Parameters for Enalaprilat and Total Drug [a]

Parameter[b]	Fasting (Mean ± *SD*)	Fed (Mean ± *SD*)	Comparison[c]
C_{max} (enalaprilat), ng/mL	154 ± 39	147 ± 36	NS
t_{max} (enalaprilat), h	3.3 ± 0.5	3.4 ± 0.5[d]	NS
$AUC_{0\text{-}24}$ (enalaprilat), ng·h/mL	1209 ± 203	1173 ± 212	NS
$AUC_{0\text{-}LSC}$ (enalaprilat), ng·h/mL	1304 ± 240	1262 ± 220	NS
Urinary recovery, 0–48 h (percent of administered enalaprilat equivalents)[d]			
Enalaprilat	30.5 ± 7.5	31.6 ± 8.8	NS
Total drug	53.1 ± 10.1	57.6 ± 12.4	NS
Urinary recovery ratio of enalaprilat/total drug, 0–48 h[d,e]	0.58	0.54	NS

[a] Following oral administration of enalapril maleate (40 mg) in healthy fasting and fed volunteers; $n = 12$; total drug was measured after hydrolysis, representing enalaprilat which was present in the urine as enalapril itself and that which was present as enalaprilat. [b] C_{max}, observed maximum serum concentration; t_{max}, time of observed maximum serum concentration; $AUC_{0\text{-}24}$ and $AUC_{0\text{-}LSC}$, area under the serum concentration–time curve from 0–24 h and 0–last observed serum concentration, respectively. [c] No significant differences (NS) were found for any comparison. The power of detecting a 20% difference in urinary recovery of enalaprilat and total drug, with $\alpha = 0.05$, is 0.82 and 0.81, respectively; posterior probability that the true difference is 20% or less is 0.97 for enalaprilat and 0.94 for total drug. [d] $n = 11$. [e] Geometric mean of individual ratios.

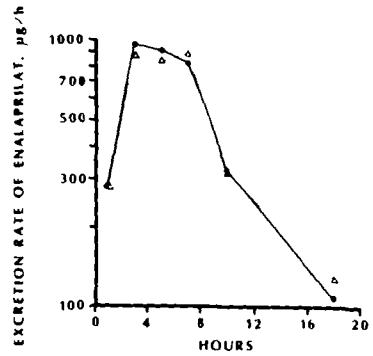

Figure 2—*Mean enalaprilat urinary excretion plots following oral administration of enalapril maleate to fasting (●) and fed (△) healthy subjects (n = 9 and 10, respectively).*

Mean diastolic blood pressure significantly decreased from predose values by 2 h after each dose, and these decreases were maintained for 4–8 h. No adverse effects were reported.

DISCUSSION

Enalapril maleate is a new nonsulfhydryl ACE inhibitor which is converted *in vivo* to an active diacid metabolite (enalaprilat). Although both enalapril and its metabolite are ACE inhibitors, it is the metabolite that exhibits the greatest potency and is the presumed active compound *in vivo*. In the present study, the effect of food on the serum concentration–time profile of enalaprilat and urinary recovery of enalaprilat and total drug (enalapril plus enalaprilat) after administration of a single dose of enalapril maleate were evaluated. This is of interest because food has been reported to decrease by 30% the extent of absorption of captopril, the currently available oral ACE inhibitor (2). In addition, maximum inhibition of ACE, as reflected by enzyme activity in serum, appears to be required for the full therapeutic effect of this class of drugs (4). Since serum ACE activity is directly related to circulating drug concentrations, this maximal degree of inhibition may not occur if drug absorption is impaired. Interestingly, food has recently been reported to decrease, by ~50%, the oral absorption of *d*-penicillamine, another sulfhydryl-containing compound (9).

This study in normal volunteers showed that a standard breakfast did not alter the serum concentration–time profile and urinary recovery of enalaprilat following a single oral dose of enalapril maleate (40 mg). We have demonstrated previously that an enalaprilat concentration of ~14 ng/mL is required to inhibit serum ACE levels by 90% (10, 11). In the current study, this serum concentration was maintained for at least 16 h after each 40-mg dose in most subjects, regardless of diet.

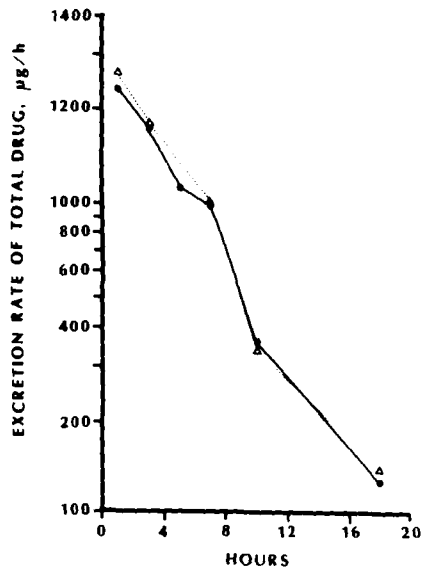

Figure 3—*Mean urinary excretion rate plots for total drug (enalaprilat measured after hydrolysis) following oral administration of enalapril maleate to fasting (●) and fed (△) healthy subjects (n = 9 and 10, respectively).*

In conclusion, the serum parameters for enalaprilat and urine parameters for enalaprilat and total drug (enalapril-enalaprilat) were similar following administration of a single enalapril maleate 40-mg tablet to healthy volunteers under fasting and nonfasting conditions. Thus, food did not appreciably alter the absorption of enalapril or the bioavailability of enalaprilat in this study.

REFERENCES

(1) R. D. Toothaker and P. G. Welling, *Annu. Rev. Pharmacol. Toxicol.*, **20**, 173 (1980).

(2) S. M. Singhvi, D. N. McKinstry, J. M. Shaw, D. A. Willard, and B. H. Migdalof, *J. Clin. Pharmacol.*, **22**, 135 (1982).

(3) R. K. Ferguson, G. A. Turini, H. R. Brunner, H. Gavras, and D. N. McKinstry, *Lancet*, **i**, 775 (1977).

(4) R. K. Ferguson, P. H. Vlasses, B. N. Swanson, P. Mojaverian, M. Hichens, and J. D. Irvin, *Clin. Pharmacol. Ther.*, **32**, 48 (1982).

(5) M. Hichens, E. L. Hand, and W. S. Mulcahy, *Ligand Quart.*, **4**, 43 (1981).

(6) J. E. Grizzle, *Biometrics*, **21**, 467 (1965).

(7) G. G. Koch, *Biometrics*, **28**, 577 (1972).

(8) B. E. Rodda and R. L. Davis, *Clin. Pharmacol. Ther.*, **28**, 247 (1980).

(9) M. A. Osman, R. B. Patel, A. Schuma, W. R. Sundstrom, and P. G. Welling, *Clin. Pharmacol. Ther.*, **33**, 465 (1983).

(10) R. K. Ferguson, P. H. Vlasses, J. D. Irvin, B. N. Swanson, and R. B. Lee, *J. Clin. Pharmacol.*, **22**, 281 (1982).

(11) B. N. Swanson, M. Hichens, P. Mojaverian, R. K. Ferguson, P. H. Vlasses, and M. Dudash, *Res. Commun. Chem. Path. Pharmacol.*, **33**, 525 (1981).

Metabolism of Salsalate in Normal Subjects

SYDNEY H. DROMGOOLE ˣ, DANIEL E. FURST, and HAROLD E. PAULUS

Received March 14, 1983, from the *Division of Rheumatology, Department of Medicine, University of California, Los Angeles, Los Angeles, CA 90024.* Accepted for publication October 26, 1983.

Abstract □ The metabolism of salsalate (I) was characterized in two normal volunteers. The drug was almost completely absorbed and was excreted primarily in the urine; only ~1% of the total dose was found in the stools. Although I is a salicylate derivative, which on hydrolysis yields two molecules of salicylic acid (II), ~7-10% of the dose was not hydrolyzed to salicylic acid and appeared in the urine either as unchanged drug or glucuronide conjugates. Thus, the incomplete availability of salicylate from salsalate that has been previously reported may not be due to incomplete absorption of the drug but to incomplete hydrolysis to salicylic acid.

Keyphrases □ Salsalate—metabolism, normal subjects □ Absorption—salsalate, normal subjects

Salsalate (I) is a salicylate derivative which on hydrolysis yields two molecules of salicylic acid (II). The results of several studies have indicated that the availability of salicylate from salsalate is lower than from either choline magnesium trisalicylate (1) or aspirin (2, 3). It has been suggested that the lower availability of salicylate from salsalate may be due to incomplete absorption (1). However, the recovery of total salicylate in the urine samples of patients receiving equivalent doses of salsalate and aspirin indicated that the absorption of the two salicylate formulations was essentially complete. The hydrolysis of salsalate to salicylate was incomplete, with <1% of the dose being excreted as unchanged salsalate and ≤13% of the dose being excreted in the urine as conjugates of salsalate (3). The only limitation of this latter study was the fact that the biological samples had been stored for several months prior to analysis, during which time salsalate (both nonconjugated and conjugated) may have partially hydrolyzed to salicylic acid.

The purpose of this study was to characterize the metabolism of salsalate in two normal volunteers following the administration of 2000 mg of salsalate containing ^{14}C-labeled salsalate.

EXPERIMENTAL SECTION

Two normal healthy male volunteers (age 29 and 35) entered into the 4-d study after initial screening procedures. The volunteers fasted for 12 h prior to and 4 h after drug administration. They ingested 2000 mg (four 500-mg capsules) of salsalate containing ^{14}C-labeled salsalate[1] (64 μCi) with water. Compound I was radiolabeled at both carboxyl positions.

Blood samples were taken just before drug ingestion, at hourly intervals up to 12 h, and then at 16, 20, 24, 30, 36, 48, 60, and 72 h following drug administration. Immediately after the blood samples were drawn into heparinized tubes, they were centrifuged, and the plasma was frozen until analysis. Urine samples were collected during the following intervals: 0-1, 1-2, 2-4, 4-6, 6-8, 8-12, 12-16, and 16-24 h. For the next 3 d, urinary output was collected as consecutive 12-h aliquots. The volume of urine and pH were recorded for each period, and aliquots were frozen in plastic containers until analysis. All stools were collected, weighed, and frozen until analysis. Due to the possibility of hydrolysis of salsalate and its conjugates to salicylic acid, all assays were completed within 2 weeks of collection.

Aliquots of plasma (0.1 mL with 0.9 mL of water) or urine (1.0 mL) were transferred into scintillation vials containing scintillation fluid[2] and counted in a scintillation counter[3]. Standards containing 500 μg of the radiolabeled salsalate[1] in propanol were also counted. All counts were corrected for quenching.

The plasma and urine samples were assayed for unchanged salsalate and salicylic acid by a previously reported HPLC technique (4). Salsalate[1], salicylic acid[4], and α-phenylcinnamic acid[4], the internal standard, were extracted from acidified plasma and urine samples. Methylene chloride[5] was used to extract plasma, whereas urine was extracted into hexane[6]. The organic phases were evaporated to dryness, redissolved in methanol (0.5 mL)[7], and analyzed by HPLC with an automatic sample injector accessory[8]. The mobile phase of methanol-1% acetic acid (60:40, v/v) was pumped at a rate of 2.0 mL/min through a 4.6 × 150-mm column[9]. Peaks were detected with a UV detector[10] (300 nm) coupled to a recorder[11] and peak integrator[12]. Plasma samples were assayed for total salicylate by HPLC after heating with HCl (18 M) overnight at 100°C. Extraction and chromatographic conditions were the same as described above for unchanged I.

Total urinary salicylate was determined by a modification of the colorimetric method described by Chiou and Onyemelukwe (5). Aliquots of urine

[1] Riker Laboratories, 3M Center, St. Paul, Minn.
[2] Ready-Sol EP; Beckman Instruments, Inc., Fullerton, Calif.
[3] Isocap 300; Scarle Analytical Inc., Des Plaines, Ill.
[4] Aldrich Chemical Co., Milwaukee, Wis.
[5] Spectroquality; Matheson, Coleman and Bell, Norwood, Ohio.
[6] Spectroquality; Mallinckrodt, St. Louis, Mo.
[7] Burdick & Jackson Laboratories, Muskegon, Mich.
[8] Model 1500; Altex Scientific, Berkeley, Calif.
[9] Ultrasphere ODS; Altex Scientific.
[10] Model 100-10 spectrophotometer; Hitachi Scientific Instruments, Mountain-View, Calif.
[11] Model 250-2, two channel; Curken Scientific, Danbury, Conn.
[12] Model 485; Varian Instrument Division, Palo Alto, Calif.

0022-3549/84/1100-1657$01.00/0

© 1984, American Pharmaceutical Association

In conclusion, the serum parameters for enalaprilat and urine parameters for enalaprilat and total drug (enalapril-enalaprilat) were similar following administration of a single enalapril maleate 40-mg tablet to healthy volunteers under fasting and nonfasting conditions. Thus, food did not appreciably alter the absorption of enalapril or the bioavailability of enalaprilat in this study.

REFERENCES

(1) R. D. Toothaker and P. G. Welling, *Annu. Rev. Pharmacol. Toxicol.*, **20**, 173 (1980).

(2) S. M. Singhvi, D. N. McKinstry, J. M. Shaw, D. A. Willard, and B. H. Migdalof, *J. Clin. Pharmacol.*, **22**, 135 (1982).

(3) R. K. Ferguson, G. A. Turini, H. R. Brunner, H. Gavras, and D. N. McKinstry, *Lancet*, **i**, 775 (1977).

(4) R. K. Ferguson, P. H. Vlasses, B. N. Swanson, P. Mojaverian, M. Hichens, and J. D. Irvin, *Clin. Pharmacol. Ther.*, **32**, 48 (1982).

(5) M. Hichens, E. L. Hand, and W. S. Mulcahy, *Ligand Quart.*, **4**, 43 (1981).

(6) J. E. Grizzle, *Biometrics*, **21**, 467 (1965).

(7) G. G. Koch, *Biometrics*, **28**, 577 (1972).

(8) B. E. Rodda and R. L. Davis, *Clin. Pharmacol. Ther.*, **28**, 247 (1980).

(9) M. A. Osman, R. B. Patel, A. Schuma, W. R. Sundstrom, and P. G. Welling, *Clin. Pharmacol. Ther.*, **33**, 465 (1983).

(10) R. K. Ferguson, P. H. Vlasses, J. D. Irvin, B. N. Swanson, and R. B. Lee, *J. Clin. Pharmacol.*, **22**, 281 (1982).

(11) B. N. Swanson, M. Hichens, P. Mojaverian, R. K. Ferguson, P. H. Vlasses, and M. Dudash, *Res. Commun. Chem. Path. Pharmacol.*, **33**, 525 (1981).

Metabolism of Salsalate in Normal Subjects

SYDNEY H. DROMGOOLE ˣ, DANIEL E. FURST, and HAROLD E. PAULUS

Received March 14, 1983, from the *Division of Rheumatology, Department of Medicine, University of California, Los Angeles, Los Angeles, CA 90024.* Accepted for publication October 26, 1983.

Abstract □ The metabolism of salsalate (I) was characterized in two normal volunteers. The drug was almost completely absorbed and was excreted primarily in the urine; only ~1% of the total dose was found in the stools. Although I is a salicylate derivative, which on hydrolysis yields two molecules of salicylic acid (II), ~7-10% of the dose was not hydrolyzed to salicylic acid and appeared in the urine either as unchanged drug or glucuronide conjugates. Thus, the incomplete availability of salicylate from salsalate that has been previously reported may not be due to incomplete absorption of the drug but to incomplete hydrolysis to salicylic acid.

Keyphrases □ Salsalate—metabolism, normal subjects □ Absorption—salsalate, normal subjects

Salsalate (I) is a salicylate derivative which on hydrolysis yields two molecules of salicylic acid (II). The results of several studies have indicated that the availability of salicylate from salsalate is lower than from either choline magnesium trisalicylate (1) or aspirin (2, 3). It has been suggested that the lower availability of salicylate from salsalate may be due to incomplete absorption (1). However, the recovery of total salicylate in the urine samples of patients receiving equivalent doses of salsalate and aspirin indicated that the absorption of the two salicylate formulations was essentially complete. The hydrolysis of salsalate to salicylate was incomplete, with <1% of the dose being excreted as unchanged salsalate and ≤13% of the dose being excreted in the urine as conjugates of salsalate (3). The only limitation of this latter study was the fact that the biological samples had been stored for several months prior to analysis, during which time salsalate (both nonconjugated and conjugated) may have partially hydrolyzed to salicylic acid.

The purpose of this study was to characterize the metabolism of salsalate in two normal volunteers following the administration of 2000 mg of salsalate containing ^{14}C-labeled salsalate.

EXPERIMENTAL SECTION

Two normal healthy male volunteers (age 29 and 35) entered into the 4-d study after initial screening procedures. The volunteers fasted for 12 h prior to and 4 h after drug administration. They ingested 2000 mg (four 500-mg capsules) of salsalate containing ^{14}C-labeled salsalate[1] (64 μCi) with water. Compound I was radiolabeled at both carboxyl positions.

Blood samples were taken just before drug ingestion, at hourly intervals up to 12 h, and then at 16, 20, 24, 30, 36, 48, 60, and 72 h following drug administration. Immediately after the blood samples were drawn into heparinized tubes, they were centrifuged, and the plasma was frozen until analysis. Urine samples were collected during the following intervals: 0-1, 1-2, 2-4, 4-6, 6-8, 8-12, 12-16, and 16-24 h. For the next 3 d, urinary output was collected as consecutive 12-h aliquots. The volume of urine and pH were recorded for each period, and aliquots were frozen in plastic containers until analysis. All stools were collected, weighed, and frozen until analysis. Due to the possibility of hydrolysis of salsalate and its conjugates to salicylic acid, all assays were completed within 2 weeks of collection.

Aliquots of plasma (0.1 mL with 0.9 mL of water) or urine (1.0 mL) were transferred into scintillation vials containing scintillation fluid[2] and counted in a scintillation counter[3]. Standards containing 500 μg of the radiolabeled salsalate[1] in propanol were also counted. All counts were corrected for quenching.

The plasma and urine samples were assayed for unchanged salsalate and salicylic acid by a previously reported HPLC technique (4). Salsalate[1], salicylic acid[4], and α-phenylcinnamic acid[4], the internal standard, were extracted from acidified plasma and urine samples. Methylene chloride[5] was used to extract plasma, whereas urine was extracted into hexane[6]. The organic phases were evaporated to dryness, redissolved in methanol (0.5 mL)[7], and analyzed by HPLC with an automatic sample injector accessory[8]. The mobile phase of methanol-1% acetic acid (60:40, v/v) was pumped at a rate of 2.0 mL/min through a 4.6 × 150-mm column[9]. Peaks were detected with a UV detector[10] (300 nm) coupled to a recorder[11] and peak integrator[12]. Plasma samples were assayed for total salicylate by HPLC after heating with HCl (18 M) overnight at 100°C. Extraction and chromatographic conditions were the same as described above for unchanged I.

Total urinary salicylate was determined by a modification of the colorimetric method described by Chiou and Onyemelukwe (5). Aliquots of urine

[1] Riker Laboratories, 3M Center, St. Paul, Minn.
[2] Ready-Sol EP; Beckman Instruments, Inc., Fullerton, Calif.
[3] Isocap 300; Scarle Analytical Inc., Des Plaines, Ill.
[4] Aldrich Chemical Co., Milwaukee, Wis.
[5] Spectroquality; Matheson, Coleman and Bell, Norwood, Ohio.
[6] Spectroquality; Mallinckrodt, St. Louis, Mo.
[7] Burdick & Jackson Laboratories, Muskegon, Mich.
[8] Model 1500; Altex Scientific, Berkeley, Calif.
[9] Ultrasphere ODS; Altex Scientific.
[10] Model 100-10 spectrophotometer; Hitachi Scientific Instruments, Mountain-View, Calif.
[11] Model 250-2, two channel; Curken Scientific, Danbury, Conn.
[12] Model 485; Varian Instrument Division, Palo Alto, Calif.

0022-3549/84/1100-1657$01.00/0

© 1984, American Pharmaceutical Association

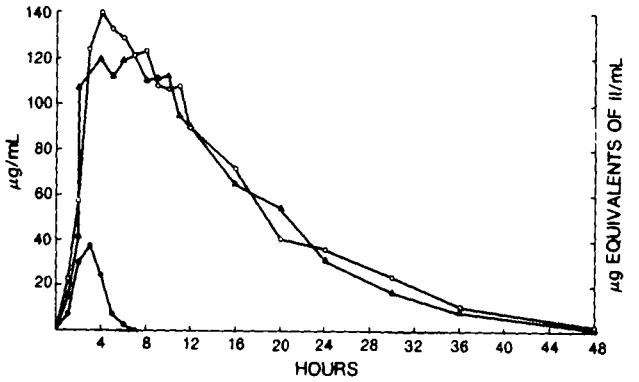

Figure 1—*Plasma levels of free salicylic acid (▲), salsalate (●), (in micrograms per milliliter), and radioactivity (○) (in microgram equivalents of salicylic acid per milliliter) in subject 1 following oral administration of 2000 mg of salsalate.*

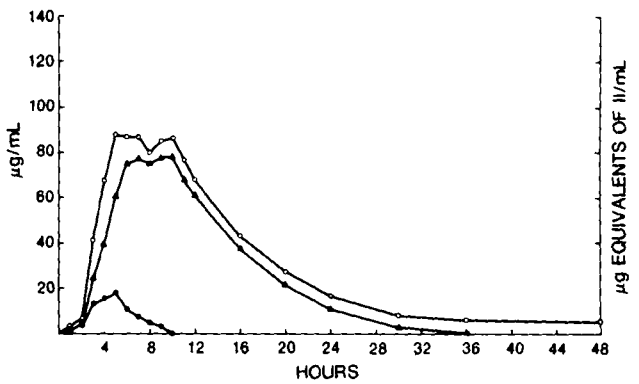

Figure 2—*Plasma levels of free salicylic acid (▲), salsalate (●), (in micrograms per milliliter), and radioactivity (○) (in microgram equivalents of salicylic acid per milliliter) in subject 2 following oral administration of 2000 mg of salsalate.*

were incubated overnight with concentrated HCl at 100°C. The tubes were then extracted with chloroform[13], an aliquot of the organic phase was shaken with the modified Trinder reagent (5), and the absorbance of the aqueous phase was measured at 540 nm. A standard curve was constructed by using known concentrations of sodium salicylate[4] from 0 to 100 mg %.

Plasma and urine samples were assayed for conjugated salsalate and salicylic acid by HPLC following incubation of the samples with β-glucuronidase[14] (5000 U/mL) in acetate buffer (pH 4.5) for 3 h at 37°C. Results of preliminary experiments indicated that partial hydrolysis of salsalate occurred during the incubation period; to correct for this hydrolysis, standards of salsalate, ranging from 20 to 300 μg/mL, were incubated and analyzed with each batch of samples. After incubation, the urine and plasma samples were analyzed for salsalate and salicylic acid by the HPLC method described above for unchanged I.

The urine samples were also assayed for nonconjugated gentisic, salicyluric, and salicylic acid levels by HPLC. Aliquots (1 mL) of standards and samples were transferred into screw-cap tubes, *o*-methoxybenzoic acid[4] (200 μg) was added as an internal standard in addition to 1.0 mL of HCl (0.6 M). The samples were extracted with ether[15] (6 mL). After centrifugation, the aqueous layer was frozen in dry ice–propanol. The ethereal phase was transferred to a tube and the solvent was removed under a stream of nitrogen at 10°C. The residue was then resuspended in 0.5 mL of mobile phase and injected into the HPLC *via* the automatic sampler. The mobile phase of methanol–1% acetic acid (15:85, v/v) was pumped at the rate of 2.0 mL/min through the reverse-phase column[9]. UV absorbance was measured at 300 nm[10]. The retention times for gentisic acid, salicyluric acid, anisic acid, and salicylic acid were 280, 600, 900, and 1190 s, respectively. A small peak was eluted between gentisic acid and salicyluric acid in the samples obtained at early times. This probably corresponds to the glucuronide(s) of salicylic acid and has been described by others (6). Under these chromatographic conditions, unchanged salsalate was not eluted.

Preliminary radioactive counting of aliquots of urine samples after HPLC indicated that not all the radioactivity could be accounted for following chromatography. This problem was resolved by using gradient elution chromatography.

Standards and urine samples (1.0 mL) were transferred into screw-cap tubes and extracted with ether[15] after acidification with 0.6 M HCl as described above. The ethereal layer was taken to dryness with nitrogen at 10°C, and the residue was resuspended in the initial mobile phase. The initial mobile phase was methanol–1% acetic acid (15:85, v/v). A solvent programmer[16] was used to change the relative pumping rates of two pumps to enable the initial phase to change linearly from its initial condition to a final composition of methanol–1% acetic acid (60:40, v/v). The gradient time was 30 min. This was followed by a 15-min elution while maintaining the final gradient conditions, after which the initial conditions were reestablished. UV absorbance was measured at 300 nm[10]. Under these conditions, the retention times were 280 s (gentisic acid), 500 s (salicyluric acid), 650 s (anisic acid), 780 s (salicylic acid), and 1800 s (salsalate). Two additional peaks were eluted at 1380 and 1590 s.

Each stool specimen was homogenized with a known amount of water. Weighed aliquots (0.5–1.0 g) were treated with the decolorizing agents perchloric acid[17] (0.4 mL) and hydrogen peroxide[18] (0.8 mL) and incubated for 24 h at 37°C, and four drops of 15% ascorbic acid[19] and 10 mL of scintillation fluid[2] were added. The treated specimens were then counted in a scintillation counter, corrected for quenching, and converted into micrograms of ^{14}C-labeled salsalate.

RESULTS AND DISCUSSION

Changes in total radioactivity of unconjugated salsalate and salicylic acid in plasma *versus* time for each subject is shown in Figs. 1 and 2. For subject 1, a peak plasma level of II (120 μg/mL) was reached after 4 h (Fig. 1), whereas with the results for subject 2, a lower peak level of 77.6 μg/mL 7 h after drug administration was attained (Fig. 3). Peak levels of I were seen in subject 1 at 3 h (37.9 μg/mL) and in subject 2 at 5 h (18.3 μg/mL).

The areas under the plasma level *versus* time curves for total radioactivity of salsalate and salicylic acid indicated that 86.6% of the area under the curve of total radioactivity was accounted for by the area under the curves of nonconjugated salsalate and salicylic acid in subject 1 and 67.3% in subject 2.

Acid hydrolysis of the plasma samples by incubation overnight at 100°C made the plasma concentrations of II congruent with the amount of radioactivity in the samples (expressed as microgram equivalents of salicylic acid per milliliter), indicating the presence of other metabolites of salicylic acid and/or salsalate in the plasma of these normal volunteers. The ratio of AUC radioactivity-$AUC_{total\ II}$ was 1.01 in subject 1 and 1.02 in subject 2.

The urinary excretion of radioactivity demonstrated that 45.8 and 56.6% of the dose was excreted after 12 h in subjects 1 and 2, respectively, whereas the amount of radioactivity in urine (expressed in microgram equivalents of salsalate) accounted for 95.5 and 101.8% of the drug dose after 84 h. Only ~1% of the total radioactivity was found in the stools of these subjects. The

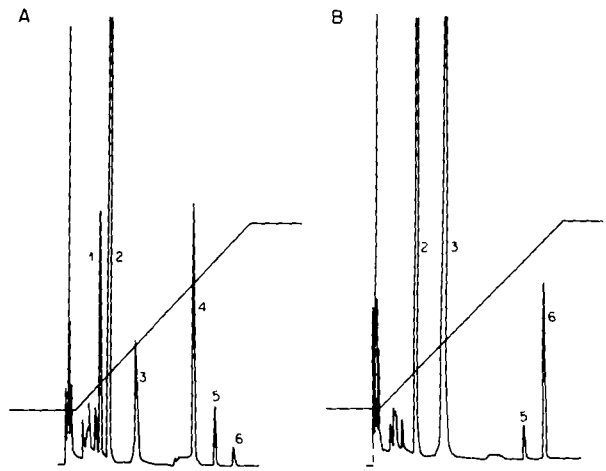

Figure 3—*A typical HPLC tracing of a urine sample before (A) and after (B) β-glucuronidase treatment (see text for explanation).*

[13] Analytical reagent; Mallinckrodt.
[14] Sigma Chemical Co., St. Louis, Mo.
[15] Nanograde; Mallinckrodt.
[16] Solvent Programmer; Altex Scientific.
[17] 70%; Eastman Kodak Co., Rochester, N.Y.
[18] 30%; Mallinckrodt.
[19] Baker Chemical Co., Phillipsburg, N.J.

Table I—Urinary Excretion of Salsalate and Its Metabolites

Compound	Urinary Excretion	
	Subject 1	Subject 2
Total radioactivity, mg equivalents of salsalate	1909.0 (95.4)[a]	2036.0 (101.8)[a]
Free salicylic acid, mg	90.5 (4.2)	50.7 (2.4)
Conjugated salicylic acid, mg	328.6 (15.4)	264.3 (12.4)
Free salsalate, mg	3.4 (0.2)	6.2 (0.3)
Conjugated salsalate, mg	136.0 (6.8)	200.0 (10.0)
Gentisic acid, mg	75.4 (3.2)	58.7 (2.5)
Salicyluric acid, mg	1514.7 (50.3)	1797.2 (59.6)
Total salicylate, mg	1961.4 (91.7)	2014.0 (96.2)

[a] Numbers in parentheses indicate the percentage of administered dose recovered in the urine.

urinary excretion of nonconjugated salsalate and salicylic acid during the study period is shown in Table I; nonconjugated salicylic acid accounted for 2–4% of the total dose, whereas <1% of the dose was excreted as nonconjugated salsalate. These results agree with those reported by Harrison *et al.* (2). Conjugates of both salsalate and salicylic acid were present in significant amounts in both volunteers (Table I). Approximately 12–15% of the dose was excreted as conjugates of salicylic acid, whereas the conjugates of salsalate accounted for 6.8 and 10% of the dose in subjects 1 and 2, respectively. The majority of the conjugates of salsalate were excreted within 12 h after the administration of the drug. A typical HPLC tracing of a urine sample before and after β-glucuronidase treatment is shown in Fig. 3. This chromatogram shows the disappearance of peak 4 and the increase in salsalate (peak 6) after incubation with glucuronidase. Peak 1 also disappeared on treatment with glucuronidase, whereas the salicylic acid peak (peak 3) increased, indicating that peak 1 was one or both of the glucuronides of salicylic acid.

The urinary excretion of nonconjugated gentisic acid, salicyluric acid, and salicylic acid is tabulated in Table I. The amount of nonconjugated gentisic acid excreted in the urine of these subjects was 2.5% (subject 1) and 3.2% (subject 2) of the total dose, whereas excretion as nonconjugated salicyluric acid accounted for 50.0% of the dose in subject 1 and 59.6% in subject 2. The total salicylate recovered in the urine (as percentage of the dose) was 91.7% in subject 1 and 96.2% in subject 2. These values do not include the gentisate excreted since this metabolite is not hydrolyzed to salicylic acid. Thus, urinary salicylate plus gentisic acid levels accounted for 94.9% (subject 1) and 98.7% (subject 2) of the administered dose of salsalate (Table I).

This study of the metabolism of salsalate in two normal volunteers clearly demonstrates the essentially complete absorption of the drug (as indicated by the almost complete recoveries of doses in the urine) and the incomplete hydrolysis of salsalate to salicylic acid (as indicated by the presence of glucuronide conjugates of salsalate in the urine). Formation of the glucuronide conjugates of salsalate may occur either during its passage through the GI tract (7) or in the liver. Regardless of the site of glucuronidation, however, in this study 7–10% of the dose was excreted as glucuronide conjugates of salsalate. Attempts to identify the structures of the glucuronide conjugates by mass spectrometry were unsuccessful. However, mass spectrometric analysis[20] of peak 4 (Fig. 3) following treatment with β-glucuronidase showed that the aglycone was salsalate.

The presence of the glucuronide conjugates, however, suggests that the lower plasma levels of salicylic acid achieved with salsalate, as compared with aspirin or choline magnesium salicylate in previous studies (1–3), are due to a decreased amount of salicylic acid in the body caused by the rapid conjugation of some salsalate (before its hydrolysis to salicylic acid) and its subsequent excretion into the urine.

Although the percentages of the dose excreted as conjugates of salsalate in the two volunteers in this study do not fully explain the 15–23% lower than expected plasma levels of salicylic acid observed in patients (3) and normal volunteers (1, 2) after the administration of salsalate, it should be pointed out that a 10% decrease in the dose of available salicylate may be accompanied by a disproportionate decrease in serum salicylate levels. Such disproportionality follows from the observation that a 50% increase in the dosage of aspirin can almost triple the serum salicylate levels (8).

It should be noted that the decreased availability is only with respect to salicylate, however, since salsalate is essentially completely absorbed and the rapid glucuronidation and excretion prevents complete hydrolysis of salsalate to salicylic acid *in vivo*, thus decreasing the amount of salicylic acid that reaches the systemic circulation.

The results of the present study in normal volunteers supports the results of our multiple dose study in patients with rheumatoid arthritis (3) and indicates that the reduced availability of salicylic acid from salsalate is due to the incomplete hydrolysis of the prodrug.

The clinical implication of these studies is that the dose of salsalate needed to achieve equal plasma salicylate levels will be greater than that predicted from an equivalent dose of aspirin. Preliminary data from multiple dose studies in normal volunteers (2, 9) suggest that the availability of salicylate from one 500-mg tablet of salsalate[21] is approximately equivalent to that available from two 325-mg tablets of aspirin. These doses contain 535 and 500 mg equivalents of salicylic acid, respectively. However, for optimal salicylate therapy of inflammatory arthritis, plasma salicylate concentrations should be determined periodically and used as the basis for dosage adjustment.

REFERENCES

(1) A. Cohen, *Curr. Ther. Res.*, **23**, 772 (1978).

(2) L. I. Harrison, M. L. Funk. O. N. Re, and R. E. Ober, *J. Clin. Pharmacol.*, **21**, 401 (1981).

(3) S. H. Dromgoole, S. Cassell, D. E. Furst, and H. E. Paulus, *Clin. Pharm. Ther.*, **34**, 539 (1983).

(4) L. I. Harrison, M. L. Funk, and R. E. Ober, *J. Pharm. Sci.*, **69**, 1268 (1980).

(5) W. L. Chiou and I. Onyemelukwe, *J. Pharm. Sci.*, **63**, 630 (1974).

(6) E. B. Cham, F. Bochner, D. M. Imhoff, D. Johns, and M. Rowland, *Clin. Chem.*, **26**, 111 (1980).

(7) W. H. Barr and S. Riegelman, *J. Pharm. Sci.*, **59**, 164 (1970).

(8) H. E. Paulus, M. Siegel, E. Mongan, R. Okun, and J. J. Calabro, *Arth. Rheum.*, **14**, 527 (1971).

(9) A. Cohen, *J. Clin. Pharmacol.*, **19**, 242 (1979).

ACKNOWLEDGMENTS

This work was supported in part by Riker Laboratories, the Clinical Research Center Grant #RR 00865, and the Arthritis Foundation.

The authors are very grateful to Dr. L. Harrison of Riker Laboratories and Dr. W. L. Stebbings of 3M Central Research Laboratories, Minn., for technical assistance in this study.

[20] Carried out at the 3M Central Research Laboratories; Model 21-491B GC–MS equipped with a solid sample probe; DuPont de Nemours and Co., Inc., Wilmington, Del.

[21] Disalcid; Riker Laboratories, Northridge, Calif.

High-Performance Liquid Chromatographic Method for the Determination of Esmolol Hydrochloride

YING-CHI LEE, DAVID MICHAEL BAASKE ˣ, and ABU S. ALAM

Received September 14, 1983, from the *Pharmaceutical Development Department, Research and Development Division, American Critical Care, McGaw Park, IL 60085.* Accepted for publication January 13, 1984.

Abstract □ A rapid high-performance liquid chromatographic method for the determination of esmolol hydrochloride, a new ultra-short-acting beta blocker, is described. The stability-indicating nature of the method was demonstrated by resolving esmolol from synthetic intermediates, potential impurities, and the product of decomposition. Reverse-phase liquid chromatography was performed with a microparticulate (10-μm) cyano-bonded silica-packed column, a fixed-wavelength UV absorbance detector (λ = 280 nm), and a mobile phase of acetonitrile–0.005 M sodium acetate–acetic acid (15:84:1) pumped at 2 mL/min. The internal standard was 2-*p*-chlorophenyl-2-methylpropanol. A percent *RSD* of <1.7% and an accuracy (100% − mean error) of >98.6% were achieved over the concentration range studied (100–500 μg/mL), with correlation coefficients >0.9996.

Keyphrases □ HPLC—determination of esmolol hydrochloride □ Esmolol hydrochloride—HPLC

Esmolol hydrochloride (methyl 3[4-[2-hydroxy-3-[(2-methylethyl)amino]propoxy]phenyl]propionate hydrochloride; I) is the first of a new class of beta blockers, known as ultra-short-acting beta blockers, to enter clinical trials. The ultra-short-acting beta blockers were designed to extend the usefulness, safety, and efficacy of beta blockers in critical cardiac therapy through controlled and titratable intravenous therapy (1). This was accomplished by designing chemical instability into the molecule. The ester functionality of the molecule is susceptible to cleavage by the nonspecific serum esterases to the free acid 3[4-[2-hydroxy-3-[(2-methylethyl)amino]-propoxy]phenyl]propionic acid.

Esmolol hydrochloride was synthesized (2) from 3-(*p*-hydroxyphenyl)propionic acid (II) *via* a four-step process (Scheme I). In this report the development and validation of a high-performance liquid chromatographic (HPLC) method for the quantitation of esmolol in the presence of synthetic intermediates (II–IV) and free acid (V) is described.

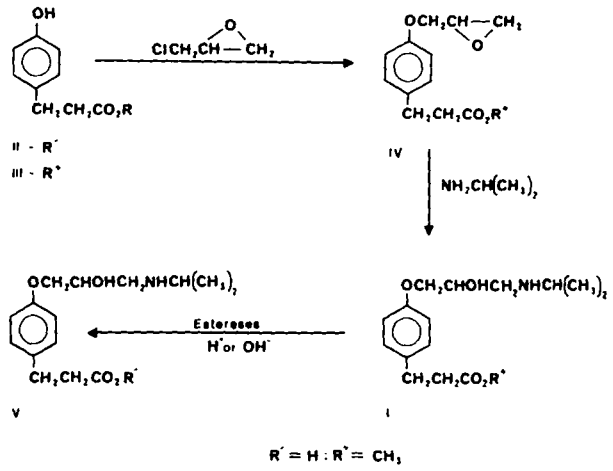

Scheme I

EXPERIMENTAL SECTION

Materials—Compounds I, III, IV, V, and VI were synthesized in this laboratory. 2-(*p*-Chloro-phenyl)-2-methyl propanol[1], compound II, glacial acetic acid[2], and sodium acetate[2] were used as received. Glass-distilled acetonitrile and methanol were used for all procedures[3]. Purified water[4] was used throughout.

Chromatography—A liquid chromatographic system (3), equipped with a fixed-wavelength UV absorbance detector[5] at 280 nm, an on-line data system[6], and a column (30 cm × 3.9 mm) packed with cyano-bonded silica (10-μm)[7], was used. Sample injections were 50 μL. Mobile phase was prepared fresh daily by thoroughly mixing 150 mL of acetonitrile, 10 mL of glacial acetic acid, and 840 mL of sodium acetate trihydrate (0.068%, w/v) buffer which was filtered through a 0.5-μm filter[8] prior to use. A constant flow rate of 2 mL/min yielded a pressure of <2000 psi.

Standard concentrations of 500, 400, 300, 200, 100, and 0 μg/mL were prepared in quadruplicate. To 1.0 mL of each standard or sample was added 750 μL of the internal standard 2-(*p*-chlorophenyl)-2-methyl propanol (4 mg/mL) in methanol–water (50:50). Peak areas were measured, and the ratios for esmolol–internal standard were calculated with the data system, yielding a calibration curve. Samples were prepared in water at 500 μg/mL.

Specificity of the Method—Esmolol hydrochloride (50 mg) was placed in each of four 100-mL volumetric flasks. Into each flask was added 75 mL of either water, 1 M HCl, 1 M NaOH, or 30% hydrogen peroxide. The flasks were gently boiled for 1 h. After cooling, the pH was adjusted to 4 with concentrated

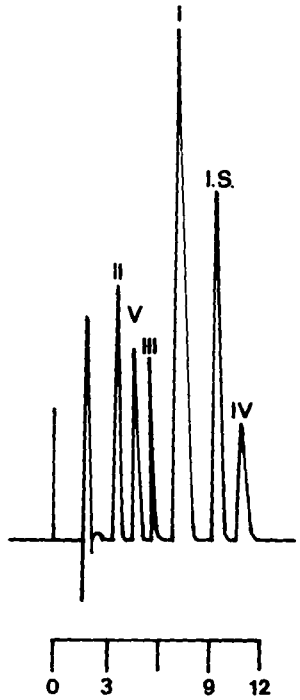

Figure 1—*Typical chromatogram showing the resolution of I from the synthetic intermediates (II–IV) and the anticipated breakdown product (V). IS, internal standard.*

[1] Aldrich Chemical Co., Milwaukee, Wis.
[2] Analytical reagent; Mallinckrodt, St. Louis, Mo.
[3] Burdick & Jackson Laboratories, Muskegon, Mich., or J. T Baker Chemical Co., Phillipsburg, N.J.
[4] Milli-Q Water Purification System; Millipore Corp., Bedford, Mass.
[5] Model LC-15; Perkin-Elmer Corp., Norwalk, Conn., or model 440; Waters Associates, Milford, Mass.
[6] HP-3354; Hewlett-Packard, Avondale, Pa.
[7] μ-Bondapak CN; Waters Associates.
[8] Millipore Corp.

0022-3549/84/1100-1660$01.00/0
© 1984, American Pharmaceutical Association

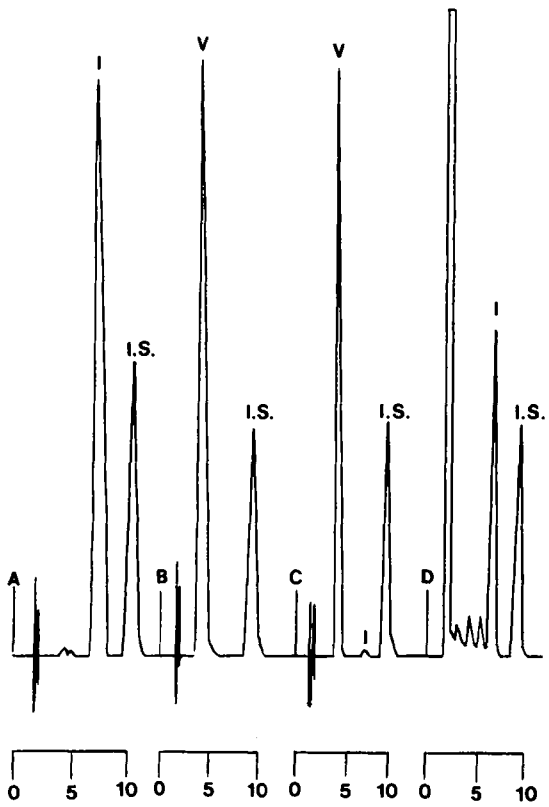

Figure 2—*Chromatogram of esmolol hydrochloride solutions boiled for 1 h. Key: (A) water, pH 5.5; (B) 1 M NaOH; (C) 1 M HCl; (D) 30% H_2O_2.*

HCl or 10 M NaOH. All flasks were brought to volume with water and analyzed.

RESULTS AND DISCUSSION

The direct measurement of the raw drug for esmolol hydrochloride content in the presence of the anticipated synthetic intermediates, the synthetic starting material, and the anticipated breakdown product is shown in Fig. 1. The detector wavelength (280 nm) was chosen to enhance visualization of all potential synthetic intermediates and not for maximum sensitivity for esmolol. The limit of quantitation for esmolol hydrochloride was ~10 μg/mL under the reported operating conditions.

Table I—Analysis of Four Experimental Lots of Esmolol Hydrochloride

Lot	Mean, %	RSD, %	Number of Determinations	Time
A	97.8	1.15	24	2 years
B	97.4	1.23	24	2 years
C	98.6	1.95	21	1 year
D	97.5	0.81	18	9 months

Applicability—The specificity of the HPLC system was tested with degraded esmolol samples. No changes in I concentration were seen in the boiled aqueous solution. After 1 h in boiling acid (1 M HCl) or base (1 M NaOH), I was almost completely converted to V, as might be expected under these conditions. Finally, boiling for 1 h in 33% hydrogen peroxide yielded several additional unidentified products (Fig. 2). In each chromatogram, it can be seen that the size of the I peak decreases with degradation. The practicality of the method was demonstrated by the analysis of four synthetic lots (Table I). The percent *RSD* values for the analysis over a 2-year period and with several analysts were consistently <2%.

Accuracy and Precision—In spite of consistently high correlation coefficients (>0.996), the peak height ratio method was not employed, as erroneous results were obtained due to tailing at higher concentrations. Curvature or tailing did not influence the peak area ratio calculations which were employed for all studies. Data generated by three separate analysts on each of 3 d yielded an accuracy >98.6%, percent *RSD* of <1.64%, and correlation coefficients >0.9996 for the calibration curves. The percent *RSD* values for a single sample were <2% (Table I).

REFERENCES

(1) J. Zaroslinski, R. J. Borgman, J. P. O'Donnell, W. G. Anderson, P. W. Erhardt, S.-T. Kam, R. D. Reynolds, R. J. Lee, and R. J. Gorczynski, *Life Sci.*, **31**, 899 (1982).

(2) P. W. Erhardt, C. M. Woo, W. G. Anderson, and R. J. Gorczynski, *J. Med. Chem.*, **25**, 1408 (1982).

(3) D. M. Baaske, N. N. Karnatz, and J. E. Carter, *J. Pharm. Sci.*, **72**, 194 (1983).

ACKNOWLEDGMENTS

The authors thank Dr. Paul W. Erhardt and Mr. Chi M. Woo for the synthetic products cited and Ms. Lori Coomans for assistance in the preparation of this manuscript.

Effect of Ethanol, Glycerol, and Propylene Glycol on the Stability of Phenobarbital Sodium

V. DAS GUPTA

Received October 18, 1983, from the *Department of Pharmaceutics, University of Houston, Houston, TX 77030.* Accepted for publication January 19, 1984.

Abstract □ The effects of ethanol, glycerol, propylene glycol, phosphate buffer, and ionic strength on the stability of phenobarbital sodium have been studied. Ethanol had the maximum stabilization effect followed by propylene glycol and glycerol when compared with the stability in water. The estimated half-lives at 50°C (pH ~ 8) were 78, 95, 109, and 127 d in water and 20% aqueous solutions of glycerol, propylene glycol, and ethanol, respectively. The effects of phosphate buffer and ionic strength were negligible.

Keyphrases □ Phenobarbital sodium—stability, effects of ethanol, glycerol, and propylene glycol □ Stability—phenobarbital, effect of solvents

It is well known that the stability of phenobarbital in liquid dosage forms depends on the pH and the vehicle. A common method to minimize degradation (1) is to use a mixed solvent of water and an organic solvent such as ethanol, glycerol, or propylene glycol. The stabilization effect of ethanol is thought to be due to a decreased dielectric constant (2), which slows down the reaction between ions of like charges, *i.e.*, the ionized form of phenobarbital and the hydroxyl ions.

An earlier report (1) indicated that it was difficult to select a stability-indicating method for the quantitation of phenobarbital. Recently, a stability-indicating assay method (3) based on HPLC has been reported which is applicable to liquid

0022-3549/84/1100-1661$01.00/0
© 1984, American Pharmaceutical Association

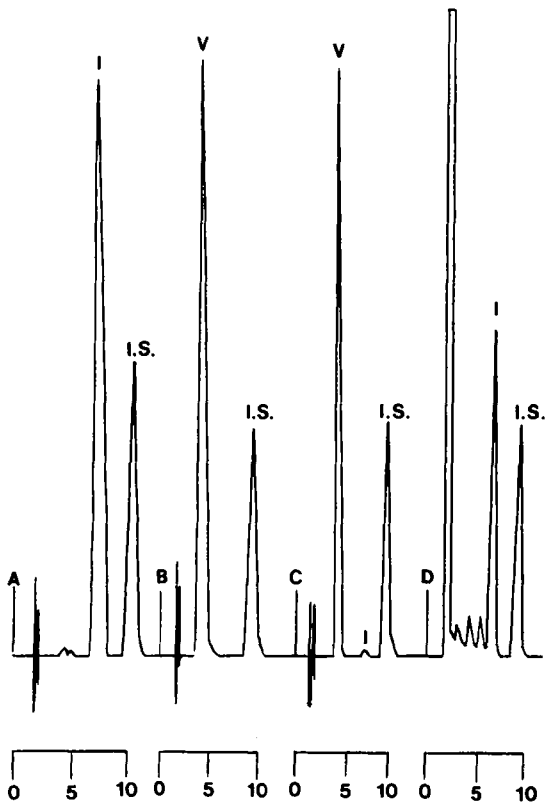

Figure 2—*Chromatogram of esmolol hydrochloride solutions boiled for 1 h. Key: (A) water, pH 5.5; (B) 1 M NaOH; (C) 1 M HCl; (D) 30% H_2O_2.*

HCl or 10 M NaOH. All flasks were brought to volume with water and analyzed.

RESULTS AND DISCUSSION

The direct measurement of the raw drug for esmolol hydrochloride content in the presence of the anticipated synthetic intermediates, the synthetic starting material, and the anticipated breakdown product is shown in Fig. 1. The detector wavelength (280 nm) was chosen to enhance visualization of all potential synthetic intermediates and not for maximum sensitivity for esmolol. The limit of quantitation for esmolol hydrochloride was ~10 μg/mL under the reported operating conditions.

Table I—Analysis of Four Experimental Lots of Esmolol Hydrochloride

Lot	Mean, %	RSD, %	Number of Determinations	Time
A	97.8	1.15	24	2 years
B	97.4	1.23	24	2 years
C	98.6	1.95	21	1 year
D	97.5	0.81	18	9 months

Applicability—The specificity of the HPLC system was tested with degraded esmolol samples. No changes in I concentration were seen in the boiled aqueous solution. After 1 h in boiling acid (1 M HCl) or base (1 M NaOH), I was almost completely converted to V, as might be expected under these conditions. Finally, boiling for 1 h in 33% hydrogen peroxide yielded several additional unidentified products (Fig. 2). In each chromatogram, it can be seen that the size of the I peak decreases with degradation. The practicality of the method was demonstrated by the analysis of four synthetic lots (Table I). The percent *RSD* values for the analysis over a 2-year period and with several analysts were consistently <2%.

Accuracy and Precision—In spite of consistently high correlation coefficients (>0.996), the peak height ratio method was not employed, as erroneous results were obtained due to tailing at higher concentrations. Curvature or tailing did not influence the peak area ratio calculations which were employed for all studies. Data generated by three separate analysts on each of 3 d yielded an accuracy >98.6%, percent *RSD* of <1.64%, and correlation coefficients >0.9996 for the calibration curves. The percent *RSD* values for a single sample were <2% (Table I).

REFERENCES

(1) J. Zaroslinski, R. J. Borgman, J. P. O'Donnell, W. G. Anderson, P. W. Erhardt, S.-T. Kam, R. D. Reynolds, R. J. Lee, and R. J. Gorczynski, *Life Sci.*, **31**, 899 (1982).

(2) P. W. Erhardt, C. M. Woo, W. G. Anderson, and R. J. Gorczynski, *J. Med. Chem.*, **25**, 1408 (1982).

(3) D. M. Baaske, N. N. Karnatz, and J. E. Carter, *J. Pharm. Sci.*, **72**, 194 (1983).

ACKNOWLEDGMENTS

The authors thank Dr. Paul W. Erhardt and Mr. Chi M. Woo for the synthetic products cited and Ms. Lori Coomans for assistance in the preparation of this manuscript.

Effect of Ethanol, Glycerol, and Propylene Glycol on the Stability of Phenobarbital Sodium

V. DAS GUPTA

Received October 18, 1983, from the *Department of Pharmaceutics, University of Houston, Houston, TX 77030.* Accepted for publication January 19, 1984.

Abstract □ The effects of ethanol, glycerol, propylene glycol, phosphate buffer, and ionic strength on the stability of phenobarbital sodium have been studied. Ethanol had the maximum stabilization effect followed by propylene glycol and glycerol when compared with the stability in water. The estimated half-lives at 50°C (pH ~ 8) were 78, 95, 109, and 127 d in water and 20% aqueous solutions of glycerol, propylene glycol, and ethanol, respectively. The effects of phosphate buffer and ionic strength were negligible.

Keyphrases □ Phenobarbital sodium—stability, effects of ethanol, glycerol, and propylene glycol □ Stability—phenobarbital, effect of solvents

It is well known that the stability of phenobarbital in liquid dosage forms depends on the pH and the vehicle. A common method to minimize degradation (1) is to use a mixed solvent of water and an organic solvent such as ethanol, glycerol, or propylene glycol. The stabilization effect of ethanol is thought to be due to a decreased dielectric constant (2), which slows down the reaction between ions of like charges, *i.e.*, the ionized form of phenobarbital and the hydroxyl ions.

An earlier report (1) indicated that it was difficult to select a stability-indicating method for the quantitation of phenobarbital. Recently, a stability-indicating assay method (3) based on HPLC has been reported which is applicable to liquid

0022-3549/84/1100-1661$01.00/0
© 1984, American Pharmaceutical Association

Table I—Stability Studies of Phenobarbital Sodium Solutions (0.5 mg/mL)

Solution	Solvent[a]	Phosphate Buffer, M	Ionic Strength[b]	Apparent $pH_{initial}$ (±0.1)	Estimated Half-Life at 50°C, d	Apparent pH_{final}[c] (±0.1)
1	—[d]	0.1	0.26	7.7	78	7.8
2	20% Ethanol	0.1	0.26	8.1	127	8.0
3	40% Ethanol	0.1	0.26	8.4	170	8.2
4	20% Glycerol	0.1	0.26	7.7	95	7.6
5	40% Glycerol	0.1	0,.26	7.7	134	7.6
6	20% Propylene glycol	0.1	0.26	7.9	109	8.0
7	40% Propylene glycol	0.1	0.26	8.2	165	8.2
8	—[d]	0.05	0.39	7.7	79	7.8
9	—[d]	0.1	0.39	7.7	77	7.8
10	—[d]	0.15	0.39	7.7	77	7.8
11	—[d]	0.1	0.26	7.7	78	7.8
12	—[d]	0.1	0.39	7.7	79	7.8
13	—[d]	0.1	0.52	7.7	80	7.8

[a] Prepared in water. [b] Adjusted with KCl. [c] After 163 d. [d] Water alone.

dosage forms such as phenobarbital elixir. The purpose of these investigations was to study the effect of ethanol, glycerol, propylene glycol, phosphate buffer concentration, and ionic strength on the stability of phenobarbital sodium using the recently developed (3) HPLC method.

EXPERIMENTAL SECTION

Chemicals, Reagents, and Apparatus—All chemicals and reagents were either USP, NF, or ACS quality. Phenobarbital sodium[1] (1) was used as received.

The chromatograph[2] was equipped with a multiple-wavelength detector[3] and a recorder[4]. A semipolar column[5] (30 cm × 4 mm i.d.) was used. The mobile phase contained 35% methanol in 0.02 M aqueous ammonium acetate. The flow rate was 3.0 mL/min, and the temperature was ambient. The sensitivity was set at 0.1 (245 nm) and the chart speed was 30.5 cm/h.

Preparation of Phenobarbital Sodium Solutions—All solutions (Table I) contained 0.5 mg/mL of phenobarbital sodium and were prepared using a simple solution method. The standard solution of phenobarbital sodium in water (0.5 mg/mL) was prepared fresh daily.

After the initial assay and pH value determination[6] the solutions were stored at 50 ± 1°C in 60-mL amber bottles[7] in an electric oven. The data were recorded again at appropriate intervals. The solutions were assayed using HPLC (3) except that the flow rate was 3.0 mL/min. The other chromatographic conditions were the same, except that no internal standard could be added since the solutions were injected into the chromatograph without dilution. The results were calculated using a previously described equation (3) and are presented in Table I and Fig. 1.

RESULTS AND DISCUSSION

Effect of Vehicle—The results (Table I) indicate that ethanol had the maximum stabilizing effect on phenobarbital sodium followed by propylene glycol and glycerol. The apparent pH values of these solutions varied slightly, although they all contained 0.1 M phosphate buffer and the ionic strength was adjusted to 0.26 with KCl. The pH-rate profile curve of phenobarbital is less sensitive to pH changes from 7.5 to 9 (4), the range used in these experiments.

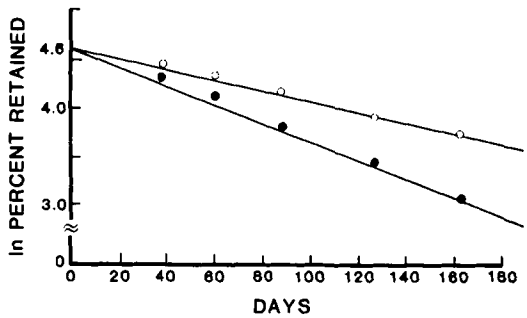

Figure 1—*First-order plots of solutions 1 and 5 (Table I). Key: (●) solution 1; (○) solution 5.*

Above pH 9, decomposition occurs readily (4). Considering this, it is obvious that the stabilizing effect of ethanol may be even better than the results indicate since the initial pH values of solutions containing ethanol (Table I) were higher than those containing propylene glycol or glycerol. Solutions containing glycerol had the lowest apparent pH values (Table I) and still had less stabilizing effect than propylene glycol and ethanol. Glycerol was better only when compared with water (Table I), which was expected. The estimated half-lives of solutions in water, 20% glycerol, 20% propylene glycol, and 20% ethanol were 78, 95, 109, and 127 d, respectively. Obviously, the stabilizing effect is inversely related to dielectric constant values of 80, 43, 32, and 25 for water, glycerol, propylene glycol, and ethanol, respectively, at 20°C. This is in agreement with earlier observations (2) that the stabilization effect is due to a decrease in the dielectric constant, which slows down the reaction between ions of like charges. Using the first-order equation (Fig. 1) and taking the activation energy value of 25 kcal/mol-deg (4), the t_{90} for solution 7 (Table I) at 25°C was determined to be ~1.8 years.

Effect of Phosphate Buffer and Ionic Strength—The phosphate buffer did not catalyze the reaction (solutions 8–10, Table I) and the effect of ionic strength was negligible (solutions 11–13). This was expected since the reaction between the un-ionized molecule of phenobarbital and the hydroxyl radical is ~250 times greater than that between the ionized form and OH^- (4).

REFERENCES

(1) W. J. Husa and B. B. Jatul, *J. Am. Pharm. Assoc. Sci. Ed.*, **33**, 217 (1944).

(2) K. Ikeda, *Chem. Pharm. Bull.*, **8**, 504 (1960).

(3) V. D. Gupta, *J. Pharm. Sci.*, **73**, 1158 (1984).

(4) K. A. Connors, G. L. Amidon, and L. Kennon, "Chemical Stability of Pharmaceuticals, A Handbook for Pharmacists," Wiley-Interscience, New York, N.Y., 1979, p. 280.

[1] American Chemical and Drug Co., Los Angeles, Calif.
[2] Model ALC202 equipped with a U6K Universal injector; Waters Associates, Milford, Mass.
[3] Spectroflow Monitor SF770; Schoeffel Instruments Corp., Ramsey, N.J.
[4] Omniscribe 5213-12; Houston Instruments, Austin, Tex.
[5] μ-Bondapak phenyl; Waters Associates.
[6] SS-3 Zeromatic pHmeter; Beckman Instruments.
[7] Brockway Glass Co., Brockway, Pa.

Spectrophotometric Method for Quantitation of Peroxides in Sorbitan Monooleate and Monostearate

ADINA MAGILL and ALLYN R. BECKER ˣ

Received September 26, 1983, from the *Preformulation Department, Syntex Research, Palo Alto, CA 94304.* Accepted for publication February 9, 1984.

Abstract □ A rapid and sensitive spectrophotometric method has been developed to quantitate the peroxides present in sorbitan monooleate and monostearate. The method relies on the peroxide conversion of iodide to iodine. The method has also been found to work for polysorbate 60.

Keyphrases □ Peroxides—sorbitan monooleate and monostearate by spectrophotometry □ Sorbitan monooleate—spectrophotometric quantitation of peroxides □ Sorbitan monostearate—spectrophotometric quantitation of peroxides

Nonionic surfactants, used extensively as emulsifying agents, are integral components of semisolid dosage forms. However, surfactants tend to form peroxides, which have caused stability problems in numerous oxidizable drugs (1-3). The formation of peroxides can also lead to chemical modifications in the surfactants themselves (*e.g.*, chain shortening) that may unfavorably modify their physical properties (1, 4, 5). Titrimetric assay methods have been developed to determine the peroxide content in surfactants, but most of these are limited to the water soluble surfactants, *e.g.*, polyoxyethylene surfactants (6, 7). One titrimetric method, that has been used to quantitate the peroxides present in fats and oils, relies on the partitioning of the desired fat or oil between an organic and aqueous layer. The fat or oil is then transferred with "constant and vigorous shaking" from the organic layer to the aqueous layer where the actual titration occurs (8). Another limitation of titrimetric quantitation of peroxides can arise when methylene blue is used as an indicator. With the yellow surfactant sorbitan monooleate, for example, the color change at the end point, from green to aqua, is extremely difficult to detect.

In the course of our studies of the stability of steroids in surfactant systems, an analytical method was needed to quantitate the peroxides that were initially present in the surfactants. This method also had to be sensitive enough to ensure that the peroxide content had been significantly reduced in each of the surfactants following a purification procedure designed to eliminate peroxides from the surfactants.

To overcome the limitations of water insolubility and a difficult titrimetric assay, we have developed a rapid and sensitive spectrophotometric method to quantitate the peroxides present in sorbitan monostearate and monooleate, two poorly water soluble surfactants. This method was also shown to work for polysorbate 60.

EXPERIMENTAL SECTION

Materials and Instrumentation—Peroxides were removed from polysorbate 60[1], sorbitan monostearate[1], and sorbitan monooleate[1] according to the method of Segal *et al.* (9), with modifications. Hexane was substituted for methylene chloride to solubilize sorbitan monooleate, and hexane with ~5% methylene chloride was used to solubilize sorbitan monostearate.

The following reagents were used: resublimed iodine[2], potassium iodide[2], sodium thiosulfate[2], sodium metabisulfite[2], reagent grade isopropyl alcohol[2], methylene blue[3], and double-distilled water. UV spectral scans and absorbances were obtained on a rapid-scanning UV-VIS spectrophotometer[4].

Titrimetric Peroxide Number Determination of Polysorbate 60 and Sorbitan Monooleate—To 2.0 g of surfactant was added 3 mL of glacial acetic acid-methylene chloride (3:2). The mixture was stirred until a clear solution was obtained. After 50 μL of a KI-saturated aqueous solution was added, the mixture was stirred for exactly 2.0 min and 5 mL of isopropyl alcohol and 100 μL of an aqueous 0.025% methylene blue solution were added. The solution was titrated with standardized sodium thiosulfate to an aqua end point.

Iodine Standards for Spectrophotometry—A 0.010 M iodine standard was prepared by dissolving iodine in an aqueous 5% KI solution. This standard solution was further diluted with the 5% KI solution to give an iodine concentration of 10^{-4}-10^{-7} M. Iodine standards containing 2% purified surfactant were also prepared as described above at an iodine concentration range of 10^{-4} to 5×10^{-6} M.

Spectrophotometric Analyses of Polysorbate 60 and Sorbitan Monooleate—Aqueous saturated KI solution (50 μL) was added to 2 g of surfactant dissolved in 3 mL acetic acid-methylene chloride (3:2) and the solution was stirred under a blanket of nitrogen for 2 min. A 5.0-mL portion of isopropyl alcohol was added and immediately 200 μL of this solution was diluted to 2.0 mL with isopropyl alcohol. The absorbance at 360 nm was then measured within 2-3 min after mixing. Two blanks were determined under the same conditions, one without surfactant, and the other without KI.

Spectrophotometric Analysis of Sorbitan Monostearate—The procedure followed for analysis of sorbitan monostearate was exactly the same as for sorbitan monooleate with one exception: prior to the final addition of 2.0 mL of isopropyl alcohol, 100 μL of methylene chloride was added to maintain the solubilization of the monooleate.

RESULTS AND DISCUSSION

This spectrophotometric method takes advantage of the iodine generated from the reaction of peroxides on iodide (6). From the stoichiometry of the reaction, 1 mol of iodine is produced for each mole of hydroperoxide present. The quantitation of iodine formed is thus a direct measure of the peroxides present in the sample[5].

In the absence of surfactant, the absorbamce at 360 nm was obtained as a function of the concentration of iodine. Beer's law was obeyed over the 10^{-4}-10^{-7} M iodine concentration range. Beer's law was also followed in the presence of purified sorbitan monostearate at an iodine concentration range of 10^{-4}-10^{-6} M at 360 nm. The molar absorptivities in the absence of surfactant and in the presence of sorbitan monostearate were 24,000 M^{-1} cm^{-1} and 27,000 M^{-1} cm^{-1}, respectively, indicating that purified surfactant had little effect on the value of the molar absorptivity at 360 nm.

Two solutions prepared for peroxide quantitation by the spectrophotometric method, one without KI and the other without surfactant, showed no absorbance at 360 nm. Therefore, the absorbance determined in samples assayed by this method is due entirely to the generation of iodine by the peroxides present in the surfactant.

To eliminate iodine fading[6], one of the complications of iodimetric assays, part of the experimental procedure was conducted under a blanket of nitrogen. This nitrogen blanket provided several minutes to obtain the final absorbance reading after the dissolution of the surfactant. When the nitrogen blanket was not used, iodine fading was detected immediately after dilution with the final portion of isopropyl alcohol.

The quantitation of peroxides is frequently expressed in terms of the peroxide number (PN). By definition, the PN is the number of equivalents of peroxide contained in 1000 g of surfactant.

[1] Emery Industries, Cincinnati, Ohio.
[2] Mallinckrodt Chemical Works, St. Louis, Mo.
[3] Matheson Coleman and Bell, East Rutherford, N.J.
[4] Model 8450A; Hewlett-Packard, Palo Alto, Calif.
[5] Tri-iodide, in equilibrium with iodine and iodide in the presence of water, is actually the species that is quantitated (6).
[6] Azaz *et al.* (6) have developed a kinetic spectrophotometric assay for peroxide quantitation in water soluble surfactants which corrects for iodine fading.

0022-3549/84/1100-1663$01.00/0
© 1984, American Pharmaceutical Association

Table I—Peroxide Number (PN) of Sorbitan Monooleate, Sorbitan Monostearate, and Polysorbate 60 Using the Spectrophotometric Method

Surfactant	Peroxide Number Before Peroxide Removal	Peroxide Number After Peroxide Removal
Sorbitan Monooleate	0.24[a]	<0.10
Sorbitan Monostearate	1.3	<0.10
Polysorbate 60	9.8[b]	<0.10

[a] By titrimetric assay the PN was determined to be 0.39. [b] By titrimetric assay the PN was determined to be 5.8.

The PN of the three surfactants in this study were determined by the spectrophotometric method before and after peroxide removal (Table I). For comparison, the PN of polysorbate 60 and sorbitan monooleate were determined before peroxide removal by the titrimetric assay.

The lower limit of <0.10 for the PN by the spectrophotometric method (Table I) was chosen because it corresponded to the lowest iodine concentration in the presence of purified surfactant used in establishing the linearity of the method. This lower limit was sensitive enough to assure that the peroxide level had been significantly reduced after extraction with sodium metabisulfite[7].

From the results shown in Table I, the titrimetric and the spectrophotometric method for polysorbate 60 and sorbitan monooleate agreed fairly well. However, the color transition at the titrimetric end point for sorbitan monooleate, from green to aqua, was difficult to observe. No such problems were encountered using the spectrophotometric method; hence, this method may provide a more accurate measure of the peroxide content of sorbitan monooleate than the titrimetric assay.

While the titrimetric assay worked well for polysorbate 60 and fairly well for sorbitan monooleate, it did not work at all for sorbitan monostearate. It was not possible to keep the sorbitan monostearate solubilized during the titration with aqueous thiosulfate using the titrimetric method. Therefore, the PN of sorbitan monostearate could only be determined using the spectrophotometric method detailed in this report.

In summary, a sensitive spectrophotometric method has been developed to quantitate the peroxides present in sorbitan monostearate and monooleate, and polysorbate 60. This method should be easily extended to include other poorly water soluble as well as water soluble surfactants.

[7] These authors feel that the lower limit of peroxide quantitation by this spectrophotometric method can be extended by 10-fold, to PN values at levels <0.01. This is based on our findings that Beer's law is valid at a 50-fold lower iodine concentration in the absence of surfactant.

REFERENCES

(1) R. Hamburger, E. Azaz, and M. Donbrow, *Pharm. Acta Helv.*, **50,** 10 (1975).

(2) J. W. McGinity, J. A. Hill, and A. L. La Via, *J. Pharm. Sci.*, **64,** 356 (1975).

(3) L. V. Coates, M. M. Pashley, and K. Tattersal, *J. Pharm. Pharmacol.*, **13,** 620 (1961).

(4) M. Donbrow, R. Hamburger, and E. Azaz, *J. Pharm. Pharmacol.*, **27,** 160 (1975).

(5) M. Donbrow, E. Azaz, and A. Pillersdorf, *J. Pharm. Sci.*, **67,** 1676 (1978).

(6) E. Azaz, M. Donbrow, and R. Hamburger, *Analyst*, **98,** 663 (1973).

(7) J. W. McGinity, T. R. Patel, A. H. Naqvi, and J. A. Hill, *Drug Dev. Comm.*, **2,** 505 (1976).

(8) Official and Tentative Methods of the American Oil Chemists' Society, Tentative Method Cd 8-53, procedure for fats and oils.

(9) R. Segal, E. Azaz and M. Donbrow, *J. Pharm. Pharmacol.*, **31,** 39 (1979).

Gas Chromatographic Method for Solvent Residues in Drug Raw Materials

F. MATSUI ˣ, E. G. LOVERING, J. R. WATSON, D. B. BLACK, and R. W. SEARS

Received August 10, 1983, from the *Bureau of Drug Research, Health Protection Branch, Health and Welfare Canada, Ottawa, Ontario, Canada K1A 0L2.* Accepted for publication February 21, 1984.

Abstract □ A gas chromatographic (GC) method for screening drug raw materials, soluble in aqueous media, for volatile solvent residues has been developed. After dissolution, separate portions of the drug are each separately extracted with *n*-octane, toluene, and ether and injected into a chromatograph equipped with a porous polymer column and a flame ionization detector. The range of extractant polarities provides chromatograms which, taken together, are free of interfering peaks from 0 to ~20 min. Peaks due to solvent residues in the drug are identified by retention time with confirmation of identity by GC-MS.

Keyphrases □ GC—solvent residues in drug raw materials, comparison with MS □ Solvent residues—drug raw materials, GC, comparison with MS

Drug raw materials are manufactured in an increasing number of countries. Whether, for a given drug, the same synthetic route is used universally or whether different routes are used, the necessarily diverse sources of raw materials, technical experience, and manufacturing conditions can lead to differences in the amount and kind of drug-related impurities (1-4). Solvent residues may also be present (1). These may be revealed by modern techniques such as liquid chromatography but, due to their volatility, not by thin-layer chromatography (a method often used to assess drug impurities). Besides being undesirable contaminants, solvent residues may interfere with the determination of drug-related impurities. The problem of solvent residues is recognized by the USP (5) which includes monographs involving, for example, tests for chloroform and ethyl acetate in colchicine, pyridine in diethylstilbestrol diphosphate, and isopropyl alcohol in dihydroxyaluminum aminoacetate. Work in this laboratory, reported herein, has shown for example, that some sulfinpyrazone and flurazepam hydrochloride raw materials are contaminated with toluene and acetone, respectively. To maintain surveillance over this situation, a method for the detection and quantitation of solvent residues in drug raw materials has been developed.

Each of three portions of an aqueous solution of the drug to be examined is individually extracted with ether, toluene, and *n*-octane, and the extracts are tested for volatile organic solvents by gas chromatography (GC). The three solvents were chosen to provide a range of polarities. This enhances the probability that any solvent residue in the drug will be substantially extracted into at least one of them. In addition, each of the three provides a different retention time range free of

0022-3549/84/1100-1664$01.00/0

© 1984, American Pharmaceutical Association

Table I—Peroxide Number (PN) of Sorbitan Monooleate, Sorbitan Monostearate, and Polysorbate 60 Using the Spectrophotometric Method

Surfactant	Peroxide Number Before Peroxide Removal	Peroxide Number After Peroxide Removal
Sorbitan Monooleate	0.24[a]	<0.10
Sorbitan Monostearate	1.3	<0.10
Polysorbate 60	9.8[b]	<0.10

[a] By titrimetric assay the PN was determined to be 0.39. [b] By titrimetric assay the PN was determined to be 5.8.

The PN of the three surfactants in this study were determined by the spectrophotometric method before and after peroxide removal (Table I). For comparison, the PN of polysorbate 60 and sorbitan monooleate were determined before peroxide removal by the titrimetric assay.

The lower limit of <0.10 for the PN by the spectrophotometric method (Table I) was chosen because it corresponded to the lowest iodine concentration in the presence of purified surfactant used in establishing the linearity of the method. This lower limit was sensitive enough to assure that the peroxide level had been significantly reduced after extraction with sodium metabisulfite[7].

From the results shown in Table I, the titrimetric and the spectrophotometric method for polysorbate 60 and sorbitan monooleate agreed fairly well. However, the color transition at the titrimetric end point for sorbitan monooleate, from green to aqua, was difficult to observe. No such problems were encountered using the spectrophotometric method; hence, this method may provide a more accurate measure of the peroxide content of sorbitan monooleate than the titrimetric assay.

While the titrimetric assay worked well for polysorbate 60 and fairly well for sorbitan monooleate, it did not work at all for sorbitan monostearate. It was not possible to keep the sorbitan monostearate solubilized during the titration with aqueous thiosulfate using the titrimetric method. Therefore, the PN of sorbitan monostearate could only be determined using the spectrophotometric method detailed in this report.

In summary, a sensitive spectrophotometric method has been developed to quantitate the peroxides present in sorbitan monostearate and monooleate, and polysorbate 60. This method should be easily extended to include other poorly water soluble as well as water soluble surfactants.

[7] These authors feel that the lower limit of peroxide quantitation by this spectrophotometric method can be extended by 10-fold, to PN values at levels <0.01. This is based on our findings that Beer's law is valid at a 50-fold lower iodine concentration in the absence of surfactant.

REFERENCES

(1) R. Hamburger, E. Azaz, and M. Donbrow, *Pharm. Acta Helv.*, **50,** 10 (1975).

(2) J. W. McGinity, J. A. Hill, and A. L. La Via, *J. Pharm. Sci.*, **64,** 356 (1975).

(3) L. V. Coates, M. M. Pashley, and K. Tattersal, *J. Pharm. Pharmacol.*, **13,** 620 (1961).

(4) M. Donbrow, R. Hamburger, and E. Azaz, *J. Pharm. Pharmacol.*, **27,** 160 (1975).

(5) M. Donbrow, E. Azaz, and A. Pillersdorf, *J. Pharm. Sci.*, **67,** 1676 (1978).

(6) E. Azaz, M. Donbrow, and R. Hamburger, *Analyst*, **98,** 663 (1973).

(7) J. W. McGinity, T. R. Patel, A. H. Naqvi, and J. A. Hill, *Drug Dev. Comm.*, **2,** 505 (1976).

(8) Official and Tentative Methods of the American Oil Chemists' Society, Tentative Method Cd 8-53, procedure for fats and oils.

(9) R. Segal, E. Azaz and M. Donbrow, *J. Pharm. Pharmacol.*, **31,** 39 (1979).

Gas Chromatographic Method for Solvent Residues in Drug Raw Materials

F. MATSUI ˣ, E. G. LOVERING, J. R. WATSON, D. B. BLACK, and R. W. SEARS

Received August 10, 1983, from the *Bureau of Drug Research, Health Protection Branch, Health and Welfare Canada, Ottawa, Ontario, Canada K1A 0L2.* Accepted for publication February 21, 1984.

Abstract □ A gas chromatographic (GC) method for screening drug raw materials, soluble in aqueous media, for volatile solvent residues has been developed. After dissolution, separate portions of the drug are each separately extracted with *n*-octane, toluene, and ether and injected into a chromatograph equipped with a porous polymer column and a flame ionization detector. The range of extractant polarities provides chromatograms which, taken together, are free of interfering peaks from 0 to ~20 min. Peaks due to solvent residues in the drug are identified by retention time with confirmation of identity by GC-MS.

Keyphrases □ GC—solvent residues in drug raw materials, comparison with MS □ Solvent residues—drug raw materials, GC, comparison with MS

Drug raw materials are manufactured in an increasing number of countries. Whether, for a given drug, the same synthetic route is used universally or whether different routes are used, the necessarily diverse sources of raw materials, technical experience, and manufacturing conditions can lead to differences in the amount and kind of drug-related impurities (1-4). Solvent residues may also be present (1). These may be revealed by modern techniques such as liquid chromatography but, due to their volatility, not by thin-layer chromatography (a method often used to assess drug impurities). Besides being undesirable contaminants, solvent residues may interfere with the determination of drug-related impurities. The problem of solvent residues is recognized by the USP (5) which includes monographs involving, for example, tests for chloroform and ethyl acetate in colchicine, pyridine in diethylstilbestrol diphosphate, and isopropyl alcohol in dihydroxyaluminum aminoacetate. Work in this laboratory, reported herein, has shown for example, that some sulfinpyrazone and flurazepam hydrochloride raw materials are contaminated with toluene and acetone, respectively. To maintain surveillance over this situation, a method for the detection and quantitation of solvent residues in drug raw materials has been developed.

Each of three portions of an aqueous solution of the drug to be examined is individually extracted with ether, toluene, and *n*-octane, and the extracts are tested for volatile organic solvents by gas chromatography (GC). The three solvents were chosen to provide a range of polarities. This enhances the probability that any solvent residue in the drug will be substantially extracted into at least one of them. In addition, each of the three provides a different retention time range free of

0022-3549/84/1100-1664$01.00/0

© 1984, American Pharmaceutical Association

Table I—Relative Retention Times of Organic Solvents

Solvent	Relative Rentention Time[a]
Methanol	0.07
Ethanol	0.12
Acetonitrile	0.14
Acetone	0.18
Dichloromethane	0.18
2-Propanol	0.19
Ether	0.21
n-Pentane	0.22
1-Propanol	0.25
Methyl ethyl ketone	0.35
Chloroform	0.35
Ethyl acetate	0.36
1,2-Dichloroethane	0.40
1-Butanol	0.46
Benzene	0.48
Carbon tetrachloride	0.50
Cyclohexane	0.53
1,1,1-Trichloroethane	0.64
Pyridine	0.79
Toluene	1.00
Dimethylformamide	1.11
Isooctane (2,2,4-trimethylpentane)	1.12
n-Butyl acetate	1.50
n-Octane	1.66
Dimethyl sulfoxide	2.29
Cyclohexanone	2.29

[a] Relative to toluene at ~9 min when these data were obtained.

main peak or impurity interference so that impurities extracted from the drug can be easily detected. Any such peaks are tentatively identified by comparison of their retention times with the known retention times of common solvents, with confirmation of identity by MS comparison with known standards.

EXPERIMENTAL SECTION

Materials and Apparatus—Ether[1] (USP) and glass-distilled toluene[2] were used as received. *n*-Octane[3] (100 mL) was passed through three silica cartridges[4] prior to use. The drug raw materials were commercially available.

The gas chromatograph[5] was equipped with a flame ionization detector and a printer–plotter mechanism (attenuation 2↑5, corresponding to 32 pA/cm). The coiled glass column (0.91 m × 4 mm i.d.), packed with a porous polymer[6] (80/100 mesh), was adapted to the chromatograph with a short length of nickel tubing. The column, injector port, and detector temperatures were 210°C; gas flow rates were: nitrogen, 60 mL/min; hydrogen, 35 mL/min; air, 400 mL/min. Columns were conditioned for 72 h at 210°C with a nitrogen flow of 60 mL/min.

Drug Dissolution—Three solutions were prepared to contain ~200 mg of drug, accurately weighed in a minimum volume of aqueous solvent. The aqueous solvent, whether acidic, basic, or neutral, was chosen on the basis of a preliminary investigation to determine the conditions of maximum solubility. Thus, hydrochloric acid solution might be selected for a basic drug such as diazepam, whereas a sodium hydroxide solution would be selected for an acidic drug such as sulfinpyrazone.

Chromatographic profiles of the ether, toluene, and *n*-octane were obtained prior to use. Samples exhibiting significant impurity peaks were either purified or rejected. To each of the three drug solutions was added either toluene (1.0 mL), *n*-octane (1.0 mL), or ether (2.0 mL). Each tube was shaken vigorously for 2 min, centrifuged, and 2 μL of the organic phase was injected into the gas chromatograph.

Prior to beginning the actual examination of drug raw materials, the retention times of a number of possible volatile contaminants were determined (Table I). If an impurity peak was found in a drug extract, a tentative identification was made by reference to Table I and verified by injection of a solution of the suspected impurity in the appropriate solvent, either ether, toluene, or *n*-octane. Confirmation was by GC–MS[7] using GC conditions as described above with an electron ionization potential of 70 eV.

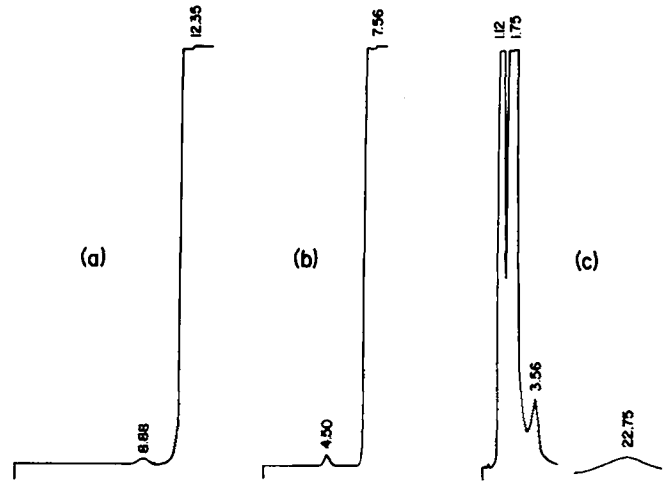

Figure 1—*Chromatograms of the extraction solvents. Key: (a) n-octane with an impurity at 8.88 min; (b) toluene with benzene at 4.5 min; (c) ether with several impurities.*

Quantitation—After identification, impurity levels were established by comparison to a three-point calibration curve. For example, for the quantitation of acetone, the calibration curve was prepared by shaking a 1-mL aliquot of each of three standard solutions of acetone in toluene (range, 1.58–0.0316 mg/mL) with the same volume of the aqueous solvent used for the dissolution of the drug raw material (Table II). Duplicate 2-μL aliquots of the organic phase representing an on-column range of 3.16–0.0632 μg acetone were chromatographed, and the response factor was calculated from the integrated area. For toluene, a three-point calibration curve was prepared in a similar manner using three standard solutions of toluene in *n*-octane (range, 0.866–0.0247 mg/mL) representing an on-column range of 1.732–0.0494 μg. Recovery of the impurity from the aqueous solution of the drug was determined by extracting a fresh sample of the drug with solvent containing a known amount of the impurity, usually one of the known solutions prepared for calibration purposes. This is equivalent to spiking the drug sample with a known amount of the impurity. Recovery, in percent, is given by: $(C_t - C_i/C_s) \times 100$, where C_t, C_i, and C_s are the area counts obtained for the spiked sample, the sample itself, and the standard solution used to spike the sample, respectively.

RESULTS AND DISCUSSION

The method was developed to screen drug raw materials for volatile organic solvent contaminants. Three portions of the material to be examined were

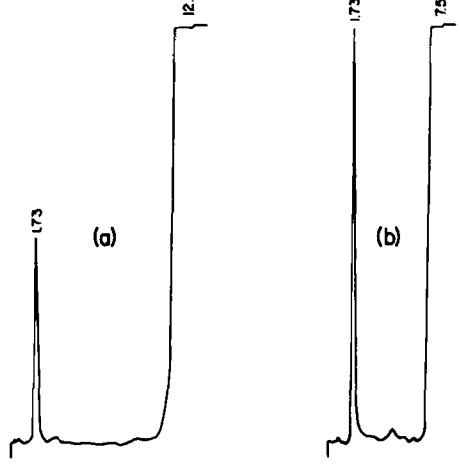

Figure 2—*Chromatograms of flurazepam extracts showing acetone at 1.73 min for the n-octane extract (a) and the toluene extract (b).*

[1] Mallinckrodt Chemical Works, St. Louis, Mo.
[2] Burdick and Jackson Inc., Muskegon, Mich.
[3] Gold Label grade; Aldrich Chemical Co., Montreal, Canada.
[4] Sep-Pak; Waters Scientific Ltd., Mississauga, Ontario, Canada.
[5] Model 5880A; Hewlett-Packard, Palo Alto, Calif.
[6] Chromosorb 106; Chromatographic Specialities, Brockville, Ontario, Canada.
[7] Model 5985; Hewlett-Packard.

Table II—Solvent Residues in Drug Raw Materials

Drug[a]	Solvent, mL	*n*-Octane[b] Residue Found	*n*-Octane[b] Level, %[c]	Toluene[b] Residue Found	Toluene[b] Level, %[c]	Ether Residue Found
Chlordiazepoxide HCl (1)	H_2O(2)	—[d]		Acetone	0.015 (90)	—
Chlorpromazine HCl (1)	H_2O (0.5)	Toluene	0.04 (101)	—		Toluene
Flurazepam HCl (8)	2.5 M HCl (0.5)	Acetone		Acetone	0–0.51 (118)	—
Furosemide (5)	2.5 M NaOH (1)	—		Acetone	0–0.05	—
Naproxen (2)	1 M NaOH (9)	Toluene	0.02–0.05 (97)	—		Toluene
Propranolol HCl (6)	H_2O (2.5)	Toluene	0–0.06 (99)	Acetone	0–0.08 (85)	Toluene
Sulfinpyrazone (4)	1 M NaOH (5)	Toluene	0–0.33 (103)	—		Toluene

[a] Number of lots analyzed in parentheses. [b] Solvent residue levels are calculated on the basis of 400 μg of drug on-column. [c] Percent recovery in parentheses. [d] None detected.

extracted separately with *n*-octane, toluene, and ether. These extracts were chosen to provide a range of polarities to facilitate the extraction of impurities from aqueous drug solution and to leave open different retention time windows in the chromatograms (Fig. 1). Although good grades of these solvents were employed, they all contain minor impurities which are evident as peaks on the chromatograms.

The method described provides for minimum detectable levels of 0.002–0.005% (with respect to sampling technique equivalent to 400 μg of drug on column) volatile solvent in drug raw material, depending upon the solvent residue and its partition ratio between the organic and aqueous phases. If lower sensitivities can be tolerated, lesser amounts of drug raw material can be used.

Typical results are presented in Table II. Acetone was found in four of six lots of propranolol hydrochloride and in four of eight lots of flurazepam hydrochloride. For flurazepam, the acetone peak is clearly evident in the chromatograms of both the *n*-octane and toluene extracts (Fig. 2), but is, as expected, much larger in the latter. The acetone level, quantitated from the toluene extract, was ~0.5% in the sample illustrated; identity was confirmed by MS. The reproducibility of the acetone determination in these samples could not be established due to insufficient sample; however, the duplicate results for one of the flurazepam samples were 0.50 and 0.48%. Toluene was found in three of four samples of sulfinpyrazone. In this case, *n*-octane proved to be a better extract than ether and, of course, toluene could not be used. The level of toluene found in one of these samples was ~0.3% with reproducibility of 3% for five determinations; identity was confirmed by MS. In addition to the drugs listed in Table II, one or more lots of the following drug raw materials was examined, with the solvent given in parentheses: acetaminophen (1 mL 2.5 M NaOH), cimetidine (2 mL 1.0 M HCl), diazepam (0.5 mL 2.5 M HCl), phenytoin sodium (1 mL H_2O), metoprolol (0.5 mL 1 M HCl), pentobarbital sodium (0.5 mL H_2O), and triamterene (5 mL HCl). No solvent residues were detected in these lots.

REFERENCES

(1) J. Schou, *Acta. Pharm. Tech.*, **1976**, Suppl. 2–19.

(2) R. C. Lawrence, E. G. Lovering, M. A. Poirier, and J. R. Watson, *J. Pharm. Sci.*, **69**, 1444 (1980).

(3) K. M. McErlane, N. M. Curran, and E. G. Lovering, *J. Pharm. Sci.*, **66**, 1015 (1977).

(4) G. R. Gordon, D. C. Ghoul, and J. H. Peters, *J. Pharm. Sci.*, **64**, 1205 (1975).

(5) "U. S. Pharmacopeia," 20th. rev., U.S. Pharmacopeial Convention, Inc., Rockville, Md., 1980.

Composite Pharmacokinetic Profiling

Keyphrases □ Pharmacokinetics—composite profiling, ceftriaxone, diazepam □ Composite profiling—pharmacokinetics, ceftriaxone, diazepam

To the Editor:

In certain patient populations, most notably neonates, it has been difficult to obtain an adequate number of blood samples to develop complete pharmacokinetic profiles of drugs due to sample-volume limitations. For this, as well as other ethical and medical reasons, the neonate has been termed a "therapeutic orphan" in that little pharmacokinetic information has been generated in this patient group. However, since the neonate represents the most physiologically dynamic patient population, it is important to understand the pharmacokinetics of drugs that are used to treat these patients. In an effort to minimize blood sampling and still develop meaningful pharmacokinetic profiles, a composite pharmacokinetic profiling approach (*e.g.*, combining blood concentrations from patients or subjects to produce a functional profile that is not possible to derive from the concentration–time data of one individual) has been investigated and will be developed in this report using simulation and curve-fitting techniques.

Crow and Gibaldi (1) have discussed the rationale for developing a composite pharmacokinetic profile by obtaining plasma concentration–time data at different times in the same patient during several dosing intervals at steady state. These authors stated that the accuracy of this composite method depends on assay variability, intrapatient pharmacokinetic variability, dosing interval reproducibility, and patient compliance. If one assumes that plasma concentration–time data among patients are normally distributed, one can apply this same rationale to developing a pharmacokinetic profile using plasma concentration–time data from several patients following single-dose administrations. This approach eliminates intrapatient pharmacokinetic variability, constancy of dosing interval, and patient compliance as variables, but adds interpatient pharmacokinetic variation. In addition, it may offer the only reasonable and perhaps the only ethical means of developing a single-dose pharmacokinetic profile of certain drugs in premature (≤2.0 kg) neonates in whom the total blood volume is ~75–80 mL/kg.

The composite profiling technique was tested by simulating blood concentration–time profiles for short and long half-life drugs that reflect both mono- and biexponential elimination characteristics following first-order absorption using complete sampling schedules. To reflect variability in real concentration–time profiles, data for 18 patients were simulated when three sampling groups were used, 20 patients were simulated when four sampling groups were used. Normally distributed error with a coefficient of variation (*CV*) of 10% was introduced into the pharmacokinetic parameters, and normally distributed error with a *CV* of 10% was introduced into the resulting concentration data. For the biexponential long half-life case, normally distributed error with a *CV* of 25% was introduced into the pharmacokinetic parameters followed by the same 10% error introduced into the resulting concentration data. These concentration–time data were then used to establish the impact of sampling times and the number of observations per time point on parameter estimations by employing the following three sampling schedules:

1. For the monoexponential short half-life drug, patients were divided into three groups of six patients each: group I was sampled at 0, 1, 4, and 12 h; group II was sampled at 0, 2, 6, and 18 h; group III was sampled at 0, 3, 8, and 24 h.
2. For the biexponential, short half-life drug, patients were divided into three groups of six patients each: group I was sampled at 0, 0.5, 3, 8, and 24 h; group II was sampled at 0, 1, 4, 12, and 24 h; group III was sampled at 0, 2, 6, 18, and 24 h.
3. For both the mono- and biexponential, long half-life drugs, patients were divided into four groups of five patients each: group I was sampled at 0, 1, 6, and 24 h; group II was sampled at 0, 2, 8, and 36 h; group III was sampled at 0, 3, 12, and 48 h; group IV was sampled at 0, 4, 18, and 72 h.

It was assumed that sampling would be limited to five or less samples per patient. These simulated data were then used as input for curve-fitting composite profiles using six, three, and one patients per group for three group sampling schedules or five, three, and one patients per group for the four group sampling schedules. Simulations and curve-fitting procedures were conducted using the nonlinear regression program, NONLIN (2).

The results of the composite curve-fits of these simulations are presented in Tables I (monoexponential elimination) and II (bioexponential elimination). If one compares the parameter values from the composite profiles to the ideal parameter values, it is clear that reasonable approximation of the "true" parameter values can be obtained by fitting the composite profile even if only one patient is included in each sampling group. The least-variable parameter is clearance (*e.g.*, the parameter of greatest interest), and good estimates of the elimination rate constants are obtained (Tables I and II). These observations are in good agreement with those of Crow and Gibaldi (1). The results of fitting the composite profiles containing normally distributed error with a *CV* of 25% in the parameter values as well as a *CV* of 10% in the resulting concentration data are presented in Table III. Good approximations of the "true" parameter values were obtained even with the introduction of normally distributed error with a *CV* of 25%, *i.e.*, two *SD* encompass 50–150% (threefold) of the mean. This observation indicates that the method is robust and can accommodate even large differences associated with interindividual variation.

Experimental data from two clinical pharmacokinetic studies were used as a final test of the proposed composite profiling technique. In the first study, 2 g of ceftriaxone was administered by intravenous infusion to 12 healthy male subjects over a 30-min interval. Blood samples were obtained during and following the infusion of drug. The subjects were divided into four groups of three subjects each: group I was sampled at 0, 10, and 40 min, 2 and 10 h; group II was sampled at 0, 20, and 50 min, 4 and 12 h; group III was sampled at 0 and 30 min, 1, 6, and 16 h; group IV was sampled at 0 and 35 min, 1.5, 8, and 24 h after starting the 30-min infusion. The *CV* for the analytical data in this study was 4.4%. In the second study 10 mg of diazepam was administered orally to 20 healthy

0022-3549/84/1100-1667$01.00/0
© 1984, American Pharmaceutical Association

Table I—Pharmacokinetic Parameters Obtained by Composite Profiling Monoexponential Elimination Data [a] Which Contained 10% *CV* Random Error in Parameters and 10% *CV* Error in the Resulting Concentrations

Study Conditions			r	C_0, μg/mL	K, h^{-1}	k_a, h^{-1}	AUC, μg·h/L	CL, L/h	Vd, L
No. of Groups	Patients Per Group	No. of Replicates							
					Short (6-h) Half-Life				
			(Ideal)	100	0.116	0.693	718	13.9	120
3	6	1	0.991	96.9	0.110	0.656	733	13.6	124
3	3	1	0.992	90.9	0.104	0.623	728	13.7	132
3	3	1	0.992	100	0.113	0.730	748	13.4	118
3	1	6	0.994 ± 0.003	102 ± 25	0.111 ± 0.013	0.740 ± 0.251	741 ± 22	13.5 ± 0.4	124 ± 15
					Long (18-h) Half-Life				
			(Ideal)	100	0.039	0.347	2276	4.39	113
4	5	1	0.993	112	0.042	0.297	2290	4.37	104
4	3	1	0.992	110	0.043	0.305	2197	4.55	106
4	1	5	0.993 ± 0.002	114 ± 10	0.043 ± 0.002	0.249 ± 0.034	2287 ± 148	4.39 ± 0.27	103 ± 7

[a] Dose = 10 mg.

Table II—Pharmacokinetic Parameters Obtained by Composite Profiling Biexponential Elimination Data [a] Which Contained 10% *CV* Error in Parameters and 10% *CV* Error in the Resulting Concentrations

Study Conditions			r	A μg/mL	α, h^{-1}	B, μg/mL	β, h^{-1}	k_a, h^{-1}	AUC, mg·h/L	CL, L/h	Vd, L
No. of Groups	Patients Per Group	No. of Replicates									
						Short (6-h) Half-Life					
			Ideal	70	0.693	30	0.116	3.00	327	30.6	264
3	6	1	0.996	52.4	0.659	31.0	0.120	3.72	315	31.7	265
3	3	1	0.997	0.914	1.34	33.7	0.126	1.48	309	32.4	257
3	3	1	0.996	43.1	0.592	30.5	0.117	10.0	326	30.7	262
3	1	6	0.998	78.5	0.798	32.0	0.119	3.53	323	31.1	261
		(*SD*)	± 0.002	± 39.9	± 0.193	± 3.7	± 0.006	± 1.41	± 22	± 2.0	± 14
						Long (18-h) Half-Life					
			Ideal	70	0.231	30	0.039	1.39	1000	10.0	256
4	5	1	0.997	58.7	0.173	28.0	0.040	1.46	980	10.2	255
4	3	1	0.998	64.9	0.172	25.9	0.039	1.40	976	10.2	262
4	1	5	0.997	65.4	0.190	27.0	0.038	1.67	999	10.0	265
		(SD)	± 0.002	± 13.9	± 0.083	± 7.7	± 0.005	± 0.69	± 61	± .6	± 31

[a] Dose = 10 mg.

Table III—Pharmacokinetic Parameters Obtained by Composite Profiling Biexponential Long Half-Life Data [a] Which Contained 25% *CV* Error in Parameters and 10% *CV* Error in the Resulting Concentrations

Study Conditions			r	A, μg/mL	α, h^{-1}	B, μg/mL	β, h^{-1}	k_a, h^{-1}	AUC, mg·h/L	CL, L/h	Vd, L
No. of Groups	Patients per Group	No. of Replicates									
			Ideal	70	0.231	30	0.039	1.39	1000	10	256
4	5	1	0.997	50.0	0.210	36.2	0.048	1.35	928	10.8	225
4	3	1	0.998	59.5	0.239	39.4	0.051	1.26	943	10.6	208
4	1	5	0.997 ± 0.002	66.9 ± 28.4	0.297 ± 0.154	37.7 ± 14.3	0.047 ± 0.005	1.26 ± 0.39	962 ± 158	10.6 ± 1.5	230 ± 48

Table IV—Pharmacokinetic Parameters Obtained by Fitting Ceftriaxone and Diazepam Data

Fitting Procedure	r	A, μg/mL	α, h^{-1}	B, μg/mL	β, h^{-1}	k_a, h^{-1}	t_{lag}, h	AUC, μg·h/mL	CL, L/h	Vd, L
					Ceftriaxone Data					
Mean of Individual Fits	0.993–0.998	101	5.20	3210	0.119	NA[a]	NA	1656	1.21	10.2
Fit of Mean Data	0.999	96	4.62	3210	0.119	NA	NA	1653	1.21	10.2
Fit of All Data	0.996	93	4.66	3150	0.121	NA	NA	1617	1.24	10.3
Composite Fit of Four Groups	0.997	84	5.90	3170	0.122	NA	NA	1624	1.23	10.1
					Diazepam Data					
Mean of Individual Fits	0.904–1.000	570	1.49	124	0.026	10.8	0.16	5088	1.96	75.6
Fit of Mean Data	1.000	592	1.51	129	0.025	3.71	0.19	5358	1.87	74.7
Fit of All Data	0.910	440	1.50	116	0.025	4.07	0.32	4797	2.08	83.2
Composite Fit of Four Groups	0.898	1450	2.03	118	0.024	2.66	0.29	5041	1.98	82.7

[a] Not applicable.

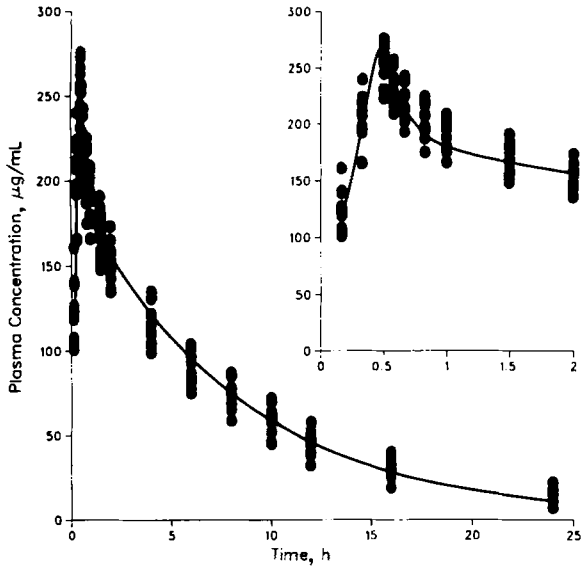

Figure 1—*All ceftriaxone plasma concentration–time data from 12 subjects together with the curve fitted using the composite pharmacokinetic profiling technique and three subjects in each of four sampling groups, as depicted in Table IV (inset).*

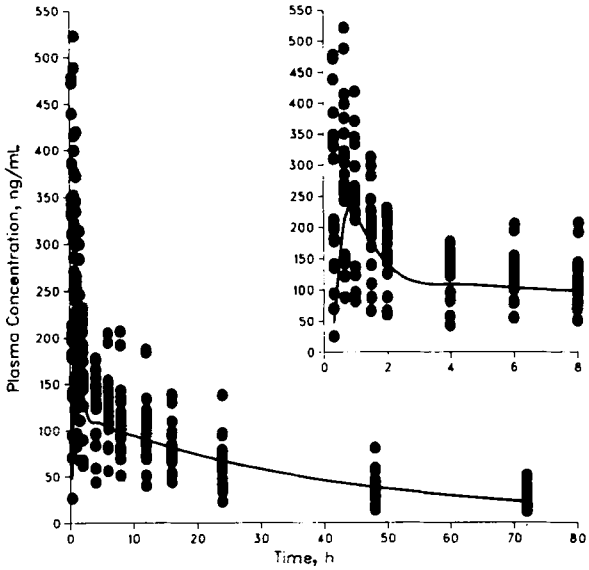

Figure 2—*All diazepam plasma concentration–time data from 20 subjects together with the curve fitted using the composite pharmacokinetic profiling technique and five subjects in each of four sampling groups, as depicted in Table IV (inset).*

subjects. Blood samples were obtained at specific times over the following 72 h. The subjects were divided into four groups of five subjects each: group I was sampled at 0, 0.33, 2, 12, and 72 h; group II was sampled at 0, 0.67, 4, 16, and 72 h; group III was sampled at 0, 1, 6, 24, and 72 h; group IV was sampled at 0, 1.5, 8, 48, and 72 h after the oral dose. The analytical *CV* for this study was 11.3%.

Four curve-fitting techniques were used to evaluate the data: (*a*) concentration–time data from the individual subjects were fitted and the mean parameters were calculated; (*b*) a single mean concentration–time profile from all subjects was fitted to determine parameter values; (*c*) all concentration–time data were fitted simultaneously to determine the parameter values; (*d*) a limited sample composite concentration–time profile was fitted to determine the parameter values. The results of these fitting procedures are presented in Table IV. In the first three of the methods, all of the concentration–time data were used in the sampling/fitting procedure, whereas in the final method, four groups of three or five patients, respectively, were used for ceftriaxone and diazepam. There was good general agreement of parameter estimates obtained by each of the four sampling/fitting techniques. The parameters A and α were variable among the four sampling/fitting procedures, and for the oral absorption of diazepam, k_a was variable as well. However, the remaining parameters for both diazepam and ceftriaxone were extremely consistent among the four methods. Again it should be noted that the clearances, volumes of distribution, and elimination rate constants show little variability. All ceftriaxone and diazepam concentration–time points, together with the composite profiling fits, are presented in Figs. 1 and 2, respectively, to show the randomness of scatter around the fitted curves.

The results of these simulations and curve-fitting procedures indicate that the composite pharmacokinetic profiling technique developed herein is a useful method that can be utilized to minimize the number of blood samples and, therefore, the total blood volume withdrawn. The application of this technique can allow for the development of pharmacokinetic profiles in patient populations, including neonates and certain disease states, in which little information has been generated due to sampling limitations. This technique has been used to develop a preliminary pharmacokinetic profile of vitamin E following an intramuscular injection to premature neonates (3).

(1) J. W. Crow and M. Gibaldi, *Drug Intell. Clin. Pharm.*, **12**, 612 (1978).

(2) C. M. Metzler, G. L. Elfring, and A. J. McEwen, *Biometrics*, **30**, 562 (1974).

(3) W. A. Colburn and R. A. Ehrenkranz, *Pediatr. Pharmacol.*, **3**, 7 (1983).

Wayne A. Colburn ˣ
Donald M. Gibson
Department of Pharmacokinetics,
Biopharmaceutics and Drug Metabolism
Hoffmann-LaRoche Inc.
Nutley, NJ 07110

Received July 20, 1983.
Accepted for publication February 15, 1984.

Disposition of Nitrofurantoin and Nitrofurazone in the Isolated Perfused Rat Kidney

Keyphrases □ Nitrofurantoin—renal metabolism, isolated perfused rat kidney □ Nitrofurazone—renal metabolism, isolated perfused rat kidney

To the Editor:

Nitrofurantoin is frequently used clinically to treat urinary tract infections, but little is known of its renal metabolism. The side effects of nitrofurantoin therapy, pulmonary and hepatic toxicities, and polyneuropathies, are thought to be a consequence of its reductive metabolic activation (1–5). The end

0022-3549/84/1100-1669$01.00/0
© 1984, American Pharmaceutical Association

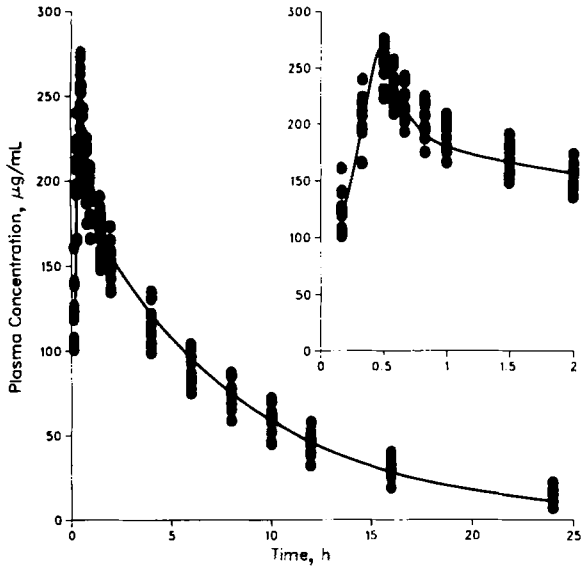

Figure 1—*All ceftriaxone plasma concentration–time data from 12 subjects together with the curve fitted using the composite pharmacokinetic profiling technique and three subjects in each of four sampling groups, as depicted in Table IV (inset).*

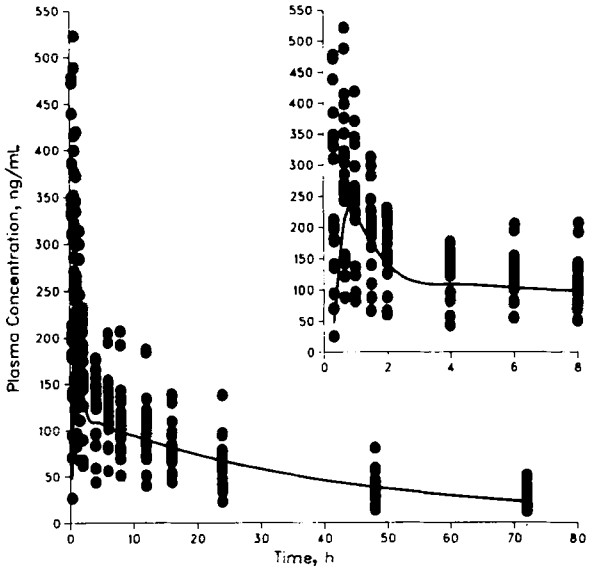

Figure 2—*All diazepam plasma concentration–time data from 20 subjects together with the curve fitted using the composite pharmacokinetic profiling technique and five subjects in each of four sampling groups, as depicted in Table IV (inset).*

subjects. Blood samples were obtained at specific times over the following 72 h. The subjects were divided into four groups of five subjects each: group I was sampled at 0, 0.33, 2, 12, and 72 h; group II was sampled at 0, 0.67, 4, 16, and 72 h; group III was sampled at 0, 1, 6, 24, and 72 h; group IV was sampled at 0, 1.5, 8, 48, and 72 h after the oral dose. The analytical *CV* for this study was 11.3%.

Four curve-fitting techniques were used to evaluate the data: (*a*) concentration–time data from the individual subjects were fitted and the mean parameters were calculated; (*b*) a single mean concentration–time profile from all subjects was fitted to determine parameter values; (*c*) all concentration–time data were fitted simultaneously to determine the parameter values; (*d*) a limited sample composite concentration–time profile was fitted to determine the parameter values. The results of these fitting procedures are presented in Table IV. In the first three of the methods, all of the concentration–time data were used in the sampling/fitting procedure, whereas in the final method, four groups of three or five patients, respectively, were used for ceftriaxone and diazepam. There was good general agreement of parameter estimates obtained by each of the four sampling/fitting techniques. The parameters A and α were variable among the four sampling/fitting procedures, and for the oral absorption of diazepam, k_a was variable as well. However, the remaining parameters for both diazepam and ceftriaxone were extremely consistent among the four methods. Again it should be noted that the clearances, volumes of distribution, and elimination rate constants show little variability. All ceftriaxone and diazepam concentration–time points, together with the composite profiling fits, are presented in Figs. 1 and 2, respectively, to show the randomness of scatter around the fitted curves.

The results of these simulations and curve-fitting procedures indicate that the composite pharmacokinetic profiling technique developed herein is a useful method that can be utilized to minimize the number of blood samples and, therefore, the total blood volume withdrawn. The application of this technique can allow for the development of pharmacokinetic profiles in patient populations, including neonates and certain disease states, in which little information has been generated due to sampling limitations. This technique has been used to develop a preliminary pharmacokinetic profile of vitamin E following an intramuscular injection to premature neonates (3).

(1) J. W. Crow and M. Gibaldi, *Drug Intell. Clin. Pharm.*, **12**, 612 (1978).

(2) C. M. Metzler, G. L. Elfring, and A. J. McEwen, *Biometrics*, **30**, 562 (1974).

(3) W. A. Colburn and R. A. Ehrenkranz, *Pediatr. Pharmacol.*, **3**, 7 (1983).

Wayne A. Colburn ˣ
Donald M. Gibson
Department of Pharmacokinetics,
Biopharmaceutics and Drug Metabolism
Hoffmann-LaRoche Inc.
Nutley, NJ 07110

Received July 20, 1983.
Accepted for publication February 15, 1984.

Disposition of Nitrofurantoin and Nitrofurazone in the Isolated Perfused Rat Kidney

Keyphrases □ Nitrofurantoin—renal metabolism, isolated perfused rat kidney □ Nitrofurazone—renal metabolism, isolated perfused rat kidney

To the Editor:

Nitrofurantoin is frequently used clinically to treat urinary tract infections, but little is known of its renal metabolism. The side effects of nitrofurantoin therapy, pulmonary and hepatic toxicities, and polyneuropathies, are thought to be a consequence of its reductive metabolic activation (1–5). The end

0022-3549/84/1100-1669$01.00/0
© 1984, American Pharmaceutical Association

products of this activating pathway are the 5-amino and cyano derivatives (6–8). Both of these metabolites have been found following anaerobic metabolism of nitrofurantoin by the 9000×*g* supernatant of rat liver and kidney homogenates (9). In addition, the cyano metabolite was detected in the perfusate and bile of isolated perfused rat livers (10), and the 5-amino derivative has been detected in the urine of male volunteers receiving an intravenous infusion or an oral tablet of nitrofurantoin (11). A third metabolite, the 4-hydroxy derivative, resulting from hydroxylation of the furan ring, has been identified (12) and detected in the urine of rats and the media of isolated perfused livers of rats induced with 3-methylcholanthrene (13–15). Unchanged nitrofurantoin in the urine accounted for 34–47% of the dose in humans (11) and 16–52% of the dose in rats (16–19).

Nitrofurazone, which is structurally similar to nitrofurantoin, is used topically as an antibacterial agent, but the frequency and severity of side effects preclude its systemic use. It is also reduced under anaerobic conditions to the analogous 5-amino and cyano derivatives (20). Furthermore, after subcutaneous injection, nitrofurazone produces kidney and liver lesions in the rat (21). Only 5–8% of a nitrofurazone dose was excreted unchanged in the urine of rats (16, 17, 22).

The available evidence suggests that, at least under *in vitro* anaerobic conditions, both nitrofurantoin and nitrofurazone are metabolized by kidney preparations. However, whole animal studies suggest that nitrofurazone is both more extensively metabolized and more toxic than nitrofurantoin.

We have studied the disposition of these two 5-nitrofurans in the isolated perfused kidney. We were particularly interested in studying the disposition of nitrofurantoin by the kidney because it controls the access of the drug to the urinary tract, and hence, the site of infection. The intact organ system allowed us to study the metabolism of nitrofurantoin by the kidney under well-oxygenated conditions without the potential confounding aspects of extrarenal, particularly hepatic, metabolism. Particular attention was directed to the known reduced metabolites of nitrofurantoin, since their presence would indicate that metabolic activation had occurred. Nitrofurazone was selected for comparison because it is structurally similar and metabolically activated to analogous derivatives; it is more toxic in general, and to the kidney in particular, than nitrofurantoin.

For each antibiotic, six rat kidneys were perfused with 6.5% bovine serum albumin dissolved in a Krebs–Henseleit buffer supplemented with glucose and eight amino acids (23). Inulin was added as a marker of the glomerular filtration rate. The 70 mL of recirculating perfusate was aerated with 95% O_2–5% CO_2, and the pH and temperature were maintained at 7.4 and 37°C, respectively. After a 20-min equilibration period, 0.1 mM nitrofurantoin or nitrofurazone dissolved in perfusate was added to the reservoir. Perfusate and urine were sampled with replacement at frequent intervals for 180 min. The pO_2 and pH were determined using a blood gas analyzer[1] and Na^+/K^+ levels were measured with a flame photometer[2]. Inulin was quantitated spectrophotometrically (24). Nitrofurantoin and nitrofurazone and their amino and cyano metabolites were quantitated by HPLC (25, 26). For nitrofurantoin the reabsorption of Na^+, fractional excretion of K^+, and the glomerular filtration rate were 90.0 ± 3.1%, 0.86 ± 0.28, and 0.39 ± 0.15 mL/min, respectively[3]. For nitrofurazone the corresponding values were 95.8 ± 1.4%, 0.49 ± 0.16, and 0.22 ± 0.07 mL/min. Although these glomerular filtration rates are low (27), suggesting a compromised preparation, subsequent studies in kidneys with improved physiological function handled both 5-nitrofurans similarly to the results reported here[4].

The concentration in the perfusate of both nitrofurantoin and nitrofurazone could be described by a one-compartment body model with first-order elimination kinetics. The total clearances[5], 0.64 ± 0.12 and 0.75 ± 0.18 mL/min for nitrofurantoin and nitrofurazone, respectively, were not significantly different. However, the fractions excreted unchanged in the urine[6] after 3 h, 0.19 ± 0.10 for nitrofurantoin and 0.02 ± 0.02 for nitrofurazone, were significantly different ($p < 0.005$). Known reduced metabolites of nitrofurantoin, the 5-amino and cyano derivatives, while not detectable in the perfusate, accounted for ~3% of the dose in the urine. Neither the 5-amino nor the cyano metabolite of nitrofurazone was detected in either the perfusate or urine. There was no evidence that the 4-hydroxy derivative of either 5-nitrofuran was formed. There appears to be net tubular reabsorption of both 5-nitrofurans since the ratios of their renal clearance to the glomerular filtration rate are <1.0 (0.39 ± 0.20 and 0.07 ± 0.06 for nitrofurantoin and nitrofurazone, respectively). These ratios could be <1.0 in the absence of tubular reabsorption if the 5-nitrofurans were highly bound to bovine serum albumin. However, only 60% of nitrofurantoin is bound to plasma proteins (11). Furthermore, nitrofurantoin, which has a pK_a of 7.2, is known to be secreted by the organic anion transport system and to be reabsorbed (28). Certainly at the pH of the urine (6.0–6.5), nitrofurantoin would be mostly un-ionized and could be reabsorbed by passive diffusion. Nitrofurazone is not ionized at the pH values encountered in this study.

At the conclusion of the 3-h experiment most of the dose of both these 5-nitrofurans is unaccounted for. Less than 15% remains in the perfusate as unchanged drug; 19% of the nitrofurantoin was excreted unchanged in the urine and ~3% as known metabolites. Thus, ~60% of the dose of nitrofurantoin is unaccounted for. For nitrofurazone, only 2% of the dose was detected in the urine. Hence, ~85% of the dose of nitrofurazone is unaccounted for. For both of these 5-nitrofurans, the fraction unaccounted for may be drug bound to tubing or chemically degraded, drug or metabolites trapped intracellularly, as yet unidentified metabolites, and/or drug covalently bound to tissue biomacromolecules after metabolic activation. The first possibility was dismissed, since identical 3-h experiments without the kidney in place resulted in no loss of either 5-nitrofuran. Some preliminary work with the 5-[2-^{14}C]nitrofurans has shown that nitrofurantoin, nitrofurazone, or their known metabolites were not detected after exhaustive extraction of homogenates of the perfused kidneys first with acetonitrile–water and then 5% trichloroacetic acid[4]. Thus, although the ^{14}C-label was found in the tissue, it would appear that neither the parent compound nor known metabolites were trapped intracellularly. Each of the remaining alternative hypotheses involve metabolism of the 5-nitrofurans. Since both the 5-amino and cyano derivatives of nitrofurantoin were detected in the urine, the drug must have been metabolically activated, and at least some of it could, therefore, have been

[1] Model C-175; Corning, Corning, N.Y.
[2] Model 450; Corning.

[3] All data is reported as mean ±*SD*, $n = 6$.
[4] B. Hoener, T. V. Zenser, B. B. Davis, and U. Bredberg, unpublished results.
[5] Dose/area under the curve.
[6] Cumulative ampunt excreted in urine/dose.

bound to biomacromolecules rather than have been further metabolized and eliminated as the end products of the activating pathway. Our preliminary work also indicates that ~5% of the ^{14}C-label is covalently bound to biomacromolecules at the end of the 3-h experiment[4]. Others have found carbon-14 bound to biomacromolecules after incubation of [2-^{14}C]nitrofurantoin with microsomal preparations from rat liver and lung (29). It is probable, therefore, that at least some portion of the dose of nitrofurantoin is covalently bound to the biomacromolecules in the perfused rat kidney with the remainder eliminated by as yet unidentified metabolic pathways. Since none of the nitrofurazone was excreted as the 5-amino or cyano metabolite, there is no direct evidence that any of the drug was reductively activated for binding to biomacromolecules. Other investigators have, however, found ^{14}C-label covalently bound to the proteins, DNA, and RNA, of the liver and kidney of rats fed [2-^{14}C]nitrofurazone (30), and our preliminary studies have found ~5% of the ^{14}C-label bound to biomacromolecules of the nitrofurazone perfused kidney[4]. The remaining 80% of the dose of nitrofurazone was accounted for by as yet unidentified metabolites in the perfusate and urine. These studies indicate that the perfused kidney does metabolize both nitrofurantoin and nitrofurazone. Furthermore, the more toxic nitrofurazone appears to be more extensively metabolized.

(1) P. L. Olive, in "Nitrofurans," G. T. Bryan, Ed., Raven, New York, N.Y., 1978, p. 131.

(2) M. R. Boyd, G. L. Catignani, H. A. Sasame, J. R. Mitchell, and A. W. Stiko, *Am. Rev. Respir. Dis.*, **120**, 93 (1979).

(3) K. G. Tolman, *Ann. Int. Med.*, **92**, 119 (1980).

(4) C. Yiannikas, J. D. Pollard, and J. G. McLeod, *Aust. N.Z. J. Med.*, **11**, 400 (1981).

(5) S. M. Cohen, in "Nitrofurans," G. T. Bryan, Ed., Raven, New York, N.Y., 1978, p. 171.

(6) J. J. Gavin, F. F. Ebetino, R. Freedman, and W. E. Waterbury, *Arch. Biochem. Biophys.*, **113**, 399 (1966).

(7) J. E. Biaglow, B. E. Jacobsen, and O. F. Nygaard, *Cancer Res.*, **37**, 3306 (1977).

(8) F. J. Peterson, R. P. Mason, J. Hovespian, and J. L. Holtzman, *J. Biol. Chem.*, **254**, 4009 (1979).

(9) M. B. Aufrere, B. Hoener, and M. Vore, *Drug Metab. Dispos.*, **6**, 403 (1978).

(10) M. B. Aufrere, "Analytical and Metabolic Studies with Nitrofurantoin," Ph.D. Thesis, University of California, San Francisco, Calif., 1978.

(11) B. Hoener and S. E. Patterson, *Clin. Pharmacol. Ther.*, **29**, 808 (1981).

(12) J. Olivard, G. M. Rose, J. M. Klein, and J. P. Hoetis, *J. Med. Chem.*, **19**, 729 (1976).

(13) H. G. Jonen, *Naunyn-Schmiedeberg's Arch. Pharmacol.*, **315**, 167 (1980).

(14) H. G. Jonen and I. Kaufman, *Biochem. Pharmacol.*, **29**, 263 (1980).

(15) H. G. Jonen, F. Oesch, and K. L. Platt, *Drug Metab. Dispos.*, **8**, 446 (1980).

(16) M. F. Paul, H. E. Paul, R. C. Bender, F. Kopko, C. M. Harrington, V. R. Ellis, and J. A. Buzard, *Antibiot. Chemother.*, **10**, 287 (1960).

(17) H. E. Paul and M. F. Paul, in "Experimental Chemotherapy," Vol. 2, R. J. Schnitzer and F. Hawking, Eds., Academic, New York, N.Y., 1964, p. 307.

(18) H. E. Paul, K. J. Hayes, M. F. Paul, and A. R. Borgmann, *J. Pharm. Sci.*, **56**, 882 (1967).

(19) M. Veronese, D. Salvaterra, D. Barzaghi, and I. Setnikar, *Arzneim.-Forsch.*, **24**, 39 (1974).

(20) K. Tatsumi, S. Kitamura, and H. Yoshimura, *Arch. Biochem. Biophys.*, **175**, 131 (1976).

(21) M. C. Dodd, *J. Pharmacol. Exp. Ther.*, **86**, 311 (1946).

(22) K. Tatsumi, T. Ou, H. Yoshimura, and H. Tsukamoto, *Chem. Pharm. Bull.*, **19**, 330 (1971).

(23) I. Berkersky, W. A. Colburn, L. Fishman, and S. A. Kaplan, *Drug Metab. Dispos.*, **8**, 319 (1980).

(24) A. Heyrovsky, *Clin. Chim. Acta.*, **1**, 470 (1956).

(25) M. B. Aufrere, B. Hoener, and M. Vore, *Clin. Chem.*, **23**, 2207 (1977).

(26) B. Hoener and J. L. Wolff, *J. Chromatogr.*, **182**, 246 (1980).

(27) F. H. Epstein, J. T. Brosnan, J. D. Tange, and B. D. Ross, *Am. J. Physiol.*, **243**, F284 (1982).

(28) M. F. Paul, R. C. Bender, and E. G. Nohle, *Am. J. Physiol.*, **197**, 580 (1959).

(29) M. R. Boyd, A. W. Stiko, and H. A. Sasame, *Biochem. Pharmacol.*, **28**, 601 (1979).

(30) K. Tatsumi, S. Kitamura, and H. Yoshimura, *Chem. Pharm. Bull.*, **25**, 2948 (1977).

Betty-ann Hoener[x]
Terry Ray Krueger
Department of Pharmacy
School of Pharmacy, 926-S
University of California
San Francisco, CA 94143

Received January 12, 1984.
Accepted for publication September 10, 1984.
We wish to thank Norwich-Eaton Pharmaceuticals, a Division of Morton Norwich, for the nitrofurantoin and nitrofurazone. We also thank Dr. Svein Øie of the Department of Pharmacy, University of California-San Francisco, for allowing us to use his perfusion apparatus. This work was supported in part by Grants GM 26691 and AI 18423 from the National Institutes of Health.

Pharmacokinetic Implications of Stereoselective Changes in Plasma-Protein Binding: Warfarin/Sulfinpyrazone

Keyphrases □ Warfarin—plasma-protein binding, stereoselective displacement, drug-drug interaction with sulfinpyrazone □ Sulfinpyrazone—plasma-protein binding, stereoselective displacement, drug-drug interaction with warfarin

To the Editor:

The intensity of the observed pharmacological response produced by any drug is invariably related, directly or indirectly, to its plasma concentration. In the systemic circulation most drugs are bound to plasma proteins, and thus an equilibrium is established between bound and free drug. Since free drug alone is the pharmacologically active agent, the drug-plasma protein interaction may not only influence overall drug disposition but also affect the magnitude and time-course of the pharmacological response. In theory, numerous models could describe the relationship between hepatic clearance and plasma protein binding. However, a widely accepted model which has been shown to explain the vast majority of empirical observations, and one which is consistent with the results to follow, is the so-called well-stirred model (1-4). For drugs exhibiting a low extraction ratio (ER <0.3), it may be shown that their observed total body clearance (CL) is directly related to their unbound fraction within plasma (f_u) (5, 6). Consequently, for low-extractration ratio drugs which are highly protein bound (>98%), a small change in the fraction of the drug bound to plasma protein will not only result in a relatively large change in f_u but also in a proportional change in CL and may thus have potentially important consequences in the in-

0022-3549/84/1100-1671$01.00/0

© 1984, American Pharmaceutical Association

bound to biomacromolecules rather than have been further metabolized and eliminated as the end products of the activating pathway. Our preliminary work also indicates that ~5% of the ^{14}C-label is covalently bound to biomacromolecules at the end of the 3-h experiment[4]. Others have found carbon-14 bound to biomacromolecules after incubation of [2-^{14}C]nitrofurantoin with microsomal preparations from rat liver and lung (29). It is probable, therefore, that at least some portion of the dose of nitrofurantoin is covalently bound to the biomacromolecules in the perfused rat kidney with the remainder eliminated by as yet unidentified metabolic pathways. Since none of the nitrofurazone was excreted as the 5-amino or cyano metabolite, there is no direct evidence that any of the drug was reductively activated for binding to biomacromolecules. Other investigators have, however, found ^{14}C-label covalently bound to the proteins, DNA, and RNA, of the liver and kidney of rats fed [2-^{14}C]nitrofurazone (30), and our preliminary studies have found ~5% of the ^{14}C-label bound to biomacromolecules of the nitrofurazone perfused kidney[4]. The remaining 80% of the dose of nitrofurazone was accounted for by as yet unidentified metabolites in the perfusate and urine. These studies indicate that the perfused kidney does metabolize both nitrofurantoin and nitrofurazone. Furthermore, the more toxic nitrofurazone appears to be more extensively metabolized.

(1) P. L. Olive, in "Nitrofurans," G. T. Bryan, Ed., Raven, New York, N.Y., 1978, p. 131.

(2) M. R. Boyd, G. L. Catignani, H. A. Sasame, J. R. Mitchell, and A. W. Stiko, *Am. Rev. Respir. Dis.*, **120**, 93 (1979).

(3) K. G. Tolman, *Ann. Int. Med.*, **92**, 119 (1980).

(4) C. Yiannikas, J. D. Pollard, and J. G. McLeod, *Aust. N.Z. J. Med.*, **11**, 400 (1981).

(5) S. M. Cohen, in "Nitrofurans," G. T. Bryan, Ed., Raven, New York, N.Y., 1978, p. 171.

(6) J. J. Gavin, F. F. Ebetino, R. Freedman, and W. E. Waterbury, *Arch. Biochem. Biophys.*, **113**, 399 (1966).

(7) J. E. Biaglow, B. E. Jacobsen, and O. F. Nygaard, *Cancer Res.*, **37**, 3306 (1977).

(8) F. J. Peterson, R. P. Mason, J. Hovespian, and J. L. Holtzman, *J. Biol. Chem.*, **254**, 4009 (1979).

(9) M. B. Aufrere, B. Hoener, and M. Vore, *Drug Metab. Dispos.*, **6**, 403 (1978).

(10) M. B. Aufrere, "Analytical and Metabolic Studies with Nitrofurantoin," Ph.D. Thesis, University of California, San Francisco, Calif., 1978.

(11) B. Hoener and S. E. Patterson, *Clin. Pharmacol. Ther.*, **29**, 808 (1981).

(12) J. Olivard, G. M. Rose, J. M. Klein, and J. P. Hoetis, *J. Med. Chem.*, **19**, 729 (1976).

(13) H. G. Jonen, *Naunyn-Schmiedeberg's Arch. Pharmacol.*, **315**, 167 (1980).

(14) H. G. Jonen and I. Kaufman, *Biochem. Pharmacol.*, **29**, 263 (1980).

(15) H. G. Jonen, F. Oesch, and K. L. Platt, *Drug Metab. Dispos.*, **8**, 446 (1980).

(16) M. F. Paul, H. E. Paul, R. C. Bender, F. Kopko, C. M. Harrington, V. R. Ellis, and J. A. Buzard, *Antibiot. Chemother.*, **10**, 287 (1960).

(17) H. E. Paul and M. F. Paul, in "Experimental Chemotherapy," Vol. 2, R. J. Schnitzer and F. Hawking, Eds., Academic, New York, N.Y., 1964, p. 307.

(18) H. E. Paul, K. J. Hayes, M. F. Paul, and A. R. Borgmann, *J. Pharm. Sci.*, **56**, 882 (1967).

(19) M. Veronese, D. Salvaterra, D. Barzaghi, and I. Setnikar, *Arzneim.-Forsch.*, **24**, 39 (1974).

(20) K. Tatsumi, S. Kitamura, and H. Yoshimura, *Arch. Biochem. Biophys.*, **175**, 131 (1976).

(21) M. C. Dodd, *J. Pharmacol. Exp. Ther.*, **86**, 311 (1946).

(22) K. Tatsumi, T. Ou, H. Yoshimura, and H. Tsukamoto, *Chem. Pharm. Bull.*, **19**, 330 (1971).

(23) I. Berkersky, W. A. Colburn, L. Fishman, and S. A. Kaplan, *Drug Metab. Dispos.*, **8**, 319 (1980).

(24) A. Heyrovsky, *Clin. Chim. Acta.*, **1**, 470 (1956).

(25) M. B. Aufrere, B. Hoener, and M. Vore, *Clin. Chem.*, **23**, 2207 (1977).

(26) B. Hoener and J. L. Wolff, *J. Chromatogr.*, **182**, 246 (1980).

(27) F. H. Epstein, J. T. Brosnan, J. D. Tange, and B. D. Ross, *Am. J. Physiol.*, **243**, F284 (1982).

(28) M. F. Paul, R. C. Bender, and E. G. Nohle, *Am. J. Physiol.*, **197**, 580 (1959).

(29) M. R. Boyd, A. W. Stiko, and H. A. Sasame, *Biochem. Pharmacol.*, **28**, 601 (1979).

(30) K. Tatsumi, S. Kitamura, and H. Yoshimura, *Chem. Pharm. Bull.*, **25**, 2948 (1977).

Betty-ann Hoener[x]
Terry Ray Krueger
Department of Pharmacy
School of Pharmacy, 926-S
University of California
San Francisco, CA 94143

Received January 12, 1984.
Accepted for publication September 10, 1984.
We wish to thank Norwich-Eaton Pharmaceuticals, a Division of Morton Norwich, for the nitrofurantoin and nitrofurazone. We also thank Dr. Svein Øie of the Department of Pharmacy, University of California-San Francisco, for allowing us to use his perfusion apparatus. This work was supported in part by Grants GM 26691 and AI 18423 from the National Institutes of Health.

Pharmacokinetic Implications of Stereoselective Changes in Plasma-Protein Binding: Warfarin/Sulfinpyrazone

Keyphrases □ Warfarin—plasma-protein binding, stereoselective displacement, drug-drug interaction with sulfinpyrazone □ Sulfinpyrazone—plasma-protein binding, stereoselective displacement, drug-drug interaction with warfarin

To the Editor:

The intensity of the observed pharmacological response produced by any drug is invariably related, directly or indirectly, to its plasma concentration. In the systemic circulation most drugs are bound to plasma proteins, and thus an equilibrium is established between bound and free drug. Since free drug alone is the pharmacologically active agent, the drug-plasma protein interaction may not only influence overall drug disposition but also affect the magnitude and time-course of the pharmacological response. In theory, numerous models could describe the relationship between hepatic clearance and plasma protein binding. However, a widely accepted model which has been shown to explain the vast majority of empirical observations, and one which is consistent with the results to follow, is the so-called well-stirred model (1-4). For drugs exhibiting a low extraction ratio (ER <0.3), it may be shown that their observed total body clearance (CL) is directly related to their unbound fraction within plasma (f_u) (5, 6). Consequently, for low-extractration ratio drugs which are highly protein bound (>98%), a small change in the fraction of the drug bound to plasma protein will not only result in a relatively large change in f_u but also in a proportional change in CL and may thus have potentially important consequences in the in-

0022-3549/84/1100-1671$01.00/0

© 1984, American Pharmaceutical Association

terpretation of the relationship between pharmacokinetic parameters and the observed pharmacological response.

Since albumin (the principal plasma binding protein for weakly acidic drugs) is chiral, its interaction with the enantiomers of racemic drugs might be expected to be different. Although stereoselective differences in protein binding have been previously noted (7–10), the implications of the phenomenon have not been generally recognized. The potential importance of stereoselective changes in plasma protein binding was demonstrated with the oral anticoagulant warfarin in its interaction with the uricosuric agent sulfinpyrazone[1]. Warfarin is administered as a racemic mixture despite the fact that the (*S*)-enantiomer is approximately five times as potent as the (*R*)-enantiomer. Moreover, the drug is highly bound (>98%) to plasma proteins.

The measurement of the free fraction of a highly bound drug such as warfarin is technically difficult due to the very low concentration of unbound drug (nanograms per milliliter at therapeutic levels). The problem is further compounded if the stereochemical composition of the free fraction is to be determined. One solution to the problem of measuring differences in enantiomeric binding is to use pseudoracemic drugs (a 1:1 mixture of (*R*)-[^{12}C]warfarin and (*S*)-[2-^{13}C]warfarin[2]) and then analyze the enatiomer concentrations by GS–MS, as previously reported (12). The advantage of this approach is that it allows an assessment of the drug in essentially the exact same form (racemate) as that which is used clinically. In addition, since MS allows differentiation of the two enantiomers within the same experiment, error can be significantly reduced. For example, the ratio, and changes in the ratio, between corresponding ions representing the (*R*)- and (*S*)-enantiomers can be measured directly without reference to internal standards or the requirement of mathematical treatment of any kind. The calculation of the degree of binding does, however, require the presence of a suitable internal standard and further data treatment.

Blood was drawn from healthy normal male volunteers and collected into flint-glass tubes containing 15% w/v potassium EDTA solution (0.1 mL), one of the few anticoagulants found to have little or no effect on drug–protein binding (13). Care was taken to avoid contact with materials that might modify the protein binding interaction in any way (14). Plasma was separated from the cellular components by centrifugation and all plasma samples were pooled. To a 12-mL plasma sample was added a methanolic solution (10 μL) of pseudoracemic warfarin to yield a final plasma concentration of 10 $\mu g \cdot mL^{-1}$. The spiked plasma samples (10 mL) were transferred into polycarbonate ultracentrifuge tubes and centrifuged at 50,000 rpm (300,000×*g*) for 20 h at 30°C. The clear supernatant (5 mL), containing unbound drug, was removed and to it was added a known amount of [phenyl-$^{2}H_5$]warfarin, the internal standard. The ultracentrifugation technique was chosen for its ability to handle relatively large plasma volumes. This feature is important as the low unbound concentration of warfarin necessitates the extraction of large volumes of plasma water to obtain sufficient amounts of the enantiomers for analysis. There are, however, practical concerns with this method. Contamination of the supernatant with albumin may result in erroneous estimates of the unbound fraction. For highly bound drugs such as warfarin, even minor contamination with albumin yields unnaturally high f_u values. Clearly, this is not the case in our investigations. Artifactual f_u values would also be readily apparent if there were any dissociation of the drug–protein complex during the centrifugation process. Although studies were undertaken to investigate the possibility, no evidence was found to suggest a concentration gradient of unbound warfarin (a result of sedimentation/layering) existed within the supernatant. Of the remaining 2 mL of spiked plasma, containing total (bound plus unbound) drug, a 1-mL sample was similarly spiked with the internal standard. The plasma and supernatant were extracted and derivatized as previously outlined for plasma samples[1]. Relative and absolute quantitation of (*R*)-[^{12}C]- and (*S*)-[2-^{13}C]warfarin was obtained by measurement of ion ratios with reference to the internal standard *via* GC–MS analysis (12).

The results of the study are shown in Table I. Although differences in the degree of binding of the two enantiomers was not significant, these differences are greatly magnified when considered in terms of the pharmacologically active free fractions. These data indicate that the (*S*)-enantiomer is more highly bound than the (*R*)-enantiomer, as previously reported (9). It is interesting to note the good agreement between our results and those reported previously, particularly in light of the different methodologies that were employed.

We have previously shown that (*R*)-warfarin has a greater distribution volume than the (*S*)-enantiomer[1]. As only free drug is available to distribute throughout the body, consideration of the present data provides an explanation for this observation: (*S*)-warfarin, being more highly bound to plasma proteins than the (*R*)-enantiomer, would be expected to have a smaller distribution volume, since it is more confined to the circulatory system. Interestingly, the ratio of the apparent volumes of distribution of the (*R*)- and (*S*)-enantiomers (V_R:V_S = 1.6) is almost identical to the unbound fraction ratio (Table I).

(*S*)-Warfarin has been shown to be about five times more potent an anticoagulant than its optical antipode. Determination of this difference, however, did not take into account the differential binding of the enantiomers (15) and thus does not reveal the true (intrinsic) difference in potency between the enantiomers. When protein binding is taken into account, the (*S*)-enantiomer has an inherent potency approximately eight times greater than that of the (*R*)-enantiomer. Clinically, it is sufficient to acknowledge the apparent differences in potency; however, the intrinsic difference in potency is important for the postulation of potential receptor sites and consideration of structure–activity relationships.

Changes in the plasma protein binding of a drug arising from multiple-drug therapy is well documented; probably, it is the most common explanation for any drug–drug interactions. Plasma is, however, an open compartment, and any drug that is displaced from plasma proteins will rapidly distribute into the tissue compartments. Consequently, the transient increase in f_u produced by the displacing drug is often of little pharmacological importance. Sulfinpyrazone is a widely used uricosuric agent, but more recently its effects on platelets has led to its use in the treatment of a variety of thromboembolic disorders. It is now well documented (16) that if warfarin and sulfinpyrazone are coadministered, the pharmacological response to warfarin is enhanced; the basis of the interaction appears to be metabolic in origin[1]. The important and poten-

[1] S. Toon, L. K. Low, W. F. Trager, R. A. O'Reilly, C. H. Motley, and A. Goulart, unpublished results.

[2] The preparation of the pseudoracemate and determination of stereochemical and isotopic purity was as previously described (11).

Table I—Enatiomeric Binding Data of Pseudoracemic Warfarin (10 μg·mL^{-1}) in the Absence and Presence of Sulfinpyrazone (15 μg·mL^{-1})

	Control	Sulfinpyrazone
(*R*):(*S*) Unbound fraction (f_u) ratio	1.58 (*SD* ± 0.15; *n* = 11)	2.25 (*SD* ± 0.26; *n* = 11)
t test		$p < 0.001$
Percentage bound[a]		
(*R*)	99.15 (*SD* ± 0.24) (f_u% = 0.85)	98.73 (*SD* ± 0.14) (f_u% = 1.27, increase of 49.41%)
(*S*)	99.47 (*SD* ± 0.16) (f_u% = 0.53)	99.42 (*SD* ± 0.10) (f_u% = 0.58, increase of 9.43%)
pesudoracemate	99.31 (f_u% = 0.69)	99.08 (f_u% = 0.92, increase of 34.06%)

[a] Calculated as the mean of the individual enantiomer binding data.

tially complicating role that stereoselective changes in protein binding play in the interaction is evident from a consideration of the equation for total body clearance which pertains to poorly extracted drugs (6):

$$CL = f_u \cdot CL'$$

Without acknowledging the stereoselective change in f_u between the two warfarin enantiomers brought about by concomitant sulfinpyrazone administration, one might incorrectly conclude that any inequivalent change in *CL* between (*R*)- and (*S*)-warfarin has its origins at the enzymatic level (as measured by the intrinsic clearance *CL'*), a result of metabolic induction or inhibition. In light of our present observations, it is apparent that stereoselective protein binding displacement of a poorly extracted drug may manifest itself as an inequivalent change in the *CL* of the two enantiomers in the absence of any dynamic change in metabolism. Sulfinpyrazone is metabolized in humans, and the plasma-protein binding of the parent drug and its metabolites have been investigated (17). Obviously, sulfapyrazone metabolites could complicate the protein binding interaction with warfarin *in vivo*; however, our evidence with volunteers who concomitantly receive warfarin and sulfinpyrazone (15) indicate this is not the case. Interestingly, sulfinpyrazone has been reported to induce the metabolism of (*R*)-warfarin while simultaneously inhibiting the metabolism of the (*S*)-enantiomer (18, 19). These conclusions were drawn from the sulfinpyrazone-induced changes in enantiomeric clearance.

(1) M. Rowland, L. Z. Benet, and G. G. Graham, *J. Pharmoacokinet. Biopharm.*, **1**, 123 (1973).

(2) K. S. Pang and M. Rowland, *J. Pharmacokinet. Biopharm.*, **5**, 625, (1977).

(3) K. S. Pang and M. Rowland, *J. Pharmacokinet. Biopharm.*, **5**, 655, (1977).

(4) K. S. Pang and M. Rowland, *J. Pharmacokinet. Biopharm.*, **5**, 681, (1977).

(5) G. R. Wilkinson and D. G. Shand, *Clin. Pharmacol. Ther.*, **18**, 377 (1975).

(6) G. Levy and A. Yacobi, *J. Pharm. Sci.*, **63**, 805 (1974).

(7) F. Karusch, *J. Am. Chem. Soc.*, **76**, 5536 (1954).

(8) W. E. Muller and U. Wollert, *Mol. Pharmacol.*, **11**, 52 (1975).

(9) A. Yacobi and G. Levy, *J. Pharmacokinet. Biopharm.*, **5**, 123 (1977).

(10) S. A. Bai, U. K. Walle, M. J. Wilson, and T. Walle, *Drug Metab. Dispos.*, **11**, 394 (1983).

(11) W. R. Porter, K. Kunze, E. J. Valente, and W. F. Trager, *J. Labelled Comp. Radiopharm.* **17**, 763 (1980).

(12) E. D. Bush, L. K. Low, and W. F. Trager, *Biomed. Mass Spectrom.*, **10**, 395 (1983).

(13) W. F. Van der Giesen and J. Wilting, *Methods Find. Exp. Clin. Pharmacol.*, **4**, 417 (1982).

(14) K. M. Giacomini, J. C. Giacomini, and R. T. Blaschke, *Biochem. Pharmacol.*, **29**, 3337 (1980).

(15) J. N. Eble, B. D. West, and K. P. Link, *Biochem. Pharmacol*, **15**, 1003 (1966).

(16) J. M. Davis and L. E. Johns, Jr., *N. Engl. J. Med.*, **299**, 955 (1978).

(17) P. Jakobson, A. K. Pedersen, and F. Andrease, *Acta Pharmacol. Toxicol.*, **51**, 243 (1982).

(18) J. O. Miners, T. Foenander, S. Wanwimolruk, A. S. Gallus, and D. J. Birkett, *Eur. J. Clin. Pharmacol.*, **22**, 327 (1982).

(19) R. A. O'Reilly, *Circulation*, **75**, 202 (1982).

Stephen Toon
William F. Trager
Department of Medicinal Chemistry
School of Pharmacy
University of Washington
Seattle, WA 98195

Received October 14, 1983.
Accepted for publication September 20, 1984.
This work was supported by Grants GM 2860 and GM 32165 from the National Institutes of Health.

Thermodynamic Studies of Tolbutamide Polymorphs

Keyphrases □ Tolbutamide—crystalline polymorphs, solubility as a function of temperature, polymorphic conversion, transition temperature

To the Editor:

Aqueous suspensions of tolbutamide were found to thicken to an unpourable state after several weeks of occasional shaking (prior to daily dosing). Samples of the same suspensions that were not shaken showed excellent stability after years of storage at ambient and elevated temperature. Microscopic examination revealed that the thickening was due to partial crystalline conversion of the original plate-like tolbutamide crystals to very fine needle-shaped crystals, which tend to form a highly flocculated structure. The crystals were identified as a polymorphic form rather than a solvate or change in habit. IR spectra and X-ray diffraction confirmed that the acicular form is identical with Burger's form III (1). The polymorphic conversion was unexpected since published solubility data suggest that form I is the more stable polymorph at room temperature (1, 2). However, a transition temperature, above which form III converts to form I, has been reported by several investigators to be somewhere between 98.5°C and 118°C (1, 3, 4). An inconsistency here is clearly apparent: form I cannot be the more stable polymorph at temperatures both above and below a transition temperature. Furthermore, the reported solubility data (1) indicating that form I is less soluble than form III at 37°C conflict with suspension stability data generated in this laboratory, which indicate that form I converts to form III at room temperature. To resolve the discrepancy between the published literature and recent observations in this laboratory, the aqueous solubilities of polymorphs I and III were determined as a function of temperature.

The form I tolbutamide used in this study was prepared for commercial use by a final recrystallization from methanol–water[1]. Form III was made by stirring an aqueous suspension

[1] Lot No. 445HS; The Upjohn Co., Kalamazoo, Mich.

0022-3549/84/1100-1673$01.00/0

© 1984, American Pharmaceutical Association

Table I—Enatiomeric Binding Data of Pseudoracemic Warfarin (10 μg·mL^{-1}) in the Absence and Presence of Sulfinpyrazone (15 μg·mL^{-1})

	Control	Sulfinpyrazone
(*R*):(*S*) Unbound fraction (f_u) ratio	1.58 (*SD* ± 0.15; *n* = 11)	2.25 (*SD* ± 0.26; *n* = 11)
t test		$p < 0.001$
Percentage bound[a]		
(*R*)	99.15 (*SD* ± 0.24) (f_u% = 0.85)	98.73 (*SD* ± 0.14) (f_u% = 1.27, increase of 49.41%)
(*S*)	99.47 (*SD* ± 0.16) (f_u% = 0.53)	99.42 (*SD* ± 0.10) (f_u% = 0.58, increase of 9.43%)
pesudoracemate	99.31 (f_u% = 0.69)	99.08 (f_u% = 0.92, increase of 34.06%)

[a] Calculated as the mean of the individual enantiomer binding data.

tially complicating role that stereoselective changes in protein binding play in the interaction is evident from a consideration of the equation for total body clearance which pertains to poorly extracted drugs (6):

$$CL = f_u \cdot CL'$$

Without acknowledging the stereoselective change in f_u between the two warfarin enantiomers brought about by concomitant sulfinpyrazone administration, one might incorrectly conclude that any inequivalent change in *CL* between (*R*)- and (*S*)-warfarin has its origins at the enzymatic level (as measured by the intrinsic clearance *CL'*), a result of metabolic induction or inhibition. In light of our present observations, it is apparent that stereoselective protein binding displacement of a poorly extracted drug may manifest itself as an inequivalent change in the *CL* of the two enantiomers in the absence of any dynamic change in metabolism. Sulfinpyrazone is metabolized in humans, and the plasma-protein binding of the parent drug and its metabolites have been investigated (17). Obviously, sulfapyrazone metabolites could complicate the protein binding interaction with warfarin *in vivo*; however, our evidence with volunteers who concomitantly receive warfarin and sulfinpyrazone (15) indicate this is not the case. Interestingly, sulfinpyrazone has been reported to induce the metabolism of (*R*)-warfarin while simultaneously inhibiting the metabolism of the (*S*)-enantiomer (18, 19). These conclusions were drawn from the sulfinpyrazone-induced changes in enantiomeric clearance.

(1) M. Rowland, L. Z. Benet, and G. G. Graham, *J. Pharmoacokinet. Biopharm.*, **1**, 123 (1973).

(2) K. S. Pang and M. Rowland, *J. Pharmacokinet. Biopharm.*, **5**, 625, (1977).

(3) K. S. Pang and M. Rowland, *J. Pharmacokinet. Biopharm.*, **5**, 655, (1977).

(4) K. S. Pang and M. Rowland, *J. Pharmacokinet. Biopharm.*, **5**, 681, (1977).

(5) G. R. Wilkinson and D. G. Shand, *Clin. Pharmacol. Ther.*, **18**, 377 (1975).

(6) G. Levy and A. Yacobi, *J. Pharm. Sci.*, **63**, 805 (1974).

(7) F. Karusch, *J. Am. Chem. Soc.*, **76**, 5536 (1954).

(8) W. E. Muller and U. Wollert, *Mol. Pharmacol.*, **11**, 52 (1975).

(9) A. Yacobi and G. Levy, *J. Pharmacokinet. Biopharm.*, **5**, 123 (1977).

(10) S. A. Bai, U. K. Walle, M. J. Wilson, and T. Walle, *Drug Metab. Dispos.*, **11**, 394 (1983).

(11) W. R. Porter, K. Kunze, E. J. Valente, and W. F. Trager, *J. Labelled Comp. Radiopharm.* **17**, 763 (1980).

(12) E. D. Bush, L. K. Low, and W. F. Trager, *Biomed. Mass Spectrom.*, **10**, 395 (1983).

(13) W. F. Van der Giesen and J. Wilting, *Methods Find. Exp. Clin. Pharmacol.*, **4**, 417 (1982).

(14) K. M. Giacomini, J. C. Giacomini, and R. T. Blaschke, *Biochem. Pharmacol.*, **29**, 3337 (1980).

(15) J. N. Eble, B. D. West, and K. P. Link, *Biochem. Pharmacol*, **15**, 1003 (1966).

(16) J. M. Davis and L. E. Johns, Jr., *N. Engl. J. Med.*, **299**, 955 (1978).

(17) P. Jakobson, A. K. Pedersen, and F. Andrease, *Acta Pharmacol. Toxicol.*, **51**, 243 (1982).

(18) J. O. Miners, T. Foenander, S. Wanwimolruk, A. S. Gallus, and D. J. Birkett, *Eur. J. Clin. Pharmacol.*, **22**, 327 (1982).

(19) R. A. O'Reilly, *Circulation*, **75**, 202 (1982).

Stephen Toon
William F. Trager
Department of Medicinal Chemistry
School of Pharmacy
University of Washington
Seattle, WA 98195

Received October 14, 1983.
Accepted for publication September 20, 1984.
This work was supported by Grants GM 2860 and GM 32165 from the National Institutes of Health.

Thermodynamic Studies of Tolbutamide Polymorphs

Keyphrases □ Tolbutamide—crystalline polymorphs, solubility as a function of temperature, polymorphic conversion, transition temperature

To the Editor:

Aqueous suspensions of tolbutamide were found to thicken to an unpourable state after several weeks of occasional shaking (prior to daily dosing). Samples of the same suspensions that were not shaken showed excellent stability after years of storage at ambient and elevated temperature. Microscopic examination revealed that the thickening was due to partial crystalline conversion of the original plate-like tolbutamide crystals to very fine needle-shaped crystals, which tend to form a highly flocculated structure. The crystals were identified as a polymorphic form rather than a solvate or change in habit. IR spectra and X-ray diffraction confirmed that the acicular form is identical with Burger's form III (1). The polymorphic conversion was unexpected since published solubility data suggest that form I is the more stable polymorph at room temperature (1, 2). However, a transition temperature, above which form III converts to form I, has been reported by several investigators to be somewhere between 98.5°C and 118°C (1, 3, 4). An inconsistency here is clearly apparent: form I cannot be the more stable polymorph at temperatures both above and below a transition temperature. Furthermore, the reported solubility data (1) indicating that form I is less soluble than form III at 37°C conflict with suspension stability data generated in this laboratory, which indicate that form I converts to form III at room temperature. To resolve the discrepancy between the published literature and recent observations in this laboratory, the aqueous solubilities of polymorphs I and III were determined as a function of temperature.

The form I tolbutamide used in this study was prepared for commercial use by a final recrystallization from methanol–water[1]. Form III was made by stirring an aqueous suspension

[1] Lot No. 445HS; The Upjohn Co., Kalamazoo, Mich.

0022-3549/84/1100-1673$01.00/0

© 1984, American Pharmaceutical Association

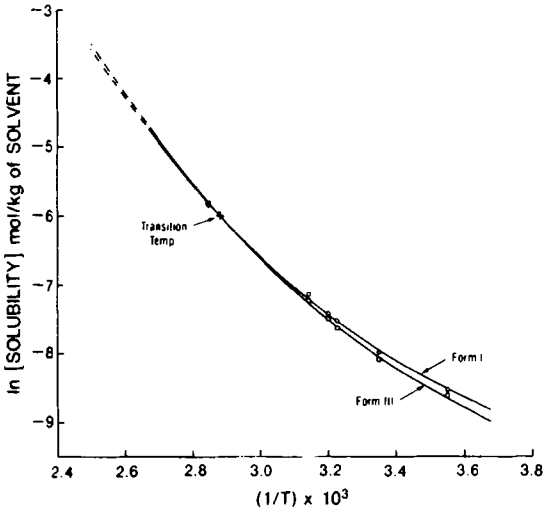

Figure 1—*Aqueous solubilities of tolbutamide forms I and III as a function of temperature.*

of form I tolbutamide (173 g in 20 L of water containing 10 g of polysorbate 80) for several days. The suspension was seeded initially with a small amount of the formulated suspension that contained some of the needle-like crystals of form III. Heating the suspension to ~40°C hastened the conversion of the plate-like form I crystals to the needle-shaped form III crystals. When conversion appeared complete by microscopic observation, the suspension was filtered on a coarse sintered glass filter, washed with deionized water, and dried at 40°C under reduced pressure. The converted crystal form was identified as form III and differentiated from form I by X-ray diffraction patterns and IR spectra which conformed with those published by Burger and others (1, 3, 4). Thermogravimetric analysis and melt solvate assays were negative for solvents. Melting points and differential scanning calorimetric thermograms corresponded to those published previously (1, 3, 4).

The aqueous solubilities of each of the two forms were obtained in the same way as reported by Burger (1). Samples of the stirred suspensions were taken periodically and assayed by UV spectrophotometry or reverse-phase HPLC at 229 nm until a constant value was obtained for several days. The solubility in octanol was determined in the same way, except that no HCl or polysorbate 80 was added. Samples were taken every hour until 4 or 5 h after apparent equilibrium.

The aqueous solubility at 37°C for form I was found to be 14.61 mg/100 mL, and that of form III was 13.03 mg/100 mL. These values are significantly different at the 95% confidence level. The aqueous solubility data in the molal units are plotted against $1/T$ in Fig. 1 (van't Hoff plot). The nonlinearity of the data is due to the wide temperature range covered, as pointed out by Grant (5). Using an iterative least-squares regression program, the solubility data for each of the forms was fit to a modified van't Hoff equation (6) as follows:

$$\ln m_{T_2} = \ln m_{T_1} + \frac{(\Delta\overline{H}_{T_1} - T_1\Delta\overline{C}p)(T_2 - T_1)}{RT_1T_2} + \frac{\Delta\overline{C}p}{R} \cdot \ln\frac{T_2}{T_1} \qquad \text{(Eq. 1)}$$

where T_2 is the temperature of interest and T_1 is an arbitrarily chosen reference temperature. In this study, T_1 was fixed at 128°C, the melting point of form I. $\Delta\overline{H}$ and $\Delta\overline{C}p$ are the differential heat of solution and the difference in heat capacity of dissolved and crystalline solute, respectively, for either form. $\Delta\overline{C}p$ is assumed constant with an arbitrary value of 84 cal/deg·mol, while the heat of solution is dependent on temperature as follows (6):

$$\Delta\overline{H}_{T_2} = \Delta\overline{H}_{T_1} + \Delta\overline{C}p(T_2 - T_1) \qquad \text{(Eq. 2)}$$

Table I—Thermodynamic Parameters Obtained from the Solubility *versus* Temperature Data (Eq. 1)

Polymorph	ln m(128°C)[a]	$\Delta\overline{H}$ (128°C), kcal/mol	$\Delta\overline{C}p$, cal/deg·mol
I	−3.52	15.0	84[b]
III	−3.44	15.4	84[b]

[a] Hypothetical value of the aqueous solubility at 128°C in units of molality. [b] Assumed to be equal in the least-squares fitting routine.

The two unknowns (heat of solution at 128°C and ln m at 128°C) are obtained from the iterative solution of Eq. 1 and are listed in Table I. The heat of solution of form I at 25°C is calculated to be 6.3 cal/deg·mol which is in good agreement with previously published data (2). The two polymorphs are enantiotropic since the solubility curves cross below the melting point. The transition temperature is estimated to be ~75°C. Below 75°C, form III has the lower solubility and is the most stable. Since the aqueous solubilities of the two forms are so close, form I may appear to be quite stable in suspensions at low temperatures, but given enough time, it will transform to the lower energy form. Above 75°C, form I has the lowest solubility and is the more stable of the two in that region.

A qualitative experiment was done to illustrate the transition point. A small quantity of form III crystals was mixed with mineral oil on a microscope slide. The mixture was heated to 100°C on a hot stage for several hours and periodically agitated by pressing and rotating the cover slip. When the temperature was reduced to 95°C and maintained, prismatic plate-like crystals, typical of form I, began to grow throughout the oil mixture while the form III clusters slowly dissolved. Then, the slide was removed from the hot stage and allowed to cool quickly to room temperature. The plates stopped growing, but fine needle-like crystals, typical to form III, began to grow. Obviously, there is a transition temperature between 25°C and 95°C.

The crystalline conversion was observed in 10 other solvents at room temperature: toluene, hexane, ethanol, chloroform, acetonitrile, methyl propyl ketone, isopropyl alcohol, tetrahydrofuran, dioxane, and octanol. The rate of conversion varied greatly with solubility, the better solvents promoting faster conversion. Since the conversion in octanol is relatively slow, it was chosen for accurate determination of polymorph solubilities. As might be expected, the solubility in octanol of form III at 30°C is significantly lower than that of form I: 19.33 mg/mL for form III and 23.54 mg/mL for form I. IR spectra were obtained on the solids remaining after the solubility study had been completed; the results confirmed the microscopic observation that no polymorphic conversion had taken place in either case during the solubility study.

The data given here present a rational explanation for the observed polymorphic change in suspensions at temperatures of <75°C. The small difference in free energy of the two polymorphic forms and the low solubilities at ambient temperature provide only a small driving force for the conversion.

This allows the preparation of apparently stable suspensions of either form. However, form I suspensions are metastable at ambient temperatures and eventually will change to form III. The conversion may be hastened by catalytic influences such as strong agitation.

(1) A. Burger, *Sci. Pharm.* **43,** 161 (1975).
(2) H. Ueda, N. Nambu, and T. Nagai, *Chem. Pharm. Bull.*, **30,** 2618 (1982).
(3) J. R. Leary, S. D. Ross, and M. J. K. Thomas, *Pharm. Weekblad. Sci. Ed.*, **3,** 62 (1981).
(4) D. L. Simmons, R. J. Ranz, N. D. Gyanchandani, and P. Picotte, *Can. J. Pharm. Sci.*, **7,** 121 (1972).
(5) D. J. W. Grant, M. Mehdizadeh, A. H.-L. Chow, and J. E. Fairbrother, *Int. J. Pharm.*, **18,** 25 (1984).
(6) G. N. Lewis and M. Randall, "Thermodynamics", 2nd ed., McGraw-Hill, New York, N.Y. 1961, p. 227.

Englebert L. Rowe [x]
Pharmacy Research
The Upjohn Company
Kalamazoo, MI 49001

Bradley D. Anderson
College of Pharmacy
University of Utah
Salt Lake City, UT 84112

Received January 12, 1984.
Accepted for publication September 20, 1984.
The authors acknowledge the IR analysis and interpretation by Mr. P. Meulman, XRD analysis by Mr. D. S. Aldrich, and assistance on the HPLC assay by Mr. W. F. Beyer, all of The Upjohn Company.

OPEN FORUM

Safety and Efficacy of Dental Sealants in the Prevention of Tooth Decay

In a recent editorial ("Coming of Age" for Device Technology), Dr. Feldmann[1] appears to be unnecessarily harsh on the use of modern dental sealants in preventing caries. The designation of such procedure as "a hoax or even a well-intended but worthless effort by dentists to protect against the ravages of caries" may have had some validity 15 or so years ago, when the early sealant materials were in developmental stages and application techniques were not well understood. Today, however, new sealants have been developed and clinically proven by dental researchers as safe and effective in preventing caries[2]. The use of sealants by dentists in the United States[3] has increased dramatically since 1974 when 37.8% of those surveyed said they offered sealant therapy; in 1982, that figure increased to 57.7%.

The National Dental Caries Prevalence Survey (1979-1980) has shown that among 5- to 17-year-old children, only 16% of the caries incidence occurred in smooth surfaces, but 84% involved chewing surfaces with pits and fissures. It is known that the chewing surfaces of children's teeth are the most susceptible to decay and derive the least benefit from fluorides. The newly developed plastic films are applied to these chewing surfaces to seal the pits and grooves, which prevents food and cariogenic bacteria being trapped and thus offers a new approach to the prevention of dental caries.

The 1983 Consensus Development Conference on the use of dental sealants in the prevention of tooth decay, sponsored by the National Institutes of Health, made the following conclusions[4]:

"The placement of sealants is a highly effective means of preventing pit and fissure caries. It is safe. It is currently underused in both private and public dental health care delivery systems. The reasons for such underuse are complex, but intensive efforts should be taken to increase sealant use. Expanding the use of sealants would substantially reduce the occurrence of dental caries in the population beyond that already achieved by fluorides and other preventive measures. Because dental caries is still a disease common to most young people in the United States and in other countries of the world, such reductions would substantially improve the health of the public and reduce the expenditures for treatment of dental disease. Practitioners, dental health agency directors, and dental educators are urged to incorporate the appropriate use of sealants into their practice and programs."

The American Dental Association Council on Dental Materials, Instruments, and Equipment, which has an acceptance program to evaluate commercially available sealants for safety and efficacy, also considers[5] "pit and fissure sealants are safe and effective as a caries prevention procedure."

G. Subba Rao
Chief Research Scientist
Division of Biochemistry
Research Institute
American Dental Association
Health Foundation
Chicago, IL 60611

[1] E. G. Feldmann, *J. Pharm. Sci.*, **73,** 713 (1984).
[2] "Emphasis: Pit and Fissure Sealant Use, An Issue Explored," *J. Am. Dent. Assoc.*, **108,** 310 (1984).
[3] "The Role of Health Professional in the Delivery of Caries Prevention," American Dental Association Health Foundation Report, Chicago, Ill., 1983.
[4] "National Institutes of Health Consensus Development Conference Statement on Dental Sealants in the Prevention of Tooth Decay," *J. Am. Dent. Assoc.*, **108,** 233 (1984).
[5] "Pit and Fissure Sealants. Report of Council on Dental Materials, Instruments, and Equipment," *J. Am. Dent. Assoc.*, **107,** 465 (1983).

Author's Response:

Apparently, Dr. Rao misunderstood or misinterpreted the message of my June issue editorial. In his letter, Dr. Rao acknowledges that classifying dental sealants as being worthless 15 or so years ago may have had validity; however, he contends that today they are considered by experts in the field to be a highly beneficial technique in protecting against dental caries.

The entire thrust of the editorial, from its title ("Coming of Age" for Device Technology), through its entire text, to the very last paragraph (which stated that ". . . what we are witnessing is truly a medical revolution"), emphasized and reemphasized that many modern medical devices, procedures, and technology now constitute valuable health advances—although this was rarely the case a generation ago. As one dramatic example, we mentioned dental sealants and praised the FDA for keeping an open mind in judging positively the current products and their application. Yes, these modern products have indeed been proven to be a safe and effective caries prevention procedure.

Over twenty-five years ago, I personally was on the ADA staff as Director of the American Dental Association's drug testing laboratory. I well remember that the biggest challenge to ADA at that time was to reverse lay, professional, and scientific thinking regarding the value of fluoridation. Until then, only the toxicity and adverse effects were generally recognized and known. But, by carefully adjusting the daily intake of fluoride, remarkable benefits could be achieved while avoiding any adverse reactions. This was one of the earlier technical revolutions in the dental field—sealants are a more recent advance.

In conclusion, we would respectfully urge Dr. Rao to read again our June editorial. Then, it should be clear to him that we have no disagreement whatsoever as to the current value of dental sealants.

Edward G. Feldmann
American Pharmaceutical Association
2215 Constitution Avenue, N.W.
Washington, DC 20037

This allows the preparation of apparently stable suspensions of either form. However, form I suspensions are metastable at ambient temperatures and eventually will change to form III. The conversion may be hastened by catalytic influences such as strong agitation.

(1) A. Burger, *Sci. Pharm.* **43,** 161 (1975).
(2) H. Ueda, N. Nambu, and T. Nagai, *Chem. Pharm. Bull.*, **30,** 2618 (1982).
(3) J. R. Leary, S. D. Ross, and M. J. K. Thomas, *Pharm. Weekblad. Sci. Ed.*, **3,** 62 (1981).
(4) D. L. Simmons, R. J. Ranz, N. D. Gyanchandani, and P. Picotte, *Can. J. Pharm. Sci.*, **7,** 121 (1972).
(5) D. J. W. Grant, M. Mehdizadeh, A. H.-L. Chow, and J. E. Fairbrother, *Int. J. Pharm.*, **18,** 25 (1984).
(6) G. N. Lewis and M. Randall, "Thermodynamics", 2nd ed., McGraw-Hill, New York, N.Y. 1961, p. 227.

Englebert L. Rowe [x]
Pharmacy Research
The Upjohn Company
Kalamazoo, MI 49001

Bradley D. Anderson
College of Pharmacy
University of Utah
Salt Lake City, UT 84112

Received January 12, 1984.
Accepted for publication September 20, 1984.
The authors acknowledge the IR analysis and interpretation by Mr. P. Meulman, XRD analysis by Mr. D. S. Aldrich, and assistance on the HPLC assay by Mr. W. F. Beyer, all of The Upjohn Company.

OPEN FORUM

Safety and Efficacy of Dental Sealants in the Prevention of Tooth Decay

In a recent editorial ("Coming of Age" for Device Technology), Dr. Feldmann[1] appears to be unnecessarily harsh on the use of modern dental sealants in preventing caries. The designation of such procedure as "a hoax or even a well-intended but worthless effort by dentists to protect against the ravages of caries" may have had some validity 15 or so years ago, when the early sealant materials were in developmental stages and application techniques were not well understood. Today, however, new sealants have been developed and clinically proven by dental researchers as safe and effective in preventing caries[2]. The use of sealants by dentists in the United States[3] has increased dramatically since 1974 when 37.8% of those surveyed said they offered sealant therapy; in 1982, that figure increased to 57.7%.

The National Dental Caries Prevalence Survey (1979-1980) has shown that among 5- to 17-year-old children, only 16% of the caries incidence occurred in smooth surfaces, but 84% involved chewing surfaces with pits and fissures. It is known that the chewing surfaces of children's teeth are the most susceptible to decay and derive the least benefit from fluorides. The newly developed plastic films are applied to these chewing surfaces to seal the pits and grooves, which prevents food and cariogenic bacteria being trapped and thus offers a new approach to the prevention of dental caries.

The 1983 Consensus Development Conference on the use of dental sealants in the prevention of tooth decay, sponsored by the National Institutes of Health, made the following conclusions[4]:

"The placement of sealants is a highly effective means of preventing pit and fissure caries. It is safe. It is currently underused in both private and public dental health care delivery systems. The reasons for such underuse are complex, but intensive efforts should be taken to increase sealant use. Expanding the use of sealants would substantially reduce the occurrence of dental caries in the population beyond that already achieved by fluorides and other preventive measures. Because dental caries is still a disease common to most young people in the United States and in other countries of the world, such reductions would substantially improve the health of the public and reduce the expenditures for treatment of dental disease. Practitioners, dental health agency directors, and dental educators are urged to incorporate the appropriate use of sealants into their practice and programs."

The American Dental Association Council on Dental Materials, Instruments, and Equipment, which has an acceptance program to evaluate commercially available sealants for safety and efficacy, also considers[5] "pit and fissure sealants are safe and effective as a caries prevention procedure."

G. Subba Rao
Chief Research Scientist
Division of Biochemistry
Research Institute
American Dental Association
Health Foundation
Chicago, IL 60611

[1] E. G. Feldmann, *J. Pharm. Sci.*, **73,** 713 (1984).
[2] "Emphasis: Pit and Fissure Sealant Use, An Issue Explored," *J. Am. Dent. Assoc.*, **108,** 310 (1984).
[3] "The Role of Health Professional in the Delivery of Caries Prevention," American Dental Association Health Foundation Report, Chicago, Ill., 1983.
[4] "National Institutes of Health Consensus Development Conference Statement on Dental Sealants in the Prevention of Tooth Decay," *J. Am. Dent. Assoc.*, **108,** 233 (1984).
[5] "Pit and Fissure Sealants. Report of Council on Dental Materials, Instruments, and Equipment," *J. Am. Dent. Assoc.*, **107,** 465 (1983).

Author's Response:

Apparently, Dr. Rao misunderstood or misinterpreted the message of my June issue editorial. In his letter, Dr. Rao acknowledges that classifying dental sealants as being worthless 15 or so years ago may have had validity; however, he contends that today they are considered by experts in the field to be a highly beneficial technique in protecting against dental caries.

The entire thrust of the editorial, from its title ("Coming of Age" for Device Technology), through its entire text, to the very last paragraph (which stated that ". . . what we are witnessing is truly a medical revolution"), emphasized and reemphasized that many modern medical devices, procedures, and technology now constitute valuable health advances—although this was rarely the case a generation ago. As one dramatic example, we mentioned dental sealants and praised the FDA for keeping an open mind in judging positively the current products and their application. Yes, these modern products have indeed been proven to be a safe and effective caries prevention procedure.

Over twenty-five years ago, I personally was on the ADA staff as Director of the American Dental Association's drug testing laboratory. I well remember that the biggest challenge to ADA at that time was to reverse lay, professional, and scientific thinking regarding the value of fluoridation. Until then, only the toxicity and adverse effects were generally recognized and known. But, by carefully adjusting the daily intake of fluoride, remarkable benefits could be achieved while avoiding any adverse reactions. This was one of the earlier technical revolutions in the dental field—sealants are a more recent advance.

In conclusion, we would respectfully urge Dr. Rao to read again our June editorial. Then, it should be clear to him that we have no disagreement whatsoever as to the current value of dental sealants.

Edward G. Feldmann
American Pharmaceutical Association
2215 Constitution Avenue, N.W.
Washington, DC 20037

This allows the preparation of apparently stable suspensions of either form. However, form I suspensions are metastable at ambient temperatures and eventually will change to form III. The conversion may be hastened by catalytic influences such as strong agitation.

(1) A. Burger, *Sci. Pharm.* **43,** 161 (1975).
(2) H. Ueda, N. Nambu, and T. Nagai, *Chem. Pharm. Bull.*, **30,** 2618 (1982).
(3) J. R. Leary, S. D. Ross, and M. J. K. Thomas, *Pharm. Weekblad. Sci. Ed.*, **3,** 62 (1981).
(4) D. L. Simmons, R. J. Ranz, N. D. Gyanchandani, and P. Picotte, *Can. J. Pharm. Sci.*, **7,** 121 (1972).
(5) D. J. W. Grant, M. Mehdizadeh, A. H.-L. Chow, and J. E. Fairbrother, *Int. J. Pharm.*, **18,** 25 (1984).
(6) G. N. Lewis and M. Randall, "Thermodynamics", 2nd ed., McGraw-Hill, New York, N.Y. 1961, p. 227.

Englebert L. Rowe [x]
Pharmacy Research
The Upjohn Company
Kalamazoo, MI 49001

Bradley D. Anderson
College of Pharmacy
University of Utah
Salt Lake City, UT 84112

Received January 12, 1984.
Accepted for publication September 20, 1984.
The authors acknowledge the IR analysis and interpretation by Mr. P. Meulman, XRD analysis by Mr. D. S. Aldrich, and assistance on the HPLC assay by Mr. W. F. Beyer, all of The Upjohn Company.

OPEN FORUM

Safety and Efficacy of Dental Sealants in the Prevention of Tooth Decay

In a recent editorial ("Coming of Age" for Device Technology), Dr. Feldmann[1] appears to be unnecessarily harsh on the use of modern dental sealants in preventing caries. The designation of such procedure as "a hoax or even a well-intended but worthless effort by dentists to protect against the ravages of caries" may have had some validity 15 or so years ago, when the early sealant materials were in developmental stages and application techniques were not well understood. Today, however, new sealants have been developed and clinically proven by dental researchers as safe and effective in preventing caries[2]. The use of sealants by dentists in the United States[3] has increased dramatically since 1974 when 37.8% of those surveyed said they offered sealant therapy; in 1982, that figure increased to 57.7%.

The National Dental Caries Prevalence Survey (1979-1980) has shown that among 5- to 17-year-old children, only 16% of the caries incidence occurred in smooth surfaces, but 84% involved chewing surfaces with pits and fissures. It is known that the chewing surfaces of children's teeth are the most susceptible to decay and derive the least benefit from fluorides. The newly developed plastic films are applied to these chewing surfaces to seal the pits and grooves, which prevents food and cariogenic bacteria being trapped and thus offers a new approach to the prevention of dental caries.

The 1983 Consensus Development Conference on the use of dental sealants in the prevention of tooth decay, sponsored by the National Institutes of Health, made the following conclusions[4]:

"The placement of sealants is a highly effective means of preventing pit and fissure caries. It is safe. It is currently underused in both private and public dental health care delivery systems. The reasons for such underuse are complex, but intensive efforts should be taken to increase sealant use. Expanding the use of sealants would substantially reduce the occurrence of dental caries in the population beyond that already achieved by fluorides and other preventive measures. Because dental caries is still a disease common to most young people in the United States and in other countries of the world, such reductions would substantially improve the health of the public and reduce the expenditures for treatment of dental disease. Practitioners, dental health agency directors, and dental educators are urged to incorporate the appropriate use of sealants into their practice and programs."

The American Dental Association Council on Dental Materials, Instruments, and Equipment, which has an acceptance program to evaluate commercially available sealants for safety and efficacy, also considers[5] "pit and fissure sealants are safe and effective as a caries prevention procedure."

G. Subba Rao
Chief Research Scientist
Division of Biochemistry
Research Institute
American Dental Association
Health Foundation
Chicago, IL 60611

[1] E. G. Feldmann, *J. Pharm. Sci.*, **73,** 713 (1984).
[2] "Emphasis: Pit and Fissure Sealant Use, An Issue Explored," *J. Am. Dent. Assoc.*, **108,** 310 (1984).
[3] "The Role of Health Professional in the Delivery of Caries Prevention," American Dental Association Health Foundation Report, Chicago, Ill., 1983.
[4] "National Institutes of Health Consensus Development Conference Statement on Dental Sealants in the Prevention of Tooth Decay," *J. Am. Dent. Assoc.*, **108,** 233 (1984).
[5] "Pit and Fissure Sealants. Report of Council on Dental Materials, Instruments, and Equipment," *J. Am. Dent. Assoc.*, **107,** 465 (1983).

Author's Response:

Apparently, Dr. Rao misunderstood or misinterpreted the message of my June issue editorial. In his letter, Dr. Rao acknowledges that classifying dental sealants as being worthless 15 or so years ago may have had validity; however, he contends that today they are considered by experts in the field to be a highly beneficial technique in protecting against dental caries.

The entire thrust of the editorial, from its title ("Coming of Age" for Device Technology), through its entire text, to the very last paragraph (which stated that ". . . what we are witnessing is truly a medical revolution"), emphasized and reemphasized that many modern medical devices, procedures, and technology now constitute valuable health advances—although this was rarely the case a generation ago. As one dramatic example, we mentioned dental sealants and praised the FDA for keeping an open mind in judging positively the current products and their application. Yes, these modern products have indeed been proven to be a safe and effective caries prevention procedure.

Over twenty-five years ago, I personally was on the ADA staff as Director of the American Dental Association's drug testing laboratory. I well remember that the biggest challenge to ADA at that time was to reverse lay, professional, and scientific thinking regarding the value of fluoridation. Until then, only the toxicity and adverse effects were generally recognized and known. But, by carefully adjusting the daily intake of fluoride, remarkable benefits could be achieved while avoiding any adverse reactions. This was one of the earlier technical revolutions in the dental field—sealants are a more recent advance.

In conclusion, we would respectfully urge Dr. Rao to read again our June editorial. Then, it should be clear to him that we have no disagreement whatsoever as to the current value of dental sealants.

Edward G. Feldmann
American Pharmaceutical Association
2215 Constitution Avenue, N.W.
Washington, DC 20037

Animal Models for Oral Drug Delivery in Man: In Situ and In Vivo Approaches. Edited by WILLIAM CROUTHAMEL and ALLEN C. SARAPU. American Pharmaceutical Association, Academy of Pharmaceutical Sciences, 2215 Constitution Ave. N.W. Washington, DC 20037. 1983. 179 pp. 15.5 × 23.5 cm. Price: $54.00.

This book is based on the symposium "Animal Models for Drug Absorption in Man" held in September 1980 at the APhA Academy of Pharmaceutical Sciences meeting in San Antonio, Texas. It contains texts from various recognized authorities in the field.

The book is divided into six chapters which discuss the mechanisms of drug absorption and techniques for studying them (Chapters 1 and 2), the use of the dog in new drug development, bioavailability testing and quality control (Chapters 3–5) and the regulatory viewpoint on the use of animals in NDA submissions (Chapter 6). In many respects, however, the most obvious division in the book is between the academic and industrial approaches to studying absorption—a distinction entirely appropriate in a subject that is of intense interest to both sides of pharmaceutical research. The text is well-argued and very readable and the rather unfortunate misspelling of 'gavage' as 'garbage' (Chapter 6) in no way reflects the general high quality of the contents.

The first two chapters (written by G. L. Amidon and N. F. H. Ho *et. al.*) are excellent and give a fairly comprehensive description of the theoretical and practical aspects of the subject. The analysis, in Chapter 2, of physiological factors controlling absorption is particularly effective.

The subsequent chapters are in some ways an anticlimax, although they do represent a useful account of industrial experiences with these models in new drug development. There are a number of examples or 'case studies' which readily illustrate the points being made, although the description of compounds in vague terms such as 'anxiolytic-type,' without structures, tends to be a little frustrating. The main criticism of this part of the book is in what it omits rather than what it includes; this may be a result of its origins as a symposium, where time is limited and a subject cannot be covered comprehensively. However, there does seem to be an overriding emphasis on the use of blood level studies in dogs when discussion of other species, such as rat and monkey, would have been of benefit. Other important considerations such as the correlation between *in situ* and *in vivo* absorption data and the crucial issue of interspecies variation in absorption also have not been given the coverage they deserve.

Nevertheless, an authoritative text on this subject is long overdue and this book is both welcome and useful. It will be of particular value to those in the pharmaceutical industry who are involved in drug design and product development. The more interested readers will be stimulated to look into the literature for some of the things the book omits and the excellent sets of references will be a useful guide for this.

Reviewed by David C. Taylor
Pharmaceutical Department
ICI Pharmaceuticals Division
Alderley Park
Macclesfield
Cheshire
U.K.

Handbook of Powder Science and Technology. By M. E. FAYED and L. OTTEN, Van Nostrand Reinhold Company, Inc., 135 West 50th Street, New York, NY 10020. 1984. 650 pp. 18 × 26 cm. Price: $79.50.

This book is intended to be a guide for quick access to a wide range of information on powder science. Actually it is not a handbook, but is a comprehensive text to which 26 authors have contributed their expertise. For a multiauthored book it is very readable.

The book is divided into 19 chapters, which are entitled: "Particle Size Analysis: Theory and Statistical Methods"; "Particle Size Measurement: Experimental Techniques"; "Particulate Characterization: Future Approaches"; "Structural Properties of Packing Particles"; "Fundamental Properties of Powders"; "Vibration of Fine Powders and Its Application"; "Size Enlargement Methods and Equipment"; "Mixing of Powders; Storage of Particulate Solids"; "Fluidization Phenomena and Fluidized Bed Technology"; "Spouting of Particulate Solids"; "Transport of Solids in Pipelines"; "Size Reduction of Solids: Crushing and Grinding Equipment"; "Sedimentation"; "Filtration of Solids from Liquid Streams"; "Cyclones"; "Electrostatic Precipitator Applications and Concepts"; "Granular Bed Filters"; "Wet Scrubber Particulate Collection".

Statistical discussion is supported by sample problems, and the validity of the calculations are discussed. Analytical instruments and processing equipment are listed, and methods of selection for specific conditions are discussed in detail. The currentness of the book is exemplified by the modern chapter on morphology of a particle and powder signature. The book contains a wealth of information on the technology of handling, measurement, separation, and use of powders.

This excellent book has an abundance of information not only for those (graduate students) who have little experience in powder technology, but also for the pharmaceutical scientists in production, research and development, and academia.

Reviewed by Eugene L. Parrott
College of Pharmacy
University of Iowa
Iowa City, IA 52242

Nucleosides, Nucleotides, and Their Biological Applications. Edited by JANET L. RIDEOUT, DAVID W. HENRY, AND LOWRIE M. BEACHAM III. Academic Press, 111 Fifth Avenue, New York, NY 10003. 1983. 327 pp. 16 × 24 cm. Price: $29.50.

The book presents the manuscripts of the 11 plenary lectures given at the Fifth International Round Table on Nucleosides, Nucleotides, and Their Biological Applications, held in Research Triangle Park, North Carolina, October 20–22, 1982. Each lecture is given its own chapter, a list of which includes "Nucleosides with Antiviral Activity", "The Chemistry and Biology of Nucleosides of Purines and Ring Analogs", "Experimental and Clinical Studies on 2′-Fluoroarabinosyl Pyrimidines and Purine-Like C-Nucleosides", "2′,5′-Oligoadenylates, Their Role in Interferon Action and Their Potential as Chemotherapeutic Agents", "Receptors for Adenosine and Adenine Nucleotides", "Analogs of 2′,5′-Oligoadenylates: Biological Probes for the Antiviral/Antitumor State of Mammalian Cells", "Synthesis of Pyrrolo[2,3-d]Pyrimidine Nucleosides by Phase Transfer Glycosylation and Their Function in Polynucleotides", "The Alkylsilyl Protecting Groups: in Particular, the *t*-Butyldimethylsilyl Group in Nucleoside and Nucleotide Chemistry", "Unusual Nucleoside Synthons and Oligonucleotide Synthesis", "Selective Modification and Deoxygenation at C-2′ of Nucleosides", and "Synthesis of Versitile C-Nucleoside Precursors and Certain C-Nucleosides".

While no attempt is made to exhaustively review all the literature in each chapter, general references are provided wherein additional reviews can be found. Each chapter is generally well written with very few typographical and/or structural errors, and all have substantial (albeit not extensive) bibliographies. The index at the end of the volume is quite detailed, including page references for specific compounds. Although the material is now almost two years old, and much new literature has been published, especially in the areas of adenosine receptors and antagonists, novel C-nucleosides, and 2′,5′-oligonucleotide synthesis, this reference is nevertheless a valuable source of information on methodology (both chemical and biological) and structural design of nucleoside/nucleotide analogues.

Reviewed by Marvin C. Pankaskie
Department of Biomedicinal Chemistry
College of Pharmacy
University of Nebraska Medical Center
Omaha, NE 68105

Animal Models for Oral Drug Delivery in Man: In Situ and In Vivo Approaches. Edited by WILLIAM CROUTHAMEL and ALLEN C. SARAPU. American Pharmaceutical Association, Academy of Pharmaceutical Sciences, 2215 Constitution Ave. N.W. Washington, DC 20037. 1983. 179 pp. 15.5 × 23.5 cm. Price: $54.00.

This book is based on the symposium "Animal Models for Drug Absorption in Man" held in September 1980 at the APhA Academy of Pharmaceutical Sciences meeting in San Antonio, Texas. It contains texts from various recognized authorities in the field.

The book is divided into six chapters which discuss the mechanisms of drug absorption and techniques for studying them (Chapters 1 and 2), the use of the dog in new drug development, bioavailability testing and quality control (Chapters 3–5) and the regulatory viewpoint on the use of animals in NDA submissions (Chapter 6). In many respects, however, the most obvious division in the book is between the academic and industrial approaches to studying absorption—a distinction entirely appropriate in a subject that is of intense interest to both sides of pharmaceutical research. The text is well-argued and very readable and the rather unfortunate misspelling of 'gavage' as 'garbage' (Chapter 6) in no way reflects the general high quality of the contents.

The first two chapters (written by G. L. Amidon and N. F. H. Ho *et. al.*) are excellent and give a fairly comprehensive description of the theoretical and practical aspects of the subject. The analysis, in Chapter 2, of physiological factors controlling absorption is particularly effective.

The subsequent chapters are in some ways an anticlimax, although they do represent a useful account of industrial experiences with these models in new drug development. There are a number of examples or 'case studies' which readily illustrate the points being made, although the description of compounds in vague terms such as 'anxiolytic-type,' without structures, tends to be a little frustrating. The main criticism of this part of the book is in what it omits rather than what it includes; this may be a result of its origins as a symposium, where time is limited and a subject cannot be covered comprehensively. However, there does seem to be an overriding emphasis on the use of blood level studies in dogs when discussion of other species, such as rat and monkey, would have been of benefit. Other important considerations such as the correlation between *in situ* and *in vivo* absorption data and the crucial issue of interspecies variation in absorption also have not been given the coverage they deserve.

Nevertheless, an authoritative text on this subject is long overdue and this book is both welcome and useful. It will be of particular value to those in the pharmaceutical industry who are involved in drug design and product development. The more interested readers will be stimulated to look into the literature for some of the things the book omits and the excellent sets of references will be a useful guide for this.

Reviewed by David C. Taylor
Pharmaceutical Department
ICI Pharmaceuticals Division
Alderley Park
Macclesfield
Cheshire
U.K.

Handbook of Powder Science and Technology. By M. E. FAYED and L. OTTEN, Van Nostrand Reinhold Company, Inc., 135 West 50th Street, New York, NY 10020. 1984. 650 pp. 18 × 26 cm. Price: $79.50.

This book is intended to be a guide for quick access to a wide range of information on powder science. Actually it is not a handbook, but is a comprehensive text to which 26 authors have contributed their expertise. For a multiauthored book it is very readable.

The book is divided into 19 chapters, which are entitled: "Particle Size Analysis: Theory and Statistical Methods"; "Particle Size Measurement: Experimental Techniques"; "Particulate Characterization: Future Approaches"; "Structural Properties of Packing Particles"; "Fundamental Properties of Powders"; "Vibration of Fine Powders and Its Application"; "Size Enlargement Methods and Equipment"; "Mixing of Powders; Storage of Particulate Solids"; "Fluidization Phenomena and Fluidized Bed Technology"; "Spouting of Particulate Solids"; "Transport of Solids in Pipelines"; "Size Reduction of Solids: Crushing and Grinding Equipment"; "Sedimentation"; "Filtration of Solids from Liquid Streams"; "Cyclones"; "Electrostatic Precipitator Applications and Concepts"; "Granular Bed Filters"; "Wet Scrubber Particulate Collection".

Statistical discussion is supported by sample problems, and the validity of the calculations are discussed. Analytical instruments and processing equipment are listed, and methods of selection for specific conditions are discussed in detail. The currentness of the book is exemplified by the modern chapter on morphology of a particle and powder signature. The book contains a wealth of information on the technology of handling, measurement, separation, and use of powders.

This excellent book has an abundance of information not only for those (graduate students) who have little experience in powder technology, but also for the pharmaceutical scientists in production, research and development, and academia.

Reviewed by Eugene L. Parrott
College of Pharmacy
University of Iowa
Iowa City, IA 52242

Nucleosides, Nucleotides, and Their Biological Applications. Edited by JANET L. RIDEOUT, DAVID W. HENRY, AND LOWRIE M. BEACHAM III. Academic Press, 111 Fifth Avenue, New York, NY 10003. 1983. 327 pp. 16 × 24 cm. Price: $29.50.

The book presents the manuscripts of the 11 plenary lectures given at the Fifth International Round Table on Nucleosides, Nucleotides, and Their Biological Applications, held in Research Triangle Park, North Carolina, October 20–22, 1982. Each lecture is given its own chapter, a list of which includes "Nucleosides with Antiviral Activity", "The Chemistry and Biology of Nucleosides of Purines and Ring Analogs", "Experimental and Clinical Studies on 2′-Fluoroarabinosyl Pyrimidines and Purine-Like C-Nucleosides", "2′,5′-Oligoadenylates, Their Role in Interferon Action and Their Potential as Chemotherapeutic Agents", "Receptors for Adenosine and Adenine Nucleotides", "Analogs of 2′,5′-Oligoadenylates: Biological Probes for the Antiviral/Antitumor State of Mammalian Cells", "Synthesis of Pyrrolo[2,3-d]Pyrimidine Nucleosides by Phase Transfer Glycosylation and Their Function in Polynucleotides", "The Alkylsilyl Protecting Groups: in Particular, the *t*-Butyldimethylsilyl Group in Nucleoside and Nucleotide Chemistry", "Unusual Nucleoside Synthons and Oligonucleotide Synthesis", "Selective Modification and Deoxygenation at C-2′ of Nucleosides", and "Synthesis of Versitile C-Nucleoside Precursors and Certain C-Nucleosides".

While no attempt is made to exhaustively review all the literature in each chapter, general references are provided wherein additional reviews can be found. Each chapter is generally well written with very few typographical and/or structural errors, and all have substantial (albeit not extensive) bibliographies. The index at the end of the volume is quite detailed, including page references for specific compounds. Although the material is now almost two years old, and much new literature has been published, especially in the areas of adenosine receptors and antagonists, novel C-nucleosides, and 2′,5′-oligonucleotide synthesis, this reference is nevertheless a valuable source of information on methodology (both chemical and biological) and structural design of nucleoside/nucleotide analogues.

Reviewed by Marvin C. Pankaskie
Department of Biomedicinal Chemistry
College of Pharmacy
University of Nebraska Medical Center
Omaha, NE 68105

Animal Models for Oral Drug Delivery in Man: In Situ and In Vivo Approaches. Edited by WILLIAM CROUTHAMEL and ALLEN C. SARAPU. American Pharmaceutical Association, Academy of Pharmaceutical Sciences, 2215 Constitution Ave. N.W. Washington, DC 20037. 1983. 179 pp. 15.5 × 23.5 cm. Price: $54.00.

This book is based on the symposium "Animal Models for Drug Absorption in Man" held in September 1980 at the APhA Academy of Pharmaceutical Sciences meeting in San Antonio, Texas. It contains texts from various recognized authorities in the field.

The book is divided into six chapters which discuss the mechanisms of drug absorption and techniques for studying them (Chapters 1 and 2), the use of the dog in new drug development, bioavailability testing and quality control (Chapters 3–5) and the regulatory viewpoint on the use of animals in NDA submissions (Chapter 6). In many respects, however, the most obvious division in the book is between the academic and industrial approaches to studying absorption—a distinction entirely appropriate in a subject that is of intense interest to both sides of pharmaceutical research. The text is well-argued and very readable and the rather unfortunate misspelling of 'gavage' as 'garbage' (Chapter 6) in no way reflects the general high quality of the contents.

The first two chapters (written by G. L. Amidon and N. F. H. Ho *et. al.*) are excellent and give a fairly comprehensive description of the theoretical and practical aspects of the subject. The analysis, in Chapter 2, of physiological factors controlling absorption is particularly effective.

The subsequent chapters are in some ways an anticlimax, although they do represent a useful account of industrial experiences with these models in new drug development. There are a number of examples or 'case studies' which readily illustrate the points being made, although the description of compounds in vague terms such as 'anxiolytic-type,' without structures, tends to be a little frustrating. The main criticism of this part of the book is in what it omits rather than what it includes; this may be a result of its origins as a symposium, where time is limited and a subject cannot be covered comprehensively. However, there does seem to be an overriding emphasis on the use of blood level studies in dogs when discussion of other species, such as rat and monkey, would have been of benefit. Other important considerations such as the correlation between *in situ* and *in vivo* absorption data and the crucial issue of interspecies variation in absorption also have not been given the coverage they deserve.

Nevertheless, an authoritative text on this subject is long overdue and this book is both welcome and useful. It will be of particular value to those in the pharmaceutical industry who are involved in drug design and product development. The more interested readers will be stimulated to look into the literature for some of the things the book omits and the excellent sets of references will be a useful guide for this.

Reviewed by David C. Taylor
Pharmaceutical Department
ICI Pharmaceuticals Division
Alderley Park
Macclesfield
Cheshire
U.K.

Handbook of Powder Science and Technology. By M. E. FAYED and L. OTTEN, Van Nostrand Reinhold Company, Inc., 135 West 50th Street, New York, NY 10020. 1984. 650 pp. 18 × 26 cm. Price: $79.50.

This book is intended to be a guide for quick access to a wide range of information on powder science. Actually it is not a handbook, but is a comprehensive text to which 26 authors have contributed their expertise. For a multiauthored book it is very readable.

The book is divided into 19 chapters, which are entitled: "Particle Size Analysis: Theory and Statistical Methods"; "Particle Size Measurement: Experimental Techniques"; "Particulate Characterization: Future Approaches"; "Structural Properties of Packing Particles"; "Fundamental Properties of Powders"; "Vibration of Fine Powders and Its Application"; "Size Enlargement Methods and Equipment"; "Mixing of Powders; Storage of Particulate Solids"; "Fluidization Phenomena and Fluidized Bed Technology"; "Spouting of Particulate Solids"; "Transport of Solids in Pipelines"; "Size Reduction of Solids: Crushing and Grinding Equipment"; "Sedimentation"; "Filtration of Solids from Liquid Streams"; "Cyclones"; "Electrostatic Precipitator Applications and Concepts"; "Granular Bed Filters"; "Wet Scrubber Particulate Collection".

Statistical discussion is supported by sample problems, and the validity of the calculations are discussed. Analytical instruments and processing equipment are listed, and methods of selection for specific conditions are discussed in detail. The currentness of the book is exemplified by the modern chapter on morphology of a particle and powder signature. The book contains a wealth of information on the technology of handling, measurement, separation, and use of powders.

This excellent book has an abundance of information not only for those (graduate students) who have little experience in powder technology, but also for the pharmaceutical scientists in production, research and development, and academia.

Reviewed by Eugene L. Parrott
College of Pharmacy
University of Iowa
Iowa City, IA 52242

Nucleosides, Nucleotides, and Their Biological Applications. Edited by JANET L. RIDEOUT, DAVID W. HENRY, AND LOWRIE M. BEACHAM III. Academic Press, 111 Fifth Avenue, New York, NY 10003. 1983. 327 pp. 16 × 24 cm. Price: $29.50.

The book presents the manuscripts of the 11 plenary lectures given at the Fifth International Round Table on Nucleosides, Nucleotides, and Their Biological Applications, held in Research Triangle Park, North Carolina, October 20–22, 1982. Each lecture is given its own chapter, a list of which includes "Nucleosides with Antiviral Activity", "The Chemistry and Biology of Nucleosides of Purines and Ring Analogs", "Experimental and Clinical Studies on 2′-Fluoroarabinosyl Pyrimidines and Purine-Like C-Nucleosides", "2′,5′-Oligoadenylates, Their Role in Interferon Action and Their Potential as Chemotherapeutic Agents", "Receptors for Adenosine and Adenine Nucleotides", "Analogs of 2′,5′-Oligoadenylates: Biological Probes for the Antiviral/Antitumor State of Mammalian Cells", "Synthesis of Pyrrolo[2,3-d]Pyrimidine Nucleosides by Phase Transfer Glycosylation and Their Function in Polynucleotides", "The Alkylsilyl Protecting Groups: in Particular, the *t*-Butyldimethylsilyl Group in Nucleoside and Nucleotide Chemistry", "Unusual Nucleoside Synthons and Oligonucleotide Synthesis", "Selective Modification and Deoxygenation at C-2′ of Nucleosides", and "Synthesis of Versitile C-Nucleoside Precursors and Certain C-Nucleosides".

While no attempt is made to exhaustively review all the literature in each chapter, general references are provided wherein additional reviews can be found. Each chapter is generally well written with very few typographical and/or structural errors, and all have substantial (albeit not extensive) bibliographies. The index at the end of the volume is quite detailed, including page references for specific compounds. Although the material is now almost two years old, and much new literature has been published, especially in the areas of adenosine receptors and antagonists, novel C-nucleosides, and 2′,5′-oligonucleotide synthesis, this reference is nevertheless a valuable source of information on methodology (both chemical and biological) and structural design of nucleoside/nucleotide analogues.

Reviewed by Marvin C. Pankaskie
Department of Biomedicinal Chemistry
College of Pharmacy
University of Nebraska Medical Center
Omaha, NE 68105

A publication of the
American Pharmaceutical Association—
the National Professional Society
of Pharmacists

JOURNAL OF PHARMACEUTICAL SCIENCES

Volume 73, 1984

JPMSAE 73(1-12) 1-1910 (1984)
ISSN 0022-3549

Sharon G. Boots
Editor

Sue A. Kruger
Production Editor

Margaret M. Madeleine
Assistant Production Editor

Karen A. Blakney
Copy Editor

Edward G. Feldmann
Contributing Editor

Samuel W. Goldstein
Contributing Editor

Patricia A. Evich
Editorial Secretary

Editorial Advisory Board

Jordan L. Cohen
Kenneth A. Connors
Louis Diamond
Ho-Leung Fung
Milo Gibaldi
Everett N. Hiestand
W. Homer Lawrence
Ian W. Mathison
Carl M. Metzler
Robert E. Notari
Paul L. Schiff, Jr.
Jane E. Shaw

Published monthly under the supervision of the Board of Trustees

The Industry–University Interface

In terms of history, it was not so very long ago—less than a century—that scientists and inventors worked in virtual isolation in their laboratories. Along with a colleague or two at most, they conducted studies and experiments that led to some of mankind's greatest achievements and discoveries.

Thanks to the motion picture industry, many of us have had an opportunity to view top quality films with star performers who portrayed the lives and major accomplishments of Madame Curie, Paul Ehrlich, Thomas Edison, Wilbur and Orville Wright, Louis Pasteur, Alexander Graham Bell, and various other such notables.

But times have changed, and dramatically so.

Today, the overwhelming proportion of research is conducted by big scientific or technical teams, at big industrial firms, or at big universities, or at big government institutions. And as the complexity of contemporary research continues to grow, even those big operations apparently are not large enough to capably handle the kind of research job that sometimes needs to be done.

Antitrust legislation often presents a hurdle for companies that might otherwise contemplate banding together in joint efforts. However, joint efforts between industry and academia do not present these same legal difficulties. This is not to say that there are no legal problems. By no means. We are aware that there are many legal considerations involved in academia–industry joint ventures that often require significant paperwork, much justification, and what usually seems to be an inordinate amount of time. But as severe as these constraints may be, they are not as severe as those presented by the antitrust laws.

Early this year, in the February issue, we already commented on this overall subject under the heading "Universities for Hire." At that time, we termed the issue of jointly sponsored Academe/Industry Research as the current "great debate" within university and some industry circles. Our conclusion then was that if all involved exercised good will, pragmatic approaches, and honest attitudes, the big concern regarding erosion of ethics and academic freedom could be averted.

Nothing dramatically new has happened since then by way of a solution to the issues and concerns that were then prevalent. However, there is growing interest in the subject as research—especially in the fields of bioengineering and biotechnology—has become increasingly complex and expensive.

Indeed, in late August of this year, the National Science Foundation released a study that it had commissioned the consulting firm of Arthur D. Little, Inc., to conduct on its behalf. The resulting report, entitled "Study of Federal Biotechnology Policy Issues," identified two top biotechnology issues meriting federal attention. One of these was the subject of university-industry relationships.

Just a few weeks earlier, the incoming President of the American Association of Colleges of Pharmacy, Robert D. Gibson of the University of California School of Pharmacy, concluded his presidential address by calling attention to the issue as one that is emerging for schools of pharmacy. He correctly noted that, for some time, it has already been a concern for other disciplines and particularly bioengineering. Now, he stated, it is developing as an issue in pharmacy schools, and he urged giving it appropriate attention *before* it became a problem, rather than *after*.

In considering the subject, Dr. Gibson listed four areas in which industry/academia joint research ventures or partnerships might impinge:

- *Suppress the free transfer of information, thereby inhibiting the advancement of the science related to pharmacy.*
- *Undermine the development of the basic sciences by diverting faculty interests to problems of immediate commercial interest.*
- *Negatively affect the quality of instruction in our schools.*
- *Distort traditional academic values and goals.*

He plans to take certain positive steps during his presidential term to face these issues and, hopefully, to develop some guidelines that might provide helpful direction to schools of pharmacy.

In the meantime, the need to work out some suitable, mutually acceptable arrangement is definitely there. Just this past March, an editorial in *Science* was entitled "Graduate Education: Signs of Trouble." The author, John Brademas, called attention to the growing problems of financing graduate education and suggested industry support as a key solution. In turn, industry has a vested interest because its future research and technical talent will come from today's graduate schools.

Finally, a group of five clinical pharmacologists from Pfizer Pharmaceuticals coauthored a "commentary" article that was published in the April 1984 issue of *Clinical Pharmacology and Therapeutics*. Appropriately, their article was titled "University and Pharmaceutical Industry Cooperation: The Need to Plan for the Future."

Their article was refreshingly candid. In the opening paragraph, they began by noting the "history of mutual mistrust" and went on to state that: "It has been said by way of hyperbole that industry wants only to pick academia's brains, whereas universities are mostly interested in picking industry's pockets. Yet the potential for gains by both sides encourages the bridging of what once seemed a wide psychologic and programmatic gap."

Proceeding then with a very balanced view of the issue, they analyzed in significant depth the specific area of joint or cooperative research projects in the area of clinical pharmacology relating to drug development. Although their emphasis was particularly directed at pharmaceutical industry relations with medical schools, their ideas and views all apply equally to pharmacy schools.

After noting a series of specific benefits deriving from collaboration—some to the university, others to industry—they concluded that, although the idea of cooperatively conducted research is far from being a new development, the need for such arrangements has recently become far more important to both "camps." Moreover, going beyond the need for such arrangements merely for survival, they see these carefully developed relationships as presenting a potentially significant new benefit for the entire health care community.

This is a view in which we fully share!

—EDWARD G. FELDMANN
American Pharmaceutical Association
2215 Constitution Avenue, NW
Washington, DC 20037

Editor's Note: Dr. Feldmann's editorials are an expression of personal opinion and do not necessarily reflect views or policies of APhA. The editorials are intended to be provocative and to stimulate thinking. Readers having reactions, either pro or con, are invited to submit them for publication in the *Open Forum* section.

JOURNAL OF PHARMACEUTICAL SCIENCES

DECEMBER 1984
VOLUME 73 NUMBER 12

RESEARCH ARTICLES

General Treatment of pH–Solubility Profiles of Weak Acids and Bases and the Effects of Different Acids on the Solubility of a Weak Base

WILLIAM H. STRENG ˣ, SWEE K. HSI, PAUL E. HELMS, and HETTY G. H. TAN

Received August 15, 1983, from the *Merrell Dow Research Institute, Merrell Dow Pharmaceuticals, Cincinnati, OH 45215.* Accepted for publication January 19, 1984.

Abstract □ The pH–solubility profile of a weak acid or base is shown to be a function of its pK_{sp}, pK_a, and uncharged species solubility. Equations are presented that can be used to calculate the solubility as a function of pH. These equations can also be used when there is added salt present. Experimental data was obtained in three cosolvent systems consisting of methanol–water and ethanol–water. Also, the effect of different acids on the solubility of a weak base is reported. A pronounced effect on the solubility by the addition of salt is explained in terms of the K_{sp}.

Keyphrases □ pH—profiles *versus* solubility, weak acids, weak bases □ Solubility—profiles *versus* pH, weak acids, weak bases

It is well known that the solubility of an acid or base is dependent on its ionization constants and the maximum solubility of the various species of the compound (1–12). In these reports, equations were presented that can be used to calculate the solubility profile as a function of pH. The pH range over which these equations are applicable are, however, limited as some only consider the pH region where the uncharged species is saturated and none consider the effects of additional salt added to the system. Introduction of salts to a saturated solution will frequently alter the solubility of the compound. This change in solubility is related to solubility product (K_{sp}) effects as well as changes in the activity coefficients. It will be shown that by combining the known expressions for solubility as a function of pH with the appropriate solubility product expression, equations can be obtained which, over a wide pH range, correlate the measured solubility data with calculated values. To perform the calculations, the ionization constant(s), uncharged species solubility, and solubility product(s) for the compound need to be known. Although these expressions are typically used for pure aqueous solvent systems, some of the experimental data reported utilized methanol–water and ethanol–water cosolvent systems and show the applicability of these equations to cosolvent systems. The effect of different pH-adjusting acids on the solubility of a weak base in water is also reported.

THEORETICAL SECTION

Expressions have been reported for the solubility of weak acids and bases as a function of pH (1–12). The number of equations required to describe the solubility over the entire pH range is dependent on the number of equilibrium constants that the compound has. Each equation, representing a different region in the solubility profile, contains a different species saturating the region[1]. For monoprotic compounds these equations are:

$$S_{1,0} = \left(\frac{1}{Y_0} + \frac{K}{Y_1\{H\}}\right)\{HD\} \qquad \text{(Eq. 1)}$$

$$S_{1,1} = \left(\frac{1}{Y_1} + \frac{\{H\}}{KY_0}\right)\{D\} \qquad \text{(Eq. 2)}$$

where $S_{m,j}$ is the total concentration of all species of compound D in solution, *i.e.*:

$$S_{m,j} = \sum_{p=0}^{m} [H_{m-p}D] \qquad \text{(Eq. 3)}$$

where m is the number of equilibrium constants, j is the region, $[H_{m-p}D]$ is the concentration of species $H_{m-p}D$, $\{H_{m-j}D\}$ is the activity (maximum solubility) of species $H_{m-j}D$, K is the equilibrium constant, $\{H\}$ is the hydrogen ion activity, and Y_i is the activity coefficient for species i (Y_0 is that of the most protonated species).

When the species which is saturated in a region is charged, the species activity in Eqs. 1 and 2 can be replaced by the corresponding solubility product which for monoprotic compounds in the presence of 1:1 electrolytes are:

$$K_{sp} = \{M\}\{D\} \quad \text{weak acid} \qquad \text{(Eq. 4)}$$

$$K_{sp} = \{HD\}\{X\} \quad \text{weak base} \qquad \text{(Eq. 5)}$$

If the compound is a weak acid, the quantity $K_{sp}/\{M\}$ would be substituted

[1] See Appendix I.

0022-3549/84/1200-1679$01.00/0
© 1984, American Pharmaceutical Association

for {D} in Eq. 2, while $K_{sp}/\{X\}$ would be substituted for {HD} in Eq. 1 for a weak base. The terms {M} and {X} are the corresponding cation and anion activities for the salt MX.

Since the solubility is dependent on species other than those of the weak acid or weak base, the addition of salts to the solution will alter the solubility. If the salt concentration is sufficiently large that the solubility product in Eqs. 4 or 5 is exceeded, there will be a decrease in the solubility. There will also be an effect on the activity coefficients since the total ionic strength will increase with the addition of a salt. This change in the activity coefficients can result in either an increase or decrease in the solubility depending on the salt concentration. When the salt concentration is not sufficiently large that the solubility product is exceeded, only the effect on the activity coefficients will be present.

An equation can be derived which can be used to determine the pH at which the solubility expression changes from one region to a second region. The derivation takes into consideration the fact that at the pH where the saturated species changes, the solution will be saturated in two species, and the resulting equation is obtained by combining the equilibrium expressions for K_a and K_{sp} with the charge balance equation[2].

The equation obtained will depend on whether the compound is a weak acid or a weak base. For a weak acid, the hydrogen ion concentration is given by:

$$\{H\} = \frac{[X] + \left[[X]^2 + 4\left(\frac{K_{sp}}{K\{HD\}Y_M} + \frac{1}{Y_H}\right)\left(\frac{K\{HD\}}{Y_D} + \frac{K_w}{Y_{OH}}\right)\right]^{1/2}}{2\left(\frac{K_{sp}}{K\{HD\}Y_M} + \frac{1}{Y_H}\right)} \quad \text{(Eq. 6)}$$

For a weak base it is:

$$\{H\} = \frac{-[M] + \left[[M]^2 + 4\left(\frac{\{D\}}{KY_{HD}} + \frac{1}{Y_H}\right)\left(\frac{KK_{sp}}{\{D\}Y_X} + \frac{K_w}{Y_{OH}}\right)\right]^{1/2}}{2\left(\frac{\{D\}}{KY_{HD}} + \frac{1}{Y_H}\right)} \quad \text{(Eq. 7)}$$

For monoprotic compounds, the total solubility given by Eqs. 1 and 2 can be rewritten to include the K_{sp} and addition of salt[3]. For a weak acid, Eq. 1 will remain the same, but Eq. 2 will become:

$$S_{1,1} = \frac{-\left([X] - \frac{\{H\}}{Y_H} + \frac{K_w}{\{H\}Y_{OH}}\right) + \left[\left([X] - \frac{\{H\}}{Y_H} + \frac{K_w}{\{H\}Y_{OH}}\right)^2 + 4\frac{K_{sp}}{Y_M Y_D}\right]^{1/2}}{2\left(\frac{KY_{HD}}{\{H\}Y_D + KY_{HD}}\right)} \quad \text{(Eq. 8)}$$

In the case of a weak base Eq. 2 remains the same while Eq. 1 becomes:

$$S_{1,0} = \frac{-\left([M] + \frac{\{H\}}{Y_H} - \frac{K_w}{\{H\}Y_{OH}}\right) + \left[\left([M] + \frac{\{H\}}{Y_H} - \frac{K_w}{\{H\}Y_{OH}}\right)^2 + 4\frac{K_{sp}}{Y_{HD}Y_X}\right]^{1/2}}{2\left(\frac{\{H\}Y_D}{KY_{HD} + \{H\}Y_D}\right)} \quad \text{(Eq. 9)}$$

A number of methods have been reported (1, 2, 4, 13–15) for determining the pK_a, pK_{sp}, and uncharged species maximum concentration. Any of these could be applied to Eqs. 1 and 8 or 2 and 9 with slight modification. It was found that when the uncharged species solubility is established, values for pK_a and pK_{sp} can be obtained by fitting calculated solubility curves to the experimental data. The calculated curves were sensitive to the values of pK_a and pK_{sp} used and could be estimated to within ± 0.01 units by this approach. In performing these calculations, it is important to realize that, whenever possible, estimations of the activity coefficients should be made. This is because typical values for the activity coefficient of a singly charged species in a solution having a total ionic strength of 0.05 M is ~0.75. Factors this large entering into the above equations will have significant effects.

[2] See Appendix II.

[3] See Appendix III.

EXPERIMENTAL SECTION

Solubility In Cosolvent Systems—The solubility of 4-[4-[(6-chloro-2-naphthalenyl)carbonyl]-1-piperidinyl]-1-(4-fluorophenyl)-1-butanone (I)[4] was determined in several solvent systems as a function of pH. Additional sodium chloride was added into several of the systems to see the effect of an added salt and determine how accurately the computer program used to calculate the solubility profiles could match the experimental data.

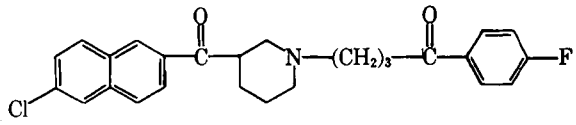

I

Solution Preparation—*85% Methanol*—Ampules were prepared containing 8.5 mL of methanol, 1.5 mL of water with 0–1.2 equivalents of HCl per equivalent of I, and 100 mg of I. In selected ampules, sodium chloride was present at concentrations of 0.01, 0.025, and 0.05 M. The ampules were sealed and placed into a 25.0°C constant-temperature bath, attached to a vibrating device, and allowed to equilibrate for 4 d. Following equilibration, the ampules were removed, and the contents were assayed.

50% Ethanol—Ampules were prepared containing 5 mL of ethanol, 5 mL of water with 0–1.2 equivalents of HCl per equivalent of I, and 100 mg of I. In selected ampules, sodium chloride was present at 0.01 and 0.05 M. The ampules were treated in the same manner as the methanol samples except they were allowed to equilibrate for 3 d.

25% Ethanol—Ampules were prepared containing 2.5 mL of ethanol, 7.5 mL of water with 0–1.2 equivalents of HCl per equivalent of I, and 100 mg of I. In selected ampules, sodium chloride was present at 0.01 and 0.05 M. The ampules were sealed and treated in the same manner as the methanol samples.

Assay Procedure—The contents of the ampules were filtered through a 0.2-μm membrane filter[5]. An appropriate aliquot was removed, and the pH of the remaining sample was measured[6]. The aliquot removed was placed in a volumetric flask and diluted with the mobile phase used in the HPLC assay. The following conditions were used in the HPLC assay: column, Partisil 10 ODS-3 (25 cm × 4.6 mm)[7]; mobile phase, acetonitrile–water (50:50) containing 0.005 M octanesulfonic acid and 0.2% acetic acid; flow rate, 120 mL/h; sample size, 10 μL (0.3–1.4 μg of I); wavelength, 246 nm[8]. The saturated concentrations were determined from the areas under the peaks, calculated with a centralized computer system[9].

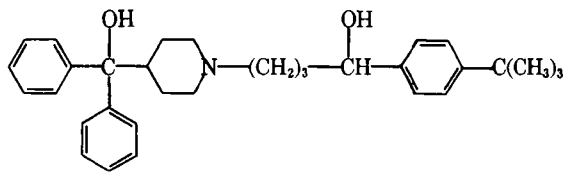

II

Effect of Different Acids on the Solubility of a Weak Base—The solubility of terfenadine, α-[4-(1,1-dimethylethyl)phenyl]-4-(hydroxydiphenylmethyl)-1-piperidinebutanol (II), was determined in water as a function of pH using lactic acid, methanesulfonic acid, hydrochloric acid, and phosphoric acid. Samples were prepared by placing 200 mg of terfenadine into washed 30-mL vials and adding 25 mL of aqueous solution containing various amounts of the selected acids. The vials were capped with a polytef-laminated rubber stopper (previously autoclaved in water to remove any extractable materials) and sealed with aluminum ferrules. The samples were placed in a sonic water bath maintained at 25°C and allowed to equilibrate for 4 d.

[4] MDL 17,214; Merrell Dow Pharmaceutical.

[5] Fluoropore filter; Millipore Corp.

[6] Model 4500 with a Radiometer GK 2321C combination electrode; Beckman Instruments.

[7] Whatman Chemical Separation, Inc.

[8] SpectroMonitor III; Laboratory Data Control.

[9] Computer Automated Laboratory System run on a Hewlett-Packard Computer/Disc system; Computer Inquiry Systems, Inc.

After equilibration, the lactic acid and phosphoric acid samples were prefiltered through filter paper[10], followed by filtration through a disposable 0.45-μm membrane filter[11]. This was necessary due to a gel formation with these acids at high concentrations. The hydrochloric acid and methanesulfonic acid solutions were filtered through disposable 0.45-μm membrane filters[11].

After filtering, the pH of the solutions was measured[12], and the solutions were assayed. To obtain peaks of reasonable area, some samples were injected directly and others were diluted with 1% aqueous acetic acid solution. The conditions were: column, μ-Bondapak C-18[13]; mobile phase, acetonitrile–water containing 20% 1 M phosphate buffer (pH 7) and 1.2% diethylamine (50:50, v/v); flow rate, 2 mL/min[14]; injection volume, 50 μL[15]; wavelength, 235 nm[8]. The saturated concentrations were determined from areas under the peaks using a centralized computer system[9].

RESULTS AND DISCUSSION

The results of the cosolvent solubilities are shown in Figs. 1–3. Adjustments to the measured pH were needed due to changes in the standard state with the cosolvent systems used (16). These corrections were 0.13 in 85% methanol, −0.17 in 50% ethanol, and −0.02 in 25% ethanol.

Using Eqs. 2 and 9, the pH–solubility profiles were calculated (lines in Figs. 1–3). The calculations were made using the Davies equation (17) for the activity coefficients:

$$-\log Y_i = AZ_i^2\left(\frac{\sqrt{I}}{1+\sqrt{I}} - 0.2I\right) \qquad \text{(Eq. 10)}$$

where A is a constant for a given temperature and solvent system, Z_i is the charge on the ion, and I is the total ionic strength. Since the calculations are complex and would require a significant amount of time to hand calculate, a computer program was written to solve the equations[16].

In Table I, the values for pK_a, pK_{sp}, and the uncharged species solubility for each solvent system are given. There is good correlation between the calculated curves (Figs. 1–3) and the observed solubility. Also shown in these figures is the dependence of the solubility of I on chloride ion. In 85% methanol at pH 5, the solubility decreases by 26, 46, and 61% in the presence of 0.01, 0.025, and 0.05 M chloride ion, respectively. A 0.05 M sodium chloride solution is about one-third the concentration of an isotonic saline solution (0.154 M). Calculations at pH 5 indicate a solubility of ~1.2 mg/mL in a 0.15 M sodium chloride solution, which would be a decrease of 80% in the solubility compared with no added sodium chloride. Similar decreases in solubility were calculated for the 50 and 25% ethanol solutions at pH 5; however, the percentage decrease is greater in these solutions, ~90 and 98% in 50 and 25% ethanol, respectively (Table II).

Inspection of the curves in Figs. 1–3 reveals the following about the solubility profile of a weak base. As the solution pH increases there is initially an increase in the solubility followed by a region in which there is little change. With a further increase in pH, there is again an increase in the solubility until a maximum is obtained. Finally, after reaching the maximum, there is a rapid decrease in the solubility.

This behavior in the profile can be explained by considering the various equilibria and species which are present in solution. Initially, the increase in solubility is due to a decrease in the anion concentration (Cl^-). This effect is subject to the solubility product (Eq. 5), where the solubility is given by Eq. 9. The total anion concentration is approximately equal to the sum of the concentrations of the weak-base protonated species and the hydrogen ion. As the pH increases, the hydrogen-ion concentration becomes very small compared with the weak-base protonated species. When this occurs, there will be little change in the solubility with pH. The maximum shown in these curves is due to the presence of both the charged and uncharged species of the weak base. The increase in solubility up to the maximum is due to an increase in the weak base uncharged species concentration up to its maximum. The rapid decrease in solubility after the maximum is due to a decrease in the weak base charged species concentration. These concentrations are controlled by the equilibrium constant. The total solubility at pH values greater than the maximum is given by Eq. 2. As the maximum solubility of the weak base uncharged species decreases, the height of the maximum will decrease (see Figs. 1 and 3). This is because at the maximum, the solution is saturated in both the weak base charged and uncharged species. Finally, the differences shown between the curves for a specific solvent system at pH values greater than the maxima are due to activity coefficient effects. If all activity coefficients were equal to one, the curves after the maxima would be superimposable.

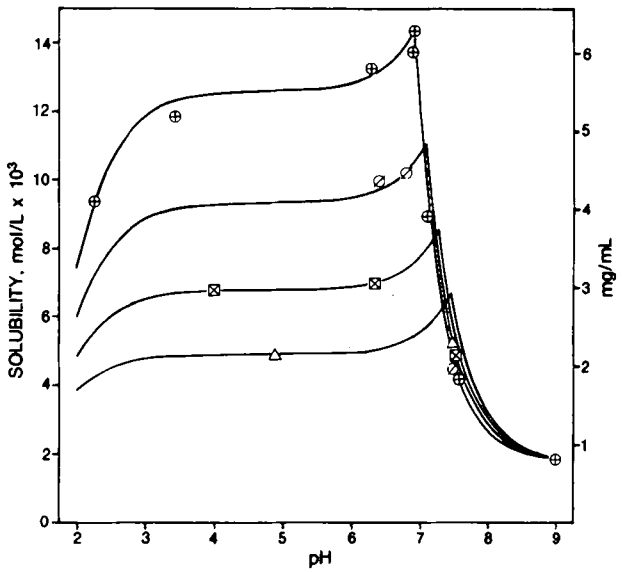

Figure 1—*pH–solubility profile of I with hydrochloric acid (solvent system, 85% methanol–water). Effect of salt on the solubility of I. Key: (⊕) no NaCl added; (Ø) 0.01 M NaCl; (□) 0.025 M NaCl; (△) 0.05 M NaCl.*

It is not possible to make direct comparisons of the pK_a value with those reported in the literature for similar compounds because of the solvent systems used. Decreases of >1 in the pK_a values compared with pure water for weak bases have been reported with 80% ethanol (18). Literature pK_a values for *N*-substituted piperidine compounds are typically 9–10 in pure water (19). This indicates that the values reported here are not unreasonable.

The pK_{sp} values used for the solubility of terfenadine with phosphoric, hydrochloric, methanesulfonic, and lactic acids are 5.6, 4.8, 4.6, and 4.05, respectively. The pK_{sp} value is largest for phosphoric acid and smallest for lactic acid. The higher the value of pK_{sp}, the lower the solubility of that salt; therefore, the solubility of terfenadine will be lowest in solutions pH-adjusted with phosphoric acid and will be highest in those solutions adjusted with lactic acid. The solubility profiles of terfenadine using these four acids are shown in Fig. 4. There is a maximum solubility between pH 4.5 and pH 5.5. The

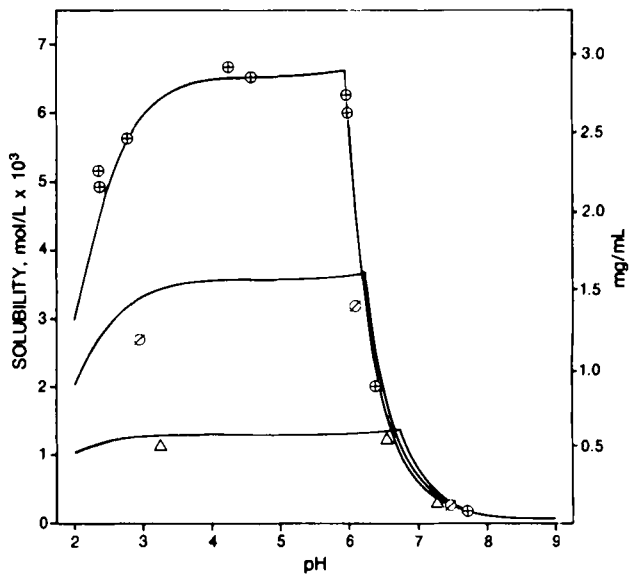

Figure 2—*pH–solubility profile of I with hydrochloric acid (solvent system, 50% ethanol–water). Effect of salt on the solubility of I. Key: (⊕) no NaCl added; (Ø) 0.01 M NaCl; (△) 0.05 M NaCl.*

[10] No. 2; Whatman.
[11] Gelman Aerodisc.
[12] Century SS-1 pH meter with an Orion combination single glass electrode; Beckman Instruments.
[13] Waters Associates.
[14] 6000A pump; Waters Associate.
[15] WISP auto injector; Waters Associates.
[16] A copy of the program can be obtained by writing the authors. It is written in Extended BASIC and was run on a PDP 11-70 computer.

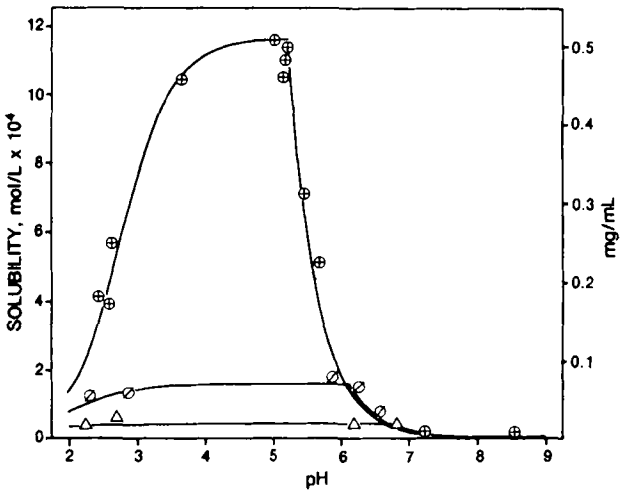

Figure 3—*pH-solubility profile of I with hydrochloric acid (solvent system, 25% ethanol-water). Effect of salt on the solubility of I. Key: (⊕) no NaCl added; (Φ) 0.01 M NaCl; (△) 0.05 M NaCl.*

decrease in solubility at higher pH is due to the solutions being saturated with respect to the uncharged form of terfenadine. At low pH, the terfenadine is forced out of solution due to the presence of additional anion from the pH adjustment.

Utilizing these pK_{sp} values, calculations were made to show the effects of the addition of sodium chloride to hydrochloric acid–terfenadine solutions and monobasic sodium phosphate to phosphoric acid–terfenadine solutions (Figs. 5 and 6). There is a pronounced effect on the solubility with the addition of even low concentrations of salts to these solutions.

These studies show the dependence of the solubility of a weak base on the pK_{sp}, pK_a, and maximum solubility of the uncharged species. Equations were presented which permit the calculation of pH-solubility profiles knowing the above constants. The effect of added salt is also shown where the solubility was significantly reduced on the addition of sodium chloride.

APPENDIX I

The derivation of Eqs. 1 and 2 and those for polyprotic compounds have been reported in detail elsewhere (1-12). They can be obtained by considering Eq. 3, the standard proton dissociation expressions, and individual species. For a monoprotic compound, Eq. 3 becomes:

$$S_{1,j} = [HD] + [D] \qquad \text{(Eq. 3a)}$$

In region $j = 0$ the HD species is saturated and, therefore, substitution of the equilibrium expression Eq. 3b into Eq. 3a for [D] will result in Eq. 3c:

$$K = \frac{\{H\}[D]}{\{HD\}} = \frac{\{H\}[D]Y_1}{\{HD\}} \qquad \text{(Eq. 3b)}$$

$$S_{1,0} = [HD] + \frac{K\{HD\}}{Y_1\{H\}} \qquad \text{(Eq. 3c)}$$

It is actually the activity of the species which is constant and not the concentration. Therefore, Eq. 3c should be expressed as Eq. 1:

Table I—Equilibrium and Solubility Constants of I

Solvent	pK_{sp}	pK_a	[A], mol/L	[A], μg/mL
85% Methanol	4.08	7.65	1.76×10^{-3}	771
50% Ethanol	4.51	7.81	7.5×10^{-5}	32.8
25% Ethanol	5.91	8.27	1×10^{-6}	0.44

Table II—Effect of Sodium Chloride On the Solubility of I at pH 5

Solvent	Solubility Without NaCl, μg/mL[a]	Solubility With NaCl, μg/mL[a]
85% Methanol	5520	1200
50% Ethanol	2870	272
25% Ethanol	509	7.8

[a] Concentration of NaCl is 0.15 M, approximately isotonic saline.

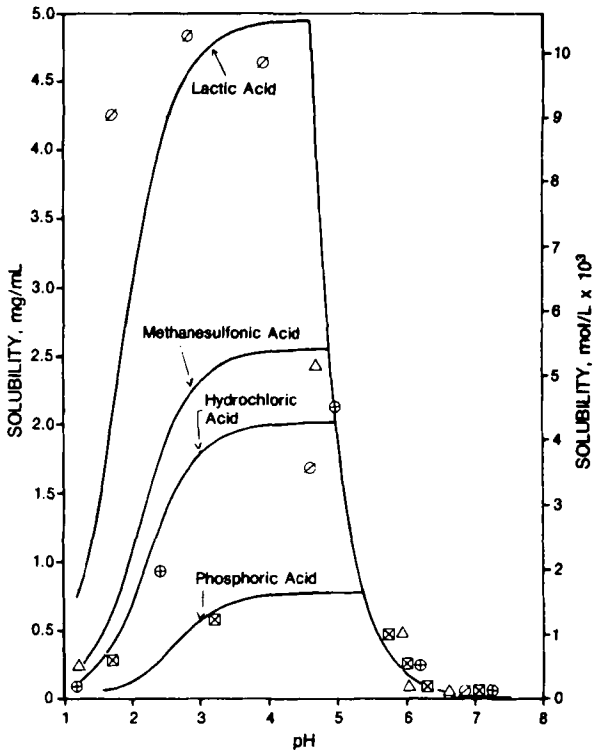

Figure 4—*pH-solubility profile of terfenadine with different acids. Effect of different acids on the solubility of terfenadine. Key: (Φ) lactic acid; (△) methanesulfonic acid; (⊕) hydrochloric acid; (□) phosphoric acid.*

$$S_{1,0} = \left(\frac{1}{Y_0} + \frac{K}{Y_1\{H\}}\right)\{HD\} \qquad \text{(Eq. 1)}$$

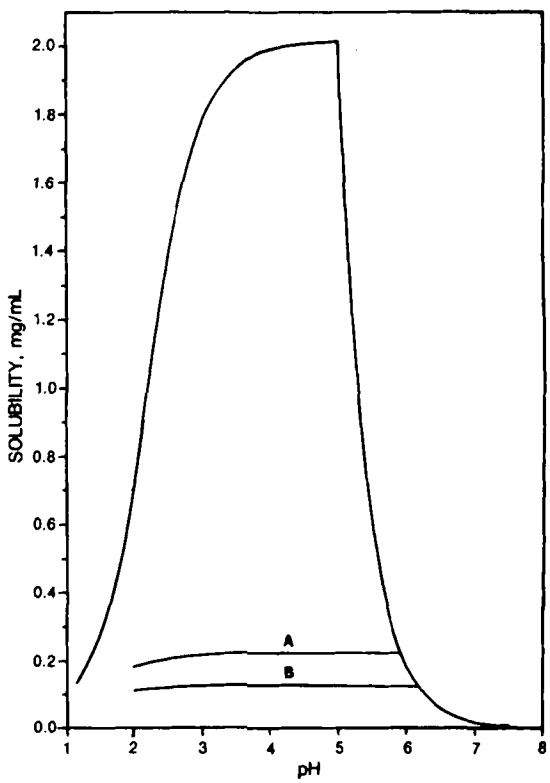

Figure 5—*pH-solubility profile of terfenadine with hydrochloric acid and salt. Calculated solubility profiles of terfenadine in solution with 0.05 M NaCl (A) and 0.1 M NaCl (B).*

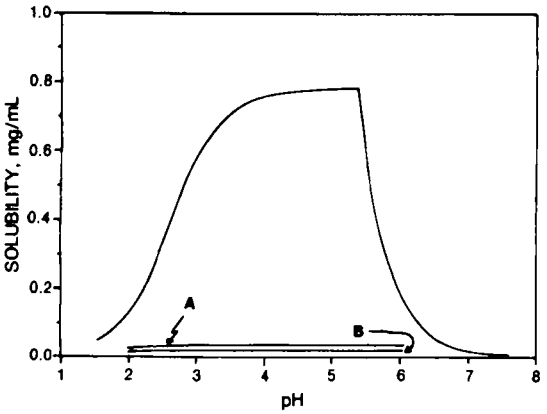

Figure 6—*pH-solubility profile of terfenadine with phosphoric acid and salt. Calculated solubility profiles of terfenadine in solution with 0.05 M NaH_2PO_4 (A) and 0.1 M NaH_2PO_4 (B).*

Similarly, Eq. 2 can be obtained by substituting the equilibrium expression into Eq. 3a for [HD], where in this case the region corresponds to $j = 1$.

Equations 1 and 2 can be generalized into the equation:

$$S_{m,j} = \sum_{j=0}^{m} \frac{\{H\}^j}{Y_0}\left[\left(\prod_{\alpha=0}^{j}\frac{1}{K_\alpha}\right)\left(1 + Y_0\sum_{i=1}^{m}\frac{1}{\{H\}^i Y_i}\prod_{t=1}^{i}K_t\right)\right]\{H_{m-j}D\} \quad \text{(Eq. 11)}$$

where $K_0 = 1$, and the other symbols are defined as above. This expression allows the determination of all equations necessary to describe the pH-solubility profile of any compound with protons that dissociate. For example, with a diacidic compound in which $m = 2$, the following equations are obtained:

$$S_{2,0} = \left(\frac{1}{Y_0} + \frac{K_1}{\{H\}Y_1} + \frac{K_1K_2}{\{H\}^2Y_2}\right)\{H_2D\} \quad \text{(Eq. 12)}$$

$$S_{2,1} = \left(\frac{1}{Y_1} + \frac{\{H\}}{K_1Y_0} + \frac{K_2}{\{H\}Y_2}\right)\{HD\} \quad \text{(Eq. 13)}$$

$$S_{2,2} = \left(\frac{1}{Y_2} + \frac{\{H\}^2}{K_1K_2Y_0} + \frac{\{H\}}{K_2Y_1}\right)\{D\} \quad \text{(Eq. 14)}$$

These equations are applicable to both weak acids and weak bases with appropriate charge assignments made to the activity coefficients and species.

APPENDIX II

The pH of maximum solubility for a monoprotic weak acid in the presence of added salt can be determined as follows[17]. For the equilibria:

$$HD \rightleftharpoons H + D \quad \text{(Eq. 6a)}$$

the equilibrium expression is given by Eq. 3b, and the solubility product is given by:

$$K_{sp} = \{M\}\{D\} \quad \text{(Eq. 4)}$$

where the added salt is MX. The charge balance equation is:

$$[M] + [H] = [OH] + [D] + [X] \quad \text{(Eq. 6b)}$$

Rearranging Eq. 3b yields:

$$\{H\} = \frac{K\{HD\}}{\{D\}} \quad \text{(Eq. 6c)}$$

Substituting for {D} from Eq. 4 into Eq. 6c gives:

$$\{H\} = \frac{K\{HD\}\{M\}}{K_{sp}} \quad \text{(Eq. 6d)}$$

Substituting for {M} from the charge balance equation (Eq. 6b) into Eq. 6d:

$$\{H\} = \frac{K\{HD\}}{K_{sp}}([D] + [X] + [OH] - [H])\,Y_M \quad \text{(Eq. 6e)}$$

Further substitution into Eq. 6e for [D] (from the equilibrium expression) and for [OH] from:

$$K_w = \{H\}\{OH\} \quad \text{(Eq. 6f)}$$

(the ionization constant product of water) results in:

$$\{H\} = \frac{K\{HD\}}{K_{sp}}\left(\frac{K\{HD\}}{HY_1} + [X] + \frac{K_w}{\{H\}Y_{OH}} - \frac{\{H\}}{Y_H}\right)Y_M \quad \text{(Eq. 6g)}$$

Rearranging Eq. 6g results in the quadratic equation:

$$\{H\}^2\left(\frac{K_{sp}}{K\{HD\}Y_m} + \frac{1}{Y_H}\right) - \{H\}[X] - \left(\frac{K\{HD\}}{Y_D} + \frac{K_w}{Y_{OH}}\right) = 0 \quad \text{(Eq. 6h)}$$

Solving Eq. 6h for {H} results in the desired equation for a monoprotic weak acid:

$$\{H\} = \frac{[X] + \left[[X]^2 + 4\left(\frac{K_{sp}}{K\{HD\}Y_M} + \frac{1}{Y_H}\right)\left(\frac{K\{HD\}}{Y_D} + \frac{K_w}{Y_{OH}}\right)\right]^{1/2}}{2\left(\frac{K_{sp}}{K\{HD\}Y_M} + \frac{1}{Y_H}\right)} \quad \text{(Eq. 6)}$$

A similar procedure is followed for a monoprotic weak base, but the solubility product is given by Eq. 5 and the charge balance is given by:

$$[M] + [H] + [HD] = [OH] + [X] \quad \text{(Eq. 7a)}$$

Substitution for {HD} from Eq. 5 is made into Eq. 6c and into the resulting equation for {X}. On rearranging and solving the resulting quadratic expression, Eq. 7 is obtained.

APPENDIX III

The equation for the total solubility of a monoprotic weak acid (Eq. 8) in the region saturated by the charged species D can be derived as follows[17]. Starting with Eq. 2 and substituting for {D} from Eq. 4 gives:

$$S_{1,1} = \left(\frac{1}{Y_D} + \frac{\{H\}}{KY_{HD}}\right)\frac{K_{sp}}{\{M\}} \quad \text{(Eq. 8a)}$$

Substituting into Eq. 8a for {M} from the charge balance equation 6b) results in:

$$S_{1,1} = \left(\frac{1}{Y_D} + \frac{\{H\}}{KY_{HD}}\right)K_{sp}/([D] + [X] + [OH] - [H])Y_M \quad \text{(Eq. 8b)}$$

Substituting Eq. 2 into Eq. 8b for [D], the ionization product constant of water (Eq. 6f) for [OH], and the hydrogen ion activity for [H] gives:

$$S_{1,1} = \left(\frac{1}{Y_D} + \frac{\{H\}}{KY_{HD}}\right)K_{sp}\Bigg/\Bigg(\frac{S_{1,1}}{\left(\frac{1}{Y_D} + \frac{\{H\}}{KY_{HD}}\right)Y_{HD}} + [X] + \frac{K_w}{\{H\}Y_{OH}} - \frac{\{H\}}{Y_H}\Bigg)Y_M \quad \text{(Eq. 8c)}$$

Equation 8c can be rearranged to the quadratic equation:

$$S_{1,1}^2\left[\frac{1}{\left(\frac{1}{Y_D} + \frac{\{H\}}{KY_{HD}}\right)Y_{HD}}\right] + S_{1,1}\left([X] + \frac{K_w}{\{H\}Y_{OH}} - \frac{\{H\}}{Y_H}\right) - \frac{K_{sp}}{Y_M}\left(\frac{1}{Y_D} + \frac{\{H\}}{KY_{HD}}\right) = 0 \quad \text{(Eq. 8d)}$$

Solving Eq. 8d for $S_{1,1}$ results in:

$$S_{1,1} = \frac{-\left([X] - \frac{\{H\}}{Y_H} + \frac{K_w}{\{H\}Y_{OH}}\right) + \left[\left([X] - \frac{\{H\}}{Y_H} + \frac{K_w}{\{H\}Y_{OH}}\right)^2 + 4\frac{K_{sp}}{Y_MY_D}\right]^{1/2}}{2\left(\frac{KY_{HD}}{\{H\}Y_D + KY_{HD}}\right)} \quad \text{(Eq. 8)}$$

A similar procedure is followed for a monoprotic weak base to arrive at Eq. 9. Substitutions are made in Eq. 1 for {HD} (from Eq. 5) and for [X] (from

[17] The charges on the ions have not been included in these equations: H and M are +1; OH, D, and X are −1.

the charge balance equation, Eq. 7a). On solving the quadratic equation, Eq. 9 is obtained.

REFERENCES

(1) S. F. Kramer and G. L. Flynn, *J. Pharm. Sci.*, **61**, 1896 (1972).

(2) D. F. Peck and L. Z. Benet, *J. Pharm. Sci.*, **67**, 12 (1978).

(3) Z. T. Chowhan, *J. Pharm. Sci.*, **67**, 1257 (1978).

(4) R. U. Nesbitt, Jr. and B. S. Sandmann, *J. Pharm. Sci.*, **67**, 1012 (1978).

(5) H. A. Krebs and J. C. Speckman, *J. Chem. Soc.*, **1945**, 593.

(6) F. S. Horn and J. Autin, *J. Am. Pharm. Assoc. Sci. Ed.*, **45**, 608 (1956).

(7) H. B. Kostenbauder, F. B. Gable, and A. N. Martin, *J. Am. Pharm. Assoc. Sci. Ed.*, **42**, 210 (1953).

(8) H. L. Johnson and H. L. Leland, *J. Am. Chem. Soc.*, **60**, 1439 (1938).

(9) S. Glasstone, *J. Chem. Soc.*, **119**, 1689 (1921).

(10) E. Berl and G. Austerweil, *Z. Elektrochem.*, **13**, 165 (1907).

(11) H. Goldschmidt and M. Eckardt, *Z. Physikal. Chem.* **56**, 385 (1906).

(12) J. B. Bogardus and R. K. Blackwood, Jr., *J. Pharm. Sci.*, **68**, 188 (1979).

(13) A. L. Green, *J. Pharm. Pharmacol.*, **19**, 10 (1967).

(14) I. Setnikar, *J. Pharm. Sci.*, **55**, 1190 (1966).

(15) R. H. Levy and M. Rowland, *J. Pharm. Sci.*, **60**, 1155 (1971).

(16) R. G. Bates, "Determination of pH, Theory and Practice," Wiley, New York, N.Y., 1973, p. 244.

(17) J. N. Butler, "Ionic Equilibrium: A Mathematical Approach," Addison-Wesley, Reading, Mass., 1964, p. 437.

(18) R. G. Bates, "Determination of pH, Theory and Practice," Wiley, New York, N.Y., 1973, p. 222.

(19) D. D. Perrin, "Dissociation Constants of Organic Bases in Aqueous Solution," Butterworth, London, 1965 (Supplement, 1972).

Pharmacokinetics of Gliclazide in Healthy and Diabetic Subjects

KUNIO KOBAYASHI *x, MASAKO KIMURA *, TAKAFUMI SAKOGUCHI *, AYUMI HASE *, AKIRA MATSUOKA *, and SHIGEO KANEKO ‡

Received May 2, 1983, from the **Department of Clinical Pathology and Clinical Laboratory, Hyogo College of Medicine, Nishinomiya 663, Japan* and ‡*Shinko Hospital, Kobe 651, Japan.* Accepted for publication December 2, 1983.

Abstract □ The pharmacokinetics of total and free gliclazide, 1-(3-azabicyclo[3,3,0]oct-3-yl)-3-(*p*-tolylsulfonyl)urea, a potential hypoglycemic drug, was studied in healthy (n = 12) and diabetic (n = 12) subjects. The serum level of gliclazide was determined by a high-performance liquid chromatographic method (HPLC). The free fraction of gliclazide was obtained from serum by an ultrafiltration technique using a collodion membrane. The mean adsorption of gliclazide to the membrane was ~50% when the membrane was used more than twice. Therefore, the gliclazide level in the filtrate was corrected by doubling the apparent value. The ratio of gliclazide-protein binding remained constant at ~92% in serum after administration to healthy and diabetic subjects. The mean pharmacokinetic parameters of elimination rate (k_e), time to reach the peak level (t_{max}), elimination half-life ($t_{1/2}$), and volume of distribution (Vd) were 0.07 h^{-1}, 2.8 h, 12.3 h, and 17.4 L, respectively. The parameters did not differ significantly between healthy and diabetic subjects or between single and successive administrations; moreover, they did not differ between the free and total drug level. Although there were intersubject variations, the therapeutic effects of oral administration of gliclazide on serum glucose and insulin levels were found in four diabetic patients. The results of this study show that the pharmacokinetics of the total gliclazide level reflect those of the free gliclazide in serum.

Keyphrases □ Gliclazide—protein binding in healthy and diabetic human serum □ Pharmacokinetics—serum gliclazide level after administration in healthy and diabetic subjects □ Ultrafiltration—protein binding of gliclazide in healthy and diabetic human serum

The pharmacokinetic study of serum drug levels is important in the assessment of intrinsic properties of a drug (*e.g.*, absorption, distribution, metabolism, and excretion) to plan effective drug administration. Sulfonylureas, such as tolbutamide and chlorpropamide, bind to several circulating serum proteins (1). In particular, serum albumin strongly interacts with many sulfonylureas (2–4) and other drugs (5). Moreover, free sulfonylureas are the forms that exert the pharmacological effect of hypoglycemic activity (6–8). Therefore, the pharmacokinetics of the free sulfonylurea level in blood may be useful in programming drug administration.

The drug level in a protein-free solution must be measured to determine the free drug level in blood. Ultrafiltration (9), equilibrium dialysis (2, 3, 10), and gel filtration (11) techniques have been used to measure free drug level. Equilibrium dialysis has been commonly used to study the binding of drugs and proteins, but the time required to reach equilibration (8–24 h) is a major disadvantage. Due to simplicity, convenience, and speed, an ultrafiltration technique was used to separate the protein-free phase from serum in the present study.

In this study, a sensitive high-performance liquid chromatographic (HPLC) method (12) was used to determine the total and free levels of gliclazide (13), during a pharmacokinetic study.

EXPERIMENTAL SECTION

Subjects—Twelve male volunteers (age, 32–42 years; weight, 54–72 kg) served as test subjects. All were healthy according to clinical examinations and routine tests. Twelve patients (seven males, five females; age, 35–76 years; weight, 45–80 kg) were patients with maturity-onset diabetes mellitus (FBS: 121–302 mg/100 mL). They did not have impaired renal function, nor hepatic or endocrine disease.

Methods of Drug Administration—One tablet containing 40 mg of gliclazide[1] was administered orally before breakfast to the healthy subjects who had fasted overnight. Blood samples were obtained without an anticoagulant before and at 1, 2, 3, 4, 6, 10, and 24 h after drug administration. After the blood had clotted, the tube was centrifuged at 2500 rpm for 10 min and the supernatant serum was separated. All serum samples were stored at −20°C until use. The volunteers had regular mealtimes throughout the experiment. Twelve diabetic patients were orally administered two tablets containing 40 mg of gliclazide (therapeutic dose) in the morning; eight of them continued to take the drug (40 mg × 2) daily for 7 d. Blood samples were obtained as

[1] Dainippon Pharmaceutical Industries Co., Osaka, Japan.

0022-3549/84/1200-1684$01.00/0

© 1984, American Pharmaceutical Association

the charge balance equation, Eq. 7a). On solving the quadratic equation, Eq. 9 is obtained.

REFERENCES

(1) S. F. Kramer and G. L. Flynn, *J. Pharm. Sci.*, **61**, 1896 (1972).

(2) D. F. Peck and L. Z. Benet, *J. Pharm. Sci.*, **67**, 12 (1978).

(3) Z. T. Chowhan, *J. Pharm. Sci.*, **67**, 1257 (1978).

(4) R. U. Nesbitt, Jr. and B. S. Sandmann, *J. Pharm. Sci.*, **67**, 1012 (1978).

(5) H. A. Krebs and J. C. Speckman, *J. Chem. Soc.*, **1945**, 593.

(6) F. S. Horn and J. Autin, *J. Am. Pharm. Assoc. Sci. Ed.*, **45**, 608 (1956).

(7) H. B. Kostenbauder, F. B. Gable, and A. N. Martin, *J. Am. Pharm. Assoc. Sci. Ed.*, **42**, 210 (1953).

(8) H. L. Johnson and H. L. Leland, *J. Am. Chem. Soc.*, **60**, 1439 (1938).

(9) S. Glasstone, *J. Chem. Soc.*, **119**, 1689 (1921).

(10) E. Berl and G. Austerweil, *Z. Elektrochem.*, **13**, 165 (1907).

(11) H. Goldschmidt and M. Eckardt, *Z. Physikal. Chem.* **56**, 385 (1906).

(12) J. B. Bogardus and R. K. Blackwood, Jr., *J. Pharm. Sci.*, **68**, 188 (1979).

(13) A. L. Green, *J. Pharm. Pharmacol.*, **19**, 10 (1967).

(14) I. Setnikar, *J. Pharm. Sci.*, **55**, 1190 (1966).

(15) R. H. Levy and M. Rowland, *J. Pharm. Sci.*, **60**, 1155 (1971).

(16) R. G. Bates, "Determination of pH, Theory and Practice," Wiley, New York, N.Y., 1973, p. 244.

(17) J. N. Butler, "Ionic Equilibrium: A Mathematical Approach," Addison-Wesley, Reading, Mass., 1964, p. 437.

(18) R. G. Bates, "Determination of pH, Theory and Practice," Wiley, New York, N.Y., 1973, p. 222.

(19) D. D. Perrin, "Dissociation Constants of Organic Bases in Aqueous Solution," Butterworth, London, 1965 (Supplement, 1972).

Pharmacokinetics of Gliclazide in Healthy and Diabetic Subjects

KUNIO KOBAYASHI *x, MASAKO KIMURA *, TAKAFUMI SAKOGUCHI *, AYUMI HASE *, AKIRA MATSUOKA *, and SHIGEO KANEKO ‡

Received May 2, 1983, from the **Department of Clinical Pathology and Clinical Laboratory, Hyogo College of Medicine, Nishinomiya 663, Japan* and ‡*Shinko Hospital, Kobe 651, Japan.* Accepted for publication December 2, 1983.

Abstract □ The pharmacokinetics of total and free gliclazide, 1-(3-azabicyclo[3,3,0]oct-3-yl)-3-(*p*-tolylsulfonyl)urea, a potential hypoglycemic drug, was studied in healthy (n = 12) and diabetic (n = 12) subjects. The serum level of gliclazide was determined by a high-performance liquid chromatographic method (HPLC). The free fraction of gliclazide was obtained from serum by an ultrafiltration technique using a collodion membrane. The mean adsorption of gliclazide to the membrane was ~50% when the membrane was used more than twice. Therefore, the gliclazide level in the filtrate was corrected by doubling the apparent value. The ratio of gliclazide-protein binding remained constant at ~92% in serum after administration to healthy and diabetic subjects. The mean pharmacokinetic parameters of elimination rate (k_e), time to reach the peak level (t_{max}), elimination half-life ($t_{1/2}$), and volume of distribution (Vd) were 0.07 h^{-1}, 2.8 h, 12.3 h, and 17.4 L, respectively. The parameters did not differ significantly between healthy and diabetic subjects or between single and successive administrations; moreover, they did not differ between the free and total drug level. Although there were intersubject variations, the therapeutic effects of oral administration of gliclazide on serum glucose and insulin levels were found in four diabetic patients. The results of this study show that the pharmacokinetics of the total gliclazide level reflect those of the free gliclazide in serum.

Keyphrases □ Gliclazide—protein binding in healthy and diabetic human serum □ Pharmacokinetics—serum gliclazide level after administration in healthy and diabetic subjects □ Ultrafiltration—protein binding of gliclazide in healthy and diabetic human serum

The pharmacokinetic study of serum drug levels is important in the assessment of intrinsic properties of a drug (*e.g.*, absorption, distribution, metabolism, and excretion) to plan effective drug administration. Sulfonylureas, such as tolbutamide and chlorpropamide, bind to several circulating serum proteins (1). In particular, serum albumin strongly interacts with many sulfonylureas (2–4) and other drugs (5). Moreover, free sulfonylureas are the forms that exert the pharmacological effect of hypoglycemic activity (6–8). Therefore, the pharmacokinetics of the free sulfonylurea level in blood may be useful in programming drug administration.

The drug level in a protein-free solution must be measured to determine the free drug level in blood. Ultrafiltration (9), equilibrium dialysis (2, 3, 10), and gel filtration (11) techniques have been used to measure free drug level. Equilibrium dialysis has been commonly used to study the binding of drugs and proteins, but the time required to reach equilibration (8–24 h) is a major disadvantage. Due to simplicity, convenience, and speed, an ultrafiltration technique was used to separate the protein-free phase from serum in the present study.

In this study, a sensitive high-performance liquid chromatographic (HPLC) method (12) was used to determine the total and free levels of gliclazide (13), during a pharmacokinetic study.

EXPERIMENTAL SECTION

Subjects—Twelve male volunteers (age, 32–42 years; weight, 54–72 kg) served as test subjects. All were healthy according to clinical examinations and routine tests. Twelve patients (seven males, five females; age, 35–76 years; weight, 45–80 kg) were patients with maturity-onset diabetes mellitus (FBS: 121–302 mg/100 mL). They did not have impaired renal function, nor hepatic or endocrine disease.

Methods of Drug Administration—One tablet containing 40 mg of gliclazide[1] was administered orally before breakfast to the healthy subjects who had fasted overnight. Blood samples were obtained without an anticoagulant before and at 1, 2, 3, 4, 6, 10, and 24 h after drug administration. After the blood had clotted, the tube was centrifuged at 2500 rpm for 10 min and the supernatant serum was separated. All serum samples were stored at −20°C until use. The volunteers had regular mealtimes throughout the experiment. Twelve diabetic patients were orally administered two tablets containing 40 mg of gliclazide (therapeutic dose) in the morning; eight of them continued to take the drug (40 mg × 2) daily for 7 d. Blood samples were obtained as

[1] Dainippon Pharmaceutical Industries Co., Osaka, Japan.

0022-3549/84/1200-1684$01.00/0

© 1984, American Pharmaceutical Association

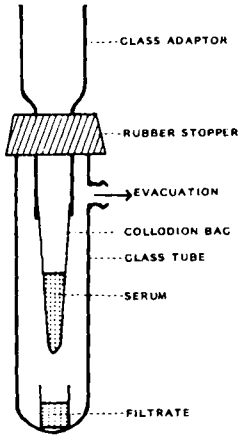

Figure 1—*Ultrafiltration assembly.*

described for the healthy subjects before drug administration and at 1, 2, 4, 6, 8, 12, and 24 h or 2, 6, and 24 h after administration.

Ultrafiltration—Ultrafiltration was performed using the apparatus shown in Fig. 1. A collodion bag[2] with an M_r cutoff of 13,200 was soaked in distilled water overnight before use. The serum samples (3 mL) were ultrafiltrated under reduced pressure (40 mm Hg) at room temperature (25–27°C). The extent of drug–membrane binding was assessed with the same apparatus by substituting 0.066 M phosphate buffer (pH 7.4) containing various concentrations of gliclazide (3–20 μg/mL) for serum. The concentration of free gliclazide in the filtrate (1–2 mL) was determined by HPLC (12). The same collodion bag was used repeatedly by washing with distilled water. Gliclazide level in the filtrate was corrected by doubling the apparent concentration based on the results of a drug-absorption experiment.

Measurements of Serum Gliclazide and Blood Glucose and Insulin Levels—The serum gliclazide level was determined by HPLC[3] (12). The free gliclazide level in the serum was found by determining the level in the filtrate that had passed through a collodion membrane filter at room temperature (25–27°C). Blood glucose and insulin (immunoreactive insulin) levels were measured with an autoanalyzer[4] and a single-antibody RIA (polyethylene glycol method) (14), respectively.

Calculations—Several pharmacokinetic parameters including the elimination rate (k_e, h^{-1}), the elimination half-life ($t_{1/2}$, h), and the area under the serum drug concentration curve (AUC_{0-24}, $\mu g \cdot h \cdot mL^{-1}$) from 0 to 24 h were calculated by conventional methods, and the peak level (C_{max}, μg/mL) and the time to reach the peak level (t_{max}, h) were graphically estimated from the decay curve. The volume of distribution (Vd) was calculated from the following equation proposed by Gibaldi *et al.*: $Vd = \text{dose}/\int_0^\infty C_p dt \cdot k_e^{-1}$, where dose, C_p, $\int_0^\infty C_p dt$, and k_e are the dose of administered drug, the serum level of drug, the area under the serum concentration curve ($AUC_{0-\infty}$), and the elimination rate, respectively. The Student's t test was used for statistical comparisons.

RESULTS AND DISCUSSION

The ultrafiltration techniques using a membrane filter[5] and a collodion membrane were tested for the measurement of free drug level. We chose a collodion membrane for the ultrafiltration because it was more convenient for multisample measurements and was more mechanically stable than other membranes. Many drugs, including sulfonylureas, are adsorbed on the membrane filter during ultrafiltration. We found that the degree of drug adsorption varies with use. We examined the recovery of gliclazide that had filtered through the collodion membrane (Table I). When a fresh membrane was used for the ultrafiltration, the mean recovery of gliclazide in the filtrate was ~27% of the original concentration (3–20 μg/mL). The recovery of gliclazide remained at ~50% when the membrane was used more than twice. If a constant amount of gliclazide was adsorbed in the membrane, the recovery would decrease with low concentrations, but this was not observed; thus, even when the gliclazide concentration was low, the binding constant between the drug and membrane filter remained the same. Based on the result from the drug-absorption experiment, the free gliclazide level in serum was measured by ultrafiltrating the serum sample (using the collodion membrane one time). The gliclazide level in the filtrate was corrected by doubling the apparent concentration.

Table I—Effect of Reuse of Collodion Membrane on Recovery of Gliclazide

	Recovery of Drug in Filtrate, %[b]				
	Original Conc. of Gliclazide, μg/mL				
n[a]	3	5	10	20	Mean ± *SD*
1	31.1	24.5	24.3	28.3	27.1 ± 3.3
2	51.1	45.6	51.4	49.8	49.5 ± 2.7
3	53.7	47.9	50.3	48.5	50.1 ± 2.6
4	56.7	40.6	--	51.5	49.6 ± 8.2
5	50.0	30.7	–	55.8	45.5 ± 13.1

[a] Number of times membrane was used for ultrafiltration. [b] Each value represents the mean of 2–4 experiments. The ultrafiltration was carried out at room temperature (25–27°C).

Although it is known that the pharmacological activity of a sulfonylurea is exerted by free drug in the blood (6), to our knowledge no information on the pharmacokinetics of free sulfonylurea level in the serum has been reported. The decay curve and the pharmacokinetic data for the free gliclazide levels in healthy and diabetic subjects are demonstrated in the present paper. The decay curves of total and free gliclazide levels in the healthy volunteers orally administered the drug (40 mg of gliclazide) are shown in Fig. 2. Individual variation in serum gliclazide level and the time to reach the peak level (t_{max}) was large. The mean values of t_{max} for the total and free gliclazide levels in the healthy subjects were 2.8 and 2.7 h, respectively (Table II). The C_{max} and AUC_{0-24} for the total gliclazide level in the healthy subjects were 2.8 μg/mL and 37.2 $\mu g \cdot h \cdot mL^{-1}$ (40 mg of gliclazide). The mean ratio of free drug level (D_f) to total drug level (D_t) was ~8% during the 24-h period after gliclazide administration. We have reported that the value of C_{max} for the free gliclazide level was 0.11 μg/mL (4) which was half the amount in the present study (0.22 μg/mL). The apparent gliclazide concentration in the filtrate was not corrected, in the former study, for the amount adsorbed to the collodion membrane during ultrafiltration.

Decay curves of blood gliclazide level in diabetic patients who took single and successive administrations of the drug (80 mg/d) are shown in Fig. 3. The decay curve in the single administration had a profile similar to that of the healthy subjects, except for the C_{max} and the drug level 24 h after drug administration. In the case of successive oral administrations of the drug for 7

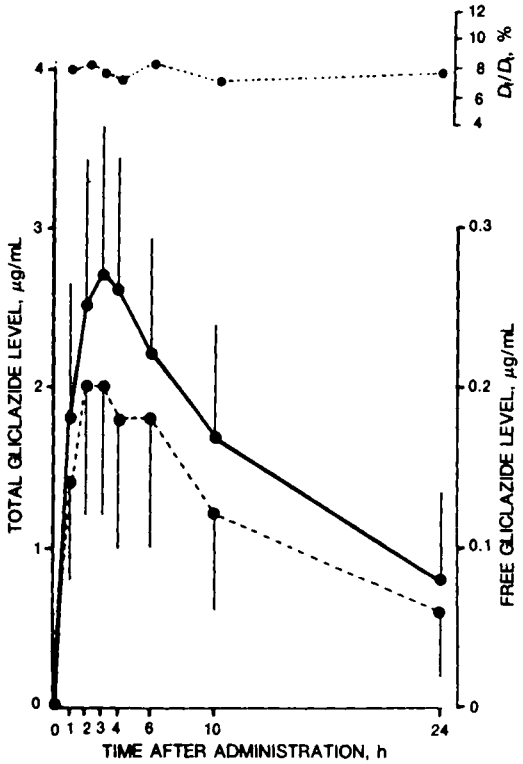

Figure 2—*Decay curves of total (—) and free gliclazide levels (---) in healthy subjects (n = 6). Each point represents the mean; the bar, SD.*

[2] Collodion bags, SM-13200; Sartorius GmbH, 3400 Göttingen, FRG.
[3] High-pressure liquid chromatograph, TRIROTAR-II; Japan Spectroscopic Co., Ltd., Tokyo, Japan.
[4] Autoanalyzer-II; Technicon Instruments Co., Tarrytown, N.Y.
[5] YMB membrane MPS-1; Micropartition system; Amicon, Ltd., Mass.

Table II—Pharmacokinetic Parameters Obtained after Oral Administration of Gliclazide [a]

Method of Administration	Parameters						
	k_e, h^{-1}	C_{max}, μg/mL	t_{max}, h	$t_{1/2}$, h	AUC_{0-24}, μg·h·mL^{-1}	Vd_β, L	n
			Healthy Subject				
Single Dose							
D_t	0.07 ± 0.03	2.8 ± 0.8	2.8 ± 0.9	12.3 ± 6.0	37.2 ± 13.1	17.4 ± 6.7	12
D_f	0.07 ± 0.04	0.22 ± 0.06	2.7 ± 0.8	12.0 ± 0.8	2.8 ± 1.16		6
			Diabetic Subject				
Single Dose							
D_t	0.07 ± 0.02	4.5 ± 2.2	3.0 ± 1.9	11.6 ± 5.2	71.8 ± 6.8	17.9 ± 8.3	12
Successive Dose							
D_t	0.07 ± 0.01 [b]	7.7 ± 2.0 [c]	3.3 ± 1.5 [b]	11.4 ± 2.7 [b]	92.5 ± 19.5 [d]	14.2 ± 7.9	8

[a] Values are mean ± *SD*. [b] Not significantly different from single dose. [c] Significantly different from single dose ($p < 0.1$). [d] Significantly different from single dose ($p < 0.01$).

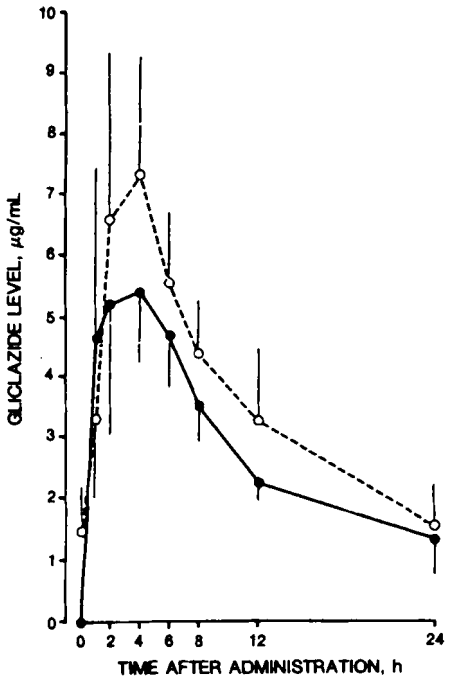

Figure 3—*Decay curves of total gliclazide level in diabetic patients. Each point represents the mean* ± SD *in seven patients who were administered a single dose of gliclazide (80 mg) (●), and four patients who took successive administration of gliclazide (80 mg/d) for 7 d (○).*

d, t_{max} = 3.3 h, was longer compared with 3.0 h for the single administration. The subjects also had higher levels of C_{max} (7.7 μg/mL) and AUC_{0-24} (92.5 μg·h·mL^{-1}) (Table II).

The decay curves of total and free serum gliclazide levels were examined in diabetic patients (Figs. 4A and B). A perfect decay curve for the free gliclazide level in the diabetic patients was not obtained because the amount of serum sample required for the ultrafiltration could not be repeatedly taken. Thus, the pharmacokinetic parameters could not be obtained by computer calculation (Table II). From the available data, the value of t_{max} for total drug level in the diabetic patients was almost equal to that in the healthy volunteers.

The total gliclazide levels reached a maximum (~7.7 μg/mL) 2 h after successive administration, which was higher than that obtained by single administration (4.5 μg/mL at 6 h). The values of C_{max} for free gliclazide levels were nearly equal for the different administration methods (0.47–0.55 μg/mL). The ratio of free drug level (D_f) to total drug level (D_t) in the diabetic subjects administered a single dose was ~8–9%, but the ratio in the diabetic subjects administered successive doses was lower (~7%).

The apparent volume of distribution (Vd) is important in the pharmacokinetic characterization of drugs. However, the calculation of volume of distribution is based on many assumptions and cannot, therefore, be estimated with a high degree of accuracy. Gibaldi *et al.* demonstrated that the volume of distribution was identical to the apparent volume of distribution obtained from the area under the serum concentration curve (AUC) determined by the equation for a two-compartment (α and β) open system (15). The volume of distribution (Vd_β) of gliclazide in healthy and diabetic subjects was 14.2–17.9 L (Table II). There was large intersubject variation in Vd but this could be due to variations in total adsorption that is known to occur with sulfonylureas. The distribution of gliclazide with high protein binding was expected to be confined more to the serum or extracellular fluid volume, as is the case of tolbutamide and chlorpropamide (16).

Effects of oral administration of gliclazide on blood glucose and insulin levels in four diabetic patients (A, B, C, and D) are summarized in Table III. The range of fasting blood glucose levels for the patient was 100–302 mg/100 mL. Although there are intersubject variations, the values of 24-h cumulative blood glucose levels were lowered by the administration of gliclazide (Δ, −177 to −1081 mg/100 mL, determined eight times in 24 h). On the other hand,

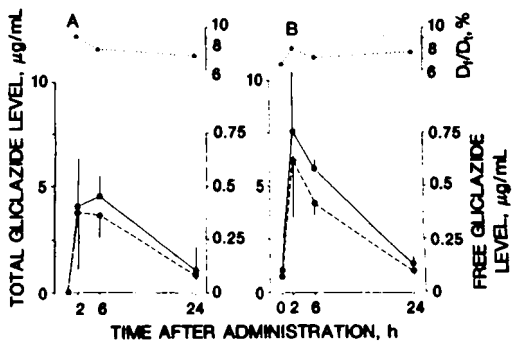

Figure 4—*Decay curves of total (—) and free gliclazide levels (- - -) in diabetic patients, who took single (A) and successive administrations (B) of gliclazide. Each point represents the mean* ± SD *in 3–4 diabetic patients.*

Table III—Effect of Oral Administration of Gliclazide on Blood Glucose and Insulin Levels in Diabetic Patients

Subject	FBS, mg/100 mL [a]	ΣBS, mg/100 mL [a]			ΣIRI, μU/mL [a]			ΣDrug, μg/mL [a]
		Predose	Postdose	Δ	Predose	Postdose	Δ	
A	302	3511	2430	−1081	128	221	+93	35.8
B	100	885	708	−177	—	—	—	26.1
C	224	2153	1406	−747	97	127	+30	24.7
C* [b]	224	2153	1176	−977	97	133	+36	32.2
D	121	1633	1075	−558	—	—	—	31.9

[a] FBS shows the fasting blood glucose level. ΣBS, ΣIRI, and ΣDrug, respectively, shows the sum level of blood glucose, immunoreactive insulin, and serum gliclazide determined eight times through 24 h. [b] C* is a diabetic patient administered gliclazide successively for 7 d.

the values of 24-h cumulative blood insulin levels were increased by the administration of the drug (Δ, 30-93 μU/mL), resulting in the stimulation of insulin release from pancreatic B cells in all cases. The difference between single and successive administration on cumulative blood glucose levels and cumulative blood insulin levels was not significant in patient C (Table III, footnote *b*).

REFERENCES

(1) K. Kakemi, H. Sezaki, T. Komuro, K. Ikeda, and H. Kishi, *Chem. Pharm. Bull.*, **18**, 2386 (1970).

(2) H. Wishinsky, E. J. Glasser, and S. Perkal, *Diabetes*, **11** (Suppl.), 18 (1962).

(3) S. Goto, H. Yoshitomi, and M. Nakase, *Chem. Pharm. Bull.*, **26**, 472 (1978).

(4) K. Kobayashi, M. Kimura, T. Sakoguchi, Y. Kitani, M. Hata, and A. Matsuoka, *J. Pharm. Dyn.*, **4**, 436 (1981).

(5) M. Nakagaki, N. Koga, and H. Terada, *Yakugaku Zasshi*, **83**, 536 (1963).

(6) R. Tompsett, S. Shultz, and W. McDermott, *J. Bacteriol.*, **53**, 581 (1947).

(7) A. H. Anton, *J. Pharmacol. Exp. Ther.*, **129**, 282 (1960).

(8) H. Neurat and K. Bailey, "The Proteins," vol. I, part B, Academic, New York, N.Y., 1953.

(9) V. P. Shah, S. M. Wallace, and S. Riegelman, *J. Pharm. Sci.*, **63**, 1364 (1974).

(10) M. J. Crooks and K. F. Brown, *J. Pharm. Sci.*, **62**, 1904 (1973).

(11) J. P. Hummel and W. J. Dreyer, *Biochim. Biophys. Acta*, **63**, 530 (1962).

(12) M. Kimura, K. Kobayashi, M. Hata, A. Matsuoka, H. Kitamura, and Y. Kimura, *J. Chromatogr.*, **183**, 467 (1980).

(13) L. G. Beregi, "Gliclazide and the Treatment of Diabetes," H. Keen, A. D. S. Caldwell, M. Murphy, and C. Bowker, Eds., Royal Society of Medicine, London, 1980, pp. 5-8.

(14) K. Kobayashi, T. Mochizuki, T. Ichiki, M. Hata, and A. Matsuoka, *Acta Med. Hyogoensia*, **3**, 283 (1978).

(15) M. Gibaldi, R. Nagashima, and G. Levy, *J. Pharm. Sci.*, **58**, 193 (1969).

(16) P. C. Johnson, R. H. Hennes, T. Driscoll, and K. M. West, *Ann. N.Y. Acad. Sci.*, **74**, 459 (1959).

ACKNOWLEDGMENTS

The authors are grateful to Dr. James E. Chaney of the College of Pharmacy, University of Kentucky for suggestions and reviewing our manuscript.

Secondary Antithyroid Action of Drugs in Relation to Structure

J. BUXERAUD ˣ, A. C. ABSIL, and C. RABY

Received July 13, 1982, from the *Department of Chimica Therapeutica, Faculty of Medicine and Pharmacy, 87032 Limoges Cedex, France.* Accepted for publication November 29, 1983.

Abstract □ Molecular interactions between iodine and disulfiram, clomethiazole, and tolnaftate were investigated by electron spectroscopy. Iodine forms charge transfer complexes with these molecules, with 1:1 stoichiometry and of the n-σ type. The formation constants were compared with those obtained with antithyroid molecules. Only disulfiram appears to have any effect on the intrathyroid cycle of iodine.

Keyphrases □ Charge transfer complexes—iodine and disulfiram, clomethiazole, tolnaftate □ Disulfiram—charge transfer complexes with iodine □ Clomethiazole—charge transfer complexes, iodine □ Tolnaftate—charge transfer complexes, iodine

It has been shown that molecules possessing an NCS moiety can form charge transfer complexes with iodine (1, 2). Both qualitative and quantitative studies have shown that certain antithyroid drugs (those possessing the NCS function) form charge transfer complexes involving the transfer of charge from the pair of free electrons on the nitrogen and/or the sulfur atoms to the antibonding orbital of the iodine (3, 4). The intensity of this action can be determined from the complex formation constant and the thermodynamic parameters. A correlation has been demonstrated between the constant (K_c) and antithyroid activity (5). A structure-activity relationship has been developed to classify all known antithyroid molecules (6). Iodine fixation by complex formation is one action mechanism of synthetic antithyroid agents.

Synthetic antithyroid drugs can also inhibit peroxidase (7). This enzyme is necessary for the oxidation of circulating iodine, for its integration into thyroglobulin, and for coupling monoiodotyrosines and diiodotyrosines to form triiodotyronines (T_3) and tetraiodothyronines (T_4). While antithyroid agents display variable activity towards peroxidase, they can all complex iodine, so that the latter is unavailable for thyroid hormone synthesis.

This NCS function is found in many drugs belonging to other therapeutic classes. Hence, if we hope to understand biological activity it is important to investigate the possible formation of complexes between these molecules (tolnaftate, disulfiram, and clomethiazole) and iodine. This can help determine whether these molecules possess secondary antithyroid activity.

EXPERIMENTAL SECTION

Materials—An ultrapure iodine was prepared by sublimation and stored in a desiccator containing P_2O_5. Disulfiram[1] [tetraethylthioperoxydicarbonic diamide (I)], tolnaftate[2] [*O*-2-napthyl-*m*,*N*-dimethylthiocarbanilate (II)], and clomethiazole[3] [5-(2-chloroethyl)-4-methylthiazole (III)] were pharmaceutical grade; purity was determined by HPLC[4]. UV-grade carbon tetrachloride[5] was used.

UV and visible spectra were recorded on a double-beam spectrophotometer[6] equipped with a Peltier effect thermoelectric cell holder. Hellma quartz cells with a path length of 1 cm were employed.

Methods—The glassware was thoroughly dried with dry nitrogen to eliminate any effects due to hydration of the complex solutions. Volumetric solutions were prepared from initial solutions obtained by weighing. The spectra were recorded immediately after solution preparation.

[1] Millot; Solac Laboratories, Paris, France.
[2] Unicet; Cetrane Laboratories, Levallois-Perret, France.
[3] Debat Laboratories, Paris, France.
[4] Model 244 U/45; Waters, S.A. Paris, France.
[5] Merck uvasol Art. 2209; E. Merck, Darmstadt.
[6] Model 554 UV-Vis; Perkin-Elmer.

0022-3549/84/1200-1687$01.00/0

© 1984, American Pharmaceutical Association

the values of 24-h cumulative blood insulin levels were increased by the administration of the drug (Δ, 30-93 μU/mL), resulting in the stimulation of insulin release from pancreatic B cells in all cases. The difference between single and successive administration on cumulative blood glucose levels and cumulative blood insulin levels was not significant in patient C (Table III, footnote *b*).

REFERENCES

(1) K. Kakemi, H. Sezaki, T. Komuro, K. Ikeda, and H. Kishi, *Chem. Pharm. Bull.*, **18**, 2386 (1970).

(2) H. Wishinsky, E. J. Glasser, and S. Perkal, *Diabetes*, **11** (Suppl.), 18 (1962).

(3) S. Goto, H. Yoshitomi, and M. Nakase, *Chem. Pharm. Bull.*, **26**, 472 (1978).

(4) K. Kobayashi, M. Kimura, T. Sakoguchi, Y. Kitani, M. Hata, and A. Matsuoka, *J. Pharm. Dyn.*, **4**, 436 (1981).

(5) M. Nakagaki, N. Koga, and H. Terada, *Yakugaku Zasshi*, **83**, 536 (1963).

(6) R. Tompsett, S. Shultz, and W. McDermott, *J. Bacteriol.*, **53**, 581 (1947).

(7) A. H. Anton, *J. Pharmacol. Exp. Ther.*, **129**, 282 (1960).

(8) H. Neurat and K. Bailey, "The Proteins," vol. I, part B, Academic, New York, N.Y., 1953.

(9) V. P. Shah, S. M. Wallace, and S. Riegelman, *J. Pharm. Sci.*, **63**, 1364 (1974).

(10) M. J. Crooks and K. F. Brown, *J. Pharm. Sci.*, **62**, 1904 (1973).

(11) J. P. Hummel and W. J. Dreyer, *Biochim. Biophys. Acta*, **63**, 530 (1962).

(12) M. Kimura, K. Kobayashi, M. Hata, A. Matsuoka, H. Kitamura, and Y. Kimura, *J. Chromatogr.*, **183**, 467 (1980).

(13) L. G. Beregi, "Gliclazide and the Treatment of Diabetes," H. Keen, A. D. S. Caldwell, M. Murphy, and C. Bowker, Eds., Royal Society of Medicine, London, 1980, pp. 5-8.

(14) K. Kobayashi, T. Mochizuki, T. Ichiki, M. Hata, and A. Matsuoka, *Acta Med. Hyogoensia*, **3**, 283 (1978).

(15) M. Gibaldi, R. Nagashima, and G. Levy, *J. Pharm. Sci.*, **58**, 193 (1969).

(16) P. C. Johnson, R. H. Hennes, T. Driscoll, and K. M. West, *Ann. N.Y. Acad. Sci.*, **74**, 459 (1959).

ACKNOWLEDGMENTS

The authors are grateful to Dr. James E. Chaney of the College of Pharmacy, University of Kentucky for suggestions and reviewing our manuscript.

Secondary Antithyroid Action of Drugs in Relation to Structure

J. BUXERAUD ˣ, A. C. ABSIL, and C. RABY

Received July 13, 1982, from the *Department of Chimica Therapeutica, Faculty of Medicine and Pharmacy, 87032 Limoges Cedex, France.* Accepted for publication November 29, 1983.

Abstract □ Molecular interactions between iodine and disulfiram, clomethiazole, and tolnaftate were investigated by electron spectroscopy. Iodine forms charge transfer complexes with these molecules, with 1:1 stoichiometry and of the n-σ type. The formation constants were compared with those obtained with antithyroid molecules. Only disulfiram appears to have any effect on the intrathyroid cycle of iodine.

Keyphrases □ Charge transfer complexes—iodine and disulfiram, clomethiazole, tolnaftate □ Disulfiram—charge transfer complexes with iodine □ Clomethiazole—charge transfer complexes, iodine □ Tolnaftate—charge transfer complexes, iodine

It has been shown that molecules possessing an NCS moiety can form charge transfer complexes with iodine (1, 2). Both qualitative and quantitative studies have shown that certain antithyroid drugs (those possessing the NCS function) form charge transfer complexes involving the transfer of charge from the pair of free electrons on the nitrogen and/or the sulfur atoms to the antibonding orbital of the iodine (3, 4). The intensity of this action can be determined from the complex formation constant and the thermodynamic parameters. A correlation has been demonstrated between the constant (K_c) and antithyroid activity (5). A structure-activity relationship has been developed to classify all known antithyroid molecules (6). Iodine fixation by complex formation is one action mechanism of synthetic antithyroid agents.

Synthetic antithyroid drugs can also inhibit peroxidase (7). This enzyme is necessary for the oxidation of circulating iodine, for its integration into thyroglobulin, and for coupling monoiodotyrosines and diiodotyrosines to form triiodotyronines (T_3) and tetraiodothyronines (T_4). While antithyroid agents display variable activity towards peroxidase, they can all complex iodine, so that the latter is unavailable for thyroid hormone synthesis.

This NCS function is found in many drugs belonging to other therapeutic classes. Hence, if we hope to understand biological activity it is important to investigate the possible formation of complexes between these molecules (tolnaftate, disulfiram, and clomethiazole) and iodine. This can help determine whether these molecules possess secondary antithyroid activity.

EXPERIMENTAL SECTION

Materials—An ultrapure iodine was prepared by sublimation and stored in a desiccator containing P_2O_5. Disulfiram[1] [tetraethylthioperoxydicarbonic diamide (I)], tolnaftate[2] [*O*-2-napthyl-*m*,*N*-dimethylthiocarbanilate (II)], and clomethiazole[3] [5-(2-chloroethyl)-4-methylthiazole (III)] were pharmaceutical grade; purity was determined by HPLC[4]. UV-grade carbon tetrachloride[5] was used.

UV and visible spectra were recorded on a double-beam spectrophotometer[6] equipped with a Peltier effect thermoelectric cell holder. Hellma quartz cells with a path length of 1 cm were employed.

Methods—The glassware was thoroughly dried with dry nitrogen to eliminate any effects due to hydration of the complex solutions. Volumetric solutions were prepared from initial solutions obtained by weighing. The spectra were recorded immediately after solution preparation.

[1] Millot; Solac Laboratories, Paris, France.
[2] Unicet; Cetrane Laboratories, Levallois-Perret, France.
[3] Debat Laboratories, Paris, France.
[4] Model 244 U/45; Waters, S.A. Paris, France.
[5] Merck uvasol Art. 2209; E. Merck, Darmstadt.
[6] Model 554 UV-Vis; Perkin-Elmer.

0022-3549/84/1200-1687$01.00/0

© 1984, American Pharmaceutical Association

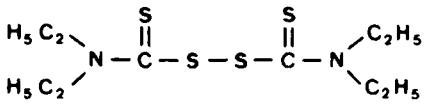

I

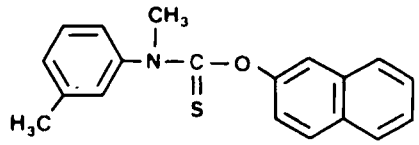

II

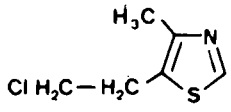

III

For all equilibrium constant calculations, a series of complex solutions were used with a constant iodine concentration and a variable donor concentration. The solutions were dilute ($\sim 10^{-4}$ M for iodine, $< 5 \times 10^{-2}$ M for tolnaftate and clomethiazole, and $< 4 \times 10^{-3}$ M for disulfiram). Optical densities were determined at three temperatures, 10°C, 20°C, and 30°C (± 0.1°C).

RESULTS

Visible Region— Iodine in solutions of carbon tetrachloride displayed an absorption peak at 515 nm. The donors displayed negligible absorption in the 350–700-nm region. All the complex solution spectra showed a disturbance of the visible band of the halogen consisting of a hypsochromic displacement ($\Delta\lambda$) of the $\pi g \rightarrow \tau_0$ transition of iodine (Fig. 1).

The stability of the complexes was examined by making new recordings after 24 h. Each of the three systems exhibited new absorption bands at 290 and 360 nm, characterizing the presence of I_3^- ions. The changes were greater with higher donor concentrations.

The 1:1 stoichiometry of the complexes was confirmed by analysis of the absorption bands, the accuracy of measurements, and the isosbestic points observed. However, this stoichiometry was checked experimentally by Job's method of continuous variations (8). To do this, the optical densities of the series of complex solutions with constant donor and iodine concentrations were recorded. A correction was made by subtracting from the optical densities recorded, the optical densities of donor and iodine solutions of the same concentration as in the complex solution:

$$A_{corr} = A_{obs} - \epsilon_D \cdot [D] - \epsilon_{I_2} \cdot [I_2] \qquad \text{(Eq. 1)}$$

where A_{corr} is the corrected optical density of the complex, A_{obs} is the optical density of the donor–iodine mixture, ϵ_D and ϵ_{I_2} are the molar absorption coefficients of the donor and iodine, and [D] and [I_2] are the donor and acceptor concentrations, respectively.

The curve obtained by plotting these optical densities for each complex solution against the iodine molar fractions displays a maximum for equal donor and iodine concentrations. The position of the maximum and the perfect symmetry of the curve confirms the presence of a complex with 1:1 stoichiometry and excludes the presence of higher-order complexes (Fig. 2).

The formation constants (K_c) and the absorption coefficients (ϵ_c) of the three donor–iodine systems investigated are given in Table I. These values were determined by using:

$$K_c = \frac{[C]}{([A_0] - [C])([D_0] - [C])} \qquad \text{(Eq. 2)}$$

where [C] is the complex concentration, [A_0] the initial iodine concentration, and [D_0] is the initial donor concentration. [C] can be replaced by the term d_c/ϵ_c leading to:

$$\frac{[A_0][D_0]}{d_c} = \left([A_0] + [D_0] - \frac{d_c}{\epsilon_c}\right) \cdot \frac{1}{\epsilon_c} + \frac{1}{K_c \epsilon_c} \qquad \text{(Eq. 3)}$$

where, at the wavelength investigated, d_c is the absorption of the complex only, ϵ_c is the molar absorption coefficient of the complex, and K_c is the complex formation constant. Equation (3) was resolved by computer using the least-squares method. Graphic representation of the term $[A_0][D_0]/d_c$ as a function of $[A_0] + [D_0] - (d_c/\epsilon_c)$ produces a line with a slope of $1/\epsilon_c$ and an intercept of $1/K_c$ (Fig. 3).

Graphic representation of $R \log K_c$ *versus* $1/T$ yields a line whose slope provides the value of $\Delta H°$, and the intercept determines the value of $\Delta S°$ (Fig.

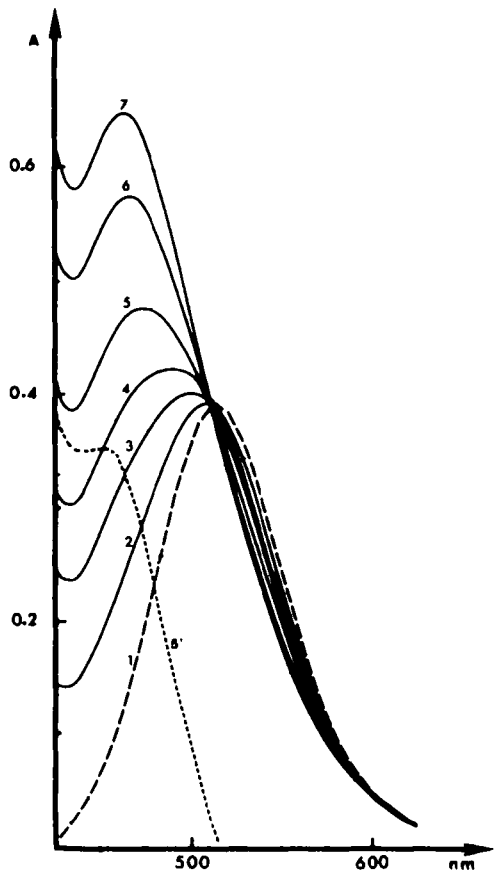

Figure 1—*Visible absorption spectra of disulfiram–iodine complex (solvent, carbon tetrachloride, temperature 20 ± 0.1°C). Key: (1) 4.242 × 10^{-4} M iodine; (2) 4.242 × 10^{-4} M iodine and 0.434 × 10^{-4} M disulfiram; (3) 4.242 × 10^{-4} M iodine and 0.868 × 10^{-3} M disulfiram; (4) 4.242 × 10^{-4} M iodine and 1.216 × 10^{-3} M disulfiram; (5) 4.242 × 10^{-4} M iodine and 1.737 × 10^{-3} M disulfiram; (6) 4.242 × 10^{-4} M iodine and 2.605 × 10^{-3} M disulfiram; (7) 4.242 × 10^{-4} M iodine and 3.473 × 10^{-3} M disulfiram; (5′) absorption curve of complex obtained for solution 5 by placing a 4.242 × 10^{-4} M iodine solution in the reference beam.*

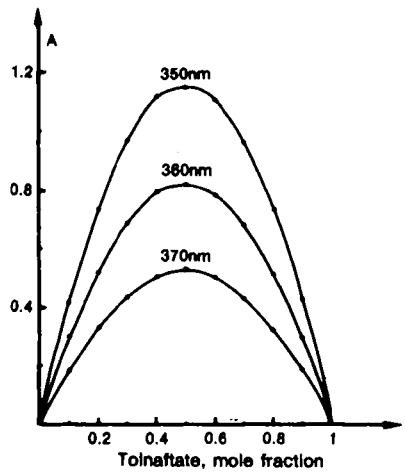

Figure 2—*Determination of stoichiometry of the tolnaftate–iodine complex by the method of continuous variations (solvent, carbon tetrachloride, temperature 20 ± 0.1°C). For each complex solution, the sum of tolnaftate and iodine concentrations is constant and equal to 18.8 × 10^{-4} M.*

Table I—Formation Constants and Molar Extinction Coefficients for Iodine Complexes in Solution in Carbon Tetrachloride[a]

Donor	nm	C, $L \cdot M^{-1} cm^{-1}$ [e]	Complex Formation Constant (K_c), $L \cdot M^{-1}$ [e]	Mean K_c
Tolnaftate[b]	455	57.38	2136	
	460	57.07	2110	
	465	55.78	2040	
	470	57.88	1855	56.65 ± 0.96
	475	55.76	1692	
	480	55.69	1466	
	485	56.56	1209	
Disulfiram[c]	460	300.51	2599	
	465	298.39	2484	
	470	288.81	2340	296.78 ± 4.44
	475	298.36	2068	
	480	298.45	1799	
	485	292.40	1520	
	490	300.51	1195	
Clomethiazole[d]	410	24.96	1231	
	415	24.84	1305	
	420	24.84	1337	
	425	25.32	1343	25.00 ± 0.19
	430	25.17	1321	
	435	24.83	1283	
	440	25.07	1203	

[a] At 20 ± 0.1°C. [b] Six different tolnaftate-I_2 solutions; $[I_2]$ 4.438 × 10^{-4} M; [tolnaftate] varied from 0.229 × 10^{-2} M to 1.836 × 10^{-2} M. [c] Six different disulfiram-I_2 solutions; $[I_2]$ 4.242 × 10^{-4} M; [disulfiram] varied from 0.434 × 10^{-3} M to 3.473 × 10^{-4} M. [d] Five different clomethiazole-I_2 solutions; $[I_2]$ 4.580 × 10^{-4} M; [clomethiazole] varied from 1.093 × 10^{-2} M to 5.467 × 10^{-2} M. [e] Values were calculated from absorption data in the visible region.

4). The thermodynamic parameters related to the formation of the complex are given in Table II.

Ultraviolet Region—The donors displayed strong absorption in the UV region (Table III), whereas iodine exhibited weak absorption. The high values of the molar extinction coefficients of the complexes in this spectral region permit the use of much lower donor concentrations than those required for the visible spectra.

The absorption bands due to the intermolecular charge transfer around 300 nm are superimposed on iodine and especially for donor absorption (Fig. 5). Analysis of these bands is therefore inaccurate and is limited only to qualitative results. Charge transfer bands, calculated graphically, are located at ~338 nm for the tolnaftate-iodine complex, at 310 nm for the disulfiram-iodine complex, and at 276 nm for the clomethiazole-iodine complex. The absorption intensity of the charge transfer bands increases with donor concentration and declines sharply with increasing temperature (Fig. 6). After 24 h the spectra

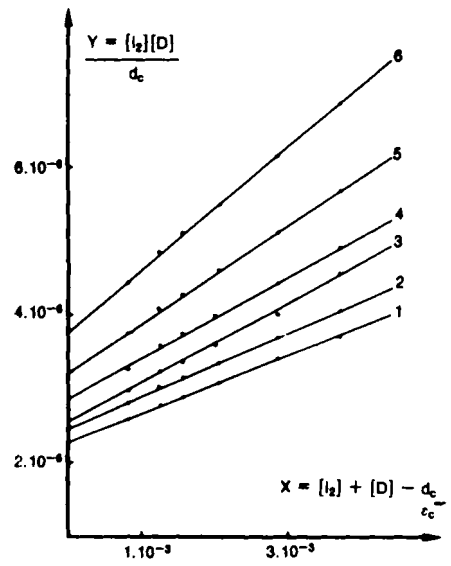

Figure 3—*Graphic representation of Eq. 3 obtained for the disulfiram-iodine complex. Lines 1, 2, 3, 4, 5, and 6 were obtained at 460, 470, 475, 480, 485, and 490 nm, respectively:* $x = [I_2] + [D] - d_c/\epsilon_c$ *and* $y = [I_2][D]/d_c$.

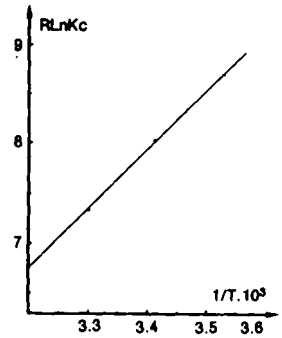

Figure 4—*Determination of the thermodynamic parameters of the tolnaftate-iodine complex. The linear regression line has the equation* y = 5.8 x − 11.77 (r = 0.999).

Table II—Thermodynamic Parameters Obtained for the Iodine Complexes

	$-\Delta H°$, kcal · mol^{-1}	$-\Delta S°$, cal · mol^{-1} K^{-1}	$-\Delta G°_{293}$, kcal · mol^{-1}
Tolnaftate[a]	5.80 ± 0.12	11.79 ± 0.42	2.35 ± 0.01
Disulfiram[b]	6.96 ± 0.30	12.48 ± 1.04	3.32 ± 0.01
Clomethiazole[c]	7.08 ± 0.14	17.76 ± 0.50	1.87 ± 0.005

[a] $[I_2]$ 4.438 × 10^{-4} M; [tolnaftate] varied from 0.229 × 10^{-2} M to 1.836 × 10^{-2} M. [b] $[I_2]$ 4.242 × 10^{-4} M; [disulfiram] varied from 0.434 × 10^{-3} M to 3.473 × 10^{-4} M. [c] $[I_2]$ 4.580 × 10^{-4} M; [clomethiazole] varied from 1.093 × 10^{-2} M to 5.467 × 10^{-2} M.

Table III—Molar Extinction Coefficients of Donors Obtained in the Ultraviolet Region[a]

Donor	λ_{max}, nm	log ϵ_{max}
Tolnaftate	263	4.38
	320.5	2.92
Disulfiram	259	4.53
Clomethiazole	256.4	3.42

[a] Solvent: carbon tetrachloride; temperature: 20 ± 0.1°C.

displayed the appearance of two new bands at 290 and 360 nm, respectively, characteristic of the formation of I_3^- ions in the complex solutions. Graphic extrapolation for the disulfiram-iodine complex (Fig. 5) helped to reveal the

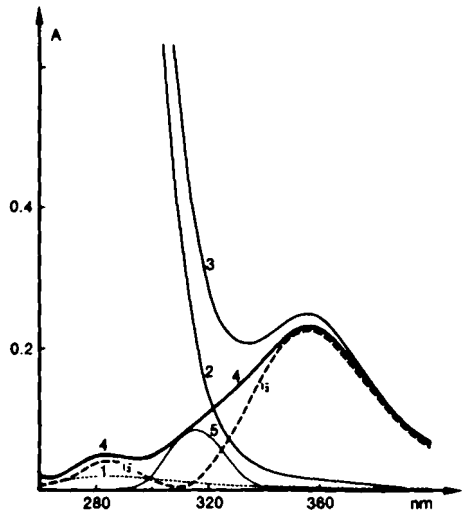

Figure 5—*Ultraviolet spectra of the disulfiram-iodine complex. Key: (1)* 4.242 × 10^{-4} *M iodine; (2)* 4.342 × 10^{-5} *M disulfiram; (3)* 4.242 × 10^{-4} *M iodine and* 4.342 × 10^{-5} *M disulfiram; (4) spectral recording obtained by placing a* 4.242 × 10^{-4} *M iodine solution and a* 4.342 × 10^{-5} *M disulfiram solution in the reference beam; (5) charge transfer band obtained by graphic extrapolation.*

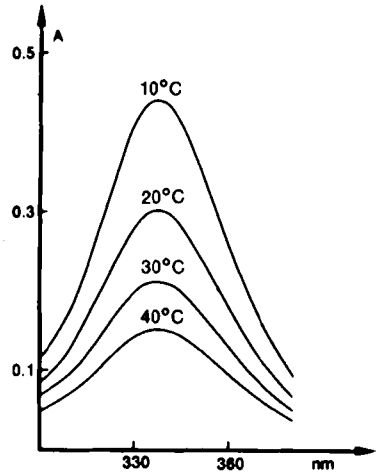

Figure 6—*Variation of the charge transfer band of a tolnaftate–iodine complex solution with temperature (4.438 × 10^{-4} M iodine and 4.682 × 10^{-4} M tolnaftate).*

three absorption bands located at 290 and 360 nm (I_3^- ions) and 310 nm (charge transfer band).

DISCUSSION

Spectroscopic observations in the visible and UV regions confirm the n-σ character of the charge transfer complexes formed by iodine with disulfiram, tolnaftate, and clomethiazole. The 1:1 stoichiometry of these complexes is confirmed by analysis of the absorption bands, measurement accuracy, isosbestic points observed, and Job's method of continuous variations.

In agreement with Mulliken (9) and Popov and Deskin (10), the formation of I_3^- ions is caused by the conversion of an outer complex into an inner complex, releasing I^- ions which act on the free molecular iodine:

1. Disulfiram + I_2 ⇄ disulfiram-I_2 (outer complex)
2. Disulfiram-I_2 ⇄ disulfiram-I^+I^-
3. Disulfiram-I^+I^- ⇄ (disulfiram-I)$^+$ + I^- (inner complex)
4. I^- + I_2 ⇄ I_3^-

Reaction 2 occurs slowly, while the other three reactions display rapid kinetics.

Table IV—Comparison of Formation Constants of Iodine Complexes Obtained with Antithyroid Drugs and with Clomethiazole, Tolnaftate, and Disulfiram

	K_c at 20°C, L · mol^{-1}	Solvent
Potassium thiocyanate	94 (at 22°C)[a]	H_2O
2-Thiazoline-2-thiol	2527 ± 118[a]	CCl_4
Thiourea	8825 ± 505[a]	CH_2Cl_2
Tetramethylthiourea	13215 ± 1150[a]	*n*-Heptane
2-Mercapto-1-methylimidazole	23194 ± 667[a]	CCl_4
Clomethiazole	25.00 ± 0.19	CCl_4
Tolnaftate	56.65 ± 0.96	CCl_4
Disulfiram	296.78 ± 4.44	CCl_4

[a] From Ref. 5.

The formation constants K_c of the iodine complexes of tolnaftate, disulfiram, and clomethiazole were compared with those obtained for antithyroid molecules (Table IV).

Antithyroid compounds are stronger donors for iodine than tolnaftate, disulfiram, and clomethiazole. Only disulfiram displayed a constant higher than that of potassium thiocyanate, whose antithyroid action is well known. Without totally inhibiting the synthesis of thyroid hormones, disulfiram appears to diminish this formation and interferes with it, causing the formation of a goiter. This property has been reported in a clinical study (11).

REFERENCES

(1) C. Raby and J. Buxeraud, *Bull. Soc. Chim. Fr.*, **10**, 439 (1978).

(2) C. Raby, J. Claude, J. Buxeraud, and C. Moesch, *Bull. Soc. Chim. Fr.*, **5**, 217 (1981).

(3) J. Buxeraud and C. Raby, *C. R. H. Acad. Sci.*, Ser. C, **286**, 565 (1978).

(4) C. Raby, J. Claude, C. Moesch, and J. Buxeraud, *C. R. H. Acad. Sci.*, Ser. C, **288**, 319 (1979).

(5) J. Buxeraud, Pharmaceutical Sciences Thesis, Limoges, France (1978).

(6) C. Raby and J. Buxeraud, *Eur. J. Med. Chem. Chim. Ther.*, **15**, 425 (1980).

(7) A. Taurog, *Endocrinology*, **98**, 1031 (1976).

(8) P. Job, *Ann. Chim. (Paris)*, **9**, 113 (1928).

(9) R. S. Mulliken, *J. Phys. Chem.*, **56**, 801 (1952).

(10) A. I. Popov and W. Deskin, *J. Am. Chem. Soc.*, **80**, 2976 (1958).

(11) A. Telkka and E. Kivalo, *Quart. J. Stud. Alcohol.*, **20**, 789 (1959).

Kinetic Study of the Hydrolysis of 1-(4-Nitrophenyl)-3-methyltriazene in Aqueous Solution and in the Presence of Surfactants

CYNTHIA EBERT, LUCIA LASSIANI, PAOLO LINDA *x, MARA LOVRECICH, CARLO NISI, and FULVIO RUBESSA

Received June 3, 1983, from the *Istituto di Chimica Farmaceutica*, and the **Istituto di Chimica, Università di Trieste, Italy.* Accepted for publication February 16, 1984.

Abstract □ The hydrolysis of 1-(4-nitrophenyl)-3-methyltriazene in aqueous solution has been studied over a pH range of 3–14. The effect of the anionic and cationic surfactants (sodium lauryl sulfate and hexadecyltrimethylammonium bromide) on the rate of hydrolysis was investigated. The quaternary ammonium bromide causes a rate decrease at all pH values studied, while sodium lauryl sulfate enhances the acid-catalyzed hydrolysis and decreases the observed rate constants in the pH-independent region. The results are discussed in terms of the current theory of micellar effects.

Keyphrases □ 1-(4-Nitrophenyl)-3-methyltriazene—kinetic study of the hydrolysis, effects of sodium lauryl sulfate and hexadecyltrimethylammonium bromide

The hydrolysis of arylmonoalkyltriazenes has been studied extensively (1–3). These substances are important as *in vivo* metabolites of the corresponding aryldialkyltriazenes, a class of compounds possessing antitumor (4–6), carcinogenic (7–9), and mutagenic (10–12) activity.

The pH-rate profiles in aqueous solution of various 1-aryl-3-methyltriazenes (1) and 1-phenyl-3-propyltriazenes (3) show two different regions; the rate of hydrolysis decreases sharply with increasing pH and then becomes almost constant. The plateau region is shifted to lower pH values by electron-withdrawing substituents in the aryl moiety. It has been postulated that the acid-catalyzed reaction involves an alkanediazonium ion as an intermediate or a protonated triazene as a discrete intermediate whose formation is rate determining. In the pH-independent region, a mechanism consisting of a simple unimolecular heterolysis of a nitrogen–nitrogen bond with anilide ion departing from an alkanediazonium ion was formulated (3).

Furthermore, the influence of serum albumins on the rates of some arylmonomethyltriazenes in buffered aqueous solution was also investigated (13). It was shown that the presence of these proteins in solution caused a marked reduction in the decomposition rates of the triazenes. The experimental results were interpreted by assuming that the substrates interact rapidly and reversibly with a binding site on the protein and that they cannot decompose when bound to this site.

The aim of the present work was to complete the pH–rate profile for a representative triazene, 1-(4-nitrophenyl)-3-methyltriazene (I), above pH 10 since systematic data of kinetic runs in this pH region were lacking. Furthermore, we studied the influence of the addition of cationic and anionic surfactants, above their critical micelle concentration (CMC), on the decomposition rate. During the past decade studies of this phenomenon have been stimulated by the hope that a micellar-catalyzed reaction might provide a basic model for interpretation of some aspects of enzymatic catalysis since micelles can be regarded as a model for enzymes and biomembranes (14–16). The effect of the micelles on drug stability has been recently reviewed (17).

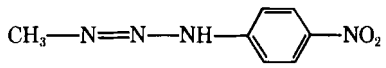

EXPERIMENTAL SECTION

Materials—1-(4-Nitrophenyl)-3-methyltriazene (I) was prepared as described previously (18), mp 112–113°C [lit. (18) mp 111–113°C]. Hexadecyltrimethylammonium bromide and sodium lauryl sulfate were purified by methods described previously (19). The buffers used were: formate (pH 3.0–4.2), succinate (pH 4.5–6.0), phosphate (pH 6.5–8.0), borate (pH 9.0), carbonate (pH 10.0–11.0), and phosphate (pH 11.0–12.0).

Kinetic Methods—The triazene was dissolved in acetonitrile to give a 2×10^{-2} M stock solution which was stored in the refrigerator. This solution (10 μL) was added to a volume of the buffer in a quartz cell thermostated at 25 ± 0.1°C to obtain a concentration of the substrate on the order of 10^{-5} M. The ionic strength was kept constant at 0.01. The pH values were determined with a digital pH-meter[1] at the temperature of the kinetic run for reactions in water. The analytical pH was used for reactions in the presence of surface-active agents—as the apparent pH in micelles. The decomposition reactions were followed spectrophotometrically[2] at 350 nm when the disappearance of protonated or neutral triazene was followed, or at 470 nm when anionic triazene was present. These wavelengths were chosen to permit maximum variation and minimum interference with the spectrum of the decomposition product. The spectrum at the end of the reaction was coincident with that of *p*-nitroaniline. Absorbances were recorded as a function of time. Pseudo-first-order rate constants were calculated using a least-squares method. Correlation coefficients were between 0.994 and 0.999.

RESULTS AND DISCUSSION

Hydrolysis in Aqueous Solution—Figure 1 shows the dependence on pH of the first-order rate constant for the decomposition of I which is consistent with that obtained for 1-(4-nitrophenyl)-3-propyltriazene by Sinnot *et al.* (3). Two routes for the triazene decomposition were confirmed: a pH-independent pathway and an acid-catalyzed reaction with a negative slope (~1, Table I). The acid-catalyzed reaction pathway was interpreted as an $A\text{-}S_E2(N)$ reaction involving a transition state in which the proton is almost completely transferred and little N—N bond-breaking has occurred, whereas the pH-independent reaction was considered as an S_N1 reaction on nitrogen without participation of water (3).

Above pH 12.5, a third region was observed with a negative slope (~1); in this case the formation of the anionic triazene was shown by a change in the visible spectrum (Fig. 2). We suggest that the decrease in log k_{obs} in this pH region is essentially due to the diminution of the reactive neutral triazene involved in the acid–base equilibrium.

The suggested overall mechanism of the reaction is described in Scheme I, where T is the unprotonated, TH^+ the protonated, and T^- the deprotonated, triazene.

$$T^- + H^+ \underset{K_2}{\rightleftharpoons} T + H^+ \underset{K_1}{\rightleftharpoons} TH^+ \xrightarrow{k_1} \text{products}$$

$$\downarrow k_2$$

$$\text{products}$$

Scheme I

[1] pHM84 Radiometer or 632 Metrohm pH meters.
[2] Model 552 and Lambda 5 spectrophotometers; Perkin-Elmer.

0022-3549/84/1200-1691$01.00/0
© 1984, American Pharmaceutical Association

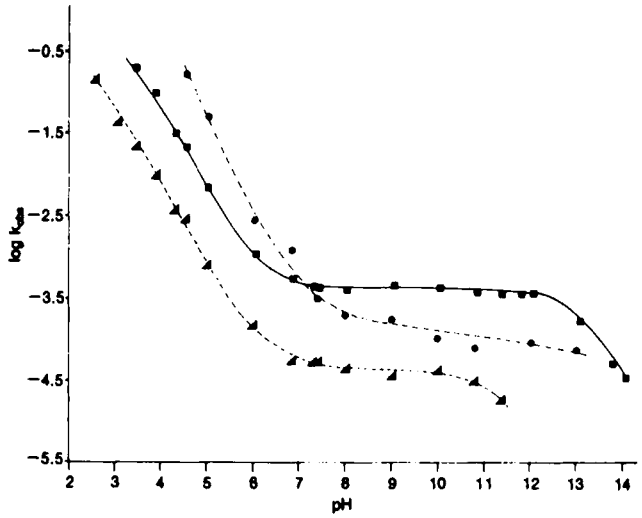

Figure 1—*Log k_{obs}-pH profile of I. Key: (■) in buffered aqueous solution at 25°C and μ = 0.01, calculated according to Eq. 1; (▲) in presence of 2 × 10^{-2} M hexadecyltrimethylammonium bromide; (●) in presence of 2 × 10^{-2} M sodium lauryl sulfate.*

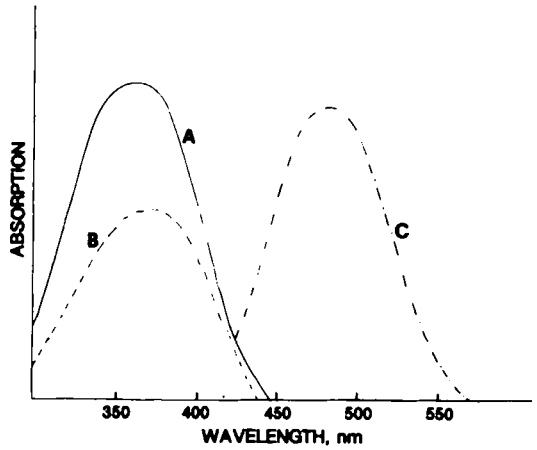

Figure 2—*Changes in visible absorption spectra in buffered aqueous solution. Key: (A) neutral triazene, pH 8.45 (I); (B) p-nitroaniline, pH 8.45; (C) the anionic form of triazene, 1M NaOH (I).*

Equation 1 represents the rate law for the mechanistic scheme:

$$k_{obs} = \frac{k_1[H^+]^2 + k_2K_1[H^+]}{[H^+]^2 + K_1[H^+] + K_1K_2} \qquad \text{(Eq. 1)}$$

The curve fitting of this equation is reported in Fig. 1 according to the following parameters: $k_1 = 0.5\ s^{-1}$; $k_2 = 3.5 \times 10^{-4}\ s^{-1}$; $K_1 = 7.9 \times 10^{-4}$ M; $K_2 = 1.0 \times 10^{-13}$ M. The estimated value of $pK_2 = 13.0$ is reasonable as compared, for example, with the $pK_a = 12.31$ measured for the deprotonation of *p*-nitroformanilide (20).

Inhibition of Hydrolysis by Hexadecyltrimethylammonium Bromide—Cationic micelles of hexadecyltrimethylammonium bromide inhibit the hydrolysis rate at any pH value considered (Table II). As expected, cationic micelles of hexadecyltrimethylammonium bromide inhibit the acid hydrolysis of I. The variation of rate constant with surfactant concentration is generally based on the assumption that substrate, in this case triazene (T), is distributed between the aqueous and micellar pseudophases, with the first-order rate constants designated as $k_{w'}$ and $k_{m'}$. The micellar surfactant concentration, $[D_n]$, is assumed to be the total surfactant concentration [D] less that of monomeric surfactant which is assumed to be given by critical micelle concentration (CMC), so that $[D_n] = [D] - CMC$; K_s is the equilibrium constant for substrate binding.

$$T + D_n \underset{}{\overset{K_s}{\rightleftharpoons}} TD_n$$

$$\downarrow k_{w'} \qquad \downarrow k_{m'}$$

products products

$$K_s = \frac{[TD_n]}{[T][D_n]}$$

Scheme II

Following Scheme II the relation between k_{obs} and $[D_n]$ is shown by:

$$k_{obs} = \frac{k_{w'} + k_{m'}K_s[D_n]}{1 + K_s[D_n]} \qquad \text{(Eq. 2)}$$

and its rearrangement gives:

$$\frac{1}{k_{w'} - k_{obs}} = \frac{1}{k_{w'} - k_{m'}} + \frac{1}{(k_{w'} - k_{m'})K_s([D] - CMC)} \qquad \text{(Eq. 3)}$$

By plotting $1/(k_{w'} - k_{obs})$ against $1/([D] - CMC)$ it is possible to calculate

Table I—Kinetic Data of the Pseudo-First-Order Decomposition of I [a]

Buffer Conc.	Buffer	Final pH	k_{obs}, $s^{-1} \times 10^4$ H_2O	Hexadecyltrimethylammonium Bromide 2×10^{-2} M	Sodium Lauryl Sulfate 2×10^{-2} M
0.0032	HCl	2.50	—	1490	—
0.016	Sodium chloroacetate	3.02	—	447	—
0.030	Sodium formate	3.42	1720	227	—
0.017	Sodium formate	3.85	837	99	—
0.013	Sodium formate	4.26	271	38.6	—
0.012	Sodium succinate	4.50	181	29.8	1760
0.076	Sodium succinate	5.00	58.8	8.29	537
0.040	Sodium succinate	6.00	9.33	1.56	29.8
0.0059	Sodium phosphate	6.82	4.71	0.58	13.0
0.0044	Sodium phosphate	7.30	3.75	0.56	4.67
0.0042	Sodium phosphate	7.40	3.63	0.57	3.40
0.0036	Sodium phosphate	8.00	3.44	0.47	2.14
0.027	Sodium borate	9.00	3.91	0.38	1.90
0.057	Sodium carbonate	10.00	3.60	0.45	1.14
0.025	Sodium carbonate	10.80	3.30	0.34	0.88
0.0022	Sodium hydroxide	11.35	3.07	0.20	—
0.0056	Sodium hydroxide	11.75	3.07	—	—
0.010	Sodium hydroxide	12.02	3.11	0.032	1.04
0.10	Sodium hydroxide	13.00	1.41	—	0.84
0.50	Sodium hydroxide	13.70	0.44	—	—
1.0	Sodium hydroxide	14.00	0.29	—	—

[a] In buffered aqueous solution and in the presence of hexadecyltrimethylammonium bromide and sodium lauryl sulfate at 25°C.

Table II—Rate of Hydrolysis of 1-(4-Nitrophenyl)-3-methyltriazene in the Presence of Hexadecyltrimethylammonium Bromide

Hexadecyltrimethylammonium Bromide, M × 10^3	k_{obs}, s^{-1} × 10^4 [a]			
	pH 4.50	pH 7.30	pH 8.45	pH 12.02
–	181	3.75	3.61	3.11
1	—	3.44	—	0.20
2	164	2.27	3.31	0.091
3	135	—	2.77	0.057
4	107	1.67	2.48	0.050
6	79.5	—	2.04	0.048
8	63.1	—	1.35	0.037
10	52.7	0.82	0.88	0.038
20	29.8	0.56	0.61	0.032

[a] Values determined at 25°C and μ = 0.01.

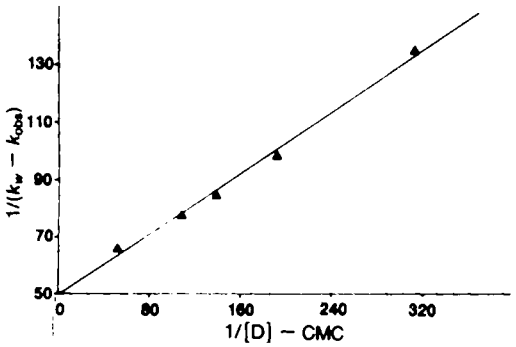

Figure 3—*The effect of hexadecyltrimethylammonium bromide on* k_{obs} *at pH 4.50 according to Eq. 2.*

$k_{w'}$, $k_{m'}$, and K_s. However, this plot is sensitive to CMC values and, as previously shown, this problem can be solved by assuming CMC as an adjustable parameter (21); a representative plot is shown in Fig. 3.

At pH 4.50 the best fit is obtained by taking CMC = 8 × 10^{-4} M, which is identical to the value determined by the surface tension method (22); then K_s = 180 M^{-1}. Similar treatment with data obtained at pH 7.30, 8.45, and 12.02 gives the results listed in Table III. Under these conditions $k_{m'}$ is very small relative to $k_{w'}$. From the estimated binding constants and pH-rate profile in micelles, it can be observed that the substrate in its neutral form is moderately bound to hexadecyltrimethylammonium bromide micelles while the anionic form, which is present at pH 12.02, is strongly bound (K_s = 35,000 M^{-1}). Also, the equilibrium between neutral triazene and its anionic form is strongly shifted by hexadecyltrimethylammonium bromide toward the anionic form, *i.e.*, the apparent pK_a value of triazene is changed by stabilization of the anionic form by cationic micelles. These effects of micelles on equilibria have been previously reported by Bunton *et al.* (23).

Hydrolysis in Presence of Sodium Lauryl Sulfate—The anionic sodium lauryl sulfate micelles enhance the rate of acid-catalyzed hydrolysis by a factor of ~10 at pH 4.5–6.0, as shown in Table I. Otherwise, sodium lauryl sulfate inhibits the uncatalyzed reaction by a smaller factor (~2).

For a given hydrogen ion concentration, the rate constants go through a maximum with increasing concentration of the anionic surfactant (Table IV). At pH 4.50 the largest enhancement occurs at 2 × 10^{-2} M sodium lauryl sulfate and the rate constant is approximately 10-fold higher than that determined in water.

The kinetic micellar effect could be interpreted by separation of the contributions of the reaction in the aqueous and micellar pseudophases, as reported (21). The quantitative treatment requires knowledge of the binding constant of triazene with micellar sodium lauryl sulfate. Unfortunately, we cannot measure or estimate K_s. However, the results in the acid-catalyzed region confirm the importance of the stabilization of the protonated form of the triazene in anionic micelles causing a change in its pK_a value.

The "Uncatalyzed" Reaction in Presence of Sodium Lauryl Sulfate and Hexadecyltrimethylammonium Bromide—The inhibition caused by both anionic and cationic micelles is not surprising since the transition state for the S_N1 decomposition of the triazene should have a strong zwitterionic character and, therefore, should be destabilized in the less polar micellar medium, whereas the initial state should be stabilized. Inhibitory effects by hexadecyltrimethylammonium bromide micelles have been previously found in the S_N1 reaction of 1-bromo-2-phenylpropane (24) and of 3-bromo-3-phenyl propionate ion (25) and by both hexadecyltrimethylammonium bromide and sodium lauryl sulfate on the S_N1 reaction of α-phenylallyl butanoate (26). These effects are comparable to the well-known effects of solvent on S_N1 reactions (27, 28).

Table III—Binding Constants and Micellar Rate Constants Calculated in Presence of Hexadecyltrimethylammonium Bromide

pH	K_s, M^{-1}	CMC, M × 10^3	$k_{w'} - k_{m'}$, s^{-1}	$k_{w'} = k_{obs(w)}$, s^{-1}
4.50	180	0.8	2.1 × 10^{-2}	1.81 × 10^{-2}
7.30	440	0.4	3.5 × 10^{-4}	3.75 × 10^{-4}
8.45	70	0.8	6.0 × 10^{-4}	3.61 × 10^{-4}
12.02	35000	0.2	3.1 × 10^{-4}	3.11 × 10^{-4}

Table IV—Rate of Hydrolysis of 1-(4-Nitrophenyl)-3-methyltriazene in the Presence of Sodium Lauryl Sulfate

Sodium Lauryl Sulfate, M × 10^3	k_{obs}, s^{-1} × 10^2 [a]
—	1.81
4	2.16
6	5.2
8	10.3
10	13.7
20	17.6
30	17.2
40	17.5
50	15.2
60	13.6
80	15.0

[a] Values at 25°C, μ = 0.01, and pH 4.50.

REFERENCES

(1) N. S. Isaacs and E. Rannala, *J. Chem. Soc., Perkin Trans. 2*, **1974**, 899 and 902.

(2) V. Zvěřina, M. Remeš, J. Diviš, J. Marhold, and M. Matrka, *Collect. Czech. Chem. Commun.*, **38**, 251 (1973).

(3) C. C. Jones, A. Kelly, M. L. Sinnott, P. J. Smith, and G. T. Tzotzos, *J. Chem. Soc., Perkin Trans. 2*, **1982**, 1655.

(4) T. A. Connors, P. M. Goddard, K. Merai, W. C. J. Ross, and D. E. V. Wilman, *Biochem. Pharmacol.*, **25**, 241 (1976).

(5) M. Julliard and G. Vernin, *Ind. Eng. Chem. Prod. Res. Dev.*, **20**, 287 (1981).

(6) T. Giraldi, C. Nisi, T. A. Connors, and P. M. Goddard, *J. Med. Chem.*, **20**, 850 (1977).

(7) H. Druckrey, *Xenobiotica*, **3**, 271 (1973).

(8) R. Preussmann, S. Ivankovic, C. Landschütz, J. Gimmy, E. Flohr, and U. Griesbach, *Z. Krebsforsch.*, **86**, 285 (1974).

(9) S. Ivankovic, R. Port, and R. Preussmann, *Z. Krebsforsch.*, **86**, 307 (1976).

(10) G. F. Kolar, R. Fahrig, and E. Vogel, *Chem. Biol. Interact.*, **9**, 365 (1974).

(11) C. Malaveille, G. F. Kolar, and H. Bartsch, *Mutat. Res.*, **36**, 1 (1976).

(12) V. H. Venger, C. Hansch, G. J. Hatheway, and Y. U. Amrein, *J. Med. Chem.*, **22**, 473 (1979).

(13) F. Delben, S. Paoletti, G. Manzini, and C. Nisi, *J. Pharm. Sci.*, **70**, 892 (1981).

(14) J. H. Fendler and E. J. Fendler, "Catalysis in Micellar and Macromolecular Systems," Academic, New York, N.Y., 1975.

(15) "Reaction Kinetics in Micelles," E. H. Cordes, Ed., Plenum, New York, N.Y., 1973.

(16) K. L. Mittal, "Micellization, Solubilization and Microemulsions," Vol. 2, Plenum, New York, N.Y., 1977.

(17) P. Linda, F. Rubessa, and G. Savelli, *La Chimica et L'Industria*, **63**, 333 (1981).

(18) T. P. Ahern and K. Vaughan, *J. Chem. Soc., Chem. Commun.*, **1973**, 701.

(19) C. A. Bunton, L. S. Romsted, and H. J. Smith, *J. Org. Chem.*, **43**, 4299 (1978).

(20) J. Kavalek and V. Sterba, *Coll. Czech. Chem. Commun.*, **40**, 1176 (1975).

(21) A. Cipiciani, P. Linda, G. Savelli, and C. A. Bunton, *J. Org. Chem.*, **46**, 911 (1981).
(22) M. J. Schick, *J. Am. Oil Chem. Soc.*, **43**, 681 (1966).
(23) C. A. Bunton, L. S. Romsted, and L. Sepulveda, *J. Phys. Chem.*, **84**, 2611 (1980) and references cited therein.
(24) V. Gani, G. Lapinte, and P. Viout, *Tetrahedron Lett.*, **1973**, 4435.
(25) C. A. Bunton, A. Kanego, and M. J. Minch, *J. Org. Chem.*, **37**, 1388 (1972).
(26) C. Lapinte and P. Viout, *Tetrahedron Lett.*, **1972**, 4221.
(27) C. A. Bunton, "Nucleophilic Substitution at a Saturated Carbon Atom," Elsevier, New York, N.Y., 1963.
(28) C. K. Ingold, "Structure and Mechanism in Organic Chemistry," Cornell University Press, Ithaca, N.Y., 1968.

ACKNOWLEDGMENTS

Thanks are due the Italian National Research Council for financial support, Prof. G. Savelli for helpful discussion, and the referee for useful suggestions.

Kinetics and Mechanism of Enzymatic Hydrolysis of Pivampicillin Monolayers

O. VALLS, M. ALVAREZ, A. ALSINA, and S. GARCÍA FERNANDEZ ˣ

Received May 19, 1982, from the *Department of Physical-Chemistry, Faculty of Pharmacy, University of Barcelona, Spain.* Accepted for publication October 17, 1983.

Abstract □ A study of the enzymatic hydrolysis of pivampicillin (an insoluble penicillin) extended as a monolayer on the aqueous interface at a constant surface pressure has been performed. Penicillinase promotes intensive hydrolysis of the pivampicillin monolayers, inducing their solubility. However, no action was observed with dog liver esterase. The hydrolytic process, which was dependent on the film surface pressure and on the quantity of the injected enzyme, is of the Michaelis-Menten type in two dimensions.

Keyphrases □ Pivampicillin—enzymatic kinetics, surface monolayers, penicillinase, esterases □ Kinetics—enzymatic, pivampicillin, surface monolayers, Michaelis-Menten

The catalytic action of an enzyme can generally be measured by the quantity of transformed substance or by the product generated per unit of time. The processes of enzymatic kinetics in bulk materials are usually Michaelis-Menten in character (1). Under these conditions, both soluble substrates and enzyme-substrate complexes are in a homogeneous system. However, insoluble substrates are normally in the form of micellar aggregates, which act as the real substrate. In such cases, study of the kinetics is complicated by the difficulty of knowing the concentration of substrate in contact with the enzyme.

This difficulty can be overcome by extending the insoluble substrate as a monolayer film over an aqueous mass which contains the soluble enzyme. Under these conditions, all the molecules of substrate are equally exposed to the action of the enzyme. Thus, it is possible to quantitate the amount of substrate in contact with the enzyme (by controlling its surface concentration in the film) and the amount of enzyme reacting with the surface (by controlling its concentration in the subphase). This system makes it possible to obtain information about action of the enzyme sites in the substrate molecules.

The first studies of enzymatic kinetics using the surface monolayer technique were performed by Hughes (2) in 1935. Measuring the decrease in surface potential during the hydrolysis process, Hughes observed that the hydrolysis rate of lecithin in monomolecular films catalyzed by phospholipase A_2 decreased when the surface concentration of the lecithin molecules in the interface increased. This method is, however, subject to significant errors in interpretation.

Since that time, several authors have used the monolayer technique to measure the activity of lipolytic processes catalyzed by lipases and phospholipases. Short-chain phospholipids and triglycerides were used as substrates so that the reaction products would be soluble and, therefore, diffuse into the aqueous subphase, leaving the monolayer. Garner and Smith (3) performed these determinations in a constant area, measuring the decrease of the monolayer surface pressure as the substrate was dissolved by the lipolytic effect of the enzyme. An inherent difficulty of this method is that the surface concentration of the film molecules vary continually during the process; therefore, the decrease of the surface pressure is linear with respect to time only in the first moment. Lagocki *et al.* (4), Dervichian (5), and Verger and de Haas (6) used methods with constant pressure, measuring the kinetic rate by the decrease of the area covered by the film (directly connected with the number of substrate molecules which escape from the surface).

The method of "zero-order trough" or "two-compartment trough" proposed by Verger and de Haas (6) is particularly interesting. In this method the enzymatic reaction takes place in a different compartment than the one which acts as a substrate reservoir. In this way, the number of the substrate molecules in the reaction compartment can be kept constant during the entire process. The process develops in a pseudo-zero-order manner, *i.e.*, the decrease of the monolayer area is proportional to time, yielding a straight line, the course and slope of which give the rate of the kinetic process.

Kinetic studies have been performed on monolayers of insoluble penicillins (7). The penicillin molecules are transformed by hydrolysis into soluble products that leave the monolayer and dissolve in the aqueous subphase. The number of hydrolyzed molecules can be determined by the monolayer surface decrease, maintaining a constant surface pressure at all times (Fig. 1).

For this type of study, pivampicillin is a particularly interesting test drug. It is a penicillin which is insoluble in neutral solutions and soluble in acidic media. Pivampicillin is activated by esterases, which transform it into ampicillin (8), and it is

0022-3549/84/1200-1694$01.00/0
© 1984, American Pharmaceutical Association

(21) A. Cipiciani, P. Linda, G. Savelli, and C. A. Bunton, *J. Org. Chem.*, **46**, 911 (1981).
(22) M. J. Schick, *J. Am. Oil Chem. Soc.*, **43**, 681 (1966).
(23) C. A. Bunton, L. S. Romsted, and L. Sepulveda, *J. Phys. Chem.*, **84**, 2611 (1980) and references cited therein.
(24) V. Gani, G. Lapinte, and P. Viout, *Tetrahedron Lett.*, **1973**, 4435.
(25) C. A. Bunton, A. Kanego, and M. J. Minch, *J. Org. Chem.*, **37**, 1388 (1972).
(26) C. Lapinte and P. Viout, *Tetrahedron Lett.*, **1972**, 4221.
(27) C. A. Bunton, "Nucleophilic Substitution at a Saturated Carbon Atom," Elsevier, New York, N.Y., 1963.
(28) C. K. Ingold, "Structure and Mechanism in Organic Chemistry," Cornell University Press, Ithaca, N.Y., 1968.

ACKNOWLEDGMENTS

Thanks are due the Italian National Research Council for financial support, Prof. G. Savelli for helpful discussion, and the referee for useful suggestions.

Kinetics and Mechanism of Enzymatic Hydrolysis of Pivampicillin Monolayers

O. VALLS, M. ALVAREZ, A. ALSINA, and S. GARCÍA FERNANDEZ ˣ

Received May 19, 1982, from the *Department of Physical-Chemistry, Faculty of Pharmacy, University of Barcelona, Spain.* Accepted for publication October 17, 1983.

Abstract □ A study of the enzymatic hydrolysis of pivampicillin (an insoluble penicillin) extended as a monolayer on the aqueous interface at a constant surface pressure has been performed. Penicillinase promotes intensive hydrolysis of the pivampicillin monolayers, inducing their solubility. However, no action was observed with dog liver esterase. The hydrolytic process, which was dependent on the film surface pressure and on the quantity of the injected enzyme, is of the Michaelis-Menten type in two dimensions.

Keyphrases □ Pivampicillin—enzymatic kinetics, surface monolayers, penicillinase, esterases □ Kinetics—enzymatic, pivampicillin, surface monolayers, Michaelis-Menten

The catalytic action of an enzyme can generally be measured by the quantity of transformed substance or by the product generated per unit of time. The processes of enzymatic kinetics in bulk materials are usually Michaelis-Menten in character (1). Under these conditions, both soluble substrates and enzyme-substrate complexes are in a homogeneous system. However, insoluble substrates are normally in the form of micellar aggregates, which act as the real substrate. In such cases, study of the kinetics is complicated by the difficulty of knowing the concentration of substrate in contact with the enzyme.

This difficulty can be overcome by extending the insoluble substrate as a monolayer film over an aqueous mass which contains the soluble enzyme. Under these conditions, all the molecules of substrate are equally exposed to the action of the enzyme. Thus, it is possible to quantitate the amount of substrate in contact with the enzyme (by controlling its surface concentration in the film) and the amount of enzyme reacting with the surface (by controlling its concentration in the subphase). This system makes it possible to obtain information about action of the enzyme sites in the substrate molecules.

The first studies of enzymatic kinetics using the surface monolayer technique were performed by Hughes (2) in 1935. Measuring the decrease in surface potential during the hydrolysis process, Hughes observed that the hydrolysis rate of lecithin in monomolecular films catalyzed by phospholipase A_2 decreased when the surface concentration of the lecithin molecules in the interface increased. This method is, however, subject to significant errors in interpretation.

Since that time, several authors have used the monolayer technique to measure the activity of lipolytic processes catalyzed by lipases and phospholipases. Short-chain phospholipids and triglycerides were used as substrates so that the reaction products would be soluble and, therefore, diffuse into the aqueous subphase, leaving the monolayer. Garner and Smith (3) performed these determinations in a constant area, measuring the decrease of the monolayer surface pressure as the substrate was dissolved by the lipolytic effect of the enzyme. An inherent difficulty of this method is that the surface concentration of the film molecules vary continually during the process; therefore, the decrease of the surface pressure is linear with respect to time only in the first moment. Lagocki *et al.* (4), Dervichian (5), and Verger and de Haas (6) used methods with constant pressure, measuring the kinetic rate by the decrease of the area covered by the film (directly connected with the number of substrate molecules which escape from the surface).

The method of "zero-order trough" or "two-compartment trough" proposed by Verger and de Haas (6) is particularly interesting. In this method the enzymatic reaction takes place in a different compartment than the one which acts as a substrate reservoir. In this way, the number of the substrate molecules in the reaction compartment can be kept constant during the entire process. The process develops in a pseudo-zero-order manner, *i.e.*, the decrease of the monolayer area is proportional to time, yielding a straight line, the course and slope of which give the rate of the kinetic process.

Kinetic studies have been performed on monolayers of insoluble penicillins (7). The penicillin molecules are transformed by hydrolysis into soluble products that leave the monolayer and dissolve in the aqueous subphase. The number of hydrolyzed molecules can be determined by the monolayer surface decrease, maintaining a constant surface pressure at all times (Fig. 1).

For this type of study, pivampicillin is a particularly interesting test drug. It is a penicillin which is insoluble in neutral solutions and soluble in acidic media. Pivampicillin is activated by esterases, which transform it into ampicillin (8), and it is

0022-3549/84/1200-1694$01.00/0
© 1984, American Pharmaceutical Association

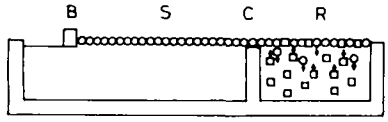

Figure 1—*Schematic of the work principle of the enzymatic hydrolysis process. Key: (B) mobile barrier; (S) reservoir of the substrate (penicillin); (C) communication channel between compartments; (R) reaction compartment.*

quickly inactivated by the action of β-lactamase enzymes secreted by penicillin-resistant microorganisms, *i.e.*, penicillinase (9). A previous study (7) with this antibiotic verified that stable monolayers can be obtained which, through the activity of hydrolytic agents, become soluble and pass into the aqueous subphase. It is possible, therefore, to perform kinetic studies on a monolayer of pivampicillin.

The results of the acid and alkaline hydrolysis of monomolecular films of pivampicillin and the first results of hydrolysis by β-lactamases have been presented previously (7). In the present study the kinetic processes of hydrolysis by an esterase and β-lactamase on monomolecular films of pivampicillin are amplified and debated.

EXPERIMENTAL SECTION

For this study a surface manometer, designed and built in our laboratory based on the pseudo-zero-order system proposed by Verger *et al.* (6), was used; this manometer was described in detail in a previous work (10). It has a barostatic system, allowing the maintenance of constant pressure and the direct registration of the variation of the monolayer area through time. Sörensen buffer (pH 7) was used as the base liquid of the film, filling both sections of the trough (11). The buffer was prepared with twice-distilled water, potassium phosphate[1], and disodium phosphate[1].

Purified technical-quality pivampicillin[2] was used for preparation of the substrate monolayer; a 10^{-5} M solution of this substance in 20% absolute ethanol–80% petroleum ether (bp 40–60°C) was used. The solvent evaporated spontaneously within ~60 s after extension, leaving a monomolecular film of the antibiotic over the aqueous surface. In each case, a variable volume of solution was spread; the resulting film was compressed, reducing its surface until the desired surface pressure for the kinetic studies was obtained. The initial surface concentration (C) of the substrate molecules in the film was calculated from the amount of penicillin extended and the total area (in cm^2) occupied initially by the film in both compartments.

While under constant agitation, 10–100 μL of enzyme solution was injected under the monolayer in the reaction compartment. The injected enzymes were an esterase and a penicillinase. The esterase used (type I from dog liver) is a carboxyesterase (E.C. 3.1.1.1)[3]. One unit of this enzyme hydrolyses 1.0 μmol of ethyl butyrate/min at pH 8 and 25°C. The enzyme (100 U/mg of protein) was used in a buffered phosphate solution at pH 8, at a concentration of 1000 IU/mL. The penicillinase, from *Bacillus cereus* (40,000 IU/mg), is a penicillinamide β-lactamhydrolase (E.C. 3.5.2.6)[4]. One international unit inactivates 1 U of penicillin/min at pH 7 and 25°C. It was used in a buffered phosphate solution at pH 7, at a concentration of 400,000 IU/cm^3.

The recording of the kinetic process (variation of the film area against time) started immediately after enzyme addition and continued for 60–120 min. The number of hydrolyzed molecules was calculated from the displacement of the mobile barrier, taking into account that a 1-cm displacement corresponds to a surface decrease of 17.5 cm^2 and to a number of hydrolyzed molecules equal to 17.5C (molecules/cm^2). A linear representation was obtained in the zero-order trough by plotting the number of hydrolyzed molecules against time. The type of slope allowed us to calculate the velocity of the hydrolytic process (molecules·cm^{-2}·min^{-1}).

RESULTS

The injection of dog liver esterase under the monolayer of pivampicillin, at final concentrations from 100 to 10,000 IU/100 mL of subphase and at starting film pressures from 1×10^{-3} to 2×10^{-2} N·m^{-1}, produced neither solubilization of the monolayer nor a real decrease of the starting pressure of the film over a 2-h period. After the injection of the enzyme, however, the surface pressure of the monolayer increased. This demonstrates penetration of the esterase in the penicillin film, but without a hydrolytic effect on pivampicillin.

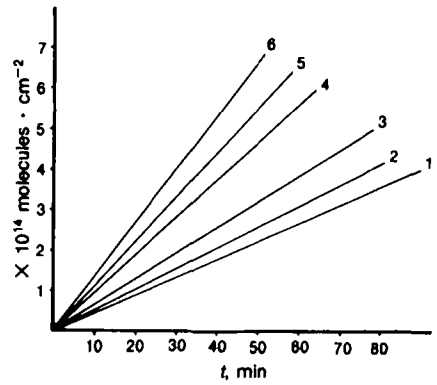

Figure 2—*Activity of the hydrolysis of pivampicillin films by penicillinase (4000 IU) at different film surface pressures. Key: (1) 4.2 × 10^{-3} N·m^{-1}; (2) 6.7 × 10^{-3} N·m^{-1}; (3) 8.4 × 10^{-3} N·m^{-1}; (4) 12.4 × 10^{-3} N·m^{-1}; (5) 13.9 × 10^{-3} N·m^{-1}; (6) 16.7 × 10^{-3} N·m^{-1}.*

The injection of penicillinase produced a rapid hydrolysis and solubilization of the pivampicillin, which manifested itself in a decrease in the monolayer area at constant surface pressure, after the short induction time (τ) necessary for the enzyme to penetrate the monolayer. The rate at which the substrate molecules leave the surface depends on the surface pressure of the film and the quantity of the enzyme injected.

In all cases, the activity of the process (hydrolyzed molecules by unit of surface), after the induction time (τ), was directly proportional to time, *i.e.*, it was a pseudo-zero-order process. As a result, the graphic representation of the activity against time was a straight line during the initial 60 min, after which the line curved slightly as the process decreased.

Figure 2 shows the hydrolytic activity (in hydrolyzed molecules per square centimeter of monolayer surface) in the reaction compartment *versus* time at different surface pressures after the injection of 4000 IU of penicillinase. After a short induction time (τ) the curve straightened until the final stage of the process. When the surface pressure of the film increases, the reaction rate also increases, tending to stabilize at high pressures (Fig. 3).

The activity of the hydrolytic process is strongly influenced by the amount of injected enzyme. This can be seen in Fig. 4, where the hydrolyzed substance is set against time, at a constant surface pressure of 4.2 × 10^{-3} N·m^{-1}, for different amounts of injected penicillin in the reaction compartment (4000–12,000 IU). As can be seen in Fig. 5, the reaction rate (hydrolyzed molecules per milliliter and per minute) increases with the amount of enzyme, giving a straight line.

The induction time (τ) decreases when the surface pressure of the film increases, stabilizing at high pressures (Fig. 6). The induction time also decreases when the amount of injected enzyme increases.

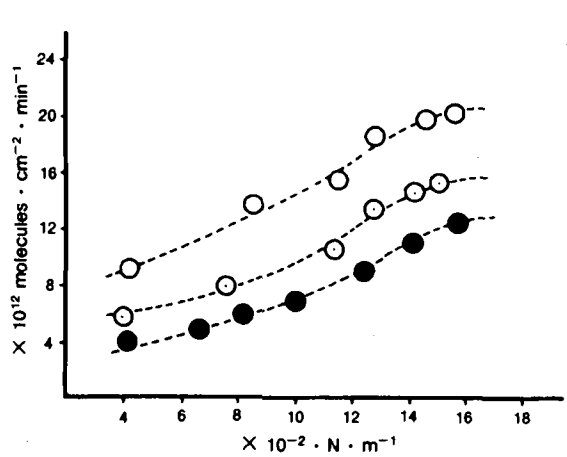

Figure 3—*Hydrolysis velocity of pivampicillin films as a function of the film surface pressure after the injection of different quantities of penicillinase. Key: (○) 12,000 IU; (⊙) 8000 IU; (●) 4000 IU.*

[1] The highest purity obtainable; E. Merck, Darmstadt, F.R.G.
[2] Obtained and purified by Antibiótics, S.A., León, Spain.
[3] Sigma Chemical Co., St. Louis, Mo.
[4] Serva Feinbiochemica, Heidelberg, F.R.G.

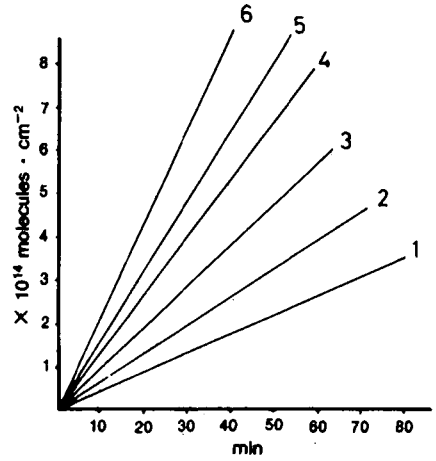

Figure 4—*Activity of the hydrolytic process of pivampicillin films by injecting different amounts of penicillinase. Key: (1) film at 4.2 × 10⁻³ N·m⁻¹, injection of 4000 IU; (2) film at 4.2 × 10⁻³ N·m⁻¹, injection of 8000 IU; (3) film at 4.2 × 10⁻³ N·m⁻¹, injection of 12,000 IU; (4) film at 16.7 × 10⁻³ N·m⁻¹, injection of 4000 IU; (5) film at 16.7 × 10⁻³ N·m⁻¹, injection of 8000 IU; (6) film at 16.7 × 10⁻³ N·m⁻¹, injection of 12,000 IU.*

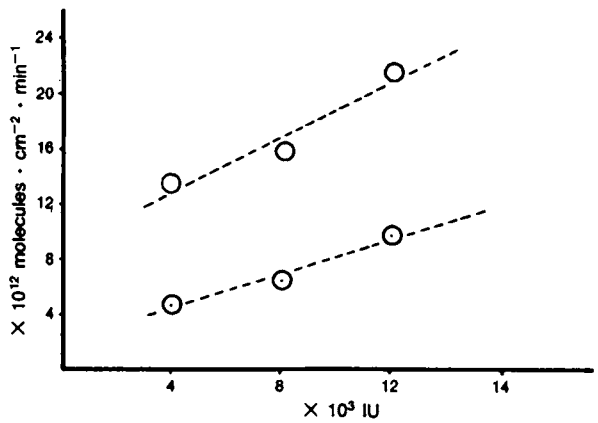

Figure 5—*Hydrolysis velocity of pivampicillin films at surface pressures of 4.2 × 10⁻³ (⊙) and 16.7 × 10⁻³ N·m⁻¹ (○) as a function of the amount of injected enzyme.*

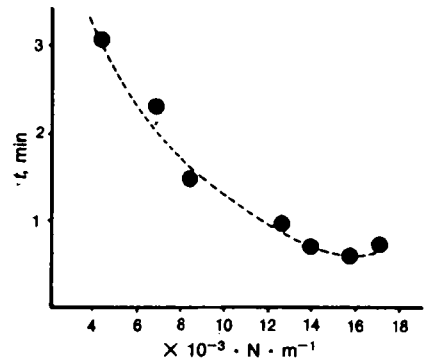

Figure 6—*Induction time of the hydrolysis of pivampicillin films after the injection of 4000 IU of penicillinase as a function of the film surface pressure.*

DISCUSSION

The pivampicillin molecule has two points especially sensitive to the hydrolytic process (Scheme I): the ester bond which forms the nucleus of 6-aminopenicillanic acid with the pivaloyl alcohol, and the β-lactamic bond of the 6-aminopenicillanic acid. Hydrolysis of the ester bond is produced through the effect of the blood esterases once the antibiotic has been absorbed, converting the antibiotic into active ampicillin, while the nonactive pivaloic ester (pivampicillin) is better absorbed through the digestive tract than the ampicillin itself (8).

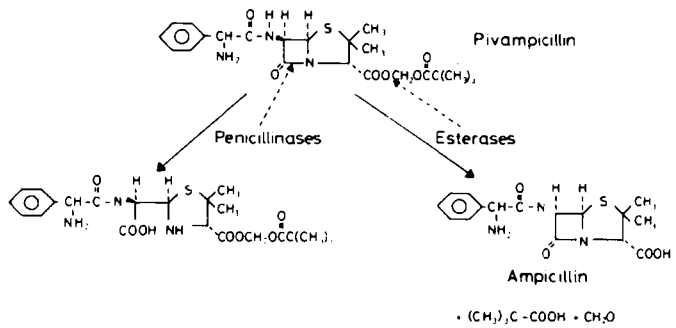

Scheme I—Hydrolysis process of the pivampicillin by esterases and penicillinases.

The *in vitro* studies with bulk material performed by Yokota *et al.* (12) seem to indicate that the enzyme responsible for this hydrolytic process is a carboxyesterase (E.C. 3.1.1.1). But the results reported in the present study indicate that this enzyme is inactive, even when tested at very high concentrations. This fact can be interpreted in different ways: (*a*) lack of specificity of the enzyme with the substrate, which would contradict the results obtained by Yokota; (*b*) liberation of insoluble products, which is not very likely because the pivaloic alcohol and the ampicillin are extraordinarily soluble under the current experimental conditions; or (*c*) inactivation of the esterase enzyme in the interface (the more probable of the three interpretations). The latter would be in agreement with the results obtained in 1958 by Sarda and Desnuelle (13), who, using triacetin as a substrate in the monolayer, found very low hydrolytic activity for the esterase compared with that of the pancreatic lipase normally used in kinetic studies of lipolysis. Finally, the possibility exists that the ester group, due to the relatively large size of the molecule of pivampicillin, must be situated in the air–water interface in order to be reached by the enzyme molecules penetrating the monolayer from the aqueous subphase.

Compared with this poor hydrolytic esterase effect, the penicillinase produced a quick hydrolysis of the pivampicillin, with a rupture of the β-lactamic bond and solubilization of the penicillin, which let the monolayer pass into the aqueous subphase. Pivampicillin is normally considered more resistant than ampicillin to the action of β-lactamase enzymes, but more sensitive than other "resistant" penicillins. The resistance of pivampicillin to the penicillinase is due to the steric effect that results from the esterification of the ampicillin carboxyl group. This chemical modification makes access of the enzyme to the active site in the β-lactamic nucleus more difficult (9). In spite of this, β-lactamase has been shown in this report to be very active in the monolayer, producing hydrolysis of all the molecules in a few minutes.

The process for enzymatic reactions in monolayers, according to a general scheme proposed by Verger *et al.*, (14), takes place in three stages. In the first stage, the enzyme penetrates the monolayer in a reversible process, with a penetration constant K_p and a desorption constant K_d; with time an equilibrium is reached, so that the amount of the enzyme penetrated is equal to that desorbed. In the second stage, also reversible, an enzyme–substrate complex (of the Michaelis–Menten type) is made, with a formation constant K_m. Finally, the enzyme–substrate complex is broken, freeing the enzyme (which remains in the monolayer) and the soluble reaction product(s) (which dissolves in the aqueous subphase), with a velocity regulated by a catalytic constant K_{cat}.

This model has been discussed based on the results obtained by Dervichian (15). However, it adapts well to the results obtained in studying the enzyme kinetics of penicillin hydrolysis in monolayers by penicillinases.

At the beginning of this process, the penicillinase has to penetrate the monolayer, improving the velocity of reaction until it reaches an equilibrium between the adsorption and desorption of enzyme molecules, and the number of molecules which exist in the monolayer remains constant. This requires an induction time (τ), after which the reaction rate is constant (a pseudo-zero-order process).

The results obtained fit also with the equation proposed by Verger *et al.* (14):

$$V_m = \frac{K_{cat} E_0 S}{K_d / K_p \cdot K_m}$$

where V_m is the velocity of the process under steady-state conditions, *i.e.*, when the concentration of the intermediate products remains constant and, thus, the velocities of formation and decomposition of the enzyme-substrate complex are equal; E_0 is the enzyme concentration in the subphase; S is the surface concentration of substrate in the monolayer; K_m is the Michaelis-Menten interfacial constant ($K_{cat} + K_d/K_p$); and K_p and K_d are the penetration and desorption constants of the enzyme. As can be seen in this equation, the hydrolysis rate of the pivampicillin must increase proportionately with the increase of the enzyme concentration, which agrees with the results shown in Fig. 5.

The increase of the reaction rate with increasing surface pressure in the monolayer can be interpreted only when the increase in the pressure causes a higher surface concentration. One must remember, however, that the increase of surface pressure reduces the penetration capacity of the enzyme in the monolayer, as shown by Verger *et al.* (16) using radioactive enzymes. These two phenomena are the reason that a pressure of maximum activity can normally be reached, varying according to the enzyme and substrate used, after which the velocity of reaction decreases. In the process of the hydrolysis of pivampicillin by penicillinase, it has been impossible to reach this maximum value. However, using Fig. 4, one can assume that this maximum is found at $1.7\text{-}1.8 \times 10^{-2}$ N·m^{-1}.

Finally, one fact in this study that might be considered paradoxical is the decrease of the induction time (τ) when the surface pressure of the monolayer is increased (Fig. 6). That is, the enzyme penetrates more quickly in monolayers which are tightly compacted than in the monolayers in which the molecules of penicillin are free, leaving large intermolecular spaces. This effect can be interpreted as a result of the improvement of the "quality of the interface," especially as to the packing of the substrate molecules, which [as was demonstrated by Slotboom *et al.* (17)] influence the kinetic parameters of the enzyme, especially increasing the value of the penetration constant K_p.

REFERENCES

(1) L. Michaelis and M. L. Menten, *Biochem. J.*, **49**, 333 (1913).

(2) A. H. Hughes, *Biochem. J.*, **29**, 437 (1935).

(3) C. W. Garner and L. C. Smith, *Biochim. Biophys. Acta*, **39**, 672 (1970).

(4) J. W. Lagocki, N. D. Bayd, J. H. Law, and F. J. Kezdy, *J. Am. Chem. Soc.*, **92**, 2923 (1970).

(5) D. G. Dervichian, *Biochimie*, **53**, 25 (1971).

(6) R. Verger and G. H. de Haas, *Chem. Phys. Lipids*, **10**, 127 (1973).

(7) O. Valls, A. Alsina, and M. Alvarez, *Anal. Reale Acad. Farm.* **47**, 51 (1981).

(8) W. von Daefne, E. Drederiksen, E. Gundersen, F. Lund, P. Mork, H. J. Petersen, K. Roholt, L. Tybring, and W. O. Gottfredsen, *J. Med. Chem.* **13**(4), 607 (1978).

(9) J. P. Hou and J. W. Poole, *J. Pharm. Sci.*, **62**, 787 (1973).

(10) O. Valls, A. Alsina, and M. Alvarez, *Cien. Ind. Farm.* **1**, 23 (1982).

(11) J. Sörensen, *Biochem. Zeits*, **21**, 131 (1909).

(12) T. Yokota, *et al.*, *Jap. J. Pharmacol.*, **24**, suppl. 78 (1974).

(13) L. Sardá and P. Desnuelle, *Biochim. Biophys. Acta*, **30**, 513 (1958).

(14) R. Verger, M. C. E. Mieras, and G. H. de Haas, *J. Biol. Chem.*, **248**, 4023 (1973).

(15) D. G. Dervichian, *Biochimie*, **53**, 25 (1971).

(16) R. Verger, J. Rietsch, M. C. E. Dam-Mieras, and G. H. de Haas, *J. Biol. Chem.*, **251**(10), 3128 (1976).

(17) A. J. Slotboom, R. Verger, H. M. Verheij, P. H. M. Baartmans, L. L. M. van Deenen, and G. H. de Haas, *Chem. Phys. Lipids*, **17**, 128 (1976).

Time-Dependent Elimination of Cinoxacin in Rats

MASAHIRO KOIKE ˣ, RYO NORIKURA, KENJI MIZOJIRI, and KOICHI SUGENO

Received May 19, 1983, from *Shionogi Research Laboratories, Shionogi & Co., Ltd., Osaka, Japan.* Accepted for publication March 8, 1984.

Abstract □ The effect of the variation of urinary pH on the pharmacokinetics of the acidic antibacterial agent, cinoxacin (pK_a 4.60), was examined. Urinary pH of 24-h fasted rats remained at about pH 6 during the daytime, while that of nonfasted rats was high (about pH 7.5) in the morning and gradually decreased to a pH similar to that of the fasted rat in the afternoon. The free fraction of cinoxacin in fasted rat sera in the morning was similar to that in nonfasted rats despite the longer half-life of cinoxacin in fasted rats. In the afternoon the free fraction was slightly different despite similar cinoxacin elimination in fasted and nonfasted rats. These findings seemed to exclude the contribution of protein binding from the causes of increased cinoxacin elimination in nonfasted rats in the morning. Elimination rate constants of cinoxacin obtained with a one-compartment open model correlated well with urinary pH 30 min after injection, suggesting that the urinary pH plays a more important role in cinoxacin elimination. When cinoxacin was orally administered to fasted rats at 11:00, the area under the plasma concentration-time curve was threefold larger than in nonfasted rats. As found with the intravenous administration, this difference may be explained by the prolonged half-life caused by decreased urinary pH after fasting. This study revealed the time-dependent elimination of cinoxacin in nonfasted rats, which is related to physiological change of urinary pH caused by food intake.

Keyphrases □ Cinoxacin—time-dependent elimination, effect of fasting, urinary pH, rats □ Urinary pH—effect of fasting on cinoxacin elimination, diurnal alteration, rats

The chronopharmacological aspects of drugs have been discussed in many review articles (1-3). Some attribute these phenomena to the diurnal oscillation of pharmacological sensitivity to drugs (4) and others to the diurnal variance of plasma levels (or levels at the receptor site) without alteration of the sensitivity to the drugs. Alteration of plasma levels can be expressed by pharmacokinetic parameters such as absorption, distribution, metabolism, and excretion (5-9). Circadian rhythms of hepatic drug-metabolizing ability have been especially well investigated (10-13), but the causes of the rhythmicity in absorption, distribution, and excretion have not been thoroughly investigated in spite of being frequently described (9).

We noticed a diurnal rhythm of urinary pH in normally fed rats and found that the rhythm disappeared with fasting. We tried to clarify the effect of such diurnal alteration of urinary pH and fasting on the pharmacokinetics of drugs in the rat. The model compound was cinoxacin (1-ethyl-1,4-dihydro-4-oxo[1,3]dioxolo[4,5-*g*]cinnoline-3-carboxylic acid). Cinoxacin is an acidic (pK_a 4.60), antibacterial agent, which is excreted almost completely unchanged in rat urine (14, 15).

EXPERIMENTAL SECTION

Materials—Male Sprague-Dawley rats, weighing 240–270 g, were purchased commercially[1] and were housed in group cages with wooden chips on the floor in a room with constant temperature (24 ± 1°C) and humidity (55

[1] Clea Japan, Inc., Tokyo, Japan.

0022-3549/84/1200-1697$01.00/0

© 1984, American Pharmaceutical Association

where V_m is the velocity of the process under steady-state conditions, *i.e.*, when the concentration of the intermediate products remains constant and, thus, the velocities of formation and decomposition of the enzyme-substrate complex are equal; E_0 is the enzyme concentration in the subphase; S is the surface concentration of substrate in the monolayer; K_m is the Michaelis-Menten interfacial constant ($K_{cat} + K_d/K_p$); and K_p and K_d are the penetration and desorption constants of the enzyme. As can be seen in this equation, the hydrolysis rate of the pivampicillin must increase proportionately with the increase of the enzyme concentration, which agrees with the results shown in Fig. 5.

The increase of the reaction rate with increasing surface pressure in the monolayer can be interpreted only when the increase in the pressure causes a higher surface concentration. One must remember, however, that the increase of surface pressure reduces the penetration capacity of the enzyme in the monolayer, as shown by Verger *et al.* (16) using radioactive enzymes. These two phenomena are the reason that a pressure of maximum activity can normally be reached, varying according to the enzyme and substrate used, after which the velocity of reaction decreases. In the process of the hydrolysis of pivampicillin by penicillinase, it has been impossible to reach this maximum value. However, using Fig. 4, one can assume that this maximum is found at $1.7\text{-}1.8 \times 10^{-2}$ N·m^{-1}.

Finally, one fact in this study that might be considered paradoxical is the decrease of the induction time (τ) when the surface pressure of the monolayer is increased (Fig. 6). That is, the enzyme penetrates more quickly in monolayers which are tightly compacted than in the monolayers in which the molecules of penicillin are free, leaving large intermolecular spaces. This effect can be interpreted as a result of the improvement of the "quality of the interface," especially as to the packing of the substrate molecules, which [as was demonstrated by Slotboom *et al.* (17)] influence the kinetic parameters of the enzyme, especially increasing the value of the penetration constant K_p.

REFERENCES

(1) L. Michaelis and M. L. Menten, *Biochem. J.*, **49**, 333 (1913).

(2) A. H. Hughes, *Biochem. J.*, **29**, 437 (1935).

(3) C. W. Garner and L. C. Smith, *Biochim. Biophys. Acta*, **39**, 672 (1970).

(4) J. W. Lagocki, N. D. Bayd, J. H. Law, and F. J. Kezdy, *J. Am. Chem. Soc.*, **92**, 2923 (1970).

(5) D. G. Dervichian, *Biochimie*, **53**, 25 (1971).

(6) R. Verger and G. H. de Haas, *Chem. Phys. Lipids*, **10**, 127 (1973).

(7) O. Valls, A. Alsina, and M. Alvarez, *Anal. Reale Acad. Farm.* **47**, 51 (1981).

(8) W. von Daefne, E. Drederiksen, E. Gundersen, F. Lund, P. Mork, H. J. Petersen, K. Roholt, L. Tybring, and W. O. Gottfredsen, *J. Med. Chem.* **13**(4), 607 (1978).

(9) J. P. Hou and J. W. Poole, *J. Pharm. Sci.*, **62**, 787 (1973).

(10) O. Valls, A. Alsina, and M. Alvarez, *Cien. Ind. Farm.* **1**, 23 (1982).

(11) J. Sörensen, *Biochem. Zeits*, **21**, 131 (1909).

(12) T. Yokota, *et al.*, *Jap. J. Pharmacol.*, **24**, suppl. 78 (1974).

(13) L. Sardá and P. Desnuelle, *Biochim. Biophys. Acta*, **30**, 513 (1958).

(14) R. Verger, M. C. E. Mieras, and G. H. de Haas, *J. Biol. Chem.*, **248**, 4023 (1973).

(15) D. G. Dervichian, *Biochimie*, **53**, 25 (1971).

(16) R. Verger, J. Rietsch, M. C. E. Dam-Mieras, and G. H. de Haas, *J. Biol. Chem.*, **251**(10), 3128 (1976).

(17) A. J. Slotboom, R. Verger, H. M. Verheij, P. H. M. Baartmans, L. L. M. van Deenen, and G. H. de Haas, *Chem. Phys. Lipids*, **17**, 128 (1976).

Time-Dependent Elimination of Cinoxacin in Rats

MASAHIRO KOIKE ˣ, RYO NORIKURA, KENJI MIZOJIRI, and KOICHI SUGENO

Received May 19, 1983, from *Shionogi Research Laboratories, Shionogi & Co., Ltd., Osaka, Japan.* Accepted for publication March 8, 1984.

Abstract □ The effect of the variation of urinary pH on the pharmacokinetics of the acidic antibacterial agent, cinoxacin (pK_a 4.60), was examined. Urinary pH of 24-h fasted rats remained at about pH 6 during the daytime, while that of nonfasted rats was high (about pH 7.5) in the morning and gradually decreased to a pH similar to that of the fasted rat in the afternoon. The free fraction of cinoxacin in fasted rat sera in the morning was similar to that in nonfasted rats despite the longer half-life of cinoxacin in fasted rats. In the afternoon the free fraction was slightly different despite similar cinoxacin elimination in fasted and nonfasted rats. These findings seemed to exclude the contribution of protein binding from the causes of increased cinoxacin elimination in nonfasted rats in the morning. Elimination rate constants of cinoxacin obtained with a one-compartment open model correlated well with urinary pH 30 min after injection, suggesting that the urinary pH plays a more important role in cinoxacin elimination. When cinoxacin was orally administered to fasted rats at 11:00, the area under the plasma concentration-time curve was threefold larger than in nonfasted rats. As found with the intravenous administration, this difference may be explained by the prolonged half-life caused by decreased urinary pH after fasting. This study revealed the time-dependent elimination of cinoxacin in nonfasted rats, which is related to physiological change of urinary pH caused by food intake.

Keyphrases □ Cinoxacin—time-dependent elimination, effect of fasting, urinary pH, rats □ Urinary pH—effect of fasting on cinoxacin elimination, diurnal alteration, rats

The chronopharmacological aspects of drugs have been discussed in many review articles (1-3). Some attribute these phenomena to the diurnal oscillation of pharmacological sensitivity to drugs (4) and others to the diurnal variance of plasma levels (or levels at the receptor site) without alteration of the sensitivity to the drugs. Alteration of plasma levels can be expressed by pharmacokinetic parameters such as absorption, distribution, metabolism, and excretion (5-9). Circadian rhythms of hepatic drug-metabolizing ability have been especially well investigated (10-13), but the causes of the rhythmicity in absorption, distribution, and excretion have not been thoroughly investigated in spite of being frequently described (9).

We noticed a diurnal rhythm of urinary pH in normally fed rats and found that the rhythm disappeared with fasting. We tried to clarify the effect of such diurnal alteration of urinary pH and fasting on the pharmacokinetics of drugs in the rat. The model compound was cinoxacin (1-ethyl-1,4-dihydro-4-oxo[1,3]dioxolo[4,5-*g*]cinnoline-3-carboxylic acid). Cinoxacin is an acidic (pK_a 4.60), antibacterial agent, which is excreted almost completely unchanged in rat urine (14, 15).

EXPERIMENTAL SECTION

Materials—Male Sprague-Dawley rats, weighing 240–270 g, were purchased commercially[1] and were housed in group cages with wooden chips on the floor in a room with constant temperature (24 ± 1°C) and humidity (55

[1] Clea Japan, Inc., Tokyo, Japan.

0022-3549/84/1200-1697$01.00/0

© 1984, American Pharmaceutical Association

Table I—Biochemical Examination of Rat Sera [a]

Examination	Sera at 09:30		Sera at 15:30	
	Fasted, $n = 5$	Nonfasted, $n = 6$	Fasted, $n = 6$	Nonfasted, $n = 4$
Total bilirubin, mg/dL	0.34 ± 0.06[b]	0.17 ± 0.05	0.32 ± 0.04[b]	0.18 ± 0.05
Albumin, g/dL	3.12 ± 0.11[c]	3.22 ± 0.07[d]	3.35 ± 0.15	3.40 ± 0.08
Total protein, g/dL	5.38 ± 0.15[d]	5.60 ± 0.21[c]	5.92 ± 0.27	5.90 ± 0.12
Non-esterified fatty acid[e], mEq/L	0.52 ± 0.08[b,c]	0.15 ± 0.05[d]	0.58 ± 0.11[b]	0.26 ± 0.10

[a] Mean ± *SD*. [b] Significant difference at $p < 0.01$ compared with nonfasted rats. [c] Significant difference at $p < 0.05$ compared with sera at 15:30. [d] Significant difference at $p < 0.01$ compared with sera at 15:30. [e] Calculated as oleic acid.

± 5%). Under a 12-h light-dark cycle, rats were given free access to solid animal chow[2] and water. One-half of the rats were transferred to a cage with a stainless steel net floor (mesh size: 1.5 × 1.5 cm) 24 h prior to drug administration to prevent coprophagy (± 1) and deprived of chow but not water. Cinoxacin was obtained commercially[3]. ^{14}C-Labeled cinoxacin was synthesized by the method of Nagasaki *et al.* (16). Its specific activity was 37.2 μCi/mg and radiochemical purity was >98%. All other chemicals were of reagent grade.

Animal Experiments—Fasted and nonfasted rats, under light ether anesthesia, were catheterized in the right external jugular vein by Upton's method (17) and urine-collecting adapters were attached to their penises. The animals were then placed in individual cages[4] and left for >2 h to eliminate the effect of ether. Next, 20 mg/kg of ^{14}C-labeled or unlabeled cinoxacin (10 mg/mL of aqueous solution with an equivalent amount of sodium hydroxide) was intravenously administered *via* the caudal vein. At 12:00, [^{14}C]cinoxacin was used and at 15:00, unlabeled cinoxacin was used. The rats were periodically forced to void urine by using ether. Blood was taken *via* the catheter and immediately centrifuged to obtain the plasma. In the case of oral administration, [^{14}C]cinoxacin was used and blood sampling was done nonserially. Twenty mg/kg of [^{14}C]cinoxacin (10 mg/mL of aqueous solution prepared similarly to the intravenous injection) was orally administered and blood samples were taken *via* the aorta after abdominal incision under light ether anesthesia. Cinoxacin in plasma was determined by fluorometry (15) and the urinary pH was measured. When ^{14}C-labeled cinoxacin was administered, radioactivity was measured with a liquid scintillation counter[5]. Diurnal changes of urinary pH in noncatheterized rats were measured as described above without cinoxacin administration.

Biochemical Examination of Serum and Protein Binding—At 09:30 and 15:30, fasted and nonfasted rats were lightly anesthetized with ether and blood was withdrawn *via* the aorta after an abdominal incision. Serum was obtained by centrifugation using a serum separation aid[6]. Total bilirubin, albumin, and total protein in the serum were determined with an autoanalyzer[7] and nonesterified fatty acids were determined with a kit[8]. Free cinoxacin in the serum was measured with an ultrafiltration method *in vitro*. Five microliters of cinoxacin (6.0 mg/mL, pH 7.4 phosphate buffer solution) was added to 2 mL of the serum to make a final concentration of 15 μg/mL. After this mixture had been left for 1 h at 25°C, the serum was centrifuged in a membrane cone[9]. The free cinoxacin in the filtrate was determined by fluorometry.

Calculation of Pharmacokinetic Parameters and Statistical Analysis—The cinoxacin elimination rate constant in plasma was calculated using MULTI (18), a nonlinear least-squares program, based on a one-compartment open model. For statistical analyses, the paired *t* test and regression analysis were used.

RESULTS AND DISCUSSION

The rat which we usually use as an experimental animal takes food exclusively at night and rarely during the daytime. Biological rhythmicity probably exists based on the food intake rhythm. The effect of food and diet on pharmacokinetic parameters, *e.g.*, absorption, distribution, metabolism, and excretion, have been reviewed (19-21). Therefore, time-dependent pharmacokinetics may be considered in relation to the rhythmicity of food intake. We examined the alteration of cinoxacin pharmacokinetics as a function of time and feeding.

[2] Type CA-1; Clea Japan, Inc.
[3] Eli Lilly Co., Indianapolis, Ind.
[4] Ballman cage Model KN-326; Natsume Seisakusho, Tokyo, Japan.
[5] Model 1215 Rackbeta; LKB-Wallac, Turku, Finland.
[6] Separaid; HATCO International, Los Angeles, Calif.
[7] Model SMA plus MICRO; Technicon Instruments Corp., N.Y.
[8] NEFA Test-C *Wako;* Wako Pure Chemical Industries, Ltd., Osaka, Japan.
[9] Centriflo CF-25; Amicon Corp., Lexington, Mass.

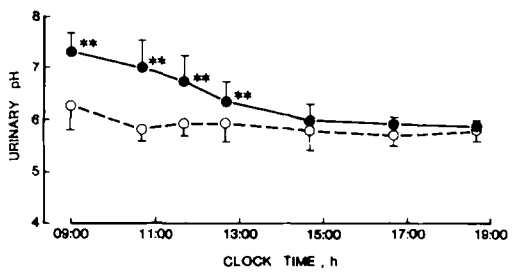

Figure 1—*Diurnal variance of urinary pH in fasted and nonfasted rats. The means and* SD *values from 15 rats are shown. Key: (●) nonfasted rats; (○) fasted rats; (**) significantly different from fasted rats at* $p < 0.01$.

In fasted and nonfasted rats, at either 09:30 or 15:30, serum was examined for factors affecting the protein binding of drugs (22-24). As shown in Table I, total bilirubin and nonesterified fatty acids increased markedly with fasting both in the morning and afternoon. Furthermore, a slight increase was observed in the afternoon in albumin, total protein, and nonesterified fatty acids in fasted and nonfasted rats. These results alerted us to the possibility that protein binding might be changed by time and feeding.

Next, we examined the diurnal rhythm of urinary pH and the effect of feeding. As shown in Fig. 1, urinary pH in fasted rats was constant during the daytime, whereas in nonfasted rats it was high in the morning and decreased slightly in the afternoon to the level of the fasted rats. This variance of urinary pH is likely to affect the renal excretion rate for drugs with pK_a values similar to urinary pH (25).

We selected cinoxacin as a model compound to investigate the effect of this variance of physiological parameters on pharmacokinetics. Renal excretion of cinoxacin is reported to be dependent on urinary pH because of renal reabsorption (26-29).

Table II shows serum protein binding of cinoxacin *in vitro*. Significant differences were detected between the serum of fasted and nonfasted rats at 15:30 but not at 09:30. Though the extent of the difference was small, it could affect the cinoxacin pharmacokinetics. Therefore, we investigated the cinoxacin elimination from plasma after intravenous administration in fasted and nonfasted rats in the morning and afternoon. Figure 2 shows the time course of plasma levels of cinoxacin after intravenous administration at 12:00 to fasted and nonfasted rats having different urinary pH values. As expected, plasma elimination was slower in fasted rats than nonfasted rats, and urinary excretion during the initial 1 h in fasted and nonfasted rats was 45.8 and 73.7% and at 2 h, 62.6 and 83.8% of the dose, respectively (data not shown). These results suggest that cinoxacin elimination was rapid especially in nonfasted rats, and the elimination was affected by minor difference of urinary pH at the time of and for at least 1 h after drug administration. This can be easily explained by greater renal reabsorption due to lower urinary pH in fasted rats (26-29).

On the other hand, when cinoxacin was injected at 15:00, it was similarly eliminated from plasma in both rat groups (Fig. 3), in spite of different serum protein binding ratios between fasted and nonfasted rats (Table II). This

Table II—*In Vitro* Serum Protein Binding of Cinoxacin in Rats

Rat	Unbound fraction, %[a]	
	Sera at 09:30	Sera at 15:30
Fasted	6.36 ± 0.38[b]	6.65 ± 0.25[c,d]
Nonfasted	6.54 ± 0.45[c]	6.00 ± 0.47[b]

[a] Percent of total concentration (15 μg/mL) ± *SD*. [b] $n = 5$. [c] $n = 6$. [d] Significant difference at $p < 0.05$ compared with sera in nonfasted rats at 15:30.

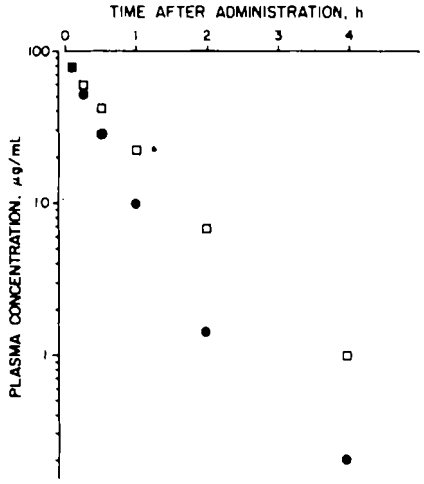

Figure 2—*Average plasma levels of cinoxacin after intravenous administration of 20 mg/kg of [^{14}C]cinoxacin to three fasted or nonfasted rats at 12:00. Key (□) fasted rats; (●) nonfasted rats.*

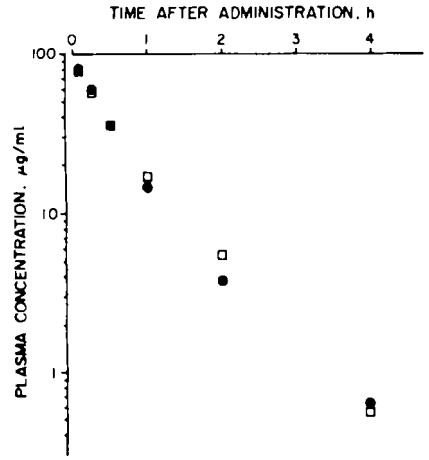

Figure 3—*Average plasma levels of cinoxacin after intravenous administration of 20 mg/kg of unlabeled cinoxacin to three fasted or nonfasted rats at 15:00. Key: (□) fasted rats; (●) nonfasted rats.*

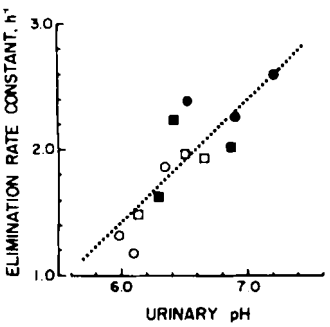

Figure 4—*Correlation between urinary pH 30 min after administration of 20 mg/kg of ^{14}C-labeled or unlabeled cinoxacin and elimination rate constant obtained from fasted or nonfasted rats at 12:00 or 15:30. Key: (●) nonfasted rats at 12:00; (○) fasted rats at 12:00; (■) nonfasted rats at 15:00; (□) fasted rats at 15:00.*

suggests that urinary pH plays a more important role than protein binding in cinoxacin elimination from the plasma. As previously described, cinoxacin elimination in nonfasted rats administered at 12:00 was rapid (Fig. 2) and >70% of the dose was excreted in urine until 13:00; furthermore, a higher pH

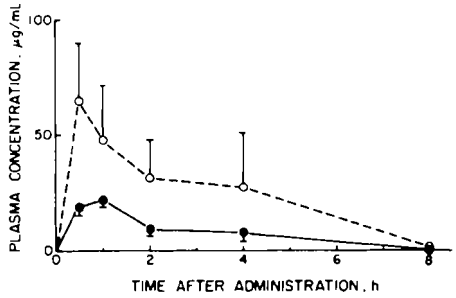

Figure 5—*Plasma levels of cinoxacin after oral administration of 20 mg/kg of [^{14}C]cinoxacin in fasted or nonfasted rats at 11:00. Means and* SD *values from three rats. Key: (○) fasted rats; (●) nonfasted rats.*

in urine was maintained at least until ~13:00 (Fig. 1). These results accounted for the faster elimination in nonfasted rats than fasted rats administered the drug at 12:00.

We investigated the correlation between urinary pH 30 min after intravenous administration and the elimination rate constant calculated from the values in Figs. 2 and 3. Figure 4 shows a significant correlation between the elimination rate constant obtained with the one-compartment open model and the urinary pH ($r = 0.8427$, $p < 0.01$). As the slope of the regression line is 1.033, if urinary pH decreases from 7 to 6, the elimination rate constant decreases from 2.43 to 1.40. Thus, diurnal variance of urinary pH in normally fed rats has an important effect on cinoxacin elimination, though in fasted rats changes in cinoxacin elimination do not arise because urinary pH remains constant during the daytime.

Figure 5 shows the plasma levels of cinoxacin orally administered to fasted and nonfasted rats at 11:00. As expected, higher plasma levels were observed in fasted rats. The area under the plasma concentration–time curve (AUC) calculated by the trapezoidal rule was 125.8 μg·h/mL in fasted rats and 40.9 μg·h/mL in nonfasted rats. The larger AUC in fasted rats is due to the lower urinary pH and in addition, a higher peak level may be partly attributable to a faster gastric emptying rate, as mentioned by Watanabe *et al.* (30).

REFERENCES

(1) A. Reinberg and F. Halberg, *Annu. Rev. Pharmacol.*, **11**, 455 (1971).

(2) A. Reinberg, *Arzneim.-Forsch.*, **28**, 1861 (1978).

(3) F. Halberg, H. F. Kabat, and P. Klein, *Am. J. Hosp. Pharm.*, **37**, 101 (1980).

(4) W. Nelson and F. Halberg, *Neuropharmacology*, **12**, 509 (1973).

(5) I. H. Patel, R. H. Levy, and J. S. Lockard, *J. Pharm. Sci.*, **66**, 650 (1977).

(6) G. E. Poley, C. A. Shively, and E. S. Vessl, *Clin. Pharmacol. Ther.*, **24**, 726 (1978).

(7) B. Brugueroile, M. Valli, L. Bouyard, G. Jadot, and P. Bouyard, *Eur. J. Drug Metab. Pharmacokinet.*, **6**, 189 (1981).

(8) W. R. Ritschel, G. Bykadi, E. J. Norman, and P. W. Lucker, *Arzneim.-Forsch.*, **30**, 1535 (1981).

(9) A. Reinberg and M. H. Smolensky, *Clin. Pharmacokinet.*, **7**, 401 (1982).

(10) F. M. Radzialowski and W. F. Bousquet, *J. Pharmacol. Exp. Ther.*, **163**, 229 (1968).

(11) T. L. Holcslaw, T. S. Miya, and W. S. Bousquet, *J. Pharmacol. Exp. Ther.*, **195**, 320 (1975).

(12) J. M. Tredger and R. S. Chhabra, *Xenobiotica*, **7**, 481 (1977).

(13) K. Püschel, T. Mätzsch, and H. Von Mayersbach, *Arch. Toxicol.*, **48**, 199 (1981).

(14) M. Nakamura and K. Sugeno, *Chemotherapy (Tokyo)*, **28** (s-4), 567 (1980).

(15) Y. Tochino, K. Sugeno, M. Doteuchi, H. Okabe, R. Norikura, and H. Tanaka, *Chemotherapy (Tokyo)*, **28** (s-4), 73 (1980).

(16) T. Nagasaki, Y. Katsuyama, and H. Minato, *J. Label. Comp. Radiopharm.*, **12**, 409 (1976).

(17) R. A. Upton, *J. Pharm. Sci.*, **64**, 112 (1975).

(18) K. Yamaoka, Y. Tanigawara, T. Nakagawa, and T. Uno, *J. Pharm. Dyn.*, **4**, 879 (1981).

(19) P. G. Welling, *J. Pharmacokinet. Biopharm.*, **5**, 291 (1977).

(20) A. Melander, *Clin. Pharmacokinet.*, **3**, 337 (1978).

(21) R. D. Toothaker and P. G. Welling, *Annu. Rev. Pharmacol. Toxicol.*, **20**, 173 (1980).

(22) E. S. Pepper and W. D. Wosilait, *Res. Commun. Chem. Pathol. Pharmacol.*, **18**, 275 (1977).
(23) S. Kitazawa and T. Komuro, *Chem. Pharm. Bull.*, **25**, 141 (1977).
(24) S. K. Chakrabarti and J. Brodeur, *Can. J. Physiol. Pharmacol.*, **58**, 205 (1980).
(25) A. Johnston, C. D. Burgess, S. J. Warrington, J. Wadsworth, and N. A. Hamer, *Br. J. Clin. Pharmacol.*, **8**, 349 (1979).
(26) K. S. Israel, H. R. Black, R. L. Nelson, M. K. Brunson, J. F. Nash, G. L. Brier, and J. D. Wolney, *J. Clin. Pharmacol.*, **18**, 491 (1978).
(27) J. F. Quay, R. F. Childers, D. W. Johnson, J. F. Nash, and J. F. Stucky III, *J. Pharm. Sci.*, **68**, 227 (1979).
(28) N. Rodriguez, P. O. Madsen, and P. G. Welling, *Antimicrob. Agents Chemother.*, **15**, 465 (1981).
(29) R. H. Barbhaiya, A. U. Gerber, W. A. Craig, and P. G. Welling, *Antimicrob. Agents Chemother.*, **21**, 472 (1982).
(30) J. Watanabe, H. Okabe, K. Mizojiri, H. Yamada, and R. Yamamoto, *Chem. Pharm. Bull.*, **25**, 2147 (1977).

ACKNOWLEDGMENTS

The authors thank Dr. Y. Yoshizaki for the biochemical examinations of rat sera.

Determination of Benzalkonium Chloride by Gas Chromatography

Z. R. CYBULSKI

Received November 25, 1983, from the *Physical Chemistry Department, Fisons plc, Pharmaceutical Division, Loughborough, LE11 ORH, UK.* Accepted March 7, 1984.

Abstract □ A new, simple, and useful approach for the analysis of benzalkonium chloride is presented. A gas chromatograph (GC) has been used to pyrolyze benzalkonium chloride in a specific and reproducible manner to yield two tertiary amines for each homologue of benzalkonium chloride present. These are separated by GC and are used to determine the homologue composition of the benzalkonium chloride. These determinations can be made with an analysis time of 25 min/sample.

Keyphrases □ Benzalkonium chloride—determination by GC □ GC—determination of benzalkonium chloride

Benzalkonium chloride is used in pharmaceuticals as an antimicrobial preservative and is a mixture of homologous compounds (I), where the R group represents an *n*-alkyl chain which can vary from 10–18 carbon atoms. The relative amounts of the different *n*-alkyl species in benzalkonium chloride solutions greatly affect the antimicrobial spectrum and activity on the mixture (1). The current methods for analysis of benzalkonium chloride solutions according to the USP (2) rely upon titrimetric analysis of the total alkylbenzyldimethylammonium chloride based upon potassium iodate equivalents. Additionally, the ratio of *n*-alkyl components of benzalkonium chloride can be determined by microhydrogenation followed by solvent extraction and gas chromatography (GC). The ratio of alkyl components is then calculated and must meet specific USP requirements. These requirements state that the C_{12} homologue must comprise at least 40% of the total benzalkonium chloride content and that the C_{14} homologue must be at least 20%. Furthermore, these two homologues together must comprise not less than 70% of the total content.

Other methods have been reported for the determination of benzalkonium chloride, for example, ion-pairing techniques (3–5), direct titration involving tetraphenylboron sodium (6) and iodate (7). Later methods of analysis have included MS using laser ionization (8), chemical ionization (9), and HPLC (10).

GC methods include one based on a modified Hofmann degradation of benzalkonium chloride with subsequent analysis of the formed benzyldimethylamine and the corresponding alkene (11). Another method involves chemical derivatization of the benzalkonium chloride to introduce specific functional groups into the derivatives which are amenable to GC with enhanced detectability using electron capture and nitrogen-specific thermionic detecting systems (12).

The procedure presented here determines directly the alkyl chain-length ratios of benzalkonium chloride species in samples of benzalkonium chloride in an easy, sensitive, and reliable operation.

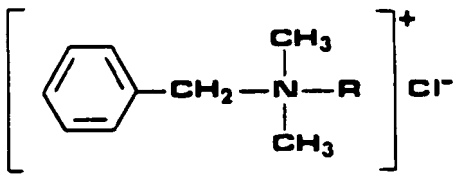

(I)

EXPERIMENTAL SECTION

Apparatus—Measurements were carried out using a GC[1] fitted with a flame ionization detector. The column used was a 0.9 m (2 mm i.d.) glass column packed with OV17 (3%) on Chromosorb W HP (80/100 mesh). A 10-μL syringe[2] was used to inject samples. The chromatograms were recorded on a potentiometric recorder[3] and peak area measurements were obtained using an integrator[4].

Mass spectrometric measurements for identification of the GC pyrolysis products were conducted using a spectrometer[5] operating in the electron impact ionization mode. The mass spectrometric data was handled by a data system[6].

Reagents, Solvents, and Standards—The carrier gas for the GC work was nitrogen; for MS work, the carrier gas was helium. The commercial samples of benzalkonium chloride were obtained from various manufacturers. Samples of benzalkonium chloride for analysis were prepared as solutions in methanol (0.5%). For confirmation, a benzalkonium chloride standard was obtained[7]. Individual pure benzalkonium chloride standards were examined with R = C_{14}, C_{16}, and C_{18}. The standards were also examined as solutions in methanol (0.5%).

[1] Model 204; Pye-Unicam.
[2] S.G.E.
[3] Model 2S; Servoscribe.
[4] Model 3390A; Hewlett Packard.
[5] Models MS30 and MS50; Kratos.
[6] Model DS55; Kratos.
[7] USP Convention Sample.

0022-3549/84/1200-1700$01.00/0
© 1984, American Pharmaceutical Association

(22) E. S. Pepper and W. D. Wosilait, *Res. Commun. Chem. Pathol. Pharmacol.*, **18**, 275 (1977).
(23) S. Kitazawa and T. Komuro, *Chem. Pharm. Bull.*, **25**, 141 (1977).
(24) S. K. Chakrabarti and J. Brodeur, *Can. J. Physiol. Pharmacol.*, **58**, 205 (1980).
(25) A. Johnston, C. D. Burgess, S. J. Warrington, J. Wadsworth, and N. A. Hamer, *Br. J. Clin. Pharmacol.*, **8**, 349 (1979).
(26) K. S. Israel, H. R. Black, R. L. Nelson, M. K. Brunson, J. F. Nash, G. L. Brier, and J. D. Wolney, *J. Clin. Pharmacol.*, **18**, 491 (1978).
(27) J. F. Quay, R. F. Childers, D. W. Johnson, J. F. Nash, and J. F. Stucky III, *J. Pharm. Sci.*, **68**, 227 (1979).
(28) N. Rodriguez, P. O. Madsen, and P. G. Welling, *Antimicrob. Agents Chemother.*, **15**, 465 (1981).
(29) R. H. Barbhaiya, A. U. Gerber, W. A. Craig, and P. G. Welling, *Antimicrob. Agents Chemother.*, **21**, 472 (1982).
(30) J. Watanabe, H. Okabe, K. Mizojiri, H. Yamada, and R. Yamamoto, *Chem. Pharm. Bull.*, **25**, 2147 (1977).

ACKNOWLEDGMENTS

The authors thank Dr. Y. Yoshizaki for the biochemical examinations of rat sera.

Determination of Benzalkonium Chloride by Gas Chromatography

Z. R. CYBULSKI

Received November 25, 1983, from the *Physical Chemistry Department, Fisons plc, Pharmaceutical Division, Loughborough, LE11 ORH, UK.* Accepted March 7, 1984.

Abstract □ A new, simple, and useful approach for the analysis of benzalkonium chloride is presented. A gas chromatograph (GC) has been used to pyrolyze benzalkonium chloride in a specific and reproducible manner to yield two tertiary amines for each homologue of benzalkonium chloride present. These are separated by GC and are used to determine the homologue composition of the benzalkonium chloride. These determinations can be made with an analysis time of 25 min/sample.

Keyphrases □ Benzalkonium chloride—determination by GC □ GC—determination of benzalkonium chloride

Benzalkonium chloride is used in pharmaceuticals as an antimicrobial preservative and is a mixture of homologous compounds (I), where the R group represents an *n*-alkyl chain which can vary from 10–18 carbon atoms. The relative amounts of the different *n*-alkyl species in benzalkonium chloride solutions greatly affect the antimicrobial spectrum and activity on the mixture (1). The current methods for analysis of benzalkonium chloride solutions according to the USP (2) rely upon titrimetric analysis of the total alkylbenzyldimethylammonium chloride based upon potassium iodate equivalents. Additionally, the ratio of *n*-alkyl components of benzalkonium chloride can be determined by microhydrogenation followed by solvent extraction and gas chromatography (GC). The ratio of alkyl components is then calculated and must meet specific USP requirements. These requirements state that the C_{12} homologue must comprise at least 40% of the total benzalkonium chloride content and that the C_{14} homologue must be at least 20%. Furthermore, these two homologues together must comprise not less than 70% of the total content.

Other methods have been reported for the determination of benzalkonium chloride, for example, ion-pairing techniques (3–5), direct titration involving tetraphenylboron sodium (6) and iodate (7). Later methods of analysis have included MS using laser ionization (8), chemical ionization (9), and HPLC (10).

GC methods include one based on a modified Hofmann degradation of benzalkonium chloride with subsequent analysis of the formed benzyldimethylamine and the corresponding alkene (11). Another method involves chemical derivatization of the benzalkonium chloride to introduce specific functional groups into the derivatives which are amenable to GC with enhanced detectability using electron capture and nitrogen-specific thermionic detecting systems (12).

The procedure presented here determines directly the alkyl chain-length ratios of benzalkonium chloride species in samples of benzalkonium chloride in an easy, sensitive, and reliable operation.

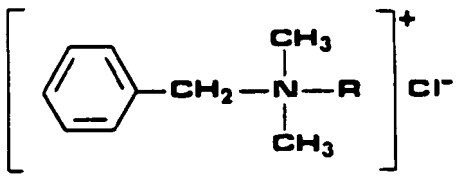

(I)

EXPERIMENTAL SECTION

Apparatus—Measurements were carried out using a GC[1] fitted with a flame ionization detector. The column used was a 0.9 m (2 mm i.d.) glass column packed with OV17 (3%) on Chromosorb W HP (80/100 mesh). A 10-μL syringe[2] was used to inject samples. The chromatograms were recorded on a potentiometric recorder[3] and peak area measurements were obtained using an integrator[4].

Mass spectrometric measurements for identification of the GC pyrolysis products were conducted using a spectrometer[5] operating in the electron impact ionization mode. The mass spectrometric data was handled by a data system[6].

Reagents, Solvents, and Standards—The carrier gas for the GC work was nitrogen; for MS work, the carrier gas was helium. The commercial samples of benzalkonium chloride were obtained from various manufacturers. Samples of benzalkonium chloride for analysis were prepared as solutions in methanol (0.5%). For confirmation, a benzalkonium chloride standard was obtained[7]. Individual pure benzalkonium chloride standards were examined with R = C_{14}, C_{16}, and C_{18}. The standards were also examined as solutions in methanol (0.5%).

[1] Model 204; Pye-Unicam.
[2] S.G.E.
[3] Model 2S; Servoscribe.
[4] Model 3390A; Hewlett Packard.
[5] Models MS30 and MS50; Kratos.
[6] Model DS55; Kratos.
[7] USP Convention Sample.

0022-3549/84/1200-1700$01.00/0
© 1984, American Pharmaceutical Association

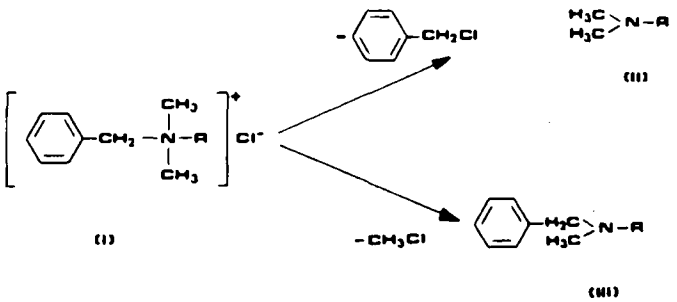

Scheme I—Gas chromatography pyrolysis products of benzalkonium chloride (I).

Assay—All benzalkonium chloride samples were dissolved in methanol to give 0.5% solutions which were used for the GC determinations. The optimum conditions for programmed GC were as follows: the oven start temperature was 100°C and this was programmed at 8.0°C/min up to 280°C; the flame ionization detector temperature was set at 350°C; the injection port temperature was 250°C; the carrier gas flow-rate was 40 mL/min. The injection size was 2 μL. The flame ionization detector sensitivity was 6.4×10^{-9} *A* full scale deflection.

Table I—MS Data on the GC Pyrolysis Products of Pure C_{14} Benzalkonium Chloride

GC Peak Retention time, min	Molecular Ion, *m/z*	Base Peak, *m/z*	Identity of Compound
0.8	126/128	91	Benzyl Chloride
5.2	241	58	Dimethylalkylamine (II) R = C_{14}
13.0	317	134	Benzylmethylalkylamine (III) R = C_{14}

Table II—Analysis of USP Benzalkonium Chloride Sample

Homologue	Label Claim, %	Found, %
C_{10}	0.8	0.0
C_{12}	41.5	41.3
C_{14}	49.1	50.5
C_{16}	8.7	8.2
C_{18}	0.0	0.0

RESULTS AND DISCUSSION

It has been shown previously (14) that when certain quaternary ammonium halides are pyrolyzed they yield tertiary amines. Benzalkonium chloride samples, when analyzed using the conditions described, yield two tertiary amines for each homologue of benzalkonium chloride present (Scheme I). The MS data supporting the structure of the pyrolysis products of the pure C_{14} benzalkonium chloride homologue are shown in Table I.

The method was applied to mixtures of benzalkonium chlorides. Using the retention times of the pyrolysis products of pure benzalkonium chloride homologues, the distribution of benzalkonium chloride was determined in a USP convention sample. The result is shown in Table II.

As there are two compounds formed for each homologue present, there are three possible methods available for calculating the percentage distribution of benzalkonium chloride homologues:

Method 1—Determination of the ratio of the responses for pyrolysis products (dimethylalkylamines) (II).

Method 2—Determination of the ratio of the responses for pyrolysis products (benzylmethylalkylamines) (III).

Method 3—Ratio of the sum of the responses determined for the corresponding pyrolysis products II and III.

Table III shows the reproducibility of the assay using the USP convention sample. The results of all three methods for calculating the homologue distribution are shown.

Since there is considerable variation in homologue composition between samples of benzalkonium chloride from different commercial sources, one commercial sample was analyzed by the new procedure. The chromatogram of the sample is shown in Fig. 1 and the homologue distribution and reproducibility data are presented in Table IV.

This assay was also conducted using nonpolar silicone phases such as SE-30, OV-1, and OV-101 (all 0.9 m columns with 3% loadings). The results obtained were reproducible for benzalkonium chloride samples which were composed predominantly of the C_{12}, C_{14}, and C_{16} homologues, although they proved to be unsuitable in cases where the C_{18} homologue was present as the C_{18} dimethylalkylamine could not be resolved from the C_{12} benzylmethylalkylamine. To demonstrate the ability of the described system to separate the pyrolysis products, a commercial sample was spiked with pure C_{18} benzalkonium chloride homologue. The resulting chromatogram is shown in Fig. 2.

Freshly packed OV-17 columns required considerable conditioning before they were suitable for use. New columns appeared to adsorb the dimethylalkylamine degradation products strongly resulting in poor peak shape (*i.e.*, considerable peak tailing). This was overcome by conditioning the columns by silylation and repeated injection with a benzalkonium chloride sample, such

Table III—Assay Reproducibility of the USP Sample

Sample	C_{12}	C_{14}	C_{16}	Total[a]
		Method 1		
1	40.8	51.0	8.3	100.0
2	41.4	50.4	8.2	105.1
3	41.2	50.6	8.2	99.5
4	41.3	50.4	8.2	101.2
5	41.3	50.4	8.1	102.4
Mean	41.2	50.6	8.2	101.6
CV	± 0.21	± 0.23	± 0.06	± 2.00
		Method 2		
1	42.1	50.0	7.8	100.0
2	42.0	49.8	8.2	106.3
3	42.1	50.0	7.9	100.0
4	42.0	49.8	8.2	103.9
5	42.0	50.2	7.8	103.6
Mean	42.0	50.0	8.0	102.8
CV	± 0.05	± 0.15	± 0.18	± 2.44
		Method 3		
1	41.0	50.8	8.2	100.0
2	41.5	50.8	8.2	105.3
3	41.4	50.5	8.2	99.6
4	41.4	50.3	8.2	101.4
5	41.4	50.5	8.1	102.6
Mean	41.3	50.5	8.2	101.8
CV	± 0.17	± 0.19	± 0.04	± 2.06

[a] Total response relative to sample 1 (100%).

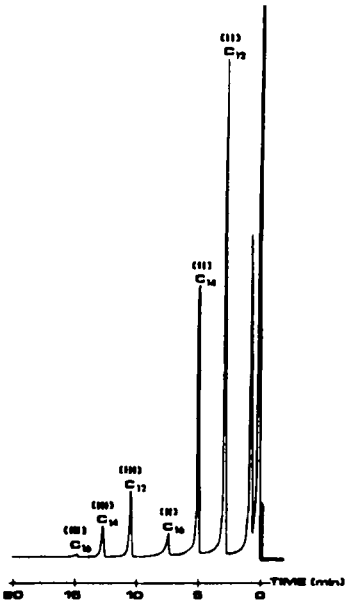

Figure 1—*Chromatogram of a commercial benzalkonium chloride sample.*

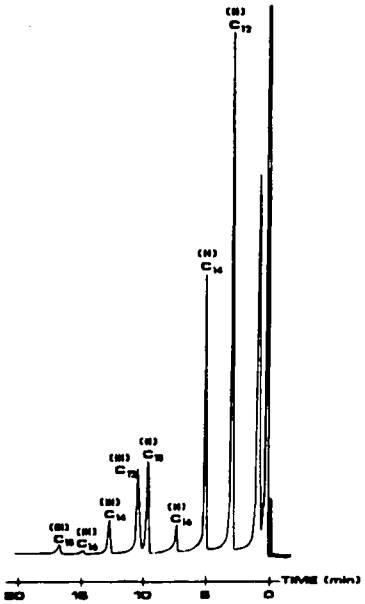

Figure 2—*Chromatogram of a commercial benzalkonium chloride sample spiked with C_{18} benzalkonium chloride homologue.*

Table IV—Assay Reproducibility of Commercial Sample

Sample	C_{12}	C_{14}	C_{16}	Total
		Method 1		
1	58.4	34.9	6.7	100.0
2	58.7	34.7	6.6	103.7
3	59.8	33.8	6.4	105.1
4	58.7	34.7	6.5	104.7
5	58.9	34.5	6.6	101.9
Mean	58.9	34.5	6.6	103.1
CV	± 0.48	± 0.38	± 0.10	± 1.89
		Method 2		
1	58.8	34.7	6.5	100.0
2	58.9	34.4	6.6	103.0
3	58.9	34.5	6.6	100.9
4	59.1	34.3	6.6	105.0
5	59.0	34.4	6.6	99.9
Mean	58.9	34.5	6.6	101.8
CV	± 0.10	± 0.14	± 0.04	± 1.97
		Method 3		
1	58.5	34.9	6.6	100.0
2	58.7	34.7	6.6	103.6
3	59.6	33.9	6.5	104.5
4	58.8	34.7	6.5	104.7
5	58.9	34.5	6.6	101.6
Mean	58.9	34.5	6.6	102.8
CV	± 0.37	± 0.34	± 0.05	± 1.81

as the USP convention standard, until an adequate peak shape was achieved from all thermal degradation products.

REFERENCES

(1) E. I. Valko and A. S. DuBois, *J. Bacteriol.*, **50,** 481 (1945).

(2) "The United States Pharmacopeia," 20th rev., U.S. Pharmacopeial Convention, Rockville, Md., 1980, pp. 1211-1212.

(3) M. E. Auerbach, *Anal. Chem.*, **15,** 492 (1943).

(4) E. L. Colichman, *Anal. Chem.*, **19,** 430 (1947).

(5) L. G. Chatten and K. O. Okamura, *J. Pharm. Sci.*, **62,** 1328 (1973).

(6) L. D. Metcalfe, R. J. Martin, and A. A. Schmitz, *J. Am. Oil Chem. Soc.*, **43,** 355 (1966).

(7) E. R. Brown, *J. Pharm. Pharmacol.*, **15,** 379 (1963).

(8) K. Balasanmugam and D. M. Hercules, *Anal. Chem.*, **55,** 146 (1983).

(9) N. N. Daoud, P. A. Crooks, R. Speak, and P. Gilbert, *J. Pharm. Sci.*, **72,** 290 (1983).

(10) R. C. Meyer, *J. Pharm. Sci.*, **69,** 1148 (1980).

(11) E. C. Jennings and H. Mitchner, *J. Pharm Sci.*, **56,** 1590 (1967).

(12) S. L. Abidi, *J. Chromatogr.*, **200,** 216 (1980).

(13) P. Choi, W. J. Criddle, and J. Thomas, *Analyst*, **104,** 451 (1979).

(14) H. H. Laycock and B. A. Mulley, *J. Pharm. Pharmacol.*, **18,** Suppl. 9S (1966).

ACKNOWLEDGMENTS

The author thanks Fisons plc for the provision of facilities for this work and Miss Kim McAllister for assistance in the GC and MS experiments.

Determination of Partition Coefficients of Glucocorticosteroids by High-Performance Liquid Chromatography

J. C. CARON ˣ and B. SHROOT

Received April 7, 1983, from the *Centre International de Recherches Dermatologiques, Sophia Antipolis, 06565 Valbonne, France.* Accepted for publication February 24, 1984.

Abstract □ Two high-performance liquid chromatographic (HPLC) techniques have been used for the determination of the lipophilicity of 50 glucocorticosteroids. For a log P range of 1 to 3, we used a persilylated octadecylsilane phase saturated with 1-octanol, which was eluted with 1-octanol saturated phosphate buffer (pH = 7). For log P values ≥3.00, the same phase was used without 1-octanol saturation and was eluted with different methanol-buffer mixtures. These two procedures allowed the determination of log P values ranging from 1.00 to >5.00. Good agreement was found between these procedures and others described in the literature. The effect of different structural changes in the glucocorticosteroid molecule on the lipophilicity is discussed.

Keyphrases □ Glucocorticosteroids--partition coefficients, determination by two HPLC methods □ HPLC--partition coefficients of glucocorticosteroids determination with and without 1-octanol □ Partition coefficients--1-octanol-water, glucocorticosteroids

The determination of 1-octanol-water partition coefficients is of particular interest in drug design for several reasons, but primarily because it governs absorption and transport to the site of action (1). Attempts have been made to calculate the partition coefficient of a given compound (2–4), but these theoretical approaches cannot take into account all the physicochemical properties of the molecule, especially the stereochemistry. It is thus advantageous to experimentally determine the lipophilicity of the compounds of interest. For this purpose, several methods have been proposed, of which the shake-flask technique (5) and the TLC method (6) are the most widely used. More recently, high-performance liquid chromatographic (HPLC) has been proposed for this purpose (7, 9) and we selected reverse-phase HPLC as a rapid and reliable method for the determination of log P. Log P is defined as the logarithm of the partition coefficient, $P = C_s/C_w$, where C_s and C_w are the equilibrium concentrations of a solute in the organic (usually 1-octanol) and aqueous (usually a buffer) phase, respectively.

EXPERIMENTAL SECTION

Materials - Hydrocortisone and its derivatives[1], triamcinolone acetonide[2], and other glucocorticosteroids[3] were used as received. Phenol, aniline, acetanilide, quinoline, anisole, benzene, *p*-chlorophenol, 4-methylquinoline, 3-bromoquinoline, phenazine, and acridine were analytical grade[4]. Pyridine, pyridine-*N*-oxide, 1-octanol, ethanol, trimethylchlorosilane, and hexamethyldisilazane were also analytical grade[5]. The HPLC columns used (stainless steel, 4.6 mm id) were of different lengths (5, 10, 15, 20, and 30 cm)[6], and packed with C_{18} Corasil[7] (particle size, 37–50 μm). The HPLC apparatus consisted of a pump[8], a valve injector[9], a UV-visible detector[10] fixed at 254 nm, and a strip chart recorder[11].

[1] Gist-Brocades.
[2] Léderlé.
[3] Glaxo.
[4] Aldrich.
[5] Fluka.
[6] Chrompack.
[7] Waters Associates.
[8] Model 6000A; Waters Associates.
[9] 7000 psi; Valco.
[10] Model M440; Waters Associates.
[11] Omniscribe.

Methods—Two systems have been used for the determination of log P, depending on the lipophilicity of the compound studied.

Log P Range, 0.93 to 3.00 (a)--The method of Mirrless *et al.* (7) was used with minor modifications. The HPLC column was dry packed with a persilylated octadecylsilane phase and saturated with 1-octanol by successive injections of 250 μL of alcohol under pressure until droplets appeared at the outlet of the column. The column was then flushed with 1-octanol-saturated phosphate buffer (0.01 M, pH 7) until the eluate appeared clear. The column was then attached to the detector and elution was continued until a stable baseline was obtained (1–2 h).

Samples were dissolved in ethanol at a concentration of 0.2% (w/v) and 10 μL was injected *via* the valve injector. Pyridine-*N*-oxide was used as a nonretained solute for the determination of the void volume of the column, measured as the elution time on the recorder.

We determined the correlation between log P and log k' for 11 standards of known log P (9) (aniline, acetanilide, quinoline, benzene, anisole, *p*-chlorophenol, phenol, 4-methylquinoline, 3-bromoquinoline, phenazine, and acridine) for a given flow rate and length of column. The capacity factor, k', is defined as: $(t_r - t_0)/t_0$ where t_r is the retention time of the compound and t_0 is the retention time of a nonretained solute.

The calibration curve obtained by the HPLC 1-octanol saturation method, for a given column length and flow rate, is shown in Fig. 1. There is good linear correlation between log P obtained by the shake-flask method (7) and log k' ($r = 0.994$) which is expressed as: $\log P_{SF} = 1.024 \log k' + 0.775$. The slope is near unity and indicates that the HPLC elution process emulates a true 1-octanol-buffer partition.

To determine the log P of steroids, three standards appropriate to the log P range under investigation were run twice a day. The reproducibility between days appeared to be >2% in the k'. For each unknown compound, the average of three determinations of the elution time was used to determine k', and again the *SD* was >2%. The log P of steroids ≤3.00 log P units was determined in this way.

The use of a 5-cm column with a flow rate of 4 mL/min results in retention times of 1–30 min for a log P range of 1–3 using the octanol saturation method. Under these conditions, it is calculated that a compound with a log P = 4 would have a retention time of 280 min; if log P = 5, a retention time of 2670 min would be anticipated. Long retention times for log P values >3 under these experimental conditions lead to peak broadening with a resultant loss in resolution, accuracy, and sensitivity. In addition, high flow rates lead to a rapid

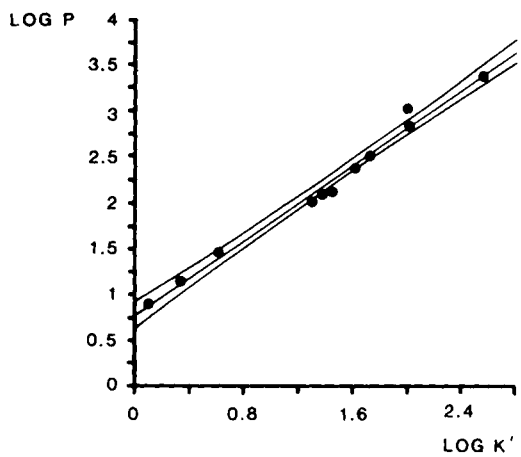

Figure 1 - *Standard calibration curve. Conditions: column length, 20 cm; flow rate, 1 mL/min. The curved lines show the 95% confidence limits.*

0022-3549/84/1200-1703$01.00/0
© 1984, American Pharmaceutical Association

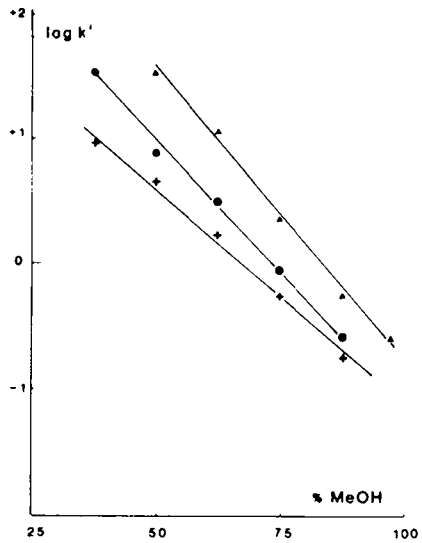

Figure 2—*Correlation between log* k' *and percent methanol (v/v). Key: (●) triamcinolone acetonide; (▲) hydrocortisone-21-butyrate; (+) prednisolone.*

wash out of the 1-octanol coating of the column, the frequent replacement of which considerably reduces the convenience of the procedure. These points led us to the idea of the solvent mixture method for the determination of log P values >3.00 (9, 10).

Log P Values of 3.00 and Above (b)—For the measurement of these log P values, a 20-cm column, filled with the same persilylated octadecylsilane phase, was used but without the 1-octanol coating. Elution was performed with at least five different methanol–buffer mixtures, and the retention time for any given solvent composition was determined for each compound (standards and unknown). An extrapolation of the logarithm of the capacity factor to 0% of organic solvent gives an estimation of the lipophilicity of the molecules studied (Fig. 2).

The proportions of methanol for each compound were chosen to keep the log k' <1.5 so that retention times could be precisely determined ($t_r \leq 45$ min). These proportions were usually kept between 45 and 95% of methanol. For five different methanol buffer mixtures, the correlation between log k' and the proportion of methanol was linear; the correlation coefficient was always >0.98 (for the majority of the steroids, $r \approx 0.99$). Figure 2 shows examples of such correlations for prednisolone, triamcinolone acetonide, and hydrocortisone-21-butyrate, which cover two decades of log P.

RESULTS AND DISCUSSION

By the first procedure, we determined the log P of 12 steroids in the range 1.21–2.88 for which the log P was reported in the literature (11). A good correlation was obtained ($r = 0.951$): $\log P_{SF} = 1.011 \log P_{HPLC} + 0.072$.

Using the second procedure, extrapolation to 0% methanol gave a measure of the partition between the buffer and the octadecylsilane phase, which is

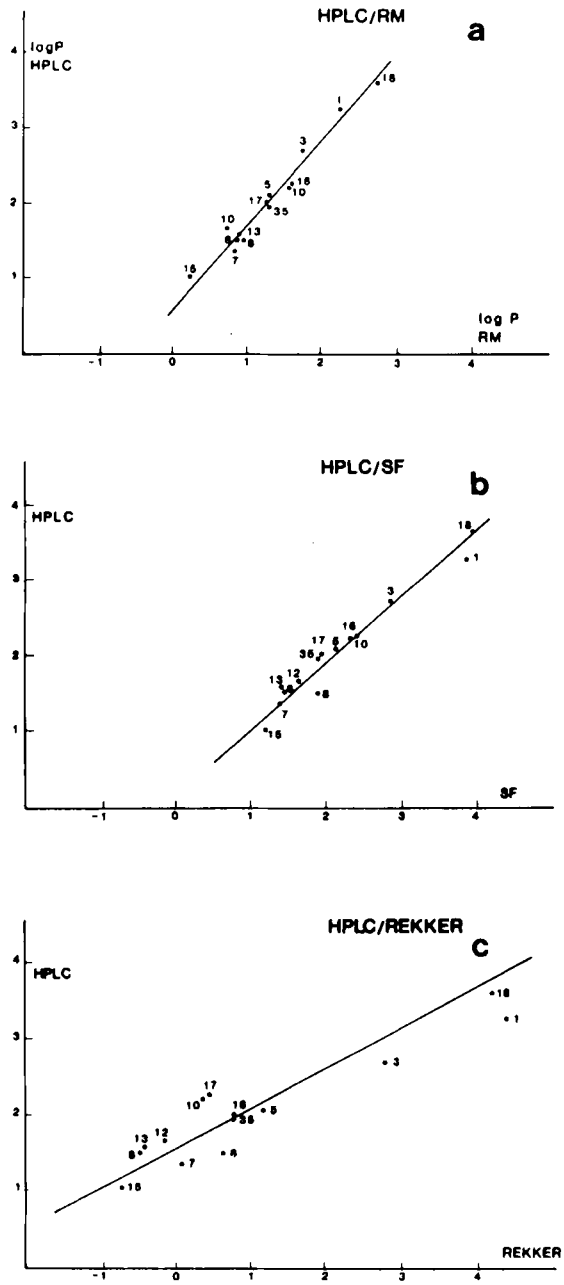

Figure 3—*Correlation between log P determined by HPLC*$_{1\text{-octanol}}$ *and (a) the* R_m *method (r = 0.983); (b) the shake-flask method (r = 0.980); (c) the Rekker method (r = 0.914).*

Table I—Log P Values for the Glucocorticosteroids Obtained by Different Methods

Steroid	$HPLC_{1\text{-octanol}}$	R_m[a]	Shake Flask[b]	Rekker[c]
Cortisone	1.50	0.88	1.47	0.64
Triamcinolone	1.02	0.24	1.21	−0.90
Prednisone	1.36	0.84	1.46	0.07
Hydrocortisone	1.50	0.96	1.93	−0.47
Prednisolone	1.58	0.90	1.42	−0.41
9α-F-hydrocortisone	1.67	0.73	1.68	−0.14
Dexamethasone	1.95	1.30	1.93	0.78
Betamethasone	2.01	1.26	1.98	0.78
Corticosterone	2.06	1.27	2.17	1.17
Hydrocortisone-21-acetate	2.21	1.58	2.37	0.39
Triamcinolone acetonide	2.27	1.63	2.44	0.46
Deoxycorticosterone	2.70	1.78	2.88	2.79
Progesterone	3.26	2.28	3.87	4.40
Betamethasone-17-valerate	3.60	2.77	3.94	3.22

[a] Ref. 10. [b] The correlation between the shake-flask and R_m method was 0.963; between the shake-flask and Rekker method, 0.914. Ref. 9. [c] Ref. 3.

Table II—Log P of Glucocorticosteroids Determined by the Solvent Mixture Method [a]

	Log P by Procedure *b*	$\Delta^{1,2}$ [b]	R_1	R_2	R_3	R_4	R_5
Progesterone	3.26	−	H	H	H	H	H
17α-Hydroxyprogesterone	2.74	−	H	H	H	OH	H
Deoxycorticosterone	2.70	−	H	H	H	H	OH
Cortexolone	2.04	−	H	H	H	OH	OH
Corticosterone	2.06	−	H	OH	H	H	OH
Cortisone	1.50	−	H	=O	H	OH	OH
Prednisone	1.36	+	H	=O	H	OH	OH
Hydrocortisone	1.50	−	H	OH	H	OH	OH
Hydrocortisone-17-butyrate	3.18	−	H	OH	H	OCOPr	OH
Hydrocortisone-21-acetate	2.21	−	H	OH	H	OH	OCOMe
Hydrocortisone-21-butyrate	2.91	−	H	OH	H	OH	OCOPr
9α-Fluorohydrocortisone	1.67	−	F	OH	H	OH	OH
Prednisolone	1.58	+	H	OH	H	OH	OH
9α-Fluoroprednisolone	1.51	+	F	OH	H	OH	OH
Triamcinolone	1.02	+	F	OH	OH	OH	OH
Triamcinolone acetonide	2.27	+	F	OH	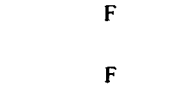		OH
Betamethasone	2.01	+	F	OH	Me	OH	OH
Betamethasone-17-valerate	3.60	+	F	OH	Me	OCOBu	OH
Betamethasone-21-valerate	3.87	+	F	OH	Me	OH	OCOBu
Betamethasone-17,21-divalerate	5.26	+	F	OH	Me	OCOBu	OCOBu
21-Deoxybetamethasone	2.35	+	F	OH	Me	OH	H
21-Deoxybetamethasone-17-propionate	3.09	+	F	OH	Me	OCOEt	H
Clobetasol	2.48	+	F	OH	Me	OH	Cl
Clobetasol-17-propionate	3.18	+	F	OH	Me	OCOEt	Cl
Clobetasol-17-butyrate	3.63	+	F	OH	Me	OCOPr	Cl
Clobetasol-17-propionate (Cl)	3.28	+	Cl	OH	Me	OCOEt	Cl
Clobetasol-17-propionate (F)	3.34	+	H	OH	Me	OCOEt	Cl
Clobetasone	2.61	+	F	=O	Me	OH	Cl
Clobetasone-17-propionate	3.46	+	F	=O	Me	OCOEt	Cl
Clobetasone-17-butyrate	3.76	+	F	=O	Me	OCOPr	Cl
Clobetasone-17-propionate (F)	3.30	+	H	=O	Me	OCOEt	Cl
Clobetasone-17-propionate (H)	3.09	+	F	=O	Me	OCOEt	H
Clobetasone-17-propionate (Br)	3.55	+	F	=O	Me	OCOEt	Br
9α-Fluorocortisone	1.37	−	F	=O	H	OH	OH
Dexamethasone	1.95	+	F	OH	Me	OH	OH
Nandrolone	2.62	−	H	H	H	OH	—
Betamethasone-21-butyrate	3.55	+	F	OH	Me	OH	OCOPr
Hydrocortisone-17-valerate	3.79	−	H	OH	H	OCOBu	OH
Hydrocortisone-17-propionate	2.70	−	H	OH	H	OCOEt	OH
Prednisone-17-acetate	2.43	+	H	=O	H	OCOMe	OH
Cortisone-17-acetate	2.45	−	H	=O	H	OCOMe	OH
Hydrocortisone-21-propionate	2.80	−	H	OH	H	OH	OCOEt
Hydrocortisone-17-acetate	2.30	−	H	OH	H	OCOMe	OH
Hydrocortisone-21-valerate	3.62	−	H	OH	H	OH	OCOBu
Prednisone-17-valerate	3.82	+	H	=O	H	OCOBu	OH
Betamethasone-21-propionate	3.06	+	F	OH	Me	OH	OCOEt
Betamethasone-21-acetate	2.77	+	F	OH	Me	OH	OCOMe

[a] These values are the means calculated from our experimental data and are not to be used to predict the lipophilicity changes induced by structure modification. [b] 1,2 refers to an olefinic bond between C_1 and C_2.

not, in fact, a true 1-octanol–buffer partition. When we compared these log k' 0% with the log P of the steroids determined by the saturation method, we obtained a linear relationship expressed as: log P (procedure *b*) = 0.939 log k' (procedure *a*) + 0.147 which validates the postulate that this procedure can be used for log P determinations >3 units, if closely related standards are used for the calibration. The main advantages of this method are the rapidity and ease of use, compared with the saturation method, but it also may allow us to determine log P values up to 6.

Listed in Table I are the log P values obtained by the 1-octanol saturation HPLC method, the shake-flask technique (11), the R_m values of Biaggi *et al.* (12), and hydrophobicity calculated by the Rekker method (3). R_m is defined as $R_m = \log (1/R_f - 1)$ and is related to the lipophilicity by log P = log K + R_m where K is a constant for the system. R_f is the usual measure of the migration of a compound in TLC.

Figure 3 shows the correlation between $HPLC_{1\text{-octanol}}$ and the 3 other methods for the 14 steroids of Table I. The agreement between $HPLC_{1\text{-octanol}}$ and shake flask and R_m methods is better than the correlation with the calculated hydrophobicity (Rekker). This is due to the fact that the Rekker method gives only an approximation and, like all results based upon calculations, it cannot take into account all the physicochemical properties of a molecule which are responsible for its lipophilicity (3).

We have used these 14 steroids as standards to determine, by the solvent mixture method, the log P of the glucocorticosteroids listed in Table II. The effect of the different structural changes on the lipophilicity of the steroids

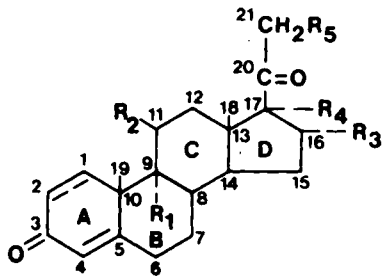

A ring = $\Delta^{1,2}$
R_1 = H, F
R_2 = H, OH, =O
R_3 = H, OH, CH_3
R_4 = H, OH, ester
R_5 = H, OH, ester, Cl

can be determined by examining pairs of compounds differing by only one substituent.

The changes induced by the introduction of a double bond at C_1—C_2, the substitution of the hydrogen atom by a fluorine at C_9, or by changing from hydroxyl to carbonyl at C_{11} have only little effect on lipophilicity. However, changes at C_{16}, C_{17}, and C_{21} have a more significant effect on lipophilicity. The substitution of the C_{16} hydrogen atom by a methyl group induces a small increase in the lipophilicity (±0.50). At C_{17}, the substitution of H by OH only slightly modifies the lipophilicity, but the esterification of the hydroxyl group leads to an increase of the lipophilicity. Changing from OH to acetate increases the log P by 0.89 ± 0.15 (n = 4). A further increase in the chain length of the ester increases the log P with an increment of 0.46 ± 0.12 (n = 5) per carbon

atom. The C_{21} position shows the same tendency. Here the log P value changes by 0.42 ± 0.22 (n = 6) per carbon atom with increasing chain length. The introduction of a chlorine atom in place of OH causes only a slight increase in the log P value.

The two HPLC methods described for the determination of the lipophilicity of glucocorticosteroids are more rapid than the shake-flask method, and are more convenient than the TLC procedure.

REFERENCES

(1) E. J. Lien, *Ann. Rev. Pharmacol. Toxicol.*, **21**, 31 (1981).

(2) C. Hansch and T. Fujita, *J. Am. Chem. Soc.*, **86**, 1616 (1964).

(3) R. F. Rekker, in "The Hydrophobic Fragmental Constant", W. Th. Nauta and R. F. Rekker, Eds., Elsevier, Amsterdam-Oxford-New York, 1977.

(4) P. Ahmad, C. A. Fyfe, and A. Mellors, *Biochem. Pharmacol.*, **24**, 1103 (1975).

(5) C. Hansch, *Acc. Chem. Res.*, **2**, 232 (1969).

(6) C. B. Boyce and B. V. Milborrow, *Nature (London)*, **5010**, 537 (1965).

(7) M. S. Mirrless, S. J. Moulton, C. T. Murphy, and P. J. Taylor, *J. Med. Chem.*, **19**, 615 (1976).

(8) T. Hanai and J. Hubert, *J. Chromatogr.*, **239**, 527 (1982).

(9) S. F. Unger, J. R. Cook, and J. S. Hollenberg, *J. Pharm. Sci.*, **67**, 1364 (1978).

(10) T. Yamana, A. Tsuji, E. Miyamoto, and O. Kubo, *J. Pharm. Sci.*, **66**, 747 (1977).

(11) A. Leo, C. Hansch, and D. Elkins, *Chem. Rev.*, **71**, 521 (1971).

(12) G. L. Biaggi, A. M. Barbaro, O. Gandolfi, M. C. Guerra, and G. Cantelli-Forti, *J. Med. Chem.*, **18**, 873 (1975).

Stability-Indicating Assay for Phenylbutazone: High-Performance Liquid Chromatographic Determination of Hydrazobenzene and Azobenzene in Degraded Aqueous Phenylbutazone Solutions

H. FABRE ˣ, N. HUSSAM-EDDINE, and B. MANDROU

Received December 30, 1982, from the *Laboratoire de Chimie Analytique, Faculté de Pharmacie, 34060 Montpellier Cedex, France.* Accepted for publication February 2, 1984.

Abstract □ A high-performance liquid chromatographic method was developed for the simultaneous determination of azobenzene, hydrazobenzene, and four other decomposition products in phenylbutazone injectable formulations. Separation was achieved on a C_{18} column, with 0.1 M Tris-citrate buffer (pH 5.25) and acetonitrile (52:48), at a flow rate of 2 mL/min and a detection wavelength of 237 nm. Diphenylamine was used as an internal standard. The limit of quantitation is 0.5% (with respect to phenylbutazone) of each degraded product. The detectability is 2.4×10^{-3} μg for azobenzene and 1.5×10^{-3} μg for hydrazobenzene. The limit of quantitation may be lowered to 0.1% (with respect to phenylbutazone) for azobenzene and hydrazobenzene in the presence of the two major decomposition products, which have been determined in commercially available injectable formulations. A higher sensitivity was obtained for azobenzene using the mobile phase 0.1 M Tris-citrate buffer (pH = 5.25) and acetonitrile (40:60) with detection at 314 nm. Under these conditions, 0.025% (with respect to phenylbutazone) of azobenzene is quantitated.

Keyphrases □ Phenylbutazone—HPLC, stability-indicating assay, degradation products □ Azobenzene—HPLC determination □ Hydrazobenzene—HPLC determination

The sodium salt of phenylbutazone (I) in aqueous solution undergoes hydrolysis and, to a small extent, oxidation and decarboxylation according to degradation Scheme I (1). Among these degradation products, some are of particular interest because of their deleterious effects: 4-butyl-4-hydroxy-1,2-diphenyl-3,5-pyrazolidinedione (II) may be involved in allergic reactions (2); hydrazobenzene (VIII) and azobenzene (IX) are suspected carcinogens (3). Despite their toxicity, no analytical method has been proposed for the identification and quantification of VIII and IX in phenylbutazone formulations. Only separation on chromatographic columns and identification by TLC have been reported as evidence for the presence of IX in commercial injections after prolonged storage (4). The present study was undertaken to complete preliminary work (5, 6); the conditions used previously in the high-performance liquid chromatographic (HPLC) procedure (6) did not allow the determination of VIII and IX within acceptable time. In this report, an improved, rapid, and sensitive HPLC procedure is presented that allows simultaneous determination of trace levels of II, III, IV, VI, VIII, and IX and a monitoring of the stability of I in injections.

EXPERIMENTAL SECTION

Materials and Reagents—Compounds I, II, III, IV, and VI were used as received[1]. Compounds VIII and IX, diphenylamine (DPA), Tris, and citric acid were analytical reagent grade. HPLC-grade acetonitrile, distilled-in-glass grade methanol, and water were also used. Injectable formulations were commercial formulations[2] (600 mg of the sodium salt of phenylbutazone, 6 mg of dibucaine, propylene glycol, and water per 3 mL of solution).

The HPLC[3] was equipped with a variable-wavelength UV detector[4]. The separation was carried out on a laboratory-made column (15 cm × 4.0 mm) containing microsilica particulate-bonded (5-μm) octadecylsilane[5]. The mobile phase A was 0.1 M Tris-citrate buffer (pH 5.25) and acetonitrile (52:48). The citrate buffer was filtered through a 0.45-μm filter[6], and the mixture was deaerated before use.

Standard Solutions—An initial mixed stock solution was prepared in the mobile phase using I (200 μg/mL) and II, III, IV, VI, VIII, and IX (100 μg of each/mL). This solution was suitably diluted in the mobile phase to give standard solutions. An internal standard solution (diphenylamine, 500 μg/mL in the mobile phase) was added to each diluted standard solution to give a 100-μg/mL concentration of diphenylamine. The final concentration range was from 5 to 160 μg/mL for I and from 2.5 to 80 μg/mL for II-IV, VI, VIII, and IX.

Test Solutions—Recovery studies were carried out on laboratory-prepared injections similar to commercial formulations with the following amounts

[1] Gifts from Geigy Laboratories, Basel, Switzerland.
[2] Butazolidine; Geigy.
[3] SP 8000; Spectra Physics.
[4] SF 770; Schoeffel.
[5] Lichrosorb RP-18; Merck, Darmstadt, W. Germany.
[6] Sartorius.

0022-3549/84/1200-1706$01.00/0

© 1984, American Pharmaceutical Association

atom. The C_{21} position shows the same tendency. Here the log P value changes by 0.42 ± 0.22 (n = 6) per carbon atom with increasing chain length. The introduction of a chlorine atom in place of OH causes only a slight increase in the log P value.

The two HPLC methods described for the determination of the lipophilicity of glucocorticosteroids are more rapid than the shake-flask method, and are more convenient than the TLC procedure.

REFERENCES

(1) E. J. Lien, *Ann. Rev. Pharmacol. Toxicol.*, **21**, 31 (1981).

(2) C. Hansch and T. Fujita, *J. Am. Chem. Soc.*, **86**, 1616 (1964).

(3) R. F. Rekker, in "The Hydrophobic Fragmental Constant", W. Th. Nauta and R. F. Rekker, Eds., Elsevier, Amsterdam-Oxford-New York, 1977.

(4) P. Ahmad, C. A. Fyfe, and A. Mellors, *Biochem. Pharmacol.*, **24**, 1103 (1975).

(5) C. Hansch, *Acc. Chem. Res.*, **2**, 232 (1969).

(6) C. B. Boyce and B. V. Milborrow, *Nature (London)*, **5010**, 537 (1965).

(7) M. S. Mirrless, S. J. Moulton, C. T. Murphy, and P. J. Taylor, *J. Med. Chem.*, **19**, 615 (1976).

(8) T. Hanai and J. Hubert, *J. Chromatogr.*, **239**, 527 (1982).

(9) S. F. Unger, J. R. Cook, and J. S. Hollenberg, *J. Pharm. Sci.*, **67**, 1364 (1978).

(10) T. Yamana, A. Tsuji, E. Miyamoto, and O. Kubo, *J. Pharm. Sci.*, **66**, 747 (1977).

(11) A. Leo, C. Hansch, and D. Elkins, *Chem. Rev.*, **71**, 521 (1971).

(12) G. L. Biaggi, A. M. Barbaro, O. Gandolfi, M. C. Guerra, and G. Cantelli-Forti, *J. Med. Chem.*, **18**, 873 (1975).

Stability-Indicating Assay for Phenylbutazone: High-Performance Liquid Chromatographic Determination of Hydrazobenzene and Azobenzene in Degraded Aqueous Phenylbutazone Solutions

H. FABRE ˣ, N. HUSSAM-EDDINE, and B. MANDROU

Received December 30, 1982, from the *Laboratoire de Chimie Analytique, Faculté de Pharmacie, 34060 Montpellier Cedex, France.* Accepted for publication February 2, 1984.

Abstract □ A high-performance liquid chromatographic method was developed for the simultaneous determination of azobenzene, hydrazobenzene, and four other decomposition products in phenylbutazone injectable formulations. Separation was achieved on a C_{18} column, with 0.1 M Tris-citrate buffer (pH 5.25) and acetonitrile (52:48), at a flow rate of 2 mL/min and a detection wavelength of 237 nm. Diphenylamine was used as an internal standard. The limit of quantitation is 0.5% (with respect to phenylbutazone) of each degraded product. The detectability is 2.4×10^{-3} μg for azobenzene and 1.5×10^{-3} μg for hydrazobenzene. The limit of quantitation may be lowered to 0.1% (with respect to phenylbutazone) for azobenzene and hydrazobenzene in the presence of the two major decomposition products, which have been determined in commercially available injectable formulations. A higher sensitivity was obtained for azobenzene using the mobile phase 0.1 M Tris-citrate buffer (pH = 5.25) and acetonitrile (40:60) with detection at 314 nm. Under these conditions, 0.025% (with respect to phenylbutazone) of azobenzene is quantitated.

Keyphrases □ Phenylbutazone—HPLC, stability-indicating assay, degradation products □ Azobenzene—HPLC determination □ Hydrazobenzene—HPLC determination

The sodium salt of phenylbutazone (I) in aqueous solution undergoes hydrolysis and, to a small extent, oxidation and decarboxylation according to degradation Scheme I (1). Among these degradation products, some are of particular interest because of their deleterious effects: 4-butyl-4-hydroxy-1,2-diphenyl-3,5-pyrazolidinedione (II) may be involved in allergic reactions (2); hydrazobenzene (VIII) and azobenzene (IX) are suspected carcinogens (3). Despite their toxicity, no analytical method has been proposed for the identification and quantification of VIII and IX in phenylbutazone formulations. Only separation on chromatographic columns and identification by TLC have been reported as evidence for the presence of IX in commercial injections after prolonged storage (4). The present study was undertaken to complete preliminary work (5, 6); the conditions used previously in the high-performance liquid chromatographic (HPLC) procedure (6) did not allow the determination of VIII and IX within acceptable time. In this report, an improved, rapid, and sensitive HPLC procedure is presented that allows simultaneous determination of trace levels of II, III, IV, VI, VIII, and IX and a monitoring of the stability of I in injections.

EXPERIMENTAL SECTION

Materials and Reagents—Compounds I, II, III, IV, and VI were used as received[1]. Compounds VIII and IX, diphenylamine (DPA), Tris, and citric acid were analytical reagent grade. HPLC-grade acetonitrile, distilled-in-glass grade methanol, and water were also used. Injectable formulations were commercial formulations[2] (600 mg of the sodium salt of phenylbutazone, 6 mg of dibucaine, propylene glycol, and water per 3 mL of solution).

The HPLC[3] was equipped with a variable-wavelength UV detector[4]. The separation was carried out on a laboratory-made column (15 cm × 4.0 mm) containing microsilica particulate-bonded (5-μm) octadecylsilane[5]. The mobile phase A was 0.1 M Tris-citrate buffer (pH 5.25) and acetonitrile (52:48). The citrate buffer was filtered through a 0.45-μm filter[6], and the mixture was deaerated before use.

Standard Solutions—An initial mixed stock solution was prepared in the mobile phase using I (200 μg/mL) and II, III, IV, VI, VIII, and IX (100 μg of each/mL). This solution was suitably diluted in the mobile phase to give standard solutions. An internal standard solution (diphenylamine, 500 μg/mL in the mobile phase) was added to each diluted standard solution to give a 100-μg/mL concentration of diphenylamine. The final concentration range was from 5 to 160 μg/mL for I and from 2.5 to 80 μg/mL for II-IV, VI, VIII, and IX.

Test Solutions—Recovery studies were carried out on laboratory-prepared injections similar to commercial formulations with the following amounts

[1] Gifts from Geigy Laboratories, Basel, Switzerland.
[2] Butazolidine; Geigy.
[3] SP 8000; Spectra Physics.
[4] SF 770; Schoeffel.
[5] Lichrosorb RP-18; Merck, Darmstadt, W. Germany.
[6] Sartorius.

0022-3549/84/1200-1706$01.00/0

© 1984, American Pharmaceutical Association

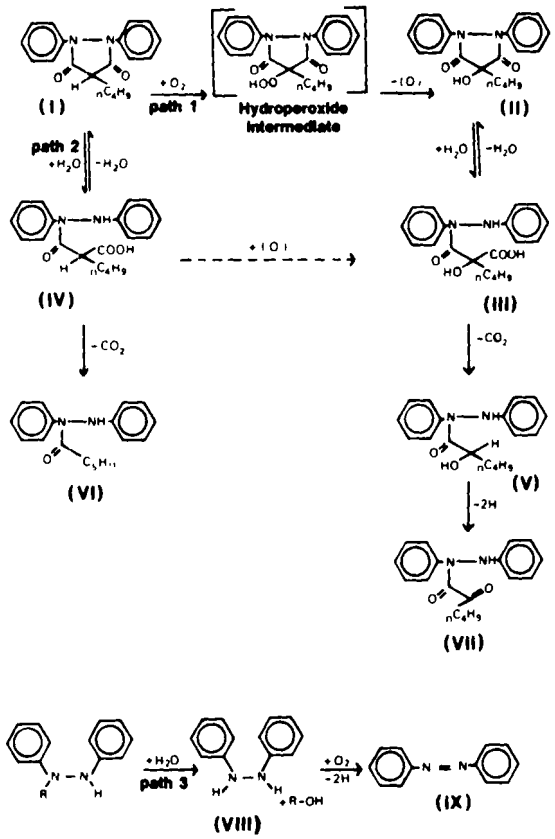

Scheme I—Degradation pathways of phenylbutazone according to Ref. 1. Key: (I) phenylbutazone; (II) 4-butyl-4-hydroxy-1,2-diphenyl-3,5-pyrazolidinedione; (III) 3-hydroxy-2-oxohexanoic acid 1,2-diphenylhydrazide; (IV) 3-carboxy-2-oxohexanoic acid 1,2-diphenylhydrazide; (V) 2-hydroxyhexanoic acid 1,2-diphenylhydrazide; (VI) hexanoic acid 1,2-diphenylhydrazide; (VII) 2-oxohexanoic acid 1,2-diphenyl hydrazide; (VIII) hydrazobenzene; (IX) azobenzene.

added: 1% (with respect to I) of II–IV, VI, VIII, and IX; 0.5% (with respect to I) of II–IV, VI, VIII, and IX; 0.2% (with respect to I) of VIII and IX in the presence of 3% (with respect to I) of III and IV; 0.1% (with respect to I) of VIII and IX in the presence of 3% (with respect to I) of III and IV. These prepared solutions and the commercial injections were diluted in the mobile phase and internal standard solution was added to match the calibration graph.

A 10-μL aliquot of each standard solution and 10 μL of test solution were injected in duplicate onto the chromatograph. The apparatus was operated at ambient temperature. The flow rate was 2 mL/min, the pressure was 140 ± 2 bars, and the detector was set at 237 nm or 314 nm, with a sensitivity of 0.1 AUFS.

RESULTS AND DISCUSSION

Specimen chromatograms of a standard solution recorded at 237 nm (suitable wavelength for simultaneous determination of I–IV, VI, VIII, and IX) and 314 nm (maximum absorbance wavelength for IX in the mobile phase) are shown in Figs. 1 and 2, respectively. A better sensitivity for IX and a negligible absorbance of I–IV, VI, and VIII is observed at 314 nm. Diphenylamine may be used as an internal standard at 237 and 314 nm. An excipient blank was injected. No interference was observed at these wavelengths.

Chromatographic Parameters—Table I lists the chromatographic data for phenylbutazone and its main decomposition products, expressed as the capacity factor k', the theoretical plate height H, the asymmetry factor A_s (7) under the conditions used in the present study (mobile phase A). To check the efficiency of acetonitrile on the selectivity, a modified mobile phase 0.1 M Tris-citrate buffer (pH 5.25)–acetonitrile–methanol (52:30:18) was used. No separation efficiency was obtained and a dramatic increase in the capacity factors and increased pressure (p = 218 bars) were observed.

Comparative data using mobile phase B, 0.1 M Tris-citrate buffer (pH 5.25) and acetonitrile (60:40) and the conditions used in a previous paper (flow rate,

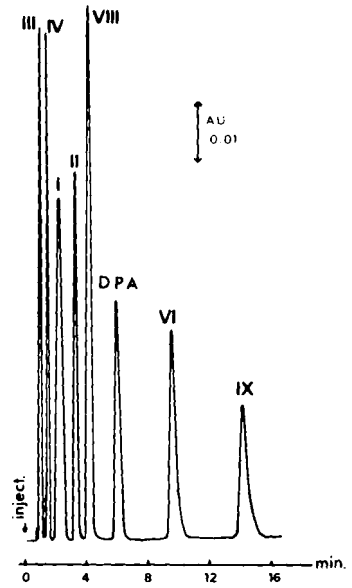

Figure 1—*Chromatogram of a standard solution of I (97.0 μg/mL), II (44.0 μg/mL), III (36.0 μg/mL), IV (40.0 μg/mL), VI (54.4 μg/mL), VIII (56.0 μg/mL), IX (48.0 μg/mL), and DPA (82.5 μg/mL). The mobile phase was 0.1 M Tris-citrate buffer (pH 5.25)–acetonitrile (52:48); flow rate was 2 mL/min, and pressure was 140 bars. Detector sensitivity was 0.1 AUFS, chart recorder speed was 0.5 cm/min, and λ was 237 nm.*

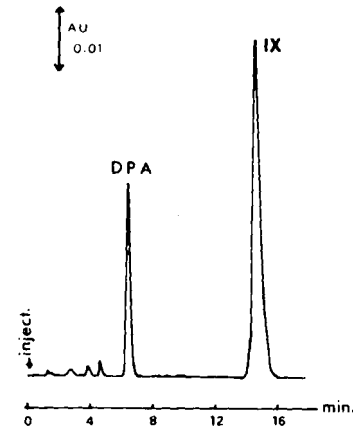

Figure 2—*Chromatogram of a standard solution recorded at 314 nm. Standard solution and conditions were the same as in Fig. 1.*

2.0 mL/min) (6), are given in Table I. Mobile phase B could not achieve the separation within an acceptable time. Accordingly, mobile phase A was chosen for the simultaneous determination of the degradation compounds.

Stability Studies—Hydrazobenzene (VIII) has been reported (1) to undergo easy oxidation into azobenzene and *trans*-azobenzene (IX) is susceptible to isomerization into *cis*-azobenzene under photolytic conditions (8). The stability of I–IV, VI, VIII, and IX was tested by separately injecting onto the chromatograph, at different time intervals, a solution of each compound (0.12

Table I—Chromatographic Data of Phenylbutazone and Its Main Decomposition Products

Compound	Mobile Phase A			Mobile Phase B
	k'	H, mm	A_s	k'
I	1.914	0.616	1.10	4.700
II	3.276	0.042	1.40	9.000
III	0.086	0.216	1.40	0.560
IV	0.569	0.118	1.43	1.740
VI	11.948	0.028	1.21	38.820
VIII	4.603	0.032	1.33	12.380
IX	19.983	0.024	1.37	55.040
DPA	7.138	0.027	1.37	—

Table II—Minimum Detectable Amount and Sensitivity for Phenylbutazone and Its Main Decomposition Products

Compound	Minimum Detectable Amount, μg[a]		Sensitivity	
	λ = 237 nm	λ = 314 nm	λ = 237 nm	λ = 314 nm
I	4.8×10^{-3}	—	11.377	—
II	1.8×10^{-3}	—	14.740	—
III	1.1×10^{-3}	—	14.296	—
IV	1.2×10^{-3}	—	14.385	—
VI	4.5×10^{-3}	—	16.387	—
VIII	1.5×10^{-3}	—	19.214	—
IX	6.0×10^{-3}	2.40×10^{-3}	14.739	37.305

[a] Determined in the presence of I (20 μg).

mg·mL^{-1}) in the mobile phase. After 3 h at ambient temperature, under diffused light, no decomposition was observed for I–IV and VI. Only 1.37% of VIII was oxidized and no isomerization of IX was observed. Under chromatographic conditions used in this study, the retention time of *cis*-azobenzene relative to *trans*-azobenzene was 0.25 min.

Linearity of response was demonstrated for each solute by plotting the peak area ratio of solute to the internal standard against the solute concentration, from mixed standard solutions with equivalent concentration of degradation compound. The calibration graphs were linear for each compound with a correlation coefficient >0.998 in all instances. Each calibration graph intersected the origin. A similar correlation was obtained using the peak heights instead of the peak area.

Repeatability was assessed by five replicate determinations of a standard solution (80 μg/mL for I and 40 μg/mL for each degradation product) and a laboratory prepared injection with 3% of each degradation compound (with respect to I). For the standard solutions the data, expressed as the *CV*, were 1.57% (I), 2.86% (II), 1.88% (III), 3.85% (IV), 5.54% (VI), 2.22% (VIII), and 2.86% (IX). For the laboratory-prepared injection, the data were 0.59% (I), 1.66% (II), 1.00% (III), 0.67% (IV), 0.67% (VI), 1.75% (VIII), and 1.35% (IX).

The detectability [amount (μg) that gives a peak height equal to twice the background for the maximum on-column level tolerable for I] and the sensitivity (change in the area value, measured at the maximum detector sensitivity, resulting from a concentration change of one unit in μg/mL) were evaluated at 237 and 314 nm (Table II). The best wavelength for the detection of azobenzene is 314 nm.

The recovery studies on laboratory prepared injectable formulations with and without added amounts of degradation products are given in Table III. To determine trace amounts of decomposition products, a high concentration of phenylbutazone (2 mg/mL) had to be injected and a blank determination

Table III—Recovery Data from Laboratory Prepared Injectable Formulation

		Amount Added, mg	Amount Found, mg	Relative Error, %
Placebo +	I	600.00	588.06	−1.99
	I	600.00	591.14	−1.48
	II	6.00	5.85	−2.5
	III	6.00	5.76	−4.06
Placebo +	IV	6.00	5.74	−4.30
	VI	6.00	6.26	+4.37
	VIII	6.00	5.85	−2.47
	IX	6.00	6.05	+0.79
	I	600.00	603.60	+0.60
	II	3.00	2.85	−4.89
	III	3.00	3.08	+2.86
Placebo +	IV	3.00	2.99	−0.37
	VI	3.00	3.15	+4.95
	VIII	3.00	3.16	+5.31
	IX	3.00	3.21	+6.95
	I	600.00	584.58	−2.57
	III	18.00	16.89	−6.16
Placebo +	IV	18.00	17.78	−1.20
	VIII	1.2	1.27	+5.83
	IX	1.2[a]	1.16	−3.33
	I	600.00	592.80	−1.20
	III	18.00	19.36	+7.57
Placebo +	IV	18.00	17.68	−1.75
	VIII	0.6	0.656	+9.33
	IX	0.6[a]	0.588	−2.00

[a] Determined at 314 nm.

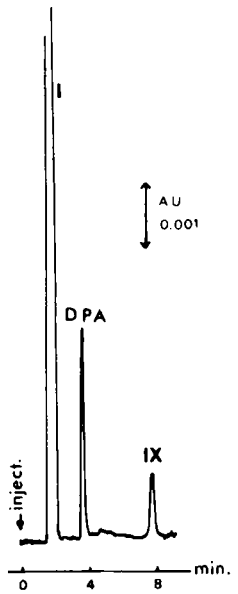

Figure 3—*Chromatogram of a laboratory-prepared injectable formulation of I (2.180 mg/mL), IX (0.525 μg/mL), and spiked with DPA (4.975 μg/mL). The mobile phase was 0.1 M Tris-citrate buffer (pH 5.25) and acetonitrile (40:60). Flow rate was 2.0 mL/min and pressure was 127 bars. Detector sensitivity was 0.01 AUFS, chart recorder speed was 0.5 cm/min, and λ was 314 nm.*

corresponding to an equal concentration of phenylbutazone had to be carried out. Recovery data presented in Table III are corrected from the blank determination. It must be noted that 0.5% (with respect to I) is the limit of quantitation for II because of the resolution between I and II in the presence of a large amount of I. The recovery studies for the two carcinogenic compounds (VIII and IX) were carried out at lower limits in the presence of the main degradation products (III and IV) determined in commercially available injectable formulations (5, 6) within the limit of validity. From Table III, 0.1% (with respect to I) may be estimated as the lowest limit of quantitation for VIII at 237 nm with acceptable accuracy. At 314 nm, where I, III, and IV are not interfering, the limit of quantitation of IX could be lowered to 0.05% (with respect to I).

To increase the detectability and the sensitivity for azobenzene, a more eluting mobile phase C [0.1 M Tris-citrate buffer–acetonitrile (40:60)] was used. Standard solutions of IX were prepared using mobile phase C as follows: 100 μg/mL of DPA was added to make an internal standard of 5 μg/mL. The concentration of IX ranged from 0.3 to 2.0 μg/mL. Good linearity was observed for the calibration graph ($r > 0.999$). The chromatogram of a laboratory-prepared injection with added amount 0.025% (with respect to I) of IX is given in Fig. 3. The recovery was 107.04% by peak area and 94.53% by peak height measurements. The detectability was 1.3×10^{-3} μg.

Commercial Injectable Formulation Analysis—Commercial injection samples issued from two different batches, within the limit of validity, were analyzed with the mobile phases A and C. For one sample, I was 99.73% of the declared value, III was 0.92% (with respect to I), and IV was 5.32% (with respect to I). For the second sample, I was 100.00%, III was 0.8% (with respect to I), and IV was 3.77%. Neither hydrazobenzene nor azobenzene were detected in these two batches.

CONCLUSIONS

The proposed method allows the detection of hydrazobenzene and azobenzene at trace levels: 1.5×10^{-3} μg for VIII, 2.4×10^{-3} μg for IX with mobile phase A, and 1.3×10^{-3} μg for IX with mobile phase C. The resolution obtained for these two carcinogenic substances from phenylbutazone and its two major decomposition products usually found in injections, allows the simultaneous determination of 0.1% of each with satisfactory accuracy. Due to the high toxicity of hydrazobenzene and azobenzene, such an assay should be carried out as a stability-indicating assay for the phenylbutazone injectable formulations susceptible to hydrolysis.

REFERENCES

(1) D. V. C. Awang, A. Vincent, and F. Matsui, *J. Pharm. Sci.*, **62**, 1673 (1973).

(2) H. Bundgaard, *Arch. Pharm. Chemi.*, **6**, 223 (1978).
(3) N. Irving Sax, "Dangerous Properties of Industrial Materials," 5th ed., Van Nostrand, New York, N.Y., 1979.
(4) E. Pawelczyk and R. Wachowiak, *Diss. Pharm. Pharmacol.*, **21**, 492 (1969).
(5) H. Fabre and B. Mandrou, *J. Pharm. Sci.*, **70**, 460 (1981).
(6) H. Fabre, B. Mandrou, and H. Eddine, *J. Pharm. Sci.*, **71**, 120 (1982).
(7) J. J. Kirkland, W. W. Yau, H. J. Stoklosa, and C. H. Dilks, *J. Chromatogr. Sci.*, **15**, 303 (1977).
(8) V. Grignard, "Traité de Chimie Organique, Vol. 15," Masson, Paris, 1948, p. 342.

Autoxidation and Hydrolysis Kinetics of the Sodium Salt of Phenylbutazone in Aqueous Solution

H. FABRE ˣ, N. HUSSAM-EDDINE, D. LERNER *, and B. MANDROU

Received June 8, 1983, from the *Laboratoire de Chimie Analytique, Faculté de Pharmacie* and the **Laboratoire de Chimie Physique Appliquée, Ecole Nationale Supérieure de Chimie, 34060 Montpellier Cedex, France.* Accepted for publication February 16, 1984.

Abstract □ The present investigation offers experimental results concerning the degradation kinetics of the sodium salt of phenylbutazone based on a reliable HPLC procedure. The method allows the simultaneous determination of the parent compound and its main decomposition products. The degradation kinetics at 37°C were compared at pH 7.9 and 10.0 and under oxygen and nitrogen atmospheres. Parallel tests were carried out in the dark and under photolytic conditions for the aforementioned conditions. The influence of traces of iron and a chelating agent of iron on the degradation was studied. At pH 7.9 and pH 10.0 the main degradation products are 3-hydroxy-2-oxohexanoic acid 1,2-diphenylhydrazide and 3-carboxy-2-oxohexanoic acid 1,2-diphenylhydrazide. Azobenzene is formed only at pH 10.0. At pH 7.9, in the dark, the degradation proceeds with a lag phase. In contrast, no lag phase is observed under photolytic conditions. The process of autoxidation and hydrolysis is catalyzed by traces of iron both in the dark and under irradiation conditions. An unexpected increase in the degradation is observed in the presence of iron(III) and EDTA in aerobic conditions and under irradiation.

Keyphrases □ Phenylbutazone—autoxidation, hydrolysis, degradation, degradation products, effects of light and pH

Numerous accounts on the stability of phenylbutazone (I) in drugs have been reported (1–7). A degradation pathway has been suggested which involves oxidation and hydrolysis (4). Furthermore, Schmid (8) has shown that the hydrolysis of I to IV is reversible.

Kinetics of the degradation of the sodium salt of phenylbutazone in aqueous solution have been previously investigated (9, 10) using UV spectrophotometry. The procedure was only valid for the determination of the parent compound; the kinetics of formation of the degradation products were not evaluated.

Since II, VIII, and IX (see *Scheme I* of the immediately preceding paper for the structures of the degradation products) have been suspected to have noxious properties (11, 12) it is useful to investigate, under different conditions, the degradation kinetics of I together with the formation of all its decomposition products. In the present work, a reliable HPLC procedure (13) has been used to follow simultaneously the kinetics of the breakdown of the parent compound and the formation of six main degradation compounds, using experimental conditions which complement previous work (9, 10).

EXPERIMENTAL SECTION

Materials, Reagents, and Solutions—Phenylbutazone and its decomposition products (II[1], III[1], IV[1], VI[1], VIII, and IX) were used as received (see *Scheme I* of the immediately preceding paper for the structures of the degradation products). All chemicals were analytical reagent grade and water was glass distilled.

The study was conducted at pH 7.9 or 10.0 using a 3.24×10^{-3} M concentration of I and an ionic strength of $\mu = 0.5$. The solutions were prepared in 0.2 M ammonium acetate buffer (when a buffer effect was studied at pH 7.9 the buffer concentrations were 0.1, 0.2, and 0.3 M). The experiments were carried out at pH 7.9 and 10.0 without additives, and at pH 7.9 in the presence of iron and iron and EDTA.

For each set of experiments, the sodium salt of phenylbutazone solution (solution A) was prepared in a volumetric flask (100 mL) by dissolving phenylbutazone (100 mg) in a minimum amount of concentrated NaOH (~4 M). Solution A was then added to a volume of 100 mL as described below.

For experiments at pH 7.9 and 10.0, without additives, an acetic acid solution was added to solution A to get a 0.2 M (or 0.1 M, or 0.3 M) final acetate concentration. The pH was adjusted[2] to 7.9 or 10.0 with ammonium hydroxide. Potassium chloride and water were added to a volume of 100 mL to have an ionic strength of $\mu = 0.5$.

For experiments in the presence of iron, a saturated solution of iron(III) chloride in the buffer was prepared by shaking (in a water bath at 40°C) iron(III) chloride in the buffer for 48 h. The filtered solution was added to solution A to make 100 mL. The iron concentration was determined in the filtrate by atomic absorption spectrophotometry[3] using a graphite furnace. The concentrations of the solution was 0.008×10^{-3} M iron(III).

For experiments in the presence of iron and EDTA, an appropriate amount of EDTA was added to an aliquot of the solution described above. The concentrations of the solutions were 0.008×10^{-3} M and 10.52×10^{-3} M with respect to iron(III) and EDTA.

Sample Processing—For each experiment, 3-mL aliquots of the solution were transferred to 10-mL standard antibiotic vials. The vials were closed with a rubber seal. The solutions were bubbled for 3 min with either oxygen or nitrogen through the rubber cap using inlet and outlet syringe needles.

Sets of vials corresponding to the different experiments were placed in the same incubator at 37 ± 1°C. The ceiling of the incubator was fitted with a distributed light source delivering a radiative power ~1% of that emitted by the sun on a bright day. The amount of near UV and visible radiation received by the solutions was estimated using actinometry[4] and was found to be 800 $\mu W/cm^2$. The set of vials to be studied in the dark was enclosed in a light-tight

[1] Gifts from Geigy Laboratories, Basel, Switzerland. These compounds were described in G. Pawelczyk and R. Wachowiak, *Diss. Pharm. Pharmacol.*, **20**, 653 (1968).
[2] Potentiograph Metrohm E 436.
[3] Model 420 equipped with an H.G.A. graphite furnace; Perkin-Elmer.
[4] In a first step, the spectral power distribution of a lamp was measured by means of a calibrated spectroradiometer. Then, a graph of the yield in Fe^{2+} ions *versus* lamp power was obtained using potassium ferrioxalate actinometry. Actinometer preparation and final titration followed the Parker and Hatchard procedure (C. A. Parker and C. G. Hatchard, *J. Phys. Chem.*, **63**, 22 (1959); see also C. A. Parker in "Photoluminescence of Solutions," American Elsevier, New York, N.Y. 1968, p. 210). The irradiation step only was different, since we used the full spectrum of the lamp. The last step was the measurement of the actual sample in the incubator. Once the absorbed power was measured, yield was obtained following standard procedures using the power distribution of the lamp, the yield *versus* wavelength quantum yield change of the actinometer, and the absorption curve of the sample.

0022-3549/84/1200-1709$01.00/0
© 1984, American Pharmaceutical Association

(2) H. Bundgaard, *Arch. Pharm. Chemi.*, **6**, 223 (1978).
(3) N. Irving Sax, "Dangerous Properties of Industrial Materials," 5th ed., Van Nostrand, New York, N.Y., 1979.
(4) E. Pawelczyk and R. Wachowiak, *Diss. Pharm. Pharmacol.*, **21**, 492 (1969).
(5) H. Fabre and B. Mandrou, *J. Pharm. Sci.*, **70**, 460 (1981).
(6) H. Fabre, B. Mandrou, and H. Eddine, *J. Pharm. Sci.*, **71**, 120 (1982).
(7) J. J. Kirkland, W. W. Yau, H. J. Stoklosa, and C. H. Dilks, *J. Chromatogr. Sci.*, **15**, 303 (1977).
(8) V. Grignard, "Traité de Chimie Organique, Vol. 15," Masson, Paris, 1948, p. 342.

Autoxidation and Hydrolysis Kinetics of the Sodium Salt of Phenylbutazone in Aqueous Solution

H. FABRE ˣ, N. HUSSAM-EDDINE, D. LERNER *, and B. MANDROU

Received June 8, 1983, from the *Laboratoire de Chimie Analytique, Faculté de Pharmacie* and the **Laboratoire de Chimie Physique Appliquée, Ecole Nationale Supérieure de Chimie, 34060 Montpellier Cedex, France.* Accepted for publication February 16, 1984.

Abstract □ The present investigation offers experimental results concerning the degradation kinetics of the sodium salt of phenylbutazone based on a reliable HPLC procedure. The method allows the simultaneous determination of the parent compound and its main decomposition products. The degradation kinetics at 37°C were compared at pH 7.9 and 10.0 and under oxygen and nitrogen atmospheres. Parallel tests were carried out in the dark and under photolytic conditions for the aforementioned conditions. The influence of traces of iron and a chelating agent of iron on the degradation was studied. At pH 7.9 and pH 10.0 the main degradation products are 3-hydroxy-2-oxohexanoic acid 1,2-diphenylhydrazide and 3-carboxy-2-oxohexanoic acid 1,2-diphenylhydrazide. Azobenzene is formed only at pH 10.0. At pH 7.9, in the dark, the degradation proceeds with a lag phase. In contrast, no lag phase is observed under photolytic conditions. The process of autoxidation and hydrolysis is catalyzed by traces of iron both in the dark and under irradiation conditions. An unexpected increase in the degradation is observed in the presence of iron(III) and EDTA in aerobic conditions and under irradiation.

Keyphrases □ Phenylbutazone—autoxidation, hydrolysis, degradation, degradation products, effects of light and pH

Numerous accounts on the stability of phenylbutazone (I) in drugs have been reported (1–7). A degradation pathway has been suggested which involves oxidation and hydrolysis (4). Furthermore, Schmid (8) has shown that the hydrolysis of I to IV is reversible.

Kinetics of the degradation of the sodium salt of phenylbutazone in aqueous solution have been previously investigated (9, 10) using UV spectrophotometry. The procedure was only valid for the determination of the parent compound; the kinetics of formation of the degradation products were not evaluated.

Since II, VIII, and IX (see *Scheme I* of the immediately preceding paper for the structures of the degradation products) have been suspected to have noxious properties (11, 12) it is useful to investigate, under different conditions, the degradation kinetics of I together with the formation of all its decomposition products. In the present work, a reliable HPLC procedure (13) has been used to follow simultaneously the kinetics of the breakdown of the parent compound and the formation of six main degradation compounds, using experimental conditions which complement previous work (9, 10).

EXPERIMENTAL SECTION

Materials, Reagents, and Solutions—Phenylbutazone and its decomposition products (II[1], III[1], IV[1], VI[1], VIII, and IX) were used as received (see *Scheme I* of the immediately preceding paper for the structures of the degradation products). All chemicals were analytical reagent grade and water was glass distilled.

The study was conducted at pH 7.9 or 10.0 using a 3.24×10^{-3} M concentration of I and an ionic strength of $\mu = 0.5$. The solutions were prepared in 0.2 M ammonium acetate buffer (when a buffer effect was studied at pH 7.9 the buffer concentrations were 0.1, 0.2, and 0.3 M). The experiments were carried out at pH 7.9 and 10.0 without additives, and at pH 7.9 in the presence of iron and iron and EDTA.

For each set of experiments, the sodium salt of phenylbutazone solution (solution A) was prepared in a volumetric flask (100 mL) by dissolving phenylbutazone (100 mg) in a minimum amount of concentrated NaOH (~4 M). Solution A was then added to a volume of 100 mL as described below.

For experiments at pH 7.9 and 10.0, without additives, an acetic acid solution was added to solution A to get a 0.2 M (or 0.1 M, or 0.3 M) final acetate concentration. The pH was adjusted[2] to 7.9 or 10.0 with ammonium hydroxide. Potassium chloride and water were added to a volume of 100 mL to have an ionic strength of $\mu = 0.5$.

For experiments in the presence of iron, a saturated solution of iron(III) chloride in the buffer was prepared by shaking (in a water bath at 40°C) iron(III) chloride in the buffer for 48 h. The filtered solution was added to solution A to make 100 mL. The iron concentration was determined in the filtrate by atomic absorption spectrophotometry[3] using a graphite furnace. The concentrations of the solution was 0.008×10^{-3} M iron(III).

For experiments in the presence of iron and EDTA, an appropriate amount of EDTA was added to an aliquot of the solution described above. The concentrations of the solutions were 0.008×10^{-3} M and 10.52×10^{-3} M with respect to iron(III) and EDTA.

Sample Processing—For each experiment, 3-mL aliquots of the solution were transferred to 10-mL standard antibiotic vials. The vials were closed with a rubber seal. The solutions were bubbled for 3 min with either oxygen or nitrogen through the rubber cap using inlet and outlet syringe needles.

Sets of vials corresponding to the different experiments were placed in the same incubator at 37 ± 1°C. The ceiling of the incubator was fitted with a distributed light source delivering a radiative power ~1% of that emitted by the sun on a bright day. The amount of near UV and visible radiation received by the solutions was estimated using actinometry[4] and was found to be 800 $\mu W/cm^2$. The set of vials to be studied in the dark was enclosed in a light-tight

[1] Gifts from Geigy Laboratories, Basel, Switzerland. These compounds were described in G. Pawelczyk and R. Wachowiak, *Diss. Pharm. Pharmacol.*, **20**, 653 (1968).
[2] Potentiograph Metrohm E 436.
[3] Model 420 equipped with an H.G.A. graphite furnace; Perkin-Elmer.
[4] In a first step, the spectral power distribution of a lamp was measured by means of a calibrated spectroradiometer. Then, a graph of the yield in Fe^{2+} ions *versus* lamp power was obtained using potassium ferrioxalate actinometry. Actinometer preparation and final titration followed the Parker and Hatchard procedure (C. A. Parker and C. G. Hatchard, *J. Phys. Chem.*, **63**, 22 (1959); see also C. A. Parker in "Photoluminescence of Solutions," American Elsevier, New York, N.Y. 1968, p. 210). The irradiation step only was different, since we used the full spectrum of the lamp. The last step was the measurement of the actual sample in the incubator. Once the absorbed power was measured, yield was obtained following standard procedures using the power distribution of the lamp, the yield *versus* wavelength quantum yield change of the actinometer, and the absorption curve of the sample.

0022-3549/84/1200-1709$01.00/0
© 1984, American Pharmaceutical Association

box. The contents of the vials were mixed by a gentle motion once a day.

Analytical Procedure—The samples were analyzed by HPLC on a home-made Lichrosorb RP 18 column (5 μm, 15 cm × 0.4 cm) under the chromatographic conditions previously described[5,6] (13). A wavelength of 237 nm was selected for the detection of I–IV, VI, and VIII; 314 nm was used for IX. Determinations were carried out in duplicate on two separate vials withdrawn at suitable time intervals. The samples were assayed immediately after dilution with the mobile phase. The reaction was stopped at 50% completion. At this point, 0.315 mL of oxygen was consumed of the 7 mL present in the vial (on the average) since the total oxidation of 3.0 mg of I requires 0.63 mL of oxygen. The observed differences between the values measured for a duplicate pair of vials were ~3% for I for 95% of the samples. For the remaining 5%, differences as high as 5%, and rarely 10%, were noted. We tentatively attribute the latter to defective sealing and/or degradation of the stopper which permitted entry of oxygen. At the end of each experiment pH values were measured: no significant variation was observed.

RESULTS AND DISCUSSION

All experiments relate to 3.24×10^{-3} M solutions of I in a 0.2 M acetate buffer at an ionic strength of 0.5 μ and a temperature of 37°C, except where otherwise stated.

Aerobic Conditions—*Qualitative Results*—Typical chromatograms of phenylbutazone solutions withdrawn at ~30–40% decomposition level (at pH 7.9) under photolytic conditions are given in Figs. 1a and b. The chromatogram obtained at pH 10.0 is similar with one exception: product U_2 is not present in the latter. The same decomposition pattern for the identified products was obtained in the dark.

At pH 7.9, the main decomposition product is III; IV is formed in a smaller amount. Compound II is detected but is not quantifiable because it is readily hydrolyzed to III which is the major degradation product in aerobic conditions. Compound VI was not detected because it probably is not formed in our working temperature range (8, 14). No authentic samples of V and VII were available to identify on the chromatogram, but under our experimental conditions, the decarboxylation of III leading to V and VII seems improbable.

Two unknown degradation products (U_1 and U_2) are found at a low and nearly constant level. Product U_1 is detectable after 15% decomposition of I under illumination; U_2 is detectable after 20 and 25% decomposition of I under illumination and in the dark, respectively. Based on starting product I, the percent yields of U_1 and U_2 are supposed to have the same molecular absorption coefficient as I, and are, respectively, 0.7% (pH 7.9) or 1.15% (pH 10) and 0.56% (pH 7.9). Products VIII and IX are not involved in the pH range near neutrality (4) and are not formed.

At pH 10.0, the main decomposition product is III; IV is formed in a smaller amount and, as expected at this pH value, IX appears but at trace levels after 25% decomposition of I (Fig. 2). Both in the dark and under photolytic conditions, IX is present as *trans*-azobenzene (relative retention time of *trans*- to *cis*-azobenzene is 2.9 min with the mobile phase described in footnote 6). Although a photostationary mixture of *cis*- and *trans*-azobenzene should be formed under illumination, the competing thermal isomerization efficiency (*cis* to *trans*) at 37°C and the low incident light flux result in undetectable amounts of the *cis* isomer (15). These observations for experiments at pH 7.9 and 10.0 are in good agreement with degradation Scheme I of the immediately preceding paper.

Quantitative Results—Kinetics of decomposition of phenylbutazone were studied at two different pH values (7.9 and 10.0). The influence of pH on the degradation is shown in Figs. 3a (in the dark) and b (under irradiation). The degradation pattern under irradiation at both pH values, and in the dark at pH 10.0, results in a single straight line. In contrast, at pH 7.9 in the dark, two linear relationships are observed; the effect is more evident with product III. In the dark and under irradiation, the degradation of I is faster at pH 7.9 than at 10.0. The formation of III is a sensitive function of pH, in contrast to IV. This means that only degradation pathway 1 is dependent on pH.

In the dark, attempts to determine the reaction order at pH 7.9, by a graphical method, show that the degradation process does not follow a simple order and that a complex reaction is involved. A fractional order probably occurs in the dark at pH 7.9. The half-lives (Table I) show an acceleration of the degradation at pH 7.9 compared with pH 10.0. At pH 10.0, zero-order kinetics are observed ($r = 0.994$).

Under photolytic conditions, the degradation process follows zero-order kinetics at pH 7.9 ($r = 0.994$) and at pH 10.0 ($r = 0.999$). The rate constants

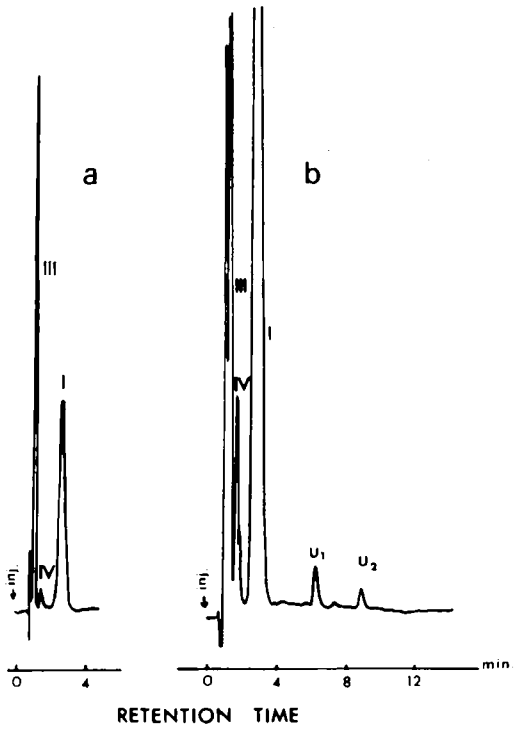

Figure 1—*Chromatograms of a 2.34 × 10^{-3} M phenylbutazone solution diluted 1 to 20 (a) and diluted 1 to 2 (b), withdrawn at ~30–40% degradation at pH 7.9. Kinetic determinations were made in aerobic conditions and under irradiation, determined at 237 nm.*

calculated from the slopes and the half-lives given in Table I clearly show an increase of the degradation at pH 7.9 compared with pH 10.0.

In contrast to pH 7.9, where the sum of I and its decomposition products is always ~100% (with respect to the initial concentration of I), this sum is lowered to 90% at pH 10.0. This apparent loss under photolytic conditions can be explained by the formation of non-UV-absorbing species.

The influence of the buffer concentration on the decomposition was carried out at pH 7.9 in the dark and under irradiation. No significant differences were found between the slopes obtained for each concentration. The influence of a buffer concentration change which could be expected to appear in the hydrolysis step is negligible.

The influence of light on the kinetic behavior of phenylbutazone solution without additives at pH 7.9 and 10.0 is shown in Figs. 4a and b, respectively.

Figure 2—*Chromatogram of a undiluted 2.34 × 10^{-3} M phenylbutazone solution withdrawn at ~30–40% degradation at pH 10.0. Kinetic conditions are the same as Fig. 1. Detection wavelength was at 314 nm.*

[5] Mobile phase: 0.1 M Tris-citrate buffer (pH 5.25)–acetonitrile (52:48); flow rate: 2.0 mL/min.

[6] Mobile phase: 0.1 M Tris-citrate buffer (pH 5.25)–acetonitrile (40:60); flow rate: 2.0 mL/min.

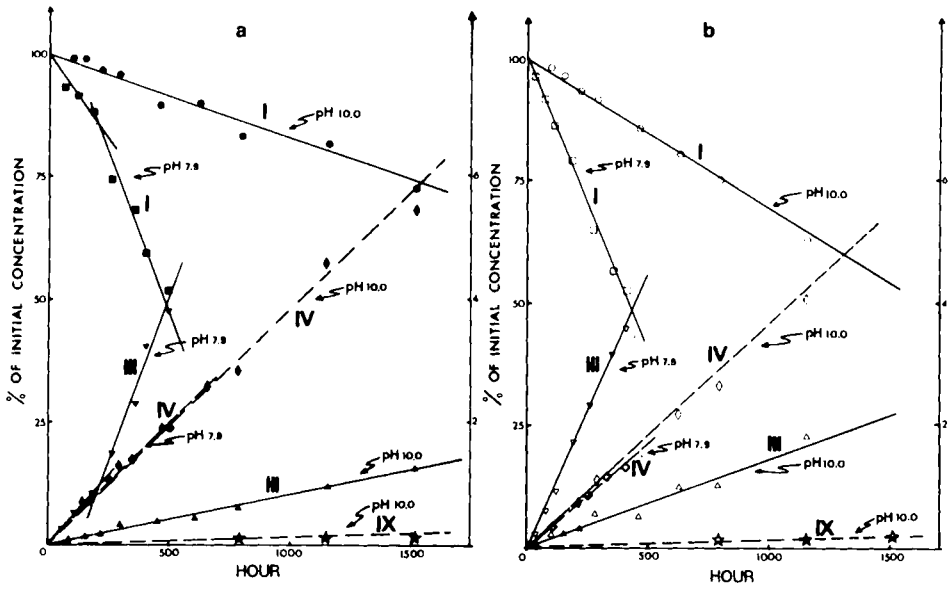

Figure 3—*Influence of pH on the percentage of I, III, IV, and IX as a function of time during the decomposition of phenylbutazone in aerobic conditions in the dark (a) and under photolytic conditions (b) (open symbols). Key: at pH 7.9—(■) I; (▼) III; (◆) IV; and at pH 10.0—(●) I; (▲) III; (♦) IV; (★) IX. (Right ordinate refers to IV and IX.)*

Table I—Half-lives ($t_{1/2}$) and Rate Constants (k) under the Degradation of Phenylbutazone under Aerobic Conditions

		$t_{1/2}$, h		k, g/L/h
pH	Additive	In the Dark	Under Irradiation	Under Irradiation
10.0	None	3000	1500	0.034
7.9	None	473	458	0.120
7.9	Iron	300	220	0.234
7.9	Iron + EDTA	450	170	0.281

Exposure to light increases the decomposition of I. (Compare half-lives in the dark and under irradiation at both pH values in Table I.)

For decomposition in the dark at pH 7.9 (Fig. 4a), the process shows a lag phase which is not observed under photolytic conditions. This induction phase suggests that radical formation is even taking place in the dark. At pH 7.9, 1 in 10^3 phenylbutazone sodium salt molecules [p$K \sim 4.6$ (16)] is in its acid form. In this form, the proton available next to the carbonyl group could be the site of the homolytic process. As the presence of oxygen is necessary to observe a photochemical degradation, it seems likely that some activated form of molecular oxygen is involved. The primary species would be either singlet $^1O_2$ or superoxide $O_2^{\cdot}$. The latter, in aqueous solution, would first react to give $^{\cdot}OOH$ radicals. These could be identical to the species generated in the thermal activation and explain why the observed decomposition products distribution is the same (10). The activation of molecular oxygen could be sensitized by I since the latter absorbs part of the exciting light.

At pH 10.0 no lag time is observed in the dark in the decomposition process, but the same pattern as for pH 7.9 for the evolution of III and IV is observed (Figs. 4a and b).

In the course of our kinetic run, we observed that the rate of formation of IV is not affected by irradiation at both pH values studied (Figs. 4a and b) whereas that of III is increased. In the presence of oxygen, the effect of light is to cause the reaction to proceed faster along path 1.

The influence of the additives iron and EDTA was investigated at pH 7.9. Figures 5a (in the dark) and b (under photolytic conditions) show the influence of traces of iron(III) alone and in the presence of EDTA, compared with the kinetics without iron. These graphs and the calculated values of rate constants and half-lives (Table I) show the catalytic role of iron(III) on the decomposition.

EDTA is a strong complexing agent for iron at pH 7.9. As can be seen, a large increase in the degradation is observed in the presence of iron(III) and EDTA, under irradiation (Figs. 5a and b, Table I). This result is unexpected since EDTA is used in commercial formulations for its "stabilization properties." Similar accelerating effects on the degradation rates have been previously observed with another chelating agent in the oxidation kinetics of epinephrine, carried out in the dark (17). The effect of EDTA in our system cannot be elucidated at present. Recent studies (18) have shown that the well-known decomposition of peroxides by iron(III) EDTA involves formation of active $^{\cdot}OH$ radicals.

Anaerobic Conditions—Determinations were carried out with nitrogen bubbled samples to compare with the oxygen-flushed samples. The results given in Table II show that in the presence of nitrogen, the degradation is largely decreased compared with the degradation in aerobic conditions, at

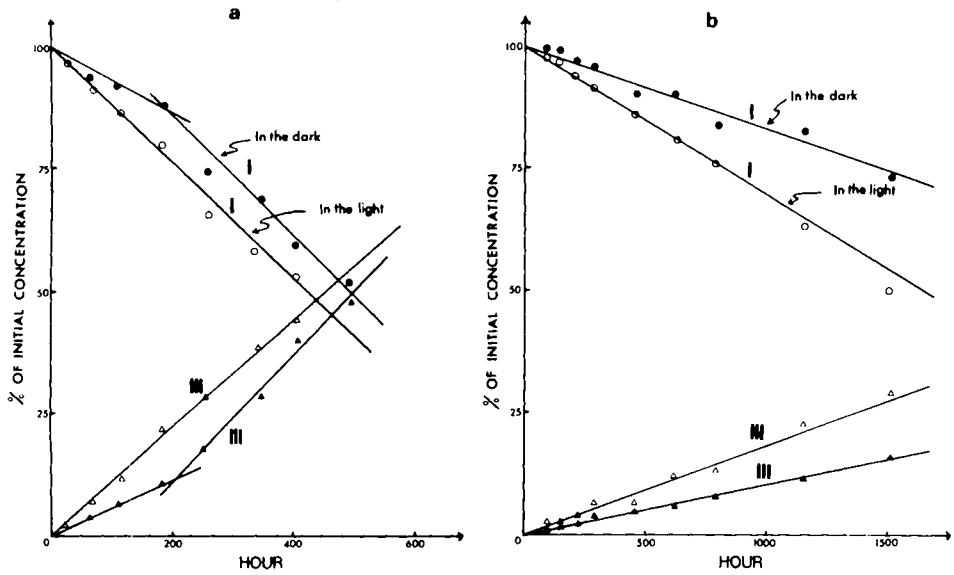

Figure 4—*Influence of light on the decomposition of phenylbutazone in aerobic conditions at pH 7.9 (a) and pH 10.0 (b).*

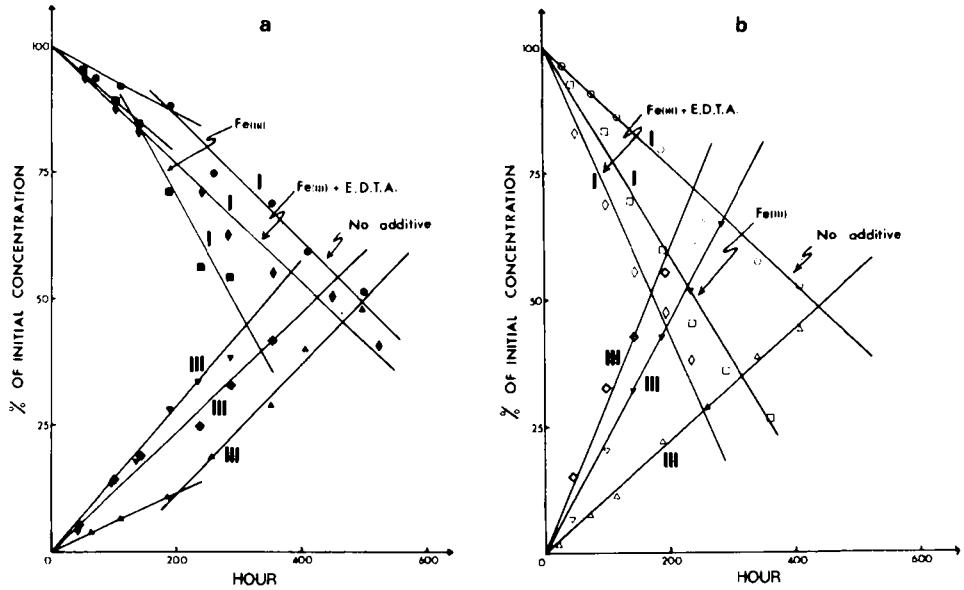

Figure 5—*Influence of iron(III) (0.008 × 10^{-3} M) in the presence of EDTA (10.52 × 10^{-3} M) on the decomposition of phenylbutazone at pH 7.9, in aerobic conditions in the dark (a) and under photolytic conditions (b) (open symbols). Key: without additive—(●) I; (▲) III; with iron—(■) I; (▼) III; with iron and EDTA—(♦) I; (◆) III.*

Table II—Comparative Degradation of Phenylbutazone (I) at Different Time Intervals

pH	Time, h	Compound[a]	Initial Concentration of I, %, with N_2		Initial Concentration of I, %, with O_2	
			In the Dark	Under Irradiation	In the Dark	Under Irradiation
		I	100.49	97.23	94.50	91.50
7.9	71	III	N.D.[d]	N.D.	4.00	7.50
		IV	0.35	0.34	0.24	0.24
		I	100.47	97.88	87.50	77.00
7.9	191	III	N.D.	N.D.	10.00	21.00
		IV	1.06	1.02	0.72	0.64
		I	98.36	97.40	66.00	57.50
7.9	357	III	0.67	1.27	31.00	39.50
		IV	1.82	1.68	1.40	1.22
		I	98.22	93.72	—	—
7.9	520.50	III	0.70	1.35	—	—
		IV	2.62	2.52	—	—
		I	95.25	90.16	88.00[b]	78.50[c]
10.0	699	III	0.45	0.93	7.00[b]	12.50[c]
		IV	2.14	2.06	2.70[b]	2.60[c]
		IX	N.D.	N.D.	N.D.	N.D.
		I	91.84	85.22	72.44	47.98
		III	0.81	1.92	16.13	9.87
10.0	1510	IV	6.38	6.08	5.24	4.37
		IX	N.D.	N.D.	0.064	0.14

[a] See Scheme I. [b] Calculated from Fig. 3a. [c] Calculated from Fig. 3b. [d] Not detected.

both pH values. In these samples, the main degradation route is 2 which, through hydrolysis, leads to IV. Compound III is also formed in small amounts. (The formation of III might be due to the fact that the deaerating procedure is not totally effective.) The removal of oxygen shows up clearly in the variation of the ratio IV:III in the dark as well as under irradiation (Table II).

The effect of additives (Table III) can be analyzed as follows: iron(III) alone induces some degradation whereas the addition of iron(III) and EDTA has no clear stabilizing effect in the dark. The effect of light is only to increase decomposition when it exists in the dark.

Table III—Effect of Additives on the Decomposition of Phenylbutazone under Anaerobic Conditions

Time, h	Additive	Phenylbutazone Remaining, %	
		In the Dark	Under Irradiation
	None	100.47	98.88
191	Iron	98.88	90.45
	Iron + EDTA	98.58	96.59
	None	98.22	93.72
530	Iron	83.00	78.52
	Iron + EDTA	92.30	90.76

CONCLUSIONS

The results we obtained at pH 7.9 and pH 10.0 are in good agreement with the general degradation scheme proposed by Awang *et al.* (4): evidence for two main degradation paths corresponding to hydrolysis (path 2) and autoxidation followed by hydrolysis (path 1) have been disclosed by HPLC analysis.

Kinetic results in aerobic conditions showed that only the oxidation path is affected by pH. This agrees with the findings of Pawelczyk and Wachowiak (2). In the dark at pH 7.9, a lag phase is observed. This was not found by Pawelczyk and Wachowiak who worked at a higher temperature which offset the induction time. This means that one cannot use data obtained between 60°C and 100°C to predict the shelf life of phenylbutazone samples.

The influence of light as well as the catalytic effect of iron traces have been shown to increase the rate of degradation of I through the oxidation pathway. HPLC analysis permitted the determination of trace amount of IX. We have found that it would only be formed at pH 10.0 and after ~25% decomposition of I. Compound IX, a potential carcinogen, could be formed in pharmaceutical formulations where autoxidation and hydrolysis are found at such pH conditions; the problem could arise for injections. In fact, Pawelczyk and Wachowiak report the formation of IX in injectable formulations, but only beyond their storage limit (3). In tablet and capsules, hydrolysis would be so impeded that formation of IX is highly improbable. Compound IX has been detected

in solid formulations only after sustained heating at 60°C after a prolonged storage time (5).

REFERENCES

(1) H. D. Beckstead, K. K. Kaistha, and S. J. Smith, *J. Pharm. Sci.*, **57**, 1952 (1968).

(2) E. Pawelczyk and R. Wachowiak, *Acta Pol. Pharm.*, **26**, 425 (1969).

(3) E. Pawelczyk and R. Wachowiak, *Acta Pol. Pharm.*, **26**, 433 (1969).

(4) D. V. C. Awang, A. Vincent, and F. Matsui, *J. Pharm. Sci.*, **62**, 1673 (1973).

(5) F. Matsui, D. L. Robertson, P. Lafontaine, H. Kolasinski, and E. G. Lovering, *J. Pharm. Sci.*, **67**, 646 (1978).

(6) S. L. Ali and T. Strittmatter, *Pharm. Ztg.*, **123**, 720 (1978).

(7) H. Fabre, B. Mandrou, and H. Eddine, *J. Pharm. Sci.*, **71**, 120 (1982).

(8) R. W. Schmid, *Helv. Chim. Acta*, **53**, 2239 (1970).

(9) E. Pawelczyk and R. Wachowiak, *Diss. Pharm. Pharmacol.*, **21**, 491 (1969).

(10) E. Pawelczyk and R. Wachowiak, *Diss. Pharm. Pharmacol.*, **22**, 475 (1970).

(11) H. Bundgaard, *Arch. Pharm. Chemi.*, **6**, 223 (1978).

(12) N. Irving Sax, "Dangerous Properties of Industrial Materials," 5th ed., Van Nostrand, New York, N.Y., 1979.

(13) H. Fabre, N. Hussam-Eddine, and B. Mandrou, *J. Pharm. Sci.*, **73**, 1706 (1984).

(14) J. Slingsby and D. A. Zuck, *Can. J. Pharm. Sci.*, **7**, 115 (1972).

(15) G. Zimmerman, L. Y. Chow, and U. J. Paik, *J. Am. Chem. Soc.*, **80**, 3528 (1958).

(16) K. G. Mooney, M. Rodriguez-Gaxiola, M. Mintun, K. J. Himmelstein, and V. J. Stella, *J. Pharm. Sci.*, **70**, 1358 (1981).

(17) T. D. Sokoloski and T. Higuchi, *J. Pharm. Sci.*, **51**, 172 (1962).

(18) N. P. Bird, D. Cummins, and K. C. Francis, 3rd Int. Conf. on Mechanisms of Reactions in Solutions, Kent, Canterbury, July 1982.

ACKNOWLEDGMENTS

Abstracted in part from a dissertation presented by N. Hussam-Eddine to the Faculté de Pharmacie, Montpellier in partial fulfillment of the Doctor of Philosophy degree requirements.

Controlled Long-Term Release of Small Peptide Hormones Using a New Microporous Polypropylene Polymer: Its Application for Vasopressin in the Brattleboro Rat and Potential Perinatal Use

JENNEKE KRUISBRINK and GERARD J. BOER ˣ

Received June 13, 1983, from the *Netherlands Institute for Brain Research, Meibergdreef 33, 1105 AZ Amsterdam, The Netherlands.* Accepted for publication January 25, 1984.

Abstract □ Based on drug release by microporous hollow fibers and the recent introduction of microporous polymers, a new technique was developed for controlled delivery of peptides. Small-diameter microporous polypropylene tubing, lumen-loaded with microgram quantities of vasopressin, and coated with collodion, releases vasopressin after *in vitro* immersion slowly (1–100 ng/d) and constantly for months. The mechanism of pseudo-zero-order delivery is based on high adsorption of vasopressin, keeping the void volume concentration of dissolved vasopressin constant, which is consequently a constant driving force of outward diffusion. The collodion coating prevents the entry of proteinaceous compounds which would result in rapid desorption of vasopressin. The present delivery module provides a lasting release for other peptides as well (lysine-vasopressin, oxytocin, α-melanocyte-stimulating hormone and, to a lesser extent, Met-enkephalin). The microporous polymer-collodion device is biocompatible and, loaded with vasopressin, successfully alleviates the diabetes insipidus of Brattleboro rats deficient for vasopressin. Subcutaneous implantation normalized diuresis for a period of 60 d and constant urine vasopressin excretion is observed. When the commercially available osmotic minipump is too large for implantation, the small size of the present controlled-delivery system allows peptide treatment of young and immature laboratory rats, even if located *in utero*.

Keyphrases □ Controlled drug delivery—vasopressin, microporous polymers, Brattleboro rat □ Vasopressin—controlled drug delivery, microporous polymers, Brattleboro rat □ Brattleboro rat—vasopressin, controlled delivery, microporous polymers

Peptide hormones and many other substances must be administered in a long-term continuous fashion and within a specified range of concentrations in order to bring about physiological changes. Effective dosages can be given by injections, but because of the short half-life of hormone peptides, high doses often have to be administered, resulting in a sawtooth pattern of peptide levels. As a consequence, side effects frequently occur. Several controlled-release techniques have been developed, ensuring a continuous and constant application for a variety of substances (1–5). Most of these techniques are based either on the principle of: (*a*) constant diffusion of substances (mostly hydrophobic steroids and drugs) through polymer matrices (6) or (*b*) constant delivery of a liquid volume containing the physiologically active agents from an osmotically active core (3). A widely used osmotic minipump—an example of the second approach—has the advantage that it is suitable for all types of compounds (including peptide hormones). However, because of its size, implantation cannot be performed in small laboratory animals or fetuses.

Recently we encountered problems when vasopressin supplementation had to be given to vasopressin-deficient newborn Brattleboro rats (7). Based on the possibilities of drug release by the use of hollow fibers (6) and the recent introduction of a new microporous polymer matrix[1] (8, 9), a technique has now been developed through which controlled delivery of peptides can be obtained. It is small enough to allow the use in immature rats. Preliminary results both on the development and on the applications of the present technique have been partially in-

[1] Accurel polypropylene.

0022-3549/84/1200-1713$01.00/0

© 1984, American Pharmaceutical Association

in solid formulations only after sustained heating at 60°C after a prolonged storage time (5).

REFERENCES

(1) H. D. Beckstead, K. K. Kaistha, and S. J. Smith, *J. Pharm. Sci.*, **57**, 1952 (1968).

(2) E. Pawelczyk and R. Wachowiak, *Acta Pol. Pharm.*, **26**, 425 (1969).

(3) E. Pawelczyk and R. Wachowiak, *Acta Pol. Pharm.*, **26**, 433 (1969).

(4) D. V. C. Awang, A. Vincent, and F. Matsui, *J. Pharm. Sci.*, **62**, 1673 (1973).

(5) F. Matsui, D. L. Robertson, P. Lafontaine, H. Kolasinski, and E. G. Lovering, *J. Pharm. Sci.*, **67**, 646 (1978).

(6) S. L. Ali and T. Strittmatter, *Pharm. Ztg.*, **123**, 720 (1978).

(7) H. Fabre, B. Mandrou, and H. Eddine, *J. Pharm. Sci.*, **71**, 120 (1982).

(8) R. W. Schmid, *Helv. Chim. Acta*, **53**, 2239 (1970).

(9) E. Pawelczyk and R. Wachowiak, *Diss. Pharm. Pharmacol.*, **21**, 491 (1969).

(10) E. Pawelczyk and R. Wachowiak, *Diss. Pharm. Pharmacol.*, **22**, 475 (1970).

(11) H. Bundgaard, *Arch. Pharm. Chemi.*, **6**, 223 (1978).

(12) N. Irving Sax, "Dangerous Properties of Industrial Materials," 5th ed., Van Nostrand, New York, N.Y., 1979.

(13) H. Fabre, N. Hussam-Eddine, and B. Mandrou, *J. Pharm. Sci.*, **73**, 1706 (1984).

(14) J. Slingsby and D. A. Zuck, *Can. J. Pharm. Sci.*, **7**, 115 (1972).

(15) G. Zimmerman, L. Y. Chow, and U. J. Paik, *J. Am. Chem. Soc.*, **80**, 3528 (1958).

(16) K. G. Mooney, M. Rodriguez-Gaxiola, M. Mintun, K. J. Himmelstein, and V. J. Stella, *J. Pharm. Sci.*, **70**, 1358 (1981).

(17) T. D. Sokoloski and T. Higuchi, *J. Pharm. Sci.*, **51**, 172 (1962).

(18) N. P. Bird, D. Cummins, and K. C. Francis, 3rd Int. Conf. on Mechanisms of Reactions in Solutions, Kent, Canterbury, July 1982.

ACKNOWLEDGMENTS

Abstracted in part from a dissertation presented by N. Hussam-Eddine to the Faculté de Pharmacie, Montpellier in partial fulfillment of the Doctor of Philosophy degree requirements.

Controlled Long-Term Release of Small Peptide Hormones Using a New Microporous Polypropylene Polymer: Its Application for Vasopressin in the Brattleboro Rat and Potential Perinatal Use

JENNEKE KRUISBRINK and GERARD J. BOER ˣ

Received June 13, 1983, from the *Netherlands Institute for Brain Research, Meibergdreef 33, 1105 AZ Amsterdam, The Netherlands.* Accepted for publication January 25, 1984.

Abstract □ Based on drug release by microporous hollow fibers and the recent introduction of microporous polymers, a new technique was developed for controlled delivery of peptides. Small-diameter microporous polypropylene tubing, lumen-loaded with microgram quantities of vasopressin, and coated with collodion, releases vasopressin after *in vitro* immersion slowly (1–100 ng/d) and constantly for months. The mechanism of pseudo-zero-order delivery is based on high adsorption of vasopressin, keeping the void volume concentration of dissolved vasopressin constant, which is consequently a constant driving force of outward diffusion. The collodion coating prevents the entry of proteinaceous compounds which would result in rapid desorption of vasopressin. The present delivery module provides a lasting release for other peptides as well (lysine-vasopressin, oxytocin, α-melanocyte-stimulating hormone and, to a lesser extent, Met-enkephalin). The microporous polymer-collodion device is biocompatible and, loaded with vasopressin, successfully alleviates the diabetes insipidus of Brattleboro rats deficient for vasopressin. Subcutaneous implantation normalized diuresis for a period of 60 d and constant urine vasopressin excretion is observed. When the commercially available osmotic minipump is too large for implantation, the small size of the present controlled-delivery system allows peptide treatment of young and immature laboratory rats, even if located *in utero*.

Keyphrases □ Controlled drug delivery—vasopressin, microporous polymers, Brattleboro rat □ Vasopressin—controlled drug delivery, microporous polymers, Brattleboro rat □ Brattleboro rat—vasopressin, controlled delivery, microporous polymers

Peptide hormones and many other substances must be administered in a long-term continuous fashion and within a specified range of concentrations in order to bring about physiological changes. Effective dosages can be given by injections, but because of the short half-life of hormone peptides, high doses often have to be administered, resulting in a sawtooth pattern of peptide levels. As a consequence, side effects frequently occur. Several controlled-release techniques have been developed, ensuring a continuous and constant application for a variety of substances (1–5). Most of these techniques are based either on the principle of: (*a*) constant diffusion of substances (mostly hydrophobic steroids and drugs) through polymer matrices (6) or (*b*) constant delivery of a liquid volume containing the physiologically active agents from an osmotically active core (3). A widely used osmotic minipump—an example of the second approach—has the advantage that it is suitable for all types of compounds (including peptide hormones). However, because of its size, implantation cannot be performed in small laboratory animals or fetuses.

Recently we encountered problems when vasopressin supplementation had to be given to vasopressin-deficient newborn Brattleboro rats (7). Based on the possibilities of drug release by the use of hollow fibers (6) and the recent introduction of a new microporous polymer matrix[1] (8, 9), a technique has now been developed through which controlled delivery of peptides can be obtained. It is small enough to allow the use in immature rats. Preliminary results both on the development and on the applications of the present technique have been partially in-

[1] Accurel polypropylene.

0022-3549/84/1200-1713$01.00/0

© 1984, American Pharmaceutical Association

corporated in other publications (10–12); this paper describes the method in full detail.

EXPERIMENTAL SECTION

Materials—The new microporous polymer matrix[1] has a large void volume, consisting of cells interconnected by small pores (8, 9, 12). In the present study, polymer matrix polypropylene tubing[2] (P 78/15/2; wall void volume 71%, cell and pore size of ~5 and 0.5 μm, and an o.d. and i.d. of 1.6 and 0.9 mm, respectively) was used. Vasopressin[3] (465 U/mg), lysine-vasopressin, Met-enkephalin[5], oxytocin[6], α-melanocyte-stimulating hormone[6], and [^{3}H]-Met-enkephalin[7] (50 Ci/mmol) were obtained commercially. [^{125}I-Tyr]-vasopressin was prepared (13) with a specific activity of 0.5–1.0 Ci/mmol.

Test Tube Experiments—Microporous polymer tubing (2 cm; one end heat-sealed with a mini-soldering iron) filled with ethanol (a few minutes under reduced pressure) was either immersed in an aqueous vasopressin solution for wall-loading (1 mg/mL, 24 h) or in water (1 h) for lumen-loading using a syringe (7 or 22 μg of vasopressin in 7.5 μL). The tubing was then mounted on a serum filter tube so that 1.5 cm of the closed end was immersed or, after heat-sealing the other end, was completely immersed. In the final stage a lumen-loaded double-closed preparation was enfilmed with collodion[8]: the tubing was dipped three times in the collodion solution [0.05 g/mL ether–ethanol, 3:1 (v/v)] and air dried between dippings (12). As a control for this final procedure, vasopressin was made in 2% agar and sucked into silicon tubing containing a strand of suture silk running through its lumen. A 1.5-cm rod was prepared with the outer dimensions of the microporous polymer tubing which could also be coated with collodion (6 dips).

Release of vasopressin was followed at 37°C in 1 mL of distilled water 10% swine serum containing 0.01% sodium azide or 0.5% bovine serum albumin. The volume was replaced daily. When release during 1 d was followed, 25-μL samples were drawn. Samples were stored at −20°C until an RIA for vasopressin was carried out (14, 15). Degradation of the vasopressin immunoreaction in water, serum, and albumin media (water, 0.5 ng–0.5 mg/mL; albumin and serum, 7 ng/mL) was determined during 24-h incubation at 37°C.

Microporous polymer-collodion devices were prepared (containing 7 μg of lysine-vasopressin, oxytocin, and α-melanocyte-stimulating hormone) and daily release was followed radioimmunologically in 10% serum (14–16). The tritiated form of Met-enkephalin (7 μg; final specific activity, 1.2 μCi/mmol) was applied and the release was followed by counting radioactivity.

Animal Experiments—Homozygous (HOM) Brattleboro rats (~140 g), congenitally deficient for vasopressin[9] (17), were kept under standard conditions in metabolism cages (18). After a control period of 3 d, in which the rats showed diabetes insipidus, the animals received subcutaneously, under light ether anaesthesia, microporous polymer-collodion tubing loaded with 7.5, 22, or 220 μg of vasopressin. Vasopressin release was followed in duplicate animals by measuring daily urine production and osmolality and by the assay of urine-excreted vasopressin (see above).

For comparison, single HOM Brattleboro male rats received: a 22-μg vasopressin-loaded microporous polymer without collodion enfilming; a 22-μg vasopressin-agar-collodion preparation; a minipump[10] filled with 22 μg of vasopressin in saline (pumping rate was 0.4 μL/h, *i.e.*, 1000 ng/d); or daily subcutaneous injections of vasopressin tannate[11] (0.5 U/100 g). Finally, a male Wistar rat received a microporous polymer-collodion implant containing 22 μg ^{125}I]-vasopressin (1 mCi/mmol), to follow urine excretion of iodine-125 (drinking water contained 0.1% KI).

Perinatal Implantations—HOM Brattleboro pups (age, 5 d) (7) received subcutaneously a water-filled microporous polymer-collodion tubing (1.5 cm) with a 0.7-mm diameter (P 17/80/2) or the dimensions used above. The largest tubing, placed longitudinally to the animal's spine, was checked daily by palpation, and, at 1 month of age, all pups were sacrificed and an attempt was made to locate the tubing.

The uterus of pregnant (18th day of gestation) Wistar rats was exposed for fetal operation according to Swaab and Honnebier (19). A small diameter microporous polymer-collodion preparation, 0.5- or 1-cm in length inserted into a 19-gauge needle, was placed through the uterine wall underneath the skin of the back of the fetus. Implants were performed on several fetuses within the exposed uterus. Ten days after birth the offspring were sacrificed and the location of the microporous polymer implant was examined.

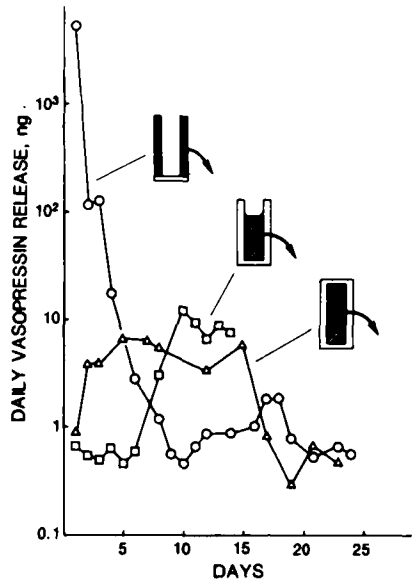

Figure 1—*Vasopressin levels measured in daily renewed 1-mL water volumes containing a microporous polymer polypropylene tubing loaded with the drug (shaded area). Data were taken from single representative experiments. Key: (○) 21 μg, wall-filled end-sealed tubing; (□) 15 μg/5 μL, lumen-filled end-sealed tubing; (△) 7 μg/7.5 μL, lumen-filled double end-sealed tubing.*

RESULTS

Test Tube Experiments with Vasopressin—From the different loading procedures of the microporous polymer polypropylene tubing, the most continuous and constant release of vasopressin on water immersion was reached after lumen loading with double-end-closed tubing (Fig. 1). On wall filling, vasopressin ran out almost asymptotically whereas the lumen-filled open

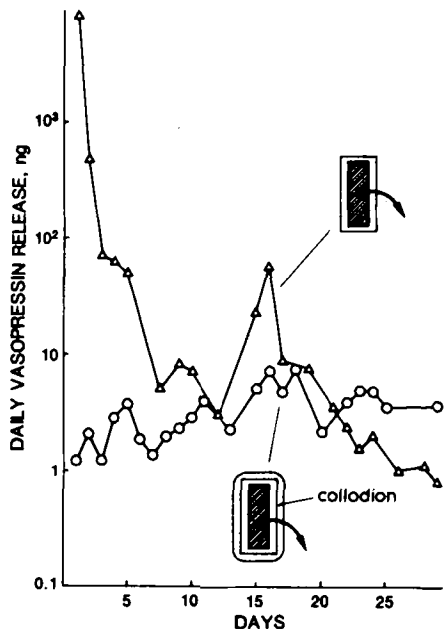

Figure 2—*Effect of collodion coating on vasopressin level in daily renewed 10% swine serum on immersion of a vasopressin-microporous polymer-collodion preparation (7 μg). Key: (△) without collodion; (○) with collodion; (▨) drug.*

[2] Kindly supplied by Mr. D. Heitmann (ENKA Research Institute, Obernburg, FRG).
[3] Grade VIII, lot 99C-1352; Sigma, St. Louis, Mo.
[4] Grade IV; Sigma.
[5] UCB, Brussels, Belgium.
[6] Organon, Oss, The Netherlands.
[7] NEN, Doorn, The Netherlands.
[8] Parlodion; Schuchardt.
[9] CPB/TNO, Rijswijk, The Netherlands.
[10] Model 2002; Alzet.
[11] Pitressin tannate; Parke-Davis.

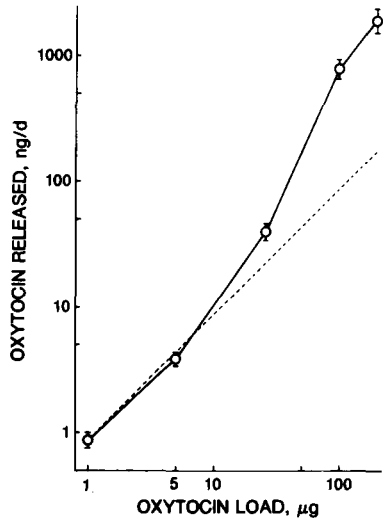

Figure 3—*Daily release of oxytocin from microporous polymer polypropylene-collodion tubing as a function of the amount of oxytocin brought into the tubing lumen. The medium is 1 mL of 0.5% albumin, renewed daily. Data are from duplicate incubations assayed over a period of 30 d. Vertical bars indicate* ± SEM; *the dashed line is the linear relationship.*

tubing had a 5-d delay before a period of rather constant release. The enveloped vasopressin preparation total release was small: ~1% of the original vasopressin load after 2 weeks. Since aqueous vasopressin loses only 20% of its activity during the same period, a strong adsorption of vasopressin onto the large internal polypropylene surface (~100 m^2/g) (9) was presumed. This contention was supported by the 300% accumulation of radioactivity of the microporous polymer polypropylene after immersion for 1 h in a ^{125}I-vasopressin solution, and the enhancement of total release (≤70%) asymptotically when surface active (0.05% Triton X-100) and/or absorption-competitive proteinaceous compounds (concentration dependent from 0.025 to 1.0% gelatin) were coloaded with vasopressin (not shown). Since incubation in 10% serum (*i.e.*, entry of externally present proteinaceous compounds) showed the rapid depletion of vasopressin as well (Fig. 2), it was therefore necessary for *in vivo* application to abolish or suppress the effect of external agents. Enveloping the vasopressin-microporous polymer preparation with cellulose dialysis membrane or an exclusion filter[12] (both permeable to vasopressin) did not prevent the asymptotic release peak (data not shown). However, after coating with nitrocellulose (collodion), the constant release of vasopressin reappeared in serum solution (Fig. 2). This enfilming was therefore applied in all subsequent studies. With a 7-μg load, daily released amounts of 2–10 ng of vasopressin were found for at least 50 d. Higher loads increased the release rate, but the relation between loading and average first month daily release shows a progressive enhancement for the heterologous oxytocin (Fig. 3). For the highest load (200 μg), constancy of release was lost; instead, a slowly asymptotically decreasing release was seen over the 30-d period.

Concentration of vasopressin in the release medium as a function of time during the first 3 d of immersion and on day 15 showed similar daily logarithmic curves (maximum reached by 6 h in serum, Fig. 4). Incubations in 0.5% albumin, started in the presence of external vasopressin (≤200 ng/mL) showed that with external concentrations <50 ng/mL, a release of vasopressin

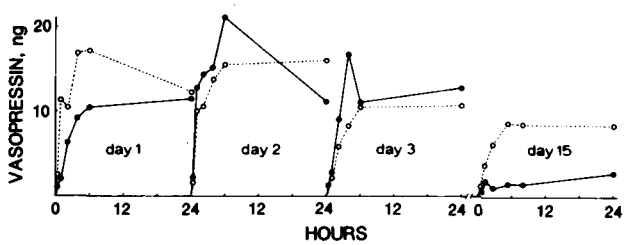

Figure 4—*Daily time course of vasopressin content in 1 mL of 10% serum on immersion of a vasopressin-microporous polymer-collodion device (7 μg) during the first 3 d and on day 15 (duplicate incubations).*

[12] Amicon UM-2.

Table I—Release and Uptake of Vasopressin by Microporous Polymer–Collodion Tubing in an Albumin Medium [a]

	Vasopressin in Medium, ng/mL	Vasopressin in Medium (by RIA), ng/mL	
		0 h	24 h
Vasopressin-microporous polymer			
	200	187 ± 16	66 ± 13
	100	93 ± 9	59 ± 9
	50	40 ± 7	31 ± 7
	10	6.1 ± 0.5	34 ± 7
	0	0	30 ± 5
Medium [b]	200	197	164
	50	42	37

[a] Tubing loaded with vasopressin (7 μg) in a 0.5% albumin medium at 37°C. Data ± *SEM* are averages of duplicate findings assayed on 3 subsequent days ($n = 6$). [b] Duplicate assays were performed on a single day for the medium, showing no marked degradation of vasopressin.

is seen; with external concentrations >50 ng/mL, vasopressin is taken up from the medium by the microporous polymer device (Table I).

The mean thickness of the collodion layer around the tubing was 45 μm (*SEM*, 2) as measured under a microscope in random 30-μm cryostat cross sections of eight preparations. A collodion bag of similar shape and thickness (42 μm, *SEM*, 2; measured in three preparations) around vasopressin in agar shows a total wash-out of vasopressin in 10% serum within a few days, while without collodion this occurs even more rapidly (data not shown).

Test Tube Experiments With other Peptides—The *in vitro* results with vasopressin were similarly obtained with lysine-vasopressin- and oxytocin-loaded microporous polymer-collodion devices, while the release pattern of α-melanocyte-stimulating hormone showed an initial lag-phase of 5 d (Fig. 5). Met-enkephalin was not adsorbed to the polypropylene (in a water medium, 70% of the load released asymptotically within 4 d) but when microporous polymer tubing was covered with collodion, the release rate was considerably retarded.

Application in the Brattleboro Rat—Immediately after implantation of the vasopressin-microporous polymer-collodion preparation, diuresis decreased from 60–70 mL of urine/100 g of body weight/d to normal (heterozygous) levels of 5–15 mL. Urine osmolality concomitantly increased from 200 to >1000 mOsm/kg H_2O (Fig. 6 A–C; Table II). A load of 7.5 μg of vasopressin reduced diuresis for 30 d, after which it slowly reached pre-implantation diabetes insipidus values at day 60. The period of low urine production increased to 35–45 and 50–80 d for the 22- and 220-μg vasopressin-filled microporous polymer tubing, respectively, with urine osmolalities of ~1500 mOsm/kg of H_2O (Table II). Return to preimplantation values became immediate after surgical removal of the implants (Fig. 6B, C). The removal was carried out under ether anesthesia. The connective tissue enveloping the implant was not attached and no signs of infection or growth abnormalities were seen.

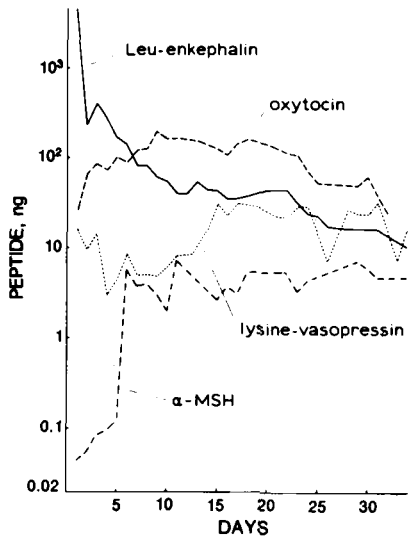

Figure 5—*Daily* in vitro *release in 10% serum medium of several neuropeptides from the microporous polymer-collodion delivery module filled with 7 μg/7.5 μL solutions.*

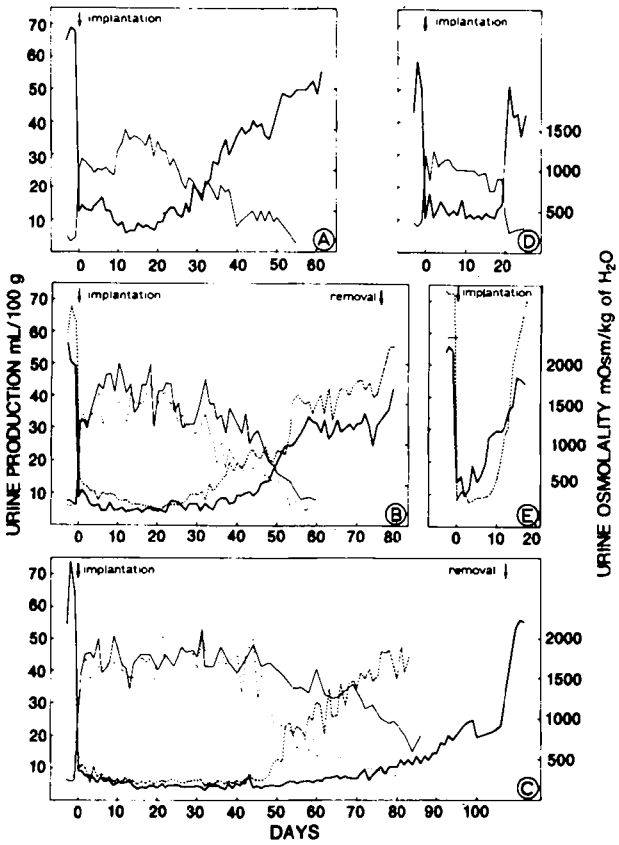

Figure 6—*Urine production (thick lines) and osmolality (thin lines) in male Brattleboro rats after implantation of different vasopressin-releasing preparations. Key: (A–C), duplicate subcutaneous implants of a microporous polymer-collodion device loaded with 7, 22, and 220 μg of vasopressin respectively (removal of the implant is indicated in B and C); (D) subcutaneous implanted osmotic minipump loaded with 22 μg of vasopressin (release rate, 1 μg/d); (E) implantation of a microporous polymer device without collodion enfilming (——) or of an agar cylinder with collodion ensheathment (·····) containing 22 μg of vasopressin.*

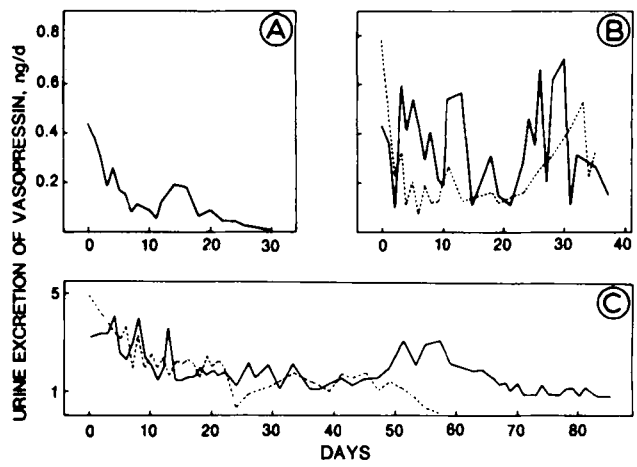

Figure 7—*Vasopressin excretion in the daily urine of Brattleboro rats after implantation of vasopressin-microporous polymer-collodion preparations containing 7 (A), 22 (B), and 220 μg of vasopressin (C) (Figs. 6A–C).*

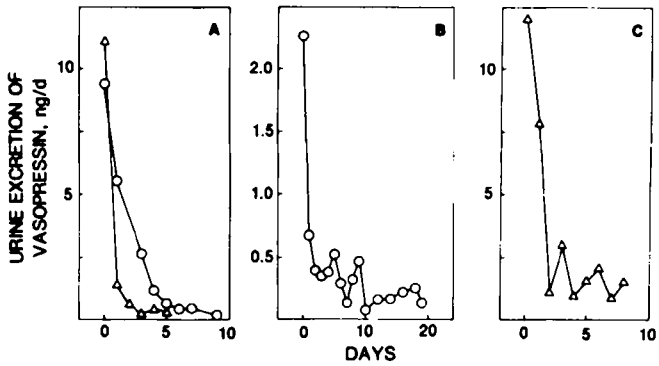

Figure 8—*Vasopressin excretion in the daily urine of Brattleboro rats after implantation of (A) a vasopressin-microporous polymer device with no collodion (△) and a vasopressin-agar-collodion preparation (○) (both with a 22-μg load; cf. Fig. 6E) and (B) an osmotic minipump (1 μg/d; cf. Fig. 6D), and after (C) daily vasopressin tannate injections (0.5 U/100 g of body weight).*

The implantation of an agar-collodion preparation and a microporous polymer tubing without collodion, both containing 22 μg of vasopressin, gave only short periods of low urine production (Fig. 6E). An osmotic minipump filled with 22 μg of vasopressin alleviated the diabetes insipidus for 20 d but not to control levels. (Fig. 6B, D; Table II).

The use of the microporous polymer technique gave reasonably constant amounts of vasopressin in daily urine during the periods of constant low diuresis (Fig. 7). Daily excreted quantities increased with the load of vasopressin, but not proportionally (Table II). Vasopressin excretion using microporous polymer without collodion or an agar-collodion preparation showed rapidly decreasing curves toward undetectable levels (Fig. 8A). Excretion of vasopressin in the first few days appeared to be somewhat higher (Fig. 7), which was also observed when the osmotic minipump or daily injections of vasopressin tannate were used (Fig. 8B, C).

To quantify the actual *in vivo* release, microporous polymer-collodion tubing filled with ^{125}I-vasopressin (22 μg) was used. Daily excretion of radioactivity with the urine was ~1% for 40 d (compare with Fig. 7B). After removal of the implant, 47% of its radioactivity was still present, giving an almost complete recovery of the label.

Perinatal Implantation Trials—Five-day-old pups always survived the implantation well, but the 1.5-cm microporous polymer preparation did not allow the sutured incision to heal if the tubing was not placed at a safe distance

Table II—Diuretic Changes and Urine Vasopressin Excretion of Homozygous Brattleboro Rats After Subcutaneous Implantation of Vasopressin Delivery Devices

	Load, μg	Period, d[a]	Diuresis, mL/100 g/d	Urine Osmolality, mOsm/kg	Vasopressin Urine Excretion, ng/d
Microporous polymer	7.5	30	10.8 ± 0.6[e]	1140 ± 40[e]	0.16 ± 0.03[e]
	22	35–46	7.3 ± 0.3[e]	1430 ± 30	0.30 ± 0.04
	220	52–82	6.2 ± 0.2	1550 ± 30	1.9 ± 0.1[e]
Minipump	22	20	12.6 ± 0.5[e]	1000 ± 30[e]	0.40 ± 0.12
Vasopressin tannate[b]	—	10	5.4 ± 0.4	1270 + 40[e]	1.6 ± 0.3[e]
Pre-operative values[c]			67.5 ± 2.6[e]	255 ± 25[e]	—[f]
Heterozygous controls[d]			5.8 ± 0.7	1440 ± 60	0.44 ± 0.09

[a] Period of the drug-polymer-implanted animals taken as the period of urine output <12 mL/100 g/d and urine osmolality >800 mOsm/kg (Fig. 6). The first day peak values were not taken for the calculation of average values (see text and Fig. 6). [b] Injections (0.5 U/100 g) for 10 d. [c] Mean of all Brattleboro rats used (n = 10), measured 3 d prior to vasopressin treatment. [d] Nineteen animals taken from a prior study (7). [e] Significantly different from heterozygous rat control data, using Student's t test ($p < 0.05$). [f] Not detectable.

from the incision. Consequently, the implant was lost. Occasionally, skin tension at the site of the rough and hard ends of the implant caused injuries, and the implant was lost. However, when still present after 6 d, it remained *in situ* without further problems. These problems were not encountered when we used small-diameter (0.7 mm) microporous polymer tubing.

The subcutaneous deposition of a small implant into rat fetuses (18th day of gestation) by needle penetration through the uterus, chorion, and amnion appeared to be possible, since delivery normally took place 4 d later. The pups were sacrificed 10 d after birth and of 10 implants, 4 were localized subcutaneously, 3 were found between the rib muscles, and 3 were lost.

DISCUSSION

Mechanism of the Microporous Polymer–Collodion Delivery Module—In this study a long-lasting and rather constant release of vasopressin from microporous polymer polypropylene-collodion preparation was realized. Apparently the vasopressin, adsorbed on the large internal surface of the microporous polymer polypropylene, forms a stock from which it is gradually freed on immersion. The constant release period might be explained by a small change in the adsorption equilibrium-determined concentration of vasopressin in the void volume of the tubing, since only small amounts of vasopressin are released. This constant concentration consequently will be a constant drive for outward diffusion causing the pseudo-zero-order release rate. Such a mechanism is reinforced by: the logarithmic time release in a constant volume (the release stops when inside and outside aqueous concentrations are the same, Fig. 4); and the increase and decrease of external vasopressin concentration to a fixed level on immersion of a (high) vasopressin-loaded device in solutions of, respectively, lower and higher vasopressin (release or uptake until equilibrium is reached, Table I). It should be emphasized that such a state of equilibrium is maintained even in 10% serum (Fig. 4), in which considerable degradation of vasopressin occurs. The proposed mechanism also explains that a slowly declining release replaces the constancy of liberation of vasopressin when either the release rate is enhanced by coloading with gelatin (12) or the load is in excess of the adsorption capacity of the polypropylene surface (200 μg of oxytocin, Fig. 3). In both cases, according to Langmuir absorption kinetics, the concentration of vasopressin in the void volume of the microporous polymer polypropylene will be relatively high and on release not replenished from the adsorbed stock. Consequently, the device empties itself quickly, which diminishes release rate more noticeably with time. A period of pseudo-zero-order release is finally reached regardless, *i.e.*, when the adsorbed stock is below the maximum capacity[13].

The collodion layer apparently prevents the rapid entry of many proteinaceous surfactants that could otherwise desorb vasopressin. Like vasopressin, oligopeptides from a medium will pass this membrane but in the opposite direction and will possibly enhance desorption. Comparing the curves in Figs. 1 and 2, this is not noticeable for 10% serum immersion, but *in vivo* (a wider variety of tissue compounds) this might be different (see below). The necessity of both microporous polymer and collodion for long-lasting release is shown when vasopressin preparations are implanted in Brattleboro rats in the absence of one or the other (Figs. 6B and E). Collodion itself, therefore, does not stipulate the constant hormone delivery, although it will undoubtedly influence release rate because of its thickness (6, 20, 21).

On the basis of this mechanism, the microporous polymer polypropylene–collodion preparation should prove applicable to any peptide, provided it sufficiently adsorbs to the polypropylene. This was true for oxytocin, lysine-vasopressin, and α-melanocyte-stimulating hormone, although constant release was not achieved for Met-enkephalin. The extent to which polypropylene adsorbs a peptide will depend on the hydrophobicity of the peptide (*i.e.*, its constituent amino acids). If polypropylene does not act properly for less hydrophobic peptides, perhaps appropriate internal surface coating or the use of other microporous polymers might give the required surface interaction.

Determination of Release Rate—Because dynamic equilibrium is reached in constant-volume incubations *in vitro*, the actual *in vivo* release should be higher. Assuming the body to be an infinite medium (outside vasopressin concentration is always zero), the release rate measured directly after the onset of *in vitro* incubation might be extrapolated and considered to be the release rate present *in vivo*. Such a calculation, on the basis of several curves as presented in Fig. 4, gives a release of 1–2% of the vasopressin load each day. This fits the radioactivity data on daily *in vivo* urine excretion (~1%) of iodinated vasopressin for 40 d. However, in general, *in vivo* rates cannot be derived easily from the release patterns *in vitro* and should be determined *in vivo*, *e.g.*, by implants with [^{3}H]vasopressin.

Vasopressin Release in the Brattleboro Rat—Long-term reduction of diabetes insipidus and reasonably constant excretion of vasopressin for several weeks were achieved by vasopressin implants (Fig. 7; note that compared with Fig. 2, vasopressin data are not expressed on a logarithmic scale). The higher excretion in the first few days was due to adaptation, probably at the level of the kidney (22, 23), since it was also seen with injected or minipump-driven vasopressin treatment (Fig. 8B, C). Assuming that ~1% vasopressin was extruded daily from the implant for 40 d, the 67% remaining in the stock should have a lower release rate. Since vasopressin urine excretion in rats is independent of infusion rate (24), the vasopressin excretion in Brattleboro rats should decline over time. The present data do not show such an effect. Only a twofold decrease occurs during the first 40 d for the 220-μg loaded implant and no decrease is observed for the 22-μg load (Fig. 7B, C). For high loads, *i.e.*, high release rates, the expected 1–2% of release per day is therefore an overestimation, probably due to the assumption of a zero subcutaneous concentration. In fact, a concentration gradient is to be expected around the vasopressin implant, which inhibits release (21) (it also could not account for the preparation acting over 100 d; Fig. 7C). In contrast to *in vitro* release (Fig. 4), the *in vivo* release indicated by daily urine vasopressin excretion appeared to be lowered with vasopressin tubing load (Table II). This additionally points to a protracted subcutaneous release of vasopressin. The rapidly decreasing release rate with the use of low-vasopressin contents of the microporous polymer tubing (Fig. 7A) is less easy to explain. Inactivation of the lower vasopressin stock may have a relatively higher threshold, or a tight encirclement of the tubing by connective tissue may be more effective in reducing the escape of vasopressin into the blood (25).

Daily injection of 100 mU of vasopressin tannate (*i.e.*, ~200 ng of vasopressin as a long-acting preparation) is shown to be the substitution dose of the Brattleboro rats (22). Normalization of diuresis ≥40 d, was brought about by implantation of a 22-μg vasopressin-loaded microporous polymer–collodion device (Table II) from which <220 ng/d is extruded. An approximately fivefold higher treatment (but supplied by an osmotic minipump) decreased urine production to near normal levels (Table II) (26). The present device, therefore, not only yielded a better alleviation of the diabetes insipidus (Table II), but also considerably prolonged the period with a more efficient use of vasopressin. Perhaps differences in release surface (entire surface of tubing *versus* small orifice of minipump) cause this effect, which could result in a different rate of uptake.

Concluding Remarks—The microporous polymer–collodion delivery module appears to be biocompatible and can be used as an implant in adult rats. Its use requires a simple operation and treatment is easily terminated. When the commercially available osmotic minipump is too large for implantation, the size of the microporous polymer delivery system allows peptide treatment of young and immature laboratory rats. The potential of the present device, moreover, is underlined by the possibility of prenatal application with smaller-sized microporous polymer tubing. The release properties of this 0.7-mm diameter tubing have been examined only in pilot studies, but did give a lasting release for vasopressin *in vitro* as well[14].

The adsorption-based mechanism of the constant delivery makes the microporous polymer technique a novice in the field of polymer monolith or membrane-controlled drug delivery systems (5, 6, 21). Whenever adsorption can be introduced on the typical microporous structure of microporous polymer and protection against the rapid desorption from outside compounds is possible, the device will provide a constant and lasting release for other peptides and possibly for other physiological compounds and pharmaceuticals as well.

REFERENCES

(1) F. A. Kincl, G. Benagiano, and I. Angee, *Steroids*, **11**, 673 (1968).

(2) W. J. Tze, F. C. Wong, L. M. Chen, and S. O'Young, *Nature* (*London*), **264**, 466 (1976).

(3) F. Theeuwes, *J. Pharm. Sci.*, **64**, 1987 (1975).

(4) W. Dames, F. Joo, and J. R. Wolff, *Brain Res.*, **36**, 259 (1979).

(5) H. Benson, B. Harley, and E. E. Schmitt, in "Kirk-Othmer Encyclopaedia of Chemical Technology, Vol. 17," Wiley, New York, N.Y., 1980, p. 290.

(6) I. Cabasso, in "Kirk-Othmer Encyclopaedia of Chemical Technology, Vol. 12," Wiley, New York, N.Y., 1980, p. 492.

(7) G. J. Boer, H. B. M. Uylings, A. J. Patel, K. Boer, and R. Kragten, *Ann. N.Y. Acad. Sci.*, **394**, 703 (1982).

(8) W. Worthy, *Chem. Eng. News*, **56**, 23 (1978).

(9) K. Schneider, *Kunststoffe*, **71**, 183 (1981).

(10) G. J. Boer and D. F. Swaab, in "Application of Behavioural Phar-

[13] Boer and Kruisbrink, in preparation.

[14] Boer and Kragten, unpublished results.

macology in Toxicology," G. Zbinden, V. Cuomo, G. Racagni, and B. Weiss, Eds., Raven Press, New York, N.Y., 1983, p. 251.
(11) D. F. Swaab and G. J. Boer, *J. Develop. Physiol.*, **5**, 67 (1983).
(12) G. J. Boer, J. Kruisbrink, and H. Van Pelt-Heerschap, *J. Endocrinol.*, **98**, 147 (1983).
(13) F. C. Greenwood, W. H. Hunter, and J. S. Glover, *Biochem. J.* **89**, 114 (1963).
(14) J. Dogterom, D. F. Swaab, and Tj. B. Van Wimersma Greidanus, *Neuroendocrinology*, **24**, 108 (1977).
(15) J. Dogterom, Tj. B. Van Wimersma Greidanus, and D. De Wied, *Am. J. Physiol.*, **234**, E 463 (1978).
(16) A. J. Thody, R. J. Penny, M. D. Clark, and C. Taylor, *J. Endocrinol.*, **67**, 385 (1975).
(17) H. Valtin and H. A. Schroeder, *Am. J. Physiol.*, **206**, 425 (1964).
(18) D. F. Swaab, G. J. Boer, and J. W. L. Nolten, *Acta Endocrinol., Suppl.*, **177**, 80 (1973).
(19) D. F. Swaab and W. J. Honnebier, *J. Obstet. Gynaecol.*, **80**, 589 (1973).
(20) T. J. Roseman and W. I. Higuchi, *J. Pharm. Sci.*, **59**, 353 (1970).
(21) R. W. Baker and H. K. Lonsdale, in "Controlled Release of Biologically Active Agents," A. C. Tanguary and R. E. Lacey, Eds., Plenum Press, New York, N.Y., 1974, p. 15.
(22) J. Mohring, B. Mohring, A. Schomig, H. Schomig-Brekner, and D. Haack, *Am. J. Physiol.*, **227**, 921 (1974).
(23) W. Kriz and L. Bankir, *Ann. N.Y. Acad. Sci.*, **394**, 424 (1982).
(24) M. Ginsburg, in "Handbook of Experimental Pharmacology Vol. XXIII," B. Berde, Ed., Springer-Verlag, Berlin, FRG, 1968, p. 286.
(25) J. Folkman and D. M. Long, Jr., *Ann. N.Y. Acad. Sci.*, **111**, 857 (1964).
(26) S. W. T. Cheng and W. G. North, *Ann. N.Y. Acad. Sci.*, **394**, 473 (1982).
(27) R. Kragten and G. J. Boer, *J. Endocrinol.*, **94**, Suppl., 29P (1982).

ACKNOWLEDGMENTS

The authors thank J. van Heerikhuize and R. Kragten for their practical assistance in parts of the study; the members of our project group Brain-Endocrine Interactions; and Drs. J. Lakeman (Organon BV, Oss, The Netherlands); A. J. Mul (Intervet International, Boxmeer, The Netherlands); W. Heuvelsland and J. J. van Aarsten (AKZO Research Centre, Arnhem, The Netherlands); C. R. Nederveen (AKZO Chemie, Amersfoort, The Netherlands); and D. Heitmann (ENKA Research Centre, Obernburg, West Germany) for their stimulating advice. This study was financially supported by the ENKA Research Institute (Obernburg, West Germany). We also gratefully thank Dr. H. Swanson and Mr. P. van Nieuwkoop for editing the manuscript.

Sustained-Release Characteristics of a New Implantable Formulation of Disulfiram

MICHAEL PHILLIPS *§x **and JOSEPH D. GRESSER** ‡¶

Received November 7, 1983, from the **Division of Internal Medicine, Georgetown University Hospital, Washington, DC 20007* and *‡Dynatech Research and Development Company, Cambridge, MA 02139.* Accepted for publication March 1, 1984. Present addresses: §Division of General Medicine and Clinical Pharmacology, The Chicago Medical School, North Chicago, IL 60064 and ¶Key Pharmaceuticals, Inc., Miami Beach, FL 33169.

Abstract □ The object of this study was to evaluate the sustained-release characteristics of a new formulation of disulfiram. Solid rods (500 mg) made of a composite of 80% poly(glycolic-co-L-lactic acid) and 20% ^{14}C-labeled disulfiram were implanted subcutaneously in five Wistar CD-1 rats; a control group received 100 mg of ^{14}C-labeled disulfiram subcutaneously. Excretion of radiolabeled material in the urine and feces was monitored for 88 d. Sustained mobilization of drug was observed in the copolymer–disulfiram implant group, reaching a peak value 30 d after implantation. The control group exhibited first-order kinetics of drug mobilization. At necropsy, there was no encapsulation of the residual rods. The copolymer–disulfiram composite performed as a true sustained-release system, and improved formulations may have clinical applications in the treatment of alcoholic humans.

Keyphrases □ Disulfiram—sustained-release implantable formulation, rats, poly(glycolic-co-L-lactic acid) □ Sustained-release formulations—implantable disulfiram, poly(glycolic-co-L-lactic acid), rats

Disulfiram is widely prescribed to discourage alcoholics from drinking alcohol, since the two drugs interact to produce a subjectively unpleasant experience characterized by facial flushing, nausea, tachycardia, and hypotension (1–4). The effectiveness of disulfiram as a treatment for alcoholism is severely limited by the willingness of patients to take the drug every day; many stop taking their tablets so that they might resume drinking alcohol as soon as the effects have worn off (5). Frequent failures of treatment with the orally administered drug have stimulated interest in parenteral therapy with subcutaneously implanted disulfiram tablets, but numerous studies during the past 25 years have demonstrated that these implants have miniscule pharmacological effects, possibly due to their poor bioavailability (6–8).

However, animal studies have demonstrated that disulfiram can be rapidly mobilized from a subcutaneous site, provided that the drug is injected in an appropriate vehicle, *e.g.*, suspended in arachis oil (9) or dissolved in polyethylene glycol (10). These findings suggest that it might be possible to prepare a sustained-release disulfiram implant with a true pharmacological effect. Ideally, such a formulation would combine disulfiram with a vehicle which would deliver the drug into the circulatory system at a steady rate for several weeks or months at a time and be free of any significant local or systemic toxicity. A vehicle which appears to offer these features is a new biodegradable polymer, poly(glycolic-co-L-lactic acid) (PLGA). When implanted subcutaneously, the copolymer appears to degrade slowly into its parent monomers, lactic acid and glycolic acid, while continuously releasing any bound drug at a steady rate. *In vivo* studies of PLGA combined with contraceptives, narcotic antagonists, and antimalarials have shown that these implants can deliver the drug continuously into the circulatory system for several months at a time (11). We describe a study of the sustained-release characteristics of a new formulation of disulfiram combined with the copolymer, which was undertaken to investigate the feasibility of using such a preparation in the treatment of alcoholic humans.

0022-3549/84/1200-1718$01.00/0
© 1984, American Pharmaceutical Association

macology in Toxicology," G. Zbinden, V. Cuomo, G. Racagni, and B. Weiss, Eds., Raven Press, New York, N.Y., 1983, p. 251.
(11) D. F. Swaab and G. J. Boer, *J. Develop. Physiol.*, **5**, 67 (1983).
(12) G. J. Boer, J. Kruisbrink, and H. Van Pelt-Heerschap, *J. Endocrinol.*, **98**, 147 (1983).
(13) F. C. Greenwood, W. H. Hunter, and J. S. Glover, *Biochem. J.* **89**, 114 (1963).
(14) J. Dogterom, D. F. Swaab, and Tj. B. Van Wimersma Greidanus, *Neuroendocrinology*, **24**, 108 (1977).
(15) J. Dogterom, Tj. B. Van Wimersma Greidanus, and D. De Wied, *Am. J. Physiol.*, **234**, E 463 (1978).
(16) A. J. Thody, R. J. Penny, M. D. Clark, and C. Taylor, *J. Endocrinol.*, **67**, 385 (1975).
(17) H. Valtin and H. A. Schroeder, *Am. J. Physiol.*, **206**, 425 (1964).
(18) D. F. Swaab, G. J. Boer, and J. W. L. Nolten, *Acta Endocrinol., Suppl.*, **177**, 80 (1973).
(19) D. F. Swaab and W. J. Honnebier, *J. Obstet. Gynaecol.*, **80**, 589 (1973).
(20) T. J. Roseman and W. I. Higuchi, *J. Pharm. Sci.*, **59**, 353 (1970).
(21) R. W. Baker and H. K. Lonsdale, in "Controlled Release of Biologically Active Agents," A. C. Tanguary and R. E. Lacey, Eds., Plenum Press, New York, N.Y., 1974, p. 15.
(22) J. Mohring, B. Mohring, A. Schomig, H. Schomig-Brekner, and D. Haack, *Am. J. Physiol.*, **227**, 921 (1974).
(23) W. Kriz and L. Bankir, *Ann. N.Y. Acad. Sci.*, **394**, 424 (1982).
(24) M. Ginsburg, in "Handbook of Experimental Pharmacology Vol. XXIII," B. Berde, Ed., Springer-Verlag, Berlin, FRG, 1968, p. 286.
(25) J. Folkman and D. M. Long, Jr., *Ann. N.Y. Acad. Sci.*, **111**, 857 (1964).
(26) S. W. T. Cheng and W. G. North, *Ann. N.Y. Acad. Sci.*, **394**, 473 (1982).
(27) R. Kragten and G. J. Boer, *J. Endocrinol.*, **94**, Suppl., 29P (1982).

ACKNOWLEDGMENTS

The authors thank J. van Heerikhuize and R. Kragten for their practical assistance in parts of the study; the members of our project group Brain-Endocrine Interactions; and Drs. J. Lakeman (Organon BV, Oss, The Netherlands); A. J. Mul (Intervet International, Boxmeer, The Netherlands); W. Heuvelsland and J. J. van Aarsten (AKZO Research Centre, Arnhem, The Netherlands); C. R. Nederveen (AKZO Chemie, Amersfoort, The Netherlands); and D. Heitmann (ENKA Research Centre, Obernburg, West Germany) for their stimulating advice. This study was financially supported by the ENKA Research Institute (Obernburg, West Germany). We also gratefully thank Dr. H. Swanson and Mr. P. van Nieuwkoop for editing the manuscript.

Sustained-Release Characteristics of a New Implantable Formulation of Disulfiram

MICHAEL PHILLIPS *§x **and JOSEPH D. GRESSER** ‡¶

Received November 7, 1983, from the **Division of Internal Medicine, Georgetown University Hospital, Washington, DC 20007* and *‡Dynatech Research and Development Company, Cambridge, MA 02139.* Accepted for publication March 1, 1984. Present addresses: §Division of General Medicine and Clinical Pharmacology, The Chicago Medical School, North Chicago, IL 60064 and ¶Key Pharmaceuticals, Inc., Miami Beach, FL 33169.

Abstract □ The object of this study was to evaluate the sustained-release characteristics of a new formulation of disulfiram. Solid rods (500 mg) made of a composite of 80% poly(glycolic-co-L-lactic acid) and 20% ^{14}C-labeled disulfiram were implanted subcutaneously in five Wistar CD-1 rats; a control group received 100 mg of ^{14}C-labeled disulfiram subcutaneously. Excretion of radiolabeled material in the urine and feces was monitored for 88 d. Sustained mobilization of drug was observed in the copolymer–disulfiram implant group, reaching a peak value 30 d after implantation. The control group exhibited first-order kinetics of drug mobilization. At necropsy, there was no encapsulation of the residual rods. The copolymer–disulfiram composite performed as a true sustained-release system, and improved formulations may have clinical applications in the treatment of alcoholic humans.

Keyphrases □ Disulfiram—sustained-release implantable formulation, rats, poly(glycolic-co-L-lactic acid) □ Sustained-release formulations—implantable disulfiram, poly(glycolic-co-L-lactic acid), rats

Disulfiram is widely prescribed to discourage alcoholics from drinking alcohol, since the two drugs interact to produce a subjectively unpleasant experience characterized by facial flushing, nausea, tachycardia, and hypotension (1–4). The effectiveness of disulfiram as a treatment for alcoholism is severely limited by the willingness of patients to take the drug every day; many stop taking their tablets so that they might resume drinking alcohol as soon as the effects have worn off (5). Frequent failures of treatment with the orally administered drug have stimulated interest in parenteral therapy with subcutaneously implanted disulfiram tablets, but numerous studies during the past 25 years have demonstrated that these implants have miniscule pharmacological effects, possibly due to their poor bioavailability (6–8).

However, animal studies have demonstrated that disulfiram can be rapidly mobilized from a subcutaneous site, provided that the drug is injected in an appropriate vehicle, *e.g.*, suspended in arachis oil (9) or dissolved in polyethylene glycol (10). These findings suggest that it might be possible to prepare a sustained-release disulfiram implant with a true pharmacological effect. Ideally, such a formulation would combine disulfiram with a vehicle which would deliver the drug into the circulatory system at a steady rate for several weeks or months at a time and be free of any significant local or systemic toxicity. A vehicle which appears to offer these features is a new biodegradable polymer, poly(glycolic-co-L-lactic acid) (PLGA). When implanted subcutaneously, the copolymer appears to degrade slowly into its parent monomers, lactic acid and glycolic acid, while continuously releasing any bound drug at a steady rate. *In vivo* studies of PLGA combined with contraceptives, narcotic antagonists, and antimalarials have shown that these implants can deliver the drug continuously into the circulatory system for several months at a time (11). We describe a study of the sustained-release characteristics of a new formulation of disulfiram combined with the copolymer, which was undertaken to investigate the feasibility of using such a preparation in the treatment of alcoholic humans.

0022-3549/84/1200-1718$01.00/0
© 1984, American Pharmaceutical Association

EXPERIMENTAL SECTION

Polymer Synthesis—The general principles of poly(glycolic-co-L-lactic acid) synthesis have been described (11). It was synthesized in bulk in an evacuated glass vessel from a mixture of 90 g of L-lactide and 10 g of glycolide with 1 g of *p*-toluenesulfonic acid monohydrate as a catalyst. After deacrating the mixture to <0.05 mm Hg for 45 min, the vessel was sealed, rotated to mix the ingredients, heated at 118°C for 2 h, mixed again, then heated for 10 d at 118 ± 2°C. The resulting polymer was dissolved in tetrahydrofuran, filtered through glass wool, precipitated in distilled water, and vacuum dried. The mean molecular weight of the copolymer (34,428 ± 877) was determined by dissolving the polymer in tetrahydrofuran (5 mg/mL) and assaying by gel-permeation chromatography using an HPLC system[1] equipped with μ-Styragel columns and a differential refractive index detector.

Dilution of Radiolabeled Disulfiram—Radiolabeled (5.0 mCi) disulfiram, [1-^{14}C]bis(diethylthiocarbamoyl)disulfide[2], was diluted with 14.9991 g of unlabeled disulfiram[3] by stirring for 2 h at room temperature in 650 mL of reagent-grade ethanol[4]; 14.9860 g of diluted disulfiram was recovered after vacuum drying at 60°C for 10 d. Two samples of the diluted radiolabeled drug were assayed in triplicate for specific activity on a liquid scintillation counter[5]; the mean specific activity was 336 μCi/g.

Composite Preparation—A cosolution of ^{14}C-labeled disulfiram and PLGA (1:4, w/w) was prepared in dichlormethane and cast as a thin film on a clean glass surface. The film was adjusted to 0.06 cm (0.025 in.) in thickness with a film spreader[6], air dried, then vacuum dried at 45°C. The final dosage form was prepared by extruding rods of this composite through a 0.3175-cm die, at a temperature between 70–80°C and pressures up to 140 psi. These disulfiram–copolymer composite rods (20:80) had a mean specific activity of 62.92 ± 8.11 μCi/g.

Implantation—Two groups of animals were studied: a test group receiving the subcutaneous ^{14}C-labeled disulfiram–copolymer implant, and a control group receiving subcutaneous uncompounded ^{14}C-labeled disulfiram. Each group was comprised of five Wistar CD-1 male rats (100–200 g). After anesthesia[7] was administered a slit was cut in the skin of the interscapular region and a small subcutaneous pocket was dissected (large enough for the introduction of the 0.3175-cm diameter rods). Each rat received 500 mg of the compounded 20% rods (containing 100 mg of ^{14}C-labeled disulfiram and 400 mg of the copolymer) and the wound was closed with clips. The second group of rats served as controls and similarly received 100 mg of uncompounded powdered ^{14}C-labeled disulfiram. No attempt was made to preserve strict asepsis during these procedures.

Sample Collection and Analysis—All rats were individually housed in metabolism cages to facilitate the separate collection of urine and feces. Prior to implantation, three fecal and urine samples were collected to determine background counts. Subsequent samples of all excreted urine and feces were collected 1, 3, 7, 9, 11, 15, 18, 22, 25, 29, 32, 39, 46, 53, 60, 67, 74, 81, and 88 d after implantation. Urine samples were assayed for ^{14}C-labeled material in a liquid scintillation counter[8], and the extraction was calculated as the mass of implanted disulfiram which contained an equivalent amount of radiolabel. Feces were combusted to $^{14}CO_2$ with an oxidizer[9] and adsorbed in oxyfluor-CO_2[10] for counting. At the conclusion of the study, the rats were sacrificed and the excised rods from the experimental animals were assayed for residual drug. Pathological studies were performed on the injection sites of two animals from each group: the sites were inspected for gross changes and tissue sections were prepared (thickness, 7–10 μm), stained with hematoxylin and eosin, and examined microscopically.

Data Analysis—All data were stored on diskettes using a microcomputer[11] and software[12] to calculate the mean and standard deviation of total disulfiram excretion during each collection interval in the test and control groups. The line of best fit for the control group was calculated by the least-squares method.

RESULTS

Drug Excretion—The average daily excretion of radiolabeled material is shown for the test and control groups in Figs. 1 and 2. The combined excretion

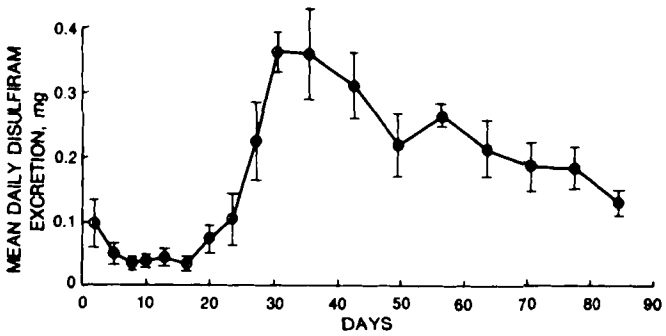

Figure 1—*Disulfiram–copolymer composite group mean daily excretion of radiolabeled metabolites in urine and feces following subcutaneous implantation. Bars indicate 1 SD.*

in urine and feces is expressed as the mass of implanted disulfiram which originally contained an equivalent amount of radiolabel. In all collection periods, the quantity of radiolabeled material in the urine was approximately 10 times greater than the amount detected in the feces. This was true for both groups of animals throughout the study. The cumulative recovery of radiolabeled material in urine and feces (expressed as a percentage of the total administered dose ±1 *SD*) was 17.41 ± 2.27% for the group receiving the disulfiram–copolymer composite and 80.54 ± 9.56% for the control group.

Residual Drug in Implanted Composite—The residual radiolabeled material in the excised composite rods accounted for an additional 55.53% (*SD* = 14.83%) of the administered dose of disulfiram. Hence, the total recovery of radiolabel from the rats receiving the disulfiram–copolymer composite accounted for 72.94% (*SD* = 14.49%) of the implanted dose. The mean weight of the rods recovered from the implantation sites was 55.53 mg (*SD* = 12.84). No residual drug was observed at the injection site in the control group.

Pathological Findings—One rat in the control group died on day 63 of the study; the cause of death was unknown. Excretion data from this animal did not deviate statistically from the others in the group and were included in the study. In the remaining animals, tissues from the injections sites were grossly and microscopically normal, with no evidence of residual drug, necrosis, or inflammatory reaction.

One rat in the test group excreted aberrantly large quantities of radiolabel during the early days of the study; at autopsy, a large abscess was found at the implantation site with no remaining rods. Data from this animal was not included in the findings reported above. The implantation sites of the remaining animals were grossly and microscopically normal, with no evidence of necrosis, inflammatory reaction, or encapsulation of the rods.

DISCUSSION

All excretion of radiolabeled material in this study was expressed in terms of the equivalent quantity of implanted disulfiram. This was not meant to imply that unchanged disulfiram was measured in the urine and feces; to the contrary, there is strong evidence that disulfiram is very rapidly metabolized in the blood and liver, and the breakdown products are promptly excreted (10, 12, 13). At least one of the metabolites, carbon disulfide, is a volatile compound excreted in the breath, which might account for some part of the discrepancy between the implanted dose and the total amount of drug recovered. The real utility of expressing excretion of radiolabel in terms of quantity of the parent drug lies in the insight it provides into the rate of mobilization of the disulfiram from the injection site.

The mobilization of drug from the disulfiram–copolymer composite (Fig. 1) demonstrates that the major objective of the study was achieved: sustained systemic delivery of disulfiram for a 3-month period. During that time, the drug was delivered continuously, although fluctuations were observed in the rate of delivery. An ideal implantable drug delivery system would achieve zero-order kinetics, *i.e.*, the rate of delivery would rapidly reach its maximal value and remain there until the supply of drug was exhausted. However, in clinical practice, even a nonideal delivery system may achieve a near-ideal pharmacological effect, provided that the rate of delivery oscillates within a defined "therapeutic window" (with upper and lower limits defined as the rates of delivery at which either toxic effects or inadequate clinical responses are observed). Consequently, even though fluctuations were observed in the rate of delivery of disulfiram from the composite implant, it could provide an acceptable therapeutic effect for a period of 3 months or longer.

The mobilization of injected powdered disulfiram in the control group provided an unexpected finding (Fig. 2), in view of the known poor bioavailability of disulfiram in subcutaneously implanted tablets. The first-order

[1] Waters Associates.
[2] Amersham.
[3] USP grade; Ayerst Laboratories.
[4] Fisher.
[5] Model LS-100C; Beckman Instruments.
[6] Boston-Bradley.
[7] Penthrane; Abbott Laboratories.
[8] Model LS-230; Beckman.
[9] Harvey Biological.
[10] New England Nuclear.
[11] TRS-80 Model 1; Radio Shack, Tandy Corporation, Ft. Worth, Tex.
[12] VisiCalc; Personal Software Inc., Sunnyvale, Calif.

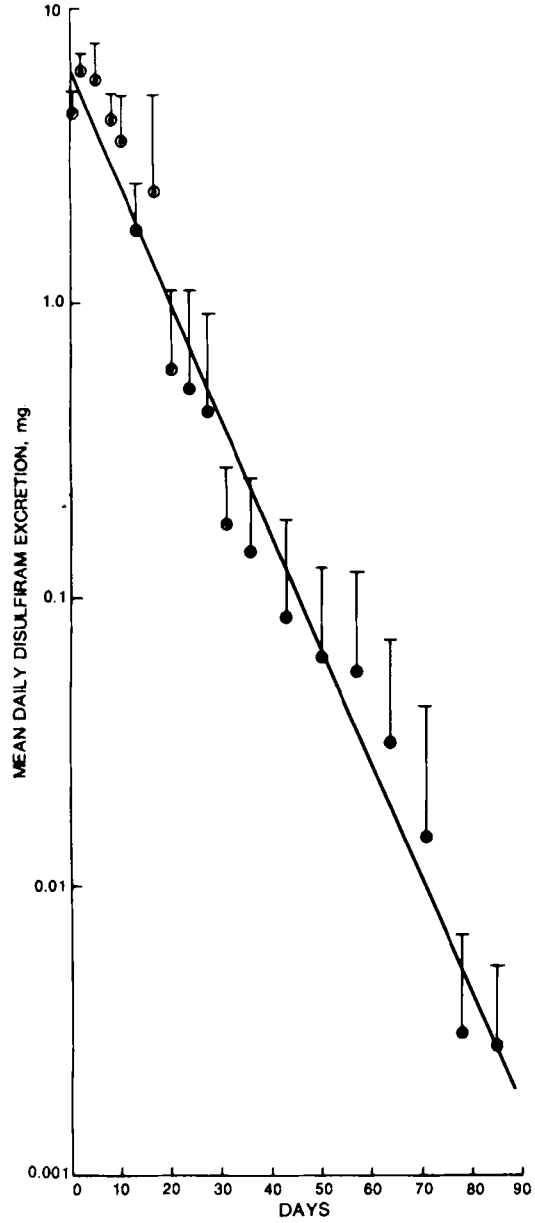

Figure 2—*Control group mean daily excretion of radiolabeled metabolites in urine and feces following subcutaneous injection of powdered disulfiram* $t_{1/2}$ = *7.53 d. Bars indicate 1* SD. (*Log* y = −0.04 x + 0.80; r^2 = 0.97; $p < 0.0001$.)

mobilization kinetics are consistent with the commonly observed kinetics of other parenterally administered drugs (14). It is possible that the bioavailability of the disulfiram was enhanced by administering it in powder form, thus greatly increasing the surface area available for the dissolution of the drug in the interstitial fluid. The long half-life of the powdered disulfiram (7.53 d) may be a function of its poor solubility in water, and raises the possibility that this preparation may also have potential clinical application.

These data demonstrate that the disulfiram–copolymer composite has the properties of a sustained-release formulation when implanted subcutaneously in rats, with no evidence of local or systemic toxicity. However, a number of factors must be taken into account before any trial of a similar material is contemplated in human subjects. First, the ratio of disulfiram to the copolymer is low, so that prohibitively large volumes of composite might be required for a prolonged period of treatment. For use in human subjects, an improved composite with a higher ratio of drug to vehicle would probably be desirable. Second, the daily dosage requirement for parenteral disulfiram is not yet known. Although patients generally require 250–500 mg of the oral drug each day to achieve a clinical effect, more research is required to determine whether or not parenteral disulfiram needs to be administered in similar quantities. Pending these advances in technology and basic knowledge, we suggest that sustained-release disulfiram implants may eventually achieve a clinical application in the treatment of alcoholic humans.

REFERENCES

(1) T. M. Kitson, *J. Stud. Alcohol*, **38,** 96 (1977).

(2) A. M. Sauter, D. Boss, and J-P. von Wartburg, *J. Stud. Alcohol*, **38,** 1680 (1977).

(3) L. Lundwall and F. Baekeland, *J. Nerv. Ment. Dis.*, **153,** 381 (1971).

(4) J. Hald and E. Jacobsen, *Lancet* **ii,** 1001 (1948).

(5) J. R. Gerrein, C. M. Rosenberg, and V. Manohar, *Arch. Gen. Psychiatry*, **28,** 798 (1973).

(6) A. Wilson, *J. Stud. Alcohol*, **36,** 555 (1975).

(7) T. M. Kitson, *J. Stud. Alcohol*, **39,** 183 (1978).

(8) B. Bergstrom, H. Ohlin, P. E. Lindblom, and J. Wadstein, *Lancet* **i,** 49 (1982).

(9) J. H. Stromme and L. Eldjarn, *Biochem. Pharmacol.*, **15,** 287 (1966).

(10) M. Phillips, *Clin. Res.*, **28,** 623A (1980).

(11) D. L. Wise, T. D. Fellmann, J. E. Sanderson, and R. L. Wentworth, in, "Drug Carriers in Biology and Medicine," G. Gregoriadis, Ed. Academic Press, New York, N.Y., 1979, pp. 237–270.

(12) S. B. Pedersen, *Arch. Pharm. Chem. Sci. Ed.*, **8,** 65 (1980).

(13) R. P. Agarwal, R. A. McPherson, and M. Phillips, *Res. Commun. Chem. Pathol. Pharmacol.*, **42,** 293 (1983).

(14) D. J. Greenblatt and J. Koch-Weser, *N. Engl. J. Med.*, **25,** 542 (1976).

ACKNOWLEDGMENTS

The authors thank Dr. John F. Howes (formerly of SISA Inc., Cambridge, Mass.) for performing the biologic assays and Ayerst Laboratories for donating the disulfiram. This study was supported by NIAAA Grant No. IR011AA05334-01.

Characterization of Drug-Loaded Poly(*d*,*l*-lactide) Microspheres

S. BENITA *x, J. P. BENOIT ‡, F. PUISIEUX ‡, and C. THIES §

Received July 11, 1983, from the *Pharmacy Department, School of Pharmacy, Hebrew University of Jerusalem, Israel, the ‡Laboratoire de Pharmacie Galenique, Faculte de Pharmacie de l'Universite Paris-Sud, Chatenay-Malabry, France, and the §Biological Transport Lab., Washington University, St. Louis, MO 63130. Accepted for publication February 23, 1984.

Abstract □ Lomustine and progesterone have been incorporated in biodegradable poly(*d*,*l*-lactide) microspheres by evaporating dichloromethane from stirred dichloromethane-in-water emulsions. Spherical microspheres with lomustine or progesterone payloads ≤23% were obtained. Higher lomustine payloads gave irregularly shaped particles. Microspheres with ≤68% progesterone were obtained, but free drug crystals formed on the surface of such microspheres. Increased agitation rates decreased mean microsphere size. Addition of drug to the dichloromethane phase increased average particle size relative to that obtained with drug-free microspheres prepared under the same experimental conditions. Complete evaporation of the dichloromethane, while the medium was continuously stirred, promoted formation of free drug crystals in the aqueous phase. Increased emulsifier concentrations did not significantly enhance drug incorporation efficiency within the microspheres. Shelf-life stability of lomustine and progesterone was reduced by incorporation in the microspheres, presumably due to their molecular dispersion in the poly(*d*,*l*-lactide).

Keyphrases □ Poly(*d*,*l*-lactide) microspheres—loaded with lomustine, progesterone, effect of emulsifier concentrations, agitation rates on formation, stability □ Microspheres—poly(*d*,*l*-lactide), progesterone, effect of emulsifier concentration, stability

Parenteral controlled-release systems which are capable of being targeted to tissue sites and to deliver their active ingredient over a long period of time are of considerable interest (1). These potential sustained-release drug-targeting dosage forms require the use of biodegradable polymers as drug carriers. Candidate biodegradable materials include gelatin (2), albumin (3, 4), poly(lactide-glycolide) copolymers (5), and polylactide (6–9). Progesterone has been incorporated in poly(*d*,*l*-lactide) microspheres in order to design an injectable long-acting delivery system. Such a dosage form administered *in vivo* yielded promising pharmacological action (10). Since little has been reported about the physical properties of such microspheres, a study of their properties as a function of the preparative conditions was carried out. Poly(*d*,*l*-lactide) microspheres containing either progesterone or lomustine were prepared. The ultimate objective is to use the latter to produce tumor embolism by intra-arterial infusion. This therapeutic method has been shown by Kato *et al.* (11), using mitomycin C microcapsules, to be an effective means of combining vascular mechanical obstruction and slow release of active mitomycin C within tumors.

EXPERIMENTAL SECTION

Materials—Poly(*d*,*l*-lactide) was supplied by D. N. Mason[1] and had a mean mol. wt. of 61,000. Two polymeric emulsifiers were used: 88% hydrolyzed polyvinyl alcohol[2] and methylcellulose (10 and 400 cps grades)[3]. Progesterone[4] and lomustine[5] [*N*-(2-chloroethyl)-*N'*-cyclohexyl-*N*-nitrosourea] were used as supplied. Dichloromethane[6], Analar grade, was employed without further purification.

Methods—Microspheres were formed at atmospheric pressure by a process similar to that described by Beck *et al.* (10). The procedure involved placing, in a 400-mL glass beaker, 250 mL of water that contained polyvinyl alcohol or methylcellulose. A solution that contained 20 mL of CH_2Cl_2, 927 mg of poly(*d*,*l*-lactide), and a known weight of drug (280–2,000 mg), was poured rapidly into the aqueous phase as it was stirred at a constant rate by a stirrer fitted with a digital revolution counter[7]. The resulting emulsion was agitated at 22° C for a known period of time during which the CH_2Cl_2 evaporated. In a few cases, the system was agitated continuously until CH_2Cl_2 evaporation was complete. This is the continuous evaporation process. For most runs, the interrupted evaporation process was used; agitation was stopped before CH_2Cl_2 evaporation was complete, the partially dried microspheres were allowed to settle, and the aqueous phase that contained the polymeric dispersing agent was replaced with deionized water by three washing and decantation steps. Once the microspheres were resuspended in emulsifier-free water, they were agitated 7–17 h so that CH_2Cl_2 evaporation could proceed to completion. Removal of the polymeric emulsifier from the aqueous phase before completion of CH_2Cl_2 evaporation minimizes formation of free drug crystals in the aqueous phase or on the surface of the microspheres (12).

On completion of CH_2Cl_2 evaporation, the microspheres were isolated by filtration, washed, and dried under reduced pressure at 22° C for 20 h. The dried microspheres were sieved and stored in a desiccator until used. The preparative parameters varied in this study include: polymeric emulsifier and emulsifier concentration, amount and type of drug incorporated in the microspheres, rate of agitation, and length of agitation. Theoretical microsphere drug contents (or payloads) specified in this paper represent the percent by weight drug carried by a microsphere if all the drug and all the poly(*d*,*l*-lactide) added to an encapsulation system were incorporated in the microspheres. Actual or measured drug contents were usually lower than the theoretical values due to drug loss to the aqueous phase during CH_2Cl_2 evaporation.

Microsphere Evaluation—*Progesterone Content*—Progesterone-loaded microspheres (30 mg) were dissolved in 2 mL of CH_2Cl_2. Ethanol (23 mL) was added to precipitate the poly(*d*,*l*-lactide). The resulting suspension was centrifuged at 20,000 rpm for 10 min. The clear supernatant was diluted with ethanol and 10 μL of the resulting solution was injected into an HPLC[8]. The chromatograph operating conditions were: C_8 reverse-phase column (10-μm spheres); methanol eluant; eluant flow rate 2 mL/min; 254 nm detector. Under these conditions, progesterone had a retention time of 97 s. The progesterone content of sample solutions was obtained from a progesterone calibration curve constructed from standard progesterone solutions.

Lomustine Content—Lomustine-loaded microspheres (30 mg) were dissolved in 2 mL of CH_2Cl_2. Ethanol (23 mL) was added to precipitate the poly(*d*,*l*-lactide). After centrifugation at 20,000 rpm for 10 min, the clear supernatant (10 μL) was subjected to HPLC analysis. The HPLC operating conditions were the same as those used for progesterone assays, except that the eluant was an acetonitrile-water mixture (75:25, v/v). The lomustine retention time was 143 s. Control experiments with cyclohexylamine and 2-chloroethanol, two known lomustine degradation products, established that neither compound gave an interfering peak within 240 s of elution. Lomustine contents of all samples were obtained from a calibration curve constructed from standard lomustine solutions.

Microscopy Studies—Optical and scanning electron microscopy were used to evaluate the drug incorporation and surface characteristics of the microspheres prepared under the various conditions used. The optical microscope[9] and the electron microscope[10] were equipped with cameras.

RESULTS AND DISCUSSION

Characterization of the Microspheres Formed—The presence of an emulsifying agent is vital to the successful formation of individual spherical microspheres by the solvent evaporation process. The emulsifiers used in this

[1] Chemical Engineering Dept., Washington University, St. Louis, Mo.
[2] Vinol 205; Air Products and Chemicals, Allentown, Pa.
[3] Methocel; Dow Chemical Co., Midland, Mich.
[4] Sigma Chemical Co., St. Louis, Mo.
[5] Roger Bellon Laboratories, Neuilly/Seine, France.
[6] J. T. Baker Chemical Co., Phillipsburg, N.J.
[7] Model RZR-2000; Heidolph Elektro, Kelheim, Germany.
[8] SP 8000; Spectra Physics, Santa Clara, Calif.
[9] American Optical, Rochester, N.Y.
[10] Model HHS-2R; Hitachi, Tokyo, Japan.

0022-3549/84/1200-1721$01.00/0
© 1984, American Pharmaceutical Association

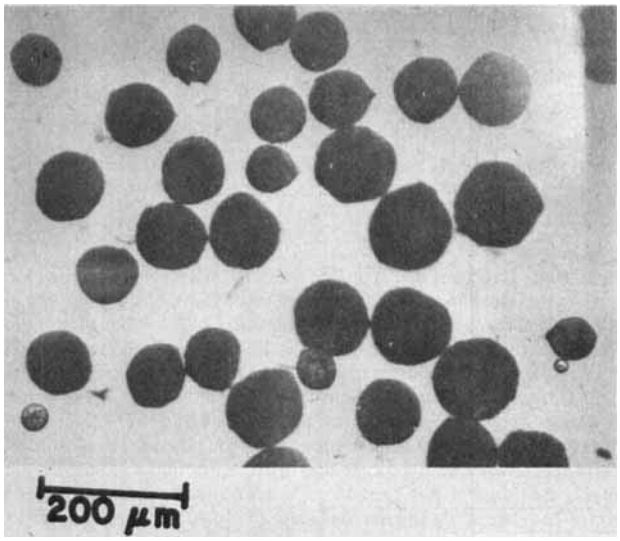

Figure 1—*Photomicrograph of lomustine-loaded microspheres prepared by the continuous evaporation process at 250 rpm with 0.05% (w/w) methylcellulose as emulsifier. Theoretical lomustine content: 35% (w/w). Magnification: 100×.*

study, partially hydrolyzed polyvinyl alcohol and methycellulose, gave suitable microspheres, although there was some difference in their performance. When lomustine was dissolved in the CH_2Cl_2 phase, along with poly(*d,l*-lactide), both emulsifiers gave spherical microspheres as long as the initial lomustine concentration was not >280 mg/20 mL of CH_2Cl_2. Higher lomustine concentrations gave irregularly shaped particles (Fig. 1).

Dichloromethane-poly(*d,l*-lactide) solutions that contained ≤2000 mg of progesterone/20 mL of CH_2Cl_2 formed stable emulsions in water when methylcellulose was the emulsifier. Higher progesterone concentrations gave misshapen particles or unstable emulsions. For this reason, poly(*d,l*-lactide) microspheres with a >68.3% (w/w) progesterone payload were not prepared. When polyvinyl alcohol was the emulsifier, solutions containing >0.5 g of progesterone/20 mL of CH_2Cl_2 consistently formed unstable emulsions. Accordingly, poly(*d,l*-lactide) microspheres with progesterone payloads >35% (w/w) were not prepared with this emulsifier.

Although polyvinyl alcohol and methylcellulose formed suitable CH_2Cl_2-in-water emulsions for a range of initial lomustine and progesterone solutions, spontaneous crystallization of these drugs occurred either in the aqueous phase or on the surface of the microspheres when either emulsifier was left in the aqueous phase until CH_2Cl_2 evaporation was complete. With lomustine, the free crystals usually appear as well-defined rods in the aqueous phase (Fig. 1). With progesterone, the free crystals also appear in the aqueous phase, but as very fine particles.

Crystal formation is eliminated or greatly reduced for 50–600-μm microspheres that have drug payloads ≤25% (w/w) if agitation is stopped well before solvent evaporation is complete and the emulsifier is removed from the aqueous phase. Solvent evaporation is then taken to completion in emulsifier-free water. If the emulsifier is removed too soon, the microspheres agglomerate because they contain too much CH_2Cl_2. If the emulsifier is removed too late, free crystals appear. Thus, there is an optimal time interval during which emulsifier removal can occur without microsphere agglomeration or free crystal formation (12). This time interval (or window) is defined experimentally for each formulation. For microspheres prepared at an agitation rate of 150 rpm, the time interval typically varied from 200 to 240 min.

Microspheres that contain ≤25% (w/w) progesterone or lomustine are spherical and have very smooth surfaces, if free crystals do not form. Figure

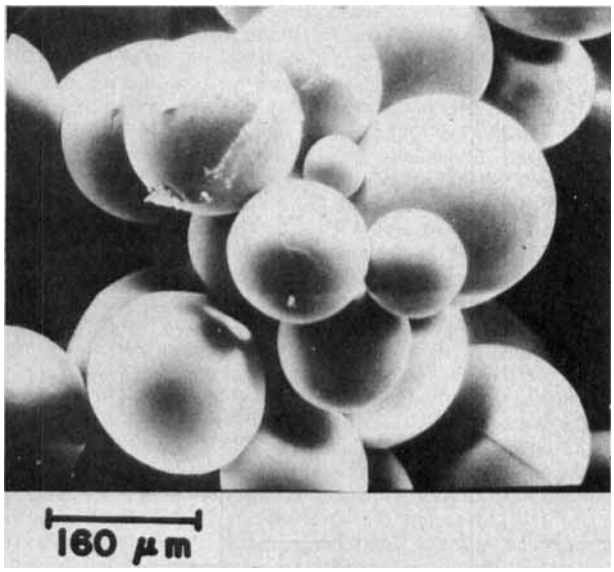

Figure 2—*Scanning electron micrograph of microspheres prepared by the interrupted evaporation process at 150 rpm with 0.27% (w/w) polyvinyl alcohol as emulsifier. Theoretical lomustine content: 23.2% (w/w). Magnification: 125×.*

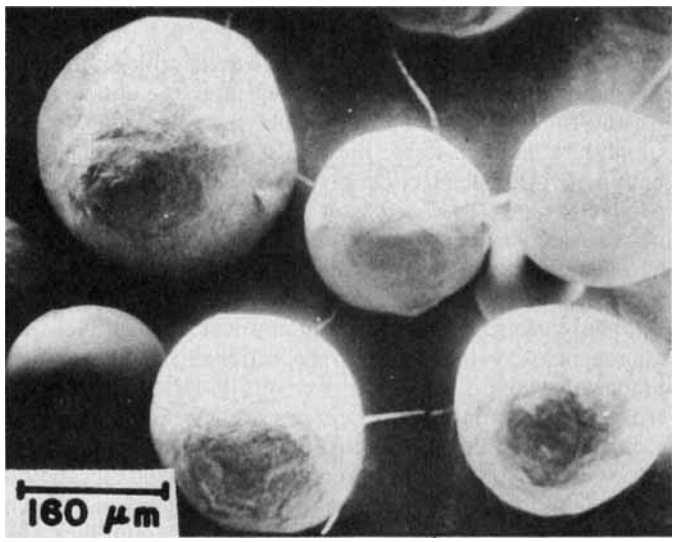

Figure 3—*Scanning electron micrograph of microspheres prepared by the continuous evaporation process at 150 rpm with 0.27% (w/w) polyvinyl alcohol as emulsifier. Theoretical lomustine content: 23.2% (w/w). Magnification: 125×.*

Table I—Drug Content of Poly(*d,l*-lactide) Microspheres Formed by the Solvent Evaporation Process [a]

Drug	Evaporation Process	Agitation Rate, rpm	Formation of Free Drug Crystals	Measured Drug Content, %[b]	Drug loss, %[c]
Lomustine	Continuous	150	+	20.2	12.9
		150	+	17.8	23.3
	Interrupted	150	−	22.0	5.2
		150	−	20.4	12.1
Progesterone	Continuous	150	+	21.4	7.6
		250	+	20.5	11.7
	Interrupted	300	−	22.3	3.9
		300	−	24.0	—

[a] All microspheres had a theoretical drug content of 23.2% (w/w) and were made with 0.27% polyvinyl alcohol as the emulsifier. [b] Mean of three determinations. [c] [(Theoretical drug content − measured drug content)/(theoretical drug content)] × 100.

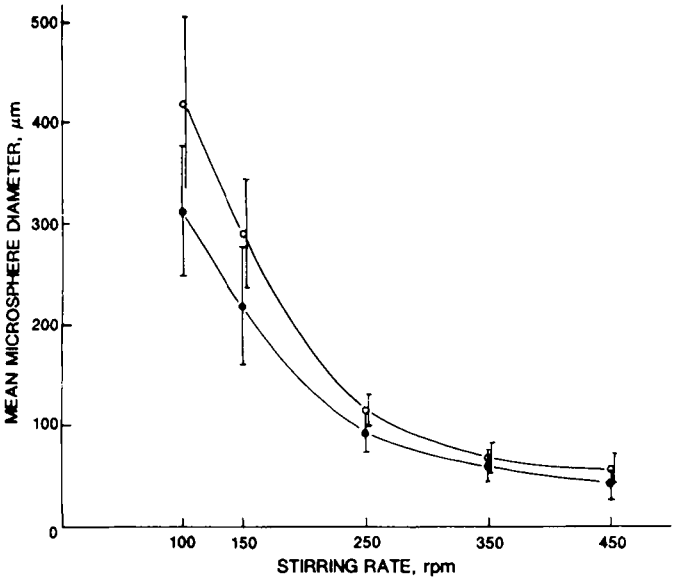

Figure 4—*Effect of stirring rate on mean size of drug-free and progesterone-loaded (23.2%, w/w) microspheres prepared with 0.27% (w/w) polyvinyl alcohol as emulsifier. Key: (●) empty microspheres; (○) progesterone-loaded microspheres.*

Table II—Effect of Stirring Rate on Lomustine Microsphere Content and Size [a]

Stirring Rate, rpm	Measured Drug Content, %[b]	Drug Loss, %[c]	Mean Particle Size, μm ± *SD*
150	20.2	12.9	289.9 ± 88.3
250	19.8	14.7	102.5 ± 25.1
350	19.7	15.1	71.0 ± 16.6
450	19.9	14.2	58.2 ± 15.6

[a] All microspheres had a theoretical content of 23.2% (w/w) lomustine and were made by the continuous evaporation process with 0.27% polyvinyl alcohol as the emulsifier. [b] Mean of three determinations. [c] [(Theoretical drug content − measured drug content)/(theoretical drug content)] × 100.

2 illustrates the type of smooth surface obtained. There is no evidence of macroscopic pores. Formation of free progesterone crystals seems to have no effect on the surface structure of poly(*d,l*-lactide) microspheres when the theoretical progesterone payload is ≤31% (w/w). This is not the case for lomustine-loaded microspheres. Figure 3 is a scanning electron micrograph of such microspheres that had a theoretical lomustine payload of 23% (w/w) and were made under conditions that allowed free lomustine crystals to form. The surface is rippled and rough. In most cases, free lomustine crystals are not visible on the surface of the microspheres.

As long as drug payloads are kept below ~25% (w/w) for lomustine and 32% (w/w) for progesterone, most free drug crystals that form either float in the water phase or are so loosely attached to the microsphere surface that they wash off during the isolation step. The loss of free drug crystals reduces the amount of lomustine or progesterone incorporated in the microspheres. Measured lomustine and progesterone losses in such cases range from 7.6 to 23.2% (Table I). Drug losses are reduced when microspheres are prepared by the interrupted evaporation process and free drug crystals do not form. However, efficiency of drug incorporation always is relatively high whether or not free crystals form. Large amounts of progesterone and lomustine are not partitioned from the CH_2Cl_2 phase into the aqueous phase during the multihour fabrication process. Since lomustine is sensitive to water, it is significant that extensive degradation did not occur during fabrication of the microspheres.

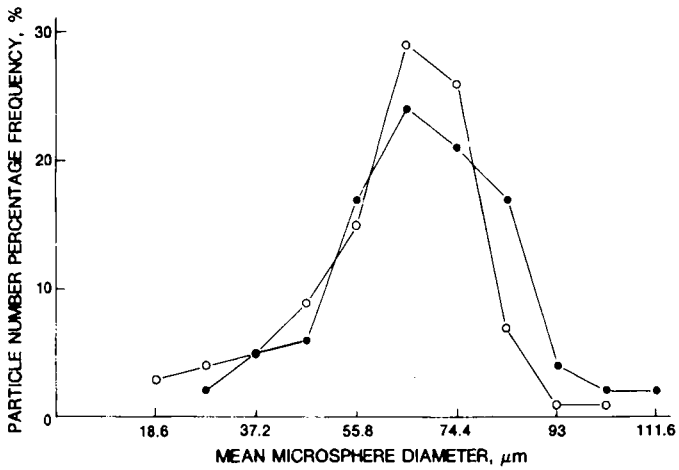

Figure 5—*Size distribution of drug-free and progesterone-loaded (23.2%, w/w) microspheres prepared at 350 rpm by the continuous evaporation process with 0.27% (w/w) polyvinyl alcohol as emulsifier. Key: (○) empty microspheres; (●) progesterone-loaded microspheres.*

Effect of Stirring Rate—Increasing the stirring rate decreases the mean diameter of the microspheres and reduces the width of the size distribution (Fig. 4, Table II). Incorporation of progesterone (23%, w/w) within the microspheres gives larger microspheres than drug-free microspheres prepared under identical conditions. However, the mean size and size distribution of drug-free and progesterone-loaded microspheres converge as the agitation rate is increased to 350 rpm (Fig. 5). The larger size of progesterone-loaded microspheres formed at lower agitation rates may reflect an increase in viscosity of the poly(*d,l*-lactide)–CH_2Cl_2 solution caused by the progesterone. Stirring rate had no detectable influence on drug content of the microspheres.

Effect of Initial Emulsifying Agent Concentration—Table III contains comments about initial polyvinyl alcohol concentration effects on microsphere properties. For a constant rate of agitation, microsphere size increased as the polyvinyl alcohol concentration increased due to an increase in viscosity of the aqueous phase. The high viscosity of the 5% (w/w) polyvinyl alcohol so-

Table III—Effect of Initial Polyvinyl Alcohol Concentration on Progesterone Microsphere Yield [a]

Polyvinyl Alcohol Concentration, %	Microsphere Recovery Yield, %[b]	Comments on Microspheres Formed
0.27	77	Individual spherical microspheres; no free crystals outside
2.7	81.6	Individual spherical microspheres; no free crystals outside
5.0	95.1	Individual spherical microspheres; no free crystals outside, but aggregation

[a] All microspheres had a theoretical payload of 23.2% (w/w) progesterone and were made by the interrupted evaporation process with 0.27% polyvinyl alcohol as the emulsifier. [b] 100 × [(Weight solid isolated microspheres recovered)/(weight of progesterone and poly(*d,l*-lactide) added to system)].

Table IV—Effect of Progesterone Payload on Microsphere Properties [a]

Theoretical Progesterone Content, %	Emulsifier	Microsphere Yield, %	Comments on Microspheres Formed
23.2	0.27% PVA[b]	81.6	Individual spherical microspheres; no free crystals outside
31.7	0.27% PVA	82.0	Individual spherical microspheres; no free crystals outside
35.0	0.27% PVA	84.2	Individuals with drug crystals embedded on the surface and outside
51.9	0.27% MC[c]	95.8	Individuals with drug crystals embedded on the surface and outside
68.3	0.27% MC	99.4	Misshapen microspheres; aggregation

[a] All microspheres prepared at 300 rpm by the interrupted evaporation process. [b] Polyvinyl alcohol. [c] Methylcellulose.

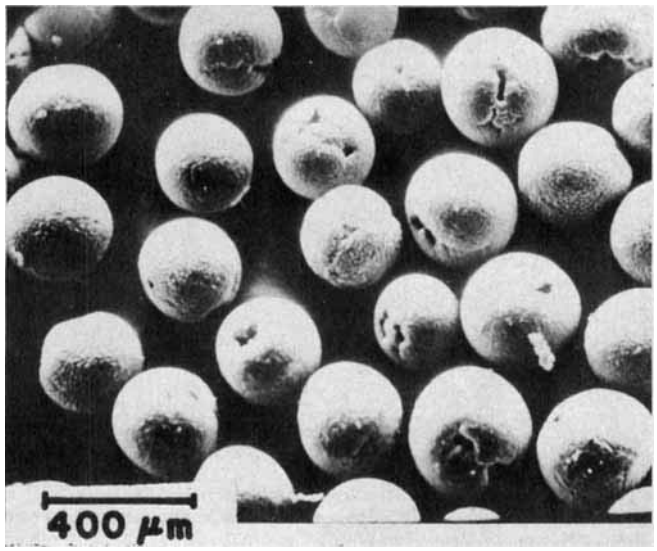

Figure 6—*Scanning electron micrograph of microspheres prepared by the continuous evaporation process at 250 rpm with 0.28% (w/w) methylcellulose (400 cps) as emulsifier. Theoretical progesterone content: 68.3% (w/w). Magnification: 50×.*

Table V—Amount of Progesterone Remaining in the Microspheres After Storage [a]

Polyvinyl Alcohol Concentration, %	Initial Mean Progesterone Content, %[b]	Mean Progesterone After Storage[b]	Progesterone Missing, %
0.27	31.7	21.5	47.4
0.27	31.7	24.8	27.8
2.5	23.6	19.0	24.2
5.0	23.2	17.8	30.3

[a] In a desiccator at 25° C for a period of 16 months. [b] Mean of three different experimental determinations.

lution hampered the washing process by prolonging microsphere sedimentation time. This led to increased microsphere aggregation.

Yields of isolated microspheres were related to final particle diameter. Microsphere batches composed of large particles were almost completely recovered. Yields of smaller particles (<100 μm) were reduced, since many small microspheres were lost during successive decantation washings.

Effect of Initial Drug Concentration—In an attempt to increase the progesterone content of the microspheres, a number of experiments were performed in which increasing amounts of progesterone were added to a fixed weight (927 mg) of poly(*d,l*-lactide). The comments in Table IV indicate that microspheres containing ≤31.7% progesterone could be prepared without appearance of free drug crystals in the aqueous phase, provided the emulsifier was removed from the system before CH_2Cl_2 evaporation was complete. Above 31.7%, free progesterone crystals appeared in the aqueous phase whether or not the emulsifier was removed. Moreover, crystals embedded in the microsphere surfaces could be distinguished. When the progesterone payload was raised to 68.3%, the microspheres remained basically spherical, but surface defects were visible (Fig. 6).

Stability Studies—Four progesterone-loaded microsphere samples were stored in a desiccator at room temperature for 16 months. They were prepared while avoiding formation of free progesterone crystals in the aqueous phase. The microspheres containing 31.7% progesterone became yellowish whereas the color of the 23.2% progesterone microspheres remained unchanged after a storage period of 16 months, even though progesterone experienced significant degradation during this period (Table V).

Lomustine microspheres, prepared by the standard procedure avoiding crystallization in the aqueous phase, were stored under different temperatures, in desiccators, and protected from light. The stability experiment results are

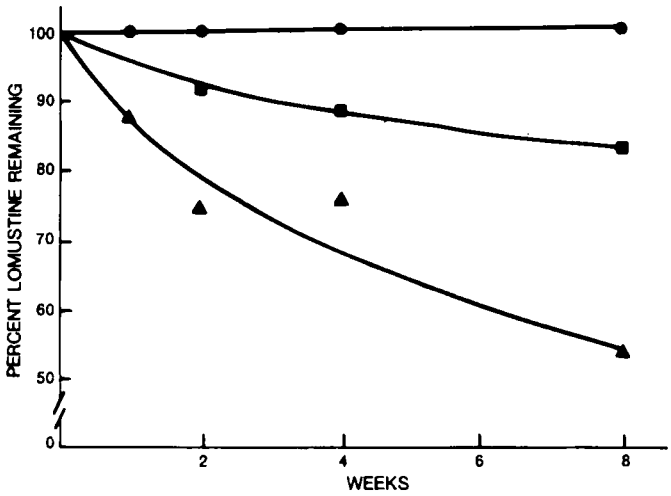

Figure 7—*Influence of storage temperature on desiccated shelf-life stability of lomustine-loaded (22.0%, w/w initially) poly(d,l-lactide) microspheres prepared by the interrupted evaporation process at 250 rpm with 0.27% (w/w) polyvinyl alcohol as emulsifier. Key, microsphere storage conditions: (●) 3° C; (■) 22° C; (▲) 37° C.*

shown in Fig. 7. At 3°C, lomustine incorporated into the microspheres remained stable for at least 8 weeks. However, degradation occurred within 8 weeks upon storage at 25° C and 37°C. The decomposition rate increased with increasing temperature. Lomustine crystals were stable over a period of 8 months at room temperature in a desiccator protected from light. Dispersing the drugs in the microspheres accelerated the degradation, probably as a result of their internal dilution within the coating polymer and chemical exposure to the polymer molecules.

REFERENCES

(1) J. K. Widder, A. E. Seney, and B. Sears, *J. Pharm. Sci.*, **71**, 379 (1982).

(2) T. Yoshioka, M. Hashida, S. Muranishi, and H. Sezaki, *Int. J. Pharm.*, **8**, 131 (1981).

(3) M. Hashida, T. Yoshioka, S. Muranishi, and H. Sezaki, *Chem. Pharm. Bull.*, **78**, 1009 (1980).

(4) Y. Morimoto, K. Sugibayashi, and Y. Kato, *Chem. Pharm. Bull.*, **29**, 1433 (1981).

(5) "Lactic-Glycolic Acid Polymers in Drug Carriers in Biology and Medicine," D. L. Wise, T. D. Fellmann, J. E. Sanderson, and R. L. Wentworth, Eds., Academic Press, Orlando, Fla., 1979.

(6) N. Mason, C. Thies, and T. J. Cicero, *J. Pharm. Sci.*, **65**, 847 (1976).

(7) L. R. Beck, D. R. Cowsar, D. H. Lewis, J. W. Gibson, and C. E. Flowers, *Am. J. Obstet. Gynecol.*, **135**, 419 (1979).

(8) N. Wakiyama, K. Juni, and M. Nakano, *Chem. Pharm. Bull.*, **30**, 2621 (1982).

(9) R. Gurny, N. A. Peppas, D. D. Harrington, and G. S. Banker, *Drug Dev. Ind. Pharm.*, **7**, 1 (1981).

(10) L. R. Beck, D. R. Cowsar, D. H. Lewis, R. J. Cosgrove, C. T. Riddle, S. L. Lowry, and T. Epperly, *Fert. Steril.*, **31**, 545 (1979).

(11) T. Kato, R. Nemoto, H. Mori, M. Takahashi, Y. Tanakawa, and M. Horada, *J. Am. Med. Assoc.*, **245**, 1123 (1981).

(12) M.-C. Bissery, F. Puisieux, and C. Thies, Proceedings of the 3rd International Conference on Pharmaceutical Technology, Paris, France, Vol. III, 233, 1983.

ACKNOWLEDGMENTS

This work was presented in part at the 3rd International Conference on Pharmaceutical Technology, 1983, Paris, France.

Quantum Chemical Approach to the Relationship Between Molecular Structure and Serotonin Receptor Binding Affinity

J. S. GÓMEZ-JERIA ˣ and D. R. MORALES-LAGOS

Received December 1, 1982, from the *Departamento de Química, Facultad de Ciencias Básicas y Farmacéuticas, Universidad de Chile, Casilla 653, Santiago, Chile.* Accepted for publication September 13, 1983.

Abstract □ We have analyzed the dependence of the serotonin receptor binding affinity on the atomic net charges, superdelocalizabilities, mass, and moment of inertia in a group of indole derivatives. The approaches employed are a new nonempirical quantitative structure-activity relationship (QSAR) method and multiple regression analyses. The results suggest that the indole derivatives interact with the receptor through a charge transfer between the phenyl ring and a counterpart in the receptor, plus some localized electrostatic interactions. Also, the fit of the equation obtained suggests that the indole derivatives have the aromatic ring placed in the same relative position during the interaction with the receptor.

Keyphrases □ Quantitative structure-activity relationships—perturbation theory, serotonin receptor binding affinity, quantum chemistry □ Serotonin—receptor binding affinity, perturbation theory, quantitative structure-activity relationship (QSAR) quantum chemistry

In recent years, there have been important advances toward a greater understanding of the activity of indole derivatives in terms of how their molecular structures might influence biological activity (1–16). It has been observed that there is a linear correlation between the potencies of tryptamine derivatives on the rat fundus and their ability to inhibit LSD (lysergide) binding to brain membranes (1, 2). This fact strongly supports the hypothesis that the conclusions based on the rat fundus receptor may hold also for the receptor in the brain.

A good correlation has been found between frontier orbital electron densities (FOED) and the ability of tryptamine derivatives to contract the rat fundus strip (3, 7). Also, it was observed (8, 9) that the position at which a high FOED was correlated with high biological potency corresponded to the sites at which the density of the highest occupied molecular orbital (HOMO) is localized in 5-hydroxytryptamine (serotonin, 5-HT), a fact that might explain the negative correlation between potency and FOED at certain atoms (1, 4). Also, the localization pattern of electron density for the HOMO and the next HOMO (NHOMO) of LSD is similar to that of 5-HT (10). These facts suggest that these molecules may interact with the receptor through a complex involving charge transfer from certain sites of the drug toward the receptor.

The patterns of the electrostatic potential maps of LSD and 5-HT show great similarities (10). The HOMO has a high influence on the electrostatic potential on the vicinities of the aromatic portion of the tryptamine derivatives (11).

Weinstein and co-workers (10, 12, 13) have suggested that a tryptamine congener attains a 5-HT-like recognition at the receptor by anchoring its side chain at the same place as 5-HT with its electrostatic vector (the vector connecting the minima through the area of the steepest change in the electrostatic potential) oriented parallel to the electrostatic vector in 5-HT. This matching is achieved by a conformational change in the side chain. For example, in the model of Weinstein and coworkers the aromatic rings of 5-HT and 6-HT are not in the same position during the interaction with the receptor (13). Also, on the basis of model complex calculations, these authors suggested that the interaction is mainly electrostatic (12), the transfer of charge being negligible.

The analysis of the photoelectron ionization potentials of LSD, some phenethylamines, and tryptamine derivatives (14, 15) has shown that not only the first ionization potential, but also the second ionization potential must be considered in order to correlate biological activity with the ionization potentials. This is consistent with the participation of the aromatic ring as an electron donor in the drug-receptor interaction, the ability of the stronger donor generally correlating with a greater activity. This study confirms the importance of the frontier orbitals, coinciding with the above points.

Glennon and Gessner (16) obtained a correlation between the binding affinities (pA_2) of some tryptamine derivatives in the 5-HT receptor of the rat stomach fundus and the ability to donate electrons in a localized charge transfer manner from the 4-position of the indole nucleus. Considering that the rat stomach fundus is an *in vitro* preparation (17, 18), the measured binding affinities will reflect only the binding energy between the drugs and the receptor. Also, as it seems that there is a certain similarity between the ability to interact with the rat fundus 5-HT receptor and 5-HT binding sites in the brain (1, 2), the study and analysis of the relations between pA_2 and the molecular electronic structure would be of a great help in a rational design of new tryptamine derivatives.

We report here the application of a new quantum-statistical approach, searching for a relationship between pA_2 and some reactivity indices.

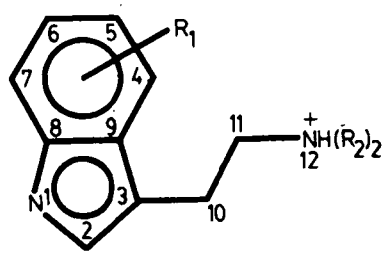

EXPERIMENTAL SECTION

Consider the weak interaction of a drug, D_i, and a macromolecular receptor, R. The model is based on the following reasonable hypotheses (19):

1. The conformation of the receptor is so strongly preferred that the binding energy is accounted for entirely in terms of local atomic interactions.
2. The total molecular partition functions can be factorized in terms of independent and uncoupled translational, rotational, vibrational, and electronic partition functions.
3. Only the electronic ground state is important in the electronic partition function.

With this model, it is possible to show formally that the drug-receptor equilibrium constant, K_i may be expressed as (19):

$$\log K_i = q + b \cdot \log M_i + c \cdot \log \sigma_i/(\mathrm{ABC})_i^{3/2}) + d\Delta E_i \quad \text{(Eq. 1)}$$

0022-3549/84/1200-1725$01.00/0
© 1984, American Pharmaceutical Association

Table I—Experimental and Calculated pA_2 Values

Compound[a]	R_1	R_2	pA_2 Calculated[b]	pA_2 Observed[c]
I	5-OH	Me	7.39	7.41
II	5-OMe	Me	7.10	7.08
III	4-OH	Me	6.65	6.84
IV	5-Me	Me	6.31	6.52
V	7-Me	Me	5.84	6.29
VI	4-NH_2	Me	6.41	6.28
VII	5-Me	H	6.63	6.86
VIII	—H	H	6.54	6.25
IX	4-OMe	Me	6.19	6.17
X[d]	—H	Me	5.98	6.04
XI[e]	—H	Me	6.02	6.03
XII[f]	—H	Me	6.04	6.02
XIII	—H	Me	6.17	6.00
XIV	6-OMe	Me	6.01	5.77
XV	5,7-$(OMe)_2$	Me	5.44	5.50
XVI	7-OMe	Me	5.19	5.33
XVII	7-OH	Me	5.19	4.88
XVIII	5,6,7-$(OMe)_3$	Me	6.04	5.98
XIX	—H	H, Me	5.87	5.97
XX	5-OMe, 7-Me	Me	6.81	6.61
XXI	5-$OCOCH_3$	Me	7.59	7.71
XXII	5-$COCH_3$	Me	5.91	5.86
XXIII	5-$OCOCH_2CH_3$	Me	7.43	7.27
XXIV	5-$OCO(CH_2)_2CH_3$	Me	7.26	7.32

[a] See Fig. 1 for the substituent position. [b] Calculated using Eq. 5. [c] Taken from Ref. 26. [d] With a methyl group in position 2. [e] With S instead of N in position 1. [f] With a methyl group in position 1.

where a, b, c, and d are constants; M, σ, and (ABC) are, respectively, the mass, the symmetry number, and the product of the three moments of inertia about the three principal axes of rotation of the ith drug molecule; and ΔE_i is the difference between the ground state energy of the complex and the energies of D_i and R, *i.e.*:

$$\Delta E_i = E_{D_iR} - (E_{D_i} + E_R) \qquad \text{(Eq. 2)}$$

In a first approach, we shall accept that, among all the components of ΔE_i the most important is the change in the electronic energy ΔE_i^e (20). Considering the interaction of the indole derivatives with the receptor as weak (*i.e.*, without the formation of covalent bonds), a perturbation treatment (21) may be performed for the evaluation of ΔE_i^e. In this way, after some approximations as the molecular structure of the receptor is unknown (22, 23), ΔE_i^e can be expressed as:

$$E_i^e = q + \sum_p (f_p Q_p^i + g_p S_p^{E,i} + h_p S_p^{N,i}) \qquad \text{(Eq. 3)}$$

where q, f_p, g_p, and h_p are constants; and Q_p^i, $S_p^{E,i}$, and $S_p^{N,i}$ are, respectively, the net charge, the electrophilic superdelocalizability, and the nucleophilic superdelocalizability of atom p in molecule i (24).

Inserting Eq. 3 into Eq. 1, we get (19):

$$\log K_i = q' + b \cdot \log M_i + c \cdot \log [\sigma_i (\mathrm{ABC})_i^{-3/2}] + \sum_p (f_q Q_p^i + g_p S_p^{E,i} + h_p S_p^{N,i}) \qquad \text{(Eq. 4)}$$

The summation on p is over a set of atoms common to all the drugs that interact with the receptor. If Eq. 4 is to be satisfied, there must exist a common set of atomic reactivity indices in all the drugs interacting with the same receptor.

We have taken the pA_2 value as a good approximation to the affinity constant of the drug-receptor complex (25). These values were selected from the literature (26) (Table I).

We employed statistical analysis to determine the set of atomic properties in an attempt to find a group of variables whose variation better explains the variation of the pA_2 values in a series of molecules. A special case of Eq. 4 has been applied with success to very different kinds of drugs (22, 27–29).

The ring geometry is displayed in Fig. 1; this geometry is similar to the one used by Inoue *et al.* (30). The bond distances for the ring substituents were taken from the literature (31).

Considering that the structure of LSD possesses both the phenylalkylamine and the indolealkylamine molecular subfragments (32), we accepted as a working hypothesis that the phenethylamine and tryptamine derivatives mimic partially or totally the LSD structure during interaction with the receptor. With this consideration, and for the sake of simplicity, we placed the amine

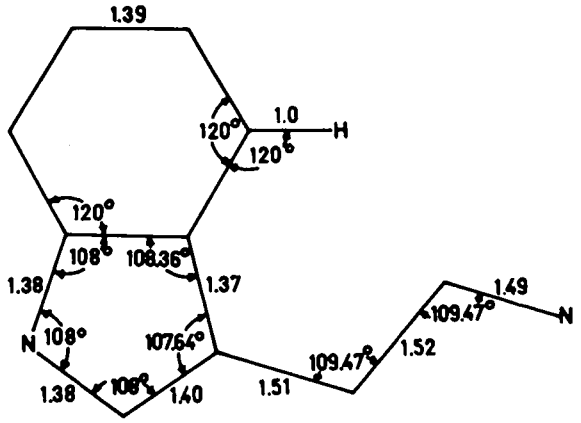

Figure 1—*Geometric parameters for the ring and the side chain.*

chain in the same plane as the phenyl ring. The net charges and the superdelocalizabilities were calculated from a CNDO/2 wave function (33).

RESULTS AND DISCUSSION

The statistical fitting of Eq. 4 was performed by means of a stepwise regression technique with pA_2 as the dependent variable. The net charges and the electrophilic superdelocalizabilities of the aromatic ring, plus the net charges and the nucleophilic superdelocalizabilities of the side-chain atoms, plus the mass and moment of inertia factors were used as independent variables (20 in all) (Table II). More than 500 combinations of variables were analyzed. The best expression found is:

$$pA_2 = 8.2812 + 3.1383Q_4 + 2.0529Q_7 + 4.8660S_5^E - 3.1825S_7^E - 2.2494S_8^E + 1.1416I \qquad \text{(Eq. 5)}$$

where $I = \log [\sigma_i/(\mathrm{ABC})_i^{3/2}]$.

This equation has a multiple correlation coefficient (r^2) of 0.97, which represents a significance of >94.1%, and a mean SD of 0.20. The analysis of variance (34) of Eq. 5 gives $F_{6,17} = 42.22$, showing the very high significance of this equation ($p < 0.0005$).

The results of the Student's t test for the significance of the coefficients are shown in Table III; the pA_2 values calculated with Eq. 5 are shown in Table I. The squared correlation matrix for the independent variables is presented in Table IV. The variables Q_4 and S_5^E appear with a relatively high r^2 value (Q_4 explaining the 62% of S_5^E). Nevertheless, considering that a certain degree of correlation between variables belonging to an aromatic system must be expected, and that these two variables have different physical meanings (the net charges representing electrostatic interactions and the electrophilic superdelocalizabilities being related to charge transfer), we think that they represent different physical processes.

Also, from the work of Topliss and Edwards (35), we can see that the relationship between the number of observations required to screen 18 variables, while keeping the probability of encountering a chance correlation with $r^2 \geq 0.9$ at the ≤1% level, is ~19. Therefore, the risk of chance correlation is very low.

The binding affinity is, therefore, related to a definite set of electronic indices. Considering the high significance of Eq. 5, we accepted that, within the accuracy of the approximations used for the determination of ΔE_i and pA_2, the results obtained suggest the existence of a direct dependence between the variation of pA_2 and those of the reactivity indices of Eq. 5.

The appearance of the total atomic electrophilic superdelocalizabilities in Eq. 5 indicates that the variation of pA_2 will depend on the relative reactivity of atoms 5, 7, and 9 toward the electrophilic components of the receptor. Also, their appearance suggests that the drug–receptor interaction has a strong orbital-controlled character (21). This is in perfect accord with the idea of a localized charge transfer from the drug to the receptor.

Remembering that S_5^E contains the contribution of the HOMO, the appearance of S_5^E is similar to that of the FOED at the 5-position. We cannot ensure that the frontier orbitals play a high significant role, because S^E, by including the other molecular orbitals, will obscure the contribution of the HOMO and NHOMO. The dependence of the variation of pA_2 on a variation of Q_4 and Q_7 indicates an electrostatic interaction between these atoms and one or more centers in the receptor.

The other index which contributes significantly is related to the molecular moment of inertia, and is defined as:

Table II—Variable Values Employed in the Statistical Analysis

Compound	Experimental pA_2	Q_4	Q_5	Q_6	Q_7	Q_8	Q_9	Q_{10}	Q_{11}	Q_{12}
I	6.2500	−0.0287	−0.0001	0.0073	−0.0244	0.1010	−0.0024	0.0028	0.1075	−0.0570
II	6.8600	−0.0528	0.0455	−0.0112	−0.0175	0.0923	0.0022	0.0032	0.1074	−0.0570
III	6.0000	−0.0285	−0.0033	0.0063	−0.0265	0.0998	−0.0027	0.0007	0.1057	0.0332
IV	7.4100	−0.0843	0.1717	−0.0511	−0.0044	0.0797	0.0157	0.0016	0.1053	0.0334
V	7.0800	−0.0864	0.1735	−0.0509	−0.0074	0.0801	0.0150	0.0016	0.1053	0.0333
VI	6.5200	−0.0519	0.0410	−0.0123	−0.0201	0.0909	0.0030	0.0021	0.0964	0.0752
VII	6.8400	0.1442	−0.0588	0.0251	0.0479	0.1158	−0.0392	−0.0085	0.0969	0.0263
VIII	6.2800	0.1400	−0.0714	0.0332	−0.0632	0.1214	−0.0524	−0.0151	0.1803	0.0089
IX	6.1700	0.1444	−0.0596	0.0231	−0.0471	0.1159	−0.0423	−0.0088	0.0989	0.0261
X	5.7700	−0.0089	−0.0537	0.1848	−0.0925	0.1174	−0.0225	0.0005	0.0964	0.0754
XI	6.2900	−0.0416	0.0028	−0.0180	0.0218	0.0808	0.0034	0.0019	0.0964	0.0750
XII	5.3300	−0.0555	0.0163	−0.0510	0.1551	0.0519	0.0154	0.0022	0.0962	0.0752
XIII	4.8800	−0.0540	0.0175	−0.0479	0.1521	0.0461	0.0168	0.0014	0.1056	0.0330
XIV	5.5000	−0.1133	0.1922	−0.1095	−0.1733	0.0319	0.0329	0.0031	0.0958	0.0754
XV	6.0400	−0.0339	−0.0020	0.0017	−0.0255	0.0949	0.0024	0.0055	0.1058	0.0331
XVI	6.0200	−0.0293	−0.0035	0.0041	−0.0251	0.0905	−0.0028	0.0016	0.1056	0.0331
XVII	6.0300	−0.0656	0.0454	−0.0282	0.0588	0.0145	0.0858	−0.0109	0.1049	0.0339
XVIII	5.9800	−0.0940	0.1471	0.0812	0.1165	0.0513	0.0140	0.0021	0.0958	0.0755
XIX	5.9700	−0.0284	−0.0022	0.0066	−0.0256	0.1001	−0.0018	0.0025	0.1045	−0.0287
XX	6.6100	−0.0992	0.1789	−0.0758	0.0402	0.0612	0.0209	0.0029	0.0960	0.0751
XXI	7.7100	−0.0939	0.1871	−0.1571	−0.0127	0.0797	0.0106	0.0032	0.1009	0.0003
XXII	5.8600	−0.0193	−0.0132	0.0225	−0.0332	0.1112	−0.0060	0.0016	0.1010	0.0007
XXIII	7.2700	−0.0939	0.1877	−0.5184	−0.0133	0.0792	0.0108	0.0033	0.1009	0.0002
XXIV	7.3200	−0.0942	0.1879	−0.1586	−0.0135	0.0790	0.0107	0.0033	0.1009	0.0002

Compound	S_4^E	S_5^E	S_6^E	S_7^E	S_8^E	S_9^E	S_{10}^N	S_{11}^N	S_{12}^N	Mass-Related Term	Moment of Inertia-Related Term
I	−4.4842	−4.4187	−4.4272	−4.4573	−4.1912	−4.3348	24.7255	21.0720	57.1031	−3.3112	−2.7062
II	−4.5953	−4.3449	−4.5129	−4.4552	−4.2362	−4.3398	24.4622	19.8324	54.6363	−3.3655	−2.8497
III	−4.5575	−4.4875	−4.4891	−4.5244	−4.2582	−4.4064	12.6679	4.4329	−37.7952	−3.4157	−2.9807
IV	−4.6877	−4.0953	−4.5876	−4.4436	−4.3075	−4.3531	20.1351	3.6279	−43.1664	−3.4685	−3.0987
V	−4.7027	−4.1367	−4.6365	−4.4630	−4.3147	−4.3632	19.5164	1.5388	−46.7765	−3.5116	−3.2093
VI	−4.6607	−4.4043	−4.5662	−4.5130	−4.2973	−4.4058	12.8513	−113.9695	−218.5616	−3.4622	−3.0917
VII	−4.1200	−4.5587	−4.4034	−4.5598	−4.1815	−4.4357	94.9910	7995.5313	15568.4297	−3.4685	−3.0082
VIII	−4.0844	−4.6561	−4.4170	−4.6543	−4.1987	−4.5106	23.9091	0.5264	−24.1683	−3.4654	−3.0058
IX	−4.1555	−4.6021	−4.4175	−4.5660	−4.1892	−4.4478	16.5885	304.8059	551.8584	−3.5116	−3.0765
X	−4.4798	−4.5784	−4.1217	−4.7075	−4.2129	−4.4580	10.1589	−77.9774	−155.0132	−3.5116	−3.2070
XI	−4.6234	−4.4846	−4.5956	−4.4391	−4.3428	−4.4111	6.9412	−176.9974	−320.2112	−3.4622	−3.0707
XII	−4.6350	−4.4200	−4.6129	−4.1407	−4.3671	−4.3477	−0.7368	−97.3377	−183.6725	−3.5086	−3.1400
XIII	−4.6367	−4.4215	−4.6052	−4.1151	−4.3493	−4.3421	17.4444	10.4940	−30.4729	−3.4685	−3.0736
XIV	−4.7826	−4.0756	−4.7632	−4.0857	−4.4261	−4.3078	16.6094	−173.3659	−315.2969	−3.5952	−3.3486
XV	−4.6018	−4.5098	−4.5304	−4.5450	−4.3035	−4.4261	42.9891	11.9697	−43.1691	−3.4622	−3.0983
XVI	−4.5798	−4.5055	−4.5108	−4.5419	−4.3104	−4.4331	25.6743	3.9224	−47.8569	−3.4622	−3.0878
XVII	−4.5536	−4.2837	−4.4861	−4.3542	−4.4048	−4.1529	29.7625	16.5035	26.0292	−3.4718	−3.0376
XVIII	−4.7039	−4.1612	−4.3536	−4.2226	−4.3643	−4.3479	18.1875	−109.3894	−210.1167	−3.6692	−3.4542
XIX	−4.5179	−4.4499	−4.4551	−4.4874	−4.2232	−4.3690	21.9919	42.8507	26.9736	−3.3655	−3.1653
XX	−4.7688	−4.1345	−4.7445	−4.3788	−4.3891	−4.3686	12.4215	−615.0073	−1042.3286	−3.5520	−3.2793
XXI	−4.7736	−4.1352	−5.3965	−4.6469	−4.4079	−4.4394	22.5130	29.9472	10.9827	−3.5872	−3.3674
XXII	−4.5132	−4.3936	−4.4493	−4.4701	−4.1739	−4.3431	20.8217	37.4708	22.6680	−3.5463	−3.2588
XXIII	−4.7839	−4.1432	−5.4065	−4.6520	−4.4140	−4.4454	22.2730	29.3867	10.2336	−3.6258	−3.4705
XXIV	−4.7894	−4.1478	−5.4149	−4.6567	−4.4182	−4.4493	22.1426	29.1086	9.8565	−3.6599	−3.5801

$$I = \log \sigma_i - (3/2)(\log A + \log B + \log C) \qquad \text{(Eq. 6)}$$

For explanatory purposes we shall examine the case where $A = Ixx$. In this case we have:

$$\log A = \log Ixx = \log \sum_i m_i(y_i^2 + z_i^2) \qquad \text{(Eq. 7)}$$

where m_i is the mass of atom i, whose coordinates are x_i, y_i, z_i. Inspection of Eq. 7 shows that these kinds of terms will appear in three cases: (*a*) when molecules differ in the nature of an atom at a certain position (m_i will be different); (*b*) when molecules differ in the position of an atom ($m_i y_i^2$ or $m_i z_i^2$ will be different); (*c*) a mixture of cases *a* and *b*. Therefore, this index can be associated with a purely positional effect and, in the case where all the molecules have a different substituent attached to the same place, with a steric effect.

Also, it is interesting to note that Eq. 5 does not include terms belonging to the side-chain atoms. There are two hypotheses explaining this fact:

1. The side chains used throughout this study are relatively constant, with the terminal amine position being primary or possessing a dimethyl group. In this case the contribution of the side chain will be almost constant, and it will be included in the constant term of Eq. 5.
2. The side chain, especially the charged nitrogen atom, only participates in the orientation and long-range recognition of these molecules by the receptor (36).

Table III—Student's *t* Test Values for Variables of Eq. 5

Variable	*t* Value	*p*
Q_4	3.20	<0.005
Q_7	3.11	<0.005
S_5^E	10.74	<0.0005
S_7^E	−9.06	<0.0005
S_9^E	−2.36	<0.025
I	4.73	<0.0005

Table IV—Squared Correlation Matrix for Varibles in Eq. 5

	Q_4	Q_7	S_5^E	S_7^E	S_9^E	I
Q_4	1.00					
Q_7	0.01	1.00				
S_5^E	0.62	0.0009	1.00			
S_7^E	0.12	0.18	0.07	1.00		
S_9^E	0.19	0.07	0.13	0.43	1.00	
I	0.19	0.0004	0.34	0.0004	0.02	1.00

Given that we are interested in the relative variation of the net charges, of the superdelocalizabilities, and of the inertia moment term, the position of the side chain will not be important if we place it in the same relative position in all the molecules considered. Also, as the pyrrole portion of the indole nucleus is relatively homogeneous in the molecules of Table I, it is not possible to determine its true importance in the regulation of the drug-receptor interaction.

Remembering that S^E is always negative, and considering only its absolute value, we may conclude that a high pA_2 is associated with: positive net charges for atoms 4 and 7; a low value of log $[\sigma/(ABC)^{3/2}]$ (which suggests a limit value for the size of the substituents); high S^E values for atoms 7 and 9, and a low S^E value for atom 5. This indicates that for atom 7 there must be an equilibrium between a positive (or slightly negative) net charge and an electronic density that participates in the interaction.

As an example of the predictive capacity of Eq. 5, we have considered the case of the 7-bromo-*N*,*N*-dimethyltryptamine. The experimental pA_2 for this compound is 6.51 (26), and Eq. 5 gives a pA_2 of 6.93.

Another problem is the solvation. It is clear that the charged groups of the drugs (*i.e.*, —$COCH_3$, —OH, *etc.*) are solvated. As we have shown[1], part of the solvation energy change calculated with the Born equation (37) is implicitly considered in the electrostatic terms of Eq. 5.

In conclusion, it seems well established that the 5-position in indole derivatives has a first-order importance in regulating pA_2, and that this regulation is associated with the availability of an electron density at this position. Our results agree with those of Weinstein and co-workers (8–10). Also, Eq. 5 shows that the ability of the ring to donate electrons is of great importance in the variation of pA_2; this agrees well with experimental (14, 15) and theoretical (10, 16) results. However, our results do not support suggestions that the charge transfer is negligible (12).

The derivation of Eq. 5 suggests very strongly that these molecules interact with the serotonergic receptor in a way such that their aromatic rings are in the same relative positions. This conclusion is in contrast with the previous suggestion that the main process in this drug-receptor interaction is the orientation of the electrostatic vector (10, 12, 13).

A question raised by this and other similar studies is why is it not possible to obtain equations with still higher multiple correlation coefficients without adding highly correlated variables. It seems that, experimental errors apart, the factors responsible are: (*a*) the method employed to obtain the reactivity indexes, especially the nucleophilic superdelocalizability (38) and (*b*) the quality of the approximations made to simplify the expression for ΔE_i^e given by perturbation theory[1].

REFERENCES

(1) J. P. Green, C. L. Johnson, H. Weinstein, S. Kang, and D. Chou, in "The Psychopharmacology of Hallucinogens," R. E. Willette and R. C. Stillman, Eds., Pergamon Press, New York, N.Y., 1978, p. 28.

(2) R. A. Glennon, *Res. Commun. Psychol. Psychiat. Behav.*, **4,** 333 (1979).

(3) J. P. Green and S. Kang, in "Molecular Orbital Studies in Chemical Pharmacology," L. B. Kier, Ed., Springer-Verlag, New York, N.Y., 1970, p. 105.

(4) C. L. Johnson and J. P. Green, *Int. J. Quant. Chem.*, **QBS1,** 159 (1974).

(5) S. Kang, C. L. Johnson, and J. P. Green, *Mol. Pharmacol.*, **9,** 640 (1973).

(6) J. P. Green, K. P. Dressler, and N. Khazan, *Life Sci.*, **12,** 475 (1973).

(7) S. Kang and J. P. Green, *Proc. Natl. Acad. Sci. USA*, **67,** 62 (1970).

(8) R. J. Batlett and H. Weinstein, *Chem. Phys. Lett.*, **30,** 441 (1975).

(9) S. Y. Chang, H. Weinstein, and D. Chou, *Chem. Phys. Lett.*, **42,** 145 (1976).

(10) H. Weinstein, R. Osman, and J. P. Green, in "Computer Assisted Drug Design," E. O. Olson and R. E. Christoffersen, Eds., American Chemical Society, Washington, D.C., 1979, p. 161.

(11) H. Weinstein, D. Chou, S. Kang, C. L. Johnson, and J. P. Green, *Int. J. Quant. Chem.*, **QBS3,** 135 (1976).

(12) H. Weinstein and R. Osman, *Int. J. Quant. Chem.*, **QBS4,** 253 (1977).

(13) H. Weinstein, R. Osman, J. P. Green, and S. Topiol, in "Chemical Applications of Atomic and Molecular Electrostatic Potentials," P. Politzer and D. G. Truhlar, Eds., Plenum Press, New York, N.Y., 1981, p. 309.

(14) L. N. Domelsmith, L. L. Munchausen, and K. N. Houk, *J. Am. Chem. Soc.*, **99,** 4311 (1977).

(15) L. N. Domelsmith, L. L. Munchausen, and K. N. Houk, *J. Med. Chem.*, **20,** 1346 (1977).

(16) R. A. Glennon an P. K. Gessner, *Res. Commun. Chem. Pathol. Pharmacol.*, **18,** 459 (1977).

(17) J. R. Vane, *Br. J. Pharmacol.*, **14,** 87 (1959).

(18) R. A. Glennon, S. M. Liebowitz, and E. C. Mack, *J. Med. Chem.*, **21,** 822 (1978).

(19) J. S. Gómez-Jeria, *Int. J. Quant. Chem.*, **23,** 169 (1983).

(20) R. Daudel, *Adv. Quant. Chem.*, **3,** 16 (1967).

(21) G. Klopman and R. F. Hudson, *Theor. Chim. Acta*, **8,** 165 (1967).

(22) F. Peradejordi, A. N. Martin, and A. Cammarata, *J. Pharm. Sci.*, **60,** 576 (1971).

(23) J. S. Gómez-Jeria and D. Morales-Lagos, *Bol. Soc. Chil. Quím.*, **27,** 44 (1982); *Chem. Abstr.*, **96,** 210320n (1982).

(24) L. Salem, "The Molecular Orbital Theory of Conjugated Systems," W. A. Benjamin, New York, N.Y., 1966, p. 330.

(25) F. G. Van den Brink, in "Kinetics of Drug Action," J. M. van Rossum, Ed., Springer-Verlag, Berlin, 1977, p. 237.

(26) R. A. Glennon, S. M. Liebowitz, and E. C. Mack, *J. Med. Chem.*, **21,** 822 (1978); R. A. Glennon and P. K. Gessner, *J. Med. Chem.*, **22,** 428 (1979); R. A. Glennon, P. K. Gessner, D. D. Godse, and B. J. Kline, *J. Med. Chem.*, **22,** 1414 (1979); R. A. Glennon, E. Schubert, J. M. Jacyno, and J. A. Rosecrans, *J. Med. Chem.*, **23,** 1222 (1980).

(27) F. Tomás and J. M. Aulló, *J. Pharm. Sci.*, **68,** 772 (1979).

(28) J. S. Gómez-Jeria and L. Espinoza, *Bol. Soc. Chil. Quím.*, **27,** 142 (1982); *Chem. Abstr.*, **96,** 195776v (1982).

(29) J. S. Gómez-Jeria, D. Morales-Lagos, and H. Chavez, "Quantum Chemical Study of Serotonin Receptor Binding Affinity," presented at the IX Latinoamerican Congress on Pharmacology and Therapeutics, Santiago, Chile, October 1982.

(30) M. Inoue, T. Sakaki, A. Wakahara, and K. Tomita, *Biochem. Biophys. Acta*, **543,** 123 (1978).

(31) H. M. Niemeyer, *Tetrahedron*, **33,** 1369 (1977).

(32) "Atlas of the Three-Dimensional Structure of Drugs," J. P. Tollenaere, H. Moorels, and L. A. Raymaekers, Eds., Elsevier, Amsterdam, 1979.

(33) J. A. Pople and D. L. Beveridge, "Approximate Molecular Orbital Theory," McGraw-Hill, New York, N.Y., 1970, p. 75.

(34) T. H. Wonnacott and R. J. Wonnacott, "Introductory Statistics for Business and Economics," Wiley, New York, N.Y., 1977.

(35) J. G. Topliss and R. P. Edwards, *J. Med. Chem.*, **22,** 1238 (1979).

(36) J. S. Gómez-Jeria and D. Morales-Lagos, "Proceedings of the XV Latinoamerican Congress on Chemistry," Puerto Rico, 1982, p. 208.

(37) M. Born, *Z. Physik*, **1,** 45 (1920).

(38) J. S. Gómez-Jeria, *J. Pharm. Sci.*, **71,** 1423 (1982).

[1] J. S. Gómez-Jeria, submitted for publication.

ACKNOWLEDGMENTS

This work has received financial support of the Departamento del Desarrollo de la Investigación, Universidad de Chile, Project Q1618-8312. We thank Mr. José López Ortíz, Director of the SESI (University of Chile) for providing free computer time.

Electrical Conductivity of a Docusate Sodium Coacervate System

CHRISTOPHER HUGHES *§ **and BERNARD ECANOW** ‡x

Received February 17, 1983, from * *Stanford University, Dept. of Biological Sciences, Stanford 94305* and the ‡ *College of Pharmacy, University of Illinois, Chicago IL 60612.* Accepted for publication August 16, 1983. § Present address: College of Medicine, University of Illinois, Chicago IL 60612.

Abstract □ The conductivity of three xanthines (caffeine, theobromine, and theophylline) and three sugars (glucose, sucrose, and glucose-6-phosphate) was measured as part of a docusate coacervate system. The conductivity of the coacervate phase was always lower than the equilibrium phase. Conductivity of xanthines showed that caffeine had the highest conductivity, followed by theobromine and theophylline. At high concentrations, these values fell and the highest conductivity was seen in samples containing theobromine, caffeine, and theophylline. For sugars at high concentrations, the lowest values of conductivity were seen in sucrose samples. Saturated theophylline samples exhibited an increased volume in the coacervate phase while the saturated sugar systems displayed a decreased coacervate phase volume. These findings are discussed with reference to various clinical parallels and thus supply evidence that coacervates can provide a useful model for human cytoplasm.

Keyphrases □ Conductivity—docusate sodium coacervate, caffeine, theobromine, theophylline, glucose, sucrose, concentration effects □ Docusate sodium—coacervate system, partition coefficients, caffeine, theobromine, theophylline, glucose, sucrose, concentration effects

Coacervates have been suggested as a model for human cytoplasm since cytoplasm is also essentially an aqueous phase of water–macromolecule colloid complexes (1, 2). Ecanow (3) has shown that coacervate systems react with more similarity to cytoplasm than do presently accepted organic solvent–water models when subjected to pH change or polar–nonpolar molecule partitioning. This report will deal with the electrical conductivity of a sodium dioctyl sulfosuccinate (docusate sodium) coacervate system as a function of pharmaceutical drug and sugar concentration. The drugs (theophylline, theobromine, and caffeine) were chosen because of their known clinical effects. The sugars (sucrose, glucose, and glucose-6-phosphate) were chosen to investigate the known phenomenon of sugar acting as a depressant at high concentrations (4).

EXPERIMENTAL SECTION

Materials and Instrumentation—All chemicals used for the HPLC analysis were used as supplied[1] and the docusate used for the preparation of the coacervate system was analytical reagent grade[2]. The sugars and xanthines were purchased from commercial sources. The liquid chromatographic apparatus used for these investigations consisted of a solvent delivery system[3], a variable-wavelength detector set at 254 nm[4], and a variable-volume injector[5]. The column used was a reverse-phase C_{18}[6] and the mobile phase consisted of acetonitrile–water (6:94, v/v). The conductivities of the samples were determined by the use of a conductivity bridge[7] and a glass dip conductivity cell[8].

Preparation of Coacervate—The docusate coacervate system was produced using the technique outlined by Acharya *et al.* (5). Solid docusate (10%, w/v) was added to distilled H_2O and mixed thoroughly. Sodium chloride was then added (2.5%) until oil-like droplets began to separate out of solution. Within a few minutes the biphasic system was obtained.

Procedure—Nine docusate sodium coacervate samples were made for each of the three drugs and eight samples were made for each of the three sugars. Each sample contained 5 mL of the coacervate plus 5 mL of the equilibrium solution. Solutions of each additive were made (100 μL) and added to the coacervate system in amounts ranging from 2.44 to 21.96 mg of chemical. Previous studies have been done to determine the partition coefficients of theophylline and theobromine in coacervate systems (6). In this study, the concentration of the drug in each phase was accurately measured by HPLC and the partition coefficients were thereby obtained for this docusate system.

Chromatographic conditions for the HPLC analysis were as follows: the flow rate was set to 3.0 mL/min with a chart speed of 10 cm/h and sensitivity set at 0.02 AUFS for the theophylline and theobromine systems. Due to the wide peaks for caffeine, the chart speed was set at 5 cm/h with a sensitivity setting of 0.005 for the detection of this compound. A 100-μL aliquot from each layer of every sample was diluted with water due to the high concentrations of the drugs in the samples and the high sensitivity of this method of analysis.

Each layer in the control sample was diluted 1:10 and run with the other samples. No concentration of any of the drugs was found in this control sample. The conductivity of each phase of this control sample was measured; these were used as control values. From the dilution of each layer, a 10-μL sample was injected into the column and chromatographed.

Standards—Standard solutions were prepared for theophylline, theobromine, and caffeine at concentrations of 10, 20, and 40 μg/mL and also injected into the column. Peak heights on the chromatogram were measured for each specimen and the concentration was determined from the respective standard curve using peak height *versus* concentration. Retention times for each of the drugs were: theophylline, 6.0 min; theobromine, 3.9 min; caffeine, 12 min.

Conductivity—The conductivity of each phase of every sample was measured 10 times and an average value for each was obtained. To ensure no contamination, the conductivity cell was rinsed completely between each measurement.

RESULTS

Partition Coefficient—The partition coefficient for each drug was obtained by plotting the concentration of the drug in the coacervate phase *versus* the concentration in the equilibrium phase (Fig. 1). The slopes of the resulting curves (in these cases, straight lines) are equal to the partition coefficients (P). For this coacervate system, the P values for these drugs are: theophylline = 1.600; caffeine = 1.522; theobromine = 1.260.

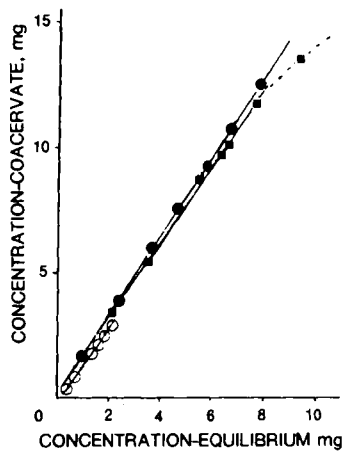

Figure 1—*Drug concentration in coacervate phases* versus *equilibrium phase. Key: (●) theophylline; (■) caffeine; (○) theobromine.*

[1] Spectrograde, A & C American Chemicals.
[2] Aldrich Chemical Co.
[3] Model 6000A; Waters Associates.
[4] Model 440; Waters Associates.
[5] Model U6K; Waters Associates.
[6] μ-Bondapak; Waters Associates.
[7] Model RC-20; Beckman Co.
[8] Model CEL-A001; Beckman Co.

0022-3549/84/1200-1729$01.00/0
© 1984, American Pharmaceutical Association

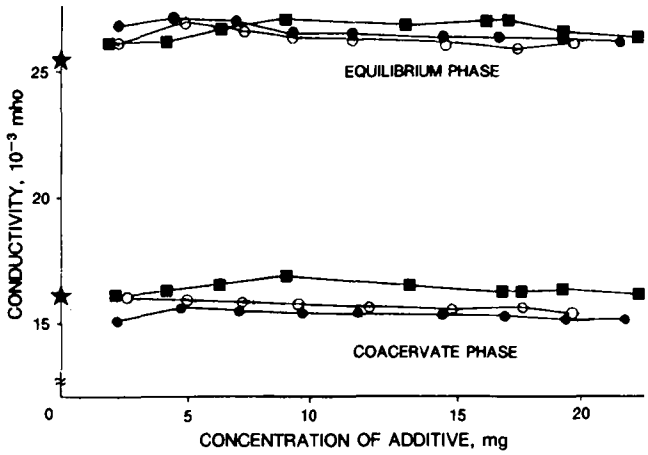

Figure 2—*Drug conductivity as a function of total concentration. Key: (●) theophylline; (■) caffeine; (○) theobromine; (★) control.*

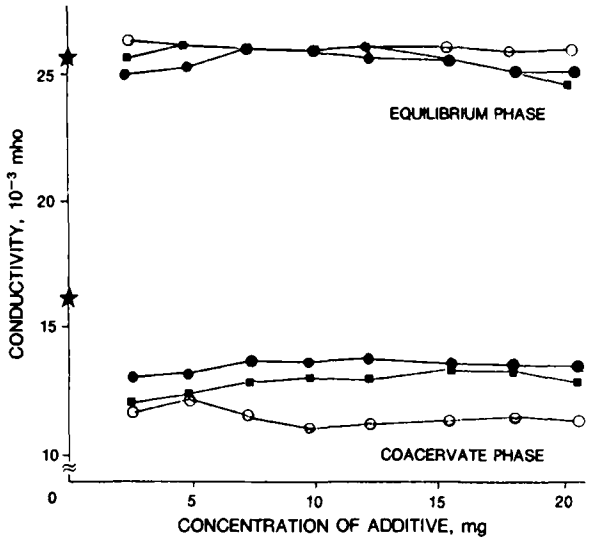

Figure 3—*Sugar conductivity as a function of total concentration. Key: (●) glucose-6-phosphate; (■) sucrose; (○) glucose; (★) control.*

Theobromine, having a low solubility constant in water, reached its saturation level in the sample containing 4.88 mg theobromine; therefore, precipitation was noted in the samples with a higher concentration of this drug. This saturation and precipitation account for the abbreviated partition coefficient graph for this drug.

Conductivity—Figures 2 (drug series) and 3 (sugar series) were obtained by plotting the electrical conductivity, measured in 10^{-3} mho, of each phase of the samples as a function of the total concentration of the additive in the system. Note that control values are indicated at the zero concentration points. In the concentration range of the drug series, the conductivity of theophylline was lowest, followed by theobromine and caffeine; for the sugar series, the lowest was glucose, then sucrose and glucose-6-phosphate. However, the conductivity did not vary significantly as a function of the concentration of the additive in the system. Therefore, samples containing additives at 2–4 times the original concentration were prepared to investigate the behavior of the coacervate system under increased concentrations.

Figures 4 and 5 are plots of conductivity *versus* total concentration of additive, but these graphs have a larger concentration scale to include the additional data mentioned above. These figures show that the high concentrations of the additives in some cases greatly affected the conductivity of the coacervate system. In the drug series, the conductivity decreased in both the coacervate and equilibrium phases and were usually lowest in theophylline and highest in theobromine, especially in the coacervate phase. A similar decrease was noted in the sugar series, with a marked change in the sucrose values. Glucose demonstrated a reversal or increase in conductivity before a later decrease with highest concentrations. These high concentrations also affected the coacervate system in other ways, as seen in the sugar samples containing 30–80 mg of additive; in these samples a clear, viscous, gel-like layer formed at the bottom of the tube. Because of the formation of this third layer, the volume of the coacervate layer decreased ~2 mL in these samples.

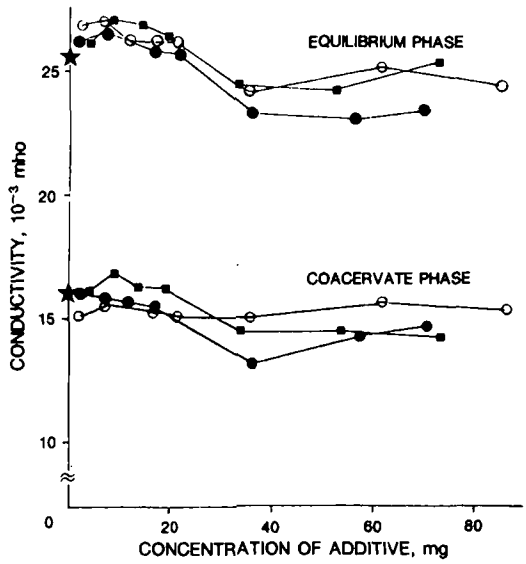

Figure 4—*Drug conductivity at increased concentrations. Key: (●) theophylline; (■) caffeine; (○) theobromine; (★) control.*

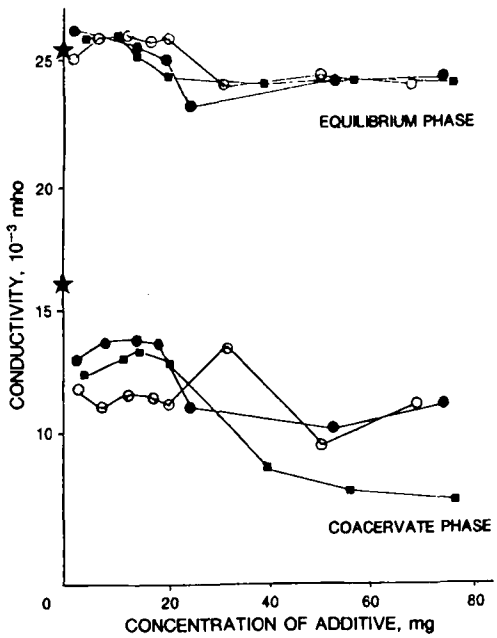

Figure 5—*Sugar conductivity at increased concentrations. Key: (●) glucose-6-phosphate; (■) sucrose; (○) glucose; (★) control.*

Table I—Coacervate Layer Volume Increases in Theophylline Samples

Sample	Theophylline Conc., mg	Coacervate Volume, mL	
		Total	Increase
1	36.41	5.6	0.6
2	57.64	6.5	1.5
3	71.03	6.8	1.8

The high-concentration theophylline series (30–80 mg) exhibited an increase in the coacervate layer volume as shown in Table I. Furthermore, the sample containing the highest concentration (71.03 mg) also had a white precipitate, indicating that the sample had reached the saturation point.

DISCUSSION

At high concentrations beyond the solubility point, sugars, like most compounds, will precipitate out of solution. However, because of the high solubility of the sugar and a strong physicochemical attraction to water, the sugar and bound water that separates as an additional phase from the rest of the system

is not a white, chalk-like powder, but rather a clear, viscous, sugar-water gel. This characteristic explains the formation of the third layer in the high-concentration sugar samples.

The increase in volume of the coacervate phase in the high-concentration theophylline samples (Table I) indicates a general increase in the structuring of this phase. In this case, the additives also act as general structure makers causing an increased nonpolarity of the equilibrium phase. This hypothesis is consistent with the decrease in electrical conductivity of these samples (Fig. 4), indicating a more structured system.

If the coacervate state is a model for human cytoplasm, then clinical parallels should be found in man. The decrease in the volume of the coacervate layer in the high-concentration sugar samples may be related to the known delayed healing of wounds in diabetics with low insulin and therefore high blood sugar levels. Ecanow *et al.* (7) have hypothesized that this delay in healing is partially caused by a rupturing of the cells in the wounded area from the high sugar concentrations acting as a structure breaker of these cells. This hypothesis is consistent with the decrease in the volume of the coacervate in the high-concentration sugar samples (acting as a structure breaker in the highly structured coacervate phase) without noticeable effect on the loosely bound equilibrium phase.

For each additive, the conductivity of the coacervate phase is reduced compared with the equilibrium phase (Figs. 2–5). This decreased conductivity of coacervates is consistent with both the hypothesis of Ecanow *et al.* (7) that conditions like malignancy occur in a nonpolar aqueous matrix (coacervate) and the findings of Lowenstein and Kanno (8) that malignant cells have a reduced action potential. Also, a low conductivity of the sugars is shown which may be related to the known depressant effect of sugars on the central nervous system, culminating in diabetic coma with high glucose concentrations (4). The effect of high concentrations of sucrose on membrane interface disorientation (structure breaking) can account for the known low absorption rate of sucrose in the intestine, compared to glucose (9).

The conductivity of caffeine was highest, followed by theobromine and theophylline (Fig. 2). These data may have a relationship to the decurarizing effects of these three drugs with caffeine showing the greatest effect, followed by theobromine and theophylline (10). With higher concentrations (Fig. 4) the conductivity was generally highest in theobromine, then caffeine and theophylline. These data may then be related to the effects of these drugs on urine production with theobromine showing the greatest effect followed by caffeine and theophylline, as reported by Scott *et al.* (11).

The increase over control values of the caffeine (Figs. 2, 4) followed by a reversal of a decrease with high concentrations (Fig. 4) finds a clinical parallel in the known increased cardiac contraction effect of caffeine at concentrations of 0.25–1.50 mM and a decreased contraction effect with concentrations >2.0 mM as reported by Guboreff and Sleator (12).

This discussion has shown a number of clinical parallels in the conductivity changes from the drug and sugar series and provides evidence in favor of the usefulness of a coacervate system as a model for human cytoplasm.

REFERENCES

(1) A. L. Oparin, "Life, Its Nature, Origin, and Development," Academic Press, New York, N.Y., 1961.

(2) H. L. Bociji and H. G. Bungenberg de Jong, "Protoplasmatologia, Biocolloids and Their Interactions," Springer-Verlag, Austria, 1956.

(3) B. Ecanow, "Models of Human Neurological Diseases," Excerpta Medica Press, Amsterdam, 1974, pp. 253–286.

(4) A. M. Harvey, R. J. Johns, and A. H. Owens, "The Principles and Practice of Medicine," Appleton-Century-Crofts, New York, N.Y., 1980, pp. 879–912.

(5) R. Acharya, B. Ecanow, and R. Balagot, *J. Colloid Interface Sci.*, **40**, 125 (1972).

(6) H. Takruri, B. Ecanow, and R. Balagot, *J. Pharm. Sci.*, **66**, 283 (1977).

(7) B. Ecanow, B. Gold, and C. Ecanow, *Physiol. Chem. Phys.*, **11**, 97 (1979).

(8) E. Lowenstein and Y. Kanno, *Nature*, **209**, 1248 (1963).

(9) G. G. Duncan, "Diseases of Metabolism," W. B. Saunders, Philadelphia, Pa, 1947, p. 23.

(10) F. A. Huidobro, *J. Pharmacol. Exp. Ther.*, **84**, 380 (1945).

(11) C. C. Scott, R. C. Anderson, and K. K. Chen, *J. Pharmacol. Exp. Ther.*, **86**, 113 (1946).

(12) T. Guboreff and W. Sleator, *J. Pharmacol. Exp. Ther.*, **148**, 202 (1965).

Urinary Metabolites of the Antiprotozoal Agent *cis*-3a,4,5,6,7,7a-Hexahydro-3-(1-methyl-5-nitro-1*H*-imidazol-2-yl)-1,2-benzisoxazole in the Rat

W. J. A. VANDENHEUVEL ˣ, B. H. ARISON, H. FLYNN, G. J. GATTO, H. E. MERTEL, and P. G. WISLOCKI

Received June 15, 1983, from *Merck Sharp & Dohme Research Laboratories, Rahway, NJ 07065.* Accepted for publication February 2, 1984.

Abstract □ ^{1}H-NMR and MS were employed to identify 13 rat urinary metabolites of ^{14}C-labeled *cis*-3a,4,5,6,7,7a-hexahydro-3-(1-methyl-5-nitro-1*H*-imidazol-2-yl)-1,2-benzisoxazole (MK-0436). The major free (unconjugated) metabolite was *cis*-3a,4,5,6,7,7a-hexahydro-3-carboxamido-1,2-benzisoxazole; it was also the second most abundant metabolite released during hydrolysis of the conjugated fraction. All other identified metabolites were hydroxylated analogues substituted at C(4)—C(7a) of the cyclohexane ring. The 4-equatorial,5-axial,7a-triol was the second most abundant metabolite excreted in an unconjugated form. Four monohydroxy (5-axial, 6-axial, 6-equatorial, 7-equatorial) metabolites of the drug were identified; they were found in the conjugated fraction only and were released by hydrolysis. The 5-axial hydroxy compound is the major conjugated metabolite and is overall the most abundant of all the metabolites. Six dihydroxy metabolites were identified: one was found exclusively in the free state, three as conjugates only (including the 7-axial,7a-diol, which is the major dihydroxy species), and two both free and conjugated. A second triol was found both free and conjugated.

Keyphrases □ *cis*-3a,4,5,6,7,7a-Hexahydro-3-(1-methyl-5-nitro-1*H*-imidazol-2-yl)-1,2-benzisoxazole—urinary metabolites, rat, NMR, MS □ Hydroxylation—conjugation, *cis*-3a,4,5,6,7,7a-hexahydro-3-(1-methyl-5-nitro-1*H*-imidazol-2-yl)-1,2-benzisoxazole, NMR, MS

Elliott and co-workers (1) reported that in the rabbit, the urinary metabolites of cyclohexane were cyclohexanol and cyclohexane-*trans*-1,2-diol (as conjugates); Renwick and Williams (2) showed that cyclohexylamine was converted to mono- and dihydroxy metabolites (free and conjugates). Testa and Jenner (3) also discussed the metabolic hydroxylation of cyclohexyl ring systems. Substituted nitroimidazoles are known to undergo hydroxylation on their hydrocarbon moieties: metronidazole is hydroxylated on the 2-methyl group (4), ipronidazole on the 2-isopropyl group (5). The antipro-

0022-3549/84/1200-1731$01.00/0

© 1984, American Pharmaceutical Association

is not a white, chalk-like powder, but rather a clear, viscous, sugar-water gel. This characteristic explains the formation of the third layer in the high-concentration sugar samples.

The increase in volume of the coacervate phase in the high-concentration theophylline samples (Table I) indicates a general increase in the structuring of this phase. In this case, the additives also act as general structure makers causing an increased nonpolarity of the equilibrium phase. This hypothesis is consistent with the decrease in electrical conductivity of these samples (Fig. 4), indicating a more structured system.

If the coacervate state is a model for human cytoplasm, then clinical parallels should be found in man. The decrease in the volume of the coacervate layer in the high-concentration sugar samples may be related to the known delayed healing of wounds in diabetics with low insulin and therefore high blood sugar levels. Ecanow *et al.* (7) have hypothesized that this delay in healing is partially caused by a rupturing of the cells in the wounded area from the high sugar concentrations acting as a structure breaker of these cells. This hypothesis is consistent with the decrease in the volume of the coacervate in the high-concentration sugar samples (acting as a structure breaker in the highly structured coacervate phase) without noticeable effect on the loosely bound equilibrium phase.

For each additive, the conductivity of the coacervate phase is reduced compared with the equilibrium phase (Figs. 2–5). This decreased conductivity of coacervates is consistent with both the hypothesis of Ecanow *et al.* (7) that conditions like malignancy occur in a nonpolar aqueous matrix (coacervate) and the findings of Lowenstein and Kanno (8) that malignant cells have a reduced action potential. Also, a low conductivity of the sugars is shown which may be related to the known depressant effect of sugars on the central nervous system, culminating in diabetic coma with high glucose concentrations (4). The effect of high concentrations of sucrose on membrane interface disorientation (structure breaking) can account for the known low absorption rate of sucrose in the intestine, compared to glucose (9).

The conductivity of caffeine was highest, followed by theobromine and theophylline (Fig. 2). These data may have a relationship to the decurarizing effects of these three drugs with caffeine showing the greatest effect, followed by theobromine and theophylline (10). With higher concentrations (Fig. 4) the conductivity was generally highest in theobromine, then caffeine and theophylline. These data may then be related to the effects of these drugs on urine production with theobromine showing the greatest effect followed by caffeine and theophylline, as reported by Scott *et al.* (11).

The increase over control values of the caffeine (Figs. 2, 4) followed by a reversal of a decrease with high concentrations (Fig. 4) finds a clinical parallel in the known increased cardiac contraction effect of caffeine at concentrations of 0.25–1.50 mM and a decreased contraction effect with concentrations >2.0 mM as reported by Guboreff and Sleator (12).

This discussion has shown a number of clinical parallels in the conductivity changes from the drug and sugar series and provides evidence in favor of the usefulness of a coacervate system as a model for human cytoplasm.

REFERENCES

(1) A. L. Oparin, "Life, Its Nature, Origin, and Development," Academic Press, New York, N.Y., 1961.

(2) H. L. Bociji and H. G. Bungenberg de Jong, "Protoplasmatologia, Biocolloids and Their Interactions," Springer-Verlag, Austria, 1956.

(3) B. Ecanow, "Models of Human Neurological Diseases," Excerpta Medica Press, Amsterdam, 1974, pp. 253–286.

(4) A. M. Harvey, R. J. Johns, and A. H. Owens, "The Principles and Practice of Medicine," Appleton-Century-Crofts, New York, N.Y., 1980, pp. 879–912.

(5) R. Acharya, B. Ecanow, and R. Balagot, *J. Colloid Interface Sci.*, **40**, 125 (1972).

(6) H. Takruri, B. Ecanow, and R. Balagot, *J. Pharm. Sci.*, **66**, 283 (1977).

(7) B. Ecanow, B. Gold, and C. Ecanow, *Physiol. Chem. Phys.*, **11**, 97 (1979).

(8) E. Lowenstein and Y. Kanno, *Nature*, **209**, 1248 (1963).

(9) G. G. Duncan, "Diseases of Metabolism," W. B. Saunders, Philadelphia, Pa, 1947, p. 23.

(10) F. A. Huidobro, *J. Pharmacol. Exp. Ther.*, **84**, 380 (1945).

(11) C. C. Scott, R. C. Anderson, and K. K. Chen, *J. Pharmacol. Exp. Ther.*, **86**, 113 (1946).

(12) T. Guboreff and W. Sleator, *J. Pharmacol. Exp. Ther.*, **148**, 202 (1965).

Urinary Metabolites of the Antiprotozoal Agent *cis*-3a,4,5,6,7,7a-Hexahydro-3-(1-methyl-5-nitro-1*H*-imidazol-2-yl)-1,2-benzisoxazole in the Rat

W. J. A. VANDENHEUVEL ˣ, B. H. ARISON, H. FLYNN, G. J. GATTO, H. E. MERTEL, and P. G. WISLOCKI

Received June 15, 1983, from *Merck Sharp & Dohme Research Laboratories, Rahway, NJ 07065.* Accepted for publication February 2, 1984.

Abstract □ ^{1}H-NMR and MS were employed to identify 13 rat urinary metabolites of ^{14}C-labeled *cis*-3a,4,5,6,7,7a-hexahydro-3-(1-methyl-5-nitro-1*H*-imidazol-2-yl)-1,2-benzisoxazole (MK-0436). The major free (unconjugated) metabolite was *cis*-3a,4,5,6,7,7a-hexahydro-3-carboxamido-1,2-benzisoxazole; it was also the second most abundant metabolite released during hydrolysis of the conjugated fraction. All other identified metabolites were hydroxylated analogues substituted at C(4)—C(7a) of the cyclohexane ring. The 4-equatorial,5-axial,7a-triol was the second most abundant metabolite excreted in an unconjugated form. Four monohydroxy (5-axial, 6-axial, 6-equatorial, 7-equatorial) metabolites of the drug were identified; they were found in the conjugated fraction only and were released by hydrolysis. The 5-axial hydroxy compound is the major conjugated metabolite and is overall the most abundant of all the metabolites. Six dihydroxy metabolites were identified: one was found exclusively in the free state, three as conjugates only (including the 7-axial,7a-diol, which is the major dihydroxy species), and two both free and conjugated. A second triol was found both free and conjugated.

Keyphrases □ *cis*-3a,4,5,6,7,7a-Hexahydro-3-(1-methyl-5-nitro-1*H*-imidazol-2-yl)-1,2-benzisoxazole—urinary metabolites, rat, NMR, MS □ Hydroxylation—conjugation, *cis*-3a,4,5,6,7,7a-hexahydro-3-(1-methyl-5-nitro-1*H*-imidazol-2-yl)-1,2-benzisoxazole, NMR, MS

Elliott and co-workers (1) reported that in the rabbit, the urinary metabolites of cyclohexane were cyclohexanol and cyclohexane-*trans*-1,2-diol (as conjugates); Renwick and Williams (2) showed that cyclohexylamine was converted to mono- and dihydroxy metabolites (free and conjugates). Testa and Jenner (3) also discussed the metabolic hydroxylation of cyclohexyl ring systems. Substituted nitroimidazoles are known to undergo hydroxylation on their hydrocarbon moieties: metronidazole is hydroxylated on the 2-methyl group (4), ipronidazole on the 2-isopropyl group (5). The antipro-

0022-3549/84/1200-1731$01.00/0

© 1984, American Pharmaceutical Association

tozoal agent *cis*-3a,4,5,6,7,7a-hexahydro-3-(1-methyl-5-nitro-1*H*-imidazol-2-yl)-1,2-benzisoxazole (MK-0436, I) is metabolized by the dog to a series of alicyclic ring hydroxylation products (6, 7). The *in vitro* [rat liver post mitochondrial fraction (S9)] metabolism of I was reported recently (8). As in the dog study, metabolite formation in all cases involved biotransformations on C(4)—C(7a) of the cyclohexane ring. Two dihydroxy and seven monohydroxy metabolites were identified; the major *in vitro* metabolite is the 5-axial hydroxy analogue. The rat urinary metabolite study reported herein was executed to allow a direct comparison of the *in vitro* and *in vivo* metabolism of I, which possesses trypanocidal activity (1, 9-12) and is reported (6)[1,2] to be converted to bioactive metabolites.

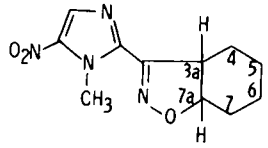

I

EXPERIMENTAL SECTION

Two Sprague-Dawley CD rats were pretreated with phenobarbital (0.1% in their drinking water) for 8 consecutive days. The animals were then dosed twice (16 h apart) at 500 mg/kg ip with I labeled with carbon-14 in the 3a- and 7a-positions (*vide infra*). Urine, collected until 24 h following the second dose of labeled I, was extracted with dichloromethane. The spent urine was incubated for 5.5 h at 37°C with β-glucuronidase and sulfatase[3] and then extracted with dichloromethane. The solvent was removed under reduced pressure to give two fractions containing the "free" and "liberated" metabolites of I (fractions 1 and 2, respectively). These fractions were subjected to TLC[4] with solvent[5] system A (toluene–ethyl acetate, 3:1) to yield partially purified metabolite fractions. Further purification was achieved by repeated use of this system and by TLC with two other solvent systems (system B: dichloromethane–methanol, 10:1; system C: trimethylpentane–2-propanol, 4:1). Metabolite zones were scraped from the plates, and metabolite fractions were isolated as described previously (8). The latter were assayed for radioactivity by use of the liquid scintillation counting technique[6].

Electron-impact[7] mass spectra (low resolution) of metabolite fractions were obtained using a 3.5-kV accelerating potential, 60-μA trap current, 70-eV ionizing energy, and 250°C source temperature. High-resolution (exact-mass)[8] mass spectrometric data were obtained using an 8-kV accelerating potential, 100-eV ionizing potential, and 200°C source temperature. Chemical-ionization[9] mass spectrometric data were obtained using methane as the reagent gas (1 Torr) and a 150-eV ionizing potential, 0.8-mA emission current, 1.8-kV electron multiplier, and 130°C source temperature. ^{1}H-NMR spectra[10] were obtained in deuterochloroform using tetramethylsilane as the internal standard. The chemical shifts and coupling patterns of H_{3a} and H_{7a} together with any new signals in the δ 3.5–5.5 ppm region (*i.e.*, diagnostic of *H*COH) were used to assign the location and stereochemistry of the hydroxyl groups of the transformation products.

Labeled I was prepared as shown in Scheme I. Ethyl [^{14}C]formate was treated with Grignard reagent prepared from 1,5-dibromopentane and magnesium to give [1-^{14}C]cyclohexanol, following the procedure of Fields *et al.* (13). Treatment of the [1-^{14}C]cyclohexanol with phthalic anhydride and *p*-toluenesulfonic acid (catalyst) then gave [1,2-^{14}C]cyclohexene (14). Reaction of the labeled cyclohexene with 1-methyl-5-nitro-1*H*-imidazol-2-hydroxyamoyl chloride (15) gave [3a,7a-^{14}C]I.

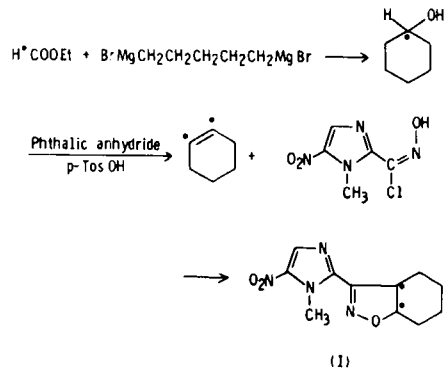

(I)

Scheme I—Synthesis outline; asterisks indicate position(s) of the ^{14}C-label.

RESULTS AND DISCUSSION

The pre- and posthydrolysis extractions resulted in the isolation of most (70%) of the total urinary radioactivity, with 70% of this associated with the posthydrolysis extraction fraction. Analytical TLC (solvent system A) of the pre- and posthydrolysis extraction fractions (1 and 2, respectively) demonstrated their multicomponent nature. The fractions were subjected to preparative-scale TLC with the same solvent system. Fraction 1 gave three major radioactive zones (R_f ~0.05, ~0.10, and ~0.27) with no evidence of more than a trace of the parent drug (R_f 0.70). The liberated metabolites (fraction 2) were subjected to preparative TLC as above; a broad, smeared zone (R_f ~0.05–0.10) and three more defined zones (R_f ~0.15, ~0.20, and ~0.28) were obtained, each of which contained drug-related species. These seven metabolite zones were further purified by TLC using solvent systems A–C to yield a total of 16 metabolites, 13 of which (accounting for >98% of the total of isolated metabolites) were identified (Table I). Five of the isolated, identified metabolites (or hydrolysis products thereof) were shown to be compounds previously identified as biotransformation products of I, and their designations (III and VI–IX, respectively) are as previously described (7, 8). The monohydroxy compounds (VI, VII, and IX) were found as rat *in vitro* metabolites (8), and III was found in dog urine (7). Compounds IX and VI were found to be the major and second most abundant rat *in vitro* metabolites, respectively. The dihydroxy metabolite VIII was found both as a rat *in vitro* metabolite (8) and a dog urinary metabolite (unconjugated) (7).

The electron-impact mass spectrometric behavior of I and several of its metabolites (those possessing hydroxyl groups on the cyclohexane ring) was discussed previously (6, 7). Not only do increases of 16 mass units in the molecular ions signify the number of oxygen atoms added to form hydroxyl groups, but the continuing presence of the fragment ions of *m/z* 153 and 195 appears to demonstrate that metabolism has occurred on the cyclohexane ring (6, 7). Thus for I and its mono-, di-, and trihydroxy metabolites, the molecular ions are *m/z* 250, 266, 282, and 298, respectively, and with these compounds the fragment ions *m/z* 153 and 195 are observed (see Table II for representative spectral data).

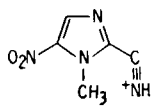

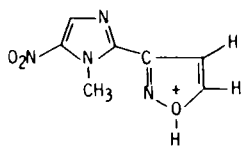

With respect to the identified rat urinary metabolites, two [the 5-equatorial,7a dihydroxy (XVI) and 4-equatorial,5-axial,7-axial trihydroxy (XVII) metabolites] were found only in the free form. Seven were found as conjugates only [the 5-axial hydroxy (IX), 6-axial hydroxy (III), 6-equatorial hydroxy (VII), 7-equatorial hydroxy (VI), 5-axial,6-equatorial dihydroxy (XVIII), 7-axial,7a dihydroxy (XIX), and 7-equatorial,7a dihydroxy (XX) metabolites]. Four of the metabolites [5-axial,7a dihydroxy (VIII), 5-axial,7-axial dihydroxy (XII), 4-equatorial,5-axial,7a trihydroxy (XXI), and the carboxamide (XXII) metabolites] were found in both free and conjugated forms. Identification of the eight newly recognized metabolites (XII and XVI–XXII; each isolated by TLC and homogeneous in three solvent systems) is discussed below (*cf.* Table I).

Metabolites XVI and XVII, under electron-impact mass spectrometry conditions, possess molecular ions of *m/z* 282 and 298, respectively, and thus these compounds are di- and trihydroxy analogues of I (for comparison, I yields

[1] B. M. Miller, R. Meurer, and W. J. A. VandenHeuvel, unpublished results.
[2] H. Skeggs, R. M. Berglund, W. J. A. VandenHeuvel, P. G. Wislocki, H. Mrozik, and F. J. Wolf, unpublished results.
[3] Each milliliter contained 1200 U of β-glucuronidase and 36,000 U of arylsulfatase; Calbiochem.
[4] Silica gel F; Brinkmann.
[5] Distilled in glass; Burdick and Jackson.
[6] Tricarb Liquid Scintillation Spectrometer and INSTA-GEL cocktail; Packard.
[7] LKB 9000.
[8] MAT 731; Varian.
[9] Model 3200; Finnigan.
[10] Model SC 300-MHz spectrometer equipped with a Fourier transform accessory; Varian.

Table I—Identified Rat Urinary Metabolites of I

Form in Urine	Compound	Fraction of Total Identified Metabolites, %[a]	R_f Values[b] A[c]	B[d]	C[e]
Free only	XVI 5 eq,7a-$(OH)_2$	1	0.02	0.57	0.35
	XVII 4 eq,5 ax,7 ax-$(OH)_3$	1	0.03	0.66	0.21
Conjugate only	IX 5 ax-OH	41	0.10	0.77	0.52
	III 6 ax-OH	1	0.09	0.78	0.36
	VII 6 eq-OH	4	0.07	0.70	0.41
	VI 7 eq-OH	9	0.20	0.82	0.53
	XVIII 5 ax,6 eq-$(OH)_2$	1	0.02	0.63	0.31
	XIX 7 ax,7a-$(OH)_2$	3	0.11	0.73	0.54
	XX 7 eq,7a-$(OH)_2$	1	0.07	0.68	0.48
Free/conjugate	XXII Amide[f]	30	0.27	0.86	0.59
	VIII 5 ax,7a-$(OH)_2$	2	0.03	0.67	0.45
	XII 5 ax,7 ax-$(OH)_2$	2	0.03	0.72	0.35
	XXI 4 eq,5 ax,7a-$(OH)_3$	3	0.08	0.70	0.44

[a] The identified metabolites account for >98% of the isolated metabolites. [b] Silica gel TLC. [c] Toluene–ethyl acetate, 3:1. [d] Dichloromethane–methanol, 10:1. [e] Trimethylpentane–2-propanol, 4:1. [f] 3a,4,5,6,7,7a-Hexahydro-3-carboxamido-1,2-benzisoxazole.

Table II—Pertinent Ions Found in the Mass Spectra[a] of I and Three of Its Urinary Metabolites

Compound	Substitution	Relative Intensity of Ion *m/z* 298	*m/z* 282	*m/z* 266	*m/z* 265	*m/z* 264	*m/z* 263	*m/z* 250	*m/z* 249	*m/z* 247	*m/z* 233	*m/z* 232	*m/z* 231	*m/z* 205	*m/z* 195	*m/z* 153	*m/z* 107
I	—	—	—	—	—	—	—	100	—	—	44	23	—	19	37	73	24
IX	5-ax-OH	—	—	35	—	—	—	—	19	17	—	—	7	—	100	60	15
XVIII	5-ax,6-eq-$(OH)_2$	—	27	—	15	12	—	—	—	18	—	—	—	—	100	41	14
XVII	4-eq,5-ax,7-ax-(OH_3)	6	—	—	—	—	3	—	—	—	—	—	—	—	100	10	5

[a] Electron-impact low-resolution[7].

a molecular ion of *m/z* 250). The presence of fragment ions *m/z* 153 and 195 in the mass spectra of the metabolites strongly suggests (6) that hydroxylation occurred on the cyclohexane ring. Pertinent NMR data for the two metabolites are as follows: XVI: δ 3.86 (m, H_{6ax}) and 3.50 ppm (dd, 11.5, 7.2, H_{3a}); XVII: δ 4.99 (dd, 11.4, H_{7a}), 4.36 (m, H_{7eq}), 4.22 (br s, H_{4ax}), and 3.80 ppm (dd, 11, 9, H_{3a}).

The hydrolysis products of XVIII–XX each exhibit molecular ions of *m/z* 282 and fragmentation patterns indicative of hydroxylation of the alicyclic ring; these metabolites are thus dihydroxy analogues of I. NMR data critical for locating the hydroxy groups and defining their stereochemistry in these compounds include: XVIII: δ 4.69 (m, H_{7a}), 4.04 (br s, H_{5eq}), 3.57 (m, H_{6ax}), and 3.74 ppm (dt, H_{3a}); XIX: δ 4.22 (dd, 6.5, 4.5, H_{7eq}), and 3.70 ppm (dd, 11, 7, H_{3a}); XX: δ 4.02 (dd, 10, 6, H_{7ax}) and 3.66 ppm (t 8.5, H_{3a}). The NMR, MS, and TLC data of XVIII match those for the synthetic 5,6-*cis* (5-axial,6-equatorial) diol of I[11].

Two of the newly identified metabolites found both free and as conjugates were also shown to be hydroxy analogues of I. Metabolites XII and XXI exhibit molecular ions of *m/z* 282 and 298, demonstrating that they are di- and trihydroxy species, respectively. The mass spectrometric fragmentation patterns for the two compounds demonstrated the general sites of substitution [C(4)—C(7a)], but NMR spectrometry once again pinpointed the exact position and stereochemistry of the hydroxyl groups. Thus, for the 5-axial,7-axial-diol (XII), the NMR data include: δ 4.60 (br d, 7, H_{7a}), 4.32 (m, H_{7eq} + H_{5eq}), and 4.02 ppm (dt, 10, 7, 7, H_{3a}). For the 4-equatorial,5-axial,7a-triol, the NMR data include: δ 4.09 (br s, H_{5eq}), 3.44 (dd, 9.0, 3.0, H_{4ax}), and 3.40 ppm (d, 9.0, H_{3a}). Metabolite XII was actually noted previously as an *in vitro* biotransformation product of I but was not identified in the earlier work (8).

Metabolite XXII is the major drug-related species in the unconjugated fraction and the second most abundant of the metabolites released from the conjugated fraction during hydrolysis. Its relatively large R_f in solvent system A suggested that it was not a hydroxy analogue of I. The mass spectrometric (electron-impact) behavior of XXII (apparent molecular ion of *m/z* 168, with none of the normally encountered metabolite fragment ions) strengthened this assumption. Chemical-ionization MS of XXII yielded a pseudomolecular ion of *m/z* 169, confirming 168 as the molecular weight of the metabolite. An exact mass determination on the molecular ion (*m/z* 168) gave an empirical formula of $C_8H_{12}N_2O_2$ (calc., 168.0898; found, 168.0905). The metabolite did not possess the UV spectral features (λ_{max} at 240 and 320 nm) characteristic of I and its hydroxy metabolites. A structure which fits all these data is presented below. NMR data [δ 6.54 and 5.39 (2, $CONH_2$), 4.58 (qn, 3.7, H_{7a}), and 3.26 ppm (q, 8.0, H_{3a})] confirmed that the metabolite is indeed *cis*-3a,4,5,6,7,7a-hexahydro-3-carboxamido-1,2-benzisoxazole.

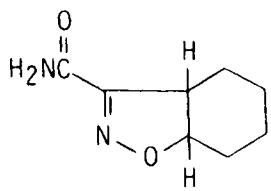

XXII

Three other rat urinary metabolites of I were partially characterized. Compound XXIII, found only in the nonconjugated form, is a dihydroxy analogue of I. Compounds XXIV and XXV, released from the conjugate fraction by hydrolysis, are both monohydroxy metabolites.

All the rat urinary metabolites of I identified (and the three isolated but only partially characterized), except one, are hydroxy analogues of the drug with substitution at C(4)—C(7a) of the cyclohexane ring. The lone exception is the carboxamide XXII which arises *via* degradation of the nitroimidazole ring. Another carboxamide, acetamide, has been found as a metabolite resulting from the *in vitro* reduction of metronidazole by xanthine oxidase (16) and the *in vivo* (turkey) metabolism of another nitroimidazole, ronidazole (17). As XXII was not found as an *in vitro* (rat liver S9) metabolite, it may arise *in vivo via* a nonhepatic metabolic route, such as reduction by gut flora.

Urinary monohydroxy metabolites of I were found only as conjugates. Compounds IX and VI (released by hydrolysis) are the two most abundant (in that order; see Table I) hydroxy metabolites of I, paralleling the rat *in vitro* situation (8). Of the two other monohydroxy metabolites, III and VII (both found as conjugates), the former was previously identified as a canine urinary metabolite (7) and the latter as a rat *in vitro* biotransformation product (8).

Although dihydroxy metabolites of I are produced by the rat both *in vitro* (free only) and *in vivo* (free and conjugated), trihydroxy metabolites XVII and XXI are found only as urinary metabolites. Compound XVII was found exclusively in the unconjugated form, whereas XXI was found both free and conjugated. The latter is the second most abundant of the metabolites excreted free.

It is clear that the alicyclic hydrocarbon moiety of I is very susceptible to hydroxylation by the rat, both *in vivo* and *in vitro*. Nine hydroxy analogues

[11] H. Mrozik and P. Eskola, unpublished data.

of I were identified as rat liver S9 *in vitro* metabolites, and this current paper reports the identification of a dozen metabolites of I in which hydroxylation occurred at C(4) - C(7a) of the cyclohexane ring. The intact animal produces not only a greater total number of and several more-extensively hydroxylated metabolites, but also effects an entirely different and quantitatively significant metabolic conversion, *i.e.*, degradation of the nitroimidazole ring. The most common metabolic transformation both *in vivo* and *in vitro*, however, is hydroxylation to form the 5-axial hydroxy metabolite. Axial hydroxyl groups at C-5 are also found in three of the dihydroxy metabolites and both of the urinary trihydroxy metabolites.

REFERENCES

(1) T. H. Elliott, D. V. Parke, and R. T. Williams, *Biochem. J.*, **72,** 193 (1959).

(2) A. G. Renwick and R. T. Williams, *Biochem. J.*, **129,** 857 (1972).

(3) B. Testa and P. Jenner, *J. Pharm. Pharmacol.*, **28,** 731 (1976).

(4) J. E. Stambaugh, L. G. Feo, and R. W. Manthei, *J. Pharmacol. Exp. Ther.*, **161,** 373 (1968).

(5) J. Fellig, A. MacDonald, E. Meseck, and H. Laurencot, *Poultry Sci.*, **48,** 1806 (1969).

(6) W. J. A. VandenHeuvel, B. H. Arison, T. W. Miller, P. Kulsa, P. Eskola, H. Mrozik, A. K. Miller, H. Skeggs, S. B. Zimmerman, and B. M. Miller, *J. Pharm. Sci.*, **68,** 1156 (1979).

(7) W. J. A. VandenHeuvel, D. Onofrey, J. S. Zweig, J. Pile, N. Kirkman-Bey, and B. H. Arison, *J. Pharm. Sci.*, **69,** 1288 (1980).

(8) W. J. A. VandenHeuvel, H. Skeggs, B. H. Arison, and P. G. Wislocki, *J. Pharm. Sci.*, **72,** 782 (1983).

(9) C. M. Malanga, J. Conroy, and A. C. Cuckler, *J. Parasitol.*, **67,** 35 (1981).

(10) F. W. Jennings, G. M. Urquhart, P. K. Murray, and B. M. Miller, *Int. J. Parasitol.*, **10,** 27 (1980).

(11) P. K. Murray, M. C. Habbersett, and R. Meurer, *Am. J. Trop. Med. Hyg.*, **32,** 1242 (1983).

(12) F. W. Jennings, G. M. Urquhart, P. K. Murray, and B. M. Miller, *Trans. R. Soc. Trop. Med. Hyg.*, **77,** 693 (1983).

(13) (a) M. Fields, M. A. Leaffer, S. Rothchild, and J. Rohan, *J. Am. Chem. Soc.*, **74,** 5498 (1958); (b) M. Fields, M. A. Leaffer, and J. Rohan, *Science*, **109,** 35 (1949) as cited in "Organic Syntheses with Isotopes," A. Murray III and D. L. Williams, Eds., Interscience, New York, N.Y., 1958, p. 102.

(14) H. Waldmann and F. Petro, *Chem. Ber.*, **1950,** 287.

(15) P. Kulsa and C. S. Rooney, U.S. Pat. No. 3,711,495 (January 16, 1973); *Chem. Abstr.*, **84,** P59471s (1976).

(16) E. J. T. Chrystal, R. L. Koch, and P. Goldman, *Mol. Pharmacol.*, **18,** 105 (1980).

(17) C. Rosenblum, N. R. Trenner, R. P. Buhs, C. B. Hiremath, F. R. Koniuszy, and D. E. Wolf, *J. Agric. Food Chem.*, **20,** 360 (1972).

ACKNOWLEDGMENTS

The authors thank Mr. H. T. Meriwether for determining the UV spectrum of metabolite XXII, Mr. J. L. Smith for establishing the empirical formula of this compound, and Mr. R. W. Walker for obtaining its chemical-ionization mass spectrum.

Acyloxyamines as Prodrugs of Anti-inflammatory Carboxylic Acids for Improved Delivery Through Skin

K. B. SLOAN*[x], S. SELK, J. HASLAM, L. CALDWELL, and R. SHAFFER

Received April 18, 1983, from the *INTER$_x$ Research Corporation, Merck Sharp and Dohme Research Laboratories, Lawrence, KS 66044.* Accepted for publication, March 21, 1984.

* Present address: Department of Medicinal Chemistry, College of Pharmacy, University of Florida, Gainesville, FL 32610.

Abstract □ An *N,N*-dialkylhydroxylamine derivative of indomethacin has been synthesized. It has been shown to improve the delivery of indomethacin through mouse skin (compared to indomethacin itself) by a factor of two, to be more effective than indomethacin in inhibiting thermal inflammation (two to three times) in animal models, but to be only as effective as indomethacin in inhibiting UV-B radiation erythema in human volunteers.

Keyphrases ■ Indomethacin—derivatives, erythema inhibition in humans, inflammation inhibition in rats, delivery vehicle comparison □ Erythema—inhibition by indomethacin derivatives in humans, inflammation inhibition in rats, delivery vehicle

It is well known that UV radiation on skin produces intense erythema, pain, and blistering (1). However, the proximal cause or causes of the response of skin to UV radiation is less than well understood. UV radiation is usually divided into three arbitrary regions: UV-A, 320–400 nm; UV-B, 320–290 nm, which is also known as sunburn UV radiation; UV-C, 290–200 nm. Regardless of the wavelength, there is a delay of onset of redness that is inversely proportional to the intensity of the radiation. Furthermore, the erythema will persist for hours or days depending directly on the intensity of the radiation. The intensity of the effect of the UV-B radiation has been shown to be particularly sensitive to treatment with nonsteroidal anti-inflammatory agents while UV-C radiation is less sensitive (2) and UV-A radiation is insensitive to nonsteroidal anti-inflammatory agents (3). For instance, topically administered indomethacin has been shown to decrease the redness, as determined visually, and the temperature, as determined by telethermometer readings, of sunburned or UV-B treated skin compared with controls (4).

Since the nonsteroidal anti-inflammatory agents are known to prevent inflammation by inhibiting prostaglandin synthesis, it was logical to suspect that prostaglandins (5) were the proximal cause of at least some of the effects of UV-B radiation because UV-B radiation was susceptible to treatment with nonsteroidal anti-inflammatory agents. Indeed, increased levels of arachidonic acid and prostaglandins E_2 and $F_{2\alpha}$ were found in human skin after treatment with UV-B (6) and UV-C radiation (7); the levels of prostaglandin E increased in a parallel manner with increased erythema over the first 4 h after exposure of guinea pig skin to UV-B radiation (8). However, after 4 h erythema scores stayed high but prostaglandin levels fell back to normal (8). Thus, oral or topical administration of indomethacin completely suppressed the elevation of the levels of the prostaglandins (9) but the erythema associated with the radiation damage was only partially suppressed compared with controls and then for only ~24 h, and the acute

0022-3549/84/1200-1734$01.00/0

© 1984, American Pharmaceutical Association

of I were identified as rat liver S9 *in vitro* metabolites, and this current paper reports the identification of a dozen metabolites of I in which hydroxylation occurred at C(4) - C(7a) of the cyclohexane ring. The intact animal produces not only a greater total number of and several more-extensively hydroxylated metabolites, but also effects an entirely different and quantitatively significant metabolic conversion, *i.e.*, degradation of the nitroimidazole ring. The most common metabolic transformation both *in vivo* and *in vitro*, however, is hydroxylation to form the 5-axial hydroxy metabolite. Axial hydroxyl groups at C-5 are also found in three of the dihydroxy metabolites and both of the urinary trihydroxy metabolites.

REFERENCES

(1) T. H. Elliott, D. V. Parke, and R. T. Williams, *Biochem. J.*, **72,** 193 (1959).

(2) A. G. Renwick and R. T. Williams, *Biochem. J.*, **129,** 857 (1972).

(3) B. Testa and P. Jenner, *J. Pharm. Pharmacol.*, **28,** 731 (1976).

(4) J. E. Stambaugh, L. G. Feo, and R. W. Manthei, *J. Pharmacol. Exp. Ther.*, **161,** 373 (1968).

(5) J. Fellig, A. MacDonald, E. Meseck, and H. Laurencot, *Poultry Sci.*, **48,** 1806 (1969).

(6) W. J. A. VandenHeuvel, B. H. Arison, T. W. Miller, P. Kulsa, P. Eskola, H. Mrozik, A. K. Miller, H. Skeggs, S. B. Zimmerman, and B. M. Miller, *J. Pharm. Sci.*, **68,** 1156 (1979).

(7) W. J. A. VandenHeuvel, D. Onofrey, J. S. Zweig, J. Pile, N. Kirkman-Bey, and B. H. Arison, *J. Pharm. Sci.*, **69,** 1288 (1980).

(8) W. J. A. VandenHeuvel, H. Skeggs, B. H. Arison, and P. G. Wislocki, *J. Pharm. Sci.*, **72,** 782 (1983).

(9) C. M. Malanga, J. Conroy, and A. C. Cuckler, *J. Parasitol.*, **67,** 35 (1981).

(10) F. W. Jennings, G. M. Urquhart, P. K. Murray, and B. M. Miller, *Int. J. Parasitol.*, **10,** 27 (1980).

(11) P. K. Murray, M. C. Habbersett, and R. Meurer, *Am. J. Trop. Med. Hyg.*, **32,** 1242 (1983).

(12) F. W. Jennings, G. M. Urquhart, P. K. Murray, and B. M. Miller, *Trans. R. Soc. Trop. Med. Hyg.*, **77,** 693 (1983).

(13) (a) M. Fields, M. A. Leaffer, S. Rothchild, and J. Rohan, *J. Am. Chem. Soc.*, **74,** 5498 (1958); (b) M. Fields, M. A. Leaffer, and J. Rohan, *Science*, **109,** 35 (1949) as cited in "Organic Syntheses with Isotopes," A. Murray III and D. L. Williams, Eds., Interscience, New York, N.Y., 1958, p. 102.

(14) H. Waldmann and F. Petro, *Chem. Ber.*, **1950,** 287.

(15) P. Kulsa and C. S. Rooney, U.S. Pat. No. 3,711,495 (January 16, 1973); *Chem. Abstr.*, **84,** P59471s (1976).

(16) E. J. T. Chrystal, R. L. Koch, and P. Goldman, *Mol. Pharmacol.*, **18,** 105 (1980).

(17) C. Rosenblum, N. R. Trenner, R. P. Buhs, C. B. Hiremath, F. R. Koniuszy, and D. E. Wolf, *J. Agric. Food Chem.*, **20,** 360 (1972).

ACKNOWLEDGMENTS

The authors thank Mr. H. T. Meriwether for determining the UV spectrum of metabolite XXII, Mr. J. L. Smith for establishing the empirical formula of this compound, and Mr. R. W. Walker for obtaining its chemical-ionization mass spectrum.

Acyloxyamines as Prodrugs of Anti-inflammatory Carboxylic Acids for Improved Delivery Through Skin

K. B. SLOAN*[x], S. SELK, J. HASLAM, L. CALDWELL, and R. SHAFFER

Received April 18, 1983, from the *INTER$_x$ Research Corporation, Merck Sharp and Dohme Research Laboratories, Lawrence, KS 66044.* Accepted for publication, March 21, 1984.

* Present address: Department of Medicinal Chemistry, College of Pharmacy, University of Florida, Gainesville, FL 32610.

Abstract □ An *N,N*-dialkylhydroxylamine derivative of indomethacin has been synthesized. It has been shown to improve the delivery of indomethacin through mouse skin (compared to indomethacin itself) by a factor of two, to be more effective than indomethacin in inhibiting thermal inflammation (two to three times) in animal models, but to be only as effective as indomethacin in inhibiting UV-B radiation erythema in human volunteers.

Keyphrases ■ Indomethacin—derivatives, erythema inhibition in humans, inflammation inhibition in rats, delivery vehicle comparison □ Erythema—inhibition by indomethacin derivatives in humans, inflammation inhibition in rats, delivery vehicle

It is well known that UV radiation on skin produces intense erythema, pain, and blistering (1). However, the proximal cause or causes of the response of skin to UV radiation is less than well understood. UV radiation is usually divided into three arbitrary regions: UV-A, 320–400 nm; UV-B, 320–290 nm, which is also known as sunburn UV radiation; UV-C, 290–200 nm. Regardless of the wavelength, there is a delay of onset of redness that is inversely proportional to the intensity of the radiation. Furthermore, the erythema will persist for hours or days depending directly on the intensity of the radiation. The intensity of the effect of the UV-B radiation has been shown to be particularly sensitive to treatment with nonsteroidal anti-inflammatory agents while UV-C radiation is less sensitive (2) and UV-A radiation is insensitive to nonsteroidal anti-inflammatory agents (3). For instance, topically administered indomethacin has been shown to decrease the redness, as determined visually, and the temperature, as determined by telethermometer readings, of sunburned or UV-B treated skin compared with controls (4).

Since the nonsteroidal anti-inflammatory agents are known to prevent inflammation by inhibiting prostaglandin synthesis, it was logical to suspect that prostaglandins (5) were the proximal cause of at least some of the effects of UV-B radiation because UV-B radiation was susceptible to treatment with nonsteroidal anti-inflammatory agents. Indeed, increased levels of arachidonic acid and prostaglandins E_2 and $F_{2\alpha}$ were found in human skin after treatment with UV-B (6) and UV-C radiation (7); the levels of prostaglandin E increased in a parallel manner with increased erythema over the first 4 h after exposure of guinea pig skin to UV-B radiation (8). However, after 4 h erythema scores stayed high but prostaglandin levels fell back to normal (8). Thus, oral or topical administration of indomethacin completely suppressed the elevation of the levels of the prostaglandins (9) but the erythema associated with the radiation damage was only partially suppressed compared with controls and then for only ~24 h, and the acute

0022-3549/84/1200-1734$01.00/0

© 1984, American Pharmaceutical Association

UV damage to epidermal cells was not affected (10). Moreover, the concentration of indomethacin used was fairly high (2.5%) and the vehicle used in all treatments contained a penetration enhancer (ethanol–propylene glycol–dimethylacetamide or dimethylformamide, 19:19:2 or 1:1:2).

Thus, although in general the treatment (oral) of sunburn with nonsteroidal anti-inflammatory agents appears promising from the point of view of increasing the minimal dose of light necessary to produce erythema (11), the lack of reports of topical activity by indomethacin without the use of penetration enhancers and its lack of effect on the long term effects of sunburn make it an unsatisfactory therapeutic agent at least from a topical delivery point of view. Therefore, in order to determine if increased delivery of indomethacin through skin would improve its therapeutic effectiveness, a number of prodrug derivatives have been prepared and evaluated (12). This paper describes the preparation and evaluation of an *N,N*-dialkylhydroxylamine derivative of indomethacin as one example of the prodrugs of anti-inflammatory carboxylic acids (13) designed to improve therapeutic effectiveness by increasing their delivery through skin.

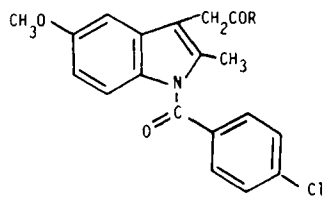

Ia, R = OH
Ib, R = Cl
Ic, R = $ON(C_2H_5)_2$

EXPERIMENTAL SECTION[1]

Preparation of 1-(4′-Chlorobenzoyl)-5-methoxy-2-methyl-3-indolylacetyl Chloride (Ib)—To a suspension of indomethacin (21.9 g, 0.061 mol) in 300 mL of benzene, 10.8 g (0.085 mol) of oxalyl chloride was added with stirring. The reaction was heated at reflux for 2 h. Then the solution was concentrated to give a residue which was triturated with 300 mL of ether. The suspension was filtered and the solid material dried to give the acid chloride as a yellow powder (18.9 g, 82% yield), mp 125–128°C. IR (KBr): 1790 and 1675 cm^{-1} (s, C=O);[1] H-NMR ($CDCl_3$): δ 7.60 (ABq, 4, J = 9 Hz, $\Delta_{\nu AB}$ = 11 Hz, ArH), 7.0–6.55 (m, 3, ArH), 4.17 (s, 2, CH_2COCl), 3.83 (s, 3, OCH_3), and 2.41 ppm (s, 3, CH_3–C=C).

Anal.—Calc. for $C_{19}H_{15}Cl_2NO_3$: C, 60.65; H, 4.02; N, 3.72. Found: C, 60.59; H, 4.08; N, 3.50.

Preparation of *N*-[1-(4′-Chlorobenzoyl)-5-methoxy-2-methyl-3-indolylacetyloxy]-*N,N*-diethylamine (Ic)—To a suspension of Ib (18.9 g, 0.048 mol) in 500 mL of ether was added *N,N*-diethylhydroxylamine (8.88 g, 0.1 mol). The mixture was stirred for 1 h at room temperature and then was filtered. The filtrate was concentrated to give solid material which was extracted with 200 mL of dichloromethane. The organic phase was washed successively with 100 mL of 0.5 M NaOH and 100 mL of water. The organic layer was separated, dried over Na_2SO_4, and concentrated to a viscous mass which was triturated with 100 mL of ether. The crystals were removed by filtration and then recrystallized from dichloromethane–ether to give 14.4 g (70% yield) of the desired product as transparent yellow prisms, mp 100–101°C. IR (KBr): 1747 cm^{-1} (s, O—C=O) and 1650 cm^{-1} (s, N—C=O); ^{1}H-NMR ($CDCl_3$): δ 7.8–7.3 (m, 4, ArH), 7.0–6.6 (m, 3, ArH), 3.83 (s, 3, OCH_3), 3.67 (s, 2, O=CCH_2), 2.89 (q, 4, J = 7 Hz, NCH_2), 2.39 (s, 3, CH_3C=C), and 1.06 ppm (t, 6, J = 7 Hz, NCH_2CH_3).

Anal.—Calc. for $C_{23}H_{25}ClN_2O_4$: C, 64.40; H, 5.88; N, 6.53. Found: C, 64.39; H, 5.86; N, 6.29.

Biological Tests—*Rat Ear Burn Test*—These results were obtained according to the method of Bronaugh *et al.* (14) where warm (51.7°C) metal cylinders were applied to the right ear of rats to cause the burn. After 1 min the burned ears were treated with 50 μL of a 0.03–0.003 M isopropyl myristate, propylene glycol solution, or a suspension of Ia or Ic. The animals were sacrificed after 10 h, circular sections of the ears were made with a leather punch, and the weights of both the right ear and the left ear pieces were determined immediately. Inflammation was determined as the increase in weight of the burned right ears compared with the weight of unburned left ears of the same animals. The percent increase in ear weight was calculated as: (weight of right ear − weight of left ear)/(weight of left ear) × 100. The percent increase in burned ear weight of animals receiving vehicle (%C) was compared with the percent weight increase in ear weight of animals receiving vehicle containing drug (%D) to give a percent inhibition of edema as follows: (%C − %D)/%C = percent inhibition of edema. The results for the comparison of indomethacin with the indomethacin hydroxylamine derivative are given in Table I.

Sunburn Test—This procedure is slightly modified from that described by Snyder (15). The differences in this procedure were the concentrations (1.1 *versus* 2.5% for Ia), amounts applied (50 *versus* 20 μL), number of applications (1 *versus* 4–19), period of observation (6 *versus* 48 h), and the fact that occlusion was used. Briefly, the test areas (4 cm^2) on the backs of human volunteers were irradiated using a bank of sunlamps. The minimum erythemal dose was determined for each subject; subsequent test exposures were 2–3 times this amount. Test formulations of Ia or Ic (0.03 M, 50 μL) or the vehicle alone were applied immediately after exposure and were partially occluded for 5 h with 2.54-cm adhesive bandages (9 spots per subject); three applications each of Ia, Ic, and vehicle in a randomized asymmetric array. Erythemal response was evaluated each hour for 6 h after exposure and graded on a scale of 0–4 (4 being a response of maximum redness). Indomethacin and Ic in the polyethylene ointment base[2] were each tested on two volunteers with the result that no difference between indomethacin and Ic could be seen (Table II). Similar results were obtained when Ia and Ic were compared in petrolatum.

Table I—Ear Burn Test: Effect of Indomethacin and Its Derivative on Inhibition of Inflammation[a]

Compound	Increase in Ear Weight, %	Inhibition of Edema	*n*
Isopropyl myristate (control)	24.1 ± 2.0	—	10
Indomethacin (0.03 M)	18.6 ± 2.0	22.8	10
Ic (0.03 M)	12.0 ± 1.6	50.2	10
Propylene glycol (control)	36.1 ± 1.8	—	18
Indomethacin			
0.03 M[b]	30.9 ± 2.3	21.6	21
0.01 M	31.9 ± 4.3	11.6	5
0.003 M	34.7 ± 3.6	3.9	16
Ic			
0.03 M[b]	28.3 ± 2.5	28.2	20
0.01 M	24.9 ± 4.0	31.0	5
0.003 M	30.5 ± 2.5	15.5	16

[a] Suspension or solutions prepared by a brief (5 min) sonication of solvent–compound mixture. Results ± *SE*. [b] Compared with a control experiment where there was 39.4 ± 2.6% increase in ear weight.

Table II—Sunburn Test: Comparison Between Indomethacin and Ic

After UV Exposure	Evaluation of Redness[a]		
	0.03 M Ic	0.03 M Indomethacin	Control
1	0	0	0
2	0.5 ± 0.8	0.8 ± 1.0	2.0 ± 1.3
3	0.7 ± 0.8	1.1 ± 0.8	2.6 ± 1.2
4	1.1 ± 0.5	1.3 ± 0.6	3.0 ± 1.1
5	1.8 ± 0.6	1.9 ± 0.8	3.5 ± 0.8
6	2.0 ± 0.6[b]	2.0 ± 0.6[b]	3.5 ± 0.8

[a] The vehicle was the polyethylene ointment base: given as 50 μL/4 cm^2 spot (n = 6). Score ± *SD*; maximum redness = 4. [b] $p < 0.005$ compared with control.

[1] TLC was run on Brinkman Polygram Sil G/UV 254. Melting points (uncorrected) were taken with a Thomas-Hoover capillary apparatus. NMR spectra were recorded on a Varian T-60 spectrometer. IR spectra were obtained on a Beckman Acculab 4 infrared spectrophotometer. Microanalyses were obtained from Midwest Microlab, Ltd., Indianapolis, Ind. The indomethacin was obtained from Sigma. The *N*-hydroxydiethylamine and the remaining reagents were obtained from Aldrich except for isopropyl myristate which was obtained from Eastman Kodak. The bulk solvents were obtained from Mallinckrodt. The mice used in the diffusion cell experiments were ICR white Swiss mice (22–25 g) from Sprague–Dawley and the diffusion cells were obtained from Kersco Engineering Consultants, Palo Alto, Calif. The HPLC system was a Waters Associates instrument using a μ-Bondapak C_{18} column. The sunlamp used was a Westinghouse FS-20.

[2] Plastibase; 5 g of polyethylene and 75 g of liquid paraffin.

Table III—Diffusion Cell Test: Comparison Between Indomethacin and Ic [a]

Hours after Application	Indomethacin Delivered, μg	
	From Indomethacin	From Ic
4	0.20 ± 0.19	0.40 ± 0.12
7	0.85 ± 0.48	1.78 ± 0.23
11	1.33 ± 0.73	2.87 ± 0.32
24	4.48 ± 1.86	8.81 ± 0.66

[a] 0.03 M in polyethylene ointment base, $n = 3$; mean ± *SD*.

Table IV—Stability of Ic in Various Solvents

Solvent	Stability (40°C)[a]	
	Amount in Solvent, mg/g	Percent Remaining
Isopropyl myristate	5[b]	79.5
Propylene glycol	3[b]	0.0
Mineral oil	1[b]	98.3
Isooctane	1	99.0
Polyethylene ointment base	10[c]	90.4
Petrolatum	10[c]	99.6

[a] After 7 d except for isopropyl myristate which was 5 d. [b] A solution of Ic. [c] A suspension of Ic.

Diffusion Cell Test—The plexiglass diffusion cells have been described previously (16) but essentially consist of a lower and an upper chamber with a side arm to allow sampling of the receptor phase (lower chamber). The mice were sacrificed by cervical dislocation. Their hair was carefully clipped and the dorsal skin removed and stretched over the receptor chamber using a rubber gasket to secure it. The receptor phase (40 mL) contained 0.9% NaCl and 0.01% thimerosal. The test formulations (0.25 mL, 0.03 M) were applied to the skin, then the entire cell was incubated at 32°C. Two-mL samples were withdrawn at the appropriate times and replaced with 2 mL of fresh receptor phase. The samples were analyzed immediately by HPLC using methanol–water with 1×10^{-3} M tetrabutylammonium perchlorate as the solvent (flow = 2.0 mL/min; absorbance at 280 nm). Samples of 500 μL were injected onto the HPLC column and eluted with a convex gradient using a commercial program[3]; 50% methanol–50% water (solvent A) and 75% methanol–25% water (solvent B) starting with 20% solvent system B and concluding with 60% solvent system B after 5 min. Under those conditions, Ia (indomethacin) had a retention time of 6.7 min while Ic had a retention time of 9.0 min. Peak heights for Ia were quantitated by comparison with standards of known concentration similarly chromatographed. In every case only Ia was observed in the receptor phase on analysis.

The comparison of the ability to deliver indomethacin from the polyethylene ointment base between indomethacin and Ic is shown in Table III. The amounts of indomethacin delivered from the application of Ic in isopropyl myristate (42.7 ± 5.4 μg of indomethacin) and petrolatum (7.9 ± 2.9 μg of indomethacin) were determined; the amounts delivered after 24 h are reported.

Physical Properties—The stability of Ic was determined by preparing solutions or suspensions of Ic in the solvents listed in Table IV. At the appropriate time samples were dissolved in or diluted with ethyl acetate and those solutions were analyzed by HPLC using the same conditions used in the diffusion cell experiments. Only Ia was observed as a decomposition product.

RESULTS AND DISCUSSION

The development of a prodrug derivative of a drug containing a specific functional group requires that the derivative of that functional group exhibit specific characteristics. The derivative should be stable enough to have a useful shelf life, yet revert quickly to the parent compound *in vivo;* the derivatizing agent should be nontoxic and impart the desired change in physicochemical properties to the parent compound. The last characteristic, in many cases, is the most difficult to predict.

N,N-Dialkylhydroxylamines appear to be attractive candidates as derivatizing agents for carboxylic acid based on the above criteria. Acyl-*N,N*-dialkylhydroxylamines are relatively stable derivatives of carboxylic acids yet are sufficiently labile to serve as activated esters in amination reactions when the reaction is catalyzed by a weak acid (17). Thus, they should be stable as long as they are kept out of contact with protic solvents, but, because they are chemically labile, they also should be labile *in vivo*. In addition, the derivatizing agents exhibit a low order of acute toxicity. *N,N*-Diethylhydroxylamine exhibits an oral LD_{LO}[4] of 1600 mg/kg in rats and a topical LD_{LO}[4] of 2000 mg/kg in rabbits (18), compared with diethylamine which exhibits an oral LD_{50} of 540 mg/kg in rats and a topical LD_{50} of 820 mg/kg in rabbits. Finally, although amines have previously been employed successfully as penetration enhancers in formulations (19, 20), derivatizing agents containing low pK_a amines [the pK_a of *N,N*-dimethylhydroxylamine is 5.2 (21) and the *O*-acylated hydroxylamine should be even less basic] have not been employed to prepare prodrugs of carboxylic acids for the purpose of improving the ability of the carboxylic acid to penetrate biological membranes. Such derivatizing agents containing a low pK_a amine group offer several potential advantages. First, the amine group generally confers to the molecule a greater ability to partition from an aqueous environment into lipids than does a carboxylic acid group (22); although it is not clear whether this tendency is due to a more favorable free energy of adsorption or dehydration contribution to the free energy of transfer, previous work (23) suggests that it is probably the latter. Second, the low pK_a amine is present in its unprotonated form (99% at pH 7.4) which is the form that undergoes partitioning (22), compared with other tertiary amines which are ~0.1% unprotonated at pH 7.4. Thus, it seemed likely that the conversion of the carboxylic acid group in nonsteroidal anti-inflammatory agents to low pK_a amine derivatives would impart the desired physical chemical properties to the derivatives.

The acylated hydroxylamine derivative (Ic) was synthesized from the reaction between Ib and two equivalents of hydroxylamine (17). Various other bases such as triethylamine or potassium carbonate were tried as substitutes for the second equivalent of hydroxylamine but the best yields were obtained with the second equivalent of hydroxylamine acting as the acid scavenger. A second route involving the use of a dehydrating agent (1,3-dicyclohexylcarbodiimide) to form the ester bond (17) has also been used to prepare these acylated hydroxylamine derivatives (13). The yields of product were generally lower using this last approach but such an approach should be more generally acceptable for carboxylic acids with sensitive functional groups.

To determine if the substitution of a carboxylic acid group by a low basicity amine group had an effect on the ability of the parent compound to penetrate biological membranes, the diethylhydroxylamine derivative of indomethacin (Ic) was compared with indomethacin in diffusion cell tests using the polyethylene ointment base as the vehicle. Almost twice as much indomethacin was delivered by the derivative Ic than by indomethacin itself (Table III, 0.03 M = ~1% Ia). In addition, only indomethacin was observed on the receptor side; no indole-chlorobenzoyl cleavage was observed. The effect of other vehicles on the delivery of indomethacin by Ic was also determined. A vehicle of petrolatum gave diffusion results that were comparable with the polyethylene ointment base (8 μg) while a vehicle of isopropyl myristate containing Ic delivered almost five times as much indomethacin as did Ic in the polyethylene ointment base. In separate experiments, ≤6% dimethylacetamide in petrolatum was used as a vehicle for the delivery of indomethacin from Ic. However, only ~25 μg of indomethacin was delivered to the receptor phase in 24 h under the best conditions using the vehicle containing the penetration enhancer compared with 42 μg of indomethacin delivered from Ic using isopropyl myristate[5]. These results show that Ic delivers indomethacin through skin better than does indomethacin.

A comparison of the stability properties of Ic in various solvents are given in Table IV. It is apparent that Ic is stable in aprotic vehicles. The relative instability of Ic in the polyethylene ointment base was attributed to acidic impurities in the ointment. The addition of an organic base such as 1-methylimidazole or inorganic bases such as magnesium oxide or zinc oxide resulted in little or no decomposition of Ic in the polyethylene ointment base being detected using the same experimental conditions[5]. In separate diffusion cell experiments zinc oxide was shown to have no effect on the delivery of indomethacin by Ic from the polyethylene ointment base vehicle[5].

The effects of Ic on inhibiting inflammation in animal models is shown in Table I. In the ear burn test, Ic was about three times as potent as indomethacin if the compounds were tested in a propylene glycol vehicle while Ic was twice as potent as indomethacin if the two compared in an isopropyl myristate vehicle. A croton oil irritation test was also used (24, 25). In that test, Ic was only marginally better than indomethacin[6], but this may have been due to the partial decomposition of Ic by the croton oil which contains an acidic component. The advantages of the ear burn model in these tests are that a comparison between vehicles can be obtained and that labile derivatives can be compared under conditions where their stability can be assured. Thus, Ic was clearly more active than indomethacin in inhibiting inflammation in animal models.

The effectiveness of Ic and indomethacin in inhibiting inflammation due

[3] The HPLC program was program 4 on a Waters Associates M660 programmer.

[4] Lowest dose at which toxic effects are observed.

[5] K.B. Sloan, unpublished results.

[6] Kanebo Company, Japan, unpublished data.

to UV-B light is shown in Table II. There was no significant difference between the two compounds at 0.03 M in petrolatum or at 0.03 M in the polyethylene ointment base. Only the results from the latter experiment are shown but the petrolatum results were essentially identical including the lag time for development of redness, although the inhibitory effect of indomethacin and Ic was apparent after 2 h, using the polyethylene ointment base formulation, instead of 3 h for the petrolatum formulation. Thus, no difference between Ic and indomethacin was observed under conditions where the diffusion cell experiments had shown that Ic delivered twice as much indomethacin through the skin as indomethacin itself (see Table III). This effect may be the result of the delivery of a maximum effective dose of indomethacin from the application of indomethacin in the polyethylene ointment base so that there was no observable effect of the excess indomethacin delivered by Ic in the polyethylene ointment base.

The initial suppression of the redness score, then the gradual approach of the redness score for the indomethacin or Ic treated areas to the redness score for the control areas after 6 h, is similar to the observations of Snyder (8) in guinea pigs and of Eaglstein *et al.* (26) in human volunteers. Thus, although an *N,N*-dialkylhydroxylamine derivative of indomethacin exhibited improved delivery of indomethacin through skin and was more effective than indomethacin in inhibiting thermal and chemical inflammation, it was no more effective than indomethacin in inhibiting the long term erythema of UV-B radiation. However, these derivatives of nonsteroidal anti-inflammatory agents may be useful in treating other inflammatory skin reactions such as allergic eczematous contact dermatitis (27) where prostaglandins have also been implicated as causative factors and insufficient nonsteroidal anti-inflammatory agent is delivered using conventional formulations and the underivatized nonsteroidal anti-inflammatory agent.

REFERENCES

(1) A. P. Warin, *Br. J. Dermatol.*, **98,** 473 (1978).

(2) W. H. Eaglstein and A. R. Marsico, *J. Invest. Dermatol.*, **65,** 238 (1975).

(3) W. L. Morison, B. S. Paul, and J. A. Parrish, *J. Invest. Dermatol.*, **68,** 120 (1977).

(4) D. S. Snyder and W. H. Eaglstein, *Br. J. Dermatol.*, **90,** 91 (1974).

(5) J. Sondergaard and M. W. Greaves, *J. Pathol.*, **101,** 93 (1970).

(6) A. K. Black, M. W. Greaves, C. N. Hensby, and N. A. Plummer, *Br. J. Clin. Pharmacol.*, **5,** 431 (1978).

(7) R. D. Camp, M. W. Greaves, C. N. Hensby, and A. P. Warin, *Br. J. Clin. Pharmacol.*, **6,** 145 (1978).

(8) D. S. Snyder, *Prostaglandins*, **11,** 631 (1976).

(9) A. K. Black, M. W. Greaves, C. N. Hensby, N. A. Plummer, and A. P. Warin, *Br. J. Pharmacol.*, **6,** 261 (1978).

(10) K. H. Kaidbey and A. K. Kurban, *J. Invest. Dermatol.*, **66,** 153 (1976).

(11) E. K. Edwards, S. N. Horwitz, and P. Frost, *Arch. Dermatol. Res.*, **272,** 263 (1982).

(12) K. B. Sloan and R. Little, European Pat. Appl., EP 39,051, November 4, 1981; *Chem. Abstr.*, **96,** 104087 (1982).

(13) K. B. Sloan, U.S. Patent, 4,206,220, June 3, 1980; *Chem. Abstr.*, **93,** 8017 (1980).

(14) R. Bronaugh, R. G. Roller, and R. Cargill, *J. Invest. Dermatol.*, **74,** 263 (1978).

(15) D. S. Snyder, *J. Invest. Dermatol.*, **64,** 322 (1975).

(16) N. Bodor, J. Zupan, and S. Selk, *Int. J. Pharm.*, **7,** 63 (1980).

(17) B. O. Handford, J. H. Jones, G. T. Young, and T. F. N. Jones, *J. Chem. Soc.*, **1965,** 6814.

(18) Registry of Toxic Effects of Chemical Substances, R. J. Lewis, Jr., and R. L. Tatken, Ed., U.S. Department of Health and Human Services, NIOSH, 1980.

(19) A. C. Allenby, N. H. Creasey, J. A. G. Edginton, J. A. Fletcher, and C. Schock, *Br. J. Dermatol. (Suppl. 4)*, **81,** 47 (1969).

(20) N. Barker and J. Hadgraft, *Int. J. Pharm.*, **8,** 193 (1981).

(21) W. P. Jencks and J. Carriuolo, *J. Am. Chem. Soc.*, **82,** 1778 (1960).

(22) A. Leo, C. Hansch, and D. Elkins, *Chem. Rev.*, **71,** 525 (1971).

(23) F. A. Vilallonga, R. J. Koftan, and J. P. O'Connell, *J. Colloid Interface Sci.*, **90,** 539 (1982).

(24) N. Bodor, K. B. Sloan, R. J. Little, S. H. Selk, and L. Caldwell, *Int. J. Pharm.*, **10,** 307 (1982).

(25) C. G. Van Amur, *Clin. Pharmacol. Ther.*, **16,** 900 (1974).

(26) W. H. Eaglstein, L. D. Ginsberg, and P. M. Mertz, *Arch. Dermatol.*, **115,** 1421 (1979).

(27) M. W. Greaves and J. Sondergaard, *Arch. Dermatol.*, **101,** 659 (1970).

ACKNOWLEDGMENTS

The authors acknowledge the contribution of R. Bronaugh who designed the ear burn test.

Microstructure of Aluminum Hydroxides and the Formation of Aluminum Dye Lakes

LYNDON L-S. WOU * and B. A. MULLEY ˣ

Received May 11, 1983, from the *Postgraduate School of Studies in Pharmacy, University of Bradford, Bradford, BD7 1DP, United Kingdom.* Accepted for publication February 22, 1984. *Present address: Beecham Pharmaceuticals Research Division, Animal Health Research Centre, Walton Oaks, Dorking Road, Tadworth, Surrey, KT20 7NT, United Kingdom.

Abstract □ The effect of processing variables on the type of aluminum hydroxide and the dye content of the resultant lakes were investigated. The solid-state structure of aluminum lakes in conjunction with the associated aluminum hydroxide was studied by electron microscopy, X-ray diffraction, and IR spectroscopy. The conditions under which the aluminum hydroxide was prepared were shown to govern the amorphous/crystalline character of the product, which was reflected in changes in particle size and surface area. A hypothesis for the interaction of the dye and aluminum hydroxide is formulated in which the amount of dye adsorbed on the aluminum hydroxide is dependent on the surface area of the microstructures present.

Keyphrases □ Aluminum hydroxides—dye lake formation □ Dye lakes—aluminum hydroxide, processing variables

FD & C aluminum lakes are widely used in edible pharmaceutical inks and to color pharmaceutical tablets, but little has been published about their nature and coloring properties. The conditions of preparation of the aluminum hydroxide, which is the substrate on which the dye is adsorbed to form the lake, have a profound effect on lake formation. The degree of alkalinity, temperature, concentration of reagents, as well as the salts used are all factors affecting the type of aluminum hydroxide formed.

The purpose of this study was to demonstrate that aluminum hydroxide, produced by methods described in lake formation processes, has properties which can be related to products described in the literature outside the laking field. The lake forming qualities of aluminum hydroxides are then evaluated in the context of the extensive fundamental work on the nature of this complex and variable material, which changes so markedly with relatively minor variations in the preparative process.

EXPERIMENTAL SECTION

Materials—Commercial FD & C dyes[1] were used in the preparation of the lakes: FD & C Blue No. 2 dye (lot No. 27390) for lake preparation No. B2; FD & C Red No. 40 dye (lot No. AA7490) for lake preparation No. R40; FD & C Yellow No. 5 dye (lot No. Z9313) for lake preparation Nos. Y5 and 1–21. Commercial lakes[1] obtained for this study were FD & C Yellow No. 5 lake (lot No. 127) and FD & C Yellow No. 6 lake (lot No. 634). Commercial aluminum hydroxides[2] were obtained as standard samples of different hydrated forms of alumina: gibbsite (lot No. RD 58/78), bayerite (lot No. RD 57/78), boehmite (lot No. RD 59/78), and pseudoboehmite (lot No. RD 60/78). All other reagents were of Analar or laboratory reagent quality.

Standard Procedures—*Preparation of Aluminum Hydroxide (Preparation No. 1)*—This method was based on the Colorcon process, which is comparable with that of Harrison (1). Sodium carbonate solution (0.96 M, 1800 mL) was added in a dropwise manner at 25°C to aqueous aluminum sulfate solution (0.16 M, 1600 mL) at 10–12 mL/min with continuous vigorous stirring. At pH 6.9, addition was halted. The precipitate was stirred slowly for 30 min and kept at pH 6.9 by adding sodium carbonate solution as necessary. The precipitate was washed until sulfate-free (barium chloride test).

Preparation of FD & C Yellow No. 5 Lake (Preparation No. Y5)—FD & C Yellow No. 5 (71 g) was dissolved in distilled water (1400 mL) at 35°C. The dye solution was passed through a filter into the aluminum hydroxide slurry (prepared in the above process) and stirred for 15 min at 20–25°C. Aluminum chloride solution (5.25 M, 69 mL) was added to the slurry at a rate not exceeding 1 g/min; the final pH was 3.8–4.0. The slurry was stirred slowly overnight. The following morning a few drops of suspended lake were spotted on filter paper to test for bleeding of the dye from the lake. The lake was washed until a 10-mL sample of wash water was no more turbid than the original water by the silver nitrate test. The lake (yield 140 g) was air dried in an oven at 50°C overnight.

Preparation of FD & C Blue No. 2 Lake (Preparation No. B2)—The method was the same as for Yellow No. 5 lake except that FD & C Blue No. 2 (70 g) was dissolved in distilled water (4700 mL) at 55°C. The dye solution was passed through a filter into the slurry and stirred for 15 min at 45–50°C. Aluminum chloride solution (5.25 M, 69 mL) was rapidly added to the slurry; the pH at the end was 4.0–4.1. The yield was 152 g.

Preparation of FD & C Red No. 40 Lake (Preparation No. R40)—The method is the same as for Yellow No. 5 lake except that FD & C Red No. 40 (86 g) was dissolved in distilled water (1400 mL) at 35°C. The yield was 150 g.

Preparation of Aluminum Hydroxide Under Different Conditions—Variations in the processing parameters during aluminum hydroxide precipitation were made by altering the following factors: pH, temperature, aging time, concentration of reagents, presence of sulfate, and nature of aluminum salts and bases. FD & C Yellow No. 5 was the dye used for lake formation in these experiments.

Preparations From Aluminum Sulfate—Since aluminum sulfate is the salt normally used for preparing the aluminum hydroxide substrate for lake formation, this was taken as a starting point for variations in processing parameters to be made. For preparation Nos. 1–4, sodium carbonate solution (1 M or 2 M) was added in a dropwise manner (10 mL/min) into aluminum sulfate solution (0.2 M) varying pH, temperature, and aging time (Table I). Lakes were formed in each case from the sulfate-free precipitate by the standard procedure. For preparation Nos. 5 and 6, sodium carbonate solution (2 M) was added to the aluminum sulfate solution (0.33 M) at 5.5 mL/min until the pH was 10.8, with a large excess of base added to preparation 5. Lakes were formed from the sulfate-free precipitate. By using sodium hydroxide solution (2 M) as the base in preparation 7, the pH of the resulting precipitate was taken up to 12.3. The standard procedure for the preparation of aluminum hydroxide was followed for preparations 9 and 10 except that the sulfate was not removed before lake formation (No. 9) and the precipitation stopped at pH 4.5 (No. 10). For preparations 11–13, sodium carbonate (1 M) and/or sodium hydrogen carbonate solutions (1 M) were added in a dropwise manner into an aluminum sulfate solution (0.2 M) at 10 mL/min until pH 6.9 was reached (Table I).

Preparations From Aluminum Chloride and Nitrate (Nos. 14–20)—Sodium hydroxide (2 M or 4 M) or sodium carbonate solution (2 M) was added to the aluminum chloride solution (0.67 M or 0.5 M) or aluminum nitrate solution (0.67 M or 0.2 M) at 10 mL/min with pH of precipitation and aging conditions given in Table I.

Preparation From Commercial Gibbsite (No. 21)—An attempt was made to form lakes from gibbsite using the standard procedure. After the excess dye was washed off, a slightly yellow grainy material was left.

Lake Analysis—*Dye Content*—Spectrophotometric analysis was used to determine the dye content of the lakes (2). For all lakes, except FD & C Blue No. 2, a sample (200 mg) in distilled water (200 mL) was boiled (3 min) with sodium hydrogen tartrate (3 g). The solution was cooled and diluted suitably for spectrophotometric analysis by scanning the visible spectrum from 400 to 700 nm. A similar process was used for FD & C Blue No. 2, except that more tartrate (6 g) was required.

Moisture—The methods employed were the Karl Fischer method[3] (3) and

[1] Colorcon Inc., West Point, Pa.
[2] Laporte Industries Ltd., Widnes, Cheshire, United Kingdom.
[3] Baird and Tatlock Manual Apparatus; Chadwell Heath, Essex, United Kingdom.

0022-3549/84/1200-1738$01.00/0
© 1984, American Pharmaceutical Association

Table I—Effect of Preparation on Type of Aluminum Hydroxide and Lake Obtained (FD & C Yellow No. 5)

Preparation	Concentration, M: Aluminum Salt	Concentration, M: Base	Temp., °C	pH	Aging	Aluminum Hydroxide	Dye in Lake, %	Moisture, %: Karl Fischer	Moisture, %: Dried at 135°C	Hardness[a]
1	Aluminum sulfate 0.2	Sodium carbonate 1.0	20	9	14 d, 20°C	Amorphous	35.6	17.7	19.0	2
2	0.2	1.0	20	7.4	2 h, 70°C	Amorphous, Pseudo-boehmite	29.2	17.0	17.8	6
3	0.2	1.0	20	10	14 d, 20°C	Bayerite, <30% Boehmite	34.1	12.5	15.6	6
4	0.2	2.0	60	10	7 d, 60°C; 21 d, 20°C	Boehmite	39.9	15.9	15.1	2
5	0.33	2.0 (large excess)	20	10.8	21 d, 20°C	Amorphous, Boehmite (poorly crystallized Gibbsite)	36.3	15.6	21.1	9
6	0.33	2.0	20	10.8	21 d, 20°C	Boehmite	51.1	6.9	14.6	9
7	0.33	Sodium hydroxide 2.0	20	12.3	21 d, 20°C	Bayerite	7.7	3.5	2.5	1p
9	0.2	Sodium carbonate 1.0	20	6.9	No sulfate washing	Amorphous	21.5	6.9	10.9	2
10	0.2	1.0	20	4.5		Amorphous	31.9	6.4	11.7	2
11	0.2	Sodium carbonate + Sodium bicarbonate 1.0	20	6.9		Amorphous	39.3	15.7	15.4	2
12	0.2	Sodium bicarbonate 1.0	20	6.9		Amorphous	39.5	13.5	14.5	2
13	0.2	Sodium carbonate 1.0	20	6.9		Amorphous	39.3	11.2	12.3	2
14	Aluminum nitrate 0.67	2.0	20	10.5	21 d, 20°C	Boehmite	38.1	10.8	16.4	9
15	0.67	Sodium hydroxide 2.0	20	12.3	3 months, 20°C	Gibbsite	22.6	5.9	5.1	1p
17	0.2	2.0	60	12.2	33 d	Boehmite, (Bayerite,) (Gibbsite)	4.8	3.7	3.1	1p
18	Aluminum chloride 0.67	Sodium carbonate 2.0	20	10.8	19 d, 20°C	Boehmite, (Bayerite)	47.2	14.3	17.8	9
19	0.67	Sodium hydroxide 2.0	20	12.3	3 months 20°C	Gibbsite	7.9	3.0	2.7	1p
20	0.5	Sodium hydroxide 4.0	60	11.8	35 d, 20°C	Gibbsite (plates)	20.4	4.4	4.8	1p
						Gibbsite + Bayerite (powder)	14.4	8.2	5.4	1p
21	Seeding from sodium aluminate solution (Laporte)					Gibbsite crystals	0.004	~0.7	0.2	g

[a] Hardness, an arbitrary scale where 0 is very soft, 9 is extremely hard, g is granular (like sand), and p is powdery.

weight loss on drying, in which samples (0.5 g) were dried to constant weight in a hot air oven at 10°C intervals, up to 135°C (4).

Chloride—The procedure was adapted from a potentiometric titration method (5). The lake sample was dissolved in nitric acid prior to titration against silver nitrate.

Sulfate—A gravimetric method (6) was used. The lake sample was boiled with sodium hydrogen tartrate to form a solution before the addition of barium chloride solution. Chloride and sulfate analyses were done only on the standard lakes.

Physical Investigation of Lakes—*Scanning Electron Microscopy*[4]—Specimens were mounted on aluminum stubs and gold coated.

Transmission Electron Microscopy[5]—Specimens were prepared by dispersing (1 min) powdered samples in methanol using an ultrasonic bath. A drop of the dispersion was put on a copper specimen support grid which had previously been coated with a thin carbon film.

Infrared Spectroscopy[6]—Pressed disks of potassium bromide (150 mg) containing finely ground sample (1 mg) were used to record the IR spectra.

X-ray Diffraction—The X-ray powder diffraction patterns were taken on an automated diffractometer[7] equipped with a scintillation detector and pulse-amplitude discrimination, using monochromatic CuK_α radiation.

Nitrogen Gas Adsorption—Two methods were used for the determination

[4] Cambridge Stereoscan 150; Cambridge Instrument Co., United Kingdom.
[5] EMMA-4 Electron Microscope; AEI Scientific Apparatus Ltd., Manchester, United Kingdom.
[6] Unicam SP 1000 Infra-red Spectrophotometer; Pye Unicam Ltd., Cambridge, United Kingdom.
[7] Siemens AG Kristalloflex 4 Diffractometer; Karlsruhe, West Germany.

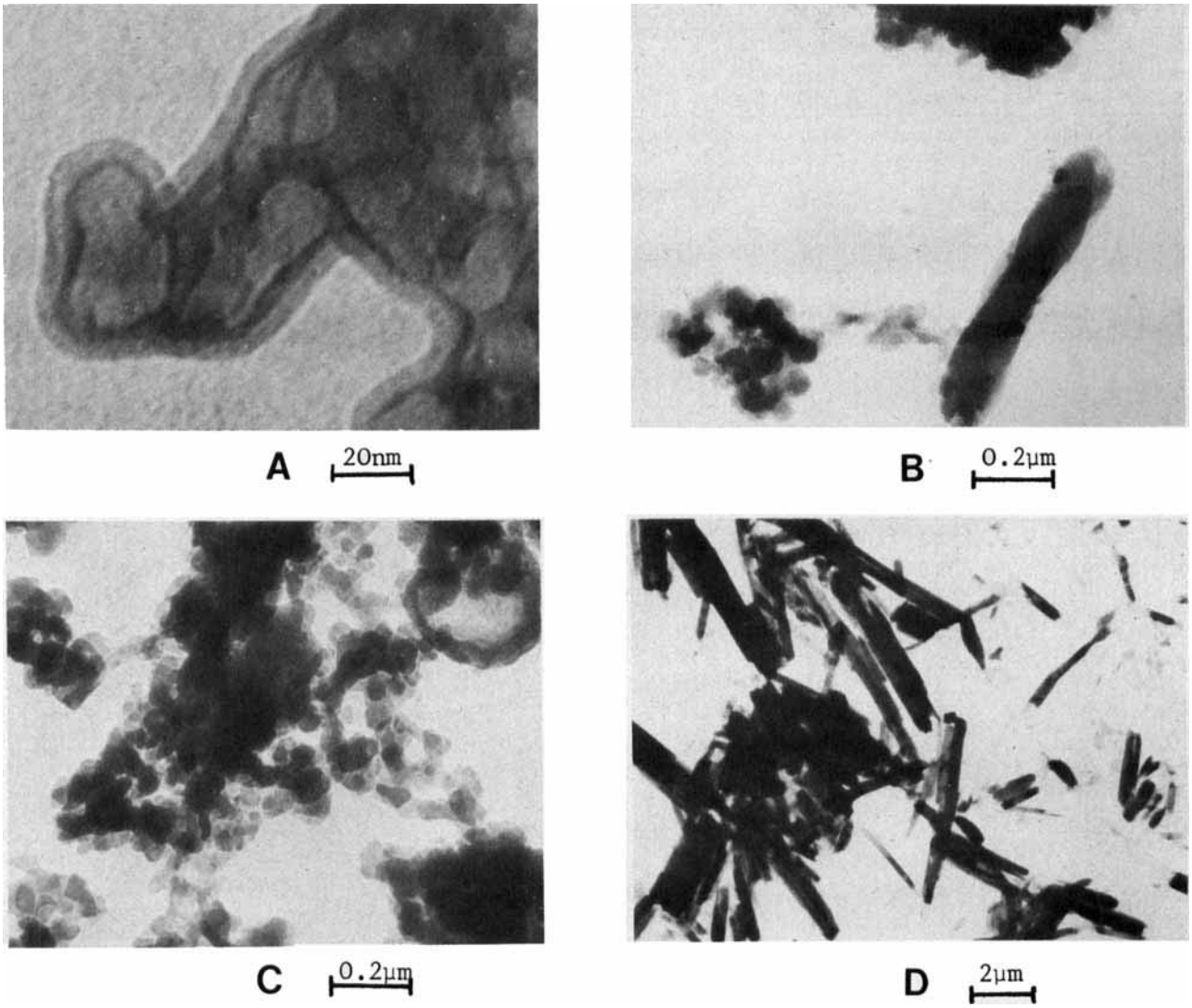

Figure 1—*Transmission electron photomicrographs of precipitated aluminum hydroxide (A), FD & C Blue No. 2 lake (B), FD & C Yellow No. 5 lake (C), and FD & C Blue No. 2 dye (D).*

of the surface area of lakes: the static method[8] using a high-vacuum system and the dynamic method[9].

RESULTS

Aluminum Hydroxide Substrate—Electron microscopy clarifies the morphology of amorphous precipitated aluminum hydroxide, which was freshly prepared (preparation No. 1). With transmission electron microscopy, the agglomerated particulate material, visible at lower magnifications, are composed of 0.1–0.2-μm diameter aggregated entities, which are primary particles of 10 nm × 20–30 nm. Each primary particle is composed of finer units, spherules of 2.5–5-nm diameter and possibly even smaller (as shown in Fig. 1A). The precipitate is thus composed of extremely fine particles (spherules) which are fairly homogeneous. This evidence, by transmission electron microscopy, is a considerable help in dispelling speculation on the structure of the gel. Electron diffraction gave a diffuse halo indicating an amorphous material. With scanning electron microscopy (photographs not shown), the precipitate appears as agglomerated material (~1.6 μm), apparently composed of 0.15-μm particles; also present is particulate material (~60 nm). When the same precipitate was dispersed for 85 h on a paint conditioner[10] in an ethanolic shellac solution, the specimen gave the appearance of 0.3–0.7 μm clusters; the smaller clusters seemed to be composed of spherical particles (40–80 nm) in groups.

The morphology of the various known samples of aluminum hydroxides showed the following features in increasing order of crystallinity as indicated from the diffractograms. Pseudoboehmite (RD 60/78) appears as a more compact gel with a more definite form than amorphous aluminum hydroxide (preparation No. 1). Boehmite (RD 59/78) contains more agglomerated material than pseudoboehmite. Bayerite (57/78) consists of a more organized and substantial material with a more definite outline. Gibbsite (RD 58/78) has a crystalline morphology.

IR spectra were obtained for amorphous aluminum hydroxide, pseudoboehmite, boehmite, bayerite, gibbsite, and aluminum hydroxides Nos. 1–20. Good agreement between the spectra for the nonamorphous hydroxides and literature data (7) was observed. Amorphous aluminum hydroxide (Fig. 2) was almost featureless and many of the aluminum hydroxides (Nos. 1–20) were virtually identical. Others were crystalline forms or these mixed with the amorphous variety, and could be identified from the spectra (*e.g.*, gibbsite has strong bands at 3550, 3490, 1020 cm^{-1}; bayerite at 3580, 3450, 765 cm^{-1}; boehmite at 3320, 3100, 1080 cm^{-1}). Selected spectra in Fig. 2 show a standard prepared amorphous form, a standard boehmite and No. 4, a standard bayerite, and No. 7, and a standard gibbsite and No. 19.

X-ray powder diffraction patterns (Fig. 3) were obtained for the preparations and complement the IR spectra. Amorphous aluminum hydroxide was devoid of lines, while the crystalline forms had the lines at the appropriate angles from which the d-spacings could be related to literature data (8). Figure 3 shows a prepared amorphous form, a standard boehmite and No. 4, a standard bayerite and No. 7, and a standard gibbsite and No. 19.

Aluminum Lakes—Chemical analyses for the standard lakes are tabulated in Table II for dye, sulfate, chloride, and moisture content with an indication of hardness (on an arbitary scale, in which 0 represents a very soft lake and 10 is a very hard lake). For the FD & C Yellow No. 5 lakes made under dif-

[8] Orr Surface Area Pore-Volume Analyzer Model 2100; Micromeritics Instrument Corp., Coulter Electronics Ltd., Dunstable, United Kingdom.
[9] Quantasorb Surface Area Analyzer; Quantachrome Corp., Greenvale, N.Y.
[10] Red Devil Inc., Union, N.J.

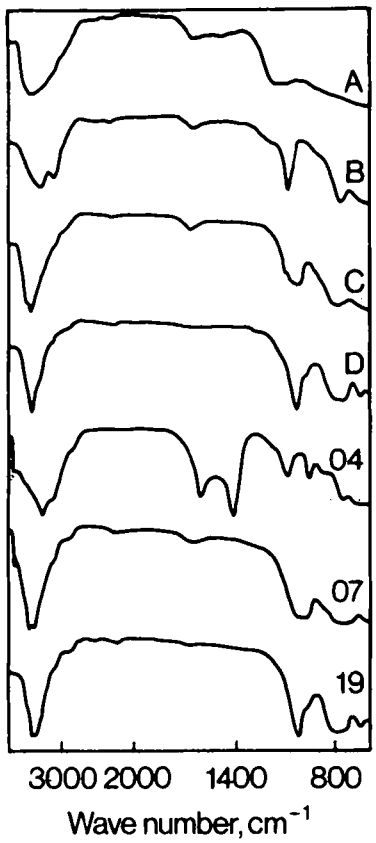

Figure 2—*IR spectra standard of aluminum hydroxides. Key: (A) amorphous; (B) boehmite; (C) bayerite; (D) gibbsite and experimental preparations (Nos. 4, 7, and 19).*

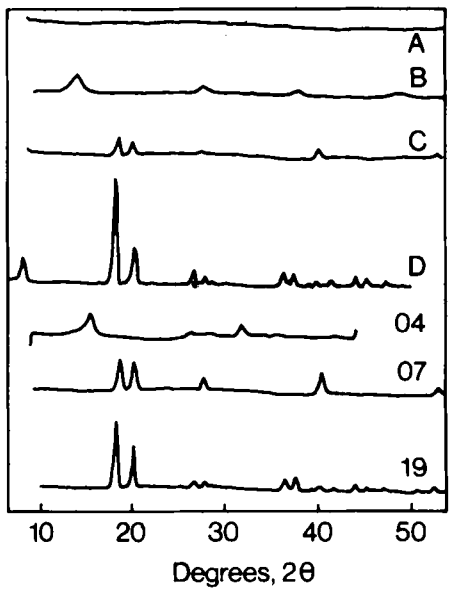

Figure 3—*X-ray diffraction pattern of standard aluminum hydroxides. Key: (A) amorphous; (B) boehmite; (C) bayerite; (D) gibbsite, and experimental preparations (Nos. 4, 7, and 19).*

ferent experimental conditions, the dye and moisture contents with an indication of hardness are shown in Table I. The importance of washing off the sulfate from the aluminum hydroxide substrate is apparent from lake preparation No. 9. The sulfate must compete with dye anions and reduce the dye content of the resulting lake. This has been noted by various patent holders (9).

Transmission electron microscopy shows that the morphology of the FD & C aluminum lakes have a definite similarity to the amorphous aluminum hydroxide (preparation No. 1) but with a denser appearance, presumably caused by a tightly packed layer of dye molecules. FD & C Blue No. 2 lake (B2) contains features of homogeneous "hydroxide" particles as well as cigar-shaped particles (Fig. 1B). FD & C Red No. 40 lake (R40) contains features of homogeneous "hydroxide" particles as well as some U- or oval-shaped particles. FD & C Yellow No. 5 lake (Y5) (Fig. 1C) and FD & C Yellow No. 6 lake (lot No. 634) both have the homogeneous "hydroxide" particles, reminiscent of amorphous aluminum hydroxide. Electron diffraction of the above four lakes gave a diffuse halo indicating the presence of amorphous material. FD & C Blue No. 2 dye (Z7390) appeared as cigar-shaped crystals (Fig. 1D). Electron diffraction gave an array of spots indicating a crystalline material.

Energy dispersive analysis gave a semiquantitative analysis of submicrometer features which conventional forms of analyses cannot do (Table III). Elements lighter than sodium were not detected. For the lakes, the "hydroxide" particles, which are morphologically similar to the amorphous aluminum hydroxide, have a fairly constant composition. The cigar-shaped particles associated with the Blue No. 2 lake and the U- or oval-shaped particles associated with the Red No. 40 lake have a higher sulfur-to-aluminum content. These particulate materials probably originate from the respective dyestuffs and not from the aluminum hydroxide. The composition of the lakes in terms of the ratio of sulfur to aluminum is in broad agreement with the dye content to aluminum hydroxide ratio (corrected for water content) from bulk chemical analysis.

IR spectra were obtained for FD & C Yellow No. 5 dye and lakes Nos. Y5 (preparations 1–21), FD & C Blue No. 2 dye and lake No. B2, FD & C Red No. 40 dye and lake No. R40, and FD & C Yellow No. 6 dye and lake No. 634. The corresponding lakes of amorphous aluminum hydroxide (Y5), boehmite No. 4, bayerite No. 7, and gibbsite No. 19 are depicted in Fig. 4. The composition of other preparations deduced from the spectra are shown in Table I. The spectra of the lakes show a weakening of the intensity for many of the bands compared with the corresponding dyes, indicating some immobilization of the groups. Frequencies with intensities attenuated after lake formation were found at 1415, 1130, 1040, 1010, 720, 695, and 650 cm^{-1} for FD & C Yellow No. 5 lake (No. Y5). There were also minor band shifts from 1190 and 1220 cm^{-1} to 1140 and 1180 cm^{-1}, respectively. These bands are attributable to sulfonate groups (10). There are, however, no new bands in the IR spectra of the lakes; the spectra are additives of those of the dye and aluminum hydroxide substrate.

All the dyes gave strong X-ray powder diffraction patterns. However, the same dyes "laked" on amorphous aluminum hydroxide gave patterns surprisingly devoid of crystalline structure, having only a "memory" of the derived dye. It was found that the crystal structure of the experimentally prepared lakes closely reflect the crystalline state of the substrate. The diffractograms of the corresponding lakes of amorphous aluminum hydroxide No. Y5, boehmite No. 4, bayerite No. 7, and gibbsite No. 19 are shown in Fig. 5. When the boehmite substrate was "laked" (*i.e.*, exposed to pH 3.8 and dye added) the resulting lakes are essentially amorphous forms such as Nos. 4, 5, 6, 14,

Table II—Chemical Analyses of Standard Lakes

FD & C Dye Lake	Dye, %	Sulfate, %	Chloride, %	Moisture, %		Hardness[a]
				Karl Fischer	Dried at 135°C	
Blue No. 2, (Preparation No. B2)	31.5	5.3	0.17	17.3	17.0	4
Red No. 40 (Preparation No. R40)	45.1	2.7	0.03	14.9	14.4	5
Yellow No. 5 (Preparation No. Y5)	37.6	4.8	< 0.01	12.4	14.7	2
Yellow No. 6 (Lot No. 634)	38.2	5.5	< 0.01	19.2	18.6	1

[a] An arbitrary scale: 0 is very soft and 10 is very hard.

Table III—Energy Dispersive Analysis

Sample FD & C Dye	Element	Peak Integral	Relative Proportion[a]	Proportion of atoms	
Blue No. 2 dye	Na	1225	53.3	31	3
(Lot No. Z7390)	S	1102	34.4	20	2
	Cl	60	1.7	1	
Blue No. 2 lake:	Na	292	12.7	1	
(Preparation No. B2)	Al	1761	65.2	5.1	4.3
'Hydroxide' particle	S	498	15.6	1.2	1
'Cigar' particle	Na	539	23.4	1	
	Al	1817	67.3	2.9	1.8
	S	1163	36.3	1.6	1
Red No. 40 dye	Na	1078	46.9	4.6	1
(Lot No. AA7490)	Si	288	10.3	1	
	S	1174	41.9	4.1	1
Red No. 40 lake:	Na	47	2.1	1	
(Preparation No. R40)	Al	1376	51.0	24.3	3.7
'Hydroxide' particle	S	443	13.8	6.6	1
'U' type particle	Na	47	2.1	1	
	Al	1321	48.9	23.3	2.9
	S	529	16.5	7.9	1
Yellow No. 5 dye:	Na	2204	95.8	75.4	1.9
(Lot No. Z9313)	Cl	45	1.3	1	
	S	1586	49.6	39	1
Yellow No. 5 lake:	Al	991	36.7	11.8	5.1
(Preparation No. Y5)	Si	87	3.1	1	
	S	227	7.1	2.3	1
Yellow No. 6 lake:	Na	49	2.1	1	
(Lot No. 634)	Al	1743	64.6	30.3	3.0
	S	695	21.7	10.2	1

[a] Divided by atomic weight.

and 18. Under the acidic conditions of the lake formation process, the boehmitic structure is probably destroyed or modified to an amorphous form of aluminum hydroxide to which the dye is adsorbed. In contrast, the bayerite and gibbsite forms are resistant to phase changes during lake formation. A summary of the effect of preparation method on the type of aluminum hydroxide and the lake obtained is given in Table I.

Gas adsorption results were obtained for the surface areas of aluminum lakes and the substrate of amorphous aluminum hydroxides (Table IV). The Quantasorb gives a favorable comparison with the static method for the specific surface area of a Yellow No. 5 lake (lot No. 127).

DISCUSSION

The conditions of preparation have a profound effect on the type of aluminum hydroxide produced and this in turn influences the dye content and physical properties of the resulting lakes. By means of two complementary techniques, X-ray diffraction and IR spectroscopy, it is possible to decide the type of aluminum hydroxide present.

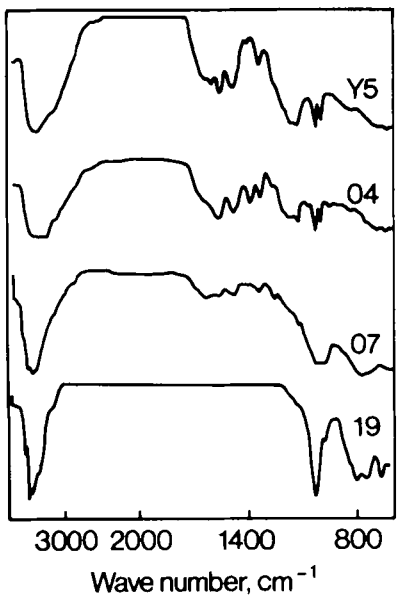

Figure 4—*IR spectra of experimentally prepared FD & C Yellow No. 5 dye and lakes Nos. Y5, 4, 7, and 19.*

An amorphous aluminum hydroxide gel was produced by the standard method of lake preparation (No. Y5) of aluminum hydroxide from aluminum sulfate and sodium carbonate at pH 6.9. An amorphous product was also obtained from the same reagents at pH 9 with 14 d aging at room temperature (No. 1) and at pH 4.5 (No. 10). When sodium bicarbonate was employed as a base (No. 12) or mixed with sodium carbonate (No. 11) an amorphous gel was prepared. The resulting lakes had a dye content of 36–39% dye (Table I). The preparation (No. 10) with the gel precipitated at pH 4.5 and had a slightly lower dye content of 32%; this may be because some of the aluminum ions were still in solution and the gel was not fully formed. The X-ray patterns for the gel and resultant lakes were featureless.

Petz (11) studied the structure of amorphous aluminum hydroxide gels by radial distribution functions computed from X-ray measurements. He found that the Al^{3+} ion is coordinated by an octahedral arrangement of oxygen sites and the relationship between the remaining oxygens is essentially the same as in water. An "icelike" quasi-lattice was postulated. Recently, Oka *et al.* (12) considered amorphous anodic alumina films to contain AlO_5 coordination polyhedra as well as AlO_4 tetrahedra and AlO_6 octahedra. These polyhedra are envisaged to be arranged in a mixture of two conformations, one of which is a crystalline modification of γ-Al_2O_3 within a short range of radial distance of <0.45 nm and the other is a conformation with randomly arranged coordination polyhedra.

Transmission electron microscopy of amorphous precipitated aluminum hydroxide gel shows "primary" particles of 10 nm × 20–30 nm existing as aggregated entities of 0.1–0.2-μm diameter, but each "primary" particle is apparently composed of still finer spherules of 2.5–5-nm diameter and possibly

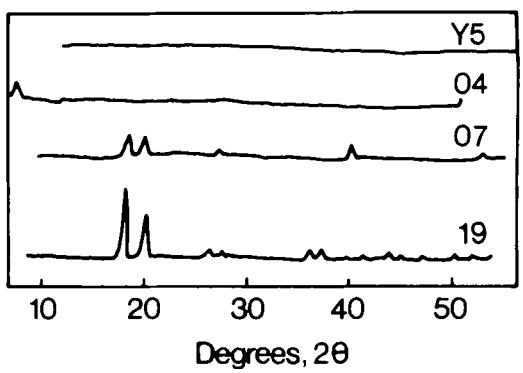

Figure 5—*X-ray diffraction patterns of experimentally prepared FD & C Yellow No. 5 dye and lakes Nos. Y5, 4, 7, and 19.*

Table IV—Surface Area Measurements of Aluminum Lakes and Their Aluminum Hydroxide Substrate

Sample	Surface Area, m^2/g
	Static Method
FD & C Yellow No. 5 Lake (Lot No. 127)	13.6
	Quantasorb
FD & C Yellow No. 5 Lake (Lot No. 127)	14.1
FD & C Yellow No. 5 Lake (Preparation No. Y5)	33.0
FD & C Yellow No. 6 Lake (Lot No. 634)	27.0
FD & C Blue No. 2 Lake (Preparation No. B2)	27.5
FD & C Red 40 Lake (Preparation No. R40)	18.2
Amorphous Aluminum Hydroxide (Preparation No. 1)	114

even smaller (Fig. 1A). This is in accordance with Lippens and Steggerda (13), who are of the opinion that amorphous material consists of spherical particles 2–5 nm in diameter, loosely aggregated to bigger units.

From the nitrogen adsorption results, the standard lakes have specific surface areas less than one-third of that for the substrate amorphous aluminum hydroxide (Table IV). This may be interpreted as follows: the adsorbed layer of dye molecules on the surface of the aluminum hydroxide envelopes the micropores (pores with radii $< \sim 1.5$ nm) and probably some of the mesopores (intermediate pores with radii of 1.5–100 nm). Thus, in the lakes, nitrogen can only be adsorbed on the dye-enveloped aluminum hydroxide, which is "smoother" since the larger dye molecules are either blanketing the micropores so that there are fewer sites for adsorption or else steric hindrance repels the nitrogen molecules, resulting in a considerable reduction in the measured specific surface area.

X-ray diffraction of the FD & C dyes, *i.e.*, Blue No. 2, Red No. 40, and Yellow Nos. 5 and 6, all show a large number of sharp lines, indicating the dyes are highly crystalline. However, lake formation of the same dyes with amorphous aluminum hydroxide gives a rather diffuse X-ray pattern in the region of the sharp lines of the dyes. The lakes are thus amorphous. Electron diffraction, associated with transmission electron microscopy, also gives the same results. Electron diffraction enables small, identifiable regions of a few cubic micrometers to be examined, whereas X-ray diffraction needs several cubic millimeters of sample, although the information obtained by the latter is more accurate.

Kiel and Heertjes (14) found that the calcium–aluminum lake of alizarin shows four sharp lines on a powder X-ray diagram indicating that the substance is highly crystalline. Furthermore, its IR spectra had some new bands, which the alizarin did not exhibit.

The IR spectra of the FD & C dyes have a number of peaks of strong intensity while the corresponding lakes have attenuated absorption bands. Since the bands attributed to sulfonate groups are immobilized, the IR spectra indicate that in all the lakes used, the sulfonate group is involved in bonding the dye to the aluminum hydroxide. This conclusion is in agreement with Cummings *et al.* (15), who suggested that the adsorbed dye anions forming the monolayer could be composed of monodispersed anions, each orientated with all the sulfonate groups as close as possible to the surface. The adsorption mechanism is probably an exchange of chloride ions for the adsorbed anions, but there may also be some covalent bonding occurring. In the laking process, pretreatment of the substrate with an acid covers the surface with anions that may be either covalently bound or present as ions. The anion may be replaced by dye anion, and it is this reaction that is the basis of the alumina dyeing process (16, 17). Under the laking conditions (pH 3.8–4.0) the aluminum hydroxide particles are positively charged enabling interaction to take place with anionic dyes. The importance of the surface charge on aluminum hydroxide particles and its dependence on pH has been recently studied (18–21).

Boehmite was produced from aluminum sulfate and sodium carbonate under alkaline conditions, but the condition of pH 7.4 for 2 h at 70°C produced pseudoboehmite, which was boehmite in an excess of amorphous gel (No. 2). Preparations at pH 10 and aging under various conditions also produced boehmite (Nos. 3, 4, 5, and 6). Aluminum nitrate and aluminum chloride, precipitated with sodium carbonate under alkaline conditions (pH 10), also produced a boehmitic gel (Nos. 14 and 18, respectively). Some of the boehmites produced lakes with a higher dye content than with the amorphous gels, *e.g.*, No. 6 contains 51% and No. 18 47% dye content but these were both very hard (Table I).

There is controversy in the literature concerning the mechanism by which aluminum hydroxide gels change during the aging process. The term "aging" is used to connote all irreversible structural or textural changes in the colloidal system which may occur after flocculation or gelation (22). Aging is a complex phenomenon. Water plays a key role in all the aging mechanisms. The poorly organized flocculated hydroxide prepared from salts of hydrated cations usually contains large quantities of molecular water (22). Baker and Pearson (23) propose that it is not a large conceptual step from the hydrolytic polymers in aluminum salt solutions [the dimer, $Al_2(H_2O)_8(OH)_2^{4+}$, for example] to the small boehmite-like crystallites capable of giving an X-ray diffraction pattern. Thus, pseudoboehmite is nothing more than an aggregate of ultra small boehmite-like crystallites, and a boehmitic pattern in crystallites as small as ~2.5 nm can be detected. The end point of the hydrolytic polymerization may be either an infinite series of chains (*i.e.*, the boehmitic-like materials) or ring structures (*i.e.*, gibbsite or bayerite).

Serna *et al.* (24) have found that sulfate and carbonate anions both show evidence of coordination with the surface aluminum cations. The carbonate interaction appears to be the strongest and is believed to be responsible for the relatively high degree of stability of carbonate-containing aluminum hydroxide gel. This could explain why the gel from sodium carbonate did not age beyond boehmite at pH 10. Only Baker and Pearson's (23) chain structure could be formed and not the ring structure. It is interesting to see from the X-ray diffraction patterns that the boehmite degenerated to various amorphous forms after lake formation, although IR spectroscopy still detected the boehmite.

On aging of the precipitate at pH ~12, gibbsite is formed from sodium hydroxide with aluminum nitrate (No. 15), and similarly with aluminum chloride (No. 19). However, at 60°C with aging, some less well crystallized material is formed: sodium hydroxide with aluminum nitrate (No. 17) forms gibbsite with bayerite and boehmite, while sodium hydroxide with aluminum chloride (No. 20) forms gibbsite and bayerite. It is noteworthy that the aged product of aluminum sulfate precipitated with sodium hydroxide at pH 12 is in the form of bayerite (No. 7). The reason may be that the sulfate coordinates to the aluminum and inhibits crystallization to the gibbsite phase. The aluminum nitrate and chloride salts, precipitated with sodium hydroxide at pH 12 with aging, both crystallize to the same end product, gibbsite. This is in line with the hypothesis that the rate of aluminum hydroxide crystallization is inversely related to the tendency of anion inclusion in aluminum hydroxide precipitates (25). The precipitation at 60°C to produce a mixed product (gibbsite plus bayerite or boehmite) happens since at elevated temperature there is a "fast" transformation to a boehmitic structure which only slowly, with aging, crystallizes to the trihydroxides.

The lakes containing gibbsite or bayerite have a much lower dye content than the amorphous lakes [lake Nos. 7, 17, and 19 contain 8, 5, and 8%, respectively, while gibbsite crystals (No. 21) adsorb a negligible amount of dye (Table I)]. This may be explained from surface area considerations. Crystalline gibbsite evidently has the least surface area available for adsorption of dye since most of the aluminum atoms are incorporated in the crystal lattice and are unavailable for adsorption. The morphology of gibbsite from transmission electron microscopy consists of straight edges and hexagonal shapes. Lippens (26) prepared gibbsite crystals in the form of hexagonal platelets of diameter 0.3 μm, and rod-shaped crystals 10×3 μm^2. Hence the surface area was quite small. Bayerite particles range from ~50 to 100 nm upwards, forming larger aggregates. Lippens (26) found that the surface area of bayerite was 6–75 m^2/g and his micrographs showed bayerite particles, called somatoids, which had a variable size, with the width being mostly smaller than 0.5 μm with a length 3–10 times the width. In contrast, Lippens and Steggerda (13) found the surface area of gelatinous boehmite to be ~200–500 m^2/g. An amorphous gel of spherical particles of 2–5-nm diameter would be expected to give a surface area of ~1000 m^2/g, but Lippens and Steggerda (13) were unable to measure the surface area by the nitrogen Brunauer, Emmett, and Teller (BET) method, since it was found that the surface was not accessible to nitrogen.

Recently, Pyman and Posner (27) have questioned the meaning of the term "surface area," since amorphous materials generally have large surface areas of 50–1000 m^2/g, a considerable pore structure which is frequently microporous, and contain appreciable quantities of water, both adsorbed onto the surface and incorporated into the structure. They suggest that assignment of a specific surface area to amorphous materials should be related to the purpose for which the surface is to be used and that the value is dependent on the method. With lakes formed from the amorphous aluminum hydroxide gel, which are believed to be composed of spherules 2.5–5 nm in diameter from the transmission electron microscopy work, the envisaged surface area of 1000 m^2/g may be regarded as an effective surface area from the viewpoint of the dye anions. Such a surface is not accessible to nitrogen adsorption, which gives a lower surface area value of 114 m^2/g $Al(OH)_3$ (Table IV). It appears that nitrogen envelopes the 10–30 nm particles without being able to reach the spherules of 2.5–5 nm.

From these considerations the following picture of lake formation is proposed. In aluminum lakes, the amount of dye adsorbed on the aluminum hydroxide is dependent on its surface area. The dye molecules are envisaged to form a monolayer on the surface of amorphous aluminum hydroxide spherules of 2.5–5-nm diameter, which provides sufficient surface area to account for

the 30–40% dye content of aluminum lakes. Direct evidence for the existence of these spherules comes from the highest power transmission electron micrographs. This conclusion is supported by the work of Lippens and Steggerda (13) who have also described amorphous aluminum hydroxide gel as being composed of 2–5-nm diameter spherical particles, loosely aggregated to form larger units. Further it agrees with the results of Bye and Chigbo (28) where they found weakly bonded flocs of apparently isometric particles of ~5 nm.

The quantity of dye adsorbed in terms of mmol dye/g Al_2O_3 [notation after de Boer *et al.* (29)] is readily calculated from the lake dye content. Since aluminum hydroxide has a variable water content, the formula $2Al(OH)_3$ may be written as $Al_2O_3 \cdot 3H_2O$, and Al_2O_3 is expressed as that equivalent amount of aluminum hydroxide with no water content. For aluminum lakes, the quantity of dye adsorbed was found to be ~2 mmol/g Al_2O_3 for Blue No. 2 and Yellow No. 5 and ~3 mmol/g Al_2O_3 for Yellow No. 6 and Red No. 40. Giles *et al.* (16) have made studies of dye adsorption on anodic films and found that for disulfonated dyes there was a maximum adsorption of ~0.2 mmol/g corresponding to ~100 m^2/g, the adsorbed dye molecule generally being orientated "edge-on." Since aluminum lakes contain about 10 times more dye than the anodic films of Giles, this suggests that the surface area of substrate covered would be in the order of 1000 m^2/g and is consistent with the spherule size of 2.5–5-nm diameter. However, the nitrogen gas adsorption results give a surface of area of amorphous aluminum hydroxide gel compatible with a "primary" particle size of 10 nm × 20–30 nm. The surface of the 2.5–5-nm diameter spherules is presumably inaccessible to nitrogen and thus the smallest particle penetrable by nitrogen may contain many crystallites. Baker and Pearson (23) suggested that the packing of these crystallites reduces the accessible surface to nitrogen. It may be firmly concluded that the evidence points to the dye being surface adsorbed on very small particles, mainly <50 nm.

These experiments provide good evidence that the fully amorphous type of aluminum hydroxide is the best form for lake formation confirming what is empirically known within the industry. It is also evident that the gel should be washed free of sulfate ion before laking to avoid interference with dye adsorption. The conditions under which the aluminum hydroxide is prepared governs the degree of amorphous/crystalline character of the product, which is reflected in changes in particle size and surface area of the aluminum hydroxide. This then controls the amount of dye taken up. Although lakes can be formed from boehmite, the product is usually hard and glassy; thus the product is unsuitable for industrial use. The crystalline trihydroxides, bayerite and gibbsite, produced under aging conditions, take up considerably less dye. Gibbsite crystals take up a negligible amount of dye. To prevent lake formation failure, aging conditions, which are likely to produce the crystalline forms of aluminum hydroxide, should be avoided.

REFERENCES

(1) A. W. C. Harrison, "The Manufacture of Lakes and Precipitated Pigments," revised by J. S. Remington and W. Francis, Leonard Hill Ltd., London, 1957, pp. 180–182.

(2) "Official Methods of Analysis of the Association of Official Analytical Chemists," 11th ed., W. Horwitz, Ed., Association of Official Analytical Chemists, Washington, 1970, p. 591.

(3) "British Standard Methods for the Determination of Water," Karl Fischer Method, B.S. 2511, British Standards Institution, London, 1970.

(4) "Specifications for Identity and Purity of Food Additives," vol. 2, Food and Agriculture Organization of the United Nations/World Health Organization, Rome, 1963, p. 121.

(5) "British Standard Methods for the Analysis of Water-Soluble Coal-Tar Dyes Permitted for Use in Foods," B.S. 3210, British Standards Institution, London, 1960, p. 14.

(6) A. I. Vogel, "A Textbook of Quantitative Inorganic Analysis Including Elementary Instrumental Analysis," 3rd ed., Longmans, London, 1961, reprinted 1972, pp. 462–465.

(7) H. W. Van der Marel and H. Beutelspacher, "Atlas of Infrared Spectroscopy of Clay Minerals and Their Admixtures," Elsevier, Amsterdam, The Netherlands, 1976, pp. 194–195.

(8) "Selected Powder Diffraction Data for Minerals," 1st ed., Joint Committee on Powder Diffraction Standards (JCPDS), Publication DBM-1-23, Philadelphia, 1974.

(9) F. J. Curtis, U.S. Pat. No. 2,053,208 (1936).

(10) L. G. Bellamy, "The Infra-red Spectra of Complex Molecules," Vol. 1, 3rd ed., Chapman and Hall, London, 1975, pp. 394–408.

(11) J. I. Petz, *J. Chem. Phys.*, **48,** 909 (1968).

(12) Y. Oka, T. Takahashi, K. Okada, and S. Iwai, *J. Non-Cryst. Solids*, **30,** 349 (1979).

(13) B. C. Lippens and J. J. Steggerda, "Physical and Chemical Aspects of Adsorbents and Catalysts," B. G. Linsen, Ed., Academic, London, 1970, pp. 171–211.

(14) E. G. Kiel and P. M. Heertjes, *J. Soc. Dyers Colour*, **79,** 21 (1963).

(15) T. Cummings, H. C. Garven, C. H. Giles, S. M. K. Rahman, J. G. Sneddon, and C. E. Stewart, *J. Chem. Soc.*, **1959,** 535.

(16) C. H. Giles, H. V. Mehta, S. M. K. Rahman, and C. E. Stewart, *J. Appl. Chem.*, **9,** 457 (1959).

(17) C. H. Giles and K. V. Datye, *Trans. Inst. Met. Finish.*, **40,** 113 (1963).

(18) C. J. Serna, J. L. White, and S. L. Hem, *Soil Sci. Soc. Am. Proc.*, **41,** 1009 (1977).

(19) A. Tentorio, E. Matijevic, and J. P. Kratohvil, *J. Colloid Interface Sci.*, **77,** 418 (1980).

(20) J. R. Feldkamp, D. N. Shah, S. L. Meyer, J. L. White, and S. L. Hem, *J. Pharm. Sci.*, **70,** 638 (1981).

(21) D. N. Shah, J. R. Feldkamp, J. L. White, and S. L. Hem, *J. Pharm. Sci.*, **71,** 266 (1982).

(22) G. C. Bye and K. S. W. Sing, in "Particle Growth in Suspensions," A. L. Smith, Ed., Academic, London, 1973, pp. 29–45.

(23) B. R. Baker and R. M. Pearson, *J. Catal.*, **33,** 265 (1974).

(24) C. J. Serna, J. L. White, and S. L. Hem, *J. Pharm. Sci.*, **67,** 1144 (1978).

(25) G. J. Ross and R. C. Turner, *Soil Sci. Soc. Am. Proc.*, **35,** 389 (1971).

(26) B. C. Lippens, Ph.D. Thesis, University of Technology, Delft, The Netherlands, 1961, Chap. 1.

(27) M. A. F. Pyman and A. M. Posner, *J. Colloid Interface Sci.*, **66,** 85 (1978).

(28) G. C. Bye and G. O. Chigbo, *J. Appl. Chem. Biotechnol.*, **23,** 589 (1973).

(29) J. H. de Boer, G. M. M. Houben, B. C. Lippens, W. H. Meijs, and W. K. A. Walrave, *J. Catal.*, **1,** 1 (1962).

ACKNOWLEDGMENTS

The award to L. L-S. Wou of a research scholarship by Colorcon, Inc. is gratefully acknowledged. The authors thank Dr. K. Marshall for advice and help. The technical assistance of Mr. G. Cliff (Department of Metallurgy, University of Manchester) with electron microscopy and Dr. G. Hornung (Department of Earth Sciences, University of Leeds) with X-ray diffractometry is appreciated.

Determination of Trimipramine and Metabolites in Plasma by Liquid Chromatography with Electrochemical Detection

RAYMOND F. SUCKOW [x] **and THOMAS B. COOPER** *

Received November 28, 1983, from the *Analytical Psychopharmacology Laboratory, Nathan S. Kline Institute for Psychiatric Research, Orangeburg, NY 10962* and the **New York State Psychiatric Institute, 722 West 168th Street, New York, NY 10032.* Accepted for publication March 9, 1984.

Abstract □ A procedure for the determination of trimipramine, the demethyl, 2-hydroxy, and 2-hydroxy demethyl metabolites in plasma by liquid chromatography with electrochemical detection is described. A 1-mL plasma sample is made alkaline with a carbonate buffer (pH 9.8) and extracted with 20% ethyl acetate in *n*-heptane. After back-extraction into an acid phosphate buffer, an aliquot is injected onto a reverse-phase trimethylsilyl-packed column and eluted with a phosphate buffer–acetonitrile mobile phase (65:35) containing *n*-butylamine. The peaks were detected at +1.1 V *versus* the silver–silver chloride reference electrode. The method provides absolute recoveries of 60–91% and a day-to-day precision of <9% for all compounds. The minimum quantifiable level for all compounds was 3 ng/mL. Steady-state plasma concentration data for 29 depressed patients receiving either 75 mg or 150 mg/d is reported.

Keyphrases □ Trimipramine—metabolite detection, HPLC, electrochemical detection, human plasma □ HPLC—electrochemical detection, trimipramine and its metabolites

Trimipramine (I) is a relatively recent addition to the structurally related dibenzazepine class of tricyclic antidepressants. It differs chemically from the prototype imipramine by a replacement of the *n*-propyl side chain with a 2-methyl propyl group. A review of its clinical use has been presented (1).

Trimipramine has been included in many tricyclic antidepressant methodologies either as an internal standard or for the purpose of demonstrating its chromatographic separation from other tricyclic antidepressants. Presently, there are two reports of its quantitation in plasma with respect to its therapeutic use. One method does not include its metabolites nor present any clinical data derived from its measurement (2). Another report (3) describes a GC procedure and its application to the pharmacokinetics of trimipramine only.

Since trimipramine is structurally very similar to imipramine one might expect its metabolic profile to be similar. We therefore developed an HPLC assay that will separate and quantitate I and its known major metabolites—the demethyl metabolite (II), the 2-hydroxy metabolite (III) and the 2-hydroxy demethyl metabolite (IV). Fixed-dose steady-state plasma concentration data for 29 patients are reported.

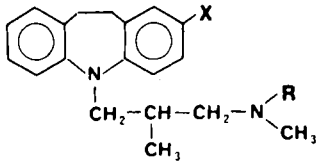

I: X = H, R = CH_3
II: X = H, R = H
III: X = OH, R = CH_3
IV: X = OH, R = H

EXPERIMENTAL SECTION

Apparatus and Reagents—Chromatography was performed using a dual piston solvent delivery pump[1] and an automatic sampler[2]. The column was 25 cm × 4.6 mm i.d. packed with 5-μm particle size trimethyl silyl material[3]. The detector system consisted of a thin-layer flow through electrochemical transducer[4]. The potential and current response were monitored by an amperometric controller[5] and recorder[6] and interfaced with a laboratory data acquisition system[7]. An aluminum column temperature control block was devised to fit the column and the temperature controlled by a circulating water bath[8]. Voltammograms were performed by a cyclic voltammetry instrument[9] and recorded on an X-Y recorder[10]. The potential was scanned from 0.0 to +1.3 V *versus* silver–silver chloride reference electrode at 180 mV/s. Glassy carbon was used as the working electrode.

Phosphoric acid[11], monobasic potassium phosphate[11], sodium carbonate[11], and potassium bicarbonate[11] were all analytical reagent grade. Acetonitrile-UV[12], *n*-heptane[11], *n*-butylamine[11], and β-glucuronidase[13] were used as received. Ethyl acetate[11] was purified through a silica-packed column prior to use. Distilled water was passed through a water purification system[14] before use.

Standards—One milligram (free base) per milliliter of stock solutions of trimipramine maleate (I)[15], the demethyl metabolite (maleate salt) (II)[15], the 2-hydroxy metabolite (fumarate salt) (III)[15], the 2-hydroxy demethyl metabolite (fumarate salt) (IV)[15], the didemethyl metabolite (maleate salt) (V)[15], and mianserin hydrochloride (VI)[16] were prepared in 0.01 M HCl. All stock solutions were further diluted with 0.01 M HCl to give working solutions of 1 μg/mL. Working standards of III and IV were prepared as 10 μg/mL for conjugate studies.

Standard curves were prepared containing five levels of spiked samples: 25, 50, 100, 200, and 400 ng/mL of I and II, and 12.5, 25, 50, 100, and 200 ng/mL of III and IV. For total III and IV, 100, 250, 500, 1000, and 2000 ng/mL spiked samples were prepared.

Extraction—The internal standard, mianserin (75 μL = 75 ng), and 0.5 mL of 0.6 M potassium bicarbonate–sodium carbonate buffer (pH 9.8) were added to 1.0 mL of plasma sample. Seven milliliters of 20% v/v ethyl acetate in *n*-heptane was added, the contents were mixed for 15 min and then centrifuged at 1500×*g* for 10 min. The organic layer was transferred to a 15-mL tapered centrifuge tube containing 0.25 mL of acidic phosphate buffer (0.025 M KH_2PO_4 adjusted to pH 2.5 with 85% H_3PO_4). After mixing for 10 min and centrifuging at 1500×*g* for 10 min, the organic layer was discarded and the aqueous portion was transferred to a small glass vial[17] and capped. Suitable aliquots were injected for chromatographic separation.

For the analysis of the 2-hydroxy and 2-hydroxy demethyl metabolites III and IV (total, free and conjugated), the pH of 0.5 mL of plasma was adjusted to 4.7 with the addition of 0.5 mL of 0.2 M KH_2PO_4. Then, 25 μL of β-glucuronidase solution was added to each tube and the mixture was incubated for 24 h at room temperature. Fifty microliters of 2 M NaOH, 50 μL (500 ng) of internal standard, mianserin, 0.5 mL of carbonate buffer, and 7 mL of 20% v/v ethyl acetate in *n*-heptane were added and the extraction was carried out as previously described. Standards containing III and IV were treated in the manner described above (including the incubation procedure).

[1] Model 6000A; Waters Associates, Milford, Mass.
[2] WISP 710B; Waters Associates.
[3] LC-1, Supelco; Bellefonte, Pa.
[4] TL-5A; Bioanalytical Systems, West Lafayette, Ind.
[5] Metrohm Model E-611 V/A Detector; Brinkmann Instruments Inc., Westbury, N.Y.
[6] Omniscribe Model B-5217B-2; Houston Instruments, Austin, Tex.
[7] PDP 11/34; Digital Equipment Corp., Maynard, Mass.
[8] Model FE; Haake Co., Saddlebrook, N.J.
[9] Model CV-1B; Bioanalytical Systems.
[10] Model 7034A; Hewlett Packard, Palo Alto, Calif.
[11] Fisher Scientific Co., Fair Lawn, N.J.
[12] Burdick-Jackson Laboratories, Muskegon, Mich.
[13] Glusulase; Endo Laboratories, Garden City, N.Y.
[14] Milli-Q; Millipore Corp., Bedford, Mass.
[15] Ives Laboratories Inc., New York, N.Y.
[16] Organon Laboratories, West Orange, N.J.
[17] Low Volume Inserts; Waters Associates.

0022-3549/84/1200-1745$01.00/0
© 1984, American Pharmaceutical Association

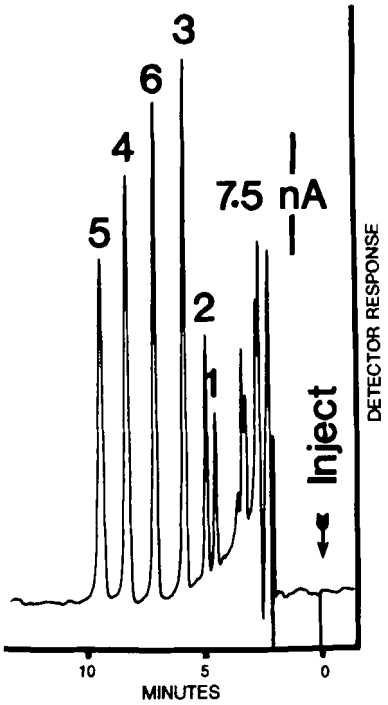

Figure 1—*A chromatogram of a spiked 1-mL plasma extract containing 25 ng each of III and IV (2 and 1) and 50 ng each of I, II, and V (5, 4, and 6). Actual patient samples showed little or no V (6). Mianserin (3) is the internal standard.*

Chromatographic Conditions—The mobile phase consisted of 0.05 M monobasic potassium phosphate-acetonitrile (65:35) with the addition of 1.2 mL/L of *n*-butylamine and 1.0 mL/L of phosphoric acid. The mixture was filtered and deaerated prior to use. The flow rate was 1.5 mL/min and the column temperature was set at 32°C. Detector potential was set at +1.10 V *versus* silver-silver chloride reference electrode.

Quantitation—All determinations were performed by calculating the peak height ratios of each compound to the internal standard. A linear regression analysis for each of the standard curves was performed by a computer program resulting in the calculations of slope, *x*-intercept, correlation coefficient, and standard error.

RESULTS AND DISCUSSION

Trimipramine (I) and its major metabolites (II, III, and IV) were separated in a single chromatogram in <10 min. Figure 1 illustrates a typical chromatogram of a spiked plasma sample. A blank plasma extract showed no endogenous interfering peaks.

The optimum oxidation potential of I–IV was determined by cyclic voltammetry. The presence of the 2-hydroxy groups on III and IV lowers the oxidation potential from that of the parent compound I. This profile, not surprisingly, resembles that of imipramine and its major analogous metabolites (4). Proposed mechanisms for the electrochemical oxidation of these compounds have been presented (5–7). The electrochemical oxidation profile for mianserin has been reported with the optimum being ~ +1.1 V *versus* the silver-silver chloride reference electrode (8).

The precision of this method was determined by spiking eight 1.0-mL aliquots of drug-free plasma with various levels of drug and metabolites. After the addition of 75 ng of internal standard, the samples were processed as described. The percent relative standard deviation for various levels are reported in Table I. Day-to-day accuracy was checked after runs over 7 consecutive days. The linear regression slopes as well as the quality control samples were assessed and are presented in Tables II and III.

Table I—Within-Run Variability of Trimipramine and Its Metabolites [a]

Concentration, ng/mL	*RSD*, %			
	I	II	III	IV
400	3.7	7.0		
200			2.1	4.4
100	1.6	3.7		
50			3.0	3.8
25	4.9	12.2		
20			3.7	5.2
5	5.1	9.6	10.4	12.1

[a] $n = 8$.

Table II—Linear Regression Data for the Standard Curve [a]

Compound	Slope, ng/mL	*x*-intercept, ng/mL	*r*
I	75.4 ± 2.58	1.63 ± 1.08	0.9999 ± 0.0001
II	63.1 ± 5.28	1.92 ± 4.22	0.9997 ± 0.0002
III	51.2 ± 3.28	1.72 ± 1.88	0.9995 ± 0.0005
IV	85.5 ± 7.47	1.21 ± 2.11	0.9992 ± 0.0015

[a] Data (mean ± *SD*) computed from seven consecutive standard curves.

Table III—Quality Control Data [a]

Compound	Amount added, ng/mL	Amount found, ng/mL	*RSD*, %
I	100	101	4.4
II	100	98	9.3
III	50	52	8.0
IV	50	51	6.5

[a] Data computed from quality control samples analyzed on seven consecutive days.

Table IV—Recovery of Trimipramine and Its Metabolites [a]

Compound	200 ng		25 ng	
	Percent	*RSD*, %	Percent	*RSD*, %
I	74	6.0	71	7.5
II	79	6.5	72	9.9
III	91	7.0	83	6.6
IV	60	6.4	59	5.7

[a] From 1 mL of plasma; $n = 8$.

The absolute recovery was determined by preparing a solution of known concentrations of all compounds, I–IV. The internal standard was added to each solution and the sample injected into the chromatograph. The same standards were added to 1 mL of plasma and processed routinely except for the internal standard. To the final acid extract, 75 ng of internal standard was added, mixed, and injected. The difference between the ratios of the standards to internal standard in processed sample *versus* the direct injection samples gave a measure of overall recovery (Table IV).

The absolute sensitivity ($S/n = 3$) of this method was 0.5-ng injected for all compounds (I–IV). In practical terms, however, the lowest quantifiable levels were ~3 ng/mL of plasma. Linearity was checked up to 500 ng.

Interfering peaks occurred in samples from patients receiving imipramine, desipramine, chlorimipramine, chlorpromazine, amoxapine, loxapine, trazodone, and haloperidol. Other tricyclic and tetracyclic antidepressants such as amitriptyline, nortriptyline, protriptyline, doxepin, and maprotiline do not interfere since they are not electroactive under these conditions. Some commonly used benzodiazepines (flurazepam, diazepam, and chlordiazepoxide) also do not interfere because they do not respond electrochemically at these conditions. This selectivity is one advantage of the electrochemical detector over a UV detector at the frequently used wavelength of 254 or 214 nm.

The extraction procedure was developed specifically for the simultaneous recovery of I–IV as well as VI. The pH of the plasma must be between 9–10 for optimum recovery of III and IV. The use of 20% v/v ethyl acetate in *n*-heptane was sufficiently polar enough to extract III and IV and at the same time did not cause variability in recoveries of I, II, and VI as was frequently encountered when using a 5–10% v/v isoamyl alcohol in *n*-heptane mixture or when using methyl *tert*-butyl ether.

When hydrolyzing plasma for the preparation of samples for the measurement of the total (conjugated and unconjugated) III and IV, an attempt was made to prevent decomposition of these hydroxy metabolites by the addition of an antioxidant. A previous report (9) indicated that the addition of ascorbic acid to the plasma hydrolysis buffer prevented a rapid decomposition of 2-hydroxydesipramine. We found this to be true not only for 2-hydroxydesipramine but for 2-hydroxyimipramine. However, the two hydroxy metabolites of trimipramine did not appear to be susceptible to this decomposition. Thus, no ascorbic acid was added to the hydrolysis buffer.

To check the validity of this assay, 100 samples were randomly selected and analyzed for I by GC with a nitrogen detector using a modified procedure developed initially for imipramine (10). The correlation coefficient between the two methods was 0.980, with HPLC = 0.942 (GC) −1.6.

Plasma samples from 29 different patients receiving either 75 or 150 mg/d

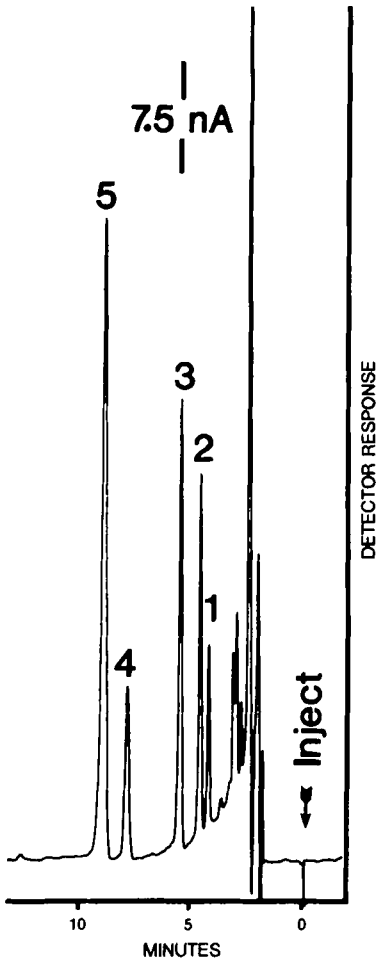

Figure 2—*A chromatogram of an extract of 1 mL of plasma from a patient receiving 150 mg/d of trimipramine. Concentrations were: I (5), 111 ng/mL; II (4), 25 ng/mL; III (2), 40 ng/mL; IV (1), 32 ng/mL.*

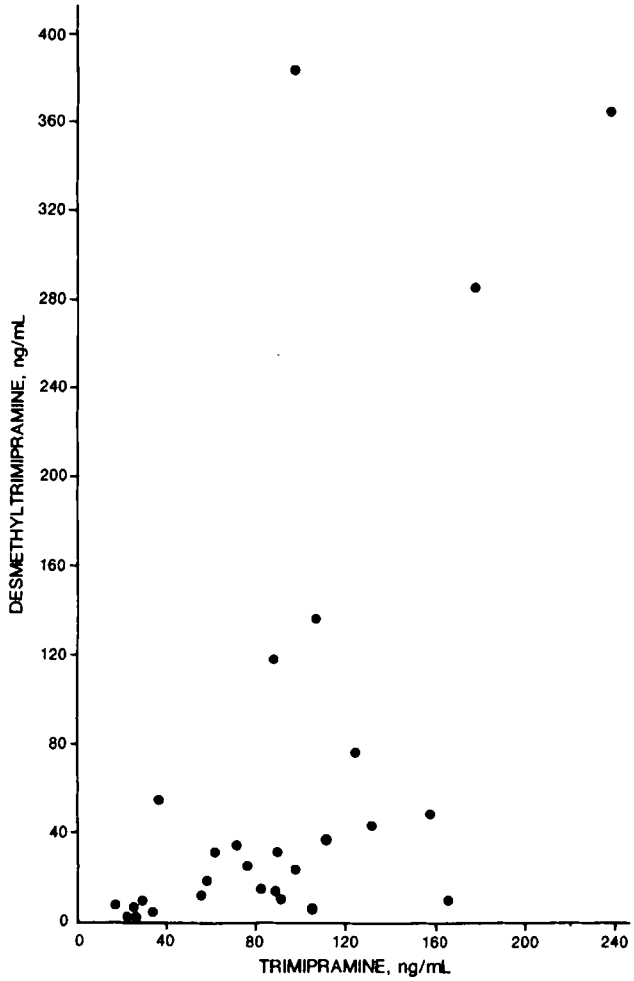

Figure 3—*Plasma concentrations of trimipramine I and the demethyl metabolite II in 28 patients. All patients were at steady state receiving either 75 or 150 mg of trimipramine (r = 0.62).*

were analyzed for trimipramine and its major metabolites (II, III, and IV). A typical chromatogram from one of these patients is shown in Fig. 2. In several patients who exhibited a relatively high level of II (>200 ng), another peak appeared at a retention time of ~7.0 min. This peak was identified as the didemethyl metabolite (V) by comparison with the retention time of a standard solution of V. A chromatogram of a spiked sample containing V as well as the other standards I–IV and VI is depicted in Fig. 1. Although never accurately quantitated, V was never found in any significant (>10 ng/mL) levels in over 120 samples tested.

To date, no clinical plasma concentrations for I and its major metabolites (II–IV) have been reported. From our preliminary data, we found that I undergoes the same metabolic pathway as imipramine: namely I is demethylated as well as hydroxylated in the 2-position, conjugated as the glucuronide, and excreted. Other minor pathways may exist for I such as *N*-oxidation, side-chain dealkylation, and others that again resemble the imipramine pathway. Metabolite II is also hydroxylated and, in a few instances, further demethylated to the primary amine (V).

Table V—Mean Data From 29 Patients Receiving 75 or 150 mg/d of Trimipramine [a]

Variables in Plasma	Mean, ng/mL	Range, ng/mL
I	86	11–241
II	65[b]	3–382
III (u)[d]	16	3–40
IV (u)	17[b]	3–49
III (T)[d]	379[b]	58–1126
IV (T)	317[b]	63–800
Ratios		
II/I	0.61[b]	0.07–3.71
III(u)/III(T)	0.04[b]	0.02–0.08
IV(u)/IV(T)	0.05[c]	0.01–0.10
III(u)/I	0.26	0.02–0.75
IV(u)/II	0.86	0.02–1.67

[a] n = 29; patient ages, 18–65. [b] n = 28. [c] n = 27. [d] Key: (u) unconjugated; (T) total.

Plasma concentrations of I and its metabolites (II–IV) varied widely among the 29 depressed patients (14 receiving 75 mg; 15 receiving 150 mg/d of I). This variability has been demonstrated for other tricyclic antidepressants such as imipramine, amitriptyline, *etc.* Table V lists the means, ranges, and various ratios for these 29 depressed patients. Demethylation of I does not appear to occur as readily as with imipramine or amitriptyline since it was reported that the ratios of the demethylated metabolites to the parent drug of both these compounds were 1.0–1.6 and 1.0 (11–13), respectively. The difference in the side chain probably accounts for this retardation in demethylation of I. A correlation between I and II is illustrated in Fig. 3.

The mean ratio of unconjugated III to I was 0.26, which is similar to the reported ratio of 2-hydroxyimipramine to imipramine (0.18–0.25) (12, 13). However, the ratio of unconjugated IV to II was 0.86 which is greater than that found for 2-hydroxydesipramine to desipramine (0.50) (12, 13). This increase in ratio of IV/II may occur because of the existence of an additional demethylation pathway from III to IV. Of the 29 patients, 3 were found to have a ratio of unconjugated III + IV/II + I ≤0.03 which could indicate the portion of the population that is considered deficient in the ability to hydroxylate (14). There was no correlation between either unconjugated III and I or unconjugated IV and II. This finding differs from the weak to moderate correlation between 2-hydroxyimipramine and imipramine and 2-hydroxydesipramine and desipramine reported by DeVane and Jusko (13) and Suckow and Cooper (4). Four to five percent of the total plasma hydroxy metabolites are unconjugated. Bock *et al.* (9) has reported 8% of the total plasma 2-hydroxydesipramine metabolite as unconjugated. This analytical procedure has sufficient sensitivity for single dose pharmacokinetic studies of trimipramine and its metabolites in plasma.

REFERENCES

(1) E. C. Settle and F. J. Ayd, *J. Clin. Psychiatry*, **41**, 266 (1980).
(2) S. H. Wong and S. L. Stolarum, *Clin. Chem.*, **27**, 1101 (1981).
(3) G. Caille, J. G. Besner, Y. Lacasse, and M. Vezina, *Biopharm. Drug Dispos.*, **1**, 187 (1980).
(4) R. F. Suckow and T. B. Cooper, *J. Pharm. Sci.*, **70**, 257 (1981).
(5) M. Neptune, R. L. McCreery, and A. A. Manian, *J. Med. Chem.*, **22**, 196 (1979).
(6) S. N. Frank and A. J. Bard, *J. Electrochem. Soc.*, **122**, 898 (1975).
(7) E. Bishop and W. Hussein, *Analyst*, **109**, 73 (1984).
(8) R. F. Suckow, T. B. Cooper, F. M. Quitkin, and J. W. Stewart, *J. Pharm. Sci.*, **71**, 889 (1982).
(9) J. L. Bock, J. C. Nelson, S. Gray, and P. I. Jatlow, *Clin. Pharmacol. Ther.*, **33**, 322 (1983).
(10) T. B. Cooper, D. Allen, and G. M. Simpson, *Psychopharmacol. Commun.*, **1**, 445 (1975).
(11) J. L. Bock, E. Giller, S. Gray, and P. Jatlow, *Clin. Pharmacol. Ther.*, **31**, 609 (1982).
(12) W. Z. Potter, H. M. Calil, T. A. Sutfin, A. P. Zavadil, W. J. Jusko, J. Rappoport, and F. K. Goodwin, *Clin. Pharmacol. Ther.*, **31**, 393 (1982).
(13) C. L. DeVane and W. J. Jusko, *Drug Intell. Clin. Pharm.*, **15**, 263 (1981).
(14) A. Mahgoud, J. R. Idle, L. G. Pringe, R. Lancaster, and R. L. Smith, *Lancet*, **ii**, 584 (1977).

ACKNOWLEDGMENTS

This work was supported in part by New York State Health Research Council Grant No. 14-081. The authors gratefully acknowledge a grant-in-aid from Ives Laboratory Inc., New York, N.Y. in support of this work. We thank Dr. G. M. Simpson, Department of Psychiatry, Medical College of Pennsylvania for permission to publish steady-state plasma level results from his clinical study.

Gas Chromatographic Analysis of Cetiedil, a Candidate Antisickling Agent, in Human Plasma With Nitrogen-Sensitive Detection

JAMES D. HENDERSON ˣ, VIPUL N. MANKAD, THOMAS M. GLENN, and YOUNG W. CHO

Received May 24, 1982, from the *Departments of Pharmacology and Pediatrics, University of South Alabama, College of Medicine, Mobile, AL 36688.* Accepted for publication August 24, 1983.

Abstract □ In this report a sensitive gas chromatographic assay for cetiedil, a candidate antisickling agent, in human plasma is described. After a triple extraction procedure, cetiedil was analyzed without derivatization with a nitrogen-phosphorus detector (with papaverine used as the internal standard.) Cetiedil was measured in plasma samples taken from human volunteers administered the drug intravenously.

Keyphrases □ Gas chromatography—cetiedil, human plasma, nitrogen-phosphorus detector □ Antisickling agents—cetiedil, GC analysis in human plasma, nitrogen-phosphorus detector □ Cetiedil—antisickling agent, GC analysis in human plasma, nitrogen-phosphorus detector

At present there is no pharmacological agent available to prevent or attenuate the sequelae of sickle cell crisis. For acute crisis, analgesics, hydration, and symptomatic care remain the standard therapy. In 1977, Cabannes reported on the clinical use of cetiedil citrate monohydrate for management of the painful thromboembolic crises characteristic of sickle cell disease (1).

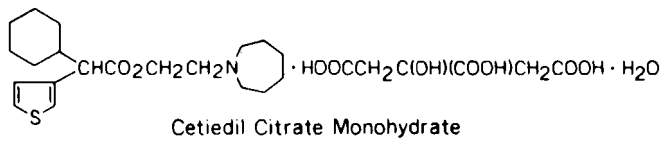

Cetiedil Citrate Monohydrate

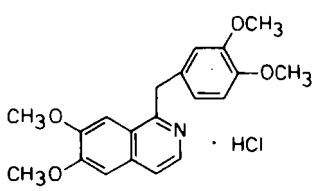

Papaverine Hydrochloride

Cetiedil[1] was first introduced for the treatment of peripheral and cerebral vascular disease (2). Subsequent studies have demonstrated that this vasoactive agent was also active in erythrocytes, in that it could prevent or reverse sickling by altering the permeability characteristics of the erythrocyte membrane (3–5). Several of its pharmacological properties (vasodilation, anticoagulation, analgesia, and inhibition of platelet aggregation) would be favorable for management of the thromboembolic episodes associated with sickle cell disease (6–8).

In this report, a reliable and sensitive gas chromatographic (GC) assay for cetiedil in human plasma, employing a triple extraction procedure and a nitrogen-phosphorus detector is described. The assay is similar to a previously reported method for analysis of papaverine in blood samples (9).

EXPERIMENTAL SECTION

Chemicals—Cetiedil citrate monohydrate[2] (white powder) and papaverine hydrochloride[3] were used without further purification. All solvents[4] were either nanograde or organic residue-analysis grade. All other reagents were certified ACS reagent grade.

Chromatographic Conditions—The gas chromatograph[5] was equipped with a nitrogen-phosphorus detector. A glass column (1.5 m × 2 mm i.d.) packed with 2% OV-101 on Chromosorb W HP 100–120-mesh support[6] was conditioned overnight (300°C). High-temperature septa[5] and graphite ferrules[6] were used. Air, helium, and hydrogen of the highest purity available[7]

[1] Stratene; Laboratoire Innothera, Arcueil, France.
[2] Johnson and Johnson Baby Products Co., Skillman, N.J.
[3] Sigma Chemical Co., St. Louis, Mo.
[4] American Scientific Products, Hanrahan, La.
[5] Model Sigma 3B; Perkin-Elmer, Norwalk, Conn.
[6] Supelco, Bellefonte, Pa.
[7] Air Products, Mobile, Ala.

0022-3549/84/1200-1748$01.00/0

© 1984, American Pharmaceutical Association

REFERENCES

(1) E. C. Settle and F. J. Ayd, *J. Clin. Psychiatry*, **41**, 266 (1980).
(2) S. H. Wong and S. L. Stolarum, *Clin. Chem.*, **27**, 1101 (1981).
(3) G. Caille, J. G. Besner, Y. Lacasse, and M. Vezina, *Biopharm. Drug Dispos.*, **1**, 187 (1980).
(4) R. F. Suckow and T. B. Cooper, *J. Pharm. Sci.*, **70**, 257 (1981).
(5) M. Neptune, R. L. McCreery, and A. A. Manian, *J. Med. Chem.*, **22**, 196 (1979).
(6) S. N. Frank and A. J. Bard, *J. Electrochem. Soc.*, **122**, 898 (1975).
(7) E. Bishop and W. Hussein, *Analyst*, **109**, 73 (1984).
(8) R. F. Suckow, T. B. Cooper, F. M. Quitkin, and J. W. Stewart, *J. Pharm. Sci.*, **71**, 889 (1982).
(9) J. L. Bock, J. C. Nelson, S. Gray, and P. I. Jatlow, *Clin. Pharmacol. Ther.*, **33**, 322 (1983).
(10) T. B. Cooper, D. Allen, and G. M. Simpson, *Psychopharmacol. Commun.*, **1**, 445 (1975).
(11) J. L. Bock, E. Giller, S. Gray, and P. Jatlow, *Clin. Pharmacol. Ther.*, **31**, 609 (1982).
(12) W. Z. Potter, H. M. Calil, T. A. Sutfin, A. P. Zavadil, W. J. Jusko, J. Rappoport, and F. K. Goodwin, *Clin. Pharmacol. Ther.*, **31**, 393 (1982).
(13) C. L. DeVane and W. J. Jusko, *Drug Intell. Clin. Pharm.*, **15**, 263 (1981).
(14) A. Mahgoud, J. R. Idle, L. G. Pringe, R. Lancaster, and R. L. Smith, *Lancet*, **ii**, 584 (1977).

ACKNOWLEDGMENTS

This work was supported in part by New York State Health Research Council Grant No. 14-081. The authors gratefully acknowledge a grant-in-aid from Ives Laboratory Inc., New York, N.Y. in support of this work. We thank Dr. G. M. Simpson, Department of Psychiatry, Medical College of Pennsylvania for permission to publish steady-state plasma level results from his clinical study.

Gas Chromatographic Analysis of Cetiedil, a Candidate Antisickling Agent, in Human Plasma With Nitrogen-Sensitive Detection

JAMES D. HENDERSON ˣ, VIPUL N. MANKAD, THOMAS M. GLENN, and YOUNG W. CHO

Received May 24, 1982, from the *Departments of Pharmacology and Pediatrics, University of South Alabama, College of Medicine, Mobile, AL 36688.* Accepted for publication August 24, 1983.

Abstract □ In this report a sensitive gas chromatographic assay for cetiedil, a candidate antisickling agent, in human plasma is described. After a triple extraction procedure, cetiedil was analyzed without derivatization with a nitrogen-phosphorus detector (with papaverine used as the internal standard.) Cetiedil was measured in plasma samples taken from human volunteers administered the drug intravenously.

Keyphrases □ Gas chromatography—cetiedil, human plasma, nitrogen-phosphorus detector □ Antisickling agents—cetiedil, GC analysis in human plasma, nitrogen-phosphorus detector □ Cetiedil—antisickling agent, GC analysis in human plasma, nitrogen-phosphorus detector

At present there is no pharmacological agent available to prevent or attenuate the sequelae of sickle cell crisis. For acute crisis, analgesics, hydration, and symptomatic care remain the standard therapy. In 1977, Cabannes reported on the clinical use of cetiedil citrate monohydrate for management of the painful thromboembolic crises characteristic of sickle cell disease (1).

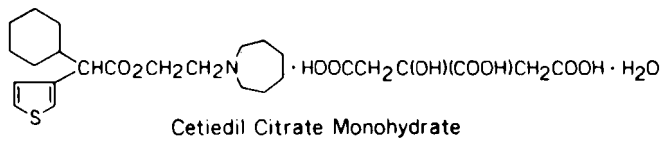

Cetiedil Citrate Monohydrate

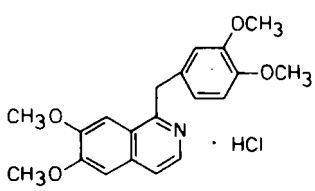

Papaverine Hydrochloride

Cetiedil[1] was first introduced for the treatment of peripheral and cerebral vascular disease (2). Subsequent studies have demonstrated that this vasoactive agent was also active in erythrocytes, in that it could prevent or reverse sickling by altering the permeability characteristics of the erythrocyte membrane (3–5). Several of its pharmacological properties (vasodilation, anticoagulation, analgesia, and inhibition of platelet aggregation) would be favorable for management of the thromboembolic episodes associated with sickle cell disease (6–8).

In this report, a reliable and sensitive gas chromatographic (GC) assay for cetiedil in human plasma, employing a triple extraction procedure and a nitrogen-phosphorus detector is described. The assay is similar to a previously reported method for analysis of papaverine in blood samples (9).

EXPERIMENTAL SECTION

Chemicals—Cetiedil citrate monohydrate[2] (white powder) and papaverine hydrochloride[3] were used without further purification. All solvents[4] were either nanograde or organic residue-analysis grade. All other reagents were certified ACS reagent grade.

Chromatographic Conditions—The gas chromatograph[5] was equipped with a nitrogen-phosphorus detector. A glass column (1.5 m × 2 mm i.d.) packed with 2% OV-101 on Chromosorb W HP 100–120-mesh support[6] was conditioned overnight (300°C). High-temperature septa[5] and graphite ferrules[6] were used. Air, helium, and hydrogen of the highest purity available[7]

[1] Stratene; Laboratoire Innothera, Arcueil, France.
[2] Johnson and Johnson Baby Products Co., Skillman, N.J.
[3] Sigma Chemical Co., St. Louis, Mo.
[4] American Scientific Products, Hanrahan, La.
[5] Model Sigma 3B; Perkin-Elmer, Norwalk, Conn.
[6] Supelco, Bellefonte, Pa.
[7] Air Products, Mobile, Ala.

0022-3549/84/1200-1748$01.00/0

© 1984, American Pharmaceutical Association

were used. Operating conditions were as follows: isothermal column temperature, 252°C; injection port temperature, 300°C; detector temperature, 300°C; carrier gas (helium) flow, 20 mL/min; air flow, 54 mL/min; hydrogen flow, 1.5 mL/min; range 1; and attenuation, 2–8. Injections (0.5–2 μL[8]) were made directly on column, the chart[9] speed was 1.3 cm/min.

Glassware Preparation—All glassware was washed in phosphate-free detergent[10] and rinsed with glass-distilled acetone. Silanization was accomplished by treatment with a 5% solution of dimethyldichlorosilane[11] in toluene, followed by rinsing in methanol. (Due to the toxicity of the silanizing agent, it is best handled with gloves and safety glasses in a well-ventilated hood. Addition of methanol produces fumes of hydrogen chloride gas if excess silanizing agent is present.) The glassware was then sonicated[12] in dichloromethane.

Internal Standard—Papaverine hydrochloride (55 ± 1 mg) was accurately weighed and transferred to a 125-mL separatory funnel. Glass-distilled water (25 mL) was added to dissolve the powder; the free base was formed by the addition of 10 M KOH (2 mL) and extracted with dichloromethane (3 × 30 mL). The combined extracts were filtered through anhydrous sodium sulfate (1 kg washed with 6 × 200 mL of methylene chloride) and brought to 100.0 mL (stock solution I). A total of 1 mL of stock solution I was diluted to 100.0 mL with dichloromethane (stock solution II). A total of 5 mL of stock solution II was placed in a 1000-mL volumetric flask and evaporated under a nitrogen[7] stream. 2-Propanol (50 mL) was added to dissolve the residue, and the volume was brought to the mark with *n*-heptane (working internal standard solution).

Cetiedil Standard Solutions—Cetiedil citrate monohydrate (16.0 mg, equivalent to 10.0 mg of free base) was dissolved in water and diluted to 200.0 mL (50 μg/mL). Serial dilutions with water gave working standard solutions of 10, 20, 40, 80, and 160 ng/mL.

Buffer Solution—Boric acid (12.4 g) and potassium chloride (14.9 g) were dissolved in water and diluted to 1 L. Of this solution, 50 mL was adjusted to pH 7.0 with 0.2 M KOH and diluted to 200 mL with water.

Extraction Procedure[13]—*Standards for Calibration Curve*—Buffer solution (pH 7, 4 mL) and blank plasma[14] (2.0 mL) were added to each of six 35-mL centrifuge tubes[15]. To one tube was added 1.0 mL of water; to each of the remaining tubes was added a 1.0-mL aliquot of each of the cetiedil working standard solutions, respectively. After addition of working internal standard solution (20.0 mL) to each tube, the mixtures were shaken at highest speed[16] (30 min) and centrifuged (30 min at 2500 rpm)[17]. The top layer was transferred to another tube containing 1 M HCl (3 mL)[18]. The mixtures were vortexed at highest speed (1 min) and centrifuged, and the top layer was discarded. The acidic extract was washed with *n*-heptane (5 mL) by vortexing for 30 s, centrifuging, and discarding the top layer. To each tube was added 10 M KOH (0.5 mL); after cooling to room temperature, dichloromethane (4 mL) was added. The mixtures were vortexed (1 min) and centrifuged, and the top layer was discarded. The organic layer was transferred directly[19] to a 5-mL vial[6], and the solutions were evaporated[20] to dryness under a nitrogen stream at 40°C. After rinsing the vial walls with dichloromethane (100 μL) and evaporating, the residue was dissolved in 2-propanol (10 μL), and an aliquot was injected.

Subject Samples—The procedure described above was followed for subject samples, except that 2.0 mL of the plasma was used in place of the blank plasma, and 1.0 mL of water was used in place of the cetiedil standard solution.

Calculations—The ratio of peak height of cetiedil to peak height of papaverine was determined for each of the calibration standards; linear regression analysis of these ratios *versus* the known cetiedil concentrations gave a slope and intercept, from which the equation for a straight line was obtained. Cetiedil concentrations in subject samples were obtained by substitution of the experimentally determined peak height ratio into the equation for the standard curve prepared for analysis of every set of samples.

Plasma Level Studies—Three adult male volunteers were admitted[21] to the study after signing informed-consent releases[22]. The subjects received a 0.15-mg/kg dose of cetiedil citrate monohydrate injectable[2] as a 30-mm intravenous infusion[23], followed by a 72-h observation period. Blood samples were obtained through a catheter placed in the arm contralateral to the infusion drip at 0 (prior to infusion), 5, 10, 15, 30, and 45 min and 1, 1.5, 2, 4, and 6 h postinfusion; the catheter was kept patent with heparinized saline. Before each blood collection, dead-space volume heparin solution was removed. After each collection, the catheter was refilled with heparinized saline (33 U of heparin/mL). Samples were collected into heparinized tubes[24] and centrifuged; the plasma was separated and stored at −15°C until assayed.

RESULTS

Standard Curve—In Fig. 1 is shown a typical chromatogram obtained for the analysis of unchanged cetiedil, with papaverine as internal standard. There

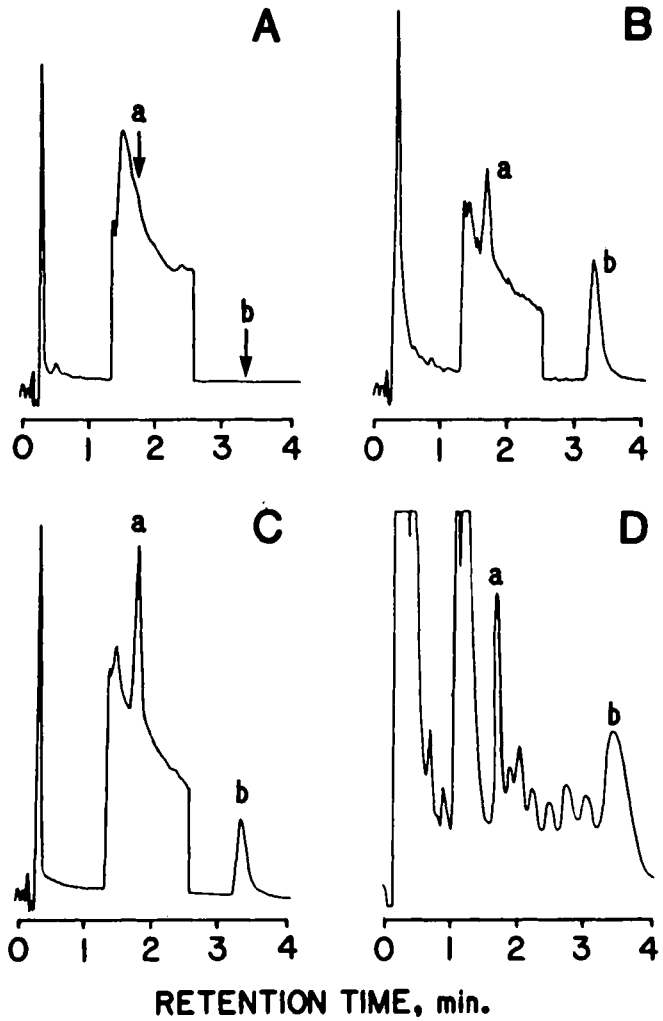

Figure 1—*Typical chromatograms of drug-free plasma carried through the procedure: (A) drug-free plasma to which 5 ng/mL of cetiedil (a) and papaverine (b) were added; (B) plasma from a subject receiving cetiedil; (C) with papaverine as the internal standard; (D) effects of filtration through sodium sulfate with possible contributions from contaminated solvents or glassware. The sudden jumps in the base line are due to programmed changes in recorder attenuation.*

[8] Model 701-RNWG, 10 μL; Hamilton, Decatur, Ga.
[9] Speedomax XL Flatbed; Leeds and Northrup, North Wales, Pa.; or 3390A Reporting Integrator; Hewlett-Packard, Avondale, Pa.
[10] Liquinox; Alconox Products, New York, N.Y.
[11] Kodak Laboratory Chemicals, Rochester, N.Y.
[12] Branson Ultrasonic Cleaner; Fisher Scientific Co., Atlanta, Ga.
[13] Preliminary unpublished work on this procedure was conducted at Cooper Laboratories, Inc.; Analytical Testing Procedure No. 78-15.
[14] Both heparinized and citrated plasma from volunteers gave identical results.
[15] Bellco Glass Co., Vineland, N.J.
[16] Wrist-Action Shaker (setting 10); Burrell, Pittsburgh, Pa.
[17] The long centrifugation time was needed for separation of an interface layer present after shaking. Small amounts of this layer may still be present after separation; great care must be taken to avoid any transfer since particulates may form on addition of HCl.
[18] Washed with 3 × 100 mL of 5% isopropanyl alcohol-toluene.
[19] Filtration through anhydrous sodium sulfate (even after extensive washing with dichloromethane) is not recommended since this procedure consistently produced spurious peaks.
[20] N-Evap; Organomation Associates, Northborough, Mass.
[21] Clinical Pharmacology Research Unit, University of South Alabama College of Medicine, Mobile, Ala.
[22] Both the consent form and the study protocol were approved by the Committee for Protection of Human Subjects and the Scientific Review Committee, University of South Alabama College of Medicine.
[23] Intravenous Infusion Delivery Set; Travenol Laboratories, Deerfield, Ill., and Dialaflo; Sorensen, Salt Lake City, Utah.
[24] Vacutainer; Becton, Dickinson and Co., Rutherford, N.J.

Table I—Cetiedil Determination in Human Plasma [a]

Cetiedil Added, ng/mL	Cetiedil Determined, ng/mL	*SD*	*n*
5	4.99	0.43	4
10	4.87	0.84	8
	11.45	1.63	5
20	19.54	2.66	5
	22.60[b]	1.43	5
40	49.76	4.05	5
200	181.35	16.14	8

[a] Different concentrations of cetiedil were added to drug-free plasma, and samples were then analyzed by the procedure described in the text. [b] Using 4 mL of blank plasma.

were no interfering peaks at the retention times for cetiedil or papaverine. The retention times for cetiedil and papaverine were 1.7 and 3.3 min, respectively. There was a linear relationship between the ratios of the peak height of cetiedil to the peak height of papaverine and the corresponding concentrations of cetiedil. The resulting general equation for the standard curve as described above ($y = 0.119x - 0.0259$) was linear ($r = 0.984$; $n = 37$) over the concentration range of 5–80 ng/mL, where y was the peak height ratio, and x was cetiedil concentration.

Precision—The precision of the method was determined by adding different concentrations of cetiedil and analyzing samples of each concentration by the described procedure (Table I). The average coefficient of variation over the concentration range of 5–200 ng/mL was 11%.

Reproducibility—To determine the day-to-day reproducibility, five different cetiedil concentrations were added to drug-free plasma, and the samples were analyzed over a period of 3 months (Table II). The average day-to-day coefficient of variation over the concentration range of 5–80 ng/mL was 16.3%. These results also indicate that cetiedil in plasma samples was stable for at least 3 months when kept frozen.

Recovery—2-Propanol solutions of cetiedil citrate were prepared so that injection of 1 μL would give a peak representing complete recovery of cetiedil from extracted plasma samples. The ratio of cetiedil peak height from the extracted samples to the standard solutions gave an average cetiedil recovery of 67.5 ± 15.5% over a concentration range of 10–80 ng/mL. Papaverine recovery was determined similarly (57.4 ± 5.2%).

Sensitivity—At an added cetiedil concentration of 0.5 ng/mL, the cetiedil peak was not routinely detected under optimal conditions (chromatograph attenuation, 2; injection volume, 2.0 μL). At 1 ng/mL, cetiedil peaks were detectable; however, the determined value was 2.56 ± 0.09 ng/mL ($n = 5$). This unacceptably large value may reflect nonlinearity of the standard curve at <5 ng/mL. When 2.0 mL of plasma was used, 5.0 ng/mL (average *CV*, 12.9%; Table I) was the sensitivity limit. From the general standard curve equation ($y = 0.0119x - 0.0259$), the theoretical sensitivity limit of the procedure would be 2.18 ng/mL. This large value may indicate that the plasma background was producing a significant amount of signal. Alternatively, the tailing of the solvent peak under maximal detection conditions may contribute to the large amount of background signal.

Plasma Level Studies—In Fig. 2 is shown the decline of unchanged cetiedil in human plasma after a 30-min intravenous infusion at a dose of 0.15 mg/kg in three subjects. The disposition of cetiedil is described by a two-compartment model (10).

DISCUSSION

The described procedure is sensitive and reproducible over a 5–80 nanogram per milliliter range. Detector response was linear over a wide concentration range. When kept in the dark at −15°C, the samples remained stable for at least 3 months without any added preservative. Standard solutions were kept in the dark at room temperature and remained stable for at least 2 weeks. All glassware were silanized to minimize drug losses.

In summary, this report, along with many other recent studies, illustrates the utility of the nitrogen-phosphorus detector in measuring drug levels over a 5–80 nanogram per milliliter range. Although combined GC-MS may provide greater sensitivity and require less time for sample analysis, such instrumentation is not universally available. Application of the nitrogen-sensitive detection technique to measurement of the candidate antisickling agent cetiedil has provided preliminary information regarding its plasma levels in humans.

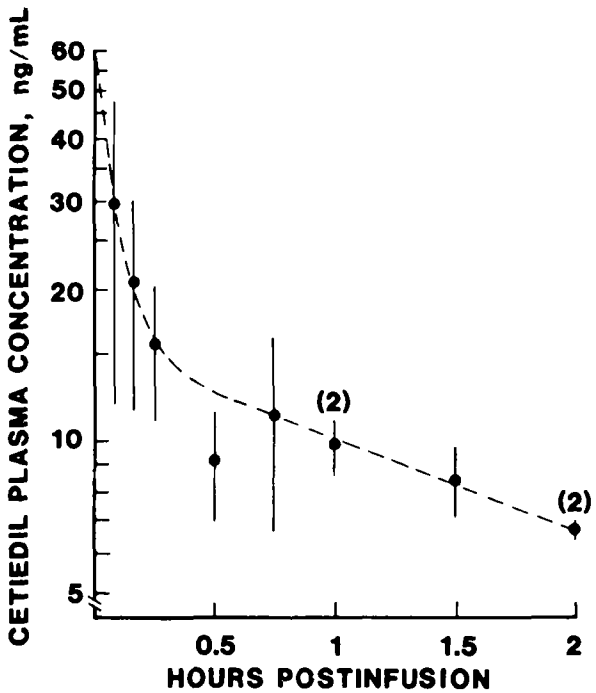

Figure 2—*Plasma level decline of unchanged cetiedil after an intravenous infusion of 0.15 mg/kg;* n = *3 unless otherwise indicated by numbers in parentheses.*

REFERENCES

(1) R. Cabannes, "Preliminary Study on the Effects of Cetiedil in Acute Episodes of Sickle Cell Anemia," Presented at the International Symposium of Vascular Disease, Rome, Italy, February 1977, and at the Sickle Cell Conference, Washington, D.C., November 1977.

(2) J. M. Casteight, *Quest. Med.*, **28**, 1025 (1975).

(3) L. J. Benjamin, G. Kokkini, and C. M. Peterson, *Blood*, **55**, 265 (1980).

(4) T. Asakura, S. T. Ohnishi, K. Adachi, M. Ozguc, K. Hashimoto, M. Singer, M. O. Russell, and E. Schwartz, *Proc. Natl. Acad. Sci. U.S.A.* **77**, 2955 (1980).

(5) L. R. Berkowitz and E. P. Orringer, *J. Clin. Invest.*, **68**, 1215 (1981).

(6) J. A. Simaan and D. M. Avialo, *J. Pharmacol. Exp. Ther.*, **198**, 176 (1976).

Table II—Reproducibility of Cetiedil Determination over Time [a]

Amount of Cetiedil Added, ng/mL	Concentration of Cetiedil Found, ng/mL						
	1 d	3 d	5 d	7 d	30 d	90 d	Mean ± *SD*[b]
5	7.1	5.7	5.4	5.4	5.6	5.2	5.64 ± 0.82
10	12.2	11.2	6.0	9.2	11.2	8.6	9.75 ± 2.25
20	22.3	20.6	18.4	28.4	24.8	22.8	22.86 ± 3.46
40	49.2	42.3	36.1	46.0	57.4	42.4	45.58 ± 7.26
80	96.6	84.9	80.7	111.4	100.0	84.1	92.93 ± 11.82

[a] Different concentrations of cetiedil were added to drug-free plasma and kept frozen in aliquots. Each aliquot was thawed on the day of analysis. [b] Reproducibility at 10 months could be demonstrated only at cetiedil concentrations of 5 ($n = 4$), 20 ($n = 3$), and 40 ($n = 3$) ng/mL; the respective determined mean ± *SD* values were 4.05 ± 0.46, 19.74 ± 2.15, and 32.76 ± 6.25 ng/mL. Determined values for 10 and 80 ng/mL were 71–75% of the theoretical added values.

(7) D. M. Avialo, *Drug Info. J.*, **10**, 36 (1976).
(8) L. Savi and P. Pola, *Minerva. Medica.* **69**, 4401 (1978).
(9) V. Bellia, J. Jacob, and H. T. Smith, *J. Chromatogr.*, **161**, 231 (1978).
(10) S. Niazi, in "Textbook of Biopharmaceutics and Clinical Pharmacokinetics," Appleton-Century-Crofts, New York, N.Y., 1979, p. 174.

ACKNOWLEDGMENTS

This study was supported by a grant from Johnson and Johnson, Inc.

The authors thank Ms. Robin Yunker (Head Nurse), Ms. Patricia Hamill, Mr. Richard Swansburg, Ms. Carolyn Williams, and Mr. William Parrish on the staff of the Clinical Pharmacology Research Unit, for their expert assistance, and Mr. Frank Vogtner for preparing the figures. The technical assistance of Ms. Ellen Runnlund is greatly appreciated. The authors also acknowledge Mr. V. Bellia and Mr. T. Smith, Cooper Laboratories, for preliminary development and description of assay conditions.

Radiopaque Liposomes: Effect of Formulation Conditions on Encapsulation Efficiency

S. BENITA *[x], P. A. POLY [‡], F. PUISIEUX [‡], and J. DELATTRE [§]

Received May 27, 1983, from the **Pharmacy Department, School of Pharmacy, Hebrew University of Jerusalem, Jerusalem 91120, Israel,* [‡]*Laboratoire de Pharmacie Galenique, Faculte de Pharmacie de Paris-Sud, 92290 Chatenay-Malabry, France,* and [§]*Laboratoire de Biochimie, Faculte de Pharmacie, 63100 Clermont Ferrant, France.* Accepted for publication, September 14, 1983.

Abstract □ Liposomes containing sodium ioxitalamate were prepared by sonication. Suitable amounts of purified soybean phosphatidylcholine and cholesterol were used at various molar ratios. Stearylamine or dicetylphosphate were added to this lipid composition when charged liposomes were required. After sonication and removal of unencapsulated solute, this manufacturing process yielded small multilamellar vesicles as confirmed by electron microscopy. These liposomes did not exhibit a narrow range of size distribution; the mean particle size varied from 135 to 145 nm. With respect to the efficiency of encapsulation, two parameters were distinguishable: the volume of encapsulated aqueous space per unit of lipid weight and the percentage of the contrast agent added that became encapsulated in the liposomes. Investigation of the preparative parameters revealed that increased molar ratios of cholesterol yielded higher aqueous volume and iodine contents in the liposomes, which were attributed to a reduction of the liposome permeability to the contrast agent. However, the inclusion of cholesterol into the bilayer liposomal membrane was limited, probably by solubility restrictions. Negatively and positively charged liposomes had higher rates of encapsulation than did neutral liposomes. This result was expected since efficient encapsulation of polar compounds requires formation of large aqueous spaces within the vesicles per mole of lipids. Increase of the lipid fractions at a constant ratio of phosphatidylcholine–cholesterol, with all the other factors kept constant, reduced the aqueous volume entrapped per millimole of lipid and, consequently, the iodine content in the liposomes. However, an increase in the initial sodium ioxitalamate concentration diminished the aqueous volume entrapped in the liposomes but increased the iodine content.

Keyphrases □ Liposomes—radiopaque, effect of formulation conditions on encapsulation efficiency □ Formulations—radiopaque liposomes, effect on encapsulation efficiency □ Encapsulation—radiopaque liposomes, effect of formulation conditions

The possibility of utilizing liposomes as vehicles for therapeutic agents had been widely considered over the last 16 years. The potential applications have been extensively reported and clearly summarized (1–3). The ultimate goal has been the targeting of drugs and other biologically active ingredients to specific cells within the body. However, this cannot be easily accomplished since it has been shown in numerous reports that intravenously injected liposomes localize predominantly in the liver, spleen, and other organs rich in cells of the reticuloendothelial system (4).

The specific hepatic uptake can be exploited to design a selective delivery system based on liposomes containing sodium ioxitalamate, which is a water-soluble iodinated contrast agent characterized by its high iodine content (57%). The radiopaque agent, sodium ioxitalamate (I), is primarily used for urography because of its pharmacokinetic properties, (5, 6); however, side

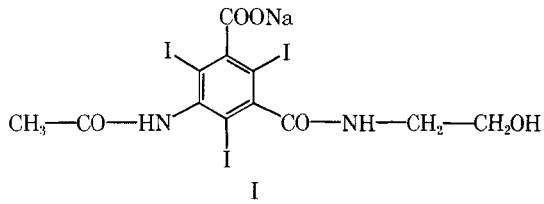

I

effects, allergic reactions, and intolerance have been reported. The preparation of liposomes containing the radiopaque agent is, therefore, also aimed at reducing or avoiding these adverse reactions since selective liver uptake enables administration of smaller amounts of radiopaque agent for a similar or even improved diagnostic result. The liposomal preparation will probably be able to produce a visible contrast enhancement of the liver, which will help improve the diagnostic accuracy of computerized tomography of this organ. Some attempts, including the preparation of brominated radiopaque liposomes (7) and the encapsulation of diatrizoic acid salts within liposomes (8), have already been performed, yielding preliminary results that are promising. However, this interesting approach is limited by the amount of contrast agent that can be entrapped in the aqueous phase of liposomes and the potential release of the opaque ingredient from the liposomes. The objective of this study, therefore, is to incorporate the contrast agent within liposomes and to investigate some of the physical and chemical factors which may control the efficiency of the encapsulation rate. The results of such an investigation offer the possibility of optimizing liposome formulation, enabling a high encapsulation rate and, consequently, an increase in the opacification of the liposomes caused by their high iodine content.

0022-3549/84/1200-1751$01.00/0
© 1984, American Pharmaceutical Association

(7) D. M. Avialo, *Drug Info. J.*, **10**, 36 (1976).
(8) L. Savi and P. Pola, *Minerva. Medica.* **69**, 4401 (1978).
(9) V. Bellia, J. Jacob, and H. T. Smith, *J. Chromatogr.*, **161**, 231 (1978).
(10) S. Niazi, in "Textbook of Biopharmaceutics and Clinical Pharmacokinetics," Appleton-Century-Crofts, New York, N.Y., 1979, p. 174.

ACKNOWLEDGMENTS

This study was supported by a grant from Johnson and Johnson, Inc.

The authors thank Ms. Robin Yunker (Head Nurse), Ms. Patricia Hamill, Mr. Richard Swansburg, Ms. Carolyn Williams, and Mr. William Parrish on the staff of the Clinical Pharmacology Research Unit, for their expert assistance, and Mr. Frank Vogtner for preparing the figures. The technical assistance of Ms. Ellen Runnlund is greatly appreciated. The authors also acknowledge Mr. V. Bellia and Mr. T. Smith, Cooper Laboratories, for preliminary development and description of assay conditions.

Radiopaque Liposomes: Effect of Formulation Conditions on Encapsulation Efficiency

S. BENITA *[x], P. A. POLY [‡], F. PUISIEUX [‡], and J. DELATTRE [§]

Received May 27, 1983, from the **Pharmacy Department, School of Pharmacy, Hebrew University of Jerusalem, Jerusalem 91120, Israel,* [‡]*Laboratoire de Pharmacie Galenique, Faculte de Pharmacie de Paris-Sud, 92290 Chatenay-Malabry, France,* and [§]*Laboratoire de Biochimie, Faculte de Pharmacie, 63100 Clermont Ferrant, France.* Accepted for publication, September 14, 1983.

Abstract □ Liposomes containing sodium ioxitalamate were prepared by sonication. Suitable amounts of purified soybean phosphatidylcholine and cholesterol were used at various molar ratios. Stearylamine or dicetylphosphate were added to this lipid composition when charged liposomes were required. After sonication and removal of unencapsulated solute, this manufacturing process yielded small multilamellar vesicles as confirmed by electron microscopy. These liposomes did not exhibit a narrow range of size distribution; the mean particle size varied from 135 to 145 nm. With respect to the efficiency of encapsulation, two parameters were distinguishable: the volume of encapsulated aqueous space per unit of lipid weight and the percentage of the contrast agent added that became encapsulated in the liposomes. Investigation of the preparative parameters revealed that increased molar ratios of cholesterol yielded higher aqueous volume and iodine contents in the liposomes, which were attributed to a reduction of the liposome permeability to the contrast agent. However, the inclusion of cholesterol into the bilayer liposomal membrane was limited, probably by solubility restrictions. Negatively and positively charged liposomes had higher rates of encapsulation than did neutral liposomes. This result was expected since efficient encapsulation of polar compounds requires formation of large aqueous spaces within the vesicles per mole of lipids. Increase of the lipid fractions at a constant ratio of phosphatidylcholine–cholesterol, with all the other factors kept constant, reduced the aqueous volume entrapped per millimole of lipid and, consequently, the iodine content in the liposomes. However, an increase in the initial sodium ioxitalamate concentration diminished the aqueous volume entrapped in the liposomes but increased the iodine content.

Keyphrases □ Liposomes—radiopaque, effect of formulation conditions on encapsulation efficiency □ Formulations—radiopaque liposomes, effect on encapsulation efficiency □ Encapsulation—radiopaque liposomes, effect of formulation conditions

The possibility of utilizing liposomes as vehicles for therapeutic agents had been widely considered over the last 16 years. The potential applications have been extensively reported and clearly summarized (1–3). The ultimate goal has been the targeting of drugs and other biologically active ingredients to specific cells within the body. However, this cannot be easily accomplished since it has been shown in numerous reports that intravenously injected liposomes localize predominantly in the liver, spleen, and other organs rich in cells of the reticuloendothelial system (4).

The specific hepatic uptake can be exploited to design a selective delivery system based on liposomes containing sodium ioxitalamate, which is a water-soluble iodinated contrast agent characterized by its high iodine content (57%). The radiopaque agent, sodium ioxitalamate (I), is primarily used for urography because of its pharmacokinetic properties, (5, 6); however, side

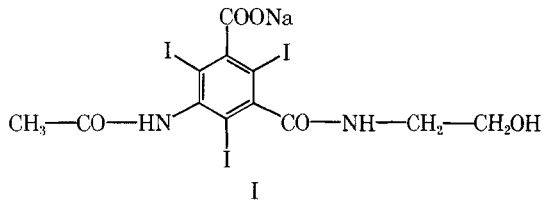

I

effects, allergic reactions, and intolerance have been reported. The preparation of liposomes containing the radiopaque agent is, therefore, also aimed at reducing or avoiding these adverse reactions since selective liver uptake enables administration of smaller amounts of radiopaque agent for a similar or even improved diagnostic result. The liposomal preparation will probably be able to produce a visible contrast enhancement of the liver, which will help improve the diagnostic accuracy of computerized tomography of this organ. Some attempts, including the preparation of brominated radiopaque liposomes (7) and the encapsulation of diatrizoic acid salts within liposomes (8), have already been performed, yielding preliminary results that are promising. However, this interesting approach is limited by the amount of contrast agent that can be entrapped in the aqueous phase of liposomes and the potential release of the opaque ingredient from the liposomes. The objective of this study, therefore, is to incorporate the contrast agent within liposomes and to investigate some of the physical and chemical factors which may control the efficiency of the encapsulation rate. The results of such an investigation offer the possibility of optimizing liposome formulation, enabling a high encapsulation rate and, consequently, an increase in the opacification of the liposomes caused by their high iodine content.

0022-3549/84/1200-1751$01.00/0
© 1984, American Pharmaceutical Association

EXPERIMENTAL SECTION

Materials—Soybean phosphatidylcholine[1] was purified by the method of Singleton *et al.* (9), and the purity was ascertained by a TLC analytical method (10). Stearylamine and dicetylphosphate were obtained commercially[2]. Cholesterol[3] was purified by two recrystallizations. Sodium ioxitalamate was used as supplied[4].

Methods—*Preparation of Liposomes*—Suitable amounts of purified phosphatidylcholine and cholesterol in various molar ratios were dissolved in 20 mL of chloroform to which stearylamine or dicetylphosphate was added when charged liposomes were required. The lipid mixture was deposited as a thin film on the walls of a round-bottomed flask by rotary evaporation under reduced pressure at 30°C. Twenty-five milliliters of an aqueous solution of sodium ioxitalamate at a given concentration was poured into the flask, shaken by continuous rotation for 30 min at 30°C, and allowed to stand over a 2-h period. The liposomal dispersion obtained was then sonicated[5] for 3 min under a nitrogen atmosphere at 0°C for homogenization. Sonication promoted conversion of the large multilamellar vesicles (MLV) into smaller liposomes which were separated from the excess of free sodium ioxitalamate by gel filtration on a coarse Sephadex G-50 column. The liposomes were mainly collected from fractions three to six after the void volume was eluted; they were identified by the presence of turbidity in the different samples collected. The liposome size was then measured[6].

Drug Encapsulation Efficiency—After vesicle preparation and removal of the unencapsulated solute, the amount of encapsulated compound could be determined. With respect to the efficiency of encapsulation, two parameters can be distinguished: first, the volume of encapsulated aqueous space per millimole of lipid and, second, the percentage of the compound added which becomes encapsulated in the liposomes. The latter, when expressed in percent iodine content of the liposomes, in fact represents a measure of the probable opacification ability of the liposomal preparation. The first parameter, which is defined as the encapsulation capacity (EC), is a function of liposome size and number of lamellae per particle. EC represents the fraction of aqueous volume entrapped per millimole of lipids and is calculated by (11):

$$EC = \frac{C_e}{C_0} \cdot \frac{1}{C_l} \qquad \text{(Eq. 1)}$$

where C_0 is the initial sodium ioxitalamate concentration, C_e is the final concentration found, and C_l is the lipid concentration in the liposomes. In contrast, the molar fraction of drug entrapped per mole of lipid is calculated by the simple ratio of the molar concentration of sodium ioxitalamate to the molar concentration of lipids determined in the liposomes. Obviously, the second parameter, which is defined as the entrapment efficiency or drug content (DC), depends on EC, but in addition, it also depends on the lipid concentration in the vesicles. DC is expressed by (in percent):

$$DC = \frac{W_c}{W_c + W_l} 100 \qquad \text{(Eq. 2)}$$

where W_c is the amount of drug found in the liposomes, and W_l is the amount of lipids which form the bilayer membrane found experimentally in the liposomes. The sodium ioxitalamate amount entrapped was determined with a liquid chromatograph[7] consisting of a pump[7], an injector[7], and a UV detector[7] fixed at 254 nm. The stationary phase was C_{18}[8], and the eluant was methanol–water (70:30) containing 1% tetrabutylammonium phosphate, supplied at a flow rate of 1 mL/min. A portion of the liposomal preparation was diluted with water (1:100) before injection. The amount of contrast agent in the liposomal preparation was calculated by using a calibration curve based on standard solutions determined under identical experimental conditions. No interference of the phospholipid fragments by the HPLC method was observed. The phospholipids in the liposomal preparation were assayed by using a phospholipid B test[9] based on a colorimetric reaction (12). No disturbance of the colorimetric reaction was detected as a result of the presence of sodium ioxitalamate, proving that the concentrations of the phospholipid found were correct. For stearylamine-, dicetylphosphate-, and cholesterol-incorporated liposomes which were eluted through the gel column, the original molar ratio to lecithin on mixing was assumed to be maintained (11). All the calculations on drug encapsulation efficiency were carried out on the basis of this assumption. Each batch of liposomes was triplicated. The different values reported are the average of six experimental measurements since the property determinations of each liposome batch were duplicated.

[1] Epikuron 200; Lecithos, Saint Maur, France.
[2] Sigma Chemical Co., St. Louis, Mo.
[3] Rhône-Poulenc, Paris, France.
[4] Guerbet Aulnay-sous-Bois, France.
[5] Model B-30 sonifier; Branson.
[6] Nanosizer; Coulter.
[7] 480-HPLC composed of a 6000A pump, a U6K injector, and a 480-UV detector; Waters Associates, Milford, Mass.
[8] μ-Bondapak; Waters Associates.
[9] Wako Chemical, Osaka, Japan.

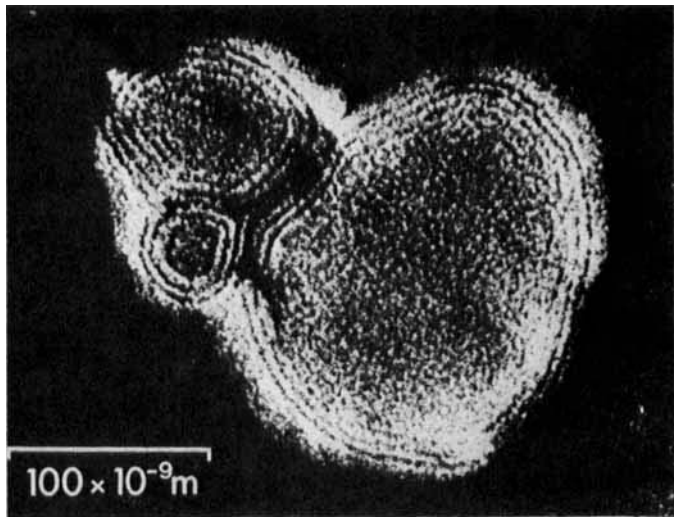

Figure 1—*Electron micrograph of multilamellar liposomes produced by the method described in the text (initial conditions: phosphatidylcholine, 500 mg; cholesterol, 70 mg in 20 mL of chloroform; 25 mL of sodium ioxitalamate aqueous solution equivalent to 100 mg of iodine/mL).*

RESULTS AND DISCUSSION

Water-soluble compounds entrapped within liposomes are found in the internal aqueous compartments of these particles (13) owing to their low affinity and solubility in the lipids which constitute the liposomal membrane. Thus, efficient encapsulation of polar compounds requires formation of large aqueous spaces within the MLV. The manufacturing process used in this study yielded, after sonication and removal of unencapsulated solute, small MLV, as confirmed by electron microscopic examinations (Fig. 1). These liposomes did not exhibit a narrow range of size distribution, and their mean particle size varied from 135 to 145 nm[6]. Polydispersity index values were obtained during routine liposome size measurements and ranged from 3 to 5, which indicated, according to the manufacturer's instructions, a distribution range, by diameter, of 2:1 in the liposome samples.

In preliminary studies, the influence of the phospholipid characteristics on liposome properties was investigated. The chemical purity of the phosphatidylcholine source, which might slightly affect the chemical composition, had little effect on solute retention or particle size of the liposomes formed. The entrapped volume of the total internal aqueous phase remained practically constant, irrespective of the phosphatidylcholine used. In spite of these results, purified soybean phosphatidylcholine, as compared with commercial soybean phosphatidylcholine, was preferred for liposomes production since fewer adverse toxic reactions would be expected after parenteral administration of such liposomes in future animal experiments.

Effect of Cholesterol Concentration—Increased initial molar ratios of cholesterol, with respect to the phosphatidylcholine concentration, yielded higher aqueous volumes and iodine contents in the liposomes (Table I). This was attributed to a reduction in the liposome permeability to the contrast agent

Table I—Influence of Initial Cholesterol Concentration on Liposome Properties [a]

Soybean Phosphatidylcholine–Cholesterol, Molar Ratio	Encapsulation Capacity, mL/mmol	Iodine Content, %[b]	Molar Fraction of Drug Entrapped/mol of Lipid, × 10^2 [c]
8:0	0.78	9.5	20.42
8:2	1.00	11.89	20.79
8:4	1.41	15.97	29.05
8:8	1.52	16.87	29.01

[a] Conditions: 500 mg of phosphatidylcholine, 4.325 g of sodium ioxitalamate, with various amounts of cholesterol. [b] Calculated according to Eq. 2 by using only the molar fraction weight of iodine contained in the sodium ioxitalamate molecule. [c] The ratio was calculated according to the experimental results by using the analytical methods described in the text.

Table II—Influence of a Positive Charge, Stearylamine, or Negative Charge, Dicetylphosphate, on the Liposome Properties[a]

Liposome Composition, Molar Ratio	Mean Particle Size, nm[b]	Encapsulation Capacity, mL/mmol	Iodine Content, %[c]	Molar Fraction of Drug Entrapped/mol of Lipid, $\times 10^2$ [d]
Soybean phosphatidylcholine-cholesterol, 8:2	140	1.00	11.89	20.79
Soybean phosphatidylcholine-cholesterol-stearylamine, 8:2:1	128	1.22	14.03	24.84
Soybean phosphatidylcholine-cholesterol-stearylamine, 8:2:2	145	1.33	15.25	29.87
Soybean phosphatidylcholine-cholesterol-dicetylphosphate, 8:2:1	138	1.19	13.87	25.29
Soybean phosphatidylcholine-cholesterol-dicetylphosphate, 8:2:2	144	1.43	16.25	27.76

[a] Conditions: 500 mg of phosphatidylcholine, 4.325 g of sodium, ioxitalamate, with various amounts of cholesterol. [b] The polydispersity index in all the measurements performed was 4. [c] Calculated according to Eq. 2 by using only the molar fraction weight of iodine contained in the sodium ioxitalamate molecule. [d] The ratio was calculated according to experimental results by using the analytical methods described in the text.

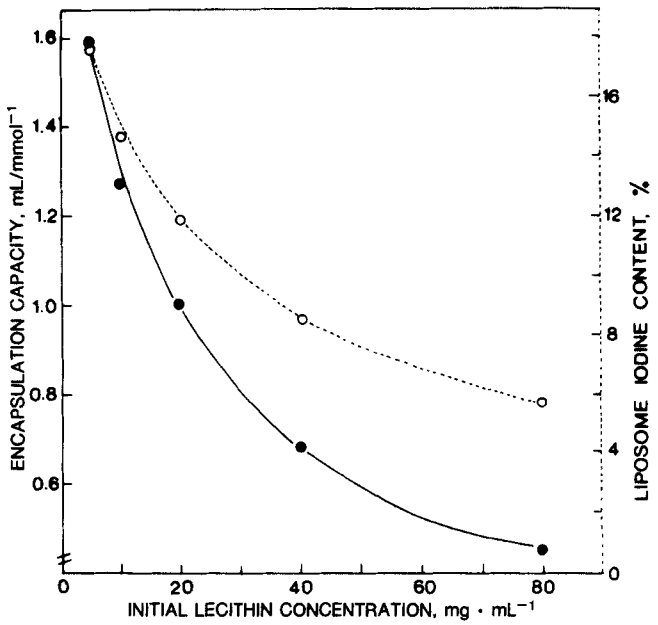

Figure 2—*Effect of initial phosphatidylcholine concentration on encapsulation capacity (●) and iodine content (○) of the liposomes prepared.*

(14). In addition to its barrier-controlling property, the incorporation of cholesterol was found to provide more physical stability against the ultrasonic vibration force as compared with that of the cholesterol-free liposomes (11). This effect might reduce precocious sodium ioxitalamate release during liposome size homogenization by sonication. However, the concentration of radiopaque agent entrapped in the liposome augmented and reached a maximum (*i.e.*, a plateau) with increasing cholesterol molar ratio (Table I). This phenomenon could be expected since the inclusion of cholesterol into the bilayer liposomal membrane is limited, probably as a result of solubility restrictions which were corroborated by the existence in the highest initial cholesterol concentration of a crystallization process, which is attributed to an excess of cholesterol after vesicle formation.

Effect of Electric Charge on the Surface of the Bilayer Membrane—Various concentrations of stearylamine (cationic substance) or dicetylphosphate (anionic substance) were included in the liposomal bilayer membranes, rendering the surface electrically charged. This resulted in a repulsion and, hence, an increase in the distance between the different bilayers, which appear to be very close to one another in neutral liposomes (Fig. 1); consequently, more hydrophilic solute can be trapped in the aqueous compartments than in neutral liposomes. Negatively and positively charged liposomes gave larger amounts of radiopaque agent and higher rates of aqueous volume encapsulation than did neutral liposomes, confirming the previous hypothesis (Table II). It should be noted that an increase in the charge membrane concentration (*i.e.*, the stearylamine or dicetylphosphate concentration) while all the other factors were kept constant enhanced the sequestration volume capacity and iodine content of the liposomes, indicating that the interlamellar spacing within the vesicles depended on the extent of bilayer ionization. No significant difference with respect to the various properties (Table II) could be detected between negatively or positively charged liposomes at an ionic compound concentration of ~10 mol%. However, a distinct increase in the encapsulation capacity was observed in negatively charged liposomes, as compared with positively charged liposomes (Table II), at an ionic compound concentration of ~20 mol%. This effect could be attributed to a minimization of the leakage during liposome production due to electrostatic repulsion between the similar negative charges of the lipid membranes and the entrapped ioxitalamate ion (15). This electrostatic repulsion reduced the diffusion of the contrast agent through the bilayer membrane. It is interesting to note that in contrast with previous reports (16), the addition of charged lipid in excess of 10 mol% of the total lipid mixture increased volume entrapment (Table II). Moreover, no marked particle size alteration (Table II) was observed among the various species of liposomes, and enlargement of the space between the lamellae did not contribute to an increase in the final liposome size.

Effect of Initial Phosphatidylcholine Concentration on Liposome Properties—It is a well-accepted fact that MLV possess a low encapsulation capacity as compared with LUV (17). The preparation method previously described yielded mainly liposomes of the MLV type, which were characterized by a large core lamella and adjacent bilayer membranes separated by small aqueous spaces. It could be considered that these resulting MLV have a similar encapsulation ability to LUV since the main part of the sequestered solution volume should be stored inside of the core space. Therefore, any variable experimental factor which could modify the physical characteristics of these MLV liposomes alters their encapsulation capacity. An increase in the phospholipid concentration at a constant ratio of cholesterol-phosphatidylcholine reduced the aqueous volume entrapped per millimole of lipid and, subsequently, the iodine content in the liposomes (Fig. 2). These results indicate that although all the other experimental factors were kept constant, larger phosphatidylcholine concentrations produced liposomes of the MLV type consisting of a larger number of lamellae per single vesicle, even if the sonication time was maintained constant during the preparation process in all the different liposome batches. It appeared that fewer liposomes were

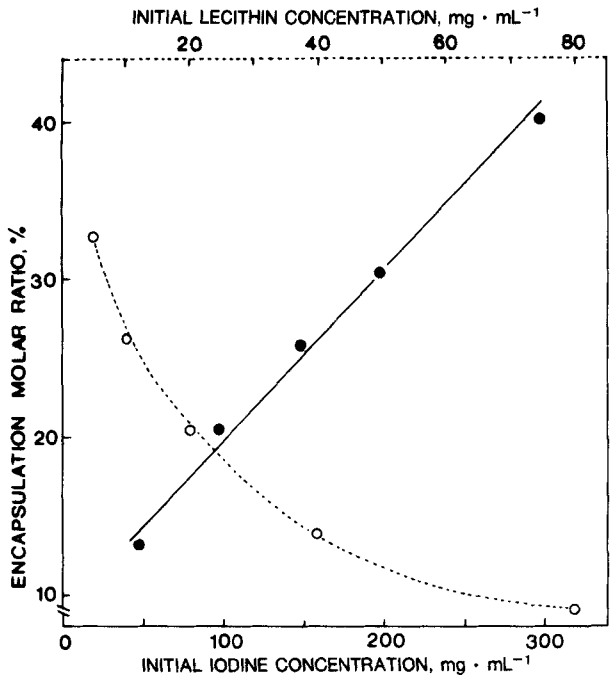

Figure 3—*Effect of initial iodine concentration (●) and initial phosphatidylcholine concentration (○) on the sodium ioxitalamate encapsulation molar ratio.*

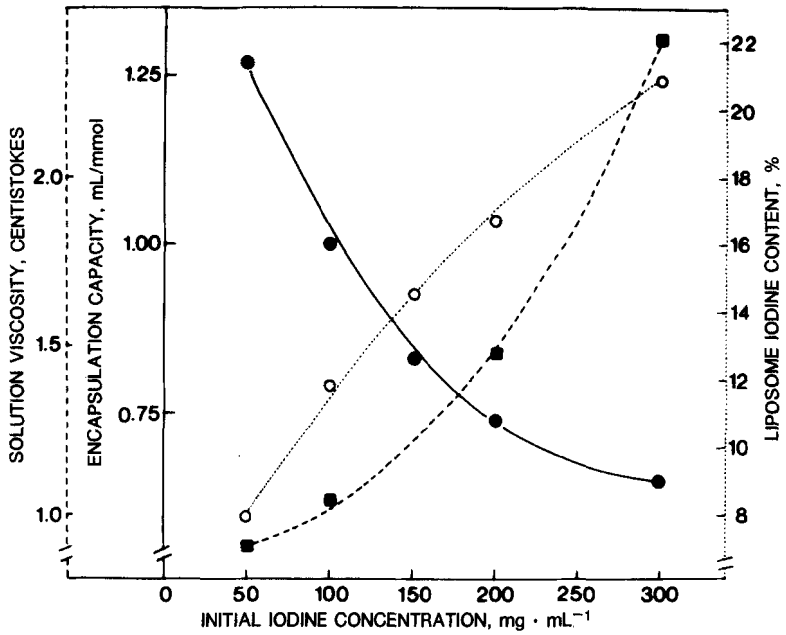

Figure 4—*Effect of initial iodine concentration on encapsulation capacity (●), iodine content of liposomes (○), and viscosity of the aqueous solution (■).*

formed in proportion to the initial amount used, but more membranes were produced per single particle by increasing the initial phosphatidylcholine concentration. Thus, the effective volume entrapped within these liposomes diminished, and since the radiopaque agent concentration remained unchanged, it resulted in a reduction in the iodine content, as seen in Fig. 2. It should be noted that an identical parallel decrease between the encapsulation volume capacity (Fig. 2) and the encapsulation molar ratio (Fig. 3) was observed. The plot obtained yielded a curved line that fell sharply at the beginning and moderately on approaching the highest phosphatidylcholine concentrations (Fig. 3), indicating probable formation of smaller interlamellar spaces within the liposomes and supporting the fact that the polar compound sodium ioxitalamate is found totally in the aqueous compartments of the MLV. No part of it was bound to the lipid membrane, as was reported for some other water-soluble drugs (13).

Effect of Initial Sodium Ioxitalamate (or Iodine Equivalent) Concentration—Dependence of the different liposome properties on the initial radiopaque agent concentration was examined. A plot of the volume encapsulation capacity against the initial iodine concentration yielded a curved line that fell almost linearly initially and curved off at the highest iodine concentration (Fig. 4). Obviously, the iodine content of these liposomes was enhanced, but the iodine encapsulation efficiency decreased with increasing initial contrast agent concentration (Fig. 4); no linear relationship was observed. Since fixed amounts of lipids were used, the decrease in EC was probably caused by other experimental factors which were affected by the initial sodium ioxitalamate concentration. Some of these factors, *e.g.*, the ionic strength or the viscosity of the dispersion medium, might alter the physical characteristics of the vesicles formed (*i.e.*, the size and the number of bilayers per particle). However, in a previous report, it has been shown that no variation in trapped volume within neutral liposomes was observed over a full range of salt concentrations corresponding to an increase in the ionic strength of the aqueous phase (15). Therefore, the explanation should be sought elsewhere. Apparently, the viscosity of the dispersion medium affected the encapsulation ability of the vesicles. Viscosity measurements of the different sodium ioxitalamate solutions were carried out with a viscometer[10] according to the British Pharmacopoeia (18). The relationship of the sodium ioxitalamate concentration effects on encapsulation capacity, iodine content, and viscosity of the aqueous phase are more clearly evident when seen graphically (Fig. 4). The encapsulation capacity function follows an inverse pattern to that of viscosity; it is clearly indicated that the sequestration ability falls off, whereas the viscosity increases drastically with increasing contrast agent concentration. It seems that the liposome entrapment process reflects fundamental changes arising from the viscosity variation of the dispersion medium. The reasons for this are not clear, but it might be due to any or all of the following factors. By raising the viscosity the shape of the vesicles formed is probably altered, thus increasing the proportion of spheroids (oblate or prolate) to spheres. If it is assumed that the surface area of these vesicles remains almost constant, then the volume of these spheroids diminishes as compared with that of the spheres. Consequently, a reduction in volume encapsulation ability should be expected, as was observed experimentally (Fig. 4). This solution is in reasonable agreement with the electron microscopic observations. Other factors which should be considered that account for an encapsulation capacity decrease are the formation of a vesicle structure that is not tightly closed at higher viscosities, enhancement of permeation (*i.e.*, loss) of the trapped ionic compound through the membrane, and a diminution in the hydration extent of the head groups which reduce the electrostatic interactions with increasing medium viscosity, leading to smaller distances between the lamellae within the liposomes. It is interesting to note that the sodium ioxitalamate encapsulation molar ratio increased linearly with the initial equivalent iodine concentration, whereas it declined nonlinearly with the initial phosphatidylcholine concentration (Fig. 3). These results indicate that the radiopaque agent incorporated within the liposomes was not influenced by the moderate lack of volume encapsulation efficiency on approaching the maximal contrast agent concentrations.

Finally, it can be concluded that any variable factor which can affect the vesicle volume encapsulation ability determines the properties of the radiopaque liposomes formed. However, by choice of suitable experimental parameters, full efficiency can be achieved without altering the fundamental characteristics of the liposomes.

[10] Ostwald.

REFERENCES

(1) D. Papahadjopoulos, *Ann. N.Y. Acad. Sci.*, **308**, 1 (1978).

(2) G. Gregoriadis, *N. Engl. J. Med.*, **295**, 704 (1976); G. Gregoriadis, *N. Engl. J. Med.*, **295**, 765 (1976).

(3) F. Puisieux and S. Benita, *Biomedicine*, **36**, 4 (1982).

(4) F. Roerdink, J. Dijkstra, G. Hartman, B. Balscher, and G. Scherphof, *Biochim. Biophys. Acta*, **677**, 79 (1981).

(5) D. Gardeur, J. Lautron, J. C. Millard, N. Berger, and J. Metzger, *J. Comput. Assit. Tomogr.*, **4**, 178 (1980).

(6) R. Nagel, W. Leistenschneider, V. Peck, and V. Claus, *Aktuel Urol.*, **8**, 207 (1977).

(7) V. J. Caride, H. D. Sostman, J. Twickler, H. Zacharis, S. C. Orphanoudakis, and C. C. Jaffe, *Invest. Rad.*, **17**, 381 (1982).

(8) A. Havron, S. E. Seltzer, A. D. Michael, and P. Shulkin, *Radiology*, **140**, 507 (1981).

(9) W. S. Singleton, M. S. Gray, M. L. Brown, and J. L. White, *J. Am. Oil Chem. Soc.*, **42**, 53 (1965).

(10) A. Legrand, J. Delattre, F. Paolaggi, L. Michael, M. Tescher, and M. L. Girard, *Pathol. Biol.*, **24**, 160 (1976).

(11) T. Yotsuyanagi, M. Nonomura, and K. Ikeda, *J. Parent. Sci. Technol.*, **35**, 271 (1981).

(12) M. Takayama, S. Ktoh, T. Nagasaki, and I. Tanimizu, *Clin. Chim. Acta*, **79**, 93 (1977).

(13) R. L. Juliano and D. Stamp, *Biochim. Biophys. Acta*, **586**, 137 (1979).
(14) J. DeGier, J. G. Mandersloot, and L. L. M. Van Deeneen, *Biochim. Biophys. Acta*, **173**, 143 (1969).
(15) D. A. Tyrrell, T. D. Heath, C. M. Colley, and B. E. Ryman, *Biochim. Biophys. Acta*, **457**, 259 (1976).
(16) A. D. Bangham, J. DeGier, and G. D. Geville, *Chim. Phys. Lipids*, **1**, 225 (1967).
(17) H. Hauser, *I. Trends Pharm. Sci.*, **7**, 274 (1982).
(18) "The British Pharmacopoeia," Her Majesty's Stationary Office, London, England, 1973.

ACKNOWLEDGMENTS

Part of this investigation was presented at the 3rd International Conference on Pharmaceutical Technology, Paris, 1983.

Gastric and Intestinal Absorption of Captopril in Acutely and Chronically Treated Rats: Comparison with Salicylic Acid

PETER J. WORLAND ˣ, OLAF H. DRUMMER, and BEVYN JARROTT

Received December 12, 1983, from the *University of Melbourne, Department of Medicine, Clinical Pharmacology and Therapeutics Unit, Austin Hospital, Heidelberg, Victoria, 3084, Australia.* Accepted for publication April 4, 1984.

Abstract □ The gastric and intestinal absorption of captopril, an orally active angiotensin-converting enzyme inhibitor was determined using rat *in situ* gastric pouch and intestinal loop techniques and compared with the absorption of another acidic drug, salicylic acid, whose absorption has been well established from both gastric and intestinal sites. Captopril absorption was determined at two initial intraluminal concentrations in acute (untreated) rats and in rats that had been chronically treated with captopril. Salicylic acid absorption was determined at one concentration in acute rats. During the 40-min experimental period, captopril absorption at the 4.6 mM dose from the gastric pouch was 17.0 ± 1.8% and 17.9 ± 5.4% in acute and chronically treated rats, respectively, and 33.6 ± 9.2% and 23.7 ± 7.6%, respectively, from the intestinal loop. At the 11.5 mM dose the captopril absorption in 40 min was 13.7 ± 2.7% and 17.3 ± 4.2% from the gastric pouch of acutely and chronically treated rats, respectively, and 17.8 ± 4.2% and 22.9 ± 3.3%, respectively, from the intestinal loop. As similar fractions of the different administered doses were absorbed from the respective gastric and intestinal sites in both acutely and chronically treated rats, the absorption process of captopril appears to be principally by passive diffusion and unaffected by chronic administration of captopril. In comparison, salicylic acid was absorbed more rapidly and to a greater extent from both the gastric and intestinal preparations. The percent of salicylic acid absorbed into the plasma at the 11.5 mM dose was 44.8 ± 4.4% and 65.3 ± 5.3% from the gastric and intestinal preparations, respectively. It is concluded that gastric absorption of captopril does occur, but its relative importance to intestinal absorption is dependent on the transit time from the gastric to intestinal site.

Keyphrases □ Captopril—*in situ* absorption, comparison with salicylic acid, rats □ Salicylic acid—*in situ* absorption, comparison with captopril, rats

Captopril, 1-[(2*S*)-3-mercapto-2-methylpropionyl]-pyrrolidine-2-carboxylic acid is the first orally effective, antihypertensive drug in a new class of angiotensin-converting enzyme inhibitors. This drug contains a reactive thiol group postulated to be necessary for its binding to the Zn^{2+} of the angiotensin-converting enzyme (1). However, this functional group also reacts to form low molecular weight disulfide conjugates of captopril in tissues such as liver and kidney (2, 3). Captopril also forms covalent links with plasma proteins *via* disulfide linkages with thiol-containing residues (4) and this may explain the extensive tissue binding of captopril (3). Possible significant alterations in the pharmacokinetics of captopril, particularly following chronic treatment, could result from tissue uptake saturation and binding processes.

Several studies on the disposition of captopril in humans and laboratory animals (3, 5–8) have found an early appearance of captopril in the plasma following oral administration with peak drug levels usually occurring within 1 h. As captopril is a structural derivative of the amino acid proline, there exists the possibility that it could be a substrate for an amino acid transport process that rapidly transports captopril across the gut wall. Additionally, the acidic nature of the drug would, according to the pH partition hypothesis (9), allow passive absorption from the highly acidic gastric site prior to entry into the intestinal absorptive sites. Recently, a clinical study with captopril observed much higher blood levels of the drug following chronic treatment than acute captopril administration, suggesting an increase in the rate and extent of absorption and bioavailability (5). However, no studies to date have directly examined whether changes in the absorption rate occur during chronic therapy.

The definition of the sites and processes involved in the absorption of captopril into the systemic circulation has an important place in the description of the disposition of captopril. In this study, the recently described *in situ* gastric pouch and *in situ* intestinal loop preparations (10, 11) have been utilized to investigate captopril absorption at these sites using acute (untreated) rats and rats chronically treated with captopril over 40 d. These techniques offer the advantage of allowing direct determination of drug traversing the gut wall and also enable the quantitation of any metabolites that may be produced that contribute to a "first pass" effect from either the gastric or intestinal sites. For comparison, we have included in the study the acidic drug salicylic acid, which is known to be readily absorbed from both sites (12).

EXPERIMENTAL SECTION

Materials—Captopril[1], captopril disulfide dimer[1], and salicylic acid[2] were used in the experiments. For the measurement of captopril using a gas chromatographic-mass spectrometric (GC–MS) assay, 3-(3-mercapto-2-methyl-propionyl)-4-thiazolidine carboxylic acid[3] (YS-980) was used as an

[1] E. R. Squibb & Sons Pty. Ltd., N.J.
[2] Pharmacopoeial purity.
[3] Courtesy of Dr. J. Iwao, Santen Pharmaceutical, Osaka, Japan.

0022-3549/84/1200-1755$01.00/0
© 1984, American Pharmaceutical Association

(13) R. L. Juliano and D. Stamp, *Biochim. Biophys. Acta*, **586**, 137 (1979).
(14) J. DeGier, J. G. Mandersloot, and L. L. M. Van Deeneen, *Biochim. Biophys. Acta*, **173**, 143 (1969).
(15) D. A. Tyrrell, T. D. Heath, C. M. Colley, and B. E. Ryman, *Biochim. Biophys. Acta*, **457**, 259 (1976).
(16) A. D. Bangham, J. DeGier, and G. D. Geville, *Chim. Phys. Lipids*, **1**, 225 (1967).
(17) H. Hauser, *I. Trends Pharm. Sci.*, **7**, 274 (1982).
(18) "The British Pharmacopoeia," Her Majesty's Stationary Office, London, England, 1973.

ACKNOWLEDGMENTS

Part of this investigation was presented at the 3rd International Conference on Pharmaceutical Technology, Paris, 1983.

Gastric and Intestinal Absorption of Captopril in Acutely and Chronically Treated Rats: Comparison with Salicylic Acid

PETER J. WORLAND ˣ, OLAF H. DRUMMER, and BEVYN JARROTT

Received December 12, 1983, from the *University of Melbourne, Department of Medicine, Clinical Pharmacology and Therapeutics Unit, Austin Hospital, Heidelberg, Victoria, 3084, Australia.* Accepted for publication April 4, 1984.

Abstract □ The gastric and intestinal absorption of captopril, an orally active angiotensin-converting enzyme inhibitor was determined using rat *in situ* gastric pouch and intestinal loop techniques and compared with the absorption of another acidic drug, salicylic acid, whose absorption has been well established from both gastric and intestinal sites. Captopril absorption was determined at two initial intraluminal concentrations in acute (untreated) rats and in rats that had been chronically treated with captopril. Salicylic acid absorption was determined at one concentration in acute rats. During the 40-min experimental period, captopril absorption at the 4.6 mM dose from the gastric pouch was 17.0 ± 1.8% and 17.9 ± 5.4% in acute and chronically treated rats, respectively, and 33.6 ± 9.2% and 23.7 ± 7.6%, respectively, from the intestinal loop. At the 11.5 mM dose the captopril absorption in 40 min was 13.7 ± 2.7% and 17.3 ± 4.2% from the gastric pouch of acutely and chronically treated rats, respectively, and 17.8 ± 4.2% and 22.9 ± 3.3%, respectively, from the intestinal loop. As similar fractions of the different administered doses were absorbed from the respective gastric and intestinal sites in both acutely and chronically treated rats, the absorption process of captopril appears to be principally by passive diffusion and unaffected by chronic administration of captopril. In comparison, salicylic acid was absorbed more rapidly and to a greater extent from both the gastric and intestinal preparations. The percent of salicylic acid absorbed into the plasma at the 11.5 mM dose was 44.8 ± 4.4% and 65.3 ± 5.3% from the gastric and intestinal preparations, respectively. It is concluded that gastric absorption of captopril does occur, but its relative importance to intestinal absorption is dependent on the transit time from the gastric to intestinal site.

Keyphrases □ Captopril—*in situ* absorption, comparison with salicylic acid, rats □ Salicylic acid—*in situ* absorption, comparison with captopril, rats

Captopril, 1-[(2*S*)-3-mercapto-2-methylpropionyl]-pyrrolidine-2-carboxylic acid is the first orally effective, antihypertensive drug in a new class of angiotensin-converting enzyme inhibitors. This drug contains a reactive thiol group postulated to be necessary for its binding to the Zn^{2+} of the angiotensin-converting enzyme (1). However, this functional group also reacts to form low molecular weight disulfide conjugates of captopril in tissues such as liver and kidney (2, 3). Captopril also forms covalent links with plasma proteins *via* disulfide linkages with thiol-containing residues (4) and this may explain the extensive tissue binding of captopril (3). Possible significant alterations in the pharmacokinetics of captopril, particularly following chronic treatment, could result from tissue uptake saturation and binding processes.

Several studies on the disposition of captopril in humans and laboratory animals (3, 5–8) have found an early appearance of captopril in the plasma following oral administration with peak drug levels usually occurring within 1 h. As captopril is a structural derivative of the amino acid proline, there exists the possibility that it could be a substrate for an amino acid transport process that rapidly transports captopril across the gut wall. Additionally, the acidic nature of the drug would, according to the pH partition hypothesis (9), allow passive absorption from the highly acidic gastric site prior to entry into the intestinal absorptive sites. Recently, a clinical study with captopril observed much higher blood levels of the drug following chronic treatment than acute captopril administration, suggesting an increase in the rate and extent of absorption and bioavailability (5). However, no studies to date have directly examined whether changes in the absorption rate occur during chronic therapy.

The definition of the sites and processes involved in the absorption of captopril into the systemic circulation has an important place in the description of the disposition of captopril. In this study, the recently described *in situ* gastric pouch and *in situ* intestinal loop preparations (10, 11) have been utilized to investigate captopril absorption at these sites using acute (untreated) rats and rats chronically treated with captopril over 40 d. These techniques offer the advantage of allowing direct determination of drug traversing the gut wall and also enable the quantitation of any metabolites that may be produced that contribute to a "first pass" effect from either the gastric or intestinal sites. For comparison, we have included in the study the acidic drug salicylic acid, which is known to be readily absorbed from both sites (12).

EXPERIMENTAL SECTION

Materials—Captopril[1], captopril disulfide dimer[1], and salicylic acid[2] were used in the experiments. For the measurement of captopril using a gas chromatographic-mass spectrometric (GC–MS) assay, 3-(3-mercapto-2-methyl-propionyl)-4-thiazolidine carboxylic acid[3] (YS-980) was used as an

[1] E. R. Squibb & Sons Pty. Ltd., N.J.
[2] Pharmacopoeial purity.
[3] Courtesy of Dr. J. Iwao, Santen Pharmaceutical, Osaka, Japan.

0022-3549/84/1200-1755$01.00/0
© 1984, American Pharmaceutical Association

internal standard (3). Other chemicals required for the GC–MS assay were obtained as described previously (3) and all other chemicals were analytical reagent grade.

***In Situ* Gut Preparations**—Male Wistar–Kyoto rats (215–300 g) that had access to food and water *ad libitum* were used for both gastric and intestinal absorption experiments. The gastric pouches were prepared as previously described (10). Briefly, following anesthetizing the animal with pentobarbital sodium (50 mg/kg ip), a jugular vein cannula was implanted for administering heparin (3000 IU/kg) and for whole blood replacement. A cannula for the collection of systemic blood samples was placed into the carotid artery. The esophagus, pylorus, pyloric blood vessels, and the branches of the gastroepiploic blood vessels were ligated. Gastric contents were removed *via* a small incision made in the rat forestomach and the pouch was rinsed clean with saline. Remaining fluid was removed with an absorbent tissue. After transposition of the stomach, and exposing the left gastric vein, a 21-gauge needle attached to a 15-cm length of polyethylene tubing (0.75-mm i.d., 1.45-mm o.d.) was inserted into the vein to allow collection of the venous blood draining the pouch. The drug was then administered *via* a syringe tied into the incision made earlier in the forestomach.

A slight modification of the method previously described by Worland and Ilett (11) was used for preparing the *in situ* intestinal loops. Slightly larger sections (length, 8–10 cm) of jejunum were selected and the same size needle (21 gauge) and cannula length (15 cm) employed for the gastric pouches were used to cannulate the vein leading away from the *in situ* loop. Blood samples were collected from the *in situ* gut preparation over 4-min intervals for a total of 40 min for all experiments.

To maintain blood flow through the *in situ* gut preparations, heparinized whole blood replacement was given *via* the jugular vein at 0.7 mL/min using a peristaltic pump[4]. The blood collected immediately prior to the experiment from donor rats was continually mixed during the replacement by a gently oscillating reservoir.

The stomach and intestine were able to adjust the pH of the administered drug in saline solutions to the physiological relevant values (~1.0 and 6.3, respectively) within a 5-min period.

Captopril was prepared at concentrations of 4.6 or 11.5 mM in normal saline (0.9% NaCl) within 2 min of being administered in a 0.5-mL volume to the isolated gut preparations. These concentrations of captopril were chosen as they approximate doses of 2 mg/kg and 5 mg/kg which are known to be pharmacologically active when given orally to rats (1). Salicylic acid was given in a 0.5-mL volume in normal saline only at a concentration of 11.5 mM.

Rat Treatment—Rats were treated with 1 mg/kg of captopril by gavage twice daily for 40 d prior to the absorption experiment; the last dose was given 14 h prior to the experiment. The male Wistar–Kyoto rats used in the study were 250–300 g at the time of the experiment.

Determination of Captopril and Salicylic Acid Levels—For the assay of free captopril using GC–MS, an aliquot of the blood sample (200 μL) was taken immediately after sample collection and added to glass extraction tubes containing 2 mg of *N*-ethylmaleimide (20 mg/mL solution in water). Internal standard (4 μg of 1-mg/mL solution in acetone) was included. The determination of total captopril (free captopril and disulfide conjugates) was obtained following reduction of disulfide bonds using the reducing agent dithiothreitol (3). Samples were also assayed for the *S*-methyl metabolite of captopril (3, 13). At the completion of the experiment, the gut tissue used for either the gastric pouch or the intestinal loop was rinsed with saline, blotted, and then finely minced in 5 volumes of phosphate buffer (0.05 M, pH 7.4). It was then homogenized with a homogenizer[5] for 45 s and an aliquot was taken to assay total captopril. Salicylic acid levels were determined from plasma collected from the *in situ* gut preparations using HPLC as described (10).

Data Analysis—The BMDP statistical software package (14) was used for the analysis of variance (ANOVA, one- and two-way). A significant difference was assumed at the $p < 0.05$ level in all statistical tests. The results are expressed as the mean ± *SEM* of four experiments.

RESULTS AND DISCUSSION

Captopril has previously been observed to be rapidly absorbed into the systemic circulation following oral administration (3, 5–8), and the gastric absorption of captopril, an acidic drug ($pK_a = 3.7$)[6] could be expected to contribute to its early appearance in systemic blood samples. In addition to passive absorption of captopril from either the gastric or intestinal regions, there is the possibility of an active absorption process in the small intestine principally intended for amino acids, but capable of transporting captopril as it is a structural derivative of the amino acid proline. The experiments reported herein have utilized *in situ* gastric pouch and intestinal loop preparations to directly determine the absorption of captopril from both the gastric and intestinal sites as represented by these *in situ* gut preparations. Although these preparations can only approximate the real situation, as the animal is anesthetized and the absorption site is necessarily restricted to either the stomach or a section of jejunum, they do allow a direct comparative measurement of drug absorption and drug metabolism across the gut wall from the respective regions.

Table I—Percent of Administered Captopril Dose in Effluent Venous Blood from *In Situ* Gut Preparations[a]

Initial Intraluminal Concentration, mM	Gastric Pouch		Intestinal Loop	
	Total Captopril	Disulfide Conjugates	Total Captopril	Disulfide Conjugates
4.6				
Acute	17.0 ± 1.8	5.4 ± 2.7	33.6 ± 9.2	3.1 ± 1.8
Chronic	17.9 ± 5.4	1.7 ± 1.4	23.7 ± 7.6	0.4 ± 0.2
11.5				
Acute	13.7 ± 2.7	1.5 ± 1.0	17.8 ± 4.2	1.9 ± 1.4
Chronic	17.3 ± 4.2	6.7 ± 4.9	22.9 ± 3.3	1.1 ± 1.0

[a] Taken over 40 min. Results presented as mean percent ± *SEM* ($n = 4$).

The percentages of captopril doses absorbed into the blood draining the *in situ* gut preparations are shown in Table I. No significant differences between the acutely and chronically treated rats were observed in either the gastric or intestinal preparations at either initial intraluminal concentrations of 4.6 or 11.5 mM. Also, the extent of disulfide conjugates appearing as metabolites from the gastric or intestinal sites at either initial concentration of captopril were not different. Captopril (detection limit, 1 ng) was not detected in systemic blood samples obtained at the completion of the experiment (40 min) indicating that the collected blood from the *in situ* gut preparation contained only absorbed drug and its metabolite produced during the absorption from the tissue or within the blood draining the tissue. A similar percentage of administered dose, to either the gastric or the intestinal preparation, was absorbed at the two concentrations; this suggests that the predominant absorption mechanism is a passive process at these doses. The significant absorption from the gastric preparation suggests that gastric absorption contributes to the early appearance of captopril in the plasma observed after oral administration of the drug (3, 5–8).

The extent of disulfide formation was small and variable. Earlier work on the biotransformation of captopril in blood by Wong *et al.* (15) has shown that, following the addition of captopril to whole rat blood and immediately attempting to stabilize the free drug with *N*-ethylmaleimide, ~17% of added captopril was covalently bound to whole blood components. Similar results were obtained by Park *et al.* (4). In our experiments the sample collection period from the gastric pouch and intestinal loop was 4 min and it would seem plausible that the extent of disulfide formation observed has occurred entirely

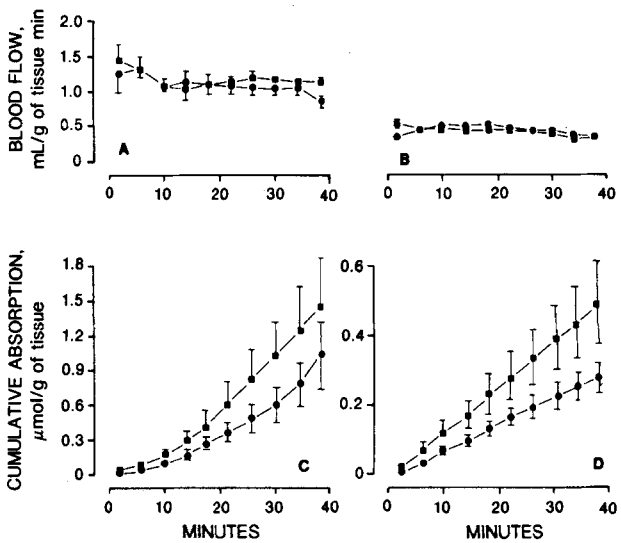

Figure 1—*Blood flow from* in situ *gut sections of rats receiving a single dose of captopril and the cumulative absorption of captopril at 4.6 mM (●) and 11.5 mM (■) initial intraluminal concentration for the intestinal (A, C) and gastric regions (B, D). Results are mean* ± SEM (n = 4)*; error bars are not shown if less than symbol size.*

[4] Manostat, N.Y.
[5] Polytron PT-10; Kinematica, Lucerne, Switzerland.
[6] E. R. Squibb & Sons Pty. Ltd. representative, personal communication.

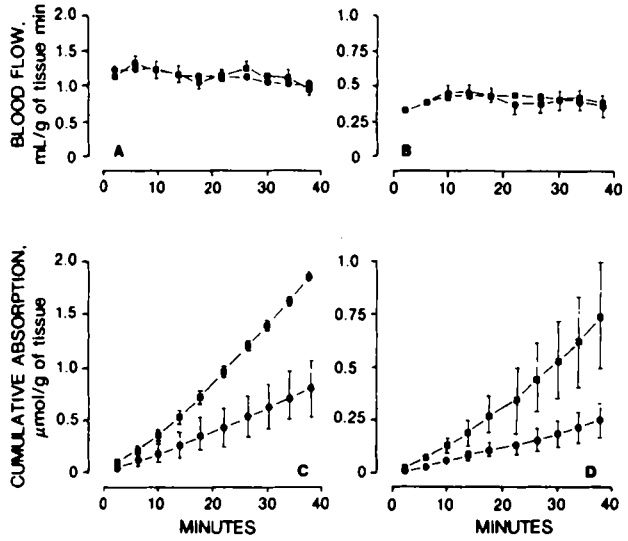

Figure 2—*Blood flow from* in situ *gut sections of rats chronically treated with captopril and the cumulative absorption of captopril at 4.6 mM (●) and 11.5 mM (■) initial intraluminal concentrations for the intestinal (A, C) and the gastric regions (B, D). Results are mean ± SEM (n = 4); error bars are not shown if less than symbol size.*

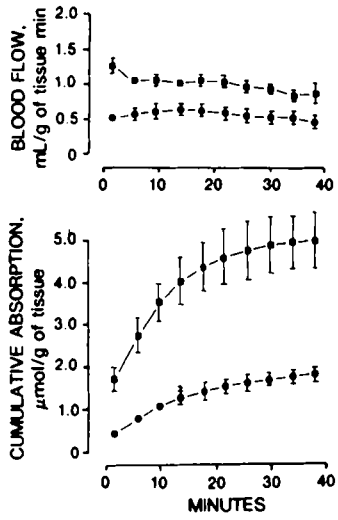

Figure 3—*Blood flow from the* in situ *gastric (●) and intestinal (■) preparations and the cumulative absorption of salicylic acid at 11.5 mM initial intraluminal concentration into the plasma. Results are mean ± SEM (n = 4); error bars are not shown if less than symbol size.*

within the blood and not the gut wall. The *S*-methyl metabolite of captopril was not detected in the blood draining from either the gastric or intestinal preparation. This metabolite has been detected in human and animal studies following oral administration of captopril (3, 13, 16), but does not appear to be produced from either the gastric or intestinal site during the absorption process.

Blood flow through the intestinal tissue has been demonstrated to be an important factor in the absorption of drugs (17-20) particularly when movement of the drug across lipoidal barriers is not the rate-limiting step. In order to eliminate possible changes in the absorption rate that may have resulted from variable blood flow, replacement blood was delivered at a constant rate throughout the experiment. The blood flow rates from the gastric pouch and intestinal loop preparations that had been given captopril are shown in the upper panels of Figs. 1 and 2. The blood flow rates did not vary significantly during the experiments and were not affected by either the dose of captopril or the chronic treatment with captopril. On the standardized basis of blood flow per gram of wet weight tissue, the blood flow from intestinal loops was two- to threefold greater than that of the gastric pouches. The weights of the intestinal segments used for the captopril (and salicylic acid) experiments were not significantly different between groups (overall mean weight, 0.74 g). Similarly, the weights of the gastric pouches (overall mean weight 1.59 g for the captopril and salicylic acid experiments) were not significantly different between groups as tested by an ANOVA (one-way).

The lower panels of Figs. 1 and 2 show the cumulative absorption of captopril during the experiments using the acutely and chronically treated rats at the two doses. The graphs are plotted on a standardized basis of per unit wet tissue weight to show differences in the capacity for absorption between the gastric and intestinal tissue. On this standardized basis, the intestinal tissue absorbed a significantly greater amount of captopril than the gastric tissue (ANOVA, two-way, $p < 0.001$) and the magnitude of the difference in the amount of captopril absorbed was similar to the difference observed in blood flow from the two sites. The back extrapolation of the terminal phase of the intestinal absorption plots from the acutely treated rats suggests a lag phase for absorption in the early period of the experiment. This phase was not as prominent in the corresponding gastric absorption and intestinal absorption plots obtained from the chronically treated rats.

Table II—Gut Tissue Concentrations of Total Captopril [a]

Initial Intraluminal Concentration, mM	Gastric Pouch	Intestinal Loop
4.6		
Acute	381.3 ± 78.0 (24.5%)[b]	1515.6 ± 199.6 (49.3%)
Chronic	278.5 ± 46.8 (23.3%)	1390.0 ± 278.6 (42.7%)
11.5		
Acute	389.2 ± 78.0 (10.9%)	1192.8 ± 238.4 (15.0%)
Chronic	597.0 ± 194.5 (16.7%)	1374.6 ± 382.4 (17.2%)

[a] In nmol/g of tissue wet weight, determined at the completion of the absorption experiments. Results presented as mean ± *SEM* ($n = 4$). [b] Values in parentheses represent the amount in the tissue as a percentage of the dose administered.

Gut tissue concentrations of total captopril were determined at the completion of the experiment. The total captopril concentrations in the gut walls from either the gastric or the intestinal tissue were not different after different doses. This suggests a saturation of tissue uptake of captopril and is perhaps more clearly shown as a percentage of administered dose. At the higher administered dose a lower percentage of the dose is found within the gut wall (Table II).

The results of this study demonstrate that in rats the rate of captopril absorption from both the gastric and intestinal sites is unchanged after chronic captopril treatment, supporting a previous report that indicated pretreatment of mice for a minimum of 14 d did not affect the extent of absorption or bioavailability of captopril as assessed by urinary excretion (21). However, these rodent studies do not conform with a report of captopril kinetics in hypertensive patients (5) in which greater plasma levels of the drug were achieved after chronic usage, suggesting a possible increase in the bioavailability of captopril.

As captopril is an acidic drug, it was of interest to compare the absorption characteristics as determined by these *in situ* gut preparations with salicylic acid, a drug whose absorption has been well studied (12, 17). The cumulative absorption of salicylic acid on the standardized basis of unit weight from the gastric and intestinal *in situ* preparations is shown in the lower panel of Fig. 3 with the respective blood flows shown in the upper panel. Significant, but small differences in blood flow were found by an ANOVA (two-way) when comparing blood flow from the intestinal loop after receiving either captopril at the two doses (acutely and chronically treated rats) or salicylic acid at the 11.5-mM dose. This was also true for blood flow from the gastric pouch. Blood flow through the intestine was less following salicylic acid administration relative to captopril ($p < 0.001$) but greater from the gastric pouch after salicylic acid than captopril ($p < 0.0001$). During the 40-min experimental period, 44.7 ± 4.4% and 65.3 ± 5.0% of the salicylic acid added to the lumen was absorbed into the plasma draining through the *in situ* stomach and intestinal preparations, respectively. The majority of this was absorbed in the first 12 min of the experiment and a lag phase for salicylic acid absorption was not evident from the absorption profiles with the collection times shown in Fig. 3. The salicylic acid absorption profiles differ markedly from those observed with captopril. This difference resulted from a greater absorption rate for salicylic acid from the gastric and intestinal loop. Twelve minutes after administration of salicylic acid ~25 and ~46% of the administered dose to the gastric and intestinal sites, respectively, had been absorbed into the plasma. In comparison, captopril absorption was only 3.3 and 2.3% of the same molar dose from the *in situ* gastric and intestinal loop preparations in 12 min. Thus for salicylic acid, the large changes in the amounts and the concentration within the gut lumen would result in a decrease in the driving force for absorption across the gut wall. For captopril, although the absorption process at the doses given suggests passive absorption, the absorption rate was not observed to decrease during the experiment. This can be expected as the intraluminal captopril concentrations would not be altering as rapidly nor to the same extent as salicylic acid within the time of the experiment.

In summary, our results have shown that the gastric absorption of captopril would contribute to the early appearance of captopril in the blood, but the intestine has a greater capacity than the stomach for the absorption of captopril and the relative magnitude of captopril absorption from the gastric site will depend on the transit rate through the stomach. Furthermore, it has been shown that chronic treatment of captopril in the rat does not increase the rate of captopril absorption from either the stomach or intestine. In comparison to salicylic acid, captopril is not as rapidly absorbed from either the stomach or intestine.

REFERENCES

(1) M. J. Antonaccio, *Ann. Rev. Pharmacol. Toxicol.*, **22**, 57 (1982), and references therein.

(2) T. Komai, T. Ikeda, K. Kawai, E. Kameyama, and H. Shindo, *J. Pharm. Dyn.*, **4**, 677 (1981).

(3) O. H. Drummer, P. J. Worland, and B. Jarrott, *Biochem. Pharmacol.*, **32**, 1563 (1983).

(4) B. K. Park, P. S. Grabowski, J. H. K. Yeung, and A. M. Breckenridge, *Biochem. Pharmacol.*, **31**, 1755 (1982).

(5) B. Jarrott, O. Drummer, R. Hooper, A. E. I. Anderson, P. J. Miach, and W. J. Louis, *Am. J. Cardiol.*, **49**, 1547 (1982).

(6) S. M. Singhvi, D. N. McKinstry, J. M. Shaw, D. A. Willard, and B. H. Migdalof, *J. Clin. Pharmacol.*, **22**, 135 (1982).

(7) A. I. Cohen, R. G. Devlin, E. Ivashkiv, P. T. Funke, and T. McCormick, *J. Pharm. Sci.*, **71**, 1251 (1982).

(8) K. L. Duchin, S. M. Singhvi, D. A. Willard, B. H. Migdalof, and D. N. McKinstry, *Clin. Pharmacol. Ther.*, **31**, 452 (1982).

(9) L. S. Schanker, *J. Med. Pharm. Chem.*, **2**, 343 (1960).

(10) P. J. Worland, O. H. Drummer, and B. Jarrott, *J. Pharmacol. Methods*, **10**, 215 (1983).

(11) P. J. Worland and K. F. Ilett, *J. Pharm. Pharmacol.*, **35**, 636 (1983).

(12) J. T. Doluisio, N. F. Billups, L. W. Dittert, E. T. Sugita, and J. V. Swintosky, *J. Pharm. Sci.*, **58**, 1196 (1969).

(13) O. H. Drummer, B. Jarrott, and W. J. Louis, *Clin. Exp. Pharmacol. Physiol.*, **Suppl 7**, 81 (1982).

(14) W. J. Dixon, M. B. Brown, L. Engelman, J. W. Frane, M. A. Hill, R. I. Jennrich, and J. D. Toporek, "BMDP Statistical Software," University of California Press, Berkeley, Calif., 1981, pp. 237–345.

(15) K. K. Wong, S.-J. Lan, and B. H. Migdalof, *Biochem. Pharmacol.*, **30**, 2643 (1981).

(16) T. Ikeda, T. Komai, K. Kawai, and H. Shindo, *Chem. Pharm. Bull.*, **29**, 1416 (1981).

(17) H. Ochsenfarht, *N.S. Arch. Pharmacol.*, **306**, 105 (1979).

(18) D. Winne, *Pharmacology*, **21**, 1 (1980).

(19) W. H. Barr and S. Riegelman, *J. Pharm. Sci.*, **59**, 154 (1970).

(20) W. G. Crouthamel, L. Diamond, L. W. Dittert, and J. T. Doluisio, *J. Pharm. Sci.*, **64**, 664 (1975).

(21) S. M. Singhvi, K. J. Kripalani, A. V. Dean, G. R. Keim, J. S. Kulesza, F. S. Meeker, Jr., J. J. Ross, Jr., J. M. Shaw, and B. H. Migdalof, *J. Pharm. Sci.*, **70**, 885 (1981).

ACKNOWLEDGMENTS

The authors thank the National Health and Medical Research Council of Australia for their financial assistance.

Pharmacokinetics of Probucol in Male Rats

JOEL F. HEEG ˣ, MICHAEL F. HISER, DARLENE K. SATONIN, and JAMES Q. ROSE

Received July 15, 1983, from the *Department of Pharmacokinetics and Drug Metabolism*, and the *Department of Bioanalytical Chemistry, Merrell Dow Research Institute-Indianapolis Center, Indianapolis, IN 46268-0470.* Accepted for publication April 5, 1984.

Abstract □ The bioavailability and pharmacokinetic behavior of 10 mg/kg of [^{14}C]probucol in an oil-water emulsion was determined after oral and intravenous administration to rats. The bioavailability of the oral formulation was ~6%. For the first 12-h interval after the intravenous bolus, plasma probucol concentrations increased after an initial decrease. This effect may be attributed to the formulation or precipitation of the drug in the vasculature. The terminal plasma half-life was 6 d. By 7 d, 45 and 4.65% of the labeled intravenous bolus was excreted in the feces and in the urine, respectively. Although most of the labeled dose was excreted in the bile, any enterohepatic recirculation that did occur did not contribute to the atypical plasma concentration *versus* time profile. The tissue distribution of the label and elimination rates in the bile differed between the two routes of administration. Either the total body burden, precipitation of the drug, or the emulsion vehicle may be responsible for the nonlinear distribution and clearance of the intravenous dose.

Keyphrases □ Bioavailability—oil-in-water emulsion, tissue distribution, probucol, biliary elimination, rats □ Probucol—bioavailability, oil-in-water emulsion, tissue distribution, biliary elimination

Probucol (I)[1], 4,4′-[(1-methylethylidene)bis(thio)]-bis[2,6-bis(1,1-dimethylethyl)]phenol, is an orally effective hypocholesterolemic drug. Its efficacy has been demonstrated in mice, rats, monkeys, and humans (1), and its chemical structure is unlike that of other hypocholesterolemic agents. There are no published pharmacokinetic studies of probucol in rats to characterize the dose-response of the drug (2) and only recently have aspects of the pharmacokinetic behavior of probucol in humans been presented (3).

The present pharmacokinetic studies were conducted in rats. Long-term toxicity and efficacy studies have been conducted in rats and other rodent and nonrodent species, and the identity of pharmacokinetic parameters that might assist interpretation of the outcome of the dose-response studies was sought.

EXPERIMENTAL SECTION

Probucol Formulations—[Ring(U)-^{14}C]probucol[2] with a specific activity of 7.58 or 34.1 μCi/mg was used for distribution and excretion studies. The compound is labeled with statistical uniformity in all positions of each ring. A radiochemical purity of >98% was determined with TLC, autoradiography, and liquid scintillation counting (LSC) techniques. Two TLC systems were used: hexane–benzene (80:20) and hexane–ether (95:5) on silica gel (0.25 mm) plates[3]. Uniformly ring-labeled [^{14}C]probucol with a specific activity of 34.1 μCi/mg and a radiochemical purity of 99.5% by HPLC and LSC techniques was used for the biliary excretion studies. Labeled probucol was mixed with nonlabeled probucol which had a chemical purity of >99.5% to provide the intended regimens of oral and intravenous probucol. The specific activities of the resultant mixtures ranged from 1.57 to 8.74 μCi/mg.

Both oral and intravenous formulations of probucol were prepared as oil-

[1] Merrell Dow Research Institute-Cincinnati Center. Available in the U.S. under the trademark Lorelco.

[2] Synthesized by D. F. Gransden and G. A. Roth, The Dow Chemical Co., Midland, Mich.

[3] Silica Gel, F-254; MCB Manufacturing Chemists, Inc., Cincinnati, Ohio.

0022-3549/84/1200-1758$01.00/0

© 1984, American Pharmaceutical Association

In summary, our results have shown that the gastric absorption of captopril would contribute to the early appearance of captopril in the blood, but the intestine has a greater capacity than the stomach for the absorption of captopril and the relative magnitude of captopril absorption from the gastric site will depend on the transit rate through the stomach. Furthermore, it has been shown that chronic treatment of captopril in the rat does not increase the rate of captopril absorption from either the stomach or intestine. In comparison to salicylic acid, captopril is not as rapidly absorbed from either the stomach or intestine.

REFERENCES

(1) M. J. Antonaccio, *Ann. Rev. Pharmacol. Toxicol.*, **22**, 57 (1982), and references therein.

(2) T. Komai, T. Ikeda, K. Kawai, E. Kameyama, and H. Shindo, *J. Pharm. Dyn.*, **4**, 677 (1981).

(3) O. H. Drummer, P. J. Worland, and B. Jarrott, *Biochem. Pharmacol.*, **32**, 1563 (1983).

(4) B. K. Park, P. S. Grabowski, J. H. K. Yeung, and A. M. Breckenridge, *Biochem. Pharmacol.*, **31**, 1755 (1982).

(5) B. Jarrott, O. Drummer, R. Hooper, A. E. I. Anderson, P. J. Miach, and W. J. Louis, *Am. J. Cardiol.*, **49**, 1547 (1982).

(6) S. M. Singhvi, D. N. McKinstry, J. M. Shaw, D. A. Willard, and B. H. Migdalof, *J. Clin. Pharmacol.*, **22**, 135 (1982).

(7) A. I. Cohen, R. G. Devlin, E. Ivashkiv, P. T. Funke, and T. McCormick, *J. Pharm. Sci.*, **71**, 1251 (1982).

(8) K. L. Duchin, S. M. Singhvi, D. A. Willard, B. H. Migdalof, and D. N. McKinstry, *Clin. Pharmacol. Ther.*, **31**, 452 (1982).

(9) L. S. Schanker, *J. Med. Pharm. Chem.*, **2**, 343 (1960).

(10) P. J. Worland, O. H. Drummer, and B. Jarrott, *J. Pharmacol. Methods*, **10**, 215 (1983).

(11) P. J. Worland and K. F. Ilett, *J. Pharm. Pharmacol.*, **35**, 636 (1983).

(12) J. T. Doluisio, N. F. Billups, L. W. Dittert, E. T. Sugita, and J. V. Swintosky, *J. Pharm. Sci.*, **58**, 1196 (1969).

(13) O. H. Drummer, B. Jarrott, and W. J. Louis, *Clin. Exp. Pharmacol. Physiol.*, **Suppl 7**, 81 (1982).

(14) W. J. Dixon, M. B. Brown, L. Engelman, J. W. Frane, M. A. Hill, R. I. Jennrich, and J. D. Toporek, "BMDP Statistical Software," University of California Press, Berkeley, Calif., 1981, pp. 237–345.

(15) K. K. Wong, S.-J. Lan, and B. H. Migdalof, *Biochem. Pharmacol.*, **30**, 2643 (1981).

(16) T. Ikeda, T. Komai, K. Kawai, and H. Shindo, *Chem. Pharm. Bull.*, **29**, 1416 (1981).

(17) H. Ochsenfarht, *N.S. Arch. Pharmacol.*, **306**, 105 (1979).

(18) D. Winne, *Pharmacology*, **21**, 1 (1980).

(19) W. H. Barr and S. Riegelman, *J. Pharm. Sci.*, **59**, 154 (1970).

(20) W. G. Crouthamel, L. Diamond, L. W. Dittert, and J. T. Doluisio, *J. Pharm. Sci.*, **64**, 664 (1975).

(21) S. M. Singhvi, K. J. Kripalani, A. V. Dean, G. R. Keim, J. S. Kulesza, F. S. Meeker, Jr., J. J. Ross, Jr., J. M. Shaw, and B. H. Migdalof, *J. Pharm. Sci.*, **70**, 885 (1981).

ACKNOWLEDGMENTS

The authors thank the National Health and Medical Research Council of Australia for their financial assistance.

Pharmacokinetics of Probucol in Male Rats

JOEL F. HEEG ˣ, MICHAEL F. HISER, DARLENE K. SATONIN, and JAMES Q. ROSE

Received July 15, 1983, from the *Department of Pharmacokinetics and Drug Metabolism*, and the *Department of Bioanalytical Chemistry, Merrell Dow Research Institute-Indianapolis Center, Indianapolis, IN 46268-0470.* Accepted for publication April 5, 1984.

Abstract □ The bioavailability and pharmacokinetic behavior of 10 mg/kg of [^{14}C]probucol in an oil-water emulsion was determined after oral and intravenous administration to rats. The bioavailability of the oral formulation was ~6%. For the first 12-h interval after the intravenous bolus, plasma probucol concentrations increased after an initial decrease. This effect may be attributed to the formulation or precipitation of the drug in the vasculature. The terminal plasma half-life was 6 d. By 7 d, 45 and 4.65% of the labeled intravenous bolus was excreted in the feces and in the urine, respectively. Although most of the labeled dose was excreted in the bile, any enterohepatic recirculation that did occur did not contribute to the atypical plasma concentration *versus* time profile. The tissue distribution of the label and elimination rates in the bile differed between the two routes of administration. Either the total body burden, precipitation of the drug, or the emulsion vehicle may be responsible for the nonlinear distribution and clearance of the intravenous dose.

Keyphrases □ Bioavailability—oil-in-water emulsion, tissue distribution, probucol, biliary elimination, rats □ Probucol—bioavailability, oil-in-water emulsion, tissue distribution, biliary elimination

Probucol (I)[1], 4,4′-[(1-methylethylidene)bis(thio)]-bis[2,6-bis(1,1-dimethylethyl)]phenol, is an orally effective hypocholesterolemic drug. Its efficacy has been demonstrated in mice, rats, monkeys, and humans (1), and its chemical structure is unlike that of other hypocholesterolemic agents. There are no published pharmacokinetic studies of probucol in rats to characterize the dose-response of the drug (2) and only recently have aspects of the pharmacokinetic behavior of probucol in humans been presented (3).

The present pharmacokinetic studies were conducted in rats. Long-term toxicity and efficacy studies have been conducted in rats and other rodent and nonrodent species, and the identity of pharmacokinetic parameters that might assist interpretation of the outcome of the dose-response studies was sought.

EXPERIMENTAL SECTION

Probucol Formulations—[Ring(U)-^{14}C]probucol[2] with a specific activity of 7.58 or 34.1 μCi/mg was used for distribution and excretion studies. The compound is labeled with statistical uniformity in all positions of each ring. A radiochemical purity of >98% was determined with TLC, autoradiography, and liquid scintillation counting (LSC) techniques. Two TLC systems were used: hexane–benzene (80:20) and hexane–ether (95:5) on silica gel (0.25 mm) plates[3]. Uniformly ring-labeled [^{14}C]probucol with a specific activity of 34.1 μCi/mg and a radiochemical purity of 99.5% by HPLC and LSC techniques was used for the biliary excretion studies. Labeled probucol was mixed with nonlabeled probucol which had a chemical purity of >99.5% to provide the intended regimens of oral and intravenous probucol. The specific activities of the resultant mixtures ranged from 1.57 to 8.74 μCi/mg.

Both oral and intravenous formulations of probucol were prepared as oil-

[1] Merrell Dow Research Institute-Cincinnati Center. Available in the U.S. under the trademark Lorelco.

[2] Synthesized by D. F. Gransden and G. A. Roth, The Dow Chemical Co., Midland, Mich.

[3] Silica Gel, F-254; MCB Manufacturing Chemists, Inc., Cincinnati, Ohio.

0022-3549/84/1200-1758$01.00/0

© 1984, American Pharmaceutical Association

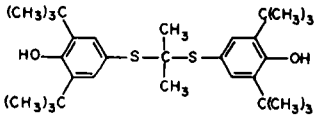

I

water emulsions. Probucol was dissolved in a saturated triglyceride from coconut oil[4]. The oil-water emulsion, like the physiologically compatible hyperalimentation emulsions, was then formulated to contain 4% glucose, 1.2% vegetable lecithin, 0.3% nonionic surfactant[5], and 15% of the saturated triglyceride containing the probucol. The mixture was sonicated[6] to form the emulsion. Because of the poor aqueous solubility of probucol, coconut oil or the above emulsion was used in previous pharmacological, toxicological, and clinical studies and in the studies reported here. All dose solutions were stored under nitrogen gas to prevent autoxidation.

Animal Maintenance and Posology—Adult male Sprague–Dawley rats were individually housed in modified, Roth-type glass metabolism chambers[7] for the separate collection of urine, feces, and expired air, or were housed in stainless-steel cages prior to sacrifice. Room air was drawn through the chambers (500–600 mL/min) and then scrubbed with a solution of ethanolamine–2-methoxyethanol (3:7) to trap any $^{14}CO_2$ as the carbamate. The rooms were temperature- and humidity-controlled and operated on a 12-h light/dark cycle. Water was provided *ad libitum* and food was withheld from the animals 4 h prior to and 4 h after dosage.

Two groups of four male rats were given a single 10-mg/kg dose of [^{14}C]probucol as an emulsion to determine the tissue distribution and the rates and routes of excretion. One group was given ~1.4 mL of the emulsion orally through stainless-steel feeding needles. The other group of rats was given ~0.3 mL iv of the emulsion over a 30-s period. The intravenous emulsion was injected into a jugular vein cannula implanted 48 h earlier. After the dose was injected, the cannula was flushed with 0.2 mL of saline.

The plasma distribution and clearance of 10 mg/kg of probucol or [^{14}C]-probucol was determined in two groups of male Sprague–Dawley rats. One group of 102 rats was given a 10-mg/kg iv dose of an 8.33-mg/mL emulsion (0.12 mL/100 g body weight) by way of a jugular cannula and a second group of 75 rats was given a single oral dose of a 1.67-mg/mL emulsion (0.6 mL/100 g body weight).

Biliary excretion studies were conducted with 11 adult male Sprague–Dawley rats. A cannula of polyethylene tubing[8] was inserted into the common bile duct, anterior to the pancreatic junction, passed subcutaneously, and exteriorized dorsally. Bile was allowed to flow continuously over a 3-d recovery period. On the second day after surgery, a jugular vein cannula was placed in six of the animals. On the third day a 10-mg/kg dose of [^{14}C]probucol emulsion was given by intravenous infusion, as described previously, to six of the rats and by oral gavage to the remaining five rats.

Sample Collection—To collect an adequate volume of blood for probucol analysis, rats were decapitated and exsanguinated at predetermined times. Following oral administration blood was collected at 0.25, 0.5, 0.75, 1, 2, 4, 6, 8, 12, 18, 24, 30, 36, 42, 48, 60, 72, 96, 120, 144, 192, 240, 288, 336, 384, 432, and 480 h postdose. Blood taken following intravenous dosing was similar except no samples were taken at 30 and 480 h and additional samples were taken at 168 h. Blood was taken from the jugular cannula or by decapitation for the biliary excretion studies. All samples were collected in heparinized containers, and the plasma fraction was stored frozen until analysis. Probucol had been shown to be stable for >16 months in frozen plasma. All analyses were completed within that time.

Urine was collected in dry ice traps, and both urine and feces were obtained every 6, 12, or 24 h and stored frozen until label analysis. The CO_2 trapping solution was changed frequently over the first 48-h test period. Tissues were harvested immediately after exsanguination and analyzed for concentrations of label activity or probucol. Bile was collected at 6-h intervals for 24 h after administration.

Sample Preparation for Probucol Analysis—*Plasma*—Plasma samples for the determination of probucol concentrations from 0.25 to 100 μg/mL were assayed by EC/GC or by HPLC and concentrations from 0.005 to 1.0 μg/mL were determined by GC/MS. All samples were fortified with aliquots of a methanolic solution containing the internal standard, 4,4′-[(1-methylbutylidene)bis(thio)]bis[2,6-bis(1,1-dimethylethyl)phenol], and the plasma protein was precipitated with methanol–acetone (3:2, v/v). After centrifugation, the liquid phase was extracted with hexane. Hexane extracts destined for HPLC were evaporated with nitrogen gas and reconstituted in methanol.

The hexane extracts destined for GC/MS were evaporated to dryness under nitrogen, reconstituted with benzene, and passed through a silica column[9]. The benzene eluant containing the probucol was evaporated to dryness under nitrogen, and the sample was reconstituted in methanol. Standard curves were prepared for all plasma samples by fortifying blank plasma with appropriate amounts of methanolic solutions of probucol prior to the above extraction schemes.

Tissue Samples—Tissues were homogenized[10] in ethanol–acetone (3:2, v/v) and diluted to 10 mL with ethanol–acetone. A 1-mL aliquot was transferred to a screw-cap test tube, and the internal standard was added along with 1 mL of hexane and 0.5 mL of water. After mixing and centrifugation, the hexane layer was evaporated to dryness with a nitrogen gas stream and the residue was reconstituted in methanol. Standard curves were prepared for tissue samples as described for plasma samples.

Instrumentation—*Electron-Capture Gas Chromatography*—The hexane extract of plasma destined for EC/GC[11] was injected directly onto a coiled glass GC column[12]. Operating conditions were as follows: carrier gas, 5% methane in argon; flow rate, 40 mL/min; injection port, 300°C; detector, 300°C; column, 270°C.

Gas Chromatography/Mass Spectrometry—The methanol extract of plasma destined for GC/MS[13] was injected onto a glass GC column[14]. Helium carrier gas at a flow rate of 20 mL/min was used. Temperatures were set as follows: injection port, 250°C; column, 280°C. The mass spectrometer was operated in the electron-impact mode. The fragment ions at *m/z* 278 (probucol) and *m/z* 306 (internal standard) were recorded by selective-ion monitoring.

Liquid Chromatography—A modular liquid chromatographic system was used in the analysis of probucol in plasma or tissue. The methanolic extracts were injected onto a reverse-phase column[15]. The HPLC system consisted of an autosampler[16], a high-pressure pump[17], and a fixed-wavelength UV (254 nm) detector[18]. The mobile phase consisted of acetonitrile, hexane, and 0.1 M ammonium acetate (900:35:65). The flow rate was 0.9 mL/min.

Analytical Recovery and Precision—The EC/GC procedure had a relative recovery of 98.4% and a relative precision at the 95% confidence level (C.L.) of 14.1%. The relative recovery of the HPLC assay was 97.2% and the relative precision was 9.6% (95% C.L.). For the lower concentrations of probucol determined by GC/MS, the relative recovery was 105.5% with a relative precision of 24% at the 95% C.L.

Sample Preparation for Radioactivity Analysis—The label activity in most of the samples was determined by direct LSC techniques. Plasma samples were prepared by the addition of 0.03–1.0 g of plasma to 0–1 mL of water; urine samples and cage washings were prepared by the addition of 0.5 mL of sample to 1 mL of water; and bile was prepared by the addition of 50 mg of bile to 1 mL of water. Ten milliliters of scintillation reagent[19,20] was then added to each sample. Exhaled $^{14}CO_2$ was trapped as the carbamate. Five milliliters of the trapping solution was then combined with 5 mL of a scintillation cocktail consisting of 120 mL of scintillation reagent[21], 220 mL of 2-methoxyethanol, and 660 mL of toluene.

Tissues were frozen in liquid nitrogen and pulverized by an electromagnetic, cryogenic impact grinding apparatus[22] (4). Samples (30–100 mg) of the pulverized tissues were added in triplicate to LSC vials containing 12 mL of scintillation fluid. A fine suspension was formed by the addition of 3 mL of water and shaking to form a sol–gel. The label activity in the samples was determined in the liquid scintillation counter[23]. External standardization was used to determine quench correction.

Aqueous fecal homogenates, equivalent to 150 mg of fecal solids, were oxidized by combustion[24] to CO_2 and trapped as the carbamate in 8 mL of a 30% solution of ethanolamine in 2-methoxyethanol. This solution was combined with 10 mL of the scintillation cocktail described earlier. Skin

[4] Noebec M-5; PVO International Inc., Boonton, N.J.
[5] Pluronic F-68; BASF Wyandotte, Wyandotte, Mich.
[6] Sonifier, Ultrasonic Cell Disruptor; Bronson Instruments, Inc., Danbury, Conn.
[7] Wyse Glass Specialties, Freeland, Mich.
[8] PE-10; Intramedic, Clay-Adams, Div. of Becton, Dickinson and Co., Parsipanny, N.J.
[9] Florisil; Fisher Scientific Co., Pittsburgh, Pa.
[10] Polytron Homogenizer; Brinkmann Instruments, Westbury, N.Y.
[11] Model 5702A equipped with a ^{63}Ni electron-capture detector; Hewlett-Packard, Avondale, Pa.
[12] 3% SP-2100 on 100/120 Supelcoport, 1.2 m × 4 mm i.d.; Supelco, Inc., Bellefonte, Pa.
[13] Finnigan 4023 GC/MS; Finnigan MAT, San Jose, Calif.
[14] 3% SP-2100 on 100/120 Supelcoport, 0.9 m × 2 mm i.d.; Supelco, Inc.
[15] Hypersil ODS, 5-μm particle size, 250 × 4.6 mm i.d.; Shanden Southern Instruments, Inc., Sewickly, Pa.
[16] WISP 710; Waters Associates, Inc., Milford, Mass.
[17] Beckman 110A; Beckman Instruments, Inc., Fullerton, Calif.
[18] Model 440; Waters Associates.
[19] Aquasol; New England Nuclear, Boston, Mass.
[20] ACS; Amersham Corp., Arlington Heights, Ill.
[21] Concifluor; Mallinckrodt Chemical Works, St. Louis, Mo.
[22] Spex Freezer/Mill, No. 6700; Spex Industries, Inc., Metuchen, N.Y.
[23] Mark III, 6880; Tracor Analytic Inc., Elk Grove Village, Ill.

samples (150 mg) were processed similarly without prior homogenization. The label activity from feces and skin was then counted with a liquid scintillation counter.

Pharmacokinetic Analysis—Since the choice of a definitive model was considered premature, model-independent techniques were used to describe the pharmacokinetic behavior of probucol. Over the sampling interval the area under the concentration-time curve (AUC) was determined by the trapezoidal rule (5). The first moment of the plasma concentration-time profile (AUMC) was determined similarly, after multiplying each concentration by its time (6). The AUC beyond the last plasma concentration value (AUC_t^∞) and the AUMC beyond that point ($AUMC_t^\infty$) were calculated by Eqs. 1 and 2, respectively. The terminal slope (β), the last plasma concentration (C_{pt}), and the time (t) when C_{pt} occurred were used in that calculation:

$$AUC_t^\infty = \frac{C_{pt}}{\beta} \quad \text{(Eq. 1)}$$

$$AUMC_t^\infty = \frac{C_{pt} \cdot t}{\beta} + \frac{C_{pt}}{\beta} \quad \text{(Eq. 2)}$$

The apparent oral (aCL_o) or systemic (CL_s) plasma clearance, the mean residence time of the drug in the plasma (MRT), and the apparent steady-state volume of distribution (Vd_{ss}) were calculated *via* Eqs. 3–6. After oral administration:

$$aCL_o = \frac{F \cdot \text{Dose}}{\text{AUC}} \quad \text{(Eq. 3)}$$

where F was the fraction of the dose absorbed and:

$$\text{MRT} = \frac{\text{AUMC}}{\text{AUC}} - \frac{1}{k_a}, \quad \text{(Eq. 4)}$$

where k_a was the absorption rate constant. After intravenous administration:

$$CL_s = \frac{\text{Dose}}{\text{AUC}} \quad \text{(Eq. 5)}$$

$$\text{MRT}_{iv} = \frac{\text{AUMC}}{\text{AUC}} \quad \text{(Eq. 6)}$$

The apparent steady-state volume of distribution (Vd_{ss}) was the product of CL_s and MRT_{iv}. The absorption was presumed to be a first-order rate phenomenon. An estimate of the absorption rate constant (k_a) was determined from a nonlinear least-squares parameter optimization computer program (NONLIN) (7) that assumed the plasma concentration-time profile of oral drug could be described by a first-order rate of absorption and biphasic first-order rates of elimination, such that $C_{p(oral)} = Ae^{-\alpha t} + Be^{-\beta t} + Me^{-k_a t}$. The half-life was calculated by dividing the ln 2 by the terminal slope (β).

A prediction of the mean plasma concentration at steady-state ($\overline{C}_p^{ss}$) was obtained from Eq. 7 which employs the accumulation ratio (8), MRT/τ, the dosage interval (τ), and the mean plasma concentration, $\overline{C}_p = (\text{AUC}/\text{MRT})$, after a single oral dose:

$$\overline{C}_p^{ss} = \frac{\text{MRT}}{\tau} \cdot \overline{C}_p \quad \text{(Eq. 7)}$$

RESULTS

The Pharmacokinetics of Probucol in Blood Plasma—After the 10-mg/kg intravenous dose, plasma probucol concentrations decreased over the first 20-min period and then increased fourfold such that concentrations of probucol over the next 12 h were greater than concentrations observed just after administration. In a separate group of rats the concentrations of label activity in plasma (expressed as microgram equivalents of probucol per milliliter) mimicked the decrease and subsequent increase in probucol concentrations (Fig. 1A). Peak concentrations of probucol were observed 8–12 h after the intravenous dose and a biexponential first-order rate of elimination of probucol from plasma then occurred. The half-life of the terminal elimination phase was 6.1 d, and the apparent systemic clearance of probucol was 21 mL/h/kg (Table I). Only 11–23% of the label concentration in plasma after the labeled intravenous dose was attributed to labeled metabolites of probucol.

After the 10-mg/kg oral dose of probucol, peak plasma concentrations of drug occurred within 2 h of administration (Fig. 1A). Initially, during the absorption phase, concentrations of probucol were greater than concentrations of label activity. This phenomenon was attributed to the fact that a different

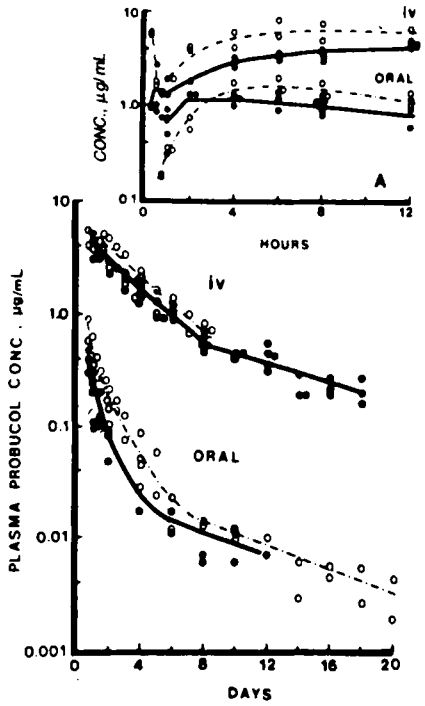

Figure 1—*Plasma concentrations of probucol (●) and [^{14}C]probucol equivalent(s) (○) after a single 10-mg/kg oil–water emulsion dose of probucol to male Sprague–Dawley rats. Inset A shows the initial 12 h of the graph in greater detail.*

group of rats was used to define the label and probucol plasma curves. The elimination of probucol from plasma consisted of two phases, and the half-life of the terminal phase was ~5.6 d. The mean residence time (MRT) of probucol was 2.36 d and the apparent oral plasma clearance was 25.0 mL/h/kg (Table I). The plasma concentration-time curve of probucol and the curve suggested by the corresponding plasma concentrations of label activity were parallel. The difference between the AUC values of the two profiles during the first 8 d indicated that 25–48% of the label activity in plasma was associated with metabolites of probucol.

Tissue Distribution—One hour after intravenous administration, 72% of the dose was found as probucol in the liver; the concentration in liver was 130–200 times the concentration in plasma (Fig. 2). After 7 d, the liver still contained more of the radioactivity (8.2%) than any other tissue studied (Table II). On day 8, 5.6% of the dose was found in the liver as unchanged drug. The half-life during the terminal phase of probucol elimination from liver was 5.5 d.

In contrast to the distribution of intravenous probucol, 7 d after the 10-mg/kg oral dose of [^{14}C]probucol, the highest concentrations of radioactivity were found in the adrenals and in brown and body fat (Table II). Concentrations in the liver after 7 d were <10% of those observed in brown fat. The largest fraction of the oral labeled dose was detected in muscle and body fat when the study was terminated (day 7). Based on reported values for body fat and muscle mass for the rat (9), these two tissues on day 7 contained 0.44 and 0.58% of the labeled dose, respectively.

Excretion—After intravenous administration, only 19% of the labeled dose was excreted in feces within the first 48 h, but after oral administration, 92% of the labeled dose was detected in feces within 48 h (Table III). By the seventh day, 94% of the labeled oral dose was recovered in the feces, in contrast to only 45% of the intravenous dose. Most of the remaining label activity from the intravenous dose was found in tissues (42.5%) (Table II). Less than 5% of the labeled intravenous dose was recovered in urine over the 7-d test period, and negligible amounts of the labeled dose were detected in CO_2.

To determine the degree to which the labeled dose was excreted in the bile, the bile duct was cannulated and animals were given [^{14}C]probucol 3 d after cannulation. After intravenous administration, 5% of the labeled dose was excreted in bile in the first 24 h, a value comparable to the 6% excreted in the feces of noncannulated rats given the intravenous dose (Table III). The rate of elimination of label in bile over the first 24-h interval after intravenous dosing appeared to be a zero-order process since ~1.3% of the labeled dose was excreted in bile during each of the 6-h collection intervals for the first 24 h (Fig. 3). Plasma drug concentrations of the bile duct-cannulated rats 12 and 24 h after intravenous dosing were comparable to the concentration of probucol in noncannulated rats (Table IV).

[24] Biological Materials Oxidizer; R. J. Harvey Instrument Corp., Hillsdale, N.J.

Table I—Parameters Describing the Pharmacokinetic Behavior of Probucol and Label Activity in Plasma of Male Sprague–Dawley Rats [a]

Parameter	Oral		Intravenous	
	Probucol	[^{14}C]Probucol Equivalents	Probucol	[^{14}C]Probucol Equivalents
A, μg/mL	1.82 ± 0.13	—	—	—
α, d^{-1}	2.00 ± 0.10	1.65 ± 0.06	—	—
B, μg/mL	0.0236 0.15	—	—	—
β, d^{-1}	0.122 ± 0.204	0.162 ± 0.107	—	—
k_a, d^{-1}	13.3 ± 1.0	—	—	—
AUC_0^t, μg/mL·d	1.01	1.61	18.2	19.2
where t = d	(12)	(12)	(18)	(8)
AUC_0^∞, μg/mL·d	1.07	1.41	19.9	(26.0)[b]
MRT, d	2.36	2.20	6.7	(6.3)[b]
Terminal $t_{1/2}$, d	5.6	5.9	6.1	(6.1)[b]
F (Fraction absorbed)	0.064	0.064	—	—
aCL_o, mL/h/kg	25.0	—	—	—
CL_s, mL/h/kg	—	—	21.0	—
Vd_{ss}, L/kg	—	—	3.38	—

[a] Given a single oral or intravenous dose of 10 mg/kg of a probucol emulsion. Data expressed as mean ± *SD*. [b] Terminal slope (β) of intravenous probucol was employed to obtain these estimates.

For the first 24 h after oral administration ~0.8% of the labeled dose was recovered in the bile of bile duct-cannulated rats (Table III), and the apparent first-order label elimination half-life during the interval was ~6 h (Fig. 3). Approximately 93.6% of the labeled dose was recovered in the feces of orally dosed noncannulated rats by day 7, and 92% of the dose was fecally excreted in the first 48 h. In the 0–24-h bile collection, only 0.8% of the labeled dose was recovered. During the 24–48-h interval, bile was not collected but must have contained <0.8% recovered in the 0–24-h interval because biliary label excretion declined in a first-order fashion during the 0–24-h interval; only 0.7% of the labeled dose was excreted in the feces during the 48–72-h collection interval (Table III). Thus, the sum of the amount of labeled dose recovered in the 0–168-h urine samples (0.3%), the amount in tissues at 168 h (3.1%), the amount excreted in the 0–24-h bile (0.8%), the amount expected to be excreted in bile during the 24–48-h interval (0–0.7%), and the amount excreted in feces during the subsequent 48–168-h interval (1.5%), provided an approximation of the absorbed labeled dose (5.7–6.4%).

DISCUSSION

Probucol is highly lipophilic (10), and tablet dosage forms are made with micronized drug. Clinical pharmacokinetic studies in healthy volunteers and in hypercholesterolemic patients after single and repeated oral doses of probucol have demonstrated aspects of the steady-state distribution and clearance of probucol (3). Although extensive studies have been conducted in the rat and monkey to elucidate the pharmacodynamic features of probucol, little is known of the bioavailability and pharmacokinetic disposition of probucol and its metabolites in these test species.

In this rat study, ~6% of the administered [^{14}C]probucol was absorbed from the oil–water emulsion. As described earlier, this approximation was the sum of all the label excreted in urine (0–168 h), bile (0–24 h), the biliary excretion estimate (24–48 h), feces (48–168 h), and residual radioactivity in tissues and carcass 7 d after dosage. Another estimate of absorption (5.3%) was obtained from a comparison of the oral and intravenous AUC values, but the apparent nonlinear distribution and/or elimination of probucol over the 0–6-d interval make this estimate less reliable (Fig. 1). Comparisons of the radioactivity in the urine and in various tissues 7 d after the oral and intravenous regimens suggest that the bioavailability of this probucol formulation was poor. A recent study suggests that the drug is selectively absorbed into the lymph rather than the portal circulation and that some oleaginous vehicles enhance its absorption (11).

Although the terminal slopes of the plasma concentration–time curves after the oral and intravenous regimens were similar, a comparison of the preterminal phase of elimination after oral and intravenous administration of probucol suggests that the disposition of the intravenous probucol is nonlinear

Table II—Radioactivity in Tissues and Excreta 7 d after the Administration of [^{14}C]Probucol to Male Sprague–Dawley Rats [a]

	Intravenous Study		Oral Study	
	μg eq/g	Percent of Dose	μg eq/g	Percent of Dose
Tissue				
Adrenal glands	98.1 ± 36.7	0.24 ± 0.052	3.22 ± 1.19	0.010 ± 0.005
Brown fat	29.7 ± 12.8	0.26 ± 0.064	2.19 ± 0.64	0.031 ± 0.011
Liver	19.5 ± 1.6	8.21 ± 0.95	0.17 ± 0.08	0.078 ± 0.037
Body fat[b]	8.4 ± 1.9	4.98 ± 1.37[c]	0.69 ± 0.36	0.44 ± 0.22[c]
Lung	7.3 ± 2.3	0.45 ± 0.15	0.08 ± 0.07	0.004 ± 0.003
Kidney	5.0 ± 0.41	0.38 ± 0.030	0.26 ± 0.10	0.021 ± 0.0064
Thymus	4.6 ± 1.2	0.13 ± 0.045	0.34 ± 0.19	0.008 ± 0.0044
Muscle	2.1 ± 0.35	7.95 ± 1.76[c]	0.13 ± 0.08	0.58 ± 0.36[c]
Skin	5.88 ± 1.67	11.32 ± 2.08	0.511 ± 0.133	1.02 ± 0.13
Tissues + carcass	—	42.43 ± 3.90	—	3.08 ± 0.45
Excreta				
Urine	—	4.65 ± 0.81	—	0.28 ± 0.09
Feces	—	45.26 ± 5.28	—	93.6 ± 1.0
Label recovery	—	92.8 ± 3.9	—	97.1 ± 0.9

[a] A 10-mg/kg single oral or intravenous dose. Data expressed as mean ± *SD* of four rats. [b] Abdominal and perirenal fat. [c] Percent dose calculated, assuming weight of fat is 7.1% or muscle is 45.5% of live body weight (9).

Table III—The Cumulative Percent of the Radioactive Dose Excreted in the Urine and Feces of Male Rats and Biliary Excretion in Bile Duct-Cannulated Male Rats [a]

Day	Intravenous			Oral		
	Urine	Feces	Bile	Urine	Feces	Bile
1	1.06 ± 0.15	6.00 ± 1.12	5.04 ± 0.90	0.095 ± 0.027	—	0.78 ± 0.20
2	2.33 ± 0.41	19.14 ± 2.89	—	0.190 ± 0.070	92.12 ± 1.26	—
3	3.48 ± 1.14	27.32 ± 2.58	—	0.228 ± 0.083	92.82 ± 1.12	—
7	4.65 ± 0.81	45.26 ± 5.28	—	0.28 ± 0.09	93.60 ± 0.96	—

[a] A 10-mg/kg [^{14}C]probucol dose. Data expressed as mean ± *SD*; n = 4 for urine and feces data; n = 5–6 for bile data.

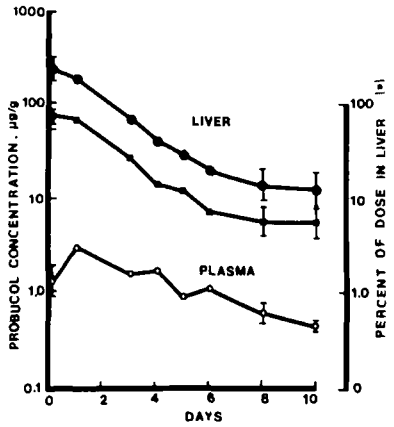

Figure 2—*Concentrations of probucol in plasma (○), liver tissue (●), or percent of dose in liver tissue (■) after a single intravenous dose of 10 mg/kg to male Sprague-Dawley rats.*

(Fig. 1). Also, the unusual decline and recurrence of probucol concentrations seen shortly after intravenous administration, but not after oral administration (Fig. 1A), suggest that the disposition of the intravenous dose may be nonlinear. Differences in the initial (0–24-h) elimination rates of radioactivity in bile and differences in the relative tissue distribution of the oral and intravenous regimens also indicate that the disposition of the intravenous [^{14}C]-probucol dose is concentration dependent.

The apparent zero-order rate of elimination of label activity in bile is seen only after intravenous administration. This may be a consequence of concentration-dependent elimination of the higher concentrations associated with the intravenous dose or the zero-order dissolution of microprecipitated drug. Since oral regimens of 100–1000 mg/kg/d in Sprague-Dawley rats did not elevate serum bilirubin (12), cholestasis is not responsible for this apparent zero-order elimination. Subsequent first-order rates of elimination of probucol and label activity from the plasma and liver tissue indicate that the zero-order rate of elimination is short-lived.

Both oral and intravenous studies indicate that an absorbed dose of probucol is excreted primarily in the feces; the elimination of label in bile duct-cannulated rats (Table III) suggests that most of the label body burden is secreted in the bile. Also, since the amount of radioactivity excreted into bile (0–24 h) is comparable to the amount of labeled dose excreted in feces after intravenous administration (0–24 h), little enterohepatic cycling may occur. The similar plasma concentrations 12 and 24 h after intravenous administration in bile duct-cannulated and noncannulated rats also indicate that enterohepatic cycling would have little effect on circulating plasma probucol concentrations.

The unusual pharmacokinetic behavior of probucol and radioactivity in plasma during the first 12 h after intravenous administration is difficult to explain (Fig. 1A). This effect (the valley in plasma concentration shortly after administration as well as concentrations of the drug from 4 to 12 h that superseded the concentration directly after injection) may be seen with drugs that undergo enterohepatic circulation; but in this study the effect may occur too fast (0–30 min) for such an explanation. Moreover, the radioactivity ex-

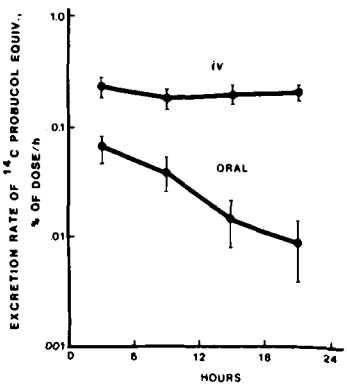

Figure 3—*Biliary excretion rates of [^{14}C]probucol equivalents from rats given a single oral (n = 5) or intravenous (n = 6) 10-mg/kg dose of [^{14}C]-probucol.*

Table IV—Plasma Probucol Concentrations Following Intravenous Administration of Probucol to Rats[a]

Hour	No Cannula	Bile Duct Cannula
12	4.5 ± 0.3 (3)	3.8 ± 1.7 (6)
24	3.5 ± 0.9 (3)	3.7 ± 0.8 (4)

[a] Dose, 10 mg/kg. Expressed as mean (µg/mL) ± *SD*; numbers in parentheses indicate number of animals.

creted in bile is similar to that recovered in feces over a 24-h collection period, and plasma concentrations in bile duct-cannulated rats are comparable to those of noncannulated rats. Consequently, significant recycling is unlikely.

Alternatively, fat and fat-containing emulsions given intravenously tend to accumulate in hepatic tissue (13) and, subsequently, are cleared in a manner comparable to the clearance of chylomicrons. In the present study, the oil from the oil-water emulsion of probucol may accumulate in the hepatic tissue, create a partititoning depot in the liver (since in this study 72% of the intravenous dose was found in the liver at 1 h), and then govern the release of probucol into the systemic circulation. The unusual behavior of the plasma concentration-time curve of carbamazapine, another compound with low aqueous solubility, during intravenous infusion is similar (14). In that study, carbamazapine was solubilized in vehicles containing high concentrations of propylene glycol and given as an infusion. A precipitous fall in plasma concentrations of carbamazapine began shortly after the infusion was initiated. Although Levy *et al.* (14) conducted several experiments to characterize the effect, no definitive explanation was found. Precipitation of the drug in plasma and subsequent redissolution was proposed.

Since the mean residence time of probucol in plasma was 2.4 d after the 10-mg/kg oral dose, with a regimen of 10 mg/kg/d less than a twofold increase in the mean plasma concentration is expected before steady-state $\overline{C}_p^{ss}$ is achieved (nonlinear distribution and/or clearance is not operative in this concentration range). The pharmacokinetic behavior of larger oral doses or an increased number of doses per day, however, may become concentration dependent (indicated by the nonlinear distribution and clearance of the intravenous plasma probucol concentrations) and exhibit another steady-state profile. Dietary and/or formulation factors may also modify the bioavailability, and hence the anticipated effects, of long-term exposure to the drug.

Although the total body clearance is known, the metabolic clearance of probucol is not. Differences between the probucol concentrations and the radiolabeled microgram equivalent concentrations of probucol in plasma indicate the presence of labeled metabolites. Studies of the metabolites of probucol, however, are limited to the characterization of ^{13}C- and ^{14}C-labeled products in the liver and adipose tissue of the rhesus monkey. In both tissues most of the ^{14}C-labeled material was probucol. Six metabolites were also identified in the fat and liver of the monkey[25].

The pharmacokinetic behavior of this formulation of probucol demonstrates not only the poor availability of such a dosage form but also the nonlinear distribution that may be a consequence of the formulation and/or the dose of probucol. This study illustrates the fate of probucol in rats and the potential for accumulation associated with repeated oral regimens of probucol. The need for further investigation of oleaginous vehicles used in preclinical studies is apparent.

REFERENCES

(1) F. N. Marshall, in "Therapeutic Selectivity and Risk/Benefit Assessment of Hypolipidemic Drugs," G. Ricci, R. Paoletti, F. Pocchiari, and D. Poggiolini, Eds., Raven, New York, N.Y., 1982, pp. 99–105.

(2) J. W. Barnhart, D. J. Rytter, and J. A. Molello, *Lipids*, **12**, 29 (1977).

(3) J. F. Heeg and H. Tachizawa, *Nouv. Presse Med.*, **40**, 2990 (1980).

(4) S. Gorzinski, M.S. Thesis, Central Michigan University (1972).

(5) M. Gibaldi and D. Perrier, "Pharmacokinetics," Dekker, New York, N.Y., 1975, pp. 293–296.

(6) K. Yamaoka, T. Nakagawa, and T. Uno, *J. Pharmacokinet. Biopharm.*, **6**, 547 (1978).

(7) C. M. Metzler, G. L. Elfring, and A. J. McEwen, "A User's Manual for NONLIN and Associated Programs," The Upjohn Company, Kalamazoo, Mich., 1974.

(8) M. Weiss, *J. Clin. Pharmacol. Ther. Toxicol.*, **19**, 82 (1981).

[25] E. M. Bargar, *et al.*, submitted for publication.

(9) W. O. Caster, J. Poncelet, A. B. Simon, and W. D. Armstrong, *Proc. Soc. Exp. Biol. Med.*, **91**, 122 (1956).
(10) P. Pignard, *Nouv. Presse Med.*, **40**, 2973 (1980).
(11) K. J. Palin, G. D. Bell, and C. G. Wilson, *J. Pharm. Pharmacol.*, **35** Suppl, 85P, (1983).
(12) J. A. Molello, C. G. Gerbig, and V. B. Robinson, *Toxicol. Appl. Pharmacol.*, **24**, 590 (1973).
(13) P. Belfrage, B. Edgren, and T. Oliverona, *Acta Physiol. Scand.*, **62**, 344 (1964).
(14) R. H. Levy, J. S. Lockard, J. R. Green, P. Friel, and L. Martis, *J. Pharm. Sci.*, **64**, 302 (1975).

ACKNOWLEDGMENTS

The authors gratefully acknowledge Ester M. Bargar, Debra Moore, William J. Caldwell, Randall S. Francisco, Douglas L. Larsen, G. Edwin Lay, Emile N. Massad, Carol J. Simmons, and James A. Vigil for their technical assistance. The authors also thank Gary E. Blau for his encouragement and advice and C. Lorraine Dimiceli for typing this manuscript.

2-Acetylpyridine Thiosemicarbazones XI: 2-(α-Hydroxyacetyl)pyridine Thiosemicarbazones as Antimalarial and Antibacterial Agents

DANIEL L. KLAYMAN *x, AI J. LIN *, JAMES M. HOCH *, JOHN P. SCOVILL *, CHRIS LAMBROS *, and ARTHUR S. DOBEK ‡

Received December 21, 1983, from the **Division of Experimental Therapeutics, Walter Reed Army Institute of Research* and the ‡*Department of Clinical Investigation, Walter Reed Army Medical Center, Washington, DC 20307.* Accepted for publication February 24, 1984.

Abstract □ A series of 2-(α-hydroxyacetyl)pyridine thiosemicarbazones was synthesized as potential antimalarial and antibacterial agents. Their synthesis was achieved by the condensation of N^4-mono- or N^4,N^4-disubstituted thiosemicarbazides with 2-(α-hydroxyacetyl)pyridine. The latter was prepared by selective bromine oxidation of (2-pyridinyl)-1,2-ethanediol. The new compounds show potent inhibitory activity against penicillin-sensitive as well as penicillin-resistant *Neisseria gonorrhoeae* (MIC, 0.5–0.004 μg/mL), against *Neisseria meningitidis* (MIC, 0.5–0.032 μg/mL), and *Staphylococcus aureus* (MIC, 0.5–2 μg/mL). Good *in vitro* antimalarial effects against *Plasmodium falciparum* (Smith strain; ID_{50}, 6.7–38 ng/mL) were observed in most of these new agents, but only 3 of 12 compounds exhibit moderate *in vivo* activity against *Plasmodium berghei*. These new agents appear to be less toxic to the host and more water soluble than the corresponding 2-acetylpyridine thiosemicarbazones.

Keyphrases □ Thiosemicarbazone derivatives—2-(α-hydroxyacetyl)pyridine thiosemicarbazones, antimalarial and antibacterial activity □ Antimalarial agents—potential, 2-(α-hydroxyacetyl)pyridine thiosemicarbazones □ Antibacterial agents—potential, 2-(α-hydroxyacetyl)pyridine thiosemicarbazones

Members of a series of N^4-mono- and N^4,N^4-disubstituted 2-acetylpyridine thiosemicarbazones (I) have been reported by us to possess antimalarial (1, 2), antibacterial (3), and antiviral (4) properties. Based on these studies, the structure–activity relationship of this class of compounds has been defined. Thus, N^4,N^4-disubstitution of the thiosemicarbazone moiety appears to be essential for optimal activity against *Plasmodium berghei* in the mouse (2) and several bacterial genera (3). Replacement of the sulfur atom with oxygen leads to inactive compounds. Furthermore, biological activity is limited to those compounds in which the ethylidene group is attached to the 2-position, rather than the 3- or 4-position, of the pyridine ring. The effects resulting from placement of a functional group on the ethylidene function, however, have not been studied. N^4,N^4-Disubstituted 2-acetylpyridine thiosemicarbazones, in particular, exhibit potent antimalarial properties *in vitro* as well as *in vivo*. Against *P. berghei* in mice, the 4-(2-pyridinyl)piperazine and 3-azabicyclo[3.2.2]nonane analogues produced cures of all infected test animals at a dosage of 80 and 160 mg/kg, respectively (2). Although potent inhibitory activity against *Plasmodium falciparum* (Smith) *in vitro* (ID_{50} = 3.6 ng/mL) was observed, 2-acetylpyridine 4,4-dimethyl-3-thiosemicarbazone shows no significant *in vivo* activity against *P. berghei* in mice due to its high host toxicity.

As antibacterial agents, 2-acetylpyridine thiosemicarbazones show excellent activity against both penicillin-sensitive and -resistant strains of *Neisseria gonorrhoeae* with MIC (minimum inhibitory concentration) values in the range of 0.002–0.062 μg/mL. These agents were also found to inhibit the growth of *Neisseria meningitidis* as well as *Staphylococcus aureus*, with the MIC in the range of 0.016–0.062 μg/mL and 0.125–0.5 μg/mL, respectively. 2-Acetylpyridine 4,4-dimethyl-3-thiosemicarbazone [I, $R^2 = N(CH_3)_2$] is by far the most potent compound against *N. gonorrhoeae* among the analogues tested, with an MIC of 0.002–0.008 μg/mL. However, the substantial toxicity observed in mice (2) has limited its potential as a clinical agent.

In the search for agents with lower toxicity, increased water-solubility, and improved structure–activity relationship, the synthesis of a new series of 2-(α-hydroxyacetyl)pyridine thiosemicarbazones (II) was undertaken. These compounds were screened for their antimalarial properties as well as their antibacterial activity.

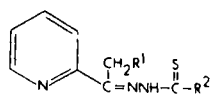

I, $R^1 = H$
II, $R^1 = OH$

0022-3549/84/1200-1763$01.00/0
© 1984, American Pharmaceutical Association

(9) W. O. Caster, J. Poncelet, A. B. Simon, and W. D. Armstrong, *Proc. Soc. Exp. Biol. Med.*, **91**, 122 (1956).
(10) P. Pignard, *Nouv. Presse Med.*, **40**, 2973 (1980).
(11) K. J. Palin, G. D. Bell, and C. G. Wilson, *J. Pharm. Pharmacol.*, **35** Suppl, 85P, (1983).
(12) J. A. Molello, C. G. Gerbig, and V. B. Robinson, *Toxicol. Appl. Pharmacol.*, **24**, 590 (1973).
(13) P. Belfrage, B. Edgren, and T. Oliverona, *Acta Physiol. Scand.*, **62**, 344 (1964).
(14) R. H. Levy, J. S. Lockard, J. R. Green, P. Friel, and L. Martis, *J. Pharm. Sci.*, **64**, 302 (1975).

ACKNOWLEDGMENTS

The authors gratefully acknowledge Ester M. Bargar, Debra Moore, William J. Caldwell, Randall S. Francisco, Douglas L. Larsen, G. Edwin Lay, Emile N. Massad, Carol J. Simmons, and James A. Vigil for their technical assistance. The authors also thank Gary E. Blau for his encouragement and advice and C. Lorraine Dimiceli for typing this manuscript.

2-Acetylpyridine Thiosemicarbazones XI: 2-(α-Hydroxyacetyl)pyridine Thiosemicarbazones as Antimalarial and Antibacterial Agents

DANIEL L. KLAYMAN *x, AI J. LIN *, JAMES M. HOCH *, JOHN P. SCOVILL *, CHRIS LAMBROS *, and ARTHUR S. DOBEK ‡

Received December 21, 1983, from the **Division of Experimental Therapeutics, Walter Reed Army Institute of Research* and the ‡*Department of Clinical Investigation, Walter Reed Army Medical Center, Washington, DC 20307.* Accepted for publication February 24, 1984.

Abstract □ A series of 2-(α-hydroxyacetyl)pyridine thiosemicarbazones was synthesized as potential antimalarial and antibacterial agents. Their synthesis was achieved by the condensation of N^4-mono- or N^4,N^4-disubstituted thiosemicarbazides with 2-(α-hydroxyacetyl)pyridine. The latter was prepared by selective bromine oxidation of (2-pyridinyl)-1,2-ethanediol. The new compounds show potent inhibitory activity against penicillin-sensitive as well as penicillin-resistant *Neisseria gonorrhoeae* (MIC, 0.5–0.004 μg/mL), against *Neisseria meningitidis* (MIC, 0.5–0.032 μg/mL), and *Staphylococcus aureus* (MIC, 0.5–2 μg/mL). Good *in vitro* antimalarial effects against *Plasmodium falciparum* (Smith strain; ID_{50}, 6.7–38 ng/mL) were observed in most of these new agents, but only 3 of 12 compounds exhibit moderate *in vivo* activity against *Plasmodium berghei*. These new agents appear to be less toxic to the host and more water soluble than the corresponding 2-acetylpyridine thiosemicarbazones.

Keyphrases □ Thiosemicarbazone derivatives—2-(α-hydroxyacetyl)pyridine thiosemicarbazones, antimalarial and antibacterial activity □ Antimalarial agents—potential, 2-(α-hydroxyacetyl)pyridine thiosemicarbazones □ Antibacterial agents—potential, 2-(α-hydroxyacetyl)pyridine thiosemicarbazones

Members of a series of N^4-mono- and N^4,N^4-disubstituted 2-acetylpyridine thiosemicarbazones (I) have been reported by us to possess antimalarial (1, 2), antibacterial (3), and antiviral (4) properties. Based on these studies, the structure–activity relationship of this class of compounds has been defined. Thus, N^4,N^4-disubstitution of the thiosemicarbazone moiety appears to be essential for optimal activity against *Plasmodium berghei* in the mouse (2) and several bacterial genera (3). Replacement of the sulfur atom with oxygen leads to inactive compounds. Furthermore, biological activity is limited to those compounds in which the ethylidene group is attached to the 2-position, rather than the 3- or 4-position, of the pyridine ring. The effects resulting from placement of a functional group on the ethylidene function, however, have not been studied. N^4,N^4-Disubstituted 2-acetylpyridine thiosemicarbazones, in particular, exhibit potent antimalarial properties *in vitro* as well as *in vivo*. Against *P. berghei* in mice, the 4-(2-pyridinyl)piperazine and 3-azabicyclo[3.2.2]nonane analogues produced cures of all infected test animals at a dosage of 80 and 160 mg/kg, respectively (2). Although potent inhibitory activity against *Plasmodium falciparum* (Smith) *in vitro* (ID_{50} = 3.6 ng/mL) was observed, 2-acetylpyridine 4,4-dimethyl-3-thiosemicarbazone shows no significant *in vivo* activity against *P. berghei* in mice due to its high host toxicity.

As antibacterial agents, 2-acetylpyridine thiosemicarbazones show excellent activity against both penicillin-sensitive and -resistant strains of *Neisseria gonorrhoeae* with MIC (minimum inhibitory concentration) values in the range of 0.002–0.062 μg/mL. These agents were also found to inhibit the growth of *Neisseria meningitidis* as well as *Staphylococcus aureus*, with the MIC in the range of 0.016–0.062 μg/mL and 0.125–0.5 μg/mL, respectively. 2-Acetylpyridine 4,4-dimethyl-3-thiosemicarbazone [I, $R^2 = N(CH_3)_2$] is by far the most potent compound against *N. gonorrhoeae* among the analogues tested, with an MIC of 0.002–0.008 μg/mL. However, the substantial toxicity observed in mice (2) has limited its potential as a clinical agent.

In the search for agents with lower toxicity, increased water-solubility, and improved structure–activity relationship, the synthesis of a new series of 2-(α-hydroxyacetyl)pyridine thiosemicarbazones (II) was undertaken. These compounds were screened for their antimalarial properties as well as their antibacterial activity.

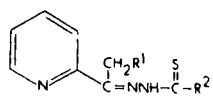

I, $R^1 = H$
II, $R^1 = OH$

0022-3549/84/1200-1763$01.00/0
© 1984, American Pharmaceutical Association

BACKGROUND

The preparation of the target compounds involved the synthesis of the unknown key intermediate, 2-(α-hydroxyacetyl)pyridine (III), followed by its condensation with an appropriately substituted thiosemicarbazide. The method used to convert 2,6-diacetylpyridine to 2,6-bis(α-hydroxyacetyl)-pyridine was applied to 2-acetylpyridine (IV) (Scheme I). In the procedure reported by Moriarty *et al.* (5), 2,6-diacetylpyridine was treated with iodosobenzene diacetate under KOH–MeOH catalysis to give a moderate yield of the corresponding dimethyl ketal. The latter was hydrolyzed to 2,6-bis(α-hydroxyacetyl)pyridine by the action of *p*-toluenesulfonic acid in acetone.

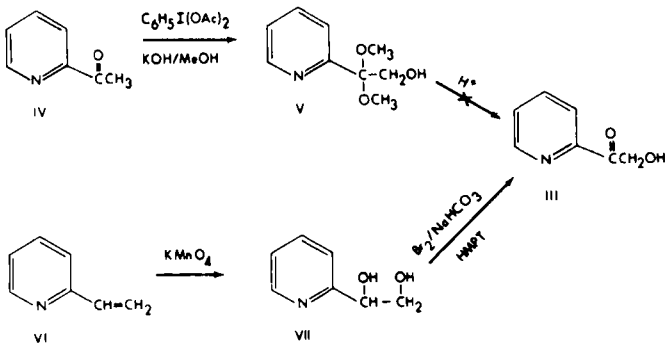

Scheme I

In our case, IV was readily converted to the corresponding ketal (V); however, the recommended technique for hydrolysis to III gave unchanged material. The use of acetic, hydrochloric, or hydriodic acids under a variety of conditions also gave either starting material or decomposition products.

An alternate avenue which was investigated involved the oxidation of 2-vinylpyridine (VI) to (2-pyridinyl)-1,2-ethanediol (VII) by potassium permanganate according to a procedure of Furuyama *et al.* (6). Further oxidation of VII to III was achieved in 35% yield using Br_2–$NaHCO_3$ with hexamethylphosphoramide serving as the coreactant. This method had been reported (7) to selectively oxidize secondary alcohols to their corresponding ketones in the presence of a primary hydroxy group. The product (III), a low-melting solid, was found to be best purified on a silica gel flash column.

Condensation of III with the appropriate thiosemicarbazides gave the desired thiosemicarbazones (IIa,d–k) in moderate yield (*cf.* Table I). Three of the thiosemicarbazides, precursors of IIe, f, and k, had not been reported previously and were prepared by a new procedure in which 4-methyl-4-phenyl-3-thiosemicarbazide [VIII (8)] is heated under reflux with a secondary amine (Scheme II). This transamination reaction gave better yields of N^4,N^4-disubstituted thiosemicarbazides (IX) than the older method involving an amine displacement reaction of methyl hydrazinecarbodithioate (9).

The hydrazone of III, *i.e.*, X, reacted with methyl and phenyl isothiocy-

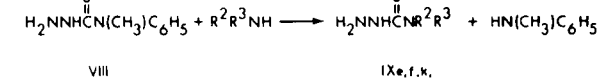

Scheme II

Table I—2-(α-Hydroxyacetyl)pyridine Thiosemicarbazones

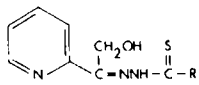

Compound	R	mp, °C	Method[a,b]	Yield, %	Formula
IIa	NH_2	81–83[c]	A	55	$C_8H_{10}N_4OS$
IIb	$NHCH_3$	165–166[d]	B	30	$C_9H_{12}N_4OS$
IIc	NHC_6H_5	140–141[c]	B	30	$C_{14}H_{14}N_4OS$
IId	$N(CH_3)_2$	132–134[e]	A	90	$C_{10}H_{14}N_4OS$
IIe	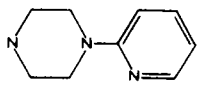	147–149[c]	C	43	$C_{17}H_{20}N_6OS$
IIf	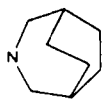	133–135[c]	A	35	$C_{16}H_{22}N_4OS$
IIg		185–186[f]	A	60	$C_{12}H_{16}N_4OS$
IIh	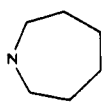	128–129[g]	C	50	$C_{14}H_{20}N_4OS$
IIi		163–165[h]	A	33	$C_{12}H_{16}N_4O_2S$
IIj		134–136[g]	A	50	$C_{13}H_{18}N_4OS$
IIk	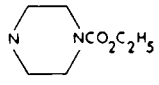	122–124[c]	C	50	$C_{15}H_{21}N_5O_3S$

[a] Key: (A) reaction of III with a thiosemicarbazide prepared by the reaction of methyl hydrazinecarbodithioate with an amine; (B) reaction of 2-(α-hydroxyacetyl)pyridine hydrazone with an isothiocyanate; (C) reaction of III with thiosemicarbazides IXe, h, k. [b] ^1H-NMR ($CDCl_3$): IIa–c, N^2-H (~14.5 ppm), $-CH_2-$ (d, ~4.6 ppm); IId–k, N^2-H (~15.3 ppm), $-CH_2-$ (s, ~4.7 ppm). [c] EtOAc. [d] Dimethylformamide–$CHCl_3$. [e] EtOAc–MeOH. [f] Dimethylformamide–MeOH. [g] CH_3CN. [h] $CHCl_3$–EtOH.

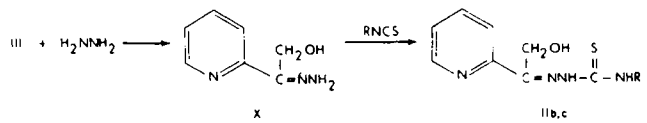

X IIb,c

Scheme III

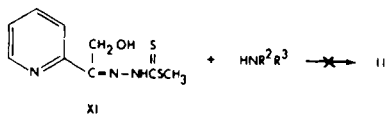

XI II

Scheme IV

anates to give the corresponding N^4-monosubstituted thiosemicarbazones (IIb,c) (Scheme III).

Another route for the preparation of II which was considered was the displacement of the $-SCH_3$ function of XI with either primary or secondary amines. Although this method (1, 2) proved to be useful for the synthesis of 2-acetylpyridine thiosemicarbazones, in the case of the α-hydroxy analogue, the reaction of carbodithioate (XI) with amines gave little or no product (Scheme IV).

A determination and comparison of the water solubility at 37°C of α-hydroxylated 2-acetylpyridine thiosemicarbazones with analogues lacking the hydroxy group revealed that appreciable hydrophilic enhancement occurred. For example, IId and f increased water solubility 1.3-fold and 7.5-fold, respectively, by having the α-hydroxy group present in the molecule.

It is of interest to note that while the N^4,N^4-disubstituted 2-acetylpyridine thiosemicarbazones exist in three tautomeric forms in $CDCl_3$, as indicated by NMR spectral data (10), only a single tautomer was observed for both N^4-mono- and N^4,N^4-disubstituted 2-(α-hydroxyacetyl)pyridine thiosemicarbazones. The C-methyl protons of 2-acetylpyridine N^4,N^4-dimethylthiosemicarbazone [I, $R^2 = N(CH_3)_2$] are seen as an unequal triplet centered at δ 2.5 ppm ($CDCl_3$) and the thiosemicarbazone NH proton appears as three peaks, *i.e.*, at δ 15, 14.5, and 8 ppm. These data suggest that the N^4, N^4-disubstituted 2-acetylpyridine thiosemicarbazones form three tautomers in $CDCl_3$. However,the N^4-monosubstituted 2-acetylpyridine thiosemicarbazones exist solely as a single *E*-isomer, with N^2 proton resonance at $\delta \sim 8$ ppm. The methylene protons of the N^4,N^4-disubstituted 2-(α-hydroxyacetyl)-pyridine thiosemicarbazones and those of the unsubstituted (IIa) and monosubstituted (IIb,c) analogues resonate as a singlet and as doublets, respectively, at $\delta \sim 4.7$ ppm. The NH proton on N^2 appears in all analogues as a singlet at $\delta \sim 15$ ppm. The NMR data suggest that the 2-(α-hydroxyacetyl)pyridine thiosemicarbazones exist primarily as the *Z*-isomer with NH forming an internal hydrogen bond with the pyridine ring nitrogen, as shown in XII. Furthermore, the lack of coupling between the methylene protons and

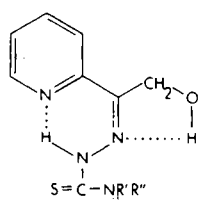

XII

the hydroxyl on the N^4,N^4-disubstituted thiosemicarbazones suggests that the hydroxyl function forms another internal hydrogen bond with the N^1 nitrogen atom of the thiosemicarbazone function. The fact that a coupling between methylene protons and the hydroxyl exists in IIa–c indicates that the hydroxyl function of unsubstituted and monosubstituted analogues is not involved in hydrogen bond formation as seen in the N^4,N^4-disubstituted thiosemicarbazones IId–k. A substantial downfield chemical shift of the proton on N^2 of thiosemicarbazones as a result of internal hydrogen bonding has been reported (11–13).

EXPERIMENTAL SECTION[1]

(2-Pyridinyl)-1,2-ethanediol (VII)—2-Vinylpyridine (VI, 75.6 g, 0.72 mol) was dissolved in 900 mL of acetone, and the solution was cooled in an ice bath to 0–5°C. A chilled solution of $KMnO_4$ (75.9 g, 0.48 mol) and $MgSO_4$ (28.8 g, 0.24 mol) in 1.5 L of H_2O was added slowly with agitation[2] to the 2-vinylpyridine solution at such a rate as to maintain the temperature of the mixture at ~5°C. After addition of all the $KMnO_4$ solution (1.5 h), the mixture was stirred at 5°C for 1 h and then at ambient temperature overnight.

A small amount of hydroquinone was added to the resulting thick, dark-brown slurry which was then filtered through diatomaceous earth[3]. The filtrate was concentrated to ~200 mL, and 750 mL of 95% EtOH was added. The filter cake was extracted with 500 mL of 95% EtOH, and the filtrate and extract were combined and stored overnight at 5°C. The mixture was filtered to remove K_2SO_4, and the filtrate was then concentrated under reduced pressure to a volume of 250 mL. The crude VII (37.1 g, 37% yield) was collected and recrystallized from MeOH–CH_3CN to give light-brown crystals, mp 93–96°C. Further recrystallization from EtOH–CH_3CN gave colorless crystals of (2-pyridinyl)-1,2-ethanediol, mp 94–96°C [lit. (14) mp 97°C].

2-(α-Hydroxyacetyl)pyridine (III)—(2-Pyridinyl)-1,2-ethanediol (10.8 g, 77.7 mmol) was suspended in 600 mL of CH_2Cl_2. To the suspension was added 3.8 g of hexamethylphosphoramide and 132 mL of 16% aqueous $NaHCO_3$ solution. The mixture was cooled to 0–5°C with an ice bath and to the mixture Br_2 (18 g, 112.5 mmol) in 60 mL of CH_2Cl_2 was added in a dropwise manner with vigorous stirring. The mixture was stirred at room temperature until the Br_2 was consumed (8–12 h). The organic layer was separated, and the aqueous layer was extracted twice with CH_2Cl_2. The organic layer and extracts were combined, dried over Na_2SO_4, and evaporated to dryness under reduced pressure. The oil was purified on a silica gel flash column, using CH_3CN as eluant to give 3.8 g (36% yield) of III. Recrystallization of III from benzene–cyclohexane gave colorless needles, mp 68–70°C, which gradually turned brown on standing. IR (KBr): 3280, 1710, 1585, 1438, 1222, 1005, 975, 776, and 625 cm^{-1}; ^{1}H-NMR ($CDCl_3$): δ 3.40 (br s, 1, OH), 5.09 (s, 2, CH_2), 7.45 and 8.12 (m, 3, ArH), and 8.68 ppm (d, 1, ArH).

Condensation of III with N^4,N^4-Disubstituted Thiosemicarbazides—2-(α-Hydroxyacetyl)pyridine (III) (2.2 g, 16 mmol) and 16 mmol of an N^4, N^4-disubstituted thiosemicarbazide were heated under reflux in 60 mL of MeOH, with two drops of glacial HOAc as catalyst, for 1.5 h. The solvent was evaporated to dryness under reduced pressure, and the crude product was recrystallized.

2-(α-Hydroxyacetyl)pyridine Hydrazone (X)—2-(α-Hydroxyacetyl)pyridine (2 g, 14.6 mmol) and 85% hydrazine hydrate (2 mL, 53.8 mmol) in 30 mL of MeOH were heated under reflux for 3.5 h. The solvent was evaporated to dryness under reduced pressure, and the resulting oil was extracted several times with hot C_6H_6. The C_6H_6 extracts were combined, dried over Na_2SO_4, and evaporated to a small volume. The crystals of X which formed were collected (1.2 g, 54% yield) and recrystallized from C_6H_6 to give light-straw needles, mp 113–115°C; ^{1}H-NMR ($CDCl_3$): δ 3.60 (br s, 1, OH), 4.57 (s, 2, CH_2O), 7.18–7.87 (m, 3, pyridinyl-H), 8.41 (br s, 2, NH_2), and 8.65 ppm (d, 1, pyridinyl H).

2-(α-Hydroxyacetyl)pyridine 4-Methylthiosemicarbazone (IIb)—2-(α-Hydroxyacetyl)pyridine hydrazone (X) (1.5 g, 10 mmol) and 0.75 g (10 mmol) of methyl isothiocyanate were heated in CH_3CN under reflux for 2 h. The solvent was evaporated to dryness under reduced pressure, and the residue was recrystallized. 2-(α-Hydroxyacetyl)pyridine 4-phenylthiosemicarbazone (IIc) was made in a similar manner using phenyl isothiocyanate.

3-Azabicyclo[3.2.2]nonane-3-thiocarboxylic Acid Hydrazide (IXf)—A solution of 5 g (27.6 mmol) of 4-methyl-4-phenylthiosemicarbazide (8) in 10 mL of EtOH was combined with 3.43 g (27.6 mmol) of 3-azabicyclo[3.2.2]-nonane, and the solution was heated under reflux for 5 h. The mixture was chilled; the crystals which separated were collected and recrystallized from EtOH. This afforded 3.36 g (61% yield) of colorless rods of 3-azabicyclo[3.2.2]nonane-3-thiocarboxylic acid hydrazide, mp 164–165°C dec.; IR (KBr): 3244, 2930, 2860, 1604, 1515, 1343, 1216, 1009, and 975 cm^{-1}.

1-(2-Pyridinyl)piperazine-4-thiocarboxylic acid hydrazide (IXc) was prepared by the method described above in 47% yield, mp 184–185°C (from EtOH). 1-Carbethoxypiperazine-4-thiocarboxylic acid hydrazide (IXk) was prepared by the method described above in 63% yield, mp 158–159°C (from EtOH).

Methyl 3-[1-(2-pyridinyl)-2-hydroxyethylidene]hydrazinecarbodithioate (XI)—Compound III (0.25 g, 1.8 mmol) and methyl hydrazinecarbodithioate (1) (0.23 g, 1.8 mmol) in 25 mL of MeOH containing one drop of HOAc was heated on a steam bath for 1.5 h. The solvent was evaporated under reduced pressure and the yellow solid obtained was recrystallized from C_6H_6 to give 0.36 g (85% yield) of XI as yellow needles, mp 122–124°C.

Solubility Determination—A saturated solution of the thiosemicarbazone,

[1] Melting points were taken on a Thomas-Hoover capillary melting point apparatus and are uncorrected. Microanalyses were performed by Spang Microanalytical Laboratory, Eagle Harbor, Mich. Analytical results were ±0.3% of the calculated values. IR spectra of solid samples were obtained in KBr disks on a Perkin-Elmer Model 283 spectrophotometer. ^{1}H-NMR spectra were run on a JEOL-FX90Q spectrometer using Me_4Si as an internal standard.

[2] A "Vibro-mixer" was found to be the most efficient.

[3] Celite.

prepared by suspending an excess quantity of the compound in distilled H_2O, was shaken in a constant-temperature bath at 37°C for 24 h, and then a 5-mL portion of the supernatant was lyophilized to constant weight. Solubilities were as follows: 2-acetylpyridine 4,4-dimethylthiosemicarbazone, 0.96 mg/mL; *N,N*-hexamethylene-2-[1-(2-pyridinyl)ethylidene]hydrazinecarbothioamide, 0.04 mg/mL; IId, 1.28 mg/mL; IIh, 0.30 mg/mL.

Antimalarial Studies—*In Vitro*—Antimalarial activity of the new compounds was evaluated *in vitro* against a chloroquine-resistant *P. falciparum* (Smith) by assessing the inhibition of uptake of [G-^{3}H]hypoxanthine by the parasites. A detailed procedure was given in a previous report from this laboratory (15).

In Vivo—The compounds described herein were tested[4] against a drug-sensitive strain of *P. berghei* (strain KBG 173) in mice. Five mice per dose level were infected by the intraperitoneal administration of parasitized erythrocytes. Untreated infected animals, which served as controls, died (on the average) after 6.2 d. A candidate drug was given 72 h after the mice were infected and was judged to be toxic if the infected mice died before day 6, inactive if they died between day 6 and day 12, active if the mean survival time of 6.2 d was at least doubled, and curative if the mice survived 60 d postinfection. Compounds which were active or curative at a dose of 40 mg/kg were retested at several lower dose levels, but results are not reported unless extension of mouse survival time was observed. Details of the test procedure were given in the first paper in this series and by Osdene *et al.* (16).

Antibacterial Studies—*Organisms*—Five clinical isolates of *S. aureus* were obtained from the Clinical Microbiology Laboratory, Walter Reed Army Medical Center. Five *N. meningitidis* and 25 *N. gonorrhoeae* isolates were obtained from the collections of the Department of Bacterial Diseases, Walter Reed Army Institute of Research, and the Centers for Disease Control, Atlanta, Georgia.

Testing Procedure—The standard agar plate dilution method using Mueller Hinton agar, as described by Washington and Sutter (17), was utilized to determine the MIC values of the test compounds against the *S. aureus* and *N. meningitidis* isolates tested. The *N. gonorrhoeae* isolates were similarly tested, but with GC agar plus 1% of a modified defined supplement (18). This supplement consisted of 81 mL of aqueous solution A (containing 40.5 g of dextrose and 0.002 g of cocarboxylase) which was mixed with 19 mL of aqueous solution B [83 mg of $Fe(NO_3)_3 \cdot 9H_2O$ and 1 g of L-glutamine]. It was then filter-sterilized and kept frozen until used.

The *S. aureus* inoculum was standardized after a 1–2-h incubation in Mueller Hinton broth by adjusting the turbidity to that of a 0.5 MacFarland standard (17) representing 10^7–10^8 colony-forming units (CFU)/mL, and then further diluted 20-fold in Mueller Hinton broth. The inocula of the two *Neisseria* species were standardized by suspending agar plate colonies of overnight growth in Mueller Hinton broth for *N. meningitidis* and GC broth plus 1% modified defined supplement for *N. gonorrhoeae* in order to approximate the turbidity of an overnight broth culture. The inocula were then further diluted 200-fold in the appropriate broth.

Because of the poor water solubility of the test compounds, it was necessary to dissolve them initially in dimethyl sulfoxide. The control plates also contained the highest concentration of Me_2SO present in each particular dilution series. Further dilutions were done with Mueller Hinton broth or, in the case of *N. gonorrhoeae* testing, with GC broth plus modified defined supplement (19). The concentrations of the test compounds were twofold dilutions from 32 to 0.25 μg/mL for *S. aureus* and from 1 to 0.002 μg/mL for the two *Neisseria* species.

The standardized bacterial inocula were applied to the thiosemicarbazone-containing agar plates and the controls using a Lidwell apparatus (20). Cultures were incubated under appropriate atmospheric conditions for 24 h at 37°C and read. The MIC for each compound was the lowest concentration of that compound which still inhibited all visible bacterial growth on the agar surface.

[4] Tests performed at the Dr. Leo Rane Laboratory, University of Miami, Miami, Fla.

RESULTS AND DISCUSSION

Antimalarial Activity—The *in vitro* antimalarial studies (Table II) of the 2-(α-hydroxyacetyl)pyridine thiosemicarbazones and the 2-acetylpyridine thiosemicarbazones indicated that, except for IIe, f, and j, the latter compounds had greater inhibitory properties against *P. falciparum*. The lower toxicity of the 2-(α-hydroxyacetyl)pyridine thiosemicarbazones to mice was evident in the *in vivo* antimalarial screen (Table II). Similarly, these compounds, in general, were less efficacious as antimalarials than their corresponding 2-acetylpyridine thiosemicarbazones. Compound IIj showed low levels of activity, whereas the best compound of the series was IIf, which showed two of five cures and no toxicity at a dose of 320 mg/kg. However, the corresponding compound with identical N^4,N^4-substitution showed three of five mouse cures at a dose of 40 mg/kg. It appears that α-hydroxylation

Table II—Antimalarial Activities *In Vitro* and *In Vivo* of 2-(α-Hydroxyacetyl)pyridine Thiosemicarbazones (II)

Compound	ID_{50}, ng/mL *P. falciparum* (Smith)[a]	Increase in Mean Survival Time, d[b] 40 mg/kg	80 mg/kg	160 mg/kg	320 mg/kg	640 mg/kg
IIa	>135	0.0		T(1/5)[c]		T(5/5)
IIb	54.0	0.0		0.0		0.0
IIc	38.0	0.6		0.0		0.0
IId	6.7	0.0		0.0		T(5/5)
IIe	13.0	0.2		0.8		0
IIf	15.0	1.2	0.6	4.4	C(2/5)	C(2/5)
IIg	23.0	−0.2	0.6	3.8	5.2,T(1/5)	0.4,T(2/5)
IIh	8.4	1.0	1.6	3.8	4.0,T(1/5)	2.0,T(2/5)
IIi	34.0	0.0	T(1/5)	1.6,T(1/5)	1.6,T(1/5)	0.6,T(2/5)
IIj	4.1	1.6	3.4	1.8,T(1/5)	1.4,T(2/5)	C(1/5),T(3/5)
IIk	23.0	0.0	T(3/5)	T(3/5)	T(1/5)	T(4/5)

[a] Determined in semiautomated test described in Ref. 15. [b] Test performed in Swiss mice infected with *P. berghei*. [c] (T) toxic, (C) cure; see *Experimental Section* for details.

Table III—Antibacterial Properties *In Vitro* of 2-(α-Hydroxyacetyl) (II) and 2-Acetylpyridine Thiosemicarbazones (I)

Compound	*N. gonorrhoeae* MIC, μg/mL II	*N. gonorrhoeae* MIC, μg/mL I[a]	*N. meningitidis* MIC, μg/mL II	*N. meningitidis* MIC, μg/mL I[a]	*S. aureus* MIC, μg/mL II	*S. aureus* MIC, μg/mL I[a]
IIa	>1	0.25–0.5	>1	>1	>32	>16
IIb	0.125–1	0.5	>1	0.5–1	>32	>16
IIc	0.032–0.25	0.032–0.25	0.5–1	0.25–>1	>32	8
IId	0.004–0.016	0.002–0.008	0.062–0.125	0.062–0.125	4	>16
IIe	0.016–0.062	0.004–0.031	0.125–0.25	0.062–0.25	2	2–4
IIf	0.008–0.016	0.008–0.031	0.062	0.031–0.125	0.5–1	0.25
IIg	0.004–0.016	0.008–0.062	0.062–0.125	0.016–0.031	1–4	0.5
IIh	0.004–0.016	0.016–0.062	0.032–0.062	0.031–0.125	0.5–1	2
IIi	0.032–0.125	—[b]	0.5–>1	—[b]	>32	—[b]
IIj	0.004–0.016	0.016–0.062	0.032–0.062	0.031–0.062	0.5–1	0.5
IIk	0.062–0.5	0.004–0.031	>1	0.062–0.25	8–32	>16

[a] *cf.* Ref. 3. [b] Not tested in earlier study.

of the acetyl group had an overall negative effect on the antimalarial potency of this series of thiosemicarbazones.

Antibacterial Activity—In the assessment of the antibacterial activity of the 2-(α-hydroxyacetyl)pyridine thiosemicarbazones (Table III), the strong inhibitory effect of the 2-acetylpyridine thiosemicarbazones seen against *N. gonorrhoeae* and *N. meningitidis* (3) was also observed here. Most of the 2-(α-hydroxyacetyl)pyridine compounds had MIC values of <0.1 μg/mL against these bacterial species, and in a few instances the degree of inhibition was slightly superior to that observed with the 2-acetylpyridine thiosemicarbazones.

Against *S. aureus*, several of the 2-(α-hydroxyacetyl)pyridine thiosemicarbazones, *i.e.*, IIf, h, and j, had MIC values of 0.5–1 μg/mL. Again, there were several instances in which inhibitory activity superior to the 2-acetylpyridine thiosemicarbazones (*i.e.*, in IId, e, h, and k) was seen.

CONCLUSIONS

The biological data for the newly synthesized 2-(α-hydroxyacetyl)pyridine thiosemicarbazones indicates that N^4,N^4-disubstitution provides optimal *in vivo* and *in vitro* antimalarial and antibacterial activities. The introduction of a hydroxy function into the α-position of 2-acetylpyridine thiosemicarbazones results in compounds with increased solubility, decreased host toxicity, and in some instances, improvement of antimalarial and antibacterial activity *in vitro*. However, this is offset by the concomitant decrease in *in vivo* antimalarial effects. These results suggest that pharmacological parameters, such as tissue distribution and the rate of metabolism, play an essential role in determining the *in vivo* antimalarial activity, as well as host toxicity, of this series of compounds.

REFERENCES

(1) D. L. Klayman, J. F. Bartosevich, T. S. Griffin, C. J. Mason, and J. P. Scovill, *J. Med. Chem.*, **22**, 855 (1979).

(2) D. L. Klayman, J. P. Scovill, J. F. Bartosevich, and C. J. Mason, *J. Med. Chem.*, **22**, 1367 (1979).

(3) A. S. Dobek, D. L. Klayman, E. T. Dickson, Jr., J. P. Scovill, and E. C. Tramont, *Antimicrob. Agents Chemother.*, **18**, 27 (1980).

(4) C. Shipman, Jr., S. H. Smith, J. C. Drach, and D. L. Klayman, *Antimicrob. Agents Chemother.*, **19**, 682 (1981).

(5) R. M. Moriarty, H. Hu, and S. C. Gupta, *Tetrahedron Lett.*, **22**, 1283 (1981).

(6) T. Furuyama, K. Mori, and R. Wakasa, *Bull. Chem. Soc. Jpn.*, **45**, 1924 (1972).

(7) M. Al Neirabeyeh, J.-C. Ziegler, and B. Gross, *Synthesis*, **1976**, 811.

(8) B. Stanovnik and M. Tišler, *J. Org. Chem.*, **25**, 2234 (1960).

(9) R. S. McElhinney, *J. Chem. Soc.*, **1966**, 950.

(10) J. P. Scovill, D. L. Klayman, A. J. Lin, and N. Acton, "Abstract of Papers, 29th Congress of IUPAC," Cologne, Germany, June 1983, p. 323.

(11) I. Antonini, F. Claudi, P. Franchetti, M. Grifantini, and S. Martelli, *J. Med. Chem.*, **20**, 447 (1977).

(12) I. Antonini, F. Claudi, G. Cristalli, P. Franchetti, M. Grifantini, and S. Martelli, *Eur. J. Med. Chem.*, **14**, 89 (1979).

(13) T. L. Lemke, T. W. Shek, L. A. Cates, L. K. Smith, L. A. Cosby, and A. C. Sartorelli, *J. Med. Chem.*, **20**, 1351 (1977).

(14) T. Furuyama, Japan. Patent No. 7,225,351 (1972); *Chem. Abstr.*, **77**, 75135 (1972).

(15) C. Lambros, G. E. Childs, J. D. Notsch, J. P. Scovill, D. L. Klayman, and D. E. Davidson, Jr., *Antimicrob. Agents Chemother.*, **22**, 981 (1982).

(16) T. S. Osdene, P. B. Russell, and L. Rane, *J. Med. Chem.*, **10**, 431 (1967).

(17) J. A. Washington II and V. L. Sutter, in "Manual of Clinical Microbiology," E. H. Lennette, A. Balows, W. J. Hausler, Jr., and J. P. Truant, Eds., American Society for Microbiology, Washington, D.C., pp. 453–458.

(18) L. A. White and D. S. Kellogg, Jr., *Appl. Microbiol.*, **13**, 171 (1965).

(19) P. Gerhardt and C. G. Hedén, *Proc. Soc. Exp. Biol. Med.*, **105**, 49 (1960).

(20) O. M. Lidwell, *Mon. Bull. Minist. Health G.B.*, **18**, 49 (1959).

ACKNOWLEDGMENTS

Contribution No. 1695 to the Army Research Program on Drug Development. Paper X: D. L. Klayman, C. J. Mason, and J. P. Scovill, *Arzneim.-Forsch.*, in press.

Kinetics and Mechanism of the Alkaline Hydrolysis of Maleimide

M. NIYAZ KHAN

Received August 23, 1983, from the *Department of Chemistry, Bayero University, Kano, Nigeria.* Accepted for publication March 21, 1984.

Abstract □ The kinetics of hydrolysis of maleimide was carried out within the $[OH^-]$ range of 2.46×10^{-6} to 2.0 M at 30°C. The observed pseudo-first-order rate constants, k_{obs}, follow the empirical equation: $k_{obs} = (A_1[OH^-] + A_2[OH^-]^2)/(1 + A_3[OH^-])$. Both ionized and un-ionized forms of maleimide have been suggested to be involved in hydrolysis. The nucleophilic attacks by hydroxide ion at the carbonyl carbon of both ionized and un-ionized maleimide and by water at the carbonyl carbon of ionized maleimide to form tetrahedral intermediates are considered to be the rate-determining steps. The observed results obtained at different 1,4-dioxane–water compositions have revealed an increase in k_{obs} with a decrease in 1,4-dioxane content which could be attributed to the higher polarity of the transition state compared with the reactant state.

Keyphrases □ Maleimide—kinetics, mechanism of hydrolysis □ Hydrolysis maleimide, effect of temperature

Many compounds containing an imide group act as drugs (1). *N*-Ethylmaleimide is of interest because of its rapid and Michael-type reaction with the sulfhydryl group of proteins (2, 3). Usually, the alkaline hydrolysis of amides and imides have been found to occur by a stepwise mechanism involving the tetrahedral intermediate (I) (4). Biechler and Taft (5) were the first to propose an additional oxydianionic tetrahedral intermediate (II) in the alkaline hydrolysis of trifluoroacetanilide. Later, II was found to exist in many acyl transfer reactions where the acyl substrates contained electron-withdrawing substituents and hydrolytic conditions covered a reasonable range of $[OH^-]$ (6). Recently, we have observed II in the alkaline hydrolysis of methyl-*o*-methoxybenzoate (7). In the continuation of our work on mechanistic studies on aqueous cleavage of amides (8) and imides (9) in a highly alkaline medium, we initiated this study to determine if an intermediate (II) exists and to study the nature of the rate-determining step.

0022-3549/84/1200-1767$01.00/0

© 1984, American Pharmaceutical Association

of the acetyl group had an overall negative effect on the antimalarial potency of this series of thiosemicarbazones.

Antibacterial Activity—In the assessment of the antibacterial activity of the 2-(α-hydroxyacetyl)pyridine thiosemicarbazones (Table III), the strong inhibitory effect of the 2-acetylpyridine thiosemicarbazones seen against *N. gonorrhoeae* and *N. meningitidis* (3) was also observed here. Most of the 2-(α-hydroxyacetyl)pyridine compounds had MIC values of <0.1 μg/mL against these bacterial species, and in a few instances the degree of inhibition was slightly superior to that observed with the 2-acetylpyridine thiosemicarbazones.

Against *S. aureus*, several of the 2-(α-hydroxyacetyl)pyridine thiosemicarbazones, *i.e.*, IIf, h, and j, had MIC values of 0.5–1 μg/mL. Again, there were several instances in which inhibitory activity superior to the 2-acetylpyridine thiosemicarbazones (*i.e.*, in IId, e, h, and k) was seen.

CONCLUSIONS

The biological data for the newly synthesized 2-(α-hydroxyacetyl)pyridine thiosemicarbazones indicates that N^4,N^4-disubstitution provides optimal *in vivo* and *in vitro* antimalarial and antibacterial activities. The introduction of a hydroxy function into the α-position of 2-acetylpyridine thiosemicarbazones results in compounds with increased solubility, decreased host toxicity, and in some instances, improvement of antimalarial and antibacterial activity *in vitro*. However, this is offset by the concomitant decrease in *in vivo* antimalarial effects. These results suggest that pharmacological parameters, such as tissue distribution and the rate of metabolism, play an essential role in determining the *in vivo* antimalarial activity, as well as host toxicity, of this series of compounds.

REFERENCES

(1) D. L. Klayman, J. F. Bartosevich, T. S. Griffin, C. J. Mason, and J. P. Scovill, *J. Med. Chem.*, **22**, 855 (1979).

(2) D. L. Klayman, J. P. Scovill, J. F. Bartosevich, and C. J. Mason, *J. Med. Chem.*, **22**, 1367 (1979).

(3) A. S. Dobek, D. L. Klayman, E. T. Dickson, Jr., J. P. Scovill, and E. C. Tramont, *Antimicrob. Agents Chemother.*, **18**, 27 (1980).

(4) C. Shipman, Jr., S. H. Smith, J. C. Drach, and D. L. Klayman, *Antimicrob. Agents Chemother.*, **19**, 682 (1981).

(5) R. M. Moriarty, H. Hu, and S. C. Gupta, *Tetrahedron Lett.*, **22**, 1283 (1981).

(6) T. Furuyama, K. Mori, and R. Wakasa, *Bull. Chem. Soc. Jpn.*, **45**, 1924 (1972).

(7) M. Al Neirabeyeh, J.-C. Ziegler, and B. Gross, *Synthesis*, **1976**, 811.

(8) B. Stanovnik and M. Tišler, *J. Org. Chem.*, **25**, 2234 (1960).

(9) R. S. McElhinney, *J. Chem. Soc.*, **1966**, 950.

(10) J. P. Scovill, D. L. Klayman, A. J. Lin, and N. Acton, "Abstract of Papers, 29th Congress of IUPAC," Cologne, Germany, June 1983, p. 323.

(11) I. Antonini, F. Claudi, P. Franchetti, M. Grifantini, and S. Martelli, *J. Med. Chem.*, **20**, 447 (1977).

(12) I. Antonini, F. Claudi, G. Cristalli, P. Franchetti, M. Grifantini, and S. Martelli, *Eur. J. Med. Chem.*, **14**, 89 (1979).

(13) T. L. Lemke, T. W. Shek, L. A. Cates, L. K. Smith, L. A. Cosby, and A. C. Sartorelli, *J. Med. Chem.*, **20**, 1351 (1977).

(14) T. Furuyama, Japan. Patent No. 7,225,351 (1972); *Chem. Abstr.*, **77**, 75135 (1972).

(15) C. Lambros, G. E. Childs, J. D. Notsch, J. P. Scovill, D. L. Klayman, and D. E. Davidson, Jr., *Antimicrob. Agents Chemother.*, **22**, 981 (1982).

(16) T. S. Osdene, P. B. Russell, and L. Rane, *J. Med. Chem.*, **10**, 431 (1967).

(17) J. A. Washington II and V. L. Sutter, in "Manual of Clinical Microbiology," E. H. Lennette, A. Balows, W. J. Hausler, Jr., and J. P. Truant, Eds., American Society for Microbiology, Washington, D.C., pp. 453–458.

(18) L. A. White and D. S. Kellogg, Jr., *Appl. Microbiol.*, **13**, 171 (1965).

(19) P. Gerhardt and C. G. Hedén, *Proc. Soc. Exp. Biol. Med.*, **105**, 49 (1960).

(20) O. M. Lidwell, *Mon. Bull. Minist. Health G.B.*, **18**, 49 (1959).

ACKNOWLEDGMENTS

Contribution No. 1695 to the Army Research Program on Drug Development. Paper X: D. L. Klayman, C. J. Mason, and J. P. Scovill, *Arzneim.-Forsch.*, in press.

Kinetics and Mechanism of the Alkaline Hydrolysis of Maleimide

M. NIYAZ KHAN

Received August 23, 1983, from the *Department of Chemistry, Bayero University, Kano, Nigeria.* Accepted for publication March 21, 1984.

Abstract □ The kinetics of hydrolysis of maleimide was carried out within the $[OH^-]$ range of 2.46×10^{-6} to 2.0 M at 30°C. The observed pseudo-first-order rate constants, k_{obs}, follow the empirical equation: $k_{obs} = (A_1[OH^-] + A_2[OH^-]^2)/(1 + A_3[OH^-])$. Both ionized and un-ionized forms of maleimide have been suggested to be involved in hydrolysis. The nucleophilic attacks by hydroxide ion at the carbonyl carbon of both ionized and un-ionized maleimide and by water at the carbonyl carbon of ionized maleimide to form tetrahedral intermediates are considered to be the rate-determining steps. The observed results obtained at different 1,4-dioxane–water compositions have revealed an increase in k_{obs} with a decrease in 1,4-dioxane content which could be attributed to the higher polarity of the transition state compared with the reactant state.

Keyphrases □ Maleimide—kinetics, mechanism of hydrolysis □ Hydrolysis maleimide, effect of temperature

Many compounds containing an imide group act as drugs (1). *N*-Ethylmaleimide is of interest because of its rapid and Michael-type reaction with the sulfhydryl group of proteins (2, 3). Usually, the alkaline hydrolysis of amides and imides have been found to occur by a stepwise mechanism involving the tetrahedral intermediate (I) (4). Biechler and Taft (5) were the first to propose an additional oxydianionic tetrahedral intermediate (II) in the alkaline hydrolysis of trifluoroacetanilide. Later, II was found to exist in many acyl transfer reactions where the acyl substrates contained electron-withdrawing substituents and hydrolytic conditions covered a reasonable range of $[OH^-]$ (6). Recently, we have observed II in the alkaline hydrolysis of methyl-*o*-methoxybenzoate (7). In the continuation of our work on mechanistic studies on aqueous cleavage of amides (8) and imides (9) in a highly alkaline medium, we initiated this study to determine if an intermediate (II) exists and to study the nature of the rate-determining step.

0022-3549/84/1200-1767$01.00/0

© 1984, American Pharmaceutical Association

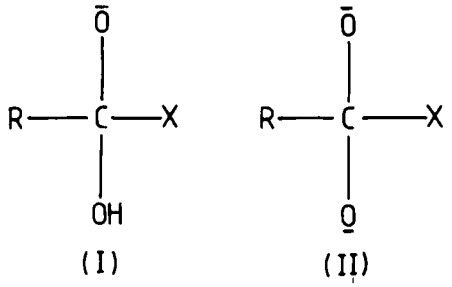

(I) (II)

EXPERIMENTAL SECTION

Materials—Reagent grade maleimide, 2-amino-2-methyl-1,3-propanediol and Tris were obtained commercially[1]. All other reagent grade chemicals were obtained commercially[2] and were used without further purification. Glass-distilled water was used throughout the studies. Buffer solutions were prepared by partial neutralization.

Kinetic Measurements—For a typical kinetic run, 47.5 mL of a mixture containing sodium hydroxide or buffer solutions of desired pH and potassium chloride to maintain the ionic strength was incubated at 30°C in a thermostatic water bath[3] for ~10–15 min. The reaction was started by adding 2.5 mL of 0.0125 M solution of maleimide prepared in 100% 1,4-dioxane. An aliquot (~2.5 mL) was withdrawn from the mixture and was quickly transferred to a 3-mL quartz cuvette kept preincubated (30°C) in the thermostatic cell holder of a spectrophotometer[4]. The temperature was maintained electronically by a temperature-control unit of the spectrophotometer[4]. The progress of the reaction was followed by monitoring the disappearance of maleimide spectrophotometrically[4] at 300 nm.

The observed pseudo-first-order rate constants, k_{obs}, were calculated from:

$$A_{obs} = E_{app}X_0 \exp(-k_{obs}t) + A_\infty \qquad \text{(Eq. 1)}$$

where X_0 is the initial concentration of substrate; A_{obs} and A_∞ are the absorbance values at any time t and $t = \infty$, respectively; and E_{app} represents the apparent molar extinction coefficient. The nonlinear least-squares technique[5] was used to calculate three unknown parameters (k_{obs}, E_{app}, and A_∞) from Eq. 1. The calculated values of A_∞ were compared with the corresponding A_{obs} obtained after ~10 half-lives of the reactions; they were almost the same. Most of the kinetic runs were carried out for more than 6 half-lives and fitting of the observed data to Eq. 1 was good for all runs. Maleamic acid and maleic acid are expected to have similar extinction coefficients at 300 nm and therefore, the hydrolysis of maleamic acid could not complicate the simple first-order kinetics. Furthermore, the bimolecular rate constant for alkaline hydrolysis was found to be 2.2×10^{-4} M^{-1} s^{-1} at 65°C (10). This indicates that the rate constant obtained at even the highest [OH^-] (2.0 M) and at 30°C, is nearly 70-fold larger than the corresponding rate constant for the hydrolysis of maleamic acid obtained at 65°C.

Because of the low aqueous solubility of maleimide, its pK_a was determined with a spectrophotometric technique (11). The value of the ionization constant, K_a, was 3.30 (±0.53) $\times 10^{-10}$ M at 30°C.

Product Characterization—A typical absorption wavelength for a cyclic imide group is 300 nm, while an amide group generally does not absorb here. Therefore a decrease in absorption peak at 300 nm should demonstrate the cleavage of the imide bond. We carried out experiments, described below, to determine the quantitative yield of the suspected product, maleamic acid.

One milliliter of 0.0125 M maleimide at 30°C was added to a mixture (total volume 19 mL) containing 0.03 M NaOH. The mixture (1 mL) was withdrawn at 25 min and was analyzed for ammonia by the nesslerizing technique (8, 12). The analysis revealed the absence of any detectable amount of ammonia formed within the 25-min period. After more than 12 half-lives of the first step of hydrolysis (25 min), 1.0 mL of 10.5 M HCl was added to the mixture. The mixture was made acidic because the acid-catalyzed hydrolysis of maleamic acid is substantially accelerated due to intramolecular carboxyl group participation (13). The recovery of ammonia was 95% at 300 min, 99% at ~21 h, and ~99% at ~41 h. Similar results were obtained for another reaction carried out at 0.2 M NaOH (other conditions similar to those described above). To substantiate the observation that no detectable ammonia formed within 25 min after the start of the reaction in basic medium, we performed a kinetic run at 30°C with a mixture containing 2.0 M NaOH and 6.25×10^{-4} M maleimide. The reaction was carried out for >72 h; the observed pseudo-first-order rate constant was 1.62 (±0.19) $\times 10^{-3}$ min^{-1} which could be compared with the literature value (25.8×10^{-3} min^{-1}) obtained at 65°C (10). To determine the rate constant for acid-catalyzed hydrolysis of the intermediate product maleamic acid, we carried out a kinetic run containing 5.952×10^{-4} M maleimide and 0.03 M NaOH at 30°C. After 24 min, 1.0 mL of 10.5 M HCl was added to the mixture. The reaction was followed for more than 10 half-lives; the observed pseudo-first-order rate constant was 5.34 (±0.04) $\times 10^{-3}$ min^{-1}. This result could be compared with the literature values 5.28×10^{-3} min^{-1} (14) and 3.16×10^{-3} min^{-1} (12).

We also carried out the hydrolysis of maleimide in the presence of 1.0 M HCl at 30°C. The observed result has shown the absence of any detectable amount of ammonia formed within 525 min after the start of the reaction and only ~14, ~37, and ~46% ammonia was recovered at 23, 73, and 97 h, respectively. This indicates that the acid-catalyzed hydrolysis of maleimide is much slower than the base-catalyzed hydrolysis.

RESULTS

The alkaline hydrolysis of maleimide was carried out within the hydroxide ion concentration range 2.460×10^{-6}–2.0 M at 30°C. The range 2.460×10^{-6}–5.382×10^{-4} M was attained by carbonate, 2-amino-2-methyl-1, 3-propanediol and Tris buffer solutions while the range of 0.002–2.0 M was maintained by sodium hydroxide solution. The ionic strength of the reaction medium was kept constant at 1.0 M in the presence of buffer components and 2.0 M in presence of sodium hydroxide. The observed pseudo-first-order rate constants at pH 8.57 and 8.08 (Table I) were obtained in the presence of 0.5 M carbonate buffer. The contribution of buffer catalysis to k_{obs} at these pH values could be assumed to be negligible compared with both OH^- and water catalyses because even within the 10.42–9.37 pH range the increase in total buffer concentration from 0.1 to 0.7 M has increased k_{obs} only by 6–18%. The observed data as summarized in Table I were found to be best fitted to the empirical:

$$k_{obs} = \frac{A_1[OH^-] + A_2[OH^-]^2}{1 + A_3[OH^-]} \qquad \text{(Eq. 2)}$$

Table I—Effect of Hydroxide Ion Concentration on the Aqueous Cleavage of Maleimide [a]

[OH^-], M	$10^3 k_{obs}$, s^{-1}	$10^3 k^b_{calcd}$, s^{-1}
2.460×10^{-6} [d]	0.1514 ± 0.0058 [c]	0.1730
3.243×10^{-6}	0.1750 ± 0.0030	0.2270
6.872×10^{-6}	0.3300 ± 0.0055	0.4650
7.603×10^{-6}	0.3124 ± 0.0023	0.5111
1.352×10^{-5}	0.6510 ± 0.0190	0.8630
2.276×10^{-5}	0.9310 ± 0.0480	1.346
4.800×10^{-5}	2.059	2.346
7.711×10^{-5}	2.633 ± 0.042	3.184
1.207×10^{-4}	4.057	4.013
2.000×10^{-4}	5.484	4.910
5.382×10^{-4}	7.312	6.247
0.002 [d]	7.558 ± 0.102	7.094
0.01	7.643 ± 0.017	7.475
0.03	7.989 ± 0.030	7.758
0.05	8.106 ± 0.037	8.001
0.07	7.954 ± 0.047	8.238
0.10	8.509 ± 0.031	8.590
0.30	10.79 ± 0.02	10.92
0.50	13.08 ± 0.026	13.25
0.70	15.04 ± 0.13	15.58
1.00	18.32 ± 0.13	19.07
1.20	20.38 ± 0.09	21.39
1.40	23.12 ± 0.20	23.72
1.50	25.11 ± 0.22	24.89
1.70	27.42 ± 0.20	27.21
1.80	28.56 ± 0.25	28.38
1.90	29.98 ± 0.24	29.54
2.00	31.44 ± 0.18	30.70

[a] $[Maleimide]_0 = 6.25 \times 10^{-4}$ M, 30°C. Unless otherwise stated the ionic strength was kept constant at 2.0 M; 5% 1,4-dioxane in the mixture. [b] Calculated from Eq. 2 with calculated values of A_1, A_2, and A_3 as mentioned in the text. [c] Error limits are standard deviations. [d] Calculated from pH values by: $[OH^-] = 10^{pH} \cdot K_w/\upsilon OH^-$. The activity coefficient (υOH^-) was calculated from: $\log \upsilon OH^- = -0.52Z^2[(\mu^{1/2}/1 + \mu^{1/2}) - 0.2\mu]$ (15) where μ is the ionic strength. The ionic strength was kept constant at 1.0 M for all mixtures containing buffer solutions of required pH.

[1] Aldrich Chemical Co., Milwaukee, Wis.
[2] BDH Chemicals Limited, Poole, England.
[3] Gallenkamp.
[4] Model 35 UV-VIS; Beckman Instruments International S.A., Geneva, Switzerland.
[5] The nonlinear and linear least-squares computer programs were developed in BASIC and the computations were carried out on VAX-11 and Commodore Professional 3016 computers.

Table II—Effect of Water–1,4-Dioxane Mixed Solvent on the Aqueous Cleavage of Maleimide [a]

1,4-Dioxane, % (v/v)	$10^3 k_{obs}$, s^{-1}
5	10.68 ± 0.030[b]
10	9.219 ± 0.049
15	7.612 ± 0.017
20	6.572 ± 0.024
25	5.467 ± 0.012
30	4.580 ± 0.012
40	3.217 ± 0.010
50	2.223 ± 0.026
60	1.573 ± 0.004
70	1.199 ± 0.011

[a] Conditions: $[Maleimide]_0 = 6.25 \times 10^{-4}$ M, 30°C, μ = 0.1 M, $[NaOH]_0$ = 0.03 M. [b] Error limits are standard deviations.

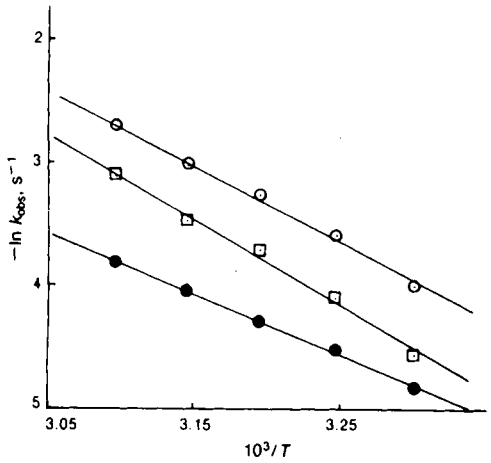

Figure 1—*Temperature dependence of* k_{obs} *for* k_1 *step* (●), ($k_1 + k_2$) *step* (⊙), *and* k_2 *step* (⊡). *The solid lines are drawn through the least-squares calculated points using the Arrhenius equation.*

where A_1, A_2, and A_3 are unknown parameters. The values of A_1, A_2, and A_3 were calculated from Eq. 2 by the use of a nonlinear least-squares technique and the respective values thus obtained were: 72.2 ± 9.1 $M^{-1} s^{-1}$, 113.0 ± 15.6 $M^{-2} s^{-1}$, and 9709.5 ± 1299.2 M^{-1}. The fitting of observed data to Eq. 2 is evident from the standard deviations of calculated unknown parameters as well as from the calculated values of rate constants (Table I).

The effect of solvent on hydrolysis was studied at 30°C with organic cosolvent prepared by mixing 1,4-dioxane and water by volume. The hydroxide ion concentration and ionic strength were kept constant at 0.03 M and 0.1 M, respectively. The observed data are summarized in Table II. The increase in k_{obs} with an increase in the dielectric constant (*i.e.*, increase of water content) of reaction medium cannot be explained by simple electrostatic theory (16) because under the experimental conditions employed, the proposed reaction mechanism involves a neutral and an anionic molecule. In the absence of any correct theoretical model which could be used to explain such rate dependence on mixed solvents and to assess, qualitatively, the effect of the solvating power of the mixed solvents on the rate of hydrolysis, we checked the fitting of the observed data with the empirical Grunwald-Winstein equation: $\log k_{obs} = \log k_0 + mY$ (18). Although the data were not in full agreement with the mY equation, the value of m was ~0.29 (determined by drawing a straight line through the observed points obtained within the mixed solvent range of 30-50%[6]).

[6] The plot of $\log k_{obs}$ *versus* Y was found to be a smooth nonlinear curve with initial and final slopes of ~0.17 and ~0.48, respectively.

Table IV—Effect of Ionic Strength on Hydrolytic Cleavage of Maleimide [a]

Ionic Strength, M	$[OH^-]$ = 0.03 M $10^3 k_{obs}$, s^{-1}	$[OH]$ = 1.0 M $10^3 k_{obs}$, s^{-1}
1.0	8.882 ± 0.064	18.73 ± 0.70
1.5	8.932 ± 0.049	20.58 ± 0.24
2.0	7.989 ± 0.030	18.32 ± 0.13
3.0	8.226 ± 0.073	21.78 ± 0.21
3.5	7.958 ± 0.077	—
4.0	—	23.35 ± 0.23

[a] Conditions: $[Maleimide]_0 = 6.25 \times 10^{-4}$ M, 30°C.

The effect of temperature on rate of hydrolysis was studied at 30–50°C, at 0.03 M, and 1.0 M hydroxide ion concentrations, keeping ionic strength constant at 2.0 M. The observed data are shown graphically in Fig. 1. The observed pseudo-first-order rate constants were found to follow Eyring and Arrhenius equations (7) and the activation parameters calculated from these equations with linear and nonlinear least-squares techniques are summarized in Table III. The activation parameters obtained at 0.03 M NaOH are attributed to only the k_1 step because the k_2 step has negligible contribution at 0.03 M NaOH. Similarly, the activation parameters obtained at 1.0 M NaOH are attributed to both k_1 and k_2 steps.

The ionic strength effect of hydrolysis was studied at two different $[OH^-]$

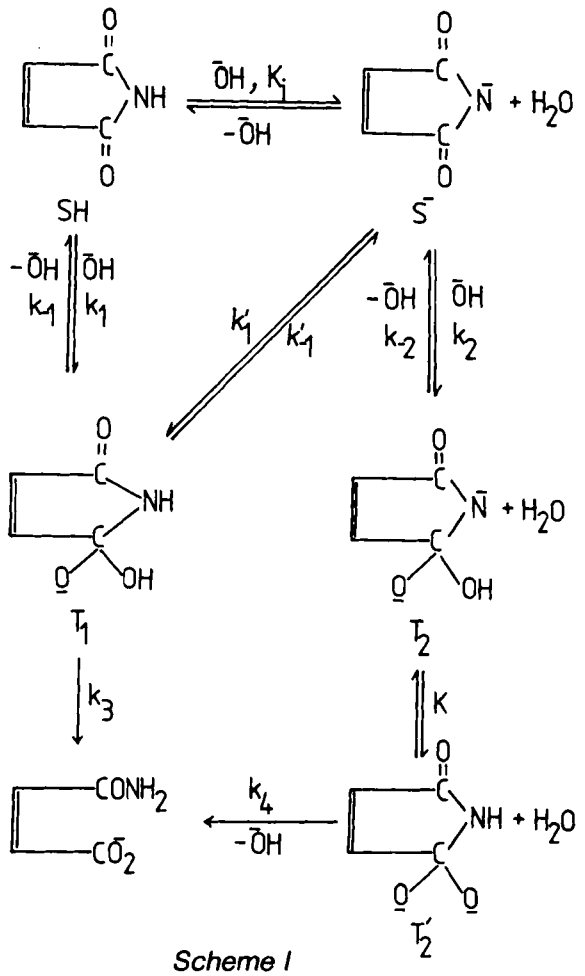

Scheme I

Table III—Activation Parameters of Hydrolytic Cleavage of Maleimide [a]

Reaction step	ΔF^* kcal/mole[b]	ΔH^*, kcal/mol	$-\Delta S^*$, cal/deg.mol	E_a, kcal/mol	ln A, s^{-1}	R_{ms}, 10^3 s^{-1} [c]
k_1[d]	20.69	8.88 ± 0.22[e]	38.8 ± 0.7[e]	9.70 ± 0.25[e]	11.31 ± 0.40	1.222
($k_1 + k_2$)[f]	20.19	11.20 ± 0.47	29.4 ± 1.5	12.22 ± 0.54	16.34 ± 0.86	5.723
k'_2[g]	20.54	12.54 ± 0.73	26.1 ± 2.3	13.78 ± 0.81	18.37 ± 1.30	12.892

[a] Conditions: $[Maleimide]_0 = 6.25 \times 10^{-4}$ M, μ = 2.0 M. [b] ΔF^* was calculated from the relationship $k_{obs} = (K_B T/h) \exp(-\Delta F^*/RT)$ at 30°C. [c] $R_{ms} = [\Sigma_{i=1}(k_{obs_i} - k_{calcd_i})^2/(N-2)]^{1/2}$. [d] At 0.03 M NaOH. [e] Error limits are standard deviations. [f] At 1.0 M NaOH. [g] k'_2 (s^{-1}) was obtained from the relationship: $k'_2 = k_{obs}$ at 1.0 M NaOH $- k_{obs}$ at 0.03 M NaOH where $k'_2 = k_2[OH^-]$.

(0.03 and 1.0 M) within the ionic strength ranging from 1.0 to 4.0 M. The observed results are summarized in Table IV.

DISCUSSION

The linear variation of k_{obs} with $[OH^-]$ occurred at a pH much higher than the pK_a of maleimide. This revealed that the alkaline hydrolysis of maleimide was not a simple second-order process, but followed a complex rate law. The simplest mechanism which could explain the observed results may be shown in Scheme I. The intermediates T_1, T_2, and T_2' were considered short-lived chemical species and hence application of steady state approximation resulted in the kinetic equation:

$$k_{obs} = \frac{k_3(k_1 + k_1'K_i'[H_2O])[OH^-]}{(1 + K_i'[OH^-])(k_{-1} + k_{-1}' + k_3)} + \frac{k_4k_2KK_i'[OH^-]^2}{(1 + K_i'[OH^-])(k_{-2} + k_4K)} \quad \text{(Eq. 3)}$$

where $K_i' = K_i/[H_2O] = K_a/K_w$ with $K_a = [S^-]a_H/[SH]$.

Recently, Jencks *et al.* (19) demonstrated that in the nucleophilic substitution reactions, the rate of expulsion of the leaving group depends largely on the push provided by groups other than the leaving group attached to the same atom and the pull provided by the leaving group. Thus, in Scheme I, the

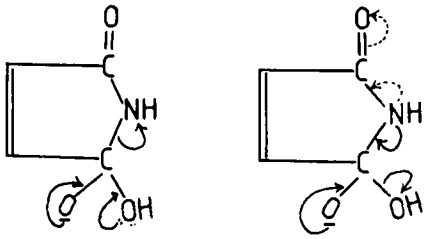

III IV

rate constant, k_3, should be considerably larger than k_{-1} and k_{-1}' because the push provided by the alcoholic oxygen atom to expel the amidic nitrogen atom would be larger than the push provided by the amidic nitrogen atom (since the nonbonded electrons on the nitrogen atom are not localized to the extent that they are localized on the alcoholic oxygen atom) to expel the alcoholic oxygen atom from T_1, as shown in III and IV. Furthermore, although the ionization constants of the conjugate acids of leaving groups involved in k_{-1}, k_{-1}', and k_3 steps are almost the same[7] (20), the high carbon basicity of oxygen compared with that of nitrogen would make k_3 larger than k_{-1} and k_{-1}'. These conclusions thus reveal that $k_3 \gg (k_{-1} + k_{-1}')$ and similarly $k_4K \gg k_{-2}$. Hence, application of these assumptions reduce Eq. 3 to:

$$k_{obs} = \frac{(k_1 + k_1'K_i'[H_2O])[OH^-] + k_2K_i'[OH^-]^2}{1 + K_i'[OH^-]} \quad \text{(Eq. 4)}$$

Equation 4 is similar to Eq. 2 with $A_1 = (k_1 + k_1'K_i'[H_2O])$, $A_2 = k_2K_i'$, and $A_3 = K_i'$. The rate constant k_2 (A_2/A_3) was found to be 0.0116 M^{-1} s^{-1} and K_a was calculated from A_3 with a known value of K_w (1.449×10^{-14} M^2) (21). The value thus obtained (1.41×10^{-10} M) is comparable with the experimentally observed value of 3.3×10^{-10} M. The values of A_1/A_3 (7.44×10^{-3} s^{-1}) and A_2/A_3 are considerably larger than the respective values of 6.64×10^{-5} s^{-1} and 25.68×10^{-5} M^{-1} s^{-1} obtained at 80°C in the hydrolytic cleavage of succinimide (22) and 19.1×10^{-5} s^{-1} and 83.9×10^{-5} $M^{-1}s^{-1}$ obtained at 80°C in the hydrolysis of 3,3-methylethylsuccinimide (23).

The present data are not sufficient to differentiate between a concerted process with transition state V and a stepwise process (Scheme II) involved

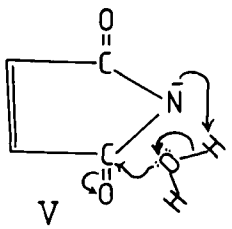

V

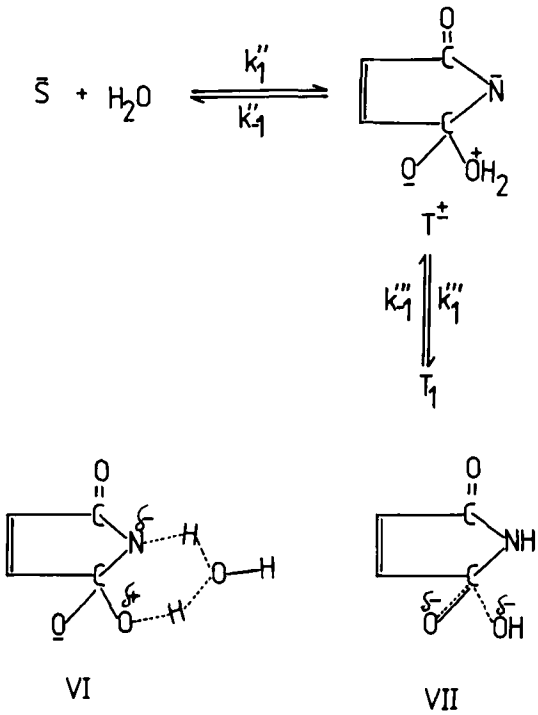

VI VII

Scheme II

in the conversion of S^- to T_1. However, as Jencks (24) has pointed out, the concerted process should be expected to occur if the lifetime of an intermediate is shorter than that of a molecular vibration of 10^{-13} s. Classical one-step concerted S_N2 and E_2 mechanisms have been challenged by the proposal that such reactions occur through a stepwise mechanism (24); therefore, we prefer Scheme II for the conversion of S^- to T_1. It has been concluded in the aminolysis of maleimide[8] that k_{-1}'' is larger than k_1'' even when the leaving group in k_{-1}'' step is a cationic amine. It is therefore obvious that in Scheme II, k_{-1}'' should be larger than k_1'' because the acidity of H_2O^+— is much larger than $>NH_2^+$. However, the high leaving ability of H_2O^+—, compared with $>NH_2^+$ from $T^\pm$—, caused by the difference in their respective acidity, could partially be offset by larger basicity toward carbon of oxygen nucleophiles than of amine nucleophiles, for a given basicity toward the proton (25). These conclusions lead to k_1'' as the rate-determining step. The proton transfer in the k_1'' step is presumably taking place through a proton switch mechanism (26).

In previous related studies (27), the formation of the oxydianionic tetrahedral intermediate, T_2, was assumed to occur by an equilibrium:

$$T_1 \overset{OH^-,\,K'}{\rightleftharpoons} T_2' \quad \text{(Eq. 5)}$$

Such an equilibrium is most likely to be significant if the nucleophilic attack to form T_1 is not the rate-determining step.

The significantly low value of the Grunwald-Winstein coefficient ($m \simeq 0.29$) indicates that the rate is not sensitive to the solvating power of the organic cosolvent. However, the increase in rate of hydrolysis with increase in water concentrations of the mixed solvents reveals that the transition state involved is more polar than the reactants (28). The solvent effect was studied at 0.03 M NaOH where the contribution of the k_2 step compared with the k_1 step was most likely negligible. It is therefore conceivable to assume that the k_1' step should be dominant over the k_1 step in the formation of T_1 (Scheme I) because the transition state of the k_1' step (VI) is apparently more polar than that of the k_1 step (VII) and because the ionic reactant of the k_1 step is presumably more strongly solvated than that of the k_1' step in a polar solvent.

The sufficiently large negative value of ΔS^* for the k_1' step must be attributed to the necessity for the proper orientation of more than one water molecule in the transition state (29); this could be expected if the transition state involved is highly polar. It is interesting to note that the ΔS^* for the k_1' step is ~12.7 e.u. more negative compared with that for the k_2 step while the ΔH^* for the k_2 step is ~3.66 kcal/mol larger than that for the k_1' step. These observations are consistent with the proposed transition states VI and VII. As expected from the proposed mechanism, the k_1' step has been found to be

[7] The pK_a of acetamide [15.4 (20a), 17.1 (20b)] and the value of K_a/K_w of ~7 for succinamic acid (22) indicate that the acidity of the amide group is not much different from water.

[8] Unpublished observations.

insensitive to the ionic strength while a change in ionic strength from 1.0 to 4.0 M resulted in an increase of ~25% in k_{obs} obtained at 1.0 M NaOH.

REFERENCES

(1) V. Stella and T. Higuchi, *J. Pharm. Sci.*, **62**, 968 (1973) and reference therein.

(2) E. Friedmann, D. H. Marrian, and I. Simon-Reuss, *Br. J. Pharmacol.*, **4**, 105 (1949); *Biochim. Biophys. Acta*, **9**, 61 (1952); E. Friedmann, *Bull. Soc. Chim. Biol.*, **31**, 506 (1949).

(3) T.-C. Tsao and K. Bailey, *Biochim. Biophys. Acta*, **11**, 102 (1953).

(4) C. O'Connor, *Quart. Rev. Chem. Soc.*, **24**, 553 (1970); M. L. Bender, *Chem. Rev.*, **60**, 53 (1960).

(5) S. S. Biechler and R. W. Taft, *J. Am. Chem. Soc.*, **79**, 4927 (1957).

(6) M. Komiyama and M. L. Bender, *Bioorg. Chem.*, **7**, 133 (1978); R. M. Pollack and T. C. Dumsha, *J. Am. Chem. Soc.*, **97**, 377 (1975); F. Kezdy and A. Bruylants, *Bull. Soc. Chim. Belg.*, **69**, 602 (1960); F. M. Menger and J. A. Donohue, *J. Am. Chem. Soc.*, **95**, 432 (1973); E. G. Sander, *J. Am. Chem. Soc.*, **91**, 3629 (1969); M. N. Khan and A. A. Khan, *Indian J. Chem.*, **13**, 485 (1975).

(7) M. N. Khan and T. O. Olagbemiro, *J. Org. Chem.*, **47**, 3695 (1982).

(8) M. N. Khan, R. Ahmad, and A. A. Khan, *Indian J. Chem.*, **14A**, 961 (1976); R. Ahmad, M. N. Khan, and A. A. Khan, *Indian J. Chem.*, **14A**, 807 (1976); M. N. Khan and A. A. Khan, *J. Chem. Soc., Perkin Trans. 2*, **1978**, 1176.

(9) M. N. Khan and A. A. Khan, *J. Chem. Soc., Perkin Trans. 2*, 796, 1093 (1979); *J. Chem. Soc., Perkin Trans. 2*, **1976**, 1009; *Indian J. Chem.*, **21A**, 365 (1982).

(10) R. J. E. Talbot, in "Comprehensive Chemical Kinetics," vol. 10, C. H. Bamford and C. F. H. Tipper, Eds., Elsevier, Amsterdam, The Netherlands, 1972, pp. 274, 275.

(11) M. N. Khan, *J. Org. Chem.*, **48**, 2046 (1983).

(12) G. Dahlgren and N. L. Simmerman, *J. Phys. Chem.*, **69**, 3626 (1965).

(13) R. Kluger and J. Chin, *J. Am. Chem. Soc.*, **104**, 2891 (1982); A. J. Kirby and P. W. Lancaster, *J. Chem. Soc. Perkin Trans. 2*, **1972**; 1206.

(14) M. F. Aldersley, A. J. Kirby, P. W. Lancaster, R. S. McDonald, and C. R. Smith, *J. Chem. Soc., Perkin Trans. 2*, **1974**, 1487.

(15) M. N. Khan and L. Malspeis, *J. Org. Chem.*, **47**, 2731 (1982).

(16) A. A. Frost and R. G. Pearson, "Kinetics and Mechanism," Wiley-Interscience, New York, N.Y., 1961, chap. 7.

(17) E. Grunwald and S. Winstein, *J. Am. Chem. Soc.*, **70**, 846 (1948).

(18) A. H. Fainberg and S. Winstein, *J. Am. Chem. Soc.*, **78**, 2770 (1956).

(19) M. J. Gresser and W. P. Jencks, *J. Am. Chem. Soc.*, **99**, 6963 (1977); 6970 (1977); D. J. Hupe and W. P. Jencks, *J. Am. Chem. Soc.*, **99**, 451 (1977).

(20) (a) G. B. Barlin and D. D. Perrin, *Quart. Rev. Chem. Soc.*, **20**, 75 (1966). (b) I. T. Ibrahim and A. Williams, *J. Chem. Soc. Perkin Trans. 2*, **1982**, 1459.

(21) C. D. Ritchie, D. J. Wright, D-S. Huang, and A. A. Kamego, *J. Am. Chem. Soc.*, **97**, 1163 (1975).

(22) M. N. Khan and A. A. Khan, *J. Org. Chem.*, **40**, 1793 (1975).

(23) G. J. Yakatan and T. Fun, *Drug Dev. Ind. Pharm.*, **3**, 315 (1977).

(24) W. P. Jencks, *Accounts Chem. Res.*, **13**, 161 (1980).

(25) N. Gravitz and W. P. Jencks, *J. Am. Chem. Soc.*, **96**, 489, 499, 507 (1974).

(26) E. Grunwald, C. F. Jumper, and S. Meiboom, *J. Am. Chem. Soc.*, **85**, 522 (1963); Z. Luz and S. Meiboom, *J. Am. Chem. Soc.*, **85**, 3923 (1963); S. Rosenberg, S. M. Silver, J. M. Sayer, and W. P. Jencks, *J. Am. Chem. Soc.*, **96**, 7986 (1974); R. Kluger and C.-H. Lam, *J. Am. Chem. Soc.*, **100**, 2191 (1978).

(27) A. Bruylant and F. Kezdy, *Rec. Chem. Progr.*, **21**, 213 (1960); R. H. DeWolfe and R. C. Newcomb, *J. Org. Chem.*, **36**, 3870 (1971).

(28) K. J. Laidler, "Chemical Kinetics," McGraw-Hill, New York, N.Y., 1965.

(29) J. C. Tillett and D. E. Wiggins, *Tetrahedron Lett.*, **14**, 91 (1971).

ACKNOWLEDGMENTS

The author is very grateful to the Research and Higher Degrees Committee of Bayero University for a research grant to purchase the UV-visible spectrophotometer.

Dissolution at Porous Interfaces VI: Multiple Pore Systems

H. GRIJSEELS *, D. J. A. CROMMELIN ˣ, and C. J. DE BLAEY ‡

Received February 3, 1983, from the *Department of Pharmaceutics, University of Utrecht, 3511 GH Utrecht, The Netherlands.* Accepted for publication March 21, 1984. Present addresses: *Gist-brocades N.V., P.O. Box 43, 7940 AA Meppel, The Netherlands and ‡Royal Dutch Society for the Advancement of Pharmacy, 2514 JL The Hague, The Netherlands.

Abstract □ With the aid of rapidly dissolving sodium chloride particles, cubic pores were made in the surface of a theophylline tablet. The influence of the pores on the dissolution rate of the surface was investigated in a rotating disk apparatus. Like the drilled pores used in earlier studies, downstream on the surface they caused a turbulent flow regimen with the development of a trough due to enhanced erosion. The phenomenon of a critical pore diameter, discovered with single, drilled pores, seems to be applicable to the cubic pores investigated in this study, although a higher degree of surface coverage with pores caused complications, probably due to particles bordering one another and forming larger pores. The behavior of the porous surfaces at different rotation speeds was studied. Due to the presence of pores the laminar character of the boundary layer flow changes to turbulent, which induces locally an increased dissolution flux in the wake of a pore.

Keyphrases □ Dissolution rates—pore effects, theophylline □ Pore effects—influence on dissolution rate, theophylline

The promoting effect of pores on the dissolution rate of a tablet surface and the effects of individual pores drilled into a dissolving surface have been reported (1–5). The objective of this study was to investigate the changes in dissolution rate of a solid surface when several pores, which can not be considered to act individually, are present. The hydrodynamic conditions around each pore will be influenced by surrounding pores and, as a consequence of the interaction of the turbulent zones behind the pores, the erosion troughs will overlap.

Pores can be drilled into a tablet surface by a drilling technique (1–5), but this method is not feasible for a large number of pores, and an alternative procedure was followed in this study. Sodium chloride particles, characterized by an almost cubic shape, were embedded in the surface of a theophylline tablet. In the dissolution experiment, the sodium chloride particles rapidly dissolved leaving (cubic) pores in the slowly dissolving theophylline surface. In this way a surface was easily supplied with a large number of pores.

0022-3549/84/1200-1771$01.00/0

© 1984, American Pharmaceutical Association

insensitive to the ionic strength while a change in ionic strength from 1.0 to 4.0 M resulted in an increase of ~25% in k_{obs} obtained at 1.0 M NaOH.

REFERENCES

(1) V. Stella and T. Higuchi, *J. Pharm. Sci.*, **62**, 968 (1973) and reference therein.

(2) E. Friedmann, D. H. Marrian, and I. Simon-Reuss, *Br. J. Pharmacol.*, **4**, 105 (1949); *Biochim. Biophys. Acta*, **9**, 61 (1952); E. Friedmann, *Bull. Soc. Chim. Biol.*, **31**, 506 (1949).

(3) T.-C. Tsao and K. Bailey, *Biochim. Biophys. Acta*, **11**, 102 (1953).

(4) C. O'Connor, *Quart. Rev. Chem. Soc.*, **24**, 553 (1970); M. L. Bender, *Chem. Rev.*, **60**, 53 (1960).

(5) S. S. Biechler and R. W. Taft, *J. Am. Chem. Soc.*, **79**, 4927 (1957).

(6) M. Komiyama and M. L. Bender, *Bioorg. Chem.*, **7**, 133 (1978); R. M. Pollack and T. C. Dumsha, *J. Am. Chem. Soc.*, **97**, 377 (1975); F. Kezdy and A. Bruylants, *Bull. Soc. Chim. Belg.*, **69**, 602 (1960); F. M. Menger and J. A. Donohue, *J. Am. Chem. Soc.*, **95**, 432 (1973); E. G. Sander, *J. Am. Chem. Soc.*, **91**, 3629 (1969); M. N. Khan and A. A. Khan, *Indian J. Chem.*, **13**, 485 (1975).

(7) M. N. Khan and T. O. Olagbemiro, *J. Org. Chem.*, **47**, 3695 (1982).

(8) M. N. Khan, R. Ahmad, and A. A. Khan, *Indian J. Chem.*, **14A**, 961 (1976); R. Ahmad, M. N. Khan, and A. A. Khan, *Indian J. Chem.*, **14A**, 807 (1976); M. N. Khan and A. A. Khan, *J. Chem. Soc., Perkin Trans. 2*, **1978**, 1176.

(9) M. N. Khan and A. A. Khan, *J. Chem. Soc., Perkin Trans. 2*, 796, 1093 (1979); *J. Chem. Soc., Perkin Trans. 2*, **1976**, 1009; *Indian J. Chem.*, **21A**, 365 (1982).

(10) R. J. E. Talbot, in "Comprehensive Chemical Kinetics," vol. 10, C. H. Bamford and C. F. H. Tipper, Eds., Elsevier, Amsterdam, The Netherlands, 1972, pp. 274, 275.

(11) M. N. Khan, *J. Org. Chem.*, **48**, 2046 (1983).

(12) G. Dahlgren and N. L. Simmerman, *J. Phys. Chem.*, **69**, 3626 (1965).

(13) R. Kluger and J. Chin, *J. Am. Chem. Soc.*, **104**, 2891 (1982); A. J. Kirby and P. W. Lancaster, *J. Chem. Soc. Perkin Trans. 2*, **1972**; 1206.

(14) M. F. Aldersley, A. J. Kirby, P. W. Lancaster, R. S. McDonald, and C. R. Smith, *J. Chem. Soc., Perkin Trans. 2*, **1974**, 1487.

(15) M. N. Khan and L. Malspeis, *J. Org. Chem.*, **47**, 2731 (1982).

(16) A. A. Frost and R. G. Pearson, "Kinetics and Mechanism," Wiley-Interscience, New York, N.Y., 1961, chap. 7.

(17) E. Grunwald and S. Winstein, *J. Am. Chem. Soc.*, **70**, 846 (1948).

(18) A. H. Fainberg and S. Winstein, *J. Am. Chem. Soc.*, **78**, 2770 (1956).

(19) M. J. Gresser and W. P. Jencks, *J. Am. Chem. Soc.*, **99**, 6963 (1977); 6970 (1977); D. J. Hupe and W. P. Jencks, *J. Am. Chem. Soc.*, **99**, 451 (1977).

(20) (a) G. B. Barlin and D. D. Perrin, *Quart. Rev. Chem. Soc.*, **20**, 75 (1966). (b) I. T. Ibrahim and A. Williams, *J. Chem. Soc. Perkin Trans. 2*, **1982**, 1459.

(21) C. D. Ritchie, D. J. Wright, D-S. Huang, and A. A. Kamego, *J. Am. Chem. Soc.*, **97**, 1163 (1975).

(22) M. N. Khan and A. A. Khan, *J. Org. Chem.*, **40**, 1793 (1975).

(23) G. J. Yakatan and T. Fun, *Drug Dev. Ind. Pharm.*, **3**, 315 (1977).

(24) W. P. Jencks, *Accounts Chem. Res.*, **13**, 161 (1980).

(25) N. Gravitz and W. P. Jencks, *J. Am. Chem. Soc.*, **96**, 489, 499, 507 (1974).

(26) E. Grunwald, C. F. Jumper, and S. Meiboom, *J. Am. Chem. Soc.*, **85**, 522 (1963); Z. Luz and S. Meiboom, *J. Am. Chem. Soc.*, **85**, 3923 (1963); S. Rosenberg, S. M. Silver, J. M. Sayer, and W. P. Jencks, *J. Am. Chem. Soc.*, **96**, 7986 (1974); R. Kluger and C.-H. Lam, *J. Am. Chem. Soc.*, **100**, 2191 (1978).

(27) A. Bruylant and F. Kezdy, *Rec. Chem. Progr.*, **21**, 213 (1960); R. H. DeWolfe and R. C. Newcomb, *J. Org. Chem.*, **36**, 3870 (1971).

(28) K. J. Laidler, "Chemical Kinetics," McGraw-Hill, New York, N.Y., 1965.

(29) J. C. Tillett and D. E. Wiggins, *Tetrahedron Lett.*, **14**, 91 (1971).

ACKNOWLEDGMENTS

The author is very grateful to the Research and Higher Degrees Committee of Bayero University for a research grant to purchase the UV-visible spectrophotometer.

Dissolution at Porous Interfaces VI: Multiple Pore Systems

H. GRIJSEELS *, D. J. A. CROMMELIN ˣ, and C. J. DE BLAEY ‡

Received February 3, 1983, from the *Department of Pharmaceutics, University of Utrecht, 3511 GH Utrecht, The Netherlands.* Accepted for publication March 21, 1984. Present addresses: *Gist-brocades N.V., P.O. Box 43, 7940 AA Meppel, The Netherlands and ‡Royal Dutch Society for the Advancement of Pharmacy, 2514 JL The Hague, The Netherlands.

Abstract □ With the aid of rapidly dissolving sodium chloride particles, cubic pores were made in the surface of a theophylline tablet. The influence of the pores on the dissolution rate of the surface was investigated in a rotating disk apparatus. Like the drilled pores used in earlier studies, downstream on the surface they caused a turbulent flow regimen with the development of a trough due to enhanced erosion. The phenomenon of a critical pore diameter, discovered with single, drilled pores, seems to be applicable to the cubic pores investigated in this study, although a higher degree of surface coverage with pores caused complications, probably due to particles bordering one another and forming larger pores. The behavior of the porous surfaces at different rotation speeds was studied. Due to the presence of pores the laminar character of the boundary layer flow changes to turbulent, which induces locally an increased dissolution flux in the wake of a pore.

Keyphrases □ Dissolution rates—pore effects, theophylline □ Pore effects—influence on dissolution rate, theophylline

The promoting effect of pores on the dissolution rate of a tablet surface and the effects of individual pores drilled into a dissolving surface have been reported (1–5). The objective of this study was to investigate the changes in dissolution rate of a solid surface when several pores, which can not be considered to act individually, are present. The hydrodynamic conditions around each pore will be influenced by surrounding pores and, as a consequence of the interaction of the turbulent zones behind the pores, the erosion troughs will overlap.

Pores can be drilled into a tablet surface by a drilling technique (1–5), but this method is not feasible for a large number of pores, and an alternative procedure was followed in this study. Sodium chloride particles, characterized by an almost cubic shape, were embedded in the surface of a theophylline tablet. In the dissolution experiment, the sodium chloride particles rapidly dissolved leaving (cubic) pores in the slowly dissolving theophylline surface. In this way a surface was easily supplied with a large number of pores.

0022-3549/84/1200-1771$01.00/0

© 1984, American Pharmaceutical Association

EXPERIMENTAL SECTION

Materials—Theophylline monohydrate[1] was used as supplied. Sodium chloride was classified by sieving. Both compounds met the requirements of the European Pharmacopoeia (6).

Particle Size Determinations—The size distribution of the sieve fractions of sodium chloride particles was determined by microscopic examination. As nearly all particles had a cubic shape, the edge of each particle was measured as its characteristic diameter. Cumulative log-probability plots of the particle distribution data gave straight lines, from which the geometric mean diameter (d_g) and the geometric standard deviation (σ_g) of each fraction were obtained. The specific gravity (ρ) of sodium chloride is 2.17×10^3 kg·m^{-3} (7) and since on the whole the shape of the particles is cubic, d_g was used to compute the number of particles per unit weight by:

$$n = \frac{1}{\rho d_g^3} \qquad \text{(Eq. 1)}$$

Disk Preparation—Tablets with a 15.0-mm diameter and varying thicknesses were compressed individually using a hydraulic press. The flat surfaces of each tablet were perfectly smooth without rims or ridges, which was achieved by using an appropriate set of die and punches. After inserting the lower punch in the die, a quantity of theophylline powder, sufficient to obtain a tablet with a thickness of 2–4 mm, was poured into the die. Next, the upper punch was mounted and the powder was precompressed at 2000 N for 10 s. After removing the upper punch, a small amount of sodium chloride was put on the theophylline surface. The particles were carefully spread over the surface to obtain a homogeneous distribution. The actual compression was then performed at 12,000 N for ≥30 s. At this compressional force the sodium chloride crystals did not break or disintegrate (checked microscopically). This procedure provided tablets with an upper surface consisting of intact cubic sodium chloride particles embedded in a theophylline matrix.

Dissolution Rate Measurements—The rotating disk apparatus for determining the dissolution rate of the tablet surfaces has been described in detail (2). In this study the rotation speed of the mounted disk varied between 100 and 340 rpm. The concentrations of sodium chloride and theophylline were measured continuously and simultaneously. The quantity of dissolved sodium chloride was monitored by a conductivity cell[2] mounted in the vessel. The theophylline concentration was measured by circulating the solution through a spectrophotometer[3] equipped with a flow cell (10-mm path length) and set at a wavelength of 270 nm. An internal calibration of both measuring systems was performed by the preaddition method described previously (1).

To be sure that dissolved sodium chloride had no influence on the absorbance of theophylline, increasing amounts of solid sodium chloride were added to a theophylline solution: no change in absorbance was noticed and, conversely, adding solid theophylline to a sodium chloride solution had no effect on the measured conductance. The dissolution rate of a smooth theophylline surface into bulk solutions with different concentrations of sodium chloride was measured and, for the sodium chloride concentrations relevant to this study, the dissolution rate of theophylline was not affected by the amount of sodium chloride in the solution.

After a short initial period, during which the sodium chloride particles dissolved, the theophylline dissolution curves were straight up to ≥15 min. This was sufficient to obtain an accurate value for the dissolution rate. Dissolution data were collected at regular time intervals by a microcomputer[4]. After the experiment, the dissolution rate of the theophylline surface was computed from the least-squares regression line of those data that were obtained after the sodium chloride had dissolved completely, *i.e.*, after the conductance of the solution had reached a constant level (in all cases within 60 s). At that moment only a negligible quantity of theophylline had dissolved (~5–10% of the final amount), implying that the shape of the created pores had hardly changed during this initial period. The conductance of the solution was measured after complete dissolution of the embedded sodium chloride; from this measurement the number of crystals originally present in the surface, which equals the number of created pores, was calculated.

RESULTS AND DISCUSSION

The erosion pattern of a tablet after the dissolution rate experiment (Fig. 1), is the result of two processes. First, dissolution of the sodium chloride particles creates cubic pores. Due to the presence of these pores in the surface troughs develop, which are the consequence of an enhanced theophylline dissolution in the wake of the pores and which extend along a spiral trajectory in the theophylline surface (2).

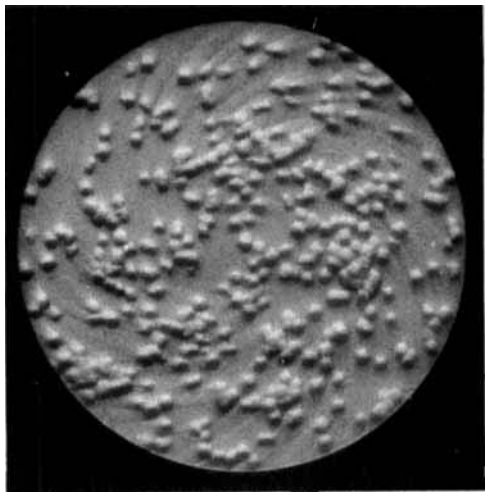

Figure 1—*The surface of a theophylline tablet after a dissolution experiment of ~15 min. Pores were created by sodium chloride particles (d_g = 308 μm), embedded in the surface.*

The dissolution rates of porous theophylline surfaces were determined at a rotation speed of 160 rpm using a varying number of sodium chloride particles of different sizes. Porous surfaces were made with the five sieve fractions listed in Table I. In all experiments the maximum coverage of the theophylline surface by sodium chloride particles remained <25%.

For each sieve fraction the dissolution rate of a theophylline surface with n pores (R_n) was measured at various values of n. In Fig. 2, I_n, the difference between the dissolution rates of a smooth surface (R_0) and a surface with n pores (R_n), is plotted as a function of the number of pores. Since the dissolution rate of a smooth theophylline surface at 160 rpm is 14.9 μg·s^{-1}, the largest pores can cause the dissolution rate to increase >50% at this rotation speed.

Figure 2 demonstrates that I_n is not only dependent on the number of pores but also on the pore size. This is not surprising in view of previous findings (1–5). It was established (3) that the critical pore diameter (the diameter a single pore must exceed to cause an increase of the dissolution rate) is related to the friction velocity v_f in the boundary layer at the rotating disk surface according to:

$$d_{crit} = 2.7 \frac{\nu}{v_f} \qquad \text{(Eq. 2)}$$

where ν is the kinematic viscosity of the solvent (mm^2·s^{-1}).

The friction velocity is a hydrodynamic variable that, for a rotating disk surface, can be computed from (8, 9):

$$v_f = 0.89 \nu^{1/4} x^{1/2} \omega^{3/4} \qquad \text{(Eq. 3)}$$

where x is the distance from the surface center (mm) and ω is the angular velocity (s^{-1}). Equation 3 implies that at the edge of the dissolving surface the friction velocity has a maximum value and, from Eq. 2, the critical pore diameter has a minimum value. With a rotation speed of 160 rpm the critical pore diameter at the edge (calculated from Eqs. 2 and 3) is ~0.13 mm. Nearer the disk center d_{crit} is larger, *e.g.*, at 2.5 mm from the surface edge a value of 0.19 mm was measured (3).

These considerations made it unlikely that the sodium chloride fractions with a d_g of ~ ≤130 μm would cause an increase in the dissolution rate. Even the 198-μm fraction could only increase the dissolution rate on a limited part

Table I—Sieve Fraction Data of Sodium Chloride

Sieve Fraction, μm	Geometric Mean Diameter (d_g), μm	Geometric *SD* (σ_g)	Calculated Particle Number (n)[a]
71–100	88	1.28	676
100–160	128	1.23	220
160–250	198	1.18	59
250–400	308	1.16	15.8
400–500	419	1.15	6.3

[a] Number of particles/mg sodium chloride.

[1] OP6, Utrecht, The Netherlands.
[2] PW9510; Philips.
[3] UV100-02; Shimadzu.
[4] Apple II plus.

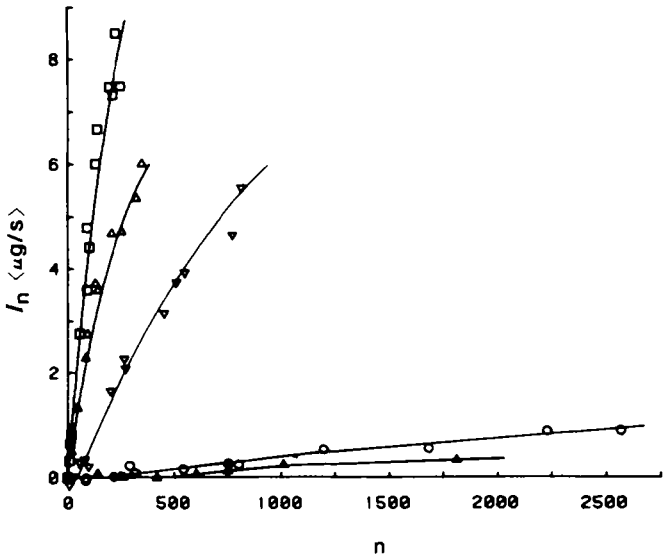

Figure 2—*Effect of number and size of pores on the increase in dissolution rate of the theophylline surface with respect to a smooth surface (160 rpm). Key: particles with a geometric mean diameter of (□) 419 μm; (△) 308 μm; (▽) 198 μm; (○) 128 μm; (▲) 88 μm.*

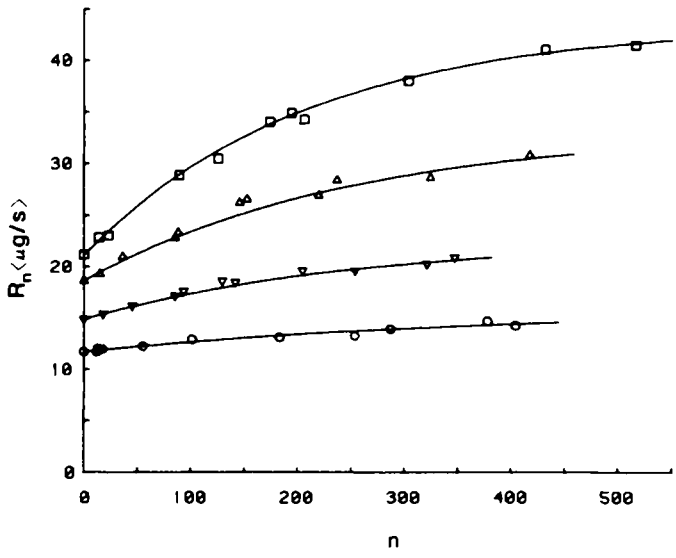

Figure 3—*Dissolution rate of a theophylline surface at different rotation speeds as a function of the number of sodium chloride particles used to create pores. Geometric mean diameter of the particles: 308 μm. Key: (□) 340 rpm; (△) 250 rpm; (▽) 160 rpm; (○) 100 rpm. Each symbol represents an individual experiment. Lines were computed by Eq. 7.*

of the surface; only particles positioned in a region of the tablet surface where d_{crit} is less than ~0.20 mm can cause a change in the dissolution rate. The more particles present in the surface, the more likely it is that somewhere a pore exceeds the local critical size. In the 198-μm fraction, the dissolution rate increases considerably with n, provided that n exceeds a minimum value of 30–40 particles (Fig. 2).

A second possible explanation for the shape of the lines in Fig. 2 must be mentioned. Single particles that create pores equal to or smaller than the local critical size, will not raise the dissolution rate, but when the number of particles in the surface increases, it is more likely that at least two particles lie against each other and together create a larger pore when the sodium chloride dissolves. The presence of these larger pores might be the reason that, at higher values of n, the two smallest particle fractions (128 and 88 μm) also cause a slight increase in the dissolution rate compared with a smooth surface.

The influence of the rotation velocity of the disk surface on the dissolution rate was investigated using the 308-μm particles. The relationship between dissolution rate and number of particles was determined at four different revolution speeds (Fig. 3). No linear relation exists between those two variables, but for every rotation speed the dissolution rate (R_n) increases asymptotically with increasing n to a maximum value. This leads to the assumption that for a certain number of pores a maximum dissolution rate (R_{max}) exists. The corresponding maximum increase of the dissolution rate, I_{max}, is defined by:

$$I_{max} = R_{max} - R_0 \qquad \text{(Eq. 4)}$$

Suppose that the relation between I_n and n can be described by the first-order equation:

$$\frac{d(I_{max} - I_n)}{dn} = -k(I_{max} - I_n) \qquad \text{(Eq. 5)}$$

then we obtain by rearranging and integrating:

$$\ln\left(1 - \frac{I_n}{I_{max}}\right) = -kn \qquad \text{(Eq. 6)}$$

A semilogarithmic plot of $(1 - I_n/I_{max})$ *versus* n should result in a straight line with a slope $-k$ and passing through the origin, provided that the assumption of a first-order relationship in Eq. 5 is justified. Since the value of I_{max} in Eq. 5 was unknown, an iterative calculation of the linear regression coefficients of the data $\ln(1 - I_n/I_{max})$ *versus* n was performed. New values for I_{max} were chosen until the best correlation coefficient was obtained. The computed coefficients were used to fit the data in Fig. 3 according to:

$$R_n = R_0 + I_n = R_0 + I_{max}(1 - e^{-kn}) \qquad \text{(Eq. 7)}$$

The points in Fig. 3 are fitted well by the lines obtained from these computations, so the assumption of a first-order relation appears to be a good approximation.

Table II—Dissolution Rates[a] of Theophylline Surfaces With Cubic Pores

Pores	Rotation Speed, rpm (ω) 100 (10.47)	160 (16.76)	250 (26.78)	340 (35.60)	p[b]	r[c]
0	11.74	14.91	18.60	21.15	0.49	0.9993
10	11.85	15.20	19.18	22.20	0.51	0.9998
20	11.95	15.49	19.73	23.19	0.54	1.0000
30	12.06	15.76	20.26	24.15	0.57	1.0000
40	12.16	16.02	20.77	25.05	0.59	1.0000
50	12.25	16.27	21.26	25.92	0.61	0.9999
75	12.49	16.86	22.41	27.90	0.65	0.9997
100	12.70	17.39	23.44	29.67	0.69	0.9996
125	12.91	17.88	24.38	31.23	0.72	0.9995
150	13.10	18.32	25.22	32.62	0.74	0.9994
200	13.44	19.08	26.68	34.95	0.78	0.9994
250	13.74	19.72	27.87	36.78	0.80	0.9994
300	14.00	20.24	28.84	38.22	0.82	0.9995
350	14.23	20.67	29.63	39.35	0.83	0.9995
400	14.44	21.02	30.28	40.25	0.83	0.9995

[a] Calculated by means of Eq. 7 with the coefficients of the best fit through the experimental data. Pore size, 308 μm. [b] Exponent in Eq. 8, slope, computed from a log-log plot. [c] Correlation coefficient of the log-log plot.

The actual nature of the hydrodynamic conditions at the tablet surface can be determined from the relationship between the dissolution rate and the angular velocity of the rough pellet surface. The relationship between R_n and angular velocity (ω) can be written in the form (10):

$$R_n \sim \omega^p \qquad \text{(Eq. 8)}$$

At smooth rotating disk surfaces, p = 0.5 under laminar conditions and p = 0.9 in a completely turbulent flow pattern. At a rough rotating disk surface, consisting of a regular, geometric pattern of pyramids, the following results were obtained (11-14): with a pyramid height of >1 mm the mass flux varied with $\omega^{0.67}$. But when the height of the roughness elements diminished, the exponent of ω increased from 0.67 to >0.9 (14). The experimental data collected in Fig. 3 were used to investigate the effect of the presence of pores on the hydrodynamics at the tablet surface. Since the dissolution rates can be compared only for equal values of n at the different rotation speeds, interpolated values of R_n were calculated by Eq. 7 from the best fit of the experimental data for various numbers of pores at each rotation speed (Table II). A linear regression analysis of the plot of log R_n *versus* log ω for any number of pores was performed on the data collected in Table II. The slopes of these plots correspond to p in Eq. 8. Exponent p increases from ~0.5 at $n = 0$ (smooth surface) to 0.8-0.9 for surfaces with >250 pores. This confirms earlier observations that, due to the presence of pores, the flow regimen in the boundary layer near the surface shows a transition from laminar to turbulent, resulting in a changed dissolution mechanism of the surface.

REFERENCES

(1) H. Grijseels and C. J. de Blaey, *Int. J. Pharm.*, **9**, 337 (1981).

(2) H. Grijseels, L. van Bloois, D. J. A. Crommelin, and C. J. de Blaey, *Int. J. Pharm.*, **14**, 299 (1983).

(3) H. Grijseels, D. J. A. Crommelin, and C. J. de Blaey, *Int. J. Pharm.* **14**, 313 (1983).

(4) H. Grijseels, B. T. J. M. Harden, and C. J. de Blaey, *Pharm. Weekbl.* **5**, 88 (1983).

(5) H. Grijseels and C. J. de Blaey, *Int. J. Pharm.*, **16**, 295 (1983).

(6) "European Pharmacopoeia," 1st ed., Maisonneuve S.A., Sainte-Ruffine, France, Vol. I, 1969, p. 331; vol. II, 1971, p. 384.

(7) "The Merck Index," 9th ed., Merck & Co., Inc., Rahway, N.J., 1976, p. 1111.

(8) H. Schlichting, "Boundary Layer Theory," McGraw-Hill, New York, N.Y., 1968, pp. 94 and 511.

(9) C. Deslouis, B. Tribollet, and L. Viet, *Electrochim. Acta*, **25**, 1027 (1980).

(10) V. G. Levich, "Physicochemical Hydrodynamics," Prentice Hall, N.J., 1962, pp. 70 and 152.

(11) M. Meklati, M. Daguenet, and G. Cognet, *C. R. Acad. Sci., Paris*, **274**, 1373 (1972).

(12) M. Meklati and M. Daguenet, *J. Chim. Phys.*, **70**, 1102 (1973).

(13) M. Meklati and M. Daguenet, *J. Chim. Phys.*, **72**, 262 (1975).

(14) L. Mollet and M. Daguenet, *J. Chim. Phys.*, **78**, 61 (1981).

Interaction of Povidone with Aromatic Compounds V: Relationship of Binding Tendency in a Macromolecular Solution Treated as a Pseudo Two Phase and a Monophase

J. A. PLAIZIER-VERCAMMEN

Received November 12, 1982, from the *Faculteit Geneeskunde en Farmacie, Vrije Universiteit Brussel, B-1090 Brussels, Belgium.* Accepted for publication April 13, 1984.

Abstract □ The pseudo-two-phase model is proposed to correlate complex formation of ligand molecules with povidone with partition coefficients (log P or II constants). The conditions which permit the use of the pseudo-two-phase model for binding of ligand onto macromolecules are determined. This model seems to be a more rational choice than the frequently used complex formation model (monophase). This is demonstrated theoretically and confirmed experimentally. The advantages of the use of such a model are also discussed.

Keyphrases □ Povidone—interaction with aromatic compounds, pseudo-two-phase and monophase systems, salicylic acid, complex formation □ Pseudo-two-phase model—compared with monophase, complex formation aromatic compounds with macromolecules

The important role of lipophilicity of ligand molecules and hydrophobic bonding in complex formation of a series of ligand molecules with povidone has been previously investigated; ligand molecules in the nonionic state showed a higher complexing tendency than those in the ionic state, (1-3). Complex formation of ligand molecules with povidone was explained in terms of hydrophobic bonding (1, 4-8). In earlier work, we studied the complexing tendency of ligand molecules in the nonionic and ionic state, and the importance of the hydrophobic bonding especially for nondissociated molecules was confirmed (9). The correlation observed between the solubility of the ligand molecule in solvent mixtures and its binding to povidone (10) also provided support for the occurrence of complex formation by hydrophobic interactions.

Hansch *et al.* (11) showed that complex formation by hydrophobic bonding of neutral organic molecules with macromolecules, such as serum albumin, can often be correlated with partition coefficients (log P or π constants) (12, 13) between 1-octanol and water. This correlation was found for phenols and serum albumin, barbiturates and homogenized rabbit brain (14), penicillin and serum albumin (15), aniline derivatives and nylon and rayon (16), and phenols and mitochondrial protein (17).

These results, correlated with octanol-water partition coefficients (log P), are expressed either as $1/C$ (11) (where C represents the molar concentration of ligand to produce a one-to-one complex of ligand and macromolecule), as log $B\%$ [percent bound ligand (14)], or as log B/F (15), where B refers to bound and F to free ligand concentrations, respectively. The methods for expressing complex formation are not comparable. As indicated by Bird and Marshall (15), B/F is a more rational choice than $B\%$ for correlating the results with log P, because B/F is analogous to an organic solvent-water partition coefficient. Moreover, as opposed to the other expressions, B is not a linear function of the association constants.

However, the use of the B/F expression has a disadvantage; one must work at a constant macromolecular concentration in order to compare the B/F expressions for the individual ligand molecules with the log P or π values. This implies that one must expect errors in the results obtained for ligand mol-

0022-3549/84/1200-1774$01.00/0

© 1984, American Pharmaceutical Association

The actual nature of the hydrodynamic conditions at the tablet surface can be determined from the relationship between the dissolution rate and the angular velocity of the rough pellet surface. The relationship between R_n and angular velocity (ω) can be written in the form (10):

$$R_n \sim \omega^p \qquad \text{(Eq. 8)}$$

At smooth rotating disk surfaces, p = 0.5 under laminar conditions and p = 0.9 in a completely turbulent flow pattern. At a rough rotating disk surface, consisting of a regular, geometric pattern of pyramids, the following results were obtained (11-14): with a pyramid height of >1 mm the mass flux varied with $\omega^{0.67}$. But when the height of the roughness elements diminished, the exponent of ω increased from 0.67 to >0.9 (14). The experimental data collected in Fig. 3 were used to investigate the effect of the presence of pores on the hydrodynamics at the tablet surface. Since the dissolution rates can be compared only for equal values of n at the different rotation speeds, interpolated values of R_n were calculated by Eq. 7 from the best fit of the experimental data for various numbers of pores at each rotation speed (Table II). A linear regression analysis of the plot of log R_n *versus* log ω for any number of pores was performed on the data collected in Table II. The slopes of these plots correspond to p in Eq. 8. Exponent p increases from ~0.5 at $n = 0$ (smooth surface) to 0.8-0.9 for surfaces with >250 pores. This confirms earlier observations that, due to the presence of pores, the flow regimen in the boundary layer near the surface shows a transition from laminar to turbulent, resulting in a changed dissolution mechanism of the surface.

REFERENCES

(1) H. Grijseels and C. J. de Blaey, *Int. J. Pharm.*, **9**, 337 (1981).

(2) H. Grijseels, L. van Bloois, D. J. A. Crommelin, and C. J. de Blaey, *Int. J. Pharm.*, **14**, 299 (1983).

(3) H. Grijseels, D. J. A. Crommelin, and C. J. de Blaey, *Int. J. Pharm.* **14**, 313 (1983).

(4) H. Grijseels, B. T. J. M. Harden, and C. J. de Blaey, *Pharm. Weekbl.* **5**, 88 (1983).

(5) H. Grijseels and C. J. de Blaey, *Int. J. Pharm.*, **16**, 295 (1983).

(6) "European Pharmacopoeia," 1st ed., Maisonneuve S.A., Sainte-Ruffine, France, Vol. I, 1969, p. 331; vol. II, 1971, p. 384.

(7) "The Merck Index," 9th ed., Merck & Co., Inc., Rahway, N.J., 1976, p. 1111.

(8) H. Schlichting, "Boundary Layer Theory," McGraw-Hill, New York, N.Y., 1968, pp. 94 and 511.

(9) C. Deslouis, B. Tribollet, and L. Viet, *Electrochim. Acta*, **25**, 1027 (1980).

(10) V. G. Levich, "Physicochemical Hydrodynamics," Prentice Hall, N.J., 1962, pp. 70 and 152.

(11) M. Meklati, M. Daguenet, and G. Cognet, *C. R. Acad. Sci., Paris*, **274**, 1373 (1972).

(12) M. Meklati and M. Daguenet, *J. Chim. Phys.*, **70**, 1102 (1973).

(13) M. Meklati and M. Daguenet, *J. Chim. Phys.*, **72**, 262 (1975).

(14) L. Mollet and M. Daguenet, *J. Chim. Phys.*, **78**, 61 (1981).

Interaction of Povidone with Aromatic Compounds V: Relationship of Binding Tendency in a Macromolecular Solution Treated as a Pseudo Two Phase and a Monophase

J. A. PLAIZIER-VERCAMMEN

Received November 12, 1982, from the *Faculteit Geneeskunde en Farmacie, Vrije Universiteit Brussel, B-1090 Brussels, Belgium.* Accepted for publication April 13, 1984.

Abstract □ The pseudo-two-phase model is proposed to correlate complex formation of ligand molecules with povidone with partition coefficients (log P or II constants). The conditions which permit the use of the pseudo-two-phase model for binding of ligand onto macromolecules are determined. This model seems to be a more rational choice than the frequently used complex formation model (monophase). This is demonstrated theoretically and confirmed experimentally. The advantages of the use of such a model are also discussed.

Keyphrases □ Povidone—interaction with aromatic compounds, pseudo-two-phase and monophase systems, salicylic acid, complex formation □ Pseudo-two-phase model—compared with monophase, complex formation aromatic compounds with macromolecules

The important role of lipophilicity of ligand molecules and hydrophobic bonding in complex formation of a series of ligand molecules with povidone has been previously investigated; ligand molecules in the nonionic state showed a higher complexing tendency than those in the ionic state, (1-3). Complex formation of ligand molecules with povidone was explained in terms of hydrophobic bonding (1, 4-8). In earlier work, we studied the complexing tendency of ligand molecules in the nonionic and ionic state, and the importance of the hydrophobic bonding especially for nondissociated molecules was confirmed (9). The correlation observed between the solubility of the ligand molecule in solvent mixtures and its binding to povidone (10) also provided support for the occurrence of complex formation by hydrophobic interactions.

Hansch *et al.* (11) showed that complex formation by hydrophobic bonding of neutral organic molecules with macromolecules, such as serum albumin, can often be correlated with partition coefficients (log P or π constants) (12, 13) between 1-octanol and water. This correlation was found for phenols and serum albumin, barbiturates and homogenized rabbit brain (14), penicillin and serum albumin (15), aniline derivatives and nylon and rayon (16), and phenols and mitochondrial protein (17).

These results, correlated with octanol-water partition coefficients (log P), are expressed either as $1/C$ (11) (where C represents the molar concentration of ligand to produce a one-to-one complex of ligand and macromolecule), as log $B\%$ [percent bound ligand (14)], or as log B/F (15), where B refers to bound and F to free ligand concentrations, respectively. The methods for expressing complex formation are not comparable. As indicated by Bird and Marshall (15), B/F is a more rational choice than $B\%$ for correlating the results with log P, because B/F is analogous to an organic solvent-water partition coefficient. Moreover, as opposed to the other expressions, B is not a linear function of the association constants.

However, the use of the B/F expression has a disadvantage; one must work at a constant macromolecular concentration in order to compare the B/F expressions for the individual ligand molecules with the log P or π values. This implies that one must expect errors in the results obtained for ligand mol-

0022-3549/84/1200-1774$01.00/0

© 1984, American Pharmaceutical Association

ecules with a low or a high tendency for complex formation (18). The $1/C$ expression offers the advantage over the B/F expression in that it is directly related to the association constant and is independent of the macromolecular concentration. However, for the determination of $1/C$, a series of ligand concentrations must be investigated to determine the concentration of ligand (F) where $r = 1$ [r is defined as mole of bound ligand/mole of macromolecule (11)]. Moreover, expressions used to correlate complex formation to log P values suffer from the fact that notations such as T (total ligand), F (free ligand), and B (bound ligand) calculated from a monophasic point of view (the theory of complex formation) are correlated to the same notations, calculated from a biphasic point of view (partition theory), but have different significance.

The purpose of this report was to investigate the possibilities of expressing complex formation of ligand molecules with macromolecules from a pseudo-two-phase point of view. For this purpose, we have regarded the macromolecular solution both as a true solution (monophase) and as a pseudo two phase comparable with a biphase. We have theoretically investigated the expression of results calculated according to the theory of complex formation in partition terms, and the relationship of the two systems. The theory is experimentally verified with two different experiments and the possibilities and limitations of the two systems are discussed.

EXPERIMENTAL SECTION

Materials and Methods—Povidone[1] was used as the macromolecule and salicylic acid[2] was used as the ligand molecule. The buffer employed was a phosphate buffer (pH 7.00) (19) containing dibasic sodium phosphate and monobasic potassium phosphate. Ultrafiltration was used to investigate the ligand-macromolecule interactions. Previously described equipment was employed (20). The concentration of unbound ligand was determined spectrophotometrically in the ultrafiltrate. The spectrophotometric measurements were performed at 296 nm with a double-beam spectrophotometer[3] after appropriate dilution.

Partial Specific Volume—The partial specific volume ($\overline{V}_2^\circ$) (21, 22) of povidone in water and phosphate buffer (pH 7.00) is calculated from the density increment with all other components at constant chemical potential using the equation:

$$\overline{V}_2^\circ = \frac{1}{\rho'}\left[1 - \left(\frac{\Delta_\rho}{\Delta C_2}\right)_m^\circ\right] \qquad \text{(Eq. 1)}$$

where $\overline{V}_2^\circ$ is the partial specific volume; C_2 is the povidone concentration; $\Delta_\rho/\Delta C_2$ is the density increment with respect to component 2; and ρ' is the buffer density. The densities of the macromolecular solution and the solvent were measured with a digital precision density meter[4], calibrated with air and solvent, at 25°C. In a second method, the partial specific volume was determined using a pycnometer.

Determination of the Binding Tendency—A solution containing salicylic acid and 2.50% povidone in a phosphate buffer (pH 7.00) was prepared. Ultrafiltration was carried out at 25°C, several ultrafiltrate fractions (~0.5-1.0 mL each) were collected, and the free ligand concentration in each sample was determined spectrophotometrically. The volume of the sample was calculated by weighing the sample and determining its density.

RESULTS AND DISCUSSION

Treatment of Povidone Solutions as Pseudo Two Phase—The question of homogeneity or heterogeneity of macromolecules in solution is still a point of discussion. Some authors (23, 24) consider that macromolecular dispersions are monophasic (homogeneous), while other authors (25, 26) believe they are clearly biphasic (heterogeneous). In fact, the problem of phases is a problem of scale. A phase dispersed in another phase ceases to exist, as such, when its degree of division reaches the molecular level. At any point along the chain, a macromolecule has a molecular size in two of the spatial dimensions and a macromolecular size in the third.

The "pseudo-two-phase" model (27, 28) was used by a number of investigators (29-33) to describe aqueous micellar solutions in general and solubilization in particular (28, 34). Such a model leads one to think of the solubilized dispersion as being distributed or partitioned between the micelles ("micellar phase") and the external "aqueous phase."

The elementary requirement that these "phases" be mechanically separable is satisfied, since such a separation can be effected with dialysis or ultrafiltration. Moreover, these micellar solutions are consistent with the Gibbs phase rule for two-phase systems; the intensive properties of the aqueous phase are nearly constant with overall surfactant concentration above the critical micellar concentration at constant temperature and pressure. The pseudo-two-phase treatment of micelles has gained strong support from the ultrafiltration and solubilization studies of Hutchinson *et al.* (30), which showed the number of free detergent molecules to be nearly constant above the micelle point.

The pseudo-two-phase model is useful if the micelles are both large and do not interact; these requirements, if they are fulfilled, should be reflected in the distribution coefficient, being independent of the surfactant concentration for a given micellar composition. All these requirements and limitations, valid for the micellar solutions, are also fulfilled in the case of macromolecular solutions. Moreover, macromolecular solutions are seen as gel particles (35) and occupy a definite volume in solution, indicated as their partial specific volume (21, 22).

Povidone, like other nonionic macromolecules, contains separate hydrophobic and polar groups, making it comparable to nonionic tensides. A molecular model of the povidone molecules showed that the polar pyrrolidone ring and the hydrophobic paraffin backbone were both accessible for the ligand molecules (36). Taking into account these considerations, we thought the pseudo-two-phase model, describing micellar solutions, could also be used for describing macromolecular solutions.

Relationship Between Binding Results, Expressed in a Monophasic (Complex Formation) and a Pseudo-Two-Phasic System (Partition)—According to the theory of complex formation (monophase) (18, 23, 37-39) the following equation is valid:

$$T = B + F \qquad \text{(Eq. 2)}$$

where T, B, and F represent the molarities of total, bound, and free ligand and are calculated on the total volume (V_T) of the solution.

Complex formation can be studied as a function of either macromolecule concentration or ligand concentration. In the first method, the ratio of T to F can be expressed as a function of the amount of povidone (40-42):

$$\frac{T}{F} = a g_{PVP} + 1 \qquad \text{(Eq. 3)}$$

where g_{PVP} is grams of povidone and a is a constant.

The second method permits the calculation of intrinsic binding constants (k) and the number of binding sites (n) on the macromolecule:

$$r = \frac{B}{g_{PVP}} = \frac{nkF}{1 + kF} \qquad \text{(Eq. 4)}$$

For isotherms of several ligand molecules with povidone, a straight line was obtained by plotting r as a function of F (3, 9, 43, 44). This finding implies that at $kF \ll 1$, $1/n$ equals zero or n is infinite, indicating a nearly infinitely large number of adsorption sites (9, 20). So Eq. 4 reduces to:

$$r = \frac{B}{g_{PVP}} = nkF \qquad \text{(Eq. 5)}$$

If both equations are valid, the constant a of Eq. 3 equals nk of Eq. 5.

According to the pseudo-two-phase model (partition), the general equation for partition between two phases is valid:

$$Kd = \left(\frac{T'V'_T - F \cdot V_F}{F}\right) \cdot \left(\frac{1}{V_B}\right) \qquad \text{(Eq. 6)}$$

where:

$$B' = T' - F, \qquad \text{(Eq. 7)}$$

Kd is the partition coefficient between "the pseudo or macromolecule phase" and the aqueous or "outer" phase; T' is the concentration (in molarity) of the aqueous phase before partition; V'_T is the volume of the aqueous phase before partition; F is the concentration (in molarity) of the aqueous phase after equilibrium (*i.e.*, the free ligand concentration); V_F is the volume of the "outer" or aqueous phase after equilibrium; B' is the concentration of ligand in the pseudo or macromolecule phase (*i.e.*, the bound ligand concentration); V_B is the volume of the "pseudophase," in our case, the volume occupied by

[1] Polyvinylpyrrolidone (Kollidon K 90); BASF, Brussels, Belgium.
[2] E. Merck, Darmstadt, F.R.G.
[3] Model 124; Perkin-Elmer.
[4] Digital density meter DMA 40; Anton Parr.

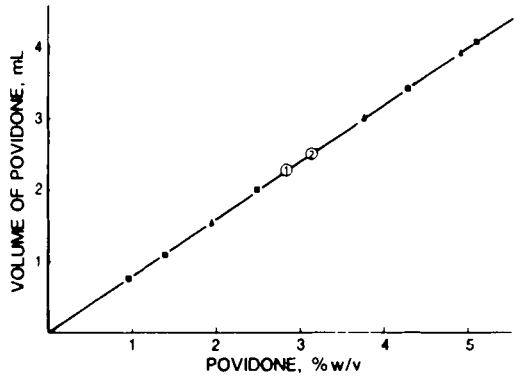

Figure 1—*Volume increment of povidone in water (1) and phosphate buffer (2) solution as a function of its weight.*

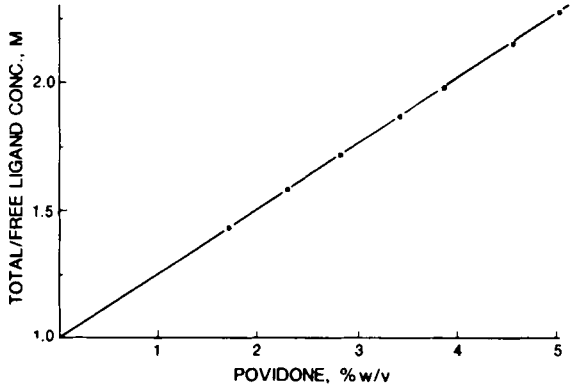

Figure 2—*Complexing tendency of salicylic acid onto povidone. Salicylic acid, 7.60 × 10⁻³ M; pH 7.00; ionic strength, 0.25; 25°C.*

povidone in solution. The partial specific volume of povidone was taken. As $V'_T = V_F$, Eq. 6 can be written:

$$Kd = \left(\frac{T' - F}{F}\right)\frac{V_F}{V_B} \qquad \text{(Eq. 8)}$$

As in the pseudo-two-phase system, T' represents the total concentration of the "outer" or aqueous phase and the relationship between total concentration in the monophase and pseudo-two-phase system is given by:

$$T' = T\left(\frac{V'_T}{V_T - V'_B}\right) \qquad \text{(Eq. 9)}$$

By comparing Eqs. 2, 7, and 9, it is noted that B' expressed in a pseudo-two-phasic system is larger than B expressed in a monophasic system. Further, we can write:

$$V_B = b \cdot g_{PVP} \qquad \text{(Eq. 10)}$$

where g is grams of povidone used in the experiment and b is the volume occupied by one gram of povidone in solution.

Substitution of Eqs. 9 and 10 in Eq. 8 gives:

$$Kd = \left(\frac{\frac{T \cdot V_T}{V_T - b \cdot g_{PVP}} - F}{F}\right) \cdot \left(\frac{V_T - b \cdot g_{PVP}}{b \cdot n \cdot g_{PVP}}\right) \qquad \text{(Eq. 11)}$$

resulting in:

$$\frac{T}{F} = \left(\frac{b \cdot g_{PVP}}{V_T}\right) \cdot (Kd - 1) + 1 \qquad \text{(Eq. 12)}$$

or:

$$\frac{B}{F} = \left(\frac{b \cdot g_{PVP}}{V_T}\right) \cdot (Kd - 1) \qquad \text{(Eq. 13)}$$

Therefore, a plot of T/F as a function of g_{PVP} results in a straight line with slope, b/V_T $(Kd - 1)$ and an intercept of 1. The slope is equal to the slope a of Eq. 3 or nk of Eq. 5.

The relationship between Kd and a, the slope of Eq. 3, or nk of Eq. 5 can be calculated from Eqs. 3, 5, and 12 and results in:

$$Kd = a\frac{V_T}{b} + 1 = nk\frac{V_T}{b} + 1 \qquad \text{(Eq. 14)}$$

From Eq. 14, it can be concluded that the linear relationship between T/F and g_{PVP}, which is found using the theory of complex formation (Eqs. 3 and 5), can be directly correlated with the pseudo-two-phase theory. This holds true for all povidone concentrations.

It has only been assumed that $V_B = V_{PVP}$ is a linear function of g_{PVP}. The linearity has been investigated using a pycnometer and is graphically represented in Fig. 1. The volume occupied by povidone is indeed a linear function of g_{PVP}. From the slope of the line, the b value was calculated and equals 0.80 mL/g (*i.e.*, every gram of povidone occupies a volume of 0.80 mL). This holds true for both water and phosphate buffer. The partial specific volume, calculated from density increments of povidone solutions using Eq. 1, agreed with the results obtained with a pycnometer.

Comparison of Results in a Macromolecular Solution Treated as Monophase and Pseudo Two Phase—To verify the results experimentally, 100-mL solutions containing a constant concentration of salicylic acid as ligand (7.60×10^{-3} M) and different amounts of povidone were prepared in a phosphate buffer (pH 7.00). From the monophasic point of view, and according to Eq. 2, $T = 7.60 \times 10^{-3}$ M and $V_T = 100$ mL.

Ultrafiltration was carried out and the free ligand concentration (F) was determined. The results calculated from the mono- and pseudo-two-phasic points of view (Eqs. 2, 3, and 11) are presented in Table I and Fig. 2.

The slope of the straight lines, T/F, as a function of the povidone concentration was 0.260. The corresponding Kd value, according to Eq. 13 where $V_T = 100$ mL and $b = 0.80$, was 33.50. The mean of the Kd values from the data of Table I, calculated according to Eq. 11, was 33.11. The Kd values agree quite well.

The results of binding onto povidone can be interpreted from the monophasic as well as from the pseudo-two-phasic point of view. The results calculated in one system can easily and correctly be expressed in the other system by use of a simple equation. The calculated Kd values are independent of the macromolecular concentration, as can be expected with partition between two phases. The Kd values offer the advantage above the B/F and $1/C$ determinations, to correlate with log P constants (11, 14, 15) so that the desired information can be obtained from one experiment and the macromolecular concentration can be varied from one ligand to another to minimize the error in the results obtained for ligand molecules with a low or high complexing tendency (18).

Table I—Complexing Tendency of Salicylic Acid Onto Povidone [a]

Povidone, %	Monophase				Pseudo Two Phase					
	T [b]	F	B	T/F	T'	F	B'	V_{PVP}	V_{H_2O}	Kd
1.70	0.00760	0.00530	0.00230	1.43	0.00770	0.00530	0.00240	1.36	98.64	32.91
2.27	0.00760	0.00478	0.00282	1.59	0.00774	0.00478	0.00296	1.82	98.18	33.49
2.81	0.00760	0.00444	0.00316	1.71	0.00777	0.00444	0.00333	2.25	97.75	32.66
3.39	0.00760	0.00404	0.00356	1.88	0.00781	0.00404	0.00377	2.71	97.29	33.49
3.84	0.00760	0.00384	0.00376	1.98	0.00784	0.00384	0.00400	3.07	96.93	32.87
4.53	0.00760	0.00352	0.00408	2.16	0.00789	0.00352	0.00437	3.62	96.38	32.98
5.01	0.00760	0.00331	0.00429	2.30	0.00792	0.00331	0.00461	4.01	95.99	33.34

[a] Calculations were made using Eqs. 2, 3, and 11. The total concentration of salicylic acid was 7.60×10^{-3} M; the pH was 7.00; the ionic strength was 0.25; the temperature was 25°C. [b] T, B, and F are molarities of total, bound, and free ligands, respectively; T', B', and Kd are molar concentrations of the aqueous phase before partition, the bound ligand concentration, and the partition coefficient between the "pseudo" and aqueous phase, respectively.

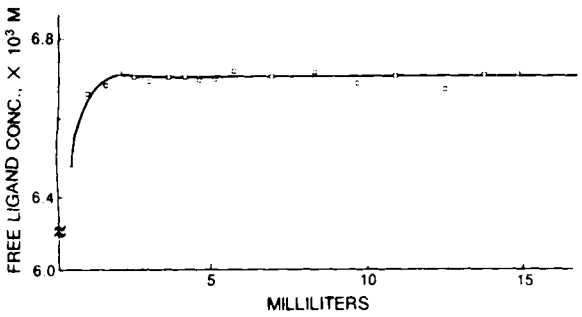

Figure 3—*Determination of the free ligand concentration of salicylic acid in the successive ultrafiltrate samples. Salicylic acid, 1.00 × 10⁻² M; povidone, 2.50%; pH 7.00; 25°C.*

Determination of the Complexing Tendency in Successive Ultrafiltrate Samples—The free ligand concentrations of successive fractions were determined from a solution containing salicylic acid (1.00×10^{-2} M) and 2.50% povidone dissolved in a buffer (pH 7.00) (Fig. 3). The free ligand concentrations in the successive aliquots remain constant, although the volume of the solution is more than halved while the povidone concentration is more than doubled.

The constancy of the free ligand concentration in the successive aliquots was tested in terms of the mono- and pseudo-two-phase models. The results are consistent with a pseudo-two-phase model. According to the partition theory (and Eq. 6), F corresponds to the concentration of the "outer" or the aqueous phase, in opposition to the theory of complex formation. Since we are dealing with concentrations and not with amounts, the free ligand concentration (F) at equilibrium is not changed by eliminating a portion of the "outer" or aqueous phase.

On the other hand, with complex formation, all results are expressed as the total volume of the solution. Therefore, the concentration of the macromolecule will increase due to solvent elimination during ultrafiltration. However, the change in total volume must simultaneously also affect the other factors. This change in the concentration of total ligand, total povidone concentration, bound ligand, and especially free ligand was theoretically investigated. These effects are considered first for a 1:1 complex:

$$M_F + F \rightleftarrows ML \qquad \text{(Eq. 15)}$$

$$k = \frac{(ML)}{(M_F) \cdot (F)} \qquad \text{(Eq. 16)}$$

where ML is the concentration of bound ligand or bound macromolecule, M_F is the free concentration of macromolecule, and F is the free ligand concentration. If T and M_T represent the total concentration of ligand and macromolecule, respectively, we may write:

$$M_F = M_T - T + F \qquad \text{(Eq. 17)}$$

so:

$$k = \frac{T - F}{(M_T - T + F) \cdot (F)} \qquad \text{(Eq. 18)}$$

Expressing Eq. 18 in terms of concentration (w/v), with the volume before ultrafiltration as V_0, then Eq. 18 can be written:

$$k = \frac{\frac{m_T}{V_0} - \frac{m_F}{V_0}}{\left(\frac{m_{M_T}}{V_0} - \frac{m_T}{V_0} + \frac{m_F}{V_0}\right)\left(\frac{m_F}{V_0}\right)} \qquad \text{(Eq. 19)}$$

where m_T, m_F, and m_{M_T} are the mass of total ligand, free ligand, and mac-

Table II—Changes in Povidone Concentration of Total, Free, and Bound Ligand as a Function of Successive Eliminated Ultrafiltrate Fractions

	dv[a]	$V_0 - \Sigma dv$[b]	Povidone, M × 10⁷ [c]	T, M × 10⁴ [d]	F, M × 10⁴ [e]	B, M × 10⁴ [f]	r[g]	Amount F Eliminated, g × 10⁵	ΣF Eliminated, g × 10⁵
Before	—	25	357	100.0	—	—	—	—	—
After	0.51	—	357	100.0	64.7	35.3	98.88	45.6	45.6
Before	—	24.49	365	100.7	—	—	—	—	—
After	0.50	—	365	100.7	66.6	34.1	93.42	46.0	91.6
Before	—	23.99	372	101.4	—	—	—	—	—
After	0.47	—	372	101.4	66.8	34.6	93.01	43.3	135
Before	—	23.52	380	102.1	—	—	—	—	—
After	0.53	—	380	102.1	67.1	35.0	92.11	49.1	184
Before	—	22.99	388	102.9	—	—	—	—	—
After	0.48	—	388	102.9	67.0	35.9	92.53	44.4	228
Before	—	22.51	397	103.7	—	—	—	—	—
After	0.51	—	397	103.7	66.9	36.8	92.70	47.1	275
Before	—	22.00	406	104.6	—	—	—	—	—
After	0.58	—	406	104.6	67.0	37.6	92.61	53.7	329
Before	—	21.42	417	105.6	—	—	—	—	—
After	0.59	—	417	105.6	67.0	38.6	92.57	54.6	384
Before	—	20.83	429	106.7	—	—	—	—	—
After	0.51		429	106.7	66.9	39.8	92.71	47.1	431
Before	—	20.32	439	107.7	—	—	—	—	—
After	0.48	—	439	107.7	66.9	40.8	92.87	44.4	475
Before	—	19.84	450	108.7	—	—	—	—	—
After	0.60	—	450	108.7	67.1	41.6	92.36	55.6	531
Before	—	19.24	464	110.0	—	—	—	—	—
After	1.21	—	464	110.0	67.0	43.0	92.61	112.0	643
Before	—	18.03	495	112.8	—	—	—	—	—
After	1.38	—	495	112.8	67.1	45.7	92.40	127.9	771
Before	—	16.65	536	116.6	—	—	—	—	—
After	1.35	—	536	116.6	66.8	49.8	92.96	124.6	896
Before	—	15.30	584	121.0	—	—	—	—	—
After	1.25	—	584	121.0	67.0	54.0	92.46	115.7	1012
Before	—	14.05	635	125.8	—	—	—	—	—
After	1.54	—	635	125.8	66.6	59.2	93.23	141.7	1154
Before	—	12.51	714	133.1	—	—	—	—	—
After	1.27	—	714	133.1	67.0	66.1	92.58	117.5	1272
Before	—	11.24	794	140.5	—	—	—	—	—
After	1.08	—	794	140.5	67.0	73.5	92.59	99.9	1372
Before	—	10.16	879	148.3	—	—	—	—	—

[a] Volume of the eliminated ultrafiltrate fraction. [b] $V_0 - \Sigma dv$ = volume remaining in the ultrafiltrate cell. [c] Povidone concentration in the ultrafiltrate cell, calculated according to Eq. 22. [d] Total ligand concentration in the ultrafiltrate cell, calculated according to Eq. 21. [e] F = free ligand concentration, determined in the ultrafiltrate fraction. [f] $B = T - F$ = bound ligand concentration. [g] r = moles of ligand bound/mole of macromolecule.

romolecule, respectively, or:

$$k = \frac{m_T - m_F}{(m_{M_T} - m_T + m_F)\left(\frac{m_F}{V_0}\right)} \quad \text{(Eq. 20)}$$

After eliminating a volume fraction dv, with mass dm, the total ligand concentration is also changed and equals:

$$T = \frac{m_T - dm}{V_0 - dv} \quad \text{(Eq. 21)}$$

and the total macromolecular concentration:

$$M_T = \frac{m_{M_T}}{V_0 - dv} \quad \text{(Eq. 22)}$$

the free ligand concentration is changed to:

$$F = x_F/(V_0 - dv) \quad \text{(Eq. 23)}$$

where x_F, the mass of free ligand, *a priori* is not known. The new equilibrium is then:

$$k = \frac{\frac{m_T}{V_0 - dv} - \frac{dm}{V_0 - dv} - \frac{x_F}{V_0 - dv}}{\left(\frac{m_{M_T}}{V_0 - dv} - \frac{m_T}{V_0 - dv} + \frac{dm}{V_0 - dv} + \frac{x_F}{V_0 - dv}\right) \cdot \left(\frac{x_F}{V_0 - dv}\right)} \quad \text{(Eq. 24)}$$

or:

$$k = \frac{m_T - dm - x_F}{(m_{M_T} - m_T + dm + x_F)\left(\frac{x_F}{V_0 - dv}\right)} \quad \text{(Eq. 25)}$$

The intrinsic binding constants before and after eliminating free ligand concentration must be equal. This is the case if:

$$\frac{m_F}{V_0} = \frac{x_F}{V_0 - dv} = \frac{dm}{dv} \quad \text{(Eq. 26)}$$

i.e., the free ligand concentrations before and after ultrafiltration are identical. This is also true for complex formation in general. In the equation, $r = nkF/(1 + kF)$ (18, 23, 37, 38), nk and F are constants, then r, the amount of bound ligand per mole of macromolecule, should also be constant.

The results from Fig. 3, were calculated according to Eqs. 21 and 22 (Table II). The results are given before and after the removal of a volume fraction. The molarity of povidone (Col. 4), as well as the total (Col. 5), and bound (Col. 7) ligand concentrations increase according to Eqs. 21 and 22, while the free ligand concentration (Col. 6) and r, the mole bound ligand/macromolecule ratio remain constant (Col. 8). Consequently, the results correspond to Eq. 26.

Using somewhat different calculations, the same conclusions were found in a study of the binding of manganese to concanavalin A (45). In the first aliquots (to ~2 mL), the free ligand concentrations are somewhat lower than in the following aliquots, resulting in an overestimation of B (Fig. 3 and Table II). This effect was also noted in experiments with other ligand molecules. This observation must be attributed to a dilution effect of the membrane, which is immersed in a buffer solution before use. Therefore, the first sample must always be eliminated to obtain correct values of B and F. We can conclude that the experiments are in accordance with the treatment of a macromolecular solution as a pseudo two phase as well as a monophase model.

Another important conclusion can be made. Some authors consider ultrafiltration as suspect due to changes in the macromolecular concentration during the experiment which disturb the binding equilibrium (46). The use of small aliquots of filtrate should overcome this objection (47, 48). Indeed, binding equilibrium is disturbed by removing small aliquots of filtrate, but the intrinsic binding constant must be a constant. From Eq. 26 it is seen that this is the case if free ligand concentrations are identical before and after ultrafiltration, whatever the volume fraction of filtrate taken; therefore, it is not necessary to take small aliquots of filtrate.

Indeed, since the free ligand concentration in the filtrate was constant, regardless of the volume fraction of filtrate taken, the concentration of bound ligand is also unchanged since it is calculated by subtracting the free from the total ligand concentration. The treatment of macromolecular solutions as a pseudo two phase is also generally applicable if Eqs. 3 and 5 are fulfilled.

It is expected that the treatment of a macromolecule solution as a pseudo two phase and calculation of partition coefficient (Kd) will have advantages over the theory of complex formation and will be useful to study and interpret complex formation between macromolecules and ligand molecules as a function of the pK_a and dissociation of the ligand and the pH of the solvent. This investigation will be reported in a following paper.

REFERENCES

(1) G. Jürgensen and P. Speiser, *Acta Pharm. Suec.*, **4,** 185 (1967).

(2) W. Scholtan, *Arzneim.-Forsch.*, **14,** 469 (1964).

(3) J. A. Plaizier-Vercammen and R. E. De Nève, *J. Pharm. Sci.*, **70,** 1252 (1981).

(4) E. Ullmann, K. Thoma, and P. Mohrschulz, *Arch. Pharm.*, **302,** 756 (1969).

(5) M. J. Cho, A. G. Mitchell, and M. Pernarowski, *J. Pharm. Sci.*, **60,** 720 (1971).

(6) R. Voigt, H. H. Schultze, and S. Keipert, *Pharmazie*, **31,** 863 (1976).

(7) S. Keipert, I. Korner, and R. Voigt, *Pharmazie*, **31,** 790 (1976).

(8) P. Molyneux and H. P. Frank, *J. Am. Chem. Soc.*, **83,** 3169 (1961).

(9) J. A. Plaizier-Vercammen and R. E. De Nève, *J. Pharm. Sci.*, **71,** 552 (1982).

(10) J. A. Plaizier-Vercammen, *J. Pharm. Sci.*, **72,** 1042 (1983).

(11) C. Hansch, K. Kiehs and G. L. Lawrence, *J. Am. Chem. Soc.*, **87,** 5770 (1965).

(12) T. Fujita, J. Iwasa, and C. Hansch, *J. Am. Chem. Soc.*, **86,** 5175 (1964).

(13) J. Iwasa, T. Fujita, and C. Hansch, *J. Med. Chem.*, **8,** 150 (1965).

(14) C. Hansch and S. M. Anderson, *J. Med. Chem.*, **10,** 745 (1967).

(15) A. E. Bird and A. C. Marshall, *Biochem. Pharmacol.*, **16,** 2275 (1967).

(16) C. Hansch and F. Helmer, *J. Polym. Sci.*, **6,** 3295 (1968).

(17) E. C. Weinbach and J. Garbus, *J. Biol. Chem.*, **240,** 1811 (1965).

(18) J. Steinhardt and J. A. Reynolds, "Multiple Equilibria in Proteins," Academic Press, New York, N.Y., 1969.

(19) "Tables Scientifiques," 6th ed., J. R. Geigy, Ed., Documenta Geigy, Basel, Switzerland, 1962.

(20) J. A. Plaizier-Vercammen and R. E. De Nève, *J. Pharm. Sci.*, **69,** 1403 (1980).

(21) D. W. Kupke, in "Principles and Techniques of Protein Chemistry," part C, S. J. Lach, Ed., Academic Press, New York, N.Y., 1973.

(22) J. T. Yang, *Adv. Protein Chem.*, **16,** 322 (1961).

(23) Ch. Tanford, "Physical Chemistry of Macromolecules," Wiley, New York, N.Y., 1966.

(24) H. G. Bungenberg de Jong, in "Colloid Science," vol. II, H. R. Kruyt, Ed., Elsevier, New York, N.Y., 1949.

(25) S. Glasstone, "Textbook of Physical Chemistry," 2nd ed., Macmillan, New York, N.Y., 1972.

(26) B. Testa and J. C. Etter, *Pharm. Acta Helv.*, **51,** 253 (1976).

(27) P. Mukerjee, *Adv. Colloid Interface Sci.*, **1,** 241 (1967).

(28) S. J. Dougherty and J. C. Berg, *J. Colloid Interface Sci.*, **18,** 110 (1974).

(29) E. D. Goddard and G. C. Benson, *Can. J. Chem.*, **35,** 986 (1957).

(30) E. Hutchinson, A. Inaba, and L. G. Bailey, *Z. Phys. Chem. N.F.*, **5,** 344 (1955).

(31) E. Matijević and B. A. Pethica, *Trans. Faraday Soc.*, **54,** 587 (1958).

(32) K. Shinoda and E. Hutchinson, *J. Phys. Chem.*, **66,** 577 (1962).

(33) G. Stainsby and A. E. Alexander, *Trans. Faraday Soc.*, **46,** 587 (1950).

(34) D. G. Hall and B. A. Pethica, in "Nonionic Surfactants," M. J. Shick, Ed., Dekker, New York, N.Y., 1967.

(35) B. Vollmert, "Grundriss der Makromolekularen Chemie," Springer Verlag, Berlin, 1962.

(36) H. P. Frank, S. Barkin, and F. R. Eirich, *J. Phys. Chem.*, **61,** 1375 (1957).

(37) I. M. Klotz, in "The Proteins," vol. I, part B, H. Neurath and K. Bailey, Eds., Academic Press, New York, N.Y., 1953.

(38) J. T. Edsall and J. Wyman, "Biophysical Chemistry," vol. I, Academic Press, New York, N.Y., 1958.

(39) R. M. Rosenberg and I. M. Klotz, in "A Laboratory Manual of Analytical Methods of Protein Chemistry," vol. II, P. Alexander and R. J. Block, Eds., Pergamon Press, New York, N.Y., 1960.

(40) C..K. Bahal and H. B. Kostenbauder, *J. Pharm. Sci.*, **53,** 1027 (1964).

(41) S. M. Blaug and P. S. Ebersman, *J. Pharm. Sci.*, **53,** 35 (1964).

(42) N. K. Patel and N. E. Foss, *J. Pharm. Sci.*, **53,** 94 (1964).

(43) W. Scholtan, *Makromol. Chem.*, **11,** 131 (1953).

(44) T. Higuchi and R. Kuramoto, *J. Am. Pharm. Assoc. Sci. Ed.*, **43**, 398 (1954).
(45) J. A. Sophianopoulos, S. J. Durham, A. J. Sophianopoulos, H. L. Ragsdale, and W. P. Cropper, *Arch. Biochem. Biophys.*, **187**, 132 (1978).
(46) P. F. Cooper and G. C. Wood, *J. Pharm. Pharmacol.*, **20**, 150S (1968).
(47) W. Bennett and W. Kirby, *J. Lab. Clin. Med.*, **66**, 721 (1965).
(48) J. Ruedy and W. Chernicki, *Can. J. Physiol. Pharmacol.*, **46**, 829 (1968).

ACKNOWLEDGMENTS

Abstracted from a thesis submitted by Dr. J. A. Plaizier-Vercammen to the Vrije Universiteit Brussel, in partial fulfillment of the Doctor in Philosophy degree requirements. Presented at the FIP Congrès at Vienna, September 1981 and at the Povidone Symposium, Lexington, Kentucky, April 1983.

The author wishes to thank Mr. G. Hoogewijs for helpful discussion, Mr. G. Bultinck for technical assistance, and BASF Brussels for batches of povidone.

Improved Competitive Indicator Methods for the Study of α-Cyclodextrin Complexes

DAVID D. PENDERGAST * and KENNETH A. CONNORS ˣ

Received January 6, 1984, from the *School of Pharmacy, University of Wisconsin, Madison, WI 53706.* Accepted for publication March 9, 1984. • Present address: The Upjohn Company, Kalamazoo, MI 49001.

Abstract □ The competitive indicator method for studying molecular complexes is extended to systems forming 1:1 (SL) and 1:2 (SL_2) complexes of substrate (S) and ligand (L). A modification is described for slightly soluble substrates, in which the presence of solid substrate establishes a constant concentration of uncomplexed substrate. These methods are applied to complexes of α-cyclodextrin with some aromatic substrates, with methyl orange as the indicator in acid solution; nitrazine yellow is introduced as an indicator for these studies in basic solution.

Keyphrases □ α-Cyclodextrin—competitive indicator methods, methyl orange, nitrazine yellow □ Competitive indicator methods—α-cyclodextrin, methyl orange, nitrazine yellow complexes

The cyclodextrins are naturally occurring cyclic oligosaccharides possessing a central cavity into which smaller molecules may "partition," forming noncovalently bonded inclusion complexes. The physical and chemical properties of the included molecule (the substrate or guest) may be altered by complexation with the cyclodextrin (the ligand or host). This phenomenon has attracted much recent attention, in part because of its potential applications in drug dosage forms (1–3). Among the properties of a drug that can be affected by cyclodextrin complexation are its solubility, dissolution rate, chemical stability, and bioavailability.

Systematic studies in this laboratory have been designed to provide information on the stoichiometry and thermodynamic stability of cyclodextrin complexes, with the goal of understanding structure-stability relationships and thus developing predictive capability. It has been necessary, in these studies, to make use of several experimental techniques for the measurement of complex stability constants and in some instances to develop new methods. One technique that has been found useful is the so-called "competitive indicator" method. In this technique, an equilibrium is established between the ligand (cyclodextrin) and an indicator whose absorption spectrum differs significantly in its complexed and uncomplexed forms. This equilibrium is then perturbed by the addition of a substrate, which competes with the indicator for the ligand. By measuring the spectral change produced by this perturbation, the stability constant for the substrate–ligand complex can be deduced. The methyl orange–α-cyclodextrin equilibrium was exploited in this way by Broser and co-workers (4) to study the adrenalin–α-cyclodextrin complex and by Casu and Ravà (5) to study a series of substituted benzoic acids. The method was recently improved in this laboratory and was applied to the study of the α-cyclodextrin complexes of some phenols (6). All of these applications have made use of methyl orange as the indicator in acidic solution and have been limited to the study of 1:1 complexes between substrate and ligand.

Our most recent work has required three new capabilities of the competitive indicator method: (*a*) that it be applicable to systems containing both 1:1 (SL) and 1:2 (SL_2) complexes, where S and L represent substrate and ligand respectively; (*b*) that it be applicable to slightly soluble substrates; (*c*) that it be applicable in alkaline medium. The present paper describes extensions to the theory and practice of the method that permit its application in these circumstances.

THEORETICAL SECTION

Standard Competitive Indicator Method—Attention is restricted to systems containing a 1:1 complex IL of indicator I with ligand plus the 1:1 (SL) and 1:2 (SL_2) complexes of substrate with ligand. The average number of ligand molecules bound per substrate molecule ($\bar{n}$) is:

$$\bar{n} = \frac{\Sigma(\text{L bound to S})}{\Sigma(\text{all S})} \qquad \text{(Eq. 1)}$$

The mass balance equations for S and L are:

$$S_t = [S] + [SL] + [SL_2] \qquad \text{(Eq. 2)}$$

$$L_t = [L] + [SL] + 2[SL_2] + [IL] \qquad \text{(Eq. 3)}$$

where S_t and L_t are the (known) total concentrations of substrate and ligand. Further define the quantity P as Σ (L bound to S) can be defined by:

$$P = [SL] + 2[SL_2] = L_t - [L] - [IL] \qquad \text{(Eq. 4)}$$

Combining Eqs. 1, 3, and 4:

$$\bar{n} = \frac{P}{S_t} \qquad \text{(Eq. 5)}$$

The equilibrium constants in this system are given by:

$$K_{11} = \frac{[SL]}{[S][L]} \qquad \text{(Eq. 6)}$$

$$K_{12} = \frac{[SL_2]}{[SL][L]} \qquad \text{(Eq. 7)}$$

$$K_I = \frac{[IL]}{[I][L]} \qquad \text{(Eq. 8)}$$

Combining Eqs. 5, 6, and 7 yields:

0022-3549/84/1200-1779$01.00/0
© 1984, American Pharmaceutical Association

(44) T. Higuchi and R. Kuramoto, *J. Am. Pharm. Assoc. Sci. Ed.*, **43**, 398 (1954).
(45) J. A. Sophianopoulos, S. J. Durham, A. J. Sophianopoulos, H. L. Ragsdale, and W. P. Cropper, *Arch. Biochem. Biophys.*, **187**, 132 (1978).
(46) P. F. Cooper and G. C. Wood, *J. Pharm. Pharmacol.*, **20**, 150S (1968).
(47) W. Bennett and W. Kirby, *J. Lab. Clin. Med.*, **66**, 721 (1965).
(48) J. Ruedy and W. Chernicki, *Can. J. Physiol. Pharmacol.*, **46**, 829 (1968).

ACKNOWLEDGMENTS

Abstracted from a thesis submitted by Dr. J. A. Plaizier-Vercammen to the Vrije Universiteit Brussel, in partial fulfillment of the Doctor in Philosophy degree requirements. Presented at the FIP Congrès at Vienna, September 1981 and at the Povidone Symposium, Lexington, Kentucky, April 1983.

The author wishes to thank Mr. G. Hoogewijs for helpful discussion, Mr. G. Bultinck for technical assistance, and BASF Brussels for batches of povidone.

Improved Competitive Indicator Methods for the Study of α-Cyclodextrin Complexes

DAVID D. PENDERGAST * and KENNETH A. CONNORS ˣ

Received January 6, 1984, from the *School of Pharmacy, University of Wisconsin, Madison, WI 53706.* Accepted for publication March 9, 1984. • Present address: The Upjohn Company, Kalamazoo, MI 49001.

Abstract □ The competitive indicator method for studying molecular complexes is extended to systems forming 1:1 (SL) and 1:2 (SL_2) complexes of substrate (S) and ligand (L). A modification is described for slightly soluble substrates, in which the presence of solid substrate establishes a constant concentration of uncomplexed substrate. These methods are applied to complexes of α-cyclodextrin with some aromatic substrates, with methyl orange as the indicator in acid solution; nitrazine yellow is introduced as an indicator for these studies in basic solution.

Keyphrases □ α-Cyclodextrin—competitive indicator methods, methyl orange, nitrazine yellow □ Competitive indicator methods—α-cyclodextrin, methyl orange, nitrazine yellow complexes

The cyclodextrins are naturally occurring cyclic oligosaccharides possessing a central cavity into which smaller molecules may "partition," forming noncovalently bonded inclusion complexes. The physical and chemical properties of the included molecule (the substrate or guest) may be altered by complexation with the cyclodextrin (the ligand or host). This phenomenon has attracted much recent attention, in part because of its potential applications in drug dosage forms (1–3). Among the properties of a drug that can be affected by cyclodextrin complexation are its solubility, dissolution rate, chemical stability, and bioavailability.

Systematic studies in this laboratory have been designed to provide information on the stoichiometry and thermodynamic stability of cyclodextrin complexes, with the goal of understanding structure-stability relationships and thus developing predictive capability. It has been necessary, in these studies, to make use of several experimental techniques for the measurement of complex stability constants and in some instances to develop new methods. One technique that has been found useful is the so-called "competitive indicator" method. In this technique, an equilibrium is established between the ligand (cyclodextrin) and an indicator whose absorption spectrum differs significantly in its complexed and uncomplexed forms. This equilibrium is then perturbed by the addition of a substrate, which competes with the indicator for the ligand. By measuring the spectral change produced by this perturbation, the stability constant for the substrate–ligand complex can be deduced. The methyl orange–α-cyclodextrin equilibrium was exploited in this way by Broser and co-workers (4) to study the adrenalin–α-cyclodextrin complex and by Casu and Ravà (5) to study a series of substituted benzoic acids. The method was recently improved in this laboratory and was applied to the study of the α-cyclodextrin complexes of some phenols (6). All of these applications have made use of methyl orange as the indicator in acidic solution and have been limited to the study of 1:1 complexes between substrate and ligand.

Our most recent work has required three new capabilities of the competitive indicator method: (*a*) that it be applicable to systems containing both 1:1 (SL) and 1:2 (SL_2) complexes, where S and L represent substrate and ligand respectively; (*b*) that it be applicable to slightly soluble substrates; (*c*) that it be applicable in alkaline medium. The present paper describes extensions to the theory and practice of the method that permit its application in these circumstances.

THEORETICAL SECTION

Standard Competitive Indicator Method—Attention is restricted to systems containing a 1:1 complex IL of indicator I with ligand plus the 1:1 (SL) and 1:2 (SL_2) complexes of substrate with ligand. The average number of ligand molecules bound per substrate molecule ($\bar{n}$) is:

$$\bar{n} = \frac{\Sigma(\text{L bound to S})}{\Sigma(\text{all S})} \qquad \text{(Eq. 1)}$$

The mass balance equations for S and L are:

$$S_t = [S] + [SL] + [SL_2] \qquad \text{(Eq. 2)}$$

$$L_t = [L] + [SL] + 2[SL_2] + [IL] \qquad \text{(Eq. 3)}$$

where S_t and L_t are the (known) total concentrations of substrate and ligand. Further define the quantity P as Σ (L bound to S) can be defined by:

$$P = [SL] + 2[SL_2] = L_t - [L] - [IL] \qquad \text{(Eq. 4)}$$

Combining Eqs. 1, 3, and 4:

$$\bar{n} = \frac{P}{S_t} \qquad \text{(Eq. 5)}$$

The equilibrium constants in this system are given by:

$$K_{11} = \frac{[SL]}{[S][L]} \qquad \text{(Eq. 6)}$$

$$K_{12} = \frac{[SL_2]}{[SL][L]} \qquad \text{(Eq. 7)}$$

$$K_I = \frac{[IL]}{[I][L]} \qquad \text{(Eq. 8)}$$

Combining Eqs. 5, 6, and 7 yields:

0022-3549/84/1200-1779$01.00/0
© 1984, American Pharmaceutical Association

$$\bar{n} = \frac{K_{11}[L] + 2K_{11}K_{12}[L]^2}{1 + K_{11}[L] + K_{11}K_{12}[L]^2} \quad \text{(Eq. 9)}$$

Equation 9 is the classical expression for the Bjerrum formation function, which occurs in the study of metal ion coordination complexes. It can be rearranged into the linear plotting form (7, 8):

$$\frac{\bar{n}}{(1-\bar{n})[L]} = K_{11} + K_{11}K_{12}[L]\frac{(2-\bar{n})}{(1-\bar{n})} \quad \text{(Eq. 10)}$$

To use Eq. 10, the quantities $\bar{n}$ and [L] are needed. These are obtained by spectrophotometric measurements at a wavelength at which the indicator absorbs light, but neither the substrate nor the ligand absorbs.

The ratio [I]/[IL] is labeled Q; this quantity is evidently inversely proportional to the free ligand concentration:

$$Q = \frac{[I]}{[IL]} = \frac{1}{K_I[L]} \quad \text{(Eq. 11)}$$

Combination of a mass balance on the indicator with Eqs. 4 and 8 gives:

$$P = L_t - \frac{1}{QK_I} - \frac{I_t}{Q+1} \quad \text{(Eq. 12)}$$

where I_t is the total indicator concentration. Moreover, Q is experimentally measurable by use of Eq. 13, where ϵ_I and ϵ_{IL} are the molar absorptivities of the indicator in the uncomplexed and complexed forms, respectively, and ϵ is the apparent molar absorptivity in a solution containing both forms:

$$Q = \frac{\epsilon - \epsilon_{IL}}{\epsilon_I - \epsilon} \quad \text{(Eq. 13)}$$

Thus, $\bar{n}$ can be experimentally measured. These symbols were introduced to achieve consistency with the earlier development (6); Eq. 10 becomes:

$$\frac{PQK_I}{S_t - P} = K_{11} + \frac{K_{11}K_{12}}{K_I} \cdot \frac{1}{Q} \cdot \frac{(2S_t - P)}{(S_t - P)} \quad \text{(Eq. 14)}$$

P and Q can be measured, S_t is known, and K_I can be determined in a separate experiment, so the stability constants K_{11} and K_{12} can be obtained from the slope and intercept of a plot according to Eq. 14. If $K_{12} = 0$, the slope of this line will be zero, and a simpler plotting form, Eq. 15, results, as was shown earlier (6).

$$\frac{S_t}{P} = 1 + \frac{K_I}{K_{11}}Q \quad \text{(Eq. 15)}$$

Solubility: Competitive Indicator Method— For substrates of low solubility, it is difficult to establish accurate values of S_t for use in the aforementioned competitive indicator method, and the following useful modification has been devised. The experiment is carried out by varying total ligand concentration, L_t, but by maintaining the free substrate concentration [S] constant at its saturation solubility S_o; this is accomplished by establishing the equilibria in the presence of solid substrate. Then Eq. 4 can be written:

$$P = K_{11}S_o[L] + 2K_{11}K_{12}S_o[L]^2 \quad \text{(Eq. 16)}$$

Substituting from Eq. 11 for [L] and rearranging gives:

$$\frac{PQK_I}{S_o} = K_{11} + \frac{2K_{11}K_{12}}{K_IQ} \quad \text{(Eq. 17)}$$

Thus, a plot of PQK_I/S_o against $1/Q$ should be linear.

This combined solubility-competitive indicator method can be extended to include systems in which a 1:1 substrate-indicator complex SI is formed, provided the stability constant, K_{SI}, can be independently measured and a wavelength can be selected such that the molar absorptivities of SI and I are equal. The analysis (9) shows that Eq. 17 remains applicable but Q and P must be evaluated by Eqs. 18 and 19, which may be compared with Eqs. 11 and 12.

$$Q = \frac{\epsilon - \epsilon_{IL}}{(\epsilon_I - \epsilon)(1 + K_{SI}S_o)} \quad \text{(Eq. 18)}$$

$$P = L_t - \frac{1}{K_IQ} - \frac{I_t}{1 + Q + QK_{SI}S_o} \quad \text{(Eq. 19)}$$

EXPERIMENTAL SECTION

Materials—α-Cyclodextrin[1] was dried for 3 h at 105°C. The methyl orange indicator was purified by the method of Lin and Connors (6). Nitrazine yellow indicator[2] (C.I. 14890) was recrystallized from water to a constant molar absorptivity of 4.045×10^4 at λ_{max} 588 nm; it was dried for 3 h at 105°C before use. Substrates were from commercial sources and were recrystallized before use (9). Buffer components were of reagent grade. Spectrophotometric[3] and pH[4] measurements were made at 25.0°C.

Procedures—*Measurement of* Q—Throughout a study, the total indicator concentration, I_t, is held constant; hence, absorptivities in Eq. 11 can be replaced by absorbances:

$$Q = \frac{A - A_{IL}}{A_I - A} \quad \text{(Eq. 20)}$$

A_I is readily measured in a solution of the indicator in the absence of ligand. A_{IL} is obtained as the product $\epsilon_{IL}I_t$; ϵ_{IL} is found as follows. In a solution containing only indicator and ligand, the mass balance on ligand is:

$$L_t = [L] + [IL] \quad \text{(Eq. 21)}$$

This, combined with Eq. 8 and the mass balance on indicator, gives:

$$[I] = \frac{I_t}{1 + K_I[L]} \quad \text{(Eq. 22)}$$

An iterative process is used. First, the assumption is made that $[L] = L_t$, and Eq. 22 is solved for [I] (making use of an independently measured value of K_I). Then, [IL] is found from the mass balance $I_t = [I] + [IL]$, and this is used in Eq. 21 to produce a refined estimate of [L]. This process is repeated until no change in [L] is noted in the fourth decimal place. The absorbance of the solution (path length = 1 cm) is $A = \epsilon_I[I] + \epsilon_{IL}[IL]$, hence:

$$\epsilon_{IL} = \frac{A - \epsilon_I[I]}{[IL]} \quad \text{(Eq. 23)}$$

This provides the information necessary to evaluate Q with Eq. 20.

Standard Method—Methyl orange studies were conducted in 0.10 M HCl, whereas nitrazine yellow studies were carried out in 0.05 M Tris buffer at pH 9.2 with the ionic strength adjusted to 0.10 M with NaCl. Portions of stock solutions of indicator, substrate, and ligand were added to 10-mL volumetric flasks to produce a series of solutions having constant indicator concentration ($2\text{-}4 \times 10^{-5}$ M) with substrate and ligand concentration varying as required by optimization considerations (to be described). In some instances, the substrate and ligand were weighed directly into the flasks. After equilibration of the solutions at 25.0°C, the absorbances were measured at the wavelength of maximal spectral shift.

Solubility Method—Indicator solutions containing varied ligand concentrations were prepared in 10-mL volumetric flasks. Each of these was transferred to a 15.5-mL vial containing solid substrate (in excess of its total solubility). After the vials were sealed, they were rotated end-over-end at 32 rpm in a 25.0°C water bath for 24 h. They were then placed upright in the 25°C bath for time sufficient for the solid substrate to settle. The clear solution was aspirated and its absorbance was measured at 25°C.

Data Treatment—Equations 14, 15, and 17 are linear, and the slopes and intercepts of these plots were obtained by conventional linear least-squares analysis. The variances of the stability constant estimates were then found by a propagation of errors treatment (9). Although in each of these equations the variable playing the role of x, the "independent" variable, has measurable uncertainty associated with it, the y variable possesses greater uncertainty; hence, the usual linear regression treatment is suitable.

If treatment according to Eq. 14 showed that the slope was not significantly different from zero, then the data were analyzed by means of Eq. 15.

Optimization of Conditions—For a system containing only a 1:1 (SL) complex, the quantity $\bar{n} = P/S_t$ can range from 0 to 1, whereas for a system capable of forming both SL and SL_2, $\bar{n}$ can range from 0 to 2. Thus, $\bar{n}$ is a useful indication of the extent of the binding isotherm that has been examined. In a 1:1 system, $\bar{n}$ is equal to f_{11}, the fraction of substrate present as the 1:1 complex, but in a 1:1 + 1:2 system, $\bar{n} = f_{11} + 2f_{12}$.

From Eq. 14, it is clear that the quantity $(S_t - P)$ control the reliability of the plotting variables. Combining Eqs. 2 and 4 gives:

$$S_t - P = [S] - [SL_2] \quad \text{(Eq. 24)}$$

Thus, $(S_t - P)$ may be positive, zero, or negative, whereas $2S_t - P$ must be positive, as must the other variables and parameters in Eq. 14. Therefore, data points plotted according to Eq. 14 must lie in either the first or third quadrants, with the point at $S_t = P$ being indeterminate. Points in the first and third quadrants correspond to the conditions $\bar{n} < 1$ and $\bar{n} > 1$, respectively. In the present studies, all systems appeared in the first quadrant.

The experimental data consist of absorbance values, which are bounded

[1] Sigma Chemical Co.
[2] Aldrich Chemical Co.
[3] Cary Varian Model 2200 or Perkin-Elmer Model 559 spectrophotometer.
[4] Orion Model 701A pH meter with Corning semi-micro combination electrode (catalog number 476050).

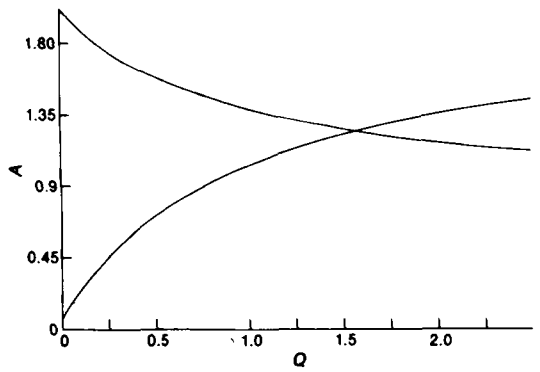

Figure 1—*Relationship between absorbance, A, and corresponding Q value (Eq. 20) for hypothetical indicator–α-cyclodextrin systems. Methyl orange (positive slope), $I_t = 4.17 \times 10^{-5}$ M; nitrazine yellow (negative slope), $I_t = 3.92 \times 10^{-5}$ M.*

by the limits A_I and A_{IL}. With Eq. 20 these are converted to Q values, which may range from 0 to ∞. The relationship between absorbance values, A, and corresponding Q values is shown in Fig. 1 for typical solutions of methyl orange and nitrazine yellow. At large Q values, the slope is so small that a small absorbance error results in a large error in Q. At low Q values, a small absorbance error results in a small absolute but large relative error in Q. These effects can be quantified by differentiating Eq. 20 to find dQ/dA. In the present work it was decided, for systems containing both 1:1 and 1:2 equilibria, to exclude data points having Q values outside the range 0.3–2.5.

According to Eq. 11, Q is uniquely related to free ligand concentration (for a given indicator). Thus, the limits placed on Q establish corresponding limits on [L]. To extend these limits in order to examine a greater range of the binding isotherm, it would be necessary to have available a series of indicators with different K_I values.

For a given indicator and substrate, each pair of plotting variables in Eq. 14 is associated with a unique Q ([L]), which may be realized by innumerable combinations of I_t, S_t, and L_t. It is necessary to limit these quantities to values that will give acceptable uncertainties in P and in $S_t - P$. This is done as follows:

1. Choose I_t such that A_I or A_{IL} (whichever is larger) ≈ 2.
2. Select a series of Q values in the 0.3–2.5 range and for each Q calculate the corresponding [L] with Eq. 11.
3. With preliminary estimates of K_{11} and K_{12}, calculate $\bar{n}$ values for each [L] value, using Eq. 9. Reject any systems giving $\bar{n}$ values ~ >0.7.
4. For each acceptable [L] value, choose L_t such that $L_t \geq 2[L]$. Calculate P with Eq. 12.
5. For each set of conditions, calculate S_t from $S_t = P/\bar{n}$.

Often it will be satisfactory to work with a fixed S_t and simply calculate the desired L_t levels from Eq. 25, which is obtained from Eqs. 5 and 12:

$$L_t = \bar{n}S_t + [L] + \frac{I_t}{Q+1} \qquad \text{(Eq. 25)}$$

S_t should be chosen such that $L_t \geq 2[L]$.

This procedure will result in data points in the first quadrant when plotted according to Eq. 14. All Q values will be in the desired range and the errors in P and $S_t - P$ will be acceptable. If the required S_t values exceed the solubility of the substrate, the solubility-competitive indicator method should be used.

RESULTS AND DISCUSSION

Indicator Properties.—A requirement of these competitive indicator methods is that the indicator must form only a 1:1 complex with the ligand. This imposes limits on acceptable indicator structures. However, indicator selection is greatly facilitated by adopting a point of view provided by a recently proposed binding site model of cyclodextrin complex formation (10, 11). To ensure only 1:1 complex formation, it is sufficient that the indicator possess only one potential binding site capable of entering the cyclodextrin cavity. For α-cyclodextrin, there is considerable evidence that uncharged substituents on an aromatic (benzene) ring, either *meta* or *para* to another group, can act as binding sites, but that charged groups have little affinity for the cavity. By inspection of indicator structures, it is therefore possible to identify likely candidates, and in this way nitrazine yellow was selected. Methyl orange has long been used (in strongly acid medium) (4). The structures of methyl orange (I) and nitrazine yellow (II) are shown:

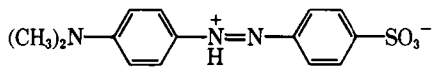

I

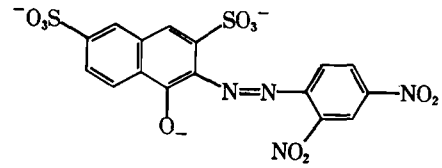

II

A second requirement is that the indicator must exhibit a significant spectral change upon complexation with α-cyclodextrin. In Table I, the properties of these indicators pertinent to these studies are gathered. The K_I values were determined by a Benesi-Hildebrand treatment; the result for methyl orange is in excellent agreement with that reported by Lin and Connors (6). Several pieces of evidence are consistent with the assumption that nitrazine yellow forms only a 1:1 complex with α-cyclodextrin: (*a*) the K_I value is independent of wavelength; (*b*) there is a single isosbestic point (at 590 nm); (*c*) graphical treatment of a matrix of spectrophotometric data (12, 13) provides evidence

Table I—Properties of Indicators in Aqueous α-Cyclodextrin Solutions [a]

Indicator	pH	Analytical Wavelength, nm	Molar Absorptivities: Free (ϵ_I)	Molar Absorptivities: Complexed (ϵ_{IL})	Equilibrium Constant K_I, M^{-1} [b]
Methyl orange	1.0	508	47,980	1,465	664 (4.7)
Nitrazine yellow	9.2	634.5	19,500	50,980	74.3 (0.9)

[a] At 25°C, ionic strength 0.10 M. [b] *SD* in parentheses.

Table II—Stability Constants Measured with Methyl Orange and Nitrazine Yellow Indicators [a]

Substrate	Competitive Indicator Method [b]	K_{11}, M^{-1}	K_{12}, M^{-1}
	Methyl Orange Indicator		
1,4-Dimethoxybenzene	Standard	55.3 (22)	208 (90)
1,4-Dimethoxybenzene	Solubility	75.4 (2.6)	221 (8.6)
4-Nitrobenzoic acid	Solubility	320 (12)	26.9 (6.5)
4-Cyanobenzoic acid	Standard	485 (11)	57 (4.7)
	Nitrazine Yellow Indicator		
Benzoate ion		12.8 (0.2)	
3-Nitrobenzoate ion		124.5 (9.1)	
4-Nitrobenzoate ion		60.0 (3.0)	

[a] At 25°C and ionic strength 0.10 M. *SD* are in parentheses. [b] Methods as described in text.

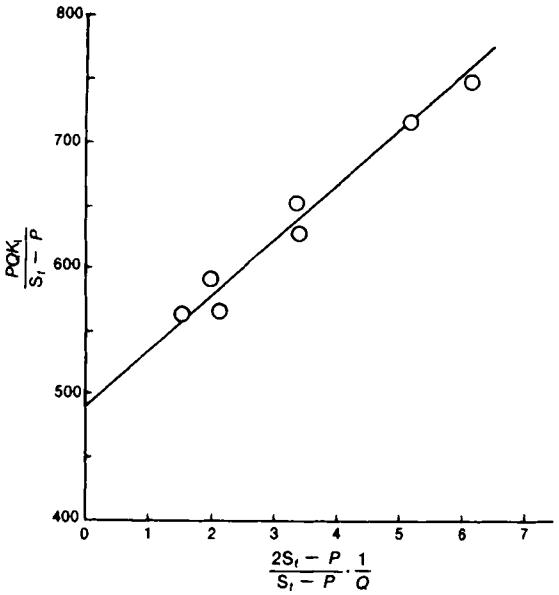

Figure 2—*Plot of Eq. 14 for the methyl orange- 4-cyanobenzoic acid-α-cyclodextrin system. $I_t = 3.0 \times 10^{-5}$ M; S_t varies from 2.3 to 6.3 × 10^{-3} M; L_t varies from 2.5 to 6.6 × 10^{-3} M.*

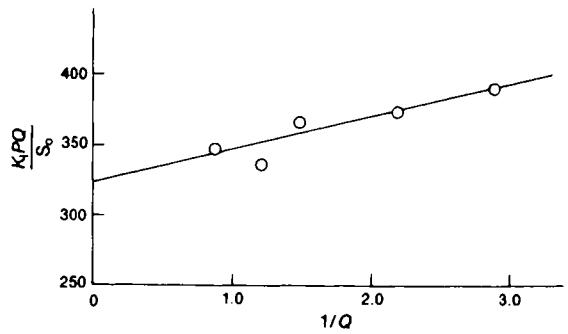

Figure 3—*Plot of Eq. 17 for the methyl orange-4-nitrobenzoic acid-α-cyclodextrin system. $I_t = 4.8 \times 10^{-5}$ M; $S_0 = 9.68 \times 10^{-4}$ M; L_t varies from 1.8 to 6.0 × 10^{-3} M.*

for the existence of only two indicator species in solution, presumably I and IL.

Stability Constant Results—These new modifications, consisting of the standard competitive indicator method for 1:1 + 1:2 systems, the solubility-competitive indicator method, and the introduction of nitrazine yellow as an indicator in basic media, were applied to the study of some substrates of interest in our systematic investigation of α-cyclodextrin complexation. The reference methods were UV spectrophotometry, potentiometry (11), and solubility (14, 15). Methyl orange was the indicator in studies (at pH 1.0) of 1,4-dimethoxybenzene, 4-nitrobenzoic acid, and 4-cyanobenzoic acid; nitrazine yellow (at pH 9.2) was employed to study the anions of benzoic, 3-nitrobenzoic, and 4-nitrobenzoic acids.

Table II lists the results. In basic medium, the carboxylate anions do not form 1:2 complexes, so the nitrazine yellow data were processed with Eq. 15. The systems studied with methyl orange in acidic medium showed both 1:1 and 1:2 complex formation, so Eqs. 14 and 17 were used. Figure 2 is a plot of Eq. 14, the standard competitive indicator method and Fig. 3 shows a plot of Eq. 17, the solubility-competitive indicator method. Table III compares the stability constants obtained by these competitive indicator methods with values obtained by other techniques. It is apparent that the competitive indicator approach is measuring the same quantity as the other methods. It must be pointed out that some of these systems, especially those in acidic media, are difficult to study, in part because of their limited solubilities. The 1,4-dimethoxybenzene system is especially interesting. The initial result on this system was obtained by the classical solubility method (14, 15), and it yielded the extremely unusual observation that $K_{12} > K_{11}$ (with rather large uncertainties in the stability constants). Application of the two new competitive indicator methods described in this paper gave results that were entirely consistent; this type of independent confirmation is useful. The only discordant result in Table III is K_{12} for 4-cyanobenzoic acid by the standard competitive indicator method. This is thought to be a consequence of the particular combination of the indicator and the substrate, possibly caused by the formation of a substrate-indicator complex. The low solubility of 4-nitrobenzoic acid did not permit a reliable application of the standard method, but preliminary results indicated behavior similar to that observed with 4-cyanobenzoic acid. Spectroscopic observations of more soluble benzoic acids in the presence of methyl orange showed small shifts in the spectrum of the indicator suggestive of the formation of complexes. It therefore seems possible that SI complexes may lead to systematic errors in methyl orange-substituted benzoic acid systems. The solubility competitive indicator method appears to be less susceptible to these errors.

CONCLUSIONS

These results have usefully extended the competitive indicator method to systems containing both 1:1 and 1:2 complexes. It may be noted that the theoretical basis is general, although the applications reported here were to complexes of α-cyclodextrin. Nitrazine yellow has been found effective for studies in alkaline solution.

The competitive indicator method will seldom be viewed as the "method of choice" when other techniques are available, for the following reasons. The addition of another complex former, namely the indicator, complicates the equilibrium system. In this system, the formation of the SL complex generates a perturbation whose observation provides information about K_{11}. The presence of complex SL_2 produces a further perturbation that gives an estimate of K_{12}. Thus, the information about K_{12} is a consequence of a perturbation

Table III—Comparison of Stability Constants by Various Methods

Substrate	Method	K_{11}, M^{-1}	K_{12}, M^{-1}	Ref.
1,4-Dimethoxybenzene	Std. comp. ind.[a]	55.3	208	This work
	Sol. comp. ind.[b]	75.4	221	This work
	Solubility	55.8	193	9
4-Nitrobenzoic acid	Sol. comp. ind.	320	26.9	This work
	Solubility	277	29.6	9
	Potentiometric	350	20.2	11
	Potentiometric	293	25.9	9
	Potentiometric	331	25.1	9
4-Cyanobenzoic acid	Std. comp. ind.	485	57	This work
	Potentiometric	471	25.0	11
	Potentiometric	428	24.1	9
	Potentiometric	441	26.2	9
Benzoate	Std. comp. ind.	12.8	—	This work
	Potentiometric	11.2	—	11
	Potentiometric	10.5	—	16
3-Nitrobenzoate	Std. comp. ind.	124.5	—	This work
	Potentiometric	94.2	—	9
	Potentiometric	126		16
4-Nitrobenzoate	Std. comp. ind.	60.0	—	This work
	Spectrophotometry	75.7	—	9
	Spectrophotometry	81.0	—	11

[a] Standard comparative indicator. [b] Solubility comparative indicator.

of a perturbation. Despite this limitation, the competitive indicator method has one notable feature that will often make it a valuable resource, namely, it allows observations to be made of a substrate whose own properties do not provide quantitative measures of complex formation; the indicator spectral change is a surrogate property.

REFERENCES

(1) W. Saenger, *Angew. Chem. Intern. Ed.*, **19**, 344 (1980).

(2) J. Szejtli, Ed., "Proceedings of the First International Symposium on Cyclodextrins," Akadémiai Kiadó, Budapest, 1982 (D. Reidel Publishing Co., Dordrecht, Holland).

(3) J. Szejtli, "Cyclodextrins and their Inclusion Complexes," Akadémiai Kiadó, Budapest, 1982.

(4) V. Lautsch, W. Bandel, and W. Broser, *Z. Naturforsch.*, **11B**, 282 (1956).

(5) B. Casu and L. Ravà, *Ric. Sci.*, **36**, 733 (1966).

(6) S.-F. Lin and K. A. Connors, *J. Pharm. Sci.*, **72**, 1333 (1983).

(7) F. J. C. Rossotti and H. S. Rossotti, *Acta Chem. Scand.*, **9**, 1166 (1956).

(8) F. J. C. Rossotti and H. S. Rossotti, "The Determination of Stability Constants," McGraw-Hill, New York, N.Y., 1961, p. 108.

(9) D. D. Pendergast, Ph.D. thesis, University of Wisconsin-Madison, 1983.

(10) T. W. Rosanske and K. A. Connors, *J. Pharm. Sci.*, **69**, 564 (1980).

(11) K. A. Connors, S.-F. Lin, and A. B. Wong, *J. Pharm. Sci.*, **71**, 217 (1982).

(12) J. S. Coleman, L. P. Varga, and S. H. Mastin, *Inorg. Chem.*, **9**, 1015 (1970).

(13) F. R. Hartley, C. Burgess, and R. M. Alcock, "Solution Equilibria," Ellis Horwood Ltd., Chichester, 1980, chap. 2.

(14) T. Higuchi and K. A. Connors, *Adv. Anal. Chem. Instrum.*, **4**, 117 (1965).

(15) K. Iga, A. Hussain, and T. Kashihara, *J. Pharm. Sci.*, **70**, 108 (1981).

(16) R. Gelb, L. Schwartz, B. Cardelino, H. Fuhrman, R. Johnson, and D. Laufer, *J. Am. Chem. Soc.*, **103**, 1750 (1981).

ACKNOWLEDGMENTS

Some of the potentiometric data were contributed by Stuart Sonnedecker. This work was supported by a grant from The Upjohn Company.

Metabolism of Meperidine in Several Animal Species

S. Y. YEH

Received June 4, 1983, from the *National Institute on Drug Abuse, Addiction Research Center, Lexington, KY 40583.* Accepted for publication February 8, 1984. Present address: NIDA, P.O. Box 5180, Baltimore, MD 21224.

Abstract □ Four new meperidine metabolites were identified by GC–MS in the urine of rats, guinea pigs, rabbits, cats, and dogs. In addition to known meperidine metabolites, 4-ethoxycarbonyl-4-phenyl-1,2,3,4-tetrapyridine (dehydronormeperidine; IV, the *N*-hydroxydehydro derivative of normeperidine (X), the dihydroxy derivative of meperidine (XII), and the dihydroxy derivative of normeperidine (XIII) were identified. The possible role of the *N*-hydroxy derivative of normeperidine (IX) in the pharmacological interaction of meperidine (I) with MAO inhibitors, seen selectively in the rabbit (and humans), is discussed. Following the administration of the *p*-hydroxy derivative of meperidine (VII), the major metabolite was conjugated VII. Trace amounts of the *p*-hydroxy derivative of normeperidine (VIII), the methoxy hydroxy derivative of meperidine (XI), XII, and XIII also were detected as metabolites of VII. The degree of *N*-demethylation of VII, both *in vitro* and *in vivo*, was small.

Keyphrases □ Meperidine—TLC, GC–MS, identification of metabolites, interaction with monoamine oxidase inhibitors □ Monoamine oxidase inhibitors—metabolites of meperidine, TLC, GC–MS

Meperidine is extensively metabolized by humans and animals. The major metabolites of meperidine identified in the urine of rats, guinea pigs, dogs, and humans are normeperidine and (1-methyl-4-phenyl-4-piperidine carboxylic) and (4-phenyl-4-piperidine carboxylic) acids (1–12), while the minor metabolites are the *p*-hydroxy derivative of meperidine (5), the *N*-oxide of meperidine (5, 6), the methoxy hydroxy derivative of meperidine (7), and the *N*-hydroxy derivative of normeperidine (7). In the urinary excretion studies of meperidine and its metabolites [normeperidine, and (1-methyl-4-phenyl-4-piperidine carboxylic) and (4-phenyl-4-piperidine carboxylic) acid], the amount of each excreted by the rabbit was found to be low (16–53% of the administered dose) when compared with other species (13). Of this total, meperidine and normeperidine accounted for only ~0.4 and 4–8.5%, respectively, of the administered dose. The remainder of the dose excreted represented unidentified metabolites. Severe interaction between monoamine oxidase inhibitors (MAOI) and meperidine have been observed in rabbits and humans, but seldom observed in other species (14–16). The purpose of this study was to identify new metabolites in rabbits and other species which might contribute to the severe interaction of meperidine and MAOI observed in the rabbit. The metabolism of the *p*-hydroxy derivative of meperidine (VII) was also investigated in a preliminary study in the rat in an attempt to determine if VII is metabolized *in vivo* to VIII.

EXPERIMENTAL SECTION

Drugs—Meperidine hydrochloride[1], normeperidine hydrochloride[1], and the *p*-hydroxy derivative of meperidine[2] (5) were obtained commercially. The *N*-oxide of meperidine was synthesized as follows. Meperidine hydrochloride (200 mg) was dissolved in 2 mL of water, basified with ammonium hydroxide, and extracted with benzene. After removal of the solvent under reduced pressure, the residue was dissolved in 1 mL of absolute ethanol, and 1 mL of 30% H_2O_2 was added. The solution was heated in a water bath at 70°C for 2 h. At that time, TLC showed no starting material. The solution was transferred to a dish and evaporated to near dryness on a steam bath. The residue was dissolved in isopropyl alcohol and transferred to a 15-mL centrifuge tube. The solvent was removed under a stream of nitrogen, to give a white liquid. Ether was added to the residue to give a white precipitate. The mixture was refrigerated and centrifuged, and the liquid phase was transferred to another centrifuge tube. By repeating this treatment, two products were obtained: ether-soluble material and a white precipitate. The solid material was recrystallized from absolute ethanol to yield 18 mg of white crystals, mp 173–175°C. The solid material showed a single spot on TLC (R_f 0.37 and

[1] Sterling-Winthrop Co., Rensselaer, N.Y.

[2] Professor C. Lindberg, Biomedical Center, University of Uppsala, Uppsala, Sweden.

0022-3549/84/1200-1783$01.00/0
© 1984, American Pharmaceutical Association

of a perturbation. Despite this limitation, the competitive indicator method has one notable feature that will often make it a valuable resource, namely, it allows observations to be made of a substrate whose own properties do not provide quantitative measures of complex formation; the indicator spectral change is a surrogate property.

REFERENCES

(1) W. Saenger, *Angew. Chem. Intern. Ed.*, **19**, 344 (1980).

(2) J. Szejtli, Ed., "Proceedings of the First International Symposium on Cyclodextrins," Akadémiai Kiadó, Budapest, 1982 (D. Reidel Publishing Co., Dordrecht, Holland).

(3) J. Szejtli, "Cyclodextrins and their Inclusion Complexes," Akadémiai Kiadó, Budapest, 1982.

(4) V. Lautsch, W. Bandel, and W. Broser, *Z. Naturforsch.*, **11B**, 282 (1956).

(5) B. Casu and L. Ravà, *Ric. Sci.*, **36**, 733 (1966).

(6) S.-F. Lin and K. A. Connors, *J. Pharm. Sci.*, **72**, 1333 (1983).

(7) F. J. C. Rossotti and H. S. Rossotti, *Acta Chem. Scand.*, **9**, 1166 (1956).

(8) F. J. C. Rossotti and H. S. Rossotti, "The Determination of Stability Constants," McGraw-Hill, New York, N.Y., 1961, p. 108.

(9) D. D. Pendergast, Ph.D. thesis, University of Wisconsin-Madison, 1983.

(10) T. W. Rosanske and K. A. Connors, *J. Pharm. Sci.*, **69**, 564 (1980).

(11) K. A. Connors, S.-F. Lin, and A. B. Wong, *J. Pharm. Sci.*, **71**, 217 (1982).

(12) J. S. Coleman, L. P. Varga, and S. H. Mastin, *Inorg. Chem.*, **9**, 1015 (1970).

(13) F. R. Hartley, C. Burgess, and R. M. Alcock, "Solution Equilibria," Ellis Horwood Ltd., Chichester, 1980, chap. 2.

(14) T. Higuchi and K. A. Connors, *Adv. Anal. Chem. Instrum.*, **4**, 117 (1965).

(15) K. Iga, A. Hussain, and T. Kashihara, *J. Pharm. Sci.*, **70**, 108 (1981).

(16) R. Gelb, L. Schwartz, B. Cardelino, H. Fuhrman, R. Johnson, and D. Laufer, *J. Am. Chem. Soc.*, **103**, 1750 (1981).

ACKNOWLEDGMENTS

Some of the potentiometric data were contributed by Stuart Sonnedecker. This work was supported by a grant from The Upjohn Company.

Metabolism of Meperidine in Several Animal Species

S. Y. YEH

Received June 4, 1983, from the *National Institute on Drug Abuse, Addiction Research Center, Lexington, KY 40583.* Accepted for publication February 8, 1984. Present address: NIDA, P.O. Box 5180, Baltimore, MD 21224.

Abstract □ Four new meperidine metabolites were identified by GC–MS in the urine of rats, guinea pigs, rabbits, cats, and dogs. In addition to known meperidine metabolites, 4-ethoxycarbonyl-4-phenyl-1,2,3,4-tetrapyridine (dehydronormeperidine; IV, the *N*-hydroxydehydro derivative of normeperidine (X), the dihydroxy derivative of meperidine (XII), and the dihydroxy derivative of normeperidine (XIII) were identified. The possible role of the *N*-hydroxy derivative of normeperidine (IX) in the pharmacological interaction of meperidine (I) with MAO inhibitors, seen selectively in the rabbit (and humans), is discussed. Following the administration of the *p*-hydroxy derivative of meperidine (VII), the major metabolite was conjugated VII. Trace amounts of the *p*-hydroxy derivative of normeperidine (VIII), the methoxy hydroxy derivative of meperidine (XI), XII, and XIII also were detected as metabolites of VII. The degree of *N*-demethylation of VII, both *in vitro* and *in vivo*, was small.

Keyphrases □ Meperidine—TLC, GC–MS, identification of metabolites, interaction with monoamine oxidase inhibitors □ Monoamine oxidase inhibitors—metabolites of meperidine, TLC, GC–MS

Meperidine is extensively metabolized by humans and animals. The major metabolites of meperidine identified in the urine of rats, guinea pigs, dogs, and humans are normeperidine and (1-methyl-4-phenyl-4-piperidine carboxylic) and (4-phenyl-4-piperidine carboxylic) acids (1–12), while the minor metabolites are the *p*-hydroxy derivative of meperidine (5), the *N*-oxide of meperidine (5, 6), the methoxy hydroxy derivative of meperidine (7), and the *N*-hydroxy derivative of normeperidine (7). In the urinary excretion studies of meperidine and its metabolites [normeperidine, and (1-methyl-4-phenyl-4-piperidine carboxylic) and (4-phenyl-4-piperidine carboxylic) acid], the amount of each excreted by the rabbit was found to be low (16–53% of the administered dose) when compared with other species (13). Of this total, meperidine and normeperidine accounted for only ~0.4 and 4–8.5%, respectively, of the administered dose. The remainder of the dose excreted represented unidentified metabolites. Severe interaction between monoamine oxidase inhibitors (MAOI) and meperidine have been observed in rabbits and humans, but seldom observed in other species (14–16). The purpose of this study was to identify new metabolites in rabbits and other species which might contribute to the severe interaction of meperidine and MAOI observed in the rabbit. The metabolism of the *p*-hydroxy derivative of meperidine (VII) was also investigated in a preliminary study in the rat in an attempt to determine if VII is metabolized *in vivo* to VIII.

EXPERIMENTAL SECTION

Drugs—Meperidine hydrochloride[1], normeperidine hydrochloride[1], and the *p*-hydroxy derivative of meperidine[2] (5) were obtained commercially. The *N*-oxide of meperidine was synthesized as follows. Meperidine hydrochloride (200 mg) was dissolved in 2 mL of water, basified with ammonium hydroxide, and extracted with benzene. After removal of the solvent under reduced pressure, the residue was dissolved in 1 mL of absolute ethanol, and 1 mL of 30% H_2O_2 was added. The solution was heated in a water bath at 70°C for 2 h. At that time, TLC showed no starting material. The solution was transferred to a dish and evaporated to near dryness on a steam bath. The residue was dissolved in isopropyl alcohol and transferred to a 15-mL centrifuge tube. The solvent was removed under a stream of nitrogen, to give a white liquid. Ether was added to the residue to give a white precipitate. The mixture was refrigerated and centrifuged, and the liquid phase was transferred to another centrifuge tube. By repeating this treatment, two products were obtained: ether-soluble material and a white precipitate. The solid material was recrystallized from absolute ethanol to yield 18 mg of white crystals, mp 173–175°C. The solid material showed a single spot on TLC (R_f 0.37 and

[1] Sterling-Winthrop Co., Rensselaer, N.Y.

[2] Professor C. Lindberg, Biomedical Center, University of Uppsala, Uppsala, Sweden.

0022-3549/84/1200-1783$01.00/0
© 1984, American Pharmaceutical Association

0.40) after development with the respective solvent systems as stated below. Elemental analyses of the crystalline product showed: C, 58.18; H, 7.12; N, 4.90. The respective theoretical values for the derived *N*-oxide VI were: C, 68.44; H, 7.98; N, 5.32.

The solvent was removed under a stream of nitrogen to give 95 mg of a white oil. TLC of the oil on instant thin-layer chromatography (ITLC)[3] showed a single spot [R_f 0.70, ethyl acetate–ammonium hydroxide (17:1) or R_f 0.54, benzene–methanol–diethylamine (48:1:1)] and visualized by spraying with iodoplatinate reagent. Treatment with 10% sodium bisulfite solution of both the liquid and the crystalline materials gave meperidine as evidenced by TLC R_f values.

GC–MS identification of VI was performed by solid probe or by injection on a 0.9-m column packed with 3% OV-17 coated on 60/80-mesh Gas Chrom Q after treatment with or without trimethylsilylimidazole in pyridine. The MS of the aforementioned oil (solid probe) showed a molecular ion at *m/z* 264 (M + H), and ions at *m/z* 276 (M + CH_3), *m/z* 292 (M + C_2H_5), *m/z* 248 (M − O_2), *m/z* 246 (M − H_2O), and *m/z* 234, indicative of the *N*-oxide of meperidine. The MS of the aforementioned solid material, mp 173–175°C (solid probe) showed a molecular ion at *m/z* 246 (M + H), and ions at *m/z* 262 (M + CH_3), *m/z* 274 (M + C_2H_5), and *m/z* 232, indicative of 4-ethoxycarbonyl-1-methyl-4-phenyl-1,2,3,4-tetrahydropyridine, a thermal-dehydrated product of the *N*-oxide of meperidine. Landberg and Bogentoft (17) have synthesized 4-ethoxycarbonyl-1-methyl-4-phenyl-1,2,3,4-tetrahydropyridine, and compared its MS with that of VI. In addition, the MS of meperidine, *m/z* 248 (M + H), *m/z* 264 (M + CH_3), *m/z* 276 (M + C_2H_5), and *m/z* 234, 218, and 149, were also observed. This appears to indicate that VI underwent thermal decomposition and loss of an oxygen atom. Chromatograms of both the aforementioned oily and solid materials, treated with or without trimethylsilylimidazole and injected on the column, showed two peaks. The retention time and the MS of the major peak corresponded to meperidine. The minor peak showed the MS of 4-ethoxycarbonyl-1-methyl-4-phenyl-1,2,3,4-tetrahydropyridine. These observations confirmed the reports in the literature (6, 7, 17). The IR[4] of the oily VI showed strong bonds at 2970, 1710 (ester C=O), 1430, 1213 [N—O stretching as shown in 4-methylpyridine *N*-oxide (18)], 1182, and 1130 cm^{-1}. ^{1}H-NMR ($CDCl_3$)[4] of the oily VI showed peaks at δ 2.6, 4.6, 6.4, and 6.7 ppm. Mitchar *et al.* (6) reported that the NMR spectrum of VI showed a characteristic downfield shift of the CH_3 group from δ 7.7 ppm of meperidine base to δ 6.4 ppm due to the inductive influence of the oxygen atom. Due to the limited amount of the material, a boiling point was not measured. Phillipson *et al.* (19) have investigated *N*-oxide of morphine, codeine, and thebaine and observed that each alkaloid forms two *N*-oxides, which have been separated and characterized by NMR and MS and reduced to the parent alkaloid.

The *N*-hydroxy derivative of normeperidine (IX) was synthesized by oxidation of normeperidine with *m*-chloroperbenzoic acid (7, 20). TLC of the product [benzene–methanol–diethylamine (48:1:1), visualized by spraying with iodoplatinate or ammoniacal silver nitrate reagent] showed two spots, one with an R_f value (equal to 0.24) corresponding to that of authentic normeperidine. The other spot (R_f 0.44), a black spot after spraying with ammoniacal silver nitrate, was due to the *N*-hydroxy derivative of normeperidine. Chromatography of the product, treated with trimethylsilylimidazole and injected on a 0.9-m column packed with 3% OV-17 coated on 60/80-mesh Gas Chrom Q and column temperature programmed from 160°C to 250°C at 10°C min, showed two major peaks with several minor peaks. One of the major peaks had a retention time and MS corresponding to that of authentic normeperidine. The other major peak (R_f 4.5) had a molecular ion at *m/z* 322 (M + H), with ions at *m/z* 350 (M + C_2H_5), *m/z* 306 (M − CH_3), *m/z* 232 [M − $(CH_3)_3SiOH$], and *m/z* 214, indicative of IX (7). Attempts to purify the IX failed. The crude product was used qualitatively to identify IX in the biological fluids.

Animal Experiments—Collection of urine samples from rats, guinea pigs, rabbits, dogs, and cats administered meperidine (20–35 mg/kg) has been described (13). The *p*-hydroxy derivative of meperidine (40 mg/kg sc) was administered to one rat (250 g), and urine was collected from a stainless steel metabolism cage for 24 h. All urine was frozen until drug analysis.

Extraction of Meperidine, the *p*-Hydroxy Derivative of Meperidine, and Their Metabolites—Meperidine, VII, and their metabolites were extracted from urine according to described procedures (20). On evaporation of the extract to dryness, the residues were used for TLC and GC–MS studies. For GC–MS studies, the residue was derivatized with trimethylsilylimidazole in pyridine[5] according to the procedure described previously (21).

Hydrolysis of Conjugated Meperidine Metabolites—Aliquots (0.5–2 mL) of urine samples were adjusted to pH 6 with acetic acid, buffered with 0.5 mL of 0.5 M sodium acetate buffer at pH 4.8, and incubated with 50 μL a solution of 9725 U of β-glucuronidase–4210 U of sulfatase[6] at 37°C for 18–20 h. After incubation, the solution was adjusted to pH 9–10 with sodium hydroxide solution, buffered with 0.1 mL of concentrated ammonium hydroxide, and extracted with ether as described previously (20).

Thin-Layer Chromatography—TLC identification of meperidine and its metabolites was by silica gel pre-coated TLC plates[7]. The chromatograms were developed with benzene–methanol–diethylamine (48:1:1) and visualized by spraying with ammoniacal silver nitrate solution for detection of IX or developed with ethyl acetate–methanol–ammonium hydroxide (17:2:1) and sprayed with iodoplatinate reagent for detection of I, II, VII, and VI (20).

Gas Chromatography–Mass Spectrometry—Chemical-ionization MS data were obtained from a gas chromatograph–mass spectrometer[8] equipped with an interactive data system[9]. The GC column consisted of a 91 cm × 2 mm glass column packed with 3% OV-17 coated on 80/100-mesh Gas Chrom Q. The temperature of the injector and ion source were 160°C and 100°C, respectively. Two temperature programs were employed: hold at 150°C for 3.33 min, followed by programming to 250°C at 6°C/min (referred to as column A) and program from 160°C to 250°C at 10°C/min (referred to as column B). Methane, with a flow rate giving an ion chamber pressure of ~1000 μm, was used as the carrier gas as well as the chemical-ionization reagent gas in the ion source. Other specifications of the MS were described elsewhere (21).

Drug and metabolites were identified by comparison of spectra with authentic standards. Other metabolites (Scheme I) were tentatively assigned structures based on MS.

RESULTS AND DISCUSSION

Thin-Layer Chromatographic Identification of Meperidine Metabolites—The limit of detection of I, II, VI, VII, and IX by TLC was ~10–25 μg/sample. In general, meperidine was found in the urinary extracts of all species studied, except the rabbit. Normeperidine was found in the urine of the rat and guinea pig, but not in the urine of the rabbit, cat, and dog. Metabolites VI and VII were not observed by TLC analysis.

TLC of extracts of rabbit urine visualized with ammoniacal silver nitrate solution showed two black spots with R_f values of 0.50 and 0.44, whereas that of a dog showed one black spot, R_f 0.50. The spot at R_f 0.50 corresponds to

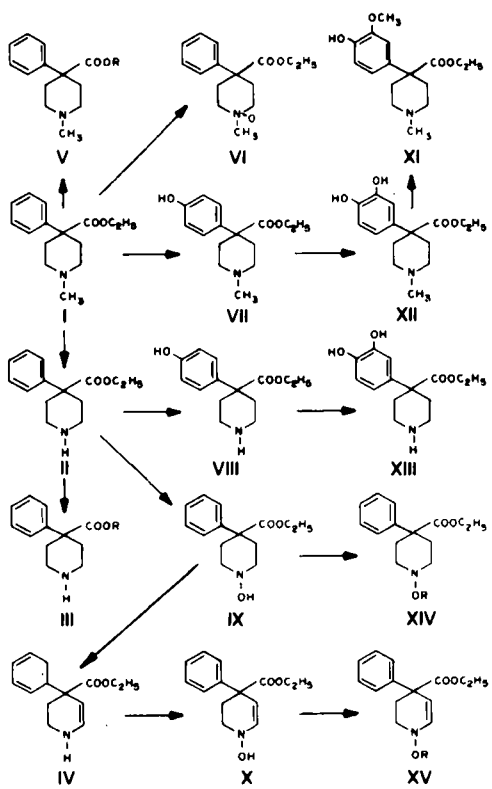

Scheme I—Metabolic pathways of meperidine.

[3] Gelmen Instrument Co., Ann Arbor, Mich.

[4] The author thanks Mr. William F. Rencher, Jr., College of Pharmacy, University of Kentucky, for the excellent IR and NMR spectra.

[5] Pierce Chemical Co., Rockford, Ill.

[6] Glusalase; Endo Laboratories, Garden City, N.Y.

[7] Quantum Industries, Fairfield, N.J.

[8] Model 3300; Finnegan, Sunnyvale, Calif.

[9] Model 6000; Finnegan.

Table I—TLC Identification of Meperidine Metabolites in the Urine of Several Species [a]

Compounds	R_f
I	0.78
II	0.33
VI	0.03
VII	0.17
IX	0.50
Extracts from urine	
Rat	0.78, 0.33
Guinea pig	0.78, 0.33
Rabbit	0.50, 0.44
Cat	0.78
Dog	0.78, 0.50

[a] Quantum Industries, Fairfield, N.J. Chromatogram was developed with benzene–methanol–diethylamine (48:1:1), or ethyl acetate–methanol–ammonium hydroxide (17:2:1).

that of authentic IX. The other spot was possibly due to X (detailed in the GC–MS identification). Metabolite IX was not seen in the TLC analysis of the urine of the rat, guinea pig, and cat (Table I).

Gas Chromatographic–Mass Spectrometric Identification of Meperidine Metabolites—Chemical-ionization GC–MS characteristics of peaks observed in the urinary extracts are compared with known standards, and previously unidentified peaks were assigned to new metabolites (Table II). Meperidine metabolites, the number of times the metabolite was identified, and the number of urine samples examined are listed in Table III.

Identification of Metabolites of Meperidine—Meperidine (I) and metabolites [*i.e.*, II, VI (detected as its thermal decomposition product, 4-ethoxycarbonyl-1-methyl-4-phenyl-1,2,3,4-tetrahydropyridine), IX, and VII (as the trimethylsilyl derivatives)] were identified in urine samples by comparison of retention times and spectra with authentic materials. The *N*-hydroxy metabolite of normeperidine was detected in urine samples only after enzymatic hydrolysis, suggesting that this material is excreted only in the conjugated form. In addition to the known metabolites, some new metabolites of meperidine were tentatively identified.

4-Ethoxycarbonyl-4-phenyl-1,2,3,4-tetrahydropyridine (Dehydronormeperidine) (IV)—This metabolite appeared at 3.75 min in the chromatogram of the extract of rabbit urine. The MS of the metabolite contains a pseudomolecular ion at *m/z* 232 (M + H) and ions at *m/z* 260 (M + C_2H_5), *m/z* 186 (232 − C_2H_5OH), and *m/z* 158 (232 − C_2H_5OH − CO). Also, the retention time of this metabolite bears the same relationship to normeperidine as does dehydromeperidine to meperidine. This metabolite was detected in all urine samples except those of the female rat, cat, and guinea pig (Table III). Based on the structure of the *N*-hydroxy derivative of normeperidine, the olefinic bond of dehydronormeperidine was arbitrarily assigned to positions 2 and 3.

Formation of dehydronormeperidine *in vivo* could occur either through the dehydration of the *N*-hydroxy derivative of normeperidine, observed to be a major metabolite in the urine of the rabbit, or by dehydration of the 2-hydroxy or 3-hydroxy derivatives of normeperidine. *In vivo* formation of the latter metabolites is plausible since analogues of these metabolites [the 2-hydroxy-*N*-nitro derivative of piperidine, a metabolite of the *N*-nitro derivative of piperidine (22) and the 3-hydroxy and 4-hydroxy derivatives of piperidine, major metabolites of piperidine in the rat (23)] have been reported. Formation of dehydronormeperidine by dehydration of the *N*-hydroxy derivative of normeperidine during GC–MS was considered possible; however, this was ruled out since the *N*-hydroxy derivative of dehydronormeperidine also has been observed in the urine (see below). If dehydronormeperidine is formed by dehydration of the *N*-hydroxy derivative of normeperidine, then the *N*-hydroxy derivative of dehydronormeperidine should not be detected.

N-Hydroxy Derivative of Dehydronormeperidine (X)—In the GC–MS analysis of rabbit urine, this metabolite (as the trimethylsilyl derivative) appeared at 5.2 min (Fig. 1). The MS of the metabolite shows a molecular ion at *m/z* 320 with abundant ions at *m/z* 348 (M + C_2H_5), *m/z* 304 (M − CH_3), *m/z* 246 (320 − C_2H_5OH − CO), *m/z* 230 [320 − $(CH_3)_3SiOH$], *m/z* 202 (230 − C_2H_4), and *m/z* 156 [246 − $(CH_3)_3SiOH$]. This metabolite was not detected in the urine without enzymatic hydrolysis, suggesting that the metabolite exists only in the conjugated form. Formation of the *N*-hydroxy de-

Table II—Chemical Ionization GC–MS Characteristics of Peaks Observed in the Urinary Extracts

Compound	Retention Time (R_t), min[a] Column A	Column B	Ions, *m/z*[b] Molecular $(m + H)^+$	Fragment $(m + C_2H_5)^+$	Fragment $(m - CH_3)^+$	Others
I	2.0	1.1	248(100)	276(15)		174(10)
VI[c]	2.8	1.6	246(100)	274(15)		172(80)
II	3.2	1.9	234(100)	262(15)	218(30)	160(10)
IV	3.8	2.1	232(100)	260(18)		158(45)
IX	4.8	2.5	322(80)	350(15)	306(70)	232(100), 158(25)
X	5.2	3.1	320(100)	348(10)	304(20)	246(35), 202(30), 156(15)
VII	7.7	3.8	336(100)	364(18)	304(25)	262(5)
VIII	8.5	4.5	322(100)	350(18)	306(20)	248(4), 212(15)
XII		4.8	424(70)	452(3)	408(60)	
XIII		4.9	410(85)	438(15)	394(100)[d]	320(80)
XI		4.9	366(95)	394(100)[d]	350(40)	

[a] Column A temperature was held at 150°C for 3.33 min and then raised to 250°C at 6°C/min. Column B was programmed from 160°C to 250°C at 10°C/min. [b] Relative intensity is in parentheses. [c] This compound was thermally decomposed through GC–MS to form 4-ethoxycarbonyl-1-methyl-4-phenyl-1,2,3,4-tetrahydropyridine (17). [d] The relative intensity appeared to be the sum of two metabolites.

Table III—Meperidine Metabolites Identified in the Urine of Several Species by GC–MS

Species	Metabolites II	IV	VI	IX	X	VII	VIII	XI	XII	XIII
Rat										
Male	5/5[a]	2/5	4/5	5/5	2/5	5/5	5/5	2/3	2/3	0/3
Female	5/5	0/5	2/5	5/5	0/5	5/5	5/5	3/5	1/5	0/5
Guinea pig										
Male	5/5	2/3	5/5	5/5	3/5	2/3	2/3	0/3	0/3	0/3
Female	4/4	0/4	3/4	3/4	2/4	1/4	—[b]	—	—	—
Rabbit										
Male	2/2	2/2	0/2	2/2	2/2	2/2	2/2	2/2	2/2	2/2
Female	2/2	2/2	0/2	2/2	2/2	2/2	2/2	—	—	—
Cat										
Male	2/2	2/2	2/2	0/2	0/2	2/2	0/2	0/2	0/2	0/2
Female	2/2	0/2	2/2	0/2	0/2	1/2	1/2	0/2	0/2	0/2
Dog										
Male	1/1	1/1	1/1	1/1	1/1	1/1	1/1	1/1	0/1	0/1
Female	1/1	1/1	1/1	1/1	1/1	1/1	1/1	1/1	0/1	0/1

[a] Number of times the metabolite was detected/number of urine samples examined. [b] Not examined.

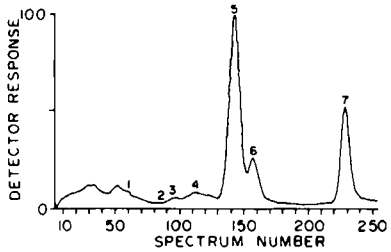

Figure 1—*GC-MS analysis of the extract of enzymatic hydrolyzed urine of a rabbit administered meperidine. The chromatogram was obtained using column A (see Table II). Key: (1) I; (2) VI; (3) II; (4) IV; (5) IX; (6) XV; (7) VII.*

rivative of dehydronormeperidine may be through *N*-hydroxylation of dehydronormeperidine.

p-*Hydroxy Derivative of Normeperidine* (*VIII*)—This metabolite (as the trimethylsilyl derivative) has the same molecular ion as the trimethylsilyl derivative of the *N*-hydroxy derivative of normeperidine, but the mass spectral characteristics and retention time (R_t = 4.5 min) are different. The MS of this peak showed a molecular ion at *m/z* 322 (M + H) and ions at *m/z* 350 (M + C_2H_5), *m/z* 306 (M − CH_3), *m/z* 248 (322 − C_2H_5OH − CO), and *m/z* 212. Since the retention time of this material is longer than that of the *p*-hydroxy derivative of meperidine, and *p*-hydroxylation of aromatic rings is a predominant metabolic pathway for this type of compound, it is reasonable to assume that this material is VIII. It is reasonable to assume that the hydroxyl group is in the *para* position based on the isolation of the *p*-hydroxy derivative of meperidine from urine (5).

The *in vitro* synthesis of VIII for use as a standard was attempted by incubating VII with rat liver homogenate and the NADPH-generating system used for *N*-demethylation of meperidine (24). After incubation, the medium was pooled, adjusted to pH 10 with sodium hydroxide solution, buffered with 1 mL of 40% K_2HPO_4 solution, and extracted. The extracted residue was dissolved in methanol and chromatographed on TLC. No spots other than those of VII and NADP were observed.

Biosynthesis of VIII has also been attempted without success by administration of VII to a rat. An aliquot of the urine of rat administered VII was hydrolyzed with β-glucuronidase-sulfatase[6] and extracted. The residue was derivatized with trimethylsilylimidazole and analyzed by GC-MS. No peak corresponding to VIII was observed.

Dihydroxy Derivative of Meperidine (*XII*)—The integrated total-ion-current chromatogram obtained by column B was scanned for *m/z* 424 the molecular ion of XII (as the trimethylsilyl derivative). A peak was localized at retention time 4.8 min (Fig. 2). The MS of this peak represents a mixture of at least two, probably three compounds, including XII and VIII both as the trimethylsilyl derivatives. The MS showed a molecular ion at *m/z* 424 (M + H) and ions at *m/z* 452 (M + C_2H_5) and *m/z* 408 (M − CH_3), which were tentatively identified as XII as the trimethylsilyl derivative. The formation of XII could result from oxide formation and hydroxylation of both the aromatic and piperidyl rings of the meperidine molecule. Based on the MS, it is difficult to assign positions to the hydroxyl groups in XII; however, *in vitro* hydroxylation of other opiates and phenolic compounds leads to *meta-para* hydroxylation (25). The MS showed a molecular ion at *m/z* 322 (M + H) and ions at *m/z* 350 (M + C_2H_5) and *m/z* 306 (M − CH_3), identified as VIII as the trimethylsilyl derivative. The MS also showed a molecular ion at *m/z* 234 (M + H) and ions at *m/z* 262 (M + C_2H_5) and *m/z* 248 (M − CH_3), which appear to be from normeperidine.

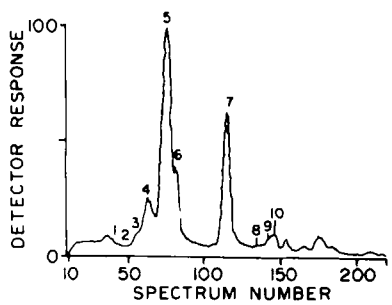

Figure 2—*GC-MS analysis of the extract of enzymatic hydrolyzed urine of a rabbit administered meperidine. The chromatogram was obtained using column B (see Table II). Key: (1–7) as in Fig. 1 legend; (8) VIII; (9) XII; (10) XI and XIII.*

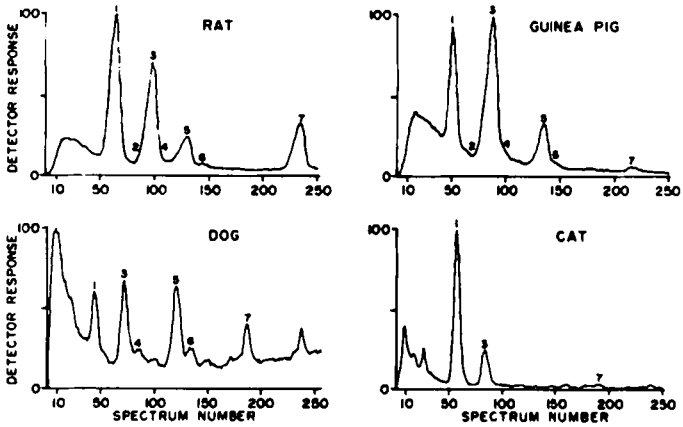

Figure 3—*GC-MS analysis of the extract of enzymatic hydrolyzed urine samples of animals administered meperidine, obtained using column A. The peaks are as listed in Fig. 1.*

Dihydroxy Derivative of Normeperidine (*XIII*) *and Methoxy Hydroxy Derivative of Meperidine* (*XI*)—The integrated total-ion-current chromatogram was scanned for *m/z* 410, indicative of XIII as the trimethylsilyl derivative. A peak with retention time at 5.0 min was located which overlapped another metabolite. One is due to XIII as the trimethylsilyl derivative, which has molecular ion at *m/z* 410 (M + H) and ions at *m/z* 438 (M + C_2H_5) and *m/z* 320 [410 − $(CH_3)_3SiOH$]. The other is due to XI as the trimethylsilyl derivative, which has molecular ion at *m/z* 366 (M + H) and ions at *m/z* 394 (M + C_2H_5) and *m/z* 350 (M − CH_3).

Formation of XI could result from hydroxylation to form a catechol, followed by methylation with catechol methyltransferase. Evidence for this metabolic pathway has been demonstrated *in vitro* for opiates and other phenolic compounds (25) and *in vivo* for naltrexone (26, 27).

Although the position of the hydroxyl and methoxy groups could not be assigned based on the MS, a reasonable assignment could be made based on the structure of the methoxy hydroxy derivative of naltrexone (isolated from urine), whose structure is secure (26). Therefore, it is reasonable to assign the structure for XI as illustrated in Scheme I.

Based on the ratio of meperidine to its metabolites observed in the total-ion-current chromatogram, it appears that IX was a major metabolite in the rabbit, while normeperidine was found in minor amounts (Fig. 1). On the other hand, normeperidine was found to be a major metabolite in the other species studied, while IX was minor (Fig. 3). As mentioned previously, severe interaction between MAOI and meperidine has been observed in humans and rabbits, but has seldom been observed in other species. The role of IX in the interaction between MAOI and meperidine observed in rabbits is not well understood.

Other major metabolites of meperidine, the corresponding free and conjugated carboxylic acids of V and III (4, 13), are not extracted by the assay used here.

Identification of Metabolites of the *p*-Hydroxy Derivative of Meperidine in the Urine of the Rat—The integrated total-ion-current chromatogram and MS of the extract (as the trimethylsilyl derivative) of an enzymatically hydrolyzed urine sample of a rat administered VII are shown in Fig. 4. The chromatogram showed a major peak and several small peaks. The retention time and MS of the major peak correspond to that of VII as the trimethylsilyl derivative. Minor metabolites of VII were also identified.

p-*Hydroxy and Dihydroxy Derivatives of Normeperidine*—The peak with retention time at 4.7 min was apparently due to a mixture of the *p*-hydroxy and dihydroxy derivatives of normeperidine, both as the trimethylsilyl derivatives (Fig. 4). The MS with a molecular ion at *m/z* 322 (M + H) and ions

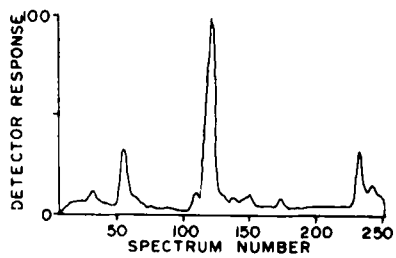

Figure 4—*GC-MS analysis of the extract of enzymatic hydrolyzed urine of a rat administered VII, obtained using column A. The peaks were identified as VII, VIII and XIII, and XI and XII.*

at m/z 350 (M + C_2H_5), m/z 306 (M − CH_3), m/z 276 (322 − C_2H_5OH), and m/z 248 (322 − C_2H_5OH − CO) was attributed to VIII as the trimethylsilyl derivative. The MS with a molecular ion at m/z 410 (M + H) and ions at m/z 438 (M + C_2H_5) and m/z 394 (M − CH_3) was attributed to XIII as the trimethylsilyl derivative. The concentration of XIII was low but detectable. Formation of VIII was apparently through *N*-demethylation of VII. Compound XIII appears to be formed *in vivo* by hydroxylation of VIII.

Methoxy Hydroxy and Dihydroxy Derivatives of Meperidine -The peak with retention time at 5.0 min was apparently due to a mixture of XI and XII, both as the trimethylsilyl derivatives (Fig. 4). The MS with a molecular ion at m/z 366 (M + H) and ions at m/z 394 (M + C_2H_5), m/z 350 (M − CH_3), and m/z 292 (366 − C_2H_5OH − CO) was attributed to XI as the trimethylsilyl derivative. The MS with a molecular ion at m/z 424 (M + H), and ions at m/z 452 (M + C_2H_5) and m/z 408 (M − CH_3) was attributed to XII as the trimethylsilyl derivative. Formation of XII and XI *in vivo* apparently occurs first by hydroxylation of VII and then by methylation of one of the hydroxyl groups. Evidence for this metabolic pathway has been mentioned above (26, 27).

Metabolites XII, VIII, XIII, and XI were not detected in the urine of rats administered either meperidine or VII without enzymatic hydrolysis, suggesting that these metabolites exist only in the conjugated form. The peak with retention time at 1.0 min has a MS with a molecular ion at m/z 306 (M + H) and ions at m/z 334 (M + C_2H_5) m/z 290 (M − CH_3), and m/z 232 (306 − C_2H_5OH − CO). The peak with retention time at 8 min showed a molecular ion at m/z 364 (M + H) and ions at m/z 392 (M + C_2H_5) and m/z 348 (M − CH_3). Peaks at 1.9, 3.6, 5.8, and 7.7 min were also observed in the extract of the control urine, indicating that these are due to natural urinary products and from the enzyme source.

N-Demethylation is a major metabolic pathway for biotransformation of meperidine, but plays only a minor role on the metabolism of VII. This is probably due to the fact that VII has a phenolic group available for conjugation. Conjugation has been shown to be a major metabolic pathway for compounds having both *N*-methyl tertiary amine and phenolic groups, such as morphine (28). In addition, *N*-demethylation of a compound depends on its lipid solubility, *N*-demethylation taking place to a greater degree with more lipid-soluble compounds (29). That the *p*-hydroxy derivative of meperidine (VII), a more polar compound than meperidine, would yield less of VIII than meperidine would yield normeperidine is understandable.

REFERENCES

(1) J. J. Burns, B. L. Berger, P. A. Lief, A. Wollack, E. M. Papper, and B. B. Brodie, *J. Pharmacol. Exp. Ther.*, **114,** 289 (1955).

(2) N. P. Plotnikoff, E. L. Way, and H. W. Elliott, *J. Pharmacol. Exp. Ther.*, **117,** 414 (1956).

(3) A. M. Asatoor, D. R. London, M. D. Milne, and M. L. Simenhoff, *Br. J. Pharmacol.*, **20,** 285 (1963).

(4) I. W. Wainer and J. E. Stambaugh, *J. Pharm. Sci.*, **67,** 116 (1978).

(5) C. Lindberg, C. Bogentoft, U. Bondesson, and B. Danielsson, *J. Pharm. Pharmacol.*, **27,** 975 (1975).

(6) M. Mitchard, M. J. Kendall, and K. Chan, *J. Pharm. Pharmacol.*, **24,** 915 (1972).

(7) W. G. Stillwell, C. S. Myron, and J. T. Steward. *Res. Commun. Chem. Pathol. Pharmacol.*, **14,** 605 (1976).

(8) N. P. Plotnikoff, H. W. Elliott, and E. L. Way, *J. Pharmacol. Exp. Ther.*, **104,** 377 (1952).

(9) V. R. Jenkins II, W. M. Talbert, and P. V. Dilts, Jr., *Obs. Gyn.*, **39,** 254 (1972).

(10) T. J. Goehl and C. Davison, *J. Pharm. Sci.*, **62,** 907 (1973).

(11) L. E. Mather and G. T. Tucker, *J. Pharm. Sci.*, **63,** 306 (1974).

(12) U. Klotz, T. S. McHorse, G. R. Wilkinson, and S. Schender, *Clin. Pharmacol. Ther.*, **16,** 667 (1974).

(13) S. Y. Yeh, H. A. Krebs, and A. Changchit, *J. Pharm. Sci.*, **70,** 867 (1981).

(14) S. Y. Yeh and C. L. Mitchell, *J. Pharmacol. Exp. Ther.*, **179,** 642 (1971) and references cited therein.

(15) S. Y. Yeh and C. W. Gorodetzky, *Toxicol. Appl. Pharmacol.*, **24,** 387 (1973) and references cited therein.

(16) S. Y. Yeh, B.-L. Chang, H. A. Krebs, and C. W. Gorodetzky, *J. Pharmacol. Exp. Ther.*, **209,** 125 (1978) and references cited therein.

(17) C. Lindberg and C. Bogentoft, *Acta Pharm. Suec.*, **12,** 507 (1975).

(18) K. Nakanishi, "Infrared Absorption Spectroscopy-Practice," Holden-Day, San Francisco, Calif., 1962, p. 210.

(19) T. D. Phillipson, S. S. Handa, and S. W. El-Dabbas, *Phytochemistry*, **15,** 1297 (1976).

(20) S. Y. Yeh and H. A. Krebs, *J. Pharm. Sci.*, **70,** 482 (1981).

(21) S. Y. Yeh, H. A. Krebs, and C. W. Gorodetzky, *J. Pharm. Sci.*, **68,** 133 (1979).

(22) K.-H. Leung, K. K. Park, and M. C. Archer, *Res. Commun. Chem. Pathol. Pharmacol.*, **19,** 201 (1978).

(23) Y. Okano, T. Miyata, S. H. Hung, T. Motoya, M. Kataoka, K. Takahama, and Y. Kase, *Jpn. J. Pharmacol.*, **28,** 41 (1978).

(24) D. H. Clouet, *J. Pharmacol. Exp. Ther.*, **144,** 354 (1964).

(25) J. Daly, J. K. Inscoe, and J. Axelrod, *J. Med. Chem.*, **8,** 153 (1965).

(26) E. J. Cone, C. W. Gorodetzky, W. D. Darwin, F. I. Carroll, G. A. Brine, and C. D. Welch, *Res. Commun. Chem. Pathol. Pharmacol.*, **20,** 413 (1978).

(27) K. Verebely, M. A. Chedekel, S. J. Mule, and D. Rosenthal, *Res. Commun. Chem. Pathol. Pharmacol.*, **12,** 67 (1975).

(28) S. Y. Yeh, *J. Pharmacol. Exp. Ther.*, **192,** 201 (1975).

(29) R. E. McMahon, *J. Med. Pharm. Chem.*, **4,** 67 (1961).

ACKNOWLEDGMENTS

The author sincerely thanks Mr. H. A. Krebs for technical assistance and Ms. W. M. Roberts for her aid in the preparation of this manuscript.

Biological Activity of the Hypolipidemic Agent, N^2-*n*-Butylindazolone

I. H. HALL ˣ, W. L. WILLIAMS, JR., S. D. WYRICK, and P. J. VOORSTAD

Received February 6, 1984, from the *Division of Medicinal Chemistry and Natural Products, School of Pharmacy, University of North Carolina at Chapel Hill, Chapel Hill, NC 27514.* Accepted for publication March 30, 1984.

Abstract □ Previously, a series of *N*-substituted indazolone derivatives proved to be effective hypolipidemic agents in rodents. The most effective agent, N^2-*n*-butylindazolone, at 20 mg/kg/d was shown to suppress the levels of cytoplasm acetyl coenzyme A required for cholesterol and fatty acid synthesis as well as *sn*-glycerol-3-phosphate acyl transferase and phosphatidate phosphohydrolase activities. Lipid content of the liver, small intestine, and serum lipoprotein fractions was lowered, whereas lipid content was increased in fecal excretions by drug treatment for 14 d. The absorption of orally administered cholesterol from the intestine was severely reduced after drug administration. The mode of action of N^2-*n*-butylindazolone appears to be similar to cyclic imides possessing hypolipidemic activity.

Keyphrases □ N^2-*n*-Butylindazolone—hypolipidemic activity in rodents, cholesterol and triglycerides reduction □ Antihyperlipidemic agents—N^2-*n*-butylindazolone, activity in rodents, cholesterol and triglycerides reduction

A series of *N*-substituted indazolone derivatives were previously screened for hypolipidemic activity in mice and were observed to be potent hypolipidemic agents at the low dose of 20 mg/kg/d (1). *N*-Substitutions of four carbon atom chain lengths in the indazolone (1) as well as in the phthalimide (2) and saccharin (2) series afforded the best hypolipidemic activity. Thus, N^2-*n*-butylindazolone (I) was selected for a more in-depth investigation of its effects on lipid synthesis and distribution in rodents.

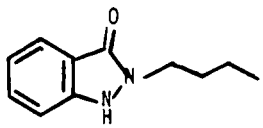

I

EXPERIMENTAL SECTION

The N^2-*n*-butylindazolone was synthesized by the method of Schwartz *et al.* (3). The details of the synthesis and physical characteristics have been reported previously (1).

Antihyperlipidemic Screens in Normal Rodents—N^2-*n*-Butylindazolone was suspended in 1% carboxymethylcellulose–water, homogenized, and administered to CF_1 male mice (~25 g) intraperitoneally for 16 d or to Sprague–Dawley male rats (~350 g) orally by an intubation needle for 14 d. On days 9 and 14 or 16, blood was obtained by tail vein bleeding and the serum was separated by centrifugation for 3 min. The serum cholesterol levels were determined by a modification of the Liebermann–Burchard reaction (4). Serum was also collected on day 14 or 16 and the triglyceride content was determined by a commercial kit[1].

Testing in Hyperlipidemic Mice—CF_1 male mice (~25 g) were placed on a commercial diet[2] which produced a hyperlipidemic state. After the serum cholesterol and triglyceride levels were observed to be elevated, the mice were administered test drugs at 20 mg/kg/d intraperitoneally for an additional 14-d period. Serum cholesterol and triglyceride levels were measured.

Animal weights were obtained periodically during the experiments and were expressed as a percentage of the animal's weight on day zero. After dosing for 14 d with test drugs, selected organs were excised, trimmed of fat, and weighed.

The acute toxicity (LD_{50} values) (5) was determined in CF_1 male mice by administering test drugs at 100 mg–2 g/kg ip as a single dose. The number of deaths were recorded over a 7-d period for each group.

In vitro enzymatic studies were determined using 10% homogenates of CF_1 male mouse liver with 50–200 μM of test drug. *In vivo* enzymatic studies were determined using 10% liver homogenates (prepared in 0.25 M sucrose + 0.001 M ethylenediaminetetraacetic acid, pH 7.2) from CF_1 male mice obtained after administering the agents at a 10–60 mg/kg/d i.p. dose for 16 d. The enzyme activities were determined by following literature procedures (2) for: acetyl coenzyme A (CoA) synthetase (6); ATP-dependent citrate lyase (7); mitochondrial citrate exchange (8, 9); cholesterol side-chain oxidation (10); 3-hydroxy-3-methylglutaryl coenzyme A reductase (HMG CoA reductase) (11, 12); acetyl CoA carboxylase activity (13); fatty acid synthetase activity (14); *sn*-glycerol-3-phosphate acyl transferase activity (15); phosphatidate phosphohydrolase activity (16).

Rat Studies—In Sprague–Dawley rats that had been administered test drugs in 14 d, the liver, small intestine, and fecal materials (24-h collection) were removed, extracted (17, 18), and analyzed for cholesterol levels (4), triglyceride levels[3], neutral lipid content (19), and phospholipid content (20).

Sprague–Dawley rats (~400 g) were administered test agents for 14 d orally. On day 13, 10 μCi of [^{3}H]cholesterol was administered, orally in rats, and according to procedures described previously (2), tissue samples were combusted[4] or plated on filter paper, dried and digested for 24 h in base[5] at 40°C, and counted[6]. Results were expressed as disintegration/min (dpm) per total organ.

Sprague–Dawley rats (~400 g) were administered the test drug intraperitoneally for 14 d at 20 mg/kg/d. On day 13, 10 μCi of [1,2-^{3}H]cholesterol (40.7 Ci/mmol) was administered to the rat, orally. Twenty-four hours later, the blood was collected and the serum was separated by centrifugation (21).

Sprague–Dawley male rats (~350 g) were treated with test drugs at 20 mg/kg/d orally for 14 d. After anesthetizing the animal, the bile duct was cannulated as previously described (2). [1,2-^{3}H]Cholesterol (40.7 mCi/mmol) (10 μCi) was administered orally 18 h prior to commencing the surgery. The bile was collected over the next 6 h and the volume (mL) measured. Aliquots were counted[6] and analyzed for [^{3}H]cholesterol content (4).

Sprague–Dawley male rats (~350 g) were administered test drugs at 20 mg/kg/d orally. Blood was collected from the abdominal vein and lipoprotein fractions were obtained by the method of Hatch and Lees (22) and Havel *et al.* (23). Each fraction was analyzed for cholesterol (4), triglyceride[3], neutral lipids (19), phospholipids (20), and protein levels (24).

RESULTS

N^2-*n*-Butylindazolone proved to be a potent hypolipidemic agent in mice and rats after intraperitoneal and oral administration, respectively. In mice, the dose affording the maximal lowering effect was 20 mg/kg/d, reducing serum cholesterol 53% and serum triglyceride levels 56%. This dose was slightly less effective in rats, lowering the levels of cholesterol 44% and triglycerides 53% (Table I).

Examination of *in vitro* enzymatic activities in CF_1 mice (Table II) demonstrated that mitochondrial citrate exchange was effectively reduced 34% at 100 μM and 43% at 200 μM. *In vitro* ATP-dependent citrate lyase activity was suppressed 35% at 200 μM. Acetyl CoA synthetase activity was lowered 46% at 100 μM and 49% at 200 μM. HMG CoA reductase activity was reduced 28% at the lower concentration (50 μM) but returned to more normal levels of activity at 100–200 μM. Cholesterol side-chain oxidation was reduced

[1] Hycel Triglyceride Test Kit; Fisher.
[2] Basal Atherogenic Test Diet; U.S. Biochemical Corp.
[3] Triglyceride Kit (bmc); Bio-Dynamics.
[4] Tissue-Oxidizer; Packard.
[5] Hyamine Hydroxide; New England Nuclear.
[6] Fisher Scintiverse in a Packard Scintillation Counter.

0022-3549/84/1200-1788$01.00/0
© 1984, American Pharmaceutical Association

Table I—Hypolipidemic Activity of N^2-*n*-Butylindazolone in Male CF_1 Mice and Sprague–Dawley Rats [a]

Compound	Mice (Intraperitoneal Dose)			Rats (Oral Dose)		
	Serum Cholesterol		Serum Triglyceride	Serum Cholesterol		Serum Triglyceride
	Day 9	Day 16	Day 16	Day 9	Day 14	Day 14
N^2-*n*-Butylindazolone						
10 mg/kg/d	86 ± 7[b]	58 ± 6[c]	64 ± 6[c]	—	—	—
20 mg/kg/d	86 ± 6[b]	47 ± 4[c]	44 ± 4[c]	92 ± 8	56 ± 6[c]	47 ± 5[c]
40 mg/kg/d	72 ± 6[c]	56 ± 5[c]	50 ± 4[c]	—	—	—
60 mg/kg/d	67 ± 6[c]	55 ± 4[c]	50 ± 4[c]	—	—	—
Control (1% Carboxymethylcellulose)	100 ± 7[d]	100 ± 6[e]	100 ± 7[f]	100 ± 8[g]	100 ± 7[h]	100 ± 7[i]

[a] Expressed as percent of control (mean ± *SD*); $n = 6$. [b] $p \leq 0.010$. [c] $p \leq 0.001$. [d] 118 mg %. [e] 122 mg %. [f] 137 mg %. [g] 73 mg %. [h] 78 mg %. [i] 110 mg %.

Table II—*In Vitro* Effects of N^2-*n*-Butylindazolone on CF_1 Mouse Liver-Enzyme Activities [a]

Enzyme Assay	Control	50 μM	100 μM	200 μM
Mitochondrial citrate exchange	100 ± 7[d]	71 ± 6[c]	66 ± 5[c]	57 ± 6[c]
ATP-dependent citrate lyase	100 ± 6[e]	101 ± 7	78 ± 6[c]	65 ± 6[c]
Acetyl CoA synthetase	100 ± 6[f]	73 ± 6[c]	54 ± 7[c]	51 ± 5[c]
HMG CoA reductase	100 ± 9[g]	72 ± 5[c]	81 ± 7[b]	92 ± 8
Cholesterol side-chain oxidation	100 ± 5[h]	—	71 ± 6	—
Acetyl CoA carboxylase	100 ± 6[i]	91 ± 7	90 ± 6	90 ± 7
Fatty acid synthetase	100 ± 8[j]	91 ± 7	85 ± 7	73 ± 6[c]
sn-Glycerol-3-phosphate acyl transferase	100 ± 7[k]	73 ± 6[c]	45 ± 5[c]	53 ± 5[c]
Phosphatidate phosphohydrolase	100 ± 7[l]	100 ± 8	74 ± 6[c]	57 ± 7[c]

[a] Expressed as percent of control (mean ± *SD*); $n = 6$. [b] $p \leq 0.01$. [c] $p \leq 0.001$. [d] 30.8% exchange of mitochondrial citrate. [e] 30.5 mg of citrate hydrolyzed/g wet tissue/20 min. [f] 28.5 mg of acetyl CoA formed/g wet tissue/20 min. [g] 384,900 dpm of cholesterol formed/g wet tissue/60 min. [h] 6080 dpm of CO_2 formed/g wet tissue/18 h. [i] 32,010 dpm/g wet tissue/30 min. [j] 37,656 dpm/g wet tissue/20 min. [k] 537,800 dpm/g wet tissue/20 min. [l] 16.7 μP_i/g wet tissue/15 min.

29% at 100 μM. The activities of regulatory enzymes of triglyceride synthesis, *sn*-glycerol-3-phosphate acyl transferase and phosphatidate phosphohydrolase were significantly inhibited by N^2-*n*-butylindazolone. The former was inhibited 55% at 100 μM and 47% at 200 μM. The latter was suppressed 26% at 100 μM and 43% at 200 μM. The effects of N^2-*n*-butylindazolone on *in vivo* enzyme activities of mouse liver (Table III) were a 38% suppression of acetyl CoA synthetase activity at 60 mg/kg/d and a 20% inhibition of HMG CoA reductase activity at 10 mg/kg/d. Acetyl CoA carboxylase activity was suppressed 20–30% for all of the doses tested. Fatty acid synthetase activity was reduced 25% at 20 mg/kg, but the agent had no effect at other doses. Phosphatidate phosphohydrolase activity was reduced in a dose-dependent manner with 60 mg/kg/d resulting in a 59% reduction. *sn*-Glycerol-3-phosphate acyl transferase activities were inhibited >20% at 10 and 20 mg/kg/d.

Lipid content was lowered 20% in the liver and 65% in the small intestine after dosing rats 20 mg/kg/d for 14 d. Cholesterol content in the liver was lowered to 29%, triglyceride level and neutral lipids were reduced 21 and 34%, respectively; phospholipid content was elevated 24%. In the small intestine, cholesterol, triglycerides, and neutral lipid levels were lowered 27, 84, and 80%, respectively. In the feces, lipid content and cholesterol levels were elevated 5% and 8% which is not significant, but there were elevations in the levels of neutral lipids and phospholipids which were significantly different from the control (Table IV).

The serum lipoprotein fractions obtained from rats treated for 2 weeks showed decreased cholesterol, triglyceride, and neutral lipid levels in all four lipoprotein fractions. Phospholipid levels were generally not affected with the exception of the high density lipoprotein which had a 14% reduction (Table IV).

[^{3}H]Cholesterol distribution after 2-weeks dosing in rats showed that cholesterol was not accumulated in the brain, lung, heart, liver, or spleen. On the other hand, higher concentrations of cholesterol were found in the small intestine (52%), large intestine (129%), chyme (80%), and feces (60%) when compared with control values. Bile excretion studies showed a 28% increase in [^{3}H]cholesterol excretion in the bile on day 14, and studies also demonstrated a 95% suppression of absorption of [^{3}H]cholesterol from the intestine after oral administration over a 24-h period (Table V).

Organ weights of the control and treated animals did not differ significantly although those of the treated animals were slightly lower. The weight of the control and treated animals increased 9.76% and 5.86%, respectively, over two weeks. Daily food intake (g/d) was 30.39 for the control and 28.75 for the treated group. Adrenal weights were not altered by drug treatment indicating that there was no compensating hypertrophy of the adrenal cortex to produce increased steroidogenesis.

Data in Tables I–V are expressed as percent of control ± *SD*. The probable significance level (p) between each test group and the control group was determined by the t test.

DISCUSSION

In comparing the mode of action of N^2-substituted indazolone to *N*-substituted cyclic imides and derivatives [e.g., phthalimide (2), saccharin (2), and 1′,8′-naphthalimide (25)], some similarities exist. All of these agents inhibit mitochondrial citrate exchange decreasing the availability of the key intermediate, acetyl CoA, which is required for fatty acid and cholesterol synthesis. All of the *N*-substituted imides block the two regulatory enzymes of triglyceride synthesis (*sn*-glycerol-3-phosphate acyl transferase and phosphatidate phosphohydrolase) and showed marginal inhibition of HMG CoA reductase, the regulatory enzyme of cholesterol synthesis. Differences which exist between *N*-substituted indazolone and *N*-substituted saccharin, phthalimide, and 1′,8′-naphthalimide cyclic imides include marginal inhibition

Table III—*In Vivo* Effects of N^2-*n*-Butylindazolone on CF_1 Mouse Liver-Enzyme Activities [a]

Compound	ATP-Dependent Citrate Lyase	Acetyl CoA Synthetase	HMG CoA Reductase	
N^2-*n*-Butylindazolone				
10 mg/kg/d	97 ± 8	99 ± 7	80 ± 7[c]	
20 mg/kg/d	100 ± 6	98 ± 6	91 ± 7	
40 mg/kg/d	101 ± 7	91 ± 7	91 ± 6	
60 mg/kg/d	92 ± 7	62 ± 5[c]	98 ± 8	
Control (1% carboxymethylcellulose)	100 ± 8[e]	100 ± 7[f]	100 ± 6[g]	
	Acetyl CoA Carboxylase	Fatty Acid Synthetase	Phosphatidate Phosphohydrolase	*sn*-Glycerol-3-Phosphate Acyl Transferase
N^2-*n*-Butylindazolone				
10 mg/kg/d	77 ± 6[c]	93 ± 7	75 ± 7[c]	79 ± 6[c]
20 mg/kg/d	69 ± 5[c]	75 ± 6[c]	68 ± 6[c]	72 ± 7[c]
40 mg/kg/d	78 ± 5[c]	94 ± 7	58 ± 5[c]	84 ± 8[b]
60 mg/kg/d	80 ± 6[c]	102 ± 8	41 ± 5[c]	88 ± 7
Control (1% carboxymethylcellulose)	100 ± 5[i]	100 ± 6[j]	100 ± 7[l]	100 ± 7[k]

[a] See legend for Table II.

Table IV—*In Vivo* Effects of N^2-*n*-Butylindazolone on Lipid Levels in Liver, Small Intestine, Feces, Bile, and Serum Lipoprotein Fractions of Rats[a]

	Lipid, mg	Cholesterol	Triglycerides	Neutral Lipids	Phospholipids	Proteins
Liver						
Control	100 ± 8	100 ± 7[d]	100 ± 6[e]	100 ± 7[f]	100 ± 9[g]	100 ± 8[h]
Treated	80 ± 7[b]	71 ± 6[c]	81 ± 5[c]	66 ± 6[c]	124 ± 8	102 ± 8
Small intestine						
Control	100 ± 7	100 ± 6[i]	100 ± 7[j]	100 ± 8[k]	100 ± 8[l]	100 ± 7[m]
Treated	35 ± 4[c]	73 ± 6[c]	16 ± 3[c]	20 ± 4[c]	75 ± 6[c]	104 ± 6
Feces						
Control	100 ± 8	100 ± 7[n]	100 ± 6[o]	100 ± 8[p]	100 ± 8[q]	100 ± 8[r]
Treated	105 ± 7	107 ± 8	114 ± 5[c]	125 ± 7[c]	131 ± 7[c]	76 ± 7
Serum lipoprotein						
Chylomicron						
Control	—	100 ± 7[s]	100 ± 5[t]	100 ± 7[u]	100 ± 7[v]	100 ± 6[w]
Treated	—	66 ± 6[c]	65 ± 4[c]	70 ± 7	102 ± 8	108 ± 7
Very low-density lipoprotein						
Control	—	100 ± 7[x]	100 ± 6[y]	100 ± 7[z]	100 ± 8[aa]	100 ± 5[bb]
Treated	—	33 ± 3[c]	42 ± 5[c]	60 ± 6[c]	107 ± 9	88 ± 6
Low-density lipoprotein						
Control	—	100 ± 6[cc]	100 ± 7[dd]	100 ± 8[ee]	100 ± 9[ff]	100 ± 7[gg]
Treated	—	33 ± 2[c]	78 ± 5[c]	67 ± 6[c]	115 ± 6	92 ± 6
High-density lipoprotein						
Control	—	100 ± 6[hh]	100 ± 7[ii]	100 ± 6[jj]	100 ± 7[kk]	100 ± 7[ll]
Treated	—	23 ± 2[c]	34 ± 4[c]	60 ± 5[c]	86 ± 6[b]	106 ± 7

[a] After 14 d of dosing, expressed as percent of control (mean ± *SD*), $n = 6$. [b] $p \leq 0.010$. [c] $p \leq 0.001$. [d] 24.03 mg cholesterol/g tissue. [e] 44.11 mg neutral lipid/g tissue. [f] 6.37 mg triglyceride/g tissue. [g] 7.19 mg. [h] 4.5 mg protein/g wet tissue. [i] 7.82 mg/g. [j] 6.98 mg/g. [k] 1.12 mg/g. [l] 2.06 mg/g. [m] 42 mg/g. [n] 28.47 mg/g. [o] 33.94 mg/g. [p] 1.86 mg/g. [q] 1.39 kg/g. [r] 6.99 mg/g. [s] 337 μg/mL. [t] 67 μg/mL. [u] 420 μg/mL. [v] 149 μg/mL. [w] 184 μg/mL. [x] 190 μg/mL. [y] 98 μg/mL. [z] 22 μg/mL. [aa] 26 μg/mL. [bb] 50 μg/mL. [cc] 210 μg/mL. [dd] 10 μg/mL. [ee] 45 μg/mL. [ff] 41 μg/mL. [gg] 122 μg/mL. [hh] 544 μg/mL. [ii] 620 μg/mL. [jj] 27 μg/mL. [kk] 153 μg/mL. [ll] 657 μg/mL.

Table V—Effects of N^2-*n*-Butylindazolone on [^{3}H]Cholesterol Distribution in Rats[a]

Organ	Organ Weight, g		Total Organ dpm	
	Control	Treated	Control	Treated
Brain	1.866	1.766	29,115	12,956
Lung	1.766	1.667	15,350	12,838
Heart	1.333	1.001	24,582	21,868
Liver	12.000	11.682	47,429	25,756
Kidney	2.900	2.466	5,875	5.191
Spleen	0.566	0.666	19,388	15,988
Adrenal	0.036	0.034	—	—
Stomach	2.066	2.100	11,375	40,005
Small intestine	8.333	8.400	15,291	37,298
Large intestine	4.100	5.000	47,109	108,044
Chyme	5.866	3.233	102,772	185,024
Feces	5.702	6.566	320,454	512,301

[a] 24 h after administration for 14 d; $n = 6$.

of fatty acid synthesis at the lower doses by the *N*-substituted indazolone; the latter agent also suppresses appetite. The *N*-substituted indazolone did lower lipid levels in the liver and small intestine of the rat with increased lipid levels in the fecal material after 14 d of dosing. Lower levels of cholesterol, triglycerides, and neutral lipids of the four blood lipoprotein fractions were evident after drug therapy. The *N*-substituted indazolone derivatives more consistently lowered lipid content of the four lipoprotein fractions when compared with cyclic imides. Whereas the ratio of cholesterol level of high density lipoprotein to low density lipoprotein probably did not change significantly, lower levels were noted in both lipoprotein fractions. Supposedly, lower levels of cholesterol in the low density fraction and higher levels of cholesterol in high density lipoprotein fraction protect against lipid deposition in the atherogenic plaque of the blood vessel and leads to clearance of lipoproteins from the blood.

Like *N*-substituted cyclic imides, [^{3}H]cholesterol distribution and excretion was altered by N^2-*n*-butylindazolone. First, after oral administration of cholesterol, GI tract absorption over a 24-h period was reduced markedly. Second, there was less cholesterol in the major organs, *e.g.*, brain, liver, heart, lung, and kidney. Third, drug therapy resulted in larger amounts of labeled cholesterol being excreted by the fecal route compared with the control. Fourth, the increase in fecal [^{3}H]cholesterol may reflect the decreased absorption of cholesterol caused by the drug and the increase in biliary excretion. The *N*-substituted indazolone derivatives appeared to be more effective than cyclic imides in reducing cholesterol absorption and appeared to be slightly less effective in reducing liver regulatory enzyme activity than cyclic imides. For example, phthalimide and saccharin reduced cholesterol absorption 56% and 33%, respectively, whereas N^2-*n*-butylindazolone resulted in a 95% reduction. However, phosphatidate phosphohydrolase activity was reduced 97% by phthalimide at 60 mg/kg/d and 70% by saccharin at 100 mg/kg/d, whereas N^2-*n*-butylindazolone at 60 mg/kg/d only lowered the activity 59%, its maximum effect. Thus, the modes of action of cyclic imides in lowering body lipids vary from compound to compound, usually affecting the same biochemical parameter but having different magnitudes of response. All of the tested cyclic imides to date appear to have multiple sites in metabolism on which they act to lower serum lipid levels in the body.

In conclusion, N^2-*n*-butylindazolone appears to be a potent hypolipidemic agent and, like cyclic imides tested, more potent than clofibrate which is commercially available. The therapeutic index was well within safe utilization of the compound and the compound[7] effectively suppressed both serum cholesterol and triglyceride levels.

REFERENCES

(1) S. D. Wyrick, P. J. Voorstad, G. H. Cocolas, and I. H. Hall, *J. Med. Chem.*, **27**, 768 (1984).

(2) I. H. Hall, P. J. Voorstad, J. M. Chapman, Jr., and G. H. Cocolas, *J. Pharm. Sci.*, **72**, 845 (1983).

(3) J. Schwatz, F. Hanziker, and W. Michealis, *Helv. Chim. Acta*, **47**, 1986 (1964).

(4) A. T. Ness, J. V. Pastewka, and A. C. Peacock, *Clin. Chim. Acta*, **10**, 229 (1964).

(5) J. T. Litchfield, Jr. and F. Wilcoxon, *J. Pharmacol. Exp. Ther.*, **96**, 99 (1949).

(6) A. G. Goodridge, *J. Biol. Chem.*, **248**, 4218 (1973).

(7) M. Hoffman, L. Weiss, and O. H. Wieland, *Anal. Biochem.*, **84**, 441 (1978).

(8) B. H. Robinson, G. R. Williams, M. L. Halperin, and C. C. Leznoff, *Eur. J. Biochem.*, **15**, 263 (1970).

(9) B. H. Robinson and G. R. Williams, *Biochim. Biophys. Acta*, **216**, 63 (1970).

(10) D. Kritchevsky and S. A. Tepper, *Atherosclerosis*, **18**, 93 (1973).

(11) G. T. Haven, J. R. Krzemien, and T. T. Nguyen, *Res. Commun. Chem. Pathol. Pharmacol.*, **6**, 253 (1973).

(12) F. Wada, K. Hirata, and Y. Sakameto, *J. Biochem. (Tokyo)*, **65**, 71 (1969).

(13) M. D. Greenspan and J. M. Lowenstein, *J. Biol. Chem.*, **243**, 6273 (1968).

(14) R. O. Brady, R. M. Bradley, and E. G. Trams, *J. Biol. Chem.*, **235**, 3093 (1960).

(15) R. G. Lamb, S. D. Wyrick, and C. Piantadosi, *Atherosclerosis*, **27**, 147 (1977).

[7] The LD_{50} was >2 g/kg ip.

(16) R. D. Mavis, J. N. Finkelstein, and B. P. Hall, *J. Lipid Res.*, **19**, 467 (1978).
(17) J. Folch, M. Lees, and G. H. C. Stanley, *J. Biol. Chem.*, **226**, 497 (1957).
(18) E. G. Bligh and W. J. Dyer, *Can. J. Biochem. Physiol.*, **37**, 911 (1959).
(19) J. H. Bragdon, *J. Biol. Chem.*, **190**, 513 (1951).
(20) C. P. Stewart and E. B. Henday, *Biochem. J.*, **29**, 1683 (1935).
(21) A. Adam, J. van Cantfort, and J. Gielen, *Lipids*, **11**, 610 (1976).
(22) F. T. Hatch and R. S. Lees, *Adv. Lipid Res.*, **6**, 33 (1968).
(23) R. J. Havel, H. A. Eder, and J. H. Bragdon, *J. Clin. Invest.*, **34**, 1395 (1955).
(24) O. H. Lowry, N. J. Rosebrough, A. L. Farr, and R. J. Randall, *J. Biol. Chem.*, **193**, 265 (1951).
(25) I. H. Hall, J. M. Chapman, Jr., P. J. Voorstad, and G. H. Cocolas, *J. Pharm. Sci.*, **73**, 956 (1984).

ACKNOWLEDGMENTS

This research was financially supported by National Heart, Lung and Blood Institute Grant 2R01 HL25680. The authors thank Michele Tousignant and MacDonald Bowden for their technical assistance.

Estimation of Tris(2-butoxyethyl) Phosphate in Biological Fluids: Novel Intersubject Variability in Recovery from Human Serum

GAIL D. ANDERSON, ALFRED T. ELVIN, and DAVID LALKA ˣ

Received July 25, 1983, from the *Department of Pharmaceutics, School of Pharmacy, State University of New York at Buffalo, Amherst, NY 14260* and the *Clinical Pharmacokinetics Laboratory, Buffalo General Hospital, Buffalo, NY 14203.* Accepted for publication April 13, 1984.

Abstract □ Tris(2-butoxyethyl) phosphate (I), a plasticizer commonly found in evacuated blood collection tubes, displaces many basic drugs from their binding sites on serum proteins and causes them to redistribute from serum into red blood cells (*i.e.*, artificially lowering serum or plasma drug concentration). Thus, the ability to quantitate I in serum or plasma may be helpful in establishing the suitability of various lots of evacuated blood collection tubes for use in drug level monitoring and pharmacokinetic studies. In the process of establishing a minor modification of an assay which has been reported, remarkable and reproducible interindividual variability ($n = 10$) in the slope of standard curves was observed (range, 0.0143–0.0486). This variability appeared to be caused by differences in the recovery of I from the serum of these individuals. The source of this difference seemed to be related to serum lipoprotein concentration since the slope of standard curves was highly correlated with serum triglyceride concentration ($r = -0.800$) as well as with the sum of serum triglyceride and cholesterol concentrations ($r = -0.881$). These observations suggest that the examination of interindividual differences in the recovery of drugs and related compounds from serum should be a routine part of assay development.

Keyphrases □ Tris(2-butoxyethyl) phosphate—recovery variability, human serum, correlation to lipoprotein, triglyceride and cholesterol levels

Tris(2-butoxyethyl) phosphate (I), a plasticizer found in the rubber stoppers of many evacuated blood collection tubes and in some catheter materials, has been shown to significantly displace basic drugs such as propranolol (1), quinidine (2), lidocaine (3), imipramine (4), and alprenolol (4) from their binding sites on α_1-acid glycoprotein (the principal base binding protein in human serum). Spuriously low (typically 25%) plasma or serum concentrations accompany this displacement due to increased partitioning of the drugs into red blood cells (1, 3). Artifacts related to this phenomenon may pervade much of the published data describing the pharmacokinetics of this type of compound. Furthermore, this artifact may adversely affect therapeutic drug monitoring. Specifically, it is likely that different lots of evacuated blood collection tubes cause varying amounts of "displacing activity" (3) and that different lots of tubes may be used to collect blood during a hospital admission. Thus, the capacity to approximate the concentration of I in plasma or serum samples is important.

A second reason to examine the analysis of I in biological fluids was that preliminary studies in this laboratory suggested remarkable intersubject variability in the slopes of standard curves for I in human serum. It is well known that the recovery of some compounds is dependent upon the biological fluid (urine, blood, serum, *etc.*) being extracted. For example the lidocaine metabolites, monoethyl-glycinexylidide and glycinexylidide, have a significantly lower recovery from serum than from urine (5). The present text describes the evidence for large (approximately threefold) interindividual differences in the recovery of I from serum, provides preliminary observations regarding the plasma constituents which exhibit covariance with these interindividual differences, and presents a description of analytical methods which allow the estimation of I in serum samples.

EXPERIMENTAL SECTION

Tris(2-butoxyethyl) phosphate[1] and dioctyl phthalate[1] were used as received. All solvents were spectral or HPLC grade.

Standard Assay of I in Serum—The concentration of I in serum samples was determined using a minor modification of a previously published procedure (4). The original extraction method was modified by increasing the organic to aqueous phase volume ratio from 2:1 to 10:1. To a 0.50-mL serum sample was added 5 mL of dichloromethane containing 1.0 μg/mL of dioctyl phthalate as an internal standard. The mixture was agitated on a fixed-angle rotary mixer (20 rpm) for 10 min and centrifuged (1000×*g*). The organic phase was transferred to a clean tube and evaporated to dryness. The residue was redissolved in 25 μL of ethyl acetate, and 1 μL was injected into a gas chromatograph equipped with flame-ionization detectors[2]. This instrument contained glass columns (122 × 0.2 cm) packed with 3% OV-101 on 80/100-mesh chromosorb W(HP)[3]. Helium was used as a carrier gas at a flow rate of 30 mL/min. The analysis was run isothermally at a column temperature of 220°C with injector and detector temperatures of 250°C. The flow rates of hydrogen and air were 30 and 300 mL/min, respectively.

[1] Aldrich Chemical Company, Inc., Milwaukee, Wis.
[2] Model 5730A; Hewlett Packard.
[3] Alltech Associates, Arlington Heights, Ill.

0022-3549/84/1200-1791$01.00/0
© 1984, American Pharmaceutical Association

(16) R. D. Mavis, J. N. Finkelstein, and B. P. Hall, *J. Lipid Res.*, **19**, 467 (1978).
(17) J. Folch, M. Lees, and G. H. C. Stanley, *J. Biol. Chem.*, **226**, 497 (1957).
(18) E. G. Bligh and W. J. Dyer, *Can. J. Biochem. Physiol.*, **37**, 911 (1959).
(19) J. H. Bragdon, *J. Biol. Chem.*, **190**, 513 (1951).
(20) C. P. Stewart and E. B. Henday, *Biochem. J.*, **29**, 1683 (1935).
(21) A. Adam, J. van Cantfort, and J. Gielen, *Lipids*, **11**, 610 (1976).
(22) F. T. Hatch and R. S. Lees, *Adv. Lipid Res.*, **6**, 33 (1968).
(23) R. J. Havel, H. A. Eder, and J. H. Bragdon, *J. Clin. Invest.*, **34**, 1395 (1955).
(24) O. H. Lowry, N. J. Rosebrough, A. L. Farr, and R. J. Randall, *J. Biol. Chem.*, **193**, 265 (1951).
(25) I. H. Hall, J. M. Chapman, Jr., P. J. Voorstad, and G. H. Cocolas, *J. Pharm. Sci.*, **73**, 956 (1984).

ACKNOWLEDGMENTS

This research was financially supported by National Heart, Lung and Blood Institute Grant 2R01 HL25680. The authors thank Michele Tousignant and MacDonald Bowden for their technical assistance.

Estimation of Tris(2-butoxyethyl) Phosphate in Biological Fluids: Novel Intersubject Variability in Recovery from Human Serum

GAIL D. ANDERSON, ALFRED T. ELVIN, and DAVID LALKA ˣ

Received July 25, 1983, from the *Department of Pharmaceutics, School of Pharmacy, State University of New York at Buffalo, Amherst, NY 14260* and the *Clinical Pharmacokinetics Laboratory, Buffalo General Hospital, Buffalo, NY 14203.* Accepted for publication April 13, 1984.

Abstract □ Tris(2-butoxyethyl) phosphate (I), a plasticizer commonly found in evacuated blood collection tubes, displaces many basic drugs from their binding sites on serum proteins and causes them to redistribute from serum into red blood cells (*i.e.*, artificially lowering serum or plasma drug concentration). Thus, the ability to quantitate I in serum or plasma may be helpful in establishing the suitability of various lots of evacuated blood collection tubes for use in drug level monitoring and pharmacokinetic studies. In the process of establishing a minor modification of an assay which has been reported, remarkable and reproducible interindividual variability ($n = 10$) in the slope of standard curves was observed (range, 0.0143–0.0486). This variability appeared to be caused by differences in the recovery of I from the serum of these individuals. The source of this difference seemed to be related to serum lipoprotein concentration since the slope of standard curves was highly correlated with serum triglyceride concentration ($r = -0.800$) as well as with the sum of serum triglyceride and cholesterol concentrations ($r = -0.881$). These observations suggest that the examination of interindividual differences in the recovery of drugs and related compounds from serum should be a routine part of assay development.

Keyphrases □ Tris(2-butoxyethyl) phosphate—recovery variability, human serum, correlation to lipoprotein, triglyceride and cholesterol levels

Tris(2-butoxyethyl) phosphate (I), a plasticizer found in the rubber stoppers of many evacuated blood collection tubes and in some catheter materials, has been shown to significantly displace basic drugs such as propranolol (1), quinidine (2), lidocaine (3), imipramine (4), and alprenolol (4) from their binding sites on α_1-acid glycoprotein (the principal base binding protein in human serum). Spuriously low (typically 25%) plasma or serum concentrations accompany this displacement due to increased partitioning of the drugs into red blood cells (1, 3). Artifacts related to this phenomenon may pervade much of the published data describing the pharmacokinetics of this type of compound. Furthermore, this artifact may adversely affect therapeutic drug monitoring. Specifically, it is likely that different lots of evacuated blood collection tubes cause varying amounts of "displacing activity" (3) and that different lots of tubes may be used to collect blood during a hospital admission. Thus, the capacity to approximate the concentration of I in plasma or serum samples is important.

A second reason to examine the analysis of I in biological fluids was that preliminary studies in this laboratory suggested remarkable intersubject variability in the slopes of standard curves for I in human serum. It is well known that the recovery of some compounds is dependent upon the biological fluid (urine, blood, serum, *etc.*) being extracted. For example the lidocaine metabolites, monoethyl-glycinexylidide and glycinexylidide, have a significantly lower recovery from serum than from urine (5). The present text describes the evidence for large (approximately threefold) interindividual differences in the recovery of I from serum, provides preliminary observations regarding the plasma constituents which exhibit covariance with these interindividual differences, and presents a description of analytical methods which allow the estimation of I in serum samples.

EXPERIMENTAL SECTION

Tris(2-butoxyethyl) phosphate[1] and dioctyl phthalate[1] were used as received. All solvents were spectral or HPLC grade.

Standard Assay of I in Serum—The concentration of I in serum samples was determined using a minor modification of a previously published procedure (4). The original extraction method was modified by increasing the organic to aqueous phase volume ratio from 2:1 to 10:1. To a 0.50-mL serum sample was added 5 mL of dichloromethane containing 1.0 μg/mL of dioctyl phthalate as an internal standard. The mixture was agitated on a fixed-angle rotary mixer (20 rpm) for 10 min and centrifuged (1000×*g*). The organic phase was transferred to a clean tube and evaporated to dryness. The residue was redissolved in 25 μL of ethyl acetate, and 1 μL was injected into a gas chromatograph equipped with flame-ionization detectors[2]. This instrument contained glass columns (122 × 0.2 cm) packed with 3% OV-101 on 80/100-mesh chromosorb W(HP)[3]. Helium was used as a carrier gas at a flow rate of 30 mL/min. The analysis was run isothermally at a column temperature of 220°C with injector and detector temperatures of 250°C. The flow rates of hydrogen and air were 30 and 300 mL/min, respectively.

[1] Aldrich Chemical Company, Inc., Milwaukee, Wis.
[2] Model 5730A; Hewlett Packard.
[3] Alltech Associates, Arlington Heights, Ill.

0022-3549/84/1200-1791$01.00/0
© 1984, American Pharmaceutical Association

Table I—Serum Biochemistry and Characteristics of the Tris(2-butoxyethyl) Phosphate Standard Curves Observed in Normal Volunteers

Subject	Standard Curve Slope	Standard Curve r	Serum α_1-Acid Glycoprotein Conc., mg/dL	Serum Albumin Conc., g/dL	Serum Triglyceride Conc., mg/dL	High-Density Lipoprotein Cholesterol Conc., mg/dL	Serum Cholesterol Conc., mg/dL	Sum of Serum Triglyceride and Cholesterol Conc., mg/dL
1	0.04855	0.970	57	4.6	32	52	155	187
2	0.03290	0.996	58	4.7	55	93	187	242
3	0.03225	0.997	63	—	30	69	192	222
4	0.02985	0.989	86	4.6	65	49	198	263
5	0.02290	0.991	88	5.0	166	52	212	378
6	0.02280	0.980	74	4.7	181	49	169	350
7	0.02035	0.966	80	5.0	95	48	193	288
8	0.01865	0.972	61	4.7	291	56	139	430
9	0.01655	0.993	71	4.9	193	56	258	451
10	0.01425	0.984	110	4.5	275	50	204	479

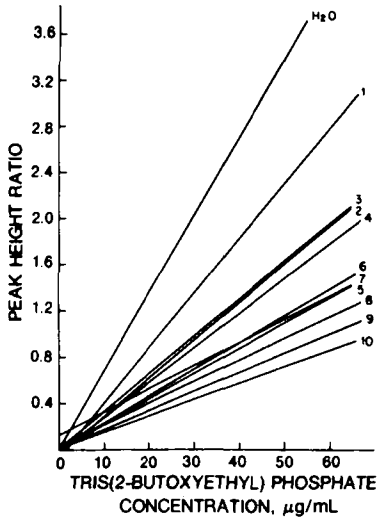

Figure 1—*The intersubject variability of peak height ratio [tris(2-butoxyethyl) phosphate/dioctyl phthalate] as a function of the concentration of tris(2-butoxyethyl) phosphate added to human serum with different normal volunteers. The identification number of each volunteer is given at the end of each standard curve.*

Preparation of Standard Curves for I—Serum samples for use in the preparation of standard curves were drawn into glass syringes. Ten normal adult volunteers (eight males and two females) ranging in age from 23 to 37 years served as study subjects. Each volunteer gave 50 mL of blood to allow the construction of standard curves for I (0, 10, 20, 30, 40, and 50 μg/mL) as well as to perform the battery of biochemical tests intended to identify the basis for the interindividual differences in standard curve slope (see below). Compound I was added to serum samples as a methanol solution[4]. Peak height ratios were plotted *versus* concentrations of I. Linear least-square regression analysis was used to determine the slopes, y-intercepts, and correlation coefficients of the lines of best fit. Repeated standard curves and single-concentration quality-control checks performed on numerous occasions were consistent with the interindividual slope differences observed in this study.

External Standard Experiments—In an effort to determine if the intersubject differences in the standard curves were due to variable recovery of the internal standard (dioctyl phthalate)[1], this compound was added as an external standard and as an internal standard to separate aliquots of serum from subjects 2 and 9 (concentration of I was 30 μg/mL). One set of the samples was extracted and assayed as described above with the exception of the transfer of an exact volume (3.0 mL) of organic phase to a clean tube. The other set of serum samples from the same subjects was extracted with 5 mL of blank dichloromethane (without internal standard) and 3.0 mL of this organic phase was transferred to a clean tube. Five micrograms of dioctyl phthalate in 1.0 mL of dichloromethane was added as an external standard. Blank dichloromethane (1.0 mL) was added to the control samples. All samples were then assayed as described above.

Effect of Alteration of Extraction Conditions—*Overview*—The primary objective of the following experiments was to establish a method which minimized or eliminated the intersubject differences in the extraction of I from serum. Pooled serum samples from individuals known to exhibit high recovery (subjects 1-3) or low recovery (subjects 8-10) of I were used for this series of studies.

Multiple Extraction Experiment—The assay procedure for I was modified to include repeated extractions of 0.5 mL of serum with dichloromethane (5.0 mL × 3). The first organic phase was transferred to a clean test tube leaving the aqueous phase in the original test tube. An additional 5 mL of dichloromethane (without internal standard) was added to the aqueous phase. This sample was then rotary mixed for 10 min, centrifuged, and transferred as described above. This procedure was repeated a third time and the pooled dichloromethane extracts containing I and internal standard were evaporated to dryness and chromatographed as described[5].

Ethyl Acetate Experiment—Serum samples (0.25 mL) were extracted as described above except that 5 mL of ethyl acetate containing 0.5 μg/mL of dioctyl phthalate was used instead of dichloromethane. Evaporation of the organic phase and GC was then performed as described above.

Assay of Serum Triglycerides, Total Cholesterol, High-Density Lipoprotein Cholesterol, Albumin, and α_1-Acid Glycoprotein—Serum concentrations of cholesterol, high-density lipoprotein cholesterol, and triglycerides were determined by previously described methods (7, 8). Serum albumin concentrations were determined using an auto analyzer[6] and the concentration of α_1-acid glycoprotein in serum was determined using a radial immunodiffusion assay[7]. This last procedure was performed in a manner to yield a coefficient of variation of 9.5%.

Statistical Analysis—All data are presented as population mean ± *SD* unless indicated otherwise. The quality of the various standard curves was estimated using linear regression analysis.

RESULTS AND DISCUSSION

Using the standard assay procedure described above, the lower limit of detection for I was 1 μg/mL and standard curves were linear to at least 50 μg/mL (standard curves were performed using single determinations at six concentrations; see above). A linear relationship between peak height ratio and serum concentrations of I was observed in all subjects. The range of correlation coefficients was 0.965-0.999 (mean = 0.984). A greater than threefold intersubject variability in slopes of standard curves was observed with a range of 0.0142-0.0486 (Table I, Fig. 1).

Addition of dioctyl phthalate as an external standard confirmed that the intersubject variability was related to the extraction of I and not the internal standard. The data presented in Table II demonstrate that a threefold range of slopes exists between "high" and "low" extraction sera independent of when the dioctyl phthalate is introduced. The diminished peak height ratio observed

[4] Preliminary studies indicated that initial evaporation of the methanol using either a stream of nitrogen or a 50°C water bath caused a loss >50% of I (*i.e.*, as estimated from reduction in peak height ratio). Later studies comparing samples dried at room temperature (18 h) to those prepared by the addition of I as a methanol solution yielded essentially identical results (*i.e.*, standard curves). The data from this series of studies were all obtained with serum samples containing <5% methanol (v/v).

[5] A number of other alterations in the extraction procedure, including protein precipitation with trichloroacetic acid and dilution of serum with distilled water, were also evaluated as methods to reduce the intersubject variability in the recovery of I. These approaches were all unsuccessful.

[6] Model SMA-2; Technicon Corporation.

[7] M-partigen; Calbiochem-Behring Corp., La Jolla, Calif.

Table II—Influence of Selected Treatments on the Peak Height Ratio of Tris(2-butoxyethyl) Phosphate to Dioctyl Phthalate

	Peak Height Ratio from High-Extraction Serum	Peak Height Ratio from Low-Extraction Serum	Peak Height Ratio from High-Extraction Serum/ Peak Height Ratio from Low-Extraction Serum
		External Standard Experiment[a]	
Internal standard (control)	1.17 ± 0.0600	0.396 ± 0.0295	2.96
External standard	0.614 ± 0.0483	0.225 ± 0.0177	2.73
		Multiple Extraction Experiment[b]	
	0.871 ± 0.152	0.685 ± 0.118	1.27

[a] The serum used in this study was from subject 2 (high extraction) and subject 9 (low extraction). [b] The serum used in these studies were prepared by pooling serum from subjects 1, 2, and 3 (high extraction) and 8, 9, and 10 (low extraction).

Table III—Intersubject Variability in Peak Height Ratio When Ethyl Acetate is Used in Place of Dichloromethane[a]

Subject	Peak Height Ratio
2	1.1232 ± 0.1435
3	1.7668 ± 0.1319
5	1.5404 ± 0.0680
8	1.8942 ± 0.0400
9	1.1761 ± 0.0162
10	1.6229 ± 0.0235

[a] All serum samples contained I at a concentration of 30 μg/mL.

in the external standard component of this study is presumably related, at least in part, to the incomplete recovery of dioctyl phthalate when it is used as an internal standard.

The results of the experiments utilizing repeated extraction to eliminate the intersubject difference in the recovery of I are also presented. Multiple extractions with dichloromethane substantially reduced the intersubject variability in the peak height ratio of I/dioctyl phthalate (Table II). However, this procedure was substantially more laborious than the standard procedure. Replacing dichloromethane with ethyl acetate (Table III) did result in elimination of much of the variability. Though this assay still has limitations, it appears to be the best procedure presently available (*i.e.*, assuming that blank serum which could be used to prepare an individual's own standard curve is unavailable). The use of ethyl acetate as the organic phase for the extraction of I from serum samples eliminates much of the intersubject variability and enables investigators to ensure the absence of I from study samples.

The chemical basis for this variability has not been established. However, highly significant correlations were found between the slope of the individual standard curves and serum concentrations of triglycerides ($r = -0.80$, $p < 0.005$) and triglycerides plus cholesterol ($r = -0.881$, $p < 0.0025$). A much weaker correlation was also found between the standard curve slope and serum concentration of α_1-acid glycoprotein ($r = -0.578$, $p < 0.05$). However, significant covariance existed between α_1-acid glycoprotein concentration and the sum of triglycerides and cholesterol serum concentrations ($r = -0.563$, $p < 0.05$)[8]. There was no significant correlation between the standard curve slope and albumin ($r = -0.292$), total cholesterol ($r = -0.403$), or high-density lipoprotein cholesterol concentrations ($r = -0.289$). Based on the observation that the addition of α_1-acid glycoprotein to serum did not affect the extraction of I[8], it is presumed that the correlation between concentration of this protein and the slope of the individual standard curves is fortuitous (*i.e.*, it was observed because α_1-acid glycoprotein exhibited covariance with triglyceride concentrations, an indicator of the concentration of very low-density lipoproteins). The precise nature of the chemical basis for the intersubject variability in serum extraction of I cannot be established on the basis of the present series of experiments. However, given the lipophilic characteristics of I, it is reasonable to assume that association with or dissolution in lipoproteins plays a major role.

Part of the overall significance of these results lies in the widespread use of pooled serum by research investigators and analytical laboratories. The use of pooled serum in the preparation of standard curves for I could have resulted in a greater than threefold error in estimates of the concentration of I in serum of certain individuals. This variability in serum extraction observed with tris(2-butoxyethyl) phosphate may occur with other highly lipophilic compounds. Indeed, it has been observed recently that bis(2-ethylhexyl) phthalate behaves in a very similar manner (9). Therefore, it is necessary to rule out possible serum-dependent extractability during the early stages of assay development for at least certain classes of compounds.

Based upon the results of the present study, the use of ethyl acetate would appear to be the best approach to minimizing assay error due to intersubject variability in the extraction of I if a relatively simple assay is to be utilized.

[8] When α_1-acid glycoprotein (the gift of Dr. Kenneth Piafsky of the University of Toronto) was added to serum, the recovery of I was not altered.

REFERENCES

(1) R. H. Cotham and D. G. Shand, *Clin. Pharmacol. Ther.*, **18,** 535 (1975).

(2) K. M. Kessler, R. C. Leech, and J. F. Spann, *Clin. Pharmacol. Ther.*, **25,** 204 (1979).

(3) P. J. McNamara, R. L. Slaughter, J. A. Pieper, M. G. Wyman, and D. Lalka, *Anesth. Analg.*, **60,** 395 (1981).

(4) O. Borga, K. M. Piafsky, and O. G. Nilsen, *Clin. Pharmacol. Ther.*, **22,** 539 (1977).

(5) K. K. Adjepon-Yamoah and L. F. Prescott, *J. Pharm. Pharmacol.*, **26,** 889 (1974).

(6) D. J. Edwards, D. Lalka, F. Cerra, and R. L. Slaughter, *Clin. Pharmacol. Ther.*, **31,** 64 (1982).

(7) G. R. Warnick and J. J. Albers, *J. Lipid Res.*, **19,** 65 (1978).

(8) G. E. Mott and M. L. Rogers, *Clin. Chem.*, **24,** 354 (1978).

(9) G. Pollack, "The Contribution of Metabolites to Pharmacologic Effect," Ph.D. Thesis, State University of New York at Buffalo, 1984.

ACKNOWLEDGMENTS

Supported in part by Grant GM-20852 and Training Grant GM-07145 from the National Institute of General Medical Sciences, National Institutes of Health. The authors wish to thank Dr. Arthur Kruski of the University of Texas Health Science Center at San Antonio for the quantitative estimation of serum triglycerides, cholesterol, and high-density lipoprotein cholesterol.

Concentration-Dependent Enhancement of 1-Dodecylazacycloheptan-2-one on the Percutaneous Penetration Kinetics of Triamcinolone Acetonide

D. S-L. CHOW ˣ, I. KAKA, and T. I. WANG

Received October 7, 1983, from the *Department of Pharmaceutics, College of Pharmacy, University of Houston, Houston, TX 77004.* Accepted for publication December 5, 1983.

Abstract □ The enhancing effect of 1-dodecylazacycloheptan-2-one (I) on the penetration kinetics of triamcinolone acetonide (II) and the possible mechanisms of enhancement were studied using nonreinforced and reinforced silicone elastomer membranes and full-thickness hairless mouse skin as penetration barriers. Lactam I, at test concentrations of 0.1–10%, significantly promoted the extent and the rate of penetration of the acetonide II. Regardless of the barrier used the effect was concentration dependent, but the penetration profiles were different. The enhancement with synthetic membranes was attributed solely to the effect of lactam I doubling the diffusion constant (D), which resulted in the increase of the permeability coefficient (K_p) and the shortening of the lag time (τ); the partition coefficient (K_m), however, was not affected. With mouse skin, I exerted effects on both D and K_m. Compound I potentiated the retention of II in skin (a reservoir effect) about sevenfold; however, the enhancing reservoir effect was independent of the concentration of I. Pretreatment with I was found to be more efficient than the coapplication of I and II in the vehicle. The coexistence of I and II was not required for the enhancement, and the reduced enhancing efficiency suggested an interaction between I and II in the vehicle. Penetration impedance was observed after exposure to I with skin, but not with synthetic membranes. Interaction of I with the skin component, or the coexistence of I and II in the skin, could be responsible for such an impedance.

Keyphrases □ Penetration kinetics—triamcinolone acetonide, influence of 1-dodecylazacycloheptan-2-one, concentration dependence □ Mechanisms of enhancement—reservoir effect, diffusion constant, partition coefficient, promotion of skin hydration □ 1-Dodecylazacycloheptan-2-one—influence on penetration kinetics of triamcinolone acetonide, concentration dependence

1-Dodecylazacycloheptan-2-one[1] (I) enhances the biological activity of various topically active agents (antibiotics and antifungals, glucocorticoids, and antipsoriatic agents) using corresponding bioassays, the zonal inhibition of microorganism growth, vasoconstriction, and lesion clearance, respectively (1, 2). The enhancing effect of I was observed with concentrations as low as 1% (1, 2), which is much lower than that required with other enhancers, such as urea, dimethyl sulfoxide, and *N*,*N*-dimethylformamide. In addition, lactam I causes practically no irritation to human skin even at concentrations >50% (2). In the light of these advantages, this substance is a promising new enhancer for topical pharmaceutical formulations.

Therapeutic activity of a topical agent is known to be the result of drug release from the dosage form, penetration of released molecules through skin barrier, and intrinsic activity of the penetrating agent at the target sites (3). The reported enhancement may be due to the I effect on any one or combination of the three components. A few studies have attempted to evaluate the I effect on the individual processes. Using triamcinolone acetonide (1), methanol (4), 8-bromoadenosine 3′,5′-hydrogenphosphate (8-bromo-cAMP; III)[2], 9-β-D-arabinofuranosyladenine (vidarabine, ara-A; IV) (5), arabinofuranosyladenine 5′-valerate (ara-A-5′-valerate; V) (6), 5-fluorouracil, indomethacin, and hydroquinone (2), the enhancing effects of I have been demonstrated to be on the penetration process, with (6) or without the mechanism of drug release. Stoughton (1) reported that percutaneous penetration of triamcinolone acetonide (II) in the presence of 10% I (within 7 and 24 h) was 10- and 5-fold higher than that without I. Greater enhancement was observed with 5-fluorouracil and indomethacin at I concentrations of 1.8–45%, yet only a two- to threefold increase was observed with hydroquinone at 2 and 5% I (2). Stoughton also found that in the case of III, the same level of penetration enhancement induced by 1% I was barely achievable with 50% dimethylformamide[2].

Behl *et al.* (4) demonstrated that the permeability of methanol was promoted 200–400-fold by I (asymptotically with I concentrations) with maximal enhancement at 10–25% I. Vaidyanathan *et al.* (5) showed that I enhanced the delivery of IV with systematic increase in the presence of 0.1–3% I. The permeability of IV with 3% I was 1.4×10^{-7} cm/s, 10-fold greater than the control. The absolute amount that penetrated at 24 h was a 170-fold increase over the control value with 3% I and a 42-fold increase with 0.1%. Vaidyanathan *et al.* (6) also reported that 20% I promoted the total fluxes of IV and V from a suspension with emulsified I or from gel formulation, 20-fold greater than those found using dimethyl sulfoxide as the vehicle. Nevertheless, no complete profile of the penetration due to I has been established. In addition, the mechanisms of such enhanced penetrations have not been elucidated in terms of the modifications of I on the basic parameters of percutaneous penetration kinetics [other than the permeability coefficient (5)]: lag time, diffusion constant, and partition coefficient.

Penetration enhancement appeared to be dependent on the concentration of I. The extent of II penetration increased with increasing I up to 10%; further increase of I (40%) diminished the extent of enhancement (1). The highest level of enhancement on 5-fluorouracil penetration was achieved with 1.8% I among test cencentrations, 1.8, 9, and 45%. With indomethacin as a penetrant, 2% I exerted an effect similar to that of 8%; both were higher than that of 24%. Similarly, 2% I had a greater effect on hydroquinone penetration than 5% I (2). Optimal enhancement was also observed with methanol (4) at 10–25% I. The enhancing effect of I on biological activity, determined either by the vasoconstriction assay or other bioassays, seemed to be concentration dependent as well (1, 2), and the pattern of such a dependence also seemed to vary with test compounds. For instance, erythromycin and clindamycin had increasing antibacterial effect with increasing I, while glucocorticoids and fusidic acid gave the greatest biological effect with the lowest examined concentrations of I (1–3%). Therefore, we attempted to characterize such a dependence and to explore its possible mechanism.

One of the most frequently prescribed topical glucocorti-

[1] Azone; Nelson Research and Development Co., Irvine, Calif.
[2] R. B. Stoughton, unpublished data, personal communication, 1981.

0022-3549/84/1200-1794$01.00/0
© 1984, American Pharmaceutical Association

coids, II (7), was selected for the study. Unlike antifungal and other antimicrobial agents, glucocorticoids exert pharmacological effects only after the agents have penetrated through the skin barrier and reached the target cells in the epidermis and dermis. In regard to therapeutic efficacy, bioavailability of the active ingredient at the site of target cells is of more concern than the concentration of the drug in the dosage form. The importance of the bioavailability of glucocorticoids in various topical drug-delivery systems has received attention from both the pharmaceutical and medical communities during the past decade. However, vehicles in use are still inefficient or only marginally effective in providing satisfactory bioavailability (8, 9). Maibach studied the percutaneous penetration of radioactively labeled hydrocortisone in 18 subjects at a dose of 4 $\mu g/cm^2$ and found that only ~1% of the dose was actually absorbed from the forearm of a normal subject (10). This problem of low bioavailability of glucocorticoids called for an urgent need to develop more efficient systems for delivering this therapeutically useful agent.

This study is intended to evaluate the penetration enhancement of II by I (in terms of the modifications of I on the individual penetration parameters) and to elucidate the possible mechanisms of concentration-dependent effects of I using an *in vitro* penetration study with excised full-thickness hairless mouse skin. In addition, two synthetic, nonreinforced and reinforced, silicone elastomer membranes were evaluated for use as artificial skin models.

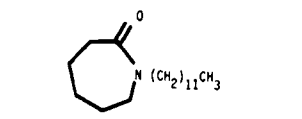

I

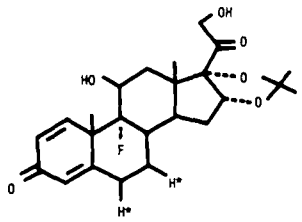

II

EXPERIMENTAL SECTION

Materials—Compound I[3] was used as supplied. Tritiated II[4] in benzene-ethanol (9:1), with a specific activity of 37.0 Ci/mmol, was used as the penetrant. Test solutions of II [3.01×10^{-10} mol/mL in propylene glycol[5] (11)], with or without 0.1, 0.5, 1, 2, 3, 4, 5, 8, and 10% (v/v) I were prepared with methanol[6] as an intermediate solvent (12).

Skin Preparation and Synthetic Membranes—Skin preparations from homozygous Hr/Hr hairless mice (HRS/J strain)[7] (age, 2–4 months) were used. The skin of all animals appeared normal and was free of bites, scratches, or bruises. The mice were sacrificed by ether inhalation, and the skin was dissected. Full-thickness skin was used for the penetration study. Tritiated water[8] served as a standard penetrant to check the intactness of the skin preparation. The thickness of the skin preparation was measured with a micrometer[9]. Membranes of silicone elastomer[10], nonreinforced and reinforced with plain weave fabric of polyethylene terephthalates, were 127.0 and 177.8 μm thick, respectively.

***In Vitro* Penetration Study**—The skin sample or synthetic membrane was mounted between the donor and receptor chambers of the Franz diffusion cell[11] (5 mL) with a 9 mm i.d. O-ring flange. The stratum corneum was exposed to ambient conditions, and the dermal side was oriented toward the saline-phosphate buffer (pH 7.4) (13), simulating the physiological pH of the dermis [pH 7.3–7.4 (14)], in the receptor chamber.

Prior to the application of the test sample, the solution in the receptor chamber was equilibrated by circulating water through a jacket surrounding the chamber at 32°C, which was chosen to reflect the temperature of the stratum corneum (15). The solution in the receptor chamber was stirred with a polytef-coated magnetic bar driven by a magnetic stirrer. A sample (0.2 mL) of II test solution, with or without I, was spread across the exposed stratum corneum surface of the mounted skin. Aliquots of saline-phosphate buffer containing the penetrated II (0.2 mL) were withdrawn from the side-arm of the receptor chamber; this volume was replaced with fresh buffer at 32°C. Samples were taken every 30 min for the initial 2 h and hourly thereafter to 12 h. The amount of II penetrated was measured by liquid scintillation counting of the withdrawn diffusate (0.2 mL in 4 mL of xylene-based cocktail[12]).

The reservoir effect of the skin to retain II was examined after the 12-h penetration study. The exposed skin was blotted dry, dissolved in 1 mL of quaternary ammonium hydroxide tissue solubilizer[13] at 55°C for 2 h, and decolorized with 0.1 mL of 30% hydrogen peroxide[14] for 30 min. The radioactivity in the solubilized skin was monitored by liquid scintillation counting in 10 mL of toluene-based cocktail[15]. The background counts and quenching effects of blank diffusate aliquot and solubilized skin were negligible. No quench correction was employed.

Data Analysis (16, 17)—The penetration parameters of II [lag time (τ), permeability coefficient through the membrane (K_p), diffusion constant within the membrane (D), and partition coefficient between the membrane and the vehicle (K_m)] were calculated from the penetration data. The penetration profiles were constructed by plotting the total amount of II penetrated *versus* time. The x-intercept of the extrapolated linear region of the curve gives τ. D was calculated from τ with known thickness of the penetration barrier (δ), using Eq. 1. The slope of the linear portion of the profile, determined by linear regression analysis, was J_s. K_p was calculated by dividing J_s by the employed concentration of II, C_s (Eq. 2), and K_m was calculated with Eq. 3:

$$\tau = \delta^2/6D \qquad \text{(Eq. 1)}$$

$$J_s = (K_m \cdot D \cdot C_s)/\delta = K_p C_s \qquad \text{(Eq. 2)}$$

$$K_p = (K_m \cdot D)/\delta \qquad \text{(Eq. 3)}$$

The significance of the difference in parameter values among groups with and without I was tested by a nonpaired Student's t test.

RESULTS AND DISCUSSION

Effects of I on Penetration Profiles and Kinetic Parameters of II—The penetration profiles of II, with and without I, through the nonreinforced and reinforced silicone elastomer membrane and full-thickness hairless mouse skin for 12 h, are shown in Figs. 1, 2, and 3, respectively. Regardless of the type of membrane used, both the extent and the rate of II penetration through the membrane were significantly enhanced with I. The penetration profiles through synthetic membranes always consisted of a lag phase followed by the linear rise. This profile was obtained with hairless mouse skin only when the concentration of I was ≤2% (Fig. 3). With I > 2%, the steady-state penetration was somewhat impeded after 8 h of exposure to I, as reflected by the plateau in the profile. The impedance was noticed only with the skin; this cautioned the use of synthetic membranes as artificial skin models for studies of I.

The percentage of II penetration at 12 h through synthetic membranes increased from two- to fourfold the control value with increasing concentrations of I (0.1, 2, and 10%, Table I). A different concentration dependence was observed with hairless mouse skin (Table II). Compound I effectively

[3] Azone, lot 0486K0610; kindly supplied by Nelson Research and Development Co.
[4] Lot 1227-060 and 14611-204; New England Nuclear, Boston, Mass.
[5] Lot A-6M04; MCB, Norwood, Ohio.
[6] OmniSolv, glass distilled; MCB, Gibbstown, N.J.
[7] Jackson Laboratory, Bar Harbor, Me.
[8] Lot 272-980, 2.16×10^6 dpm/mL; New England Nuclear, Boston, Mass.
[9] Hi-precision, Model 221; the Starrett Co., Athol, Mass.
[10] Silastic sheets, Lot H049156 (nonreinforced) and H021446 (reinforced); Dow Corning Co., Midland, Mich.
[11] FDC 108 series with FDC 128 manifold and FDC-127 magnetic bar; Crown Glass Co., Somerville, N.J.
[12] Aquasol-2, 079AT1; New England Nuclear.
[13] Protosol, 092PR1; New England Nuclear.
[14] Analytical Reagent, Lot KJGP; Mallinckrodt Inc., Paris, Ky.
[15] Econofluor, 231EC1; New England Nuclear.

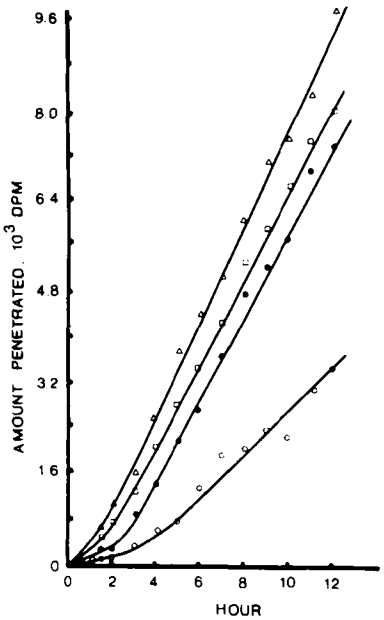

Figure 1—*Penetration profiles of II through nonreinforced silicone elastomer membrane with various concentrations of I. Key: (○) 0%; (●) 0.1%; (□) 2%; (△) 10%.*

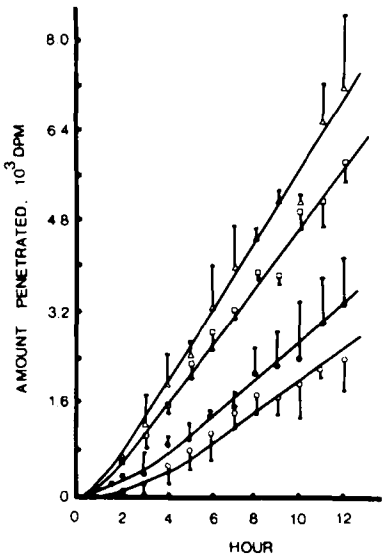

Figure 2—*Penetration profiles of II through reinforced silicone elastomer membrane with various concentrations of I. Key: (○) 0%; (●) 0.1%; (□) 2%; (△) 10%, (n = 3 each).*

elevated the percent of II penetrated through the skin with concentrations >0.5% ($p < 0.02$). Penetration increased 8-, 28-, and 124-fold over that observed without I, at 0.5, 1, and 2-3% I, respectively. However, increased concentrations of I (4-10%) reduced the promotion ($p < 0.005$, except $p < 0.1$ with 5% I) to 76-98-fold the control value (*i.e.*, only 61-79% of the maximum enhancement achieved at 2-3% I). This was a result of late-stage penetration impedance.

The steady-state penetration rate of II (J_s) through nonreinforced silicone elastomer membrane was doubled with as low as 0.1% I, but increases to 2 and 10% did not further promote the penetration rate. Similar results were observed with reinforced membrane, except that the effective concentration was >0.1% (Table I). The J_s value of II through the hairless mouse skin was also concentration dependent (Table II). The rate was 3.38×10^{-18} mol/cm^2/s without I, doubled with 0.1% I, and drastically increased 14-, 46-, and 138-fold with 0.5, 1, and 2-3% I, respectively. Increasing I to 4% reduced the effect to ~66% of the observed maximal enhancement (4.67×10^{-16} mol/cm^2/s) with 2-3% I) or ~90-fold greater than the control penetration rate. Relatively constant penetration rates ($3.05\text{-}3.38 \times 10^{-16}$ mol/cm^2/s) were obtained with I concentrations of 4-10% (Table II).

The effect of I on the gross penetration process can be explained by individual parameters of penetration kinetics as shown in Tables I and II. With synthetic membranes τ values were not appreciably altered with 0.1% I, but were shortened to about one-half with I concentrations of 2 and 10%. K_p values similarly increased with J_s values as a function of I concentrations. Since K_m values were not significantly affected by test concentrations of I, the increase in K_p and reduction in τ were due solely to the I effect of increasing D in synthetic membranes.

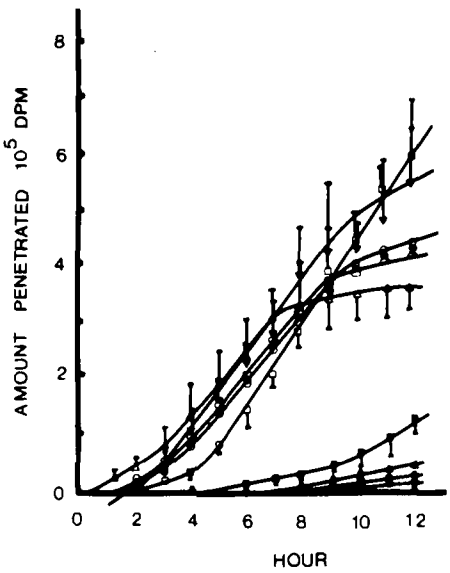

Figure 3—*Penetration profiles of II through full-thickness hairless mouse skin with various concentrations of I. Key: (○) 0%, n = 6; (●) 0.1%, n = 3; (▲) 0.5%, n = 1; (■) 1%, n = 4; (□) 2%, n = 6; (▼) 3%, n = 2; (●) 4%, n = 4; (○) 5%, n = 4; (◯) 8%, n = 8; (△) 10%, n = 7.*

Table I—Percutaneous Penetration Parameters of Triamcinolone Acetonide Through Silicone Elastomer Membranes with Various Concentrations of 1-Dodecylazacycloheptan-2-one (I)

I, %	Percent Penetrated at 12 h	Penetration Rate (J_s), 10^{-18} mol/cm^2/s[a]	Lag Time (τ), h	Permeability Coefficient, (K_p), 10^{-8} cm/s[b]	Diffusion Constant (D), 10^{-9} cm^2/s[c]	Partition Coefficient (K_m), 10^{-2} [d]
			Nonreinforced Membrane			
0	0.04	1.97	2.27	0.73	3.29	2.82
0.1	0.07	4.32	2.04	1.60	3.66	5.55
2.0	0.12	4.42	1.23	1.63	6.07	3.43
10.0	0.14	5.02	1.06	1.86	7.04	3.35
			Reinforced Membrane			
0	0.06	1.41	1.96	0.53	0.75	1.24
0.1	0.15	1.87	1.82	0.69	0.80	1.53
2.0	0.16	3.08	0.98	1.14	1.49	1.36
10.0	0.20	3.72	1.09	1.38	1.34	1.83

[a] J_s = slope/(A × 3600 × specific activity × 10^6 × 2.2 × 10^6), where slope was in the unit of dpm/h, A = 0.636 cm^2, and specific activity of tritiated II was 37 Ci/mmol. [b] $K_p = J_s/C_s$, where $C_s = 3.01 \times 10^{-10}$ mol/mL. [c] $D = \delta^2/6\tau$, where δ was 127 μm (0.005″) as reported by the manufacturer for nonreinforced membrane and δ was 177.8 μm (0.007″) for reinforced membrane. [d] $K_m = K_p\delta/D$.

Table II—Percutaneous Penetration Parameters of Triamcinolone Acetonide Through Full-Thickness Hairless Mouse Skin with Various Concentrations of 1-Dodecylazacycloheptan-2-one (I)

I, %	n	Percent Penetrated at 12 h	Penetration Rate (J_s), 10^{-16} mol/cm^2/s[a]	Lag Time (τ), h	Permeability Coefficient (K_p), 10^{-6} cm/s[b]	Diffusion Constant (D), 10^{-8} cm^2/s[c]	Partition Coefficient (K_m)[d]	Adjusted Diffusion Constant (D'), 10^{-10} cm^2/s[c]	Adjusted Partition Coefficient (K_m')[d]
0	6	0.11 ± 0.05	0.04	>12	0.01	<1.25	0.06-0.46	<0.62	0.81-6.57
0.1	3	0.18 ± 0.04	0.07	>12	0.03	<1.25	0.12-0.46	<0.62	1.65-6.57
0.5	1	0.88	0.46	7.20	0.17	2.09	0.46	1.03	6.57
1.0	4	3.14 ± 1.12	1.56	7.46	0.58	2.02	1.64	0.99	23.43
2.0	6	13.57 ± 1.22	4.65	4.39	1.72	3.43	2.86	1.69	40.71
3.0	2	12.59 ± 3.56	4.67	3.11	1.73	4.84	2.04	2.38	29.08
4.0	4	10.75 ± 0.73	3.07	2.08	1.14	7.23	0.90	3.56	12.81
5.0	4	10.27 ± 4.07	3.14	2.13	1.16	7.06	0.94	3.48	13.33
8.0	8	9.54 ± 1.85	3.38	2.43	1.25	6.18	1.15	3.04	16.45
10.0	7	8.32 ± 0.09	3.05	1.48	1.13	10.20	0.63	5.01	9.03

[a] J_s = slope/(A × 3600 × specific activity × 10^6 × 2.2 × 10^6), where slope was in the unit of dpm/h, A = 0.636 cm^2, and specific activity of tritiated II was 37 Ci/mmol. [b] $K_p = J_s/C_s$, where $C_s = 3.01 \times 10^{-10}$ mol/mL. [c] $D = \delta^2/6\tau$, where δ was measured as 570 μm for full-thickness skin, and D' was similarly calculated with δ estimated as 40 μm for hydrated stratum corneum. [d] $K_m = K_p\delta/D$, and K_m' was similarly calculated with D'.

With hairless mouse skin, τ values were significantly shortened from >12 h to 7.20, 4.39, and 1.48 h by increasing I from 0 to 0.5, 2, and 10%, respectively (Table II). K_p values gradually increased from 1.25×10^{-8} cm/s to a maximum of 1.73×10^{-6} cm/s (a 138-fold increase over the control value) by increasing I to 2-3%. Values then declined with I ≥4%, leveling off at 66% of maximum ($1.13-1.25 \times 10^{-6}$ cm/s, Table II). D and K_m values were calculated first with the measured full-thickness of the skin (570 ± 104 μm, n = 15). However, since the major penetration barrier of the skin is in the stratum corneum (18, 19), the derivations of D and K_m, considering the skin a uniform and invariant cellular matrix, might have overestimated D values, yet underestimated K_m values. A second attempt was therefore made to estimate D' and K_m', using the literature thickness value (20) for fully hydrated stratum corneum (40 μm). The D' value thus obtained with no I ($< 6.2 \times 10^{-11}$ cm^2/s) was similar to the literature values for steroids [ranging from 2×10^{-11} for progesterone to 3×10^{-13} cm^2/s for hydrocortisone (21)]. The K_m' value obtained without I, 0.81-6.57, was comparable to the literature value of 5 for hydrocortisone (19).

Unlike the cases with synthetic membranes, I exerted effects on both D' and K_m' (Table II). D' was significantly promoted with I at as low as 0.5%; the extent of enhancement increased with increased I concentrations. On the other hand, K_m' increased with increasing I up to a maximum of sevenfold greater than the control value with 2% I while further increase in I from 3 to 10% reduced the enhancement from 67 to 21% of the maximum. The reduction in τ was a result of promoting D', whereas the increase in K_p was the net activity of I effects on D' and K_m'. With ≤2% I, both parameters were increased with increasing I; however, with I concentrations of ≥3%, K_m' dwindled from the maximum value, offsetting the I promoting effect on D'. The less favored partitions of II to stratum corneum with 3-10% I in vehicle, as compared with that at 2% I, dominated other effects of I and accounted for the decline in K_p at these high concentrations of I.

***In Vitro* Pretreatment of Hairless Mouse Skin with I**—To determine whether the coexistence of I and II in the vehicle is essential for penetration enhancement and impedance, the excised hairless mouse skin was pretreated *in vitro* with I prior to the penetration of II (instead of coapplication of I and II). Compound I (0.2 mL) in propylene glycol (2% or 10%), was applied on the skin mounted on the diffusion cell for 8 h. After the removal of I, 0.2 mL of II in propylene glycol without I was applied and the penetration profile was monitored. Controls were samples with pretreatments of 0.2 mL of propylene glycol for 8 h, followed by 0.2 mL of II with 0, 2, 4, 5, and 10% I.

The penetration profiles of II with I pretreatment in propylene glycol or with propylene glycol alone were established (Fig. 4), and the penetration parameters were evaluated (Table III). The 8 h contact of skin with propylene glycol, a skin-hydrating solvent, did not appreciably alter, or only marginally increased, the percent penetrated and K_p of II ($p > 0.2$, except for 0% I which had a significant increase, $p < 0.025$). Pretreatment of the skin with 2 or 10% I in propylene glycol, on the other hand, significantly augmented the I enhancements on the extent (percent penetrated), rate (J_s), and K_p of the penetration of II ($0.05 < p < 0.1$). [Compare the paired values C and B (obtained with the skin pretreatment of propylene glycol) or C and A (obtained without any skin pretreatment) in Table III.] The τ values were drastically shortened to 0.7 h after pretreatment with 2 or 10% I, as a result of the substantial promotion of D' within the skin by an 8-h pretreatment. Two percent I was as effective as 10% for pretreatment in increasing D', and significantly more effective than 10% ($p < 0.001$) in enhancing other parameters; both 2 and 10% pretreatments were more effective ($0.05 < p < 0.1$) than the coexistence of II and I of corresponding concentrations in the vehicle (Table III). This observation suggested that the penetration enhancement did not require the coexistence of I and II in the vehicle. Actually, penetration was more efficiently promoted with pretreatment of I than with coapplication of I and II, suggesting a possible interaction between I and II in the vehicle (unfavorable for the penetration process at the I concentrations tested). K_m values were low and of the magnitude obtained with coexisting 0.5% I; therefore, the great extent of penetration enhancement with pretreatment was mainly due to the D' promotion by I.

In addition, the previously reported penetration impedance of II with ≥3% I, still occurred with pretreatment of 10% I, and a similar onset of the impedance (~8 h) was observed (Fig. 4). With the pretreatment of 2% I, no plateau of the penetration profile (similar to that with coexisting 2% I) was evident after 12 h of penetration (Fig. 4). These observations suggested that 8-h skin exposure to I alone was unable to induce the penetration impedance; otherwise the impedance should have been observed from the initiation of the penetration study after pretreatment. Pretreatment of I, without the coexistence of I and II in the vehicle, could still bring about the impedance, again at 8 h after penetration began. The observations that coexistence in the vehicle (and consequently the simultaneous penetration of I and II) was not essential, yet I alone could not cause the impedance, suggested that the coexistence of II and a sufficient amount of I in the reservoir site (probably the stratum corneum of the skin) might be responsible for the observed penetration impedance by an as yet undefined mechanism.

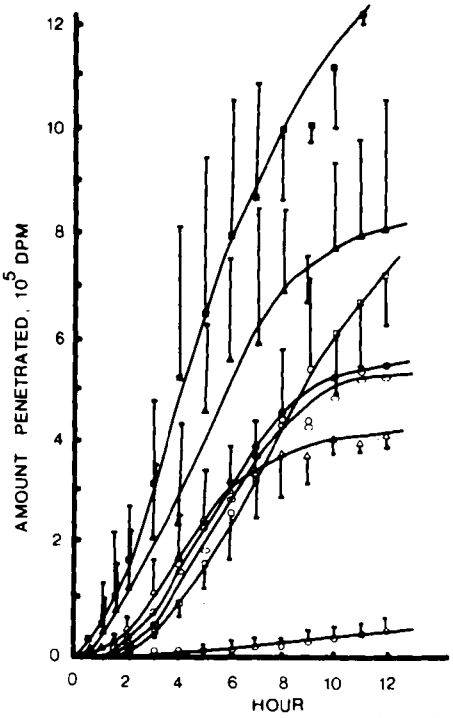

Figure 4—*Penetration profiles of II through full-thickness hairless mouse skin pretreated with I or propylene glycol for 8 h. Key: open symbols, pretreated with propylene glycol; (○) 0% I, n = 2; (□) 2% I, n = 2; (◯) 4% I, n = 1; (○) 5% I, n = 1; (△) 10% I, n = 2. Solid symbols, pretreated with I: (■) 2%, n = 3; (▲) 10%, n = 10.*

Table III—Effect of Pretreatments on Percutaneous Penetration Parameters of Triamcinolone Acetonide Through Full-Thickness Hairless Mouse Skin

1-Dodecyl-azacyclo-heptan-2-one, %	Pre-treatment[a]	n	Percent Penetrated at 12 h	Penetration Rate (J_s), 10^{-16} mol/cm^2/s[b]	Lag Time (τ), h	Permability Coefficient (K_p), 10^{-6} cm/s[c]	Diffusion Constant (D), 10^{-8} cm^2/s[d]	Partition Coefficient (K_m)[e]	Adjusted Diffusion Constant (D'), 10^{-10} cm^2/s[d]	Adjusted Partition Coefficient (K_m')[e]
0	A	6	0.11 ± 0.05	0.04	>12	0.01	<1.25	0.06-0.46	<0.62	0.81-6.57
	B	2	1.06 ± 0.73	0.33	>7.20	0.12	<2.09	~0.33	<1.03	~4.74
2	A	6	13.57 ± 1.22	4.65	4.39	1.72	3.43	2.86	1.69	40.71
	B	2	16.50 ± 2.16	5.21	2.97	1.93	5.10	2.17	2.49	30.95
	C	3	30.28 ± 4.97	8.61	0.69	3.19	21.80	0.83	10.74	11.89
4	A	4	10.75 ± 0.73	3.07	2.08	1.14	7.23	0.90	3.56	12.81
	B	1	12.13	5.24	2.28	1.94	6.60	1.68	3.25	23.89
5	A	4	10.27 ± 4.07	3.14	2.13	1.16	7.06	0.94	3.48	13.33
	B	1	12.57	4.53	1.80	1.68	8.40	1.15	4.12	16.33
10	A	7	8.32 ± 0.90	3.05	1.48	1.13	10.20	0.63	5.01	9.03
	B	2	9.53 ± 0.90	3.94	1.27	1.46	11.84	0.70	5.83	10.01
	C	10	18.51 ± 4.37	5.78	0.77	2.14	19.54	0.62	9.62	8.90

[a] Key: (A) II with I as penetrant, without any pretreatment. Data were abstracted from Table II; (B) skin pretreated with propylene glycol for 8 h and II with I as penetrant; (C) skin pretreated with I for 8 h and II alone as the penetrant. [b] J_s = slope/(A × 3600 × specific activity × 10^6 × 2.2 × 10^6), where slope was in the unit of dpm/h, A = 0.636 cm^2, and specific activity of tritiated II was 37 Ci/mmol. [c] $K_p = J_s/C_s$, where C_s = 3.01 × 10^{-10} mol/mL. [d] $D = \delta^2/6\tau$, where δ was measured as 570 μm for full-thickness skin, and D' was similarly calculated with δ estimated as 40 μm for hydrated stratum, corneum. [e] $K_m = K_p\delta/D$, and K_m' was similarly calculated with D'.

Table IV—Influence of 1-Dodecylazacycloheptan-2-one on Reservoir Effect of Hairless Mouse Skin in Retaining Triamcinolone Acetonide

I, %	n	Recovery at 12 h, % Skin	Diffusate	Total
0	4	1.4 ± 0.5	0.1 ± 0.1	1.5 ± 0.5
1	3	9.8 ± 4.2	3.1 ± 1.1	12.9 ± 4.3
2	4	8.9 ± 3.1	13.6 ± 1.2	22.5 ± 3.3
5	3	10.6 ± 3.3	10.3 ± 4.1	20.9 ± 5.3
8	2	10.6 ± 5.6	9.5 ± 1.9	20.1 ± 5.9
10	2	8.4 ± 4.2	8.3 ± 0.9	16.7 ± 4.3
Mean		9.7		
SD		3.5		
0[a]	1	3.3	1.1 ± 0.7	4.4 ± 0.7
2[a]	2	33.1 ± 2.2	30.3 ± 5.0	63.4 ± 5.5
10[a]	2	19.5 ± 3.6	18.5 ± 4.4	38.0 ± 5.7

[a] Pretreatment for 8 h.

Reservoir Effect—The so-called "reservoir effect" has been reported qualitatively or semiquantitatively for various topically applied glucocorticoids (19). The stratum corneum retains the penetrated drug molecules and makes the agents available for additional absorption even when the drug administration is ceased. To examine the I effect on the reservoir effect of II in hairless mouse skin, the II retentions in skin after 12-h penetration (with various concentrations of I) were evaluated. The presence of I in the vehicle significantly promoted the retention of II in full-thickness skin ($0.05 < p < 0.1$); the mean was 9.7 ± 3.5%, as compared with that without I, 1.4 ± 0.5% (Table IV). However, the enhancing effect was independent of the concentration of I. With the concentrations of I studied (1-10%), the II retained in the skin ranged from 8.4 ± 4.2% to 10.6 ± 5.6% (Table IV); variations were insignificant ($p > 0.7$).

The pretreatment of the skin with 2 or 10% I for 8 h further increased the I enhancing effect on II reservoir in the skin, from 8.9 ± 3.1% to 33.1 ± 2.2% for 2% I ($p < 0.001$) and from 8.4 ± 4.2% to 19.5 ± 3.6% ($0.1 < p < 0.2$) for 10% I (Table IV).

The promotion of skin hydration has been reported as a major mechanism of penetration enhancement induced by 8 M urea and dimethyl sulfoxide, as evidenced by the respective 280 and 150% weight gain of the epidermis (22). The possible I-induced hydration of stratum corneum was accordingly explored. The weights of skin samples, with an area of 0.636 cm^2, in contact with various concentrations of I for 12 h were measured (mean, 108.3 ± 17.7 μg; range, 84.9–146.5 μg; n = 12) and were not significantly different ($p > 0.6$) from the samples without I (mean, 103.5 ± 16.8 μg; range, 84.3 − 124.8 μg; n = 4).

Another possible mechanism of leaching out normally impermeable components of stratum corneum (lipoprotein or phospholipid) and leaving a permeable channel for easier penetration, reported by Allenby *et al.* (22) for urea and dimethyl sulfoxide, was not explored for I.

CONCLUSIONS

The penetration profiles of II with I through synthetic membranes were different from those through hairless mouse skin. This observation cautioned the use of synthetic membranes as skin models in the study of I.

Compound I significantly enhanced the extent of II penetration through hairless mouse skin, from 7-fold with 0.5% I, to 124-fold with 2-3% I, and then leveled off at 76-98-fold with 4-10% I. A similar pattern was obtained for the I enhancement on the penetration rate of II; a 2-fold increase with 0.1%, increasing to 138-fold with 2-3% and leveling off at 90-fold with 4-10%. The enhancing effect on the penetration of II was dependent on the concentration of I. With I concentrations >2%, penetration impedance was observed after an 8-h skin exposure to I. Optimal concentration of I on the penetration of II was 2% (v/v). Compound I exerted increasing promoting effects on the diffusion constant of II within the stratum corneum with increasing concentrations of I, manifested by the continuous reduction in lag time. On the other hand, I increased the partition coefficient of II between stratum corneum and propylene glycol with an optimal concentration of 2%. Further increment in I >2% diminished the enhancing effect.

Compound I potentiated the retention of II in skin (reservoir effect) about sevenfold; however, such an increase was independent of the concentration of I. The difference between the weights of the skin samples with and without I contact was insignificant, suggesting that the promotion of skin hydration was not a major mechanism in the penetration enhancement induced by I.

The pretreatment of I was found to be more efficient than coapplication of I and II in the vehicle. The pretreatment of skin with 2 or 10% for 8 h further augmented the enhancing effect of I on the extent and the rate of II penetration, and on the reservoir effect, due to the substantial promotion of the diffusion constant; also, pretreatment with 2% I was more effective than with 10% I. The observations indicated that coexistence of I and II was not required for penetration enhancement and that there was a possible interaction between I and II in the vehicle to lessen the enhancing efficiency.

The penetration impedance after 8-h skin exposure to I was observed only with skin, not with synthetic membranes. Interaction of I with the skin component could be responsible for such an impedance. In the pretreatment study, the penetration impedance after 8 h was still observed with 10% I, suggesting that I and II were required to coexist (not in the vehicle but probably in the stratum corneum) to elicit this impedance.

REFERENCES

(1) R. B. Stoughton, *Arch. Dermatol.*, **118**, 474 (1982).

(2) R. B. Stoughton and W. O. McClure, "Azone Enhances Percutaneous Absorption," American Academy of Dermatology, Nelson Research and Development Co. (1983).

(3) M. Katz and B. J. Poulsen, *J. Soc. Cosmetic Chem.*, **23**, 565 (1972).

(4) C. Behl, N. H. Bellantone, and J. Pei, "Abstracts, 130th Annual Meeting," American Pharmaceutical Association, Washington, D.C., April 1983, abstr. 31.

(5) R. Vaidyanathan, G. L. Flynn, and W. I. Higuchi, "Abstracts, 33rd National Meeting of the Academy of Pharmaceutical Sciences," American Pharmaceutical Association, Washington, DC, November 1982, abstr. 97.

(6) R. Vaidyanathan, G. L. Flynn, and W. I. Higuchi, "Abstracts, 33rd National Meeting of the Academy of Pharmaceutical Sciences," American Pharmaceutical Association, Washington, DC, November 1982, abstr. 98.

(7) R. B. Stoughton, in "Recent Advances in Dermatopharmacology,"

P. Frost, E. C. Gomez, and N. Zarias, Eds., Spectrum Publications, Inc., New York, N.Y., 1977, pp. 105–120.
(8) B. Idson, *Pharm. Technol.* **November,** 70 (1981).
(9) K. K. Kraning and G. F. Odland, *J. Invest. Dermatol.*, **73,** 395 (1979).
(10) H. I. Maibach, *Dermatologica*, **152** (Suppl. 1), 11 (1976).
(11) B. J. Poulsen, *Br. J. Dermatol.*, **82** (Suppl. 6), 49 (1970).
(12) J. Brotherton, *Cytobios*, **3,** 225 (1971).
(13) T. J. Franz, *J. Invest. Dermatol.*, **64,** 190 (1975).
(14) G. L. Flynn, H. Durrheim, and W. I. Higuchi, *J. Pharm. Sci.*, **70,** 52 (1981).
(15) N. Barker and J. Hadgraft, *Int. J. Pharm.*, **8,** 193 (1981).
(16) P. H. Dugard, in "Advances in Modern Toxicology, Vol. 4, Dermatotoxicology and Pharmacology," F. N. Marzulli and H. I. Maibach, Eds., Wiley, New York, N.Y., 1976, pp. 525–550.
(17) T. Higuchi, *J. Soc. Cosmetic Chem.*, **11,** 85 (1960).
(18) B. Idson, *J. Pharm. Sci.*, **64,** 901 (1975).
(19) R. J. Scheuplein and I. H. Blank, *Physiol. Rev.*, **51,** 702 (1971).
(20) R. J. Scheuplein, *J. Invest. Dermatol.*, **48,** 79 (1967).
(21) R. J. Scheuplein, I. H. Blank, G. J. Brauner, and D. J. MacFarlane, *J. Invest. Dermatol.*, **52,** 63 (1969).
(22) A. C. Allenby, N. H. Creasey, J. A. G. Edginton, J. A. Fletcher, and C. Schock, *Br. J. Dermatol.*, **81** (Suppl. 4), 47 (1969).

ACKNOWLEDGMENTS

This research was supported by a Research Initiation Grant, University of Houston and Biomedical Research Support Grant, National Institutes of Health. Presented in part at the 130th Annual Meeting of APhA, New Orleans, La., April 1983. The authors acknowledge the supply of Azone given by Nelson Research and Development Co. and the assistance of the University of Houston Word Processing Center in preparing the manuscript.

Pectin–Gelatin Complex Coacervates II: Effect of Microencapsulated Sulfamerazine on Size, Morphology, Recovery, and Extraction of Water-Dispersible Microglobules

JEAN N. McMULLEN *[x], DAVID W. NEWTON [‡], and CHARLES H. BECKER [§]

Received May 11, 1982, from the **Faculty of Pharmacy, University of Montreal, Montreal, Quebec H3C 3J7, Canada*, the [‡]*Department of Pharmaceutics, College of Pharmacy, University of Nebraska Medical Center, Omaha, NE 68105*, and the [§]*College of Pharmacy, University of Florida, Gainesville, FL 32610.* Accepted for publication March 23, 1984.

Abstract □ Spherical medicated microglobules were prepared by complex coacervation of Type A gelatin with pectin, having nominal diameters of 5, 10, and 25 μm and containing 37.3, 44.9, and 45.2% (w/w) sulfamerazine, respectively. They were recovered as water-insoluble powders and were spontaneously revertible to highly disperse systems when reconstituted in water or physiological electrolyte solution. The conditions affecting microglobule formation were studied. For complete formation, the crystals must be dispersed at ≥pH 5. The effect of the sulfamerazine mass added on microglobule morphology, yield, and contents were investigated. As much as 37.3, 44.5, and 69.1% (w/w) sulfamerazine in 5-, 10- and 25-μm microglobules could be formed without loss of spherical shape. The microglobule yield *versus* drug-to-colloid ratio curves were nonlinear below the critical drug-to-colloid ratio for loss of sphericity. Addition of sulfamerazine suppressed coacervation by 10–15% but it had no significant effect on microglobule size. The extraction of medicated microglobules in various media demonstrated the existence of a porous matrix that required hydration to facilitate extraction of the microglobular drug. Fifteen percent of the encapsulated sulfamerazine was extracted from 25-μm microglobules as opposed to 9% from 10-μm microglobules after equilibration for 24 h in replacement electrolyte solution.

Keyphrases □ Microencapsulation—pectin–gelatin coacervates, sulfamerazine □ Coacervates—pectin–gelatin, sulfamerazine, microglobules, recovery, size

Little consideration of the morphological character of complex coacervate-coated particles appears in the pharmaceutical literature until Newton *et al.* (1) produced spherical microglobules of uniform size with centrally located drug. The process of medicated microglobule formation is to be differentiated from microencapsulation; the latter usually yields nonspherical particles. Complex coacervates of gelatin–acacia or gelatin–pectin readily wet and surround suspended particles and emulsified droplets. On cooling and denaturation with formaldehyde, the liquid coacervate droplets congeal, forming microglobules that are recoverable as water-dispersible powders after flocculation in 2-propanol (1, 2).

Certain physicochemical conditions for preparing and recovering nonmedicated microglobules from type A gelatin–pectin complex coacervates were detailed previously (2). The purpose of this investigation was to characterize conditions for sulfamerazine microglobule formation in complex coacervates of pectin and gelatin, yielding microglobules of uniform size with centrally located drug that were recoverable as a dry powder. Medicated microglobules with diameters of <10 μm, spontaneously revertible to a polydisperse system in aqueous fluids, were sought for potential use in parenteral dosage forms.

EXPERIMENTAL SECTION

Materials—Type A gelatin[1] and pectin NF[2] were used in sols containing 1% benzyl alcohol for preservation. Sulfamerazine USP[3], micronized powder (≤5 μm); formaldehyde solution, USP; glycerin, 99.6%; 2-propanol, 99%; replacement electrolyte solution[4]; collagenase B[5]; pancreatin[5]; and pepsin[6] were used as received. Other reagents were of analytical reagent grade.

Preparation and Recovery of Microglobules – The method of preparation and recovery of microglobules employed by McMullen *et al.* (2) was used. Coacervates were prepared at 45°C from 40.0-g batches stirred by a magnetic stirrer at a speed sufficient to produce a vortex without air bubbles. Appropriate weights of 2% (w/w) stock solutions of pectin and gelatin were individually adjusted to the mixing pH (pH 8–10) with 1.0 M NaOH at 45°C to

[1] 275 Bloom, isoelectric point 8.6; Fisher Scientific Co., Fair Lawn, N.J.
[2] Sunkist Growers Inc., Ontario, Calif.
[3] Matheson, Coleman & Bell, Norwood, Ohio.
[4] Normosol-R pH 7.4; Abbott Laboratories, North Chicago, Ill.
[5] Calbiochem, San Diego, Calif.
[6] Wilson Labs, Chicago, Ill.

0022-3549/84/1200-1799$01.00/0
© 1984, American Pharmaceutical Association

P. Frost, E. C. Gomez, and N. Zarias, Eds., Spectrum Publications, Inc., New York, N.Y., 1977, pp. 105–120.
(8) B. Idson, *Pharm. Technol.* **November,** 70 (1981).
(9) K. K. Kraning and G. F. Odland, *J. Invest. Dermatol.*, **73,** 395 (1979).
(10) H. I. Maibach, *Dermatologica*, **152** (Suppl. 1), 11 (1976).
(11) B. J. Poulsen, *Br. J. Dermatol.*, **82** (Suppl. 6), 49 (1970).
(12) J. Brotherton, *Cytobios*, **3,** 225 (1971).
(13) T. J. Franz, *J. Invest. Dermatol.*, **64,** 190 (1975).
(14) G. L. Flynn, H. Durrheim, and W. I. Higuchi, *J. Pharm. Sci.*, **70,** 52 (1981).
(15) N. Barker and J. Hadgraft, *Int. J. Pharm.*, **8,** 193 (1981).
(16) P. H. Dugard, in "Advances in Modern Toxicology, Vol. 4, Dermatotoxicology and Pharmacology," F. N. Marzulli and H. I. Maibach, Eds., Wiley, New York, N.Y., 1976, pp. 525–550.
(17) T. Higuchi, *J. Soc. Cosmetic Chem.*, **11,** 85 (1960).
(18) B. Idson, *J. Pharm. Sci.*, **64,** 901 (1975).
(19) R. J. Scheuplein and I. H. Blank, *Physiol. Rev.*, **51,** 702 (1971).
(20) R. J. Scheuplein, *J. Invest. Dermatol.*, **48,** 79 (1967).
(21) R. J. Scheuplein, I. H. Blank, G. J. Brauner, and D. J. MacFarlane, *J. Invest. Dermatol.*, **52,** 63 (1969).
(22) A. C. Allenby, N. H. Creasey, J. A. G. Edginton, J. A. Fletcher, and C. Schock, *Br. J. Dermatol.*, **81** (Suppl. 4), 47 (1969).

ACKNOWLEDGMENTS

This research was supported by a Research Initiation Grant, University of Houston and Biomedical Research Support Grant, National Institutes of Health. Presented in part at the 130th Annual Meeting of APhA, New Orleans, La., April 1983. The authors acknowledge the supply of Azone given by Nelson Research and Development Co. and the assistance of the University of Houston Word Processing Center in preparing the manuscript.

Pectin–Gelatin Complex Coacervates II: Effect of Microencapsulated Sulfamerazine on Size, Morphology, Recovery, and Extraction of Water-Dispersible Microglobules

JEAN N. McMULLEN *[x], DAVID W. NEWTON [‡], and CHARLES H. BECKER [§]

Received May 11, 1982, from the **Faculty of Pharmacy, University of Montreal, Montreal, Quebec H3C 3J7, Canada*, the [‡]*Department of Pharmaceutics, College of Pharmacy, University of Nebraska Medical Center, Omaha, NE 68105*, and the [§]*College of Pharmacy, University of Florida, Gainesville, FL 32610.* Accepted for publication March 23, 1984.

Abstract □ Spherical medicated microglobules were prepared by complex coacervation of Type A gelatin with pectin, having nominal diameters of 5, 10, and 25 μm and containing 37.3, 44.9, and 45.2% (w/w) sulfamerazine, respectively. They were recovered as water-insoluble powders and were spontaneously revertible to highly disperse systems when reconstituted in water or physiological electrolyte solution. The conditions affecting microglobule formation were studied. For complete formation, the crystals must be dispersed at ≥pH 5. The effect of the sulfamerazine mass added on microglobule morphology, yield, and contents were investigated. As much as 37.3, 44.5, and 69.1% (w/w) sulfamerazine in 5-, 10- and 25-μm microglobules could be formed without loss of spherical shape. The microglobule yield *versus* drug-to-colloid ratio curves were nonlinear below the critical drug-to-colloid ratio for loss of sphericity. Addition of sulfamerazine suppressed coacervation by 10–15% but it had no significant effect on microglobule size. The extraction of medicated microglobules in various media demonstrated the existence of a porous matrix that required hydration to facilitate extraction of the microglobular drug. Fifteen percent of the encapsulated sulfamerazine was extracted from 25-μm microglobules as opposed to 9% from 10-μm microglobules after equilibration for 24 h in replacement electrolyte solution.

Keyphrases □ Microencapsulation—pectin–gelatin coacervates, sulfamerazine □ Coacervates—pectin–gelatin, sulfamerazine, microglobules, recovery, size

Little consideration of the morphological character of complex coacervate-coated particles appears in the pharmaceutical literature until Newton *et al.* (1) produced spherical microglobules of uniform size with centrally located drug. The process of medicated microglobule formation is to be differentiated from microencapsulation; the latter usually yields nonspherical particles. Complex coacervates of gelatin–acacia or gelatin–pectin readily wet and surround suspended particles and emulsified droplets. On cooling and denaturation with formaldehyde, the liquid coacervate droplets congeal, forming microglobules that are recoverable as water-dispersible powders after flocculation in 2-propanol (1, 2).

Certain physicochemical conditions for preparing and recovering nonmedicated microglobules from type A gelatin–pectin complex coacervates were detailed previously (2). The purpose of this investigation was to characterize conditions for sulfamerazine microglobule formation in complex coacervates of pectin and gelatin, yielding microglobules of uniform size with centrally located drug that were recoverable as a dry powder. Medicated microglobules with diameters of <10 μm, spontaneously revertible to a polydisperse system in aqueous fluids, were sought for potential use in parenteral dosage forms.

EXPERIMENTAL SECTION

Materials—Type A gelatin[1] and pectin NF[2] were used in sols containing 1% benzyl alcohol for preservation. Sulfamerazine USP[3], micronized powder (≤5 μm); formaldehyde solution, USP; glycerin, 99.6%; 2-propanol, 99%; replacement electrolyte solution[4]; collagenase B[5]; pancreatin[5]; and pepsin[6] were used as received. Other reagents were of analytical reagent grade.

Preparation and Recovery of Microglobules – The method of preparation and recovery of microglobules employed by McMullen *et al.* (2) was used. Coacervates were prepared at 45°C from 40.0-g batches stirred by a magnetic stirrer at a speed sufficient to produce a vortex without air bubbles. Appropriate weights of 2% (w/w) stock solutions of pectin and gelatin were individually adjusted to the mixing pH (pH 8–10) with 1.0 M NaOH at 45°C to

[1] 275 Bloom, isoelectric point 8.6; Fisher Scientific Co., Fair Lawn, N.J.
[2] Sunkist Growers Inc., Ontario, Calif.
[3] Matheson, Coleman & Bell, Norwood, Ohio.
[4] Normosol-R pH 7.4; Abbott Laboratories, North Chicago, Ill.
[5] Calbiochem, San Diego, Calif.
[6] Wilson Labs, Chicago, Ill.

0022-3549/84/1200-1799$01.00/0
© 1984, American Pharmaceutical Association

give the desired pectin-to-gelatin ratio. The gelatin solution was added to the pectin solution with stirring and after 2 min the pH was lowered by addition of 0.5 M HCl to pH 5, then to the pH of coacervation (pH_c). After stirring for 30 min, 5 mL of 37% (w/w) HCHO was added and stirred for 30 min under ambient conditions. After 15–20 h, the suspension was centrifuged and the supernatant was decanted. The microglobules were resuspended in 5 mL of glycerin with a vortex mixer and 35 mL of isopropyl alcohol was slowly added as a flocculating agent while mixing. The flocculated microglobules were then filtered, washed with two 100-mL portions of isopropyl alcohol and dried for 15–20 h in an oven at 36°C ± 1°C. Pectin and gelatin sol concentrations of 2.0% were selected on the basis of earlier studies (2), which demonstrated optimum yield at this concentration. The pH of mixing (pH_m)[7], pH of coacervation (pH_c)[8], and colloid ratio were varied to yield microglobules of desired morphology and size (2).

Effect of pH—A sulfamerazine sample (0.8 g) was added to 40.0-g coacervate batches at three pH_m values, at pH 5.0, and at several pH_c values. The system was stirred for 3 min before addition of 0.5 M HCl except when sulfamerazine was added at pH_c, and the recovery procedure was completed as for nonmedicated microglobules (2). Each batch was evaluated for the extent of microencapsulation of the sulfamerazine particles and for microglobule morphology. The sulfamerazine content was determined for selected batches and the particle size was analyzed using a microscopic count technique. To produce a batch of medicated microglobules having a mean diameter of ~5 μm, it was necessary to modify the procedure to eliminate sulfamerazine crystals >2–3 μm. In this case, a sample of sulfamerazine (1.87 g) was added to a 40.0-g batch at the selected pH_m, stirred to disperse the crystals, and centrifuged at 1000 rpm for 3 min. The supernatant was transferred to a 50-mL beaker and the coacervation procedure was resumed.

Effect of Mass of Sulfamerazine—Samples of sulfamerazine (≤3.2 g) were added (at pH_m 10.0) to 40.0-g coacervate batches having a pectin–gelatin colloid ratio of 30:70. Coacervates formed at pH_c of 3.8 and produced microglobules of 25 μm. Samples of sulfamerazine (1.2 g) were added (at pH_m 10.0) to 40.0-g batches having a pectin–gelatin colloid ratio of 33:67. Coacervates formed at pH_c 4.5 and produced microglobules of 10 μm. The recovered batches were evaluated for morphology, total yield, and sulfamerazine content.

Observed Extent of Extraction and Digestion of Microglobules in Aqueous Media—Microglobules (~100 mg) containing 41% (w/w) of sulfamerazine were placed in 20-mL type I glass vials containing 10 mL, respectively, of simulated gastric fluid[9]; 0.1 M HCl, simulated intestinal fluid[9]; 0.1 M NaOH; collagenase B solution, 20 U/mL at pH 7.0 in 0.05 M Tris[10] and 0.005 M calcium chloride (3); replacement electrolyte solution[4]; or distilled water. The vials were sealed with pretreated rubber closures, crimped with aluminum caps and rotated at 25 ± 3 rpm at 37°C in an apparatus similar to that used by Souder and Ellenbogen (4). The suspensions were observed visually and microscopically at 7.5, 15, 30, 60, and 120 min to determine the effect of extraction with the various media on morphology and contents of the microglobules.

Determination of Sulfamerazine Released from Microglobules Extracted with Aqueous Media—Accurately weighed 10-mg samples of microglobules [25-μm average diameter containing 33% (w/w) sulfamerazine] were extracted in 10-mL portions of replacement electrolyte solution and distilled water in 20-mL type I glass vials sealed with pretreated rubber closures and rotated at 25 ± 3 rpm at 37°C. The suspensions were sampled at 0.5, 1.0, 2.0, 4.0, 8.0, and 20.0 h, filtered through a 0.22-μm micropore filter membrane[11], and assayed. Similarly, 10-μm microglobules containing 47% (w/w) sulfamerazine were extracted in replacement electrolyte solution only.

Determination of Sulfamerazine Released from Microglobules Extracted with Aqueous Acetone Solutions—Accurately weighed 50-mg samples of microglobules (25-μm average diameter) containing 41% (w/w) sulfamerazine were extracted for 15 min in 10 mL of aqueous acetone solutions of 0–100% (v/v) acetone in 10% increments. Each sample was filtered through a 0.25-μm membrane[12], 5 mL of filtrate was transferred to a 25-mL volumetric flask, and the solvent was evaporated to dryness. Each sample was brought to volume with 0.1 M NaOH and assayed spectrophotometrically.

Assay of Sulfamerazine Content in Microglobules—Batches of microglobules were washed with acetone, 100 mL/1.0 g of drug originally added, to dissolve any superficial drug. An accurately weighed 100-mg microglobule sample was transferred to a 100-mL volumetric flask and brought to volume with 0.1 M NaOH. A 10-mL aliquot was filtered using a 0.22-μm membrane[11]; 1.0 mL of the filtrate was transferred to a 50-mL volumetric flask and brought to volume with 0.1 M NaOH. The absorbance was read at 255 nm against a blank of 0.1 M NaOH. The concentration (mg/mL) was calculated from a standard (Beer's) curve.

Microglobule Formation of Various Drugs—Samples (0.8 g) of hydrocortisone acetate, chloramphenicol, barium sulfate, aluminum powder, phenobarbital, and cod liver oil were added (at pH_m 10.0) to 40.0-g batches having a pectin–gelatin colloid ratio of 30:70 and coacervates formed (pH_c 3.8). After recovery as a dry powder, each batch was examined microscopically at 1000× for microglobule morphology.

Table I—Effect of pH of Addition on Microencapsulation of Sulfamerazine

Pectin–Gelatin Colloid Ratio	pH_m	pH_c	Appearance[a]		
			pH_m	pH 5	pH_c
50:50	8	3.4	A	A	N
	9	3.4	P	A	N
	10	3.2	E	E	P
40:60	8	3.8	A	A	N
	9	3.8	E	P	N
	10	3.8	E	E	P
33:67	8	3.9	P	A	N
	9.5	4.6	E[b]	E	P
	10	4.5	E[c]	E	P
30:70	8	4.0	P	A	N
	9	3.8	E	E	P
	10	3.8	E[d]	E	P
25:75	8	4.4	P	A	N
	9	4.2	E	E	P
	10	3.8	E	E	P

[a] N is no affinity between drug and microglobules; A is surface adsorption; P is partial microencapsulation; E is complete microencapsulation. [b] Mean is 5.7 μm; SD = 0.93; 37.3% w/w sulfamerazine. [c] Mean is 9.2 μm; SD = 1.01; 44.9% w/w sulfamerazine. [d] Mean is 25.5 μm; SD = 4.3; 45.2% w/w sulfamerazine.

RESULTS AND DISCUSSION

Effect of pH of Addition on Microglobule Formation of Sulfamerazine—The results of studies carried out to determine the stage to add and disperse sulfamerazine are summarized in Table I. When the drug was added at the endpoint pH (pH_c), complete microencapsulation was never obtained for any of the colloid ratio–pH_m combinations studied. This confirms the highly stable nature of pectin–gelatin complex coacervate microglobules reported in a previous paper (2) which precluded their coalescence at temperatures well above the gelation point of gelatin. Adding the drug at the starting pH (pH_m) or at pH 5 resulted in uniform and complete microencapsulation in most cases (except pH_m 8). This information indicates that the drug is not included within microglobules by a surface-active phenomena of wetting and spreading as reported for the gelatin–acacia system (1, 2, 5, 6) but probably by entrapment; the adsorbed colloids on the surface react to form a coacervate layer as the pH is lowered below 5. In the cases where adsorption or partial microencapsulation was noted for the addition of drug at pH_m and pH 5 for batches with a starting pH of 8 and 9, the microglobule size was either equal to or smaller than the crystals to be formed. Consequently the forces of cohesion stabilizing the microglobules to a set size precluded the complete coating of irregularly shaped particles. It was possible to obtain medicated microglobules having mean diameters of 5.7, 9.2, and 25.5 μm as pictured in Fig. 1 containing 37.3, 44.9, and 45.2% (w/w) sulfamerazine, respectively.

Effect of Mass of Sulfamerazine—The effect of mass of sulfamerazine on 10-μm and 25-μm microglobules is plotted in Figs. 2 and 3, respectively, and demonstrated in the photomicrographs (Fig. 4). The spherical nature of the microglobules was maintained at ≤69% (w/w) sulfamerazine content for the 25-μm microglobules and ≤45.5% (w/w) for the 10-μm microglobules. Above these values the spherical shape was lost as a result of the increasing volume of suspended particles being coated by a constant volume of coacervate. It is interesting to note that the curves of yield *versus* drug-to-total colloid ratio became linear with the loss of microglobule sphericity. There was a 10–15% suppression in coacervate yield as shown by the curve for calculated colloid yield[13] *versus* drug-to-colloid ratio (Figs. 2 and 3). This can be attributed to

[7] Century SS-1 pH meter; Beckman Instruments, Fullerton, Calif.
[8] Miniature glass 476031 and Calomel 476017 electrodes; Corning Scientific Products Co., Medfield, Mass.
[9] Simulated TS as per "The United States Pharmacopeia," 19th rev. U.S. Pharmacopeial Convention, Rockville, Md., 1975, p. 765.
[10] THAM; Fisher Scientific Co.
[11] 0.22-μm MF filter; Millipore Corp., Bedford, Mass.
[12] 0.25-μm UG filter; Millipore Corp.
[13] Percent suppression = [Coacervate yield (0% Drug) − Coacervate Yield (x% Drug)/Coacervate Yield (0% Drug)] × 100.

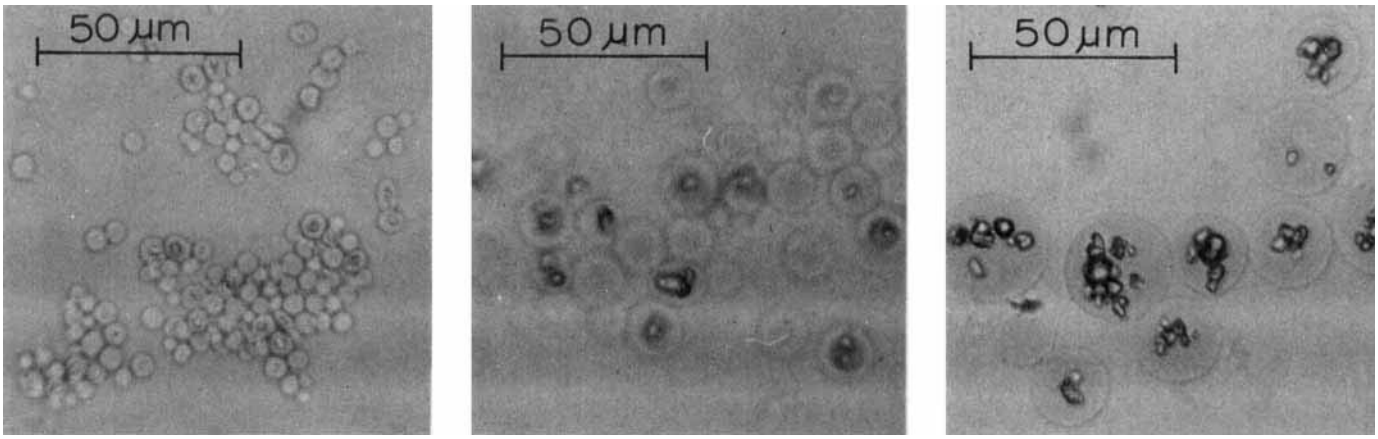

Figure 1—*Pectin–gelatin microglobules having nominal size of 5, 10, and 25 μm containing 37.3, 44.9, and 45.2% (w/w) sulfamerazine.*

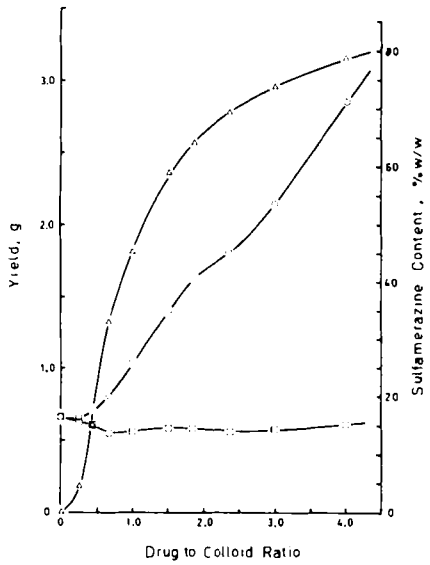

Figure 2—*Effect of mass of sulfamerazine on total dry yield, content, and coacervate yield of 25-μm microglobules. Key: (○) dry yield; (□) coacervate yield (dry yield − sulfamerazine content); (△) sulfamerazine content, % (w/w).*

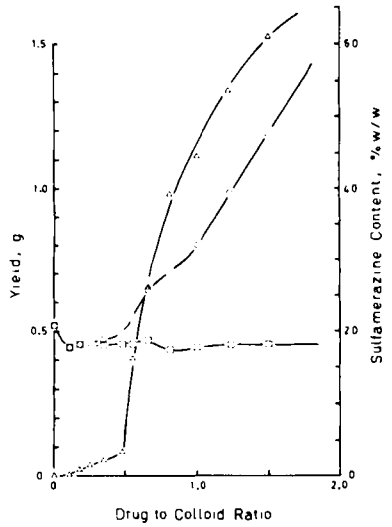

Figure 3—*Effect of mass of sulfamerazine on total dry yield, content, and coacervate yield of 10-μm microglobules. Key: (○) dry yield; (□) coacervate yield (dry yield − sulfamerazine content); (△) sulfamerazine content, % (w/w).*

salt suppression by the slight amount of dissolved sulfamerazine at pH_c, which would insulate ionic groups on pectin and gelatin and decrease their reactivity (7). For both systems the curves of percent sulfamerazine in dry product *versus* drug-to-colloid ratio show a lag phase (more pronounced in Fig. 3) resulting from the initial saturation of the equilibrium liquid with sulfamerazine.

Extraction and Digestion of Microglobules—The results of extraction studies on microglobules containing 41% (w/w) sulfamerazine are summarized in Table II. Extraction with collagenase B seems to digest the gelatin portion (3, 8) of the microglobules as evidenced by their change to near transparency in ~2 h. They completely fragmented after 8 h, having released their sulfamerazine crystals and the fragments and crystals were visible after 24 h of extraction. Complete microglobule digestion was observed with gastric and intestinal fluid test solution only. No apparent morphological change in the appearance of the microglobules was observed during extraction in 0.1 M HCl, 0.1 M NaOH, replacement electrolyte, or distilled water.

The extractions in 0.1 M HCl and 0.1 M NaOH are of particular interest in that these seem to suggest the presence of a highly porous matrix which,

Table II—Effect of Extraction on Morphology and Contents of Microglobules

Extraction Medium[a]	Minimum Time, h		Microscopic Appearance of Suspension[c]
	Digestion	Dissolution	
Collagenase B (20 u/mL)	8.0	NS[b]	f, u
Gastric fluid	8.0	0.25	d, s
Intestinal fluid	0.25	NS	d, u
0.1 M HCl	NS	0.5	i, s
0.1 M NaOH	NS	0.5	i, s
Replacement electrolyte solution (pH 7.4)	NS	NS	i, u
Distilled water	NS	NS	i, u

[a] 37°C. [b] Not sufficient time through 24 h of extraction. [c] i is intact microglobules; f is fragmented microglobules; d is digested microglobules; u is sulfamerazine crystals; s is sulfamerazine in solution.

Table III—Effect of Extraction with Acetone–Water Solutions on Microglobules[a]

Amount, % v/v	Sulfamerazine Solubility, g/10 mL	Sulfamerazine Dissolved, g/10 mL	Sulfamerazine Extracted, %
0	0.0009	0.0010	4.9
10	0.0031	0.0028	13.7
20	0.0078	0.0066	32.2
30	0.0130	0.0115	56.1
40	0.0296	0.0156	76.1
50	0.0564	0.0156	76.1
60	0.0808	0.0157	76.6
70	0.1356	0.0148	72.2
80	0.2148	0.0146	71.2
90	0.2814	0.0115	56.1
100	0.1342	0.0021	10.2

[a] Containing 41.0% (w/w) sulfamerazine (0.0205 g/10 mL).

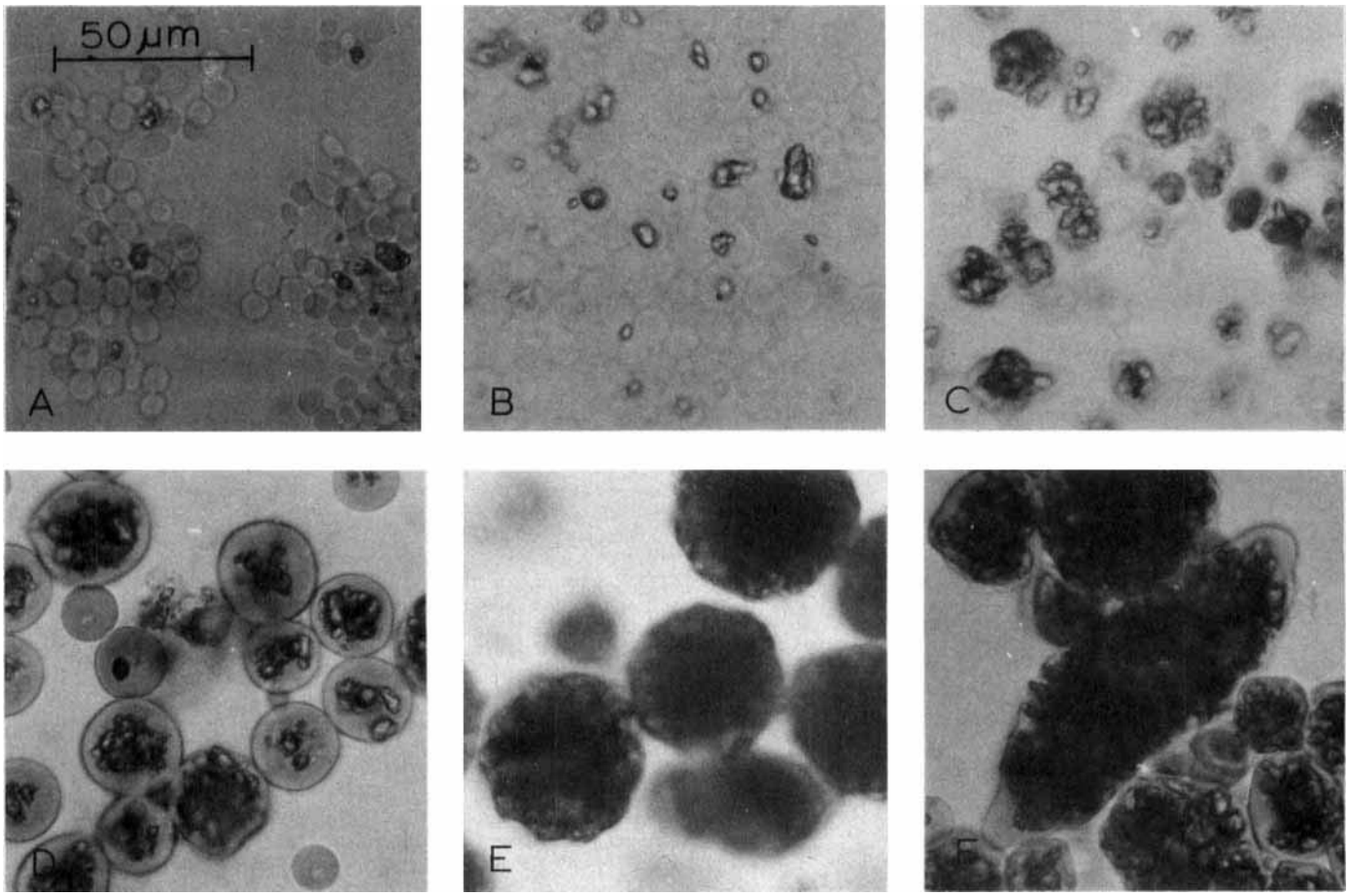

Figure 4—*Effect of mass of sulfamerazine on morphology of 10-μm microglobules containing 16.2% (A), 39.1% (B), and 53.6% (w/w) (C) sulfamerazine; 25-μm microglobules containing 30.5% (D), 58.5% (E), and 73.5% (w/w) (F) sulfamerazine.*

once the microglobules are hydrated, permits the formation and subsequent diffusion out of the microglobules of the soluble hydrochloride or sodium salts of sulfamerazine, respectively. The dependence on hydration for the pore or

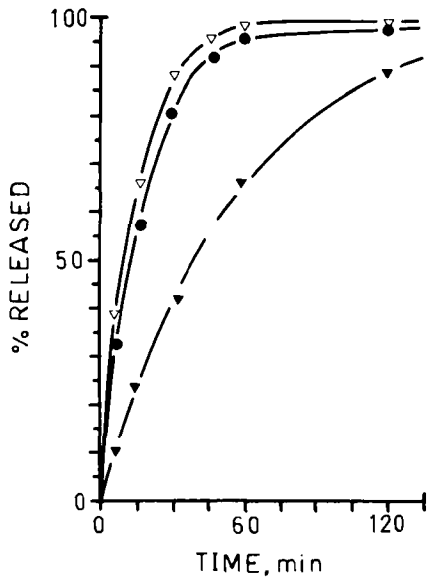

Figure 5—*Effect of extraction with replacement electrolyte solution and distilled water on 10- and 25-μm microglobules. Key: 25-μm microglobules containing 33% (w/w) sulfamerazine extracted in (▼) replacement electrolyte solution and (▽) distilled water; (●) 10-μm microglobules containing 47% (w/w) sulfamerazine extracted in replacement electrolyte solution.*

channel formation was confirmed by extraction of microglobules with aqueous acetone solutions of various concentrations. These results (Table III) indicate that with ≤30% acetone, the amount released is limited by the solubility of sulfamerazine in the binary mixture. For greater concentrations of acetone (≤60%) the microglobules are sufficiently hydrated to allow as much as a 76% release of the drug. At still higher concentrations, the amount of sulfamerazine released decreases although its solubility increases to a maximum at ~90% acetone. The higher acetone concentrations are accompanied by a progressive morphological change from uniform smooth microglobules with a smooth surface to smaller microglobules with a wrinkled surface, an indication of progressive dehydration of the hydrophilic colloids. In pure acetone the extraction of 10.2% of the sulfamerazine from the microglobules is attributed to solubilization of sulfamerazine imbedded superficially in the microglobules (1).

Determination of Sulfamerazine Released from Microglobules Extracted with Aqueous Media—The curves plotted in Fig. 5 demonstrate rapid dissolution of sulfamerazine from the microglobule matrix. The dissolution profile is first order with half-lives of 38.7 min and 9.8 min for 25-μm microglobules in replacement electrolyte and distilled water, respectively, and 12.2 min for 10-μm microglobules in replacement electrolyte. The reduced dissolution rate for microglobules containing sulfamerazine in replacement electrolyte as opposed to distilled water can be attributed to reduced hydration of the microglobule matrix. The higher dissolution rate for sulfamerazine from the 10-μm microglobules in replacement electrolyte results from the higher surface area. These results indicate a very porous matrix which would be more suitable to high molecular weight drugs, drugs microencapsulated as an oil or waxy dispersion, or drugs chemically linked to the polymer matrix.

Microencapsulation of Various Drugs—For successful drug microencapsulation by complex coacervates of pectin and gelatin, the solubility of the drug in the equilibrium liquid and the coacervate must be sufficiently low, it must not have any surfactant activity (9), it must have adequate stability in alkaline and acidic media, and it must have a uniform particle size lower than the desired microglobule size to maintain a spherical shape. Various organic and

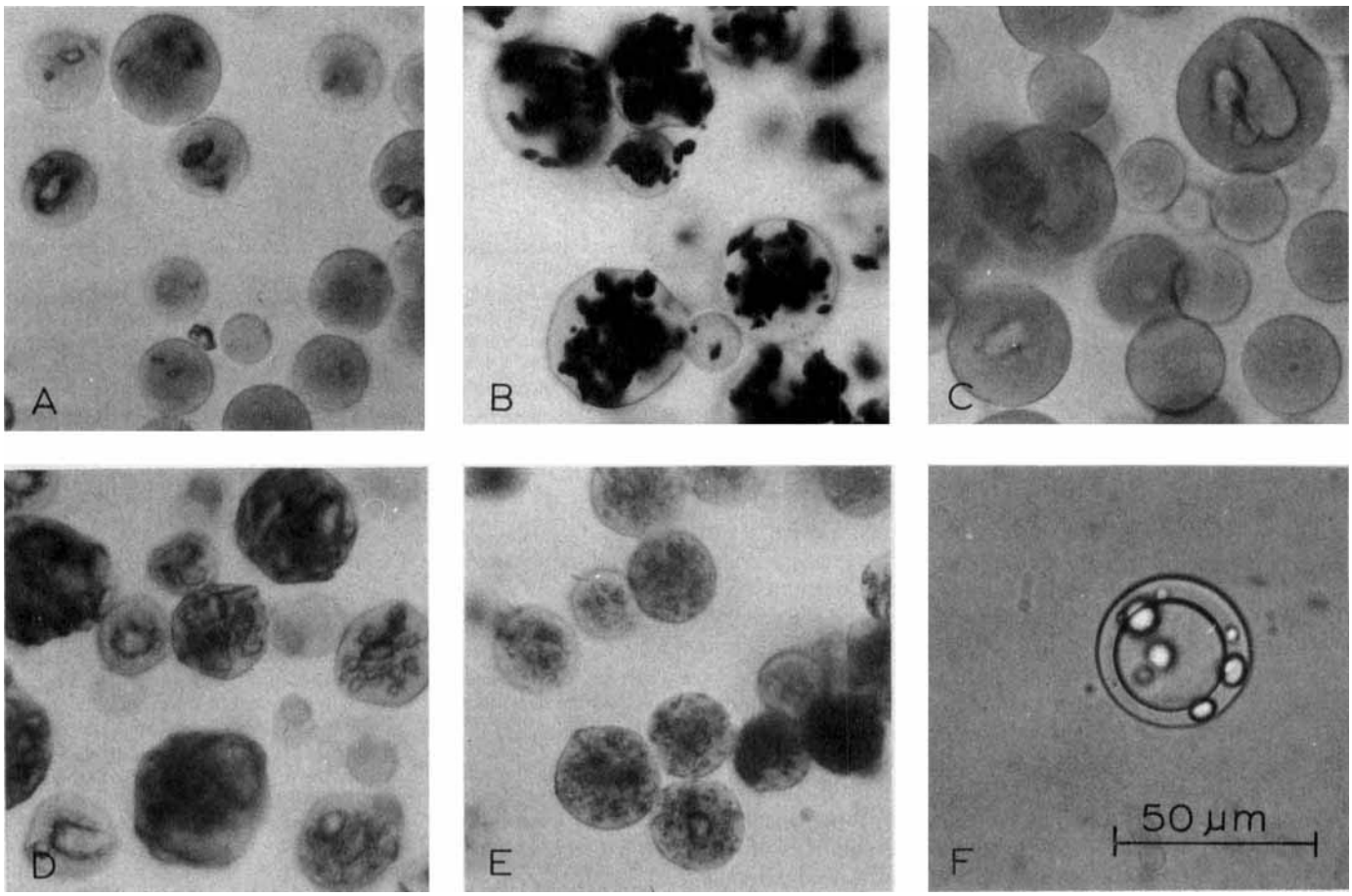

Figure 6—*Pectin-gelatin microglobules containing an undetermined amount of chloramphenicol (A), aluminum powder (B), phenobarbital (C), hydrocortisone acetate (D), barium sulfate (E), and cod liver oil (F).*

inorganic substances complying with these requirements were successfully microencapsulated (Fig. 6).

REFERENCES

(1) D. W. Newton, J. N. McMullen, and C. H. Becker, *J. Pharm. Sci.*, **66**, 1327 (1977).

(2) J. N. McMullen, D. W. Newton, and C. H. Becker, *J. Pharm. Sci.*, **71**, 628 (1982).

(3) "Methods in Enzymology," vol. V, S. P. Colowick and N. O. Kaplan, Eds., Academic Press, New York, N.Y., 1962, pp. 659-665.

(4) J. C. Souder and W. C. Ellenbogen, *Drug Stand.*, **26**, 77 (1958).

(5) "Colloid Science," Vol. II, H. R. Kruyt, Ed., Elsevier, New York, N.Y., 1949, pp. 433-450.

(6) G. N. Paradisis and E. L. Parrott, *J. Clin. Pharmacol.*, **8**, 54 (1968).

(7) "Colloid Science," vol. II, H. R. Kruyt, Ed., Elsevier, New York, N.Y., 1949, pp. 338-384.

(8) "Enzyme Handbook," vol. II, T. E. Barman, Ed., Springer-Verlag, New York, N.Y., 1969, pp. 636, 637.

(9) L. A. Luzzi and R. J. Gerraughty, *J. Pharm. Sci.*, **56**, 634 (1967).

ACKNOWLEDGMENTS

Presented at the Annual Meeting of the Association of Faculties of Pharmacy of Canada, Ottawa, Canada, May 1982. The authors thank Mrs. Ginette Simard for her assistance in preparing this manuscript and Mr. Simon Béchard for his technical assistance.

DC Polarographic Reduction of Chloroguanide Hydrochloride

F. VICENTE-PEDRÓS ˣ, F. TOMÁS-VERT, and J. VERA-SÁNCHEZ *

Received September 24, 1982, from the *Departamento de Química Física, Facultad de Química, Universidad de Valencia, Burjasot-Valencia* and the **Departamento de Química Física, Facultad de Ciencias, Murcia, Spain.* Accepted for publication February 29, 1984.

Abstract □ Chloroguanide hydrochloride, an antimalarial drug, shows one well-defined DC polarographic wave in Britton–Robinson buffered media. In the pH range 3–9 the observed reduction wave is related to the reduction of the two azomethine centers on the monoprotonated biguanide group (BH^+). The effects of pH and other experimental variables on the limiting current and half-wave potentials as well as the reduction mechanism are discussed.

Keyphrases □ Polarography—proguanil hydrochloride, effect of pH □ Proguanil hydrochloride—DC polarographic reduction

The different pharmacological and physical properties of each biguanide derivative depend on the chemical nature of the substituent radicals joined to the biguanide group. Nevertheless, in addition to its chemical properties, the specific applications for biguanides also depend on the solubility and surface-active characteristics (1–4).

The present study concerns results which have been obtained with the antimalarial (5) and antirheumatic (6–10) substance, chloroguanide hydrochloride [1-(*p*-chlorophenyl)-5-isopropylbiguanide hydrochloride] in Britton–Robinson media.

The general difficulties encountered in reducing the biguanide group of other monoprotonated biguanides on the dropping mercury electrode (11, 12) are associated with the great delocalization of its π-electronic system, as is the case of guanidine derivatives (13) since the π electrons are delocalized over the entire area of this monoprotonated or basic group. Under these circumstances, the particular behavior of chloroguanide should be associated with the configuration of its biguanide group. The X-ray studies have demonstrated, for this monohydrochloride in solid form, ~60° angle between the two "guanidine planes" (14), whereas this angle is substantially lower for other biguanides (15, 16). This leads us to speculate that chloroguanide shows a polarographic wave, like chlorhexidine (17–19), that is independent of the guanidine planes. The angle is larger than that in other cationic biguanides that do not show polarographic waves having the characteristics (12, 20) described in this work.

EXPERIMENTAL SECTION

The polarographic waves were obtained with a polarograph[1]. A digital pH meter[2] with a combined glass-reference electrode was utilized which enabled us to attain a pH precision of 0.01 pH unit. Thermostabilization was achieved with a ±0.1° C precision, using a cryostat[3] and a thermostat[4]. In the three-electrode coulometric cell, the working cathode was a mercury pool, the auxiliary electrode was platinum, and the reference electrode was Ag/AgCl, $KCl_{(s)}$.

The chloroguanide hydrochloride was used as supplied[5], mp 238 ± 2° C, and showed one spot on TLC. The UV and IR spectra were obtained with spectrophotometers[6]. Nonaqueous tritration in acetic media (21) was used to confirm the purity. The chemicals used to prepare the buffered solutions were analytical reagent grade; water was distilled and the mercury was double-distilled.

The polarographic measurements were carried out on freshly prepared samples in a total volume of 25 mL. Purified N_2 was passed through all sample solutions (7 min) for deaeration. Other polarographic conditions were: mercury flow, m = 0.88 ± 0.02 mg·s^{-1}; controlled drop time, τ = 0.6 s; depolarizer concentration (chloroguanide hydrochloride), $C = 4 \times 10^{-4}$ M; temperature, T = 298 K; and Britton–Robinson buffer mixture, I = 0.5 M. The diffusion current (i_d) was measured as shown in Fig. 1.

RESULTS AND DISCUSSION

Chloroguanide is electroactive in Britton–Robinson buffered solutions over the pH range studied, 3–9. The polargrams show one reduction wave (Fig. 1).

The drop time effect on the cathodic waves (Table I) is shown by slopes $\Delta E_{1/2}/\Delta \ln \tau = 22 \pm 2$ mV and $\Delta \ln i_l/\Delta \ln \tau = 0.18 \pm 0.02$, two characteristics of the diffusion-controlled processes (22). Also, the effects of both the mercury pressure and chloroguanide concentration on the diffusion current of the wave shows that this current appears to be diffusion controlled at every pH examined. The limiting current intensity remains essentially constant at pH 3.5–6.5 and decreases at pH > 6.5 (Fig. 2). The decreasing current intensity has the form of a dissociation curve with an apparent polarographic pK_s = 8.3 [pK_s = pH, where $i_l = i_d/2$ (23)]. To verify the pK_a value, a spectrophotometric study (24) of this compound was performed: pK_{a1} = 2.3 ± 0.1 and pK_{a2} = 10.4 ± 0.2. The pK_s value is apparently affected by the double layer structure. Due to this change, the overall absorptivities of the protonated and unprotonated forms are different. From the dependence of the half-wave potentials of quasi-diffusion kinetic surface waves on pH (Fig. 2), the K_a values cannot be determined directly, as was possible for quasi-diffusion kinetic volume waves (25).

The number of electrons involved in the electroreduction process at different pH values have been estimated by substituting the values of c, τ, m, and the x conductometric coefficient of diffusion, D° [5×10^{-6} cm^2·s^{-1} (26)] in the Ilkovic equation (22). In moderately acidic media the height of the cathodic

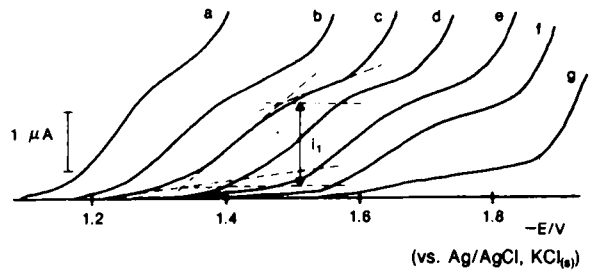

Figure 1—*DC polarograms of chloroguanide in Britton–Robinson buffer at pH 3.01 (a), 3.99 (b), 4.88 (c), 5.75 (d), 6.76 (e), 7.53 (f), and 8.55 (g). Conditions:* $C = 4 \times 10^{-4}$ *M; I = 0.5 M;* T = *298 K; m = 0.88 mg·s*$^{-1}$*;* τ = *0.6 s.*

Table I—Effect of the Drop Time (τ) on the Wave [a]

τ, s	i_l, μA	$-E_{1/2}$, mV
0.4	1.65	1503
0.6	1.75	1489
0.8	1.91	1482
1.0	2.06	1476
1.2	2.10	1470
1.4	2.24	1469
2.0	2.38	1460
3.0	2.54	1449

[a] pH 5.78. Conditions: depolarizer concentration, $C = 4 \cdot 10^{-4}$ M; temperature, T = 298 *K*; mercury flow, m = 0.88 mg·s^{-1}; ionic strength, I = 0.5 M.

[1] Polarecord E-506; Metrohm, S.A.
[2] Radiometer.
[3] Heto 03T623.
[4] Heto 05E623.
[5] Paludrine; I.C.I. Farma S.A.
[6] Model SP-8-11, Pye Unicam was used to obtain UV spectra and a Model 281; Perkin-Elmer was used for IR spectra.

0022-3549/84/1200-1804$01.00/0
© 1984, American Pharmaceutical Association

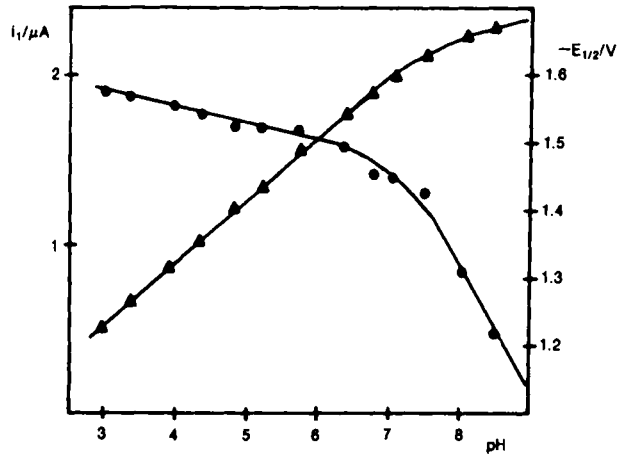

Figure 2—*pH-Dependence of limiting current and half-wave potentials. Key: (●) i_l; (▲) $E_{1/2}$. (Conditions: see Fig. 1).*

wave corresponds to the uptake of 4 electrons. Controlled-potential coulometry with a mercury pool electrode, performed at a controlled-applied potential corresponding to the plateau of the polarographic curve, verified a consumption of 4 electrons per molecule at all values of pH studied.

Plotting $E_{1/2}$ of the wave *versus* pH in the 3-7 range (Fig. 2) gives a straight line of slope, $\Delta E_{1/2}/\Delta pH = 93 \pm 2$ mV. From this slope, the number of H^+ ions (z_{H^+}) in the rate-determining step can be calculated using the following equation (27):

$$z_{H^+} = \frac{\alpha n_a \Delta E_{1/2}}{59 \Delta pH} \qquad \text{(Eq. 1)}$$

By substituting the value of αn_a, obtained from the slope of log $(i/i_l - i)$ *versus* $-E$ plots, the z_{H^+} values are ~1.0 (Table II). The most probable number of electrons (n_a) in the rate-determining step is one electron.

The addition of dimethylformamide to chloroguanide solutions decreases the absolute value of $E_{1/2}$ (Table III). This shows the strong influence exerted by the Helmholtz double layer around the electrode on the cathodic mechanism. The addition of gelatin in amounts $<6 \times 10^{-3}$ % by weight prevents registration of these waves. The electrocapillary curves (τ *versus* E) shows a slight adsorption of the monoprotonated chloroguanide on the dropping mercury electrode (DME) at the wave potentials (18). The wave has a surface character.

The ionic strength decreases the i_l values and causes displacement of the $E_{1/2}$ to more negative values (Table IV), whereas the effect of the decreased buffering capacity (Table V) is lower than that produced by variation of the ionic strength.

On the other hand, the energies of activation, Q, which are calculated by the following equation (28):

$$i_d = Ae^{-Q/RT} \qquad \text{(Eq. 2)}$$

are higher than typical for diffusion-controlled processes. Therefore, the value at pH 5.34 is $Q = 3.8 \pm 0.1$ kcal·mol^{-1} and at pH 7.11, the value is $Q = 4.1 \pm 0.1$ kcal·mol^{-1}. This slight dependence on pH values coincides with an increased irreversibility when pH is increased (Fig. 1). The $E_{1/2}$ values remain nearly constant at pH 7.11, when T is varied from 0°C to 50°C, which should be related to the fact that the first single electron transfer is not exceedingly slow.

As Hollek (29) has indicated, the adsorption of a depolarizer or a reaction product on the DME is a potential cause for deviation of the $\Delta E_{1/2}/\Delta pH$ value from −60 mV/pH unit. Therefore, although the $\Delta E_{1/2}/\Delta pH$ surface waves

Table II—Polarographic Data for Chloroguanide [a]

pH	i_l, μA	$-E_{1/2}$, mV	$n_a\alpha$	Number of H^+ ions, z_{H^+}
3.01	1.85	1224	0.86	1.33
3.99	1.83	1307	0.65	1.01
4.88	1.69	1400	0.60	0.93
5.75	1.70	1493	0.64	0.99
6.73	1.43	1576	0.79	1.22
7.53	1.31	1630	0.72	1.12
8.55	0.45	1665	0.67	1.04

[a] Conditions: $\tau = 0.6$ s; others as described in Table I.

Table III—Effect on Cathodic Waves of Dimethylformamide in Britton-Robinson Buffer Mixtures [a]

Dimethylformamide, % (v/v)	i_l, μA	$-E_{1/2}$, mV	$n_a\alpha$
0.0	2.07	1538	0.78
0.1	2.05	1539	0.80
0.2	2.05	1539	0.81
0.3	2.07	1538	0.75
1.0	2.05	1531	0.69
2.0	1.98	1519	0.68
4.0	1.71	1488	0.88
8.0	1.80	1489	1.15

[a] Conditions: pH = 6.40; $\tau = 0.6$ s; $C = 5.6 \times 10^{-4}$ M; others as described in Table I.

Table IV—Effect of Ionic Strength on $E_{1/2}$ [a]

I,M	i_l, μA	$-E_{1/2}$, mV	$n_a\alpha$
0.5	2.13	1545	0.75
1.4	2.04	1598	0.79
1.9	1.70	1599	0.80
2.3	1.64	1602	0.78

[a] Conditions: pH = 6.45; $\tau = 0.6$ s; $C = 5.6 \times 10^{-4}$ M; others as described in Table I.

Table V—Effect of Buffering Capacity on Waves [a]

[acids], mol·L^{-1}	i_l, μA	$-E_{1/2}$, mV
0.10	2.13	1545
0.07	2.05	1560
0.05	2.00	1568
0.04	1.95	1569

[a] $\tau = 0.6$ s. Total concentrations: [acetic] = [boric] = [phosphoric]. Conditions: I = 0.5 M (with KCl); others as described in Table I.

are smaller than the slope of their plots on semilogarithmic coordinates, the absolute value of $\Delta E_{1/2}/\Delta pH$ for surface waves is larger than the $\Delta E_{1/2}/\Delta pH$ volume for surface waves. Since the rate of the previous surface reaction is sufficiently high in chloroguanide reduction, the i_l value of the kinetic wave is close to the diffusion intensity. Under these conditions, the wave has a well-defined limiting current plateau, and the wave height is determined by the Ilkovic equation. The wave is a quasi-diffusion surface wave.

The biguanide group reduction is made evident by UV spectroscopy, since the chloroguanide absorption $\pi \rightarrow \pi^*$ transition at 232 and 251 nm decreases when chloroguanide is fully reduced, and a single band with one maximum value (~256 nm) is registered. This means a decrease of the electronic delocalization, and a new transition ($n \rightarrow \pi^*$) appears with a maximum absorption value at ~290 nm. This is a typical example of a reduced substance obtained when the two azomethine groups have been transformed into the corresponding amine groups, as Schultz (30) confirmed with the chemical reduction of chloroguanide using a zinc amalgam.

Based on the experimental results, the reduction of the biguanide group is likely to take place as shown in Scheme I:

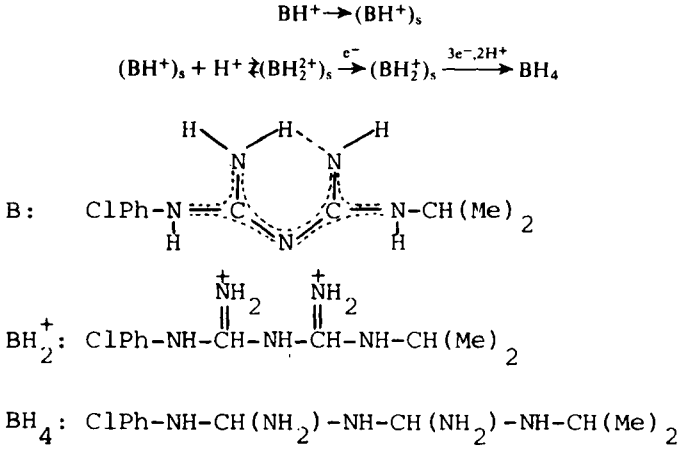

Scheme I

As stated earlier, this reduction seems to take place through an intermediate $(BH_2^+)_s$ which disappears quickly with the complete reduction of the double bonds at the potentials at which the polarographic wave is detected. The *p*-chlorophenyl substituent in chloroguanide seems to be transformed into a state of reduced electron delocalization with respect to the other biguanides. Perhaps as is the case in the solid state (14), the monoprotonated molecule-cation, (BH^+), which exists at physiological pH in solution, is present as a result of a certain independence of the guanidine groups, as occurs with other efficient antimalarial drugs which show the independent imine groups (31).

The polarographic method can be applied for the analytical determination of chloroguanide at pH 3-7 in buffered media. The plots of i_d *versus* C give linear calibrations at 10^{-5}–5×10^{-3} M concentrations. For example, at pH 5.01: $i_d(\mu A) = (4.25 \times 10^3) \cdot C\ (\text{mol} \cdot \text{L}^{-1})(SD = 5 \times 10^{-3})$.

The assay is rapid and has great sensitivity. The lowest sensitivity limit recorded is 0.05–0.1 $\mu g \cdot mL^{-1}$. At $\tau = 0.6$ s the limit of detection is less favorable than in conventional DC polarography because the ratio of charging current to faradic current increases when drop time decreases (32).

Any substance having a half-wave potential within the range of ±100 mV with respect to the $E_{1/2}$ of chloroguanide produces an overlapping of both waves. Also, the presence of gelatin, Triton X-100, or another strongly absorbable substance on the DME produces interferences since the chloroguanide electroreduction is a heterogeneous process.

REFERENCES

(1) F. Kurzer and D. Pitchfort, *Fortschr. Chem. Forsch.*, **10,** 759 (1968).

(2) J. M. Tanzer, A. M. Slee, and B. A. Kamay, *Antimicrob. Agents Chemother.*, **12,** 721 (1977).

(3) V. D. Warner, D. M. Lynch, and R. S. Ajemian, *J. Pharm. Sci.*, **65,** 1070 (1976).

(4) V. D. Warner, D. M. Lynch, K. Kwan Kim, and G. L. Grunewald, *J. Med. Chem.*, **22,** 359 (1977).

(5) F. H. S. Curd and F. L. Rose, *J. Chem. Soc.*, 729 (1946).

(6) M. S. Manku and D. F. Horrobin, *Prostaglandins*, **12,** 789 (1976).

(7) J. P. Famay, J. Fontaine, and J. Reuse, *J. Pharm. Pharmacol.*, **29,** 761 (1977).

(8) D. F. Horrobin and M. S. Maku, *Br. Med. J.*, **1,** 651 (1978).

(9) E. C. Huskisson, *Handb. Exp. Pharmacol.*, **50**(II), 399 (1979).

(10) J. Fontaine, C. O. Quédraogo, J. P. Famay, and J. Reuse, *Arch. Int. Pharmacodyn. Ther.*, **242,** 300 (1979).

(11) W. U. Malik and R. N. Goyal, *Talanta*, **23,** 705 (1976).

(12) F. Vicente, J. Trijueque, F. Tomás, *Quim. Ind. (Biblao)* **29,** 619 (1982).

(13) G. C. Whitnack and S. S. Clair Gautz, *J. Electrochem. Soc.*, **106,** 422 (1952).

(14) C. J. Brown, *J. Chem. Soc., A*, **1,** 60 (1967).

(15) G. Schwarzenbach, R. Gunt, and G. Anderegg, *Helv. Chim. Acta*, **37,** 937 (1954).

(16) R. Ernst and F. W. Cagle, *Acta Crystallogr. B*, **33,** 235 and 237 (1977).

(17) F. Vicente, F. Tomás, and M. A. Nuñez-Flores, IV Reunion de Química (Sanitaria), A.N.Q.E., Vol. II, 57, Madrid (1981).

(18) F. Vicente, Doctoral Thesis, Universidad de Valencia (1981).

(19) F. Vicente, F. Tomás, and J. Vera, Libro de actas de La VI Reunion Latinoamericana de Electroquímica y Corrosion, vol. II, 500, Oaxtopec, México (1983).

(20) F. Vicente, J. Trijueque, and F. Tomás, *J. Pharm. Sci.*, **72,** 565 (1983).

(21) H. E. Stagg, *J. Pharm. Pharmacol.*, **1,** 391 (1949).

(22) S. G. Mairanovskii, "Catalytic and Kinetic Waves in Polarography," Plenum, New York, N.Y. 1968, p. 2.

(23) H. A. Jaffe and M. Orchi, "Theory and Applications of Ultraviolet Spectroscopy," John Wiley, New York, N.Y., 1962, p. 536.

(24) M. Heyrovsky and S. Vavricka, *J. Electroanal. Chem.*, **36,** 203 (1972).

(25) E. Laviron, *Bull. Soc. Chim. Fr.*, 2350 (1961).

(26) J. Trijueque, F. Vicente, and F. Tomás, V Encontro de Química, Communication C. 31.46, S.P.Q., Porto (1982).

(27) J. Heyrovský and J. Kunta, "Principles of Polarography," Academic Press, New York, N.Y., 1966, p. 557.

(28) M. V. Susic, D. A. Markovic, and N. N. Hercigonja, *J. Electroanal. Chem.*, **41,** 122 (1973).

(29) L. Holleck, *Naturwiss.*, **43,** 13 (1956).

(30) R. C. Schultz, *J. Amer. Pharm. Assoc. Sci. Ed.*, **38,** 84 (1949).

(31) A. Burger, "Química Medica," vol. II, Aguilar, Madrid, Spain, 1955, p. 289.

(32) A. J. Bard and L. R. Faulkner, "Electrochemical Methods: Fundamentals and Applications," John Wiley, New York, N.Y., 1982, pp. 147-156.

Design of a Slow-Release Capsule Using Laser Drilling

N. K. JAIN ˣ and S. U. NAIK

Received August 29, 1983, from the *Pharmaceutics Laboratory, Pharmacy Department, Faculty of Technology & Engineering, M. S. University of Baroda, Baroda, India.* Accepted for publication December 13, 1983.

Abstract □ Conventional hard gelatin capsules were made GI-tract resistant by formalin vapor treatment. The residual formalin content was 80 μg/capsule 24 h after treatment, which decreased with increased storage time. An *in vitro* GI-tract resistance test was performed by exposing the capsules to simulated gastric fluid for 4 h and then to simulated intestinal fluid for 4 h at 37°C. The resistance was further confirmed by *in vivo* X-ray studies in human volunteers. Minute pores were drilled on the hardened shells of the capsules with a carbon dioxide gas laser. This permitted the slow passage of the encapsulated tetracycline hydrochloride when subjected to 0.1 M HCl in *in vitro* dissolution studies. *In vitro* drug release from these capsules followed zero-order kinetics after an initial lag period of 30 min. The factors influencing the *in vitro* release rate of tetracycline hydrochloride from these capsules are discussed.

Keyphrases □ Gelatin capsules–drug release, GI-tract resistance, laser-drilled design □ Laser-drilled capsules–drug release, GI-tract resistance, X-ray studies

The potential application of the laser in the fields of communication, industry, military science, chemistry, biology, and medicine has been well established and well documented (1). The possible use of the laser in designing a controlled-release capsule dosage form has been recently reported (2). Theeuwes *et al.* (3) reported the use of automated laser drilling in making exit pores for indomethacin in the design of an elementary osmotic pump.

Conventional hard-gelatin capsules normally disintegrate rapidly and the encapsulated drug exhibits a cube-root dissolution pattern (4). Exposure to formalin vapors causes the cross-linkage of the gelatin molecule, resulting in an unpre-

0022-3549/84/1200-1806$01.00/0

© 1984, American Pharmaceutical Association

As stated earlier, this reduction seems to take place through an intermediate $(BH_2^+)_s$ which disappears quickly with the complete reduction of the double bonds at the potentials at which the polarographic wave is detected. The *p*-chlorophenyl substituent in chloroguanide seems to be transformed into a state of reduced electron delocalization with respect to the other biguanides. Perhaps as is the case in the solid state (14), the monoprotonated molecule-cation, (BH^+), which exists at physiological pH in solution, is present as a result of a certain independence of the guanidine groups, as occurs with other efficient antimalarial drugs which show the independent imine groups (31).

The polarographic method can be applied for the analytical determination of chloroguanide at pH 3-7 in buffered media. The plots of i_d *versus* C give linear calibrations at 10^{-5}–5×10^{-3} M concentrations. For example, at pH 5.01: $i_d(\mu A) = (4.25 \times 10^3) \cdot C\ (\text{mol} \cdot \text{L}^{-1})(SD = 5 \times 10^{-3})$.

The assay is rapid and has great sensitivity. The lowest sensitivity limit recorded is 0.05–0.1 $\mu g \cdot mL^{-1}$. At $\tau = 0.6$ s the limit of detection is less favorable than in conventional DC polarography because the ratio of charging current to faradic current increases when drop time decreases (32).

Any substance having a half-wave potential within the range of ±100 mV with respect to the $E_{1/2}$ of chloroguanide produces an overlapping of both waves. Also, the presence of gelatin, Triton X-100, or another strongly absorbable substance on the DME produces interferences since the chloroguanide electroreduction is a heterogeneous process.

REFERENCES

(1) F. Kurzer and D. Pitchfort, *Fortschr. Chem. Forsch.*, **10,** 759 (1968).

(2) J. M. Tanzer, A. M. Slee, and B. A. Kamay, *Antimicrob. Agents Chemother.*, **12,** 721 (1977).

(3) V. D. Warner, D. M. Lynch, and R. S. Ajemian, *J. Pharm. Sci.*, **65,** 1070 (1976).

(4) V. D. Warner, D. M. Lynch, K. Kwan Kim, and G. L. Grunewald, *J. Med. Chem.*, **22,** 359 (1977).

(5) F. H. S. Curd and F. L. Rose, *J. Chem. Soc.*, 729 (1946).

(6) M. S. Manku and D. F. Horrobin, *Prostaglandins*, **12,** 789 (1976).

(7) J. P. Famay, J. Fontaine, and J. Reuse, *J. Pharm. Pharmacol.*, **29,** 761 (1977).

(8) D. F. Horrobin and M. S. Maku, *Br. Med. J.*, **1,** 651 (1978).

(9) E. C. Huskisson, *Handb. Exp. Pharmacol.*, **50**(II), 399 (1979).

(10) J. Fontaine, C. O. Quédraogo, J. P. Famay, and J. Reuse, *Arch. Int. Pharmacodyn. Ther.*, **242,** 300 (1979).

(11) W. U. Malik and R. N. Goyal, *Talanta*, **23,** 705 (1976).

(12) F. Vicente, J. Trijueque, F. Tomás, *Quim. Ind. (Biblao)* **29,** 619 (1982).

(13) G. C. Whitnack and S. S. Clair Gautz, *J. Electrochem. Soc.*, **106,** 422 (1952).

(14) C. J. Brown, *J. Chem. Soc., A*, **1,** 60 (1967).

(15) G. Schwarzenbach, R. Gunt, and G. Anderegg, *Helv. Chim. Acta*, **37,** 937 (1954).

(16) R. Ernst and F. W. Cagle, *Acta Crystallogr. B*, **33,** 235 and 237 (1977).

(17) F. Vicente, F. Tomás, and M. A. Nuñez-Flores, IV Reunion de Química (Sanitaria), A.N.Q.E., Vol. II, 57, Madrid (1981).

(18) F. Vicente, Doctoral Thesis, Universidad de Valencia (1981).

(19) F. Vicente, F. Tomás, and J. Vera, Libro de actas de La VI Reunion Latinoamericana de Electroquímica y Corrosion, vol. II, 500, Oaxtopec, México (1983).

(20) F. Vicente, J. Trijueque, and F. Tomás, *J. Pharm. Sci.*, **72,** 565 (1983).

(21) H. E. Stagg, *J. Pharm. Pharmacol.*, **1,** 391 (1949).

(22) S. G. Mairanovskii, "Catalytic and Kinetic Waves in Polarography," Plenum, New York, N.Y. 1968, p. 2.

(23) H. A. Jaffe and M. Orchi, "Theory and Applications of Ultraviolet Spectroscopy," John Wiley, New York, N.Y., 1962, p. 536.

(24) M. Heyrovsky and S. Vavricka, *J. Electroanal. Chem.*, **36,** 203 (1972).

(25) E. Laviron, *Bull. Soc. Chim. Fr.*, 2350 (1961).

(26) J. Trijueque, F. Vicente, and F. Tomás, V Encontro de Química, Communication C. 31.46, S.P.Q., Porto (1982).

(27) J. Heyrovský and J. Kunta, "Principles of Polarography," Academic Press, New York, N.Y., 1966, p. 557.

(28) M. V. Susic, D. A. Markovic, and N. N. Hercigonja, *J. Electroanal. Chem.*, **41,** 122 (1973).

(29) L. Holleck, *Naturwiss.*, **43,** 13 (1956).

(30) R. C. Schultz, *J. Amer. Pharm. Assoc. Sci. Ed.*, **38,** 84 (1949).

(31) A. Burger, "Química Medica," vol. II, Aguilar, Madrid, Spain, 1955, p. 289.

(32) A. J. Bard and L. R. Faulkner, "Electrochemical Methods: Fundamentals and Applications," John Wiley, New York, N.Y., 1982, pp. 147-156.

Design of a Slow-Release Capsule Using Laser Drilling

N. K. JAIN ˣ and S. U. NAIK

Received August 29, 1983, from the *Pharmaceutics Laboratory, Pharmacy Department, Faculty of Technology & Engineering, M. S. University of Baroda, Baroda, India.* Accepted for publication December 13, 1983.

Abstract □ Conventional hard gelatin capsules were made GI-tract resistant by formalin vapor treatment. The residual formalin content was 80 μg/capsule 24 h after treatment, which decreased with increased storage time. An *in vitro* GI-tract resistance test was performed by exposing the capsules to simulated gastric fluid for 4 h and then to simulated intestinal fluid for 4 h at 37°C. The resistance was further confirmed by *in vivo* X-ray studies in human volunteers. Minute pores were drilled on the hardened shells of the capsules with a carbon dioxide gas laser. This permitted the slow passage of the encapsulated tetracycline hydrochloride when subjected to 0.1 M HCl in *in vitro* dissolution studies. *In vitro* drug release from these capsules followed zero-order kinetics after an initial lag period of 30 min. The factors influencing the *in vitro* release rate of tetracycline hydrochloride from these capsules are discussed.

Keyphrases □ Gelatin capsules–drug release, GI-tract resistance, laser-drilled design □ Laser-drilled capsules–drug release, GI-tract resistance, X-ray studies

The potential application of the laser in the fields of communication, industry, military science, chemistry, biology, and medicine has been well established and well documented (1). The possible use of the laser in designing a controlled-release capsule dosage form has been recently reported (2). Theeuwes *et al.* (3) reported the use of automated laser drilling in making exit pores for indomethacin in the design of an elementary osmotic pump.

Conventional hard-gelatin capsules normally disintegrate rapidly and the encapsulated drug exhibits a cube-root dissolution pattern (4). Exposure to formalin vapors causes the cross-linkage of the gelatin molecule, resulting in an unpre-

0022-3549/84/1200-1806$01.00/0

© 1984, American Pharmaceutical Association

dictable decrease in solubility of these capsules (5). The objectives of this study were: (*a*) to prepare GI-tract resistant hard-gelatin capsules by formalin vapor treatment and to confirm their resistance by *in vitro* and *in vivo* studies; (*b*) to make minute pores on the hardened shells of the capsules by laser drilling to allow the contents to release slowly through these minute pores; (*c*) to report on the different factors that are likely to influence the *in vitro* drug release rate from these capsules.

EXPERIMENTAL SECTION

Preparation of GI-Tract Resistant Capsules—The conventional hard-gelatin capsules were exposed to formalin vapor under normal temperature and pressure conditions. After the vapor contact time, the capsules were dried in an oven at 50°C. The formalin vapor contact time and drying time were optimized with respect to GI-tract resistance, residual formalin content, drilling requirements, physical characteristics of the capsules, *etc.*, by trial experiments.

Residual Formalin Content—The analytical procedure used to determine the residual formalin content was based on the method of Macfadyan (6). The method involves the spectrocolorimetric measurement (at 490 nm) of the violet color produced when 1.0 mL of the sample, containing ~2–3 μg of formalin with 9.0 mL of 0.2% (w/v) solution of chromotropic acid[1] in 80% (v/v) sulfuric acid, was heated on a boiling-water bath for 30 min.

The sample was prepared by placing one formalin-treated capsule in each of the three clean, dry, 20.0-mL vials containing 10.0 mL of distilled water. After closing with rubber stoppers and sealing with aluminum seals, the vials were agitated on a mechanical agitator for 1.0 h. The saturation solubility of the formalin capsule in 10.0 mL of distilled water was optimized with respect to agitation time by trial experiments. A sample (1.0 mL) was withdrawn from each vial with a syringe, and the residual formalin content was determined. The average content of the three vials was reported as the residual formalin content.

***In Vitro* GI-Tract Resistance Test**—The studies were carried out by the rotating-basket method (7). A flask containing 900.0 mL of simulated gastric fluid as the dissolution medium (8) was immersed in a constant-temperature bath at 37 ± 0.5°C. The empty formalin-treated capsule (with laser drilled pores on the body) was then inserted, and the basket was rotated at 100 rpm for 4 h. At the end of 4.0 h, 900.0 mL of the simulated gastric fluid was replaced by the same quantity of simulated intestinal fluid (8), and the experiment was repeated for 4.0 h.

***In Vivo* X-ray Studies**—Two human male volunteers (age, 27 and 29 years; weight, 65.5 and 71.5 kg.) were selected for the study. The subjects had no history of GI disease and neither used any medication regularly. Both volunteers were asked to abstain from alcoholic beverages for 48 h preceding each experiment and fasted overnight. At 8:30 a.m. one capsule containing 250.0 mg of barium sulfate (band sealed with a suitable GI-tract resistant material) was administered orally with ~25.0 mL of water. Volunteers were allowed to take food 4.0 h after administration of the capsule. X-ray photographs were taken at 0.5, 1.0, 2.0, 4.0, 6.0, and 8.0 h after capsule administration.

Laser Drilling—A CO_2 (CW/pulsed) laser[2] (Fig. 1) was used to drill small pores into the hardened shells of the capsules. This laser can be operated in continuous or pulsed modes. In the pulsed mode, the pulse width of the laser can be varied from 100 μs to 1 s, and the frequency can be varied from 1 to 1000 pulses/s. Pulse width and frequency variations changed the diameter of the drilled pores and the number of drilled pores, respectively. The laser was internally pulsed through an electronically controlled trigger switch. This type of pulsing provides a power output four to five times the average output, depending on the pulse width selected. This laser system had well-insulated high-voltage terminals and an automatic switch to ground the capacitor bank when switching off or tripping off the power supply; the power supply and the coolant flow were interlocked.

In this investigation, laser-drilled capsules were studied with respect to variation in the number of drilled pores, diameter of the drilled pores, and the drilling pattern of the pores. To vary the number of pores, the capsule was mounted on a linear drive (speed, 2 mm/s). By changing the laser frequency and keeping the power and pulse width (220 μs) constant, 25, 50, 75, and 100 pores with an SD_2 size distribution were drilled on the body of the capsule shell.

[1] P.B. No. 6136; Loba-Chemie, Indoaustranal Co., Bombay, India.
[2] 50W CO_2 Laser model JI.S-C-101; designed and developed by Laser Division, Jyoti Ltd., Baroda, India.

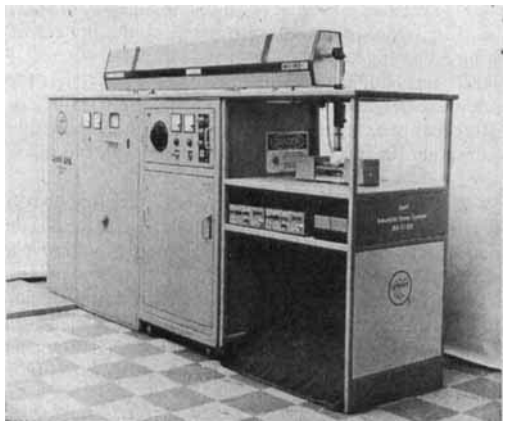

Figure 1—*Carbon dioxide gas laser with a linear drive.*

Table I—Pulse Width Variations with Corresponding Pore Size Distributions and Average Diameters

Pore Size Distribution	Pulse Width, μs	Average Pore Diameter, μm	
		dln[a]	*dg*[b]
SD_1	100	83–88	78.50 ± 1.57
SD_2	220	103.60	100.00 ± 1.41
SD_3	300	160.20	155.00 ± 1.52
SD_4	420	207.80	205.00 ± 1.38

[a] Statistical length-number mean diameter. [b] Geometric mean diameter from the probability plot (±*SD*).

The pores were placed equidistant in three lines with an almost equal number of pores per line.

For the study of diameter variation, 50 drilled pores with size distributions of SD_1, SD_2, SD_3, and SD_4, with an average length-number mean diameter (*dln*) equal to 83.58, 103.60, 160.20, and 207.80 μm, respectively [determined by the optical microscopic method (9)], were obtained by varying the pulse width of the laser and keeping the frequency constant at 1 pulse/s (Table I). The variation in the pore drilling pattern was studied with 50-pore capsules (of SD_2 distribution) on the body only and on both the cap and body. Laser-drilled pores on the hardened shells of the capsules are shown in Fig. 2.

Factors Influencing Release Rate—GI-tract resistant capsules with 50 laser-drilled pores (SD_2 size distribution) on the body, containing tetracycline hydrochloride[3] (as a model drug) and band sealed with GI-tract resistant seals, were used for the study. The average weight of the filled capsules was determined by weighing 10 capsules. Friability testing of the capsules was done on a friabilator[4] (10). The bulk density of the sample was determined by the

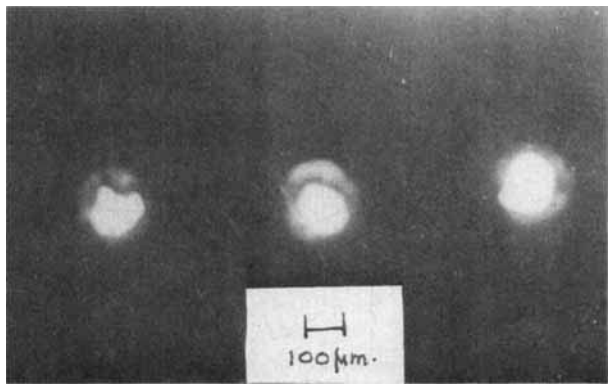

Figure 2—*Different sizes of laser-drilled pores on the hardened capsule shell.*

[3] Synbiotics, Wadi Wadi, Baroda, India.
[4] Roche.

standard three-tap method suggested by Butler and Ransey (11). The particle size and size distribution analyses were made by the optical microscopic method (9), by preparing a suspension of the sample in glycerol.

To study the effect of diluents, capsules containing 250.0 mg of tetracycline hydrochloride were prepared using lactose or microcrystalline cellulose as diluent. Differences in bulk density between the drug and the diluents were taken into consideration when calculating the fill weight of individual capsules.

The effect of powder properties such as particle size and distribution and bulk density were studied by using capsules filled with three powder samples with different characteristics. The original sample of tetracycline hydrochloride (sample I) was screened through a 360-mesh standard sieve; an oversized fraction (sample II), and an undersized fraction, which was pulverized with a pestle and mortar (sample III), were also used for the study. Tetracycline hydrochloride capsules were prepared by filling tetracycline hydrochloride with 2.0% talc or 1.0% magnesium stearate to study the effect of common lubricants.

Saturated solutions of dioctyl sodium sulfosuccinate[5] and polysorbate 80[6] in alcohol were sprayed separately on the tetracycline hydrochloride to give 0.5% (w/w) and 1.0% (w/w) of these wetting agents uniformly distributed in the dried (at 40°C) tetracycline hydrochloride. These samples were used to study the effect of wetting agents.

***In Vitro* Dissolution Rate Studies**—The dissolution rate studies were carried out by a method similar to that used in the *in vitro* GI-tract resistance test. However, the dissolution medium was 0.1 M HCl, 5.0-mL samples were withdrawn at 30-min intervals and the volume of the dissolution medium was maintained by replacing an equal volume of the medium after each withdrawal. The samples were analyzed at 353 nm using a spectrocolorimeter[7].

RESULTS AND DISCUSSION

All the samples tested for *in vitro* GI-tract resistance showed resistance in both simulated gastric and intestinal fluids. The capsules remained intact throughout the GI tract in the X-ray studies, confirming *in vivo* resistance in the subjects tested. Figure 3 shows the position of the capsule in the GI tract at 0.5, 1.0, 2.0, 4.0, 6.0, and 8.0 h after the capsule was administered in one of the subjects. The capsule remained in the stomach for more than 1.0 h; 2.0 h after administration, the capsule was seen in the duodenal area of the small intestine. The capsule was traced intact in the ileum after 4.0 h, in the colon after 6.0 h, and finally in the rectum at 8.0 h. The residual formaldehyde content after 24.0 h of treatment was 80 μg/capsule, which reduced to 68 and 60 μg/capsule after 15 and 30 d of storage, respectively.

The number of drilled pores considerably influenced the release rate of tetracycline hydrochloride from the capsule (Fig. 4). A plot of percentage of

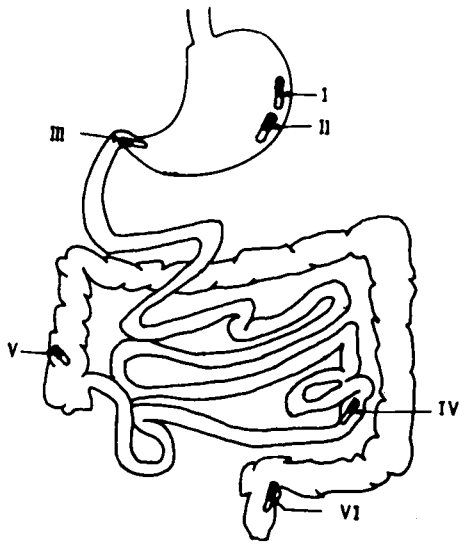

Figure 3—*Schematic representation of the position of the capsule in the GI tract (detected by X-ray photography) after capsule administration. Key: (I) 0.5 h; (II) 1.0 h; (III), 2.0 h; (IV) 4.0 h, (V) 6.0 h; (VI) 8.0 h.*

[5] Doxinate; Hoescht Aktiengeselschaft, Badvilbel, F.R.G.
[6] Tween 80; Atlas Chemical Co., Wilmington, Del.
[7] Model VSU2-P; C.Z. Spectrophotometer, F.R.G.

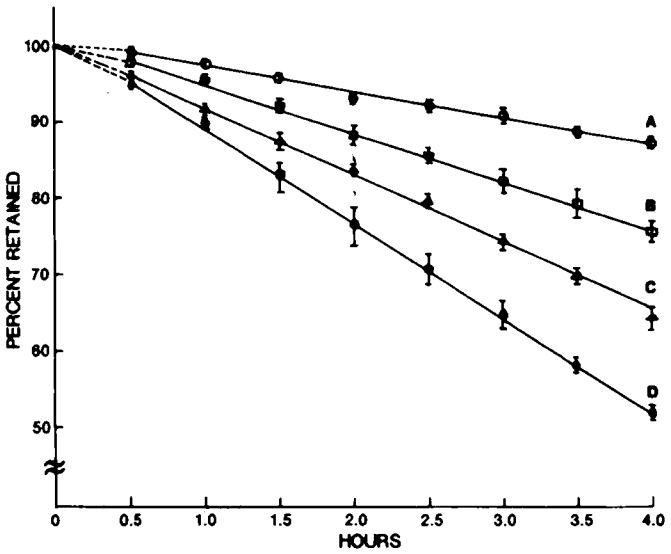

Figure 4—*Effect of variation in number of drilled pores, n (with SD_2 type of size distribution) on percent drug retained as a function of time. Key: (A) n = 25; (B) n = 50; (C) n = 75; (D) n = 100.*

the drug retained against time indicates that the drug release follows a zero-order pattern after an initial lag period of 30 min in all cases. This lag period may be attributed to the time required for the dissolution fluid to penetrate the capsule, wet and dissolve the drug, and finally allow the drug to pass through the pores.

The slope values were calculated by (12):

$$\alpha = \frac{\{\sum xy - (\sum x \cdot \sum y/n)\}}{\{\sum x^2 - [(\sum x)^2/n]\}} \qquad \text{(Eq. 1)}$$

where α is the slope, x is the time (in hours), and y is the percentage drug retained. Since the release follows zero-order kinetics, the slope represents the rate of the release (k_n) and n indicates the number of pores drilled. The calculated values of k_{25}, k_{50}, k_{75}, and k_{100} were 3.30, 6.32, 8.92, and 12.27%/h, respectively. The variations in number of drilled pores were in the ratio of 1:2:3:4; the release rate constant, k_n, showed a similar ratio. This indicates a proportionate increase in the release rate of the drug with an increase in the number of drilled pores (n).

The effect of pore size and size distribution on the release rate constant of tetracycline hydrochloride is shown in Fig. 5 for the size distribution ranges SD_1, SD_2, SD_3, and SD_4. The statistical mean diameter of each size distribution was calculated by (12):

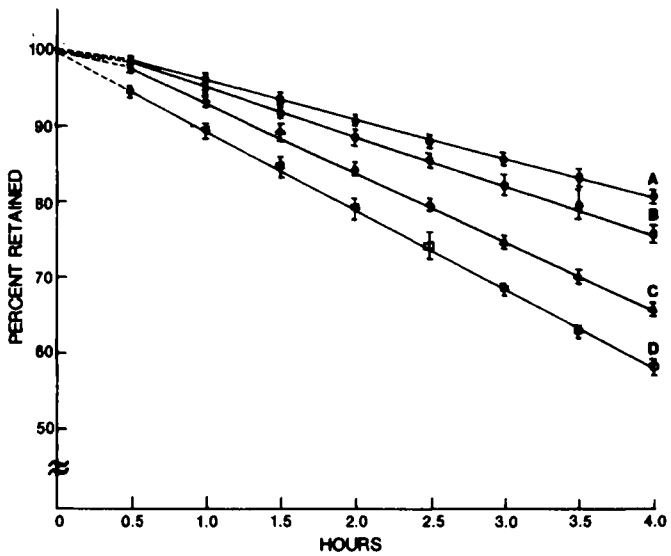

Figure 5—*Effect of variation in size distribution of drilled pores on percent drug retained as a function of time. Key: (A) SD_1; (B) SD_2; (C) SD_3; (D) SD_4.*

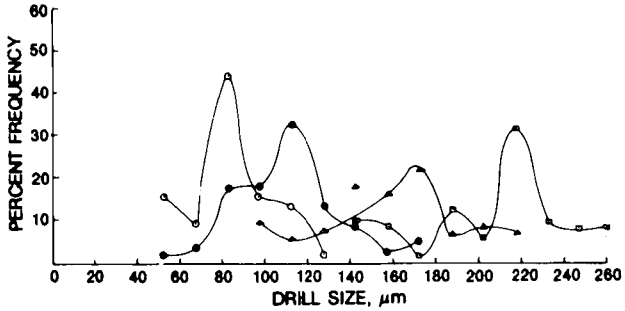

Figure 6—*Frequency distribution plots of different size ranges of drilled pores. Key: (⊙) SD_1; (●) SD_2; (▲) SD_3; (⊡) SD_4.*

$$d_{mean} = \left(\frac{\sum nd^{p+f}}{\sum nd^f}\right)^{1/p} \quad \text{(Eq. 2)}$$

where n is the number of pores in a size range whose midpoint, d, is one of the equivalent arithmetic, geometric, or harmonic mean diameters; p is the index related to size of an individual pore, since d raised to the power $p = 1$ or $p = 2$ is an expression of the pore length or surface, respectively. The frequency with which the pores in a certain size range occur is expressed by nd^f. When the frequency index has values of 0, 1, or 2 the size frequency distribution is expressed in terms of total number, length, or surface of pores, respectively. The frequency distribution and the log probability plots of SD_1, SD_2, SD_3, and SD_4 pore size distributions are shown in Figs. 6 and 7, respectively. The arithmetic length-number mean diameters, *dln*, were calculated by (12):

$$dln = \frac{\sum nd}{\sum n} \quad \text{(Eq. 3)}$$

and were 83.58, 103.60, 160.20, and 207.80 μm. These values correlated well with the corresponding geometric mean diameters of 78.50, 100.00, 155.00, and 205.00 μm obtained from the log probability plot. The respective standard deviations calculated from the slopes of the lines were 1.57, 1.41, 1.52, and 1.38. The total surface area available for the release of the drug with 50 pores on the body of the capsule for each of the four groups was 1.10, 1.68, 4.03, and 6.78 cm^2/capsule. The calculated release rate constants indicate that the drug was released at the rate of 5.04, 6.32, 8.96, and 10.60%/h for the respective release areas. The release rate followed zero-order kinetics after an initial lag period of 30 min in all cases, except the capsules with SD_4 pore size distribution had no lag period. Such a deviation for larger pore sizes may be due to a decrease in the time required for the dissolution fluid to penetrate the capsule with a larger surface area. The capsules with pores of SD_1 and SD_2 size distributions showed a loss of <0.8%/capsule when subjected to friability tests, unlike the capsules with SD_3 and SD_4 distributions, where the loss was >1%/capsule.

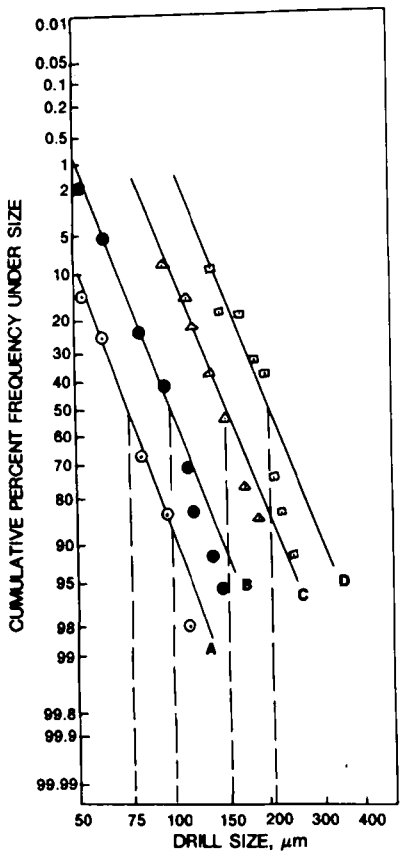

Figure 7—*Log probability plots of different size ranges of drilled pores. Key: (A) SD_1; (B) SD_2; (C) SD_3; (D) SD_4.*

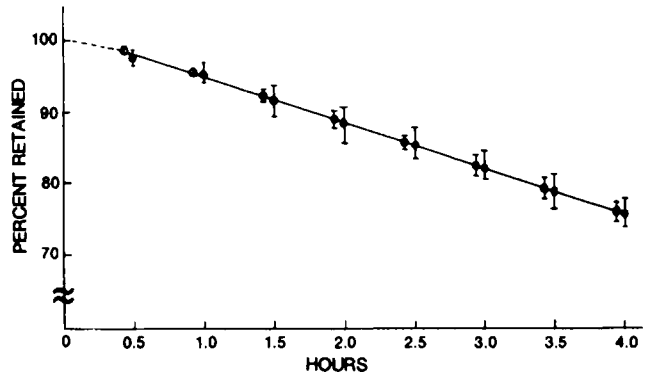

Figure 8—*Influence of variation in pattern of drilling on percent drug retained as a function of time. Key: (○) only body drilling; (●) cap and body drilling.*

The variation in drilling pattern did not show statistically significant differences ($t = 0.037$, $d = 16$, $p < 0.01$) in release rates of the drug (Fig. 8). The higher standard deviations observed in the values for cap and body drilling as compared with body drilling alone may be attributed to incomplete drilling when the comparatively thicker cap and body surface was drilled simultaneously.

The release rate of the drug from the capsule was considerably affected by the powder characteristics, *i.e.*, bulk density and particle size distribution, of the encapsulated drug samples I, II, and III. The bulk densities were 0.61, 0.60, and 0.73 g/cm^3. Average length number mean diameters (*dln*) were 51.20, 95.74, and 23.30 μm and showed release rates of 6.32, 5.00, and 8.11%/h, respectively (Fig. 9). This probably indicates an increase in release rate with decreased particle size of the encapsulated drug. The frequency distributions and log probability plots of the three samples are shown in Figs. 10 and 11, respectively. The aforementioned statistical diameters correlated well with the geometric mean diameters (*dg*) of 48.50, 85.0, and 17.50 μm, respectively, obtained from the log probability plot. The corresponding standard deviations calculated from each slope were 3.03, 1.67, and 2.8.

Figures 12 and 13 show the effect of different additives on the release rate of the drug from the capsules. The use of lactose and microcrystalline cellulose

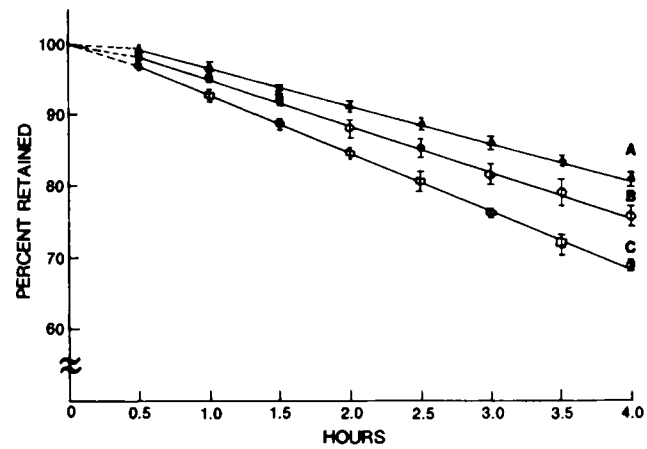

Figure 9—*Effect of particle size and size distribution of the encapsulated drug sample on percent drug retained as a function of time. Key: (A) sample I; (B) sample II; (C) sample III.*

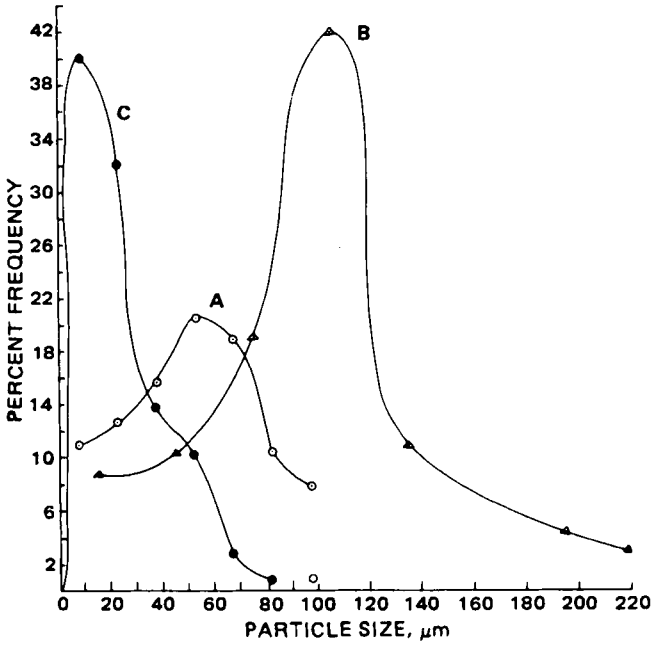

Figure 10—*Frequency distribution plots of different samples of powder. Key: (A) sample I; (B) sample II; (C) sample III.*

as diluents and magnesium stearate and talc as lubricants did not significantly affect the release rate of the drug. Of the two wetting agents used, dioctyl sodium sulfosuccinate showed a statistically significant enhancement of the release rate, unlike polysorbate 80 which showed some enhancement but was not statistically significant. Table II is the analysis of variance (13) to compare the effect of additives on the release rate of the drug. The calculated F ratio is higher than the F value obtained from the table (13) ($f_1 = 6, f_2 = 56, p =$ 0.05) which clearly indicates that the samples do not have the same release rate *i.e.*, they are statistically different. To determine which samples are different from each other, a least-significant procedure (13) was applied; Table III shows the ranked means. The calculated value of 5% allowance is 7.05

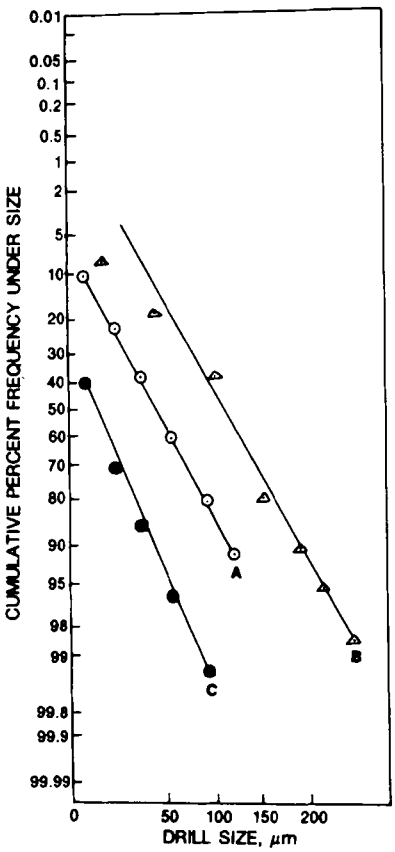

Figure 11—*Log probability plots of different samples of powder. Key: (A) sample I; (B) sample II; (C) sample III.*

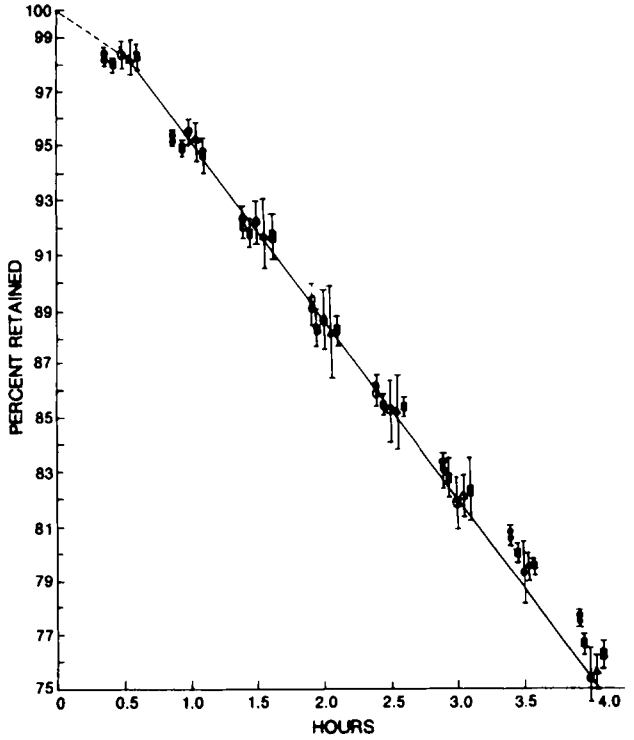

Figure 12—*Effect of common capsule additives on percent drug retained as a function of time. Key: (○) drug only; (△) with microcrystalline cellulose; (□) with lactose; (●) with talc; (⚉) with magnesium stearate.*

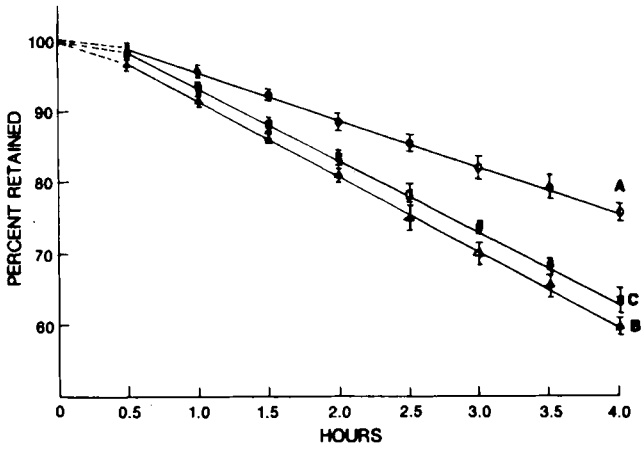

Figure 13—*Effect of wetting agents on percent drug retained as a function of time. Key: (A) drug only; (B) with dioctyl sodium sulfosuccinate; (C) with polysorbate 80.*

Table II—Analysis of Variance

Source of Variation	Degrees of Freedom	Sum of Squares	Mean Squares	F Ratio	F Value[a]
Among the treatments	$t - 1 = 6$	3990.93	665.16	11.88	2.25[b]
Within the treatments	$\Sigma ni - 1 = 56$	3135.68	55.99		
Total	$N - 1 = 62$				

[a] From the tables. [b] F value at $f_1 = 6$, $d_2 = 56$, and $p = 0.05$; $\bar{x} = 5457.87$, $\bar{x}^2 = 479957.48$, $N = 63$, $\Sigma ni - 1 = 56$, and $t = 7$.

Table III—Ranked Means [a]

Drug	Talc	Magnesium Stearate	Microcrystalline Cellulose	Lactose	Polysorbate 80	Dioctyl Sodium Sulfosuccinate
88.48	88.70	89.10	83.54	88.38	82.78	80.53

[a] Any two means not underscored by the same line are statistically significantly different; $t = 2.00$, $S_2 = 55.99$, $ni = 9$, $n = 9$, degrees of freedom = 56, $p = 0.05$, and 5% allowance = 7.05.

which indicates dioctyl sodium sulfosuccinate has a statistically significant difference in release rate than the other additives studied ($p = 0.05$, $t = 2.0$, $S_2 = 55.99$, $n_1 = 9$, degrees of freedom = 56).

CONCLUSIONS

GI-tract resistant hard-gelatin capsules were prepared by formalin treatment. The contents of the capsule were released slowly through minute laser-drilled pores. Variations in number and diameter of drilled pores changed the rate of release of the drug from these capsules. Common additives like lactose, microcrystalline cellulose, magnesium stearate, and talc did not significantly affect the rate of release of the drug; neither did variations in drilling patterns. The presence of dioctyl sodium sulfosuccinate significantly affected the release rate; although polysorbate 80 enhanced the release, the effect was not statistically significant.

The results of the present investigation clearly indicate that the technique of laser drilling could be successfully used in designing slow-release capsule dosage forms. A proportionate increase in release rate with the number of pores drilled and with increased average diameter of the pores suggests the possibility of using the laser technique to design controlled-release capsule dosage forms.

REFERENCES

(1) A. Lytel, "Introduction to Lasers & Masers," Buckinghamshire, England, 1965, p. 103.

(2) *Laser Focus*, **16**(7), 26 (1980).

(3) F. Theeuwes, D. Swanson, P. Wong, P. Bonsen, V. Place, K. Heimlick, and K. C. Kwan, *J. Pharm. Sci.*, **72**, 253 (1983).

(4) J. T. Carstensen, "Pharmaceutics of Solids and Solid Dosage Forms," Wiley, New York, N.Y., 1977, p. 145.

(5) L. Lachman, H. A. Lieberman, and J. L. Kanig, "The Theory and Practice of Industrial Pharmacy," 2nd ed., Lea and Febiger, Philadelphia, Pa., 1976, p. 404.

(6) H. Macfadyan, *J. Biol. Chem.*, **158**, 107 (1945).

(7) "The United States Pharmacopeia," 19th rev., U.S. Pharmacopeial Convention, Rockville, Md., 1975, p. 651.

(8) "The United States Pharmacopeia," 19th rev., U.S. Pharmacopeial Convention, Rockville, Md., 1975, p. 765.

(9) A. N. Martin J. Swarbrick, and A. Cammarata, "Physical Pharmacy," 2nd ed., Lea & Febiger, Philadelphia, Pa., 1970, pp. 468-493.

(10) L. Lachman, H. A. Lieberman, and J. L. Kanig, "The Theory and Practice of Industrial Pharmacy," 2nd ed., Lea and Febiger, Philadelphia, Pa., 1976, p. 347.

(11) A. Q. Butler and J. R. Ransey, Jr., *Drug Standards*, **20**, 217 (1952).

(12) J. T. Carstensen, "Theory of Pharmaceutical Systems," vol. I, Academic Press, New York, N.Y., 1972, p. 16.

(13) "Remington's Pharmaceutical Sciences," 14th ed., Mack Publishing Co., Easton, Pa., 1970, pp. 122-140.

ACKNOWLEDGMENTS

The authors gratefully acknowledge the Laser Division and the management of Jyoti Ltd., Baroda, India, for providing laser facilities and guidance; Dr. O. D. Gulati and Dr. N. A. Dave, Radiology Department, Medical College, Baroda, for providing X-ray facilities and guidance; M/s Sarabhai Chemicals, a Division of Ambalal Sarabhai Enterprises, Baroda, India, for supplying free gift samples of the drug and hard-gelatin capsules; and Professor S. S. Merh, Department of Geology, Faculty of Science, M. S. University of Baroda, Baroda, India, for providing photomicrograph facilities.

Degradative Behavior of Cadralazine in Aqueous Solution

MARCO VISCONTI ˣ, LUISA CITERIO, MASSIMILIANO BORSA, and GIORGIO PIFFERI

Received February 24, 1983, from the *ISF—Laboratories for Biomedical Research, Milan, Italy.* Accepted for publication February 16, 1984.

Abstract □ The degradation of cadralazine in aqueous solution was investigated in relation to pH, concentration, and temperature, under aerobic and anaerobic conditions in light and dark. The appearance of three main degradation products was also studied. Drug disappearance was dependent on temperature, pH, concentration, and oxygen and followed three different mechanistic pathways: thermal, hydrolytic, and oxidative. The individual rate constants were determined by nonlinear regression fitting.

Keyphrases □ Cadralazine—degradation kinetics, antihypertensive agent, identification of oxidative, hydrolytic, and thermal degradation products □ Antihypertensive agent—cadralazine, degradation kinetics, identification of oxidative, hydrolytic, and thermal degradation products □ Degradation kinetics—cadralazine, antihypertensive agent

Cadralazine, ethyl 6-[ethyl-(2-hydroxypropyl)amino]-3-pyridazinecarbazate (I) (1), is a new potent peripheral vasodilator (2, 3) which has been shown to be active in hypertensive patients (4–11). Like the chemically related antihypertensive drugs hydralazine (12) and pildnalazine (13), cadralazine is stable in the solid state, whereas it is susceptible to decomposition in water.

A study was therefore initiated to identify the degradation products of I; it was performed in stress conditions that are different than the physiological ones, in order to accelerate the decomposition processes. Further investigations were conducted to establish the kinetics of cadralazine degradation. The effects of pH, temperature, drug concentration, and other factors on cadralazine decomposition and on the appearance rate of the main degradation products were also investigated.

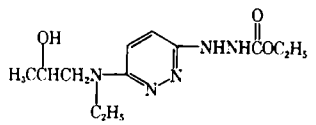

I

EXPERIMENTAL SECTION[1]

Cadralazine (I), the working standard (14) [MS: *m/z* 283 (37), 238 (100), 210 (50), 192 (53) and 164 (60)] was used as received. 6-[Ethyl-(2-hydroxypropyl)amino]-1,2,4-triazolo[4,3-*b*]pyridazin-3(2*H*)-one (II) was synthesized according to the method of Parravicini *et al.* (1) [MS: *m/z* 237 (12), 192 (38), and 164 (100)]. *N*-Ethyl-*N*-(2-hydroxypropyl)-6-oxo-3(1*H*)-pyridazinylamine (III), synthesized by the hydrolysis of 6-chloro-*N*-ethyl-*N*-(2-hydroxypropyl)-3-pyridazinylamine (15) by a literature method (13), was obtained as a white powder, mp 106–107°C; MS[2]: *m/z* 197 (15% $M^{\ddagger}$), 152 [100, $(M - CH_3CHOH)^+$], 139 (20), and 124 (40); ^{1}H-NMR[3] (60 Hz, Me_2SO-d_6): δ 7.25 and 6.78 (ABq, 2, *J* = 10 Hz, H-5 and H-4), 4.25 (br s, 1, OH), 4.00 (m, 1, CH), 3.46 (q, 2, *J* = 6.5 Hz, NCH_2CH_3), 3.22 (d, 2, *J* = 6.5 Hz, NCH_2CH), 1.15 (d, 3, *J* = 5.3 Hz, CH_3CH), and 1.10 ppm (t, 3, *J* = 6.5 Hz, CH_2CH_3).

Anal.—Calc. for $C_9H_{15}N_3O_2$: C, 54.81; H, 7.66; N, 21.30. Found: C, 54.56; H, 7.82; N, 21.51.

N-Ethyl-*N*-(2-hydroxypropyl)-3-pyridazinylamine (IV), synthesized by hydrogenolysis of 6-chloro-*N*-ethyl-*N*-(2-hydroxypropyl)-3-pyridazinylamine (15) by a literature method (13), was obtained as a pale-yellow oil; MS[2]: *m/z* 181 (22% $M^{\ddagger}$), 136 [100, $(M - CH_3CHOH)^+$], 123 (30), and 108 (90); ^{1}H-NMR[3] (60 Hz, $CDCl_3$): δ 8.44 (dd, 1, *J* = 4.6, 1.0 Hz, H-6), 7.18 (dd, 1, *J* = 4.6, 9.5 Hz, H-5), 6.90 (dd, 1, *J* = 9.5, 1.0 Hz, H-4), 5.00 (br s, 1, OH) 4.10 (m, 1, CH), 3.56 (d, 2, *J* = 6.2 Hz, NCH_2CH), 3.53 (q, 2, *J* = 7.0 Hz, NCH_2CH_3), 1.22 (d, 3, *J* = 7.0 Hz, CH_3CH), and 1.18 ppm (t, 3, *J* = 7.0 Hz, CH_2CH_3).

Anal.—Calc. for $C_9H_{15}N_3O$: C, 59.66; H, 8.34; N, 23.19. Found: C, 60.00; H, 8.04; N, 23.34.

Ethyl 2-[6-[ethyl-(2-hydroxypropyl)amino]-3-pyridazinyl]azocarboxylate (V) was synthesized according to Gaviraghi *et al.* (16) [MS: *m/z* 283 (28), 238 (48), 237 (32), 181 (36), and 136 (100)]. The following internal standards were used: 1-[3,4,5-trimethoxythiobenzoyl]-4-methylpiperazine hydrochloride (VI) synthesized according to Farina *et al.* (17) and (L)-α-(3,4,5-trimethoxythiobenzamido)caprolactam (VII) synthesized according to Farina *et al.* (18). All the compounds synthesized gave the expected NMR and mass spectral data.

Identification of the Degradation Products—Aliquots (25 mL) of a 0.1% (w/v) cadralazine (I) solution in phosphate buffer (pH 7.4) were kept overnight at 80°C in a water bath under constant tungsten light, then extracted three times with 40 mL of chloroform. The organic layer was evaporated to dryness, and the residue was dissolved in 5 mL of methanol; 200 μL of the solution was spotted and eluted on silica gel plates with the following eluants: chloroform–methanol–water (95:10:1), chloroform–methanol–water (70:27:5), 1-butanol–acetic acid–water (80:20:20), benzene–methanol (80:20), tetrahydrofuran–methanol (96:4); on aluminum oxide plates with methyl ethyl ketone–methanol–chloroform (40:5:55); on silanized silica gel plates with benzene–ethyl acetate–acetonitrile–methanol (35:45:15:5). The spots were detected under UV light, scraped, examined by MS[2] and compared with synthetic samples.

Decomposition Rate of Cadralazine—The degradations were performed on 0.1% solution of cadralazine buffered at pH 3.0, 5.0, 7.4, and 10.0, and stored at 30 ± 0.1°C, 50 ± 0.1°C, and 80 ± 0.1°C in air and light; analogous solutions buffered at pH 0.2 and 1 were followed at 50 ± 0.1°C in the same conditions. Degradations at pH 7.4 and 10 were also studied at 80°C in a nitrogen atmosphere (both in light and in the dark) and in a dark and aerobic atmosphere. Solutions of 0.093, 0.93, 5.15, 10.3, and 18.3 mg/mL of cadralazine in acetate buffer (pH 5.0) were tested at 80 ± 0.1°C in a light and aerobic atmosphere. All samples were taken at various intervals. The internal standard VI was added, and the samples were suitably diluted and assayed by TLC–photodensitometry[4] at 254 nm as previously described (19).

Appearance Rate of II, III, and IV—The appearance rates of II, III, and IV were tested on 0.1% solutions of cadralazine buffered at pH 7.4 and 10.0, submitted to decomposition at 80 ± 0.1°C in an aerobic or a nitrogen atmosphere, in light or dark. Quantitation was performed by adding VII (an internal standard for II and III) and VIII (an internal standard for IV) to the samples. The undiluted solutions were assayed by TLC–photodensitometry as previously described (19).

RESULTS AND DISCUSSION

Characterization of the Degradation Products—TLC of the degraded cadralazine mixture in several eluant systems indicated the presence of four major and three minor compounds. The degradation products were isolated (TLC) and characterized by comparison of their R_f values and MS data with those of authentic samples of I–V (1, 16). The four major compounds were identical with cadralazine (I) (1), triazolone II (1), pyridazinone III, pyridazine IV; one of the minor compounds was the azocarboxylate V (16, 20). Two

[1] All reagents and solvents were analytical grade. Hydrochloric acid–potassium chloride buffer (Normex, pH 0.2 and 1.0, respectively), sodium citrate buffer (pH 3.0), potassium phthalate buffer (pH 5.0), sodium acetate buffer (pH 5.0), potassium phosphate buffer (pH 7.4), and sodium borate buffer (pH 10.0) were purchased from Carlo Erba, Milan, Italy. Sodium chloride was added to all buffers to a constant ionic strength (μ = 0.115). TLC plates silica gel 60 F 254, HPTLC silica gel 60 F 254, silanized silica gel 60 F 254, and aluminum oxide type E F 254 were obtained from Merck, Darmstadt, West Germany.

[2] Varian Mat 112 spectrometer (70 eV, 1.5 mA).

[3] Perkin-Elmer R12B.

[4] Camag TLC scanner; Camag, Switzerland, equipped with a Perkin-Elmer 56 recorder.

0022-3549/84/1200-1812$01.00/0
© 1984, American Pharmaceutical Association

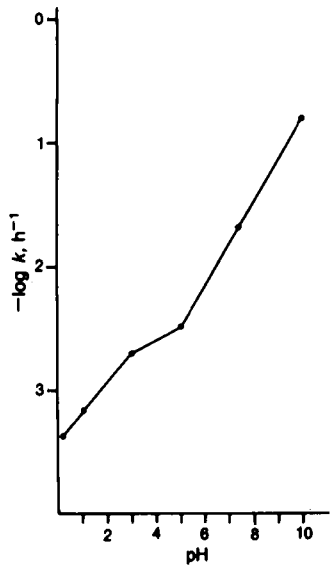

Figure 1—*The pH-rate profile of cadralazine (0.1%, w/v) in aqueous solutions at 50°C.*

of the minor products were not identified. Compounds II, III, IV, and V were treated under the same conditions used for cadralazine degradation, and no decomposition was found except for V, which rapidly converted to III and IV.

Order of Reaction—Semilogarithmic plots of residual concentrations of cadralazine *versus* time exhibited good linearity ($r^2 > 0.98$) for experiments at all pH levels studied. The disappearance of cadralazine from aqueous solutions followed pseudo-first-order kinetics under the experimental conditions. The degradation rate constants of cadralazine were computed by the least-squares linear regression method. The calculated pseudo-first-order rate constants at fixed concentration of cadralazine (0.1%, w/v), buffer ionic strength ($\mu = 0.115$) and temperature (50 ± 0.1°C) were: 4.17×10^{-4} h^{-1} at pH 0.2; 6.72×10^{-4} h^{-1} at pH 1; 2.00×10^{-3} h^{-1} at pH 3; 3.17×10^{-3} h^{-1} at pH 5; 2.14×10^{-2} h^{-1} at pH 7.4; 0.1570 h^{-1} pH 10.

pH Dependency—The pH-rate profile for the degradation of cadralazine was constructed from the logarithm of the pseudo-first-order rate constants and the pH values at 50 ± 0.1°C. The buffering capacities of all the solutions were sufficient to keep constant pH values (±0.05) throughout the experiment. The pH-rate profile (Fig. 1) showed a sigmoid curve superimposed on one branch of a V-graph and revealed a profound degradation rate increase in the neutral and basic pH region, where cadralazine was in the neutral form. In the acidic pH region, the degradation rate appeared low, whereas between pH 3 and 5 it was less sensitive to pH changes. At pH 7.4 and 50°C, the apparent first-order rate constant was 2.14×10^{-2} h^{-1}, which corresponds to a half life of ~32.4 h.

Concentration Effect—The effect of cadralazine concentration on its degradation constant was investigated at 80°C in pH 5 acetate buffer. As shown in Fig. 2, the highest concentrations stabilized the solutions of cadralazine.

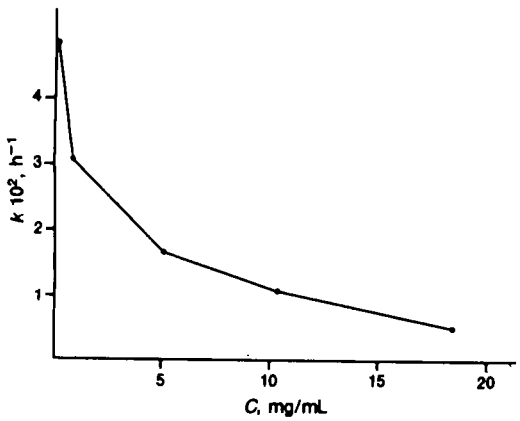

Figure 2—*Influence of cadralazine concentration on the rate degradation constants at 80°C and pH 5.0.*

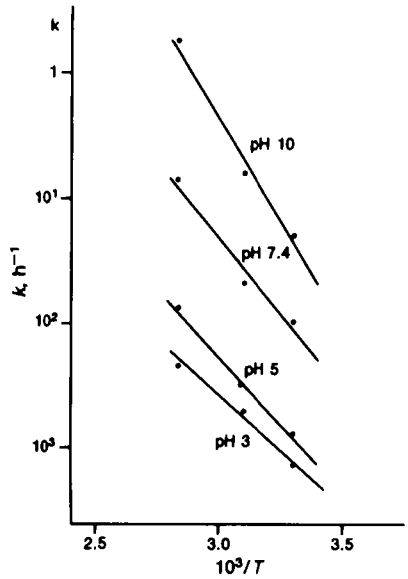

Figure 3—*Arrhenius plot depicting the temperature dependency of cadralazine degradation.*

Table I—Arrhenius Parameters for Degradation of Cadralazine

pH	$E^{\neq}$, kcal/mol	log A	r^2
3	7.72	2.46194	0.976
5	10.12	4.38242	0.997
7.4	11.00	5.89449	0.963
10	15.36	9.74349	0.983

Influence of Temperature, Light, and Air on Cadralazine—The Arrhenius plots of the pseudo-first-order rate constant (k) at varying temperatures (30, 50, and 80 ± 0.1°C) at different pH levels (10, 7.4, 5, and 3) are shown in Fig. 3. The apparent Arrhenius parameters for the disappearance of cadralazine, calculated from the regression equations, are reported in Table I. The degradation of cadralazine was greatly influenced by the presence of air and, to a lesser extent, by light, as shown in Fig. 4.

Light, pH and Air Effects on Formation of II, III and IV—The appearance rate of triazolone II at pH 7.4 and 80°C (Fig. 5A) was independent of the presence of air or light, whereas its formation rate was moderately pH dependent. Moreover, it has been reported that II is obtained from I by thermal cyclization (1). The weak influence of pH and the independence of the formation of II from light and air suggests that the mechanism of formation of II may be essentially thermal in degradative conditions.

In contrast, the appearance rate of pyridazinone III (Fig. 5B) was independent of the presence of air, greatly dependent on pH, and moderately influenced by the presence of light. This excludes an oxidative mechanism in its formation and suggests a hydrolytic pathway.

Finally, pyridazine IV was not detected in the absence of air, whereas its formation was independent of light, and moderately related to the increase in pH (Fig. 5C). This behavior is essentially in agreement with an oxidative reaction.

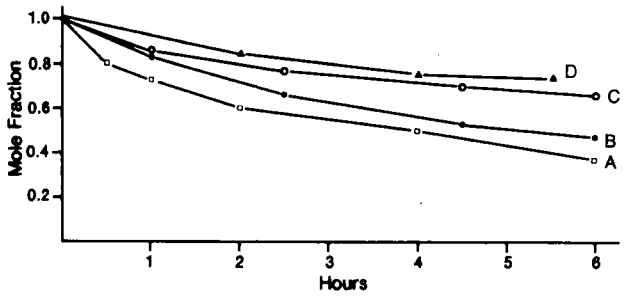

Figure 4—*Experimental time-concentration profile of cadralazine at 80°C and pH 7.4 in light and air (A), dark and air (B), light and nitrogen (C), and dark and nitrogen (D).*

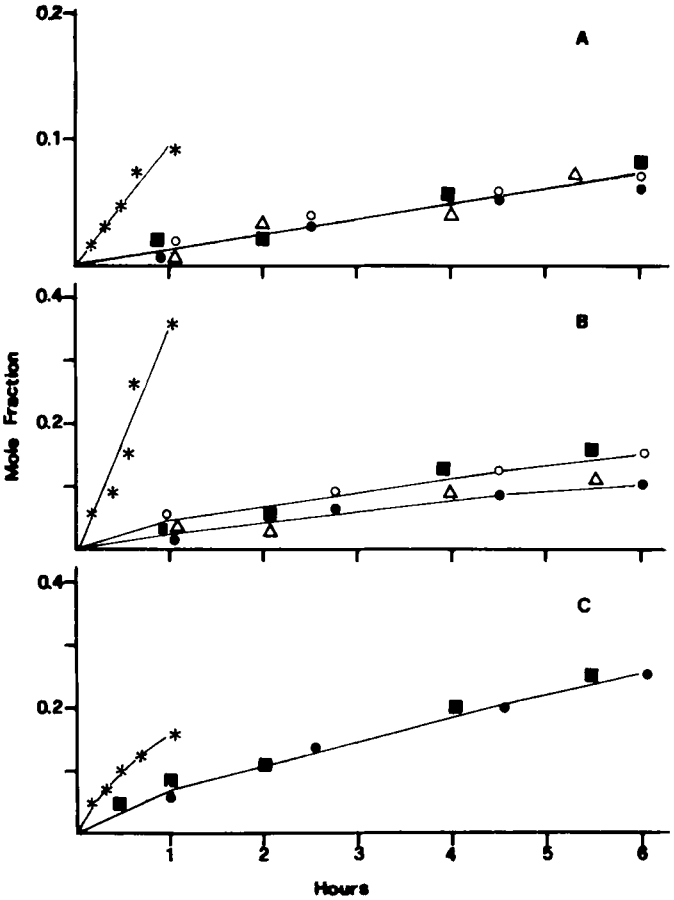

Figure 5—*Experimental time-concentration profile of II (A), III (B), and IV (C) at 80°C in pH 10, light and air (*), pH 7.4, light and air (■), light and nitrogen (○), dark and air (●), and dark and nitrogen (▲). No traces of IV were found at pH 7.4 in light and nitrogen, or in dark and nitrogen.*

Possible Degradation Pathway—The degradation of cadralazine yields triazolone II, pyridazinone III, pyridazine IV, and minor quantities of azocarboxylate V. Cadralazine decomposition at pH 7.4 and 80°C can be hypothesized as a combination of three parallel reactions (Scheme I). On the basis of this hypothesis, the disappearance of cadralazine can be described as a pseudo-first-order process expressed by:

$$-\frac{d[I]}{dt} = (k_2 + k_3 + k_4)[I] = k_1[I] \qquad \text{(Eq. 1)}$$

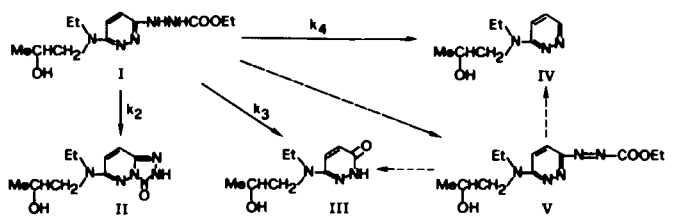

Scheme I—Proposed degradation pattern of cadralazine in aqueous solution.

Table II—Rate Constants for Cadralazine Degradation [a]

Constant	k, h^{-1} [b]	r^2
k_1	0.1346 ± 0.0190	0.989
k_2	0.0179 ± 0.0047	0.994
k_3	0.0452 ± 0.0049	0.990
k_4	0.0744 ± 0.0050	0.997
$k_2 + k_3 + k_4$	0.1375	

[a] Determined at pH 7.4, 80°C. [b] Confidence limits of ±95%.

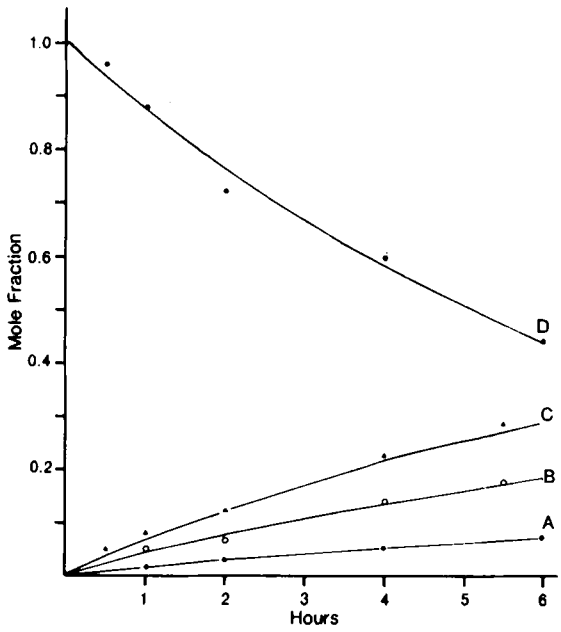

Figure 6—*Time-concentration profile of cadralazine (A) and its degradation products II (B), III (C), and IV (D) in an aqueous solution (0.1%, w/v) of cadralazine at pH 7.4 incubated at 80°C. The experimental data are superimposed on calculated curves.*

Rate expressions describing the appearance of II, III, and IV take similar forms (pseudo-first-order reactions):

$$\frac{d[II]}{dt} = k_2[I] \qquad \text{(Eq. 2)}$$

$$\frac{d[III]}{dt} = k_3[I] \qquad \text{(Eq. 3)}$$

$$\frac{d[IV]}{dt} = k_4[I] \qquad \text{(Eq. 4)}$$

These differential equations can be solved and the amount of each component in the mixture can be expressed as the mole fraction of the initial concentration of cadralazine as a function of time:

$$\frac{[I]}{[I]_0} = e^{-k_1 t} \qquad \text{(Eq. 5)}$$

$$\frac{[II]}{[I]_0} = \frac{k_2}{k_1}(1 - e^{-k_1 t}) \qquad \text{(Eq. 6)}$$

$$\frac{[III]}{[I]_0} = \frac{k_3}{k_1}(1 - e^{-k_1 t}) \qquad \text{(Eq. 7)}$$

$$\frac{[IV]}{[I]_0} = \frac{k_4}{k_1}(1 - e^{-k_1 t}) \qquad \text{(Eq. 8)}$$

Initial conditions were defined so that at $t = 0$ the amount of cadralazine was equal to $[I]_0$, and no degradation products were present, *i.e.*, [II], [III], and [IV] were equal to zero.

Equations 5–8 were used to calculate simultaneously k_1, k_2, k_3, and k_4 from the experimental data derived from the degradation of I carried out at 80°C and pH 7.4, in air and light, using a nonlinear regression program (NOLIN). The values obtained for k_i and their 95% confidence limits are reported in Table II. The quality of the fit between experimental and theoretical concentrations is shown in Fig. 6. The accuracy of the calculated k_i was demonstrated by comparing the pseudo-first-order rate constant k_1, determined experimentally, with the sum of the individually calculated rate constants $k_2 + k_3 + k_4$.

The minor compound, V, was not considered in the kinetic study, because its yield was small, near the range of detectability. However, this product could be a possible intermediate in the formation of III and IV.

REFERENCES

(1) F. Parravicini, G. Scarpitta, L. Dorigotti, and G. Pifferi, *Il Farmaco, Ed. Sci.*, **34**, 299 (1979).

(2) G. Pifferi, F. Parravicini, G. Scarpitta, and C. Semeraro, VIth In-

ternational Symposium on Medicinal Chemistry, Brighton, September 1978, Abstr. 817.

(3) C. Semeraro, L. Dorigotti, S. Banfi, and C. Carpi, *J. Cardiovasc. Pharmacol.*, **3**, 455 (1981).

(4) L. Muiesan, G. Romanelli, E. Agabiti-Rosei, L. Alicandri, M. Beschi, M. Castellano, R. Fariello, A. Geri, L. Platto, P. Beggi, M. Motolese, and G. Muiesan, IXth World Congress of Cardiology, Moscow, June 1982.

(5) L. Corea, M. Bentivoglio, P. Beggi, and M. Motolese, IXth World Congress of Cardiology, Moscow, June 1982.

(6) M. Motolese, A. Magagna, B. Abdel-Mag, S. Lucarini, L. Graziadei, and A. Salvetti, IXth World Congress of Cardiology, Moscow, June 1982.

(7) F. V. Costa, R. Caldari, A. M. Marata, E. Strocchi, E. Ambrosioni, and B. Magnani, IXth Scientific Meeting of the International Society of Hypertension, Mexico City, February 1982.

(8) P. Van Brummelen, F. R. Bühler, W. Kiowski, P. Bolli, and O. Bertel, *Int. J. Clin. Pharmacol. Biopharm.*, **17**, 380 (1979).

(9) F. W. Amann and F. R. Bühler, *Clin. Eur.*, **18**, 1028 (1979).

(10) G. C. Lavezzaro, D. Gastaldo, P. Noussan, M. Bensoni, J. Parini, and P. F. Angelino, *Minerva Cardioangiol.*, **29**, 527 (1981).

(11) P. F. Angelino, M. Bensoni, D. Gastaldo, M. Minelli, J. Parini, and G. C. Lavezzaro, *Minerva Cardioangiol.*, **30**, 69 (1982).

(12) A. R. Schulert, *Arch. Int. Pharmacodyn.*, **132**, 1 (1961).

(13) P. Ventura, F. Parravicini, L. Simonotti, R. Colombo, and G. Pifferi, *J. Pharm. Sci.*, **70**, 334 (1981).

(14) L. Citerio, M. Visconti, M. Borsa, and G. Pifferi, *Boll. Chim. Farm.*, **120**, 222 (1981).

(15) G. Pifferi, F. Parravicini, C. Carpi, and L. Dorigotti, *J. Med. Chem.*, **18**, 741 (1975).

(16) G. Gaviraghi, M. Pinza, and G. Pifferi, *Synthesis*, **8**, 608 (1981).

(17) C. Farina, M. Pinza, A. Gamba, and G. Pifferi, *Eur. J. Med. Chem.*, **14**, 27 (1979).

(18) C. Farina, R. Pellegata, M. Pinza, and G. Pifferi, *Arch. Pharm.*, **314**, 108 (1981).

(19) T. Crolla, L. Citerio, M. Visconti, and G. Pifferi, *High-Resol. Chromatogr. Chromatogr. Commun.*, **6**, 445 (1983).

(20) L. Simonotti, F. Parravicini, and G. Pifferi, Vth National Congress of Mass Spectrometry, Rende, September 1980, Abstr. p. 34.

ACKNOWLEDGMENTS

The authors thank Prof. Emilio Rocca, University of Milan, for his help with the computer simulations and Dr. M. T. Riccaboni for her secretarial assistance in the preparation of this manuscript.

Binding Parameters of Interactions of Monomer–Polymer Systems Based on Quenching of Their Completely Overlapped Fluorescence: A Theory

HANNA N. BORAZAN

Received March 3, 1983, from the *Department of Pharmaceutical Chemistry, College of Pharmacy, University of Baghdad, Baghdad, Republic of Iraq.* Accepted for publication September 12, 1983.

Abstract □ A theory is presented which describes the interactions between completely overlapping fluorescing monomer–polymer systems and affords a method to calculate binding parameters. The theory is based on the assumptions that the complex formed from the fluorescing binding site and the monomer molecule does not fluoresce and that the fluorescence intensity is linearly related to concentration. The relationships derived from this theory have provided a sensitive and easy method for calculating the number of binding sites on a polymer molecule from only three emission-intensity values. The theory has been tested on systems containing trimethoprim–serum albumins and found to yield results which are consistent with a curve-fitting approach to the experimental data. This reflects the validity of the theoretical model presented and the various assumptions and approximations made.

Keyphrases □ Monomer–polymer systems—binding parameters, overlapped fluorescence quenching □ Binding parameters—overlapped fluorescence quenching, monomer–polymer system □ Fluorescence quenching—binding parameters, monomer–polymer systems

Fluorescence quenching has been applied to the study of complex formation (1); for example, the interactions of amino acids containing aromatic nuclei and their amines, and oligopeptides containing aromatic amino acids with nucleic acids, were studied by this method (2, 3). Recently, Koumriqian (4) and Borazan and Koumriqian (5) have applied the technique to study interactions between catecholamines and polyadenylic acid. In these studies, the emissions of the polynucleotides were negligible compared with those of the monomers. It was, therefore, easy to derive equations for calculating the binding parameters using the fraction remaining from the fluorescence intensity of the monomers or the observed quantum yield.

However, due to the inherent properties of many systems, both the monomers and polymers in the binary mixtures exhibit almost complete emission overlap over a wide range of excitation and emission wavelengths. Examples for such systems can be found in the fluorescence quenching studies of the interactions of steroids–polynucleotides (6), antineoplastics–polynucleotides (7), and antibacterials–serum albumins (8). Thus, these types of systems impose a difficult problem when analyzing the experimental data to calculate the binding constants. These authors (6–8) have applied an empirical approach involving a curve-fitting technique to analyze the fluorescence data.

The present study is concerned with a theoretical treatment which utilizes the fluorescence technique in situations where complete fluorescence overlap is taking place. This allowed us to determine the number of fluorescing binding sites on a polymer molecule available to the monomer molecules and to calculate the equilibrium constant for the process.

THEORETICAL SECTION

To calculate the binding constants for an interaction between a monomer, M, and a binding site on a polymer, Pb, the following simple mathematical model was assumed:

$$M + Pb = MPb \qquad \text{(Eq. 1)}$$

where MPb, is the complex formed. When using the fluorescence technique to calculate the binding parameters, the solution of the problem is straight-

0022-3549/84/1200-1815$01.00/0
© 1984, American Pharmaceutical Association

ternational Symposium on Medicinal Chemistry, Brighton, September 1978, Abstr. 817.

(3) C. Semeraro, L. Dorigotti, S. Banfi, and C. Carpi, *J. Cardiovasc. Pharmacol.*, **3**, 455 (1981).

(4) L. Muiesan, G. Romanelli, E. Agabiti-Rosei, L. Alicandri, M. Beschi, M. Castellano, R. Fariello, A. Geri, L. Platto, P. Beggi, M. Motolese, and G. Muiesan, IXth World Congress of Cardiology, Moscow, June 1982.

(5) L. Corea, M. Bentivoglio, P. Beggi, and M. Motolese, IXth World Congress of Cardiology, Moscow, June 1982.

(6) M. Motolese, A. Magagna, B. Abdel-Mag, S. Lucarini, L. Graziadei, and A. Salvetti, IXth World Congress of Cardiology, Moscow, June 1982.

(7) F. V. Costa, R. Caldari, A. M. Marata, E. Strocchi, E. Ambrosioni, and B. Magnani, IXth Scientific Meeting of the International Society of Hypertension, Mexico City, February 1982.

(8) P. Van Brummelen, F. R. Bühler, W. Kiowski, P. Bolli, and O. Bertel, *Int. J. Clin. Pharmacol. Biopharm.*, **17**, 380 (1979).

(9) F. W. Amann and F. R. Bühler, *Clin. Eur.*, **18**, 1028 (1979).

(10) G. C. Lavezzaro, D. Gastaldo, P. Noussan, M. Bensoni, J. Parini, and P. F. Angelino, *Minerva Cardioangiol.*, **29**, 527 (1981).

(11) P. F. Angelino, M. Bensoni, D. Gastaldo, M. Minelli, J. Parini, and G. C. Lavezzaro, *Minerva Cardioangiol.*, **30**, 69 (1982).

(12) A. R. Schulert, *Arch. Int. Pharmacodyn.*, **132**, 1 (1961).

(13) P. Ventura, F. Parravicini, L. Simonotti, R. Colombo, and G. Pifferi, *J. Pharm. Sci.*, **70**, 334 (1981).

(14) L. Citerio, M. Visconti, M. Borsa, and G. Pifferi, *Boll. Chim. Farm.*, **120**, 222 (1981).

(15) G. Pifferi, F. Parravicini, C. Carpi, and L. Dorigotti, *J. Med. Chem.*, **18**, 741 (1975).

(16) G. Gaviraghi, M. Pinza, and G. Pifferi, *Synthesis*, **8**, 608 (1981).

(17) C. Farina, M. Pinza, A. Gamba, and G. Pifferi, *Eur. J. Med. Chem.*, **14**, 27 (1979).

(18) C. Farina, R. Pellegata, M. Pinza, and G. Pifferi, *Arch. Pharm.*, **314**, 108 (1981).

(19) T. Crolla, L. Citerio, M. Visconti, and G. Pifferi, *High-Resol. Chromatogr. Chromatogr. Commun.*, **6**, 445 (1983).

(20) L. Simonotti, F. Parravicini, and G. Pifferi, Vth National Congress of Mass Spectrometry, Rende, September 1980, Abstr. p. 34.

ACKNOWLEDGMENTS

The authors thank Prof. Emilio Rocca, University of Milan, for his help with the computer simulations and Dr. M. T. Riccaboni for her secretarial assistance in the preparation of this manuscript.

Binding Parameters of Interactions of Monomer–Polymer Systems Based on Quenching of Their Completely Overlapped Fluorescence: A Theory

HANNA N. BORAZAN

Received March 3, 1983, from the *Department of Pharmaceutical Chemistry, College of Pharmacy, University of Baghdad, Baghdad, Republic of Iraq.* Accepted for publication September 12, 1983.

Abstract □ A theory is presented which describes the interactions between completely overlapping fluorescing monomer–polymer systems and affords a method to calculate binding parameters. The theory is based on the assumptions that the complex formed from the fluorescing binding site and the monomer molecule does not fluoresce and that the fluorescence intensity is linearly related to concentration. The relationships derived from this theory have provided a sensitive and easy method for calculating the number of binding sites on a polymer molecule from only three emission-intensity values. The theory has been tested on systems containing trimethoprim–serum albumins and found to yield results which are consistent with a curve-fitting approach to the experimental data. This reflects the validity of the theoretical model presented and the various assumptions and approximations made.

Keyphrases □ Monomer–polymer systems—binding parameters, overlapped fluorescence quenching □ Binding parameters—overlapped fluorescence quenching, monomer–polymer system □ Fluorescence quenching—binding parameters, monomer–polymer systems

Fluorescence quenching has been applied to the study of complex formation (1); for example, the interactions of amino acids containing aromatic nuclei and their amines, and oligopeptides containing aromatic amino acids with nucleic acids, were studied by this method (2, 3). Recently, Koumriqian (4) and Borazan and Koumriqian (5) have applied the technique to study interactions between catecholamines and polyadenylic acid. In these studies, the emissions of the polynucleotides were negligible compared with those of the monomers. It was, therefore, easy to derive equations for calculating the binding parameters using the fraction remaining from the fluorescence intensity of the monomers or the observed quantum yield.

However, due to the inherent properties of many systems, both the monomers and polymers in the binary mixtures exhibit almost complete emission overlap over a wide range of excitation and emission wavelengths. Examples for such systems can be found in the fluorescence quenching studies of the interactions of steroids–polynucleotides (6), antineoplastics–polynucleotides (7), and antibacterials–serum albumins (8). Thus, these types of systems impose a difficult problem when analyzing the experimental data to calculate the binding constants. These authors (6–8) have applied an empirical approach involving a curve-fitting technique to analyze the fluorescence data.

The present study is concerned with a theoretical treatment which utilizes the fluorescence technique in situations where complete fluorescence overlap is taking place. This allowed us to determine the number of fluorescing binding sites on a polymer molecule available to the monomer molecules and to calculate the equilibrium constant for the process.

THEORETICAL SECTION

To calculate the binding constants for an interaction between a monomer, M, and a binding site on a polymer, Pb, the following simple mathematical model was assumed:

$$M + Pb = MPb \qquad \text{(Eq. 1)}$$

where MPb, is the complex formed. When using the fluorescence technique to calculate the binding parameters, the solution of the problem is straight-

0022-3549/84/1200-1815$01.00/0
© 1984, American Pharmaceutical Association

forward if one of the reactants does not fluoresce. In the present theoretical treatment, however, one case of concern is when both the monomer and binding site fluoresce at a given set of excitation and emission wavelengths (fluorescence overlap). Another source of concern is the quenching of the emissions of the interacting species when the complex is formed. It is assumed in the following derivations that the polymer molecule contains n fluorescing binding sites and that the emission intensity is linearly related to concentration. When working with dilute solutions:

$$\text{concentration} = \text{constant} \times \text{fluorescence intensity} \qquad \text{(Eq. 2)}$$

Accordingly:

$$I_{obs}^{\lambda} = I_M^{\lambda} + I_{Pb}^{\lambda,\Sigma} \qquad \text{(Eq. 3)}$$

where I_{obs}^{λ} and I_M^{λ} are the observed and free monomer emission intensities and $I_{Pb}^{\lambda,\Sigma}$ is the fluorescence intensity of the polymer sites without a bound substrate. The summation sign, Σ, is used to emphasize that the fluorescence originates from different sites on one polymer molecule.

I_{obs}^{λ} can be related to the total unquenched emission intensity, as:

$$I_{obs}^{\lambda} = \beta_{tot} I_{tot}^{\lambda} = \beta_M I_{M,0}^{\lambda} + \beta_{Pb} I_{Pb_0}^{\lambda,\Sigma} \qquad \text{(Eq. 4)}$$

β_{tot}, β_M, and β_{Pb} are the fractions of remaining fluorescence intensities for the total emission, monomer, and binding sites, and $I_{M,0}^{\lambda}$ and $I_{Pb_0}^{\lambda,\Sigma}$ are the initial emission intensities of the monomer and polymer binding sites. Therefore, from Eqs. 3 and 4:

$$I_M^{\lambda} = \beta_M I_{M,0}^{\lambda} \qquad \text{(Eq. 5)}$$

$$I_{Pb}^{\lambda,\Sigma} = \beta_{Pb} I_{Pb,0}^{\lambda,\Sigma} \qquad \text{(Eq. 6)}$$

According to Eq. 1, the concentration of the complex (MPb) can be expressed in three different ways:

$$(MPb) = (M_0) - (M) \qquad \text{(Eq. 7)}$$

$$(MPb) = (Pb_0) - (Pb) \qquad \text{(Eq. 8)}$$

$$(MPb) = n(P_0) - n(P) \qquad \text{(Eq. 9)}$$

where (M_0) and (M) are the initial and free concentrations of the monomer, respectively; (Pb_0) and (Pb) are the concentrations of the initial and the remaining free polymer binding sites, respectively; and (P_0) and (P) represent the total and free concentrations of the polymer, respectively.

According to the assumption presented in Eq. 2, one can easily verify the following equations:

$$(M) = \beta_M (M_0) \qquad \text{(Eq. 10)}$$

$$(Pb) = \beta_{Pb} (Pb_0) \qquad \text{(Eq. 11)}$$

$$(P) = \beta_{Pb} (P_0) \qquad \text{(Eq. 12)}$$

It is evident from Eqs. 10–12, that β_M and β_{Pb} are essentially equal to the fractions which remain free of interaction. Combining Eqs. 5, 7, and 10:

$$(MPb) = (M_0)\left(1 - \frac{I_M^{\lambda}}{I_{M,0}^{\lambda}}\right) \qquad \text{(Eq. 13)}$$

and Eqs. 6, 9, and 12:

$$(MPb) = n(P_0)\left(1 - \frac{I_{Pb}^{\lambda,\Sigma}}{I_{Pb_0}^{\lambda,\Sigma}}\right) \qquad \text{(Eq. 14)}$$

Equating Eqs. 13 and 14, substituting for $I_{Pb}^{\lambda,\Sigma}$ (Eq. 3), and rearranging equations:

$$I_M^{\lambda} = \frac{(M_0) I_{Pb_0}^{\lambda,\Sigma} I_{M,0}^{\lambda} - n(P_0) I_{M,0}^{\lambda} (I_{Pb_0}^{\lambda,\Sigma} - I_{obs}^{\lambda})}{n(P_0) I_{M,0}^{\lambda} + (M_0) I_{Pb_0}^{\lambda,\Sigma}} \qquad \text{(Eq. 15)}$$

Rearranging Eq. 3 and combining with Eq. 6:

$$\beta_{Pb} = \frac{I_{obs}^{\lambda} - I_M^{\lambda}}{I_{Pb_0}^{\lambda,\Sigma}} \qquad \text{(Eq. 16)}$$

Substituting for I_M^{λ} (Eq. 15) into Eq. 16:

$$\beta_{Pb} = \frac{(M_0) I_{obs}^{\lambda} - (M_0) I_{M,0}^{\lambda} + n(P_0) I_{M,0}^{\lambda}}{n(P_0) I_{M,0}^{\lambda} + (M_0) I_{Pb_0}^{\lambda,\Sigma}} \qquad \text{(Eq. 17)}$$

According to the mathematical model presented in Eq. 1, the equilibrium constant expression, K, can be written as:

$$K = \frac{(MPb)}{(M)(Pb)} \qquad \text{(Eq. 18)}$$

Incorporating Eqs. 9 and 12 into Eq. 7:

$$(M) = (M_0) - n(P_0)(1 - \beta_{Pb}) \qquad \text{(Eq. 19)}$$

The equilibrium constant equation (Eq. 18) can be written in the following form after substituting for (MPb) (Eqs. 9 and 12), M (Eq. 19), and for (Pb) (Eqs. 11 and 12):

$$K = \frac{\left[\frac{1 - \beta_{Pb}}{\beta_{Pb}}\right]}{[(M_0) - n(P_0)(1 - \beta_{Pb})]} \qquad \text{(Eq. 20)}$$

Thus, the value of n must be determined in addition to the other experimental parameters in order to solve for β_{Pb} (Eq. 17) and K (Eq. 20).

In principle, one may be able to arrive at the values of n by performing a curve-fitting technique through assigning values to n and calculating the equilibrium constant, K, at different concentration levels to minimize percent variation (6–8). Thus, the present investigation is undertaken to study the problem from a fundamental point of view, in the hope of arriving at the exact relationships controlling such complicated systems. This can be done through optimizing the K expression (Eq. 20) with respect to n, *i.e.*:

$$\frac{\partial K}{\partial n} = 0 \qquad \text{(Eq. 21)}$$

Therefore, Eq. 20 should lead to the following:

$$[(M_0) - n(P_0) + n(P_0)\beta_{Pb}] \frac{1}{\beta_{Pb}^2} \frac{d\beta_{Pb}}{dn} + \left[\frac{1 - \beta_{Pb}}{\beta_{Pb}}\right]\left[-(P_0) + (P_0)\beta_{Pb} + n(P_0)\frac{d\beta_{Pb}}{dn}\right] = 0 \qquad \text{(Eq. 22)}$$

Rearranging Eq. 22 and setting it up in an integral form, we can write:

$$\int \frac{\gamma d\beta_{Pb}}{(1 - \beta_{Pb})^2 n} - \int \frac{d\beta_{Pb}}{(1 - \beta_{Pb})^2} + \int \frac{2\beta_{Pb} d\beta_{Pb}}{(1 - \beta_{Pb})^2} - \int \frac{\beta_{Pb}^2 d\beta_{Pb}}{(1 - \beta_{Pb})^2} - \int \frac{\beta_{Pb}}{n} dn = 0 \qquad \text{(Eq. 23)}$$

where:

$$\gamma = \frac{(M_0)}{(P_0)} \qquad \text{(Eq. 24)}$$

Eq. 17 can be rearranged to yield n in terms of intensities and concentrations:

$$n = \frac{(M_0)(I_{obs}^{\lambda} - I_{M,0}^{\lambda}) - (M_0)\beta_{Pb} I_{Pb_0}^{\lambda,\Sigma}}{(P_0)\beta_{Pb} I_{M,0}^{\lambda} - (P_0) I_{M,0}^{\lambda}} \qquad \text{(Eq. 25)}$$

To simplify the notations, set:

$$a = I_{obs}^{\lambda} - I_{M,0}^{\lambda} \qquad \text{(Eq. 26)}$$

$$b = I_{Pb_0}^{\lambda,\Sigma} \qquad \text{(Eq. 27)}$$

$$c = I_{M,0}^{\lambda} \qquad \text{(Eq. 28)}$$

$$\beta = \beta_{Pb} \qquad \text{(Eq. 29)}$$

Therefore, Eq. 25 can be written in the following form:

$$n = \frac{\gamma(b\beta - a)}{c(1 - \beta)} \qquad \text{(Eq. 30)}$$

Taking the differential of Eq. 30:

$$dn = \frac{\gamma b d\beta}{c(1 - \beta)} + \frac{\gamma bc\beta d\beta}{c^2(1 - \beta)^2} - \frac{\gamma ac d\beta}{c^2(1 - \beta)^2} \qquad \text{(Eq. 31)}$$

Substituting for n (Eq. 30) and dn (Eq. 31) into Eq. 23:

$$c \cdot \int \frac{d\beta}{(1 - \beta)(b\beta - a)} - \int \frac{d\beta}{(1 - \beta)^2} + 2 \cdot \int \frac{\beta d\beta}{(1 - \beta)^2} - \int \frac{\beta^2 d\beta}{(1 - \beta)^2} - b \cdot \int \frac{\beta d\beta}{(b\beta - a)} - b \cdot \int \frac{\beta^2 d\beta}{(1 - \beta)(b\beta - a)} + a \cdot \int \frac{\beta d\beta}{(1 - \beta)(b\beta - a)} = 0 \qquad \text{(Eq. 32)}$$

The above integrals can be evaluated to yield the following (9, 10):

$$c \cdot \int \frac{d\beta}{(1 - \beta)(b\beta - a)} = \frac{c}{b - a} \cdot \ln \frac{(b\beta - a)}{(1 - \beta)} \qquad \text{(Eq. 33)}$$

$$\int \frac{d\beta}{(1 - \beta)^2} = \frac{1}{1 - \beta} \qquad \text{(Eq. 34)}$$

$$2 \cdot \int \frac{\beta\, d\beta}{(1-\beta)^2} = 2 \cdot \ln(1-\beta) + \frac{2}{1-\beta} \quad \text{(Eq. 35)}$$

$$\int \frac{\beta^2 d\beta}{(1-\beta)^2} = \beta + 2 \cdot \ln(1-\beta) + \frac{1}{1-\beta} \quad \text{(Eq. 36)}$$

$$b \cdot \int \frac{\beta\, d\beta}{(b\beta - a)} = \beta + \frac{a}{b} \cdot \ln(b\beta - a) \quad \text{(Eq. 37)}$$

$$b \cdot \int \frac{\beta^2\, d\beta}{(1-\beta)(b\beta - a)} = -\beta - \frac{a+b}{b} \cdot \ln(b\beta - a) + \frac{b}{b-a} \cdot \ln \frac{(b\beta - a)}{(1-\beta)} \quad \text{(Eq. 38)}$$

$$a \cdot \int \frac{\beta\, d\beta}{(1-\beta)(b\beta - a)} = \frac{a^2}{b(b-a)} \cdot \ln(b\beta - a) - \frac{a}{b-a} \cdot \ln(1-\beta) \quad \text{(Eq. 39)}$$

Substituting for the integral values (Eqs. 33-39) into Eq. 32:

$$\left[\frac{c}{b-a} - \frac{a}{b}\right] \cdot \ln(b\beta - a) - \left[\frac{c}{b-a} - 1\right] \cdot \ln(1-\beta) - \beta = 0 \quad \text{(Eq. 40)}$$

One can easily verify that Eq. 40 holds for $|b\beta - a|$, and when expressing it in its original notations (Eqs. 26-29) it yields the following:

$$\left[\frac{I_{M,0}^{\lambda}}{I_{Pb_0}^{\lambda,\Sigma} + I_{M,0}^{\lambda} - I_{obs}^{\lambda}} - \frac{I_{obs}^{\lambda} - I_{M,0}^{\lambda}}{I_{Pb_0}^{\lambda,\Sigma}}\right] \cdot \ln\left|I_{Pb_0}^{\lambda,\Sigma}\beta_{Pb} + I_{M,0}^{\lambda} - I_{obs}^{\lambda}\right| - \left[\frac{I_{obs}^{\lambda} - I_{Pb_0}^{\lambda,\Sigma}}{I_{Pb_0}^{\lambda,\Sigma} + I_{M,0}^{\lambda} - I_{obs}^{\lambda}}\right] \cdot \ln(1-\beta_{Pb}) - \beta_{Pb} = 0 \quad \text{(Eq. 41)}$$

RESULTS AND DISCUSSION

Solving the nonlinear equation (Eq. 41) is a difficult task using conventional mathematical methods. An approximate solution to the problem is obtained by expanding the logarithmic terms and expressing the equation in terms of the power series of β. This method yields highly approximate results because terms having exponents greater than four are omitted. Higher order equations are almost impossible to solve, however, if one seeks better results. Thus, the most reasonable technique remaining is to solve Eq. 41 numerically with a programmable calculator.

To test the theory, experimental data involving fluorescence quenching studies, where complete emission overlap characterizes the systems, were taken from Saoud (8). His investigation was concerned with interactions between trimethoprim and serum albumins taken from different species. The measured emission intensity data were computed into the coefficients of the natural logarithms of Eq. 41, while the equation is solved by assigning values to β and calculating the value of the equation $[F(\beta)]$. Obviously, the acceptable solution is $F(\beta) = 0$. In all cases, β is solved to 1×10^{-6}. The value of $|F(\beta)|$ that corresponds to this level of accuracy ranged from 3.6×10^{-5} to 6.6×10^{-7}. The results are summarized in Table I.

Applying Eq. 25, the value of β_{Pb}^1 yields unrealistic results, since negative values of the number of binding sites are obtained. Thus the values of β_{Pb}^2 are the ones taken as a base for calculating the binding parameters. It is evident from Table I that as the monomer-polymer ratio is increased by 400%, the equilibrium constant varies only in the range from 8.5 to 19.8%. Furthermore, the estimated difference in the number of binding sites for the same magnitude of increase in the ratio is found to be 20.3–57.8%. These variations reflect the combined effects of the experimental errors, the inherent factors in the systems themselves, and the various assumptions and approximations made. For example, it was assumed in the derivations presented in the theory that all of the binding sites are independent (no site-site interaction took place), equivalent, and fluorescing. Based upon different physical methods, deviations from linearity of the Scatchard plots are reported in the literature. The explanations given include site-site interactions (11, 12), competitive binding between fluorescing and nonfluorescing binding sites, and the presence of nonequivalent binding sites (13).

Saoud (8) has applied Eq. 17 to calculate β_{Pb} by assigning values to the number of binding sites, n. The best n value is the one that generates the least variation in K. Indeed, the n values obtained by the author that induce minimum variation in K were close to the values obtained from Eq. 41. This gives supporting evidence to the validity of the relationships derived in this theory.

It may be concluded that the present theory has provided a powerful tool to calculate the binding parameters for the monomer-polymer interactions

Table I—Fractions Which Remain Free of Binding Interactions on the Polymer and Monomer Molecules Together with Number of Binding Sites and the Equilibrium Constants for the Interactions of Trimethoprim with Serum Albumins [a]

$(M_0)/(P_0) \times 10^{-2}$ [b]	β^1_{Pb}	β^2_{Pb}	β_M	n	K, $M^{-1} \times 10^{-5}$
		Trimethoprim-Human Serum Albumin[c]			
0.69013	0.646359	0.742452	0.952831	12.64	3.64061
1.38026	0.457742	0.580798	0.970633	9.67	3.71803
2.07039	0.323637	0.464287	0.978571	8.28	3.93036
2.76052	0.215785	0.371481	0.982130	7.85	4.30678
Mean				9.61	3.89895
± SD, %				24.92	8.54
		Trimethoprim-Camel Serum Albumin[c]			
0.69013	0.708736	0.783187	0.950220	15.85	2.91337
1.38026	0.530511	0.628165	0.968354	11.75	3.05642
2.07039	0.397371	0.511137	0.975151	10.52	3.26931
2.76052	0.286506	0.413516	0.978418	10.16	3.62393
Mean				12.07	3.21576
± SD, %				23.57	11.05
		Timethoprim-Bovine Serum Albumin[c]			
0.69013	0.735330	0.812953	0.909549	33.37	2.52964
1.38026	0.570280	0.647819	0.958704	16.18	2.83529
2.07039	0.426571	0.514425	0.967674	13.78	3.25150
2.76052	0.313160	0.405888	0.974813	11.70	3.75388
Mean				18.76	3.09258
± SD, %				57.76	19.79
		Trimethoprim-Rat Serum Albumin[c]			
0.69013	0.797670	0.840868	0.963713	15.74	1.96373
1.38026	0.642249	0.709530	0.972037	13.29	2.10580
2.07039	0.488334	0.577188	0.975292	12.10	2.50365
2.76052	0.375465	0.475640	0.980032	10.51	2.81223
Mean				12.91	2.34635
± SD, %				20.26	18.08

[a] In 1 mM aqueous cacodylate buffer, pH 7, based on fluorescence data taken from Ref. 8. [b] The concentration of the albumins was 1.449×10^{-8} M and the measurements were at 25°C. [c] The excitation wavelength was 290 nm and the emission intensities were measured at 335 nm for human serum albumin, 345 nm for camel serum albumin, 352 nm for bovine serum albumin, and 340 nm for rat serum albumin.

from fluorescence quenching, even when a complete overlap in their emission properties is taking place. The method is sensitive and easy, where only three experimental values are necessary to calculate the number of fluorescing binding sites on the polymer: the emissions of the two pure components and the emissions of a mixture containing equimolar concentrations of the components.

REFERENCES

(1) R. Foster, "Organic Charge Transfer Complexes," Academic Press, London, England, 1969, pp. 82–89.

(2) C. Helene, T. Montenay-Garestier, and J. L. Dimicoli, *Biochim. Biophys. Acta*, **254**, 349 (1971).

(3) C. Helene, H. Borazan, J. L. Dimicoli, J. C. Maurizot, M. Durand, and J. J. Toulme, "Proceedings of the 23rd Annual Meeting of the Societe de Chimie Physique over the Dynamic Aspects of Conformation Changes in Biological Macromolecules", Orleans, France, 1973, p. 349.

(4) S. N. Koumriqian, M. Sc. Thesis, University of Baghdad, Baghdad, Iraq, 1981.

(5) H. N. Borazan and S. N. Koumriqian, *J. Pharm. Sci.*, **72**, 1450 (1983).

(6) A. J. Qasir, M. Sc. Thesis, University of Baghdad, Baghdad, Iraq, 1982.

(7) M. E. Zia, M. Sc. Thesis, University of Baghdad, Baghdad, Iraq, 1982.

(8) M. D. Saoud, M. Sc. Thesis, University of Baghdad, Baghdad, Iraq, 1982.

(9) G. A. Korn and T. M. Korn, "Mathematical Handbook for Scientists and Engineers," McGraw-Hill, New York, N.Y., 1968, pp. 928–932.

(10) "CRC Standard Mathematical Tables," W. H. Beyer and S. M. Selby, Eds., CRC Press, Cleveland, Ohio, 1976, pp. 345–346.

(11) M. Durand, J. C. Maurizot, H. N. Borazan, and C. Helene, *Biochemistry*, **14**, 563 (1975).

(12) M. Durand, H. N. Borazan, J. C. Maurizot, J. L. Dimicoli, and C. Helene, *Biochimie*, **58**, 395 (1976).

(13) T. L. Miller, S. L. Willett, M. E. Moss, J. Miller, and B. A. Belinka, Jr., *J. Pharm. Sci.*, **71**, 173 (1982).

ACKNOWLEDGMENTS

The author thanks the University of Baghdad for financial support of this work.

Hypolipidemic Activity of 4-Pyrimidinecarboxylic Acids in CF_1 Mice

I. H. HALL ˣ, G. H. COCOLAS, and W. L. WILLIAMS, JR.

Received September 19, 1983, from the *Division of Medicinal Chemistry and Natural Products, School of Pharmacy, University of North Carolina at Chapel Hill, Chapel Hill, NC 27514.* Accepted for publication February 16, 1984.

Abstract □ A series of 4-pyrimidinecarboxylic acids were evaluated for hypolipidemic activity in mice at 20–30 mg/kg/d ip. A number of these derivatives were observed to be active at this dose. Substitution of the hydroxyl group in position 2 and 6 of the 4-pyrimidinecarboxylic acid with a sulfhydryl and an amino group, respectively, led to a compound which produced a >40% reduction of serum cholesterol and triglyceride levels in mice. Similarly, a compound which was substituted with an amino group in position 2 and an isobutyl group in position 5 led to equally potent activity as a hypolipidemic agent.

Keyphrases □ 4-Pyrimidinecarboxylic acids—antihypolipidemic activity, mice □ Antihypolipidemic agents—4-pyrimidinecarboxylic acids, activity in mice

Windmueller and co-workers (1–4) demonstrated that 1% orotic acid (2,6-dihydroxy-4-pyrimidinecarboxylic acid) in the diet of rats decreased plasma lipids. Ravi Subbiah (5) later showed that both serum cholesterol and triglycerides were reduced in rats treated with 1% orotic acid, but there was an increase in cholesterol, fatty acid, and triglyceride levels in the liver with a decrease in cholesterol excretion into the bile and feces. Subsequent studies showed that orotic acid reduced the serum lipoprotein fractions, *i.e.*, low-density lipoprotein, very low-density lipoprotein, and high-density lipoprotein (6–8) induced hyperlipidemic states in animals (7). Protein synthesis required for the apoprotein was not inhibited; rather, there was an inability to incorporate the lipid with the apoprotein for the lipoprotein fractions by the liver (6). The present study deals with the structure modification of orotic acid to yield other 4-pyrimidinecarboxylic acids which hopefully will possess hypolipidemic activity at a relatively low dose.

EXPERIMENTAL SECTION

Source of Compounds—Orotic acid was commercially available[1]. The chemical synthesis and physical characteristics of the 4-pyrimidinecarboxylic acids have been previously reported in the literature (9–11). Chemical syntheses were conducted by these methods and melting points are reported in Table I. Melting points were determined on a melting point apparatus[2] and are uncorrected.

Hypolipidemic Activity—Test compounds were suspended in 1% carboxymethylcellulose–water, homogenized, and administered intraperitoneally to CF_1 male mice (~25 g) for 16 d. On days 9 and 16, blood was obtained by tail vein bleeding and the serum was separated by centrifugation for 3 min. The serum cholesterol was determined by a modification of the Liebermann–Burchard reaction (12). Serum triglyceride levels were determined in blood collected on day 16 by a commercial kit[3]. The data for these assays is presented as a percent of control ± *SD*; the probability level was calculated by the Student's *t* test. Clofibrate[4] at 150 mg/kg/d was used as a standard for comparisons in the hypolipidemic screens.

[1] Aldrich Chemical Company.
[2] Mel-Temp.
[3] Bio Dynamics/bmc.
[4] Ayerst Laboratories.

Table I—Chemical Structure and Physical Characteristics of 4-Pyrimidinecarboxylic Acids

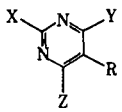

Compound	X	Y	Z	R	Melting Point, °C	Reference for Synthetic Procedure
I	OH	OH	COOH	CH_3		
II	NH_2	OH	COOH	CH_3	300–301	(10)
III	SH	OH	COOH	CH_3	297–300	(11)
IV	OH	SO	COOH	CH_3	317–319	(11)
V	SH	NH_2	COOH	CH_3	241–243	(9)
VI	NH_2	SH	COOH	CH_3	282–283	(11)
VII	NH_2	NH_2	COOH	C_2H_5	252–253	(9)
VIII	NH_2	NH_2	COOH	n-C_3H_7	243–244	(9)
IX	NH_2	NH_2	COOH	n-C_4H_9	245–246	(9)
X	NH_2	NH_2	COOH	iso-C_4H_9	238–239	(9)
XI	NH_2	NH_2	COOH	$C_6H_5CH_2$	248–249	(9)
XII	NH_2	NH_2	COOH	p-$CH_3OC_6H_4$	248–249	(9)
XIII	OH	NH_2	COOH	iso-C_4H_9	249–250	(9)
XIV	OH	NH_2	COOH	p-$CH_3OC_6H_4$	356–357	(9)
XV	SH	NH_2	COOH	C_2H_5	238–239	(9)
XVI	SH	NH_2	COOH	n-C_3H_7	233–234	(9)
XVII	SH	NH_2	COOH	n-C_4H_9	216–217	(9)
XVIII	SH	NH_2	COOH	$C_6H_5CH_2$	277–279	(9)
XIX	SH	NH_2	COOH	p-$CH_3OC_6H_4$	283–286	(9)
XX	C_2H_5S	OH	COOH	C_2H_5	232–233	(10)
XXI	SH	OH	CH_2OH	CH_3	297–300	(11)

0022-3549/84/1200-1819$01.00/0
© 1984, American Pharmaceutical Association

Table II—Hypolipidemic Activity of 4-Pyrimidinecarboxylic Acids in CF_1 Male Mice [a]

Compound	Dose mg/kg/d ip	Serum Cholesterol Levels Day 9	Serum Cholesterol Levels Day 16	Serum Triglyceride Levels Day 16
I	20	91 ± 5	68 ± 3[b]	82 ± 6
	30	94 ± 4	76 ± 4[b]	65 ± 5[b]
II	20	84 ± 4[b]	82 ± 4[b]	76 ± 6[b]
	30	78 ± 3[b]	77 ± 3[b]	56 ± 6[b]
III	20	80 ± 5[b]	75 ± 5[b]	74 ± 6[b]
	30	61 ± 4[b]	66 ± 3[b]	58 ± 5[b]
IV	20	75 ± 5[b]	65 ± 3[b]	68 ± 5[b]
V	20	76 ± 5[b]	56 ± 3[b]	48 ± 4[b]
VI	20	69 ± 5	66 ± 4[b]	59 ± 6[b]
VII	20	95 ± 5	73 ± 5[b]	71 ± 5[b]
VIII	20	101 ± 5	60 ± 4[b]	57 ± 5[b]
IX	20	73 ± 4[b]	78 ± 3[b]	89 ± 7
X	20	103 ± 5	74 ± 4[b]	53 ± 6[b]
XI	20	99 ± 6	73 ± 3[b]	68 ± 6[b]
XII	20	68 ± 4[b]	71 ± 4[b]	81 ± 7
XIII	20	81 ± 3[b]	56 ± 5[b]	43 ± 4[b]
XIV	20	81 ± 3[b]	73 ± 4[b]	73 ± 5[b]
XV	20	79 ± 6[b]	68 ± 5[b]	63 ± 3[b]
XVI	20	78 ± 5	71 ± 5[b]	94 ± 6
XVII	20	97 ± 7	68 ± 3[b]	74 ± 7[b]
XVIII	20	82 ± 8	69 ± 4[b]	50 ± 4[b]
XIX	20	80 ± 5[b]	64 ± 3[b]	80 ± 5[b]
XX	20	70 ± 6[b]	56 ± 3[b]	64 ± 3[b]
XXI	20	84 ± 5	79 ± 4[b]	55 ± 4[b]
Clofibrate	150	88 ± 4	87 ± 5	75 ± 5[b]
1% Carboxymethylcellulose		100 ± 6	100 ± 5	100 ± 7

[a] As mean ± *SD* percent of control; $n = 6$. [b] $p \leq 0.001$.

RESULTS AND DISCUSSION

A number of the 4-pyrimidinecarboxylic acid derivatives demonstrated potent hypolipidemic activity at 20 mg/kg/d ip in mice (Table II). Compounds I, IV, V, VI, VIII, XIII, XV, XVII, XVIII, XIX, and XX afforded ≥30% reduction of the serum cholesterol level at 20 mg/kg/d after dosing for 16 d and III produced a similar reduction at 30 mg/kg/d. Compounds IV, V, VI, VIII, X, XI, XIII, XV, XVIII, XX, and XXI resulted in ≥30% reduction of serum triglycerides after dosing for 16 d. Compounds I, II, and III were also effective at this level at a dose of 30 mg/kg/d. Compounds V and XIII appeared to be the most effective in this dose range with a >40% reduction of both serum lipids. Those carboxylic acids with a methyl group in the 5 position and a sulfhydryl group substituted in the 2 or 6 position (IV, V, and VI) at a dose of 20 mg/kg/d, and III at a dose of 30 mg/kg/d, resulted in lowering of both serum cholesterol and triglyceride levels after dosing for 16 d.

When positions 2 and 6 were substituted with an amino group while varying the R group substitutions, the *n*-propyl derivative (VIII) resulted in the best hypolipidemic activity of this series, with a 40% reduction of serum cholesterol and a 43% reduction of serum triglycerides after dosing for 16 d at 20 mg/kg/d. Compound X, with a substitution of isobutyl in position 5, was also active with a 26 and 47% reduction of cholesterol and serum triglycerides, respectively.

Substitution of a hydroxyl group in the 2 position, an amino in the 6 position with an isobutyl in position 5 (compound XIII) resulted in one of the best activities, with a 44% reduction of serum cholesterol and a 57% reduction of serum triglycerides. Of those compounds with a substituted aromatic ring in the 5 position, compound XVIII with a sulfhydryl group in position 2 and an amino group in position 6 resulted in a reduction of 31% in serum cholesterol and 50% in serum triglycerides. Compound XV, similar to XVIII but with an ethyl group substituted in the 5 position, also afforded good activity with a 32% reduction of serum cholesterol and a 37% reduction in triglyceride levels. Compound XX with a substituted sulfhydryl group in position 2, a hydroxyl group in the 6 position, and an ethyl group in the 5 position also afforded good activity by lowering serum cholesterol levels 44% and triglyceride levels 36% on day 16.

Substitution of an alcohol in place of a carboxylic acid group in position 4, with the same substitutions on 2, 6, and 5 (compare XXI to III) resulted in approximately the same degree of reduction of serum cholesterol at a dose of 20 mg/kg/d (20–25%), but the serum triglycerides were reduced from 26% to 45% with XXI at a dose of 20 mg/kg/d.

These studies have shown that a number of substituted 4-pyrimidinecarboxylic acids are potent hypolipidemic agents when compared with clofibrate at 150 mg/kg in rodents (Table II). Further studies are currently being conducted to establish the effects of the more potent derivatives on lipid metabolism and liver and serum lipoprotein levels. It would be desirable if the new agents did not cause lipid deposition in the hepatocyte, resulting in fatty livers similar to the observed effect of orotic acid on diet (2, 5).

Orotic acid is known to have no effect on cholesterol-7-α-hydroxylase activity and thus does not affect bile excretion of cholesterol (5); however, it does decrease mitochondrial fatty acid oxidation and acetyl-CoA dehydrogenase but not β oxidation by the peroxisomal system (13). A more in-depth study of orotic acid derivatives is required to assess their usefulness as hypolipidemic agents.

REFERENCES

(1) H. G. Windmueller, *Biochem. Biophys. Res. Commun.*, **11**, 496 (1963).

(2) H. G. Windmueller, *J. Biol. Chem.*, **239**, 330 (1964).

(3) H. G. Windmueller and A. G. Spaeth, *J. Biol. Chem.*, **241**, 2891 (1966).

(4) H. G. Windmueller and R. I. Levy, *J. Biol. Chem.*, **242**, 2246 (1967).

(5) M. T. Ravi Subbiah, *J. Steroid Biochem.*, **9**, 775 (1978).

(6) P. S. Roheim, S. Switzer, A. Girard, and H. A. Eder, *Biochem. Biophys. Res. Commun.*, **20**, 416 (1965).

(7) R. Fears and A. M. Umpleby, *Biochem. Soc. Trans.*, **6**, 602 (1978).

(8) L. A. Pottengen and G. Getz, *J. Lipid Res.*, **12**, 450 (1971).

(9) S. Borodkin, S. Jonsson, G. H. Cocolas, and R. L. McKee, *J. Med. Chem.*, **10**, 248 (1967).

(10) S. Borodkin, S. Jonsson, G. H. Cocolas, and R. L. McKee, *J. Med. Chem.*, **10**, 290 (1967).

(11) H. L. Wheeler and D. F. McFarland, *Am. Chem. J.*, **43**, 19 (1910).

(12) A. T. Ness, J. V. Pastewka, and A. C. Peacock, *Clin. Chim. Acta*, **10**, 229 (1964).

(13) S. Miyazawa, S. Furuta, and T. Hashimoto, *Biochim. Biophys. Acta*, **711**, 494 (1982).

ACKNOWLEDGMENTS

The authors thank P. J. Voorstad, MacDonald Bowden, and Walter Spivey for their technical assistance. Research support for this project was from the National Institute of Health, Grant No. HL25680.

Determination of Dextromethorphan in Biological Fluids by Liquid Chromatography by Using Semi-microbore Columns

RAJA G. ACHARI ˣ, HEINZ M. EDERMA, DAVID CHIN, and STANLEY R. OLES

Received August 23, 1983, from *Bristol-Myers Products Research and Development Center, Hillside, NJ 07207.* Accepted for publication February 3, 1984.

Abstract □ A sensitive, specific procedure for the determination of dextromethorphan in plasma and urine in dogs is described. The use of a semi-microbore column, 2.1 mm i.d. × 25 cm resulted in a detection limit of 1 ng/mL in plasma and 25 ng/mL in urine. Plasma (3 mL) is extracted in CCl_4 and the drug is back-extracted with 3% acetic acid. The chromatographic separation is carried out using a 5-μm particle size octadecyl-bonded column, and the drug is monitored by a fluorescence detector. The results after 10-mg oral administrations of dextromethorphan to dogs are provided.

Keyphrases □ Dextromethorphan—HPLC determination, semi-microbore column, dog plasma, urine

Dextromethorphan is a widely used synthetic antitussive agent. Due to significant first-pass hepatic metabolism, only a trace amount of unmetabolized drug is found in circulation, usually <5 ng/mL after oral administration (1, 2). Previous reports of dextromethorphan analysis involved electron-capture GC, nitrogen-phosphorus detection GC and RIA (1–3). There has been no report in the literature on the assay of dextromethorphan in biological fluids by high-performance liquid chromatography (HPLC) due to a lack of sensitivity of the instrument at this level. We report here an HPLC method for determining dextromethorphan using semi-microbore columns capable of measuring the drug in amounts as low as 1 ng/mL.

EXPERIMENTAL SECTION

Materials—All chromatographic solvents were HPLC grade, reagents were ACS, U.S.P., or N.F. quality and were used as received without further purification. Dextromethorphan HBr[1] was U.S.P. grade and was used as received. The apparatus was a modular unit consisting of a reciprocating pump[2], a fluorescence detector[3], an autoinjector[4], and a strip-chart recorder[5]. All columns were prepacked and octadecylsilane bonded[6]. The average particle size of the packing material was 5 μm. The mobile phase was acetonitrile–water (45:55) containing 0.01 M monobasic ammonium phosphate and 0.005 M sodium lauryl sulfonate. The pH was adjusted to 3.0 using phosphoric acid. The flow rate was maintained at 300 μL/min.

Sample Preparation—*Plasma Extraction Procedure*—Plasma (3 mL) was transferred into a screw-cap disposable tube (16 mm × 125 mm), 0.5 mL of 6 M HCl was added, and the mixture was vortexed; 10 M NaOH (0.4 mL) was then added and mixed until a clear mixture was obtained. Immediately, 10 mL of CCl_4 was added and the mixture was first handshaken gently a few times and then shaken for 30 min on a mechanical horizontal shaker. After a 10-min centrifugation at 2500 rpm, the top aqueous layer of the sample was completely removed by suction and discarded. The organic layer was poured into a 20 × 150 mm wide-mouth test tube. The carbon tetrachloride layer (8 mL) was transferred into another 16 × 125 mm disposable screw-cap tube. (In this step, it is essential to avoid having any of the residual aqueous layer enter the pipette.) Acetic acid (3%) was added (0.5 mL) and shaken for 30 min on a horizontal shaker. The tube was centrifuged for 5 min at 2500 rpm and a portion of the acid layer was removed for analysis.

A urine sample (5 mL) was diluted to 50 mL with 3% acetic acid. The diluted urine was injected directly into the liquid chromatograph for dextromethorphan analysis. Three healthy beagle dogs (weight, ~10 kg) were dosed orally with 10 mg of dextromethorphan hydrobromide in a physiological saline solution. Blood (8 mL) was withdrawn with a heparinized syringe at predose, 0.5, 1, 2, 4, 8, and 24 h after dosing. The blood was immediately centrifuged and the plasma was extracted for dextromethorphan analysis as described above. Urine samples were collected over a 24-h period and pooled.

Standard Curve and Calibration—Aqueous solutions of dextromethorphan hydrobromide were added to blank plasma samples such that the plasma contained 1–5 ng/mL of dextromethorphan hydrobromide. These standard plasma samples were extracted as described under sample preparations. Calibration curves were plotted using peak height *versus* the plasma drug concentration using the least-squares method. The concentrations of the drug in samples were interpolated from the standard curve.

Aqueous solutions of dextromethorphan hydrobromide were added to the blank urine samples to yield concentrations of 50–500 ng/mL dextromethorphan hydrobromide. These samples were diluted 5–50 mL with 3% acetic acid solution.

RESULTS AND DISCUSSION

Dextromethorphan has a UV maximum at 280 nm, so the initial experiments were carried out at this wavelength. The detection limit at 280 nm was not satisfactory for plasma analysis. By changing the wavelength to 200 nm, a 20-fold increase in sensitivity was obtained, but endogenous materials from plasma interfered. Since dextromethorphan has good fluorescent properties, the detection mode was changed from UV to fluorescence. Although the detection limit by fluorescence was similar to that by UV at 200 nm, the specificity improved significantly. The plasma blank showed no interference due to endogenous substances in the dextromethorphan elution region of the chromatogram. The use of semi-microbore columns (2.1 mm i.d.) increased the sensitivity of dextromethorphan fivefold with conventional 4.6 mm i.d. columns.

The chromatograms of the extracts of both human plasma and canine plasma were identical. For this reason, pooled human plasma was used to obtain a standard curve for dog plasma analysis since blank dog plasma was in short supply. Figure 1 shows the chromatograms of unspiked and dextromethorphan hydrobromide-spiked (1 ng/mL) human plasma. Figure 2 shows the chromatograms of dog urine blank and that spiked with 50 ng/mL. The detection limit in the urine samples is ~20 ng/mL.

Linearity—A linearity study was conducted on plasma samples by spiking with known amounts of dextromethorphan hydrobromide; levels of 0, 1, 2, 3, and 5 ng/mL were investigated. Between-day variation was examined by an analysis of variance of slopes and intercepts from 11 standard curves run over a period of 3 weeks. The slopes of these curves had an *RSD* of ±8.7%. This variation is not unusual and is related to a slight change in the chromatographic column performance over a period of time. A small interference is indicated by a positive intercept which amounted to an equivalent of 0.30 ng/mL of dextromethorphan hydrobromide. The data are summarized in Table I.

A linearity study on the urine sample was done by spiking blank urine with dextromethorphan hydrobromide at levels of 50–500 ng/mL. A correlation coefficient of 0.9996 was found. This much improved correlation for the urine standards as compared to the plasma standards is due to the fact that no extraction was involved in urine standards.

Absolute Recovery of Dextromethorphan from Biological Fluids—Recovery studies of dextromethorphan from spiked plasma were carried out. Recovery data were calculated against an unextracted standard (Table II). A small interference was found in the blank plasma and this peak height was subtracted from the sample peak height for the calculation of the recovery data. The *RSD* values were ~7–9% at the 2–5 ng/mL level, and 15% at 1 ng/mL, which is about the lower limit of detection by this method.

[1] Hoffman-La Roche, Nutley, N.J.
[2] Model 6000; Waters Associates, Milford, Mass.
[3] Model GM 970; Kratos, Ramsey, N.J.
[4] Model WISP 710; Waters Associates.
[5] Model 56; Perkin-Elmer Corp., Norwalk, Conn.
[6] 2.1 mm × 25 cm, packed with Partisil ODS-3; Alltech Assoc., Deerfield, Ill.

0022-3549/84/1200-1821$01.00/0
© 1984, American Pharmaceutical Association

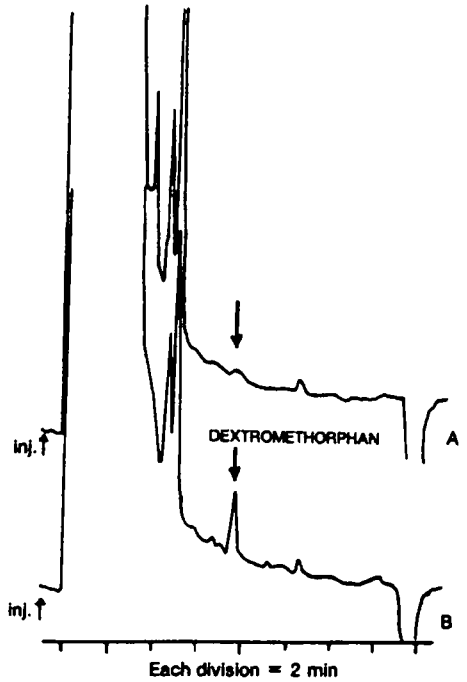

Figure 1—*Chromatograms of plasma blank (A) and plasma spiked with 1 ng/mL of dextromethorphan hydrobromide (B). Arrows indicate dextromethorphan elution areas.*

Recoveries of dextromethorphan hydrobromide from urine samples were essentially 100% since the fluorescence responses in the spiked urine samples were similar to those of the aqueous standards at the same concentration. The results were expected since there was no simple extraction involved. The urine samples were simply diluted with 3% acetic acid solution and then injected into the HPLC system.

Dextromethorphan Level After Oral Administration To Dogs—A typical plasma dextromethorphan concentration *versus* time curve in dogs after 1 mg/kg oral administration is shown in Fig. 3. These results compare well with those found by Barnhart and Massad (1, 4) who found 2.1 ng/mL peak maximum in dog plasma after 1 mg/kg oral administration. No detectable

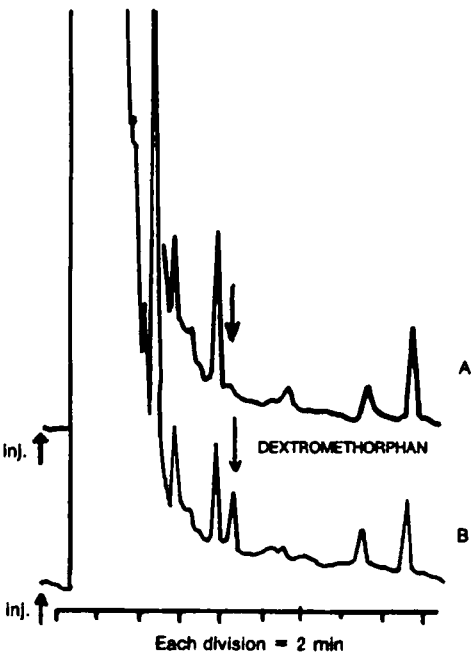

Figure 2—*Chromatograms of dog urine blank (A) and urine spiked with dextromethorphan hydrobromide at 50 ng/mL (B). Arrows indicate dextromethorphan elution areas.*

Table I—Between-Day Variation of Dextromethorphan Linearity [a]

n	ng/mL	Peak Height, mm ± *SD*
9	0	4.3 ± 1.4
8	1	15.6 ± 1.4
9	2	29.6 ± 1.3
9	3	44.1 ± 3.7
11	5	72.7 ± 6.3

[a] The regression yielded $r = 0.9965$ and $y = 13.8x + 3.2$.

Table II—Recovery of Dextromethorphan From Plasma

n	Spiked Plasma, ng Dextromethorphan Hydrobromide/mL	Recovery, % ± *SD*
8	1	41.1 ± 5.8
9	2	48.7 ± 3.8
9	3	51.6 ± 3.3
11	5	53.3 ± 4.6

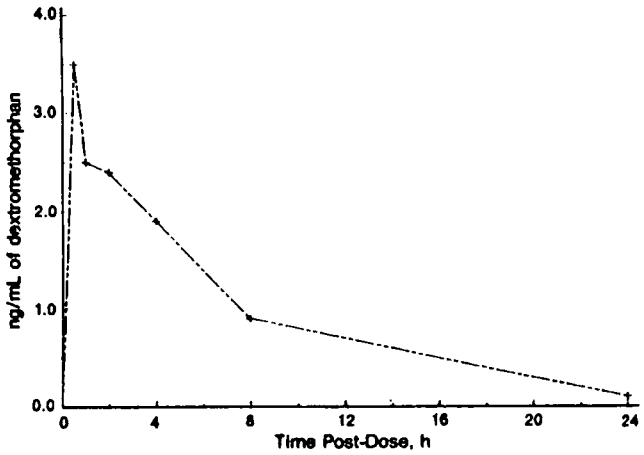

Figure 3—*Plasma dextromethorphan concentration* versus *time curve in the dog after 1-mg/kg oral administration of dextromethorphan hydrobromide.*

amount of dextromethorphan was found in pooled urine. This finding is also consistent with that found by Barnhart and Massad who recovered only a trace of the drug (0.12% of the total dose) after a 1.073 mg/kg oral administration.

The method described above is simple, accurate, and specific for determining dextromethorphan in plasma and urine. The use of semi-microbore columns allows detection limits of 1 ng of dextromethorphan/mL of plasma and 20 ng/mL of urine.

REFERENCES

(1) J. W. Barnhart and E. N. Massad, *J. Chromatogr.*, **163,** 390 (1979).

(2) J. E. O'Brien, O. N. Hinsvark, W. R. Newman, L. P. Amsel, J. E. Giering, and F. E. Leaders, Jr., *Proc. 9th Mat. Res. Symp.*, National Bureau of Standards, April 1978, Gaithersburg, Md.

(3) R. Dixon, J. Carbone, E. Mohacsi, and C. Perry, *Res. Commun. Chem. Pathol. Pharmacol.*, **22,** 243 (1978).

(4) J. W. Barnhart, *Toxicol. Appl. Pharmacol.*, **55,** 43 (1980).

ACKNOWLEDGMENTS

The authors wish to thank Mr. J. Zyracki and W. Williams of the Bristol-Myers Toxicology Department for drug administration and withdrawal of blood from the dogs. We also wish to thank Mr. J. Zyracki and Mr. R. Rafft for many helpful discussions regarding animal experiments.

Presented at the 130th Annual Meeting of the American Pharmaceutical Association, April 1983, New Orleans, La.

Determination of Flurbiprofen in Human Serum by Reverse-Phase High-Performance Liquid Chromatography with Fluorescence Detection

K. S. ALBERT *x, W. R. GILLESPIE *, A. RAABE ‡, and M. GARRY ‡

Received September 6, 1983, from *The Upjohn Company, Kalamazoo, MI 49001 and ‡Hazelton Raltech, Inc., Madison, WI 53707. Accepted for publication February 8, 1984.

Abstract □ A reverse-phase high-performance liquid chromatographic method is described for the determination of flurbiprofen in human serum. Flurbiprofen is extracted from hydrochloric acid-acidified serum with pentane–ether (80:20). An octadecylsilane column was used with a mobile phase of acetonitrile–water–phosphoric acid (650:350:0.5, v/v/v). A fluorescence detector with excitation at 250 nm and emission at 315 nm provided a quantifiable peak for 0.1 μg/mL of flurbiprofen in 0.5 mL of plasma. A comparison between UV and fluorescence detection systems is presented. The method is applicable to human bioavailability and pharmacokinetic studies with flurbiprofen.

Keyphrases □ Flurbiprofen– HPLC detection compared with fluorescence detection, human serum

Flurbiprofen [(±)-2-(2-fluoro-4-biphenylyl)propionic acid] is an orally active, nonsteroidal, anti-inflammatory drug found to be effective in the treatment of rheumatoid arthritis (1–3). We have developed a simple, sensitive, specific, and rapid analytical procedure to measure levels of flurbiprofen (0.1–10 μg/mL) in serum generated in clinical studies. Previous methods either required specialized sample preparation apparatus (4) or time-consuming TLC separation followed by derivatization and GC analysis (5). Investigations into the fluorescence of flurbiprofen suggested that sufficient sensitivity and selectivity could be achieved by employing reverse-phase high-performance liquid chromatography (HPLC) with fluorescence detection. Liquid–liquid extraction proved to be a satisfactory sample preparation technique and 4-biphenylacetic acid exhibited partition and fluorescence characteristics similar enough to flurbiprofen to be used as an internal standard. A method for measuring up to 0.1 μg/mL in 0.5 mL of plasma is described herein.

EXPERIMENTAL SECTION

Reagents and Materials—Reagents were at least analytical reagent grade quality. Acetonitrile[1], methanol[1], and pentane[1] were distilled in glass. Deionized water was supplied[2]. Stock solutions of 4-biphenylacetic acid[3] and flurbiprofen[4] were prepared at 1 mg/mL in methanol. Anhydrous ether[5], phosphoric acid[5] and 1 M hydrochloric acid[6] were used as supplied. The ether was monitored daily for peroxide formation.

Instrumentation—A fluorescence detector[7], solvent pump[8], and an autoinjector[8] were used for the routine chromatographic analysis. A variable-wavelength UV detector[9] was used for comparison with the fluorescence detector. A recorder[10] and an integrator[11] were used for data acquisition. A two-speed reciprocating shaker[12] and centrifuge[13] were used in the sample preparation.

Chromatographic Conditions—Chromatography took place on a 0.46 cm i.d. × 25-cm column packed with octadecylsilane bonded to microparticulate silica (6 μm)[14]. A guard column[15], 0.46 cm × 3 cm, packed with octadecylsilane bonded to microparticulate silica (5 μm), preceded the analytical column. The mobile phase was acetonitrile–water–phosphoric acid (650:350:0.5, v/v/v) filtered through a 0.45-μm membrane[16].

The flow rate was 1.0 mL/min, the column temperature was ambient, and the column back pressure was ~1000 psi. The injection volume was 20 μL, and the run time was 8 min. The retention times for flurbiprofen and 4-biphenylacetic acid were 5.0 min and 6.1 min, respectively. The settings for the fluorescence detector were: excitation wavelength, 250 nm; emission wavelength, 315 nm; slit width, 5 nm; range, 3.0; photomultiplier gain, normal; response, normal; output to recorder, 1 V; output to integrator, 10 mV.

Sample Preparation—Appropriate spiking solutions of flurbiprofen in methanol were prepared from the 1-mg/mL stock solution. A methanolic solution (10 μg/mL) of the internal standard (4-biphenylacetic acid) was prepared from the 1-mg/mL stock solution.

The appropriate standard spiking solution (50 μL for standard tubes) or 50 μL of methanol (for controls, samples, and the blanks) was added to culture tubes (16 × 125 mm) equipped with polytef-lined screw caps. Internal standard (50 μL), 0.5 mL serum, and 0.5 mL of 1 M hydrochloric acid was added to the tube and the contents were mixed on a vortex mixer. Pentane–ether (80:20, 10 mL) was added, the tube was shaken at high speed for 10 min and then centrifuged at 2000 rpm for 10 min. The organic layer was transferred to an empty culture tube (16 × 125 mm), and it then was evaporated under nitrogen in a water bath maintained at 30°C. When dry, the residue was dissolved in 5.0 mL of acetonitrile by mixing on a vortex mixer. A portion of the solution was transferred to a vial for autoinjection.

Two normal healthy male adult volunteers were administered flurbiprofen. These volunteers fasted 9 h before and 4 h after administration. One 50-mg film-coated flurbiprofen tablet was administered with ~188 mL of water, and blood (7 mL) was drawn by venipuncture into blood collection tubes[17] just before drug administration (0 h) and at 0.5, 1, 2, 3, 4, 6, 8, 12, 16, 24, and 30 h. Serum was harvested from the blood samples immediately after collection and kept frozen until assayed by the above procedure.

Calculations—Data were processed by a data system[11] using computer-generated, baseline-corrected peak heights. Peak height ratio curves (concentration flurbiprofen/concentration internal standard) were established and checked daily with standards to ensure acceptable slope and y-intercept values.

The apparent elimination rate constant for each subject, λ_z, was determined from a least-squares regression fit of the terminal log-linear region of the semilogarithmic plasma concentration–time curves. Area under the concentration–time curve, AUC_∞, was estimated by the trapezoidal rule with extrapolation to infinity. Apparent clearance after oral dosing, CL/F, was calculated from the expression:

$$CL/F = \frac{\text{Dose}}{AUC_\infty} \qquad \text{(Eq. 1)}$$

Apparent volume of distribution, Vd/F was calculated according to:

$$Vd/F = \frac{\text{Dose}}{\lambda_z AUC_\infty} = \frac{CL/F}{\lambda_z} \qquad \text{(Eq. 2)}$$

[1] Burdick and Jackson Laboratories, Muskegon, Mich.
[2] Milli-Q; Millipore Corp., Bedford, Mass.
[3] Aldrich Chemical Co., Milwaukee, Wis.
[4] Supplied by The Upjohn Co., Kalamazoo, Mich.
[5] Mallinckrodt, Inc., St. Louis, Mo.
[6] Fisher Scientific, Pittsburgh, Pa.
[7] Model 650-105; Perkin-Elmer, Norwalk, Conn.
[8] Model 1081B; Hewlett Packard, Palo Alto, Calif.
[9] Model LDC Spectromonitor III; Milton Roy Co., Riviera, Fla.
[10] Linear Instruments Corp., Irvine, Calif.
[11] Model 3356; Hewlett Packard, Avondale, Pa.
[12] Eberback Corp., Ann Arbor, Mich.
[13] International Equipment Corp., Needham, Mass.
[14] Zobax ODS; DuPont, Wilmington, Del.
[15] Brown Laboratories, Santa Clara, Calif.
[16] Millipore Corp.
[17] Vacutainer without anticoagulant.

0022-3549/84/1200-1823$01.00/0
© 1984, American Pharmaceutical Association

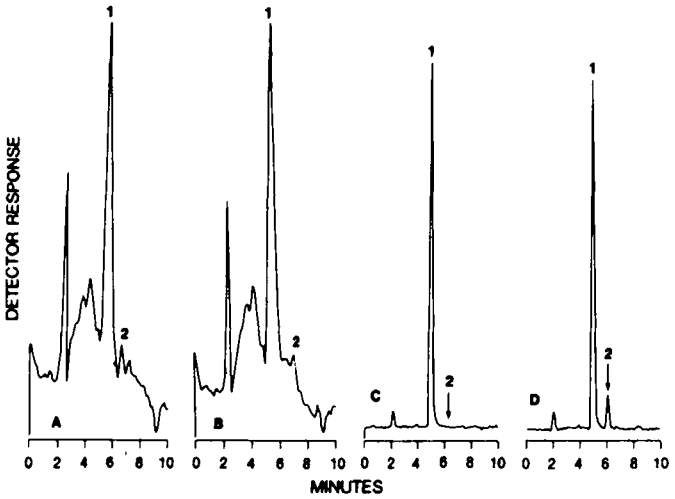

Figure 1—*Reverse-phase high-performance liquid chromatograms of serum extracts using UV (A,B) and fluorescence (C,D) detection. Serum was spiked with 4-biphenylacetic acid (A,C) or 4-biphenylacetic acid and flurbiprofen (0.1 μg/mL serum concentration) (B,D). Key: (1) 4-biphenylacetic acid; (2) flurbiprofen.*

Table I—Flurbiprofen Data Used in Constructing Standard Curves

Theoretical Conc., μg/mL	Mean Experimental Value, μg/mL[a]	*SD*	*RSD*, %
0	< 0.10		
0.10	0.099	0.0107	10.8
0.30	0.301	0.0162	5.38
0.60	0.597	0.0343	5.74
1.00	0.993	0.0395	3.98
3.00	3.020	0.156	5.17
6.00	5.980	0.075	1.25
10.0	10.00	0.230	2.28
Curve	Slope	Intercept	*r*
1	0.8562	−0.0090	0.9999
2	0.8289	−0.0205	0.9998
3	0.8336	−0.0026	0.9997
4	0.8479	0.0145	0.9989
Mean	0.8417	−0.0044	0.9996
SD	0.0126	0.0146	0.00046

[a] Mean of eight values, *i.e.*, samples analyzed in duplicate on four successive days.

Table II—Recoveries of 4-Biphenylacetic Acid and Flurbiprofen from Human Serum

Amount Added, μg/mL	Amount Found, μg/mL	Recovery, %
	4-Biphenylacetic Acid	
1.0	0.967	96.7
1.0	0.906	90.6
1.0	1.003	100.3
1.0	0.965	96.5
1.0	0.952	95.2
1.0	0.903	90.3
Mean		94.9
SD		3.9
	Flurbiprofen	
0.10	0.093	92.6
0.10	0.095	94.6
1.00	1.05	104.5
1.00	1.01	101.1
10.0	9.77	97.7
10.0	9.36	93.6
Mean		97.4
SD		4.7

RESULTS AND DISCUSSION

A comparison of chromatograms with UV and fluorescence detection (Fig. 1) of blank and flurbiprofen-spiked serum illustrates the sensitivity and selectivity of the fluorescence assay. The blank (Fig. 1C) reveals no interfering peaks and the peak height of the flurbiprofen at required limit of sensitivity is adequate for quantitation. Because of the interferences evident in the chromatograms from UV detection, fluoresence is the preferred detection technique.

The precision and linearity of the method was investigated. A standard curve (eight points) was analyzed on 4 consecutive days. Table I summarizes the experimental data. The low deviation from linearity within each curve and the low relative standard deviation for the different runs demonstrates the efficacy of the method.

Table II summarizes the recovery results for flurbiprofen and internal standard (4-biphenylacetic acid) from spiked serum as compared with direct injection of standards prepared from stock solutions. The integrator peak height information was used in the calculations (*i.e.*, no internal standards were used). The results of 97.4 + 4.7% for flurbiprofen and 94.9 + 3.9% for 4-biphenylacetic acid show the essential quantitative recovery from serum.

The strong native fluorescence of flurbiprofen allowed achievement of the desired sensitivity of 0.1 μg/mL without approaching the design capability limits of the detector. Likewise, the amount of acetonitrile added to dissolve the extract residue in the sample preparation was chosen for convenience and can be decreased significantly, thus increasing the assay sensitivity. The limit of quantitation might also be improved by increasing the volume of solution injected.

The serum concentration–time profiles resulting from the administration of single oral 50-mg doses of flurbiprofen to two human subjects are shown in Fig. 2. Estimates of selected pharmacokinetic parameters are presented in Table III. The results are consistent with previously published reports describing flurbiprofen pharmacokinetics (6).

In conclusion, a sensitive, precise, and specific HPLC method with fluorescence detection has been described for the detection of 0.1 μg/mL of flurbiprofen in 0.5 mL of plasma. The method is readily applicable to routine analysis of plasma samples from bioavailability–pharmacokinetic studies in humans. Moreover, because of the strong native fluoresence of flurbiprofen,

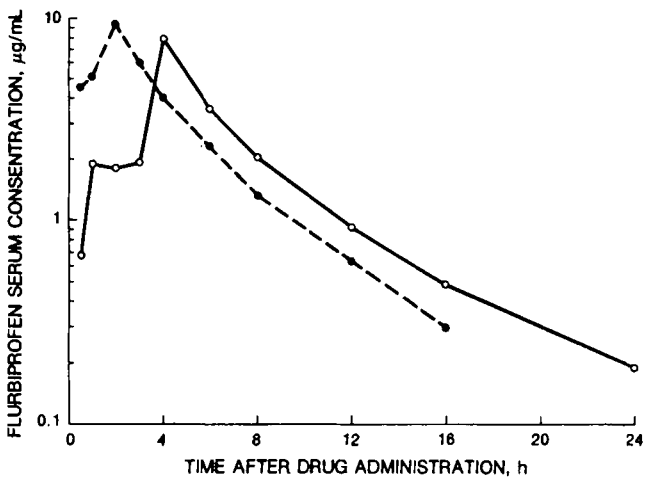

Figure 2—*Flurbiprofen serum concentrations following the administration of single oral 50-mg doses to two adult volunteers. Key: (○) subject 1; (●) subject 2.*

Table III—Flurbiprofen Pharmacokinetics Following the Administration of Single Oral 50-mg Doses to Two Adult Volunteers

	Subject 1	Subject 2
Age, years	26	30
Body weight, kg	80.7	62.6
Peak concentration, μg/mL	8.01	9.44
Peak time, h	4	2
Area under the concentration–time curve, μg·h/mL	39.8	41.2
Apparent clearance, mL/h/kg	15.6	19.4
Apparent distribution volume, mL/kg	131	104
Apparent elimination rate constant, h^{-1}	0.118	0.186

the sensitivity of the method can no doubt be extended making it an attractive technique for studying the bioavailability and pharmacokinetics of flurbiprofen in pediatric populations where small sample volumes and lower doses are required.

REFERENCES

(1) S. S. Adams and K. F. McCullough, 7th European Rheumatology Congress, London, England, Abstr. 32.2 (1971).

(2) I. M. Chalmers, B. J. Cathcart, E. B. Kumar, W. Carson Dick, and W. W. Buchanan, *Ann. Rheum. Dis.*, **31**, 319 (1972).

(3) I. M. Chalmers, M. A. Bell, and W. W. Buchanan, *Ann. Rheum. Dis.*, **32**, 58 (1973).

(4) B. G. Snider, L. J. Beaubein, D. J. Sears, and P. D. Rahn, *J. Pharm. Sci.*, **70**, 1347 (1981).

(5) D. G. Kaiser, S. R. Shaw, and G. J. Vangiessen, *J. Pharm. Sci.*, **63**, 567 (1974).

(6) P. C. Risdall, S. S. Adams, E. L. Crampton, and B. Marchant, *Xenobiotica*, **8**, 691 (1978).

Direct, Simultaneous Determination of Propranolol and Its 4-Hydroxy Metabolite by Liquid Chromatography

G. TAMAI, I. MORITA, T. MASUJIMA, H. YOSHIDA, ˣ and H. IMAI

Received August 3, 1983, from the *Institute of Pharmaceutical Sciences, Hiroshima University School of Medicine, Hiroshima 734, Japan.* Accepted for publication November 28, 1983.

Abstract □ Propranolol and its active 4-hydroxy metabolite are determined by direct injection of spiked plasma samples onto a protein-coated ODS liquid chromatographic column. The recovery of propranolol and the 4-hydroxy metabolite is essentially quantitative and the reproducibility is good. The reproducibility and simplicity may be superior to the conventional HPLC analyses which include pretreatment, *i.e.*, solvent extraction or deproteinization.

Keyphrases □ Protein-coated ODS column—reverse-phase, direct injection analysis of plasma sample □ Propranolol—analysis and its 4-hydroxy metabolite, plasma

Propranolol, a β-adrenergic blocking drug, is widely used for the treatment of cardiac arrhythmia, sinus tachycardias, hypertension (1), and other pathological states (2, 3). The therapeutic drug level of propranolol is considered to be in the range of 50–100 ng (193–386 pmol)/mL of plasma (4). The 4-hydroxy metabolite, formed by hydroxylation of propranolol (5), has been reported to be an equipotent β-adrenergic blocker (6). Thus, for drug level monitoring, both propranolol and the 4-hydroxy derivative should be determined. Determination of propranolol (7, 8) and the 4-hydroxy metabolite using a reverse-phase HPLC method including sample pretreatment, such as solvent extraction or deproteinization has been reported previously (9–11). We reported that the protein-coated ODS column had no affinity for proteins, but did have an affinity for small hydrophobic molecules (12). The simultaneous plasma determination of propranolol and the 4-hydroxy metabolite reported herein is rapid and reproducible, and deproteinization can be carried out by the direct injection of plasma samples onto a protein-coated ODS liquid chromatographic column.

EXPERIMENTAL SECTION

Chemicals and Reagents—Propranolol hydrochloride[1], the 4-hydroxy metabolite (as the hydrochloride)[2], and bovine serum albumin[3] were obtained commercially. All other chemicals were analytical reagent grade.

Preparation of the Protein-Coated Octadecylsilane Column—An ODS column (pore size, 10-nm) was packed by the balanced-slurry method (slurry solvent, chloroform; purge solvent, 50% methanol). After the ODS column was equilibrated with phosphate-buffered saline (pH 7.4), 6% bovine serum albumin solution was injected to saturate the column. After the column was equilibrated with 0.1 M phosphate solution (pH 3.0), bovine serum albumin solution (6%) was again injected, and the column was then washed with absolute methanol. This procedure was repeated several times. The same procedure was repeated, using dialyzed rabbit plasma instead of the bovine serum albumin solution. The column treated by the aforementioned procedure is referred to as the protein-coated ODS column below.

Liquid Chromatographic Apparatus—An HPLC apparatus with a single plunger pump[4] and a sample injector[5] was assembled in our laboratory. For stepwise elution, solvent switching was performed by a solvent selector[6] and controlled by a sequence programmer[7]. For double-column analysis, a flow-direction switch valve[8] was placed between the precolumn and the analytical column. The valve was controlled by the sequence programmer[7]. Two fluorometers[9] were used in series: one for detection of propranolol (Ex, 297 nm; Em, 347 nm); the other for the 4-hydroxy metabolite (Ex, 327 nm; Em, 427 nm).

Preparation of Standard and Sample Solutions—A stock solution of propranolol and the 4-hydroxy metabolite containing 2% sodium metabisulfite (13) was prepared in distilled water at 10^{-5} M. Heparinized human and rabbit plasma samples were obtained by centrifuging whole blood (1000×*g*, at 25°C, for 10 min) and filtering[10] to remove solid materials. A plasma sample (0.25 mL) with or without propranolol and the 4-hydroxy derivative at the drug monitoring level, was injected onto the column. If the pressure of the column increased during successive analyses, the inlet filter of the column was washed with 1 M NaOH.

Single-Column Analysis—An ODS column of 100 mm × 6 mm i.d.[11] (particle size 5 μm, pore size 10 nm) was protein-coated and then used at room temperature. The protein-coated ODS column was equilibrated with phosphate-buffered saline (flow rate, 2 mL/min). The plasma sample spiked with propranolol and its 4-hydroxy derivative (0.25 mL) was injected onto the column. After eluting plasma proteins and hydrophilic components with phosphate-buffered saline for 5 min, the column was washed with phosphate-buffered saline containing 22% acetonitrile for 4 min. Propranolol and the 4-hydroxy derivative were then eluted with 0.1 M citrate buffer (pH 4.0) containing 22% acetonitrile.

[1] Supplied by Sumitomo Chemicals, Osaka, Japan.
[2] Supplied by I.C.I. Pharmaceutical Ltd., Osaka, Japan.
[3] Fraction V Powder; Sigma, St. Louis, Mo.
[4] Model INTD18-40-3S2K; Toyo Soda, Tokyo, Japan.
[5] Model 7125; Rheodyne, Calif.
[6] Model 8V; Kyowa Seimitsu, Tokyo, Japan.
[7] Model SCY-PO; Omron, Tokyo, Japan.
[8] Model 7010; Rheodyne.
[9] Model RF-530; Shimadzu, Kyoto, Japan.
[10] Millex-HA; Millipore Corp., Bedford, Mass.
[11] Shodex ODSpak; Showa Denko, Tokyo, Japan.

0022-3549/84/1200-1825$01.00/0

© 1984, American Pharmaceutical Association

the sensitivity of the method can no doubt be extended making it an attractive technique for studying the bioavailability and pharmacokinetics of flurbiprofen in pediatric populations where small sample volumes and lower doses are required.

REFERENCES

(1) S. S. Adams and K. F. McCullough, 7th European Rheumatology Congress, London, England, Abstr. 32.2 (1971).

(2) I. M. Chalmers, B. J. Cathcart, E. B. Kumar, W. Carson Dick, and W. W. Buchanan, *Ann. Rheum. Dis.*, **31**, 319 (1972).

(3) I. M. Chalmers, M. A. Bell, and W. W. Buchanan, *Ann. Rheum. Dis.*, **32**, 58 (1973).

(4) B. G. Snider, L. J. Beaubein, D. J. Sears, and P. D. Rahn, *J. Pharm. Sci.*, **70**, 1347 (1981).

(5) D. G. Kaiser, S. R. Shaw, and G. J. Vangiessen, *J. Pharm. Sci.*, **63**, 567 (1974).

(6) P. C. Risdall, S. S. Adams, E. L. Crampton, and B. Marchant, *Xenobiotica*, **8**, 691 (1978).

Direct, Simultaneous Determination of Propranolol and Its 4-Hydroxy Metabolite by Liquid Chromatography

G. TAMAI, I. MORITA, T. MASUJIMA, H. YOSHIDA, ˣ and H. IMAI

Received August 3, 1983, from the *Institute of Pharmaceutical Sciences, Hiroshima University School of Medicine, Hiroshima 734, Japan.* Accepted for publication November 28, 1983.

Abstract □ Propranolol and its active 4-hydroxy metabolite are determined by direct injection of spiked plasma samples onto a protein-coated ODS liquid chromatographic column. The recovery of propranolol and the 4-hydroxy metabolite is essentially quantitative and the reproducibility is good. The reproducibility and simplicity may be superior to the conventional HPLC analyses which include pretreatment, *i.e.*, solvent extraction or deproteinization.

Keyphrases □ Protein-coated ODS column—reverse-phase, direct injection analysis of plasma sample □ Propranolol—analysis and its 4-hydroxy metabolite, plasma

Propranolol, a β-adrenergic blocking drug, is widely used for the treatment of cardiac arrhythmia, sinus tachycardias, hypertension (1), and other pathological states (2, 3). The therapeutic drug level of propranolol is considered to be in the range of 50–100 ng (193–386 pmol)/mL of plasma (4). The 4-hydroxy metabolite, formed by hydroxylation of propranolol (5), has been reported to be an equipotent β-adrenergic blocker (6). Thus, for drug level monitoring, both propranolol and the 4-hydroxy derivative should be determined. Determination of propranolol (7, 8) and the 4-hydroxy metabolite using a reverse-phase HPLC method including sample pretreatment, such as solvent extraction or deproteinization has been reported previously (9–11). We reported that the protein-coated ODS column had no affinity for proteins, but did have an affinity for small hydrophobic molecules (12). The simultaneous plasma determination of propranolol and the 4-hydroxy metabolite reported herein is rapid and reproducible, and deproteinization can be carried out by the direct injection of plasma samples onto a protein-coated ODS liquid chromatographic column.

EXPERIMENTAL SECTION

Chemicals and Reagents—Propranolol hydrochloride[1], the 4-hydroxy metabolite (as the hydrochloride)[2], and bovine serum albumin[3] were obtained commercially. All other chemicals were analytical reagent grade.

Preparation of the Protein-Coated Octadecylsilane Column—An ODS column (pore size, 10-nm) was packed by the balanced-slurry method (slurry solvent, chloroform; purge solvent, 50% methanol). After the ODS column was equilibrated with phosphate-buffered saline (pH 7.4), 6% bovine serum albumin solution was injected to saturate the column. After the column was equilibrated with 0.1 M phosphate solution (pH 3.0), bovine serum albumin solution (6%) was again injected, and the column was then washed with absolute methanol. This procedure was repeated several times. The same procedure was repeated, using dialyzed rabbit plasma instead of the bovine serum albumin solution. The column treated by the aforementioned procedure is referred to as the protein-coated ODS column below.

Liquid Chromatographic Apparatus—An HPLC apparatus with a single plunger pump[4] and a sample injector[5] was assembled in our laboratory. For stepwise elution, solvent switching was performed by a solvent selector[6] and controlled by a sequence programmer[7]. For double-column analysis, a flow-direction switch valve[8] was placed between the precolumn and the analytical column. The valve was controlled by the sequence programmer[7]. Two fluorometers[9] were used in series: one for detection of propranolol (Ex, 297 nm; Em, 347 nm); the other for the 4-hydroxy metabolite (Ex, 327 nm; Em, 427 nm).

Preparation of Standard and Sample Solutions—A stock solution of propranolol and the 4-hydroxy metabolite containing 2% sodium metabisulfite (13) was prepared in distilled water at 10^{-5} M. Heparinized human and rabbit plasma samples were obtained by centrifuging whole blood (1000×*g*, at 25°C, for 10 min) and filtering[10] to remove solid materials. A plasma sample (0.25 mL) with or without propranolol and the 4-hydroxy derivative at the drug monitoring level, was injected onto the column. If the pressure of the column increased during successive analyses, the inlet filter of the column was washed with 1 M NaOH.

Single-Column Analysis—An ODS column of 100 mm × 6 mm i.d.[11] (particle size 5 μm, pore size 10 nm) was protein-coated and then used at room temperature. The protein-coated ODS column was equilibrated with phosphate-buffered saline (flow rate, 2 mL/min). The plasma sample spiked with propranolol and its 4-hydroxy derivative (0.25 mL) was injected onto the column. After eluting plasma proteins and hydrophilic components with phosphate-buffered saline for 5 min, the column was washed with phosphate-buffered saline containing 22% acetonitrile for 4 min. Propranolol and the 4-hydroxy derivative were then eluted with 0.1 M citrate buffer (pH 4.0) containing 22% acetonitrile.

[1] Supplied by Sumitomo Chemicals, Osaka, Japan.
[2] Supplied by I.C.I. Pharmaceutical Ltd., Osaka, Japan.
[3] Fraction V Powder; Sigma, St. Louis, Mo.
[4] Model INTD18-40-3S2K; Toyo Soda, Tokyo, Japan.
[5] Model 7125; Rheodyne, Calif.
[6] Model 8V; Kyowa Seimitsu, Tokyo, Japan.
[7] Model SCY-PO; Omron, Tokyo, Japan.
[8] Model 7010; Rheodyne.
[9] Model RF-530; Shimadzu, Kyoto, Japan.
[10] Millex-HA; Millipore Corp., Bedford, Mass.
[11] Shodex ODSpak; Showa Denko, Tokyo, Japan.

0022-3549/84/1200-1825$01.00/0

© 1984, American Pharmaceutical Association

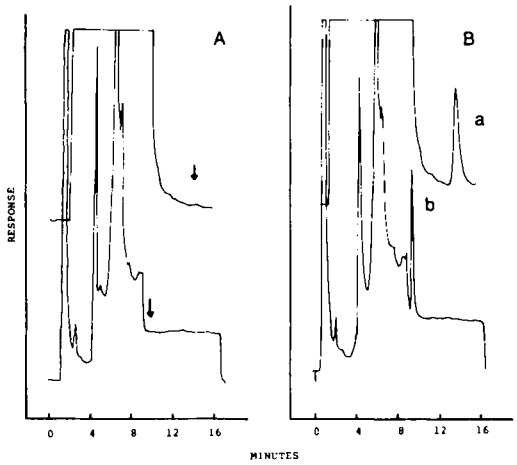

Figure 1—*Chromatograms obtained by a single protein-coated ODS column. Key: (A) human plasma blank; (B) human plasma sample spiked with propranolol (a) (Ex 297 nm, Em 347 nm) and the 4-hydroxy metabolite (b) (Ex 327 nm, Em 427 nm). Samples were 100 pmol of drug/0.25 mL of plasma.*

Double-Column Analysis—A protein-coated ODS column, 60 mm × 4 mm i.d.[12] (particle size 20 μm, pore size 10 nm), was used as the precolumn at room temperature. A 60 mm × 4 mm i.d. column[13] (particle size 5 μm, pore size 10 nm) was used as the analytical column at 35°C. The precolumn was equilibrated with phosphate-buffered saline (flow rate, 1.2 mL/min). A 0.25-mL plasma sample spiked with propranolol and the 4-hydroxy metabolite was injected onto the precolumn. Plasma proteins and hydrophilic compounds were eluted with phosphate-buffered saline for 5 min, and then the column was washed with phosphate-buffered saline containing 15% acetonitrile for 2 min. After being washed with 0.1 M citrate buffer (pH 4.0) containing 5% acetonitrile for 4 min, the precolumn was connected to the analytical column which was equilibrated with 0.1 M citrate buffer (pH 4.0) containing 15% acetonitrile. The propranolol and 4-hydroxy derivative retained on the precolumn were eluted with 0.1 M citrate buffer (pH 4.0, containing 15% acetonitrile) through the analytical column (flow rate, 1.7 mL/min). For elution from the analytical column, the 15% acetonitrile concentration was suitable for separatory elution. Chromatograms obtained by the flow-through and back-flush methods were compared.

RESULTS AND DISCUSSION

Determination By the Single-Column Technique—Propranolol, a basic drug [pK_a 9.45 (14)], has an affinity for ODS resin at pH 7.4. After the protein-coated ODS column was equilibrated with phosphate-buffered saline, a plasma sample (0.25 mL) spiked with propranolol and the 4-hydroxy metabolite (100–400 pmol/mL of plasma) was injected onto the column. Plasma proteins and hydrophilic compounds were eluted by phosphate-buffered saline, but propranolol and the 4-hydroxy metabolite were retained on the column. It was confirmed that the 4-hydroxy metabolite was eluted by phosphate-buffered saline containing 22% acetonitrile within 7 min, and propranolol was eluted after 30 min. The column was then washed with phosphate-buffered saline containing 22% acetonitrile for 4 min. Propranolol and the 4-hydroxy metabolite were eluted with 0.1 M citrate buffer (pH 4.0) containing 22% acetonitrile. In Fig. 1 are shown chromatograms of a human plasma blank and a plasma sample spiked with propranolol and the 4-hydroxy derivative. A calibration curve is shown in Fig. 2. The recoveries were 101.8 and 101.4%, respectively, with good reproducibilities (*CV*, 1.6 and 1.2%, respectively; n = 5). The practical drug monitoring level of propranolol and the 4-hydroxy metabolite was determined with good reproducibility and recovery. The levels of propranolol and the 4-hydroxy metabolite, analyzed by the present method, were totals in plasma, regardless if free or bound to proteins [binding of propranolol to plasma proteins has been reported to be as high as 90–96% (15)]. In the determination of propranolol with a single protein-coated ODS column, at least 50 samples were analyzed without deterioration of the column.

Determination By the Double-Column Technique—Representative chromatograms showing the separation of propranolol and the 4-hydroxy metabolite by the flow-through and back-flush methods are shown in Figs. 3 and 4. With the flow-through method, a slight peak broadening was observed after 150 successive analyses (Fig. 3). The reason might be due to reduced efficiency of the precolumn. With the back-flush method, sharp chromatograms were obtained and 150 successive analyses could be performed without deterioration of the column (Fig. 4). Propranolol was concentrated at the top of the precolumn by eluting with phosphate-buffered saline containing 15% acetonitrile. Both methods gave quantitative recoveries of propranolol and 4-hydroxy

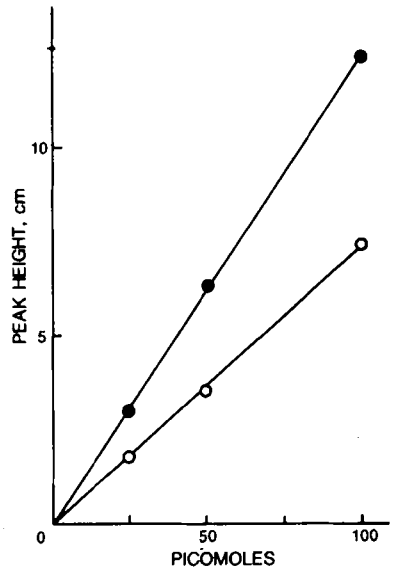

Figure 2—*Calibration curve obtained by a single protein-coated ODS column. Key: (○) propranolol; (●) 4-hydroxy metabolite.*

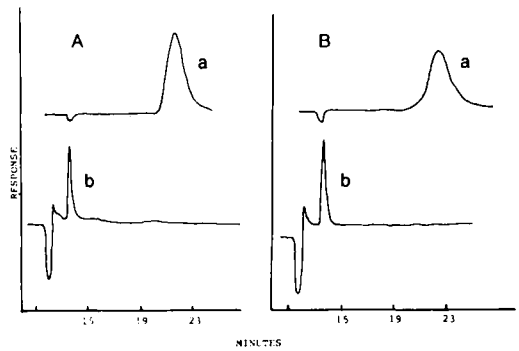

Figure 3—*Chromatograms obtained by the flow-through method. Key: (A) chromatogram of first analysis; (B) chromatogram after 150 successive analyses. The eluate from the analytical column was monitored for propranolol (a) and the 4-hydroxy metabolite (b).*

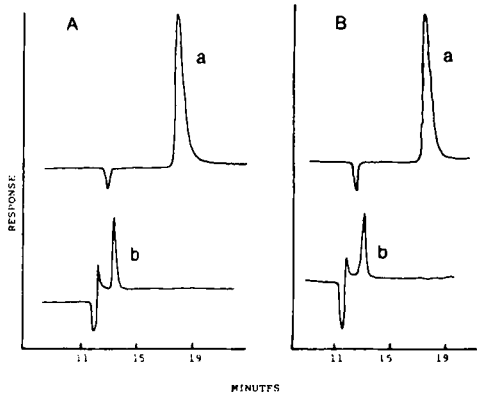

Figure 4—*Chromatograms obtained by the back-flush method. Key: (A) chromatogram of first analysis; (B) chromatogram after 150 successive analyses. The eluate from the analytical column was monitored for propranolol (a) and the 4-hydroxy metabolite (b).*

[12] Gel 3050; Hitachi, Tokyo, Japan.
[13] TSK gel ODS-120T; Toyo Soda, Tokyo, Japan.

Table I—Comparison of Deproteinization Methods [a]

Deproteinization Method	Recovery, %	CV, %
Protein-coated ODS column	100.1	0.9
5% Acetonitrile	101.0	3.2
5% Trichloroacetic acid	25.9	4.0

[a] Conditions: 300 ng of propranolol/mL of plasma; injection of 100 μL of plasma; $n = 5$.

metabolite; therefore, an internal standard was not required. By using a flow direction switching valve, the deterioration of the analytical column was minimized. At least 150 successive analyses with almost no column deterioration were carried out by the back-flush method.

Table I shows the comparison of the methods of deproteinization. Note that in the present method the deproteinization was performed at the initial stage after the injection of sample onto the column. In comparison with common HPLC analyses that include pretreatment, *i.e.*, solvent extraction or deproteinization, the proposed method proved superior in simplicity and accuracy.

REFERENCES

(1) D. G. Shand, *N. Engl. J. Med.*, **293**, 280 (1975).

(2) A. Mitrani, M. Oettinger, E. G. Abinader, M. Sharf, and A. Klein, *Br. J. Obstet. Gynaecol.*, **82**, 651 (1975).

(3) R. B. Weber and O. M. Reinmuth, *Neurology*, **22**, 366 (1972).

(4) A. S. Nies and D. G. Shand, *Circulation*, **52**, 6 (1975).

(5) J. W. Paterson, M. E. Conolly, C. T. Dolley, A. Hayes, and R. G. Cooper, *Pharmacol. Clin.*, **2**, 127 (1970).

(6) J. D. Fitzgerald and S. R. O'Donnell, *Br. J. Pharmacol.*, **43**, 222 (1971).

(7) G. Nygard, W. H. Shelver, and S. K. W. Khalil, *J. Pharm. Sci.*, **68**, 379 (1979).

(8) M. Simon and R. Terry, *Ther. Drug Monitor.*, **1**, 265 (1979).

(9) R. L. Nation, G. W. Peng, and W. L. Chiou, *J. Chromatogr.*, **145**, 429 (1978).

(10) S. R. Parinam, C. Q. Louise, and S. M. Hiltrud, *Clin. Chim. Acta*, **88**, 355 (1978).

(11) D. W. Schneck, J. F. Pritchard, and A. H. Hayes, *Res. Commun. Chem. Pathol. Pharmacol.*, **24**, 3 (1979).

(12) H. Yoshida, I. Morita, T. Masujima, and H. Imai, *Chem. Pharm. Bull.*, **30**, 2287 (1982).

(13) J. F. Pritchard, D. W. Schneck, and A. H. Hayes, *J. Chromatogr.*, **162**, 47 (1979).

(14) W. Sadee' and G. C. Beelen, "Drug Level Monitoring," Wiley-Interscience, New York, N.Y., 1980.

(15) T. P. Moyer and S. G. Sheps, *Ther. Drug Monitor.*, **3**, 217 (1981).

Determination of "Brompton's Cocktails" by Circular Dichroism

W. MARC ATKINSON, JOHN M. BOWEN, and NEIL PURDIE ˣ

Received November 21, 1983, from the *Chemistry Department, Oklahoma State University, Stillwater, OK 74078.* Accepted for publication February 23, 1984.

Abstract □ Circular dichroism spectropolarimetry has been applied to the simultaneous determination of chiral compounds in binary mixtures without separation or sample preparation steps. A strategy which uses data measured at equivalent wavelength pairs simplifies the calculations. Correspondence is within ±2% of the compositions of prepared standard mixtures.

Keyphrases □ Circular dichroism—spectropolarimetry, UV absorption, Brompton's solutions, *R*-(−)-cocaine hydrochloride, morphine sulfate, (±)-methadone, (−)-fructose, β-cyclodextrin □ Brompton's solutions—circular dichroism, spectropolarimetry, UV absorption

A medically approved practice used to relieve the physical distress from chronic pain, such as is experienced by some terminally ill cancer patients, is to administer a mixture of controlled, addictive substances in an oral preparation commonly referred to as "Brompton's cocktails." Cocaine is common to all preparations. Other components differ, but are most often either morphine or (±)-methadone. The mixture is served in a fruit-flavored alcohol base.

Although documented evidence for the abuse of this prescription is limited at this time, the potential exists. We have developed a simple protocol for a rapid direct determination of the drugs by circular dichroism (CD) spectropolarimetry which requires no separation or sample prepreparation. We have previously reported data for opium alkaloids (1, 2), *R*-(−)-cocaine (3, 4), (+)-lysergide (D-LSD) (5), and tetracycline (6). The CD technique focuses only on those components which absorb light and which are simultaneously chiral. Chirality may be either intrinsic to the molecule (1–6) or induced by its complexation with a chiral substrate molecule (4).

By being able to focus on only the CD-active components, the problem of deconvoluting the cumulative UV spectra of the mixtures is considerably simplified. Absorption by the other CD-inactive components only affects the signal-to-noise ratio of the detector.

EXPERIMENTAL SECTION

Standard samples of *R*-(−)-cocaine hydrochloride[1], morphine sulfate[1], and (±)-methadone[2] were used without further purification. The fruit-flavored syrups commonly used contain (−)-fructose. Standard (−)-fructose[3] was obtained commercially. In-house standard mixtures were prepared by weight. Samples of unknown composition were either blind in-house preparations, or were provided[4]. Chirality is induced into (±)-methadone by complexation with the chiral cyclic oligosaccharide β-cyclodextrin[5] present in large excess in aqueous solution, $\sim 10^{-2}$ M.

CD measurements were made on an automatic recording spectropolarimeter[6], and data analyses were made on the ancillary data processor[7]. Daily calibration of the ellipticity scale was made against a standard solution of androsterone in dioxane, as recommended. Samples were diluted with the appropriate volume of dilute hydrochloric acid or water, usually 1:10.

[1] Mallinckrodt Inc.
[2] Drug Enforcement Administration.
[3] Fisher Scientific.
[4] Arizona Department of Public Safety and the local hospital pharmacy.
[5] Kodak.
[6] Model 500A; JASCO.
[7] Model DP-500N.

0022-3549/84/1200-1827$01.00/0

© 1984, American Pharmaceutical Association

Table I—Comparison of Deproteinization Methods [a]

Deproteinization Method	Recovery, %	CV, %
Protein-coated ODS column	100.1	0.9
5% Acetonitrile	101.0	3.2
5% Trichloroacetic acid	25.9	4.0

[a] Conditions: 300 ng of propranolol/mL of plasma; injection of 100 μL of plasma; $n = 5$.

metabolite; therefore, an internal standard was not required. By using a flow direction switching valve, the deterioration of the analytical column was minimized. At least 150 successive analyses with almost no column deterioration were carried out by the back-flush method.

Table I shows the comparison of the methods of deproteinization. Note that in the present method the deproteinization was performed at the initial stage after the injection of sample onto the column. In comparison with common HPLC analyses that include pretreatment, *i.e.*, solvent extraction or deproteinization, the proposed method proved superior in simplicity and accuracy.

REFERENCES

(1) D. G. Shand, *N. Engl. J. Med.*, **293**, 280 (1975).

(2) A. Mitrani, M. Oettinger, E. G. Abinader, M. Sharf, and A. Klein, *Br. J. Obstet. Gynaecol.*, **82**, 651 (1975).

(3) R. B. Weber and O. M. Reinmuth, *Neurology*, **22**, 366 (1972).

(4) A. S. Nies and D. G. Shand, *Circulation*, **52**, 6 (1975).

(5) J. W. Paterson, M. E. Conolly, C. T. Dolley, A. Hayes, and R. G. Cooper, *Pharmacol. Clin.*, **2**, 127 (1970).

(6) J. D. Fitzgerald and S. R. O'Donnell, *Br. J. Pharmacol.*, **43**, 222 (1971).

(7) G. Nygard, W. H. Shelver, and S. K. W. Khalil, *J. Pharm. Sci.*, **68**, 379 (1979).

(8) M. Simon and R. Terry, *Ther. Drug Monitor.*, **1**, 265 (1979).

(9) R. L. Nation, G. W. Peng, and W. L. Chiou, *J. Chromatogr.*, **145**, 429 (1978).

(10) S. R. Parinam, C. Q. Louise, and S. M. Hiltrud, *Clin. Chim. Acta*, **88**, 355 (1978).

(11) D. W. Schneck, J. F. Pritchard, and A. H. Hayes, *Res. Commun. Chem. Pathol. Pharmacol.*, **24**, 3 (1979).

(12) H. Yoshida, I. Morita, T. Masujima, and H. Imai, *Chem. Pharm. Bull.*, **30**, 2287 (1982).

(13) J. F. Pritchard, D. W. Schneck, and A. H. Hayes, *J. Chromatogr.*, **162**, 47 (1979).

(14) W. Sadee' and G. C. Beelen, "Drug Level Monitoring," Wiley-Interscience, New York, N.Y., 1980.

(15) T. P. Moyer and S. G. Sheps, *Ther. Drug Monitor.*, **3**, 217 (1981).

Determination of "Brompton's Cocktails" by Circular Dichroism

W. MARC ATKINSON, JOHN M. BOWEN, and NEIL PURDIE ˣ

Received November 21, 1983, from the *Chemistry Department, Oklahoma State University, Stillwater, OK 74078.* Accepted for publication February 23, 1984.

Abstract □ Circular dichroism spectropolarimetry has been applied to the simultaneous determination of chiral compounds in binary mixtures without separation or sample preparation steps. A strategy which uses data measured at equivalent wavelength pairs simplifies the calculations. Correspondence is within ±2% of the compositions of prepared standard mixtures.

Keyphrases □ Circular dichroism—spectropolarimetry, UV absorption, Brompton's solutions, *R*-(−)-cocaine hydrochloride, morphine sulfate, (±)-methadone, (−)-fructose, β-cyclodextrin □ Brompton's solutions—circular dichroism, spectropolarimetry, UV absorption

A medically approved practice used to relieve the physical distress from chronic pain, such as is experienced by some terminally ill cancer patients, is to administer a mixture of controlled, addictive substances in an oral preparation commonly referred to as "Brompton's cocktails." Cocaine is common to all preparations. Other components differ, but are most often either morphine or (±)-methadone. The mixture is served in a fruit-flavored alcohol base.

Although documented evidence for the abuse of this prescription is limited at this time, the potential exists. We have developed a simple protocol for a rapid direct determination of the drugs by circular dichroism (CD) spectropolarimetry which requires no separation or sample prepreparation. We have previously reported data for opium alkaloids (1, 2), *R*-(−)-cocaine (3, 4), (+)-lysergide (D-LSD) (5), and tetracycline (6). The CD technique focuses only on those components which absorb light and which are simultaneously chiral. Chirality may be either intrinsic to the molecule (1–6) or induced by its complexation with a chiral substrate molecule (4).

By being able to focus on only the CD-active components, the problem of deconvoluting the cumulative UV spectra of the mixtures is considerably simplified. Absorption by the other CD-inactive components only affects the signal-to-noise ratio of the detector.

EXPERIMENTAL SECTION

Standard samples of *R*-(−)-cocaine hydrochloride[1], morphine sulfate[1], and (±)-methadone[2] were used without further purification. The fruit-flavored syrups commonly used contain (−)-fructose. Standard (−)-fructose[3] was obtained commercially. In-house standard mixtures were prepared by weight. Samples of unknown composition were either blind in-house preparations, or were provided[4]. Chirality is induced into (±)-methadone by complexation with the chiral cyclic oligosaccharide β-cyclodextrin[5] present in large excess in aqueous solution, $\sim 10^{-2}$ M.

CD measurements were made on an automatic recording spectropolarimeter[6], and data analyses were made on the ancillary data processor[7]. Daily calibration of the ellipticity scale was made against a standard solution of androsterone in dioxane, as recommended. Samples were diluted with the appropriate volume of dilute hydrochloric acid or water, usually 1:10.

[1] Mallinckrodt Inc.
[2] Drug Enforcement Administration.
[3] Fisher Scientific.
[4] Arizona Department of Public Safety and the local hospital pharmacy.
[5] Kodak.
[6] Model 500A; JASCO.
[7] Model DP-500N.

0022-3549/84/1200-1827$01.00/0

© 1984, American Pharmaceutical Association

Table I—Circular Dichroism Spectral Characteristics [a]

Compound	Characteristic[b]	Wavelength, nm	[θ], degree/M-cm
Morphine Sulfate	λ^-_{max}	286	−66
	λ^o	263	0
	λ^+_{max}	244	372
Cocaine hydrochloride	λ^+_{max}	278	11.5
	λ^o	262	0
	λ^-_{max}	245	−55
(−)-Fructose	λ^+_{max}	273	0.3[d]
	λ^o	235	0
(±)-Methadone[c]	λ^+_{max}	290	9.6[e]
	λ^+_{max}	273	6.4[e]
	λ^+_{max}	266	5.6[e]

[a] For 0.1 M HCl aqueous solutions. [b] λ^+_{max} and λ^-_{max} are wavelengths of the maximum positive or negative signals. λ^o is the wavelength of zero ellipticity. [c] In β-cyclodextrin solution only. [d] Value is calculated for total sugar although only the open-chain form is CD active in the 220–350-nm region. [e] Values for 1:1 complex with β-cyclodextrin.

Table II—Determinations of Binary Mixtures [a]

Sample[b]	Cocaine	Morphine	(−)-Fructose	(±)-Methadone	λ Pairs
S1	1.06 (1.05)	—	—	(0.98)	—
S2	2.31 (2.32)	—	—	(1.55)	—
S3	1.72 (1.74)		9.65 (9.87)	—	7
S4	2.61 (2.55)	—	15.94 (16.23)	—	4
S5	4.15 (4.18)	—	15.04 (14.23)	—	6
S6	2.22 (2.24)	3.44 (3.28)	—	—	6
S7	5.78 (5.81)	1.59 (1.56)	—	—	6
S8	2.95 (2.99)	1.06 (1.05)	—	—	6
B1	0.95 (1)[c]	1.53 (1.5)[c]	—	—	10
B2	0.98 (1)[c]	1.55 (1.5)[c]	—	—	7
B3	1.08 (1)[c]	—	133[d]	present	7
B4	1.01 (1)[c]	—	137[d]	present	6
B5	0.95 (1)[c]	1.46 (1.5)[c]	119[d]	—	6

[a] In mg/mL. Data in parentheses are calculated from known weights. [b] S represents an in-house preparation and B represents an externally supplied Brompton's solution. [c] Figures correspond with pharmacist's recipe. [d] Results are for (−)-fructose in fruit-flavored additives; no composition given.

(−)-Fructose solutions have low ellipticities (7, 8), so solution concentrations were as high as 0.2 M.

RESULTS AND DISCUSSION

CD spectral parameters for the four compounds are collected in Table I. Molar ellipticity [θ] values calculated from the slopes of the respective Beer's law calibration curves at the reported wavelength maxima are also presented. Significant spectral overlap is observed for mixtures of *R*-(−)-cocaine and morphine and *R*-(−)-cocaine and (−)-fructose. The compositions of the in-house preparation of these mixtures were made to be consistent with the pharmacy prepared prescriptions which are on the order of 1.5 mg/mL of morphine sulfate and 1 mg/mL *R*-(−)-cocaine hydrochloride or (±)-methadone. If the binary mixture consists of *R*-(−)-cocaine and (±)-methadone, the problem reduces to the determination of only *R*-(−)-cocaine by direct measurement of the aqueous solution which is conveniently done at the 278 nm positive maximum for the analyte.

For binary mixtures of CD-active components, the observed ellipticity at any wavelength for a 1-cm cell is given by the expression:

$$\psi_{exp} = [\theta]_1 C_1 + [\theta]_2 C_2$$

where the subscripted [θ] and *C* terms refer to the molar ellipticities and molar concentrations of the two components, respectively. The resolution of broad UV absorption bands into positive and negative components in CD spectra offers a simpler option to the simultaneous solution of the equation which is fairly general. The equation reduces to a single unknown if data are measured at preselected wavelength pairs on the standard spectrum of either component at which the absolute values of [θ] are equal in magnitude. Experience with the blind in-house mixtures shows us that the best correspondence in determinations is obtained if the pairs are chosen from the standard spectrum of the component which has the lower [θ]; namely cocaine in mixtures with morphine, and fructose in mixtures with either cocaine or morphine. Results from the calculations and the number of wavelength pairs used are given in Table II for several binary mixtures.

Compared with the direct determination of complex mixtures by UV absorption spectrophotometry, which is commonly done using computer simulation methods, CD effectively reduces the number of analytes contributing to the overall spectrum by focusing on only those which are CD active. The number of curve-fitting parameters is reduced accordingly, and the precision in the determination of each component is improved. Matrix distortions of the CD spectra of the analyte(s) by the simultaneous absorption of energy by achiral components are not observed.

Determinations made on the unknowns obtained from external sources indicated that the preparations were within the recommended limits prescribed for administration to patients (Table II). One ternary mixture was investigated in which tampering with the prescription was suspected. The mixture was reported to consist of morphine, *R*-(−)-cocaine, and (−)-fructose in alcohol. The CD spectrum was a close replica of the mixture prepared according to the prescription. Measurements of data at wavelength pairs for (−)-fructose and the simultaneous solution of the equation for the remaining constituents yielded 1.46 mg/mL for morphine and 0.95 mg/mL for *R*-(−)-cocaine.

At its present state of development, CD spectropolarimetry offers a rapid and quantitative procedure for drug assay and as such has a useful application to product quality control. As the spectral library is extended to include more and more standards, anonymous compound recognition and identification can be anticipated. With the appropriate computer software the same simulation techniques applied to UV absorption determination of multiple-component mixtures can be applied equally well.

REFERENCES

(1) T. A. Crone and N. Purdie, *Anal. Chem.*, **53**, 17 (1981).

(2) J. M. Bowen, T. A. Crone, R. K. Kennedy, and N. Purdie, *Anal. Chem.*, **54**, 66 (1982).

(3) J. M. Bowen and N. Purdie, *Anal. Chem.*, **53**, 2237 (1981).

(4) J. M. Bowen and N. Purdie, *Anal. Chem.*, **53**, 2239 (1981).

(5) J. M. Bowen, H. A. McMorrow, and N. Purdie, *J. Forensic Sci.*, **27**, 822 (1982).

(6) J. M. Bowen and N. Purdie, *J. Pharm. Sci.*, **71**, 836 (1982).

(7) G. D. Maier, J. W. Kusiak, and J. M. Bailey, *Carbohydr. Res.*, **53**, 1 (1977).

(8) L. D. Hayward and S. J. Angyal, *Carbohydr. Res.*, **53**, 13 (1977).

ACKNOWLEDGMENTS

The authors thank the National Science Foundation for the support of this work under Grant No. NSF CHE-7909388. We are also indebted to Mr., Robert A. Jarzen of the Arizona Department of Public Safety for providing the necessary samples.

High-Performance Liquid Chromatographic Method for the Determination of Tiflamizole in Plasma

DARIEL C. RAKESTRAW ˣ **and CHARLES C. WHITNEY, JR.**

Received October 27, 1983, from *E. I. duPont de Nemours and Company, Inc., Pharmaceuticals Research and Development Division, DuPont Pharmaceuticals, Newark, DE 19714.* Accepted for publication February 24, 1984.

Abstract □ A sensitive, specific, high-performance liquid chromatographic procedure was developed for the measurement of plasma tiflamizole levels. Acidic plasma samples were extracted with three volumes of ether. The ether extracts were combined and evaporated to dryness. The residue was dissolved in acetonitrile, washed with hexane, and the acetonitrile was evaporated to dryness. The residue was dissolved in 0.5 mL of mobile phase consisting of acetonitrile and 0.007 M pH 3 sodium phosphate buffer (70:30, v/v) and then chromatographed on a octadecylsilane bonded microparticulate silica column. The assay is specific, precise, accurate, and can measure 10 ng of tiflamizole in 5 mL of plasma. The method was applied to human pharmacokinetic studies.

Keyphrases □ HPLC—tiflamizole, human plasma □ Tiflamizole—HPLC, human plasma

Tiflamizole, 4,5-bis(4-fluorophenyl)-2-[(1,1,2,2-tetrafluoroethyl)sulfonyl]-1*H*-imidazole (I), is a potent nonsteroidal antiarthritic drug that both prevents and treats adjuvant-induced arthritis in rats (1, 2). Tiflamizole is presently being evaluated in clinical studies.

The chemistry, pharmacology, and pharmacokinetics of tiflamizole were recently discussed (1–4). In the initial human studies low doses of tiflamizole were used. This required a specific and highly sensitive GC method[1] for tiflamizole analysis. However for the larger doses currently in use, the high sensitivity is not required and a simpler, more rapid method was developed. This paper describes a specific high-performance liquid chromatographic (HPLC) plasma assay for tiflamizole. The sensitivity of the method is 10 ng/mL.

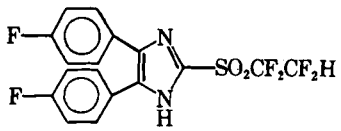

I

EXPERIMENTAL SECTION

Reagents and Apparatus—Tiflamizole[2], 1 M pH 5.3, and 0.007 M pH 3.0 sodium phosphate (monobasic), acetonitrile[3], ether[4], and hexane[3] were used without further purification. The liquid chromatograph consisted of a variable-wavelength UV detector[5] set at 280 nm, a solvent pump[6], a reporting integrator[7], a valve-loop injector[8] with a 100-μL loop, and a 0.46 cm i.d., × 25 cm octadecylsilane bonded microparticulate column[9]. The mobile phase was acetonitrile–0.007 M pH 3 sodium phosphate buffer (70:30). The flow rate was 1.5 mL/min, the column temperature was ambient, and the column back pressure was ~1000 psi. The approximate retention times of tiflamizole and naphthalene were 4.5 and 5.8 min, respectively.

[1] D. C. Rakestraw and C. C. Whitney, unpublished results.
[2] E. I. duPont de Nemours and Co., Inc., Wilmington, Del.
[3] Burdick and Jackson Laboratories, Inc., Muskegon, Mich.
[4] J. T. Baker Chemical Co., Phillipsburg, N.J.
[5] Model 852; E. I. duPont de Nemours and Co.
[6] Model 870; E. I. duPont de Nemours and Co.
[7] Model 3390 A; Hewlett-Packard, Avondale, Pa.
[8] Model SVOV-6-1XC20 Sample Injection Valve; Glenco Scientific Inc., Houston, Tex.
[9] Zorbax ODS, Part Number 880952; E. I. duPont de Nemours and Co.

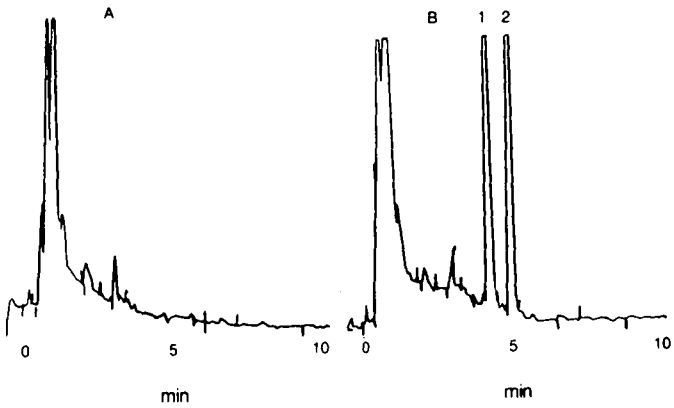

Figure 1—*Chromatograms of extracts from a plasma blank (A) and spiked (0.5 μg) plasma sample (B). Key: (1) tiflamizole; (2) naphthalene.*

Table I—Stability of Tiflamizole in Human Plasma [a]

Day	Amount Spiked, μg[b]	Amount Found, μg	*CV*, %
1	0.48	0.49	4.7
11	0.48	0.50	1.2
21	0.48	0.49	2.0
117	0.48	0.49	1.2
530	0.48	0.48	2.1

[a] Stored at −20°C. [b] $n = 3$.

Standards—Standard curves were prepared from unextracted tiflamizole standards. These standards (0.1, 0.2, 0.5, and 1 μg/mL) were prepared in a mobile phase containing 1 μg/mL of the internal standard, naphthalene, and 100 μL of each was injected into the column and chromatographed.

The peak areas of tiflamizole and naphthalene were measured and the ratio of tiflamizole/naphthalene was calculated. Linear regression least-squares fit was used to calculate the standard curve. Concentration of tiflamizole in unknown samples was determined from the peak area ratio of tiflamizole/naphthalene and the standard curve.

Extraction—A measured volume of plasma (0.5–10 mL) was transferred to a 15-mL polytef-lined screw-cap test tube[10] containing 5 mL of 1 M pH 5.3 sodium phosphate buffer. The mixture was extracted with one 10-mL and two 5-mL portions of ether. After shaking the extract for 30 min, the tube was centrifuged to separate the ether and the aqueous layers.

The organic layers were combined in another 15-mL tube and evaporated to dryness using a gentle stream of air. The residue was dissolved in 5 mL of acetonitrile and washed with three 5-mL volumes of hexane. After shaking for 20 min, the tube was centrifuged to separate the acetonitrile and hexane layers. The hexane layer was discarded by aspiration, then the acetonitrile was evaporated to dryness. The residue was dissolved in 0.5 mL of mobile phase containing 1 μg/mL of naphthalene; 100 μL was then injected into the liquid chromatograph.

Recovery Study—Control plasma samples (1 mL) spiked with 0.1, 0.2, 0.5, and 1.0 μg of tiflamizole were used to determine the extraction recovery. Control plasma samples (1 mL) spiked with 0.5 μg of tiflamizole were run concomitantly with the plasma of each subject to monitor daily recovery of tiflamizole.

Plasma Level Study—Tiflamizole (5 mg) was administered orally with ~237 mL (8 oz.) of water to 3 healthy human males, 64–76 kg, who had fasted

[10] VWR Scientific, Philadelphia, Pa.

0022-3549/84/1200-1829$01.00/0
© 1984, American Pharmaceutical Association

Table II—Recovery of Tiflamizole from Spiked Plasma

Tiflamizole, μg/mL	Recovery, %	Mean ± *SD*
0.1	90, 92, 89	90.3 ± 1.5
0.2	103, 97, 100	100.0 ± 3.0
0.5	97, 98, 99	98.0 ± 1.0
1.0	98, 100, 100	99.3 ± 1.2

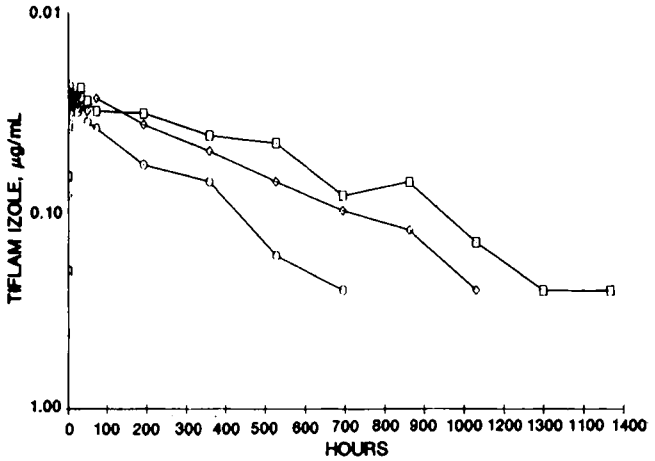

Figure 2—*Tiflamizole profiles in three healthy adult male subjects following a single oral 5-mg dose.*

overnight. Blood samples (10 mL) were withdrawn[11] prior to dosing and at specified times up to 57 d after dosing. The blood samples were centrifuged and the plasma was stored frozen in clean plastic tubes[10]. The elimination half-lives for these individuals were determined using linear regression analysis of the terminal plasma level–time data points.

[11] Heparinized vacutainers.

RESULTS AND DISCUSSION

Typical chromatograms of extracted control plasma and plasma spiked with tiflamizole are shown in Fig. 1. Tiflamizole/naphthalene peak area ratios were linear (from 0.1 to 1.0 μg/mL) and the correlation coefficients for the fit of experimental points were 0.99995. The intercepts were not significantly different from zero. There was no interference from constituents in control plasma or in the plasma from subjects or patients prior to administration of tiflamizole. Tiflamizole is stable in plasma stored at −20°C for at least 530 d. The results are shown in Table I.

Tiflamizole recoveries from spiked plasma (0.1–1.0 μg/mL) were 87.0–100% with *SD* values of 1.0–3.0% (Table II). Daily recoveries of 0.5 μg of tiflamizole spiked to 1 mL of control plasma were 99.7% ($n \simeq 131$) with a *SD* of 3.2%. Tiflamizole can be determined at levels as low as 0.01 μg/mL using 5 mL of plasma.

Figure 2 illustrates the plasma tiflamizole concentration profile in three healthy subjects given a single oral 5-mg dose. Peak concentrations of 0.36–0.61 μg/mL occurred between 4 and 12 h. The elimination half-lives were 9.9–18.0 d.

REFERENCES

(1) Thomas R. Sharpe, Saul C. Cherkofsky, Walter E. Hewes, Dewey H. Smith, Walter A. Gregory, Stephen B. Haber, Michael R. Leadbetter, and Joel G. Whitney, *J. Med. Chem.*, in press.

(2) W. E. Hewes, D. C. Rakestraw, C. C. Whitney, and V. G. Vernier, *Pharmacologist*, **24**, 23 (1983).

(3) G. S. Shotzberger, W. E. Hewes, W. Galbraith, and V. G. Vernier, *Pharmacologist*, **24**, 23 (1983).

(4) D. C. Rakestraw, C. C. Whitney, and V. G. Vernier, *Pharmacologist*, **24**, 23 (1983).

ACKNOWLEDGMENTS

The authors gratefully acknowledge the excellent technical assistance of G. W. Lynch.

Analysis of Tablets Containing Aspirin, Acetaminophen, and Ascorbic Acid by High-Performance Liquid Chromatography

R. THOMIS, E. ROETS, and J. HOOGMARTENS ˣ

Received March 25, 1983, from the *Katholieke Universiteit Leuven, Laboratorium voor Farmaceutische Chemie, Instituut voor Farmaceutische Wetenschappen, B-3000 Leuven, Belgium.* Accepted for publication February 8, 1984.

Abstract □ The high-performance liquid chromatographic method described enables the quantitation of the components and the main impurities of tablets containing aspirin, acetaminophen, and ascorbic acid. A C_8 reverse-phase column was used; the mobile phase was methanol–0.2 M phosphate buffer (pH 3.5)–water (20:10:70). Results obtained for a brand of effervescent tablets, normally aged for 5 years and stressed at 37°C, 50°C, or in 79% relative humidity at room temperature, are reported. Salicylic acid was the main product of decomposition. Diacetyl-*p*-aminophenol was observed to be formed by transacetylation.

Keyphrases □ Acetaminophen—HPLC with ascorbic acid and aspirin □ Aspirin—HPLC with acetaminophen and ascorbic acid □ Ascorbic acid—HPLC with acetaminophen and aspirin

During the last decade, phenacetin has been often replaced by acetaminophen in analgesic tablet formulations containing aspirin as the main component (1). Acetaminophen–aspirin mixtures have lower stability due to acetylation of the former by the latter, producing diacetyl-*p*-aminophenol (2, 3). This acetylation, however, was not evident in another study (4).

Tablets containing ascorbic acid were reported to be stable for over 5 years under normal storage conditions (5), but in combination with aspirin the eventual acetylation of ascorbic acid should be considered. Acetylation, in aqueous medium, of ascorbic acid by acetic anhydride has been described (6). Acetylation of other compounds present in tablet formulations,

0022-3549/84/1200-1830$01.00/0
© 1984, American Pharmaceutical Association

Table II—Recovery of Tiflamizole from Spiked Plasma

Tiflamizole, μg/mL	Recovery, %	Mean ± *SD*
0.1	90, 92, 89	90.3 ± 1.5
0.2	103, 97, 100	100.0 ± 3.0
0.5	97, 98, 99	98.0 ± 1.0
1.0	98, 100, 100	99.3 ± 1.2

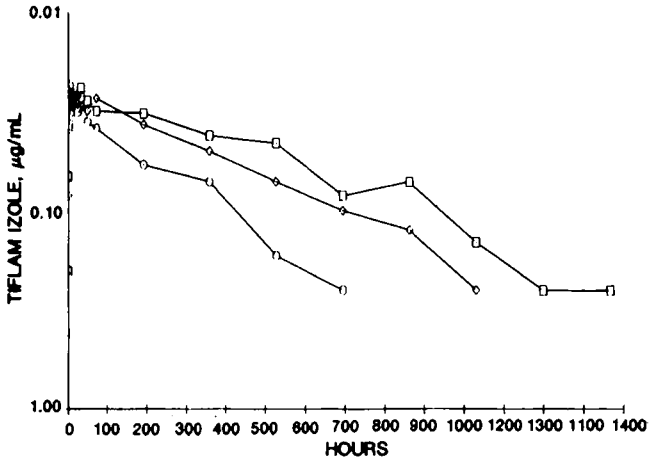

Figure 2—*Tiflamizole profiles in three healthy adult male subjects following a single oral 5-mg dose.*

overnight. Blood samples (10 mL) were withdrawn[11] prior to dosing and at specified times up to 57 d after dosing. The blood samples were centrifuged and the plasma was stored frozen in clean plastic tubes[10]. The elimination half-lives for these individuals were determined using linear regression analysis of the terminal plasma level–time data points.

[11] Heparinized vacutainers.

RESULTS AND DISCUSSION

Typical chromatograms of extracted control plasma and plasma spiked with tiflamizole are shown in Fig. 1. Tiflamizole/naphthalene peak area ratios were linear (from 0.1 to 1.0 μg/mL) and the correlation coefficients for the fit of experimental points were 0.99995. The intercepts were not significantly different from zero. There was no interference from constituents in control plasma or in the plasma from subjects or patients prior to administration of tiflamizole. Tiflamizole is stable in plasma stored at −20°C for at least 530 d. The results are shown in Table I.

Tiflamizole recoveries from spiked plasma (0.1–1.0 μg/mL) were 87.0–100% with *SD* values of 1.0–3.0% (Table II). Daily recoveries of 0.5 μg of tiflamizole spiked to 1 mL of control plasma were 99.7% ($n \simeq 131$) with a *SD* of 3.2%. Tiflamizole can be determined at levels as low as 0.01 μg/mL using 5 mL of plasma.

Figure 2 illustrates the plasma tiflamizole concentration profile in three healthy subjects given a single oral 5-mg dose. Peak concentrations of 0.36–0.61 μg/mL occurred between 4 and 12 h. The elimination half-lives were 9.9–18.0 d.

REFERENCES

(1) Thomas R. Sharpe, Saul C. Cherkofsky, Walter E. Hewes, Dewey H. Smith, Walter A. Gregory, Stephen B. Haber, Michael R. Leadbetter, and Joel G. Whitney, *J. Med. Chem.*, in press.

(2) W. E. Hewes, D. C. Rakestraw, C. C. Whitney, and V. G. Vernier, *Pharmacologist*, **24**, 23 (1983).

(3) G. S. Shotzberger, W. E. Hewes, W. Galbraith, and V. G. Vernier, *Pharmacologist*, **24**, 23 (1983).

(4) D. C. Rakestraw, C. C. Whitney, and V. G. Vernier, *Pharmacologist*, **24**, 23 (1983).

ACKNOWLEDGMENTS

The authors gratefully acknowledge the excellent technical assistance of G. W. Lynch.

Analysis of Tablets Containing Aspirin, Acetaminophen, and Ascorbic Acid by High-Performance Liquid Chromatography

R. THOMIS, E. ROETS, and J. HOOGMARTENS ˣ

Received March 25, 1983, from the *Katholieke Universiteit Leuven, Laboratorium voor Farmaceutische Chemie, Instituut voor Farmaceutische Wetenschappen, B-3000 Leuven, Belgium.* Accepted for publication February 8, 1984.

Abstract □ The high-performance liquid chromatographic method described enables the quantitation of the components and the main impurities of tablets containing aspirin, acetaminophen, and ascorbic acid. A C_8 reverse-phase column was used; the mobile phase was methanol–0.2 M phosphate buffer (pH 3.5)–water (20:10:70). Results obtained for a brand of effervescent tablets, normally aged for 5 years and stressed at 37°C, 50°C, or in 79% relative humidity at room temperature, are reported. Salicylic acid was the main product of decomposition. Diacetyl-*p*-aminophenol was observed to be formed by transacetylation.

Keyphrases □ Acetaminophen—HPLC with ascorbic acid and aspirin □ Aspirin—HPLC with acetaminophen and ascorbic acid □ Ascorbic acid—HPLC with acetaminophen and aspirin

During the last decade, phenacetin has been often replaced by acetaminophen in analgesic tablet formulations containing aspirin as the main component (1). Acetaminophen–aspirin mixtures have lower stability due to acetylation of the former by the latter, producing diacetyl-*p*-aminophenol (2, 3). This acetylation, however, was not evident in another study (4).

Tablets containing ascorbic acid were reported to be stable for over 5 years under normal storage conditions (5), but in combination with aspirin the eventual acetylation of ascorbic acid should be considered. Acetylation, in aqueous medium, of ascorbic acid by acetic anhydride has been described (6). Acetylation of other compounds present in tablet formulations,

0022-3549/84/1200-1830$01.00/0
© 1984, American Pharmaceutical Association

such as phenylephrine (7), codeine (8), or homatropine (9), has also been reported. Acetylation of proteins by aspirin was proposed as an explanation for the hypersensitivity to aspirin in humans (10).

This paper reports on the stability of an effervescent tablet from one manufacturer[1]. The tablets contain aspirin, acetaminophen, and ascorbic acid as the active components. High-performance liquid chromatography (HPLC) was chosen as the method for analysis. HPLC has been used previously for the analysis of multicomponent tablets containing aspirin and acetaminophen (11-17), but to our knowledge this is the first time that ascorbic acid was included in the analysis.

EXPERIMENTAL SECTION

Reagents and Chemicals—Some of the reference products were obtained through synthesis according to literature procedures: diacetyl-*p*-aminophenol, mp 151-154°C [lit. (2, 18) mp 152-156°C and 151-154°C]: *O*-acetyl-*p*-aminophenol, mp 79-81°C [lit. (19) mp 73-74°C and 75°C][2]. A mixture of 3-*O*-acetylascorbic acid and 2-*O*-acetylascorbic acid was obtained in solution[3] (6). Aspirin, salicylic acid, acetaminophen, and ascorbic acid were of Ph. Eur. quality. Sodium saccharin[4], *p*-hydroxybenzoic acid[4], and *p*-aminophenol[4] were of reagent quality. Formic acid[5], potassium hydrogen phosphate[5], and phosphoric acid[5] were of *pro analysi* quality. Reagent-grade methanol[6] was distilled in glass before use; water was distilled twice.

Apparatus and Operating Conditions—A high-pressure pump[7] was connected to a 10-μL loop injector[8], a column packed in-house with 10-μm C_8 reverse-phase material[9], a 254-nm fixed-wavelength detector[10], an integrator (used in the area mode)[11], and a recorder[12]. Some chromatograms were obtained with a variable-wavelength detector[13].

The mobile phase, CH_3OH-0.2 M phosphate buffer (pH 3.5)-water (20:10:70, v/v) was deaerated by sonication; the flow rate was 1 mL/min. The UV detector was set at 0.05 AUFS and the integrator at attenuation 4; the chart speed was 5 mm/min. The column was kept at room temperature (~20°C). The variable-wavelength detector was used at 280 nm.

Preparation of Sample Solutions—Two tablets (average mass, 3.45 g) were pulverized, and 1.000 g was weighed into a 50.0-mL volumetric flask. Formic acid (1.0 mL) and methanol (25 mL) were added, and the flask was mechanically shaken for 10 min. The mixture was brought to volume with methanol, 10 mL was clarified by centrifugation, and 5.0 mL of the supernatant was transferred into a 25.0-mL volumetric flask. Internal standard solution (5.0 mL) was added, and the solution was diluted to volume with water. The solution was analyzed within 1 h after preparation. A 0.0025% (w/v) solution of *p*-hydroxybenzoic acid in methanol-water (20:80) was used as the internal standard solution.

Sample and Storage Conditions—The tablets were prepared to contain 300 mg of aspirin, 200 mg of acetaminophen, and 300 mg of ascorbic acid. Sodium hydrogen carbonate, tartaric acid, citric acid, sodium saccharin, lactose, starch, dimethyl polysiloxane, povidone, and citrus oil were the excipients. Eleven batches, naturally aged 4-61 months at the time of analysis, were available. All samples were kept in their original, unopened plastic tubes; the stoppers had a drying agent. Tubes from the most recent batch were stored for 12 weeks in stressed conditions, *i.e.*, at 37°C (closed tubes), at 50°C (closed tubes), and at room temperature (~20°C) with a relative humidity of 79% (closed and open tubes).

Chromatographic Analysis—Least-squares regression lines (y, peak area ratio; x, amount injected in μg) were obtained with suitably prepared standard solutions for ascorbic acid ($y = 2.235x + 0.0005$), acetaminophen ($y = 2.717x + 0.0153$), salicylic acid ($y = 0.1226x + 0.0012$ at 254 nm, $y = 0.3774x + 0.0001$ at 280 nm), aspirin ($y = 0.2022x + 0.0010$), and diacetyl-*p*-aminophenol ($y = 2.182x + 0.0031$). The coefficient of correlation was >0.999 in all cases. When immediate analysis was impossible, standard solutions were kept at 5°C. The reproducibility was checked by a quadruple extraction of the same powdered tablet mixture and a twofold injection of each resulting solution. The mean and *CV* values obtained for the eight experiments were: ascorbic acid (107.0%, 0.9); acetaminophen (99.8%, 1.0); salicylic acid, measured at 280 nm, (0.81%, 1.8); aspirin (98.9%, 0.6); diacetyl-*p*-aminophenol (0.14%, 3.8). The results are expressed as a percentage of the label claim, except for the impurities where the mass of substance found (*e.g.*, salicylic acid) is reported as a percentage of the label content of the corresponding component (*e.g.*, aspirin).

Four tablets were retained for analysis from each tube, *i.e.*, the pair closest to the orifice and that closest to the bottom. Both pairs were extracted and the solutions were analyzed twice. Significant differences between top and bottom tablets were never found; therefore, the mean of four results is reported.

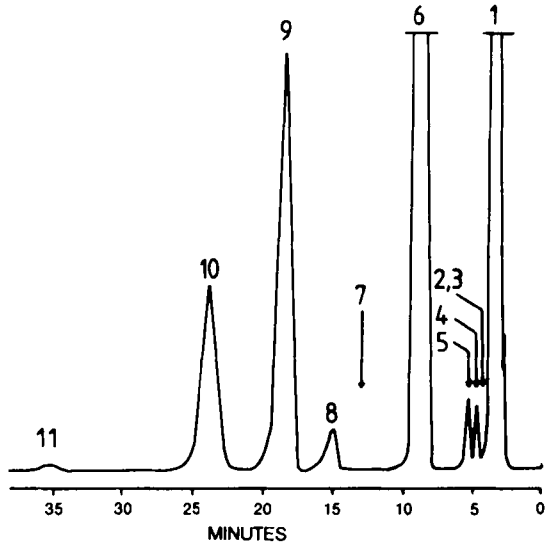

Figure 1—*Chromatogram of 45-month-old tablets; detection at 254 nm. Key: (1) ascorbic acid; (2) p-aminophenol; (3) 3-O-acetylascorbic acid; (4) 2-O-acetylascorbic acid; (5) sodium saccharin; (6) acetaminophen; (7) O-acetyl-p-aminophenol; (8) salicylic acid; (9) p-hydroxybenzoic acid (internal standard); (10) aspirin; (11) diacetyl-p-aminophenol.*

RESULTS AND DISCUSSION

A typical chromatogram, obtained for 45 month-old tablets, is shown in Fig. 1. The influence of the pH of the mobile phase on the separation of *p*-hydroxybenzoic acid, salicylic acid, and aspirin is shown in Fig. 2. A mobile phase containing methanol and a buffer (pH 3.4) was described recently for the analysis of bulk aspirin (20, 21). In all tablets examined, a small peak possibly corresponding to 2-*O*-acetylascorbic acid is present, but a peak cor-

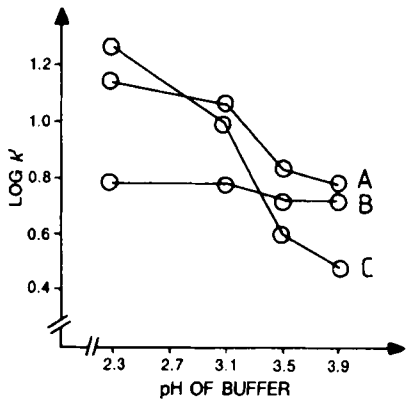

Figure 2—*Influence of the mobile phase buffer pH on the capacity factor (k') of aspirin (A), p-hydroxybenzoic acid (B), and salicylic acid (C).*

[1] S.M.B., Belgium.
[2] This product was purified by column chromatography [silica gel, dichloromethane-acetone (95:5)].
[3] The Paulssen experiment with acetic anhydride in water-dioxane was repeated and followed by HPLC for 1 h. Two secondary peaks were observed. In analogy with the published results, the 3-*O*-acetyl structure was assigned to the first (decreasing) peak (k', 0.5) and the 2-*O*-acetyl structure to the second (increasing) peak (k', 0.6).
[4] Fluka AG, Buchs, Switzerland.
[5] E. Merck, Darmstadt, F.R.G.
[6] Aldrich Europe, Beerse, Belgium.
[7] Model M 6000 A; Waters Associates, Milford, Mass.
[8] Model CV-6-UHPa-N60; Valco, Houston, Tex.
[9] LiChrosorb RP8, (25 cm × 4.6 mm i.d.); E. Merck, Darmstadt, F.R.G.
[10] Model 440; Waters Associates.
[11] Model DP88; Pye Unicam, Cambridge, England.
[12] Model BD40; Kipp & Zonen, Delft, The Netherlands.
[13] Model LC3UV; Pye Unicam.

Table I—Results of the Analysis for Different Batches of Tablets [a]

Batch Age, months	Ascorbic Acid, %	Acetaminophen, %	Diacetyl-*p*-aminophenol, %	Aspirin, %	Salicylic Acid, %[b]
4	106	99.2	0.2	98.5	0.8
9	106	99.2	0.2	99.2	1.2
13	106	100.4	0.3	97.5	1.5
20	105	100.1	0.3	97.0	2.6
24	106	99.9	0.4	95.1	3.6
34	106	98.4	0.4	93.3	4.9
37	105	99.9	0.5	92.0	6.2
45	107	99.0	0.9	76.3	18.1
49	105	99.5	0.6	87.0	9.8
55	106	98.9	0.8	80.9	14.3
61	105	99.3	0.6	88.4	9.4

[a] Percentage of label claim, except as noted in the text. [b] Measured at 280 nm.

recoveries, and since all lots were kept in the same conditions, this must be due to striking differences in the manufacturing quality.

The results obtained in stressed conditions are given in Table II. At 37°C, the USP 3% limit for salicylic acid is reached after ~1 month; at 50°C, the limit is reached after 2 weeks. In open tubes, kept at room temperature and in humid conditions such as frequently occurs in bathrooms, this limit can be reached in ~1 d. Results for the experiment with closed tubes at room temperature and in 79% relative humidity are not reported in detail since the stability was not affected, thus proving the quality of the container.

Although ascorbic acid seems to withstand moderate heating quite well, the effect of high humidity is disastrous. It should, however, be kept in mind that the stability is influenced not only by the conditions of conservation, but also by the presence of other tablet components. The hydrolysis of aspirin involves formation of acetic acid, which lowers the pH and acts as a solvent, thus facilitating reaction. The eventual influence of acetic acid formation is supported by the fact that in the 50°C experiment, ascorbic acid starts to decompose only after 4 weeks, when appreciable amounts of acetic acid have already been formed. A similar effect is observed for diacetyl-*p*-aminophenol

Table II—Results of the Analysis of Stressed Tablets [a]

Conservation Conditions	Conservation Time, weeks	Ascorbic Acid, %	Acetaminophen, %	Diacetyl-*p*-aminophenol, %	Aspirin, %	Salicylic Acid, %
Closed tube						
37°C	0	106	99.2	0.2	98.5	0.8[b]
	2	105	99.7	0.4	97.3	1.9
	4	104	99.0	0.8	96.5	2.7
	8	106	99.0	0.9	94.8	4.1
	12	105	99.2	1.1	93.0	5.4
50°C	0	106	99.2	0.2	98.5	0.8[b]
	2	107	98.9	0.8	96.0	3.0
	4	107	97.6	1.5	89.2	8.2
	8	102	98.7	1.1	59.5	30.0
	12	92	100.7	0.2	29.7	52.1
Open tube[c]	0	106	99.2	0.2	98.5	0.8[b]
	2	90	100.1	0.3	47.7	39.8
	4	33	99.3	0.2	11.4	68.4
	8	8	100.1	0.1	5.6	72.1
	12	4	100.3	0.1	0	75.9

[a] Percentage of label claim, except as noted in text. [b] Measured at 280 nm. [c] At ~20°C and 79% relative humidity.

responding to the assumed 3-*O*-acetylascorbic acid has never been detected. This substance was observed to be very unstable in solution, which confirms an earlier report (6). Quantitative determination of the ascorbic acid derivatives was not attempted since the only reference available was a solution containing a mixture of these impurities. *p*-Aminophenol, which has the same retention time as 3-*O*-acetylascorbic acid, was never detected during our experiments. Due to the rather poor separation in this area of the chromatogram, the detection limit for *p*-aminophenol was not better than 2%. *p*-Aminophenol has been reported as an impurity present in tablets containing acetaminophen, but only when codeine phosphate or magnesium stearate were also present (3); these products were not present in the tablets examined. *O*-Acetyl-*p*-aminophenol was never detected in significant amounts. Diacetyl-*p*-aminophenol was not detected at 280 nm (a more appropriate wavelength for the detection of salicylic acid, present in all the samples as the predominant impurity). Detection at ~300 nm (close to the absorption maximum for salicylic acid) was not applied due to the low absorbance of *p*-hydroxybenzoic acid, used as the internal standard. Samples were extracted with a mixture of formic acid and methanol. The presence of formic acid favors the drug release from the excipients (22). The stability at ~5°C of a solution to be analyzed was followed by HPLC, and the decrease of the content was noted: ascorbic acid, 0.003%/h; acetaminophen, 0.001%/h; aspirin, 0.02%/h; diacetyl-*p*-aminophenol, 0.001%/h. The value for aspirin corresponds well with a value reported for a chloroform–formic acid extract (22).

Table I lists the results for the naturally aged samples. No significant decrease in ascorbic acid or acetaminophen content was observed, and diacetyl-*p*-aminophenol was not formed in appreciable amounts although a small increase was observed. A linear correlation ($r = 0.983$) exists between diacetyl-*p*-aminophenol and salicylic acid formation. The formation of diacetyl-*p*-aminophenol from acetaminophen by transacetylation with aspirin has been discussed previously (3). The formation of salicylic acid is rapid. The 3.0% limit for buffered tablets of the USP XX (23) is exceeded in <2 years, and the BP 80 (24) 1.0% limit for dispersible tablets is exceeded after ~0.5 year. The decrease of aspirin is completely explained by the increase of salicylic acid. Some lots (45 and 55 months) show exceptionally high salicylic acid which, in the 50°C experiment, reaches a maximum after 4 weeks, corresponding to a minimum for acetaminophen. This maximum is followed by a rapid decrease, paralleled by an increase of acetic acid (or salicylic acid) and acetaminophen, which suggests formation of the latter through hydrolysis of diacetyl-*p*-aminophenol.

In all the stressed experiments, the loss of aspirin is completely explained by the formation of salicylic acid. This agrees with recently published results for aspirin tablets, stressed at 50°C and at 80°C, where appreciable amounts of non-salicylic-acid salicylates were only observed at the higher temperature (17).

REFERENCES

(1) A. J. M. Seegers, L. P. Jager, and J. Van Noordwijk, *J. Pharm. Pharmacol.*, **30**, 84 (1978).

(2) K. T. Koshy, A. E. Troup, R. N. Duvall, R. C. Conwell, and L. L. Shankle, *J. Pharm. Sci.*, **56**, 1117 (1967).

(3) B. G. Boggiano, R. Drew, and R. D. Hancock, *Aust. J. Pharm.*, **51**, 514 (1970).

(4) E. Kalatzis, *J. Pharm. Sci.*, **59**, 193 (1970).

(5) S. H. Rubin, E. De Ritter, and J. B. Johnson, *J. Pharm. Sci.*, **65**, 963 (1976).

(6) R. B. Paulssen, D. Chatterji, T. Higuchi, and I. H. Pitman, *J. Pharm. Sci.*, **64**, 1300 (1975).

(7) A. E. Troup and H. Mitchner, *J. Pharm. Sci.*, **53**, 375 (1964).

(8) A. L. Jacobs, A. E. Dilatush, S. Weinstein, and J. J. Windheuser, *J. Pharm. Sci.*, **55**, 893 (1966).

(9) E. Shami, J. Dudzinski, L. Lachman, and J. Tingstad, *J. Pharm. Sci.*, **62**, 1283 (1973).

(10) M. A. Schwartz and G. L. Amidon, *J. Pharm. Sci.*, **55**, 1464 (1966).

(11) I. L. Honigberg, J. T. Stewart, and M. Smith, *J. Pharm. Sci.*, **67**, 675 (1978).

(12) R. G. Baum and F. F. Cantwell, *J. Pharm. Sci.*, **67**, 1066 (1978).
(13) J. T. Stewart, I. L. Honigberg, and J. W. Coldren, *J. Pharm. Sci.*, **68**, 32 (1979).
(14) K. J. Williams, A. Li Wan Po, and W. J. Irwin, *J. Chromatogr.*, **194**, 217 (1980).
(15) V. D. Gupta, *J. Pharm. Sci.*, **69**, 110 (1980).
(16) V. D. Gupta, *J. Pharm. Sci.*, **69**, 113 (1980).
(17) V. Y. Taguchi, M. L. Cotton, C. H. Yates, and J. F. Millar, *J. Pharm. Sci.*, **70**, 64 (1981).
(18) M. H. Broyles and W. K. Easley, *J. Org. Chem.*, **25**, 2233 (1960).
(19) S. E. Hazlet and C. A. Dornfeld, *J. Am. Chem. Soc.*, **66**, 1781 (1944).
(20) M. Menouer, H. M. Ghernati, F. Bouabdallah, and M. H. Guermouche, *Analusis*, **10**, 172 (1982).
(21) M. Menouer, F. Bouabdellah, H. M. Ghermati, and M. H. Guermouche, *J. High-Resolution Chromatogr. Chromatogr. Commun.*, **5**, 267 (1982).
(22) J. Levine and J. D. Weber, *J. Pharm. Sci.*, **57**, 631 (1968).
(23) "The United States Pharmacopeia," 20th rev., U.S. Pharmacopeial Convention, Rockville, Md., 1980.
(24) "The British Pharmacopoeia 1980," H. M. Stationery Office, London, 1980.

ACKNOWLEDGMENTS

The authors thank Miss L. Van Meensel for secretarial assistance.

Effects of Benztropine Mesylate on Haloperidol-Induced Prolactin Secretion and Serum Haloperidol Levels in Rats

JACK M. ROSENBERG *x, MARTIN SIDEMAN *, INGO S. KAMPA ‡, HOWARD McGUIRE §, and LIDIJA KAMPA ¶

Received November 7, 1983, from the **Arnold & Marie Schwartz College of Pharmacy and Health Sciences, Long Island University, Brooklyn, NY 11201*, the ‡*Department of Pathology, The Valley Hospital, Ridgewood, NJ 07451*, §*Long Island University, Brooklyn, NY 11201*, and ¶*Kean College of New Jersey, Union, NJ 07087*. Accepted for publication February 22, 1984.

Abstract □ The effects of benztropine mesylate on haloperidol-induced prolactin secretion and serum haloperidol levels were investigated in 240 rats. Animals were pretreated with benztropine mesylate or saline 20 min prior to receiving haloperidol or saline. Serum prolactin and haloperidol levels were analyzed at six time periods over 150 min. There was no significant difference in prolactin levels of control animals, *i.e.*, saline pretreated/saline treated rats compared to benztropine mesylate pretreated/saline treated rats. Haloperidol caused a significant rise ($p < 0.0001$) in serum prolactin compared with controls. The prolactin concentration for the 30–150-min sampling period was significantly higher when the rats received benztropine mesylate prior to haloperidol ($p < 0.05$). There was a significant correlation ($r = 0.57, p < 0.001$) between serum haloperidol levels and serum prolactin levels in haloperidol-treated animals pretreated with either saline or benztropine mesylate. Additionally, serum haloperidol levels were not significantly different in animals pretreated with benztropine mesylate compared with those pretreated with saline. Thus, the enhancement of prolactin levels by benztropine mesylate was independent of any effect of haloperidol metabolism. This study appears to indicate that in the rat, cholinergic mechanisms exert a weak inhibitory effect on prolactin secretion under conditions of dopamine blockade.

Keyphrases □ Benztropine mesylate—prolactin secretion, serum haloperidol levels, rats □ Haloperidol—prolactin secretion, benztropine mesylate, serum levels, rats

The secretion of the anterior pituitary hormone, prolactin, appears to be dominantly regulated by a prolactin-inhibitory factor liberated by the hypothalamus as a result of afferent dopaminergic impulses (1–3). Dopamine is believed to be the major prolactin-inhibitory factor (4). In addition, prolactin release appears to be mediated to some extent by prolactin-releasing factors (5). Evidence also exists in animals that cholinergic and serotonergic mechanisms modulate the secretion of prolactin at the level of the pituitary (6–9). Although pilocarpine and physostigmine inhibited prolactin secretion in rats (8, 10, 11), no effect was observed on neuroleptic-induced prolactin secretion in this species (11). There are complex and conflicting reports concerning the effects of cholinergic blocking drugs on serum prolactin levels in humans and animals (6, 11, 12).

A fairly good correlation between the antipsychotic potency of various neuroleptics and their prolactin-stimulating effects has been demonstrated both in humans and rats (9, 13–15). Neuroleptics differ considerably in their intrinsic central anticholinergic properties (16). According to Lal *et al.* (17) such differences may account, at least in part, for variations in serum prolactin-stimulating properties found among antipsychotic agents. This suggestion was based on their demonstration in humans that intramuscularly administered benztropine mesylate, a muscarinic receptor-blocking agent, significantly enhanced the elevated prolactin levels induced by intramuscularly administered haloperidol (17). However, no attempt was made to determine if benztropine mesylate influenced prolactin secretion by altering haloperidol metabolism (17).

In this laboratory, comparison of the rank-order of reported central anticholinergic activity of nine antipsychotic drugs belonging to five chemical classes of neuroleptics appeared not to have significant effect upon either the magnitude or duration of prolactin stimulation in rats (18). However, there are no assurances that central anticholinergic threshold levels had been reached with the doses of drugs utilized.

In light of the above, it appeared desirable to further investigate the possible role of anticholinergic activity in enhancing neuroleptic-induced prolactin secretion in rats, to help clarify if a species difference exists between humans and rats in regard to this effect, and to determine if benztropine mesylate influences haloperidol plasma levels. The present investigation examined the effects of benztropine mesylate on haloperidol-induced prolactin secretion and serum haloperidol levels in rats.

EXPERIMENTAL SECTION

Two hundred and forty male Sprague–Dawley adult rats[1] (225–300 g) were divided into 24 equal groups. The rats were housed for 14 d prior to the study

[1] Taconic Farms, Germantown, N.Y.

0022-3549/84/1200-1833$01.00/0
© 1984, American Pharmaceutical Association

(12) R. G. Baum and F. F. Cantwell, *J. Pharm. Sci.*, **67**, 1066 (1978).
(13) J. T. Stewart, I. L. Honigberg, and J. W. Coldren, *J. Pharm. Sci.*, **68**, 32 (1979).
(14) K. J. Williams, A. Li Wan Po, and W. J. Irwin, *J. Chromatogr.*, **194**, 217 (1980).
(15) V. D. Gupta, *J. Pharm. Sci.*, **69**, 110 (1980).
(16) V. D. Gupta, *J. Pharm. Sci.*, **69**, 113 (1980).
(17) V. Y. Taguchi, M. L. Cotton, C. H. Yates, and J. F. Millar, *J. Pharm. Sci.*, **70**, 64 (1981).
(18) M. H. Broyles and W. K. Easley, *J. Org. Chem.*, **25**, 2233 (1960).
(19) S. E. Hazlet and C. A. Dornfeld, *J. Am. Chem. Soc.*, **66**, 1781 (1944).
(20) M. Menouer, H. M. Ghernati, F. Bouabdallah, and M. H. Guermouche, *Analusis*, **10**, 172 (1982).
(21) M. Menouer, F. Bouabdellah, H. M. Ghermati, and M. H. Guermouche, *J. High-Resolution Chromatogr. Chromatogr. Commun.*, **5**, 267 (1982).
(22) J. Levine and J. D. Weber, *J. Pharm. Sci.*, **57**, 631 (1968).
(23) "The United States Pharmacopeia," 20th rev., U.S. Pharmacopeial Convention, Rockville, Md., 1980.
(24) "The British Pharmacopoeia 1980," H. M. Stationery Office, London, 1980.

ACKNOWLEDGMENTS

The authors thank Miss L. Van Meensel for secretarial assistance.

Effects of Benztropine Mesylate on Haloperidol-Induced Prolactin Secretion and Serum Haloperidol Levels in Rats

JACK M. ROSENBERG *x, MARTIN SIDEMAN *, INGO S. KAMPA ‡, HOWARD McGUIRE §, and LIDIJA KAMPA ¶

Received November 7, 1983, from the **Arnold & Marie Schwartz College of Pharmacy and Health Sciences, Long Island University, Brooklyn, NY 11201*, the ‡*Department of Pathology, The Valley Hospital, Ridgewood, NJ 07451*, §*Long Island University, Brooklyn, NY 11201*, and ¶*Kean College of New Jersey, Union, NJ 07087*. Accepted for publication February 22, 1984.

Abstract □ The effects of benztropine mesylate on haloperidol-induced prolactin secretion and serum haloperidol levels were investigated in 240 rats. Animals were pretreated with benztropine mesylate or saline 20 min prior to receiving haloperidol or saline. Serum prolactin and haloperidol levels were analyzed at six time periods over 150 min. There was no significant difference in prolactin levels of control animals, *i.e.*, saline pretreated/saline treated rats compared to benztropine mesylate pretreated/saline treated rats. Haloperidol caused a significant rise ($p < 0.0001$) in serum prolactin compared with controls. The prolactin concentration for the 30–150-min sampling period was significantly higher when the rats received benztropine mesylate prior to haloperidol ($p < 0.05$). There was a significant correlation ($r = 0.57, p < 0.001$) between serum haloperidol levels and serum prolactin levels in haloperidol-treated animals pretreated with either saline or benztropine mesylate. Additionally, serum haloperidol levels were not significantly different in animals pretreated with benztropine mesylate compared with those pretreated with saline. Thus, the enhancement of prolactin levels by benztropine mesylate was independent of any effect of haloperidol metabolism. This study appears to indicate that in the rat, cholinergic mechanisms exert a weak inhibitory effect on prolactin secretion under conditions of dopamine blockade.

Keyphrases □ Benztropine mesylate—prolactin secretion, serum haloperidol levels, rats □ Haloperidol—prolactin secretion, benztropine mesylate, serum levels, rats

The secretion of the anterior pituitary hormone, prolactin, appears to be dominantly regulated by a prolactin-inhibitory factor liberated by the hypothalamus as a result of afferent dopaminergic impulses (1–3). Dopamine is believed to be the major prolactin-inhibitory factor (4). In addition, prolactin release appears to be mediated to some extent by prolactin-releasing factors (5). Evidence also exists in animals that cholinergic and serotonergic mechanisms modulate the secretion of prolactin at the level of the pituitary (6–9). Although pilocarpine and physostigmine inhibited prolactin secretion in rats (8, 10, 11), no effect was observed on neuroleptic-induced prolactin secretion in this species (11). There are complex and conflicting reports concerning the effects of cholinergic blocking drugs on serum prolactin levels in humans and animals (6, 11, 12).

A fairly good correlation between the antipsychotic potency of various neuroleptics and their prolactin-stimulating effects has been demonstrated both in humans and rats (9, 13–15). Neuroleptics differ considerably in their intrinsic central anticholinergic properties (16). According to Lal *et al.* (17) such differences may account, at least in part, for variations in serum prolactin-stimulating properties found among antipsychotic agents. This suggestion was based on their demonstration in humans that intramuscularly administered benztropine mesylate, a muscarinic receptor-blocking agent, significantly enhanced the elevated prolactin levels induced by intramuscularly administered haloperidol (17). However, no attempt was made to determine if benztropine mesylate influenced prolactin secretion by altering haloperidol metabolism (17).

In this laboratory, comparison of the rank-order of reported central anticholinergic activity of nine antipsychotic drugs belonging to five chemical classes of neuroleptics appeared not to have significant effect upon either the magnitude or duration of prolactin stimulation in rats (18). However, there are no assurances that central anticholinergic threshold levels had been reached with the doses of drugs utilized.

In light of the above, it appeared desirable to further investigate the possible role of anticholinergic activity in enhancing neuroleptic-induced prolactin secretion in rats, to help clarify if a species difference exists between humans and rats in regard to this effect, and to determine if benztropine mesylate influences haloperidol plasma levels. The present investigation examined the effects of benztropine mesylate on haloperidol-induced prolactin secretion and serum haloperidol levels in rats.

EXPERIMENTAL SECTION

Two hundred and forty male Sprague–Dawley adult rats[1] (225–300 g) were divided into 24 equal groups. The rats were housed for 14 d prior to the study

[1] Taconic Farms, Germantown, N.Y.

0022-3549/84/1200-1833$01.00/0
© 1984, American Pharmaceutical Association

in a temperature-controlled (23 ± 3°C) artificially illuminated (lights on from 7:00 a.m. to 7:00 p.m. daily) room. The animals were given food[2] and water *ad libitum*. Between 12:30 p.m. and 2:00 p.m., each group was injected intraperitoneally with a 2-mg/kg dose of benztropine mesylate[3] [a dose previously shown to produce a rapid onset of central anticholinergic action (19) with a duration of action of ~24 h (20)] or an equal volume of normal saline. Twenty minutes following pretreatment, 12 groups of rats received 0.5 mg/kg of haloperidol injection[4] administered intraperitoneally and the remaining animals received an equal volume of normal saline. Haloperidol was chosen because of its weak central anticholinergic effects (16). The dose utilized was previously shown in this laboratory to produce a significant increase in serum prolactin secretion above baseline levels for a period of 180 min (15).

Blood samples were obtained by decapitation from the trunk portions at 0, 30, 60, 90, 120, and 150 min after haloperidol or normal saline administration. Blood samples were allowed to stand for 10 min at 4°C; the serum was separated and stored at −20°C until prolactin and haloperidol analyses could be performed. Serum samples were analyzed for prolactin by a double-antibody competitive binding assay. Iodinated rat prolactin, prepared by a modification of the Hunter-Greenwood method (21), was obtained commercially[5]. Rat prolactin antiserum and the reference prolactin standard were supplied by the Rat Pituitary Distribution Program[6]. The procedure for prolactin analysis was modified by the use of a precipitating second antibody suspended in polymer solution[7]. All results are expressed in terms of National Institute of Arthritis, Diabetes, and Digestive Diseases and Kidney (NIADDK) rat prolactin. Each serum sample was assayed in duplicate and the mean was taken as representative of true prolactin concentration. All test and control samples were determined concurrently; the intra-assay variation was 4.2%.

Serum haloperidol concentrations were determined utilizing a commercially available RIA kit[8] according to the instructions supplied. The procedure uses a tritiated label and the bound and free haloperidol are separated by adsorption on dextran-coated charcoal. All tests and control samples were determined concurrently and the results are expressed in μg/mL. The intra-assay variation was 4.7%. Statistical significance was determined by a two-way fixed analysis of variance and factorial analysis of variance with repeated measurements (22).

RESULTS

Evaluation of serum prolactin levels over 150 min, in rats pretreated with normal saline followed by intraperitoneal injection of haloperidol (Fig. 1), indicated a significant rise in serum prolactin compared with controls (saline pretreated/saline treated rats; $F_{(1,91)} = 53.51, p < 0.0001$). Likewise, there was a significant rise in serum prolactin in the 150-min period following intraperitoneal injection of haloperidol (Fig. 1) in rats pretreated with benztropine mesylate compared with controls (benztropine pretreated/saline treated rats; $F_{(1,98)} = 74.64, p < 0.0001$). There was no significant difference in the prolactin levels of the control animals (Fig. 1), *i.e.*, saline pretreated/saline treated rats *versus* benztropine pretreated/saline treated rats over the time period of this experiment ($F_{(1,87)} = <1.0$, not significant). Additionally, there were no significant differences in the mean prolactin levels of the haloperidol-treated rats pretreated with either saline or benztropine mesylate ($F_{(1,87)} = 3.80, p > 0.05$). However, when the data were analyzed by a factorial analysis of variance the prolactin concentrations for the 30–150-min sampling period were significantly higher when the rats received benztropine mesylate prior to haloperidol than when they received saline prior to haloperidol ($F_{(1,89)} = 4.36, p < 0.05$). This approach more fully captured the interrelations between the drugs and prolactin than standard straight baseline comparisons and permitted the use of simple main effects to isolate the locus of effect on prolactin due to haloperidol within benztropine mesylate.

Table I shows the effects of benztropine mesylate and normal saline pretreatments on serum haloperidol levels over a period of 150 min. Serum haloperidol levels were not significantly different in animals pretreated with benztropine mesylate compared with animals pretreated with saline ($F_{(1,89)} < 1.0$, not significant). There was a significant correlation ($r = 0.57, p < 0.001$) between the serum prolactin and serum haloperidol levels in haloperidol-treated animals pretreated with either benztropine mesylate or saline.

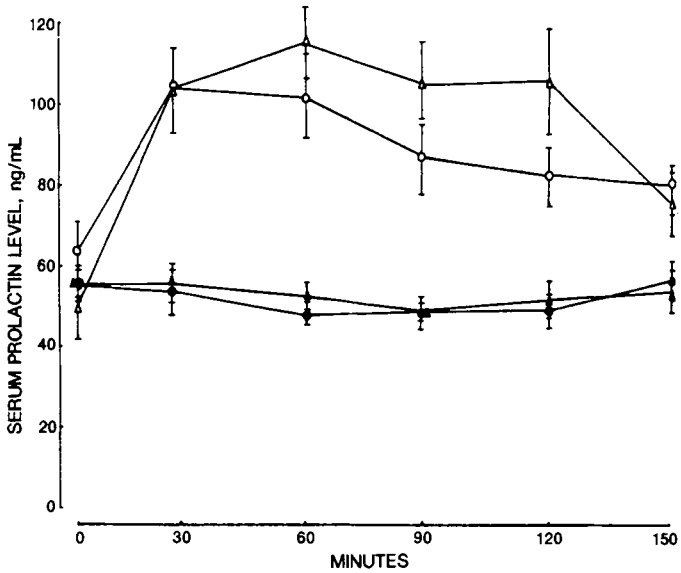

Figure 1—*Effects of pretreatment with benztropine mesylate or saline on the serum prolactin levels induced by treatment with haloperidol or saline. Each point represents a mean of 10 male rats; vertical lines show the* SEM. *Key: (●) saline pretreatment/saline treatment; (▲) benztropine mesylate pretreatment/saline treatment; (○) saline pretreatment/haloperidol treatment; (△) benztropine mesylate pretreatment/haloperidol treatment.*

DISCUSSION

Prolactin-elevating potency of neuroleptics in rats has previously been shown to correlate well with dopamine receptor blockade (23). The presence of a tuberoinfundibular cholinergic pathway has been described in rats (24). Adrenergic neurons regulating prolactin release have receptors for acetylcholine, and cholinergic neurons in the hypothalamus may terminate on adrenergic neurons (11). Pilocarpine has been shown to inhibit prolactin secretion in rats, and atropine reversed this effect (11). Atropine has been shown to potentiate neuroleptic-induced prolactin secretion in the monkey (6). These data are consistent with an inhibitory muscarinic mechanism on prolactin secretion. Although cholinergic drugs reduce prolactin secretion in the rat, after blockade of catecholamine receptors by chlorpromazine, haloperidol, or pimozide, no reduction in serum prolactin could be seen (11). Paradoxically, atropine may also reduce prolactin levels in the rat (8).

In humans it has been demonstrated that some patients who were receiving anticholinergic antiparkinsonian drugs in addition to chronic neuroleptic treatment had higher circulating prolactin concentrations than subjects on neuroleptics alone (25). However, in this laboratory previous comparisons of the rank-order of reported intrinsic central anticholinergic activity of nine antipsychotic drugs (belonging to five chemical classes of neuroleptics) with the experimentally determined rank-orders of time of maximum serum prolactin levels, magnitude of prolactin secretion at each sampling period, or the maximum serum prolactin elevation for each drug, demonstrated no significant correspondence (18). These comparisons suggested that reported intrinsic anticholinergic activity of neuroleptics did not have a significant effect upon either the magnitude or duration of prolactin stimulation produced by these drugs in rats. Although the doses of neuroleptics employed correspond well with human therapeutic dosages and produced marked prolactin stimulation, central anticholinergic activity was not experimentally determined. It is possible that anticholinergic threshold levels may not have been reached in rats with the doses utilized for some or all of the drugs; this requires further investigation.

In the present study the antimuscarinic agent, benztropine mesylate, had no effect on basal prolactin secretion in the rat but did significantly enhance the prolactin elevation promoted by haloperidol. This finding in the rat exactly corresponds to the observation in humans that intramuscularly administered benztropine mesylate did not significantly influence basal prolactin levels but did significantly enhance prolactin levels induced by intramuscularly administered haloperidol (17).

The present study also demonstrated that benztropine mesylate enhanced prolactin secretion independent of an effect on haloperidol metabolism, since pretreatment with benztropine did not significantly alter serum haloperidol levels. It appears that in both species cholinergic mechanisms have no effect on basal prolactin secretion but exert a weak inhibitory effect under conditions of dopamine receptor blockage.

[2] Purina Lab Chow; Ralston Purina Co., St. Louis, Mo.
[3] Merck Sharp and Dohme, Westport, Pa.
[4] McNeil Laboratories, Fort Washington, Pa.
[5] New England Nuclear, Boston, Mass.
[6] National Institute of Arthritis, Diabetes, Digestive Diseases and Kidney (NIADDK), Rat Pituitary Hormone Distribution Program, National Pituitary Agency, Baltimore, Md.
[7] Clinical Assays—Division of Travenol Laboratories, Cambridge, Mass.
[8] Damon Diagnostics, Needham Heights, Mass.

Table I—Effects of Benztropine Mesylate and Saline Pretreatments on Serum Haloperidol Levels

Pretreatment	Serum Haloperidol Levels, μg/mL[a]					
	0 min	30 min	60 min	90 min	120 min	150 min
Saline[b]	0.15 ± 0.05	16.92 ± 2.80	10.80 ± 1.41	8.47 ± 1.25	7.00 ± 0.78	6.60 ± 0.49
Benztropine Mesylate[c]	0.32 ± 0.30	15.71 ± 3.42	9.20 ± 1.17	8.38 ± 0.96	6.76 ± 1.04	6.20 ± 0.97

[a] Mean ± *SEM*; n = 10 animals per group. [b] 2 ml/kg ip 20 min prior to a 0.5-mg/kg ip injection of haloperidol. [c] 2 mg/kg ip 20 min prior to a 0.5-mg/kg ip injection of haloperidol.

It is unlikely that the antihistaminic properties of benztropine (26) or its inhibiting effect on the uptake of dopamine in certain brain regions (27) accounted for the reported observations. Libertun and McCann (28) found, in rats, that a dose-dependent rise in prolactin produced by histamine was blocked by the antihistamine diphenhydramine. It has also been reported that the inhibition of dopamine uptake by benztropine mesylate may potentiate the synaptic actions of dopamine (27), and dopamine has been shown to be a highly effective inhibitor of prolactin secretion (29). Lastly, although serum prolactin and serum haloperidol levels are statistically highly correlated, they should not be used interchangeably as the basis for experimental observations since >67% of the variance remains unknown.

REFERENCES

(1) A. G. Frantz and D. L. Kleinberg, *Science*, **170,** 745 (1979).

(2) M. T. Buckman and G. T. Peake, *J. Am. Med. Assoc.*, **236,** 871 (1976).

(3) I. A. Kamberi, R. S. Mical, and J. C. Porter, *Experientia*, **26,** 1150 (1970).

(4) E. Fluckiger, *Bull. Schweiz, Akad. Med. Wiss.*, **34,** 191 (1978).

(5) M. Szabo and L. A. Frohman, *Endocrinology*, **98,** 1451 (1976).

(6) R. R. Gala, M. G. Subramanian, J. A. Peters, and S. Jaques, *Hormone Res.*, **7,** 118 (1976).

(7) M. G. Subramanian and R. R. Gala, *Neuroendocrinology*, **22,** 240 (1976).

(8) B. K. McLean and M. B. Nikitovitch-Winer, *Endocrinology*, **97,** 763 (1975).

(9) E. J. Sachar, P. H. Gruen, N. Altman, F. S. Halpern, and A. G. Frantz, in "Hormones, Behavior and Psychopathology," Raven Press, New York, N.Y., 1976.

(10) H. J. Chen and J. Meites, *Endocrinology*, **96,** 10 (1975).

(11) L. Grandison and J. Meites, *Endocrinology*, **99,** 75 (1976).

(12) R. W. McCallum, J. R. Sowers, J. M. Hershman, and R. A. L. Sturdevant, *J. Clin. Endocrinol. Metab.*, **42,** 1152 (1976).

(13) H. Y. Meltzer and V. S. Fang, *Arch. Gen. Psychiat.*, **33,** 763 (1975).

(14) G. Langer, E. J. Sachar, F. S. Halpern, P. H. Gruen, and M. Solomon, *J. Clin. Endocrinol. Metab.*, **45,** 996 (1979).

(15) J. M. Rosenberg and C. A. Lau-Cam, *J. Pharm. Sci.*, **69,** 74 (1980).

(16) S. H. Snyder, D. Greenberg, and H. I. Yamamura, *Arch. Gen. Psychiat.*, **31,** 58 (1974).

(17) S. Lal, T. Mendis, P. Cervantes, H. Guyda, and J. L. DeRivera, *Neuropsychobiology*, **5,** 327 (1979).

(18) J. M. Rosenberg, H. McGuire, I. S. Kampa and C. A. Lau-Cam, *Can. J. Pharm. Sci.*, **16,** 35 (1981).

(19) H. C. Fibiger, A. P. Zis, and A. G. Phillips, *Eur. J. Pharmacol.*, **30,** 309 (1975).

(20) "1983, USP DI; Drug Information for the Health Care Provider" vol. 1, U. S. Pharmacopeial Convention Inc., Rockville, Md., p. 109.

(21) W. H. Hunter and F. C. Greenwood, *Nature (London)*, **194,** 495 (1962).

(22) B. J. Winer, "Statistical Principles in Experimental Design," 2nd ed., McGraw-Hill, New York, N.Y., 1962, pp. 776–795.

(23) P. Seeman, T. Lee, M. Chau Wong, and K. Wong, *Nature*, **261,** 171 (1976).

(24) K. A. Carson, G. B. Nemeroff, and M. S. Bone, *Brain Res.*, **129,** 169 (1977).

(25) J. L. DeRivera, S. Lal, P. Ettigi, S. Hontela, H. F. Muller, and H. G. Friesen, *Clin. Endocrinol.*, **5,** 282 (1976).

(26) J. E. F. Reynolds, "Martindale, The Extra Pharmacopoeia," The Pharmaceutical Press, 28th ed., London, England, 1982, p. 295.

(27) J. T. Coyle and S. J. Snyder, *Science*, **166,** 899 (1969).

(28) C. Libertun and S. M. McCann, *IRCS J. Med. Sci.*, **4,** 374 (1976).

(29) "The Pharmacological Basis of Therapeutics," 6th ed., A. Goodman Gilman, L. S. Goodman, and A. Gilman, Eds., Macmillan, New York, N.Y., 1980, p. 1382.

ACKNOWLEDGMENTS

The authors thank the National Institute of Arthritis, Diabetes, Digestive Diseases, and Kidney (NIADDK), Rat Pituitary Distribution Program, and Dr. A. F. Parlow for the gift of radioimmunoassay materials. We also thank McNeil Laboratories for their gift of haloperidol.

Chromatographic Separation of the C(1), C(1a), and C(2) Components of Gentamicin and the Assessment of Their Individual Binding to Serum Proteins

WILLIAM C. GRIFFITHS *x, JAMES F. BELLIVEAU ‡, CHARLENE L. BENSTED *, STEVEN G. CALABRESI *, and ISRAEL DIAMOND *

Received December 21, 1983, from the **Department of Pathology and Laboratory Medicine, Division of Biology and Medicine, Roger Williams General Hospital and Brown University, Providence, RI 02908* and the *‡Department of Chemistry, Providence College, Providence, RI 02918.* Accepted for publication March 9, 1984.

Abstract □ [^{3}H]gentamicin and [^{14}C]gentamicin samples were purified by Sephadex column chromatography and separated by an HPLC technique into the three major, medicinally active gentamicin components. These separated components were used in equilibrium dialysis studies to determine their percent binding to serum proteins. The bindings of the components were inversely related to concentrations of ionized calcium and magnesium. When dialyzed against a buffer containing physiological concentrations of the divalent cations, the binding of the C(1) component was 2.2 ± 1.0%, the binding of the C(1a) component was 1.2 ± 1.9%, and the binding of the C(2) component was 5.0 ± 2.0%. The percent bindings are not identical and, due to their low values, probably have negligible clinical significance. The radioactive composition and purity of the ^{3}H- and ^{14}C-labeled gentamicin samples differed and these may be important factors in the variance of reported gentamicin bindings.

Keyphrases □ Gentamicin—component separation serum protein binding, radiolabels, HPLC □ Serum protein binding—radiolabeled gentamicin, component separation, HPLC

Since its discovery in 1963, the use of the broad spectrum antibiotic gentamicin has found acceptance in the treatment of gram negative infections (1). Because nephrotoxicity and ototoxicity are associated with gentamicin administration, its use has been somewhat limited (2). In evaluating the pharmacokinetics and renal cortical uptake of gentamicin, its binding to serum proteins was investigated. However, reported gentamicin binding varies from 0 to 30% (3–8). Parameters which influence the binding of gentamicin to serum proteins and which must be controlled in these binding studies are the levels of ionized calcium and magnesium (6, 7) and the use of serum rather than heparinized plasma (6). However, the chemical purity of the radioactively labeled gentamicin used in some studies was not well defined. To further examine gentamicin binding to serum proteins, our study was designed to separate both ^{3}H- and ^{14}C-labeled gentamicin samples into the three major, medicinally active components [C(1), C(1a), and C(2)] and to determine the percent binding of these components to the proteins of a serum pool prepared from hospital patient samples.

EXPERIMENTAL SECTION

Gentamicin sulfate[1] and [^{14}C]gentamicin sulfate[2] (120 mg, specific activity 830 μCi/mg) were generously donated. Unlabeled gentamicin (100 mg) was tritium labeled[3] by the high-pressure gas phase technique (crude product specific activity 0.37 mCi/mg). The scintillation cocktail was commercially obtained[4]. Unless otherwise specified, all other chemicals were reagent grade. The serum used in the experiments was prepared by pooling the excess of >2000 specimens from adult hospital patients. The pool was divided into 5-mL aliquots, which were kept at −5°C until use, to a maximum of 6 months.

[1] Lot No. 1045-268-3194; Schering Corp.
[2] Lot No. 5883-118; Schering Corp.
[3] New England Nuclear, Boston, Mass.
[4] Aquasol; New England Nuclear.

Purification of Radioactive Gentamicin with Thin-Layer Chromatographic Detection—Radioactive gentamicin was partially purified with Sephadex column chromatography using a modification of the method of Mahon *et al.* (9). Aliquots (1 mL) were collected into test tubes. One microliter from each aliquot was placed into scintillation vials containing 10 mL of the scintillation fluid. The vials were counted in a liquid scintillation counter[5]. The fractions showing the highest level of radioactivity were saved and the others were discarded. The fractions containing gentamicin were identified by TLC. Aliquots (100 μL) were spotted on a silica gel TLC plate[6]. A 1-mg/mL nonradioactive gentamicin solution (25 μL) in water was used as a marker on either side of the plate. The solvent system was chloroform–17% NH_4OH–methanol–H_2O (1:2:4:1, by volume). One percent ninhydrin in ethanol was used as the visualization agent. This system separates gentamicin into three bands which correspond to the three major components of the active drug.

Liquid Chromatographic Separation into Gentamicin Components—The HPLC separation of radioactive gentamicin into its three major components was accomplished by a modification of the ion-pair method of Anhalt and Brown (10). This was done with an HPLC unit using a C_{18} column[7] with a mobile phase of 0.2 M Na_2SO_4, 0.02 M sodium pentane sulfonate, and 0.1% (v/v) acetic acid in water–methanol (97:3) at a flow rate of 2 mL/min at ambient temperature. Samples (25 μL) were injected and collected fractions were analyzed both by TLC and liquid scintillation counting.

Dialysis Studies—Equilibrium dialysis was carried out in a multicavity dialysis cell[8] (eight chambers, 1.0-mL capacity each) with cellulose dialysis membranes[9]. Human pooled serum was dialyzed against an equivalent amount of a buffer containing a radioactive gentamicin component (purified by Sephadex and HPLC) and nonradioactive gentamicin at a concentration of 10 μg/mL. Divalent cation concentrations were varied by changing the concentration of these species in the buffer from zero to four times the physiological concentrations. Divalent cation concentrations of the serum samples were varied by adding equivalent amounts of EDTA to the serum to reduce their concentrations to zero or by adding the appropriate amount of these cations to the buffer to bring the concentrations to four times the physiological value. Dialysis membranes were prepared by boiling them in distilled water three times and then soaking them overnight in the dialysis buffer of 0.05 M Tris, 0.1% sodium azide, and 0.15 M NaCl (adjusted to pH 7.4 with 1 M HCl). All dialysis experiments were equilibrated for a 48-h period in a thermally controlled (37°C) shaking waterbath[10]. Control experiments, consisting of buffer with gentamicin against buffer without gentamicin, were also run.

[5] Model 3385, TRI-CARB; Packard.
[6] LK5D, silica gel 8 nm; Whatman, Clifton, N.J.
[7] μ-Bondapak C_{18} column, Model 204; Waters.
[8] Model 348; Bel Art Products, Inc.
[9] Model No. 43020; Roche.
[10] Model 50; GCA/Precision Scientific.

Table I—Percent Radioactivity of Gentamicin Components Separated by Liquid Chromatography

Component	^{3}H-Labeled Sample[a]	^{14}C-Labeled Sample	
		Our Data[a]	Manufacturer's Data
C(1)	21%	58%	54.4%
C(1a)	42%	6%	10.4%
C(2)	37%	36%	35.2%

[a] These percentages correspond to the radioactivity of the HPLC-separated components used in the dialysis studies, not to the overall radioactive composition of the initial sample.

0022-3549/84/1200-1836$01.00/0
© 1984, American Pharmaceutical Association

Table II—Percent Binding of Gentamicin Components to Serum Proteins[a]

Serum Environment	C(1) Component		C(1a) Component		C(2) Component	
			Absence of Ca^{2+} and Mg^{2+}			
^3H-Label data	8.7 ± 3.9 (5)	$p < 0.01$	2.8 ± 1.1 (4)	$p = 0.02$	5.7 ± 3.3 (5)	$p < 0.01$
^{14}C-Label data	5.8 ± 2.2 (4)	$p < 0.01$	3.4 ± 2.9 (3)	$p = 0.02$	7.2 ± 1.5 (5)	$p < 0.01$
^3H- and ^{14}C-Label data	7.4 ± 2.4 (9)	$p < 0.01$	3.1 ± 1.0 (7)	$p < 0.01$	6.5 ± 1.4 (10)	$p < 0.01$
			Normal Ca^{2+} and Mg^{2+}			
^3H-Label data	2.1 ± 1.5 (10)	$p < 0.01$	1.5 ± 1.8 (12)	$p = 0.05$	6.8 ± 2.2 (10)	$p < 0.01$
^{14}C-Label data	2.3 ± 0.6 (5)	$p = 0.02$	0.2 ± 8.1 (4)	$p = 0.70$	1.4 ± 1.5 (5)	$p = 0.12$
^3H- and ^{14}C-Label data	2.2 ± 1.0 (15)	$p = 0.01$	1.2 ± 1.9 (16)	$p = 0.27$	5.0 ± 2.0 (15)	$p < 0.01$
			Elevated Ca^{2+} and Mg^{2+} (× 4)			
^3H data	3.6 ± 4.2 (4)	$p < 0.01$	2.3 ± 3.0 (4)	$p = 0.14$	5.1 ± 4.6 (5)	$p < 0.01$
^{14}C data	−1.1 ± 1.7 (5)	$p = 0.57$	−2.8 ± 5.3 (4)	$p = 0.11$	0.6 ± 1.2 (5)	$p = 0.12$
^3H and ^{14}C data	1.0 ± 0.8 (9)	$p = 0.46$	−0.3 ± 3.2 (8)	$p = 0.50$	2.2 ± 2.9 (10)	$p = 0.05$
			Controls			
^3H-Label data			0.8 ± 0.6 (34)			
^{14}C-Label data			−0.4 ± 1.1 (21)			
^3H- and ^{14}C-Label data			0.4 ± 0.6 (55)			

[a] All bindings are given as: mean ± 95% confidence limit (number of data points); p values are the probabilities for the t test comparing the percent binding values to the control values. Total gentamicin concentrations in serum at equilibrium were at 5 μg/mL during this study.

Liquid scintillation counting was done on the serum and buffer portions after minimizing quenching differences through a matrix equalization procedure. In this procedure, pooled serum without gentamicin was dialyzed against buffer without gentamicin to reproduce the slight changes due to the osmotic effect during dialysis. The dialyzed serum without gentamicin was added to an equal volume of radioactive buffer, and the dialyzed buffer without gentamicin was added to an equal volume of radioactive serum before counting on the liquid scintillation counter. The percentage of drug bound to the serum proteins was calculated as published by Olsen (11, 12). Radiochemical analysis of the dialysis membrane indicated that negligible binding-absorption of gentamicin had occurred to this membrane.

RESULTS AND DISCUSSION

TLC analysis of the Sephadex-enriched [^3H]gentamicin showed significant amounts of radioactive material at the origin and in locations other than those attributable to known gentamicin components, demonstrating incomplete purification.

The results of the HPLC separation of Sephadex-treated radioactive gentamicin into its components is presented in Table I. Essentially all of the radioactivity of the [^{14}C]gentamicin can be ascribed to the gentamicin components, whereas significant radioactivity (~25%) of the [^3H]gentamicin was found in HPLC fractions that contained negligible gentamicin, mostly in the fractions eluting early. Some tritiated impurities possibly also bind to serum proteins. This binding of impurities may explain the observation that a tritiated gentamicin sample, purified by Sephadex but not HPLC, gave 15, 10, and 6% binding with zero, normal, and elevated divalent cation levels as compared with 5.1, 3.6, and 3.6% for the combined bindings of the HPLC purified-separated tritiated components.

Multiple equilibrium dialysis experiments were carried out using either [^3H]gentamicin components or [^{14}C]gentamicin components. The data are summarized in Table II. There were also 34 control experiments using [^3H]gentamicin and 21 control experiments using [^{14}C]gentamicin, all run concurrently with one or another serum dialysis experiment. The criterion for assessing the difference in binding from zero of a given gentamicin component in a given environment was the comparison of the average test experiment data with the average control result, using the Student's t test.

The bindings are inversely related to concentrations of ionized calcium and magnesium as reported earlier (6, 7). In the absence of ionized calcium and magnesium in the serum pool, partially separated gentamicin components, C(1), C(1a), and C(2), all showed binding different from zero, at 7.4, 3.1, and 6.5%, respectively. In the presence of physiological concentrations of calcium and magnesium, components C(1) and C(2) showed binding. The averages were 2.2 and 5.0%, respectively. Component C(1a) showed no binding under these conditions. In the presence of calcium and magnesium concentrations which were four times the usual physiological concentrations, none of the components showed binding when average data were used. There were two discrepancies, however, in that the tritium-labeled C(1) and C(2) components showed binding at 3.6 and 5.1%, respectively. This finding is probably due either to incomplete separation of the tritiated gentamicin components from nondrug impurities, or to a large precision error. A three-way analysis of variance using the Fisher F ratio showed that the 4X physiological divalent cation, physiological divalent cation, and no divalent cation binding results were different for the C(1) component ($p < 0.001$), for the C(2) component ($p = 0.030$), but not for the C(1a) component [for which the only binding was in the absence of calcium and magnesium ($p = 0.179$)].

Several fresh serum samples, drawn from volunteers, were used in dialysis experiments and showed degrees of binding comparable to those obtained using pooled serum. The bindings of the individual gentamicin components to serum proteins are different and, due to their low values, this binding effect probably has no clinical significance. This study indicates that, besides the use of serum rather than heparinized plasma and control over the divalent cation concentrations, other significant factors in the variance of reported gentamicin bindings may be the radioactive purity and relative composition of labeled gentamicin mixtures. Thus, these factors must be better controlled or, at least, better documented in protein binding studies.

REFERENCES

(1) R. L. Jao and G. G. Jackson, *J. Am. Med. Assoc.*, **189**, 817 (1964).

(2) G. G. Jackson and G. Arcieri, *J. Infect. Dis.*, **124**, S130 (1971).

(3) R. J. Bulger, S. Sidel, and W. M. Kirby, *Ann. Intern. Med.*, **69**, 593 (1963).

(4) R. C. Gordon, C. Regamey, and W. M. Kirby, *Antimicrob. Agents Chemother.*, **2**, 214 (1972).

(5) D. R. Myers, W. M. Bennett, and G. D. Olsen, *Clin. Res.*, **24**, 133A (1976).

(6) D. R. Myers, J. DeFehr, W. M. Bennett, G. A. Porter, and G. D. Olsen, *Clin. Pharmacol. Ther.*, **23**, 356 (1978).

(7) C. H. Ramerez-Rhonda, R. K. Holmes, and J. P. Sanford, *Antimicrob. Agents Chemother.*, **7**, 239 (1975).

(8) L. J. Riff and G. G. Jackson, *J. Infect. Dis.*, **124**, S98 (1971).

(9) W. A. Mahon, J. Ezer and T. W. Wilson, *Antimicrob. Agents Chemother.*, **3**, 585 (1973).

(10) J. P. Anhalt and S. D. Brown, *Clin. Chem.*, **24**, 1940 (1978).

(11) G. D. Olsen, *Clin. Pharmacol. Ther.*, **14**, 338 (1973).

(12) G. D. Olsen, *Clin. Pharmacol. Ther.*, **17**, 31 (1975).

Determination of Nitroglycerin and Its Dinitrate Metabolites in Human Plasma by High-Performance Liquid Chromatography with Thermal Energy Analyzer Detection

A. J. WOODWARD ˣ, P. A. LEWIS, M. AYLWARD, R. RUDMAN, and J. MADDOCK

Received December 23, 1983, from *Simbec Research Ltd., Merthyr Tydfil, Mid Glamorgan, United Kingdom.* Accepted for publication March 30, 1984.

Abstract □ A highly selective and sensitive high-performance liquid chromatographic assay employing a thermal energy analyzer as the detector for nitroglycerin and its dinitrate metabolites in human plasma has been developed. Prior to chromatography the method employs a simple one-stage extraction step. Nitroglycerin and its dinitrate metabolites are then chromatographed on a 10-μm nitrile bonded phase column using an internal-external standard method. The nitroglycerin and its 1,2,3-propanetriol-1,3- and -1,2-dinitrate metabolites (glyceryl-1,3- and -1,2-dinitrate) have a retention time of 8.5, 10.5, and 11.5 min, respectively at a flow rate of 2.0 mL/min for a mobile phase of 5% v/v acetone in *n*-hexane. The limits of sensitivity were 0.05 ng/mL for nitroglycerin and 0.25 ng/mL for the dinitrate metabolites. Linearity of response was observed over the 0.1–2.0-ng/mL range for nitroglycerin and 0.5–10.0-ng/mL range for the dinitrate metabolites. Blood level data from a pilot study with human volunteers in receipt of an oral form of nitroglycerin is presented.

Keyphrases □ Nitroglycerin—HPLC, parent drug, dinitrate metabolites, human plasma □ Thermal energy analyzer—HPLC, nitroglycerin, dinitrate metabolites, human plasma

Nitroglycerin has been shown to be an effective vasodilator used prophylactically in the treatment of angina (1). The majority of published methods for the analysis of nitroglycerin in plasma employ GC with electron-capture detection (ECD) (2–4). These sensitive methods require complicated extraction procedures and careful handling to ensure reproducibility.

A recent publication (5) describes a very sensitive and rapid assay employing negative ion GC–MS; however ionization techniques are not suitable for analyses of large routine workloads due to continuous contamination of the ion source. A high-performance liquid chromatographic (HPLC) procedure with a thermal energy analyzer as detector has been reported for determining nitroglycerin and its metabolites in beagle dog blood (6). This method has been criticized (7) as being insufficiently sensitive for the determination of the compound in humans following therapeutic doses.

Our laboratories have successfully used HPLC combined with the thermal energy analyzer for the analysis of isosorbide dinitrate in human plasma (8). This report describes the development of a highly sensitive and robust procedure for the assay of nitroglycerin and its dinitrate metabolites in human plasma using similar techniques.

EXPERIMENTAL SECTION

Materials and Apparatus—Pure authentic trinitroglycerin[1] and isosorbide dinitrate[2] were used as received without purification as a standard and internal standard, respectively. 1,2,3-Propanetriol-1,2-dinitrate (glyceryl-1,2-dinitrate)[3] and 1,2,3-propanetriol-1,3-dinitrate (glyceryl-1,3-dinitrate)[3] were supplied as 10% dispersions in cornstarch and purified by extraction with a dichloromethane–ethyl acetate (1:1, v/v) solution before use. All chemicals used were Analar[4] grade. All solvents used were glass distilled[5] or HPLC[5] grade.

The HPLC pump[6] was fitted with a loop injector[7] with a 100-μL loop. The system was interfaced to a thermal energy analyzer[8] with the following conditions: furnace temperature, 575°C; argon flow rate, 15 mL/min; oxygen flow rate, 25 mL/min; range × 8. The slush bath of the instrument consisted of methanol and solid carbon dioxide pellets and was maintained at −77°C. The signal was recorded on a 10.0-mV recorder[9].

A 25-cm × 0.46-mm i.d. column containing a polar bonded-phase packing material[10], was employed at ambient temperature. The material is uniformly spherical, and each particle is ~6 μm in diameter. The mobile phase was prepared by mixing acetone and *n*-hexane in a ratio of 5:95. The solution was deaerated in an ultrasonic bath[11] and was purged with pure helium immediately prior to use. The mobile phase was pumped in an isocratic manner through the column at ambient temperature at a flow rate of 2.0 mL/min, giving a back-pressure ≃500 psi. All glassware was treated with a siliconizing agent[12] and allowed to dry prior to use.

Standard Solutions—Solutions of nitroglycerin, glyceryl-1,2-dinitrate, glyceryl-1,3-dinitrate, and isosorbide dinitrate were prepared daily and stored at 4°C. These solutions were prepared as follows; a working standard solution of nitroglycerin was prepared at a concentration of 1 mg/100 mL in *n*-hexane; the internal standard, isosorbide dinitrate, was prepared at a concentration of 10 mg/100 mL in *n*-hexane. Working standard solutions were prepared for isosorbide dinitrate, glyceryl-1,2-dinitrate, and glyceryl-1,3-dinitrate at concentrations of 100 μg/100 mL in *n*-hexane.

Plasma standards were produced by spiking 5.0-mL aliquots of fresh human plasma with appropriate volumes of the plasma standard solutions to give a range of calibrators with concentrations of nitroglycerin at 0, 0.1, 0.25, 0.5, 1.0, 1.5, and 2.0 ng/mL and glyceryl-1,2-dinitrate and glyceryl-1,3-dinitrate at 0, 0.5, 1.0, 2.5, 5.0, 7.5, and 10 ng/mL. These standards were vortex mixed for 30 s and then allowed to stand at 4°C for 15 min to equilibrate.

The range of calibrators were taken through the complete extraction procedure as described below. Calibration curves were constructed by plotting the peak height ratio of nitroglycerin and its dinitrate metabolites to isosorbide dinitrate, the internal standard, *versus* the appropriate concentrations of the compounds. Plasma samples were similarly treated and the peak height ratios referred to the appropriate calibration curve to read the concentration of nitroglycerin and its dinitrate metabolites present.

Method—All blood samples withdrawn from subjects in receipt of nitroglycerin were collected into treated glass syringes and transferred into treated glass tubes containing 250 U of heparin and 25 μL of 0.002 M silver nitrate solution. The tubes were immediately mixed by inversion and centrifuged at 1000×*g* for 10 min at 4°C.

Aliquots (5.0 mL) of the fresh plasma samples were transferred into 25.0-mL glass extraction tubes fitted with screw caps with polytef liners. Working isosorbide dinitrate internal standard solution (10 μL) was added to all tubes giving a concentration of 2.0 ng/mL of internal standard. Dichloromethane–ethyl acetate (1:1, v/v, 15.0 mL) was added to all tubes, which were then capped tightly and shaken mechanically on a horizontal shaker[13] at 250 cycles/min for 5 min. The tubes were then centrifuged at 750×*g* for

[1] 1% Trinitroglycerin solution ART 7753; E. Merck, Darmstadt, F.R.G.
[2] Kindly donated by Reed and Carnrick Inc., N.J.
[3] Kindly donated by Professor A. Beckett, Chelsea College, London.
[4] B.D.H. Ltd., Poole, Dorset, England.
[5] Rathburn Chemicals Ltd., Walkerburn, Peebleshire, Scotland.
[6] L.D.C. Constametric IIIG HPLC Pump; Milton Roy Corp., Fla.
[7] Rheodyne type 7125; Rheodyne Inc., Calif.
[8] Model 502A/LC; Analytical Instruments Division, Thermo Electron Corp., Waltham, Mass.
[9] Rikadenki Mitsui Ltd., Machinery Sales, Chessington, Surrey, England.
[10] Zorbax CN; Dupont Instruments Ltd., Stevenage, Herts., U.K.
[11] Baird and Tatlock Ltd., Romford, Essex.
[12] Surfasil; Pierce and Warriner (U.K.) Ltd., Chester, Cheshire, U.K.
[13] Braun Lab Shaker LSL; FT Scientific Ltd., Tewkesbury, England.

0022-3549/84/1200-1838$01.00/0
© 1984, American Pharmaceutical Association

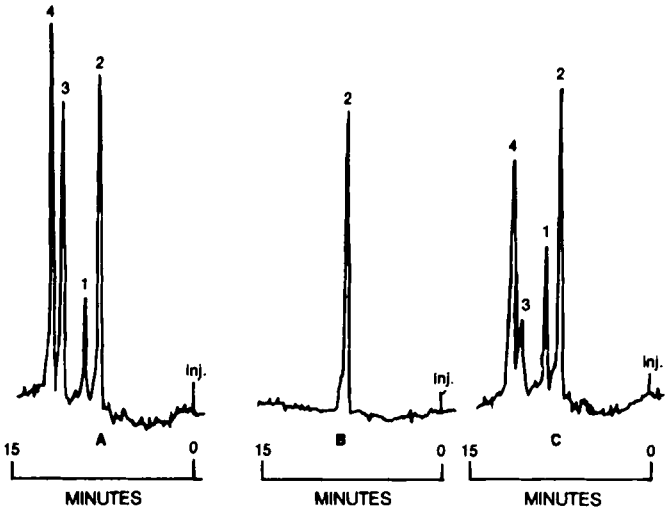

Figure 1—*Determination of nitroglycerin and its metabolites in plasma. Key: (A) spiked test plasma extract containing 0.5 ng/mL of nitroglycerin (1), 2 ng/mL of isosorbide dinitrate internal standard (2), 2.5 ng/mL of glyceryl-1,3-dinitrate (3), and 2.5 ng/mL of glyceryl-1,2-dinitrate (4); (B) spiked plasma extract containing 2 ng/mL of isosorbide dinitrate internal standard (2); (C) plasma extract from a sample withdrawn 15 min following dosing of 2 × 400-μg nitroglycerin sublingual tablets to an adult healthy volunteer indicating the presence of nitroglycerin (1), isosorbide dinitrate (2) (internal standard), glyceryl-1,3-dinitrate (3), and glyceryl-1,2-dinitrate (4).*

5 min at 0°C. The upper aqueous phases were aspirated to waste using a water pump[14] and the lower organic phases were carefully transferred to 20-mL glass vials. The organic phases were then evaporated just to dryness under a gentle stream of nitrogen at room temperature. The vials were capped and stored at −20°C. Immediately prior to analysis on the HPLC, the residues were reconstituted in 150 μL of *n*-hexane.

RESULTS AND DISCUSSION

The chromatographic conditions described were implemented to give the best compromise between chromatographic resolution and peak symmetry and relatively short retention times to permit the analysis of a large throughput of samples with good accuracy and precision. Using these HPLC conditions, isosorbide dinitrate, nitroglycerin, glyceryl-1,3-dinitrate, and glyceryl-1,2-dinitrate give retention times of 7.3, 8.5, 10.5, and 11.5 min, respectively, with a run time between each injection of 15 min.

Figure 1 illustrates a typical plasma chromatogram, chromatograms of spiked plasma samples, drug-free control plasma, and plasma following dosing of a sublingual preparation of nitroglycerin (for comparison). Standard calibration lines were constructed by plotting the peak height ratios of nitroglycerin and its dinitrate metabolites to the isosorbide dinitrate internal standard against the respective concentrations of the compounds. Linearity was found over the standard calibration ranges employed for the parent drug and metabolites. Coefficients of variation of 11.6% at 0.1 ng/mL and 6.6% at 2.0 ng/mL were found for nitroglycerin; comparable data were obtained for the metabolites. The 95% confidence limits obtained for five replicate plasma standard calibrations are shown in Table I and indicate good precision throughout the ranges employed.

Within- and between-batch reproducibility is demonstrated with the following data. Ten replicate plasma control samples were assayed on the same day for each parameter at two levels. Nitroglycerin spiked at 0.4 and 1.0 ng/mL gave mean results of 0.43 (*SD*, ± 0.06) and 1.06 (*SD*, ± 0.18). Between-batch reproducibility on a series of seven control samples for each parameter was 1.7–11.5% (mean, 6.1%) for nitroglycerin, 2.4–14.2% (mean, 6.7%) for glyceryl-1,3-dinitrate, and 3.0–9.0% (mean, 6.1%) for glyceryl-1,2-dinitrate. Spiked pooled plasma samples, when assayed after 7 and 14 d storage at −25°C, appeared not to have deteriorated on storage. Nitroglycerin determined in duplicate samples giving initial mean values of 0.26 and 0.78 ng/mL gave a mean value of 0.22 and 0.66 ng/mL at 7 d and 0.22 and 0.77 ng/mL at 14 d. Glyceryl-1,3-dinitrate and glyceryl-1,2-dinitrate were spiked at concentrations of 1.75 and 3.45 ng/mL and also proved to be stable over the 14-d period. The mean overall recoveries for nitroglycerin and its dinitrate metabolites were calculated over the calibration ranges by comparing peak height ratios for unextracted standards to those taken through the extraction procedure and corrected for the recovery of the internal standard. The recoveries were 76.4% for nitroglycerin, 70.2% for glyceryl-1,3-dinitrate, and 77.0% for glyceryl-1,2-dinitrate.

[14] Filter pump; Baird and Tatlock Ltd.

Table I—Confidence Limits of the Analysis of Spiked Plasma Standards for Nitroglycerin and Its Dinitrate Metabolites

Nitroglycerin		Glyceryl-1,2-Dinitrate		Glyceryl-1,3-Dinitrate	
ng/mL	95% Limits	ng/mL	95% Limits	ng/mL	95% Limits
0.1	0.02	0.5	0.04	0.5	0.07
0.25	0.018	1.0	0.04	1.0	0.09
0.5	0.08	2.5	0.14	2.5	0.31
1.0	0.07	5.0	0.12	5.0	0.35
1.5	0.14	7.5	0.35	7.5	0.45
2.0	0.18	10.0	0.41	10.0	0.27

The minimum detectable levels of nitroglycerin and the 1,3- and 1,2-dinitrate metabolites, determined as the lowest levels discernible over a baseline signal-to-noise ratio of 2:1, were 50, 250, and 250 pg/mL, respectively. These data demonstrate that the developed procedure is sufficiently sensitive and robust for the investigation of the pharmacokinetics of nitroglycerin in humans and further, for the first time, data on two important metabolites of the parent compound can be studied in humans.

Figure 2 illustrates plasma concentration–time profiles representing mean data obtained from 13 subjects in receipt of 800 μg (2 × 400 μg) of nitroglycerin as sublingual tablets. The data on nitroglycerin and its dinitrate metabolites is accompanied by the 95% confidence limits for the individual subject data at each time point. It can be seen that the dinitrate data can prove to be useful in monitoring the elimination of formulations which produce low plasma nitroglycerin concentrations. We have undertaken a preliminary investigation of oral controlled-release formulations and have found that the levels of nitroglycerin are extremely low, in most cases indiscernible from the base line, and yet substantial absorption has occurred as demonstrated by the levels of the two dinitrate metabolites. These findings are contradictory to data obtained by GC–ECD methods (9), where the metabolites are not measured and no data may be available to confirm the specificity of those procedures with regard to the dinitrates.

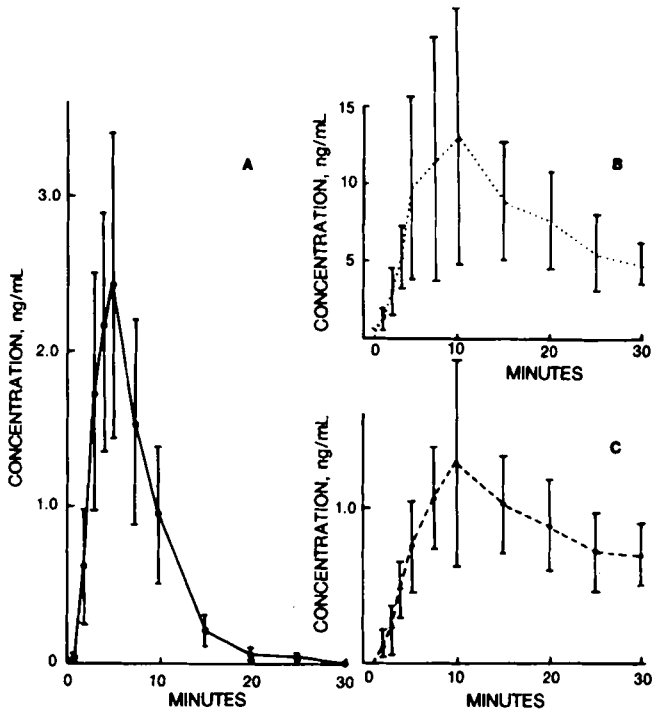

Figure 2—*Mean concentration–time plasma curves and 95% confidence limits for nitroglycerin (A) and its metabolites glyceryl-1,2-dinitrate (B) and glyceryl-1,3-dinitrate (C), for 13 subjects in receipt of 2 × 400-μg sublingual nitroglycerin tablets.*

REFERENCES

(1) F. G. Di Carlo, *Drug Metab. Rev.*, **4**, 1 (1975).
(2) M. T. Rossell and M. G. Bogaert, *J. Chromatogr.*, **64**, 364 (1972).
(3) M. T. Rossell and M. G. Bogaert, *J. Pharm. Sci.*, **62**, 754 (1973).
(4) P. S. K. Yap, E. F. McNiff, and H. Fung, *J. Pharm. Sci.*, **67**, 582 (1978).
(5) J. A. Settlage, W. Gielsdorf, and H. Jaeger, *J. High-Resolution Chromatogr. Chromatogr. Commun.* **6**, 68 (1983).
(6) R. J. Spanggord and R. G. Keck, *J. Pharm. Sci.*, **69**, 444 (1980).
(7) C. C. Wu, T. D. Sokoloski, A. M. Burkman, M. F. Blanford, and L. S. Wu, *J. Chromatogr.*, **228**, 333 (1982).
(8) J. Maddock, P. A. Lewis, A. Woodward, P. R. Massey, and S. Kennedy, *J. Chromatogr.*, **272**, 129 (1983).
(9) A. Bashir, M. J. Lewis, and A. H. Henderson, *Br. J. Clin. Pharmacol.*, **14**, 779 (1982).

ACKNOWLEDGMENTS

The authors are grateful for the cooperation and assistance of their colleagues throughout Simbec Research and are particularly grateful to Mrs. A. Franks for the preparation of this manuscript.

Antifungal Properties of 2-*n*-Alkyn-1-ols

HERMAN GERSHON *x, GAIL E. ROWE *, ROBERT C. SANTORE *, JOHN R. GILBERTSON ‡, and HERMAN LANGKAMP §

Received September 19, 1983, from the **Boyce Thompson Institute for Plant Research at Cornell University, Ithaca, NY 14853* and the ‡*Departments of Pharmacology and Physiology and* §*Microbiology, School of Dental Medicine, University of Pittsburgh, Pittsburgh, PA 15261.* Accepted for publication March 12, 1984.

Abstract □ Fourteen 2-*n*-alkynols (C_3-C_{14}, C_{16}, and C_{18}) were tested against *Aspergillus oryzae*, *Aspergillus niger*, *Trichoderma viride*, and *Myrothecium verrucaria* in Sabouraud dextrose agar at pH 5.6 and 7.0. Toxicity to *Candida albicans*, *Candida tropicalis*, *Trichophyton mentagrophytes*, and *Mucor mucedo* was determined in the same medium at pH 5.6 and 7.0 in the absence and presence of 10% beef serum. Fungitoxicity was strongly influenced by chain length, slightly by the pH of the medium, and significantly by the presence of beef serum. 2-*n*-Undecyn-1-ol was the most active member of the series, and there was marked synergism between it and ketoconazole.

Keyphrases □ *n*-2-Alkyn-1-ols—*in vitro* antifungal activity, effect of chain length, pH, adsorbents □ Antifungal activity—*n*-alkynols, *in vitro*, effect of chain length, pH, adsorbents □ Structure-activity relationships—*n*-alkynols, antifungal activity, *in vitro* □ Synergism—2-undecyn-1-ol and ketoconazole, *in vitro*, *Candida albicans* and *Candida tropicalis*

In our studies of the effect of structural modification on the fungitoxicity of alkanoic acids (1), 2-alkenoic acids (2), 2-alkynoic acids (3), 2-fluoroalkanoic acids (1), 2-bromoalkanoic acids (2), α,ω-alkanedicarboxylic acids (4), alkoxyacetic acids (5), and *n*-alkanols (6), two major physical factors were observed to influence the activities of the toxicants. These included the partition coefficient and absence or presence of adsorbents such as albumin in the growth medium. Factors that affect partition coefficients of the acids include chain length, pK_a, and pH of the medium (3). The pH of the medium had no significant effect on the activity of the alcohols, and for increased fungitoxicity, a lipophilic substituent at the terminal end of the alkanol is useful (6).

Since the alkynoic acids (3) were considerably more toxic to fungi than the alkanoic acids (1), it was of interest to compare the alkanols (6) with an analogous series of alkynols. It was reported that 1-hydroxy-2-nonyn-4-one, a metabolite from *Ischnoderma benzoinum* (Wahl.) Karst had antifungal activity (7). Also of interest was the observation that alcohol oxidase was irreversibly inhibited by propargyl alcohol and 1,4-butynediol, acetylenic alcohols (8).

The present work is concerned with a systematic evaluation of the homologous series of 2-*n*-alkyn-1-ols of chain lengths C_3-C_{14}, C_{16}, and C_{18} against eight fungi: *Aspergillus oryzae*, *Aspergillus niger*, *Trichoderma viride*, *Myrothecium verrucaria*, *Candida albicans*, *Candida tropicalis*, *Trichophyton mentagrophytes*, and *Mucor mucedo*. Since synergism was demonstrated between ketoconazole, a promising antimycotic agent (9), and amphotericin B and other fungitoxicants (10), it was also desired to determine if there would be any synergism between the most active of the alkynols and ketoconazole.

EXPERIMENTAL SECTION

Some compounds were obtained from commercial sources[1]. Literature methods were used for the preparation of the remaining alkynols: C_{12} (11), C_{14} (12), and C_{16} and C_{18} (13).

The test fungi included *A. oryzae* (ATCC 1101), *A. niger* (ATCC 1004), *T. viride* (ATCC 8678), *M. verrucaria* (ATCC 9095C), *C. albicans* (ATCC 10231), *C. tropicalis* (ATCC 9741), *T. mentagrophytes* (ATCC 9129), and *M. mucedo* (ATCC 7941) (14)[2]. The compounds were tested against *A. oryzae*, *A. niger*, *T. viride*, and *M. verrucaria* in Sabouraud dextrose agar[3] at pH 5.6 and 7.0 according to published methods (1). Graded levels of test compound dissolved in dimethyl sulfoxide (Me_2SO) were incorporated into the growth medium which was subsequently inoculated with the respective fungus. The inoculum was one drop of spore suspension. The preparation of spore suspensions of *A. niger*, *T. viride*, *M. verrucaria*, and *A. oryzae* was accomplished by growing the fungi on potato dextrose agar[3] for several weeks at 28°C in flat, wide-mouth bottles until extensive sporulation had occurred. The spores were harvested by adding 5 mL of sterile 0.85% NaCl solution to the bottles together with ~10 sterile beads, 5 mm in diameter. The spores were freed of the mycelia by shaking, and the suspension was transferred to sterile test tubes and counted in a hemocytometer. The spore concentration was adjusted to 6×10^6 spores/mL by diluting with sterile saline. Inoculations were carried out with Pasteur pipets which deliver 40 drops/mL. Incubation took place at 28°C for 5 d.

For *T. mentagrophytes*, *M. mucedo*, *C. albicans*, and *C. tropicalis* previously described methods were employed (15). Graded levels of test compound

[1] The C_3, C_5-C_{11}, and C_{13} 2-alkyn-1-ols were purchased from Farchan Labs, Willoughby, Ohio, and the C_4 alkynol was obtained from Aldrich Chemical Co., Milwaukee, Wis. Ketoconazole is a product of Janssen Pharmaceutica Inc., New Brunswick, N.J.

[2] These authors present evidence that ATCC 7941 is *Mucor cirinelloides*. We will retain the ATCC nomenclature until it is changed by the American Type Culture Collection.

[3] Difco Labs, Detroit, Mich.

0022-3549/84/1200-1840$01.00/0

© 1984, American Pharmaceutical Association

REFERENCES

(1) F. G. Di Carlo, *Drug Metab. Rev.*, **4**, 1 (1975).
(2) M. T. Rossell and M. G. Bogaert, *J. Chromatogr.*, **64**, 364 (1972).
(3) M. T. Rossell and M. G. Bogaert, *J. Pharm. Sci.*, **62**, 754 (1973).
(4) P. S. K. Yap, E. F. McNiff, and H. Fung, *J. Pharm. Sci.*, **67**, 582 (1978).
(5) J. A. Settlage, W. Gielsdorf, and H. Jaeger, *J. High-Resolution Chromatogr. Chromatogr. Commun.* **6**, 68 (1983).
(6) R. J. Spanggord and R. G. Keck, *J. Pharm. Sci.*, **69**, 444 (1980).
(7) C. C. Wu, T. D. Sokoloski, A. M. Burkman, M. F. Blanford, and L. S. Wu, *J. Chromatogr.*, **228**, 333 (1982).
(8) J. Maddock, P. A. Lewis, A. Woodward, P. R. Massey, and S. Kennedy, *J. Chromatogr.*, **272**, 129 (1983).
(9) A. Bashir, M. J. Lewis, and A. H. Henderson, *Br. J. Clin. Pharmacol.*, **14**, 779 (1982).

ACKNOWLEDGMENTS

The authors are grateful for the cooperation and assistance of their colleagues throughout Simbec Research and are particularly grateful to Mrs. A. Franks for the preparation of this manuscript.

Antifungal Properties of 2-*n*-Alkyn-1-ols

HERMAN GERSHON *x, GAIL E. ROWE *, ROBERT C. SANTORE *, JOHN R. GILBERTSON ‡, and HERMAN LANGKAMP §

Received September 19, 1983, from the **Boyce Thompson Institute for Plant Research at Cornell University, Ithaca, NY 14853* and the ‡*Departments of Pharmacology and Physiology and* §*Microbiology, School of Dental Medicine, University of Pittsburgh, Pittsburgh, PA 15261.* Accepted for publication March 12, 1984.

Abstract □ Fourteen 2-*n*-alkynols (C_3-C_{14}, C_{16}, and C_{18}) were tested against *Aspergillus oryzae*, *Aspergillus niger*, *Trichoderma viride*, and *Myrothecium verrucaria* in Sabouraud dextrose agar at pH 5.6 and 7.0. Toxicity to *Candida albicans*, *Candida tropicalis*, *Trichophyton mentagrophytes*, and *Mucor mucedo* was determined in the same medium at pH 5.6 and 7.0 in the absence and presence of 10% beef serum. Fungitoxicity was strongly influenced by chain length, slightly by the pH of the medium, and significantly by the presence of beef serum. 2-*n*-Undecyn-1-ol was the most active member of the series, and there was marked synergism between it and ketoconazole.

Keyphrases □ *n*-2-Alkyn-1-ols—*in vitro* antifungal activity, effect of chain length, pH, adsorbents □ Antifungal activity—*n*-alkynols, *in vitro*, effect of chain length, pH, adsorbents □ Structure-activity relationships—*n*-alkynols, antifungal activity, *in vitro* □ Synergism—2-undecyn-1-ol and ketoconazole, *in vitro*, *Candida albicans* and *Candida tropicalis*

In our studies of the effect of structural modification on the fungitoxicity of alkanoic acids (1), 2-alkenoic acids (2), 2-alkynoic acids (3), 2-fluoroalkanoic acids (1), 2-bromoalkanoic acids (2), α,ω-alkanedicarboxylic acids (4), alkoxyacetic acids (5), and *n*-alkanols (6), two major physical factors were observed to influence the activities of the toxicants. These included the partition coefficient and absence or presence of adsorbents such as albumin in the growth medium. Factors that affect partition coefficients of the acids include chain length, pK_a, and pH of the medium (3). The pH of the medium had no significant effect on the activity of the alcohols, and for increased fungitoxicity, a lipophilic substituent at the terminal end of the alkanol is useful (6).

Since the alkynoic acids (3) were considerably more toxic to fungi than the alkanoic acids (1), it was of interest to compare the alkanols (6) with an analogous series of alkynols. It was reported that 1-hydroxy-2-nonyn-4-one, a metabolite from *Ischnoderma benzoinum* (Wahl.) Karst had antifungal activity (7). Also of interest was the observation that alcohol oxidase was irreversibly inhibited by propargyl alcohol and 1,4-butynediol, acetylenic alcohols (8).

The present work is concerned with a systematic evaluation of the homologous series of 2-*n*-alkyn-1-ols of chain lengths C_3-C_{14}, C_{16}, and C_{18} against eight fungi: *Aspergillus oryzae*, *Aspergillus niger*, *Trichoderma viride*, *Myrothecium verrucaria*, *Candida albicans*, *Candida tropicalis*, *Trichophyton mentagrophytes*, and *Mucor mucedo*. Since synergism was demonstrated between ketoconazole, a promising antimycotic agent (9), and amphotericin B and other fungitoxicants (10), it was also desired to determine if there would be any synergism between the most active of the alkynols and ketoconazole.

EXPERIMENTAL SECTION

Some compounds were obtained from commercial sources[1]. Literature methods were used for the preparation of the remaining alkynols: C_{12} (11), C_{14} (12), and C_{16} and C_{18} (13).

The test fungi included *A. oryzae* (ATCC 1101), *A. niger* (ATCC 1004), *T. viride* (ATCC 8678), *M. verrucaria* (ATCC 9095C), *C. albicans* (ATCC 10231), *C. tropicalis* (ATCC 9741), *T. mentagrophytes* (ATCC 9129), and *M. mucedo* (ATCC 7941) (14)[2]. The compounds were tested against *A. oryzae*, *A. niger*, *T. viride*, and *M. verrucaria* in Sabouraud dextrose agar[3] at pH 5.6 and 7.0 according to published methods (1). Graded levels of test compound dissolved in dimethyl sulfoxide (Me_2SO) were incorporated into the growth medium which was subsequently inoculated with the respective fungus. The inoculum was one drop of spore suspension. The preparation of spore suspensions of *A. niger*, *T. viride*, *M. verrucaria*, and *A. oryzae* was accomplished by growing the fungi on potato dextrose agar[3] for several weeks at 28°C in flat, wide-mouth bottles until extensive sporulation had occurred. The spores were harvested by adding 5 mL of sterile 0.85% NaCl solution to the bottles together with ~10 sterile beads, 5 mm in diameter. The spores were freed of the mycelia by shaking, and the suspension was transferred to sterile test tubes and counted in a hemocytometer. The spore concentration was adjusted to 6×10^6 spores/mL by diluting with sterile saline. Inoculations were carried out with Pasteur pipets which deliver 40 drops/mL. Incubation took place at 28°C for 5 d.

For *T. mentagrophytes*, *M. mucedo*, *C. albicans*, and *C. tropicalis* previously described methods were employed (15). Graded levels of test compound

[1] The C_3, C_5-C_{11}, and C_{13} 2-alkyn-1-ols were purchased from Farchan Labs, Willoughby, Ohio, and the C_4 alkynol was obtained from Aldrich Chemical Co., Milwaukee, Wis. Ketoconazole is a product of Janssen Pharmaceutica Inc., New Brunswick, N.J.

[2] These authors present evidence that ATCC 7941 is *Mucor cirinelloides*. We will retain the ATCC nomenclature until it is changed by the American Type Culture Collection.

[3] Difco Labs, Detroit, Mich.

0022-3549/84/1200-1840$01.00/0

© 1984, American Pharmaceutical Association

Table I—Antifungal Activity of 2-*n*-Alkyn-1-ols Against *A. oryzae*, *A. niger*, *T. viride*, and *M. verrucaria* in Sabouraud Dextrose Agar [a]

$H(CH_2)_nC{\equiv}CCH_2OH$

	Level of Inhibition at pH 5.6 [b]				Antifungal	Level of Inhibition at pH 7.0				Antifungal
n	*A. oryzae*	*A. niger*	*T. viride*	*M. verrucaria*	Spectrum Index [c]	*A. oryzae*	*A. niger*	*T. viride*	*M. verrucaria*	Spectrum Index
0	0	0	0	1	1	0	0	0	1	1
1	1	1	1	1	16	1	1	1	1	16
2	1	1	1	1	16	1	1	1	1	16
3	1	1	1	1	16	1	1	1	1	16
4	2	2	1	2	28	2	2	1	2	28
5	2	2	2	2	32	2	2	2	2	32
6	2	2	2	2	32	2	2	2	2	32
7	3(60)	3(90)	3(40)	3(30)	48	3(90)	3(90)	3(40)	3(30)	48
8	3(50)	3(40)	3(40)	3(30)	48	3(50)	3(40)	3(40)	3(30)	48
9	3(40)	3(100)	3(30)	3(20)	48	3(50)	3(100)	3(30)	3(20)	48
10	0	0	0	3(30)	3	0	0	0	3(20)	3
11	0	0	0	0	0	0	0	0	0	0
13	0	0	0	0	0	0	0	0	0	0
15	0	0	0	0	0	0	0	0	0	0

[a] At 28°C for 5 d. [b] Compounds were incorporated in test medium at 10^4, 10^3, and 10^2 μg/mL. Key: (3) inhibition at all levels of compound; (2) inhibition at the two highest levels; (1) inhibition at the highest level only; (0) compound inactive at the highest level tested; numbers in parentheses are MIC values, μg/mL. [c] Antifungal spectrum index = the sum of the numbers of levels of inhibition multiplied by the number of organisms inhibited.

Table II—Antifungal Activity of 2-*n*-Alkyn-1-ols Against *C. albicans*, *C. tropicalis*, *T. mentagrophytes*, and *M. mucedo* in Sabouraud Dextrose Agar [a]

$H(CH_2)_nC{\equiv}CCH_2OH$

	Levels of Inhibition [b]																
	C. albicans				*C. tropicalis*				*T. mentagrophytes*				*M. mucedo*				
	pH 5.6		pH 7.0		pH 5.6		pH 7.0		pH 5.6		pH 7.0		pH 5.6		pH 7.0		Antifungal
	−	+	−	+	−	+	−	+	−	+	−	+	−	+	−	+	Spectrum
n	Serum	Serum	Serum	Serum	Serum	Serum	Serum	Serum	Serum	Serum	Serum	Serum	Serum	Serum	Serum	Serum	Index [c]
0	0		0		0		0		1	1	1	1	1	1	1	1	16
1	1	1	1	1	1	1	1	1	1	1	1	1	1	1	1	1	64
2	1	1	1	1	1	1	1	1	2	1	2	1	1	1	1	1	72
3	2	1	2	1	1	1	1	1	2	1	2	1	2	1	2	1	88
4	2	2	2	2	2	2	2	2	2	2	2	2	2	2	2	2	128
5	2	2	2	2	2	2	2	2	3(30)	2	3(40)	2	2	2	2	2	136
6	2	2	2	2	2	2	2	2	3(60)	3(70)	3(70)	3(70)	2	2	2	2	144
7	2	2	2	2	2	2	2	2	3(20)	3(30)	3(20)	3(40)	2	2	2	2	144
8	3(20)	3(90)	3(30)	3(90)	3(30)	3(80)	3(30)	3(90)	3(3)	3(20)	3(4)	3(30)	3(20)	3(60)	3(20)	3(40)	192
9	3(40)	2	3(40)	2	3(70)	2	3(90)	2	3(2)	3(30)	3(3)	3(30)	3(6)	3(30)	3(6)	3(50)	176
10	2	2	2	2	2	2	2	2	3(4)	3(40)	3(4)	3(50)	0		0		84
11	0		0		0		0		3(3)	2	3(5)	2	0		0		10
13	0		0		0		0		0		0		0		0		0
15	0		0		0		0		0		0		0		0		0

[a] In the presence and absence of beef serum. *C. albicans*, *C. tropicalis*, and *M. mucedo* were incubated at 37°C for 20 h and *T. mentagrophytes* at 28°C for 5 d. [b] Compounds were incorporated in test medium at 10^4, 10^3, and 10^2 μg/mL. Key: (3) inhibition at all levels of compound; (2) inhibition at the two highest levels; (1) inhibition at the highest level only; (0) compound inactive at the highest level tested; numbers in parentheses are MIC values, μg/mL. [c] Antifungal spectrum index = sum of the number of levels of inhibition multiplied by the number of organisms inhibited.

dissolved in Me_2SO were added to Sabouraud dextrose agar at pH 5.6 and 7.0 alone and supplemented with 10% beef serum[4] and inoculated with the respective fungi. Inocula for *T. mentagrophytes* and *M. mucedo* were prepared as above except that the growth media were Mycocel agar[5] and Sabouraud dextrose agar[3], respectively. One drop of spore suspension was used. The inocula of *C. albicans* and *C. tropicalis* were obtained from 20-h cultures in Sabouraud dextrose broth[3]. The cell counts ranged from 3 to 7.5 × 10^6 cells/mL. The tests with *T. mentagrophytes* were incubated at 28°C for 5 d; those with *C. albicans*, *C. tropicalis*, and *M. mucedo* were incubated for 20 h at 37°C. All tests were carried out in duplicate in "I" plate Petri dishes[6]. Data of growth or no growth were recorded.

The compounds were tested at 10^4, 10^3, and 10^2 μg/mL. Minimal inhibitory concentrations (MIC) were sought in increments of 10 μg/mL for 10–100 μg/mL and in 1-μg/mL increments for 1–10 μg/mL. The results were weighted by calculating the antifungal spectrum index which is defined as the sum of the number of levels of complete inhibition multiplied by the number of organisms inhibited at the concentrations of 10^4, 10^3, and 10^2 μg/mL (16, 17).

It should be mentioned that serum was used with the second set of four fungi because they are animal pathogens, except that *M. mucedo* is a model for a pathogenic *Mucor* species. These compounds are also being studied as potential chemotherapeutic agents in animal infections.

[4] Miles Labs, Elkhart, Ind.
[5] BBL, Cockeysville, Md.
[6] Falcon; Becton, Dickenson, and Co., Oxnard, Calif.

The effect of ketoconazole on the inhibition of 2-*n*-undecyn-1-ol of *C. albicans* and *C. tropicalis* in Sabouraud dextrose agar at pH 7.0 containing 10% human serum[3] was examined. The MIC values of ketoconazole and the undecynol were codissolved in Me_2SO and added to the agar in increments of 0.1 ranging from 1 to 0.1. The plates were incubated at 37°C for 20 h, and the MIC for the mixture was determined.

RESULTS

The results of the 2-alkyn-1-ols against *A. oryzae*, *A. niger*, *T. viride*, and *M. verrucaria* are given in Table I, and those against *C. albicans*, *C. tropicalis*, *T. mentagrophytes*, and *M. mucedo* are in Table II. The study of the effect of ketoconazole on the toxicity of 2-*n*-undecyn-1-ol to *C. albicans* and *C. tropicalis* is shown in Table III.

On comparing the activity of the alkynols at pH 5.6 and 7.0 against *A. oryzae*, *A. niger*, *T. viride*, and *M. verrucaria*, it is apparent from the antifungal spectrum indices (Table I) that the alcohols of 10–12 carbon atom chain length are most toxic. The order of toxicity of the homologous series is: 12 = 11 = 10 > 9 = 8 > 7 > 6 = 5 = 4 > 13 > 3 > 14 = 16 = 18.

The most fungitoxic alkynol against *C. albicans*, *C. tropicalis*, *T. mentagrophytes*, and *M. mucedo* was the C_{11} homologue, and the overall order of toxicity was: 11 > 12 > 10 = 9 > 8 > 7 > 6 > 13 > 5 > 4 > 3 > 14 > 16 = 18 (Table II). The data of Table III indicate that the MIC for undecynol is 120 μg/mL for both *Candida* species in the presence of human serum at pH 7.0. This level of compound is one-third higher than the corresponding MIC values

Table III—Effect of Ketoconazole (K) on the Minimal Inhibitory Concentration of 2-*n*-Undecyn-1-ol (U) Against *C. albicans* and *C. tropicalis*[a]

	C. albicans	*C. tropicalis*
U	120	120
K	50	50
U + K[b]	36 + 15	36 + 15

[a] In Sabouraud dextrose agar containing 10% human serum at pH 7.0 at 37°C for 20 h; MIC values, μg/mL. [b] Combined MIC values of U and K in increments of 1, 0.9, 0.8 . . . 0.1 parts of the mixture. The numbers represent 0.3 of the combined MIC.

using beef serum. The minimal inhibitory concentrations for ketoconazole was 50 μg/mL against both fungi. A solution containing 30% of the MIC of both compounds was completely inhibitory to both organisms.

DISCUSSION

It was demonstrated previously that in a homologous series of normal alcohols the most fungitoxic member was the C_{10} alkanol (6). In the present study, the C_{11} alkynol was the most active against the fungi. Since biological activity in a homologous series of compounds is influenced by the partition coefficient, which in turn is determined by chain length (lipophilicity) and pK_a (hydrophilicity), the longer chain length of the alkynol required for maximal activity can be rationalized as follows. Aliphatic monobasic hydroxylic compounds in water have a pK_a of 15.5, whereas 2-alkyn-1-ols have a pK_a of 13.6 in water (18). Since water solubility increases with decreasing pK_a, it requires a longer chain length to restore the necessary amphiphilicity for optimal biological activity. The pH of the growth medium has a minor effect on the activity of the test compounds. This can be observed best where low levels of toxicant were required for inhibition of the fungus. It is generally consistent in that at the higher pH more compound is needed for inhibition.

The presence of beef serum reduced the activity of the toxicant (Table II). It was most noticeable against organisms which were inhibited by low levels of compound. Although hydrogen bonding may be responsible for this in part, it is also possible that the alkynol reacted by a nucleophilic reaction with the proteins or other components of the serum.

Although it is not firmly established, the mechanism of action of the acetylenic alcohols, once penetration of the spore had taken place, is by the irreversible inhibition of the enzyme alcohol oxidase. This inhibition was demonstrated with the enzyme, *in vitro*, using propargyl alcohol (8). The lower acetylenic alcohols were not fungitoxic because they are too water soluble to penetrate the fungal spore membrane. Ketoconazole was able to potentiate the toxicity of 2-undecyn-1-ol toward the two *Candida* species (Table III). It was reported that ketoconazole inhibited ergosterol biosynthesis. Thus, it is believed to cause functional changes in the membrane, such as permeability (19).

If we compare the fungitoxicities of the most active member of each of the series of alkynoic acids (3), ω-chloroalkanols (6), alkanols (6), and alkynols by comparing the sums of the antifungal spectrum indices for *A. niger*, *T. viride*, and *M. verrucaria* at pH 5.6 and *C. albicans*, *T. mentagrophytes*, and *M. mucedo* at pH 5.6 and 7.0 with and without beef serum, the order of activity is as follows: 2-*n*-undecyn-1-ol (135) > 2-*n*-hexadecynoic acid (117) > 9-*n*-chlorononan-1-ol (111) = 10-*n*-chlorodecan-1-ol (111) > *n*-nonan-1-ol (93).

REFERENCES

(1) H. Gershon and R. Parmegiani, *J. Med. Chem.*, **10,** 186 (1967).

(2) H. Gershon, M. W. McNeil, R. Parmegiani, P. K. Godfrey, and J. M. Baricko, *Antimicrob. Agents Chemother.*, **4,** 435 (1973).

(3) H. Gershon and L. Shanks, *Can. J. Microbiol.*, **24,** 593 (1978).

(4) H. Gershon and L. Shanks, *Can. J. Microbiol.*, **22,** 1198 (1976).

(5) H. Gershon, L. Shanks, and A. DeAngelis, *J. Pharm. Sci.*, **68,** 82 (1979).

(6) H. Gershon and L. Shanks, *J. Pharm. Sci.*, **69,** 381 (1980).

(7) T. Anke, B. M. Giannetti, and W. Steglich, *Z. Naturforsch, Tiel C*, **37,** 1 (1982).

(8) C. S. Nichols and T. H. Cromartie, *Biochem. Biophys. Res. Commun.*, **97,** 216 (1980).

(9) J. Heeres and H. Van den Bossche, in "Reports in Medicinal Chemistry," vol. 17, H.-J. Hess, Ed., Academic Press, New York, N.Y., 1982, pp. 139–150.

(10) F. C. Odds, *Antimicrob. Agents Chemother.*, **22,** 763 (1982).

(11) Y. L. Tchao, *Bull. Soc. Chim.*, **53,** 682 (1933).

(12) D. E. Ames, A. N. Covell, and T. G. Goodburn, *J. Chem. Soc.*, **1963** 5889.

(13) G. Grimmer and A. Hildebrandt, *Justus Liebigs Ann. Chem.*, **685,** 154 (1965).

(14) T. M. Hammill, D. L. Secor, and B. E. Thompson, *Mycologia*, **75,** 311 (1983).

(15) H. Gershon and L. Shanks, *Can. J. Microbiol.*, **21,** 1317 (1975).

(16) H. Gershon and R. Parmegiani, *Appl. Microbiol.*, **10,** 348 (1962).

(17) H. Gershon, R. Parmegiani, and W. J. Nickerson, *Appl. Microbiol.*, **10,** 556 (1962).

(18) A. Albert and E. P. Serjeant, "Ionization Constants of Acids and Bases", Wiley, New York, N.Y., 1962, p. 129.

(19) H. Van den Bossche, G. Willemsen, W. Cools, F. Cornelissen, W. F. Lauwers, and J. M. Van Cutsem, *Antimicrob. Agents Chemother.*, **17,** 922 (1980).

An Improved Synthesis of Captopril

DOO H. NAM *, CHOON S. LEE *, and DEWEY D. Y. RYU ‡x

Received June 13, 1983, from **The Korea Advanced Institute of Science, Seoul, Korea* and the ‡*University of California, Davis, CA 95616.* Accepted for publication February 22, 1984.

Abstract □ An improved synthesis of captopril using methacrylic acid as the starting material is described. Treatment of methacrylic acid (I) with a hydrogen halide gave the 3-halogeno-2-methylpropanoic acids II and III, which were treated with thionyl chloride to yield the corresponding 3-halogeno-2-methylpropanoyl chlorides IV and V. Treatment of IV or V with L-proline yielded the *N*-(*R,S*-3-halogeno-2-methylpropanoyl)-L-prolines VI and VII, which were separated into optically pure *R*- and *S*-diastereoisomers using dicyclohexylamine. Treatment of halides of VI or VII with methanolic ammonium hydrosulfide gave captopril in 28% yield.

Keyphrases □ Captopril—new synthetic method, antihypertensive, inhibitor of angiotensin-converting enzyme □ Antihypertensive—captopril, new synthetic method

Captopril[1], an orally active hypertensive agent, is a competitive inhibitor of angiotensin I-converting enzyme (1, 2). The synthesis of captopril was first reported by Cushman *et al.* (2) in an overall yield of 12%, starting with 3-acetylthio-2-methylpropanoic acid. More recently, a facile synthesis of captopril was reported (3). This synthesis is convenient and the yield is good (26%); however, the conversion of methacrylic acid to the optically active starting material, *R*-3-hydroxy-2-methylpropanoic acid, using a microbial oxidative transformation (4, 5) is poor. We have developed a more convenient synthesis of captopril using methacrylic acid as a starting material (Scheme I).

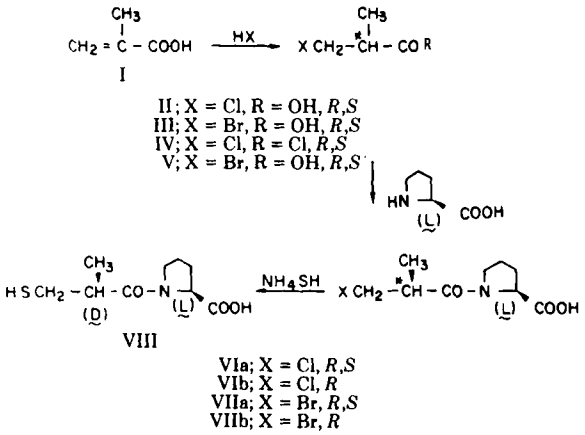

Scheme I

EXPERIMENTAL SECTION[2]

***R,S*-3-Halogeno-2-methylpropanoyl Chloride (IV, V)**—Methacrylic acid (I)[3] was treated with anhydrous hydrogen halide to give *R,S*-3-halogeno-2-methylpropanoic acid (II and III) according to the method of Groszkowski *et al.* (6); II (bp_{15} 106–107°C) and III (bp_{15} 106–108°C) were identical with the reported materials (6) by IR and NMR spectroscopy. Treatment of II and III with thionyl chloride to yield IV and V was also carried out by the procedure of Groszkowski *et al.* (6), except a small quantity of *N,N*-dimethylformamide (0.1 mol of II or III) was used as the catalyst (7). Compounds IV (bp_{45} 74–75°C) and V (bp_{30} 72–73°C) were identical with those previously reported by Horii *et al.* (8) by IR and NMR spectroscopy.

***N*-(*R*-3-Halogeno-2-methylpropanoyl)-L-proline (VI, VII)**—For the *N*-acylation of L-proline with IV or V, the procedure of Hongo *et al.* (9) was employed. L-Proline (13.8 g, 0.12 mol) was allowed to react with IV (14.1 g, 0.1 mol) or V (20.1 g, 0.1 mol) in the presence of 84 mL of 2 M NaOH at 0°C for 1 h and then at room temperature for 3 h. The mixture was acidified to pH 1.5 with concentrated hydrochloric acid, and extracted with 500 mL of ethyl acetate. The organic phase was dried over anhydrous magnesium sulfate, and the solvent was removed under reduced pressure to yield the syrupy residue (VIa[4] or VIIa[4]). This material was dissolved in acetonitrile, and dicyclohexylamine (21.7 g, 0.12 mol) was slowly added in a dropwise manner with rapid stirring and cooling in an ice bath. The product was removed by filtration to give 36.1 g of the dicyclohexylammonium salt of VIa (90% yield), mp 179–183°C (dec.), or 37.8 g of the salt of VIIa (85% yield), mp 175–180°C (dec.). The crude dicyclohexylammonium salt was dissolved in refluxing acetonitrile–dichloromethane (1:1), and the saturated solution was cooled at room temperature. The dicyclohexylammonium salt of the *R,S*-diastereoisomer of the chloro compound was obtained in 43% yield (15.5 g, white crystals), mp 184–187°C (dec.), $[\alpha]_D^{20}$ −40° (*c*, 2.0, ethanol); the salt of the *R,S*-diastereoisomer of the bromo compound was obtained in 40% yield (15.2 g, white crystals)[5], *mp* 180–183°C (dec.), $[\alpha]_D^{20}$ −44° (*c*, 2.0, ethanol). The optically purified dicyclohexylammonium salt of *R,S*-diastereoisomers dissolved in 1 M $KHSO_4$ was extracted with ethyl acetate. The extract was dried over anhydrous magnesium sulfate, and the solvent was removed under reduced pressure. The residue was crystallized from ethyl acetate–hexane (1:1) to recover 7.8 g of VIb[6] as white crystals (90% yield), mp 110–112°C, $[\alpha]_D^{20}$ −98.9° (*c*, 2.0, ethanol) [IR (KBr): 1710 (amide C=O) and 1590 cm^{-1} (amide C—N); ^{1}H-NMR ($CDCl_3$): δ 1.38 (d, 3, J = 3 Hz, —CH_3), 2.30 (m, 4, —CH_2— in proline), 3.11 (m, 1, —CH—), 3.79 (m, 4, Cl—CH_2—, N—CH_2—), 4.69 (t, 1, J = 2.3 Hz, N—CH—), and 11.30 ppm (s, 1, —COOH)] or 8.6 g of VIIb[6] as white crystals (95% yield), mp 113–115°C, $[\alpha]_D^{20}$ −103.2° (*c*, 2.0, ethanol) [IR (KBr): 1720 (amide C=O) and 1600 cm^{-1} (amide C—N); ^{1}H-NMR ($CDCl_3$): δ 1.50 (d, 3, J = 3 Hz, —CH_3), 2.33 (m, 4, —CH_2— in proline), 3.38 (m, 1, —CH—), 3.86 (m, 4, Br—CH_2—, N—CH_2—), 4.77 (t, 1, J = 2.5 Hz, N—CH—), and 11.40 ppm (s, 1, —COOH).

Anal.—Calc. for VIb ($C_9H_{14}ClNO_3$): C, 49.21; H, 6.42, N, 6.38. Found: C, 49.00; H, 6.69; N, 6.19. Calc. for VIIb ($C_9H_{14}BrNO_3$): C, 40.93; H, 5.34, N, 5.30. Found: C, 41.05; H, 5.43; N, 5.26.

***N*-(*R*-3-Mercapto-2-methylpropanoyl)-L-proline (VIII)**—To the solution of 100 mL of methanolic ammonium hydrosulfide[7], VIb (2.1 g, 0.01 mol) or VIIb (2.6 g, 0.01 mol) was added at room temperature. The resulting mixture was refluxed for 24 h with stirring under a nitrogen atmosphere. The mixture was concentrated to 20 mL under reduced pressure, acidified with 5 M HCl (pH 1), and then extracted with ethyl acetate. The organic phase was dried over anhydrous magnesium sulfate, and the solvent was removed under reduced pressure. The residue was fractionated by column chromatography using Wakogel C200 by linear gradient of methanol in ethyl acetate (0 to 100%), and the fractions positive to sodium nitroprusside were combined. Recrystallization from ethyl acetate–hexane (1:1) gave 1.86 g of VIII as white crystals from VIb or 1.95 g of VIII from VIIb, mp 105–106°C [lit. (2) mp 104–105°C; lit. (3) mp 105–106°C; $[\alpha]_D^{20}$ −128.2° (*c*, 2.0, ethanol); lit. (2) $[\alpha]_D^{22}$ −131.0°; lit. (3) $[\alpha]_D^{25}$ −129.8°], which was identical by IR and NMR spectroscopy (3) with authentic captopril[8].

RESULTS AND DISCUSSION

To develop a more convenient synthesis of captopril from methacrylic acid, the addition of hydrogen halide to methacrylic acid was attempted using the

[1] *N*-(*R*-3-mercapto-2-methylpropanoyl)-L-proline (*S,S*), SQ 14,225.

[2] Melting points were determined by using a Thomas-Hoover capillary melting point apparatus. IR spectra with a Perkin-Elmer 735B grating IR spectrometer and NMR spectra with a Varian T-60A NMR spectrometer were recorded with each sample. An Autopol III automatic polarimeter (Rudolph Research, N.J.) for the determination of optical rotation, and a Perkin-Elmer 240 elemental analyzer for elemental analysis were also employed.

[3] Methacrylic acid stabilized with 200–300 ppm of *p*-methoxyphenol was obtained from Eastman Kodak Co., Rochester, N.Y.

[4] *N*-(*R,S*-3-halogeno-2-methylpropanoyl)-L-proline.

[5] Optical resolution was performed by the preferential crystallization technique of dicyclohexylammonium salts until its optical rotation was no more increased.

[6] *N*-(*R*-3-halogeno-2-methylpropanoyl)-L-proline.

[7] Prepared by dissolving hydrogen sulfide gas in 98 mL of methanol after addition of 2 mL of concentrated ammonium hydroxide.

[8] Supplied from Squibb Institute for Medical Research, Princeton, N.J.

0022-3549/84/1200-1843$01.00/0
© 1984, American Pharmaceutical Association

method of Groszkowski *et al.* (6). The carboxylic acids (II and III) were converted to their corresponding acyl halides (IV and V) in nearly 95% yield using *N*,*N*-dimethylformamide as a catalyst (7). To avoid protecting the carboxylic function of L-proline, the direct *N*-acylation of L-proline with IV or V was carried out in 90% yield using the procedure of Hongo *et al.* (9). *N*-(*R*,*S*-3-Halogeno-2-methylpropanoyl)-L-proline (VIa or VIIa) was successfully separated into optically pure diastereoisomers using dicyclohexylamine. Treatment of halides of VIb or VIIb with methanolic ammonium hydrosulfide afforded captopril in 28% overall yield. This synthetic method is an improvement over that reported by Cushman *et al.* (12%) (2) and is more convenient than the method reported by Shimazaki *et al.* (3), which involves a fermentation step.

REFERENCES

(1) M. A. Ondetti, B. Rubin, and D. W. Cushman, *Science*, **196**, 441 (1977).

(2) D. W. Cushman, H. S. Cheung, E. F. Sabo, and M. A. Ondetti, *Biochemistry*, **16**, 5484 (1977).

(3) M. Shimazaki, J. Hasegawa, K. Kan, K. Nomura, Y. Nose, H. Kondo, T. Ohashi, and K. Watanabe, *Chem. Pharm. Bull.*, **30**, 3139 (1982).

(4) J. Hasegawa, M. Ogura, S. Hamaguchi, M. Shimazaki, H. Kawaharada, and K. Watanabe, *J. Ferment. Technol.*, **59**, 203 (1981).

(5) J. Hasegawa, M. Ogura, H. Kanema, N. Noda, H. Kawaharada, and K. Watanabe, *J. Ferment. Technol.*, **60**, 501 (1982).

(6) S. Groszkowski, J. Sienkiewicz, and L. Najman, *Farmacia*, **15**, 263 (1967).

(7) S. H. Pine, J. B. Hendrickson, C. J. Cram, and G. S. Hammond, "Organic Chemistry," 4th ed., McGraw-Hill, New York, N.Y., 1980, pp. 310–312.

(8) Z. Horii and T. Watanabe, *Yakugaku Zassi*, **81**, 1786 (1961).

(9) C. Hongo, M. Shibazaki, S. Yamada, and I. Chibata, *J. Agric. Food Chem.*, **24**, 903 (1976).

Phosphorous-Containing Analogues of Aspartame

VICTOR NELSON *§x and PRZEMSLAW MASTALERZ ‡

Received October 18, 1983, from the **Department of Chemistry and Chemical Engineering, Michigan Technological University, Houghton, MI 49931* and the ‡*Institute of Organic and Physical Chemistry, Technical University of Wroclaw, Wroclaw, Poland.* Accepted for publication March 9, 1984.

§Present address: NCI-Frederick Cancer Research Facility, Frederick, MD 21701.

Abstract □ Four analogues of aspartame (aspartylphenylalanine methyl ester) were prepared in which one of the carboxylate groups was replaced by a phosphonate group. None of the peptides so obtained was sweet, in contrast with the parent compound which is over 100 times sweeter than sucrose. These results contrast with several published reports of phosphonate analogues of amino acids and peptides which are potent inhibitors of enzymes containing acceptor sites for the parent compound.

Keyphrases □ Aspartame—phosphonate analogues, sweetness

Since the discovery in 1969 that the synthetic dipeptide aspartame (*S*-aspartyl-*S*-phenylalanine methyl ester, I) was over 100 times sweeter than sucrose (1), many analogues have been prepared to ascertain which structural features are responsible for the sweetness. Quite early it was shown that alteration of the aspartyl moiety often result in loss of sweetness, but the phenylalanine moiety can be modified significantly with retention of sweetness (1, 2). More recent work (3) has shown that there are many exceptions to this simple rule, and that the structure-taste relationships are subtle and complicated.

One modification not yet reported is the replacement of one of the two carboxylate groups with a phosphonic acid function. There are several examples in the literature of amino acid and peptide analogues in which carboxylate groups have been replaced by phosphonate groups with retention of biological activity. For example, 1-amino-2-phenylethanephosphonic acid, the phosphonic acid analogue of phenylalanine, is a competitive inhibitor of phenylalanyl-tRNA synthetase (4), 1-amino-3-phosphonobutyric acid inhibits glutamine synthetase (5), and a series of peptides incorporating 1-aminoethanephosphonic acid as the C-terminal residue are shown to have antibacterial properties (6).

These results prompted us to synthesize the following aspartame analogues as diastereomeric mixtures (Scheme I): *R*,*S*-2-amino-3-phosphonopropionyl-*S*-phenylalanine methyl ester (IV); the free acid thereof (V); *S*-aspartyl-*R*,*S*-aminobenzylmethanephosphonate diethyl ester (VIII) and its free acid (IX).

RESULTS AND DISCUSSION

The peptide analogues were made by a standard coupling method (7) from the blocked amino acids. Although other coupling methods have been used to prepare dipeptides incorporating amino phosphonic acids (8), in our hands the mixed anhydride method employing ethyl chloroformate as coupling agent (7, 9) proved most successful. Compound IV was synthesized from *S*-phenylalanine methyl ester and the *N*-benzoxycarbonyl derivative of racemic 2-amino-3-dimethylphosphonopropionic acid (II). After coupling, the fully blocked peptide was partially deblocked to the methyl carboxylate (IV) by treatment with hydrogen bromide in acetic acid. The remaining methyl group was shown to reside on the carboxylate rather than the phosphonate group by recovery of starting material after attempted reesterification with thionyl chloride and methanol, a method which esterifies carboxylic acids but not phosphonic acids. This ester was converted to the fully deblocked peptide (V) by treatment with methanolic sodium hydroxide. Compound VIII was synthesized by coupling *S*-aspartic acid in the form of its *N*-benzoxycarbonyl-γ-benzyl ester derivative (10) with the diethyl ester of racemic aminobenzylmethanephosphonic acid (VI) (11), followed by hydrogenolysis. Deblocking with hydrogen bromide in acetic acid yielded the fully deblocked peptide analogue IX. Spectral data for the blocked aminophosphonic acid (II), blocked peptides (IV and VII), and deblocked peptides (V and IX) are presented in the *Experimental Section*. No attempt was made to separate the diastereomers in each product mixture since a significantly sweet isomer could have been detected by taste in the presence of a large amount of tasteless material.

Following the method previously used for testing sweetness in aspartame analogues (1), cotton swabs were soaked in water solutions of compounds to be tested, and the solutions were sucked off the swab. Usually compounds are not considered significantly sweet unless solutions of ≤2% concentrations evoke a sweet taste. However, even with 5% solutions, each peptide was found to be tasteless or slightly bitter by three different people. The lack of sweetness in IV and V is perhaps not surprising when one considers which modifications of the aspartyl residue of aspartame have previously been found to destroy sweetness. Replacement with an α-aminomalonyl moiety (*i.e.*, removing a methylene group from the aspartyl side chain) yields a compound even sweeter than aspartame (12), while replacing the aspartate by a glutamate moiety (thus adding an extra methylene group to the side chain) destroys sweetness (1). All other modifications of the aspartyl residue have led to nonsweet compounds. This suggests (3) that the N-terminal end of the molecule must incorporate a five- or six-membered zwitterionic ring in order to exhibit

0022-3549/84/1200-1844$01.00/0

© 1984, American Pharmaceutical Association

method of Groszkowski *et al.* (6). The carboxylic acids (II and III) were converted to their corresponding acyl halides (IV and V) in nearly 95% yield using *N*,*N*-dimethylformamide as a catalyst (7). To avoid protecting the carboxylic function of L-proline, the direct *N*-acylation of L-proline with IV or V was carried out in 90% yield using the procedure of Hongo *et al.* (9). *N*-(*R*,*S*-3-Halogeno-2-methylpropanoyl)-L-proline (VIa or VIIa) was successfully separated into optically pure diastereoisomers using dicyclohexylamine. Treatment of halides of VIb or VIIb with methanolic ammonium hydrosulfide afforded captopril in 28% overall yield. This synthetic method is an improvement over that reported by Cushman *et al.* (12%) (2) and is more convenient than the method reported by Shimazaki *et al.* (3), which involves a fermentation step.

REFERENCES

(1) M. A. Ondetti, B. Rubin, and D. W. Cushman, *Science*, **196**, 441 (1977).

(2) D. W. Cushman, H. S. Cheung, E. F. Sabo, and M. A. Ondetti, *Biochemistry*, **16**, 5484 (1977).

(3) M. Shimazaki, J. Hasegawa, K. Kan, K. Nomura, Y. Nose, H. Kondo, T. Ohashi, and K. Watanabe, *Chem. Pharm. Bull.*, **30**, 3139 (1982).

(4) J. Hasegawa, M. Ogura, S. Hamaguchi, M. Shimazaki, H. Kawaharada, and K. Watanabe, *J. Ferment. Technol.*, **59**, 203 (1981).

(5) J. Hasegawa, M. Ogura, H. Kanema, N. Noda, H. Kawaharada, and K. Watanabe, *J. Ferment. Technol.*, **60**, 501 (1982).

(6) S. Groszkowski, J. Sienkiewicz, and L. Najman, *Farmacia*, **15**, 263 (1967).

(7) S. H. Pine, J. B. Hendrickson, C. J. Cram, and G. S. Hammond, "Organic Chemistry," 4th ed., McGraw-Hill, New York, N.Y., 1980, pp. 310–312.

(8) Z. Horii and T. Watanabe, *Yakugaku Zassi*, **81**, 1786 (1961).

(9) C. Hongo, M. Shibazaki, S. Yamada, and I. Chibata, *J. Agric. Food Chem.*, **24**, 903 (1976).

Phosphorous-Containing Analogues of Aspartame

VICTOR NELSON *§x and PRZEMSLAW MASTALERZ ‡

Received October 18, 1983, from the **Department of Chemistry and Chemical Engineering, Michigan Technological University, Houghton, MI 49931* and the ‡*Institute of Organic and Physical Chemistry, Technical University of Wroclaw, Wroclaw, Poland.* Accepted for publication March 9, 1984.

§Present address: NCI-Frederick Cancer Research Facility, Frederick, MD 21701.

Abstract □ Four analogues of aspartame (aspartylphenylalanine methyl ester) were prepared in which one of the carboxylate groups was replaced by a phosphonate group. None of the peptides so obtained was sweet, in contrast with the parent compound which is over 100 times sweeter than sucrose. These results contrast with several published reports of phosphonate analogues of amino acids and peptides which are potent inhibitors of enzymes containing acceptor sites for the parent compound.

Keyphrases □ Aspartame—phosphonate analogues, sweetness

Since the discovery in 1969 that the synthetic dipeptide aspartame (*S*-aspartyl-*S*-phenylalanine methyl ester, I) was over 100 times sweeter than sucrose (1), many analogues have been prepared to ascertain which structural features are responsible for the sweetness. Quite early it was shown that alteration of the aspartyl moiety often result in loss of sweetness, but the phenylalanine moiety can be modified significantly with retention of sweetness (1, 2). More recent work (3) has shown that there are many exceptions to this simple rule, and that the structure-taste relationships are subtle and complicated.

One modification not yet reported is the replacement of one of the two carboxylate groups with a phosphonic acid function. There are several examples in the literature of amino acid and peptide analogues in which carboxylate groups have been replaced by phosphonate groups with retention of biological activity. For example, 1-amino-2-phenylethanephosphonic acid, the phosphonic acid analogue of phenylalanine, is a competitive inhibitor of phenylalanyl-tRNA synthetase (4), 1-amino-3-phosphonobutyric acid inhibits glutamine synthetase (5), and a series of peptides incorporating 1-aminoethanephosphonic acid as the C-terminal residue are shown to have antibacterial properties (6).

These results prompted us to synthesize the following aspartame analogues as diastereomeric mixtures (Scheme I): *R*,*S*-2-amino-3-phosphonopropionyl-*S*-phenylalanine methyl ester (IV); the free acid thereof (V); *S*-aspartyl-*R*,*S*-aminobenzylmethanephosphonate diethyl ester (VIII) and its free acid (IX).

RESULTS AND DISCUSSION

The peptide analogues were made by a standard coupling method (7) from the blocked amino acids. Although other coupling methods have been used to prepare dipeptides incorporating amino phosphonic acids (8), in our hands the mixed anhydride method employing ethyl chloroformate as coupling agent (7, 9) proved most successful. Compound IV was synthesized from *S*-phenylalanine methyl ester and the *N*-benzoxycarbonyl derivative of racemic 2-amino-3-dimethylphosphonopropionic acid (II). After coupling, the fully blocked peptide was partially deblocked to the methyl carboxylate (IV) by treatment with hydrogen bromide in acetic acid. The remaining methyl group was shown to reside on the carboxylate rather than the phosphonate group by recovery of starting material after attempted reesterification with thionyl chloride and methanol, a method which esterifies carboxylic acids but not phosphonic acids. This ester was converted to the fully deblocked peptide (V) by treatment with methanolic sodium hydroxide. Compound VIII was synthesized by coupling *S*-aspartic acid in the form of its *N*-benzoxycarbonyl-γ-benzyl ester derivative (10) with the diethyl ester of racemic aminobenzylmethanephosphonic acid (VI) (11), followed by hydrogenolysis. Deblocking with hydrogen bromide in acetic acid yielded the fully deblocked peptide analogue IX. Spectral data for the blocked aminophosphonic acid (II), blocked peptides (IV and VII), and deblocked peptides (V and IX) are presented in the *Experimental Section*. No attempt was made to separate the diastereomers in each product mixture since a significantly sweet isomer could have been detected by taste in the presence of a large amount of tasteless material.

Following the method previously used for testing sweetness in aspartame analogues (1), cotton swabs were soaked in water solutions of compounds to be tested, and the solutions were sucked off the swab. Usually compounds are not considered significantly sweet unless solutions of ≤2% concentrations evoke a sweet taste. However, even with 5% solutions, each peptide was found to be tasteless or slightly bitter by three different people. The lack of sweetness in IV and V is perhaps not surprising when one considers which modifications of the aspartyl residue of aspartame have previously been found to destroy sweetness. Replacement with an α-aminomalonyl moiety (*i.e.*, removing a methylene group from the aspartyl side chain) yields a compound even sweeter than aspartame (12), while replacing the aspartate by a glutamate moiety (thus adding an extra methylene group to the side chain) destroys sweetness (1). All other modifications of the aspartyl residue have led to nonsweet compounds. This suggests (3) that the N-terminal end of the molecule must incorporate a five- or six-membered zwitterionic ring in order to exhibit

0022-3549/84/1200-1844$01.00/0

© 1984, American Pharmaceutical Association

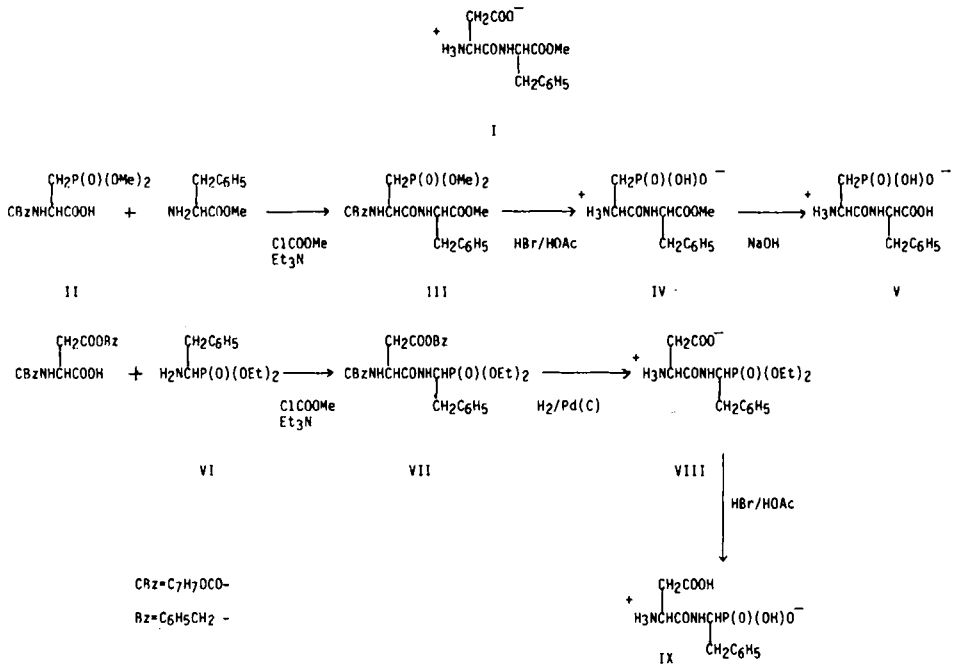

Scheme I

sweetness. According to this model, the negative carboxylate oxygen of the aspartyl moiety in aspartame is hydrogen bonded to the positive ammonium group, forming a six-membered ring. A seven-membered ring, which would be formed by a glutamate residue, is apparently too large. Since a phosphonate group is larger than a carboxylate group, replacement of the carboxylate group in the aspartyl side chain of aspartame would result in a six-membered ring larger than that in aspartame. Furthermore, the phosphonate group is pyramidal as opposed to the planar carboxylate group, so this ring could not be flat, as it is in aspartame.

Turning to the C-terminal end of aspartame, we find more leeway for modification. Many sweet analogues have been prepared incorporating a variety of amino acid esters and amides in place of phenylalanine methyl ester (13). However, in all these analogues two substituents of dissimilar size are attached to the carbon of the C-terminal residue. The orientation of the groups is always such that the large group corresponds to the benzyl side chain of aspartame and the smaller group corresponds to the methoxycarbonyl moiety. Apparently a difference in size between these two groups is important. For example, exchanging the methyl ester for the larger ethyl ester diminishes sweetness (1). Perhaps VIII and IX are not sweet because the phosphonate group, being larger than a methoxycarbonyl group, is too close in size to, or even larger than, the benzyl group. Also, it is noteworthy that replacement of the methoxycarbonyl group of aspartame with the free carboxylic acid or carboxamide destroys the sweetness. Evidently this part of the molecule must be relatively nonpolar. It is possible that both the diethylphosphonate group and the free phosphonic acid group are too polar to permit VIII and IX to be sweet.

In view of the exacting stereochemical requirements of the taste receptors it is not surprising that neither the charged, pyramidal phosphonic acid group nor the bulky diethylphosphonate group is a good replacement for the planar methylcarboxylate group of aspartame.

EXPERIMENTAL SECTION[1]

***N*-Benzyloxycarbonyl-2-*R*,*S*-amino-3-dimethylphosphonopropionic Acid (II)**—Racemic 2-amino-3-phosphonopropionic acid (14) (17 g, 0.1 mol) was stirred in water (100 mL) with KOH (33.5 g, 0.6 mol) at 0°C as a solution of carbobenzoxy chloride (35 g, excess) in ether was added in a dropwise manner. The solution was stirred overnight at room temperature, washed twice with ether, and acidified with hydrochloric acid to precipitate an oil. The aqueous layer was extracted with ethyl acetate and the combined oil and extract was dried with anhydrous sodium sulfate. Evaporation of the solvent yielded an oil, which was converted to the trimethyl ester by treatment for several hours with a methanolic solution of diazomethane according to a published method (15). After removal of volatile material, the oily triester (22.5 g, 0.065 mol) was refluxed in methanol (100 mL) with 0.55 M NaOH (118 mL, 0.065 mol) for 2 h. After evaporation of the solvent, the residue was triturated with hot ethyl acetate, dissolved in water, and neutralized with Dowex-50 (H^+). The water solution was extracted repeatedly with ethyl acetate, the combined extracts were dried, and the solvent was evaporated to yield the product as a glass (37%), which softens without melting at 150°C. TLC on silica gel (ethyl acetate–methanol, 9:1) shows one spot, R_f 0.3; ^{1}H-NMR ($CDCl_3$): δ 2.88 (m, CH_2), 4.03 (d, OCH_3), 5.48 (s, $ArCH_3$), 6.63 (m, NH), and 8.78 ppm (s, ArH); IR ($CHCl_3$): 3400–2400 (OH and NH), 1720 (C=O), 1500, 1210 (OH), and 1040 cm^{-1} (P=O).

Diethyl Aminobenzylmethanephosphonate (VI)—This material was prepared by diborane reduction (16) of the *O*-methyl oxime of diethyl phenylacetylphosphonate to give product identical with that of a published method (11).

Coupling Procedure—The blocked amino acids were coupled according to a published method (7), in which ethyl chloroformate is added to a solution of triethylamine and the blocked N-terminal amino acid in chloroform. The blocked C-terminal amino acid is added and the mixture is stirred for 12 h at room temperature.

Compound III was isolated as a thick oil in 78% yield. TLC on silica gel (ethyl acetate–methanol, 9:1) showed one spot, R_f 0.6; ^{1}H-NMR ($CDCl_3$): δ 2.73 (m, CH_2P), 3.48 (m, CHCO), 4.05 (m, OCH_3), 4.50 (m, CH), 5.05 (m, $ArCH_2$), 5.48 (s, $ArCH_2$), and 7.55 and 7.65 ppm (2 s, ArH); IR ($CHCl_3$): 2950–3420 (NH), 1680–1750 (C=O), 1500 (NH), 1190–1250 (OCH_3), and 1040 cm^{-1} (P=O).

Compound VII was isolated as a thick oil in 52% yield. TCL on silica gel (benzene–ethyl acetate, 7:3) showed one spot, R_f 0.2; ^{1}H-NMR ($CDCl_3$): δ 1.20 (m, CH_3), 3.00 (m, CH_2CO and CH), 4.03 (m, OCH_2), 4.60 (m, $ArCH_2$), 5.00 (m, $ArCH_2$ and CH), and 7.23 ppm (s, ArH); IR ($CHCl_3$): 3400 (NH), 3060 (ArH), 1740 (C=O), 1500 (NH), 1220 (OCH_2), and 1040 cm^{-1} (P=O).

Deblocking Procedures—Compound VII was deblocked to give VIII by hydrogenolysis over palladium on charcoal in methanol using 1 atm of hydrogen at room temperature. Filtration and evaporation of solvent yielded the product as a glass. Compounds III and VIII were deblocked to IV and IX, respectively, by a standard method (17) in which the blocked peptide was stirred at 60°C for 20 min in 48% hydrogen bromide–acetic acid (30 mL/g). The volatile material was evaporated, the residue was dissolved in ethanol, and the peptide was precipitated by addition of pyridine. Ester IV (0.0076 mol) was saponified to acid V by refluxing in 50 mL of methanolic sodium hydroxide (0.6 M) for 1 h. The solid so formed was isolated by filtration and

[1] NMR Spectra were obtained on a Tesla 80-MHz spectrometer, either in $CDCl_3$ with Me_4Si as standard, or in D_2O with sodium trimethylsilylpropanesulfonate as standard. IR spectra were obtained on a Specord spectrophotometer.

dissolved in aqueous acetic acid, and the product was precipitated by addition of ethanol.

Compound IV was an amorphous solid (59% yield) which did not melt up to 300°C. ^{1}H-NMR (D_2O): δ 2.50 (m, CH_2P), 3.48 (m, CHCO), 4.04 (s, OCH_3), 4.58 (m, ArCH_2), and 7.63 ppm (m, ArH). IR (KBr): 3700–2500 (NH and OH), 1680, 1740 (C=O), 1200 (OCH_3), and 1070 cm^{-1} (P=O).

Anal.—Calc. for $C_{13}H_{19}N_2O_6P \cdot 3.5\ H_2O$: N, 7.12; P, 7.87. Found: N, 6.64; P, 8.33.

Compound V was an amorphous solid (55% yield) which did not melt up to 300°C. ^{1}H-NMR (D_2O–D_2SO_4): δ 2.00–5.10 (m, aliphatic H) and 7.70 ppm (ArH); IR (KBr): 3700–2500 (NH and OH), 1650–1660 (C=O), and 1070 cm^{-1} (P=O).

Anal.—Calc. for $C_{12}H_{17}N_2O_6P$: N, 8.86; P, 9.80. Found: N, 8.18; P, 10.25.

Compound VIII was an amorphous gum which softened without melting at 90°C. TLC on silica gel (methanol) showed one spot, R_f 0.5.

Compound IX was an amorphous solid (50% yield) which did not melt up to 260°C. ^{1}H-NMR (D_2O–D_2SO_4): δ 2.75–3.88 (m, CH and CH_2), 4.38–5.25 (m, ArCH_2 and CH), and 7.62 cm^{-1} (s, ArH). IR (KBr): 2700–3500 (OH, ArH, and CH), 1700 (C=O), 1150 (C—O), and 1050 cm^{-1} (P=O).

Anal.—Calc. for $C_{12}H_{17}N_2O_6P \cdot H_2O$: N, 8.38; P, 9.26. Found: N, 8.40; P, 9.02.

REFERENCES

(1) R. H. Mazur, J. M. Schlatter, and A. H. Goldcamp, *J. Am. Chem. Soc.*, **91**, 2684 (1969).

(2) R. H. Mazur, K. A. Reuter, R. A. Switek, and J. M. Schlatter, *J. Med. Chem.*, **16**, 1284 (1973).

(3) S. A. MacDonald, C. G. Wiulson, M. Chorev, F. S. Vernacchia, and M. Goodman, *J. Med. Chem.*, **23**, 413 (1980).

(4) J. W. Anderson and L. Fowden, *Chem. Biol. Interactions*, **2**, 53 (1970).

(5) P. Mastalerz, *Arch. Immunol. Exp. Ther.*, **7**, 201 (1959).

(6) (a) J. W. Huber and W. F. Gilmore, *J. Med. Chem.*, **18**, 106 (1975); (b) J. G. Allen, F. R. Atherton, M. J. Hall, C. H. Hassall, S. W. Holmes, R. W. Lambert, L. J. Nisbet, and P. S. Ringrose, *Nature (London)*, **272**, 56 (1978); (c) J. R. Atherton, M. J. Hall, C. H. Hassall, R. W. Lambert, and P. S. Ringrose, *Microb. Agents Chemother.*, **15**, 677 (1979).

(7) J. R. Vaughn, Jr., *J. Am. Chem. Soc.*, **73**, 3547 (1951).

(8) W. F. Gilmore and H. A. McBride, *J. Pharm. Sci.*, **63**, 1087 (1974).

(9) P. Kafarski, B. Lejczak, P. Mastalerz, J. Szewszyk, and C. Wasielewski, *Can. J. Chem.*, **60**, 3081 (1982).

(10) P. M. Bryant, R. H. Moore, P. J. Pimlott, and G. T. Young, *J. Chem. Soc.*, **1959**, 3868.

(11) S. Asano, T. Kitahara, T. Ogawa, and M. Matsui, *Agric. Biol. Chem. Jpn.*, **37**, 1193 (1973).

(12) M. Fujino, M. Wakimasu, K. Tanaka, H. Aoki, and N. Nakajima, *Naturwissenschaften*, **60**, 351 (1973).

(13) M. Kawai, M. Chorev, J. Marin-Rose, and M. Goodman, *J. Med. Chem.*, **23**, 420 (1980).

(14) M. Soroka and P. Mastalerz, *Rocz. Chem.*, **50**, 661 (1976); *Chem. Abstr.*, **81**, 151443v.

(15) M. Hoffman and C. Wasielewski, *Rocz. Chem.*, **50**, 139 (1976); *Chem. Abstr.*, **84**, 180338g.

(16) K. D. Berlin, N. K. Roy, R. T. Claunch and D. Bude, *J. Am. Chem. Soc.*, **90**, 4494 (1968).

(17) R. Boissonnas and G. Preitner, *Helv. Chim. Acta.*, **36**, 875 (1953).

ACKNOWLEDGMENTS

This work was performed under an exchange program between the University of Oregon and the Technical University of Wroclaw, Wroclaw, Poland, sponsored by the National Science Foundation. The authors thank the Technical University of Wroclaw for providing facilities and financial support and the University of Oregon for allowing one of us (V.N.) to participate in the program.

Induction of Hyperpyrexia by Dihydrocurvularin, a Metabolic Product of *Penicillium gilmanii*

FREDERICK A. H. RICE ˣ and CHESTER G. CHEN

Received May 24, 1983, from the *Department of Chemistry, American University, Washington, DC 20016.* Accepted for publication March 12, 1984.

Abstract □ The previously reported rise in rectal temperature that follows the intravenous injection of the mixture of metabolic products (extractable with ether from the Czapek Dox medium on which *Penicillium gilmanii* has grown) is due to a single compound, dihydrocurvularin. Intravenous injection of 1–10 μg of dihydrocurvularin into rabbits causes a rise of at least one degree in rectal temperature of rabbits in 2–8 h. The degree of temperature rise depends more on the individual rabbit than on the quantity of dihydrocurvularin injected. Treatment with lipopolysaccharide abolishes the ability of dihydrocurvularin to cause a rise in rectal temperature. Treatment with dihydrocurvularin, however, does not abolish the ability of lipopolysaccharide to induce a temperature response or a leukocytosis. Rabbits respond to repeated treatment with dihydrocurvularin with a rise in rectal temperature that is indistinguishable from that observed on their first injection. Treatment with dihydrocurvularin does not affect differential counts or the concentration of leukocytes or red blood cells in the circulatory system.

Keyphrases □ Dihydrocurvularin—intravenous injection, hyperpyrexia, rabbits, effect of lipopolysaccharide

The intravenous injection of microgram quantities of the mixture of metabolic products elaborated by *Penicillium gilmanii* grown on a Czapek Dox medium induces a temporary rise in rectal temperature and leukocytosis in rabbits (1, 2). After extraction with ether the medium no longer induced a temperature rise but afforded a pure crystalline enolic heterocyclic compound, leucogenenol (2), of which 0.002 μg/kg, on intravenous injection, induces a temporary leukocytosis in animals (1, 3), but even milligram quantities do not induce hyperpyrexia. On the other hand, intravenous injection of microgram quantities of the mixture of compounds extractable from the culture medium with ether induces a hyperpyrexia in rabbits comparable to that observed following the injection of microgram quantities of lipopolysaccharides.

Investigations on leucogenenol established that it acted on cells in the peripheral circulation by increasing the rate at which committed cells of the bone marrow develop into functional cells such as neutrophils and lymphocytes (4–7). Undoubtedly as a consequence of its ability to increase the rate of development of cells involved in the immune response, treatment with leucogenenol enhances the immunocompetence of an animal and increases the rate at which immunosuppressed animals recover immunocompetence (8–13). Leucogenenol is also found as a thymo-thyroid hormone (14–16).

0022-3549/84/1200-1846$01.00/0

© 1984, American Pharmaceutical Association

dissolved in aqueous acetic acid, and the product was precipitated by addition of ethanol.

Compound IV was an amorphous solid (59% yield) which did not melt up to 300°C. ^{1}H-NMR (D_2O): δ 2.50 (m, CH_2P), 3.48 (m, CHCO), 4.04 (s, OCH_3), 4.58 (m, ArCH_2), and 7.63 ppm (m, ArH). IR (KBr): 3700–2500 (NH and OH), 1680, 1740 (C=O), 1200 (OCH_3), and 1070 cm^{-1} (P=O).

Anal.—Calc. for $C_{13}H_{19}N_2O_6P \cdot 3.5\ H_2O$: N, 7.12; P, 7.87. Found: N, 6.64; P, 8.33.

Compound V was an amorphous solid (55% yield) which did not melt up to 300°C. ^{1}H-NMR (D_2O–D_2SO_4): δ 2.00–5.10 (m, aliphatic H) and 7.70 ppm (ArH); IR (KBr): 3700–2500 (NH and OH), 1650–1660 (C=O), and 1070 cm^{-1} (P=O).

Anal.—Calc. for $C_{12}H_{17}N_2O_6P$: N, 8.86; P, 9.80. Found: N, 8.18; P, 10.25.

Compound VIII was an amorphous gum which softened without melting at 90°C. TLC on silica gel (methanol) showed one spot, R_f 0.5.

Compound IX was an amorphous solid (50% yield) which did not melt up to 260°C. ^{1}H-NMR (D_2O–D_2SO_4): δ 2.75–3.88 (m, CH and CH_2), 4.38–5.25 (m, ArCH_2 and CH), and 7.62 cm^{-1} (s, ArH). IR (KBr): 2700–3500 (OH, ArH, and CH), 1700 (C=O), 1150 (C—O), and 1050 cm^{-1} (P=O).

Anal.—Calc. for $C_{12}H_{17}N_2O_6P \cdot H_2O$: N, 8.38; P, 9.26. Found: N, 8.40; P, 9.02.

REFERENCES

(1) R. H. Mazur, J. M. Schlatter, and A. H. Goldcamp, *J. Am. Chem. Soc.*, **91**, 2684 (1969).

(2) R. H. Mazur, K. A. Reuter, R. A. Switek, and J. M. Schlatter, *J. Med. Chem.*, **16**, 1284 (1973).

(3) S. A. MacDonald, C. G. Wiulson, M. Chorev, F. S. Vernacchia, and M. Goodman, *J. Med. Chem.*, **23**, 413 (1980).

(4) J. W. Anderson and L. Fowden, *Chem. Biol. Interactions*, **2**, 53 (1970).

(5) P. Mastalerz, *Arch. Immunol. Exp. Ther.*, **7**, 201 (1959).

(6) (a) J. W. Huber and W. F. Gilmore, *J. Med. Chem.*, **18**, 106 (1975); (b) J. G. Allen, F. R. Atherton, M. J. Hall, C. H. Hassall, S. W. Holmes, R. W. Lambert, L. J. Nisbet, and P. S. Ringrose, *Nature (London)*, **272**, 56 (1978); (c) J. R. Atherton, M. J. Hall, C. H. Hassall, R. W. Lambert, and P. S. Ringrose, *Microb. Agents Chemother.*, **15**, 677 (1979).

(7) J. R. Vaughn, Jr., *J. Am. Chem. Soc.*, **73**, 3547 (1951).

(8) W. F. Gilmore and H. A. McBride, *J. Pharm. Sci.*, **63**, 1087 (1974).

(9) P. Kafarski, B. Lejczak, P. Mastalerz, J. Szewszyk, and C. Wasielewski, *Can. J. Chem.*, **60**, 3081 (1982).

(10) P. M. Bryant, R. H. Moore, P. J. Pimlott, and G. T. Young, *J. Chem. Soc.*, **1959**, 3868.

(11) S. Asano, T. Kitahara, T. Ogawa, and M. Matsui, *Agric. Biol. Chem. Jpn.*, **37**, 1193 (1973).

(12) M. Fujino, M. Wakimasu, K. Tanaka, H. Aoki, and N. Nakajima, *Naturwissenschaften*, **60**, 351 (1973).

(13) M. Kawai, M. Chorev, J. Marin-Rose, and M. Goodman, *J. Med. Chem.*, **23**, 420 (1980).

(14) M. Soroka and P. Mastalerz, *Rocz. Chem.*, **50**, 661 (1976); *Chem. Abstr.*, **81**, 151443v.

(15) M. Hoffman and C. Wasielewski, *Rocz. Chem.*, **50**, 139 (1976); *Chem. Abstr.*, **84**, 180338g.

(16) K. D. Berlin, N. K. Roy, R. T. Claunch and D. Bude, *J. Am. Chem. Soc.*, **90**, 4494 (1968).

(17) R. Boissonnas and G. Preitner, *Helv. Chim. Acta.*, **36**, 875 (1953).

ACKNOWLEDGMENTS

This work was performed under an exchange program between the University of Oregon and the Technical University of Wroclaw, Wroclaw, Poland, sponsored by the National Science Foundation. The authors thank the Technical University of Wroclaw for providing facilities and financial support and the University of Oregon for allowing one of us (V.N.) to participate in the program.

Induction of Hyperpyrexia by Dihydrocurvularin, a Metabolic Product of *Penicillium gilmanii*

FREDERICK A. H. RICE ˣ and CHESTER G. CHEN

Received May 24, 1983, from the *Department of Chemistry, American University, Washington, DC 20016.* Accepted for publication March 12, 1984.

Abstract □ The previously reported rise in rectal temperature that follows the intravenous injection of the mixture of metabolic products (extractable with ether from the Czapek Dox medium on which *Penicillium gilmanii* has grown) is due to a single compound, dihydrocurvularin. Intravenous injection of 1–10 μg of dihydrocurvularin into rabbits causes a rise of at least one degree in rectal temperature of rabbits in 2–8 h. The degree of temperature rise depends more on the individual rabbit than on the quantity of dihydrocurvularin injected. Treatment with lipopolysaccharide abolishes the ability of dihydrocurvularin to cause a rise in rectal temperature. Treatment with dihydrocurvularin, however, does not abolish the ability of lipopolysaccharide to induce a temperature response or a leukocytosis. Rabbits respond to repeated treatment with dihydrocurvularin with a rise in rectal temperature that is indistinguishable from that observed on their first injection. Treatment with dihydrocurvularin does not affect differential counts or the concentration of leukocytes or red blood cells in the circulatory system.

Keyphrases □ Dihydrocurvularin—intravenous injection, hyperpyrexia, rabbits, effect of lipopolysaccharide

The intravenous injection of microgram quantities of the mixture of metabolic products elaborated by *Penicillium gilmanii* grown on a Czapek Dox medium induces a temporary rise in rectal temperature and leukocytosis in rabbits (1, 2). After extraction with ether the medium no longer induced a temperature rise but afforded a pure crystalline enolic heterocyclic compound, leucogenenol (2), of which 0.002 μg/kg, on intravenous injection, induces a temporary leukocytosis in animals (1, 3), but even milligram quantities do not induce hyperpyrexia. On the other hand, intravenous injection of microgram quantities of the mixture of compounds extractable from the culture medium with ether induces a hyperpyrexia in rabbits comparable to that observed following the injection of microgram quantities of lipopolysaccharides.

Investigations on leucogenenol established that it acted on cells in the peripheral circulation by increasing the rate at which committed cells of the bone marrow develop into functional cells such as neutrophils and lymphocytes (4–7). Undoubtedly as a consequence of its ability to increase the rate of development of cells involved in the immune response, treatment with leucogenenol enhances the immunocompetence of an animal and increases the rate at which immunosuppressed animals recover immunocompetence (8–13). Leucogenenol is also found as a thymo-thyroid hormone (14–16).

0022-3549/84/1200-1846$01.00/0

© 1984, American Pharmaceutical Association

Having established that the effect of the mixture of metabolic products of *P. gilmanii* on circulating leukocytes is due to a single compound, leucogenenol, we turned our attention to identifying the compound(s) that induce a rise in rectal temperature of rabbits.

Raistrick and Rice (17) reported the isolation of 2,3-dihydro-3,6-dihydroxy-2-methyl-4-pyrone and curvularin from those metabolic products of *P. gilmanii* that are extractable from the culture medium by ether. Therefore, either or both of these compounds could be responsible for the temperature rise observed when the mixture of compounds extracted from the culture medium with ether is injected intravenously into rabbits (1). Accordingly, rabbits were treated with 2,3-dihydro-3,6-dihydroxy-2-methyl-4-pyrone and with curvularin (I) in quantities up to 100 μg/kg, and the effect on rabbit rectal temperature was measured. Neither compound had any effect; therefore, it was apparent that a hitherto unrecognized compound(s) was present in the ether-extractable metabolic products.

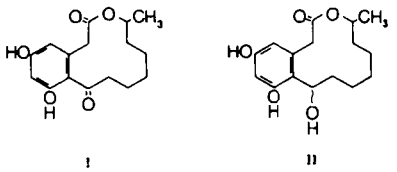

I

II

RESULTS AND DISCUSSION

Preparative TLC following column chromatography of the ether-extractable metabolic products afforded curvularin (I), $C_{16}H_{20}O_5$, and a compound, $C_{16}H_{22}O_5$, in yields of ~35 mg and ~3 mg, respectively, from 1800 mL of culture medium. The compound $C_{16}H_{22}O_5$ induced a rise in the rectal temperature of rabbits when injected 1-10 μg/kg iv. Individually, or as a mixture, the other ether-extractable compounds did not affect rabbit rectal temperature.

The difference in molecular formula of $C_{16}H_{22}O_5$ from that of curvularin ($C_{16}H_{20}O_5$) and the similarity of their IR spectra suggested that $C_{16}H_{22}O_5$ resulted from the reduction of curvularin (I) to dihydrocurvularin (II). Accordingly, curvularin was reduced with sodium borohydride to yield two isomers of dihydrocurvularin (R_f 0.4 and 0.6, EtOAc) one of which (R_f 0.4) was found to be identical with that isolated from the metabolic products of *P. gilmanii*. It was not possible to identify the configuration of the isomers. Injection of either isomer of dihydrocurvularin induces a rise in the rectal temperature of rabbits. The naturally occurring isomer of R_f 0.4 was used for further biological studies.

Figure 1 shows the effect of the injection of 3 μg/kg iv of dihydrocurvularin (R_f 0.4) on the rectal temperature of rabbits. Unlike lipopolysaccharides, repeated dihydrocurvularin injections produce a rise in rectal temperature indistinguishable from that observed on initial injection (Fig. 1). The time required for the rabbit to show a maximum rise in rectal temperature varies with the animal. In a group of 12 rabbits, 8 showed a maximum rise in rectal temperature at ~6 h while 4 rabbits showed a maximum rise at ~2 h. No significant differences in the degree or time of temperature rise were observed when 1, 3, or 10 μg/kg of dihydrocurvularin was injected in groups of rabbits. Injection of 0.1 μg/kg of dihydrocurvularin had no significant effect on rectal temperature.

There are no significant changes in differential blood cell counts made at half-hour intervals for 24 h following treatment with dihydrocurvularin, nor do the rabbits show a leukocytosis or change in red blood cell counts in their peripheral circulation.

For some unexplained reason, previous treatment with lipopolysaccharide prevents a rise in temperature following injection of dihydrocurvularin. Since rabbits respond to treatment with dihydrocurvularin with either an immediate or delayed temperature rise, it was considered important to consider the two groups separately. Accordingly, rabbits were first treated with dihydrocurvularin, then with lipopolysaccharide, and then with dihydrocurvularin. None of the rabbits that responded with either an immediate or delayed temperature response responded to treatment with dihydrocurvularin 2 d or 1 or 2 weeks following their treatment with lipopolysaccharide. All the rabbits showed a maximum increase in rectal temperature 6-8 h after their initial injection with

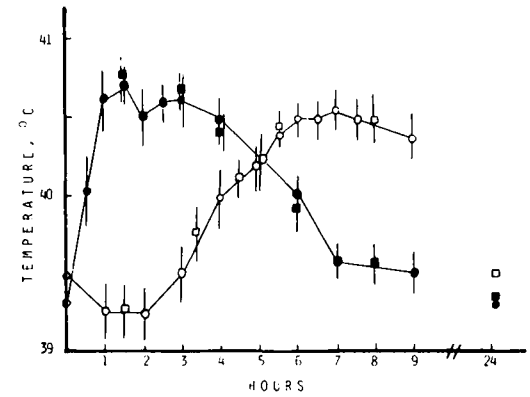

Figure 1—*Effect of the intravenous injection of dihydrocurvularin on the rectal temperature of rabbits injected with 3 μg/kg iv of dihydrocurvularin dissolved in pyrogen-free isotonic saline at a concentration of 10 μg/mL. Key: (●) initial injection; (■) reinjected 48 h later; (○) initial injection; (□) reinjected 7 d later. Vertical bars represent* SD. *Animals that responded with an increase in rectal temperature in 2 h (n = 4) were considered as one group; the remaining animals (n = 8) were considered as a second group. Before treatment rabbits showed a mean diurnal variation of 0.2 ± 0.1°C.*

lipopolysaccharide as well as the expected leukocytosis (18). Treatment with dihydrocurvularin had no significant effect on the response to lipopolysaccharide. On the other hand, none of the rabbits that were treated again with lipopolysaccharide 1 or 2 weeks following their initial injection showed a significant increase in rectal temperture.

It is possible that dihydrocurvularin could be of considerable use for investigating the effect of increased temperatures on physiological responses, as a tool to elucidate the mechanism of temperature regulation, as an important tool to study the role of fever (possibly isolated from other effects of leukocyte endogenous mediator) on the pathogenesis of infection, and possibly as a therapeutic agent.

EXPERIMENTAL SECTION[1]

Solvents and other chemicals were redistilled or recrystallized as appropriate before use. Evaporation of solutions to lesser volumes or to dryness were carried out under reduced pressure in a rotary evaporator at 40-50°C (bath temperature). Where indicated, solutions were filtered under suction through a medium-porosity fritted glass Buchner funnel. Compounds were recrystallized until they showed a single peak on GC.

Rectal temperatures were taken with a telethermometer[2] and pyrogen-free isotonic saline solutions[3] were used for injection in the marginal ear vein of rabbits. Smears of peripheral blood, obtained from the marginal ear vein opposite the one used for injection, were made and the cells examined and enumerated in the usual manner. White blood cells and red blood cells were counted with a Coulter counter[4].

Groups of six rabbits (New Zealand White) (~2.5 kg) were used to determine the ability of each compound or mixture of compounds to induce hyperpyrexia. Prior to treatment rabbits showed a mean diurnal variation of 0.2 ± 0.1°C. The rabbit was weighed and then injected intravenously in the marginal ear vein with the calculated quantity (usually 1-10 μg) of the metabolic compound or compounds dissolved in 1-5 mL of pyrogen-free isotonic saline. Rectal temperatures were recorded at half-hour intervals for 12 h and again at 24 h. A rise of temperature of 1°C was considered significant. Standard deviations were not calculated for the experiments that led to the isolation of the compound that induces a temperature rise in rabbits. However, if one or more rabbits failed to respond with a significant rise in temperature, the experiment was repeated using greater quantities (≤100 μg) of the compound or mixture of compounds being investigated.

[1] Melting points were determined with a Kofler micro hot stage apparatus. UV spectra were determined with a Perkin-Elmer 323 spectrophotometer. IR spectra were determined with the Perkin-Elmer 727 spectrometer, and optical rotations were measured with a Perkin-Elmer 141 spectrometer using a 1-dm tube holding approximately 1 mL. GC were obtained on a Perkin-Elmer 900 gas chromatograph programmed from 200°C to 300°C at 12°C/min, using a flame detector and a column (30.48 cm × 2 mm i.d.) packed with 1% OV-17 on Gas-Chrom Q (18-100 mesh). Florisil (80-100 mesh) obtained from Fisher Scientific Co., Fair Lawn, N.J. was used for column chromatography and precoated silica gel plates (2000 μm, 20 × 20 cm), made fluorescent by the addition of zinc silicate (Anal Tech., Newark, Del.), were used for preparative TLC with the indicated solvents.

[2] Model 43; Yellow Springs Instrument Co., Yellow Springs, Ohio.

[3] Cutter Laboratories, Berkeley, Calif.

[4] Model F.

Isolation of Curvularin and Dihydrocurvularin—*Penicillium gilmanii* was grown as previously reported (1) at room temperature on Czapek Dox medium containing added zinc and copper ions (19) for ~6 weeks. The medium (1800 mL) then was separated from the mycelia by filtration through fluted filter paper[5] and continuously extracted[6] with ether (500 mL) for ~8 h. The ether extract was dried over anhydrous sodium sulfate, filtered, and evaporated to ~25 mL. The solution was then allowed to flow under gravity through a column (15 × 2 cm) of Florisil previously washed with absolute ethanol (500 mL) and ether (500 mL) and still wet with ether. An additional 200 mL of anhydrous ether was allowed to flow through the column followed by 100 mL of ethyl acetate. The ether and ethyl acetate that had flowed through the column was evaporated to dryness. The combined weight was ~1 g. The dry residue was dissolved in 10 mL of isotonic saline and ~1 mL/kg was injected into each of six rabbits. There was no significant rise in the rectal temperature of the rabbits.

The column was then eluted with dioxane (250 mL) which was evaporated to dryness and separated into four fractions by preparative TLC using ethyl acetate as the developing agent. Zones were made visible under UV light. Each zone (R_f 0.8, 0.45, 0.1, and 0.0) was scraped off the plate and its contents eluted with dioxane.

The contents of the zone with R_f 0.8 on evaporation to dryness appeared as a crystalline mass (35 mg) which on recrystallization from ether or ethyl acetate yielded ~30 mg of curvularin as white needles, mp 209°C [lit. (17) mp 205°C]. There was no depression in melting point on admixture with authentic curvularin. Curvularin sublimed unchanged at 140°C (bath temperature) under reduced pressure (0.05 mm Hg); $[\alpha]_{589}^{22}$ −35°, $[\alpha]_{578}^{22}$ −37°, $[\alpha]_{546}^{22}$ −45°, $[\alpha]_{436}^{22}$ −128°, $[\alpha]_{365}^{22}$ −240° (*c*, 1, EtOH); λ_{max}(EtOH): 273 nm (ε 8000) and 303 nm (ε 7100). The MS[13] (70 eV) showed M^+ 292.

Anal.—Calc. for $C_{16}H_{20}O_5$: C, 65.7; H, 6.9. Found: C, 65.8; H, 6.9.

The contents of the zone with R_f 0.45 on evaporation to dryness yielded a syrup (3 mg) which crystallized from dichloromethane to give white needles (~2 mg), mp 175°C; $[\alpha]_{589}^{22}$ −38°, $[\alpha]_{546}^{22}$ −44°, $[\alpha]_{436}^{22}$ −64°, $[\alpha]_{365}^{22}$ −61° (*c*, 1, EtOH); λ_{max} (EtOH): 284 nm (ε 2800); IR (KBr) ν_{max}: 3440 s, 3390 s, 3260 m, 2970 m, 2950 s, 2930 s, 2910 s, 2850 m, 1740 s, 1630 s, and 1460 s cm^{-1}. The MS[7] (70 eV) showed M^+ 294 with clusters of major peaks at 276, 180, 161, and 147; CI − NH_3: M^+ 294.

Anal.—Calc. for $C_{16}H_{22}O_5$: C, 65.3; H, 7.5. Found: C, 65.3; H, 7.5.

Intravenous injection of the contents of the zone with R_f 0.45 induced a febrile response. On elution and evaporation to dryness zones with R_f 0.1 and 0.0 yielded syrups. Injection of rabbits with either fraction (1–20 μg/kg iv) did not induce a febrile response. The fractions were not investigated further.

Sodium Borohydride Reduction of Curvularin to Dihydrocurvularin—An excess (25 mg) of sodium borohydride was added to a cooled (ice water) solution of 50 mg of curvularin in absolute ethanol (5 mL) and set aside at room temperature. Water (2.5 mL) and acetic acid (2.5 mL) then was added and after standing at room temperature for several hours, the solution was evaporated to dryness and the solid residue was extracted with dioxane (5 × 5 mL). The dioxane extract was filtered and evaporated to dryness to yield a thick syrup, which on preparative TLC (ethyl acetate) showed two compounds with R_f 0.45 and 0.65, which were scraped off the plate and eluted with dioxane.

Evaporation of the eluate of the zone with R_f 0.45 yielded dihydrocurvularin (II) as a syrup (20 mg) which crystallized from dichloromethane (~15 mg), mp 175°C, which showed no depression on admixture with the naturally occurring compound of the same R_f given above. The optical rotation, IR spectrum, UV spectrum, and MS were identical with those of the naturally occurring dihydrocurvularin of R_f 0.45.

Anal.—Calc. for $C_{16}H_{22}O_5$: C, 65.3; H, 7.5; M^+, 294. Found: C, 65.3; H, 7.5; M^+, 294.

Evaporation of the eluate of the zone with R_f 0.65 afforded isodihydrocurvularin as a crystalline mass of needles (30 mg), which on recrystallization from ethyl acetate (weight ~20 mg) had mp 186°C. The melting point was depressed on admixture with dihydrocurvularin. $[\alpha]_{589}^{22}$ −40°, $[\alpha]_{578}^{22}$ −41°, $[\alpha]_{546}^{22}$ −45°, $[\alpha]_{436}^{22}$ −66°, $[\alpha]_{365}^{22}$ −63°, (*c*, 1, EtOH). The IR and UV spectra were essentially indistinguishable from the corresponding spectra of dihydrocurvularin. Intravenous injection into rabbits induced a febrile response. The compound was not investigated further.

Effect of Dihydrocurvularin on Rectal Temperatures and Circulating Blood Cells—Twelve rabbits (weight, ~2.5 kg) selected at random from 50 animals were injected in the marginal ear vein with 3 μg/kg iv of synthetic dihydrocurvularin dissolved (10 μg/mL) in pyrogen-free isotonic saline. At half-hour intervals thereafter rectal temperatures were recorded and, in addition, a sample of blood (~0.4 mL) was taken from the marginal ear vein opposite to that used for injection. Smears of the blood were made on microscope slides, stained with Wright's stain, and differential counts were made in the usual manner. Additionally, the concentration of white and red blood cells was determined with a Coulter counter. Means and standard deviations were calculated from the results obtained from 4 of the 12 rabbits whose rectal temperatures rose within 2 h; means and standard deviations were also calculated from results obtained from the remaining 8 rabbits. The experiment was repeated using 0.1, 1, 3, and 10 μg/kg of dihydrocurvularin.

Effect on the Temperature Response of Repeated Treatment with Dihydrocurvularin—Each of the 12 rabbits that were injected with 3 μg/kg of dihydrocurvularin were reinjected with 3 μg/kg of dihydrocurvularin 24 h later, and their rectal temperatures were recorded at half-hour intervals for 12 h. At 2-d intervals for 2 weeks, each rabbit was reinjected with 3 μg/kg of dihydrocurvularin, and again their rectal temperatures were recorded at half-hour intervals for 12 h.

Effect of Lipopolysaccharide on the Temperature Rise Induced by Dihydrocurvularin—Each of six rabbits (group I) was injected with 3 μg/kg iv of dihydrocurvularin, and their rectal temperatures were measured at half-hour intervals for 12 h and again at 24 h as described above. Two days later each rabbit, and each of six additional rabbits (group II), received 1 μg/kg iv of lipopolysaccharide (*Escherichia coli* preparation, L-3129[8]), and their rectal temperatures were again recorded. Two days following their treatment with lipopolysaccharide each rabbit in group I was injected with 3 μg/kg iv of dihydrocurvularin and again their rectal temperatures were recorded at half-hour intervals as described. One week and 2 weeks later each rabbit in group I received 3 μg/kg iv of dihydrocurvularin, and each rabbit in group II received 1 μg/kg of lipopolysaccharide. Rectal temperatures were again recorded. Differential and white blood cell counts were made only on the rabbits that were treated with lipopolysaccharide.

REFERENCES

(1) F. A. H. Rice, *Proc. Soc. Exp. Biol. Med.*, **123,** 189 (1966).

(2) F. A. H. Rice, *J. Chem. Soc.*, **1971,** 2599.

(3) F. A. H. Rice, *J. Infect. Dis.*, **118,** 76 (1968).

(4) F. A. H. Rice and J. H. Darden, *J. Infect. Dis.*, **118,** 289 (1968).

(5) F. A. H. Rice, J. Connolly, K. Aziz, and J. D. McCurdy, *J. Infect. Dis.*, **123,** 117 (1971).

(6) F. A. H. Rice, J. D. McCurdy, and K. Aziz, *Proc. Soc. Exp. Biol. Med.*, **136,** 56 (1971).

(7) G. C. Fossati, D. Fumarola, E. Cerra, and E. Cavalieri, *Riv. Emoter. Immunoematol.*, **16,** 91 (1969).

(8) F. A. H. Rice and R. Ciavarra, *Proc. Soc. Exp. Biol. Med.*, **137,** 567 (1971).

(9) F. A. H. Rice, R. Ciavarra, and T. Borsos, *Proc. Soc. Exp. Biol. Med.*, **140,** 471 (1972).

(10) F. A. H. Rice, N. D. Das, and M-J. Koo, *Proc. Soc. Exp. Biol. Med.*, **141,** 222 (1972).

(11) F. A. H. Rice and M-J. Koo, *J. Immunol.*, **127,** 1601 (1981).

(12) F. A. H. Rice, J. Lepick, and P. Hepner, *Radiat. Res.*, **42,** 164 (1970).

(13) F. A. H. Rice and J. D. McCurdy, *J. Immunol.*, **128,** 1769 (1982).

(14) F. A. H. Rice and B. Shaikh, *Biochem. J.*, **116,** 709 (1970).

(15) F. A. H. Rice, B. Shaikh, and C. G. Chen, *Johns Hopkins Med. J.*, **135,** 336 (1974).

(16) F. A. H. Rice, J. D. McCurdy, and C. Oresajo, *Am. J. Physiol.*, **238,** E540 (1980).

(17) H. Raistrick and F. A. H. Rice, *J. Chem. Soc.*, **1971,** 3069.

(18) E. G. Young and F. A. H. Rice, *J. Lab. Clin. Med.*, **29,** 735 (1944).

(19) G. Smith, *Trans. Br. Mycol. Soc.*, **32,** 280 (1949).

[5] Whatman No. 1.

[6] Soxlet.

[7] LKB 9000.

[8] Sigma Chemical Co., St. Louis, Mo.

Laser Raman Investigation of Drug–Polymer Conjugates: Sulfathiazole–Povidone Coprecipitates

BARBARA A. BOLTON and PARAS N. PRASAD ˣ

Received June 6, 1983, from the *Department of Chemistry, State University of New York at Buffalo, Buffalo, NY 14214.* Accepted for publication April 12, 1984.

Abstract □ Laser Raman spectroscopy is used for the investigation of the drug-polymer conjugates, sulfathiazole-povidone. Specifically, Raman spectra, both in the lattice vibration and the intramolecular vibration regions, are used to characterize various polymorphic forms of sulfathiazole. It is found that sulfathiazole exists in two unsolvated forms, untreated sulfathiazole and another form grown from propanol. The crystals grown from ethanol include varying amounts of ethanol depending on the growth condition. The nature of the povidone-sulfathiazole coprecipitates of various compositions are studied. We find no evidence of any new polymorphic form of sulfathiazole in these coprecipitates. The coprecipitates are found to consist of one of the unsolvated forms of sulfathiazole.

Keyphrases □ Sulfathiazole-conjugate with povidone, laser Raman spectroscopy □ Povidone-conjugate with sulfathiazole, laser Raman spectroscopy

The potential of a polymer matrix to produce a high-energy form of a drug has been realized for a long time. Interest in drug-polymer conjugates stems from the fact that the bioavailability of a drug, and therefore its therapeutic utility, can be increased. The strength and the specificity of interactions between a drug and a polymer play important roles in determining the lattice energy of the drug-polymer conjugate and, thus, the dissolution rate of the drug. The dissolution rate of one drug-polymer conjugate, sulfathiazole-povidone, has been studied by Simonelli *et al.* (1, 2). Povidone produced a high-energy form of the drug which exhibited much faster dissolution than the previously known polymorphic forms of sulfathiazole. When a drug is present in a polymer matrix, its enhanced dissolution rate may be derived from any of the following: (*a*) chemical attachment to the polymer; (*b*) existence of a metastable form of the drug stabilized by specific interactions with polymer; (*c*) the reduction of particle size and crystallinity due to the presence of the polymer. For the sulfathiazole-povidone conjugate, the drug does not appear to chemically bond with the polymer (2). The nature and the effect of the sulfathiazole–povidone interaction on enhancement of dissolution rates is not fully understood.

In this paper we present the investigation of the sulfathiazole-povidone conjugate by the technique of laser Raman spectroscopy. Raman spectroscopy provides spectra of both lattice vibrations (phonons) and intramolecular vibrations (3-5). Phonon spectra provide valuable information on the crystalline interactions; they are used to characterize the crystalline modifications and the effect of various external perturbations (including interactions with a matrix). The intramolecular vibrations are used to study the chemical stability of the various forms (5). These probes are based on the principle that a physical transformation in the solid state shows a dominant effect on the phonon motions but only a small effect on the intramolecular vibrations. On the other hand, a chemical change leads to a change both in the phonon spectra and in the spectra of intramolecular vibrations (6).

Laser Raman spectroscopy was used for the following investigations of sulfathiazole and sulfathiazole-povidone conjugates: (*a*) to identify and characterize the various polymorphic forms of sulfathiazole; (*b*) to determine if povidone produces a high-energy polymorphic form of sulfathiazole that is different from the known polymorphic forms; (*c*) to study the nature and strength of interaction between the drug and the polymer.

EXPERIMENTAL SECTION

Sulfathiazole was grown from ethanol solution by using two different procedures: slow growth at room temperture to generate large crystals, or rapid growth from a warm ethanol solution. The latter method was used by Higuchi *et al.* to produce their polymorphic form I (7). Sulfathiazole was also grown from 1-propanol[1] (80°C and room temperature) and 2-butanol[2] (room temperature) solutions as well as from the melt. The sulfathiazole-povidone[3] conjugates were prepared by the alcohol-evaporation method described by Simonelli *et al.* (1).

Raman spectra were obtained using a double monochromator[4] and the 514.5-nm line of a coherent radiation argon ion laser. Spectra were taken at room temperatures. Direct current detection was used.

RESULTS AND DISCUSSIONS

Polymorphic Forms of Sulfathiazole—Higuchi *et al.* have reported two polymorphic forms of sulfathiazole (7). The recrystallization of sulfathiazole from a warm ethanol solution gave form I. The second form of sulfathiazole was obtained either from the melt, or from a 1-propanol or 2-butanol solution. The room temperature Raman phonon spectra of four sulfathiazole samples are shown in Fig. 1. The phonon spectra obtained were for untreated sulfathiazole (A), rapidly recrystallized from warm ethanol (B), slowly recrystallized from ethanol (C) and recrystallized from 1-propanol (D), respectively. Sulfathiazole B phonon spectra appear to correlate with the phonon spectra of the untreated sulfathiazole. But there are some notable differences. The weak band at 82.0 cm^{-1} of sulfathiazole A splits into a doublet at 81.5 and 89.5 cm^{-1} in the sulfathiazole B spectrum. Additionally, the doublet at 135.0 and 145.0 cm^{-1} in the sulfathiazole A spectrum shifts to 134.5 and 139.5 cm^{-1} for the ethanol-grown sample. We carefully compared the intramolecular vibrations of sulfathiazole A and sulfathiazole B. In the 200–650 cm^{-1} and 900–1600 cm^{-1} regions, the vibrational spectra of sulfathiazole B were essentially similar to that of sulfathiazole A. However, the spectral region 650–900 cm^{-1} showed the following changes (Fig. 2): an extra band was observed at 878.5 cm^{-1} in the sulfathiazole B spectrum; the 681.5, 733.0, and 838.0 bands of pure sulfathiazole shifted to 684.5, 730.0, and 842.5 cm^{-1}, respectively, in the sulfathiazole B spectrum. The observed internal vibration at 878.5 cm^{-1} was identified as belonging to the solvent, ethanol. When frequency shifts are small (<3 cm^{-1}) the interaction between two components is generally weak and of a van der Waals type. In the ethanol-grown sulfathiazole, the observed shifts were ≥3 cm^{-1}. These results may indicate specific interaction between the solvent and some functional group of the drug, *i.e.*, hydrogen bonding. Our analysis was not able to detect the O—H stretching of the ethanol due to its broad and weak nature. However, we found these ethanol-sulfathiazole crystals to be stable for >6 months.

The third phonon spectrum (Fig. 1C) is of sulfathiazole grown slowly from ethanol. New bands were observed at 22.0, 24.5, 27.5, 64.0, and 126.5 cm^{-1}. In addition to these extra features, a comparison of the 30–70 cm^{-1} region for the sulfathiazole B and the sulfathiazole C samples reveal shifts to higher frequencies in the sulfathiazole C spectrum. Again, an inspection of the intramolecular vibrations for the sulfathiazole C sample shows the ethanol band (~878 cm^{-1}) and shifting of bands in the spectral region from 650 to 900

[1] J. T. Baker Co.
[2] Aldrich Chemical Co.
[3] Mol. wt. 10,000; GAF Corp.
[4] Model 14018; Spex.

0022-3549/84/1200-1849$01.00/0
© 1984, American Pharmaceutical Association

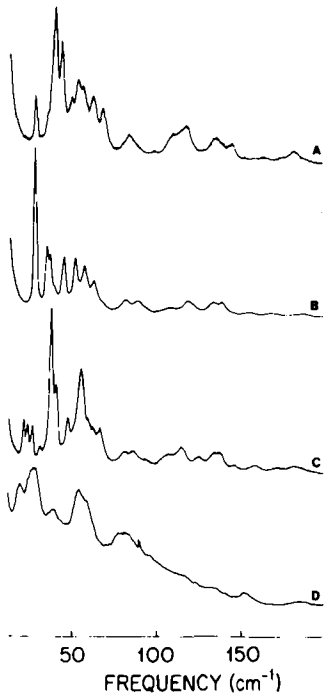

Figure 1—*Room temperature phonon spectra of four sulfathiazole samples. Key: (A) untreated sulfathiazole; (B) sulfathiazole rapidly recrystallized from warm ethanol; (C) sulfathiazole slowly recrystallized from ethanol; (D) sulfathiazole recrystallized from 1-propanol.*

cm^{-1}, similar to what was observed in the sulfathiazole B spectrum. We have also found that some ethanol-grown crystals exhibit phonon features which are in between that observed for sulfathiazole B and sulfathiazole C (*i.e.*, smaller shifts and fewer peaks than the sulfathiazole C spectrum). The ethanol band (~878 cm^{-1}) was present in all spectra of sulfathiazole grown from ethanol.

The results indicate that sulfathiazole incorporates the solvent (ethanol) into its crystal lattice and thus forms a solvate. The differences we observed in the phonon spectra of the various ethanol solvates may be due to varying intake of the solvent by the drug lattice. In other words, sulfathiazole and ethanol do not crystallize in one fixed stoichiometry.

The phonon spectrum of sulfathiazole grown from the 1-propanol solution is also shown (Fig. 1D). The phonon spectrum of this polymorph is distinctly different from the phonon spectra of sulfathiazole A or the ethanol solvates. Only five broad features are observed in the 10–100-cm^{-1} region. Identical broad phonon spectra were also obtained for crystals grown from the 2-butanol solution and from the melt. The intramolecular region 200–1600 cm^{-1} of the sulfathiazole D crystals were compared with that observed for sulfathiazole A. Some notable differences were observed: two new bands were observed at

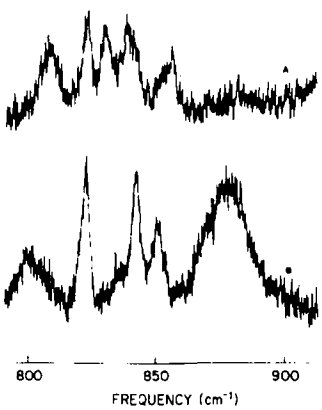

Figure 2—*The 800–900 cm^{-1} internal vibration regions are compared for the untreated sulfathiazole (A) and the sulfathiazole sample rapidly recrystallized from warm ethanol (B). In spectrum B, the broad peak at 878.5 cm^{-1} belongs to the solvent, ethanol.*

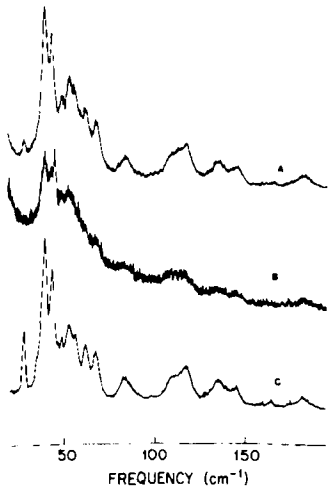

Figure 3—*Phonon spectra of the conjugates having sulfathiazole–povidone weight ratios of 10:1 (A) and 1:1 (B) are compared with the phonon spectra of untreated sulfathiazole (C).*

552.0 and 1502.0 cm^{-1} in the sulfathiazole D spectrum; the 304.0 and 649.5 cm^{-1} bands of pure sulfathiazole shifted to 288.0 and 656.5 cm^{-1} in the sulfathiazole D spectrum; the doublet, 632.5 and 638.5 cm^{-1}, in pure sulfathiazole shifted to 630.0 and 635.5 cm^{-1}. The extra features at 552.0 and 1502.0 cm^{-1} were also present in the 2-butanol-grown sulfathiazole spectra and in some of the drug–polymer conjugates (see next section) that were grown from ethanol. Thus, we do not attribute these new features to the solvent, 1-propanol. The appearance of new features and the shifting of peaks are believed to result from the formation of a different polymorph of sulfathiazole. From the broad nature of phonon bands, it appears that this polymorphic form is more disordered than the ethanol solvate.

Sulfathiazole–Povidone Conjugates—The phonon and the intramolecular vibrational spectra at room temperature were obtained for conjugates having sulfathiazole–povidone weight ratios of 10:1, 5:1, 3:1, 1:1, and 1:2. The phonon spectra of the conjugates 10:1, 1:1, and the sulfathiazole A sample are shown in Fig. 3. The phonon spectra of the 10:1 and 5:1 conjugates were essentially identical with that of sulfathiazole A. The only observable change is that the 27.5-cm^{-1} phonon band decreases in intensity as the weight ratio of sulfathiazole to povidone decrease. A decrease in the weight ratio of sulfathiazole to povidone appears to decrease the resolution of the phonon bands. This can be seen with the phonon spectrum of the 1:1 weight ratio. The 27.5 cm^{-1} transition is no longer visible. This poorly resolved spectrum still correlates with the spectrum of sulfathiazole A. The intramolecular vibrations of the 5:1 and 1:1 conjugates consisted of essentially unperturbed sulfathiazole bands. Also, the ethanol band (~878 cm^{-1}) was not present in either spectra. Therefore, we find no evidence of any chemical interaction between the drug and the polymer. Sulfathiazole appears in an unsolvated form even though the conjugate was precipitated from ethanol.

The phonon spectra of the conjugates 3:1, 1:2, and that of sulfathiazole grown from 1-propanol are shown in Fig. 4. The broad phonon features of the 3:1 conjugate correlates with those observed in the sulfathiazole D spectrum. The intramolecular vibrations of the 3:1 conjugate also correlate with the sulfathiazole D internal vibrations. Thus, sulfathiazole is present in the 3:1 conjugate as the polymorph grown from propanol. Again, no specific interactions between the polymer and the drug were observed.

The phonon spectrum of the 1:2 conjugate (Fig. 4) has a broad transition at 48 cm^{-1} and a weak broad feature at 57 cm^{-1}. While the phonon region of povidone is not shown in Fig. 4, the phonon spectrum of the 1:2 conjugate correlates with that of povidone. Thus, at ratios ≥1:2, the phonon spectra are dominated by povidone. With the lower ratios of sulfathiazole to povidone, the intermolecular vibrations of sulfathiazole were so weak that even the most intense vibrations were barely visible. No correlation of the 1:2 conjugate spectrum could be made. A 1:1 conjugate was prepared by rapidly cooling a sulfathiazole–povidone solution. The phonon spectrum of this conjugate was also dominated by povidone. However, the intramolecular vibrations were observed. Sulfathiazole was present in the 1:1 conjugate as the polymorphic form obtained from 1-propanol.

Simonelli *et al.* have correlated the dissolution rates of sulfathiazole–povidone conjugates to povidone weight fractions (2). They found two plateaus at low povidone weight fractions. They concluded that the lower plateau (lower dissolution rate) resulted from form I (sulfathiazole grown from warm ethanol) being present in the drug–polymer conjugates. Our results of the phonon

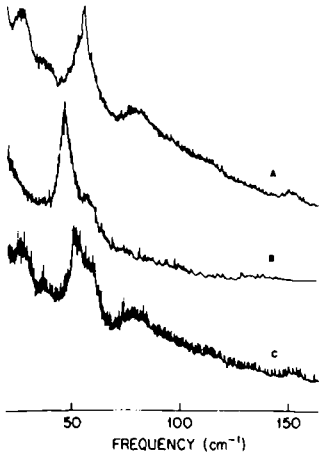

Figure 4—*Phonon spectra of the conjugates having sulfathiazole–povidone weight ratios of 3:1 (A) and 1:2 (B) are compared with that of sulfathiazole grown from propanol (C).*

and intramolecular vibrations have shown that at low povidone weight fractions (10:1, 5:1, and 1:1 conjugates), sulfathiazole was not present as the ethanol solvate but as the unsolvated sulfathiazole. In the sulfathiazole–povidone conjugate region 3:1–1:1.5, a second (higher dissolution rates) plateau was observed. Simonelli *et al.* postulated that the initial rate of dissolution exhibited at the higher plateau could rise from the presence of a new higher energy form of sulfathiazole. However, this higher energy form of sulfathiazole exhibited much faster dissolution than the previously known polymorphic forms of sulfathiazole. In the sulfathiazole–povidone region 3:1–1:1, we observed two different kinds of phonon and intramolecular spectra, one belonging to the sulfathiazole A form and the other being the polymorphic form obtained from propanol. The method of preparation (*i.e.*, temperature and/or concentration of solution) probably determines which of the two forms of sulfathiazole is present in the conjugates with drug–polymer ratios of 3:1–1:1.5. No other crystalline forms of sulfathiazole were observed in the drug–polymer conjugates. We therefore attribute the higher dissolution rate observed to arise from the particle size reduction of the drug in the presence of the polymer, whereby the increased effective surface area leads to an enhanced dissolution rate.

REFERENCES

(1) A. P. Simonelli, S. C. Mehta, and W. I. Higuchi, *J. Pharm. Sci.*, **58,** 538 (1969).

(2) A. P. Simonelli, S. C. Mehta, and W. I. Higuchi, *J. Pharm. Sci.*, **65,** 355 (1976).

(3) J. C. Bellows, F. P. Chen, and P. N. Prasad, *Drug Dev. Ind. Pharm.*, **3,** 451 (1977).

(4) D. E. Resetarits, K. C. Cheng, B. A. Bolton, P. N. Prasad, E. Shefter, and T. R. Bates, *Int. J. Pharm.*, **2,** 113 (1979).

(5) B. A. Bolton and P. N. Prasad, *J. Pharm. Sci.*, **70,** 789 (1981).

(6) P. N. Prasad, J. Swiatkiewicz, and G. Eisenhardt, *Appl. Spectrosc. Rev.*, **18,** 59 (1982).

(7) W. I. Higuchi, P. D. Bernardo, and S. C. Mehta, *J. Pharm. Sci.*, **56,** 200 (1967).

ACKNOWLEDGMENTS

This research was supprted by Air Force Office of Scientific Research Grant AFOSR 820118.

Electrostatic Effects in Acylation of Hemoglobin by Aspirins

SOLOMON E. MASSIL, GUEY-YUEH SHI, and IRVING M. KLOTZ ˣ

Received October 24, 1983, from the *Department of Chemistry, Northwestern University, Evanston, IL 60201.* Accepted for publication April 11, 1984.

Abstract □ Carboxylate substituents added to the salicylate ring increase the effectiveness of a variety of aspirins and diaspirins in acylating hemoglobin. Even more effective are a series of monoesters of dicarboxylate derivatives. Bis(5-carbomethoxysalicyl)fumarate and -succinate at 5 mM concentrations modify ~100% of the hemoglobin in solution and should alter the aggregation behavior of sickle hemoglobin.

Keyphrases □ Diaspirin—hemoglobin, sickle cell anemia, carboxylate substituents □ Hemoglobin—carboxylate-substituted diaspirins, acylation, sickle cell anemia

Previous studies have shown that aspirin and its analogues are capable of acylating hemoglobin (1). Acetylsalicylate, the prototype monoester, tends to transfer its acetyl group largely to the βLys[1] 59 and βLys 144 residues. These are in areas of the protein with a high local concentration of cationic side chains; *e.g.*, βLys 59 is part of a surface constellation constituted of βLys residues 59, 61, 65, and 66. The double-headed bissalicylates, in turn, preferentially go to the β-cleft of hemoglobin. In this canyon, both β chains contribute their βVal 1, βHis 2, βLys 82, and βHis 143 residues to provide a highly cationic environment.

In view of these observations, it seemed likely that even greater acylation of hemoglobin might be achieved with salicylate esters carrying additional negative charges. Furthermore, different structural dispositions of anionic charges on the reagents might lead to alternative specificities in binding to and acylation of Lys residues in hemoglobin. These might be directed toward placing substituents near βVal 6 or near βPhe 85 or βLeu 88 of hemoglobin S, residues evidently at a contact interface in sickled hemoglobin (2, 3). Therefore, several aspirin analogues with added substituents, particularly anionic ones, have been prepared. These substances are members of different classes of compounds: substituted monosalicylates [substituted carboxyphenyl acetates (I–V)]; substituted bissalicylates of succinic acid [bis(substituted carboxyphenyl)succinates (VI, VII, X, and XI)], of fumaric acid [bis(substituted carboxyphenyl)fumarates (VIII and IX)], or of anhydromethylene citric acid [bis(substituted

[1] Key: (Lys) lysine; (Val) valine; (His) histidine; (Phe) phenylalanine; (Leu) leucine.

0022-3549/84/1200-1851$01.00/0
© 1984, American Pharmaceutical Association

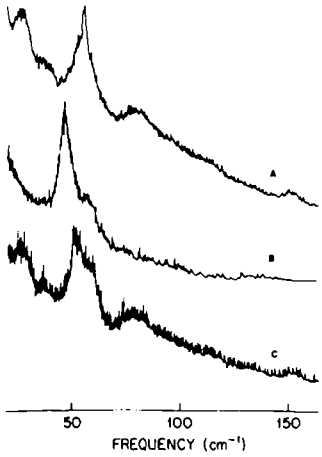

Figure 4—*Phonon spectra of the conjugates having sulfathiazole–povidone weight ratios of 3:1 (A) and 1:2 (B) are compared with that of sulfathiazole grown from propanol (C).*

and intramolecular vibrations have shown that at low povidone weight fractions (10:1, 5:1, and 1:1 conjugates), sulfathiazole was not present as the ethanol solvate but as the unsolvated sulfathiazole. In the sulfathiazole–povidone conjugate region 3:1–1:1.5, a second (higher dissolution rates) plateau was observed. Simonelli *et al.* postulated that the initial rate of dissolution exhibited at the higher plateau could rise from the presence of a new higher energy form of sulfathiazole. However, this higher energy form of sulfathiazole exhibited much faster dissolution than the previously known polymorphic forms of sulfathiazole. In the sulfathiazole–povidone region 3:1–1:1, we observed two different kinds of phonon and intramolecular spectra, one belonging to the sulfathiazole A form and the other being the polymorphic form obtained from propanol. The method of preparation (*i.e.*, temperature and/or concentration of solution) probably determines which of the two forms of sulfathiazole is present in the conjugates with drug–polymer ratios of 3:1–1:1.5. No other crystalline forms of sulfathiazole were observed in the drug–polymer conjugates. We therefore attribute the higher dissolution rate observed to arise from the particle size reduction of the drug in the presence of the polymer, whereby the increased effective surface area leads to an enhanced dissolution rate.

REFERENCES

(1) A. P. Simonelli, S. C. Mehta, and W. I. Higuchi, *J. Pharm. Sci.*, **58,** 538 (1969).

(2) A. P. Simonelli, S. C. Mehta, and W. I. Higuchi, *J. Pharm. Sci.*, **65,** 355 (1976).

(3) J. C. Bellows, F. P. Chen, and P. N. Prasad, *Drug Dev. Ind. Pharm.*, **3,** 451 (1977).

(4) D. E. Resetarits, K. C. Cheng, B. A. Bolton, P. N. Prasad, E. Shefter, and T. R. Bates, *Int. J. Pharm.*, **2,** 113 (1979).

(5) B. A. Bolton and P. N. Prasad, *J. Pharm. Sci.*, **70,** 789 (1981).

(6) P. N. Prasad, J. Swiatkiewicz, and G. Eisenhardt, *Appl. Spectrosc. Rev.*, **18,** 59 (1982).

(7) W. I. Higuchi, P. D. Bernardo, and S. C. Mehta, *J. Pharm. Sci.*, **56,** 200 (1967).

ACKNOWLEDGMENTS

This research was supprted by Air Force Office of Scientific Research Grant AFOSR 820118.

Electrostatic Effects in Acylation of Hemoglobin by Aspirins

SOLOMON E. MASSIL, GUEY-YUEH SHI, and IRVING M. KLOTZ ˣ

Received October 24, 1983, from the *Department of Chemistry, Northwestern University, Evanston, IL 60201.* Accepted for publication April 11, 1984.

Abstract □ Carboxylate substituents added to the salicylate ring increase the effectiveness of a variety of aspirins and diaspirins in acylating hemoglobin. Even more effective are a series of monoesters of dicarboxylate derivatives. Bis(5-carbomethoxysalicyl)fumarate and -succinate at 5 mM concentrations modify ~100% of the hemoglobin in solution and should alter the aggregation behavior of sickle hemoglobin.

Keyphrases □ Diaspirin—hemoglobin, sickle cell anemia, carboxylate substituents □ Hemoglobin—carboxylate-substituted diaspirins, acylation, sickle cell anemia

Previous studies have shown that aspirin and its analogues are capable of acylating hemoglobin (1). Acetylsalicylate, the prototype monoester, tends to transfer its acetyl group largely to the βLys[1] 59 and βLys 144 residues. These are in areas of the protein with a high local concentration of cationic side chains; *e.g.*, βLys 59 is part of a surface constellation constituted of βLys residues 59, 61, 65, and 66. The double-headed bissalicylates, in turn, preferentially go to the β-cleft of hemoglobin. In this canyon, both β chains contribute their βVal 1, βHis 2, βLys 82, and βHis 143 residues to provide a highly cationic environment.

In view of these observations, it seemed likely that even greater acylation of hemoglobin might be achieved with salicylate esters carrying additional negative charges. Furthermore, different structural dispositions of anionic charges on the reagents might lead to alternative specificities in binding to and acylation of Lys residues in hemoglobin. These might be directed toward placing substituents near βVal 6 or near βPhe 85 or βLeu 88 of hemoglobin S, residues evidently at a contact interface in sickled hemoglobin (2, 3). Therefore, several aspirin analogues with added substituents, particularly anionic ones, have been prepared. These substances are members of different classes of compounds: substituted monosalicylates [substituted carboxyphenyl acetates (I–V)]; substituted bissalicylates of succinic acid [bis(substituted carboxyphenyl)succinates (VI, VII, X, and XI)], of fumaric acid [bis(substituted carboxyphenyl)fumarates (VIII and IX)], or of anhydromethylene citric acid [bis(substituted

[1] Key: (Lys) lysine; (Val) valine; (His) histidine; (Phe) phenylalanine; (Leu) leucine.

0022-3549/84/1200-1851$01.00/0
© 1984, American Pharmaceutical Association

carboxyphenyl)4-oxo-1,3-dioxolane-5,5-diacetate (XII–XV)]. The extent of modification of hemoglobin by these compounds has been explored.

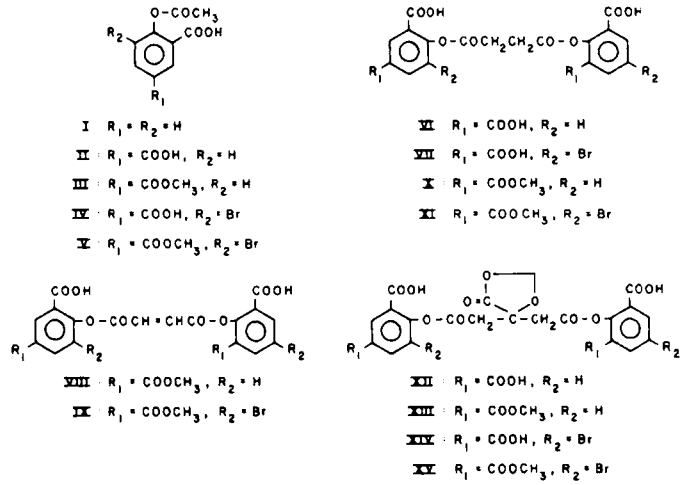

RESULTS AND DISCUSSION

Chemistry—Some of the compounds (Table I) proved to be very elusive. One of the key intermediates, 4-hydroxy-5-bromo-isophthalic acid monomethyl ester could not be obtained from the diester by conventional methods (4), which in this case produced the diacid. However, the simple procedure of stirring the diester in an appropriate alkaline solution yielded the desired monoester, from which V and IX could be prepared. The bisfumarates of the diacids 4-hydroxy-isophthalic and its 5-bromo analogue were so sensitive to traces of water in the environment that they could not be isolated even though their presence was established (TLC) in the dry solvent in which their synthesis was carried out. In contrast, the corresponding monoesters were comparatively stable.

As mentioned previously (5), the methylene citrate derivatives had to be protected under petroleum ether in the cold, but they were sufficiently stable to carry out modification experiments if they were added quickly to the hemoglobin solution.

Activity—A comparison (Table I) of aspirin (I) with its doubly anionic analogue 4-(acetyloxy)-1,3-benzenedicarboxylic acid (II) shows that the extent of modification of hemoglobin is significantly greater for the latter. This increase was expected for the doubly charged reagent. To our surprise, however, the monomethyl ester, 4-(acetyloxy)-1,3-benzenedicarboxylic acid 1-methyl ester (III), is much more effective than either analogue I or II. We conclude, therefore, that the presence of the added carbomethoxy moiety is much more influential than the additional charge. Evidently this second electron-withdrawing group in the *para* position to the acetoxy substituent activates the latter substantially so that it is much more effective in transferring its acetyl radical to the hemoglobin. The dipole of the $-COOCH_3$ moiety may also provide some electrostatic interaction with a cationic locus on the protein.

A bromo substituent on the aromatic ring, producing IV, also increases effectiveness (compared with II) of the aspirin analogue in modifying hemoglobin. This effect of the polarizable bromine atom has been seen previously (1). A particularly marked increase in modification is manifested with the monoanionic monoester V, the bromo analogue of III. Again we see that the *para* carbomethoxy substituent has a marked activating effect on the acetoxy group.

Turning to the bissalicylates, we find similar substituent effects, even more marked in these diaspirins. Bissalicyl succinate, the single-COOH reference analogue of VI, at 5 mM concentration modifies ~15% of hemoglobin (1, 6). In contrast, the additional —COOH provided by VI increases the degree of modification to almost 80%. An additional bromo substituent increases the reactivity even further, as is evident with VII (Table I).

It has been shown previously (5, 6) that the fumarate diaspirin, bis(2-carboxyphenyl)fumarate, is more effective than the corresponding salicylate derivative. This superiority is maintained in the present series of compounds. Thus, VIII is more reactive than X, and IX is better than XI. With all of these compounds the extent of modification of hemoglobin is very high.

In the methylene citric acid series (XII–XV), the beneficial effects of the $-COOCH_3$ substituent continue to be expressed. Thus, XIII is superior to XII, and XV is better than XIV.

The shifts in p_{50} values (oxygen pressure at half-saturation of hemoglobin) provide some insight into the location of the acyl group affixed by the aspirin

Table I—Modification of Hemoglobin by Salicylates

Compound	Conc., mM	Percent Modification of Oxyhemoglobin A, 1 mM	p_{50} for Oxygen Binding, mm Hg: Without Inositol Hexaphosphate	p_{50} for Oxygen Binding, mm Hg: With 2 mM Inositol Hexaphosphate
None	—	—	5	40
Aspirin; 2-(acetyloxy)-benzoic acid (I)	20	26	5	34
	10	15	4	35
	5	8	4	36
4-(Acetyloxy)-1,3-benzenedicarboxylic acid (II)[a]	20	39	5	21
	10	23	4	30
	5	10	4	36
4-(Acetyloxy)-1,3-benzenedicarboxylic acid 1-methyl ester (III)	10	70	5	22
	5	43	5	32
4-(Acetyloxy)-5-bromo-1,3-benzenedicarboxylic acid (IV)	10	68	7	28
	5	48	7	36
4-(Acetyloxy)-5-bromo-1,3-benzenedicarboxylic acid 1-methyl ester (V)	10	83	7	20
	5	60	7	28
Bis(2,4-dicarboxyphenyl)-succinate (VI)[b,f]	5	78	6	14
	1	31	6	38
Bis(6-bromo-2,4-dicarboxyphenyl)succinate (VII)[b,c,f]	5	86	5	11
		86	6	12
	1	46	6	40
		39	7	35
Bis(4-carbomethoxy-2-carboxyphenyl)-fumarate (VIII)[b,f]	5	97	6	7
	1	45	7	36
Bis(6-bromo-4-carbomethoxy-2-carboxyphenyl)-fumarate (IX)[b,d,f]	5	98	4	7
		100		
		100		
	1	61	5	26
		49		
		58		
Bis(4-carbomethoxy-2-carboxyphenyl)-succinate (X)[b,f]	5	77	7	12
		81		
	1	33	6	39
		34		
Bis(6-bromo-4-carbomethoxy-2-carboxyphenyl)-succinate (XI)[b,e,f]	5	63	6	24
		74		
	1	17	6	37
		24		
Bis(2,4-dicarboxyphenyl)4-oxo-1,3-dioxolane-5,5-diacetate (XII)	5	41	6	33
	1	13	7	39
Bis(4-carbomethoxy-2-carboxyphenyl)4-oxo-1,3-dioxolane-5,5-diacetate (XIII)	5	76	7	23
	1	34	7	38
Bis(6-bromo-2,4-dicarboxyphenyl)4-oxo-1,3-dioxolane-5,5-diacetate (XIV)	5	40	6	34
	1	15	7	38
Bis(6-bromo-4-carbomethoxy-2-carboxyphenyl)-4-oxo-1,3-dioxolane-5,5-diacetate (XV)	5	94	6	23
	1	42	7	38

[a] Some qualitative experiments with this compound have been described by Kokkini *et al.* (11). [b] Satisfactory analytical data (±0.4% for C, H) were reported for each of these compounds. [c] Calc. for Br, 26.44; found, 25.82. [d] Calc. for Br, 25.36; found 24.91. [e] Calc. for Br, 25.28; found 24.83. [f] Melting points (°C): VI, 228–230; VII, 212–213; VIII, 200–202; IX, 233–235; X, 179–181; XI, 178–180.

reagent. If p_{50} is shifted back to near 40 mm (Table I) when inositol hexaphosphate is added to the hemoglobin solution, then this effector is clearly able to enter the β-cleft of the protein to shift the conformation to the low-affinity form. As has been shown previously (1), the diaspirins are capable of denying inositol phosphate access to the β-cleft by forming a covalent blocking bridge across the portal. It is apparent that these features of the double-headed aspirins are maintained in the current series of compounds (VI–XI), all of which, at least at a concentration of 5 mM, keep p_{50} from returning to the normal value in the presence of inositol hexaphosphate. The

two most striking agents in this regard are the monomethyl esters VIII and IX, which at 5 mM concentration keep p_{50} in the presence of inositol hexaphosphate at essentially the same value as in its absence. Thus, these two compounds are essentially 100% effective in blocking access to the β-cleft. The bis(carbomethoxysalicyl)fumarate (VIII), devoid of the bromo substituent, should be a particularly attractive compound from a pharmacological viewpoint for testing as an antisickling agent.

EXPERIMENTAL SECTION[2]

3-Bromo-5-carbomethoxy Salicylic Acid—Partial hydrolysis of 5-bromo-4-hydroxy-isophthalic acid dimethyl ester was affected by stirring the mixture of diester (2.0 g) with 25 mL of 33% KOH in methanol and 25 mL of water for several hours at room temperature. The unchanged diester in suspension was removed by filtration. The filtrate was cooled and acidified with 1 M HCl. The resulting precipitate was removed by filtration and then recrystallized from dilute ethanol to give the monoester, mp 237–238°C. IR: 1720 cm^{-1}; ^{1}H-NMR (Me_2SO-d_6): δ 3.85 (3, s, —$COOCH_3$) and 8.0–8.4 ppm (2, t, ArH).

Anal.—Calc. for $C_9H_7BrO_5$: C, 39.30; H, 2.57; Br, 29.05. Found: C, 39.34; H, 2.58; Br, 29.18.

Preparation of Substituted Isophthalic Acids and Methyl Esters—*4-(Acetoxy)-isophthalic Acid (II) and 4-Acetoxy-isophthalic Acid 1-Methyl Ester (III)*—These compounds were prepared as described in the literature (4).

4-(Acetoxy)-5-bromo-isophthalic Acid (IV)—Compound IV was prepared in a manner similar to that in the literature (4) for II and was recrystallized from chloroform–petroleum ether, mp 197–199°C. ^{1}H-NMR (Me_2SO-d_6): δ 2.45 (3, s, —$OCOCH_3$), 8.4 (2, t, ArH), and 11.61 ppm (br s, 2, 2-COOH).

Anal.—Calc. for $C_{10}H_7BrO_6$: C, 39.63; H, 2.33. Found: C, 39.74; H, 2.32.

4-Acetoxy-5-bromo-isophthalic Acid Monomethyl Ester (V)—Ester V was also prepared by a procedure (4) analogous to that used for III and was recrystallized from chloroform–petroleum ether, mp 133–135°C. IR: 1725 cm^{-1}; ^{1}H-NMR ($CDCl_3$-Me_2SO-d_6): δ 2.37 (3, s, —$OCOCH_3$), 3.92 (3, s, $COOCH_3$), and 8.34–8.53 ppm (2, d, ArH).

Anal.—Calc. for $C_{11}H_9BrO_6$: C, 41.67; H, 2.86; Br, 25.20. Found: C, 41.40; H, 2.80; Br, 25.75.

General Method for the Synthesis of Bissuccinates (VI and VII)—Sodium hydride (0.06 mol) was added to a solution of substituted salicylic acid (0.02 mol) in 30 mL of dry tetrahydrofuran, and the mixture was stirred overnight at room temperature. Succinyl chloride (0.01 mol) was dissolved in a minimum quantity of tetrahydrofuran (~5 mL) and added in a dropwise manner, over a period of 0.5 h, to the stirred suspension of sodium salt of the substituted salicylate. The resulting mixture was further stirred for an additional day. After removal of solvent under reduced pressure, the gummy residue was treated with ethyl acetate and acidified with aqueous 1 M HCl while being cooled in an ice bath. The organic layer was removed, washed with cold saturated NaCl solution, and dried over $MgSO_4$. After removal of solvent, the residue was recrystallized from a mixture of ethyl acetate–petroleum ether. Properties of the compounds obtained (VI and VII) are summarized in Table I.

General Method for the Synthesis of Bisfumarates and Bissuccinates (VIII–XI)—To a stirred mixture of substituted salicylic acid (2.0 mmol) and *N,N*-dimethylaniline (6.2 mmol) in 80 mL of dry benzene was added in a dropwise manner fumaryl or succinyl chloride (1.02 mmol) dissolved in 20 mL of benzene. The resultant mixture was stirred overnight at room temperature. After removal of the solvent under reduced pressure, the residue was suspended in 50 mL of ethyl acetate and extracted several times with ice-cold 1 M HCl (50 mL) and once with water (50 mL). The organic layer was dried ($MgSO_4$), filtered, and evaporated under reduced pressure. The residue was further recrystallized from either ethanol or a mixture of ethyl acetate–petroleum ether. The compounds obtained (VIII–XI) are listed in Table I. ^{1}H-NMR spectra were consistent with the structures.

General Method for the Synthesis of Biscitrates (XII–XV)—The preparations of XII–XV were described in a previous publication (5).

Hemoglobin Experiments—Whole blood (with anticoagulant) was obtained from local hospitals. Hemolysate was prepared by the method of Drabkin (7) except that chloroform was used to facilitate separation of the membranes. Hemolysate from normal adults was used without further purification. After freezing in liquid nitrogen, the hemolysate and hemoglobin samples were stored at −80°C. Hemoglobin concentrations in solution were measured after conversion to the cyanomet derivative (8).

Chemical modifications with the acylating compounds were performed with 1–5-fold molar ratio of reagent to hemoglobin for the bissalicylate esters and with a 5–20-fold molar excess for the monosalicylates. The reactions were carried out in 0.1 M Tris-HCl buffer, pH 7.3, which the hemoglobin had been dialyzed against. All reactions were performed with oxyhemoglobin. Modification reactions were initiated by suspending the compound in buffer, partially dissolving it, and adding hemoglobin within 30 s. Stirring was continued for 2 h at 37°C. The reaction mixture was then dialyzed overnight against cold 0.13 M glycine (pH 6.0).

The extent of modification of the hemoglobin was assessed by isoelectric focusing (9, 10) in a flat gel[3] using the procedures described by the manufacturer, with the following alterations. A 1-mm gel (instead of 3 mm) was prepared between a glass plate (bottom) and a piece of plexiglass (top) with a polytef gasket between plates. The gel composition for 100 mL of solution was 4 g (0.56 M) of acrylamide[4], 0.16 g (0.01 M) of *N,N'*-methylenebisacrylamide[5], 5 g (0.54 M) of glycerol, 5.4 mL of ampholytes, pH 6.5–9[6], 1.8 mL of ampholytes, pH 6–8[7], 0.05 g (4.3 mM) of *N,N,N',N'*-tetramethylethylenediamine[4], and 0.05 g (2.2 mM) of ammonium persulfate[8]. All hemoglobin samples were saturated with gaseous CO and made 0.01 M in NaCN; 2.5 μL was then applied to the gel surface on small pieces of filter paper. The anolyte was 1 M H_3PO_4; 2 M NaOH served as catholyte. Isoelectric focusing was carried out at 10°C for ~90 min with a power level of 30 W. Immediately after the power was turned off, the gel was fixed in an aqueous solution of 10 g/100 mL (0.6 M) of trichloroacetic acid[9] and 6 g/100 mL (0.2 M) of 5-sulfosalicylic acid[10] for 20–30 min, and then placed for 30–60 min in a preservative solution of water–ethanol–acetic acid–glycerol (35:5:1:1). After the gel had dried overnight, the modification pattern in each reaction channel was analyzed by recording a densitometric scan with a soft laser scanning densitometer with an integrator[11]. Oxygen affinities of chemically modified and unmodified hemoglobins were determined in the presence and in the absence of 2 mM inositol hexaphosphate[12] using an oxygenator[13].

REFERENCES

(1) I. M. Klotz, D. N. Haney, and L. C. King, *Science*, **213**, 724 (1981).

(2) B. C. Wishner, K. B. Ward, E. E. Lattman, and W. E. Love, *J. Mol. Biol.*, **98**, 179 (1975).

(3) B. Magdoff-Fairchild and C. C. Chiu, *Proc. Natl. Acad. Sci. USA*, **76**, 223 (1979).

(4) S. E. Hunt, J. I. Jones, and A. S. Lindsey, *J. Chem. Soc.*, **1956**, 3099.

(5) S. E. Massil, G.-Y. Shi, and I. M. Klotz, *J. Pharm. Sci.*, **73**, 418 (1984).

(6) R. H. Zaugg, J. A. Walder, R. Y. Walder, J. M. Steele, and I. M. Klotz, *J. Biol. Chem.*, **255**, 2816 (1980).

(7) D. L. Drabkin, *J. Biol. Chem.*, **164**, 703 (1946).

(8) O. W. Van Assendelft, "Spectrophotometry of Haemoglobin Derivatives," Charles C Thomas, Springfield, Ill., 1970.

(9) H. F. Bunn, *Ann. N.Y. Acad. Sci.*, **209**, 345 (1973).

(10) P. G. Righetti and J. W. Drysdale, in "Laboratory Techniques in Biochemistry and Molecular Biology," vol. 5, Part 2, T. S. Work and E. Work, Eds., Elsevier, Amsterdam, 1976.

(11) G. Kokkini, K. K. Bhargava, L. J. Benjamin, R. W. Grady, C. M. Peterson, and A. Cerami, in "Development of Therapeutic Agents for Sickle Cell Disease," J. Rosa, Y. Beuzard, and J. Hercules, Eds., Elsevier/North Holland, Amsterdam, 1979, pp. 111–117.

ACKNOWLEDGMENTS

This work was supported in part by Grant No. HL-22719 from the National Heart, Lung, and Blood Institute of the National Institutes of Health. S.E.M. was on leave from Makhteshim Chemical Works, Ltd., Beer-Sheva, Israel.

[2] Elemental analyses were performed by Micro-Tech Laboratories, Skokie, Ill. IR spectra were obtained with a Perkin-Elmer 283 spectrometer. ^{1}H-NMR spectra were recorded using Varian EM-360 (60 MHz) and JEOL-FX-270 spectrometers, and chemical shifts are listed as δ values in ppm relative to $(CH_3)_4Si$ as internal standard. Melting points were determined with a Buchi capillary apparatus and are uncorrected. The 4-hydroxy-isophthalic acid (or 5-carboxysalicylic acid) used herein as a starting material was purchased from the Chemolog Co., N.Y.

[3] LKB 2117 Multiphor instrument with a Savant power source.
[4] Eastman.
[5] Aldrich Chemical Co.
[6] Pharmacia.
[7] LKB.
[8] Bio-Rad.
[9] Mallinckrodt.
[10] Baker.
[11] Zeineh; BioMed Instruments.
[12] Sigma Chemical Co.
[13] Hemoscan; American Instruments.

Bromo-6-methoxy-8-aminoquinolines: Preparation and ^{13}C-NMR Assignments

JAMES D. McCHESNEY ˣ, S. SARANGAN, and CHARLES D. HUFFORD

Received April 26, 1982, from the *Department of Pharmacognosy, School of Pharmacy, The University of Mississippi, University, MS 38677.* Accepted for publication January 25, 1984.

Abstract □ Preparation of all possible monobromo-6-methoxy-8-aminoquinolines is reported. These materials provided an opportunity to assess the effect of bromine substitution on ^{13}C-NMR chemical shift patterns. An explanation of the isomerization of 5-bromo-6-methoxy-8-acetamidoquinoline to 7-bromo-6-methoxy-8-aminoquinoline during hydrolysis is presented.

Keyphrases □ Bromine substitution—^{13}C-NMR chemical shifts, bromoaminoquinoline isomerization □ Bromoaminoquinolines—^{13}C-NMR chemical shifts, isomerization, bromine substitution

Various isomers of bromo-6-methoxy-8-aminoquinoline were required as intermediates in connection with syntheses of deuterated derivatives of the antimalarial drug primaquine (I) (1). Primaquine, 6-methoxy-8-(4-amino-1-methylbutyl)-aminoquinoline, is used for the radical cure of vivax malaria and, in combination with other antimalarial drugs such as chloroquine, for prophylaxis in endemic areas (2).

An obvious route of preparation of these bromoaminoquinolines should involve the reduction of the corresponding bromo nitro compounds. Examination of the literature showed that while 3-bromo-6-methoxy-8-aminoquinoline had indeed been prepared by this method (3), the 5-bromo derivative had been obtained by the bromination of 6-methoxy-8-acetaminoquinoline and the subsequent hydrolysis of the acetyl group (4). Reduction of 5-bromo-6-methoxy-8-nitroquinoline gave poor yields of the amino compound (4). The 7-bromo compound was prepared by a rather unusual transformation of the 5-bromo derivative in refluxing 10% hydrobromic acid (4). The 2- and 4-bromo derivatives have not been previously reported.

The present work describes the preparation of these two unknown compounds as well as a study of the ^{1}H- and ^{13}C-NMR spectra of all these monobromo and the 5,7-dibromo-6-methoxy-8-aminoquinolines. In addition we have reexamined the unusual transformation of the 5-bromo isomer into the 7-bromo material. The reduction of the various bromo-8-nitroquinolines was examined to develop an efficient nitro reduction without accompanying debromination.

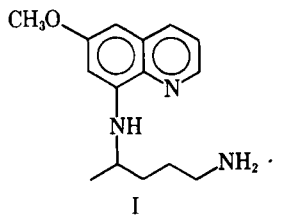

I

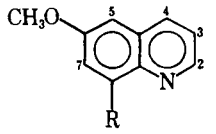

II: R = NO_2
III: R = NO_2, 2-Br
IV: R = NO_2, 3-Br
V: R = NO_2, 4-Br
VI: R = NH_2
VII: R = NH_2, 2-Br
VIII: R = NH_2, 3-Br
IX: R = NH_2, 4-Br
X: R = NH_2, 5-Br
XI: R = NH_2, 7-Br
XII: R = NH_2, 5-Br, 7-Br
XIII: R = $NHCOCH_3$, 2-Br

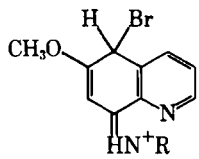

EXPERIMENTAL SECTION[1]

6-Methoxy-8-nitroquinoline (II)—Nitrobenzene (50 mL) was added slowly with stirring to fuming sulfuric acid (30% sulfur trioxide, reagent grade, 150 mL) at room temperature. The mixture was stirred at 60–65°C for ~8 h (until a drop of the mixture was found to be miscible when poured into water). The "sulfo mix" (5) was then added slowly with vigorous stirring to a paste of 2-nitro-4-methoxyaniline (85 g, 0.5 mol), glycerol (230 g, 2.5 mol), and water (230 mL). The resulting mixture was heated gradually in an oil bath to 130–135°C and kept at that temperature for 6 h. The color of the mixture changed from orange-red to dark brown. The mixture was allowed to cool, was poured into crushed ice, and then neutralized with 10% NaOH. The solid material was removed by filtration, washed with water, and dried. Recrystallization from chloroform gave 64.0 g (63% yield) of II as straw-colored crystals, mp 158–160°C [lit. (6) mp 158–160°C].

2-Bromo-6-methoxy-8-nitroquinoline (III)—1-Methyl-6-methoxy-8-nitroquinoline-2-one (7) (7.0 g, 0.03 mol) and phosphorus oxybromide (17.3 g, 0.113 mol) were heated at 120–125°C for 6 h. The mixture was cooled, poured into crushed ice, and neutralized with excess ammonium hydroxide. The pale-yellow solid was removed by filtration, washed, and dried. Recrystallization from ethanol gave 6.7 g (80% yield) of III as pale-yellow needles, mp 228–230°C.

Anal.—Calc. for $C_{10}H_7BrN_2O_3$: C, 42.23; H, 2.49; N, 9.89. Found: C, 42.08; H, 2.60; N, 9.90.

4-Bromo-6-methoxy-8-nitroquinoline (V)—In a similar manner, 4-hydroxy-6-methoxy-8-nitroquinoline (3.3 g, 0.015 mol) (8) was treated with phosphorus oxybromide (5.8 g, 0.02 mol) in quinoline to give V as yellow crystals (chloroform), 3.1 g (64% yield), mp 191–193°C.

Anal.—Calc. for $C_{10}H_7BrN_2O_3$: C, 42.23; H, 2.49; N, 9.89. Found: C, 42.52; H, 2.70; N, 10.20.

General Procedure for Nitro Group Reduction—The nitro compound (~10 mmol) was dissolved in concentrated hydrochloric acid (~30 mL), and the solution was cooled in an ice-salt bath. The ice-cold solution was added slowly with vigorous stirring to an ice-cold solution of stannous chloride (anhydrous, 98%, ~10 g) in 30 mL of concentrated hydrochloric acid. The resulting mixture was stirred at 0–5°C for 1 h and then poured into crushed ice. The mixture was made alkaline with concentrated ammonium hydroxide and extracted with ethyl acetate (5 × 50 mL). The combined organic layers were washed

[1] The ^{1}H-NMR spectra (90 MHz) were recorded on a Varian EM 390 spectrometer using Me_2SO-d_6 as solvent and tetramethylsilane as an internal standard. The ^{13}C-NMR spectra (15.03 MHz) were recorded on a JEOL-FX60 FT spectrometer using Me_2SO-d_6 as solvent and tetramethylsilane as internal standard. NMR data are reported as δ values (ppm). Mass spectra were obtained using a Finnigan 3200 GC–MS coupled to an INCOS data system. HPLC was accomplished on a μ-Bondapak C_{18} reverse-phase column and a mobile phase of 2.2 g of potassium dihydrogen phosphate, 3.3 g of potassium hydrogen phosphate, 1.2 L of distilled water, and 2.8 L of HPLC-quality methanol. TLC was accomplished on silica G (254) precoated plates; GC was done on base-deactivated 3% OV-17 packed on a 183 m × 0.6 cm o.d. glass column with flame-ionization detection on a Beckman GC-65, with a flow rate of 30 mL/min of nitrogen. All compounds gave satisfactory elemental analyses. Starting compounds were prepared by literature procedures or purchased from Aldrich unless otherwise noted.

0022-3549/84/1200-1854$01.00/0
© 1984, American Pharmaceutical Association

twice with water and once with saturated brine, dried over anhydrous sodium sulfate, and concentrated under reduced pressure. Recrystallization was from ethanol.

2-Bromo-6-methoxy-8-aminoquinoline (VII)—The aforementioned 2-bromo-6-methoxy-8-nitroquinoline (4.2 g, 0.015 mol) dissolved in concentrated hydrochloric acid (25 mL) was added to stannous chloride (15 g, 0.066 mol) dissolved in concentrated hydrochloric acid (25 mL). This afforded 3.44 g (90% yield) of colorless crystals, mp 88–90°C. ^{1}H-NMR: δ 8.00 (1, d, J = 8 Hz, H-4), 7.50 (1, d, J = 8 Hz, H-3), 6.51 (2, br s, H-5 and H-7), and 3.83 ppm (3, s, OCH_3); ^{13}C-NMR: 159.2 (s, C-6), 145.5 (s, C-8), 138.1 (d, C-4), 134.9 and 134.7 (s, C-2 and C-8), 128.8 (s, C-4a), 125.8 (d, C-3), 101.0 (d, C-7), 93.8 (d, C-5), and 55.1 ppm (q, OCH_3).

Anal.—Calc. for $C_{10}H_9BrN_2O$: C, 47.45; H, 3.58; N, 11.07. Found: C, 47.54; H, 3.68; N, 11.27.

3-Bromo-6-methoxy-8-aminoquinoline (VIII)—3-Bromo-6-methoxy-8-nitroquinoline (5.6 g, 0.02 mol) dissolved in concentrated hydrochloric acid (30 mL) was added to stannous chloride (20 g, 0.089 mol) dissolved in concentrated hydrochloric acid (30 mL). This afforded 4.57 g (90% yield) of colorless needles, mp 95–96°C [lit. (3) mp 95–96°C]. ^{1}H-NMR: δ 8.58 (1, d, J = 2 Hz, H-2), 8.31 (1, d, J = 2 Hz, H-4), 6.67 (1, d, J = 2 Hz, H-5 or H-7), 6.55 (1, d, J = 2 Hz, H-5 or H-7), and 3.91 ppm (3, s, OCH_3); ^{13}C-NMR: 159.8 (s, C-6), 146.3 (s, C-8), 144.6 (d, C-2), 135.7 (d, C-4), 132.8 (s, C-8a), 131.1 (s, C-4a), 117.5 (s, C-3), 100.4 (d, C-7), 93.0 (d, C-5), and 55.1 ppm (q, OCH_3).

4-Bromo-6-methoxy-8-aminoquinoline (IX)—The aforementioned 4-bromo-6-methoxy-8-nitroquinoline (4.2 g, 0.015 mol) dissolved in concentrated hydrochloric acid (25 mL) was added to stannous chloride (15 g, 0.066 mol) dissolved in concentrated hydrochloric acid (25 mL). The resulting mixture was stirred at 0–5°C for 1 h, poured into crushed ice, and neutralized to pH 8–9 with concentrated ammonium hydroxide. A solid (4-bromo-6-methoxy-8-aminoquinoline hydrochloride) separated and was removed by filtration and recrystallized from ethanol. This afforded 3.3 g (76% yield) of IX as pale-yellow needles, mp 98–100°C. ^{1}H-NMR: δ 8.35 (1, d, J = 5 Hz, H-2), 7.73 (1, d, J = 5 Hz, H-3), 6.63 (2, br s, H-5 and H-7), and 3.90 ppm (3, s, OCH_3); ^{13}C-NMR: 160.1 (s, C-6), 147.2 (s, C-8), 143.8 (d, C-2), 135.2 (s, C-8a), 131.3 (s, C-4), 129.0 (s, C-4a), 125.7 (d, C-3), 100.2 (d, C-7), 92.1 (d, C-5), and 55.1 ppm (q, OCH_3).

Anal.—Calc. for $C_{10}H_9BrN_2O$·HCl: C, 41.48; H, 3.48; N, 9.67. Found: C, 41.00; H, 3.00; N, 9.64.

5-Bromo-6-methoxy-8-aminoquinoline (X)—5-Bromo-6-methoxy-8-nitroquinoline (9) (1.5 g, 0.005 mol) dissolved in concentrated hydrochloric acid (10 mL) was added to stannous chloride (5 g, 0.022 mol) dissolved in concentrated hydrochloric acid (10 mL). This afforded 1.16 g (92% yield) of colorless needles, mp 152–153°C [lit. (4) mp 153–154°C]. ^{1}H-NMR: δ 8.73 (1, dd, $J_{2,3}$ = 5 Hz, $J_{2,4}$ = 2 Hz, H-2), 8.37 (1, dd, $J_{4,2}$ = 2 Hz, $J_{4,3}$ = 8 Hz, H-4), 7.63 (1, dd, $J_{3,2}$ = 5 Hz, $J_{3,4}$ = 8 Hz, H-3), 7.03 (1, s, H-7), and 3.91 ppm (3, s, OCH_3); ^{13}C-NMR: 155.0 (s, C-6), 146.7 (s, C-8), 144.8 (d, C-2), 134.0 (s, C-8a), 133.2 (d, C-4), 128.0 (s, C-4a), 123.1 (d, C-3), 96.3 (d, C-7), 89.9 (s, C-5), and 56.4 ppm (q, OCH_3).

5-Bromo-6-methoxy-8-acetaminoquinoline (XIII)—6-Methoxy-8-acetaminoquinoline (3.2 g, 0.015 mol) was dissolved in glacial acetic acid (30 mL). Pyridinium hydrobromide perbromide (4.8 g, 0.015 mol) was added slowly, and the mixture was stirred at room temperature for 2 h. The solution was cooled in an ice bath and neutralized with excess concentrated ammonium hydroxide. The precipitate was removed by filtration and washed with ice-cold water; the dried material was recrystallized from ethyl alcohol to give 3.4 g (77% yield) of colorless needles, mp 167–169°C [lit. (4) mp 167–169°C].

7-Bromo-6-methoxy-8-aminoquinoline (XI)—The method of Lauer *et al.* (4) was used to give material with mp 110–112°C [lit. (4) mp 111.5–112.5°C]. ^{1}H-NMR: δ 8.63 (1, dd, $J_{2,3}$ = 5 Hz, $J_{2,4}$ = 2 Hz, H-2), 8.13 (1, dd, $J_{4,2}$ = 2 Hz, $J_{4,3}$ = 8 Hz, H-4), 7.47 (1, dd, $J_{3,2}$ = 5 Hz, $J_{3,4}$ = 8 Hz, H-3), 6.83 (s, H-5), and 4.00 ppm (3, s, OCH_3); ^{13}C-NMR: 154.2 (s, C-6), 145.5 (d, C-2), 143.8 (s, C-8), 134.9 (d, C-4), 134.1 (s, C-8a), 128.1 (s, C-4a), 122.3 (d, C-3), 95.6 (s, C-7), 93.5 (d, C-5), and 56.1 ppm (q, OCH_3).

5,7-Dibromo-6-methoxy-8-aminoquinoline (XII)—The method of Lauer *et al.* (4) was used to give off-white crystals from ethanol, mp 86–87°C [lit. (4) mp 87–88°C]. ^{1}H-NMR: δ 8.77 (1, dd, $J_{2,3}$ = 5 Hz, $J_{2,4}$ = 2 Hz, H-2), 8.33 (1, dd, $J_{4,2}$ = 2 Hz, $J_{4,3}$ = 8 Hz, H-4), 7.63 (1, dd, $J_{3,2}$ = 5 Hz, $J_{3,4}$ = 8 Hz, H-3), and 3.91 ppm (3, s, OCH_3); ^{13}C-NMR: 152.6 (s, C-6), 147.7 (d, C-2), 144.4 (s, C-8), 135.3 (s, C-8a), 134.6 (d, C-4), 126.7 (s, C-4a), 123.6 (d, C-3), 99.1 (s, C-7), 98.0 (s, C-5), and 60.5 ppm (q, OCH_3).

RESULTS AND DISCUSSION

2-Bromo-6-methoxy-8-nitroquinoline (III) was obtained by treatment of 1-methyl-6-methoxy-8-nitroquinoline-2-one with phosphorus oxybromide. The quinoline-2-one derivative was prepared in two steps from 6-methoxy-8-nitroquinoline (7). 6-Methoxy-8-nitroquinoline (II) may be prepared in good yield by the use of "sulfo mix" (5) in place of arsenic pentoxide (10), the duration of reaction being shorter and the workup of the reaction being comparatively easier. 4-Bromo-6-methoxy-8-aminoquinoline (V) was made from the corresponding 4-hydroxy compound (8).

The unexpected result of isomerization of the 5-bromo isomer into the 7-bromo isomer, which was reported previously (4), was confirmed; the spectral data clearly distinguish the 5- and 7-bromo isomers. A clue to the explanation of this result is the observed rapid exchange of the hydrogen atoms at both C-5 and C-7. This suggests that protonation occurs at C-5 of the highly activated ring to form an iminium intermediate (XIV). Nucleophilic attack of this material by bromide ion would generate 6-methoxy-8-acetaminoquinoline and molecular bromine. Subsequent bromination of the 6-methoxy-8-acetaminoquinoline may proceed at C-5 to regenerate the starting bromo isomer, or alternatively, since C-7 is also activated, bromination may take place at C-7 to generate the isomeric product. Since protonation seems to be favored at C-5, this process should ultimately transform all of the 5-bromo derivative to the 7-bromo substance (4).

With all the bromo-8-nitroquinolines in hand, we turned our attention to the formation of the 8-aminoquinolines. The reduction of the nitro to an amino group caused several problems. It was found that use of either 10% palladium on charcoal or Raney Nickel-catalyzed reduction with hydrazine hydrate in refluxing ethanol resulted in considerable hydrogenolysis of the bromo group. Catalytic hydrogenation with Raney Nickel (50 psi, room temperature) also gave inconsistent results with the bromonitro compounds. Hence, a detailed study was undertaken to find the best method for the reduction of the nitro group without accompanying hydrogenolysis of the bromo substituent. The reduction was attempted under three different pH conditions (neutral, basic, and acidic), and the course of the reduction was monitored by GC; and bromoaminoquinolines were well separated from 6-methoxy-8-aminoquinoline and the starting nitro derivatives. It was found that reduction with stannous chloride in concentrated hydrochloric acid at low temperature for a period of 1 h gave the best results in all the cases examined. Longer reaction times resulted in extensive hydrogenolysis especially in the case of the 2- and 5-bromo derivatives. Hydrazine hydrate reduction catalyzed by Raney Nickel at room temperature gave satisfactory results only in the case of 3- and 4-bromo compounds. Raney Nickel-catalyzed reduction with hydrogen gas at 50 psi and room temperature for ≥6 h gave fair to poor yields of bromoamino compounds. Shorter duration of hydrogenation resulted in incomplete reduction and the recovery of the starting bromonitro compounds. Thus, the stannous chloride–hydrochloric acid method was found to be the best, and yields ranging from 85 to 95% could be achieved in all the cases. 5,7-Dibromo-6-methoxy-8-aminoquinoline (XII) was prepared as reported earlier (4).

The ^{1}H-NMR data of all these compounds are readily assigned by simple chemical-shift theory and coupling patterns. Since little data is available concerning the effects of bromine on carbon resonances, the complete assignments of the ^{13}C-NMR data were also examined.

The use of long-range coupling patterns of quinoline derivatives can be used to confirm assignments (11). The fully coupled ^{13}C-NMR spectra of 6-methoxy-8-aminoquinoline (III) readily confirms those assignments listed. The protons of the amino group also show long-range coupling to C-7 just like that observed for primaquine (12). This coupling can be removed by exchange using deuterium oxide, and the C-7 signal appears as the expected doublet of doublets (J = 158.2, 5.9 Hz). The carbon atom at the 5-position, on the other hand, remains unchanged after exchange [dt (J = 162.1, 4.9 Hz)]. The carbon atom at the 4a-position appears as a doublet (J = 6.8 Hz), C-6 as a quartet (J = 3.9 Hz), C-8 as a singlet, and C-8a as a complex multiplet. The coupling patterns for C-2, C-3, and C-4 appear just as for quinoline (11).

The assignments of the signals for the various bromo derivatives (VII–XI) were made using chemical-shift theory, single-frequency off-resonance decoupling, and long-range coupling patterns in the proton-coupled spectrum. Introduction of a bromine substituent in benzenes causes a shielding of the substituted carbon (5–6 ppm) and a deshielding of the *ortho* carbon (3–4 ppm) (13). The *meta* and *para* effects are much smaller. This general trend appears to hold for the substituted carbon and the protonated carbons of the bromoquinolines as well. The shift of the nonprotonated *ortho* carbon, on the other hand, is in the opposite direction (shielded) by several ppm. It is also interesting to compare the 5,7-dibromo derivative (XII) with VI, X, and XI. The C-7 signal in XII appears at nearly the same place as in VI, whereas C-5 is deshielded by ~5 ppm. Also, C-5 in X appears near 90 ppm, while in XII it appears at 98 ppm, showing that introduction of a bromine at C-7 (*meta* position) causes a deshielding effect of ~8 ppm. Comparison of C-7 in XII and XI shows a deshielding effect of only ~2 ppm. Clearly, we can conclude that one must be careful in drawing any generalizations with bromine substituents, particularly in highly substituted systems.

REFERENCES

(1) J. D. McChesney and S. Sarangan, *J. Labelled Cmpd. Radiopharm.*, **20**, 53 (1983).

(2) L. H. Schmidt, *Annu. Rev. Microbiol.*, **23**, 427 (1969).

(3) R. H. Baker, S. W. Tinsley, Jr., D. Butler, and B. Riegel, *J. Am. Chem. Soc.*, **72**, 393 (1950).

(4) W. M. Lauer, C. J. Claus, R. W. Von Korff, and S. A. Sundet, *J. Am. Chem. Soc.*, **74**, 2080 (1952).

(5) "Reagents for Organic Synthesis," vol. 2, M. Fieser and L. Fieser, Eds., Wiley-Interscience, New York, N.Y., 1969, p. 391.

(6) "Beilstein's Handbüch der Organische Chemie," vol. 21, Springer-Verlag, Berlin-Heidelberg-New York, 1978, p. 54.

(7) W. A. Wetter and C. D. Blanton, Jr., *J. Med. Chem.*, **17**, 620 (1974).

(8) B. Riegel, G. R. Luppin, B. H. Adelson, R. J. Jackson, C. J. Albosetti, Jr., R. M. Dodson, and R. H. Baker, *J. Am. Chem. Soc.*, **68**, 1264 (1946).

(9) W. M. Lauer, C. Rondestvedt, R. T. Arnold, N. L. Drake, J. Van Hook, and J. Tinker, *J. Am. Chem. Soc.*, **68**, 1546 (1946).

(10) "Organic Synthesis," coll. vol. III, E. C. Horning, Ed., Wiley, New York, N.Y., 1955, pp. 568–572.

(11) S. R. Johns and R. I. Willing, *Aust. J. Chem.*, **29**, 1617 (1976).

(12) A. M. Clark, C. D. Hufford, and J. D. McChesney, *Antimicrob. Agents Chemother.*, **19**, 337 (1981).

(13) G. C. Levy, R. L. Lichter, and G. L. Nelson, "Carbon-13 Nuclear Magnetic Resonance Spectroscopy," Wiley-Interscience, New York, N.Y., 1980.

ACKNOWLEDGMENTS

Supported by the UNDP/World Bank/World Health Organization Special Programme for Research and Training in Tropical Diseases.

Determination of the Structure of a Synthetic Impurity in Guaifenesin: Modification of a High-Performance Liquid Chromatographic Method for Phenylephrine Hydrochloride, Phenylpropanolamine Hydrochloride, Guaifenesin, and Sodium Benzoate in Dosage Forms

GARY W. SCHIEFFER ˣ, WARREN O. SMITH, GWEN S. LUBEY, and DANIEL G. NEWBY

Received October 13, 1983, from the *Analytical Chemistry Division, Norwich Eaton Pharmaceuticals, Inc., Norwich, NY 13815.* Accepted for publication March 12, 1984.

Abstract □ An impurity present in all commercial guaifenesin-containing dosage forms examined was isolated and identified as 2-(2-methoxyphenoxy)1,3-propanediol (VI). The eluant of a previously developed stability-indicating liquid chromatographic method for phenylephrine hydrochloride (I), phenylpropanolamine hydrochloride (II), and guaifenesin (III) was modified to yield a better separation between phenylpropanolamine and the impurity. The method was expanded to include sodium benzoate (IV), a preservative found in some liquid formulations.

Keyphrases □ Guaifenesin—synthetic impurity, HPLC with phenylephrine hydrochloride, phenylpropanolamine hydrochloride, and sodium benzoate

A stability-indicating reverse-phase high-performance liquid chromatographic (HPLC) method for phenylephrine hydrochloride (I), phenylpropanolamine hydrochloride (II), and guaifenesin (III), primarily in capsule formulations, was recently presented (1). However, on further examination of a wide variety of capsule, tablet, and liquid formulations from various manufacturers, it became evident that all chromatograms of products containing III (and even standard III solutions) yielded an impurity that eluted immediately following the II peak. In early method development work involving the capsule formulations, the peak area of this III impurity was only slightly more than 2% of the area of II (~0.2% of the III area) and barely discernable in the tail of the II peak (*cf.* Fig. 2 of Ref. 1). The separation was sufficient to yield good analytical data. However, impurity peak areas were later observed in other commercial formulations that were >20% of the area of the II peak. Because of the relatively large amount of the III impurity in some formulations, the ubiquitous nature of the impurity, and the danger of loss of resolution between II and the impurity for less efficient columns, both elucidation of the impurity structure and modification of the chromatographic eluant system to yield better resolution between II and the impurity were sought.

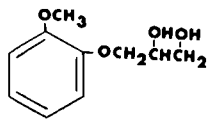

III

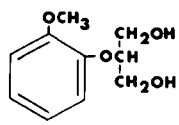

VI

EXPERIMENTAL SECTION

Reagents and Chemicals—All reagents and chemicals were ACS, USP or NF quality and were used without further purification. Compounds I, II, and III were used as received[1].

2-(2-Methoxyphenoxy)-1,3-propanediol (VI) was synthesized according to a literature procedure (2). Recrystallization from ethyl acetate–hexane, yielded a white powder, mp 62–64°C [lit. (2) mp 61–62°C]. IR (KBr): 3325 (O—H), 3041 (ArC—H), 3000–2850 (aliphatic C—H), 2837 (methoxy C—H), 1600–1450 (Ar deformations), 1240 and 1100–1000 (C—O), and 750 cm^{-1} (1,2-substituted Ar ring C—H, out of plane deformation); ^{1}H-NMR (acetone-d_6): δ 7.07 (ArH), 4.25 (—OCH), 3.87 (—OCH_3) and 3.85 ppm (—CH_2OH).

The *para* isomer of III, 3-(4-methoxyphenoxy)-1,2-propanediol, was pre-

[1] Norwich Eaton Pharmaceuticals, Inc.

0022-3549/84/1200-1856$01.00/0

© 1984, American Pharmaceutical Association

REFERENCES

(1) J. D. McChesney and S. Sarangan, *J. Labelled Cmpd. Radiopharm.*, **20**, 53 (1983).

(2) L. H. Schmidt, *Annu. Rev. Microbiol.*, **23**, 427 (1969).

(3) R. H. Baker, S. W. Tinsley, Jr., D. Butler, and B. Riegel, *J. Am. Chem. Soc.*, **72**, 393 (1950).

(4) W. M. Lauer, C. J. Claus, R. W. Von Korff, and S. A. Sundet, *J. Am. Chem. Soc.*, **74**, 2080 (1952).

(5) "Reagents for Organic Synthesis," vol. 2, M. Fieser and L. Fieser, Eds., Wiley-Interscience, New York, N.Y., 1969, p. 391.

(6) "Beilstein's Handbüch der Organische Chemie," vol. 21, Springer-Verlag, Berlin-Heidelberg-New York, 1978, p. 54.

(7) W. A. Wetter and C. D. Blanton, Jr., *J. Med. Chem.*, **17**, 620 (1974).

(8) B. Riegel, G. R. Luppin, B. H. Adelson, R. J. Jackson, C. J. Albosetti, Jr., R. M. Dodson, and R. H. Baker, *J. Am. Chem. Soc.*, **68**, 1264 (1946).

(9) W. M. Lauer, C. Rondestvedt, R. T. Arnold, N. L. Drake, J. Van Hook, and J. Tinker, *J. Am. Chem. Soc.*, **68**, 1546 (1946).

(10) "Organic Synthesis," coll. vol. III, E. C. Horning, Ed., Wiley, New York, N.Y., 1955, pp. 568–572.

(11) S. R. Johns and R. I. Willing, *Aust. J. Chem.*, **29**, 1617 (1976).

(12) A. M. Clark, C. D. Hufford, and J. D. McChesney, *Antimicrob. Agents Chemother.*, **19**, 337 (1981).

(13) G. C. Levy, R. L. Lichter, and G. L. Nelson, "Carbon-13 Nuclear Magnetic Resonance Spectroscopy," Wiley-Interscience, New York, N.Y., 1980.

ACKNOWLEDGMENTS

Supported by the UNDP/World Bank/World Health Organization Special Programme for Research and Training in Tropical Diseases.

Determination of the Structure of a Synthetic Impurity in Guaifenesin: Modification of a High-Performance Liquid Chromatographic Method for Phenylephrine Hydrochloride, Phenylpropanolamine Hydrochloride, Guaifenesin, and Sodium Benzoate in Dosage Forms

GARY W. SCHIEFFER ˣ, WARREN O. SMITH, GWEN S. LUBEY, and DANIEL G. NEWBY

Received October 13, 1983, from the *Analytical Chemistry Division, Norwich Eaton Pharmaceuticals, Inc., Norwich, NY 13815.* Accepted for publication March 12, 1984.

Abstract □ An impurity present in all commercial guaifenesin-containing dosage forms examined was isolated and identified as 2-(2-methoxyphenoxy)1,3-propanediol (VI). The eluant of a previously developed stability-indicating liquid chromatographic method for phenylephrine hydrochloride (I), phenylpropanolamine hydrochloride (II), and guaifenesin (III) was modified to yield a better separation between phenylpropanolamine and the impurity. The method was expanded to include sodium benzoate (IV), a preservative found in some liquid formulations.

Keyphrases □ Guaifenesin—synthetic impurity, HPLC with phenylephrine hydrochloride, phenylpropanolamine hydrochloride, and sodium benzoate

A stability-indicating reverse-phase high-performance liquid chromatographic (HPLC) method for phenylephrine hydrochloride (I), phenylpropanolamine hydrochloride (II), and guaifenesin (III), primarily in capsule formulations, was recently presented (1). However, on further examination of a wide variety of capsule, tablet, and liquid formulations from various manufacturers, it became evident that all chromatograms of products containing III (and even standard III solutions) yielded an impurity that eluted immediately following the II peak. In early method development work involving the capsule formulations, the peak area of this III impurity was only slightly more than 2% of the area of II (~0.2% of the III area) and barely discernable in the tail of the II peak (*cf.* Fig. 2 of Ref. 1). The separation was sufficient to yield good analytical data. However, impurity peak areas were later observed in other commercial formulations that were >20% of the area of the II peak. Because of the relatively large amount of the III impurity in some formulations, the ubiquitous nature of the impurity, and the danger of loss of resolution between II and the impurity for less efficient columns, both elucidation of the impurity structure and modification of the chromatographic eluant system to yield better resolution between II and the impurity were sought.

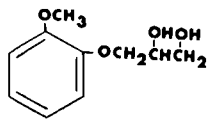

III

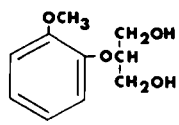

VI

EXPERIMENTAL SECTION

Reagents and Chemicals—All reagents and chemicals were ACS, USP or NF quality and were used without further purification. Compounds I, II, and III were used as received[1].

2-(2-Methoxyphenoxy)-1,3-propanediol (VI) was synthesized according to a literature procedure (2). Recrystallization from ethyl acetate–hexane, yielded a white powder, mp 62–64°C [lit. (2) mp 61–62°C]. IR (KBr): 3325 (O—H), 3041 (ArC—H), 3000–2850 (aliphatic C—H), 2837 (methoxy C—H), 1600–1450 (Ar deformations), 1240 and 1100–1000 (C—O), and 750 cm^{-1} (1,2-substituted Ar ring C—H, out of plane deformation); ^{1}H-NMR (acetone-d_6): δ 7.07 (ArH), 4.25 (—OCH), 3.87 (—OCH_3) and 3.85 ppm (—CH_2OH).

The *para* isomer of III, 3-(4-methoxyphenoxy)-1,2-propanediol, was pre-

[1] Norwich Eaton Pharmaceuticals, Inc.

0022-3549/84/1200-1856$01.00/0

© 1984, American Pharmaceutical Association

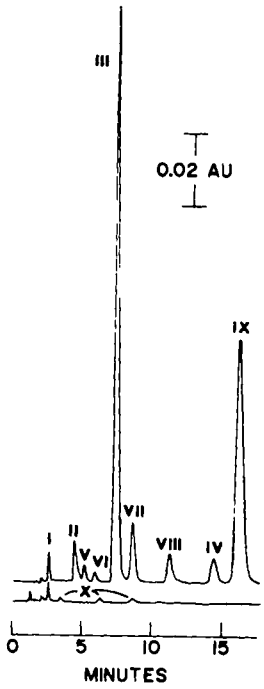

Figure 1—*Chromatogram of 40 μg/mL of phenylephrine hydrochloride (I), 400 μg/mL of phenylpropanolamine hydrochloride (II), 1.8 mg/mL of guaifenesin (III), 40 μg/mL of benzoic acid (IV), and possible impurities and degradants: 1 μg/mL of α-aminopropiophenone (V), 20 μg/mL of 2-(2-methoxyphenoxy)-1,3-propanediol (VI), 4 μg/mL of* m*-hydroxybenzaldehyde (VII), 100 μg/mL of guaiacol (VIII), 40 μg/mL of benzaldehyde (IX), and forced degraded phenylephrine hydrochloride products (X).*

pared according to a general procedure for synthesis of α-glyceryl phenyl ethers (3). Recrystallization from ethyl acetate–hexane yielded a white powder, mp 80–82°C [lit. (4) mp 76–78°C]. IR (KBr): 818 cm^{-1} (*para*-substituted benzene ring); otherwise, the spectrum was similar to that for III.

Degradation products of I were formed by storing I in 0.5 M KOH at 80–90°C for 1 week (1).

Apparatus—The HPLC apparatus described previously (1) was used. The system used for quantitative assay of I, II, III, and the preservative sodium benzoate [as benzoic acid (IV)] consisted of an absorbance detector at 254 nm, a 20-μL loop injector, and a C_8 column[2] pumped at 2.0 mL/min with an eluant containing 50 mL of methanol, 170 mL of acetonitrile, 755 mL of water, and 25 mL of pentanesulfonic acid sodium salt in glacial acetic acid[3]. The resulting eluant was 5 mM in ion-pairing salt and 1.7% in acetic acid. The HPLC system used for collection of the impurity consisted of a C_{18} column[4] with water–methanol (80:20) as eluant at a 1.5-mL/min flow rate. To collect the impurity, 10 fractions from 100-μL injections of a 107-mg/mL aqueous solution of III were collected from the chromatographic region just prior to the elution of the III peak. The combined fractions were evaporated to a total volume of 1 mL.

A GC apparatus[5] was used with a photoionization detector at 10.2 eV and a 1.8 m × 2 mm i.d. glass column packed with 3% OV-17 on Chromasorb G-HP. Both III and the collected impurity were treated with *n*-butylboronic acid for 30 min. One microliter or less of both derivatized and underivatized solutions were injected at a column temperature of 200°C and nitrogen flow rate of 25 mL/min.

^{1}H-NMR spectra were obtained on an 80-MHz Fourier-transform instrument[6]. Samples were dissolved in 99.96 atom-%D hexadeuterated acetone with tetramethylsilane as internal standard. IR spectra were obtained from KBr pellets with a Fourier-transform instrument[7].

Standard Solution Preparation—The final HPLC method used aqueous standard solutions containing 0–0.1 μg/mL of I, 0.24–0.45 μg/mL of II, 2–5.6 μg/mL of III, and 0–0.12 μg/mL of IV, depending on the label claim of the dosage form assayed.

Sample Preparation—For the capsule and tablet samples not containing I, 200 or 300 mg of ground sample was leached with water or mobile phase and diluted to 50 mL. For capsule samples containing I, to obtain a more homogenous sample, 1–1.3 g of ground sample was leached with water and diluted to 250 mL. The samples were injected directly after a 10-min sonication and 5-min centrifugation at 2500 rpm. For the liquid samples, 4.0–25.0 mL (depending on label claim) was diluted to 250 mL with water and then injected directly.

Table I—Area Linearity

Parameter	Phenylephrine Hydrochloride	Phenylpropanolamine Hydrochloride	Guaifenesin	Sodium Benzoate[a]
Correlation coefficient	0.99996	0.99997	0.9999	0.9999
Standard error of the estimate ($S_{y/x}$)	270	800	24,000	3700
Intercept, %[b]	−0.3	0.7	1.4	1.4
Variation, %[c]	0.7	0.6	1.2	1.2

[a] As benzoic acid. [b] (y-Intercept/$\bar{y}$) × 100, where $\bar{y}$ is the average y. [c]($S_{y/x}$ / $\bar{y}$) × 100.

RESULTS AND DISCUSSION

Elucidation of Impurity Structure—Gas chromatograms of both derivatized and underivatized III and collected impurity samples revealed that cyclic butylboronate derivatization increased the retention time of both compounds by ~50%. This indicated that, like III, the impurity required two hydroxyl groups, no more than one carbon atom apart, for formation of the cyclic butylboronate derivative (5). Logical possibilities included the *para* isomer of III and 2-(2-methoxyphenoxy)-1,3-propanediol (VI). The former was immediately excluded since it was found to possess nearly the same HPLC retention time as III.

^{1}H-NMR of both the collected impurity and the synthesized compound (VI) in hexadeuterated acetone yielded practically identical spectra, provided the concentration of the synthesized compound was dilute (≤1 mg/mL)[8]. Intermolecular hydrogen bonding resulted in peak shifts in the spectra at higher concentrations.

The collected impurity sample was lyophilized to remove the eluant and pressed into a KBr pellet. The IR spectrum of the impurity was practically identical to that of the synthesized compound, again provided that the concentration of the synthetic compound was low enough to minimize hydrogen bonding effects[8].

HPLC of the synthesized compound using both C_8 and C_{18} columns yielded a retention time identical to that for the impurity observed in III samples. The ratio of molar absorptivities of III to VI at 254 nm was found to be 1:1.

Modification of the Liquid Chromatographic Stability-Indicating Assay—Any HPLC system developed should be specific for the analytes I, II, III, and IV with respect to the following known and postulated impurities and degradation products (1): α-aminopropiophenone (V), a precursor and postulated (but so far undetected) trace impurity of II; 2-(2-methoxyphenoxy)-1,3-propanediol (VI), the identified III impurity; *m*-hydroxybenzaldehyde (VII), an observed degradation product of I; guaiacol (VIII), an observed hydrolysis product of III; benzaldehyde (IX), an observed hydrolysis product of II; forced-degradation products of I (X).

To achieve the desired resolution between II and VI and maintain the separation from the above compounds, the organic modifier of the original eluant system (1) was changed from 30% methanol to 5% methanol and 17% acetonitrile (Fig. 1). The separation was maintained on several C_8 columns, including one that had seen heavy use. An internal standard was not deemed necessary, due to the high precision obtained with fixed-loop injectors.

The linearity data for I, II, III, and IV, determined by plotting peak areas *versus* standard weights, are presented in Table I. Linearity was observed over the ranges of 0.4–3.4 μg for I, 3.3–31 μg for II, 14.5–138 μg for III, and 1–9.3 μg for IV.

Assay of 12 synthetic capsule samples made by spiking placebo with solutions containing known amounts of standard I, II, and III at levels of 50–150% of the theoretical values yielded average recoveries and *RSD* values of 99.8

[2] Whatman Partisil-10.
[3] PIC-B5; Waters Associates.
[4] μ-Bondapak C_{18}; Waters Associates.
[5] HNU Model 401.
[6] Bruker WP-80.
[7] Nicolet MX-1.
[8] Spectra furnished on request.

Table II—HPLC Assay of Capsule [a] and Liquid [b] Samples

Sample Weight or Volume	Phenylephrine Hydrochloride, mg/g	Phenylpropanolamine Hydrochloride, mg/g or mL	Guaifenesin, mg/g or mL	Sodium Benzoate, mg/mL[c]
Weight, g				
0.651	9.61	82.6	375	
0.661	9.61	85.0	382	
0.666	9.34	83.7	376	
1.046	9.36	82.2	373	
1.078	9.73	81.7	371	
1.303	9.48	82.2	373	
1.331	9.65	84.0	375	
1.328	9.45	83.9	375	
1.927	9.45	84.0	375	
1.922	9.54	84.3	375	
1.137	9.83	82.9	365	
1.912	9.62	83.4	365	
Mean, mg/g	9.56	83.7	372	
RSD, %	1.5	0.6	1.4	
Volume, mL				
15.0		2.52	19.3	1.16
20.0		2.51	19.1	1.15
25.0		2.48	19.1	1.14
30.0		2.50	19.2	1.15
35.0		2.50	19.2	1.16
Mean, mg/mL		2.50	19.2	1.15
RSD, %		0.6	0.5	0.7

[a] Entex Capsules, Norwich Eaton Pharmaceuticals, Inc. Label is 9.4 mg/g for phenylephrine hydrochloride, 85 mg/g for phenylpropanolamine hydrochloride, and 377 mg/g for guaifenesin. [b] Head & Chest Liquid, Procter & Gamble. Label is 2.56 mg/mL for phenylpropanolamine hydrochloride, 20 mg/mL for guaifenesin, and 1.20 mg/mL for sodium benzoate. [c] As benzoic acid.

Table III—HPLC Assay of Various Commercial Dosage Forms

Dosage Form	Phenylephrine Hydrochloride		Phenylpropanolamine Hydrochloride		Guaifenesin		2-(2-Methoxyphenoxy)-1,3-propanediol, % of Guaifenesin Conc.
	Assay, mg/mL	Label, %	Assay, mg/mL or g	Label, %	Assay, mg/mL or g	Label, %	
Liquid[a]	—	—	2.36	94.4	19.5	97.7	1.5
Liquid[b]	—	—	9.0	99.9	31.6	105.2	2.3
Liquid[c]	—	—	2.52	99.8	20.0	99.8	0.2
Liquid[d]	—	—	1.26	100.3	9.8	97.9	0.3
Liquid[e]	—	—	2.66	106.4	9.8	97.7	2.0
Capsule[f]	9.56	101.7	83.7	98.5	372	98.7	0.2
Tablet[g]	—	—	39.2	100.2	299	97.9	0.2

[a] Triaminic (Dorsey). [b] Naldecon Ex (Bristol). [c] Robitussin CF (A. H. Robins). [d] Dorcol (Dorsey). [e] Vicks Formula 44D (Vicks). [f] Entex Capsules (Norwich Eaton Pharmaceuticals, Inc.); from Table II. [g] Head & Chest Tablets (Procter & Gamble).

± 1.1%, 99.7 ± 1.2%, and 99.3 ± 1.0%, respectively. Similarly, assays of 12 synthetic liquid samples for II, III, and IV yielded average recoveries and *RSD* values of 99.7 ± 1.5%, 100.1 ± 1.5%, and 100.5 ± 1.5%, respectively.

The assay results for I, II, III, and IV in several commercial dosage forms representing liquid, tablet, and capsule preparations are presented in Tables II and III. In addition, assay values for VI (as percentage of III concentration) in seven different formulations from six different manufacturers are also presented in Table III. The impurity VI was observed in each formulation examined at concentrations ranging from 0.2 to 2.3% of the III concentration.

The widespread distribution of VI in formulations containing III prompted assessment of the potential toxicity of VI. According to literature data (16), when administered to mice, impurity VI is actually less toxic [mean paralyzing dose (PD_{50}) = 800 mg/kg, mean lethal dose (LD_{50}) = 1710 mg/kg] than III (PD_{50} = 320 mg/kg, LD_{50} = 1200 mg/kg). This information, coupled with the similarity in structure between III and VI, indicates the potential toxicity of VI is minimal.

REFERENCES

(1) G. W. Schieffer and D. E. Hughes, *J. Pharm. Sci.*, **72,** 55 (1983).

(2) J. Gierer and I. Kunze, *Acta. Chemica Scand.* **15,** 803 (1961).

(3) K. A. Kilpatrick and J. P. Lambooy, *Proc. Soc. Exp. Biol. Med.*, **126,** 237 (1967).

(4) K. Thomae, French Patent No. 1,445,013, 1966; *Chem. Abstr.*, **69,** 21920u (1968).

(5) "Handbook of Derivatives for Chromatography," K. Blau and G. King, Eds., Hayden & Son, Ltd., London, 1978, pp. 270-272.

(6) F. M. Berger, C. V. Hubbard, and B. J. Ludwig, *Proc. Soc. Exp. Biol. Med.*, **82,** 532 (1953).

ACKNOWLEDGMENTS

The authors are grateful to J. Glover for the synthesis of 2-(2-methoxyphenoxy)-1,3-propanediol and 3-(4-methoxyphenoxy)-1,2-propanediol and to A. Bramer for the sample assays.

Ethylene–Vinyl Acetate Copolymer Microspheres for Controlled Release of Macromolecules

MICHAEL V. SEFTON *, LARRY R. BROWN ‡, and ROBERT S. LANGER ‡x

Received May 26, 1983, from the *Department of Chemical Engineering and Applied Chemistry, University of Toronto, Toronto, Ontario M5S 1A4, the ‡Department of Nutrition and Food Science and Whitaker College of Health Sciences and Technology, Massachusetts Institute of Technology, Cambridge MA 02139 and the Department of Surgery, Children's Hospital Medical Center, Boston MA 02115. Accepted for publication March 26, 1984.

Abstract □ A simple technique has been devised for preparing ethylene–vinyl acetate copolymer microspheres containing macromolecular drugs. Beads with good sphericity were formed by a simple extrusion process that can easily be repeated by any laboratory without special equipment. The extruded droplets gelled on immediate contact with cold ethanol in a dry ice–ethanol bath. The ethanol also served to remove the solvent and harden the microspheres as they warmed to room temperature. Release of bovine serum albumin followed the expected trends, *i.e.*, initial linearity with the square root of time and faster release rates with greater drug loading.

Keyphrases □ Microencapsulation—ethylene–vinyl acetate copolymer microspheres, release kinetics, sustained release systems □ Ethylene–vinyl acetate copolymer microspheres—drug delivery, release kinetics

Monolithic systems composed of ethylene–vinyl acetate copolymer have been used for the controlled delivery of macromolecular drugs such as insulin (1), heparin (2), enzymes (3), DNA (2), tumor angiogenesis factor (2) and its inhibitor (4), and has provided a basis for various bioassays (5–7) and chemotactic studies (8). In all these cases, the drug and polymer solution were mixed together and cast as a film on a precooled plate to yield a matrix device in the form of a slab (~5 × 5 cm, 0.75–1.75 mm thick), which could be further divided into 1 × 1 cm squares (9). These systems have been designed to release at decreasing rates (9), constant rates (10), and increasing rates (11).

A new procedure is described here for making nearly spherical beads of ethylene–vinyl acetate copolymer for controlled release of macromolecular drugs. Such microspheres may prove to be useful as an injectable dosage form. In addition, the simplicity of the technique may facilitate its widespread application in new areas.

EXPERIMENTAL SECTION

Microsphere Preparation—Microsphere preparation is shown diagrammatically in Fig. 1. Ethylene–vinyl acetate copolymer[1] (40% vinyl acetate) was washed in water and ethanol[2] (12) and dissolved in methylene chloride[3] to give a 10% (w/v) solution. Bovine serum albumin[4] was sieved[5] to give 106–150-μm particles. The polymer solution (2 mL) was added to a weighed amount of powder in a 5-mL glass vial[6] and the mixture was vortexed[7] to give a uniform suspension. The mixture was quickly drawn into a disposable 3-mL syringe[8] *via* a 1.27-cm 16-gauge needle[9] that had been trimmed to a blunt end with a standard machine shop grinder wheel. After vortexing again for a few seconds, the suspension was carefully extruded through the same 16-gauge needle drop by drop into 20 mL of cold unstirred absolute ethanol in a 50-mL beaker immersed in a dry ice–ethanol bath (−78°C). The mixture gelled virtually immediately on contact with the cold ethanol in the near-spherical shape of the droplets, and the hard, gelled spheres sank to the bottom of the beaker. The mixture was extruded as quickly as possible drop by drop to minimize methylene chloride evaporation and plugging of the needle. It was also found that extrusion was facilitated by conducting it outside of a fume hood. Microspheres were prepared with loadings of 10–50% protein by weight.

After 5–10 min, the beaker containing the microspheres was removed from the dry ice bath and allowed to warm to room temperature. The microspheres turned white as the solvent was extracted into the ethanol. After ≥1 h, the liquid was replaced with ~10 mL of fresh ethanol and set aside overnight in a 20-mL glass vial[6]. The ethanol was decanted and the microspheres were dried for 4–5 h in a vacuum desiccator. The duration of the various process steps were not considered critical as long as solvent and ethanol removal was largely complete. For example, removal of the microspheres from the cold ethanol immediately after extrusion caused the microspheres to agglomerate since insufficient methylene chloride had been removed for the microspheres to remain gelled at room temperature.

Release Kinetics—A 30–50-mg aliquot of microspheres was weighed and placed in a vial containing 10 mL of saline (0.154 M NaCl[10]) at room temperature (23°C). The liquid was sampled periodically and the concentration of protein was determined spectrophotometrically[11] at 280 nm. Each sample was returned to the vial after measurement. Release was monitored in duplicate for a period of 6 d; release values were within ≤10% of the mean.

Bead Characterization—Dry microspheres were sliced with a razor blade, mounted on studs using silver paint, sputter coated, and examined by scanning electron microscopy[12]. Average bead diameter was estimated with the aid of a metallograph microscope[13] at low magnification (15×).

RESULTS AND DISCUSSION

The formation of polymer microspheres by precipitation of a polymer solution in contact with a nonsolvent is a standard microencapsulation technique (13). A process based on this technique and the extrusion of the polymer solution in a dropwise manner into a nonsolvent for the preparation of controlled-release formulations was patented by Sternberg *et al.* (14). This procedure did not work for our system: the extruded droplets of methylene

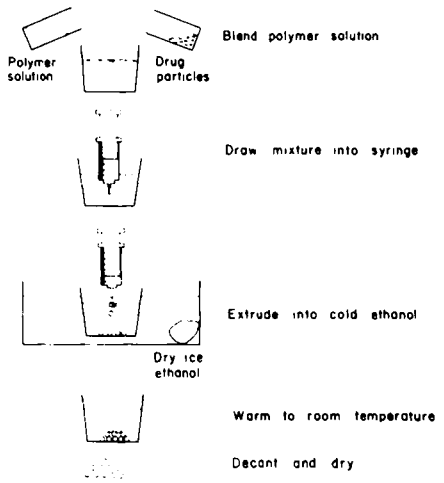

Figure 1—*Schematic illustration of microsphere preparation.*

[1] Elvax 40; DuPont Chemical Co., Wilmington, Del.
[2] U.S. Industrial Chemicals, New York, N.Y.
[3] Reagent grade; Mallinckrodt, St. Louis, Mo.
[4] Sigma Chemical Co., St. Louis, Mo.
[5] American Standard Sieves, Nos. 40, 60, and 200; Dual Manufacturing Co., Chicago, Ill.
[6] Wheaton Scientific Co., Millville, N.J.
[7] Scientific Instruments, Springfield, Mass.
[8] Becton, Dickinson and Co., Rutherford, N.J.
[9] Perfektum, Popper & Sons, New Hyde Park, N.Y.
[10] USP grade; Mallinckrodt.
[11] Model 250; Gilford Instrument Laboratories, Oberlin, Ohio.
[12] ISI DS 130; International Scientific Instruments, Santa Clara, Calif.
[13] Reichert MEF, Austria.

0022-3549/84/1200-1859$01.00/0
© 1984, American Pharmaceutical Association

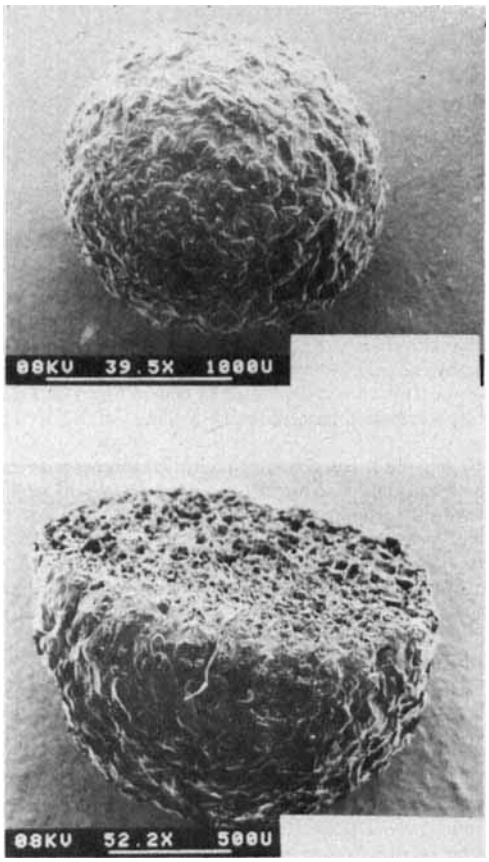

Figure 2—*Scanning electron micrographs of a whole microsphere, and a microsphere sliced with a razor blade, both containing 50% (w/w) albumin.*

chloride solution of polymer-containing dispersed protein lost their shape on contact with ethanol at room temperature; the polymer precipitated as a shapeless coagulum on the bottom of the beaker. Regularly shaped beads could be formed only by extruding into cold ethanol. Presumably, the polymer solution gelled rapidly on contact with the cold ethanol, preserving the shape of the droplets and giving time for the methylene chloride to slowly diffuse into the surrounding ethanol.

Beads prepared from 10% polymer in methylene chloride were almost perfectly spherical immediately after formation in cold ethanol. As the beads warmed and methylene chloride was removed, the polymer became softer and more easily deformed. The beads flattened slightly and became more ellipsoidal; this was accentuated for the beads with low loadings of albumin [*i.e.*, <20% (w/w) albumin]. The softness of the beads with lower albumin loadings was noted particularly when they were dry; it was difficult to handle the beads with forceps or a spatula without further changing their shape. Since these lower loading beads were also tacky (in the "dry" state), they stuck to the walls of glass or plastic containers and further increased handling difficulties. Scanning electron micrographs of beads containing 50% (w/w) bovine serum albumin are shown in Fig. 2, illustrating the sphericity of these beads.

When a 5% solution of ethylene–vinyl acetate copolymer in methylene chloride was used to fabricate the microspheres, it was less viscous than the 10% solution and, therefore, easier to use in making microspheres with high drug loading. However, this 5% solution resulted in beads with poorly defined shapes. Beads with 50% drug loading were teardrop shaped while smaller loadings (<20%) resulted in large aggregates of irregularly shaped beads. It appeared that the low ratio of polymer to solvent in these beads resulted in a slower cold ethanol solidification process than when beads were made from a 10% polymer solution. Consequently, the beads could be deformed and changed shape while the newly formed beads sank to the bottom of the cold ethanol. The beads with 50% loading were not as easily deformed so that only a small tail was produced while the beads with lower loadings were still tacky at the bottom of the cold ethanol and stuck to the previously formed beads. The most desirable shape was obtained with the 10% solution; thus, kinetic studies were conducted with the beads made from this solution. An intermediate concentration may be a better compromise between low polymer–drug mixture viscosity and good bead shape, particularly for higher drug loadings.

Table I—Estimated Microsphere Diameter

Loading, % (w/w)	Diameter, mm[a]
10	1.11
20	1.17
30	1.43
50	1.37

[a] Average of 10–20 beads; precision = ±0.07 mm.

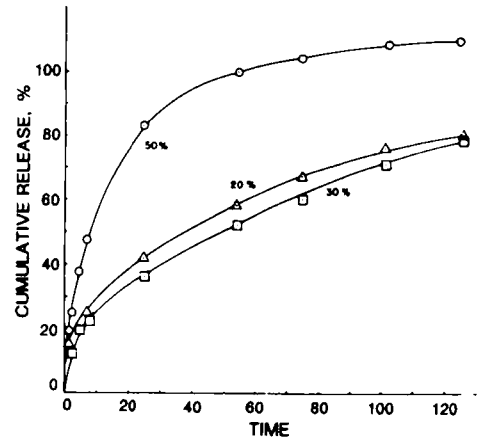

Figure 3—*Cumulative release of albumin from ethylene-vinyl acetate microspheres. Values are the mean of two measurements; release values were within ≤10% of the mean.*

The average size of microspheres made from a 10% solution are listed in Table I. As expected, the less drug in the microspheres and therefore the more polymer and solvent, the smaller (in general) the microspheres. Although the initial bead size was determined by the extruding needle diameter (16-gauge needle, 1.19 mm i.d. × 1.65 mm o.d.), the lower loading microspheres shrank more in the cold ethanol since there was more solvent to remove. The microspheres were reasonably uniform in size despite the crude nature of the extrusion process: the variation in bead size was less than the ±0.07-mm precision of the metallograph measurements. It is expected that greater microsphere uniformity could be obtained with better blending of the drug and polymer solution and by using a syringe pump to extrude the drug–polymer mixture at a constant rate.

Only to a limited extent can smaller microspheres be prepared effectively by using a smaller gauge needle, or by using a lower polymer concentration. For example, microspheres with 30% albumin were ~1.20 mm in diameter when prepared with a 20-gauge needle. However, viscosity effects and the need to grind the drug into even finer particles limit this approach, while some deterioration in bead shape may need to be tolerated if less concentrated polymer solutions are used. Smaller beads may be prepared more readily by a vibratory prilling process (15) or by blowing droplets off the end of a needle by a coaxial air stream (16). In the latter case it would be necessary to prevent the volatile methylene chloride from evaporating before the droplets leave the needle.

Typical release kinetics are shown in Fig. 3 as a plot of cumulative release against time. The release kinetics for 10% loading were not included because of the irregular shape of the beads and the difficulties in handling them.

The kinetic data is consistent with previous studies with this macromolecule-controlled release system (3). Cumulative release is generally greater at any time (*i.e.*, faster release rate) with higher drug loadings. This is presumed to result from the greater porosity of the polymer matrix at higher drug loadings (9). The seemingly faster initial release for the 20% albumin-loaded spheres compared with the 30% loaded matrices (Fig. 3) was not considered statistically significant. The release of albumin from the beads was relatively rapid with one-half of the content released in 50 h. In retrospect, such a release rate might have been predicted on the basis that a 1.0-cm thick slab of similar composition released one-half of its drug from a single face in 28 d (17). The differences in the time to release half of their content are completely attributable to the differences in the sizes and shapes of the two matrix preparations (especially the sizes).

The particle sizes of the albumin particles (106–150 μm) were ≤15% of the diameter of the microspheres themselves. It is probable that a significant portion of the albumin merely dissolved from the surface of the bead when the microspheres were placed into release media. Thus, this early burst of drug

from the microsphere can be primarily attributed to dissolution of drug from the surface with a minor contribution of matrix diffusion of albumin. To slow the release rate to levels practical for long term therapy, the beads can be coated with polymer containing no drug. A sevenfold decrease in release rate was observed after coating insulin-containing slabs with 20% ethylene-vinyl acetate solution (9).

The microsphere preparation technique can be used for other drugs and polymers other than ethylene-vinyl acetate, but it is important that the polymer-solvent solutions have glass transition temperatures > −78°C. Nonsolvents for the polymer, other than ethanol, could be used as long as they do not freeze at −78°C. In addition, the low-temperature nature of the process makes it ideally suited for thermally labile compounds that cannot be processed at the higher temperatures of conventional prilling processes [*e.g.*, 60°C for gelatin encapsulation (18)].

REFERENCES

(1) H. Creque, R. Langer, and J. Folkman, *Diabetes*, **29**, 37 (1980).

(2) R. Langer and J. Folkman, *Nature (London)*, **263**, 747 (1976).

(3) R. Langer and J. Folkman, in "Polymeric Delivery Systems," Midland Macromolecular Monograph, Vol. 5, R. J. Kostelnik, Ed., Gordon and Breach, New York, N.Y., 1978, pp. 175–196.

(4) R. Langer, H. Brem, M. Klein, K. Falterman, and J. Folkman, *Science*, **193**, 70 (1976).

(5) S. Brem, I. Preis, R. Langer, H. Brem, J. Folkman, and A. Patz, *Am. J. Opthamol.*, **84**, 323 (1977).

(6) D. Gospodarowicz, M. Balecki, and T. K. Thakral, *Exp. Eye Res.*, **28**, 501 (1979).

(7) M. E. Plishkin, S. M. Girzberg, and M. Carp, *Transplantation*, **29**, 255 (1980).

(8) R. Langer, M. Fefferman, P. Gryska, and K. Bergman, *Can. J. Microbiol.*, **26**, 274 (1980).

(9) W. D. Rhine, D. S. T. Hsieh, and R. Langer, *J. Pharm. Sci.*, **69**, 265 (1980).

(10) D. S. T. Hsieh, W. Rhine, and R. Langer, *J. Pharm. Sci.*, **72**, 17, (1983).

(11) R. Langer, W. Rhine, D. S. T. Hsieh, and J. Folkman, *J. Membr. Sci.*, **7**, 333 (1980).

(12) R. Langer, in "Immunological Techniques, Methods in Enzymology Vol. 73," H. Van Vunakis and J. R. Langone, Eds., 1981, p. 57.

(13) A. Kondo, "Microcapsule Processing and Technology," Dekker, New York, N.Y., 1979.

(14) S. Sternberg, H. J. Bixler, and A. S. Michaels, U.S. Patent 3,639,306, February 1 (1972).

(15) W. E. Yates and N. B. Akesson, Proceedings 1st International Conference on Liquid Atomization and Spray Systems, Tokyo, Japan, 1978, pp. 181–185.

(16) S. Wagaosa, H. Matsui, N. Tokuoka, and G. T. Sato, Proceedings 1st International Conference on Liquid Atomization and Spray Systems, Tokyo, Japan, 1978, pp. 29–36.

(17) R. Bawa, R. Siegel, B. Marasca, M. Karel, and R. Langer, *J. Controlled Release*, in press.

(18) J. E. Vandergaer, in "Microencapsulation: Processes and Applications," J. E. Vandergaer, Ed., Plenum Press, New York, N.Y., 1974, pp. 21–37.

ACKNOWLEDGMENTS

The authors acknowledge the financial support of an NIH Grant GM 26698.

Comparison of ^{99m}Tc-*N*-Pyridoxyl-5-Methyltryptophan and ^{99m}Tc-*N*-(3-Bromo-2,4,6-trimethylacetanilide)-Iminodiacetate as Hepatobiliary Radiopharmaceuticals in Rats

ALAN R. FRITZBERG *§x, DUANE C. BLOEDOW ‡, DENNIS ESHIMA *, and DENNIS L. JOHNSON *

Received June 13, 1983, from the **Department of Radiology, University of Colorado, Health Sciences Center, Denver, CO 80262* and the ‡*School of Pharmacy, University of Colorado, Boulder, CO 80309.* Accepted for publication March 21, 1984. §Present address: NeoRx Corporation, Seattle, WA 98119.

Abstract □ ^{99m}Tc - *N* - (3-bromo-2,4,6-trimethylacetanilide)iminodiacetate (I) and ^{99m}Tc-*N*-pyridoxyl-5-methyl-tryptophan (II) have been described as having optimal properties as hepatobiliary radiopharmaceuticals. This study compared specificity for hepatobiliary excretion, blood disappearance, rates of biliary appearance, and pharmacokinetic parameters including hepatic clearance, volumes of distribution, and mean residence times in normal and sulfobromophthalein-treated rats. The specificity of I was higher as indicated by 94% in the bile at 90 min compared to 91% for II in normal rats and a urine excretion of 0.3% for I compared with 1.9% for II. In sulfobromophthalein-treated animals, urine excretion increases were only to 0.5 and 3.0% for I and II, respectively. In control rats, blood disappearance was similar for both I and II, but II disappeared faster in treated animals. The clearance of II was 70 mL/min/kg in normal and 47 mL/min/kg in treated rats; clearance of I was 51 and 30 mL/min/kg in normal and treated rats, respectively. Volumes of distribution were larger for II. Compound I was superior in specificity while II was superior in clearance and excretion kinetics.

Keyphrases □ Hepatobiliary radiopharmaceuticals—^{99m}Tc-labeled compounds compared, sulfobromophthalein-treated and normal rats □ Radiopharmaceuticals—^{99m}Tc-labeled hepatobiliary compounds compared, sulfobromophthalein-treated and normal rats □ Sulfobromophthalein—effect on hepatobiliary radiopharmaceuticals, rats

Efforts to develop an optimal ^{99m}Tc-labeled hepatobiliary agent (I) have followed either a series beginning with ^{99m}Tc-labeled pyridoxylidene glutamate (2) or ^{99m}Tc-*N*-(2,6-dimethylacetanilide)iminodiacetate (3). These studies have resulted in improvements in hepatobiliary specificity, kinetics, and resistance to transport competition from elevated bilirubin levels. The currently "best" agents, based on animal and clinical studies, are ^{99m}Tc-*N*-(3-bromo-2,4,6-trimethylacetanilide)iminodiacetate (I) (4, 5) and ^{99m}Tc-*N*-pyridoxyl-5-methyltryptophan (II) (6).

To try to answer the question of which agent is superior, short of clinical paired comparisons in normal volunteers and patients, we have carried out detailed studies in rats. These studies were designed to compare rates of blood disappearance, rates of biliary appearance, specificity for hepatobiliary excretion, hepatic clearance of the complexes, and ability of the

© 1984, American Pharmaceutical Association

from the microsphere can be primarily attributed to dissolution of drug from the surface with a minor contribution of matrix diffusion of albumin. To slow the release rate to levels practical for long term therapy, the beads can be coated with polymer containing no drug. A sevenfold decrease in release rate was observed after coating insulin-containing slabs with 20% ethylene-vinyl acetate solution (9).

The microsphere preparation technique can be used for other drugs and polymers other than ethylene-vinyl acetate, but it is important that the polymer-solvent solutions have glass transition temperatures > −78°C. Nonsolvents for the polymer, other than ethanol, could be used as long as they do not freeze at −78°C. In addition, the low-temperature nature of the process makes it ideally suited for thermally labile compounds that cannot be processed at the higher temperatures of conventional prilling processes [*e.g.*, 60°C for gelatin encapsulation (18)].

REFERENCES

(1) H. Creque, R. Langer, and J. Folkman, *Diabetes*, **29**, 37 (1980).

(2) R. Langer and J. Folkman, *Nature (London)*, **263**, 747 (1976).

(3) R. Langer and J. Folkman, in "Polymeric Delivery Systems," Midland Macromolecular Monograph, Vol. 5, R. J. Kostelnik, Ed., Gordon and Breach, New York, N.Y., 1978, pp. 175–196.

(4) R. Langer, H. Brem, M. Klein, K. Falterman, and J. Folkman, *Science*, **193**, 70 (1976).

(5) S. Brem, I. Preis, R. Langer, H. Brem, J. Folkman, and A. Patz, *Am. J. Opthamol.*, **84**, 323 (1977).

(6) D. Gospodarowicz, M. Balecki, and T. K. Thakral, *Exp. Eye Res.*, **28**, 501 (1979).

(7) M. E. Plishkin, S. M. Girzberg, and M. Carp, *Transplantation*, **29**, 255 (1980).

(8) R. Langer, M. Fefferman, P. Gryska, and K. Bergman, *Can. J. Microbiol.*, **26**, 274 (1980).

(9) W. D. Rhine, D. S. T. Hsieh, and R. Langer, *J. Pharm. Sci.*, **69**, 265 (1980).

(10) D. S. T. Hsieh, W. Rhine, and R. Langer, *J. Pharm. Sci.*, **72**, 17, (1983).

(11) R. Langer, W. Rhine, D. S. T. Hsieh, and J. Folkman, *J. Membr. Sci.*, **7**, 333 (1980).

(12) R. Langer, in "Immunological Techniques, Methods in Enzymology Vol. 73," H. Van Vunakis and J. R. Langone, Eds., 1981, p. 57.

(13) A. Kondo, "Microcapsule Processing and Technology," Dekker, New York, N.Y., 1979.

(14) S. Sternberg, H. J. Bixler, and A. S. Michaels, U.S. Patent 3,639,306, February 1 (1972).

(15) W. E. Yates and N. B. Akesson, Proceedings 1st International Conference on Liquid Atomization and Spray Systems, Tokyo, Japan, 1978, pp. 181–185.

(16) S. Wagaosa, H. Matsui, N. Tokuoka, and G. T. Sato, Proceedings 1st International Conference on Liquid Atomization and Spray Systems, Tokyo, Japan, 1978, pp. 29–36.

(17) R. Bawa, R. Siegel, B. Marasca, M. Karel, and R. Langer, *J. Controlled Release*, in press.

(18) J. E. Vandergaer, in "Microencapsulation: Processes and Applications," J. E. Vandergaer, Ed., Plenum Press, New York, N.Y., 1974, pp. 21–37.

ACKNOWLEDGMENTS

The authors acknowledge the financial support of an NIH Grant GM 26698.

Comparison of ^{99m}Tc-*N*-Pyridoxyl-5-Methyltryptophan and ^{99m}Tc-*N*-(3-Bromo-2,4,6-trimethylacetanilide)-Iminodiacetate as Hepatobiliary Radiopharmaceuticals in Rats

ALAN R. FRITZBERG *§x, DUANE C. BLOEDOW ‡, DENNIS ESHIMA *, and DENNIS L. JOHNSON *

Received June 13, 1983, from the **Department of Radiology, University of Colorado, Health Sciences Center, Denver, CO 80262* and the ‡*School of Pharmacy, University of Colorado, Boulder, CO 80309.* Accepted for publication March 21, 1984. §Present address: NeoRx Corporation, Seattle, WA 98119.

Abstract □ ^{99m}Tc - *N* - (3-bromo-2,4,6-trimethylacetanilide)iminodiacetate (I) and ^{99m}Tc-*N*-pyridoxyl-5-methyl-tryptophan (II) have been described as having optimal properties as hepatobiliary radiopharmaceuticals. This study compared specificity for hepatobiliary excretion, blood disappearance, rates of biliary appearance, and pharmacokinetic parameters including hepatic clearance, volumes of distribution, and mean residence times in normal and sulfobromophthalein-treated rats. The specificity of I was higher as indicated by 94% in the bile at 90 min compared to 91% for II in normal rats and a urine excretion of 0.3% for I compared with 1.9% for II. In sulfobromophthalein-treated animals, urine excretion increases were only to 0.5 and 3.0% for I and II, respectively. In control rats, blood disappearance was similar for both I and II, but II disappeared faster in treated animals. The clearance of II was 70 mL/min/kg in normal and 47 mL/min/kg in treated rats; clearance of I was 51 and 30 mL/min/kg in normal and treated rats, respectively. Volumes of distribution were larger for II. Compound I was superior in specificity while II was superior in clearance and excretion kinetics.

Keyphrases □ Hepatobiliary radiopharmaceuticals—^{99m}Tc-labeled compounds compared, sulfobromophthalein-treated and normal rats □ Radiopharmaceuticals—^{99m}Tc-labeled hepatobiliary compounds compared, sulfobromophthalein-treated and normal rats □ Sulfobromophthalein—effect on hepatobiliary radiopharmaceuticals, rats

Efforts to develop an optimal ^{99m}Tc-labeled hepatobiliary agent (I) have followed either a series beginning with ^{99m}Tc-labeled pyridoxylidene glutamate (2) or ^{99m}Tc-*N*-(2,6-dimethylacetanilide)iminodiacetate (3). These studies have resulted in improvements in hepatobiliary specificity, kinetics, and resistance to transport competition from elevated bilirubin levels. The currently "best" agents, based on animal and clinical studies, are ^{99m}Tc-*N*-(3-bromo-2,4,6-trimethylacetanilide)iminodiacetate (I) (4, 5) and ^{99m}Tc-*N*-pyridoxyl-5-methyltryptophan (II) (6).

To try to answer the question of which agent is superior, short of clinical paired comparisons in normal volunteers and patients, we have carried out detailed studies in rats. These studies were designed to compare rates of blood disappearance, rates of biliary appearance, specificity for hepatobiliary excretion, hepatic clearance of the complexes, and ability of the

© 1984, American Pharmaceutical Association

agents to compete with sulfobromophthalein as a member of the dye anion and bilirubin pathway for hepatobiliary excretion.

EXPERIMENTAL SECTION

Radiopharmaceutical Preparation—Kits for the preparation of I for animal use were obtained as a gift[1]. They were prepared by the addition of 2–3 mL of generator eluate saline containing [^{99m}Tc]pertechnetate at a concentration of ~5 mCi/mL. The percent of ^{99m}Tc-radioactivity bound to the ligand was determined by TLC[2]. Saturated sodium chloride was used to develop silicic acid strips (R_f of pertechnetate = 1, R_f of I = 0–0.2) for the determination of free [^{99m}Tc]pertechnetate. An acetonitrile–water mixture (3:1) was used to develop silica gel strips (R_f of pertechnetate and I = 1, R_f of insoluble radioactive material = 0) for the determination of insoluble activity. The percent bound was calculated as 100 − (percent [^{99m}Tc]pertechnetate + percent insoluble radioactivity). Values were ≥98%. The ligand of II was supplied[3]. The preparation of kits for II was performed essentially as described (6). Radioactivity was added to a thawed kit (~30–50 mCi to 1.0 mL of kit volume) and the vial was heated in a boiling water bath for 30 min. At that time, small amounts of free pertechnetate were sometimes present. A 250-μL aliquot was therefore purified by HPLC to remove any free pertechnetate or insoluble radioactive material. Chromatographic conditions were: 0.01 M sodium phosphate buffer (pH 6) and acetonitrile with a gradient of 20–70% acetonitrile programmed over 20 min at a flow rate of 1.0 mL/min on an ODS column[4]. Fractions from three different peaks were collected without fractionation at 8–10 mL eluate volume [these fractions were shown to contain stereoisomeric chelate isomers that were only slightly different in their biological properties (7)]. The eluate was collected in a tube containing 1.5 mg of freshly dissolved ascorbic acid, as an antioxidant stabilizer, in 1 mL of water. Fifteen- to twenty-fold dilutions were made with saline containing 1 mg/mL ascorbic acid. The final injection volume of 0.25 mL contained ~50 μCi.

Animal Studies—Male Sprague–Dawley rats (300–430 g) were anesthetized with sodium pentobarbital. Catheters were placed in the femoral vein for injections, hydration, and infusions and in the carotid artery for blood sampling. The common bile duct was cannulated and bile was collected in tubes in a fraction collector. The body temperature of the rats was maintained at 37°C with external heat from a lamp. For competitive studies, sulfobromophthalein was infused at a transport maximum level of 2.5 μmol/min/kg for 15 min prior to and for 60 min postinjection of the radiopharmaceutical (8). The infusion flow rate was 0.1 mL/min. Urine normally was retained in the bladder during the 90-min studies. At that time the bladder was tied off, removed, and counted together with portions of the urinary tract that might contain urine. Bile and urine samples were counted in a well counter with appropriate dose standards. Total blood volume was assumed to be 7% of body weight (9). Blood samples of 0.3–0.4 mL were taken at 1, 2, 3, 4, 5, 6, 9, 12, 15, 20, 25, 45, 60, 75, and 90 min postinjection. Bile samples were collected at 0 and 2 min and then at 4-min intervals to 90 min postinjection.

Pharmacokinetic Calculations—Blood radioactivity concentration (cpm/mL of blood) *versus* time curves for each animal were used to calculate distribution volume, blood clearance, and mean residence time using standard methods (10, 11). All comparisons were made using Student's *t* test (12).

RESULTS

The preparations of II were purified by HPLC to remove unbound label as pertechnetate. This was necessary because the presence of small amounts of oxygen during the heating period decomposed some of the chelate and reoxidized the technetium. The isomeric chelated forms were not separated since they have been shown to have small *in vivo* differences (7) and ultimate use of this preparation in clinical situations would not involve HPLC purification (hence no possibility for separation of chelate forms).

Blood disappearance curves for the radioactivities of I and II under normal and sulfobromophthalein conditions are shown in Figs. 1 and 2. In control rats, II levels were somewhat lower in the first 5 min while I levels were slightly lower afterwards. Both compounds are rapidly cleared with <1% of the injected dose remaining in the blood at 14 min for I and at 18 min for II. In rats treated with sulfobromophthalein the blood disappearance of both compounds was slowed; however, the disappearance of II was faster than that of I at all times.

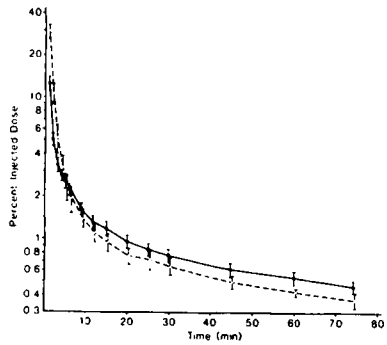

Figure 1—*Disappearance of radioactivity from I (- -○- -) and II (-●-) from blood of normal rats. Data are plotted as mean* ± SEM (n = 5) *and represent percent of injected dose remaining in total blood.*

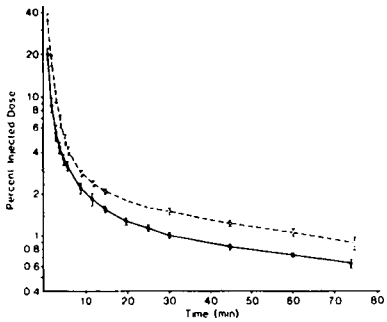

Figure 2—*Disappearance of radioactivity from I (- -○- -) and II (-●-) from the blood of rats treated with sulfobromophthalein. Data are plotted as mean* ± SEM (n = 5) *and represent percent of injected dose remaining in total blood.*

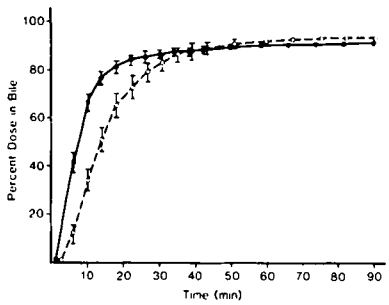

Figure 3—*Comparative rates of appearance of radioactivity from I (- -○- -) and II (-●-) in bile in normal rats. Data are plotted as mean* ± SEM *of percent of injected dose.*

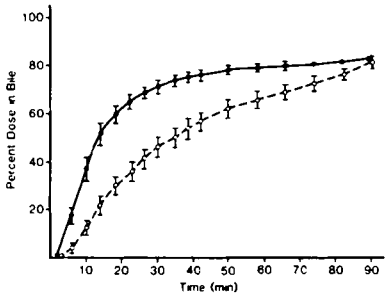

Figure 4—*Comparative rates of appearance of radioactivity of I (- -○- -) and II (-●-) in bile of rats treated with sulfobromophthalein. Data are mean* ± SEM (n = 5) *percent of injected dose.*

Bile cumulative radioactivity curves for the radiopharmaceuticals are shown in Figs. 3 and 4. In normal rats II appeared significantly faster. Forty-one percent of the dose of II was found in the bile by 6 min compared with 12%

[1] E. R. Squibb & Sons, New Brunswick, N.J.
[2] Gelman ITLC, Ann Arbor, Mich.
[3] Nihon Medi-Physics, Takarazuka, Japan.
[4] Beckman-Altex gradient system with 5-μm ultrasphere ODS column, Berkeley, Calif.

Table I—Excretion and Pharmacokinetic Parameters of Hepatobiliary Agents in Control and Treated Rats [a]

Radiopharmaceutical	Urine Excretion, %[b]	Biliary Excretion, %[b]	CL_t, mL/min/kg	Vd, mL/kg	Mean Residence Time, min
I					
Control	0.27 ± 0.08	93.86 ± 1.13	50.8 ± 4.6	743 ± 73[c]	14.6 ± 0.56[c]
Sulfobromophthalein	0.47 ± 0.08	81.02 ± 1.48	29.5 ± 0.93[c]	564 ± 36	19.2 ± 1.00
II					
Control	1.89 ± 0.25	91.45 ● 1.30	70.0 ± 8.0	1695 ± 209	24.1 ± 0.51
Sulfobromophthalein	3.00 ± 0.39	81.98 ± 1.17	46.8 ± 2.7	1042 ± 88	22.1 ± 0.89

[a] Data are mean ± *SEM*. [b] Urine and biliary excretion are percent injected dose at 90 min postinjection. [c] Statistically significant difference ($p < 0.05$) from II (sulfobromophthalein).

for I. Comparative values at 10 min were 66 and 34%; by 40 min, equivalent percentages of each had been excreted. The high final values indicate the high specificity of both compounds.

In sulfobromophthalein-treated animals the rates of appearance of radioactivity in the bile were significantly decreased. Moreover, the differences between compounds I and II were more marked in treated animals than controls. Over the first 20 min II appeared at a lower rate than in the normal animals, but essentially at the same rate as I in normal animals.

Quantitative comparisons of renal and hepatobiliary excretion of the complexes and pharmacokinetic parameters are shown in Table I. Both agents exhibited high specificity for hepatobiliary excretion. However, the percentage of I (94.9%) was higher than II (91.4%) in bile. This was consistent with a lower renal excretion of I (0.27% compared with 1.89% for II). In animals treated with sulfobromophthalein, biliary excretion was reduced for both radiopharmaceuticals to ~82% at 90 min. Conversely, renal excretion at 90 min was increased for both, but only by a small percentage (from 0.3 to 0.5% for I and from 1.9 to 3.0% of the injected dose for II).

Statistically, the blood clearances for I and II were not significantly different for the controls ($p < 0.05$). Since both agents are highly specific for hepatobiliary excretion, the correction of blood clearances for renal clearances was considered negligible. The magnitude of clearances for the two agents indicates efficient hepatobiliary excretion of both agents at rates which would depend primarily on hepatic blood flow. The clearances of both II and I were reduced in the presence of sulfobromophthalein. In this case the difference in clearance values was statistically significant ($p < 0.05$). The distribution volume for II was greater than that for I ($p < 0.05$) and the volumes of both compounds were decreased during the administration of sulfobromophthalein.

The mean residence time (MRT) for II was greater than the MRT for I ($p < 0.05$). The MRT is directly related to distribution volume and inversely related to blood clearance (MRT = distribution volume/blood clearance). Thus, although the hepatobiliary excretion (blood clearance) of II is more efficient than that of I, the II distribution volume is greater, resulting in a greater MRT for II. Caution should be exercised however, since interpretations of MRT values are difficult if the clearing organ (in this case the liver) is also responsible for significant distribution of the compound (13).

DISCUSSION

Both of the ^{99m}Tc-labeled hepatobiliary agents evaluated here are the result of the synthesis and biological study of a long series of chelating agents beginning with *N*-(2,6-dimethylacetanilide)iminodiacetate for I and pyridoxylidene glutamate for II. They both rate highly with regard to the clinical objectives of rapid hepatocyte uptake from the blood, short hepatocyte transit times, high specificity for hepatobiliary excretion, and ability to be taken up and excreted by the liver with high specificity in the presence of bilirubin or other competing transport pathway members. The questions of this study are whether or not one agent is significantly superior and whether or not a comparative evaluation in animals can indicate which will be superior in clinical use.

In this study sulfobromophthalein was used as a model for the determination of the ability of these technetium complexes to be taken up and excreted by the liver in the jaundiced or hyperbilirubinemic patient. A more direct way would have been to use bilirubin. However, it has been difficult to achieve sufficiently high serum bilirubin levels for significant effects on the transport of ^{99m}Tc-labeled iminodiacetate radiopharmaceuticals without causing toxic reactions (14, 15). The secretion of bilirubin is competitively inhibited by sulfobromophthalein (16) and many examples of similar effects on the transport of bilirubin and sulfobromophthalein are known (17). In addition, studies in isolated hepatocytes, in which sulfobromophthalein and bilirubin were separately added, both were reported to have comparable effects on the uptake of ^{99m}Tc-labeled iminodiacetate complexes by the hepatocytes (14).

Short hepatocyte transit times result in a "bolus" effect on the passage of radioactivity from liver to bile. This effect allows imaging of the hepatic ducts superimposed on the liver and often provides information on the location of problems in the biliary ductule network (14). The data from these studies demonstrate that with similar blood disappearance rates and thus hepatic uptake,the more rapid biliary excretion of II results in an advantage in bile-to-liver ratio comparisons.

Under normal liver function conditions the blood disappearance rates of both agents were similar. The bile appearance of II was significantly faster and indicates a shorter hepatocyte transit time for II. Final values of collected activity in the bile were consistent with their reported specificities for hepatobiliary excretion (4, 6).

Studies in which the transport capacity of the liver was stressed by sulfobromophthalein resulted in greater differences between the complexes. Under this condition the blood percent dose values for II were lower at all times and biliary excretion differences were more marked than in normal control studies. Thus, II was superior in its uptake and excretion in competition with sulfobromophthalein and, as such, appears to have a higher affinity for the transport proteins.

The results of these studies support a small specificity superiority for I and a significant kinetic superiority for II as hepatobiliary radiopharmaceuticals. However, species differences are well known (18) and it must be emphasized that there is still a need to compare these agents in humans.

REFERENCES

(1) A. R. Fritzberg and W. C. Klingensmith, *J. Nucl. Med.*, **23,** 543 (1982).

(2) R. J. Baker, J. C. Bellen, and P. M. Ronai, *J. Nucl. Med.*, **16,** 720 (1975).

(3) E. Harvey, M. Loberg, and M. Cooper, *J. Nucl. Med.*, **16,** 533 (1975).

(4) A. D. Nunn, M. D. Loberg, and R. A. Conley, *J. Nucl. Med.*, **24,** 423 (1983).

(5) W. C. Klingensmith, A. R. Fritzberg, V. M. Spitzer, D. C. Cuni, M. R. Williamson, and J. P. Gerhold, *Radiology*, **146,** 181 (1983).

(6) M. Kato-Azuma, *J. Nucl. Med.*, **23,** 517 (1982).

(7) M. Kato-Azuma, H. Ueda, and M. Hazue, *J. Nucl. Med.*, **24,** 127 (1983).

(8) D. Dhumeaux, P. Berthelot, A. M. Preaux, S. Erlanger, and R. Fauvert, *Rev. Eur. Etud. Clin. Biol.*, **15,** 279 (1970).

(9) "United States Pharmacopeia," 20th rev., U.S. Pharmacopeial Convention, Inc., Rockville, M.D., 1980, p. 764.

(10) K. Yamaoka, T. Nakagawa, and T. Uno, *J. Pharmacokinet. Biopharm.*, **6,** 547 (1978).

(11) L. Z. Benet and R. L. Galeazzi, *J. Pharm. Sci.*, **68,** 1071 (1979).

(12) A. Goldstein, in "Biostatistics: An Introductory Text," A. Goldstein, Ed., MacMillan, New York, 1964, pp. 61 and 62.

(13) W. J. Jusko, in "Applied Pharmacokinetics," W. E. Evans, J. J. Schentag, and W. J. Jusko, Eds., Applied Therapeutics, Inc., San Francisco, 1980, p. 662.

(14) M. D. Loberg, A. D. Nunn, and D. W. Porter, in "Nuclear Medicine Annual 1981," L. M. Freeman and H. S. Weissmann, Eds., Raven Press, New York, 1981, pp. 1-33.

(15) A-L. Jansholt, D. R. Vera, K. A. Krohn, and R. C. Stadalnik, "Radiopharmaceuticals II, Proc. 2nd Intl. Symp. on Radiopharmaceuticals," V. J. Sodd, D. R. Hoogland, D. R. Allen, and R. D. Ice, Eds., Society of Nuclear Medicine, New York, 1979, pp. 555 564.

(16) T. Hargreaves, *Q. J. Exp. Physiol.*, **51,** 184 (1966).

(17) J. D. Ostrow, in "The Liver," F. F. Becker, Ed., Dekker, New York, 1974, Ch. 11, pp. 303-369.

(18) R. L. Smith, "The Excretory Function of Bile," Chapman and Hall, London, 1973, pp. 73.

Agonist–Antagonist Actions and Stereoselectivity of Optical Pairs of Some *N*-Substituted α-*N*-Normetazocines

MARIO D. ACETO *, EVERETTE L. MAY *x, LOUIS S. HARRIS *, ARTHUR E. JACOBSON ‡, and HIROYOSHI AWAYA *§

Received November 21, 1983, from the *Department of Pharmacology, Medical College of Virginia, Virginia Commonwealth University, Richmond, VA 23298 and the ‡National Institutes of Health, Bethesda, MD 20205. Accepted for publication March 21, 1984. §Present address: 1-Ku Maragouchi Onoda, Yamaguchi 756 Japan

Abstract □ α-(−)-, (+)-, and (±)-*N*-4-Methylpentyl-, (−)- and (+)-*N*-*cis*-3-chloroallyl-, and (−)- and (+)-*N*-propynyl-*N*-normetazocine (I, II, and III, respectively) have been prepared from α-(−)-, (+)-, and (±)-*N*-normetazocine (IV) and tested for antinociceptive activity in mice and in morphine-dependent rhesus monkeys. The results obtained with Ia and b somewhat resemble the results obtained with the corresponding phenazocine isomers, whereas those observed with IIa and b more nearly correspond with those reported for (+)- and (−)-*N*-allyl-*N*-normetazocine (SKF 10,047; NANM). The propynyl isomers (IIIa and b) display profiles of activity more closely like the corresponding isomers of metazocine. Evidence is considered which suggests that some of the (+)-isomers merit closer scrutiny in animal and human studies.

Keyphrases □ α-Normetazocine—alkylation, optical pairs, antagonism, antinociception, psychotomimetic, mice, morphine-dependent rhesus monkeys □ Antagonists—α-normetazocine, alkylation, antinociception, psychotomimetic, mice, morphine-dependent rhesus monkeys

N-Substituted *N*-normetazocines of the α-series[1] (1) have attained importance not only in current medicine[2] but also in behavioral studies (2) and as receptor probes (3). Optical pairs are of particular interest (2–4). The present note describes the chemistry and some basic pharmacology of three optical pairs and one racemate belonging to the α-series.

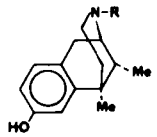

I: R = $(CH_2)_3CHMe_2$
II: R = $CH_2CH{=}CHCl$ (Cis)
III: R = $CH_2C{\equiv}CH$
IV: R = H

a = (+), b = (−), c = (±)

EXPERIMENTAL SECTION

Chemistry[3]—The compounds were synthesized by alkylation of α-*N*-normetazocine (IV) using a tetrahydrofuran–dimethylformamide solvent mixture[4] and the halides 4-methylpentyl bromide for I, *cis*-1,3-dichloropropene for II, and propynyl chloride for III. Potassium carbonate or potassium bicarbonate was the hydrogen bromide or hydrogen chloride acceptor. Antipodes IIa and IIb were also prepared by optical resolution of α-(±)-3-*cis*-chloropropenyl-*N*-normetazocine (IIc) (5)[5] with *d*- and *l*-mandelic acids.

Mouse Antinociception Tests—Male mice weighing 20–30 g were used. All drugs were administered as salts, dissolved in distilled water, and administered subcutaneously in a volume of 0.1 mL/10 g of body weight. At least three doses per curve were tested and 6–10 animals per dose were used. ED_{50} values were calculated using computerized probit analysis.

Tail-Flick (TF) Tests—The procedure and modification (6) have been described. Briefly, the mouse tail was placed in a groove which contained a slit under which was a photoelectric cell. When the heat source or noxious stimulus was turned on, it focused on the tail and the animal responded by flicking its tail out of the groove. Thus, light passed through the slit and activated the photocell which, in turn, stopped the recording timer. The apparatus was calibrated so that control mice would flick their tails in 2–4 s. Mice were injected subcutaneously with drug and tested 20 min later. Vehicle controls were also tested.

In the antagonism experiments (tail-flick *versus* morphine), the antagonists were administered subcutaneously 10 min before morphine, and the animals were tested 20 min later.

Phenylquinone (PPQ) Abdominal Stretching Test (7)—The mice were injected subcutaneously with drugs and 10 min later received 2 mg/kg of a fresh *p*-phenylquinone solution intraperitoneally. The mice were then placed in cages in groups of two. At 10 min after the phenylquinone injection, the total number of stretches per group were counted within a 1-min period. A stretch was characterized by an elongation of the body, development of tension in the muscles in the abdominal region, and extension of the forelimbs. The antinociceptive response was expressed as the percent inhibition of the phenylquinone-induced stretching response. Appropriate controls were used.

Hot Plate (HP) Assay (8)—The hot plate was held at a constant 55°C *via* a refluxing 1:1 mixture of ethyl formate and acetone. Mice were placed on the hot plate, and activity was noted as a delay of ≥5 s but no more than 30 s beyond the control time for the movement of the hind limb of the mouse, over at least two consecutive time periods. The mice were tested at 5, 10, 20, 30, 60 min, and longer if necessary, until responses returned to control levels.

Dependent Rhesus Monkey—In the single-dose substitution (SDS) test, for the most part, the recommendations of Seevers (9) and Seevers and Deneau (10) were utilized. A brief description of the procedure, including modifications (11), is as follows. Male and female rhesus monkeys (*Macaca mulatta*) weighing 2.5–7.5 kg were used. The animals were housed in pens, four or five to a group, and received 3 mg/kg sc of morphine every 6 h. This dose schedule was reported to produce maximal physical dependence (10). All the animals had received morphine for ≥3 months. A minimal, 2-week, wash-out and recuperation period was allowed for each animal between tests. The SDS test was initiated by the subcutaneous injection of the test drug or control substances (morphine and vehicle water, respectively) into the animals in a group that had not received morphine for 14–15 h and showed definite signs of withdrawal. Each animal was randomly allocated to one of four or five treatments: (*a*) two or three dose levels of the compound under investigation; (*b*) the morphine control, 3.0 mg/kg; (*c*) the vehicle control, 1 mL/kg. The animals were scored for suppression of withdrawal signs during a 2.5-h ob-

[1] α-Metazocine is 2′-hydroxy-2,5,9α-trimethyl-6,7-benzomorphan. For a comprehensive review and alternative chemical names for the 6,7-benzomorphans see Ref. 1.

[2] Pentazocine (see Refs. 1 and 5) is marketed as Talwin for both oral and parenteral use; phenazocine (Ref. 13) is sold in England as Narphen.

[3] Melting points (capillary, uncorrected, Table III) were taken in a Thomas–Hoover apparatus; mass spectral (molecular weights in agreement with theory) and C, H, and N data (Table III) are from the Section on Instrumentation and Analytical Services, National Institutes of Health. Optical rotations (Table III) were taken in a Perkin-Elmer 261 instrument using methanol as a solvent with the exception of IIIa and IIIb (bases) which were in ethanol. Rotation temperatures were 21–26°C. Free bases were recrystallized from acetone or acetone–hexane; hydrobromide salts were recrystallized from methanol–acetone. All compounds crystallized as white needles or prisms.

[4] This solvent mixture was suggested by Dr. H. Merz, C. H. Boehringer Sohn, Ingelheim, West Germany, who also kindly supplied 1,3-*cis*-dichloropropene.

[5] Compound IIc was supplied by Dr. A. E. Soria, Sterling-Winthrop Research Institute, Rensselaer, N.Y.

0022-3549/84/1200-1864$01.00/0
© 1984, American Pharmaceutical Association

Table I—Antinociceptive and Narcotic Antagonist Data for *N*-Substituted α-Normetazocine and Standards [a]

Compound	Antinociceptive Activity (ED_{50}), mg/kg sc			Antagonistic Activity (AD_{50}), mg/kg sc
	Tail-Flick Test	*p*-Phenylquinone Test	Hot Plate Test	Tail-Flick *versus* Morphine
Ia[b]	Inactive	16.3 (3.7-45.8)	70% at 100.0	Inactive
Ib[b]	20.6 (9.9-42.4)	0.9 (0.3-3.1)	3.1 (2.4-4.1)	Inactive
Ic[c]	10.8 (3.1-37.3)	5.1 (2.5-10.4)	8.3 (6.0-11.4)	Inactive
IIa[b]	Inactive	55% at 30	30% at 50.0	23.9 (17.6-32.6)
IIb[b]	Inactive	1.7 (0.5-5.9)	20% at 20.0	0.004 (0.002-0.008)
IIIa[b]	Inactive	Inactive	10% at 20.0	Inactive
IIIb[b]	Inactive	0.2 (0.1-0.4)	50% at 20.0	0.03 (0.1-0.7)
Morphine[d]	5.8 (5.7-5.9)	0.2 (0.2-0.3)	1.0 (0.8-1.1)	Inactive
Nalorphine[c]	Inactive	0.6 (0.3-1.4)	9.9 (5.7-17.1)	2.6 (0.7-9.8)

[a] Range of values is in parentheses. [b] Hydrobromide salt. [c] Hydrochloride salt. [d] Sulfate salt.

servation period. The observer was "blind" regarding the allocation of treatments. At the end of the study, the data were grouped according to dose and drug, and the results were analyzed using the Mann-Whitney U-test (12).

Precipitated Withdrawal (PPTW) Test in Rhesus-Monkeys—The PPTW test was performed under the conditions described above for the SDS test, except that the animals of a group were challenged 2 or 3 h after the last dose of morphine. Naloxone at a dose of 0.05 mg/kg sc served as the positive control.

(±)-5,9α-Dimethyl-2′-hydroxy-2-(4-methylpentyl)-6,7-benzomorphan (Ic)—A mixture of 2.0 g of IVc (1, 13), 1.6 g of 4-methylpentyl bromide, 2.5 g of potassium bicarbonate, 4 mL of tetrahydrofuran, and 8 mL of dimethylformamide[4] was stirred at reflux for 2-3 h, cooled, diluted with 20-25 mL of water, and extracted with 30-40 mL of ether. The ether was washed twice with water, dried (sodium sulfate), and evaporated to dryness giving 1.9 g of Ic, mp 138.0-138.5°C after recrystallization[3].

The hydrochloride salt of Ic was prepared in acetone with hydrogen chloride. Compounds Ia and Ib were similarly prepared using IVa and IVb, respectively (14). The hydrobromide salts were prepared in acetone-33% hydrogen bromide in acetic acid.

Similarly, IIa and IIb were synthesized from IVa and IVb and *cis*-1,3-dichloropropane[4], and IIIa and IIIb were obtained from IVa and IVb and propynyl chloride; they were characterized as free bases and hydrobromide salts. Compounds IIa and IIb were also characterized as *d*- and *l*-mandelate salts, respectively.

Optical Resolution of α-(±)-2-(3-*cis*-Chloropropenyl)-5,9-dimethyl-2′-hydroxy-6,7-benzomorphan (IIc)—A mixture of 4.3 g of IIc (5)[5], 2.6 g of *d*-mandelic acid, and 75 mL of absolute ethanol was heated until a solution was obtained and allowed to stand at room temperature for 4-5 h to give 2.5 g of the *d*-mandelate salt of IIa, mp 181-186°C. This was dissolved in 40 mL of boiling absolute ethanol. This solution deposited 2.0 g of pure IIa *d*-mandelate after standing overnight at room temperature. It was converted to 1.2 g of the base IIa by dissolving in boiling methanol (10 mL)-water (5 mL) and treating the solution with 5 mL of concentrated ammonium hydroxide, mp 136.0-138.5°C after a recrystallization from acetone-hexane.

Table II—Effects of *N*-Substituted Normetazocine in the Morphine-Dependent Rhesus Monkey

Compound	Single-Dose Substitution Test, mg/kg sc	Precipitated Withdrawal Test, mg/kg sc
Ia[a]	Did not substitute (3.0-12.0)	Weak activity; convulsions (6.0-18.0)
Ib[a]	Substituted completely (1.5-3.0)	Not tested
Ic[a]	Did not substitute; convulsions (12.0)	Not tested
IIa[a]	Did not substitute (0.25-4.0)	Did not precipitate withdrawal, 1.0-12.0 mg/kg
IIb[a]	Did not substitute (0.125-0.5)	Precipitated withdrawal (0.015-1.0)
IIIa[a]	Partial brief substitution (1.25-10.0)	Not tested
IIIb[a]	Did not substitute (0.015-0.25)	Precipitated withdrawal (0.125-0.5)
Morphine[b]	Substituted (3.0)	Did not precipitate withdrawal, (1.5-6.0)
Nalorphine[c]	Did not substitute (0.1-1.0)	Precipitated withdrawal (0.5)

[a] Hydrobromide salt. [b] Sulfate salt. [c] Hydrochloride salt.

The filtrates from isolation and recrystallization of the *d*-mandelate salt above were combined and evaporated to dryness under reduced pressure. The residue in warm methanol was treated with dilute ammonium hydroxide, affording 2.7 g of a mixture of IIa and IIb. This mixture, 1.7 g of *l*-mandelic acid and 30 mL of absolute ethanol, was heated to solution and left at room temperature for 4.5 h, affording 1.9 g of the *l*-mandelate salt of IIb, mp 181-186°C. This was dissolved in 20 mL of boiling absolute ethanol. The solution was concentrated to 12-15 mL and allowed to stand at room temperature overnight, affording 1.6 g of pure IIb *d*-mandelate which was converted to base IIb with methanol ammonium hydroxide as described for IIa above. Bases IIa and IIb and their mandelate salts were identical to those obtained from IVa and IVb, respectively, and *cis*-1,3-dichloropropene.

RESULTS

The different *N*-substituted normetazocines showed dissimilar profiles of activity (Tables I and II). None of the isomers nor the racemate of the *N*-4-methylpentyl-substituted normetazocine (Ia-c) showed antagonist activity *versus* morphine antinociception. Both the (−)-isomer and racemate were active in the TF, PPQ, and HP tests; the (−)-isomer was more potent than the racemate. In morphine-dependent monkeys, none of the compounds precipitated withdrawal and only the (−)-isomer substituted for morphine. The (+)-isomer and racemate produced convulsions, precluding testing at higher doses. Regarding the *N*-substituted chloroalkyl isomers, both IIa and b antagonized morphine antinociception; the (−)-isomer was clearly the more potent, ~50 times more so than nalorphine. Neither isomer was active in the TF or HP tests. In the PPQ test, the (−)-isomer was decidedly the more active antipode. Both isomers antagonized morphine antinociception; again, the (−)-isomer was far more potent. Neither isomer substituted for morphine in the addicted monkeys: the (−)-isomer, as expected, precipitated withdrawal, the (+)-isomer did not.

Finally, with the *N*-propynyl-substituted (+)- and (−)-normetazocines (IIIa,b) the following results were obtained. The (+)-isomer showed very weak activity in the HP test only and was devoid of antagonist activity. However, it partially substituted for morphine in addicted monkeys. The (−)-isomer showed weak agonist activity in the HP test and was equipotent with morphine in the PPQ test. As an antagonist, the (−)-isomer was much more active than nalorphine.

DISCUSSION

Results obtained with the 4-methylpentyl (I) isomers are vaguely reminiscent of those obtained with phenazocine antipodes (13), potency differences notwithstanding[6]. In both series, (−)-isomers supported morphine dependence although, relatively, a much larger dose of (−)-phenazocine was needed. Neither (+)-isomer would substitute for morphine, and with Ia severe tremors were noted. In retrospect, (+)-phenazocine, nearly as potent as morphine in the HP test, should have been tested more extensively.

Observations noted with the *N*-chloroallyl isomers (IIa,b) are quantitatively similar to those reported (15) for (+)- and (−)-*N*-allyl-*N*-normetazocine (NANM); IIb is a very powerful antagonist. It is interesting to note that Brady and co-workers recently showed (2) in rats and squirrel monkeys trained to discriminate the psychotomimetic phencyclidine hydrochloride (PCP) from saline that the (+)-isomer of NANM produced dose-dependent responses appropriate for PCP. The (−)-isomer did not produce responses appropriate for PCP at any dose. These data suggest a separation of psychotomimetic and

[6] Phenazocine is α-(±)-*N*-phenethyl-substituted *N*-normetazocine. It and its antipodes are 20-30 times more potent antinociceptively than corresponding I compounds.

Table III—Optical Rotation, Melting Points, and Analyses

Compound	$[\alpha]_D$	Concentration	mp, °C	Formula[a]
Ia	+100.1°	0.70	130-131	$C_{20}H_{31}NO$
Ia·HBr	+71.2°	0.87	229 230	$C_{20}H_{32}BrNO$
Ib	−99.5°	0.78	130-131	$C_{20}H_{31}BrNO$
Ib·HBr	+69.9°	0.67	229-230	$C_{20}H_{32}BrNO$
IIa	+115.8°	0.62	138-139[b]	—
IIa·HBr	+69.3°	0.49	199-200	$C_{17}H_{23}BrClNO$
IIa·*d*-Mandelate	+100.0°	0.78	186.0-187.5	—
IIb	−115.4°	0.95	137.0-138.5[c]	—
IIb·HBr	−68.9°	0.47	198-200	$C_{17}H_{23}BrClNO$
IIb·*l*-Mandelate	−99.7°	0.57	186-188	—
IIIa	+124.0°	0.23	167-169	—
IIIa·HBr	+90.9°	0.34	210-211	$C_{17}H_{22}BrNO$
IIIb	−124.0°	0.21	167-169	—
IIIb·HBr	−90.2°	0.35	210-211	$C_{17}H_{22}BrNO$
Ic	—	—	138.0-138.5	$C_{20}H_{31}NO$
Ic·HCl·H_2O	—	—	139-140	$C_{20}H_{32}ClNO·H_2O$

[a] All compounds were analyzed for C, H, and N; all values were within 0.4% of theoretical value. [b] Another crystalline modification melted at 115°C with gas evolution. [c] Another crystalline modification melted at 189-190°C.

analgesic effects. Whether in humans (−)-NANM or the chloroallyl *N*-substituted derivative are free of psychotomimetic effects remains to be shown. The racemate (IIc) was reported in 1964 (5), as was IIIc whose antipodes (IIIa,b) displayed profiles of activity reminiscent of *N*-methyl-6,7-benzomorphans of the α-series. This series was unique in two respects: (*a*) (+)-isomers substituted partially or completely for morphine; (*b*) the more antinociceptively potent (HP test) (−)-isomers would not. In fact, like IIIb, the (−)-isomers of this *N*-methyl series precipitated abstinence signs in morphine-dependent monkeys (4), yet two were more morphine-like than nalorphine-like in humans (16). In view of these different profiles of activity in animals and the remarkable separation of morphine-like effects in different species, these compounds [especially the (+)-isomers] deserve more extensive testing, perhaps in humans.

The exploitation of these differences may expand our knowledge of the basic mechanisms involved and possibly lead to a development of an ideal analgesic. It is also evident that studies with racemates may at times be misleading and that whenever possible pure optical isomers should be used.

REFERENCES

(1) D. A. Palmer and M. J. Strauss, *Chem. Rev.*, **77**, 1 (1977).

(2) K. T. Brady, R. L. Balster, and E. L. May, *Science*, **215**, 178 (1982).

(3) E. T. Iwamoto and W. E. Martin, *Med. Res. Rev.*, **1**, 411 (1981); S. H. Snyder, *Sci. Am.*, **236**, 44 (1977).

(4) J. H. Ager, A. E. Jacobson, and E. L. May, *J. Med. Chem.*, **12**, 288 (1969).

(5) S. Archer, N. F. Albertson, L. S. Harris, A. K. Pierson, and J. G. Bird, *J. Med. Chem.*, **7**, 123 (1964).

(6) F. E. D'Amour and D. L. Smith, *J. Pharmacol. Exp. Ther.*, **72**, 74 (1941); W. L. Dewey, L. S. Harris, J. F. Howes, and J. A. Nuite, *J. Pharmacol. Exp. Ther.*, **175**, 435 (1970).

(7) J. Pearl and L. S. Harris, *J. Pharmacol. Exp. Ther.*, **154**, 319 (1966).

(8) N. B. Eddy and D. Leimbach, *J. Pharmacol. Exp. Ther.*, **107**, 385 (1953); L. Atwell and A. E. Jacobson, *Lab. Anim.*, **7**, 42 (1978); A. E. Jacobson and E. L. May, *J. Med. Chem.*, **8**, 563 (1965).

(9) M. H. Seevers, *J. Pharmacol. Exp. Ther.*, **56**, 157 (1936).

(10) M. H. Seevers and G. A. Deneau, "Physiological Pharmacology I," W. S. Root and F. G. Hofman, Eds., Academic Press, New York, N.Y., 1963, p. 565.

(11) M. D. Aceto, W. L. Dewey, J. K. Chang, and N. M. Lee, *Eur. J. Pharmacol.*, **83**, 139 (1982).

(12) A. Seigel, "Nonparametric Statistics for the Behavioral Sciences," McGraw-Hill, New York, 1956.

(13) E. L. May and M. B. Eddy, *J. Org. Chem.*, **24**, 1435 (1959).

(14) B. F. Tullar, L. S. Harris, R. L. Perry, A. K. Pierson, A. E. Soria, W. F. Wetteran, and N. F. Albertson, *J. Med. Chem.*, **10**, 383 (1967).

(15) M. D. Aceto and E. L. May, *Eur. J. Pharmacol.*, **91**, 267 (1983).

(16) D. R. Jasinski in, "Drug Addiction I, Assessment of the Abuse Potentiality of Morphine (Methods used in Man)," W. R. Martin, Ed., Springer-Verlag, New York, 1977, chap. 3.

ACKNOWLEDGMENTS

Thanks are due F. T. Grove, R. Jones, and S. Tucker for their excellent technical contribution. This work was supported by Grant DA-00490 and Contract 271-81-3830, National Institute on Drug Abuse.

9α- and 9β-Hydroxyphenylmorphans

HIROYOSHI AWAYA *§, EVERETTE L. MAY *x, ARTHUR E. JACOBSON ‡, and MARIO D. ACETO *

Received November 25, 1983, from the **Department of Pharmacology, Medical College of Virginia, Virginia Commonwealth University, Richmond, VA 23298* and the ‡*National Institutes of Health, Bethesda, MD 20205.* Accepted for publication March 21, 1984. §Present address: 1-Ku Marugouchi Onoda, Yamaguchi 756 Japan.

Abstract □ Platinum-oxide hydrogenation of 5-*m*-methoxyphenyl-2-methyl-9-oxomorphan (I) gave the 9α-hydroxy racemate (II) whose phenolic analogue (III) is a strong antinociceptive agent, fully supportive of morphine dependence in rhesus monkeys. The di-*O*-acetyl derivative (VI) of III was similar to III in its profile of activity. The diastereoisomer of III (VII), obtained by hydrogenation of the methobromide of I (IV), extrusion of methyl bromide, and *O*-demethylation of the resultant free base (VIII), was almost inactive antinociceptively and did not suppress withdrawal symptoms in morphine-dependent monkeys. The orientation of the C-9 hydroxyl groups was deduced from spectral data and by analogy.

Keyphrases □ 9α- and 9β-Hydroxyphenylmorphans—hydrogenation, diastereoisomer spectral data, synthesis □ Antinociceptive activity—9α- and 9β-hydroxyphenylmorphans, potency, withdrawal symptoms, substitution for morphine, antagonism

The introduction of a 9α-methyl group (1) into 5-*m*-hydroxyphenyl-2-methylmorphan (IX) (2), whose antipodes are strong antinociceptive agents showing a separation of morphine-like effects (1, 3), gives low-potency antagonists without appreciable pain-relieving properties. It was desired to determine the effect of hydroxyl substitution in the 9-position of IX. One of the two possible diastereoisomers (VII) resulting from such substitution would be similar to the very potent (10 times morphine) oxymorphone (4) with respect to 9-OH—N geometry. The synthesis of VII and its diastereoisomer (III) and some pharmacological findings are presented herein.

RESULTS AND DISCUSSION

Chemistry—When bicyclic ketone I (free base of hydrochloride salt) was hydrogenated in ethanol (platinum oxide), addition of hydrogen was stereoselective; the 9α-alcohol (II) was isolated in 98% yield. To obtain the 9β-alcohol (VIII), the methobromide of I (IV) was similarly hydrogenated, giving V which was converted to free base VIII pyrolytically (Scheme I).

Hydroxyl assignments are based principally on IR spectral data, which indicated strong 9-OH N bonding for VIII. Only free hydroxyl absorption and 9-OH-π bonding were seen for II. The ^{1}H-NMR data also appeared to support these assignments (see C-9 H values for ^{1}H-NMR and IR maxima in the *Experimental Section*). Finally, this stereochemical pattern of addition of hydrogen to the carbonyl group of I would be similar to that observed in the benzomorphan series (5) and for 5-*m*-methoxyphenyl-2-methyl-9-methylenemorphan (1).

Phenols III and VII were prepared from II and VIII, respectively, with boiling 48% hydrobromic acid or with boron tribromide in methylene chloride (6). Diacetate VI resulted from treatment of III with acetic anhydride containing a little pyridine.

Pharmacology—As recorded in Table I, the 9α-hydroxy racemate (III) is comparable to morphine in antinociceptive activity in mice by the tail-flick (TF) (7), *p*-phenylquinone-writhing (PPQ) (7), hot-plate (HP) (8), and Nilsen (9) tests, while the 9β-isomer (VII) had low-order potency in the PPQ test only. Compound III fully supported morphine dependence in rhesus monkeys at 1–16 mg/g, but VII, as expected, did not substitute for morphine at 3–18 mg/kg (10). The antinociceptive potency of the di-*O*-acetyl derivative of III (VI) was similar to that of the parent III in the TF, PPQ, and HP tests. In opiate-dependent monkeys, VI completely suppressed abrupt withdrawal at 10.0 mg/kg[1]. It was reported earlier (11) that VI did not suppress withdrawal at 1–10 mg/kg, results that seem inconsistent with the antinociceptive profiles

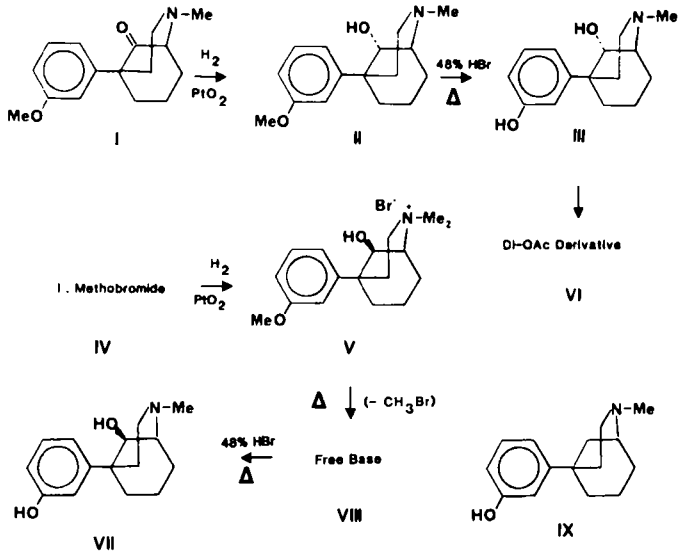

Scheme I

of activity of VI and its precursor III. None of the three racemates (III, VI, and VII) elicited properties of antagonism in the opiate-dependent monkey (10, 11) or in the TF *versus* morphine test (10).

It seems noteworthy that VII, with 9-OH—N geometry similar to that of oxymorphone (4) is relatively inactive. It would therefore be of interest to synthesize the 14α-hydroxy epimer of oxymorphone which would correspond to the very active III.

EXPERIMENTAL SECTION[2]

9α-Hydroxy-5-*m*-methoxyphenyl-2-methylmorphan (II) Hydrochloride—Compound I (1.0 g, 3.9 mmol) in 60 mL of methanol was hydrogenated (Parr apparatus, 30 psig, 25°C) with 0.15 g of platinum oxide during 2 h. The filtered solution was evaporated to dryness under reduced pressure giving 0.98 g of II, mp 98–100°C (from ether–petroleum ether). IR ($CHCl_3$): 3650 w (free OH) and 3570 m cm^{-1} (OH-π bonding); ^{1}H-NMR ($CDCl_3$): δ 2.52 (3, s, N—CH_3), 3.81 (3, s, O—CH_3), and 4.32 ppm (1, d, J = 3 Hz, C-9). The hydrochloride salt (from acetone–hydrogen chloride) crystallized from methanol–ether in prisms, mp 225–227°C. ^{1}H-NMR (Me_2SO-d_6): δ 2.80 (3, s, N—CH_3), 3.75 (3, s, O—CH_3) and 5.51 ppm (1, d, J = 3 Hz, C-9); EI-MS: m/z 261 (M^+ − HCl).

Anal.—Calc. for $C_{16}H_{24}ClNO_2 \cdot 0.25\ H_2O$: C, 63.6; H, 8.2; N, 4.6. Found: C, 63.6; H, 8.4; N, 4.4.

9α-Hydroxy-5-*m*-hydroxyphenyl-2-methylmorphan (III)—The hydrochloride salt of II (0.5 g, 2.0 mmol) was added to 5 mL of nearly boiling 48% hydrobromic acid. The solution was refluxed for 12–15 min, cooled, and made alkaline with ammonium hydroxide. The liberated base was dissolved in chloroform (6–8 mL, three extractions). On standing for 30 min, the combined extracts deposited 200 mg of III, mp 193–196°C. From the filtrate and chloroform washings of the precipitate, an additional 140 mg of III separated after cooling to 0°C, total yield 80%. It was nearly pure [TLC: R_f 0.25, silica gel, chloroform–methanol–ammonium hydroxide (90:9:1)] and was recrystallized by dissolving 200 mg in 200 mL of boiling acetone, filtering the hot

[1] Unpublished results.

[2] Melting points (uncorrected) were taken in a Thomas-Hoover capillary apparatus. IR and NMR spectra were obtained with a Beckman Aculab 8 and a 60-MHz Hitachi-Perkin Elmer Model R-24, respectively. Mass and analytical data are from the Section on Microanalytical Services and Instrumentation (Dr. David Johnson, Chief), National Institutes of Health.

0022-3549/84/1200-1867$01.00/0
© 1984, American Pharmaceutical Association

Table I—Antinociceptive Data for 9-Hydroxyphenylmorphans and Morphine

Compound	Antinociceptive Activity (ED_{50}), mg/kg sc			
	Tail-Flick Test	*p*-Phenylquinone Test	Hot Plate Test	Nilsen Test
III[a]	3.5 (2.5–5.0)	0.2 (0.07–0.4)	1.9 (1.5–2.6)	2.7 (2.2–3.2)
VI[b]	7.3 (3.6–14.7)	1.0 (0.3–3.1)	2.0 (1.4–2.8)	—
VII[c]	Inactive[d]	8.6 (4.2–17.6)	Inactive[e]	—
Morphine[f]	5.8 (5.7–5.9)	0.23 (0.20–0.26)	1.0 (0.8–1.1)	1.3 (1.0–1.7)

[a] Hydrochloride salt. [b] Hydrobromide salt. [c] *dl*-Mandelate salt. [d] Essentially inactive; 46% of mice affected at 60 mg/kg. [e] Essentially inactive; 30% of mice affected at 100 mg/kg. [f] Sulfate salt.

solution, concentrating the filtrate to 4 mL, and cooling to 5°C. The yield was 140 mg, mp 197–198°C.

Anal.—Calc. for $C_{15}H_{21}NO_2 \cdot 0.5\ H_2O$: C, 72.8; H, 8.5; N, 5.7. Found: C, 72.8; H, 8.4; N, 5.7.

The hydrochloride salt of III (acetone–hydrogen chloride) was recrystallized from methanol–acetone, mp 225.5–227.0°C. EI-MS: *m/z* 247 ($M^+ - HCl$).

Anal.—Calc. for $C_{15}H_{22}ClNO_2$: Cl, 12.5. Found: Cl, 12.2.

By the method of Rice (5), III could be obtained equally well from II, using boron tribromide.

9α-Acetoxy-5-*m*-acetoxyphenyl-2-methylmorphan (VI) Hydrobromide—Acetic anhydride (20 mL), 0.7 g (2.8 mmol) of III (hydrochloride salt) and a drop of pyridine were refluxed for 1 h. The cooled mixture was poured into 50 mL of ice water, made alkaline by careful addition of potassium carbonate (stirring), and extracted with chloroform–ethanol (10:1, 4 × 25 mL). The combined extracts were washed twice with water, dried (sodium sulfate), and evaporated under reduced pressure to afford 0.62 g (68%) of oily VI which, in acetone, was converted to 0.63 g of the hydrobromide salt with 32% hydrogen bromide–acetic acid. It was recrystallized from acetone–methylene chloride, mp 220–223°C. IR (Nujol): 1760 and 1750 cm^{-1}; EI-MS: *m/z* 331 ($M^+ - HBr$).

Anal.—Calc. for $C_{19}H_{26}BrNO_4$: C, 55.4; N, 6.4; N, 3.4. Found: C, 55.4; H, 6.6; N, 3.3.

9β-Hydroxy-5-*m*-hydroxyphenyl-2-methylmorphan (VII) *dl*-Mandelate—The methobromide (IV) (2) of I (0.5 g, 1.4 mmol) in 30 mL of methanol was hydrogenated (0.15 g of platinum oxide, 23–25°C, 30 psig) for 42 h. The filtered solution was evaporated to dryness under reduced pressure to afford 0.56 g of hygroscopic solid, which was dissolved in 5 mL of 1-nonanol. The solution was refluxed for 5 min under nitrogen, cooled, diluted with 20 mL of ether, and extracted with 20 mL of 10% hydrochloric acid in four portions. The combined extracts were made basic with ammonium hydroxide and extracted with 50 mL of ether in four portions. The ether was washed twice with water, dried (sodium sulfate), and evaporated to dryness under reduced pressure (0.3 mm, 18 h) giving 0.23 g (55% yield) of VIII, mp 68–70°C. IR ($CHCl_3$): 3640 w (free OH), 3560 w (OH–π bonding), and 3400 s cm^{-1} (OH—N bonding); ^1H-NMR ($CDCl_3$): δ 2.40 (3, s, N—CH_3), 3.80 (3, s, O—CH_3), and 4.14 ppm (1, d, J = 4 Hz, C-9); EI-MS: *m/z* 261 (M^+), 244, 232, and 218.

To this base was added 5 mL of hot 48% hydrobromic acid. The solution was refluxed for 10 min, cooled, poured into 20 mL of saturated saline, made alkaline with ammonium hydroxide, and extracted with 50 mL of ether in four portions. The extracts were washed twice with saturated saline, dried (sodium sulfate), and evaporated giving 0.18 g of VII. Treatment of VII with 0.11 g (1 equivalent) of *dl*-mandelic acid in acetone furnished 0.25 g (14% based on starting IV) of the *dl*-mandelate salt of VII, which crystallized from methanol–acetone as a hemihydrate, mp 93–94°C; EI-MS: *m/z* 247 (M^+ – mandelic acid).

Anal.—Calc. for $C_{23}H_{29}NO_5 \cdot 0.5\ H_2O$: C, 67.6; H, 7.4; N, 3.5. Found: C, 67.2; H, 7.2; N, 3.3.

REFERENCES

(1) H. Awaya, E. L. May, M. D. Aceto, H. Merz, M. E. Rogers, and L. S. Harris, *J. Med. Chem.*, **27**, 536 (1984).

(2) E. L. May and J. G. Murphy, *J. Org. Chem.*, **20**, 1197 (1955).

(3) E. L. May and M. Takeda, *J. Med. Chem.*, **13**, 805 (1980); T. G. Cochran, *J. Med. Chem.*, **17**, 987 (1974); M. E. Rogers and E. L. May, *J. Med. Chem.*, **17**, 1328 (1974).

(4) U. Weiss, *J. Am. Chem. Soc.*, **77**, 5891 (1955); T. B. Zalucky and G. Hite, *J. Med. Pharm. Chem.*, **3**, 615 (1961); A. E. Jacobson, E. L. May, and L. J. Sargent, in "Medicinal Chemistry," 3rd ed., A. Burger, Ed., Wiley-Interscience, New York, N.Y., 1970, chap. 49.

(5) H. Kugita and E. L. May, *J. Org. Chem.*, **26**, 1954 (1961).

(6) K. C. Rice, *J. Med. Chem.*, **20**, 164 (1977).

(7) W. L. Dewey, L. S. Harris, J. F. Howes, and J. A. Nuite, *J. Pharmacol. Exp. Ther.*, **179**, 652 (1970).

(8) N. B. Eddy and D. Leimbach, *J. Pharmacol. Exp. Ther.*, **107**, 385 (1953); A. E. Jacobson and E. L. May, *J. Med. Chem.*, **8**, 563 (1965).

(9) T. D. Perrine, L. Atwell, I. B. Tice, A. E. Jacobson, and E. L. May, *J. Pharm. Sci.*, **61**, 86 (1972).

(10) M. D. Aceto, L. S. Harris, and E. L. May, in "Problems of Drug Dependence, 1983," L. Harris, Ed., National Institute on Drug Abuse Research Monograph Series 49, U.S. Government Printing Office, Washington, D.C., 1983, pp. 404 and 413.

(11) J. H. Woods, J. L. Katz, F. Medzihradsky, C. B. Smith, and G. D. Winger, in "Problems of Drug Dependence, 1982," L. Harris, Ed., National Institute on Drug Abuse Research Monograph Series 43, U.S. Government Printing Office, Washington D.C., 1982, p. 508.

ACKNOWLEDGMENTS

Gratitude is expressed to Dr. Herbert Merz, C. H. Boehringer Sohn, Ingelheim, West Germany, for a generous supply of compound I and to S. Tucker, F. T. Grove, and R. Jones for excellent technical assistance. This research was performed under Grant No. 5-21527 and Contract No. 271-81-3830, National Institute on Drug Abuse.

Effects of Solvent Medium on Solubility IV: Comparison of the Hydrophilic–Lipophilic Character Exhibited by Functional Groups in Ethanol–Water and Ethanol–Cyclohexane Mixtures

RUBEN H. MANZO ˣ, AMELIA A. AHUMADA, and ERNESTINA LUNA

Received November 3, 1983, from the *Departamento de Farmacia, Facultad de Ciencias Químicas, Universidad Nacional de Córdoba, Suc. 16, C.C. 61, 5016 Córdoba, Argentina.* Accepted for publication April 13, 1984.

Abstract □ Solvent effects on the solubility of a set of structurally related solid compounds (A_x, A_y, *etc.*) in ethanol-water (system 1) and ethanol-cyclohexane (system 2) are compared by the equation, $\log S_y = P_y \log S_x + C$. For a given structural change, $A_x \rightarrow A_y$, it yields the respective medium-effects parameters, P_{y1} and P_{y2}. They are used to compare the sensitivity of both solvent systems with the structural changes in the substrates by the equation, $\Delta_{12} = (P_{y1} - 1) - (1 - P_{y2})$. Structural changes involving the full replacement of the hydrogen atoms bonded to either O or N afford $\Delta_{12} < 0$, while those involving solely an increase in the alkyl chain of the substrates yield $\Delta_{12} > 0$. A structural change where the donor-acceptor capacity of hydrogen bonding is maintained yields a Δ_{12} approaching zero.

Keyphrases □ Solubility—effects of solvent medium, hydrophilic-lipophilic character, ethanol-water, ethanol-cyclohexane □ Hydrophilic-lipophilic character—effects of solvent medium, ethanol-water, ethanol-cyclohexane, solubility

In previous papers of this series (1-3) Eq. 1 has been used successfully to correlate solvent effects with solubility equilibria:

$$\log S_y = P_y \log S_x + C \qquad \text{(Eq. 1)}$$

S_y and S_x are, respectively, two sets of solubility data of a pair of structurally related compounds, A_y and A_x, which arise from measurements in the same set of adequately selected solvent conditions. This linear free energy relationship (LFER) affords the medium effect parameter P_y, which in a given system of solvents measures the difference in hydrophilicity (or lipophilicity) between A_y and A_x. Equation 1 has been used to measure the hydrophilic-lipophilic character exhibited by a variety of functional groups in ethanol-water mixtures (3).

A theoretical model to rationalize solvent effects on solubility was developed (1). In two-solvent systems, each consisting of binary mixtures of increasing lipophilicity, one (system 1) in which the solubility of both substrates (A_x and A_y) increases, and the other (system 2) in which the solubilities decrease as the lipophilicity of the mixtures is raised, the model predicts the following: in system 1, P_y will be higher than unity when A_y is more lipophilic than A_x and *vice versa;* in system 2, P_y will be lower than unity when A_y is more lipophilic than A_x and higher than unity in the reverse situation.

This paper deals with the comparison of the sensitivity of two-solvent systems with a variety of structural changes in the substrates. Thus, if the sensitivities of systems 1 and 2 to a given structural change ($A_x \rightarrow A_y$) are the same, the following relation between P_{y1} and P_{y2} would be expected to hold (1):

$$(P_{y1} - 1) = (1 - P_{y2}) \qquad \text{(Eq. 2)}$$

which is conveniently expressed as:

$$(P_{y1} - 1) - (1 - P_{y2}) = \Delta_{12} = 0 \qquad \text{(Eq. 3)}$$

However, when the solvent systems have different sensitivities to the structural change, Δ_{12} becomes different from zero, having a positive value when system 1 is more sensitive than system 2, and a negative value in the reverse situation.

In this paper, the former measurements of solvent effects in ethanol-water mixtures (2,3), now system 1, were extended to a nonaqueous medium consisting of ethanol-cyclohexane mixtures which were selected as system 2. System 2 forms a less structured environment of lower dielectric constant than system 1 and the hydroxyl groups are less disponible and freer to interact with the substrates through hydrogen bonding.

EXPERIMENTAL SECTION

The compounds of the basic structure p-X_1—C_6H_4—X_2 were used for the solubility measurements. The numbers assigned to each compound in a previous paper (3) were maintained. The corresponding X_1 and X_2 are, respectively: H_2N—, —$COOCH_3$ (I); H—, —$NHCOCH_3$ (III); HO—, —$NHCOCH_3$ (IV); $(CH_3)_2N$—, —$COOCH_3$ (VII); CH_3O—, —$NHCOCH_3$ (X); C_2H_5O—, —$NHCOCH_3$ (XI); CH_3COO—, —$NHCOCH_3$ (XII); H—, —$N(CH_3)COCH_3$ (XIII); H_2N—, —$COOC_2H_5$ (XIV); H_2N—, —$COO(CH_2)_2CH_3$ (XV); HO—, —$COO(CH_2)_2CH_3$ (XVI).

Preparation and physical constants of I, III, IV, VI, VII, XV, and XVI were reported (2, 3); X and XII were prepared through acetylation, X from *p*-anisidine (4), and XII from IV (5). The following were commercially available: XI[1], XIV[1], and XIII[2]. The melting points for these compounds were: X, mp 127.0-127.5°C (water) [lit. (6) mp 129-131°C]; XI, mp 134-135°C (ethanol-water, 50:50) [lit. (6) mp 134-135°C]; XII, mp 153.0-154.5°C (water) [lit. (5) mp 152-156°C]; XIII, mp 99.0-99.5°C (water) [lit. (6) mp 101-102°C]; XIV, mp 88-89°C (ethanol-water, 15:85) [lit. (6) mp 88-90°C]. 5,5′-Diethylbarbituric acid (barbital) (XVII)[1], mp 189-191°C (water), and 5-ethyl-5-isoamylbarbituric acid (amobarbital) (XVIII), mp 155.5-156.5°C (ethanol-water, 20:80), were also used. Compound XVIII was extracted with chloroform from commercial tablets[3].

Solvent mixture preparations and solubility determinations have been reported (2, 3). Solubility data of XVII and XVIII in ethanol-water mixtures (0-70% ethanol) were taken from Breon and Paruta (7).

RESULTS AND DISCUSSION

Solubility data of the structurally related derivatives p-X_1—C_6H_4—X_2 in systems 1 and 2 are reported in Table I with data of a pair of barbituric acid derivatives (XVII and XVIII). The data of p-X_1—C_6H_4—X_2 derivatives complement previously reported results (2, 3, 7). The solubility of all compounds of the set is raised with increasing amounts of ethanol in system 1 and lowered by the increase of the cyclohexane content in system 2.

To incorporate low solubility values into the data set of system 2, measurements were performed in mixtures having cyclohexane content as high as 94 and 96%. P_{y1} and P_{y2} were obtained from the correlation of the solubility data according to Eq. 1, and are reported in Table II. These values can be used to compare the sensitivity of both solvent systems with a variety of structural changes in the substrates.

[1] Sigma Chemical Co.
[2] BDH.
[3] Quait N; Química Ariston S.A.

0022-3549/84/1200-1869$01.00/0
© 1984, American Pharmaceutical Association

Table I—Solubility in Systems 1 and 2 at 25°C

Solvent Composition		Solubility, mg/g_{soln}									
		III	IV	VI	X	XI	XII	XIII	XIV	XVII	XVIII
					System 2 (Ethanol-Cyclohexane)						
4	96	16.6	0.529	27.6	2.36	0.717			11.0	2.44	16.6
6	94	26.8	1.57		3.67	3.13	1.38	91.4	16.8	5.84	31.9
8	92	35.4	2.65	35.1	6.11	5.01	2.16		24.2		
10	90	47.7	4.50	39.5	8.35	6.55	3.10	131	34.2	10.7	53.5
15	85	90.3	9.45	47.5	15.2	12.7	5.66	168	49.6	15.9	86.4
20	80	96.5	18.4	58.3	20.4	16.1	9.80	190	73.4	24.3	111
25	75	140	26.1	60.6	27.1	23.4	11.1	222	110		
30	70	195	39.0	69.6	34.1	26.6	15.3	260	132	39.3	185
40	60	214	64.7	78.9	47.9	32.6	19.4	296	191	57.6	236
50	50	241	92.3	82.7	72.6	46.9		423	362	70.9	
60	40	246	117							78.6	
					System 1 (Ethanol-Water)						
0	100				2.24	0.502	2.20	26.5	1.37		
10	90				3.29	0.824	3.06	46.4	1.63		
20	80				3.37	1.15	3.51	78.3	3.08		
30	70				8.99	2.31	5.28	196	8.06		
40	60				11.3	5.08	12.6	295	23.8		
50	50				28.6	12.7	26.6	423	56.5		
60	40				42.6	19.1	31.6		110		
70	30				64.2	34.1	50.7		176		

Table II—Correlation of Solubility Data According to Eq. 1 [a]

Compounds Correlated	n	Range	P_y	Intercept	r
System 2		CH, %			
XII/IV	8	94-60	0.717	−0.698	0.995
XII/III	8	94-60	1.11	−1.34	0.997
VI/I	6	96-50	0.393	−0.144	0.994
XI/III	8	94-50	1.06	−0.981	0.992
XI/IV	9	94-50	0.638	−0.454	0.993
XIII/III	7	94-60	0.592	0.242	0.990
IV/III	12	96-30	1.71	−0.836	0.995
XI/X	10	96-50	0.922	−0.221	0.997
X/IV	10	96-50	0.664	−0.274	0.997
X/III	10	96-50	1.11	−0.841	0.993
XIV/I	7	96-50	1.10	0.690	0.996
XV/XIV	8	96-50	0.908	0.281	0.994
XVIII/XVII	6	94-60	0.926	0.576	0.997
System 1		Water, %			
XII/IV	8	100-30	0.971	−1.07	0.985
XII/III	7	100-30	0.827	−0.860	0.992
XI/III	8	100-30	1.66	−1.05	0.990
XI/IV	8	100-30	1.36	−1.31	0.992
XIII/III	6	100-50	1.26	0.942	0.998
XI/X	6	90-30	1.17	−0.226	0.997
X/IV	7	100-30	1.13	−0.847	0.992
X/III	8	100-30	0.957	−0.667	0.988
XIV/I	8	100-30	1.22	0.297	0.999
XV/XIV	8	100-30	1.25	0.126	0.998
XVIII/XVII	8	100-30	2.19	−2.15	0.998

[a] Solubility data in molality units were used in all cases except those of the correlation XVIII/XVII in system 1, which were taken from Ref. 7 and are expressed in mg/mL. However, as previously discussed (1), P_y obtained by using different units to express solubility, remains essentially unchanged. It should be emphasized that all the solubility data of barbituric derivatives reported in Ref. 7 can be correlated according to Eq. 1.

Table III contains Δ_{12} values of some relevant structural changes. They were grouped under the headings of the structural change involved after clearly defined patterns were recognized.

$\Delta_{12} < 0$—Inspection of Table III reveals that a structural change ($A_x \rightarrow A_y$) involving the full replacement of the hydrogen atoms bonded to either O or N affords a negative value of Δ_{12} (correlations 1-4). Therefore, the sensitivity of system 2 to such structural modification is greater than that of system 1. One reason for this behavior might be that an aqueous medium, such as system 1, has a number of ways to interact with both A_x and A_y structures due to its high donor-acceptor capacity toward hydrogen bonding. System 2, having a lower ability to produce specific interactions, has an enhanced sensitivity toward a structural change involving the full replacement of the hydrogen atoms and thus the number of potential interactions are limited.

$\Delta_{12} > 0$—A structural change which solely involves the increase of the alkyl chain yields a positive value of Δ_{12}. This behavior was observed with chain extensions of ether, ester, and barbituric acid derivatives (correlations 5-8). Consequently, in this situation system 1 appears to be more sensitive than system 2. This could be explained by considering that an increase in the size of the hydrocarbon moiety of a substrate is better accepted by a less rigid system such as 2 than by a highly structured system such as 1.

Δ_{12} Approaching Zero—For a structural change like —OH→ —NH_2, where the donor-acceptor capacity toward hydrogen bonding is maintained, a similar sensitivity in both systems is expected. From the values reported previously (2), a random value of Δ_{12} approaching zero (−0.04) is calculated for such a structural change.

On the other hand, the direct comparison of the structural difference —OH → —OC_2H_5 between two pharmacologically related drugs, IV (acetaminophen) and XI (phenacetin), affords a Δ_{12} of zero. This result can be seen as a consequence of two opposite effects: the hydrogen atom replacement generates a negative Δ_{12} for —OH→—OCH_3, as occurs in IV→X (correlation

Table III—Sensitivity of Systems 1 and 2 to Structural Changes

Structural Change, $A_x \rightarrow A_y$	Compounds	Δ_{12}
$\Delta_{12} \neq 0$		
Full Replacement of H		
$-OH \rightarrow -OCH_3$	X/IV	−0.21
$-OH \rightarrow -OOCCH_3$	VIII/VII	−0.69
	XII/IV	−0.31
$-NH_2 \rightarrow -N(CH_3)_2$	VI/I	−0.28
$-NH-OCCH_3 \rightarrow -N(CH_3)-OCCH_3$	XIII/III	−0.15
Chain Extension		
$-OCH_3 \rightarrow -OC_2H_5$	XI/X	+0.11
$-COOCH_3 \rightarrow -COOC_2H_5$	XIV/I	+0.32
$-COOC_2H_5 \rightarrow -COO(CH_2)_2CH_3$	XV/XIV	+0.16
$-C_2H_5 \rightarrow -(CH_2)_2CH(CH_3)_2$	XVIII/XVII	+1.12
$\Delta_{12} \cong 0$		
Changes Which Preserve H		
$-NH_2 \rightarrow -OH$	VII/I	−0.09
	XVI/XV	+0.05
Hydrogen Replacement Plus Chain Extension		
$-OH \rightarrow -OC_2H_5$	XI/IV	0.00

1); the chain extension $-OCH_3 \rightarrow -OC_2H_5$ (X→XI) generates a positive Δ_{12} (correlation 5). Obviously, the extent of the affinity of a functional group for a given medium is the result of a number of well-defined molecular interactions usually described as specific, nonspecific, solvophobic, *etc.* (8).

Because of the importance of the hydrophilic-lipophilic concept, considerable effort has been made to measure such properties from partition coefficient or solubility measurements (9, 10) and more recently from solvent effects on solubility (2, 3).

The results discussed here show that functional groups may exhibit different hydrophilic-lipophilic properties in different environments, *i.e.*, XVIII appears to be 16-fold more lipophilic than XVII in ethanol-water, but only ~1.2-fold more lipophilic in ethanol-cyclohexane. Thus, it is now clear that the order of hydrophilic strength of different functional groups in ethanol-water reported previously (3) should be quite different from the order of the same groups in ethanol-cyclohexane.

Just as Hammett pointed out the ambiguity of the concepts of acidity and basicity (11), the inherent ambiguity of the hydrophilic-lipophilic concept should be emphasized. However, Eq. 1 appears to be a useful tool to obtain information about the hydrophilic-lipophilic properties of different solvent media.

REFERENCES

(1) R. H. Manzo, *J. Pharm. Pharmacol.*, **34**, 486 (1982).

(2) R. H. Manzo, *An. Assoc. Quim. Argentina*, **71**, 47 (1983).

(3) R. H. Manzo, A. A. Ahumada, and E. Luna, *J. Pharm. Sci.*, **73**, 1094 (1984).

(4) "Organic Syntheses, Vol. 3," E. C. Horning, Ed., Wiley, New York, N.Y., 1960, p. 661.

(5) K. T. Koshy, A. E. Troup, R. N. Duvall, R. C. Conwell, and L. L. Shankle, *J. Pharm. Sci.*, **56**, 1117 (1967).

(6) "The Merck Index," 9th ed., Merck & Co. Inc., Rahway, N.J., 1976.

(7) T. L. Breon and A. N. Paruta, *J. Pharm. Sci.*, **59**, 1306 (1970).

(8) C. Reichardt, "Solvent Effects in Organic Chemistry," Monographs in Modern Chemistry, Vol. 3, Weinheim, Verlag Chemie, FRG, 1979, pp. 5–36.

(9) A. Leo, C. Hansch, and D. Elkins, *Chem. Rev.*, **71**, 525 (1971).

(10) R. F. Rekker and H. M. de Kort, *Eur. J. Med. Chem. Chim. Ther.*, **14**, 479 (1979).

(11) L. P. Hammett, "Physical Organic Chemistry," 2nd ed., McGraw-Hill, New York, N.Y., 1970, pp. 262–313.

ACKNOWLEDGMENTS

The authors thank the Consejo de Investigaciones Científicas y Tecnológicas de la Provincia de Córdoba for financial support (Grants 064/82 and 185/83). A.A.A. thanks the CONICET (R.A.) for a fellowship. This paper was presented at the "3° Reunion Argentina de Fisico-Química Orgánica," La Plata, Argentina, September 1983.

Synthesis and Evaluation of Novel *N*-Substituted *N'*-(3-Hydroxy-17-oxoestra-1,3,5(10)-trien-2- and -4-yl)thiourea Derivatives for Binding to the Estrogen Receptor and Cytotoxic Activity on MCF-7 Cells

A.-MOHSEN M. E. OMAR *x, OMAIMA M. ABOULWAFA *, and G. LECLERCQ ‡

Received October 25, 1982, from the **Pharmaceutical Chemistry Department, Faculty of Pharmacy, University of Alexandria, Alexandria Egypt* and the ‡*Laboratoire de Cancérologie Mammaire, Service de Médecine, Institut Jules Bordet, 1000 Brussels, Belgium.* Accepted for publication October 26, 1983.

Abstract □ A novel series of estrone derivatives having a free 3-phenolic group with the 2- or 4-position substituted with a thiourea function was synthesized. None of the products showed significant binding to the estrogen receptor, and the cytotoxic activity on MCF-7 cells for VII and X was weak.

Keyphrases □ Estrone 2- and 4-thiourea derivatives—free phenolic group, synthesis, binding to the estrogen receptor, cytotoxic activity □ Steroidal thiourea derivatives—2- or 4-position of estrone, synthesis binding to the estrogen receptor, cytotoxic activity

Several types of compounds containing structural modifications of steroidal and nonsteroidal estrogens were synthesized during past years, in the hope of developing agents with a high binding affinity to the estrogen receptor (1, 2) and reduced estrogenic properties. These, in accordance with their capabilities in antagonizing the action of estradiol at the estrogen receptor (3), can be used as antiestrogens (4–9) or as cytotoxic agents with selective activity against the hormone-dependent tumor cells (10–13). In connection with an extensive program studying the effect of structural modifications on the biological activity of hormones, a variety of modified steroids were synthesized and tested for antiestrogenic (14), endocrinological (15–17), and anticancer (15, 17, 18) properties. As a supplemental investigation, a novel series of estrone thiourea derivatives (V–XI) were synthesized to check their binding to

© 1984, American Pharmaceutical Association

Table III—Sensitivity of Systems 1 and 2 to Structural Changes

Structural Change, $A_x \rightarrow A_y$	Compounds	Δ_{12}
$\Delta_{12} \neq 0$		
Full Replacement of H		
$-OH \rightarrow -OCH_3$	X/IV	−0.21
$-OH \rightarrow -OOCCH_3$	VIII/VII	−0.69
	XII/IV	−0.31
$-NH_2 \rightarrow -N(CH_3)_2$	VI/I	−0.28
$-NH-OCCH_3 \rightarrow -N(CH_3)-OCCH_3$	XIII/III	−0.15
Chain Extension		
$-OCH_3 \rightarrow -OC_2H_5$	XI/X	+0.11
$-COOCH_3 \rightarrow -COOC_2H_5$	XIV/I	+0.32
$-COOC_2H_5 \rightarrow -COO(CH_2)_2CH_3$	XV/XIV	+0.16
$-C_2H_5 \rightarrow -(CH_2)_2CH(CH_3)_2$	XVIII/XVII	+1.12
$\Delta_{12} \cong 0$		
Changes Which Preserve H		
$-NH_2 \rightarrow -OH$	VII/I	−0.09
	XVI/XV	+0.05
Hydrogen Replacement Plus Chain Extension		
$-OH \rightarrow -OC_2H_5$	XI/IV	0.00

1); the chain extension $-OCH_3 \rightarrow -OC_2H_5$ (X→XI) generates a positive Δ_{12} (correlation 5). Obviously, the extent of the affinity of a functional group for a given medium is the result of a number of well-defined molecular interactions usually described as specific, nonspecific, solvophobic, *etc.* (8).

Because of the importance of the hydrophilic-lipophilic concept, considerable effort has been made to measure such properties from partition coefficient or solubility measurements (9, 10) and more recently from solvent effects on solubility (2, 3).

The results discussed here show that functional groups may exhibit different hydrophilic-lipophilic properties in different environments, *i.e.*, XVIII appears to be 16-fold more lipophilic than XVII in ethanol-water, but only ~1.2-fold more lipophilic in ethanol-cyclohexane. Thus, it is now clear that the order of hydrophilic strength of different functional groups in ethanol-water reported previously (3) should be quite different from the order of the same groups in ethanol-cyclohexane.

Just as Hammett pointed out the ambiguity of the concepts of acidity and basicity (11), the inherent ambiguity of the hydrophilic-lipophilic concept should be emphasized. However, Eq. 1 appears to be a useful tool to obtain information about the hydrophilic-lipophilic properties of different solvent media.

REFERENCES

(1) R. H. Manzo, *J. Pharm. Pharmacol.*, **34**, 486 (1982).

(2) R. H. Manzo, *An. Assoc. Quim. Argentina*, **71**, 47 (1983).

(3) R. H. Manzo, A. A. Ahumada, and E. Luna, *J. Pharm. Sci.*, **73**, 1094 (1984).

(4) "Organic Syntheses, Vol. 3," E. C. Horning, Ed., Wiley, New York, N.Y., 1960, p. 661.

(5) K. T. Koshy, A. E. Troup, R. N. Duvall, R. C. Conwell, and L. L. Shankle, *J. Pharm. Sci.*, **56**, 1117 (1967).

(6) "The Merck Index," 9th ed., Merck & Co. Inc., Rahway, N.J., 1976.

(7) T. L. Breon and A. N. Paruta, *J. Pharm. Sci.*, **59**, 1306 (1970).

(8) C. Reichardt, "Solvent Effects in Organic Chemistry," Monographs in Modern Chemistry, Vol. 3, Weinheim, Verlag Chemie, FRG, 1979, pp. 5–36.

(9) A. Leo, C. Hansch, and D. Elkins, *Chem. Rev.*, **71**, 525 (1971).

(10) R. F. Rekker and H. M. de Kort, *Eur. J. Med. Chem. Chim. Ther.*, **14**, 479 (1979).

(11) L. P. Hammett, "Physical Organic Chemistry," 2nd ed., McGraw-Hill, New York, N.Y., 1970, pp. 262–313.

ACKNOWLEDGMENTS

The authors thank the Consejo de Investigaciones Científicas y Tecnológicas de la Provincia de Córdoba for financial support (Grants 064/82 and 185/83). A.A.A. thanks the CONICET (R.A.) for a fellowship. This paper was presented at the "3° Reunion Argentina de Fisico-Química Orgánica," La Plata, Argentina, September 1983.

Synthesis and Evaluation of Novel *N*-Substituted *N'*-(3-Hydroxy-17-oxoestra-1,3,5(10)-trien-2- and -4-yl)thiourea Derivatives for Binding to the Estrogen Receptor and Cytotoxic Activity on MCF-7 Cells

A.-MOHSEN M. E. OMAR *x, OMAIMA M. ABOULWAFA *, and G. LECLERCQ ‡

Received October 25, 1982, from the **Pharmaceutical Chemistry Department, Faculty of Pharmacy, University of Alexandria, Alexandria Egypt* and the ‡*Laboratoire de Cancérologie Mammaire, Service de Médecine, Institut Jules Bordet, 1000 Brussels, Belgium.* Accepted for publication October 26, 1983.

Abstract □ A novel series of estrone derivatives having a free 3-phenolic group with the 2- or 4-position substituted with a thiourea function was synthesized. None of the products showed significant binding to the estrogen receptor, and the cytotoxic activity on MCF-7 cells for VII and X was weak.

Keyphrases □ Estrone 2- and 4-thiourea derivatives—free phenolic group, synthesis, binding to the estrogen receptor, cytotoxic activity □ Steroidal thiourea derivatives—2- or 4-position of estrone, synthesis binding to the estrogen receptor, cytotoxic activity

Several types of compounds containing structural modifications of steroidal and nonsteroidal estrogens were synthesized during past years, in the hope of developing agents with a high binding affinity to the estrogen receptor (1, 2) and reduced estrogenic properties. These, in accordance with their capabilities in antagonizing the action of estradiol at the estrogen receptor (3), can be used as antiestrogens (4–9) or as cytotoxic agents with selective activity against the hormone-dependent tumor cells (10–13). In connection with an extensive program studying the effect of structural modifications on the biological activity of hormones, a variety of modified steroids were synthesized and tested for antiestrogenic (14), endocrinological (15–17), and anticancer (15, 17, 18) properties. As a supplemental investigation, a novel series of estrone thiourea derivatives (V–XI) were synthesized to check their binding to

© 1984, American Pharmaceutical Association

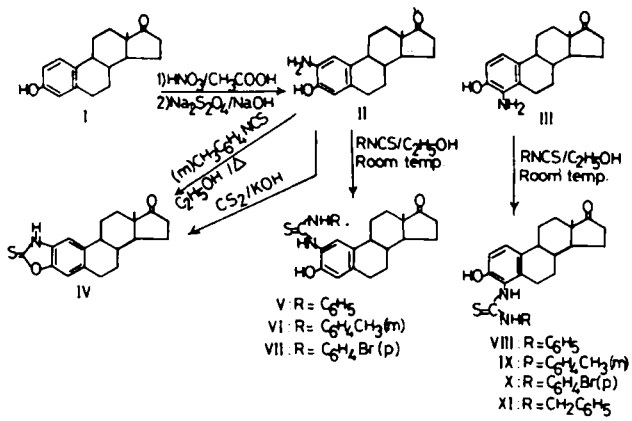

Scheme I

the estrogen receptor and *in vitro* cytotoxic activity on the growth of cells from the estrogen receptor-positive breast cancer cell line MCF-7.

RESULTS AND DISCUSSION

Chemistry—The synthesis of *N*-substituted *N'*-(3-hydroxy-17-oxoestra-1,3,5(10)-trien-2-yl)thioureas (V–VII) and the corresponding *N*-substituted *N'*-(3-hydroxy-17-oxoestra-1,3,5(10)-trien-4-yl)thioureas (VIII–XI) was accomplished as shown in Scheme I. The 2- and 4-aminoestrones (II and III, respectively), prepared by nitration of estrone (19) and reduction of the produced 2- and 4-mononitroestrones as previously reported (20), were allowed to react at room temperature with the equivalent amount of the selected arylisothiocyanate derivatives in ethanol or ethanol–acetone to give the estrone-2-thiourea derivatives (V–VII). The attempt to crystallize VI from boiling ethanol led to the elimination of *m*-toluidine and the formation of 2'-thio-17-oxoestra-1(10),4-dieno[2,3-*d*]oxazoline (IV). The same oxazoline derivative IV was obtained when equimolar amounts of 2-aminoestrone (II) and *m*-tolylisothiocyanate were heated in boiling ethanol for a short period or, as previously reported for other heat-sensitive thioureas (21), when VI was heated above its melting point. The separation of the estrone-4-thiourea derivatives (VIII–XI), on the other hand, necessitated the evaporation of the mixture to dryness, without application of heat, and then purifying the residues by precipitation from different cold solvent systems (Table I). *N*-Benzyl-*N'*-(3-hydroxy-17-oxoestra-1,3,5(10)-trien-4-yl)thiourea (XI) was found to be insensitive to heat; hence, its preparation and purification were carried out in boiling ethanol. The structures of V–XI were confirmed by elemental analysis, IR, ^{1}H-NMR spectra (Table I), and (for VII and X) MS.

Biological Screening—The relative binding affinity of the steroidal thioureas (V–XI) was evaluated by measuring their ability to inhibit the binding of tritiated estradiol to the cytoplasmic estrogen receptor, obtained from immature rat uteri (2, 10). The steroidal thiourea derivatives (V–VII) did not produce any inhibition of binding, indicating that they were totally devoid of binding affinity. Compounds VIII–XI produced only a slight inhibition, indicative of a weak (most probably insignificant) binding affinity (≤0.1%). Moreover, VII and X were evaluated *in vitro* for their inhibition of the growth of cells from the estrogen receptor-positive breast cancer (MCF-7) cell line (12). As shown in Table II, at a concentration of 10^{-6} M, both compounds produced a slight inhibition of the growth of MCF-7 cells. These effects were only significant ($p < 0.05$) in the case of VII. In addition, the combination of varying molar concentrations of estradiol with the two thioureas (at a concentration of 10^{-6} M) did not suppress the growth inhibition of MCF-7 cells (Table II), indicating that the estrogen receptor was not involved in this weak antitumor activity exhibited by VII and X (12). This behavior totally contrasted with the inhibited growth of MCF-7 cells produced by 1-[2-[*p*-(3,4-dihydro-6-methoxy-2-phenylnaphth-1-yl)phenoxy]ethyl]pyrrolydine hydrochloride (nafoxidine)[1], which was suppressed by addition of estradiol (*cf.*, footnote *b* in Table II). Such a slight inhibition of the growth of MCF-7 cells by the thioureas is consistent with their lack of binding affinity for the estrogen receptor. The presence of the thiourea function, although fulfilling the polar structural requirements for association with the receptor (4, 8, 10), seems to be bulky spatial arrangement as compared with several nitrogen mustard functions (23). Hence, the product was sterically hindered from fitting in the estrogen receptor sites (6).

[1] Lot 100A; The Upjohn Co.

Table I—Synthesized Estrone-2- and -4-thiourea Derivatives (V–XI)

Compound	Yield, %	mp, °C	Molecular[a] Formula	^{1}H-NMR (δ), ppm[b]
V	81	186–188[c]	$C_{25}H_{28}N_2O_2S$	0.87 (s, 3, C(18)—CH_3), 6.62 (s, 1, C(4)-H), 7.30 (br m 5, ArH), 7.71 (s, 1, C(1)—H), 8.81 (s, 2, NHCSNH, disappearing on deuteration), 9.47 (s, 1, OH, lost on deuteration).
VI	96	174–176[c]	$C_{26}H_{30}N_2O_2S$	0.86 (s, 3, C(18)—CH_3), 2.3 (s, 3, tolyl-CH_3), 6.75 (s, 1, C(4)—H), 7.1 (m, 4, ArH), 7.49 (s, 1, C(1)—H), 8.38 (s, 1, tolyl-NH, lost on deuteration), 8.51 (s, 1, NH, lost on deuteration), 8.86 (s, 1, OH).
VII	86	187–189[c]	$C_{25}H_{27}BrN_2O_2S$	0.86 (s, 3, C(18)—CH_3), 6.62 (s, 1, C(4)—H), 7.35 (d, 2, J = 10 Hz, ArH), 7.52 (d, 2, J = 10 Hz, ArH), 7.72 (s, 1, C(1)—H), 8.94 (s, 2, NHCSNH, lost on deuteration), 9.6 (s, 1, OH).
VIII	89	140–142[d]	$C_{25}H_{28}N_2O_2S$	
IX	95	163–165[d]	$C_{26}H_{30}N_2O_2S$	0.88 (s, 3, C(18)—CH_3), 2.36 (s, 3, (tolyl-CH_3), 6.89 (d, 1, J = 8 Hz, C(2)—H), 7.10–7.41 (m, 6, ArH + C(1)—H + tolyl-NH), 8.02 (br s, 1, NH, lost on deuteration).
X	89	161–163[e]	$C_{25}H_{27}BrN_2O_2S$	
XI	87	165–167[f]	$C_{26}H_{30}N_2O_2S$[g]	0.87 (s, 3, C(18)—CH_3), 4.79 (d, 2, J = 6 Hz, $C_6H_5CH_2$, becoming singlet at 4.77 on deuteration), 6.20 (m, 1, benzyl-NH, lost on deuteration), 6.83 (d, 1, J = 8 Hz, C(2)—H), 7.18 (d, 1, J = 8 Hz, C(1)-H), 7.25 (s, 5, ArH), 7.78 (s, 1, NH, lost on deuteration).

[a] Compounds V–XI were analyzed for C, H, and N; unless otherwise noted, all values were within ±0.4% of the theoretical value. [b] In $CDCl_3$ or Me_2SO-d_6 plus D_2O. [c] The compounds solidified and remelted at 310°C. [d] Recrystallized from benzene–petroleum ether (bp 60–80°C). [e] Recrystallized from chloroform–petroleum ether (bp 60–80°C). [f] Recrystallized from ethanol–water. [g] Calc.: C, 71.86; N, 6.45. Found: C, 71.40; N, 6.00.

EXPERIMENTAL SECTION[2]

***N*-Substituted *N'*-(3-Hydroxy-17-oxoestra-1,3,5(10)-trien-2-yl)thioureas (V–VII)**—A solution of 2-aminoestrone (II) (200 mg, 0.7 mmol) was dissolved in hot absolute ethanol (15 mL), allowed to cool to room temperature, and then treated with the solution of one molar equivalent of the appropriate arylisothiocyanate derivative in absolute ethanol (5 mL). The solution was allowed to stand at room temperature overnight. The resulting crystals were removed by filtration and washed with petroleum ether. The yields, physical constants, and ^{1}H-NMR spectral data of the products are presented in Table I.

2'-Thio-17-oxoestra-1(10),4-dieno[2,3-d]oxazoline (IV)—A solution of equimolar amounts of 2-aminoestrone (II) and *m*-tolylisothiocyanate (0.87

[2] All melting points are uncorrected. IR spectra were measured as Nujol mulls on a Beckman 4210 Spectrophotometer. ^{1}H-NMR and MS were measured on a Perkin-Elmer R32 and an AEI-MS-50, respectively.

Table II—Growth Inhibition of MCF-7 Cells by VII and X Alone or Combined with Estradiol

Compound	Molarity	DNA, μg[a]			
		Alone	Estradiol 10^{-8} M	Estradiol 10^{-7} M	Estradiol 10^{-6} M[b]
Control		9.1 ± 1.8 (100)			
VII[c]	10^{-8}	9.6 ± 1.3 (105)			
	10^{-7}	9.6 ± 1.2 (105)			
	10^{-6}	6.9 ± 0.7 (76)	6.6 ± 0.9 (72)	6.0 ± 1.1 (66)	5.7 ± 0.3 (63)
X	10^{-8}	9.0 ± 1.0 (99)			
	10^{-7}	7.8 ± 0.7 (86)			
	10^{-6}	7.6 ± 1.4 (83)	9.6 ± 1.0 (105)	7.7 ± 1.0 (84)	7.4 ± 0.5 (81)

[a] Experiments were performed in quadruplicate; the results are given as mean ± *SD*. The percent of control is given in parentheses. [b] Inhibition produced by 5×10^{-7} M nafoxidine alone was 6.2 ± 0.6 (68); the value after addition of 10^{-8} M estradiol was 7.6 ± 0.8 (83). [c] Variance analysis showed that VII produced a significant growth inhibition at 10^{-6} M ($p < 0.05$); this effect was not suppressed by estradiol. The slight inhibition of X was not significant ($p > 0.10$).

mmol) in ethanol (15 mL) was heated at reflux for 30 min. The solution was concentrated and the product, obtained after cooling, was recrystallized from ethanol to give IV as white shiny scales (95% yield), mp 308–310°C. Compound IV was also produced when thiourea VI was heated in ethanol for recrystallization, or heated above its melting point for a short time. The mixed melting point with a sample of IV, prepared from 2-aminoestrone (II), carbon disulfide, and potassium hydroxide [as previously reported (21)] showed no depression. IR and ^{1}H-NMR spectra of IV obtained from both sources were superimposable. IR (mineral oil): ν 1730 (C=O), 1595 (C=C, Ar), 1510, 1495, 1140, and 930 cm^{-1} (NCS amide I, II, III, and IV bands, respectively); ^{1}H-NMR ($CDCl_3$ + D_2O): δ 0.92 (s, 3, C(18)—CH_3), 7.05–7.30 (two m, 2, ArH), and 10.55 ppm [br s (diffuse), oxazoline-H, exchangeable].

***N*-Substituted *N'*-(3-Hydroxy-17-oxoestra-1,3,5(10)-trien-4-yl) thioureas (VIII–XI)**—A solution of 4-aminoestrone (III) (200 mg, 0.7 mmol) and the equivalent amount of the isothiocyanate derivative in a mixture of absolute ethanol (15 mL) and acetone (5 mL) was allowed to stand at room temperature for 24–30 h. The solvent was evaporated to dryness without application of heat. The oily residues were dissolved in cold benzene or chloroform (10 mL); the precipitates were removed by filtration and treated with petroleum ether to give the thiourea derivatives (VIII–X) as white amorphous solids. The benzyl derivative XI was prepared by heating at reflux a mixture of 4-aminoestrone (III) (250 mg, 0.87 mmol) and benzylisothiocyanate (130 mg, 0.87 mmol) in absolute ethanol (30 mL) for 30 min. The solution was concentrated to 10 mL, water was added in a dropwise manner, and the solution was allowed to stand overnight to deposit colorless needles. The application of this method to prepare thioureas VIII–X gave impure products. The yields, physical constants, and ^{1}H-NMR spectral analyses are recorded in Table I. IR data for the thiourea derivatives (V–XI) (mineral oil): ν 3340–3310, 3310–3120 (NH), 3120–3050 (OH), 1730–1700 (C=O), 1595–1580 and 1490–1485 (C=C, Ar), 1540–1515, 1340–1330, 1165–1140, and 950–920 cm^{-1} (NCS amide mixed vibrational I, II, III, and IV bands, respectively); MS for VII: *m/z* (relative abundance %); M^+ absent, 216 (100), 214 (100), 174 (24), 173 (48), 172 (29), 171 (48), 134 (26), 93 (56), 87 (19), 86 (19), 77 (18), 65 (76); MS for X: 216 (100), 214 (100), 173 (21), 171 (21), 157 (19), 155 (19), 135 (27), 84 (60), 76 (15), 75 (21).

Relative Binding Affinity for the Estrogen Receptor—The ability of the compounds to bind to the uterine estrogen receptors was estimated according to a previously described experimental procedure (24). Briefly, uterine estrogen receptor cytosol was incubated at 18°C for 30 min with 5×10^{-9} M [^{3}H]estradiol (saturation amount) in the absence or presence of increasing amounts of the test compound (X) or unlabelled estrone (control). After incubation, unbound compounds were removed by dextran-coated charcoal and bound [^{3}H]estradiol was measured. The relative concentration of unlabelled estrone and test compound required to achieve 50% inhibition of the estradiol binding gave the relative binding affinity ($RBA_X = ([I_{50}]\text{estrone}/[I_{50}]_X) \times 100$).

Effect of VII and X on the Growth of MCF-7 Breast Cancer Cells—The action of the compounds on MCF-7 cell growth was estimated by measuring the amounts of DNA after 120 h of culture in the absence or presence of the test compound. In practice, MCF-7 cells were grown at 37°C in closed flasks (75 cm^2) containing Earle's minimal essential medium supplemented with L-glutamine (0.6 mg/mL), gentamicin (40 μg/mL), penicillin (100 μg/mL), streptomycin (100 μg/mL) and 10% fetal calf serum. At confluency, the cells were removed by trypsinization (0.05% trypsin, 0.025% EDTA) and suspended ($\sim 1 \times 10^5$ cells/mL) in the growth medium supplemented with charcoal-stripped fetal calf serum (0.5% charcoal and 0.005% dextran in 1.5 mL of medium, incubated overnight at 4°C). They were then plated in 35-mm Petri dishes containing this medium and cultured at 37°C in a 95% air–5% CO_2 atmosphere. After 24 h, the compounds (solvent: ethanol at the final concentration of 0.1%) were added to the culture dishes. After 48 h, the medium was replaced by fresh medium containing the drugs. The cultures were then grown for an additional 72-h period before final harvest. Both at 24 h (compound addition) and 144 h (end of experiment) the cells were washed twice with 2 mL of Earle's base before being suspended in 1.5 mL of trypsin–EDTA. Total DNA of the collected cells was precipitated in 0.5 M perchloric acid and evaluated by the diphenylamine method (25). The control was run in parallel, without the drug (solvent only added).

REFERENCES

(1) S. G. Korenman, *J. Clin. Endocrinol.*, **28,** 127 (1968).

(2) S. G. Korenman, *Steroids*, **13,** 163 (1969).

(3) J. H. Clark, E. J. Peck, Jr., and J. N. Anderson, *Nature (London)*, **251,** 44 (1974).

(4) E. R. Clark and V. C. Jordan, *Br. J. Pharmacol.*, **57,** 487 (1977).

(5) V. C. Jordan, B. Haldemann, and K. E. Allen, *Endocrinology*, **108,** 1353 (1981).

(6) E. R. Clark and A. M. McCracken, *J. Pharm. Pharmacol.*, **23,** 339 (1971).

(7) T. Tatee, K. E. Carlson, J. A. Katzenellenbogen, D. W. Robertson, and B. S. Katzenellenbogen, *J. Med. Chem.*, **22,** 1509 (1979).

(8) D. W. Robertson, J. A. Katzenellenbogen, J. R. Hayes, and B. S. Katzenellenbogen, *J. Med. Chem.*, **25,** 167 (1982).

(9) B. S. Katzenellenbogen and E. R. Ferguson, *Endocrinology*, **97,** 1 (1975).

(10) G. Leclercq and J. C. Heuson, *Anticancer Res.*, **1,** 217 (1981).

(11) E. R. DeSambre and L. Y. Arbogast, *Cancer Res.*, **34,** 1971 (1974).

(12) M. Lippman, G. Bolan, and K. Huff, *Cancer Res.*, **36,** 4595 (1976).

(13) T. S. Tsai and B. S. Katzenellenbogen, *Cancer Res.*, **37,** 1537 (1977).

(14) E. R. Clark, A.-M. M. E. Omar, and G. Prestwich, *J. Med. Chem.*, **20,** 1096 (1977).

(15) A.-M. M. E. Omar, S. M. El-Khawass, A. B. Makar, N. M. Bakry, and T. T. Daabees, *Pharmazie*, **33,** 577 (1978).

(16) S. M. El-Khawass, A.-M. M. E. Omar, T. T. Daabees, and F. M. Sharaby, *Pharmazie*, **35,** 143 (1980).

(17) E. A. Ibrahim, A.-M. M. E. Omar, M. A. Khalil, A. B. Makar, and T. T. Daabees, *Pharmazie*, **35,** 810 (1980).

(18) A.-M. M. E. Omar, A. M. Farghaly, A. A. B. Hazzaa, and N. H. Eshba, *Pharmazie*, **35** 809 (1980).

(19) A. J. Tomson and J. P. Horwitz, *J. Org. Chem.*, **24,** 2056 (1959).

(20) S. Kraychy, *J. Am. Chem. Soc.*, **81,** 1702 (1959).

(21) A.-M. M. E. Omar, Sh. A. Shams El-Dine, and A. A. B. Hazzaa, *Pharmazie*, **28,** 682 (1973).

(22) C. Djerassi, J. M. Budzikiewicz, and J. Chamberlin, *J. Am. Chem. Soc.*, **84,** 4544 (1962).

(23) H. Hamacher, *Arzneim. Forsch.*, **29,** 463 (1979).

(24) G. Leclercq, M. C. Deboel, and J. C. Heuson, *Int. J. Cancer*, **18,** 750 (1976).

(25) J. Burton, *Biochem. J.*, **62,** 315 (1956).

ACKNOWLEDGMENTS

Partially supported by the Pharco Pharmaceuticals, Cairo, Egypt. Biological tests were supported by a grant from the Fonds Cancérologique de la Caisse Générale d'Epargne et de Retraite de Belgique to Dr. G. Leclercq.

Liquid Chromatographic Microassay for Carbamazepine and Its 10,11-Epoxide in Plasma

Keyphrases □ Carbamazepine—carbamazepine 10,11-epoxide, HPLC □ Carbamazepine 10,11-epoxide—HPLC with carbamazepine

To the Editor:

MacKichan (1) has developed a high-performance liquid-chromatographic assay (HPLC) to measure carbamazepine and one of its active metabolites the corresponding 10,11-epoxide in plasma and saliva using double internal standardization. The double internal standard technique provides a more accurate means of quantitating these substances, since the concentrations of the parent compound and metabolite can vary in the same biological specimen by an order of magnitude or more. The HPLC technique described herein is a micronization of the assay developed by MacKichan and allows carbamazepine and its 10,11-epoxide to be accurately quantitated in biological specimens of 100 μL.

The HPLC system utilized in this procedure consists of a liquid chromatograph with an integrative data system and absorbance detector[1]. Injections were made with an auto injector[2] onto a reverse-phase column[3] equipped with a 70 × 6 mm stainless steel precolumn[4] packed with reverse-phase packing material[5]. A μ-Bondapak phenyl column was employed in these analyses since this column is routinely used in our laboratory. The tribasic sodium phosphate and chloroform used in the extraction procedure were ACS certified[6]. All solvents used in the mobile phase were HPLC grade. The carbamazepine[7], the 10,11-epoxide[7], lorazepam[8], and the *N*-demethyl derivative of diazepam[9] were gifts.

A methanolic solution of carbamazepine and the 10,11-epoxide (400 μg/mL) was employed in the preparation of the following plasma standards: 0.5, 1.0, 2.5, 5.0, 10.0, 15.0, and 30.0 μg/mL. Stock solutions of lorazepam and the *N*-demethyl derivative of diazepam were prepared in methanol at a concentration of 100 μg/mL. These solutions were then combined and diluted with distilled deionized water to create an internal standard solution containing lorazepam and the *N*-demethyl derivative of diazepam at concentrations of 10 and 15 μg/mL.

The extraction procedure is a scaled-down version of the extraction process outlined by MacKichan (1). Samples of plasma (100 μL) and an aliquot of the internal standard solution (50 μL) were added to disposable glass test tubes. Each tube was vortexed to mix the internal standard and sample. To this mixture, 100 μL of an aqueous saturated solution of tribasic sodium phosphate was added and vigorously vortexed for 10 s. Chloroform (2 mL) was then added to the tubes, which were then vigorously vortexed (30 s). The samples were centrifuged (10 min at 1500 rpm) and the aqueous phase was aspirated. The organic phase was decanted into clean test tubes and evaporated to dryness under reduced pressure at 42°C. The residues were reconstituted with 100 μL of mobile phase and ~50 μL was injected onto the column. UV absorbance was monitored at 254 nm. The mobile phase consisted of a deionized water–acetonitrile–methanol mixture (62:35:3). The addition of methanol to the mobile phase rectified some peak broadening which was encountered with the phenyl column. The chromatograms resulting from the injection of blank human plasma, human plasma with internal standards added, as well as human plasma with carbamazepine, the 10,11-epoxide, lorazepam, and the *N*-demethyl derivative of diazepam are presented in Fig. 1. All of the peaks were well resolved from each other and from endogenous components of plasma with the exception of the 10,11-epoxide peak which possessed a minor interference similar to that observed by MacKichan (1). This interfering peak can be seen in Fig. 1A and B and poses no appreciable problem with regard to quantitation of the epoxide, representing the equivalent of 0.2 μg/mL of epoxide. The retention times for the epoxide, carbamazepine, lorazepam, and the *N*-demethyl derivative of diazepam were 4.1, 5.7, 6.7, and 8.9 min, respectively.

The mean extraction recovery was 80.3% for carbamazepine and 73.3% for the corresponding 10,11-epoxide, which is lower than the essentially complete recovery of carbamazepine and the epoxide by the method of MacKichan (1). These lower recoveries may be, in part, related to the greater percentage of tribasic sodium phosphate and methanol in the extraction procedure compared with the original method. The approximate sensitivity limits for the assay are 0.1 μg/mL for carbamazepine and 0.3 μg/mL for the epoxide, based on a signal-to-noise ratio of 2.5. The calibration plot is linear in the 0.5–30 μg/mL range. Intraday and interday variability studies, based on six replicate measurements for a period of 6 d at concentrations of 1.0 and 30.0 μg/mL, have demon-

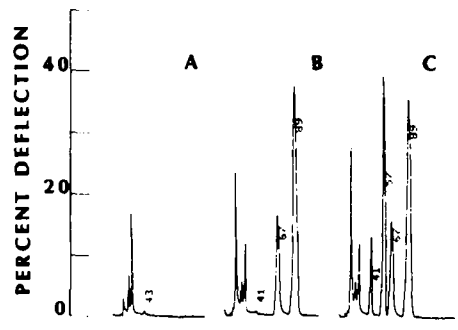

Figure 1—*Chromatograms of a blank human plasma extract (A), a plasma extract with 500 ng of lorazepam (peak 67) and 750 ng of the N-demethyl derivative of diazepam (peak 89) added (B), and a plasma extract containing 10 μg/mL of the 10,11-epoxide of carbamazepine (peak 41) and carbamazepine (peak 57) and 500 ng of lorazepam (peak 67) and 750 ng of the N-demethyl derivative of diazepam (peak 89) added (C). Detector and recorder responses for each chromatogram are 10 mV and 0.005 A full scale. The numbers beside each peak represent its retention time in tenths of minutes.*

[1] Models SP 8000B and SP 8300; Spectraphysics, Santa Clara, Calif.
[2] WISP 710B; Waters Associates, Milford, Mass.
[3] μ-Bondapak phenyl column (30 cm × 2.9 mm i.d., 10 μm particles; Waters Associates.
[4] Crawford (Swagelok-316).
[5] Bondapak C_{18}/Corasil; 37–50 μm.
[6] Fisher Scientific, King of Prussia, Pa.
[7] Tegretol; Ciba-Geigy Corporation, Summit, N.J.
[8] Wyeth Laboratories, Philadelphia, Pa.
[9] Hoffmann-LaRoche, Inc., Nutley, N.J.

0022-3549/84/1200-1874$01.00/0
© 1984, American Pharmaceutical Association

strated assay coefficients of variation of <8.5% for both compounds.

In summary, this micronized assay provides a means for simultaneous analysis of carbamazepine and its 10,11-epoxide from small volumes of plasma. This is of particular value when analyzing samples from pediatric patient populations. In addition, this assay makes possible quantitation of these compounds in the biological fluids of many laboratory animals, where constraints may exist on the volume of blood that can be collected.

(1) J. J. MacKichan, *J. Chromatogr.*, **181**, 373 (1980).

Dennis M. Grasela
Mario L. Rocci, Jr.[x]
Department of Pharmacy
Philadelphia College of Pharmacy and Science
Division of Clinical Pharmacology
Jefferson Medical College
Philadelphia, PA 19107

Received September 29, 1983
Accepted for publication October 15, 1984.

OPEN FORUM

The Ulcerogenic Potential of Copper Aspirinate Seems to be More Imaginary than Real

Alich *et al.*[1] interpreted the appearance of an intravenously injected protein-bound dye in the gastric mucosa and submucosa of rats given $Cu(II)SO_4$, $Cu(II)_2$(aspirinate)$_4$, or $Cu(II)SO_4$ plus aspirin administered with or without dihydroxyaluminum glycinate and magnesium carbonate buffer as erosions. Leakage of the protein-bound dye from the vasculature was suggested as due to damaged blood vessels. Appearance of the protein-bound dye in the mucosa and submucosa in association with the above treatments does not provide evidence of either erosions or vascular damage.

Appearance of the protein-bound dye in the mucosa and submucosa of copper compound-treated rats is more likely due to leakage associated with absorption-induced hyperemia, as shown for the vehicle control, and the quantity of protein-bound dye found in these two tissues is more likely due to the amount of copper-containing compounds absorbed and their subsequent formation of quaternary dye-protein-copper complexes which produced colorations of varying intensity. Copper sulfate, which is not lipid soluble, was poorly absorbed in the time course of this experiment while more of the lipid-soluble copper aspirinate was absorbed[2]. The combination of aspirin plus copper probably produced an aspirin- and/or salicylate-copper complex as a result of the 10-min sonication, and these complexes were nearly equally well absorbed following instillation. Appearance of the dye-protein-copper complexes in the mucosa and submucosa in association with absorption of administered copper compounds is also consistent with the poor agreement between the two "lesion" grading techniques found when aspirin was administered without a copper-containing compound.

Alich *et al.*[1] suggested that, in general, the presence of buffer had no significant effect on the extent of "damage" produced under these experimental conditions. Exception is also taken to this suggestion since it seems clear that there was a statistically significant reduction in coloration in the group given the buffered copper aspirinate preparation. This reduction in coloration is consistent with a reduction in absorption of copper complex following the formation of an insoluble form of copper, $CuCO_3$, or some other nonabsorbable form of copper during the 10-min sonication of a suspension containing 27 μmol of $Cu(II)_2$(aspirinate)$_4$, 71 μmol of $MgCO_3$, and 22 μmol of dihydroxyaluminum glycinate/mL. The formation of $Cu(II)$(glycinate)$_2$, $Cu(II)$(salicylate)$_2$, and $Cu(II)_2$(aspirinate)$_4$ during the 10-min sonication of buffer, aspirin, and $CuSO_4$ may have only partially overcome the effects of $MgCO_3$ when the copper plus aspirin preparation was used. The absorption of copper when it was given as $CuSO_4$ also appeared to have been impeded by the buffer.

In their discussion of the existing literature pertaining to effects of $Cu(II)_2$(aspirinate)$_4$, Alich *et al.*[1] further reduce the credibility of their interpretation of their results as indicating gastric erosions and vascular damage. They did point out that Williams *et al.*[2] found no gastric erosions with $Cu(II)_2$(aspirinate)$_4$, but failed to mention that Williams *et al.*[2] had used doses of 115, 345, 690, and 1380 mg of $Cu(II)_2$(aspirinate)$_4$/kg of body weight, doses much greater than the 115-mg/kg dose used in their study[1].

Alich *et al.*[1] did point out that Williams *et al.*[2] reported "some evidence" of hemorrhage without gastric erosions in rats given $Cu(II)_2$(aspirinate)$_4$, but failed to mention that this hemorrhage which was observed at 345, 690, and 1380 mg/kg was not observed at 115 mg/kg. Alich *et al.*[1] offered no rationale as to how this hemorrhage, which occurred in the absence of gastric erosions, was relevant to their gastric study or in any way supported their interpretation of their results. We have determined the $LD_{50/7}$ of $Cu(II)_2$(aspirinate)$_4$ to be 895 ± 222 and 977 ± 297 mg/kg, respectively, in male and female rats using doses ranging up to 1500 mg/kg. Doses of 1000 and 1500 mg/kg did not produce gastric ulcers but did produce diarrhea. A diarrheal-inducing bolus may cause intestinal bleeding, but this cannot be mistaken for gastric bleeding, and these doses are much greater than the 115-mg/kg dose used by Alich *et al.*[1]. We have also reported results of our chronic toxicity study of $Cu(II)_2$(aspirinate)$_4$ in rats given 100 mg/kg *for 5 d/week* for 3 months[3]. No gastric histopathology was found at the light microscopic level with this more challenging treatment regimen.

Alich *et al.*[1] incorrectly indicated that we had reported that aspirin was an active antiulcer agent in the Shay rat[4]. They also failed to notice that we reported a reduction in gastric acid secretion in response to treatment of the Shay rat with copper complexes and not an accumulation of gastric acid following pyloric ligation as they indicated. The antisecretory effects of copper complexes have been confirmed and extended by others[5-8]. These results support the suggestion that antisecretory activity, in part, accounts for their mechanism of antiulcer activity. Alich *et al.*[1] also overlooked the report by Hayden *et al.*[9] that $Cu(II)_2$(aspirinate)$_4$ prevents aspirin-potentiated ulcers in the Shay rat.

Alich *et al.*[1] questioned the significance of data obtained in nonfasted rats in comparison with their data, but failed to recognize that our Shay rat preparation, like theirs, includes fasting.

Alich *et al.*[1] did point out that Rainsford and Whitehouse[10] reported the production of ulcers in rats with $Cu(II)_2$(aspirinate)$_4$ (200 mg/kg), but overlooked the response to that report which pointed out that those studies were flawed by the use of an inappropriate suspending agent, which has the potential of removing the copper from the administered complex, and the solution of copper complexes in 20 mM hydrochloric acid, which has the potential of destroying the "dissolved" complex and freeing the ulcerogenic ligand[11].

Alich *et al.*[1] did point out that Boyle *et al.*[12] found an antiulcer effect for $Cu(II)_2$(aspirinate)$_4$, but failed to mention that the dose was 345 mg/kg, a dose 3 times as large as their 115-mg/kg dose, and dismissed their results for specious reasons, the inclusion of both number and size of lesions in their assessment of the ulcerogenicity of aspirin.

Alich *et al.*[1] also pointed out that the results reported by Lewis[13,14] and Brown *et al.*[15] were "about the same for free aspirin and $Cu(II)_2$(aspirinate)$_4$" and indicated that the method used for quantitation of was less than state of the art, but failed to mention that doses of 300 mg/kg were used.

The significance of $Cu(II)_2$(aspirinate)$_4$-induced gastric irritation, even if it did occur with doses of 100 mg/kg and higher, remains obscure since the antiulcer dose of this compound is 5–10 mg/kg[4,9,13]. The 10-mg/kg dose has also been shown to markedly increase the rate of interstitial tissue repair in the surgically induced ulcer using histochemical techniques and light microscopy[13].

0022-3549/84/1200-1875$01.00/0
© 1984, American Pharmaceutical Association

strated assay coefficients of variation of <8.5% for both compounds.

In summary, this micronized assay provides a means for simultaneous analysis of carbamazepine and its 10,11-epoxide from small volumes of plasma. This is of particular value when analyzing samples from pediatric patient populations. In addition, this assay makes possible quantitation of these compounds in the biological fluids of many laboratory animals, where constraints may exist on the volume of blood that can be collected.

(1) J. J. MacKichan, *J. Chromatogr.*, **181**, 373 (1980).

Dennis M. Grasela
Mario L. Rocci, Jr.[x]
Department of Pharmacy
Philadelphia College of Pharmacy and Science
Division of Clinical Pharmacology
Jefferson Medical College
Philadelphia, PA 19107

Received September 29, 1983
Accepted for publication October 15, 1984.

OPEN FORUM

The Ulcerogenic Potential of Copper Aspirinate Seems to be More Imaginary than Real

Alich *et al.*[1] interpreted the appearance of an intravenously injected protein-bound dye in the gastric mucosa and submucosa of rats given $Cu(II)SO_4$, $Cu(II)_2$(aspirinate)$_4$, or $Cu(II)SO_4$ plus aspirin administered with or without dihydroxyaluminum glycinate and magnesium carbonate buffer as erosions. Leakage of the protein-bound dye from the vasculature was suggested as due to damaged blood vessels. Appearance of the protein-bound dye in the mucosa and submucosa in association with the above treatments does not provide evidence of either erosions or vascular damage.

Appearance of the protein-bound dye in the mucosa and submucosa of copper compound-treated rats is more likely due to leakage associated with absorption-induced hyperemia, as shown for the vehicle control, and the quantity of protein-bound dye found in these two tissues is more likely due to the amount of copper-containing compounds absorbed and their subsequent formation of quaternary dye-protein-copper complexes which produced colorations of varying intensity. Copper sulfate, which is not lipid soluble, was poorly absorbed in the time course of this experiment while more of the lipid-soluble copper aspirinate was absorbed[2]. The combination of aspirin plus copper probably produced an aspirin- and/or salicylate-copper complex as a result of the 10-min sonication, and these complexes were nearly equally well absorbed following instillation. Appearance of the dye-protein-copper complexes in the mucosa and submucosa in association with absorption of administered copper compounds is also consistent with the poor agreement between the two "lesion" grading techniques found when aspirin was administered without a copper-containing compound.

Alich *et al.*[1] suggested that, in general, the presence of buffer had no significant effect on the extent of "damage" produced under these experimental conditions. Exception is also taken to this suggestion since it seems clear that there was a statistically significant reduction in coloration in the group given the buffered copper aspirinate preparation. This reduction in coloration is consistent with a reduction in absorption of copper complex following the formation of an insoluble form of copper, $CuCO_3$, or some other nonabsorbable form of copper during the 10-min sonication of a suspension containing 27 μmol of $Cu(II)_2$(aspirinate)$_4$, 71 μmol of $MgCO_3$, and 22 μmol of dihydroxyaluminum glycinate/mL. The formation of $Cu(II)$(glycinate)$_2$, $Cu(II)$(salicylate)$_2$, and $Cu(II)_2$(aspirinate)$_4$ during the 10-min sonication of buffer, aspirin, and $CuSO_4$ may have only partially overcome the effects of $MgCO_3$ when the copper plus aspirin preparation was used. The absorption of copper when it was given as $CuSO_4$ also appeared to have been impeded by the buffer.

In their discussion of the existing literature pertaining to effects of $Cu(II)_2$(aspirinate)$_4$, Alich *et al.*[1] further reduce the credibility of their interpretation of their results as indicating gastric erosions and vascular damage. They did point out that Williams *et al.*[2] found no gastric erosions with $Cu(II)_2$(aspirinate)$_4$, but failed to mention that Williams *et al.*[2] had used doses of 115, 345, 690, and 1380 mg of $Cu(II)_2$(aspirinate)$_4$/kg of body weight, doses much greater than the 115-mg/kg dose used in their study[1].

Alich *et al.*[1] did point out that Williams *et al.*[2] reported "some evidence" of hemorrhage without gastric erosions in rats given $Cu(II)_2$(aspirinate)$_4$, but failed to mention that this hemorrhage which was observed at 345, 690, and 1380 mg/kg was not observed at 115 mg/kg. Alich *et al.*[1] offered no rationale as to how this hemorrhage, which occurred in the absence of gastric erosions, was relevant to their gastric study or in any way supported their interpretation of their results. We have determined the $LD_{50/7}$ of $Cu(II)_2$(aspirinate)$_4$ to be 895 ± 222 and 977 ± 297 mg/kg, respectively, in male and female rats using doses ranging up to 1500 mg/kg. Doses of 1000 and 1500 mg/kg did not produce gastric ulcers but did produce diarrhea. A diarrheal-inducing bolus may cause intestinal bleeding, but this cannot be mistaken for gastric bleeding, and these doses are much greater than the 115-mg/kg dose used by Alich *et al.*[1]. We have also reported results of our chronic toxicity study of $Cu(II)_2$(aspirinate)$_4$ in rats given 100 mg/kg *for 5 d/week* for 3 months[3]. No gastric histopathology was found at the light microscopic level with this more challenging treatment regimen.

Alich *et al.*[1] incorrectly indicated that we had reported that aspirin was an active antiulcer agent in the Shay rat[4]. They also failed to notice that we reported a reduction in gastric acid secretion in response to treatment of the Shay rat with copper complexes and not an accumulation of gastric acid following pyloric ligation as they indicated. The antisecretory effects of copper complexes have been confirmed and extended by others[5-8]. These results support the suggestion that antisecretory activity, in part, accounts for their mechanism of antiulcer activity. Alich *et al.*[1] also overlooked the report by Hayden *et al.*[9] that $Cu(II)_2$(aspirinate)$_4$ prevents aspirin-potentiated ulcers in the Shay rat.

Alich *et al.*[1] questioned the significance of data obtained in nonfasted rats in comparison with their data, but failed to recognize that our Shay rat preparation, like theirs, includes fasting.

Alich *et al.*[1] did point out that Rainsford and Whitehouse[10] reported the production of ulcers in rats with $Cu(II)_2$(aspirinate)$_4$ (200 mg/kg), but overlooked the response to that report which pointed out that those studies were flawed by the use of an inappropriate suspending agent, which has the potential of removing the copper from the administered complex, and the solution of copper complexes in 20 mM hydrochloric acid, which has the potential of destroying the "dissolved" complex and freeing the ulcerogenic ligand[11].

Alich *et al.*[1] did point out that Boyle *et al.*[12] found an antiulcer effect for $Cu(II)_2$(aspirinate)$_4$, but failed to mention that the dose was 345 mg/kg, a dose 3 times as large as their 115-mg/kg dose, and dismissed their results for specious reasons, the inclusion of both number and size of lesions in their assessment of the ulcerogenicity of aspirin.

Alich *et al.*[1] also pointed out that the results reported by Lewis[13,14] and Brown *et al.*[15] were "about the same for free aspirin and $Cu(II)_2$(aspirinate)$_4$" and indicated that the method used for quantitation of was less than state of the art, but failed to mention that doses of 300 mg/kg were used.

The significance of $Cu(II)_2$(aspirinate)$_4$-induced gastric irritation, even if it did occur with doses of 100 mg/kg and higher, remains obscure since the antiulcer dose of this compound is 5–10 mg/kg[4,9,13]. The 10-mg/kg dose has also been shown to markedly increase the rate of interstitial tissue repair in the surgically induced ulcer using histochemical techniques and light microscopy[13].

0022-3549/84/1200-1875$01.00/0
© 1984, American Pharmaceutical Association

Alich *et al.*[1] claimed that many possible variables introduced by others had been eliminated from their studies, but failed to recognize that they had introduced new variables that others had not introduced and that their results are subject to an alternative interpretation. As it turns out, this is the second paper coauthored by Alich and Wittmers on the subject of $Cu(II)_2(aspirinate)_4$ wherein conclusions were not supported by the evidence provided. In an earlier paper[14] these authors contended that salicylic acid was a contaminant of $Cu(II)_2(aspirinate)_4$, but failed to provide evidence in support of this contention[15]. The present contention by Alich *et al.* that $Cu(II)_2(aspirinate)_4$ causes erosions and vascular leakage at a dose of 100 mg/kg is not supported by evidence and it is also clearly inconsistent with results reported by ourselves and others they cited. Results obtained by Alich *et al.*[1] may be better interpreted in terms of absorption of copper compounds.

John R. J. Sorenson
University of Arkansas
College of Pharmacy
Little Rock, AR 72205

[1] A. A. Alich, V. J. Welch, and L. E. Wittmers, Jr., *J. Pharm. Sci.*, **72**, 1457 (1983).
[2] D. A. Williams, D. T. Waltz, and W. O. Foye, *J. Pharm. Sci.*, **65**, 126 (1976).
[3] J. R. J. Sorenson, T. M. Rolniak, and L. W. Chang, *Inorg. Chim. Acta*, **91**, L31 (1984).
[4] J. R. J. Sorenson, *J. Med. Chem.*, **19**, 135 (1976).
[5] F. Marletta, E. Rizzarelli, A. Mangiameli, M. Alberghina, A. Brogna, S. Sammartano, and A. Blasi, *Rend. Gastroenterol.* **9** Suppl. 1, 35 (1977).
[6] F. Marletta, E. Rizzarelli, A. Mangiameli, M. Alberghina, A. Brogna, S. Monaco, S. Sammartano, and A. Blasi, "The XIVth International Congress on Internal Medicine," October 1978, pp. 132 and 133.
[7] R. Goburdhun, K. Gulrez, H. Haruna, and G. B. West, *J. Pharmacol. Meth.*, **1**, 109 (1978).
[8] G. B. West, *J. Pharmacol. Meth.*, **8**, 33 (1982).
[9] L. J. Hayden, G. Thomas, and G. B. West, *J. Pharm. Pharmacol.* **30**, 244 (1978).
[10] K. D. Rainsford and M. W. Whitehouse, *J. Pharm. Pharmacol.*, **28**, 83 (1976).
[11] J. R. J. Sorenson, *J. Pharm. Pharmacol.*, **29**, 450 (1977).
[12] E. Boyle, P. C. Freeman, A. C. Goudie, F. R. Mangan, and M. Thompson, *J. Pharm. Pharmacol.*, **28**, 865 (1976).
[13] S. F. Townsend and J. R. J. Sorenson, in "Trace Elements in the Pathogenesis and Treatment of Inflammatory Conditions," Agents and Actions Suppl. 8, K. D. Rainsford, K. Brune, and M. W. Whitehouse, Eds., Birkhauser, Basel, 1981, pp. 389–398.
[14] A. A. Alich and L. E. Wittmers, Jr., *J. Pharm. Sci.*, **69**, 725 (1980).
[15] J. R. J. Sorenson, *J. Pharm. Sci.*, **70(3)**, IV (1981).

Response to: "The Ulcerogenic Potential of Copper Aspirinate Seems to be More Imaginary than Real"

Dr. John Sorenson has responded to a paper in which we showed that when intact rat stomachs were subjected to aspirin or copper aspirinate under normal conditions of absorption, and when mucosal damage was highlighted with a protein-binding dye, observations differed from those made on Shay-prepared rats by Sorenson[1]. Our data indicated that copper aspirinate gave much larger superficial lesion indices and slightly smaller deep lesion indices than aspirin alone[2]. Dr. Sorenson's article contains several comments deserving of our response.

1. Dr. Sorenson, in taking exception to our results, makes frequent reference to studies which employed the Shay rat as a model. As we indicated in our paper, the Shay rat is quite a different model from ours. We attempted to approximate normal conditions under which drugs are presented to and absorbed from the stomach. We wish to reiterate that our model is different from the Shay model, and appears to produce different results. Since the Shay rat has frequently been used by other laboratories, an effort was made to refer to such data where appropriate.

2. Dr. Sorenson interprets the lesion index graphs incorrectly. The lesion index does not measure depth of color, but sums over the number of lesions of each diameter within one of the two color groups. Therefore, the index gives a number related to total area of mucosa damaged for each kind of lesion. Our paper indicates that the two color groups were independently verified by microscopic examination to be deep and superficial erosions, the deep erosions being a very dark blue, the superficial a royal blue. Dr. Sorenson hypothesizes that the color in the mucosa is caused by a dye-protein-copper complex formed when the copper is absorbed into the mucosa and the dye-protein complex leaves the vascular system. While this is an interesting hypothesis, it does not account for all of our results portrayed in Fig. 1A and B of our paper[2]. Dr. Sorenson's hypothesis may be possible or appropriate in A, for the sets of data containing Cu(II), but does not account for the lesion index in the controls or in those rats treated with aspirin. Likewise, in B of Fig. 1, the hypothesis may fit the last two sets of bars, but not the copper sulfate control or the rats treated with aspirin. Our observations from past work indicate that Cu(II) is absorbed into the mucosa whether complexed or not. In 1- or 2-h experimental periods similar to those described in our paper, but in which no dye was used, mucosal tissue exposed to copper-containing compounds, became a uniform grey-blue color and yielded extremely high values for copper analysis indicating that copper was absorbed into the tissue[3].

In any case, the amounts of copper present in our experiments would be too small to account for the extent of the coloration of the lesions. Likewise the hypothesis does not explain why there are two distinct shades of blue. Finally, the hypothesis cannot be applied to all the data presented in the paper.

3. Sorenson states that appearance of the protein-dye complex in the mucosa under the conditions of our experiment "does not provide evidence of either erosions or vascular damage." He attributes the leakage to absorption-induced hyperemia. Under normal physiological conditions, Pontamine Sky Blue 6BX, and other protein-binding dyes, do not leak from the vascular system in any significant amount[4]. The protein movement from the vascular volume into the interstitial space is very slow, as indicated by the small permeability coefficients for molecules of this size range. All animals in our experiments were sacrificed 10 min post dye injection. The discussion in our paper details the damage to blood vessels which allows leakage of the protein–dye complex into the tissue. Use of a protein-bound dye to aid assessment of mucosal damage is not unique with us. Dr. Sorenson is aware of the papers of West and co-workers[5,6] who also used this method.

4. Dr. Sorenson, commenting on our observations of hemorrhage in the absence of visible erosions, claims we ". . . offered no rationale as to how this hemorrhage which occurred in the absence of erosions was relevant to their gastric study or in any way supported their interpretation of their results." Sorenson appears not to have understood the description of Robins' work[7]. Robins observed (electron microscope) that prior to the appearance of visible mucosal erosions, and within minutes of being placed in the stomach, aspirin caused small blood vessels to develop fenestrations and later to break down completely[7]. These observations lend support to our suggestion that bleeding occurs prior to the appearance of visible lesions. Our paper describes samples which were found, on microscopic examination, to have no lesions, but by the dye method to present superficial erosions. The extravascular accumulation of the protein-dye complex in these cases indicated that the capillary endothelium was damaged prior to the development of the lesions. We also observed complete ischemia in the centers of a number of erosions, suggesting that the circulation was severely disrupted in these areas within the 2-h exposure to the drug.

5. Dr. Sorenson refers to a reduction in gastric acid secretion in response to the treatment of the Shay rat with copper complexes. The Sorenson reference given[8] contains no mention of the measurement of acid secretion. Further, other references described inhibition of acid secretion in Shay rats by copper–amino acid complexes[9,10]. Since controls were also Shay rats, it is not possible to determine whether the acid secretion was more or less than that in a non-Shay rat. It does not appear legitimate to extrapolate such results, in Shay rats, treated with copper–amino acid complexes, to non-Shay rats treated with copper aspirinate. West and co-workers (whose work Sorenson uses to buttress his arguments in this discussion) did not find the Shay-prepared rat to be the perfect model for testing activities of drugs[6].

6. Dr. Sorenson proposes that the complex of copper aspirinate is formed by the 10-min sonication of the Cu^{2+} and aspirin mixture to be placed in the stomach. He also proposes that $CuCO_3$ or "some other nonabsorbable form of copper" is formed from copper aspirinate during the sonication in the buffered system. This is an interesting proposal, the decomposition appearing more plausible than the formation of the complex (although in our thermal analysis experiments decomposition is not observed below 265°C). In any case, it does not seem to be legitimate to propose two opposite effects by the same sonication.

7. Dr. Sorenson states that we "incorrectly indicated" that he had reported that aspirin was an active antiulcer agent in the Shay rat. Our reference is to a specific paper[1], in which the statement is made (on p. 139): "Aspirin and anthranilic acid were active at 225 mg/kg ig. Again, if this is real activity in this model then these two compounds lack potency. The question as to whether or not these are irritant-induced or false positive results remains to be answered."

0022-3549/84/1200-1876$01.00/0
© 1984, American Pharmaceutical Association

Alich *et al.*[1] claimed that many possible variables introduced by others had been eliminated from their studies, but failed to recognize that they had introduced new variables that others had not introduced and that their results are subject to an alternative interpretation. As it turns out, this is the second paper coauthored by Alich and Wittmers on the subject of $Cu(II)_2(aspirinate)_4$ wherein conclusions were not supported by the evidence provided. In an earlier paper[14] these authors contended that salicylic acid was a contaminant of $Cu(II)_2(aspirinate)_4$, but failed to provide evidence in support of this contention[15]. The present contention by Alich *et al.* that $Cu(II)_2(aspirinate)_4$ causes erosions and vascular leakage at a dose of 100 mg/kg is not supported by evidence and it is also clearly inconsistent with results reported by ourselves and others they cited. Results obtained by Alich *et al.*[1] may be better interpreted in terms of absorption of copper compounds.

John R. J. Sorenson
University of Arkansas
College of Pharmacy
Little Rock, AR 72205

[1] A. A. Alich, V. J. Welch, and L. E. Wittmers, Jr., *J. Pharm. Sci.*, **72**, 1457 (1983).
[2] D. A. Williams, D. T. Waltz, and W. O. Foye, *J. Pharm. Sci.*, **65**, 126 (1976).
[3] J. R. J. Sorenson, T. M. Rolniak, and L. W. Chang, *Inorg. Chim. Acta*, **91**, L31 (1984).
[4] J. R. J. Sorenson, *J. Med. Chem.*, **19**, 135 (1976).
[5] F. Marletta, E. Rizzarelli, A. Mangiameli, M. Alberghina, A. Brogna, S. Sammartano, and A. Blasi, *Rend. Gastroenterol.* **9** Suppl. 1, 35 (1977).
[6] F. Marletta, E. Rizzarelli, A. Mangiameli, M. Alberghina, A. Brogna, S. Monaco, S. Sammartano, and A. Blasi, "The XIVth International Congress on Internal Medicine," October 1978, pp. 132 and 133.
[7] R. Goburdhun, K. Gulrez, H. Haruna, and G. B. West, *J. Pharmacol. Meth.*, **1**, 109 (1978).
[8] G. B. West, *J. Pharmacol. Meth.*, **8**, 33 (1982).
[9] L. J. Hayden, G. Thomas, and G. B. West, *J. Pharm. Pharmacol.* **30**, 244 (1978).
[10] K. D. Rainsford and M. W. Whitehouse, *J. Pharm. Pharmacol.*, **28**, 83 (1976).
[11] J. R. J. Sorenson, *J. Pharm. Pharmacol.*, **29**, 450 (1977).
[12] E. Boyle, P. C. Freeman, A. C. Goudie, F. R. Mangan, and M. Thompson, *J. Pharm. Pharmacol.*, **28**, 865 (1976).
[13] S. F. Townsend and J. R. J. Sorenson, in "Trace Elements in the Pathogenesis and Treatment of Inflammatory Conditions," Agents and Actions Suppl. 8, K. D. Rainsford, K. Brune, and M. W. Whitehouse, Eds., Birkhauser, Basel, 1981, pp. 389–398.
[14] A. A. Alich and L. E. Wittmers, Jr., *J. Pharm. Sci.*, **69**, 725 (1980).
[15] J. R. J. Sorenson, *J. Pharm. Sci.*, **70(3)**, IV (1981).

Response to: "The Ulcerogenic Potential of Copper Aspirinate Seems to be More Imaginary than Real"

Dr. John Sorenson has responded to a paper in which we showed that when intact rat stomachs were subjected to aspirin or copper aspirinate under normal conditions of absorption, and when mucosal damage was highlighted with a protein-binding dye, observations differed from those made on Shay-prepared rats by Sorenson[1]. Our data indicated that copper aspirinate gave much larger superficial lesion indices and slightly smaller deep lesion indices than aspirin alone[2]. Dr. Sorenson's article contains several comments deserving of our response.

1. Dr. Sorenson, in taking exception to our results, makes frequent reference to studies which employed the Shay rat as a model. As we indicated in our paper, the Shay rat is quite a different model from ours. We attempted to approximate normal conditions under which drugs are presented to and absorbed from the stomach. We wish to reiterate that our model is different from the Shay model, and appears to produce different results. Since the Shay rat has frequently been used by other laboratories, an effort was made to refer to such data where appropriate.

2. Dr. Sorenson interprets the lesion index graphs incorrectly. The lesion index does not measure depth of color, but sums over the number of lesions of each diameter within one of the two color groups. Therefore, the index gives a number related to total area of mucosa damaged for each kind of lesion. Our paper indicates that the two color groups were independently verified by microscopic examination to be deep and superficial erosions, the deep erosions being a very dark blue, the superficial a royal blue. Dr. Sorenson hypothesizes that the color in the mucosa is caused by a dye-protein-copper complex formed when the copper is absorbed into the mucosa and the dye-protein complex leaves the vascular system. While this is an interesting hypothesis, it does not account for all of our results portrayed in Fig. 1A and B of our paper[2]. Dr. Sorenson's hypothesis may be possible or appropriate in A, for the sets of data containing Cu(II), but does not account for the lesion index in the controls or in those rats treated with aspirin. Likewise, in B of Fig. 1, the hypothesis may fit the last two sets of bars, but not the copper sulfate control or the rats treated with aspirin. Our observations from past work indicate that Cu(II) is absorbed into the mucosa whether complexed or not. In 1- or 2-h experimental periods similar to those described in our paper, but in which no dye was used, mucosal tissue exposed to copper-containing compounds, became a uniform grey-blue color and yielded extremely high values for copper analysis indicating that copper was absorbed into the tissue[3].

In any case, the amounts of copper present in our experiments would be too small to account for the extent of the coloration of the lesions. Likewise the hypothesis does not explain why there are two distinct shades of blue. Finally, the hypothesis cannot be applied to all the data presented in the paper.

3. Sorenson states that appearance of the protein-dye complex in the mucosa under the conditions of our experiment "does not provide evidence of either erosions or vascular damage." He attributes the leakage to absorption-induced hyperemia. Under normal physiological conditions, Pontamine Sky Blue 6BX, and other protein-binding dyes, do not leak from the vascular system in any significant amount[4]. The protein movement from the vascular volume into the interstitial space is very slow, as indicated by the small permeability coefficients for molecules of this size range. All animals in our experiments were sacrificed 10 min post dye injection. The discussion in our paper details the damage to blood vessels which allows leakage of the protein–dye complex into the tissue. Use of a protein-bound dye to aid assessment of mucosal damage is not unique with us. Dr. Sorenson is aware of the papers of West and co-workers[5,6] who also used this method.

4. Dr. Sorenson, commenting on our observations of hemorrhage in the absence of visible erosions, claims we ". . . offered no rationale as to how this hemorrhage which occurred in the absence of erosions was relevant to their gastric study or in any way supported their interpretation of their results." Sorenson appears not to have understood the description of Robins' work[7]. Robins observed (electron microscope) that prior to the appearance of visible mucosal erosions, and within minutes of being placed in the stomach, aspirin caused small blood vessels to develop fenestrations and later to break down completely[7]. These observations lend support to our suggestion that bleeding occurs prior to the appearance of visible lesions. Our paper describes samples which were found, on microscopic examination, to have no lesions, but by the dye method to present superficial erosions. The extravascular accumulation of the protein-dye complex in these cases indicated that the capillary endothelium was damaged prior to the development of the lesions. We also observed complete ischemia in the centers of a number of erosions, suggesting that the circulation was severely disrupted in these areas within the 2-h exposure to the drug.

5. Dr. Sorenson refers to a reduction in gastric acid secretion in response to the treatment of the Shay rat with copper complexes. The Sorenson reference given[8] contains no mention of the measurement of acid secretion. Further, other references described inhibition of acid secretion in Shay rats by copper–amino acid complexes[9,10]. Since controls were also Shay rats, it is not possible to determine whether the acid secretion was more or less than that in a non-Shay rat. It does not appear legitimate to extrapolate such results, in Shay rats, treated with copper–amino acid complexes, to non-Shay rats treated with copper aspirinate. West and co-workers (whose work Sorenson uses to buttress his arguments in this discussion) did not find the Shay-prepared rat to be the perfect model for testing activities of drugs[6].

6. Dr. Sorenson proposes that the complex of copper aspirinate is formed by the 10-min sonication of the Cu^{2+} and aspirin mixture to be placed in the stomach. He also proposes that $CuCO_3$ or "some other nonabsorbable form of copper" is formed from copper aspirinate during the sonication in the buffered system. This is an interesting proposal, the decomposition appearing more plausible than the formation of the complex (although in our thermal analysis experiments decomposition is not observed below 265°C). In any case, it does not seem to be legitimate to propose two opposite effects by the same sonication.

7. Dr. Sorenson states that we "incorrectly indicated" that he had reported that aspirin was an active antiulcer agent in the Shay rat. Our reference is to a specific paper[1], in which the statement is made (on p. 139): "Aspirin and anthranilic acid were active at 225 mg/kg ig. Again, if this is real activity in this model then these two compounds lack potency. The question as to whether or not these are irritant-induced or false positive results remains to be answered."

0022-3549/84/1200-1876$01.00/0
© 1984, American Pharmaceutical Association

These are the major points relevant to this study on which we would differ from Dr. Sorenson's interpretation of our work. It is somewhat difficult to respond to some of his statements because no data is given to support the claims made. For example, Dr. Sorenson challenges the widely accepted use of a protein-binding dye and proposes in its place an "absorption-induced" hyperemia; no substantiating evidence is presented. He proposes a difference in the rate of absorption of the different copper-containing species, giving as evidence only an oleyl alcohol/water partition coefficient for copper aspirinate/aspirin[11]. He proposes both formation and decomposition of copper complexes by sonication, again with no evidence given. Dr. Sorenson states that we neglected to report, in our survey of experiments, that he had pointed out in print[12] that a Rainsford and Whitehouse paper was flawed by the use of an inappropriate suspending agent[13]. No supporting evidence was given.

In conclusion, this challenge of our results is not a legitimate one. We believe that under the experimental conditions employed, copper aspirinate does not appear to be less damaging than aspirin. Further work is in process on the mechanism and characteristics of the gastric mucosal damage inflicted by the copper complex of aspirin as well as that of aspirin in combination with copper.

After consideration of Dr. Sorenson's concerns, as well as a review of the literature, we believe that a more thorough comparison of models is warranted. West and co-workers[5,6] have compared mucosal damage from aspirin and copper aspirinate in the stress-induced, Shay, and drug-induced ulcer models. A study is planned to compare these with the unstressed model in which the ulcers or erosions are caused by the presentation of the drug under study.

A. A. Alich[x]
College of St. Scholastica
Department of Chemistry
Duluth, MN 55811

L. E. Wittmers, Jr.
School of Medicine
University of Minnesota-Duluth
Department of Physiology
Duluth, MN 55812

[1] J. R. J. Sorenson, *J. Med. Chem.*, **19**, 135 (1976).
[2] A. A. Alich, V. J. Welsh, and L. E. Wittmers, Jr., *J. Pharm. Sci.*, **72**, 1457 (1983).
[3] Unpublished results.
[4] E. M. Renkin, *Acta Physiol. Scand.*, **463 Suppl.**, 81 (1979).
[5] G. B. West, *J. Pharmacol. Meth.*, **8**, 33 (1982).
[6] L. H. Hayden, G. Thomas, and G. B. West, *J. Pharm. Pharmacol.*, **30**, 244 (1978).
[7] P. G. Robins, *Br. J. Exp. Pathol.*, **61**, 497 (1980).
[8] J. R. Sorenson, T. M. Rolniak, and L. W. Chang, *Inorg. Chim. Acta (Lett.)*, **91**, L31 (1984).
[9] F. Marletta, F. Rizzarelli, A. Mangiameli, M. Alberghina, A. Brogna, S. Sammartano, S. Monaco, and A. Blasi, "XIVth International Congress on Internal Medicine," Rome, 1978, Abstr. p. 132.
[10] M. Alberghina, A. Brogna, A. Mangiameli, F. Marletta, F. Rizzarelli and S. Sammartano, *Il. Farmaco—Ed. Sci.*, **37**, 805 (1982).
[11] D. A. Williams, D. T. Walz, and W. O. Foye, *J. Pharm. Sci.*, **65**, 126 (1976).
[12] J. R. J. Sorenson, *J. Pharm. Pharmacol.*, **29**, 450 (1977).
[13] K. D. Rainsford and M. W. Whitehouse, *J. Pharm. Pharmacol.*, **28**, 83 (1976).

Pharmaceutical Company Data on Drugs in Breast Milk

The World Health Organization Regional Office for Europe has recently established a Working Group to produce a monograph describing the present state of information about drug excretion in breast milk and the hazards, if any, to the suckling infant. The Group is currently reviewing published literature but is aware that other data may be maintained by drug companies in internal files. The Group would welcome the opportunity to evaluate such information with a view to including it in the monograph. Drug companies which have in their possession unpublished data on excretion of drugs in breast milk are asked to contact:

P.N. Bennett, MD FRCP
School of Pharmacy and Pharmacology
University of Bath
Claverton Down
Bath
Avon BA2 7AY
England

ERRATA

In the article "Determination of Pantothenic Acid in Multivitamin Pharmaceutical Preparations by Reverse-Phase High-Performance Liquid Chromatography" (1), the following should be noted:

On page 114, Figures 1 and 2 were transposed.

(1) T. J. Hudson and R. J. Allen, *J. Pharm. Sci.*, **73**, 113 (1984).

In the article "Diaspirins of Methylenecitric Acid" (1), the following correction should be made:

On page 419, in the last line in Table I the compound name should read [Bis(3,5-dibromo-2-carboxyphenyl)fumarate].

(1) S. E. Massil, G.-Y. Shi, and I. M. Klotz, *J. Pharm. Sci.*, **73**, 418 (1984).

In the article "Physicochemical Model for Dose-Dependent Drug Absorption" (1), the following correction should be made:

On page 1278, in the *Appendix*, the last line should read $R_i = k_{ai} f_{ui} \times C_i V_i$.

(1) J. B. Dressman, D. Fleisher, and G. L. Amidon, *J. Pharm. Sci.*, **73**, 1274 (1984).

0022-3549/84/1200-1877$01.00/0
© 1984, American Pharmaceutical Association

These are the major points relevant to this study on which we would differ from Dr. Sorenson's interpretation of our work. It is somewhat difficult to respond to some of his statements because no data is given to support the claims made. For example, Dr. Sorenson challenges the widely accepted use of a protein-binding dye and proposes in its place an "absorption-induced" hyperemia; no substantiating evidence is presented. He proposes a difference in the rate of absorption of the different copper-containing species, giving as evidence only an oleyl alcohol/water partition coefficient for copper aspirinate/aspirin[11]. He proposes both formation and decomposition of copper complexes by sonication, again with no evidence given. Dr. Sorenson states that we neglected to report, in our survey of experiments, that he had pointed out in print[12] that a Rainsford and Whitehouse paper was flawed by the use of an inappropriate suspending agent[13]. No supporting evidence was given.

In conclusion, this challenge of our results is not a legitimate one. We believe that under the experimental conditions employed, copper aspirinate does not appear to be less damaging than aspirin. Further work is in process on the mechanism and characteristics of the gastric mucosal damage inflicted by the copper complex of aspirin as well as that of aspirin in combination with copper.

After consideration of Dr. Sorenson's concerns, as well as a review of the literature, we believe that a more thorough comparison of models is warranted. West and co-workers[5,6] have compared mucosal damage from aspirin and copper aspirinate in the stress-induced, Shay, and drug-induced ulcer models. A study is planned to compare these with the unstressed model in which the ulcers or erosions are caused by the presentation of the drug under study.

A. A. Alich[x]
College of St. Scholastica
Department of Chemistry
Duluth, MN 55811

L. E. Wittmers, Jr.
School of Medicine
University of Minnesota-Duluth
Department of Physiology
Duluth, MN 55812

[1] J. R. J. Sorenson, *J. Med. Chem.*, **19**, 135 (1976).
[2] A. A. Alich, V. J. Welsh, and L. E. Wittmers, Jr., *J. Pharm. Sci.*, **72**, 1457 (1983).
[3] Unpublished results.
[4] E. M. Renkin, *Acta Physiol. Scand.*, **463 Suppl.**, 81 (1979).
[5] G. B. West, *J. Pharmacol. Meth.*, **8**, 33 (1982).
[6] L. H. Hayden, G. Thomas, and G. B. West, *J. Pharm. Pharmacol.*, **30**, 244 (1978).
[7] P. G. Robins, *Br. J. Exp. Pathol.*, **61**, 497 (1980).
[8] J. R. Sorenson, T. M. Rolniak, and L. W. Chang, *Inorg. Chim. Acta (Lett.)*, **91**, L31 (1984).
[9] F. Marletta, F. Rizzarelli, A. Mangiameli, M. Alberghina, A. Brogna, S. Sammartano, S. Monaco, and A. Blasi, "XIVth International Congress on Internal Medicine," Rome, 1978, Abstr. p. 132.
[10] M. Alberghina, A. Brogna, A. Mangiameli, F. Marletta, F. Rizzarelli and S. Sammartano, *Il. Farmaco—Ed. Sci.*, **37**, 805 (1982).
[11] D. A. Williams, D. T. Walz, and W. O. Foye, *J. Pharm. Sci.*, **65**, 126 (1976).
[12] J. R. J. Sorenson, *J. Pharm. Pharmacol.*, **29**, 450 (1977).
[13] K. D. Rainsford and M. W. Whitehouse, *J. Pharm. Pharmacol.*, **28**, 83 (1976).

Pharmaceutical Company Data on Drugs in Breast Milk

The World Health Organization Regional Office for Europe has recently established a Working Group to produce a monograph describing the present state of information about drug excretion in breast milk and the hazards, if any, to the suckling infant. The Group is currently reviewing published literature but is aware that other data may be maintained by drug companies in internal files. The Group would welcome the opportunity to evaluate such information with a view to including it in the monograph. Drug companies which have in their possession unpublished data on excretion of drugs in breast milk are asked to contact:

P.N. Bennett, MD FRCP
School of Pharmacy and Pharmacology
University of Bath
Claverton Down
Bath
Avon BA2 7AY
England

ERRATA

In the article "Determination of Pantothenic Acid in Multivitamin Pharmaceutical Preparations by Reverse-Phase High-Performance Liquid Chromatography" (1), the following should be noted:

On page 114, Figures 1 and 2 were transposed.

(1) T. J. Hudson and R. J. Allen, *J. Pharm. Sci.*, **73**, 113 (1984).

In the article "Diaspirins of Methylenecitric Acid" (1), the following correction should be made:

On page 419, in the last line in Table I the compound name should read [Bis(3,5-dibromo-2-carboxyphenyl)fumarate].

(1) S. E. Massil, G.-Y. Shi, and I. M. Klotz, *J. Pharm. Sci.*, **73**, 418 (1984).

In the article "Physicochemical Model for Dose-Dependent Drug Absorption" (1), the following correction should be made:

On page 1278, in the *Appendix*, the last line should read $R_i = k_{ai} f_{ui} \times C_i V_i$.

(1) J. B. Dressman, D. Fleisher, and G. L. Amidon, *J. Pharm. Sci.*, **73**, 1274 (1984).

0022-3549/84/1200-1877$01.00/0
© 1984, American Pharmaceutical Association

These are the major points relevant to this study on which we would differ from Dr. Sorenson's interpretation of our work. It is somewhat difficult to respond to some of his statements because no data is given to support the claims made. For example, Dr. Sorenson challenges the widely accepted use of a protein-binding dye and proposes in its place an "absorption-induced" hyperemia; no substantiating evidence is presented. He proposes a difference in the rate of absorption of the different copper-containing species, giving as evidence only an oleyl alcohol/water partition coefficient for copper aspirinate/aspirin[11]. He proposes both formation and decomposition of copper complexes by sonication, again with no evidence given. Dr. Sorenson states that we neglected to report, in our survey of experiments, that he had pointed out in print[12] that a Rainsford and Whitehouse paper was flawed by the use of an inappropriate suspending agent[13]. No supporting evidence was given.

In conclusion, this challenge of our results is not a legitimate one. We believe that under the experimental conditions employed, copper aspirinate does not appear to be less damaging than aspirin. Further work is in process on the mechanism and characteristics of the gastric mucosal damage inflicted by the copper complex of aspirin as well as that of aspirin in combination with copper.

After consideration of Dr. Sorenson's concerns, as well as a review of the literature, we believe that a more thorough comparison of models is warranted. West and co-workers[5,6] have compared mucosal damage from aspirin and copper aspirinate in the stress-induced, Shay, and drug-induced ulcer models. A study is planned to compare these with the unstressed model in which the ulcers or erosions are caused by the presentation of the drug under study.

A. A. Alich[x]
College of St. Scholastica
Department of Chemistry
Duluth, MN 55811

L. E. Wittmers, Jr.
School of Medicine
University of Minnesota-Duluth
Department of Physiology
Duluth, MN 55812

[1] J. R. J. Sorenson, *J. Med. Chem.*, **19**, 135 (1976).
[2] A. A. Alich, V. J. Welsh, and L. E. Wittmers, Jr., *J. Pharm. Sci.*, **72**, 1457 (1983).
[3] Unpublished results.
[4] E. M. Renkin, *Acta Physiol. Scand.*, **463 Suppl.**, 81 (1979).
[5] G. B. West, *J. Pharmacol. Meth.*, **8**, 33 (1982).
[6] L. H. Hayden, G. Thomas, and G. B. West, *J. Pharm. Pharmacol.*, **30**, 244 (1978).
[7] P. G. Robins, *Br. J. Exp. Pathol.*, **61**, 497 (1980).
[8] J. R. Sorenson, T. M. Rolniak, and L. W. Chang, *Inorg. Chim. Acta (Lett.)*, **91**, L31 (1984).
[9] F. Marletta, F. Rizzarelli, A. Mangiameli, M. Alberghina, A. Brogna, S. Sammartano, S. Monaco, and A. Blasi, "XIVth International Congress on Internal Medicine," Rome, 1978, Abstr. p. 132.
[10] M. Alberghina, A. Brogna, A. Mangiameli, F. Marletta, F. Rizzarelli and S. Sammartano, *Il. Farmaco—Ed. Sci.*, **37**, 805 (1982).
[11] D. A. Williams, D. T. Walz, and W. O. Foye, *J. Pharm. Sci.*, **65**, 126 (1976).
[12] J. R. J. Sorenson, *J. Pharm. Pharmacol.*, **29**, 450 (1977).
[13] K. D. Rainsford and M. W. Whitehouse, *J. Pharm. Pharmacol.*, **28**, 83 (1976).

Pharmaceutical Company Data on Drugs in Breast Milk

The World Health Organization Regional Office for Europe has recently established a Working Group to produce a monograph describing the present state of information about drug excretion in breast milk and the hazards, if any, to the suckling infant. The Group is currently reviewing published literature but is aware that other data may be maintained by drug companies in internal files. The Group would welcome the opportunity to evaluate such information with a view to including it in the monograph. Drug companies which have in their possession unpublished data on excretion of drugs in breast milk are asked to contact:

P.N. Bennett, MD FRCP
School of Pharmacy and Pharmacology
University of Bath
Claverton Down
Bath
Avon BA2 7AY
England

ERRATA

In the article "Determination of Pantothenic Acid in Multivitamin Pharmaceutical Preparations by Reverse-Phase High-Performance Liquid Chromatography" (1), the following should be noted:

On page 114, Figures 1 and 2 were transposed.

(1) T. J. Hudson and R. J. Allen, *J. Pharm. Sci.*, **73**, 113 (1984).

In the article "Diaspirins of Methylenecitric Acid" (1), the following correction should be made:

On page 419, in the last line in Table I the compound name should read [Bis(3,5-dibromo-2-carboxyphenyl)fumarate].

(1) S. E. Massil, G.-Y. Shi, and I. M. Klotz, *J. Pharm. Sci.*, **73**, 418 (1984).

In the article "Physicochemical Model for Dose-Dependent Drug Absorption" (1), the following correction should be made:

On page 1278, in the *Appendix*, the last line should read $R_i = k_{ai} f_{ui} \times C_i V_i$.

(1) J. B. Dressman, D. Fleisher, and G. L. Amidon, *J. Pharm. Sci.*, **73**, 1274 (1984).

0022-3549/84/1200-1877$01.00/0
© 1984, American Pharmaceutical Association

X-ray Crystallography and Drug Action. Edited by A. S. HORN and C. J. DE RANTER. Oxford University Press, 200 Madison Avenue, New York, NY 10016. 1984. 514 pp. 16 × 24 cm. Price: $59.00.

The International School of Crystallography at the Ettore Majorana Centre in Erice, Sicily, sponsors an annual week-long course devoted to one of the various interdisciplinary subdivisions of crystallography. In the spring of 1983, the ninth course was devoted to the subject of X-ray crystallography and drug action. This book is a collection of the twenty-seven papers presented at the course.

The first six papers are general reviews of the ways in which the results of both small molecule and macromolecular crystal structure determinations are applied to problems in pharmaceutical chemistry. Discussions of selected basic principles of crystal structure determination and of quantum chemical calculations are included. They are technically sound, but not so rigorous as to encourage a noncrystallographer to pass on to the next paper. The last four papers in the book are similarly comprehensive in their coverage of aspects of graphics and molecular modeling.

Most of the volume is devoted to presentations of research studies of a variety of biological systems. Pharmacologists, biochemists, and crystallographers interact in many mutually supportive ways. Two papers on the dihydrofolate reductase-thymidylate synthetase system as a therapeutic target for the treatment of a variety of diseases describe this relationship with exceptional clarity. Analgesics and neuroactive drugs are treated with similar thoroughness. The remaining presentations are so broad in scope that no summary of reasonable length could do them justice.

As with any effort involving many authors, there are places where this book falls short of its potential. The reader is denied the benefit of summaries of what must have been exciting discussions after each presentation. No single paper is concerned primarily with polymorphism, an omission which will disappoint pharmaceutical chemists. Perhaps an even more serious omission is that, with several of the contributions discussing enantiomeric effects upon drug activity, crystallographic studies of spontaneous resolution in drugs are not even considered in the review papers.

From a technical point of view, the book is extremely well produced. The typescripts provided by the authors are generally clear. Very few typographical errors were discovered. For the most part, the figures are well done and clearly labeled. A few of the stereoscopic pairs are so closely set that some individuals may encounter difficulty in achieving stereopsis, even with the aid of a viewer. The subject index could have been more complete and consistent, particularly with reference to citations of drugs by name. Computer programs are indexed by name rather than by function. This is unnecessarily confusing, since the former might well be obscure to the noncrystallographer, as well as being unrelated to the latter.

When one considers the price of this volume in relation to others of similar coverage, it is certainly modestly priced. Even with the omissions and technical shortcomings noted, the overall strength of the discussions of structure activity relationships in proteins, enzymes, and their complexes with smaller molecules makes this book a worthwhile addition to the personal library of most pharmaceutical chemists.

Reviewed by Wilson H. De Camp
Division of Drug Chemistry
Food and Drug Administration
Washington, DC 20204

Fungal Metabolites. Vol. II. By W. B. TURNER and D. C. ALDRIDGE. Academic Press, 111 Fifth Avenue, New York, NY 10003. 1983. 631 pp. 16 × 23.5 cm. Price: $80.00.

As a frequent and happy user of the first volume of *Fungal Metabolites* by Turner, it was a great pleasure to see the publication of this second volume in 1983. The first volume, published in 1971, is an extensive compilation of secondary (specific) metabolites of fungi organized into chapters largely on the basis of their biogenesis. Volume II is essentially a 10-year update that includes nearly 2,000 new metabolites. Chapters 1 and 2 from Volume I dealt with primary and secondary metabolism, and aspects of cultivation and secondary metabolism. These chapters are not included as separate topics in the new book, but the few developments in these areas are covered in other sections where appropriate. References to labeling experiments used in Volume I have been deleted, but Volume II contains much new important information on carbon-13 isotopic labeling experiments extensively utilized during the past decade in the elucidation of biosynthetic pathways.

The 1983 edition of *Fungal Metabolites* is divided into seven chapters of varying length. Chapters describe groups of metabolites which are: not from acetate (40 pp.—215 references); from fatty acids (10 pp.—59 references); from polyketides (168 pp.—731 references); from terpenes (141 pp.—593 references); from tricarboxylic acid cycle intermediates (16 pp.—75 references); from amino acids (72 pp.—389 references); miscellaneous compounds (37 pp.—180 references); and an addendum chapter (62 pp.—281 references). References for all but the last chapter date largely in the 1970's with a few citations from the 1960's and 1980. The addendum chapter is essentially an update of information on all classes of fungal metabolites covered in earlier chapters, and it includes literature citations from 1980, 1981, and a few into 1982.

The bulk of this book is loaded with useful illustrations and references, and the text provides good concise coloring for the structures shown. The empirical formula, organism, and subject indices make the book practically useful. This is especially so, since the authors took great care to maintain the same organization used in the original volume. It is also easy to cross-reference between the two volumes. This is an outstanding reference-work and it is a must for any laboratory seriously engaged in research on the topic of fungal metabolites.

Reviewed by John P. Rosazza
College of Pharmacy
University of Iowa
Iowa City, IA 52242

Pattern Recognition Approaches To Data Interpretation. By DIANE D. WOLFF and MICHAEL L. PARSONS. Plenum Press, 233 Spring St., New York, NY 10013. 1983. 223 pp. 17 × 26 cm. Price: $29.50.

This book is a "how to" description of the use of multivariate statistical packages in the evaluation of large arrays of chemical data. The authors focus primarily on techniques popularized in recent years under the general term, "pattern recognition" with a major emphasis on how to use and interpret ARTHUR (B. R. Kowalski, Laboratory of Chemometrics, Seattle, WA), SPSS (SPSS, Inc., Chicago, IL), and BMDP (Health Sciences Computing Facility, Los Angeles, CA). SAS (SAS Institute Inc., Cary, NC) and CLUSTAN (Scotland) are described to a somewhat lesser degree. The book is intended for investigators with little or no prior experience with data analysis nor with the above-mentioned statistical packages. Program descriptions, strengths, and implementation are linked to the particular versions of the packages used by the authors. For example, users of the 1977 and later versions of the ARTHUR program would be advised to refer to the manuals for those programs for program description and implementation and to the book for suggestions on problem statement, analysis, and interpretation.

Through the example of a single set of pollution data, the authors take the reader through the steps of data analysis from problem statement and data coding to final evaluation. The numerical techniques described and applied to the pollution data include data mapping, supervised and unsupervised learning algorithms, and univariate and bivariate statistics. The excellent discussion and demonstration of preliminary data evaluation and variable relationships is the major strength of this book. A minor weakness is that the opinions expressed by the authors concerning the utility-specific numerical techniques seem to be based on their experiences rather than rigorous statistical studies. The comparison of numerical techniques available in two or more packages will certainly be valued by chemists who are uncertain as to which packages better address a particular application.

Pattern Recognition Approaches to Data Interpretation is a long overdue addition to the wealth of monographs on chemometrics published over the past few years. It is unique in its applications oriented approach. The book is a recommended reader for novices and a resource for more experienced investigators.

Reviewed by Alice Harper
Department of Chemistry
University of Texas at El Paso
El Paso, TX 79968

X-ray Crystallography and Drug Action. Edited by A. S. HORN and C. J. DE RANTER. Oxford University Press, 200 Madison Avenue, New York, NY 10016. 1984. 514 pp. 16 × 24 cm. Price: $59.00.

The International School of Crystallography at the Ettore Majorana Centre in Erice, Sicily, sponsors an annual week-long course devoted to one of the various interdisciplinary subdivisions of crystallography. In the spring of 1983, the ninth course was devoted to the subject of X-ray crystallography and drug action. This book is a collection of the twenty-seven papers presented at the course.

The first six papers are general reviews of the ways in which the results of both small molecule and macromolecular crystal structure determinations are applied to problems in pharmaceutical chemistry. Discussions of selected basic principles of crystal structure determination and of quantum chemical calculations are included. They are technically sound, but not so rigorous as to encourage a noncrystallographer to pass on to the next paper. The last four papers in the book are similarly comprehensive in their coverage of aspects of graphics and molecular modeling.

Most of the volume is devoted to presentations of research studies of a variety of biological systems. Pharmacologists, biochemists, and crystallographers interact in many mutually supportive ways. Two papers on the dihydrofolate reductase-thymidylate synthetase system as a therapeutic target for the treatment of a variety of diseases describe this relationship with exceptional clarity. Analgesics and neuroactive drugs are treated with similar thoroughness. The remaining presentations are so broad in scope that no summary of reasonable length could do them justice.

As with any effort involving many authors, there are places where this book falls short of its potential. The reader is denied the benefit of summaries of what must have been exciting discussions after each presentation. No single paper is concerned primarily with polymorphism, an omission which will disappoint pharmaceutical chemists. Perhaps an even more serious omission is that, with several of the contributions discussing enantiomeric effects upon drug activity, crystallographic studies of spontaneous resolution in drugs are not even considered in the review papers.

From a technical point of view, the book is extremely well produced. The typescripts provided by the authors are generally clear. Very few typographical errors were discovered. For the most part, the figures are well done and clearly labeled. A few of the stereoscopic pairs are so closely set that some individuals may encounter difficulty in achieving stereopsis, even with the aid of a viewer. The subject index could have been more complete and consistent, particularly with reference to citations of drugs by name. Computer programs are indexed by name rather than by function. This is unnecessarily confusing, since the former might well be obscure to the noncrystallographer, as well as being unrelated to the latter.

When one considers the price of this volume in relation to others of similar coverage, it is certainly modestly priced. Even with the omissions and technical shortcomings noted, the overall strength of the discussions of structure activity relationships in proteins, enzymes, and their complexes with smaller molecules makes this book a worthwhile addition to the personal library of most pharmaceutical chemists.

Reviewed by Wilson H. De Camp
Division of Drug Chemistry
Food and Drug Administration
Washington, DC 20204

Fungal Metabolites. Vol. II. By W. B. TURNER and D. C. ALDRIDGE. Academic Press, 111 Fifth Avenue, New York, NY 10003. 1983. 631 pp. 16 × 23.5 cm. Price: $80.00.

As a frequent and happy user of the first volume of *Fungal Metabolites* by Turner, it was a great pleasure to see the publication of this second volume in 1983. The first volume, published in 1971, is an extensive compilation of secondary (specific) metabolites of fungi organized into chapters largely on the basis of their biogenesis. Volume II is essentially a 10-year update that includes nearly 2,000 new metabolites. Chapters 1 and 2 from Volume I dealt with primary and secondary metabolism, and aspects of cultivation and secondary metabolism. These chapters are not included as separate topics in the new book, but the few developments in these areas are covered in other sections where appropriate. References to labeling experiments used in Volume I have been deleted, but Volume II contains much new important information on carbon-13 isotopic labeling experiments extensively utilized during the past decade in the elucidation of biosynthetic pathways.

The 1983 edition of *Fungal Metabolites* is divided into seven chapters of varying length. Chapters describe groups of metabolites which are: not from acetate (40 pp.—215 references); from fatty acids (10 pp.—59 references); from polyketides (168 pp.—731 references); from terpenes (141 pp.—593 references); from tricarboxylic acid cycle intermediates (16 pp.—75 references); from amino acids (72 pp.—389 references); miscellaneous compounds (37 pp.—180 references); and an addendum chapter (62 pp.—281 references). References for all but the last chapter date largely in the 1970's with a few citations from the 1960's and 1980. The addendum chapter is essentially an update of information on all classes of fungal metabolites covered in earlier chapters, and it includes literature citations from 1980, 1981, and a few into 1982.

The bulk of this book is loaded with useful illustrations and references, and the text provides good concise coloring for the structures shown. The empirical formula, organism, and subject indices make the book practically useful. This is especially so, since the authors took great care to maintain the same organization used in the original volume. It is also easy to cross-reference between the two volumes. This is an outstanding reference-work and it is a must for any laboratory seriously engaged in research on the topic of fungal metabolites.

Reviewed by John P. Rosazza
College of Pharmacy
University of Iowa
Iowa City, IA 52242

Pattern Recognition Approaches To Data Interpretation. By DIANE D. WOLFF and MICHAEL L. PARSONS. Plenum Press, 233 Spring St., New York, NY 10013. 1983. 223 pp. 17 × 26 cm. Price: $29.50.

This book is a "how to" description of the use of multivariate statistical packages in the evaluation of large arrays of chemical data. The authors focus primarily on techniques popularized in recent years under the general term, "pattern recognition" with a major emphasis on how to use and interpret ARTHUR (B. R. Kowalski, Laboratory of Chemometrics, Seattle, WA), SPSS (SPSS, Inc., Chicago, IL), and BMDP (Health Sciences Computing Facility, Los Angeles, CA). SAS (SAS Institute Inc., Cary, NC) and CLUSTAN (Scotland) are described to a somewhat lesser degree. The book is intended for investigators with little or no prior experience with data analysis nor with the above-mentioned statistical packages. Program descriptions, strengths, and implementation are linked to the particular versions of the packages used by the authors. For example, users of the 1977 and later versions of the ARTHUR program would be advised to refer to the manuals for those programs for program description and implementation and to the book for suggestions on problem statement, analysis, and interpretation.

Through the example of a single set of pollution data, the authors take the reader through the steps of data analysis from problem statement and data coding to final evaluation. The numerical techniques described and applied to the pollution data include data mapping, supervised and unsupervised learning algorithms, and univariate and bivariate statistics. The excellent discussion and demonstration of preliminary data evaluation and variable relationships is the major strength of this book. A minor weakness is that the opinions expressed by the authors concerning the utility-specific numerical techniques seem to be based on their experiences rather than rigorous statistical studies. The comparison of numerical techniques available in two or more packages will certainly be valued by chemists who are uncertain as to which packages better address a particular application.

Pattern Recognition Approaches to Data Interpretation is a long overdue addition to the wealth of monographs on chemometrics published over the past few years. It is unique in its applications oriented approach. The book is a recommended reader for novices and a resource for more experienced investigators.

Reviewed by Alice Harper
Department of Chemistry
University of Texas at El Paso
El Paso, TX 79968

X-ray Crystallography and Drug Action. Edited by A. S. HORN and C. J. DE RANTER. Oxford University Press, 200 Madison Avenue, New York, NY 10016. 1984. 514 pp. 16 × 24 cm. Price: $59.00.

The International School of Crystallography at the Ettore Majorana Centre in Erice, Sicily, sponsors an annual week-long course devoted to one of the various interdisciplinary subdivisions of crystallography. In the spring of 1983, the ninth course was devoted to the subject of X-ray crystallography and drug action. This book is a collection of the twenty-seven papers presented at the course.

The first six papers are general reviews of the ways in which the results of both small molecule and macromolecular crystal structure determinations are applied to problems in pharmaceutical chemistry. Discussions of selected basic principles of crystal structure determination and of quantum chemical calculations are included. They are technically sound, but not so rigorous as to encourage a noncrystallographer to pass on to the next paper. The last four papers in the book are similarly comprehensive in their coverage of aspects of graphics and molecular modeling.

Most of the volume is devoted to presentations of research studies of a variety of biological systems. Pharmacologists, biochemists, and crystallographers interact in many mutually supportive ways. Two papers on the dihydrofolate reductase-thymidylate synthetase system as a therapeutic target for the treatment of a variety of diseases describe this relationship with exceptional clarity. Analgesics and neuroactive drugs are treated with similar thoroughness. The remaining presentations are so broad in scope that no summary of reasonable length could do them justice.

As with any effort involving many authors, there are places where this book falls short of its potential. The reader is denied the benefit of summaries of what must have been exciting discussions after each presentation. No single paper is concerned primarily with polymorphism, an omission which will disappoint pharmaceutical chemists. Perhaps an even more serious omission is that, with several of the contributions discussing enantiomeric effects upon drug activity, crystallographic studies of spontaneous resolution in drugs are not even considered in the review papers.

From a technical point of view, the book is extremely well produced. The typescripts provided by the authors are generally clear. Very few typographical errors were discovered. For the most part, the figures are well done and clearly labeled. A few of the stereoscopic pairs are so closely set that some individuals may encounter difficulty in achieving stereopsis, even with the aid of a viewer. The subject index could have been more complete and consistent, particularly with reference to citations of drugs by name. Computer programs are indexed by name rather than by function. This is unnecessarily confusing, since the former might well be obscure to the noncrystallographer, as well as being unrelated to the latter.

When one considers the price of this volume in relation to others of similar coverage, it is certainly modestly priced. Even with the omissions and technical shortcomings noted, the overall strength of the discussions of structure activity relationships in proteins, enzymes, and their complexes with smaller molecules makes this book a worthwhile addition to the personal library of most pharmaceutical chemists.

Reviewed by Wilson H. De Camp
Division of Drug Chemistry
Food and Drug Administration
Washington, DC 20204

Fungal Metabolites. Vol. II. By W. B. TURNER and D. C. ALDRIDGE. Academic Press, 111 Fifth Avenue, New York, NY 10003. 1983. 631 pp. 16 × 23.5 cm. Price: $80.00.

As a frequent and happy user of the first volume of *Fungal Metabolites* by Turner, it was a great pleasure to see the publication of this second volume in 1983. The first volume, published in 1971, is an extensive compilation of secondary (specific) metabolites of fungi organized into chapters largely on the basis of their biogenesis. Volume II is essentially a 10-year update that includes nearly 2,000 new metabolites. Chapters 1 and 2 from Volume I dealt with primary and secondary metabolism, and aspects of cultivation and secondary metabolism. These chapters are not included as separate topics in the new book, but the few developments in these areas are covered in other sections where appropriate. References to labeling experiments used in Volume I have been deleted, but Volume II contains much new important information on carbon-13 isotopic labeling experiments extensively utilized during the past decade in the elucidation of biosynthetic pathways.

The 1983 edition of *Fungal Metabolites* is divided into seven chapters of varying length. Chapters describe groups of metabolites which are: not from acetate (40 pp.—215 references); from fatty acids (10 pp.—59 references); from polyketides (168 pp.—731 references); from terpenes (141 pp.—593 references); from tricarboxylic acid cycle intermediates (16 pp.—75 references); from amino acids (72 pp.—389 references); miscellaneous compounds (37 pp.—180 references); and an addendum chapter (62 pp.—281 references). References for all but the last chapter date largely in the 1970's with a few citations from the 1960's and 1980. The addendum chapter is essentially an update of information on all classes of fungal metabolites covered in earlier chapters, and it includes literature citations from 1980, 1981, and a few into 1982.

The bulk of this book is loaded with useful illustrations and references, and the text provides good concise coloring for the structures shown. The empirical formula, organism, and subject indices make the book practically useful. This is especially so, since the authors took great care to maintain the same organization used in the original volume. It is also easy to cross-reference between the two volumes. This is an outstanding reference-work and it is a must for any laboratory seriously engaged in research on the topic of fungal metabolites.

Reviewed by John P. Rosazza
College of Pharmacy
University of Iowa
Iowa City, IA 52242

Pattern Recognition Approaches To Data Interpretation. By DIANE D. WOLFF and MICHAEL L. PARSONS. Plenum Press, 233 Spring St., New York, NY 10013. 1983. 223 pp. 17 × 26 cm. Price: $29.50.

This book is a "how to" description of the use of multivariate statistical packages in the evaluation of large arrays of chemical data. The authors focus primarily on techniques popularized in recent years under the general term, "pattern recognition" with a major emphasis on how to use and interpret ARTHUR (B. R. Kowalski, Laboratory of Chemometrics, Seattle, WA), SPSS (SPSS, Inc., Chicago, IL), and BMDP (Health Sciences Computing Facility, Los Angeles, CA). SAS (SAS Institute Inc., Cary, NC) and CLUSTAN (Scotland) are described to a somewhat lesser degree. The book is intended for investigators with little or no prior experience with data analysis nor with the above-mentioned statistical packages. Program descriptions, strengths, and implementation are linked to the particular versions of the packages used by the authors. For example, users of the 1977 and later versions of the ARTHUR program would be advised to refer to the manuals for those programs for program description and implementation and to the book for suggestions on problem statement, analysis, and interpretation.

Through the example of a single set of pollution data, the authors take the reader through the steps of data analysis from problem statement and data coding to final evaluation. The numerical techniques described and applied to the pollution data include data mapping, supervised and unsupervised learning algorithms, and univariate and bivariate statistics. The excellent discussion and demonstration of preliminary data evaluation and variable relationships is the major strength of this book. A minor weakness is that the opinions expressed by the authors concerning the utility-specific numerical techniques seem to be based on their experiences rather than rigorous statistical studies. The comparison of numerical techniques available in two or more packages will certainly be valued by chemists who are uncertain as to which packages better address a particular application.

Pattern Recognition Approaches to Data Interpretation is a long overdue addition to the wealth of monographs on chemometrics published over the past few years. It is unique in its applications oriented approach. The book is a recommended reader for novices and a resource for more experienced investigators.

Reviewed by Alice Harper
Department of Chemistry
University of Texas at El Paso
El Paso, TX 79968